ANGEWANDTE CHEMIE

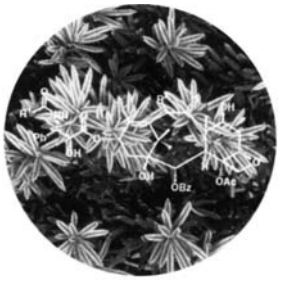
A Journal of the Gesellschaft Deutscher Chemiker

International Edition in English

1994
33/1
Page 1–130

COVER PICTURE

The cover picture shows the structural formula of taxol, $R^1 = Ph$, $R^2 = OAc$, superimposed on the needles of the European yew (photograph: S. C. Wilson, TIME–LIFE Magazine, USA). The source of this cytostatic agent till now has been the bark of the Pacific yew; however, about 3000 trees had to be sacrificed to obtain enough taxol to treat 500 patients. As a rapidly regenerable source of a precursor of taxol, the yew needles can help to remedy the situation, since the 10-deacetylbaccatin III isolable from them can be converted into, for instance, taxotere ($R^1 = t$BuO, $R^2 = OH$) or taxol. Nevertheless, more abundant taxol sources and methods to make taxol accessible by semisynthesis or total synthesis are being sought. The fascinating history of taxol, unfolding along the highly interwoven boundary between medicine, cellular biology, and organic chemistry, is summarized by Nicolaou et al. on pages 45–66.



REVIEWS

Contents

Is EXAFS spectroscopy a promising method? Yes, because the element-specific determination of local structures in situ is possible, regardless of the sample's physical state and even at very high dilution. In addition to the principle limitations of this method (differentiation cannot be made between neighboring elements in the periodic table, different backscatterers present at similar distances cannot yield unambiguous results), technical problems (only a few synchrotron radiation sources, data analysis only possible with extensive simulation programs) hinder the development. Although this method has not been in use for very long it has afforded interesting results, for example, in catalysis and the structural characterization of biological systems.

H. Bertagnolli,*
T. S. Ertel* 15–44

X-Ray Absorption Spectroscopy of Amorphous Solids, Liquids, and Catalytic and Biochemical Systems—Capabilities and Limitations

© VCH Verlagsgesellschaft mbH, D-69451 Weinheim, 1994

0570-0833/94/0101-0003 $ 10.00+.25/0

ANGEWANDTE CHEMIE

A Journal of the Gesellschaft Deutscher Chemiker

International Edition in English

Advisory Board: H. Brunner (Chairman), K. Cammann, G. Ertl, H. Offermanns, H. Paulsen, H.-J. Quadbeck-Seeger (Deputy Chairman), C. Rüchardt, H. Rudolph, W. Saenger, K. Sandhoff, D. Seebach, A. Simon, G. Wegner, E.-L. Winnacker

Editorial Office
Tel.: Int. + 6201/606-315 • Telefax: Int. + 6201/606-331 or -328
Telex: 465516 vchwh d • E-Mail: Z16@DHDURZ2 in Earn Bitnet

Postal address: Postfach 101161, D-69451 Weinheim (FRG)

Deliveries (also for courier services): Pappelallee 3, D-69469 Weinheim (FRG)

Editor: Peter Gölitz

Associate Editors: Neville A. Compton, Rachel H. Schmidt-Radde, Karen J. Schneider; Gerhard Karger (Book Editor)

Editorial Assistants: Jutta Göhrig, Eva Schweikart

Secretary: Claudia Heilmann • **Production:** Margitta Schmitt

Subscriptions: Beate Geiß (Tel. ext. 199) • **Marketing:** Ingrid Smieja (ext. 146)

Advertising: Norbert Schippel (ext. 312, fax ext. 328)

Publishers: VCH Verlagsgesellschaft/Verlag I
Postfach 101161, D-69451 Weinheim (FRG)

Managing Directors: Hans Dirk Köhler, Dr. Karlheinz Köpfer

Department Manager: Dr. Eva-Elisabeth Wille

Advertising and Marketing Manager: Rainer J. Roth • **Advertising Administration:** Maria Merkl

Bank connections (Bank, Acc. no., Bank identification code): Volksbank Weinheim, 11024807, 67092300; Dresdner Bank AG, 7511880, 67080050; Deutsche Bank, 5813209, 67070010; Bezirkssparkasse Weinheim, 00003662, 67052385; BW-Bank, 5113840200, 67020020; Postgiro-Frankfurt, 145314-600, 50010060; Postgiro-Karlsruhe, 21755-754, 66010075.

No. of issues: 22 per year

Valid price list for advertisements: No. 35 of October 1, 1993.

Subscription rates (including postage and handling charges): Annual subscription DM 1190.00, single issue DM 90.00. Subscription rates for members of the German Chemical Society (GDCh): regular members DM 288.00, student members DM 128.00.

Orders may be placed through your bookseller or—for members of the GDCh only—directly at the publishers:
Germany: Contact the Marketing Department.

Switzerland: VCH Verlags-AG, Hardstrasse 10, Postfach, CH-4020 Basel, Tel. (061) 271 06 06, Telex 911 527 DMS CH, Telefax (061) 271 0618.

United Kingdom: VCH Publishers (UK) Ltd., 8 Wellington Court, Wellington Street, Cambridge CB1 1HW, England, Tel. (0223) 321111, Telex 825372 turpin g, Telefax (0223) 313221.

USA and Canada: VCH Publishers Inc., 303 NW 12th Avenue, Deerfield Beach, FL 33442-1788; Telex 5101011104 VCHPUB; Telefax (305) 428-8201; Tel. (305) 428-5566 or (800) 422-8824.

Delivery: By direct mail (printed matter) or through booksellers. • **Change of address:** Please notify your bookseller or the publishers immediately. • **Cancellation of subscriptions:** The publishers must be notified not later than three months before the end of the calendar year.

Authors who wish to publish in *Angewandte Chemie International Edition* should consult the current "Notice to Authors", which is printed in the first issue of every year immediately after the Table of Contents, before they draft their manuscript.

Angewandte Chemie International Edition in English is the English version of *Angewandte Chemie*.

Registered names, trademarks, etc., used in this journal, even when not marked as such, are not to be considered unprotected by law.

All rights reserved (including those of translation into foreign languages). No part of this issue may be reproduced in any form—by photoprint, microfilm, or any other means—nor transmitted or translated into a machine language without the express written consent of the publishers.

This journal was carefully produced in all its parts. Nevertheless, authors, editor, and publisher do not warrant the information contained therein to be free of errors. Readers are advised to keep in mind that statements, data, illustrations, procedural details, or other items may inadvertently be inaccurate.

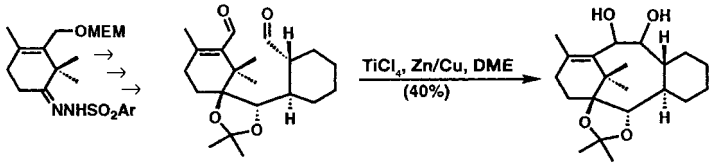
Valid for users in the USA: The appearance of the code at the bottom of the first page of an article in this journal (serial) indicates the copyright owner's consent that copies of the article may be made for personal or internal use, or for the personal or internal use of specific clients. This consent is given on the condition, however, that the copier pay the stated per-copy fee through the Copyright Clearance Center, Inc., for copying beyond that permitted by Sections 107 or 108 of the U.S. Copyright Law. This consent does not extend to other kinds of copying, such as a copying for general distribution, for advertising or promotional purposes, for creating new collective works, or for resale. For copying from back volumes of this journal see 'Permissions to Photo-Copy: Publisher's Fee List' of the CCC.

Printed in the Federal Republic of Germany by Konrad Triltsch Druck und Verlagsanstalt Würzburg GmbH. Printed on acid-free paper, bleached without the use of chlorine.

© VCH Verlagsgesellschaft mbH, D-69451 Weinheim, Federal Republic of Germany, 1994.

For the USA and Canada: ANGEWANDTE CHEMIE International Edition in English (ISSN 0570-0833) is published twice monthly except in August and December (22 issues) and distributed by VCH Publishers, Inc., 303 NW 12th Avenue, Deerfield Beach, FL 33442-1788; Telefax (305) 428-8201; Telephone (305) 428-5566 or (800) 367-8249. Annual subscription price: US$ 840/$895 (airmail) including postage and handling charges for institutions and $ 160/$ 190 (airmail) for individuals whose institution already subscribes, or who are retired or self-employed consultants. Second-Class Postage Paid at Deerfield Beach, FL. **POSTMASTER:** Send address changes to Angewandte Chemie IE, 303 NW 12th Avenue, Deerfield Beach, FL 33442-1788. Printed in the Federal Republic of Germany.

A promising antineoplastic chemotherapeutic but hampered by severely limited availability, taxol is described here together with its biological effects and the efforts to increase its accessibility through chemical synthesis. The challenges for the synthetic chemist lie in the eight-membered ring, the densely packed nature of the molecule, and the many oxygen functionalities. An arbitrarily chosen example of an approach to the ABC ring system of taxol is the sequence from **1** through several steps to **2** and finally to **3**.



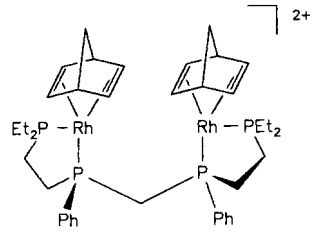
1 **2** **3**

K. C. Nicolaou,* W.-M. Dai, R. K. Guy 45–66

Chemistry and Biology of Taxol

HIGHLIGHTS

A breakthrough in tailor-made homogeneous catalysts has been achieved by Stanley et al., who synthesized the *rac*-Rh_2 complex **1** with a new tetraphosphane ligand, which catalyzes the hydroformylation of olefins with a high activity and extremely selectively. The combination of these important catalytic properties is traced back to the intramolecular interaction of the two Rh centers fixed by the ligand matrix.

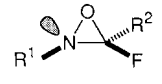


1

G. Süss-Fink* 67–69

Cooperativity in Rh_2 Complexes: High Catalytic Activity and High Regioselectivity in the Hydroformylation of Olefins

The functionalization of hydrocarbons by selective oxidation is of great technical importance. Two new, effective reagents, (perfluoroalkyl)oxaziridines **1a, b**, hydroxylate the C–H bonds at tertiary C atoms with high selectivity and in good yield. It remains to be seen if they are more economical and efficient than the tried-and-true dioxiranes and $RuCl_3/NaIO_4$.



1

a: $R^1 = C_4F_9$ $R^2 = C_3F_7$

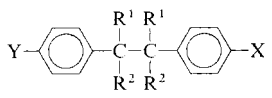
b: $R^1 = C_6F_{13}$ $R^2 = C_5F_{11}$

O. Reiser* 69–72

Oxidation of Weakly Activated C–H Bonds

COMMUNICATIONS

What is the functional relationship between the kinetics and thermodynamics for an elementary reaction in solution? This fundamental question was investigated for unimolecular fragmentations of C–C bonds in radical ions of bibenzylic substrates such as **1**. A Marcus-type free-energy relationship with a parabolic shape fitted the data well. The results imply that mesolytic cleavages have low intrinsic barriers (about 3 kcal mol^{-1}).

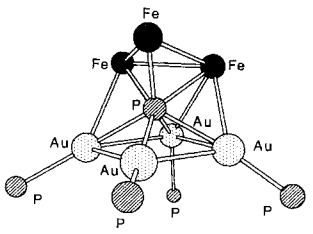


1: R^1, R^2 = Me, Et, Bu, CN, MeO
X, Y = H, MeO, CF_3, NO_2, CN, NMe_2

P. Maslak,* T. M. Vallombroso, W. H. Chapman, Jr., J. N. Narvaez 73–75

Free-Energy Relationship for Mesolytic Cleavage of C–C Bonds

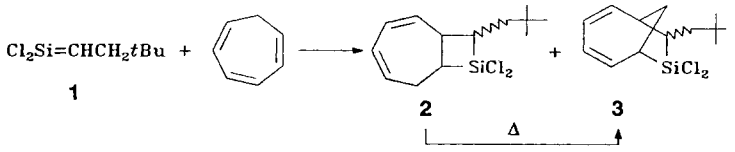
The seven-coordinate phosphorus atom in the title compound is bound to a slightly distorted square-planar Au_4 array (see structure on the right). Despite the fact that the phosphorus atom is donating all but two of its electrons to the Fe_3 cluster, it is still able to act as a nucleus for the aggregation of four gold fragments.



D. L. Sunick, P. S. White, C. K. Schauer* 75–77

A Cluster-Bound Triply-Bridging Phosphorus Atom Coordinated to Four $(Ph_3P)Au^+$ Units: $[Fe_3(CO)_9P\{Au(PPh_3)\}_4][BAr_4]$

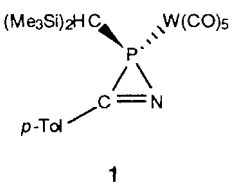
Silabicyclo[4.2.1]nonadienes 3 are two of the products of the reaction of silene **1** and cycloheptatriene. Besides these unusual [6+2] cycloadducts, the [2+2] cycloadducts also arise, which isomerize into **3** upon heating. The [4+2] and [2+2] adducts of 1,3-cycloheptadiene and **1** form competitively; the [2+2] cycloadducts rearrange to give the Diels–Alder products.



W. Ziche, C. Seidenschwarz, N. Auner,* E. Herdtweck, N. Sewald 77–80

Competing Reactions of Silenes: [2+2], [4+2], and [6+2] Cycloadditions with Cycloheptadiene and Cycloheptatriene

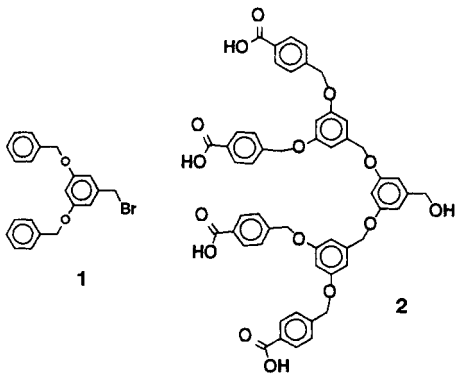
A novel compound with an unsaturated three-membered ring, 2*H*-1-aza-2-phosphirene, is present in complex **1**. This unusual ligand is formed in a surprisingly simple way in the reaction of the corresponding amino(aryl)-carbenepentacarbonyltungsten(0) complex with [bis(trimethylsilyl)methylene]chlorophosphane. The crucial step is the rearrangement of 2-aza-1-phospha-4-tungsta-1,3-butadiene to give the 2*H*-1-aza-2-phosphirene tungsten complex.



R. Streubel,* J. Jeske, P. G. Jones, R. Herbst-Irmer 80–82

Synthesis of the First 2*H*-1-Aza-2-phosphirene Complexes

An accelerated route to the synthesis of dendritic macromolecules through the use of fractal components larger than the repeating unit is described. The first-generation bromide **1** and the second-generation novel branched AB_4 monomer **2** can be used to prepare a highly regular fifth-generation poly(ether ester) dendrimer ($M_r = 9371$) in only three synthetic steps.



K. L. Wooley, C. J. Hawker, J. M. J. Fréchet* 82–85

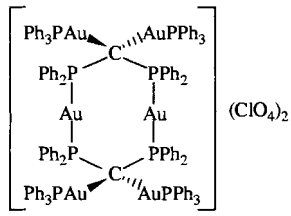
A "Branched-Monomer Approach" for the Rapid Synthesis of Dendimers

When $Ag_7O_8NO_3$ is heated in an O_2-free atmosphere between 300 and 930 K, its AgO units (300–480 K) are transformed into Ag_2O units (480–580 K) and ultimately into metallic Ag. A strongly chemisorbed O_γ species is found on the Ag surface at temperatures between 580 and 900 K which participates in the catalytic oxidation of methanol to give formaldehyde. The various O species were characterized by Raman spectroscopy.

B. Pettinger, X. Bao, I. Wilcock, M. Muhler, R. Schlögl, G. Ertl 85–87

Thermal Decomposition of Silver Oxide Monitored by Raman Spectroscopy: From AgO Units to Oxygen Atoms Chemisorbed on the Silver Surface

The pale yellow, air- and moisture-stable hexanuclear Au^I complex **1** contains a central $Au_2C_2P_4$ eight-membered ring with two additional $AuPPh_3$ groups coordinated to each peripheral carbon atom. The Au–Au distances in **1** are short and all Au atoms linearly coordinated.

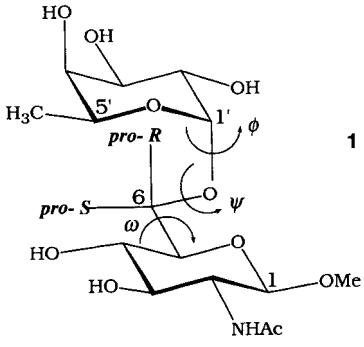


1

E. J. Fernández, M. C. Gimeno, P. G. Jones, A. Laguna,* M. Laguna, J. M. López-de-Luzuriaga 87–88

A Hexanuclear Gold(I) Complex: $[\{(Ph_3PAu)_2C(PPh_2AuPPh_2)\}_2](ClO_4)_2$

A significant preference for the (1 → 6) linkage, but not for a particular conformation with regard to this bond is shown by the agglutinin from *Aleuria aurantia* when it binds to carbohydrates with the fucose residue. This is revealed by NMR spectroscopic studies on the rather flexible disaccharide **1**, which showed that at least members of two major conformational families, *gg* and *gt*, are bound.

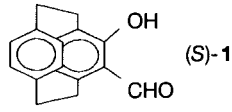


1

T. Weimar, T. Peters* 88–91

Aleuria aurantia Agglutinin Recognizes Multiple Conformations of α-L-Fuc-(1 → 6)-β-D-GlcNAc-OMe

A chiral analogue of salicylaldehyde, namely the [2.2]paracyclophane derivative **1**, was synthesized and resolved into enantiomers. The potential use of the new recoverable chiral auxiliary is illustrated by the asymmetric synthesis of some β-hydroxy-α-amino acids.

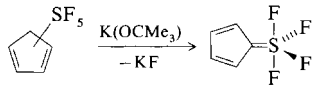


(*S*)-**1**

V. Rozenberg, V. Kharitonov, D. Antonov, E. Sergeeva, A. Aleshkin, N. Ikonnikov, S. Orlova, Y. Belokon' 91–92

Scalemic 2-Formyl-3-hydroxy[2.2]paracyclophane: A New Auxiliary for Asymmetric Synthesis

A rigid trigonal-bipyramidal arrangement of substituents and consequently a rigid C=S bond are found in thione **2** at temperatures up to 180 °C. Compound **2** does not occur in the resonance-stabilized ylide-type resonance structure with an aromatic five-membered ring. It is formed by elimination of HF from cyclopentadiene **1**, the anion of which should display a diverse coordination chemistry.

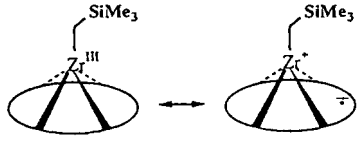


1 **2**

A. Klauck, K. Seppelt* 93–95

(Pentafluoro-λ⁶-sulfanyl)cyclopentadiene and Cyclopentadienylidenetetrafluoro-λ⁶-sulfane

The unusual stability of [(OEP)-$ZrCH_2SiMe_3$] (**1**), which formally contains a Zr^{III} center and is formed by reaction of [(OEP)Zr-$(CH_2SiMe_3)_2$] with H_2, is best explained by considering two resonance structures, a Zr^{III} metal-based radical and a zwitterionic porphyrin radical anion. OEP (octaethylporphyrin) is denoted by a circle in the formulas shown on the right.

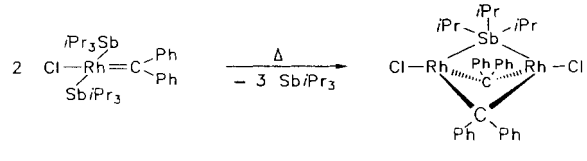


1

H. Brand, J. Arnold* 95–97

Facile Reduction of a Dialkyl Zirconium(IV) Octaethylporphyrin (OEP) Complex by H_2: Crystal Structure and Spectroscopic Characterization of $[(OEP)ZrCH_2SiMe_3]$

Not only CO, NO, and related molecules but also stibanes SbR_3 can act as bridging ligands in dinuclear complexes. Compound **2**, the first compound of this type, which is accessible upon thermolysis of **1** and characterized by X-ray structure analysis, is remarkably stable. The $SbiPr_3$ ligand is easily displaced by stibanes SbR_3 containing smaller substituents R (Me, Et) and also by $CNtBu$ without disturbing the carbene bridges.



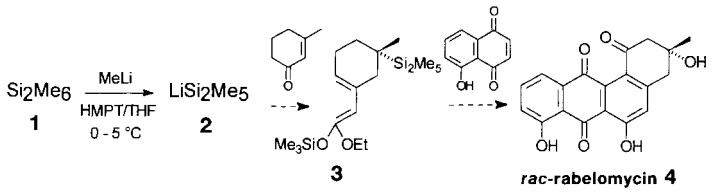
1 **2**

P. Schwab, N. Mahr, J. Wolf, H. Werner* 97–99

Trialkylstibanes as Bridging Ligands: Synthesis and Structure of the Dinuclear Complexes $[Rh_2Cl_2(\mu\text{-}SbiPr_3)(\mu\text{-}CR_2)_2]$

 © VCH Verlagsgesellschaft mbH, D-69451 Weinheim, 1994 0570-0833/94/0101-0007 $ 10.00+.25/0

To hold the position for a labile hydroxyl group and to direct a regioselective deprotonation, the Si_2Me_5 group is introduced in the diene component **3**, from which the antibiotic *rac*-rabelomycin (**4**) is accessible through cycloaddition and subsequent photooxygenation. This procedure emphasizes the usefulness of the pentamethylsilyllithium **2**, readily prepared from disilane **1**, for the synthesis of tertiary alcohols.

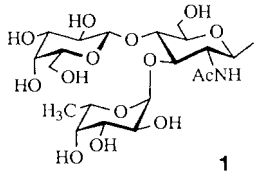


1 2 3 *rac*-rabelomycin **4**

K. Krohn,*
K. Khanbabaee 99–100

First Total Synthesis of (±)-Rabelomycin

As a tumor-associated cell–antigen mimic, Lewis^x trisaccharide determinant **1** was constructed with the azide function as anomeric protecting group with the aid of a 4-Mpm-protected (Mpm = methoxyphenylmethyl) fucosyl donor. Exchange of the OMpm functions for OAc groups furnishes a Lewis^x trisaccharide stable enough against acid attack for glycopeptide synthesis. A glycopeptide with two Lewis^x antigen side chains was deblocked and coupled to bovine serum albumin as well as to KLH (keyhole limpet hemocyanin). These synthetic glycoproteins simulate biantennary Lewis^x antigen structures.

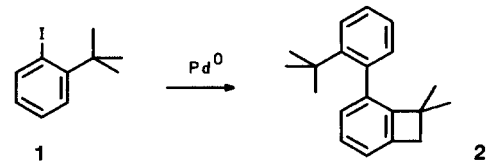


1

K. von dem Bruch,
H. Kunz* 101–103

Synthesis of *N*-Glycopeptide Clusters with Lewis^x Antigen Side Chains and Their Coupling to Carrier Proteins

The *tert*-butyl group of 1 is surprisingly reactive in the presence of palladium catalysts. A domino coupling affords 1,2-dihydrocyclobutabenzene **2** in good yield (75%). The observed C–H activation can also be used for cross coupling reactions.

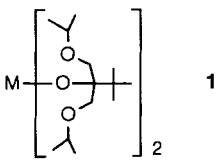


1 **2**

G. Dyker* 103–105

Palladium-Catalyzed C–H Activation of *tert*-Butyl Groups: A Simple Synthesis of 1,2-Dihydroxyclobutabenzene Derivatives

At low temperatures and without decomposition, alkaline-earth alkoxides **1** (M = Ca, Sr, Ba) and an analogous cadmium complex sublime under vacuum, which makes these compounds possible candidates for chemical vapor deposition (CVD) techniques, for example, for the preparation of high-temperature superconductors. The high volatility of these alkoxides is in part a consequence of their unusually low degree of aggregation.

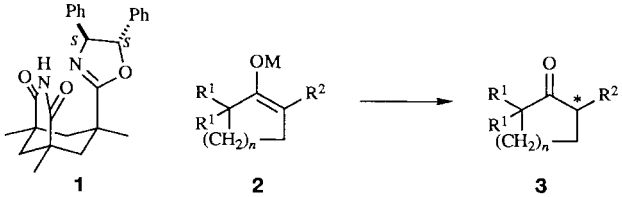


1

W. A. Herrmann,*
N. W. Huber,
T. Priermeier 105–107

Solvent-Free Volatile Alkoxides of the Alkaline-Earth Elements

From Kemp's tricarboxylic acid the (*S*,*S*)-imide **1** and its enantiomer, as well as related imides, were synthesized. With this new chiral reagent, lithium enolates of α-monoalkylated cycloalkanones can be protonated. For instance, **2** can be transformed into **3**.

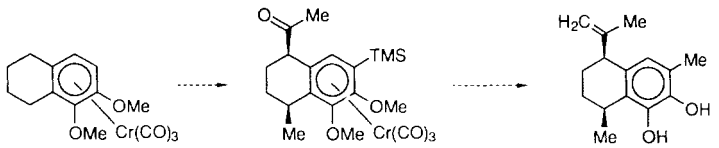


1 **2** **3**

A. Yanagisawa,
T. Kuribayashi, T. Kikuchi,
H. Yamamoto* 107–109

Enantioselective Protonation of Simple Enolates: Chiral Imide as a Chiral Proton Source

With complete diastereoselectivity and no loss of absolute stereochemical information, the chiral synthetic building block **1** is converted into **2**, an advanced intermediate in the total synthesis of the antiinfective sesquiterpene **3**. The reactivity of arene–$Cr(CO)_3$ complexes is crucial to the synthetic strategy. TMS = $SiMe_3$.

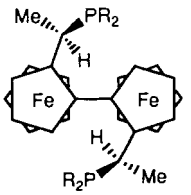


1 **2** **3**

H.-G. Schmalz,* M. Arnold, J. Hollander, J. W. Bats 109–111

The Total Synthesis of *cis*-7,8-Dihydroxy-11,12-dehydrocalamenene by Regio- and Diastereoselective Alkylation of Chiral η^6-Arenetricarbonylchromium Complexes: An Unexpected Case of Nucleophilic Aromatic *tele*-Substitution with Methoxide as a Leaving Group

Not bulky substituents but flexible alkyl groups led to the hitherto highest enantioselectivities for the asymmetric hydrosilylation of simple ketones catalyzed by diphosphane–rhodium complexes. The reduction of acetophenone in the presence of the diphosphane ligand **1**, R = *n*Pr, *n*Bu, gave 92% *ee*, whereas with **1**, R = Ph and R = *i*Pr, *ee* values of only 15% and 1%, respectively, were achieved.

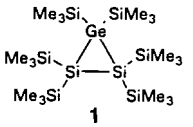


1

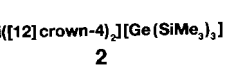
M. Sawamura, R. Kuwano, Y. Ito* 111–113

trans-Chelating Chiral Diphosphane Ligands Bearing Flexible *P*-Alkyl Substituents (AlkylTRAPs) and their Application to the Rhodium-Catalyzed Asymmetric Hydrosilylation of Simple Ketones

The disilagermirane 1 is obtained in good yields from $(Me_3Si)_3SiLi(thf)$ and $GeCl_2$. The germyllithium compound **2** was also prepared; its anion, the higher homologue of the Si starting material for **1**, might prove to be a versatile building block for a great variety of mixed three-membered rings containing the heavier elements of group 14.



1

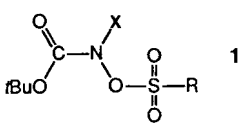


2

A. Heine, D. Stalke* 113–115

Synthesis and Structure of the Disilagermirane $R_2Ge(SiR_2)_2$ and the Solvent-Separated Ion Pair $[Li([12]crown\text{-}4)_2][GeR_3]$; R = $SiMe_3$

The N–O bond in 1 lengthens by roughly 6 pm when the neutral compound (X = H) is N-lithiated (X = Li). This key result of the first crystal structure analysis of a nitrenoid explains the facile replacement of the OR groups in nitrenoids $R^1(Li)OR^2$ by nucleophiles like R′Li and is in accord with calculational predictions. In the solid state **1** (X = Li) occurs as a Li-linked dimer with three Li-coordinating THF molecules, one of which bridges the two Li centers. R = 2,4,6-trimethylphenyl.

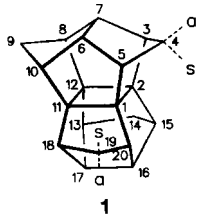


1

G. Boche,* C. Boie, F. Bosold, K. Harms, M. Marsch 115–117

[(*N*-Lithio-*N*-mesitylsulfonyloxy-*tert*-butylcarbamate)$_2$ · $(thf)_3$]: Crystal Structure of a Nitrenoid

Isopagodanes like the "square", D_{2d}-symmetric $C_{20}H_{20}$ [1.1.1.1] skeleton 1 may serve as precursors to unusual cage ions of very special geometry. The synthetic strategy for pagodanes could not be directly applied to isopagodanes. A detour, in which a [2+2] photocycloaddition replaced the unsuccessful [6+6] photocycloaddition, was ultimately successful.



1

M. Wollenweber, R. Pinkos, J. Leonhardt, H. Prinzbach* 117–120

Isopagodanes—Precursors of Unusual Cage Ions

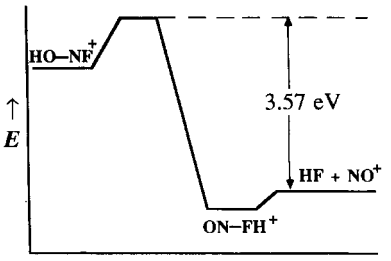
In a new reaction of tresyl chloride ($CF_3CH_2SO_2Cl$) the nucleophilic attack on the tresylate is not between the activating group and the trifluoroethanesulfonate as expected, but between the sulfonate and the trifluoroethyl group. The coupling of alkylamines with "tresylated" agarose Ⓐ, for example, thus gives sulfamates [Eq. (a)].

$$Ⓐ\text{–}CH_2\text{–}O\text{–}SO_2CH_2CF_3 + R\text{–}NH_2 + 3\,NaOH \longrightarrow Ⓐ\text{–}CH_2\text{–}O\text{–}SO_2\text{–}NH\text{–}R + CH_3COOH + 3\,NaF + H_2O \quad (a)$$

A. Demiroglou, C. Bandel-Schlesselmann, H. P. Jennissen* 120–123

A Novel Reaction Sequence for the Coupling of Nucleophiles to Agarose with 2,2,2-Trifluoroethanesulfonyl Chloride

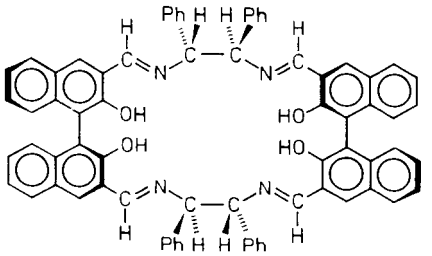
2.68 + 0.10 eV, the largest value by far for the kinetic energy release (KER) in the decomposition of metastable, singly charged ions was detected by mass spectrometry for the fragmentation of $HONF^+$. Thus, the exceptionally large KER predicted by a theoretical analysis of the potential energy surface (calculated energy profile shown on the right) was also confirmed experimentally.



F. Cacace, F. Grandinetti,*
F. Pepi 123–125

An Extraordinarily Violent Molecular Dissociation: The Unprecedented Kinetic Energy Release in the Decomposition of $HONF^+$, a Singly Charged Metastable Ion

The 24-membered macrocycle 1 is surprisingly generated from (*S*)-2,2′-dihydroxy-1,1′-binaphthyl - 3,3′ - dialdehyde [(*S*)-(**2**)] and (*R*,*R*)-1,2-diamino-1,2-diphenylethane, whereas in the same reaction (*R*)-**2** yields the polymeric Schiff base as expected. Macrocycle **1** can be used for an economical and simple enantiomeric resolution of **2**.



1

H. Brunner,*
H. Schiessling 125–126

Dialdehyde + Diamine—Polymer or Macrocycle?

* Author to whom correspondence should be addressed

BOOKS

Nanostructures Based on Molecular Materials · W. Göpel, C. Ziegler — *T. Bein* 127

Magnetic Resonance Microscopy · B. Blümich, W. Kuhn — *H. Post* 128

New Books — **129**

Author Index 11 — **Preview 130**

The following reviews will appear in future issues:

The Structure Correlation Method and Reaction Paths for Pentacoordinated Metal Complexes
T. Auf der Heyde

Digitalis Research in Berlin-Buch: Retrospective and Perspective Views
K. R. H. Repke et al.

Fluorinated Isocyanides—More than Ligands with Unusual Properties
D. Lentz

Rates of Cation–Nucleophile Reactions: Reactivity Scales for Categorizing Polar Organic and Organometallic Reactions
H. Mayr, M. Patz

Organizing Principle and Theory of Perilinear Reactions
R. Herges

Chemistry and Biology of Taxol

Kyriacos Costa Nicolaou,* Wei-Min Dai, and Rodney Kiplin Guy

One can view plants as a reference library of compounds waiting to be searched by a chemist who is looking for a particular property. Taxol, a complex polyoxygenated diterpene isolated from the Pacific Yew, *Taxus brevifolia*, was discovered during extensive screening of plant materials for antineoplastic agents during the late 1960s. Over the last two decades, interest in and research related to taxol has slowly grown to the point that the popular press now seems poised to scoop each new development. What was once an obscure compound, of interest only to the most masochistic of synthetic chemists and an equally small number of cellular biologists, has become one of the few organic compounds, which, like benzene and aspirin, is recognizable by name to the average citizen. In parallel, the scientific study of taxol has blossomed. Physicians are currently studying its effects on nearly every known neoplasm. Biologists are using taxol to study the mechanisms of cell function by observing the effects of its interactions with the cellular skeletal systems. Synthetic chemists, absorbed by the molecule's unique and sensitive structure and functionality, are exploring seemingly every available pathway for its synthesis. Indeed, the demand for taxol has risen so in the last five years that alternative sources to the extraction of *T. brevifolia* are being vigorously pursued. Because of the rapidly expanding scope of research in the multifaceted study of taxol, those who are interested in the field may find acquisition of a reasonable base of knowledge an arduous task. For this reason, this account attempts to bring together, for the first time, in a cogent overview the chemistry and biology of this unique molecule.

1. Introduction

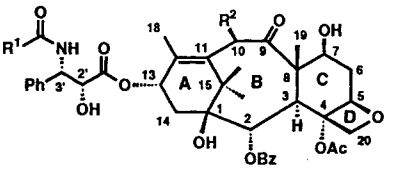
Cancer, a disease characterized by unregulated proliferation of cells, is a growing public health problem whose estimated worldwide new incidence is about six million cases per year.[1] In the United States, cancer is second only to heart disease as cause of death.[2] The seriousness of the problem was recognized in the United States in the mid-1960s, studied by the Yarbourogh commission, and addressed legislatively in 1971 by the passage of the National Cancer Act, which attempted to invigorate cancer research through a directed increase in funding.[3] The long-term result of this legislation was the establishment of several national cancer centers and a significant increase in basic research activities aimed at understanding and treating cancer.[4] Considerable progress has been made towards controlling several forms of cancer through a combination of prevention and therapy.[5] Some types of cancer, however, have not yet yielded to the onslaught of research, and breast cancer, in particular, remains a major issue of both scientific[6] and public[7] concern.

Many of the gross causes of cancer, such as dietary, environmental, and occupational exposure to certain chemical substances or forms of electromagnetic radiation, have been elucidated through epidemiological studies.[8] These results have led to a number of prevention programs aimed at reducing exposure to carcinogenic agents (e.g., the US national "Smoke Out" program) and stimulated some controversy over the level of risk involved in such exposures.[9] The biological pathways through which these agents exert their activity as well as the mechanisms of carcinogenesis and metastasis are less well understood and remain the subject of much study and debate.[10] Currently, for example, both genetic[11] and signal transduction[12] models are used to explain carcinogenesis. Although metastasis is well understood at the level of individual tissues, much work remains to be done before the signaling for or the individual biochemical events involved in metastasis can be interrupted.[13]

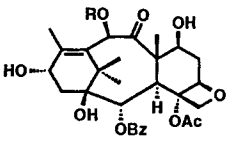
In the early 1960s the National Cancer Institute (NCI) began an ongoing program to discover new drugs by releasing protocols[14] for widespread screening of substances and extracts from various origins for antineoplastic activity.[15] Following the NCI initiative, United States Forest Service botanist

[*] Prof. Dr. K. C. Nicolaou,
Department of Chemistry, MB-210A, The Scripps Research Institute
10666 North Torrey Pines Road, La Jolla, CA 92037 (USA)
and
Department of Chemistry, University of California
San Diego, B-014, La Jolla, CA 92093-0314 (USA)
Telefax: Int. code + (619)554-6738
Dr. W.-M. Dai
Department of Chemistry
The Hong Kong University of Science & Technology
Clear Water Bay, Kowloon (Hong Kong)
Mr. R. K. Guy,
Department of Chemistry, The Scripps Research Institute, La Jolla (USA)

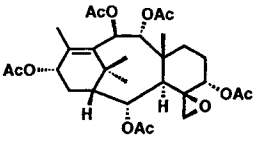
A. Barclay collected samples of the bark of the pacific yew, *Taxus brevifolia* Nutt, from an Oregon forest in 1962.[16] These samples were sent by the NCI to Wani and Wall, chemists at the Research Triangle Institute in North Carolina. Initial screening of a crude extract of the bark showed cytotoxic activity against leukemia cells and inhibitory action against a variety of tumors. Several years later, the active component of the extract, taxol (**1**, Fig. 1), was isolated by Wall et al. The compound was subjected to an X-ray crystallographic analysis carried out at Duke University, which revealed its molecular structure, including absolute stereochemistry.[17] The beauty of the molecular architecture and the highly congested nature of taxol are appreciated by inspection of molecular models (Fig. 2). Of the more than 110000 compounds from 35000 plant species tested between 1960 and 1981, taxol proved the most interesting.[18] Nevertheless, further investigation of taxol languished for almost a decade due, primarily, to difficulty of extraction from the natural source, problems with the murine screening system, and a belief that taxol was simply another microtubule-destabilizing agent like colchicine and the vinca alkaloids.[19] However, interest in the compound reemerged and rapidly acquired strong momentum when Horwitz et al. at the Albert Einstein College of Medicine reported that taxol did indeed act on microtubules but with a unique mode: it stabilized microtubules instead of destabilizing them like all other known agents.[20]



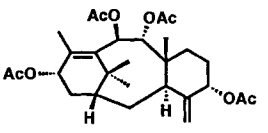
1: Taxol, R^1 = Ph, R^2 = OAc
2: Taxotere, R^1 = *t*BuO, R^2 = OH



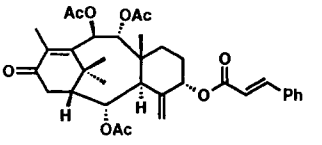
3:10-Deacetylbaccatin III, R = H
4: Baccatin III, R = Ac



5: Baccatin I



6: Taxusin



7: Taxinine

Fig. 1. The taxane family of diterpenoids. Included are the clinically relevant taxol (**1**) and Taxotere (**2**), their commercial precursors 10-deacetylbaccatin III (**3**) and baccatin III (**4**), and some representative taxanes (**5**–**7**), to demonstrate the rich structural variety of the class.



K. C. Nicolaou



W.-M. Dai



R. K. Guy

K. C. Nicolaou was born in Cyprus and received his Ph.D. degree from the University of London under F. Sondheimer and P. Garratt. After postdoctoral work at Columbia University with T. Katz and at Harvard University with E. J. Corey, in 1976 he joined the faculty at the University of Pennsylvania, where he was promoted to Rhodes-Thompson Professor of Chemistry. In 1989 he accepted joint appointments as Professor of Chemistry at the University of California San Diego and as Darlene Shiley Professor of Chemisty and Chairman of the Department of Chemistry at the Scripps Research Institute. His awards include a Guggenheim Fellowship, a Humboldt Senior American Scientist Award, and the American Chemical Society Award for Creative Work in Synthetic Organic Chemistry. Nicolaou's research interests focus on chemical synthesis, molecular design and recognition, and the biological function of molecules.

W.-M. Dai was born in 1957 in Ninghai, China. He received his B. S. in 1982 from Hangzhou University (China), his M.S. in 1984 at the Shanghai Institute of Organic Chemistry, Academia Sinica under Professor W.-S. Zhou, and his Ph.D in 1990 from Kyoto University (Japan) on asymmetric synthesis utilizing chiral tin(II) enolates, and its application in the total synthesis of alkaloids. He then joined Professor Nicolaou's group as Research Associate. In September 1992 he accepted a teaching post at the Department of Chemistry of the Hong Kong University of Science and Technology. His research interests include the development of novel asymmetric reactions and the synthesis of natural products and biomedically interesting molecules. He is currently engaged in the design, synthesis, and study of novel enediynes.

R. K. Guy, born in 1968 in Ft. Rucker, Alabama, USA, obtained his BA in Chemistry from Reed College, Portland Oregon. He then worked in the Synthetic Development Laboratory of the Almaden Research Center of IBM, San Jose, California on photoresist materials until 1992. At present he is an Office of Naval Research Predoctoral Fellow at the Scripps Research Institute and involved in the total synthesis of taxol program with Professor Nicolaou.

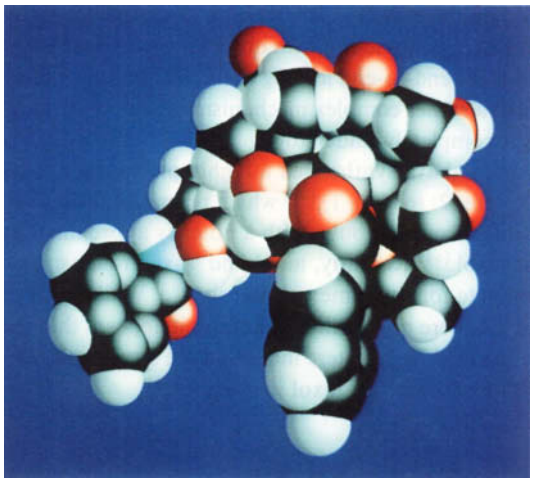


Fig. 2. A space-filling model of taxol (MM2, macromodel).

2. The Biological Role of Taxol

2.1. Taxol and Microtubules

Microtubules are involved in many aspects of cellular biology. They are used by the cell to form a static structure, called the cytoskeleton, which helps shape the cell[21] and position the organelles.[22] The dynamic properties of microtubules are used to transmit cellular signals,[23] reorganize organelles,[24] and move the cell.[25] As will be discussed below, they are an absolute necessity for cell division, a process in which they play a central role. Because of their versatility, usage, and importance to growing cells, microtubules have been called "the most strategic subcellular targets of anticancer chemotherapeutics."[26] Figure 3 summarizes the present state of knowledge about the taxol–microtubule connection.

Microtubules are primarily composed of two subunits: α- and β-tubulin, structurally similar protein isofamilies of approximately 440 amino acids each with a molecular weight of about

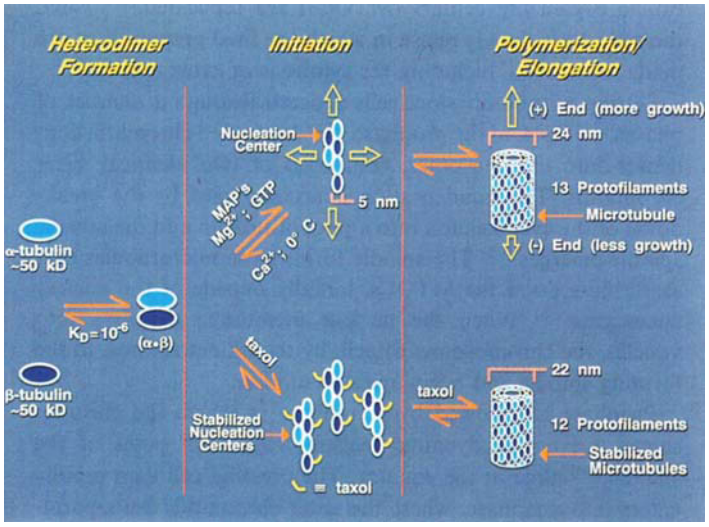


Fig. 3. Microtubule formation and the mechanism of action of taxol. For explanation, see text.

50 kD.[27] The tubulin genes are highly conserved,[28] and there is a 35–40 % homology between the α and β types.[29] Both isofamilies are subject to a variety of posttranslational modifications giving rise to a large number of similar proteins within any given cell. Whether the various cellular functions of microtubules are due to individual tubulins or related groups of tubulins is still unclear.[30] The tubulin dimer binds two molecules of guanosine 5′-triphosphate (GTP), an event involved in the assembly of microtubules. One of the GTP molecules binds exchangeably to a site of the β subunit, called the *E*-site,[31] whereas the other molecule binds tightly to another site, presumed to be on the α subunit and called the *N*-site.[32] The remainder of the mass (up to 20%) of a microtubule is made up by heterogeneous microtubule-associated proteins (MAPs), whose structure and function vary with both organism and tissue.[33]

The tubulin dimer is the binding target of a number of drugs that inhibit the polymerization of tubulin. Although the binding site has been localized to the β subunit for some of these drugs, notably colchicine,[34] most of the others appear to bind to multiple, as yet undefined sites.[35] Competition experiments have shown that colcemid, podophyllotoxin, and nocodazole all bind to the colchicine site, while the vinca alkaloids, vinblastine and vincristine, bind to a different site.[36]

The initial event in the polymerization of microtubules is the formation of a heterodimer comprising one molecule of α-tubulin and one molecule of β-tubulin, which has a dissociation constant K_D of about 10^{-6}.[37] In the presence of magnesium ions and GTP, these dumbbell-shaped heterodimers then join in a head-to-tail fashion to give the nucleation center for protofilament formation. Concomitant growth both along and perpendicular to the axis of the initial protofilament then occurs until the growing molecule curls along the axis of the protofilaments, and the edge filaments join to give a microtubule.[38] From this point, the growth occurs only at the ends of the tubule.

A normal microtubule from brain tubulin is composed of 13 protofilaments and has a diameter of about 24 nm. The protofilaments are assembled in a slightly staggered manner, which gives the microtubule a left-handed three-start helix (in which, in any horizontal unit plane three filaments start).[39] In this configuration, the filaments are aligned in a helical fashion such that one complete turn of the helix results in a vertical rise of three tubulin subunits. The grooves between the protofilaments of the resulting microtubule are much more pronounced on its outer than on the inner surface.[40] The filamentous structure of the microtubule is overlaid with MAPs, some of which appear to have a stimulatory effect on polymerization.[33] Typically, equilibria are set up at both ends of the microtubule with constant loss and gain of tubulin subunits. Often the relative rates of loss/gain at the two ends are different, which gives the microtubule a growing polarity. The faster growing end is termed the "plus" pole and the more slowly growing end the "minus" pole.[41]

In general, microtubules are not static structures. After a certain period of growth, the microtubule and free tubulin will reach relative concentrations corresponding to the equilibrium constant. At this point, disassembly and growth are precariously balanced; this is termed the critical concentration.[42] When the relative tubulin concentration is below the value required for equilibrium, spontaneous assembly will not occur. The tubulin

system then is capable of rapid rearrangement. A number of models, of which the dynamic instability model is currently the most widely accepted, have been proposed[43] to explain this behavior.[44] According to this hypothesis, only tubulin with bound GTP is able to add to the growing end of the microtubule, and the microtubule maintains a "cap" of tubulin·GTP complex. GTP hydrolysis is assumed to be an ongoing background process, and it is proposed that, when a microtubule loses its cap, rapid disassembly ensues. Thus, the model claims that while the mass of assembled microtubules will remain constant, they are represented by constantly growing or shrinking tubules, not by static structures. Establishing the existence of the cap has proven difficult, and the model is currently in dispute.[45]

In 1979 Horwitz et al. demonstrated that taxol affects the tubulin–microtubule equilibrium.[20] Taxol decreases both the critical concentration of tubulin (to almost 0 mg mL^{-1}) and the induction time for polymerization, either in the presence or absence of GTP, MAPs, and magnesium. The microtubules formed by taxol induction proved morphologically distinct from those formed in the control experiments. They exhibited a shorter average length and resistance both to cooling and to ionic calcium, which normally depolymerize microtubules. It was only with the combination of cooling and calcium ions, or cooling and high ionic-strength buffers that taxol-stabilized microtubules could be induced to depolymerize.[46] Changing the pH of the medium to above 7.6 also induced depolymerization,[47] although this may have been due to hydrolysis of the C13 side chain of taxol.[48] Attempts to remove taxol from both microtubules and tubulin after depolymerization indicated that it binds much more strongly to the intact microtubule than to the tubulin dimer and that the molecule does not permanently modify tubulin during the binding interaction.

The maximum effects of taxol occur at a stoichiometry of 1:1 taxol:tubulin dimer.[49] Subsequently, through the use of the tritiated compound, the same workers proved that taxol binds specifically and reversibly to a polymerized form of tubulin with an apparent binding constant K_{app} of 10^{-6}.[50] It was postulated that the effects of taxol were caused by an increase in nucleation events.

The binding site of taxol appears to be distinct from that of other anti-microtubule agents[51] and common MAPs.[52] However, it has been suggested that some spatial overlap exists between the colchicine and taxol binding sites.[53] In addition, taxol does not affect the binding or the hydrolysis of GTP.[54] More recently, the binding site of taxol has been localized to the β subunit of tubulin through direct photoaffinity labeling[55] and analysis of the binding profiles of strains of algae with mutations in tubulin genes.[56] Efforts to locate the binding site more closely are currently under way.[57]

Careful examination of the X-ray scattering patterns and electron microscopy images of microtubules formed by taxol induction revealed several gross structural differences between these tubules and tubules formed in control experiments (see Fig. 3).[58] Taxol induction produces tubules that have a mean diameter of about 22 nm as opposed to 24 nm for those produced by MAP induction and that are composed of 12 protofilaments rather than 13. Time-resolved X-ray scattering data support the idea that taxol promotes sideways growth of tubules in the nucleation center as well as lengthening along the protofilament axis. Taken in conjunction with observations showing that taxol promotes the end-to-end joining of microtubules,[59] these results point to a rather complex mechanism of action for taxol that is not yet completely understood.

French workers have synthesized a highly promising analog of taxol, Taxotere (**2**, see Fig. 1),[60] which promotes the assembly and stability of microtubules with a potency approximately twice that of taxol.[61] Recently, taxol and Taxotere have been shown to compete for the same binding site.[62] While most of the effects of Taxotere mirror those of taxol, it appears that the microtubules formed by Taxotere induction are structurally different from those formed by taxol induction.[63]

2.2. Taxol and the Cell Cycle

Cells have a characteristic life cycle which is depicted schematically in Figure 4. Some of the approximately 10^{13} cells in a human body, such as neurons, are unable to replicate and exist in a state called terminal differentiation. The cells of other tissues spend most of their time in a nonproliferative state called quiescence, or G_0, which is outside the cell cycle.[64] These cells replicate at different rates: skeletal muscle cells less than once a year, liver cells about once a year, and stem cells of the gut about twice a day. They can remain quiescent for long periods and yet switch to rapid proliferation when more cells are needed, such as during the healing of a wound. The different rates of cellular proliferation are related primarily to the fraction of cells in the cell cycle, not to the relative time needed to traverse the cycle. Quiescent cells can be induced to reenter the cell cycle at G_1 either through the action of tissue-specific growth factors[65] or through the influence of internal controls related to differentiation states. While normal cells are inhibited towards proliferation when their population density is high, cancerous cells often lack these control mechanisms and continue to replicate in conditions that normally induce quiescence.[66]

Once induced to reenter the cell cycle, the cells pass through G_1 and initiate, through a complex enzymatic cascade,[67] the S phase.[68] During this phase the DNA, histones, and microtubule organizing centers (MTOCs) are replicated.[69] Next, the cell enters the G_2 phase in which the final preparations are made for mitosis, including the synthesis of extra tubulin.[70]

During mitotic division, cells proceed through a number of phases.[71] First, in the prophase, the duplicated chromatin condenses into chromosomes, composed of two identical sister chromatids. This condensation is accompanied by the breakdown of the cytoskeleton into a pool of tubulin and the mitotic spindle emerges.[72] The spindle forms from microtubules that assemble around the MTOCs, initially outside of the nuclear membrane.[73] When the nuclear membrane dissolves into vesicles, the chromosomes attach, by their kinetochores, to the forming spindle and begin agitated motion.

Prophase is followed by metaphase in which the chromosomes, driven by dynamic tension from both poles of the spindle,[74] align at the equator. The dividing cell then rapidly enters into anaphase, where the sister chromatids are separated,[75] each containing one copy of the genetic message of the chromosome. The chromatids separate slowly, at about

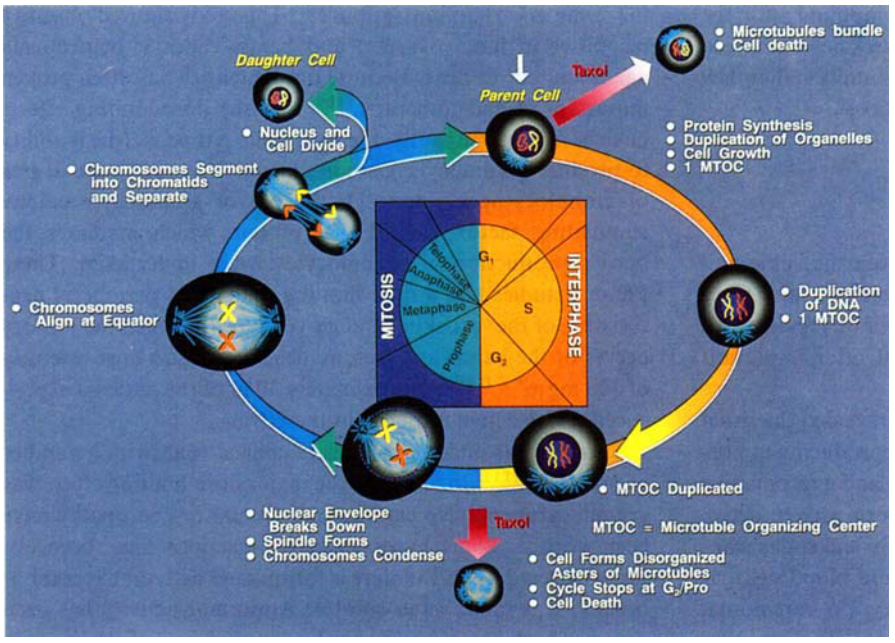


Fig. 4. Taxol and the cell cycle. For explanation, see text.

1 μm min^{-1}. Concomitantly, the poles of the spindle are pushed apart by other microtubules.

Finally, the cell enters telophase during which the chromatids arrive at the poles of the spindle, the nuclear envelope reassembles, and the organelles and cytosol segregate in a process known as cytokinesis. The resulting separated daughter and parent cells continue to grow and synthesize new proteins before either entering G_0 or traversing the cycle.

The events in the cell cycle proceed through a linear pathway in which the initiation of late events require the completion of the early events. Normal cells have control mechanisms, called checkpoints, which enforce this ordering.[76] An example of such a checkpoint is that, when a chromosome is slow to line up at the spindle equator during metaphase, anaphase is delayed until the chromosome arrives.[77] When these checkpoints are abolished, the cell may die or undergo catastrophic alterations to its normal metabolism. Tumor cells are often deficient in checkpoints.

When Horwitz et al. extended their studies on taxol to in vitro cell culture systems, they found that this agent caused HeLa[78] cells to arrest at the transition from interphase to mitosis, (G_2/Pro, see Fig. 4).[79] Morphologically, these cells exhibited unnatural "bundles" of microtubules and no mitotic spindle. Moreover, the investigation showed that taxol inhibited the motility of fibroblasts without affecting their ability to form podia.

These studies were rapidly extended by a number of groups, who found that taxol affects microtubules in all phases of the cell cycle. Cells arrested in mitosis exhibit "asters",[80] which are star-shaped microtubule formations that are not organized around MTOCs and that are formed reversibly.[81] In the other phases of the cell cycle, taxol causes the generally irreversible formation of bundles of microtubules, visually reminiscent of a log jam.[82] The net effect of these phenomena is a sequestration of tubulin as stable structures. The resulting absence of free tubulin prevents the assembly of a normal mitotic spindle. It may be that the cancerous cells lack a checkpoint to detect the absence of a spindle and attempt to continue the cell cycle, which leads to cell death. Other vital cell processes that depend upon microtubules may also be prevented, or checkpoints missed, and the cell remains in interphase. Recent studies have shown that taxol can inhibit the transition of cells out of the quiescent state.[83] Studies with leukemia cell lines indicated that cells may freeze at interphase points in taxol-sensitive lines.[84] Not surprisingly, some fungal cells are also sensitive to taxol.[85]

Taxol has been implicated in the disturbance of many cellular phenomena that are not directly related to cell division. For example, taxol inhibits the locomotion of Walker 256 carcinoma cells,[86] the slow transportation of tubulin, actin, and polypeptides in axons,[87] the intracellular transportation of steroids in MLTC-1 cells,[88] and the immunoreactivity of τ-MAPs in neurons.[89] It should be noted that microtubules are involved in all of these phenomena.

Most intriguing are taxol's effects on protein secretion, a process in which microtubules are intimately involved.[90] The agent inhibits the secretion of insulin from pancreatic cells,[91] catecholamine from adrenal medullary cells,[92] plasma proteins from rat liver cells,[93] and prothrombinase from platelets.[94] In each of these cases, the effect appears to be specific and does not inhibit overall protein secretion. Interestingly, taxol has been shown to increase the secretion of tumor necrosis factor alpha (TNF-α) and interleukin-1 from macrophages in a manner similar to that of bacterial lipopolysaccharide (LPS), an action which may contribute to the antineoplastic activity of taxol.[95] These observations led to the recognition that LPS selectively and specifically binds β-tubulin and MAP-2.[96] The taxol-induced inhibition of collagenase secretion has been linked to a blockage of metastasis of prostate tumor cells (PC-3 ML) in SCID mice.[97]

Likewise, Taxotere has been shown to be active against a wide range of tumor cell lines.[98] As with the microtubule studies, the in vitro cytotoxicity effects of Taxotere are higher than those of

taxol at equivalent doses. The effects of the compound upon the various microtubule-mediated cellular processes have not been reported but one may make the reasonable assumption that they will be similar to those described above for taxol.

2.3. Clinical Applications of Taxol

The clinical usage of taxol has recently been the subject of excellent reviews by Rowinsky et al.[99] Therefore, and since much of the clinical data is beyond the scope of this review, this section will only highlight these studies and offer important recent results.

Preclinical studies on mice, rats, and dogs revealed the usual toxic effects of mitosis inhibitors on tissues reproducing at normal rates, including the blood, lymph, gut, and reproductive systems. Prior to clinical trials, taxol had been proven active against murine B16, L1210, P388, and P1534 leukemias, cancers characterized by overproduction of white blood cells. It also had a demonstrable effect upon Walker 256 carcinoma, sarcoma 180, and Lewis lung tumor cell lines.[100] Taxol was also proven efficacious against a number of leukemias and solid tumors in xenografts (tissue transplanted from one species to another), including those in breast, ovary, brain, and lung.[101] Recently, taxol has proven useful as sensitizer for radiation treatment against cultured astrocytoma cells, which normally serve a structural element in the nervous system.[102] Presumably this effect arises since it holds the cells at G_2/Pro, a phase in which they are known to be quite sensitive to ionizing radiation.[103]

These promising early results led to wide spread Phase I clinical trials in which the clinical safety was established. Initially the trials were hampered by acute hypersensitivity reactions that may be attributable to the vehicle of administration required for solubilization, Cremaphor, a polyoxyethylated castor oil that is known to cause histamine release.[104] Effective protocols, including prophylactic pretreatment with antihistamines[105] and longer infusion times,[105] have emerged to essentially circumvent this problem. In later trials, neutropenia, the inability to produce a certain class of granular white blood cells, has emerged as the major dose-limiting effect, although irregular heart beat rhythms (cardiac arrhythmias),[106] and neuropathy, the deadening of sensory nerves, have also been observed. Due to the sensitivity of the blood to agents which inhibit cellular proliferation and that of the nervous system to cytotoxins, these were not unexpected side effects. In vivo antineoplastic effect was demonstrated with a number of cancers including leukemia, breast, ovarian, and lung tumors, and melanoma. The dose recommendations emerging from these studies were generally in the range of 200–250 mg m^{-2} (of body surface area), administered in about 3 L of isotonic solution over a period of 6–24 hours. Recently several groups have disclosed the development of immunoassays for measuring plasma concentrations of taxol.[107]

Several Phase I trials involving the co-administration of taxol with other drugs are currently under way. Studies with cisplatin, a chemotherapeutic that acts directly upon DNA, have given promising results and demonstrated that the best application sequence is that of taxol (135–170 mg m^{-2}) followed by cisplatin (75 mg m^{-2}) administration.[108] This study showed objective responses in lung, ovarian, and breast cancers; neutropenia again limited the dose. Because dose intensity has often proven important in chemotherapy,[109] and the dose-limiting effects have been predominantly due to granulocytopenia (the inability to produce granulocytes), studies aimed at lowering the degree of granulocytopenia through the use of granulocyte colony stimulating factor (G-CSF), a protein which increases the body's production of granulocytes, were undertaken. These Phase I studies had a dose-limiting toxicity of peripheral neuropathy, of the "stocking and glove" type (in which the sensory nerves of the hands and feet are deadened), at a dose intensity of 300 mg m^{-2}.[110] Approximately 30% of the patients experienced an objective response in these trials.

Taxotere has undergone Phase I clinical trials with a number of protocols.[111] In all cases, the major dose-limiting effect was granulocytopenia. No cardiac arrhythmias or neuropathy have been evident. Some hypersensitivity reactions have been observed, even though Taxotere is formulated without Cremaphor because it is more water-soluble. Antitumor activity has been noted in both breast and ovarian cancers. Phase II studies with Taxotere in which the efficacy of the drug may be established are currently under way.

Phase II clinical trials, limited to those neoplasms that showed preclinical effects because of restricted availability of the drug, have proven the efficacy of treating several cancers with taxol. In the case of ovarian cancer, taxol gave a response with manageable side effects in 30–35% of the cases.[112] These results, which represent the highest reported salvage rate for ovarian cancer, are particularly significant since these patients showed resistance to other therapies.[113] Initial trials involving patients with metastatic breast cancer gave a 56% response rate with manageable granulocytopenia as the dose-limiting side effect.[114] Responses of between 20 and 50% have been demonstrated with non-small-cell lung cancer.[115] A recent Phase II study indicated positive results with G-CSF-mediated dose escalation (30% objective response increases to 60%) in the treatment of recurrent ovarian cancer.[116] This suggests that, in those cases where the dose-limiting toxicity is granulocytopenia, G-CSF co-administration protocols are warranted. These favorable results recently led the Food and Drug Administration (FDA) of the United States to approve taxol for the treatment of patients suffering from advanced recurrent ovarian cancer.[117] It is almost certain that taxol, and very likely Taxotere, will soon be approved for the treatment of other cancers.

2.4. The Issue of Supply

As mentioned above, large scale clinical trials with taxol have been hampered for a long time by relatively low supplies of the drug.[118] Taxol is currently produced by a somewhat tedious extraction from the bark of the Pacific Yew, *Taxus brevifolia* Nutt (Fig. 5a). This extraction, when carried out under good manufacturing practice (GMP) guidelines, is the only method which is currently approved by the FDA as a source of taxol.[119]

The history and biology of the Pacific Yew have recently been reviewed.[120] The yew is a coniferous tree which usually grows

in the understory of old-growth stands of conifer or hardwood (Fig. 5a presents a typical setting). The majority of the trees grow in the coastal regions of the Pacific Northwest from Annette Island, Alaska, to Mendicino County, California, as well as the Cascade Range of Washington and Oregon, the western slopes of the Rockies, and the Lewis Range of Montana. The tree grows slowly and typical mature specimens rarely exceed 12 m in height and 60 cm in diameter. Because of their slow growth and a tendency to grow in dispersed microsites within the larger old-growth ecosystem, the density of the yew is quite low. Prior to the advent of taxol, the trees were regarded primarily as scrub and rarely taken during primary logging operations. Instead they were burned in place during slash disposal fires.



Fig. 5. a) The Pacific Yew, *Taxus brevifolia*. b) The European ornamental shrub *Taxus baccata* (photographs by S. C. Wilson TIME-LIFE Magazine, USA).

To obtain one kilogram of taxol, 10 000 kilograms of bark are required, which, in turn, requires the sacrifice of about 3000 trees. Because of the relatively large amount of taxol needed to treat a patient (under current protocols almost two grams), this kilogram of taxol is enough to treat only 500 patients. A number of groups including SRI International,[121] the Forest Service,[122] and Weyerhaeuser[123] have been exploring the factors that cause variance in taxol concentrations from tree to tree to find growing conditions that will optimize the yield of available taxol from each tree. The Weyerhaeuser group is currently growing the yew in plantations and expect to be producing commercial quantities of taxol by 1994.[124]

The two currently most promising options for large-scale production of taxol are cell culture and semisynthesis. Bristol–Myers Squibb has recently announced that they will begin production of taxol through a semisynthetic route following the methods of Holton's semisynthesis and Hauser's extraction process (see Section 3.5).[125] This route proceeds through the coupling of a suitable side-chain equivalent with a 7-protected baccatin III intermediate obtainable in large quantities from *T. baccata* (Fig. 5b) and currently provided by the Indena company.[119] Taxotere is currently produced by attaching a synthetic side chain to 10-deacetyl baccatin III (**3** in Fig. 1), which is readily available from the European Yew, *T. baccata*, in yields approaching 1 kg of **3** from 3000 kg of needles.[126]

Cell culture has already been used to produce ^{14}C labeled taxol from ^{14}C sodium acetate.[127] The USDA (United States Department of Agriculture) has received a patent for the production of taxol from cultured callus cells of *T. brevifolia*.[128] They have licensed this process to Phyton Catalytic, who estimates that they will begin commercial production within two to five years.[129] The advantage of this system is that the major secretion product of the cells is taxol, which reduces the purification to an ether extraction of the medium. ESCAgenetics has also announced technology for producing high levels of taxol in plant cell cultures, and they project large-scale production in the near future.[130] Additionally, callus cultures of *T. cuspidata* and *T. canadensis* have been sustained in a taxol-producing system for over two months.[131] A fungus, indigenous to *T. brevifolia*, that produces small amounts of taxol has recently been isolated and cultured.[132]

3. Synthetic Approaches to Taxol and Taxol Systems

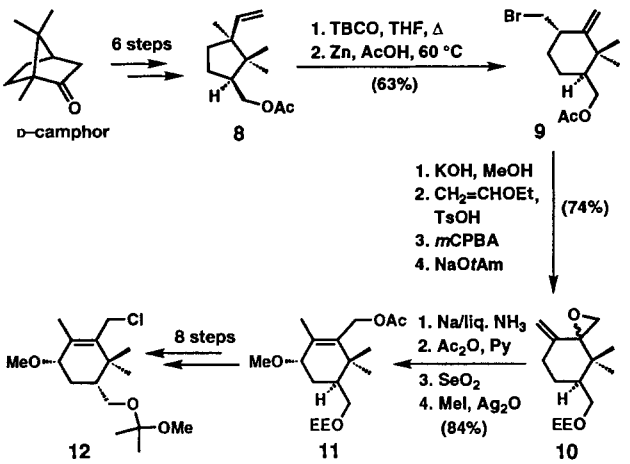
As a target for chemical synthesis, taxol presents a plethora of potential problems. Perhaps most obvious is the challenge presented by the central B ring, an eight-membered carbocycle. Such rings are notoriously difficult to form because of both entropic and enthalpic factors. The normally high transannular strain of an eight-membered ring is further increased in this case by the presence of the geminal dimethyl groups, which project into the interior of the B ring. Then the *trans*-fused C ring with its angular methyl group and another ring (A ring), which is a 1,3 C_3 bridge, must be introduced. The A ring includes a somewhat problematic bridgehead alkene formally forbidden in a six-membered ring by Bredt's rule. If assembling the carbon skeleton alone is not a daunting enough task, one should consider the high degree of oxygenation that must be introduced in a manner which allows the differential protection of five alkoxy groups in a minimum of three orthogonal classes. Additionally, some of the functionality is quite sensitive to environmental conditions. The oxetane ring, for example will open under acidic or nucleophilic conditions, and the 7-hydroxyl group, if left unprotected, will epimerize under basic conditions.

From the time of its structural elucidation, the challenge posed by taxol's unusual molecular architecture and sensitive functionality has fascinated synthetic organic chemists. Despite the many attempts to synthesize taxol, the molecule still remains inaccessible by total synthesis. Much elegant work, however, has been reported in the area. The fruits of these endeavors include the development of new synthetic methodology and strategies, the synthesis of model systems, and the construction of intermediates for projected total and partial syntheses of the natural product. Because an excellent review by Swindell on the synthetic efforts through the middle of 1991 exists,[133] this section will only provide highlights of the synthetic chemistry related to taxol and emphasize the more recent developments. These efforts are discussed under the following subsections: approaches directed at the assembly of the ring A of taxol (Section 3.1), strategies towards the construction of rings C and CD of taxol (Section 3.2), efforts to join the various rings of taxol and the more convergent strategies towards the taxane skeleton (Section 3.3), methods for production of the taxol and Taxotere side

chains (Section 3.4), and semisynthetic approaches to taxol and Taxotere (Section 3.5).

3.1. Approaches to the A Ring System of Taxol

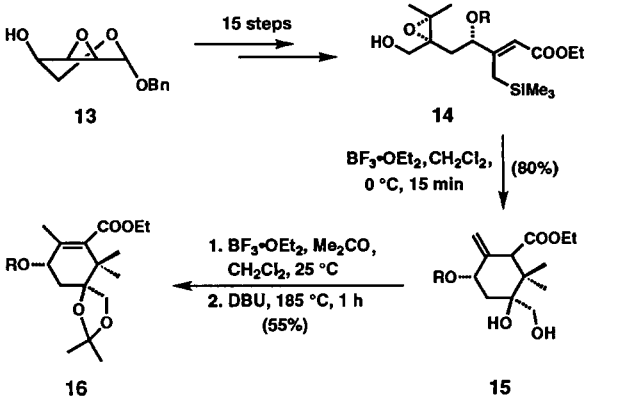
One of the earliest approaches to the ring A of taxol was that of Kitagawa et al.,[134] in which a Wagner-Meerwein rearrangement, induced by a bromonium ion, converted cyclopentane ring **8** into cyclohexane skeleton **9** (Scheme 1). Compound **9** was then transformed into intermediates **11** and **12** in several steps by standard methodology.



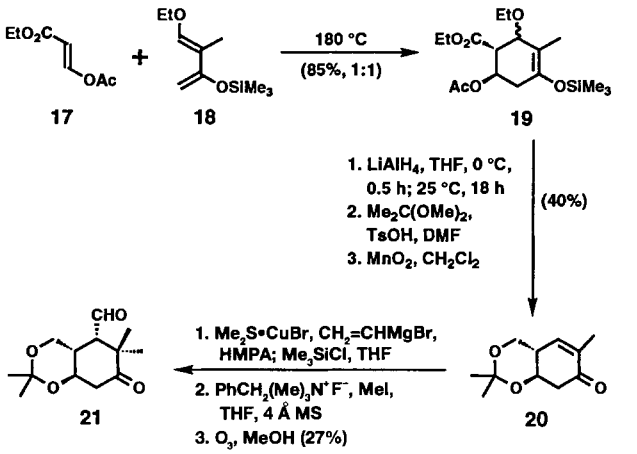
Scheme 1. Kitagawa's approach to the A ring system of taxol by ring enlargement (1980 and 1984). TBCO = 2,4,4,6-tetrabromocyclohexa-2,5-dienone, Ts = *p*-toluenesulfonyl, *m*CPBA = *m*-chloroperbenzoic acid, *t*Am = *t*BuCH$_2$, EE = ethoxyethyl, Py = pyridine.

An elegant approach to the A ring of taxol was reported by Frejd et al. in 1987.[135] This method (Scheme 2) involved a Lewis acid promoted cyclization of epoxysilane **14**, prepared from **13**, to afford the key cyclohexane system **15**. Further elaboration of this intermediate provided compound **16**.

Clark's group[136] reported a synthesis of the A ring system **21** based on a Diels–Alder reaction (Scheme 3). After the cycloaddition process to assemble the cyclohexene ring, the final carbon



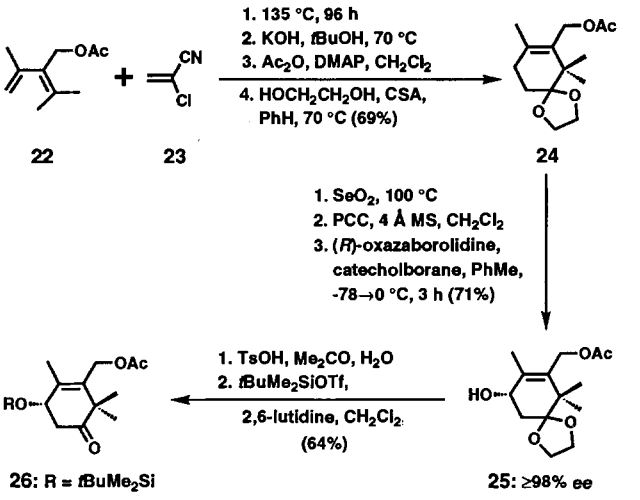
Scheme 2. Frejd's approach to the A ring system by intramolecular cyclization (1987). DBU = 1,8-diazabicyclo[5.4.0]undec-7-ene, R = *t*BuMe$_2$Si.



Scheme 3. Clark's approach to the A ring system through a Diels–Alder reaction (1987). DMF = dimethylformamide, HMPA = hexamethylphosphoric triamide, MS = molecular sieves.

framework was produced through further elaboration and a carefully controlled Gilman reaction. While this procedure had the advantage of brevity, it lacked stereocontrol and required the use of unstable starting materials.

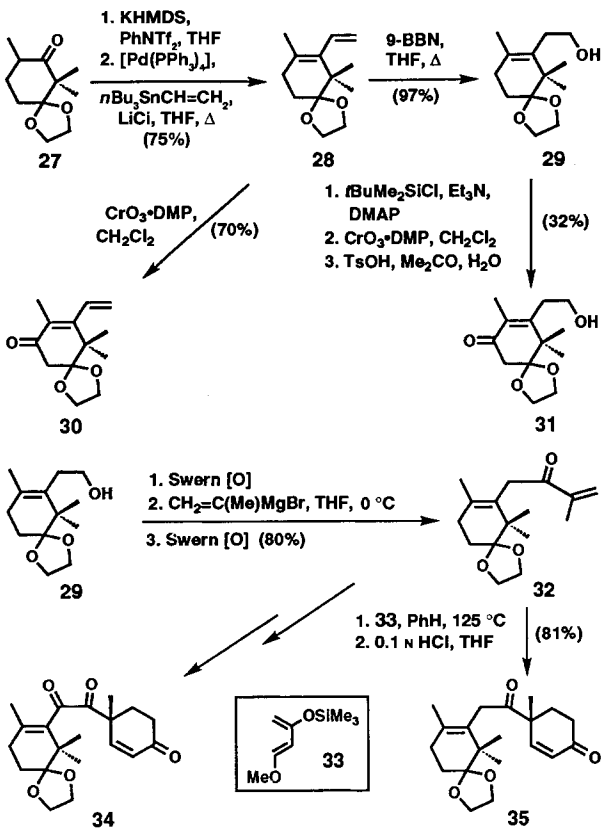
Our own Diels–Alder based strategy[137] for the construction of the A ring is shown in Scheme 4. In this rather simple ap-



Scheme 4. Nicolaou's approach to the A ring system through Diels–Alder reactions (1992). DMAP = 4-dimethylaminopyridine, CSA = camphorsulfonic acid, PCC = pyridinium chlorochromate, Tf = trifluoromethanesulfonyl.

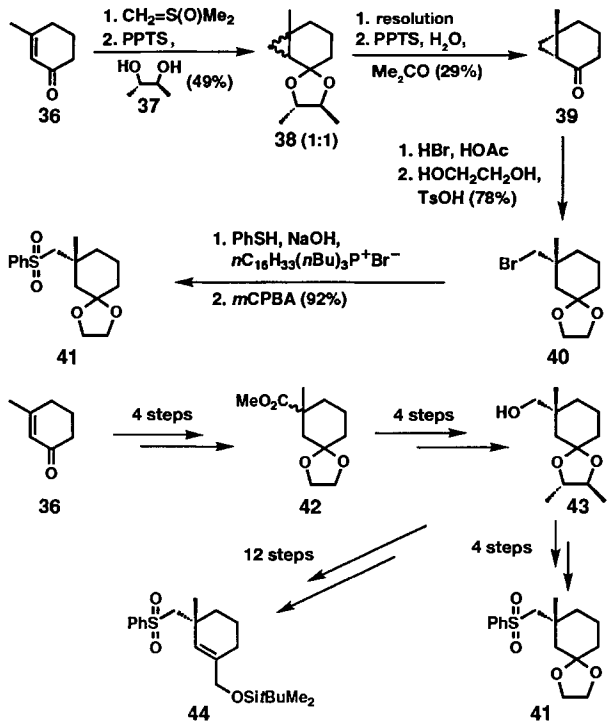
proach the readily available Diels–Alder partners **22** and **23** reacted in a regiospecific manner to afford, after further elaboration, cyclohexene derivative **24**. This intermediate was then smoothly and efficiently transformed into ring A intermediates **25** and **26**. Strategies for the coupling of these systems with fragments containing the C ring of taxol are discussed in Section 3.3.

Scheme 5 depicts the approach of Danishefsky, Queneau et al.[138] to taxol A ring intermediates and model coupling reactions. In this study the known starting material **27**[221] was converted into intermediates **30** or **31** by Stille coupling and subsequent oxidation with chromium(VI) oxide or other



Scheme 5. The Danishevsky–Bornmann approach to A ring systems (1992). HMDS = hexamethyldisilazide, 9-BBN = 9-borabicyclo[3.3.1]nonane, DMP = 3,5-dimethylpyrazole.

standard manipulations. A Diels–Alder reaction of **32** with Danishefsky's diene (**33**) to form **35** demonstrated a possible route for the attachment of the C ring; another potential scenario is the transformation of **32** into **34** in three steps.

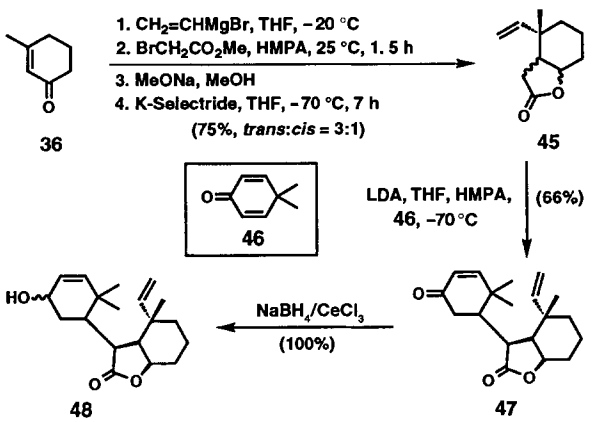


Scheme 6. Kitagawa's approach to the C ring system of taxol (1984). PPTS = pyridinium-*p*-toluenesulfonic acid.

3.2. Approaches to the C and CD Ring Systems of Taxol

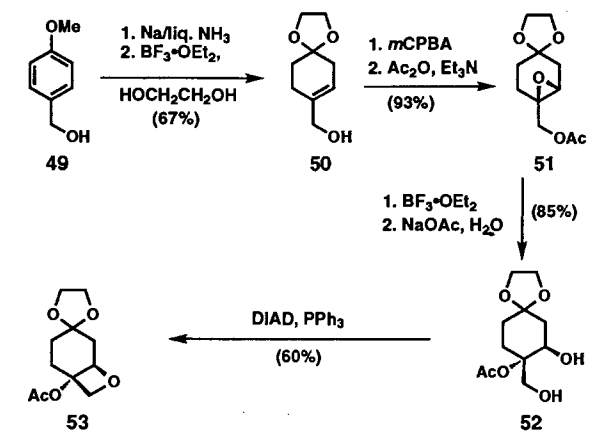
Simple model systems for the C ring such as **41** and **44** (Scheme 6) have been synthesized by Kitagawa et al.[139] Compounds **39**–**44**, enriched in the several enantiomers, were obtained through resolution of diastereomeric **38**, which was produced by cyclopropanation of **36** with dimethylsulfoxonium methylide and treatment with **37**. A phenylsulfonyl group was built into the final intermediates to allow for modeling of coupling reactions.

Fetizon et al. demonstrated construction of C ring model system **45** (Scheme 7).[140] Conjugate addition of vinyl magnesium bromide to **36**, followed by enolate trapping with methyl bromoacetate, hydrolysis, and selective reduction gave **45**. A clever approach to ring A–C model systems **47** and **48** was demonstrated by coupling **46** to **45** under basic conditions.



Scheme 7. Fetizon's approach to the A ring system and the B-seco skeleton (1984). K-Selectride = potassium tri-*sec*-butylborohydride, LDA = lithium diisopropylamide.

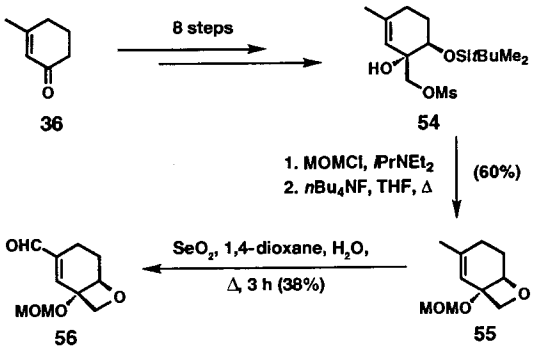
Berkowitz et al. were the first to report a CD ring model system (Scheme 8).[141] Birch reduction of **49** followed successively by protection of the resulting ketone, allylic epoxidation,



Scheme 8. Berkowitz's approach to the CD ring system (1985 and 1987). DIAD = diisopropylazodicarboxylate.

protection, directed epoxide opening, and acyl group migration gave the key intermediate **52**. Finally, an intramolecular Mitsunobu reaction was used to construct the oxetane functionality of **53**.

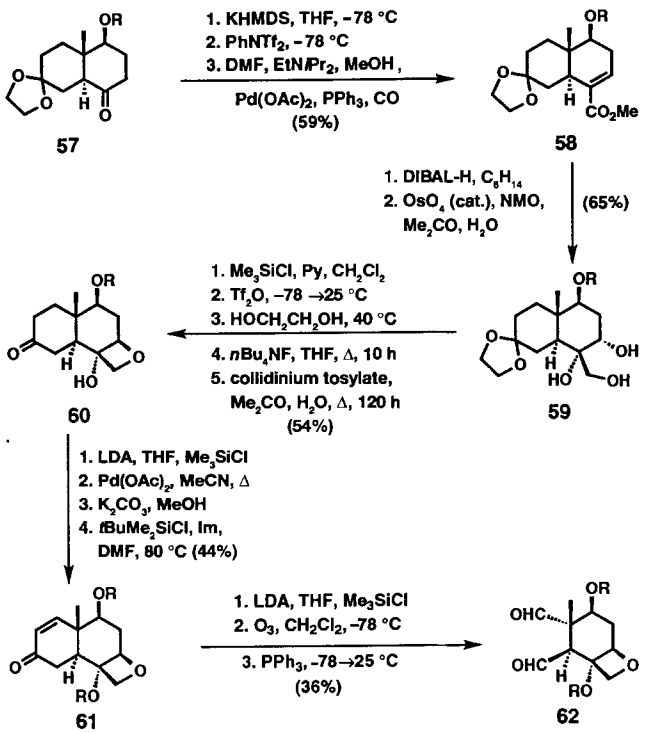
In a different approach, Clark et al.[136] demonstrated the construction of the CD model systems **55** and **56** (Scheme 9).



Scheme 9. Clark's approach to the CD ring system (1987). MOM = methoxymethyl.

Compound **36** was converted into **54** by oxidation of the trimethylsilyl enolate, protection of the resulting alcohol, Petersen olefination, vicinal dihydroxylation, and selective mesylation. The oxetane **55** was formed by an intramolecular S_N2 type mesylate displacement reaction (**54** → **55**). Finally, allylic oxidation of **55** gave **56**.

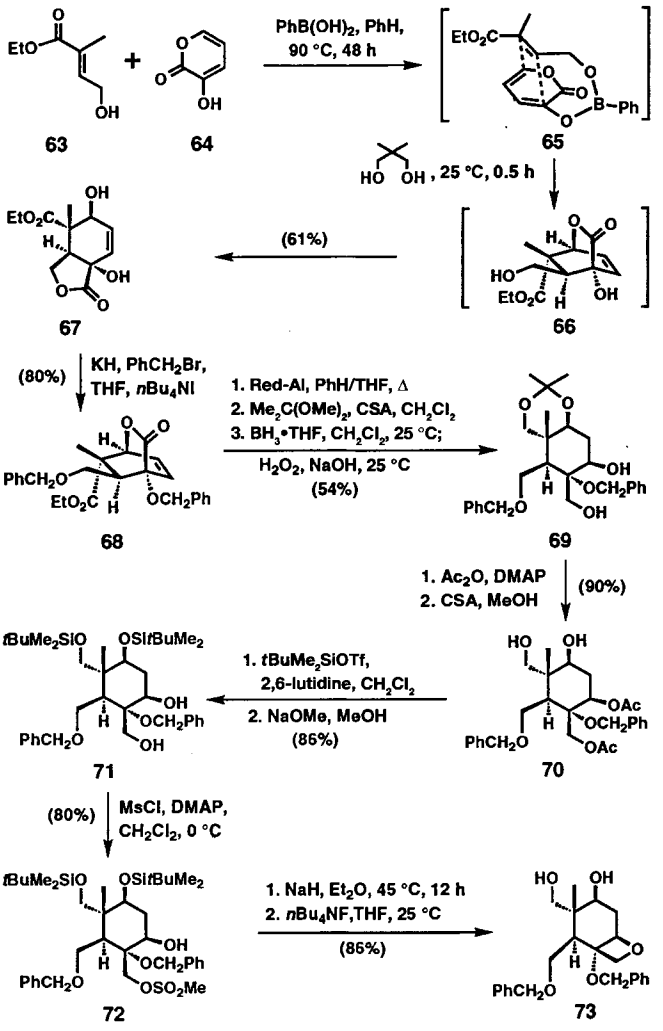
A fully functionalized CD ring system of taxol was synthesized by the Magee–Danishefsky team (Scheme 10).[142] In this effort the Wieland–Miescher ketone was converted into its



Scheme 10. The Magee–Danishefsky approach to CD ring systems (1992). R = tBuMe$_2$Si, DIBAL-H = diisobutylaluminum hydride, NMO = N-methylmorpholine N-oxide, Im = imidazole, collidine = 2,4,6-trimethylpyridine.

derivatives **57**–**61**. Key transformations in this sequence included a palladium-catalyzed carbonylation, vicinal dihydroxylation, intramolecular displacement of the triflate group to form the oxetane ring, and the formation of an enone through Ito's palladium-mediated process. Compound **61** was converted into **62** by ozonolysis of an intermediate silyl vinyl ether.

In our laboratories a strategy was developed for the construction of the CD ring system **73** (Scheme 11)[143] that took advantage of a boron-mediated Diels–Alder reaction[144] between dienophile **63** and 3-hydroxy-2-pyrone (**64**). The initial product

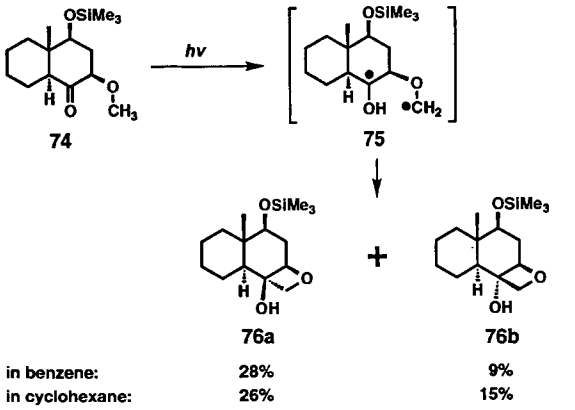


Scheme 11. Nicolaou's approach to the CD ring system through a Diels–Alder reaction (1992). Red-Al = sodium bis(methoxyethoxy)aluminum dihydride, Ms = methanesulfonyl.

of this reaction, compound **66**, spontaneously rearranged to bicycle **67**, which was transformed into **68** and thence sequentially to **69**, **70**, **71**, and **72**. Finally, the oxetane ring was fused onto the C ring by internal nucleophilic displacement of a mesylate group by an alkoxide (**72** → **73**). This flexible strategy allows entry into a variety of C and CD ring systems suitably protected and functionalized for coupling reactions with appropriate A ring systems.

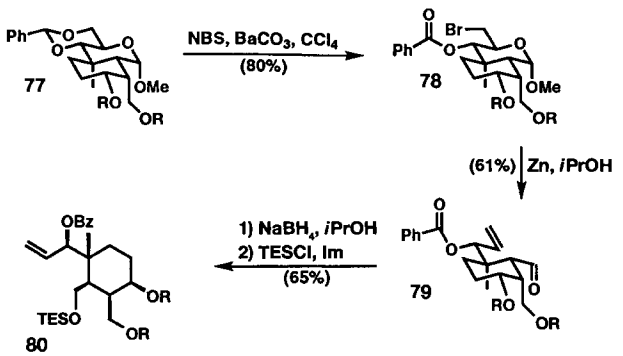
Wender and Rawlins have recently reported model studies of a Norrish Type II photolysis of α-methoxyketone **74** directed at

the production of the oxetane ring of taxol (Scheme 12).[145] Unfortunately, and despite the elegance of the method, the yields of the resulting oxetane were rather low, and the predominant stereochemistry corresponded to the undesired *trans* oxetane.



Scheme 12. Wender's photolytic entry into the CD ring model system (1992).

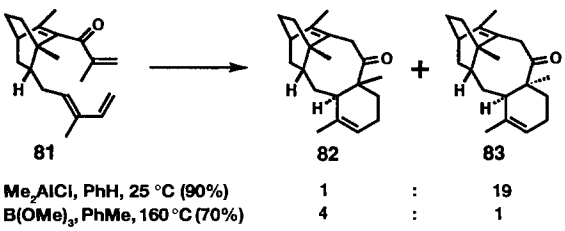
Jenkins et al. have synthesized a functionalized C ring model system (Scheme 13) for use in his convergent approach to the taxane skeleton (see Scheme 17 in Section 3.3).[146] The protected methoxypyranose derivative **77** was converted by a rather clever application of the Vasella fragmentation into the aldehyde **79** and then reduced and protected to give the C ring model **80**. This model can be easily converted into a number of Diels–Alder precursors.



Scheme 13. Jenkin's functionalized C ring model system (1993). R = tBuPh$_2$Si, NBS = *N*-bromosuccinimide, TES = triethylsilyl.

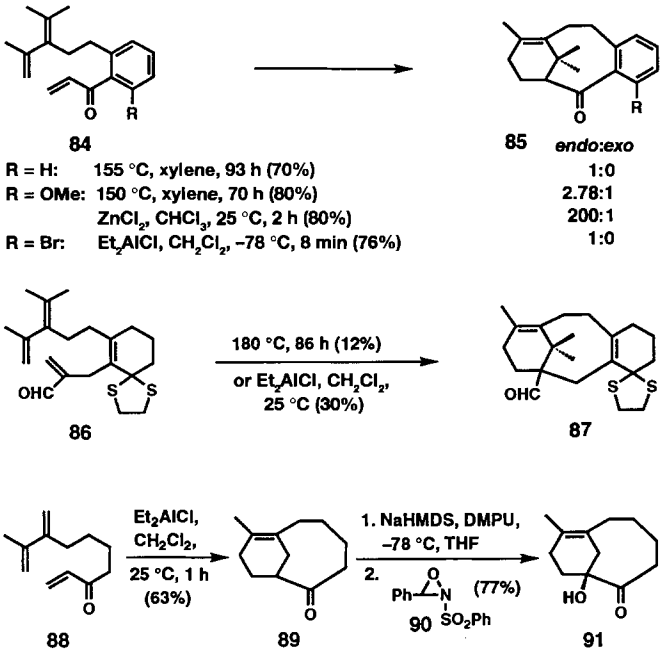
3.3. Approaches to the Taxol Skeleton

One of the earliest and most impressive attempts to construct a taxol-type skeleton was that of Sakan and Craven, who in 1983 reported the intramolecular Diels–Alder reaction shown in Scheme 14.[147] The uncatalyzed reaction gave the desired product **82** but as an intractable mixture with by-products. Catalysis of the crucial Diels–Alder reaction by a strong Lewis acid (Me_2AlCl) gave predominantly the undesired stereoisomer. Finally, success was gained through the addition of $B(OMe)_3$, which gave, in a clean conversion, predominantly the desired product.

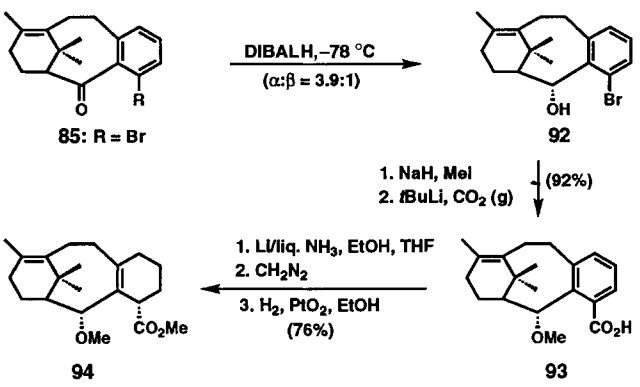


Scheme 14. Sakan's approach to the taxol skeleton through a Diels–Alder reaction (1983). The desired isomer is **82**.

Similarly but independently, Shea and his collaborators developed a number of intramolecular versions of the Diels–Alder reaction starting with **84**, **86**, and **88** and leading to taxol skeleton models **85**, **87**, and **91** as shown in Scheme 15.[148] Atropisomers were observed in these series of compounds. The same group has also demonstrated the viability of establishing the C15 hydroxyl group through trapping of the bridgehead enolate with Davis's reagent. The Diels–Alder product **85** was trans-



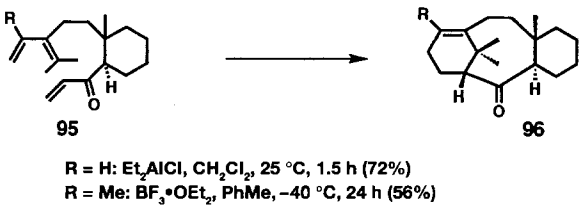
Scheme 15. Shea's approach to the taxol skeletons through a Diels–Alder reaction (1983, 1986, 1988, and 1992). DPMU = *N*,*N*′-dimethyl-*N*,*N*′-propylene urea.



Scheme 16. Shea's approach to taxol skeletons through a Diels–Alder reaction/Birch reduction (1992).

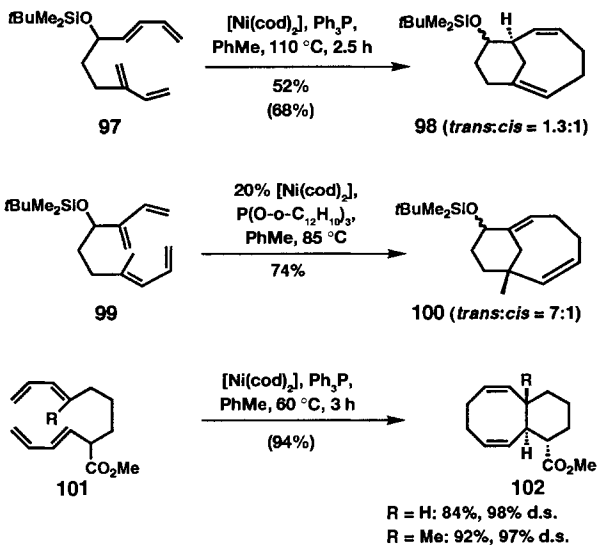
formed into taxol model system **94** possessing the ABC ring skeleton (Scheme 16).[149]

Scheme 17 outlines Jenkins' intramolecular Diels–Alder approach to the taxol skeleton.[150] This methodology was developed concurrently with Shea's and provided entries to compounds such as **96**. Recently, Jenkins et al. synthesized a more functionalized C-ring analog for use in this methodology (see Scheme 13 in Section 3.2).



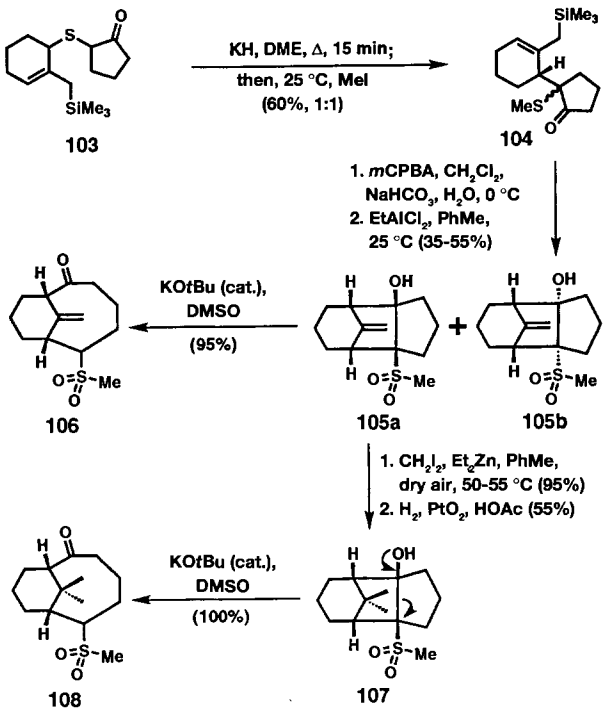
Scheme 17. Jenkin's approach to taxol skeletons through a Diels–Alder reaction (1984–1989).

As part of studies involving nickel-catalyzed cycloadditions of bis(diene)s, the Wender group developed approaches to AB and BC ring model systems **98**, **100**, and **102** (Scheme 18).[151] While these methods provided a relatively unsubstituted system, they did demonstrate the feasibility of forming the B ring of taxol with a direct [4 + 4] cycloaddition process.

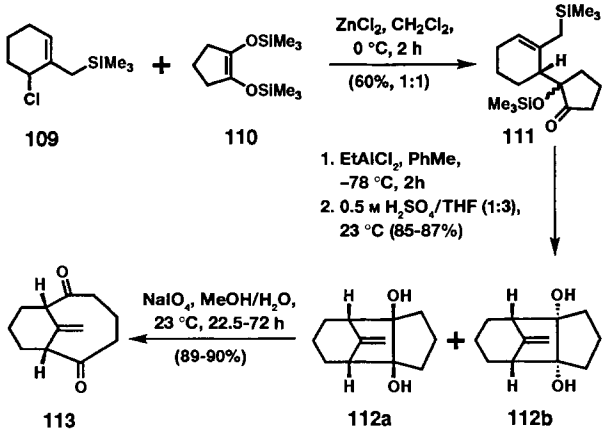


Scheme 18. Wender's approach to the AB and BC ring systems through a [4 + 4] addition (1987). COD = 1,5-cyclooctadiene, $P(O\text{-}o\text{-}C_{12}H_{10})_3$ = tri-*o*-biphenyl phosphite, d.s. = diastereoselectivity. The percentages in parentheses indicate how much starting material was consumed.

Two clever approaches to taxol model systems were reported by Trost et al. In the first approach, shown in Scheme 19, a fragmentation reaction of hydroxy sulfones **105a,b** and **107** leading to the eight-membered ring systems **106** and **108** was utilized.[152] This reaction takes advantage of the stabilization, provided by the sulfone group, of the carbanion intermediates involved. In the second approach, depicted in Scheme 20, an oxidative cleavage of diols **112a,b** led to the formation of a similar bicyclic skeleton (**113**).[153]

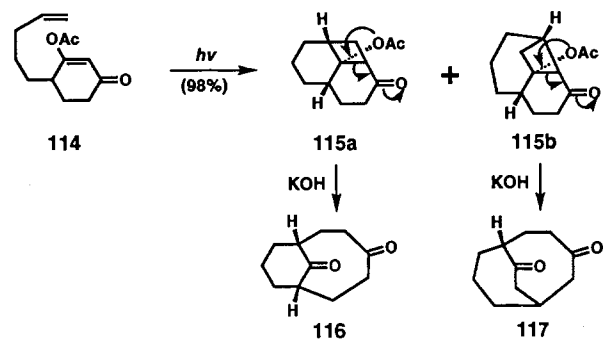


Scheme 19. Trost's approach to the AB ring systems through a fragmention (1982). DME = dimethoxyethane, DMSO = dimethylsulfoxide.



Scheme 20. Trost's approach to the AB ring system through an oxidative cleavage reaction (1984).

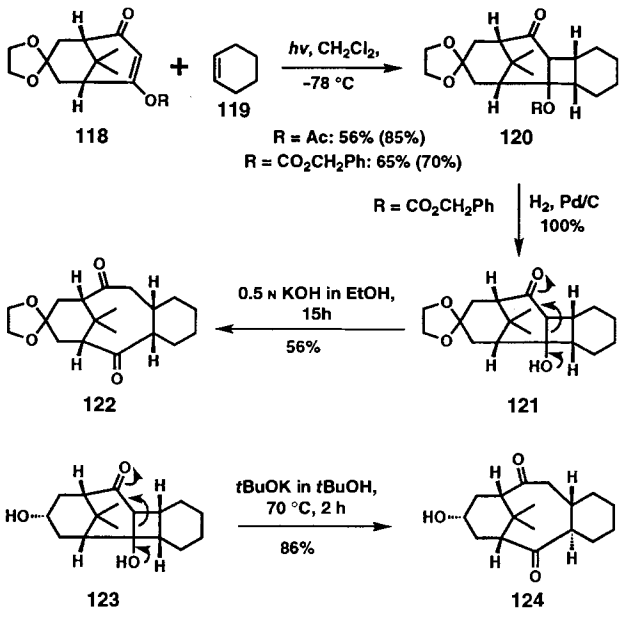
An approach based on a retroaldol type fragmentation was reported by Pattenden in 1983 (Scheme 21).[154] In this strategy,



Scheme 21. Pattenden's approach to the AB ring system through a retroaldol cleavage reaction (1983).

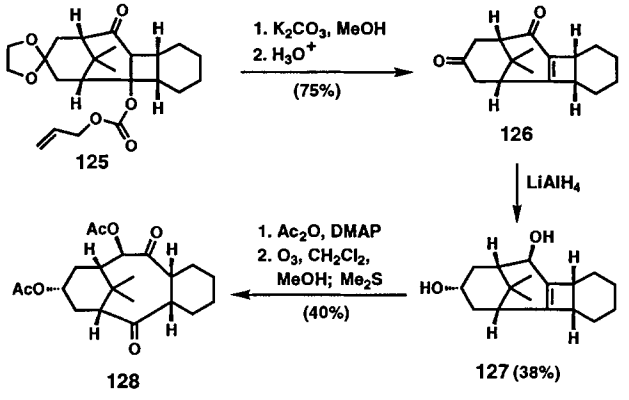
β-acetoxy ketones **115a,b**, derived from the intramolecular [2 + 2] photocycloaddition of **114**, were converted into **116** and **117**, respectively, under the influence of KOH. Unfortunately, the nonregioselective nature of the photocycloaddition reaction led to a mixture of products.

Retroaldol and oxidative ring expansion were also utilized by Blechert et al. in the synthesis of a number of interesting taxoids with biological activity (Schemes 22–24). Substrates **121** and

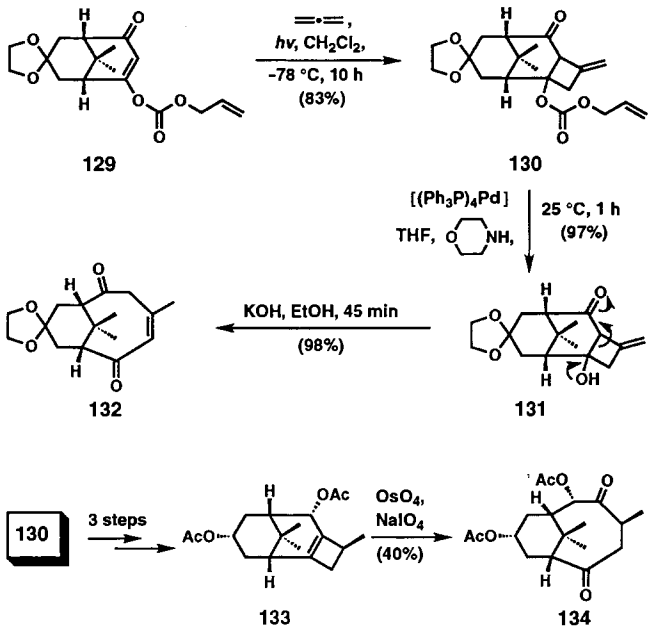


Scheme 22. Blechert's approach to taxol systems through a retroaldol cleavage reaction (1984 and 1991). The percentages in parentheses indicate how much starting material was consumed.

123,[155] and **131**,[156] derived from intermolecular [2 + 2] photocycloaddition reactions and subsequent manipulations, were subjected to basic conditions and afforded tricyclic model systems **122** and **124** (Scheme 22), and **132** (Scheme 24), respectively, on retroaldol-type fragmentations. In an alternative approach, oxidative cleavage of compounds **127**[157] and **133** gave **128** (Scheme 23) and **134** (Scheme 24), respectively. These highly promising ring expansion strategies have the potential of de-



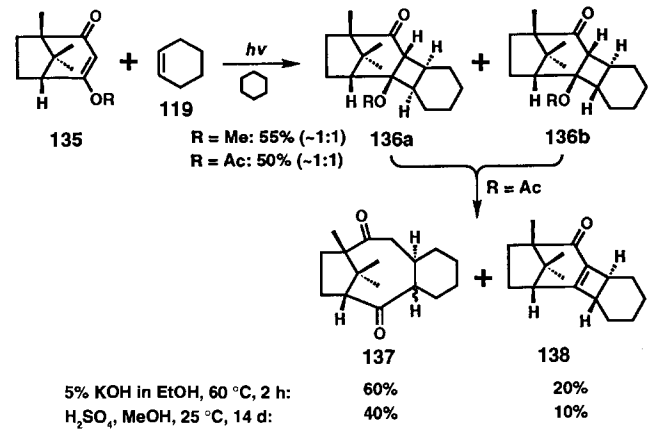
Scheme 23. Blechert's approach to the taxol skeleton through oxidative ring expansion (1992). The reduction of **126** yields isomers of **127** in 33% yield.



Scheme 24. Blechert's approach to the AB ring system through retroaldol cleavage and oxidative ring expansion (1992).

livering important pointers for the design of mimics of taxol and even the natural product itself.

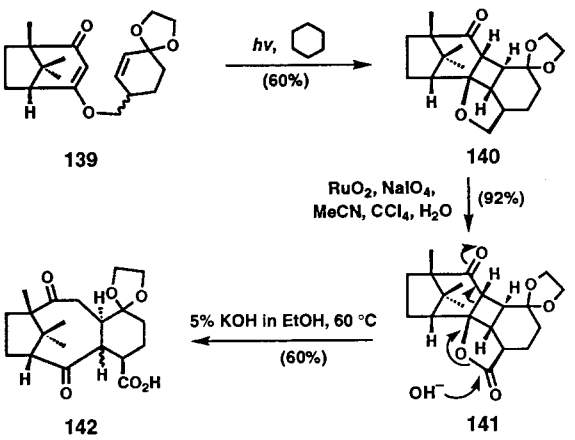
Berkowitz et al. also provided examples of the approach through photocycloaddition–retroaldol reactions to the construction of taxol model systems **137** and **142**, starting from **135** and **139** (Schemes 25 and 26).[158] These models have 5-mem-



Scheme 25. Berkowitz's first approach to the BC ring system through intramolecular photocycloaddition and retroaldol cleavage (1985).

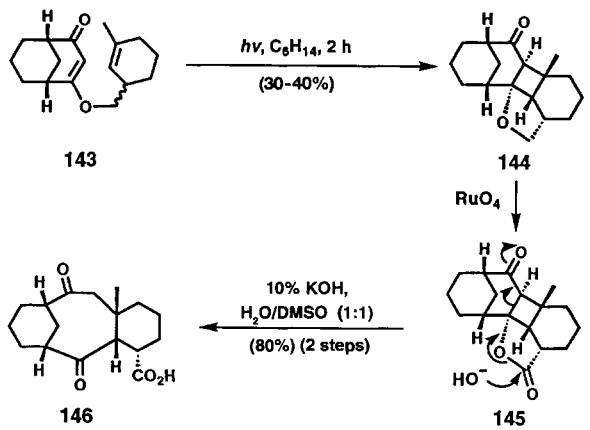
bered A-ring frameworks that, while not functionalized appropriately for conversion to the cyclohexene ring present in the natural product, could provide interesting biological mimics of taxol.

A further example of a synthesis of the taxoid skeleton through photocycloaddition–retroaldol reactions was reported by Inouye's group (Scheme 27).[159] This study could prove particularly useful because of its success in the difficult step of installing the tertiary methyl group and proper functionality for



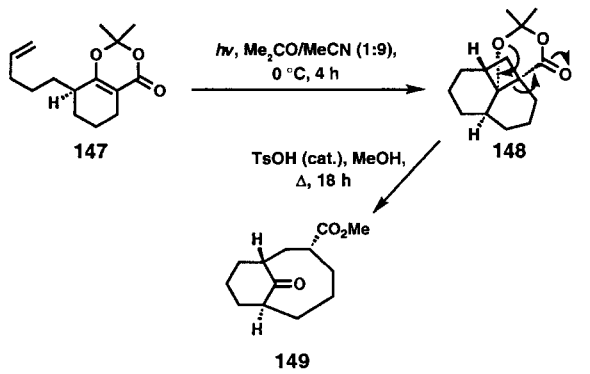
Scheme 26. Berkowitz's second approach to the BC system through intramolecular photocycloaddition and retroaldol cleavage (1985).

further elaboration, even though the synthesized model **146** lacked the *gem* dimethyl groups of taxol.



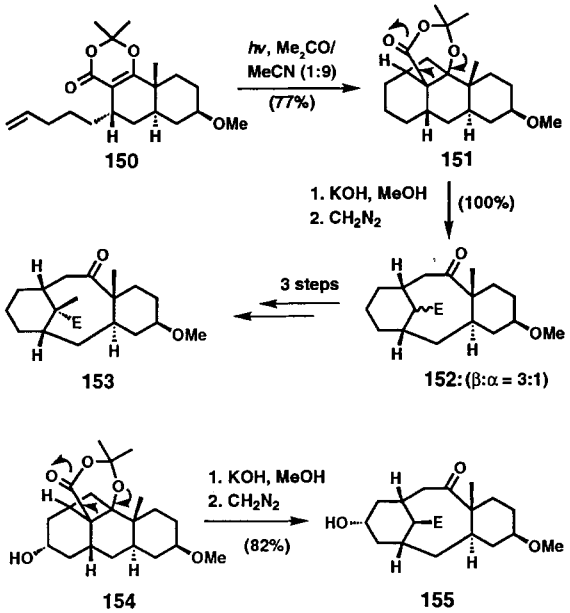
Scheme 27. Inouye's approach to the taxol skeleton through retroaldol cleavage (1985). The yield of **144** is relatively small, because only one isomer of **143** reacts. The other isomer was recovered unchanged.

The Winkler group's studies were also based on photocycloaddition/retroaldol strategies and led to interesting and promising results. As shown in Scheme 28,[160] the original



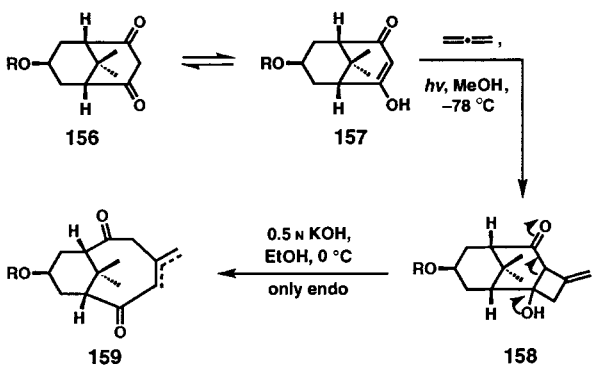
Scheme 28. Winkler's approach to the AB ring system through retroaldol cleavage (1986).

model system **148** was converted into AB ring system **149** by acidic treatment. In a subsequent study, treatment of compounds **151** and **154** with base provided, after methylation, taxol frameworks **153** and **155**, respectively (Scheme 29).[161] These systems could also prove amenable to fruitful elaboration.



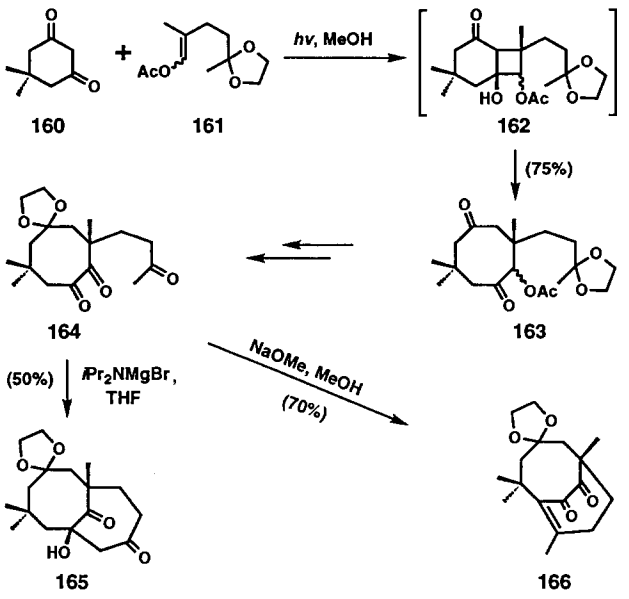
Scheme 29. Winkler's approach to the taxol skeleton through retroaldol cleavage (1989 and 1992). E = CO_2Me

The work of the Fetizon laboratory, depicted in Scheme 30, also involved a combination of photocycloaddition and retroaldol reactions and provided rapid access to interesting taxoid skeletons **159**.[162] The same group reported an unsuccessful

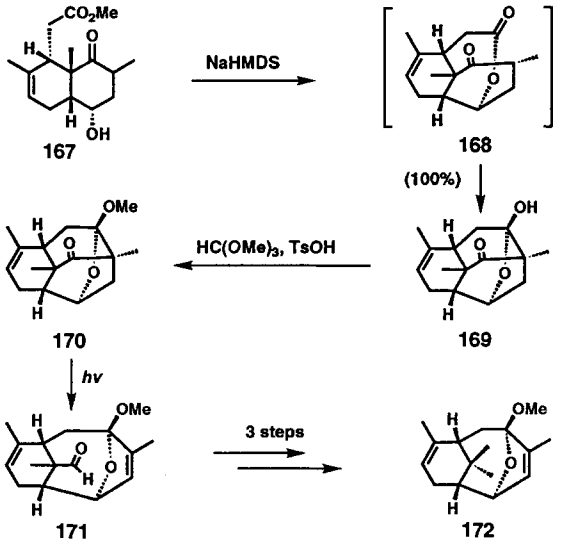


Scheme 30. Fetizon's approach to the taxol AB ring systems through retroaldol cleavage (1987). **156**–**158**, R = PhCO, MOM; **159**, R = H: only endocyclic double bonds (yield 35%), R = MOM: 43% of the product has endo- and 29% exocyclic double bonds.

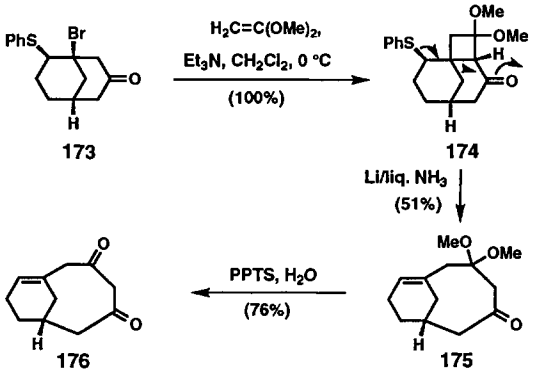
attempt[163] to prepare the taxol BC ring system by aldol condensation of **164** (Scheme 31). Additionally, ketoester condensation of **168** (Scheme 32)[164] followed by methylation furnished product **170**, which was further elaborated to the AB ring framework by a Norrish II photolytic reaction to provide **172** via **171**.



Scheme 31. Fetizon's approach to the AB ring system through a combination of photochemistry and aldol reactions (1992).

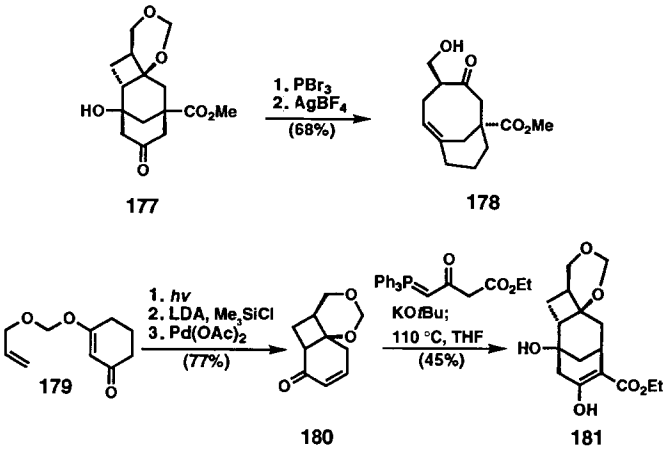


Scheme 32. Fetizon's approach to the AB ring system through ketoester condensation and photolysis (1992).



Scheme 33. Kraus's approach to the AB ring system through reductive cleavage (1987).

Kraus et al. have reported two photocycloaddition–reductive cleavage approaches to the AB ring model systems (Scheme 33 and 34). The first method[165] involves in situ generation of an enone from **173** followed by trapping as **174** with ketene dimethyl acetal. Treatment of **174** with Li/liquid ammonia gave the ring-opened product **175**, which upon deprotection led to **176**. In the second approach,[166] the tetracycle **177** is fragmented by generation of the bridgehead bromide followed by Lewis acid treatment to give bicycle **178**. To move to a more functionalized system, the enone **179** is subjected to intramolecular photocyclization with the vinyl ether to give, after oxidation, tricyclic enone **180**. The enone is then further annulated to give tetracycle **181**. The authors intend to perform a fragmentation analogous to that of **177** on this substrate.

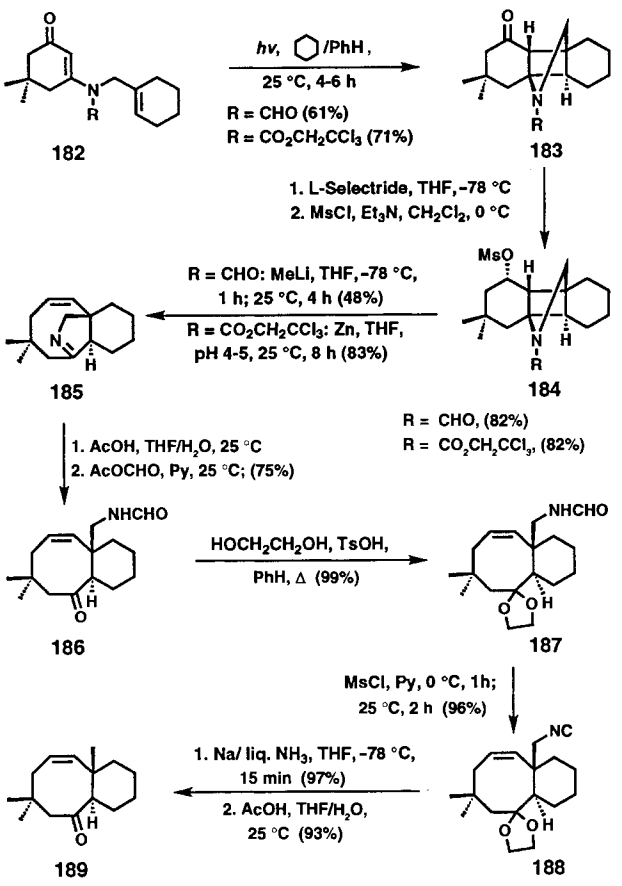


Scheme 34. Kraus's approach to an AB ring system (1993).

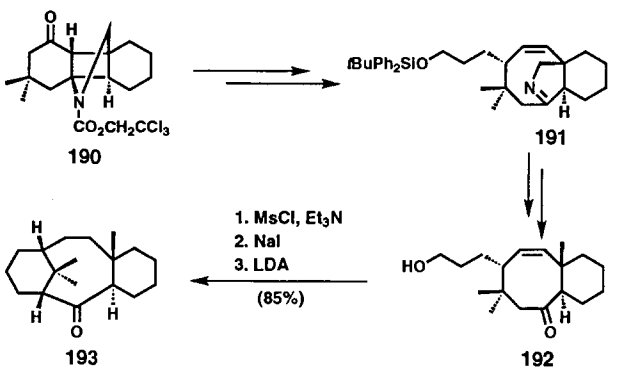
The Swindell group has been very successful in preparing a number of advanced taxol intermediates by a variety of methods. In general, Swindell's strategy involves initial photoinduced construction of a polycyclic system such as **183**, which is then elaborated further to give the desired ring frameworks as shown in Scheme 35.[167] Thus, an amide fragmentation of **184** formed the eight-membered ring system **185**, which was further converted into the BC ring model compound **189** via intermediates **186**–**188**.

In another approach by Swindell et al. (Scheme 36), intramolecular alkylation of **192**, derived from the photoproduct **190** (=**183**, R = $CO_2CH_2CCl_3$) in two sets of seven steps, provided an entry into taxol ABC model system **193**.[168] Alternatively, an aldol reaction was employed to construct ring A (**198** → **199**, Scheme 37) along the route to the advanced ABC ring skeletons **199** and **201** starting from photoadduct **194**.[169] In the same study, highly advanced taxol skeletons such as **205** were constructed (Scheme 38) by photoaddition, amide fragmentation, and aldol condensation.

A reductive fragmentation reaction was used by Ghosh et al. to establish the eight-membered ring compound **207** (Scheme 39) starting with compound **206**.[170] Subsequent ring expansion of **208**, derived from **207**, gave the AB ring skeleton **209**.



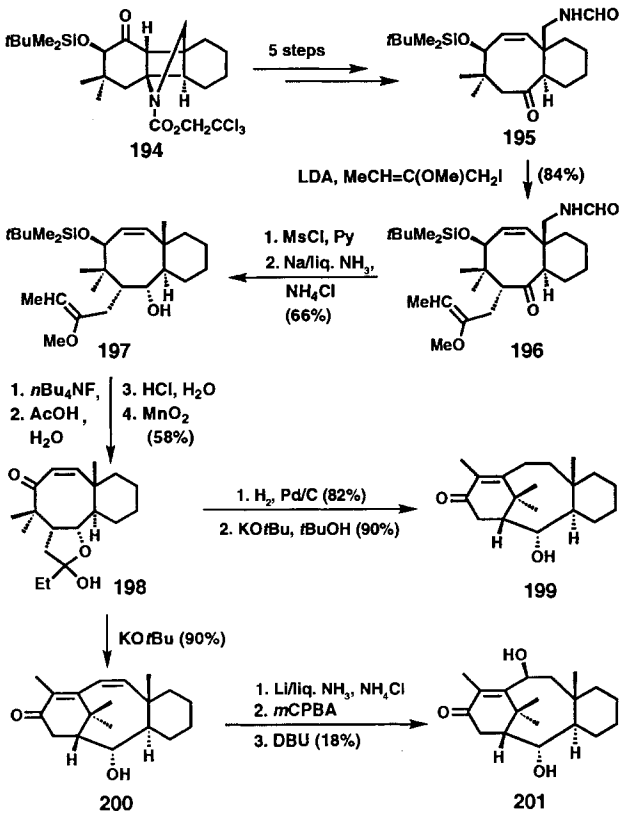
Scheme 35. Swindell's approach to the BC ring system through amide fragmentation (1984 and 1987). L-Selectride = lithium tri-*sec*-butylborohydride.



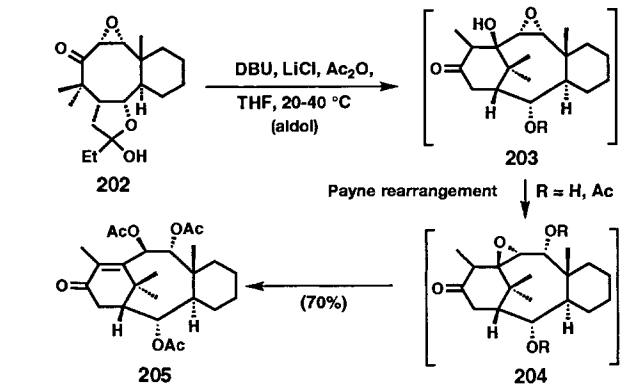
Scheme 36. Swindell's approach to the ABC taxol skeleton through amide fragmentation (1987).

An interesting application of the Grob fragmentation for the synthesis of an AB ring system was devised by Yamada et al. (Scheme 40).[117] In this study, tricyclic substrate **211**, derived from **210** in 17 steps, was converted in eight steps into hydroxy mesylate **212**. Treatment of **212** with potassium hydride followed by methylation furnished **213** in high yield.

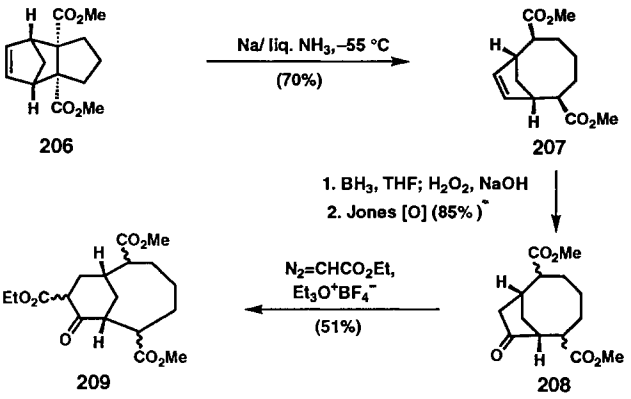
The Holton laboratory has reported a number of advanced studies concerning taxol, including a total synthesis of taxusin (**6**, see Fig. 1), in which they employed the naturally occurring β-patchouline oxide as starting material. Two of these approaches use a hydroxyepoxide fragmentation process as the



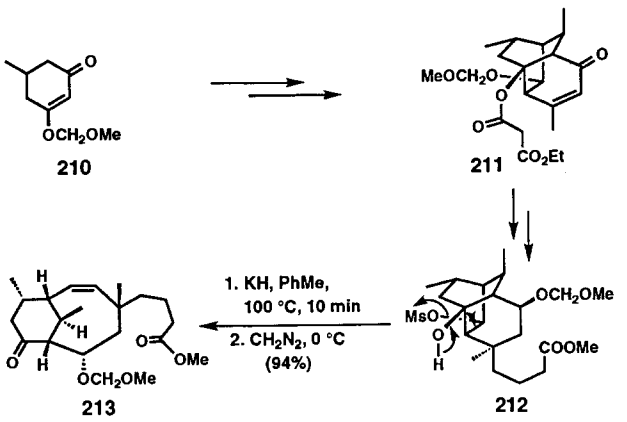
Scheme 37. Swindell's approach to the advanced taxol skeletons through amide fragmentation (1990).



Scheme 38. Swindell's approach to the highly advanced ABC skeleton through amide fragmentation (1990).

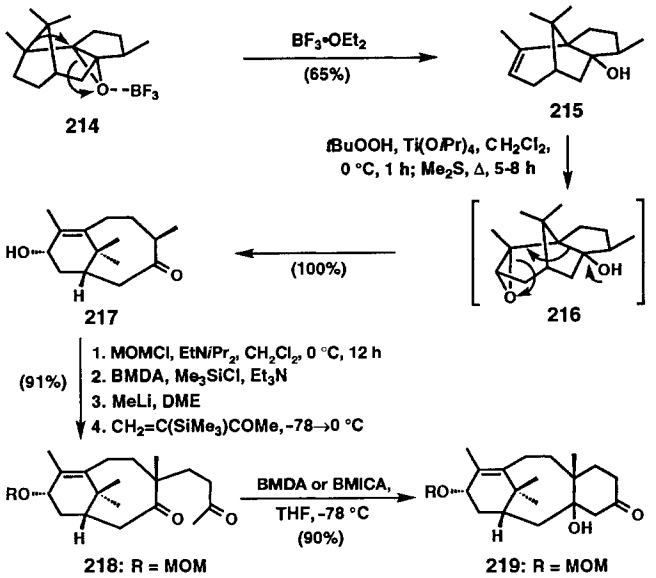


Scheme 39. Ghosh's approach to the AB ring system through reductive cleavage (1990).



Scheme 40. Yamada's approach to the AB ring system through Grob fragmentation (1984).

key step to secure AB ring systems. In the first approach, patchouline oxide (**214**) is subjected to Lewis acid mediated epoxide opening/rearrangement, and the resulting hydroxy alkene is epoxidized to give **217**. An intramolecular aldol condensation within **218** derived from **217** established the ABC ring framework **219** of taxol (Scheme 41).[172] The same strategy was

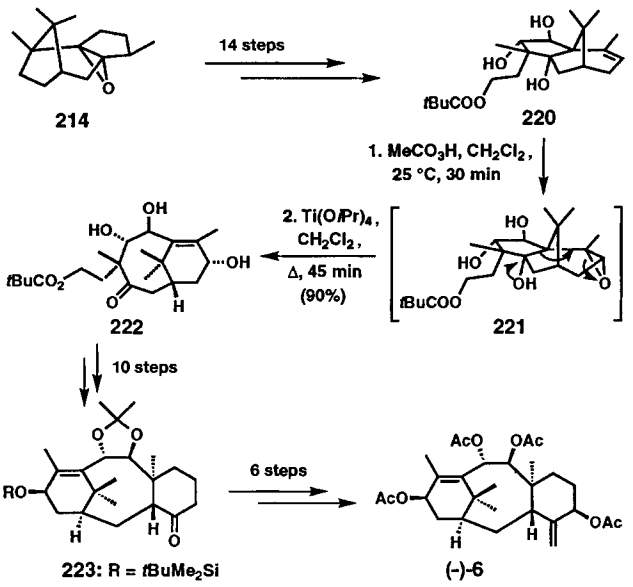


Scheme 41. Holton's approach to the taxol skeleton through fragmentation (1984). MgBr(NRR'), R = R' = *i*Pr (BMDA); R = *i*Pr, R' = cyclohexyl (BMICA).

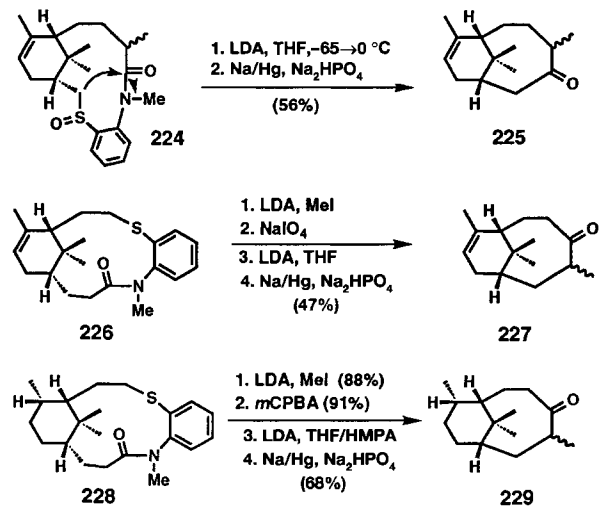
applied to compound **222** (Scheme 42) leading to a total synthesis of the nonnatural enantiomer of (−)-taxusin [(−)-**6**].[173]

An elegant ring-contraction method has been applied to the synthesis of taxol model systems **225**, **227**, and **229** by Ohtsuka et al.[174] As shown in Scheme 43, this approach involves a base-induced rearrangement after which a sulfoxide moiety is excised by reductive C–S bond cleavage, leading to the eight-membered ring.

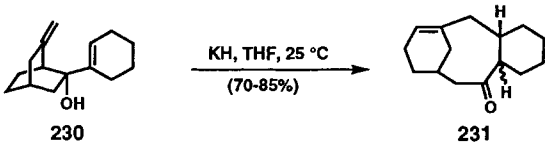
An interesting approach to the taxol skeleton **231** based on an oxy-Cope rearrangement reaction of **230** was published by Martin et al. in 1982 (Scheme 44).[175] This approach is most notable



Scheme 42. Holton's approach to the synthesis of (−)-taxusin [(−)-**6**] (1988).



Scheme 43. Ohtsuka's approach to the AB ring systems through ring contraction (1984, 1986, and 1988).

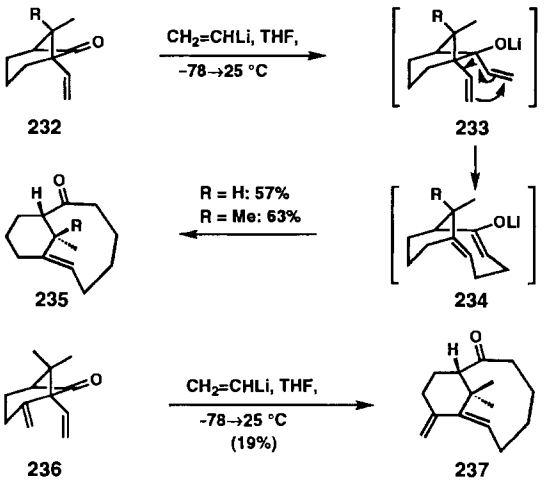


Scheme 44. Martin's approach to the taxol skeleton through anionic or oxy-Cope rearrangement (1982).

for its brevity: it establishes the ABC ring system in four steps from readily available (3-oxocyclohexyl)acetic acid.

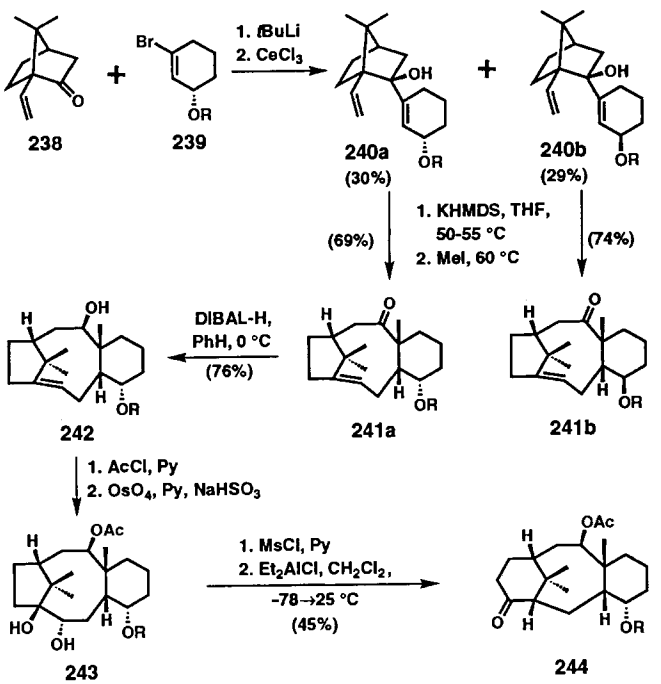
The approach of Snider et al. to model systems **235** and **237** also involved oxy-Cope rearrangements (Scheme 45).[176] While these approaches provide for functionalization at the AB ring junctures, they do not lead to the tricyclic carbon skeleton.

Paquette's group reported a particularly interesting anionic oxy-Cope rearrangement route to the taxol skeleton (Scheme



Scheme 45. Snider's approach to the AB ring systems through anionic oxy-Cope rearrangement (1991).

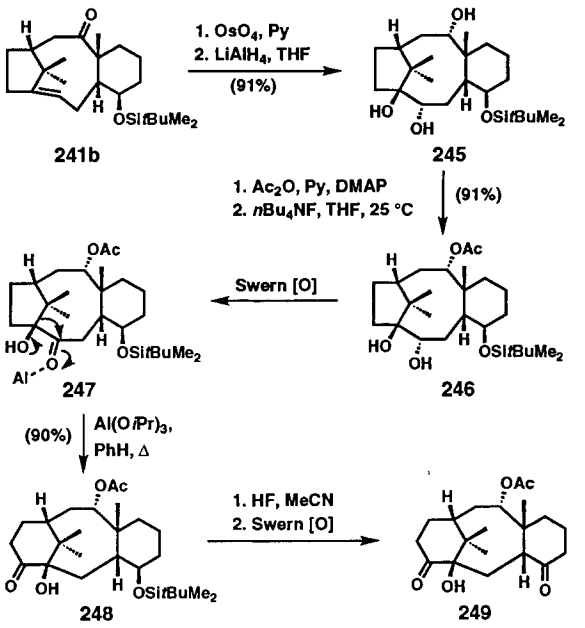
46). Base treatment of isomers **240a,b** gave rearrangement products **241a,b**; **241a** was converted into diol **243** via **242**. Pinacol-type rearrangement of **243** afforded the ABC ring skeleton **244**.[177] An α-hydroxyketone rearrangement of **247**, prepared



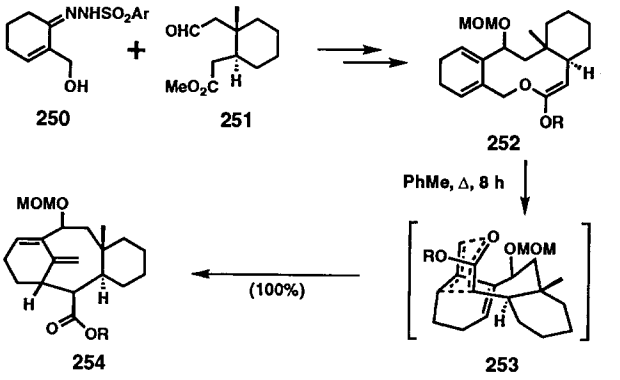
Scheme 46. Paquette's approach to the taxol skeleton through an oxy-Cope rearrangement (1989–1991). R = tBuMe$_2$Si.

from the isomeric diol **246** from **241b**, was also reported by the Paquette group to furnish the advanced model system **249** (Scheme 47).[178]

A clever approach to the taxol skeleton based on an intramolecular Claisen rearrangement in which a 10-membered ring is contracted to an eight-membered ring was reported by Funk (**252** → **253** → **254**, Scheme 48). The ten-membered ring was synthesized from **250** and **251** in seven steps.[179] This



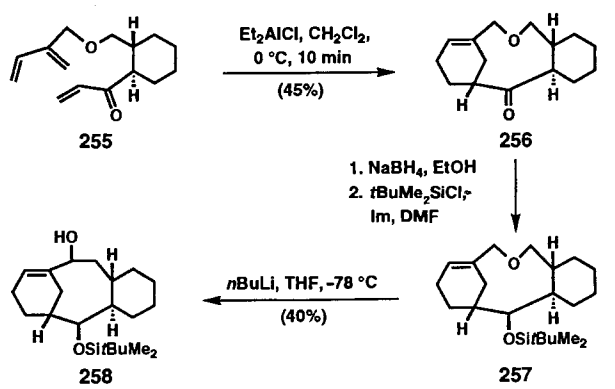
Scheme 47. Paquette's approach to the taxol skeletons through an α-hydroxyketone rearrangement (1992).



Scheme 48. Funk's approach to the taxol skeleton through an intramolecular Claisen rearrangement (1988). Ar = triisopropylbenzene, R = tBuMe$_2$Si.

method provides the ABC system with the troublesome angular methyl group already installed.

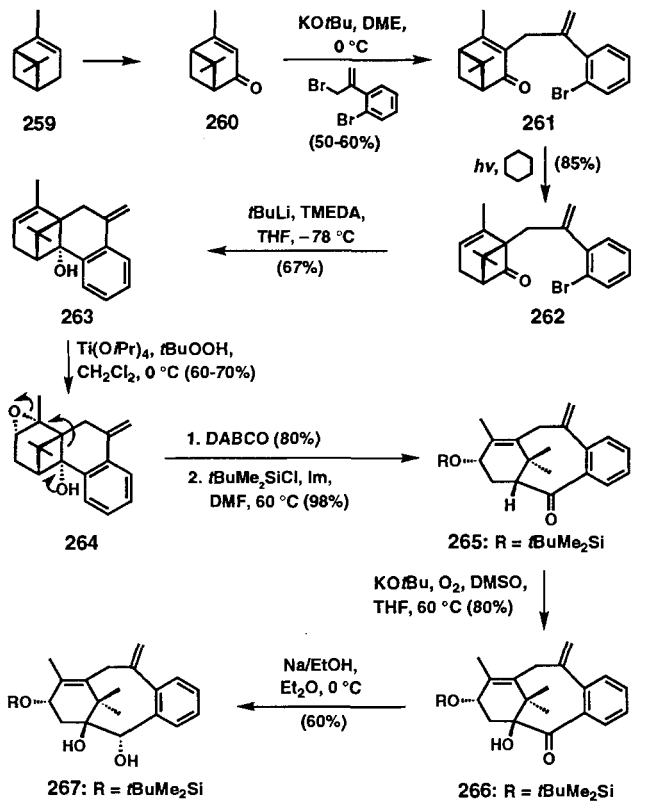
Another interesting strategy towards the taxol skeleton (Scheme 49) based on a Wittig rearrangement was recently pub-



Scheme 49. Yadav's approach to the taxol skeleton through an intramolecular Wittig rearrangement (1991).

lished by Yadav's group.[180] This approach began with an intramolecular Diels–Alder reaction to construct the A ring model system **256**, which was converted into **257** by standard chemistry. Treatment of **257** with base resulted in a contraction of the nine-membered ring to the eight-membered ring **258**.

An elegant strategy towards the taxol skeleton was recently reported from the Wender group (Scheme 50). In this sequence,



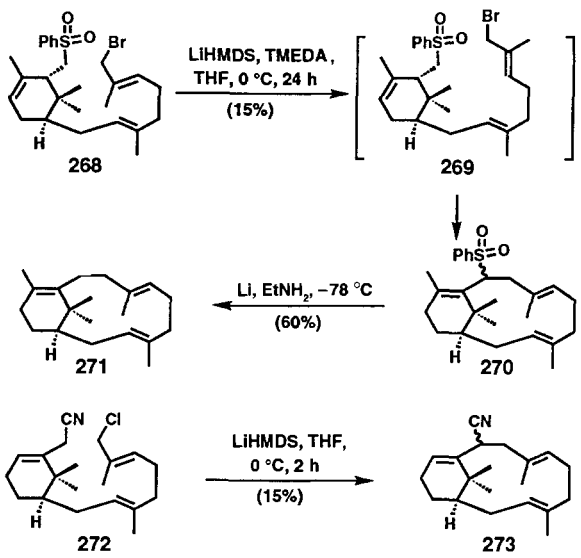
Scheme 50. Wender's approach to the taxol skeleton through rearrangement (1992). TMEDA = *N,N,N',N'*-tetramethylethylenediamine, DABCO = 1,4-diazabicyclo[2.2.2]octane.

(+)-pinene (**259**) was utilized as a cheap starting material for hydroxyepoxide **264**, which then underwent base-induced fragmentation to afford the tricyclic system **265**. Further elaboration led to the more advanced intermediates **266** and **267** (Scheme 50).[181] Final functionalization of these intermediates to taxol, the ultimate goal of these studies, still remains elusive.

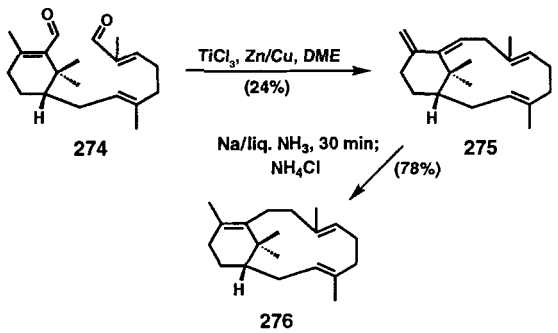
Two approaches to BC secotaxol skeletons **271** and **273** reported by Kato are shown in Scheme 51.[182] Both involved intramolecular alkylation reactions, in which the bromosulfone **269** and chloronitrile **272** were used to construct the 12-membered seco ring systems **271** (after desulfurization) and **273**, respectively. These compounds are analogs of verticillene, a putative biosynthetic precursor to taxol.

The strategy of Pattenden et al. towards taxoids (Scheme 52) relied on a McMurry-type, intramolecular, reductive pinacol coupling reaction of the dialdehyde **274** to form the macrocyclic ring **275**. This intermediate was further transformed into (*E,E*)-verticillene (**276**) by reduction with Na in liquid ammonia.[183]

In the pioneering work of Kende et al., a McMurry cyclization reaction was successfully applied to form the B ring system

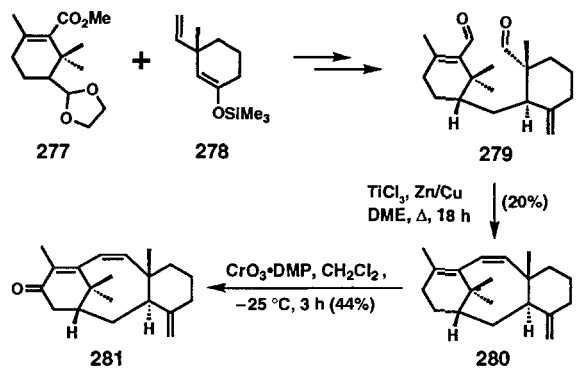


Scheme 51. Kato's approach to the BC secotaxol skeleton through intramolecular alkylation (1978 and 1981).



Scheme 52. Pattenden's approach to the BC secotaxol skeleton through intramolecular reductive coupling (1985 and 1990).

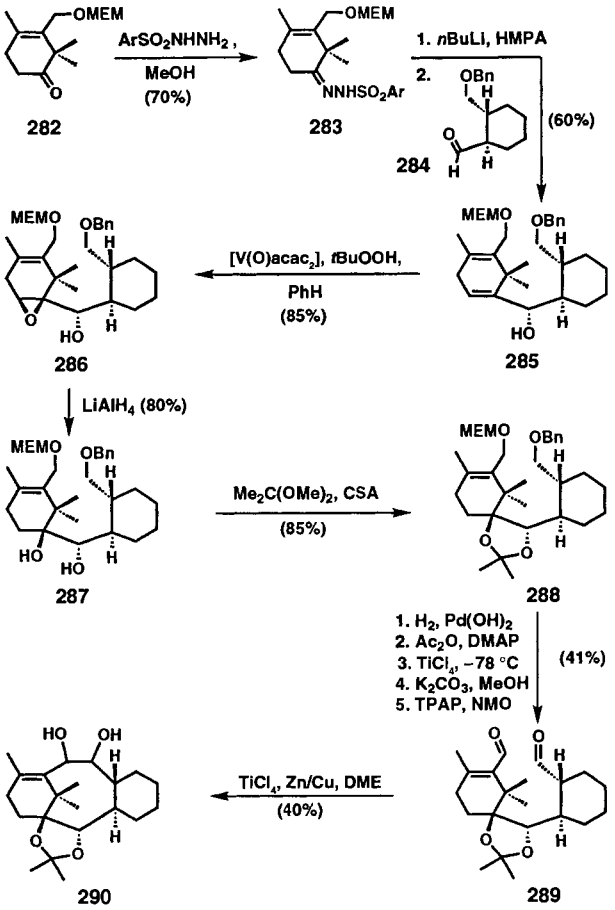
280 from the dialdehyde **279**, obtained from **277** and **278** in twelve steps, as shown in Scheme 53.[184] The low yield of the intramolecular coupling reaction was attributed primarily to competing intramolecular 1,4-addition of the intermediate diketyl.



Scheme 53. Kende's approach to the taxol skeleton through intramolecular McMurry cyclization (1986). DMP = 3,5-dimethylpyrazole.

A variety of coupling reactions between A and C ring systems have been carried out in our laboratories. Dithiane and Stille

coupling reactions were demonstrated to be feasible. The hydrazone–vinyllithium chemistry, illustrated in Scheme 54, was found to be exceptionally efficient in coupling A ring and C ring fragments.[185] Addition of the vinyllithium species, generated from **283**, to the aldehyde **284** gave **285**, which was converted into the diol **287** by regioselective epoxidation and subsequent regioselective reduction. Protection of the diol as **288** and further standard chemistry provided the dialdehyde **289**. An intramolecular coupling reaction within **289** gave the diol **290**. We are currently attempting to apply this technology to the total synthesis of taxol.



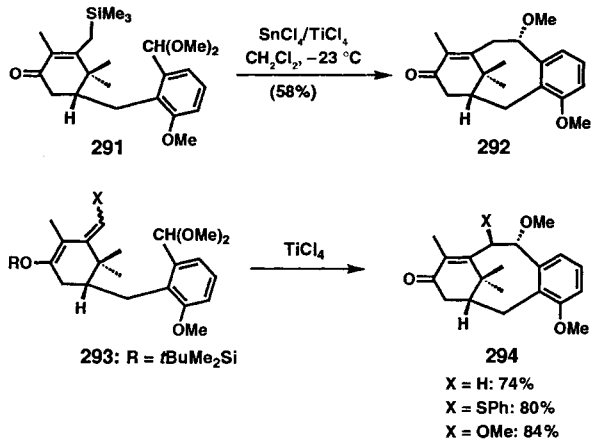
Scheme 54. Nicolaou's approach to the taxol skeleton through intramolecular cyclization (1992). Ar = 2,4,6-triisopropylphenyl, Bn = benzyl, acac = acetylacetonate, TPAP = tetra-*n*-propylammonium perruthenate.

Kuwajima's elegant studies in the taxol area employing acid-promoted intramolecular alkylation reactions culminated in the synthesis of several advanced intermediates (Scheme 55).[186] These workers have carried out careful surveys of the appropriate conditions for these cyclizations and prepared taxoids such as **292** and **294**.

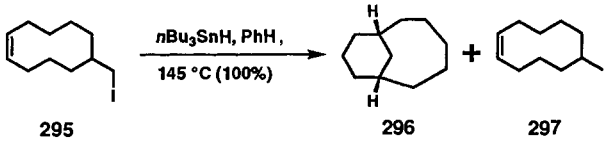
Radical-based approaches to taxol model systems have also been reported. In an attempt by Winkler et al.,[187] a simple cyclic iodoalkene **295** was used to form the AB ring fragment **296** (Scheme 56). Pattenden et al., on the other hand, were able to prepare the ABC ring skeleton **301** through a tandem radical sequence as shown in Scheme 57.[188]

A recent report from Cha's group delineates the synthesis of taxol AB ring model compounds **308a,b** based on a formal [4 + 3] diene–oxyallyl cycloaddition reaction as shown in Scheme 58.[189] The adduct **304**, obtained from **302** and **303**, was subjected to ring expansion (**304** → **305** for A ring), followed by further manipulation to give ketone **306**. Beckmann rearrangement then led to compounds **307a,b** which were converted into the targeted intermediates **308a,b**. Even though the efficiency of the last step needs further improvement, the strategy does provide a novel approach to the bicyclic AB system.

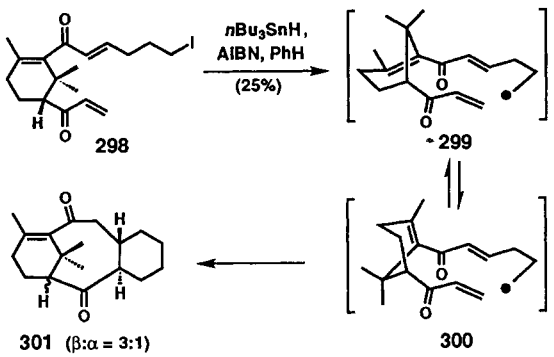
Wang's group has recently disclosed a sequential anionic condensation strategy for establishing the B ring (Scheme 59).[190] Thus, A ring model **309** was condensed with the zinc cuprate formed from **310**. After manipulation, the B ring was closed by applying an intramolecular version of the same method to give **313**. Finally, the C ring was added with a Diels–Alder reaction to give **315**.



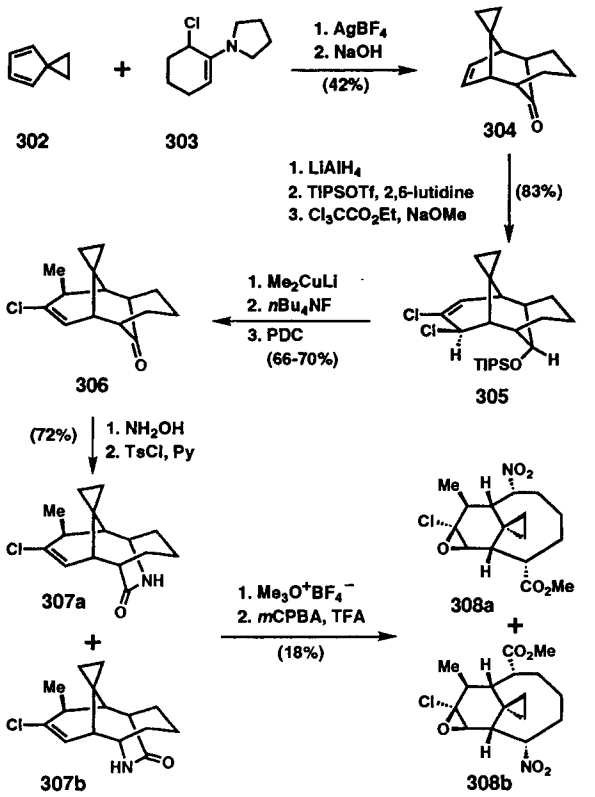
Scheme 55. Kuwajima's approach to taxol skeletons through intramolecular alkylation (1989).



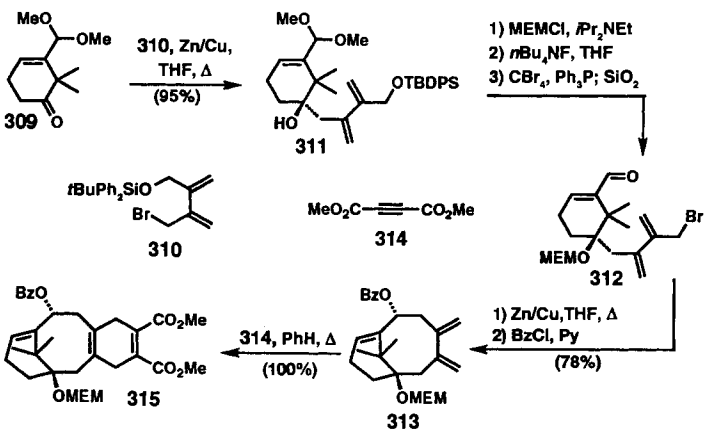
Scheme 56. Winkler's approach to the AB ring system through intramolecular radical cyclization (1989). Product ratio **296**:**297** = 4.1:1.



Scheme 57. Pattenden's approach to the taxol skeleton through intramolecular radical cyclization (1992). AIBN = 2,2'-azobis(isobutyronitrile).



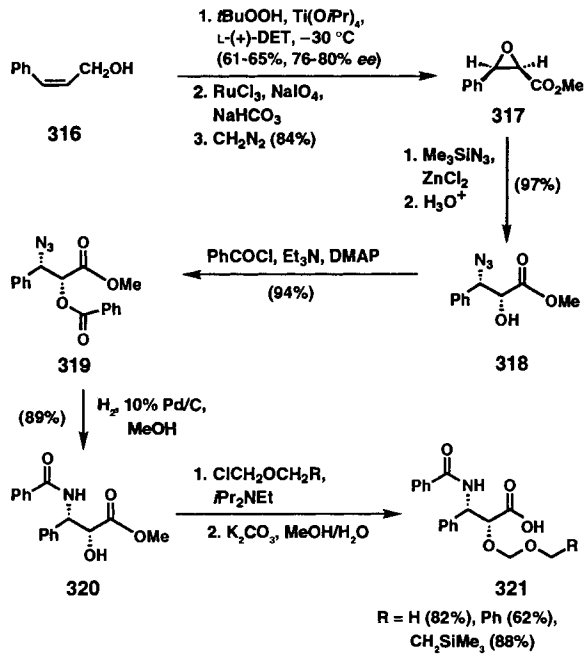
Scheme 58. Cha's approach to AB ring systems through [4 + 3] diene–oxyallyl cycloaddition (1992). TIPS = triisopropylsilyl, PDC = pyridinium dichromate, TFA = trifluoroacetic acid. Product ratio **308a**:**308b** = 3:2.



Scheme 59. Wang's approach to the ABC ring system through sequential anionic condensation (1993). MEM = methoxyethoxymethyl, Bz = benzoyl.

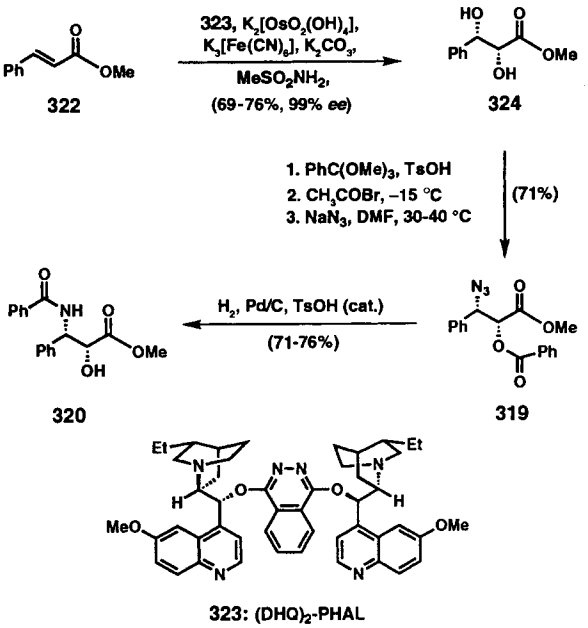
3.4. Approaches to the Taxol Side Chain

Greene et al. were the first to synthesize the taxol side-chain derivatives **321**, starting from *cis*-cinnamyl alcohol (**316**), for coupling with taxol's polycyclic framework (Scheme 60).[191] Although this strategy relied on the use of Sharpless asymmetric epoxidation to establish the two stereocenters in the molecule, the enantiomeric excess of the product was not particularly high (76–80% *ee*). An alternative route employing Sharpless asymmetric dihydroxylation reaction was later developed by the same group to produce the enantiomerically pure epoxide **317**.[192]



Scheme 60. Greene's approach to the taxol side chain through an epoxidation (1986). DET = diethyl tartrate.

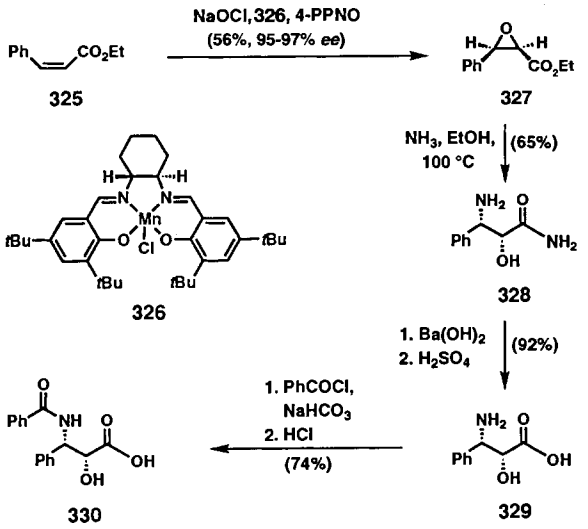
Sharpless and Kolb[193] have applied their latest version of the chiral catalyst $(DHQ)_2$-PHAL (**323**) to the asymmetric dihydroxylation of **322** to give optically enriched **324** in 99% *ee* (Scheme 61). Diol **324** was then converted into the known side-chain derivative **320** via azide **319** in four steps.



Scheme 61. Sharpless's approach to the taxol side chain through asymmetric dihydroxylation (1992).

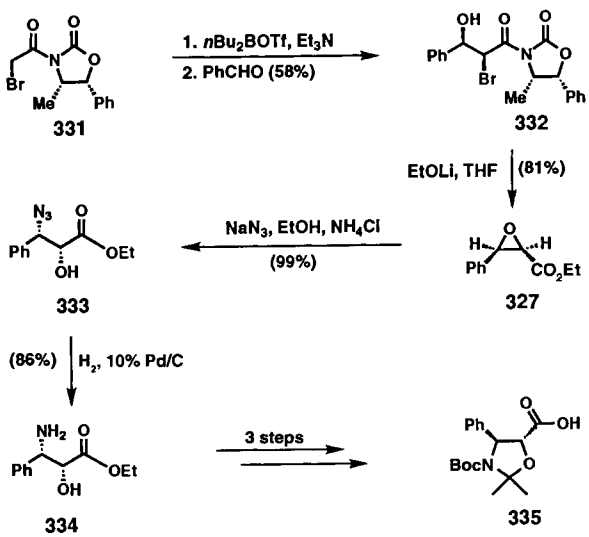
Jacobsen and Deng reported an efficient entry to compound **330** (the free acid of **320**) based on the asymmetric epoxidation

reaction of cinnamate ester **325** that is catalyzed by the chiral catalyst **326**, developed by his group (Scheme 62).[194] This method apparently offers the advantages of both brevity and low cost.



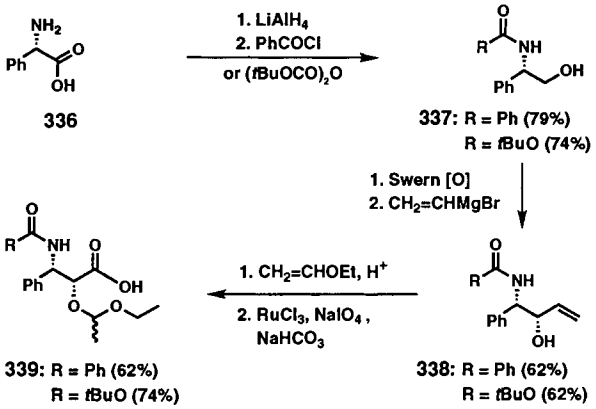
Scheme 62. Jacobsen's approach to the taxol side chain through an epoxidation (1992). 4-PPNO = 4-phenylpyridine *N*-oxide. Besides **327**, 13% of its *trans* isomer is formed from **325**.

Commerçon et al. used a method based on an Evans-type auxiliary-controlled aldol condensation of chiral imide **331** with benzaldehyde. Treatment of **332** with base afforded the known epoxide **327** (Scheme 63), which was then converted by standard chemistry into the protected taxol side-chain equivalent **335**.[195]



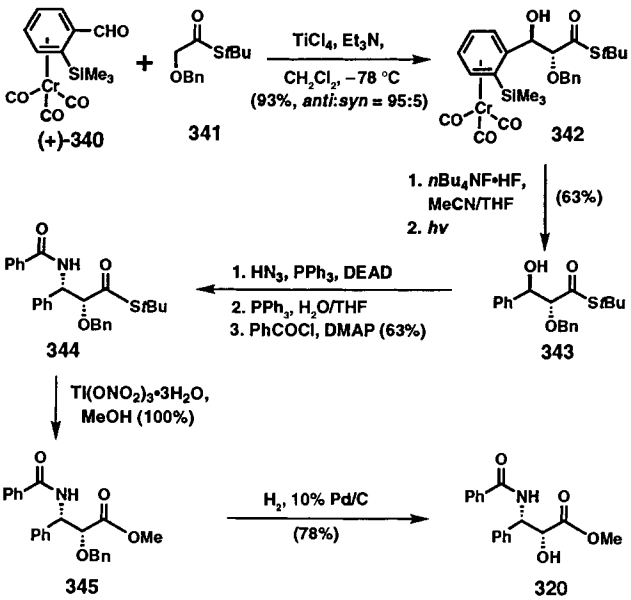
Scheme 63. Commerçon's approach to the taxol side chain through epoxidation (1992). boc = *tert*-butoxycarbonyl.

Greene et al. also introduced a method for the synthesis of the taxol side chain starting with an amino acid (Scheme 64).[196] Reduction, protection, oxidation, and homologation of (*S*)-(+)-phenylglycine (**336**) by standard methods led to the synthesis of compound **339** suitable for synthesis of taxol and Taxotere. A recent synthesis of the Taxotere side chain was achieved by dilithiation of Boc-protected benzylamine.[196b]



Scheme 64. Greene's approach to the taxol side chain starting from phenylglycine (1992).

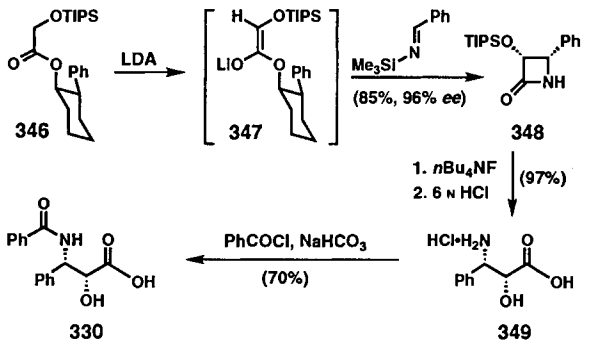
Hanaoka et al.[197] reported an interesting aldol condensation with the chiral chromium(0) complex of a benzaldehyde derivative [(+)-**340**] with **341** to form enantiomerically enriched **342** (Scheme 65). Following standard chemistry, **342** was transformed into the known ester **320**.



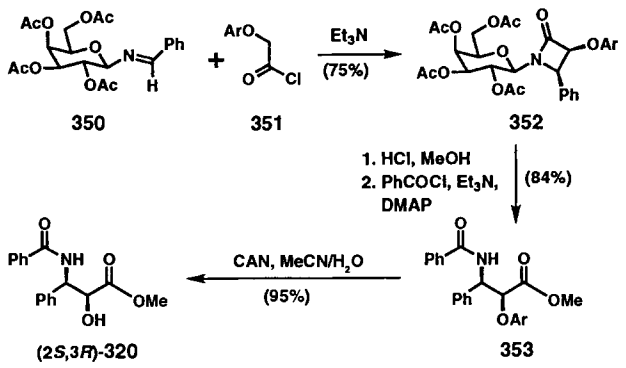
Scheme 65. Hanaoka's approach to the taxol side chain through aldol condensation (1992). DEAD = diethyl azocarboxylate.

β-Lactams have proven to be excellent precursors of the taxol side chain in several procedures. Scheme 66 shows Ojima's synthesis[198] of β-lactam **348** employing chiral ester enolate **347**. Subsequent manipulation of **348** led to the formation of the known hydroxy acid **330**.

An elegant synthesis of β-lactam **352** in optically active form by Georg et al. was based on the use of a carbohydrate chiral auxiliary (Scheme 67).[199] This approach resulted in the preparation of the nonnatural (2*S*,3*R*) enantiomer **320** of the taxol side chain in relatively few steps.

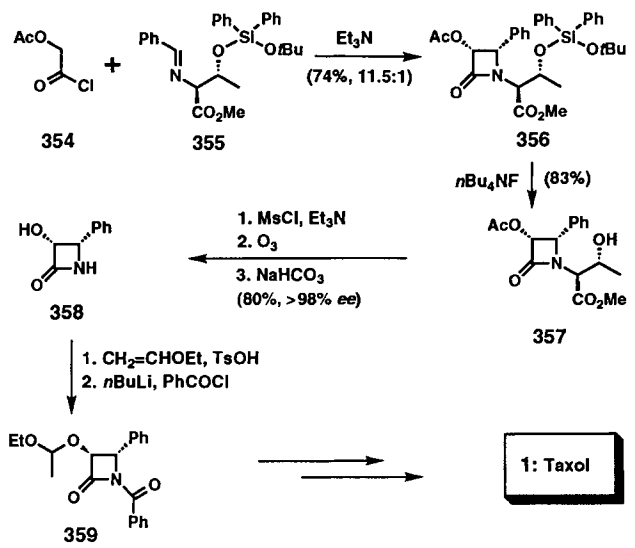


Scheme 66. Ojima's approach to the taxol side chain via a β-lactam (1992).



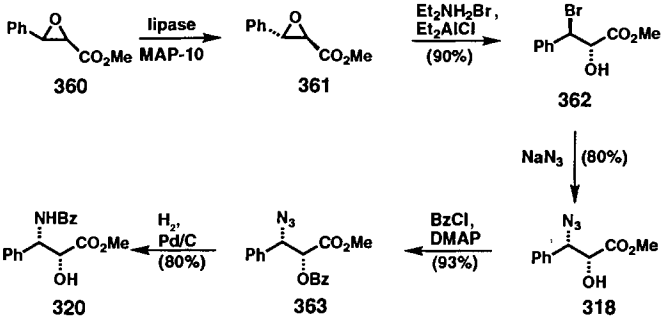
Scheme 67. Georg's approach to the taxol side chain via β-lactam (1992). Ar = 4-methoxyphenyl, CAN = ammonium cerium(IV) nitrate.

Farina's synthesis of β-lactam **359** was also based on the use of a chiral imine, **355**, prepared from an amino acid derivative (Scheme 68).[200] Following condensation of **354** with **355**, a reaction sequence was developed to remove the chiral auxiliary from the product (**357** → **358**). The protected β-lactam **359** was then treated with a baccatin III derivative to furnish taxol (see Section 3.5, Scheme 72). Racemic taxol side chain was also synthesized by Palomo et al.[201] according to a β-lactam strategy.



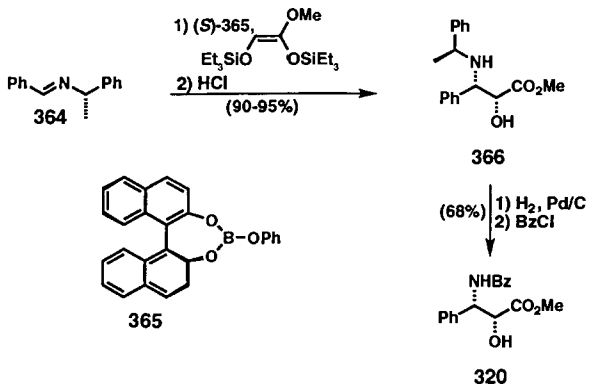
Scheme 68. Farina's approach to the taxol side chain via a β-lactam (1992). The ratio of the two *cis* compounds is 11.5:1.

Chen et al. have recently employed the enzymatic resolution of a chiral epoxy ester (**360**) to produce, after manipulation, the side-chain analog **320** (Scheme 69).[202] Techniques involving enzymatic resolution of other racemic substrates have also been used for the production of the taxol side chain.[203]



Scheme 69. Chen's approach to the taxol side chain via an enzymatic resolution of a racemate (**360** → **361**) (1993).

Yamamoto et al. have recently disclosed the synthesis of an enantiomerically enriched mixture of side-chain analog **320** (Scheme 70).[204] Their method centers around the aldol condensation of **364** with an enol ether under the mediation of chiral Lewis acid **365**.



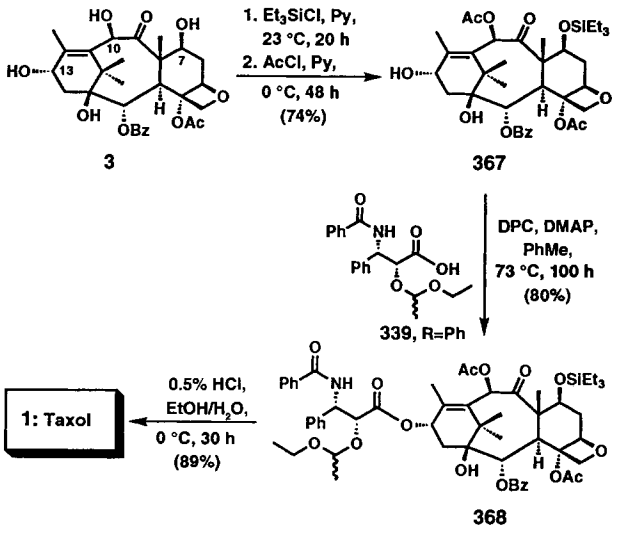
Scheme 70. Yamamoto's approach to the taxol side chain (1993).

3.5. Semisynthesis of Taxol and Analogs

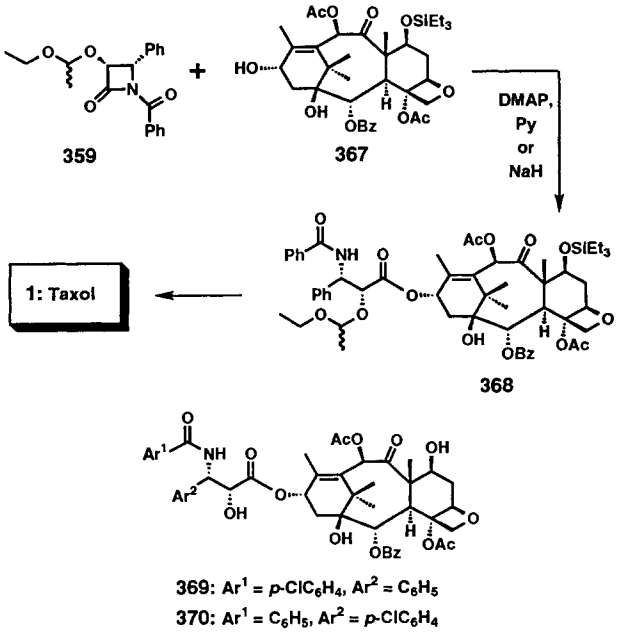
Despite the many efforts made by scientists during the past two decades, taxol still remains inaccessible by total synthesis. To circumvent the problem of direct extraction from the bark of yew trees, a method for the large scale production of taxol from renewable yew needles and twigs was sought.[125] 10-Deacetylbaccatin III (**3**, see Fig. 1) possesses the basic skeleton and functionality of taxol, and can be isolated from yew needles and twigs in significantly higher yield than taxol itself. This compound has attracted wide attention as a potential starting material for the semisynthesis of taxol and its analogs such as Taxotere.[61b] Since the side chain of taxol is readily available in enantiomerically enriched form by chemical synthesis, the remaining task is reduced to regioselective formation of the C13

ester bond. Several processes have been developed for this purpose.

The groups of Potier and Greene achieved the first successful semisynthesis of taxol[60a] after several preliminary attempts.[205] They found that the four hydroxy groups in **3** exhibited different reactivities towards acylation. Thus, **3** was first converted into its C7- and C10-protected derivative **367** (Scheme 71), which was then coupled with the side-chain equivalent **339** (R = Ph) under the influence of DPC-DMAP. These extreme conditions were essential for ester formation because of the steric hindrance around the C13 hydroxyl group. Acidic treatment of compound **368** provided taxol in high yield. This semisynthesis of taxol from **3** has served as the standard protocol for other modified procedures developed later.



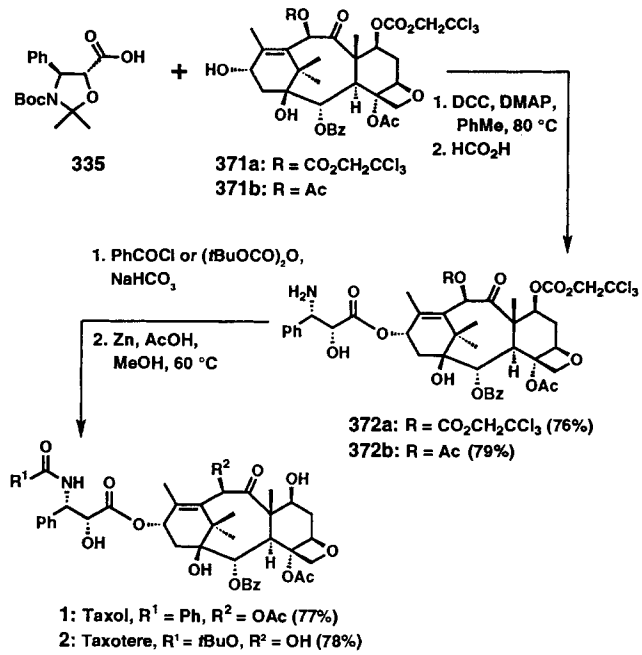
Scheme 71. Potier and Greene's semisynthesis of taxol (1988). DPC = di-2-pyridyl carbonate.



Scheme 72. Holton and Ojima's semisynthesis of taxol (1990–1992).

Holton was successful in coupling baccatin III derivative **367** with optically active β-lactam **359**, made by optical resolution of racemic material, to form the same compound, **368** (Scheme 72).[206] Ojima's group has recently prepared **359** in optically active form by asymmetric reaction analogous to that described in Scheme 66.[198] The combination of Holton's and Ojima's procedures provided another semisynthesis of taxol in a few steps.[198, 200, 203] The same methodology was employed by the groups of Georg and Himes in the preparation of biologically active taxol analogs **369** and **370** with modified side chains.[207]

Commerçon et al. synthesized taxol (**1**) and Taxotere (**2**) by coupling derivatives **371a,b** of baccatin III (**4**) with the side-chain equivalent **335** (Scheme 73).[195] Side chain **335** was prepared by them as described in Scheme 63. The free amines **372a,b**, obtained from this coupling reaction, were then subjected to acylations to provide, after removal of the trichloroethoxycarbonyl group, **1** and **2** in good yields.



Scheme 73. Commerçon's semisynthesis of taxol and Taxotere (1992). DCC = dicyclohexylcarbodiimide.

4. Structure–Activity Relationships

Despite taxol's prospects as an anticancer agent and the global excitement surrounding its potential therapeutic value, several problems associated with the drug still hamper its widespread usage. Central among them is the issue of formulation. As discussed in Section 2.3, taxol's low water solubility ($0.03\ mg\,mL^{-1}$)[208] forces its formulation in a Cremaphor vehicle, which has several difficulties associated with its use. The development of a water-soluble analog or prodrug of taxol could circumvent this problem and greatly facilitate the administration of taxol. In a broader sense, better understanding of

the structure–activity relationships (SARs) of taxol and its derivatives will be pivotal in the design and synthesis of new generations of taxol-based antitumor agents with improved physical, chemical, and biological profiles. Major contributions to the understanding of taxol's SARs have been made by Potier's group in France and Kingston's group in the United States. Readers interested in the details of these studies are referred to Kingston's[209] and Potier's[210] recent review articles. In the following sections, the latest developments and the most important taxol derivatives will be discussed, beginning with the synthesis of water-soluble analogs of taxol.

4.1. Improvement of Water Solubility

As indicated in Figure 6, the C13 side chain is critical for maintaining the biological properties of taxol. The C2′ hydroxyl group is also important, although not as crucial, since acylation results in loss of microtubule stabilization but not cytotoxicy. (This phenomenon, may, however, be explained by ester hydrolysis within the cell.) The C7 hydroxyl group is a good site for derivatization, since blocking of this position causes only minimal loss of activity. A number of derivatives carrying groups at the C2′, C7, or both hydroxyls have been synthesized, including carboxylic acid salts, basic moieties, and other designed functionalities. The most important contributions are discussed below.

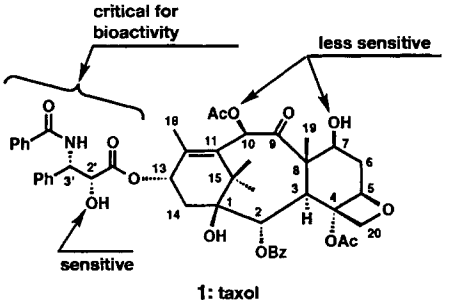


Fig. 6. The significance of selected structural sites for designing taxol analogs and prodrugs.

Deutsch et al. reported a number of taxol compounds (for example, **373**–**375**, Fig. 7),[211] functionalized at C2′, which exhibited improved water solubility. Aqueous solutions of up to 1% of compounds **373**–**375** were obtained. The biological actions of these compounds were also impressive. In assays with B16 melanoma cells, they demonstrated cytotoxicity comparable and even exceeding that of taxol. In particular, compound **375** had a rate of five out of ten cures in mice at dosages of 10 mg kg^{-1}. In the MX-1 breast xenograft test, complete tumor disappearance results were obtained at doses of 40 and 20 mg kg^{-1}, and all surviving mice were tumor free. These compounds may suffer, however, from their tendency to release taxol rapidly in aqueous media and thus cause precipitation problems.

Stella and collaborators have reported the preparation of a series of methanesulfonate salts of derivatives of taxol with amino acids in C2′ and C7 positions whose water solubilities are

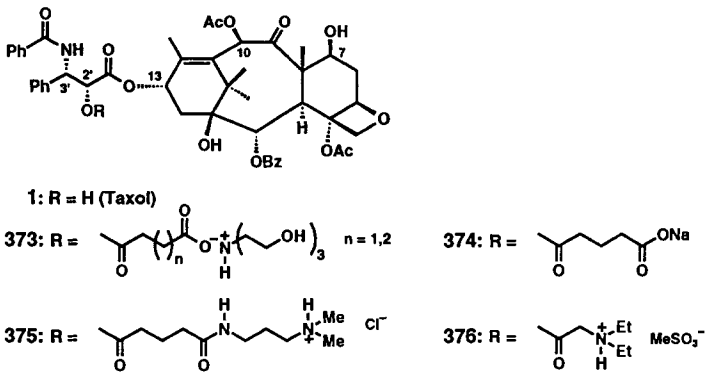


Fig. 7. Structures of water-soluble and biologically active taxol derivatives; Deutsch (1989), Stella (1992).

greater than 2 mg mL^{-1}.[212] For example, they found that the C2′-modified taxol **376** exhibited similar potency to taxol in inhibiting B16 melanoma cell proliferation and as an antitumor agent against breast carcinoma xenografts in mice. The mechanism of action of these water-soluble taxol derivatives was assumed to involve the in vivo release of taxol, an assumption that is supported by the similarity of their biological profiles to those of the natural product.

More recently, our group has been successful in the design and synthesis of two new types of biologically active taxol analogs.[213] The design of these compounds relied on the proposed mechanisms of releasing taxol from its prodrugs (Fig. 8).

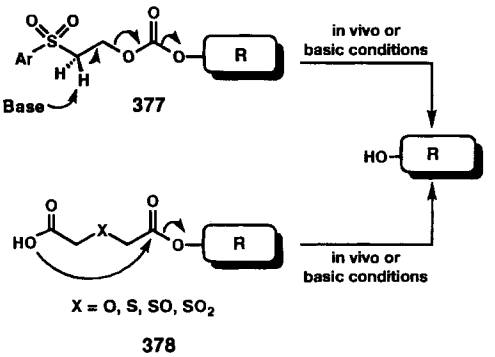


Fig. 8. Proposed mechanism of taxol release from designed protaxols (Nicolaou, 1993). R = taxol residue.

In the first type, the 2-arylsulfonyl ethoxycarbonyl group in **377** was conceived to allow the regeneration of taxol through a base-induced β-elimination reaction. In the second type, the monoester **378** of a dicarboxylic acid was planned to provide the opportunity for cleaving the ester bond through an intramolecular hydrolysis with a assumed cyclic transition state. A polar group X, such as an ether oxygen atom or sulfonyl group, linking the two carboxylic moieties was introduced in order to improve the water solubility of the molecule. These mechanisms allow for the activation of the drug in vivo in the basic microenvironment of certain tumor cells,[214] while maintaining stability in the relatively neutral environment of the fluid systems of the body. To utilize these principles, the derivatives **379**–**384** (Fig. 9) were designed and synthesized in one to three steps from

taxol. Compounds **379–381** exhibited markedly improved water solubility (≈ 1 mg mL^{-1}) and considerable stability at neutral pH and ambient temperature. At basic pH, however, these compounds readily release taxol at a rate depending upon the pH and the medium. In vitro cytotoxicity and microtubule polymerization studies showed profiles consistent with the controlled release of taxol into the system. These profiles demonstrate the high potential for use of these compounds as water soluble prodrugs of taxol in therapy.

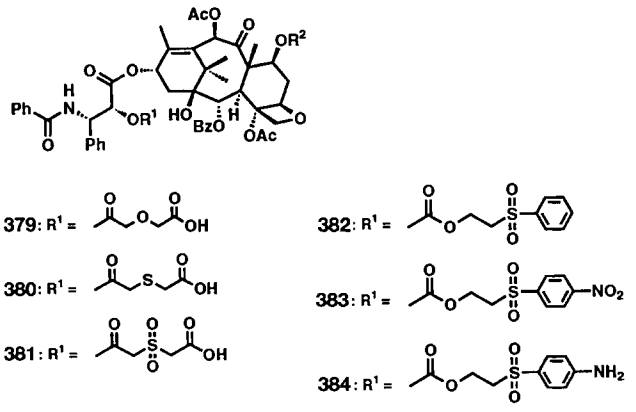


Fig. 9. Designed protaxols (Nicolaou, 1993). $R^2 = H$.

4.2. The Effect of Side-Chain Structures

As indicated in Figure 6, the side chain of taxol plays an important role in the biological functions of this antitumor agent. Protection of the C 2′ hydroxyl group results in major loss of activity but, as discussed in the previous section, those derivatives which possess labile groups in this position exhibit prodrug biological profiles. Structural modifications of the taxol side chain have been recently reported by both the Potier and Swindell groups.[215] These studies revealed a number of interesting features, which are summarized in Figure 10. Important findings include the following: a) the C 3′ acyl group is critical, although the amide's aryl group may be substituted by other aryl or alkyl groups; b) the C 3′ aryl group is required—a replacement by a methyl group reduces the activity 19-fold; c) the C 3′-bound nitrogen can be replaced by an oxygen atom without significant loss of activity; d) one of the C 2′ or C 3′ polar functionalities can be removed without significant effect, but the removal of both or interchange of their positions causes dramatic loss of activity; e) the (2′*S*,3′*R*) isomer is significantly less active than the natural (2′*R*,3′*S*) isomer, but the (2′*S*,3′*S*) and (2′*R*,3′*R*) isomers show comparable activity to that of the natural product.

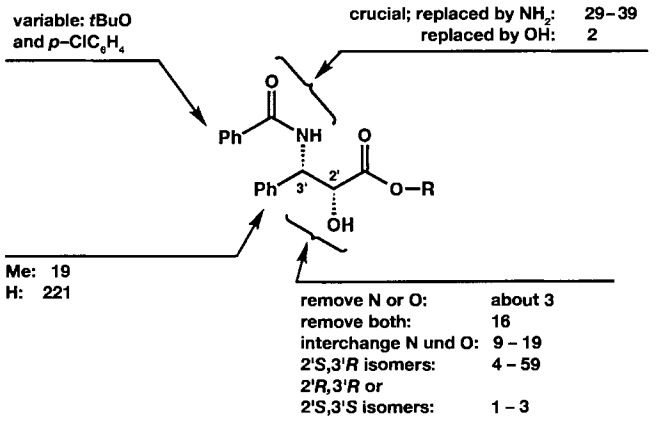


Fig. 10. Effects of structural modifications of the taxol side chain; Potier (1991), Swindell (1991). The numbers indicate the factor by which the activity is decreased.

The role of the taxol side chain in affecting biological activity has not yet been fully determined. However, the structure–activity relationships observed in the studies discussed above have revealed several key features about the mechanism of action of taxol. Based on the fact that the side chain is inactive by itself but essential to the activities of the intact taxol molecule, it is suspected that the principle recognition partner is the taxane skeleton itself. The taxol side chain may be preorganized through hydrogen bonding and may fit into a hydrophobic cleft on the taxane binding site, which stabilizes the drug–tubulin interaction. The details of this mechanism need further exploration. Further studies are needed to elucidate the molecular basis of the mechanism of action of taxol fully.

4.3. Modifications of the Taxol Skeleton

A variety of taxol derivatives, modified on the taxane skeleton, have been prepared by Kingston et al.[216] Figure 11 highlights the effects of structural changes on the biological action of the drug on microtubules. Specifically, these workers have observed that modifications at the C 2, C 7, and C 10 positions have insignificant effects on the biological action of the drug, ranging from doubled to halved activity. The oxetane ring, on the other hand, has proven crucial for maintaining the activity: ring opening led to drastic decrease in both tubulin disassembly (activity

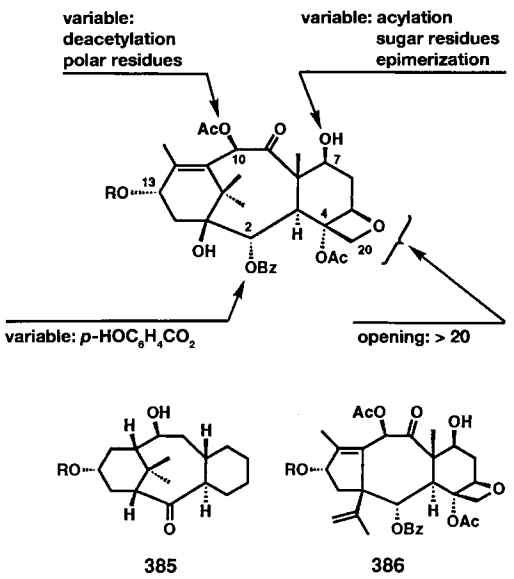


Fig. 11. Taxol derivatives and analogs with modified or rearranged skeletons (Kingston, 1991). See text.

smaller by more than a factor of 20) and cytotoxicity against KB cells ($>10^5$ times smaller IC_{50} values).

Interestingly, the structurally simplified taxane **385** (R = taxol side chain) and taxane analog (**386**) with a contracted A ring,[216] which both possess a properly functionalized side chain, inhibit tubulin depolymerization. Further study in this area could open up new avenues for the design and synthesis of taxol-like compounds. Modification of the taxol skeleton is currently a hot research topic, and several recent efforts have led to the preparation of a number of additional taxane skeletons derived from baccatin III (**4**).[217] Most recently Chen's group has disclosed some studies centered around deleting substituents on the taxol skeleton.[218] This group showed that deletion of the *O*-acetyl group in the 10 position has little if any affect upon the activity. However, deletion of the *O*-benzoyl group in the 2 position causes a drastic reduction in its bioactivity.

One should keep in mind that the different testing systems used by various groups may give different data. Relative values, indexed to taxol, are the most useful for comparison. The correlation between cytotoxicity and antimicrotubular activity has been fairly well established and, with a few exceptions, the trends are usually parallel.

5. Summary and Outlook

The cellular mechanisms by which taxol exerts its effects are beginning to come to light. These studies, as well as those which focus on the supracellular effects of taxol, should remain an area of active study in the coming years. Since the safety and efficiency of taxol and Taxotere are now proven in clinical trials, the way is paved for large-scale evaluations of the clinical usefulness and efficiency of taxol in treating specific neoplasms. At the same time, studies of the synergistic effects of taxol and other drugs may provide even more exciting leads. At the moment these studies are hindered by the lack of a steady and copious stock of taxol. One should expect extensive action in the arena of taxol supply until an efficient, inexpensive, and proprietary process for the production of taxol is developed.

Only a few natural products have excited the extensive level of synthetic effort invested in taxol. While the likelihood of a practical synthetic route for the total synthesis of taxol being developed is relatively low, these studies are sure to provide a wealth of information about taxol's SARs and expand the frontiers of synthetic chemistry. Another exciting prospect is the design and synthesis of simpler biologically active mimics of taxol. With so many groups hard at work, the attainment of a total synthesis of taxol is merely a question of time.

Taxol and its relatives are emerging as yet another class of naturally occurring substances, like the enediyne antitumor antibiotics[218] and the macrocyclic immunophillin ligands,[219] that combine novel molecular architecture, important biological activity, and fascinating mode of action. As such, taxol is bound to continue to stimulate synthetic chemists, molecular designers, molecular and cellular biologists, and clinicians. This deliberate merging of chemistry and biology promises to lead to exciting ventures and discoveries.

We wish to thank our talented collaborators, C. Claiborne, H. Ueno, C. K. Hwang, M. Kerr, J. J. Liu, Y. Mizuno, M. Nakada, C. Riemer, K. Shibayama, E. Sorensen, and Z. Yang for the stimulating discussions and their contributions. We thank J. Hightower and K. Boyd for the art work and M. Egan and S. Conley for undertaking the task of proofreading the manuscript and double-checking the references. Much credit is due to S. Reed for his exacting, informative, and educational comments on the biological sections of this manuscript. Additionally, we wish to thank R. Kelsey of the National Forest Service for a helpful conversation concerning the biology of T. brevifolia. For financial assistance we thank the National Institutes of Health, USA, and the Office of Naval Research, USA.

Received: March 4, 1993 [A 928 IE]
German version: *Angew. Chem.* **1994**, *106*, 38

Addendum

Since the submission of the final version of this article (6/93), more than 100 articles concerning taxol have appeared in the literature. This addendum addresses those that were indexed in Chemical Abstracts Online or Medline by November 15, 1993. The following is a list of those that the authors deem to be both within the scope of this review and particularly important.

Concerning a) microtubules: K. E. Sawin, S. A. Endow, *Bioessays*, **1993**, *15*, 399–407; R. F. Luduena, *Mol. Biol. Cell* **1993**, *4*, 455–457; b) the microtubule organizing center: M. D. Rose, S. Biggino, L. L. Satterwhite, *Curr. Op. Cell Biol.* **1993**, *5*, 105–115.

Concerning the biological effects of taxol: a) the cell cycle: N. M. Lopes, E. G. Adams, T. W. Pitts, B. K. Bhoyan, *Cancer Chemother. Pharmacol.* **1993**, *32*, 235–242; b) metastasis: M. L. Stracke, M. Sorough, L. A. Liotta, E. Schiffmann, *Kidney Int.* **1993**, *43*, 151–157; c) radiation sensitivity: P. B. Schiff, *PCT Int. Appl.* WO 9314787 A1 (August 5, 1993); H. Choy, F. F. Rodriguez, S. Koester, S. Hilsenbeck, D. D. Van Hoff, *Cancer* **1993**, *71*, 3774–3778; A. Steren, B. U. Sevin, J. Perras, R. Ramus, R. Angioli, H. Nguyen, O. Koechli, H. E. Auerette, *Gynecol. Oncol.* **1993**, *50*, 89–93, d) lipopolysaccharide imitation: C. L. Manthey, N. Qureshi, P. L. Stuetz, S. N. Vogel, *J. Exp. Med.* **1993**, *178*, 695–702; e) the pharmacology of taxol: G. N. Kumar, K. V. Walle, K. N. Bhalla, T. Walle, *Res. Commun. Chem. Pathol. Pharmacol.* **1993**, *80*, 337–344; f) the state of art in the clinic: D. Bissit, S. B. Kaye, *Eur. J. Cancer 29A* **1993**, 1228–1231; Paclitaxel (taxol) Investigators Workshop, *Sem. Oncol.* **1993**, *20* (4 Suppl. 3) 1–60.

Concerning the production of taxol through cell culture: A. G. Fett-Neto, S. J. Melanson, K. Sakata, F. Dicosmo, *Bio/Technology* **1993**, *11*, 731–734; R. J. Smith, T. L. Addams, C. R. Burton, R. W. Stahlhut, *PCT Int. Appl.* WO 9310253 A1 (May 27, 1993).

Concerning the synthesis of a) taxoids as photoaffinity label: G. I. Georg, G. C. Hattiman, *Bioorg. Med. Chem. Lett.* **1992**, *2*, 735–738; A. Chatterjee, J. S. Williamson, J. K. Zjawiony, J. R. Peterson, *ibid.* **1992**, *2*, 91–94; b) prodrugs of taxol: D. G. I. Kingston, Z. Y. Zhao, EP-A 537905 (April 21, 1993); c) the taxol CD ring system: R. C. A. Isaacs, M. J. DiGrandi, S. J. Danishefsky, *J. Org. Chem.*, **1993**, *58*, 3938–3941.

Studies on the structure–activity relationships of taxol: a) deletion of the C7 OH group: A. G. Chaudhory, J. M. Rimoldi, D. G. I. Kingston, *J. Org. Chem.* **1993**, *58*, 3798–3799; b) insertion of a C9 OH group: L. L. Klein, *Tetrahedron Lett.* **1993**, *34*, 2047–2050; c) formation of side-chain analogs: G. I. Georg, Z. S. Cheruvallah, *Bioorg. Med. Chem. Lett.* **1992**, *2*, 295–298.

[1] D. M. Parkin, E. Läärä, C. S. Muir, *Int. J. Cancer* **1988**, *41*, 184-197.
[2] U. S. Bureau of the Census, *Statistical Abstract of the United States: 1991* (111. Ausgabe) Washington, DC, USA, **1991**, p. 81 (Nr. 118).
[3] C. Vanchieri, *J. Natl. Cancer Inst.* **1990**, *82*, 1872-1875.
[4] a) W. W. Shingleton, *Arch. Surg. (Chicago)* **1989**, *124*, 43–45; b) P. Reizenstein, J. Ponten, *Biomed. Pharmacother*, **1984**, *38*, 282–284.
[5] R. Doll, *Eur. J. Cancer* **1990**, *26*, 500–508.
[6] A. I. Holleb, *Ca-Cancer J. Clin.* **1991**, *41*, 69–70.
[7] K. J. Smigel, *J. Natl. Cancer Inst.* **1992**, *84*, 10–11.
[8] C. S. Muir, *Cancer Res.* **1990**, *50*, 6441–6448.
[9] B. N. Ames, L. S. Gold, *Angew. Chem.* **1990**, *102*, 1233–1246; *Angew. Chem. Int. Ed. Engl.* **1990**, *29*, 1197–1208.
[10] See the Supplement 16G of *J. Cell. Biochem.* **1992**, an issue dedicated to "Intermediate Biomarkers of Precancer and Their Application in Chemoprevention".
[11] J. M. Bishop, *Science* **1987**, *235*, 305–311.
[12] H. M. Schüller, *Biochemm. Pharmacol.* **1991**, *42*, 1511–1523.
[13] a) I. R. Hart, A. Saini, *Lancet* **1992**, *339*, 1453–1457; b) D. G. Brodland, J. A. Zitelli, *J. Am. Acad. Dermatol.* **1992**, *27*, 1–8.
[14] *Cancer Chemother. Rep.* **1962**, *25*, 1–66.
[15] a) M. R. Grever, S. A. Schepartz, B. A. Chabner, *Semin. Oncol* **1992**, *19*, 622–638; b) J. S. Driscoll, *Cancer Treat. Rep.* **1984**, *68*, 63–76; c) S. Marsoni, R. Wittes, *ibid.* **1984**, *68*, 77–85.
[16] T. Junod, *Life* **1992**, *15* (May), 71–76.
[17] M. C. Wani, H. L. Taylor, M. E. Wall, P. Coggon, A. T. McPhail, *J. Am. Chem. Soc.* **1971**, *93*, 2325–2327.
[18] S. Borman, *Chem. Eng. News* **1991**, *69*, 11–18.
[19] D. A. Fuchs, R. K. Johnson, *Cancer Treat. Rep.* **1978**, *62*, 1219–1222.
[20] S. B. Horwitz, J. Fant, P. B. Schiff, *Nature* **1979**, *277*, 665–667.
[21] B. R. Brinkley, *Cold Spring Harbor Symp. Quant. Biol.* **1982**, *46*, 1029–1040.
[22] E. H. Ball, J. J. Singer, *Proc. Natl. Acad. Sci. USA* **1982**, *79*, 123–126.
[23] M. M. Rasenick, N. Wang, K. Yan, *Adv. Second Messenger Phosphoprotein Res.* **1990**, *24*, 381–386.
[24] M. S. Cooper, A. H. Cornell-Bell, A. Chernjawsky, J. W. Dani, S. J. Smith, *Cell* **1990**, *61*, 135–145.
[25] J. M. Scholey, *Nature* **1990**, *343*, 118–120.
[26] E. K. Rowinsky, R. C. Donehower, *Pharmacol. Ther.* **1991**, *52*, 35–84.
[27] K. F. Sullivan, *Annu. Rev. Cell Biol.* **1988**, *4*, 687–716.
[28] a) R. G. Burns, C. Surridge, *FEBS Lett.* **1990**, *271*, 1–8; b) D. W. Cleveland, K. F. Sullivan, *Annu. Rev. Biochem.* **1985**, *54*, 141–150; c) E. C. Raff, *J. Cell. Biol.* **1984**, *99*, 1–10.
[29] M. Little, T. Seehaus, *Comp. Biochem. Physiol. B* **1988**, *90*, 655–670.
[30] R. F. Ludueña, A. Banerjee, I. A. Khan, *Curr. Opin. Cell. Biol.* **1992**, *4*, 53–57.
[31] a) R. L. Geahlen, B. E. Haley, *Proc. Natl. Acad. Sci. USA* **1977**, *74*, 4375–4377; b) *J. Biol. Chem.* **1979**, *254*, 11982–11987.
[32] a) R. C. Weisenberg, G. G. Borisy, E. W. Taylor, *Biochemistry* **1968**, *7*, 4466–4479; b) B. M. Spiegelman, S. M. Penningroth, M. W. Kirshner, *Cell* **1977**, *12*, 587–600.
[33] a) J. B. Olmsted, *Annu. Rev. Cell Biol.* **1986**, *2*, 421–457; b) A. Matus, *Curr. Opin. Cell Biol.* **1990**, *2*, 10–14; c) G. Wiche, C. Oberkanins, A. Himmler, *Int. Rev. Cytol.* **1991**, *124*, 217–273; d) J. B. Olmsted, *Curr. Opin. Cell Biol.* **1991**, *3*, 52–58.
[34] V. D. Lee, B. Huang, *Plant Cell* **1990**, *2*, 1051–1057.
[35] L. Wilson, *Life Sci.* **1975**, *17*, 303–309.
[36] R. Bai, G. R. Pettit, E. Hamel, *J. Biol. Chem.* **1990**, 17141–17149.
[37] A. D. Bershadsky, J. M. Vasiliev, *Cytoskeleton*, Plenum, New York, **1989**, pp. 100–107.
[38] D. L. Purich, D. Kristofferson, *Adv. Protein Chem.* **1984**, *36*, 133–212.
[39] L. A. Amos in *Microtubules* (Eds.: K. Roberts, J. Hyams), Academic Press, New York, **1979**, pp. 2–64.
[40] H. P. Erickson, *J. Cell Biol.* **1974**, *60*, 153–167.
[41] a) L. T. Haimo, *Methods Cell Biol.* **1982**, *24*, 189–206; b) P. R. Burton, R. H. Himes, *J. Cell Biol.* **1978**, *77*, 120–133; c) E.-M. Mandelkow, E. Mandelkow, *J. Mol. Biol.* **1979**, *129*, 135–148.
[42] D. L. Purich, D. Kristofferson, *Adv. Protein Chem.* **1984**, *36*, 133–212.
[43] L. U. Cassimeris, R. A. Walker, N. K. Pryer, E. D. Salmon, *Bioessays* **1987**, *7*, 149–154.
[44] a) H. P. Erickson, E. T. O'Brien, *Annu. Rev. Biophys. Biophys. Chem.* **1992**, *21*, 145–146; b) V. I. Gelfand, A. D. Bershadsky, *Annu. Rev. Cell Biol.* **1991**, *7*, 93–116; c) E. D. Salman in *Mitosis* (Eds.: J. S. Hyams, B. R. Brinkley), Academic Press, New York, **1989**, p. 119–181.
[45] M. Caplow, *Curr. Opin. Cell Biol.* **1992**, *4*, 58–65.
[46] C. A. Collins, R. B. Vallee, *J. Cell Biol.* **1987**, *105*, 2847–2854.
[47] I. Ringel, S. B. Horwitz, *J. Pharmacol. Exp. Ther.* **1991**, *259*, 855–860.
[48] I. Ringel, S. B. Horwitz, *J. Pharmacol. Exp. Ther.* **1987**, *242*, 692–698.
[49] a) P. B. Schiff, S. B. Horwitz, *Biochemistry* **1981**, *20*, 3247–32542; b) *Bristol-Myers Cancer Symp.* **1984**, *2*, 483–501.
[50] J. Parness, S. B. Horwitz, *J. Cell Biol.* **1981**, *91*, 479–487.
[51] N. Humar, *J. Biol. Chem.* **1981**, *256*, 10435–10441.
[52] a) R. B. Vallee, *J. Cell Biol.* **1982**, 435–442; b) R. B. Vallee, C. A. Collins, *Methods Enzymol.* **1986**, *134*, 116–127.
[53] W. D. Howard, S. N. Timasheff, *J. Biol. Chem.* **1988**, *263*, 1342–1346.
[54] M.-F. Carlier, D. Pantaloni, *Biochemistry* **1981**, *20*, 1918–1922.
[55] S. Rao, S. B. Horwitz, I. Ringel, *J. Natl. Cancer Inst.* **1992**, *84*, 785–788.
[56] a) M. J. Schibler, B. Huang, *J. Cell. Biol.* **1991**, *113*, 605–614; b) F. R. Cabral, R. C. Brady, M. J. Schibler, *Ann. NY Acad. Sci.* **1986**, *466*, 745–756; c) M. J. Schibler, F. R. Cabral, *Can. J. Biochem. Cell. Biol.* **1985**, *63*, 503–510; d) *J. Cell Biol.* **1986**, *102*, 1522–1531.
[57] J. M. Carboni, V. Farina, S. Rao, S. I. Hauck, S. B. Horwitz, I. Ringel, *J. Med. Chem.* **1993**, *36*, 513–515.
[58] J. M. Andreu, J. Bordas, J. F. Diaz, J. G. de Ancos, R. Gil, F. J. Medrano, E. Nogales, E. Pantos, E. Towns-Andrews, *J. Mol. Biol.* **1992**, *226*, 169–184.
[59] R. C. Williams, Jr., L. A. Rone, *J. Biol. Chem.* **1987**, *264*, 1663–1670.
[60] a) J. N. Denis, A. E. Greene, D. Guénard, F. Gueritte-Voegelein, L. Mangatal, P. Potier, *J. Am. Chem. Soc.* **1988**, *110*, 5917–5919; b) L. Mangatal, M. T. Adeline, D. Guénard, F. Gueritte-Voegelein, P. Potier, *Tetrahedron* **1989**, *45*, 4177–4190.
[61] a) I. Barasoain, C. De Ines, F. Duz, J. M. Andreia, V. Peyrot, D. Leynadier, P. Garcia, C. Briand, G. De Suusa, R. Rahmani, *Proc. Am. Assoc. Cancer Res.* **1991**, *32*, 329 (AO: 1952); b) I. Ringel, S. B. Horwitz, *J. Natl. Cancer Inst.* **1991**, *83*, 288–291.
[62] J. F. Díaz, J. M. Andreu, *Biochemistry* **1993**, *32*, 2747–2755.
[63] V. Fromes, P. Guonon, M. C. Bissery, A. Fellous, *Proc. Am. Assoc. Cancer Res.* **1992**, *33*, 511 (Abstract 3055).
[64] A. B. Pardee, *Science*, **1989**, *249*, 603–609.
[65] a) T. F. Deuel, *Annu. Rev. Cell Biol.* **1987**, *3*, 443–492; b) F. Cross, H. Weintraub, J. Roberts, *ibid.* **1989**, *5*, 341–396.
[66] A. B. Pardee, *Cancer Res.* **1987**, *47*, 1488–1491.
[67] a) D. O. Morgan, *Curr. Opin. Genet. Dev.* **1992**, *2*, 33–37; b) C. Norbury, P. Nurse, *Annu. Rev. Biochem.* **1992**, *61*, 441–470; c) L. H. Hartwell, *Genetics* **1991**, *129*, 975–980; d) A. W. Murray, M. W. Kirschner, *Science* **1989**, *246*, 614–621.
[68] R. A. Laskey, M. P. Fairman, J. J. Blow, *Science* **1989**, *249*, 609–614.
[69] A. B. Pardee, R. Dubrow, J. L. Hamlin, R. F. Hamlin, R. F. Kletzien, *Annu. Rev. Biochem.* **1978**, *47*, 715–750.
[70] J. A. Snyder, J. R. McIntosh, *Annu. Rev. Biochem.* **1976**, *45*, 699–720.
[71] a) J. R. McIntosh, *Trends Biochem. Sci.* **1984**, *9*, 195–198; b) C. Mazia in *The Cell, Vol. III* (Eds.: J. Brachat, A. E. Mirsky), Academic Press, London, **1961**, p. 77–412.
[72] a) J. R. McIntosh, M. P. Koonce, *Science* **1989**, *249*, 622–628; b) R. Kuriyama, C. Nislow, *Bioessays* **1992**, *14*, 81–88.
[73] a) M. Kirschner, T. Mitchison, *Cell* **1986**, 329–342; b) W. M. Saxton, *J. Cell Biol.* **1984**, *99*, 2175–2186.
[74] J. R. McIntosh, C. M. Pfarr, *J. Cell Biol.* **1991**, *115*, 577–585.
[75] G. Gorbsky, *Bioessays* **1992**, *14*, 73–80.
[76] L. H. Harwell, T. A. Weinert, *Science* **1989**, *249*, 629–634.
[77] C. L. Rieder, S. P. Alexander in *Aneuploidy, Mechanisms of Origin* (Ed.: M. A. Resnich), Liss, New York, **1989**.
[78] Like most of the cancer cell lines, HeLa cells are the result of culturing cells harvested from a human being. The HeLa line came into being when cancerous cells were removed from the cervix of Henrietta Lacks on February 9, 1951, in Baltimore. Henrietta Lacks died in October of that year: L. Oliwenstein, *Discover* **1992**, December, 34–35.
[79] P. B. Schiff, S. B. Horwitz, *Proc. Natl. Acad. Sci. USA* **1980**, *77*, 1561–1565.
[80] a) M. De Brabander, G. Geuens, R. Nuydens, R. Willebroards, J. De May, *Cell Biol. Int. Rep.* **1981**, *5*, 913–920; b) *Cold Spring Harbor Symp. Quant. Biol.* **1982**, *46*, 219–226; c) J. J. Manfredi, J. Parness, S. B. Horwitz, *J. Cell Biol.* **1982**, *94*, 688–696; d) G. Schatten, H. Schatten, T. H. Bestor, R. J. Balczon, *ibid.* **1982**, *94*, 455–465; e) B. Herman, M. A. Langerin, *Eur. J. Cell Biol.* **1983**, *31*, 034–045; f) J. Mole-Bajer, A. S. Bajer, *J. Cell Biol.* **1983**, *96*, 527–540; g) J. J. Manfredi, S. B. Horwitz, *Pharmacol. Ther.* **1984**, *25*, 83–125.
[81] M. De Brabander, G. Geuens, R. Nuydens, R. Willebroards, J. De May, *Proc. Natl. Acad. Sci. USA* **1981**, *78*, 5608–5612.
[82] a) K. Hausmann, M. Linnenbach, D. J. Patterson, *J. Ultrastruct. Res.* **1983**, *82*, 212–220; b) D. F. Albertini, B. Herman, P. Sherline, *Eur. J. Cell Biol.* **1984**, *82*, 212–220; c) P. F. Turner, R. L. Margolis, *J. Cell Biol.* **1984**, *99*, 940–946; d) J. J. Manfredi, J. Fant, S. B. Horwitz, *Eur. J. Cell Biol.* **1986**, *42*, 126–134.
[83] a) K. L. Crossin, D. H. Carney, *Cell* **1981**, *27*, 341–350; b) R. L. Ball, D. H. Carney, T. Albrecht, *Exp. Cell Res.* **1990**, *191*, 37–44.
[84] E. K. Rowinsky, R. C. Donehower, R. J. Jones, R. W. Tucker, *Cancer Res.* **1988**, *48*, 4093–4100.
[85] D. H. Young, E. L. Michelotti, C. S. Swindell, N. E. Krauss, *Experientia* **1992**, *48*, 882–885.
[86] H. U. Keller, A. Zimmerman, *Invasion Metastasis* **1986**, *6*, 33–43.
[87] Y. Komiya, T. Tashiro, *Cell Motil. Cytoskeleton* **1988**, *11*, 151–156.
[88] W. E. Rainey, R. E. Kramer, J. I. Mason, J. W. Shay, *J. Cell Physiol.* **1985**, *123*, 17–24.
[89] M. P. Mattson, *Brain Res.* **1992**, *582*, 107–118.

[90] P. F. Hall in *Cellular Regulation of Secretion and Release* (Ed.: M. P. Conn), Academic Press, New York, **1982**, pp. 194–227.
[91] S. L. Howell, C. S. Hii, S. Shaikh, M. Thyhurst, *Biosci. Rep.* **1982**, *2*, 795–801.
[92] a) D. B. McKay, A. S. Schneider, *J. Pharmacol. Exp. Ther.* **1984**, *231*, 102–108; b) D. B. McKay, R. S. Aronstram, A. S. Schneider, *Mol. Pharmacol.* **1985**, *28*, 10–16; c) J. Thuret-Carnahan, J.-L. Bossu, A. Feltz, K. Langly, D. Aunis, *J. Cell Biol.* **1985**, *100*, 1863–1874; d) D. B. Mc Kay, *J. Pharmacol. Exp. Ther.* **1989**, *248*, 1302–1307.
[93] a) K. Oda, Y. Ikehara, *Biochem. Biophys. Res. Common.* **1982**, *107*, 561–567; b) S. S. Kaufman, D. J. Tuma, J. A. Vanderhoof, *Toxicol. Appl. Pharmacol.* **1986**, *82*, 233–238.
[94] M. Crook, *Biochem. Soc. Trans.* **1991**, *19*, 47S.
[95] a) A. H. Ding, F. Porteu, E. Sanchez, C. F. Nathan, *Science* **1990**, *248*, 370–372; b) C. Bogdan, A. H. Ding, *J. Leukocyte Biol.* **1992**, *52*, 119–121; c) S. Williams, D. G. Mutch, L. Xu, J. L. Collins, *Am. J. Obstet. Gynecol.* **1992**, 1870–1876.
[96] A. Ding, E. Sanchez, M. Tancinco, C. J. Nathan, *J. Immunol.* **1992**, *148*, 2853–2858.
[97] M. D. Stearns, M. Wang, *Cancer Res.* **1992**, *52*, 3776–3781.
[98] a) M. Aapro, B. Braakhuis, M. Dietel, A. Hanauske, B. Hill, L. Kelland, P. Lelieveld, R. Silvestrini, W. Zoli, *Proc. Am. Assoc. Cancer Res.* **1992**, *33*, 516 (Abstract 3086); b) S. D. Harrison, Jr., D. J. Dykes, R. V. Shephard, D. P. Griswold, Jr., M. C. Bissery, *ibid.* **1992**, *33*, 526 (Abstract 3144); c) M. C. Bissery, D. Guénard, F. Gueritte-Voegelein, F. Lavelle, *Cancer Res.* **1991**, *51*, 4845–4852; d) M. C. Bissery, M. Bayssas, F. Lavelle, *Proc. Am. Assoc. Cancer Res.* **1991**, *32*, 417 (2475); e) F. Lavelle, C. Fizames, F. Gueritte-Voegelein, D. Guénard, P. Potier, *ibid.* **1989**, *30*, 566 (2254).
[99] a) E. K. Rowinsky, L. A. Cazenave, R. C. Donehower, *J. Natl. Cancer Inst.* **1990**, *82*, 1247–1259; b) E. K. Rowinsky, R. C. Donehower, *ibid.* **1991**, *83*, 1778–1781; c) E. K. Rowinsky, N. Onetto, R. M. Canetta, S. G. Arbuck, *Semin. Oncol.* **1992**, *19*, 646–662.
[100] *National Cancer Institute Clinical Brochure: Taxol (NSC1259973)*, NCI, Division of Cancer Treatment, Bethesda, MD, USA **1983**, 6–12.
[101] a) J. Riondel, M. Jacrot, F. Picot, H. Beriel, C. Mouriquand, P. Potier, *Cancer Chemother. Pharmacol.* **1986**, *17*, 137–142; b) M. Jacrot, J. Riondel, F. Picot, D. Leroux, C. Mouriquand, H. Beriel, P. Potier, *C.R. Seances Acad. Sci. Ser. 3* **1983**, *247*, 597–600.
[102] a) R. B. Tishler, P. B. Schiff, C. R. Geard, E. J. Hall, *Int. J. Radiat. Oncol. Biol. Phys.* **1992**, *22*, 613–617; b) R. B. Tishler, C. R. Geard, E. J. Hall, P. B. Schiff, *Cancer Res.* **1992**, *52*, 3495–3497; c) T. K. Hei, E. J. Hall, *ibid.* **1993**, *53*, 1368–1372.
[103] W. K. Sinclair, *Radiat. Res.* **1968**, *33*, 620–643.
[104] R. B. Weiss, R. C. Donehower, P. H. Wiernik, T. Ohnuma, R. J. Gralla, D. L. Trump, J. R. Baker, Jr., D. A. Van Echo, D. D. Von Hoff, B. Leyland-Jones, *J. Clin. Oncol.* **1990**, *8*, 1263–1268.
[105] T. Brown, K. Havlin, G. Weiss, J. Cagnola, J. Koeller, J. Kuhn, J. Rizzo, J. Craig, J. Phillips, D. Von Hoff, *J. Clin. Oncol.* **1991**, *9*, 1261–1267.
[106] E. K. Rowinsky, W. P. McGuire, T. Guarnieri, J. S. Fisherman, M. C. Christian, R. C. Donehower, *J. Clin. Oncol.* **1991**, *9*, 1704–1712.
[107] a) J.-G. Leu, B.-X. Chen, P. B. Schiff, B. F. Erlanger, *Cancer Res.* **1993**, *53*, 1388–1391; b) P. G. Grothaus, T. J. G. Raybould, G. S. Bignami, C. B. Lazo, J. B. Byrnes, *J. Immunol. Methods* **1993**, *158*, 5–15.
[108] E. K. Rowinsky, M. R. Gilbert, W. G. McGuire, D. A. Noe, L. B. Grochow, A. A. Forastiere, D. S. Ettinger, B. G. Lubejko, B. Clark, S. E. Sartorius, D. R. Cornblath, C. B. Hendricks, R. C. Donehower, *J. Clin. Oncol.* **1991**, *9*, 1692–1703.
[109] a) L. Levin, W. Hryniuk, *Semin. Oncol.* **1987**, 15, 756–767; b) W. Hryniuk, M. N. Levine, *J. Clin. Oncol.* **1986**, *4*, 1162–1170.
[110] G. Sarosy, E. Kohn, D. A. Stone, M. Rothenberg, J. Jacob, D. O. Adamo, F. P. Ognibene, R. E. Cunnion, E. Reed, *J. Clin. Oncol.* **1992**, *10*, 1165–1170.
[111] a) R. Pazdur, R. A. Newman, B. M. Newman, A. Fuentes, J. Benvenuto, B. Bready, D. Moore, Jr., I. Jaiyesimi, F. Vreeland, M. M. G. Bayssas, M. N. Raber, *J. Natl. Cancer Inst.* **1992**, *84*, 1781–1788; b) R. Pazdur, D. H. Ho, Y. Lassere, B. Bready, I. H. Kvakoff, M. N. Raber, *Proc. Am. Soc. Clion. Oncol.* **1992**, *11*, 111 (Abstract 265); c) H. Burris, R. Irvin, J. Kuhn, S. Kalter, L. Smith, D. Shaffer, G. Rodriguez, G. Weiss, J. Eckardt, F. Vreeland, M. M. G. Bayssas, D. Von Hoff, *ibid.* **1992**, *11*, 137 (Abstract 369); d) D. Bissett, J. Cassidy, A. Setanoians, G. A. Chadwick, P. Wilson, S. B. Kaye, D. J. Kerr, *Proc. Am. Assoc. Cancer Res.* **1992**, *33*, 526 (Abstract 3145); e) R. Bruno, J. C. Vergniol, G. Montay, N. Le Bail, A. Frydman, M. Clavel, M. Marty, *ibid.* **1992**, *33*, 261 (Abstract 1561); f) D. de Valeriola, C. Brassinne, M. Piccart, E. Tomiak, J. Kerger, A. Awada, C. Ravoet, S. Lips, V. Auzannet, N. Le Bail, R. Bruno, J. Klastersky, *ibid.* **1992**, *33*, 261 (Abstract 1561).
[112] a) W. P. McGuire, E. K. Rowinsky, N. B. Rosensheim, F. C. Grumbine, D. S. Ettinger, D. K. Armstrong, R. C. Donehower, *Ann. Intern. Med.* **1989**, *111*, 273–279; b) T. Thigpen, J. Blessing, H. Ball, S. Hummel, R. Barret, *Proc. Annu. Meet. Am. Soc. Clin. Oncol.* **1990**, *9*, (Abstract 604).
[113] R. F. Ozols, *Curr. Probl. Cancer* **1992**, *16*, 63–126.
[114] F. A. Holmes, R. S. Walters, R. L. Theriault, A. D. Forman, L. K. Newton, M. N. Raber, A. U. Buzdar, D. H. Frye, G. N. Hortobagyi, *J. Natl. Cancer Inst.* **1991**, *83*, 1797–1805.
[115] a) W. K. Murphey, R. J. Winn, F. V. Fossella, D. M. Shin, H. E. Hynes, H. M. Gross, E. Davila, J. T. Leimert, H. M. Dhingra, M. N. Raber, I. H. Krakoff, W. K. Hong, *Proc. Annu. Meet. Am. Soc. Clin. Oncol.* **1992**, *11*, 294 (Abstract 985); b) A. Chang, K. Kim, J. Glick, T. Anderson, D. Karp, D. Johnson, *ibid.* **1992**, *11*, 293 (Abstract 981).
[116] G. Sarosy, E. Kohn, C. Link, D. Adamo, P. Davis, F. Ognibene, B. Goldspiel, M. Cristian, E. Reed, *Proc. Annu. Meet. Am. Soc. Clin. Oncol.* **1992**, *11*, 226 (Abstract 716).
[117] a) *Chem. Eng. News* **1992**, *70* (47), 17; b) *Science* **1993**, *259*, 181.
[118] E. Blume, *J. Natl. Cancer Inst.* **1991**, *83*, 1054–1056.
[119] G. M. Cragg, K. M. Snader, *Cancer Cells* **1991**, *3*, 233–235.
[120] a) H. Hartzell, Jr., *The Yew Tree A Thousand Whispers*, Hulogosi, Eugene, OR, USA, **1991**; b) C. L. Bolsinger, A. E. Jaramillo in *Silvics of North America: Vol. 1., Conifers*, (Eds.: R. M. Burns, B. H. Honkala), USDA: Forest Service, Washington, DC, USA, pp. 573–579.
[121] N. Vidensek, P. Lim, A. Campbell, C. Carlson, *J. Nat. Prod.* **1990**, *53*, 1609–1610.
[122] R. G. Kelsey, N. C. Vance, *J. Nat. Prod.* **1992**, *55*, 912–917.
[123] N. C. Wheeler, K. Jech, S. Masters, S. W. Brobst, A. B. Alvarado, A. J. Hoover, K. M. Sader, *J. Nat. Prod.* **1992**, *55*, 432–440.
[124] S. Bormann, *Chem. Eng. News* **1992**, *70* (41), 30–32.
[125] a) D. McCormick, *Bio/Technology* **1993**, *11*, 26; b) R. A. Holton, *Workshop on Taxol and Taxus: Current and Future Perspectives*, National Cancer Institute, Bethesda, MD, USA, 26. June 1990.
[126] M. Colin, D. Guénard, F. Gueritte-Voegelein, P. Poiter, *US-A 4924012*, **1991**.
[127] G. A. Strobel, A. Stierle, F. J. G. M. van Kuijk, *Plant Sci.* **1992**, *84*, 65–74.
[128] A. A. Christen, D. M. Gibson, J. Bland, *US-A 5019504*, **1992**.
[129] S. M. Edgington, *Bio/Technology* **1991**, *9*, 933–938.
[130] E. Blume, *J. Natl. Cancer Inst.* **1991**, *83*, 1054–1056.
[131] A. G. Fett-Neto, F. DiCosmo, W. F. Reynolds, K. Sakata, *Bio/Technology* **1992**, *10*, 1572–1575.
[132] a) A. Stierle, G. Strobel, D. Stierle, *Science* **1993**, *260*, 214–216; b) R. Stone, *ibid.* **1993**, *260*, 154–155.
[133] C. S. Swindell, *Org. Prep. Proced. Int.* **1991**, *23*, 465–543.
[134] a) I. Kitagawa, S. Tsujii, H. Fujioka, A. Kajiwara, Y. Yamamoto, H. Shibuya, *Chem. Pharm. Bull.* **1984**, *32*, 1294–1302; b) I. Kitagawa, H. Shibuya, H. Fujioka, A. Kajiwara, S. Tsujii, Y. Yamamoto, A. Takagi, *Chem. Lett.* **1980**, 1001–1004; c) I. Kitagawa, H. Shibuya, H. Fujioka, Y. Yamamoto, A. Kajiwara, K. Kitamura, A. Miyao, T. Hakoshima, K. Tomita, *Tetrahedron Lett.* **1980**, *21*, 1963–1966.
[135] L. Pettersson, T. Frejd, G. Magnusson, *Tetrahedron Lett.* **1987**, *28*, 2753–2756.
[136] J. Lin, M. M. Nikaido, G. Clark, *J. Org. Chem.* **1987**, *52*, 3745–3752.
[137] K. C. Nicolaou, C.-K. Hwang, E. J. Sorensen, C. F. Clairborne, *J. Chem. Soc. Chem. Commun.* **1992**, 1117–1118.
[138] a) Y. Queneau, W. J. Krol, W. G. Bornmann, S. J. Danishefsky, *J. Org. Chem.* **1992**, *57*, 4043–4047; b) *ibid.* **1993**, *58*, 798.
[139] H. Shibuya, S. Tsujii, Y. Yamamoto, H. Miura, I. Kitagawa, *Chem. Pharm. Bull.* **1984**, *32*, 3417–3427.
[140] R. Z. Andriamialisoa, M. Fetizon, I. Hanna, C. Pascard, T. Prange, *Tetrahedron* **1984**, *40*, 4285–4295.
[141] a) W. F. Berkowitz, A. S. Amarasekara, *Tetrahedron Lett.* **1985**, *26*, 3663; b) W. F. Berkowitz, A. S. Amarasekara, J. J. Perumattam, *J. Org. Chem.* **1987**, *52*, 1119–1124.
[142] T. V. Magee, W. G. Bornmann, R. C. A. Isaacs, S. J. Danishefsky, *J. Org. Chem.* **1992**, *57*, 3274–3276.
[143] K. C. Nicolaou, J. J. Liu, C.-K. Hwang, W.-M. Dai, R. K. Guy, *J. Chem. Soc. Chem. Commun.* **1992**, 1118–1120.
[144] K. Narasaka, S. Shimada, K. Osoda, N. Iwasawa, *Synthesis* **1991**, 1171–1172.
[145] P. A. Wender, D. B. Rawlins, *Tetrahedron* **1992**, *48*, 7033–7048.
[146] a) R. V. Bonnert, J. Howarth, P. R. Jenkins, N. J. Lawrence, *J. Chem. Soc. Perkin Trans. 1* **1991**, 1225–1228; b) R. V. Bonnert, M. J. Davis, J. Howarth, P. R. Jenkins, N. J. Lawrence, *ibid.* **1992**, 27–30; c) A. N. Boa, J. Clark, P. R. Jenkins, N. J. Lawrence, *J. Chem. Soc. Chem. Commun.* **1993**, 151–152.
[147] K. Sakan, B. M. Craven, *J. Am. Chem. Soc.* **1983**, *105*, 3732–3734.
[148] a) K. J. Shea, P. D. Davis, *Angew. Chem.* **1983**, *95*, 422–423; *Angew. Chem. Int. Ed. Engl.* **1983**, *22*, 419–420; *Angew. Chem. Suppl.* **1983**, 564–570; b) K. J. Shea, J. W. Gilman, C. D. Haffner, T. K. Dougherty, *J. Am. Chem. Soc.* **1986**, *108*, 4953–4956; c) K. J. Shea, C. D. Haffner, *Tetrahedron Lett.* **1988**, *29*, 1367–1370; d) K. J. Shea, S. T. Sakata, *ibid.* **1992**, *33*, 4264–4264.
[149] R. W. Jackson, R. G. Higby, J. W. Gilman, K. J. Shea, *Tetrahedron* **1992**, *48*, 7013–7032.
[150] a) P. A. Brown, P. R. Jenkins, J. Fawrett, D. R. Russel, *J. Chem. Soc. Chem. Commun.* **1984**, 253–255; b) P. A. Brown, P. R. Jenkins, *J. Chem. Soc. Perkin Trans. 1* **1986**, 1303–1309; c) R. V. Bonnert, P. R. Jenkins, *J. Chem. Soc. Chem. Commun.* **1987**, 1540–1541; d) R. V. Bonnert, P. R. Jenkins, *J. Chem. Soc. Perkin Trans. 1* **1989**, 413–418.
[151] a) P. A. Wender, M. J. Tebbe, *Synthesis* **1991**, 1089–1094; b) P. A. Wender, M. L. Snapper, *Tetrahedron Lett.* **1987**, *28*, 2221–2224; c) P. A. Wender, N. C. Ihle, *ibid.* **1987**, *28*, 2451–2454; see also: P. A. Wender, N. C. Ihle, *J. Am. Chem. Soc.* **1986**, *108*, 4678–4679.

[152] B. M. Trost, H. Hiemstra, *J. Am. Chem. Soc.* **1982**, *104*, 886–887.
[153] B. M. Trost, M. J. Fray, *Tetrahedron Lett.* **1984**, *25*, 4605–4608.
[154] M. J. Begley, M. Mellor, G. Pattenden, *J. Chem. Soc. Perkin Trans. 1* **1983**, 1905–1912.
[155] a) H. Neh, S. Blechert, W. Schnick, M. Jansen, *Angew. Chem.* **1984**, *96*, 903–904; *Angew. Chem. Int. Ed. Engl.* **1984**, *23*, 905–906; b) S. Blechert, A. Kleine-Klausing, *ibid.* **1991**, *103*, 428–430 and **1991**, *30*, 412–414.
[156] R. Kaczmarek, S. Blechert, *Tetrahedron Lett.* **1986**, *27*, 2845–2848.
[157] S. Blechert, R. Muller, M. Beitzel, *Tetrahedron* **1992**, *48*, 6953–6964.
[158] W. F. Berkowitz, J. Perumattam, A. Amarasekara, *Tetrahedron Lett.* **1985**, *26*, 3665–3668.
[159] T. Kojima, Y. Inouye, H. Kakisawa, *Chem. Lett.* **1985**, 323–326.
[160] J. D. Winkler, J. P. Hey, P. G. Williard, *J. Am. Chem. Soc.* **1986**, *108*, 6425–6427.
[161] a) J. D. Winkler, D. Subrahmanyam, R. P. Hsung, added as corrigendum: *Tetrahedron* **1993**, *49*, 291) *ibid.* **1992**, *48*, 7049–7056; b) J. D. Winkler, C.-S. Lee, L. Rubo, C. L. Muller, P. J. Squattrito, *J. Org. Chem.* **1989**, *54*, 4491–4493; see also: J. D. Winkler, J. P. Hey, S. D. Darling, *Tetrahedron Lett.* **1986**, *27*, 5959–5962.
[162] M. Benchikh le-Hocine, D. Do Khac, M. Fetizon, I. Hanna, R. Zeghdoudi, *Synth. Commun.* **1987**, *17*, 913–918; for a five-membered substrate, see M. Benchikh le-Hocine, D. Do Khac, M. Fetizon, *ibid.* **1992**, *22*, 245–255; see also M. Fetizon, I. Hanna, R. Zeghdoudi, *ibid.* **1986**, *16*, 1–9; G. Aranda, J.-M. Bernassau, M. Fetizon, I. Hanna, *J. Org. Chem.* **1985**, *50*, 1156–1161.
[163] M. Benchikh le-Hocine, D. Do Khac, M. Fetizon, *Synth. Commun.* **1992**, *22*, 1871–1882.
[164] M. Benchikh le-Hocine, D. Do Khac, M. Fetizon, F. Guir, Y. Guo, T. Prange, *Tetrahedron Lett.* **1992**, *33*, 1443–1446.
[165] G. A. Kraus, P. J. Thomas, Y.-S. Hon, *J. Chem. Soc. Chem. Commun.* **1987**, 1849–1850.
[166] G. A. Kraus, D. Zheng, *Synlett* **1993**, 71–72.
[167] a) C. S. Swindell, S. J. deSolms, J. P. Springer, *Tetrahedron Lett.* **1984**, *25*, 3797–3800; b) C. S. Swindell, S. J. deSolms, *ibid.* **1984**, *25*, 3801–3804; c) C. S. Swindell, B. P. Patel, S. J. deSolms, J. P. Springer, *J. Org. Chem.* **1987**, *52*, 2346–2355; see also: F. M. Schell, P. M. Cook, S. W. Hawkinson, R. E. Cassady, W. E. Thiessen, *ibid.* **1979**, *44*, 1380–1382.
[168] C. S. Swindell, B. P. Patel, *Tetrahedron Lett.* **1987**, *28*, 5275–5278.
[169] C. S. Swindell, B. P. Patel, *J. Org. Chem.* **1990**, *55*, 3–5.
[170] G. Saha, A. Bhattacharya, S. S. Roy, S. Ghosh, *Tetrahedron Lett.* **1990**, *31*, 1483–1484.
[171] H. Nagaoka, K. Ohsawa, T. Takata, Y. Yamada, *Tetrahedron Lett.* **1984**, *25*, 5389–5392.
[172] R. A. Holton, *J. Am. Chem. Soc.* **1984**, *106*, 5731–5732.
[173] R. A. Holton, R. R. Juo, H. B. Kim, A. D. Williams, S. Harusawa, R. E. Lowenthal, S. Yogai, *J. Am. Chem. Soc.* **1988**, *110*, 6558–6560.
[174] a) Y. Ohtsuka, T. Oishi, *Heterocycles* **1984**, *21*, 371; b) *Tetrahedron Lett.* **1986**, *27*, 203–206; c) *Chem. Pharm. Bull.* **1988**, *36*, 4711–4721, 4722–4736.
[175] S. F. Martin, J. B. White, R. Wagner, *J. Org. Chem.* **1982**, *47*, 3190–3192.
[176] B. B. Snider, A. J. Allentoff, *J. Org. Chem.* **1991**, *56*, 321–328; see also: P. A. Zucker, J. A. Lupia, *Synlett* **1990**, 729–730.
[177] a) L. A. Paquette, K. D. Combrink, S. W. Elmore, R. D. Rogers, *J. Am. Chem. Soc.* **1991**, *113*, 1335–1344; b) S. W. Elmore, K. D. Combrink, L. A. Paquette, *Tetrahedron Lett.* **1991**, *32*, 6679–6682; c) see also: L. A. Paquette, D. T. DeRussy, N. A. Pegg, R. T. Taylor, T. M. Zydowsky, *J. Org. Chem.* **1989**, *54*, 4576–4581; L. A. Paquette, C. A. Teleha, R. T. Taylor, G. D. Maynard, R. D. Rogers, J. C. Gallucci, J. P. Springer, *J. Am. Chem. Soc.* **1990**, *112*, 265–277; L. A. Paquette, N. A. Pegg, D. Toops, G. D. Maynard, R. D. Rogers, *ibid.* **1990**, *112*, 277–283; N. A. Pegg, L. A. Paquette, *J. Org. Chem.* **1991**, *56*, 2461–2468.
[178] a) L. A. Paquette, S. W. Elmore, K. D. Combrink, E. R. Hickey, R. D. Rogers, *Helv. Chim. Acta* **1992**, *75*, 1755–1771; b) L. A. Paquette, K. D. Combrink, S. W. Elmore, M. Zhao, *ibid.* **1992**, *75*, 1772–1791.
[179] R. L. Funk, W. J. Daily, M. Parvez, *J. Org. Chem.* **1988**, *53*, 4141–4143.
[180] J. S. Yadav, R. Ravishankar, *Tetrahedron Lett.* **1991**, *32*, 2629–2632.
[181] P. A. Wender, T. P. Mucciaro, *J. Am. Chem. Soc.* **1992**, *114*, 5878–5879.
[182] a) T. Kumagai, F. Tse, T. Uyehara, T. Kato, *Chem. Lett.* **1981**, 25–27; b) T. Kato, H. Takayanagi, T. Suzuki, T. Uyehara, *Tetrahedron Lett.* **1978**, 1201–1204.
[183] M. J. Begley, C. B. Jackson, G. Pattenden, *Tetrahedron* **1990**, *46*, 4907–4924; see also: C. B. Jackson, G. Pattenden, *Tetrahedron Lett.* **1985**, *26*, 3393–3396.
[184] A. S. Kende, S. Johnson, P. Sanfilippo, J. C. Hodges, L. N. Jungheim, *J. Am. Chem. Soc.* **1986**, *108*, 3513–3515.
[185] K. C. Nicolaou, Z. Yang, E. Sorensen, M. Nakada, *J. Chem. Soc. Chem. Commun.* **1993**, 1024–1026.
[186] a) Y. Horiguchi, T. Furukawa, I. Kuwajima, *J. Am. Chem. Soc.* **1989**, *111*, 8277–8279; b) T. Furukawa, K. Morihira, Y. Horiguchi, I. Kuwajima, *Tetrahedron* **1992**, *48*, 6975–6984; c) Y. Kataoka, Y. Nakamura, K. Morihira, H. Arai, Y. Horiguchi, I. Kuwajima, *Tetrahedron Lett.* **1992**, *33*, 6979–6982.
[187] J. D. Winkler, V. Sridar, M. G. Siegel, *Tetrahedron Lett.* **1989**, *30*, 4943–4946.
[188] S. A. Hitchcock, G. Pattenden, *Tetrahedron Lett.* **1992**, *33*, 4843–4846; corrigendum: *ibid.* **1992**, *33*, 7448.
[189] J. Oh, J.-R. Choi, J. K. Cha, *J. Org. Chem.* **1992**, *57*, 6664–6667.
[190] Z. Wang, S. E. Warder, H. Perrier, E. L. Grimm, M. A. Bernstein, R. G. Ball, *J. Org. Chem.* **1993**, *58*, 2931–2932.
[191] J. N. Denis, A. E. Greene, A. A. Serra, M.-J. Luche, *J. Org. Chem.* **1986**, *51*, 46–50.
[192] J.-N. Denis, A. A. Correa, A. E. Greene, *J. Org. Chem.* **1990**, *55*, 1957–1959.
[193] K. B. Sharpless, H. C. Kolb, *US-Patent*, pending.
[194] L. Deng, E. N. Jacobsen, *J. Org. Chem.* **1992**, *57*, 4320–4323.
[195] A. Commerçon, D. Bezard, F. Bernard, J. D. Bourzat, *Tetrahedron Lett.* **1992**, *33*, 5185–5188.
[196] a) J.-N. Denis, A. Correa, A. E. Greene, *J. Org. Chem.* **1991**, *56*, 6939–6942; b) A. M. Kanazawa, A. Correa, J.-N. Denis, M.-J. Luche, A. E. Greene, *ibid.* **1993**, *58*, 255–257.
[197] C. Mukai, I. J. Kim, M. Hanaoka, *Tetrahedron Asymmetry* **1992**, *3*, 1007–1010.
[198] a) I. Ojima, I. Habus, M. Zhao, G. Georg, L. R. Jayasinghe, *J. Org. Chem.* **1991**, *56*, 1681–1683; b) I. Ojima, I. Habus, M. Zhao, M. Zucco, Y. H. Park, C. M. Sun, T. Brigaud, *Tetrahedron* **1992**, *48*, 6985–7012.
[199] G. I. Georg, P. M. Mashava, E. Akgun, M. W. Milstead, *Tetrahedron Lett.* **1991**, *32*, 3151–3154; see also [207].
[200] V. Farina, S. I. Hauck, D. G. Walker, *Synlett* **1992**, 761–763.
[201] a) C. Palomo, J. M. Aizpurua, M. C. Lopez, N. Aurrekoetxea, M. Oiarbide, *Tetrahedron Lett.* **1990**, *31*, 6425–6428; b) C. Palomo, A. Arrieta, F. P. Cossio, J. M. Aizpurua, A. Mielgo, N. Aurrekoetxea, *ibid.* **1990**, *31*, 6429–6432.
[202] D.-M. Gou, Y.-C. Liu, C.-S. Chen, *J. Org. Chem.* **1993**, *58*, 1287–1289.
[203] H. Honig, P. Seufer-Wasserthal, H. Weber, *Tetrahedron* **1990**, *46*, 3841–3850.
[204] K. Hattori, M. Miyata, H. Yamamoto, *J. Am. Chem. Soc.* **1993**, *115*, 1151–1152.
[205] a) V. Senilh, F. Gueritte, D. Guénard, M. Colin, P. Potier, *C. R. Seances Acad. Sci. Ser. 2* **1984**, *299*, 1039–1045; b) F. Gueritte-Voegelein, V. Senilh, B. David, D. Guénard, P. Potier, *Tetrahedron* **1986**, *42*, 4451–4460.
[206] R. A. Holton, *EP-A 400971*, **1990**.
[207] G. I. Georg, Z. S. Cheruvallavth, R. H. Himes, M. R. Mejillano, *Bioorg. Med. Chem. Lett.* **1992**, *2*, 295–298.
[208] C. S. Swindell, N. E. Krauss, S. B. Horwitz, I. Ringel, *J. Med. Chem.* **1991**, *34*, 1176–1184. Different numbers have been obtained ranging from 0.7 $\mu g\,mL^{-1}$ to $<0.05\ mg\,mL^{-1}$.
[209] a) D. G. I. Kingston, G. Samaranayake, C. A. Ivey, *J. Nat. Prod.* **1990**, *53*, 1–12; b) D. G. I. Kingston, *Pharmacol. Ther.* **1991**, *52*, 1–34.
[210] a) P. Potier, *Chem. Soc. Rev.* **1992**, 113–119; b) D. Guénard, F. Gueritte-Voegelein, P. Potier, *Acc. Chem. Res.* **1993**, *26*, 160–167.
[211] H. M. Deutsch, J. A. Glinski, M. Hernandes, R. D. Haugwitz, V. L. Narayanan, M. Suffness, L. H. Zalkow, *J. Med. Chem.* **1989**, *32*, 788–792.
[212] A. E. Mathew, M. R. Mejillano, J. P. Nath, R. H. Himes, V. J. Stella, *J. Med. Chem.* **1992**, *35*, 145–151.
[213] K. C. Nicolaou, C. Riemer, M. Kerr, D. Rideout, W. Wrasidlo, *Nature* **1993**, *364*, 464–466.
[214] H. G. Keizer, H. Joenje, *J. Natl. Cancer Inst.* **1989**, *81*, 706–709.
[215] a) F. Gueritte-Voegelein, D. Guénard, F. Lavelle, M.-T. Le Goff, L. Mangatal, P. Potier, *J. Med. Chem.* **1991**, *34*, 992–998; b) C. S. Swindell, N. E. Krauss, S. B. Horwitz, I. Ringel, *ibid.* **1991**, *34*, 1176–1184.
[216] G. Samaranayke, N. F. Magri, C. Jitrangsri, D. G. I. Kingston, *J. Org. Chem.* **1991**, *56*, 5114–5119.
[217] a) A. Wahl, F. Gueritte-Voegelein, D. Guénard, M.-T. Le Goff, P. Potier, *Tetrahedron* **1992**, *48*, 6965–6974; b) V. Farina, S. Huang, *Tetrahedron Lett.* **1992**, *33*, 3979–3981.
[218] a) S. H. Chen, J.-M. Wei, V. Farina, *Tetrahedron Lett.* **1993**, *34*, 3205–3206; b) S.-H. Chen, C. Fairchild, S. W. Mamber, V. Farina, *J. Org. Chem.* **1993**, *58*, 2927–2928.
[219] K. C. Nicolaou, W.-M. Dai, *Angew. Chem.* **1991**, *103*, 1453–1506; *Angew. Chem. Int. Ed. Engl.* **1991**, *30*, 1387–1430.
[220] a) S. L. Schreiber, *Chem. Eng. News* **1992**, *70* (43), 22–32; b) M. K. Rosen, S. L. Schreiber, *Angew. Chem.* **1992**, *104*, 413–429; *Angew. Chem. Int. Ed. Engl.* **1992**, *31*, 384–400.
[221] a) J. Detering, H.-D. Martin, *Angew. Chem.* **1988**, *100*, 714–716; *Angew. Chem. Int. Ed. Engl.* **1988**, *27*, 695–698; b) J. R. Hargreves, P. W. Hickmott, B. J. Hopkins, *J. Chem. Soc. C.* **1968**, 2599–2603.

X-Ray Absorption Spectroscopy of Amorphous Solids, Liquids, and Catalytic and Biochemical Systems—Capabilities and Limitations

Helmut Bertagnolli* and Teja S. Ertel*

Although the effect on which X-ray absorption spectroscopy (EXAFS spectroscopy) is based has been known for about 70 years, up until about 20 years ago it had not found any application. The reasons for this were on the one hand the shortage of efficient X-ray sources, and on the other hand the lack of a suitable theoretical description. With the advent of synchrotron radiation the situation has changed completely. Today, EXAFS spectroscopy is applied to a variety of very different problems and used more and more frequently to answer chemical questions. The extraordinary behavior of EXAFS spectroscopy that allows the determination of local structures in almost any mixture, independent of the sample's physical state as well as element-specifically with high sensitivity, carries with it the danger that the amount of the obtainable structural information will be overestimated. A realistic estimate of the capability of EXAFS spectroscopy has in the meantime been achieved for crystalline materials, but not for amorphous materials. In this case the viewpoints range from complete rejection to overinterpretation of the EXAFS spectrum. In this article an attempt is made to show how EXAFS spectroscopy can be applied in the investigation of noncrystalline materials. First, the measurement techniques, data analysis procedures, and the simulation of EXAFS spectra are explained. Starting with the simplest systems, the amorphous metals and nonmetals, and using representative but not necessarily current examples, an explanation is given of the structural information provided by EXAFS spectroscopy, of how the local environment about the two components can be determined in binary systems, and of how even the crystallization process and structural changes can be investigated in chemical reactions. Thereafter, EXAFS studies on solutions, molecular liquids, and melts are presented. The final section is concerned with typical applications of EXAFS spectroscopy, the investigation of homogeneous and heterogeneous catalysts as well as the elucidation of active sites in enzymes.

1. Theoretical Foundations

A monochromatic X-ray beam of energy E is attenuated by the passage through a material of thickness d according to Equation (a).[1] $I_0(E)$ and $I(E)$ are the intensity of the incident and transmitted beams, respectively. $\mu(E)$ is the linear absorption coefficient. Its dependence on E is depicted in Figure 1a. $\mu(E)$ decreases with increasing E of the incident X-rays until a threshold is reached at which the energy is sufficient to remove an electron from an inner shell. At this threshold, $\mu(E)$ increases abruptly. Beyond this point, $\mu(E)$ resumes its steady decrease. More precise measurements of the absorption coefficient indicate that the curve shown in Figure 1a is typical only for isolated atoms. When other atoms are in the vicinity of the absorbing atom, the absorption coefficient shows small oscillations up to about 1000 eV above the absorption edge. This is shown schematically in Figure 1b.

$$\frac{I(E)}{I_0(E)} = e^{-\mu(E)d} \qquad \text{(a)}$$

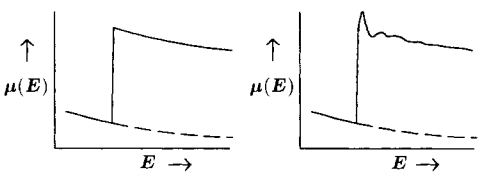


Fig. 1. Graph of the absorption coefficient $\mu(E)$ for an isolated atom (left) and for an atom surrounded by backscattering atoms (right).

This fine structure has been known for a long time—H. Fricke[2] and G. Hertz[3] discovered it in 1920—but the effect could not be explained satisfactorily by theory at the time. R. de L. Kronig[4, 5] already had the correct fundamental ideas in the 1930s, but the interpretation remained confusing until the 1970s when D. E. Sayers, E. A. Stern, and F. W. Lytle[6, 7] formulated

[*] Prof. Dr. H. Bertagnolli, Dr. T. S. Ertel
Institut für Physikalische Chemie der Universität
Pfaffenwaldring 55, D-70550 Stuttgart (FRG)
Telefax: Int. code + (711)685-4443

 © VCH Verlagsgesellschaft mbH, D-69451 Weinheim, 1994 0570-0833/94/0101-0045 $ 10.00+.25/0

when D. E. Sayers, E. A. Stern, and F. W. Lytle[6, 7] formulated a theory that has remained generally accepted until today. This theory will be briefly outlined below.

The probability for absorption of an X-ray photon by an electron of an inner shell is dependent on the initial and final states of the excited electron. The initial state is that of the core electron, while the final state is more difficult to describe. The absorption of X-ray radiation generates a photoelectron that can be considered as a spherical wave originating from the absorbing atom. This wave is then backscattered by the neighboring atoms. The final state is therefore the superposition of the original and backscattered waves. The resulting constructive and destructive interference leads to the oscillations in the absorption coefficient.

This qualitative description indicates that the oscillations in the absorption coefficient μ are dependent on the distance r_j, the number of neighboring atoms N_j, and the type of backscattering atom j. The backscattering ability of atom j is characterized by the backscattering amplitude F_j, while the effect of j on the phase is determined by the phase shift φ_{ij}. In addition, the finite lifetime of the photoelectron—equivalent to an additional damping with a mean free path length of λ_j—must be taken into account as well as the fact that the backscattering atoms are distributed around a mean distance due to thermal vibrations and static disorder. A good approximation for this distribution is a Gaussian function with a mean square deviation of σ_j^2. In analogy to X-ray and neutron diffraction, the quantity σ_j^2 is called a Debye–Waller-like factor. This terminology indicates that σ_j^2 also contains contributions stemming from the static disorder. This fine differentiation will be ignored in this review and σ_j^2 will be called—as is customary—simply the Debye–Waller factor.

According to the above considerations, precise measurements of the energy dependence of the X-ray absorption coefficient make it possible to determine the local environment around the element which absorbs the X-rays. Methods which are based on this principle are categorized as X-ray absorption spectroscopy or X-ray absorption fine structure (XAFS) spectroscopy. The energy range close the absorption edge is called XANES (X-ray absorption near edge structure), while the range about 30–1000 eV from the edge is called EXAFS (extended X-ray absorption fine structure). XANES yields information about the spatial arrangement of backscatterers. The corresponding theory has not yet been completely developed and, therefore, mostly only qualitative comparisons are employed. In contrast, the theory for EXAFS has evolved to such an extent that reliable conclusions about local structures are possible. Since the positions of the K and L edges are dependent on the element in question, the suitable choice of incident X-ray energies makes it possible to excite one specific element and, hence, to probe its environment. This method is therefore element-specific, independent of the physical state of the sample, and can be employed even for low concentrations of absorbing atoms.

In order to determine the relationship between the quantities characterizing the local environment around the absorbing atom and the X-ray absorption coefficient $\mu(E)$, it is necessary to correct and normalize the modulation of $\mu(E)$ for the background absorption $\mu_0(E)$ [Eq. (b)].[8] The next step is to convert

$$\chi(E) = \frac{\mu(E) - \mu_0(E)}{\mu_0(E)} \qquad \text{(b)}$$

the function $\chi(E)$ into the function $\chi(k)$, in which k is the magnitude of the photoelectron wave vector. k can be calculated





Helmut Bertagnolli, born in 1943 in Baden-Baden, studied chemistry at the Universität Freiburg and received his doctorate there in 1974 in the field of physical chemistry with Prof. Zimmermann. Subsequently, he moved to the Universität Karlsruhe, where he habilitated in 1979 with a work on the scattering of polarized neutrons on ^1H-containing molecular liquids. In 1981 he took up a professorship at the Universität Würzburg; since 1993 he has held the newly founded chair of physcial chemistry at the Universität Stuttgart. The main focus of his research interest lies in the study of the amorphous state, which he characterizes primarily with X-ray and neutron diffraction as well as EXAFS spectroscopy and interprets with statistical mechanical calculations and reverse-Monte-Carlo simulations.

Teja Sebastian Ertel, born in München in 1965, studied chemistry from 1984 to 1985 at the Ludwig-Maximilians Universität München and from 1985 to 1989 at the Universität Würzburg. He received his doctorate in 1992 under the supervision of Prof. Bertagnolli. During his studies he was supported by scholarships from the Stiftung Stipendien-Fonds des Verbands der Chemischen Industrie. In the same year he received the research prize awarded by the Braintrust Gesellschaft für Forschungstransfer München. Since April 1992 he has been working with the aid of a grant from the Dr. Leni Schöninger-Stiftung at the Universität Stuttgart on the structural elucidation of amorphous materials with the help of various spectroscopic techniques.

according to Equation (c) from the energy E of the incident

$$k = \sqrt{\frac{8\pi^2 m_e}{h^2}(E - E_0)} \qquad \text{(c)}$$

X-ray photon and the position of the absorption edge E_0. The mass of the electron is denoted by m_e, h stands for Planck's constant. Equation (d) relates the resulting EXAFS function

$$\chi(k) = \sum_j \frac{N_j}{kr_j^2} \cdot F_j(k) \cdot e^{-2\sigma_j^2 k^2} e^{-\frac{2r_j}{\lambda_j(k)}} \cdot \sin[2kr_j + \varphi_{ij}(k)] \qquad \text{(d)}$$

$\chi(k)$ to the quantities that characterize the environment of the absorbing atom.[6, 7]

The EXAFS function in k space contains all necessary information, however, it is not readily visualized. Fourier transformation of $\chi(k)$ yields a radial distribution function $F(r)$, which has maxima at $R_j = r_j - \alpha_j$ and therefore indicates the distribution of the backscatterers [Eq. (e)]. Generally, only the magni-

$$F(r) = \frac{1}{\sqrt{2\pi}} \int_{k_{min}}^{k_{max}} \chi(k) \cdot k^n w(k) \exp(i2kr)\, dk \qquad \text{(e)}$$

tude of $F(r)$ is plotted, called either the modulo function of the Fourier transformed EXAFS function or simply the structure function $|F(r)|$. During data interpretation it must be taken into account that all maxima are shifted to lower distances—typical shifts are between 0.2–0.3 Å. As the functions are only transformed in the interval $k_{max} - k_{min}$, non-real peaks can appear in the transformed functions. These peaks can be strongly dampened by the use of a window function $w(k)$, which defines the interval to be transformed as well as the weighting of all points. A typical example for $w(k)$ is a step function. While this type of function has the highest resolution, it is not always possible to avoid truncation effects. The use of a Gaussian step function lets the sides of the window slope gently downward at the edges and truncation effects are rarely observed.

The multiplication of the EXAFS function by k^n ($n = 1-3$) is performed to compensate the decrease of $\chi(k)$ with increasing k. This decrease is caused by the functional form of the backscattering amplitude $F_j(k)$ and the factor $\exp(-2\sigma^2 k^2)$. B. K. Teo and P. A. Lee[9] proposed $n = 1$ for backscatterers with atomic number $Z > 57$, $n = 2$ for elements with $36 < Z < 57$, and $n = 3$ for $Z < 36$. Weighting with k^3 requires very high data quality, as for high k values the signal-to-noise ratio is especially unfavorable. This weighting scheme has the advantage, however, that the EXAFS oscillations are evenly weighted over the entire k region. Moreover, the use of different weighting schemes makes it possible to distinguish heavy elements from light ones.

To develop a feel for the characteristics of the EXAFS functions and their Fourier transforms, the structure functions, it is useful to examine some theoretical curves. Figure 2a shows the k^3-weighted $\chi(k)$ function of an Fe–C pair with a typical distance of 2.0 Å (as in ferrocene), coordination number $N_j = 1$, and $\sigma_j = 0.05$ Å, by using theoretical backscattering amplitudes and phases from A. G. McKale et al.[10] The Fourier transformed function (Fig. 2b) shows a maximum which is clearly shifted to smaller distances. This maximum is asymmetric due to the finite transformation interval. Figure 2c shows the EXAFS function of an Fe–Br unit, using the same parameters. A comparison with Figure 2a indicates that the amplitude is significantly larger (also note the different scales). This trend can be generalized: lighter elements are weaker backscatterers, and are therefore more difficult to detect than heavy elements.

How can the element type be recognized? According to Equation (d), the backscattering amplitude and phase are element-specific quantities. The backscattering amplitude is the envelope in the EXAFS function, which results in the clearly different Figures 2a and 2c. The Fourier transformed functions, on the other hand, do not give any indications of the presence of different elements.

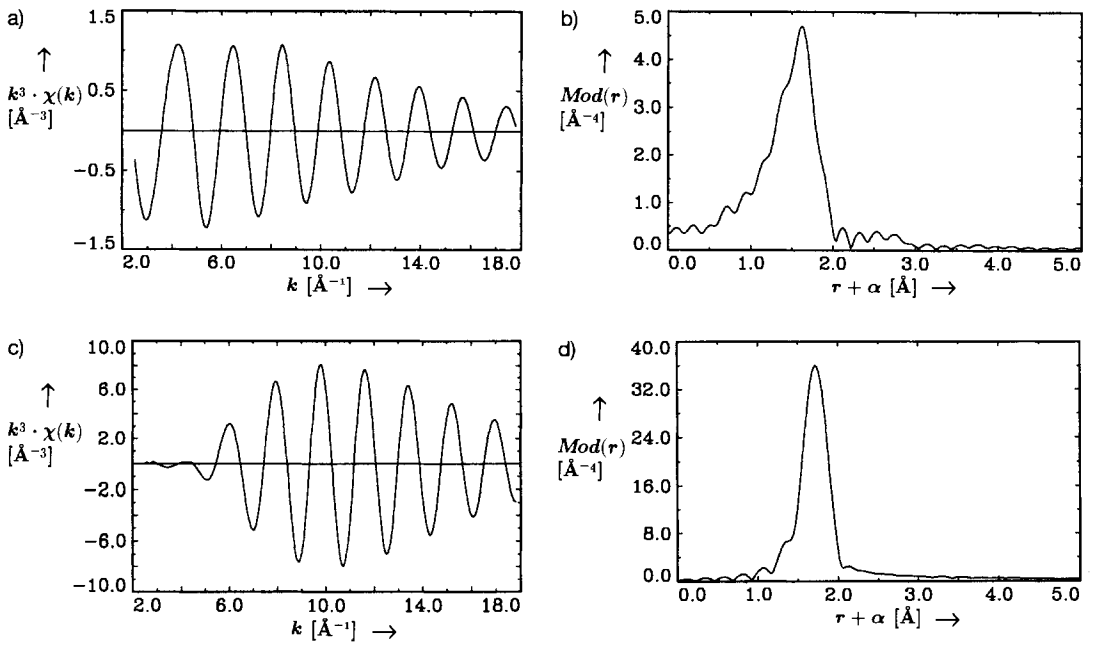


Fig. 2. Theoretical EXAFS functions (a, c) and their Fourier transforms (b, d) for an Fe–C (a, b) and an Fe–Br (c, d) absorber–backscatterer pair. The EXAFS functions were calculated employing McKale amplitude and phase functions [10], by using the following structural parameters: absorber–backscatterer distances $r_{Fe-C} = 2.0$, $r_{Fe-Br} = 2.0$ Å, coordination numbers $N_C = 1.0$ and $N_{Br} = 1.0$, Debye–Waller factors $\sigma_C = 0.05$ and $\sigma_{Br} = 0.05$ Å.

The theoretical calculation of backscattering amplitudes and phases was a problem for a long time and was one of the main reasons why EXAFS spectroscopy did not find wide application. The first extensive calculations of backscattering amplitudes and phases stem from B. K. Teo and P. A. Lee[9] and were based on an electron–atom scattering theory from P. A. Lee and G. Beni.[11] In this theory, the spherical wave originating from the absorbing atom was approximated by a planar wave. This approximation is valid as long as the effective atom size is small compared to the interatomic distance. In the meantime, a number of powerful program packages are available for the calculations, which use spherical waves.[10] A commonly used program is EXCURV90 and its later versions, which was developed by the Science and Engineering Research Council (SERC), Daresbury Laboratory, Warrington, UK. This program uses a formalism by S. J. Gurman et al.[12] to calculate theoretical backscattering amplitudes and phases, as well as the quantity $\lambda_j(k)$ which characterizes the lifetime of the photoelectron. This formalism is based upon an electron scattering theory by P. A. Lee and J. B. Pendry.[13] Moreover, this program is also capable of including multiple scattering effects.[14] In 1986, J. J. Rehr et al. began the development of the program FEFF, which to date allows the most accurate theoretical calculations of mean free wavelengths $\lambda_j(k)$ and amplitude and phase functions for any given pair of absorbing and backscattering atoms.[15, 16]

At this point it must be noted, that the backscattering amplitudes of neighboring elements in the periodic table are only slightly different. This makes an unambiguous differentiation of neighboring elements nearly impossible. In general, however, there is sufficient additional information about the sample to enable identification of the elements involved, provided the theoretically calculated backscattering parameters do correctly model the actual backscattering behavior. Very different chemical environments can lead to deviations. In such cases, it is necessary to employ model compounds.

It is always preferable to use backscattering amplitudes and phases that were obtained from model compounds. In these cases, one measures the EXAFS spectrum of a compound with a precisely known structure. The coordination number N_j and the distance to the absorbing atom r_j are known, and the Debye–Waller factor can be estimated from X-ray data, vibrational frequencies, and variable temperature measurements. The backscattering amplitudes and phases can be then determined from the experimental spectrum. However, not all compounds with known structures are suitable as model compounds, even if they are chemically similar to the system under study. To be suitable, the system must posses a well-defined coordination sphere, that is, the contribution of each term must be clearly separable from all others (cf. Eq. (d)). Model compounds of this kind are very difficult to find and in many cases, the use of calculated backscattering parameters is required.

In most cases, different pairs of atoms at various distances are present and the corresponding EXAFS functions overlap. The overlap of the functions of an Fe–C and an Fe–Br pair with absorber–backscatter distances of 2.0 and 3.5 Å, respectively, is shown in Figure 3a. The Fourier transformed function has separate peaks (Fig. 3b). In such favorable cases, each single peak can be selected separately by a window function and backtransformed from the spatial domain (function $|F(r)|$) to the impulse domain (function $\chi(k)$). The result is shown in Figures 3c and 3d. In comparison to Figures 2a and 2c, it can be seen that the contribution of the Fe–C pair is reproduced. The Fe–Br unit shows the same envelope, but a different period due to the increased Fe–Br distance from 2.0 to 3.5 Å. This example demonstrates how the Fourier filter technique can be used to determine the contribution of a backscatterer. The envelope of the filtered function indicates the type of backscatterer, the amplitude yields the coordination number and the Debye–Waller factor, while the period shows the distance to the absorbing atom.

Figure 3a shows a nearly ideal case. In reality, frequently several distances of comparable magnitude are present. In Figure 4a the results from the overlap of two contributions is shown, an Fe–C and an Fe–Br unit, with $r_{Fe-C} = 2.0$ Å and

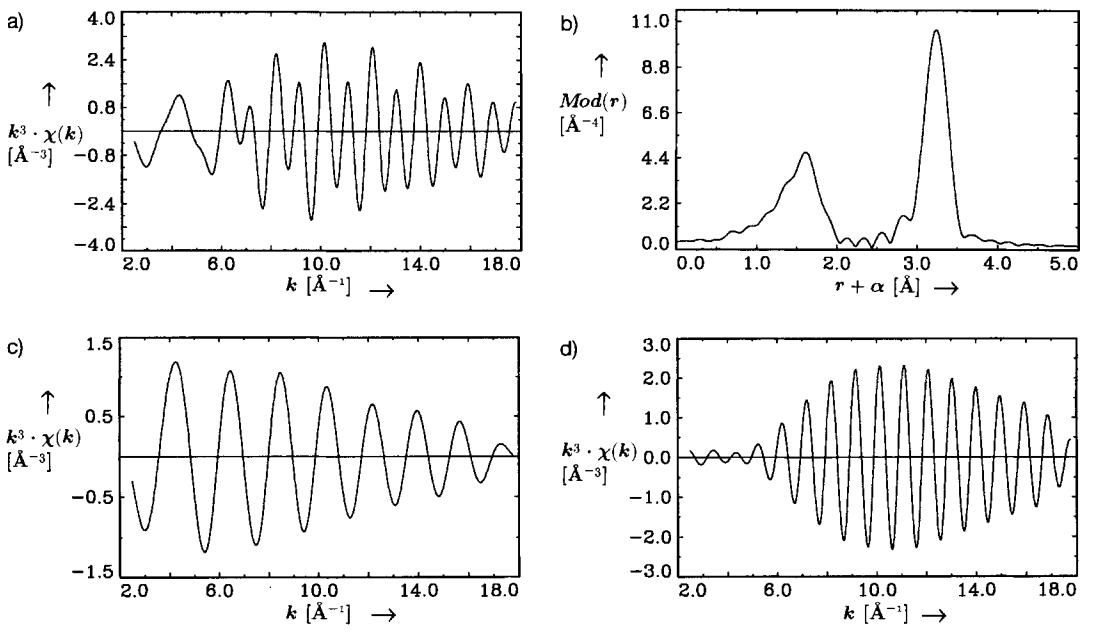


Fig. 3. Theoretical EXAFS function (a) and its Fourier transform (b) for a superpositioned Fe–C and Fe–Br absorber–backscatterer pair. The EXAFS function was calculated employing McKale amplitude and phase functions [10], by using the following structural parameters: absorber–backscatterer distances $r_{Fe-C} = 2.0$, $r_{Fe-Br} = 3.5$ Å, coordination numbers $N_C = 1.0$ and $N_{Br} = 1.0$, Debye–Waller factors $\sigma_C = 0.05$ and $\sigma_{Br} = 0.05$ Å. The EXAFS function was Fourier filtered in the range of 0.5 to 2.5 Å (c) and 2.5 to 4.5 Å (d).

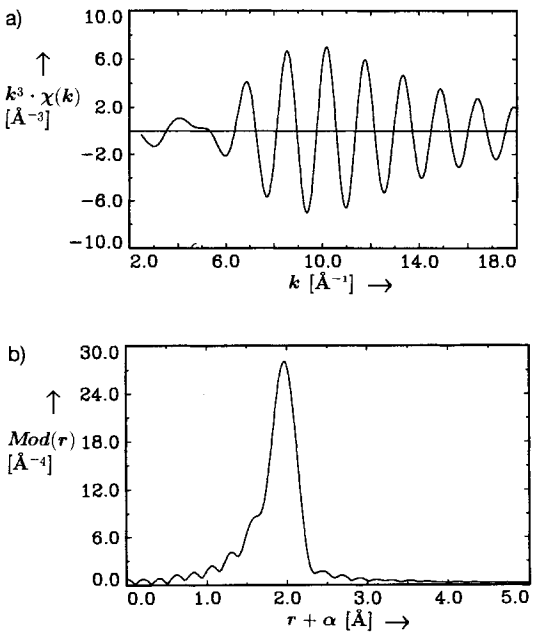


Fig. 4. Theoretical EXAFS function (a) and its Fourier transform (b) for a superpositioned Fe–C and Fe–Br absorber–backscatterer pair. The EXAFS function was calculated employing McKale amplitude and phase functions [10], by using the following structural parameters: absorber–backscatterer distances $r_{Fe-C} = 2.0$, $r_{Fe-Br} = 2.25$ Å, coordination numbers $N_C = 1.0$ and $N_{Br} = 1.0$, Debye–Waller factors $\sigma_C = 0.05$ and $\sigma_{Br} = 0.05$ Å.

$r_{Fe-Br} = 2.25$ Å. As can be clearly seen from the envelope, the contribution of the Br backscatterer dominates, while that of the carbon backscatterer is not discernible. The Fourier transformed function (Fig. 4b) indicates the carbon only as a weak shoulder and a separation into independent coordination spheres is impossible. In such cases, it is necessary to simultaneously fit two shells. Since each shell requires at least three parameters—distance, coordination number, and Debye–Waller factor—the number of parameters increases rapidly with the use of multiple shells. A useful strategy for such cases is to initially fit the experimental EXAFS function to a single shell. If the agreement is poor, the prospect of the presence of a different backscatterer should be explored. If this possibility can be excluded, the existence of another shell can be assumed. In this manner, successive shells can be constructed. In each case, it is necessary to determine the contribution to the total function. If it is small enough to be within experimental error, it is usually better to simply ignore it. In order to analyze the significance of newly added shells of backscatterers, the program EXCURV90 includes a test in which the improvement of a fitting index makes it possible to judge whether the addition of another shell is useful. The fitting of multiple shells frequently leads to overinterpretation of EXAFS measurements and this practice has on occasion led to criticism of the method in general.

Nevertheless, the fitting of a theoretical function to experimental data is in most cases the only way to interpret EXAFS spectra. When appropriate care is taken, the results are very reliable. Distances can be determined with an accuracy of up to 1%, coordination numbers can be ascertained to within 10–30%. When model compounds, optimized measurements, and highly accurate data analysis are employed, the error boundary for the coordination numbers can be significantly reduced.

2. Measurement Fundamentals and Techniques

As can be gleaned from Equation (a), the quantity to be measured by X-ray absorption spectroscopy is the X-ray absorption coefficient $\mu(E)$. The most common technique involves the direct measurement of $\mu(E)$. In order to obtain monochromatic X-rays, a continuous spectrum is employed. According to Bragg's law [Eq. (f)],[17] (λ = wavelength of the incident X-

$$n\lambda = 2d\sin\vartheta \qquad (f)$$

rays; d = interplanar spacing of the crystal; 2ϑ = scattering angle, n = order of diffraction ($n = 1,2,3\ldots$)) a crystal double monochromator, with the second crystal at a slight angle to the first one, selects a beam of wavelength λ, while simultaneously suppressing beams with wavelengths $\lambda/2$, $\lambda/3$, etc. The absorption coefficient is found according to Equation (a) by measuring the intensity of the X-rays before and after the sample. The energy of the incident radiation is adjusted by a stepwise change of the incident angle of the monochromator. The experimental setup is schematically shown in Figure 5a. The sample to be measured, a reference compound, which in many cases is used for calibration purposes, and the ionization chambers for the intensity measurements are arranged in a line. The sample is located between the first and second ionization chamber, and the reference compound is located between the second and third chamber. Typical measurement times are 20–60 minutes, when synchrotron radiation is used. Rapid rotation of the monochromator can reduce these times to a few seconds,[18] however, the experimental effort is increased drastically. The acronym for this measuring technique is QEXAFS (Q = quick). The continuous X-ray spectrum can also be used directly. It is split up by Bragg reflection on a crystal and, after passage through the sample, can be measured by using an array detector.[19,20] This measurement principle is depicted in Figure 5c and is called DEXAFS (D = dispersive).

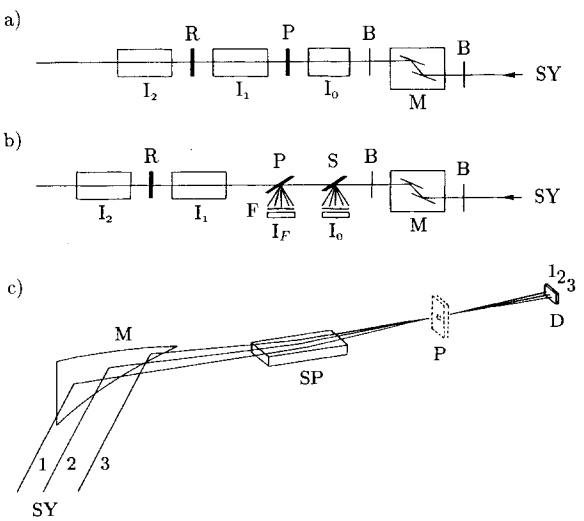


Fig. 5. Experimental setup for transmission (a), fluorescence (b), and energy-dispersive (c) EXAFS measurements (SY = synchrotron radiation, 1,2,3 = beam paths, M = monochromator, I_0,I_1,I_2 = ionization chambers, D = detector (diode array), S = scattering sample, P = sample, R = reference sample, B = slit, F = filter, SP = mirror).

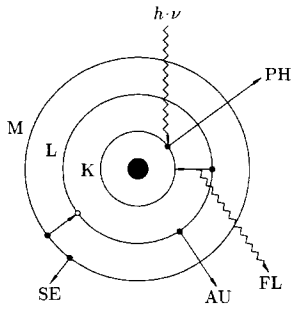


Fig. 6. Subsequent decay processes after creation of a hole in the electron shell by absorption of X-rays $h\nu$ (PH = photoelectron, AU = Auger electron, SE = secondary electron, FL = fluorescence radiation).

Since the absorption of X-rays is linked to the creation of an electron vacancy, it is possible to use all subsequent decay processes to determine the absorption coefficient (Fig. 6). An electron from an outer shell can fill the vacancy, accompanied by the emission of fluorescence radiation (FL) or Auger electrons (AU). These two emissions are competing processes. The fluorescence yield increases with increasing atomic number and this process has the advantage that the background radiation can be removed by using suitable filters, which increases the sensitivity of the method. A typical setup for fluorescence measurements is shown in Figure 5b. In general, the emitted fluorescence is measured at a right angle to the incident beam; the sample is therefore rotated by 45°.

The detection of Auger electrons yields the same structural information as a transmission EXAFS experiment or the fluorescence method described above. Auger measurements are advantageous in situations in which the fluorescence method fails due to low quantum yields—in the case of K-edge measurements for elements with $Z < 30$, and $Z < 80$ for L-edge experiments. Due to the small mean free wavelength of the emitted electrons (ca. 100 Å), the Auger method is especially suited for the study of surfaces (SEXAFS, S = surface). A thorough description of this method can be found in [21]. It is also possible, in principle, to directly detect the photoelectrons generated. This is difficult, however, because their spatial distribution changes with the energy of the incident X-ray beam. This effect can be effectively circumvented by detecting all electrons produced by cascading processes. This includes the Auger and photoelectrons as well as secondary electrons created by inelastic scattering of photoelectrons and the fluorescence radiation.

Three types of devices are available for the detection of X-ray photons: ionization chambers, scintillation counters, and solid-state detectors (Ge, Si, Li-doped Si). The determining criteria for the choice of detector are its energy resolution and recovery period. The energy resolution is defined as the full signal width at half height. The recovery period or dead time is determined by the decay rate of the process used for detection and determines the maximum possible count rate. Ionization chambers have virtually no dead times and can therefore detect high photon intensities with an energy resolution of about 3000 eV. Scintillation counters have a lower resolution and recovery periods between 1.4 (plastic scintillators) and 230 ns (NaI(Tl) scintillator). Solid-state detectors are characterized by a very high energy resolution of 150–400 eV with very short recovery periods. Their maximum count rate is the lowest of the three types, because the semiconductor material used is damaged by high photon fluxes.[22]

EXAFS measurements require an X-ray source which provides a continuous spectrum. The most suitable source is synchrotron radiation, but the bremsstrahlung of conventional X-ray sources can be employed as well.[23–25] In this case, the intensity is lower by a factor of 10^3.[26] This can be partly compensated by the use of focusing X-ray optics and rotating anodes. The experimental effort and financial outlay are enormous, however, and the quality of the obtained spectra is much lower than those obtained with synchrotron radiation. This situation might change once it is possible to better focus X-rays; preliminary experiments in this area have been performed.[27]

Which elements are suitable for an EXAFS study is determined by the spectral region of the X-ray source. If a typical range of 4–26 keV for synchrotron radiation is assumed, K-edge measurements can be used for elements from $Z = 20$ (Ca) to 47 (Ag), while the L_{III} edge can be used for elements from $Z = 51$ (Sb) to 92 (U). Due to the overlap with L_{II} spectra, elements 51 (Sb) to 59 (Pr) are only partially suitable for measurements using the L_{III} edge. Only starting with Nd is there an energy gap of 514 eV between the L_{III} and L_{II} absorption edges and an EXAFS function with a k range of 10 $Å^{-1}$ can be obtained. This leaves a gap between Ag and Nd, which contains important elements such as Sn, Sb, and I. These elements might become accessible for K-edge measurements if it were possible to extend the spectral range of synchrotron radiation to 50 keV. For elements lighter than calcium it is necessary to employ soft X-rays and high-vacuum techniques. This strongly limits the study of liquid samples.

3. Data Analysis

While the measurement of the X-ray absorption coefficient appears to be simple in principle, this is definitely not the case for the data analysis—shown schematically in Figure 7. Extensive discussions of the analysis can be found in references [8, 28]. A few examples shall suffice here to illustrate the main problems. As can be gleaned from Equation (b), the modulation of the X-ray absorption coefficient is normalized for the background absorption $\mu_0(E)$. There is no exact theoretical expression for $\mu_0(E)$, which must therefore be determined empirically. A number of procedures for this are discussed in the literature, for instance the approximation by a polynomial or a spline function.[8] Even though there are criteria for the choice of background, the determination of $\mu_0(E)$ is a critical aspect. The EXAFS oscillations can be dampened too much if $\mu_0(E)$ matches the experimental data too closely. The exact position of E_0—not to be confused with its absolute value—is also not known because E_0 depends on the chemical environment of the absorbing atom. E_0 is necessary (cf. Eq. (c)) for the conversion of the energy E to the magnitude of the wave vector k. These difficulties can be surmounted when model compounds are available for the data analysis.

4. Applications of EXAFS Spectroscopy

Since the nearly coincident development of powerful X-ray sources in the form of synchrotron radiation and the theoretical

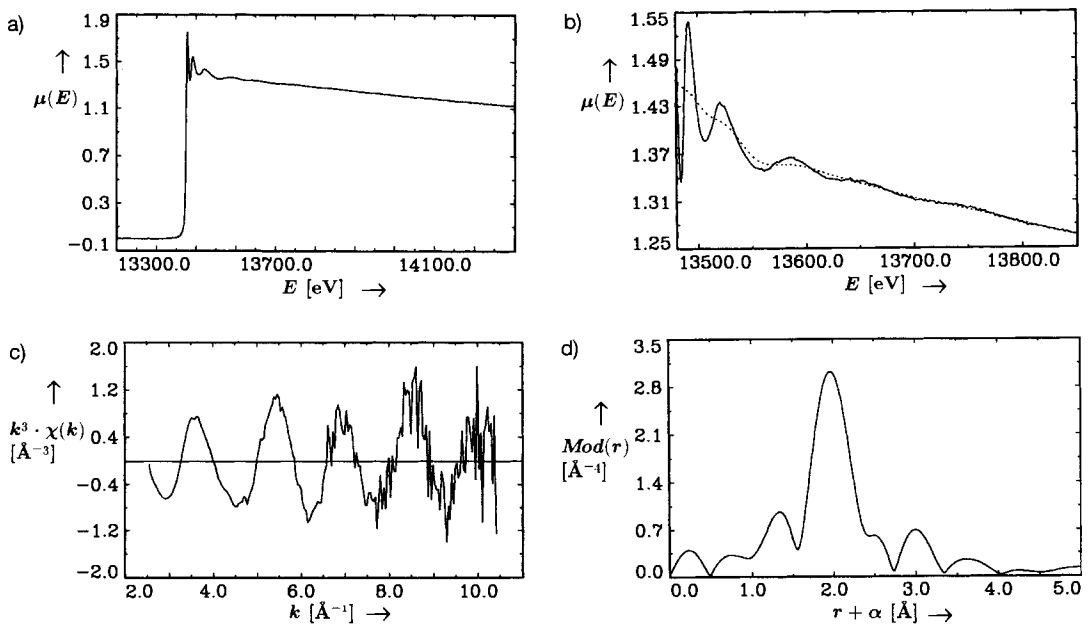


Fig. 7. a) Absorption spectrum $\mu(E)$ after edge correction and removal of pre-edge absorption; b) absorption spectrum $\mu(E)$ (solid line) and background $\mu_0(E)$ (dotted line); c) k^3-weighted EXAFS function and d) modulo function Mod(r) of the Fourier transformed $k^3\chi(k)$ function for methylmagnesium bromide in diethyl ether.

advances in the interpretation of EXAFS spectra, EXAFS spectroscopy has been employed for the study of a variety of very different systems. A Chemical Abstracts literature search for the period up to and including 1992 using the term EXAFS yielded 3423 references. Most of them refer to the study of crystalline systems, for which such powerful methods as X-ray or neutron diffraction are available for structural characterization. In these cases, EXAFS only served to verify the results of conventional methods, or at best to supplement those results. Work of this type will not be discussed in this review. The discussion here will be limited to studies which use the specific advantages of EXAFS, that is, the selective determination of structures in noncrystalline systems. In spite of this limitation, it is impossible to present a complete review. This article deliberately uses representative, not necessarily current examples to demonstrate how EXAFS spectroscopy can be utilized and what kind of limitations are encountered.

4.1. Amorphous Solids

4.1.1. Amorphous Metals and Nonmetals

Atomic systems such as amorphous selenium or germanium are the simplest chemical systems with respect to chemical composition. The determination of local order in these compounds is very important for the understanding of their physical properties and is very amenable to EXAFS studies. These measurements yield coordination numbers, distances to nearest neighbors, and the Debye–Waller term $e^{-2k^2\sigma^2}$. These quantities can then be compared with their analogues in the crystalline phase. The term $e^{-2k^2\sigma^2}$ contains static and dynamic contributions stemming from the static disorder and thermal vibrations, respectively. With increasing temperature, the thermal vibrations of the atoms around their equilibrium positions can become anharmonic and the distribution of atoms becomes asymmetric. Careful variable-temperature EXAFS measurements can yield information about this phenomenon. For amorphous Ge[29] it was found that the short-range local order is not different from the crystalline phase and that the atom distribution is symmetric. The covalent bonds between Ge atoms appear to maintain much of the local order. EXAFS measurements on amorphous Se below and above the glass transition temperature yield a coordination number of 2.[30] This indicates that the atomic arrangement of the Se atoms as chains or Se_8 rings remains intact.

The variation of another thermodynamic variable, namely pressure, is much more difficult to achieve. There is one report[31] that describes studies of amorphous germanium under pressure. The reason behind this study was the observation that amorphous Ge is a semiconductor at ambient pressure, while it shows metallic properties at 6 GPa. Figure 8 shows the Fourier transformed EXAFS functions of amorphous Ge at pressures of 0.0 and 8.9 GPa and, for comparison, of crystalline germanium. In contrast to the EXAFS function of the crystalline phase, the amorphous sample does not show any higher coordination shells. No phase transition from amorphous to crystalline was observed for this sample. It is interesting to note how the pres-

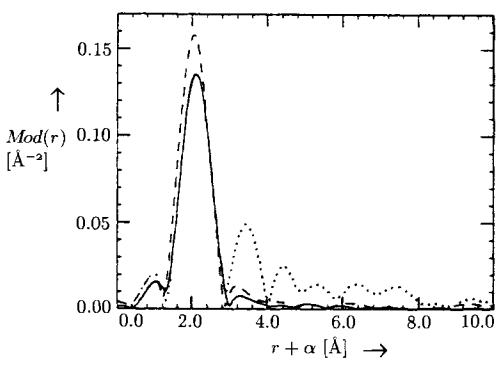


Fig. 8. Modulo function of the Fourier transformed $k\chi(k)$ function (Ge–K absorption edge, $k = 4.0$–10.0 Å^{-1}, multiplied by a Gaussian window function) of amorphous germanium at 0.0 GPa (solid line) and 8.9 GPa (dashed line), as well as of crystalline germanium at 0.0 GPa (dotted line) [31].

sure in the sample was measured. A careful analysis of the pressure dependence of the EXAFS spectrum of a copper foil showed that the variation in nearest neighbor distances and the Debye–Waller factors allow an estimation of the pressure to within 0.2 GPa.[32] For the Ge experiment, a copper foil was measured together with the sample permitting the pressure to be determined.

4.1.2. Amorphous Alloys and Binary Systems

For the systems discussed so far, it was sufficient to use an atomic pair distribution function $g(r)$, which gives a measure of the probability of finding another atom at distance r. For multiatom systems consisting of m atoms, a set of $m \times (m+1)/2$ functions $g_{\alpha\beta}(r)$ is required, which indicate the probability of finding an atom of type β at a distance r from an atom of type α. If standard X-ray or neutron diffraction methods are used to determine the structure, $m \times (m+1)/2$ independent experiments are necessary. In spite of isotopic substitution techniques for neutron diffraction—which are also limited by the small number of suitable isotopes—and the exploitation of anomalous dispersion effects for X-ray diffraction, the determination of the complete set of atomic pair distribution functions is possible only in exceptional cases and only for simple systems. Cases like this are especially suited for EXAFS spectroscopy, as only the environment of the absorbing atom can contribute to the structure function, which reduces the number of atom pair correlation functions to m. It should not be overlooked, however, that because of the finite lifetime of the photoelectron the detectable correlations between atoms are significantly shorter in EXAFS spectroscopy than in the diffraction methods.

The study of amorphous $Ni_{64}Zr_{36}$ serves as an example for the comparison of EXAFS results with those from neutron diffraction experiments.[33] This system allows EXAFS measurements on the K edge of Ni and Zr. The structure functions show only one peak and are consistent with the neutron data if an asymmetric distribution is assumed. The fact that conventional diffraction methods are superior to EXAFS spectroscopy for the determination of long-range correlations can be shown by using a study of amorphous $Ga_{48}As_{52}$.[34] The atom pair distributions determined from anomalous X-ray diffraction show correlations up to distances of 6 Å, while the EXAFS spectra exhibit only one maximum, and do not show any indications of the higher order.[35]

On the other hand, EXAFS spectroscopy has great advantages in cases where minute changes in the first coordination shell are to be detected, for instance for the study of homo- versus hetero-association in binary systems. Fe–K-edge measurements of amorphous $Fe_{0.30}Y_{0.70}$ indicated the tendency of iron atoms to form Fe clusters which are imbedded in an amorphous matrix of yttrium atoms.[36] Amorphous $Cu_{24}Zr_{76}$ supposedly also contains Cu clusters, since fewer Cu–Zr and more Cu–Cu pairs were found than were expected on purely statistical grounds.[37] EXAFS measurements of the As and Se edges indicate that amorphous As_2Se_3 behaves in a similar fashion.[38] The authors of that study differentiate between As–Se and As–As pairs; it is important to recall, however, that it is difficult for EXAFS spectroscopy to distinguish between neighboring elements in the periodic table. In another study that examined the As_xSe_{1-x} ($0.20 \leq x \leq 0.57$) system,[39] the authors admit that EXAFS spectroscopy is definitely not accurate enough to determine the exact ratio of hetero- to homoatomic bonds in As_xSe_{1-x}. For amorphous III/V compounds, the appearance of bonds between the same elements is the dominant defect type, which also strongly effects the electronic properties. Measurements of amorphous InP[40] showed that about one third of all bonds occur between chemically identical elements, indicating that the system is partially chemically disordered.

More of a curiosity is the EXAFS study of alloy formation by mechanical grinding.[41] In agreement with other X-ray studies, the Fe–K-edge EXAFS spectra of a mixture of 75 atom% Fe and 25 atom% C indicate the partial destruction of the crystalline phase and the formation of an amorphous phase which has a short-range order identical to that of cementite Fe_3C.

Light-induced changes in the short-range order can also be studied by EXAFS spectroscopy.[42–44] The effects are very small, however, and are of the same magnitude as measurement uncertainties. For $GeSe_2$,[42] a change in the coordination number upon irradiation has been postulated, while for $As_{50}Se_{50}$ films no structural changes within the first coordination shell could be detected.[44]

4.1.3. Structural Changes upon Crystallization

The previously mentioned sensitivity of EXAFS spectroscopy to changes in the immediate surroundings of the absorbing atom can be employed to determine the crystallization behavior of amorphous samples.[45–47] The studies of thulium/chromium/aluminum oxyhydroxides are an especially instructive example.[48] The samples were prepared by the stoichiometric precipitation of the oxyhydroxides, heating to a certain temperature, and subsequent cooling.

The EXAFS spectra, measured on the L_{III} edge of Tm, and their Fourier transforms are shown in Figure 9. In the vicinity of

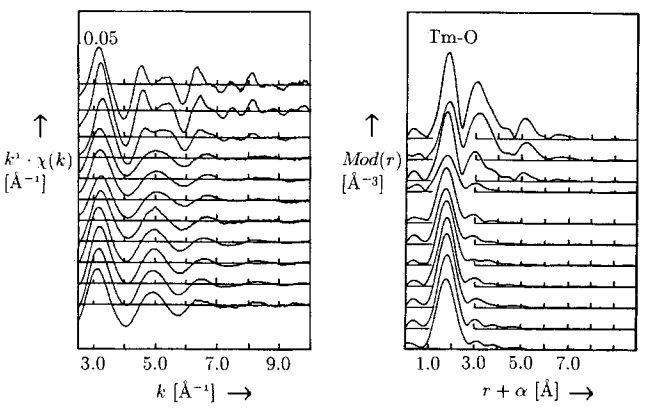


Fig. 9. k-weighted EXAFS functions (left; Tm-L_{III} absorption edge) and modulo functions of the Fourier transformed $k^2\chi(k)$ functions (right) (k = 2.0–9.0 Å, multiplied by Kaiser-Bessel window functions) of 3Tm/2Cr/3Al/xO at the temperatures 1180, 845, 817, 750, 650, 555, 460, 365, 270, 175, and 60 °C (from top to bottom) [48].

the crystallization temperature, the structure functions show the existence of further coordination shells. A definite jump in the Tm–O bond length and a less well-defined change in the coordi-

nation number are observed as well. These data are interpreted to mean that initially Tm(O)OH releases water, forming Tm_2O_3, and then spontaneously reacts at the crystallization temperature to give $Tm_3Cr_2Al_3O_{12}$. During this process, the coordination number of Tm initially decreases from eight to six, and then rises back to eight again.

4.1.4. Structural Changes Induced by Chemical Reactions

EXAFS spectroscopy is also used to determine structural changes that are brought about by chemical reactions. An example is the study of the reaction of amorphous MoS_3 with lithium. This reaction leads to amorphous compounds of the composition Li_xMoS_3 ($0 \leq x \leq 4$).[49] The Fourier transforms of the Mo–K-edge EXAFS spectra of MoS_3, $LiMoS_3$, Li_2MoS_3, Li_3MoS_3, and Li_4MoS_3 are shown in Figure 10. The structure function of MoS_3 shows two maxima. The one at 1.9 Å is assigned to Mo–S, the one at 2.4 Å to a Mo–Mo distance. These assignments are consistent with the results from other X-ray studies on binuclear Mo compounds, once the phase shift is taken into account. The reaction of MoS_3 with lithium leads to a decrease in the maximum assigned to the Mo–Mo distance until the composition Li_2MoS_3 is reached. At higher Li concentrations, a dramatic increase of this peak is observed, which has been interpreted by the authors as a significant structural change involving the formation of Mo clusters.

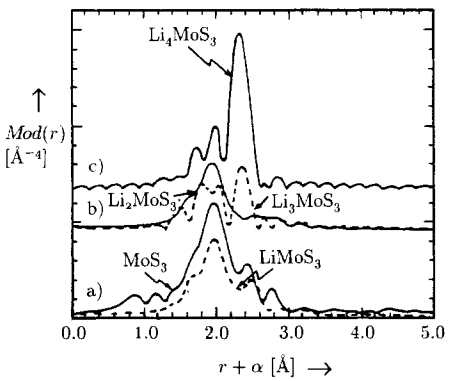


Fig. 10. Modulo function of the Fourier transformed $k^3\chi(k)$ function (Mo–K absorption edge, $k = 4.0$–18.0 Å^{-1}) of untreated MoS_3 (a, solid line), $LiMoS_3$ (a, dashed line), Li_2MoS_3 (b, solid line), Li_3MoS_3 (b, dashed line), and Li_4MoS_3 (c, solid line) [49].

4.1.5. Liquid Crystals

EXAFS spectroscopy can also contribute to the structural elucidation of liquid crystals.[50] In these studies, the short-range order in the liquid phase is compared with that in the crystal. It was shown that in the case of the Cu salts of fatty acids with 6, 12, 18, and 22 C atoms, the crystalline and mesophases have the same short-range order.

4.2. Liquids

X-ray and neutron diffraction methods have been used to study the structure of liquids for about 60 and 30 years, respectively. As has been mentioned in section 4.1.2., diffraction methods have the disadvantage that they can only provide a weighted sum of all atom pair distribution functions, with the scattering ability of each atom pair acting as the weighting factor. The selective determination of the short-range order around specific atom types is only rarely possible—and only then when associated with isotopic substitution methods which require a great deal of effort. This type of study lends itself to EXAFS spectroscopy. The first EXAFS study on a liquid system was published in 1975,[51] but the majority of EXAFS studies of this kind have taken place since 1978.

4.2.1. Solutions of Ionic Compounds

For solutions of salts with concentrations less than 0.1 M it is fairly difficult to employ diffraction methods to determine the structure of the hydration shell because the majority of the scattering is due to solvent molecules. The use of EXAFS spectroscopy is an obvious choice and the first EXAFS studies on solutions of ionic compounds were indeed performed in the mentioned concentration range. The primary goal was to determine the distances of the water molecules of hydration to the cations and anions of the dissolved salts (Table 1). Most subsequent studies dealt with concentrated aqueous solutions of 1:1 and 1:2 electrolytes; mostly halides of Ni, Cu, and Zn were examined. It was postulated that these salts possess a direct metal–halogen bond in addition to the metal–water coordination. There were also indications of cation–cation interactions similar to those found in the corresponding crystalline salts (Table 2).

Table 1. Distances d between cations/anions in dilute solutions of salts and the oxygen atom of the water molecules in the first hydration shell. c = concentration.

Compound	c [mol L^{-1}]		d [Å]	Ref.
$CuBr_2$	0.1	Cu-O	1.97 ± 0.08	[51]
		Br-O	3.14 ± 0.10	[51]
$Ni(NO_3)_2 \cdot 6(H_2O)$	0.1	Ni-O	2.05	[52]
$Ni(NO_3)_2 \cdot 6(H_2O)$	0.1	Ni-O	2.06 ± 0.01	[53]
$Co(NO_3)_2 \cdot 6(H_2O)$	0.1	Co-O	2.08 ± 0.01	[53]
$Cr(NO_3)_3 \cdot 6(H_2O)$	0.1	Cr-O	2.01 ± 0.01	[53]

The measurements were soon extended to more complex solutions of ionic compounds and mixtures of different electrolytes in water. For example, in saturated aqueous mixtures of $ZnCl_2$ and LiCl or $CaCl_2$ it was postulated that there are partially linked, tetrahedral $[ZnCl_4]^{2-}$ units with Zn–Cl distances of 2.24 ± 0.01 Å (LiCl) and 2.25 ± 0.01 Å ($CaCl_2$).[60] The observation that Zn–O backscatterers are also present at 1.89 ± 0.05 Å (LiCl) and 1.92 ± 0.08 Å ($CaCl_2$) led the authors to the conclusion that a partial substitution of Cl in the tetrahedral $[ZnCl_4]^{2-}$ units by H_2O had taken place. The EXAFS measurements on the environment of the Ca^{2+} ions yielded an octahedral solvation by water molecules with a Ca–O distance of 2.45 Å. No metal–halogen association was observed. In the case of mixtures of $CoCl_2$ and $NiCl_2$ in water (0.5 M, enriched in Cl^- by addition of HCl gas), both cations were found to have

Table 2. Qualitative summary of EXAFS results obtained for aqueous solutions of salts at various concentrations. c = concentration, c_s = saturation concentration.

Salt	c [mol L^{-1}]	Results	Ref.
RbBr	saturated 1.0–6.0	determination of Rb^+-OH_2, Br^--OH_2 and Rb-Br	[54]
$MnCl_2$	0.1–4.95	octahedral $[MnCl_{(6-n)}(H_2O)_n]^{(n-4)+}$ species	[55]
$MnBr_2$	1.6–5.2	octahedral $[MnBr_{(6-n)}(H_2O)_n]^{(n-4)+}$ species	[56]
$NiCl_2$	2.78, 3.74	completely hydrated Ni^{2+} ions; Ni–O distances: 2.06 Å (2.78 M), 2.07 Å (3.74 M). Indications of Cl^- present in the second coordination shell of the Ni^{2+} ion	[57]
$NiCl_2$	0.5, 4.0	No or only few Ni–Cl bonds present	[57]
$NiBr_2$	0.4, 4.0	No or only few Ni–Br bonds present	[57]
$CuCl_2$	0.05, 4.86	Cu–Cl bonds present at high concentrations	[57]
$CuBr_2$	0.05–4.5	50% of Cu^{2+} ions are bound in planar $CuBr_4$ units, which are also found in the crystal	[57, 58]
$CuBr_2$	3.3, 4.4	various mononuclear $[CuBr_n(H_2O)_{n-6}]^{2-n+}$ species	[59]
$ZnCl_2$	saturated	Zn^{2+} ions are present in linked $ZnCl_4^{2-}$ tetrahedra, Cl^- is partially substituted by OH_2 (Zn–Cl 2.23 Å, Zn–O 1.92 Å)	[60]
$ZnBr_2$	8.08	Zn^{2+} ions are present in linked $ZnBr_4^{2-}$ tetrahedra, Br^- is partially substituted by OH_2	[57]
$CdBr_2$	saturated, 0.75 c_s, 0.5 c_s, 0.25 c_s, 0.10 c_s, 0.02 c_s	chains of $CbBr_4^{2-}$ or $CdBr_3^-$ units (cf. Fig. 11)	[61]

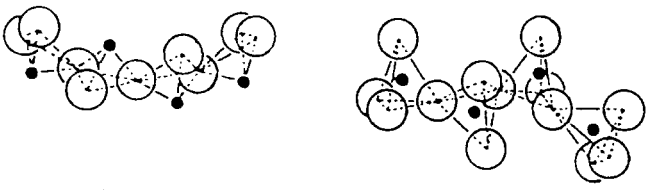


Fig. 11. Models for the local structure of $CdBr_2$ in aqueous solutions. Left: chains of $CdBr_3^-$ pyramids, right: chains of $CdBr_4^{2-}$ tetrahedra [61]. White spheres = Br^-, black spheres = Cd^{2+} ions.

metal–halogen bonds. The tendency for the formation of chloro complexes was higher for the Co^{2+} ions than for Ni^{2+} ions.[62]

Examples for studies of nonaqueous electrolyte solutions can be found in a report about copper halides in dimethylsulfoxide, acetonitrile, pyridine, and water,[63] as well as in pyridine/water mixtures.[64] The determination of the environment of the Ag^+ ions in the N-donor solvents ammonia, pyridine, and acetonitrile[65] also falls into this category. The comparison of EXAFS spectroscopic results of $[UO_2([18]crown-6)](ClO_4)_2$ in the solid state and dissolved in acetonitrile indicated that in solution only two thirds of the UO_2^{2+} ions are present as crown ether complexes, while the remaining UO_2^{2+} ions are coordinated by the acetonitrile solvent molecules. The solvent is apparently capable of removing the UO_2^{2+} ions from the crown ether environment.[66]

4.2.2. *Solutions of Grignard Reagents and of Chloro Complexes*

Upon close examination, it turns out that the majority of EXAFS studies on solutions can be attributed to the field of homogeneous catalysis. This leaves only very few studies that deal with conventional solutions. This group is meant to encompass systems that cannot be classified as solutions of ionic compounds or as belonging to the field of homogeneous catalysis. An example is the study of the structure of Grignard compounds in solution.[67, 68] In spite of their importance in preparative chemistry, their structures in solution had remained uncertain[69] and there have been intense controversies about their correct description. Even though there had been many studies of Grignard compounds, there was basically no information about intra- and intermolecular distances in these reagents in solutions. By using Br–K-edge EXAFS measurements for methyl-, ethyl-, and phenylmagnesium bromide in diethyl ether (3.12 M, 3.04 M, 2.96 M, respectively) and for vinylmagnesium bromide in tetrahydrofuran (1.56 M), it was possible to show that the Grignard compounds methyl-, ethyl-, and phenylmagnesium bromide are present in diethyl ether in the form of tetrahedral monomers as well as octahedral dimers. The amount of dimeric species was 60 ± 7%, 62 ± 8%, and 33 ± 9% for the three compounds. These systems can be described by equilibrium (g). In the case of methyl- and ethylmagnesium bromide, the

$$2\,RMgBr(Et_2O)_2 + 2\,Et_2O \rightleftharpoons RMg(Et_2O)_3Br_2(Et_2O)_3MgR \qquad (g)$$

equilibrium lies more on the right, while for phenylmagnesium bromide it lies more on the side of the monomers. In tetrahydrofuran, vinylmagnesium bromide forms octahedral monomers. No indications for associative tendencies were found. These results are summarized, together with the distances determined by EXAFS spectroscopy, in Figure 12.

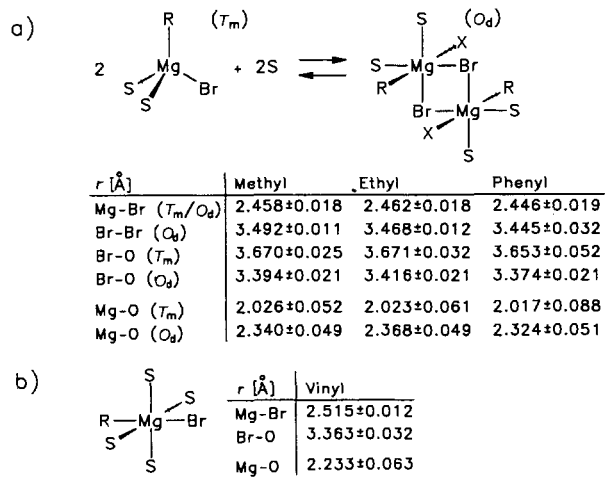


Fig. 12. Equilibrium and structural models for the Grignard compounds a) methyl-, ethyl-, and phenylmagnesium bromide in diethyl ether (3.12, 3.04, 2.96 M; dimer content (O_d) 60±7, 62±8, 33±9%, respectively; distance r[Å]; R = Me, Et, Ph, S = Et_2O, X = Me, Et, Ph, Et_2O) and b) for vinylmagnesium bromide in THF (1.56 M; distance r[Å]; R = vinyl, S = THF) [68].

A study that falls into the conventional solution category dealt with the structure of $[MeEtim]_2[MCl_4]$ ([MeEtim]$^+$ = 1-methyl-3-ethylimidazolium; M = Mn, Co, Ni) in the ionic liquid [MeEtim]-Cl-$(AlCl_3)_x$.[70] The chemical and physical properties of these solutions are primarily determined by the amount x of $AlCl_3$. Liquids with a content of more than 50 mol% $AlCl_3$ are classified as acidic, those with less as basic. For the basic

solutions, a fourfold coordination of the metal center (M = Mn, Co, Ni) by Cl^- ions was found (Mn–Cl = 2.38, Co–Cl = 2.27, Ni–Cl = 2.25 Å), indicating the presence of species of the type $[MCl_4]^{2-}$ in solution. In acidic solutions, however, the immediate environment of the metal atom contains six Cl atoms at very different distances (Mn–Cl = 2.54, Co–Cl = 2.44, Ni–Cl = 2.38) as well as three Al atoms (Mn–Al = 3.33, Co–Al = 3.24, Ni–Al = 3.19 Å). This clearly suggests the presence of complexes of the type $[M(AlCl_4)_3]^-$. The $[AlCl_4]^-$ ligand is bound to the metal center in a bidentate fashion and there appears to be no evidence, in contrast to earlier assumptions, for the chelate-type binding of $[Al_2Cl_7]^-$ species.

4.2.3. *Metal and Semimetal Melts*

The first studies on metal melts were performed to investigate asymmetry effects during the analysis of EXAFS functions. E. D. Crozier and A. J. Seary, for example, studied solid and molten zinc in a temperature range of 273 to 782 K.[71] It turned out that the distribution of the nearest backscatterers is asymmetric at high temperatures. When this asymmetry is neglected and the analysis is performed by using a symmetric distribution function (Debye model), errors occur in the determination of the absorber–backscatterer distance r and the Debye–Waller factor σ. The use of an anharmonic oscillator model, on the other hand, leads to more reliable values for r and σ, with the Debye–Waller factor being about 20% higher than for the symmetric distribution.

Variable temperature studies of crystalline orthorhombic α-gallium, metastable monoclinic β-gallium, and liquid gallium showed that there are very similar short-range orders in the liquid and the crystalline β-structure.[72] The Ga–Ga distances in the first coordination shell are 2.44 and 2.68 Å for the α- and β-forms, respectively. Measurements on tin in a temperature range of 50 to 291 °C were performed to observe structural changes in the immediate vicinity of the Sn atom during the solid–liquid phase transition.[73] The analysis of the EXAFS function, taking asymmetry effects into account, indicated that during the phase transition, the distances increase, but the coordination geometry of the solid state is maintained (four short and two long Sn–Sn distances, Table 3).

Table 3. Sn–Sn distances in the first and second coordination spheres in the element tin at different temperatures (N = coordination number of the Sn atoms) [73].

T [°C]	$r_{Sn-Sn(1)}$ [Å] ($N = 4$)	$r_{Sn-Sn(2)}$ [Å] ($N = 2$)	T [°C]	$r_{Sn-Sn(1)}$ [Å] ($N = 4$)	$r_{Sn-Sn(2)}$ [Å] ($N = 2$)
50	2.997	3.170	232 [a]		
100	2.985	3.156	248	2.974	3.190
150	2.986	3.188	291	3.019	3.282
200	2.978	3.178			

[a] melting point.

An EXAFS study by K. Tamura et al. dealt with Se, Te, and Se–Te mixtures in various phases.[74] Figure 13a shows the Fourier transformed EXAFS functions of crystalline, liquid, and gaseous Se at different temperatures. It is apparent that the intensity of the maximum for the shortest Se–Se bond within a Se_x chain decreases with increasing temperature. An especially strong bond contraction can be observed during the transition to the gaseous phase. At 80 K, it is possible to determine the shortest interchain Se–Se distance (3.38 Å) and the distance to the next-nearest neighbor within a chain (3.73 Å). These values are in good agreement with those obtained from other X-ray studies (3.436 and 3.716 Å, respectively). The authors assume the lack of the maxima for these distances at higher temperatures is due to the greater static and thermal disorder (chain rotation around the Se–Se bonds).

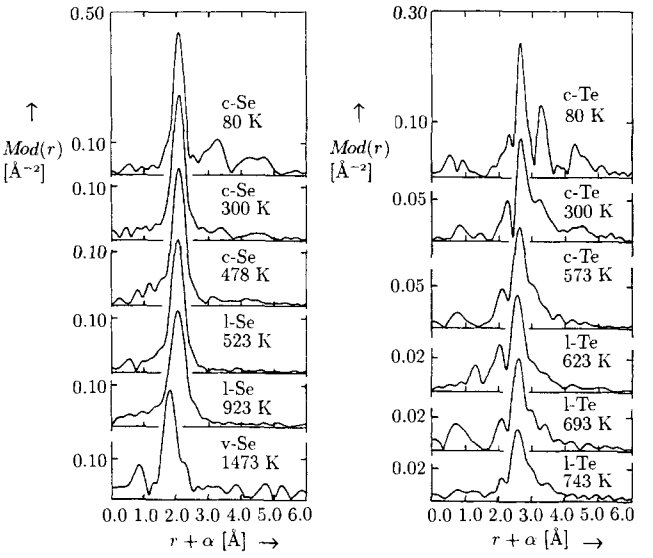


Fig. 13. k-weighted Fourier transformed EXAFS function of crystalline (c-Se), liquid (l-Se), and gaseous (v-Se) selenium (left) and crystalline (c-Te), as well as liquid (l-Te) tellurium (right) at different temperatures [74].

Figure 13b shows the corresponding EXAFS functions of crystalline and liquid tellurium. At first glance, the situation with Te appears to be similar to that found for Se. For crystalline tellurium, the shortest intrachain Te–Te distance at 80 K is found to be 2.84 Å, which is in excellent agreement with the value of 2.835 Å determined by crystallography. The peaks of the structure function at 3.3 and 4.4 Å can be assigned to interchain distances. The next-nearest intrachain distance also contributes to the peak at 4.4 Å. As was found for selenium, at higher temperature these distances can no longer be detected. In the liquid phase of Te, however, two distances are observed, 2.8 and 3.0 Å, while solid Te only showed one distance in that range at 2.84 Å. The authors' explanation for this lies in a chain structure with alternating longer and shorter Te–Te distances. This phenomenon is assumed to be caused by a weakening of the bond by the free electron pairs of neighboring chains (Fig. 14). These results do not support conclusions about a possible threefold coordination of Te atoms, which would result in an As-like pyramidal geometry. This had been postulated by many authors for liquid Te. The investigation of liquid Se–Te mixtures ($Se_{80}Te_{20}$, $Se_{50}Te_{50}$, $Se_{30}Te_{70}$, and $Se_{20}Te_{80}$) was performed by using EXAFS spectra from both absorption edges. The Se–Se distance was found to increase in these compounds with increasing Te content. In addition, the number of longer Te–Te bonds within a chain increases with increasing temperature and Te

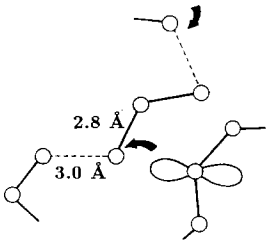


Fig. 14. Schematic structural model for liquid Te, consisting of Te_x chain molecules with shorter and longer bonds. The charge transfer of the lone pair in the neighboring Te_x chain affects a weakening of the covalent bond [74].

content. The authors interpret this as an indication for a semiconductor–metal phase transition.

4.2.4. Salt Melts

There are only a few EXAFS investigations of salt melts, probably due to the amount experimental effort involved. J. Wong and F. W. Lytle studied vitreous and liquid $ZnCl_2$ (melting point 593 K) in the temperature ranges of 120 to 573 K and 603 to 673 K, respectively.[75] Crystalline α-$ZnCl_2$ was used as model compound. It was found that in both the liquid and vitreous phases, the Zn^{2+} ion was surrounded by 5.1 ± 0.8 Cl^- ions at a distance of 2.34 ± 0.01 Å. This is more in accordance with the molecular dynamics calculations of L. V. Woodstock et al. ($N_{Cl} = 4.7$)[76] than with X-ray diffraction results obtained by M. Imoaka et al. ($N_{Cl} = 4.0$).[77] Based on the Debye–Waller factors obtained at different temperatures it appears that the motion of the Zn^{2+} ions is decoupled from their nearest Cl^- neighbors. This effect is especially strong below the glass transition temperature of 375 K. In contrast, EXAFS measurements of vitreous GeO_2 (temperature range 128 to 848 K), which were performed for comparison purposes, indicate strong coupling between the motion of the Ge atoms and the four closest oxygen atoms.

In order to study the salt–metal transition, the two systems RbBr and $Rb_{0.8}(RbBr)_{0.2}$ were examined at 700 °C at the Br–K absorption edge.[78] The coordination number of Rb was calibrated by measuring the EXAFS spectrum of crystalline RbBr at 20 °C. The most important result of this work was that the Rb coordination number decreases from six for liquid RbBr to four in $Rb_{0.8}(RbBr)_{0.2}$.

4.2.5. Molecular Liquids

In 1987, B. X. Yang and J. Kirz performed the first and so far only EXAFS study of liquid water,[79] by using the O–K absorption edge. Due to the low energy of the X-rays employed (500 to 1000 eV), this type of experiment is very laborious and data analysis is difficult. A comparison of the Fourier transformed EXAFS function with atom pair correlation functions $g_{OO}(r)$ and $g_{OH}(r)$ obtained by combining X-ray, neutron, and electron diffraction data of heavy water[80, 81] is shown in Figure 15. The maximum at 2.6 Å can definitively be assigned to an O–O absorber–backscatterer pair. Of interest is the peak at 1.0 Å, which, based on comparison with the $g_{OH}(r)$ function, is assigned by the authors to an H backscatterer rather than an artifact stemming from an incorrect background correction. Usually, H atoms are not observable in EXAFS spectra due to their low backscattering ability (only one electron). The authors note that the backscattering amplitude and phase of the oxygen atom is strongly modified by the H atoms located between the absorbing O atom and the backscattering O atom.

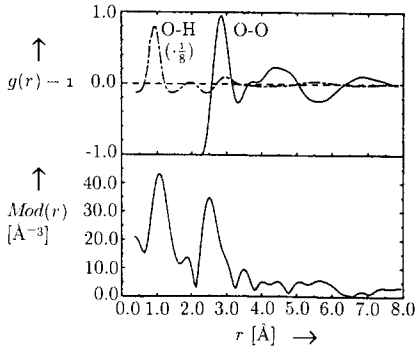


Fig. 15. Top: Atom pair correlation functions (solid line $g_{OO}(r)-1$, dashed/dotted line $(g_{OH}(r)-1)/8$) of D_2O [80,81]. Bottom: k^2-weighted Fourier transformed EXAFS functions of H_2O [79].

The EXAFS study of liquid bromobenzene exemplifies the detailed information that can be obtained through a combination of EXAFS spectroscopy and X-ray and neutron diffraction.[82] The analysis of the EXAFS spectrum indicates a strong interaction between Br atoms and a second one between Br atoms and the aromatic π electron system. It was, however, impossible to unambiguously deduce the relative orientation of the bromobenzene molecules from the observed distances and coordination numbers. This proved possible when using X-ray and neutron diffraction. Figure 16 shows the model for the short-range order in liquid bromobenzene, which is consistent with the results from EXAFS spectroscopy and X-ray and neutron diffraction methods.

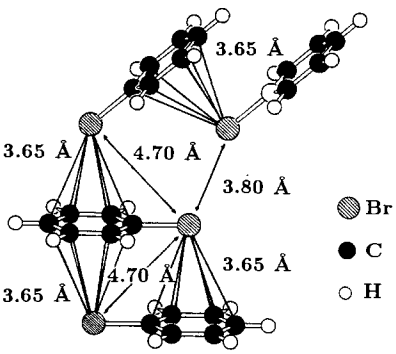


Fig. 16. Three-dimensional structural model for liquid bromobenzene, based on results from EXAFS spectroscopy, and X-ray and neutron diffraction techniques [82].

4.3. Catalysis

The examination of catalysts is one of the main applications of EXAFS spectroscopy. The growing number of available synchrotron sources has over the years led to an enormous increase in the number of publications on this topic. Apart from a number of review articles,[83–85] the biannual reports of the International Conference on X-ray Absorption Fine Structure (EXAFS

and XANES) (since 1986) give an excellent overview of the various applications of EXAFS spectroscopy for catalyst research.[86-88] Since a more thorough discussion of surface studies would go beyond the scope of this article, the reader is referred to two good reviews in the literature.[89, 90]

4.3.1. Heterogeneous Catalysis

The vast majority of all EXAFS studies deals with heterogeneous catalytic systems. In general, heterogeneous catalysts consist of porous oxides, for instance aluminum oxide or silicone oxide, with very large specific surface areas on which extremely finely divided clusters of active metals are adsorbed or chemically bound. The carrier materials are usually loaded with approximately one weight percent of metal. This very low degree of loading, together with the interference from the carrier material, makes the application of conventional spectroscopic methods for the investigation of catalytically active species very difficult. On the other hand, the element specificity and high sensitivity of EXAFS spectroscopy make it comparatively easy to gain information about the environment of the metal atoms.

The properties of catalysts consisting of small metal clusters are critically dependent on the degree of dispersion of the metal.[91, 92] The degree of dispersion is defined as the ratio of metal atoms on the surface to the total number of metal atoms in the cluster. It is typically greater than 0.5, corresponding to a particle size of about 20 Å and a total number of less than 100 atoms per cluster. G. H. Via et al. have studied finely divided osmium, iridium, and platinum clusters on SiO_2 and Al_2O_3 to obtain information about the degree of dispersion, morphology, and size of these metal clusters.[93] The comparison of the EXAFS spectra of the finely divided metal catalysts with those of the pure metals showed that the oscillations of the EXAFS functions are significantly weaker for the catalysts than for the pure metals. In the metal clusters of the catalyst, the metal–metal distances are reduced, the Debye–Waller factor is increased, and the coordination number of the metal centers with respect to the metal–metal bonds (metal–metal coordination number) is decreased (Table 4). The coordination numbers here are clearly averages, as metal atoms can occupy different positions in the cluster (in the interior, on edges, or at corners). In addition, chemisorption studies yielded degrees of dispersion between 0.7 and 1.0. Using the very simplified assumption of cubic clusters (fcc structure), this degree of dispersion led to an average cluster size of 8–15 Å and a corresponding average coordination number of 5–9, in good agreement with the coordination numbers of 7–10 determined by EXAFS spectroscopy (Table 4).

Table 4. Structural parameters (metal–metal distances r, coordination numbers N, Debye–Waller factors σ) for finely divided Os, Ir, and Pt clusters on SiO_2 and Al_2O_3 [93]. The corresponding values for the pure metal are given in parentheses.

Metal	Carrier	r [Å]	N	δ [Å]
Os	SiO_2	2.702 (2.705)	8.3 (12)	0.054 (0.027)
Ir	SiO_2	2.712 (2.714)	9.9 (12)	0.060 (0.030)
Ir	Al_2O_3	2.704 (2.714)	9.9 (12)	0.061 (0.030)
Pt	SiO_2	2.774 (2.775)	8.0 (12)	0.061 (0.044)
Pt	Al_2O_3	2.758 (2.775)	7.2 (12)	0.075 (0.044)

Further similar EXAFS studies by R. B. Gregor and F. W. Lytle, which tested structural models for metal clusters, indicated disc-like structures for osmium clusters, cubic structures for copper, ruthenium, and iridium clusters, while platinum showed different cluster shapes which depended on the preparative conditions.[94] Based on EXAFS results, J. H. Sinfelt et al. reported that the determinations of the degree of dispersion using chemisorption techniques have only limited validity.[95]

The "life cycle" of a metal catalyst can be characterized by three stages: preparation, stationary state and aging, and regeneration. The preparation phase can also be divided into these three steps: impregnation of the carrier material (for instance with isolated complex ions on the oxide surface), drying and annealing (calcination) (removal of water and ionic components stemming from preceding steps), and reduction with hydrogen.

The separate steps of the preparation phase have been studied especially intensively. A nice example is the EXAFS study of a Pd/Al_2O_3 catalyst.[96] Palladium acetylacetonate was used as precursor and deposited onto Al_2O_3 as carrier, followed by drying at 100 °C. The analysis of the EXAFS spectra of the pure $[Pd(acac)_2]$ solution yielded four oxygen atoms at 1.96 Å. The coordination number increases to five in the dried sample. The only possible explanation for this observation is that the metal atom becomes embedded in an octahedral coordination site on the Al_2O_3 surface with concomitant loss of an acetylacetonate moiety. During the annealing step the precursor decomposes further and loses the second acetylacetonate ligand. Annealing at temperatures of 300 to 700 °C leads to an increasing growth of the oxide phase of PdO. This is clearly observable due to the appearance of a second coordination shell (Pd–Pd distance in PdO) in the radial distribution curves of the EXAFS function. The quantitative analysis of the first coordination shell confirms the existence of 4 to 4.5 oxygen atoms with a Pd–O distance of 2.00 Å, which is nearly identical to the Pd–O distance in the structure of pure PdO.

Using palladium nitrate instead of $Pd(acac)_2$ as precursor leads to a catalyst that shows, after annealing under analogous conditions, a Pd–O amplitude that is 2/3 smaller than the one observed for the acetylacetonate sample. This indicates a higher degree of dispersion and hence catalyst activity, since these two quantities are usually correlated. This application clearly demonstrates the sensitivity of the EXAFS method, which in this case enables the development of criteria for precursor selection to target and control specific catalyst properties. It was also possible to demonstrate that with increased loading, the oxide phase becomes more completely formed.

The determination of structural differences between the reduced and nonreduced states of catalysts will be illustrated by using an investigation of a Cu/ZnO catalyst for methanol synthesis.[97] This study dealt with annealed Cu/ZnO catalysts containing different Cu/Zn ratios (10:90, 20:80, 33:67). To gain an insight into the species present, the structural parameters of the model compounds Cu, CuO, Cu_2O, and ZnO were also measured (Table 5). A comparison of the results of the EXAFS analysis of the annealed Cu/ZnO catalysts (Table 6) with those of the model compounds indicates that based on the observed

Table 5. Structural parameters (absorber–backscatterer distances r, coordination numbers N) for the model compounds for Cu/ZnO catalysts [97]. AB = absorber–backscatterer pair.

Model	AB	r [Å]	N	Model	AB	r [Å]	N
Cu (Metal)	Cu-Cu	2.56	12	Cu_2O	Cu-O	1.84	2
CuO	Cu-O	1.96	4		Cu-Cu	3.02	12
	Cu-Cu	3.00	4	ZnO	Zn-O	1.99	4
					Zn-Zn	3.22	12

Cu–O, Cu–Cu, and Cu–Zn distances, Cu^{2+} ions are present in a CuO-like phase, and also substitute Zn in the ZnO lattice. This study yielded the first positive proof of such a Cu–Zn exchange in annealed nonreduced catalysts. An analogous analysis for the reduced state showed that Cu^0 atoms are in a Cu metal-like environment, while the Cu^+ ion surroundings are Cu_2O-like (Table 6). Initially, the observed average Cu–Zn distance at

Table 6. Structural parameters (absorber–backscatterer distances r, coordination numbers N) for annealed and for reduced Cu/ZnO catalysts ($Cat_{cal.}$ and $Cat_{red.}$, respectively) [97]. AB = absorber–backscatterer pair.

Catalyst	AB	$r_{cal.}$ ($r_{red.}$) [Å]	N ($cat_{cal.}$)
Cu/Zn (10:90)	Cu-O	1.97 (1.86)	4
	Cu-Cu	2.99 (2.53)	3
	Cu-Zn	3.22 (2.25)	10
Cu/Zn (20:80)	Cu-O	1.98 (1.80)	4
	Cu-Cu	2.99 (2.55)	4
	Cu-Zn	3.19 (2.20)	8
Cu/Zn (33:67)	Cu-O	2.00 (1.79)	4
	Cu-Cu	3.01 (2.57)	4
	Cu-Zn	3.26 (2.27)	5

2.24 ± 0.04 Å was difficult to explain. It was possible to exclude replacement of Zn lattice atoms in ZnO by Cu^+ ions, as had been observed for the nonreduced sample. The authors concluded that, in all probability, Cu^+ ions occupy interstitial locations in ZnO. This conclusion is in accordance with all EXAFS results as well as with structural considerations.

The influence of gases on the structural properties of finely divided metal clusters was studied by D. C. Kroningsberger et al.[98] Using an Ir/Al_2O_3 catalyst as example, they were able to show that removal of chemisorbed hydrogen leads to an increased disorder in the Ir clusters and to a reduction in the metal–metal distances. The adsorption of O_2 at 77 K takes place at the surface of the iridium particles. The Ir–O(adsorbed) bonds are of the same type as the bonds of Ir atoms to the O atoms of the carrier material after hydrogen removal. Increasing the temperature to 100 K leads to significant changes in the EXAFS spectrum. It is possible to demonstrate a second, shorter Ir–O distance and a decrease in the Ir–Ir coordination number. This indicates the beginning of the oxidation of the Ir clusters.

In addition to heterogeneous catalysts containing only one type of metal, heterodi- and -trimetallic catalysts play a crucial role, especially in the petroleum industry. EXAFS spectroscopy makes it possible to gain some interesting insights. For example, for the monometallic catalyst H_2PtCl_6 on a carrier, it was found that the drying process does not affect the structure of the $PtCl_6^{2-}$ complex and the slow formation of PtO_2 is observed first during annealing.[99] On the other hand, in a bimetallic Pt/Rh catalyst (made from chlorinated precursors) the platinum is already in a PtO_2 environment after drying. The presence of the Rh metal reduces the temperature necessary to convert H_2PtCl_6 into PtO_2 by several hundred degrees.[100] A systematic investigation using different degrees of impregnation for Pt/Rh or Pt/Re, and Cl led to the following explanation. The Al_2O_3 carrier material employed has two different binding sites: a small number of tight binding sites with Al–O bonds strong enough to resist exchange of O by Cl atoms and a larger number of weaker binding sites with Al–O bonds which permit this exchange. It was observed that an increase in the proportion of Rh or Re metal led to a decrease in the Cl coordination number of platinum and a concomitant increase in the O coordination number. Rhodium and rhenium therefore selectively bind to the sites with stronger Al–O bonds, forcing the Pt atoms to occupy the weaker binding sites.

An EXAFS study of a Pt/Re bimetallic catalyst at different temperatures indicated that the rhenium centers—in contrast to the platinum centers—are not completely reduced (Fig. 17). The

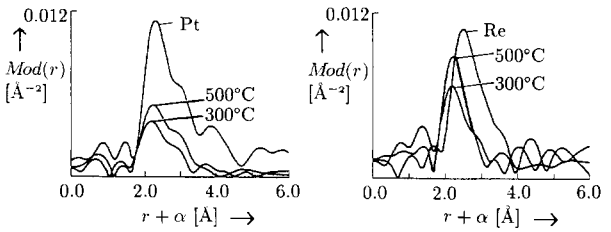
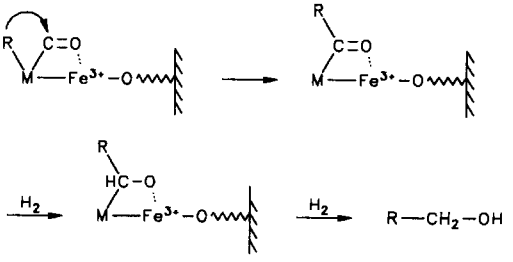


Fig. 17. Fourier transformed EXAFS functions, measured at the Pt-L_{III} (left) and Re-L_{III} (right) absorption edges, of pure platinum and rhenium, respectively, as well as those of bimetallic catalysts reduced at 300 and 500 °C [101].

Re atoms remain partially attached to the carrier by Re–O bonds and act in turn as carrier for platinum clusters.[101] A study employing a variety of analytical methods (EXAFS, FT-IR, ^{57}Fe Mössbauer, and ^{129}Xe NMR spectroscopy as well as transmission electron microscopy (TEM)), examined Rh/Fe, Pt/Fe, and Ir/Fe bimetallic catalysts on SiO_2. Based on the EXAFS data, the authors postulated M-Fe^{3+}-O bonds (M = Rh, Pt, Ir).[102] The M clusters, about 10 Å in size (^{57}Fe Mössbauer spectroscopy), are attached to the SiO_2 carrier by Fe atoms. In this case, the additional metal Fe plays an important role in determining the high activity and selectivity for the catalytic



Scheme 1. Proposed mechanism for the formation of CH_3OH and CH_3CH_2OH under the influence of Rh/Fe, Pt/Fe, and Ir/Fe bimetallic catalysts [102]. R = H, CH_3; M = Rh, Pt, Ir.

preparation of CH_3OH and CH_3CH_2OH from CO and H_2 (Fischer–Tropsch reaction). As an explanation for the role played by iron, the authors presented the mechanistic proposal shown in Scheme 1.

In addition to the analysis of the EXAFS range in the absorption spectrum, the shape of the absorption edge itself can yield valuable information about the structure of catalysts. An example can be found in the study of a SiO_2 catalyst impregnated with titanium oxide.[103] Based on the comparison of the XANES region of differently loaded catalysts with those of the anatase and rutile modifications of TiO_2, it was possible to show that only a selective formation of an anatase-like TiO_2 structure is taking place on the carrier material. The analysis of the EXAFS function of this system confirms this result.

The structure of the L_{III} absorption edge of metals like platinum and rhenium is strongly dependent on the chemical environment of the metal atoms. The reduction of a catalyst can be followed by using the changes in the XANES region. In situ studies of Pt catalysts under realistic chemical and physical conditions (temperature increase of 6 °C min^{-1}, constant H_2 flux) demonstrated that the reduction process is complete after 60 minutes (Fig. 18).[104] Energy-dispersive EXAFS studies are

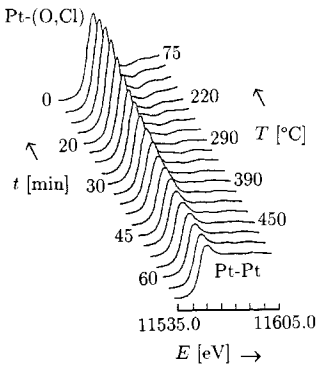


Fig. 18. Changes in the Pt–L_{III} absorption edge as a function of time and temperature, induced by in situ reduction of a 1.5 wt% monometallic platinum catalyst. The immediate coordination sphere of the Pt center consists initially of O and Cl backscatterers. After 60 minutes, the Pt–L_{III} absorption edge is nearly identical with that of pure platinum [101].

able to follow processes with much faster kinetics. Examples are studies of the activation, poisoning, and regeneration of Pt/Cu and Ir/Cu catalysts.[105, 106]

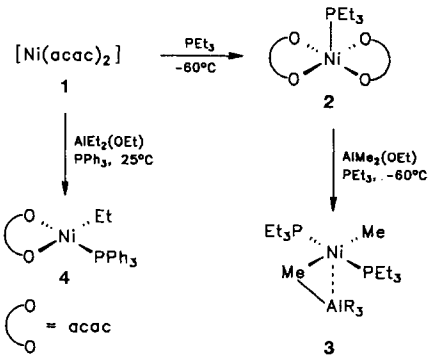
4.3.2. *Homogeneous Catalysis*

Compared to heterogeneous catalysts, homogeneous ones have the advantage that they can be reproducibly prepared and specifically tailored by variation of the ligands. EXAFS studies in this area are fairly rare and hence not as multifaceted as for heterogeneous catalysts. It is therefore possible to organize them according the catalyzed reaction type.

J. Evans et al. investigated the structure of the alkene metathesis catalyst $[(\eta\text{-}C_5H_5)_2Ti(CH_2AlMe_2)]$ in the solid state as well as in a frozen toluene solution.[107] Based on the EXAFS analysis, no significant structural differences could be observed.

The complexes $[NiX_2(PR_3)_2]$ (X = Cl, Br; R = Ph, Et) can act as precursors for alkene oligomerization and polymerization catalysts. Parameters obtained from EXAFS spectroscopy of polycrystalline samples agree within 3% with those found by X-ray structure determinations. The structure of complexes dissolved in toluene remains unchanged in this case as well.[107]

The same workers did more extensive studies on the activation of these complexes with Lewis acids, and obtained remarkable results.[108] Specifically, the $Al_2Me_3Cl_3$- and $AlEt_3$-activated oligomerization of propene by $[NiCl_2(PEt_3)_2]$ was studied. Initially, model reactions (Scheme 2) were studied by EXAFS spectroscopy to determine to what extent it is possible to gain information about the environment of the Ni atoms in similar systems (for structural parameters, see Table 7). The addition of



Scheme 2. Schematic representation of the studied model reactions, also showing simplified structural models of the complexes formed (**2**–**4**) [108]. Hacac = pentane-2,4-dione.

PEt_3 to trimeric $[Ni(acac)_2]$ (**1**) in diethyl ether leads, at −60 °C, to the disappearance of the Ni–Ni interaction. The paramagnetic pentacoordinated adduct **2** is formed in the process. Further reaction with $AlMe_2(OEt)$ at the same temperature enables the isolation of $[Ni(Me)_2(PEt_3)_2]$ after workup.[109] Even in solution, the analysis of the EXAFS spectrum yields two carbon atoms and two phosphorous atoms at distances of 1.91 and 2.12 Å, respectively, from the nickel center. In addition, a Ni–Al distance of 2.97 Å is detected. The sum of the covalent radii of Ni and Al atoms is 2.4 Å, which is considerably shorter than the observed distance. The authors proposed structure **3**, with a Ni-C-Al interaction, as a possible explanation. The EXAFS study of the preparation of $[Ni(Et)(acac)(PEt_3)]$ (**4**) (an intermediate in the alkylation reaction of the Ni center) in toluene yielded structural parameters similar to those obtained from an X-ray diffraction study of the crystalline compound.[110] These experiments clearly indicate the ease of following in situ reac-

Table 7. Structural parameters (Ni-backscatterer distances r, coordination numbers N) for various model reactions studied by EXAFS [108]. B = backscatterer.

Solution	B	r [Å] [a]	N [b]
$[Ni(acac)_2]/PEt_3$ in Et_2O	O	2.01	4.2
at −60 °C (**2**)	P	2.42	1.2
	C	2.88	3.6
$[Ni(acac)_2]/PEt_3/AlMe_2(OEt)$	C	1.91	2.2
in Et_2O at −60 °C (**3**)	P	2.12	1.9
	Al	2.97	0.9
$[Ni(acac)_2]/PPh_3/AlEt_2(OEt)$	O	1.88	–
in toluene at 25 °C (**4**)	C	1.97	–
	P	2.13	–

[a] Stated error for the absorber–backscatterer distances 1.5%. [b] Stated error for the coordination numbers ±0.3.

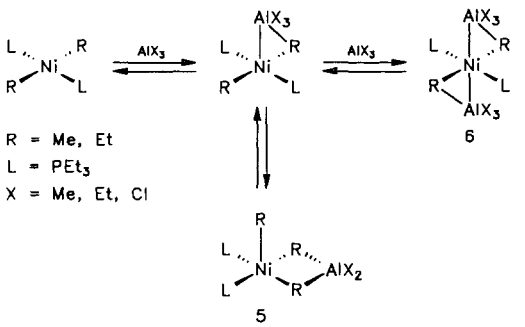
tions and obtaining meaningful structural information about the environment of the nickel centers.

Solutions of $[NiCl_2(PEt_3)_2]$, activated by $Al_2Me_3Cl_3$ or $AlEt_3$, in *p*-fluorotoluene showed, after reaction with propene, a product distribution of 4:2:1 for the C_6:C_9:C_{12} oligomers (determined by GC-MS). The C_6 fraction was primarily composed of 2,3-dimethylbutene, 4-methylpent-1-ene, and 2-methylpent-2-ene. Activation with $ZnEt_2$ leads to face-centered cubic Ni clusters. This was unambiguously shown by EXAFS spectroscopy, which yielded Ni–Ni distances of 2.45, 4.32, 4.14, and 4.87 Å. The solution had only a very limited catalytic activity. The structural parameters (Table 8) for the $Al_2Me_3Cl_3$-activated system indicate the primary presence of complexes of type **5** (Scheme 3). Assuming the existence of a planar Ni-C-Al bridge

Table 8. Structural parameters (Ni-backscatterer distances *r*, coordination numbers *N*) for activated solutions of the alkene oligomerization catalyst in *p*-fluorotoluene at −40 °C [108]. B = backscatterer.

Solution	B	*r* [Å]	*N* [b]	Solution	B	*r* [Å] [a]	*N* [b]
$NiCl_2(PEt_3)_2$/	C	1.91	2.7	$NiCl_2(PEt_3)_2AlEt_3$/	C	1.86	2.0
$Al_2Me_3Cl_3$	P	2.21	2.0	propene	P	2.15	2.0
	Al	2.96	1.1		Al	2.93	2.2
	Cl	4.38	2.0				
$NiCl_2(PEt_3)_2/AlEt_3$	C	1.93	2.2				
	P	2.20	2.1				
	Al	2.98	1.5				
	Cl	4.40	2.2				

[a] Stated error for the absorber–backscatterer distances 1.5%. [b] Stated error for the coordination numbers ±0.3.

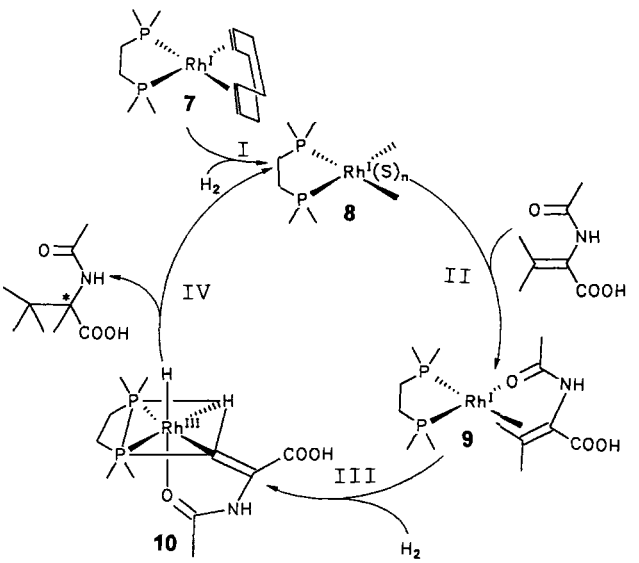


Scheme 3. Equilibria and structural models for different solutions of the alkene oligomerization catalyst (see Table 8) [108].

with terminal Cl atoms at the Al atom and using the found Ni–Al and Ni–Cl distances, the authors determined Ni-C-Al and Cl-Al-Cl bond angles of 95 and 118°, respectively. The $AlEt_3$-activated system looks somewhat different. Based on the observed Ni–C and Ni–Al coordination numbers, complexes of type **6** form the majority, while only small quantities of **5** are present. The addition of propene to the $[NiCl_2(PEt_3)_2]/AlEt_3$ solution leads to a change in the original EXAFS spectrum. The disappearance of the Ni–Cl distances and the decrease in the Ni–C distance to 1.86 Å are especially remarkable. The influence of the alkene apparently reduces the concentration of species of type **5** dramatically. Finally, it should be mentioned that this study provides the first direct evidence for a Ni-C-Al interaction in solution.

Hydrogenation catalysts have also been studied by EXAFS spectroscopy. For instance, J. Goulon et al. examined nickel and cobalt 2-ethylhexanoate in benzene before and after reduction by $AlEt_3$.[111] The observed Ni–O and Ni–C distances in solution before reduction indicate that four carboxylic acid groups are bound to the metal atom in a monodentate fashion. After the addition of $AlEt_3$, metal–metal distances are observed that are very similar to those in the pure metal, indicating the formation of amorphous, metal-like clusters. The authors note that the detected metal–carbon bonds play a significant role in the catalytic activity of these compounds. A very similar study, performed by C. Esselin et al. with nickel and iron acetylacetonates in benzene, which were reduced by $AlEt_3$ and $GaEt_3$, gave essentially identical results.[112]

The most interesting and extensive study in the area of hydrogenation catalysts has been performed by B. R. Stults et al.[113] They examined optically active rhodium complexes of the type $[Rh(P-P)L]^+X^-$ and $[Rh(P)_2L]^+X^-$ for the asymmetric hydrogenation of the prochiral alkene 2-acylamino-3-methylbut-2-enoic acid. Based on results from previous studies (using X-ray structure determinations, ^{13}C and ^{31}P NMR spectroscopy in solution, and solid-state ^{13}C NMR spectroscopy) and those of other workers, the authors had already proposed the catalytic cycle shown in Scheme 4.[114, 115] EXAFS spectroscopy was



Scheme 4. Proposed catalytic cycle for the asymmetric hydrogenation of prochiral olefins [113].

supposed to yield structural information about solution species formed under realistic reaction conditions. To achieve this goal, a number of crystallographically characterized Rh complexes was examined in solution and in the solid state (Table 9). The distances obtained agreed very well with those obtained by the crystal structure determinations. In general, it was observed that the crystalline compounds had shorter Rh–P and Rh–C distances, which the authors attributed to crystal packing forces.

The compounds $[Rh(dipamp)(cod)]^+$ and $[Rh(camp)_2(cod)]^+$ (for abbreviations see Table 9) were studied in situ in methanol after a 30-minute treatment with H_2. For the interme-

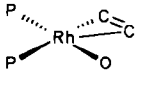
Table 9. Lengths of the Rh–X bonds in Rh complexes determined by EXAFS and X-ray diffraction studies [113]. XSA = X-ray structure analysis. soln. = solution.

Compound [a]		Bond length [Å]		
		XSA	EXAFS	
			solid	soln.
[Rh(diphos)(cod)]$^+$	Rh-P	2.28	2.29	2.33
	Rh-C	2.25	2.22	2.32
[Rh(dipamp)(cod)]$^+$	Rh-P	2.27	2.28	2.28
	Rh-C	2.20	2.22	2.34
[Rh(diphos)(amb)]	Rh-P	2.27	2.27	
	Rh-P	2.23	2.23	
	Rh-C	2.22	2.28	
	Rh-O	2.11	2.12	
[Rh(dipamp)(amb)]	Rh-P		2.29	
	Rh-P		2.26	
	Rh-C		2.28	
	Rh-O		2.01	
[Rh(dipamp)$_2$]	Rh-P	2.31	2.30	2.29
[Rh(acac)$_3$]	Rh-O	1.99	2.03	2.07
[Rh(diop)(nbd)]$^+$	Rh-P	2.30	2.29	2.34
	Rh-C	2.22	2.19	2.36
[Rh(camp)$_2$(cod)]$^+$	Rh-P	2.35	2.32	2.34
	Rh-C	2.20	2.10	2.30
[Rh(L)(cod)]$^+$	Rh-P	2.26	2.27	2.34
	Rh-C	2.26	2.26	2.30

[a] diphos = bis(1,2-diphenylphosphino)ethane, dipamp = (*R*,*R*)-1,2-ethanediylbis[(*o*-methoxyphenyl)phenylphosphene], diop = (*R*,*R*)-isopropylidene-2,3-dihydroxy-1,4-bis(diphenylphosphino)butane, camp = (*R*)-*o*-anisylmethylcyclohexylphosphane, L = *cis*-bis(diphenylphosphino)ethylene, cod = 1,5-cyclooctadiene, amb = 2-acylamino-3-methylbut-2-enoic acid, nbd = bicyclo[2.2.1]heptadiene, Hacac = pentane-2,4-dione.

diate **8** (Scheme 4) with dipamp and camp ligands, the analysis of the EXAFS spectra yielded Rh–P distances of 2.34 and 2.35 Å and Rh–O distances (coordinated solvent) of 2.34 and 2.36 Å, respectively. The coordination number was two in all cases. After addition of 2-acylamino-3-methylbut-2-enoic acid to [Rh(dipamp)$(CH_3OH)_2$]$^+$, the following structural parameters were found for **9**: Ph–P1 = 2.36, Rh–P2 = 2.29, Rh–C = 2.26, and Rh–O = 1.86 Å. Scheme 5 shows the proposed structure of the square-planar rhodium complex, which has been confirmed by X-ray structure determinations.[116] The different Rh–P distances are attributed to the position of the P atoms *cis* or *trans* to the alkene and to the O atom. The very short Rh–O distance of 1.86 Å is remarkable when compared to the crystalline compound (2.01 Å, Table 9). The analysis of the EXAFS spectra of [Rh(camp)$_2$$(CH_3OH)_2$]$^+$ in the presence of 2-acylamino-3-methylbut-2-enoic acid was not successful; apparently a large number of different catalyst–substrate species is formed. This is due to the monodentate nature of camp, as opposed to bidentate dipamp, which leads to rapid isomerization in this case. This was also confirmed by NMR experiments.

Finally, a study of the hydroformylation catalyst Na[$(NCCH_2)Co(COOCH_3)(CO)_3$] in methanol should be mentioned here.[117] Na[$Co(CO)_4$] was used as model compound. In solution, the complex has a trigonal-bipyramidal structure, with three C atoms at a distance of 1.83 and two C atoms at a distance of 2.13 Å from the Co atom.



Scheme 5. Schematic representation of the structural model of the square-planar rhodium complex [Rh(dipamp)(amb)] in methanol, based on EXAFS results [113].

4.4. Biochemistry

To demonstrate the application of EXAFS spectroscopy to biological problems, the studies of photosystem II, blue copper proteins, superoxide dismutase, and cytochrome c oxidase will be used as examples.

4.4.1. Photosystem II

Nearly all oxygen required for the energy supply in animals and aerobic bacteria stems from the ability of plants to convert water into the life-sustaining O_2 molecule. This ability is directly linked to photosystem II (PS II). A manganese-containing enzyme complex—the so-called oxygen-evolving complex (OEC)—bound to the thylacoide membrane of chloroplasts catalyzes the oxidation of water to molecular oxygen. In this process, every reaction center in PS II acts independently and accepts, in a stepwise manner, four electrons. Using kinetic studies, it was possible to distinguish five intermediate states of the manganese complex, called S_0 to S_4, with S_0 representing the most reduced state. The stable, resting state of the OEC is the S_1 state.

Even though it has been known since 1970 that four specifically bound manganese ions are required for OEC activity,[118] there is controversy over the structure of the cluster and the Mn oxidation states during the electron transfer reaction. In a series of studies[119–127] it was found that in the S_1 state the Mn atoms are surrounded by N or O atoms—it is difficult to distinguish between these two elements—at an average distance of 1.75 and 2.15 Å. In addition, there is a Mn–Mn distance at 2.7 Å. Based on the comparison with binuclear Mn model compounds, the short Mn–(N,O) distance was assigned to a μ-oxo bridge between two Mn centers, while the longer distance was assigned to terminal nonbridging N- and/or O-containing ligands. An additional indication for the presence of a binuclear or multinuclear cluster is the observed Mn–Mn distance of 2.7 Å. However, due to low data quality, the presence of a cluster of higher nuclearity could not be excluded. In addition, the oxidation states of the Mn centers remained unclear. EPR measurements led to the conclusion that μ-oxo-bridged Mn^{III}/Mn^{IV} and Mn^{II}/Mn^{III} dimers are present.[128, 129] A precise analysis of the very broad XANES signal indicated the presence of Mn^{III}/Mn^{IV} centers. No significant changes in the immediate vicinity of Mn ions were observed during the transition to the S_2 state. Even though it is known that inorganic cofactors, such as chloride ions, are required for O_2 production,[130, 131] no indication for Cl coordination to the Mn centers was found.

J. E. Penner-Hahn et al.[132] also investigated the S_1 state of OEC. They were able to significantly improve data quality by increasing the Mn concentration in the sample, accumulating spectra, and by using a solid-state detector array. But even with this improvement it remained impossible to determine whether the Cl^- ions were coordinated to the Mn centers or not. These authors, in contrast to earlier results by other groups, did not find a Mn-(N,O) distance of 1.75 Å, but, in rough agreement with the earlier results, they did observe two O backscatterers at approximately 1.9 and 2.1 Å, two Mn backscatterers at 2.7 Å and, additionally, another Mn atom at 3.3 Å. The presence of two Mn backscatterers at 2.7 Å, together with the analysis of the

XANES spectra and a comparison of EPR spectra, led the authors to propose a trinuclear $Mn^{II}/Mn^{III}/Mn^{IV}$ cluster and a mononuclear Mn^{III} cluster. Three Mn^{III} centers in the trinuclear cluster and one Mn^{III} center in the mononuclear cluster were also in accordance with the EXAFS and EPR results. This oxidation state assignment would require a very distorted environment about the Mn center in order to explain the very broad structure of the XANES signal.

4.4.2. Blue Copper Proteins

Another group of electron carriers in photosynthetic and bacterial redox chains consists of the so-called blue or type I copper proteins. The best known examples are plastocyanin, azurin, stellacyanin, umecyanin, amicyanin, and rusticyanin. The type I copper proteins share a common structural unit, consisting of two histidine and one cystine ligand in a distorted trigonal geometry. The coordination sphere of the Cu center is completed by axial bonds to sulfur atoms (methionine) and in part by oxygen atoms from the peptide chain.

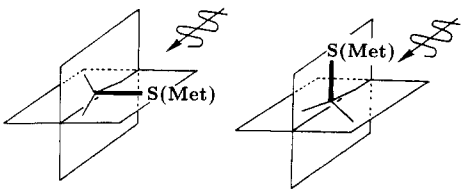
Even though these proteins are by now fairly well structurally characterized, there are still uncertainties regarding the relationship between the redox potential and the Cu coordination environment. In this context, the length of the axial Cu–S(Met) bond appears to play a central role.[133] A large number of EXAFS studies—for instance, the first determination of the bond length of the short Cu–S(Cys) contact[134]—has been performed on this system. Their results are summarized in Table 10.

Table 10. Summary of EXAFS studies of type I copper proteins. Cond. = conditions.

Protein	Cond.	Cu-N(His) [Å]	Cu-S(Cys) [Å]	Cu-S(apical) [Å]	Ref.
rusticyanin	ox.	1.99	2.16	2.84	[135]
(*Thiobacillus ferrooxidans*)	red.	2.07	2.17	2.80	
plastocyanin	ox.	2.05	2.12	–	[136]
(*Phaseolus vulgaris*)	red.	2.05	2.22	–	
azurin	ox., pH 9.1	1.95	2.23	–	[137]
(*Pseudomonas*	ox., pH 4.1	1.95	2.19	–	
aeruginosa)	red., pH 9.2	1.89/2.05	2.21	2.74	
	red., pH 5.5	1.89/2.04	2.24	2.70	
stellacyanin	ox.	1.93	2.21	–	[136]
(*Rhus vernificera*)	red.	1.98	2.25	2.66	
umecyanin	ox.	1.99	2.13	–	[138]
(*Amorarcia laphatifolia*)	red.	2.03	2.21	–	
amicyanin	ox., pH 9.2	1.89/2.01	2.11	–	[139]
(*Thiobacillus*	ox., pH 5.2	1.86/1.95	2.13	–	
versutus)	red., pH 8.9	1.86/2.18	2.19	–	
	red., pH 6.6	1.89	2.18	2.41	

It was mainly possible to demonstrate the existence of two Cu–N(His) contacts between 1.86 to 2.07 Å and a Cu–S(Cys) contact between 2.12 to 2.24 Å. Reduction to the Cu^{I} form leads to a small but significant increase in the Cu–N(His) bonds to an average of 2.05 Å. The Cu–S(Cys) bond remains nearly unchanged by the reduction.

The exact determination of the axial Cu–S(Met) contact by using EXAFS spectroscopy has so far not been successful. In 1982, the research group of R. A. Scott attempted to isolate the contribution of the axial Cu–S(Met) distance to the EXAFS function by using polarized synchrotron radiation and varying the orientation of plastocyanin single crystals (*Populus nigra*) with respect to the polarization vector of the incident X-rays.[140] In the unit cell of plastocyanin, four Cu–S(Met) bonds are aligned parallel to the crystallographic *c* axis.[141] When the *c* axis of the crystal is oriented parallel to the direction of the polarization of the incident beam, the EXAFS function should primarily contain the contribution of the S(Met) backscatterers. If, however, the *b* axis is parallel to the direction of polarization, the contributions of N(His) and S(Cys) backscatterers to the total EXAFS function should be especially high (Scheme 6). The results of this study are in very good agreement with crystallographic data for the Cu–N(His) and Cu–S(Cys) bonds. However, there was no indication for any contribution from the methionine sulfur atom. This was explained by the uncorrelated motion of the atoms involved. The authors stated that the Debye–Waller factor was so large as to make the determination of the Cu–S(Met) distance by EXAFS techniques practically impossible, because the amplitude of any absorber–backscatterer contribution would be dampened too strongly.



Scheme 6. Schematic representation of the orientation of the Cu–S(Met) bond in plastocyanin with respect to the polarization direction of the incident synchrotron radiation. Left: The crystallographic *c* axis and the Cu–S(Met) bond are parallel to the beam polarization. Right: The crystallographic *b* axis is parallel to the beam polarization.

A later study of azurine (*Pseudomonas aeruginosa*)[137] also demonstrated that there are circumstances that make the detection of actual bond lengths by EXAFS spectroscopy difficult or impossible. In the oxidized form of the enzyme, there is destructive interference between the Cu–S(Met) shell and a shell containing imidazole C atoms. This interference does not allow the contribution of the Cu–S(Met) shell to be observed. In the reduced enzyme, however, it was possible to observe this contribution at 2.70 ± 0.05 Å. The reduction and the related shortening of the Cu–S(Met) bond indicate that the methionine ligand plays a central role in the determination of the redox potential.

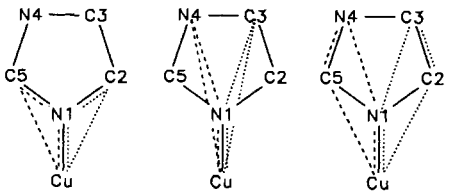
4.4.3. Superoxide Dismutase

The Cu/Zn superoxide dismutase (Cu/Zn SOD) belongs to the group of type II copper proteins. In contrast to type I Cu proteins, the coordination sphere of type II Cu proteins consists mainly of atoms with low atomic numbers, such as N (histidine) and O atoms (water and O-containing amino acids). Cu/Zn SOD catalyzes the conversion of the superoxide radical to oxygen and hydrogen peroxide, $2H^+ + 2O_2^{\bullet -} \rightarrow O_2 + H_2O_2$. In the crystalline state, the Cu atom in this enzyme is surrounded by four imidazole ligands (histidine) in a flattened tetrahedral ge-

ometry. One of these imidazole ligands forms an N bridge to the neighboring Zn atom. One of the enzyme's characteristics is its ability to bind small anionic ligands, for instance the substrate $O_2^{\cdot-}$ or inhibitors like CN^-, in a surface site between the Cu^{II} center and an arginine residue.[142]

Earlier EXAFS studies on the environment of the Cu ions, using differently prepared samples, indicated the presence of four imidazole ligands at 2.00 Å and an additional solvent molecule at 2.23 Å for native SOD in aqueous solution.[143] These results are in very good agreement with the crystal structure analysis. In the freeze-dried enzyme,[144] the Zn atom is surrounded by three imidazole N atoms at 2.01 Å and one O(Asp) atom at 2.04 Å. Attempts to fit farther-removed C and N atoms, which contribute significantly to the EXAFS function, led to the reduction of some distances by about 0.5 Å. Neither for the used model compounds nor for the actual enzyme samples, was it possible to obtain a convincing fit in the low k range, where multiple scattering effects are particularly significant.

A later study[145] dealt with the native enzyme and its complexes with cyanide and azide ions. Due to the inclusion of multiple scattering effects, it was possible to fit the higher coordination shells very well. It was necessary, however, to assume that the distances between the Cu atom and the C2 and the C5 atoms of the imidazole ring are different. The same assumption was made for the C3 and N4 atoms. The distances obtained indicate an inclination of the imidazole ring of 5–10° with respect to the Cu–N1 axis (Scheme 7). The idealized geometry corresponds to a square pyramid around the Cu atom, with four N atoms at the corners of the basal plane and one axial O atom (from a solvent molecule).



Scheme 7. Atom numbering scheme as well as examples for scattering pathways of multiple-scattering contributions within the imidazole ring.

The characterization of the complexes of SOD with CN^- and N_3^- ions as model substrates presents a very good opportunity to study the structural changes after $O_2^{\cdot-}$ coordination. The analysis of the EXAFS function of the SOD complex with azide ions indicates an equatorial coordination of the N_3^- ion to the Cu atom, presumably in a square pyramidal geometry. A Cu–N(azide) distance and three Cu–N(His) distances of 1.99 Å were observed, as well as a Cu–N(His) contact of 2.27 Å. The coordination of the azide ion leads to a shift of an imidazole ligand from an equatorial to an axial position. The angle between the Cu–N(azide) axis and the molecular axis of the azide ion is less than 135°.

The SOD complex with CN^- ions shows a Cu–C(CN) bond length of 1.97 Å, also indicating an equatorial coordination of the cyanide ion. The CN^- binding also leads to a shortening of the three Cu–N(His) bonds to 1.95 Å. In contrast to the SOD complex with N_3^-, in which an axially coordinated imidazole group with a Cu–N distance of 2.27 Å is retained, the Cu atom in the CN^--SOD complex is surrounded by only four ligands. No additional Cu–imidazole contact could be demonstrated by EXAFS spectroscopy. It appears that the cyanide ion replaces a histidine residue and leads to a higher asymmetry in the orientation of the imidazole ring than is found in the native enzyme.

4.4.4. Cytochrome c Oxidase

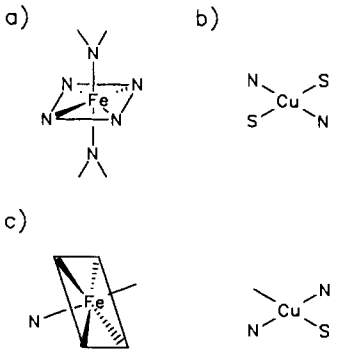
Cytochromes are electron-transfer proteins that contain iron phorphyrin moieties. They only exist in aerobic cells. During their catalytic cycle, in all cytochromes the Fe^{II} centers are oxidized to Fe^{III} centers and can therefore no longer be oxidized by molecular oxygen. An exception to this is cytochrome c oxidase which contains additional copper ions. It is the last member in the mitochondrial respiratory chain. Its function is the transfer of four electrons to oxygen, thereby reducing it to water in the process. Each of the four metal centers (two Fe and two Cu) can accept one electron. The Fe(heme a) and Cu_A centers are located in a magnetically insulating environment and are about 12 Å apart. The Fe(heme a_3) and the Cu_B center are a magnetically coupled pair. It is assumed that the oxidized enzyme accepts electrons from heme a and transports them through the Cu_A center to the binuclear heme a_3/Cu_B unit, where the O_2 binding supposedly takes place as well.[146, 147]

EXAFS studies that employ Fe and Cu absorption edges are promising in this case. However, the Fe, as well as the Cu atoms, are present in chemically different environments. The measured EXAFS spectrum is therefore a superposition of the spectra of the Fe center in heme a and heme a_3, or of the Cu ions in the form of Cu_A and Cu_B. Early XAS studies dealt only with a comparison between the absorption edge of the enzyme with those of model compounds.[148, 149] It was found, that the position and the structure of the Cu edge is barely affected by oxidation or reduction. This led to the conclusion, that one of the Cu centers retains its Cu^I oxidation state during oxidation.

The first EXAFS study indicated the average environment around both Cu centers consisted of 1–1.5 S atoms at 2.27 Å and two nitrogen atoms at 1.97 Å.[150] Somewhat later, L. Powers et al.[151] assumed, based on earlier work,[148] that Cu_B is a type I copper center like that found in stellacyanin. Therefore, they subtracted the experimentally determined spectrum of oxidized stellacyanin from the spectrum of oxidized cytochrome c oxidase in order to obtain the EXAFS spectrum of the Cu_A center. In this fashion, it was possible to identify two nitrogen atoms at 1.97 Å and two sulfur atoms at 2.23 Å. The Fe-edge EXAFS spectrum also led to the identification of sulfur backscatterers, a fact that led to the assumption of a sulfur bridge between Fe(heme a_3) and the Cu_B center. These results were later questioned, however. First, no contribution of bridging sulfur atoms could be deduced from the EXAFS spectrum of active cytochrome c oxidase.[152] Second, the EXAFS spectrum of the enzyme did not yield indications about a short Cu–S contact, which is certainly present in stellacyanin.[153] Therefore, the method of L. Powers et al.[151] for obtaining a "pure" Cu_A spectrum was no longer tenable. Even the stated Cu–Fe distance of 3.8 Å in reference [151] is contrary to the 3.0 Å given in reference [153]. Moreover, it was shown that

different enzyme preparation methods yielded different EXAFS spectra.[154, 155]

The most recent study dealt with a form of the enzyme from which the Cu_A center has been selectively removed and which retains up to 75% of its activity.[156] The thus obtained Cu_B EXAFS spectrum yielded three N or O atoms and one S or Cl atom as backscatterers, but no short Cu–S contact was found. This conclusively demonstrated that a stellacyanin-like Cu_B configuration can be excluded. According to these results, the Cu_B center is coordinated by three histidine and one cystine molecule. A—potentially bridging—Cl atom is also possible. The subtraction of the Cu-edge EXAFS spectrum of the Cu_A-depleted enzyme from that of the native enzyme yields selectively the environment of the Cu_A atom. Cu_A is surrounded by two N/O atoms at a distance of 1.97 $\pm$ 0.02 Å and two S atoms at a distance of 2.28 $\pm$ 0.02 Å. This indicates the coordination of two histidine and two cystine molecules to the Cu_A center (Scheme 8). Metal-metal contacts in the Cu_A-depleted enzyme



Scheme 8. Proposed structures for the metal centers in cytochrome c oxidase. a) heme a, b) Cu_A, c) heme a_3-Cu_B. The Cu–S distances in Cu_A and heme a_3-Cu_B are 2.28 Å, the Cu–N distances 1.97 Å.

have so far not been reported in the literature. Fe-edge EXAFS investigations of this enzyme modification have also not yet been reported. Other studies have dealt with the cytochromes b_2,[157] cytochrome P-450-CAM,[158] and the effect of cyanide binding to cytochrome c oxidase.[154]

5. Outlook

Is EXAFS spectroscopy a promising new technique? On first glance, the answer is yes. The element-specific determination of local structures is possible, independent of the sample's physical state and even at very high dilution. The action of catalysts can be investigated and reactions can be studied in situ. On second glance, the answer is no. Experiments must rely on synchrotron radiation, as the laboratory EXAFS methods are not yet far enough developed. This necessitates long-term planning of experiments, short beam times, and dependence on the research policy of the operator. The analysis of spectra is difficult; interpretation is only possible with the help of extensive spectral simulations, which is in contrast to many common spectroscopic techniques. Compared to these efforts, the information obtained is minimal.

Neither of these viewpoints does justice to EXAFS spectroscopy. Its utilization is only sensible when detailed information about the immediate short-range order around a specific atom type is necessary, and when this information is not accessible by other spectroscopic techniques. Even then it is wrong to expect too much of EXAFS spectroscopy. If the short-range order is characterized by a broad distance distribution, or if different backscatterers are present at similar distances, EXAFS spectroscopy cannot yield unambiguous results. As long as these limitations are kept in mind, and systems to be studied are selected accordingly, EXAFS spectroscopy, in combination with other techniques, can supply new observations—maybe even key information. The future will show the potential of this method. The experimental conditions are improving, that is the access to a synchrotron radiation source: in mid-1994 the European Synchrotron source in Grenoble is supposed to begin operation.

We wish to thank the Sonderforschungsbereich 347 ("Selective Reactions Metal-Activated Molecules") and the Dr. Leni-Schöniger Stiftung for financial support. We are grateful for the conscientious reading of this manuscript by Dr. Dieter Leicht and Mr. Uwe Kolb. Ms. Diana Müller is acknowledged for her assistance in preparing the illustrations. A special thanks goes to Ms. Sabine Hückmann who worked on the biological section of this review.

Received: February 24, 1993 [A 927IE]
German version: *Angew. Chem.* **1994**, *106*, 15
Translated by Dr. Wolf Christian Wilisch, Pasadena, CA (USA).

[1] C. Gerthsen, H. Kneser, H. Vogel, *Physik*, 15. ed., Springer, Berlin, **1986**, p. 604.
[2] H. Fricke, *Phys. Rev.* **1920**, *16*, 202.
[3] G. Hertz, *Z. Phys.* **1920**, *3*, 19.
[4] R. de L. Kronig, *Z. Phys.* **1931**, *70*, 317.
[5] R. de L. Kronig, *Z. Phys.* **1932**, *75*, 468.
[6] D. E. Sayers, E. A. Stern, F. W. Lytle, *Phys. Rev. Lett.* **1971**, *27*, 1204.
[7] F. W. Lytle, D. E. Sayers, E. A. Stern, *Phys. Rev. B* **1975**, *11*, 4825.
[8] B. K. Teo, *EXAFS: Basic Principles and Data Analysis*, Springer, Berlin, **1986**.
[9] B. K. Teo, P. A. Lee, *J. Am. Chem. Soc.* **1979**, *101*, 2815.
[10] A. G. McKale, B. W. Veal, A. P. Paulikas, *J. Am. Chem. Soc.* **1988**, *110*, 3763.
[11] P. A. Lee, G. Beni, *Phys. Rev. B* **1977**, *15*, 2862.
[12] S. J. Gurman, N. Binstedt, I. Ross, *J. Phys. C* **1984**, *17*, 143.
[13] P. A. Lee, J. B. Pendry, *Phys. Rev. B* **1975**, *11*, 2795.
[14] S. J. Gurman, N. Binstedt, I. Ross, *J. Phys. C* **1986**, *19*, 1845.
[15] J. J. Rehr, R. C. Albers, C. R. Natoli, E. A. Stern, *Phys. Rev. B* **1986**, *34*, 4350.
[16] J. J. Rehr, J. Mustre de Leon, S. I. Zabinsky, R. C. Albers, *J. Am. Chem. Soc.* **1991**, *113*, 5135.
[17] G. H. Stout, L. H. Jensen, *X-Ray Structure Determination*, Wiley, New York, **1989**, p. 24.
[18] R. Frahm, *Physica B* **1989**, *158*, 342.
[19] M. Hagelstein, S. Cunis, R. Frahm, W. Niemann, P. Rabe, *Physica B* **1989**, *158*, 324.
[20] A. Fontaine, E. Dartyge, J. P. Itie', A. Fucha, A. Polain, H. Tolentino, G. Tourillon, *Top. Curr. Chem.* **1989**, *151*, 179.
[21] a) *X-Ray Absorption: Principles, Application, Techiques of EXAFS, SEXAFS and XANES* (*Chem. Anal. N.Y.* **1988**, *92*); b) J. Stöhr in [21a], p. 443.
[22] E. P. Bertin, *Introduction to X-Ray Spectrometric Analysis*, Plenum, New York, **1985**.
[23] W. Thulke, R. Haensel, P. Rabe, *Rev. Sci. Instrum.* **1983**, *54*, 277.
[24] K. Tohji, Y. Udagawa, T. Kawasaki, K. Masuda, *Rev. Sci. Instrum.* **1983**, *54*, 1482.
[25] P. Brinkgreve, T. M. J. Maas, D. C. Koningsberger, J. B. A. D. van Zon, M. H. C. Jansen, A. C. M. E. van Kalmhout, M. P. A. Viegers in *EXAFS- and Near Edge Structure III* (*Springer Proc. Phys.* **1984**, *2*, 517).
[26] D. C. Koningsberger in [21a], p. 163.
[27] I. Amato, *Science* **1991**, *252*, 208.
[28] D. E. Sayers, B. A. Bunker in [21a], p. 211.
[29] E. D. Crozier in *EXAFS-Spectroscopy, Techniques and Applications* (Eds.: B. K. Teo, D. C. Joy), Plenum, New York, **1981**.
[30] M. Federico, G. Galli, S. Magazu, D. Majolino, *Nuova Chim.* **1988**, *10*, 425.
[31] J. Freund, R. Ingalls, E. D. Crozier, *J. Phys. Chem.* **1990**, *94*, 1087.
[32] J. Freund, R. Ingalls, E. D. Crozier, *Phys. Rev. B* **1989**, *39*, 12537.
[33] A. Sadoc, Y. Calvayrac, *J. Non Cryst. Solids* **1986**, *88*, 242.

[34] D. Udron, M.-L. Thèye, D. Raoux, A.-M. Flank, P. Lagarde, J.-P. Gaspard, *J. Non Cryst. Solids* **1991**, *137/138*, 131.
[35] M.-L. Thèye, A. Gheorghiu, H. Launois, *J. Phys. C* **1980**, *13*, 6569.
[36] T. I. Morrison, C. L. Foiles, D. M. Pease, N. J. Zaluzec, *Phys. Rev. B* **1987**, *36*, 3739.
[37] A. Sadoc, J. C. Lasjaunias, *J. Phys. F* **1985**, *15*, 1021.
[38] A. M. Flank, D. Bazin, H. Dexpert, P. Lagarde, C. Hervo, J. Y. Barraud, *J. Non Cryst. Solids* **1987**, *91*, 306.
[39] V. Mastelaro, H. Dexpert, S. Benazeth, R. Ollitrault-Fichet, *J. Solid State Chem.* **1992**, *96*, 301.
[40] A. M. Flank, P. Lagarde, D. Udron, S. Fisson, A. Gheorghiu, M. L. Thèye, *J. Non Cryst. Solids* **1987**, *97/98*, 435.
[41] T. Nasu, C. C. Koch, K. Nagoka, N. Itoh, M. Sakurai, K. Suzuki, *Mater. Sci. Eng. A* **1991**, *134*, 1385.
[42] L. F. Gladden, S. R. Elliot, G. N. Greaves, S. Cummings, T. Rayment, *J. Non Cryst. Solids* **1985**, *77/78*, 1199.
[43] H. C. Gerritsen, H. van Brug, F. Bijkerk, K. Murakami, M. J. van der Wiel, *J. Appl. Phys.* **1986**, *60*, 1774.
[44] S. R. Elliot, A. V. Kolobov, *Philos. Mag. B* **1990**, *61*, 853.
[45] R. Frahm, R. Haensel, P. Rabe, *J. Phys. Condens. Matter* **1989**, *1*, 1521.
[46] G. Kh. Tagabilev, V. K. Fyodorov, D. I. Kochubey, S. N. Gusenko, J. B. Kekalo, Yu. A. Skakov, *Nucl. Instrum. Methods Phys. Res. Sect. A* **1991**, *308*, 251.
[47] H. Yamashita, H. Mizutani, T. Tanaka, T. Funabiki, S. Yoshida, *J. Non Cryst. Solids* **1987**, *95/96*, 419.
[48] H. Niemann, A. Torkler, M. A. Denecke, W. Gunsser, W. Niemann, *J. Solid State Chem.* **1991**, *93*, 154.
[49] R. A. Scott, A. J. Jacobson, R. R. Chianelli, W.-H. Pan, E. I. Stiefel, K. O. Hodgson, S. P. Cramer, *Inorg. Chem.* **1986**, *25*, 1461.
[50] P. Maldivi, D. Guillon, A.-M. Giroud-Godquin, J.-C. Marchon, H. Abied, H. Dexpert, A. Skoulios, *J. Chim. Phys. Phys. Chim. Biol.* **1989**, *86*, 1651.
[51] P. Eisenberger, B. M. Kincaid, *Chem. Phys. Lett.* **1975**, *24*, 133.
[52] D. R. Sandstrom, W. H. Dodgen, F. W. Lytle, *J. Chem. Phys.* **1977**, *67*, 473.
[53] D. R. Sandstrom, B. R. Stults, R. B. Greegor in *EXAFS Spectroscopy: Techniques and Applications* (Eds.: B. K. Teo, D. C. Joy), Plenum, New York, **1981**, p. 139.
[54] H. Bertagnolli, T. S. Ertel, M. Hoffmann, R. Frahm, *Ber. Bunsenges. Phys. Chem.* **1991**, *95*, 704.
[55] B. Beagley, C. A. McAuliffe, S. P. B. Smith, E. W. White, *J. Phys. Condens. Matter* **1991**, *3*, 7919.
[56] D. R. Sandstrom, *J. Chem. Phys.* **1979**, *71*, 2381.
[57] P. Lagarde, A. Fontaine, D. Raoux, A. Sadoc, P. Migliardo, *J. Chem. Phys.* **1980**, *72*, 3061.
[58] A. Fontaine, P. Lagarde, D. Raoux, M. P. Fontana, G. Maisano, P. Migliardo, F. Wanderlingh, *Phys. Rev. Lett.* **1978**, *41*, 504.
[59] J. M. Fine, Ph. D. Thesis, Washington State University, **1981**.
[60] G. Galli, S. Magazu, D. Majolino, P. Migliardo, M. C. Billissent-Funel, F. Aliotta, C. Vasi, *Nouvo Cimento Soc. Ital. Fis. D* **1990**, *12*, 197.
[61] A. Sadoc, P. Lagarde, G. Vlaic, *J. Phys. C* **1985**, *18*, 23.
[62] A. Corrias, A. Musinu, G. Pinna, *Chem. Phys. Lett.* **1985**, *120*, 295.
[63] I. Persson, M. Sandstroem, A. T. Steel, M. J. Zapatero, R. Aadesson, *Inorg. Chem.* **1991**, *30*, 4075.
[64] K. Ozutsumi, T. Kawashima, *Polyhedron* **1992**, *11*, 169.
[65] T. Yamaguchi, H. Wakita, M. Nomura, *J. Chem. Soc. Chem. Commun.* **1988**, 433.
[66] A. Dejean, P. Charpin, G. Folcher, P. Rigny, A. Navaza, G. Tsoucaris, *Polyhedron* **1987**, *6*, 189.
[67] T. S. Ertel, H. Bertagnolli, S. Hückmann, U. Kolb, D. Peter, *Appl. Spectrosc.* **1992**, *46*, 690.
[68] T. S. Ertel, H. Bertagnolli, *GIT Fachz. Lab.* **1992**, *9*, 901.
[69] E. C. Ashby, *Quart. Rev.* **1967**, *21*, 259.
[70] A. J. Dent, K. R. Seddon, T. Welton, *J. Chem. Soc. Chem. Commun.* **1990**, 315.
[71] E. D. Crozier, A. J. Seary, *Can. J. Phys.* **1980**, *58*, 1388.
[72] J. P. Badiali, L. Bosio, R. Cortes, P. Bondot, G. Loupias, J. Petiau, *J. Phys. Colloq.* **1980**, *C8*, 211.
[73] B. R. Orton, G. K. Malra, A. T. Steel, *J. Phys. F Met. Phys.* **1987**, *17*, L45.
[74] K. Tamura, M. Inui, M. Yao, H. Endo, S. Hosokawa, H. Hoshino, Y. Katayamam, K. Maruyama, *J. Phys. Condens. Matter* **1991**, *3*, 7495.
[75] J. Wong, F. W. Lytle, *J. Non Cryst. Solids* **1980**, *37*, 273.
[76] L. V. Woodstock, C. A. Angell, P. Cheeseman, *J. Chem. Phys.* **1976**, *65*, 1565.
[77] M. Imaoka, Y. Konagaya, H. Hasegawa, *Yogyo Kyokaishi* **1971**, *79*, 97.
[78] J. F. Jal, J. Dupuy, A. Sadoc, *J. Phys. Colloq.* **1985**, *C9* (1), 107.
[79] B. X. Yang, J. Kirz, *Phys. Rev. B* **1987**, *36*, 1361.
[80] E. Kalman, G. Palinkas, P. Kovacs, *Mol. Phys.* **1977**, *34*, 505.
[81] E. Kalman, G. Palinkas, P. Kovacs, *Mol. Phys.* **1977**, *34*, 525.
[82] H. Bertagnolli, T. Engelhardt, B. Lengeler, *Ber. Bunsenges. Phys. Chem.* **1987**, *91*, 1287.
[83] J. C. J. Bart, G. Vlaic, *Adv. Catal.* **1985**, *34*.
[84] F. W. Lytle, G. H. Via, J. H. Sinfelt in *Synchrotron Radiation Research* (Eds.: H. Winik, S. Doinach), Plenum, New York, **1980**, p. 401.
[85] P. A. Lee, P. H. Citrin, P. Eisenberger, B. M. Kincaid, *Rev. Mod. Phys.* **1981**, *53*, 769.
[86] *J. Phys. Colloq.* **1986**, *C8* (1), 219–343 (Proceedings of 4th International Conference on EXAFS and Near Edge Structure).
[87] *Physica B (Amsterdam)* **1988**, *158*, 135–215 (Proceedings of Fifth International Conference on X-Ray Absorption Fine Structure, Seattle).
[88] *X-Ray Absorption Fine Structure* (Ed.: S. S. Hasnain), Ellis Horwood, New York, **1991**, pp. 445–566.
[89] J. M. White, *Science* **1982**, *218*, 429.
[90] J. Haase, *Chem. Unserer Zeit* **1992**, *26*, 219.
[91] J. H. Sinfelt, *Prog. Solid State Chem.* **1975**, *10*, 75.
[92] J. H. Sinfelt, *Science* **1977**, *195*, 641.
[93] G. H. Via, J. H. Sinfelt, F. W. Lytle, *J. Chem. Phys.* **1979**, *71*, 690.
[94] R. B. Greegor, F. W. Lytle, *J. Catal.* **1980**, *63*, 476.
[95] J. H. Sinfelt, G. H. Via, F. W. Lytle, *J. Chem. Phys.* **1978**, *68*, 2009.
[96] E. Lesage-Rosenberg, G. Vlaic, H. Dexpert, P. Lagarde, E. Freund, *Appl. Catal.* **1986**, *22*, 211.
[97] G. Sankar, S. Vasudevan, C. N. R. Rao, *J. Chem. Phys.* **1986**, *85*, 2291.
[98] D. C. Koningsberger, F. B. M. Duivenvoorden, B. J. Kip, D. E. Sayers, *J. Phys. Colloq.* **1986**, *C8* (1), 255.
[99] P. Lagarde, T. Murata, G. Vlaic, E. Freund, H. Dexpert, J. P. Bournonville, *J. Catal.* **1983**, *84*, 333.
[100] D. Bazin, H. Dexpert, P. Lagarde, J. P. Bournonville, *J. Catal.* **1986**, *110*, 209.
[101] D. Bazin, H. Dexpert, P. Lagarde, *Top. Curr. Chem.* **1988**, *145*, 69.
[102] M. Ichikawa, L.-F. Rao, T. Kimura, A. Fukuoka, *J. Mol. Catal.* **1990**, *62*, 15.
[103] T. M. Salama, T. Tanaka, T. Yamaguchi, K. Tanabe, *Surf. Sci.* **1990**, *227*, L100.
[104] E. Dartyge, A. Fontaine, A Jucha, D. E. Sayers in *EXAFS and Near Edge Structure III* (*Springer Proc. Phys.* **1984**, *2*, 472).
[105] D. E. Sayers, D. Bazin, H. Dexpert, A. Jucha, E. Dartyge, A. Fontaine, P. Lagarde in *EXAFS and Near Edge Structure III* (*Springer Proc. Phys.* **1984**, *2*, 209).
[106] G. Maire, F. Garin, P. Bernhardt, P. Girard, J. L. Schmitt, E. Dartyge, H. Dexpert, A. Fontaine, A. Jucha, P. Lagarde, *Appl. Catal.* **1986**, *26*, 305.
[107] J. Evans, J. T. Gauntlett, H. Leach, *J. Phys. Colloq.* **1986**, *C8* (1), 327.
[108] J. M. Corker, J. Evans, *J. Chem. Soc. Chem. Commun.* **1991**, *16*, 1104.
[109] T. Yamamoto, M. Takamatsu, A. Yamamoto, *Bull. Chem. Soc. Jpn.* **1982**, *55*, 325.
[110] F. A. Cotton, B. A. Frenz, D. L. Hunter, *J. Am. Chem. Soc.* **1974**, *96*, 4820.
[111] J. Goulon, E. Georges, C. Goulon-Ginet, Y. Chauvin, D. Commereuc, H. Dexpert, E. Freund, *Chem. Phys.* **1984**, *83*, 357.
[112] C. Esselin, E. Bauer-Grosse, J. Goulon, C. Williams, Y. Chauvin, D. Commereuc, E. Freund, *J. Phys. Colloq.* **1986**, *C8* (1), 243.
[113] B. R. Stults, R. M. Friedman, K. Koenig, W. S. Knowles, R. B. Greegor, F. W. Lytle, *J. Am. Chem. Soc.* **1981**, *103*, 3235.
[114] W. S. Knowles, B. D. Vineyard, M. J. Sabacky, B. R. Stults, *Fundam. Res. Homogeneous Catal.* **1979**, *3*, 537.
[115] B. R. Stults, *EXAFS and Single Crystal Studies of Asymetric Homogeneous Catalysis*, Am. Soc. Chem. Jpn. Chem. Congr., Honolulu, **1979**.
[116] A. S. C. Chan, J. J. Pluth, J. Halpern, *Inorg. Chim. Acta* **1979**, *37*, 477.
[117] G. Vlaic, J. C. J. Bart, M. Foa, F. Francalanci, R. Clement, *J. Organomet. Chem.* **1985**, *287*, 369.
[118] B. Kok, B. Forbush, M. McGloin, *Photochem. Photobiol.* **1970**, *11*, 457.
[119] J. A. Kirby, A. S. Robertson, J. P. Smith, A. C. Thompson, S. R. Cooper, M. P. Klein, *J. Am. Chem. Soc.* **1981**, *103*, 5529.
[120] J. A. Kirby, D. Goodin, T. Wydrynski, A. S. Robertson, M. P. Klein, *J. Am. Chem. Soc.* **1981**, *103*, 5537.
[121] D. Goodin, V. K. Yachandra, R. D. Britt, K. Sauer, M. P. Klein, *Biochim. Biophys. Acta* **1984**, *767*, 209.
[122] J. Cole, V. K. Yachandra, R. D. Guiles, A. E. McDermott, R. D. Britt, S. L. Dexheimer, K. Sauer, M. P. Klein, *Biochim. Biophys. Acta* **1987**, *890*, 395.
[123] V. K. Yachandra, R. D. Guiles, A. McDermott, R. D. Britt, S. L. Dexheimer, K. Sauer, M. P. Klein, *Biochim. Biophys. Acta* **1986**, *850*, 324.
[124] J. L. Cole, V. K. Yachandra, A. E. McDermott, R. D. Guiles, R. D. Britt, S. L. Dexheimer, K. Sauer, M. P. Klein, *Biochemistry* **1987**, *26*, 5967.
[125] V. K. Yachandra, R. D. Guiles, A. McDermott, J. L. Cole, R. D. Britt, S. L. Dexheimer, K. Sauer, M. P. Klein, *Biochemistry* **1987**, *26*, 5974.
[126] V. K. Yachandra, R. D. Guiles, A. McDermott, R. D. Britt, J. Cole, S. L. Dexheimer, K. Sauer, M. P. Klein, *J. Phys. Colloq.* **1986**, *C8* (1), 1121.
[127] A. E. McDermott, V. K. Yachandra, R. D. Guiles, J. L. Cole, S. L. Dexheimer, R. D. Britt, K. Sauer, M. P. Klein, *Biochemistry* **1988**, *27*, 4021.
[128] G. C. Dismukes, D. Ferris, P. Watnick, *Photochem. Photobiophys.* **1982**, *3*, 243.
[129] L. E. Andreasson, O. Hansson, T. Vanngard, *Chem. Scr.* **1983**, *21*, 71.
[130] S. Theg, P. Jursinic, P. H. Homann, *Biochim. Biophys. Acta* **1984**, *766*, 636.
[131] S. Itoh, C. T. Yerkes, H. Koike, H. H. Robinson, A. R. Crofts, *Biochim. Biophys. Acta* **1984**, *766*, 612.
[132] J. E. Penner-Hahn, R. M. Fronko, V. L. Pecoraro, C. F. Yocum, S. D. Betts, N. R. Bowlby, *J. Am. Chem. Soc.* **1990**, *112*, 2549.
[133] E. W. Ainscough, A. G. Bingham, A. M. Brodie, W. R. Ellis, H. B. Gray,

T. M. Loehr, J. E. Plowman, G. E. Norris, E. N. Baker, *Biochemistry* **1987**, *26*, 71.
[134] T. D. Tullius, P. Frank, K. O. Hodgson, *Proc. Natl. Acad. Sci. USA* **1978**, *75*, 4069.
[135] S. D. Holt, B. Piggott, W. J. Ingledew, M. C. Feiters, G. P. Diakun, *FEBS Lett.* **1990**, *269*, 117.
[136] M. C. Feiters, S. Dahlin, B. Reinhammar, *Biochim. Biophys. Acta* **1988**, *955*, 250.
[137] C. M. Groeneveld, M. C. Feiters, S. S. Hasnain, J. Van Rijn, J. Reedijk, G. W. Canters, *Biochim. Biophys. Acta* **1986**, *873*, 214.
[138] S. K. Chapman, W. H. Orme-Johnson, J. McGinnis, J. D. Sinclair-Day, A. G. Sykes, P. I. Ohlsson, K. G. Paul, *J. Chem. Soc. Dalton Trans.* **1986**, 2063.
[139] A. Lommen, K. I. Pandya, D. C. Koningsberger, G. W. Canters, *Biochim. Biophys. Acta* **1991**, *1076*, 439.
[140] R. A. Scott, J. E. Hahn, S. Doniach, H. C. Freeman, K. O. Hodgson, *J. Am. Chem. Soc.* **1982**, *104*, 5364.
[141] P. M. Colman, H. C. Freemau, J. M. Guss, M. Murata, V. A. Norris, R. A. M. Ramshaw, M. P. Venkatappa, *Nature* **1978**, *272*, 319.
[142] J. A. Tainer, E. D. Getzoff, J. S. Richardson, D. C. Richardson, *Nature* **1983**, *306*, 284.
[143] N. J. Blackburn, S. S. Hasnain, N. Binsted, G. P. Diakun, C. D. Garner, P. F. Knowles, *Biochem. J.* **1984**, *219*, 985.
[144] N. J. Blackburn, S. S. Hasnain, G. P. Diakun, P. F. Knowles, N. Binsted, C. D. Garner, *Biochem. J.* **1983**, *213*, 756.
[145] N. J. Blackburn, R. W. Strange, L. M. McFadden, S. S. Hasnain, *J. Am. Chem. Soc.* **1987**, *109*, 7162.
[146] B. Malmstrom in *Metal Ion Activation of Dioxygen* (Ed.: T. G. Spiro), Wiley-Interscience, New York, **1980**, pp. 181–207.
[147] J. Gelles, S. I. Chan, *Biochemistry* **1985**, *24*, 3963.
[148] L. Powers, W. E. Blumberg, B. Chance, C. H. Barlow, J. S. Leigh, J. Smith, T. Yonetani, S. Vik, J. Peisach, *Biochim. Biophys. Acta* **1979**, *546*, 520.
[149] V. W. Hu, S. I. Chan, G. S. Brown, *Proc. Natl. Acad. Sci. USA* **1977**, *74*, 3821.
[150] R. A. Scott, S. P. Cramer, R. W. Shaw, H. Beinert, H. B. Gray, *Proc. Natl. Acad. Sci. USA* **1981**, *78*, 664.
[151] L. Powers, B. Chance, Y. Ching, P. Angiolillo, *Biophys. J.* **1983**, *344*, 465.
[152] B. Chance, C. Kumar, L. Powers, Y. Ching, *Biophys. J.* **1983**, *44*, 353.
[153] R. A. Scott, J. R. Schwartz, S. P. Cramer, *Biochemistry* **1986**, *25*, 5546.
[154] R. A. Scott, J. R. Schwartz, S. P. Cramer, *J. Inorg. Biochem.* **1985**, *23*, 199.
[155] A. Naqui, C. Kumar, Y. Ching, L. Powers, B. Chance, *Biochemistry* **1984**, *23*, 6222.
[156] P. M. Li, J. Gelles, S. I. Chan, R. J. Sullivan, R. A. Scott, *Biochemistry* **1987**, *26*, 2091.
[157] I. Ascone, J. Goulon, A. Bianconi, M. Tegoni, F. Labeyrie, *J. Phys. Colloq.* **1986**, *C8*, 1143.
[158] J. H. Dawson, L. Kau, J. E. Penner-Hahn, M. Sono, K. M. Eble, G. S. Bruce, L. P. Hager, K. O. Hodgson, *J. Am. Chem. Soc.* **1986**, *108*, 8114

How do they fit so much in?



Keep up with the latest developments in all areas of chemistry.
Order your own personal subscription.

Just fax

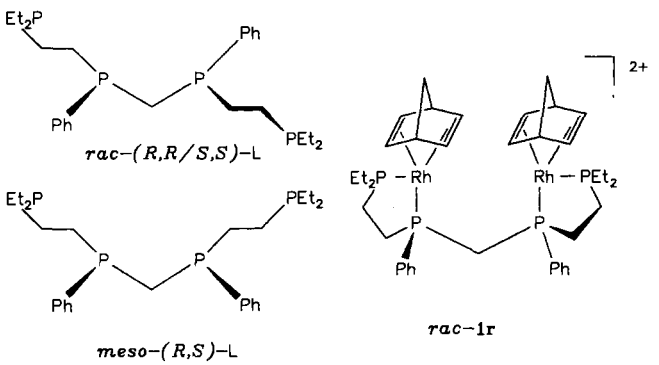
USA	Fax: (3 05)	428-82 01
UK	Fax: (02 23)	31 32 21
Japan	Fax: (03)	38 16 37 58
Rest of world	Fax: (0 11 49)	62 01-606-184

VCH

Cooperativity in Rh_2 Complexes: High Catalytic Activity and High Regioselectivity in the Hydroformylation of Olefins

Georg Süss-Fink*

An important step forward in the search for catalytically active polynuclear metal complexes has been made by George G. Stanley's group: The bimetallic complex cations *rac*-$[Rh_2(nbd)_2L]^{2+}$ **1r** and *meso*-$[Rh_2(nbd)_2L]^{2+}$ **1m** (nbd = norbornadiene) which were isolated as tetrafluoroborates (Scheme 1),[1] were obtained by reacting bis(norbornadiene)rhodium tetrafluoroborate with a new tetraphosphane ligand L which exists in *R,R*, *S,S* and *R,S* forms and can be separated into racemic (*R,R*/*S,S*) and *meso* structures (*R,S*).[2]



Scheme 1. The tetraphosphane ligand L and the hydroformylation-active dirhodium complex **1r**.

The racemic complex **1r**, whose structure was determined by single-crystal X-ray crystallography, is an excellent hydroformylation catalyst for olefins such as propylene, 1-hexene, and 1-octene, combining high activity with high regioselectivity. Up to 12000 catalytic cycles (10 cycles per minute) were achieved in a single batch run without observing any decomposition of the catalyst. The conversion of alkene to aldehyde for the hydroformylation of 1-hexene was 85%, and the *n*/*i* ratio was 96.5 : 3.5.[1] The combination of high activity and high selectivity can be explained by cooperativity between both metal centers in the catalytically active bimetallic complex.

The hydroformylation of olefins is the world's most important homogeneous catalytic industrial process with more than six million tonnes of oxo products produced each year.[3] Besides the problem of chemical selectivity, the hydroformylation of higher olefins raises the question of regioselectivity depending on whether the formyl group is added to the terminal or to the inner carbon atom of the double bond. This results in a ratio of linear to branched product (*n*/*i* ratio of the aldehyde formed) [Eq. (a) and (b)]. The industrial processes are all based on monometallic cobalt or rhodium complexes.

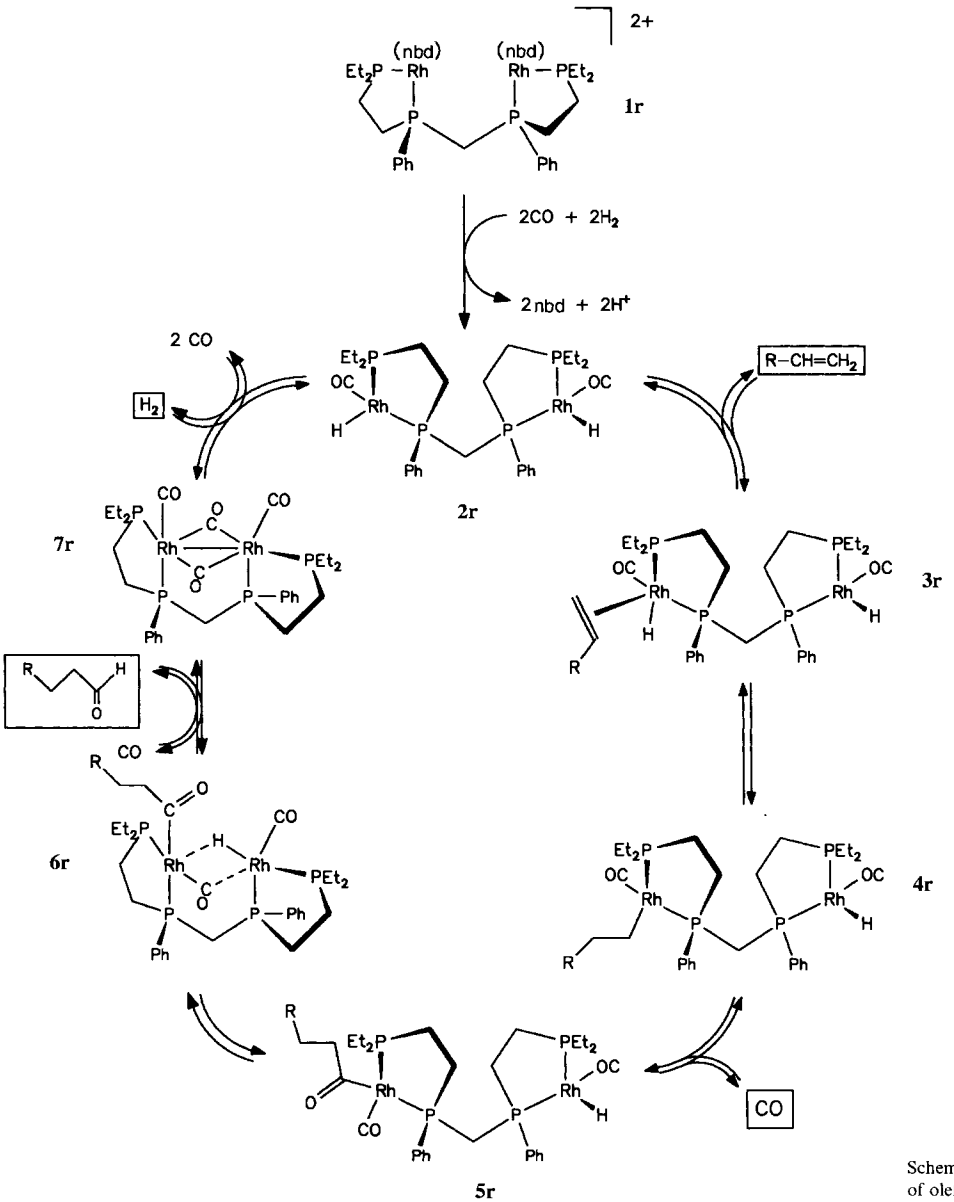
$$R\text{-}CH{=}CH_2 + CO + H_2 \longrightarrow \begin{cases} R\text{-}CH_2CH_2\text{-}CHO \quad \textit{n}\text{-aldehyde} & \text{(a)} \\ R\text{-}CH(CHO)\text{-}CH_3 \quad \textit{i}\text{-aldehyde} & \text{(b)} \end{cases}$$

Ever since transition metal clusters have been discussed as catalysts,[4] there have been many attempts to develop polynuclear catalytically active complexes in which the metal centers interact during formation of the target molecule ("cooperativity") to control activity and selectivity. In this way, a highly selective hydroformylation catalyst for propylene was found in the cluster anion $[HRu_3(CO)_{11}]^-$ (linear to branched product ratio of butyraldehyde 98.6 : 1.4), however, its activity is very low with only 57 catalytic cycles in 66 h.[5] The high selectivity and low activity suggest that the catalytic process occurs via a sterically demanding, intact trimetallic structure, for which there is experimental evidence.[6] In contrast to $[HRu_3(CO)_{11}]^-$, the tetrametallic neutral cluster $[Rh_4(CO)_{12}]$ yields high catalytic conversions (84000 cycles) for hydroformylation of 1-hexene, however, the selectivity is unfavorable (*n*/*i* 54: 46).[7] Accordingly, evidence for a catalytic route via monometallic rhodium complex fragments was found.[8] The catalyst **1r** described by Stanley et al. is the only polynuclear metal complex as yet which compares favorably with the hydroformylation catalysts used industrially.

The combination of high catalytic activity and high regioselectivity results from the interaction of the two rhodium centers of **1r** during the hydroformylation cycle (Scheme 2). Under synthesis gas pressure, the complex cation **1r** used as a catalyst precursor is converted into the neutral complex **2r** which is regarded as the active species. Norbornadiene and protons are eliminated in the process. The coordinately unsaturated species **2r** (both Rh atoms have 16 valence electrons) reacts on addition of an olefin to give **3r**, and by insertion of the olefin ligand in the Rh–H bond forms **4r**. The alkyl complex **4r** is converted into

[*] Prof. Dr. G. Süss-Fink
Institut de Chemie, Université de Neuchâtel
Avenue de Bellevaux 51, CH-2000 Neuchâtel (Switzerland)
Telefax: Int. code + (38) 214081

 © VCH Verlagsgesellschaft mbH, D-69451 Weinheim, 1994 0570-0833/94/0101-0067 $ 10.00+.25/0

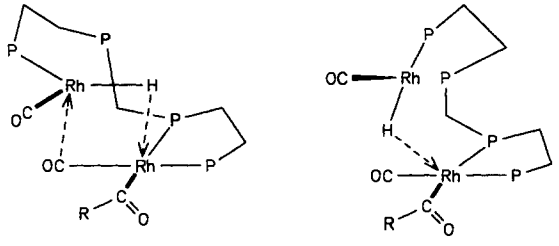


Scheme 2. Proposed catalytic cycle of hydroformylation of olefins with **1r** as catalyst precursor.

the corresponding acyl complex **5r** by incorporation of CO. In what is generally believed to be the rate-determining step, **5r** rearranges into **6r** in which a hydrido and a carbonyl ligand are arranged semi-bridging between the two rhodium atoms. The doubly carbonyl-bridged complex **7r** forms on aldehyde elimination. This is reconverted with hydrogen into the active species **2r** with elimination of carbon monoxide, thus, completing the cycle.

The key step in the catalysis cycle proposed by Stanley et al. is the transfer of the hydrido ligand from one rhodium atom to the other in the bimetallic complex **6r**, in which the interaction of both metal centers is the greatest ("cooperativity") (Scheme 3). The most important evidence for this hypothesis is the observation that if the bimetallic complex **2m** (meso form), a diastereomer of **2r**, is used as the catalyst precursor, the activity and selectivity drop drastically. The meso form **6m** can only form a singly bridged species on hydride transfer because the terminal CO group is unfavorably oriented at the acyl-bound Rh atom. It is assumed that the interaction of the Rh centers across the carbonyl bridge in **6r** favors intramolecular hydride transfer. This assumption was confirmed by SYBYL molecular modeling investigations (molecular dynamics minimizations).

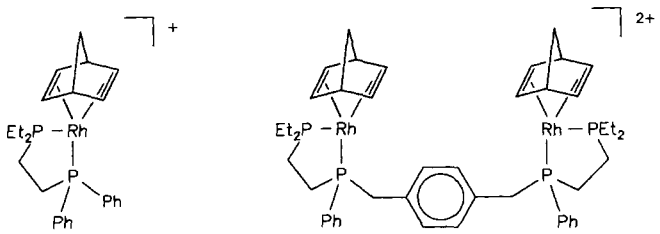
Stanley et al. have attempted to verify the hypothesis of intramolecular hydride transfer in the bimetallic hydroformyla-



Scheme 3. Intramolecular hydride transfer in complexes **6r** (left) and **6m** (right). The complexes are shown without the aldehyde ligands.

 © VCH Verlagsgesellschaft mbH, D-69451 Weinheim, 1994 0570-0833/94/0101-0068 $ 10.00+.25/0

tion catalyst through a well-designed systematic investigation. For this, the monometallic complex **8** ("half" complex) and the bimetallic complex **9** ("spacer" complex), both of which are analogous to **1r**, as well as other similar complexes were synthesized. All these model complexes either do not catalyze the hydroformylation or catalyze the hydroformylation with only very low activity and selectivity. Complexes **8** and **9** are comparable



8 **9**

to **1r** both electronically and sterically; however, an intramolecular hydride transfer is not possible either in the monometallic complex **8** or in the bimetallic complex **9**, in which both the Rh atoms are kept further apart by phenylene spacers, which explains the difference in catalytic characteristics compared to **1r**. Finally, the isolation and characterization of the bimetallic complex **7r** (postulated in the catalytic cycle) from the reaction of **1r** with CO and H_2, suggestive of a sensitive equilibrium between **2r** and **7r**, adds additional support to the mechanism proposed by Stanley et al.

The results of Stanley et al. indicate that a breakthrough in the development of tailor-made homogeneous catalysts may be expected. It now seems possible to fix two or more cooperating metal centers in the geometry required for a particular catalytic process with the aid of a suitable ligand matrix, with the aim of controlling selectivity and activity of the catalyst.

German version: *Angew. Chem.* **1994**, *106*, 71

[1] M. E. Broussard, B. Juma, S. G. Train, W.-J. Peng, S. A. Laneman, G. G. Stanley, *Science* **1993**, *260*, 1784.
[2] S. A. Laneman, F. R. Fronczek, G. G. Stanley, *J. Am. Chem. Soc.* **1988**, *110*, 5585.
[3] K. Weissermel, H.-J. Arpe, *Chimie organique industrielle*, 1st edition, Masson, Paris, **1981**, p. 113; *Industrielle Organische Chemie*, 2nd edition, Verlag Chemie, Weinheim, **1978**, p. 120.
[4] B. F. G. Johnson, J. Lewis, *Pure Appl. Chem.* **1975**, *44*, 43; E. L. Muetterties, *Bull. Soc. Chim. Belg.* **1975**, *84*, 959; *Science* **1977**, *196*, 839.
[5] G. Süss-Fink, G. F. Schmidt, *J. Mol. Chem.* **1987**, *42*, 361.
[6] G. Süss-Fink, G. Herrmann, *J. Chem. Soc. Chem. Commun.* **1985**, 735.
[7] R. Lazzaroni, P. Pertici, S. Bertozzi, G. Fabrizi, *J. Mol. Catal.* **1990**, *58*, 75.
[8] C. Fyhr, M. Garland, *Organometallics* **1993**, *12*, 1753.

Oxidation of Weakly Activated C–H Bonds**

Oliver Reiser*

The selective oxidation of alkanes remains a challenge in organic synthesis. The development of economical processes for the functionalization of hydrocarbons is of tremendous technical importance. In nature such reactions are mediated efficiently by various enzymes. The systems related to cytochrome P-450, which for example detoxify lipid-soluble compounds in the human liver,[1] have received the most attention.

The fundamental problem in the functionalization of saturated hydrocarbons is that their components, carbon and hydrogen, do not have lone electron pairs, and the molecules do not have orbitals of sufficient energy that are easily accessible. Thus, very reactive reagents and/or extreme reaction conditions are typically required, for example for the oxidation of alkanes. However, the initial products are almost always more reactive than the starting compounds, and undesired side reactions may occur.

Other complications arise if the molecule to be oxidized contains different types of C–H bonds. Since formation of tertiary radicals and carbenium ions is favored and they are also more stable than their secondary and primary analogues, functionalization processes that proceed via these intermediates generally have the selectivity for C atoms in the order tertiary > secondary > primary. For steric reasons, however, the attack of bulky reagents at primary C atoms may be preferred; the best example here is the oxidative addition of transition metal complexes.

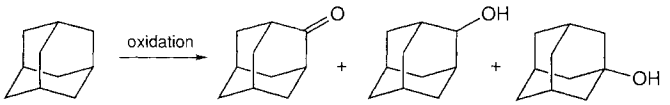
The metal-mediated oxyfunctionalization of organic compounds, of olefins in particular, is becoming increasingly important.[2] Research on metal catalysts that activate elemental oxygen and make it usable as a selective oxidizing agent is therefore especially worthwhile. Inspired by the enzyme cytochrome P-450, in which the active center is an oxoiron(IV) unit, researchers have examined numerous iron-containing reagents for the oxidation of alkanes. For example, the so-called Gif systems[3]

[*] Dr. O. Reiser
Institut für Organische Chemie der Universität
Tammannstrasse 2, D-37077 Göttingen (FRG)
Telefax: Int. code (551)39-9475

[**] This work was supported by the Deutsche Forschungsgemeinschaft (Habilitation fellowship).

 © VCH Verlagsgesellschaft mbH, D-69451 Weinheim, 1994 0570-0833/94/0101-0069 $ 10.00+.25/0

developed by Barton et al., which consist essentially of air, catalytic amounts of iron and/or zinc, acetic acid (HOAc), pyridine (py), and water, oxidize adamantane (**1**) to give adamantanone (**2**) as the major product along with 2- (**3**) and 1-adamantanol (**4**) as side products.



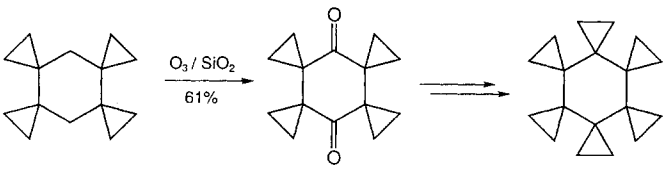
1 **2** **3** **4**

The oxidizing species are postulated to be $[Fe^{II}Fe^{III}_2O(OAc)_6(py)_{3.5}]$[4] and $C_5H_4NO^+$,[5] in keeping with the necessity of a nitrogen base component such as pyridine. Apparently these species attack C–H bonds on secondary C atoms in marked preference to those on primary and tertiary C atoms. Mechanistic studies suggest that the oxidation yielding ketones like **2** does not proceed via the corresponding alcohols **3** and **4**. Turnover rates of over 3000 and almost quantitative reactions have been achieved with several Gif reagents. One disadvantage is that the reactions can be conducted only up to 10–15% conversion to avoid considerable amounts of side products.

The allotropic form of oxygen, ozone, can also be employed for the oxidation of saturated hydrocarbons. The reactivity of ozone without additional reagents is not sufficient for the preparative functionalization of alkanes in solution; however, its reactivity is increased substantially by the addition of iron(III) chloride[6] or antimony pentafluoride.[7] The dry ozonation variant[8] of Mazur et al.,[9] by which alkanes are hydroxylated at tertiary C atoms with high selectivities and yields, was shown to be especially useful. According to this method, silica gel is coated with roughly 1 wt% of the substrate, cooled to −78 °C, saturated with ozone, and subsequently allowed to warm to room temperature within 0.5–2 h. Adamantane (**1**) is converted almost quantitatively into 1-adamantanol (**4**) in this way (Table 1), and this method of oxyfunctionalization has been applied successfully even on certain steroids.[10]

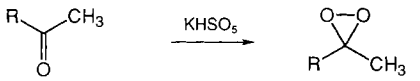
The selective oxidation of hydrocarbons by dry ozonation is not restricted to reaction at tertiary C atoms: the CH_2 groups adjacent to a cyclopropane ring are smoothly converted into carbonyl groups. This "cyclopropyl activation" can be explained by the well-known ability of the cyclopropyl group to effectively stabilize a neighboring R_3C^+ center. Although in the oxidation of alkanes with ozone the first intermediate, the hydrotrioxide,[11] does not arise from carbenium ions, the effect of polarity upon attack of the electronegative ozone molecule, either as a radical or by 1,3-dipolar addition, at the C–H bond certainly leads to development of a positive charge on the pertinent C atom.[11] Dry ozonation was the first efficient method for the α-functionalization of cyclopropylidene hydrocarbons and served as the key step in the first synthesis of [6]rotane (**7**) via the tetraspiro hydrocarbon **5**.[12]

The ketonation of cyclopropylidene hydrocarbons with ruthenium tetraoxide (generated in situ from $RuCl_3$ and $NaIO_4$ in CH_3CN/CCl_4/aqueous phosphate buffer)[13] proved to be more convenient and better suited for large-scale reactions. This oxidation of organic substrates originally developed by K. B. Sharpless et al.[14] for the oxidative cleavage of alkenes can also be applied for the selective hydroxylation of tertiary C–H groups;[13c,d] for example, adamantane (**1**) is converted into 1-adamantanol (**4**) in 75% yield.[13d]



5 **6** **7**

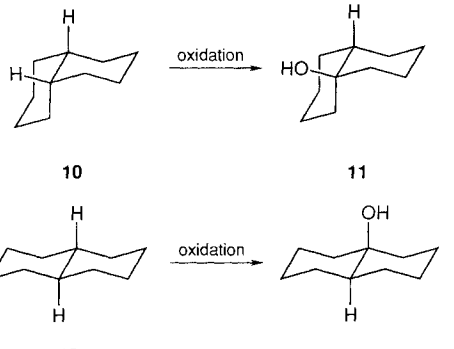
Since the development of a handy, even large-scale method for the generation of dimethyldioxirane (**9a**), it has become known best as a reagent for the epoxidation of double bonds.[15] Its application for the selective hydroxylation of C–H bonds at tertiary C atoms is less well known. For example, the reaction of **1** with **9a** as the oxidizing agent provides **4** with only minor amounts (<3%) of side products.[16] Oxidations with **9a** pro-



8a: R = CH_3 **9a**: R = CH_3

8b: R = CF_3 **9b**: R = CF_3

ceed stereoselectively with retention, as the reactions with *cis*-decalin (**10**) and *trans*-decalin (**12**) demonstrate. Remarkably, the oxidation of **10** is faster than that of **12**: after a reaction time of 17 h **11** had been formed in 84% yield, **13** in only 20%. This



10 **11**

12 **13**

indicates that the oxidation of equatorial positions is preferred to that of axial positions (Table 1).

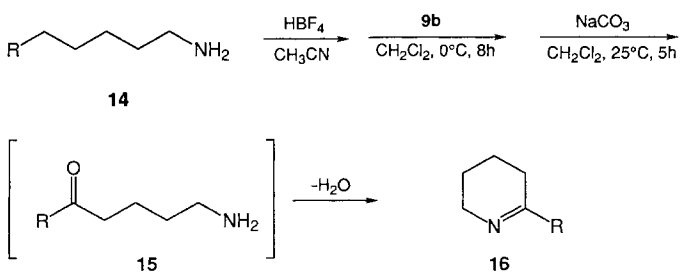
 © VCH Verlagsgesellschaft mbH, D-69451 Weinheim, 1994 0570-0833/94/0101-0070 $ 10.00+.25/0

An oxidizing agent up to 7000 times more reactive than **9a** is methyl(trifluoromethyl)dioxirane (**9b**), which not only hydroxylates tertiary C–H positions (Table 1) but also converts secondary C–H groups into carbonyl functions. As an illustration, the oxidation of cyclohexane at −22 °C afforded cyclohexanone in yields of over 98% in only 18 min.[17] With this reagent not only the monohydroxylation of adamantane (**1**) providing **4** proceeds in excellent yield, but also the two-, three-, and even four-fold hydroxylation of the bridgehead positions of adamantane.[18]

Table 1. Comparison of reagents for the oxidation of adamantane (**1**) and decalins **10** and **12**.

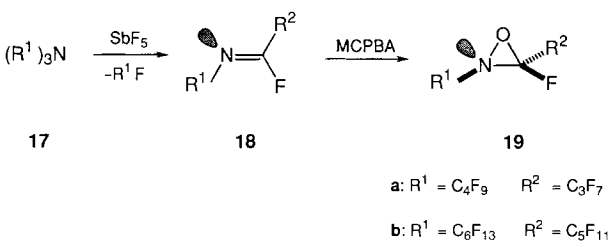
Substrate	Oxidation agent	Product	t [h]/ T [°C]	Yield [%]
1	O_3/SiO_2	**4**	0.5/−78 → 25	99
1	$RuCl_3/NaIO_4$	**4**	3–7/90	75
1	**9a**	**4**	18/22	87
1	**9b**	**4**	1 min/−22	92
1	$F_2/H_2O/CH_3CN$	**4**	−/0	80
1	**19a**	**4**	<1/25	90
1	**19b**	**4**	<1/25	90
10	O_3/SiO_2	**11**	0.5/−78 → 25	99
10	**9a**	**11**	17/22	84
10	**9b**	**11**	0.2/−22	91
10	**19a**	**11**	few/25	85
10	**19b**	**11**	few/25	88
12	O_3/SiO_2	**13**	0.5/−78 → 25	72
12	**9a**	**13**	17/22	20
12	**9b**	**13**	0.1/−22	61
12	**19a**	**13**	many/25	73

Remarkably, **9b** is stable towards acids like trifluoroacetic acid, trifluoromethanesulfonic acid, and sulfuric acid. Based on this observation, Asensio et al. employed **9b** for the oxidation of tertiary C–H positions in the presence of amino groups.[19] Their trick was protecting the amino group as an ammonium tetrafluoroborate by treatment with tetrafluoroboric acid. In the subsequent reaction with **9b**, the C–H bond at a tertiary C atom, which must be at least two C atoms removed from the ammonium group, is converted into a hydroxyl or acetamido function in excellent yield. C–H bonds on secondary C atoms in acyclic amines such as **14** (R = Me, Et, Pr) may also be oxidized in this way to afford the corresponding ketones **15**; the oxygen insertion takes place exclusively at the ε-methylene group. The authors explain the excellent selectivity by the coordination of **9b** to the ammonium group by hydrogen bonding.



Hydroxylation of C–H bonds on tertiary C atoms can be conducted with solutions of fluorine in aqueous acetonitrile.[20] This reagent appears particularly attractive for the synthesis of ^{18}O-labeled compounds; for example, [^{18}O]-1-adamantanol ([^{18}O]-**4**) is prepared in over 80% yield by using a solution of F_2 in acetonitrile and $H_2{}^{18}O$.

The newest reagents for the oxyfunctionalization of hydrocarbons are the di(perfluoroalkyl)oxaziridines **19**,[21] which can be synthesized from commercially available tri(perfluoroalkyl)amines **17** on a large scale[21b] in two steps. The reaction of **17** with antimony pentafluoride produces α-fluoroketimines **18**, which are then epoxidized with *m*-chloroperbenzoic acid (MCPBA) to give **19**. Compound **19** can be purified by vacuum



distillation and stored indefinitely at room temperature. Solutions of hydrocarbons such as **1**, **10**, and **12** in chloroform, carbon tetrachloride, or trichlorofluoromethane are readily monohydroxylated at their tertiary C atoms with only minimal amounts of side products. In addition to the high selectivity for tertiary C atoms over secondary, **19** shows a marked preference for the oxidation of equatorial over axial positions and a high stereospecificity for retention of configuration of the C atoms oxidized (Table 1). The authors propose the concerted O insertion into a C–H bond as the mechanism, since in the reaction of **19** with **1** in CCl_4 no chlorine-containing trapping products are formed from **1** via intermediate radicals, as is observed for the oxidation of **1** in CCl_4 with ozone.

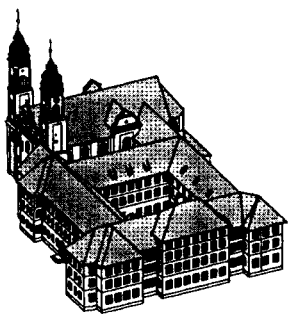
It remains to be seen if the range of application of this latest oxidizing agent for hydrocarbons will surpass that of the other reagents. Besides the selectivity of these reagents, their price, accessibility, and convenient and safe handling are important criteria for application. Based on price and efficiency, the $RuCl_3/NaIO_4$ system and the dioxiranes seem to be ahead of their more recent competitors.

German version: *Angew. Chem.* **1994**, *106*, 73

[1] H. L. Holland, *Organic Synthesis with Oxidative Enzymes*, VCH, New York, **1991**.
[2] See also J. Sundermeyer, *Angew. Chem.* **1993**, *105*, 1195–1197; *Angew. Chem. Int. Ed. Engl.* **1993**, *32*, 1144–1146, and references therein.
[3] D. H. R. Barton, E. Csuhai, N. Ozbalik, *Tetrahedron* **1990**, *46*, 3743–3752, and references therein.
[4] D. H. R. Barton, M. J. Gastiger, W. B. Motherwell, *J. Chem. Soc. Chem. Commun.* **1983**, 731–733.
[5] See R. H. Crabtree, A. Habib in *Comprehensive Organic Chemistry* (Eds.: S. Ley, B. M. Trost), Pergamon, Oxford, **1991**, p. 13ff.
[6] T. M. Hellman, G. A. Hamilton, *J. Am. Chem. Soc.* **1974**, *96*, 1530–1535.
[7] a) G. A. Olah, G. K. S. Prakash, J. Sommer, *Superacids*, Wiley, New York, **1985**, p. 315ff, and references therein; b) N. Yoneda, T. Kiuchi, T. Fukuhara, A. Suzuki, G. A. Olah, *Chem. Lett.* **1984**, 1617.

 © *VCH Verlagsgesellschaft mbH, D-69451 Weinheim, 1994* *0570-0833/94/0101-0071 $ 10.00+.25/0*

[8] Reviews: a) A. de Meijere, *Nachr. Chem. Tech. Lab.* **1979**, *27*, 177–182; b) E. Keinan, T. H. Varkony in *The Chemistry of Peroxides* (Eds.: S. Patai), Wiley, New York, **1983**, p. 649ff.
[9] Z. Cohen, E. Keinan, Y. Mazur, T. H. Varkony, *J. Org. Chem.* **1975**, *40*, 2141–2142.
[10] Z. Cohen, E. Keinan, Y. Mazur, A. Ulman, *J. Org. Chem.* **1976**, *41*, 2651–2652.
[11] a) M. Zarth, A. de Meijere, *Chem. Ber.* **1985**, *118*, 2429–2449; b) A. de Meijere, F. Wolf, *Methoden Org. Chem. (Houben-Weyl)* 4th ed., Vol. E13, **1988**, pp. 971–990, and references therein.
[12] a) E. Proksch, A. de Meijere, *Angew. Chem.* **1976**, *88*, 802–803; *Angew. Chem. Int. Ed. Engl.* **1976**, *15*, 761–762; b) *Tetrahedron Lett.* **1976**, 4851–4854.
[13] a) T. Hasegawa, H. Niwa, K. Yamada, *Chem. Lett.* **1985**, 1385–86, and references therein; b) B. Waegell, J.-L. Coudret, S. Zöllner, A. de Meijere, unpublished; J.-L. Coudret, planned dissertation, Universite d'Aix Marseille III; c) A. Tenaglia, E. Terranova, B. Waegell, *Tetrahedron Lett.* **1989**, *30*, 5271–5274; d) H. J. Carlsen, *Synth. Commun.* **1987**, *17*, 19–23.
[14] P. H. J. Carlsen, T. Katsuki, V. S. Martin, K. B. Sharpless, *J. Org. Chem.* **1981**, *46*, 3936–3938.
[15] a) W. Adam, L. P. Hadjiarapoglou, R. Curci, R. Mello in *Organic Peroxides* (Ed.: W. Ando), Wiley, New York, **1992**, pp. 195–219ff; b) R. Curcin in *Adv. Oxygenated Processes*, (Ed.: A. L. Baumstark), JAI, Greenwich, CT, USA, Vol. 2, **1990**, pp. 1–59.
[16] R. W. Murray, R. Jeyaraman, L. Mohon, *J. Am. Chem. Soc.* **1986**, *108*, 2470–2472.
[17] R. Mello, M. Fiorentino, C. Fusco, R. Curci, *J. Am. Chem. Soc.* **1989**, *111*, 6749–6757.
[18] R. Mello, L. Cassidei, M. Fiorentino, R. Curci, *Tetrahedron Lett.* **1990**, *31*, 3067–3070.
[19] G. Asensio, M. E. Gonzalez-Nunez, C. B. Bernadini, R. Mello, W. Adam, *J. Am. Chem. Soc.* **1993**, *115*, 7250–7253.
[20] S. Rozen, M. Brand, M. Kol, *J. Am. Chem. Soc.* **1989**, *111*, 8325–8326.
[21] a) D. D. Desmarteau, A. Donadelli, V. Montanari, V. A. Petrov, G. Resnati, *J. Am. Chem. Soc.* **1993**, *115*, 4897–4898; b) V. A. Petrov, D. D. DesMarteau, *J. Org. Chem.* **1993**, *58*, 4754–4755.



CMCD 4

Computational Methods in Chemical Design
Molecular Modeling: Theory and Experiment

Kloster Irsee, May 16 to 20, 1994

The symposium and FEBS course follow the previous three successful meetings on Molecular Modeling and Computer Graphics held in Elmau. The aim continues to bring together investigators interested in elucidating, at the molecular level, interrelationships between structure, physical, chemical and biological properties of molecular materials. "Computational Methods" is intended to be a connecting theme, drawing together various disciplines associated with structural chemistry, as for example: solid state and solution studies, theoretical methods and new developments in computer applications and computer graphics.

Topics: Bio-Crystallography; Protein Modeling; Molecular Recognition and Ligand-Receptor Interactions; Molecular Solid State Systems including Crystal Engineering, Intermolecular Interactions, and Solid State Reactions; Synchrotron Studies, Neutron Diffraction, and Solid State NMR; Polymer Modeling; New Concepts in Structural, Theoretical, and Computational Chemistry; Demonstrations of Hard- and Software.

Invited Speakers: Tore Brinck, Stephen Byrn, Zbigniew Dauter, Gautam Desiraju, Angelo Gavezzotti, Jenny P. Glusker, Andrew D. Hamilton, Gerard Harbison, Kenneth D. M. Harris, William L. Jorgensen, Gerhard Klebe, Jan Kroon, Loes Kroon-Batenburg, Leslie Leiserowitz, Arthur Lesk, Christine Orengo, James Pflugrath, Douglas Rohrer, Mark A. Spackman, John J. Stezowski, a. o.

For more information and the Second Circular please contact: Prof. Dr. Carl Krüger, Max-Planck-Institut für Kohlenforschung, Röntgenlabor, Postfach 10 13 53, D 45466 Mülheim an der Ruhr, Germany, Tel.: +49 - 208 - 3062175, FAX: +49 - 208 - 3062981, E-mail: <krueger@mpi-muelheim.mpg.d400.de>

Free-Energy Relationship for Mesolytic Cleavage of C–C Bonds**

Przemyslaw Maslak,* Thomas M. Vallombroso, William H. Chapman, Jr., and Javier N. Narvaez

A full understanding of an elementary reaction must include the functional dependence of the reaction rate (kinetics) on the driving force (thermodynamics), which should include all pertinent variables such as stereoelectronic factors and medium effects. Unimolecular dissociations of radical ions into radicals and ions (mesolytic scissions)[1] provide an opportunity to develop such a quantitative theory for a bond-breaking process. We present here the experimentally determined free-energy relationship for mesolytic cleavages of C–C bonds in π radical ions spanning a range of over 40 kcal mol^{-1} for the driving force and over 17 powers of ten for the rate constants. We show that these fragmentations have low intrinsic barriers if the stereoelectronic factors are optimal, and that a parabolic, Marcus-type free-energy relation may be fitted to the data.

The unpaired electron in the π radical ion resides in a π-type orbital localized on one bonding partner of the scissile bond. The fragmentation reaction is accompanied by the redistribution of electron density to the forming fragments according to one of the modes of electron apportionment[2] [Equations (a)–(d)]. As illustrated by the curved arrows, the processes described by Equations (a) and (c) formally correspond to homolysis; the alternatives (b) and (d) are equivalent to heterolysis.

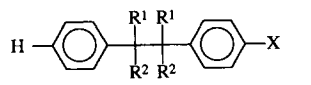
$$^{-\bullet}A\text{–}B \longrightarrow A^- + B^\bullet \quad \text{(a)}$$

$$^{-\bullet}A\text{–}B \longrightarrow A^\bullet + B^- \quad \text{(b)}$$

$$^{+\bullet}A\text{–}B \longrightarrow A^+ + B^\bullet \quad \text{(c)}$$

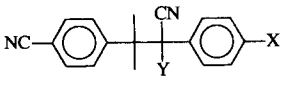
$$^{+\bullet}A\text{–}B \longrightarrow A^\bullet + B^+ \quad \text{(d)}$$

We have prepared[1, 3, 4] a series of directly observable radical ions of substrates containing two benzylic units (**1**–**5**) that undergo unimolecular C–C bond scissions according to Equations (a)–(d). The radical ions were designed to provide optimal overlap of the π system bearing the unpaired electron with the scissile C–C bond.[3–5] In all cases probed,[3, 4] the C–C bond cleavage reactions were irreversible under the reaction conditions, as was found in experiments with stereochemically pure *erythro*/*threo* or *meso*/*dl* radical ion precursors. The kinetic data (Table 1) for mesolysis were obtained[3, 4] in polar media to exclude aggregation and ion pairing, by ESR and UV/VIS spectroscopy, flash photolysis, pulse radiolysis, time-resolved fluorescence spectroscopy, and cyclic voltammetry (CV). The primary fragments observed corresponded to the thermodynamically predicted apportionment of electrons.[3, 4] In all cases, the isolated products were consistent with fragmentation of the central C–C bond.[3, 4]



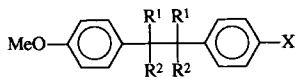
1: X = NO_2 **2**: X = NMe_2

a: $R^1 = R^2$ = Me
b: $R^1 = (CH_2)_5 = R^2$
c: R^1 = Me, R^2 = Et (*erythro*)
d: R^1 = Me, R^2 = Pr (*erythro*)
e: R^1 = Me, R^2 = *i*Bu (*erythro*)
f: $R^1 = R^2$ = Et
g: $R^1 = R^2$ = Bu
h: $R^1 = R^2$ = Pr



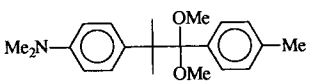
3

a: Y = Me, X = MeO
b: Y = Me, X = H
c: Y = Me, X = CF_3
d: Y = CN, X = MeO
e: Y = CN, X = H



4

a: $R^1 = R^2$ = Me, X = MeO
b: R^1 = Me, R^2 = Et, X = MeO (*meso*)
c: $R^1 = R^2$ = Et, X = MeO
d: $R^1 = R^2$ = Me, X = CN
e: $R^1 = R^2$ = Me, X = H



5

The evaluation of the thermodynamics of mesolytic processes was based on a simple thermodynamic cycle.[1, 6, 7] Regardless of the mode [(a)–(d)] of cleavage, the free energy of mesolysis ΔG_m is a function of the free energy of homolysis ΔG_h of the compound A–B and the difference in redox potentials of A–B and the ionic fragment produced ($\Delta G_m = \Delta G_h - 23.06\,\Delta E$, where $\Delta E = E^o_{AB} - E^o_{A^\bullet}$ (or $E^o_{B^\bullet}$) for cleavages of radical cations, and $\Delta E = E^r_{A^\bullet}$ (or $E^r_{B^\bullet}$) $- E^r_{AB}$ for cleavages of radical anions). The thermodynamic factors determine where the unpaired electron is initially localized[3, 4] (A or B), and which of the cleavage modes (homolytic or heterolytic) takes place.[3, 4]

In our systems ΔG_h has been approximated by experimentally accessible $\Delta G_h^{\ddagger}$. The approximation is valid ($\pm$ 3 kcal mol^{-1}) if the radical coupling has only a small activation barrier (that is, the reaction is diffusion-limited) and the thermolysis is carried out under conditions selected to minimize recombination within the solvent cage.[8] These conditions have been established for our compounds.[3, 4] The redox potentials of the radical ions and the ionic fragments have been determined by a technique[9] based on the curvature of the Marcus equations for electron transfer between the electrode and species of interest that gives results comparable to those obtained by other methods.[7]

The kinetic and thermodynamic data at 300 K (Table 1) were used to construct the free-energy relationships of Figure 1. The slope of the solid line corresponds to unity; that is, it depicts endergonic reactions with no kinetic "overhead". The overhead is defined here as the difference between $\Delta G_m^{\ddagger}$ and ΔG_m and represents the barrier to the reverse (exergonic) reaction (that is,

[*] Prof. Dr. P. Maslak, T. M. Vallombroso, Dr. W. H. Chapman, Jr., Dr. J. N. Narvaez
Department of Chemistry, The Pennsylvania State University
University Park, PA 16802 (USA)
Telefax: Int. code + (814)863-8403

[**] This research was supported by the National Science Foundation.

 © VCH Verlagsgesellschaft mbH, D-69451 Weinheim, 1994 0570-0833/94/0101-0073 $ 10.00+.25/0

Table 1. Kinetic and thermodynamic data for mesolysis of **1**–**5**.

Cmpd. [a]	lg (k_m) (300 K)	Method [b]	$\Delta G_h^{\neq}$ [kcal mol^{-1}] [c]	E^{τ}_{AB} [d] [V]	E^{0}_{AB} [d] [V]	$E^{\tau}_{A(B)}$ [d] [V]	$E^{0}_{A(B)}$ [d] [V]
1c	−7.4	ESR [e]	42.0	−1.098		−0.355	
1d	−7.0	ESR [e], UV [e]	40.3	−1.094		−0.382	
1e	−4.7	ESR [e], UV [e]	35.0	−1.083		−0.378	
1f	−3.2	ESR [e], UV [e], CV [e, f]	34.5	−1.080		−0.372	
1g	−2.5	ESR [e], CV [e]	32.0	−1.067		−0.384	
1h	−2.7	ESR [e]	31.5	−1.052		−0.374	
2a	−0.2	ESR [f, g, i], CV [f, g]	42.3		0.715		−0.460
2b	0.7	CV [f]	42.2		0.700		−0.501
2c	1.3	ESR [g], CV [f, g]	40.5		0.724		−0.460
2d	1.6	ESR [g], CV [g]	39.2		0.674		−0.453
2e	1.8	ESR [g], CV [f, g]	35.5		0.655		−0.420
2f	5.2	FP [g]	33.0		0.682		−0.411
2g	5.7	FP [g], CV [h]	31.6		0.613		−0.471
2h	5.6	FP [g], CV [h]	31.4		0.659		−0.434
3a	5.9	Q [f], PR [f, j], CV [l]	38.7	−2.177		−0.744	
3b	7.0	Q [f], PR [f, j]	39.7	−2.168		−0.596	
3c	8.6	Q [f], PR [f, j]	40.0	−2.105		−0.327	
3d	9.6	Q [f]	35.2	−1.836		0.223	
3e	≥10.5	Q [f]	33.8	−1.815		0.416	
4a	8.8	Q [g], TRF [k]	41.7		1.518		−0.091
4b	9.1	Q [g], TRF [k]	41.0		1.510		−0.094
4c	9.6	Q [g], TRF [k]	34.0		1.382		0.038
4d	6.4	Q [g], FP [i]	41.7		1.548		−0.091
4e	7.4	Q [g], TRF [k]	41.7		1.508		−0.091
5	0.2	CV [i]	44.1		0.772		−0.460

[a] Radical ion precursor. [b] Method for determination of kinetic parameters (the rates determined by different methods were in good agreement): ESR = activation parameters determined by ESR spectroscopy, UV = rate determined by UV/VIS spectroscopy at one temperature, CV = activation parameters determined by cyclic voltammetry (all solvents specified included 0.1 M tetramethylammonium perchlorate, tetrabutylammonium perchlorate or lithium perchlorate), FP = activation energies determined by flash photolysis, Q = rates determined by quantum yield quenching experiments at one temperature, PR = rates determined by pulse radiolysis at one temperature, TRF = rates determined by time-resolved fluorescence at one temperature. The solvents used are given in footnotes. [c] Free energy of activation for homolysis of the radical ion presursor determined in xylene or decalin in the presence of excess of thiophenol or 1,4-cyclohexadiene as radical traps (calculated at 300 K). [d] Redox potentials (versus SCE) established by the procedure of ref. [9]. [e] Me_2SO. [f] CH_3CN. [g] CH_2Cl_2/MeOH. [h] PrCN/EtBr. [i] CH_2Cl_2. [j] MeOH. [k] Et_2O. [l] NH_3(liq).

bond-forming coupling of radicals and ions). The examination of Figure 1 yields the following important conclusions: 1) The line through the experimental points in the endergonic region is apparently parallel to the no-overhead line, which implies that the kinetics of these processes closely follows their thermodynamics. 2) The overheads (the vertical separations between the experimental points and the solid line) are small (2–4 kcal mol^{-1}). These observations indicate that the large accelerations[10] of mesolytic bond scissions relative to the homolytic processes in A–B molecules have thermodynamic origins and that the energetic costs of reorganization to attain the transition state (TS) are low.

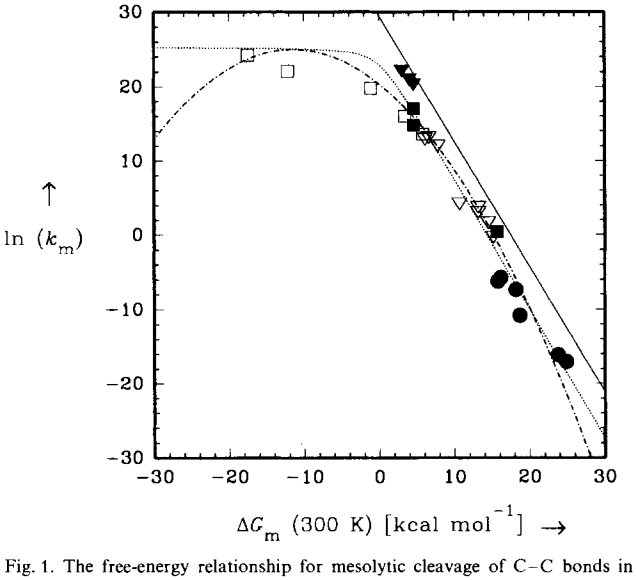


Fig. 1. The free-energy relationship for mesolytic cleavage of C–C bonds in π radical ions of **1c**–**h** (●), **2** (▽), **3** (□), **4a**–**c** (▼), **4d**, **e** and **5** (■). Kinetic measurements were carried out in Me_2SO ($\mathbf{1}^{\bullet-}$), CH_3CN ($\mathbf{3}^{\bullet-}$, $\mathbf{2}^{\bullet+}$), or CH_2Cl_2/MeOH ($\mathbf{2}^{\bullet+}$, $\mathbf{4}^{\bullet+}$, $\mathbf{5}^{\bullet+}$). Addition of electrolytes to these solutions had little effect on the observed rate constants k_m. The solid line represents a hypothetical reaction with no kinetic overhead ($k_m = (k_bT/h)\exp(-\Delta G_m/(RT))$, that is, one with only the thermodynamic barrier). The broken lines are the best fit lines for parabolic and hyperbolic (Weller-type)[11] functions.

A general parabolic and a hyperbolic (Weller-type)[11] equation (broken curves) were fitted to the experimental data. The expected shape of such a relation depends on the shape of the free-energy function. The obvious choices include linear (which is only an approximation), quadratic (Marcus type)[12] or hyperbolic (Weller type).[11] There are precedences for these possibilities in chemistry, and it has been shown that all three can be derived from a unified qualitative treatment based on the Hammond postulate and energy-surface crossing models.[13] The particularly appealing choice is the quadratic, one-parameter, Marcus-type equation (e),[12] in which $\Delta G_0^{\neq}$ is the intrinsic barrier that contains the relevant internal and solvent "reorganization" contributions to the activation energy.[12] It was originally derived for electron-transfer reactions. Recently, analogous models based on a Morse curve description of bond cleavage were developed for dissociative electron-transfer cases and for mesolytic reactions of radical ions.[14]

$$\Delta G_m^{\neq} = \Delta G_0^{\neq}[1 + \Delta G_m/(4\Delta G_0^{\neq})]^2 \quad \text{(e)}$$

Combining the Marcus expression with the Eyring equation ($\ln(k_m/T) = \ln(C) - \Delta G_m^{\neq}/(RT)$) yields Equation (f). The terms

$$\ln(k_m/T) = [\ln(C) - \Delta G_0^{\neq}/(RT)] - \Delta G_m/(2RT) - \Delta G_m^2/(16RT\Delta G_0^{\neq}) \quad \text{(f)}$$

 © VCH Verlagsgesellschaft mbH, D-69451 Weinheim, 1994 0570-0833/94/0101-0074 $ 10.00+.25/0 Angew. Chem. Int. Ed. Engl. 1994, 33, No. 1

in square brackets reflect a combination of stereoelectronic and statistical factors as well as the energetic costs associated with reorganization of the substrate and solvent to reach the transition state. The term linear in ΔG_m is independent of C and $\Delta G_o^{\ddagger}$. The intrinsic barrier in the quadratic term determines the width of the parabola and the location of the maximum (k_{max} at $\Delta G_m = -4\Delta G_o^{\ddagger}$). Importantly, the best fit, second-order polynomial shown in Figure 1 has the first-order coefficient of 0.81 mol kcal^{-1}, almost equal to that uniquely defined by Equation (f) [$(2RT)^{-1} = 0.84$ mol kcal^{-1}, at 300 K]. This implies that the data are described well by a unique one-parameter, Marcus-type free-energy relationship.

The fit of a parabolic function to the data in Figure 1 spanning a range of over 40 kcal mol^{-1} for the driving force confirms that the intrinsic barrier for mesolytic cleavages is low ($\Delta G_o^{\ddagger} \approx 3$ kcal mol^{-1}). In this treatment any errors in the determination of ΔG_m would shift the curve to the left or right, but the small deviations of the experimental data from a theoretical curve are possibly due to the fact that different modes of cleavage are included. The different modes are expected to differ in the extent of charge delocalization in the transition state and thus have different degrees of TS stabilization.[2-4] Closer scrutiny of this plot indicates that it may contain *four related* data sets corresponding, in order of decreasing intrinsic barriers, to homolytic radical anion cleavage [**1**; Equation (a)], homolytic radical cation cleavage [**2**, **4d** and **e**, **5**; Equation (c)], heterolytic radical anion cleavage [**3**; Equation (b)], and heterolytic radical cation cleavage [**4a** and **c**; Equation (b)]. We are currently testing this hypothesis and searching for the "inverted region" to confirm the parabolic shape of the free-energy relationship for mesolytic cleavage of single bonds.

Received: July 24, 1993 [Z 6232 IE]
German version: *Angew. Chem.* **1994**, *106*, 110

[1] P. Maslak, J. N. Narvaez, *Angew. Chem.* **1990**, *102*, 302; *Angew. Chem. Int. Ed. Engl.* **1990**, *29*, 283.
[2] P. Maslak, R. D. Guthrie, *J. Am. Chem. Soc.* **1986**, *108*, 2628, 2637.
[3] P. Maslak, S. L. Asel, *J. Am. Chem. Soc.* **1988**, *110*, 8260; P. Maslak, W. H. Chapman, Jr., *J. Chem. Soc., Chem. Commun.* **1989**, 1809; *Tetrahedron* **1990**, *46*, 2715; *J. Org. Chem.* **1990**, *55*, 6334; W. H. Chapman, Jr., Ph.D. Dissertation, The Pennsylvania State University, **1992**.
[4] P. Maslak, J. N. Narvaez, *J. Chem. Soc. Chem. Commun.* **1989**, 138; P. Maslak, J. N. Narvaez, J. Kula, D. Malinski, *J. Org. Chem.* **1990**, *55*, 4550; P. Maslak, J. Kula, J. N. Narvaez, *ibid.* **1990**, *55*, 2277; P. Maslak, J. Kula, *Mol. Cryst. Liq. Cryst.* **1991**, *194*, 293; P. Maslak, J. Kula, J. E. Chateauneuf, *J. Am. Chem. Soc.* **1991**, *113*, 2304; J. N. Narvaez, Ph.D. Dissertation, The Pennsylvania State University, **1993**.
[5] The dihedral angle between the aromatic plane and that containing the scissile bond and the aromatic carbon to which the benzylic carbon is connected is near 90°. P. Maslak, J. N. Narvaez, M. Parvez, *J. Org. Chem.* **1991**, *56*, 602.
[6] D. D. M. Wayner, V. D. Parker, *Acc. Chem. Res.* **1993**, *26*, 287.
[7] See for example: D. D. M. Wayner, D. J. McPhee, D. Griller, *J. Am. Chem. Soc.* **1988**, *110*, 132; D. D. M. Wayner, B. A. Sim, J. J. Dannenberg, *J. Org. Chem.* **1991**, *56*, 4853; E. M. Arnett, S. Venimadhavan, *J. Am. Chem. Soc.* **1991**, *113*, 6967; S. Venimadhavan, K. Amarnath, N. G. Harvey, J.-P. Cheng, E. M. Arnett, *ibid.* **1992**, *114*, 221; F. G. Bordwell, A. V. Satish, *ibid.* **1992**, *114*, 10173; X.-M. Zhang, F. G. Bordwell, *ibid.* **1992**, *114*, 9787; V. D. Parker, K. Handoo, F. Roness, M. Tilset, *ibid.* **1991**, *113*, 7493; V. D. Parker, *Acta Chem. Scand.* **1992**, *46*, 307.
[8] C. Rüchardt, H.-D. Beckhaus, *Angew. Chem.* **1980**, *92*, 417; *Angew. Chem. Int. Ed. Engl.* **1980**, *19*, 429; *ibid.* **1985**, *97*, 531 and **1985**, *24*, 529; *Top. Curr. Chem.* **1986**, *130*, 1; G. Kratt, H.-D. Beckhaus, C. Rüchardt, *Chem. Ber.* **1984**, *117*, 1748; G. Kraft, H.-D. Beckhaus, W. Bernlohr, C. Rüchardt, *Thermochim. Acta* **1983**, *62*, 279; X. L. Huang, J. J. Dannenberg, *J. Org. Chem.* **1991**, *56*, 6367.
[9] R. J. Klingler, J. K. Kochi, *J. Am. Chem. Soc.* **1982**, *104*, 4186; *ibid.* **1981**, *103*, 5839.
[10] For a recent review on redox activation see: M. Chanon, M. Rajzmann, F. Chanon, *Tetrahedron* **1989**, *46*, 6193.
[11] D. Rehm, A. Weller, *Isr. J. Chem.* **1970**, *8*, 259; *Pure Appl. Chem.* **1968**, *16*, 115.
[12] R. A. Marcus, *Discuss. Faraday Soc.* **1960**, *29*, 21; *Annu. Rev. Phys. Chem.* **1964**, *15*, 155; *J. Chem. Phys.* **1965**, *43*, 679; L. Eberson, *Electron Transfer Reactions in Organic Chemistry*, Springer, New York, **1987**; R. Marcus, N. Sutin, *Biochim. Biophys. Acta* **1985**, *811*, 265; P. Suppan, *Top. Curr. Chem.* **1991**, *163*, 95.
[13] J. R. Murdoch, *J. Am. Chem. Soc.* **1983**, *105*, 2159.
[14] J.-M. Savéant, *J. Am. Chem. Soc.* **1987**, *109*, 6788; *ibid.* **1992**, *114*, 10595; C. P. Andrieux, J.-M. Savéant, D. Zann, *Nouv. J. Chim.* **1984**, *8*, 107.

A Cluster-Bound Triply-Bridging Phosphorus Atom Coordinated to Four $(Ph_3P)Au^+$ Units: $[Fe_3(CO)_9P\{Au(PPh_3)\}_4][BAr_4]$**

Deborah L. Sunick, Peter S. White, and Cynthia K. Schauer*

Attractive interactions between metal centers in formally closed-shell d^{10} complexes have been the subject of numerous experimental and theoretical studies.[1] Gold(I), in particular, displays a pronounced tendency to self-associate,[2] and an accurate theoretical description of the $Au^I \cdots Au^I$ attraction requires inclusion of electron correlation and relativistic effects.[3, 4] Such attractive interactions between Au^I ions result in stabilization of the hypercoordinate central atom in a remarkable series of heteroatom-centered gold clusters, $L[Au(PR_3)]_n^{m+}$ (for L = C, n = 5–6;[5] for L = N, n = 5;[6] and for L = P, n = 5–6[7]) that have recently been reported by Schmidbaur et al.

Gold(I) fragments also interact strongly with transition metal carbonyl clusters, and many new clusters have been prepared by the replacement of cluster-bound hydride ligands by $(Ph_3P)Au^+$ units.[8] In the vast majority of cases, a single $(PPh_3)Au$ unit will occupy the same coordination site as the ligand it replaced, but the structures of clusters with more than one $(PR_3)Au$ fragment are dictated by the favored formation of $Au \cdots Au$ bonds. We recently reported the synthesis of the cluster **1**,[9] where the $(Ph_3P)Au$ fragment interacts exclusively with the phosphorus heteroatom of the cluster. This initial μ_3-$PAu(PPh_3)$ interaction

$[(\mu\text{-H})_2Fe_3(CO)_9\{\mu_3\text{-PAu}(PPh_3)\}]$ **1**
$[(\mu\text{-H})Fe_3(CO)_9P\{Au(PPh_3)\}_2]$ **2**
$[Fe_3(CO)_9P\{Au(PPh_3)\}_3]$ **3**

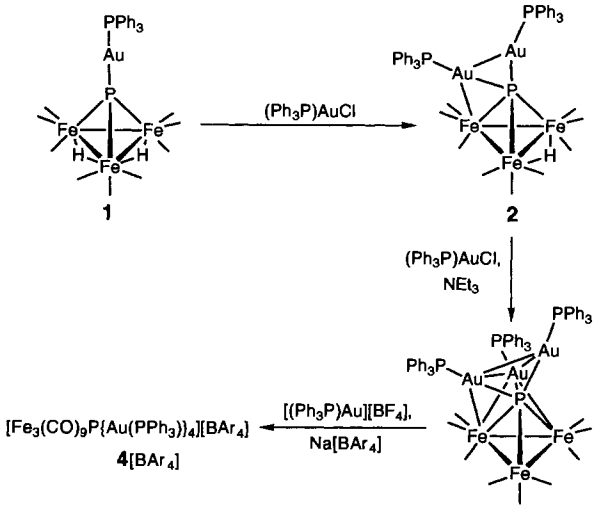
acts as a nucleus for the aggregation of cationic gold fragments, and sequential replacement of the cluster-bound hydride ligands in **1** by $(Ph_3P)Au^+$ fragments produces **2** (with a coordinated $[Au_2(PPh_3)_2]^{2+}$ unit) and **3** (with a coordinated triangular $[Au_3(PPh_3)_3]^{3+}$ unit) (see Scheme 1).[10] An analysis of the X-ray structure of the trigold cluster **3** suggested that there is sufficient space to coordinate a fourth Au^I fragment to the central phosphorus atom. We report here the synthesis and structural characterization of **4**[BAr_4] (Ar = 3,5-$(CF_3)_2C_6H_3$), a

[*] Prof. C. K. Schauer, D. L. Sunick, Dr. P. S. White
Department of Chemistry, The University of North Carolina at Chapel Hill
Chapel Hill, NC 27599-3290 (USA)
Telefax: Int. code + (919)962-2388

[**] Partial financial support was provided by a Presidential Young Investigator Award from the National Science Foundation (CHEM-8958027). Partial funds for equipping the single-crystal X-ray diffraction facility at UNC-CH were provided by the National Science Foundation (CHE-8919288). D. L. S. was supported, in part, by a fellowship from the Department of Education. We thank Frank Rix and Prof. Maurice Brookhart for providing a sample of $Na^+[BAr_4]^-$ (Ar = 3,5-$(CF_3)_2C_6H_3$).

 © VCH Verlagsgesellschaft mbH, D-69451 Weinheim, 1994 0570-0833/94/0101-0075 $ 10.00+.25/0

cluster that serves to bring together studies in the areas of heteroatom-centered gold clusters and gold-derivatized transition metal clusters. Of importance in the successful synthesis of **4** is the stability and solubility afforded by the $[BAr_4]^-$ counterion.



Scheme 1.

Following the strategy employed by Schmidbaur et al., $[(Ph_3P)Au][BF_4]$, prepared by reaction of $(Ph_3P)AuCl$ with $Ag[BF_4]$, is employed as an aurating agent. Upon treatment of the Au_3 cluster **3** with a solution of $[(Ph_3P)Au][BF_4]$ in THF, a new deep purple color is observed. The pattern of infrared CO stretching frequencies is shifted by 20 cm^{-1} to higher energy, and the $^{31}P\{^1H\}$ NMR spectrum shows a quintet at $\delta = 82.4$ ($^2J_{P,P} = 129$ Hz), with a corresponding doublet at $\delta = 49.0$ for the phosphane ligands, all suggesting formation of the desired Au_4 cluster. Solutions of $4[BF_4]$, however, decomposed over 1–2 hours, even at $-50\,^\circ C$, to regenerate **3**, together with unidentified gold-containing products. The anion $[BAr_4]^-$ has been recently employed as a replacement for $[BF_4]^-$ to impart increased stability and solubility to cationic, highly electrophilic transition metal complexes.[11] In an attempt to isolate a more soluble and stable salt of **4**, a sample of **3** and 1 equiv of $Na^+[BAr_4]^-$ is treated with $[(Ph_3)Au][BF_4]$. After removal of the solvent, the $[BAr_4]^-$ salt of **4** can be extracted into Et_2O; salts are left behind as by-products. The solubility of $4[BAr_4]$ in ether is especially impressive since the Au_3 cluster **3** is nearly completely insoluble in Et_2O. Crystals of $4[BAr_4]$ are isolated from Et_2O/pentane in 56% yield.

Solutions of $4[BAr_4]$ in THF or CH_2Cl_2 are stable for a day; however, the tetragold cluster **4** readily transfers one $(Ph_3P)Au^+$ fragment in stoichiometric reactions with $[(Ph_3P)_2N]^+\,Cl^-$ or PPh_3 in CH_2Cl_2 solution to regenerate the trigold cluster **3**. To test the possible role of the $[BF_4]^-$ counterion on the low stability of $4[BF_4]$, a solution of $4[BAr_4]$ in THF was added to a flask containing 3 equiv of dry $[NBu_4]^+[BF_4]^-$. At room temperature, complete decomposition of **4** to **3** takes place within 45 minutes, which strongly suggests that $[BF_4]^-$ can be a reactive counterion toward polyaurated cations.

The $^{31}P\{^1H\}$ NMR data for **1**–**4** are summarized in Table 1. At room temperature, sharp, coupled resonances are observed for the central phosphorus atoms (P_c) and the PPh_3 ligands in **1**–**4**, indicating that intermolecular exchange of $(Ph_3P)Au^+$ fragments is not rapid. For the phosphorus-centered gold clusters $[P\{Au(PPh_3)\}_5]^{2+}$ and $[P\{Au(PPh_3)\}_6]^{3+}$,[7] low-temperature ^{31}P NMR spectroscopy was required to observe two-bond P_c-PPh_3 coupling. Successive substitution of gold fragments for hydride ligands in **1** results in a decrease in the average $^2J_{P,P}$ value from 314 Hz in **1** to 129 Hz in **4**, together with a progressive upfield shift of the ^{31}P NMR chemical shift for P_c from $\delta = 390.3$ in **1** to 82.4 in **4**. Similar trends are observed upon addition of a $(Ph_3P)Au^+$ fragment to the pentagold cluster $[P\{Au(PPh_3)\}_5]^{2+}$ ($\delta = 122$ for P_c, $^2J_{P,P} = 186$ Hz) to produce $[P\{Au(PPh_3)\}_6]^{3+}$ ($\delta = -166$ for P_c, $^2J_{P,P} = 167$ Hz).[7] The four gold-bound phosphane ligands in **4** are still equivalent in the $-100\,^\circ C$ ^{31}P NMR spectrum; however, the resonance for P_c is shifted by more than 20 ppm upfield.

Table 1. $^{31}P\{^1H\}$ NMR data for gold clusters **1**–**3** and **4**$[BAr_4]$. The measurements were performed at 25 °C.

	Cmpd	Solvent	$\delta(P_c)$	$\delta(PPh_3)$	$^2J(P,P)$ [Hz]
1		C_6H_6	390.3 (d)	40.8 (d)	314
2		CH_2Cl_2	253.3 (t)	45.3 (d)	192
3		CH_2Cl_2	125.7 (quart)	45.1 (d)	147
4	$[Fe_3(CO)_9P\{Au(PPh_3)\}_4]^+$	$[D_8]$THF	82.4 (quint)	49.0 (d)	129
4	(−100 °C)	$[D_8]$THF	58.9 (quint)	47.7 (d)	130

The structure of $4[BAr_4]$ was determined by a single-crystal X-ray diffraction study (Fig. 1),[12] and consists of a slightly distorted square-planar $[Au_4(PPh_3)_4]^{4+}$ unit ($Au\cdots Au$ = 2.976(1)–3.224(2) Å) coordinated to the $[Fe_3(CO)_9P]^{3-}$ cluster framework. The dihedral angle between the Fe_3 plane and the Au_4 plane is 30°. Three of the four $(Ph_3P)Au^+$ fragments in the Au_4 unit are strongly bound to the central phosphorus atom ($Au-P_c$ = 2.357(6)–2.427(6) Å), while the third $(Ph_3P)Au^+$ fragment (Au3) is at a distance of 2.694(6) Å. Three of the four Au^I ions in the Au_4 square also interact with Fe1 and Fe2 in the Fe_3 triangle: Au3 bridges the Fe1–Fe2 edge, while Au2 and Au4 interact with Fe2 and Fe1, respectively (Fig. 2, right). The stepwise construction of the Au_4 array in **4** can be accessed by evaluating the structures of **2**–**4**. In the digold cluster **2** one $(Ph_3P)Au^+$ fragment (Au1) is bound to the cluster exclusively through P_c, while the second $(Ph_3P)Au^+$ unit (Au2) bridges an

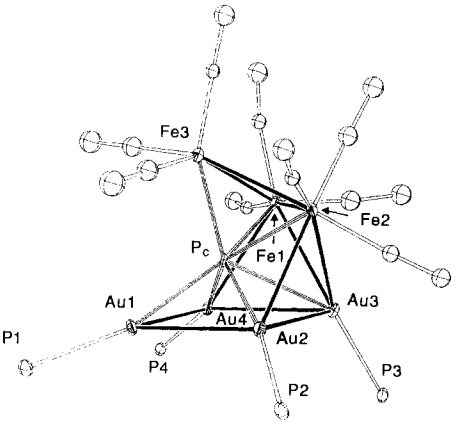


Fig. 1. ORTEP drawing (ellipsoids represent 30% probability) of the structure of the cation **4**. Phenyl rings have been omitted for clarity. Selected distances [Å]: Au1-Au2 2.976(1), Au1-Au4 2.992(2), Au2-Au3 3.224(2), Au3-Au4 2.980(1), Au1-P1 2.302(6), Au1-P_c 2.357(6), Au2-Fe2 2.729(3), Au2-P2 2.299(6), Au2-P_c 2.427(6), Au3-Fe1 2.690(3), Au3-Fe2 2.830(4), Au3-P3 2.287(6), Au3-P_c 2.694(6), Au4-Fe1 2.786(3), Au4-P4 2.296(6), Au4-P_c 2.412(6), Fe1-Fe2 2.674(5), Fe1-Fe3 2.632(5), Fe2-Fe3 2.670(5), Fe1-P_c 2.296(7), Fe2-P_c 2.278(7), Fe3-P_c 2.220(7).

 © VCH Verlagsgesellschaft mbH, D-69451 Weinheim, 1994 0570-0833/94/0101-0076 $ 10.00+.25/0

Fe–P edge. The structure of the trigold cluster **3** (Fig. 2 left) is simply derived from addition of a third $(Ph_3P)Au^+$ fragment (Au3) to a Fe_2P face of the cluster As can be seen by comparing the two structures in Figure 2, **4** is formally constructed by "insertion" of Au4 into the Au1–Au3 bond.

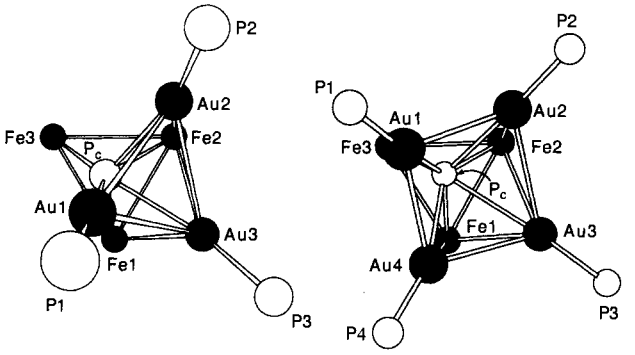


Fig. 2. View onto the Fe_3 plane of the ball and stick drawings of the $Fe_3P[Au_3P_3]$ core of **3** (left) and $Fe_3P[Au_4P_4]$ core of **4** (right).

A C_{4v} symmetry structure (with a square-planar array of Au^I ions) instead of T_d symmetry structure was recently predicted to be the most stable for the hypothetical $[P\{Au(PH_3)\}_4]^+$ cluster,[4e] and is observed experimentally for $[As\{Au(PPh_3)\}_4]^+$.[13] Given the large number of possible other arrangements of gold atoms involving different modes of bonding to the Fe_3 triangle, the configuration adopted by the $[Au_4(PPh_3)_4]^{4+}$ fragment in **4** is likely governed by the stability of the nearly square-planar arrangement of Au^I ions. Remarkably, the geometry of the Au_4 array in **4** is similar to that adopted in the related monoarylphosphorus dication, $[(o\text{-tolyl})P\{Au(PPh_3)\}_4]^{2+}$ (Au···Au = 2.97(5), Au–P_c = 2.37(1), Au–PPh_3 = 2.293(7) Å).[14] Thus, **4** can be viewed either as a $[\{Au(PPh_3)\}_4]^{4+}$ derivative of the $[Fe_3(CO)_9(\mu_3\text{-}P)]^{3-}$ cluster or as an $Fe_3(CO)_9$ derivative of $[P\{Au(PPh_3)\}_4]^+$, in which bonding to the Fe_3 array requires six electrons from the P^{3-} ion. Such a cluster is not readily amenable to classical bonding descriptions.

Experimental Procedure

Reactions were performed under purified nitrogen with standard Schlenk techniques.

4[BAr_4]: Solid samples of purple-red **3** (57.5 mg, 0.031 mmol) and $Na^+[BAr_4]^-$ (27.4 mg, 1 equiv) were combined in a flask, and a freshly prepared solution of [$(Ph_3P)Au$][BF_4] [14] in 10 mL of THF (prepared from 0.031 mmol each of Ag[BF_4] and $(Ph_3P)AuCl$ in the dark) at −70 °C was filtered onto the solids. A new deep purple color was observed as **3** dissolved. After stirring for 5 min, conversion to **4** was complete (as indicated by IR spectroscopy). The solvent was removed under vacuum and **4**[BAr_4] was extracted into Et_2O. The solution was filtered, and then layered with pentane to yield crystals of **4**[BAr_4]. Isolated yields: 56 mg (57%). ^1H NMR (300 MHz, [D_8]THF): δ = 7.9, 7.7 (br s, Ar protons) 7.25, 7.50 (m, Au(PPh_3)); IR (Et_2O): ν_{CO} = 2041 cm^{-1} vs, 1993 vs, 1983 s, 1974 m, 1936 w, br; correct elemental analysis for $C_{113}H_{72}Au_4BF_{24}Fe_3O_9P_5$.

Received: July 13, 1993 [Z 6210 IE]
German version: *Angew. Chem.* **1994**, *106*, 108

[1] M. Jansen, *Angew. Chem.* **1987**, *99*, 1136; *Angew. Chem. Int. Ed. Engl.* **1987**, *26*, 1098.
[2] S. S. Pathaneni, G. R. Desiraju, *J. Chem. Soc. Dalton Trans.* **1993**, 319.
[3] A. Görling, N. Rösch, D. E. Ellis, H. Schmidbaur, *Inorg. Chem.* **1991**, *30*, 3986.
[4] a) P. Pyykkö, J.-P. Desclaux, *Acc. Chem. Res.* **1979**, *12*, 276; b) P. Pyykkö, *Chem. Rev.* **1988**, *88*, 563; c) P. Pyykkö, Y. Zhao, *Angew. Chem.* **1991**, *103*, 622; *Angew. Chem. Int. Ed. Engl.* **1991**, *30*, 604; d) J. Li, P. Pyykkö, *Chem. Phys. Lett.* **1992**, *197*, 586; e) *Inorg. Chem.* **1993**, *32*, 2630.
[5] a) F. Scherbaum, A. Grohmann, B. Huber, C. Krüger, H. Schmidbaur, *Angew. Chem.* **1988**, *100*, 1602; *Angew. Chem. Int. Ed. Engl.* **1988**, *27*, 1544; b) F. Scherbaum, A. Grohmann, G. Müller, H. Schmidbaur, *ibid.* **1989**, *101*, 464 and **1989**, *28*, 463; c) O. Steigelmann, P. Bissinger, H. Schmidbaur, *ibid.* **1990**, *102*, 1473 and **1990**, *29*, 1399.
[6] A. Grohmann, J. Riede, H. Schmidbaur, *Nature* **1990**, *345*, 140.
[7] a) H. Schmidbaur, G. Weidenhiller, O. Steigelmann, *Angew. Chem.* **1991**, *103*, 442; *Angew. Chem. Int. Ed. Engl.* **1991**, *30*, 433; b) E. Zeller, H. Schmidbaur, *J. Chem. Soc. Chem. Commun.* **1993**, 69.
[8] a) K. P. Hall, D. M. P. Mingos, *Prog. Inorg. Chem.* **1984**, *32*, 237; b) I. D. Salter, *Adv. Organomet. Chem.* **1989**, *29*, 249.
[9] D. L. Sunick, P. S. White, C. K. Schauer, *Organometallics* **1993**, *12*, 245.
[10] D. L. Sunick, P. S. White, C. K. Schauer, *Inorg. Chem.*, in press.
[11] M. Brockhart, B. Grant, A. F. Volpe, Jr., *Organometallics* **1992**, *11*, 3920.
[12] **4**[BAr_4] · 1.5 Et_2O: a = 12.918(3), b = 19.863(9), c = 23.256(4) Å, α = 89.94(2), β = 91.57(2), γ = 94.31(3)° at −150 °C. Space group $P\bar{1}$ (Z = 2). Least squares refinement of 729 least squares parameters and 7934 reflections converged at R (R_w) = 0.066 (0.069). Further details of the crystal structure investigation are available on request from the Director of Cambridge Crystallographic Data Centre, 12 Union Road, GB-Cambridge CB21EZ (UK), on quoting the full journal citation.
[13] E. Zeller, H. Beruda, A. Kolb, P. Bissinger, J. Riede, H. Schmidbaur, *Nature* **1991**, *352*, 141.
[14] H. Schmidbaur, E. Zeller, G. Weidenhiller, O. Steigelmann, H. Beruda, *Inorg. Chem.* **1992**, *31*, 2370.

Competing Reactions of Silenes: [2 + 2], [4 + 2], and [6 + 2] Cycloadditions with Cycloheptadiene and Cycloheptatriene**

Wolfgang Ziche, Claudia Seidenschwarz, Norbert Auner,* Eberhardt Herdtweck, and Norbert Sewald

Dedicated to Professor Ernst Otto Fischer on the occasion of his 75th birthday

(Hetero)olefins usually undergo [2 + 2] and [4 + 2] cycloadditions, while examples of thermal [6 + 2] cycloadditions are comparatively rare.[1] "Dichloroneopentylsilene" **1** is a

$Cl_2Si{=}CHCH_2tBu$ **1**

building block for synthetic organosilicon chemistry, which is characterized by a highly polar Si=C bond and a strongly electrophilic silicon atom. These properties are mainly responsible for its unique reactivity: on the one hand, **1** reacts with relatively unreactive dienes like naphthalene[2] and furans[3] to give Diels–Alder adducts and, on the other hand, it undergoes [2 + 2] cycloadditions with disubstituted acetylenes to give silacyclobutenes.[4] The reaction of **1** with 1,3-butadienes leads selectively to monosilacyclobutanes,[5] and upon treatment of **1** with 1,3-cyclohexadiene the [2 + 2] and [4 + 2] cycloadditions compete with each other;[6] in both cases the [2 + 2] adducts are converted thermally into Diels–Alder and retro-ene products. We report here on the cycloadditions of **1** with 1,3-cycloheptadiene and 1,3,5-cycloheptatriene.

[*] Prof. N. Auner, Dr. W. Ziche, Dr. C. Seidenschwarz, Dr. E. Herdtweck, Dr. N. Sewald
Anorganisch-chemisches Institut der Technischen Universität München
Lichtenbergstrasse 4, D-85747 Garching (FRG)
Telefax: Int. code + (89) 3209-3743

[**] Silaheterocycles, Part 30. This work was supported by the Volkswagen-Stiftung, the Deutsche Forschungsgemeinschaft, and the Fonds der Chemischen Industrie. – Part 29: W. Ziche, V. Popkova, C. Seidenschwarz, N. Sewald, E. Herdtweck, N. Auner, *Organometallics*, submitted.

Reaction of silene **1**, prepared in situ from trichlorovinylsilane and *t*BuLi, with cycloheptadiene produces a mixture of the [2 + 2] and [4 + 2] cycloadduct isomers, **2** and **3**, respectively, which is not separable by distillation.[7] To separate the structural isomers the mixture was treated with phenylmagnesium bromide. In this reaction only the two chloro substituents of the [2 + 2] adducts are replaced by two phenyl groups giving **4**. This selective reactivity is analogous to that of the corresponding cyclohexadiene adducts[6] and is attributed to the angles at the silicon atom in the monosilacyclobutane subunits (see also Fig. 1).[8–10] Compound **4** was recrystallized from pentane and shown by X-ray structure analysis (Fig. 1) to be the diphenyl-substituted [2 + 2] isomer (*E*)-**4**.[8]

(*E*/*Z*)- **2**

exo/*endo*- **3**

4

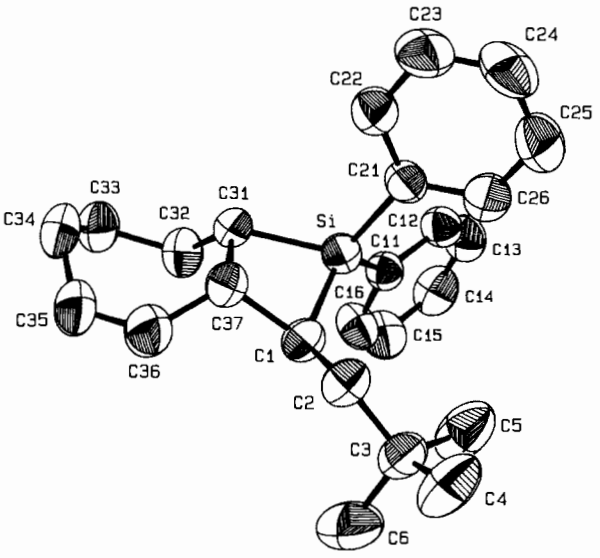


Fig. 1. Crystal structure of (*E*)-**4** (ORTEP representation). Selected distances [pm] and angles [°]: Si-C1 188.0(1), SiC31 188.4(1), Si-C11 187.3(1), Si-C21 187.5(1), C1-C2 152.4(1), C1-C37 158.9(1), C31-C37 156.4(1), C1-SiC31 79.45(5), Si-C1-C37 85.88(7), Si-C31-C37 86.44(7), C1-C37-C31 99.46(9), C11-Si-C21 110.48(5), C31-C37-C36 118.52(11), Si-C1-C2 126.72(9), Si-C31-C32 118.51(9).

The most striking structural features of (*E*)-**4** are the nonplanar central silacyclobutane unit and the small endocyclic angles; the angle at silicon (79.45°) is significantly smaller than at the opposite carbon atom (99.46°). These values are normal for silacyclobutane derivatives.[9]

Surprisingly, the reaction of **1** with 1,3,5-cycloheptatriene leads to four [2 + 2] (**5**) and two [6 + 2] cycloadducts (**6**) (Scheme 1, for relative amounts see Table 1).

Table 1. Selected spectroscopic data[a] for (*E*)-**4**, **5**, **6**, and *endo*-**7**.

(*E*)-**4**: ^{1}H NMR: δ = 0.78 (s, 9H), 0.80–2.20 (m, 8H), 2.50 (m, 2H), 3.00 (m, 1H), 5.47 (m, 1H), 5.55 (m, 1H), 7.35–7.45 (m, 4H), 7.55–7.67 (m, 6H); ^{13}C NMR: δ = 25.07, 26.40, 26.91 (CH_2), 29.86 ($C(CH_3)_3$), 30.65 ($C(CH_3)_3$), 43.96 (CH_2-$C(CH_3)_3$), 28.01, 29.62, 43.95 (CH), 133.15, 136.60 (C), 125.39, 127.82, 127.83, 125.60, 133.62, 135.95, 135.96, 136.12, 136.13 (CH); ^{29}Si NMR: δ = 2.3 ((*Z*)-**4**: 5.4); MS (70 eV): *m*/*z*: 360 (M^+, 3%), 209 ($Ph_2SiCHCH_2^+$, 100), 183 (Ph_2SiH^+, 39), 266 ($M^+ - C_7H_{10}$, 36), 292 ($M^+ - C_6H_6$, 11), 293 ($M^+ - C_6H_5$, 3).

5: ^{29}Si NMR: δ = 12.6 (27%), 13.3 (5), 17.5 (4), 18.4 (32); GC-MS: *m*/*z*: (M^+, 3%), 217 ($M^+ - t$Bu, 8), 181 ($M^+ - C_7H_9$, 5), 91 ($C_7H_7^+$, 55), 57 (*t*Bu, 100).

(*E*)-*cis*-**5**: ^{1}H NMR: δ = 0.90 (s, 9H; $C(CH_3)_3$), 1.37, 1.56 (CH_2-$C(CH_3)_3$), 2.10 (m, 1H; Si-C*H*-CH_2tBu), 2.40 (m, 1H; Si-CH), 2.45 (m, 1H; Si-CH-C*H*), 2.22 (m, 2H; CH_2), 5.72–6.00 (m, 4H; CH=CH–CH=CH); ^{13}C NMR: δ = 29.75 ($C(CH_3)_3$), 30.26 ($C(CH_3)_3$), 26.84 (CH_2), 41.60, 46.74, 48.04 (CH), 42.46 (CH_2-$C(CH_3)_3$), 125.17, 127.31, 135.24, 135.75 (=CH); ^{29}Si NMR: δ = 18.4.

(*Z*)-*cis*-**5**: ^{1}H NMR: δ = 0.90 (s, 9H; $C(CH_3)_3$), 1.37, 1.56 (CH_2-$C(CH_3)_3$), 1.70 (m, 1H; Si-C*H*-CH_2tBu), 1.95 (m, 1H; Si-CH), 2.21 (m, 1H; Si-CH-C*H*), 2.34, 2.57 (m, 2H; CH_2), 5.68–5.90 (m, 4H; CH=CH–CH=CH); ^{13}C NMR: δ = 29.75 ($C(CH_3)_3$), 30.96 ($C(CH_3)_3$), 31.41 (CH_2), 40.04, 42.24, 43.40 (CH), 43.29 (CH_2-$C(CH_3)_3$), 124.79, 124.98, 134.16, 135.02 (=CH); ^{29}Si NMR: δ = 12.6.

(*E*)/(*Z*)-*trans*-**5**: ^{13}C NMR: δ = 29.75 ($C(CH_3)_3$), 30.57, 30.77 ($C(CH_3)_3$), 36.81, 40.33 (CH_2-$C(CH_3)_3$), 25.90, 31.27 (CH_2), 36.09, 38.31, 39.59, 40.44, 43.33, 54.04 (CH), 124.90, 128.52, 128.62, 132.78, 134.41, 135.15, 135.30 (=CH); ^{29}Si NMR: δ = 13.3, 17.5.

endo-**6**: ^{1}H NMR: δ = 0.90 (s, 9H; $C(CH_3)_3$), 1.58 (m, 2H; CH_2-$C(CH_3)_3$), 1.84 (m, 1H; Si-C*H*-CH_2tBu), 1.98 (m, 1H; CH_2), 2.19 (m, 1H; CH_2), 2.51 (m, 1H; Si-CH), 2.95 (m, 1H; Si-CH-C*H*), 5.65, 5.69, 5.80, 5.93 (div. m, 4H, CH=CH–CH=CH); ^{13}C NMR: δ = 29.71 ($C(CH_3)_3$), 30.89 ($C(CH_3)_3$), 31.77 (CH_2), 33.89 (Si-CH), 37.54 (CH_2-$C(CH_3)_3$), 44.90 (Si-CH-CH), 46.35 (Si-CH-CH_2tBu), 123.56, 123.54, 126.39, 134.07 (=CH); ^{29}Si NMR: δ = 46.5 (22%); MS (70 eV): *m*/*z*: 274 (M^+, 6%), 239 (M^+ – Cl, 6), 217 ($M^+ - t$Bu, 5), 181 ($M^+ - C_7H_9$, 15), 91 ($C_7H_7^+$, 56), 57 (*t*Bu, 100).

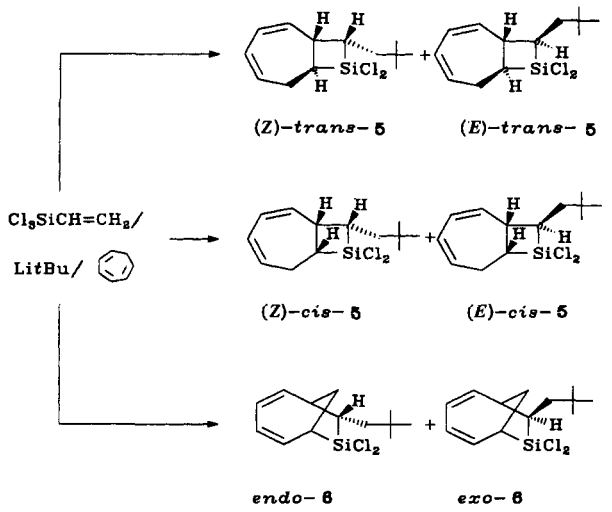
exo-**6**: ^{1}H NMR: 0.90 (s, 9H; $C(CH_3)_3$), 1.22, 1.62 (m, 2H; CH_2-$C(CH_3)_3$), 1.34 (m, 1H; Si-C*H*-CH_2tBu), 1.75 (m, 1H; CH_2), 2.10 (m, 1H; CH_2), 1.34 (m, 1H; Si-CH), 2.46 (m, 1H; Si-CH-C*H*), 5.65, 5.73, 5.83, 5.90 (div. m, 4H, CH = CH – CH = CH); ^{13}C NMR: δ = 29.75 ($C(CH_3)_3$), 31.66 ($C(CH_3)_3$), 29.04 (CH_2), 34.51 (Si-CH), 45.08 (CH_2-$C(CH_3)_3$), 47.52 (Si-CH-CH), 42.74 (Si-CH-CH_2tBu), 123.51, 123.89, 132.40, 133.35 (=CH); ^{29}Si NMR: δ = 41.7 (10%); MS (70 eV): *m*/*z* see *endo*-**6**.

endo-**7**: ^{1}H NMR: δ = 0.84 (s, 9H; $C(CH_3)_3$), 1.50 (dd, *J* = 14.6, 3.0 Hz, 1H; CH_2-$C(CH_3)_3$), 1.85 (dd, *J* = 14.6, 14.6 Hz, 1H; CH_2-$C(CH_3)_3$), 2.05–2.30 (m, 3H; CH_2, Si-C*H*-CH_2tBu), 2.62 (m, 1H; Si-CH), 3.18 (m, 1H; Si-CH-C*H*), 5.50, 5.75–5.95 (m, 4H, CH=CH–CH=CH), 7.15–7.40 (m, 6H; m-Ph, p-Ph), 7.50–7.55 (m, 4H, o-Ph); ^{13}C NMR: δ = 29.90 ($C(CH_3)_3$), 32.02 ($C(CH_3)_3$), 34.72, 38.28 (CH_2), 31.32, 41.19, 46.48 (CH), 123.70, 132.43 (=C), 121.56, 126.65, 127.06, 127.17, 127.73, 127.93, 129.13, 129.20, 134.18, 134.87, 135.47, 135.72, 136.93, 137.90 (=CH); ^{29}Si NMR: δ = 17.5; MS (70 eV): *m*/*z*: 358 (M^+, 29%), 301 ($M^+ - t$Bu, 14), 279 ($M^+ - C_6H_7^+$, 32), 209 ($M^+ - t$Bu – C_7H_8, 74), 183 (Ph_2SiH^+, 100), 105 ($C_8H_9^+$, 29), 57 (*t*Bu, 100).

[a] ^{1}H NMR: $CDCl_3$, 100, 270, and 360 MHz; ^{13}C NMR: 25.14 MHz, $CDCl_3$, ^{29}Si NMR: 53.64 MHz, $CDCl_3$. GC-MS at 70 eV.

The ^{29}Si NMR chemical shifts of the products, before and after distillation, allow clear assessment of the type of cycloadducts formed. The signals for **5** lie between δ = 12.6 and 18.4, characterizing these compounds as the [2 + 2] cycloadducts. For **6** the signals at δ = 41.7 and 46.5 have chemical shifts typical of dichlorosilacyclopentanes, thus identifying the two compounds as the *exo*/*endo* [6 + 2] cycloadduct isomers. Formation of both the [6 + 2] and the [2 + 2] cycloadducts by a concerted process is forbidden by the Woodward–Hoffmann rules.[11] No [4 + 2] cycloadducts are formed in the reaction sequence shown in Scheme 1; their ^{29}Si NMR signals would be expected in the region $\delta \approx$ 25–30.[6]

 © VCH Verlagsgesellschaft mbH, D-69451 Weinheim, 1994 0570-0833/94/0101-0078 $ 10.00+.25/0



Scheme 1. Reaction of **1** with 1,3,5-cycloheptatriene.

The separation of the structural isomers of **5** and **6** into individual components was successfully achieved in a chemical fashion:

- When a mixture of **5** and **6** was stored at room temperature for several months, *endo/exo*-**6** (*endo/exo* 75/25) was formed exclusively. Thermolysis of this mixture in solution (toluene 110 °C, 120 h) or neat (200 °C, 120 h) significantly accelerated the isomerization of **5** into **6**. The *endo/exo* ratio for **6** was then 85/15. Compound **6** was characterized by 2D NMR spectroscopy.
- Derivatizing **5**/**6** with phenylmagnesium bromide gave almost selective isomerization to the diphenyl-substituted [6 + 2] cycloadduct, *endo*-**7**, which is crystalline and was characterized by X-ray structure analysis (Fig. 2).[12]

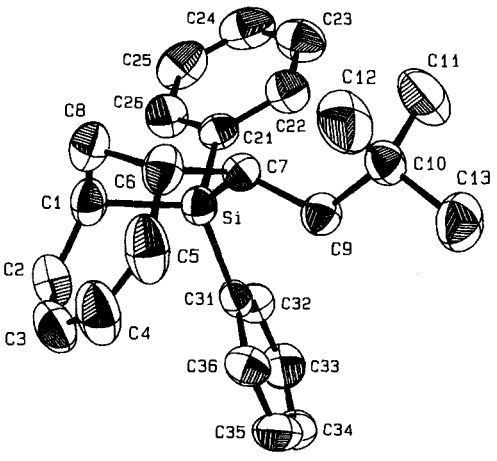
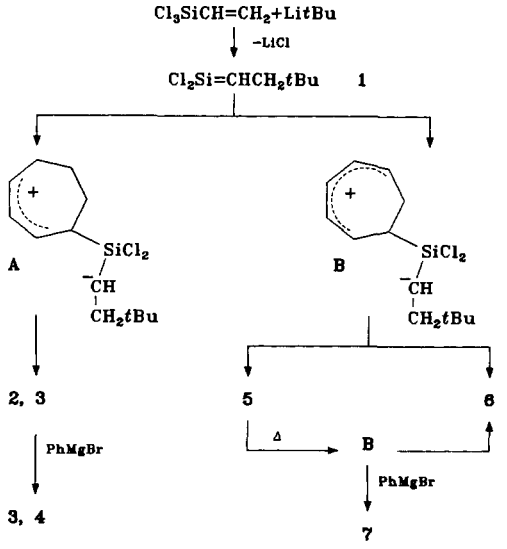


Fig. 2. Crystal structure of *endo*-**7** (ORTEP representation). Selected distances [pm] and angles [°]: Si-C1 190.3(1), Si-C7 190.3(1), Si-C21 187.4(1), Si-C31 186.9(1), C7-C9 153.3(1), C6-C7 155.8(1), C5-C6 149.1(2), C1-C2 148.1(2), C1-C8 153.0(1), C6-C8 153.8(1), C1-Si-C7 96.35(6), Si-C7-C6 103.79(8), Si-C7-C9 118.49(9), Si-C1-C2 113.92(10), C2-C1-C8 113.93(14), C5-C6-C7 114.03(13).

As is clear from Fig. 2, the *endo* isomer of the [6 + 2] cycloadduct **7** shows no striking structural features; the C6–C7 bond length is 155.9(2) pm, a little longer than the average of the other C–C bond lengths ($d = 151.9$ pm). The bicyclo[4.2.1]-2,4-nonadiene unit is somewhat distorted in comparison to the analogous all-carbon framework as a consequence of the larger atomic radius of the Si atom.[13]

The [2 + 2] and [6 + 2] cycloadditions of silene **1** reported here, as well as the isomerizations, can be explained in terms of zwitterionic intermediates (Scheme 2). The strongly polarized



Scheme 2. Possible reaction pathways for the formation and rearrangement of the cycloadducts of **1**.

and electrophilic silene **1** attacks one of the terminal carbons in the conjugated π-electron system of cycloheptadiene and cycloheptatriene, forming the zwitterions **A** and **B**, respectively. Carbocation **B** is more effectively stabilized than **A** by greater delocalization, which thereby allows more time for stereochemical orientation of the dipolar system and a number of possible modes of ring closure. The attack of the carbanion at the terminal carbon atom of the cationic propenyl and pentadienyl moieties leads in both cases to rapid ring closure, giving the [2 + 2] cycloadducts **2** and **5** preferentially. Competing with this is the formation of the Diels–Alder adduct **3**, in a slower step, and the [6 + 2] cycloadduct **6**, which is mainly produced as the thermodynamically more stable *endo* isomer.[14] The greater stability of **B** is also confirmed by the fact that the (*Z*) [2 + 2] adduct **5** does not thermally isomerize to give the retro-ene compound. This isomerization was observed for the related compounds formed from **1** with butadienes,[5] 1,3-cyclohexadiene,[6] and 1,3-cycloheptadiene.[15]

These results open up wide-ranging possibilities for the transformation of the regiospecific but stereoisomeric [2 + 2] adducts of silene **1** into stereochemically pure products with nucleophilic reagents. In this way the whole process becomes stereoselective.

Experimental Procedure

5/**6**: A solution of *t*BuLi (1.7 M in pentane, 36.0 mL, 60.0 mmol) was added dropwise to a mixture of $Cl_3SiCH{=}CH_2$ (9.6 g, 60.0 mmol) and 1,3-cycloheptatriene (11.0 g, 119.6 mmol) in pentane (500 mL) at −78 °C. After the mixture was allowed to warm to room temperature, it was stirred for another 12 h. After filtration the mixture was distilled to give a mixture of **5**/**6** (100 °C, 10^{-2} mbar) as a colorless viscous liquid (9.3 g, 34.0 mmol, 56.6% yield).

4: A mixture of **2**/**3** (2.76 g, 10.0 mmol, prepared analogously to **5**/**6**) was added to phenylmagnesium bromide (60.0 mmol) in THF (50 mL) and heated at reflux for 60 h. The solvent was then distilled off and the residue extracted with pentane. **3** (105 °C, 10^{-2} mbar; 0.85 g, 3.0 mmol, 30% yield) and **4** (185 °C, 10^{-2} mbar; 1.19 g, 3.3 mmol, 33% yield; E/Z = 66/34) were isolated by distillation. (*E*)-**4** solidified in the receiving flask and was recrystallized from pentane to give a white solid (m.p. 85 °C).

7: The derivatization of **5**/**6** with phenylmagnesium bromide (3.40 g, 12.5 mmol) followed that of **4**. Compound **7** was isolated as a thick oil by distillation (200 °C, 10^{-2} mbar), which crystallized in the receiving flask. Recrystallization from pentane gave pure **7** as a white solid (3.58 g, yield 83.3%, m.p. 97 °C).

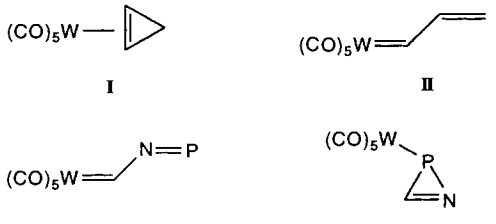
Received: July 21, 1993 [Z 6224 IE]
German version: *Angew. Chem.* **1994**, *106*, 93

[1] K. Mach, H. Antropiusová, L. Petrusová, V. Hanus, F. Turecek, *Tetrahedron* **1984**, *40*, 3295.
[2] N. Auner, C. Seidenschwarz, N. Sewald, E. Herdtweck, *Angew. Chem.* **1991**, *103*, 425; *Angew. Chem. Int. Ed. Engl.* **1991**, *30*, 444.
[3] N. Auner, A. Wolff, *Chem. Ber.* **1993**, *126*, 575.
[4] N. Auner, C. Seidenschwarz, E. Herdtweck, *Angew. Chem.* **1991**, *103*, 1172; *Angew. Chem. Int. Ed. Engl.* **1991**, *30*, 1151; N. Auner, C.-R. Heikenwälder, C. Wagner, *Organometallics* **1993**, *12*, 4135.
[5] N. Sewald, W. Ziche, A. Wolff, N. Auner, *Organometallics* **1993**, *12*, 4123.
[6] N. Auner, C. Seidenschwarz, N. Sewald, *Organometallics* **1992**, *11*, 1137.
[7] Nonetheless the assignment of the NMR signals to the individual isomers is possible by comparison to the NMR data from the cycloadducts of **1** with cyclohexadiene[6]; the ^{29}Si NMR spectrum in particular can be used to determine the product type (**2**: δ = 16.45, 16.47 and **3**: δ = 28.90, 29.70) as well as the relative proportions of the individual stereoisomers (*E*)/(*Z*)-**2**, and *exo*/*endo*-**3**). (*E*)/(*Z*) describes the position of the neopentyl group on the silacyclobutanes relative to the vicinal bond of the annulated ring; *exo*/*endo* denotes the stereochemistry of the neopentyl group in the [4 + 2] and [6 + 2] cycloadducts; and *cis*/*trans* refers to the stereochemistry of the fusion of the seven- and four-membered rings in **5**.
[8] X-ray crystal structure analysis of (*E*)-**4** ($C_{25}H_{32}Si$), M = 360.6; colorless prisms (0.51 × 0.18 × 0.26 mm^3); triclinic space group, $P\bar{1}$ (no. 2), a = 993.6(1), b = 1055.5(1), c = 1152.2(1) pm, α = 69.51(1), β = 85.13(1), γ = 76.42(1)°, 25 reflections with high diffraction angles ($2\theta_{min/max}$ = 79.7°/96.8°), V = 1100 × 10^6 pm^3, Z = 2, ρ_{calc} = 1.086 g cm^{-3}, F_{000} = 392, μ = 9.4 cm^{-1}. A crystal suitable for X-ray analysis was mounted in a capillary with perfluorinated polyether. Data were collected on an Enraf-Nonius CAD-4 four-circle diffractometer. Intensity data for 4381 reflections were collected at room temperature (21 ± 1) °C with graphite-monochromated $Cu_{K\alpha}$ radiation, λ = 154.184 pm, $\theta/2\theta$-Scan, 1.0° < θ < 70.0°. From these data 594 reflections with negative intensities were removed. After correction for minor decomposition (99 h, −7.1%) and an empirical absorption correction (8 Psi-scan data, $C_{min/max}$ = 0.959/1.000) there remained, after averaging 414 reflections (R_m = 0.010(F)), 3580 independent reflections. One reflection, obviously a measurement error, was discounted. The structure was solved using a combination of direct and indirect methods, difference-Fourier maps and full-matrix least-squares techniques. All heavy atoms were refined with anisotropic parameters and all hydrogen atom positions with isotropic parameters. Refinement lead to convergence with R = 0.065 and R_w = 0.048 for 3579 reflections and 363 variables. A difference map showed no residual electron density outside + 0.70 and −0.35 e Å^{-3}. All calculations were performed on a micro-Vax-3100 computer with the STRUX IV program package (MULTAN 11/82, ORTEP-II, PLATON, SCHAKAL, SDP and SHELX-86)[16]. Further details of the crystal structure investigation may be obtained from the Fachinformationszentrum Karlsruhe, D-76344 Eggenstein-Leopoldshafen (FRG) on quoting the depository number CSD-56657, the names of the authors, and the journal citation.
[9] E. S. Mastryukov, O. V. Dorofeeva, L. V. Vilkov, B. N. Sivin, S. J. Sivin, *Zh. Strukt. Khim.* **1975**, *16*, 473; E. S. Mastryukov, O. V. Dorofeeva, L. V. Vilkov, N. A. Tarasenko, *J. Mol. Struct.* **1975**, *27*, 216; O. A. D'yachenko, Yu. A. Sokolova, L. O. Atovmyan, N. V. Ushakov, *Izv. Akad. Nauk SSSR Ser. Khim.* **1985**, *34*, 937.
[10] B. Rempfer, G. Pfafferott, H. Oberhammer, N. Auner, J. E. Boggs, *Acta Chem. Scand. Ser. A* **1988**, *42*, 352.
[11] R. B. Woodward, R. Hoffmann, *J. Am. Chem. Soc.* **1965**, *87*, 395.
[12] X-ray crystal structure analysis of **7** ($C_{25}H_{30}Si$), M = 358.6; colorless crystal fragments; triclinic space group, $P\bar{1}$ (no. 2), a = 993.0(2), b = 1067.8(3), c = 1123.5(2) pm, α = 92.69(1), β = 101.31(1), γ = 113.86(1)°, 25 reflections with high diffraction angles ($2\theta_{min/max}$ = 35.0°/42.9°), V = 1058 × 10^6 pm^3, Z = 2, ρ_{calc} = 1.126 g cm^{-3}, F_{000} = 392, μ = 1.1 cm^{-1}. A crystal suitable for X-ray analysis was mounted in a capillary with perfluorinated polyether. Data were collected on an Enraf-Nonius CAD-4 four-circle diffractometer. Intensity data for 3934 reflections were collected at room temperature (21 ± 1) °C with graphite-monochromated $Mo_{K\alpha}$ radiation, λ = 71.073 pm, ω-scan, 1.0° < θ < 25.0°. From these data 647 reflections with negative intensity were removed; there remained 3115 independent reflections. One reflection, obviously a measurement error, was ignored. The structure was solved using a combination of direct, difference-Fourier maps and full-matrix least-squares techniques. All heavy atoms were refined with anisotropic parameters and all hydrogen atom positions with isotropic parameters. Refinement lead to convergence with R = 0.058 and R_w = 0.029 for 3114 reflections and 355 variables. A difference-Fourier map showed no residual electron density outside + 0.26 and −0.35 e Å^{-3}.
[13] To the best of our knowledge the crystal structure of the parent compound, bicyclo[4.2.1]-2,4-nonadiene, has not been recorded. Structural comparisons: P. Berno, A. Ceccon, F. Daprà, A. Gambaro, A. Venzo, P. Ganis, G. Valle, *J. Organomet. Chem.* **1986**, *301*, 161; Z. Goldschmidt, H. E. Gottlieb, E. Genizi, D. Cohen, I. Goldberg, *ibid.* **1986**, *301*, 337; M. Parvez, K. S. Feldman, B. J. Kosmider, *Acta Crystallogr. Sect. C* **1987**, *43*, 1410.
[14] For force-field calculations on the relative stability of the cycloadducts of **1**/cyclohexadiene see ref.[6]. Preliminary results of the force-field calculations on (*E*)/(*Z*)-*cis*/*trans*-**5** show that all four isomers have approximately the same stability.
[15] C. Seidenschwarz, Dissertation, Technische Universität München, **1991**.
[16] W. Scherer, P. Kiprof, E. Herdtweck, R. E. Schmidt. M. Birkhan, W. Massa, *"Strux IV"*, program system for the manipulation of X-ray data, Technische Universität München and Universität Marburg, **1987** and **1990**.

Synthesis of the First 2*H*-1-Aza-2-phosphirene Complexes**

Rainer Streubel,* Jörg Jeske, Peter G. Jones, and Regine Herbst-Irmer

The elucidation of the mechanisms of preparatively important reactions is fascinating, but also often very time-consuming. The rearrangement **I** → **II** of a η^2-cyclopropene into a vinyl carbene complex during the insertion of an alkyne into the metal–carbene carbon bond of an arylidene(pentacarbonyl)-tungsten(0) complex was verified only recently,[1] although this reaction sequence has long been utilized in preparative work.[2] In attempting to synthesize the first derivatives of 2-aza-1-phospha-4-tungsta-1,3-butadiene (**III**), which is isolobal with **II**, we have now surprisingly obtained exclusively 2*H*-1-aza-2-phosphirene tungsten complexes of type **IV**, which are isomeric with **III** (Scheme 1).



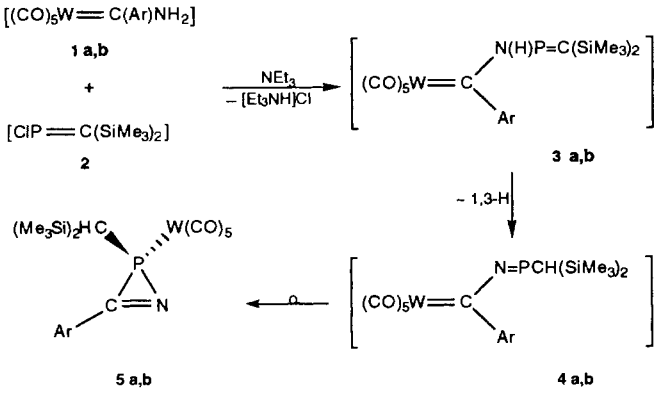
Scheme 1.

To the best of our knowledge neither 2*H*-1-aza-2-phosphirenes nor their cyclic isomers are known, nor have there been previous reports of complexes containing these three-membered rings as ligands.[3]

[*] Dr. R. Streubel, Dipl.-Chem. J. Jeske, Prof. Dr. P. G. Jones
Institut für Anorganische und Analytische Chemie der
Technischen Universität
Postfach 3329, D-38023 Braunschweig (FRG)
Telefax: Int. code + (531)391-5387
Dr. R. Herbst-Irmer
Institut für Anorganische und Analytische Chemie der Universität Göttingen

[**] This work was supported by the Fonds der Chemischen Industrie and BASF AG, Ludwigshafen.

The reaction of amino(aryl)carbene tungsten complexes **1a,b**[4] with chloro[bis(trimethylsilyl)methylene]phosphane (**2**)[5] in the presence of triethylamine under mild conditions gave the 2*H*-1-aza-2-phosphirene-2-pentacarbonyltungsten complexes **5a,b** (Scheme 2). These were isolated from pentane in good yields as yellow crystalline solids.



Scheme 2. Proposed reaction sequence for the formation of the 2*H*-1-aza-2-phosphirene tungsten complexes **5a,b**. **1a**, **3a–5a**: Ar = *p*-tolyl; **1b**, **3b–5b**: Ar = *p*-anisyl.

Table 1. Selected spectroscopic data of **5a,b** and **6** [a].

5a: ^{1}H NMR: $\delta = 0.10$ (s, 9H, $SiMe_3$), 0.29 (s, 9H, $SiMe_3$), 0.71 (d, ^2J(H,P) = 2.8 Hz, 1H, PCH), 2.48 (s, 3H, *p*-CH_3), 7.43 (d, ^3J(H,H) = 8.1 Hz, 2H, *m*-H), 7.91 (d, ^3J(H,H) = 8.1 Hz, 2H, *o*-H); ^{13}C{^{1}H} NMR: $\delta = 1.35$ (d, ^3J(C,P) = 3.13 Hz, $SiMe_3$), 2.14 (d, ^3J(C,P) = 3.04 Hz, $SiMe_3$), 22.02 (s, Ph-CH_3), 27.44 (d, ^1J(C,P) = 24.24 Hz, PCH), 123.79 (d, ^2J(C,P) = 15.08 Hz, Ph), 129.62 (s, Ph), 130.47 (s, Ph), 145.30 (s, Ph), 191.44 (d, ^1J(C,P) = 1.44 Hz, PCN), 195.91 (dd, ^2J(C,P) = 9.11 Hz, ^1J(C,W) = 125.93 Hz, *cis*-CO), 197.87 (d, ^2J(C,P) = 35.91 Hz, *trans*-CO); ^{31}P{^{1}H} NMR: $\delta = -111.19$ (d, ^1J(P,W) = 293.09 Hz).

5b: ^{1}H NMR: $\delta = 0.05$ (s, 9H, $SiMe_3$), 0.31 (s, 9H, $SiMe_3$), 0.71 (d, ^2J(H,P) = 2.77 Hz, 1H, PCH), 3.09 (s, 3H, OCH_3), 6.57 (d, ^3J(H,H) = 8.82 Hz, 2H, *m*-H), 7.89 (d, ^3J(H,H) = 8.82 Hz, 2H, *o*-H); ^{13}C{^{1}H} NMR: $\delta = 1.32$ (d, ^3J(C,P) = 3.18 Hz, $SiMe_3$), 2.15 (d, ^3J(C,P) = 3.20 Hz, $SiMe_3$), 27.47 (d, ^1J(C,P) = 24.32 Hz, PCH), 54.98 (s, OCH_3), 115.39 (s, Ph), 119.08 (d, ^2J(C,P) = 15.0 Hz, Ph), 131.85 (s, Ph), 164.54 (s, Ph), 190.27 (d, ^1J(C,P) = 3.05 Hz, PCN), 196.53 (dd, ^2J(C,P) = 9.03 Hz, ^1J(C,W) = 126.01 Hz, *cis*-CO), 198.09 (d, ^2J(C,P) = 35.38 Hz, *trans*-CO); ^{31}P{^{1}H} NMR: $\delta = -115.1$ (d, ^1J(P,W) = 292.5 Hz).

6: ^{1}H NMR: $\delta = 0.10$ (s, 9H, $SiMe_3$), 0.44 (s, 9H, $SiMe_3$), 0.88 (d, ^2J(H,P) = 1.73 Hz, 1H, PCH), 2.51 (s, 3H, *p*-CH_3), 7.53 (d, ^3J(H,H) = 8.19 Hz, 2H, *m*-H), 8.04 (d, ^3J(H,H) = 8.19 Hz, 2H, *o*-H); ^{13}C{^{1}H} NMR: $\delta = 1.49$ (d, ^3J(C,P) = 3.06 Hz, $SiMe_3$), 2.94 (d, ^3J(C,P) = 3.81 Hz, $SiMe_3$), 21.90 (s, Ph-CH_3), 30.18 (d, ^1J(C,P) = 31.33 Hz, PCH), 122.86 (d, ^2J(C,P) = 12.88 Hz, Ph), 128.98 (s, Ph), 130.30 (s, Ph), 146.14 (s, Ph), 195.17 (s, *cis*-CO), 196.31 (s, *trans*-CO), 197.39 (s, *cis*-CO), 199.39 (d, ^2J(C,P) = 40.71 Hz, *trans*-CO), 201.64 (d, ^1J(C,P) = 1.44 Hz, PCN); ^{31}P{^{1}H} NMR: $\delta = -62.0$ (d, ^1J(P,W) = 305.02 Hz).

[a] All spectra of **5a** and **6** in $CDCl_3$ and of **5b** in C_6D_6, 25 °C; ^{1}H NMR: 200 MHz, ^{13}C NMR: 50.3 MHz, ^{31}P NMR: 81.0 MHz; the deuterated solvent was used as internal standard and 85% H_3PO_4 as external standard.

Even though none of the intermediates could be isolated or detected spectroscopically, the reaction sequence for the formation of the 2*H*-azaphosphirene tungsten complexes **5a,b** summarized in Scheme 2 still seems plausible. The first step is the formation of the P–N bond to give the 3-aza-2-phospha-5-tungsta-1,4-pentadiene derivatives **3a,b** with the loss of triethylammonium chloride. A subsequent 1,3 hydrogen shift in **3a,b** leads to the formation of the P–N double bond of the bis(trimethylsilyl)methyl-substituted 2-aza-1-phospha-4-tungsta-1,3-butadienes **4a,b**—similar 1,3-hydrogen shifts have already been exploited to synthesize a bis(trimethylsilyl)methyl-substituted iminophosphane[6] and (1-dialkylaminopropylidene)aminocarbene complexes.[7] An immediate valence-isomerization of compounds **4a,b**, possibly via a metallacyclic intermediate, leading to the formation of the C–N double bond, and a subsequent shift of the pentacarbonyltungsten fragment to the phosphorus atom, affords the 2*H*-azaphosphirene complexes **5a,b**. The composition and constitution of compounds **5a,b** are confirmed by elemental analyses, mass spectrometric and IR[8] and NMR spectroscopic investigations (Table 1). The phosphorus atoms in **5a,b** each show one resonance signal in the high-field region of the ^{31}P NMR spectrum (**5a**: $\delta = -111.19$ (^1J(P,W) = 293.09 Hz), **5b**: $\delta = -115.1$ (^1J(P,W) = 292.5 Hz)). The large values of the ^1J(P,W) coupling constants are characteristic for direct bonding of the $[W(CO)_5]$ fragment to the phosphorus atom. The ^{13}C NMR signal of the imine-carbon atom (**5a**: $\delta = 191.44$ (^1J(C,P) = 1.44 Hz); **5b**: $\delta = 190.27$ (^1J(C,P) = 3.05 Hz) is significantly shifted downfield in comparison to the corresponding signals of 3-aryl-2*H*-azirines.[9] The values of the ^1J(C,P) coupling constants of **5a,b** are remarkably small; 1-aryl-1*H*-phosphirine complexes show the same phenomenon.[10]

The proposed constitution of the compounds **5a,b** was confirmed for **5a** by a single-crystal X-ray structure analysis. There are two independent molecules in the asymmetric unit, which, however, do not differ significantly.[11] As shown in Figure 1, the 2*H*-1-aza-2-phosphirene unit in **5a** is characterized by a short C1–N1 bond (126.5(11) and 126.2(11) pm), similar to that observed in 2*H*-azirine palladium complexes. As a result of this short C1–N1 bond in **5a**, a very acute endocyclic angle (41.6(4) and 41.8(4)°) occurs at the phosphorus atom. The very short C1–C3 single bond (145.8(12) and 147.0(12) pm) clearly indicates a π interaction between the two ring systems in **5a** (interplanar angle 2° and 3°). The question then arises whether it is possible to stabilize or destabilize the 2*H*-1-aza-2-phosphirine unit by using suitable substituents at the phenyl ring, and thereby to induce isomerizations of this ring.

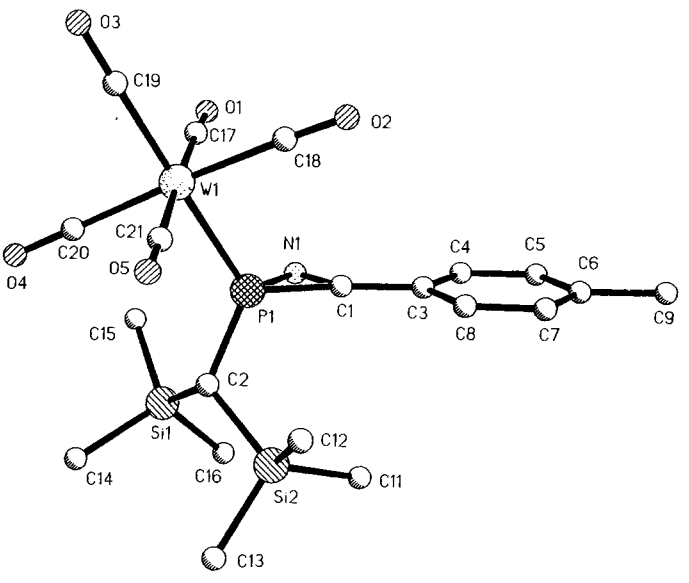
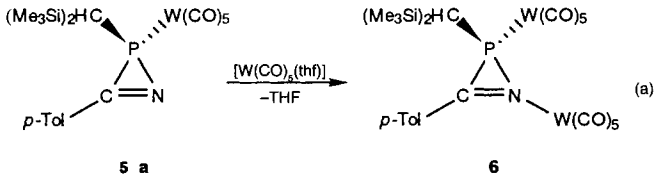


Fig. 1. One of the two independent molecules of **5a** in the crystal. Selected bond lengths [pm] and angles [°] (values for both molecules): P1-C1 176.5(9), 174.9(9), P1-C2 180.1(8), 180.3(8), P1-N1 179.3(8), 178.9(9), P1-W1 247.0(2), 247.9(2), N1-C1 126.5(11), 126.2(11), C1-C3 145.8(12), 147.0(12); C1-P1-N1 41.6(4), 41.8(4), C1-N1-P1 68.0(5), 67.4(6), N1-C1-P1 70.4(6), 70.8(6), N1-C1-C3 134.5(8), 132.6(8), C3-C1-P1 154.9(7), 156.6(6).

 © VCH Verlagsgesellschaft mbH, D-69451 Weinheim, 1994 0570-0833/94/0101-0081 $ 10.00+.25/0

The reaction of **5a** with $[W(CO)_5(thf)]$ illustrates the nucleophilic character of the 2 *H*-azaphosphirene complex **5a**.[1,2] The reaction leads smoothly and with retention of the three-membered ring to the orange-colored 1,2-bis(pentacarbonyltungsten)-1-aza-2-phosphirene derivative **6** [Eq. (a)].



(a)

5a **6**

The η^1 coordination of the $[W(CO)_5]$ fragment at the nitrogen atom not only has a considerable deshielding effect on the two other ring atoms, but also on the phenyl-carbon atoms in **6** (cf. NMR data in Table 1). Both the NMR signal of the phosphorus and that of the carbon atom in the three-membered ring of **6** are shifted significantly downfield in comparison to the corresponding signals of **5** (**5a**, **6**: $\delta^{31}P = -111.19, -62.0$; $\delta^{13}C = 191.44, 201.64$); furthermore, the values of the exocyclic $^1J(C,P)$ and $^1J(P,W)$ coupling constants are considerably higher.

As these results show, amino(aryl)carbene tungsten complexes can be used for the synthesis of new phospha heterocycles. The development of additional methods for the synthesis of 2 *H*-1-aza-2-phosphirenes and investigations into the reactivity of this new ring system are planned.

Experimental Procedure

General procedure for the preparation of **5a,b**: A solution of **1a,b** (1.5 mmol) in Et_2O (15 mL) was treated with **2** (0.34 g, 1.5 mmol) and NEt_3 (5 mL) under nitrogen at room temperature and stirred for two days. The orange reaction mixture was concentrated to dryness under reduced pressure. The residue was treated with pentane (30 mL), subsequently filtered and the filtration residue washed twice with pentane (5 mL). The filtrate was concentrated to 10 mL under reduced pressure and cooled to −30 °C. The resulting crystalline solid was washed with a little pentane and then the remaining solvent was removed under high vacuum (10^{-3} mbar). **5a**: yellow crystals, yield 49%, m.p. 104–105 °C (decomp); **5b**: yellow-orange crystals, yield 45%, m.p. 103–104 °C (decomp).

6: **5a** (0.6 g, 0.95 mmol) in THF (20 mL) was treated at 0 °C with a $[W(CO)_5(thf)]$ solution (100 mL, 0.095 M) and stirred at this temperature for 0.5 h. The reaction solution was concentrated to 15 mL under reduced pressure and stirred for a further two hours at room temperature. Subsequently, the solution was concentrated to dryness, the residue taken up in pentane (50 mL), filtered, and concentrated to dryness again. If the residue was taken up in Et_2O (15 mL), **6** remained in the residue. The solid was separated from the solution, washed twice with a little pentane and subsequently dried under high vacuum. Orange powder, yield 69%, m.p. 121 °C (decomp).

Received: August 6, 1993 [Z 6264 IE]
German version: *Angew. Chem.* **1994**, *106*, 115

[1] H. Fischer, J. Hofmann, E. Mauz, *Angew. Chem.* **1991**, *103*, 1013; *Angew. Chem. Int. Ed. Engl.* **1991**, *30*, 998.
[2] K. H. Dötz, *Angew. Chem.* **1984**, *96*, 573; *Angew. Chem. Int. Ed. Engl.* **1984**, *23*, 587, and references therein.
[3] 1 *H*-Diphosphirenes are known both in the uncomplexed (a) and the complexed (b) form: a) E. Niecke, R. Streubel, M. Nieger, D. Stalke, *Angew. Chem.* **1989**, *101*, 1708; *Angew. Chem. Int. Ed. Engl.* **1989**, *28*, 1673; b) R. Streubel, N. H. Tran Huy, L. Ricard, F. Mathey, *Phosphorus, Sulfur Silicon Relat. Elem.* **1993**, *77*, 229.
[4] The amino(aryl)carbene tungsten complexes **1a**, **b** were prepared according to known procedures: E. O. Fischer, H. J. Kollmeier, *Chem. Ber.* **1971**, *104*, 1339.
[5] R. Appel, A. Westerhaus, *Tetrahedron Lett.* **1981**, *22*, 4957.
[6] R. Streubel, E. Niecke, *Chem. Ber.* **1990**, *123*, 1245.
[7] K. H. Dötz, *Chem. Ber.* **1980**, *113*, 3597.
[8] Selected IR spectroscopic and MS data of **5a**, **b** and **6**–**5a**: IR (CH_2Cl_2): $\tilde{\nu}$ = 2073 s (C=O), 1985 s (C=O), 1960–1919 vs, b (C=O), 1602 m (C=N) cm^{-1}; MS (EI, 70 eV, ^{184}W): m/z = 631 (M^+). **5b**: IR (CH_2Cl_2): $\tilde{\nu}$ = 2072 s (C=O), 1984 s (C=O), 1964–1912 vs, b (C=O), 1600 m (C=N) cm^{-1}; MS (EI, 70 eV, ^{184}W): m/z = 647 (M^+). **6**: IR (CH_2Cl_2): $\tilde{\nu}$ = 2078 s (C=O), 2065 s (C=O), 1996 s (C=O), 1964–1913 vs, b (C=O), 1603 m (C=N) cm^{-1}. Correct elemental analysis for **5a**, **b** and **6**.
[9] A. Hassner, C. A. Bunnell, K. Haltiwanger, *J. Org. Chem.* **1978**, *43*, 57.
[10] a) F. Mercier, F. Mathey, *Tetrahedron Lett.* **1986**, *27*, 1323; b) F. Mathey, *Chem. Rev.* **1990**, *90*, 997.
[11] Crystal structure analysis of **5a**: $C_{20}H_{26}NO_5PSi_2W$, monoclinic, space group *Cc*, a = 1393.4(5), b = 1392.1(3), c = 2714.1(9) pm, β = 99.58(3)°, V = 5.191(3) nm^3, Z = 8, μ = 4.6 mm^{-1}, T = −130 °C. A yellow crystal (ca. 0.4 × 0.4 × 0.4 mm) was mounted in inert oil (RS 3000, donated by Riedel de Haën). 6276 intensities to $2\theta_{max}$ = 55° were measured with $Mo_{K\alpha}$ radiation on a Stoe-STADI4 diffractometer, of which 6208 were independent after an absorption correction and 6198 were used for all calculations (program SHELXL-93: G. M. Sheldrick, Universität Göttingen **1993**). The structure was solved by heavy atom methods and refined anisotropically on F^2. H atoms were included with a riding model. The final $wR(F^2)$ value was 0.069, with a conventional $R(F)$ 0.032 for 555 parameters and 262 restraints. The structure is characterized by a marked pseudosymmetry; the intenstity statistics and the largest peaks of the Patterson function indicate the centrosymmetric space group *C2/c*, in which, however, only the position of the W atom could be determined. The structure could only be extended in *Cc* (with two independent molecules); the choice of the space group was then confirmed by an *x*-refinement [H. D. Flack, *Acta Crystallogr. Sect A* **1983**, *39*, 876], in which *x* was refined to the value −0.002(8). Further details of the crystal structure investigation may be obtained from the Fachinformationszentrum Karlsruhe, D-76344 Eggenstein-Leopoldshafen (FRG) on quoting the depository number CSD-400333, the names of the authors, and the journal citation.
[12] W. Strohmeier, F. J. Müller, *Chem. Ber.* **1969**, *102*, 3608.

A "Branched-Monomer Approach" for the Rapid Synthesis of Dendimers**

Karen L. Wooley, Craig J. Hawker, and Jean M. J. Fréchet*

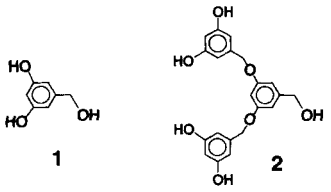
The reactivities[1] and properties[2] of dendritic macromolecules are currently being examined both out of scientific curiosity and for potential commercial applications. This has created a demand for the rapid production of dendrimers. However, both of the methods employed in the synthesis of the "perfect" dendritic macromolecules, the "divergent-"[3] and "convergent-growth"[4] approaches, involve stepwise, tedious, and time-consuming processes. Improvements have been made for the convergent growth approach. In an accelerated double-stage process[5] several growth steps are eliminated through the use of large dendritic core molecules (hypercores), allowing the preparation of high molecular weight compounds. Alternatively, in a "two-monomer approach"[6] two generations can be grown in one pot without intermediate purification steps. We now report on the use of more highly functionalized "branched monomers" in the convergent growth approach as a means for the accelerated synthesis of dendrimers.

Conceptually, the simplest repeating unit or "fractal component" used in the convergent growth process is replaced by a larger fractal component of the next generation. Therefore instead of a classical AB_2 monomer (e.g. **1**) a larger AB_4 monomer of the next generation (e.g. **2**) is employed. Use of the larger monomer preserves the convergent-growth concept with a single reactive group (the benzylic hydroxyl group) at the focal point

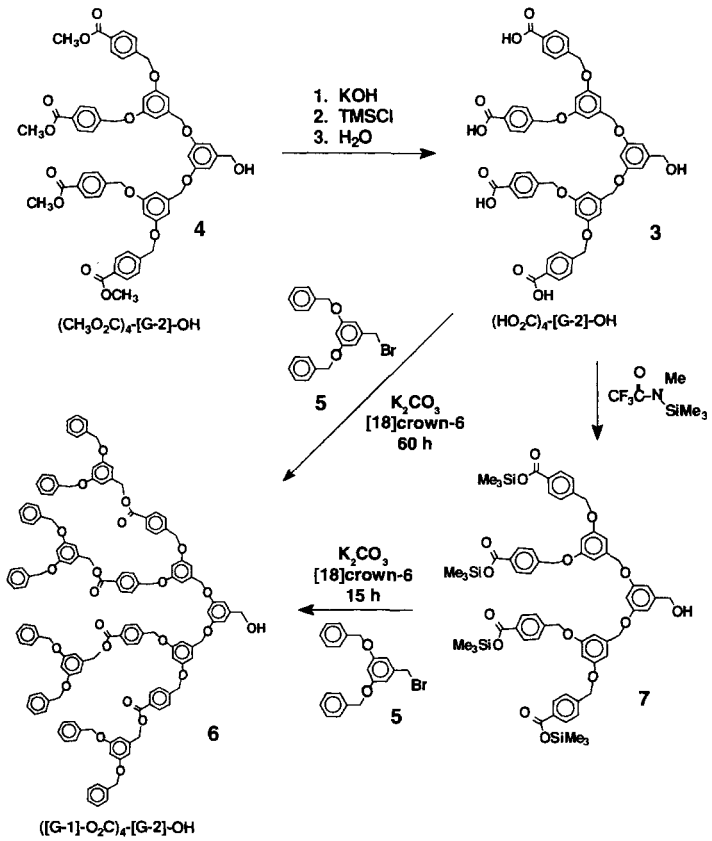
[*] Prof. Dr. J. M. J. Fréchet, Dr. K. L. Wooley, Dr. C. J. Hawker
Baker Laboratory, Department of Chemistry
Cornell University
Ithaca, NY 14853-1301 (USA)
Telefax: Int. code + (607)255-4137

[**] Financial support of this project was provided by the National Science Foundation (DMR-9224421 and 9121654), the Department of Education (fellowship for K. W.), and the Australian Research Council (fellowship for C. H.).

while maintaining the branching pattern and flexibility of the final dendrimer, and reducing the number of steps required to reach higher generations. In view of difficulties encountered in the preparation of **2** in high yield, the branched monomer **3** was selected for this study.



Preparation of **3** required protection of its carboxy groups as methyl esters. Complete hydrolysis of the starting material $(CH_3O_2C)_4$-[G-2]-OH **4**[7] with potassium hydroxide in a mixed-solvent system of water, ethanol, and 1,4-dioxane at reflux furnished the tetracarboxylate (Scheme 1). Neutralization with glacial acetic acid resulted in precipitation of a partially protonated species, which is insoluble in organic solvents. However, upon addition of chlorotrimethylsilane to a slurry of the collected precipitate in THF, the soluble trimethylsilyl ester of **3** (compound **7**) was formed. Precipitation of this intermediate into water gave the desired tetracarboxylic acid **3**.



Scheme 1. Preparation of branched monomers **3** and **7** and their use in the preparation of a third-generation dendrimer.

As shown in Scheme 1, reaction of the branched monomer **3** with the first-generation dendritic bromide **5** in the presence of potassium carbonate gave a third-generation dendritic benzyl ether **6**, containing four internal ester linkages, in 85% yield after purification by flash chromatography. Because the generation number correlates with the number of layers of monomer units, each generation growth step performed with the second-generation branched monomer **3** results in an increase in size of two generations. Alcohol **6** is a dendritic trilayer block copolymer, since in its construction an outer concentric layer of ether groups surrounds an inner layer of ester groups as well as two layers of ether linkages. It should be noted that the purity of the branched monomer is critical if high yields of pure dendrimer are to be obtained.

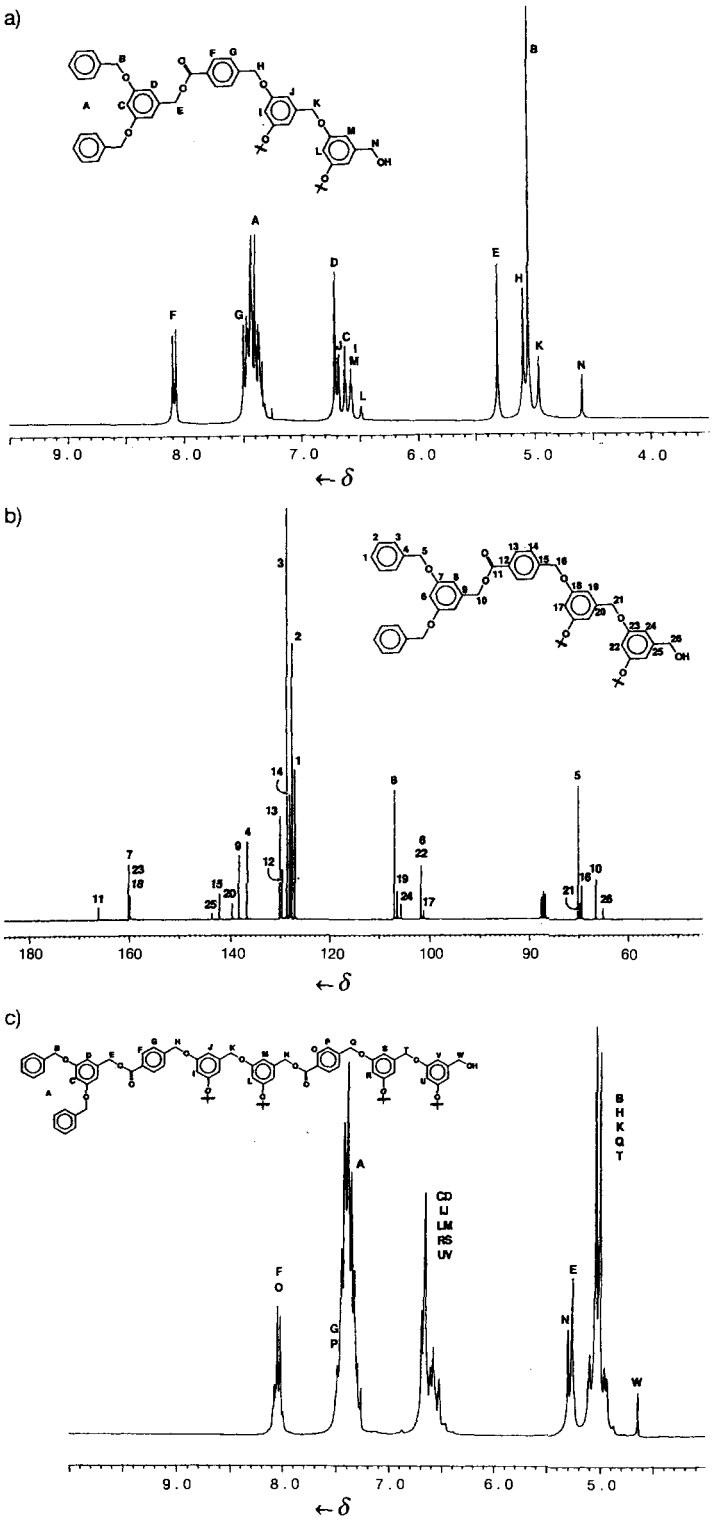


Fig. 1. a) ^{1}H NMR spectrum (300 MHz, $CDCl_3$) of **6**; b) ^{13}C NMR spectrum (75 MHz, $CDCl_3$) of **6**; c) ^{1}H NMR spectrum (300 MHz, $CDCl_3$) of **9**.

 © VCH Verlagsgesellschaft mbH, D-69451 Weinheim, 1994 0570-0833/94/0101-0083 $ 10.00+.25/0

The reaction between **3** and **5** was found to be quite slow, requiring approximately 60 hours to reach greater than 90% completion. This most likely results from the low solubility of **3** in the basic reaction mixture and its possible aggregation through hydrogen bonding. To increase the efficiency of the synthesis and reduce the reaction time, the tetracarboxylic acid **3** was treated with *N*-methyl-*N*-(trimethylsilyl)trifluoroacetamide to give the branched tetrakis(trimethylsilyl) monomer **7**, which was not isolated but treated in situ with the first-generation bromide **5** in the presence of potassium carbonate and [18]crown-6 (Scheme 1). In this way, the desired third-generation alcohol **6** was obtained with 90% conversion after heating at reflux for only 15 hours. Both the ^{1}H and ^{13}C NMR spectra of **6** were extremely well-resolved, and all of the protons and carbon atoms in the structure could be identified and assigned (Fig. 1).

Activation of the focal-point group through transformation of benzylic alcohol **6** to give benzylic bromide **8** was performed with carbon tetrabromide and triphenylphosphane in 91% yield. Coupling of the third-generation dendrimer **8** to the branched monomer **7** generated in situ to afford the fifth-generation dendrimer **9** (Scheme 2) was monitored by gel permeation chromatography (GPC) and found to be roughly 40% complete after 17 hours. Unfortunately, the yield of **9** could not be increased under the conditions selected. This decrease in yield in the coupling reactions leading to higher generation dendrimers was observed previously[4] in the preparation of a sixth-generation dendrimer by the convergent-growth process and is thought to be partly sterically induced, and partly the result of less effective coupling reactions. Despite this shortcoming, the efficiency of this branched-monomer approach is apparent in the synthesis of the dendritic block copolymer **9** which has a molecular weight of 9371, contains eight layers of phenyl rings, and is obtained in only three steps with an overall yield of 31% from the first-generation bromide **5**, which has two layers of phenyl rings and a molecular weight of only 383. In the traditional convergent-growth approach with 3,5-dihydroxybenzyl alcohol as the monomer[4] [G-5]-OH was obtained in 50% overall yield from [G-1]-Br as a result of improved Williamson-type couplings, but the synthesis required seven steps!

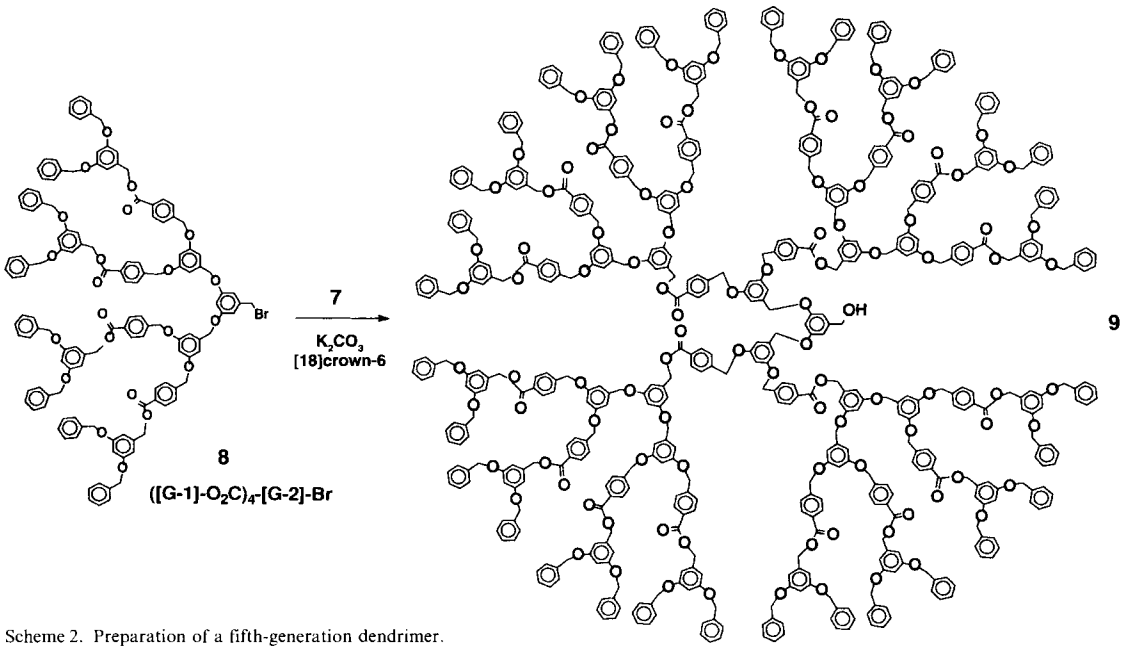
As shown in Figure 1c, resonances in the ^{1}H NMR spectrum of **9** are broad compared to those of **6**. Although much fine structure has been lost, important characterization information remains. In particular, one-half of the quartet (AB_q) from the *para*-substituted aromatic rings of the branched monomer units is observed at $\delta = 7.9-8.1$, two resonances at $\delta = 5.25$ and 5.29 are found for the methylene groups of the two layers of benzyl esters, and the benzylic protons of the focal-point group resonate at $\delta = 4.63$.

The synthesis of dendritic poly(ether/ester) layer block copolymers by a novel, rapid branched-monomer approach has been demonstrated. These dendritic macromolecules are interesting since hydrolyzable ester linkages are placed in discrete layers within the structure, such that cleavage or degradation of the dendrimer yielding water-soluble fragments may be possible. By judicious choice of the starting material and the branched monomer a large variety of functionalized dendritic macromolecules and block copolymers can be synthesized.

Experimental Procedure

$(HO_2C)_4$-[G-2]-OH **3**: To a solution of **4** [7] (1.27 g, 1.3 mmol) in 1,4-dioxane (30 mL) was added aqueous KOH (1.10 g, 19.6 mmol, in 12 mL H_2O). The mixture was heated at reflux, 95% ethanol (15 mL) and additional H_2O (18 mL) were added to form a one-phase reaction mixture, and heating was continued for 20 h. The mixture was allowed to cool to room temperature, glacial acetic acid (5 mL) was added, and the precipitate was collected by suction filtration. Upon addition of trimethylsilyl chloride to the slurry of partially protonated product in THF, trimethylsilyl esters formed and the product dissolved. After 20 min at room temperature, the mixture was concentrated under reduced pressure and added to H_2O to give the fully protonated product as precipitate. This precipitate was collected by suction filtration, dissolved in THF, filtered, and concentrated providing tetracarboxylic acid **3** as a white solid, which yellowed with storage over a period of weeks. Yield 96%; T_g 89 °C; m.p. 203–205 °C; ^{1}H NMR ([D$_8$]THF) δ 4.18 (br, 1H; CH_2OH), 4.46 (s, 2H; CH_2OH), 4.96 (s, 4H; $ArCH_2O$), 5.10 (s, 8H; HO_2CPhCH_2), 6.45 (t, 1H, $J = 2$ Hz; ArH), 6.56 (d, 2H, $J = 2$ Hz; ArH), 6.58 (t, 2H, $J = 2$ Hz; ArH), 6.70 (d, 4H, $J = 2$ Hz; ArH), 7.47, 7.97 (AB_q, 16H, $J = 8$ Hz; HO_2CPhH); IR: $\tilde{\nu} = 3500-2400$, 1693, 1597, 1450, 1423, 1373, 1317, 1292, 1160, 1051, 1020 cm^{-1}.

([G-1]-$O_2C)_4$-[G-2]-OH **6**: To a solution of **3** (0.20 g, 0.22 mmol, 1.0 equiv) in THF (25 mL) under nitrogen at room temperature was added *N*-methyl-*N*-(trimethylsilyl)trifluoroacetamide (0.25 mL, 0.27 g, 1.3 mmol, 5.9 equiv). After 30 min the THF solution was heated at reflux and then **5** (0.42 g, 1.1 mmol, 5 equiv), potassium carbonate (0.30 g, 2.2 mmol, 10 equiv), and [18]crown-6 (0.03 g, 0.11 mmol, 0.5 equiv) were added. The reaction was monitored by GPC. After completion the



Scheme 2. Preparation of a fifth-generation dendrimer.

 © VCH Verlagsgesellschaft mbH, D-69451 Weinheim, 1994 0570-0833/94/0101-0084 $ 10.00+.25/0

reaction mixture was evaporated to dryness under reduced pressure and the residue partitioned between water and methylene chloride. The aqueous layer was extracted three times with CH_2Cl_2, and the extracts were combined, dried over $MgSO_4$, and then concentrated under reduced pressure. The crude product was purified by flash chromatography ($CH_3OH/CH_3COOH/CH_2Cl_2$ 2:1:97) to afford **6** as a colorless glass. Yield 85%; T_g 34 °C; ^{1}H NMR ($CDCl_3$) see Fig. 1a; IR: $\tilde{\nu}$ = 3550–3350, 3200–2800, 1719, 1597, 1497, 1453, 1416, 1375, 1343, 1319, 1273, 1215, 1161, 1105, 1061, 1030, 1020 cm^{-1}.

([G-1]-$O_2C)_4$-[G-2]-Br **8**: To a solution of **6** (0.43 g, 0.20 mmol, 1.0 equiv) in THF (20 mL) was added carbon tetrabromide (0.13 g, 0.4 mmol, 2 equiv) and triphenylphosphane (0.10 g, 0.4 mmol, 2 equiv), and the reaction mixture was stirred at room temperature under nitrogen. The progress of the reaction was monitored by thin-layer chromatography. The reaction was quenched by addition of water and CH_2Cl_2. The aqueous layer was extracted three times with CH_2Cl_2, and the extracts were dried over $MgSO_4$ and concentrated under reduced pressure. The crude product was purified by precipitation into ether followed by flash chromatography (2% ether/CH_2Cl_2) to yield **8** as a colorless glass. Yield 91%; T_g 34 °C; ^{1}H NMR ($CDCl_3$) δ 4.35 (s, 2H; CH_2Br), 4.94 (s, 4H; ArCH_2O-), 5.03 (s, 16H; $PhCH_2$), 5.09 (s, 8H; RO_2CPhCH_2), 5.28 (s, 8H; ArCH_2O_2C), 6.4–6.8 (m, 21H; ArH), 7.2–7.6 (m, 40H; PhH), 7.46, 8.05 (AB_4, 16H, J = 8 Hz, RO_2CPhH); IR: $\tilde{\nu}$ = 3200–2800, 1719, 1597, 1499, 1453, 1416, 1373, 1343, 1321, 1273, 1215, 1160, 1105, 1061, 1019 cm^{-1}.

(([G-1]-$O_2C)_4$-[G-2])$_4$-[G-2]-OH **9**: Same procedure as for **6**, however with **8** instead of **5**. The crude product was purified by flash chromatography (3% methanol/CH_2Cl_2) to afford **9** as a colorless glass; T_g 38 °C; ^{1}H NMR ($CDCl_3$) see Fig. 1c; IR: $\tilde{\nu}$ = 3600–3400, 3000–2800, 1719, 1597, 1497, 1453, 1416, 1373, 1343, 1273, 1215, 1159, 1105, 1061, 1019 cm^{-1}.

Received: July 15, 1993 [Z 6215IE]
German version: *Angew. Chem.* **1994**, *106*, 123

[1] C. J. Hawker, J. M. J. Fréchet, *J. Chem. Soc. Perkin Trans. 1* **1992**, 2459; G. R. Newkome, C. N. Moorefield, *Polym. Prepr. Am. Chem. Soc. Div. Polym. Chem.* **1993**, *34*, 75; L. Lochmann, K. L. Wooley, P. T. Ivanova, J. M. J. Fréchet, *J. Am. Chem. Soc.* **1993**, *115*, 7043.

[2] T. H. Mourey, S. R. Turner, M. Rubinstein, J. M. J. Fréchet, C. J. Hawker, K. L. Wooley, *Macromolecules* **1992**, *25*, 2401; K. L. Wooley, C. J. Hawker, J. M. Pochan, J. M. J. Fréchet, *ibid.* **1993**, *26*, 1514; G. R. Newkome, J. K. Young, G. R. Baker, R. L. Potter, L. Audoly, D. Cooper, C. D. Weis, K. Morris, C. S. Johnson, *ibid.* **1993**, *26*, 2394; Y. Guo, K. H. Langley, F. E. Karasz, *ibid.* **1992**, *25*, 4902; C. J. Hawker, K. L. Wooley, J. M. J. Fréchet, *J. Am. Chem. Soc.* **1993**, *115*, 4375; P. M. Saville, J. W. White, C. J. Hawker, K. L. Wooley, J. M. J. Fréchet, *J. Phys. Chem.* **1993**, *97*, 293; N. J. Turro, J. K. Barton, D. A. Tomalia, *Acc. Chem. Res.* **1991**, *24*, 332.

[3] G. R. Newkome, C. N. Moorefield, *Adv. Dendritic Macromol.* **1993**, *1*, 1; H. Mekelburger, W. Jaworek, F. Vögtle, *Angew. Chem.* **1992**, *104*, 1609; *Angew. Chem. Int. Ed. Engl.* **1992**, *31*, 1571; H. B. Mekelburger, K. Rissanen, F. Vögtle, *Chem. Ber.* **1993**, *126*, 1161; D. A. Tomalia, A. M. Naylor, W. A. Goddard III, *Angew. Chem.* **1990**, *102*, 119; *Angew. Chem. Int. Ed. Engl.* **1990**, *29*, 138.

[4] C. J. Hawker, J. M. J. Fréchet, *J. Chem. Soc. Chem. Commun.* **1990**, 1010; C. J. Hawker, J. M. Fréchet, *J. Am. Chem. Soc.* **1990**, *112*, 7638.

[5] K. L. Wooley, C. J. Hawker, J. M. J. Fréchet, *J. Am. Chem. Soc.* **1991**, *113*, 4252.

[6] R. Spindler, J. M. J. Fréchet, *J. Chem. Soc. Perkin Trans. 1* **1993**, 913.

[7] C. J. Hawker, K. L. Wooley, J. M. J. Fréchet, *J. Chem. Soc. Perkin Trans. 1* **1993**, 1287.

Thermal Decomposition of Silver Oxide Monitored by Raman Spectroscopy: From AgO Units to Oxygen Atoms Chemisorbed on the Silver Surface

Bruno Pettinger, Xinhe Bao, Ian Wilcock, Martin Muhler, Robert Schlögl, and Gerhard Ertl*

In studies on the catalytic partial oxidation of methanol on silver surfaces it was recently found that the interaction of oxygen at nearly atmospheric pressure with silver at elevated temperatures (> 700 K) leads to the formation of a very stable species, which was identified as O atoms chemisorbed on the surface of the distorted Ag lattice. It is also this species that enters the catalytic oxidation reaction.[1, 2] In order to compare this species, which is associated with metallic silver, to silver oxides, the thermal decomposition of the latter in an oxygen-free atmosphere over the temperature range 300 to 930 K was investigated by Raman spectroscopy. The starting compound was $Ag_7O_8NO_3$ (**1**); in contrast to ordinary silver oxide, which exhibits a pronounced tendency for formation of carbonates in the surface region, **1** is rather stable to the attack of carbon-containing impurity compounds in the gas phase.[3]

Steel-gray $Ag_7O_8NO_3$ powder was prepared by anodic oxidation in a glove box.[4] The experiments were performed in a reaction cell we had constructed which was connected to a Raman spectrometer (SPEX Triplemate) and a diode array detector (OMA II from EG & G).[5, 6] In order to minimize temperature gradients, the powder was pressed into a thin sheet on a silver support which was mounted in a stainless steel sample holder connected to a cylindrical oven. The temperature was monitored by a thermocouple attached to the holder.

Silver oxides are rather sensitive to photochemical reduction and reoxidation, which hampers Raman spectroscopic investigations, in particular, of Ag_2O.[7–9] Hence we reduced the intensity of the laser excitation (λ_{ex} = 514.5 nm) to about 20 mW, and noticeable light-induced changes of the sample were no longer observed.

Raman spectra of **1** reflecting the chemical changes upon heating are reproduced in Figure 1. At T = 300 K the spectrum exhibits essentially only a band at 410 cm^{-1}, which is characteristic for the AgO unit in **1**, and an additional shoulder at around

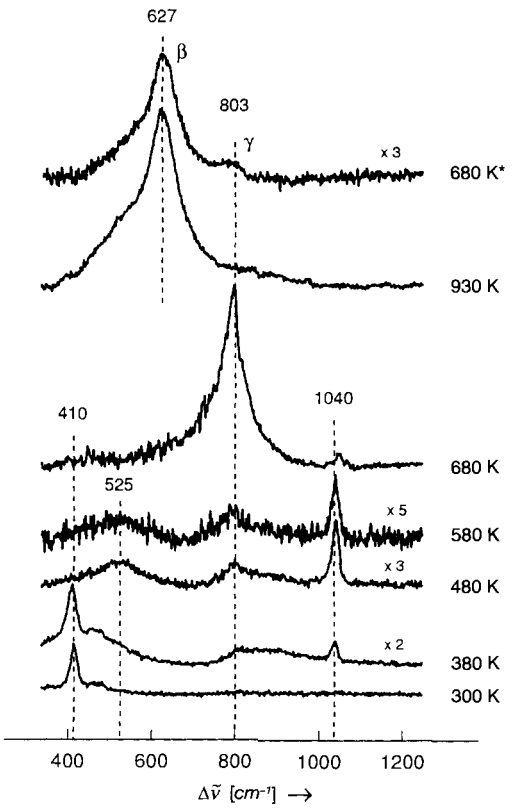


Fig. 1 Raman spectra recorded during the decomposition of $Ag_7O_8NO_3$ (**1**) under a nitrogen atmosphere (1 bar N_2) at different temperatures. The spectrum labeled 680 K* was obtained from a sample of **1** that was first heated to 930 K and then cooled to 680 K.

[*] Dr. B. Pettinger, Dr. X. Bao, Dr. I. Wilcock, Dr. M. Muhler, Prof. R. Schlögl, Prof. G. Ertl
Fritz-Haber-Institut der Max-Planck-Gesellschaft
Faradayweg 4–6, D-14195 Berlin (FRG)
Telefax: Int. code + (30)8327595

450 cm^{-1}. The assignment of the band at 410 cm^{-1} is based on the results of previous IR and Raman studies of related compounds (410 $cm^{-1} \leq \nu \leq 430\ cm^{-1}$).[7, 9]

When the temperature is increased to 380 K, the intensity of the band at 410 cm^{-1} decreases. Simultaneously the shoulder at roughly 450 cm^{-1} becomes more pronounced, and additional features between 800 and 1040 cm^{-1} emerge. The latter peak is attributed to the presence of NO_3^- ions which segregate from the lattice and become more Raman intense. The assignment of the feature growing in around 800 cm^{-1} will be discussed later. Heating to 480 K causes the band at 410 cm^{-1} to disappear completely, the broad peak at approximately 450 cm^{-1} to shift continuously to 525 cm^{-1}, and the other features to become more pronounced. When the temperature is increased further to 580 K the situation remains essentially unchanged.

In conflicting reports *on* the spectral data of Ag_2O various bands ranging from 200 to 2000 cm^{-1} are listed.[10-12] From an IR study in vacuo Allen and Scaife[11] concluded that a single band at approximately 530 cm^{-1} is representative of Ag_2O. Since the O atoms in the Ag_2O lattice are located at sites of inversion, first-order Raman scattering is forbidden and the intensity of this band is expected to be rather weak.[7] In addition, Ag_2O undergoes photochemical reoxidation readily upon irradiation with laser light. The absence of the band at 410 cm^{-1} in the spectra recorded at 480 and 580 K prompts us to attribute the band at 525 cm^{-1} to Ag_2O. It decreases in intensity when the temperature is increased to about 600 K, which is the typical temperature for the decomposition of Ag_2O to metallic silver.[4, 13, 14] The relatively high stability of this entity in the present study is presumably a consequence of the specific geometric and electronic structure provided by the presence of the NO_3^- ions.

The continuous shift of the peak initially at 450 cm^{-1} to 525 cm^{-1} with progressing thermal decomposition is attributed to the increasing oxygen deficiency in the AgO lattice and the resulting changes in the coordination of the Ag^+ ions. This contradicts the previous assignment of this shoulder as a satellite peak of AgO.[7] Our conclusion is in line with more recent reports about the importance of oxygen deficiency on the properties of this compound.[15, 16]

The thermal decomposition of silver oxide to bulk silver in an oxygen-free atmosphere is complete at 680 K as is evident from the pronounced increase in intensity of the peak at 803 cm^{-1}. The same Raman band has been found in previous investigations in which a Ag(111) single-crystal surface was exposed to oxygen for long periods at elevated temperature.[1, 2] Investigations with a combination of various techniques led to the conclusion that this band is due to an atomic oxygen species strongly chemisorbed *on* the reconstructed silver surface.

Thermal decomposition of the silver oxide apparently creates a state of the surface similar to that generated by interaction of O_2 with metallic Ag at high temperatures. Apart from reconstruction of the topmost atomic layer into a extended superstructure, the surface becomes rough on a μm-scale with formation of facets.[1] As a consequence, the Raman scattering cross section of chemisorbed oxygen is strongly enhanced (by a factor of about 10^3). Thus, this O species (referred to as O_γ) gives rise to a high-intensity band, although it is confined to the surface layer and hence its amount is much lower than that of an O species in a bulk phase.

The O_γ species *on* the Ag surface are always associated with O_β species *below* the surface, which are characterized by a band at about 630 cm^{-1} in the Raman spectrum.[2, 6] High surface concentrations of the O_γ atoms reduce the Raman cross section for the O_β species to the extent that the corresponding band is not discernible in the spectrum. However, this feature appears after further heating to 930 K, at which temperature the chemisorbed O_γ atoms recombine and desorb. Compared to the Raman line of the O_β species of single-crystal silver surfaces, this band exhibits a significantly larger band width and asymmetry on its low-frequency side. These spectral differences must be attributed to the amorphous/polycrystalline structure of the sample; in other words, the environment of the O_β species is less ordered. The oxygen atoms in the bulk represent a resevoir for the creation of O_γ atoms at the surface. When the temperature is lowered to 680 K, the O atoms diffuse to the surface, and the band at 803 cm^{-1} is reestablished. The intensity of this band is low at the beginning of this process but increases with time.

The band for the O_β species at roughly 630 cm^{-1} is distinctly different from those for AgO and Ag_2O at 410 and 530 cm^{-1}, respectively. Chemisorbed O atoms on the undisturbed Ag surface (i.e. no subsurface O_β species are present) exhibit a Raman band at approximately 950 cm^{-1}; these O atoms recombine and desorb around 600 K, reflecting their relatively low thermal stability. It is the much more stable O_γ species that is present on the surface during the catalytic transformation of methanol to formaldehyde, which is carried out industrially at around 900 K.[17]

The stepwise thermal decomposition of $Ag_7O_8NO_3$ (**1**) thus proceeds by transformation of AgO into Ag_2O structural units and finally into metallic silver, which exhibits a reconstructed surface with strongly chemisorbed O atoms (γ state) that communicate with oxygen atoms in the subsurface region (β state). All states are characterized by distinctly different frequencies for the Ag–O vibrations. It was possible to identify the corresponding band of Ag_2O, amongst others, by Raman spectroscopy for the first time.

Received: August 18, 1993 [Z 6293 IE]
German version: *Angew. Chem.* **1994**, *106*, 113

[1] X. Bao, J. V. Barth, G. Lehmpfuhl, R. Schuster, Y. Uchida, R. Schlögl, G. Ertl, *Surg. Sci.* **1993**, *284*, 14.
[2] X. Bao, M. Muhler, B. Pettinger, R. Schlögl, G. Ertl, *Catal. Lett.* **1993**, im Druck.
[3] I. Náray-Szabó, G. Argay, D. Szabó, *Acta Crystallogr.* **1965**, *19*, 180.
[4] I. Náray-Szabó, K. Popp, *Z. Anorg. Allg. Chem.* **1963**, *322*, 286.
[5] B. Pettinger, A. Friedrich, U. Tiedemann, *J. Electroanal. Chem. Interfacial Electrochem.* **1990**, *280*, 49.
[6] X. Bao, B. Pettinger, G. Ertl, R. Schlögl, *Ber. Bunsenges. Phys. Chem.* **1993**, *97*, 322.
[7] J. C. Hamilton, J. C. Farmer, R. J. Anderson, *J. Electrochem. Soc.* **1986**, *133*, 739.
[8] N. Iwaraki, Y. Sasaki, Y. Nishina, *Surf. Sci.* **1988**, *198*, 524.
[9] H. Matsuta, K. Hirokawa, *Appl. Spectrosc.* **1989**, *43*, 239.
[10] S. S. Nandra, J. Bandekar, A. L. Cholli, *Appl. Spectrosc.* **1991**, *45*, 1183.
[11] J. A. Allen, P. H. Scaife, *Aust. J. Chem.* **1966**, *19*, 715.
[12] T. L. Slager, B. J. Lindgren, A. J. Mallmann, R. G. Greenler, *J. Phys. Chem.* **1972**, *76*, 940.
[13] A. F. Wells, *Structural Inorganic Chemistry*, Clarendon, Oxford, **1984**, p. 1099.
[14] M. Schmalz, Ph.D. Thesis, Technische Universität Berlin, **1992**.
[15] A. N. Mansour, S. Dallek, C. R. Anderson, *Physica B* **1989**, *158*, 519.
[16] A. N. Mansour, *J. Phys. Chem.* **1990**, *94*, 1006.
[17] *Ullmanns Encycl. Tech. Chem. 4th ed. 1972–1984*, **1982**, *21*, 311.

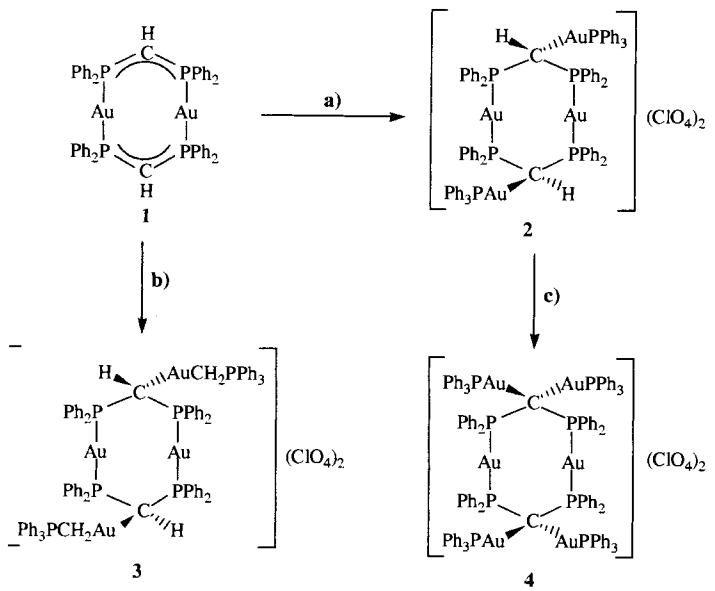
 © VCH Verlagsgesellschaft mbH, D-69451 Weinheim, 1994 0570-0833/94/0101-0086 $ 10.00+.25/0

A Hexanuclear Gold(I) Complex: $[\{(Ph_3PAu)_2C(PPh_2AuPPh_2)\}_2](ClO_4)_2$**

Eduardo J. Fernández, M. Concepción Gimeno, Peter G. Jones, Antonio Laguna*, Mariano Laguna, and José M. Lopez-de-Luzuriaga

Linearly coordinated gold(I) complexes often display short inter- or intramolecular contacts of about 3 Å between the formally closed-shell (d^{10}) metal centers. This phenomenon is termed "aurophilicity" and is considered to arise from relativistic effects.[1-3] Here we report the synthesis and structure of a new hexanuclear gold complex (**4**) containing three pairs of gold atoms linked by such short contacts. The ligand involved is bis(diphenylphosphino)methanediide, which acts as an eight-electron donor bonded to four gold atoms; the only previously known example in which this ligand bridges four metal centers is the mercury acetate complex $[Hg_2(OAc)_2\{(Ph_2P)C\}\{Hg(OAc)\}_2]$.[4]

The starting complex was the dinuclear methanide **1** (Scheme 1), first prepared by Schmidbaur et al.,[5] which is a suitable precursor for tetranuclear complexes.[6] Complex **1** reacts with $[Au(PPh_3)(tht)]ClO_4$[7] or $[Au(CH_2PPh_3)(tht)]ClO_4$[8] in molar ratio 1:2 in dichloromethane, displacing the tetrahydrothiophene (tht) ligand to give solutions from which the colorless air- and moisture-stable complexes **2** and **3**, respectively, can be isolated in 90% yield. The *trans* configuration of the H atoms attached to the central $Au_2P_4C_2$ ring in **2** and **3** is assumed from the analogous arrangement in $[\{Au(PPh_2)_2CH(AuC_6F_5)\}_2]$.[6]



Scheme 1. Synthesis of the hexanuclear complex **4**. a) $[Au(PPh_3)(tht)]ClO_4$; b) $[Au(CH_2PPh_3)(tht)]ClO_4$; c) $[Au(acac)(PPh_3)]$.

Solutions of **2** and **3** in acetone show conductivities typical of 1:2 electrolytes. Their IR spectra show ν(Au–C) bands at 590 (m; **2**) or 570 (m; **3**) cm^{-1}. The NMR spectra[9] are consistent with the proposed structures in Scheme 1. The $^{31}P\{^1H\}$ NMR spectra show two resonances, one for the P atoms in the central eight-membered ring and one for the PPh_3 groups; the spectrum of **3** shows two singlets, that of **2** a triplet and quintet, probably because of virtual coupling between the two different phosphorus atoms. The ^1H NMR signal of the CH group in the central eight-membered ring appears as a triplet at $\delta = 5.38$ (**2**) or as a multiplet at $\delta = 3.63$ (**3**), indicating that the CH proton is more shielded in **3**.

The reaction of **2** with $[Au(acac)PPh_3]$[10] in molar ratio 1:2 leads after 10 d at room temperature to the pale yellow complex **4**, an air- and moisture-stable solid and 1:2 electrolyte, in 87% yield. (No analogous reaction was observed with **3**). The acetylacetonate (acac) ligand is able to deprotonate the CH group of the methanide ligand, whereby acetylacetone is formed and the methanediide C atom can coordinate to the $[AuPPh_3]^+$ fragment. The IR spectrum of **4** shows a ν(Au–C) band at 590 (m) cm^{-1}; the $^{31}P\{^1H\}$ NMR spectrum shows two singlets, one for the PPh_3 and one for the PPh_2 groups.

Crystals of **4** suitable for X-ray diffraction studies[11] were obtained from dichloromethane/hexane. Figure 1 shows the structure of the cation of **4**, which contains an eight-membered $Au_2P_4C_2$ cycle with two additional $AuPPh_3$ groups coordinated to each peripheral carbon atom. Crystallographic inversion symmetry imposes a chair configuration. Short gold–gold contacts are observed [Au1···Au1′ (transannular) 2.920(2), Au2···Au3 2.987(2) Å], and all gold atoms are linearly coordinated (maximum deviation 5°).

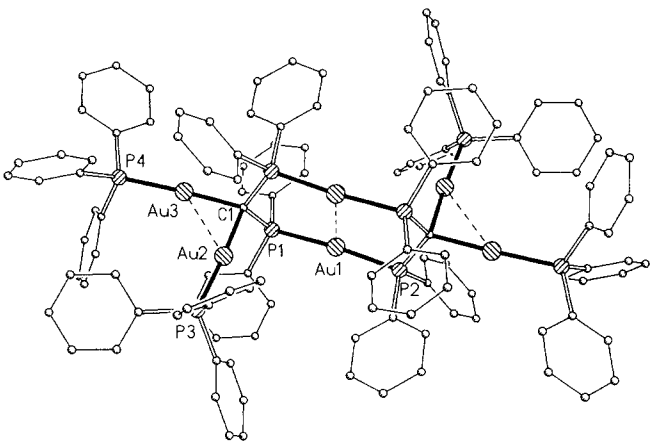


Fig. 1. The cation of complex **4** in the crystal. Radii are arbitrary. H atoms are omitted for clarity. Selected bond lengths [Å] and angles [°]: Au3-C1 2.104(10), Au2-C1 2.112(10); P2-Au1-P1 175.0(1), P3-Au2-C1 176.1(3), C1-Au3-P4 177.2(3); other values see text.

The $(PPh_3Au)_2C$ moiety has been observed in other complexes, and a three-center, two-electron (3c-2e) bonding system has been postulated for the Au_2C group[12-15] on the basis of the small Au-C-Au angle [Au3-C1-Au2 90.2(4)° in **4**], the slightly shortened P–C bonds [P1-C1 1.810(10), P2-C1′ 1.757(11) Å in **4**; compare with P–CH_2 1.83(1), 1.80(1) Å in $[Au_2(dppm)_2]^{2+}$[16]], and the large angle opposite the CAu_2

[*] Prof. Dr. A. Laguna, Dr. M. C. Gimeno, Prof. Dr. M. Laguna
Departamento de Química Inorgánica
Instituto de Ciencia de Materiales de Aragón
Universidad de Zaragoza-C. S. I. C.
E-50009 Zaragoza (Spain)
Dr. E. J. Fernández, J. M. Lopez de Luzuriaga
Departamento de Química, Universidad de la Rioja
Obispo Bustamente 3, E-26001 Logroño (Spain)
Prof. Dr. P. G. Jones
Institut für Anorganische und Analytische Chemie
der Technischen Universität
Postfach 3329, D-38023 Braunschweig (FRG)

[**] This work was supported by the Dirección General de Investigación Científica y Técnica (PB91-0122) the Instituto de Estudios Riojanos and the Fonds der Chemischen Industrie.

group [P2′-C1-P1 112.7(6)° in **4**, probably constrained by the geometric requirements of the ligand]. The Au–P bonds to the PPh_2 groups, Au1–P1 2.329 and Au1–P2 2.325(3) Å are slightly longer than in $[\{Au(PPh_2)_2CH(AuC_6F_5)\}_2]$[6] with 2.309 and 2.305 Å, whereas the Ph_3P–Au distances Au2–P3 2.273 and Au3–P4 2.279(3) Å may be considered as normal values.

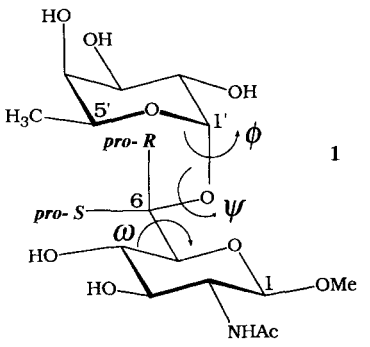
Received: July 14, 1993 [Z 6212 IE]
German version: *Angew. Chem.* **1994**, *106*, 96

[1] H. Schmidbaur, *Gold Bull. Gold Pat. Dig.* **1990**, *23*, 11-21.
[2] H. Schmidbaur, *Interdiscip. Sci. Rev.* **1992**, *17*, 213-220.
[3] P. Pyykkö, *Chem. Rev.* **1988**, *88*, 563-594.
[4] M. Luser, P. Peringer, *Organometallics* **1984**, *3*, 1916-1917.
[5] H. Schmidbaur, J. R. Mandl, *Angew. Chem.* **1977**, *89*, 679-680; *Angew. Chem. Int. Ed. Engl.* **1977**, *16*, 640-641.
[6] R. Usón, A. Laguna, M. Laguna, M. C. Gimeno, P. G. Jones, C. Fittschen, G. M. Sheldrick, *J. Chem. Soc. Chem. Commun.* **1986**, 509-510.
[7] R. Usón, A. Laguna, M. Laguna, J. Jiménez, M. P. Gómez, A. Sainz, P. G. Jones, *J. Chem. Soc. Dalton Trans.* **1990**, 3457-3463.
[8] C. J. Aguirre, M. C. Gimeno, A. Laguna, M. Laguna, J. M. López-de-Luzuriaga, F. Puente, *Inorg. Chim. Acta* **1993**, *208*, 31-36.
[9] All complexes were satisfactorily characterized by elemental analysis (C,H) and IR spectroscopy. NMR spectra in $CDCl_3$: **2**: $\delta(^1H) = 7.98-6.55$ (m,Ph), 5.38 (t, CH, $J(PH)$ 3.5 Hz); $\delta(^{31}P) = 40.1$ (q, PPh_3, $J(PP)$ 6.9 Hz), 41.8 (t, PPh_2). **3**: $\delta(^1H) = 7.72-7.08$ (m, Ph), 3.63(m, CH), 1.03 (d, CH_2, $J(PH)$ 13.2 Hz); $\delta(^{31}P) = 30.8$ (s, PPh_3), 38.4 (s, PPh_2). **4**: $\delta(^{31}P) = 39.22$ (s, PPh_3), 53.26 (s, PPh_2).
[10] D. Gibson, B. F. G. Johnson, J. Lewis, *J. Chem. Soc. A* **1970**, 367-369.
[11] Crystal data: $4 \cdot 2CH_2Cl_2$, $C_{124}H_{104}Au_6Cl_6O_8P_8$, $P\bar{1}$, $a = 11.103(4)$, $b = 15.266(5)$, $c = 18.424(6)$ Å, $\alpha = 81.68(3)$, $\beta = 80.18(3)$, $\gamma = 86.11(3)°$, $V = 3042(2)$ Å^3, $Z = 1$, $\mu = 7.5$ mm^{-1}, $T = -100$ °C. A colorless tablet $0.6 \times 0.2 \times 0.05$ mm was mounted in inert oil (type RS3000, donated by Riedel de Haën). Using $Mo_{K\alpha}$ radiation on a Siemens R3 diffractometer, 13478 reflections were measured to $2\theta_{max} = 50°$, of which after absorption corrections 10742 were unique (R_{int} 0.044) and 10711 used for all calculations (program SHELXL-92). The structure was solved by the heavy-atom method and refined on F^2 with Au, P, Cl, and O anisotropic and idealized phenyl rings. H atoms were included with a riding model. The final $wR(F^2)$ was 0.137, with conventional $R(F)$ 0.047 for 255 parameters and 60 restraints. Further details of the crystal structure invesigation may be obtained from the Fachinformationszentrum Karlsruhe, 76344 Eggenstein-Leopoldshafen (FRG), on quoting the depository number CSD 400261, the names of the authors, and the journal citation.
[12] P. Braunstein, H. Lehner, D. Matt, A. Tiripicchio, M. Tiripicchio-Camellini, *Angew. Chem.* **1984**, *96*, 307-308; *Angew. Chem. Int. Ed. Engl.* **1984**, *23*, 304-305.
[13] B. F. G. Johnson, J. Lewis, P. R. Raithby, A. Sanders, *J. Organomet. Chem.* **1984**, *260*, C29-C32.
[14] J. Vicente, M. T. Chicote, J. A. Cayuelas, J. Fernández-Baeza, P. G. Jones, G. M. Sheldrick, P. Espinet, *J. Chem. Soc. Dalton Trans.* **1985**, 1163-1168.
[15] E. J. Fernández, M. C. Gimeno, P. G. Jones, A. Laguna, M. Laguna, J. López-de-Luzuriaga, *J. Chem. Soc. Dalton Trans.* **1992**, 3365-3370.
[16] H. Schmidbaur, A. Wohlleben, U. Schubert, A. Frank, G. Huttner, *Chem. Ber.* **1977**, *110*, 2751-2757.

Aleuria aurantia Agglutinin Recognizes Multiple Conformations of α-L-Fuc-(1 → 6)-β-D-GlcNAc-OMe**

Thomas Weimar and Thomas Peters*

The molecular mechanisms underlying specific recognition reactions between oligosaccharides and receptor proteins such as antibodies and lectins have been the subject of numerous studies during past years.[1] Here, we report the use of 2D transferred NOE (TRNOE) experiments[2] to study the complexation of an α-L-fucose-specific lectin, *Aleuria aurantia* agglutinin (AAA),[3] with a synthetic *N*-glycoprotein-type disaccharide α-L-Fuc-(1 → 6)-β-D-GlcNAc-OMe (**1**).[4] Disaccharide **1** is a rather flexible molecule which samples at least two distinct regions in conformational space roughly characterized by different values for the exocyclic dihedral angle ω (O6-C6-C5-O5), *gt* ($\omega = 60°$), and *gg* ($\omega = -60°$). Additional variation of the dihedral angles ϕ (H1′-C1′-O1′-C6) and ψ (C1′-O1′-C6-C5) leads to a complex conformational equilibrium in **1**. Because of the high selectivity of AAA for disaccharide **1** as compared to α-(1 → 2)-, α-(1 → 3)-, or α-(1 → 4)-linked fucose residues,[3c] selection of a single conformer of **1** upon binding appears reasonable. However, TRNOE experiments and specific line-broadening effects indicate flexibility of the reducing β-D-GlcNAc unit in liganded **1**.



1

^1H NMR spectra of free **1** and **1** complexed with AAA were recorded in D_2O at 600 MHz[5] (Fig. 1). For free **1** the amount of *gg*, *gt*, and *tg* conformers could be estimated on the basis of vicinal coupling constants $J_{5,6\text{-}pro\text{-}R}$ (5.7 Hz) and $J_{5,6\text{-}pro\text{-}S}$ (2.0 Hz). Assignments of prochiral protons H6-*pro-R* and H6-*pro-S* were assumed to be analogous to D-glucose.[6] Different parametrizations[7-9] of the Karplus relation gave the following *gg*:*gt*:*tg* ratios: 56:43:1,[7] 66:37:−3,[8] and 58:54:−12.[9] Regardless of the parametrization used, *gg* orientations were found to be preferred over *gt*, and *tg* orientations could be almost excluded. In the presence of lectin (Fig. 1b) it was observed that all resonances of **1** were broadened, but those of the fucose residue were significantly more broadened to an extent that even spin-spin couplings in the order of 7 Hz (C6′ methyl protons) could no longer be resolved (cf. Fig. 1a and 1b).[10] This could be explained by faster transverse relaxation of a more immobilized fucose residue, or by an incomplete averaging of slightly different chemical shifts for free and complexed molecules, or both. Both explanations would indicate a fucose residue bound more tightly than the *N*-acetyl glucosamine residue. This conclusion was further substantiated by the results of NOESY[11] experiments for free and liganded **1**.

For free disaccharide **1** positive NOEs were observed because of fast molecular tumbling (Fig. 2a). The NOE patterns observed can only be understood on the basis of a complex conformational equilibrium about the glycosidic linkage. Nevertheless, conformers can roughly be categorized as belonging to the *gg* or *gt* family. Strong interglycosidic NOEs were observed between H1′ and H6-*pro-S* and H6-*pro-R* and between H5′ and H6-*proS* (Fig. 2a). Additionally, several medium to weak interglycosidic NOEs were observed (Fig. 2a: H1′/H5, H1′/H4, H5′/H5, H5′/H4, H5′/OMe).

The NOEs observed for disaccharide **1** in the presence of AAA were negative (Fig. 2b), a clear indication of transferred NOEs (TRNOEs). TRNOEs reflect the conformation of the ligand in the bound state. Since the mixing time used (100 ms) was rather short, spin diffusion is unlikely to play a role. Qual-

[*] Priv.-Doz. Dr. T. Peters, Dr. T. Weimar
Institut für Biophysikalische Chemie der Universität, Biozentrum
Marie-Curie-Strasse 9, Gebäude N 230, D-60439 Frankfurt am Main (FRG)
Telefax: Int. code + (69)5800-9632

[**] This work was supported by the Deutsche Forschungsgemeinschaft (Sonderforschungsbereich 169) and the Fonds der Chemischen Industrie. T. P. thanks NATO for a research grant (CRG.890356).

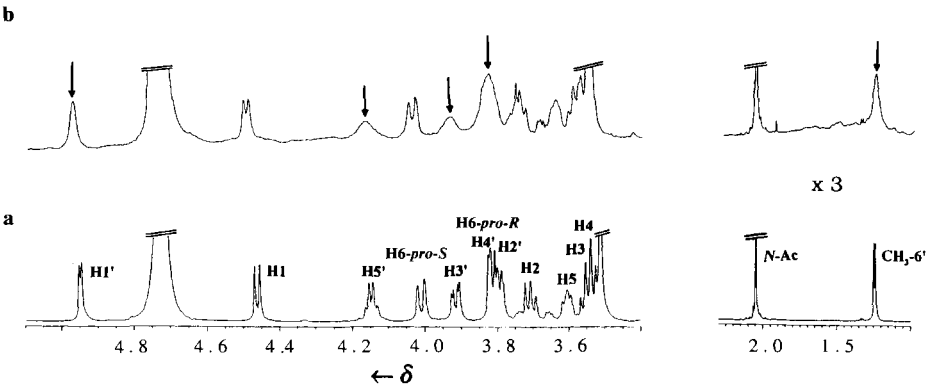


Fig. 1. ^{1}H NMR spectra of free and liganded **1** recorded in D_2O at 303 K and 600 MHz. a) ^{1}H NMR spectrum of free **1** (10 mg dissolved in 0.5 mL D_2O, 52 mM). b) ^{1}H NMR spectrum of **1** (0.64 mg, 1.7 μmol) in the presence of AAA (4 mg, 0.11 μmol), dissolved in 0.5 mL D_2O (3.4 mM **1**, 0.22 mM AAA). Broadened fucose resonances are indicated by arrows.

itatively, strong interglycosidic TRNOEs (H1′/H6-*pro-R*, H1′/H6-*pro-S*, H5′/H6-*pro-S*) matched corresponding NOEs observed for unliganded **1** (cf. Fig. 2a and 2b), only the comparison of weak and medium effects revealed differences. For instance, free **1** showed dipole-dipole contacts of medium intensity between H5′ and protons H5 and H4 (Fig. 2a). For bound **1** only a rather weak TRNOE between H5′ and H4 and assumption leads to contradictions. If one single conformer was selected upon binding, the orientation about the C5–C6 linkage had to be *gt* because strong TRNOEs of similar magnitude were observed between H4 and both protons at C6, H6-*pro-R* and H6-*pro-S* (Fig. 2b). This can neither be expected for *gg* nor for *tg* conformations which both place one of the protons H6 at a distance of about 4 Å to H4, which is above the upper distance

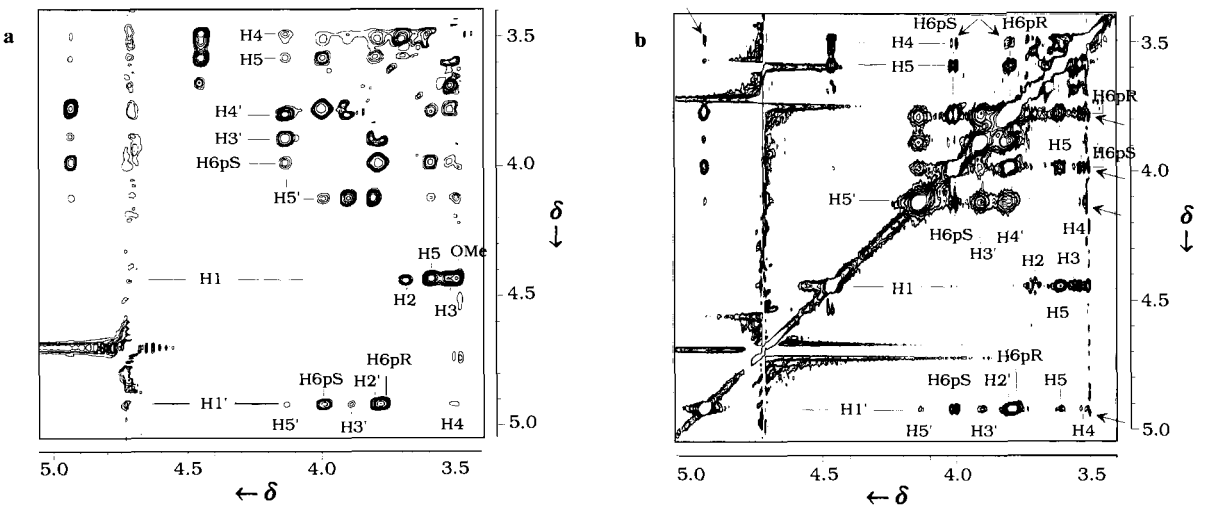


Fig. 2. 2D NOESY ^{1}H NMR spectra (600 MHz, 303 K, D_2O) of free and liganded **1**. Sample concentrations were as in Figure 1. 512 experiments were performed in t_1 with 2 K data points each to yield a final data matrix after 2D Fourier transform of 2 K × 1 K data points. Prior to Fourier transformation the data matrix was multiplied with $\pi/3$ shifted squared sine bell functions in both directions, t_1 and t_2. A third-order baseplane correction (UXNMR, standard Bruker software) was applied after 2D Fourier transform and phase correction. Protons H6-*pro-S* and H6-*pro-R* are abbreviated as H6pS and H6pR, respectively. a) Free **1**. The mixing time was 900 ms and 32 scans were recorded for each experiment. The relaxation delay was 4.0 s. NOEs are positive and only positive levels are shown. b) Liganded **1**. The mixing time was 100 ms and 150 scans were recorded for each experiment. The relaxation delay was 1.5 s. The cross peaks are negative and represent transferred NOEs (TRNOEs) which reflect the bound conformation of **1**. TRNOEs labeled with arrows indicate the presence of *gt and gg* conformations of **1** in the bound state (see text for details).

no TRNOE between H5′ and H5 was observed. For the following qualitative discussion it is useful to have a gauge which defines an upper limit for proton–proton distances up to which TRNOEs may be expected. The weak intraglycosidic TRNOE between H1′ and H5′ which corresponds to a H1′–H5′ distance of 3.7 Å can serve as such a standard. Thus, if a TRNOE is observed the corresponding distance will be assumed to be $\leq$3.7 Å.

Is it possible to explain the TRNOEs observed with a model which assumes that **1** is bound as a single conformer with a fixed orientation of the (1 → 6) linkage? It is easily shown that this limit as estimated above. On the other hand, weak TRNOEs between H1′ and H4 and between H5′ and H4 (Fig. 2b) are expected only for *gg* conformers. This is easily checked by simple model building: both proton pairs, H1′/H4 and H5′/H4, cannot be brought closer than about 4.5 and 6.0 Å, respectively, with the C5–C6 bond locked in a *gt* conformation. These two TRNOEs are also incompatible with a *tg* conformation of the C5–C6 linkage. Table 1 gives a summary of the TRNOEs discussed and their pertinence to *gt*, *gg*, and *tg* conformations of the C5–C6 bond. Evidently both *gt* and *gg* conformers are bound by AAA. Additionally, Metropolis Monte Carlo (MMC)

Table 1. TRNOEs observed in liganded **1** and their relation to *gt*, *gg*, and *tg* orientations at the C5–C6 bond. "+/–" indicates that a TRNOE can/cannot be observed in this conformation.

Conformation	TRNOE		
	H4/H6-*pro-S* and H4/H6-*pro-R* (strong)	H1′/H4 (weak)	H5′/H4 (weak)
gt	+	–	–
gg	–	+	+
tg	–	–	–

simulations[12] of unliganded **1** yielded minima **A**–**D**[13] which represent major conformations within the *gt* and *gg* family (Fig. 3). All *tg* conformations possess a high energy mainly because of unfavorable van der Waals interactions and thus play no significant role (vide supra). On the basis of our experimental findings these simulations support the understanding of the complex conformational equilibrium of **1** for both the liganded and the unliganded form: the TRNOE H1′/H4 can only be expected for the region around minimum **D** (*gg* family), the one between H5′ and H4 only for the region around minimum **B** (*gg* family), and the one between H5′ and H5 only for the region around minimum **A** (*gt* family). On the whole, it appears that multiple conformations of **1** are bound by AAA which is consistent with the observation of specific line broadenings described above.

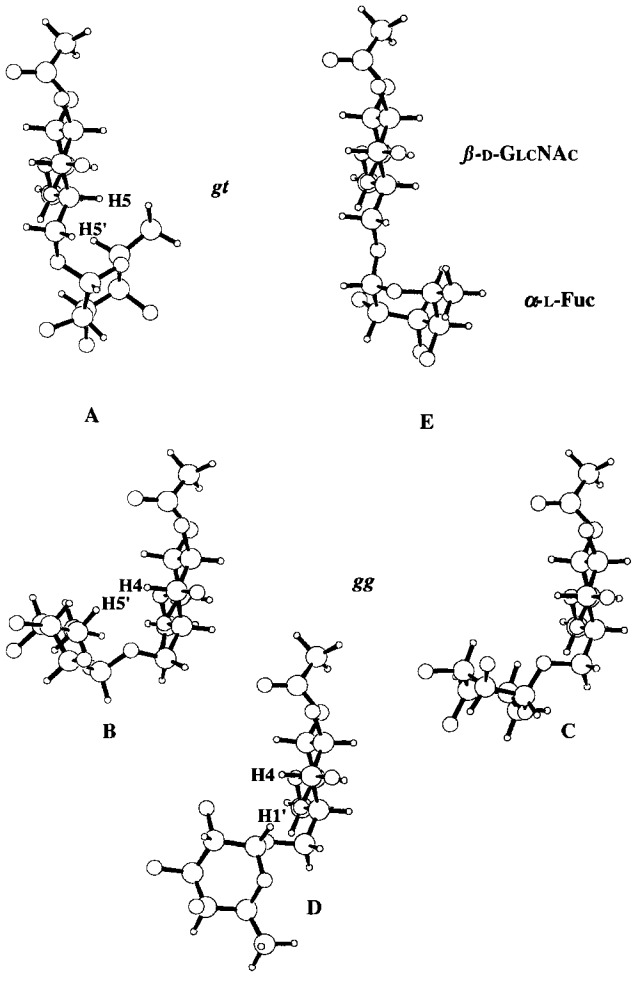


Fig. 3. Ball and stick models (plot program Schakal-88B, E. Keller, University of Freiburg, **1988**) of the major minimum energy conformations **A**–**D** [13] of **1** portraying the *gt* and *gg* conformational families.

It is concluded that although AAA specifically recognizes the (1 → 6)-linked fucose in **1**,[3c] the orientation of this linkage is not fixed in liganded **1**; the reducing *N*-acetyl glucosamine unit having relatively more conformational freedom than the fucose residue. Because of the differences that were observed between the weak to medium interglycosidic NOE and TRNOE patterns it can be assumed that the conformational equilibrium of **1** is disturbed upon binding to AAA. There are two other studies where the binding of (1 → 6)-linked disaccharides to a monoclonal antibody k is disturbed upon binding to AAA. There are two other studies where the binding of (1 → 6) linked disaccharides to a monoclonal antibody[14] and to lectin[15] was investigated. In one case it was found that a monoclonal antibody binds the saccharide, methyl *O*-β-D-galactopyranosyl-(1 → 6)-4-deoxy-4-fluoro-β-D-galactopyranoside, in a single well-defined conformation which does not belong to any of the major conformational families identified for the free disaccharide.[14] In the other case of β-methylmelibiose (α-D-Gal-(1 → 6)-β-D-Glc-OMe) binding to Ricin B,[15] it was concluded that a predominant conformer of the free disaccharide is selected upon binding. We suggest that specific recognition of flexible carbohydrate epitopes by receptor proteins may involve rather different binding modes, not necessarily involving selection of a single conformer.

Received: July 14, 1993
Revised: August 20, 1993 [Z 6211 IE]
German version: *Angew. Chem.* **1994**, *106*, 79

[1] a) F. A. Quiocho, *Curr. Top. Microbiol. Immunol.* **1988**, 135–148; b) R. U. Lemieux, *Chem. Soc. Rev.* **1989**, *18*, 347–374; c) D. R. Bundle, N. M. Young, *Curr. Opin. Struct. Biol.* **1992**, *2*, 666–673; d) L. A. Lasky, *Science* **1992**, *258*, 964–969.

[2] a) G. M. Clore, A. M. Gronenborn, *J. Magn. Reson.* **1982**, *48*, 402–417; b) *ibid.* **1983**, *53*, 423–442.

[3] a) N. Kochibe, K. Furukawa, *Biochemistry* **1980**, *19*, 2841–2846; b) K. Yamashita, N. Kochibe, T. Ohkura, I. Ueda, A. Kobata, *J. Biol. Chem.* **1985**, *8*, 4688–4693; c) H. Debray, J. Montreuil, *Carbohydr. Res.* **1989**, *185*, 15–26; d) F. Fukumori, N. Takeuchi, T. Hagiwara, K. Ito, N. Kochibe, A. Kobata, Y. Nagata, *FEBS Lett.* **1989**, *250*, 153–156; e) Y. Nagata, F. Fukumori, H. Sakai, T. Hagiwara, Y. Hiratsuka, N. Kochibe, A. Kobata, *Biochem. Biophys. Acta* **1991**, *1076*, 187–190. f) AAA was purchased from Boehringer Mannheim, Germany. In solution the lectin forms a dimer with a molecular weight of 36 kD for each subunit. AAA was dissolved in a phosphate buffer according to [3e]. H_2O was exchanged against D_2O by repeated lyophilization and dissolving in D_2O.

[4] T. Peters, T. Weimar, *Liebigs Ann. Chem.* **1991**, 237–242.

[5] ^{1}H NMR for free **1** (Bruker AMX 600 spectrometer, 600 MHz, D_2O, 303 K, δ(HDO) = 4.722): δ = 4.94 (d, J(1′,2′) = 3.9 Hz, H1′), 4.46 (d, J(1,2) = 8.6 Hz, H1), 4.14 (dq, J(4′,5′) < 1.0, J(5′,6′) = 6.6 Hz, H5′), 4.01 (dd, J(5,6-*pro-S*) = 2.0, J(6-*pro-S*,6-*pro-R*) = 12.0 Hz, H6-*pro-S*), 3.92 (dd, J(2′,3′) = 10.4, J(3′,4′) = 3.3 Hz, H3′), 3.82 (dd, H4′), 3.80 (dd, J(5,6-*pro-R*) = 5.7 Hz, H6-*pro-R*), 3.79 (dd, H2′), 3.71 (dd, J(2,3) = 9.8 Hz, H2), 3.60 (ddd, H5), 3.50–3.60 (m, H3, H4), 3.51 (s, OMe), 2.04 (s, NAc), 1.24 (d, C6′-Me).

[6] a) Y. Nishida, H. Hori, H. Ohrui, H. Meguro, J. Uzawa, D. Reimer, V. Sinnwell, H. Paulsen, *Tetrahedron Lett.* **1988**, *29*, 4461–4464; b) H. Ohrui, Y. Nishida, M. Watanabe, H. Hori, H. Meguro, *ibid.* **1985**, *26*, 3251–3254.

[7] J. A. Gerlt, A. V. Youngblood, *J. Am. Chem. Soc.* **1980**, *102*, 7433–7438.

[8] D. G. Streefkerk, M. J. A. de Bie, J. F. G. Vliegenthart, *Tetrahedron* **1973**, *29*, 833–844.

[9] C. A. G. Haasnoot, F. A. A. M. De Leeuw, C. Altona, *Tetrahedron* **1980**, *36*, 2783–2792.

[10] After completion of all experiments ethylenediaminetetraacetate (edta) was added and a ^{1}H NMR spectrum was obtained to make sure that the line broadening effects were not due to specific complexation of the carbohydrate with impurities of cations such as Ca^{2+}. Since AAA has no Ca^{2+} or other metal ion binding sites it can be assumed that edta efficiently removes such impurities from the protein surface.

 © VCH Verlagsgesellschaft mbH, D-69451 Weinheim, 1994 0570-0833/94/0101-0090 $ 10.00+.25/0

[11] D. Marion, K. Wüthrich, *Biochem. Biophys. Res. Commun.* **1983**, *113*, 967–974.
[12] a) T. Peters, B. Meyer, R. Stuike-Prill, R. Somorjai, J.-R. Brisson, *Carbohydr. Res.* **1993**, *238*, 49–73; b) T. Weimar, B. Meyer, T. Peters, *J. Biomol. NMR* **1993**, *3*, 399–414; c) L. Poppe, R. Stuike-Prill, B. Meyer, H. van Haalbeek, *ibid.* **1992**, *2*, 109–136; d) R. Stuike-Prill, B. Meyer, *Eur. J. Biochem.* **1990**, *194*, 903–919.
[13] The simulations for **1** were performed according to the published procedure [12] with a temperature parameter of 303 K and 2×10^6 macro steps. Maximum step lengths were 20° (ϕ), 20° (ψ), 25° (ω), and 2.5° (τ = C1′-O1′-C6), leading to an overall acceptance ratio of 0.48. Five minima could be identified: $\phi = 49°$, $\psi = 91°$, $\omega = 50°$ (minimum **A**, $E_{rel} = 0.00$ kcal mol^{-1}); $\phi = 49°$, $\psi = 124°$, $\omega = -80°$ (minimum **B**, $E_{rel} = 0.20$ kcal mol^{-1}); $\phi = 55°$, $\psi = 149°$, $\omega = -61°$ (minimum **C**, $E_{rel} = 0.56$ kcal mol^{-1}), $\phi = 55°$, $\psi = -122°$, $\omega = -65°$ (minimum **D**, $E_{rel} = 1.90$ kcal mol^{-1}); $\phi = 55°$, $\psi = -176°$, $\omega = 56°$ (minimum **E**, $E_{rel} = 2.19$ kcal mol^{-1}). See also Figure 3.
[14] C. P. J. Claudemanns, L. Lerner, G. D. Daves, Jr., P. Kovác, R. Venable, A. Bax, *Biochemistry* **1990**, *29*, 10906–10911.
[15] V. L. Bevilacqua, K. Yangmee, J. H. Prestegard, *Biochemistry* **1992**, *31*, 9339–9349.

Scalemic 2-Formyl-3-hydroxy[2.2]paracyclophane: A New Auxiliary for Asymmetric Synthesis**

Valeria Rozenberg, Vladimir Kharitonov, Dimitri Antonov, Elena Sergeeva, Andrei Aleshkin, Nickolai Ikonnikov, Svetlana Orlova, and Yuri Belokon'*

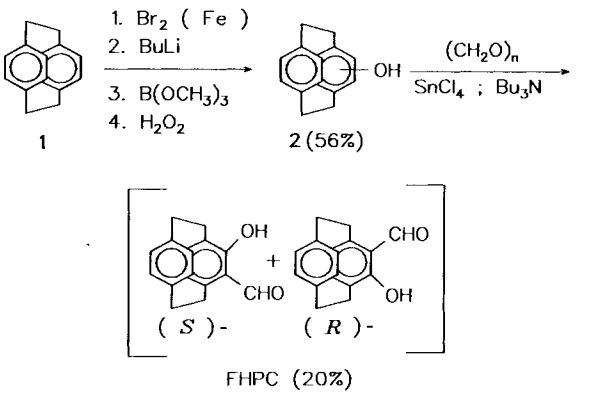
Among the most successful chiral ligands employed in asymmetric synthesis, catalyzed or promoted by transition metals, are molecules with planar chirality, such as derivatives of ferrocene.[1] These feature prominently as chiral ligands in palladium-catalyzed Grignard cross-coupling reactions,[1a] palladium-catalyzed allylic alkylation reactions,[1b] gold-catalyzed aldol condensations of α-isocyanoacetates,[1c] and hydrogenation of enamides.[1d] Chiral arenechromium complexes have been used in many stoichiometric asymmetric reactions,[2a] and also very recently to catalyze the addition reactions of organozinc compounds to aldehydes.[2b] Furthermore, a chiral pyridoxal derivative was shown to function as an auxiliary in the asymmetric synthesis of amino acids.[3]

Unfortunately, the compounds with planar chirality derived from arene or cyclopentadiene transition metal complexes are either readily oxidized or are unstable under certain reaction conditions.

We have therefore investigated whether other compounds with planar chirality, derived from [2.2]paracyclophane, are also suitable as chiral auxiliaries, since here the starting material is very stable towards light, oxidation, acids, bases, and relatively high temperatures.[4] We report here the synthesis and resolution of 2-formyl-3-hydroxy[2.2]paracyclophane (FHPC), a chiral analogue of salicylaldehyde, as well as an example of its application as a chiral auxiliary for the synthesis of β-hydroxy-α-amino acids.

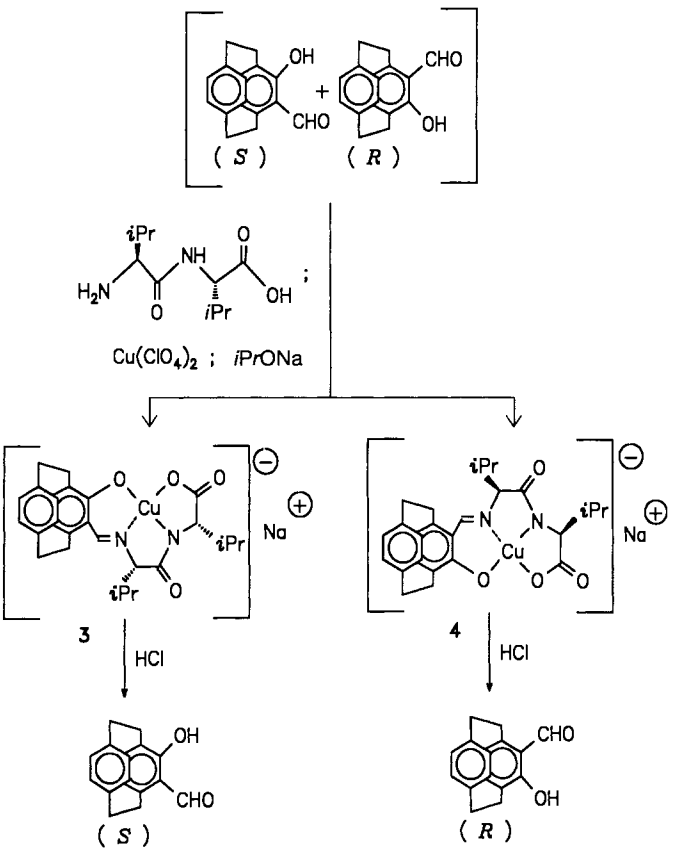
[*] Prof. Dr. Y. Belokon', Dr. V. Rozenberg, Dr. V. Kharitonov, Dipl.-Chem. D. Antonov, Dipl.-Chem. E. Sergeeva, Dipl.-Chem. A. Aleshkin, Dr. N. Ikonnikov, Dipl.-Chem. S. Orlova
117813, Institute of Organo-Element Cmpds
Russian Academy of Sciences
Moscow, Vavilov 28 (Russia)
Telefax: Int. code + (095)135-5085

[**] This work was supported by the Russian Science Foundation.



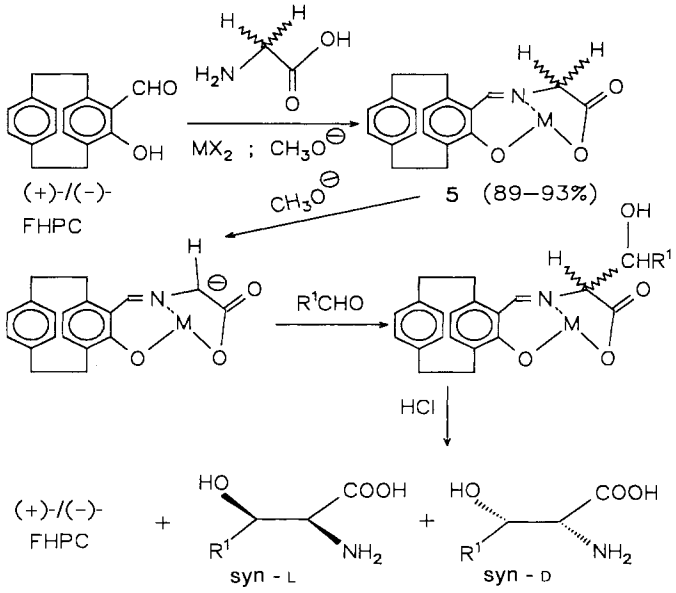
Scheme 1. Synthesis of racemic FHPC.

Racemic FHPC was synthesized in a multistep reaction (Scheme 1): bromination of the parent paracyclophane **1**, Li–Br exchange,[5] reaction of the organometallic intermediate with trimethylborate, and oxidation with H_2O_2 furnished the phenol **2**.[6] The *ortho* formylation with $(CH_2O)_n$, catalyzed by $SnCl_4$ and Bu_3N, gave the expected racemic FHPC.[7] The differing solubility of the diastereomeric Cu^{II} complexes (**3** and **4**) of the Schiff bases derived from (*S*)-FHPC and (*R*)-FHPC and (*S*)-valyl-(*S*)-valine in 2-propanol were used for the resolution of racemic FHPC (Scheme 2). The diastereoisomers can be separated by chromatography on SiO_2. The enantiomers of FHPC were recovered from the complexes with aqueous HCl (Scheme 2); their enantiomeric purity reached 94%, as determined by ^{1}H NMR spectroscopy in which [Eu(hfc)$_3$] was employed as a shift reagent.



Scheme 2. Resolution of racemic FHPC.

 © VCH Verlagsgesellschaft mbH, D-69451 Weinheim, 1994 0570-0833/94/0101-0091 $ 10.00+.25/0



Scheme 3. Asymmetric synthesis of β-hydroxy-α-aminoacids employing scalemic FHPC. $MX_2 = Cu(OAc)_2$; R^1 = *i*Pr, Ph.

Scalemic FHPC can now be used for the asymmetric synthesis of β-hydroxy-α-amino acids, as shown in Scheme 3. This involves the condensation of the chiral Cu^{II} complexes **5** of the Schiff bases, derived from (+)- or (−)-FHPC and glycine, with isobutyraldehyde or benzaldehyde. The enantiomeric purity of the isolated amino acids was greater than 90%, and the *syn*/*anti* ratio was over 30:1 (see Table 1). FHPC was recovered almost quantitatively and with unchanged optical purity from the reaction mixture.

Table 1. Condensation reaction of **5** with isobutyraldehyde and benzaldehyde in MeOH, catalyzed by MeONa under Ar, $T = 50\,^{\circ}C$.

R^1 in R^1CHO	$[a]_D^{25}$ of FHPC	t [h]	*syn*/*anti*	*ee* [%] [a]
*i*Pr	+513 [b]	1.5	28/1	90(L)
*i*Pr	+513	4.5	33/1	92(L)
*i*Pr	+513	7.5	58/1	93(L)
*i*Pr	− 505 [c]	1.3	13/1	94(D)
*i*Pr	− 505	4.5	20/1	96(D)
*i*Pr	− 505	7.5	15/1	98(D)
Ph	+513	0.5	[d]	77(L)

[a] GLC enantiomeric analyses of the *syn*-β-hydroxy-α-amino acids were performed on a Chirasil-Val-type phase [13], by using their *N*-trifluoroacetylisopropyl esters. Experimentally observed enantiomeric excesses *ee* of the amino acids were recalculated, assuming 100% *ee* of the chiral auxiliary FHPC. The chemical yields were in the range of 60–80%. [b] The analysis of the ^1H NMR spectrum (with $[Eu(hfc)_3]$ as a shift reagent) gave an enantiomeric purity of 86%. [c] The analysis of the ^1H NMR spectrum (with $[Eu(hfc)_3]$ as a shift reagent) gave an enantiomeric purity of 85%. [d] The amount of *anti* isomer was too small to carry out any meaningful measurements.

In our opinion FHPC compares favorably with other stoichiometric chiral auxiliaries currently used for the asymmetric syntheses of β-hydroxy-α-amino acids.[8]

Moreover, we believe that scalemic FHPC could also be used in numerous reactions, catalyzed by metal complexes of the salicylaldehyde-derived Schiff bases.[8–11] Cyclopropanation,[9] oxidation of sulfides,[10] epoxidation of olefins,[11] and silylcyanation of aldehydes[12] are just several examples of catalytic reactions in which the chiral analogue of salycilaldehyde might be used either to improve the enantiomeric excess of the reactions or to simplify the synthetic procedure.

Experimental Procedure

Synthesis of FHPC: The formylation of **2** in 20% yield was carried out according to a literature method for the *ortho* formylation of phenols [7]. M.p. 201–204 °C. ^1H NMR (200 MHz, C_6D_6, 25 °C): $\delta = 2.24$–3.62 (m, 8H; CH_2), 5.98 (d, $^3J(H,H) = 8$ Hz, 1H), 6.16–6.26 (m, 2H), 6.30 (d, $^3J(H,H) = 8$ Hz, 1H), 6.40 (dd, $^3J(H,H) = 8$, $^4J(H,H) = 1.8$ Hz, 1H), 7.00 (dd, $^3J(H,H) = 8$, $^4J(H,H) = 1.8$ Hz, 1H), 9.47 (s, 1H; CHO), 12.61 (s, 1H; OH); UV/VIS (benzene): $\lambda_{max}(\varepsilon) = 304(4493)$, 399 nm (2310); IR ($CDCl_3$): $\tilde{\nu} = 1630\ cm^{-1}$ (C = O); correct C,H analyses.

Resolution of racemic FHPC into enantiomers: The diastereoisomeric complexes **3** and **4** were obtained by heating FHPC (0.347 g, 1.38 mmol), *i*PrONa (13.8 mL of 0.3 N solution in *i*PrOH), $Cu(ClO_4)_2 \cdot 6H_2O$ (0.512 g, 1.38 mmol) and (*S*)-valyl-(*S*)-valine (0.298 g, 1.38 mmol) in *i*PrOH (15 mL) under reflux for 3 h. The reaction mixture was cooled down and left overnight at room temperature. The resulting precipitate of [(+)-FHPC-(*S*)-Val-(*S*)-Val]Cu^{II} (0.14 g, 0.32 mmol, 23%) was filtered off and treated (see below) to give 0.060 g (0.24 mmol, 17% based on the initial racemic FHPC) (+)-FHPC ($[a]_D^{25} = +513$ ($c = 0.2$ in benzene), 86% *ee*). The filtrate was concentrated to dryness and the residue chromatographed on SiO_2 (Kieselgel-60, $d = 1.9$ cm, $l = 20$ cm). Partially resolved, unreacted FHPC (0.030 g, 0.12 mmol, 8.6%, $[a]_D^{25} = +253$ ($c = 0.2$ in benzene), 40% *ee*) was eluted with benzene/methanol (10/1) as the first fraction. Elution with MeOH/AcOEt furnished 0.25 g (0.57 mmol, 43%) of [(−)-FHPC-(*S*)-Val-(*S*)-Val]Cu^{II} whicb was treated to give 0.060 g (0.24 mmol, 17%) of (−)-FHPC ($[a]_D^{25} = -505$ ($c = 0.2$ in benzene), 85% *ee*). More careful chromatographic separation may afford (−)-FHPC with 94% *ee* ($[a]_D^{25} = -556$ ($c = 0.2$ in benzene)).

Synthesis of **5**: Condensation of (+)-FHPC or (−)-FHPC (0.15 g, 0.595 mmol) with glycine (0.05 g, 0.67 mmol) and $Cu(OAc)_2 \cdot H_2O$ (0.14 g, 0.7 mmol) in MeONa (5.2 mL of 0.23 N solution in MeOH) under argon afforded **5**, which was purified on a Sephadex LH-20 column (benzene/methanol 3/1). The yield was 89–93% (0.206–0.215 g, 0.53–0.55 mmol).

Synthesis of β-hydroxyleucene and phenylserine: To (+)- or (−)-**5** (0.027 g, 0.59 mmol) was added a solution of MeONa (6 mL of 0.28 N solution in MeOH), followed by isobutyraldehyde (0.22 mL, 2.36 mmol) [or benzaldehyde (0.24 mL, 2.36 mmol)] under argon. The mixture was stirred at 50 °C for several hours and the reaction mixture was worked up as described below.

General procedure for the recovery of FHPC and amino acids from the Cu^{II} complexes: To a solution of the complex in MeOH was added 2 N HCl (8–10 mol equiv) and the mixture was heated to reflux until FHPC precipitated from the solution. The mixture was extracted with benzene, and FHPC was purified on SiO_2 (benzene). The amino acids were obtained from the aqueous solution by ion-exchange chromatography on Dowex-50 (H^+).

Received: July 6, 1993 [Z 6190 IE]
German version: *Angew. Chem.* **1994**, *106*, 106

[1] a) T. Hayashi, M. Konishi, M. Fukushima, T. Mise, M. Kagotani, M. Tajika, M. Kumada, *J. Am. Chem. Soc.* **1982**, *104*, 180–186; b) T. Hayashi, *Pure Appl. Chem.* **1988**, 7–12; c) A. Togni, S. Pastor, *J. Org. Chem.* **1990**, *55*, 1649–1664; d) W. Cullen, F. Einstein, C. Huang, A. Willis, E. Yeh, *J. Am. Chem. Soc.* **1980**, *102*, 988–993.
[2] a) S. G. Davies, R. F. Newton, J. M. Williams, *Tetrahedron Lett.* **1989**, *30*, 2967–2970; J. Blagg, S. G. Davies, *J. Chem. Soc. Chem. Commun.* **1985**, 653–654; b) M. Uemura, R. Miyaka, K. Nakayama, M. Shiro, Y. Hayashi, *J. Org. Chem.* **1993**, *58*, 1238–1244.
[3] M. Ando, I. Watanabe, H. Kuzuhara, *Bull. Chem. Soc. Jpn.* **1990**, *63*, 88–90.
[4] S. Rosenfeld, P. Keehn, *The Cyclophanes, Vol. 1, 2*, Academic Press, New York, **1983**.
[5] H. J. Reich, D. J. Cram, *J. Am. Chem. Soc.* **1969**, *91*, 3534–3543.
[6] a) W. Hoffmann, K. Ditrich, *Synthesis* **1983**, 107–109; b) K. Krohn, H. Rieger, H. Hopf, D. Barrett, P. G. Gones, D. Doring, *Chem. Ber.* **1990**, *123*, 1729–1732.
[7] G. Casiraghi, G. Casnati, G. Puglia, G. Sartori, G. Terenghi, *J. Chem. Soc. Perkin Trans. 1* **1980**, 1862–1865.
[8] R. Williams, *Synthesis of Optically Active α-Amino Acids*, Pergamon, Oxford, **1989**.
[9] T. Aratani, *Pure Appl. Chem.* **1985**, *57*, 1839–1844.
[10] S. Colonna, A. Manfredi, M. Spadoni, L. Casella, M. Gullotti, *J. Chem. Soc. Perkin Trans. 1* **1987**, 71–73.
[11] E. Jacobsen, W. Zhang, A. Muci, J. Ecker, L. Deng, *J. Am. Chem. Soc.* **1991**, *113*, 7063–7064.
[12] M. Hayashi, Y. Miyamoto, T. Inoue, N. Oguni, *J. Org. Chem.* **1993**, *58*, 1515–1522.
[13] M. V. Saporovskaya, L. M. Volkova, V. A. Pavlov, *Zh. Anal. Khim.* **1989**, *44*, 525–528.

 © VCH Verlagsgesellschaft mbH, D-69451 Weinheim, 1994 0570-0833/94/0101-0092 $ 10.00+.25/0

(Pentafluoro-λ^6-sulfanyl)cyclopentadiene and Cyclopentadienylidenetetrafluoro-λ^6-sulfane**

Axel Klauck and Konrad Seppelt*

Dedicated to Professor Hans Bock on the occasion of his 65th birthday

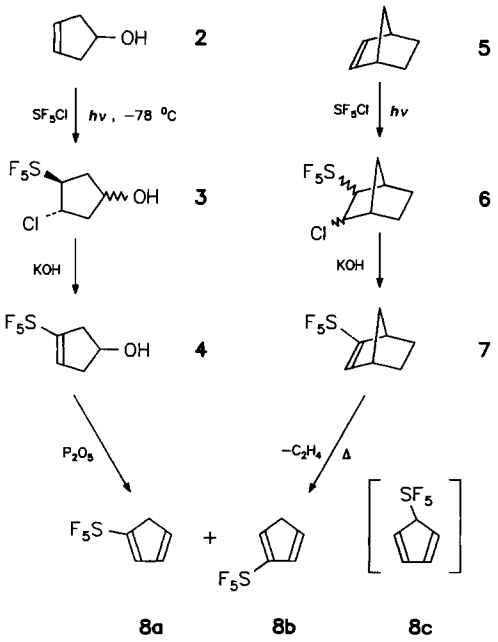
The alkylidene sulfur tetrafluorides $R_2C{=}SF_4$ have a short and rigid C–S bond with anisotropic electron density distribution such that it can reasonably be referred to as a C–S double bond.[1] We wondered if the same would be true for cyclopentadienylidenetetrafluoro-λ^6-sulfane (**1**), since the equilibrium could lie in the direction of the ylide-type resonance structure because of aromatization. Since the torsion at the C–S bond is linked to the conformational equilibration of the different fluorine atoms, this question can be answered qualitatively by using ^{19}F NMR spectroscopy.[1]



1 ?

The parent compound cyclopentadienethione is an unstable compound,[2] which can only be stabilized by introducing substituents that exert large steric and electronic effects.[3] The steric and electronic protection afforded by four fluorine substituents at the sulfur atom should make compound **1** sufficiently stable for its thorough investigation. In this regard one only needs to consider the stability of $H_2C{=}SF_4$[1] versus $H_2C{=}S$.[4]

The synthetic route to **1** initially requires the preparation of (pentafluoro-λ^6-sulfanyl)cyclopentadiene **8**, which can form three isomers and which is in itself a worthwhile target compound on account of its expected high reactivity. We prepared **8** by two routes, from 3-cyclopenten-1-ol (**2**) and from norbornene (**5**). As with almost all syntheses of highly fluorinated organosulfur compounds, the first step involves the radical addition of SF_5Cl to a C–C double bond.



It is clear from the NMR data (^1H, ^{13}C, ^{19}F) of **8** that the isomers **8a** and **8b** formed in a ratio of about 60:40. The assignment of the spectra to **8a** and **8b** is based on the different $^{13}C{-}^{19}F$ coupling constants and is not totally certain. Evidence for the formation of **8c** was not observed. The related trifluoromethylcyclopentadiene occurs in a corresponding isomer ratio of 70:30.[5] Since the isomers are easily interconverted through a [1,5]-sigmatropic hydrogen shift, we assume that the ratio **8a**:**8b**:**8c** of 60:40:0 also reflects the relative stabilities. Compounds **8a, b** have the typical properties of cyclopentadienes. Interestingly the mixture dimerizes to give a single product **12**, whose structure was determined by a single-crystal X-ray analysis (Fig. 1). Since the dimer is formed from two molecules of **8a** and is obtained in high yield without any other dimers present according to NMR spectroscopy, the conversion **8a** $\rightleftharpoons$ **8b** is essential. The exclusive formation of this one enantiomer pair from 32 theoretically possible ones can be explained only by the combination of steric and electronic effects of the large and rigid SF_5 groups.[6] In contrast trifluoromethylcyclopentadiene dimerizes to produce a mixture of four isomers.[5]

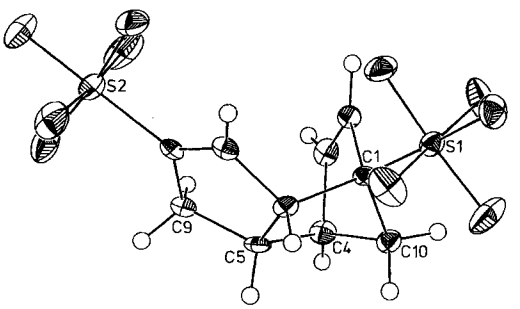
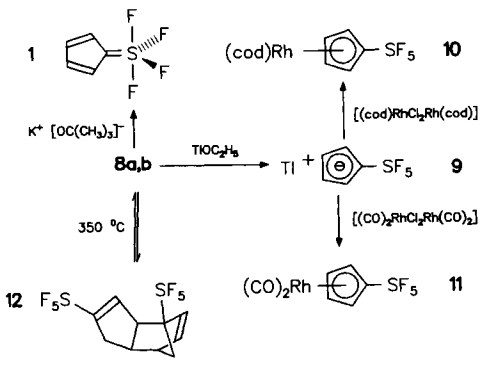


Fig. 1. Crystal structure of the dimer **12**. $a = 935.1(1)$, $b = 1083.8(2)$, $c = 1292.9(2)$ pm, $\beta = 91.77(2)°$, $V = 1310.3(3) \times 10^6$ pm^3, $T = -143$ °C, $P2_1/c$, $Z = 4$; 1883 measured, 1718 unique reflections, of which 1613 had $F > 3\sigma(F)$, 229 parameters; all non-hydrogen atoms refined anisotropically; $R = 0.033$, $R_w = 0.030$; full matrix, SHELX 76 and 86[11].

The reaction of **8a, b** with thallium ethanolate gives thallium (pentafluoro-λ^6-sulfanyl)cyclopentadienylide (**9**), which was isolated as the crystalline THF adduct. In its NMR spectrum only a single anion of **9** is observed. The crystal structure analysis of **9**·THF reveals the bent chain of rings linked through the Tl^+ ions, which is typical for thallium cyclopentadienides.[7] The coordination number at the thallium center is increased by the coordinated THF molecule (Fig. 2). The Tl–C distances indicate a largely ionic compound.[7]



[*] Prof. Dr. K. Seppelt, Dipl.-Chem. A. Klauck
Institut für Anorganische und Analytische Chemie der Freien Universität
Fabeckstrasse 34–36, D-14195 Berlin (FRG)
Telefax: Int. code + (30) 838-2424

[**] This work was supported by the Deutsche Forschungsgemeinschaft and the Fonds der Chemischen Industrie. We thank Hoechst AG, Frankfurt, for fluorinated solvents.

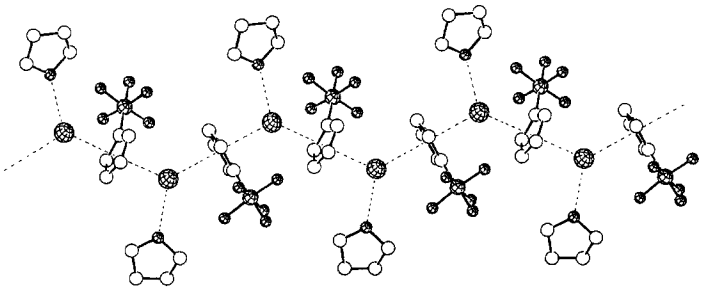


Fig. 2. Crystal structure of **9**·THF. The hydrogen atoms have been omitted for clarity. $a = 1214.4(5)$, $b = 1015.7(4)$, $c = 1075.1(3)$ pm, $\beta = 113.95(3)°$, $V = 1212.1(8) \times 10^6$ pm^3, $T = -143\,°C$, $P2_1/c$, Z = 4; 4181 measured reflections, 2646 unique reflections, of which 2373 had $F > 3\sigma(F)$, 185 parameters; all non-hydrogen atoms refined anisotropically; $R = 0.035$, $R_w = 0.026$. Tl–C 302.7(6)–314.9(5), Tl–O 287.7(4) pm[11].

Starting from **9** many organometallic cyclopentadienyl complexes should now be accessible by simple metathesis reactions. In this way, for example, the complexes **10** (cod = 1,5-cyclooctadiene) and **11** were produced. The crystal structure analysis of **10** shows it to be a typical η^5-cyclopentadienyl complex (Fig. 3).

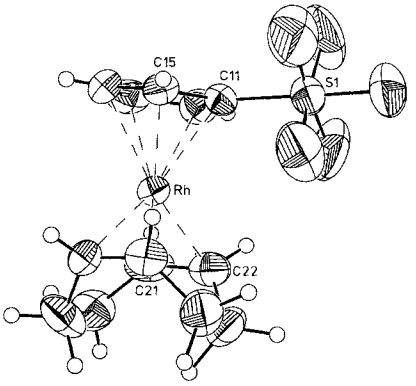


Fig. 3. Crystal structure of **10**. $a = 917.4(1)$, $b = 1318.2(1)$, $c = 1177.4(2)$ pm, $\beta = 101.84(2)°$, $V = 1386(3) \times 10^6$ pm^3, $T = 20\,°C$, $P2_1/c$, Z = 4. 2335 measured reflections, 2184 unique reflections, of which 1934 had $F > 3\sigma(F)$, 226 parameters, all non-hydrogen atoms refined anisotropically; $R = 0.036$, $R_w = 0.031$. Rh–C(Cp) 220.9(6)–228.1(6), Rh–C(cod) 207.9(6)–209.9(6) pm[11].

Disturbances in the fivefold symmetry of the cyclopentadienyl unit arising from the SF_5 group are evident only to a small degree in the Rh–C bond lengths. In spite of repeated efforts we have not succeeded in synthesizing the corresponding ferrocene, even though the formation of bis(trifluoromethyl)ferrocene from $FeCl_2$ and $Tl(CF_3C_5H_4)$ is possible.[8]

The deliberate fluoride abstraction from **8** by elimination of KF from the intermediate $K^+(C_5H_4SF_5)^-$ at $-55\,°C$ gives **1** as a yellow liquid, which is stable as a diluted solution for several days at room temperature. Compound **1** was characterized by ^1H and ^{19}F NMR spectroscopy as well as by mass spectrometry. If one ignores the small HF coupling in the ^{19}F NMR spectrum, the A_2B_2 system known for alkylidene sulfur tetrafluorides is observed. This spin system does not coalesce to a single line even when a highly dilute sample is heated to 180 °C. From this one can conclude that the zwitterionic mesomeric resonance structure is not significant despite the potential stabilization of the aromatic five-membered ring. It is known that the axial and equatorial fluorine atoms of alkyltetrafluorosulfonium cations $R-SF_4^+$ exchange even at $-80\,°C$.[9] In our proposed structure for **1** the plane of the five-membered ring is coplanar with the axial fluorine atoms, and the structure is rigid in analogy to the known alkylidene sulfur tetrafluoride.[1]

Experimental Procedure

3 (Mixture of isomers): In a glass ampule 1.87 g (22.2 mmol) **2**[10], 1.70 g CCl_3F, and 3.64 g (22.4 mmol) $SClF_5$ were irradiated with a high-pressure Hg vapor lamp at $-78\,°C$ for ca. 16 h. The volatile components were removed at 80 °C/0.1 mbar leaving 3.55 g (65%) **3**. M.p. $-65\,°C$; ^{19}F NMR (84 MHz, $CDCl_3$): 2 sets of AB_4-type signals in the ratio 70:30. $\delta = 85.3$, 61.0 ($^2J(AB) = 143.3$ Hz), 85.3, 60.1 ($^2J(AB) = 143.2$ Hz); IR: strong bands at 3386, 906, 847 (vs), 750, 651, 596 cm^{-1}.

4: 2.25 g (9.12 mmol) **3** reacted at room temperature within several h upon stirring with 2.50 g powdered KOH in 50 mL ether. After neutralization, extraction with ether, drying with $MgSO_4$, and fractional condensation (25 °C/−78 °C/−196 °C) in dynamic vacuum at 10^{-3} mbar, 1.07 g (56%) **4** was isolated in the trap at −78 °C. M.p. 5 °C; ^{19}F NMR ($CDCl_3$): AB_4 type, $\delta = 85.26$, 62.82 ($^2J(AB) = 145.8$ MHz); IR: strong bands at 3352, 824 (vs), 774, 663 cm^{-1}.

8 (from **3**): 3.87 g (18.4 mmol) **4** was layered with P_2O_5 in a glass flask. The reaction vessel was attached to a cold trap system (−78 °C/−196 °C) and warmed to 50 °C. 2.60 g (73%) **8a**, **b** was obtained in the trap at −78 °C under a dynamic vacuum. M.p. −75 °C; ^{19}F NMR ($CDCl_3$): two sets of AB_4-type signals in the ratio 60:40, $\delta = 86.44$, 67.92 ($^2J(AB) = 150.1$ Hz, isomer A), 84.84, 65.09 ($^2J(AB) = 146.5$ Hz, isomer B); IR(gas): strong bands at 1097, 893 (vs), 871 (vs), 805 (vs), 673, 605 cm^{-1}; ^1H NMR (250 MHz, $CDCl_3$): $\delta = 3.2$ (isomer B), 3.5 (isomer A), (-CH_2-), 6.4–6.5, 6.6–6.7, 6.8, 7.0; $^{13}C\{^1H\}$ NMR ($CDCl_3$): 40.6 (B), 42.7 ($J(CF_{eq}) = 2.0$ Hz, A), 128.8 ($J(CF_{eq}) = 3.5$ Hz), 129.8, 133.4–135.2, 155 (-$C(SF_5)$, A and B); MS (*m/z*: 192 (M^+, 98.2%), 173 ($[C_5H_5SF_4]^+$, 15.0%), and smaller fragments.

6: In a sealed glass ampule 1.50 g (15.9 mmol) **5** dissolved in 2.8 g CCl_3F reacted with 2.85 g (17.5 mmol) $SClF_5$ under irradiation with a high-pressure Hg vapor lamp. Fractional condensation (25 °C/−78 °C/−196 °C) in dynamic vacuum gave 4.00 g (98%) **6** in the trap at −78 °C. M.p. 5.5 °C; ^{19}F NMR ($CDCl_3$): AB_4 type, $\delta = 85.7$, 58.8 ($^2J(AB) = 141.6$ Hz); IR: strong bands at 2917, 1305, 890 (vs), 869 (vs), 831 (vs), 814 (vs), 797 (vs), 786 (vs), 758, 636 (vs), 590 cm^{-1}.

7: A mixture of 3.50 g (13.6 mmol) **6** and 10 g finely powdered KOH in 50 mL pentane was heated at reflux for two weeks. Fractional condensation (25 °C/−78 °C/−196 °C) in dynamic vacuum gave 2.36 g (79%) pure **7** in the trap at −78 °C. M.p. −52 °C; ^{19}F NMR ($CDCl_3$): AB_4 type, $\delta = 85.5$, 64.3 ($^2J(AB) = 148.9$ Hz); IR: strong bands at 2977, 2929, 1309, 1067, 917, 831 (vs), 791 (vs), 770 (vs), 686, 658 (vs), 597 (vs) cm^{-1}.

8 (from **5**): 0.42 g (1.9 mmol) **7** was pyrolyzed at 10^{-3} mbar and 400 °C in a glass tube, and the volatile components were fractionally distilled in a cold-trap system (−78 °C/−196 °C). 0.10 g (27%) **8** was isolated in the trap at −78 °C.

9: 0.44 g (1.8 mmol) $Tl(OC_2H_5)$ was dissolved in 50 mL dry THF (or pentane, Et_2O, EtOH) and cooled to −196 °C. 0.36 g (1.9 mmol) **8** was added by condensation. The mixture was slowly warmed to −20 °C. Recrystallization from THF at −78 °C gave 0.51 g (61%) **9**·THF. M.p. 65 °C (decomp); ^{19}F NMR ([D_8]THF): AB_4 type, $\delta = 95.9$, 79.3 ($^2J(AB) = 150.4$ Hz); ^1H NMR ([D_8]THF): $\delta = 5.9$, 6.5; MS (*m/z*): 396 ([*M*]$^+$, 6.7%), 332 ([$TlSF_5$]$^+$, 0.6), 225 ([TlHF]$^+$, 1.4), 205 (Tl^+, 100.0) and smaller fragments; IR: strong bands at 1522 (vs), 1036, 903, 849 (vs), 839 (vs), 800 (vs), 757 (vs), 658 cm^{-1}.

10: On addition of 235 mg (0.477 mmol) $[Rh_2Cl_2(cod)_2]$ to a suspension of 0.64 g (1.45 mmol) **9** in 30 mL THF at −78 °C, an orange solution and a precipitate of TlCl was obtained. The solvent was removed under vacuum, the residue dissolved in pentane and centrifuged to give after recrystallization 0.28 g (0.70 mmol, 74%) **10**. M.p. 89.4 °C; ^{19}F NMR ($CDCl_3$): AB_4 type, $\delta = 76.0$, 87.8 ($^2J(AB) = 148.9$ Hz); $^{13}C\{^1H\}$ NMR ($CDCl_3$): $\delta = 31.9$ ($^1J(CRh) = 0.5$ Hz), 66.6 ($^1J(CRh) = 13.9$ Hz), 84.9 ($^1J(CRh) = 4.0$ Hz, $J(CF_{eq}) = 4.0$ Hz), 87.2 ($^1J(CRh) = 3.5$ Hz, $J(CF_{eq}) = 1.3$ Hz), 93.3 ($^2J(CF_{eq}) = 11.4$, $^1J(CRh) = 3.1$, $^2J(CF_{ax}) = 1.1$ Hz); MS (*m/z*): 402 (*M*$^+$, 100%), 372 ($[C_{11}H_{10}F_5RhS]^+$, 4.4), 348 ($[C_9H_{10}F_5RhS]^+$, 3.4), 275 ($[C_{13}H_{16}Rh]^+$, 10.1), and smaller fragments; IR: strong bands at 901, 871 (vs), 826 (vs), 785 (vs), 775 (vs), 734, 625, 587 cm^{-1}.

11: 0.30 g (0.78 mmol) $[Rh_2Cl_2(CO)_4]$ in THF reacted with 1.2 g (3.0 mmol) **9** at −78 °C, whereupon the solution turned red. The reaction mixture was warmed to room temperature, the THF removed in vacuo and replaced with pentane, and the resulting solution centrifuged. Fractional condensation of the crude product (25 °C/−78 °C/−196 °C) under a dynamic vacuum gave 0.40 g (71%) in the trap at −78 °C. M.p. −3 °C; ^{19}F NMR ($CDCl_3$) : AB_4 type, $\delta = 74.9$, 83.2 ($^2J(AB) = 146.5$ Hz); ^1H NMR ($CDCl_3$): $\delta = 5.45$ ($^3J(HH) = {}^2J(HRh) = 2.45$ Hz, $J(CF_{eq}) = 1$ Hz), 5.87 ($^3J(HH) = {}^2J(HRh) = 2.45$ Hz, $^{13}C\{^1H\}$ NMR ($CDCl_3$): $\delta = 86.92$ ($J(CF_{eq}) = 4.0$, $^1J(CRh) = 0.7$ Hz), 87.22 ($J(CF_{eq}) = 1.8$ Hz), 123.67 ($^2J(CF_{eq}) = 23.6$, $^1J(CRh)/^2J(CF_{ax}) = 2.6/4.4$ Hz), 188.28 ($^1J(CRh) = 84.84$, $^4J(CF_{eq}) = 1.3$ Hz); MS (*m/z*): 349.89064 calc. 349.89073 (*M*$^+$, 84.4%), 322 ([M − CO]$^+$, 68.4), 294 ([M − 2CO]$^+$, 13.5), 223 ([M − SF_5]$^+$, 6.2), and smaller fragments; IR: strong bands at 2061 (vs), 1999 (vs), 906, 852 (vs), 798 (vs), 670, 599, 570, 514, 493 cm^{-1}.

12 (Dimer of **8**): 0.26 g (1.4 mmol) **8** at 25 °C produced 0.25 g (0.65 mmol, 96%) **12** after several days. M.p. 31.6 °C; ^{19}F NMR ($CDCl_3$) : two sets of AB_4-type signals, $\delta = 86.12$, 62.22, 83.51, 59.13 ($^2J(AB) = 146.5$, 141.6 Hz); $^{13}C\{^1H\}$ NMR ($CDCl_3$): $\delta = 35.83$ ($^3J(CF_{eq}) = 2.4$ Hz), 41.05, 42.35 ($J(CF_{eq}) = 2.0$ Hz), 54.78 ($J(CF_{eq}) = 3.4$ Hz), 55.83 ($J(CF_{eq}) = 2.0$ Hz), 102.03 ($^2J(CF_{eq}) = 11.2$, $^2J(CF_{ax}) = 1.5$ Hz),

 © VCH Verlagsgesellschaft mbH, D-69451 Weinheim, 1994 0570-0833/94/0101-0094 $ 10.00+.25/0 Angew. Chem. Int. Ed. Engl. 1994, 33, No. 1

133.04 ($J(CF_{eq})$ = 5.9 Hz), 133.30 ($J(CF_{eq})$ = 1.7 Hz), 134.36 ($J(CF_{eq})$ = 4.4 Hz), 157.60 ($^2J(CF_{eq})$ = 15.1, $^2J(CF_{ax})$ = 2.0 Hz); MS (*m/z*): 384 (M^+, 1.1%), 257 ($[M-SF_5]^+$, 1.5), 192 ($[C_5H_5SF_5]^+$, 100.0), and smaller fragments; IR: strong bands at 914, 842 (vs), 797 (vs) 779 (vs), 734, 718, 662, 592 cm^{-1}.

1: 0.65 g (3.4 mmol) **8** was added to a solution of 0.380 g (3.39 mmol) $K(OCMe_3)$ in 30 mL dry pentane by condensation. The reaction mixture was stirred at −78 °C until the starting material signals in the ^{19}F NMR spectrum disappeared. The solution was yellow at −60 °C; when the temperature increased the solution became brown then black. After removal of the volatile components under high vacuum and several fractional condensations at different temperatures under dynamic vacuum, 0.14 g (24%) **1** was obtained. ^{19}F NMR (CD_2Cl_2): A_2B_2 type, δ = 63.7, 55.3 ($^2J(AB)$ = 167.0 Hz); ^1H NMR (500 MHz, CD_2Cl_2): δ = 6.53, 6.57; MS (*m/z*): 171.99683 (calc. 171.99699) (M^+, 100.0%), 150 ($[C_5HSF_3]^+$, 10.0), 115 ($[C_2H_2SF_3]^+$, 1.9), 89 ($[SF_3]^+$, 16.6), and smaller fragments; IR (gas): 3155 (vw), 3091 (vw), 2982 (w), 1602 (w), 1458 (m), 1399 (w), 1369 (m), 1249 (vs), 1089 (s), 1062 (w), 1028 (m), 911 (s), 867 (vs), 832 (vs), 798 (vs), 672 (s) cm^{-1}. UV/VIS: λ_{max} = 250 nm.

Received: July 21, 1993 [Z 6223 IE]
German version: *Angew. Chem.* **1994**, *106*, 98

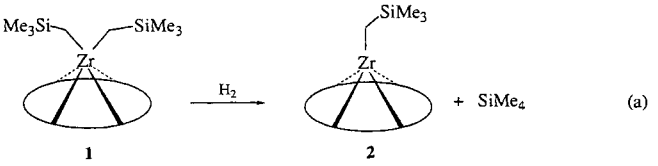
[1] K. Seppelt, *Angew. Chem.* **1991**, *103*, 399–413; *Angew. Chem. Int. Ed. Engl.* **1991**, *30*, 361–374.
[2] R. Schulz, A. Schweig, *Angew. Chem.* **1981**, *93*, 603–605; *Angew. Chem. Int. Ed. Engl.* **1981**, *20*, 570–572.
[3] R. Gompper, H. Glöckner, *Angew. Chem.* **1984**, *96*, 48–49; *Angew. Chem. Int. Ed. Engl.* **1984**, *23*, 53–54.
[4] D. R. Johnson, F. X. Powell, W. H. Kirchhoff, *J. Mol. Spectrosc.* **1971**, *39*, 136–145; H. W. Kroto, R. J. Suffolk, *Chem. Phys. Lett.* **1972**, *15*, 545–548; M. E. Jacox, D. E. Milligan, *J. Mol. Spectrosc.* **1975**, *58*, 142–157; B. Solouki, P. Rosmus, H. Bock, *J. Am. Chem. Soc.* **1976**, *98*, 6054–6055.
[5] T. Olsson, O. Wennerström, *Acta Chem. Scand. Ser. B* **1978**, *32*, 293–296.
[6] D. Ginsburg, *Tetrahedron* **1983**, *39*, 2095–2135; R. B. Woodward, R. Hoffmann, *Angew. Chem.* **1969**, *81*, 797–870; *Angew. Chem. Int. Ed. Engl.* **1969**, *8*, 781–853.
[7] a) E. Frasson, F. Mengus, C. Panattoni, *Nature* **1963**, *199*, 1087–1089; b) H. Werner, H. Otto, H. J. Kraus, *J. Organomet. Chem.* **1986**, *315*, C57–C60; c) M. B. Freeman, L. G. Sneddon, J. C. Huffmann, *J. Am. Chem. Soc.* **1977**, *99*, 5194–5196; d) S. Harvey, C. L. Raston, B. W. Skelton, A. H. White, M. F. Lappert, G. Srivastava, *J. Organomet. Chem.* **1987**, *328*, C1–C6; thallium cyclopentadienides not found as polymers or oligomers: H. Schumann, C. Janiak, M. A. Khan, J. J. Zuckerman, *ibid.* **1988**, *354*, 7–13; H. Schumann, C. Janiak, J. Pickardt, U. Börner, *Angew. Chem.* **1987**, *99*, 788–789; *Angew. Chem. Int. Ed. Engl.* **1987**, *26*, 789–790.
[8] P. G. Gassmann, C. H. Winter, *J. Am. Chem. Soc.* **1986**, *108*, 4228–4229.
[9] J. Wessel, G. Kleemann, K. Seppelt, *Chem. Ber.* **1983**, *116*, 2399–2407.
[10] A. Maercker, R. Geuß, *Chem. Ber.* **1973**, *106*, 773–797.
[11] Further details of the crystal structure investigations may be obtained from the Fachinformationszentrum Karlsruhe, Gesellschaft for wissenschaftlich-technische Information mbH, D-76344 Eggenstein-Leopoldshafen (FRG) on quoting the depository number CSD-57634, the names of the authors, and the journal citation.

Facile Reduction of a Dialkyl Zirconium(IV) Octaethylporphyrin (OEP) Complex by H_2: Crystal Structure and Spectroscopic Characterization of $[(OEP)ZrCH_2SiMe_3]$**

Holger Brand and John Arnold*

During our recent studies of the homogeneous catalytic hydrogenation of olefins by $[(OEP)ZrR_2]$ (OEP = octaethylporphyrin, R = alkyl) we observed degradation of the catalyst in the absence of olefin to a green paramagnetic compound that we have now isolated in pure form for $R = CH_2SiMe_3$ and show here to be the reduced monoalkyl complex $[(OEP)ZrCH_2SiMe_3]$ (**2**).[1–3] Formally, this compound contains Zr in the +III oxidation state which is remarkable since: i) alkylzirconium(III) compounds are extremely rare,[4] and ii) reduction of Zr^{IV} to Zr^{III} by H_2 is, to the best of our knowledge, unprecedented. A combination of spectroscopic techniques shows, however, that this simple view of the complex does not fully account for the observed data, and that a more accurate picture is obtained by considering a second resonance form involving a neutral Zr^{IV}–porphyrin radical anion.[5] As similar arguments were made some time ago by Reed et al. to explain related data for reduced iron porphyrins, our results provide an interesting comparison between early transition metal porphyrin radicals with these more well-studied late metal derivatives.[6, 7]

Reaction of $[(OEP)Zr(CH_2SiMe_3)_2]$ (**1**)[1] with H_2 (1 atm) in toluene at 20 °C results in a color change from red to green and affords a quantitative yield of $[(OEP)ZrCH_2SiMe_3]$ (**2**) after filtration and removal of the solvent [Eq. (a), OEP is denoted as a circle]. Crystallization from pentane at −40 °C gave blue crystals of analytically pure **2** suitable for X-ray crystallography. The crystal structure of **2** (Fig. 1) shows the zirconium atom to be five-coordinate with the alkyl group in the axial position.[8] The zirconium atom is displaced by 0.63 Å out of the mean plane generated by the four nitrogen atoms, towards the carbon atom of the alkyl group. This value is similar in magnitude to the related five-coordinated (OEP)Sc compounds[9, 10] but is significantly smaller than that for the dialkyl precursor **1** (in which the Zr is displaced by 0.93 Å[1]) and related *cis*-coordinated (OEP)Zr derivatives.[2] This is no doubt due to relief of steric strain brought about by the loss of the *cis* ligand, a view which is further supported by the shortening of the Zr–C bond in **2** (2.216(8) Å) relative to that in **1** (2.287(4) Å). A slight lengthen-



(a)

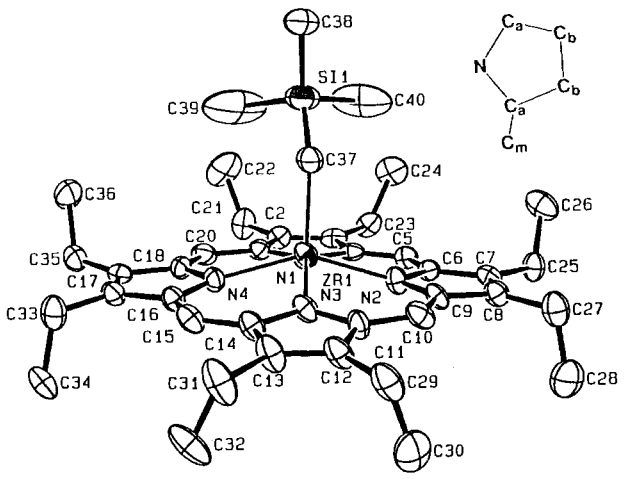


Fig. 1. Crystal structure (ORTEP) of one of the two independent molecules of $[(OEP)ZrCH_2SiMe_3]$ (**2**) with thermal ellipsoids drawn at the 50% probability level. Hydrogen atoms have been omitted for clarity. Selected bond lengths [Å] and angles [°]: Si1-C37 1.846(8); Zr1-N1 2.152(6); Zr1-N2 2.146(6); Zr1-N3 2.143(6); Zr1-N4 2.160(6); Zr1-C37-Si1 124.1(4).

[*] Prof. Dr. J. Arnold, H. Brand
Department of Chemistry, University of California
Berkeley, CA 94720 (USA)
Telefax: Int. code + (510)642-8369

[**] We thank the donors of the Petroleum Research Fund, administered by the American Chemical Society and the Exxon Education Foundation for funding, and Prof. S. Strauss, Fort Collins, Colorado, for helpful discussions.

 © VCH Verlagsgesellschaft mbH, D-69451 Weinheim, 1994 0570-0833/94/0101-0095 $ 10.00+.25/0

ing of $N-C_a$ and C_b-C_b and shortening of C_a-C_b bonds is apparent when the average bond lengths in the porphyrin core of **2** are compared with those of other d^0 transition metal OEP derivatives (Table 1). Similar results have been reported for reduced Fe–porphyrin compounds and these have been rationalized in terms of partial population of the porphyrin LUMO of e symmetry.[7, 11]

Table 1. Comparison of average bond lengths [a].

Compound	$N-C_a$	C_a-C_b	C_b-C_b	C_a-C_m
2 [b]	1.395(7)	1.428(11)	1.373(7)	1.388(12)
(OEP)M derivates [c]	1.382(7)	1.447(6)	1.361(6)	1.390(9)

[a] These are averaged values with the calculated standard deviations given in parentheses. [b] Data from the two independent molecules in the unit cell. [c] Averaged values from $[(OEP)ZrMe_2]$, $[(OEP)ZrCl_2]$, $[(OEP)Zr(O\,t\,Bu)_2]$ (all ref. [2]), **1** (ref. [1]), and [(OEP)ScMe] (ref. [10]).

The UV/VIS, ^{1}H NMR, and EPR spectra of **2** are shown in Figure 2. The UV/VIS spectrum shows a Soret band (Fig. 2A) that is reduced in intensity relative to that in the spectrum of the starting material **1** and extra bands at 458 and above 600 nm, typical of a porphyrin radical anion.[6, 12] In comparison, most of the isoelectronic d^1 Ti–porphyrin compounds display a "normal" UV/VIS spectrum, since the single electron in these species resides in a metal d_{xy} orbital.[13, 14] We note, however, that if back-bonding from the axial ligand to the metal raises the energy of this orbital,[15, 16] green porphyrin radical anions are observed.[17, 18]

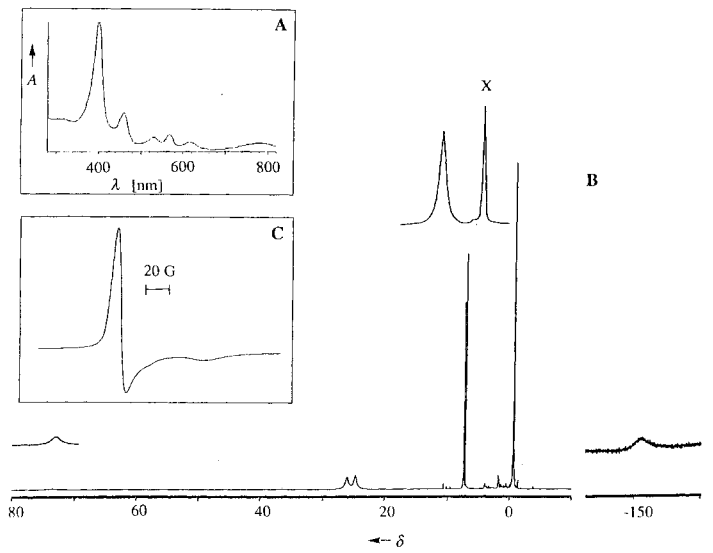
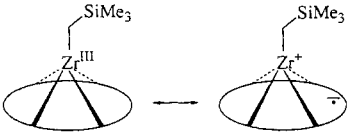


Fig. 2. A) UV/VIS, B) ^{1}H NMR, and C) EPR spectra of **2**. A = absorbance.

The ^{1}H NMR spectrum (Fig. 2B) provides more information about the electronic nature of **2**. The proton resonances have been assigned by integration and by selective deuteration at the *meso* positions,[19] and follow Curie–Weiss behavior between 5 and 80 °C. The large upfield shift and temperature dependence of the signal corresponding to the *meso* hydrogen atoms is indicative of high spin density at the *meso* carbon atoms.[20, 21] Since the methylene protons of the CH_2SiMe_3 group also experience a strong, temperature-dependent paramagnetic shift (down field in this case) there must also be considerable spin density at the Zr atom.[20, 21] This ambiguity of spin density is best explained by assuming single occupancy of a molecular orbital of e symmetry,[7, 11] delocalized over the porphyrin ring *and* the transition metal. Such an orbital has the right symmetry to overlap with the metal d_{xz} and d_{yz} orbitals, and its wave function has a large coefficient at the *meso* carbon atoms.

No EPR signal is detected at 293 K; however, at 77 K an isotropic signal typical of a metal-centered radical, with $g_\perp = 2.001$ G and $g_\parallel = 1.989$ G, is observed (Fig. 2C).[22] The fact that an isotropic signal with no ^{14}N hyperfine coupling[14, 17, 23, 24] is observed at low temperature, yet no signal is detected at 293 K is also consistent with single occupation of an e orbital and not of the metal d_{xy} orbital as is the case with a Ti^{III} system. Porphyrin radical anions of late transition metals show g values around the spin only value; in these compounds the electron is confined to the porphyrin ring since the metal d_{xz} and d_{yz} orbitals are occupied.[25] The electronic structure of $[(OEP)ZrCH_2SiMe_3]$ (**2**) is therefore best described by two resonance formulae, a Zr^{III} metal-based radical *and* a zwitterionic porphyrin radical anion.



2

Experimental Procedure

Toluene (25 mL) was vacuum transferred onto $[(OEP)ZrCl_2] \cdot 0.5$ toluene (0.500 g, 0.675 mmol) [2] and $LiCH_2SiMe_3$ (0.127 g, 1.350 mmol). After 2 h all the starting materials were dissolved and H_2 (1 atm) was admitted, resulting in a color change to dark green. The solution was filtered after 2 h and the volatiles were removed under reduced pressure. The compound was crystallized from pentane to afford blue crystals: M.p. 100 °C (decomp.); ^{1}H NMR (C_6D_6, 300 MHz): $\delta = 73.5$ (2H, br s, $h_{1/2} = 610$ Hz; CH_2Si), 26.1 (8H, br s, $h_{1/2} = 250$ Hz, CH_2CH_3), 24.7 (8H, br s, $h_{1/2} = 250$ Hz, CH_2CH_3), 7.39 (9H, s, $h_{1/2} = 15.4$ Hz; $Si(CH_3)_3$), −0.64 (24H, s, $h_{1/2} = 25$ Hz; CH_2CH_3), −154 (br s, $h_{1/2} = 3000-3500$ Hz, *meso*-H); UV/VIS (pentane): λ_{max} (ε) = 316 (14100), 398 (56200), 458 (15800), 530 (9300), 566 (10700), 614 (7600), 786 (6600); MS (70 eV): m/z 711 (50%, M^+); μ_{eff} (C_6D_6) = 1.88 BM; EPR ($C_6H_{11}CH_3$, 77 K): $g_\perp = 2.001$, $g_\parallel = 1.964$; Anal. calcd. for $C_{47}H_{55}N_4SiZr$: C, 67.55; H, 7.79; N, 7.88; found: C, 67.58; H, 7.78; N, 7.87.

Received: July 30, 1993 [Z 6246 IE]
German version: *Angew. Chem.* **1994**, *106*, 119

[1] H. Brand, J. Arnold, *J. Am. Chem. Soc.* **1992**, *114*, 2266.
[2] H. Brand, J. Arnold, *Organometallics* **1993**, *12*, 6355.
[3] For other accounts on zirconium porphyrins see: J. W. Buchler, in *The Porphyrins* (Ed.: D. Dolphin), Academic Press, New York, **1978**, *Vol 1*, Chapter 10; B. D. Berezin, T. N. Lomova, *Russ. J. Inorg. Chem.* **1981**, *26*, 203; K. Kim, W. S. Lee, H.-J. Kim, S.-H. Cho, G. S. Girolami, P. A. Gorlin, K. S. Suslick, *Inorg. Chem.* **1991**, *30*, 2652; K. Shibata, T. Aida, S. Inoue, *Tetrahedron Lett.* **1992**, *33*, 1077; K. Shibata, T. Aida, S. Inoue, *Chem. Lett.* **1992**, 1173; H.-J. Kim, D. Whang, K. Kim, Y. Do, *Inorg. Chem.* **1993**, *32*, 360.
[4] D. J. Cardin, M. F. Lappert, C. L. Raston, *Chemistry of Organo-Zirconium and Organo-Hafnium Compounds*, Wiley, New York, **1986**.
[5] J. W. Buchler, L. Puppe, K. Rohbock, H. H. Schneehage, *Ann. N. Y. Acad. Sci.* **1973**, *206*, 116.
[6] C. A. Reed, *Adv. Chem. Ser.* **1982**, *No. 201*, 333.
[7] T. Mashiko, C. A. Reed, K. J. Haller, R. Scheidt, *Inorg. Chem.* **1984**, *23*, 3192.
[8] Crystal data for **2**: $a = 12.837(3)$, $b = 13.728(2)$, $c = 24.178(5)$ Å, $\alpha = 75.560(15)$, $\beta = 83.900(18)$, $\gamma = 68.289(16)°$, $V = 3833.2(15)$ Å^3, space group $P\bar{1}$, $Z = 4$. The structure was solved by Patterson methods leaving the final residuals for 832 variables refined against the 6237 data for which $F^2 > 3\sigma|F^2|$ were $R = 0.0525$, $R_w = 0.0625$ and GOF = 1.74. The structure consists of two crystallographically independent molecules of the compound packed tightly into a triclinic unit cell. Only one of the two molecules is discussed in the text. Further details of the crystal structure analysis are available on request from the Director of the Cambridge Crystallographic Data Centre, University

Chemical Laboratory, 12 Union Road, GB-Cambridge CB21EZ (UK) on quoting the full journal citation.
[9] J. Arnold, C. G. Hoffman, *J. Am. Chem. Soc.* **1990**, *112*, 8620.
[10] J. Arnold, C. G. Hoffman, D. Y. Dawson, *Organometallics* **1993**; in press.
[11] This is equivalent to the e_g orbital (for D_{4h} symmetry) as described by the four-orbital diagram in: M. Gouterman in *The Porphyrins* (Ed.: D. Dolphin), Academic Press, New York, **1978**, *Vol. III*, Chapter 1, p 93.
[12] A reviewer pointed out that the peaks in the UV/VIS spectrum may in fact result from a mixture of the following species: $(OEP)Zr^{IV}$, $(OEPH)Zr^{IV}$, $(OEPH_2)Zr^{IV}$, and $(H_2OEP)Zr^{IV}$ formed by disproportionation and subsequent protonation and rearrangement. At such high dilution we cannot rule out such reactions, however, we note that the relative intensities of the peaks are reproducible and that an identical UV/VIS spectrum is produced by generation of $[(OEP)ZrCH_2SiMe_3]$ (**2**) from $[(OEP)Zr(CH_2SiMe_3)_2]$ (**1**) and dihydrogen in situ in the UV cell. For explanation of the nomenclature used and the UV/VIS features for the species mentioned above see ref. [5].
[13] J.-C. Marchon, J.-M. Latour, C. J. Boreham, *J. Mol. Cat.* **1980**, *7*, 227.
[14] J.-M. Latour, J.-C. Marchon, M. Nakajima, *J. Am. Chem. Soc.* **1979**, *101*, 3974.
[15] C. Ratti, P. R. A. Tabard, R. Guilard, *J. Chem. Soc. Chem. Commun.* **1989**, 69.
[16] A. Dedieu, M.-M. Rohmer, H. Veillard, A. Veillard, *Nouv. J. Chem.* **1979**, *3*, 653.
[17] A. Deronzier, J. M. Latour, *Nouv. J. Chem.* **1984**, *8*, 393.
[18] T. Malinski, D. Chang, J.-M. Latour, J.-C. Marchon, M. Gross, A. Giraudeau, K. M. Kadish, *Inorg. Chem.* **1984**, *23*, 3947.
[19] The signal at $\delta = -154$ was absent in the ^1H NMR spectrum of $[(meso\text{-}D_4\text{-}OEP)ZrCH_2SiMe_3]$.
[20] F. A. Walker, G. N. La Mar, *Ann. N. Y. Acad. Sci.* **1973**, *206*, 328.
[21] G. N. La Mar, F. N. Walker in *The Porphyrins* (Ed.: D. Dolphin), Academic Press, New York, **1978**, *Vol. IV*, Chapter 2.
[22] Virtually identical results were obtained by measuring the EPR spectra of three different crops; the average value is reported here.
[23] W. C. Lin in *The Porphyrins* (Ed.: D. Dolphin), Academic Press, New York, **1978**, *Vol. IV*, Chapter 7.
[24] B. B. Wayland, B. B. Olson, Z. U. Siddiqui, *J. Am. Chem. Soc.* **1976**, *98*, 94.
[25] J. Fajer, M. S. Davis in *The Porphyrins* (Ed.: D. Dolphin), Academic Press, New York, **1978**, *Vol. IV*, Chapter 4.

Trialkylstibanes as Bridging Ligands: Synthesis and Structure of the Dinuclear Complexes $[Rh_2Cl_2(\mu\text{-}Sb\mathit{i}Pr_3)(\mu\text{-}CR_2)_2]$**

Peter Schwab, Norbert Mahr, Justin Wolf, and Helmut Werner*

Dedicated to Professor Carl Krüger on the occasion of his 60th birthday

Owing to recent investigations particularly by Huttner et al.[1] the existence of dinuclear transition metal complexes containing Sb, SbR, and SbR_2 units as bridging ligands is well established.[2] In contrast, stibanes SbR_3 as well as arsanes AsR_3 and phosphanes PR_3 were considered to be able only to form terminal $M-ER_3$ bonds.[3] We have now discovered the first examples of SbR_3-bridged dinuclear complexes which are not only easily accessible but are also surprisingly thermally stable.

The carbenerhodium(I) compounds **1**–**3**, prepared from *trans*-$[RhCl(C_2H_4)(Sb\mathit{i}Pr_3)_2]$ and diaryldiazomethanes,[4] react on warming in benzene by partial loss of the $Sb\mathit{i}Pr_3$ ligands to give complexes **4**–**6** in about 80% yield. Complexes **4**–**6** are red crystalline solids which are soluble in C_6H_6 and CH_2Cl_2 and thermally decompose only above 180 °C. The composition was confirmed by elemental analysis. The spectroscopic data of **4**–**6** differ significantly from those of the mononuclear compounds **1**–**3** insofar as in the ^1H NMR spectra the signal of the SbC*H* protons appears at *higher* field than that of the $SbCHCH_3$ protons [see Table 1 and cf. **1**: $\delta(SbCH) = 2.08$ (sept, $J(H,H) = 7.3$ Hz), $\delta(SbCHCH_3) = 1.31$ (d, $J(H,H) = 7.3$ Hz)], while in the ^{13}C NMR spectra the Sb*C*H resonance is observed at *lower* field than that of the $SbCHCH_3$ carbon atoms [see Table 1 and cf. **1**: $\delta(SbCH) = 19.07$ (d, $J(RhC) = 3.4$ Hz), $\delta(SbCHCH_3) = 21.90$ (s)]. Another characteristic feature is that in compound **1** the phenyl groups are spectroscopically equivalent, whereas in compound **4** they are different, as is illustrated by the double set of signals for the C_6H_5 carbon atoms. The ^{13}C NMR spectrum of **6** reveals that all three possible isomers with

Table 1. Selected spectroscopic data (omitting the ^1H and ^{13}C NMR data for aryl groups) for compounds **4**–**9** and **12**–**14**.

4: ^1H NMR (400 MHz, C_6D_6): $\delta = 1.12$ (d, $^3J(HH) = 7.2$ Hz; $SbCHCH_3$), 0.79 (sept, $^3J(HH) = 7.2$ Hz; $SbCHCH_3$); ^{13}C NMR (100.6 MHz, C_6D_6): $\delta = 186.95$ (t, $^1J(RhC) = 26.3$ Hz; RhCRh), 22.98 (s; $SbCHCH_3$), 21.90 (s; $SbCHCH_3$).

5: ^1H NMR (200 MHz, $CDCl_3$): $\delta = 1.20$ (d, $^3J(HH) = 6.9$ Hz; $SbCHCH_3$), 1.00 (sept, $^3J(HH) = 6.9$ Hz; $SbCHCH_3$); ^{13}C NMR (50.3 MHz, $CDCl_3$): $\delta = 188.30$ (t, $^1J(RhC) = 26.2$ Hz; RhCRh), 22.97 (s, $SbCHCH_3$), 21.87 (s, $SbCHCH_3$).

6: ^1H NMR (200 MHz, $CDCl_3$): $\delta = 1.23$ (d, $^3J(HH) = 6.4$ Hz; $SbCHCH_3$), 0.97 (sept, $^3J(HH) = 6.4$ Hz; $SbCHCH_3$); ^{13}C NMR (50.3 MHz, $CDCl_3$): $\delta = 188.00$, 187.85, 187.79 (all t, $^1J(RhC) = 25.6$ Hz; RhCRh), 23.08 (s; $SbCHCH_3$), 21.87 (s; $SbCHCH_3$).

7: ^1H NMR (200 MHz, $CDCl_3$): $\delta = 1.23$ (d, $^3J(HH) = 6.9$ Hz; $SbCHCH_3$), 0.98 (sept, $^3J(HH) = 6.9$ Hz; $SbCHCH_3$); ^{13}C NMR (50.3 MHz, $CDCl_3$): $\delta = 188.31$, 187.50 (both t, $^1J(RhC) = 26.5$ Hz; RhCRh), 21.88 (s; $SbCHCH_3$), 21.01 (s; $SbCHCH_3$).

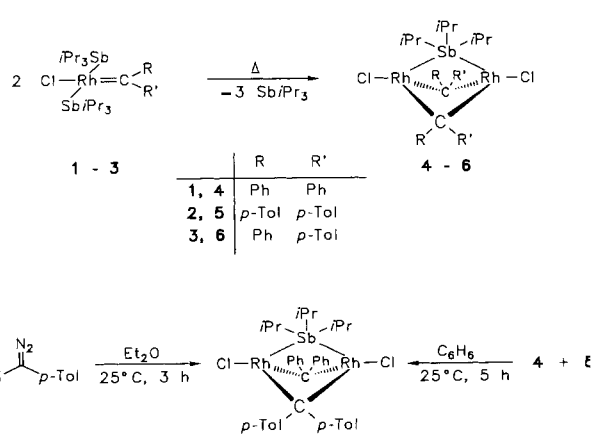
8: ^1H NMR (400 MHz, $CDCl_3$). $\delta = 0.84$ (s; $SbCH_3$); ^{13}C NMR (100.6 MHz, $CDCl_3$): $\delta = 187.43$ (t, $^1J(RhC) = 26.1$ Hz; RhCRh), 13.84 (s; $SbCH_3$).

9: ^1H NMR (400 MHz, $CDCl_3$): $\delta = 1.48$ (q, $^3J(HH) = 7.8$ Hz; $SbCH_2CH_3$), 0.95 (t, $^3J(HH) = 7.8$ Hz; $SbCH_2CH_3$); ^{13}C NMR (100.6 MHz, $CDCl_3$): $\delta = 182.99$ (t, $^1J(RhC) = 25.7$ Hz; RhCRh), 12.67 (s; $SbCH_2CH_3$), 10.68 (s; $SbCH_2CH_3$).

12: MS (70 eV): m/z (%) = 692 (M^+), 609 ($M^+ - CNtBu$); IR (KBr): $\tilde{\nu} = 1890\ cm^{-1}$ (C≡N); ^1H NMR (200 MHz, $CDCl_3$): $\delta = 1.54$ (s; $CNCCH_3$).

13: MS (70 eV): m/z (%) = 668 (M^+), 603 ($M^+ - C_5H_5$), 538 ($M^+ - 2C_5H_5$), 502 ($M^+ - CPh_2$), 336 ($M^+ - 2CPh_2$); ^1H NMR (400 MHz, C_6D_6): $\delta = 4.30$ (br, $A_5XX'A'_5$ spin system; C_5H_5). For ^{13}C NMR see ref. [6].

14: MS (70 eV): m/z (%) = 724 (M^+), 659 ($M^+ - C_5H_5$), 594 ($M^+ - 2C_5H_5$), 530 ($M^+ - C(p\text{-Tol})_2$), 336 ($M^+ - 2C(p\text{-Tol})_2$); ^1H NMR (400 MHz, C_6D_6): $\delta = 4.39$ (br, $A_5XX'A'_5$ spin system; C_5H_5); ^{13}C NMR (100.6 MHz, C_6D_6): $\delta = 187.83$ (t, $^1J(RhC) = 42.8$ Hz; RhCRh), 88.42 (triplet-like, $A_5XX'A'_5$- spin system; C_5H_5).



Scheme 1.

[*] Prof. Dr. H. Werner, Dipl.-Chem. P. Schwab, Dipl.-Chem. N. Mahr, Dr. J. Wolf
Institut für Anorganische Chemie der Universität
Am Hubland, D-97074 Würzburg (FRG)
Telefax: Int. code + (931)888-4605

[**] This work was supported by the Deutsche Forschungsgemeinschaft (Sonderforschungsbereich 347), the Fonds der Chemischen Industrie, and Degussa AG.

 © VCH Verlagsgesellschaft mbH, D-69451 Weinheim, 1994 0570-0833/94/0101-0097 $ 10.00+.25/0

different orientations of the aryl groups are present. The more unsymmetrical complex **7** which contains two different carbene ligands (see Scheme 1) is formed either on treatment of **1** with di(*p*-tolyl)diazomethane or on reaction of equimolar amounts of **4** and **5**. In the latter case the yield is quantitative.

The X-ray crystal structure analysis of **4**[5] (Fig. 1) confirms the hitherto unknown capability of trialkylstibanes to behave as bridging ligands, that is to form *two* M–Sb bonds. The Rh–Rh distance (2.5349(5) Å) is relatively short and is indicative of a direct metal–metal interaction. Equally short Rh–Rh bond

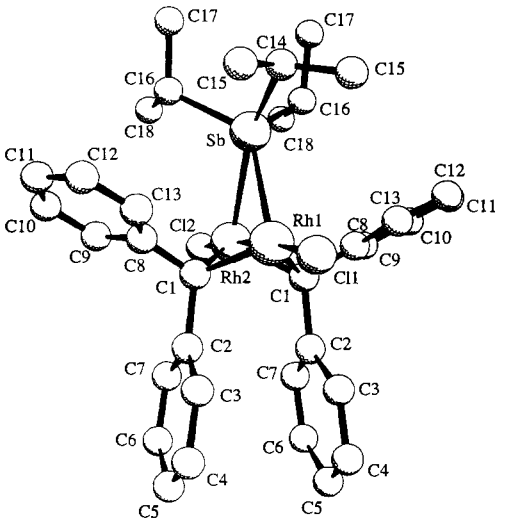
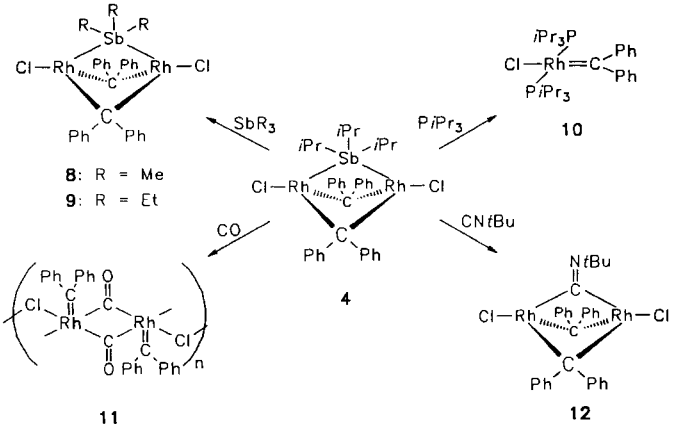


Fig. 1. Crystal structure of **4**. Selected bond lengths [Å] and angles [°]: Sb-Rh1 2.6868(5), Sb-Rh2 2.6695(5), Rh1-Rh2 2.5349(5), Rh1-Cl1 2.300(1), Rh1-C1 2.003(1), Rh2-Cl2 2.294(1), Rh2-C1 2.007(3); Rh1-Sb-Rh2 56.49(1), Sb-Rh1-Rh2 61.41(1), Sb-Rh2-Rh1 62.10(1), Sb-Rh1-C1 90.24(9), Sb-Rh2-C1 90.59(9), Rh1-Rh2-Cl2 176.35(4), Rh2-Rh1-Cl1 175.45(4), C1-Rh1-C1 87.7(2), C1-Rh2-C1 87.3(2), Rh1-C1-Rh2 78.5(1), Rh1-Rh2-C1 50.63(9), Rh2-Rh1-C1 50.9(1), Rh1-C1-C2 115.5(2), Rh1-C1-C8 114.8(2), Rh2-C1-C2 114.5(2), Rh2-C1-C8 118.4(2), C2-C1-C8 111.5(3).

lengths have been found in other carbene-bridged dirhodium complexes of the type $[Rh_2Cl_2(py)_2(\mu\text{-}CO)(\mu\text{-}CPh_2)_2]$[6] and $[(C_5H_5)_2Rh_2(\mu\text{-}CO)(\mu\text{-}CPh_2)_2]$.[7] Noteworthy are the significantly larger (ca. 0.1 Å) Rh–Sb distances in **4** compared with those in **1**,[4] which is in agreement with the bridging position of the Sb*i*Pr$_3$ ligand. The Cl-Rh-Rh-Cl unit is almost linear; the somewhat slight bending away from the Sb atom is possibly due to the steric repulsion between the chloro ligands and the bulky isopropyl groups.

A series of interesting reactions of compounds **4** is outlined in Scheme 2. We note in particular the smooth and almost quantitative exchange of the stibane ligand which provides a route to other SbR_3-bridged dinuclear rhodium complexes. Compound **8** is even more stable than **4** and decomposes only above 240 °C.

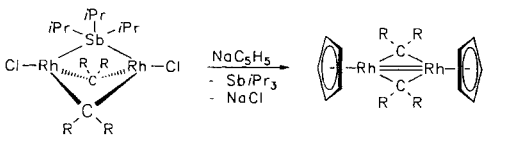
Attempts to replace the Sb*i*Pr$_3$ ligand in **4** by a bridging P*i*Pr$_3$ unit failed. Compound **4** reacts with one equivalent of triisopropylphosphane to give the mononuclear carbenerhodium(I) complex **10** in 25% yield.[4] However, compound **10** may be obtained almost quantitatively by reaction of **4** with four equivalents of P*i*Pr$_3$. Treatment of **4** with CO also leads to the displacement of the stibane accompanied by cleavage of the $Rh(CPh_2)Rh$ bridges. The resulting polymeric complex **11** was previously prepared by Sonogashira et al.[8] from $[\{Rh(CO)_2Cl\}_2]$ and diphenylketene; the structure of the reaction product from **11** and NaC_5H_5, namely $[(C_5H_5)_2Rh_2(\mu\text{-}CO)(\mu\text{-}CPh_2)_2]$ has been determined by X-ray analysis.[7] In



Scheme 2.

contrast to the reaction with CO, treatment of **4** with *tert*-butylisonitrile leads to a displacement of Sb*i*Pr$_3$ by the CN*t*Bu ligand; in this process, the carbene bridges remain intact.

The lower stability of the $Rh(SbR_3)Rh$ bridges over the $Rh(CPh_2)Rh$ bridges is equally illustrated in the reactions of **4** and **5** with NaC_5H_5. In these reactions, the dinuclear complexes **13** and **14**, respectively, (see Scheme 3) are formed in excellent yields (89%); compound **13** is also accessible by thermolysis of $[(C_5H_5)_2Rh_2(\mu\text{-}CO)(\mu\text{-}CPh_2)_2]$.[6–8]



Scheme 3.

The conversion of **13** on treatment with Sb*i*Pr$_3$ to the mononuclear carbene complex $[(C_5H_5)Rh(=CPh_2)(SbiPr_3)]$, which was recently prepared by us from **1** and NaC_5H_5,[4] was not successful. We assume that the attack of the bulky stibane upon the Rh–Rh double bond is significantly hindered by the four phenyl groups of the bridging carbene ligands.

Experimental Procedure

4: A solution of **1** (98 mg, 0.12 mmol) in benzene (10 mL) was stirred for 4 h at 60 °C. After cooling to room temperature, the solvent was removed. The residue was washed with pentane and dissolved in ether (10 mL). The product mixture was separated by chromatography on Al_2O_3 (neutral, activity grade V, 3 cm column) with ether/benzene (1:2). The red fraction was evaporated to dryness, and the residue was recrystallized from acetone (−78 °C) to give red crystals which were stable in air for short periods. Yield 42 mg (81%); m.p. 190 °C (decomp). Compounds **5** and **6** were prepared in a similar way. Yield about 78%. **5**: m.p. 190 °C (decomp); **6**: m.p. 178 °C (decomp).

7: a) A solution of **1** (81 mg, 0.10 mmol) in ether (10 mL) was treated with a solution of di(*p*-tolyl)diazomethane (22 mg, 0.10 mmol) in ether (5 mL) and stirred for 3 h at room temperature. The solvent was removed, the residue repeatedly washed with pentane and dried in vacuum; red microcrystalline solid. Yield 34 mg (76%); m.p. 183 °C (decomp). b) A solution of **4** (47 mg, 0.06 mmol) and **5** (49 mg, 0.06 mmol) in benzene (10 mL) was stirred for 5 h at room temperature, and was then worked up as described for a). Yield 93 mg (96%).

8: A solution of **4** (82 mg, 0.10 mmol) in benzene (10 mL) was treated with $SbMe_3$ (16 µL, 0.10 mmol) and stirred for 30 min at room temperature. The solvent was removed, the residue was washed with pentane and dissolved in benzene (2 mL). The solution was chromatographed on Al_2O_3 (see **4**) with C_6H_6/CH_2Cl_2 (1:1) and from the red fraction dark red crystals were isolated which were stable in air for short periods. Yield 66 mg (89%); m.p. 242 °C (decomp). Compound **9** was prepared analogously; yield 87%; m.p. 152 °C (decomp).

 © VCH Verlagsgesellschaft mbH, D-69451 Weinheim, 1994 0570-0833/94/0101-0098 $ 10.00+.25/0

12: A solution of **4** (71 mg, 0.08 mmol) in benzene (10 mL) was treated with CN*t*Bu (9 μL, 0.08 mmol) and stirred for 1 h at room temperature. The solvent was removed, the residue repeatedly washed with acetone and dried in vacuum. An orange-red solid was isolated which was stable in air for short periods; yield 56 mg (98%); m.p. 222 °C (decomp).

13: A solution of **4** (87 mg, 0.10 mmol) in THF (15 mL) was treated with NaC_5H_5 (44 mg, 0.50 mmol) and stirred for 1 h at room temperature. The solvent was removed, the residue was extracted with pentane/benzene (1:1; 3 mL), and the solution chromatographed on Al_2O_3 (see **4**). With ether a violet fraction was eluted from which after evaporation of the solvent and recrystallization from ether/pentane violet needles were isolated; yield 53 mg (80%); m.p. 208 °C (decomp). Compound **14** was prepared analogously; yield 78%; m.p. 132 °C (decomp).

Received: July 31, 1993 [Z 6251 IE]
German version: *Angew. Chem.* **1994**, *106*, 82

[1] a) U. Weber, L. Zsolnai, G. Huttner, *J. Organomet. Chem.* **1984**, *260*, 281–291; b) G. Huttner, U. Weber, B. Sigwarth, O. Scheidsteger, H. Lang, L. Zsolnai, *ibid.* **1985**, *282*, 331–348.

[2] a) A. R. Barron, A. M. Cowley, R. A. Jones, C. M. Nunn, D. L. Westmoreland, *Polyhedron* **1988**, *7*, 77–78; b) A. L. Balch, V. J. Catalano, M. A. Chatfield, J. K. Nagle, M. M. Olmstead, P. E. Reedy, Jr., *J. Am. Chem. Soc.* **1991**, *113*, 1252–1258.

[3] a) W. Levason, C. A. McAuliffe, *Phosphine, Arsine and Stibine Complexes of the Transition Elements*, Elsevier, Amsterdam, **1977**; b) W. Levason, C. A. McAuliffe, *Acc. Chem. Res.* **1978**, *11*, 363–368; c) N. R. Champness, W. Levason, M. Webster, *Coord. Chem. Rev.*, in press.

[4] P. Schwab, N. Mahr, J. Wolf, H. Werner, *Angew. Chem.* **1993**, *105*, 1498–1500; *Angew. Chem. Int. Ed. Engl.* **1993**, *32*, 1480–1482.

[5] Crystals from THF/2-propanol; crystal size 0.3 × 0.2 × 0.2 mm; orthorhombic, space group *Pnma* (no. 62), $Z = 4$; $a = 17.730(7)$, $b = 13.008(1)$, $c = 14.919(1)$ Å; $V = 3441.0(7)$ Å^3, $\rho_{calcd} = 1.660$ g cm^{-3}; max. $2\theta = 54°$ ($Mo_{K\alpha}$, $\lambda = 0.70930$ Å, graphite monochromator, $\omega/2\theta$-Scan, $T = 293$ K); 4264 reflections measured, 4028 independent, 2777 observed [$F_o > 3\,\sigma(F_o)$]. Lorentzian polarization correction ($\mu = 19.0$ cm^{-1}), direct methods (SHELXS-86), refinement with program package SDP (Enraf-Nonius), position of hydrogen atoms calculated according to ideal geometry (C-H distance 0.95 Å), refined with the riding model; $R = 0.027$, $R_w = 0.033$; reflex/parameter ratio 13.16; residual electron density +0.738/−0.554 eÅ^{-3}. Further details of the X-ray structure analysis are available on request from the Fachinformationszentrum Karlsruhe, D-76344 Eggenstein-Leopoldshafen (FRG), on quoting the depository number CSD-57659, the names of the authors, and the journal citation.

[6] T. Yamamoto, A. R. Garber, J. R. Wilkinson, C. B. Boss, W. E. Streib, L. J. Todd, *J. Chem. Soc. Chem. Commun.* **1974**, 354–356.

[7] H. Ueda, Y. Kai, N. Yasuoka, N. Kasai, *Bull. Chem. Soc. Jpn.* **1977**, *50*, 2250–2254.

[8] P. Hong, N. Nishii, K. Sonogashira, N. Hagihara, *J. Chem. Soc. Chem. Commun.* **1972**, 993.

First Total Synthesis of (±)-Rabelomycin**

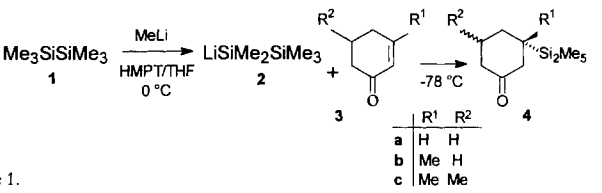
Karsten Krohn* and Karamali Khanbabaee

Dedicated to Professor Ulrich Wannagat on the occasion of his 70th birthday

Rabelomycin (**9**), known since 1970,[1] is a structurally simple member of the rapidly expanding class of angucyclin antibiotics.[2] The name angucyclins was given to the class on the basis of the analogy with the anthracyclins and the angular benz[*a*]-anthracene framework.[3] In particular, angucyclin antibiotics are characterized by antifungal,[4] antiviral,[5] enzyme inhibitory,[6] and antitumor activity.[7] Most of the biologically active compounds, which include **9**, carry a labile tertiary hydroxyl group β to the C1 carbonyl group. This inherent lability is one of the reasons that, with the exception of the biomimetically oriented urdamycin-B synthesis of Yamaguchi et al.,[8] no total synthesis of angucyclins is known.

We now present the first synthesis of racemic rabelomycin (*rac*-**9**), in which the synthetic problem is solved in a simple and productive manner with the help of a Diels–Alder reaction and a new type of photooxygenation of a nonfunctionalized C-atom. Previously, only model compounds lacking the tertiary hydroxyl group could be prepared with the Diels–Alder reaction.[9, 10]

Retrosynthetic analysis yielded a diene (OH instead of Si_2Me_5 in **6**, see Scheme 2) which, as preliminary experiments indicated, is probably extremely labile and, furthermore, not easily accessible. We therefore had the idea of replacing the hydroxyl group in the diene with a substituent that is a poorer leaving group. Our original intention was to use the dimethylphenylsilyl group, which could be replaced by a hydroxyl group in a later step.[11] However, to study the Michael addition of lithiated silanes to Michael acceptors such as 3-methylcyclohexenone, the cheaper trimethylsilyllithium was chosen. This reagent is prepared by Still by treatment of hexamethyldisilane (**1**) with methyllithium in hexamethylphosphoric triamide (HMPT).[12] However, on carrying out the reaction on a larger scale, it was discovered that the C–Si bond and not the Si–Si bond in **1** is broken, leading to the formation of pentamethyldisilyllithium (**2**, Scheme 1). This result is in agreement with an observation of Hudrlik[13a] and was recently confirmed for cyclic silanes by Allred et al.[13b] Under the conditions described in the Experimental Section the cleavage of the C–Si bond in hexamethyldisilane by alkyllithium compounds to afford **2** is a general reaction which takes place not only with methyllithium in ether, but also, for example, with *n*-butyllithium. Obviously, the negative charge on the silicon is stabilized by the second silicon atom in the α position. This effective stabilization is also noticeable in the reactivity of the species. The "soft" anion adds to the α,β-unsaturated carbonyl compounds cyclohexenone (**3a**), 3-methylcyclohexenone (**3b**), and 3,4-dimethylcyclohexenone (**3c**) to give exclusively the 1,4 addition products (Scheme 1).[14a] The adducts **4a**–**4c** that are formed are chiral, and further evidence for the presence of a $SiMe_2SiMe_3$ unit is provided by the splitting of the signal of the diastereotopic methyl groups in the $SiMe_2$ group in both the ^1H and ^{13}C NMR spectra (see Experimental for **4b**).



Scheme 1.

Thus, the reagent is already sufficiently selective towards 1,4-addition that the formation of silylcuprates, through the addition of copper salts to the reagent (cf. ref. [11]), is not necessary. The reagent even adds smoothly to sterically hindered enones. The easily accessible pentamethyldisilyllithium (**2**) is a new synthetic reagent, whose usefulness in the synthesis of tertiary alcohols is demonstrated by this first synthesis of rabelomycin.

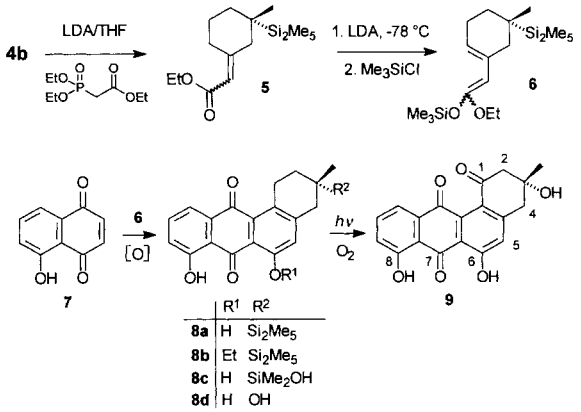
The first advantage of having a silyl group on the tertiary carbon atom is shown in the next step of the synthesis. Chain

[*] Prof. K. Krohn, Dipl.-Chem. K. Khanbabaee
Fachbereich Chemie und Chemietechnik der Universität-Gesamthochschule
Warburger Strasse 100, D-33098 Paderborn (FRG)
Telefax: Int. code + (5251) 60-3245

[**] Synthetic Angucyclins, Part 2. This work was supported by the Deutsche Forschungsgemeinschaft and the Fonds der Chemischen Industrie. Part 1: K. Krohn, F. Ballwanz, W. Baltus, *Liebigs Ann. Chem.* **1993**, 991–913.

extension of the β-silylketone **4b** to the unsaturated ester **5** in a Wittig-Horner reaction with triethylphosphonoacetate can be carried out without the risk of a base-catalyzed β elimination in 95% yield. The presence of two signals in the ^{29}Si NMR spectrum at $\delta = -7.63$ ($SiMe_2$) and at $\delta = -19.51$ ($SiMe_3$) confirms that the Si–Si bond survives the transformation intact.[15]

The silyl group provides a further benefit in the next step through its property of destabilizing anions in the β position to the silicon atom. Theoretically, two regioisomeric dienolates can be formed by the deprotonation of **5** with lithium diisopropylamine (LDA). Our plan assumed, however, that proton abstraction α to the tertiary carbon atom in **5** would be suppressed by a combination of the steric shielding afforded by the methyl and silyl groups and the β-effect of the silicon. This expectation was completely fulfilled, and after selective enolate formation with LDA and trapping with trimethylsilyl chloride only the desired regioisomer of the diene **6** (76%) could be isolated. The subsequent Diels–Alder reaction proceeded regiospecifically to give a 1:1 mixture of the phenol **8a** (32%) and the ethyl ether **8b** (33%) (Scheme 2). However, the formation of



Scheme 2.

this mixture is not a disadvantage, since the ethyl ether can be quantitatively converted into the phenol by treatment with aluminum trichloride. Under these conditions the Si–Si bond is also cleaved, and after hydrolytic workup the silanol **8c** is obtained (76% over both steps). Alternatively, the Si–Si bond can be cleaved under mild conditions with bromine.[14b] Silyl groups with electronegative substituents can be oxidatively replaced with hydroxyl groups.[11b] In this way **8c** could be converted into the tertiary alcohol 1-deoxyrabelomycin (**8d**, 78%) by mild treatment with potassium fluoride and hydrogen peroxide.[16]

Due to the initially mentioned instability of the tertiary alcohol, the introduction of the oxygen at C1 of **8d** was carried out in the last step of the synthesis. The oxygenation of **8d** to give rabelomycin **9** was successfully carried out in a new type of photooxygenation, in which a dilute solution of **8d** was exposed to daylight (70%). This photochemical introduction of oxygen at the angular benzylic position at C1 to form labile β-hydroxyketones has already proved successful in the synthesis of angucyclin analogues.[17] This reaction will, in our opinion, be an important step in future angucyclin syntheses, because base-catalyzed oxygenation[10] of compounds with tertiary hydroxyl groups such as **8d** invariably leads to decomposition.

Experimental Section

Preparation of **2** and Michael addition to **3b** to form **4b**: A solution of hexamethyldisilane (50.0 mL, 0.34 mol) in HMPT (200 mL) was cooled to 0 °C and treated with a 5% solution of methyllithium in ether (88 mL, 0.2 mol) under nitrogen. After 15 min dry THF (0.5 L) was added over 10 min, the reaction mixture cooled to −78 °C, followed by treatment with a solution of **3b** (16.5 g, 0.15 mol) in dry THF (100 mL). After 15 min the reaction was quenched by the addition of dry methanol (20 mL), and the mixture then warmed to 0 °C. The product was extracted with *n*-pentane (1 L), the pentane solution washed twice with water (a total of 1 L) and dried over magnesium sulfate. The solution was concentrated under vacuum, and the residue fractionally distilled under oil pump vacuum; yield 21.2 g (58%) (95–99 °C; 1.3 Torr), colorless oil. ^{1}H NMR (200 MHz, $CDCl_3$): $\delta = -0.07$ (s; 3H, $SiMe_2$), 0.08 (s; 3H, $SiMe_2$), 0.00 (s; 9H, $SiMe_3$), 0.86 (s; 3H, CH_3), 1.39–1.47 (m; 1H), 1.61–1.80 (dt; 1H), 1.84–1.94 (m; 3H), 2.14–2.35 (m; 3H); ^{13}C NMR (50 MHz, $CDCl_3$): $\delta = -5.57$ (prim.), −5.42 (prim.), −0.94 (3 × prim.), 20.46 (prim.), 22.95 (sec.), 27.02 (quat.), 32.12 (sec., 41.46 (sec.), 49.55 (sec.) 213.31 (quat.) (Assignments from DEPT).

Photooxygenation of **8d** to **9**: A solution of **8d** (30 mg, 0.092 mmol) in dichloromethane (6 mL) was exposed to diffuse daylight for 10 hours in three NMR tubes. After plate chromatographic purification on silica gel (dichloromethane:ether = 80:20) orange crystals of **9** were obtained from the fraction of medium polarity. (22 mg, 70%); M.p. 192 °C (decomp.); (ref. [1] for (+)-rabelomycin: M.p. 193 °C (decomp.). ^{1}H NMR (400 MHz, $CDCl_3$): $\delta = 1.49$ (s; 3H, CH_3), 2.95 (d, $J_{2e,2a} = 15$ Hz; 1H, 2-H_e), 3.04 (d, $J_{2e,2a} = 15$ Hz; 1H, 2-H_a), 3.08 (s; 2H, 4-H_2), 6.99 (s; 1H, 5-H), 7.25 (dd, $J_{9,11} = 2.0$, $J_{9,10} = 7.3$ Hz; 1H, 9-H), 7.65 (dd, $J_{9,11} = 2.0$, $J_{9,10} = 7.3$ Hz; 1H, 11-H), 7.67 (t, $J_{9,10} = J_{9,11} = 7.3$ Hz; 1H, 10-H), 11.65 (s; 1H, -OH), 12.30 (s; 1H, OH); ^{13}C NMR: $\delta = 30.05$ (prim.), 44.26 (sec.), 53.89 (sec.), 76.95 (quat.), 115.03 (quat.), 116.83 (quat.), 120.10 (tert.), 122.04 (tert.), 124.02 (tert.), 128.04 (quat.), 135.46 (quat.), 137.82 (tert.), 138.06 (quat.), 150.63 (quat.), 162.06 (quat.), 163.77 (quat.), 183.19 (quat.), 192.57 (quat.), 196.05 (quat.). MS (160 °C) *m/z* (%): 338 (13) [M^+], 321 (25), 320 (100) [$M^+ - H_2O$], 310 (54), 305 (15), 295 (21), 292 (25), 281 (23), 280 (94).

Received: June 12, 1993
Revised: September 1, 1993 [Z 6138 IE]
German version: *Angew. Chem.* **1994**, *106*, 100

[1] W.-C. Liu, W. L. Parker, D. S. Slusarchyk, G. L. Greenwood, S. F. Graham, E. Meyers, *J. Antibiot.* **1970**, *23*, 437–441.
[2] J. Rohr, R. Thiericke, *Nat. Prod. Rep.* **1992**, *9*, 103–137.
[3] H. Drautz, H. Zähner, J. Rohr, A. Zeeck, *J. Antibiot.* **1986**, *39*, 1657–1669.
[4] T. Oki, O. Tenmyo, M. Hirano, K. Tomatsu, H. Kamai, *J. Antibiot.* **1990**, *43*, 763–770.
[5] S. Kondo, S. Gomi, D. Ikeda, M. Hamada, T. Takeuchi, H. Iwai, J. Seki, H. Hoshino, *J. Antibiot.* **1991**, *44*, 1228–1236.
[6] K. Ohta, E. Mizuta, H. Okazaki, T. Kishi, *Chem. Pharm. Bull.* **1984**, *32*, 4350–4359.
[7] J. H. Wilton, D. C. Cheney, G. C. Hokanson, J. C. French, H. Cun-heng, J. Clardy, *J. Org. Chem.* **1985**, *50*, 3936–3938.
[8] M. Yamaguchi, T. Okuma, A. Horiguchi, C. Ikeura, T. Minami, *J. Org. Chem.* **1992**, *57*, 1647–1649.
[9] a) A. Guingant, M. M. Barreto, *Tetrahedron Lett.* **1987**, *28*, 3107–3110; b) K. Kim, J. Reibenspies, G. Sulikowski, *J. Org. Chem.* **1992**, *55*, 5557–5559.
[10] J. A. Valderrama, R. Araya-Maturana, M. F. González, R. Tapia, F. Fariña, M. C. Paredes, *J. Chem. Soc. Perkin Trans. 1* **1991**, 555–559.
[11] a) D. J. Ager, I. Fleming, *J. Chem. Soc. Chem. Commun.* **1978**, 177–178; b) I. Fleming, R. Henning, H. Plaud, *ibid.* **1984**, 29–31.
[12] W. C. Still, *J. Org. Chem.* **1976**, *41*, 3063–3064.
[13] a) P. F. Hudrlik, M. A. Waugh, A. M. Hudrlik, *J. Organomet. Chem.* **1984**, *271*, 69–76; b) A. L. Allred, R. T. Smart, D. A. Van Beek, *Organometallics* **1992**, *11*, 4225–4230.
[14] a) K. Krohn, P. Ritzenhoff, unpublished; b) G. Pilcher, M. L. P. Leitão, Y. Meng-Yan, R. Walsh, *J. Chem. Soc. Faraday Trans.* **1991**, *87*, 841–846.
[15] We thank Prof. H. Marsmann (Universität-Gesamthochschule Paderborn), for recording the ^{29}Si NMR spectra
[16] T. H. Chan, K. T. Nwe, *J. Org. Chem.* **1992**, *57*, 6107–6111.
[17] K. Krohn, F. Ballwanz, W. Baltus, *Liebigs Ann. Chem.* **1993**, 911–913.

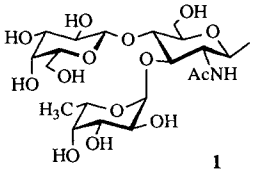
 © VCH Verlagsgesellschaft mbH, D-69451 Weinheim, 1994 0570-0833/94/0101-0100 $ 10.00+.25/0

Synthesis of *N*-Glycopeptide Clusters with Lewis^x Antigen Side Chains and Their Coupling to Carrier Proteins**

Karsten von dem Bruch and Horst Kunz*

Dedicated to Professor Erich Wünsch on the occasion of his 70th birthday

The trisaccharide determinant 3-*O*-α-fucosyl-*N*-acetyllactosamine (**1**), known as the Lewis^x antigen, has been found both in glycoproteins and in membrane glycolipids of mammalian cells.[1] It is formed during embryonic development and cell differentiation at the 8-cell stage by α-1,3-fucosylation of the I determinant as SSEA-1 antigen (SSEA = stage-specific embryonic antigen), and later it is almost completely masked by further fucosylation (Lewis^y antigen) and/or sialylation.[1, 2] The glycan with an α(2-3)- or α(2-6)-sialylated galactose unit (sialyl Lewis^x) is widely distributed and is an important signal in cell–cell recognition by lectins responsible for cellular adhesion (E-selectin, ELAM-1).



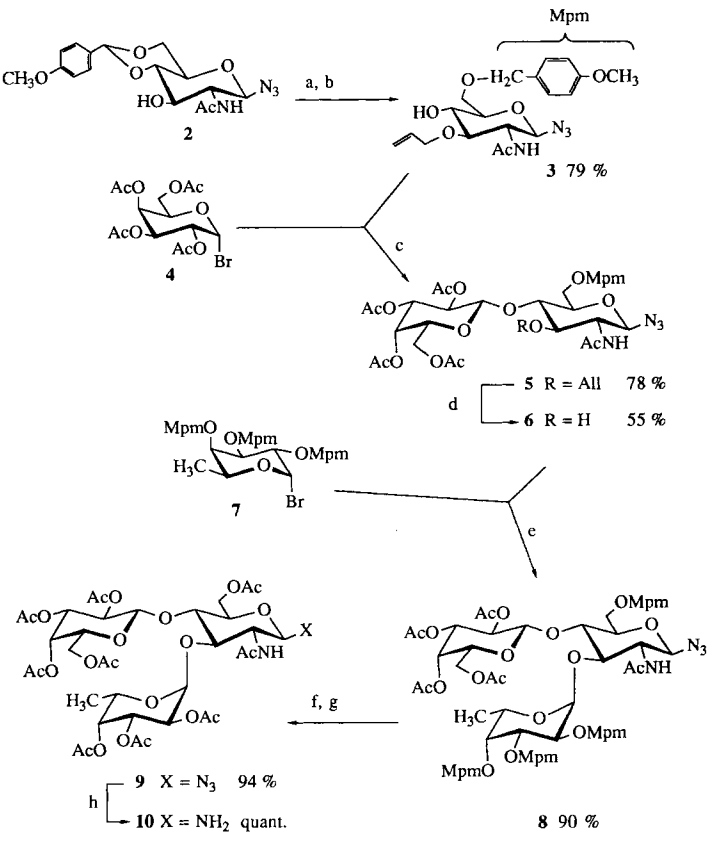
1

The recognition of sialyl Lewis^x by E-selectin leads, for example, during inflamation to the recruitment of neutrophilic granulocytes and their subsequent invasion into the focus of inflammation.[3] In contrast to sialyl Lewis^x antigen, in healthy adults the occurrence of the Lewis^x antigen is confined to certain specific regions such as the kidney tubules, gastrointestinal epithelial cells, and cells of the spleen and brain.[4, 5]

In tumors the degree of accumulation of Lewis^x antigen in the cell membrane has been shown to correspond directly to the extent of loss of cell–cell recognition, which normally acts to control growth. Therefore, glycoconjugates with Lewis^x antigen structure are of special interest as tumor-associated antigens. Because cluster structures show increased antigenicity[6] and in addition, in natural glycoproteins the antennary oligosaccharide side chains enable a multiple presentation of the saccharide determinants, our aim was the synthesis of glycopeptides with two Lewis^x antigen side-chains, which can simulate a biantennary Lewis^x antigen structure.

We have used two methodological principles during the synthesis of the Lewis^x trisaccharide: a) An azide function serves as an anomeric protective group for the glucosamine unit and at the same time as precursor for the anomeric amino group, required later for the formation of the *N*-glycosidic linkage to the peptide. b) The α-fucose was added in the Mpm-protected form (Mpm = 4-methoxyphenylmethyl) to achieve the acid stability necessary for formation of the glycosidic linkage.[7] The Mpm groups can be selectively removed in the presence of the azido function and replaced by acetyl groups.[7, 8]

The 4,6-(4-methoxybenzylidene)-protected *N*-acetylglucosaminylazide **2**[7, 8] was converted into the corresponding 3-*O*-allyl ether with allyl bromide in the presence of barium hydroxide[9] in dimethylformamide (DMF). The allyl ether was then converted into the glucosaminazide **3** containing a selectively deblocked 4-OH function through a regioselective reductive acetal opening[10] by treatment with sodium cyanoborohydride/trifluoroacetic acid (Scheme 1). Since 6-*O*-Mpm groups are labile in acid, the glycosylation of **3** required carefully chosen conditions. The glycosylation with 2,3,4,6-tetra-*O*-acetyl-galactopyranosyl bromide (**4**)[11] (1.2 equiv) with silver trifluoromethanesulfonate (2.3 equiv) in the presence of 2,6-di-*tert*-butylpyridine (1 equiv) was successful and afforded the β-glycoside **5**. An alternative procedure in the presence of mercury cyanide, which was used successfully in the synthesis of the Lewis^a glycopeptide,[12] yielded the unwanted orthoester only. The allyl ether cleavage was achieved by isomerization with palladium chloride and sodium acetate[13] in acetic acid. The azido function was stable under these conditions; however, the lability of the Mpm groups in acidic milieu reduced the yield of **6**. The allyl cleavage can be optimized by using a lactosamine analogue of **5** that has benzoyl groups in position 6 instead of Mpm groups; the synthesis of this derivative, however, requires two additional steps. The α-fucoside unit was added as the Mpm-protected fucopyranosyl bromide (**7**),[12] which was treated with the acceptor **6** in a stereoselective in situ anomerization procedure[14] to give the protected Lewis^x trisaccharide **8**.



Scheme 1. a) CH_2=CH-CH_2Br, $Ba(OH)_2$/DMF; b) $NaCNBH_3$, CF_3COOH, DMF; c) AgOTf, 2,6-*t*Bu-pyridine, CH_2Cl_2, toluene 1:1) d) $PdCl_2$, NaOAc, AcOH, 50 °C; e) Et_4NBr, 2,6-*t*Bu-pyridine, CH_2Cl_2/DMF 1:1; f) $(NH_4)_2Ce(NO_3)_6$, CH_3CN/H_2O 9:1; g) Ac_2O, pyridine; h) H_2/Raney Ni, *i*PrOH, 20 °C.

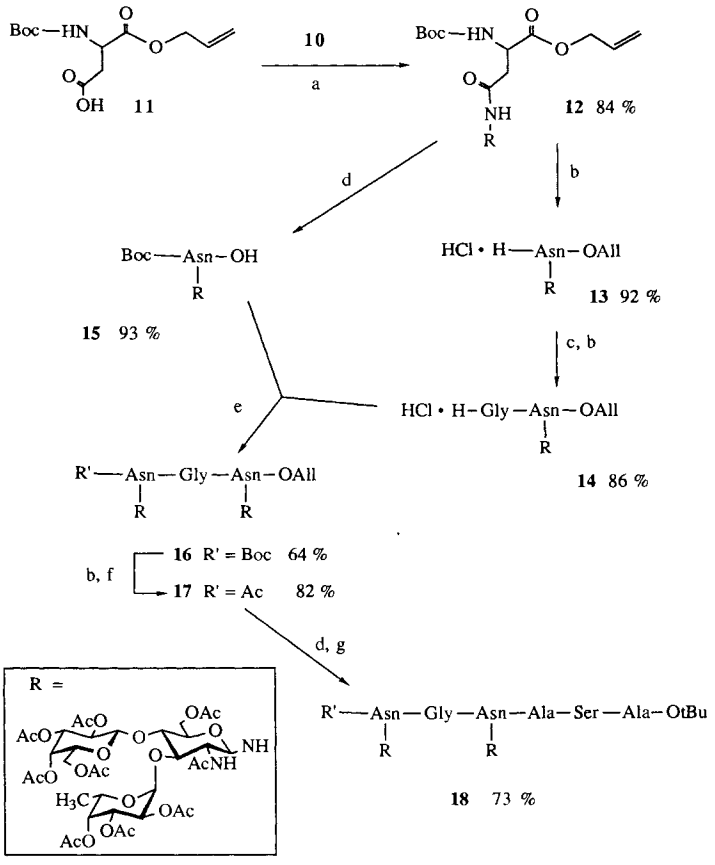
With cerium ammonium nitrate[10b] the Mpm groups can be removed from **8** without affecting the azide function.[7, 12] Acetylation of the deblocked OH groups yielded the *O*-acetyl-protected Lewis^x azide **9**. Catalytic hydrogenation of **9** with neutral Raney nickel in isopropyl alcohol yielded the trisaccha-

[*] Prof. Dr. H. Kunz, Dr. K. von dem Bruch
Institut für Organische Chemie der Universität
J.-J.-Becher-Weg 18–20, D-55099 Mainz (FRG)
Telefax: Int. code + (6131)39-4786

[**] This work was supported by the Bundesministerium für Forschung und Technologie and the Fonds der Chemischen Industrie. K. von dem Bruch thanks the Fonds der Chemischen Industrie for a Ph.D. grant and Hoechst AG for a Ph.D. student prize.

ridamine **10**.[15] These conditions were designed to prevent a O → N acyl transfer.

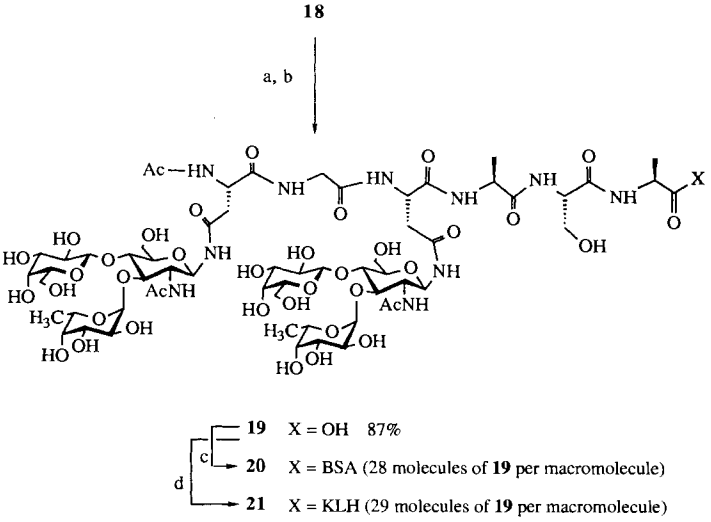
The protected trisaccharidamine was coupled with α-allyl Boc-asparaginate (**11**)[16] to yield the *N*-glycosylasparagine conjugate **12**; isobutyl-2-isobutoxy-1,2-dihydroquinoline-1-carboxylate (IIDQ)[17] proved itself as condensation agent. The Boc groups can be completely and selectively removed from **12** without saccharide cleavage by using HCl/diethyl ether. This demonstrates that the *O*-acetyl protective groups stabilize the *O*-glycosidic bonds against attack by acids.[7] Chain extension of the product **13** and removal of the Boc groups yielded the N-deblocked Lewis^x dipeptide allyl ester **14** in an overall yield of 86%. Alternatively, the allyl ester **12** was selectively cleaved by Rh^I-catalyzed isomerization.[16] Condensation of **15** and **14** under the influence of the water-soluble 1-ethyl-3-(3-dimethylamino)propylcarbodiimide (EDC) in the presence of 1-hydroxybenzotriazole (HOBt)[18] gave a tripeptide linked to two Lewis^x units (**16**).



Scheme 2. a) IIDQ, CH_2Cl_2; b) HCl/Et_2O; c) Et(iPr_2)N, Boc-Gly-OH, IIDQ, CH_2Cl_2; d) [(Ph_3P)$_3$RhCl], EtOH/H_2O 9:1, 70 °C; e) Et(iPr_2)N, EtN=C=N(CH_2)$_3$$NMe_2$ (EDC), HOBt, CH_2Cl_2; f) Ac_2O/pyridine; g) TBTU, HOBt, H-Ala-Ser-Ala-O*t*Bu, CH_3CN.

Replacement of the Boc groups with the biocompatible *N*-acetyl groups, another Rh^I-catalyzed allyl ester cleavage on **17**, and condensation of the product with a spacer tripeptide ester under the influence of *O*-(1*H*-benzotriazol-1-yl)-*N*,*N*,*N*′,*N*′-tetramethyluronium tetrafluoroborate (TBTU)[19] led to the glycohexapeptide **18**, which has two Lewis^x side chains suitably placed to simulate biantennary presentation.

For deblocking, first the C-terminal *tert*-butyl ester of **18** was cleaved by formic acid. The *O*-acetyl groups were removed by Zemplén saponification by using a very dilute sodium methanolate solution in methanol,[20] which gave a pH of 8.5 on moist pH paper. The glycohexapeptide **19** obtained with two Lewis^x antigen side chains was purified by gel-filtration chromatography on Sephadex G15 and characterized by high-field NMR as well as fast atom bombardment mass spectrometry (FAB-MS).[21] The coupling of the Lewis^x glycopeptide **19** to bovine serum albumin (BSA) to give the synthetic glycoprotein antigen **20** was carried out analogously to a procedure already used with T antigen glycopeptides[22] involving the use of water-soluble carbodiimide/*N*-hydroxysuccinimide[23] in water at a pH of 5.7. To test the antibodies induced against **20**, a second neoglycoprotein (**21**) was created from **19** and hemocyanin from *Megathura crenulata* (KLH, keyhole limpet hemocyanin). The content



Scheme 3. a) HCOOH, 20 °C; b) MeOH/NaOMe, pH 8.5 with air-moist pH paper; c) bovine serum albumin (BSA), EDC, *N*-hydroxysuccinimide, water, pH 5.7; d) KLH, EDC, *N*-hydroxysuccinimide, water, pH 5.7.

of Lewis^x antigen glycopeptide **19** in the glycoproteins was determined photometrically according to the phenol–sulfuric acid method.[24] The assay was calibrated with completely deblocked Lewis^x trisaccharidazide from **9** as standard. It was found that both glycoproteins contain about 30 molecules of synthetic Lewis^x antigen glycopeptide per protein molecule. Thus, clearly defined glycoconjugates that imitate glycoproteins with biantennary Lewis^x determinant structure are now available as models for immunological investigations of tumor-associated recognition signals.

Received: August 6, 1993 [Z6263IE]
German version: *Angew. Chem.* **1994**, *106*, 87

[1] H. C. Gooi, T. Feizi, A. Kapadia, B. B. Knowles, D. Solter, M. J. Evans, *Nature* **1981**, *292*, 156.
[2] H. C. Gooi, *Eur. J. Immunol.* **1983**, *13*, 306.
[3] a) M. L. Phillips, E. Nudelman, F. C. A. Gaeta, M. Perez, A. K. Singhal, S.-I. Hakomori, J. C. Paulson, *Science* **1990**, *250*, 1130; b) M. J. Polley, M. L. Phillips, E. Wagner, E. Nudelman, A. K. Shinghal, S.-I. Hakomori, J. C. Paulson, *Proc. Natl. Acad. Sci. USA*, **1991**, *88*, 6224.
[4] N. Fox, I. Damjanov, B. B. Knowles, D. Solter, *Cancer Res.* **1983**, *43*, 669.
[5] E. F. Hounsell, *Chem. Soc. Rev.* **1987**, *16*, 161.
[6] Y. C. Lee et al. (see for example: R. T. Lee, Y. C. Lee, *Glycoconjugate J.* **1987**, *4*, 317) have shown that the galactose receptor of hepatocytes shows several orders of maginitude greater affinity for di- and trivalent galactosamine and galactose ligands than for the corresponding monovalent analogues.
[7] H. Kunz, C. Unverzagt, *Angew. Chem.* **1988**, *100*, 1763; *Angew. Chem. Int. Ed. Engl.* **1988**, *27*, 1697.
[8] C. Unverzagt, H. Kunz, *J. Prakt. Chem.* **1992**, *334*, 570.
[9] J. C. Jacquinet, P. Sinay, *J. Org. Chem.* **1977**, *42*, 720.

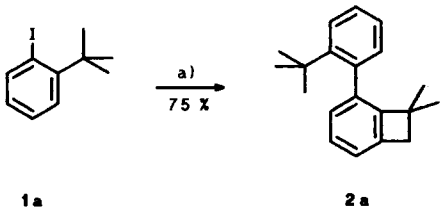
[10] a) P. J. Garegg, H. Hultberg, S. Wallin, *Carbohydr. Res.* **1982**, *108*, 97; b) R. Johansson, B. Samuelsson, *J. Chem. Soc. Perkin Trans 1* **1984**, 2371.
[11] a) H. Ohle, W. Marecek, W. Bourjan, *Ber. Dtsch. Chem. Ges.* **1929**, *62*, 833; b) L.-F. Tietze, T. Eicher, *Reaktionen und Synthesen im organisch-chemischen Praktikum*, Thieme, Stuttgart **1981**, p. 483.
[12] J. März, H. Kunz, *Synlett* **1992**, 589.
[13] R. Bose, R. Scheffold, *Angew. Chem.* **1976**, *88*, 578; *Angew. Chem. Int. Ed. Engl.* **1976**, *15*, 558.
[14] R. U. Lemieux, J. I. Haymi, *Can. J. Chem.* **1965**, *43*, 2162.
[15] H. Kunz, W. Pfrengle, K. Rück, W. Sager, *Synthesis* **1991**, 1039, and references therein.
[16] H. Waldmann, H. Kunz, *Liebigs Ann. Chem.* **1983**, 1712.
[17] Y. Kiso, H. Yajima, *J. Chem. Soc. Chem. Commun.* **1972**, 942.
[18] W. König, R. Geiger, *Chem. Ber.* **1970**, *103*, 788.
[19] R. Knorr, A. Trzeciak, W. Bannwarth, D. Gillessen, *Tetrahedron Lett.* **1983**, *24*, 1927.
[20] S. Peters, T. Bielefeldt, M. Meldal, K. Bock, H. Paulsen, *J. Chem. Soc. Perkin Trans 1* **1992**, 1163.
[21] **19**: Amorphous solid, m.p. 225 °C (decomp); $[\alpha]^{20} = -53.5$ ($c = 1$, water); $R_f = 0.33$ (MeOH/AcOH 50:1); FAB-MS (glycerol, negative ionization): m/z 1595.2 ($M-1$); ^{1}H NMR (400 MHz, D_2O): $\delta = 5.07$ (d, 2H, $J_{1,2} = 2.4$ Hz, H-1, Fuc), 4.81–4.68 (m, 4H, 2 × H-1, GlcNAc, 2 × H-5, Fuc), 4.43 (d, 2H, $J_{1,2} = 7.8$ Hz, H-1, Gal), 4.41 (t, 1H, $J_{\alpha\beta} = 5.3$ Hz, α-H, Ser), 4.32, 4.18 (2, q, 1H, $J_{\alpha\beta} = 7.2$ Hz, α-H, Ala); ^{13}C NMR (100.6 MHz, D_2O): $\delta = 101.8$ (C-1, Gal), 98.6 (C-1, Fuc), 78.1 (C-1, GlcNAc), 61.1 (β-C, Ser), 55.4 (α-C, Ser), 54.6 (C-2, GlcNAc), 50.3 (α-C, Asn), 49.92, 49.85 (α-C, Ala), 42.7 (α-C, Gly), 36.78, 36.52 (β-C, Asn), 22.2 (CH_3CONH, GlcNAc), 21.9 (CH_3CONH, terminal AcNH), 17.05, 16.49 (CH_3, Ala), 15.3 (CH_3, Fuc).
[22] H. Kunz, S. Birnbach, *Angew. Chem.* **1986**, *98*, 354; *Angew. Chem. Int. Ed. Engl.* **1986**, *25*, 360.
[23] a) E. Wünsch, F. Drees, *Chem. Ber.* **1966**, *99*, 110; b) F. Weygand, D. Hoffmann, E. Wünsch, *Z. Naturforsch. B* **1966**, *21*, 426.
[24] M. Dubois, K. A. Gilles, J. K. Hamilton, P. A. Rebes, F. Smith, *Anal. Chem.* **1956**, *28*, 350.

Palladium-Catalyzed C–H Activation of *tert*-Butyl Groups: A Simple Synthesis of 1,2-Dihydrocyclobutabenzene Derivatives**

Gerald Dyker*

Metalation reactions are often chosen to activate C–H bonds which would otherwise be too unreactive. In this context special mention should be made of transition metals in catalytic reactions. Whereas the palladium catalyzed C–H activation at sp^2 carbon centers is now established as a key step in the selective functionalization of alkenes and arenes,[1] such reactions at sp^3 hybridized carbon atoms, which could open up many synthetic possibilities, have hardly been examined.[2] A new domino coupling reaction is described here in the course of which a palladium-catalyzed C–H activation at a *tert*-butyl group is observed for the first time.

1-*tert*-Butyl-2-iodobenzene (**1a**)[3] is condensed with palladium catalysis to give the strained 1,2-dihydrocyclobutabenzene derivative **2a** in 75% yield. (Scheme 1; for the spectroscopic data of this and other new compounds see Table 2).[4] For a similar coupling reaction of 2-iodoanisole[2a] it is still not clear whether the heteroatom makes a decisive contribution towards the C–H activation or not. The findings now presented confirm the generality of the reaction principle that the intramolecular

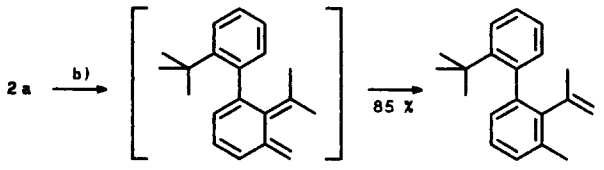


1a **2a**

Scheme 1. Homo coupling of **1a**: a) 2.5 mol% $[Pd(OAc)_2]$, K_2CO_3, nBu_4NBr, *N,N*-dimethylformamide (DMF), N_2, 4 d, 105–110 °C.

C–H activation at alkyl groups is not dependent upon additional activation by a heteroatom.

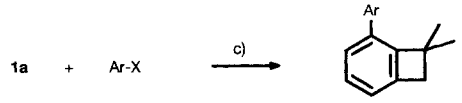
In order to confirm the structure of **2a** chemically, it was thermolyzed at 200 °C (Scheme 2). From this reaction the substituted biphenyl **4** is formed as a result of a pericyclic reaction cascade (1. ring opening to give the *ortho*-quinone compound **3**; 2. [1,5]hydrogen shift with rearomatization).[5]



3 **4**

Scheme 2. Thermolysis of **2a**: b) 1,2-dichlorbenzene, 24 h, 200 °C.

The range of applications offered by this new annelation reaction was explored by experiments involving cross coupling reactions. The aryl halides **1b–g** were added in excess as the second coupling components (Scheme 3). Whereas with 4-bromotoluene (**1b**) und 4-bromoanisole (**1c**) (X = Br) the coupled products **2b** and **2c**, respectively, were produced in satisfactory yields (Table 1), the domino coupling process was inhibited by the more reactive aryl halides 4-iodoanisoles **1c, d** (X = I) and



1b-g (5 equiv) **2b-g**

Scheme 3. Cross coupling of **1a** with the aryl halides **1b–g**; c) 10 mol% $[Pd(OAc)_2]$, K_2CO_3, nBu_4NBr, DMF, N_2, 4 d, 105–110 °C. Ar see Table 1.

Table 1. Cross coupling of **1a** with aryl halides **1b–g** to produce the corresponding 1,2-dihydrocyclobutabenzene derivatives **2**.

Coupling partner	Ar	X	Yield [a] [%]
1b	4-methylphenyl	Br	56
1c	4-methoxyphenyl	Br	59
		I	0
1d	3-methoxyphenyl	Br	37
1e	ethyl phenyl-4-carboxylate	Br	0
1f	4-nitrophenyl	Br	0
1g	2-naphthyl	Br	11

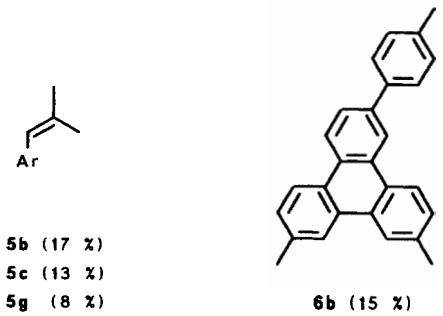
[a] Yield of **2**, isolated by flash chromatography.

[*] Dr. G. Dyker
Institut für Organische Chemie der Technischen Universität
Hagenring 30, D-38106 Braunschweig (FRG)
Telefax: Int. code + (531)391-5388

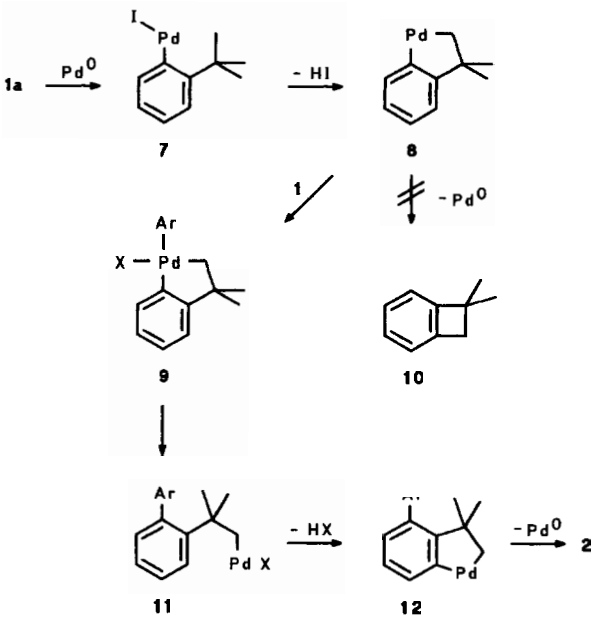
[**] Transition Metal-Catalyzed Annelation Reactions, Part 5. This work was supported by the Fonds der Chemischen Industrie and the Volkswagen-Stiftung. Part 4: G. Dyker, *J. Org. Chem.* **1993**, *58*, 6426–6428.

ethyl 4-bromobenzoate (**1e**). In this case the palladium-catalyzed Ullmann reaction [6] of **1c** (X = I) and **1e** predominates; 1-*tert*-butyl-2-iodobenzene (**1a**) hardly reacts.

Vinyl arenes **5**[7] and the triphenylene derivative **6b** (Table 2) were isolated as the side products of the cross coupling reactions (Scheme 4). These products are indicative of a multistep formation mechanism. A possible mechanism for the main reaction shall now be discussed which can be developed in accordance with the experimental results and in analogy to the similar coupling reaction of 2-iodoanisole[2c] (Scheme 5). The cyclometalation of **7** to give **8**, in which the intramolecular C–H activation at the *tert*-butyl group is postulated as the decisive reaction step, might initiate a $Pd^{II}-Pd^{IV}-Pd^{II}$ catalytic cycle[8] involving **9** and **11** as additional reactive intermediates. The formation of 1,2-dihydrocyclobutabenzene **10** by the reductive elimination of Pd^0 from **8** was not detected. Apparently the aryl substituent of **12** exerts the required steric influence to facilitate the formation of the strained 1,2-dihydrocyclobutabenzene derivatives **2**.

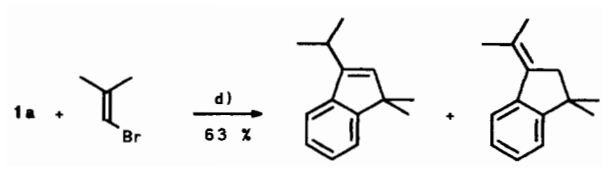


Scheme 4. Side products of the cross coupling of **1a** with the aryl halides **1b**, **1c**, **1g**. Ar see Table 1.



Scheme 5. Possible mechanism for the coupling reaction of **1a** to afford **2**. Pd^0 complexes were postulated as the active catalysts.

The bromoolefin **13** is also suitable as a coupling component (Scheme 6). In this case the domino process is terminated by ring closure, resulting in the formation of indene derivatives **14**[9] and **15**.



13 (10 equiv) 14 (9:1) 15

Scheme 6. Cross coupling of **1a** with vinyl bromide (**13**); d) 10 mol% $[Pd(OAc)_2]$, K_2CO_3, nBu_4NBr, DMF, N_2, 3 d, 105–110 °C.

The palladium-catalyzed C–H activation of *tert*-butyl neighboring groups described here for the first time is a new fundamental process for cross coupling reactions, which should allow the simple synthesis of selectively substituted 1,2-dihydrocyclobutabenzene and indene derivatives. The variation of neighboring groups, in particular the inclusion of silyl groups, with a

Table 2. Selected physical and spectroscopic data [a] of the compounds **2a–2d**, **2g**, **4**, **6b**, **14**, and **15** [4].

2a: Colorless oil; ^1H NMR: $\delta = 1.22$ (s, 3H), 1.23 (s, 9H), 2.01 (s, 3H), 2.92 (d, $^2J = 13.5$ Hz, 1H; H_A-7), 2.95 (d, $^2J = 13.5$ Hz, 1H; H_B-7), 7.00–7.05 (m, 3H), 7.10–7.16 (m, 2H), 7.28 (m_t, 1H), 7.54 (m_d, 1H); ^{13}C NMR: $\delta = 26.39$ (q), 27.77 (q), 33.03 (q), 36.67 (s), 44.95 (t; C-7), 46.00 (s; C-8), 122.00 (d), 124.42 (d), 125.70 (d), 127.11 (d), 127.40 (d), 128.70 (d), 132.98 (d), 127.89 (s), 139.62 (s), 141.46 (s), 147.78 (s), 150.78 (s)

2b: Colorless needles, m.p. 67–68 °C; ^1H NMR: $\delta = 1.46$ (s, 6H; $C(CH_3)_2$), 2.39 (s, 3H), 2.96 (s, 2H; H-7), 7.05 (m, 1H), 7.22 (m_d, 2H), 7.24–7.26 (m, 2H), 7.41 (m_d, 2H); ^{13}C NMR: $\delta = 21.19$ (q), 27.23 (q), 44.73 (t; C-7), 46.05 (s; C-8), 122.23 (d), 126.35 (d), 127.54 (d), 128.07 (d), 129.13 (d), 136.39 (s), 136.45 (s), 136.76 (s), 142.23 (s; C-6), 151.14 (s; C-1)

2c: Colorless solid m.p. 53 °C; ^1H NMR: $\delta = 1.46$ (s, 6H; $C(CH_3)_2$), 2.96 (s, 2H; H-7), 3.85 (s, 3H; OCH_3), 6.95 (m, 2H; H-3′, H-5′), 7.03 (m, 1H), 7.21–7.27 (m, 2H), 7.45 (m, 2H; H-2′, H-6′); ^{13}C NMR: $\delta = 27.00$ (q), 44.50 (t; C-7), 45.80 (s; C-8), 55.11 (q), 113.65 (d; C-3′, C-5′), 121.78 (d), 125.94 (d), 127.36 (d), 129.05 (d; C-2′, C-6′), 131.58 (s), 142.04 (s; C-6), 150.74 (s; C-1), 158.70 (s; C-4′)

2d: Colorless oil; ^1H NMR: $\delta = 1.47$ (s, 6H; $C(CH_3)_2$), 2.97 (s, 2H; H-7), 3.85 (s, 3H; OCH_3), 6.88 (m, 1H), 7.04–7.12 (m, 3H), 7.24–7.28 (m, 2H), 7.32 (m, 1H); ^{13}C NMR: $\delta = 27.24$ (q), 44.74 (t; C-7), 45.08 (s; C-8), 55.31 (q), 112.74 (d), 113.74 (d), 120.74 (d), 122.63 (d), 126.44 (d), 127.56 (d), 129.36 (d), 136.34 (s), 140.75 (s), 142.28 (s), 151.22 (s), 159.62 (s)

2g: Colorless solid, m.p. 91 °C; ^1H NMR: $\delta = 1.49$ (s, 6H; $C(CH_3)_2$), 3.00 (s, 2H; H-7), 7.10 (m_d, 1H; H-5), 7.31 (m_t, 1H; H-4), 7.39 (m_d, 1H; H-3), 7.45–7.53 (m, 2H; H-6′, H-7′), 7.67 (dd, $J = 8.5$, 1.7 Hz, 1H; H-3′), 7.84–7.91 (m, 3H; H-4′, H-5′, H-8′), 7.97 ("s", 1H; H-1′); ^{13}C NMR: $\delta = 27.30$ (q; CH_3), 44.77 (t; C-7), 46.16 (s; C-8), 122.60 (d; C-5), 125.89 (d; C-6′), 126.21 (d; C-7′), 126.66 (d; C-3′), 126.68 (d; C-3), 126.94 (d; C-1′), 127.68 (d; C-4), 127.69 (d; C-5′), 127.93 (d; C-4′), 128.15 (d; C-8′), 132.53 (s; C-4a′), 133.54 (s; C-8a′), 136.43 (s; C-2), 136.79 (s; C-2′), 142.31 (s; C-6), 151.56 (s; C-1)

4: Colorless oil; ^1H NMR: $\delta = 1.17$ (s, 9H), 1.74 (s, br, 3H; Vinyl-CH_3), 2.32 (s, 3H; aryl-CH_3), 4.76 (m, 1H), 5.08 (m, 1H), 6.99 (m_d, 1H; H-6′), 7.03 (m_d, 1H; H-6), 7.07 (m_t, 1H; H-5′), 7.09 (m_t, 1H; H-5), 7.17 (m_d, 1H; H-4), 7.25 (m_t, 1H; H-4′), 7.52 (m_d, 1H; H-3′); ^{13}C NMR: $\delta = 20.50$ (q, aryl-CH_3), 24.54 (q; br [b]; vinyl-CH_3), 33.30 (q), 37.01 (s), 116.63 (t, br) 123.88 (d; C-5′), 124.97 (d; C-5), 126.85 (d; C-4′), 128.31 (d; C-3′), 128.40 (d; C-6), 128.71 (d; C-4), 133.14 (d; C-6′), 134.99 (s; C-3), 139.47 (s; C-1′), 141.74 (s), 144.11 (s), 147.35 (s; C-2′)

6b: Colorless solid, m.p. 182 °C, crystallized from ether/pentane; ^1H NMR: $\delta = 2.44$ (s, 3H; phenyl-CH_3), 2.61 (s, 6H), 7.32 ("d", 2H; H-3′, H-5′), 7.46 (m, 2H, H-6, H-11), 7.69 (m_d, 2H; H-2′, H-6′), 7.81 (dd, $J = 8.4$, 1.9 Hz, 1H; H-3), 8.42 (s, br, 2H; H-8, H-9), 8.51 ("d", "J" = 8.4 Hz, 1H; H-5), 8.58 ("d", "J" = 8.4 Hz, 1H; H-12), 8.61 ("d", "J" = 8.4 Hz, 1H; H-4), 8.76 ("d", "J" = 1.9 Hz, 1H; H-1).
14: ^1H NMR: $\delta = 1.25$ (d, $J = 6.8$ Hz, 6H), 1.28 (s, 6H), 2.84 (sept. d, $J = 6.8$, 1.1 Hz, 1H), 5.99 (d, $J = 1.1$ Hz, 1H), 7.14–7.32 (m, 4H).
15: ^1H NMR: $\delta = 1.26$ (s, 6H), 1.87 (s, 3H), 2.07 (s, 3H), 2.51 (s, br, 2H), 7.14–7.32 (m, 3H), 7.52 (m_d, 1H)

[a] ^1H NMR: 400.1 MHz, $CDCl_3$, TMS; ^{13}C NMR: 100.6 MHz, $CDCl_3$. [b] A number of ^{13}C NMR signals of **4** are very broad, a singlet could not be detected.

 © VCH Verlagsgesellschaft mbH, D-69451 Weinheim, 1994 0570-0833/94/0101-0104 $ 10.00+.25/0

view to explaining the relationship between the structural parameters and the course of the coupling reaction are the subject of investigations that are currently in progress.

Experimental Procedure

2a: A mixture of **1a** (520 mg, 2 mmol), $[Pd(OAc)_2]$ (11 mg, 0.05 mmol), K_2CO_3 (1.1 g, 8.0 mmol), and nBu_4NBr (645 mg 2.0 mmol) in DMF (10 mL) was stirred for 4 d at 105–110 °C under nitrogen in a closed reaction vessel. After the addition of water (50 mL), the mixture was extracted three times with ether (50 mL), the organic phase filtered through silica gel, and the solvent distilled off. The least polar fraction ($R_f = 0.34$) was isolated by flash chromatography (silica gel, petroleum ether). Kugelrohr distillation at 100 °C/0.1 Torr afforded **2a** as a colorless oil (197 mg, 75%).

Received: July 1, 1993 [Z 6182 IE]
German version: *Angew. Chem.* **1994**, *106*, 117

[1] a) R. F. Heck, *Org. React. N. Y.* **1982**, *27*, 345–390; b) S. J. Tremont, H. U. Rahman, *J. Am. Chem. Soc.* **1984**, *106*, 5759–5760.
[2] a) A. Sen, *Platinum Met. Rev.* **1991**, *35*, 126–132; b) *Acc. Chem. Res.* **1988**, *21*, 421–428; c) G. Dyker, *Angew. Chem.* **1992**, *104*, 1079–1081; *Angew. Chem. Int. Ed. Engl.* **1992**, *31*, 1023–1025.
[3] M. S. Lesslie, U. J. H. Mayer, *J. Chem. Soc.* **1961**, 611–618.
[4] The new compounds **2a**, **2b**, **2c**, **2d**, **2g**, **4**, and **6b** were fully characterized by spectroscopic methods (IR, UV, ^1H NMR, ^{13}C NMR), mass spectrometric data, and elemental analysis; the NMR signals of **2g**, **4**, and **6b** were assigned from 2D NMR Spectra (HH-COSY, CH-COSY, COLOC) and the NOE experiments; ^1H NMR data were obtained for **15** (selected data are given in Table 2).
[5] T. Kametani, M. Tsubuki, Y. Shiratori, Y. Kato, H. Nemoto, M. Ihara, K. Fukumoto, F. Satoh, H. Inoue, *J. Org. Chem.* **1977**, *42*, 2672–2676.
[6] G. Dyker, *J. Org. Chem.* **1993**, *58*, 234–238.
[7] D. A. R. Happer, B. E. Steenson, *J. Chem. Soc. Perkin Trans. 2* **1988**, 19–24.
[8] a) A. J. Canty, *Platinum Met. Rev.* **1993**, *37*, 2–7; b) *Acc. Chem. Res.* **1992**, *25*, 83–90.
[9] H. A. Staab, C. M. Wittig, P. Naab, *Chem. Ber.* **1978**, *111*, 2965–2981.

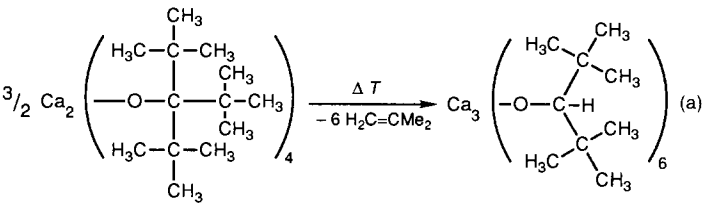
Solvent-Free Volatile Alkoxides of the Alkaline-Earth Elements**

Wolfgang A. Herrmann,* Norbert W. Huber, and Thomas Priermeier

Since the discovery of oxidic high-temperature superconductors interest in volatile calcium, strontium, and barium alkoxides of type $M(OR)_2$ has increased.[1a–c] These compounds are needed for the deposition of thin oxide layers of the respective elements from the gas phase. As cadmium is used as a substitute for yttrium (up to 30 atom%) in YBaCu-type superconductors, cadmium alkoxides also deserve attention.[1d]

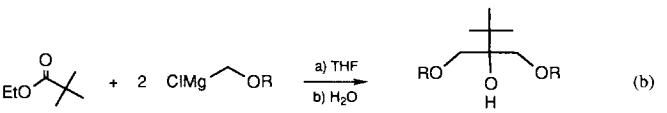
How are volatile $M(OR)_2$ compounds obtained? The widely employed concept of steric shielding of reactive molecular centers by means of bulky ligands has not been particularly successful in the chemistry of the metals in question. Even ligands as sterically demanding as $^-OSi(C_6H_5)_3$ form oligo- and polynuclear complexes of low volatility[2] sometimes still containing solvent.

Complexes with the ligand "tritox" ($^-OCtBu_3$) are less stable as a result of steric crowding.[3] Upon sublimation above 185 °C and 10^{-3} mbar, the new complex $[Ca_2(tritox)_4]$ decomposes to give $[Ca_3(ditox)_6]$[4] (ditox = $^-OCHtBu_2$) and isobutene according to Equation (a).



In our approach to the problem, donor functionality and steric bulk are combined within the same ligand.[5] We have prepared a series of donor-functionalized alkoxy ligands and, after adjusting them to charge and ionic radius of the metal in question, used them to synthesize the most volatile alkoxides of the alkaline-earth elements and of cadmium known so far.

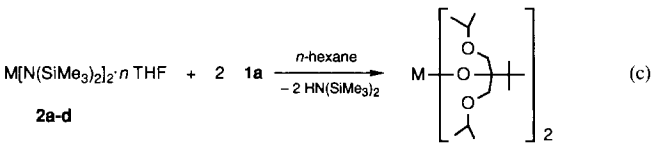
The trifunctional alcohols **1a**,**b** are obtained from common precursors in 75% yield after distillation [Eq.(b)]. The metal



1a : R = $CH(CH_3)_2$
1b : R = C_2H_5

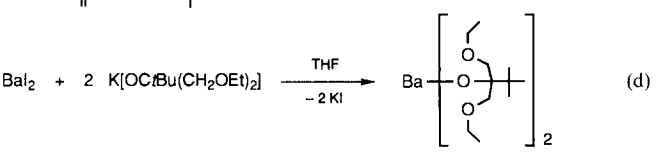
amides **2a–c** react with **1a** at room temperature in *n*-hexane according to Equation (c) and form alkoxides **3a–c** almost quantitatively. Alternatively, the barium derivatives, in particular, can be obtained by transmetalation [Eq.(d)], or directly from metallic barium [Eq.(e)].

The colorless metal complexes **3a–c** and **4c** have excellent solubility even in nonpolar solvents like *n*-pentane. Elemental analyses and NMR spectroscopic data show them to be solvent-free, a rarity for this type of compounds.[6] Their most remark-

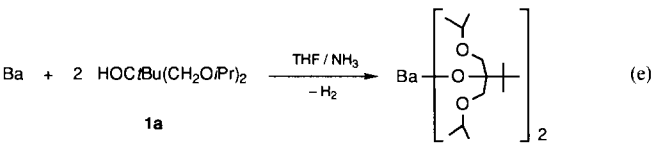


2a-d **3a-d**

2,3	a	b	c	d
M	Ca	Sr	Ba	Cd
n	2	2	2	0



4c



1a **3c**

[*] Prof. Dr. W. A. Herrmann, N. W. Huber, T. Priermeier
Anorganisch-chemisches Institut der Technischen Universität München
Lichtenbergstrasse 4, D-85747 Garching (FRG)
Telefax: Int. code + (89) 3209-3473

[**] This work was supported by the Bundesministerium für Forschung und Technologie and the Zentralforschung der Hoechst AG. N. W. H. thanks the Fonds der Chemischen Industrie for a doctoral fellowship. We thank Dipl.-Chem. F.-R. Klingan for carrying out the NMR investigations.

able property, however, is the high volatility reflected by the sublimation temperatures of 150 °C (**3a**, **4c**), 170 °C (**3b**), and 185 °C (**3c**) at 10^{-2} mbar. The compounds are thermally stable under these conditions and do not leave a significant residue. A thermogravimetric study carried out on **3c** shows that the residue at 600 °C/6 mbar (resulting from traces of moisture in the measuring apparatus) is less than 3 wt%. From chemical ionization (CI) mass spectra and single-crystal X-ray structure analyses we find that the new alkaline-earth metal alkoxides are dimeric both in the gas phase and in the solid state in spite of their high volatility (possibly also a consequence of molecular shape).

As an example, the crystal structure of the calcium complex **3a** (Fig. 1)[7] shows that three alkoxy groups serve as μ-O ligands bridging the two metal centers. Peripheral ether-type oxygen atoms complete the coordination sphere, such that both metal centers achieve the favorable coordination number (CN) 6 through coordinative and ionic bonds. We attribute the extreme pyramidality at the oxygen atoms of the three bridging alkoxy ligands as well as the bending of the terminal Ca2-O41-C405 unit to the steric hindrance within the chelate structure.

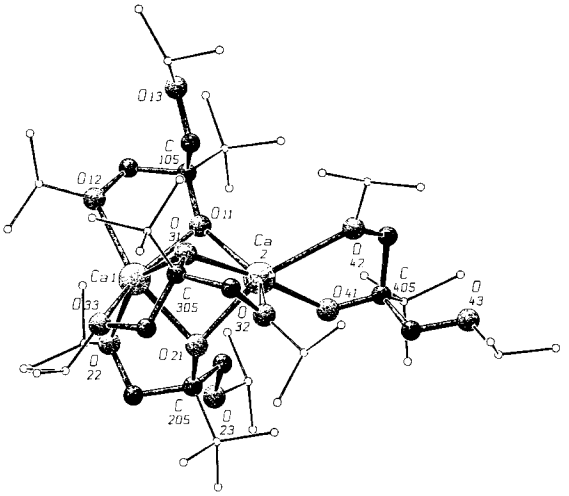


Fig. 1. Molecular structure of the binuclear calcium alkoxide **3a** at −110 °C (SCHAKAL plot). For clarity, the isopropyl and *tert*-butyl groups are only sketched. Selected distances [pm] and angles [°]: Ca2–O41 218.1(4), Ca1–μO 226.9(8), Ca2–μO 236.2(8), Ca1–O_{ether} 246.9(9), Ca2–O_{ether} 259.4(6), Ca1–Ca2 312.3(2); Ca2-O41-C405 132.1(4), Ca1-μO-Ca2 84.8(2), μO-Ca1-μO 81.2(3), μO-Ca2-μO 77.4(2); sum of the angles at O11: 343.3(6), at O21: 343.1(6), at O31: 331.0(6).

The few volatile alkoxides of the alkaline-earth metals reported previously do not have well-defined sublimation temperatures. They are much less volatile, and because of the unfavorable choice of ligands (e.g. containing silicon or fluorine), they cannot serve as molecular precursors for superconductors.[8]

Though the concept presented here does not use commercially available ligands, it can be generalized nonetheless. Thus, **3d**, the first volatile cadmium alkoxide, is synthesized following Equation (c).[9, 10] Crystalline **3d** is also composed of dimeric units, but in the gas phase it is a monomer according to CI mass spectra.

Each cadmium atom is coordinated by five oxygen atoms which form a distorted trigonal bipyramid. The metal atoms are bridged by two alkoxy groups, and the μO-Cd-μO planes are tilted by an angle of 19° with respect to each other, resulting in a coordination number of 3. The coordination sphere (CN 5) is completed by two axial donor functions from ether-type atoms. As in **3c** the alkoxy ligands in **3d** have strongly pyramidalized bridging oxygen atoms and narrow Cd-O_{term}-C angles.

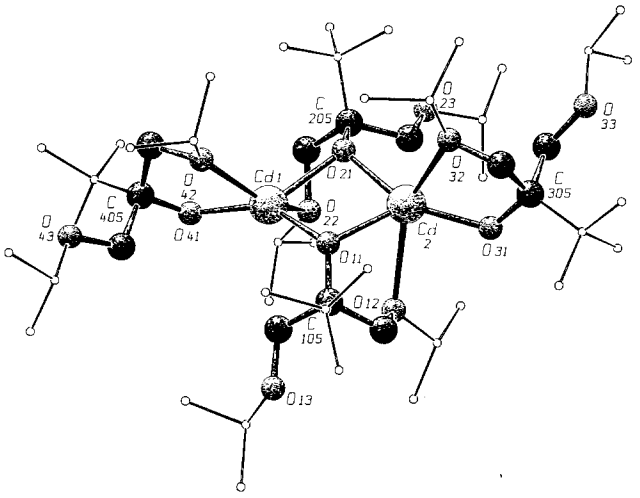


Fig. 2. Molecular structure of the binuclear cadmium alkoxide **3d** at −80 °C (SCHAKAL plot). The disorder of two of the isopropyl groups (see ref. [7]) is not shown. Selected distances [pm] and angles [°]: Cd–O_{term} 206.2(11), Cd–μO 218.2(13), Cd–O_{ether} 251.8(15), Cd1–Cd2 328.6(1); Cd-O_{term}-C 120.9(9), Cd1-μO-Cd2 97.7(4), μO-Cd-μO 80.4(4), sum of the angles around O11: 340.6(7), around O21: 342.9(8).

Our results show that stable metal alkoxides with little tendency toward aggregation and with high volatility can be obtained easily and economically by using tailored ligands. With **1a** as the ligand, we have also prepared the first volatile alkoxides $M(OR)_2$ of divalent manganese, iron, and cobalt (sublimation temperatures: 70–90 °C/10^{-2} mbar), which will be reported on in due course.[10]

Experimental Procedure

1a: To a solution of $ClMgCH_2OCH(CH_3)_2$ (0.26 mol) in THF (150 mL) at −10 °C was added $EtOCOCMe_3$ (8.46 g, 65 mmol) dropwise within 30 min. After stirring for 20 h, the reaction mixture was poured onto ice (50 g), neutralized with aqueous NH_4Cl, and extracted with diethyl ether (3 × 100 mL). The ether phase was washed with aqueous $NaHCO_3$ and H_2O, and subsequently dried with $MgSO_4$. After removal of the ether under vacuum, the residue was distilled at 76 °C/7 mbar. Yield: 11.53 g (76%). – **1b** was prepared analogously, but the reaction was conducted at −20 °C for 3 d (b.p. 52–56 °C/2 mbar, yield: 78%). The batch size can be increased without any loss in yield.

3c: To a solution of **2c** (2.02 g, 3.35 mol) in 35 mL *n*-hexane at −30 °C was added dropwise **1a** (1.56 g, 6.69 mmol). The mixture was stirred for 16 h at 25 °C. After removal of the solvent under vacuum, the colorless product was sublimed at 185 °C/10^{-2} mbar. Yield: > 98%.

4c: A mixture of potassium alkoxide (0.86 g, 3.54 mmol; prepared from KH and **1b** in THF) and BaI_2 (0.69 g, 1.77 mmol) was charged with 50 mL THF (added by vacuum condensation). The pure white suspension was stirred for 16 h at 25 °C. The solvent was removed under vacuum and the product dried under vacuum for 3 h. The isolated product was charged with 50 mL *n*-pentane (added by vacuum condensation), and after stirring for another 15 h the suspension was filtered. The filtrate was concentrated under vacuum, and **4c** was obtained as a yellowish oily product which crystallized upon standing. Yield: 0.55 g (57%).

3d: To a solution of **2d** (1.00 g, 2.30 mol) in 20 mL *n*-hexane at −30 °C was added **1a** (1.07 g, 4.60 mmol) dropwise. The mixture was stirred for 11 h at 25 °C. The solvent was removed under vacuum, and the colorless crystalline product was sublimed at 95 °C/10^{-2} mbar. Yield: > 98%.

Received: June 18, 1993 [Z6149IE]
German version: *Angew. Chem.* **1994**, *106*, 102

[1] a) L. G. Hubert-Pfalzgraf, *New J. Chem.* **1987**, *11*, 663–675; b) D. C. Bradley, *Chem. Rev.* **1989**, *89*, 1317–1322; c) L. G. Hubert-Pfalzgraf, *Appl. Organomet. Chem.* **1992**, *6*, 627–643; d) M. T. Andreas, A. I. Kingon, *Chem. Mater.* **1991**, *3*, 428–431.

[2] a) K. G. Caulton, M. H. Chisholm, S. R. Drake, W. E. Streib, *Angew. Chem.* **1990**, *102*, 1492–1493; *Angew. Chem. Int. Ed. Engl.* **1990**, *29*, 1483–1485; b) S. R. Drake, D. J. Otway, *J. Chem. Soc. Chem. Commun.* **1991**, 517–519.

[3] a) H. A. Stecher, A. Sen, A. L. Rheingold, *Inorg. Chem.* **1989**, *28*, 3280–3282; b) W. A. Herrmann, R. Anwander, M. Kleine, W. Scherer, *Chem. Ber.* **1992**, *125*, 1971–1979; c) R. Papiernik, L. G. Hubert-Pfalzgraf, M. C. Massiani,

Polyhedron **1991**, *10*, 1657–1662; d) B. D. Murray, H. Hope, P. P. Power, *J. Am. Chem. Soc.* **1985**, *107*, 169–173.

[4] Dimeric $[Ca(OCtBu_3)_2]$ is synthesized from **2a** and $HOCtBu_3$ by analogy to Equation (c); colorless crystals, moderately soluble in *n*-pentane, readily soluble in toluene and diethyl ether. Warming under high vacuum (185 °C/10^{-3} mbar) gives a moderate yield of trimeric $[Ca(OCHtBu_2)_2]$ as a colorless sublimate, soluble in toluene and THF. The properties of the sublimate are identical to those of a sample prepared from **2a** and $HOCHtBu_2$. The trimeric structure of $[Ca(OCHtBu_2)_2]$ results from chemical ionization (CI) mass spectrometry.

[5] a) W. A. Herrmann, N. W. Huber, R. Anwander, T. Priermeier, *Chem. Ber.* **1993**, *126*, 1127–1130; b) W. A. Herrmann, R. Anwander, M. Denk, *ibid.* **1992**, *125*, 2399–2405.

[6] For a comprehensive review of the literature see: a) W. S. Rees, D. A. Moreno, *J. Chem. Soc. Chem. Commun.* **1991**, 1759–1760; b) P. B. Hitchcock, M. F. Lappert, G. A. Lawless, B. Royo, *ibid.* **1990**, 1141–1142; c) F. G. N. Cloke, P. B. Hitchcock, M. F. Lappert, G. A. Lawless, B. Royo, *ibid.* **1991**, 724–726; d) S. R. Drake, D. J. Otway, M. B. Hursthouse, K. M. A. Malik, *Polyhedron* **1992**, *11*, 1995–2007; e) A. P. Purdy, C. F. George, J. H. Callahan, *Inorg. Chem.* **1991**, *30*, 2812–2819.

[7] **3a** ($C_{52}H_{108}Ca_2O_{12}$; $M = 1005.57$) crystallizes at −30 °C from *n*-hexane in the orthorhombic space group *Pbca* (No.61), $Z = 8$, $a = 3043.8(4)$, $b = 2003.2(3)$, $c = 1997.6(3)$ pm, $V = 12180 \times 10^6$ pm^3, $\varrho_{calcd} = 1.097$ g cm^{-3}, $F(000) = 4448$; $Mo_{K\alpha}$ radiation, −110 °C, Enraf-Nonius CAD-4 diffractometer, ω scan (max. 60 s), 8219 measured reflections of which 4696 with $I > 2.5\sigma(I)$ were used in the refinements. Structure solution by direct methods, no intensity correction, no absorption correction. $R = \Sigma(||F_o| - |F_c||)/\Sigma|F_o| = 0.063$; $R_w = [\Sigma w(|F_o| - |F_c|)^2/\Sigma w|F_o|^2]^{1/2} = 0.070$, residual electron density: +0.35 e Å^{-3}. – **3d** ($C_{52}H_{108}Cd_2O_{12}$; $M = 1150.23$) crystallizes at −30 °C from *n*-hexane in the triclinic space group $P\bar{1}$ (No. 2), $Z = 2$, $a = 1342.3(2)$, $b = 1438.0(2)$, $c = 1714.0(3)$ pm, $\alpha = 75.15(1)$, $\beta = 88.32(1)$, $\gamma = 80.87(1)°$, $V = 3157 \times 10^6$ pm^3, $\varrho_{calcd} = 1.210$ g cm^{-3}, $F(000) = 1224$; $Cu_{K\alpha}$ radiation, −80 °C, Enraf-Nonius CAD-4 diffractometer, $\omega/2\theta$ scan (max. 90 s), 9661 measured reflections of which 6825 with $I > 2.0\sigma(I)$ were used in the refinements. Structure solution by Patterson methods, intensity correction and absorption correction. $R = \Sigma(||F_o| - |F_c||)/\Sigma|F_o| = 0.077$; $R_w = [\Sigma w(|F_o| - |F_c|)^2/\Sigma w|F_o|^2]^{1/2} = 0.076$, residual electron density: +1.18 e Å^{-3}. The structure exhibits a resolvable orientational disorder of the isopropyl groups at O23 and O42. Further details of the crystal structure investigation may be obtained from the Fachinformationszentrum Karlsruhe, Gesellschaft für wissenschaftlich-technische Information mbH, D-76344 Eggenstein-Leopoldshafen, on quoting the depository number CSD-57715, the names of the authors, and the journal citation.

[8] For a current summary see: T. P. Hanusa, *Chem. Rev.* **1993**, *93*, 1023–1036. Our experience shows the sublimation data (80 °C/1 Torr) given for $[Ba_2(OSitBu_3)_4 \cdot THF]$ to be those of the free ligand. See S. R. Drake, W. E. Streib, K. Folting, M. H. Chisholm, K. G. Caulton, *Inorg. Chem.* **1992**, *31*, 3205–3210.

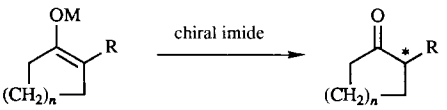
[9] All other known cadmium alkoxides are nonvolatile: a) S. Boulmaaz, R. Papiernik, L. G. Hubert-Pfalzgraf, J. Vaissermann, J. Daran, *Polyhedron*, **1992**, *11*, 1331–1336; b) S. C. Goel, M. Y. Chiang, W. E. Buhro, *J. Am. Chem. Soc.* **1990**, *112*, 6724–6725; c) H. W. Roesky, M. Scholz, M. Noltemeyer, *Chem. Ber.* **1990**, *123*, 2303–2309.

[10] W. A. Herrmann, N. W. Huber, *Chem. Ber.*, in press.

Enantioselective Protonation of Simple Enolates: Chiral Imide as a Chiral Proton Source**

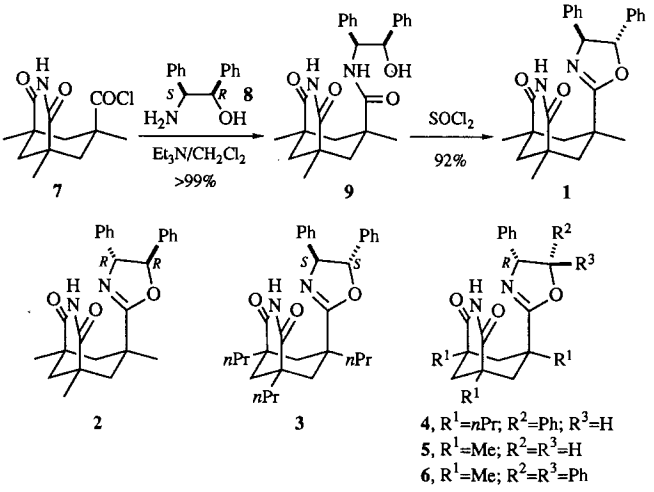
Akira Yanagisawa, Takeshi Kuribayashi, Tetsuo Kikuchi, and Hisashi Yamamoto*

The enantioselective protonation of prochiral enolates is one of the most effective methods of preparing optically active α-substituted carbonyl compounds. Numerous successes have been reported in the last twenty years; however, most of these have used substrates bearing polar substituents such as amino, hydroxyl, or phenyl groups,[1–3] and few succeeded in the asymmetric induction of simple enolates.[4] Here, we report a general solution to this problem in which we use the new chiral proton sources, (*S,S*)-imide **1** and (*R,R*)-imide **2**, which possess an asymmetric 2-oxazoline ring, and describe their application to the enantioselective protonation of metal enolates derived from α-monoalkylated cycloalkanones [Eq. (a)].



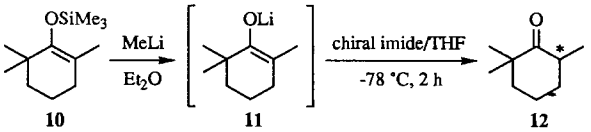
(a)

Selective *C*-protonation is expected to occur in the reaction of an enolate with an imide because of the relatively weak acidity of the imide proton.[5] The chiral imide was prepared (see Scheme 1) from a readily available derivative of Kemp's tricarboxylic acid[6] in two steps and in more than 90% overall yield. The synthesis avoided the cumbersome resolution step. The imide acid chloride **7**[7] was condensed with (1*R*,2*S*)-2-amino-1,2-diphenylethanol (**8**) to afford amide **9** (>99% yield), and cyclization to form a 2-oxazoline ring with thionyl chloride completed the synthesis of (*S,S*)-imide **1** ($[\alpha]_D^{26} = -21.9$ ($c = 0.73$ in $CHCl_3$)).[8, 9]



Scheme 1. Top: Synthesis of (*S,S*)-imide **1**. Bottom: Structural formulas of the (*R,R*)-imide **2** and the imides **3**–**6**.

Using the chiral imides derived from a variety of amino alcohols, we examined the asymmetric protonation reaction of lithium enolate [Eq. (b)].[10] Treatment of lithium enolate **11**, gener-



(b)

ated from the silyl enol ether **10** and methyllithium in diethyl ether,[10] with (*S,S*)-imide **1** (1 equiv) in THF at −78 °C for 2 h afforded (*R*)-2,2,6-trimethylcyclohexanone (**12**) with 87% *ee* (Table 1, entry 1). Use of the enantiomer (*R,R*)-imide **2** afforded (*S*)-**12** with a similar enantioselectivity (entry 2). Substitution of the methyl groups of **1** with *n*-propyl groups[11] had no effect

[*] Prof. H. Yamamoto, Dr. A. Yanagisawa, T. Kuribayashi, T. Kikuchi
School of Engineering, Nagoya University
Chikusa, Nagoya 464-01 (Japan)
Telefax: Int. code + (52)783-2373

[**] This work was supported by the Ministry of Education, Science, and Culture of the Japanese Government.

Table 1. Protonation of the lithium enolate **11** with chiral imides **1**–**6** [a].

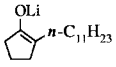
Entry	Imide	*ee* [%] [b]	Configuration [c]
1	**1**	87	*R*
2	**2**	88	*S*
3	**3**	88	*R*
4	**4**	60	*S*
5	**5**	54	*S*
6	**6**	85	*S*

[a] Yields of isolated **12** were 97–60%. [b] Determined by GC analysis with chiral column (Chrompack). [c] Determined by comparison with published data; (*R*)-isomer (46% *ee*): $[\alpha]_{578}^{RT} = -36.3$ ($c = 1.8$ in $CHCl_3$) [4b]. Observed $[\alpha]_D$ value of (*R*)-isomer (69% *ee*): $[\alpha]_D^{22} = -41.0$ ($c = 3.1$ in $CHCl_3$). RT = room temperature.

(compare entries 1 and 3). The *cis* arrangement of the two phenyl groups of imide **4** decreased the enantioselectivity (compare entries 2 and 4). The configuration of the product **12** was reflected by the absolute configuration of the C4 stereogenic center of the oxazoline ring (entries 2, 4, 5, and 6). Consequently, (*S,S*)-imide **1** and (*R,R*)-imide **2** were found to be the most effective proton sources.

Selected results of the reaction of various lithium enolates with (*S,S*)-imide **1** or (*R,R*)-imide **2** are summarized in Table 2.

Table 2. Enantioselective protonation of lithium enolates with **1** and **2** [a].

Entry	Lithium enolate	Imide	Ketone [b] *ee* [%]	Configuration
1		**1**	68 [c]	*R* [d]
2		**2**	70 [c]	*S* [d]
3		**1**	87 [e]	*R* [f]
4		**2**	88 [e]	*S* [f]
5		**1**	96 [c]	*R* [g]
6		**2**	97 [c]	*S* [g]
7		**1**	78 [c]	–

[a] Unless otherwise noted, lithium enolate was generated from the corresponding silyl enol ether (1 equiv) and MeLi (1.2 equiv) in diethyl ether at room temperature. The protonation was carried out by adding a chiral imide (1.2 equiv) in THF at −78 °C (duration 2 h). [b] Yields of isolated products were 94–45%, depending on the generation of the enolate anion. The only by-product is the starting silyl enol ether. [c] Determined by HPLC analysis of the α-methyl-α-trifluoromethylphenylacetic acid (MTPA) ester of *trans*-2-methylcyclohexanol derived from the corresponding ketone by reduction ($NaBH_4/CH_3OH$) and esterification. [d] Determined by comparison with published data; pure (*S*)-isomer: $[\alpha]_D = +14$ ($c = 0.23$ in MeOH) [12]. Observed value of (*R*)-isomer (36% *ee*): $[\alpha]_D^{24} = -5.9$ ($c = 0.50$ in MeOH). [e] Determined by GC analysis with chiral column (CHROMPACK). [f] See footnote [b] in Table 1. [g] Observed $[\alpha]_D$ value of (*S*)-isomer (93% *ee*): $[\alpha]_D^{25} = +77.3$ ($c = 1.2$ in Et_2O). Reported $[\alpha]_D$ value of (*S*)-isomer (97% *ee*): $[\alpha]_D^{24} = +81.0$ ($c = 1.0$ in Et_2O) [13].

The following features are characteristic: 1) The (*R*)- and (*S*)-enriched ketones could be prepared with equal optical purity with either (*S,S*)-imide **1** or (*R,R*)-imide **2**. 2) The existence of two methyl groups at the C6 position of the enolate of 2-methylcyclohexanone raised the enantioselectivity (entries 1–4). 3) An exceedingly high *ee* was achieved with the enolate of a cyclopentanone that possessed a long alkyl chain (entries 5 and 6).

A proposed model of the transition state of this protonation is shown in Figure 1. The lithium atom of the enolate coordinates to both the nitrogen atom of the 2-oxazoline ring and the oxygen atom of the imide. An eight-membered ring that avoids steric repulsion between a phenyl substituent of oxazoline ring and the alkyl ring of the enolate is formed. Thus, (*S,S*)-imide **1** protonates selectively at the *si* face of the lithium enolate. In addition, steric bulkiness of alkyl substituents at the C6 position seems beneficial for the enantioface discrimination. Further study on asymmetric protonation with this chiral imide and its precise reaction mechanism is currently underway.

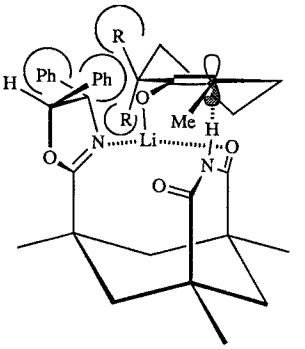


Fig. 1. Proposed model of the transition state of the asymmetric protonation of lithium enolates with (*S,S*)-imide **1**.

Experimental Procedure

Silyl enol ether **10** was derived from 2,2,6-trimethylcyclohexanone (**12**). To a solution of **10** (104 mg, 0.49 mmol) in dry Et_2O (2.5 mL) at 0 °C was added a solution of MeLi (1.5 M, 0.35 mL, 0.53 mmol) in Et_2O under argon atmosphere [10]. After the reaction mixture had been stirred for 2 h at 20 to 25 °C, protonation was carried out at −78 °C by addition of a solution of (*S,S*)-imide **1** (211 mg, 0.51 mmol) in dry THF (2.5 mL). The reaction solution was held at −78 °C for 2 h. Then a saturated NH_4Cl solution (10 mL) was added, and the organic material was extracted twice with Et_2O (2 × 10 mL). The combined extracts were dried over anhydrous Na_2SO_4 and concentrated in vacuo. The crude product was purified by column chromatography on silica gel (hexane/Et_2O, 5:1) to afford (*R*)-(−)-**12** [4b] (59 mg, 86% yield) with 87% *ee*. The imide **1** was recovered without significant loss of optical purity.

Received: July 14, 1993
Revised: September 14, 1993 [Z 6213 IE]
German version: *Angew. Chem.* **1994**, *106*, 129

[1] Reviews: a) L. Duhamel, P. Duhamel, J.-C. Launay, J.-C. Plaquevent, *Bull. Soc. Chim. Fr. II* **1984**, 421; b) H. Waldmann, *Nachr. Chem. Tech. Lab.* **1991**, *39*, 413.

[2] Recent reports: a) U. Gerlach, S. Hünig, *Angew. Chem.* **1987**, *99*, 1323; *Angew. Chem. Int. Ed. Engl.* **1987**, *26*, 1283; b) C. Fehr, J. Galindo, *J. Am. Chem. Soc.* **1988**, *110*, 6909; c) D. Potin, K. Williams, J. Rebek, Jr., *Angew. Chem.* **1990**, *102*, 1485; *Angew. Chem. Int. Ed. Engl.* **1990**, *29*, 1420; d) O. Piva, J.-P. Pete, *Tetrahedron Lett.* **1990**, *31*, 5157; e) O. Piva, R. Mortezaei, F. Henin, J. Muzart, J.-P. Pete, *J. Am. Chem. Soc.* **1990**, *112*, 9263; f) F. Henin, J. Muzart, J.-P. Pete, A. M'boungou-M'passi, H. Rau, *Angew. Chem.* **1991**, *103*, 460; *Angew. Chem. Int. Ed. Engl.* **1991**, *30*, 416; g) F. Henin, J. Muzart, J.-P. Pete, O. Piva, *New J. Chem.* **1991**, *15*, 611; h) E. Vedejs, N. Lee, *J. Am. Chem. Soc.* **1991**, *113*, 5483; i) F. Hénin, J. Muzart, *Tetrahedron: Asymmetry* **1992**, *3*, 1161; j) A. Kumar, R. V. Salunkhe, R. A. Rane, S. Y. Dike, *J. Chem. Soc. Chem. Commun.* **1991**, 485; k) S. Takeuchi, N. Miyoshi, Y. Ohgo, *Chem. Lett.* **1992**, 551; l) S. Takeuchi, N. Miyoshi, K. Hirata, H. Hayashida, Y. Ohgo, *Bull. Chem. Soc. Jpn.* **1992**, *65*, 2001; m) T. Yasukata, K. Koga, *Tetrahedron: Asymmetry* **1993**, *4*, 35; n) T. Haubenreich, S. Hünig, H.-J. Schulz, *Angew. Chem.* **1993**, *105*, 443; *Angew. Chem. Int. Ed. Engl.* **1993**, *32*, 398; o) C. Fehr, I. Stempf, J. Galindo, *ibid.* **1993**, *105*, 1091, 1093 and **1993**, *32*, 1042, 1044.

[3] For enantioselective protonation reactions by catalytic antibodies, see: a) I. Fujii, R. A. Lerner, K. D. Janda, *J. Am. Chem. Soc.* **1991**, *113*, 8528; b) J.-L. Reymond, K. D. Janda, R. A. Lerner, *ibid.* **1992**, *114*, 2257.

[4] a) H. Hogeveen, L. Zwart, *Tetrahedron Lett.* **1982**, *23*, 105; b) M. B. Eleveld, H. Hogeveen, *ibid.* **1986**, *27*, 631; c) K. Matsumoto, H. Ohta, *ibid.* **1991**, *32*, 4729; d) K. Fuji, K. Tanaka, H. Miyamoto, *Tetrahedron: Asymmetry* **1993**, *4*, 247.

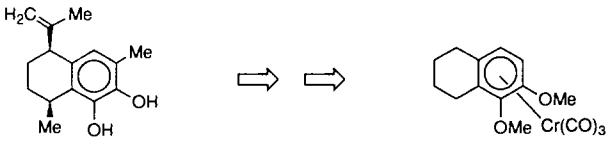
[5] Perhaps C-protonation must distinctly predominate over O-protonation to achieve the highly enantioselective protonation. For example, the pK_a value of succinimide is 9.5: *The Merck Index*, 11th ed., Merck & Co. Inc., USA **1989**, 1399.

[6] a) D. S. Kemp, K. S. Petrakis, *J. Org. Chem.* **1981**, *46*, 5140; b) J. Rebek, Jr., B. Askew, M. Killoran, D. Nemeth, F.-T. Lin, *J. Am. Chem. Soc.* **1987**, *109*, 2426. c) Recently Curran and Rebek reported asymmetric radical reactions on using an imide chiral auxiliary prepared from Kemp's tricarboxylic acid: J. G. Stack, D. P. Curran, J. Rebek, Jr., P. Ballester, *ibid.* **1991**, *113*, 5918; J. G. Stack, D. P. Curran, S. V. Geib, J. Rebek, Jr., P. Ballester, *ibid.* **1992**, *114*, 7007.
[7] B. Askew, P. Ballester, C. Buhr, K. S. Jeong, S. Jones, K. Parris, K. Williams, J. Rebek, Jr., *J. Am. Chem. Soc.* **1989**, *111*, 1082.
[8] The oxazoline ring was formed by inversion at the carbon atom carrying the hydroxyl group: J. Sicher, M. Pánková, *Collect. Czech. Chem. Commun.* **1955**, *20*, 1409.
[9] $[\alpha]_D$ value of (*R,R*)-imide **2**: $[\alpha]_D^{26} = +24.7$ ($c = 0.73$ in $CHCl_3$).
[10] Review: E. W. Colvin, *Silicon in Organic Synthesis*, Butterworth, London, **1981**, p. 217.
[11] a) K.-S. Jeong, A. V. Muehldorf, J. Rebek, Jr., *J. Am. Chem. Soc.* **1990**, *112*, 6144; b) K. S. Jeong, T. Tjivikua, A. Muehldorf, G. Deslongchamps, M. Famulok, J. Rebek, Jr., *ibid.* **1991**, *113*, 201.
[12] C. Beard, C. Djerassi, J. Sicher, F. Sipos, M. Tichy, *Tetrahedron* **1963**, *19*, 919.
[13] A. Mori, H. Yamamoto, *J. Org. Chem.* **1985**, *50*, 5444.

The Total Synthesis of *cis*-7,8-Dihydroxy-11,12-dehydrocalamenene by Regio- and Diastereoselective Alkylation of Chiral η^6-Arenetricarbonylchromium Complexes: An Unexpected Case of Nucleophilic Aromatic *tele*-Substitution with Methoxide as a Leaving Group**

Hans-Günther Schmalz,* Markus Arnold, Jens Hollander, and Jan W. Bats

In the course of our work on chiral transition metal π complexes as synthetic building blocks[1] we have found an efficient total synthetic route to the potential antiinfective sesquiterpene *cis*-7,8-dihydroxy-11,12-dehydrocalamenene (**1**).[2] Our synthetic strategy (Scheme 1) is founded on the chemistry of η^6-benzene–$Cr(CO)_3$ derivatives.[3] Starting with the chiral complex **2**, all three side chains are introduced by successive deprotonation–alkylation steps during which both the increased acidity of the complexed ligand (especially in the benzylic positions)[4] and the steric shielding effect of the $Cr(CO)_3$ fragment are exploited.

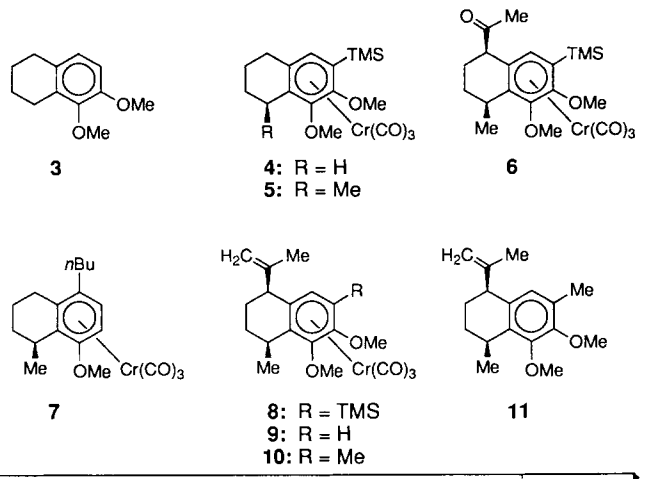


1 **2**

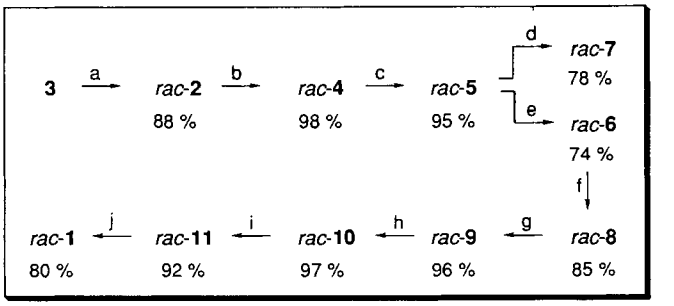
Scheme 1.

The synthetic route was first worked out and optimized employing racemic compounds (Scheme 2).[5] The complex *rac*-**2** was obtained by direct complexation of 5,6-dimethoxytetralin (**3**)[6] with $[Cr(CO)_6]$ under standard conditions.[7] After protection of the (relatively) acidic aryl position adjacent to the methoxy substituent by silylation (*rac*-**2** → *rac*-**4**), benzylic methylation of *rac*-**4** led with complete regio- and diastereoselectivity to *rac*-**5**, whose constitution and relative configuration were established by a crystal structure analysis (Fig. 1).[8] The conversion of *rac*-**5** into the acylated compound *rac*-**6** was also achieved in good yield though only when *sec*-butyllithium (*s*BuLi) was employed as base and hexamethylphosphoric acid triamide (HMPT) was not used as cosolvent. In contrast, treatment of *rac*-**5** with *n*BuLi in THF/HMPT unexpectedly gave high yields of *rac*-**7**,[9] which can be considered as the product of a nucleophilic aromatic *tele* substitution[*] with methoxide as the leaving group (see below). For the further transformation of *rac*-**6** in the direction of the target compound it was next methylenated by the method of Lombardo.[10] After fluoride-induced desilylation, the still-missing methyl group was introduced by *ortho* deprotonation/alkylation. Oxidative decomplexation with iodine in ether yielded *rac*-**11**, which was finally deprotected by treatment with thioethanolate[11] to provide *rac*-**1**[12] (overall yield from *rac*-**2**: ca. 40% over 8 steps!).

The selective formation of *rac*-**6** or *rac*-**7**, which can be controlled by the choice of reaction conditions, deserves a comment: With *n*BuLi *rac*-**5** probably undergoes nucleophilic addition to give the anionic intermediate *rac*-**12**, whereas with the stronger base *s*BuLi (and in the absence of HMPT as the cosolvent which promotes nucleophilic addition[13b]) the intermediate deprotonated at the benzylic position, *rac*-**13**, is formed (Scheme 3).[14]



3 **4**: R = H, **5**: R = Me **6** **7** **8**: R = TMS, **9**: R = H, **10**: R = Me **11**

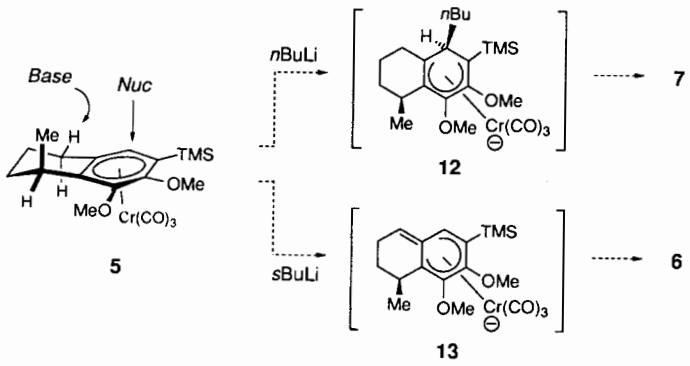


Scheme 2. Synthesis of *rac*-**1**. a) 1.1 equiv. $[Cr(CO)_6]$, nBu_2O/THF (10:1), reflux, 45 h; b) *n*BuLi, THF, −60 °C → −40 °C, 30 min, then Me_3SiCl, 0 °C, 1 h; c) *n*BuLi, THF/HMPT, −60 °C, 10 min, 0 °C, 2 h, then MeI, −40 °C, 10 min, 0 °C, 1 h; d) *n*BuLi, THF/HMPT, −40 °C → 0 °C, 2 h, then CH_3COCl, −70 °C → 0 °C, 0.5 h; e) *s*BuLi, THF, −65 °C, 10 min, −10 °C, 2.5 h, then CH_3COCl, −25 °C, 10 min, 25 °C, 0.5 h; f) CH_2Br_2/Zn/$TiCl_4$, THF, 0 °C → 25 °C, 25 °C, 2.5 h; g) nBu_4NF, THF, room temperature, 3 h; h) *n*BuLi, THF, −50 °C → −30 °C, 1.5 h, then MeI, −30 °C → −10 °C, 20 min; i) I_2, Et_2O, 25 °C, 1 h; j) NaSEt, DMF, reflux, 20 h. For selected physical and spectroscopic data see Table 1.

The conversion of *rac*-**4** into *rac*-**5** is a rare example of a nucleophilic aromatic *tele* substitution[*] in which the entering group takes a position more than one atom distant from the position to which the leaving group was attached.

[*] Dr. H.-G. Schmalz, Dipl.-Chem. M. Arnold, Dipl.-Chem J. Hollander, Dr. J. W. Bats
Institut für Organische Chemie der Universität
Marie-Curie-Strasse 11, D-60439 Frankfurt am Main (FRG)
Telefax: Int. code + (69) 5800-9250

[**] This work was supported by the Volkswagenstiftung and the Fonds der Chemischen Industrie. We thank Prof. G. Quinkert, Frankfurt, for his support.



Scheme 3. Mechanistic consideration: benzylic deprotonation versus nucleophilic addition.

The surprising ease with which *rac*-**5** is nucleophilically attacked under conditions that lead to smooth benzylic deprotonation in the case of *rac*-**4** can be explained: The crystal structure of *rac*-**5** shows the saturated six-membered ring in a half-chair conformation with the benzylic methyl substituent in a pseudo-axial position (Fig. 1 top).[8] The only benzylic H atom available for deprotonation (*exo* to the $Cr(CO)_3$ group) is thus in a pseudo-equatorial position. Its abstraction should therefore be relatively disfavored for stereoelectronic reasons.[14] The crystal structure shows further that the $Cr(CO)_3$ tripod prefers an eclipsed conformation (relative to three C atoms of the arene ring; Fig. 1, bottom) such that one of the CO ligands is located exactly "under" the ring atom attacked by *n*BuLi. That this attack should be comparatively favorable is inferred from investigations that have shown that (charge-controlled) nucleophilic additions to arene–$Cr(CO)_3$ complexes occur especially readily at those ring atoms whose charge density is lowered by eclipsing CO ligands.[13, 15] In this way the originally unexpected reactivity of *rac*-**5** towards *n*BuLi can be attributed to the structurally well-established interplay of two stereoelectronic effects (disfavored benzylic deprotonation and facilitated nucleophilic addition).[16]

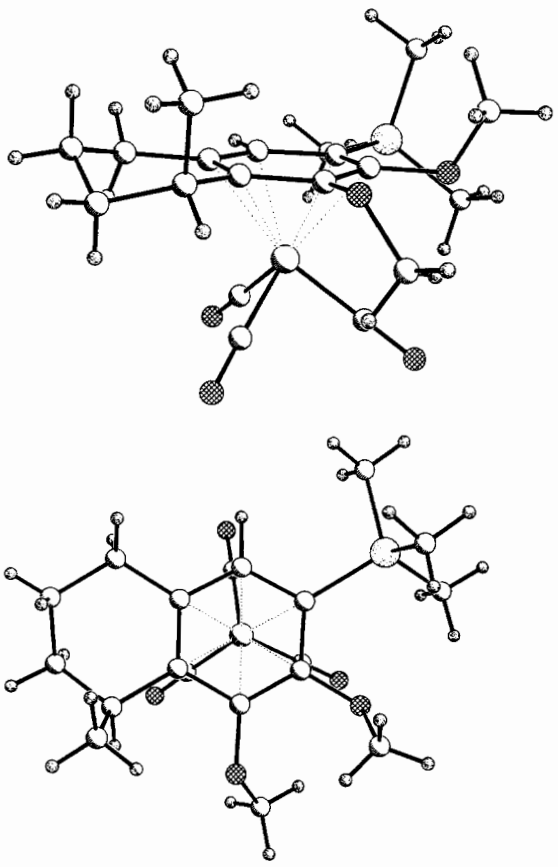


Fig. 1. Two views of the crystal structure of *rac*-**5**.

Table 1. Characteristic data for compounds **2**, **5**, **6**, *rac*-**7**, and *rac*-**8**. ^1H NMR: $CDCl_3$, int. TMS; ^{13}C NMR: 63 MHz, $CDCl_3$, int. TMS, DEPT experiments as well.

2: M.p. 101–102 °C; $[\alpha]_D^{20} = +299$ ($c = 0.445$ in $CHCl_3$); ^1H NMR (250 MHz): $\delta = 1.62-1.93$ (m, 4H), 2.51 (m, 2H), 2.78 (m, 2H), 3.81 (s, 3H), 3.87 (s, 3H), 5.08 (d, 1H, $J = 6.9$ Hz), 5.29 (d, 1H; $J = 6.9$ Hz); ^{13}C NMR: $\delta = 21.6$ (CH_2), 21.8 (CH_2), 23.5 (CH_2), 27.8 (CH_2), 56.2 (CH_3), 65.1 (CH_3), 74.0 (CH), 91.8 (CH), 101.7, 110.1, 135.3, 156.8, 234.6.

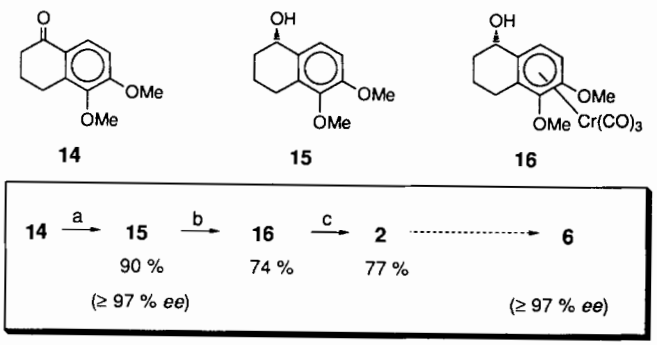
5: M.p. 124 °C; ^1H NMR (250 MHz): $\delta = 0.35$ (s, 9H), 1.31 (d, 3H, $J = 7.0$ Hz), 1.62–1.82 (m, 3H), 1.90–2.03 (m, 1H), 2.49 (m, 2H), 3.18 (m, 1H), 3.76 (s, 3H), 3.85 (s, 3H), 5.25 (s, 1H); ^{13}C NMR: $\delta = -0.4$ (CH_3), 16.9 (CH_2), 20.9 (CH_3), 26.9 (CH_2), 27.8 (CH), 28.4 (CH_2), 60.5 (CH_3), 65.2 (CH_3), 90.7, 98.9 (CH), 101.8, 117.3, 127.7, 138.3, 234.3.

6: M.p. 148–150 °C; $[\alpha]_D^{20} = -64.4$ ($c = 0.371$ in $CHCl_3$); ^1H NMR (250 MHz): $\delta = 0.33$ (s, 9H), 1.29 (d, 3H, $J = 7.0$ Hz), 1.55–1.81 (m, 2H), 2.04–2.16 (m, 2H), 2.25 (s, 3H), 3.19 (m, 1H), 3.63 (m, 1H), 3.80 (s, 3H), 3.86 (s, 3H), 5.07 (s, 1H); ^{13}C NMR: $\delta = -0.6$ (CH_3), 20.7 (CH_3), 21.7 (CH_2), 27.6 (CH_2), 27.7 (CH), 28.5 (CH_3), 51.1 (CH), 60.5 (CH_3), 65.3 (CH_3), 90.8, 98.6, 99.3 (CH), 116.9, 131.6, 139.9, 208.8, 233.7.

rac-**7**: ^1H NMR (270 MHz): $\delta = 0.94$ (t, 3H, $J = 7.0$ Hz), 1.22 (d, 3H, $J = 7.0$ Hz), 1.32–1.91 (m, 8H), 2.09 (m, 1H), 2.37–2.59 (m, 1H), 2.65 (m, 1H), 2.85 (m, 1H), 3.18 (m, 1H), 3.68 (s, 3H), 4.96 (d, 1H, $J = 6.8$ Hz), 5.35 (d, 1H, $J = 6.8$ Hz); ^{13}C NMR: $\delta = 13.9$ (CH_3), 16.5 (CH_2), 19.9 (CH_3), 22.7 (CH_2), 24.6 (CH_2), 27.3 (CH), 28.2 (CH_2), 31.2 (CH_2), 32.6 (CH_2), 55.8 (CH_3), 73.6 (CH), 92.7 (CH), 105.6, 107.3, 110.0, 139.8, 234.5.

rac-**8**: M.p. 116–120 °C; ^1H NMR (270 MHz): $\delta = 0.32$ (s, 9H), 1.32 (d, 3H, $J = 7.0$ Hz), 1.60 (s, 3H), 1.67–1.75 (m, 3H), 2.05 (m, 1H), 3.18 (m, 1H), 3.30 (m, 1H), 3.78 (s, 3H), 3.85 (s, 3H), 4.88 (br s, 2H), 5.41 (s, 1H); ^{13}C NMR: $\delta = -0.1$ (CH_3), 18.3 (CH_3), 20.9 (CH_3), 22.6 (CH_2), 27.8 (CH_2), 28.1 (CH), 46.1 (CH), 60.4 (CH_3), 65.4 (CH_3), 90.6, 98.6 (CH), 102.9, 114.7 (CH_2), 117.5, 146.9, 234.0.

We have shown that our strategy is also suitable for the synthesis of nonracemic compounds by the preparation of **6** (Scheme 4). Ionic hydrogenation[18] of the *endo*-tetralol com-



Scheme 4. Enantioselective preparation of **6**. a) CBS reduction [1,19], THF, 25 °C; b) 1.1 equiv $[Cr(CO)_6]$, cat. THF, nBu_2O/heptane (1:1), reflux, 27 h, removal of a small amount of *exo* diastereoisomer by flash chromatography; c) $HSiEt_3$, F_3CCO_2H, CH_2CH_2, −10 °C, 1 h, 25 °C, 2 h.

plex **16**,[1] which is prepared from **14** by enantioselective reduction (→ **15**)[1, 19] and diastereoselective complexation, provided the chiral synthetic building block **2** with high enantiomeric purity. The transformation of **2** into **6** was then achieved (without racemization) under the conditions worked out in the

 © VCH Verlagsgesellschaft mbH, D-69451 Weinheim, 1994 0570-0833/94/0101-0110 $ 10.00+.25/0

racemic series.[20] Thus, the absolute stereochemical information brought into the synthetic scheme by the chiral metal complex could be transferred without any loss to the two newly generated chiral centers.

The synthesis presented here is attractive because it has only a few steps and a remarkably high efficiency (total yield, selectivity), and it opens up an easy route to multi-gram quantitites of optically active 7,8-dihydroxy-11,12-dehydrocalemenene derivatives with a given absolute configuration. The underlying concept[21] has proved to be very effective and will now be used in the enantioselective synthesis of other compounds.[1b]

Received: June 28, 1993 [Z 6177 IE]
German version: *Angew. Chem.* **1994**, *106*, 77

[1] a) H.-G. Schmalz, B. Millies, J. W. Bats, G. Dürner, *Angew. Chem.* **1992**, *104*, 640–643; *Angew. Chem. Int. Ed. Engl.* **1992**, *31*, 631–633; b) H.-G. Schmalz, J. Hollander, M. Arnold, G. Dürner, *Tetrahedron Lett.* **1993**, *34*, 6259–6262.

[2] S. Wahyuono, J. J. Hoffmann, R. B. Bates, S. P. McLaughlin, *Phytochemistry* **1991**, *30*, 2175–2182.

[3] a) M. F. Semmelhack, *Ann. N. Y. Acad. Sci.* **1977**, *295*, 36–51; b) J. P. Collman, L. S. Hegedus, J. R. Norton, R. G. Finke, *Principles and Applications of Organotransition Metal Chemistry*, University Science Books, Mill Valley, CA, USA, **1987**, Chapter 20; c) V. N. Kalinin, *Russ. Chem. Rev.* **1987**, *56*, 682–700; d) M. Uemura, *Adv. Met.-Org. Chem.* **1991**, *2*, 195.

[4] a) S. G. Davies, S. J. Coote, C. L. Goodfellow, *Adv. Met.-Org. Chem.* **1991**, *2*, 1, and references therein; b) S. G. Davies, *J. Organomet. Chem.* **1990**, *400*, 223–234, and references therein.

[5] All new compounds were characterized by the usual spectroscopic methods (see also Table 1) and gave correct elemental analyses.

[6] Prepared in 99% yield from **14** (H_2, Pd-C, EtOH/2 N HCl, 4.5 bar, 15 h).

[7] C. A. L. Mahaffy, P. L. Pauson, *Inorg. Synth.* **1979**, *19*, 154.

[8] X-ray crystal structure analysis of *rac*-**5**: Enraf-Nonius CAD4 diffractometer, $Cu_{K\alpha}$ radiation, $2\theta_{max} = 120°$, empirical absorption correction with DIFABS; structure determination with direct methods (SHELXS); the position of one hydrogen atom of each of the two methoxy groups was determined from a difference synthesis. All other hydrogen atoms were placed at calculated positions without refinement. $C_{19}H_{26}CrO_5Si$, monoclinic, space group $P2_1/n$, $a = 10.266(3)$, $b = 18.422(6)$, $c = 11.764(4)$ Å, $\beta = 108.41°$, $V = 2111(2)$ Å^3, $Z = 4$, $\rho_{calc} = 1.304$ g cm^{-3}, $\mu = 52.9$ cm^{-1}; 3128 independent reflections, of which 3015 with $I > 0$ were used; $R = 0.058$, $R_w = 0.056$. The residual electron density was less than 0.38 e Å^{-3}. Further details of the crystal structure investigation are available on request from The Director of the Cambridge Crystallographic Centre, 12 Union Road, Cambridge CB2 1EZ (UK), on quoting the full journal citation.

[9] The constitution of *rac*-**7** was confirmed by nuclear Overhauser enhancement (NOE) NMR measurements.

[10] L. Lombardo, *Tetrahedron Lett.* **1982**, *23*, 4293–4296; *Org. Synth.* **1987**, *65*, 81; the time required for the preparation of the reagent can be reduced considerably by using ultrasound (4 h at 0 °C vs. 3 d at 5 °C).

[11] G. I. Feutrill, R. N. Mirrington, *Tetrahedron Lett.* **1970**, 1327–1328.

[12] The ^{1}H NMR data for *rac*-**1** and *rac*-**11** agree with those in ref.[2].

[13] a) M. F. Semmelhack in *Compr. Org. Synth., Vol. 4* (Eds.: B. M. Trost, I. Fleming), Pergamon, Oxford, **1991**, p. 517, and references therein; b) M. F. Semmelhack, H. T. Hall, Jr., R. Farina, M. Yoshifuji, G. Clark, T. Barbar, K. Hirotsu, J. Clardy, *J. Am. Chem. Soc.* **1979**, *101*, 3535–3544; c) E. P. Kündig, V. Desobry, D. P. Simmons, E. Wenger, *ibid.* **1989**, *111*, 1804–1814, and references therein.

[14] We assume the lithiated species to be structure **13**, in which the deprotonated center is part of a new double bond[4a]. During the deprotonation, the C–H bond to be broken should be as parallel as possible to the aryl π orbitals so that the developing p orbital can be stabilized early (see P. Deslongchamps, *Stereoelectronic Effects in Organic Chemistry*, Pergamon, Oxford, **1983**, *365*, 243–267, and references therein.

[15] B. Ohlson, C. Ullenius, S. Jagner, C. Grivet, E. Wenger, E. P. Kündig, *J. Organomet. Chem.* **1989**, *365*, 243–267, and references therein.

[16] The transformation of the initial nucleophile adduct *rac*-**12** into *rac*-**7** could take place in analogy to the mechanism suggested by Rose-Munch et al.[17] (for nucleophilic *tele* substitution on halobenzene–$Cr(CO)_3$ derivatives). Nevertheless, the selective formation of *rac*-**7** is remarkable for several reasons. Not only is the smooth attack of the nucleophile adjacent to the bulky TMS group unique, but also the complete regioselectivity of the methoxide expulsion and the ease with which the methoxide acts as a leaving group. Further investigations are in progress to clarify these phenomena and to determine the synthetic potential of nucleophilic addition to *rac*-**5** and analogous compounds.

[17] a) F. Rose-Munch, E. Rose, A. Semra, *J. Chem. Soc. Chem. Commun.* **1986**, 1108–1109; *ibid.* **1987**, 942–943; F. Rose-Munch, E. Rose, A. Semra, L. Mignon, J. Garcia-Oricain, C. Knobler, *J. Organomet. Chem.* **1989**, *363*, 297–309; F. Rose-Munch, E. Rose, A. Semra, C. Bois, *ibid.* **1989**, *363*, 103–121.

[18] a) Review: D. N. Kursanov, Z. N. Parnes, N. M. Loim, *Synthesis* **1974**, 633; b) M. F. Semmelhack, J. Bisaha, M. Czarny, *J. Am. Chem. Soc.* **1979**, *101*, 768–770.

[19] a) E. J. Corey, R. K. Bakshi, S. Shibata, *J. Am. Chem. Soc.* **1987**, *109*, 5551–5553; b) E. J. Corey, R. K. Bakshi, S. Shibata, C. P. Chen, V. K. Singh, *ibid.* **1987**, *109*, 7925–7926; b) We have found that the enantioselectivity of the Corey–Bakshi–Shibata (CBS) reduction of **14** as described in ref. [1] can even be increased (from 94 to 97% *ee*) if the $BH_3 \cdot Me_2S$ reagent is added slowly by means of a syringe pump.

[20] The *ee* values given were determined by ^{1}H NMR spectroscopy (with $Eu(hfc)_3$ in $CDCl_3$); **15** was employed as the acetate. The conversion of **15** into **6** (Scheme 4) was performed without recrystallization steps so that a possible (partial) racemization would have been recognized.

[21] A completely different strategic concept for the synthesis of (exclusively racemic) monohydroxycalamenenes also using arene–$Cr(CO)_3$ complexes for relative stereocontrol at the benzylic positions was followed by Uemura: a) M. Uemura, K. Isobe, K. Take, Y. Hayashi, *J. Org. Chem.* **1983**, *48*, 3855–3858; b) M. Uemura, K. Isobe, Y. Hayashi, *Chem. Lett.* **1985**, 91–94.

trans-Chelating Chiral Diphosphane Ligands Bearing Flexible *P*-Alkyl Substituents (AlkylTRAPs) and their Application to the Rhodium-Catalyzed Asymmetric Hydrosilylation of Simple Ketones

Masaya Sawamura, Ryoichi Kuwano, and Yoshihiko Ito*

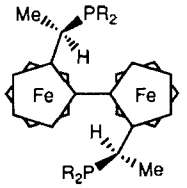
The design and synthesis of new chiral ligands for transition metals are essential for the development of catalytic asymmetric synthesis.[1, 2] We recently showed that the *trans*-chelating chiral diphosphane ligand PhTRAP (Fig. 1a)[3] is an excellent ligand for the rhodium-catalyzed asymmetric Michael addition of 2-cyanopropionates.[4] The concave chiral surroundings provided by the four Ph groups on the *trans*-positioned phosphorus atoms in the ligand are crucial for high enantioselectivity. Most chiral phosphane ligands to date were designed to bear bulky and conformationally rigid substituents such as Ph or cyclohexyl groups on the phosphorus atoms in order to force the resulting chiral environment to extend to the reaction site.[5] However, molecular modeling studies of TRAP–metal complexes suggested that the bulkiness and rigidity of the substituents on phosphorus atom are not always required for asymmetric reactions and may contribute negatively when the substituents are too large for the effective interaction of reactants and catalyst. This prompted us to synthesize new TRAPs bearing less bulky and more flexible alkyl substituents.

The new *trans*-chelating chiral peralkyldiphosphanes[6] (*R*,*R*)-(*S*,*S*)-*n*BuTRAP, -*n*PrTRAP, and -*i*PrTRAP (Fig. 1a), which bear different alkyl groups instead of the Ph groups of PhTRAP, were synthesized in four steps and in 25–34% overall yield from the readily available (*R*)-*N*,*N*-dimethyl-1-ferrocenylethylamine by essentially same procedure as that used for PhTRAP.[3] The X-ray crystal structure of *trans*-[RhCl(CO)-{(*R*,*R*)-(*S*,*S*)-*n*BuTRAP}] (Fig. 1b)[7] reveals that Rh has a nearly planar coordination geometry with a P-Rh-P bite angle of 164.4°. The conformation of the ligand is essentially C_2-symmetric, and the four *n*Bu groups are arranged in a C_{2v}-symmet-

[*] Prof. Dr. Y. Ito, Dr. M. Sawamura, R. Kuwano
Department of Synthetic Chemistry and Biological Chemistry
Faculty of Engineering, Kyoto University
Sakyo-Ku, Kyoto 606-01 (Japan)
Telefax: Int. code + (75)753-5668

 © VCH Verlagsgesellschaft mbH, D-69451 Weinheim, 1994 0570-0833/94/0101-0111 $ 10.00+.25/0

a



R = *n*Pr: (*R*,*R*)-(*S*,*S*)-*n*PrTRAP
R = *n*Bu: (*R*,*R*)-(*S*,*S*)-*n*BuTRAP
R = *i*Pr: (*R*,*R*)-(*S*,*S*)-*i*PrTRAP
R = Ph: (*R*,*R*)-(*S*,*S*)-PhTRAP

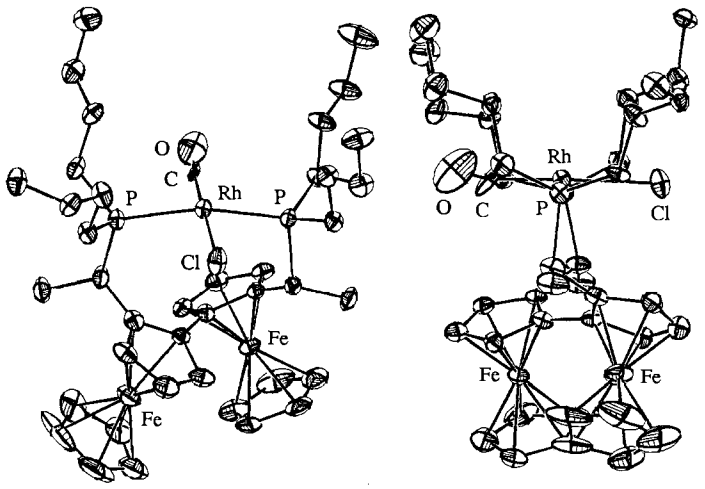
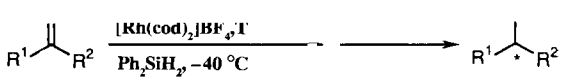


Fig. 1. a) The new (*R*,*R*)-(*S*,*S*)-TRAPs. b) ORTEP plots (two views) of the X-ray crystal structure of *trans*-[RhCl(CO){(*R*,*R*)-(*S*,*S*)-*n*BuTRAP}] (ellipsoids at the 30% probability level). The structure with 0.55 occupancy is shown. In the structure with 0.45 occupancy the Cl and CO ligands are interchanged.

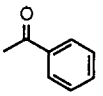
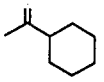
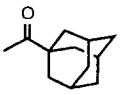
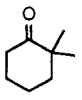
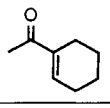
ric fashion with the exception of one of the four terminal carbon atoms (Fig. 1b). The torsion angle between the two linked Cp rings is 123°. The chloro and carbonyl groups on rhodium, which may be replaced by a prochiral substrate in a catalytic asymmetric reaction, are completely buried in the chiral cavity created by the biferrocenyl backbone and the *n*Bu groups, suggesting that the alkylTRAPs may display a high degree of chiral recognition.

Indeed, *n*PrTRAP and *n*BuTRAP were found to be excellent chiral ligands for the rhodium-catalyzed asymmetric hydrosilylation of simple ketones.[8, 9] Thus, to a solution of the catalyst precursor prepared in situ by mixing $[Rh(cod)_2]BF_4$ (0.01 mmol) (cod = cyclooctadiene) and (*R*,*R*)-(*S*,*S*)-TRAP (0.011 mmol) in THF or dimethoxyethane (DME) (1 mL) at room temperature, was added ketone (1.0 mmol) and diphenylsilane (1.5 mmol) at −40 °C. The mixture was stirred at this temperature until the reaction was complete, and the resulting silyl ether was then solvolyzed [Eq. (a)]. The *trans*-chelating ligands bearing prima-



ry alkyl groups on phosphorus atoms, *n*BuTRAP and *n*PrTRAP, were equally effective in the hydrosilylation of acetophenone (Table 1, runs 1, 2) in terms of both enantioselectivity (92% *ee*, *S*) and catalytic activity. This indicates that the terminal Me groups of *n*BuTRAP are not important for stereoselectivity. On the other hand, the reduction of acetophenone in the presence of *i*PrTRAP and PhTRAP, which carry bulkier substituents on the phosphorus atoms, was much less

Table 1. Asymmetric hydrosilylation of ketones catalyzed by TRAP–Rh complexes [a].

Run	Ketone	Ligand [b]	Time [h]	Yield [%] [c]	*ee* [%]	config. [d]
1		*n*BuTRAP	11	88 [f]	92 [j]	*S*
2		*n*PrTRAP	5	89 [f]	92 [j]	*S*
3		*i*PrTRAP	48	78 [f]	1 [j]	*S*
4		PhTRAP	9	85 [f]	15 [j]	*S*
5 [e]		*n*BuTRAP	10	62 [g]	80 [k]	*S*
6		*n*BuTRAP	48	92 [g]	91 [k]	*S*
7						
8			12	71 [g, i]	95 [j]	*S*

[a] Reactions were carried out in THF unless otherwise noted. The mol ratio $[Rh(cod)_2]BF_4$/TRAP/ketone/Ph_2SiH_2 was 1/1.1/100/150. [b] (*R*,*R*)-(*S*,*S*)-TRAP was used. [c] No starting material was recovered after workup; hydrosilylation was almost quantitative. [d] Determined by optical rotation. [e] DME was used as solvent. [f] Isolated yield by preparative thin-layer chromatography. [g] Isolated yield by medium-pressure liquid chromatography. [h] Isolated yield by bulb-to-bulb distillation. [i] Obtained with traces of 1-cyclohexylethanol, which seems to be produced during the methanolysis of the silyl ether. [j] Determined by GLC analysis of the alcohol with Chiraldex G-TA. [k] Determined by HPLC analysis of *N*-(3,5-dinitrophenyl)carbamate with Sumichiral OA-4500. [l] Determined by GLC analysis of trifluoroacetate with Chiraldex G-TA.

enantioselective (1% *ee*, *R*, and 15% *ee*, *S*, respectively; runs 3, 4). These results suggest that the chiral environment created by the *trans*-spanning biferrocenyl backbone of the ligands is the critical element for stereocontrol. *n*BuTRAP was also effective in the reduction of hindered saturated ketones (runs 5–7). Reaction of 1-acetylcyclohexene gave allylic alcohols with 95% *ee* accompanied by traces (<1% by gas-liquid chromatography (GLC)) of the 1,4-reduction product (run 8). To the best of our knowledge, *n*BuTRAP and *n*PrTRAP are the first chiral phosphane ligands effective for the rhodium-catalyzed asymmetric hydrosilylation of simple ketones lacking secondary coordinating functional groups.[8]

Received: August 6, 1993 [Z 6262 IE]
German version: *Angew. Chem.* **1994**, *106*, 92

[1] Reviews: a) *Catalytic Asymmetric Synthesis* (Ed.: I. Ojima), VCH, New York, **1993**; b) I. Ojima, N. Clos, C. Bastos, *Tetrahedron* **1989**, *45*, 6901–6939; c) R. Noyori, M. Kitamura in *Modern Synthetic Methods, Vol. 5* (Ed.: R. Scheffold), Springer, Berlin, **1989**, pp. 115–198.

[2] For examples of ligands having large bite angles see: a) B. M. Trost, D. L. Van Vranken, *Angew. Chem.* **1992**, *104*, 194–196; *Angew. Chem. Int. Ed. Engl.* **1992**, *31*, 228–230; b) B. M. Trost, D. L. Van Vranken, C. Bingel, *J. Am. Chem. Soc.* **1992**, *114*, 9327–9343.

[3] M. Sawamura, H. Hamashima, Y. Ito, *Tetrahedron Asymmetry* **1991**, *2*, 593–596.

[4] M. Sawamura, H. Hamashima, Y. Ito, *J. Am. Chem. Soc.* **1992**, *114*, 8295–8296.

[5] Chiral phospholane ligands developed in the past few years: a) M. J. Burk, J. E. Feaster, R. L. Harlow, *Organometallics* **1990**, *9*, 2653–2655; b) M. J. Burk, R. L. Harlow, *Angew. Chem.* **1990**, *102*, 1511–1513; *Angew. Chem. Int. Ed. Engl.* **1990**, *29*, 1462–1464; c) M. J. Burk, J. E. Feaster, R. L. Harlow, *Tetrahedron Asymmetry* **1991**, *2*, 569–592; d) M. J. Burk, *J. Am. Chem. Soc.* **1991**, *113*, 8518–8519; e) M. J. Burk, J. E. Feaster, *ibid.* **1992**, *114*, 6266–6267; f) *Tetrahedron Lett.* **1992**, *33*, 2099–2102.

 © VCH Verlagsgesellschaft mbH, D-69451 Weinheim, 1994

[6] General name for these diphosphanes: (*S,S*)-2,2″-bis[(*R*)-1-(dialkylphosphino)ethyl]-1,1″-biferrocene.

[7] *trans*-[RhCl(CO){(*R,R*)-(*S,S*)-*n*BuTRAP}] was prepared from $[RhCl(CO)_2]_2$ and (*R,R*)-(*S,S*)-*n*BuTRAP: m.p. 222–225 °C (decomp); $[\alpha]_D^{20} = -760.1$ ($c = 0.321$ in $CHCl_3$); ^1H NMR (200 MHz, $CDCl_3$, TMS) $\delta = 0.81-1.00$ (m, 12H), 1.10–2.38 (m, 30H), 2.88 (quint., $J = 7$ Hz, 1H), 3.08 (quint., $J = 7$ Hz, 1H), 4.03–4.09 (m, 2H), 4.28 (s, 5H), 4.31 (s, 5H), 4.35–4.45 (m, 4H); $^{31}P\{^1H\}$ NMR (81 MHz, $CDCl_3$, 85% H_3PO_4) $\delta = 27.27$ (dd, $^2J(P,P) = 341$, $^1J(P,Rh) = 119$ Hz), 32.56 (dd, $^2J(P,P) = 341$, $^1J(P,Rh) = 119$ Hz). Orange crystals for the X-ray crystal structure were grown from CH_2Cl_2/EtOH by solvent diffusion techniques; crystal data: orthorhombic, $P2_12_12_1$ (no. 19), $a = 13.74(1)$, $b = 23.34(2)$, $c = 12.96(1)$ Å, $V = 4158(7)$ Å^3, $Z = 4$, $\lambda(Mo_{K\alpha}) = 0.71073$ Å; MAC Science MXC3 diffractometer. The structure was solved by direct methods and by Fourier synthesis using the Crystan-GM program package. The atoms of disordered chloro and carbonyl ligands were located at positions defined by difference Fourier synthesis for 0.55/0.45 occupancy. Hydrogen atoms were not included in the calculation. R; $R_w = 0.069$; 0.066 for 4996 reflections. Further details of the crystal structure investigation are available on request from the Director of the Cambridge Crystallographic Data Centre, 12 Union Road, GB-Cambridge CB2 1EZ (UK), on quoting the full journal citation.

[8] The enantioselectivities in the asymmetric hydrosilylation of simple ketones lacking secondary coordinating functional groups catalyzed by chiral rhodium–phosphane complexes still remain at most about 60%, but high enantioselectivities over 80% are obtained with α- and γ-keto esters, see: a) I. Ojima, T. Kogura, M. Kumagai, *J. Org. Chem.* **1977**, *42*, 1671–1679; b) I. Ojima, T. Kogure, *Tetrahedron Lett.* **1974**, 1889–1892; c) I. Ojima, T. Kogure, M. Kumagai, S. Horiuchi, T. Sato, *J. Organomet. Chem.* **1976**, *122*, 83–97; d) K. Yamamoto, T. Hayashi, M. Kumada, *ibid.* **1973**, *54*, C45–C47; e) T. Hayashi, K. Yamamoto, K. Kasuga, H. Omizu, M. Kumada, *ibid.* **1976**, *113*, 127–137; f) for a review see I. Ojima, K. Hirai in *Asymmetric Synthesis, Vol. 5* (Ed.: J. D. Morrison), Academic Press, New York, **1985**, Chapter 4. For an intramolecular version see reference [5f].

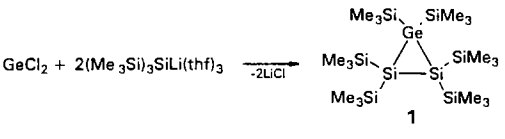
[9] High enantioselectivities have been achieved in the rhodium-catalyzed asymmetric hydrosilylation of simple ketones by using nitrogen-based chiral ligands: a) H. Brunner, R. Becker, G. Rieple, *Organometallics* **1984**, *3*, 1354–1359; b) H. Brunner, A. Kürzinger, *J. Organomet. Chem.* **1988**, *346*, 413–424; c) H. Brunner, U. Obermann, *Chem. Ber.* **1989**, *122*, 499–507; d) H. Brunner, P. Brandl, *J. Organomet. Chem.* **1990**, *390*, C81–C83; e) *Tetrahedron Asymmetry* **1991**, *2*, 919–930; f) S. Gladiali, L. Pinna, G. Delogu, E. Graf, H. Brunner, *ibid.* **1990**, *1*, 937–942; g) H. Nishiyama, H. Sakaguchi, T. Nakamura, M. Horihata, M. Kondo, K. Itoh, *Organometallics* **1989**, *8*, 846–848; h) H. Nishiyama, M. Kondo, T. Nakamura, K. Itoh, *ibid.* **1991**, *10*, 500–508; i) H. Nishiyama, S. Yamaguchi, M. Kondo, K. Itoh, *J. Org. Chem.* **1992**, *57*, 4306–4309; j) H. Nishiyama, S.-B. Park, K. Itoh, *Tetrahedron Asymmetry* **1992**, *3*, 1029–1034; k) H. Nishiyama, S. Yamaguchi, S.-B. Park, K. Itoh, *ibid.* **1993**, *4*, 143–150.

Synthesis and Structure of the Disilagermirane $R_2Ge(SiR_2)_2$ and the Solvent-Separated Ion Pair $[Li([12]crown-4)_2][GeR_3]$; (R = $SiMe_3$)**

Andreas Heine and Dietmar Stalke*

Up until the beginning of the 1980s three-membered ring systems of the heavier elements of group 14 were considered unobtainable, and in fact even today not many of these compounds are known. However, the use of very bulky ligands stabilizes these tricyclic systems kinetically and protects the reactive center with an organic layer. This prevents further reaction and dimerization. In 1981 Masamune et al.[1] isolated the unprecedented hexakis(2,6-dimethylphenyl)cyclotrisilane by reduction of dichlorobis(2,6-dimethylphenyl)silane with lithium naphthalenide. In a related reaction Weidenbruch et al.[2] obtained the even more sterically crowded hexa-*tert*-butylcyclotrisilane. Hexakis(2,6-dimethylphenyl)-[3] and hexa-*tert*-butylcyclotrigermane[4] have also been obtained by reductive cyclization of diorganodihalogengermanes with lithium naphthalenide. To date six cyclotrisilanes[1, 2, 5–7] and four cyclotrigermanes[3, 4] have been structurally characterized.[8] Recently Baines et al.[9] published the structure of the siladigermirane $Mes_2Si(GeMes_2)_2$, which was also synthesized by reductive cyclization.[10] Three-membered ring systems containing silicon have also been thoroughly investigated by MO calculations.[11–13]

We report here on the synthesis and structure of **1**, the first disilagermirane. Compound **1** was synthesized from germanium dichloride and tris(trimethylsilyl)silyllithium at −78 °C [Eq. (a)].[14, 15]



(a)

The reaction mechanism for the formation of **1** has not been confirmed unequivocally. It seems possible, however, that initially a germylene is formed intermediately by simultaneous LiCl elimination and migration of two Me_3Si groups. The $(Me_2Si)_2Ge$: then reacts with the intermediately formed disilene $(Me_3Si)_2Si{=}Si(SiMe_3)_2$ to give **1**. This seems feasible, since stable dialkylgermylenes have been synthesized and characterized previously.[16–18] This reaction provides a novel and easy access to mixed tricyclic ring systems containing heavier elements of group 14. We are currently trying to synthesize other derivatives from the reaction of $EHal_2$ (E = Ge, Sn, Pb; Hal = Cl, Br) with $(Me_3Si)_3ELi$ (E = Si, Ge, Sn).

Compound **1** has D_{3h} symmetry[19] (Fig. 1). The three ring atoms lie on a crystallographic mirror plane. A threefold axis is perpendicular to the mirror plane intersecting the center of the $GeSi_2$ triangle. This causes a disorder of the single germanium atom over all three ring positions; however the disorder could be solved and refined reasonable well. The site occupation factor of the Ge atom converged at 1/3. As expected the two exocyclic Ge–Si distances (235.6 pm) are shorter than the endocyclic Ge–Si distances (239.1 pm). This is also valid for the Si–Si distances (236.6 pm exocyclic, 237.7 pm endocyclic). The Si–Si and Si–Ge distances in the three-membered ring are consistent with the results of recently published ab initio calcula-

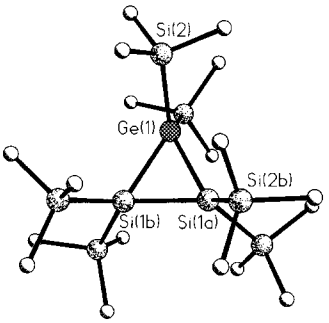


Fig. 1. Structure of **1** in the solid state. Selected bond lengths [pm] and angles [°]: Ge(1)-Si(2) 235.6(4), Ge(1)-Si(1a) 239.1(1), Si(1a)-Si(2b) 236.6(5), Si(1a)-Si(1b) 237.7(14); mean exocyclic Si-Si-Si angle 105.2(3), mean exocyclic Si-Ge-Si angle 105.8(3)°.

[*] Priv.-Doz. Dr. D. Stalke, Dr. A. Heine
Institut für Anorganische Chemie der Universität
Tammannstasse 4, D-37077 Göttingen (FRG)
Telefax: Int. code + (551)39-2582

[**] This work was supported by the Deutsche Forschungsgemeinschaft and the Fonds der Chemischen Industrie. We thank one of the referees for valuable comments.

tions.[12] In comparison, the endocyclic Si–Si distances in hexakis(2,6-dimethylphenyl)cyclotrisilane are 238 pm and 242 pm,[1] whereas in the sterically even more crowded hexa-*tert*-butylcyclotrisilane they are 251 pm.[2] The Ge–Ge bond lengths in $[(2,6\text{dimethylphenyl})_2\text{Ge}]_3$[3] and $(t\text{BuGe})_3$[4] are 254 pm and 256 pm, respectively.

In order to obtain, for example, hexakis(trimethylsilyl)-digermastannirane in analogy to the reaction described above, we synthesized tris(trimethylsilyl)germyllithium-([12]crown-4)$_2$ (**2**). The preparation of **2** [Eq. (b)][20] was carried out analogously to that of the silicon compound,[14, 15] the only difference being the presence of [12]crown-4.

$$(Me_3Si)_4Ge + MeLi \xrightarrow[2\text{ d stirring}]{[12]\text{crown-4}} \underset{\mathbf{2}}{[Li([12]\text{crown-4})_2][Ge(SiMe_3)_3]} + Me_4Si \qquad (b)$$

Compound **2** crystallizes as expected as a solvent-separated ion pair.[19] In Figure 2 only the structure of the $[Ge(SiMe_3)_3]$ anion is depicted. The mean Ge–Si bond length (236.7 pm) is in good agreement with the exocyclic Ge–Si bond in **1** (235.6 pm). The Ge–Si distance in $[Cp^*Cl_2HfGe(SiMe_3)_3]$ ($Cp^* = C_5Me_5$),[21] the only other known structurally characterized compound with this moiety, is 240.9 pm.

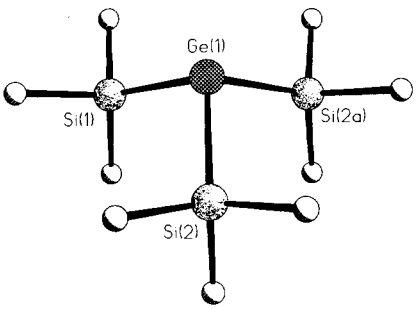


Fig. 2. Structure of the anion in **2**. Selected bond lengths [pm] and angles [°]: Ge(1)-Si(1) 236.6(1), Ge(1)-Si(2) 236.9(1); Si(1)-Ge(1)-Si(2) 102.66(3), Si(2)-Ge(1)-Si(2a) 100.53(4).

The most remarkable structural feature in the anion of **2** is the Si-Ge-Si angle (average of 101.6°; Ge1, Si1, and C2 lie on a crystallographic mirror plane, so that there are only two independent angles). This angle is more acute than the Si-Si-Si angle in the tris(trimethylsilyl)silyllithium derivatives $R_3SiLi(thf)_3$ (102.1°)[15] and $R_3SiLi\text{-}(dme)_{1.5}$ (104°),[22] (R = $SiMe_3$, dme = dimethoxyethane), which both crystallize as contact ion pairs. The reason for this is the increasing energetic separation of *ns* and *np* orbitals for the heavier elements of the group. This decreases the participation of electrons in s orbitals in σ bonds. Therefore, in the $[Ge(SiMe_3)_3]$ anion the three orthogonal p orbitals are chiefly used for bonding to the three Me_3Si substituents, whereas the lone pair possesses mainly s character. Recent investigations on $Ph_3SnLi(pmdeta)$[23] and $Ph_3PbLi(pmdeta)$,[24] (pmdeta = $(Me_2NCH_2CH_2)_2NMe$) show that with increasing atomic number this effect becomes more pronounced (C-E-C- angle in $Ph_3E\text{-}Li$; E = Sn: 96.1° and for E = Pb: 94.3°). The reduction in the Si-Ge-Si angle in the $[Ge(SiMe_3)_3]$ anion is even more remarkable, because the steric demand of a $(thf)_3Li$ group such as in $(Me_3Si)_3SiLi(thf)_3$ on the Si-Si-Si angle[25] as well as a (pmdeta)Li group such as in $Ph_3SnLi(pmdeta)$ and $Ph_3PbLi(pmdeta)$ on the C-Sn-C and C-Pb-C angles, respectively, are not applicable for the $[Ge(SiMe_3)_3]$ anion. The Si-Ge-Si angle in $(Me_3Si)_3GeLi(thf)_3$ should be even smaller for these reasons. In $Ge(pz)_3Na(thf)_3$ (pz = pyrazol-1-yl) the germanium atom is likewise not coordinated by the alkali metal, because the sodium atom is coordinated by the three pyrazolyl ligands, which decreases the N-Ge-N angle to 96.2°.[26]

Experimental Procedure

1: A solution of $GeCl_2$ (0,3 g, 2.1 mmol) in *n*-hexane (25 mL) was cooled to −78 °C and treated with $(Me_3Si)_3SiLi(thf)_3$ (2,0 g, 4.2 mmol). The solution was warmed to 0 °C and stirred for 12 h. The solvent was removed under reduced pressure (10^{-2} bar) and the solid residue taken up in *n*-pentane (25 mL). The insoluble components were filtered off and the solution was cooled to −90 °C. After 2 d colorless crystalline plates were obtained that were suitable for X-ray diffraction. Yield: 0.57 g (48%), decomposition at $T \geq 140$ °C. ^{1}H NMR (C_6D_6, 25 °C): $\delta = 0.43$ (s, 36H; $Si(SiMe_3)_2$), 0.45 (s, 18H; $Ge(SiMe_3)_2$); ^{29}Si NMR (C_6D_6, 25 °C): $\delta = -6.65$ ($Si(SiMe_3)_2$), −22.1 ($Ge(SiMe_3)_2$), −159.98 ($Si(SiMe_3)_2$; IR: $\tilde{\nu}$[cm^{-1}] = 1260 m, 1243 m, 1093 m, 1021 m, 838 vs; FI-MS: *m/z* (%): 568 (100) [M^+].

2: To a solution of (1.35 g, 3.7 mmol) $(Me_3Si)_4Ge$ in *n*-hexane (25 mL) was added [12]crown-4 (1.3 mL) and slowly methyllithium (2.5 mL, 4 mmol) in Et_2O. The white suspension was stirred for 24 h at room temperature and then THF (5 mL) was added to dissolve the white precipitate. The solution was stirred for an additional 24 h and subsequently stored at −35 °C. After approximately 7 d colorless needles were obtained that were suitable for X-ray diffraction. ^{1}H NMR ([D$_8$]toluene, 25 °C): $\delta = 0.27$ (s, $Ge(SiMe_3)_3$), 3.59 (s,$[O(CH_2)_2]_4$); ^{7}Li NMR ([D$_8$]toluene, 25 °C): $\delta = 0.27$ (s).

Received: May 26, 1993
Revised version: August 11, 1993 [Z 6048 IE]
German version: *Angew. Chem.* **1994**, *106*, 121

[1] S. Masamune, Y. Hanzawa, S. Murakami, T. Bally, J. J. Blount, *J. Am. Chem. Soc.* **1982**, *104*, 1150.
[2] A. Schäfer, M. Weidenbruch, K. Peters, H. G. von Schnering, *Angew. Chem.* **1984**, *96*, 311; *Angew. Chem. Int. Ed. Engl.* **1984**, *23*, 302.
[3] S. Masamune, Y. Hanzawa, D. J. Williams, *J. Am. Chem. Soc.* **1982**, *104*, 6136.
[4] M. Weidenbruch, F.-T. Grimm, M. Herrndorf, A. Schäfer, K. Peters, H. G. von Schnering, *J. Organomet. Chem.* **1988**, *341*, 335.
[5] J. C. Dewan, S. Murakami, J. T. Snow, S. Collins, S. Masamune, *J. Chem. Soc. Chem. Commun.* **1985**, 892.
[6] H. Watanabe, M. Kato, T. Okawa, Y. Nagai, M. Goto, *J. Organomet. Chem.* **1984**, *271*, 225.
[7] M. Weidenbruch, K. L. Thorn, S. Pohl, W. Saak, *J. Organomet. Chem.* **1987**, *329*, 151.
[8] Review: T. Tsumuraya, S. A. Batcheller, S. Masamune, *Angew. Chem.* **1991**, *103*, 916; *Angew. Chem. Int. Ed. Engl.* **1991**, *30*, 902.
[9] K. H. Baines, J. A. Cooke, N. C. Payne, J. J. Vittal, *Organometallics* **1992**, *11*, 1408.
[10] K. H. Baines, J. A. Cooke, *Organometallics* **1991**, *10*, 3419.
[11] W. W. Schoeller, T. Dabisch, *J. Chem. Soc. Chem. Commun.* **1985**, 1706.
[12] P. von R. Schleyer, A. F. Sax, J. Kalcher, R. Janoschek, *Angew. Chem.* **1987**, *99*, 374; *Angew. Chem. Int. Ed. Engl.* **1987**, *26*, 364.
[13] D. A. Horner, R. S. Grev, H. F. Schaefer III, *J. Am. Chem. Soc.* **1992**, *114*, 2093.
[14] H. Gilman, C. L. Smith, *J. Organomet. Chem.* **1967**, *8*, 245; *ibid.* **1968**, *14*, 91.
[15] A. Heine, R. Herbst-Irmer, G. M. Sheldrick, D. Stalke, *Inorg. Chem.* **1993**, *32*, 2694.
[16] D. G. Goldberg, D. H. Harris, M. F. Lappert, K. M. Thomas, *J. Chem. Soc. Chem. Commun.* **1976**, 261.
[17] P. B. Hitchcock, M. F. Lappert, S. J. Miles, A. J. Thorne, *J. Chem. Soc. Chem. Commun.* **1984**, 480.
[18] P. Jutzi, A. Becker, H. G. Stammler, B. Neumann, *Organometallics* **1991**, *10*, 1647.
[19] Crystal Data of **1**: $C_{18}H_{54}Si_8Ge$, $M = 567.9$, rhombohedral, space group $R\bar{3}c$, $a = b = 1051.4(1)$, $c = 5435.4(11)$ pm, $V = 5.203$ nm^3, $Z = 6$, $\varrho_{calcd} = 1.087$ Mg m^{-3}, $F(000) = 1836$, $\lambda = 71.073$ pm, $T = -120$ °C, $\mu(Mo_{K\alpha}) = 1.165$ mm^{-1}, crystal size: $0.5 \times 0.5 \times 0.3$ mm, $8° \leq 2\theta \leq 55°$; of the 3513 collected reflections 1339 were independent and used for refinement; largest difference peak and hole: 550 e nm^{-3}, $R1(F > 4\sigma(F)) = 0.028$ and $wR2 = 0.066$ (all data) with $R1 = \Sigma|F_o - F_c|/\Sigma F_o$ and $wR2 = (\Sigma w(F_o^2 - F_c^2)^2/\Sigma w(F_o^2)^2)^{0.5}$; **2**: $C_{25}H_{59}LiO_8Si_3Ge$, $M = 651.5$, monoclinic, space group $P2_1/m$, $a = 939.4(1)$, $b = 1433.5(2)$, $c = 1395.7(3)$ pm, $\beta = 104.56(1)°$, $V = 1.819$ nm^3, $Z = 2$, $\varrho_{calcd} = 1.189$ Mg m^{-3}, $F(000) = 700$, $\lambda = 71.073$ pm, $T = -80$ °C, $\mu(Mo_{K\alpha}) = 0.978$ mm^{-1}, crystal size: $0.5 \times 0.4 \times 0.4$, $8° \leq 2\theta \leq 55°$; of the 7864 reflections collected 4370 were independent and used for refinement, largest differ-

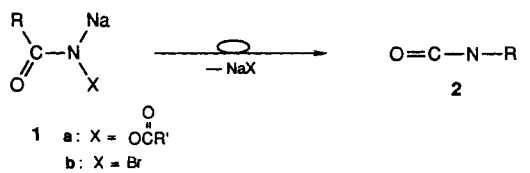
ence peak and hole: 310 e nm^{-3}, $R1$ ($F > 4\sigma(F)$) = 0.040 and $wR2$ = 0.095 (all data); R values as defined above. Data of both structures were collected on a Stoe-Siemens-AED diffractometer. The intensities of the rapidly cooled crystals in an oil drop [27] were collected by the $2\theta/\omega$ method. Both structures were solved by direct methods (SHELXS-90) [28] and refined by full-matrix least-squares on F^2 [29]. The silicon/germanium disorder in **1**, which is caused by symmetry could be resolved. The refinement of occupancy for the central silicon atoms and the germanium atom resulted in values of 2/3 and 1/3, respectively. The refinement in the space group $C2/c$ was not successful. Due to the disorder of the crown ether molecule caused by the mirror plane, two crown ether molecules with an occupancy of 1/2 each were refined. 1–2 and 1–3 distances of chemically equivalent bonds were refined by using distance restraints. Further details of the crystal structure investigations are available on request from the Director of the Cambridge Crystallographic Data Centre, 12 Union Road, GB-Cambridge CB2 1EZ (UK), by quoting the full journal citation.

[20] A. G. Brook, F. Abdesaken, H. Söllradl, *J. Organomet. Chem.* **1986**, *299*, 9.
[21] J. Arnold, D. M. Roddick, T. D. Tilley, A. C. Rheingold, S. J. Geib, *Inorg. Chem.* **1988**, *27*, 3510.
[22] G. Becker, H.-M. Hartmann, A. Münch, H. Riffel, *Z. Anorg. Allg. Chem.* **1985**, *530*, 29.
[23] D. Reed, D. Stalke, D. S. Wright, *Angew. Chem.* **1991**, *103*, 1539; *Angew. Chem. Int. Ed. Engl.* **1991**, *30*, 1459.
[24] D. R. Armstrong, M. G. Davidson, D. Moncrieff, D. Stalke, D. S. Wright, *J. Chem. Soc. Chem. Commun.* **1992**, 1413.
[25] A. Heine, D. Stalke, *Angew. Chem.* **1993**, *105*, 90; *Angew. Chem. Int. Ed. Engl.* **1993**, *32*, 121.
[26] A. Steiner, D. Stalke, *J. Chem. Soc. Chem. Commun.*, in press.
[27] T. Kottke, D. Stalke, *J. Appl. Crystallogr.* **1993**, *26*, 615.
[28] G. M. Sheldrick, *Acta Crystallogr. Sect. A* **1990**, *46*, 467.
[29] G. M. Sheldrick, SHELXL-93, Universität Göttingen, **1993**.

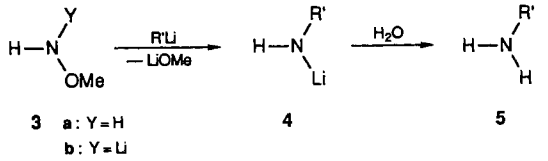
[(*N*-Lithio-*N*-mesitylsulfonyloxy-*tert*-butylcarbamate)$_2$·(thf)$_3$]: Crystal Structure of a Nitrenoid**

Gernot Boche,* Christiane Boie, Ferdinand Bosold, Klaus Harms, and Michael Marsch

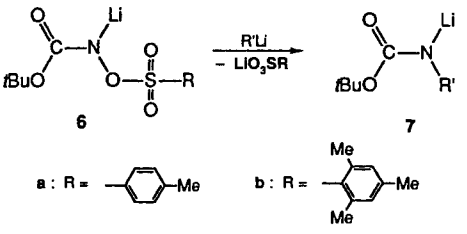
Nitrenoids **1** and their reactions have been known for a very long time. In 1872 Lossen described compounds of type **1a**,[1, 2a, b] which like compounds **1b**[2a, b, 3] prepared by Hofmann in 1881, are converted into isocyanates **2** by the shift of the R group to the N atom and α elimination of NaX.



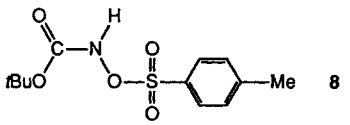
The observation made by Schverdina and Kotscheschkov in 1938 was particularly remarkable and long not understood: in the amination of organolithium compounds R'Li the *electrophilic* species is not *O*-methylhydroxylamine (**3a**) but rather the N-lithiated species **3b**. Primary amines **5** are then obtained via **4**.[4] The dimerization of a nitrenoid,[5] which proceeds analogously, and its α elimination to provide a nitrene[6] were also described. What are the structural requirements for these nitrenoid reactions?



One of the insights obtained from quantum chemical calculations of **3b** and its reaction with R'Li[7] was that the N–O bond in **3b** is bridged by Li and *longer* than the related bond in its nonlithiated counterpart **3a**. This would explain the relatively facile cleavage of the N–OCH$_3$ bond in **3b**[8] and the N–X bonds in other nitrenoids such as **1a,b**. In 1991 Genet, Mallart, Greck, and Piveteau showed that nitrenoids of type **6** are also suited for the electrophilic amination of R'Li to give **7**.[9] The corresponding Boc-protected primary amine is obtained from protonation of **7**.



We report here on the crystal structure of *N*-lithium *N*-mesitylsulfonyloxy-*tert*-butylcarbamate (**6b**), which crystallizes as a dimer with three equivalents of THF, and we compare this structure to that of the dimer of the nonlithiated *N*-toluenesulfonyloxy-*tert*-butylcarbamate (**8**). Compound **6b** is the first nitrenoid characterized by X-ray structure analysis.[10]



The two anions in [(**6b**)$_2$(thf)$_3$] (Fig. 1) are linked by two Li cations, such that Li1 (Li1A) is bound to N1A (N1) and O4 (O4A). The strong donor O4A prevents the bridging of, for example, the N1–O3 bond by Li1A. The two Li centers are tetracoordinate; each interacts with two terminal (O6, O6A) and one shared THF molecule (O7), an unusual type of THF coordination. It is amazing that the oxygen atoms O1 (O1A) and O2 (O2A) of the sulfonyloxy unit are not bound to lithium, considering their excellent donor properties.[11, 8] The shortening of the N1–C10 bond in [(**6b**)$_2$(thf)$_3$] to 133.1(4) pm relative to the analogous bond in (**8**)$_2$ (N1–C8, 140.6(7) pm, Fig. 2) and the lengthening of the C10–O4 bond in [(**6b**)$_2$(thf)$_3$] (123.9(4) vs. 120.6(7) pm for C8–O4 in (**8**)$_2$) are as expected. In [(**6b**)$_2$(thf)$_3$] C10 has planar coordination, in (**8**)$_2$ C8 (sum of angles 360.0 and 359.8°, respectively). O3 in [(**6b**)$_2$(thf)$_3$] is almost in the plane formed by N1, C10, O4, and O5 (torsion

[*] Prof. Dr. G. Boche, C. Boie, F. Bosold, Dr. K. Harms, M. Marsch
Fachbereich Chemie der Universität
D-35032 Marburg (FRG)

[**] This research was supported by the Deutsche Forschungsgemeinschaft (SFB 260) and the Fonds der Chemischen Industrie.

 © VCH Verlagsgesellschaft mbH, D-69451 Weinheim, 1994 0570-0833/94/0101-0115 $ 10.00+.25/0

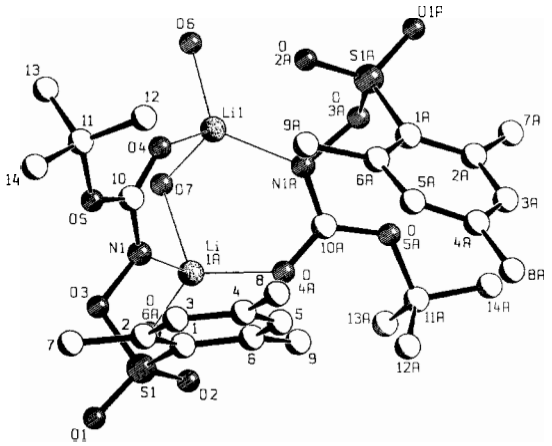


Fig. 1. Crystal structure of $[(\mathbf{6b})_2(thf)_3]$[11]; for clarity only the O atoms O6, O7, and O6A of the three THF molecules are shown; the C atoms are numbered. Important bond lengths [pm] and angles [°]: N1-O3 148.5(3), C10-N1 133.1(4), C10-O4 123.9(4), C10-O5 134.7(3), N1-Li1A 201.5(6), Li1-O4 189.5(5), Li1-O6 195.9(6), Li1-O7 215.9(6); N1-C10-O4 119.3(2), O4-C10-O5 123.0(5), O5-C10-N1 117.7(3); O3-N1-C10-O5 3.9(3), O3-N1-C10-O4 −176.1(2); Li1A-N1-C10-O4 −2.0(5).

angle O3-N1-C10-O5 3.9(3)°), whereas O3 in $(\mathbf{8})_2$ projects 46(2) pm out of the plane defined by N1, C8, O4, and O5. Dimer $(\mathbf{8})_2$ is held together by two hydrogen bonds (N1–H1 88(5) pm, H1–O4A 199.8(5) pm, N1–O4A 287.3(5) pm[19]). The following changes in bond lengths are important for the reactivity of **6b**: 1) C10–O5 in $[(\mathbf{6b})_2(thf)_3]$ is 5 pm longer than C8–O5 in $(\mathbf{8})_2$. Thus **6b** should eliminate LiO*t*Bu relatively easily to give

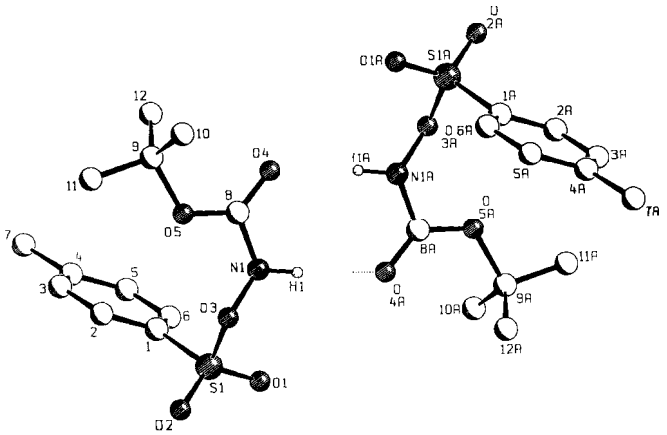


Fig. 2. Crystal structure of $(\mathbf{8})_2$[17]; the C atoms are numbered. Important bond lengths and distances [°]: N1-O3 142.3(5), C8-N1 140.6(7), C8-O4 120.6(7), C8-O5 129.7(6), N1-H1 88(5), H1-O4A 200(5), N1-O4A 287.3(5); N1-C8-O4 118.2(5), O4-C8-O5 129.8(5), O5-C8-N1 111.8(5), N1-H1-O4A 174.2(47); O3-N1-C8-O5 −23.9(6), O3-N1-C8-O4 160.5(4).

the corresponding isocyanate. The analogous formation of a ketene from Li ester enolates by elimination of LiOR is as well known as the corresponding lengthening of the C–OR bond in these compounds.[20] 2) The lengthening of the N1–O3 bond by 6.2 pm relative to that in the neutral compound $(\mathbf{8})_2$ has particular significance for the nitrenoid character of **6b**. This structural change is in accord with the remarkably facile substitution of the RSO_3^- group in **6b** (as well as other leaving groups X^- in nitrenoids) by R′Li, is supported by the previously mentioned calculations,[7] and is analogous to the results from studies on carbenoids $R_2C(Li)X$ (X = Hal, OR), for which the facile replacement of X^- by R′Li is also accompanied by the lengthening of the C–X bond.[8]

Experimental Procedure

$[(\mathbf{6b})_2(thf)_3]$: *N*-mesitylsulfonyloxy-*tert*-butylcarbamate (164 mg, 0.52 mmol) was dissolved in THF/pentane (2 mL, 1/1), cooled to −78 °C, and treated with *n*BuLi in hexane (0.33 mL, 1.6 M). After 48 h at −50 °C colorless prisms of $[(\mathbf{6b})_2(thf)_3]$ suitable for X-ray structure analysis had formed. Yield: 115 mg (52%).

$(\mathbf{8})_2$: A solution of *tert*-butyl-*N*-hydroxycarbamate (7.5 g, 56.5 mmol) and *p*-toluenesulfonic chloride (10.7 g, 56.5 mmol) in anhydrous diethyl ether (ca. 450 mL) at 0 °C was treated with a solution of triethylamine (7.9 mL, 0.1 mol) in anhydrous diethyl ether (5.0 mL). The reaction mixture was stirred for 30 min at 0 °C and the ammonium salt formed removed by filtration. The solvent was removed on a rotary evaporator and the resulting yellow solid washed with petroleum ether until it was colorless[21]. Recrystallization of the crude product from diethyl ether produced colorless crystals after four days at 20 °C that were suitable for X-ray structure analysis. Yield: 12.2 g (75%).

Received: September 1, 1993 [Z 6329 IE]
German version: *Angew. Chem.* **1994**, *106*, 90

[1] W. Lossen, *Justus Liebigs Ann. Chem.* **1872**, *161*, 347–362.
[2] Review: a) P. A. S. Smith in *Molecular Rearrangements* (Ed.: P. De Mayo), Interscience Publ., New York, **1962**, pp. 457–591; b) carbonylnitrenes: W. Lwowski in *Nitrenes* (Ed.: W. Lwowski), Interscience Publ., New York, **1970**, pp. 185–224; for more on sulfonylnitrenes see: D. S. Breslow in [2b]; pp. 245–303.
[3] A. W. Hofmann, *Chem. Ber.* **1881**, *14*, 2725–2736.
[4] a) N. I. Schverdina, Z. Kotsheschkov, *J. Gen. Chem. USSR Engl. Transl.* **1938**, *8*, 1825; b) more recent research: P. Beak, B. J. Kokko, *J. Org. Chem.* **1982**, *47*, 2822–2823; B. J. Kokko, P. Beak, *Tetrahedron Lett.* **1983**, *24*, 561–564; P. Beak, A. Basha, B. Kokko, *J. Am. Chem. Soc.* **1984**, *106*, 1511–1512; P. Beak, A. Basha, B. Kokko, D. Loo, *ibid.* **1986**, *108*, 6016–6023; c) for an excellent review of the electrophilic amination of "carbanions": E. Erdik, M. Ay, *Chem. Rev.* **1989**, *89*, 1947–1980.
[5] G. Boche, C. Meier, W. Kleemiss, *Tetrahedron Lett.* **1988**, *29*, 1777–1780.
[6] F. Bosold, G. Boche, W. Kleemiss, *Tetrahedron Lett.* **1988**, *29*, 1781–1784.
[7] a) G. Boche, H.-U. Wagner, *J. Chem. Soc. Chem. Commun.* **1984**, 1591–1592; b) D. R. Armstrong, R. Snaith, G. T. Walker, *ibid.* **1985**, 789–791; c) M. L. McKee, *J. Am. Chem. Soc.* **1985**, *107*, 859–864.
[8] We showed recently that the C–OR bond in α-lithiated ethers RCHLi–OR ("Li/OR carbenoids"), which also undergo R′/OR exchange, is also longer than the C–OR bond in the corresponding ethers: a) G. Boche, A. Opel, M. Marsch, K. Harms, F. Haller, J. C. W. Lohrenz, c. Thümmler, W. Koch, *Chem. Ber.* **1992**, *125*, 2265–2273; b) G. Boche, F. Bosold, J. C. W. Lohrenz, A. Opel, P. Zulauf, *ibid.* **1993**, *126*, 1873–1885; c) see also the analogous structure of a Li/Cl carbenoid: G. Boche, M. Marsch, A. Müller, K. Harms, *Angew. Chem.* **1993**, *105*, 1081–1082; *Angew. Chem. Int. Ed. Engl.* **1993**, *32*, 1032–1033.
[9] J. P. Genet, S. Mallart, C. Greck, E. Piveteau, *Tetrahedron Lett.* **1991**, *32*, 2359–2362.
[10] For the crystal structure analysis of chloramine-T (sodium *N*-chloro-4-methylbenzenesulfonamide) see: M. M. Olmstead, P. P. Power, *Inorg. Chem.* **1986**, *25*, 4057–4058. The N–Cl bond is not lengthened, and the Na^+ ion is not bound to the nitrogen atoms. Chloramine-T reacts like a nitrenoid with nucleophiles such as thioethers, but "chlorine" is also transferred. In addition chloramine-T is a strong oxidizing agent. b) Review: M. M. Campbell, G. Johnson, *Chem. Rev.* **1978**, *78*, 65–79.
[11] Crystallographic data for $[(\mathbf{6b})_2(thf)_3]$ ($C_{20}H_{32}LiNO_{6.5}S$, $M = 429.47$): orthorhombic, space group *Pbcn*, $a = 1182.5(2)$, $b = 2126.8(8)$, $c = 1859.7(4)$ pm, $Z = 8$, $\rho_{calc} = 1.220\ g\,cm^{-3}$, $\mu(Cu_{K\alpha}) = 1.530\ cm^{-1}$. Data recorded at 190 K with an Enraf-Nonius CAD4 diffractometer ($Cu_{K\alpha}$ radiation, $\lambda = 1.54187$ Å, graphite monochromator); 2939 measured independent reflections, solution by direct methods with the Siemens SHELXTL-PLUS (VMS) program package, refinement of F^2 with all data with SHELXL-93, $wR2 = 0.1727$ for all data, ($w = 1/[\sigma^2(F_o^2) + (0.1131\,P)^2 + 4.0929\,P]$) with $P = (F_o^2 + 2F_c^2)/3$; the conventional R value for 2701 reflections with $I > 2\sigma(I)$ was 0.0591; all non-hydrogen atoms were refined anisotropically, H atoms were refined as "riding" at calculated positions and with sets of common temperature factors. All calculations were conducted on a Micro-VAX II and a VAX 6000-420 [12–16].
[12] Siemens SHELXTL-PLUS (VMS), Version 4.21, Siemens Analytical X-Ray Instruments Inc., Madison, **1990**.
[13] A. L. Spek, PLATON 92, Program for Geometrical Analysis of Crystal Structures, Utrecht, **1992**.
[14] E. Keller, SCHAKAL-88B, A FORTRAN Program for the Graphic Representation of Molecular and Crystallographic Models, Freiburg, **1988**.
[15] G. M. Sheldrick, SHELXL-93, Program for Refinement of Crystal Structures, Göttingen, **1993**.

[16] Further details of the crystal structure investigations may be obtained from the Fachinformationszentrum Karlsruhe, D-76344 Eggenstein-Leopoldshafen (FRG) on quoting the depository numbers CSD-400302[11] and CSD-400303[17].

[17] Crystallographic data for $(\mathbf{8})_2$ ($C_{12}H_{17}NO_5S$, $M = 287.3$): monoclinic, space group $P2_1/c$, $a = 937.00(1)$, $b = 2047.8(1)$, $c = 810.3(1)$ pm, $\beta = 110.81(1)°$, $Z = 4$, $\rho_{calc} = 1.313\ g\,cm^{-3}$, $\mu(Cu_{K\alpha}) = 2.134\ cm^{-1}$. Data recorded at 263K with an Enraf-Nonius CAD4 diffractometer ($Cu_{K\alpha}$ radiation, $\lambda = 1.54178$ Å, graphite monochromator); 1694 measured reflections, of which 1494 were independent ($R_{int} = 0.0694$), 1329 with $F > 4\sigma(F)$ were considered observed. Solution by direct methods and refinement of F with the Siemens SHELXTL-PLUS (VMS) program package, $R = 0.0573$, $wR = 0.0640$ ($w = 1/\sigma^2(F)$); all non-hydrogen atoms were refined anisotropically, "aromatic" H atoms and N–H were found, the other H atoms were placed at calculated positions. All calculations were conducted on a Micro-VAXII and a VAX 6000-420[12–16].

[18] a) G. Boche, *Angew. Chem.* **1989**, *101*, 286–306; *Angew. Chem. Int. Ed. Engl.* **1989**, *28*, 277–297; b) F. Bosold, P. Zulauf, M. Marsch, K. Harms, J. C. W. Lohrenz, G. Boche, *ibid.* **1991**, *103*, 1497–1499 and **1991**, *30*, 1455–1457.

[19] The crystallographically determined N–H distances in hydrogen bonds are always too short (by ca. 12 pm) such that the H1–O4A distance here is too long: R. Taylor, O. Kennard, *Acta Crystallogr. Sect. B* **1983**, *39*, 133–138.

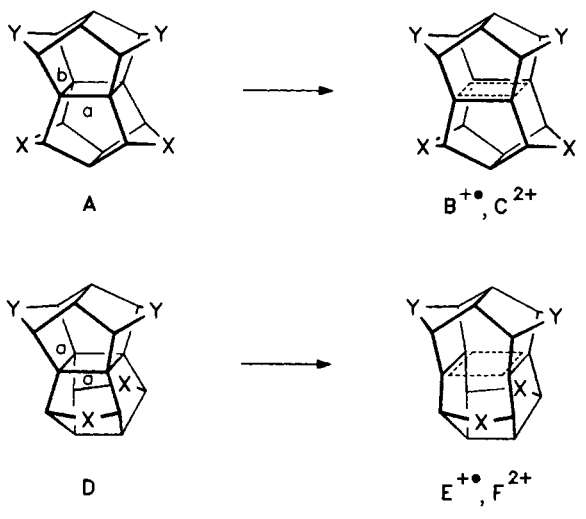
[20] D. Seebach, R. Amstutz, T. Laube, W. B. Schweizer, J. D. Dunitz, *J. Am. Chem. Soc.* **1985**, *107*, 5403–5409.

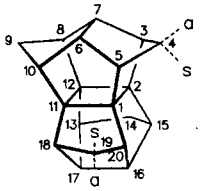
[21] In analogy to the preparation of *O*-(mesitylsulfonyl)hydroxylamine by J. G. Krause, *Synthesis* **1972**, 140.

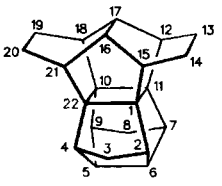
Isopagodanes—Precursors of Unusual Cage Ions**

Markus Wollenweber, Rolf Pinkos, Jürgen Leonhardt, and Horst Prinzbach*

The highly strained, polycyclic pagodanes **A** have a high preparative potential, notably as intermediates in the synthesis of dodecahedranes[1] and of the unusual radical cations **B** and dications **C**.[2] The "isopagodanes" **D**[4] were expected to contribute significant information for the quantitative evaluation of the factors responsible for the nature and extent of the transannular electron delocalization (σ-homoaromaticity[2, 3]) in these cage ions. By rotating the two "halves" of the molecules by 90° with respect to each other, D_{2d} symmetry is enforced in the [1.1.1.1] and [2.2.2.2] skeletons (X = Y = CH_2 and $(CH_2)_2$, respectively). A favorable structure is thus provided for the formation of the corresponding ions **E** and **F** in potentially square configurations. According to calculations, the analogous ions **B**/**E** and **C**/**F** should differ considerably with regard to the influence exerted by the bridges X and Y on stability and nature of bonding.[5, 6] We report here on a versatile approach to the synthesis of compounds of type **D** and, in particular, on the preparation of the parent [1.1.1.1] and [2.2.1.1] skeletons **1** and **2**.[7] Compounds **1** and **2** are expected to resemble the pagodane analogues[1] as far as strain energy and rigidity as well as high thermal stability are concerned. MMX calculations predict strain energies for **1** and **2** of 113.8 and 103.6 kcal mol^{-1}, respectively.




1


2

As can be seen from Scheme 1, our original conceptual approach to the construction of isopagodanes **L** → **D**, subdivided into three stages, had been designed in close analogy with the optimized pagodane route **G** → **A**.[8] The prerequisites were seemingly fulfilled when dienes of type **G** (including isodrin) could be "metathesized" efficiently to give dienes **L**. However, an a priori analysis of the individual steps had to take into consideration that the frameworks **L** and **M**, in contrast to **G** and **H**, are conformationally mobile. Even in the favored "closed" conformations the distance between the π systems in **L** and **M** is larger than in **G** and **H**.[4] The chances of success in the two key steps—the benzo/benzo photocycloaddition **M** → **N** and the domino Diels–Alder addition **N** → **O**—were further jeopardized by the fact that very minor structural changes, X = $(CH_2)_2$ for example, are sufficient to prevent the model reaction **H** → **I** from taking place.[4, 9] Moreover, **N** could not be expected to have the high structure-specific kinetic stability of the *syn-o,o'*-dibenzo compound **I** (X = CH_2, $\Delta H^{\neq}(206\,°C) = 37.8$ kcal mol^{-1}; $\Delta S^{\neq} = 2.9$ cal mol^{-1} K^{-1})[10], which was essential for step **I** → **K**.

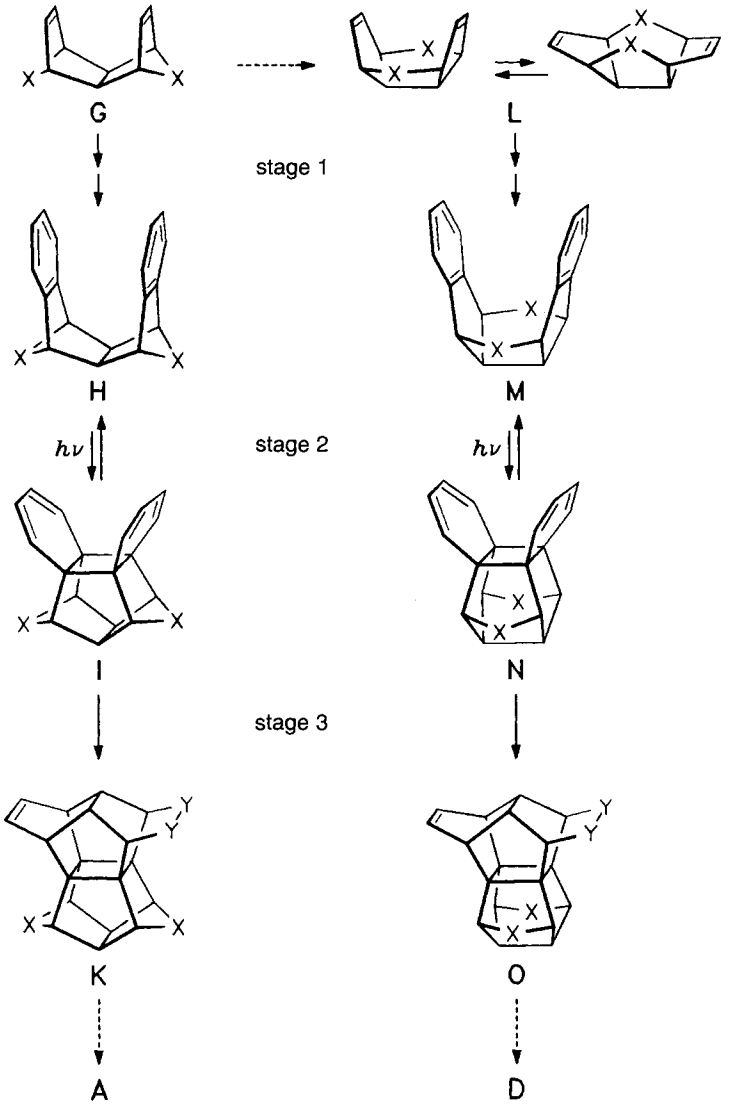
Experimentally, the analogy to the pagodane route did indeed end with the attempt to bring about photochemical four-membered ring formation in the dibenzo compound **3** (**M**, X = CH_2)[4] to give **4**. Compound **3** remained unchanged under widely varied conditions of direct irradiation (with poly- and monochromatic light) and sensitized irradiation. No adduct (e.g. **6**) was detected on irradiation at low temperatures (−70 °C) in the presence of 4-methyl-1,2,4-triazoline-3,5-dione. Equilibration of **3** with **4** as a very low-percentage equilibrium component was thus thought to be unlikely, especially in view of the fact that the photoadduct in the photoequilibrium **H** ⇌ **I** (X = CH_2, 7:3) was trapped almost quantitatively by use of the above reagent.[9]

Eventually, a way out of this dilemma was found with the reaction sequence **3** → **[5]** → **7** → **9** → **11(12)** → **4** (Scheme 2)—

[*] Prof. Dr. H. Prinzbach, Dr. M. Wollenweber, Dr. R. Pinkos, J. Leonhardt
Chemisches Laboratorium der Universität
Institut für Organische Chemie und Biochemie
Albertstrasse 21, D-79104 Freiburg (FRG)
Telefax: Int. code + (761) 203-5987

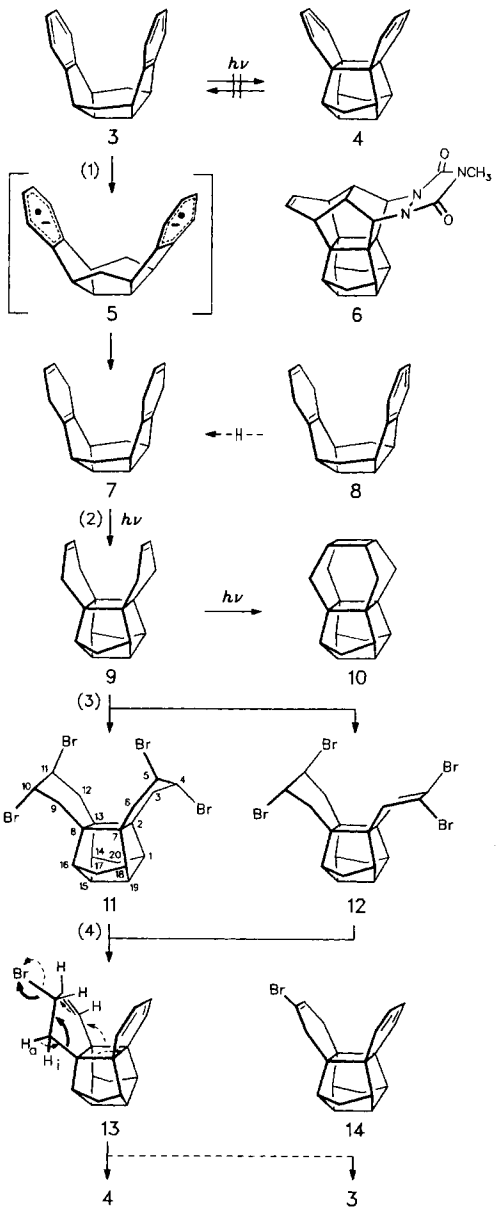
[**] This work was supported by the Deutsche Forschungsgemeinschaft, the Fonds der Chemischen Industrie, and BASF AG. We thank Dr. D. Hunkler and Dr. J. Wörth for recording the NMR and mass spectra, Priv.-Doz. Dr. R. Schwesinger and Dipl.-Chem. R. Link for their help regarding the use of the new phosphazene bases, and G. Leonhardt-Lutterbeck for competent technical assistance.

 © VCH Verlagsgesellschaft mbH, D-69451 Weinheim, 1994 0570-0833/94/0101-0117 $ 10.00+.25/0



Scheme 1.

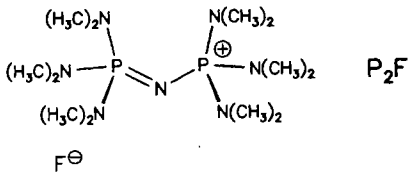
the transannular four-membered ring formation was brought about through a geometrically less demanding $[2_\pi + 2_\pi]$ photocycloaddition. The double Birch reduction of **3** to **7** (possibly via the diradical anion **5**), which had failed in the case of the dibenzo analogue **H**[11] (X = CH_2; the distance between the two benzene rings is here shorter than in **3**), was achieved in the presence of very high ethanol concentrations; however, overreduction of **3** was unavoidable. A procedure was provisionally adopted by which the reaction was stopped at around 90% conversion. After chromatographic separation **7** was then isolated in approximately 65% yield [with respect to converted **3**, colorless crystals, UV (*n*-hexane): $\lambda_{max}(\varepsilon) = 198$ nm (7520), $\varepsilon_{254} \approx 1$]. Byproduct **8** was not reduced to **7** when subjected to analogous conditions. However, dehydrogenation of **8** back to **3** by irradiation in acetone (Solidex filter, high-pressure Hg lamp, 0 °C) or, preferably, by reaction with 2,3-dichloro-5,6-dicyano-1,4-benzoquinone (DDQ) proved possible, thus allowing **8** to be recycled. A selective $[2_\pi + 2_\pi]$ cycloaddition of **7** to give **9** could not be effected by using carbonyl-containing sensitizers with various triplet energies; dehydrogenation providing **8** and **3** was the main reaction observed with acetone, xanthone, or benzophenone. On irradiation in benzene the addition **7** → **9** did take place, but the following step **9** → **10** was comparatively rapid, and some dehydrogenation also occurred. Direct irradiation with monochromatic 254-nm light proved to be more selective despite the fact that **7** has a low extinction coefficient at this wavelength; the reaction was stopped at around 90% conversion, because polymerization became increasingly detractive with longer reaction times. After chromatographic separation from the relatively small quantities of **8** and **10**, cycloadduct **9** [λ_{max}(*n*-hexane) = 196 nm (ε = 6170)] was isolated in 74% yield (with respect to reacted **7**). Titration with bromine resulted in quantitative addition to give an approximately 1:1 mixture of tetrabromides **11** (C_2) and **12** (C_s), which was used in the next step without further purification. Transannular Br_2 addition was obviously not competing. Fears that the kinetic instability of pho-

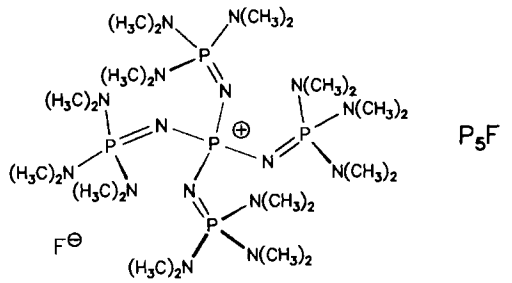


Scheme 2. (1) 150 mL NH_3, 600 mg (2.32 mmol) **3** in 64 mL ether and 34 mL (580 mmol) ethanol, 4.53 g (650 mmol) Li, −78 °C, 1 h, 12% **3**, 58% **7**, 12% 4,5-dihydro-**7**, 12% **8**; (2) 835 mg (3.18 mmol) **7**, 250 mL cyclohexane, Rayonet reactor (254 nm), 3.5 h, 12% **8**, 12% **7**, 6% **10**, 65% **9**; (3) 0.1 M Br_2 solution in CH_2Cl_2, −78 °C, 100%; (4) 2.46 g (2.59 mmol) 80% P_2F in 10 mL THF, 164 mg (0.28 mmol) **11**/**12** in 6 mL THF, N_2 atmosphere, −78 °C, 1 h, up to 80% **4**.

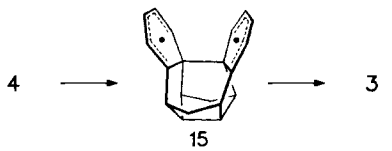
 © VCH Verlagsgesellschaft mbH, D-69451 Weinheim, 1994 0570-0833/94/0101-0118 $ 10.00+.25/0

toadducts of type **N** might lead to complications in step **11/12** → **4** with its multiple HBr eliminations proved to be well justified. The necessary temperatures were either too high (potassium *tert*-butoxide/dimethyl sulfoxide (DMSO), 1,5-diazabicyclo[4.3.0]non-5-ene (DBN)/THF), or other elimination pathways leading back to **3** or to **14** were favored (*tert*-butyl-P_4 base,[12] −78 °C). A breakthrough was accomplished with the "naked" fluoride recently developed by Schwesinger et al.;[13] under these conditions **4** was formed rapidly even at −78 °C. By using carefully prepared batches of base (2.3 equivalents P_5F or P_2F per HBr), **4** could be secured reproducibly on a gram scale in yields of up to 80% besides **3**. It was established that **3** does not arise from





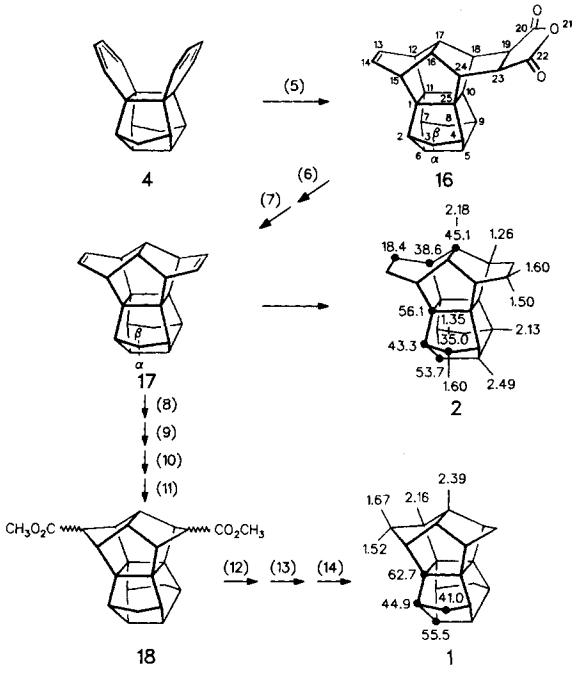
4; a plausible mechanism is a competing 1,8-HBr-(*cis*)-elimination in **13**. The thermally labile compound **4** could be purified by rapid chromatography on deactivated silica gel. Evidence for the C_{2v} symmetry of **4** includes the six signals observed in its ^{1}H NMR spectrum. The UV spectrum (*n*-hexane) with $\lambda_{max}(\varepsilon) = 292$ nm (2570) confirms the presence of the σ-coupled tetraene chromophore. Upon treatment with acid, irradiation (with 254-nm light instantaneously; with 350–400-nm light within hours), and upon heating in benzene, **4** was smoothly converted into **3** [$t_{1/2}$(24 °C) = 32.7 h, $t_{1/2}$(44 °C) = 97.5 min, $t_{1/2}$(50 °C) = 26.2 min; $E_a = 23.9 \pm 1.5$ kcal mol^{-1}]. The activation energy for this cleavage, in good agreement with the enthalpy of formation calculated for the intermediate diradical **15** (Scheme 3,



Scheme 3. The enthalpies of formation ΔH_f° for **4**, **15**, and **3** derived from MM2 calculations are 112.5, 133.0, and 37.7 kcal mol^{-1}, respectively.

MM2),[4] is approximately 10 kcal mol^{-1} less than the value quoted above for the **I** isomer and comparable with the fragmentation barriers of *syn*- and *anti*-*o*,*o*'-dibenzene (E_a = 26.7 and 24.8 kcal mol^{-1}, respectively).[14]

The addition of maleic anhydride (MA) to **4** provides the entry into the third stage of our synthesis (Scheme 4). Because of the limits set by the lability/reactivity of the reactants, the following procedure was adopted: The fluoride base was extracted from the crude solution from the HBr elimination step (mixture of **4** and **3**). The solution was concentrated in vacuo below room temperature and the solid residue mixed thoroughly with approximately 30 equivalents of freshly sublimed, finely ground MA. After rapid heating to 100 °C the domino adduct **16** formed in yields of 50–60% (based on **11/12**) was separated from **3** without loss of material; no adduct other than **16** could be detected (TLC, ^{1}H NMR). The oxidative degradation of **16** to give the [2.2.1.1]isopagodadiene **17** turned out to be problematic. A yield of only a few percent was obtained under the conditions optimized for the pagodane route. However, with a modified two-step procedure the yield was increased to 70–75%. The catalytic hydrogenation of **17** to give the parent [2.2.1.1] skeleton **2** and the twofold ring contraction **17** → **18** proceeded as expected.[8] Nearly equal proportions of the three possible methyl esters **18** emerged from the photo-Wolff rearrangement in methanol/CH_2Cl_2; the final protonation at C-4(9) of the intermediate ketene is clearly not sterically controlled. In a deviation from the model reaction scheme[8] the ester was converted into **1** according to the method of Barton et al.[16] (The overall yield for the sequence of saponification, formation of the acid chloride, esterification, and thermolysis approached ca. 50%.)



Scheme 4. (5) Molten MA, 100 °C, 15 min, 22% **3**, 50–60% **16**; (6) KOH, methanol/H_2O (1:1), reflux, 1 h, 100%; (7) Cu_2O, 2,2'-dipyridyl, quinoline a) room temperature, 7 d, b) 185 °C, 17 h, 72% **17**; (8) BH_3·THF, 25 °C, 4 h; NaOH, H_2O_2, 25 °C, 18 h, 100% crude product; (9) CrO_3, acetone, H_2SO_4, 25 °C, 1 h, 56%; (10) NaH, THF, HCO_2CH_3, methanol (cat.), 25 °C, 22 h; glacial acetic acid, 4-methylphenylsulfonylazide, triethylamine, CH_2Cl_2, 25 °C, 30 h, 52%; (11) methanol/CH_2Cl_2 (10:1), high-pressure Hg lamp, Duran filter, 25 °C, 45 min, 98% **18**; (12) KOH, ethanol, H_2O, reflux 3 h, 72%; (13) oxalyl chloride, dimethylformamide (DMF), toluene, 100%; (14) sodium mercaptopyridine-1-oxide, 4-dimethylaminopyridine (DMAP), *tert*-butylthiol, toluene, reflux, 3 h, 68% **1**. – The numbers shown on the skeletons of **1** and **2** are the ^{1}H and ^{13}C NMR chemical shifts (δ values).

The four (8:4:4:4) ^{1}H NMR and four ^{13}C NMR signals confirm the D_{2d} symmetry of **1**. The H,H coupling constants ($J_{3,4a} \approx J_{3,4s} \approx 1$, $J_{4a,4s} = 10.0$, $J_{3,7} \approx 4$ Hz) are generally somewhat smaller than the calculated values (MM2). The smaller

 © VCH Verlagsgesellschaft mbH, D-69451 Weinheim, 1994 0570-0833/94/0101-0119 $ 10.00+.25/0

chemical shifts observed for the carbon atoms of the cyclobutane ring in **2** point to the (calculated) reduction in strain.

The colorless crystals of **2** melt at 198 °C without decomposition, those of **1** at 90–92 °C. In the mass spectra of **1** and **2** a dominant molecular ion peak and only weak fragmentation peaks are observed.

The key step in the synthesis of pagodanes, the benzo/benzo photocycloaddition, exhibits a very subtle dependency on structure. For that reason it was necessary to modify the original synthetic scheme for the isopagodanes, which had been designed by direct analogy with the pagodane route. The reaction sequence described above, which starts from **3** (and thus originally from isodrin) and leads to the parent [2.2.1.1]- and [1.1.1.1]isopagodane skeletons, can also be applied to the synthesis of functionalized derivatives. Preliminary results from electrochemical and ESR studies are stimulating in that they reveal one of the astonishing peculiarities of the isopagodane series: In line with calculations,[6] **2** undergoes two-electron oxidation via a cyclically delocalized radical cation **E** to give a dication **F**, which is persistent enough to allow observation of the two-electron reduction.[5, 17]

Received: July 23, 1993 [Z 6161 IE]
Publication delayed on authors' request.
German version: *Angew. Chem.* **1994**, *106*, 84

[1] W.-D. Fessner, H. Prinzbach (*The Pagodane Route to Dodecahedranes*) in *Cage Hydrocarbons* (Ed.: G. A. Olah), Wiley, New York **1990**, p. 353; G. Lutz, R. Pinkos, B. A. R. C. Murty, P. R. Spurr, W.-D. Fessner, J. Wörth, H. Fritz, L. Knothe, H. Prinzbach, *Chem. Ber.* **1992**, *125*, 1741; J.-P. Melder, R. Pinkos, H. Fritz, J. Wörth, H. Prinzbach, *J. Am. Chem. Soc.* **1992**, *114*, 10213; R. Pinkos, J.-P. Melder, K. Weber, D. Hunkler, H. Prinzbach, *ibid.* **1993**, *115*, 7173.

[2] H. Prinzbach, B. A. R. C. Murty, W.-D. Fessner, J. Mortensen, J. Heinze, G. Gescheidt, F. Gerson, *Angew. Chem.* **1987**, *99*, 488; *Angew. Chem. Int. Ed. Engl.* **1987**, *26*, 457; T. Drewello, W.-D. Fessner, A. J. Kos, C. B. Lebrilla, H. Prinzbach, P. von R. Schleyer, H. Schwarz, *Chem. Ber.* **1988**, *121*, 187; G. K. Surya Prakash, V. V. Krishnamurthy, R. Herges, R. Bau, H. Yuan, G. Olah, W.-D. Fessner, H. Prinzbach, *J. Am. Chem. Soc.* **1988**, *110*, 7764.

[3] K. Weber, H. Prinzbach, R. Schmidlin, F. Gerson, G. Gescheidt, *Angew. Chem.*, **1993**, *105*, 907; *Angew. Chem. Int. Ed. Engl.* **1993**, *32*, 875.

[4] G. Sedelmeier, W.-D. Fessner, R. Pinkos, C. Grund, B. A. R. C. Murty, D. Hunkler, G. Rihs, H. Fritz, C. Krüger, H. Prinzbach, *Chem. Ber.* **1986**, *119*, 3442; B. A. R. C. Murty, P. R. Spurr, R. Pinkos, C. Grund, W.-D. Fessner, D. Hunkler, H. Fritz, W. R. Roth, H. Prinzbach, *Chimia* **1987**, *41*, 32; J.-P. Melder, F. Wahl, H. Fritz, H. Prinzbach, *ibid.* **1987**, *41*, 426.

[5] M. Wollenweber, Dissertation, Universität Freiburg, **1993**.

[6] R. Herges, H. Neumann, W.-D. Fessner, H. Prinzbach, unpublished.

[7] The new compounds were characterized by elemental analyses and by spectroscopic data (^{1}H NMR, ^{13}C NMR, IR, and MS). Names and numbering for the polycycles were generated using the POLCYC program written by G. Rücker and C. Rücker (*Chimia* **1990**, *44*, 116).

[8] W.-D. Fessner, G. Sedelmeier, P. R. Spurr, G. Rihs, H. Prinzbach, *J. Am. Chem. Soc.* **1987**, *109*, 4626; J.-P. Melder, H. Prinzbach, *Chem. Ber.* **1991**, *124*, 1271.

[9] M. Wollenweber, D. Hunkler, M. Keller, L. Knothe, H. Prinzbach, *Bull. Soc. Chim. Fr.* **1993**, *130*, 32.

[10] W. von E. Doering, W. R. Roth, R. Breuckmann, H. J. Figge, L. Figge, H. W. Lennartz, W.-D. Fessner, H. Prinzbach, *Chem. Ber.* **1988**, *121*, 1.

[11] R. Thiergardt, M. Keller, M. Wollenweber, H. Prinzbach, *Tetrahedron Lett.*, **1993**, *21*, 3397.

[12] R. Schwesinger, H. Schlemper, *Angew. Chem.* **1987**, *99*, 1212; *Angew. Chem. Int. Ed. Engl.* **1987**, *26*, 1164; R. Schwesinger, *Nachr. Chem. Techn. Lab.* **1990**, *38*, 1214.

[13] R. Schwesinger, R. Link, G. Thiele, H. Rotter, D. Honert, H.-H. Limbach, F. Männle, *Angew. Chem.* **1991**, *103*, 1376; *Angew. Chem. Int. Ed. Engl.* **1991**, *30*, 1372.

[14] J. F. M. Oth, H. Röttele, G. Schröder, *Tetrahedron Lett.* **1970**, *11*, 61; J. A. Berson, R. F. Davis, *J. Am. Chem. Soc.* **1972**, *94*, 3658; N. C. Yang, T. Noh, H. Gan, S. Halfon, B. J. Hrnjez, *ibid.* **1988**, *110*, 5919.

[15] W.-D. Fessner, C. Grund, H. Prinzbach, *Tetrahedron Lett.* **1989**, *30*, 3133; F.-G. Klärner, U. Artschwager-Perl, W.-D. Fessner, C. Grund, R. Pinkos, J.-P. Melder, H. Prinzbach, *ibid.* **1989**, *30*, 3137; T. Otten, H. Müller-Bötticher, D. Hunkler, H. Fritz, H. Prinzbach, *ibid.* **1992**, *33*, 4153.

[16] D. H. R. Barton, D. Crich, W. B. Motherwell, *Tetrahedron* **1985**, *41*, 3901.

[17] Unpublished research in collaboration with Prof. Dr. J. Heinze and A. Forsthuber (Freiburg, Germany) as well as with Prof. Dr. F. Gerson and Dr. G. Gescheidt (Basel, Switzerland).

A Novel Reaction Sequence for the Coupling of Nucleophiles to Agarose with 2,2,2-Trifluoroethanesulfonyl Chloride**

Anastasios Demiroglou,
Cornelia Bandel-Schlesselmann
and Herbert P. Jennissen*

Sulfonyl chlorides such as tosyl chloride and 2,2,2-trifluoroethanesulfonyl chloride (tresyl chloride[11]) are among the most widely employed nucleophilic reagents. Over ten years ago tresyl chloride was also introduced in the synthesis of supports for affinity chromatography[2] and is now widely used for the activation of solid phases containing primary hydroxyl groups for subsequent coupling with primary amines or thiols.[3–14] Equation (a) was proposed to describe the tresylation of a solid support, for example, the polysaccharide agarose (tresyl agarose, tresyl Sepharose).[2] The subsequent coupling of amines and thiols to tresyl Sepharose was thought to follow Equations (b)

$$\text{-}CH_2\text{-}OH + ClSO_2CH_2CF_3 \xrightarrow{\text{pyridine}} \text{-}CH_2\text{-}O\text{-}SO_2CH_2CF_3 + HCl \quad (a)$$

$$\text{-}CH_2\text{-}O\text{-}SO_2CH_2CF_3 + R\text{-}SH \longrightarrow \text{-}CH_2\text{-}S\text{-}R + HOSO_2CH_2CF_3 \quad (b)$$

$$\text{-}CH_2\text{-}O\text{-}SO_2CH_2CF_3 + R\text{-}NH_2 \longrightarrow \text{-}CH_2\text{-}NH\text{-}R + HOSO_2CH_2CF_3 \quad (c)$$

and (c), respectively;[2] however, these reactions, in which 2,2,2-trifluoroethanesulfonic acid acts as the leaving group, were never proven.[2–5, 10] The unexpected protein binding properties of thioalkyl agaroses prepared by the tresyl chloride method[14–16] prompted us to reinvestigate the putative reaction mechanism [Eqs.(a)–(c)] by performing systematic elemental analyses of the synthesized alkyl Sepharose products. We found that the elemental analyses of the coupling products obtained from tresylated agarose are not in agreement with Equations (b) and (c),[16] which we show here to be wrong.

A typical analysis of the coupling products obtained from Sepharose 4B activated with tresyl chloride is shown in Table 1. In experiments 1–5 the covalent tresylation of Sepharose can be easily followed by an elemental sulfur analysis. These results are in accord with those reported by Mosbach and Nilsson.[1] In the SIMS analyses for experiments 1 and 2 a signal corresponding to the fluorine of the tresyl residue was also detected. Coupling with butanethiol (expts 1–5) leads to a reduction of the SIMS fluorine signal by a factor of 45 in experiment 1 and by a factor of 10 in experiment 2, which is still in agreement with a release of the 2,2,2-trifluoroethanesulfonic acid moiety. However, the further product analysis (Table 1) shows that the elemental sulfur content does not remain constant after the coupling as ex-

[*] Prof. Dr. H. P. Jennissen, A. Demiroglou, C. Bandel-Schlesselmann
Institut für Physiologische Chemie
der Universität-Gesamthochschule
Hufelandstrasse 55, D-45122 Essen (FRG)
Telefax: Int. code + (201) 723-4694

[**] This work was supported by the Bundesministerium für Forschung und Technologie (Förderkennzeichen: 07024610) and by the European Community (EC Joint Research Project CI1*-CT91-0888). We are indebted to Dipl.-Ing. H. Bandmann (Institut für Organische Chemie der Universität-Gesamthochschule, Essen) for the measurement of the ^{1}H and ^{19}F NMR spectra, to Dr. M. K. Otto and Prof. Dr. J. Wissler (Fraunhofer Institut für Grenzflächen und Bioverfahrenstechnik, Stuttgart) for the determination of inorganic fluoride, to Dr. C. Plog (Dornier GmbH, Friedrichshafen) for the secondary ion mass spectrometry (SIMS) measurements, G. Brauner and V. Hiltenkamp (Institut für Mikroanalytik, der Universität-Gesamthochschule, Essen) for the elemental nitrogen and sulfur analysis, and Dr. E. Logemann (Freiburg) for discussions.

 © VCH Verlagsgesellschaft mbH, D-69451 Weinheim, 1994 0570-0833/94/0101-0120 $ 10.00+.25/0

Table 1. Analysis of the products obtained from the coupling of tresyl chloride activated Sepharose with butanethiol and butylamine[a].

Experiment	Starting material tresyl Sepharose			Reaction with	Product				
	Sulfur analysis	SIMS analysis [b]			Elemental analysis		Incorporated butyl residues	SIMS analysis [b]	
		F^- intensity	F^-/CH_2		sulfur	nitrogen	^{14}C analysis	F^- intensity	F^-/CH_2
	[μg-atom/g dry gel]				[μg-atom/g dry gel]		[μmol/g dry gel]		
1	328	2070	0.487	butanethiol	697	0	426	46	0.006
2	863	3874	ND	butanethiol	1628	0	604	382	ND
3	251	ND	ND	butanethiol	488	0	328	ND	ND
				butylamine	ND	ND	342	ND	ND
4	906	ND	ND	butanethiol	1933	0	1073	ND	ND
				butylamine	850	814	871	ND	ND
5	992	ND	ND	butanethiol	2023	0	1151	ND	ND
				butylamine	907	1000	957	ND	ND

[a] Activation of Sepharose 4B with tresyl chloride and the coupling with butanethiol and with amine are described in ref. [14] and in the text. For elemental analysis (S,N) see Experimental Procedure, and for ^{14}C tracer see ref. [22]. For further details see Experimental Procedure and the text. ND: not determined. [b] The control values for unsubstituted Sepharose 4B (see Table 2, expt 1) have been subtracted.

pected. In fact it increases by roughly a factor of 2 in all the experiments. The increase in sulfur content of the gel corresponds to the amount of ^{14}C-butyl thiol incorporated covalently, which indicates that the ratio of original tresyl chloride sulfur to alkylthiol sulfur is 1:1. A very similar result was obtained when butylamine was coupled to tresyl Sepharose (expts 3–5). Here the sulfur content before and after coupling is practically constant, whereas the nitrogen content and ^{14}C-butyl amine incorporation are stoichiometric. Similar results were obtained when the coupling was conducted at pH 8.0 under the conditions described in ref.[2], rather than in NaOH solution (pH 13.3). These experiments demonstrate that the sulfur atom of tresyl chloride is not part of the leaving group in the coupling reaction.

Table 2 shows that alkaline treatment (0.5 M NaOH, 24 h) alone leads to a loss of fluorine atoms, as reflected by the decrease in the intensity of the SIMS signal by a factor of 70 (expts 2 and 3), whereas the sulfur content is unaffected (expts 3 and 4). ^{14}C-Butanethiol cannot be coupled to alkali-treated tresyl Sepharose (expt 3). Alkali treatment of the coupling product, butyl Sepharose, for 24 hours results in a relatively small loss of 14–17% of sulfur and ^{14}C-butyl residues. This indicates that the covalent bond between the matrix and the alkyl residues is quite stable.

Since impurities in the employed tresyl chloride could be excluded (the ^1H NMR and ^{19}F NMR spectra of tresyl chloride show only the expected quartet and triplet, respectively, indicating 99% purity), a novel leaving group had to be involved. One possibility was that 1,1,1-trifluoroethane, an insoluble and practically inert gas, was released. However, manometric measurements in a Warburg apparatus[16] of various tresyl Sepharoses during alkaline hydrolysis disproved gas development. Therefore the liquid phase obtained after NaOH hydrolysis of tresyl Sepharose and after coupling of butanethiol and butylamine was analyzed by ^{19}F NMR spectroscopy. Only one singlet at $\delta = -119.5$ to -119.7 in scans covering a range from $\delta = +115$ to -235 is evident (Fig. 1A–D), demonstrating that inorganic fluoride is the only fluorine product of the hydrolysis of tresyl Sepharose under the conditions examined. The additional peak at $\delta = -75.5$ in Figure 2D is due to a contamination in the butylamine employed for coupling. This contamination accounts for 6.7% of the total F^- signal.

After the ^{19}F NMR analyses had proved that the fluoride ion is the only fluorine product released from tresyl Sepharose, quantitative F^- determinations were performed (Table 3). Fluoride was found to be generated in a F/S ratio of approximately 3:1, which demonstrates the quantitative conversion of organic into inorganic fluoride (Table 3). The appearance of fluoride during the hydrolysis of tresyl Sepharose was also recently noted by Ohata et al.[17] However, the "classical" reaction sequence of tresyl chloride activation and coupling [Eqs. (a)–(c)] was not queried by this group.

Table 2. SIMS Fluoride analysis of tresyl and butyl Sepharose before and after treatment with NaOH[a].

Experiment	Sepharose starting material			Reaction with	Product			
	Sulfur analysis	SIMS analysis			Sulfur analysis	Incorporated butyl residues	SIMS analysis	
		F^- intensity	F^-/CH_2			^{14}C analysis	F^- intensity	F^-/CH_2
	[μg-atom/g dry gel]				[μg-atom/g dry gel]	[μmol/g dry gel]		
1. Sepharose 4B control	0	30	0.010	–	–	–	–	–
2. tresyl Sepharose	469 [b]	2824		NaOH	ND	–	40	ND
3. tresyl Sepharose	328	2070	0.497	NaOH [c]	294 [d]	9	29	0.007
4. butyl Sepharose	1628	382		NaOH	1359	522 [e]	134	ND

[a] Sepharose 4B was activated and coupled with butanethiol as described in the Experimental Procedure, in the text, and in the legend to Table 1; ND = not determined. The gels were incubated in 0.5 M NaOH for 24 h. For further details on the analysis of the gels see the Experimental Procedure, the text, and the legend to Table 1. SIMS analysis: In experiments 2–4 the control values for unsubstituted Sepharose (expt 1) were substracted. [b] Calculated from the incorporation of ^{14}C butanethiol (605 μmol/g dry gel) and the ratio of 1.29/1 for tresyl Sepharose for butyl residues incorporated/elemental sulfur analyzed (expt 1, Table 1). [c] Reaction with NaOH was followed by coupling with butanethiol. [d] Calculated based on the dry weight of the corresponding tresyl Sepharose. [e] Before treatment with NaOH the amount of incorporated ^{14}C-butanethiol was 604 μmol/g dry gel (see expt 2, Table 1).

Table 3. Determination of inorganic fluoride in the liquid phase after the coupling of Sepharose tresylate with butanethiol and butylamine[a].

Experiment	Starting material tresyl Sepharose Sulfur analysis [mg-atom/g dry gel]	Reaction with	Elemental analysis sulfur [mg-atom/g dry gel]	Elemental analysis nitrogen [mg-atom/g dry gel]	Product analysis Incorporated butyl residues ^{14}C analysis [mmol/g dry gel]	Inorganic fluoride [mmol/g dry gel]
1	1.67	NaOH	2.01	0	–	5.80
2	1.67	butanethiol	3.50	0	1.96	5.11
3	1.67	butylamine	1.81	1.73	1.58	5.77

[a] For further details on preparative and analytical procedures (determination of inorganic fluoride) see the Experimental Procedure, legends to Tables 1 and 2, Figure 1, and the text.

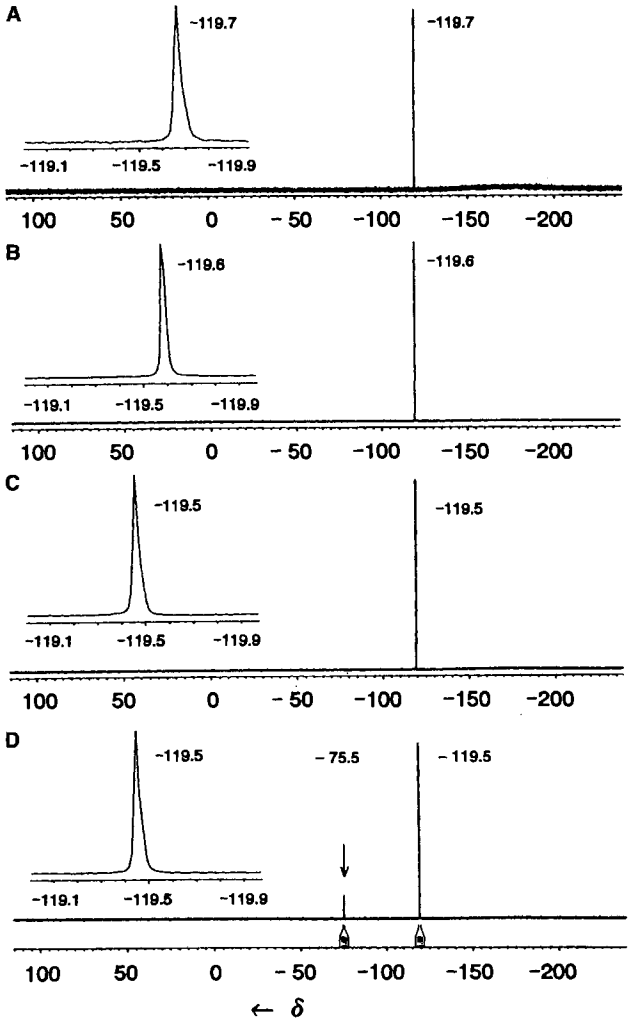


Fig. 1. ^{19}F NMR spectra of the liquid phase obtained from reaction mixtures of tresyl Sepharose in alkaline medium. The spectra were measured with $CFCl_3$ as external standard. The inserted spectra were measured with a resolution of 30 Hzcm^{-1}. The numbers refer to the chemical shifts. The arrow in D indicates the signal due to a contaminant of the butylamine solution. For further details see Table 3 and the text. A) 48 mM NaF in 1 M NaOH; B) liquid phase of tresyl Sepharose (1.67 mg-atom sulfur/g dry gel) after hydrolysis in 0.5 M NaOH; C) liquid phase of tresyl Sepharose (1.67 mg-atom sulfur/g dry gel) after coupling in 0.21 M butanethiol and 0.5 M NaOH; D) liquid phase of tresyl Sepharose (1.67 mg-atom sulfur/g dry gel) after coupling in 0.21 M butylamine and 0.5 M NaOH.

The question now remained what organic residue constitutes the leaving group in the tresyl chloride reaction. In this context the papers of Jones[19] and Buxton et al.[20] are of great interest, since they showed that in alkaline media the trifluoromethyl groups of *o*- and *p*-substituted benzotrifluorides[19] and α-trifluoromethylpropionic acid[20, 21] undergo a combined addition–elimination reaction with the formation of a carboxyl group and sodium fluoride. We therefore infer from their work that acetic acid is the organic product formed during the coupling reaction.

We conclude from the data presented here that during the reaction of tresyl Sepharose with nucleophilic agents in alkaline medium an addition–elimination reaction takes place generating acetic acid and fluoride ion. Equations (d)–(f) describe the novel reaction of tresyl Sepharose in alkali with thiols and amines in which esters of sulfuric acid (checked by acid titration), *S*-alkylthiosulfuric acid, and *N*-alkylamidosulfuric acid are produced, respectively.

$$|\text{-CH}_2\text{-O-SO}_2\text{CH}_2\text{CF}_3 + 3\text{NaOH} \longrightarrow |\text{-CH}_2\text{-O-SO}_3\text{H} + \text{CH}_3\text{COOH} + 3\text{NaF} \quad \text{(d)}$$

$$|\text{-CH}_2\text{-O-SO}_2\text{CH}_2\text{CF}_3 + \text{R-SH} + 3\text{NaOH} \longrightarrow |\text{-CH}_2\text{-O-SO}_2\text{-S-R} + \text{CH}_3\text{COOH} + 3\text{NaF} + \text{H}_2\text{O} \quad \text{(e)}$$

$$|\text{-CH}_2\text{-O-SO}_2\text{CH}_2\text{CF}_3 + \text{R-NH}_2 + 3\text{NaOH} \longrightarrow |\text{-CH}_2\text{-O-SO}_2\text{-NH-R} + \text{CH}_3\text{COOH} + 3\text{NaF} + \text{H}_2\text{O} \quad \text{(f)}$$

Experimental Procedure

Preparative Methods: The conditions for the activation of agarose (Sepharose 4B, Pharmacia/LKB Freiburg) with tresyl chloride (Fluka, Neu Ulm) are described in ref.[14]. For environmental reasons anhydrous acetone was used in the incubation mixture instead of anhydrous dioxane[14]. Tresyl Sepharose was coupled to butanethiol and butylamine according to the general procedure described in ref.[14]. In a typical preparation 10 g (wet weight) of tresyl Sepharose was added to 18 mL of 0.43 M thiol or 0.43 M amine in 1 M NaOH in a closed flask. The final concentrations in the mixture after addition of Sepharose were 0.28 M for both thiol and amine and 0.64 M for NaOH. The mixtures with the thiols were incubated for 60 min at room temperature, those with the amines for 60 min at 5 °C. Practically identical results were obtained when the amines were coupled at room temperature. After coupling the gel was washed on a Büchner funnel with ca. 20 vol water, acetone/water (1:3, v/v), acetone/water (3:1, v/v), and finally with pure acetone until the thiol or amine smell had disappeared. A reversal of this washing procedure was used to transfer the gel back into aqueous medium.

For the alkaline hydrolysis 15 g tresyl Sepharose (wet weight[22]) was added to 15 mL 1 M NaOH and incubated at room temperature between 2.5 and 24 h. In the initial experiments the reaction mixture was incubated for 24 h until it was found that the reaction was complete after 1–2.5 h. The solid phase (gel) was then separated from the liquid phase on a Büchner funnel for separate analysis. All other methods concerning the preparation and handling of agarose are given in ref.[14].

Analytical Methods: 1. Elemental sulfur and nitrogen analysis (double analysis) was performed by gas chromatography on a Carlo Erba Strumentzione Elemental Analyzer model 1106. 2. ^1H NMR spectra were recorded on a high-resolution Bruker AMX-300 NMR spectrometer (282 MHz) in $CDCl_3$. The ^{19}F NMR spectra were recorded on the same instrument with $CFCl_3$ as external standard (max. resolution: 30 Hzcm^{-1} for the spectra inserted in Fig. 1). 3. Fluoride was determined with a modified flow injection halide sensor based on a lanthanum fluoride solid-phase electrode[23]. The sensitivity exceeded 10^{-7} M fluoride. 4. The SIMS analyses were carried out with a Belzers SIMS apparatus with a QMG 511. The Ar^+ ions (3 keV, 10^{-9} A/0.1 cm^2) were directed towards the sample in an angle of 60°. There was charge compensation by an additional electron beam. The Sepharose bead samples were lyophilized and affixed to conducting solvent-free, double-sided adhesive tape.

 © VCH Verlagsgesellschaft mbH, D-69451 Weinheim, 1994 0570-0833/94/0101-0122 $ 10.00+.25/0 Angew. Chem. Int. Ed. Engl. 1994, 33, No. 1

The mass spectrum was obtained for positive and negative secondary ions in a range of 0–100. 5. The degree of substitution of the gel was monitored by adding 0.05–0.25 μCi mL^{-1} *n*-[1-^{14}C]-butanethiol (NEN)[14] or *n*-[1-^{14}C]-butylamine (Hoechst AG) to the coupling mixture (as described in ref.[22]). The amount of coupled alkyl residues was determined by liquid scintillation counting[22] after acid hydrolysis of the *n*-[1-^{14}C]-butyl-labeled agarose (colorless hydrolysate). Analyses were done in triplicate.

Received: July 6, 1993 [Z 6200 IE]
German version: *Angew. Chem.* **1994**, *106*, 126

[1] R. K. Crossland, W. E. Wells, V. J. Shiner, Jr., *J. Am. Chem. Soc.* **1971**, *93*, 4217–4219.
[2] K. Mosbach, K. Nilsson, *Biochem. Biophys. Res. Commun.* **1981**, *102*, 449–457.
[3] K. Nilsson, P. O. Larsson, *Anal. Biochem.* **1983**, *134*, 60–72.
[4] K. Nilsson, K. Mosbach, *Biotechnol. Bioeng.* **1984**, *26*, 1146–1154.
[5] K. Nilsson, K. Mosbach, *Methods Enzymol.* **1984**, *104*, *Part C*, 56–69.
[6] C. F. Mandenius, S. Welin, B. Danielsson, I. Lundstroem, K. Mosbach, *Anal. Biochem.* **1984**, *137*, 106–114.
[7] W. H. Scouten, W. van den Tween, D. Delhaes, H. Kranenberg, M. Dekker, *J. Chromatogr.* **1986**, *376*, 289–298.
[8] K. I. Allam, M. Ehrat, D. Cecchini, B. A. Warden, R. W. Giese, *Anal. Biochem.* **1987**, *162*, 171–177.
[9] P. Wikstroem, P. O. Larsson, *J. Chromatogr.* **1987**, *388*, 123–134.
[10] K. Nilsson, K. Mosbach, *Methods Enzymol.* **1987**, *135*, *Teil B*, 65–78.
[11] K. Ernst-Cabrera, M. Wilchek, *J. Chromatogr.* **1987**, *397*, 187–196.
[12] S. Tay, E. W. Merrill, E. W. Salzman, J. Lindon, *Biomaterials* **1989**, *10*, 11–15.
[13] M. A. Desai, A. Lyddiatt, *Bioseperation* **1990**, *1*, 43–58.
[14] A. Demiroglou, H. P. Jennissen, *J. Chromatogr.* **1990**, *521*, 1–17.
[15] H. P. Jennissen, A. Demiroglou, *J. Chromatogr.* **1992**, *597*, 93–100.
[16] A. Demiroglou, H. P. Jennissen, *Biol. Chem. Hoppe-Seyler* **1993**, *374*, 763.
[17] T. Ohata, Y. Tairyo, S. Takitani, *Chromatographia* **1993**, *35*, 321–324.
[18] O. Warburg, *Stoffwechsel der Tumoren*, Springer, Berlin, **1926**.
[19] R. G. Jones, *J. Am. Chem. Soc.* **1947**, *69*, 2346–2350.
[20] W. M. Buxton, M. Stacey, J. C. Tatlow, *J. Chem. Soc. London*, **1954**, *1054*, 366–374.
[21] M. Hudlický, *Organic Fluorine Chemistry*, Plenum, New York, **1971**, 110.
[22] H. P. Jennissen, L. M. G. Heilmeyer, Jr., *Biochemistry* **1975**, *14*, 454–460.
[23] W. Wiesner, M. K. Otto, K. D. Kulbe, *Ann. N. Y. Acad. Sci.* **1990**, *589*, 705–711.

An Extraordinarily Violent Molecular Dissociation: The Unprecedented Kinetic Energy Release in the Decomposition of $HONF^+$, a Singly Charged Metastable Ion**

Fulvio Cacace, Felice Grandinetti,* and Federico Pepi

The kinetic energy associated with the separation of the fragments from the decomposition of a metastable species constitutes an integral component of the reaction dynamics and is therefore of fundamental interest.[1] In the case of charged species the translational energy of the fragments can be measured with experimental techniques such as mass-analyzed ion kinetic energy (MIKE) spectrometry,[2–5] whose application has provided a large amount of data and has proved a useful tool in the determination of the structures of ions.[6]

The kinetic energy release (KER) spans over several orders of magnitude, from a few hundredths of the one eV to large energies of 10 eV and above, measured in the decomposition of certain multiply charged ions. The latter, however, generally undergo charge-separation reactions, and their KER is not simply related to the intrinsic dynamics of the dissociation reaction, since most of the translational energy of the charged fragments arises from their coulombic repulsion.[7] The KER associated with the decomposition of a singly charged ion provides a more direct insight into the potential energy hypersurface of the decomposing species.

A survey of the experimental results, customarily expressed by the $T_{1/2}$ energy calculated from the metastable peaks widths at their half heights, indicates that the KER associated with the decomposition of singly charged ions falls in general well below 2 eV, rarely exceeding 1.5 eV. This is hardly surprising, since large translational energies of the fragments require a combination of several factors, including a much higher stability of the fragments with respect to their parent, a high barrier for the dissociation, and a partition of the energy released that favors the translational over the rotational and/or internal degrees of freedom of the fragments.

The loss of HX from simple ions containing the $(X-N-Y)H^+$ moiety (X, Y = O or F) which leads to metastable ions $(N-Y)^+$ is characterized by an appreciable barrier for the reverse reaction and by a large KER, for example in the case of protonated nitric acid,[8] nitrogen trifluoride,[9] methyl[10] and ethyl nitrate.[11]

A recent theoretical study of a closely related system has pointed to the large exothermicity of the unimolecular dissociation (shown in [Eq. (a)]) estimated to be 68 kcal mol^{-1} (2.95 eV)

$$H-O-N-F^+ \longrightarrow HF + NO^+ \qquad (a)$$

at the (CISD + Q) (CISD + Q = configuration interaction limited to single and double excitations corrected for unlinked quadruple excitations) level of theory with a double-zeta plus polarization quality basis set.[12] This has prompted a reinvestigation of the system at the GAUSSIAN-1 level of theory,[13] aimed at evaluating the barrier for dissociation [Eq. (a)]. The results summarized in Table 1, and illustrated in Figures 1 and 2 agree quite well with those from the previous theoretical study with regard to the exothermicity of the dissociation [Eq. (a)] and indicate, in addition, that the barrier for the dissociation process, which requires molecular reorganization, is as high as 24.2 kcal mol^{-1}. The latter is an interesting finding, showing that the total energy released in the decomposition of those $HONF^+$ ions which are sufficiently excited to overcome the barrier exceeds 80 kcal mol^{-1}, some 3.5 eV. Furthermore, the nature of the NO^+ and HF fragments suggests that only a limited fraction of the energy released should be partitioned in

Table 1. GAUSSIAN-1 absolute energies [Hartree] and relative stabilities, ΔE [kcal mol^{-1}] of the investigated $(F,H,N,O)^+$ ions and their fragments.

Species (*n*) [a]	*E* (GAUSSIAN-1)	ΔE (298 K)
1 (0)	−229.65430	0
2 (0)	−229.65002	+2.7
3 (0)	−229.66528	−6.9
4 (0)	−229.76601	−70.1
TS1 (1, −1266 cm^{-1})	−229.61015	+27.7
TS2 (1, −1844 cm^{-1})	−229.61143	+26.9
TS3 (1, −1656 cm^{-1})	−229.57292	+51.1
TS4 (1, −1821 cm^{-1})	−229.61207	+26.5
NO^+	−129.39882	−55.5
HF	−100.34679	

[a] *n* = number of imaginary frequencies; frequency.

[*] Dr. F. Grandinetti,[+] Prof. Dr. F. Cacace, Dr. F. Pepi
Università di Roma "La Sapienza"
P. le Aldo Moro, 5 I-00185 Roma (Italy)
Telefax: Int. code + (6)4991-3888
[+] Permanent address:
Dipartimento di Scienze
Ambientali, Università della Tuscia, V.S.C. De Lellis,
I-01100 Viterbo (Italy)

[**] This work was supported by the Italian Ministero dell'Università e della Ricerca Scientifica e Tecnologica (MURST) and Consiglio Nazionale Ricerche (CNR).

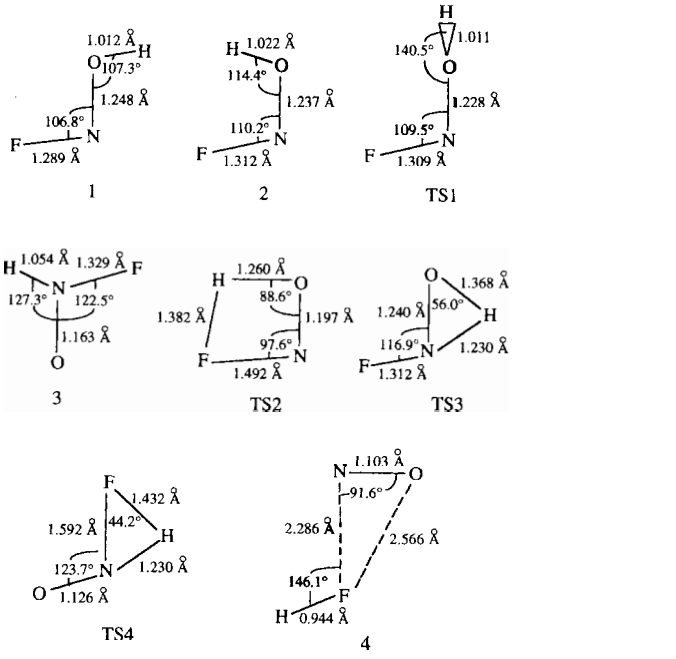


Fig. 1. MP2(FU)/6-31G* optimized geometries (see Experimental Procedure) of the species of interest.

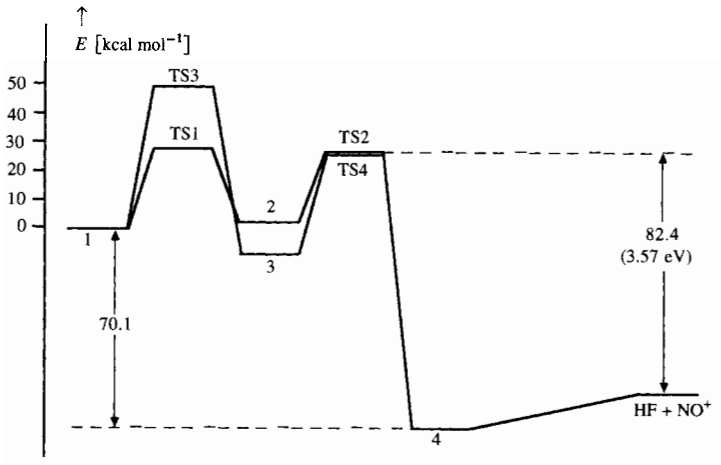


Fig. 2. Schematic energy profile of dissociation of $HONF^+$ [Eq. (a)]

their rotational and/or internal degrees of freedom, which justifies the expectation of an exceptionally large KER.

In order to verify the above-mentioned theoretical predictions experimentally, a suitable route must be found to ions of the required H-O-N-F^+ structure, containing excess internal energy sufficient to allow decomposition according to Equation (a). $HONF^+$ ions have been successfully obtained upon ionization of a NF_3/H_2O mixture, under chemical ionization (CI) conditions. A plausible explanation for the formation of $HONF^+$ is based on the reaction sequence summarized in Equations (b)–(d).

$$NF_3 + e \longrightarrow NF_2^+ + F^\cdot + 2\,e \quad (b)$$

$$NF_2^+ + H_2O \longrightarrow [H_2O{-}NF_2]^+_{exc} \quad (c)$$

$$[H_2O{-}NF_2]^+_{exc} \longrightarrow [HONF]^+_{exc} + HF \quad (d)$$

The adduct from the highly exothermic reaction (c) dissociates yielding $HONF^+$ ions of the desired structure, containing, as required, excess internal energy. In fact, apart from the evidence provided by the formation route, the H-O-N-F connectivity of the ions obtained from Equation (d) is demonstrated by their collisionally activated dissociation (CAD) spectrum, which displays signals for the fragments NO^+ (56.2%), NF^+ (31.1%), NOH^+ (9.7%), OH^+ (1.8%), and N^+ (1.2%). The fact that the $HONF^+$ ions are formed in an excited state is suggested by the considerable (1.36 eV) KER of dissociation [Eq. (d)], since it is most reasonable to assume that a proportionately large amount of energy is deposited into the internal degrees of freedom of the $HONF^+$ fragment. Moreover, a fraction of the energy of the ionizating electrons may contribute to excited $HONF^+$ ions.

The MIKE spectrum of the $HONF^+$ ions obtained from the sequence (b)–(d), displays the single transition [Eq. (a)], whose KER ($T_{1/2} = 2.68 \pm 0.1$ eV) fully meets, and perhaps exceeds, the theoretically based expectations, being unprecedented for the decomposition of a metastable monocation (Fig. 3). From

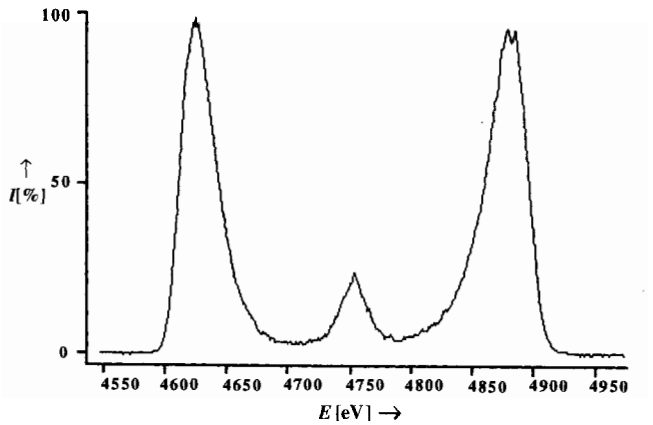


Fig. 3. The NO^+ peak from the decomposition of the metastable $HONF^+$ [Eq. (a)]. The kinetic energy of the precursor ion is 7921 eV. I = relative intensity.

the study of a large number of simple ions, it has been found that $T_{1/2}$ generally exceeds the mean kinetic energy release by 15–20%.[5] Under this assumption, the mean kinetic energy of the fragments would account for 60 to 70% of the total energy released from process (a) which in Figure 2 corresponds to the energy difference of about 3.57 eV, between **TS2** and the separate NO^+ and HF fragments; the remaining fraction is contained in their rotational and internal degrees of freedom. The narrow gaussian component of Figure 3, centered at $m/z = 30$, can be ascribed to the decomposition of metastable ions **4** formed from the isomerization of $HONF^+$ ions, and stabilized by collisional deactivation in the ion source. From Figure 2, and consistent with the MIKE spectrum, the fragmentation of **4** into NO^+ and HF is a simple bond cleavage, occurring with no energy barrier, for the reverse reaction.

In conclusion, apart from the intrinsic interest of (X–N–Y)H^+ systems, several of which play an important role in such fields as chemical reactivity and catalysis, environmental, flame, and atmospheric chemistry, the present results underline the powerful interplay between high-level calculations and MIKE spectrometry in gathering direct insights into relevant details of the potential energy hypersurface of simple ions in the gas phase.

Experimental Procedure

MIKE and CAD spectra of the $(F,H,N,O)^+$ ions were recorded by using a ZAB-2F mass spectrometer from VG Micromass Ltd. Typical operating conditions of the CI

 © VCH Verlagsgesellschaft mbH, D-69451 Weinheim, 1994 0570-0833/94/0101-0124 $ 10.00+.25/0

source were as follows: bulk gas pressure 0.1–0.2 Torr, source temperature 180 °C, emission current 1 mA, repeller voltage 0 V, electron energy 100 eV. The MIKE spectra were recorded by using an accelerating potential of 8 KeV at a typical energy resolution of 8×10^3, and represent the average of at least 100 scans. CAD spectra were taken by admitting He into the collision cell at such a pressure to reduce the main beam intensity to 30% of its initial value.

Computational Details: Ab initio quantum-mechanical calculations were performed by using a RISC/6000 version of the GAUSSIAN 92 program package [14]. The standard internal 6-31G* [15a], 6-311G** [15b], 6-311 + G** [16], and 6-311G** (2 df) [16] basis sets were employed. Geometry optimizations were performed in the full space of the coordinates by analytical gradient-based techniques [17], in the framework of the second-order Møller-Plesset perturbation theory [18], with the 6-31G* basis set. The MP2 method was used with full (FU) electron correlation (including inner-shell electrons). The geometries obtained (Fig. 1) in this way are denoted by MP2(FU)/6-31G*. The corresponding vibrational frequencies were computed for all of the species investigated, in order to characterize them as true minima, transition structures, or higher order saddle points on the potential energy hypersurface. The zero-point energy of the various species was accounted for in this way. The GAUSSIAN-1 procedure, as outlined in ref. [13], was employed to obtain the total energies of the investigated species.

Received: June 15, 1993 [Z 6143 IE]
German version: *Angew. Chem.* **1994**, *106*, 104

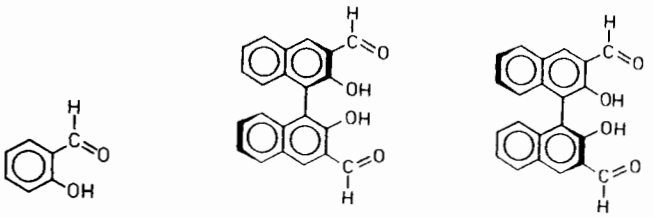
[1] K. C. Smyth, T. W. Shannon, *J. Chem. Phys.* **1969**, *51*, 4633.
[2] J. H. Beynon, R. G. Cooks, *Res. Dev.* **1971**, *22*, 26.
[3] J. H. Homes, A. D. Osborne, *Int. J. Mass Spectrom. Ion Phys.* **1979**, *32*, 35.
[4] J. E. Szulejko, A. Mendez Amaya, R. P. Morgan, A. G. Brenton, J. H. Beynon, *Proc. R. Soc. London A* **1980**, *373*, 1.
[5] B. A. Runpf, P. J. Derrick, *Int. J. Mass. Spectrom. Ion Processes* **1988**, *82*, 239.
[6] J. L. Holmes, *Org. Mass Spectrom.* **1985**, *20*, 169.
[7] B. Brehm, G. De Frenes, *Adv. Mass Spectrom.* **1979**, *8*, 138.
[8] F. Cacace, M. Attinà, G. de Petris, M. Speranza, *J. Am. Chem. Soc.* **1990**, *112*, 1014.
[9] F. Grandinetti, J. Hrušák, D. Schröder, S. Karrass, H. Schwarz, *J. Am. Chem. Soc.* **1992**, *114*, 2806.
[10] G. de Petris, *Org. Mass Spectrom.* **1990**, *25*, 83.
[11] G. de Petris, *Org. Mass Spectrom.* **1990**, *25*, 557.
[12] C. Meredith, R. A. Davy, H. F. Schaefer III, *J. Chem. Phys.* **1990**, *93*, 1215.
[13] J. A. Pople, M. Head-Gordon, D. J. Fox, K. Raghavachari, L. A. Curtiss, *J. Chem. Phys.* **1989**, *90*, 5622.
[14] M. J. Frisch, G. W. Trucks, M. Head-Gordon, P. M. W. Gill, M. W. Wong, J. B. Foresman, B. G. Johnson, H. B. Schlegel, M. A. Robb, E. S. Replogle, R. Gomperts, J. L. Andres, K. Raghavachari, J. S. Binkley, C. Gonzalez, R. L. Martin, D. J. Fox, D. J. Defrees, J. Baker, J. J. P. Stewart, J. A. Pople, Gaussian 92, Revision A, Gaussian, Inc., Pittsburgh, PA, **1992**.
[15] a) P. C. Hariharan, J. A. Pople, *Chem. Phys. Lett.* **1972**, *66*, 217; b) R. Krishnann, J. S. Binkley, R. Seeger, J. A. Pople, *ibid.* **1980**, *72*, 4244.
[16] M. J. Frisch, J. A. Pople, J. S. Binkley, *Chem. Phys. Lett.* **1984**, *80*, 3265.
[17] H. B. Schlegel, *J. Comput. Chem.* **1982**, *3*, 214.
[18] C. Møller, M. S. Plesset, *Phys. Rev.* **1934**, *46*, 86.

Dialdehyde + Diamine—Polymer or Macrocycle?

Henri Brunner* and Hubert Schiessling

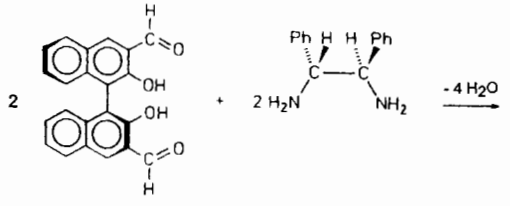
Dedicated to Professor Otto J. Scherer on the occasion of his 60th birthday

Schiff bases derived from salicylaldehyde (**1**) and primary amines are common chelating ligands in complex chemistry.[1] Optically active salicylaldiminates have, for some time, also been employed successfully in enantioselective catalysis (e.g. cyclopropanation).[2] The optically active compounds (*R*)-**2** and (*S*)-**2** contain two salicylaldehyde residues in a chiral binaphthyl system.[3,4] The synthesis of 2,2′-dihydroxy-1,1′-binaphthyl-3,3′-dialdehyde (**2**) proceeds by 1,1′-coupling of the commercially available 3-hydroxy-2-naphthoic acid, acetylation of the phenolic OH groups, reduction of the acid chloride, and cleavage of the protecting groups, in an overall yield of about 20%.[3] Enantiomeric resolution takes place at the 2,2′-dihydroxy-1,1′-binaphthyl-3,3′-dicarboxylic acid stage.[5]

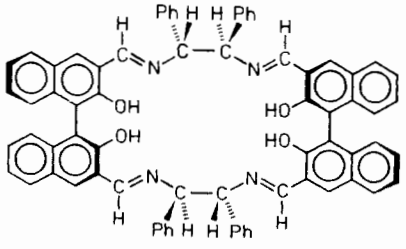


1 (*R*)-**2** (*S*)-**2**

The condensation of salicylaldehyde (**1**) with the difunctionalized amine 1,2-diaminoethane yields the known tetradentate salen ligand. In contrast to the monofunctionalized aldehyde **1**, the binaphthyl derivatives **2** are difunctionalized, and should therefore react with (*R*,*R*)-1,2-diamino-1,2-diphenylethane[6,7] (**3**) to give polymeric Schiff bases. This supposition is confirmed by the reaction of (*R*)-**2** with **3**, but not by the reaction of (*S*)-**2** with **3**, in which two molecules of dialdehyde undergo condensation with two molecules of diamine to form the 24-membered macrocycle **4**. Compound **4** is a yellow solid that may be purified by chromatography on silica gel.[8] An *m*/*z* value of 1037 in the mass spectrum confirms the above formulation. Obviously during the condensation of (*R*)-**2** with **3**, the ends of the growing chain are so far apart from one another that the anticipated polymer forms, whereas in the reaction of (*S*)-**2** with **3**, the 24-membered ring closes.



(*S*)-**2** **3**



4

A simple enantiomeric separation exploits the observation that with the given optically active diamine **3**, only the *S* enantiomer of aldehyde **2** gives rise to a macrocycle, whereas the *R*

[*] Prof. Dr. H. Brunner, Dipl.-Chem. H. Schiessling
Institut für Anorganische Chemie der Universität
D-93040 Regensburg (FRG)
Telefax: Int. code + (941)943-4439

 © VCH Verlagsgesellschaft mbH, D-69451 Weinheim, 1994 0570-0833/94/0101-0125 $ 10.00+.25/0

enantiomer forms a polyimine. When the products of the reaction of (*R*)-**2** and (*S*)-**2** with **3** are subjected to column chromatography on silica gel, the macrocycle formed from the reaction of (*S*)-**2** with **3** is eluted with dichloromethane/toluene as an orange band, whilst the polyimine arising from (*R*)-**2** is left as a residue on the column. Stirring of **4** with hydrochloric acid liberates (*S*)-**2**, which may then be isolated enantiomerically pure.

The large-scale synthesis of racemic **2** is achieved from the commercially available 1,1′-binaphthyl-2,2′-diol.[9] This is first methylated with NaH/dimethylsulfate, and then formylated *ortho* to the methoxy groups with BuLi/DMF/HCl, before the methoxy groups are cleaved with boron trichloride. With the procedure described, **2** may be obtained optically pure without laborious recrystallization. This new enantiomeric separation of **2** is considerably less costly than the original synthetic route.[3]

The new macrocycle **4** should be able to form complexes of defined stereochemistry with up to four metal centers on both sides of the molecule.

Experimental Procedure

4: Racemic **2** (4.39 g, 12.8 mmol) and **3** (2.80 g, 13.2 mmol) were stirred together in dichloromethane (100 mL) at room temperature for 24 h. Monitoring by thin-layer chromatography (dichloromethane as eluent) showed complete consumption of **2**. The solvent was removed, and the residue chromatographed on silica in portions of 1 g (column 1 m × 3 cm, dichloromethane/toluene 9:1, temperature −18 °C). The band containing the macrocycle **4** is distinguished by its orange color. Yield: 1.40 g (1.35 mmol; 42% based on a single enantiomer of **2**); yellow powder, turning brown >270 °C. Macrocycle **4** contains approximately 0.5 moles of dichloromethane, which is in agreement with the ^{1}H NMR spectrum and elemental analysis. MS (FD, CH_2Cl_2): 1037 MH^+; ^{1}H NMR ($CDCl_3$, 250 MHz, TMS): δ = 12.62 (s, 4H), 8.42 (s, 4H), 7.34–6.72 (m, 40H), 4.96 (s, 4H): IR (KBr): $\nu_{C=N}$ = 1635 cm^{-1}.

2: For the liberation of (*S*)-**2**, the yellow powder **4** is dissolved in dichloromethane (50 mL) and stirred for 24 h with 5 *N* HCl (100 mL), after which the dichloromethane is distilled off. The dialdehyde (*S*)-**2** is then filtered off and washed free of acid. Purification is accomplished by column chromatography on silica/dichloromethane, with the isolation of 830 mg (2.42 mmol, 90%) (*S*)-**2**, $[\alpha]_{20}^{D} = -250$ (literature value: −248 [3]), (c = 0.3, CH_2Cl_2).

After elution of **4**, the polyimine can be washed from the column with acetone. Liberation of aldehyde from the polyimine with 5 *N* HCl affords a mixture containing all of the (*R*)-**2** and 50–60% of the (*S*)-**2** initially present.

Received: August 10, 1993 [Z6269IE]
German version: *Angew. Chem.* **1994**, *106*, 130

[1] F. A. Cotton, G. Wilkinson, *Inorganic Chemistry*, Verlag Chemie, Weinheim, **1982**, p. 140, and references therein.
[2] T. Aratani, *Pure Appl. Chem.* **1985**, *57*, 1839.
[3] H. Brunner, J. Goldbrunner, *Chem. Ber.* **1989**, *122*, 2005.
[4] H. Brunner, K. Wutz, *New J. Chem.* **1992**, *16*, 57.
[5] K. Weil, W. Kuhn, *Helv. Chim. Acta* **1944**, *27*, 1848.
[6] E. J. Corey, R. Imwinkelried, S. Pikul, Yi Bin Xiang, *J. Am. Chem. Soc.* **1989**, *111*, 5493.
[7] K. Saigo, N. Kubota, S. Takebayashi, M. Hasegawa, *Bull. Chem. Soc. Jpn.* **1986**, *59*, 931.
[8] Compared with similar imines, the macrocycle **4** has notably enhanced resistance towards hydrolysis, which makes possible its purification by column chromatography on silica.
[9] L. F. Tietze, T. Eicher, *Reaktionen und Synthesen*, Thieme, Stuttgart, **1981**, p. 394.



Nanostructures Based on Molecular Materials. Edited by *W. Göpel* and *C. Ziegler*. VCH Verlagsgesellschaft/VCH Publishers, Weinheim/New York, 1992. X, 377 pp., hardcover DM 168.00.—ISBN 3-527-28416-8/1-56081-210-9

The control of structure and function of materials on the nanometer scale is becoming increasingly feasible and important. Scientists are fascinated by the prospects of molecule-based electronics, electrooptic elements, and sensor structures rivalling nature in size and selectivity. The notion of molecule-based nanostructures was the theme of a workshop held in Germany (in Monrepos Castle, Ludwigsburg) in October 1991, from which this book was developed. As with many emerging areas of interdisciplinary scientific activity, a definition of what constitutes nanostructures based on molecular materials is difficult. The scope of this book emphasizes the design of molecules for "molecular electronics", and their assembly in Langmuir–Blodgett (LB) films. Several additional contributions deal with liquid crystals, photoelectric processes, nonlinear optical systems, and sensors. Other fields of research activity on nanostructures, such as self-assembled monolayers, host–guest chemistry in layered compounds and zeolites, organic inclusion chemistry, and nanocomposites, are not covered in detail. However, for those interested in a current overview of concepts and realized systems in molecular electronics, this book is a valuable resource. Most articles provide short reviews (some quite brief) on the author's research, with references to the original literature. Many readers would probably have appreciated a subject index.

An overview of the topics of the book (Göpel) presents an optimistic view on the rapid development of nanometer structures on a broad basis, including the controlled preparation of 0–3 dimensional structures, scanning probe microscopies, and important applications such as those mentioned above, as well as catalysts, ordered polymers, and membranes. The important difference between bottom-up approaches (based on molecular assemblies) and top-down approaches (based on high resolution patterning of solids and films) is also emphasized.

Electron transfer, both at low field ("molecular wires"), and resulting from optical or redox excitations, plays a key role in concepts of molecular electronic devices. Proteins from the photosynthetic center can teach us about electron transfer paths and how they can be turned on (Ulstrup). Once important features of the photosynthetic reaction center are understood, one can attempt to mimic its molecular machinery for solar energy conversion. Fujihira describes elegant developments in this field, including the assembly of electron acceptor (viologen), sensitizer (porphyrin), and donor (ferrocene) functions in LB heterostructures, and photoelectric conversion by these structures. Ambitious information processing schemes based on organic nanostructures functioning as molecular shift registers (electric field and optically driven) are described by Wilson. Layers that are of nanometer scale in one dimension only can be assembled with present technology, and can be interfaced to existing silicon devices; they can reduce space charge effects. Light driven molecular triads that represent cellular automata could form the building blocks of computing networks, as discussed by Roth. Problems such as the probability of errors as a function of energy differences of the electronic states involved might require the design of sophisticated triads where the center group can be modulated.

The transition from conventional microelectronics towards molecule-based electronics is envisaged as occurring through an increasing contribution of molecular components to the total system (Näbauer). Molecular electronics is expected to make possible greater integration, lower power consumption, and faster switching times, and to allow simplified fabrication. This latter assertion remains to be demonstrated, given the inherent problem of how to interface with individual moleules. Lithographic techniques have recently been refined to such an extent that quantum dots and wires could be fabricated (Jay), and similar techniques should make it possible to pattern thin films of organic molecules, provided the lithographic technique is compatible with the organic systems.

Molecules with second-order and third-order optical nonlinearities can be understood and possibly predicted from quantum chemical calculations (Bredas, Ratner). Various push–pull molecules with high first-order hyperpolarizability and polyacetylene oligomers with third-order response are described. In many cases the theoretical predictions of trends are in reasonable agreement with experiment. Elegant self-assembly techniques have been used by Marks to form multilayer thin films for second harmonic generation.

In addition to wires, molecular switches are basic components of potential molecular electronic devices. A collaboration between several groups described by Schaumburg et al. aims at developing molecules which can change under external influence to a metastable state with suitable lifetimes and distinct properties that permit "read" operations. Interesting examples include photo redox switches (e.g., ferrocene-Ru(bpy)$_3$ changes its fluorescence on oxidation), and push–pull systems containing bianthrone for optical switching.

As mentioned above, this book emphasizes the Langmuir–Blodgett technique as a means of fabricating molecular-scale thin films. Peterson discusses the role of parasitic capacitance, defects, and other parameters in films intended as rectifiers, and proposes optimized structures based on poly(phenylenevinylene) for this purpose. Supramolecular assemblies based on LB films of amphiphilic porphyrins and phthalocyanines, made by using ordering principles to achieve face-to-face dimers and flat ionic networks, are discussed by Palacin. LB films are also of interest for aligning liquid crystals (Wei). New developments in the design of ferroelectric liquid crystals and LB films with spontaneous polarization are reported by Blinov.

Molecule-based materials that have a small band gap and an intrinsic conductivity, and can be doped to form n- and p-type materials, are classified as intrinsic molecular semiconductors (Andre). An example is the radical lutetium bisphthalocyanine, which has been used in field effect transistors. Discotic mesophases are interesting liquid crystalline systems that offer enormous flexibility in the design and physical properties of the disk-like cores which are stacked together. For example, phthalocyanines with alkyl side chains form a spine of aromatic cores favoring one-dimensional charge transport (Simon), while binuclear complexes of fatty acids with transition metals have related but distinct features (Marchon). The latter can also form lyotropic mesophases and gels in hydrocarbon solvents.

The last part of the book adds several useful articles on methods for the characterization of complex structures such as

This section contains book reviews and a list of new books received by the editor. Book reviews are written by invitation from the editor. Suggestions for books to be reviewed and for book reviewers are welcome. Publishers should send brochures or (better) books to the Book Editor, Dr. Gerhard Karger, Redaktion Angewandte Chemie, Postfach 101161, D-69451 Weinheim, Federal Republic of Germany. The editor reserves the right of selecting which books will be reviewed. Uninvited books not chosen for review will not be returned.

those described earlier. These include current–voltage measurements of partially ordered metal/functionalized polythiophene/metal structures (Umbach), and the characterization and modification of molecular materials by scanning tunneling microscopy (Rabe). The morphology and electronic structure of conducting polymers and the structure and dynamics of monolayers of long-chain alkyl derivatives are being studied with the latter technique. Investigations of molecular packing, epitaxy with the substrate, defect and domain mobility, and the ability to modify materials on the nanometer scale will be of critical importance for the rational design of thin film structures. An important aspect of nanoscale materials is their chemical characterization, e.g., to obtain information about composition, valence states, and molecular energy levels. Photoemission spectroscopy provides detailed information on these aspects, with nanometer vertical sensitivity and lateral resolution at the micron scale. A useful overview of the technique and examples, including conjugated polymer films on metals, is given by Salaneck. The final chapter by Göpel deals with the preparation of molecular thin film structures by vapor deposition and their characterization under ultra-high vacuum (UHV) conditions, in particular the changes of structural and electronic properties observed when one varies the coverage from submonolayer to monolayer and multilayer thickness, and on exposure to gases such as oxygen. Electron energy loss, photoemission spectroscopy, and conductivity measurements of molecular sandwich structures such as phthalocyanine films are discussed.

In summary, this book provides a timely overview of research activities and concepts in the field of molecular electronics and will be useful to readers with various interests.

Thomas Bein
Department of Chemistry
Purdue University, Indiana (USA)

Magnetic Resonance Microscopy. Edited by *B. Blümich* and *W. Kuhn*. VCH Verlagsgesellschaft, Weinheim, 1992. X, 604 pp., hardcover DM 268.00.—ISBN 3-527-28403-6

Magnetic resonance (MR) microscopy is an old idea which has only recently started to attract increasing interest. It arose out of the rapid development of MR tomography for medical applications, but it was not until quite late that efforts to adapt the MR imaging principle to observe small volumes with high spatial resolution were begun. The technique that has developed from this work not only gives high resolution in the μm range, but has the further advantage of "speed". Thus, unlike routine MR imaging in medicine, it is possible to obtain images from substances with large natural linewidths (solids in the extreme case) with useful spatial resolution. These two properties of an MR microscope make possible a wide variety of applications.

This book collects together the papers presented at the first International Conference on MR Microscopy, held in September 1991 in Heidelberg. Thus it is not a textbook in the conventional sense, but gives a picture of the state of the art in this relatively new field. The contributions are grouped in five chapters.

The first chapter deals with the fundamental principles of forming images of substances with large natural linewidths. All the authors are concerned with the same subject, and consequently some repetition is unavoidable. In the second article of this chapter W. S. Veeman gives a lucid explanation of the problems of MR imaging of solids and the various approaches to solving them. Readers with a particular interest in the theory are well served by the article by R. Kimmich, which explains in detail many different ways of generating three-dimensional images. Those who make the effort to work carefully through this article will then have an understanding of how "simple" experiments can yield images of solid samples, and how even chemical shift imaging is possible. The chapter ends with two interesting articles on imaging by electron spin resonance (ESR).

The second chapter is concerned with applications of the various imaging techniques to polymers and other solid-like substances, and indicates the present limitations on resolution. Although there is much repetition, the articles contain important information, for example on the problem of artefacts caused by inclusions in solids, which can make the experiments difficult to perform successfully. There are also interesting contributions describing dynamic studies of processes such as photopolymerization and the imaging of "chemical waves".

The third chapter deals with measurements of flow and diffusion. Everyone involved in carrying out flow and diffusion experiments (including routine tomography measurements) will benefit from the help with theoretical and experimental problems offered by these articles.

The fourth chapter shows, with examples of the images obtained, how the high resolution capability of MR microscopy is being applied to studies of plants.

The book concludes with a chapter showing how the high spatial resolution of MR microscopes and the very high sensitivity attainable by using high magnetic field strengths can be used in biomedical research. Possible applications include those based on imaging of heteronuclides, and localized spectroscopy of very small volumes (also by ESR spectroscopy).

Who will benefit from this book? Newcomers to MR microscopy will not find it easy to get to grips with the methodology if they start here; they should first learn something about conventional MR imaging before reading this book. On the other hand, the reader wishing to learn about the potential uses of an MR spectrometer for the imaging of small specimens will find all the relevant techniques and experiments described here. This book cannot, of course, offer a systematic and exhaustive treatment of the capabilities and problems along the lines of a textbook. Here it might have been useful if the editor had supplied an introduction or a summary at the end of each chapter. Also the omission of the names of the authors of the individual contributions from the list of contents is rather unhelpful.

Hans Post
Bruker Medizintechnik
Rheinstetten (FRG)

 © VCH Verlagsgesellschaft mbH, D-69451 Weinheim, 1994 0570-0833/94/0101-0128 $ 10.00+.25/0

New Books

Oxygen in Catalysis. (Chemical Industries Series 43). Edited by **A. Bielanski, J. Haber.** Marcel Dekker, Washington, **1993.** 488 pp., hardcover, $ 145.–. —ISBN 0-8247-8320-4

Shape Selective Catalysis in Industrial Applications. (Chemical Industries Series 36). Edited by **N. Y. Chen, W. E. Garwood, F. G. Dwyer.** Marcel Dekker, Washington, **1993.** 320 pp., hardcover, $ 125.–.—ISBN 0-8247-7856-1

Gesundheit für Mensch und Tier - Warum Tierversuche noch nötig sind. (Serie Piper aktuell). By **G. Küsters, R. Geursen.** Piper, München, **1993.** 184 pp, paperback, DM 19.90.—ISBN 3-492-11896-8

Beer and Wine Production. Analysis, Characterization, and Technological Advances. (ACS Symposium Series No. 536). Edited by **B. H. Gump, D. J. Pruett.** American Chemical Society, Washington, **1993.** 280 pp, hardcover, $ 59.95.—ISBN 0-8412-2714-4

Solid-State Physics. An Introduction to Theory and Experiment. By **H. Ibach, H. Lüth.** Springer Verlag, Heidelberg, **1993.** 341 pp., paperback, DM 59.–.—ISBN 3-540-56841-7

Fundamentals of Photoinduced Electron Transfer. By **G. J. Kavarnos.** VCH, Weinheim/New York, **1993.** 359 pp., hardcover, DM 105.–/$ 75.–.—ISBN 3-527-27856-1/0-89573-751-5

Molecular Magnetism. By **O. Kahn.** VCH, Weinheim/New York, **1993.** 380 pp., hardcover, DM 154.–/$ 95.–. —ISBN 3-527-89566-3/1-56081-566-3

Die Tenside. Edited by **K. Kosswig, H. Stache.** Carl Hanser, München, **1993.** 528 pp, hardcover, DM 178.–.—ISBN 3-446-16201-1

Inorganic Biochemistry. An Introduction. By **J. A. Cowan.** VCH, Weinheim/New York, **1993.** 349 pp., hardcover, DM 69.–/$ 39.50.—ISBN 3-527-89537-X/1-56081-537-X

Directory of Chemicals and their Suppliers - Europe 1993/1994. Econ, Düsseldorf, **1993.** 280 pp., paperback, DM 478.–.—ISBN 3-430-12106-X

Capillary Zone Electrophoresis. (Electrophoresis Library). By **F. Foret, L. Krivankova, P. Bocek.** VCH, Weinheim/New York, **1993.** 346 pp., hardcover, DM 228.–/$ 145.–.—ISBN 3-527-30019-8/1-56081-765-8

The World of Physical Chemistry. By **K. J. Laidler.** Oxford University Press, Oxford, **1993.** 476 pp, hardcover, £ 55.–.—ISBN 0-19-855597-0

Shikimic Acid. Metabolism and Metabolites. By **E. Haslam.** Wiley, Chichester, **1993.** 387 pp., hardcover, £ 75.–.—ISBN 0-471-93999-4

Colloid-Polymer Interactions. Particulate, Amphihilic, and Biological Surfaces. (ACS Symposium Series 532). Edited by **P. Dubin, P. Tong.** American Chemical Society, Washington, **1993.** 290 pp., hardcover, $ 74.95. —ISBN 0-8412-2696-2

Praktikum der technischen Chemie. By **P. Kripylo, F. Vogt.** Deutscher Verlag für Grundstoffindustrie, Leipzig, **1993.** 275 pp., hardcover, DM 62.–.—ISBN 3-342-00669-2

Chaos in Chemistry and Biochemistry. Edited by **R. J. Field, L. Györgyi.** World Scientific, Singapore, **1993.** 289 pp., hardcover, $ 58.–.—ISBN 981-02-1024-8

Activated Metals in Organic Synthesis. By **P. Cintas.** CRC Press, Boca Raton, USA/London, **1993.** 236 pp., hardcover, $ 59.95./£ 40.–.—ISBN 0-8493-7863-X

Der clevere Organiker. Leitfaden zm Erfolg in der Synthese. By **H. J. E. Loewenthal, E. Zass.** Johann Ambrosius Barth, Heidelberg, **1993.** 228 pp., hardcover, DM 48.–.—ISBN 3-335-00360-8

Structures and Conformations of Non-Rigid Molecules. Edited by **J. Laane, M. Dakkouri, B. van der Veken, H. Oberhammer.** Kluwer, Dordrecht, the Netherlands, **1993.** 656 pp., hardcover, Dfl. 395.–.—ISBN 0-7923-2415-3

Quanten. Begriffe und Konzepte für Chemiker. By **P. W. Atkins.** VCH, Weinheim, **1993.** 427 pp., hardcover/softcover, DM 128.–/68.–.—ISBN 3-527-29082-6/3-527-28423-0

Scale-up Methodology for Chemical Processes. By **J.-P. Euzen, P. Trambouze, J.-P. Wauquier.** Editions Technip, Paris, **1993.** 244 pp., hardcover, FF 420.–. —ISBN 2-7108-0646-0

Process Risk Managment Systems. By **W. F. Kenney.** VCH, Weinheim/New York, **1993.** 373 pp., hardcover, DM 96.–/$ 59.95.—ISBN 3-527-28116-9/1-56081-045-9

Gas Chromatographic Environmental Analysis. Principles, Techniques, Instrumentation. By **F. Bruner.** VCH, Weinheim/New York, **1993.** 233 pp., hardcover, DM 98.–/$ 65.–.—ISBN 3-527-28042-1/1-56081-011-4

Guardians of Science. Fairness and Reliability of Peer Review. By **H.-D. Daniel.** VCH, Weinheim/New York, **1993.** 118 pp., hardcover, DM 78.–/$ 50.–.—ISBN 3-527-29041-9/1-56081-751-8

Thermal Analysis of Materials. By **R. F. Speyer.** Marcel Dekker, New York, **1993.** 304 pp., hardcover, $ 99.75.—ISBN 0-8247-8963-6

Chemistry and Chemical Engineering. (Memofix). By **E. Althaus, M. Jakubith.** VCH, Weinheim/New York, **1993.** 342 pp., paperback, DM 68.–/$ 45.–.—ISBN 3-527-29004-4/1-56081-281-8

Efficiency in Research, Development and Production: *The Statistical Design and Analysis of Chemical Experiments.* By **L. Davies.** Royal Society of Chemistry, Cambridge, **1993.** 180 pp., paperback, £ 19.50.—ISBN 0-85186-137-7

Thin Film Coating. Edited by **H. Benkreira.** Royal Society of Chemistry, Cambridge, **1993.** 218 pp., hardcover, £ 45.–.—ISBN 0-85186-695-6

Cyclophane Chemistry. By **F. Vögtle.** Wiley, Chichester, **1993.** 501 pp., hardcover, £ 100.–.—ISBN 0-471-93199-3

Supplement S: The chemistry of sulphur-containing functional groups. (The chemistry of functional groups). Edited by **S. Patai, Z. Rappaport.** Wiley, Chichester, **1993.** 1122 pp., hardcover, £ 320.–.—ISBN 0-471-93046-6

The Chemistry of the Copper and Zinc Triads. Edited by **A. J. Welch, S. K. Chapman.** Royal Society of Chemistry, Cambridge, **1993.** 255 pp., hardcover, £ 47.50.— ISBN 0-85186-715-4

Cluster Ions. (Wiley Series in Ion Chemistry and Physics). Edited by **C.-Y. Ng, T. Baer, I. Powis.** Wiley, Chichester, **1993.** 479 pp., hardcover, £ 80.–.—ISBN 0-471-93830-0

Frontiers in Nonlinear Optics. Edited by **H. Walther, N. Koroteev, M. O. Scully.** Institute of Physics Publishing, Bristol, **1993.** 294 pp., hardcover, £ 55.–.—ISBN 0-7503-0218-6

Principles of Organic Synthesis, Third Edition. By **R. O. C. Norman, J. M. Coxon.** Chapman & Hall, London, **1993.** 811 pp., paperback, £ 22.50.—ISBN 0-7514-0126-9

Handbook of Industrial Surfactants. Gower, Hants, Great Britain, **1993.** 905 pp., hardcover, £ 125.–.— ISBN 0-566-07457-5

Genetic Engineering of Microorganisms. Edited by **A. Pühler.** VCH, Weinheim/New York, **1993.** 178 pp., paperback, DM 38.–/$ 25.–.—ISBN 3-527-30039-2/1-56081-826-3

Chaos and Order. By **F. Cramer.** VCH, Weinheim/New York, **1993.** 249 pp., hardcover, DM 48.–/$ 30.–.— ISBN 3-527-29067-2/1-56081-812-3

The Chemistry of Natural Products, Second Edition. Edited by **R. H. Thomson.** Chapman & Hall, London, **1993.** 452 pp., hardcover, £ 79.–.—ISBN 0-7514-0014-9

Refractory Ceramics to Silicon Carbide. (Ullmann's Encyclopedia of Industrial Chemistry, Vol. A23). VCH, Weinheim/New York, **1993.** 759 pp., hardcover, DM 575.–/$ 325.– (subscription price: DM 485.–/ $ 260).—ISBN 3-527-20123-8/0-89573-173-8

Houben-Weyl. E15, Teil 1-3, En-X, In-X-Verbindungen. Edited by **K. H. Büchel, J. Falbe, H. Hagenmann et al.** Thieme, Stuttgart, **1993.** DM 6600.– (subscription price: 5940.–).—ISBN 3-13-218504-3/3-13-797604-9/ 3-13-797504-2

Virus Strategies. Molecular Biology and Pathogenesis. Edited by **W. Doerfler, P. Böhm.** VCH, Weinheim/New York, **1993.** 542 pp., hardcover, DM 268.–/$ 175.–.— ISBN 3-527-30027-9/1-56081-764-X

AIP Handbook of Modern Sensors. Physics, Designs and Applications. (Modern Instrumentation and Measurements in Physics & Engineering). By **J. Fraden.** American Institute of Physics, New York, **1993.** 552 pp., hardcover, $ 66.–.—ISBN 1-56396-108-3

Gas Source Molecular Beam Epitaxy. Growth and Properties of Phosphorus Containing III-V Heterostructures. (Springer Series in Materials Science, Vol. 26). By **M. B. Panish, H. Temkin.** Springer, Heidelberg, **1993.** 428 pp., hardcover, DM 98.–.—ISBN3-540-56540-X

Bioprocessing. (Biotechnology, Vol. 3, Second Revised Edition). Edited by **G. Stephanopoulos.** VCH, Weinheim/New York, **1993.** 816 pp., hardcover, DM 490.–/$ 365.– (subscription price: DM 390.–/$ 295.–).—ISBN 3-527-28313-7/1-56081-153-6

Carbohydrates as Organic Raw Materials II. Edited by **G. Descotes.** VCH, Weinheim/New York, **1993.** 278 pp., hardcover, DM 148.–/$ 95.–.—ISBN 3-527-30007-4/1-56081-703-8

QSAR: Hansch Analysis and Related Approaches. (Methods in Principles in Medicinal Chemistry, Vol. 1). By **H. Kubinyi.** VCH, Weinheim/New York, **1993.** 240 pp., hardcover, DM 158.–/$ 100.–.—ISBN 3-527-30035-X/1-56081-768-2

Random Walks in Biology. By **H. C. Berg.** Princeton University Press, Princeton, USA, **1993.** 148 pp., paperback, $ 12.95.—ISBN 0-691-00064-6

Lithium. (Die Bibliothek der Wissenschaft, Vol. 2). By **J. Deberitz.** Verlag Moderne Industrie, Landsberg, **1993.** 70 pp., hardcover, DM 16.80.—ISBN 3-478-93093-6

Umwelt. (Römpp Lexikon). Edited by **H. Hulpke, H. A. Koch, R. Wagner.** Thieme, Stuttgart, **1993.** 855 pp., hardcover, DM 298.– (subscription price: 268.–).—ISBN 3-13-736501-5

Catalytic Asymmetric Synthesis. Edited by **I. Ojima.** VCH, Weinheim/New York, **1993.** 476 pp., hardcover, DM 186.–/$ 110.–.—ISBN 3-527-89532-9/1-56081-532-9

Chemistry and Crystal Growth

Jürg Hulliger*

Dedicated to Professor Hanns Thomas Arend on the occasion of his 70th birthday

Single-crystal materials, along with other forms of condensed matter (ceramics, polymers, liquid crystals, etc.) are fundamental to modern technology. The basic research and production of new materials with "tailored" solid-state physical properties therefore necessitate not only chemical synthesis but also the production of single crystals of a particular morphology (either bulk or thin layer crystals) and well-defined crystal defects (doping). In this review, an attempt is made to broaden the traditional synthetic concept of chemistry to the process of single-crystal synthesis. The methods of the resulting approach, which takes into account the specific properties of solid materials, are discussed and illustrated by experimental set-ups for the solution of a range of problems in chemical crystallization. Also included is recent work on the growing of single crystals of high-temperature superconductors, organic nonlinear optical compounds, and proteins.

1. Introduction

Solve et Coagula![1]

1.1. Chemistry and Crystal Growth: The Evolution and Significance of Crystallization

The endeavor to transform liquid and gaseous substances into the solid, pure state, thereby immobilizing them (coagulation), permeates the whole of chemistry, from the early uncertain attempts of the alchemists[1, 2] to present day methods of purification and crystal growth (Fig. 1).[3, 4] Coagulation, in the modern sense, means the bonding of atoms, ions, and molecules to form supramolecular solid-state structures.[5] Therefore, the formation of crystal nuclei of molecular substances would seem to be an ideal case of molecular self-organization,[6] in which the generation of a multiplicity of system-determined morphological forms can be interpreted, for example, within the framework of pattern formation theory.[7]

In the course of the development of chemistry, chemists have been primarily concerned with the synthesis of low molecular weight and macromolecular substances and the building up of extended solid-state structures, basically by molecular accretion. This led to the fact that "crystal nucleation and growth ... remained virtual areas of darkness on the map of the chemical knowledge".[8] Somewhat belatedly, great interest in supramolecular chemistry became apparent very recently. This has been strongly motivated, for example, by the development of functional solid materials (for molecular electronics,[9] for sensors,[10] and for applications based on their mechanical and other properties[11]). Traditionally, however, the physical properties of single-crystal materials (e.g., cooperative phenomena such as magnetism,[12] ferroelectricity,[13] or superconductivity,[14] etc) did not occupy the center of interest. In this context Lüttringhaus commented:[15] "The more chemistry expanded, the more the chemist concerned himself with chemical reactions, and the less with the state of his substances. In particular, he entrusted the study of crystals to crystallographers or structural physicists."

When the anisotropy of physical phenomena in single crystals was discovered, the peculiarities of their physical properties, however, became a topic of physics. The Neumann Principle enabled an increasing number of properties represented by tensors to be qualitatively classified by point symmetry groups.[16] The direction of solid-state physics had been pointed towards the "high tech" age by important discoveries including the technologies of high frequencies, semiconductors, magnetic storage, and lasers, and by the physics of solid phases characterized by nonlinear properties. This could not have been contemplated without experiments with increasingly complex single crystals. The necessary crystal growth technique had taken its place in the field of crystal physics alongside crystallography and experimental mineralogy.

Significantly, the above passage can be found in the introduction to general laboratory practice (crystallization) in Volume 1 of the textbook *Methoden der Organischen Chemie* (Houben-

[*] Prof. Dr. J. Hulliger
Eidgenössische Technische Hochschule
Institut für Quantenelektronik
New address:
Institut für anorganische, analytische und physikalische Chemie der Universität
Freiestrasse 3, CH-3012 Bern (Switzerland)
Telefax: Int. code +(31) 631-3993

 © *VCH Verlagsgesellschaft mbH, D-69451 Weinheim, 1994* *0570-0833/94/0202-0143 $ 10.00+.25/0*

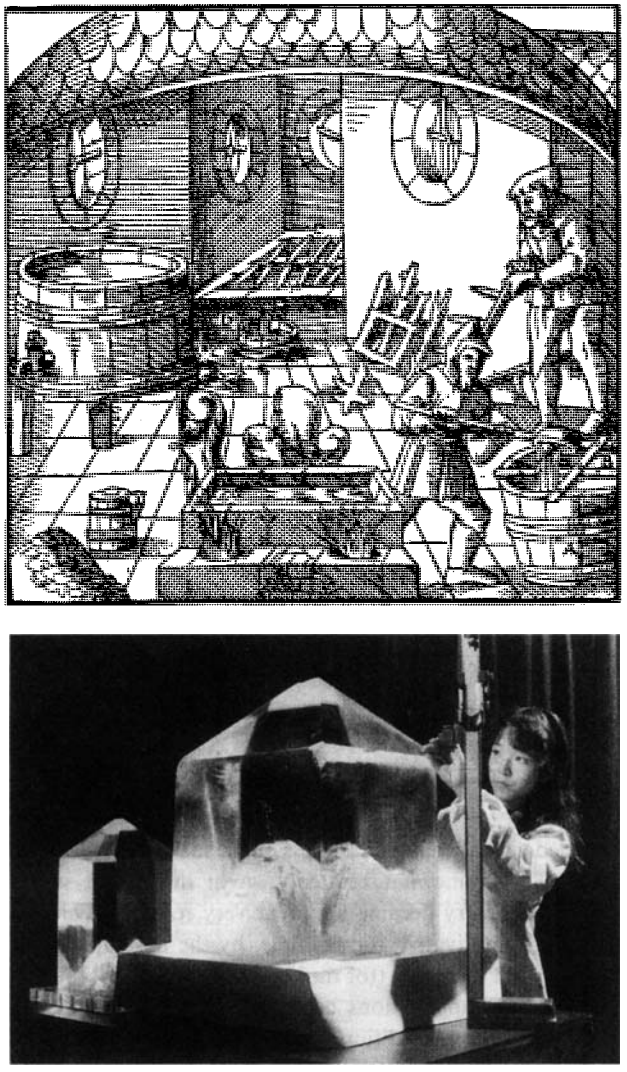
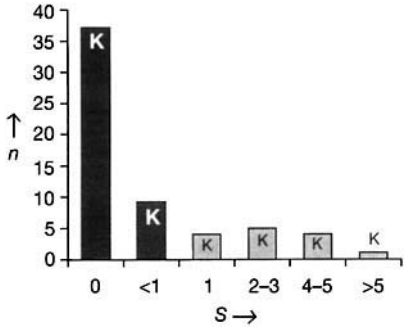


Fig. 1. Crystallization in the course of time. Top: Salt production in the Middle Ages [2c]: evaporation and crystallization of vitriol; bottom: Advanced crystal growth of large, highly pure crystals of KH_2PO_4 for optical frequency doubling [4].

Weyl);[15] crystallization had not become a theme of modern chemistry. Obviously, crystallization processes have always played an important role in chemistry, and crystallization has been exhaustively described in the older chemical literature.[17, 18] Nevertheless, crystallization, in the conventional chemical sense, is merely a useful laboratory technique even today, whereas crystal growth in the true sense, that is, the science of producing large single crystals for a particular purpose, is a topic mainly found in the field of physics research. A glance at the many general chemistry textbooks available today reinforces this impression (Scheme 1). On average, the subject of



Scheme 1. References to crystal growth in chemical textbooks: 60 recent general textbooks of organic, inorganic, and physical chemistry were searched for references to crystallization, recrystallization, and crystal growth [19]. The histogram shows the frequency of these references. S = number of pages on crystallization (K); n = number of books: out of approximately 43000 pages, about 50 pages covered this theme ($c_K \approx 0.12\%$). If the c_K value is compared with the corresponding value of 50 old *organic* chemistry textbooks, the value of c_K today is considerably smaller.

crystallization forms only about 0.1% of the total.[19] The majority of current chemistry textbooks do not describe it at all, nor do they describe the solid-state properties of the interesting types of materials mentioned above. (The review of well-known chemical journals (1968–1991) gives a similar picture.) Compared with textbooks written 20–40 years ago, the relative amount of space devoted to the special science of crystallization has clearly decreased. One can only assume that the situation with respect to solid-state chemistry could be improved; however, in a recent summary of views on the theme "Is Everything O.K. with Solid-State Chemistry?"[20] it is stated: "... there is no textbook on solid-state chemistry adequate for modern science...",[20] and the reviewer summarizes the results of an opinion poll involving 50 specialists in solid-state chemistry:

"It is high time to recognize that besides classical chemistry, which deals with individual molecules and atoms or ions,



Jürg Hulliger was born in 1953 in Zürich. He studied chemistry at the ETH, Zürich, and graduated in physical chemistry. He took his Doctorate at the anorganisch-chemisches Institut der Universität Zürich under Prof. J. H. Ammeter. After spending a year at the Pennsylvania State University, he succeeded Prof. H. Arend at the ETH, Zürich, at the Institut für Festkörperphysik (later Quantenelektronik). There, between 1987 and 1993, he led a group working on crystal growth. In 1993, he accepted the offer of a Professorship at the Institut für anorganische, analytische und physikalische Chemie der Universität Bern. His research fields are: chemistry, crystal growth, and physical properties of inorganic and organic solid materials, and the development of special methods for the synthesis of crystals and for the in situ characterization of crystal growth.

there exists chemistry where chemical transformation has a collective character. This chemistry cannot be equated with classical chemistry nor extrapolated from it."[20]

In the case of solid-state chemistry, the collective character of the process which leads to the formation of complex solids is stressed, but, even in this connection, the general importance of processes and mechanisms of crystal growth and their characterization by instrumental analysis have not been mentioned. We have to say, with no exaggeration: solid-state properties (as considered by physics) in association with crystal growth (synthesis of single crystals—as distinct from molecular synthesis or the usual kind of synthesis of solid materials) has not been the concern of chemistry, or has only been on the fringe.

On the other hand, how are developments progressing in the field of materials research (see, for example, the recently founded (1988) journal *Advanced Materials*, VCH, or papers in *Issues and Opportunities in Materials Research*[21]) whose success depends to a large extent on the contribution from chemical synthesis? The concept of crystal engineering was given an identity after 1945 by von Hippel,[22] and in its further development (Hahn,[23] Kitaigorodski,[24] Arend,[25] Willet,[26] F. Hulliger,[27] Kaldis,[28] Leiserowitz et al.,[29] Schmidt,[30] McBride et al.,[31] Desiraju,[32] Etter,[33] Fagan et al.,[6] etc.) is to be regarded as a solid-state analogue of "molecular engineering", the well-known system of synthesis. One of the great challenges of modern chemistry thus concerns the reinforcing of ways of thinking about supramolecular structures and developing methods for their construction, in particular the synthesis of single-crystal materials with "tailored" physical properties (see Tables in refs. [3, 34]).

In this context, a new topochemical subject known as nanochemistry[35] deserves special attention (see, for example, Ozin[36]). Thus, a series of methods of extremely wide application are available to the modern grower of crystals, enabling the targeted construction of solid-state structures or molecular syntheses, impossible by the classical route. These include (in addition to the possibilities discussed by Ozin,[36] and the fullerene syntheses) molecular beam epitaxy (MBE),[37] metal-organic chemical vapor deposition (MOCVD), chemical beam epitaxy (CBE)[38] CVD, or plasma-assisted deposition techniques, the Langmuir–Blodgett process,[39] and special applications of topochemistry.[40] There is also an analogy between the mechanistic concepts of molecular synthesis and controlled crystallization. Kahr et al.[31], for example, have compared the production of true growth locations of a crystal nucleus with the starting point of a radical chain reaction (see Section 2.1). The term chemospecificity in crystallization corresponds to the selective choice of a particular guest molecule, regiospecificity is shown by alteration of crystal habit, and stereospecificity in the spatial distribution of crystal defects.

Modern achievements in synthetic chemistry such as superconducting oxides,[41] magnetically-ordered organic or organometallic compounds,[42] fullerenes and their derivatives,[43] and organic, strongly nonlinear, optical compounds[44] are of interest for their distinctive solid-state physical properties. The detailed investigation of these subjects requires well-defined single crystals, and, increasingly, also epitaxial thin films. In general, a detailed investigation of the physical properties of a new substance discovered by classical synthesis is only possible after single-crystal samples of known real structure have been prepared. Single crystals, epitaxial thin films, and fibers made from an increasingly large number of different compounds are today undeniably a part of the fundamental research into material science and technology. Here, where success largely depends on an interdisciplinary method of thought and work, the elucidation of complex plans of materials research requires the interlinking of chemistry and physics. The modern science of crystal growth is active in the promising areas in which chemistry and physics overlap, that is, where growth processes are investigated, and special methods for producing solid single crystals, epitaxial layers, and fibers with tailored properties are developed.

To quote but one example: "Materials are really the key to new solid-state lasers" (Chai).[45] Following the first phase of development of solid-state lasers in the 1960s and 1970s, a more vigorous search for other matrix lattices has recently been started,[46] which, along with high power short wavelength semiconductor laser diodes, has the main aim of producing tunable light sources and "up-conversion" systems.[47] This involves, for example, the crystal growth of fluorides ($LiYF_4$, KYF_4, etc.) and oxides (silicates, garnets, etc.) as well as fluoride glasses.[48]

From today's viewpoint, the basic question for chemists is to what extent chemistry should integrate solid-state properties and single-crystal synthesis as one of its new leitmotifs into research and teaching in the future.

Single crystals play a decisive role not only in the context of complex materials research. Single-crystal X-ray structural analysis still represents the definitive proof of structure for the chemist. The discussion of molecular and other properties depends upon it, especially for a comparison with structures calculated from quantum chemistry.

Based on this outline, two subjects are dealt with in the following sections: 1) an introductory description for the chemist of the basic principles of crystallization and crystal growth from the modern viewpoint (see especially refs. [3, 34, 49]), and 2) a practical discussion of methods which can contribute to progress in mass crystallization (on the laboratory scale), or the production of small single crystals (for structural investigations), and the preparation of larger single crystals (for the investigation of the physics of the solid state).

1.2. From Crystallization to Single-Crystal Growth

Crystallization is one of the most perfect purification operations...[17b]

In practice, crystallization was, for organic chemistry, one of the most effective methods of purifying substances for a long time, especially for the separation of enantiomers (resolution of racemates). With the development of chromatography and other methods of separation (including chiral stationary phases), crystallization itself lost some importance as a laboratory technique, which must be the main reason why it is not treated at all in the newer textbooks of general chemistry, or at least only briefly, although methods for the preparation of small single crystals or polycrystalline materials, mainly for complete crystal structure analysis by X-ray or neutron diffraction, have remained in use.

The special techniques summarized in Scheme 2, for which crystallization processes were developed or used, have attained importance in chemical research and technology. Industrial crystallization is undoubtedly most important.[50] Because of the necessity for quality control of bulk production, as well as a technically feasible user-friendly crystal morphology[51, 52] and defined particle size distribution of agglomerates,[53] the process control system must be based on extensive knowledge of the mechanisms of nucleation and growth for a given hydrodynamic regime and set of surface-active agents (crystal habit modifiers[62]). In the industrial production of mainly large single crystals with defined real structure, extremely pure starting materials are required on the one hand, and very closely controlled crystal growth technology on the other (Fig. 2).[2, 4, 55, 63]

1. Industrial crystallization [50–53]
   Sales of a) polycrystalline bulk materials in which each product is estimated to exceed 10^6 t per year, for example, NaCl, urea, sugar, or zeolite Linde A with 10^5 t per year [54]; b) single-crystal production of elements (e.g., Si with no dislocations: 10^4 t per year) [55] and compounds (e.g., cubic stabilized ZrO_2: 300 t per year) [56]
2. Determination of structures of crystals and molecules
   (about 8000 new crystal structures per year)
3. Separation, purification, and purity determination of fine chemicals, pigments, and natural products
4. Racemate separation and determination of absolute configurations [29, 57]
5. Crystallization of macromolecular substances (proteins, polymers) [58, 59]
6. Measurement of physical properties by spectroscopic and other physical methods
7. Biocrystallization (also in the medical field: osteoporosis (see ref. [3]: kidney stones and gall stones)) [60]
8. Synthesis under topochemical control [40, 61]
   (e.g., cracking catalysts based on zeolites [54])

Scheme 2. Areas where crystallization processes are important in chemical research and technology.

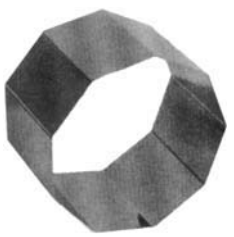
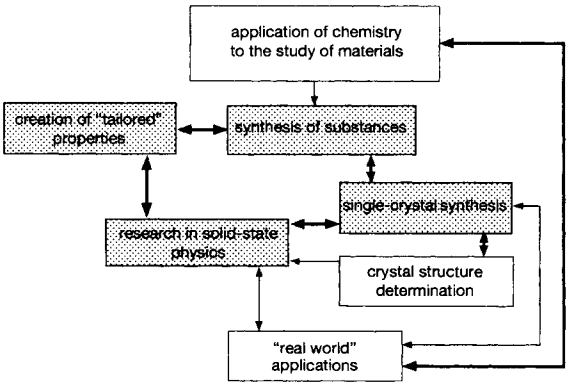


Fig. 2. Special technology ("edge-defined film-fed growth") for the economic production of silicon solar cells. Eight- or nine-sided thin-walled single crystals, several meters long, are obtained from the molten material by crystal pulling [63].

In the laboratory, the elucidation of structure has had to take second place in view of the demand for small single crystals (linear dimensions d less than one mm); about 8000 new crystal structures per year currently result either from the purification of various compounds or the separation of racemates. As a more detailed discussion of all recent relevant fields would go far beyond the scope of this article, the reader is referred to the recent literature on this subject in some cases.

To recapitulate, most types of chemical crystallization can be divided into three classes, which differ in the method used: a) large-scale production of small crystals, b) crystallization of individual single crystals (d less than one mm), and c) growth of single crystals (1 mm $\lesssim d \lesssim$ 1 m). As modern materials research and crystal growth are oriented towards the same stages of the processes, this classification will be used for the planning of Section 3. That is to say, for newly synthesized compounds, the desired solid-state properties are at first investigated with polycrystalline (for example, ceramic) and small single-crystal samples, and are then optimized (see Scheme 3) by developing specific methods of crystal growth (bulk, thin film, and fiber single crystals). From the viewpoint of materials research, the usual synthetic methods at this point give way to methods of single-crystal growth to achieve the desired solid-state properties.



Scheme 3. Chemistry and crystal growth: interlinking of the processes in materials science including single-crystal synthesis.

In view of the continually increasing number of initially poorly characterized compounds, the question of simple but effective strategies of crystallization arises. A cost estimate ("man-years investments") based on "response theory" (Tiller, 1991)[49] shows that the implementation of the "black box" assumption (a current view of crystal growth!) leads to an "art-based technology" (crystal growth = a collection of recipes) based on the multidimensional parameter space j + k, where j = the number of materials and k = the number of experimental parameters, whereas a "system approach", which always presupposes some sort of prestructuring "clustering", leads to a "science-based technology" (strategies for proceeding with a minimum of experiments). A proposed plan for an intelligently organized laboratory crystallization process is discussed from a practical point of view in Sections 3.2 and 3.3. This contains the exploratory methods of crystallization and the advanced methods of single-crystal growth.

All methods must be termed exploratory when they systematically use a phenomenological approach with a minimum of experimental work, for example, by the deliberate use of self-regulating mechanisms. In many cases, crystals produced in a first stage are used as nuclei in a second stage of advanced crystal growth. The so-called temperature-difference method of solution growth (see Section 3.2) should be regarded as a simple example of a "science-based technology". Here it should be mentioned that H. T. Arend contributed greatly to the research and development work on exploratory strategies of crystallization during the course of his activity as a crystal grower at the Eidgenössische Technische Hochschule (ETH), Zürich.

In the future, the electronic storage and handling of data concerning methods and materials should provide the chemist

with a database, in which the knowledge about crystallization is stored ("computer knowledge base for crystallization"[64]). A first attempt at this has been in existence since 1990,[64] and it is to be hoped that its usefulness and shortcomings will become apparent through continual use. However, data systems will certainly not be able to replace the specialist in the foreseeable future. If a problem is too difficult for the crystal growth expert to solve, existing electronic strategies will also fail. "The expert then falls back on his intuition and far more wide background knowledge."[64] There is another electronic data bank that stores information on the crystallization of biological macromolecules.[65] This contains data on more than 1000 crystalline forms of over 600 biological macromolecules. The use of this when attempting systematic protein crystallization (e.g. "successive automated grid searches") is discussed by Weber.[58]

In addition to the electronic media, it should not be forgotten that a rich experience of the solution of crystallization problems exists, for example, in the older organic chemical literature. This can now be extended in a methodical manner.[15, 18]

This article has so far been aimed at throwing some light on the significance of crystallization in chemistry, and preparing the reader for the specific nature of the later part of the discussion which describes experiments in modern crystal growth. After a general outline of the theory (Section 2), a very practically oriented systematic approach is set out in Section 3. In Section 4, the crystal growth of three classes of materials of topical interest is briefly discussed.

2. Fundamentals of Crystal Growth

2.1. Energetics and Kinetics of Nucleation and Volume Growth

A crystal is nothing but a large molecule.
Van Vleck[66]

Crystallization leads to the buildup of supraatomic and supramolecular ordered states, whose microscopic real structure and macroscopic morphology are determined by energetic, kinetic, and transport (mass and heat) mechanisms; thus, lattice components are attached. This means that, as a nonequilibrium process of a heterogeneous system ($\Delta G(\mathrm{N} \rightarrow \mathrm{C}) = G_\mathrm{C} - G_\mathrm{N} < 0$; C: crystal, N: nutrient phase), the final condition of a macroscopic crystal is the result of a transition process due to a local thermodynamic deviation from equilibrium, $\Delta G(x, y, z; \Delta p, \Delta T, \Delta X_i)$, the removal of the heat of crystallization, the inflow of lattice components, and the outflow of dispersive and other components which are not taken up into the lattice or are only taken up in small amounts.[49] If the crystal growth takes place at a high or low temperature (or pressure), attention must also be paid to defect equilibria on changing to normal conditions (e.g. Schottky defects[67]). It is today widely recognized that crystal growth must be regarded as a complex process (Neuhaus[68]) whose mechanism is divided into stages. This has consequences for the experimental methods of producing single crystals with "tailored" physical properties.

Kinetic effects (in processes involving a large deviation from equilibrium, e.g., in MBE or MOCVD technology[69]) make possible the buildup of heteroepitaxial layers,[70] superlattices, or mechanically strong strained thin films,[70, 71] and also affect the distribution equilibrium of dopants[49] and dominate the morphology.[72] An example of kinetically controlled crystal growth is provided by optically anomalous crystals in which a regular incorporation of foreign components or a disorientation of the lattice components disturbs the symmetry of individual growth sectors.[31]

Whereas, in the 1960s and 1970s, crystal growth was mainly studied phenomenologically,[73] during the 1980s the development of new experimental techniques for investigating growth in situ introduced the possibility of "taking a picture" at the atomic/molecular level (transmission electron microscopy (TEM),[74] reflection high-energy electron diffraction (RHEED), low-energy electron diffraction (LEED),[75] synchrotron radiation and light scattering experiments at the crystal–nutrient phase interface (CNI),[76] scanning tunneling microscopy (STM),[77] and atomic force microscopy (AFM)[78]). Light scattering experiments have shown that, for example, in a supercooled melt, the growing crystal is surrounded by a partially ordered layer that can be several μm thick, depending on the degree of supercooling.[76] In situ observations of the properties of metallic clusters (Pt, Au, Pb) in vacuo have been carried out by TEM (video recording).[79]

Turning now to the theory,[73] (for historical information, see refs. [2, 34]) the early contributions of Gibbs (1878), Wulff (1895), Volmer (1926), Kossel (1927), Stranski (1928), and others have been fundamentally extended by the discovery of the energetically favorable growth by screw dislocations (Burton, Cabrera, Frank (BCF theory) 1949[80]), the treatment of morphological stability/instability criteria (Mullins and Sekerka, 1963[81]) for the crystal–nutrient phase interface, and the incorporation of impurities into the lattice (Burton, Prim, Slichter, 1953[82]). More recently, Monte Carlo methods,[83] "molecular modeling", and ab initio simulations (for Si, GaAs, noble gases, etc.)[84] illustrate space and time aspects of the growth steps at a crystal surface. Also, progress has been made in the calculation of the expected binding energy of macroscopic (*hkl*) surfaces[85] (for the general consideration of theoretical models, see literature quoted, for example, in ref. [3, 34]).

An understanding of the mechanism of homogeneous nucleation is of fundamental interest.[53, 86] Starting from the statistically disordered nutrient phase N ($T > T_{\mathrm{equilibrium}}$), the structure-forming self-organization of the components (Fig. 3) takes place in the supercooled or supersaturated state in several stages,[87] leading to a reaction principle (with a part played by molecular recognition mechanisms) whose elementary steps, infinitely repeated, lead to the "macromolecular" crystal. Homogeneous nucleation and crystal growth can be described in analogy to chemical reactions according to Scheme 4.[49, 86a] As an illustration of stepwise buildup by nucleation, Figure 3 shows structures calculated from quantum mechanics of associates and clusters ($\mathrm{Na^+(NaCl)_n}$) up to the formation of a "first" NaCl ordered structure of a unit cell (gas phase).[87a]

In the classical capillary approximation, the transition of small molecular agglomerates to clusters (C) of increasing size leads to the formation of a phase boundary surface (outer surface), for which the cluster formation energy ΔG_C consists of a volume and surface area term. For a nucleus, assumed to be

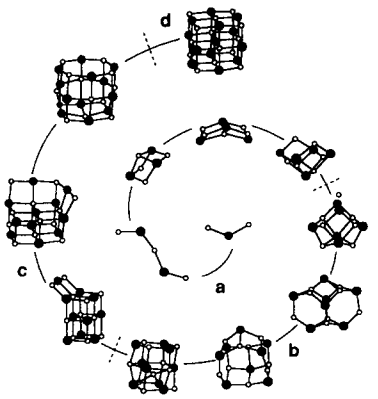


Fig. 3. Quantum-mechanical calculation of the stepwise development of structures leading to the formation of an NaCl lattice cell structure (from ref. [87a] with additions from the author). a) Small aggregates; b) cluster formation; c) transition to an NaCl lattice structure unit; d) first "unit cell".

spherical, in solution, ΔG_C[53] is described by Equation (a), where the cluster radius r^* [Eq. (b)] represents the critical size, and ΔG_C^* [Eq. (c)] represents the activation energy to overcome the critical size of the nucleus. The molar volume of the cluster is represented by v; $\sigma = (X - X_o)/X_o$ represents the relative supersaturation,[88] X_o represents the equilibrium concentration, γ represents the interface surface energy per unit area, and k_B is the Boltzmann constant.

$$\Delta G_C = \Delta G_C(r) = -\frac{4\pi}{3} r^3 [k_B T \ln(\sigma + 1)]/v + 4\pi r^2 \gamma \quad \text{(a)}$$

$$r^* = 2v\gamma/[k_B T \ln(\sigma + 1)] \quad \text{(b)}$$

$$\Delta G_C^* = 16\pi v^2 \gamma^3/[3k_B^2 T^2 \ln^2(\sigma + 1)] \quad \text{(c)}$$

The transition into growth of macroscopic crystals (Reactions 3 and 4 in Scheme 4) can take place by energy fluctuations in the system; thus, r^* and ΔG_C^* are overcome.

1) Formation of associates from monomer A

$A + A \rightleftharpoons A_2$
$A_2 + A \rightleftharpoons A_3$
...

2) Buildup of clusters

$A_n + A \rightleftharpoons A_{n+1}$
...
(coalescence of clusters also possible)

3) Formation of critical nucleus A_m^* and its growth

$A_{m-1} + A \rightleftharpoons A_m^*$
$A_m^* + A \rightleftharpoons A_{m+1}$

4) Molecular accretion on macroscopic crystal surfaces (Ω)

$\Omega + A \rightleftharpoons \Omega A$

Scheme 4. Reaction scheme for homogeneous nucleation (see text).

According to Larson et al.,[89] consideration of surface curvature anisotropy (for example, by the attachment of clusters to macroscopic surfaces) leads to a thermodynamic stabilization of small clusters with $r < r^*$. Therefore, in real systems (in the supersaturated state), there exists a specific distribution of metastable or stable but subcritical nuclei of varying size r. Since r^* depends on σ, the construction of the first ordered lattice cell does not in general lead to a production of the critical nucleus size. Statistical thermodynamic models confirm the capillary approximation [Eq. (a)] down to cluster sizes of approximately 10–30 atoms/molecules.[86a] Gas-phase experiments by Volmer et al. have shown that condensed droplets of organic compounds have a diameter of $r^* = 0.8$–1.5 nm, and $n = 30$–130 molecules,[50] which would be expected to be a realistic description of the capillary model. For liquid–solid phase systems, there is some experimental data about the size distribution and concentration of clusters, but a great lack of structural information. The size of clusters in solutions is in the range 1–10 nm, with up to 1000 molecules.[89]

According to Boltzmann statistics, the number of clusters that exist in the state with ΔG_C^* is proportional to $\exp(-\Delta G_C^*/k_B T)$. The nucleation rate J [$cm^{-3} s^{-1}$] therefore follows Arrhenius's Law. This is true when the activation energy for the diffusion is appreciably less than ΔG_C^*, as, for example, for molten materials, in which nucleation takes place just below the liquidus temperature. Including the contribution made by diffusion ΔG_D^*, J (for solutions) is given by Equation (d), in which v_L represents the molar volume of the solvent, and h is Planck's constant.

$$J = \exp(-\Delta G_D^*/k_B T) \exp(-\Delta G_C^*/k_B T)\, k_B T/h v_L \quad \text{(d)}$$

As shown by measurements by Tammann (1898) and others,[18, 34, 86b] $J(\sigma)$ can show a fairly sharp maximum, where the temperature range for maximum nucleation and that for maximum growth rate do not in general overlap to a great extent. In the crystallization of proteins, one of the main problems can be that conditions for nucleation and those for growth are optimized separately.[58]

In many systems, nucleation proceeds heterogeneously, as interactions with solid items of equipment or vessel walls reduce activation energy and nucleation temperature. If the critical nucleus size is reached, the continuing process of accretion of materials becomes the growth of macroscopic crystals (in analogy with polymerization reactions), for which various mechanisms can be effective within the CNI.[34, 73, 86b] Both experimentally and theoretically, the distinction must be made between growth on an atomically rough or smooth (in this case stepped) surface, and growth by means of screw dislocations. The step velocity v and the macroscopically measurable surface growth velocity R (R: linear or nonlinear) are functions of the supersaturation σ, and depend on the transport mechanisms; thus, lattice components are added, and are incorporated into the "kink position" preferentially for energy reasons. In the case of a growth mechanism driven by adsorption onto the growth surface and by screw dislocations (BCF Theory[80]) the growth rate R of macroscopic faces can be described (in solution) by Equation (e) where k_1 and k_2 represent kinetic, temperature-dependent constants.[90]

$$R = k_2 \sigma^2 \tanh(\sigma^{-1} k_1/k_2) \quad \text{(e)}$$

For small values of σ a parabolic rate relationship would be expected, and for larger values of σ it would be linear

(v is linearly dependent on σ). Detailed measurements[91] of $R(\sigma)$ and $v(\sigma)$ on, for example, KH_2PO_4, have shown considerable deviations from the expected parabolic relationship for small values of σ, attributed to the effect of foreign materials. Above a critical supersaturation value σ', the growth velocity R increases considerably (suppression of growth for a small deviation from equilibrium). This shows once again the importance of prior purification of materials before mechanisms of crystallization can be investigated and interpreted. Because specific impurities are active down to the ppm level, this presents no easy task for preparative and analytical chemistry. This helps to understand why, in some cases, even when seed nuclei are used and the supercooling and/or supersaturation is relatively large ($\Delta T, \sigma$), no crystal growth, or very slow crystal growth is observed. From general experience with solid materials of various types, it can be said that the problems of chemical crystallization are not with the crystal growth, but with the nucleation. This happens in many systems where nucleation takes place at a high degree of supersaturation, so that the volume growth proceeds too quickly. Separate production of seed nuclei for a later crystallization process is therefore to be recommended.

Foreign materials can reduce the rate of accretion, even without adsorption onto growth-active locations. When $k_0 < 1$ (Nernst distribution coefficient $k_0 = X_C/X_N$), the foreign material (including dispersive components) becomes concentrated in the vicinity of the growing faces,[34] which leads, for example, to a reduction in the liquidus temperature in accordance with the phase diagram of a two-component system (see Section 2.2, Fig. 6, Type I, III). Thus, when the temperature is kept constant (provided that the system is thermally homogeneous), the supercooling ΔT or the supersaturation σ decreases, and the growth proceeds more slowly. It is therefore useful to reduce the thickness of the diffusive matter transfer zone by a suitable flow profile in the nutrient phase, and thorough mixing throughout its volume. Regarding the incorporation of foreign material into the lattice, an increase in the concentration X_C due to kinetic effects is observed. Depending on the growth rate R and the hydrodynamic condition, $k_{kinetic} > k_0$, and in extreme cases reaches 1, where $X_C \approx X_N$. In analogy to the result of comparable work, the theory of Burton et al. gives the Equation (f),[82]

$$k_{kinetic} = k_{CNI}\,[k_{CNI} + (1 - k_{CNI})\exp(-R\delta/D)]^{-1} \qquad (f)$$

where D denotes the diffusion constant, δ the thickness of the crystal–nutrient interface (CNI), and k_{CNI} the Nernst distribution coefficient in the CNI (approximation: $k_{CNI} \approx k_0$).

The well-known rule that, in purification by crystallization, the crystallization process must take place slowly is therefore confirmed in one respect. Since too rapid a growth rate can lead to a macroscopic inclusion of nutrient phase, a suitably slow growth rate is always advisable (see earlier comment on nucleation at high σ values).

2.2. Phase Diagrams and a Systematic Classification for General Methods of Crystal Growth

Experimental crystal growth requires exact knowledge of the relevant phase diagram, at least in the region of existence ($\Delta p, \Delta T, \Delta X$) of the primary product to be crystallized. As the necessary thermodynamic data are known in relatively few cases, or their accuracy may be inadequate with respect to the values of p, T, X, limited-range phase diagrams often have to be specially determined under conditions comparable to those to be used in the crystal growth work (containers, purity requirements, time scales,[92] etc.). (For experimental methods, see ref. [93], and, for data, ref. [94].) In the thermoanalytical investigations, visual observation of the liquefaction and crystallization processes should be included. In this way, information is commonly obtained that may well be irrelevant in pure phase diagram work, but can be very important in crystal growth (existence of small amounts of undissolved solid materials or cloudiness, melt–solution segregation, morphological aspects, color effects during crystal growth, etc.). As an example from high-temperature solution growth, an experimental procedure is briefly described here. This was used as an exploratory technique (see Section 3.2) in the determination of growth conditions for the production of epitaxial layers of $KTa_{1-x}Nb_xO_3$.[95]

High-melting materials (e.g. ABO_3 perowskites) can be brought into solution by fluxes (that is, lower melting oxides or halides) at much lower temperatures than the melting point of the pure substances, and crystallized.[96, 97] Here, it is necessary to know at least part of the quasi-binary phase diagram (see Figs. 6, 7). Solution and crystallization processes for temperatures up to about 1200 °C can be investigated in situ by visual observation and/or thermoanalytical measurements by using the system shown schematically in Figure 4. By simultaneously using six platinum crucibles (diameter: 8 mm, $l = 15$ mm) illuminated with a fiber-optical light guide, morphological and chemical information can be obtained and color effects observed. In the case of the $KTa_{1-x}Nb_xO_3$ referred to above, this led to a simple determination of the phase diagram (Type I, see Fig. 6) with potassium fluoride as the solvent. Moreover, useful basic information for the later development of an epitaxial process[98] was obtained from experiments on $KTaO_3$ substrates, which were several mm^2 in size. The growth of the $KTa_{1-x}Nb_xO_3$ layers is accompanied by the formation of a strong blue color, noticeable even at the early stage of the growth process (Fig. 5).

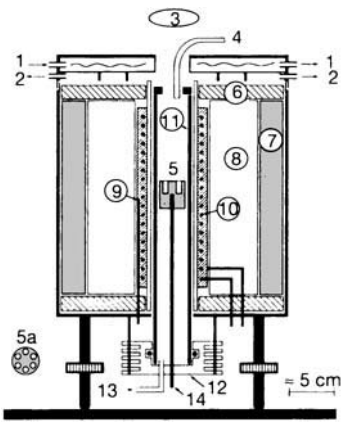


Fig. 4. Furnace for visual observation of dissolution and crystallization phenomena [95]. In the arrangement shown, six Pt crucibles can be charged with samples simultaneously. Alternative arrangement: Two crucibles + DTA. 1: Water cooling. 2: Exit for gaseous emissions. 3: Binocular microscope. 4: Quartz lamp for illuminating the samples. 5: Inconel 600 crucible container. 6–8: Insulation materials (ceramic powder and fiber materials). 9: Control thermocouple. 10: Kanthal A1 heating coil. 11: Inconel 600 or ceramic protective tube. 12: Replaceable floor plate (sealed). 13: Gas inlet. 14: Sample thermocouple. Maximum operating temperature: 1200 °C. (Example of use: see Fig. 5.)

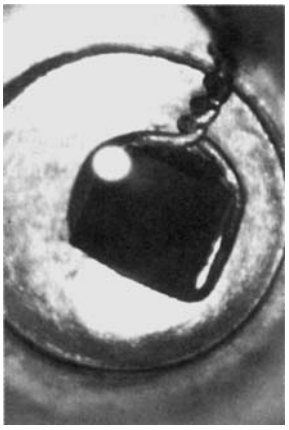


Fig. 5. In situ observation (see furnace in Fig. 4) of epitaxial growth of dark blue $KTa_{1-x}Nb_xO_3$ crystals on a $KTaO_3$ substrate from KF flux at 920 °C after 10 min (110) orientation with macroscopically rough growth surface [95]. Crucible diameter $\varnothing = 8$ mm.

Three phase diagrams (T, X, at constant p) are shown schematically in Figures 6 and 7 to help in understanding the later discussion of the crystal growth of many substances: 1) The two-component system A/B without formation of solid solutions, as a basis for solution growth from dilute or concentrated solution, 2) the melting diagram for crystal growth of a congruently melting compound AB from the pure melt or from the self-fluxing mixture (incongruently melting compounds are usually obtained from nonstoichiometric melt solutions, that is an excess of one of the components (self-fluxing mixtures)), and 3) the two-component system forming solid solutions $A_{1-x}B_x$, which requires special techniques for growing macroscopic homogeneous mixed crystals. The diagram illustrating the most commonly used solution growth method (Fig. 7) is discussed in more detail: In the A/B system (no solid solutions), to enable as wide a range of T (largest value of ΔT) on the solubility curve to be utilized practically, the eutectic temperature T_E should be reached at a low concentration of $X_{substance}$. Below the liquidus curve and adjacent to it, there is a metastable state, such that when this is crossed, spontaneous nucleation takes place. In the metastable region of the phase diagram, the reactions of Scheme 4 take place. These reactions have so far been very little investigated experimentally. A complex array of processes and conditions determine the width (ΔT) of this important zone. These include cooling velocity, hydrodynamic state, concentration of dissolved and undissolved foreign substances, type of solvent and extent of solvation, dwell times, etc. In the case of mass crystallization (see Section 3.1), the attempt should be made to cause nucleation in the system without too large a step beyond the metastable zone. If seed nuclei are used, it is advantageous to superheat the system, and then to keep it always within the metastable zone, so that controlled growth is then possible without the formation of secondary nuclei.

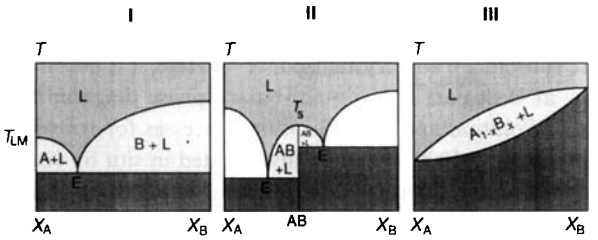


Fig. 6. (T,X) Phase diagram for two-component systems (A/B) as a basis for: solution growth of B (I; see also Fig. 7); the melt growth or flux growth of a congruently melting compound AB (II); the growth of mixed crystals $A_{1-x}B_x$ (III). L: liquid phase, E: eutectic point; T_{LM}, T_S: melting points of solvent and of substance AB, respectively.

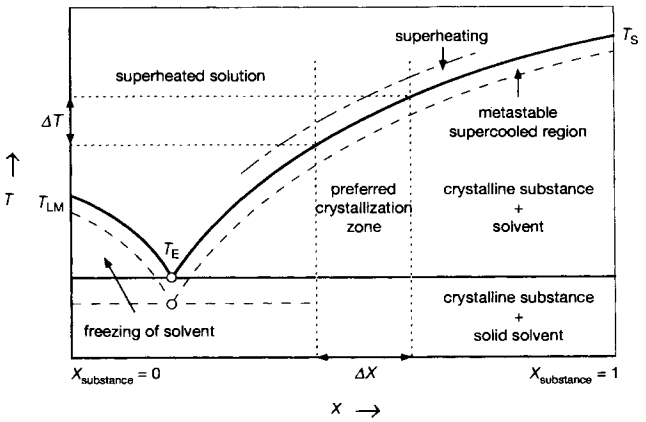


Fig. 7. Phase diagram (T,X) of solution growth, showing optimum crystallization zone (ΔT,ΔX), and metastable region of supersaturation and of superheating. The region of freezing of the solvent is shown on the left of the diagram (see Sections 3.1.1 and 4). T_{LM}, T_S: melting points of solvent and substance S, respectively; T_E: eutectic temperature.

With regard to the classification of crystallization processes to be described later, it should be said that if crystallization is regarded as a phase change of a system of one or more components, this leads to a systematization of the general methods (Laudise,[99] Arend[100]). Sections 3 and 4 give more details of individual processes.

2.3. Morphology as a Property

Growth processes lead not only to the formation of the real structure of a crystalline solid (which largely determines its physical properties), but also to the creation of a morphology, which determines the real structure by means of the growth mechanisms of the individual faces, and also creates additional properties. The scale of this effect extends to large three-dimensional crystals with specific crystal habit, two-dimensional epitaxial thin films, one-dimensional fiber crystals or whiskers, and "zero-dimensional" "quantum dots". For about 15 years, methods of two-dimensional crystallization (liquid-phase epitaxy (LPE), MBE, and MOCVD) have enabled functional semiconductor structures to be produced.[70, 71] Homo- and heteroepitaxy increasingly includes other classes of materials such as oxides (ABO_3 ferroelectric materials,[98, 101] magneto-optic garnets[102]), and even organic compounds. Also in the area of three-dimensional crystals, process control of the morphology has become important. The Stephanov process,[103] for example, enables crystals of sapphire and $LiNbO_3$ in the form of plates, tubes, and other shapes to be pulled. Silicon single crystals for solar cells have recently been produced with a profile in the form of a thin-walled polygon (see Fig. 2).[63]

In industrial mass crystallization and general crystal growth, those molecular processes are of interest which lead to the formation of a specific growth morphology. Here, the distinction

must be made between mechanisms for pure substances and those influenced by surface-active [(*hkl*)-specific or site-specific] foreign materials. For pure substances, the morphology is determined by stability/instability criteria in the crystal–nutrient interface (CNI), and is essentially controlled kinetically. Depending on the extent of supersaturation and on the mass and heat flow, polygonal, hopper-shaped, dendritic,[49] and irregular (even fractal)[7] growth is observed (Fig. 8).[72]

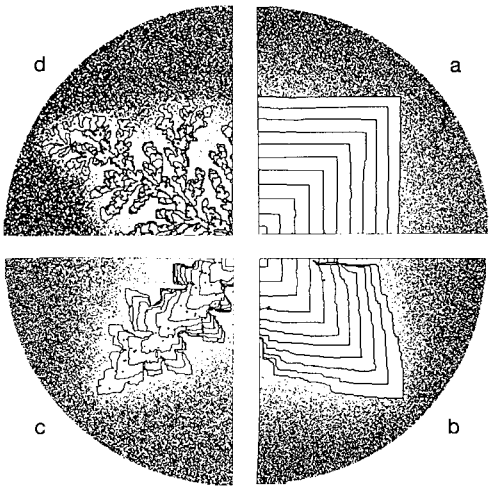


Fig. 8. Monte Carlo simulations of growth in two dimensions as a mathematical function of the driving potential (from [72]). a) Polygonal surface growth, b) transition to hopper-shaped growth, c) dendritic growth, d) irregular growth.

In general, the end morphology of a faceted crystal is determined by the slowest growing faces. The theory of Hartman and Perdok can be used to predict flat crystal surfaces ("periodic bond chains", so-called PBC vectors;[104] for new developments see ref. [85]), according to which, the (*hkl*) faces with the lowest energy of attachment of a growth layer show the lowest face growth rate R.

Even small concentrations (ppm) of suitable foreign substances can influence growth, for example, by molecular recognition mechanisms, and can retard rapidly growing surfaces. With the synthesis of tailored additives ("habit modifiers"), the formation of a desired crystal habit or form of agglomerates is realized in industrial crystallization,[52, 62b] enabling the properties of a large number of products in powder form to be controlled (purity, bulk density, dissolution rate, etc.). The activity of foreign substances is deduced experimentally from the form of the function $R(\sigma, X_{\text{foreign substance}})$. Here, it is certain that in situ atomic force microscopy will yield interesting results within the next few years.[78] As well as the effect of the foreign substance on R, the effect on the nucleation rate J is of practical as well as theoretical interest. The majority of the well-known crystallization problems in organic synthetic chemistry must to some extent be caused by small or large amounts of mainly unknown foreign substances.

Considerable progress in the understanding of molecular recognition processes achieved during the last decade,[29, 35] have, according to Davey et al., had the result that "tailor-made additives for the control of specific processes are now a reality".[62b]

3. Experimental Methods of Crystallization

Crystal growth is a science and an art. The scientists' role in the crystal growth process is that of an assistant who helps molecules to crystallize. Most molecules, after all, are very good at growing crystals. The scientific challenge is to learn how to intervene in the process in order to improve the final product.
Etter[105]

Following the classification made in Section 1, the techniques of mass crystallization and of true methods of crystal growth (exploratory and advanced) are treated separately. We shall therefore collate the crystallization techniques described in the chemical literature, briefly discuss them, and hence elucidate the basic principles of the most commonly used process of solution crystallization. The obvious consequences for methods of mass crystallization on the laboratory scale are set out in Sections 3.1 and 3.2. As examples of bulk growth, three crystal growth processes are described in Section 3.3. These are used in materials research into molecular substances for nonlinear optics.

3.1. Mass Crystallization on the Laboratory Scale

The processes listed in Sections 3.1.1–3.1.5 are described in the extensive literature on industrial crystallization[50, 106] and chemical laboratory practice :[15, 17, 18]

3.1.1. Crystallization from Solution

Crystallization from solutions has mainly two aims: the isolation of a solid, which was synthesized in solution, and the stepwise purification of a soluble solid. Isolation: Crystallization is achieved by 1. complete, usually rapid (isothermal) evaporation of the solvent (rotary evaporator); 2. partial or complete, usually slow (isothermal) evaporation of the solvent (crystallizing dishes, open to the atmosphere or in a desiccator); 3. slow or rapid reduction of the temperature of a saturated solution (without evaporation); 4. freezing of the solvent; 5. precipitation by the (isothermal) addition of reactive components or solvent components to reduce solubility (addition by diffusion or with stirring); 6. salting out by the (isothermal) addition of a strong electrolyte; 7. spray drying by rapid evaporation of the solvent by pressure reduction (flash evaporation); 8. freeze drying; 9. electrocrystallization; 10. molten salt synthesis (at high temperatures);[107] 11. hydrothermal synthesis.[108]

Here, in practice, crystallization is essentially performed more rapidly than with single-crystal growth, the purity of the substances obtained is rather less, and the crystallized material often shows inclusions of solvent. Success depends greatly on the choice of solvent,[109] and on the nature of the impurities present. Van der Sluis et al.[110] have used statistical analysis methods to determine which solvent molecules are preferentially included in the crystal lattices of known organic compounds: water to 61%, dichloromethane to 6%, benzene to 5%, methanol to 4%, acetonitrile to 2%, and dimethyl sulfoxide to

0.5%. These figures indicate the proportion of the structures that can include solvent molecules or form solvates. It should also be noted that the concentration and frequency of the inclusions are strongly dependent on the growth conditions (kinetic effects, see Section 2.1), which are usually not discussed in this connection.

Even if the aim of the crystallization is the isolation of a compound, the principle applies that the material should be purified by other methods before crystallization, and analysis for trace elements or molecules for control purposes should be included.

If a compound needs to be purified in a stepwise manner, this can be achieved by crystallization with rejection of mother liquor or by fractional crystallization with reuse of mother liquor.

3.1.2. Crystallization from the Melt

Crystals that form from molten substances can be obtained by zone melting carried out one or more times, by Bridgman techniques or by solidification of a supercooled melt. Whereas solution processes cover almost the entire range of classes of materials, melt crystallization is restricted to those that are thermally stable in the liquid state at their melting point, and where chemically inert vessels are available (a problem with high-temperature superconductors, see Section 4.2). Zone melting has been of great importance for the purification of thermally stable materials for a long time.[111] Bridgman techniques have been applied in many cases.[34]

3.1.3. Crystallization from the Gas Phase

Crystals form from the gaseous state by 1. sublimation and desublimation in a vacuum or in a gas flow, 2. chemical transport, 3. reactive deposition from the gas phase (chemical vapor deposition CVD). Quantitative crystallization from the gas phase is usually of limited application due to the low vapor pressure of the component being transported. With semiconductor materials (Si, ZnSe, ZnS, SiC, etc.), CVD is an important process.

3.1.4. Crystallization in the Solid State

Crystals form likewise from solids by 1. recrystallization, 2. devitrification (slow crystallization of supercooled organic and inorganic glasses), 3. reactive solid-state diffusion and ceramic synthesis, 4. sol-gel syntheses of ceramic materials.[112]

The crystallization of the so-called oils of organic compounds (glassy, high viscosity condensed phases), which is often described as difficult, is here discussed in more detail. The fundamental investigations of Tammann have led to the formulation of rules for the nucleation behavior of organic melts (see Section 2).[15, 18] According to these, for complex molecular materials, the temperature T_N of the maximum rate of nucleus formation J can be considerably below the temperature T_G of the maximum rate of crystal growth. As exemplified by glycerine, this difference can be as much as 65 K in exceptional cases.[34] It is generally known that many organic melts that are thermally fairly stable (benzophenone, salol, benzil, etc.) can be strongly supercooled,[113] without producing growth nuclei within a reasonably short time. As the nucleation rate J is in general reduced by dissimilar dissolved materials, prior purification and trace analysis are of the greatest importance, and active impurities must be limited to the ppm concentration range. To bring about the crystallization of analytically pure, stable, but difficult to nucleate supercooled melts (see ref. [15], therein Fig. 1, 2), the samples are preferentially heated above the melting point, slowly supercooled (1 K min^{-1} to 1 K h^{-1}), and repeatedly subjected to temperature cycling at temperatures just below the melting point (5–20 K), so that the oily substance does not completely harden in the supercooled region (insufficient diffusion, Eq. (d), Section 2.1). Slow heating and cooling, with periods of constant temperature (hours to days), at various temperatures (induction periods) can be helpful in finding the regions for T_N and T_G, which sometimes do not overlap. For most real systems (material + its surroundings), heterogeneous nucleation is more probable than homogeneous nucleation. Therefore, purification of the melts should only involve the removal of dissolved impurities. The introduction of a matrix with a similar lattice structure can lead to crystallization by heteroepitaxial processes. For other induction possibilities (e.g., by ultrasound), see references [18, 50].

3.1.5. Crystallization by the Formation of Derivatives

Several organic compounds crystallize better 1. as salts (alkali metal or ammonium salts), 2. as hydrochloride, 3. as metal–salt complex, 4. as molecular compounds (diastereomeric reaction partners for racemate separation), or 5. as inclusion compounds.[114]

3.1.6. Basic Principles of Chemical Crystallization from Solution

Although many methods are available, for most newly synthesized substances, only crystallization from solution (temperature reduction or evaporation) is used. (For a critical review of crystallization from solutions and melts, see Matz.[50]) The further development of efficient and versatile laboratory methods of solution crystallization that take advantage of established knowledge of nucleation and growth mechanisms are therefore still important for synthetic chemistry.

If one wishes to obtain crystals from solution efficiently, the following points should be taken into consideration:

1) Choice of a chemically stable two-component or multicomponent system without formation of solid solutions and with a eutectic temperature T_E for small values of $X_{substance}$ (see phase diagram in Fig. 7; solvents: see refs. [34, 109]).
2) Exclusion of components that inhibit nucleation and growth (which may include solvents).
3) Suitable concentration range for crystallization: $\approx 5\,wt\% \lesssim X_{substance} \lesssim 30\,wt\%$ (for systems showing good nucleation properties, superheating for a short period at 5–20 K above saturation temperature is recommended; otherwise not). When growing large single crystals, the $X_{substance}$ concentration should be as high as possible.
4) The optimum nucleation and growth temperatures (in particular for molecular crystals) are usually considerably below

the melting point of the pure material, and considerably above the eutectic temperature or the melting point of the pure solvent.

5) After successful nucleation (N) at $T_N < T_G$ (Fig. 7), volume growth (G) should be carried out closer to the saturation temperature (but always within the metastable region) and with increasing depletion of the solution at a temperature that is reduced in a controlled manner with thorough mixing (maintenance of constant supersaturation). The chemical laboratory equipment normally available is not suitable for these operations. A heating bath with programmable temperature is required (see Section 3.2).
6) When working with spontaneous nucleation, small amounts of insoluble solids should not be removed for the first crystallization of the compound, as these usually reduce the nucleation threshold. However, for later crystallization, solid particles can lead to macrodefects (inclusions of solution and particles), and are to be avoided.

If careful attention is paid to the complex relationships during crystallization and to systematic working methods, a solution to many difficult problems can be found, sometimes quite quickly. This implies that proficiency in crystallization should always remain a part (preferably increasing) of theoretical and practical chemical education.

This results in the following approach for chemical mass crystallization:

1) The first nuclei are prepared by exploratory methods of crystal growth (see Section 3.2).
2) Mass crystallization (on the laboratory scale) is carried out by using process control comparable to that used in growing bulk single crystals. This increases the chance (in the sense of Section 1) that the synthetic chemist will, on average, obtain significantly larger crystals than hitherto, and that (in special cases) it will be possible to use these for an initial determination of solid-state physical properties.

By this "trick of the trade", the area of interest and the experimental practice of traditional synthesis may be extended in the direction of single-crystal synthesis and solid-state properties of interesting classes of substances. So-called "exploratory" methods of crystal growth can be of further assistance, as these attempt to give maximum control of the process at minimum cost.

3.2. Exploratory Methods of Crystal Growth

Compared with the major improvements of the last decade in almost all structure-determination steps of X-ray crystallography, crystallization lags behind.
Van der Sluis et al.[115]

In Section 1 we commented on the significance of crystallization for chemistry. Crystal structure investigations must today be the largest (nonindustrial) consumer of small single crystals. The preparation of suitable samples ($d \approx 0.1-0.3$ mm, as isometric as possible) is therefore becoming more and more *the* rate-determining step. Initial attempts at designing a versatile set of apparatus for purposeful crystallization are already in existence.[100, 115, 116]

Exploratory techniques have the advantage that they require relatively simple equipment in the chemical laboratory and that only small amounts of substance are necessary. The process operation has the best possible control of crystallization parameters, preferably self-regulating. During the measurements the solution and crystallization phenomena can be visually observed. The crystals can be removed without mechanical and thermal stress and without serious surface contamination.

With the aim of applicability over as wide a range of substances as possible, the following should be considered:

1) Isothermal evaporation (Fig. 9), 2) temperature reduction (also in a gel, Fig. 10), 3) temperature difference methods (Figs. 12, 13), 4) isothermal diffusion (in droplets (Fig. 14a), using membranes (Fig. 14b), in a gel (Fig. 14c), or through a coating), 5) melt growth in capillaries, 6) sublimation/desublimation (evaporation from Knudsen cells, Fig. 17), 7) chemical transport and reactive evaporation, 8) high-temperature solution growth (see Section 2.2, Fig. 4), and 9) hydrothermal solution growth (miniaturized equipment, see Fig. 18).

For methods 1–5, it is necessary to have chambers with temperature control, homogeneous heating, and controlled atmospheres (commercial ovens are not always suitable), which incorporate visual observation by a binocular microscope, and where small crystals can be removed.

The important features of these techniques are illustrated in Figures 9, 10, and 12–19. For example, for controlled isothermal evaporation (Fig. 9), the walls of the vessels should be such that the solutions do not creep up them to a great extent (silanated glass or polytetrafluoroethylene (Teflon) should be used), unless it is intended to use this as an effective method of promoting nucleation. The junction of the walls to the floor should be

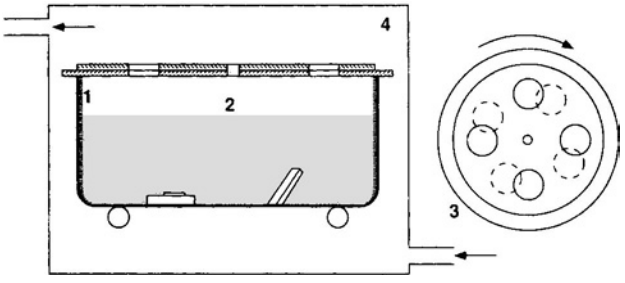


Fig. 9. Crystallization vessel with flat or slightly convex bottom for isothermal evaporation of the solvent. 1: Silanization to prevent creeping of the solution. 2: Supersaturated nutrient phase. 3: Lid with turnplate with apertures for the regulation of evaporation rate. 4: Arrangement in homogeneously heated chamber with through flow of gas and access for observation and removal of samples; T = constant.

gently rounded and it is advantageous when the floor is convex (the vessel being held vertical by standing it on a ring), and the clearance of the loosely fitting lid can be adjusted by a turnplate. A saturated solution of the substance to be crystallized should be prepared in a separate vessel at the evaporation temperature, and, before charging, 5–10 vol% solvent should be added to reduce the concentration below saturation. When the first crystals become visible, the solution is usually too strongly supersaturated, causing rapid growth to start. This should be retarded by a slight increase in temperature (if $\partial X_{substance}/\partial T > 0$). The

gas flow through the evaporation chamber should be reduced at the same time. It is recommended that the first crystals should be almost completely redissolved in the solution, so that they can then be allowed to grow slowly as has been described. The removal of small crystals ($d \approx 0.1-0.3$ mm) requires great care. A thin-walled capillary can be used with a mechanical means of applying reduced pressure (with fine adjustment), so that the small crystal brings with it a minimal amount of solution. The nutrient phase and the crystal are then ejected into a large volume of preheated liquid in which the crystallized compound is less soluble (only for stable hydrates and solvates). After a small amount of etching of the crystal, it is again picked up and transferred to the absorbent base of a preheated container, which also serves for the removal and slow cooling of the crystal. Meanwhile, the growth of the remaining crystals continues fairly undisturbed. The other crystallization methods also require an equal amount of care. In general, isothermal evaporation is the preferred choice if $\partial X_{\text{substance}}/\partial T < 0$. High-temperature variations of the method are discussed by Elwell et al.[96] and Wanklyn.[97]

Crystallization in a gel by reducing the temperature (Fig. 10 right): Crystallization from gels is usually used for sparingly soluble salts, by using counter-current diffusion.[34, 117, 118] For

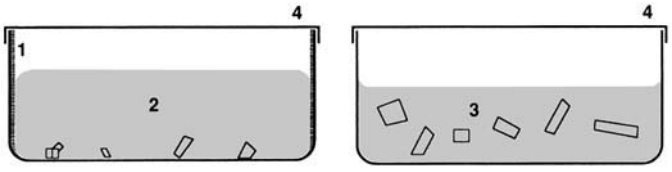


Fig. 10. Crystallization vessels for lowering the temperature of a solution (left) or of a gelled solution (right). 1: Silanization. 2: Solution. 3: Gelled solution (in superheated state). 4: Lid with observation facility (similar to Fig. 9).

substances of normal solubility, an aqueous or ethanolic/aqueous solution can, for example, be gelled in the supersaturated state by adding 5–10 vol% tetramethoxysilane (Arend et al.[119]) in the superheated state. Nucleation takes place normally in a strongly supercooled state. This is retarded by increasing the temperature, and the process then changes to slow growth of single crystals. The crystallization from gels by reducing the temperature has the advantage that phenomena associated with convection are prevented; thus, growth takes place purely by diffusional matter transfer. If gels are absent, the crystals grow preferentially at the bottom of the vessel and are fed from one direction only. For the same reason, the growing nuclei in a gel tend to be more widely separated (self-regulating mechanism), so that fewer agglomerates are produced. Typical growth times after the induction phase are weeks or months. Small crystals are picked up together with a piece of gel, and then treated in the manner already described. By using flat (closable) dishes and a relatively thin layer of gel, the continued growth of remaining crystals is possible. The gel growth method has recently been used successfully for nonlinear optical organic compounds (Fig. 11).[120a] This very simple method provides serious competition to the technique of growing molecular substances in space (removal of gravitational convection).[120b] Also, experiments with gels should be valuable for the investiga-

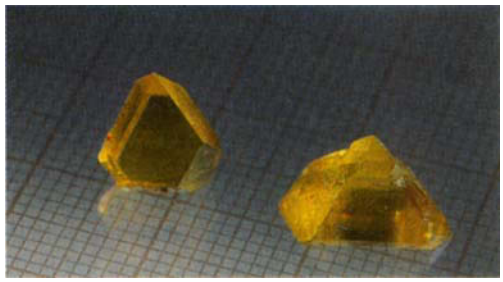


Fig. 11. Solution growth of PNP (B. Březina, ETH, Zürich): Gel growth by lowering the temperature (left: maximum crystal size $d \approx 1$ cm), and by growth in a solution moving with laminar flow (right: starting from a *b* platelet seed crystal, the crystal grew preferentially in the direction of the pyroelectrically negative pole ($\Delta T > 0$) of the polar twofold axis; see Fig. 21). Use: measurement of nonlinear optical and electro-optical effects [169].

tion of deviations from the 1:1 distribution of D and L crystals ("chiral symmetry breaking"[121]) as the mobility of secondary nuclei is here much reduced.

Temperature-difference method (Fig. 12): This system has a wide application spectrum (provided that $5 \lesssim X_{\text{substance}} \lesssim 30$ wt%, $\partial X_{\text{substance}}/\partial T > 0$[122]). The separately saturated solu-

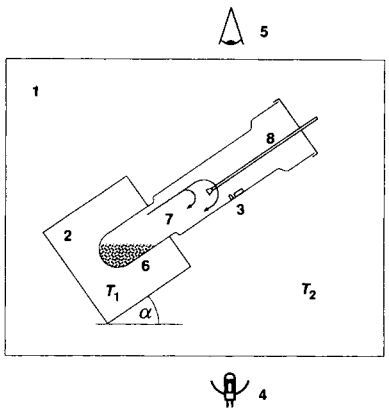


Fig. 12. Crystallization by the temperature-difference (ΔT) process (from [122], modified). Arrangement for the observation of spontaneous crystallization or growth upon nuclei. 1: Thermostatically controlled air bath. 2: *T*-controlled Al block inclined at angle $\alpha = 10-30°$ ($\Delta T = T_1 - T_2 = 1-5$ K). 3: Glass vessel with rectangular center section [123] and screw lid, 4: Cold light illumination. 5: Observation by binocular microscope. 6: Supply of solid phase. 7: Flow due to thermal convection. 8: Holder for seed crystal (eccentrically mounted) for seed-growth experiments.

tion at T_2 is placed in the glass vessel (with a small excess of solid phase at the bottom), so that, in the temperature gradient $\Delta T = T_1 - T_2 < 1-5$ K, the solution, rising by natural convection, becomes supersaturated, and begins to form nuclei spontaneously (self-regulating mechanism). The central part of the closed vessel should preferably be a smooth rectangular glass vessel (inside dimensions: 12, 15, 23 mm),[123] so that the faceted growth of the crystals is not disturbed by the curvature of the vessel wall. Two conditions are recommended to give the most favorable crystallization parameters: a) Single-sample operation, as described in Figure 11, while observing with a binocular microscope and slowly increasing ΔT, b) series operation in a crystallization matrix (Fig. 13). Around 50 crystallizing

vessels can be placed in conventionally heated cabinets fitted with the appropriate equipment. As indicated, crystallization can also be carried out by using seed nuclei. The small crystals should be removed in the manner described. Typical crystallization times can be several weeks. As this process operates after reaching a stationary state of constant supersaturation, it can also be used to produce macroscopic homogeneous single crystals of solid solutions.[122]

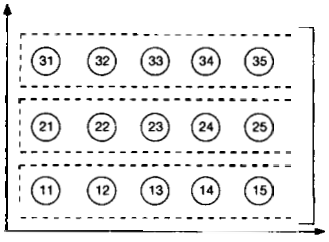


Fig. 13. Crystallization matrix for the determination of optimum growth conditions; on the y axis the temperature difference ΔT is varied and on the x axis the solvent is varied. Series arrangement using sample tubes in a matrix [123] PR_{ij} (i: ΔT, j: solvent) in a heated cabinet [122]. The temperatures of the blocks (shown by dashed lines) are individually controlled, so that a constant $\Delta T(i)$ with respect to the ambient temperature (i.e. of the heated cabinet) is obtained. The blocks have several holes (numbered) for the sample tubes PR_{ij}. ΔT influences the supersaturation and flow velocity.

Based on many years of experience (Arend, Hulliger) with a wide range of classes of substances, the chance of success of crystallization with the ΔT method is over 90%. It is possible to extend the process to large crystals[122a] and to the use of high temperatures (approximating to hydrothermal in subcritical pressure ranges).

The isothermal diffusion method (Fig. 14) also has a wide application spectrum, and the "sitting-drop" version of this is reported to be most successful.[115] Also included here is gel crystallization by counter-current diffusion of two components

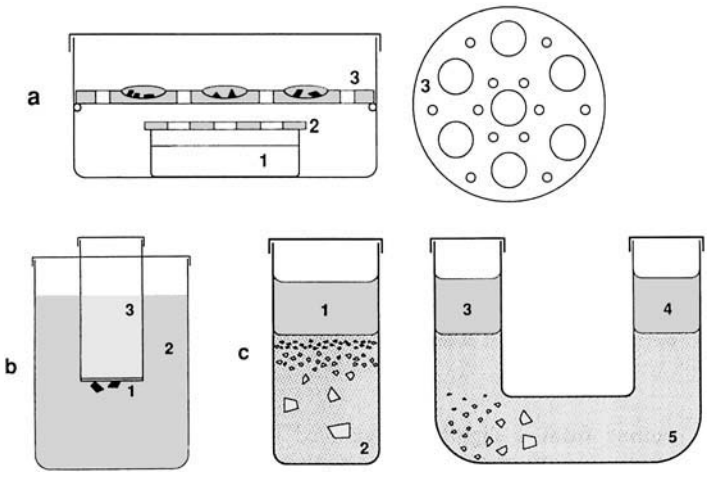


Fig. 14. Crystallization by isothermal diffusion a) "sitting drop" method. 1: Precipitating agent, 2: control of evaporation rate, 3: plate with hollows for receiving the drops (see also commercial products for protein crystallization); b) diffusion through a membrane. 1: Membrane, 2/3: solution/precipitating agent; c) two types of diffusion in the gel (see also [34, 117]): mostly unidirectional diffusion into the gel (left-hand diagram 1: precipitating agent or second component) or counter-current diffusion (right-hand diagram 3, 4: components A and B in solution), 2: gel with crystallizing substance, 5: initially pure gel.

(a slow precipitation reaction), in general using inward diffusion of components that reduce solubility or change pH (substance example:[124], see Fig. 15). It is also possible to work with the help of a **membrane.**[125]



Fig. 15. Gel growth of silver periodate by pH reduction ($AgNO_3$, H_5IO_6, and sodium silicate gel). **Yellow crystals: $Ag_2H_3IO_6$, red-brown crystals (black in photograph): Ag_2IO_5 [124].**

Melt growth in capillaries may be used if, for example, only small amounts of material are available. The cylindrical crystallizates formed can be used for X-ray work, either together with the capillary (Lindemann glass) or after etching. A modern application of melt growth in glass capillaries is in the production of nonlinear optical organic fibers (Fig. 16).[126]

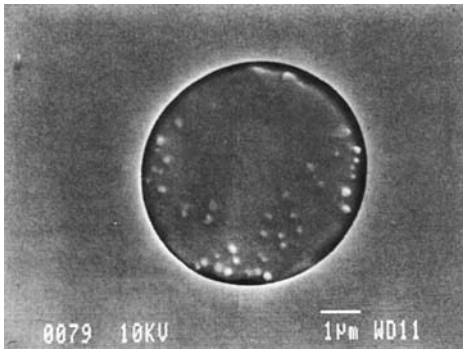


Fig. 16. Modern application of melt growth in glass capillaries. Fiber single crystal of 4-(*N*,*N*-dimethylamino)-3-acetamidonitrobenzene (DAN). Internal diameter = 6 µm. With DAN fibers, a high efficiency was obtainable in optical frequency doubling experiments (Nd:YAG, 1064 nm) (Kerkoc et al. [126]).

Sublimation and Desublimation (Fig. 17): In addition to the well-known variations of gas-phase crystallization, the technique of controlled evaporation from Knudsen cells should be mentioned here.[127] This system (Fig. 17) can be used for crystallization by forming derivatives, but particularly for producing macroscopically homogeneous solid solutions (other processes are given in ref. [34] and by Karl[111]).

Possible processes for crystal growth by using chemical transport reactions are described in the well-known work of Schäfer.[128]

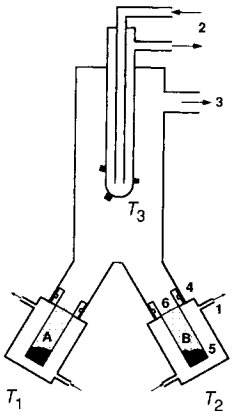


Fig. 17. Growth from the gas phase by controlled evaporation from Knudsen cells [127]. (T_1, T_2: cell temperatures, T_3: temperature of deposition (cold finger). Suitable for the growth of mixed crystals $A_{1-x}B_x$ by separate evaporation of $A(T_1)$ and $B(T_2)$, and for low temperatures (unstable compounds). 1: Inlet or outlet for heating liquid. 2: Connections for coolant. 3: To high vacuum pump with cold trap. 4: Knudsen cells sealed with O-rings. 5: Supply of solid phase. 6: Aperture for controlled evaporation rate at cell pressure $p(T)$.

The hydrothermal crystallization process involves considerable cost.[34, 129] Moret has developed a small apparatus for exploratory work (Fig. 18),[130] which was used in reactive counter-current diffusion experiments for forming single crystals of a series of compounds, including $NiFe_2O_4$, $KFeF_4$, Te_4O_9, $PbCu_6O_8$, Cu_2I_2. The construction of autoclaves, in general, is described by Laudise et al.;[131] the hydrothermal synthesis of inorganic substances by Rabenau.[108]

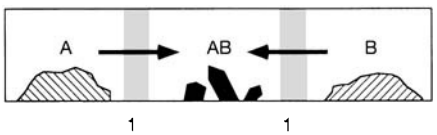


Fig. 18. Schematic diagram of a hydrothermal reactor for the synthesis of AB by counter-current diffusion of the starting materials A and B through a diaphragm (1). Miniaturized, easily operated equipment for the synthesis and single-crystal growth of small crystals is described by Moret [130]. (Reactor dimensions: $l \approx 15$ cm, internal diameter ≈ 0.7 cm; see also [108]).

This discussion of the practical aspects of exploratory crystal growth is deliberately not oriented towards particular classes of substances, but has attempted to propose a developable range of basic equipment whose design must be optimized in individual cases. The classification of processes according to substances is based only on distinctions such as low melting point, high melting point, stability/instability, etc. The substance-based approach, which corresponds more closely with chemical thought, has not proved useful in crystal growth. Chemically unimportant differences in the structure of the molecules or in associated impurities can affect crystal growth disproportionately, and can influence the choice of process decisively. The present approach should provide useful guidelines and should enable crystallization to be carried out by the most adequate means as the *last synthesis step*. It should also lead to an improvement in the reproducibility of crystallization results in the majority of cases.

3.3. Discussion of Modern Methods of Advanced Chemical Crystallization

A fairly complete overview of advanced methods used today can be obtained from the following articles: Gilman (Ed.),[132] Pamplin (Ed.),[133] Laudise,[99] Elwell et al.,[96] Dryburgh et al. (Eds.),[134] Wilke et al.,[34] Arend et al. (Eds.),[135] and Hurle et al. (Eds.).[136]

Three processes will be described in more detail. These are currently used for growing single crystals of nonlinear optical molecular crystals. Their applicability to other classes of compounds depends on specific properties which cannot be discussed in general terms.

3.3.1. *Crystallization from Slightly Supercooled Organic Melts*

Under certain conditions, the strong tendency of organic melts to supercool (Section 3.1.4) can be successfully used for the synthesis of single crystals of cm^3 dimensions, and for making single crystals that are almost perfect crystallographically. For this, pure materials are required that are sufficiently thermally stable for long periods (days or weeks). These are melted, preferably degassed, superheated (10–20 K), slightly supercooled ($\Delta T \approx 0.1$–2 K), and can then be crystallized by the complete immersion of a seed crystal. Scheffen-Lauenroth et al. and Klapper[137] have recently demonstrated the usefulness of this method with salol, benzophenone, and benzil. Using equipment similar to that shown in Figure 19 (left), a strongly nonlinear optical compound (COANP: 2-cyclo-octylamino-5-nitropyridine) could be crystallized (Fig. 19 right).[138] Crystal

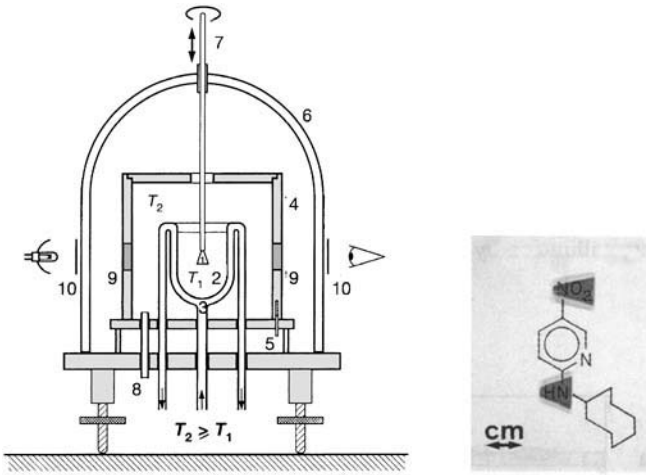


Fig. 19. Left: Crystallization from a supercooled melt (Hulliger et al. [138]). 1: Seed crystal (completely immersed: crystal pulling also possible). 2: Isothermally heated melt. 3: Glass vessel with water cooling. 4: Heating for gas atmosphere. 5: Pt-100 control thermocouple. 6: Vacuum hood. 7: Equipment for moving seed crystal (translation or rotation). 8: Inert gas inlet. 9: Red glass (protection against short wave light). 10: Polarizer, analyzer, and cold light illumination (IR filter not shown). Right: COANP single crystals (1 mm thick platelets) produced by crystal growth from slightly supercooled melts by complete immersion of the seed crystal [138]. Growth time: 1–2 weeks. Application: frequency doubling experiments and measurement of electro-optical effect [169].

pulling from a slightly supercooled melt produced cm^3-size single crystals of COANP which had not been obtainable by other methods.[139] Moreover, the same growth method has led to the discovery of the first purely organic photorefractive crystal.[139, 140] The investigation of the physical state (vitreous state and cluster formation) of supercooled COANP melts is described by Kind et al.[141] Crystal growth from supercooled melts has at least two important advantages over normal meth-

ods (zone melting and Bridgman techniques)[34]: The growing crystal is surrounded only by the liquid phase (as well as by the seed holder), and the growth takes place under virtually isothermal conditions.

3.3.2. Crystallization by Isothermal Evaporation with Resaturation

The principle of controlled isothermal evaporation and resaturation has attractive advantages compared with temperature-reduction methods. This method is 1) possible when $\partial X_{substance}/\partial T \lesssim 0$ and for relatively small values of $X_{substance}$; 2) single-crystal synthesis is possible when the evaporation temperature is constant and as low as necessary (unstable compounds). Bösch et al.[142] and Hesse et al.[143] crystallized alkali metal hyperoxides, peroxides, as well as ozonides from liquid ammonia by this technique. Fuith et al.[144] discussed the design of the apparatus shown in modified form in Figure 20 (and the growth of, for example, sulfate crystals). This apparatus is also used by the present author for organic compounds.

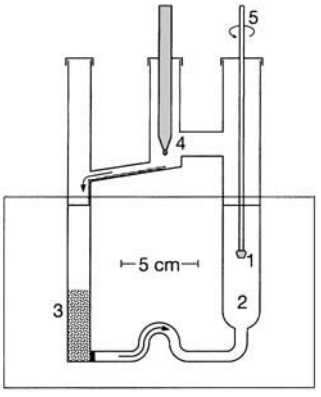


Fig. 20. Crystal growth by isothermal evaporation (arrangement placed in a thermostatically heated water bath) with resaturation (Fuith et al. [144], modified). 1: Seed crystal. 2: Solution with hydrostatic equilibration. 3: Nutrient material. 4: Cold finger (thermostat or Peltier element) for condensation of solvent. 5: Rotational movement of crystal (for relatively rapid growth).

3.3.3. Crystal Growth in Laminar Flow by Lowering the Temperature of a Solution

Convection phenomena or other uncontrolled flow conditions in the nutrient phase can reduce the width of the metastable area of supercooling[68] and lead to the formation of undesired growing crystal surfaces (defect formation and morphological instabilities).[91, 145] The hydrodynamic state of the system is more easily controlled by a directed, almost laminar flow over a seed nucleus (stationary or intermittently rotated, Fig. 21). Furthermore, thorough mixing is ensured by the careful selection of the method of propelling the solution. In some cases, growth rate by the solution process is considerably increased at increased flow velocities (several $cm\,s^{-1}$). This has been used for the relatively rapid growth of very large crystals of KH_2PO_4 (see Fig. 1).[146] Also, in cases of strongly anisotropic growth, the directed flow improves deposition on slowly growing surfaces. This should have many small-scale applications. At the present time, the author is crystallizing nonlinear optical compounds, such as 2-(*N*-(L)-prolinol)-5-nitropyridine (PNP) (Fig. 11) and 4′-dimethylamino-*N*-methyl-stilbazonium-*p*-tosylate (DAST: one of the strongest electro-optical organic compounds known today) by this method.

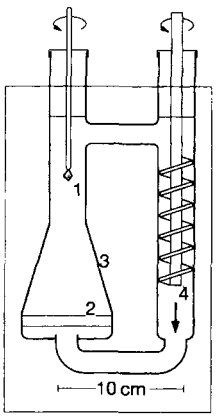


Fig. 21. Crystal growth by lowering the temperature (arrangement placed in a temperature-controlled water bath) under smooth fluid flow: 1: Seed crystal in a zone with almost laminar flow. 2: Diaphragm or glass spheres (disturbance of stream lines). 3: Cone (smoothing and compression of the flow). 4: Propulsion helix (Delrin).

4. Progress in the Single-Crystal Growth of Materials of Topical Interest

4.1. Special Literature Information

A wide-ranging review of developments in the crystal growth of approximately 2000 compounds is available in the latest edition (1988) of the highly regarded standard work of Wilke and Bohm (349-pages index of materials information and literature).[34] Another compendium will be available in 1993, namely the first handbook of crystal growth, including the newer methods and materials (MBE, MOCVD, superconductors, proteins, etc.).[136] Current work (e.g., CA selects, "crystal growth", etc.) is reported in the *Journal of Crystal Growth*, which also publishes the reports of the conferences held by the ICCG (International Conferences on Crystal Growth) that take place every 3–4 years. Journals of national speciality groups[147] may also be of interest, since they publish lists of grown crystals (special materials), and name indexes from time to time.

4.2. High-Temperature Superconductors: Oxocuprates

Up to three or four years ago oxocuprates were a class of chemical compounds no more remarkable than countless others.
Müller-Buschbaum[148]

With the discovery of the relatively high transition temperature of $La_{2-x}Ba_xCuO_4$,[149] the superconductivity of several oxides [NbO, $SrTiO_3$ (doped), $LiTi_2O_4$ ($T_c = 13.7$ K), $BaPb_xBi_{1-x}O_3$ ($T_c = 13$ K), known for quite a long time] became the center of interest of solid-state science virtually overnight.[41, 150] Where is the challenge of growing crystals of this type of material?

It was soon realized that for $La_{2-x}M_xCuO_4$ (M = Ba, Sr) and the related compounds of Y-Ba-Cu-O, Bi-Ca-Sr-Cu-O, Tl-Ca-Ba-Cu-O, etc., the controlled three- and two-dimensional crystal growth (see Section 2.3) of the oxocuprates requires detailed knowledge of the stability regions (primary crystallization fields) of incongruently melting substances within a pseudo-ternary or pseudo-quaternary phase diagram, including oxygen pressure, so that the pure compounds can be crystallized from

nonstoichiometric melt solutions.[151a] The determination of phase diagrams and the crystal growth itself are made more difficult by complex reaction equilibria that are established kinetically slowly.[152] Moreover, the Ba-Cu-O liquid phase has extremely corrosive properties, which require the development of resistant crucible materials:[153] "Corrosion of the crucible is the most basic problem for crystal growth of the high T_c superconductors" (Changkang[151a]). The determination of the phase diagram of YBCO has given very variable results (Fig. 22).[152e] Also, the use of foreign fluxing agents, in analogy to the usual process of flux growth, gives mainly negative results. Watanabe has tested nearly 100 flux compositions at various temperatures,[154a] and concludes: "The present results suggest that a more extensive and detailed search for a suitable flux may be worthwhile: but there may be no suitable flux"[154a] (apart from self-fluxing[154b]).

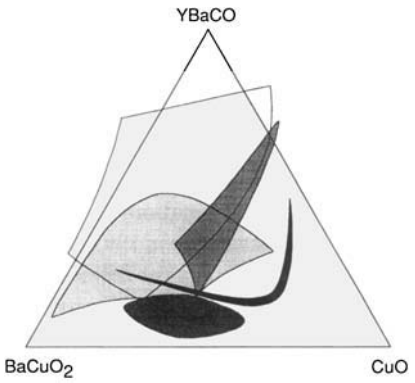


Fig. 22. Graphic design or the key to YBCO crystallization? Primary crystallization fields from the results of several authors (from [152e]).

Nevertheless, mm-size single crystals were occasionally produced. However, the still-awaited breakthrough in oxocuprate crystal growth depends on: 1) the chemical stability of liquid phases towards crucible materials yet to be developed[151b] (cold crucible processes are conceivable), 2) knowledge of the phase diagram (T, X_i, p) and of the purity of the phases (effects of impurities), 3) the establishment of equilibrium (oxygen pressure) and the homogenization of the liquid phase (mixing, superheating), 4) the control of growth kinetics within the metastable region of supercooling. The solution of the crucible problem is of the greatest importance, and not only from the practical point of view: side reactions disturb the equilibration of the oxocuprate, so that relatively narrow existence and stability regions change continuously during phase diagram or crystal growth work.

Even if all these problems were solved (including problems of phase changes during cooling), large oxocuprate crystals may soon be of minor importance technologically; this does not apply to epitaxial and polycrystalline thin films. In this area, as well as LPE,[155] gas-phase techniques[156] have mainly been used, including laser ablation,[157] RF sputtering,[158] MBE,[159] MOCVD, and even sol-gel techniques. This has stimulated developments in the epitaxy of other oxides, for example, in ferroelectricity.[101] Just as the epitaxy of other materials (semiconductors and magneto-optic garnets) was achieved in a similar way, a parallel development of substrate crystals is required for thin film growth of oxocuprates.[160]

The known hurdles in three- and two-dimensional crystal growth of oxocuprates reveal themselves primarily as a chemical problem, and high-temperature and solid-state chemistry will be able to contribute greatly to its solution. In conclusion, it may be mentioned that advances have been made in the last 12 years in the crystal growth of organic superconductors (ambient pressure, $T_c(\max) = 11.4$ K).[161, 162] The future may well have some big surprises in store directly stemming from the merging of these two worlds of chemistry (alkali metal-C_{60},...?).[163] A real challenge for crystal synthesis!

4.3. Nonlinear Optical Molecular Crystals

Special donor-substituted and acceptor-substituted π-electron systems[44] show optical frequency doubling or an electro-optical effect in crystals. These effects have appreciably higher or comparable values compared with those observed with inorganic substances known for a long time, such as $LiNbO_3$,[164] $KNbO_3$,[165] KH_2PO_4 (see Fig. 1).[4, 166]

During the past 15 years, about 300 more or less strongly hyperpolarizable organic compounds were rediscovered for modern optics. Some of these were modified existing compounds and some were newly synthesized ("molecular and crystal engineering"), and were investigated as single crystals[44] or Langmuir-Blodgett (LB) films,[39b, 167] and in the form of poled polymers.[168] In frequency doubling experiments with the Nd:YAG laser ($\lambda_0 = 1064$ nm), for three-[138, 169] and one-dimensional crystals[126, 170] (see Figs. 16, 19 right), efficiencies of over 25% producing green light were reached. Reviews of compounds, crystal growth, and optical characteristics have been published by Zyss et al.[44a] and in reference [171].

In three-dimensional crystal growth, it was necessary to work mainly with solutions (and gels) for stability reasons.[120] By the method of temperature reduction and isothermal evaporation, cm^3-sized crystals were produced of MBANP (2-(α-methylbenzylamino)-5-nitropyridine),[171c] POM (methyl-3-nitro-4-pyridine-1-oxide),[171a] NPP (N-(4-nitrophenyl)-(L/D)-prolinol),[171a] PNP,[172] DAST,[173] and other compounds. Melt growth was used only infrequently (for example, for *m*-dinitrobenzene, *m*-nitroaniline, methyl-(2,4-dinitrophenyl)-amino-2-propanoate,[171a] COANP,[138] and DAN,[126]), where the best conditions for obtaining the desired optical quality should be provided by slow growth from the homogeneously supercooled melt (see Section 3.3.1).

In analogy to other topical subjects, interest in two-dimensional crystallization is also increasing. With the achievement of growing μm-thick crystal platelets[174] in a smooth (sometimes wedge-shaped) fissure, development is clearly proceeding in the direction of heteroepitaxy from the gas phase (MBE).[175]

Faced with the wide variability of organic compounds, the salient question is not what can be achieved but whether the class of materials shows sufficient long-term stability after incorporation into an optical component. It is well known that the optical damage threshold of organic compounds is lower than with oxides or semiconductors. Also, in this field, a further chemically interesting task presents itself, namely, to find hyper-

polarizable systems that are significantly more stable photochemically and thermally than the amino- or hydroxy- and nitro- or cyano-substituted π-electron systems that have been used for a long time. Here, the resulting nonlinearity would be expected to be less, which reduces one of the important advantages compared with oxides. However, for electro-optical use, organic crystals and thin films of significantly more stable compounds should have a chance (a general discussion of application areas is given in [176]). The newly discovered photorefractive effects in organic crystals are even less researched.[140]

4.4. Protein Crystallization

Many protein crystallographers believe that the growth of protein crystals is much more complicated than the growth of inorganic crystals
Rosenberger[177]

The fact that it has taken so long to produce proteins whose crystals have sufficiently good diffraction properties (Bernal and Crowfoot, 1934) "... is undoubtedly partly due to prejudice..." (Lüttringhaus[15]) although the crystallization of hemoglobin was first reported in 1840 (McPherson, historical review).[178]

From the modern point of view, it is generally accepted that, as regards nucleation and growth behavior, proteins do not differ in principle from lower molecular weight substances.[58, 179] Some differences arise from the biological origin of the samples and the fact that a protein crystal contains 30–80 vol% combined water. Hence, crystallization is carried out from water ($T \leq 30\,^{\circ}C$), usually after adding a controlled quantity of a precipitating agent [$(NH_4)_2SO_4$, 2-methyl-2,4-pentanediol, polyethylene glycol, etc.[65, 180]] so that, for a given total system, the solubility behavior of the protein becomes a critical parameter of the process. When salts are used, the solubility decreases with increasing ionic strength. Although solubility properties have been widely researched, there is still no model that can explain what takes place when the type of precipitating agent or its concentration is changed. According to Sieker,[180] experiments on 70 proteins produced crystals with a 60% success rate, although crystals of a quality good enough for X-ray structural analysis could be produced from only 70% of the crystallizable samples after further development of the crystallization techniques used.

The main difference in behavior compared with lower molecular weight substances is that a higher degree of supersaturation ($\sigma \approx 5-20$) is often necessary, together with a long induction period (lysozyme: 1–200 days depending on the concentrations of protein and NaCl).[181] Because of the molar volume, r^* is approximately 500 times as large for proteins as for lower molecular weight substances. For some years, induction periods have been investigated with dynamic light scattering, leading to conclusions about the diffusion and size of the scattering centers. This method could also be used diagnostically to establish the effectiveness of precipitation agents.[179]

Work on the growth kinetics of macroscopic protein crystals has led to the conclusion that the rate-determining step depends on processes on the growth surface. The measured growth rates R are of the order of a few 10^{-3} cm per day. In comparison with typical R values for other solution growth processes, protein crystals do not grow appreciably more slowly. On the other hand, at the molecular level, the mass transfer rate is approximately 10^{-3} times less[116b] (a recent discussion of growth mechanisms is given by Weber[58]). One of the remaining problems in the mechanistic investigation lies with the poor reproducibility of the data. Apart from the effects of impurities (including bacteria), this is certainly associated with the slow establishment of complex equilibria (folds and water inclusions, etc.). However, the use of the atomic force microscopy (AFM) method by Durbin et al.[182] showed that the well-known BCF (see Section 2) mechanism[80] for low molecular weight materials is in fact also valid for protein crystals.

Experimental methods of protein crystallization have been described by many researchers.[58, 116b, 179, 180] In analogy to the methods described in Section 3, the following are available: 1. Isothermal diffusion, a) over the gas phase (5–50 μL, "hanging or sitting drop" method—the commonest), b) by using a membrane, c) in a gel ("hanging drop"),[183] and d) by diffusion across the interface between the protein solution and the precipitant solution, and 2. temperature reduction (rare).

In addition to the literature mentioned previously, four conference reports *Crystal Growth of Biological Macromolecules* (1985, 1987, 1989, 1992) are worthy of note.[184]

5. Summary and Future Prospects

It has become increasingly evident in the last few years that scientific aspects of crystal growth have attracted the attention of physicists, chemists, metallurgists, ceramists, materials scientists, mineralogists, geologists, as well as a small number of biologists, and that a substantial number of these people regard crystal growth as their special field of competence and interest.[185]

Although these lines were written 25 years ago, large areas of synthetic chemistry have not yet adopted crystal growth as a possible special method of synthesis for building supramolecular structures with specific physical properties. Nevertheless, the development of a large number of single-crystal materials since the general upsurge in solid-state physics and materials science has shown the way towards the possibility of a chemistry that encompasses both the classical synthesis of new compounds and the formation of single-crystal phases with interesting properties. As well as giving an account of interdisciplinary cooperation and the theoretical side of the science of crystal growth, it seemed to me that the central topic was a discussion of recent developments in the systematic practical solution of crystallization problems. Here, the distinction has been made between exploratory methods, which are as simple and self-regulating as possible, and advanced methods of crystal growth. Crystallization is no longer an "outdated laboratory technique" for the chemist, but a modern and novel method of carrying out chemical syntheses in new areas of materials research.

I should like to thank my colleagues Hermann Wüest, Marcel Ehrensperger, Lucien Pauli, Dr. Roland Gutmann, Dr. Primoz Kerkoc, and Dr. Bohuslav Březina (Prague) for their collaboration in the development of a large number of methods of crystal growth. My special thanks are due to Prof. Dr. Dr. hc Hanns Arend, who introduced me to crystal growth and who has given me great support ever since. The ETH Zürich and the Swiss National Science Foundation are acknowledged for financial support.

Received: October 5, 1992 [A 926 IE]
German version: *Angew. Chem.* **1994**, *106*, 151
Translated by R. G. Leach, Basingstoke, UK

[1] H. Gebelein, *Alchemie*, Diederichs, München, **1991**, p. 49.
[2] a) J. J. Brissot, *Acta Electron.* **1973**, *16*, 285–290; b) J. Bohm, *Cryst. Res. Technol.* **1981**, *16*, 275–292; c) G. Agricola, *De Re Metallica* (Print of the Basel issue of 1556), cited from: *Ausgewählte Werke I*, Dtsch. Verlag Wiss., Leipzig, **1956** (see also Ref. [34]).
[3] P. M. Dryburgh in *Advanced Crystal Growth* (Eds.: P. M. Dryburgh, B. Cockayne, K. G. Barraclough), Prentice Hall, New York, **1987**, pp. 1–21.
[4] T. Sasaki, A. Yokotani, *J. Cryst. Growth* **1990**, *99*, 820–826.
[5] *Supramolecular Chemistry, II. NATO Science Form* (Eds.: V. Balzani, L. De Cola), Plenum, New York, **1992**; F. Vögtle, *Supramolekulare Chemie*, Teubner, Stuttgart, **1989**.
[6] P. J. Fagan, M. D. Ward, *Spektrum Wiss.* **1992**, no. *12*, 56–62; *Sci. Am.* **1992**, *267*, 28–34; H. Bock, *Acta Nova Leopoldina* **1993**, *38*, 221–233.
[7] T. Vicsek, *Fractal Growth Phenomena*, World Scientific, Singapore, **1989**.
[8] From the Laudatio for Prof. J. M. McBride (Prelog-Medaille-Preisträger, ETH Zürich, **1992**).
[9] *Molecular Electronics (Biosensors and Biocomputers)* (Ed.: F. T. Hong), Plenum, New York, **1989**; C. R. A. Catlow, *Modelling of Structure and Reactivity in Zeolites*, Academic Press, London, **1992**; *Polymers for High Technology (Electronics and Photonics)* (*ACS Symp. Ser.* **1987**, *346*).
[10] *Sensors (a Comprehensive Survey; Chemical and Biochemical Sensors, Part I, II) Vol. 1,2* (Eds.: W. Göpel, J. Hesse, J. N. Zemel), VCH, Weinheim, **1992**.
[11] *Spektrum Wiss.* **1986**, *no. 12; Sci. Am.* **1986**, *255*, 42–177.
[12] C. Heck, *Magnetic Materials and their Applications*, Butterworth, London, **1974**; J. S. Miller, *Adv. Mater.* **1991**, *3*, 110–112.
[13] M. E. Lines, A. M. Glass, *Principles and Applications of Ferroelectrics and Related Materials*, Clarendon, Oxford, **1977**; *Landolt-Börnstein, Neue Serie 28(Ferroelektrika und verwandte Substanzen, Teilbände a (Nicht-Oxide) und b (Oxide)* (Ed.: E. Nakamura), Springer, Berlin, **1990**.
[14] P. M. Grant, *Adv. Mater.* **1990**, *2*, 232–253; W. Buckel, *Supraleitung*, VCH, Weinheim, **1990**.
[15] A. Lüttringhaus, *Methoden Org. Chem. (Houben-Weyl) 4th Ed. 1952*, vol. I/1, **1958**, pp. 345–389.
[16] J. F. Nye, *Physical Properties of Crystals (their Representation by Tensors and Matrices)*, Clarendon, Oxford, **1985**; S. Haussühl, *Kristallphysik*, Physik Verlag/Verlag Chemie, Weinheim, **1983**.
[17] a) W. Eitel, *Handbuch der Arbeitsmethoden in der anorganischen Chemie, Bd. 4*, Berlin, **1926**; b) H. Fürst, *Laboratoriumstechnik der organischen Chemie*, Akademie Verlag, Berlin, **1961**, pp. 233–271; c) *Textbook of Practical Organic Chemistry* (Eds.: B. S. Furniss, A. J. Hannaford, P. W. G. Smith, A. R. Tatchell), Wiley, New York, **1978**, pp. 135–156; d) D. D. Perrin, W. L. F. Armarego, *Purification of Laboratory Chemicals*, Pergamon, Oxford, **1988**.
[18] R. S. Tipson in *Technique of Organic Chemistry III (Part I: Separation and Purification)* (Ed.: A. Weissberger), Wiley Interscience, New York, **1966**, pp. 395–562.
[19] Inspection of current books at specialized shops, Zürich, autumn, **1991**.
[20] V. Boldyrev, *Adv. Mater.* **1992**, *4*, 70–72.
[21] J. S. Langer, *Phys. Today* **1992**, *45* (10), 24–31.
[22] A. von Hippel, *Molecular Science and Molecular Engineering*, Wiley, New York, **1959**; *Science* **1962**, *138*, 91–108.
[23] T. Hahn, *Cryst. Growth Electron. Mater. Lect. Int. Summer Sch. Cryst. Growth Mater. Res. 5th* **1985**, pp. 299–306.
[24] A. I. Kitaigorodski, *Organic Chemical Crystallography*, Consultants Bureau, New York, **1961**; *Molecular Crystals and Molecules*, Academic Press, New York, **1973**.
[25] H. Arend, *Cryst. Growth Electron. Mater. Lect. Int. Summer Sch. Cryst. Growth Mater. Res. 5th* **1985**, pp. 307–311.
[26] R. D. Willett, *Magneto-Structural Correlations in Exchange Coupled Systems (NATO ASI Ser. Scr. C* **1985**, *140*, 389–420).
[27] F. Hulliger, *Phys. Chem. Mater. Layered Struct.* **1976**, *5*, 1–392.
[28] *Curr. Top. Mater. Sci.* **1977**, *1* and subsequent issues.
[29] L. Addadi, Z. Berkovitch-Yellin, I. Weissbuch, M. Lahav, L. Leiserowitz, *Top. Stereochem.* **1986**, *16*, 1–85.
[30] G. M. Schmidt, *Pure Appl. Chem.* **1971**, *27*, 647–678.
[31] B. Kahr, J. M. McBride, *Angew. Chem.* **1992**, *104*, 1–28; *Angew. Chem. Int. Ed. Engl.* **1992**, *31*, 1–26.
[32] G. R. Desiraju, *Mater. Sci. Monogr.* **1989**, *54*.
[33] M. C. Etter, *J. Phys. Chem.* **1991**, *95*, 4601–4610; M. C. Etter, S. M. Reutzel, *J. Am. Chem. Soc.* **1991**, *113*, 2586–2598.
[34] K. T. Wilke, J. Bohm, *Kristallzüchtung*, Deutsch, Thun, **1988**.
[35] *Nanostructures Based on Molecular Materials* (Eds.: W. Göpel, C. Ziegler), VCH, Weinheim, **1992**.
[36] G. A. Ozin, *Adv. Mater.* **1992**, *4*, 612–649.
[37] A. Y. Cho, *J. Cryst. Growth* **1991**, *111*, 1–13; W. T. Tsang, *ibid.* **1991**, *105*, 1–29; R. F. C. Farrow, *ibid.* **1990**, *104*, 556–577; W. T. Tsang, *ibid.* **1991**, *107*, 960–968; *Molecular Beam Epitaxy and Heterostructures. (NATO ASI Ser. Ser. E* **1983**, *87*); T. Yoshimura, S. Tatsuura, W. Sotoyama, *Appl. Phys. Lett.* **1991**, *59*, 482–484.
[38] H. Kukimoto, *J. Cryst. Growth* **1989**, *95*, 360–362; J. O. Williams, *Adv. Mater.* **1989**, *1*, 282–292; F. W. Ainger, K. Bass, C. J. Brierley, M. D. Hudson, C. Trundle, R. W. Whatmore, *Prog. Cryst. Growth Charact.* **1991**, *22*, 183–197; A. Erbil, W. Braun, B. S. Kwak, B. J. Wilkens, L. A. Boatner, J. D. Budai, *J. Cryst. Growth* **1992**, *124*, 684–689.
[39] a) B. Tieke, *Adv. Mater.* **1990**, *2*, 222–231; H. Fuchs, H. Ohst, W. Prass, *ibid.* **1991**, *3*, 10–18; b) M. Flörsheimer, M. Küpfer, C. Bosshard, H. Looser, P. Günter, *ibid.* **1992**, *4*, 795–798.
[40] B. S. Green, R. Arad-Yellin, M. D. Cohen, *Top. Stereochem.* **1986**, *16*, 131–218; F. Toda in *Molecular Inclusion and Molecular Recognition – Clathrates II (Top. Curr. Chem.* **1988**, *149*, 211–238).
[41] A. Khurana, *Phys. Today* **1987**, *40*, 17–23; L. M. Sheppard, *Am. Ceram. Soc. Bull.* **1992**, *71*, 1242–1252; *Earlier and Recent Aspects of Superconductivity (Springer Ser: Solid State Sci.* **1990**, *90*).
[42] D. Gatteschi, O. Kahn, J. S. Miller, F. Palacio, *Adv. Mater.* **1991**, *3*, 161–163; O. Kahn, J. Kröber, C. Jay, *ibid.* **1992**, *4*, 718–728; O. Kahn, *Molecular Magnetism*, VCH, Weinheim, **1993**, in press; J. S. Miller, *Adv. Mater.* **1992**, *4*, 298–300; J. S. Miller, J. C. Calabrese, R. S. McLean, A. J. Epstein, *ibid.* **1992**, *4*, 498–501.
[43] H. W. Kroto, *Angew. Chem.* **1992**, *104*, 113–133; *Angew. Chem. Int. Ed. Engl.* **1992**, *31*, 111–129; F. Diederich, Y. Rubin, *ibid.* **1992**, *104*, 1123–1292 and **1992**, *31*, 1101–1123.
[44] a) *Nonlinear Opt. Prop. Org. Mol. Cryst.* **1987**; b) *Spec. Publ. R. Soc. Chem.* **1989**, *69*; c) *Proc. SPIE Int. Soc. Opt. Eng.* **1988**, *971*; *ibid.* **1990**, *1147*; *ibid.* **1991**, *1337*; *ibid.* **1991**, *1560*, see also vols. *682, 824, 971*.
[45] B. H. T. Chai, *Recent Developments of New Laser Crystals*, Lecture at the 10th Int. Conf. Crystal Growth, San Diego, USA, **1992**.
[46] *Growth, Charact. Appl. Laser Host Nonlinear Cryst. (Proc. SPIE Int. Soc. Opt. Eng.* **1989**, *1104*).
[47] F. E. Auzel in *Semiconductor Optoelectronics* (Ed.: M. A. Herman), Wiley, Warschau, **1978**, pp. 233–275; F. E. Auzel, *Proc. IEEE* **1973**, *61*, 758–785.
[48] M. Oomen, *Adv. Mater.* **1991**, *3*, 403–406.
[49] W. A. Tiller, *The Science of Crystallization: Macroscopic Phenomena and Defect Generation (Vol. 1), Microscopic Interfacial Phenomena (Vol. 2)*, Cambridge University Press, Cambridge, **1991**.
[50] G. Matz, *Kristallisation, Grundlagen und Technik*, Springer, Berlin, **1969**.
[51] J. Garside, *Chem. Eng. Sci.* **1985**, *40*, 3–26.
[52] *Advances in Industrial Crystallization* (Eds.: J. Garside, R. J. Davey, A. G. Jones), Butterworth/Heinemann, Oxford, **1991**.
[53] J. A. Dirksen, T. A. Ring, *Chem. Eng. Sci.* **1991**, *46*, 2399–2427.
[54] G. T. Kerr, *Spektr. Wiss.* **1989**, *no. 9*, 94–100; *Sci. Am.* **1989**, *261*, 82–87.
[55] W. Zulehner, *Mikroelek.* **1988**, *2*, 154–157; W. Lin, K. E. Benson, *Annu. Rev. Mater. Sci.* **1987**, *17*, 273–298; W. Zulehner, *J. Cryst. Growth* **1983**, *65*, 189–213.
[56] V. I. Aleksandrov, V. V. Osiko, A. M. Prokhorov, V. M. Tatarintsev, *Curr. Top. Mater. Sci.* **1978**, *1*, 421–480; J. F. Wenckus, *J. Cryst. Growth* **1993**, *128*, 13–14.
[57] J. Jacques, A. Collet, S. H. Wilen, *Enantiomers, Racemates and Resolutions*, Wiley, New York, **1981**; D. Wörsch, F. Vögtle in *Molecular Inclusion and Molecular Recognition – Clathrates I (Top. Curr. Chem.* **1987**, *140*, 21–42); S. H. Wilen in *Tables of Resolving Agents and Optical Resolutions* (Ed.: E. L. Eliel), Notre Dame, London, **1972**; S. H. Wilen, *Top. Stereochem.* **1971**, *6*, 107–176.
[58] P. C. Weber, *Adv. Protein Chem.* **1991**, *41*, 1–36.
[59] a) *Crystal Growth in Science and Technology* (*NATO ASI Ser. Ser. B* **1989**, *210*); b) C. E. Bugg in [59a], pp. 239–251; D. C. Bassett in [59a], pp. 267–273.
[60] *Inorganic Biological Crystal Growth* (Ed.: B. R. Pamplin), Pergamon, Oxford, **1981**; L. Addadi, S. Weiner, *Angew. Chem.* **1992**, *104*, 159–176; *Angew. Chem. Int. Ed. Engl.* **1992**, *31*, 153–169.
[61] J. E. D. Davies, W. Kemula, H. M. Powell, N. O. Smith, *J. Inclusion Phenom.* **1983**, *1*, 3–44; E. Weber in *Biomineralization* (Eds.: S. Mann, J. Webb, R. P. Williams), VCH, Weinheim, **1989**; E. Weber in *Molecular Inclusion and Molecular Recognition – Clathrates I (Top. Curr. Chem.* **1987**, *140*, 3–20); G. A. Ozin, S. Özkar, *Adv. Mater.* **1992**, *4*, 11–22.
[62] a) M. van der Leeden, G. van Rosmalen, K. de Vreugd, G. Witkamp, *Chem. Ing. Tech.* **1989**, *61*, 385–395; b) R. J. Davey, L. A. Polywka, S. J. Maginn in *Advances in Industrial Crystallization* (Eds.: J. Garside, R. J. Davey, A. G. Jones), Butterworth/Heinemann, Oxford, **1991**, pp. 150–165.

[63] *Mobil Solar Energy Corporation* (brochure **1992**), Billerica, MA 01821-3980, USA; F. V. Wald, *Sol. Energy Mater.* **1991**, *23*, 175–182.
[64] P. van der Sluis, A. M. F. Hezemans, J. Kroon, *J. Cryst. Growth* **1991**, *108*, 719–727.
[65] G. L. Gilliland, *J. Cryst. Growth* **1988**, *90*, 51–59.
[66] J. H. Van Vleck, *Theory of Electric and Magnetic Susceptibilities*, Oxford University Press, London, **1932**, p. 322.
[67] A. M. Stoneham, *Theory of Defects in Solids (Electronic Structure of Defects in Insulators and Semiconductors)*, Clarendon, Oxford, **1975**.
[68] A. Neuhaus, *Chem. Ing. Tech.* **1956**, *28*, 155–161.
[69] H. Watanabe, T. Mizutani, A. Usui, *Semicond. Semimet.* **1990**, *30*, 1–52.
[70] *Wiss. Z. Tech. Univ. Dresden* **1988**, *37*, 179–282; G. W. Cullen, C. C. Wang, *Heteroepitaxial Semiconductors for Semiconductor Devices*, Springer, Berlin, **1978**; R. A. McKee, F. J. Walker, J. R. Conner, E. D. Specht, D. E. Zelmon, *Appl. Phys. Lett.* **1991**, *59*, 782–784; J. S. Harris, J. N. Eckstein, E. S. Hellman, D. G. Schlom, *J. Cryst. Growth* **1989**, *95*, 607–616; J. Kwo, *ibid.* **1991**, *111*, 965–972; J. N. Eckstein, I. Bozovic, D. G. Schlom, J. S. Harris, *ibid.* **1991**, *111*, 973–977.
[71] *Interfaces, Superlattices, and Thin Films* (Eds.: J. D. Dow, I. K. Schuller), Mater. Res. Soc., Pittsburgh, **1987**; *Strained-Layer Superlattices* (*Semicond. Semimet.* **1990**, *32*); F. Nguyen-Van-Dau, P. Etienne, J. Massies, *Rev. Phys. Appl.* **1990**, *25*, 971–976.
[72] Y. Saito, T. Ueta, *Phys. Rev. A Gen. Phys.* **1989**, *40*, 3408–3419.
[73] A. A. Chernov, *Z. Phys. Chem. Leipzig* **1988**, *269*, 941–970.
[74] *Electron Microscopy in Solid State Physics* (*Mater. Sci. Monogr.* **1987**, *40*).
[75] L. C. Feldman, J. W. Mayer, *Fundamentals of Surface and Thin Film Analysis*, North-Holland, New York, **1986**; L. M. Peng, M. J. Whelan, *Surf. Sci. Lett.* **1990**, *238*, L446–L452; C. T. Foxon, *Appl. Surf. Sci.* **1991**, *50*, 28–33; M. A. van Hove, W. H. Weinberg, C. M. Chan, *Low-Energy Electron Diffraction* (*Springer Ser. Surf. Sci.* **1986**, *6*).
[76] D. A. H. Cunningham, R. J. Davey, K. J. Roberts, J. N. Sherwood, T. Shripathi, *J. Cryst. Growth* **1990**, *99*, 1065–1069; D. A. H. Cunningham, A. R. Gerson, K. J. Roberts, J. N. Sherwood, K. Wojciechowski in *Advanced Industrial Crystallization* (Eds.: J. Garside, R. J. Davey, A. G. Jones), Butterworth/Heinemann, Oxford, **1991**, pp. 105–130; R. Steininger, J. H. Bilgram, *J. Cryst. Growth* **1991**, *112*, 203–226.
[77] *Scanning Tunneling Microscopy 1 (General Principles and Applications to Clean and Adsorbate Covered Surfaces)* (Eds.: H. J. Günterodt, R. Wiesendanger), Springer, Berlin, **1992**; C. Ludwig, B. Gompf, W. Glatz, J. Peterson, W. Eisenmenger, M. Möbus, U. Zimmermann, N. Karl, *Z. Phys. B Condens. Matter* **1992**, *86*, 397–404.
[78] D. Sarid, *Scanning Force Microscopy*, Oxford University Press, Oxford, **1991**; P. E. Hillner, S. Manne, A. J. Gratz, P. K. Hansma, *Ultramicroscopy* **1992**, *42/44*, 1387–1393; J. Frommer, *Angew. Chem.* **1992**, *104*, 1325–1357; *Angew. Chem. Int. Ed. Engl.* **1992**, *31*, 1298–1328.
[79] R. Wallenberg, J. O. Bovin, D. J. Smith, *Naturwissenschaften* **1985**, *72*, 539–541; J. O. Bovin, J. O. Malm, *Z. Phys. D* **1991**, *19*, 293–298.
[80] W. K. Burton, N. Cabrera, F. C. Frank, *Philos. Trans. R. Soc. London A* **1951**, *243*, 299.
[81] W. W. Mullins, R. F. Sekerka, *J. Appl. Phys.* **1963**, *34*, 323–329.
[82] J. A. Burton, R. C. Prim, W. P. Slichter, *J. Chem. Phys.* **1953**, *21*, 1987–1991.
[83] G. H. Gilmer, *J. Cryst. Growth* **1977**, *42*, 3–10; R. F. Xiao, J. I. D. Alexander, F. Rosenberger, *Phys. Rev. B Condens. Matter* **1988**, *38*, 2447–2455.
[84] K. A. Jackson, G. H. Gilmer, D. E. Temkin, J. D. Weinberg, K. Beatty, *J. Cryst. Growth* **1993**, *128*, 127–138; G. P. Srivastava, B. Jones, *Adv. Mater.* **1992**, *4*, 482–489.
[85] See references in [62b]; E. S. Bock, D. Feil, W. J. Briels, P. Bennema, *J. Cryst. Growth* **1991**, *114*, 389–410; *Morphology of Crystals, Part A, B* (Ed.: I. Sunagawa), Reidel, Boston, **1987**.
[86] a) B. Mutaftschiev in [59a], p. 27–48; b) A. A. Chernov in *Modern Crystallography III (Crystal Growth)* (Ed.: A. Chernov), Springer, Berlin, **1984**, Chapter 2.
[87] a) T. P. Martin, *Mater. Sci.* **1988**, *6*, 2–7; b) *The Physics and Chemistry of Finite Systems: From Clusters to Crystals, Vol. I, II)* (Eds.: P. Jena, S. N. Khanna, B. K. Rao), Plenum, New York, **1991/1992**.
[88] P. M. Dryburgh, *Educ. Chem.* **1989**, *26*, 24–25.
[89] M. A. Larson, J. Garside, *J. Cryst. Growth* **1986**, *76*, 88–92.
[90] A. E. Nielson, *Croat. Chem. Acta* **1987**, *60*, 531–539.
[91] A. A. Chernov, *Contemp. Phys.* **1989**, *30*, 251–276.
[92] O. Söhnel, J. W. Mullin, *Chem. Eng. Res. Des.* **1988**, *66*, 537–540.
[93] A. Reisman, *Phase Equilibria*, Academic Press, New York, **1970**; *Phase Diagrams 1970–1978*.
[94] *Phase Diagrams for Ceramists, Vol. I.* (Ed.: M. K. Reser), Am. Ceram. Soc., Columbus, **1964** and subsequent issues; I. Barin, *Thermochemical Data of Pure Substances, Vol. 1, 2*, VCH, Weinheim, **1989**.
[95] a) J. Hulliger, R. Gutmann, *J. Cryst. Growth* **1990**, *99*, 634–637; b) R. Gutmann, J. Hulliger, H. Wüest, *Ferroelectrics* **1992**, *134*, 291–296.
[96] D. Elwell, H. J. Scheel, *Crystal Growth form High-Temperature Solutions*, Academic Press, London, **1975**.
[97] B. M. Wanklyn in *Crystal Growth* (Ed.: B. R. Pamplin), Pergamon, Oxford, **1975**, p. 217–288.
[98] R. Gutmann, J. Hulliger, *Cryst. Prop. Prep.* **1991**, *32–34*, 117–122.
[99] R. A. Laudise, *The Growth of Single Crystals*, Prentice-Hall, Engelwood Cliffs, **1970**; R. A. Laudise, *Cryst. Growth Proc. Int. Conf.* **1967**, 3–16.
[100] H. Arend in [59a], pp. 225–230.
[101] S. L. Swartz, V. E. Wood, *Condens. Mater. News.* **1992**, *1*, 4–13; *Ferroelectric Thin Films* (*Mater. Res. Soc. Symp. Proc.* **1990**, *200*).
[102] W. Tolksdorf in [59a], pp. 397–410.
[103] A. V. Stephanov, *Zh. Tekh. Fiz.* **1959**, *29*, 381–393; R. S. Feigelson in [59a], pp. 275–302; B. S. Red'kin, V. N. Kurlov, V. A. Tatarchenko, *J. Cryst. Growth* **1987**, *82*, 106–109.
[104] P. Hartman, W. G. Perdok, *Acta Crystallogr.* **1955**, *8*, 49–52; *ibid.* **1955**, *8*, 521–524; *ibid.* **1955**, *8*, 525–529.
[105] M. C. Etter, *Preprints Int. Workshop Cryst. Growth Org. Mater.*, Tokyo University, Tokyo, **1989**, pp. 1.
[106] W. Asche, *CLB Chem. Labor Biotech.* **1991**, *42*, 442–444; M. Mersmann, *Adv. Transp. Processes* **1992**, *7*, 287–318.
[107] *Molten Salt Chem. 1964*; H. Bloom, *The Chemistry of Molten Salts*, Benjamin, New York, **1967**; *Molten Salt Chemistry and Technology* (*Mater. Sci. Forum* **1992**, *73–75*).
[108] A. Rabenau, *Angew. Chem.* **1985**, *97*, 1017–1032; *Angew. Chem. Int. Ed. Engl.* **1985**, *24*, 1026–1040.
[109] C. Reichardt, *Solvents and Solvent Effects in Organic Chemistry*, VCH, Weinheim, **1988**; R. A. Horne, *Water and Aqueous Solutions*, Wiley, New York, **1972**.
[110] P. van der Sluis, J. Kroon, *J. Cryst. Growth* **1989**, *97*, 645–656.
[111] N. Karl in *Crystals 4* (Ed.: H. C. Freyhardt), Springer, Berlin **1980**, pp. 1–100.
[112] *Sol-Gel Technology for Thin Films, Fibers, Preforms, Electronics and Speciality Shapes* (Ed.: L. C. Klein), Noyes, Park Ridge, **1988**.
[113] A. Smakula, *Einkristalle (Technische Physik in Einzeldarstellungen, Bd. 14)*, Springer, Berlin, **1962**, p. 58.
[114] W. Schlenk, *Methoden Org. Chem. (Houben-Weyl) 4th ed. 1952*, Bd. I/1, **1958**, pp. 395–416.
[115] P. van der Sluis, A. F. Hezemans, J. Kroon, *J. Appl. Cryst.* **1989**, *22*, 340–344.
[116] a) P. G. Jones, *Chem. Br.* **1981**, *17*, 222–225; b) R. S. Feigelson, *J. Cryst. Growth* **1988**, *90*, 1–13; c) R. Boese, M. Nussbaumer, *Organic Crystal Chemistry* (Ed.: D. W. Jones) (*Int. Union Crystallogr. Crystallogr. Symp.* **1993**, *6*, in press (particularly for low-temperature X-ray structure determination)).
[117] H. K. Henisch, *Crystal Growth in Gels*, Pennsylvania State University Press, London, **1970**; H. K. Heinisch, *Crystals in Gels and Liesegang Rings*, Cambridge University Press, Cambridge, **1988**.
[118] M. C. Robert, F. Lefaucheux, *J. Cryst. Growth* **1988**, *90*, 358–367.
[119] H. Arend, J. J. Connelly, *J. Cryst. Growth* **1982**, *56*, 642–644.
[120] a) P. Andreazza, F. Lefaucheux, M. C. Robert, D. Josse, J. Zyss, *J. Appl. Phys.* **1990**, *68*, 8–13; B. Březina, J. Hulliger, *Cryst. Res. Technol.* **1991**, *26*, 155–160; b) A. Perigaud, F. Gonzalez, M. Cunisse, *Ann. Chim. Paris* **1991**, *16*, 133–141.
[121] D. K. Kondepudi, R. J. Kaufman, N. Singh, *Science* **1990**, *250*, 975–976.
[122] a) H. Arend, R. Perret, H. Wüest, P. Kerkoc, *J. Cryst. Growth* **1986**, *74*, 321–325; b) W. S. Wang, J. Hulliger, H. Arend, *Ferroelectrics* **1989**, *92*, 113–119.
[123] Glassware with square cross-section obtainable from SOCIETE ATA, Geneva, Switzerland.
[124] H. Arend, J. Perison, *Mater. Res. Bull.* **1971**, *6*, 1205–1210.
[125] A. H. Madjid, A. R. Vaala, J. Pedulla, W. F. Anderson, *Phys. Status Solidi A* **1972**, *12*, 575–579.
[126] P. Kerkoc, J. Hulliger, *J. Cryst. Growth* **1990**, *99*, 1023–1027.
[127] J. Hulliger, Dissertation, Universität Zürich, **1984**.
[128] H. Schäfer, *Chemische Transportreaktionen*, VCH, Weinheim, **1962**; H. Schäfer, *J. Cryst. Growth* **1971**, *9*, 17–30.
[129] *Prog. Cryst. Growth Charact.* **1991**, *21*, 1–359.
[130] J. Moret, unpublished results.
[131] R. A. Laudise, J. W. Nielson, *Solid State Phys.* **1961**, *12*, 149–222.
[132] *The Art and Science of Growing Crystals* (Ed.: J. J. Gilman), Pergamon, Oxford, **1963**.
[133] *Crystal Growth* (Ed.: B. R. Pamplin), Pergamon, Oxford **1975**.
[134] *Advanced Crystal Growth* (Eds.: P. M. Dryburgh, B. Cockayne, K. G. Barraclough), Prentice Hall, New York, **1987**.
[135] See [59a].
[136] *Handbook of Crystal Growth, Vol. I, II, III* (Ed.: D. T. J. Hurle), North-Holland, Amsterdam, **1993–1994**, in press.
[137] T. Scheffen-Lauenroth, H. Klapper, R. A. Becker, *J. Cryst. Growth* **1981**, *55*, 557–570; H. Klapper, *Universitas* **1985**, *40*, 11–20.
[138] J. Hulliger, B. Březina, M. Ehrensperger, *J. Cryst. Growth* **1990**, *106*, 605–610.
[139] J. Hulliger, K. Sutter, Y. Schumacher, B. Březina, V. A. Ivanshin, *J. Cryst. Growth* **1993**, *128*, 886–890.
[140] K. Sutter, J. Hulliger, P. Günter, *Solid State Commun.* **1990**, *74*, 867–870; J. Hulliger, Y. Schumacher, K. Sutter, B. Březina, H. Ammann, *Mater. Res. Bull.* **1991**, *26*, 887–891.
[141] R. Kind, O. Liechti, N. Korner, J. Hulliger, J. Dolinsek, R. Blinc, *Phys. Rev. B Condens. Matter* **1992**, *45*, 7697–7703.

[142] M. Bösch, W. Känzig, *Helv. Phys. Acta* **1975**, *48*, 743–785.
[143] W. Hesse, M. Jansen, W. Schnick, *Prog. Solid State Chem.* **1989**, *19*, 47–110.
[144] A. Fuith, H. W. Warhanek, *J. Cryst. Growth* **1984**, *69*, 96–100.
[145] S. Gits-Leon, F. Lefaucheux, M. C. Robert, *J. Cryst. Growth* **1978**, *44*, 345–355.
[146] G. M. Loiacono, *Ferroelectrics* **1987**, *71*, 49–60; N. P. Zaitseva, F. S. Ganikhanov, O. V. Kachalov, V. F. Efimkov, S. A. Pastukhov, V. B. Sobolev, *Kristallografiya* **1991**, *36*, 1231–1236.
[147] a) Communication of the deutschen Gesellschaft für Kristallwachstum und Kristallzüchtung (dgkk), editor: F. Wallrafen; b) Groupe française de croissance cristalline (GFCC), President: B. Mutaftschiev.
[148] H. Müller-Buschbaum, *Angew. Chem.* **1991**, *103*, 741; *Angew. Chem. Int. Ed. Engl.* **1991**, *30*, 723.
[149] J. G. Bednorz, K. A. Müller, *Z. Phys. B Condens. Matter* **1986**, *64*, 189–193.
[150] *Advances in Sperconductivity II* (Eds.: T. Ishiguro, K. Kajimura), Springer, Tokyo, **1990**.
[151] a) C. Changkang, *Prog. Cryst. Growth Charact.* **1990**, *24*, 213–267; b) M. Berkowski, P. Bowen, T. Liechti, H. J. Scheel, *J. Am. Ceram. Soc.* **1992**, *75*, 1005–1007.
[152] a) F. Holtzberg, P. Strobel, T. K. Worthington, *J. Magn. Magn. Mater.* **1988**, *76-77*, 626–630; b) H. Scheel, *J. Less Common Met.* **1989**, *151*, 199–211; c) F. Holtzberg, C. Feild, *J. Cryst. Growth* **1990**, *99*, 915–921; d) *Eur. J. Solid State Chem.* **1990**, *27*, 107–133; e) H. J. Scheel, F. Licci, *Thermochim. Acta* **1991**, *174*, 115–130.
[153] F. Licci, C. Frigeri, H. J. Scheel, *J. Cryst. Growth* **1991**, *112*, 606–610.
[154] a) K. Watanabe, *J. Cryst. Growth* **1990**, *100*, 293–296; *ibid.* **1991**, *114*, 269–278; b) Flux, for example, T. A. Vanderah, C. K. Lowe-Ma, D. E. Bliss, M. W. Decker, M. S. Osofsky, E. F. Skelton, M. M. Miller, *ibid.* **1992**, *118*, 385–395.
[155] H. J. Scheel, M. Berkowski, B. Chabot, *J. Cryst. Growth* **1991**, *115*, 19–30; C. Klemenz, H. J. Scheel, *ibid.* **1993**, in press.
[156] K. Wasa, H. Adachi, K. Hirochi, Y. Ichikawa, T. Matsushima, *J. Mater. Res.* **1991**, *6*, 1595–1604.
[157] J. T. Cheung, H. Sankur, *Crit. Rev. Solid State Mater. Sci.* **1988**, *15*, 63–109; G. Koren, A. Gupta, E. A. Giess, A. Segmüller, R. B. Laibowitz, *Appl. Phys. Lett.* **1989**, *54*, 1054–1056; R. Ramesh, A. Inam, W. K. Chan, B. Wilkens, K. Myers, K. Remsching, D. L. Hart, J. M. Tarascon, *Science* **1991**, *252*, 944–946.
[158] S. Miura, T. Yoshitake, S. Matasubara, Y. Miyasaka, N. Shohata, *Appl. Phys. Lett.* **1988**, *53*, 1967–1969.
[159] D. G. Schlom, A. F. Marshall, J. T. Sizemore, Z. J. Chen, J. N. Eckstein, I. Bozovic, K. E. von Dessonneck, J. S. Harris, J. C. Bravman, *J. Cryst. Growth* **1990**, *102*, 361–375.
[160] D. Mateika, H. Kohler, H. Laudan, E. Völkel, *J. Cryst. Growth* **1991**, *109*, 447–456; H. J. Scheel, M. Berkowski, B. Chabot, *Physica C Amsterdam* **1991**, *185–189*, 2095–2096.
[161] T. Ishiguro, K. Yamaji, *Organic Superconductors*, Springer, Berlin, **1989**.
[162] G. Saito, T. Inukai, *Nippon Kessho Seicho Gakkaishi* **1989**, *16*, 2–16; H. H. Wang, A. M. Kini, L. K. Montgomery, U. Geiser, K. D. Carlson, J. M. Williams, J. E. Thompson, D. M. Watkins, W. K. Kwok, U. Welp, K. G. Vandervoort, *Chem. Mater.* **1990**, *2*, 482–484; H. Kusuhara, T. Mishima, Y. Sakata, Y. Ueba, M. Kaji, K. Tada, *Sumitomo Electr. Tech. Rev.* **1990**, *30*, 60–65; *The Physics and Chemistry of Organic Superconductors (Proc. Phys.* **1990**, *51*).
[163] D. Jérome, *Condens. Mater. News* **1992**, *1*, 11–16.
[164] R. S. Weiss, T. K. Gaylord, *Appl. Phys. A* **1985**, *37*, 191–203; B. C. Grabmaier, E. Willibald-Riha, E. Born, *Siemens Forsch. Entwicklungsber.* **1988**, *17*, 159–164.
[165] W. Xing, H. Looser, H. Wüest, H. Arend, *J. Cryst. Growth* **1986**, *78*, 431–437; J. Hulliger, R. Gutmann, H. Wüest, *ibid.* **1993**, *128*, 897–902.
[166] Y. Nishida, A. Yokotani, T. Sasaki, K. Yoshida, T. Yamanaka, C. Yamanaka, *Appl. Phys. Lett.* **1988**, *52*, 420–421.
[167] C. Bosshard, M. Flörsheimer, M. Küpfer, P. Günter, *Opt. Commun.* **1991**, *85*, 247–253.
[168] A. Buckley, *Adv. Mater.* **1992**, *4*, 153–158; *Nonlinear Optical Effects in Organic Polymers* (*NATO ASI Ser. Ser. E* **1989**, *162*).
[169] C. Bosshard, dissertation (no. 9407), ETH, Zürich, **1991**; P. Günter, C. Bosshard, K. Sutter, H. Arend, G. Chapuis, R. J. Twieg, D. Dobrowolski, *Appl. Phys. Lett.* **1987**, *50*, 486–488; K. Sutter, C. Bosshard, W. S. Wang, G. Surmely, P. Günter, *ibid.* **1988**, *53*, 1779–1781.
[170] P. Kerkoc, M. Zgonik, K. Sutter, C. Bosshard, P. Günter, *J. Opt. Soc. Am. B Opt. Phys.* **1990**, *7*, 313–319.
[171] a) J. Badan, R. Hierle, A. Perigaud, P. Vidakovic, *Nonlinear Opt. Prop. Org. Mol. Cryst.* **1987**, *1*, 297–356; b) B. J. McArdle, J. N. Sherwood in *Advanced Crystal Growth* (Eds.: P. M. Dryburgh, B. Cockayne, K. G. Barraclough), Printice Hall, New York, **1987**, pp. 179–217; c) J. N. Sherwood, *Spec. Publ. R. Soc. Chem.* **1989**, *69*, 71–81; d) M. Samoc, J. O. Williams, D. F. Williams, *Prog. Cryst. Growth Charact.* **1981**, *4*, 149–172; e) G. J. Sloan, A. R. McGhie, *Techniques of Melt Crystallization*, Wiley, New York, **1988**; f) B. G. Penn, B. H. Cardelino, C. E. Moore, A. W. Shields, D. O. Frazier, *Prog. Cryst. Growth Charct.* **1991**, *22*, 19–51; g) R. T. Bailey, F. R. Cruickshank, D. Pugh, J. N. Sherwood, *Acta Crystallogr. Sect. A* **1991**, *47*, 145–155; H. Klapper, *Cryst. Growth Prop. Appl.* **1991**, *13*, 109–162.
[172] J. Hulliger, W. S. Wang, M. Ehrensperger, *J. Cryst. Growth* **1990**, *100*, 640–642.
[173] J. W. Perry, S. R. Marder, K. J. Perry, E. T. Sleva, *Proc. SPIE Int. Soc. Opt. Eng.* **1991**, *1560*, 302–309; J. Hulliger, unpublished results.
[174] O. Sugihara, T. Toda, T. Ogura, T. Kinoshita, K. Ssaki, *Opt. Lett.* **1991**, *16*, 702–704; T. Suhura, K. Suetomo, N. H. Hwang, N. Nishihara, *IEEE Phot. Technol. Lett.* **1991**, *3*, 241–243.
[175] U. Zimmermann, G. Schnitzler, N. Karl, E. Umbach, *Thin Solid Films* **1989**, *175*, 85–88; T. Kobayashi, *Cryst. Growth Prop. Appl.* **1991**, *13*, 1–63; M. Hara, H. Sasabe, *Oyo Butsuri* **1991**, *60*, 1243–1246; H. Tada, A. Koma, *Kagaku Kogyo* **1991**, *44*, 2109–2112.
[176] D. F. Eaton, G. R. Meredith, J. S. Miller, *Adv. Mater.* **1992**, *4*, 45–48; D. Bloor, *Spec. Publ. R. Soc. Chem.* **1989**, *69*, 3–21; D. J. Williams, *Angew. Chem.* **1984**, *96*, 637–650; *Angew. Chem. Int. Ed. Engl.* **1984**, *23*, 690–703; S. Sudo, *Nonlinear Opt.* **1990**, *1*, 213–221.
[177] F. Rosenberger, *J. Cryst. Growth* **1986**, *76*, 618–636.
[178] A. McPherson, *J. Cryst. Growth* **1991**, *110*, 1–10.
[179] R. Boistelle in *Advances in Industrial Crystallization* (Eds.: G. Garside, R. J. Davey, A. G. Jones), Butterworth/Heinemann, Oxford, **1991**, pp. 131–147.
[180] L. C. Sieker, *J. Cryst. Growth* **1988**, *90*, 31–38; A. McPherson, *Eur. J. Biochem.* **1990**, *189*, 1–23; *Crystallization of Nucleic Acids and Proteins, A Practical Approach* (Eds.: A. Ducruix, R. Giegé), IRL, Oxford, **1992**.
[181] M. Ries-Kautt, A. J. Ducruix, *J. Biol. Chem.* **1989**, *264*, 745–748.
[182] S. D. Durbin, W. E. Carlson, *J. Cryst. Growth* **1992**, *122*, 71–79.
[183] K. Provost, M. C. Robert, *J. Cryst. Growth* **1991**, *110*, 258–264.
[184] *J. Cryst. Growth* **1986**, *76*; *ibid.* **1988**, *90*; *ibid.* **1991**, *110*; *ibid.* **1992**, *122*.
[185] N. Cabrera, B. Chalmers, M. Schieber, *J. Cryst. Growth* **1967**, *1*, from the editorial.

Just what does a referee system achieve?

Regular readers of "Angewandte" are well aware that Dr. Hans-Dieter Daniel has researched this question using *Angewandte Chemie* as example. The preliminary results were presented in a communication on this topic (Issue 2/93). Now the complete analysis by Daniel is available in book form: "The Guardians of Science: Fairness and Reliability in Peer Review" by H.-D. Daniel, foreword by H. Nöth (VCH, Weinheim, 1993, ISBN 3-527-29041-9, DM 78.—).

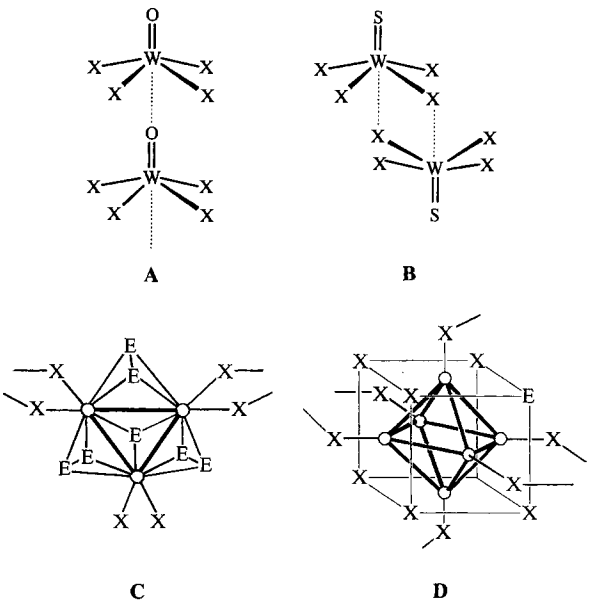
New Forms and Functions of Tellurium: From Polycations to Metal Halide Tellurides

Johannes Beck

Metal chalcogenides and metal chalcogenide halides are distinguished by their structural diversity and by their very different physical properties. Therefore, the synthesis of novel compounds from this class is always a rewarding goal for the preparatively oriented solid-state chemist. Over the past few years, many syntheses and structural investigations have stimulated the field. The emphasis of the research has been placed on selenium-rich and tellurium-rich compounds, which are characterized by directed covalent bonds between the chalcogen atoms. Compounds with novel chalcogen polycations have also become accessible during the past few years by reacting the chalcogen elements with transition metal halides, or from chemical vapor deposition in the sense of chemical transport reactions. In these compounds, tellurium differs from its lighter homologues by a pronounced tendency towards greater covalence. This article attempts to provide an overview of new developments in the field of compounds with chalcogen polycations and of metal chalcogenide halides, with an emphasis on compounds containing molybdenum and tungsten as the transition metals and tellurium as the chalcogen.

1. Introduction

Metal chalcogenide halides are ternary compounds, that is compounds containing three different chemical elements. These are formed with main group and subgroup metals, the elements oxygen to tellurium (chalcogens), and fluorine to iodine (halides). The metals behave very differently with respect to the formation of chalcogenide halides. Niobium, for example, forms a large number of such compounds with compositions like NbS_2Cl_2[1] or $Nb_2Te_2I_6$.[2] For zirconium, however, although it is the immediate neighbor of niobium in the periodic table, no halide sulfides, halide selenides, or halide tellurides are known. For the elements of group 8 (chromium, molybdenum, and tungsten), the chemistry of halide oxides, halide sulfides, and halide selenides is well-developed. Trivalent chromium forms a chloride oxide CrOCl,[3] a bromide oxide CrOBr,[4] and a bromide sulfide CrSBr,[5] all of which crystallize with the FeOCl type structure.[6] CrSBr is highly antiferromagnetic with a Neél temperature of 132 K.[5, 7] For tungsten, a large number of halide oxides, halide sulfides, and halide selenides are known, which have also been structurally characterized. Often isotypic series are encountered, in which the different halogens and/or chalcogens can replace each other without changing the structure type. An example for this are the chalcogenide halides of hexavalent tungsten. The compounds $WOCl_4$[8] and $WOBr_4$[9] are isotypic; their columnar structure is built of square pyramids of monomers associated along the W–O axis to form chains (Scheme 1, **A**). α-$WSCl_4$ and $WSBr_4$[10] form dimers held together by bridging halogen atoms (Scheme 1, **B**). In the structure of β-$WSCl_4$,[11] these dimers are "docked" by additional pyramidal $WSCl_4$ molecules. This polymorphism has so far not been



Scheme 1. Structural types of selected chalcogenide halides of molybdenum and tungsten. **A**: WOX_4 (X = Cl, Br), **B**: WSX_4 (X = Cl, Br), **C**: $Mo_3E_7X_4$ (E = S, Se; X = Cl, Br, I); **D**: $[Mo_6X_7E]X_{6/2}$ (E = S, Se, Te; X = Cl, Br, I). The metal atoms are represented by white spheres.

[*] Prof. J. Beck
Institut für Anorganische und Analytische Chemie der Universität
Heinrich-Buff-Ring 58, D-35392 Giessen (FRG)
Telefax: Int. code + (641)702-5669

 © *VCH Verlagsgesellschaft mbH, D-69451 Weinheim, 1994* *0570-0833/94/0202-0163 $ 10.00+.25/0*

observed for $WSeCl_4$, which crystallizes in the β-$WSCl_4$ type structure (Fig. 1) only.[12] All these compounds are constructed from square pyramidal monomers in which the chalcogen atom is in the apical position. The tungsten–chalcogen bonds are very short (mean W=O = 180, W=S = 210, W=Se = 220 pm), and may be formally regarded as double bonds. It is noteworthy that this series of closely related compounds ceases with the halide selenides, that is tungsten halide tellurides are unknown.

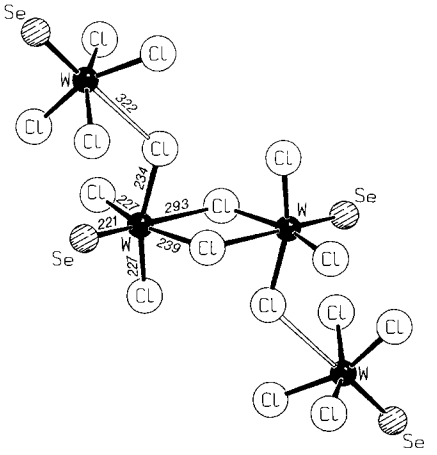


Fig. 1. Structure of $WSeCl_4$ with important distances in pm.

For molybdenum, the situation is similar. Several molybdenum halide sulfides and halide selenides are known.[13] This is exemplified by compounds of the type $Mo_3E_7X_4$ (E = S, Se; X = Cl, Br, I),[14] which feature triangular Mo_3 clusters with dichalcogenide dianions bridging the edges (Scheme 1, **C**). All compounds with E = S and Se, and X = Cl, Br, and I, have been prepared, but no corresponding tellurium compounds are known. The only known halide tellurides of the group 8 elements are derived from the cluster compounds of divalent molybdenum. One of the eight inner halogen atoms of the $[Mo_6X_8]X_4$ cluster can be substituted by a tellurium atom, which is distributed statistically over all eight possible positions[15] (Scheme 1, **D**). The $Mo_6Te_{8-y}X_y$ type compounds with X = Br, I and $0 \leq y \leq 3$, which fall into the class of the superconducting Chevrel compounds, are of special interest because of their physical properties.[16] This review reports on the authors' efforts to synthesize halide tellurides of molybdenum and tungsten. The somewhat surprising results are discussed with respect to current findings of other research groups.

2. An Initial Route to the Ternary Molybdenum/Tellurium/Halogen System: Compounds with Trihalotelluronium Ions TeX_3^+

The tetrahalides of sulfur, selenium, and tellurium have partially ionic character, which enables them to form trihalochalcogenonium ions EX_3^+ (E = S, Se, Te, X = Cl, Br and for E = Se, Te, X = I).[17] Chalcogen tetrahalides react with strong Lewis acids to form ionic adducts. The role of the halide ion acceptor can be filled not only by halides of main group elements like $AlCl_3$ or SbF_5, but by metal halides of the subgroup elements as well, such as $TiCl_4$, $NbCl_5$, $FeCl_3$, UCl_5, or $AuCl_3$. $MoOCl_3$ also proved to be a suitable Lewis acid. The compounds $SCl_3^+MoOCl_4^-$[18] and $SeCl_3^+MoOCl_4^-$[19] were obtained from MoO_3 and a mixture of SCl_2/Cl_2 or directly from $SeCl_4$ and $MoOCl_3$. This series is completed by the preparation of the corresponding tellurium compound $TeCl_3^+MoOCl_4^-$,[20] which turned out to be isostructural with $SeCl_3^+MoOCl_4^-$.

Likewise, $MoCl_4$ reacts with $TeCl_4$ and accepts two chloride ions, thus forming $MoCl_6^{2-}$. Depending on the amount of $TeCl_4$ used, two different compounds, $MoTe_2Cl_{12}$ and $MoTe_3Cl_{16}$ could be obtained.[21] Their structures feature almost ideally octahedral $MoCl_6^{2-}$ ions and trigonal-pyramidal $TeCl_3^+$ ions. Figure 2 shows a section from the structure of $MoTe_3Cl_{16}$. In addition to the three short Te–Cl distances (230–232 pm) there are three longer Te–Cl contacts (287–302 pm); the result is that

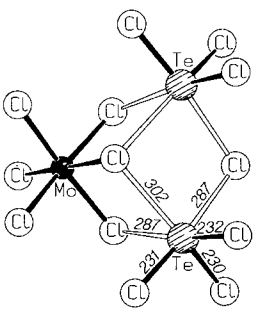


Fig. 2. A section from the structure of $MoTe_3Cl_{16}$ which can also be formulated as $(TeCl_3^+)_3(MoCl_6^{2-})(Cl^-)$. Short covalent bonds are represented by black rods, longer weak Te–Cl contacts by white rods. The Mo–Cl distances are between 224 and 249 pm, the Te–Cl bonds are given in pm.



Johannes Beck was born in 1956 in Hornberg/Schwarzwald. From 1976–1982 he studied chemistry at Tübingen, where he received his doctorate under the supervision of J. Strähle with a thesis on pentaazadienido metal complexes. Subsequently, he moved to work with H. Bärnighausen at the Universität Karlsruhe, where he completed his habilitation in 1991. In 1992 he accepted a call to the Universität Giessen to succeed R. Hoppe to the chair for Inorganic and Analytical Chemistry. His research interests include crystal structure analysis, polycations of the chalcogens, halides, oxyhalides, and chalcogenides of the transition metals, as well as metal complexes with polyazenido ligands.

each Te atom is surrounded by a distorted octahedron of Cl atoms. This distortion of the polyhedron around the Te atom is found in almost all compounds of TeX_3^+ ions and halide metalate ions and is caused by the lone pair of electrons at the Te^{4+} ion. The stereochemically active lone pair points from the Te ion towards one of the faces of the coordination polyhedron and thereby effects the typical separation into three normal and three elongated Te–X distances.[22] $MoTe_3Cl_{16}$ is thus regarded as $(TeCl_3^+)_3(MoCl_6^{2-})(Cl^-)$, and $MoTe_2Cl_{12}$ as $(TeCl_3^+)_2(MoCl_6^{2-})$. The two compounds may also be described as mixed tetrahalides $3\,TeCl_4 \cdot MoCl_4$ and $2\,TeCl_4 \cdot MoCl_4$. The chlorine atoms form closest-packed structures with different stacking sequences, in which Mo and Te atoms occupy a quarter of the tetrahedral interstices in an ordered fashion.

Although both $MoTe_2Cl_{12}$ and $MoTe_3Cl_{16}$ are ternary compounds of the Mo/Te/Cl system, they do not belong to the category of molybdenum chloride telluride compounds. In the latter one would expect not only to find Mo–Cl bonds, but also Mo–Te bonds, which occur in neither $MoTe_2Cl_{12}$ nor in $MoTe_3Cl_{16}$.

3. The Oxidation of Chalcogen Elements by Transition Metal Halides: A New Route to Chalcogen Polycations

One of the historical discoveries in the chemistry of the early nineteenth century was the observation that sulfur, selenium, and tellurium were soluble in concentrated sulfuric acid. The composition of the ensuing intensely colored solutions, however, remained unknown until the mid-1960s.[23] From preliminary investigations by the research groups of Bjerrum,[24] Gillespie,[25] and Corbett,[26] it became apparent that chalcogen polycations were responsible for the coloring. This was corroborated by the first crystal structure analyses of the tetrachloroaluminates of the Se_8^{2+}[27] and Te_4^{2+} ions.[28] Convenient preparations for these ions are the oxidation of the chalcogen elements with $S_2O_6F_2$ in HSO_3F, or with AsF_5 or SbF_5 in liquid SO_2, or the symproportionation of the chalcogen elements with a higher chalcogenide halide in the presence of a halide ion acceptor. In this way, saltlike compounds are formed whose AsF_6^-, SbF_6^-, SO_3F^-, or $AlCl_4^-$ anions, as weak conjugate bases of very strong Lewis acids, stabilize the chalcogen polycations. So far, only one compound with a halide metalate anion of a transition metal has been reported: Tellurium and $TeCl_4$ react in a $NbCl_5/NbOCl_3$ melt to form $Te_4^{2+}Nb_2OCl_{10}^{2-}$.[29] The reaction does not change the oxidation state of the niobium atom; the $NbCl_5/NbOCl_3$ mixture acts as a Lewis acid and elemental tellurium is oxidized by $TeCl_4$. A more recent finding is that chalcogen elements can be oxidized directly and selectively to chalcogen polycations by transition metal halides whose metal atoms are in high oxidation states. The metal halides are reduced to halide metalate anions and a solvent is unnecessary. Rather, the components react in sealed glass or quartz ampoules under vacuum, along a defined temperature gradient, in the sense of a chemical transport reaction. Using reaction temperatures between 150 and 250 °C and temperature gradients of approximately 20 °C, these ionic compounds are successfully deposited (mostly quantitatively) from the vapor phase in the colder part of the reaction ampoule.

3.1. Se_4^{2+} and Te_4^{2+}: Well-known Ions in New Environments

Tellurium reacts smoothly with $MoOCl_4$ or WCl_6 to form $Te_4^{2+}(MoOCl_4^-)_2$[30] and $Te_4^{2+}(WCl_6^-)_2$,[31] respectively. For selenium, the reaction with $MoOCl_4$ leads to the analogous selenium compound $Se_4^{2+}(MoOCl_4^-)_2$.[21] The structures of these compounds feature square-planar E_4^{2+} ions (E = Se, Te), which have been synthesized during the past few years with various counterions. Strong cation–anion interactions are characteristic for these saltlike compounds.

In each case four halogen or four halogen and oxygen atoms bridge the edges of the E_4 square, and additional neighboring atoms are arranged above and below the E_4 square plane.[32] Though the chalcogen–halogen distances in these compounds are longer than covalent bonds, they are often noticeably shorter than the sum of the van der Waals radii. The E_4^{2+} ions can be perceived as aromatic systems with 6π electrons and have repeatedly been subject of molecular orbital calculations.[33–35] They possess a lowest unoccupied, weakly antibonding molecular orbital, which extends above the ring edges. Partial transfer of electron density to neighboring anions causes a slight elongation of the bonds within the E_4^{2+} ion. In $Se_4^{2+}(MoOCl_4^-)_2$, such

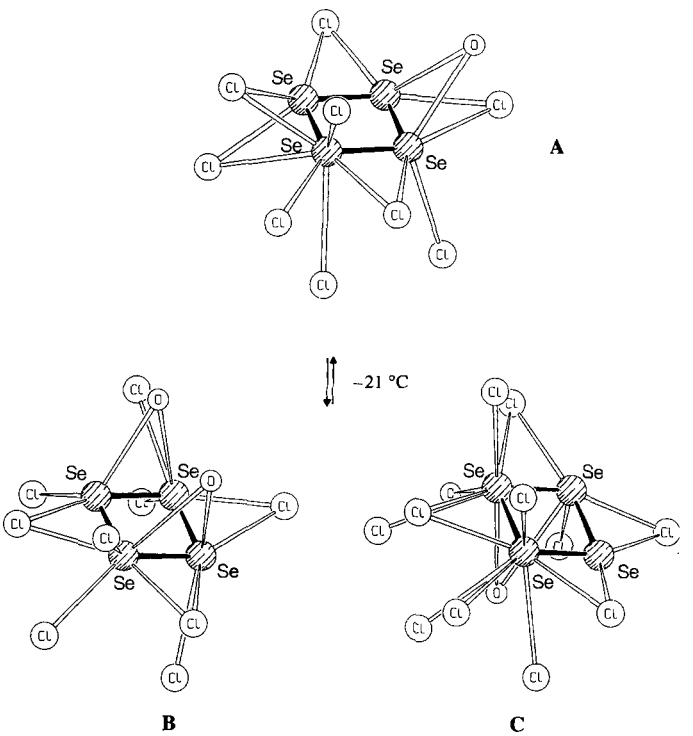
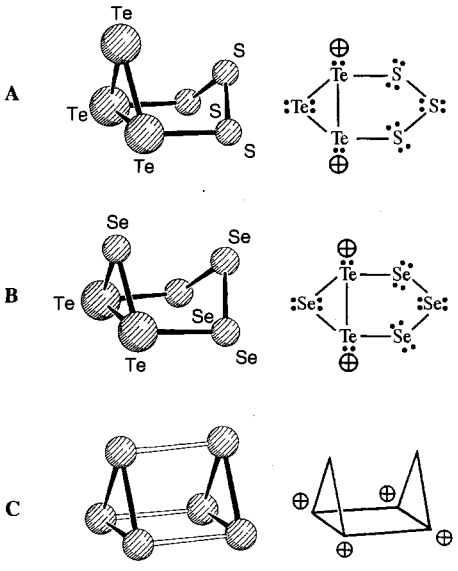


Fig. 3. Structure of the Se_4^{2+} ion in $Se_4(MoOCl_4)_2$. The Cl and O atoms from neighboring $MoOCl_4^-$ ions that are not more than 360 pm from a Se atom are represented in the structures **A**–**C**. At −21 °C, a reversible phase transition (ΔH = 0.2 kJ mol^{-1}) occurs. The room temperature phase has only one crystallographically independent Se_4^{2+} ion (**A**). In the low-temperature phase this is split into two independent cations (**B** and **C**) as a result of a doubled lattice parameter, and thus a doubled unit cell volume.

interactions are the driving force for a solid-state phase transition. Whereas the structures of the Se_4^{2+} and $(MoOCl_4^-)_2$ ions do not change, their relative orientation changes at $-21\,^{\circ}C$ in such a way that the Se centers show a higher coordination number in the low-temperature phase (Fig. 3).

3.2. Te_6^{2+}: Another Prismatic Chalcogen Polycation

The chalcogen polycations with six atoms known so far, for example, $Te_3S_3^{2+}$,[36] $Te_2Se_4^{2+}$,[37] and Te_6^{4+},[38] have structures that can be derived from a hexagonal prism (Scheme 2). In the heteroatomic ions $Te_3S_3^{2+}$ and $Te_2Se_4^{2+}$, two edges of the prism are unconnected. In both polycations there are two tellurium atoms that are three-bonded (cross-ring bond) which formally carry the positive charges, according to the Zintl–Klemm concept.[39] The Te_6^{4+} ion has six very short bonds of 267 pm between the Te atoms of the triangular faces and three very long Te–Te bonds of approximately 312 pm which link the triangular faces of the prism. If these long bonds are assigned a bond order of 2/3, this ion also obeys the Zintl–Klemm concept, which predicts four three-bonded Te atoms for Te_6^{4+} ions. In the homoatomic Te_6^{4+} ion, the four charges are distributed equally over the six Te atoms.



Scheme 2. Structures of the hexaatomic chalcogen cations $Te_3S_3^{2+}$ (**A**), $Te_2Se_4^{2+}$ (**B**), and Te_6^{4+} (**C**), and their corresponding Lewis structures. For the Te_6^{4+} ion only one of the three possible resonance structures is shown.

The Te_6^{2+} ion has been postulated several times[25, 26] but has so far not been characterized by crystal structure analysis. At 210–230 °C, tellurium and $WOCl_4$ selectively react to form Te_3WOCl_4, a compound built of discrete Te_6^{2+} ions and one-dimensional strands of $WOCl_4^-$ ions.[21] The Te_6^{2+} ion (Fig. 4) has a prismatic Te_6 structure with one prism edge, which joins the triangular faces, not connected by a bond, and only weak Te–Te contacts (mean 328 pm) in the two Te_3 triangles. The other Te–Te bonds (mean 272 pm) fall within the range of covalent

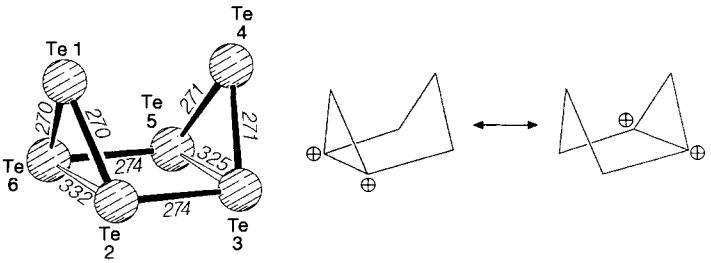


Fig. 4. Structure of the Te_6^{2+} ion in $Te_6^{2+}[(WOCl_4^-)_2]_n$, and its corresponding resonance structures; bond lengths given in pm.

Te–Te bonds. In the homoatomic Te_6^{2+} ion, the two positive charges are localized at four Te centers. This can be expressed by the resonance structures shown in Figure 4. Even though in the structure of $Te_6(WOCl_4)_2$ the Te_6^{2+} ions form strands (see Fig. 6, **A**), there is no interaction between the single polycations. The shortest interionic distance between Te atoms is 461 pm, which is longer than the sum of the van der Waals radii (440 pm).[40]

3.3. The Bicyclic Te_8^{2+} Ion: Final Member of the Homologous Series E_8^{2+} (E = S, Se, Te)

The octaatomic polycations S_8^{2+}[41] and Se_8^{2+}[27] were prepared by using the classical methods for synthesis of chalcogen polycations as AsF_6^- and $AlCl_4^-$ salts, respectively. The unusual structures of these ions, which both form eight-membered rings with weak transannular intramolecular interactions, and their bonding have already been discussed several times.[42, 43] More modern concepts of chemical bonding interpret these transannular bonds as six-center, two-electron $\pi^*-\pi^*$ bonds.[44]

The final member of the series of E_8^{2+} cations, Te_8^{2+}, was obtained in the compound $Te_8^{2+}(WCl_6^-)_2$ by reacting WCl_6 with tellurium.[45] The formation of ionic products with WCl_6 to date remains restricted to tellurium. Sulfur reacts with WCl_6 either to give $WSCl_4$ or to give the adduct $WCl_6 \cdot S_8$, depending on the reaction conditions. The structure of $WCl_6 \cdot S_8$ is built of alternate layers of neutral S_8 rings and WCl_6 molecules.[46] The reaction of selenium with WCl_6 is presently under investigation.[12] The structure of the Te_8^{2+} ion (Fig. 5) can be described as a bicyclic species consisting of two condensed five-membered rings, each of which assumes an envelope configuration. The Te–Te distances around the eight-membered ring are on average 275 pm, the transannular bond is 299 pm. The two bridgehead

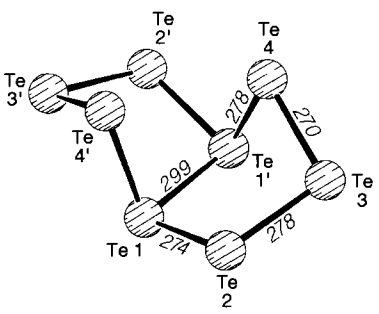


Fig. 5. Structure of the Te_8^{2+} ion in $Te_8(WCl_6)_2$. The ion has a twofold rotational axis perpendicular to the Te1–Te1′ bond. The bond lengths are given in pm.

atoms Te1 and Te1′ are three-bonded and are trigonal-pyramidally coordinated. The two positive charges in the Te_8^{2+} ion are predominantly localized at these two Te atoms. In contrast to its two lighter homologues S_8^{2+} and Se_8^{2+}, the bicyclic character in the Te_8^{2+} ion is more pronounced due to the short transannular bond. Moreover, in the structure of $Te_8(WCl_6)_2$ (Fig. 6, **B**) the association of chalcogen polycations was observed for the first time. The individual Te_8^{2+} ions are linked by Te–Te contacts of 342 pm to form a folded band. Interionic contacts of a similar size are also observed in the chainlike tellurium polyanions Te_4^{2-} and Te_5^{2-}, in which polyanionic units associate and form polymeric strands of tellurium.[47,48]

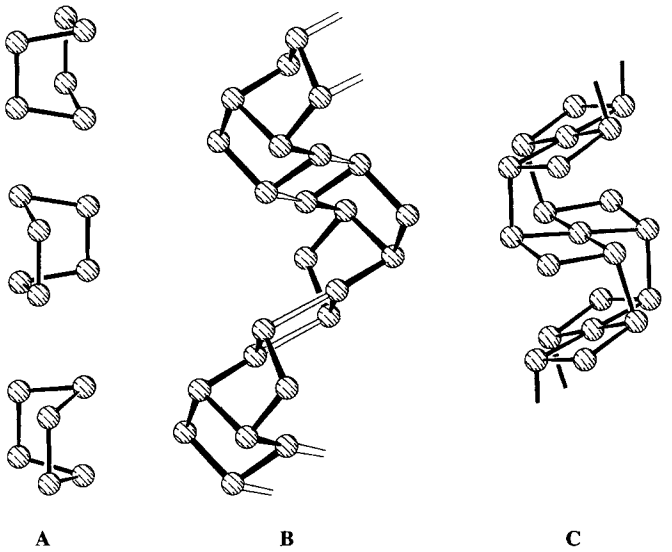


Fig. 6. The arrangement of the Te_6^{2+} (**A**), Te_8^{2+} (**B**), and $(Te_7^{2+})_n$ ions (**C**) in the structures of $Te_6(WOCl_4)_2$, $Te_8(WCl_6)_2$, and Te_7WOBr_5, respectively. This structural comparision illustrates the increase of interionic interactions, culminating in the polymeric structure (**C**).

3.4. Te_7^{2+}: A Polymeric Tellurium Polycation

The polymeric $(Te_7^{2+})_n$ tellurium cation occurs in the Te_7MOX_5 type structure, for which four examples are known so far: Te_7WOBr_5,[49] Te_7WOCl_5,[50] and Te_7NbOX_5 (X = Cl, Br).[51] These compounds are built of one-dimensional strands of square-pyramidal $(MOX_4^-)_n$ ions, isolated X^- ions, and polymeric $(Te_7^{2+})_n$ ions, in which nearly planar Te_7 units are linked to give a folded band (Fig. 7). The charge distribution in the Te_7MOX_5 type structure can be unambiguously clarified by preparing the niobium-containing compounds (but not by preparing those containing tungsten). The diamagnetism of aTe_7NbOBr_5 shows that the niobium atom is in the oxidation state + v, the $NbOBr_4^-$ group carries one negative charge, and the correct ionic formulation of the compound is $(Te_7^{2+})_n(NbOBr_4^-)_nBr^-$. Already on going from the Te_6^{2+} ion (discrete) to the Te_8^{2+} ion (significant interionic interaction), the increasing tendency towards association between the tellurium polycations becomes apparent. In the polymeric $(Te_7^{2+})_n$ ion, the Te_7 units are connected by covalent Te–Te bonds of 288 pm (see Fig. 6, **C**).

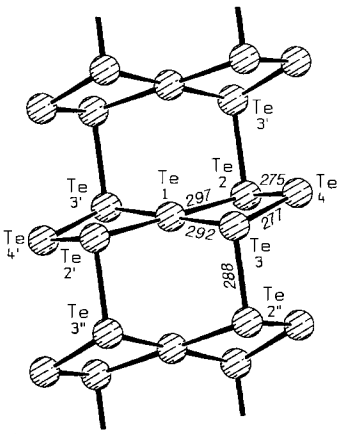
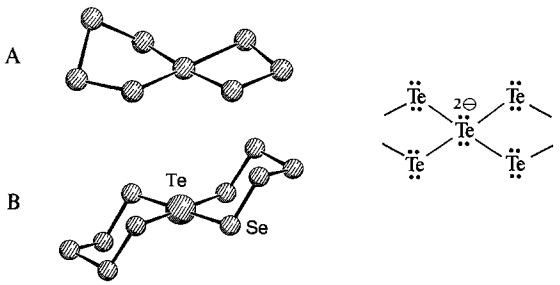


Fig. 7. Structure of the polymeric Te cation $(Te_7^{2+})_n$; bond lengths given in pm.

Structural motifs of the $(Te_7^{2+})_n$ ion are realized in various ways in compounds with tellurium polyanions.[52] Thus, for example, the central square-planar $TeTe_4^{6-}$ unit is common to the discrete Te_5^{6-} ion in Ga_2Te_5,[53] the polymeric $(Te_5^{2-})_n$ ion in Rb_2Te_5 and Cs_2Te_5,[54] the spirocyclic anions in Te_7^{2-}[55] and Te_8^{2-},[56] (Scheme 3, **A**) and the $(Te_7^{2+})_n$ ion. Compounds with the same structural motif containing selenium are also known with the spirocyclic anions $TeSe_{10}^{2-}$ (Scheme 3, **B**)[57] and Se_{11}^{2-}.[58] The $TeTe_4^{6-}$ unit contains 36 valence electrons and is isostructural with XeF_4 or ICl_4^- (Scheme 3). The Gillespie–Nyholm valence shell-electron pair repulsion model[59] regards the central tellurium atom in an ψ^2 octahedral (psedo-octahedral) coordination, in which the two lone pairs are *trans* to each other. Extended-Hückel calculations[60] interpret the bonding in terms of a three-center, four-electron model. In this model, the significant elongation of the four Te–Te bonds by approximately 8% (as compared with the sum of the covalent radii of 274 pm) can be explained in terms of the antibonding character of the highest occupied molecular orbitals.



Scheme 3. Structures of the spirocyclic anions Te_8^{2-} (**A**), $TeSe_{10}^{2-}$ (**B**), and a Lewis formula for the central $TeTe_4^{2-}$ unit.

3.5. $Te_6I_2^{2+}$ and $(Se_6I^+)_n$: A Discrete and a Polymeric Iodochalcogen Polycation

Under ambient conditions, sulfur and selenium do not form stable binary iodides. With the exception of the SeI_6^{2-} ion, no compounds with S–I or Se–I bonds were known until a few

years ago. The first successful synthesis of a neutral compound with a Se–I bond was achieved in 1987 with 2,4,6-tri-*tert*-butylphenyl(iodo)selenide.[61] Here, the bulky phenyl substituent affords kinetic stabilization. In their cationic forms, however, bound into a crystal lattice with AsF_6^- or SbF_6^- anions, S–I and Se–I bonds are stable. Since the first preparation of an (iodo)sulfur cation in $S_2I_4^{2+}(AsF_6^-)_2$ in 1980 by Passmore et al.,[62] the same group has synthesized a whole series of other cations such as S_7I^+, $[(S_7I)_2I]^{3+}$, SeI_3^+, $Se_2I_4^{2+}$, $(Se_6I^+)_n$, and $Se_6I_2^{2+}$.[63]

TeI_3^+ was hitherto the only known (iodo)tellurium cation.[64] From the reaction of Te, I, and WCl_6, another (iodo)tellurium cation, $Te_6I_2^{2+}(WCl_6^-)_2$ has now become accessible.[21] This cation is centrosymmetric and the Te atoms form a six-membered ring with chair conformation, in which the two iodine atoms are bound to the ring at positions 1 and 4 in such a way that an *endo-endo* conformation results (Fig. 8). The $Te_6I_2^{2+}$ ion

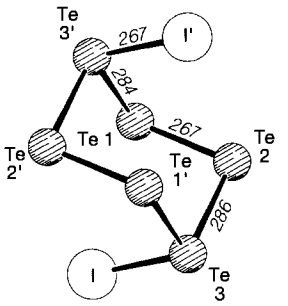


Fig. 8. Structure of the centrosymmetric $Te_6I_2^{2+}$ ion in $Te_6I_2(WCl_6)_2$; bond lengths given in pm.

is thus isostructural with its selenium analogue $Se_6I_2^{2+}$.[65] Both ions have distinctly alternating bond lengths. In the $Te_6I_2^{2+}$ ion, the Te–I bonds as well as the Te1–Te2 bonds, and the Te1′–Te2′ bonds (all 267 pm) are unusually short. Conversely, the other Te–Te bonds (mean 285 pm) are clearly longer than a Te–Te single bond (expected value 274 pm). Formally, the two positive charges are localized at the two three-bonded Te3 and Te3′ atoms. If the shortened bonds are assigned some degree of double bonding, however, delocalization ensues and the positive charges are distributed over all atoms in the cation, including the iodine atoms.[65] This interpretation is made plausible from the occurrence of several short distances between the I atoms of the cations and the Cl atoms of the WCl_6^- anions in the $Te_6I_2^{2+}(WCl_6^-)_2$ structure.

The reaction of selenium, iodine, and WCl_6 selectively leads to the polymeric (iodo)selenium cation $(Se_6I^+)_n$ in the compound $(Se_6I^+)_nWCl_6^-$.[66] The cation (Fig. 9) is an infinite one-dimensional chain of Se_6 rings in a chair conformation, connected by iodine bridges formed by *endo* iodine atoms at *para* Se ring atoms. The linear environment of the iodine atoms is best understood under the assumption of a three-center, four-electron bond. The Se–I distances (278 pm) are significantly longer than the sum of the covalent radii (250 pm). The structure of the polymeric cation is very similar to that of the corresponding cations in $(Se_6I)AsF_6$ and $(Se_6I)SbF_6$.[65] The difference lies in the identical orientation of the Se_6 rings in $(Se_6I)WCl_6$, as opposed to a twisted orientation of adjacent rings in $(Se_6I)MF_6$ (M = As, Sb).

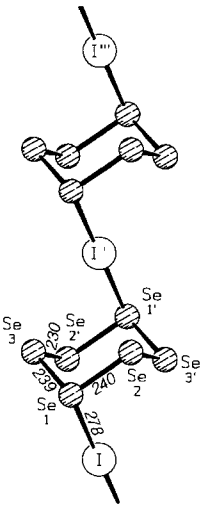


Fig. 9. Structure of the polymeric $(Se_6I^+)_n$ ion in $(Se_6I)WCl_6$. There are inversion centers at the iodine atom positions and at the centers of gravity of the Se_6 rings; bond lengths given in pm.

Has the original goal of synthesizing molybdenum and tungsten halide tellurides been achieved with the compounds presented in this section? At a first glance, the overall formulas of $MoOTe_2Cl_4$, WTe_2Cl_6, $MoOSe_2Cl_4$, $WOTe_3Cl_4$, WTe_4Cl_6, $WOTe_7Br_5$, $WOTe_7Cl_5$, $NbOTe_7Cl_5$, $NbOTe_7Br_5$, WTe_3Cl_6I, and WSe_6Cl_6I seem to suggest this. The structural principle common to all these compounds is their construction from chalcogen polycations and halide metalate anions; however, these compounds have no metal–chalcogen bonds. Thus, the compounds presented so far cannot be counted among the desired class of metal halide tellurides compounds.

4. Halogen-Containing Tellurides and Halide Tellurides of Molybdenum and Tungsten

In this section the emphasis will again be placed on compounds of the ternary system metal/tellurium/halogen (metal = molybdenum, tungsten), but which are based on structural principles totally different from those considered so far.

4.1. $MoTe_4Br$: A Molybdenum Telluride with a Chain Structure, Containing Bromine

$MoTe_4Br$ forms as crystals with a silver luster from $MoTe_2$, Te, and $TeBr_4$ at 440 °C.[21] The structure of $MoTe_4Br$ is characterized by infinite one-dimensional $Mo(Te_2)_2$ chains with intercalated bromide ions (Fig. 10). $MoTe_4Br$ is isotypic with $TaTe_4I$, which is closely related to $NbTe_4I$.[67] Mo_2 pair formation occurs along the linear molybdenum chain. The short Mo–Mo distance (300 pm) is still within the range of a metal–metal bond. For comparison, the formal Mo–Mo single bond in the structure of $[Mo_6Cl_8]Cl_4$ is 261 pm,[68] and in the structure of $MoTe_2$, in which the Mo atoms form zigzag chains, the metal–metal distance is 290 pm.[69] The larger distance of 382 pm to the adjacent Mo_2 pairs in $MoTe_4Br$ is no longer considered as a Mo–Mo interaction. This pair formation indicates that the molybdenum atoms in $MoTe_4Br$ still possess available d electrons. As expected, in $NbTe_4I$ and $TaTe_4I$, which formally con-

tain Nb^{5+} and Ta^{5+}, respectively, and thus have a d^0 configuration, the metal–metal distances within the chain are equidistant.[67]

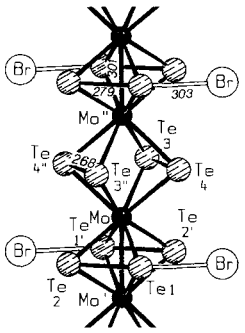


Fig. 10. A section from the $Mo(Te_2)_2$ chain in the structure of $MoTe_4Br$ with the most important bond lengths given in pm. The Mo–Te bonds range between 273 and 287 pm.

The tellurium atoms in $MoTe_4Br$ form Te_2^{2-} ions which bridge two adjacent Mo atoms in such a way that each Mo atom achieves a coordination number eight and a square antiprismatic coordination polyhedron results. The bromide ion forms close contacts to several Te atoms, of which the Te1–Br distance of 303 pm is the shortest. Since the sum of the covalent radii of Te and Br atoms is 251 pm,[40] a Te–Br bond of 303 pm is very weak, but still partially covalent. The Te–Br distances of 290 and 302 pm in the tellurium subhalide Te_2Br fall into a similar range.[70] Whether the distance between the atoms Te1 and Br in the $MoTe_4Br$ structure is regarded as a covalent Te–Br bond, or as a close contact of a bromide ion with a Te atom from a positively charged $Mo(Te_2)_2$ chain, results in two limiting ionic formulas: $(Mo^{3+})(Te_2^{2-})(Te_2Br^-)$ or $[(Mo^{5+})(Te_2^{2-})_2]^+(Br^-)$. Since $MoTe_4Br$ shows only a weak, temperature-independent paramagnetism, the coupling of unpaired electrons is very strong, and thus a decision on the oxidation state of the molybdenum centers is not possible on the basis of magnetic properties. A comparison with the isostructural $TaTe_4I$ favors the existence of Mo^{5+} ions with a d^1 configuration in $MoTe_4Br$; in $TaTe_4I$ the Ta oxidation state appears certain, since in the chain of Ta atoms there are no Ta–Ta pairs. The Te–Te bonds within Te_2 groups taking part in the short Te–halogen contacts are lengthened in both $TaTe_4I$ and $MoTe_4Br$. For $TaTe_4I$ this increase is approximately 4 pm, for $MoTe_4Br$ it is 11 pm. This shows that the Te–halogen interactions are slightly bonding, a result which was confirmed by band structure calculations on $TaTe_4I$.[67] The Te_2Br fragment is also encountered in the $[(C_5H_5)(CO)_2MoFe(CO)_3(Te_2Br)]$ complex[71] (Fig. 11), in which Te–Br distance and the Te–Te distance are 281 pm. The complex is only weakly dissociated in solution, which indicates the stability of the Te–Br bond; however, it reacts with $AgSbF_6$ to give the 1:1 electrolyte $[(C_5H_5)(CO)_2MoFe(CO)_3(Te_2)]^+SbF_6^-$.

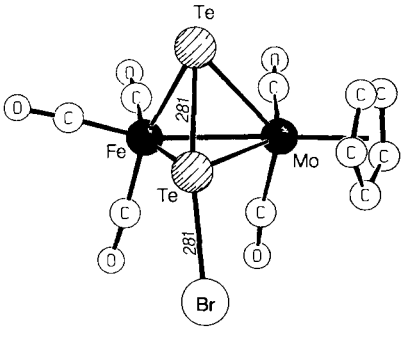


Fig. 11. Structure of the $[(C_5H_5)(CO)_2MoFe(CO)_3(Te_2Br)]$ complex [71]; bond lengths given in pm.

4.2. $MoTe_6Br_3$: A Molybdenum Telluride with Te_4^{2+} Ligands, Containing Bromine

$MoTe_6Br_3$, like $MoTe_4Br$, forms as crystals with a silver luster from $MoTe_2$, Te, and $TeBr_4$, but at a lower temperature (300 °C).[21] The structure of $MoTe_6Br_3$ (Fig. 12) is built from bromide ions and dimeric cationic complexes which can be perceived as fragments from the chain structure of $MoTe_4Br$. The dimers are centrosymmetric and consist of Mo_2 pairs (Mo–Mo distance 296 pm) bridged by two Te_2^{2-} pairs (Te1–Te2 and Te1'–Te2'). Two almost planar Te_4 rings, bound in an η^4–π fashion, complete an octacoordinate environment around each Mo atom in the form of a square antiprism. The average Te–Te bond length in the Te_4 rings is 279 pm. If the Te_4 ring is assumed to be a complexing Te_4^{2+} ion, $MoTe_6Br_3$ can be formulated ionically as $[(Mo^{3+})_2(Te_2^{2-})_2(Te_4^{2+})_2]^{6+}(Br^-)_6$. Thus far, there are only a few examples of chalcogen polycations acting as complex ligands. For instance, the reaction of $[M(CO)_6]$ (M = Mo, W) with Se_4^{2+} in liquid SO_2 affords a complex cation $[(CO)_5MSe_4M(CO)_5]^{2+}$,[72] in which the Se_4^{2+} ion is bound as an η^2 ligand along two of the edges of the four-membered ring to two $M(CO)_5$ fragments (Fig. 13, **A**). The same reaction with Te_4^{2+} yields the cationic complex $[(CO)_4M(Te_3)]^+$,[73] which contains the triangular Te_3^+ ion (unknown as a noncomplexed species) as a π-bound η^3 ligand (Fig. 13, **B**). The structure of $Nb_3OTe_8I_7$ contains complex cations, in which a Te_4^{2+} ion bridges two niobium atoms (Fig. 13, **C**).[74] The consideration of Te_4^{2+} as a ligand is also supported by the coordination of neighboring halide ions, which in $Nb_3OTe_8I_7$ (Fig. 13, **C**) and $MoTe_6Br_3$ (Fig. 12) typically bridge the edges of the Te_4 ring. In $MoTe_6Br_3$ some of these Te–Br distances are very short, and, in particular, the Te3–Br and the Te5–Br distances (mean 281 pm) must be interpreted as considerably covalent Te–Br bonds.

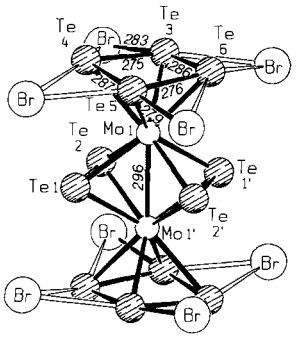


Fig. 12. Structure of the $[Mo_2(Te_2)_2(Te_4)_2]^{6+}$ complex in $MoTe_6Br_3$ with the most important bond lengths given in pm. The adjacent bromide ions which bridge the edges of the Te_4 rings are also shown. The weaker Te–Br contacts are represented by white rods. The Mo–Te bonds range between 273 and 286 pm.

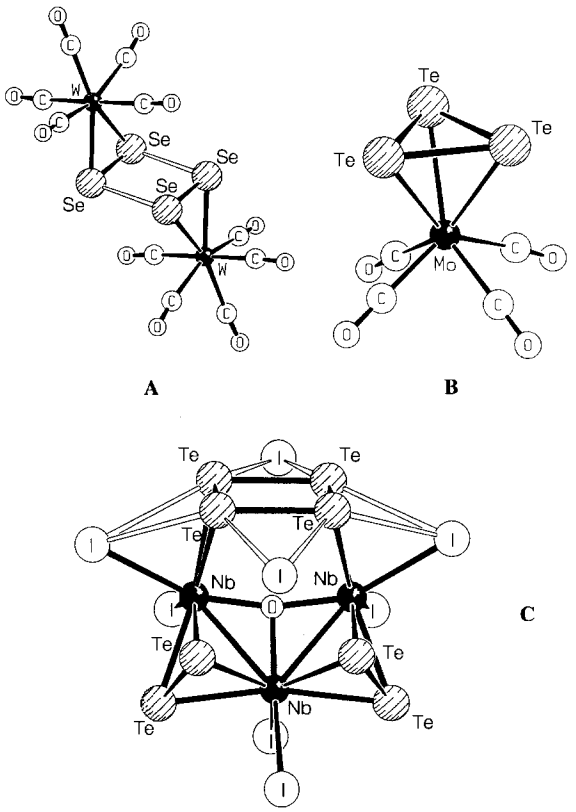


Fig. 13. Structures of compounds containing chalcogen polycations that complex metal atoms. **A**: $[(CO)_5MSe_4M(CO)_5]^{2+}$ [72], **B**: $[(CO)_4Mo(Te_3)]^+$ [73]. **C** shows a section from the $Nb_3OTe_8I_7$ structure [74].

4.3. $Mo_4Te_7X_8$ (X = Cl, Br): A Molybdenum Halide Telluride with a Structure Containing Two Different Chains

At 500 °C, the isostructural compounds $Mo_4Te_7Cl_8$ and $Mo_4Te_7Br_8$ are formed in the ternary molybdenum/tellurium/halogen (halogen = Cl, Br) system.[21] Both compounds appear as shining black needles. $Mo_4Te_7Br_8$ is a semiconductor with a small specific conductivity of 4×10^{-5} $(\Omega cm)^{-1}$ at room temperature. The structures are built from two different one-dimensional chains between which there are no significant interactions (Fig. 14). One of the chains, $(Mo_2X_7)_n$, contains only molybdenum and halogen atoms. Each Mo atom is hexacoordinated by an octahedron of six halogen atoms. The MoX_6 octahedrons connect by alternately sharing edges and faces along the chain. Furthermore, the Mo atoms form Mo_2 pairs with distances of 275 pm for X = Cl and 282 pm for X = Br. The other chain, $[Mo_2(Te_2)_3(TeX)]_n$, contains Mo atoms surrounded only by Te atoms. The Mo_2 pair formation is much less pronounced, and the Mo–Mo distances alternate only slightly with 292 and 301 pm for X = Cl and 296 and 310 pm for X = Br. Along the chain, two neighboring Mo atoms are each coordinated alternately by two μ_2-Te_2^{2-} pairs, or by one μ_2-Te_2^{2-} pair and the Te atom of a bridging TeX group. The TeX groups, hitherto unknown, are a peculiarity in the $Mo_4Te_7X_8$ structures. The Te–X distances are 244 pm for X = Cl and 260 pm for X = Br; thus, they are only slightly longer than the sum of the covalent radii of Te and Cl atoms (236 pm) and Te and Br atoms (251 pm), respectively. It is thus a reasonable to consider the TeX group as the isoelectronic tellurium analogue of the hypochlorite ion OCl^-. The ionic formula $[\{(Mo^{4+})_2(Te_2^{2-})_3(TeX^-)\}^+]_n$-$[\{(Mo^{3+})_2(X^-)_7\}^-]_n$ for $Mo_4Te_7X_8$ therefore seems appropriate.[75]

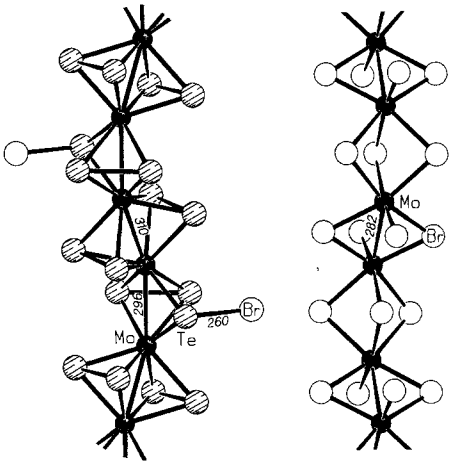


Fig. 14. Sections from the $Mo_2(Te_2)_3(TeX)$ and Mo_2X_7 chains in the structures of $Mo_4Te_7X_8$ (X = Cl, Br). The distances given pm are valid for $Mo_4Te_7Br_8$. The Mo–X bonds range from 238 to 252 pm for X = Cl, and from 251 to 268 pm for X = Br, the Mo–Te bonds are between 270 and 283 pm.

For these four new compounds from the ternary molybdenum/tellurium/halogen systems, the more or less pronounced proximity of tellurium atoms and halogen atoms is a characteristic observed in addition to the ever-present Mo–Mo interactions. With Te–Br contacts between 260 and 303 pm, a broad spectrum of distances is observed ranging from ionic contacts to covalent bonding. Since $MoTe_4Br$ and $MoTe_6Br_3$ contain only Mo–Te bonds and no Mo–Br bonds, they can be classified as bromine-containing tellurides. For $Mo_4Te_7X_8$ (X = Cl, Br), both Mo–Te and Mo–X bonds are present, so that the classification as metal halide tellurides is therefore justifiable. Admittedly, the tellurium and the halogen atoms are not bound to the same molybdenum atom—rather a separation into Mo–X chains and Mo–Te chains occurs. This may be perceived as a segregation in the solid.

4.4. $W_2O_2Te_4Br_5$: The First Tungsten Halide Telluride

$W_2O_2Te_4Br_5$ can be obtained by reacting $WOBr_4$ and tellurium at 400 °C.[21] Similar to $Mo_4Te_7X_8$, the structure of $W_2O_2Te_4Br_5$ is also composed of two different infinite one-dimensional chains (Fig. 15). In the $(WOBr_4)_n$ chains are square-pyramidal monomers which are associated through almost linear, strongly assymetric W-O-W-O bridges. The W=O distances (174 and 205 pm) are distinctly different. The second chain contains an almost linear W-O-W-O chain with identical W–O distances of 190 pm. The tungsten atoms have the coordination number seven and are pentagonal-bipyramidal surrounded. In addition to the two oxygen atoms at the apical positions, two Te_2 groups and one terminal bromine atom are coordinated to each W atom. Between the Te_2 groups of neighboring tungsten

atoms, Te–Te bonds (295 pm) exist, so that U-shaped, planar Te_4^{2-} ions are present, which each bridge one W-O-W unit. This way, for $W_2O_2Te_4Br_5$, the formal ionic formulation $[\{W^{6+}OBr(Te_4^{2-})\}^+]_n[(W^{5+}OBr_4)^-]_n$ results. Thus, in $W_2O_2Te_4Br_5$, in contrast to the previously described molybdenum compounds, for the first time, Te and Br atoms are both bound to a tungsten atom.

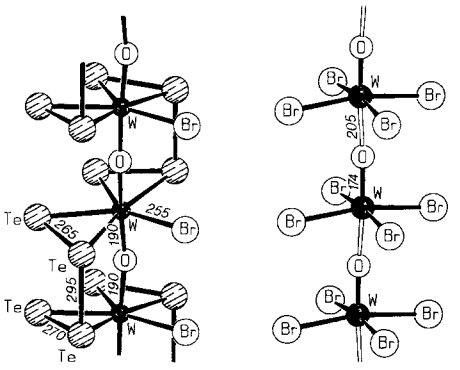


Fig. 15. Sections from the $(WOTe_4Br)_n$ and $(WOBr_4)_n$ chains in the $W_2O_2Te_4Br_5$ structure; bond lengths given in pm. The W–Br bonds in the $(WOBr_4)_n$ chain are between 248 and 255 pm, the W–Te bonds between 272 and 283 pm.

5. Summary and Outlook

The barely researched ternary M/Te/X systems with M = Mo, W and X = Cl, Br, I, turn out to be a very rich field with respect to structural chemistry, where many different structural principles are realized. Compounds such as $Mo_4Te_7X_8$ and $W_2O_2Te_4Br_5$, which simultaneously contain metal–tellurium and metal–halogen bonds and thus can be classified as halide tellurides, are still in the minority. Rather, compounds built from tellurium polycations and halide metalate anions dominate. The halide tellurides do not show the structural characteristic of terminal M=E bonds (M = Mo, W; E = O, S, Se) with a formal double bond character typical for the halide oxides, halide sulfides, and halide selenides. Apparently, this kind of bonding becomes unfavorable for the heaviest of the chalcogens used here—tellurium—and for the metal atoms in their higher oxidation states. In recent times, however, complexes with terminal tellurido ligands have become known,[76] including a tungsten complex $[WTe_2(PMe_3)_4]$ containing a linear Te=W=Te group.[77] These results have provided fresh impetus to the search for other halide tellurides of molybdenum and tungsten. The potential of the synthesis route for preparing chalcogen polycations from chalcogen elements and metal halides is by no means exhausted. The observation that different metal halides specifically generate different polycations provides hope for obtaining other new chalcogen polycations with metal halides not yet employed. Investigations with rhenium halides and uranium halides are already under way, as well as experiments to oxidize mixtures of chalcogens with suitable metal halides. It is conceivable that in this way the great number of mixed polycations, among them the octaatomic and decaatomic species $Te_2Se_6^{2+}$ and $Te_2Se_8^{2+}$,[78] respectively, synthesized in Gillespie's group, may be further increased.

The compounds available thus far raise many questions about their method of formation and their types of bonding. An interesting problem is the elucidation of the reaction mechanisms during chemical transport. For example, what is the nature of the tellurium-containing species in the gas phase above a continuously growing crystal of Te_7WOBr_5 and what effects the buildup of the polymeric tellurium substructure? Compounds such as $MoTe_4Br$ and $Mo_4Te_7Br_8$ contribute to the current topic of low-dimensional solids,[79] for which the bonding cannot be described satisfactorily by simple ionic formulas. Modern methods applied in the theory of chemical bonding will be helpful for a deeper understanding of these solids.

The results presented in this article were obtained for the most part during the authors' work on his habilitation thesis at the Universität Karlsruhe from 1988–1991. The author is very much indebted to Professor Hartmut Bärnighausen for continuous support during this period and for many helpful discussions. The results of G. Bock, T. Marschall, and J. Wetterau, my first coworkers at the Universität Giessen, have also been included in this article, and I owe them many thanks for their commitment. Thanks also go to Dr. M. Serafin for his help with the SCHAKAL plots [80] and to the Fonds der Chemischen Industrie for generous financial support.

Received: May 27, 1993 [A1IE]
German version: *Angew. Chem.* **1994**, 106, 172
Translated by Dr. U. Löchner, Heilbronn (FRG)

[1] H. G. von Schnering, W. Beckmann, *Z. Anorg. Allg. Chem.* **1966**, *347*, 231.
[2] H. F. Franzen, W. Hönle, H. G. von Schnering, *Z. Anorg. Allg. Chem.* **1983**, *497*, 13.
[3] H. Schäfer, F. Wartenpfuhl, *Z. Anorg. Allg. Chem.* **1961**, *308*, 282.
[4] M. Danot, J. Rouxel, *C. R. Seances Acad. Sci. Ser. C* **1966**, *262*, 1879.
[5] J. Beck, *Z. Anorg. Allg. Chem.* **1990**, *585*, 157.
[6] S. Goldsztaub, *Bull. Soc. Fr. Mineral.* **1935**, *58*, 49; M. D. Lind, *Acta Crystallogr. Sect. B* **1970**, *26*, 1058.
[7] O. Göser, W. Paul, H. G. Kahle, *J. Magn. Magn. Mater.* **1990**, *92*, 129.
[8] H. Hess, H. Hartung, *Z. Anorg. Allg. Chem.* **1966**, *344*, 157.
[9] U. Müller, *Acta Crystallogr. Sect. C* **1984**, *40*, 915.
[10] M. G. B. Drew, R. Mandyczewsky, *J. Chem. Soc. A* **1970**, 2815.
[11] F. A. Cotton, F. A. Kibala, R. B. W. Sandor, *Inorg. Chem.* **1989**, *28*, 2485.
[12] J. Beck, J. Wetterau, unpublished results; J. Wetterau, diploma thesis, Universität Giessen, **1993**.
[13] J. Fenner, A. Rabenau, G. Trageser, *Adv. Inorg. Chem. Radiochem.* **1979**, *23*, 329; a comprehensive review of syntheses, structures, and properties of chalcogenide halides of main group and subgroup metals, covering the literature up to 1979.
[14] J. D. Marcoll, A. Rabenau, D. Mootz, M. Wunderlich, *Rev. Chim. Miner.* **1974**, *11*, 607.
[15] C. Perrin, M. Sergent, F. Le Traon, A. Le Traon, *J. Solid State Chem.* **1978**, *25*, 197.
[16] M. Sergent, O. Fischer, M. Decroux, C. Perrin, R. Chevrel, *J. Solid State Chem.* **1977**, *22*, 87.
[17] B. Krebs, F.-P. Ahlers, *Adv. Inorg. Chem.* **1990**, *35*, 235; an exhaustive and topical review on the chalcogen halides.
[18] L. Kolditz, T. Moya, U. Calov, E. A. Kravchenko, R. Stösser, *Z. Chem.* **1981**, *21*, 38.
[19] A. Gleizes, J. Galy, *C. R. Seances Acad. Sci. Ser. C* **1978**, *286*, 29.
[20] J. Beck, *Z. Naturforsch. B* **1991**, *46*, 183.
[21] J. Beck, unpublished results.
[22] B. H. Christian, M. J. Collins, R. J. Gillespie, J. F. Sawyer, *Inorg. Chem.* **1986**, *25*, 777.
[23] R. J. Gillespie, *J. Chem. Soc. Rev.* **1979**, *8*, 315; a comprehensive review covering the known chalcogen polycations up to 1979. Their structures are treated in the context of general structural principles in the cluster chemistry of main group elements.
[24] N. J. Bjerrum, G. P. Smith, *J. Am. Chem. Soc.* **1968**, *90*, 4472; N. J. Bjerrum, *Inorg. Chem.* **1970**, *9*, 1965.
[25] J. Barr, R. J. Gillespie, R. Kapoor, K. C. Malhotra, *Can. J. Chem.* **1968**, *46*, 149; J. Barr, R. J. Gillespie, G. P. Pez, P. K. Ummat, O. C. Vaidya, *Inorg. Chem.* **1971**, *10*, 362.

[26] D. J. Prince, J. D. Corbett, B. Garbisch, *Inorg. Chem.* **1970**, *9*, 2731.
[27] R. K. McMullan, D. J. Prince, J. D. Corbett, *J. Chem. Soc. Chem. Commun.* **1969**, 1438; *Inorg. Chem.* **1971**, *10*, 1749.
[28] T. W. Couch, D. A. Lokken, J. D. Corbett, *Inorg. Chem.* **1972**, *11*, 357.
[29] M. J. Collins, R. J. Gillespie, J. W. Kolis, J. F. Sawyer, *Acta Crystallogr. Sect. C* **1987**, *43*, 2033.
[30] J. Beck, *Z. Naturforsch. B* **1990**, *45*, 1610.
[31] J. Beck, *Z. Naturforsch. B* **1990**, *45*, 413.
[32] G. Cardinal, R. J. Gillespie, J. F. Sawyer, J. E. Vekris, *J. Chem. Soc. Dalton Trans.* **1982**, 765.
[33] K. Tanaka, T. Yamabe, H. Terama-e, K. Fukui, *Inorg. Chem.* **1979**, *18*, 3591.
[34] J. J. Rothmann, L. S. Bartell, C. S. Ewig, J. R. Van Wazer, *J. Comput. Chem.* **1980**, *1*, 64.
[35] J. D. Corbett, *Inorg. Nucl. Chem. Lett.* **1969**, *5*, 81.
[36] R. J. Gillespie, W. Luk, E. Maharajh, D. R. Slim, *Inorg. Chem.* **1977**, *16*, 892.
[37] R. C. Burns, M. J. Collins, S. M. Eicher, R. J. Gillespie, J. F. Sawyer, *Inorg. Chem.* **1988**, *27*, 1807.
[38] R. C. Burns, R. J. Gillespie, W.-C. Luk, D. R. Slim, *Inorg. Chem.* **1979**, *18*, 3087; M. J. Collins, R. J. Gillespie, J. F. Sawyer, *Acta Crystallogr. Sect. C* **1988**, *44*, 405.
[39] H. G. von Schnering, *Angew. Chem.* **1981**, *93*, 44; *Angew. Chem. Int. Ed. Engl.* **1981**, *20*, 33.
[40] L. Pauling, *Die Natur der Chemischen Bindung*, Verlag Chemie, Weinheim, **1968**; *The Nature of the Chemical Bond*, Cornell University Press, Ithaca, NY, USA, **1960**.
[41] C. G. Davies, R. J. Gillespie, J. J. Park, J. Passmore, *Inorg. Chem.* **1971**, *10*, 2781.
[42] R. J. Gillespie, J. Passmore, *Adv. Inorg. Chem. Radiochem.* **1975**, *17*, 49.
[43] J. D. Corbett, *Prog. Inorg. Chem.* **1976**, *21*, 129.
[44] N. Burford, J. Passmore, J. C. Sanders, *Mol. Struct. Energ.* **1991**, *11*, 53.
[45] J. Beck, *Angew. Chem.* **1990**, *102*, 301; *Angew. Chem. Int. Ed. Engl.* **1990**, *29*, 293.
[46] F. A. Cotton, P. A. Kibala, R. B. W. Sandor, *Acta Crystallogr. Sect. C* **1989**, *45*, 1287.
[47] F. Fenske, G. Baum, H. Wolkers, B. Schreiner, F. Weller, K. Dehnicke, *Z. Anorg. Allg. Chem.* **1993**, *619*, 489.
[48] K. W. Klinkhammer, P. Böttcher, *Z. Naturforsch. B* **1990**, *45*, 141.
[49] J. Beck, *Angew. Chem.* **1991**, *103*, 1149; *Angew. Chem. Int. Ed. Engl.* **1991**, *30*, 1128.
[50] J. Beck, *Z. Anorg. Allg. Chem.* **1993**, *619*, 237.
[51] J. Beck, G. Bock, unpublished results; G. Bock, diploma thesis, Universität Giessen, **1993**.
[52] P. Böttcher, *Angew. Chem.* **1988**, *100*, 781; *Angew. Chem. Int. Ed. Engl.* **1988**, *27*, 759.
[53] M. Joulien-Pouzol, S. Jaulmes, F. Alapini, *Acta Crystallogr. Sect. B* **1977**, *33*, 2270.
[54] P. Böttcher, U. Kretschmann, *J. Less. Common. Met.* **1983**, *95*, 81; *Z. Anorg. Allg. Chem.* **1982**, *491*, 39.
[55] F. Klaiber, W. Petter, F. Hulliger, *J. Solid State Chem.* **1983**, *46*, 112.
[56] B. Schreiner, K. Dehnicke, K. Maczek, D. Fenske, *Z. Anorg. Allg. Chem.*, in press.
[57] R. Zagler, B. Eisenmann, *Z. Naturforsch. B* **1991**, *46*, 593.
[58] B. Krebs, E. Lührs, R. Willmer, F.-P. Ahlers, *Z. Anorg. Allg. Chem.* **1991**, *592*, 17; M. G. Kanatzidis, S.-P. Huang, *Inorg. Chem.* **1989**, *28*, 4667.
[59] R. J. Gillespie, R. S. Nyholm, *Quart. Rev. London* **1957**, *11*, 339.
[60] J. Bernstein, R. Hoffmann, *Inorg. Chem.* **1985**, *24*, 4100.
[61] W.-W. du Mont, S. Kubiniok, K. Peters, H. G. von Schnering, *Angew. Chem.* **1987**, *99*, 820; *Angew. Chem. Int. Ed. Engl.* **1987**,*26*, 780.
[62] J. Passmore, G. W. Sutherland, T. K. Whidden, P. S. White, *J. Chem. Soc. Chem. Commun.* **1980**, 289.
[63] T. Klapötke, J. Passmore, *Acc. Chem. Res.* **1989**, *22*, 234, and references therein; review of syntheses, structures, and bonding of the known chalcogen–halogen cations.
[64] J. P. Johnson, M. P. Murchie, J. Passmore, M. Tajik, P. S. White, C.-M. Wong, *Can. J. Chem.* **1987**, *65*, 2744; J. Passmore, G. Sutherland, P. S. White, *ibid.* **1981**, *59*, 2876.
[65] W. A. Shantha Nandana, J. Passmore, P. S. White, C.-M. Wong, *Inorg. Chem.* **1989**, *28*, 3320.
[66] J. Beck, T. Marschall, unpublished results; T. Marschall, diploma thesis, Universität Giessen, **1993**.
[67] W. Tremel, *Chem. Ber.* **1992**, *125*, 2165.
[68] H. Schäfer, H. G. von Schnering, J. Tillack, F. Kuhnen, W. Wöhrle, H. Baumann, *Z. Anorg. Allg. Chem.* **1967**, *353*, 281.
[69] B. E. Brown, *Acta Crystallogr.* **1966**, *20*, 268.
[70] R. Kniep, D. Mootz, A. Rabenau, *Z. Anorg. Allg. Chem.* **1976**, *422*, 17.
[71] L. E. Bogan, T. B. Rauchfuß, A. L. Rheingold, *Inorg. Chem.* **1985**, *24*, 3720.
[72] M. J. Collins, R. J. Gillespie, J. W. Kolis, J. F. Sawyer, *Inorg. Chem.* **1986**, *25*, 2057; C. Belin, T. Makani, J. Rozière, *J. Chem. Soc. Chem. Commun.* **1985**, 118.
[73] M. J. Collins, R. J. Gillespie, J. W. Kolis, J. F. Sawyer, *Inorg. Chem.* **1986**, *25*, 2057; A. Seigneurin, T. Makani, D. J. Jones, J. Rozière, *J. Chem. Soc. Dalton Trans.* **1987**, 2111.
[74] W. Tremel, *J. Chem. Soc. Chem. Commun.* **1992**, 126.
[75] An alternative formulation assumes neutral chains; that is the Mo atoms in both chains must have mixed-valence: $[(Mo^{3+})(Mo^{4+})(Te_2^{2-})_3(TeX^-)]_n[(Mo^{3+})(Mo^{4+})(X^-)_7]_n$. No decision between the two formulations can be made from magnetic properties, since the two $Mo_4Te_7X_8$ compounds show only a weak, temperature-independent paramagnetism.
[76] U. Siemeling, *Angew. Chem.* **1993**, *105*, 70; *Angew. Chem. Int. Ed. Engl.* **1993**, *32*, 67, and references therein.
[77] D. Rabinovich, G. Parkin, *J. Am. Chem. Soc.* **1991**, *113*, 9421.
[78] M. J. Collins, R. J. Gillespie, J. F. Sawyer, *Inorg. Chem.* **1987**, *26*, 1476.
[79] J. Rouxel, *Acc. Chem. Res.* **1992**, *25*, 328.
[80] E. Keller, SCHAKAL 92 (program for graphic representation of crystal structures), Universität Freiburg, **1992**.

How do they fit so much in?



Keep up with the latest developments in all areas of chemistry.
Order your own personal subscription.

Just fax

USA	Fax: (305)	428-8201
UK	Fax: (0223)	313221
Japan	Fax: (03)	3816 3758
Rest of world	Fax: (0 1149)	62 01-606-184

VCH

The Photochemical Activation of Carbon Dioxide Using a Nickel Complex

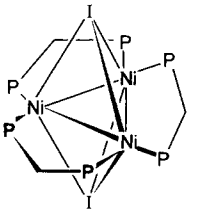
Walter Leitner

Carbon dioxide is in many ways a remarkable starting material in chemical syntheses.[1] It is cheap and easy to purify, presents no problems in handling, and is virtually nontoxic. Furthermore, its availability is almost inexhaustible since the quantity of carbon released by combustion of fossil fuels in the form of CO_2 far exceeds that used up in technical and chemical processes.[2] Of special interest in this context are processes that avoid the use of fossil fuels for the generation of the energy required for CO_2 activation.

Unlike chemists, plants are capable of synthesizing organic compounds from sunlight, CO_2, and a cosubstrate. Photosynthesis, optimized over millions of years of evolution and estimated to convert about 10^{11} tons of carbon per year, is the most important chemical process on our planet and forms the basis of life. It is only in the last ten years that man has begun to search intensively for molecular systems which allow the photochemical activation of carbon dioxide.[3]

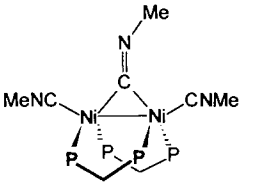
The fundamental problem of photochemical activation of CO_2 is the first step, namely the formation of the radical anion $CO_2^{\bullet -}$. For this purpose it is essential to generate the necessary powerful reducing agent through irradiation. The first successful examples of this approach were achieved with, among others, metal-free redox-active systems,[4] dipyridine complexes,[5] semiconductor materials,[6] and a combination of such components.[7] In some cases small amounts of C_2 products were detected.[6b] Kubiak et al. of Purdue University have now shown that the new and exceptionally efficient photochemical reducing agent **1** also allows photoreduction of CO_2.[8] Their findings deserve special attention since for the first time the generated $CO_2^{\bullet -}$ radical anion is available for C–C coupling reactions with cosubstrates.

Cluster **1** is a result of detailed investigations of similar bi- and trinuclear nickel complexes by the same group during the last couple of years.[9] These complexes are derived from the binuclear complex **2**, in which no iodine is present and the nickel atoms are in the zero oxidation state. The authors described this and other similar binuclear Ni^0 complexes as "cradle complexes",[9a] not knowing that they were indeed an extremely promising starting point in the photochemical activation of CO_2. Thermal, electrochemical, or photochemical excitation of **2** resulted in activation of CO_2, but reactions of $CO_2^{\bullet -}$ with the isocyanide ligands finally led via structurally interesting intermediates to the stable carbonyl complex **3**, which exhibits no further reactivity towards CO_2.[9a–b] Treatment of **2** with CH_2I_2 or NiI_2 gave the first trinuclear iodine-containing complex[9c] in a rather complicated but smooth reaction. The highly symmetrical

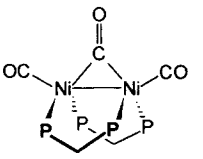


1

P⌒P = Ph_2P-(CH_2)-PPh_2



2



3

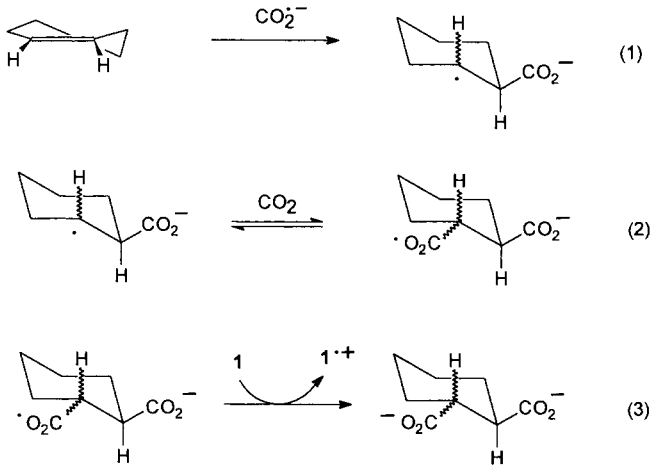
cluster **1** was obtained directly by the comproportionation of $[Ni(cod)_2]$ (cod = 1,5-cyclooctadiene) and NiI_2 in the presence of 1,2-bis(diphenylphosphino)methane (dppm). Cluster **1** finally allowed the photochemical formation of free $CO_2^{\bullet -}$, which was detected with different methods.[8]

The violet **1** can be oxidized electrochemically at $E_{1/2}$ ($\mathbf{1}^{\bullet +}/\mathbf{1}$) = −0.69 V (vs. SCE) to the green radical cation $\mathbf{1}^{\bullet +}$. Crystal structure analyses of both compounds indicate that oxidation causes negligible structural changes in the cluster. The edges of the equilateral triangle formed by the nickel atoms are bridged by dppm ligands. Both faces of the triangle are capped by a μ_3-iodo ligand. Diffuse daylight is sufficient to bring about photochemical oxidation of **1** in solvents such as THF or CH_2Cl_2. In an atmosphere of CO_2, the photolysis of a THF solution of **1** leads to the formation of CO and CO_3^{2-} in the absence of proton sources, or to HCO_2^- in the presence of toluene. These products indicate intermediate formation of $CO_2^{\bullet -}$. In addition to these classical reactions of $CO_2^{\bullet -}$, the radical anion was trapped by cyclohexene. Equations (1)–(3) demonstrate a plausible mechanism for the observed formation of cyclohexane dicarboxylic acid; the reversibility (Kolbe reaction) of step (2) readily explains the *cis*/*trans* ratio of 37:63 in the isolated product. This is the first proof of a photochemically induced

[*] Dr. W. Leitner
Max-Planck-Gesellschaft zur Förderung der Wissenschaften
Arbeitsgruppe CO_2-Chemie an der Universität
Lessingstrasse 12, D-07743 Jena (FRG)
Telefax: Int. code + (3641)635360

 © VCH Verlagsgesellschaft mbH, D-69451 Weinheim, 1994 0570-0833/94/0202-0173 $ 10.00+.25/0

C–C coupling with CO_2, and the first example of an addition of $CO_2^{\bullet-}$ to an olefinic double bond.



It is quite remarkable that once more a nickel complex can be considered a milestone in CO_2 chemistry. Since the first successful structural characterization of a CO_2 complex $[(Cy_3P)_2Ni(CO_2)]$ (Cy = cyclohexyl)[10] by Aresta et al., nickel complexes have been setting the pace in this branch of organometallic chemistry. Amine–nickel complexes have been reported recently to bind even atmospheric CO_2.[11] Other nickel complexes are versatile synthetic reagents in stoichiometric coupling reactions of CO_2 with unsaturated substrates.[12] Furthermore, nickel complexes are used as catalysts in the formation of cyclic carbonates from epoxides and CO_2,[13] and of 2-pyrones from alkynes and CO_2.[14a] The latter reaction was applied recently in the synthesis of novel polymers.[14b] Electrochemically generated Ni^0 species may also effect C–C coupling between alkynes and CO_2, and α,β-unsaturated carboxylic acids are produced under these conditions.[15]

The $\mathbf{1}/\mathbf{1}^{\bullet+}$ system, like all other approaches to the photochemical activation of CO_2, suffers from an unfavorable total energy balance. The C–C coupling has undoubtedly been proved, but, the authors do not comment on the yields or on the possibilities of realizing a catalytic cycle. Nevertheless, the opportunity of using photochemically activated **1** in some of the already mentioned reactions and the excellent work of Kubiak et al. are grounds enough for optimism that, in the near future, catalytic variations of photochemical C–C coupling reactions with CO_2 will be reported.

German version: *Angew. Chem.* **1994**, *106*, 183

[1] a) A. Behr, *Carbon Dioxide Activation by Metal Complexes*, VCH, Weinheim, **1988**; b) *Enzymatic and Model Carboxylation and Reduction Reactions for Carbon Dioxide Utilization* (Eds.: M. Aresta, J. V. Schloss) (*NATO ASI Ser. Ser. C* **1990**, *314*); c) A. Behr, *Angew. Chem.* **1988**, *100*, 681; *Angew. Chem. Int. Ed. Engl.* **1988**, *27*, 661; d) I. S. Kolomnikov, T. V. Lysak, *Russ. Chem. Rev. (Engl. Transl.)* **1990**, *59*, 344; e) D. Walther, *Nachr. Chem. Techn. Lab.* **1992**, *40*, 1214.

[2] For example, W. Seifritz, *Der Treibhauseffekt*, Hanser, München, **1991**.

[3] a) R. Ziessel in [1b], p. 79; b) M. Aresta, in *Photochemical Conversion and Storage of Solar Energy* (Eds.: E. Pellezetti, M. Schiavello), Kluwer, Dordrecht, **1991**, p. 517; c) N. S. Lewis, G. A. Shreve in *Electrochemical and Electrocatalytic Reactions of Carbon Dioxide* (Eds.: B. P. Sullivan, K. Krist, H. E. Guard), Elsevier, Lausanne, **1993**, p. 263.

[4] a) J. Hawecker, J.-M. Lehn, R. Ziessel, *Helv. Chim. Acta* **1986**, *69*, 1990; b) B. P. Sullivan, T. J. Meyer, *Organometallics* **1986**, *5*, 1500; c) H. Ishida, K. Tanaka, T. Tanaka, *Chem. Lett.* **1988**, 339; d) J.-M. Lehn, R. Ziessel, *J. Organomet. Chem.* **1990**, *382*, 157.

[5] a) M. Halmann, *Nature* **1978**, *275*, 115; b) B. R. Eggins, J. T. S. Irvine, E. P. Murphy, J. Grimshaw, *J. Chem. Soc. Chem. Commun.* **1988**, 1123; c) H. Kisch, G. Twardzik, *Chem. Ber.* **1991**, *124*, 1161; d) M. Kanemoto, T. Shiragami, C. Pac, S. Yanagida, *J. Phys. Chem.* **1992**, *96*, 3521.

[6] a) M. Bradley, T. Tysak, D. Graves, N. Vlachopoulos, *J. Chem. Soc. Chem. Commun.* **1983**, 349; b) J. Petit, P. Chartier, M. Beley, J. Sauvage, *New J. Chem.* **1987**, *11*, 751; c) M. T. Khan, N. N. M. Rao, D. Chatterjee, *J. Photochem. Photobiol. A* **1991**, *60*, 311.

[7] S. Matsuuoka, T. Kohzuki, C. Pac, S. Yanagoka, *Chem. Lett.* **1990**, 2047.

[8] D. A. Morgenstern, R. W. Wittrig, P. E. Fanwick, C. P. Kubiak, *J. Am. Chem. Soc.* **1993**, *115*, 6470.

[9] a) D. L. DeLeat, P. E. Fanwick, C. P. Kubiak, *J. Chem. Soc. Chem. Commun.* **1987**, 1412; b) D. L. DeLaet, R. del Rosario, P. E. Fanwick, C. P. Kubiak, *J. Am. Chem. Soc.* **1987**, *109*, 754; c) F. R. Lemke, D. L. DeLaet, J. Gao, C. P. Kubiak, *J. Am. Chem. Soc.* **1988**, *110*, 6904; d) K. S. Ratliff, G. K. Broeker, P. E. Fanwick, C. P. Kubiak, *Angew. Chem.* **1990**, *102*, 405; *Angew. Chem. Int. Ed. Engl.* **1990**, *29*, 395.

[10] M. Aresta, C. F. Nobile, V. G. Albano, E. Forni, M. Manassero, *J. Chem. Soc. Chem. Commun.* **1975**, 636.

[11] a) P. Moore, S. Rawle, *J. Chem. Soc. Chem. Commun.* **1992**, 1701; b) T. Tanase, S. Nitta, S. Yoshikawa, K. Kobayashi, T. Sakurai, S. Yano, *Inorg. Chem.* **1992**, *31*, 1058.

[12] a) D. Walther, E. Dinjus, *Z. Chem.* **1981**, *21*, 416; b) G. Burkhart, H. Hoberg, *Angew. Chem.* **1982**, *94*, 75; *Angew. Chem. Int. Ed. Engl.* **1982**, *21*, 76; for reviews see: c) H. Hoberg in *Carbon Dioxide as a Source of Carbon* (Eds.: M. Aresta, G. Forti) (*NATO ASI Ser. Ser. C* **1987**, *206*, p. 275); d) D. Walther, *Coord. Chem. Rev.* **1987**, *79*, 135; for recent examples see: e) H. Hoberg, A. Ballesteros, *J. Organomet. Chem.* **1991**, *411*, C16; f) D. Walther, G. Bräunlich, B. Undeutsch, W. Ludwig, *ibid.* **1992**, *427*, 395.

[13] a) R. J. De Pasquale, *J. Chem. Soc. Chem. Commun.* **1973**, 157; b) J. E. Bäckvall, O. Karlson, S. O. Ljunggren, *Tertahedron Lett.* **1980**, 4985.

[14] a) D. Walther, E. Dinjus, H. Schönberg, J. Sieler, *J. Organomet. Chem.* **1987**, *334*, 377; b) T. Tsuda, K. Maruta, Y. Kitaike, *J. Am. Chem. Soc.* **1992**, *114*, 1498.

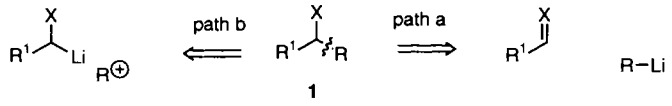
[15] a) E. Duñach, J. Périchon, *Synlett* **1990**, 143; b) S. Dérien, E. Duñach, J. Périchon, *J. Organomet. Chem.* **1990**, *385*, C43.

 © VCH Verlagsgesellschaft mbH, D-69451 Weinheim, 1994 0570-0833/94/0202-0174 $ 10.00+.25/0

Enantioselective Transformations and Racemization Studies of Heteroatom Substituted Organolithium Compounds

Varinder Kumar Aggarwal*

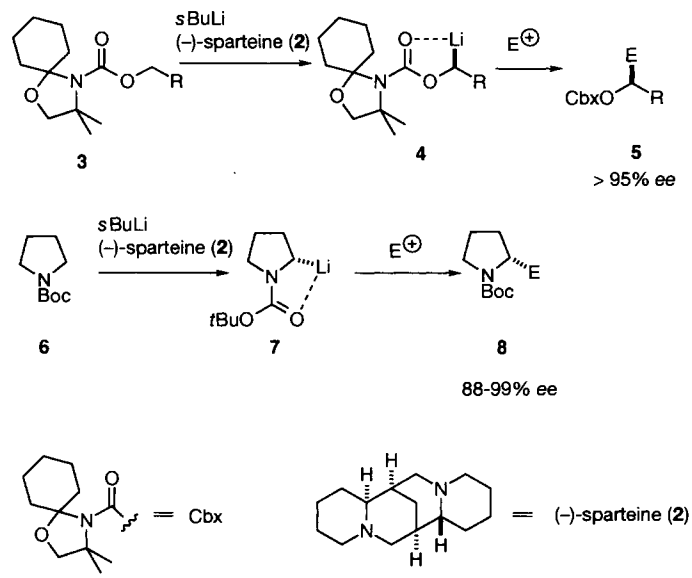
Disconnection of C–C bonds adjacent to heteroatoms is of central importance in organic synthesis. This disconnection can lead to either an organometallic reagent and a C=X group (Scheme 1, path a) or to a carbon electrophile and an α-hetero-



Scheme 1.

atom-substituted organolithium compound (path b). Both pathways can be useful for asymmetric synthesis. For successful asymmetric synthesis using path b the following traditional criteria need to be fulfilled: 1) good methods for the synthesis of the α-lithio compounds in high enantiomeric excess must be available, 2) the α-lithio compounds must be configurationally stable, and 3) either complete retention or inversion of configuration should occur upon quenching with an electrophile.

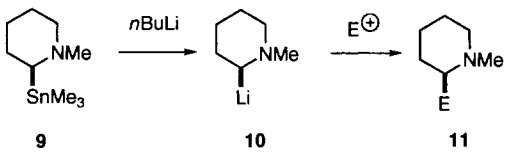
For α-alkoxy- and α-aminoorganolithium compounds there are now several processes that meet the above criteria, and the most notable examples are shown in Scheme 2. These examples utilize the chiral base derived from *s*BuLi and (–)-sparteine (**2**) to effect asymmetric deprotonation.[1–3]



Scheme 2.

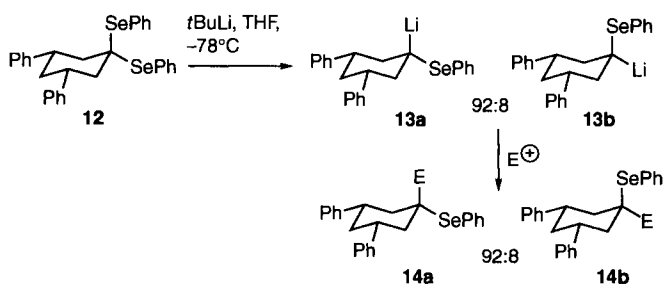
[*] Dr. V. K. Aggarwal
Department of Chemistry, Dainton Building
University of Sheffield
Sheffield S3 7HF (UK)
Telefax: Int. code + (742) 738673

In these and all other successful cases the intermediate chiral organolithium species is stabilized by chelation to a donor group.[3, 4] The only example of an α-aminoorganolithium compound that is not stabilized by chelation but is still configurationally stable has recently been discovered by Gawley et al.[5] They have shown that cyclic α-aminostannanes without chelating groups can be transmetalated with *n*BuLi, and that such α-aminoorganolithium compounds are configurationally stable at –78 °C and can be trapped with electrophiles with complete retention of stereochemistry (Scheme 3).



Scheme 3.

However, in contrast to oxygen- and nitrogen-stabilized carbanions, those stabilized by sulfur or selenium are much less configurationally stable.[6–8] Reich et al.[8] have shown that the α-lithioselenides **13a,b** rapidly equilibrate and that subsequent trapping with a range of electrophiles is faster than equilibration (Scheme 4). Consequently, the product ratio (**14a**:**14b**) reflects

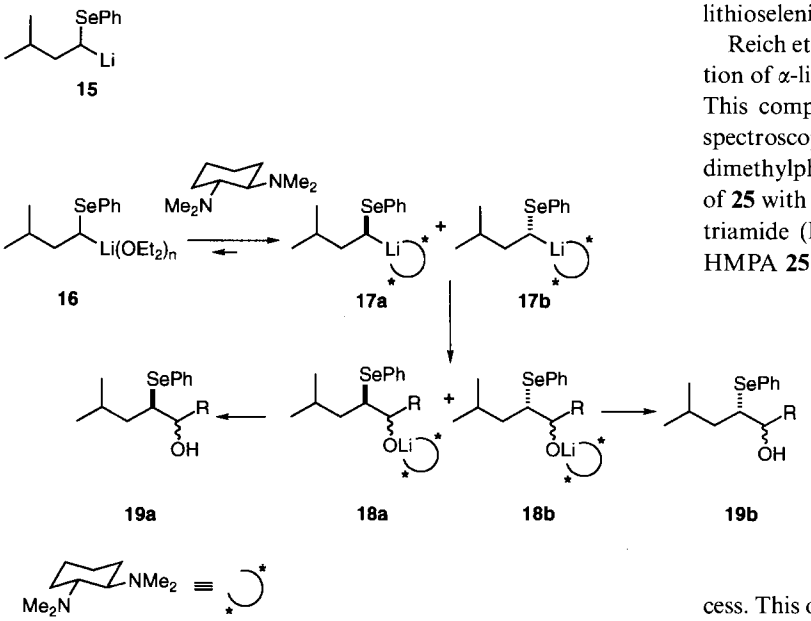


Scheme 4.

the equilibrium ratio of the α-lithioselenides **13a**/**13b**. By considering ratios of enantiomeric and diastereomeric products obtained in reactions of racemic and nonracemic α-lithioselenides **15** (see Scheme 5) with aldehydes, Hoffmann et al. have recently shown that in acyclic systems α-lithioselenides are also trapped more rapidly than they equilibrate.[9] In contrast to the above-formulated criteria, this result demonstrates the possibility of using *configurationally labile* organolithium compounds in stereoselective synthesis by forming diastereomeric complexes with chiral additives.

In this study[9] Hoffmann et al. discovered that the equilibrium constant for formation of the amino complexes **17** was large and that these complexes react with aldehydes more rapidly

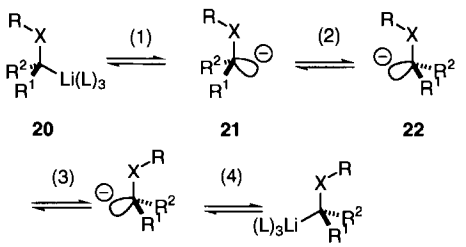
than the uncomplexed organolithium compound **16**. The ligand-induced acceleration in the rate of addition to aldehydes suggests possibilities for asymmetric catalysis. However, it was found that the intermediate **18** obtained from trapping **17** with aldehydes complexes the diamine more strongly than the α-lithioselenides **17** (Scheme 5). This means that stoichiometric amounts of diamine are required for asymmetric synthesis of **19**. The products **19** obtained showed an enantiomeric excess that was comparable to the diastereomeric ratio of **17** (7:3). This is expected when trapping of the complexed α-lithioselenides **17** is more rapid than their interconversion. If alternative diamines could be found that give rise to high thermodynamic ratios of the complexes **17a,b**, then it might be possible to obtain higher enantioselectivities. Alternatively, if trapping of the complex by electrophiles is slower than their interconversion, then higher enantioselectivities may be obtained through kinetic resolution, as has been shown by Beak et al. for a related system.[10]



Scheme 5.

Hoffmann et al.[11a] and Reich et al.[11b] have both addressed the issue of understanding the mechanism of racemization of α-lithioselenides. In α-heterosubstituted alkyllithium compounds the negative charge is partially stabilized by $n_C \rightarrow \sigma^*_{X-R}$ delocalization in the X–R bond. Thus, the starting α-lithioselenide (X = Se) **20** and the enantiomeric α-lithioselenide **24** must both possess C–Li bonds antiperiplanar to the X–R bonds. The process of racemization shown in Scheme 6 fulfills these requirements and can be discussed as a sequence of several distinct steps: 1) loss of Li from C to give either separated or contact ion pairs, 2) inversion of the pyramidal carbon atom, 3) rotation about the C–X bond, and 4) recombination of the carbanion with the Li atom.[11a]

Kinetic data for the racemization of **20**, R = Ph, R^1 = $PhCH_2$, R^2 = H, ($\Delta G^{\neq}$ = 12.4 kcal mol^{-1}, $\Delta H^{\neq}$ = 11.9 kcal mol^{-1}, $\Delta S^{\neq}$ = − 2.5 kcal mol^{-1}) has now been determined.[11a]

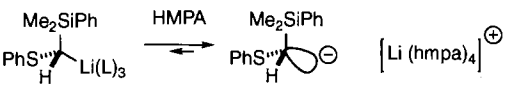


Scheme 6.

Based on comparisons with the activation energies estimated for loss of Li and inversion of pyramidal carbon, and from other observations, the authors suggested that rotation of the C–X bond was the rate-determining step (step 3). This proposal was supported by the observation that increasing substitution either at R or at the carbanion center, which reduces conformational mobility, results in greater configurational stability of the α-lithioselenide.

Reich et al. have recently studied the mechanism of racemization of α-lithioselenides using **25** as an example (Scheme 7).[11b] This compound contains several nuclei observable by NMR spectroscopy and a diastereotopic probe in the form of the dimethylphenylsilyl group. By following the ^{7}Li NMR spectrum of **25** with increasing concentrations of hexamethyl phosphoric triamide (HMPA), they found that with three equivalents of HMPA **25** was converted to the solvent-separated ion pair **26**. The diastereotopic probe showed that this species was still chiral even though significant planarization at the carbanionic center had occurred. Intuitively, one would expect the solvent-separated ion pair **26** to racemize more rapidly than the contact ion pair **25**. However, the rate of racemization is roughly twenty times slower for **26** compared to **25**, which immediately indicates that ion separation is not the rate-determining step in the racemization process. This observation fits the hypothesis that the rate-determining step is associated with rotation about the carbanion–S bond. The solvent-separated ion pair **26** should show greater $n_C \rightarrow \sigma^*_{S-R}$ delocalization than **25**, and this leads to a greater barrier to rotation about the C–S bond. Intuitively, one might expect the rate of racemization to increase with increasing concentrations of HMPA. In fact the rate of racemization is reduced. This suggests that racemization of the solvent-separated ion pair **26** might actually proceed via the contact species **25**, and recoordination of the lithium ion to carbon center, accompanied by loss of one or more HMPA molecules, explains the rate-retarding effect with increasing concentrations of HMPA.

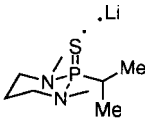
A similar effect of HMPA is seen on the rotation about the C_α–P bond in lithiated thiophosphonamides; as in the previous



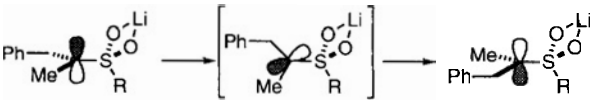
Scheme 7.

 © VCH Verlagsgesellschaft mbH, D-69451 Weinheim, 1994 0570-0833/94/0202-0176 $ 10.00+.25/0

ly discussed example, the presence of HMPA slows down the rate of rotation[12] (Scheme 8). Finally, the importance of



27 $\Delta G^{\ddagger}$ = 9.8 kcal mol^{-1} (THF)
$\Delta G^{\ddagger}$ = 11.4 kcal mol^{-1} (THF-HMPA)



28 **29** ent-**28**

a R = *t*Bu; $\Delta G^{\ddagger}$ = 13.0 kcal mol^{-1} (THF-DMPU)
b R = CF_3; $\Delta G^{\ddagger}$ = 17.3 kcal mol^{-1} (THF-DMPU)

Scheme 8.

$n \rightarrow \sigma^*$ delocalization of the carbanionic lone pair for configurational stability is underscored by a study of the mechanism of epimerization of α-lithiosulfones.[13, 14] The increasing barrier to racemization (**28a**: $\Delta G^{\ddagger} = 13.0$; **28b**: $\Delta G^{\ddagger} = 17.3$ kcal mol^{-1}) with increasing ability of the S–R group to accept negative charge is indicative of $n_C \rightarrow \sigma^*_{S-R}$ hyperconjugation in stabilizing the α-lithio species **28** and of the rate-determining step involving rotation about the C_α–S bond (Scheme 8).

These experiments clearly indicate that rotation of the C–X bond plays a dominant role in racemization of S-, Se-, and P-stabilized carbanions. If we are to extend the application of heteroatom-substituted anions in asymmetric synthesis to more general cases, this new understanding of the mechanism of racemization will play a crucial part.

German version: *Angew. Chem.* **1994**, *106*, 185

[1] D. Hoppe, F. Hintze, P. Tebben, *Angew. Chem.* **1990**, *102*, 1457; *Angew. Chem. Int. Ed. Engl.* **1990**, *29*, 1422.
[2] S. T. Kerrick, P. Beak, *J. Am. Chem. Soc.* **1991**, *113*, 9708.
[3] P. Knochel, *Angew. Chem.* **1992**, *104*, 1486; *Angew. Chem. Int. Ed. Engl.* **1992**, *31*, 1459.
[4] a) W. C. Still, C. Seekumar, *J. Am. Chem. Soc.* **1980**, *102*, 1201; b) R. J. Linderman, B. D. Griedel, *J. Org. Chem.* **1991**, *56*, 5491; c) J. Schwerdtfeger, D. Hoppe, *Angew. Chem.* **1992**, *104*, 1547; *Angew. Chem. Int. Ed. Engl.* **1992**, *31*, 1505; d) D. Hoppe, M. Paetow, F. Hintze, *ibid.* **1993**, *105*, 430 and **1993**, *32*, 394; e) W. H. Pearson, A. C. Lindbeck, J. W. Kampf, *J. Am. Chem. Soc.* **1993**, *115*, 2622; f) A. F. Burchat, J. M. Chong, S. B. Park, *Tetrahedron Lett.* **1993**, *34*, 51; g) J. M. Chong, S. B. Park, *J. Org. Chem.* **1992**, *57*, 2220.
[5] R. E. Gawley, Q. H. Zhang, *J. Am. Chem. Soc.* **1993**, *115*, 7515.
[6] P. G. McDougal, B. D. Condon, *Tetrahedron Lett.* **1989**, *30*, 789.
[7] R. W. Hoffmann, M. Julius, K. Oltmann, *Tetrahedron Lett.* **1990**, *31*, 7419.
[8] H. J. Reich, M. D. Bowe, *J. Am. Chem. Soc.* **1990**, *112*, 8994; see also A. Krief, G. Eurard, E. Badaoui, V. DeBeys, R. Dieden, *Tetrahedron Lett.* **1989**, *30*, 5635.
[9] W. Klute, R. Dress, R. W. Hoffmann, *J. Chem. Soc. Perkin Trans. 2* **1993**, 1409.
[10] P. Beak, H. Du, *J. Am. Chem. Soc.* **1993**, *115*, 2516.
[11] a) T. Ruhland, R. Dress, R. W. Hoffmann, *Angew. Chem.* **1993**, *105*, 1487; *Angew. Chem. Int. Ed. Engl.* **1993**, *32*, 1467; b) H. J. Reich, R. R. Dykstra, *ibid.* **1993**, *105*, 1489 and **1993**, *32*, 1469.
[12] S. E. Denmark, K. A. Swiss, S. R. Wilson, *J. Am. Chem. Soc.* **1993**, *115*, 3826.
[13] H. J. Gais, G. Hellmann, *J. Am. Chem. Soc.* **1992**, *114*, 4439.
[14] H. J. Gais, G. Hellmann, H. Günther, F. Lopez, H. J. Lindner, S. Braun, *Angew. Chem.* **1989**, *101*, 1061; *Angew. Chem. Int. Ed. Engl.* **1989**, *28*, 1025.



Any time, any place...

browse through one of the best chemistry journals at your leisure. To start your own personal subscription just fax

USA	Fax: (3 05)	428-82 01
UK	Fax: (02 23)	31 32 21
Japan	Fax: (03)	38 16 37 58
Rest of world	Fax: (0 1149)	62 01-606-184

VCH

The Sialyl Lewis^X Group and its Analogues as Ligands for Selectins: Chemoenzymatic Syntheses and Biological Functions

Athanassios Giannis*

White blood cells or leukocytes are components of blood that play a vital role in the immune response. Neutrophils, for example, are responsible for rapid and unspecific immune defense by ingesting invading bacteria, while B and T lymphocytes are responsible for the specific immune response. As part of the immune response leukocytes leave the blood vessels and migrate to the zone of infection and the secondary lymphatic organs. The cells leave the blood through the endothelium of the postcapillary venules in the area of the target tissue.

The complex multistage event leading to migration of leukocytes into the zone of infection occurs during normal chronic inflammation as well during acute inflammation and is mediated by a specific and regulated cell–cell recognition process between leukocytes and endothelial cells. This cell–cell recognition takes place by means of the interaction of a number of membrane-bound adhesion receptors with the corresponding membrane-bound ligands. The following receptors are known to be involved:[1] a) selectins, b) integrins, and c) members of the immunoglobulin superfamily.

The selectin family consists of three members, which are all glycoproteins and which mediate the initial stage of leukocyte adhesion (Fig. 1), namely, L, E, and P selectin. L selectin is constitutively expressed on the surface of leukocytes. It is involved in the recirculation of lymphocytes in peripherial lymph nodes as well as in the recruitment of leukocytes at the zone of inflammation. E selectin is expressed on the surface of endothelial cells a few hours after stimulation with interleukin 1 or tumor necrosis factor α. P selectin is kept in intercellular stores in blood platelets (thrombocytes) and endothelial cells. Within a few minutes of exposure to thrombin, histamin, substance P, peroxide radicals, or complement factors, P selectin is mobilized from these stores and transported to the cell surface. The exact structure of the membrane-associated carbohydrate ligand for L selectin is not known. However, it is known that the L selectin ligand is located at the postcapillary endothelium of the high endothelial venules (HEV) of the peripheral lymph nodes. According to the available data it is a sialic acid containing, sulfated, and possibly fucosylated oligosaccharide.[2]

The sialyl Lewis^X group (SLe^X) (**1** without R in Fig. 1) serves as a common ligand for all three selectins and is a component of glycosphingolipids and glycoproteins, which are also found on the surface of the leukocyte membrane. The importance of this oligosaccharide group for leukocyte adhesion was recently underlined by investigations into a hereditary disease, namely, leukocyte adhesion defiency type 2.[3] Owing to a defect in the biosynthesis of the SLe^X group, which is not understood yet in detail, the neutrophils are not able to adhere to stimulated endothelium and thus to migrate into the zone of inflammation. Patients with this condition suffer from repeated severe bacterial infections. On the other hand, there is also a series of acute and chronic diseases whose course is negatively influenced when too many leukocytes migrate to the area of the infection or in the area of the pathological process itself. These include cardiogenic shock, stroke, thrombosis, rheumatism, psoriasis, dermatitis, adult respiratory distress syndrome, bacterial meningitis, and encephalitis. In addition, metastasis formation in a number of tumors seems to be linked to the expression of SLe^X and other closely related oligosaccharides on the membrane surface of the tumor cells and the interaction of these groups with endothelial selectins. Efforts have thus been directed towards the development of adhesion blockers as new antiphlogistics, antithrombotics, immunosuppressants, and as drugs to prevent the formation of metastases.

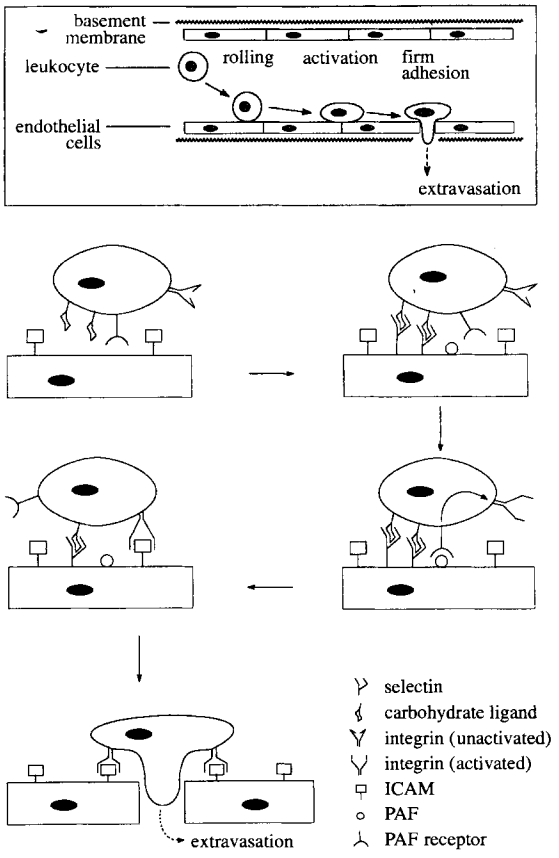


Fig. 1. Interaction between leukocytes and endothelial cells of blood vessels (modified from ref.[1e]). Top: overview; bottom: single steps with explanation of the symbols. Stimulation of endothelial cells by various mediators and factors leads to the expression of selectins and platelet-activating factor (PAF). The extravasation of leukocytes from the postcapillary venules starts with a weak, low-affinity, selectin-mediated adhesion of the leukocytes to endothelial cells, which leads to a slowing down of the leukocyte velocity (rolling). In the second phase a PAF-mediated activation of the leukocyte integrins occurs. In the third phase the activated integrins bind with high affinity to their ligands which are located on the endothelial cell surface. These ligands are called intercellular cell adhesion molecules (ICAM) and are members of the immunoglobin superfamily. The firm adhesion of the leukocyte cells to the endothelium and finally their departure from the blood vessel (extravasation) results.

[*] Priv.-Doz. Dr. A. Giannis
Institut für Organische Chemie und Biochemie der Universität
Gerhard-Domagk-Strasse 1, D-53121 Bonn (FRG)
Telefax: Int. code + (228) 73 77 78

 © VCH Verlagsgesellschaft mbH, D-69451 Weinheim, 1994 0570-0833/94/0202-0178 $ 10.00+.25/0

A topic of currently high priority is the synthesis of the SLe^X group and analogues thereof, which could act as alternative selectin ligands and thus block the interaction between endothelium and leukocytes. Such an oligosaccharide synthesis must meet a number of criteria; it must be efficient, highly regio- and stereoselective, and suitable for large-scale production. In addition, the synthesis of a potential pharmaceutical must fulfill economic and ecological requirements (e.g. reagents containing heavy metals should be avoided). The groups of J. C. Paulson and C.-H. Wong have gone a long way towards solving these problems through the development of a clever (though not uncomplicated) enzyme-catalyzed synthesis of SLe^X (Fig. 2).[4] They employ the glycosyl transferases involved in the biosynthesis of SLe^X. A number of difficulties had to be overcome before the synthesis became viable:

a) although galactosyl transferase was available, neither the Neu5Ac transferase (Neu5AcT) nor the Fuc transferase (FucT) were;
b) the pertinent glycosyl donors (sugar nucleotides) are too expensive to be used in stoichiometric amounts in large-scale synthesis;
c) the glycosyl transferases are inhibited by the final products and/or intermediates.

The first problem was overcome by cloning and expressing the genes for Neu5Ac transferase and Fuc transferase[5] in Sf9 or COS 1 cells. In this way both transferases could be produced in large amounts. A new method for cofactor regeneration in situ allowed the sugar nucleotides (UDP Gal, CMP Neu5Ac, GDP Fuc) to be easily generated and also largely suppressed the inhibition of the enzymes by the products. To enable easy isolation, the SLe^X group was synthesized as the *O*-allylglycoside **1** ($R = CH_2CHCH_2$). In the original paper the oligosaccharide was produced in mg amounts; however, in the meantime the synthesis in g amounts has apparently been achieved.[6]

^{13}C-labeled SLe^X derivatives were also synthesized for NMR spectroscopic studies. These studies showed that the SLe^X group has a folded, low-energy conformation, in which the L-fucose residue lies above the D-galactose unit. Therefore it appears that the tetrasaccharide forms a well-defined hydrophilic surface along the Neu5Ac-Gal-Fuc structural unit, while a hydrophobic region exists below the Neu5Ac-Gal-GlcNAc structural unit.

The fact that the transferases show some flexibility with regard to the glycosyl residues they will accept allowed the synthesis of a series of SLe^X analogues (Fig. 3) such as the glucal derivative **2**[7] and the di(SLe^X) derivative **3**, which were used for investigtions into structure–activity relationships.[8] The affinity of **2** for E selectin was found to be similar to that of SLe^X; in contrast, **3** proved to be a fivefold better ligand. Based on these results and the fact that the sulfatides **4** and **5** isolated from biological material demonstrated a higher affinity for E selectin,[9] Gaeta, Wong, et al. postulated the following model of the E selectin–SLe^X interaction:[8]

a) the interaction is multivalent;[10]
b) the structural elements of the SLe^X unit essential for recognition by E selectin include the carboxyl function of *N*-acetylneuraminic acid, part of the galactose residue (possibly only the 4- and 6-hydroxyl functions),[11] and the three hydroxyl

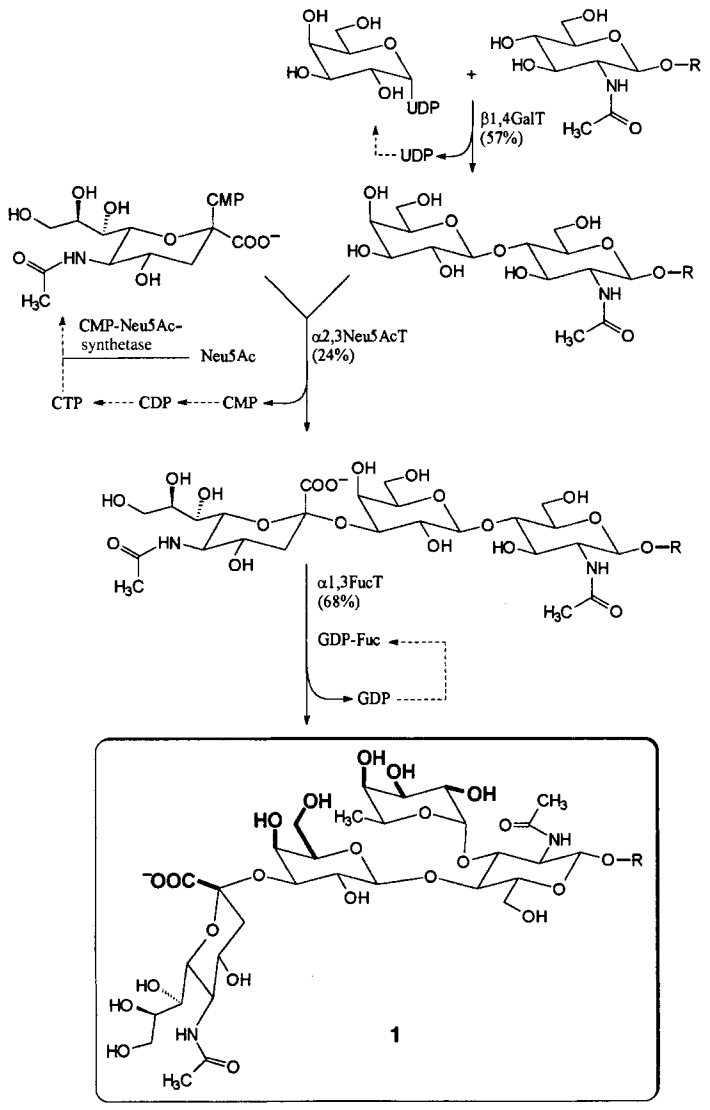


Fig. 2. Chemosynthetic SLe^X synthesis according to Paulson, Wong, et al. ($R = CH_2{-}CH{=}CH_2$).

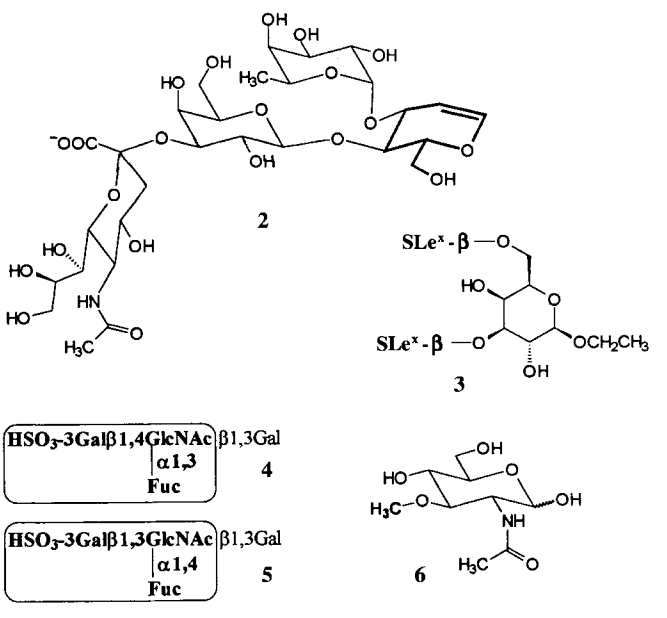


Fig. 3 Chemical structures of the selectin ligands **2**–**5** and of *N*-acetyl-3-*O*-methyl-D-glucosamine (**6**), a potent inhibitor of *N*-acetylneuraminic (sialic) acid biosynthesis.

 © VCH Verlagsgesellschaft mbH, D-69451 Weinheim, 1994 0570-0833/94/0202-0179 $ 10.00+.25/0

groups of the fucose residue. The CH_3 group of this L sugar seems to be nonessential;

c) the bioactive conformation of the oligosaccharide, in other words, its conformation when bound to E-selectin, is identical with the low-energy conformation determined in aqueous solution by NMR spectroscopy.

Direct confirmation of this last hypothesis is still lacking, since investigations into the structure of the E-selectin–SLe^X complex have not been carried out. The structure–activity relationships found are largely in accordance with those found by Tyrrell et al.[11] The pharmacophores are highlighted in the chemical formula of SLe^X-R **1** (Fig. 2).

The final confirmation of the efficacy of **1** (R = H) as an antiinflammatory drug was provided by Mulligan et al.[12] with animal models. Rats were injected with a poison isolated from cobras (cobra venom factor, CVF), which led to a P-selectin induced adhesion of neutrophils to the endothelium of blood vessels of the lungs. This in turn resulted in a massive accumulation of neutrophils in the tissues of the lungs as neutrophils left the blood vessels and invaded the surrounding tissues. The accompanying increase in the permeability of the blood vessels led to lung edemas, bleeding in the alveoli, and severe damage to the lungs. An intravenous injection of SLe^X **1** (R = H) into the animals drastically reduced the level of damage observed. The effect was dose dependent and time dependent in relation to the CVF infusion. For example, when a dose of 200 μg of SLe^X **1** (R = H) was given shortly before application of the snake venom, a 50% reduction in the amount of bleeding in the lungs and accumulation of neutrophils in lung tissues was observed compared to that in untreated animals. In contrast, the same dose given after the application of snake venom was less effective in reducing the damage. Other, nonfucosylated oligosaccharides such as Neu5Acα2,3Galβ1,4GlcNAc proved to be inactive. The fact that such a low dose induces this protective effect is surprising: a single dose of 200 μg of **1** (R = H) corresponds to a concentration of less than 1 μmol L^{-1} in the blood! The experimentally induced lung damage in rats is equivalent to adult respiratory distress syndrome in humans, which is still difficult to treat, has a high mortality rate (60%), and affects in the USA alone around 150000 people per year.[13]

Based on these results, the hope that SLe^X-containing oligosaccharides and their analogues may prove to be effective antiinflammatory drugs seems to be well founded. However, it should be borne in mind that many aspects of the selectin–leukocyte interaction remain unexplained[1d] and that the selectins have overlapping ligand specificity and indeed that a variety of compounds can serve as selectin ligands. For example, the sulfatides **4** and **5** (Fig. 3) are not only potent E-selectin ligands, they also have a high affinity for L-selectin.[9b] The discovery that the sulfooligosaccharides **4** and **5**[14] can serve as selectin ligands also indicates that the SLe^X group may be replaced by simpler analogues that would be easier to synthesize. A long-range goal is the replacement of the SLe^X group with mimetics that are effective when taken orally, have better pharmacokinetics, and are metabolically more stable.

Crucial to the development of such carbohydrate mimetics is the determination of the conformation of the carbohydrate ligand when bound to selectin, that is to say the biologically active conformation. A suitable molecule could then be created by attaching the structural units essential for recognition to an appropriate scaffold. The methods that have been developed for the construction of peptide mimetics[15] could also be applied to the design of carbohydrate mimetics. Recent results indicate that a carbohydrate structure is not an absolute requirement: screening showed that small peptides act as monosaccharide mimetics and block the interaction of the lectin concanavalin A with its carbohydrate ligands.[16] Finally, since the SLe^X-induced leukocyte adhesion could also be blocked by inhibiting the enzymes responsible for the biosynthesis of this oligosaccharide group, intensive efforts are underway to develop such inhibitors.[17] In this context it is of interest that an inhibitor of Neu5Ac biosynthesis has recently become available: the simple D-glucosamine derivative **6** (Fig. 3) is a specific and potent inhibitor of both GlcNAc kinase and ManNAc kinase (K_i = 17 and 80 μM, respectively) and thus inhibits Neu5Ac biosynthesis.[18]

These developments show clearly that "knowledge of carbohydrate synthesis, structure and function can serve the medicinal chemist well in the design of new drug candidates".[19]

German version: *Angew. Chem.* **1994**, *106*, 188

[1] For excellent reviews see: a) L. A. Lasky, *Science* **1992**, *258*, 964; b) T. A. Springer, L. A. Lasky, *Nature* **1991**, *349*, 196; c) T. A. Springer, *ibid.* **1990**, *346*, 425; d) E. C. Butcher, *Cell* **1991**, *67*, 1033; e) R. O. Hynes, A. D. Lander, *ibid.* **1992**, *68*, 303; f) L. Stoolman in *Cell Surface Carbohydrates and Cell Development* (Ed.: M. Fukuda), CRC, Boca Raton, FL, USA, **1992**, p. 71.

[2] Y. Imai, L. A. Lasky, S. D. Rosen, *Nature* **1993**, *361*, 555.

[3] A. Etzioni, M. Frydman, S. Pollack, I. Avidor, M. L. Phillips, J. C. Paulson, R. Gershoni-Baruch, *N. Engl. J. Med.* **1992**, *327*, 1789.

[4] Y. Ichikawa, Y.-C. Lin, D. P. Dumas, G.-J. Shen, E. Garcia-Junceda, M. A. Williams, R. Bayer, C. Ketcham, L. E. Walker, J. C. Paulson, C.-H. Wong, *J. Am. Chem. Soc.* **1992**, *114*, 9283.

[5] B. W. Weston, R. P. Nair, R. D. Larsen, J. B. Lowe, *J. Biol. Chem.* **1992**, *267*, 4152.

[6] S. Bormann, *Chem. Eng. News* **1992**, *70* (49), 25.

[7] Glucal derivative **2** was synthesized chemically and then converted into SLe^X-H **1** (R = H); S. D. Danishefsky, K. Koseki, D. A. Griffith, J. Gervay, J. M. Peterson, F. McDonald, T. Oriyama, *J. Am. Chem. Soc.* **1992**, *114*, 8331.

[8] S. A. DeFrees, F. C. A. Gaeta, Y.-C. Lin, Y. Ichikawa, C.-H. Wong, *J. Am. Chem. Soc.* **1993**, *115*, 7549.

[9] a) C.-T. Yuen, A. M. Lawson, W. Chai, M. Larkin, M. S. Stoll, A. C. Stuart, F. X. Sullivan, T. J. Ahern, T. Feizi, *Biochemistry* **1992**, *31*, 9126; b) P. J. Green, T. Tamatani, T. Watanabe, M. Miyasaka, A. Hasegawa, M. Kiso, C.-T. Yuen, M. S. Stoll, T. Feizi, *Biochem. Biophys. Res. Commun.* **1992**, *188*, 244.

[10] In this context the reader is referred to the efficient synthesis of *N*-glycopeptide clusters with $Lewis^X$ antigen side chains and their subsequent attachment to carrier proteins: K. von dem Bruch, H. Kunz, *Angew. Chem.* **1994**, *106*, 87; *Angew. Chem. Int. Ed. Engl.* **1994**, *33*, 101.

[11] D. Tyrrell, P. James, N. Rao, C. Foxall, S. Abbas, F. Dasgupta, M. Nashed, A. Hasegawa, M. Kiso, D. Asa, J. Kidd, B. K. Brandley, *Proc. Natl. Acad. Sci. USA* **1991**, *88*, 10372.

[12] M. S. Mulligan, J. C. Paulson, S. DeFrees, Z.-L. Zheng, J. B. Lowe, P. A. Ward, *Nature* **1993**, *364*, 149.

[13] R. C. Bone, *N. Engl. J. Med.* **1993**, *328*, 431.

[14] Sulfatides **4** and **5** were synthesized for the first time recently: K. C. Nicolaou, N. J. Bockovich, D. R. Carcanague, *J. Am. Chem. Soc.* **1993**, *115*, 8843.

[15] a) A. Giannis, T. Kolter, *Angew. Chem.* **1993**, *105*, 1303; *Angew. Chem. Int. Ed. Engl.* **1993**, *32*, 1244; b) R. A. Wiley, D. H. Rich, *Med. Res. Rev.* **1993**, *13*, 327; c) R. Hirschman, *Angew. Chem.* **1991**, *103*, 1305; *Angew. Chem. Int. Ed. Engl.* **1991**, *30*, 1278.

[16] a) K. R. Oldenburg, D. Loganathan, I. J. Goldstein, P. G. Schultz, M. A. Gallop, *Proc. Natl. Acad. Sci. USA* **1992**, *89*, 5393; b) J. K. Scott, D. Loganathan, R. B. Easley, X. Gong, I. J. Goldstein, *ibid.* **1992**, *89*, 5398.

[17] a) M. M. Palcic, L. D. Heerze, O. P. Srivastava, O. Hindsgaul, *J. Biol. Chem.* **1989**, *264*, 17174; b) S. Cai, M. R. Stroud, S. Hakomori, T. Toyokumi, *J. Org. Chem.* **1992**, *57*, 6693, and references therein; c) C.-H. Wong, D. P. Dumas, Y. Ichikawa, K. Koseki, S. J. Danishefski, B. W. Weston, J. B. Lowe, *J. Am. Chem. Soc.* **1992**, *114*, 7321.

[18] R. Zeitler, A. Giannis, S. Danneschewski, E. Henk, T. Henk, C. Bauer, W. Reutter, K. Sandhoff, *Eur. J. Biochem.* **1992**, *204*, 1165.

[19] J. H. Musser, *Annu. Rep. Med. Chem.* **1992**, *27*, 301.

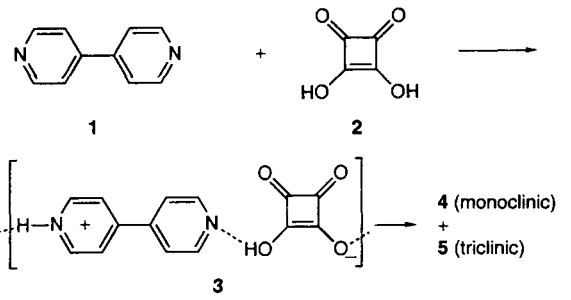
 © VCH Verlagsgesellschaft mbH, D-69451 Weinheim, 1994 0570-0833/94/0202-0180 $ 10.00+.25/0

Proton-Transfer-Dependent Reversible Phase Changes in the 4,4′-Bipyridinium Salt of Squaric Acid**

Manfred T. Reetz,* Sigurd Höger, and Klaus Harms

Proton-transfer-mediated electron transfer in organic materials is a way to regulate the electronic properties of solids.[1] Intramolecular proton transfers are responsible for the photo- and thermochromic properties of the crystal forms of *N*-salicylidene anilides.[2] Proton transfers under hydrostatic pressure in quinhydrones are known to be accompanied by changes in the absorption spectrum.[3] In the phase change of dimethyl 3,6-dichloro-2,5-dihydroxyterephthalate, the color change is associated with a proton transfer.[4] For this reason, investigations on crystal structures of self-assembling, hydrogen-bonded aggregates are gaining in importance.[5] We report here on a new hydrogen-bonded system which undergoes a thermally induced reversible single-crystal–single-crystal phase change. This process is associated with a proton transfer and a concomitant change in color.

The reaction of 4,4′-bipyridine (**1**) (colorless) and squaric acid (**2**) (colorless) in water leads to a pale yellow-brown precipitate **3** (Scheme 1).[6] On recrystallization the bulk of the material is obtained as pale ochre colored [λ_{max} (solid) = 390 nm] rectangular crystals (**4**). A few individual crystals of an additional polymorph (**5**), which appears to be slightly darker [λ_{max} (solid) = 460 nm], are also formed.[7]



Scheme 1.

The (extended) asymmetric units of salts **4** (monoclinic) and **5** (triclinic) are shown in Figure 1.[8] They consist of infinite chains connected by hydrogen bonds and are arranged in stacks. These are aligned with the crystallographic *c* axis. The position of the ordered protons in these chains can be explained by the acidity constants of both components (squaric acid: pK_1 = 1.2–1.7, pK_2 = 3.2–3.5; 4,4′-bipyridinium dihydrochloride: pK_1 = 2.73, pK_2 = 4.87).[9] Each asymmetric unit in salt **4** contains one bipyridine unit (torsion angle 24°), while two different bipyridine units are contained in **5** (C301 to C310, torsion angle 8°; C201 to C210, torsion angle 12°). Figure 2 shows a view of **4** along the stack.

Characteristic for both structures are the strong hydrogen bonds of the type N–H···O and O–H···N (Table 1). The

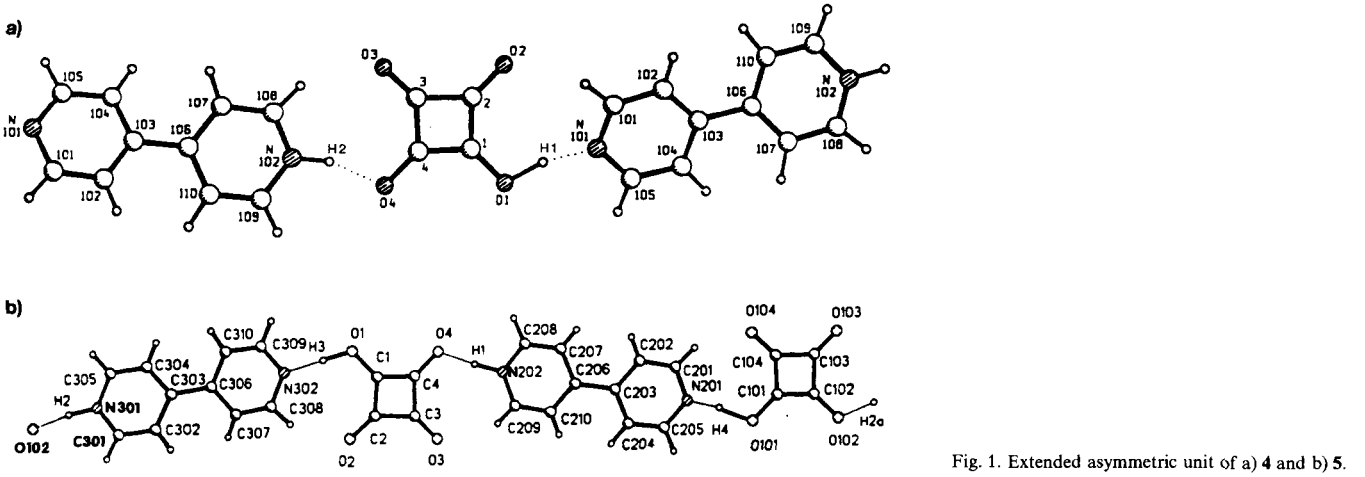


Fig. 1. Extended asymmetric unit of a) **4** and b) **5**.

atomic distances within the anions (Table 2) show that the geometry of the anions in salts **4** and **5** is strongly influenced by these hydrogen bonds. The formal mirror plane of an uncomplexed squaric acid monoanion does not occur. Such an ideal geometry is found in oxamide-dioxonium-dihydrosquarate (monodeprotonated squaric acid anion).[10] Our structures are "intermediates" between unperturbed monohydrogen squarate and free squaric acid. Thus, they are examples of the correlation

[*] Prof. Dr. M. T. Reetz, Dr. S. Höger
Max-Planck-Institut für Kohlenforschung
Kaiser-Wilhelm-Platz 1, D-45470 Mülheim an der Ruhr (FRG)
Telefax: Int. code + (208)306-2985
Dr. K. Harms
Fachbereich Chemie der Universität
Hans-Meerwein-Strasse, D-35043 Marburg (FRG)

[**] This work was supported by the Deutsche Forschungsgemeinschaft (Leibniz-Program) and the Fonds der Chemischen Industrie.

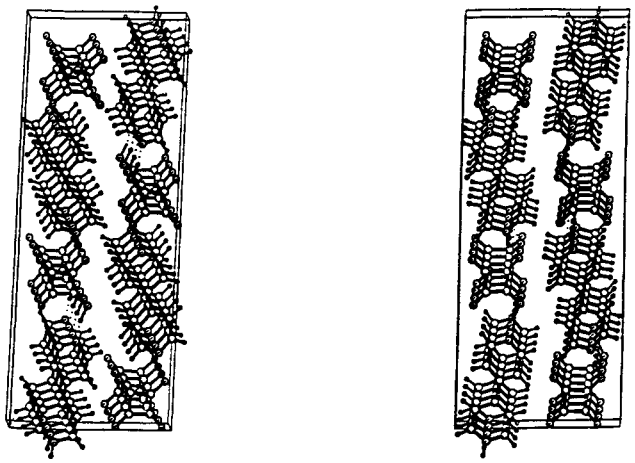


Fig. 2. View of the stacks of **4** (stereoscopic representation)

Table 1. Strong hydrogen bonds in **4** and **5**.

Crystal	Donor	H	Acceptor	D···A [Å]	D-H [Å]	H···A [Å]	Angle [°]
4	O1	H1	N101	2.613(3)	1.131(34)	1.488(35)	173.8(31)
4	N102	H2	O4	2.602(3)	1.023(2)	1.582(2)	174.3(1)
5	O1	H3	N302	2.616(4)	0.972(54)	1.666(53)	164.6(41)
5	N202	H1	O4	2.613(4)	0.974(40)	1.671(38)	161.4(33)
5	O101	H4	N201	2.572(4)	1.100(47)	1.483(46)	169.2(39)
5	N301	H2	O102	2.580(4)	1.098(45)	1.509(45)	162.9(38)

principle proposed by Bürgi and Dunitz.[11] They represent points on the reaction coordinate of the deprotonation of squaric acid.

Table 2. Atomic distances in the anions in **4** and **5**.

Crystal	X	Y	Distance [Å]	X	Y	Distance [Å]
4	C1	C2	1.443(3)	C1	O1	1.317(3)
4	C2	C3	1.500(3)	C2	O2	1.231(3)
4	C3	C4	1.481(3)	C3	O3	1.222(3)
4	C4	C1	1.414(3)	C4	O4	1.269(3)
5	C1	C2	1.451(5)	C1	O1	1.326(5)
5	C2	C3	1.489(6)	C2	O2	1.236(5)
5	C3	C4	1.485(6)	C3	O3	1.230(5)
5	C4	C1	1.397(5)	C4	O4	1.268(5)
5	C101	C102	1.403(5)	C101	O101	1.308(5)
5	C102	C103	1.471(6)	C102	O102	1.281(5)
5	C103	C104	1.480(5)	C103	O103	1.229(5)
5	C104	C101	1.464(5)	C104	O104	1.237(5)

Equally unusual is the thermally reversible phase transition of the monoclinic form **4**. On heating to 180 °C, crystals of **4** change from yellow to red. This phase transition always orginates at the end of the crystal and then moves along the length of the crystal in fractions of a second (Fig. 3, left). A determination of the orientation of the unit cell axes relative to the outer edges of the crystal reveals that the longest edge of the crystal corresponds to the shortest unit cell axis, the shortest edge (plate thickness) to the longest axis, and the plate width to the middle axis.

Differential scanning calorimetric (DSC) measurements show that this transformation is accompanied by an energy uptake of 19.8 $J g^{-1}$. When this high-temperature phase (which is still present as a single crystal) is cooled below 150 °C, the color of the crystal changes back to yellow (Fig. 3, right). The apparent reversal into the original phase is, however, not complete, since the system releases only 15.7 $J g^{-1}$ of energy. The crystal thereby

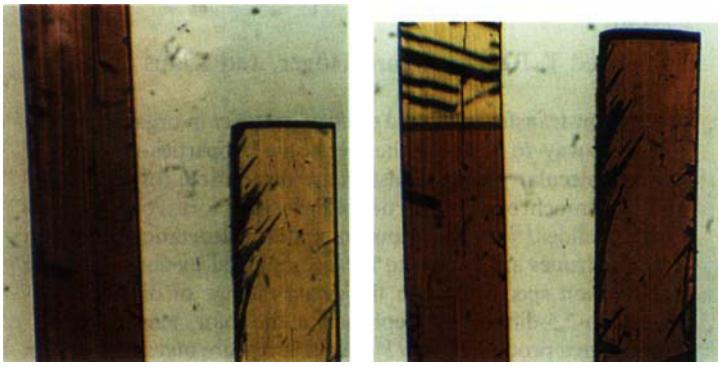


Fig. 3. Left: The initial heating of a crystal sample of **4** to 180 °C. The red crystal is already in the high-temperature modification. Right: Initial cooling below 150 °C.

fractures into several smaller pieces, and it was not possible to perform a single-crystal X-ray stucture determination on this product. When this new phase is reheated, it changes back into the red high-temperature phase at 173 °C. This change is accompanied by the uptake of 15.7 $J g^{-1}$. Subsequent cooling to below 150 °C again releases 15.5 $J g^{-1}$ and results in a transformation to the yellow modification. Further heating or cooling changes neither the transition temperature nor the energy balance. The original and the newly-formed room temperature modifications are different not only in the higher energy content of the latter (approximately 4 $J g^{-1}$), but also in the absorption coefficients in the UV region and the signal intensities in the X-ray powder diffractogram: The relative intensity of the absorption band in the UV region (maximum at 240 nm) is markedly increased in comparison with the intensity of the charge transfer (CT) band (390 nm) in the solid-state UV/VIS spectrum of the monoclinic form when it is recooled after being heated. While the ratio of the intensities of the maxima is initially approximately 3:4 (UV:CT), it changes to approximately 6:5 after the crystals have been heated; the position of the bands, however, remains unaltered. The relative intensities of the signals in the powder diffractogram also differ in going from the original sample to the heated and cooled sample. Thus, since the position of the signals is unchanged, the dimensions of the unit cell must have remained constant and only the atomic positions within this unit cell have altered. It was not possible to isolate sufficient quantities of **5** to perform analogous experiments. It is nevertheless remarkable that upon heating no color change such as that for **4** was observed for **5**.

When **3** is recrystallized from D_2O the acidic protons in **4** are replaced by deuterium. The single-crystal X-ray crystallographic examination of this form (**6**) at room temperature shows that the O1–N101 distance has increased from 2.620(3) to 2.641(4) Å when compared with the protonated form **4** at the same temperature.[8] At the same time the O4–N102 distance increases from 2.593(2) to 2.623(2) Å. This is reminiscent of the

 © VCH Verlagsgesellschaft mbH, D-69451 Weinheim, 1994 0570-0833/94/0202-0182 $ 10.00+.25/0

increase in the O–O distance of free squaric acid when it is deuterated[12] and is an indication for the presence of a double minimum potential.[13] When the deuterated form **6** is heated, no color change is observed up to the decomposition temperature of about 225 °C.

Such a strong isotope effect (increase of the phase-transition temperature) is also known for free squaric acid.[14] This supports the assumption that in our case the red high-temperature modification is formed from the yellow room temperature modification by proton transfer. This influences the electron donor–acceptor properties of the participating ions.

Preliminary experiments show that **4** also undergoes a reversible phase change under hydrostatic pressure. The solid-state UV/VIS spectrum and the X-ray powder diffractogram of a powdered sample of **4** that had been pressurized to 11 kbar for 60 s are, after relaxation, similar to those of the previously heated form.

Received: July 1, 1993
Revised version: August 23, 1993 [Z 6183 IE]
German version: *Angew. Chem.* **1994**, *106*, 193

[1] T. Mitani, *Mol. Cryst. Liq. Cryst.* **1989**, *171*, 343.
[2] T. Inabe, K. Okinawa, H. Okamoto, T. Mitani, Y. Murayama, S. Takeda, *Mol. Cryst. Liq. Cryst.* **1992**, *216*, 229.
[3] K. Nakasuji, K. Sugiura, T. Kitagawa, J. Toyada, H. Okamoto, K. Okinawa, T. Mitani, H. Yamamoto, I. Murata, A. Kawamoto, J. Tanaka, *J. Am. Chem. Soc.* **1991**, *113*, 1862.
[4] S. R. Byrn, D. Y. Curtin, J. C. Paul, *Acc. Chem. Res.* **1973**, *7*, 217; Q. C. Yang, M. F. Richardson, J. D. Dunitz, *J. Am. Chem. Soc.* **1985**, *107*, 5535; *Acta Crystallogr. Sect. B* **1989**, *45*, 312.
[5] H. Bock, W. Seitz, Z. Havlas, J. W. Bats, *Angew. Chem.* **1993**, *105*, 410; *Angew. Chem. Int. Ed. Engl.* **1993**, *32*, 411.
[6] Reaction of equimolar quantities of **1** and **2** in hot water produced after cooling a light yellow-brown precipitate **3** in essentially quantitative yield. Single crystals of **4** and **5** that were suitable for X-ray analysis were obtained by recrystallization from water. Elemental analysis ($C_{14}H_{10}N_2O_4$): calcd: C 62.21%, H 3.74%, N 10.37%; found: C 61.95%, H 3.81%, N 10.31%. M.p. ca. 225 °C (decomp).
[7] Review of polymorphs of organic solids: J. Bernstein in *Organic Solid State Chemistry* (Ed.: D. R. Desiraju), Elsevier, Amsterdam, **1987**, p. 471.
[8] X-ray crystal structure determinations ($Cu_{K\alpha}$ radiation): **4** (183 K), monoclinic, $P2_1/n$, $a = 3.758(1)$, $b = 11.196(1)$, $c = 27.351(2)$ Å; $\beta = 92.95(1)°$, $Z = 4$, $\rho_{calcd} = 1.562\ g cm^{-3}$; $R = 0.052$ ($R_w = 0.057$) for 1701 independent reflections. **5** (173 K), triclinic, $P1$, $a = 9.619(1)$, $b = 10.679(2)$, $c = 12.726(4)$ Å, $\alpha = 70.17(3)$, $\beta = 85.83(2)$, $\gamma = 70.08(1)°$, $Z = 4$, $\rho_{calcd} = 1.55\ g cm^{-3}$; $R = 0.049$ ($R_w = 0.053$) for 2859 independent reflections. **4** (293 K), monoclinic, $P2_1/n$, $a = 3.800(1)$, $b = 11.208(1)$, $c = 27.447(2)$ Å, $\beta = 92.22(1)°$, $Z = 4$, $\rho_{calcd} = 1.537\ g cm^{-3}$; $R = 0.061$ ($R_w = 0.041$) for 1734 independent reflections. **6** (293 K), monoclinic $P2_1/n$, $a = 3.793(1)$, $b = 11.175(1)$, $c = 27.581(4)$ Å, $\beta = 91.99(1)°$, $Z = 4$, $\rho_{calcd} = 1.536\ g cm^{-3}$; $R = 0.036$ ($R_w = 0.036$) for 1445 independent reflections. Further details of the crystal structure investigations may be obtained from the Fachinformationszentrum Karlsruhe, D-76344 Eggenstein-Leopoldshafen (FRG) on quoting the depository number CSD-57835, the names of the author and the journal citation.
[9] E. Patton, R. West, *J. Phys. Chem.* **1970**, *74*, 2512; L. A. Ashton, J. I. Bullock, P. N. G. Simpson, *J. Chem. Soc. Faraday Trans. 1* **1982**, 343; J. Ulstrup, *Acta Chem. Scand.* **1971**, *25*, 3397.
[10] H. Endres, M. Schendzielorz, *Acta Crystallogr. Sect. C* **1984**, *40*, 453.
[11] H. B. Bürgi, J. D. Dunitz, *Acc. Chem. Res.* **1983**, *16*, 153.
[12] D. Semmingsen, *Acta Chem. Scand. Ser. A* **1975**, *29*, 470.
[13] T. R. Singh, J. L. Wood, *J. Phys. Chem.* **1969**, *50*, 3572.
[14] F. J. Hollander, D. Semmingsen, F. F. Koetzle, *J. Chem. Phys.* **1977**, *67*, 4825.

Calicheamicin θ_1^I: A Rationally Designed Molecule with Extremely Potent and Selective DNA Cleaving Properties and Apoptosis Inducing Activity**

K. C. Nicolaou,* T. Li, Masahisa Nakada, Conrad W. Hummel, A. Hiatt, and W. Wrasidlo

A biologically active and selective enediyne[1] molecule, calicheamicin θ_1^I (**1**) (Fig. 1 A) has been rationally designed on the basis of chemical principles and the mechanism of action of the naturally occurring calicheamicin γ_1^I (**2**) (Fig. 1 A).[2] Unlike its natural counterpart, this new enediyne was designed to undergo activation under mildly basic conditions[3] by hydroxide ion (Fig. 1 B), leading to 1,4-benzenoid diradicals[4] which are capable of causing double strand cleavage of DNA. Prepared by total synthesis, calicheamicin θ_1^I (**1**) exhibits potent (concentrations $< 10^{-9}$ M) and sequence-selective (TCCT, TTTT, and CTCT sites) DNA cleavage at pH 7.5 and 37 °C, initiates programmed cell death (apoptosis)[5] at concentrations $< 10^{-10}$ M, and kills cells with potencies ($< 10^{-12}$ M) exceeding, in certain cases, those of natural calicheamicin γ_1^I (**2**),[1] CN-MRA,[6] and ricin,[7] compounds which have been claimed as some of the most toxic substances known.

Guided by the mechanism of action (Fig. 1 B) of calicheamicin γ_1^I (**2**)[8] in which a powerful nucleophile, such as a thiolate ion, initiates a cascade of reactions that leads to DNA damage,[9, 10] and with the intention of designing a molecule that would be activated under a different set of conditions, we focused on calicheamicin θ_1^I (**1**), which is equipped with a thioacetyl group instead of the trisulfide moiety as a triggering device. Compound **1** was expected to undergo ready activation by attack from oxygen nucleophiles, such as hydroxide ion (as well as from sulfur and nitrogen nucleophiles); compound **2** is normally activated by thiols. Due to the simplicity of activation of the designed compound, certain advantages were expected for calicheamicin θ_1^I (**1**) both for in vitro and in vivo action.

Although structurally related to the naturally occurring compound, the designed molecule (**1**) is unique in its projected mode of activation. Furthermore, despite the structural similarity between the natural (**2**) and designed (**1**) compounds, the targeted calicheamicin θ_1^I (**1**) could not be synthesized from the natural product (**2**) because of the overlap of the required chemistry with the mechanism of activation (and therefore destruction) of **2**. The significance of the reported findings, therefore, extend over molecular design[11] [rational mechanism of action], chemical synthesis (preparation of a highly complex molecule), and biology (impressive biological properties) (vide infra).

Calicheamicin θ_1^I (**1**) was obtained by total synthesis following a variation of the sequence recently described[12–15] for the construction of calicheamicin γ_1^I (**2**). Thus, the previously synthesized intermediate **3**[12–15] was treated with *para*-toluenesulfonic acid in aqueous tetrahydrofuran at ambient temperature

[*] Prof. Dr. K. C. Nicolaou, Dr. T. Li, M. Nakada, C. W. Hummel, A. Hiatt, W. Wrasidlo
Department of Chemistry, The Scripps Research Institute
10666 North Torrey Pines Road, La Jolla, CA 92037 (USA)
and
Department of Chemistry, University of California
San Diego, 9500 Gilman Drive, La Jolla, CA 92093 (USA).
Telefax: Int. code +(619)554-6738

[**] This work was supported by the National Institutes of Health (USA) and The Scripps Research Institute. We thank Drs. Darryl Rideout and Z. Zeng for helpful discussions, E. N. Pitsinos and Drs. H. Saimoto, K. Shibayama, Y. Mizuno, and K.-U. Baldenius for assistance in the synthetic work and Robert Merlock and Gail Hum for technical assistance on the biological assays.

 © VCH Verlagsgesellschaft mbH, D-69451 Weinheim, 1994 0570-0833/94/0202-0183 $ 10.00+.25/0

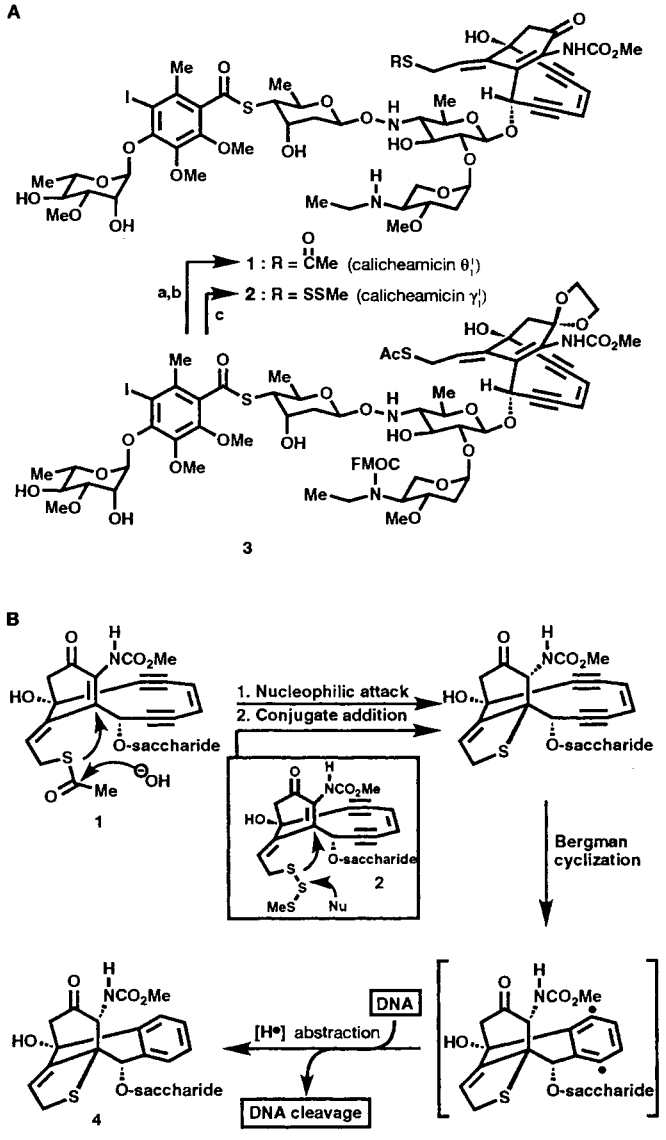


Fig. 1. A) Molecular structures of designed (θ_1^I, **1**) and natural (γ_1^I, **2**) calicheamicins and their chemical synthesis from precursor **3**. Methods: a) 2.0 equiv of TsOH · H_2O, THF/H_2O (50:1), 25 °C, 48 h, 100% (based on 57% conversion); b) Et_2NH/THF/H_2O (5:25:1), 25 °C, 2 h, 75%; c) see refs. [10–13]; FMOC = 9-fluorenylmethoxycarbonyl, Ar = aryl, eq = equatorial, ax = axial. Selected physical properties of **1**: $R_f = 0.13$ (dichloromethane/ethyl acetate/methanol = 5.5:4:0.5); $[\alpha]_D^{19}$ −147.6 ($c = 0.59$, $CHCl_3$); IR (KBr): $\nu_{max} = 3443, 2932, 1683, 1456, 1390, 1325, 1243, 1074, 959, 913\ cm^{-1}$; ^1H NMR (500 MHz, $CDCl_3$): $\delta = 6.21$ (d, $J = 1.5$ Hz, 1H, C*H*-C≡C), 6.14 (dd, $J = 9.8$, 5.1 Hz, 1H, C=C*H*-CH_2), 5.87 (d, $J = 9.5$ Hz, 1H, C*H*=CH), 5.81 (dd, $J = 9.4$, 1.6 Hz, 1H, C*H*=CH), 5.72 (d, $J = 1.5$ Hz, 1H, D-1), 5.70 (d, $J = 3.2$ Hz, 1H, E-1), 5.02 (dd, $J = 10.2$, 1.8 Hz, 1H, B-1), 4.70 (d, $J = 7.8$ Hz, 1H, A-1), 4.47 (dd, $J = 3.2$, 1.7 Hz, D-2), 4.31 (m, 1H, B-3), 4.18 (dq, $J = 9.6$, 6.1 Hz, 1H, D-5), 4.06 (dq, $J = 10.9$, 6.2 Hz, 1H, B-5), 4.03 (dd, $J = 9.7$, 9.7 Hz, 1H, A-3), 3.91–3.56 (m, 8H), 3.88 (s, 3H, $ArOCH_3$), 3.82 (s, 3H, $ArOCH_3$), 3.76 (dd, $J = 10.9$, 2.5 Hz, 1H, B-4), 3.69 (bs, 3H, $NHCO_2CH_3$), 3.63 (dd, $J = 9.5$, 9.5 Hz, 1H, D-4), 3.56 (s, 3H, CH_3O-D-ring), 3.42 (s, 3H, CH_3O-E-ring), 2.85 (AB-q, $J = 16.7$ Hz, $\Delta\nu = 259$ Hz, 2H, CH_2), 2.74 (bm, 1H, CH_2N), 2.65 (m, 1H, E-4), 2.54 (bm, 1H, CH_2N), 2.38(1H, E-2eq), 2.36 (dd, $J = 9.6$, 9.6 Hz, 1H; A-4), 2.35 (s, 3H, $ArCH_3$), 2.29 (s, 3H, CH_3CO), 2.02 (m, 1H, B-2eq), 1.76 (m, 1H, B-2ax), 1.50 (m, 1H, E-2ax), 1.40 (d, $J = 6.2$ Hz, 3H, B-6), 1.36 (d, $J = 6.2$ Hz, 3H, A-6), 1.29 (d, $J = 6.2$ Hz, 3H, D-6), 1.16 (t, $J = 7.1$ Hz, 3H, CH_3CH_2N); ^{13}C NMR (125 MHz, $CDCl_3$): $\delta = 195.3$, 192.6, 192.0, 151.5, 150.6, 143.0, 133.4, 130.2, 124.4, 123.5, 102.6, 100.9, 99.6, 99.5, 97.2, 93.5, 88.0, 82.9, 80.8, 75.7, 71.9, 71.8, 71.1, 70.4, 69.8, 69.1, 68.4, 68.3, 67.0, 61.7, 61.2, 60.9, 57.2, 56.1, 52.8, 51.6, 42.4, 36.8, 34.1, 30.5, 30.3, 29.7, 25.3, 18.9, 17.6 (2), 14.4; HRMS (FAB) calcd for $C_{56}H_{74}IN_3O_{22}S_2Cs$ (M + Cs); 1464.2035, found 1464.2211. B) Mechanism of the activation of **1**.

for 48 h. Subsequent exposure to aqueous diethylamine furnished **1** in 75% overall yield. Selected physical properties for calicheamicin θ_1^I (**1**) are summarized in the legend for Figure 1.

In order to gain insight into the DNA cleaving profile of calicheamicin θ_1^I (**1**), its ability to cut supercoiled plasmid DNA was examined and compared to that of the natural product (**2**). ΦX174 supercoiled DNA was incubated with **1** and **2** in buffer solutions of varying pH values at 37 °C and cleavage was assayed by agarose gel electrophoresis (Fig. 2). The synthetic

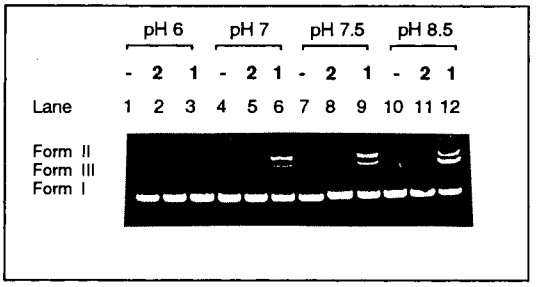


Fig. 2. Interaction of calicheamicin θ_1^I (**1**) with double stranded DNA. Agarose gel electrophoresis patterns of supercoiled ΦX174 DNA cleavage by **1** and **2**. Designed calicheamicin θ_1^I (**1**) causes double strand cleavage of supercoiled DNA with higher potencies that natural calicheamicin γ_1^I (**2**) under mildly basic conditions. Methods: Supercoiled closed circular form I ΦX174 DNA (200 ng) was incubated with 10 nM of **1** or **2** in different pH buffer solutions in a total volume of 10 μL [dimethylsulfoxide (DMSO)/4 mM Tris buffer (1:99), 4 mM ethylenediaminetetraacetic acid (EDTA)] for 12 hours at 37 °C. Electrophoresis was carried out by using 1% agarose gel with added ethidium bromide. Lanes 1, 4, 7, and 10 are controls. Form I: supercoiled DNA; Form II: nicked DNA; and Form III: linear DNA.

calicheamicin θ_1^I (**1**) exhibited double and single strand cuts at very low concentrations in neutral or basic media in the absence of any additives, overshadowing in this respect calicheamicin γ_1^I (**2**), which was essentially inactive under similar conditions. In the presence of thiols, however, **2** was the more potent compound (data not shown); an observation which is in accord with the proposed mechanism of activation for the two compounds. It is also interesting to note that the potency of **1** as a DNA cleaving agent in neutral or basic media is further potentiated by thiols as expected from the higher nucleophilicity of sulfur nucleophiles as compared to that of oxygen-centered nucleophiles.

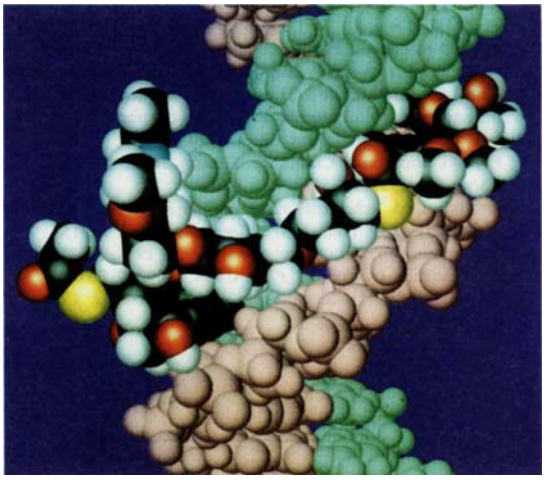
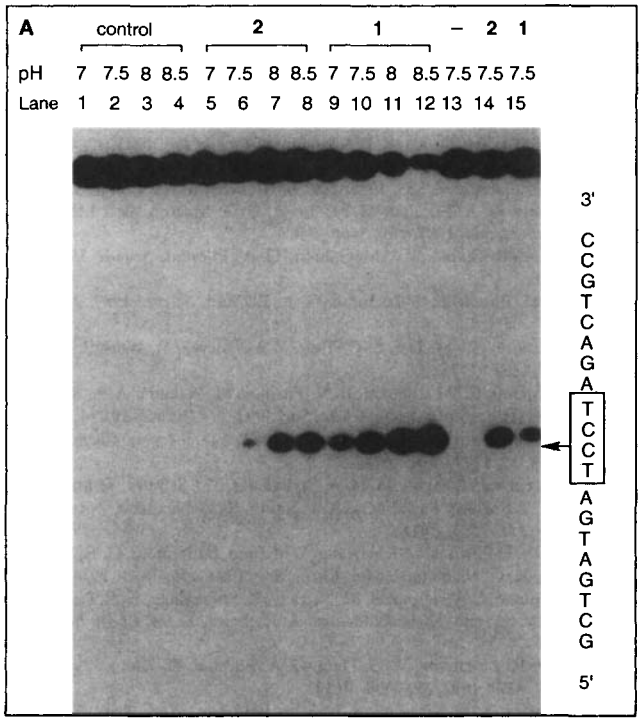
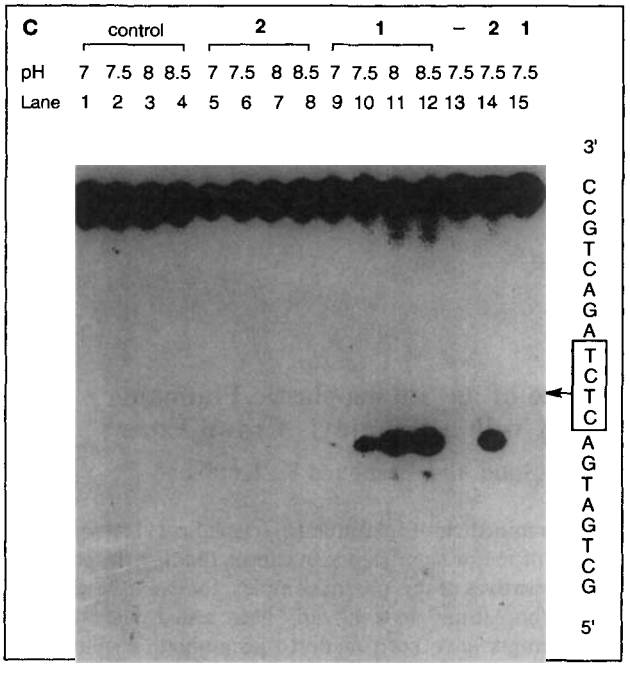


Fig. 3. Computer-generated space-filling model of calicheamicin θ_1^I (**1**) bound in the minor groove of double helical DNA along a TCCT site [Sybyl molecular modeling program; modeling and photography by Manos Pitsinos, University of California, San Diego, and The Scripps Research Institute].

 © VCH Verlagsgesellschaft mbH, D-69451 Weinheim, 1994 0570-0833/94/0202-0184 $ 10.00+.25/0





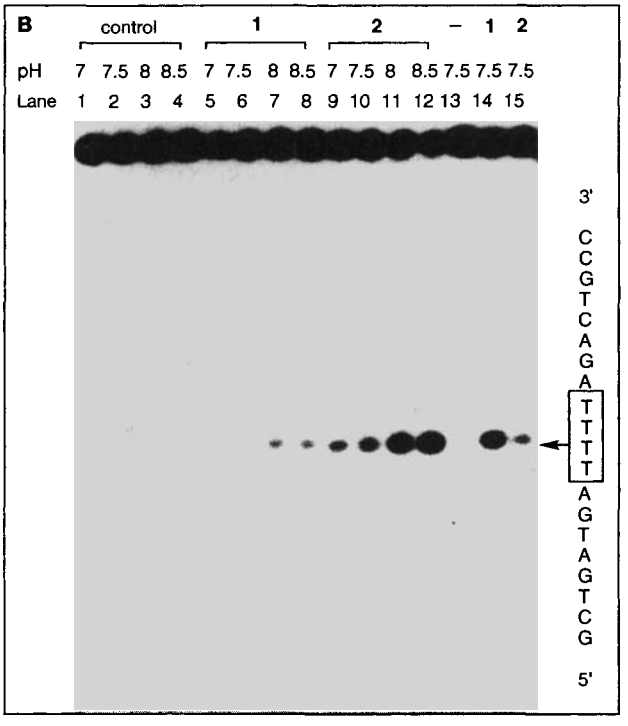


Fig. 4. Autoradiograms of denaturing gels showing selective cleavage of double stranded 5'-end-labeled 20mer DNA containing A) a TCCT/AGGA B) a TTTT/AAAA, and C) a CTCT/GAGA sequence. DNA is cleaved selectively at the designated site. Methods: The synthetic DNA duplex (100 pM, Operon Technologies) was incubated in solutions of various pH values with 400 μM **2** (lanes 5–8) or **1** (lanes 9–12) for 4 hours and with 1 μM **2** (lane 14) or 1 μM **1** (lane 15) for 20 mins followed by addition of β-mercaptoethanol (5 mM) and further incubation for 15 mins. Lanes 1–4 and 13 are controls. All incubations were carried out in 50 mM Tris · HCl buffer/DMSO (97:3) solutions at 37 °C, and the DNA in each reaction mixture was resolved by electrophoresis and autoradiography.

By analogy to its natural counterpart,[9, 10, 16] calicheamicin θ_1^I (**1**) was expected to recognize and cleave along TCCT, CTCT, and TTTT sites of helical DNA. Responsible for this striking recognition is the oligosaccharide tail of these molecules which assists them to bind tightly and selectively[17, 18] in the minor groove of double stranded DNA along these sequences (Fig. 3). Indeed this expectation was confirmed by incubating compounds **1** and **2** with three synthetic 20mers containing a TCCT, TTTT, or CTCT sequence, respectively (Fig. 4A–C). Again, it is noteworthy that **1** exhibited higher potency that **2** in the absence of additives, an order that was reversed, however, in the presence of β-mercaptoethanol as expected.

Calicheamicin θ_1^I (**1**) was tested against a broad spectrum of cell lines ranging from the relatively resistant melanoma cell line SK-MEL 28 to the highly sensitive leukemia cell line MOLT-4 and including a number of untransformed cell lines (Table 1). In

Table 1. Cytotoxicities [a] of calicheamicins θ_1^I (**1**) and γ_1^I (**2**) against a panel of cancer and untransformed cell lines.

Cell type	Cell line	IC_{50} [M]–**1**	IC_{50} [M]–**2**
	Cancer cell lines		
Breast carcinoma	BT-549	$<10^{-12}$	1.0×10^{-9}
Pancreatic carcinoma	CAPAN 1	$<10^{-12}$	1.3×10^{-9}
Lung carcinoma	H322	1.0×10^{-9}	1.7×10^{-8}
B-cell leukemia	HL-60	$<10^{-12}$	$<10^{-12}$
T-cell leukemia	MOLT-4	$<10^{-12}$	$<10^{-12}$
Colon carcinoma	HT-29	$<10^{-12}$	7.0×10^{-9}
Breast carcinoma	MCF-7	1.2×10^{-11}	4.1×10^{-8}
Ovarian carcinoma	OVCAR-3	$<10^{-12}$	2.2×10^{-9}
Lung carcinoma	UCLA-P-3	$<10^{-12}$	1.7×10^{-9}
Prostate carcinoma	PC-3	$<10^{-12}$	4.4×10^{-9}
Squamous carcinoma	SIHA	$<10^{-12}$	6.7×10^{-10}
Melanoma	SK-MEL 28	$<10^{-12}$	1.6×10^{-9}
Melanoma (metastatic)	M24 MET	$<10^{-12}$	1.0×10^{-9}
CNS cancer	U251	9.9×10^{-9}	1.1×10^{-9}
Perirenal carcinoma	786-0	$<10^{-12}$	1.0×10^{-8}
	Untransformed cell lines		
Chinese hamster ovary	CHO	4.3×10^{-9}	1.2×10^{-9}
Human mammary epithelial	HMEC	$<10^{-12}$	1.0×10^{-9}
Human dermal fibroblast	NHDF	$<10^{-12}$	1.0×10^{-9}
Peripheral blood lymphoblast	RPMI 7666	$<10^{-12}$	1.6×10^{-9}

[a] Cytotoxicities were determined by using the sulforhodamine B assay method (see ref. [20]); IC_{50} is the final molarity at which 50% of cell viability was observed after 72 h incubation under standard tissue conditions (37 °C, 5% CO_2 in air).

 © VCH Verlagsgesellschaft mbH, D-69451 Weinheim, 1994 0570-0833/94/0202-0185 $ 10.00+.25/0

several cases the synthetic compound (**1**) was found to be superior to the naturally occurring calicheamicin γ_1^I (**2**) in terms of potency (Table 1). Furthermore, experiments with other known highly cytotoxic agents such as CN-MRA[6] and ricin[7] (data not shown) revealed comparable or higher potencies for **1**. Particularly significant is the powerful effect of this compound on breast, colon, ovarian, prostate, and the SK-MEL 28 melanoma cell lines.

In order to gain further insight into the mechanism of action of **1**, cells were examined after exposure to compounds **1** and **2** for signs of apoptosis.[5, 19] Indeed, the typical signs of this phenomenon (condensed chromatin and DNA degradation into nucleosomal fragments, Fig. 5) were observed for MOLT-4 leukemia cells upon exposure to low concentrations of both **1** and **2**, with the designed calicheamicin (**1**) inflicting a more severe apoptotic morphology than the natural compound **2** (Fig. 5F and D). In addition, a higher proportion of cells were affected by compound **1** (ca. 66%) than by compound **2** (ca. 28%) under the same conditions, resulting in a more pronounced degradation of DNA (Fig. 5G and E).

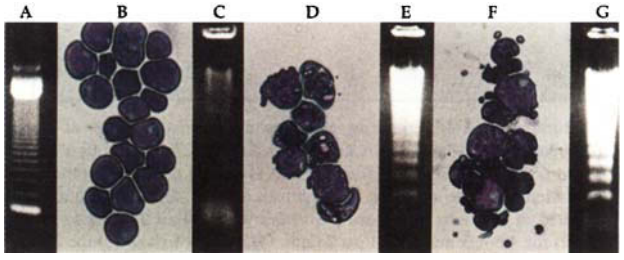


Fig. 5. Apoptotic morphology and nuclear DNA degradation induced by calicheamicin θ_1^I (**1**) and its natural counterpart, calicheamicin γ_1^I (**2**). A) Molecular weight markers consisting of multiples of a 123 base-pair fragment (Gibco BRL); B) untreated MOLT-4 leukemia cells; C) DNA extracted from untreated MOLT-4 cells; D) MOLT-4 cells incubated with 10^{-10} M **2**; E) DNA extracted from MOLT-4 cells exposed to 10^{-8} M **2**; F) MOLT-4 cells incubated with 10^{-10} M **1**; G) DNA extracted from MOLT-4 cells exposed to 10^{-8} M **1**. Methods: Solutions of calicheamicin **1** or **2** in DMSO (10^{-3} M) were diluted in culture medium to the appropriate concentrations and added to cell cultures. MOLT-4 cells (10^5) were incubated with 10^{-10} M final concentrations of **1** or **2** for apoptosis morphology assays, and with 10^{-8} M final concentrations for DNA degradation assays. After incubation for 4 h at 37 °C, cells were harvested and processed as described in ref. [18] to visualize apoptotic morphology and DNA degradation.

The described chemical and biological results demonstrate the power of organic chemistry in the design and synthesis of sophisticated molecules for specific biological actions. The availability of calicheamicin θ_1^I (**1**) by total synthesis and its highly potent and selective DNA cleaving, apoptosis-inducing, and cytotoxic properties represent significant advances in the areas of DNA cleavage and cell death. As a powerful biological tool, compound (**1**) may find useful applications in specific DNA cutting and in investigating the phenomenon of apoptosis. As a highly potent cytotoxic agent and potential antiticancer agent, calicheamicin θ_1^I (**1**) deserves further investigation. Further improvements and variations in the biological properties of **1** may result by incorporation of other designed delivery systems and activating devices.

Received: August 26, 1993 [Z 6319 IE]
German version: *Angew. Chem.* **1994**, *106*, 195

[1] K. C. Nicolaou, W.-M. Dai, *Angew. Chem.* **1991**, *103*, 1453–1481; *Angew. Chem. Int. Ed. Engl.* **1991**, *30*, 1387–1416.
[2] M. D. Lee, G. A. Ellestad, D. B. Borders, *Acc. Chem. Res.* **1991**, *24*, 235–243.
[3] J. H. Haseltine, S. J. Danishefsky, G. Schulte, *J. Am. Chem. Soc.* **1989**, *111*, 7638–7640; J. Aiyar, S. J. Danishefsky, D. M. Crothers, *ibid.* **1992**, *114*, 7552–7554.
[4] R. G. Bergman, *Acc. Chem. Res.* **1973**, *6*, 25–31.
[5] R. E. Ellis, J. Yuan, H. R. Horvitz, *Annu. Rev. Cell. Biol.* **1991**, *7*, 663–698.
[6] E. M. Acton, G. L. Tong, C. W. Mosher, R. L. Wolgemuth, *J. Med. Chem.* **1984**, *27*, 638–645.
[7] V. Raso, J. Ritz, M. Basala, S. F. Schlossman, *Cancer Res.* **1982**, *42*, 457–464.
[8] M. D. Lee, T. S. Dunne, M. M. Siegel, C. C. Chang, G. O. Morton, D. B. Borders, *J. Am. Chem. Soc.* **1987**, *109*, 3464–3466; M. D. Lee, T. S. Dunne, C. C. Chang, G. A. Ellestad, M. M. Siegel, G. O. Morton, W. J. McGahren, D. B. Borders, *ibid.* **1987**, *109*, 3466–3468.
[9] N. Zein, A. M. Sinha, W. J. McGahren, G. A. Ellestad, *Science* **1988**, *240*, 1198–1201.
[10] N. Zein, M. Porcin, R. Nilakantan, G. A. Ellestad, *Science* **1989**, *244*, 697–699.
[11] K. C. Nicolaou, W.-M. Dai, S.-C. Tsay, V. A. Estevez, W. Wrasidlo, *Science* **1992**, *256*, 1172–1178.
[12] K. C. Nicolaou, C. W. Hummel, E. N. Pitsinos, M. Nakada, A. L. Smith, K. Shibayama, H. Saimoto, *J. Am. Chem. Soc.* **1992**, *114*, 10082–10084; see also: K. C. Nicolaou, *Angew. Chem.* **1993**, *105*, 1462–1471; *Angew. Chem. Int. Ed. Engl.* **1993**, *32*, 1377–1385.
[13] R. D. Groneberg, T. Miyazaki, N. A. Stylianides, T. J. Schulze, W. Stahl, E. P. Schreiner, T. Suzuki, Y. Iwabuchi, A. L. Smith, K. C. Nicolaou, *J. Am. Chem. Soc.* **1993**, *115*, 7593–7611.
[14] A. L. Smith, E. Pitsinos, C.-K. Hwang, Y. Mizuno, H. Saimoto, G. R. Scarlato, T. Suzuki, K. C. Nicolaou, *J. Am. Chem. Soc.* **1993**, *115*, 7612–7624.
[15] K. C. Nicolaou, C. W. Hummel, M. Nakada, K. Shibayama, E. N. Pitsinos, H. Saimoto, Y. Mizuno, K.-U. Baldenius, A. L. Smith, *J. Am. Chem. Soc.* **1993**, *115*, 7625–7635.
[16] S. Walker, R. Landovitz, W. D. Ding, G. A. Ellestad, D. Kahne, *Proc. Natl. Acad. Sci., USA* **1992**, *89*, 4608–4612.
[17] R. C. Hawley, L. L. Kiessling, S. L. Schreiber, *Proc. Natl. Acad. Sci., USA* **1989**, *86*, 1105–1109.
[18] K. C. Nicolaou, S.-C. Tsay, T. Suzuki, G. F. Joyce, *J. Am. Chem. Soc.* **1992**, *114*, 7555–7557.
[19] K. C. Nicolaou, P. Stabila, B. Esmaeli-Azad, W. Wrasidlo, A. Hiatt, *Proc. Natl. Acad. Sci., USA* **1993**, *90*, 3142–3146.
[20] P. Skehan, R. Storeng, D. Scudiero, A. Monks, J. McMahon, D. Vistica, J. T. Warren, H. Bokesch, S. Kenney, M. R. Boyd, *J. Natl. Cancer Inst.* **1990**, *82*, 1107–1112.

Structure of an Antineoplastic Platinum Complex with a Bipyridyl–Crown Ether**

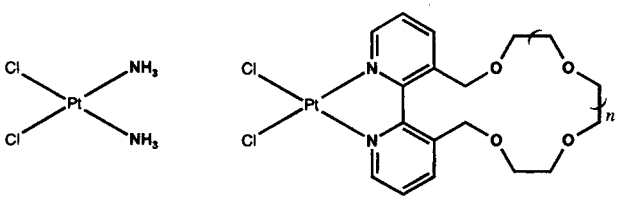
Andreas Gund and Bernhard K. Keppler*

Cis-diamminedichloroplatinum(II) (cisplatin **1**) has for a long time been of major significance in cancer therapy. In addition, several derivatives of this parent complex, for example iproplatin and carboplatin,[1] have already been tested clinically. Recently attempts have been made to accumulate cisplatin and other pharmacologically important compounds selectively in certain body tissues by binding the substances agent to carrier molecules ("drug targeting"), thereby increasing efficacy. For example, binding cisplatin to phosphonic acids that show a high affinity for the inorganic bone matrix hydroxylapatite resulted in higher accumulation and therefore increased therapeutic efficacy for bone tumors.

The same goal of reducing toxic side effects while maintaining therapeutic efficacy can also be accomplished by improving the

[*] Priv.-Doz. Dr. Dr. B. K. Keppler, Dipl.-Chem. A. Gund
Anorganisch-chemisches Institut der Universität
Im Neuenheimer Feld 270, D-69120 Heidelberg (FRG)
Telefax: Int. code + (6221) 56-4955

[**] This work was supported by the Deutsche Krebshilfe, Dr.-Mildred-Scheel-Stiftung für Krebsforschung, Bonn, and by the Fonds der Chemischen Industrie. We thank Dr. Nuber for carrying out the X-ray measurements.



1 $n = 1$ **2a** $n = 2$ **2b** $n = 3$ **2c**

Scheme 1. Cisplatin (**1**) and the pertinent structurally analogous complexes between bipyridyl-crown ether and platinum (**2a–e**).

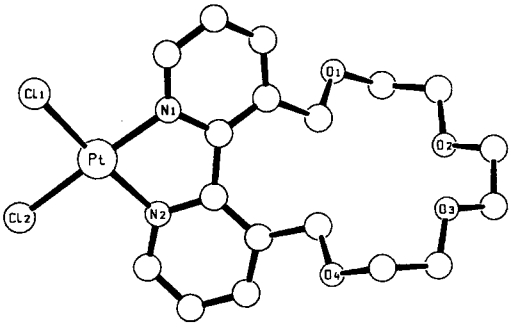


Fig. 1. SCHAKAL drawing of the crystal structure of **2a**. Selected bond lengths [pm] and angles [°]: Pt–Cl1 230.1(3), Pt–Cl2 229.5(3), Pt–N1 200.3(7), Pt–N2 202.0(8); Cl1-Pt-Cl2 89.0(1), Cl1-Pt-N1 95.6(2), Cl2-Pt-N2 95.2(2), N1-Pt-N2 80.4(3).

solubility of the complexes, by slowing down degradation processes through shielding of the platinum with bulky ligands, and by increasing membrane permeability with more lipophilic ligands. Here, crown ethers are especially promising as novel, complex building blocks, as they fulfill the last two requirements: they are bulky and soluble in both hydrophilic and lipophilic media. Complexation of platinum with bipyridyl-crown ethers yields the novel compounds **2a–c** with structures analogous to cisplatin (Scheme 1), which have shown good antitumor activity in vivo as well as in vitro. Notably, these compounds not only showed the expected activity for a human ovarian carcinoma cell line in concentrations of 10–30 $\mu g\,mL^{-1}$, but also almost complete growth inhibition in human colon and rectal cancer cell lines.[2] Two platinum complexes with crown ethers are known. In one of them, [([18]crown-6) · $\{cis$-$[PtCl_2(NH_3)_2]\}_2$ · $(MeCONMe_2)_2$],[3] two molecules of cisplatin are bound by hydrogen bonds between the ammine ligands and the oxygen atoms of the polyether [18]crown-6. In the second, [Pt(bpy)-$(NH_3)_2$(dibenzo[30]crown-10)]$(PF_6)_2$ (bpy = 2,2′-bipyridine),[4] the platinum complex forms a 1:1 adduct with dibenzo[30]-crown-10. In both cases binding of platinum to the polyether occurs through dipolar interactions. Thus, these compounds must be regarded as adducts of the metal complex with the macrocycle and therefore are probably not stable in solution. The smallest of our platinum complexes with a bipyridyl-crown ether containing four oxygen atoms (**2a**) can be prepared in water at 60 °C by reaction of K_2PtCl_4 with the appropriate macrocycle.[8] It was obtained in form of a light yellow powder, which was subsequently characterized by IR, ^1H, and ^{13}C NMR spectroscopy. The higher homologues **2b** and **2c** were prepared analogously. Crystals suitable for X-ray structure analysis were obtained as yellow needles by dissolving **2a** in warm methanol and subsequent slow evaporation of the solvent. In this way the alcohol is incorporated into the crystal lattice in a 1:1 ratio, but no interaction with platinum complex fragment or the crown ether is observed.[6] As shown in Figure 1, the platinum atom of this highly symmetrical molecule is in a square planar environment surrounded by two chloride ions and the two *cis* nitrogen atoms of the bipyridyl unit. This *cis* arrangement of pairs of groups, such as halogenide or carboxylate (that can easily be hydrolyzed under physiological conditions) and more strongly coordinating (nitrogen-containing) ligands, is an important prerequisite for tumor-inhibiting activity in these platinum compounds.

The bond lengths and angles for the bipyridyl–platinum fragment (Fig. 1) are in good agreement with those for planar [(bpy)$PtCl_2$] (red form).[7] However, in **2a** the two pyridine rings are not planar, but instead are twisted by $\theta = 31.1°$. This is a result of steric interactions in the crown ether moiety, especially between the two methylene groups, which are bonded directly to the bipyridyl fragment. In solution the two rings rapidly "flip". This process proceeds through a transition state in which the aromatic ring systems are coplanar. One can follow this racemization by dynamic ^1H NMR spectroscopy: At high temperatures at which racemization occurs, a sharp singlet is observed for the diastereotopic CH_2 protons of the two methylene groups bonded to the ring, while at low temperature a quartet (AB spin system) results. The coalescence temperature for the racemization of **2a** is 22 °C (200 MHz); this in turn translates into a value for $\Delta G^{\neq}$ of about 13.7 $kcal\,mol^{-1}$. The twofold ability of these bipyridyl-crown ether complexes to coordinate transition metal ions with the outward facing N atoms and alkali metal ions inside the cavity of the crown ether has already been studied by Rebek et al. by means of ^1H NMR spectroscopy.[8] He concluded the presence of an "allosteric effect": Binding of a transition metal ion to the outer sphere of the bipyridyl-crown ether levels the pyridine rings. This exerts an unfavorable effect on the conformation of the whole system to such an extent that the ability of the crown ether to complex cations is reduced relative to that of "deplatinated" macrocycles. This reduced tendency of compounds **2a–c** to bind alkali metal ions can also be recognized in the ^1H NMR spectrum: All signals, but in particular that of the benzylic CH_2 protons of the crown ether ($\delta = 4.6$, s, 4H), remain unchanged even several hours after addition of Li, Na, and K salts to solutions of **2a–c**. In contrast, addition of alkali metal ions to solutions of crown ethers whose bipyridyl unit has

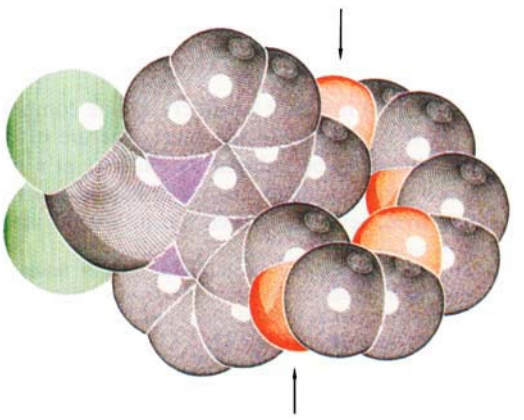


Fig. 2. Space-filling model **2a**. To perceive precise structural details a comparison with Figure 1 is necessary. The oxygen atoms O1 and O4 (arrows) face away from the crown ether cavity. Twisting of the two pyridine rings ($\theta = 31.1°$) can also be seen.

 © *VCH Verlagsgesellschaft mbH, D-69451 Weinheim, 1994* *0570-0833/94/0202-0187 $ 10.00+.25/0*

not been complexed, and which show a much larger conformational flexibility and therefore a higher binding tendency, results in a change of the benzylic CH_2 proton's singlet to a quartet (AB spin system).[8]

In a space-filling model of **2a** (Fig. 2) derived from the X-ray data, two oxygen atoms of the polyether face away from the crown ether cavity and are in an unfavorable arrangement for complexation of alkali metal ions. This model, however, certainly does not represent the structure in solution, but it shows that flexibility is decreased by complexation with platinum.

Received: June 9, 1993
Revised: August 25, 1993 [Z 6132 IE]
German version: *Angew. Chem.* **1994**, *106*, 198

[1] A. Pasini, F. Zunino, *Angew. Chem.* **1987**, *99*, 632; *Angew. Chem. Int. Ed. Engl.* **1987**, *26*, 615.
[2] A. Gund, B. K. Keppler, unpublished results.
[3] D. R. Alston, J. F. Stoddart, D. J. Williams, *J. Chem. Soc. Chem. Commun.* **1985**, *9*, 532.
[4] H. M. Colquhoun, J. F. Stoddart, D. J. Williams, J. B. Wolstenholme, R. Zarzycki, *Angew. Chem.* **1981**, *93*, 1093; *Angew. Chem. Int. Ed. Engl.* **1981**, *20*, 1051.
[5] Crystal data for **2a**: $C_{18}H_{22}N_2O_4Cl_2 \cdot CH_3OH$, crystal dimensions [mm]: $0.08 \times 0.08 \times 0.95$, monoclinic, space group $P2_1/n(14)$, $a = 14.761(5)$, $b = 9.450(6)$, $c = 17.089(9)$ Å, $\beta = 111.56°$, $V = 2217.0$ Å^3, $Z = 4$, $\rho_{calcd} = 1.88$ g cm^{-3}; $F(000) = 1224$; 5568 reflections with $3° < 2\theta < 55°$, for 3643 of which $I > 2.0\,\sigma(I)$. Structure solution and refinement for 3267 independent reflections with $I > 2.5\,\sigma(I)$ for 263 parameters. $R = 0.041$, $R_w = 0.036$, GOF = 1.76. Data were measured on an AED-II/SynTEX-R3 diffractometer with $Mo_{K\alpha}$ radiation (graphite monochromator, $\lambda = 0.71073$ Å). Hydrogen atoms were identified from the difference-Fourier map and included in the calculation of structure factors while holding thermal parameters constant. Residual electron density: max. 0.78, min. -0.83 eÅ^{-3}. Further details of the crystal structure investigation may be obtained from the Fachinformationszentrum Karlsruhe, D-76344 Eggenstein-Leopoldshafen, on quoting the depository number CSD-57880, the names of the authors, and the journal citation.
[6] The methanol can be completely removed by drying in high vacuum, as shown by elemental analysis. In the crystal the distance O(MeOH)–Cl(2) is 326 pm. For clarity, the alcohol molecule was omitted in the figures.
[7] R. S. Osborn, D. Rogers, *J. Chem. Soc. Dalton Trans.* **1974**, 1002.
[8] J. Rebek, Jr., J. E. Trend, R. V. Wattley, S. Chakravorti, *J. Am. Chem. Soc.* **1979**, *101*, 4333.

Cooperativity and Transfer of Chirality in Liquid-Crystalline Polymers**

Günter Wulff,* Harald Schmidt, Hartmut Witt, and Rudolf Zentel*

In memory of Günther Snatzke

The interest in chiral liquid-crystalline compounds is due to the fact that chirality in the superstructure of the liquid-crystalline phase can be induced by chirality at a molecular level. This can result in the formation of helical superstructures with pitches from several hundred nm to several μm. The material properties of such phases are also of particular interest, for example, the selective reflection of light by the cholesteric phase or the ferroelectricity of the smectic C* phase. Such thermotropic phases of compounds of low molecular weight are well-known, as are those of side chain polymers.[1] In the latter case, the chiral group is mainly found in the branch group.[1] It is rarely seen in the spacer[2] or in the mesogen.[3] On the other hand, thermotropic side chain polymers with chirality in the main chain are as yet unknown.

Our intention was to synthesize liquid-crystalline polyvinyl compounds, which have chirality that arises from the configuration of the main chain.[4, 5] It is thus possible to investigate the coupling and decoupling of the chiral polymer chains with the achiral mesogens. From this we found a surprisingly distinct relationship between the structure of the groups at the uniquely defined stereochemical centers of the main chain and the transfer of chirality onto the mesogens (Fig. 1).

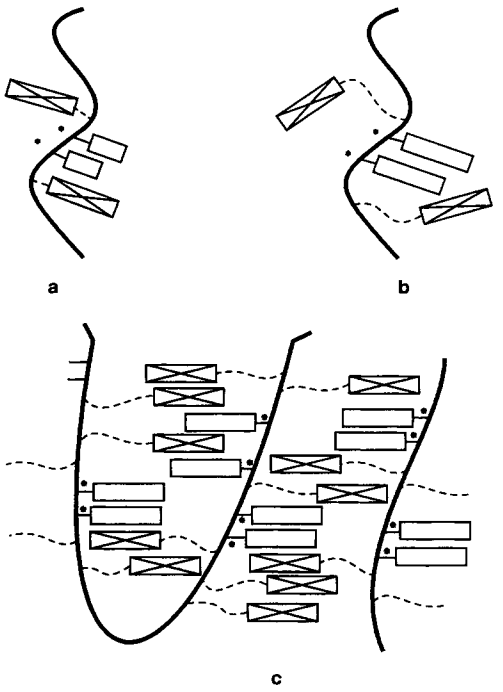
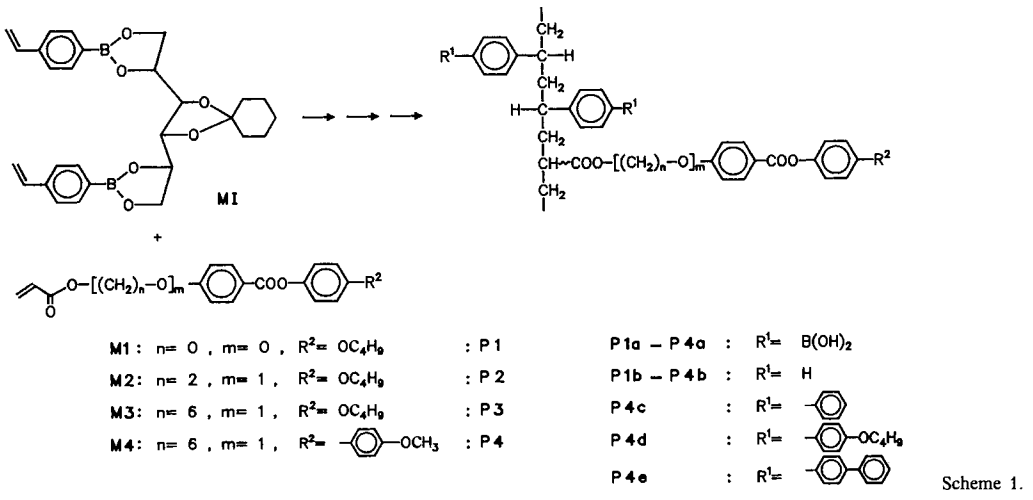


Fig. 1. Schematic representation of the configuration of the mesogen groups from the comonomer (⊠) and the substituents in the chiral diad (□) on the polymer chains. a) Behavior in solution of polymers of the type **P1b** and **P2b** with a short spacer at the mesogen and phenyl groups at the diad. The chromophore in the mesogen is placed in a preferred chiral conformation by the neighboring diad. b) Behavior in solution of polymers of the type **P4c–4e** with a long spacer at the mesogen and diad units lengthened to biphenylyl or terphenylyl groups. A transfer of chirality between the diad and the mesogen chromophore is not observed. c) Behavior in liquid-crystalline phase of polymers of the type **P4c–4e** with a long spacer at the mesogen and mesogen-like diad units. A strong inter- and intramolecular interaction and transfer of chirality occurs due to the general orientation of both groups in the liquid crystal.

Main chain chiral polyvinyl compounds were synthesized using a method[4, 5] in which chiral diads in the main chain are produced by means of a template. The optically active polymers **P1a–4a** with 4-vinylphenylboronic acid diads, which show predominantly (*S,S*) configuration, were obtained by radical cyclocopolymerization of the template monomer **MI** with the liquid-crystalline monomers **M1–M4** (Scheme 1) and subsequent removal of the template. Once the boronic acid groups have been eliminated with $AgNO_3/NH_3$, the liquid-crystalline poly-

[*] Prof. Dr. G. Wulff, Prof. Dr. R. Zentel,[+] Dr. H. Schmidt, Dr. H. Witt
Institut für Organische Chemie und Makromolekulare Chemie der Universität
Universitätstrasse 1, D-40225 Düsseldorf (FRG)
Telefax: Int. code + (211)311-4788
[+] New address:
Institut für Organische Chemie der Universität
J.-J.-Becher-Weg 18–20, D-55128 Mainz (FRG)
Telefax: Int. code + (6131)3954-23

[**] This work was supported by the Deutsche Forschungsgemeinschaft and the Fonds der Chemischen Industrie. We thank Prof. Dr. H.-G. Kuball for helpful discussions.



Scheme 1.

mers **P1b**–**4b** are obtained (Table 1). These liquid-crystalline polymers have a clearing point which is somewhat lower than and a liquid-crystalline range which is somewhat narrower than that of the homopolymers synthesized from **M1**–**M3**[6] and **M4**.[7] This is because of the influence of the non-mesogenic comonomer.

Table 1. Composition and selected properties of the newly synthesized liquid-crystalline copolymers which have chirality arising from the configuration of the main chain.

Polymer	Composition [a] mesogen/diad component (mole ratio)	$[\alpha]_{546}^{30}$	Phase transitions [b]
P1a	3:1	+2.9	
P1b		–	g 100 lc [c] 200 i
P2a	3:1	+3.8	
P2b		–	k 77s [c] 146 i
P3a	4:1	−1.9	
P3b		–	g 30 s [c] 110 i
P4a	2:1	−4.2	
P4b		–	g 65 c 105 s-n [c] 240 i
P4c	3.5:1	−17.4	g 78 n* 187 i
P4d	3.5:1	−3.2	g 85 n* 225 i
P4e	3.5:1	−11.1	g 80 n* 210 i

[a] Mole ratio of the component of mesogen monomer to the component of diad yielded by **MI** (determined by ^{1}H NMR spectroscopy). [b] Phase transitions determined by differential scanning calorimetry (DSC) (Mettler TA4000). g: glassy, k: partially crystalline, lc: liquid crystalline, not identified precisely, s: smectic, n: nematic, n*: cholesteric, i: isotropic. Parameters; temperature in °C. [c] Due to the chirality in the main chain of the polymers, chiral liquid-crystalline phases are expected. These were however difficult to determine for **P1b** and **P2b** and were not detectable for **P3b** and **P4b**.

Possible interactions between the chiral configurations in the main chain and the achiral mesogens of the side chains should be detectable by circular dichroism (CD) of the solution of polymers **P1a**–**4a** (Fig. 2). A negative Cotton effect at 230 nm was observed for the chiral diad in each case. However, in the mesogen absorption region (≈260 nm), an additional positive Cotton effect was only obtained for **P1a** (spacer $n = 0$) and **P2a** (spacer $n = 2$). For a longer spacer ($n = 6$), this effect does not occur, that is, no chiral induction takes place in the mesogen. This is consistent with earlier findings for main chain chiral polymers[5] and also with the model for the decoupling of the mesogen and polymer chain by the flexible spacer[8] (cf. Fig. 1a and 1b).

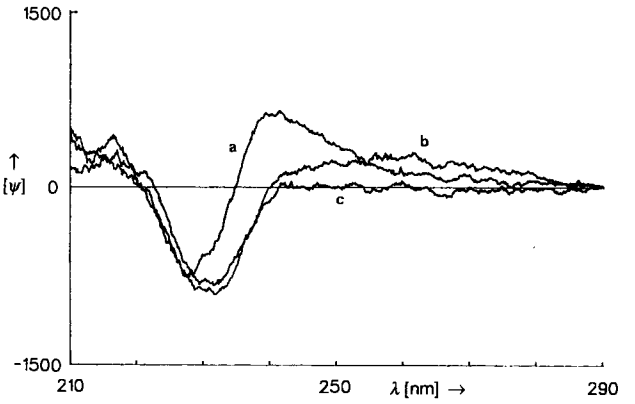


Fig. 2. Circular dichroism of polymers **P1a** (a), **P2a** (b), and **P4a** (c) in tetrahydrofuran. Polymers with a long spacer (**P4a** and almost identical spectrum for **P3a**) show no induced Cotton effect in the region of the mesogen chromophore. The specific ellipticity [Ψ] is given (unit °dm^{-1}g^{-1}mL).

Texture investigations of the liquid-crystalline phase, which should yield information about the influence of chirality of the main chain on the superstructure of the liquid-crystalline phase, were only possible for polymers with a long spacer (**P3b** and **P4b**).[9] In these cases, no chiral superstructure was observed, that is, if a chiral superstructure exists, its pitch is greater than the sample thickness and is therefore not detectable. The texture appears typically nematic and not cholesteric (Fig. 3 top). This was consistent with the results of the CD measurements, which means that for polymers with a long spacer, there is no noteworthy interaction between the chiral configuration in the main chain and the mesogen. This is the case not only in solution, but also in the densely packed liquid-crystalline phase in which van der Waals interactions would have had to take place between the mesogens and the chiral diad in the main chain. This result is all the more surprising as there is formation of distinct cholesteric textures on dissolving small amounts of chiral doping agent.[10]

In order to strengthen the interaction between the chiral structural elements in the polymer chain and the mesogen groups, the individual structural groups of the chiral diads were lengthened by the Suzuki reaction.[11] Polymers **P4c**–**4e** were

synthesized from polymer **P4a** by reaction with bromobenzene, 1-bromo-4-butoxybenzene, or 4-bromobiphenyl under Pd^0 catalysis (see Table 1). The yields of these polymer-analogous reactions are around 60–70%. The polymers thus synthesized with mesogen-like structures at the chiral diads (biphenylyl and terphenylyl groups) show distinctly cholesteric textures unlike **P3b** and **P4b** (Fig. 3 bottom). This behavior is evidence for a

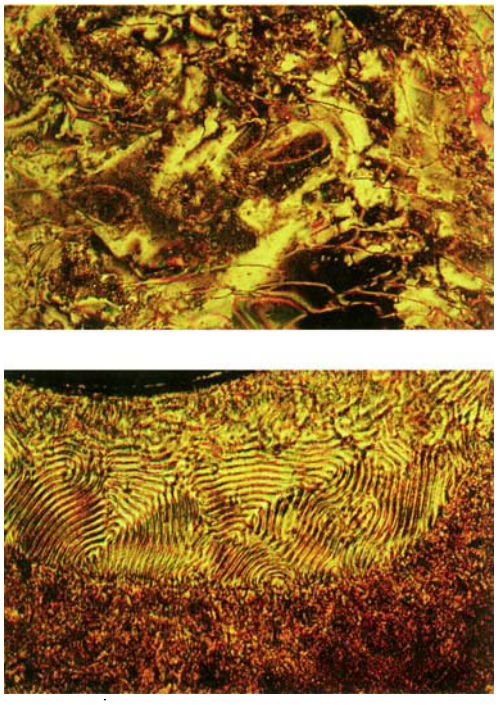


Fig. 3. Polarization microscopy photographs of (top) the schlieren texture of the nematic phase **P4b** and (bottom) the fingerprint texture of the cholesteric phase of **P4e**, synthesized from **P4a** by the Suzuki reaction. Magnification 100×.

distinct interaction between the modified chiral diads and the original mesogens in the liquid-crystalline phase. However, CD measurements in solution (Fig. 4) showed no interaction between the chiral diad and the mesogens for these polymers (**P4c–4e**).

In order to explain this discrepancy, CD measurements were carried out in bulk. For this, thin films (20–30 nm) of polymers

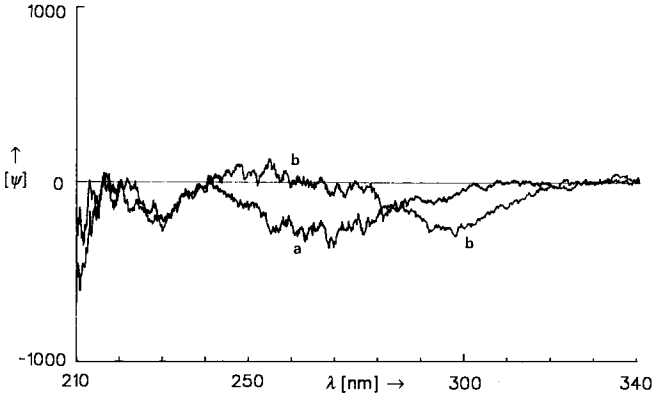


Fig. 4. Circular dichroism of polymers **P4d** (a) and **P4e** (b) in tetrahydrofuran. The weaker negative Cotton effect at 230 nm is due to unreacted 4-vinylphenylboronic acid.

P4c–4e in the cholesteric phase were tempered and then quickly cooled to room temperature. The CD spectra obtained from these films[12] (Fig. 5) differ distinctly from the solution spectra. After heating the films to temperatures above the clearing point, the CD signal disappears completely, only to reappear unaltered on cooling.[13] It can be stabilized in the glassy state by rapid cooling of the liquid-crystalline phase. We could rule out the possibility that this phenomenon may be attributed to birefringence effects by carrying out exhaustive measurements at various orientations of the films in the spectrometer, and by checking the reproducibility of the measurements for various films.[13]

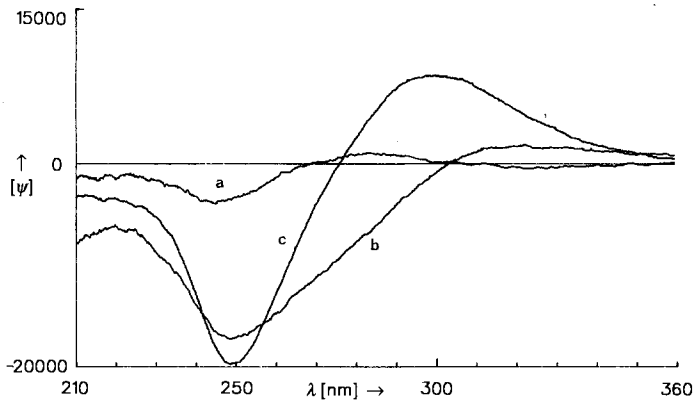


Fig. 5. Circular dichroism of polymers **P4c** (a), **P4d** (b), and **P4e** (c) measured as films. The films were tempered at 180 °C and quickly cooled. The specific ellipticity [Ψ] was calculated from the determined film thickness of 20–30 nm.

The CD signals described earlier prove unambiguously that the chromophores of the mesogens in the liquid-crystalline state are in a chiral environment. The extent to which the CD signals may be discussed at a molecular level in terms of interactions between different chromophores cannot yet be answered. Neither is it known if to some extent an existing helical superstructure in the thin films (thickness 20–30 mm compared to a pitch of a few μm) contributes to the effects described here.[14] Positive Cotton effects in the region 280–325 nm together with strongly negative Cotton effects at 245–250 nm may be interpreted as circular dichroism. The zero passage of **P4e** at 276 nm is in the region of the absorption maxima of the mesogen (268 nm) and the terphenyl (300 nm), so that it may be treated as a positive exciton couplet. In comparison to this, **P4e** in solution shows only a weak negative Cotton effect for the terphenyl diad at 300 nm (see Fig. 4).

If the textures of the liquid-crystalline phases of polymers **P3b** and **P4b** (with distyryl diads) are compared with those of polymers **P4c–4e** (with lengthened mesogen-like diads), a distinct chiral induction is detected only in those of the latter. However, both **P3b** and **P4b** as well as **P4c–4e** show no interaction between the chiral diads and the mesogen chromophore in solution by circular dichroism. This verifies a particular mechanism for the transfer of chirality through space for polymers **P4c–4e** in the liquid-crystalline phase, as is shown schematically in Figure 1c for inter- and intramolecular transfer. Figure 1c should be understood in such a way that the interaction between chiral diads and mesogens forces the latter into a helical superstructure. By comparison with CD spectra in solution, this transfer can be clearly differentiated from the conventional transfer mechanisms along the polymer chain (Fig. 1a). This differentiation was possible because optically active liquid-crystalline side chain polymers, whose chirality is derived from

 © VCH Verlagsgesellschaft mbH, D-69451 Weinheim, 1994 0570-0833/94/0202-0190 $ 10.00+.25/0 Angew. Chem. Int. Ed. Engl. 1994, 33, No. 2

the configuration of the main chain, were successfully synthesized for the first time. With such a structure, the influence of the chiral configurations on the different chromophores and on the formation of the liquid-crystalline phase may be understood separately.

Received: April 22, 1993
Revised version: August 6, 1993 [Z6026IE]
German version: *Angew. Chem.* **1994**, *106*, 240

[1] C. B. McArdle, *Side Chain Liquid Crystalline Polymers*, Blackie, Glasgow, **1989**.
[2] G. Scherowsky, U. Müller, J. Springer, W. Trapp, A. M. Levelut, P. Davidson, *Liq. Cryst.* **1989**, *5*, 1297.
[3] H. Poths, R. Zentel, S. U. Vallerien, F. Kremer, *Mol. Cryst. Liq. Cryst.* **1991**, *203*, 101.
[4] G. Wulff, *Angew. Chem.* **1989**, *101*, 22; *Angew. Chem. Int. Ed. Engl.* **1989**, *28*, 21.
[5] G. Wulff, P. K. Dhal, *Macromolecules* **1990**, *23*, 100.
[6] J. Horváth, K. Nyitrai, F. Cser, Gy. Hardy, *Eur. Polym. J.* **1985**, *21*, 251.
[7] M. Portugall, H. Ringsdorf, R. Zentel, *Makromol. Chem.* **1982**, *183*, 2311.
[8] H. Finkelmann, H. Ringsdorf, J. H. Wendorff, *Makromol. Chem.* **1978**, *179*, 273.
[9] For polymers with a shorter spacer (**P1b** and **P2b**) either the formation of a network at the high temperature required to attain the liquid-crystalline phase (**P1b**) or the high viscosity in the smectic phase (**P2b**) prevents the formation of characteristic textures.
[10] (*S,S*)-1,3-Diphenylpropanediol (a low molecular weight model for the chiral diad in polymers **P1**–**P4**) was used as a chiral doping agent. Similar results were obtained with (*R*)-mandelic acid.
[11] N. Miyaura, T. Yanagi, A. Suzuki, *Synth. Commun.* **1981**, *11*, 513.
[12] CD measurements in the polymer film have already been described by: M. M. Green, H. Ringsdorf, J. Wagner, R. Wüstefeld, *Angew. Chem.* **1990**, *102*, 1525; *Angew. Chem. Int. Ed. Engl.* **1990**, *29*, 1478.
[13] O. Thurmüller, diploma thesis Universität Düsseldorf, **1993**.
[14] A. Schönhofer, H.-G. Kuball, C. Puebla, *Chem. Phys.* **1983**, *76*, 453.

$[K([18]crown\text{-}6)]^+ [Mo_4(\mu_4\text{-}H)(OCH_2tBu)_{12}]^-$, the First Alkoxidohydrido Cluster of Molybdenum, Evidence for a Rare, if not the First, Example of a μ_4-Hydride**

Theodore A. Budzichowski, Malcolm H. Chisholm,* John C. Huffman, and Odile Eisenstein*

The dimetal hexaalkoxides $[M_2(OR)_6]$ ($M{\equiv}M$) are weakly Lewis acidic and this affords entry into all of the chemistry associated with the M–M triple bond (M = Mo, W).[1] We have recently been studying the reactions of $[M_2(OR)_6]$ compounds with a variety of anions in hydrocarbon solvents [Eq. (a)].[2]

$$[M_2(OR)_6] + [Q]^+[X]^- \rightleftharpoons [Q]^+[M_2(OR)_6X]^- \quad (a)$$

Q = NBu^n_4 or K

When X is a halide the equilibrium lies well to the left but for $X = OR^-$ it lies well to the right and salts containing the anion $[M_2(OR)_7]^-$ may be isolated.[2a] When $X = CN^-$ the equilibrium can be monitored by NMR spectroscopy and thus the strength of the bonding of CN^- to the W_2^{6+} center and to the Mo_2^{6+} center can be compared directly based on the thermodynamic parameters.[2b] The reaction involving $X = H^-$ occurs readily ($Q^+ = K^+$), but is quite different for molybdenum versus tungsten, and the nature of the products depends upon the ratio (alkoxide:hydride) of the two starting materials used. The title compound is formed by the reaction shown in Equation b

$$2\,[Mo_2(OCH_2tBu)_6] + KH/[18]crown\text{-}6 \xrightarrow[THF]{22\,^\circ C} [K([18]crown\text{-}6)]^+\,[Mo_4(\mu\text{-}H)(OCH_2tBu)_{12}]^- \quad (b)$$

and is best prepared (88% isolated crystalline yield) by using a deficiency of the hydride reagent (45 mol% $K[B(sBu)_3H]$). The reaction may be viewed to proceed in two steps. The first step formally involves addition of H^- to yellow $[Mo_2(OCH_2tBu)_6]$ to form the anionic complex $[Mo_2(OCH_2tBu)_6H]^-$, which then attacks another equivalent of coordinatively unsaturated $[Mo_2(OCH_2tBu)_6]$ to afford the Mo_4 cluster anion. It should be noted that $[Mo_2(OR)_6]$ compounds where R = *i*Pr and $R = CH_2tBu$ do not undergo cluster formation, in contrast to their tungsten analogues.[3] By ^1H NMR spectroscopy we find no evidence for the $[Mo_2(OCH_2tBu)_6H]^-$ anion which implies that the second addition of $[Mo_2(OCH_2tBu)_6]$ occurs at a much faster rate than the initial adduct formation.

The X-ray structure analysis (space group $P\bar{1}$) shows there is one unique Mo_4 cluster anion in the unit cell and two cationic $[K([18]crown\text{-}6)]^+ \cdot (THF)_2$ moieties each lying on a crystallographic inversion center.[4] It should be emphasized that there is only one potassium ion per cluster and the two independent cations are each of half weight. A difference Fourier synthesis with phases based on the non-hydrogen atoms revealed approximately one half of the hydrogen atoms of the anion, including H(A) which is in the appropriate position for a μ_4-hydride. In the first cycles of refinement its positional and thermal parameters were allowed to vary along with the non-hydrogen atoms. An ORTEP view of the anion is given in Figure 1 and the central $[Mo_4(\mu_4\text{-}H)O_{12}]$ skeleton is shown in Figure 2.

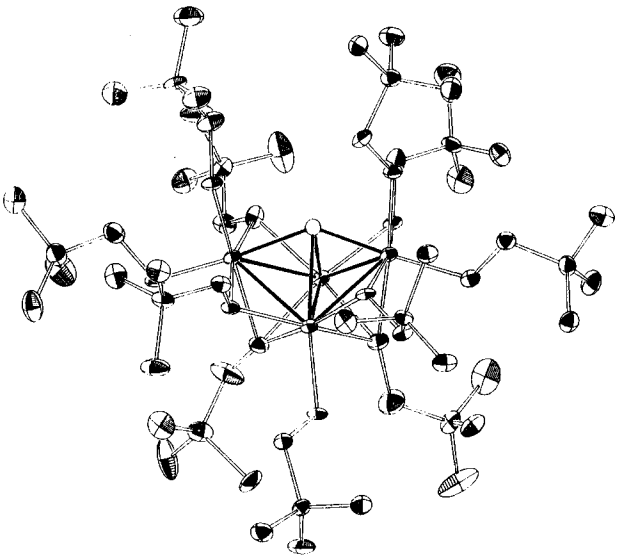


Fig. 1. ORTEP diagram for the $[Mo_4(OCH_2tBu)_{12}(\mu_4\text{-}H)]^-$ anion. Ellipsoids are at the 30% probability level, (the μ_4-hydrido ligand is shown as an arbitrary sphere). Atom labels and the terminal alkoxido ligand bound to the rear hinge Mo atom have been omitted for clarity.

[*] Prof. M. H. Chisholm, Dr. T. A. Budzichowski, Dr. J. C. Huffman
Department of Chemistry and Molecular Structure Center
Indiana University, Bloomington, IN 47405 (USA)
Telefax: Int. code + (812)855-7148
Prof. O. Eisenstein
Laboratoire de Chimie Théorique, Bâtiment 490
Université de Paris-Sud, F-91405 Orsay (France)

[**] This work was supported by the Department of Energy, Office of Basic Research, Chemistry Division, and National Science Foundation/Centre National de la Recherche Scientifique (International Grant for US/France collaboration).

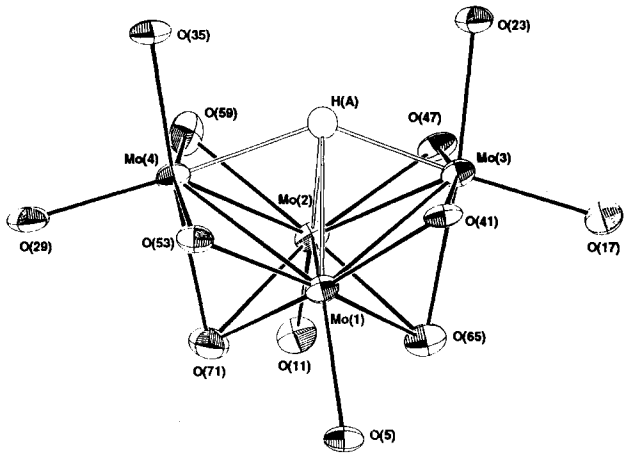


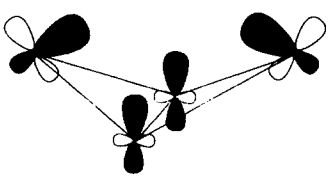
Fig. 2. ORTEP diagram of the $[Mo_4(OCH_2tBu)_{12}(\mu_4\text{-H})]^-$ anion showing only the core Mo, O, and μ_4-H atoms. Ellipsoids are at the 30% probability level and the μ_4-hydrido ligand is shown as an arbitrary sphere. Selected bond lengths [Å]: Mo(1)-H(A) 2.24(1), Mo(2)-H(A) 2.12(1), Mo(3)-H(A) 2.08(1), Mo(4)-H(A) 1.88(1), Mo(1)-Mo(2) 2.522(3), Mo(1)-Mo(3) 2.545(3), Mo(1)-Mo(4) 2.503(3), Mo(2)-Mo(3) 2.505(2), Mo(2)-Mo(4) 2.538(3), Mo-O_t (1.933–2.032, 1.983 mean), Mo-μ_2-O (2.092–2.172, 2.133 mean), Mo-μ_3-O (2.135–2.180, 2.157 mean), Mo(3)-O(17) 1.939(7), Mo(4)O(29) 1.933(7), Mo(3)-O(23) 1.996(9), Mo(4)-O(35), 1.993(8); Average *cis*-L-M-L bond angles 90.0°, *trans*-L-M-L 169.5, Mo_h-Mo_w-Mo_h 60.0 mean, Mo_w-Mo_h-Mo_w 95.7 mean, Mo_h-Mo_h-Mo_w 60.0 mean, Mo(1,2,3)-Mo(1,2,4) dihedral angle = 117.8°. w = wingtip, h = hinge.

Despite the inherent difficulties associated with locating hydrogen atom positions near transition metals by X-ray diffraction, as well as several minor disorder problems associated with this crystallographic study,[4] we are confident of the assignment of a μ_4-hydride for several reasons. Inspection of the Mo–O distances shows the expected trend d(M–O terminal) < d(Mo–μ_2-O) < d(Mo–μ_3-O) and no evidence of coordinated ROH ligands was observed.[5] Preliminary reactivity studies further support this view: The complex is inert towards tBuCH$_2$OD (10-fold excess, 40 °C, 12 h), suggesting neither hydridic behavior, which would liberate HD, nor acidic behavior, which would result in H/D exchange. Placement of the hydrido ligand within bonding distance of all four metal atoms completes a nearly octahedral coordination sphere (excluding M–M bonding) for each of the molybdenum centers, and is most reasonable considering the steric congestion within the molecule. As a structural consequence of the μ_4-hydride, the Mo_4-butterfly unit opens considerably [Mo(1,2,3)–Mo(1,2,4) dihedral angle 117.8°] compared to two structurally related analogues $[Mo_4(OiPr)_9Br_3]$ (dihedral angle 97.6°) and $[Mo_4(OiPr)_8Br_4]$ (dihedral angle 97.4°) which do not possess bonded ligands in this domain.[6] Furthermore, the nonbonded wingtip-to-wingtip distance is considerably longer for the title compound (3.741 Å) than for the other two structurally characterized Mo_4^{12+} butterfly clusters (3.284 and 3.287 Å, respectively).[6]

Since the framework of the molecule has virtual C_{2v} symmetry five groups of alkoxido ligands with relative integral intensities of 2:2:2:2:4 are found by NMR spectroscopy. All of the terminal and both of the μ_3-OR ligands lie on mirror planes but the four μ_2-OR ligands do not. The methylene protons of the latter are diastereotopic and appear as an AB quartet in the ^{1}H NMR spectrum. The signal for the hydrido ligand occurs at $\delta = -15.2$, *upfield* of Me_4Si in contrast to the signals of the hydrido ligands of all the previously characterized alkoxidohydrido tungsten clusters that are downfield from Me_4Si. Thus, the ^{1}H NMR data[7] are consistent with the maintenance of the structure found in the solid state. We have been unable to locate an IR absorption band assignable to either a μ_4-H or a μ_4-D ligand. The absorption bands associated with this moiety are either too weak to be observed or are obscured by other IR active modes of the OR ligands.

Although M_4-butterfly clusters are known to capture μ_4-carbido,[8] -nitrido,[9] and -oxido ligands,[10] to our knowledge this is the first complex with a μ_4-hydrido ligand. While there are numerous μ_2-H, μ_3-H, and μ_6-H moieties reported in the Cambridge Crystallographic Data Center, this data base does not contain the $M_4(\mu_4$-H) moiety. As a check on the viability of the proposed μ_4-hydrido ligand we investigated the possible interactions of a hydrido ligand with the hypothetical cluster $[Mo_4(OH)_{12}]$, whose structural parameters are related to those in the title compound, but which are idealized to C_{2v} symmetry.

A study of the interaction of a hydrido ligand with the model cluster $[Mo_4(OH)_{12}]$ by extended Hückel calculations[11] strongly supports the proposed μ_4 coordination of H^-. It is found to be considerably more stable than a μ_2 coordination to the molybdenum atoms of the back-bone of the butterfly. The preference for the μ_4 coordination comes from the shape of the LUMO of $[Mo_4(OH)_{12}]$ (Scheme 1). The LUMO is low in energy and has a_1 symmetry. It is therefore ideally suited to stabilize the hydrido 1 s orbital in a μ_4 position, since it can overlap with the orbitals of the four metallic centers. (The HOMO of the cluster being of a different symmetry is not affected by the coordination of the hydrido ligand.) Coordination to the backbone molybdenum atoms leads to a total overlap which is half of that with a hydrido ligand in a μ_4 position (0.32). An interesting aspect of the problem is why is the LUMO of $[Mo_4(OH)_{12}]$ low in energy (HOMO–LUMO gap 0.04 eV). The LUMO is the in-phase combination of the LUMOs localized on each metal center. Each Mo is surrounded by five ligands that are arranged in an octahedral geometry, one site (the center of the butterfly) being vacant. Such a metallic fragment is characterized by a low-lying LUMO pointing towards the empty site of the octahedron. The in-phase combination of the four LUMOs is therefore lower in energy and points toward the center of the butterfly structure.



Scheme 1. LUMO of $[Mo_4(OH)_{12}]$.

In conclusion, we find it most intriguing that addition of hydride to $[Mo_2(OCH_2tBu)_6]$ should induce the coupling of two Mo≡Mo units to give what appears to be the first example of a cluster containing $M_4(\mu_4$-H). Further studies are in progress.

Experimental Procedure

A solution of $[K([18]crown\text{-}6)]^+[B(sBu)_3H]^-$ was prepared by mixing [18]crown-6 (175 mg, 0.66 mmol) and potassium tri-*sec*-butylborohydride (0.65 mL of 1.0 M solution in diethyl ether, 0.65 mmol) in 10 mL of dry, degassed THF. This was cooled to −78 °C and added by cannula dropwise to a stirred solution of $[Mo_2(OCH_2tBu)_6]$ (1.00 g, 1.40 mmol) in 5 mL THF at −78 °C. The reaction was allowed to warm to room temperature and stirred an additional 15 minutes. The solvent was removed in vacuo to afford a dark purple microcrystalline solid, which was washed with 3 × 10 mL dry, degassed C_6H_6 and filtered to afford an 88% yield of brown product. X-ray quality crystals were grown from a THF solution by hexane diffusion. The

 © VCH Verlagsgesellschaft mbH, D-69451 Weinheim, 1994 0570-0833/94/0202-0192 $ 10.00+.25/0

reaction may also be performed with solid KH, but a substantially longer reaction time is necessary (>24 h) owing to the low solubility of this reagent. The analogous $[Mo_4(\mu_4\text{-}D)(OCH_2tBu)_{12}]^-$ anion was prepared in a similar manner from commercially available KD.

The reaction is extremely sensitive to the presence of trace amounts of H_2O. Both KH and K[B(*s*Bu$_3$)H] and H_2O react to give H_2 and KOH/K[B(*s*Bu$_3$)OH] and the latter react with $[Mo_2(OCH_2tBu)_6]$ to give the green $[Mo_4O(OCH_2tBu)_{11}]^-$ anion and pentyl alcohol. The alcohol and KH/K[B(*s*Bu$_3$)H] react to generate [KOCH$_2$*t*Bu] which in turn reacts with $[Mo_2(OCH_2tBu)_6]$ to form the purple $[Mo_2(OCH_2tBu)_7]^-$ anion [2a]. Both of these by-products have been synthesized by independent routes which will be described in a later publication.

Received: December 7, 1992
Revised version: October 4, 1993 [Z 5733 IE]
German version: *Angew. Chem.* **1994**, *106*, 203

[1] M. H. Chisholm, *Acc. Chem. Res.* **1990**, *23*, 419; *J. Organomet. Chem.* **1991**, *400*, 235; *Pure Appl. Chem.* **1991**, *63*, 665.

[2] a) T. A. Budzichowski, M. H. Chisholm, J. C. Huffman, K. G. Moodley, J. D. Martin, *Polyhedron*, **1993**, *12*, 343; b) T. A. Budzichowski, M. H. Chisholm, unpublished results.

[3] a) M. H. Chisholm, D. L. Clark, K. Folting, J. C. Huffman, *Angew. Chem.* **1986**, *98*, 1021; *Angew. Chem. Int. Ed. Engl.* **1986**, *25*, 1014; b) M. H. Chisholm, D. L. Clark, K. Folting, J. C. Huffman, M. J. Hampden-Smith, *J. Am. Chem. Soc.* **1987**, *109*, 7750; c) M. H. Chisholm, D. L. Clark, M. J. Hampden-Smith, *ibid.* **1989**, *111*, 574; d) see also preparation and structure of $[Mo_4(OMe)_2(OiPr)_{10}]$; comments on why $[W_2(OiPr)_6]_2$ dimerizes, whereas $[Mo_2(OiPr)_6]$ does not: M. H. Chisholm, C. E. Hammond, M. J. Hampden-Smith, J. C. Huffman, W. G. Van Der Sluys, *Angew. Chem.* **1987**, *99*, 937; *Angew. Chem. Int. Ed. Engl.* **1987**, *26*, 904.

[4] Crystal data for $[K([18]crown\text{-}6)]^+[Mo_4(\mu_4\text{-}H)(OCH_2tBu)_{12}]^- \cdot 2THF$. X (solvent) $T = -171\,^\circ C$; $a = 15.767(17)$, $b = 24.173(28)$, $c = 15.094(17)$ Å, $\alpha = 90.01(2)$, $\beta = 115.87(2)$, $\gamma = 91.02(3)^\circ$, $Z = 2$, $\rho_{calcd} = 1.21\ g\,cm^{-3}$, space group $P\bar{1}$. Final residuals are $R(F) = 0.075$ and $Rw(F) = 0.072$. During the refinement of the structure an area which contained numerous peaks of electron density 1.2 to 3.8 $e\,Å^{-3}$ well separated from the ions was observed. Attempts to identify this apparent solvent were unsuccessful and it was modeled by using 10 half weight carbon atoms. A disorder was present in one OR group of the cluster [O(65)–C(70)] as well, but this was easily modeled by using six half-weighted carbon atoms. Further details of the crystal structure investigation may be obtained from the Fachinformationszentrum Karlsruhe, D-76344 Eggenstein-Leopoldshafen (FRG), on quoting the depository number CSD-57854, the names of the authors, and the journal citation.

[5] M. H. Chisholm, *Polyhedron* **1983**, *2*, 681.

[6] M. H. Chisholm, D. L. Clark, R. J. Errington, K. Folting, J. C. Huffman, *Inorg. Chem.* **1988**, *27*, 2071.

[7] ^1H NMR (CD_2Cl_2, 22 °C, 500 MHz): $\delta = 4.56$ (d, $J = 11$ Hz, 4H), 4.33 (d, $J = 11$ Hz, 4H), 4.31 (s, 4H), 4.04 (s, 4H), 3.63 (s, 24H), 3.28 (s, 4H), 3.24 (s, 4H), 1.22 (s, 36H), 0.94 (s, 18H), 0.89 (s, 18H), 0.79 (s, 18H), 0.65 (s, 18H), −15.14 (s, 1H); ^{13}C NMR (CD_2Cl_2, 22 °C, 125 MHz): $\delta = 84.67$, 83.88, 81.76, 81.04, 79.11 (4:2:2:2:2 for -CH_2-), 70.54 (-OCH_2CH_2O-), 35.28, 34.79, 33.93, 33.34 (2:6:2:2 for -CMe_3), 28.90, 28.21, 28.14, 27.99, 27.49 (4:2:2:2:2 for -CH_3). IR (KBr disk or CH_2Cl_2 solution): $\tilde{\nu}$ [cm^{-1}] = 2946, 2903, 2861, 1477, 1455, 1387, 1353, 1285, 1250, 1214, 1110, 1070, 1049, 1017, 995, 965, 934, 838, 835, 753, 663, 623, 448. Correct C,H analysis.

[8] a) J. H. Davis, M. A. Beno, J. M. Williams, J. Zimmic, M. Tachikawa, E. L. Muetterties, *Proc. Natl. Acad. Sci.* **1981**, *78*, 668; b) E. M. Holt, K. H. Whitmire, D. F. Shriver, *J. Organomet. Chem.* **1981**, *213*, 125; c) J. S. Bradley, G. B. Ansell, M. E. Leonowicz, E. W. Hill, *J. Am. Chem. Soc.* **1981**, *103*, 4968.

[9] a) M. L. Blohm, W. L. Gladfelter, *Organometallics* **1985**, *4*, 45; b) D. E. Fjare, W. L. Gladfelter, *J. Am. Chem. Soc.* **1984**, *106*, 4799.

[10] a) C. K. Schauer, D. F. Shriver, *Angew. Chem.* **1987**, *99*, *Angew. Chem. Int. Ed. Engl.* **1987**, *26*, 255; b) C. K. Schauer, E. J. Voss, M. Sabat, D. F. Shriver, *J. Am. Chem. Soc. 1989*, **111**, 7662.

[11] The extended Hückel calculations were done by using the weighted H_{ij} formula (J. H. Ammeter, H.-B. Bürgi, J. C. Thibeault, R. Hoffmann, *J. Am. Chem. Soc.* **1978**, *100*, 3686). The hydrido ligand was positioned at the intersection of the two mirror planes 2 Å from the wingtip molybdenum atom (μ_4 site) or on the C_2 axis of the back-bone atoms, 2 Å away from these atoms. Atomic parameters were taken from the literature. Mo (R. H. Summerville, R. Hoffmann, *J. Am. Chem. Soc.* **1976**, *98*, 7240); Br (J. Hinze, H. H. Jaffé, *J. Chem. Phys.* **1963**, *67*, 1501); O and H (R. Hoffmann, *ibid.* **1963**, *63*, 1397).

$[Re_2I_2(CO)_6(Se_7)]$, a Coordination Compound of Elemental Selenium with a Transition Metal: a Solution- and Solid-State Study**

Alessia Bacchi, Walter Baratta, Fausto Calderazzo,* Fabio Marchetti, and Giancarlo Pelizzi

Dedicated to Professor Ernst Otto Fischer on the occasion of his 75th birthday

It has recently been found[1] that *cyclo*-octasulfur coordinates to a transition element; coordination compounds with elements in their polyatomic form are also known for dihydrogen[2] and diiodine.[3] Coordination of *cyclo*-octasulfur may be regarded as the primary stage prior to the irreversible oxidation to sulfides and metallacyclopolysulfides,[4] resulting from sulfur-sulfur bond cleavage. The first labile coordination compounds of S_8 ($[Re_2X_2(CO)_6(S_8)]$, X = Br, I) were isolated and suggested, on the basis of their chemical and spectroscopic properties,[1] to have a dinuclear structure with bridging halides and η^2-coordinated *cyclo*-octasulfur.

We now report the isolation and crystallographic characterization of $[Re_2I_2(CO)_6(Se_7)]$, which can be regarded as a coordination compound of Se_7, one of the known[5] cyclic compounds of elemental selenium. These new findings indirectly confirm the earlier structural assignment of the sulfur analogue, show that an oligonuclear cyclic form of elemental selenium can coordinate to a transition metal, and define the structural parameters of coordinated Se_7.

Treatment of a CS_2 solution of $[Re_2I_2(CO)_6(THF)_2]$[6] with elemental selenium[7] at room temperature [Eq. (a)] followed by THF removal by repeated evaporation of the volatiles in vacuo, yielded the brown crystalline diamagnetic coordination compound, which analyzed (C, H, Se) satisfactorily as $[Re_2I_2(CO)_6(Se_7)]$. In its IR spectrum, the compound has carbonyl

$$[Re_2I_2(CO)_6(THF)_2] + 7/n\,Se_n \rightleftharpoons [Re_2I_2(CO)_6(Se_7)] + 2\,THF \qquad (a)$$

stretching bands (CS_2 solution) at 2045, 2030, 1960, and 1934 cm^{-1}, in accord with a C_{2v} symmetry of the $Re_2(CO)_6$ core ($2A_1$, $2B_1$, B_2). The ^{13}C NMR spectrum of the compound in CS_2 at room temperature shows three resonances in 1:1:1 ratio at $\delta = 187$, 184, and 182, assigned to three pairs of nonequivalent carbonyl groups. Finally, the ^{77}Se NMR spectrum at room temperature in CS_2 solution (C_6D_6 lock) shows four resonances in 2:2:2:1 ratio at $\delta = 1150$, 1011, 973, and 927 (relative to $SeMe_2$ in $CDCl_3$[9]), suggesting the presence of four nonequivalent groups of selenium atoms in the molecule. In comparison, free Se_7 (in admixture with Se_6 and Se_8) is fluxional and shows a single resonance at $\delta = 998$ relative to neat $SeMe_2$.[10] The resonance at $\delta = 1150$ is assigned to the Re-bonded selenium

[*] Prof. Dr. F. Calderazzo, Dr. W. Baratta, Dr. F. Marchetti
Dipartimento di Chimica e Chimica Industriale, Sezione di Chimica Inorganica, Università di Pisa, Via Risorgimento 35, I-56126 Pisa (Italy)
Telefax: Int. code + (50)918-260
Dr. A. Bacchi, Prof. Dr. G. Pelizzi
Istituto di Chimica Generale ed Inorganica and
Centro di Studio CNR per la Strutturistica Diffrattometrica
Università di Parma (Italy)

[**] This work was supported by the Consiglio Nazionale delle Ricerche (CNR, Rome), Progetto Finalizzato Materiali Speciali per Tecnologie Avanzate and by the Ministero dell'Università e della Ricerca Scientifica e Tecnologica (MURST). We thank Prof. P. S. Pregosin, Laboratorium für Anorganische Chemie der E. T. H., Zürich, for providing NMR facilities and discussing the NMR spectra during the sabbatical of W. B.

atoms on the basis of their relaxation times. Thus, strong evidence for a dinuclear structure in solution with bridging iodides, a bidentate heptaselenium ligand, and two sets of three carbonyl groups in *fac* arrangement exists. However, only X-ray diffraction can unambiguously distinguish the two possibilities: a) a rhenium(I) complex of *cyclo*-heptaselenium, or b) a complex of rhenium(II) with a metal–metal bond and a bidentate heptaselenide ligand.

The X-ray structural analysis carried out on a single crystal of the heptane-solvated compound[11] has definitely established the former formulation. A perspective view of the molecule is shown in Figure 1. Each metal atom is in an almost octahedral

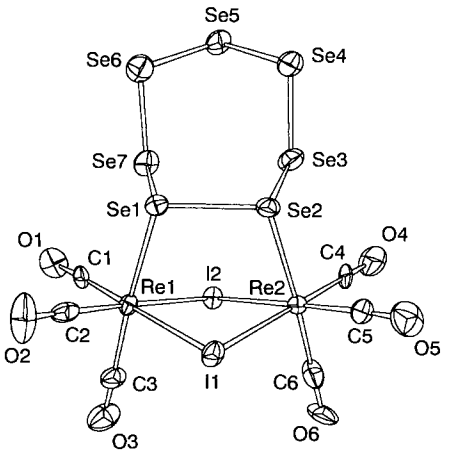


Fig. 1. ORTEP view (50% probability ellipsoids) of $[Re_2I_2(CO)_6(Se_7)]$. Ranges for bond distances in Å (number of bonds in parenthesis): Re–I(4), 2.820–2.826; Re-Se(2), 2.586–2.587; Re-C(6), 1.890–1.974; Se–Se(6), 2.309–2.346, Se1–Se2, 2.558(3). Ranges of selected bond angles [°], number of angles in parenthesis: Re-I-Re(2), 92.44–92.50; I-Re-I(2), 84.12–84.27; Re-C-O(6), 176–179; Se-Se-Se(7), 99.3–104.3.

environment coordinated to three terminal carbonyl groups, two bridging iodides, and one selenium atom of the *cyclo*-heptaselenium ligand. The Re···Re nonbonding distance is 4.077(3) Å, in agreement with the 3.90(4) Å distance in the rhenium(I) dimer $[Re_2Br_2(CO)_6(Se_2Ph_2)]$.[13] The angular distortions from ideal octahedral geometry are less than 6.5°. The Re–Se distance (average 2.586 Å) compares well with the Re–Se distance of 2.604(4) Å in the diphenyldiselenide complex.[13] The two coordination polyhedra share the two iodo ligands, and the apical selenium atoms are bonded at a distance of 2.558(3) Å. The rhenium-coordinated *cyclo*-heptaselenium ligand adopts a chairlike conformation defined by the planes Se1-Se2-Se3-Se7 (maximal deviation of atoms from best plane: $d_{max} = 0.036$ Å, plane 1), Se3-Se4-Se6-Se7 ($d_{max} = 0.016$ Å, plane 2), and Se4-Se5-Se6 (plane 3); the dihedral angles are 78.11(5)° between plane 1 and 2, and 74.90(9)° between plane 2 and 3. Plane 2 is almost parallel to the Re1-Re2-Se1-Se2 plane ($d_{max} = 0.07$ Å); the dihedral angle is 5.89(4)°. The molecular symmetry is close to C_s; the mirror plane contains the atoms Se5, I1, and I2.

To our knowledge, no examples of a discrete molecule of an allotropic modification of elemental selenium coordinated to a transition metal center have been established previously; on the other hand, selenium and tellurium complexes of d^{10} copper(I) and gold(I) halides are known,[14] which contain screw-type chalcogen ligands[15] or *cyclo*-Se_6 as ligand,[16] interconnected in the crystal lattice at bonding metal–chalcogen distances (e.g., Cu–Se bond distance 2.447(4) Å;[16a] average Cu–Se bond distance 2.460(2) Å[16b]). Copper selenide clusters stabilized by tertiary phosphanes are also known.[17] Although Se_7 does not appear to have been studied crystallographically as yet, the structural parameters of Se_7 interlayered with Se_6 in $(NEt_4^+)_2[Se_5^{2-} \cdot 1/2\ Se_6 \cdot Se_7]$ have been reported:[18] the Se_7 moiety adopts a chairlike conformation whose symmetry is approximately C_s and Se–Se bond distances range from 2.323(7) to 2.365(7) Å; the unique Se–Se bond bisected by the symmetry plane is significantly longer [2.409(7) Å]. Thus, coordination of Se_7 to a rhenium(I) center would correspond to a lengthening of the bond by only about 0.15 Å with respect to uncoordinated *cyclo*-heptaselenium. A theoretical study[19] of some selenium clusters has predicted that the chairlike conformation of Se_7 is the ground state of the molecule and that the unique Se–Se bond (2.48 Å) would be significantly longer than the others.

Experimental Procedure

IR spectra were recorded on a Perkin-Elmer FT-IR 1725 X, and NMR spectra on Bruker AC 250 and Varian Gemini 200 HVC instruments. Under a dinitrogen atmosphere the rhenium(I) complex $[Re_2I_2(CO)_6(THF)_2]$ (0.476 g, 0.507 mmol) was treated with sublimed [7] Se_n (0.345 g, 4.37 mmol for $n = 1$) in CS_2 (15 mL). The suspension was stirred in the dark for 21 h at room temperature; throughout this time, the volatiles were removed in vacuo. The dry residue was dissolved in fresh CS_2, and this operation repeated three times until the IR spectrum of the supernatant solution in the carbonyl stretching region showed that the starting metal carbonyl had disappeared. The final suspension was filtered, and the brown complex washed with heptane and dried *in vacuo* (44% yield). The *cyclo*-heptaselenium rhenium(I) complex is readily soluble in CS_2 (about 4% w/v) and stable in air if dry; by addition of THF to its CS_2 solution, a slow separation of α-Se_8 [8] was observed (Unit cell parameters: $a = 9.072$, $b = 9.097$, $c = 11.625$ Å, $\beta = 90.99°$).

Received: June 29, 1993 [Z 6175 IE]
German version: *Angew. Chem.* **1994**, *105*, 206

[1] W. Baratta, F. Calderazzo, *Organometallics* **1993**, *12*, 1489.
[2] G. J. Kubas, *Acc. Chem. Res.* **1988**, *21*, 120.
[3] J. A. M. van Beek, G. van Koten, G. P. C. M. Dekker, E. Wissing, M. C. Zoutberg, C. H. Stam, *J. Organomet. Chem.* **1990**, *394*, 659.
[4] a) L. Linford, H. G. Raubenheimer, *Adv. Organomet. Chem.* **1991**, *32*, 1; b) A. Müller, E. Diemann, *Adv. Inorg. Chem. Radiochem.* **1987**, *31*, 89; c) L. C. Roof, J. W. Kolis, *Chem. Rev.* **1993**, *93*, 1037.
[5] a) *Gmelin Handbuch der Anorganischen Chemie, Selen*, Ergänzungsband A 1, Springer, Berlin, **1979**; Ergänzungsband A 2, **1980**; b) R. Steudel, M. Papavassiliou, E.-M. Strauss, R. Laitinen, *Angew. Chem.* **1986**, *98*, 81; *Angew. Chem. Int. Ed. Engl.* **1986**, *25*, 99; c) R. Steudel in *Studies in Inorganic Chemistry, Vol. 14* (Ed.: R. Steudel), Wiley, New York, **1992**, p. 233.
[6] D. Vitali, F. Calderazzo, *Gazz. Chim. Ital.* **1972**, *102*, 587.
[7] Commercial gray selenium (20 g) was pyrolyzed in vacuo (about 10^{-2} Torr) at about 240 °C in a 1-L flask equipped with a central cold finger (cooled with liquid nitrogen). The red sublimed Se_n was scraped from the cold finger and kept at about −30 °C until it was used for the subsequent reaction with the rhenium(I) complex. A solution of the sublimed Se_n in CS_2 at room temperature slowly deposited monoclinic α-Se_8, as shown by comparison of the cell constants of the precipitate ($a = 9.068$, $b = 9.080$, $c = 11.572$ Å, $\beta = 90.75°$) with the literature data [8]. No or incomplete reaction was observed between the rhenium(I) carbonyl complex and gray elemental selenium. Commercial selenium carefully prewashed with carbon disulfide did not react.
[8] P. Cherin, P. Unger, *Acta Crystallogr. Sect. B* **1972**, *28*, 313.
[9] a) N. P. Luthra, J. D. Odom in *The Chemistry of Organic Selenium and Tellurium Compounds, Vol. 1* (Eds.: S. Patai, Z. Rappoport), Wiley, New York, **1986**; b) L. Christiaens, J. L. Piette, L. Laitem, M. Baiwir, J. Denoel, G. Llabres, *Org. Magn. Reson.* **1976**, *8*, 354.
[10] a) R. Steudel, M. Papavassiliou, W. Krampe, *Polyhedron* **1988**, *7*, 581; b) P. Pekonen, R. S. Laitinen, Y. Hiltunen, *J. Chem. Soc. Dalton Trans.* **1992**, 2885; c) R. Steudel, E.-M. Strauss, *Z. Naturforsch. B* **1981**, *36*, 1085.
[11] Data for the X-ray analysis of $[Re_2I_2(CO)_6(Se_7) \cdot 1/2\ C_7H_{16}]$: a solution of the compound in CS_2 yielded suitable single crystals after addition of heptane and slow evaporation of the volatiles; Philips PW 1100 diffractometer ($Mo_{K\alpha}$ radiation, $\lambda = 0.71073$ Å, graphite monochromator). Space group $P\bar{1}$, triclinic, $a = 10.468(6)$, $b = 10.823(10)$, $c = 11.699(7)$ Å, $\alpha = 105.66(6)$, $\beta = 95.85(6)$, $\gamma = 104.15(4)°$, $Z = 2$. Measured range $3° \le \theta \le 30°$, measured octants $\pm h$, $\pm k$, $+l$, $T = 293$ K, 7105 measured reflections. Structure solution with Patterson method [12a], structure refinement of F^2 (224 refined parameters against 7105 reflections) with SHELX92 [12b]; empirical absorption according to Walker and Stuart [12c] applied after the last isotropic refinement. Final R values: $R = 0.0573$ for 4422 observed reflections $|I \ge 2\sigma(I)|$ and 0.1172 for all

data; $wR_2 = 0.1795$ with $w = 1/|\sigma^2(F_o^2) + (0.1281\ P)|$, where $P = |\max(F_o^2, 0) + 2\ F_c^2|$; GOF = 0.955. Max./min. residual electron density 3.97/ −3.80 eÅ^{-3}. Half a heptane molecule per asymmetric unit is present, disordered about an inversion centre. Structural parameters were calculated with PARST [12d]. Extensive use was made of the Cambridge Structural Database System and of the Crystal Structure Information System (CRYSTIN, Universität Bonn). Calculations were performed on the ENCORE-GOULD-POWERNODE 6040 and ENCORE 91 computers of the Centro di Studio per la Strutturistica Diffrattometrica del CNR, Parma and on the IBM 3081 computer of CNUCE, Pisa. Further details of the crystal structure study may be obtained from the Fachinformationszentrum Karlsruhe, D-76344 Eggenstein-Leopoldshafen (FRG), on quoting the depository number CSD-57484, and journal citation.

[12] a) G. M. Sheldrick, *SHELX86, A Program for Structure Determination*, Universität Göttingen, **1986**; b) G. M. Sheldrick, *SHELX 92, A Program for Structure Refinement*, Universität Göttingen, **1992**; c) N. Walker, D. Stuart, *Acta Crystallogr. Sect. A* **1983**, *39*, 158; d) M. Nardelli, *Comput. Chem.* **1983**, *7*, 95.

[13] J. Korp, I. Bernal, J. L. Atwood, F. Calderazzo, D. Vitali, *J. Chem. Soc. Dalton Trans.* **1979**, 1492.

[14] Reviews: a) J. Fenner, A. Rabenau, G. Trageser, *Adv. Inorg. Chem. Radiochem.* **1980**, *23*, 329; b) M. J. Atherton, J. H. Holloway, *ibid.* **1979**, *22*, 171; c) A. Rabenau, H. Rau, *Inorg. Syn.* **1973**, *14*, 160; d) V. E. Fedorov, A. V. Mishchenko, V. P. Fedin, *Russian Chem. Rev. Engl. Transl.* **1985**, *54*, 408.

[15] a) J. Fenner, A. Rabenau, *Z. Anorg. Allg. Chem.* **1976**, *426*, 7; b) J. Fenner, *Acta Crystallogr. Sect. B* **1976**, *32*, 3084; c) W. Milius, A. Rabenau, *Z. Naturforsch. B.* **1988**, *43*, 243; d) P. M. Carkner, H. M. Händler, *J. Solid State Chem.* **1976**, *18*, 183.

[16] a) H. M. Händler, P. M. Carkner, *J. Solid State Chem.* **1979**, *29*, 35; b) W. Milius, A. Rabenau, *Mater. Res. Bull.* **1987**, *22*, 1493.

[17] a) D. Fenske, H. Krautscheid, S. Balter, *Angew. Chem.* **1990**, *102*, 799; *Angew. Chem. Int. Ed. Engl.* **1990**, *29*, 796; b) D. Fenske, H. Krautscheid, *ibid.* **1990**, *102*, 1513; and **1990**, *29*, 1452.

[18] J. Dietz, U. Müller, V. Müller, K. Dehnicke, *Z. Naturforsch. B* **1991**, *46*, 1293.

[19] D. Hohl, R. O. Jones, R. Car, M. Parrinello, *Chem. Phys. Lett.* **1987**, *139*, 540.

Spectroscopic and Reactivity Studies of a Copper-Containing Metallacrown**

Alexander J. Blake, Robert O. Gould, Craig M. Grant, Paul E. Y. Milne, David Reed, and Richard E. P. Winpenny*

Crown ethers were first discovered more than twenty years ago,[1] and since that time their utilization in all fields of chemistry has been extensive. More recently a related class of compounds, named metallacrowns, has begun to appear,[2] in which the carbon backbone of the macrocyclic ligand has been replaced by metal-containing entities. Recently we reported on the cation of **1**, a potentially new member of this small class of

$[Cu_6(MeL)_{12}Na][NO_3]$ **1**

compounds, a hexanuclear copper complex of 2-hydroxy-6-methylpyridine (MeLH),[3] in which a sodium cation was found at the center of a macrocyclic cavity created by a hexanuclear copper complex of MeL. Before claiming that **1** was a metallacrown, we felt that two criteria needed to be satisfied: firstly that the structure is retained in solution, and secondly that the sodium cation at the center of **1** could be replaced by another metal without gross alteration of the structure. Here we report spectroscopic studies of **1**, which indicate that the structure is largely retained in solution, and reactions of **1**, which show that the sodium can be replaced by copper or magnesium to open up further new chemistry.

Compound **1** is synthesized from the reaction of the potassium salt of MeLH and hydrated copper nitrate in the solid state, followed by crystallization from CH_2Cl/ether. X-ray structural analysis[13] (the structure of the cation is identical with that of **2** except that the central copper atom Cu1 is replaced by a sodium atom) led to the conclusion that a sodium cation was at the center of the cavity, despite the apparent absence of sodium from the reactants.[4] This is further confirmed by the mass spectrum, in which a peak is seen for $[Cu_6(MeL)_{12}Na]^+$. Interestingly, strong fragment peaks are seen for $[Cu_4(MeL)_8Na]^+$, $[Cu_3(MeL)_6Na]^+$, $[Cu_2(MeL)_4Na]^+$, $[Cu_2(MeL)_3Na]^+$, and $[Cu(MeL)_2Na]^+$; no strong peaks are seen which indicate ready loss of sodium from **1**.

^{1}H NMR spectroscopy suggests that the structure of **1** is largely retained in solution. Eight paramagnetically shifted resonances reflect the presence of two inequivalent ligand types in **1**. Six of the signals of relative intensity 1 are due to aromatic protons and are shifted to higher frequency than commonly observed. Two signals of relative intensity 3 are shifted to low frequency and are due to the methyl protons. The ^{23}Na NMR spectrum of **1** showed a single peak at $\delta = -165.2$ and with a line-width of several hundred Hz. The chemical shift range of ^{23}Na is normally quite narrow,[5] and therefore this shift is indicative of a strong influence from the paramagnetic coppers. Additionally, the linewidth is consistent with a quadrupolar sodium atom in a highly symmetrical site. Thus both ^{1}H and ^{23}Na NMR spectra are consistent with the crystal structure.

We have shown that reaction of **1** with solid lanthanum nitrate leads to a highly unusual La_8Cu_{12} metal complex.[3] We have investigated similar reactions with a series of other metal nitrate salts. Treatment of a dichloromethane solution of **1** with solid lead nitrate over a period of ten weeks at 3 °C caused the solution to darken. Unchanged lead nitrate was removed from the mixture, and very dark green crystals grown by addition of ether. X-ray structural analysis[6] shows that compound **2** has

$[Cu_6(MeL)_{12}Cu][Pb(NO_3)_4]$ **2**

formed (Fig. 1). The cation in **2** is almost identical to that in **1**, except that the Na atom in **1** has been replaced by a Cu atom.

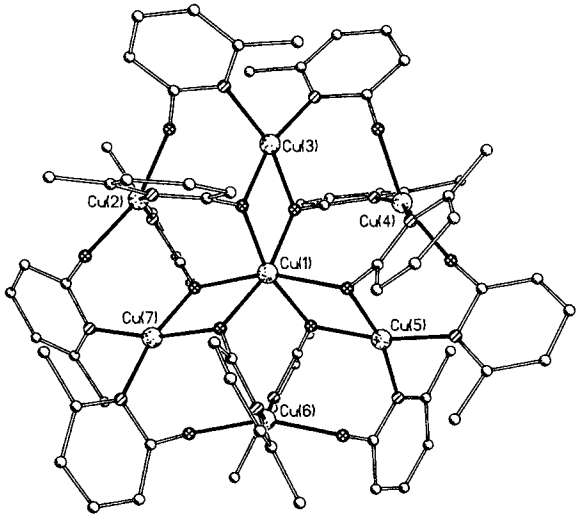


Fig. 1. The crystal structure of the heptametallic cation of **2**. Bond length ranges [Å] (average, standard deviations 0.014 Å): Cu–N 1.963–2.036, Cu1–O 1.994–2.210, other Cu–O distances 1.913–2.003.

[*] Dr. R. E. P. Winpenny, Dr. A. J. Blake, Dr. R. O. Gould, C. M. Grant, P. E. Y. Milne, Dr. D. Reed
Department of Chemistry
The University of Edinburgh
West Mains Road, GB-Edinburgh EH9 3JJ (UK)
Telefax Int. code + (031)650-4743

[**] This work was supported by the Science and Engineering Research Council.

 © VCH Verlagsgesellschaft mbH, D-69451 Weinheim, 1994 0570-0833/94/0202-0195 $ 10.00+.25/0

The metallacrown consists of six copper atoms in a six-pointed star array. Each is four coordinate, with a *trans* arrangement of 2 O and 2 N donors from MeL units for Cu2, Cu4 and Cu6, and a *cis* arrangement of the same donor set for Cu3, Cu5, and Cu7. The *cis* oxygens form the cavity in which the seventh copper atom is bound. The coordination geometry of this copper is distorted from an octahedron towards a trigonal prism. This distortion is caused by the small angle (about 74°) between each pair of oxygen atoms which bridge to the peripheral coppers, and its effect is to cause a rotation about a molecular threefold axis, so that the upper triangle of oxygens in the "trigonal prism" is twisted with respect to the lower triangle by 41° from its eclipsed position in an ideal trigonal prism rather than by the 60° required for an octahedron.

The anion of **2**—$[Pb(NO_3)_4]^{2-}$—is also, to our knowledge, new. $Sn(NO_3)_4$ has been reported[7] and contains Sn(IV) with a regular coordination geometry based on a dodecahedron. Here the anion contains Pb^{II}, and the coordination geometry is extremely irregular.

The mass spectrum of **2** shows a peak for the cation $[Cu_6(MeL)_{12}Cu]^+$ and similar structural fragments to those in the spectrum of **1**; that is, again it appears that the central metal atom is largely retained. Peaks are also seen at *m/z* greater than that of the cation, consistent with addition of fragments of the $[Pb(NO_3)_4]^{2-}$ anion. The ^1H NMR spectrum indicates that **2** is unstable in solution.[8]

To a large extent **1** did not react with solid magnesium nitrate. However, a very small number of lighter green crystals suitable for X-ray analysis[6] also formed. The crystallographic study revealed a new mixed-metal compound **3** (Fig. 2). The three cop-

$[Cu_3Mg(MeL)_6(NO_3)_2(MeLH)_2]$ **3**

per atoms in the structure retain much the same spatial arrangement as the corresponding unit in **1** and **2**; the structure resembles **1** or **2** but cut in half. The coordination geometry of magnesium is much nearer octahedral than that of the central atoms in **1** and **2**; only one angle [O3-Mg1-O3a = 72.05(11)°] differs dramatically from the expected value. As was the case in **2**, this acute angle is between two μ_2-oxygens, in this case bridging Cu1 and Mg1. The more regular geometry reflects a requirement of the metal, and perhaps explains why **3** is formed in such a low yield, and why the Mg atom is not at the center of a macrocycle: the geometrical preferences of Mg^{2+} and the conformational inflexibility of the metallacrown do not match, whereas for metal ions such as Na^+ and Cu^{2+}, which can support distorted coordination geometries, they do. Under these conditions **1** does not react with other s-block salts.

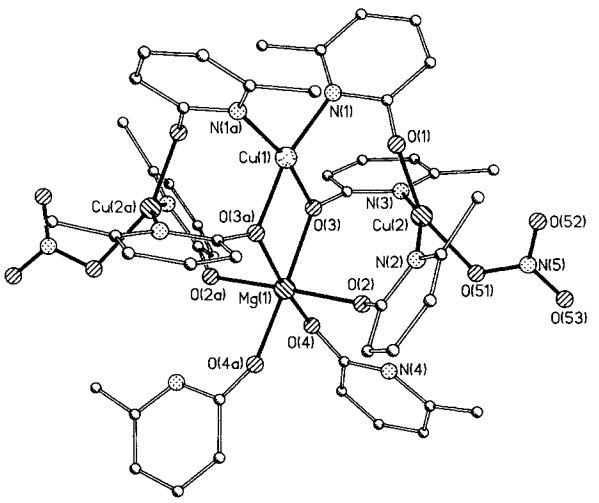


Fig. 2. The crystal structure of **3**. A crystallographic twofold axis passes through Cu1 and Mg1. Bond lengths [Å] (average standard deviations 0.03 Å): Cu1–N1 2.001, Cu1–O3 1.985, Cu2–O1 1.936, Cu2–N2 1.998, Cu2–N3 2.015, Cu2–O51 2.020, Mg1–O2 2.042, Mg1–O3 2.132, Mg1–O4 2.064. Bond angles [°] (average standard deviations 0.13°): N1-Cu1-N1A 95.75, N1-Cu1-O3 93.86, N1-Cu1-O3a 166.56, O3-Cu1-O3a 78.34, O1-Cu2-N2 91.72, O1-Cu2-N3 93.07, O1-Cu2-O51 157.41, N2-Cu2-N3 159.08, N2-Cu2-O51 90.35, N3-Cu2-O51 92.97, O2-Mg1-O2a 178.28, O2-Mg1-O3 87.77, O2-Mg1-O3a 93.62, O2-Mg1-O4 89.52, O2-Mg1-O4a 89.28, O3-Mg1-O3a 72.05, O3-Mg1-O4 89.28, O3-Mg1-O4a 89.52, O4-Mg1-O4a 89.52°.

Several aspects of the synthetic work remain to be explored. It is unclear how addition of $Pb(NO_3)_2$ to **1** leads to compound **2**. Obviously it is not merely replacement of Na^+ by Cu^{2+}, as the source of Cu must be other metallacrowns. This suggests that lead nitrate may disrupt the structure of **1** completely. Unfortunately in this case the paramagnetic nature of the compounds hinders extensive investigation of the reaction chemistry by NMR spectroscopy.

Experimental Procedure

1: Hydrated copper nitrate (6.9 mmol) and the potassium salt of MeLH (3.4 mmol) were intimately mixed. The green paste which resulted was extracted with dichloromethane (20 mL), and slow diffusion of ether vapor caused dark green cubic crystals to form. Yield (after one month): 19%. Use of NaMeL led to isolation of a light green powder, rather than to an increased yield of **1**. ^1H NMR for **1** (CD_2Cl_2): δ = 40.8, 40.4, 29.0, 22.0, 21.3, 18.3 (each a singlet of intensity 1); −6.9, −13.8 (each a singlet of intensity 3). Additional peaks due to free ligand and solvent were also observed. ^{23}Na NMR ($CDCl_3$): δ = −165.2 (s). FABMS: *m/z*: 1704, $[Cu_6(MeL)_{12}Na]^+$; 1141, $[Cu_4(MeL)_8Na]^+$; 862, $[Cu_3(MeL)_6Na]^+$; 581, $[Cu_2(MeL)_4Na]^+$; 473, $[Cu_2(MeL)_3Na]^+$; 302, $[Cu(MeL)_2Na]^+$; 131, $[(MeL)Na]^+$.

2: $Pb(NO_3)_2$ (2.8 mmol) was added to a solution of **1** (0.06 mmol) in CH_2Cl_2 (4 mL), and the reaction mixture stored at 3 °C. Over a period of ten weeks the solution changed from green to very dark green, and a yellow precipitate was noticed among the solid $Pb(NO_3)_2$. The solution was filtered through Celite, and an equal volume of ether was added to the filtrate. Long (4–7 mm) crystals of **2** formed in one day. Yield: 12% based on **1**. Slow diffusion of ether vapor leads to formation of a dark green oil rather than crystalline material. FABMS: *m/z*: 2133, $[\{Cu_6(MeL)_{12}Cu\}Pb(NO_3)_3]$; 2070, $[\{Cu_6(MeL)_{12}Cu\}Pb(NO_3)_2]^+$; 2007, $[\{Cu_6(MeL)_{12}Cu\}Pb(NO_3)]^+$; 1805, $[\{Cu_6(MeL)_{12}Cu\}(NO_3)]^+$; 1742, $[Cu_6(MeL)_{12}Cu]^+$; 1181, $[Cu_4(MeL)_8Cu]^+$; 1075, $[Cu_4(MeL)_7Cu]^+$; 1010, $[Cu_3(MeL)_7Cu]^+$; 900, $[Cu_3(MeL)_6Cu]^+$; 794, $[Cu_3(MeL)_5Cu]^+$.

3: $Mg(NO_3)_2 \cdot 6H_2O$ (2 mmol) was added to a solution of **1** (0.07 mmol) in CH_2Cl_2 (4 mL), and the reaction mixture stored at 3 °C. After eight weeks the reaction solution was filtered, and ether vapor allowed to diffuse into the green filtrate. In the main, dark green crystals of **1** were recovered, plus a very small number of light green crystals of **3**. Yield: 5%.

Received: July 26, 1993 [Z 6236 IE]
German version: *Angew. Chem.* **1994**, *106*, 208

[1] C. J. Pedersen, *J. Am. Chem. Soc.* **1967**, *89*, 2495; C. J. Pedersen, *ibid.* **1967**, *89*, 7017.

[2] M. S. Lah, V. L. Pecoraro, *J. Am. Chem. Soc.* **1989**, *111*, 7258; M. S. Lah, M. L. Kirk, W. Hatfield, V. L. Pecoraro, *J. Chem. Soc. Chem. Commun.* **1989**, 1606; M. S. Lah, V. L. Pecoraro, *Inorg. Chem.* **1991**, *30*, 878; M. S. Lah, B. R. Gibney, D. L. Tierney, J. E. Penner-Hahn, V. L. Pecoraro, *J. Am. Chem. Soc.* **1993**, *115*, 5857.

[3] A. J. Blake, R. O. Gould, P. E. Y. Milne, R. E. P. Winpenny, *J. Chem. Soc. Chem. Commun.* **1991**, 1453.

[4] Atomic absorption analysis of KMeL indicates that sodium is present as a significant impurity (about 2%), and this is consistent with the observed yield of **1** which is 19% (theoretical yield, based on one Na per twelve MeL, 24%).

[5] The ^{23}Na NMR shift range in typical solvents varies from δ = +5– −15: J. J. Dechter, *Prog. Inorg. Chem.* **1982**, *29*, 285.

[6] Crystal data for $C_{72}H_{72}Cu_7N_{16}O_{24}Pb$ (**2**): monoclinic, $P2_1/n$, a = 12.698(3), b = 23.800(9), c = 29.895(4) Å, β = 100.267(11)°, V = 8890 Å^3, M = 2197, Z = 4, ρ_{calc} = 1.642 g cm^{-3}, T = 150 K, $\mu(Mo_{K\alpha})$ = 3.62 mm^{-1}. Crystal data for $C_{48}H_{48}Cu_3MgN_{10}O_{14}$ (**3**): monoclinic, $C2/c$, a = 18.2394(12), b = 14.4374(8), c = 20.7395(12), β = 99.553(5), V = 5386 Å^3, M = 1204, Z = 4 (the molecule lies on a twofold rotation axis), ρ_{calc} = 1.485 g cm^{-3}, T = 293 K, $\mu(Mo_{K\alpha})$ = 1.26 mm^{-1}. Data were collected with a Stoë Stadi-4 diffractometer,

graphite monochromator, $Mo_{K\alpha}$ radiation, $\omega-2\theta$ scans and the learnt profile method, (W. Clegg, *Acta Crystallogr. Sect. A* **1981**, *37*, 22). Absorption corrections were applied using ψ scans. In the case of **2** the crystal was cooled by using an Oxford Cryosystems low temperature device (J. Cosier & A. M. Glazer, *J. Appl. Crystallogr.* **1986**, *19*, 105). Both structures were solved by heavy-atom methods, and all non-hydrogen atoms were refined anisotropically. The structure of **2** was refined on F^2 with SHELXL-92 (G. M. Sheldrick, SHELXL-92, gamma test version, University of Göttingen, **1993**) to give $wR2 = 0.2236$ for 8581 unique data ($2\theta \leq 45°$) [$R1 = 0.0895$ for 6036 observed reflections, $F_o > 4\,\sigma(F)$]. The structure of **3** was refined on F with SHELX-76 (G. M. Sheldrick, program for crystal structure refinement, University of Cambridge, **1976**) to give $R = 0.0369$ ($R_w = 0.0409$) for 2534 observed reflections [$2\theta \leq 45°$, $F_o > 4\,\sigma(F)$]. Further details of the crystal structure investigations are available on request from the Director of the Cambridge Crystallographic Data Centre, 12 Union Road, GB-Cambridge CB2 1EZ (UK) on quoting the full journal citation.

[7] C. D. Garner, P. Sutton, S. C. Wallwork, *J. Am. Chem. Soc.* **1967**, 1949.

[8] In CD_2Cl_2 intense peaks are seen for MeLH in addition to a large number of paramagnetically shifted peaks, eight of which are also seen for **1**. In $CDCl_3$ very intense peaks for MeLH are seen, plus the eight peaks for **1** which are very weak.

New Titanium–Boron Complexes with a Planar Tetracoordinate Carbon or a Planar Tricoordinate Phosphorus Center**

Paul Binger,* Frank Sandmeyer, Carl Krüger, Jörg Kuhnigk, Richard Goddard, and Gerhard Erker

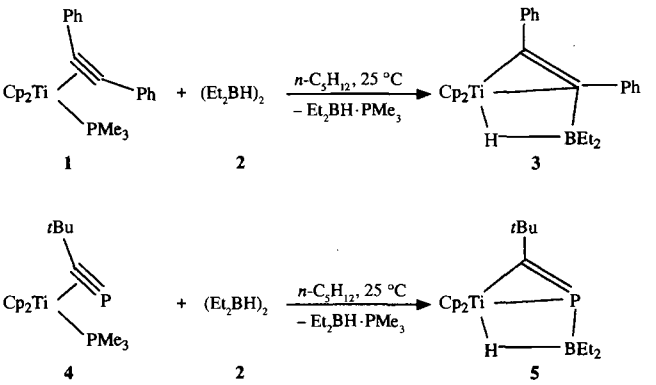
Dedicated to Professor Otto J. Scherer on the occasion of his 60th birthday

C–C double and C–C triple bonds as well as multiple bonds including heteroatoms are very rapidly hydroborated by alkyldiboranes at 0–20 °C.[1] Hydroboration also occurs in the reaction of (1-alkenyl) chlorozirconocenes with 9-borabicyclo[3.3.1]nonane (9-BBN).[2] However, nothing is known about the nature of the interaction between alkyldiboranes and alkenes or alkynes π-bonded to titanocene. In connection with the synthesis and reactivity of bimetallic complexes containing titanocene and zirconocene groups, we have now investigated the reaction of tetraethyldiborane (**2**) with diphenyl acetylene (tolane) coordinated η^2 to titanocene and the analogous reaction with *tert*-butylphosphaalkyne coordinated η^2 to titanocene.

In the reaction of the trimethylphosphane-stabilized titanocenes **1** and **4**, containing η^2-bonded tolane or phosphaalkyne ligands, respectively (see Scheme 1), with **2**, we observe no B–H addition to either the C–C or C–P triple bond. Instead a special class of dimetallabicyclopentenes is formed, the suitability of which for stabilizing unusual coordination geometries of carbon has previously been reported by Erker et al.[3] and theoretically studied by Gleiter et al.[4] Bimetallic systems, consisting of a main group element (Al, Ga) and a transition metal of the fourth subgroup (Zr, Hf), which contain a planar tetracoordinate carbon as central structural feature have recently aroused a great deal of interest.

Thus we have not only succeeded in transferring the simple synthetic method of G. Erker et al. to Ti/B complexes, but we have also been able to prepare and structurally characterize a representative of this class of compounds in which a phosphorus atom takes the position normally reserved for the planar tetracoordinate carbon atom.

The dinuclear complex **3** with a titanium and boron center is obtained in a spontaneous reaction in 94% yield from the tolane complex **1** and the equivalent amount of tetraethyldiborane (**2**) at room temperature as an orange powder (Scheme 1). Under identical conditions the dinuclear complex **5** is obtained from the phosphaalkyne complex **4** and **2** in 46% yield over 20 h (Scheme 1). The particularly remarkable feature of both reactions is that in the products **3** and **5** a Et_2BH fragment is found exclusively, even though the reagent **2** consists of an equilibrium mixture of several diboranes of the general composition $(Et_xBH_{3-x})(Et_yBH_{3-y})$ ($x = 1, 2$; $y = 1, 2$) and Et_3B.[5] A zirconium complex analogous to **3** was recently obtained from (η^2-tolane)(trimethylphosphane)zirconocene, 9-BBN, and triethylborane in about 12% yield.[6]



Scheme 1. Syntheses of the bimetallic complexes **3** and **5**.

The structures of **3** and **5** cannot be assigned unambiguously from spectroscopic data. The ^{13}C NMR shift of the planar tetracoordinate carbon atom in **3** ($\delta = 115$ ([D_8]THF, 25 °C, 75.5 MHz))[7] lies within the resonance range of aromatic carbon atoms and is not very characteristic. The NMR signal of the boron atom at $\delta = 25.2$ ([D_8]THF, 25 °C, 64.2 MHz) lies within the region for boranes with B–H bridges.[8] The X-ray structure investigations,[9] however, conclusively show the planar geometry of the five-membered skeleton in complex **3**, comprising Ti, the two olefinic C atoms, B, and H and thus confirm that **3** belongs to the class of "anti-van't Hoff/le Bel" compounds obtained by Erker et al.

The ^{31}P NMR signal of complex **5** at $\delta = 34.8$ is clearly shifted upfield in comparision to the corresponding signal of the starting material **4** ($\delta = 122.7$). The strong shielding of the phosphorus atom suggests that the lone pair of electrons on the phosphorus atom is not involved in the bonding. Thus, this type of coordination is clearly different from the known $\eta^2:\eta^1$ coordination of phosphaalkynes,[10] and from the η^1 coordination of phosphaalkenes,[11] which also may lead to planar-coordinated phosphorus. In these cases the ^{31}P NMR signals are at very low field in comparison to the signal of complex **5**. The NMR signal of the boron atom in **5** is found at $\delta = 35.6$. The boron atom is thus slightly more deshielded than in the analogous tolane complex **3**. This observation together with the high-field position of the ^{31}P NMR signal give the impression that in **5** boron serves as an electron donor to the phosphorus atom, which in turn may transfer electron density in the plane containing the σ bonds to titanium. Thus, the bonding would be clearly different from that

[*] Prof. Dr. P. Binger, Dipl.-Chem. F. Sandmeyer, Prof. Dr. C. Krüger, J. Kuhnigk, Dr. R. Goddard
Max-Planck-Institut für Kohlenforschung
Kaiser-Wilhelm-Platz 1, D-45470 Mülheim an der Ruhr (FRG)
Telefax: Int. code + (208)306-2980
Prof. Dr. G. Erker
Organisch-chemisches Institut der Universität
Corrensstrasse 40, D-48149 Münster (FRG)

[**] F. S. thanks the Fonds der Chemischen Industrie for a grant.

 © VCH Verlagsgesellschaft mbH, D-69451 Weinheim, 1994 0570-0833/94/0202-0197 $ 10.00+.25/0

calculated by Hoffmann et al.[12] for compounds with a planar tetracoordinate carbon atom, which could not function as a donor due to its electron deficiency. The results of electron density measurements as well as ab initio calculations should reveal the exact nature of the bonding.

The crystal structure analysis provides the conclusive evidence for the planar environment of the tricoordinate phosphorus atom in complex **5** (Fig. 1).[13] According to the structure

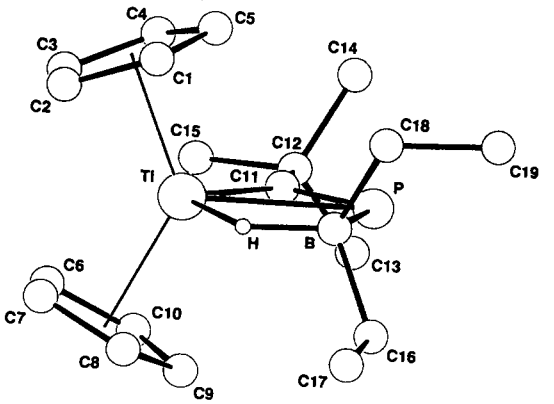
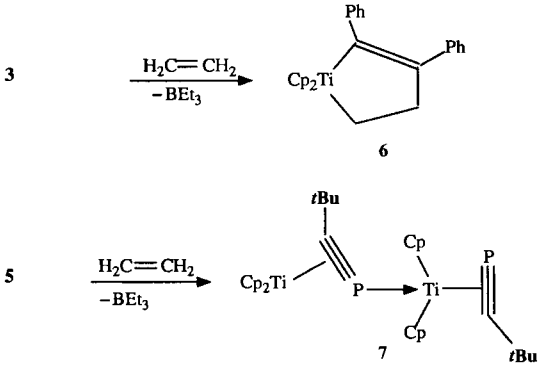


Fig. 1. Crystal structure of **5**. Selected distances [Å] and angles [°]: Ti–P 2.648(1), Ti–C11 2.099(2), Ti–H 1.81(3), P–C11 1.666(2), P–B 2.054(3), B–H 1.25(3); H-Ti-P 72.9(9), C11-Ti-P 39.0(1), B-P-Ti 64.6(1), C11-P-Ti 52.4(1), H-B-P 109(1), B-H-Ti 113(2).

analysis, the basic framework of complex **5** consists of a planar dimetallabicyclo[2.1.0]pentene unit which contains a Cp_2Ti and a Et_2B group as well as C11, P, and H as bridging ligand. The phosphaalkyne ligand is η^2 coordinated to the transition metal and η^1 coordinated to the boron atom. The phosphorus atom functions as a bridgehead atom; the three bonds emanating from it lie exactly in a plane. The bonds P–C11 (1.666(2) Å) and Ti–P (2.648(1) Å) are slightly longer than those in the starting material, whereas the Ti–C11 distance (2.099(2) Å) is clearly shorter,[10] so that this bond can be ascribed partial double bond character. The Ti-H-B unit has bond lengths similar to those found in tetrahydroborate–titanium complexes.[14] No bonding interaction is observed between the titanium atom and the boron atom (Ti–B 2.563(2) Å). Overall we have therefore proven that complex **5** has the same structural features as complex **3** and numerous known zirconium and hafnium complexes with planar tetracoordinate carbon.[3]



Scheme 2. Reactivity of the complexes **3** and **5** with ethylene.

In spite of their thermal stability, complexes **3** and **5** are highly reactive towards unsaturated substrates. Thus **3** reacts at room temperature with ethylene to form the titanacyclopentene **6** (as yet unreported), together with triethylborane (Scheme 2). Under the same conditions complex **5** disintergrates under the influence of ethylene into the components (η^2-*tert*-butylphosphaalkyne)titanocene and diethylborane; the latter reacts with ethylene to give triethylborane. The titanocene unit does not undergo oxidative coupling, instead it dimerizes to give the known dinuclear complex **7**.[10]

Experimental Procedure

3: To a suspension of **1** (1.49 g, 3.5 mmol) in pentane (55 mL) was pipetted **2** (0.85 mL, 7.0 mmol) at room temperature. The color changed to orange immediately. After 3 min the orange solid **3** was filtered off. The mother liquor was concentrated (50% volume) and cooled to −20 °C from which additional **3** was obtained (total yield 94%). IR (KBr): $\tilde{\nu}$[cm^{-1}] = 1685 (BH); ^{1}H NMR (200 MHz, [D$_8$]THF, 25 °C): δ = 7.07–6.54 (m, 10H; Ph), 5.92 (s, 10H; Cp), 1.14–0.84 (m, 10H; Et), −4.06 (broad, μ–H). Correct elemental analyses.

5: Complex **5** was prepared analogously to complex **3** from **4** (1.8 g, 5.2 mmol) and **2** (1.8 mL, 15.6 mmol) in pentane (35 mL). The mixture was stirred for 20 h at room temperature, filtered over Celite, and the mother liquor cooled to −20 °C. Compound **5** crystallized in form of orange-red platelets in 46% yield. IR (KBr): $\tilde{\nu}$[cm^{-1}] = 1700–2000 (BH, not unambiguously assignable); ^{1}H NMR (200 MHz, [D$_8$]THF, 25 °C): δ = 5.52 (s, 10H; Cp), 1.49 (s, 9H; *t*Bu), 1.15–0.83 (m, 10H; Et), the signal of the μ–H atom could not be found. Correct elemental analyses.

Received: July 27, 1993
Revised version: September 15, 1993 [Z 6238 IE]
German version: *Angew. Chem.* **1994**, *106*, 213

[1] a) H. C. Brown, *Hydroboration*, W. A. Benjamin, New York, **1962**; b) R. Köster, *Methoden Org. Chem. (Houben-Weyl) 4th ed. 1952–*, Vol. XIII/3a, **1982**, p. 51–89.
[2] F. W. Hartner, Jr., J. Schwartz, *J. Am. Chem. Soc.* **1981**, *103*, 4979.
[3] Review: G. Erker, *Comments Inorg. Chem.* **1992**, *13*, 111; *Nachr. Chem. Tech. Lab.* **1992**, *40*, 1099.
[4] a) R. Gleiter, I. Hyla-Kryspin, S. Niu, G. Erker, *Angew. Chem.* **1993**, *105*, 753; *Angew. Chem. Int. Ed. Engl.* **1993**, *32*, 754; b) Experimental electron density determination see: C. Krüger, S. Werner, *Transition Metal Carbyne Complexes* (Ed.: F. R. Kreissl) (*NATO ASI Ser. Ser. C* **1993**, *392*, 131).
[5] R. Köster, G. Griaznov, W. Larbig, P. Binger, *Justus Liebigs Ann. Chem.* **1964**, *672*, 1.
[6] G. Erker, M. Albrecht, C. Krüger, S. Werner, P. Binger, F. Langhauser, *Organometallics* **1992**, *11*, 3517.
[7] H.-O. Kalinowski, S. Berger, S. Braun, *^{13}C NMR-Spektroskopie*, Thieme, Stuttgart, **1984**.
[8] H. Nöth, B. Wrackmeyer, *NMR: Basic Princ. Prog.* **1978**, *14*.
[9] C. Krüger, F. Sandmeyer, unpublished results.
[10] P. Binger, B. Biedenbach, A. T. Herrmann, F. Langhauser, P. Betz, R. Goddard, C. Krüger, *Chem. Ber.* **1990**, *123*, 1617.
[11] a) A. M. Arif, A. H. Cowley, S. Quashie, *J. Chem. Soc. Chem. Commun.* **1985**, 428; b) D. Gudat, E. Niecke, A. M. Arif, A. H. Cowley, S. Quashie, *Organometallics* **1986**, *5*, 593; c) R. H. Neilson, R. J. Thoma, I. Vickovic, W. H. Watson, *ibid.* **1984**, *3*, 1132.
[12] R. Hoffmann, R. W. Alder, C. F. Wilcox, Jr., *J. Am. Chem. Soc.* **1970**, *92*, 4992.
[13] Data for the crystal structure analysis of **5**: Formula $C_{19}H_{30}BPTi$, M_r = 348.1, crystal dimensions: 0.07 × 0.42 × 0.53 mm, a = 7.809(1), b = 18.864(3), c = 12.696(2) Å, β = 96.72(1)°, V = 1857.5 Å^3, ρ_{calcd} = 1.24 gcm^{-3}, μ = 5.34 cm^{-1}, Z = 4, monoclinic, space group $P2_1/n$ (no. 14), Enraf-Nonius-CAD4 diffractometer, λ = 0.71069 Å, ω-2θ scan, 6052 measured reflections ($\pm h$, + k, + l), [sinθ/λ_{max}] 0.74 Å^{-1}, 5595 independent and 4486 observed reflections [$I > 2\sigma(I)$], 319 refined parameters, R = 0.052, R_w = 0.058, max. residual electron density 1.26 eÅ^{-3}, heavy-atom method, H atoms found and refined. Further details of the crystal structure investigation may be obtained from the Fachinformationszentrum Karlsruhe, D-76344 Eggenstein-Leopoldshafen (FRG) on quoting the depository number CSD-57904, the names of the authors, and the journal citation.
[14] a) K. N. Semenenko, E. B. Lobkovskii, A. I. Shumankov, *J. Struct. Chem. Engl. Transl.* **1976**, *17*, 912; b) J. A. Jensen, S. R. Wilson, A. J. Schultz, G. S. Girolami, *J. Am. Chem. Soc.* **1987**, *109*, 8094; c) K. M. Melmed, D. Coucouvanis, S. J. Lippard, *Inorg. Chem.* **1973**, *12*, 232; d) J. A. Jensen, G. S. Girolami, *J. Chem. Soc. Chem. Commun.* **1986**, 1160.

$[P_4(Cp^*Al)_6]$: A Compound with an Unusual P_4Al_6 Cage Structure**

Carsten Dohmeier, Hansgeorg Schnöckel,* Christian Robl, Uwe Schneider, and Reinhart Ahlrichs*

Recently we reported on the synthesis and characterization of pentamethylcyclopentadienylaluminum (Cp*Al, **1**), the first organometallic compound with monovalent aluminum.[1] These results were followed by a great number of investigations concerning the properties and the reaction behavior of the compound. Of particular interest was the association behavior of **1** in solution. It could be demonstrated that tetrameric **1** is in equilibrium with monomeric Cp*Al in solvents such as toluene [(Eq. (a)].[2]

$$[(Cp^*Al)_4] \rightleftharpoons 4\,Cp^*Al \qquad (a)$$

The compound $[(Cp^*Al)_4]$ in solution is thus a "continuous" source for a carbene analogous alanediyl.

At first we investigated the oxidation of **1** ($Al^I \rightarrow Al^{III}$) with white phosphorus [Eq. (b)], since the compounds between the heavy elements of the third and fifth main group are of current interest with regard to both bonding theory (e.g. in multiple bonding or cage systems[3]) and industrial applications (semiconductor precursors[4]). If **1** is allowed to react with P_4, cleavage of the P_4 tetrahedron into four P building blocks leads to the formation of $[P_4(Cp^*Al)_6]$ (**2**) in high yield according to Equation (b).[5] Compound **2** forms bright yellow air- and moisture-

$$1.5\,\underset{\mathbf{1}}{[(Cp^*Al)_4]} + P_4 \xrightarrow{\text{toluene/25 °C}} \underset{\mathbf{2}}{[P_4(Cp^*Al)_6]} \qquad (b)$$

sensitive rhombuses, which are almost insoluble in all common solvents. Thus, no indication of the structure of the species present in solution can be obtained by NMR spectroscopic methods. In contrast, the molecular structure of solid **2** (Figs. 1 and 2) is obtained by a crystal structure analysis.[6] This shows

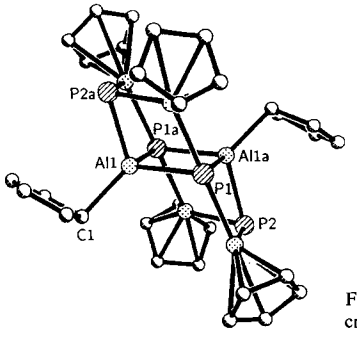


Fig. 1. Molecular structure of **2** in the crystal (methyl groups are not shown).

[*] Prof. Dr. H. Schnöckel, Dipl.-Chem. C. Dohmeier
Institut für Anorganische Chemie der Universität
Kaiserstrasse 12, D-76128 Karlsruhe (FRG)
Telefax: Int. code + (721)608-4854
Prof. Dr. R. Ahlrichs, Dipl.-Chem. U. Schneider
Institut für Physikalische Chemie der Universität
Kaiserstrasse 12, D-76128 Karlsruhe (FRG)
Priv. Doz. Dr. C. Robl
Institut für Anorganische Chemie der Universität
Meiserstrasse 1, D-80333 München (FRG)

[**] This work was supported by the Deutsche Forschungsgemeinschaft and the Fonds der Chemischen Industrie. We thank Prof. Dr. A. Schmidpeter for helpful discussions.

that centrosymmetric molecules occur, in which five edge-sharing Al_2P_2 rings form a P_4Al_6 framework alternatingly occupied with aluminum and phosphorus (Fig. 2). It can be described by two face-sharing, distorted Al_4P_4 cubes which lack two P atoms at diametral corners.[7]

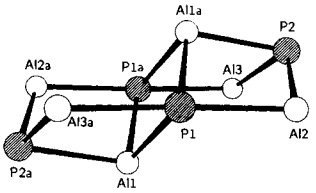


Fig. 2. P_4Al_6 framework of crystalline **2**.

The Al–P bond lengths are—depending on the coordination number of the participating atoms—between 231 pm (e.g. P2–Al2) and 242 pm (e.g. P1–Al1) (see Table 1). Thus, they vary

Table 1. Selected distances and angles in crystalline $[P_4(Cp^*Al)_6]$ (**2**), calculated molecular parameters of $[P_4(CpAl)_6]$ (**3**) (numbering corresponds to that in **2**, Fig. 2), and shared electron numbers (SEN) [12].

	2 Distance [pm]	**3** Distance [pm]	SEN
P1-Al1	242.2(2)	245.5	1.14
P1-Al2	239.4(1)	236.3	1.23
P1-Al3a	240.1(1)	236.3	1.23
P2-Al2	231.2(2)	230.9	1.41
P2-Al1a	236.0(1)	240.4	1.20
P2-Al3	230.8(2)	230.9	1.41
Al1-Al1a	310.0	319.1	0.34
Al1-Al3a	301.6	305.5	0.33
Al1···Al2	385.6	371.6	0.16
P1···P1a	371.6	373.1	–
P1···P2	364.1	365.0	–
	Angle [°]	Angle [°]	
Al3a-P1-Al2	174.3(1)	179.5	
Al1a-P1-Al1	79.7(1)	81.1	
Al1-P1-Al3a	77.4(1)	78.7	
P1-Al1-P1a	100.3(1)	98.9	
P1-Al1-P2a	99.2(1)	97.4	
P1a-Al1-P2a	99.3(1)	97.4	
P2a-Al1-C1	116.8(1)	123.5	
P1-Al2-P2	101.3(1)	102.8	
Al2-P2-Al1a	80.5(1)	80.8	
Al2-P2-Al3	117.6(1)	107.0	

about the value of 235 pm in the crystalline AlP (zinc blend structure). Depending on whether the aluminum atoms have two or three phosphorus neighbors, the Cp* groups are linked η^5 and η^1, respectively. As expected, the π-like backbonds from the Cp* ligands to aluminum are in competition with the formation of additional Al–P bonds. The σ-Al–C bond is relatively long (205.7 pm). The distance between aluminum and the π-bound C atoms (mean 227.6 pm) lies between the distances found in $[(Cp^*AlCl_2)_2]$ (ca. 222 pm)[8] and $[(Cp^*Al)_4]$ (**1**) (233.4 pm). Also of interest are the "nonbonding" Al–Al distances in **2**: five short (4×302 pm, 1×310 pm) and four long Al–Al contacts (4×386 pm), bonding interactions can be assumed for the former (see below) (d_{Al-Al} in the metal: 286 pm). In contrast, the P–P distances in **2** (364–372 pm) are found which lie in the range of van der Waals distances.

 © VCH Verlagsgesellschaft mbH, D-69451 Weinheim, 1994 0570-0833/94/0202-0199 $ 10.00+.25/0

In order to get a deeper understanding of the unexpected bonding in **2** we carried out quantum chemical calculations on the model compound $[P_4(CpAl)_6]$ (symmetry C_{2h}) **3**.[9] The calculated Al–P distances in the P_4Al_6 cage of **3** is also shown in Table 1. The discrepancy between the latter and the values determined from experiments with **2** is always less than 2%.

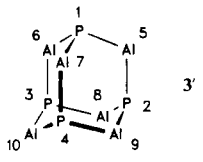
There are 32 electrons available for the bonds in the P_4Al_6 framework: two from each Cp*Al unit, five per P atom. These 16 electron pairs result in one pair of electrons for each of the 14 Al–P bonds of the framework in addition to the lone pair of electrons at the tricoordinate P atoms. If covalent bonds are assumed, the two tetracoordinate P atoms (P1/P1a) would formally carry a single positive charge and the two Al atoms Al1 and Al1a would carry a single negative charge. This would require a perfect $3s$-$3p_y$ hybridization at the P atoms (y = P1–Al2 direction), which is unusual for phosphorus (promotion energy $3s \rightarrow 3p$: 8 eV).

This model contradicts chemical intuition and is not confirmed by the analysis of the wave function. The Mulliken atomic charges[10] (P1/P1a: −1.09, P2/P2a: −0.68, Al1/Al1a: + 0.90, Al2/Al3/Al2a/Al3a: + 0.98) and the high occupation of the $3s$ orbitals on P1/P1a (1.81e) as well as on P2/P2a (1.83e) can be explained as follows: Each P atom carries a lone pair of electrons, which has predominantly s character and is only weakly delocalized in the cage.[11] Thus, **3** is an electron-deficient compound, in which 12 occupied MOs describe 14 bonds. This is also consistent with the shared electron numbers (SEN)[12] (Table 1) and thus with the significant bond contributions for the "nonbonding" Al–Al contacts.

In order to understand the bonding in **2** we investigated the adamantane-analogous isomer **3'** (Table 2) with quantum mechanical methods for comparison. The geometric parameters and the SENs are given in Table 2. Depending on the method of calculation **3** is more stable by 30 to 80 kJ mol^{-1} than **3'**.[13]

Table 2. Calculated molecular parameters of **3'** (symmetry C_{3v}).

	Distance [pm]	SEN
P1-Al5	234.7	1.39
P2-Al5	231.0	1.47
P2-Al9	237.4	1.27
Al5···Al9	361.2	0.16
Al5···Al6	353.1	0.23
Al8···Al9	378.3	0.10
P1···P3	418.7	–
P4···P3	411.3	–



3'

Apparently, the lacking or very weak Al–Al interactions in **3'** lead to the calculated destabilization in comparison to **3**. However, the difference in energy is not very large and thus a thermal rearrangement of **2** into **2'** (adamantane-analogous isomer of **2**) can be expected.[14] In this context the thermochromic properties of **2**, whose interpretation is the subject of current investigations, are of interest.

Experimental Procedure

In order to record the Raman spectrum (Bruker-FRA-106 (Nd:YAG laser 1.06 μ)) solid **2** was sealed in an evacuated tube. The KBr disk for the IR spectrum (Nicolet 520-FT-IR) was prepared in a glove box.

2: **1** (0.43 mmol, 70 mg) was dissolved in toluene (22 mL). The pale yellow solution was then slowly layered with a solution of freshly sublimed P_4 (0.39 mmol) in toluene (4 mL) at room temperature. The reaction mixture turned intense yellow within an hour. After approximately 4 d, bright yellow crystals of **2** (68 mg, 87%) were isolated. These crystals were air- and moisture-sensitive and showed thermochromic behavior (yellow↔orange) above 115 °C and sublimed at 290 °C (decomp). FT-Raman spectrum: [cm^{-1} (rel. int.)]: 2915(10), 2855(4), 2724(1), 1600(0.50), 1533(1.5), 1456(1.5), 1426(2), 1384(2), 1038(0.5), 800(1), 679(1.5), 596(3), 557(1), 502(1), 462(0.5), 431(1.5), 383(1.5), 358(2), 348(1.5), 287(1), 241(1.5), 173(2), 141(4), 113(4). – FT-IR (KBr) [cm^{-1} (rel. int.)]: 2967(5), 2916(10), 2872(7), 2850(8), 2726(1), 1661(0.5), 1596(1), 1495(2), 1442(7), 1430(6), 1375(9), 1273(4), 1143(1), 1034(3), 940(2), 850(2), 797(3), 728(1), 657(4), 623(1), 591(3), 562(1), 489(7), 455(7), 437(9), 368(5), 318(3).

Received: 30 July, 1993 [Z 6245 IE]
German version: *Angew. Chem.* **1994**, *106*, 225

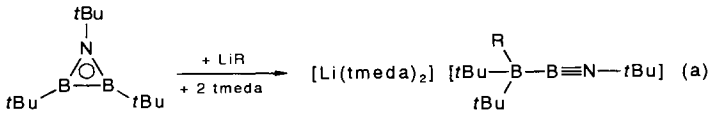
[1] C. Dohmeier, C. Robl, M. Tacke, H. Schnöckel, *Angew. Chem.* **1991**, *103*, 594; *Angew. Chem. Int. Ed. Engl.* **1991**, *30*, 564.
[2] J. Gauss, U. Schneider, R. Ahlrichs, C. Dohmeier, H. Schnöckel, *J. Am. Chem. Soc.* **1993**, *115*, 2402.
[3] See for example M. A. Petrie, P. P. Power, *Inorg. Chem.* **1993**, *32*, 1309, and references therein.
[4] See for example A. H. Cowley, R. A. Jones, *Angew. Chem.* **1989**, *101*, 1235; *Angew. Chem. Int. Ed. Engl.* **1989**, *28*, 1208.
[5] Even with great variation of the mole ratio of **1** and P_4, no other products were detected in addition to **2**.
[6] X-ray structure analysis of **2**, $C_{60}H_{90}Al_6P_4$, triclinic, space group $P\bar{1}$, $a = 1120.74(13)$, $b = 1290.80(16)$, $c = 1350.99(15)$ pm, $\alpha = 99.345(9)$, $\beta = 112.699(9)$, $\gamma = 111.496(9)°$, $V = 1569.0(3) \times 10^6$ pm^3, $Z = 2$, $\rho_{calcd} = 1.161$ g cm^{-3}, $F(000) = 588$, $\mu = 2.34$ cm^{-1} ($Mo_{K\alpha}$), 295 K, ($\omega/2\theta$) scan, $\theta_{max} = 25°$, scan speed 2.93–14.65 degree min^{-1}, scan width 1.1°, Siemens R3m/V diffractometer, graphite monochromator, 5981 reflections measured, of which 5554 symmetry independent, $R_{int} = 0.00850$; 4711 reflections with $|F| > 3\sigma_{|F|}$ regarded as observed. Calculations with SHELXTL-Plus, 303 parameters, H atoms geometrically positioned, non-hydrogen atoms refined anisotropically, numerical absorption correction; $R = 0.0816$, $R_w = 0.0715$, $R_g = 0.0572$, $w = \sigma_{|F|}^{-2}$. Limits of the final difference Fourier synthesis + 0.88/ −0.65e × 10^{-6} pm^3. Further details of the crystal structure investigation may be obtained from the Fachinformationszentrum Karlsruhe, D-76344 Eggenstein-Leopoldshafen (FRG) on quoting the depository number CSD-57696, the names of the authors, and the journal citation.
[7] An analogous linkage is observed, for example, in the double zwitterionic compound $(CH_3N)_6P_4F_8$; M. Kubjacek, K. Utvary, *Monatsh. Chem.* **1981**, *112*, 1353.
[8] H.-J. Koch, S. Schulz, H. W. Roesky, M. Noltemeyer, H.-G. Schmidt, A. Heine, R. Herbst-Irmer, D. Stalke, G. M. Sheldrick, *Chem. Ber.* **1992**, *125*, 1107.
[9] All calculations were carried out with the TURBOMOLE program (R. Ahlrichs, M. Bär, M. Häser, H. Horn, C. Kölmel, *Chem. Phys. Lett.* **1989**, *162*, 165) on IBM RISC 6000 workstations. The structure of **3** was obtained by geometry optimization at the SCF level with fully optimized basis sets for the atoms (Al, P, C: SVP; H: DZ) (A. Schäfer, H. Horn, R. Ahlrichs, *J. Chem. Phys.* **1992**, *97*, 2571).
[10] R. Mulliken, *J. Chem. Phys.* **1955**, *23*, 1833.
[11] The distorted trigonal-bipyramidal coordination at P1 and P1a here corresponds to the geometry, which is to be expected according to the VSEPR model for a PR_4^- anion (for example K. B. Dillon, A. W. G. Platt, A. Schmidpeter, F. Zwaschka, W. S. Sheldrick, *Z. Anorg. Allg. Chem.* **1982**, *488*, 7).
[12] Shared electron numbers are a measure for the covalent bond order; see for example C. Ehrhardt, R. Ahlrichs, *Theor. Chim. Acta* **1976**, *42*, 33, and references therein.
[13] The SCF method affords a stabilization of **3** by about 106 kJ mol^{-1}. This value is probably too large, since **3'** could only be optimized in C_{3v} symmetry and lowering the symmetry can lead to a stabilization of **3'**. Therefore the two corresponding isomers of $[P_4(AlCl)_6]$ (**4** and **4'**) (C_{2h} and T_d, respectively) were investigated. The SCF method affords only a stabilization of 36 kJ mol^{-1} for **4** in comparison to **4'**. In order to estimate the influence of the electron correlation on the stability additional MP2 calculations on these model examples were carried out. Here the closer packing of the C_{2h} structure leads to a greater influence of the electron correlation and thus to an additional preference of **4** by 44 kJ mol^{-1}.
[14] The thermal conversion of two P_4X_6 isomers has been reported for $[P_4(NiC_3H_7)_6]$; O. J. Scherer, K. Andres, C. Krüger, Y.-H. Tsay, G. Wolmershäuser, *Angew. Chem.* **1980**, *92*, 563; *Angew. Chem. Int. Ed. Engl.* **1980**, *19*, 571.

 © VCH Verlagsgesellschaft mbH, D-69451 Weinheim, 1994 0570-0833/94/0202-0200 $ 10.00+.25/0

(Iminoboryl)borates $[(t\mathrm{BuN}{\equiv}\mathrm{B})\mathrm{B}t\mathrm{Bu}_2\mathrm{R}]^-$ from the Azadiboriridine $\mathrm{NB}_2t\mathrm{Bu}_3$ (R = Me, Bu)

Ellen Eversheim, Ulli Englert, Roland Boese, and Peter Paetzold*

The azadiboriridine $\mathrm{NB}_2t\mathrm{Bu}_3$ (**1a**) reacts with CO[1] and BH_3[2] at the B–B bond to give unexpected products. We have now treated **1a** with the alkyllithium compounds LiMe and LiBu in the presence of *N,N,N',N'*-tetramethylethylenediamine (tmeda) and observed a B–N ring opening and the migration of one of the *t*Bu groups [Eq. (a)].



(a)

1a

2a, R = Me
2b, R = Bu

In accord with the proposed structure of the colorless, solid products **2a, b**, the ^{11}B NMR signal of **1a** ($\delta = 51.9$) is replaced by two significantly upfield-shifted signals at $\delta = 17.7, -15.9$ (**2a**) and $\delta = 16.3, -13.4$ (**2b**), whereas the two B–*t*Bu groups of each of the products remain equivalent in the ^{1}H and ^{13}C NMR spectra. The crystal structure analysis of **2b** (Fig. 1)[3] shows that in the anion a two- and a four-coordinated boron atom are bonded to each other with an interatomic distance in the range expected for B–B single bonds (1.725 Å). The length

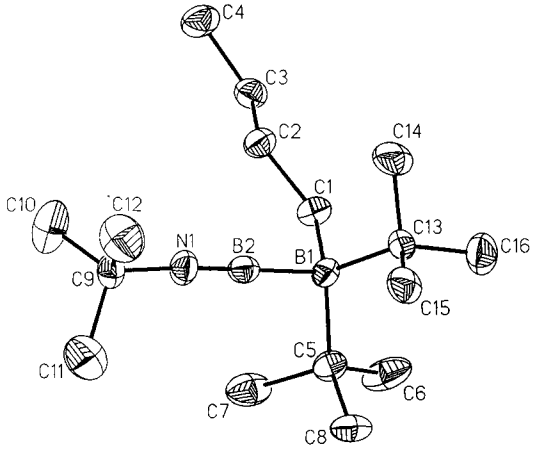


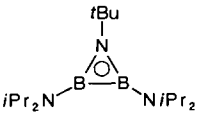
Fig. 1. Crystal structure of the anion of **2b**. Selected bond distances [Å] and angles [°]: B1-B2 1.725(5), B2-N1 1.250(5), N1-C5 1.473(4), B1-C1 1.679(5), B1-C5 1.710(5), B1-C13 1.707(5); B1-B2-N1 178.7(3), B2-N1-C9 174.7(3), C1-B1-B2 108.5(3), C5-B1-B2 107.7(3), C13-B1-B2 116.2(3).

of the B–N bond in the anion (1.250 Å) is typical for the B–N triple bond of iminoboranes.[4] Accordingly the B1-B2-N1-C9 chain deviates only slightly from linearity.

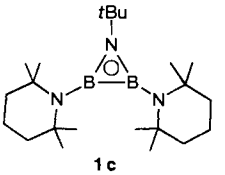
[*] Prof. Dr. P. Paetzold, E. Eversheim, Dr. U. Englert
Institut für Anorganische Chemie der Technischen Hochschule
Templergraben 55, D-52056 Aachen (FRG)
Telefax: Int. code + (241)8888-288
Priv.-Doz. Dr. R. Boese
Institut für Anorganische Chemie
der Universität-Gesamthochschule Essen (FRG)

The anions **2** are isoelectronic with alkynyl borates of the type $[\mathrm{R_3BC}{\equiv}\mathrm{CR}]^-$. However, they can also be considered adducts of the Lewis acids $\mathrm{BR}t\mathrm{Bu}_2$ with the anion $\mathrm{B}{\equiv}\mathrm{N}t\mathrm{Bu}^-$, which is isoelectronic with *tert*-butyl isocyanide $\mathrm{C}{\equiv}\mathrm{N}t\mathrm{Bu}$. We presume that $\mathrm{BN}t\mathrm{Bu}^-$ is both a strong σ donor and a π acceptor as a result of the lone pair at the boron atom and the nitrilium group, respectively, and is therefore expected to act as a strongly bound ligand in transition metal complexes. Our attempts to trap the presumably reactive anion with unsaturated complexes after separation of the $\mathrm{BR}t\mathrm{Bu}_2$ moiety by means of bases such as pyridine have been unsuccessful.

We had not expected the ring opening according to Equation (a), because atom B1 is sterically overcrowded. The crystal structure of the ring compound **1a**, from which we wanted to deduce its unexpected reactions,[1, 2] could not be determined because of disorder.[5] The azadiboriridine compounds **1b** and **1c** with B-bound amino groups, the structures of which are known,[6, 7] do not react as unexpectedly as **1a** because of their different electronic properties. Therefore, we tried to synthesize

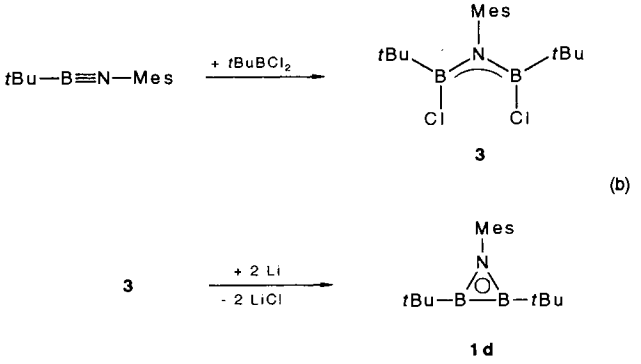


1b

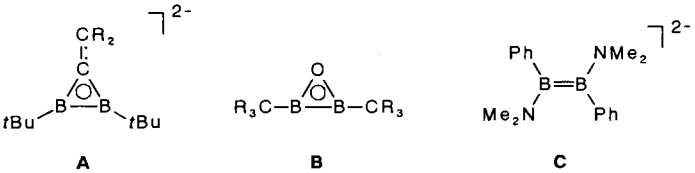


1c

a azadiboriridine with sterically demanding organic ligands which, like **1a**, would not rapidly dimerize to *nido*-diazahexaborane,[8] but in contrast to **1a** should crystallize without disorder. This was achieved by chloroboration of the known iminoborane $t\mathrm{BuB}{\equiv}\mathrm{NMes}$[9] (Mes = 2,4,6-$\mathrm{Me_3C_6H_2}$) to form compound **3** and subsequent ring closure to give **1d** in a hetero-Wurtz synthesis, as shown in Equation (b).



The crystal structure analysis (Fig. 2)[10] shows that the B–B distance of 1.558 Å in **1d** represents a particularly short B–B bond, which is comparable with the quite short bonds in the similar compounds **A** (1.58 Å),[11] **B** (1.60 Å)[12] (R = $\mathrm{SiMe_3}$),



A **B** **C**

 © VCH Verlagsgesellschaft mbH, D-69451 Weinheim, 1994 0570-0833/94/0202-0201 $ 10.00+.25/0

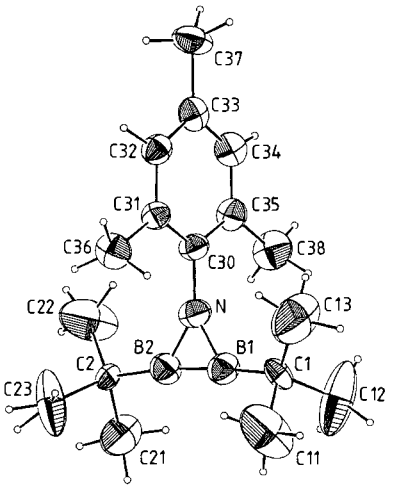


Fig. 2. Crystal structure of **1d**. Selected bond distances [Å] and angles [°]: B1-B2 1.558(9), B1-N 1.373(6), B2-N 1.356(6), B1-C1 1.483(7), B2-C2 1.482(7), N-C30 1.398(5); B1-N-B2 69.6(4), N-B1-B2 54.7(3), N-B2-B1 55.7(3), C1-B1-B2 176.0(4), C2-B2-B1 172.3(5).

and **C** (1.631 Å)[13] or in both the 2,3-diaminoazadiboriridines **1b** (1.604 Å)[6] and **1c** (1.610 Å)[7]. The B–N bonds (1.373 and 1.356 Å) and the B–C bonds (1.483 and 1.482 Å) are also rather short. All these distances in **1d** are reminiscent of corresponding structural parameters in the isoelectronic tri-*tert*-butylcyclopropenyl cation $C_3tBu_3^+$, with its short ring C–C distance of 1.372 Å and the short C–C distances of 1.485 and 1.489 Å between the ring and the *t*Bu groups.[14] The C1-B1-B2-C2 chain in molecule **1d** is essentially linear, with angles of 176.0 and 172.3°, respectively, at B1 and B2. This and the short B–B distance may be compared with similar structural features of the oxadiborirane **B**. Ab initio calculations on three-membered ring systems composed of BH, BH, and Y show an increasing shortening of the B–B bond and an increasing linearization of the HB–BH chain in the series Y = BH, CH_2, NH, O. This was rationalized in terms of the σ-bridged π-bonding model.[15] In the hypothetical parent compound H_2B-BH_2 the B–B single-bond length is calculated to be 1.71 Å, and the double bond in HB=BH to be 1.51 Å.[16] Thus the B–B distance in **1d** suggests strong double-bond character.

Preliminary experiments in NMR tubes have shown that **1d** reacts with CO, BH_3, and LiR analogously to **1a**. Apparently the structure of **1a** is closely related to that of **1d**. We are currently trying to elucidate the relationship between the unique reactivity of the triorganoazaboriridines and their structure.

Experimental

2a: A solution of methyllithium in diethyl ether (3.20 mL, 1.6 M) was added dropwise to a solution of **1a** (1.07 g, 5.17 mmol) and tmeda (1.6 mL) in THF (10 mL) at −78 °C. The mixture was stirred for 30 minutes at room temperature, volatiles were removed in vacuo (25 °C/1 Torr), and the residue was taken up in ether. At −30 °C, 2.03 g (84%) of **2a** crystallized.

NMR spectra in [D_8]THF at 25 °C; ^{1}H NMR (499.843 MHz, TMS): $\delta = -0.59$ (q, ^2J(HB) = 3.3 Hz; BMe), 0.75 (q, ^3J(HB) = 2.8 Hz; B*t*Bu$_2$), 1.13 (s; N*t*Bu), 2.14 (s; 4 NMe_2), 2.29 (s; 4 NCH_2); ^{11}B NMR (150.364 MHz, $Et_2O \cdot BF_3$): $\delta = -15.9, 17.7$ (2s, 1:1); ^{13}C NMR (125.697 MHz, TMS): $\delta = 31.1$ (q; BMe), 34.8, 36.1 (2q; *t*Bu), 46.0 (q; NMe), 50.6 (s; NC), 58.7 (t; NCH_2).

2b: Similarly 1.88 g (78%) of **2b** were obtained from 0.99 g of **1a** (4.78 mmol) and 3.00 mL of BuLi (1.6 M) in hexane.

NMR spectra (as for **2a**); ^{1}H NMR: $\delta = -0.01$ (t/q, ^3J(HH) = 7.9 Hz, ^2J(HB) = 4.3 Hz; BCH_2), 0.75 (q, ^3J(HB) = 2.4 Hz; B*t*Bu$_2$), 1.10 (t, ^3J = 7.0 Hz; Me(Bu)), 1.13 (s; N*t*Bu), 1.26, 1.38 (2m; CH_2(Bu)), 2.14 (s; NMe), 2.30 (s; NCH_2); ^{11}B NMR: $\delta = -13.4, 16.3$ (2s, 1:1); ^{13}C NMR: $\delta = 15.5$ (q; Me(Bu)), 28.1, 28.8 (2t; CH_2(Bu)), 35.1, 36.1 (2q; *t*Bu), 46.4 (q; NMe), 50.2 (s; NC), 58.6 (t; NCH_2).

3: Gas-phase thermolysis of Cl(*t*Bu)B=N(Mes)$SiMe_3$ (5.78 g, 18.7 mmol) yielded the iminoborane *t*BuB≡NMes, [9] which was frozen out at −196 °C with 5 mL of pentane. *t*BuBCl_2 [17] (2.10 g, 15.1 mmol) was added dropwise to the resulting solution at −78 °C. Distillation of this solution at 74 °C/0.003 Torr gave 4.63 g (90%) **3**.

NMR spectra in $CDCl_3$ at 25 °C (standards as for **2a**); ^{1}H NMR (80.13 MHz): $\delta = 1.01$ (s; *t*Bu), 2.18, 2.26 (2s; Me), 6.84 (s; CH); ^{11}B NMR (32.08 MHz): $\delta = 55.4$; ^{13}C NMR (67.88 MHz): $\delta = 20.0, 20.3$ (2q; Me), 29.1 (q; *t*Bu), 129.3 (d; CH), 135.3, 136.2, 140.9 (3s; Mes).

1d: Compound **3** (1.95 g, 6.20 mm) was added dropwise to a suspension of lithium powder (0.16 g, 22.4 mmol) in THF (10 mL) at −78 °C. After stirring for 1 h at −30 °C, the solvent was removed at 25 °C/10 Torr, and the residue taken up in pentane (50 mL). The filtered solution was reduced in volume. At 60 °C, 1.27 g (70%) of **1d** crystallized (m.p. 80 °C).

NMR spectra (conditions as for **3**); ^{1}H NMR: $\delta = 0.98$ (s; *t*Bu), 1.98, 2.26 (2s; Me), 6.85 (s; CH); ^{11}B NMR: $\delta = 49.3$; ^{13}C NMR: $\delta = 19.1, 20.9$ (2q; Me), 26.1 (q; *t*Bu), 128.5 (d; CH), 132.3, 134.8, 138.8 (3s; Mes).

Received: August 3, 1993 [Z 6254 IE]
German version: *Angew. Chem.* **1994**, *106*, 211

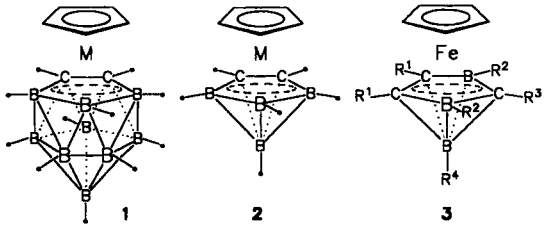
[1] P. Paetzold, B. Redenz-Stormanns, R. Boese, *Angew. Chem.* **1990**, *102*, 910–911; *Angew. Chem. Int. Ed. Engl.* **1990**, *29*, 900–902.
[2] P. Paetzold, B. Redenz-Stormanns, R. Boese, M. Bühl, P. von R. Schleyer, *Angew. Chem.* **1990**, *102*, 1059–1060; *Angew. Chem. Int. Ed. Engl.* **1990**, *29*, 1059–1060.
[3] Crystal data: $a = 10.030(2)$, $b = 11.738(2)$, $c = 15.284(3)$ Å, $\alpha = 91.88(1)$, $\beta = 90.98(1)$, $\gamma = 93.42(1)°$, $V = 1794.4(5)$ Å^3, $Z = 2$, $\rho_{calcd} = 0.919$ g cm^{-3}, $P\bar{1}$ (No. 2), Nicolet-R3m/V diffractometer; data collected at 125 K; $\mu(Mo_{K\alpha}) = 0.5$ cm^{-1}; 4492 independent reflections in the range $3 \le 2\theta \le 45°$, 3616 of which were observed ($F_o \ge 4\sigma(F)$); structure solution and refinement with 332 parameters using SHELXTL-PLUS; $R = 0.0765$, $R_w = 0.0926$, $w^{-1} = \sigma^2(F_o) + 0.0318F_o^2$ [18].
[4] P. Paetzold, C. von Plotho, G. Schmid, R. Boese, B. Schrader, D. Bougeard, U. Pfeiffer, R. Gleiter, W. Schäfer, *Chem. Ber.* **1984**, *117*, 1089–1102; M. Haase, U. Klingebiel, R. Boese, M. Polk, *ibid.* **1986**, *119*, 1117–1126.
[5] R. Boese, B. Kröckert, P. Paetzold, *Chem. Ber.* **1987**, *120*, 1913–1915.
[6] K.-H. van Bonn, P. Schreyer, P. Paetzold, R. Boese, *Chem. Ber.* **1988**, *121*, 1045–1057.
[7] F. Dirschl, E. Hanecker, H. Nöth, W. Rattay, W. Wagner, *Z. Naturforsch. B* **1986**, *41*, 32–37.
[8] P. Paetzold, B. Redenz-Stormanns, R. Boese, *Chem. Ber.* **1991**, *124*, 2435–2441.
[9] K.-H. van Bonn, T. von Bennigsen-Mackiewicz, J. Kiesgen, C. von Plotho, P. Paetzold, *Z. Naturforsch. B* **1988**, *43*, 61–68.
[10] Crystal data: $a = 8.906(3)$, $b = 23.38(1)$, $c = 9.021(3)$ Å, $\beta = 102.29(3)°$, $V = 1836(2)$ Å^3, $Z = 4$, $\rho_{calcd} = 0.9734$ g cm^{-3}, $P2_1/n$ (No. 14), ENRAF-Nonius CAD-4 diffractometer, data measured at 248 K; $\mu(Mo_{K\alpha}) = 0.5$ cm^{-1}; 4753 independent reflections in the range $6 \le 2\theta \le 60°$, 1677 of which were observed ($I \ge 2.5\sigma(I)$); structure solution with direct methods (MULTAN) [19], structure refinement with SDP for 193 parameters; $R = 0.096$, $R_w = 0.097$, $w^{-1} = \sigma^2(F_o)$ [18].
[11] H. Meyer, G. Schmidt-Lukasch, G. Baum, W. Massa, A. Berndt, *Z. Naturforsch. B* **1988**, *43*, 801–806.
[12] a) P. Paetzold, L. Géret-Baumgarten, R. Boese, *Angew. Chem.* **1992**, *104*, 1071–1072; *Angew. Chem. Int. Ed. Engl.* **1992**, *31*, 1040–1042; b) M. Bühl, H. F. Schaefer III, P. von R. Schleyer, R. Boese, *ibid.* **1993**, *105*, 1265–1266 and **1993**, *32*, 1154–1155.
[13] A. Moezzi, R. A. Bartlett, P. P. Power, *Angew. Chem.* **1992**, *104*, 1075–1076; *Angew. Chem. Int. Ed. Engl.* **1992**, *31*, 1082–1083.
[14] R. Boese, N. Augart, *Z. Kristallogr.* **1988**, *182*, 32–35.
[15] C. Liang, L. C. Allen, *J. Am. Chem. Soc.* **1991**, *113*, 1878–1884; H. Grützmacher, *Angew. Chem.* **1992**, *104*, 1358–1360; *Angew. Chem. Int. Ed. Engl.* **1992**, *31*, 1329–1331.
[16] E. Kaufmann, P. von R. Schleyer, *Inorg. Chem.* **1988**, *27*, 3987–3992.
[17] P. A. McCusker, E. C. Ashby, H. S. Makowski, *J. Am. Chem. Soc.* **1957**, *79*, 5182–5184.
[18] Further details on the crystal structure determinations can be obtained from the Fachinformationszentrum Karlsruhe, D-76344 Eggenstein-Leopoldshafen, on quoting the depository number CSD-57907.
[19] P. Main, S. J. Fiske, S. E. Hull, L. Lessinger, G. Germain, J. P. Declerq, M. M. Woolfson, *MULTAN 80, A System of Computer Program for the Automatic Solution of Crystal Structures from X-Ray Diffraction Data*, York (England), Louvain (Belgium), **1980**.

(η^5-Pentamethylcyclopentadienyl)iron Complexes with η^5-2,3,5-Tricarbahexaboranyl and η^5-2,3-Dihydro-1,3-diborolyl Ligands**

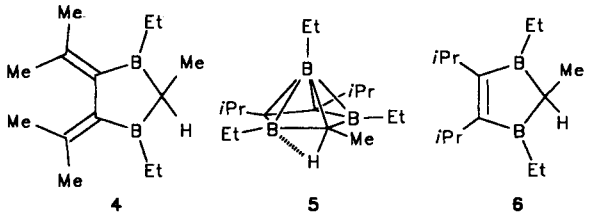
Walter Siebert,* Ralph Hettrich, and Hans Pritzkow

Dedicated to Professor M. Frederick Hawthorne on the occasion of his 65th birthday

Hawthorne et al reported the syntheses of the first complexes containing *nido*-$C_2B_9H_{11}$ ligands in 1965,[1] thus heralding the beginnings of metallacarborane chemistry which they then systematically elaborated.[2] Of the smaller carboranes, the *nido*-$C_2B_4H_6$ ligand, which contains five less BH groups, also displays a high synthetic potential.[3] The metallacarborane clusters **1** and **2** (M = Fe, Co) are well-known complexes containing these ligands, and may—if regarded as π complexes—be considered as forming a bridge to the metallocenes. The iron compounds **1**[4] and **2**[5] (M = Fe) are paramagnetic complexes (17 valence electrons (VE)), which react by taking up one additional electron to form the diamagnetic anions $\mathbf{1}^-$ and $\mathbf{2}^-$ (M = Fe), the analogues of ferrocene. The buildup of neutral 18 VE complexes requires either the substitution of the C_5H_5 ligand by C_6H_6, or the replacement of the C_2B_n carboranes ($n = 4$, 9) by the 5e ligand *nido*-$C_3B_3R_6$, which would lead to the formation of **3**. We report here on the (tricarbahexaboranyl)iron complex **3a** which is analogous to ferrocene, and on the first 16 VE iron sandwich compound **7**.



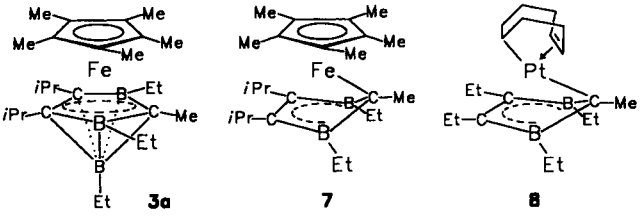
We have observed the metal-induced formation of 2,3,5-tricarbahexaboranylnickel complexes[6] by rearrangement of bis(2,3-dihydro-1,3-diborole)nickel complexes at room temperature and have recently been able to synthesize the unknown 2,3,5-tricarbahexaborane **5** by two different routes. The hydroboration of 1,3-diethyl-2-methyl-4,5-diisopropylidene-1,3-diborolane (**4**)[7] with $(HBEt_2)_2$ leads rather surprisingly to a 2:1 mixture of the carborane **5**[8] and the 1,3-diborole **6**, which can be deprotonated to the corresponding anions $(\mathbf{5}-H)^-$ and $(\mathbf{6}-H)^-$ by the action of NaH or LiMe, respectively.



[*] Prof. Dr. W. Siebert, Dr. R. Hettrich, Dr. H. Pritzkow
Anorganisch-chemisches Institut der Universität
Im Neuenheimer Feld 270, D-69120 Heidelberg (FRG)
Telefax: Int. code + (6221)56-4197

[**] This work was supported by the Deutsche Forschungsgemeinschaft (SFB 247), the Fonds der Chemischen Industrie, and the BASF AG.

A mixture of the green, air-sensitive complexes **3a** and **7** is obtained by reaction of the anions with $[(C_5Me_5)FeCl]$ (formed in situ); complex **7** can be separated from **3a** by crystallization. After separation of **5**/**6** by distillation, both complexes can also be separately synthesized and spectroscopically characterized. The ^{11}B NMR spectrum provides evidence for the presence of the 2,3,5-tricarbahexaboranyl ligand in **3a**; signals at $\delta = 6.6$ and $\delta = -1.8$ can be assigned to the basal boron atoms and the apical boron atom, respectively. The ^{11}B resonance signals are



strongly shifted in comparison to the signals for the free carborane **5** [$\delta = 22$ (2B), -36 (1B)] (the signal for the apical boron atom being shifted downfield, whereas that for the basal boron atoms is shifted upfield). This observation has also been made for other metal complexes.[8] The $\delta(^{11}B)$ value of 19.4 for the 16 VE sandwich complex **7** lies within the expected range for monofacially coordinated 1,3-diborolyl ligands; this rules out a *closo* structure with 14 framework electrons for the C_3B_2Fe framework atoms, which should be possible according to cluster formalism.

The result of the crystal structure analysis[9] on **7** confirms the sandwich arrangement with a severely folded 2,3-dihydro-1,3-diborolyl ring, in which the planes C3-C3′-B1-B1′ and B1-C2-B1′ form an angle of 41.3° (Fig. 1). The following deviations

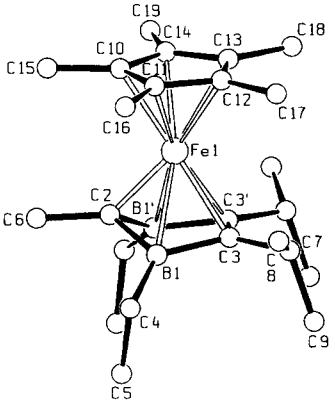


Fig. 1. Molecular structure of **7**. Selected distances [Å] and angles [°]: Fe1-B1 2.249(5), Fe1-C2 1.899(6), Fe1-C3 2.121(4), B1-C2 1.549(7), B1-C3 1.573(6), C3-C3′ 1.406(8); C2-B1-C3 110.1(4), B1-C2-B1′ 89.5(5), B1-C3-C3′ 104.3(2).

from the plane of best fit through the C_3B_2 ligands result: C2 + 0.29, B1 −0.24, C3 + 0.09, Fe +1.71 Å; the distance of the Fe1 atom to the plane through the C_5Me_5 ring is 1.73 Å. The 16 VE complex **7** has a small B1-C2-B1′ bond angle of 89.5(5)°, a short Fe1−C2 bond length of 1.899(6) Å, and a long Fe1−B1 distance of 2.249(5) Å, whereas the Fe1−C3, B1−C3, and C2−B1 bond lengths lie in the usual range. In comparison to this, a significantly larger B-C-B angle of 108.8(2)°, a longer Ni−C(B_2) bond length of 2.091(3) Å, and a shorter Ni−B distance of 2.172(3) Å was determined for the 18 VE nickel complex $[(\eta^5\text{-}C_5H_5)Ni\{\eta^5\text{-}(CEt)_2(BEt)_2CMe\}]$.[10] The position of the methyl group on C2 is quite remarkable; this atom can be

 © VCH Verlagsgesellschaft mbH, D-69451 Weinheim, 1994 0570-0833/94/0202-0203 $ 10.00+.25/0

regarded as approximately sp^3 hybridized. In contrast to **7**, the heterocycle in the corresponding 18 VE nickel complexes is only folded to the extent of 10–12°. A larger fold angle (28°) of the heterocyclic C_3B_2 ligand can be found in the 16 VE complex (η^3-cyclooctenyl)(η^5-1,3,4,5-tetraethyl-2-methyl-2,3-dihydro-1,3-diborolyl)platinum (**8**).[11] However, the $\delta(^{11}B)$ value of 50 signalizes a weaker interaction between the boron and the metal atom than that in **3a** ($\delta = 19.4$).

Complex **7** is the first structurally characterized 16 VE iron sandwich complex, which does not allow stacking with an additional $(C_5Me_5)Fe$ fragment (resulting in the formation of a triple-decker complex). This is due to the stabilizing electronic effects of the methyl groups on the C_5 ring, and the steric shielding effected by the substituents of the heterocycle. In the course of the synthesis of $[\{(\eta^5\text{-}C_5H_5)Fe\}_2\{\mu,\eta^5\text{-}(CEt)_2(BEt)_2CMe\}]$,[12] we were able to isolate a reactive green mononuclear complex, but were not able to characterize it fully. Our results show that the 16 VE iron sandwich complex **7** is stabilized by an extreme folding of the heterocycle. This folding is cancelled when the electron-poor complex reacts with addition of a $(C_5H_5)M$ (M = Fe, Co) fragment to give a triple-decker (29 or 30 VE, respectively), or is capped by a boranediyl building block (R^4B:) to formally give the carboranyl iron complex **3** (18 VE).

Experimental Procedure

3a/**7**: A mixture of **5** and **6** (0.470 g, 1 mmol of each component) was added to a suspension of NaH (0.130 g, 5.4 mmol) in THF (5 mL) at −20 °C and then stirred at room temperature for 2 h. The solution was then separated from excess NaH and added to a solution of $[(C_5Me_5)FeCl]$ at −75 °C, prepared from C_5Me_5H (0.270 g, 2.0 mmol), BuLi solution and $FeCl_2 \cdot 2THF$ (0.530 g, 2.0 mmol) in THF (10 mL).]. The reaction mixture was stirred for 20 h at 20 °C, after which Et_2O/THF was removed under vacuum. The green residue was dissolved in a mixture of 0.5 mL toluene and 0.5 mL hexane and passed through a chromatography column packed with Al_2O_3 using hexane as eluant. The green fraction obtained contained **3a**, **7**, and a small amount of $[(C_5Me_5)_2Fe]$. **7** crystallized at −30 °C after concentration of the solution.

7: Yield: 170 mg (42%); m.p. 216–218 °C (decomp); ^{1}H NMR (200 MHz, C_6D_6): $\delta = 0.42$ (m, br, 4H; BCH_2CH_3), 0.53 (t, br, 6H, $^3J(H,H) = 6$ Hz; BCH_2CH_3), 1.26 (d, 6H, $^3J(H,H) = 6.5$ Hz; $CHCH_3$), 1.45 (s, 15H; C_5CH_3), 1.91 (d, 6H, $^3J(H,H) = 6.5$ Hz; $CHCH_3$), 2.77 (s, 3H; CCH_3), 4.21 (sept. 2H; $CH(CH_3)_2$; ^{11}B NMR (29 MHz, C_6D_6): $\delta = 19.4$; ^{13}C NMR (75 MHz, C_6D_6): $\delta = 6$ (br; BCH_2), 10.0 (BCH_2CH_3), 10.5 (C_5CH_3), 20.2 (CCH_3), 23.7, 24.3 ($CH(CH_3)_2$), 33.6 ($CHCH_3$), 80.3 (C_5CH_3), 133 (br; C4,5), C2 (CCH_3, not observed); EI-MS: *m/z* (%) = 408 (M^+, 100), 393 ($M^+ - CH_3$, 4), 379 ($M^+ - C_2H_5$, 5), 365 ($M^+ - C_3H_7$, 10).

3a: Yield: 45 mg (10%) green, air-sensitive oil (isolated from the mother liquor of **7**); ^{1}H NMR (200 MHz, C_6D_6): $\delta = 0.62$ (m, br; $B(CH_2CH_3)$, 0.91 (m, br; $B(CH_2CH_3)$, 1.2–1.5 (several incompletely resolved signals), 1.63 (s; C_5Me), 1.82 (s; CCH_3), 2.12 (sept; $CHCH_3$); ^{11}B NMR (29 MHz, C_6D_6): $\delta = -1.8$ (1B), 6.6 (2B); EI-MS: *m/z* (%) = 448 (M^+, 34), 443 ($M^+ - CH_3$, 24), 420 ($M^+ - C_2H_4$, 100).

Received: August 18, 1993 [Z.6294IE]
German version: *Angew. Chem.* **1994**, *106*, 215

[1] M. F. Hawthorne, D. C. Young, P. A. Wegner, *J. Am. Chem. Soc.* **1965**, *87*, 1818.
[2] K. P. Callahan, M. F. Hawthorne, *J. Organomet. Chem.* **1975**, *100*, 97; D. M. Schubert, W. S. Rees, Jr., C. B. Knobler, M. F. Hawthorne, *Pure Appl. Chem.* **1987**, *59*, 869.
[3] R. N. Grimes in *Comprehensive Organometallic Chemistry, Vol. 1* (Eds.: G. Wilkinson, F. G. A. Stone, E. W. Abel), Pergamon, Oxford, **1982**, p. 459; *Chem. Rev.* **1992**, *92*, 251.
[4] M. F. Hawthorne, R. L. Pilling, *J. Am. Chem. Soc.* **1965**, *87*, 3987.
[5] M. Stephan, J. H. Davis, Jr., X. Meng, K. J. Chase, J. Hauss, U. Zenneck, H. Pritzkow, W. Siebert, R. N. Grimes, *J. Am. Chem. Soc.* **1992**, *114*, 5214.
[6] T. Kuhlmann, H. Pritzkow, U. Zenneck, W. Siebert, *Angew. Chem.* **1984**, *96*, 994; *Angew. Chem. Int. Ed. Engl.* **1984**, *23*, 965.
[7] M. Enders, B. Gangnus, R. Hettrich, J. Magos-Martin, M. Stephan, H. Pritzkow, W. Siebert, U. Zenneck, *Chem. Ber.* **1993**, *126*, 2197.
[8] A. Fessenbecker, A. Hergel, R. Hettrich, V. Schäfer, W. Siebert, *Chem. Ber.* **1993**, *126*, 2205.
[9] Crystal structure analysis of **7**: orthorhombic space group *Pbnm*, $a = 10.752(5)$, $b = 14.481(7)$, $c = 15.565(8)$ Å, $V = 2423$ Å^3, $Z = 4$; 2885 measured reflections ($Mo_{K\alpha}$ radiation, θ scan), of which 1705 observed ($I > 2\sigma_I$), refinement using F^2 with all reflections [13] (Fe, C, B anisotropic, H atomic positions calculated with common isotropic temperature factors), $R_w = 0.20$, $R = 0.064$ (observed reflections only). The molecule has a crystallographically imposed mirror plane, the C_5Me_5 ring is strongly disordered and was refined as a rigid ring in two positions. Further details of the crystal structure investigation may be obtained from the Fachinformationszentrum Karlsruhe, D-76344 Eggenstein-Leopoldshafen (FRG) on quoting the depository number CSD-400452, the names of the authors, and the journal citation.
[10] W. Siebert, M. Bochmann, J. Edwin, C. Krüger, Y.-H. Tsay, *Z. Naturforsch. B* **1978**, *33*, 1410; U. Fenner, Dissertation, Universität Heidelberg, **1992**
[11] H. Wadepohl, H. Römich, H. Pritzkow, W. Siebert, *Chem. Ber.* **1988**, *121*, 2103.
[12] a) W. Siebert, *Angew. Chem.* **1985**, *97*, 924; *Angew. Chem. Int. Ed. Engl.* **1985**, *24*, 953; b) H. Wadepohl, Dissertation, Universität Marburg, **1982**.
[13] G. M. Sheldrick, SHELXL 93, Universität Göttingen, **1993**.

Photoisomerization of Highly Alkylated Butadienes**

Henning Hopf,* Helmut Lipka, and Marit Traetteberg

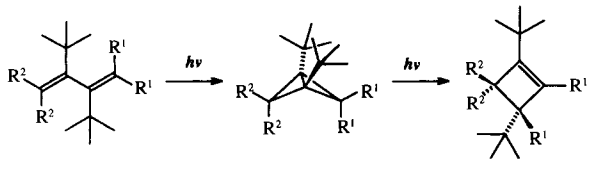
It has long been known that highly substituted acyclic 1,3-dienes prefer nonplanar molecular structures rather than the flat s-*trans* and s-*cis* conformations.[1] In contrast, how this deviation from planarity, which in the extreme case can lead to the orthogonal arrangement of the two "double bond halves", effects the chemical behavior of these compounds has hardly been investigated. With the development of a simple and versatile method for preparing highly alkylated (including *tert*-butyl-substituted) butadienes, we have recently[2] reached the stage where we are able to investigate the relationship between orthogonality and the reactivity of acyclic compounds. We report here on the photoisomerizations of selected polyalkyldienes, which were irradiated directly (450 W Hg high-pressure lamp) in dilute solutions (0.05–2%) in inert solvents (pentane, cyclohexane, etc.) at room temperature. The parent compound 1,3-butadiene rearranges under these conditions into a mixture of cyclobutene and bicyclobutane, in which the monocyclic product predominates,[3] and the yield of bicyclobutane is at best a few percent. Addition of copper(I) chloride leads to an increase in the proportion of the bicyclobutane component, without, however, making the process of any significant preparative value.[4]

The situation is quite different for polyalkylated dienes: According to X-ray structural analysis[5] and electron diffraction[6] the orthogonal 2,3-di-*tert*-butyl-1,3-butadiene (**1a**) isomerizes exclusively (60%) upon irradiation (60 min) to the bicyclobutane **2a**. The even more highly substituted butadiene **1b** is converted into the corresponding dimethyl derivative **2b**.[7]

Both photoproducts are not stable to further irradiation: **2a** rearranges to **3a**; **2b** to **3b**,[7] which are again the sole reaction products. In this ring opening the central bond of **2** is presumably broken and the resulting 1,3-diyl is then stabilized by a hydrogen shift. If one reduces the steric strain in the interior of the molecule by shifting one of the bulky susbtituents to the periphery of the diene system, as for example in *trans*-1,3-di-*tert*-butyl-1,3-butadiene (**4**), an s-*cis* conformation can appar-

[*] Prof. Dr. H. Hopf, Dr. H. Lipka
Institut der Organische Chemie der Technischen Universität
Postfach 3329, D-38023 Braunschweig (FRG)
Telefax: Int. code + (531)391-5388
Prof. Dr. M. Traetteberg
Department of Chemistry, University of Trondheim
N-7055 Dragvoll (Norway)

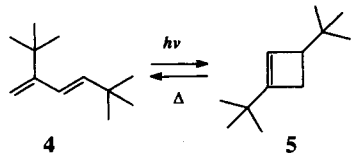
[**] Sterically Hindered Double Bond Systems; Part 3. Part 2: see ref. [2]. This work was supported by the Deutsche Forschungsgemeinschaft and the Fonds der Chemischen Industrie. We thank BASF AG for donating chemicals.



1 **2** **3**

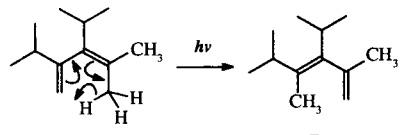
a: $R^1=R^2=H$; **b:** $R^1=H$, $R^2=CH_3$

ently be attained,[8] since the only photoproduct obtained after 45 minutes is the cyclobutene **5**,[7] which upon heating to about 200 °C is converted back into the expected product **4**.



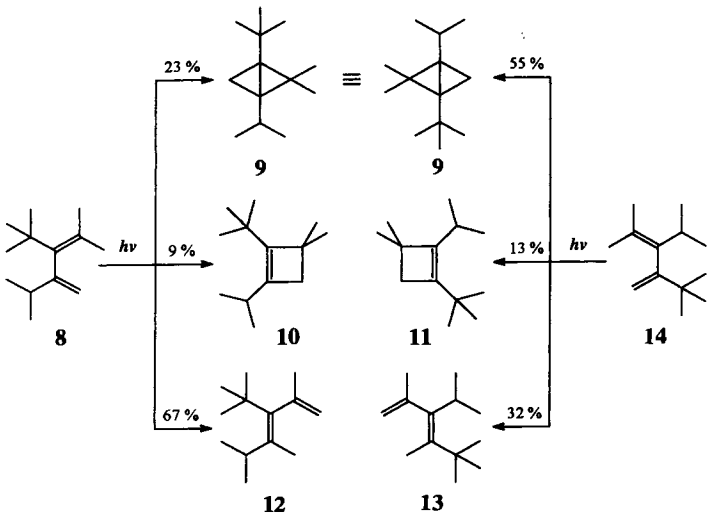
4 **5**

A third reaction pathway for highly alkylated dienes is made available, when these have terminal methyl substituents and central substituents which are not too bulky, so that an orthogonal structure is either not enforced or can be left readily via comparatively low-lying transition states. The major rearrangement product (80%) from **6** is isomer **7**,[7, 9] which results from a 1,5-hydrogen shift.



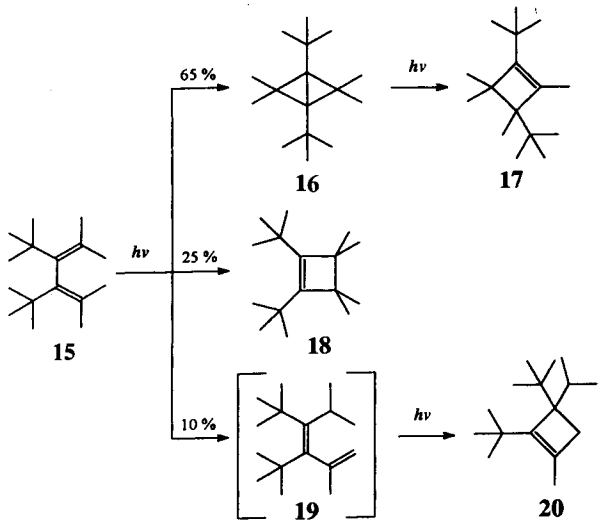
6 **7**

The variability of the diene synthesis[2] makes it possible to introduce desired alkyl groups into the four olefinic positions of the diene system, so that the contributions of each photoisomerization pathway can be controlled. Thus, irradiation of the diene **8** gives a mixture of the three photoisomers **9** (23%), **10** (9%), and **12** (67%).[10] If the isopropyl and the *tert*-butyl groups in the molecule's interior (compound **14**) are interchanged, **9** becomes the major rearrangement product (55%), while the amount of the 1,5-hydrogen migration isomer **13** is significantly reduced (32%); the amount of the cyclization product **11** (13%) is scarcely altered in comparision with **8**. From these results it can be concluded that for an arrangement of substituents as in **14** (flanking *tert*-butyl groups), the orthogonality of the starting material is much greater than in the isomer **8**, with its centrally bound *tert*-butyl substituents.



8 **9** **9** **10** **11** **12** **13** **14**

Finally, the completely substituted diene **15** is also interesting, since because of the two *tert*-butyl groups in the interior of the molecule, it should be orthogonally configurated. In fact, the bicyclobutane **16** is the major product (65%) of the photoisomerization.[7] Nevertheless, the other two rearrangements also compete; the cyclobutene **18** is formed in 25% yield and the 1,5-hydrogen shift product in 10% yield.[7] However, in this case, the primary product **19** is not isolated, but rather its cycloisomer **20**. As expected, compound **16** is not photostable; upon longer irradiation it is converted into **17** (main product) which is formally formed from **16** by the migration of a methyl group.



15 **16** **17** **18** **19** **20**

To what extent these isomerization reactions can be applied to dienes with bulky but removable substituents, (e.g. trialkylsilyl groups) is currently under investigation.[11]

Received: August 18, 1993 [Z 6295 IE]
German version: *Angew. Chem.* **1994**, *106*, 232

[1] a) K. W. F. Kohlrausch, H. Wittek, *Ber. Dtsch. Chem. Ges. B* **1942**, *75*, 227-232; b) G. Köbrich, A. Mannschreck, R. A. Misra, G. Rissmann, M. Rösner, W. Zündorf, *Chem. Ber.* **1972**, *105*, 3794-3806.
[2] H. Hopf, H. Lipka, *Chem. Ber.* **1991**, *124*, 2075-2084.
[3] R. Srinivisan, *J. Am. Chem. Soc.* **1963**, *85*, 4045-4046. More recent literature on the butadiene/cyclobutene equilibrium: K. B. Clark, W. J. Leigh, *ibid.* **1987**, *109*, 6086-6092, and references therein.
[4] Summary: J. Kopecky, *Organic Photochemistry*, VCH, New York, **1992**, p. 76 ff.
[5] W. R. Roth, O. Adamczak, R. Breuckmann, H.-W. Lennartz, R. Boese, *Chem. Ber.* **1991**, *124*, 2499-2521; dihedral angle: 84°.
[6] M. Traetteberg, H. Hopf, H. Lipka, unpublished results; dihedral angle: 82°.
[7] All new compounds were characterized by the usual spectroscopic and analytical methods.
[8] According to MM3 calculations the torsion potentials for **1** and **4** are very different; **1** shows a deep potential minimum (orthogonal configuration) with high barriers in both directions (*syn*: ca. 22 kcal mol^{-1}, *anti*: ca. 13 kcal mol^{-1}). The torsion potential curve for **4**, on the other hand, is relatively flat (maximum energy difference ca. 2 kcal mol^{-1}; M. Traetteberg, unpublished results).
[9] The configuation of **7** has not been established. NOE spectra (NOE = nuclear Overhauser effect) do not provide clear indication for an assignment of the configuration, and under the irradiation conditions it cannot be ruled out that it can undergo *E*/*Z* isomerization in a secondary reaction. In the photolysate one diastereoisomer clearly predominates (85%, NMR analysis). According to NMR spectra the by-products found are derivatives of bicyclobutane and cyclobutene.
[10] The configuration shown is derived from NOE measurements (strong interactions between the *tert*-butyl and the isopropyl groups.)
[11] Note added in proof (November 26, 1993): Bis-2,3-trimethylsilyl-1,3-butadiene also photoisomerizes to give a bicyclobutane analogous to **2**. (H. Hopf, R. Hänel, unpublished results).

 © VCH Verlagsgesellschaft mbH, D-69451 Weinheim, 1994 0570-0833/94/0202-0205 $ 10.00+.25/0

Fullerene Dications as Initiators for Gas-Phase "Ball-and-Chain" Polymerization of Ethylene Oxide; Termination by Cyclization**

Jinru Wang, Gholamreza Javahery, Simon Petrie, Alan C. Hopkinson, and Diethard K. Bohme*

Multiply charged cations of buckminsterfullerene, C_{60}^{n+}, are remarkably stable, easily generated (up to at least $n = 3$), and readily subjected to chemical reaction in the gas phase.[1] This control over the number of charges on a molecule is unique and provides an unprecedented opportunity for exploring the role of charge in directing intramolecular reactions. For example, Coulombic repulsion between two positive charges has been postulated to drive the "ball-and-chain" polymerization of 1,3-butadiene initiated by C_{60}^{2+} away from the surface of C_{60} into the surrounding space.[2, 3] An almost exponential decrease in the rate of polymerization is observed at 294 ± 2 K in helium at 0.40 ± 0.01 Torr for the proposed sequential addition leading to a chain of six units of 1,3-butadiene.[2] We report here on a second possible feature of such polymerization: termination by cyclization at chain lengths at which Coulombic repulsion is weaker than chemical forces. We have chosen to investigate this possibility experimentally with the C_{60}^{2+}-initiated polymerization of ethylene oxide which, unlike butadiene, has a strong tendency for cyclization.

Figure 1 displays the remarkable observation that a series of rapid sequential addition reactions attach up to six molecules of ethylene oxide to C_{60}^{2+} in helium buffer gas at 0.35 Torr and 294 K [Eq. (a)]. The initiation reaction of C_{60}^{2+} with ethylene

$$C_{60}(C_2H_4O)_n^{2+} + C_2H_4O \longrightarrow C_{60}(C_2H_4O)_{n+1}^{2+} \quad n = 0 - 5 \qquad (a)$$

oxide proceeds relatively slowly with a rate constant of $(5.3 \pm 1.6) \times 10^{-11}$ cm^3 molecule^{-1} s^{-1}, which corresponds to a reaction efficiency of 0.019.[4] The subsequent oligomerization reactions are characterized by larger rate coefficients: we estimate the second step to be more than ten times faster than the first step, and the rate constants drop by a factor of 2 to 3 with each successive step (in the reaction of C_{60}^{2+} with butadiene the rate constants drop by a factor of 3 to 4). Also, more significantly and unlike the case of 1,3-butadiene, the observed rate of addition of ethylene oxide shows a sharp drop at $n = 5$ by about a factor of 10. In contrast to the dication, the monocation of C_{60} did not react with ethylene oxide with a measurable specific rate ($k \leq 3 \times 10^{-13}$ cm^3 molecule^{-1} s^{-1}).

The slow first step, which is presumed to proceed in a termolecular fashion by collisional stabilization (He is the stabilizing third body) under our experimental conditions, is not atypical: we have found other oxygen-containing compounds to add slowly to C_{60}^{2+} under similar conditions. In analogy to these reactions we expect the first step to be nucleophilic addition leading to the formation of a product **I** in which the charge is formally localized on the oxygen atom.[1d] This addition is accompanied by a loss in charge delocalization energy of the C_{60}^{2+},

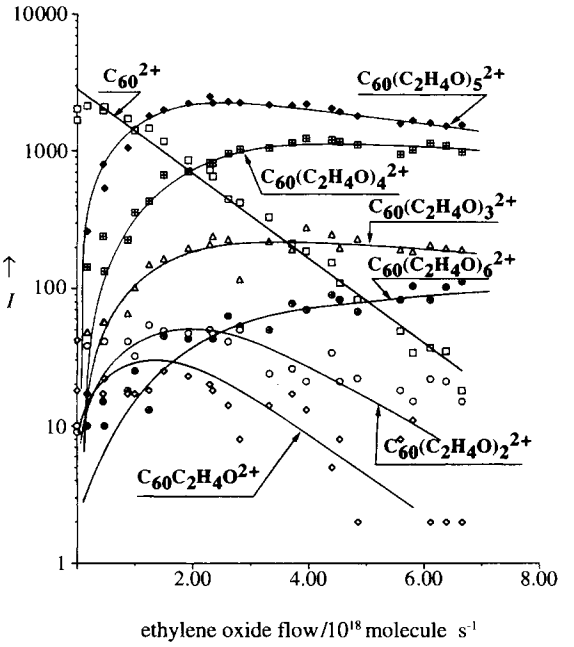
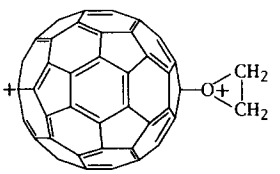
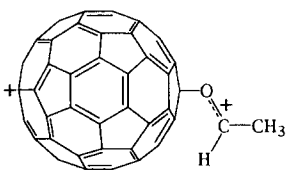


Fig. 1. Variation in the ion signals I upon addition of ethylene oxide into the reaction region of the SIFT apparatus in which C_{60}^{2+} has been established as the dominant ion in helium buffer gas. $p = 0.35$ Torr, $\bar{v} = 6.4 \times 10^3$ cm s^{-1}, $L = 47$ cm, and $T = 294$ K. C_{60}^{2+} is produced by electron impact at 60 eV of C_{60} vapor entrained in argon carrier gas. Signal intensities for the first three adducts $C_{60}(C_2H_4O)_n^{2+}$ ($n = 1, 2, 3$) at low ethylene oxide flows, suggest that the rate constants for reaction of these adducts substantially exceed that for reaction of "bare" C_{60}^{2+}. However, the signal intensities observed for these adducts at high flows ($\geq 4 \times 10^{18}$ molecules s^{-1}) are substantially higher than would be expected if these adducts reacted rapidly with ethylene oxide. This apparent discrepancy suggests that higher order adducts may undergo chemical or thermal dissociation. Alternatively, fragmentation may be induced by the electric field gradient in the vicinity of the product ion sampling nosecone, or different isomeric forms of the adducts may be present, some of which react rapidly while others remain essentially unreacted. A detailed kinetic model would require a better understanding of these factors.

which will act to disfavor association, as will the accompanying distortion at the C_{60} bonding site, which is required for tetrahedral coordination with the nucleophile.[6] If the excess energy associated with C–O bond formation is sufficiently large, we can expect subsequent ring opening and a hydride shift to generate structure **II**.[7]



I



II

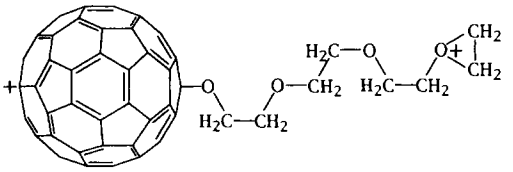
Addition of the second molecule of ethylene oxide can now occur at a site with a localized charge without a distortion requirement, which is more favorable than addition at the site of the remaining charge on the C_{60} surface (recall also that C_{60}^{+} is unreactive).[9] This would explain the considerably higher rate of addition of the second, third, and fourth molecules of ethylene oxide leading either to the propagation of a chain as indicated in structure **III** (for addition to structure **I**)[10] or as indicated in structure **IV** (for addition to structure **II**).

Coulombic repulsion between the propagated charge and the remaining charge on the surface of C_{60} will tend to drive the

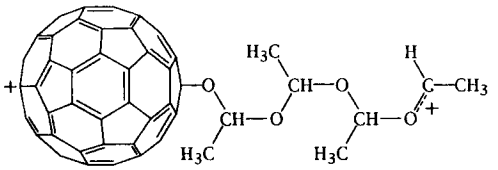
[*] Prof. Dr. D. K. Bohme, J. Wang, Dr. G. Javahery, Dr. S. Petrie, Prof. Dr. A. C. Hopkinson
Department of Chemistry and Centre for Research in Earth and Space Science
York University
North York, Ontario M3J 1P3 (Canada)
Telefax: Int. code + (416)736-5516

[**] This research was supported by the Natural Sciences and Engineering Research Council of Canada. D. K. B. thanks the Canada Council for a Killam Research Fellowship. The authors thank H. Becker and E. Uggerud for helpful discussions.

 © VCH Verlagsgesellschaft mbH, D-69451 Weinheim, 1994 0570-0833/94/0202-0206 $ 10.00+.25/0

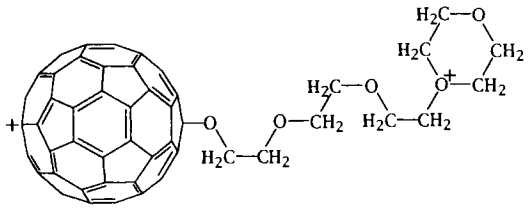


III

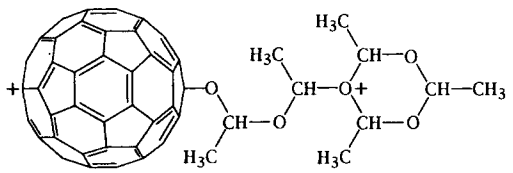


IV

molecular growth away from the surface in a similar fashion to that envisaged for the C_{60}^{2+}-induced polymerization observed with 1,3-butadiene; however, ethylene oxide oligomers should show an increasing tendency for unimolecular cyclization to form a relatively stable six-membered ring at the end of the chain as Coulombic repulsion weakens with increasing charge separation. Structures **V** and **VI** show the products of this cyclization which would inhibit further chain propagation.



V



VI

The observed discontinuity in the addition rate between the fifth and sixth addition is consistent with such a mechanism. However, while the data indicates that most chains do not contain more than five ethylene oxide units, some have six units, and termination after four and perhaps even three additions is probable also. Moreover we cannot rule out cyclization beyond dimers and trimers, to form larger rings, and the dissociation to form cyclic oligomers.

The mechanism of cationic cyclooligomerization of ethylene oxide with BF_3 in CH_2Cl_2 has been investigated in detail by Dale and Daasvatn.[11] These authors have demonstrated the requirement of a minimum chain length for direct cyclization (in the absence of Coulombic repulsion), the termination of the growing chain by direct cyclization beyond dimers and trimers, the competition between formation of a cyclic trimer and dimer, and the possible expulsion of cyclic oligomers. We are currently investigating the chemistry of C_{60}^{n+} with other small epoxides.

Experimental Procedure

The reaction of C_{60}^{2+} with ethylene oxide was monitored with a Selected-Ion Flow Tube (SIFT) apparatus [12, 13]. C_{60}^{2+} was produced by the electron bombardment of 60 eV of C_{60} vapor entrained in argon carrier gas. The dications were selected with a quadrupole mass filter, injected into a flowing helium gas at 295 ± 2 K and 0.35 ± 0.01 Torr, allowed to reach thermal equilibrium by collisions with helium atoms, and finally exposed to ethylene oxide further downstream. The progress of the reactions was followed with a second quadrupole mass filter in the usual fashion [12, 13]. The ethylene oxide had a purity of ≥99.0% (Matheson). The fullerene powder was a mixture of C_{60} and 2–12% C_{70} (Strem Chemicals).

Received: August 25, 1993 [Z 6315 IE]
German version: *Angew. Chem.* **1994**, *106*, 227

[1] a) S. Petrie, G. Javahery, J. Wang, D. K. Bohme, *J. Am. Chem. Soc.* **1992**, *114*, 9177; b) S. Petrie, G. Javahery, D. K. Bohme, *ibid.* **1993**, *115*, 1445; c) G. Javahery, S. Petrie, H. Wincel, J. Wang, D. K. Bohme, *ibid.* **1993**, *115*, 5716; d) *ibid.* **1993**, *115*, 6295; e) G. Javahery, S. Petrie, J. Wang, H. Wincel, D. K. Bohme, *ibid.* **1993**, *115*, 9701.
[2] J. Wang, G. Javahery, S. Petrie, D. K. Bohme, *J. Am. Chem. Soc.* **1992**, 114, 9665.
[3] "Ball-and-chain" systems in which the C_{60} unit and another functional group are connected by a rigid polycyclic chain have been reported recently: S. I. Kahn, A. M. Oliver, M. N. Paddon-Row, Y. Rubin, *J. Am. Chem. Soc.* **1993**, *115*, 4919.
[4] The reaction efficiency is taken to be equal to the ratio of the measured reaction rate constant to the calculated collision rate constant. The collision rate constant was calculated according to the Average Dipole Orientation (ADO) theory [5].
[5] T. Su, M. T. Bowers, *Int. J. Mass. Spectrom. Ion Phys.* **1973**, *23*, 347.
[6] S. Petrie, D. K. Bohme, *Can. J. Chem.*, in press.
[7] It is interesting to note that acetaldehyde, which might be expected to form the secondary carbocation adduct **II** directly, was observed not to add to C_{60}^{2+} with a measurable rate ($k < 1 \times 10^{-12}$ cm^3 molecule^{-1} s^{-1}) [8].
[8] S. Petrie, G. Javahery, H. Wincel, J. Wang, D. K. Bohme, *Int. J. Mass Spectrom. Ion Processes* **1993**, submitted.
[9] The observed 10-fold increase in the rate of addition of the second ethylene oxide molecule compared to the first suggests very strongly that the first addition activates the dication in some manner. The first addition most likely generates an activated site because the C_{60} substituent carries a localized charge. Previous experiments in our laboratory have shown that sequential addition to the surface of the C_{60} (to form a double-handled adduct) is characterized by essentially identical rates for the first and second addition steps [1].
[10] Addition in this manner is considered to involve concomitant ring opening of the ethylene oxide monomer previously added.
[11] J. Dale, K. Daasvatn, *Acta Chem. Scand. B* **1980**, *34*, 327.
[12] G. I. Mackay, G. D. Vlachos, D. K. Bohme, H. I. Schiff, *Int. J. Mass Spectrom. Ion Phys.* **1980**, *36*, 259.
[13] A. B. Raksit, D. K. Bohme, *Int. J. Mass Spectrom. Ion Processes* **1983/1984**, *55*, 69.

$[(Ph_3PAu)_6(dppeAu_2)(AuCl)_4Pd]$, an Icosahedral Au_{12} Cluster with a Central Pd Atom**

Martin Laupp and Joachim Strähle*

The photolysis of $[Ph_3PAuN_3]$ leads to the formation of homometallic gold clusters by reductive elimination of the azide group.[1, 2] The heterodimetal clusters $[(Ph_3PAu)_xM(CO)_y]^{n+}$ ($n = 0,1,2$) are formed in the presence of metal carbonyls. The composition of the cluster is governed by the electron requirements of the transition metal M, that tries to achieve a stable noble-gas electron configuration. This simple approach to the synthesis of new clusters, encouraged us to carry out the photolytic reaction on other azide complexes. Although the photol-

[*] Prof. Dr. J. Strähle, Dipl.-Chem. M. Laupp
Institut für Anorganische Chemie der Universität
Auf der Morgenstelle 18, D-72076 Tübingen (FRG)
Telefax: Int. code +(7071)29-2436

[**] This work was supported by the Deutsche Forschungsgemeinschaft and the Fonds der Chemischen Industrie. We thank the company Degussa, Wolfgang, for a gift of tetrachlorogold acid.

 © VCH Verlagsgesellschaft mbH, D-69451 Weinheim, 1994 0570-0833/94/0202-0207 $ 10.00+.25/0

ysis of Ag^I and Cu^I complexes does not lead to the formation of stable clusters, we could produce the cluster $[(dppe)PtCo_2(CO)_7]$ (dppe = 1,2-bis(diphenylphosphino)ethane) from the azido platinum(II) complex $[(dppe)Pt(N_3)_2]$ and $[Co_2(CO)_8]$. From $[(Ph_3P)_2Pt(N_3)_2]$, $[Ph_3PAuN_3]$, and $[Ph_3PAuCl]$ we obtained the cluster $[(Ph_3PAu)_6(AuCl)_3Pt(CO)]$.[3] In this cluster the nine gold atoms form a polyhedron which can be described as an incomplete icosahedron in which one triangular face is missing. The platinum atom is located in the center of the incomplete icosahedron and its CO ligand points towards the middle of the missing icosahedral face. Since gold-palladium clusters are relatively rare, we carried out the analagous cophotolysis with $[Ph_3PAuN_3]$ and the azido palladium complex $[(dppe)Pd(N_3)_2]$ and obtained the cluster **1**, in which the twelve gold atoms form a complete icosahedron with a palladium atom in the center. The presence of the palladium atom was confirmed by energy dispersive X-ray microanalysis and mass spectrometric analysis. Moreover, the structure refinement[4] shows that the palladium atom is in the center of the cluster.

$[(Ph_3PAu)_6(dppeAu_2)(AuCl)_4Pd]$ **1**

The photolysis product of $[(Ph_3P)_2Pd(N_3)_2]$, $[Ph_3PAuN_3]$ and $[Ph_3PAuCl]$ presumably has a structure analagous to **1**. A crystal structure analysis has not been done yet; nevertheless, the constitution of this cluster was shown by mass spectrometry to be $[(Ph_3PAu)_8(AuCl)_4Pd]$ (**2**). To date, only one cluster with a complete Au_{12} icosahedron around a central atom was known—that of $[(PhMe_2PAu)_{10}(AuCl)_2Au]^{3+}$.[5] In this cluster, the center of the icosahedron is occupied by a Au atom. We now announce the first isoelectronic clusters **1** and **2** that contain a heteroatom in the center.

The gold–palladium clusters synthesized by Pignolet et al.[6, 7] exhibit Au_6Pd and Au_8Pd polyhedra. The crystal structure analysis shows that the eight gold atoms in $[(Ph_3PAu)_8Pd]^{2+}$[6] form a crownlike structure centered by a Pd atom, whereas in $[(Ph_3PAu)_8Pd(CO)]^{2+}$ and $[(Ph_3PAu)_6\{(MeO)_3PAu\}_2Pd\{P(OMe)_3\}]^{2+}$, the eight Au atoms are arranged as hemispherical icosahedral fragment.[7]

In the photolytic synthesis of **1** [Eq. (a)], a mixture of $[Ph_3PAuN_3]$ and $[(dppe)Pd(N_3)_2]$ are irradiated for 2 h with a high-pressure Hg vapor lamp. Then $[Ph_3PAuCl]$ is added, and the irradiation continued for one hour. After chromatographic separation of the products of photolysis, deep red columnar crystals of **1**, which deteriorate very quickly out of the mother liquor, are isolated in about 15% yield.

$$8[Ph_3PAuN_3] + 4[Ph_3PAuCl] + [(dppe)Pd(N_3)_2] \longrightarrow \underset{\mathbf{1}}{[(Ph_3PAu)_6(dppeAu_2)(AuCl)_4Pd]} + 15\,N_2 + 6\,PPh_3 \quad (a)$$

During the cluster formation from mononuclear units it is curious that the diphosphane ligand is transfered to the gold atom, although the synthesis of **2** shows that the diphosphane ligand is not necessary to stabilize the cluster.

The cluster **1** lies on the C_2 axis of the monoclinic space group $C2/c$.[4] The axis passes through the Pd atom and the center of the ethylene bridge of the diphosphane ligand (Fig. 1). The Au–Au distances of 285.2(2) to 293.5(2) pm lie in the typical range for distances between peripheral gold atoms as found in the homometallic cluster $[(PhMe_2PAu)_{10}(AuCl)_2Au]^{3+}$.[5] The Pd–Au distances (272.2(2) to 276.7(1) pm) are, in contrast, clearly shorter and indicate strong bonding interaction. They resemble the Au–Au distances to the central atom in the previously mentioned homometallic Au_{13} cluster.[5]

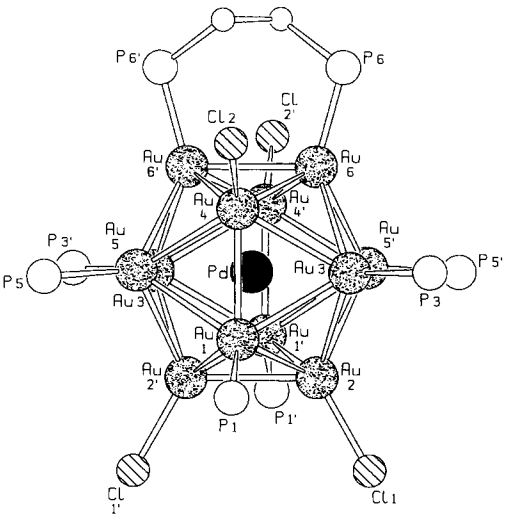


Fig. 1. Structure of **1** in crystal [12]. Only the P atoms of the phosphane ligands and in the case of dppe, only the ethylene bridge was drawn. Important interatomic distances [pm]: Au1-Au2 285.4(2), Au1-Au2' 287.3(1), Au1-Au3 289.7(2), Au1-Au4 288.9(2), Au1-Au5 291.4(1), Au2-Au2' 289.9(2), Au2-Au3 288.2(2), Au2-Au5' 293.5(2), Au3-Au4 290.2(2), Au3-Au5 290.5(1), Au3-Au6 287.4(2), Au4-Au5 287.8(1), Au4-Au6 292.0(1), Au5-Au6' 287.8(2), Pd-Au1 272.2(2), Pd-Au2 274.0(4), Pd-Au3 276.7(1), Pd-Au4 275.2(2), Pd-Au5 276.7(2), Pd-Au6 273.5(3), Au-P_{PPh_3} 229.0(8)–230.5(7), Au6-P_{dppe} 227.9(9), Au2-Cl1 237.5(7), Au4-Cl2 239.2(9).

Large homometallic gold clusters characterized by one central and n peripheral gold atoms can, according to Mingos,[8, 9] be classified by their topology as spherical type with $12n+18$ valence electrons, and as flattened toroidal type with $12n+16$ valence electrons. In the spherical clusters whose n peripheral Au atoms lie approximately on the surface of a sphere, the $10(n+1)$ nonbonding electrons are found in the fully occupied d orbitals of the $n+1$ gold atoms; $2n$ electrons are required for bonding to the ligands of the peripheral gold atoms. The remaining eight electrons are thus reserved for bonds between the metal atoms in the polyhedron. They are located in the four bonding MOs of the cluster; in the toroidal clusters six bonding MOs are required. The cluster **1** belongs to the spherical type clusters. With $12n+18 = 162$ valence electrons as well, it is isoelectronic with $[(PhMe_2PAu)_{10}(AuCl)_2Au]^{3+}$[5] and has eight bonding electrons in the polyhedron, which are contributed by the eight gold(0) centers of the $[Au_{12}]^{4+}$ polyhedra.

Experimental Procedure

1: $[(dppe)Pd(N_3)_2]$ (491 mg, 0.8 mmol) are first mixed with $[Ph_3PAuN_3]$ (423 mg, 0.8 mmol) in freshly distilled THF (70 mL) for 2 h while stirring under a weak stream of N_2 and irradiating at room temperature with a high-pressure mercury vapor lamp. The solution turns deep red. Then $[Ph_3PAuCl]$ (410 mg, 0.8 mmol) is mixed into the reaction solution, which is irradiated for another 1 h. Thereafter, the solvent is completely removed in vacuum, and the residue redissolved in CH_2Cl_2 and chromatographed in an Al_2O_3 column. A red fraction can be seperated with CH_2Cl_2/THF (1:1). This is evaporated to dryness and dissolved in CH_2Cl_2 again. After overlaying of the solution with diisopropylether, deep red columnar crystals of **1** form within 14 days at 0 °C in approximately 15% yield. The crystals presumably contain solvate molecules and because of this, deteriorate quickly outside of the solvent. The presence of Pd was confirmed by energy-dispersive X-ray microanalysis. FAB-MS: m/z (%): 4548.2 (15) $[M^+ - Cl]$, 4285.3 (30) $[M^+ - Cl - PPh_3]$, 4088.8 (100) $[M^+ - Cl - PPh_3 - Au]$, 4054.0 (40) $[M^+ - 2Cl - PPh_3 - Au]$, 3792.5 (35) $[M^+ - 2Cl - 2PPh_3 - Au]$. $^{31}P\{^1H\}$ NMR (32.39 MHz, CD_2Cl_2, −30 °C, H_3PO_4): δ = 65.05 (PPh_3), 28.74 (dppe).

 © VCH Verlagsgesellschaft mbH, D-69451 Weinheim, 1994 0570-0833/94/0202-0208 $ 10.00+.25/0 Angew. Chem. Int. Ed. Engl. 1994, 33, No. 2

2: Procedure as for the synthesis of **1**; $[(Ph_3P)_2)Pd(N_3)_2]$ is used in place of $[(dppe-Pd(N_3)_2]$ to furnish deep red crystals stable in air and in about 10% yield. FAB-MS: *m/z* (%): 4673.8 (15) $[M^+ - Cl]$, 4215.5 (40) $[M^+ - Cl - PPh_3 - Au]$, 4177.5 (100) $[M^+ - 2Cl - PPh_3 - Au]$, 3916.8 (80) $[M^+ - 2Cl - 2PPh_3 - Au]$, 3721.7 (50) $[M^+ - 2Cl - 2PPh_3 - 2Au]$, 3685.3 (35) $[M^+ - 3Cl - 2PPh_3 - 2Au]$, 3421.2 (20) $[M^+ - 3Cl - 3PPh_3 - 2Au]$.

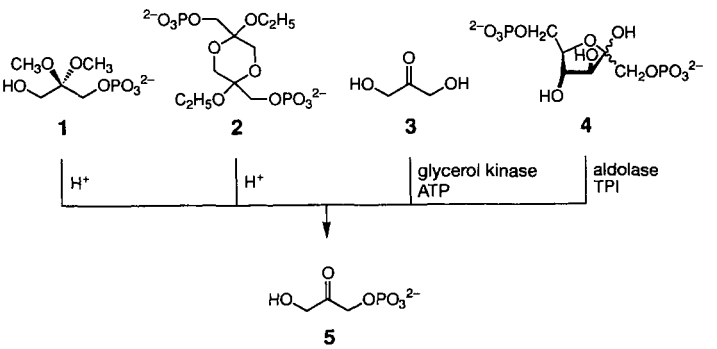
Recieved: August 19, 1993 [Z 6299 IE]
German version: *Angew. Chem.* **1994**, *106*, 210

[1] G. Beuter, A. Brodbeck, M. Holzer, S. Maier, J. Strähle, *Z. Anorg. Allg. Chem.* **1992**, *616*, 27–34.
[2] M. Holzer, J. Strähle, G. Baum, D. Fenske, *Z. Anorg. Allg. Chem.*, in press.
[3] M. Breuer, J. Strähle, *Z. Anorg. Allg. Chem.* **1993**, *619*, 1564–1574.
[4] Crystal data for **1**: *C2/c*, $a = 2953.8(8)$, $b = 1862.4(3)$, $c = 2921.8(6)$ Å, $\beta = 107.85(2)^\circ$, $Z = 4$, $R = 0.058$ for 6928 independent reflections with $I > 3\sigma(I)$ and 383 refined parameters (Enraf-Nonius CAD4 diffractometer, SDP-Plus, $Mo_{K\alpha}$ radiation, ω Scans, $3^\circ \leq \theta \leq 26^\circ$. Empirical absorption correction, solution of structure by direct methods (SHELXS 86 [10]), SDP [11]) refinement with anisotropic temperature parameters for the metal, Cl, and P atoms; H atoms were not included. The residual electron density in a final difference Fourier Synthesis could not be attributed to a solvate molecule. A test refinement with a Au atom in the center of the cluster resulted in a higher *R* value of 0.071 and the isotropic temperature factor increased from 2.15×10^4 to 6.72×10^4 pm^2. Further details of the crystal structure investigation may be obtained from the Fachinformationszentrum Karlsruhe, D-76344 Eggenstein-Leopoldshafen, on quoting the depository number CSD-57681.
[5] C. E. Briant, B. R. C. Theobald, J. W. White, L. K. Bell, D. M. P. Mingos, A. J. Welch, *J. Chem. Soc. Chem. Commun.* **1981**, 201–202.
[6] L. N. Ito, B. J. Johnson, A. M. Mueting, L. H. Pignolet, *Inorg. Chem.* **1989**, *28*, 2026–2028.
[7] L. N. Ito, A. M. P. Felicissimo, L. H. Pignolet, *Inorg. Chem.* **1991**, *30*, 988–994.
[8] D. M. P. Mingos, *Polyhedron* **1984**, *3*, 1289–1297.
[9] D. M. P. Mingos, D. J. Wales, *Introduction to Cluster Chemistry*, Prentice-Hall, London, **1990**.
[10] G. M. Sheldrick, SHELXS 86, Fortran program to determine crystal structures. Göttingen, **1986**.
[11] B. A. Frenz and Fa. Enraf-Nonius, Structure Determination Package VAXS-DP, Version 3.0, **1986**.
[12] E. Keller, SCHAKAL, Fortran program to depict crystal structures, Freiburg, **1986**.

Synthesis of Dihydroxyacetone Phosphate (and Isosteric Analogues) by Enzymatic Oxidation; Sugars from Glycerol**

Wolf-Dieter Fessner* and Gudrun Sinerius

Enzyme-catalyzed aldol additions are currently of great interest because of their broad potential for application in asymmetric syntheses.[1] In particular, the dihydroxyacetone phosphate (DHAP) dependent aldolases, which are available as a complete stereochemical set for the generation of all four possible types of diastereomeric DHAP–aldehyde adducts (D-fructose 1,6-bisphosphate aldolase = FruA, [EC 4.1.2.13]; D-tagatose 1,6-bisphosphate aldolase = TagA, [EC 4.1.2.-]; L-fuculose 1-phosphate aldolase = FucA, [EC 4.1.2.17]; L-rhamnulose 1-phosphate aldolase = RhuA, [EC 4.1.2.19]),[2] are characterized by preparative efficiency, high chiral induction for two stereocenters, and a broad substrate tolerance for the aldol acceptor component. In addition, the FucA and RhuA enzymes have the capacity for an almost complete kinetic differentiation of racemic 2-hydroxyaldehydes.[3] Problematic is the fact that DHAP **5**, the essential donor component, is commercially too expensive for preparative syntheses[4] and relatively unstable in solution. The published procedures for its chemical synthesis (acid hydrolysis of the dimethyl acetal **1**, eight steps from 3-chloro-1,2-propanediol,[5] overall yield 17%; hydrolysis of the dimeric diethyl acetal **2**, three to five steps from dihydroxyacetone, phosphorylation by diphenyl chlorophosphate,[6a] phosphoroxy chloride,[6b] or *O,O'*-dibenzyl *N,N*-diethyl phosphoramidite,[6c] up to 50% overall yield) and enzymic synthesis (phosphorylation of dihydroxyacetone **3** by glycerol kinase/ATP, 83%;[7] cleavage of fructose 1,6-bisphosphate **4** by FruA/TPI (TPI = triosephosphate isomerase), ca. 100%[8]) have serious disadvantages with respect to expenditure (number of steps, cost of reagents) and purity of product. Here we describe a novel enzymic procedure that generates **5** practically quantitatively and in high chemical purity from inexpensive starting materials and its use in situ with different DHAP aldolases in a coupled reaction with aldehydes. This procedure also proved adaptable to the synthesis of DHAP analogues modified at the phosphate group, which are likewise accepted by the aldolases.

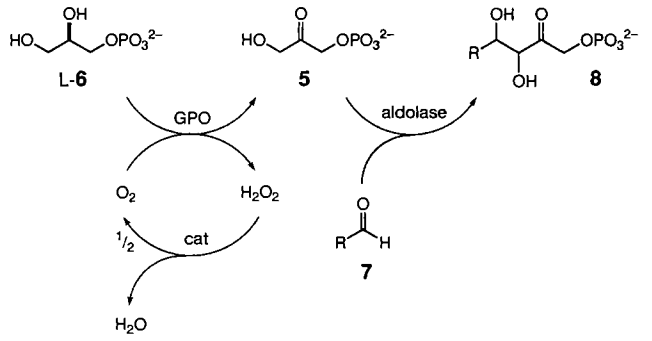


In the metabolism of several bacteria L-glycerol 3-phosphate (L-**6**) is oxidized to DHAP by a flavine-dependent glycerol phosphate oxidase (GPO, [EC 1.1.3.21]).[9] In contrast to the oxidation mediated by glycerol phosphate dehydrogenase [EC 1.1.1.8], a separate cofactor regeneration step[10] is not necessary because the reduced cofactor $FAD(H_2)$ remains tightly bound to the enzyme and is rapidly reoxidized by elemental oxygen with liberation of hydrogen peroxide. Since the latter can be used for the indirect quantification of glycerol in optical tests, GPO is a common and inexpensive enzyme. However, its obvious application to the preparative synthesis of **5** had to the best of our knowledge not been realized previously. We have found that the oxidation of L-**6** indeed proceeds smoothly and practically without competing side reactions if the buildup of a considerable stationary concentration of the coproduct H_2O_2, known to destruct enzymic activities, is suppressed by added catalase (cat, [EC 1.11.1.6]; Scheme 1). GPO exclusively oxidizes the L enantiomer,[11] which preparatively is best obtained by enzymic phosphorylation of glycerol.[7] This latter reaction, however, cannot be coupled with the oxidase reaction because of the low oxygen tolerance of glycerol kinase.

At higher concentrations **5** acts as a competitive GPO inhibitor. Out of the seven different commercial GPO preparations from at least three different organisms that we have inves-

[*] Prof. Dr. W.-D. Fessner,[+] Dipl.-Chem. G. Sinerius
Institut für Organische Chemie und Biochemie der Universität
Albertstrasse 21, D-79104 Freiburg (FRG)
[+] New address:
Institut für Organische Chemie der Technischen Hochschule
Professor-Pirlet-Strasse 1, D-52056 Aachen (FRG)
Telefax: Int. code + (241) 8888-127

[**] Enzymes in Organic Synthesis, Part 7. This research was supported by the Deutsche Forschungsgemeinschaft (Grant Fe 244/2-2), the Fonds der Chemischen Industrie, and the Wissenschaftliche Gesellschaft Freiburg. We thank Dr. P. Rasor, Boehringer Mannheim GmbH, for the generous gift of several enzymes, and Dr. W. Deck for ^{31}P NMR spectra.—Part 6: [3b].

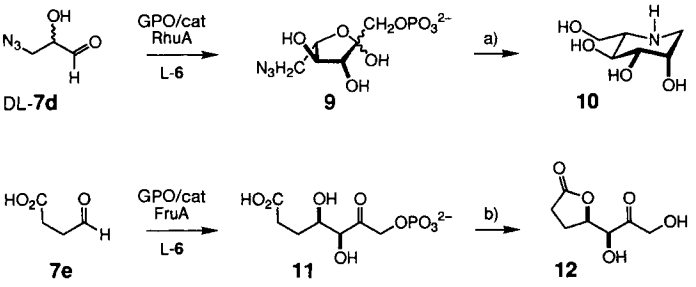


Scheme 1. Multienzymic synthesis of ketose-1-phosphates **8** from L-glycerol 3-phosphate (L-**6**).

tigated[12] the ones from *Streptococcus* species showed the lowest product inhibition (residual activity ca. 20% at 100 mM **5**). At this concentration preparative reactions can thus be run up to roughly 90–95% conversion to furnish **5** without further contaminants.[13] These particular enzyme preparations also displayed the highest stability in solution ($t_{1/2} \geq 3$ d at 25 °C; 2 U mL^{-1}),[14] which makes immobilization unnecessary, and only minimal sensitivity to higher concentrations of substrate (0.5 M), organic cations (e.g., cyclohexylammonium salts, 1.0 M), and inorganic phosphate (0.1 M; residual activity $\geq 70\%$ in each case), as well as the highest tolerance against H_2O_2 ($t_{1/2} \approx 1.5$ h at 150 mM). On the preparative scale, a sufficient oxygen supply at room temperature could be easily provided by shaking or mechanical stirring without noticeable enzyme deactivation. Scheme 1 suggested further that oxygenation could be sustained by careful addition of H_2O_2, which was indeed verified experimentally.

Rather unexpectedly, the oxidative generation of **5** could be smoothly coupled to its consumption by enzyme-catalyzed addition to aldehydes **7** (Scheme 1). This not only prevents inhibition of the GPO by **5** and thus assures rapid and quantitative conversion of L-**6**, but also suppresses almost completely any decomposition of the labile **5** since it does not accumulate. Neither the (limited) occurrence of H_2O_2 nor the application of oxygen-saturated solutions—even at an elevated oxygen partial pressure of up to 5 bar—led to the feared deactivation of the several tested DHAP aldolases from rabbit muscle (FruA) and *E. coli* (FruA, FucA, RhuA). The coupled reactions were preferably run at slightly acidic pH to assure that **5** is sufficiently stable and to maintain a high conversion rate. Compared to the established procedures[6–8] the GPO method usually furnishes adducts **8** of higher purity and in equal or higher yields. An interesting observation is that when the cyclohexylammonium salt of **6** is used, some particular aldol adducts (e.g. L-**8e**) crystallize in high yield and purity already upon concentration of the crude product solution, which significantly simplifies the work-up.

In spite of the sensitivity of aldehydes for air oxidation, this anticipated competing reaction was negligible under the usual reaction conditions; we interpret this inter alia as resulting from hydrate formation in aqueous solution. Simple (acetaldehyde, **7a**) and hydroxylated aliphatic aldehydes (glycolaldehyde, **7b**; L-glyceraldehyde, **7c**) were transformed smoothly into the known ketose phosphates[2a] (Table 1). In a one-flask reaction starting from L-**6** and racemic 3-azido-2-hydroxypropanal **7d** only the L-configurated aldehyde was converted by the RhuA as expected, owing to efficient kinetic control.[3a] The resulting pure adduct **9** was transformed into the non-naturally configurated alkaloid 1-deoxy-L-mannojirimycin **10** by dephosphorylation and hydrogenolysis (overall yield 60%; Scheme 2).[15]



Scheme 2. Chemoenzymic syntheses of 1-deoxy-L-mannojirimycin (**10**) and chiral γ-lactones like **12**. a) Acid phosphatase [EC 3.1.3.2], H_2, Pt/C; b) H_3O^+.

Particularly advantageous is the GPO reaction in combination with FruA-catalyzed conversions of anionic aldol acceptors, because in this case the thermodynamic relationships are far more favorable than those involving **4**, which is most often applied as the starting material.[1c] Thus, succinic semialdehyde **7e** and L-**6** gave adduct **11** in good yield (81%; only 40% from **4**[16]). Acidic conditions effected a cyclization furnishing the optically pure γ-lactone **12** (Scheme 2; RhuA provides *ent*-**11**/**12**, see Table 1) which, because of its differentiated funtionalization, is of interest as a potential precursor to a range of biologically active compounds.

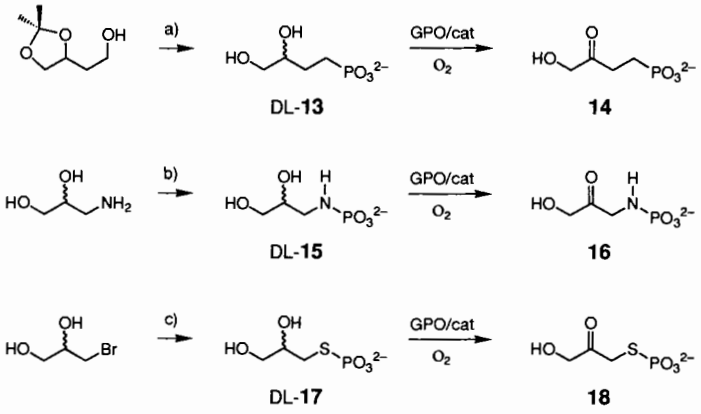
Table 1. Aldol reactions coupled with the GPO-catalyzed, in situ generation of DHAP and its analogues [a].

Aldehyde	Donor	Aldolase	Product	Yield [%]
–[b]	L-**6**	$FruA_{eco}$	D-fructose 1,6-P_2 (**4**)	95
acetaldehyde (**7a**)	L-**6**	RhuA	5-deoxy-L-*threo*-pentulose 1-P (**8a**)	70
glycolaldehyde (**7b**)	L-**6**	$FruA_{rab}$	D-*threo*-pentulose 1-P (**8b**)	84
glycolaldehyde (**7b**)	L-**6**	RhuA	L-*threo*-pentulose 1-P (**8c**)	96
glycolaldehyde (**7b**)	L-**6**	FucA	D-*erythro*-pentulose 1-P (**8d**)	93
L-glyceraldehyde (**7c**)	L-**6**	RhuA	L-fructose 1-P (**8e**)	85
L-glyceraldehyde (**7c**)	L-**6**	FucA	L-tagatose 1-P (**8f**)	86
3-azido-2-hydroxypropanal (**7d**)	L-**6**	RhuA	L-6-azido-6-deoxy-L-fructose 1-P (**9**)	70
succinic semialdehyde (**7e**)	L-**6**	$FruA_{rab}$	(4*R*,5*S*)-6-oxo-4,5,7-trihydroxyheptanoic acid 7-P (**11**)	81
succinic semialdehyde (**7e**)	L-**6**	RhuA	(4*S*,5*R*)-6-oxo-4,5,7-trihydroxyheptanoic acid 7-P (*ent*-**11**)	82
L-glyceraldehyde (**7c**)	DL-**13**	RhuA	2-deoxy-L-*arabino*-hept-3-ulose 1-phosphonate (**19**)	[c]
L-glyceraldehyde (**7c**)	DL-**15**	RhuA	1-deoxy-L-fructose 1-phosphoramidate (**20**)	[d]
L-glyceraldehyde (**7c**)	DL-**17**	RhuA	1-deoxy-L-fructose 1-phosphorothioate (**21**)	[c]

[a] Indices: eco = *Escherichia coli*, rab = rabbit muscle; P = orthophosphoric ester. Yields refer to isolated material purified by ion exchange and uniform according to ^{1}H NMR spectroscopy and thin-layer chromatography. [b] Formation of D-glyceraldehyde 3-phosphate by triosephosphate isomerase. [c] 1:1 Mixture with D-**13** or D-**17**, respectively. [d] Not determined.

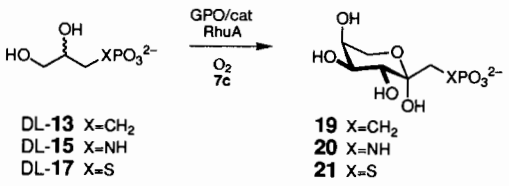
 © VCH Verlagsgesellschaft mbH, D-69451 Weinheim, 1994 0570-0833/94/0202-0210 $ 10.00+.25/0

The positive results with the GPO method suggested a possible extension to the preparation of suitable DHAP analogues. Earlier work employing FruA from rabbit muscle had shown that modification of the free hydroxymethylene moiety in **5** generally leads to a complete loss of activity, whereas phosphonate **14**, which is derived from isosteric replacement of the phosphorylated subunit in **5**, is converted in enzymic assays at 10% of the rate of the reaction of **5**.[17] Ketone **14** had been accessible previously only by a multistep route of low efficiency,[18a,d] and its preparative use restricted to the assay scale.[18b] However, phosphonate **13**,[18c,e] isosteric to diol **6**, is readily obtained by the route illustrated in Scheme 3, as are the corresponding phosphoramidate and phosphorothioate analogues **15**[19] and **17**, respectively.



Scheme 3. Chemoenzymic syntheses of isosteric DHAP analogues. a) Ph_3PBr_2/dimethylformamide (DMF), $P(OEt)_3$, Me_3SiBr, H_2O; b) ref. [19]; c) aq. Na_3PO_3S (pH 8).

Indeed, upon treatment with GPO all three compounds were converted into the corresponding DHAP analogues which, for practical reasons (hydrolytic instability[19] of **15**–**18**), were directly converted in situ by coupled aldol additions into the sugar derivatives **19**–**21** (Table 1). As expected only up to 50% of the



racemic precursors **13** and **17** was converted. Thus, the adducts were characterized only as mixtures with remaining starting material (Table 2). The analysis of the reaction of **15**/**16** was complicated by competing rapid phosphoroamidate hydrolysis and potentially competing oxidative side reactions and subsequent reactions (plausibly via enamine tautomers[20]). For a more detailed investigation of the latter system and to facilitate product isolation the synthesis of enantiomerically pure L-analogues is highly desirable.

In the last two years the GPO procedure has completely replaced the competing methods for DHAP generation for almost all types of applications in our labs. In particular, the extension of the product spectrum through the use of DHAP analogues[21] is an advantage of this procedure.

Table 2. NMR data of selected compounds [a].

12: ^{1}H NMR (pH 1.0): δ = 2.40–2.52 (m, 3-H), 2.70 (m, 2-H), 4.51 (d, 5-H), 4.54 (d, 7-H_a), 4.65 (d, 7-H_b), 5.12 (dt, 4-H), $J_{3,4}$ = 6.0, $J_{4,5}$ = 2.3, $J_{7a,7b}$ = 19.5; ^{13}C NMR (pH 1.0): δ = 23.14 (C-3), 28.71 (C-2), 66.40 (C-7), 76.47 (C-4), 81.73 (C-5), 181.84 (C-1), 211.60 (C-6)

13: ^{1}H NMR: δ = 1.42–1.80 (m, 1-, 2-H), 3.52 (dd, 4-H_a), 3.62 (dd, 4-H_b), 3.70 (m, 3-H), $J_{2,4a}$ = 6.7, $J_{2,4b}$ = 3.75, $J_{4a,4b}$ = 12.0; ^{13}C NMR: δ = 24.90 (d, C-1), 27.55 (d, C-2), 65.49 (s, C-4), 72.99 (d, C-3); $J_{C\text{-}1,P}$ = 133.1, $J_{C\text{-}2,P}$ = 2.7, $J_{C\text{-}3,P}$ = 16.0; ^{31}P NMR: δ = 24.26

14: ^{1}H NMR: δ = 1.68 (m, 1-H), 2.67 (m, 2-H), 4.73 (s, 4-H); ^{13}C NMR: δ = 25.88 (d, C-1), 32.61 (d, C-2), 67.31 (s, C-4), 203.05 (d, C-3), $J_{C\text{-}1,P}$ = 131.6, $J_{C\text{-}2,P}$ = 4.1, $J_{C\text{-}3,P}$ = 13.2; ^{31}P NMR: δ = 24.58

17: ^{1}H NMR: δ = 2.80 (ddd, 1-H_a), 2.90 (ddd, 1-H_b), 3.61 (dd, 3-H_a), 3.69 (dd, 3-H_b), 3.90 (ddd, 2-H), $J_{1a,1b}$ = 13.5, $J_{1a,P}$ = 11.2, $J_{1b,P}$ = 12.0, $J_{1a,2}$ = 6.7, $J_{1b,2}$ = 4.8, $J_{2,3a}$ = 6.0, $J_{2,3b}$ = 4.5, $J_{3a,3b}$ = 11.7; ^{13}C NMR: δ = 32.80 (s, C-1), 64.38 (s, C-3), 72.56 (s, C-2); ^{31}P NMR: δ = 16.78

18: ^{1}H NMR [b]: δ = 3.04 (d, 1-H_H), 3.60 (s, 3-H_H), 3.64 (d, 1H_K), 4.56 (s, 3-H_K), $J_{1,P(H)}$ = 13.5, $J_{1,P(K)}$ = 11.0, ketone : hydrate = 6 : 1; ^{13}C NMR: δ = 36.06 (s, C-1$_K$), 65.14 (s, C-3$_K$), 210.75 (s, C-2$_K$); ^{31}P NMR: δ = 15.55 (K)

19: ^{1}H NMR: δ = 1.70 (m, 2-H), 1.98 (m, 1-H); ^{13}C NMR: δ = 22.25 (d, C-1), 32.58 (s, C-2), 62.69 (s, C-3), 69.89, 70.46, 71.03 (3s, C-4, -5, -6), 109.36 (s, C-7), $J_{C\text{-}1,P}$ = 133.8; ^{31}P NMR: δ = 25.36

21: ^{1}H NMR: δ = 2.98 (dd, 1-H_a), 3.22 (dd, 1-H_b); ^{13}C NMR: δ = 36.95 (s, C-1), 63.81 (s, C-6), 69.30, 69.75, 70.34 (3s, C-3, -4, -5), 98.96 (s, C-2); ^{31}P NMR: δ = 16.77

[a] NMR spectra were recorded in D_2O at pH 7.0 after ion exchange giving the Na^+ salts. ^{1}H NMR data (400.1 MHz) are referenced relative to sodium 3-trimethylsilyl-[$^2H_4$]propionate (TSPNa) (δ = 0.00), ^{13}C NMR (100.6 MHz) to CH_3CN (δ = 1.30), and ^{31}P NMR (80 MHz) to D_3PO_4 (δ = 0.00); coupling constants in Hz. [b] Indices: H = hydrate, K = ketone.

Experimental Procedure

To a solution containing **6** (as its bis(cyclohexylammonium) salt; 370 mg, 1.0 mmol) and L-glyceraldehyde **7c** (110 mg, 1.2 mmol) in 10 mL of oxygen-saturated water at pH 6.8 was added 70 U of GPO, 1000 U of catalase, and 50 U of RhuA. The mixture was shaken at 20 °C under an oxygen atmosphere at 100 Upm. Conversion was monitored by enzymic assay for equivalents of DHAP produced, as well as by ^{1}H and ^{31}P NMR spectroscopy. After the solution was filtered through charcoal, the pH was adjusted to 7.5 by addition of 1.0 M cyclohexylamine in ethanol, and the solution was concentrated to dryness by rotary evaporation at $\leq$20 °C in vacuo. The solid residue was taken up in 0.5 mL of water, and the resulting solution was filtered. Anhydrous ethanol was added (2.5 mL) followed by anhydrous acetone until a faint turbidity remained. Recrystallization at 4 °C furnished the bis(cyclohexylammonium) salt of L-fructose 1-phosphate **8e** as colorless needles; chemical yield 370 mg (85%).

Received: July 22, 1993 [Z 6226 IE]
German version: *Angew. Chem.* **1994**, *106*, 217

[1] a) E. J. Toone, E. S. Simon, M. D. Bednarski, G. M. Whitesides, *Tetrahedron* **1989**, *45*, 5365–5422; b) D. G. Drueckhammer, W. J. Hennen, R. L. Pederson, C. F. Barbas, C. M. Gautheron, T. Krach, C.-H. Wong, *Synthesis* **1991**, 499–525; c) W.-D. Fessner, *Kontakte (Darmstadt)* **1992** (3), 3–9; *ibid.* **1993** (1), 23–34.

[2] a) W.-D. Fessner, G. Sinerius, A. Schneider, M. Dreyer, G. E. Schulz, J. Badía, J. Aguilar, *Angew. Chem.* **1991**, *103*, 596–599; *Angew. Chem. Int. Ed. Engl.* **1991**, *30*, 555–558; b) W.-D. Fessner, O. Eyrisch, *ibid.* **1992**, *104*, 76–78 and **1992**, *31*, 56–58.

[3] a) W.-D. Fessner, J. Badía, O. Eyrisch, A. Schneider, G. Sinerius, *Tetrahedron Lett.* **1992**, *33*, 5231–5234; b) W.-D. Fessner, A. Schneider, O. Eyrisch, G. Sinerius, J. Badía, *Tetrahedron Asymmetry* **1993**, *4*, 1183–1192.

[4] Fluka price per mmol DHAP: Li_2-**5** · H_2O = US$ 250, $Ba_{1.5}$H-**2** = US$ 27.

[5] C. E. Ballou, H. O. L. Fischer, *J. Am. Chem. Soc.* **1956**, *78*, 1659–1661.

[6] a) R. L. Colbran, J. K. N. Jones, N. K. Matheson, I. Romeza, *Carbohydr. Res.* **1967**, *4*, 355–358; b) F. Effenberger, A. Straub, *Tetrahedron Lett.* **1987**, *28*, 1641–1644; c) R. L. Pederson, J. Esker, C.-H. Wong, *Tetrahedron* **1991**, *47*, 2643–2648.

[7] D. C. Crans, G. M. Whitesides, *J. Am. Chem. Soc.* **1985**, *107*, 7019–7027.

[8] O. Meyerhof, K. Lohmann, *Biochem. Z.* **1934**, *271*, 89–110; cf. W.-D. Fessner, C. Walter, *Angew. Chem.* **1992**, *104*, 643–645; *Angew. Chem. Int. Ed. Engl.* **1992**, *31*, 614–616.

[9] The GPO from *Streptococcus faecium* is a homodimer of subunits with a molecular weight of 65000 each containing one mole of FAD; K_M (L-**6**) = 26 mM, specific activity 65 U mg^{-1}: a) T. W. Esders, C. A. Michrina, *J. Biol. Chem.* **1979**, *254*, 2710–2715; b) A. Claiborne, *ibid.* **1986**, *261*, 14398–14407.

 © *VCH Verlagsgesellschaft mbH, D-69451 Weinheim, 1994* *0570-0833/94/0202-0211 $ 10.00+.25/0*

[10] W.-D. Fessner, G. Sinerius, *Bioorg. Med. Chem.*, in press.
[11] a) In analogy with biochemical literature we have retained the stereonotation for **6** which is defined by its relationship to L-glyceraldehyde 3-phosphate. b) As evident from enzymic assays, the GPO activity is only marginally affected by D-**6** and the isomeric glycerol 2-phosphate. This suggests that either the racemate or common commercial mixtures of 1(2)-monophosphates could also be utilized instead of enantiomerically pure L-**6** as inexpensive alternatives.
[12] Commerical glycerol phosphate oxidases from *Streptococcus, Pediococcus*, and *Aerococcus* as well as from an unspecified microorganism were employed as provided by Asahi, Boehringer Mannheim, Sigma, and Toyobo.
[13] **5** can be stored at −78 °C either as the product solution adjusted to pH 3–4 or as lyophilized salts, the composition of which can be predetermined by selection of the precursor salt of L-**6**.
[14] In accordance with the often high binding constants of FAD-dependent enzymes, the stability of the oxidases is only negligibly improved by addition of FAD in the range of 1–1000 μM.
[15] K. K.-C. Liu, T. Kajimoto, L. Chen, Z. Zhong, Y. Ichikawa, C.-H. Wong, *J. Org. Chem.* **1991**, *56*, 6280–6289.
[16] G. Puttkammer, Diploma Thesis, Universität Freiburg, **1990**.
[17] N. Bischofberger, H. Waldmann, T. Saito, E. S. Simon, W. Lees, M. D. Bednarski, G. M. Whitesides, *J. Org. Chem.* **1988**, *53*, 3457–3465; M. D. Bednarski, E. S. Simon, N. Bischofberger, W.-D. Fessner, M.-J. Kim, W. Lees, T. Saito, H. Waldmann, G. M. Whitesides, *J. Am. Chem. Soc.* **1989**, *111*, 627–635.
[18] a) H. B. F. Dixon, M. J. Sparkes, *Biochem. J.* **1974**, *141*, 715–719; b) D. Stribling, *ibid.* **1974**, *141*, 725–728; c) P. R. Adams, R. Harrison, T. D. Inch, *ibid.* **1974**, *141*, 729–732; d) S. L. Goldstein, D. Braksmayer, B. E. Tropp, R. Engel, *J. Med. Chem.* **1974**, *17*, 363–364; e) J. Kabak, L. DePhilippe, R. Engel, B. Tropp, *ibid.* **1972**, *15*, 1074–1075.
[19] R. Duncan, D. G. Drueckhammer, *Tetahedron Lett.* **1993**, *34*, 1733–1736.
[20] J. E. Hodge, B. E. Fisher, *Methods Carbohydr. Chem.* **1963**, *2*, 99–107.
[21] The technique also seems to be applicable for the regiospecific introduction of isotopic labels from suitably labeled glycerol precursors.

Neutral Gold(I) Fluoride Does Indeed Exist**

Detlef Schröder, Jan Hrušák,
Inis C. Tornieporth-Oetting, Thomas M. Klapötke,
and Helmut Schwarz*

Dedicated to Professor Heinrich Nöth on the occasion of his 65th birthday

The chemistry of gold and its compounds still receives considerable attention.[1] This interest is not only caused by the potential catalytic activity of gold; it also reflects the fascinating coordination chemistry of gold(I) compounds.[2] Although several gold halides in various oxidation states are described in the literature,[1, 3] there is no unambiguous experimental evidence for the existence of the neutral AuF.[4] The only *indirect* characterization of gaseous AuF is based on the analysis of emission spectra of species generated in the etching of gold films in O_2/CF_4 and O_2/SF_6 rf glow-discharge plasmas.[5] Although the title of that contribution[5] implies that evidence for the existence of AuF had been found, in the discussion of the experimental results the authors leave no doubt that besides AuF the diatomic molecules AuO, AuO^+, and AuF^+ cannot be definitively ruled out as the emitting species, and the hope for additional investigations is explicitly expressed. Actually, it has been stated recently that "there is still no evidence for the existence of a definitively characterized gold(I) fluoride."[4b] Recent theoretical calculations, using a correlated relativistic approach, predict solitary AuF as a stable entity with a calculated bond dissociation energy of 59 kcal mol^{-1}.[6] Here for the first time, we will provide evidence for the existence of this long-sought molecule, and we also will report an estimate of the bond dissociation energy of AuF.

Neutralization–reionization mass spectrometry (NRMS) has been established as a versatile tool in the study of elusive molecules in the gas phase.[7] The inability to generate the corresponding bulk materials in the condensed phase often does not reflect an intrinsic instability of the neutral species; rather, the "non-existence" is due to facile bi- or termolecular reactions, such as isomerization, disproportionation, or solvolysis, which prevent experimental detection and characterization of the molecule in solution or in a matrix. Recently, NRMS has been successfully applied to the study of many unusual organometallic molecules, none of which is viable in the condensed phase.[7, 8]

Upon collisional activation[9] of AuF^+ with oxygen as a stationary gas, the formation of Au^+, corresponding to the loss of the fluorine ligand, is the only singly charged product observed (Fig. 1). Due to the high ionization energy of fluorine (IE(F) = 17.4 eV, IE(Au) = 9.2 eV)[16] as well as the reduced kinetic energy of the resulting fragment ion, the intensity of the signal corresponding to the fluorine cation was below the detection limit. In addition to atomic Au^+, dications are formed by charge stripping of AuF^+ in collision with oxygen. The observation that the doubly charged Au^{2+} gives rise to a signal about 25 times more intense than that of the AuF^{2+} dication indicates that the lifetime of AuF^{2+} is short; most likely upon charge stripping an electron is removed from the σ bond of AuF^+, thus making the incipient AuF^{2+} quite susceptible to fragmentation.[17] By means of high-resolution translational energy loss spectroscopy (HRTELS)[18] we ascertained that excited electronic states of AuF^+ do not contribute to the cations originating from electron impact ionization (EI) of AuF_3; this is evidenced by the absence of peaks at the high-energy side, which would result from superelastic collisions of excited AuF^+ in an HRTELS experiment (inset in Fig. 1).

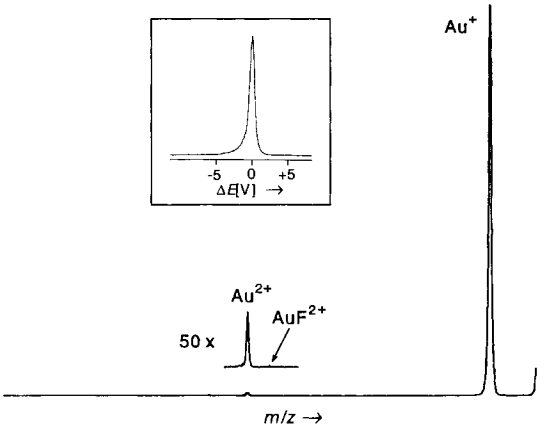


Fig. 1. Collisional activation spectrum of mass-selected AuF^+ with oxygen (70% *T*). The inset shows the HRTEL spectrum of AuF^+ with oxygen (50% *T*); see text and [9] for details.

If AuF^+ is subjected to a NRMS experiment, a distinct recovery signal is observed, which corresponds to the reionized neutral AuF molecule (Fig. 2). This provides for the first time un-

[*] Prof. Dr. H. Schwarz, Dr. D. Schröder, Dr. J. Hrušák
Institut für Organische Chemie der Technischen Universität
D-10623 Berlin (FRG)
Telefax: Int. code +(30)314-21102.
Dr. I. C. Tornieporth-Oetting, Priv.-Doz. Dr. T. M. Klapötke
Institut für Anorganische and Analytische Chemie
der Technischen Universität, Berlin

[**] This work was supported by the Deutsche Forschungsgemeinschaft and the Fonds der Chemischen Industrie.

ambiguous experimental evidence that neutral AuF is a stable gas-phase species as predicted by theory[6] and conjectured in the analysis of emission spectra.[5] From the distance between the two collision cells (10 cm) the *minimal* lifetime of neutral AuF is calculated to exceed 25 μs. The NR spectrum is dominated by a large signal corresponding to Au^+, which largely originates from the dissociation of the neutral molecule followed by reionization; furthermore, a weak signal for Au^{2+} is observed. We note in passing that also in the NR spectrum of the AuF^- anion, generated by electron import of AuF_3 in the presence of the electron-moderating agent N_2O,[19] a recovery signal corresponding to reionized AuF is observed. These NR experiments demonstrate beyond doubt that AuF resides in a potential minimum. Thus, the elusiveness of the species in the condensed phase[1] does not reflect an intrinsic instability of AuF; rather, our results point to the operation of facile intermolecular reactions, which as yet preclude the generation of bulk AuF.

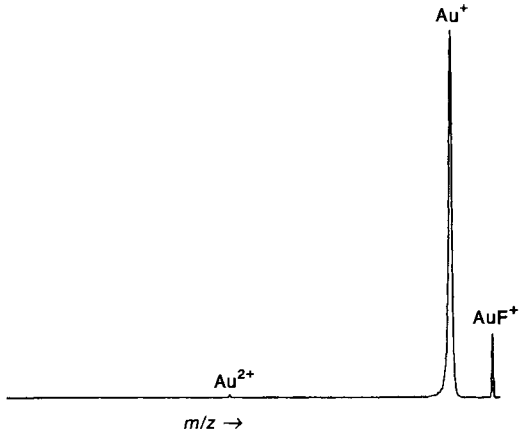
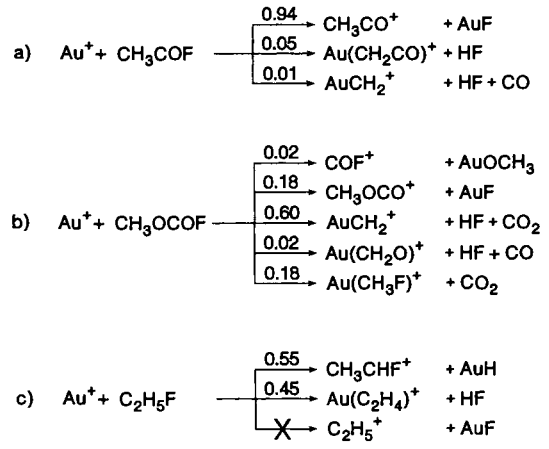


Fig. 2. Neutralization–reionization mass spectrum of mass-selected AuF^+ (xenon, 85% *T*/oxygen 85% *T*).

Once the existence of neutral AuF had been established, we were interested in the determination of the bond dissociation energy (BDE) of this molecule. One possibility of elucidating the thermochemistry of *neutral* species in a mass spectrometric setup is provided by the study of ion–molecule reactions of thermalized ions with appropriate neutral substrates. These experiments allow the determination of upper and lower bounds for the heat of formation of neutral as well as ionic species, provided thermochemical information for the remaining reaction partners is available.[16] To this end we have performed Fourier transform ion cyclotron resonance (FTICR) experiments,[9] in which thermalized Au^+ cations were subjected to reaction with various fluorine-containing organic compounds R–F (Scheme 1). Since an abstraction of a fluoride anion is believed to occur fast and without a significant barrier,[20] the occurrence of the corresponding R^+ cations permits the determination of the upper and lower limits of BDE(AuF).

When Au^+ is treated with acetyl fluoride, the predominant reaction channel corresponds to the formation of CH_3CO^+ and neutral AuF (Scheme 1a). This observation implies that BDE(AuF) > 68 kcal mol^{-1}. Similarily, neutral AuF is formed in the reaction of Au^+ with methyl fluoroformate, which yields a lower bound for BDE(AuF) of 73 kcal mol^{-1} (Scheme 1b). As other reaction channels compete effectively with this reaction, abstraction from methyl fluoroformate is believed to occur near threshold. However, because $\Delta H_f(FCO_2CH_3)$[21] is not as reliably known as $\Delta H_f(CH_3COF)$, the BDE value based on process (1b) is subject to further refinement. The observation that various other fluorinated organic compounds R–F do *not* give rise to neutral AuF and the corresponding organic cations R^+ (e.g., R=CH_3, C_2H_5, $CFCl_2$, CF_2Cl, CF_2Br, CHF_2, CF_3, *c*-C_6F_5, CH_2CH_2OH, and SF_5)[24] permits an estimate of the upper limit of BDE(AuF). An upper bound for BDE(AuF) of 85 kcal mol^{-1} results from the absence of the formation of $C_2H_5^+$ in the ion–molecule reaction of Au^+ with ethyl fluoride (Scheme 1c). Furthermore, since in this reaction $C_2H_5^+$ is not even formed if excited Au^+ cations are used, the upper bound of 85 kcal mol^{-1} will be considerably too high.



Scheme 1. Ion–molecule reactions with Au^+.

In conclusion, the existence of AuF has been unambiguously established by means of a NRMS experiment. From the results of ion–molecule reactions of thermalized Au^+ cations with various substrates, lower and upper bounds for the bond dissociation energy of AuF can be obtained, which are in reasonable agreement with the theoretical predictions.[6a,c,25]

Received: July 22, 1993
Revised version: October 14, 1993 [Z 6228 IE]
German version: *Angew. Chem.* **1994**, *106*, 223

[1] *Gmelin Handbook, Au Suppl. Vol. B1*, Springer, Berlin, **1992**.
[2] a) F. Scherbaum, A. Grohmann, B. Huber, C. Krüger, H. Schmidbaur, *Angew. Chem.* **1988**, *100*, 1600, 1602; *Angew. Chem. Int. Ed. Engl.* **1988**, *27*, 1544, 1546; b) F. Scherbaum, A. Grohmann, G. Müller, H. Schmidbaur, *ibid.* **1989**, *101*, 464 and **1989**, *28*, 463; c) A. Grohmann, J. Riede, H. Schmidbaur, *Nature* **1990**, *345*, 140; d) E. Zeller, H. Beruda, A. Kolb, P. Bissinger, J. Riede, H. Schmidbaur, *ibid.* **1991**, *352*, 141.
[3] B. G. Müller, *Angew. Chem.* **1987**, *99*, 1120; *Angew. Chem. Int. Ed. Engl.* **1987**, *26*, 1081.
[4] a) N. S. Chilingarov, M. V. Korobov, S. V. Rudometkin, A. S. Alikhanayan, L. N. Sidorov, *Int. J. Mass Spectrom. Ion Processes* **1986**, *69*, 175; b) ref. [1], p. 113.
[5] K. L. Saenger, C. P. Sun, *Phys. Rev. A* **1992**, *46*, 670.
[6] a) P. Schwerdtfeger, M. Dolg, W. H. E. Schwarz, G. A. Bowmaker, P. D. W. Boyd, *J. Chem. Phys.* **1989**, *91*, 1762; b) P. Schwerdtfeger, *J. Am. Chem. Soc.* **1989**, *111*, 7261; c) P. Schwerdtfeger, P. D. W. Boyd, A. K. Burell, W. T. Robinson, M. J. Taylor, *Inorg. Chem.* **1990**, *29*, 3593.
[7] Recent reviews: a) H. Schwarz, *Pure Appl. Chem.* **1989**, *61*, 685; b) J. L. Holmes, *Adv. Mass Spectrom.* **1989**, *11*, 53; c) J. K. Terlouw, *ibid.* **1989**, *11*, 984; d) J. L. Holmes, *Mass Spectrom. Rev.* **1989**, *8*, 513; e) F. W. McLafferty, *Science* **1990**, *247*, 925.
[8] For the application of NRMS to organometallic ions, see: a) C. B. Lebrilla, T. Drewello, H. Schwarz, *Organometallics* **1987**, *6*, 2268; b) T. Drewello, H. Schwarz, *Int. J. Mass Spectrom. Ion Processes* **1989**, *93*, 177; c) K. Eller, D.

 © *VCH Verlagsgesellschaft mbH, D-69451 Weinheim, 1994* *0570-0833/94/0202-0213 $ 10.00+.25/0*

Sülzle, H. Schwarz, *Chem. Phys. Lett.* **1989**, *154*, 443; d) T. Drewello, H. Schwarz, *ibid.* **1990**, *171*, 5; e) D. Schröder, D. Sülzle, J. Hrušák, D. K. Böhme, H. Schwarz, *Int. J. Mass Spectrom. Ion Processes* **1991**, *110*, 145; f) D. Schröder, H. Schwarz, *Organometallics* **1992**, *11*, 2296; g) D. Schröder, H. Schwarz, *Helv. Chim. Acta* **1992**, *75*, 1281; h) D. V. Zagorevskii, J. L. Holmes, *Organometallics* **1992**, *11*, 3224; i) D. V. Zagorevskii, J. L. Holmes, *Org. Mass Spectrom.* **1993**, *28*, 49; j) S. Karraß, D. Stöckigt, D. Schröder, H. Schwarz, *Organometallics* **1993**, *12*, 1449; k) D. Schröder, J. Hrušák, H. Schwarz, *Ber. Bunsenges. Phys. Chem.*, **1993**, *97*, 1085.

[9] Experimental details: All experiments were performed with a modified VG ZAB/HF/AMD four-sector mass spectrometer in *BEBE* configuration (*B* stands for magnetic and *E* for electric sector), which has been described previously [10]. The ion source was passivated by pretreatment with gaseous fluorine, generated in situ by thermolysis of AgF_2 (Alfa Ventron), and heated to 300 °C in order to minimize condensation of AuF_3 vapor on the instrument walls. Anhydrous AuF_3 was admitted to the ion source through the solid probe inlet system (sample temperature 330–380 °C) [11] and subsequently ionized by a beam of electrons (kinetic energy 70 eV) in an electron impact ion source (repeller voltage ≈ 20 V). Collisional activation was performed by colliding the beam of *B*(1) mass-selected AuF^+ cations with oxygen (70% transmission *T*); the cationic fragments were recorded by scanning *E*(1). For the NRMS study the ions of interest were mass-selected by means of *B*(1) and subjected to a double-collision experiment in the field-free region preceding *E*(1). Neutralization of the cations was brought about by collision with xenon (85% *T*); the remaining ions in the beam were deflected by a 1000 V potential, and the fast neutral species were subsequently reionized by collision with oxygen (85% *T*). The spectrum of the reionized species was recorded by scanning *E*(1). Due to the relatively low vapor pressure of AuF_3 and its readiness to undergo pyrolysis, maximum sensitivity in the collision experiments could only be achieved by using the first two sectors at a mass resolution of $m/\Delta m = 2.000$. All spectra were accumalted and processed on-line with the VG 250/11 data system, and 15–30 scans were averaged to improve the signal-to-noise ratio. Additional experiments were performed with a Spectrospin CMS 47X Fourier Transform ion cyclotron resonance (FTICR) mass spectrometer, which has been described in detail elsewhere [12]. In brief, Au^+ cations were generated in the external ion source by laser desorption/laser ionization of a pure gold target and, by using a system of electric potentials and lenses, the ions were transferred to the FTICR cell, which was situated within a 7 Tesla magnetic field. For the determination of ΔH_f, the isolated Au^+ cations were thermalized by multiple collisions with pulsed-in argon gas and reisolated by the FERETS (FERETS = front-end resolution enhancement using tailored sweeps) technique [13].

AuF_3 was prepared by treating a gold wire with an excess of elemental fluorine ($p_{F_2} = 15$ bar) in a quartz reactor at 1000 °C; since AuF_3 is extremely sensitive to atmospheric moisture, all handling was done under utmost anhydrous conditions [11]. The ion source mass spectrum of the AuF_3 so-formed was in excellent agreement with the previously reported one [14]. The organic fluorine compounds were either commercially available or synthesized and purified by well-known literature procedures [15].

[10] (a) R. Srinivas, D. Sülzle, T. Weiske, H. Schwarz, *Int. J. Mass. Spectrom. Ion Processes* **1991**, *107*, 368; (b) R. Srinivas, D. Sülzle, W. Koch, C. H. DePuy, H. Schwarz, *J. Am. Chem. Soc.* **1991**, *113*, 5970.

[11] In order to obtain maximal ion currents, the AuF_3 samples were slowly heated during the measurement (heating rate ≈ 2 (K) min^-, starting at 330 °C); this procedure represents a compromise between conditions at which AuF_2 is not volatile enough and those at which it is pyrolyzed.

[12] a) K. Eller, H. Schwarz, *Int. J. Mass Spectrom. Ion Processes* **1989**, *93*, 243; b) K. Eller, W. Zummack, H. Schwarz, *J. Am. Chem. Soc.* **1990**, *112*, 621.

[13] R. A. Forbes, F. H. Laukien, J. Wonka, *Int. J. Mass Spectrom. Ion Processes* **1988**, *83*, 23.

[14] a) M. J. Vasile, T. J. Richardson, F. A. Stevie, W. E. Falconer, *J. Chem. Soc. Dalton Trans.* **1976**, 351; see also ref. [4a].

[15] a) A. N. Nesmejanow; E. J. Kahn, *Chem. Ber.* **1934**, *67*, 370; b) E. Gryszkiewicz-Trochimowski, A. Sporzynski, J. Wnuk, *Recl. Trav. Chim. Pays-Bas* **1947**, *66*, 417; c) W. F. Edgell, L. Parts, *J Am. Chem. Soc.* **1955**, *77*, 4899.

[16] If not stated otherwise, all thermochemical data were taken from S. G. Lias, J. E. Bartmess, J. F. Liebman, J. L. Holmes, R. D. Levin, W. G. Mallard, *J. Phys. Chem. Ref. Data* **1988**, *17*, Suppl. 1.

[17] Reviews on the gas-phase chemistry of organic dications: a) W. Koch, H. Schwarz in *Structure/Reactivity and Thermochemistry of Ions* (Eds.: P. Ausloos, S. G. Lias), Reidel, Dordrecht, **1987**, p. 413; b) W. Koch, F. Maquin, D. Stahl, H. Schwarz, *Chimia* **1985**, *39*, 376; c) K. Lammertsma, P. von R. Schleyer, H. Schwarz, *Angew. Chem.* **1989**, *101*, 1313; *Angew. Chem. Int. Ed. Engl.* **1989**, *28*, 1321.

[18] P. Jonathan, Z. Hermann, M. Hamadan, A. G. Brenton, *Int. J. Mass Spectrom. Ion Processes* **1988**, *84*, 203, and references therein.

[19] K. J. van den Berg, S. Ingemann, N. M. M. Nibbering, *Org. Mass Spectrom.* **1993**, *28*, 527.

[20] For the energetics of similar halogen abstractions, see a) E. R. Fisher, L. S. Sunderlin, P. B. Armentrout, *J. Phys. Chem.* **1989**, *93*, 7375; b) E. R. Fisher, R. H. Schultz, P. B. Armentrout, *ibid.* **1989**, *93*, 7382.

[21] $\Delta H_f(FCOOCH_3)$ was estimated from the reaction $FCOOCH_3 + H_3CCOOCH_3 \rightarrow H_3COCOOCH_3 + CH_3CCOF$ which was assumed to be thermoneutral (see ref. [22]; $\Delta H_f(CH_3COCO^+)$ was taken from ref. [23].

[22] S. W. Benson, *Thermochemical Kinetics*, 2nd Ed., Wiley, New York, **1976**.

[23] M. C. Blanchette, J. L. Holmes, C. E. C. A. Hop, F. P. Lossing, R. Postna, P. J. A. Ruttnik, J. K. Terlouw, *J. Am. Chem. Soc.* **1986**, *108*, 7589.

[24] For ion–molecule reactions of Au^+ with various other substrates, see: a) W. L. Grady, M. M. Bursey, *Int. J. Mass Spectrom. Ion Phys.* **1983**, *52*, 247; b) D. A. Weil, C. L. Wilkins, *J. Am. Chem. Soc.* **1985**, *107*, 7316; c) A. K. Chowdhury, C. L. Wilkins, *ibid.* **1987**, *109*, 5336; see also: d) G. J. Leggett, M. C. Davies, D. E. Jackson, S. J. B. Tendler, *J. Phys. Chem.* **1993**, *97*, 5348.

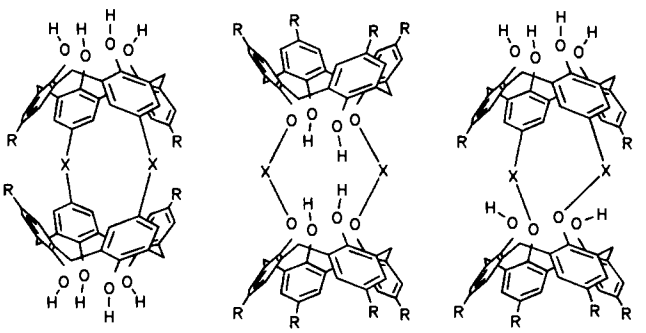
[25] According to the most recent state-of-the-art calculations, BDE(Au–F) = 71 kcal mol^{-1}, P. Schwerdtfeger, J. S. McFeaters, R. L. Stephens, M. J. Liddell, M. Dolg, B. A. Hess, *Chem. Mater.*, in press.

"Head-to-Tail" Linkage in Double Calix[4]arenes

Wojciech Wąsikiewicz, Gabriel Rokicki, Jędrzej Kiełkiewicz, and Volker Böhmer*

Calixarenes are macrocyclic compounds[1] which are readily available in large quantities, above all by condensation of *p-tert*-butylphenol with formaldehyde under alkaline conditions.[2] Numerous compounds are then accessible by substitution at the *para* positions (in some cases after prior elimination of the *tert*-butyl groups) and by reaction at the phenolic OH groups.[3] The synthesis of larger structures can also be achieved by covalently linking calixarene subunits.

Until now, the subunits have either been linked through the phenolic OH groups[4–12] or through the *para* positions.[13–15] When two calix[4]arenes in the *cone* conformation are coupled cyclically by two bridges X, two types of macrotricycles are formed in which either the two cavities (**1**)[13–15] or the two hydroxylated sides (**2**)[4, 5, 7] face each other. These alternatives can be described as "head-to-head" or "tail-to-tail" arrangements. We report here on the first double calix[4]arenes linked in a "head-to-tail" arrangement (**3**), in which both calixarenes have the same orientation. In contrast to compounds of type **1** or **2** in which the dipole moments of the calix[4]arene units cancel one another out, the dipole moments in **3** add up. This

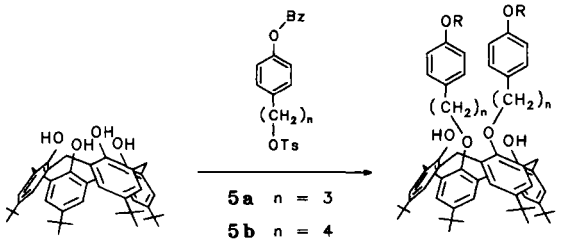


1 **2** **3**

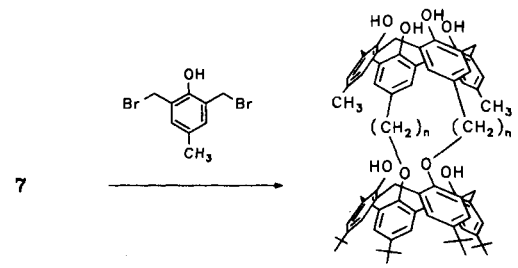
[*] Dr. V. Böhmer
Institut für Organische Chemie der Universität
J.-J.-Becher-Weg 34, SBI, D-55099 Mainz (FRG)
Telefax: Int. code + (6131)395419
Dipl.-Chem. W. Wąsikiewicz, Dr. G. Rokicki, Dr. J. Kiełkiewicz
Faculty of Chemistry
Warsaw University of Technology (Poland)

may be of significance for the potential application of similar compounds in areas such as nonlinear optics.[16]

In order to obtain stable compounds of type **3**, we chose to link the moieties by ether bonds. The synthesis was achieved by analogy with the method described for the preparation of bridged calix[4]arenes.[17] *tert*-Butylcalix[4]arene **4** reacted smoothly with tosylates **5** in a mole ratio 1:2 to give diethers **6** in yields of 89 and 70% after purification. After cleavage of the benzyl groups (H_2/Pd, 85–92%), diphenols **7** were reacted with bisbromomethylated *p*-cresol in glacial acetic acid in the presence of zinc acetate (as Lewis acid and Brønsted base). Finally, the double calix[4]arenes **8** were isolated in yields of 4–5% after a simple column-chromatographic purification.



4 **6** R = Bz, **7** R = H



7 **8**

The structures of **8a** and **8b** were confirmed by their mass and NMR spectra (see Table 1). The presence of two pairs of doublets assigned to the Ar–CH_2–Ar methylene protons shows that both calix[4]arene subunits are in the *cone* conformation.

Table 1. ^{1}H NMR data ($CDCl_3$, 400 MHz, δ values, coupling constants in Hz in parentheses) for the double calixarenes **8**.

Proton	**8a**	**8b**	
–OH	9.352	10.180	(br s, 4H)
	7.228	6.135	(s, 2H)
Ar–H	6.997	6.998	(s, 4H)
	6.980	6.897	(s, 4H)
	6.764	6.821	(s, 4H)
	6.742	6.568	(s, 4H)
Ar–CH_2–Ar	4.189 (14.0)	4.209 (13.8)	(d, 4H)
	4.116 (12.9)	4.155 (13.1)	(d, 4H)
	3.407 (14.1)	3.422 (13.9)	(d, 4H)
	3.262 (13.0)	3.205 (13.2)	(d, 4H)
–$(CH_2)_n$–	3.777	3.84	(m, 4H)
	2.338	2.591	(m, 4H)
	1.405	1.805	(m, 4H)
		1.645	(m, 4H)
–CH_3	2.209	1.897	(s, 6H)
–$C(CH_3)_3$	1.250	1.290	(s, 18H)
	0.923	0.806	(s, 18H)

This is further supported by the low-field OH signal corresponding to four protons. The rest of the spectrum is also consistent with the postulated structure: two singlets for the *tert*-butyl groups, one singlet for the methyl groups, and four singlets for the aromatic protons. Thus, the conformation adopted by **8a** and **8b** corresponds to that depicted.

A comparison of the NMR spectra of **8a** and **8b** leads to the conclusion that the hydrogen bonds in **8a** are somewhat weakened. This is an effect generally observed in *p*-bridged calixarenes with decreasing length of the bridge.[18] The distortion of the "newly formed" calixarene is also reflected in the position of the singlet corresponding to the methyl groups. Compared to the methyl groups in **8b** ($\delta = 1.90$), those in **8a** ($\delta = 2.21$) are rotated further out of the shielding region of the benzene rings below, belonging to the "original" calixarene.

We are now in the process of synthesizing further calix[4]arenes of type **3**. A different strategy in which the calix[4]arene units are synthesized prior to linkage should also allow access to compounds with three or more calixarenes in the "head-to-tail" arrangement.

Experimental Procedure

The synthesis of **8a** is described as a typical example; all compounds gave correct elemental analyses and molecular peaks with 100% relative abundance in the FD mass spectra.

6a: A solution of **4** (4.0 g, 5.4 mmol) (1:1 complex with toluene) and **5a** (4.8 g, 12.1 mmol) in anhydrous acetonitrile (180 mL) was heated under reflux with K_2CO_3 (0.82 g, 5.9 mmol) (argon, stirring). After 40 h, the solvent was removed by distillation, and the residue was taken up into CH_2Cl_2 (30 mL) and water (20 mL). The organic phase was washed with dilute hydrochloric acid and water, and then dried. The brown residue was purified by flash chromatography (silica gel, $CHCl_3$). Finally, recrystallization from acetone gave **6a** as colorless crystals (5.27 g, 89%), m.p. 194–197 °C; ^{1}H NMR ($CDCl_3$, 200 MHz): $\delta = 7.90$ (s, 2H, OH), 7.34–6.84 (*m*, 26H, ArH), 4.99 (s, 4H; O–CH_2–Ar), 3.97 (t, $J = 7$ Hz, 4H; CH_2–CH_2–Ar), 4.29 and 3.30 (d, $J = 12.9$ Hz, 4H each; Ar–CH_2–Ar), 2.94 (t, $J = 7$ Hz, 4H; Ar–O–CH_2), 2.32–2.25 (m, 4H; CH_2–CH_2–CH_2), 1.28 and 0.99 (s, 18H each; $C(CH_3)_3$).

7a: Compound **6a** (2.6 g, 2.37 mmol) was dissolved in glacial acetic acid (100 mL), and 5% Pd/C (2.1 g) was added to the solution, which was then stirred under hydrogen at room temperature and atmospheric pressure. After the mixture had been stirred vigorously for about 7 h, hydrogen was no longer taken up. After removal of the catalyst, the filtrate was concentrated by evaporation, the residue dissolved in CH_2Cl_2 (50 mL), and the resulting solution washed with $NaHCO_3$ solution. The crude product was finally purified by chromatography over a short column (silica gel, $CHCl_3$/diethyl ether 50:1) to yield **7a** as a colorless, amorphous product (1.99 g, 92%); ^{1}H NMR ($CDCl_3$, 200 MHz): $\delta = 6.68$–7.07 (m, 16H; ArH + 2H; OH), 5.50 (br s, 2H, OH), 3.96 (t, $J = 7$ Hz, 4H; CH_2–CH_2–Ar), 4.30 and 3.30 (d, $J = 12.9$ Hz, 4H each; Ar–CH_2–Ar), 2.81 (t, $J = 7$ Hz, 4H; Ar–O–CH_2), 2.28–2.23 (m, 4H; CH_2–CH_2–CH_2), 1.28 and 0.98 (s, 18H each; $C(CH_3)_3$).

Double calixarene **8a**: A solution of **7a** (1.5 g, 1.64 mmol) and 2,6-bis(bromomethyl)-4-methylphenol (0.964 g, 3.28 mmol) in glacial acetic acid (50 mL) was added dropwise with stirring to a boiling solution of zinc acetate (0.72 g) in glacial acetic acid (250 mL) over 24 h. After the mixture had refluxed for a further 45 h, the solvent was removed by distillation, and the dark green residue was taken up in $CHCl_3$ (40 mL) and water (30 mL). The organic phase was washed with $NaHCO_3$ solution and water, and was then concentrated by evaporation. Pure **8a** (75 mg, 3.9%), m.p. > 400 °C, was finally obtained by flash chromatography (silica gel, $CHCl_3$ and *n*-hexane/CH_2Cl_2 2:3) (for ^{1}H NMR see Table 1).

Received: August 13, 1993 [Z 6282 IE]
German version: *Angew. Chem.* **1994**, *106*, 230

[1] C. D. Gutsche, *Calixarenes*, The Royal Chemical Society, Cambridge, **1990**; *Calixarenes, A Versatile Class of Macrocyclic Compounds* (Eds.: J. Vicens, V. Böhmer), Kluwer, Dordrecht, **1991**.

[2] C. D. Gutsche, M. Iqbal, *Org. Synth.* **1990**, *86*, 234–237; C. D. Gutsche, B. Dhawan, M. Leonis, D. Stewart, *ibid.* **1990**, *86*, 238–242; J. H. Munch, C. D. Gutsche, *ibid.* **1990**, *86*, 243–246.

[3] Short overview: V. Böhmer, A. M. McKervey, *Chem. Unserer Zeit* **1991**, *25*, 195–207; for selective functionalization see also: J.-D. van Loon, W. Verboom, D. N. Reinhoudt, *Org. Prep. Proced. Int.* **1992**, *24*, 437–462.

[4] P. D. Beer, A. D. Keefe, A. M. Z. Slawin, D. J. Williams, *J. Chem. Soc. Dalton Trans.* **1990**, 3675.

 © *VCH Verlagsgesellschaft mbH, D-69451 Weinheim, 1994* *0570-0833/94/0202-0215 $ 10.00+.25/0*

[5] J.-D. van Loon, D. Kraft, M. J. K. Ankoné, W. Verboom, S. Harkema, W. Vogt, V. Böhmer, D. N. Reinhoudt, *J. Org. Chem.* **1990**, *55*, 5176–5179.
[6] A. M. McKervey, M. Owens, H.-R. Schulten, W. Vogt, V. Böhmer, *Angew. Chem.* **1990**, *102*, 326–328; *Angew. Chem. Int. Ed. Engl.* **1990**, *29*, 280–282.
[7] D. Kraft, J.-D. van Loon, M. Owens, W. Verboom, W. Vogt, M. A. McKervey, V. Böhmer, D. N. Reinhoudt, *Tetrahedron Lett.* **1990**, *31*, 4941–4944.
[8] Z. Asfari, R. Abidi, F. Arnaud, J. Vicens, *J. Inclusion Phenom. Mol. Recognit. Chem.* **1992**, *13*, 163–169.
[9] Z. Asfari, J. Weiss, J. Vicens, *Pol. J. Chem.* **1992**, *66*, 709–711.
[10] J. L. Atwood, S. G. Bott, C. Jones, C. L. Raston, *J. Chem. Soc. Chem. Commun.* **1992**, 1349–1351.
[11] X. Delaigue, M. W. Hosseini, A. De Cian, J. Fischer, E. Leize, S. Kieffer, A. Van Dorsselaer, *Tetrahedron Lett.* **1993**, *34*, 3285–3288.
[12] S. Arimori, T. Nagasaki, S. Shinkai, *J. Chem. Soc. Perkin Trans. 1* **1993**, 887–889.
[13] V. Böhmer, H. Goldmann, W. Vogt, J. Vicens, Z. Asfari, *Tetrahedron Lett.* **1989**, *30*, 1391–1394.
[14] A. Arduini, G. Manfredi, A. Pochini, A. R. Sicuri, R. Ungaro, *J. Chem. Soc. Chem. Commun.* **1991**, 936–937.
[15] Z. Asfari, J. Vicens, J. Weiss, *Tetrahedron Lett.* **1993**, *34*, 627–628.
[16] E. Kelderman, L. Derhaeg, G. J. T. Heesink, W. Verboom, J. F. J. Engbersen, N. F. van Hulst, A. Persoons, D. N. Reinhoudt, *Angew. Chem.* **1992**, *104*, 1107–1110; *Angew. Chem. Int. Ed. Engl.* **1992**, *31*, 1075–1077.
[17] H. Goldmann, W. Vogt, E. Paulus, V. Böhmer, *J. Am. Chem. Soc.* **1988**, *110*, 6811–6817.
[18] V. Böhmer, H. Goldmann, W. Vogt, E. F. Paulus, F. L. Tobiason, M. J. Thielman, *J. Chem. Soc. Perkin Trans. 2*, **1990**, 1769–1775.

Inversely Coordinating Silanide Ions in an Oligomeric Sodium Alcoholate**

Hans Pritzkow, Thomas Lobreyer, Wolfgang Sundermeyer,* Nicolaas J. R. van Eikema Hommes, and Paul von Ragué Schleyer

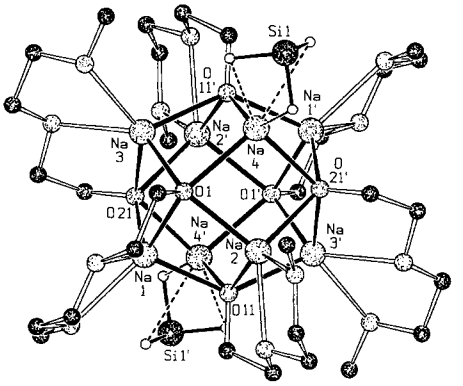
In 1961 Ring and Ritter succeeded in characterizing the molecule $KSiH_3$.[1] Their results were confirmed by Weiss et al.[2] in 1970 and extended by structural analyses on the alkali metal silanides $MSiH_3$ (M = Rb, Cs). All three compounds crystallize in the NaCl structure, and according to NMR spectroscopic studies the SiH_3 groups rotate freely at their lattice sites down to a temperature of −100 °C. Becker et al.[3] were able to detect an orthorhombic low-temperature modification of $KSiH_3$ for the first time in 1989 (β-$KSiH_3$).

In contrast, according to ab initio calculations[4] the molecule $LiSiH_3$ should have a remarkable structure with inverted C_{3v} geometry, which is favored over the conventional tetrahedral van't Hoff structure by 10 kJ mol^{-1}. Thus the silyl anion H_3Si^- is expected to bind to the lithium cation through the negatively polarized hydrogen atoms and not in the usual way. The calculated structures of the analogous $NaSiH_3$ isomers (**1a**, **b**; see Fig. 2) are very close in energy,[5, 6] but the van't Hoff structure is the more stable by about 4–8 kJ mol^{-1}. Experimental proof of these theoretically predicted molecular structures did not exist previously. We now report the X-ray crystal structure of an oligomeric sodium alcoholate to which two H_3Si^- anions are coordinated with inverted C_{3v} symmetry, as well as the ab initio calculation of a simplified model of this compound.

[*] Prof. Dr. W. Sundermeyer, Dr. H. Pritzkow, Dipl.-Chem. T. Lobreyer
Anorganisch-chemisches Institut der Universität
Im Neuenheimer Feld 270, D-69120 Heidelberg (FRG)
Telefax: Int. code + (6221)564197
Dr. N. J. R. van Eikema Hommes, Prof. P. von R. Schleyer
Institut für Organische Chemie 1 der Universität Erlangen-Nürnberg
Henkestrasse 42, D-91054 Erlangen (FRG)

[**] This work was supported by the Bundesministerium für Forschung und Technologie (project no. 0328980 A) and the Fonds der Chemischen Industrie. We thank Degussa, Messer-Griesheim, and BASF for making chemicals available.

Treatment of monosilane with dispersed sodium in diethyleneglycol dimethyl ether (diglyme) leads at 100 °C to sodium silanides of composition $NaSi(SiH_3)_nH_{3-n}$ ($n = 0-3$).[7] After about 20 days a few reproducible, colorless crystals separate as by-product from the filtered yellowish solution of the silanides. The X-ray structure analysis[9] showed that it was the sodium–oxygen cage compound $[Na_8(O_3C_5H_{11})_6(SiH_3)_2]$ (**2**, Fig. 1).[10] Apparently the methyl–oxygen bond of the solvent diglyme is cleaved by the alkali metal sodium to a small extent under these drastic conditions.[11]



2

Fig. 1. Crystal structure of the neutral complex **2** [14]. Selected distances [Å] and angles [°]: Na–Na 3.013–3.055(2), Na–$O_{alcoholate}$ 2.300–2.427(3), Na–O_{ether} 2.389–2.457(2), Na4–Si1 3.048(2), Si–H 1.38–1.42(3), Na4–H 2.52–2.67(3); H-Si-H 96.0, 97.1, 91.3(18).

The eight sodium atoms form a cube, the faces of which are capped by alcoholate oxygen atoms of the six monomethyl diethyleneglycolate ions, which are each bonded to four sodium atoms [Na–O 2.300–2.417 Å]. Together these fourteen atoms form an approximate rhombododecahedron. The two ether oxygen atoms of each monomethyl diethyleneglycolate ion are bound to a common sodium atom (Na–O 2.389–2.457 Å). Thus six of the eight sodium atoms are fivefold coordinated to oxygen atoms. The coordination of the other two sodium atoms is completed by a SiH_3^- ion. The silyl hydrogen atoms were localized in a difference Fourier synthesis, and their positions subsequently refined; they are situated on the side facing the sodium atom. The determined Na–Si distance [3.048 Å] is clearly longer than the distance calculated by us for the isolated $NaSiH_3$ molecule **1a** (2.71 Å); the Si–H distances (1.38–1.42 Å) are shorter (calculated: 1.56 Å). The SiH_3 unit forms a steep pyramid in which the H-Si-H angles vary between 91 and 96° (calculated for **1a**: 92°). The Na-Si-H angles in the crystal [57.7–62.0(13)°] are slightly larger than the calculated angles (56°). Besides the bonds to the hydrogen atoms and the interaction with the sodium atom, the silicon atom has no other contacts to neighboring atoms closer than 3.2 Å.

Although according to calculations[5, 6] the van't Hoff isomer **1b** of the monomeric, gaseous $NaSiH_3$ is more stable than the inverted isomer **1a**, for **2** the inverted structure is apparently energetically favored. To determine whether this is a contradiction of theory or whether **1a,b** are not suitable models for **2**, calculations were performed on a $[(NaOH)_3NaSiH_3]$ complex as model (that is, on a species which reflected half of the crystallographically studied sodium–oxygen cage **2**). The MP2/6-31G* geometries of the inverted structure **3a** and the van't Hoff structure **3b** are depicted in Figure 2 and contrasted with the structures of the isomeric molecules **1a** and **1b**. The Na–Si distance in **3** is longer than in the corresponding isomers of **1**,

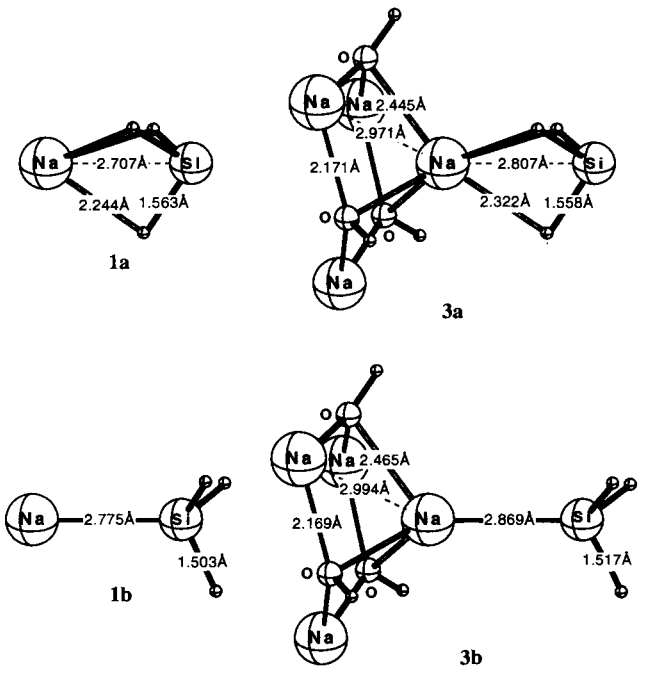


Fig. 2. Structures of **1a** and its van't Hoff isomer **1b** calculated with ab initio methods (MP2/6-31G*) and of the $[Na(OH)_3NaSiH_3]$ complexes **3a** and **3b**. Whereas **1a** is 6.5 kJ mol^{-1} less stable than **1b**, **3a** is 6 kJ mol^{-1} more stable than **3b** (data from MP4sdq/6-31* calculations).

but is still shorter than in solid **2**. Such deviations in the molecular geometry in the gas phase and in the solid state can be explained by dielectric effects in the crystal field.[12] The elongation of the bond in this case is certainly attributable to the higher coordination of the alkali metal atom in **2**. However, most important for the comparison between **3a** and **3b** are the relative energies, which show that in **3** the complexation reverses the order for stability from that found for **1**. On the highest level used for the calculations (MP4sdq/6-31G*//MP2/6-31G*), the inverted complex **3a** is 6 kJ mol^{-1} more stable than **3b**. The results of the calculations are thus in accord with the experimentally determined data.

For gaseous lithium silanide the inverted structure is, according to calculations,[4] more favorable than the van't Hoff structure on account of the contributions of the agostic Li–H interactions. In contrast, for gaseous sodium silanide the corresponding Na–H interactions are weaker, with the result that the contribution of the metal–silicon bond energy that favors the van't Hoff structure increases in importance. The inversion of stabilities in the isomeric complexes **3a** and **3b** is a consequence of the additional electrostatic interaction ($H^{\delta-}\cdots Na^{\delta+}$) of the SiH_3 group with the three sodium atoms of the $(NaOH)_3$ fragment. The preferred conformation of the SiH_3 groups in **2** is therefore attributable to these interactions.

Experimental Procedure

Sodium (10 g, 0.44 mol) was dispersed in diglyme (500 mL) at 100 °C in a reactor fitted with a hollow stirrer and baffle plate and converted into sodium silanides of the composition $NaSi(SiH_3)_nH_{3-n}$ ($n = 0-3$) by treatment with continuously added monosilane [7]. After 4 h the monosilane addition was stopped, and the contents of the reactor allowed to cool to room temperature under nitrogen. The resulting yellow solution was filtered over a G-4 frit. After about 20 days colorless crystals precipitated from the solution of sodium silanides. The solution was removed by syringe, and the crystals were selected manually.

2: ^{1}H NMR (90 MHz, $[D_{10}]$1,2-dimethoxyethane, TMS): $\delta = 3.47$ (m, 12H), 3.61 (m, 30H), 3.80 (m, 18H); ^{29}Si NMR (17.75 MHz, diglyme, C_6D_6): $\delta = -83.7$; IR (KBr): $\tilde{\nu}$[cm^{-1}] = 2878 vs, 2657 m, 2010 w, 1937 w, 1674 w, 1608 s, 1456 s, 1373 w, 1350 w, 1296 w, 1245 w, 1200 m, 1082 vs, 937 vs, 849 s, 768 w; MS (70 eV, gly = $OC_2H_5OC_2H_5OCH_3$): *m/z* (%): 875 $(Na_7(gly)_6)$, 734 $(Na_6(gly)_5)$, 591 $(Na_5(gly)_4)$, 449 $(Na_4(gly)_3$, 100%), 307 $(Na_3(gly)_2)$, 165 $(Na_2(gly))$, 121, 89, 59.

Received: August 14, 1993
Revised version: October 15, 1993 [Z6285IE]
German version: *Angew. Chem.* **1994**, *106*, 221

[1] M. A. Ring, D. M. Ritter, *J. Phys. Chem.* **1961**, *65*, 182.
[2] E. Weiss, G. Hencken, H. Kühr, *Chem. Ber.* **1970**, *103*, 2868–2872.
[3] O. Mundt, G. Becker, H.-M. Hartmann, W. Schwarz, *Z. Anorg. Allg. Chem.* **1989**, *572*, 75–88.
[4] P. von R. Schleyer, T. Clark, *J. Chem. Soc. Chem. Commun.* **1986**, 1371–1373.
[5] B. T. Luke, J. A. Pople, M.-B. Krogh-Jespersen, Y. Apeloig, J. Chandrasekhar, P. von R. Schleyer, *J. Am. Chem. Soc.* **1986**, *108*, 260–269.
[6] A. S. Zyubin, T. S. Zyubina, O. P. Charkin, P. von R. Schleyer, *Russ. J. Inorg. Chem.* **1990**, *35*, 1044.
[7] T. Lobreyer, J. Oeler, W. Sundermeyer, H. Oberhammer, *Chem. Ber.* **1993**, *126*, 665–668; see also [8].
[8] T. Lobreyer, H. Oberhammer, W. Sundermeyer, *Angew. Chem.* **1993**, *105*, 587–588; *Angew. Chem. Int. Ed. Engl.* **1993**, *32*, 586–587.
[9] **2** $(C_{30}H_{72}Na_8O_{18}Si_2)$: $M = 960.98$, space group $P2_1/n$, $a = 12.905(6)$, $b = 12.025(6)$, $c = 16.739(9)$ Å, $\beta = 94.80(3)°$, $V = 2588.5$ Å^3, $Z = 2$, four-circle diffractometer ($Mo_{K\alpha}$ radiation, ω scan, $T = -100$ °C), 4140 independent reflections (of which 3137 with $I > 2\sigma_I$). Refinement against F^2 with all reflections, non-hydrogen atoms anisotropic, hydrogen atoms in calculated positions (CH_2) or in rigid groups (CH_3) with variable C–H distances, common isotropic temperature factors for identical groups, H atoms on Si refined isotropically in found positions. $R_1 = 0.035$, $wR_2 = 0.095$ (for all reflections), 312 parameters. Residual electron density: besides a maximum of 0.4 eÅ^{-3} in the vicinity of the Si atom, between −0.17 and + 0.18 eÅ^{-3}. All calculations were performed with the program SHELXL93 [13]. Further details of the crystal structure investigation may be obtained from the Fachinformationszentrum Karlsruhe, D-76344 Eggenstein-Leopoldshafen (FRG) on quoting the depository number CSD-400477, and the journal citation.
[10] T. Lobreyer, W. Sundermeyer, H. Oberhammer, lecture at the Xth Int. Symp. Organosilicon Chem., Poznan, Poland, August 1993.
[11] A. Maercker, *Angew. Chem.* **1987**, *99*, 1002–1019, *Angew. Chem. Int. Ed. Engl.* **1987**, *26*, 972–989.
[12] M. Bühl, P. von R. Schleyer, *Angew. Chem.* **1991**, *103*, 1179; *Angew. Chem. Int. Ed. Engl.* **1991**, *30*, 1160.
[13] G. M. Sheldrick, SHELXL93, Universität Göttingen, **1993**.
[14] E. Keller, SCHAKAL88, Universität Freiburg, **1988**.

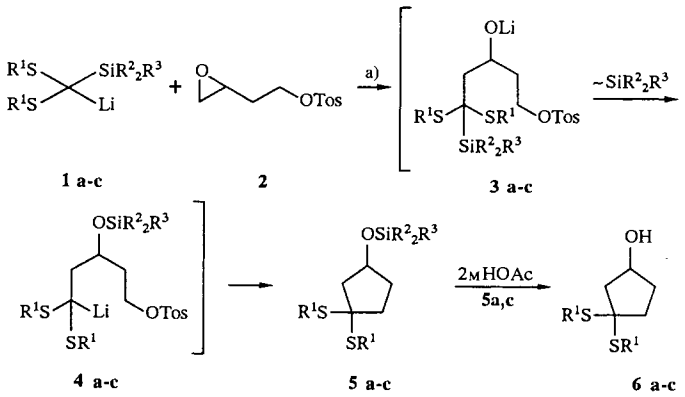
Syntheses of Cyclopentanols by a Silicon-Induced Cascade Reaction**

Michael-Ralph Fischer, Andreas Kirschning, Tycho Michel, and Ernst Schaumann*

The synthesis of chiral cyclopentane derivatives is a component of many natural product syntheses.[1] The diverse synthetic possibilities include the chemistry of the trimethylenemethane equivalent,[2, 3] ring expansion reactions of three-[4] and four-[5] membered rings as well as radical cyclization reactions.[6] Extending our work on the synthesis of cyclopropanes with the homo-Peterson reaction[6] we have now developed a simple route to cyclopentanes including optically active examples. In this route the lithium derivatives **1a–c**, which are easily obtained from silylated thioacetals,[6] react with the epoxy *para*-toluenesulfonate **2** to afford the silyl ethers **5a–c** (Scheme 1, Table 1). Apparently the carbanion of **1** attacks the unsubstituted carbon atom of the epoxide in **2** chemoselectively and regioselectively to give **3**. Finally, a 1,4-carbon to oxygen shift of

[*] Prof. Dr. E. Schaumann, M.-R. Fischer, Dr. A. Kirschning, Dipl.-Chem. T. Michel
Institute für Organische Chemie der Universität
Leibnizstrasse 6, D-38678 Clausthal-Zellerfeld (FRG)
Telefax: Int. code + (5323)72-2858

[**] This work was supported by the Fonds der Chemischen Industrie.



Scheme 1. **a**: $R^1 = R^2 = R^3 = Me$; **b**: $R^1 = R^2 = Me$, $R^3 = tBu$; **c**: $R^1 + R^1 = (CH_2)_3$, $R^2 = R^3 = Me$. Tos = 4-$MeC_6H_4SO_2$. a) $-78 \rightarrow -50\,^\circ C$.

Table 1. Reactants, yields, and selected spectroscopic data of the products.

Silyl cmpd	Epoxide	Product	Yield [%]	^1H NMR [a] δ(CHO)	^{13}C NMR [b] δ(CHO); δ(C3)
1a	**2**	**6a**	80	4.43 (m)	73.36; 63.14
1b	**2**	**5b**	46	4.38 (quin; $J = 6.2$)	72.95; 60.21
1c	**2**	**6c**	65	4.37 (m)	73.27; 53.67
7	(*S*)-**2**	**8** [c]	55	4.30 (m)	73.8; 63.8 73.7; 62.3
1a	**10** [d]	**11** [e]	49	4.21 (dt, $J = 8.8, 2.8$)	73.71; 68.19

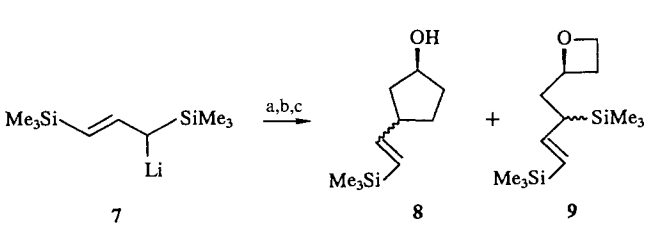
[a] ^1H NMR spectra: 400 MHz, $CDCl_3$, TMS, J(H,H) [Hz]. [b] ^{13}C NMR spectra: 100 MHz, $CDCl_3$. [c] Mixture of diastereomers (ca. 1:1), $[\alpha]_D = -26.7$ ($c = 1.04$, $CHCl_3$, 20 °C). [d] Pure diastereomer, m.p. 101 °C. [e] Pure diastereomer, m.p. 71 °C.

the silyl group (1,4-Brook rearrangement)[7, 9] to afford **4** generates a new carbanion, which displaces the *para*-toluenesulfonate group in an S_Ni reaction. The free alcohols **6a, c** can be obtained from the trimethylsilyl derivatives **5a, c** under acidic conditions.

The ease of formation of **5b** shows that the sterically demanding *tert*-butyldimethylsilyl group rearranges without problems[10] and thus may serve as a stable protecting group in subsequent reactions. However, in this case an oxetane (< 10%) was also produced in the cyclization of **3b**.

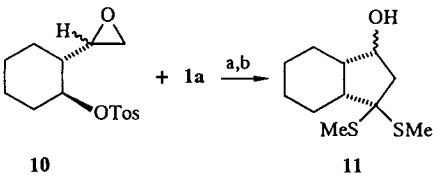
Following the same principle, the reaction of the lithium derivative **7** of a 1,3-disilylated propene with (S)-**2**[11] synthesized from (L)-hydroxysuccinic acid gives rise to a mixture (1:1) of optically active diastereomers **8**. In the second step rearrangement of the allylic trimethylsilyl group leads to a less stable carbanion, and therefore a crown ether and high temperatures are necessary. The sluggishness of silyl migration in this case causes formation of 14% of the oxetane **9** as a mixture of diastereomers from the alkoxide (Scheme 2, Table 1).

The efficiency of the cascade reaction[12] is documented in the synthesis of the annelated cyclopentane compound **11** from the



Scheme 2. a) (*S*)-**2**. b) [12]Crown-4, $-78 \rightarrow 0\,^\circ C$, ca. 2 h (monitored by TLC). c) 2 M HOAc/MeOH.

substituted epoxy *para*-toluenesulfonate **10**[13] (Scheme 3, Table 1). These reactions, which afford good yields, offer a promising alternative to the already known [4 + 1] cycloaddition reactions,[14] particularly as the reaction can be undertaken with an enantiomerically pure epoxy *para*-toluenesulfonate compound such as **2**.



Scheme 3. a) $-78 \rightarrow -40\,^\circ C$, ca. 2 h, monitored by TLC. b) 2 M HOAc/MeOH.

Experimental Procedure

3,3-Bis(methylthio)cyclopentanol **6a**: To a solution of protonated **1a** (397 mg, 2.2 mmol) in 6 mL of anhydrous THF was added *n*BuLi (2.49 mmol, 1.6 M in hexane) under an inert gas atmosphere at $-78\,^\circ C$. This solution was stirred at 0 °C for 30 min. At $-78\,^\circ C$, **2** (500 mg, 1 mmol) in 5 mL of anhydrous THF was slowly added dropwise. The yellow reaction solution was warmed to $-50\,^\circ C$ and then hydrolyzed with a mixture of ether, water, and saturated ammonium chloride solution (1:1:1). The aqueous phase was separated and extracted again with ether. The combined organic phases were dried over magnesium sulfate and concentrated in vacuo. The crude product was taken up in 0.5 mL methanol, and 0.5 mL 2 M acetic acid was added. The solution was stirred at 20 °C for 12 h, and finally the phases were separated after addition of an ether–water mixture. The organic phase was neutralized with saturated sodium hydrogen carbonate solution, washed with saturated sodium chloride solution, dried over magnesium sulfate, and concentrated in vacuo. The product was purified by column chromatography on silica gel with petroleum ether/ethyl acetate (7:1) as eluent (Table 1).

Received: July 28, 1993 [Z 6242 IE]
German version: *Angew. Chem.* **1994**, *106*, 220

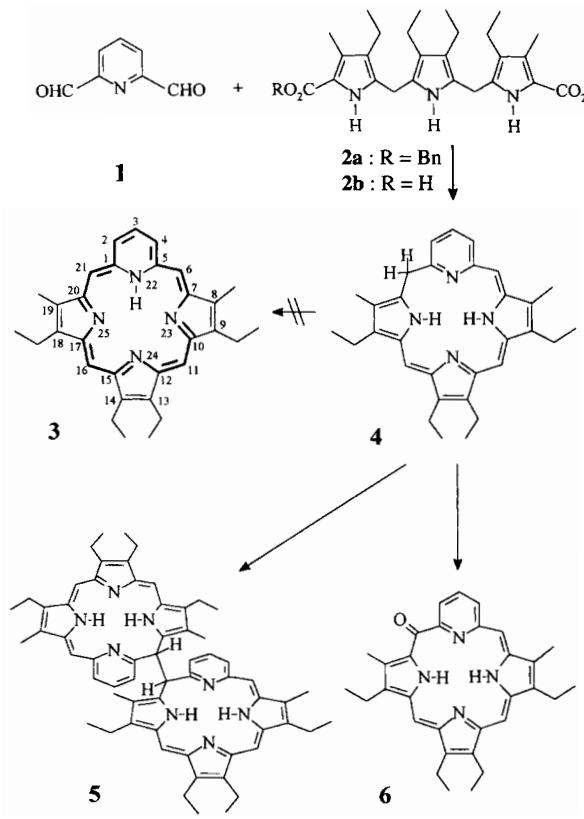
[1] T. L. Ho, *Carbocycle Construction in Terpene Synthesis*, 1st ed., VCH, Weinheim, **1988**; M. Harre, P. Raddatz, R. Walenta, E. Winterfeldt, *Angew. Chem.* **1982**, *94*, 496; *Angew. Chem. Int. Ed. Engl.* **1982**, *21*, 480; B. M. Trost, J. I. Luengo, *J. Am. Chem. Soc.* **1988**, *110*, 8239; L. A. Paquette, *Top. Curr. Chem.* **1984**, *119*, 1.
[2] B. M. Trost, *Angew. Chem.* **1986**, *98*, 1; *Angew. Chem. Int. Ed. Engl.* **1986**, *25*, 1.
[3] B. M. Trost, D. M. T. Chan, *J. Am. Chem. Soc.*, **1983**, *105*, 2315, 2326; B. M. Trost, P. Seoane, S. Mignani, M. Acemoglu, *ibid.* **1989**, *111*, 7487.
[4] a) G. Quinkert in *Selectivity—a Goal for Synthetic Efficiency* (Eds.: W. Bartmann, B. M. Trost), 1st ed., VCH, Weinheim, **1984**, p. 213; b) J. Salaün in *The Chemistry of the Cyclopropyl Group, Part 2* (Eds.: S. Patai, Z. Rappoport), 1st ed., Wiley, Chichester, **1987**, p. 849; T. Hudlicky, T. M. Kutchan, S. Naqvi, *Org. React. N.Y.* **1985**, *33*, 247; Z. Goldschmidt, B. Crammer, *Chem. Soc. Rev.* **1988**, *17*, 229.
[5] A. E. Greene, J.-P. Deprés, *J. Am. Chem. Soc.* **1979**, *101*, 4003; A. E. Greene, J.-P. Deprés, F. Coelho, T. J. Brocksom, *J. Org. Chem.* **1985**, *50*, 3943.
[6] B. Giese, *Radicals in Organic Synthesis*, 1st ed., Pergamon, Oxford, **1986**; M. Ramaiah, *Tetrahedron* **1987**, *43*, 3541; D. P. Curran, *Synthesis* **1988**, *417*, 489.
[7] E. Schaumann, C. Friese, *Tetrahedron Lett.* **1989**, *30*, 7033; E. Schaumann, A. Kirschning, F. Narjes, *J. Org. Chem.* **1991**, *56*, 717; F. Narjes, O. Bolte, D. Icheln, W. A. König, E. Schaumann, *ibid.* **1993**, *58*, 626.
[8] D. Seebach, M. Kolb, B.-T. Gröbel, *Chem. Ber.* **1973**, *106*, 2277.
[9] M. Lautens, P. H. M. Delanghe, J. B. Goh, C. H. Zhang, *J. Org. Chem.* **1992**, *57*, 3270, and references therein.
[10] The step **3b** → **4b** takes place at ca. $-10\,^\circ C$.
[11] P. A. Bartlett in *Selectivity—a Goal for Synthetic Efficiency* (Eds.: W. Bartmann, B. M. Trost), 1st ed., VCH, Weinheim, **1984**, p. 1.
[12] Cf. L. F. Tietze, U. Beifuss, *Angew. Chem.* **1993**, *105*, 137; *Angew. Chem. Int. Ed. Engl.* **1993**, *32*, 131.
[13] Preparation by boron trifluoride catalyzed ring-opening of cyclohexene oxide with trimethylsilylacetylene and subsequent desilylation with methanolic sodium hydroxide. The acetylene obtained was reduced to the alkene with Pd/$BaSO_4$/quinoline, tosylated under standard conditions in pyridine and epoxidized with *meta*-chloroperbenzoic acid in dichloromethane.
[14] F. Barrière, J. C. Barrière, D. H. R. Barton, J. Cleophax, A. Gateau-Olesker, S. D. Géro, F. Tadj, *Tetrahedron Lett.* **1985**, *26*, 3121; A. Padwa, M. A. Filipkowski, *ibid.* **1993**, *34*, 813.

 © VCH Verlagsgesellschaft mbH, D-69451 Weinheim, 1994 0570-0833/94/0202-0218 $ 10.00+.25/0

New Porphyrinoid Macrocycles Containing Pyridine

Kurt Berlin and Eberhard Breitmaier*

New structural variants of porphyrins are not only interesting as Hückel aromatic compounds and chromophores, they have potential applications as ligands and in medicine as well.[1] Thus we were encouraged to replace one five-membered ring in this macrocycle with a larger heteroarene. Exchange of a pyrrole ring in porphyrin with pyridine would provide cycle **3**, which has only one possible 18 π aromatic resonance structure. We propose the designation pyriporphin for the unsubstituted framework and the numbering shown.[2] The obvious question is whether the aromaticity of the pyridine ring is sacrificed in favor of the [18]annulene. We planned to synthesize **3** by condensation of pyridine-2,6-dicarbaldehyde (**1**) with the "tripyrranedicarboxylic acid" **2b**[3,4] and subsequent oxidation.



Pyridine-2,6-dicarbaldehyde (**1**)[5] reacted with dicarboxylic acid **2b**[3] as expected to provide the isolable, dark blue pyriporphyrinogen **4**. However, treatment of **4** with an excess of tetrachloro-*p*-benzoquinone (*p*-chloranil) did not furnish the desired pyriporphyrin **3** but the green pyriporphyrinone **6** as the single isolable product in roughly 5% yield. In contrast to the analogous oxophlorines[6] this compound does not show downfield shifts for the alkyl and *meso* protons in its ^{1}H NMR spectrum, which would indicate the enolization of the ketone and in turn 18 π aromaticity. To avoid oxidation of **4** to give pyriporphyrinone **6** we employed an equimolar amount of *p*-chloranil and obtained, in addition to **6**, a product with almost twice the molecular weight (M = 926.6) of pyriporphyrinogen **4** (M = 464.3). NMR experiments confirmed our suspicions that this compound is the didehydro dimer of **4**. After the connectivity of the rings was determined by CH-COLOC and CH-COSY experiments, the presence of a bridging C–C single bond was secured by the coupled ^{13}C NMR spectrum and NOE experiments. Selected data are listed in Table 1.

Table 1. Selected physical and spectroscopic data of **4**, **5**, and **6**[8]

4: M.p. 164–165 °C (decomp); ^{1}H NMR (400 MHz, $CDCl_3$): δ = 1.23 (4t, 12H; 9b, 13b, 14b, 18b-H), 2.23 (s, 3H; 19a-H), 2.37 (s, 3H; 8a-H), 2.66, 2.71, 2.79 (4q, 8H; 9a, 13a, 14a, 18a-H), 3.76 (s, 2H; 6-H), 6.13 (s, 1H; 11-H), 6.30 (s, 1H; 21-H), 7.02 (s, 1H; 16-H), 7.34 (d, 1H; 2-H), 7.43 (d, 1H; 4-H), 7.66 (t, ^3J(H, H) = 8.2 Hz; 1H; 3-H), 8.74, 10.09, (s br, 1H; N-H); ^{13}C NMR (100 MHz, $CDCl_3$): δ = 9.3 (C-8a), 9.7 (C-19a), 15.0, 16.1, 16.5, 17.3 (C-9b/13b/14b/18b), 17.9, 18.2, 18.3 (C-9a/13a/14a/18a), 34.8 (C-6), 90.0 (C-11), 100.8 (C-21), 111.6 (C-16), 115.5 (C-4), 116.1 (C-8), 122.6 (C-2), 128.2 (C-17), 130.5 (C-7), 132.7 (C-19), 133.9 (C-9), 136.2 (C-3), 137.8 (C-10), 139.9 (C-20), 144.7*, 145.6 (C-18), 147.0*, 148.8*, 151.3*, 155.0, 155.1 (C-1/C-5),*: (C-15/12/13/14); MS (EI, 35 eV): m/z = 464.2943 (M^+, 100%, calcd. 464.2940); UV/VIS (CH_2Cl_2): λ_{max} (log ε) = 294 (3.94), 400 (4.29), 602 (3.82), 645 (3.87).

5: M.p. 202–204 °C (decomp); ^{1}H NMR (400 MHz, $CDCl_3$): δ = 1.17, 1.28 (4t, 12H; 9b, 13b, 14b, 18b-H), 1.57 (s, 3H; 8a-H), 2.14 (s, 3H; 19a-H), 2.71 (4q, 8H; 9a, 13a, 14a, 18a-H), 4.54 (s, 1H; 6-H), 5.72 (s, 1H; 21-H), 6.05 (s, 1H; 11-H), 6.75 (d, 1H; 2-H), 6.97 (s, 1H; 16-H), 7.03 (d, 1H; 4-H), 7.06 (t, ^3J(H, H) = 8.0 Hz, 1H; 3-H), 9.05, 11.62 (s br, 1H; N-H); ^{13}C NMR (100 MHz, $CDCl_3$): δ = 8.7 (C-8a), 9.9 (C-19a), 14.9, 16.1, 16.6, 17.3 (C-9b/13b/14b/18b), 18.1, 18.2, 18.3 (C-9a/13a/14a/18a), 53.0 (C-6), 90.2 (C-11), 98.9 (C-21), 111.8 (C-16), 117.2 (C-4), 121.4 (C-8), 121.7 (C-2), 132.6 (C-19), 132.7 (C-17), 134.3 (C-3), 135.2 (C-7), 136.5 (C-10), 140.0 (C-20), 143.3 (C-15), 143.8 (C-12), 145.9 (C-9), 146.0 (C-18), 146.1 (C-13/14), 154.8 (C-1), 157.0 (C-5); MS (FAB): m/z = 927.6 (calc. 927.6) [M^+ + H], 463.3 [M^{2+}]; UV/VIS (CH_2Cl_2): λ_{max} (log ε) = 254 (4.07), 292 (4.11), 398 (4.55), 605 (4.03), 651 (4.09).

6: M.p. 155–158 °C (decomp); ^{1}H NMR (400 MHz, $CDCl_3$): δ = 1.27 (4t, 12H; 9b, 13b, 14b, 18b-H), 2.27 (s, 3H; 19a-H), 2.62 (s, 3H; 8a-H), 2.70-2.89 (4q, 8H; 9a, 13a, 14a, 18a-H), 6.17 (s, 1H; 11-H), 6.38 (s, 1H; 21-H), 7.01 (s, 1H; 16-H), 7.76 (d, 1H; 2-H), 7.95 (t, ^3J(H,H) = 8.2 Hz, 1H; 3-H), 8.15 (d, 1H; 4-H), 9.05, 9.52 (s br, 1H; N-H), ^{13}C NMR (100 MHz, $CDCl_3$): δ = 9.8 (C-19a), 12.4 (C-8a), 15.0, 15.9, 16.3, 17.0 (C-9b/13b/14b/18b), 17.7, 17.9, 18.2 (C-9a/13a/14a/18a), 89.5 (C-11), 101.7 (C-21), 107.8 (C-16), 125.8 (C-4), 128.6 (C-2), 131.4, 131.6 (C-7/8), 132.1 (C-17), 133.7 (C-9), 135.1 (C-19), 136.1 (C-3), 139.4 (C-20), 140.1 (C-10), 143.6 (C-18), 45.9 (C-15), 149.9, 152.6, 152.8 (C-12/13/14), 158.1 (C-1), 161.8 (C-5), 167.7 (C-6); MS (35 eV): m/z = 478.2721 (M^+, 100%, calcd. 478.2733); UV/VIS (CH_2Cl_2): λ_{max} (log ε) = 341 (4.16), 372 (4.25), 398 (4.26), 644 (3.94).

The formation of dimer **5** depends on the amount of oxidant used, which indicates that two radicals arising from pyriporphyrinogen **4** recombine. When lower concentrations of *p*-chloranil are used, the reaction of the radical with the oxidant to yield pyriporphyrinone **6** is just as likely as the reaction with another radical to give dimer **5**. Fuhrhop et al. reported an analogous dimerization in the oxidation of 5,15-dioxoporphodimethenes.[7]

Although two asymmetric centers are formed in the reaction of pyriporphyrinogen **4** to provide dimer **5**, only one compound is evident in the NMR spectra. This indicates that the steric requirements of the radicals determine the course of the reaction. The *anti* conformation of the *meso* compound shown in Figure 1 is sterically least hindered (Fig. 1).

Owing to the hindered rotation about this single bond, the methyl groups can only be equivalent when the conformation is symmetric. Thus most of the other possible conformations can be discounted. This assumption was confirmed by NOE differ-

[*] Prof. Dr. E. Breitmaier, K. Berlin
Institut für Organische Chemie und Biochemie der Universität
Gerhard-Domagk-Strasse 1, D-53121 Bonn (FRG)
Telefax: Int. code + (228) 735683

 © VCH Verlagsgesellschaft mbH, D-69451 Weinheim, 1994 0570-0833/94/0202-0219 $ 10.00+.25/0

ence experiments, which indicate the proximity of the marked CH_3 groups (Fig. 1) to the pyridine protons, and by the small chemical shift of the pyridine protons which reflect the anisotropy of the pyridine ring.

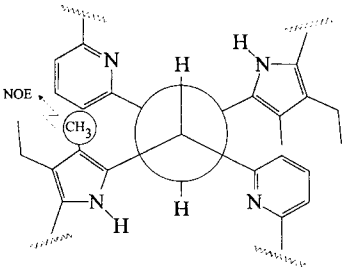


Fig. 1. Proposed configuration of the bridging C–C single bond in dimer **5**.

Experimental Procedure

Solution of **4**: Diester **2a** (635 mg, 1 mmol) was dissolved in anhydrous THF (100 mL), charged with triethylamine (0.1 mL) and 10% Pd/C (200 mg), and hydrogenated at atmospheric pressure. The catalyst was removed by filtration and washed with THF. The filtrate was then added dropwise to a solution of pyridine-2,6-dicarbaldehyde (**1**) (135 mg, 1 mmol) in dichloromethane (800 mL). Argon was bubbled through the reaction mixture before a solution of HBr in glacial acetic acid (1.8 mL, 33%) was added dropwise.

4: The solution of **4** was stirred for 20 h under argon and exclusion of light, then washed with dilute ammonia solution and water, and dried over K_2CO_3. The solvent was removed under vacuum and the residue purified by chromatography first on silica gel (ethyl acetate:cyclohexane 1:3) and then on neutral alumina (activity III; ethyl acetate:cyclohexane 1:9). The intensely colored turquoise fraction furnished dark blue, shiny, microcrystalline **4** (38 mg, 8.2%).

6: The solution of **4** (see above) was stirred under exclusion of light for 4 h then treated with *p*-chloranil (750 mg, ca. 3 mmol). After 15 min the reaction mixture was neutralized with triethylamine (2.5 mmol) and left to stand for 12 h. The solvent was removed under vacuum and the residue purified by chromatography first on silica gel (ethyl acetate:cyclohexane 1:3) then on alumina (activity III; ethyl acetate:petroleum ether 1:4) and recrystallized from dichloromethane/petroleum ether. Yield: 28 mg (5.9%) green, shiny, microcrystalline **6**.

5: The reaction was carried out analogously to that leading to **6**, but only 246 mg (1 mmol) *p*-chloranil was employed. The crude product was purified by chromatography on alumina (activity III; petroleum ether:ethyl acetate 95:5). Yield: green-black, shiny microcrystalline **5** (21 mg, 4.5%) and **6** (14 mg, 2.9%).

Received: August 13, 1993 [Z 6279 IE]
German version: *Angew. Chem.* **1994**, *106*, 229

[1] J. L. Sessler, A. K. Burrell, *Top. Curr. Chem.* **1991**, *161*, 177–273, and references therein; E. Vogel, *Pure Appl. Chem.* **1990**, *62*, 557–564; *ibid.* **1993**, *65*, 143–152, and references therein; J. L. Sessler, S. J. Weghorn, T. Morishima, M. Rosingana, V. Lynch, V. Lee, *J. Am. Chem. Soc.* **1992**, *114*, 8306; J. L. Sessler, T. D. Mody, D. A. Ford, V. Lynch, *Angew. Chem.* **1992**, *104*, 461–464; *Angew. Chem. Int. Ed. Engl.* **1992**, *31*, 452–455; M. Pohl, H. Schmickler, J. Lex, E. Vogel, *ibid.* **1991**, *103*, 1737–1741 and **1991**, *30*, 1693–1697; H. König, C. Eickmeier, M. Möller, U. Rodewald, B. Franck, *ibid.* **1990**, *102*, 1437–1439 and **1990**, *29*, 1393–1395; S. Beckmann, T. Wessel, B. Franck, W. Hönle, H. Borrmann, H. G. von Schnering, *ibid.* **1990**, *102*, 1439–1441 and **1990**, *29*, 1395–1397; T. Wessel, B. Franck, M. Möller, U. Rodewald, M. Läge, *ibid.* **1993**, *105*, 1201–1203 and **1993**, *32*, 1148–1151.

[2] A similar though not conjugated system was synthesized recently: D. Jacoby, C. Floriani, A. Chiesi-Villa, C. Rizzoli, *J. Am. Chem. Soc.* **1993**, *115*, 7025–7026.

[3] J. L. Sessler, M. R. Johnson, V. Lynch, *J. Org. Chem.* **1987**, *52*, 4394–4397.

[4] To simplify matters the trivial name tripyrrane is used here instead of 2,5-bis[(pyrrol-2-yl)methyl]pyrrole.

[5] Z. Dawoodi, M. J. Mays, *J. Chem. Soc. Dalton Trans.* **1984**, 1931–1943.

[6] R. Rusch, A. Gast, E. Breitmaier, *Liebigs Ann. Chem.* **1990**, 1157–1159.

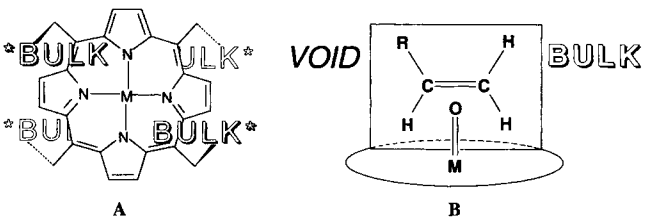
[7] J.-H. Fuhrhop, E. Baumgartner, H. Bauer, *J. Am. Chem. Soc.* **1981**, *103*, 5854–5861.

[8] K. Berlin, part of the planned dissertation (complete documentation of the NMR data).

Chiroporphyrins: An Approach to Asymmetric Catalysts with Stereocenters Near the Plane of the Porphyrin Ring**

Marc Veyrat, Olivier Maury, Frédéric Faverjon, Diana E. Over, René Ramasseul, Jean-Claude Marchon,* Ilona Turowska-Tyrk, and W. Robert Scheidt*

The utility of chiral appendages attached to *meso*-tetraarylporphyrinato ligands in the enantioselective control of metal-catalyzed epoxidation of olefins[1] has encouraged us to seek new porphyrin types that would achieve selectivity through close proximity of the substituents at the stereogenic centers to the reactive oxometal group.[2] We envisaged the possibility that a D_2-symmetric "chiroporphyrin" complex of generalized structure **A** could facilitate the oxygen transfer pathway represented by the transition-state assembly **B**.[3] In this geometry,



A B

Scheme 1. Generalized structure **A** of a chiroporphyrin catalyst and schematic representation of the structure **B** of the epoxidation transition state.

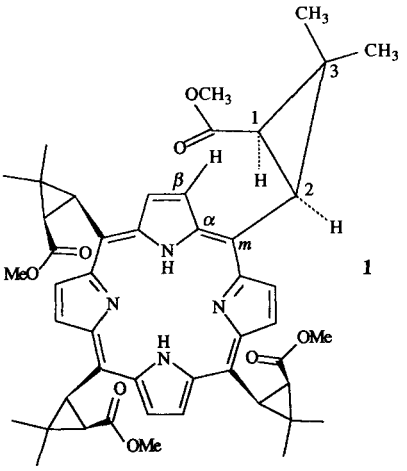
steric repulsion near the plane of the porphyrin ring between a bulky *meso* group and a substituent (R = C_6H_5) on the olefin would favor epoxidation at the *Re* face. Herein we report two chiroporphyrins of this novel class, which are obtained in a single step from pyrrole and easily available chiral aldehydes: **1** from (1*R*)-(−)-*cis*-caronaldehydic acid methyl ester, and **2** from (1*R*)-(−)-myrtenal. Among the four atropisomers that can be expected on account of the restricted rotation[4] of the bulky chiral substituents around the bonds to the *meso* carbon atoms of **1** and **2**, the D_2-symmetric $\alpha\beta\alpha\beta$ isomer appears to be the most stable and abundant. The nickel(II) complex of **2** is the first chiral porphyrin for which a crystal structure determination unambiguously establishes the distribution and symmetry of its atropisomers and their absolute configuration. Moreover, the chloromanganese(III) derivatives of **1** and **2** are efficient asym-

[*] Dr. J.-C. Marchon, Dipl.-Chem. M. Veyrat, Dipl.-Chem. O. Maury, F. Faverjon, Dr. D. E. Over, Dr. R. Ramasseul
CEA/Département de Recherche Fondamentale sur la Matière Condensée
CNRS/Laboratoire de Chimie de Coordination (URA n°1194)
SESAM, Centre d'Etudes Nucléaires de Grenoble
F-38041 Grenoble (France)
Telefax: Int. code + (76)88-5497

Prof. W. R. Scheidt, Dr. I. Turowska-Tyrk
Department of Chemistry and Biochemistry
University of Notre Dame
Notre Dame, IN 46556 (USA)
Telefax: Int. code + (219)631-6652

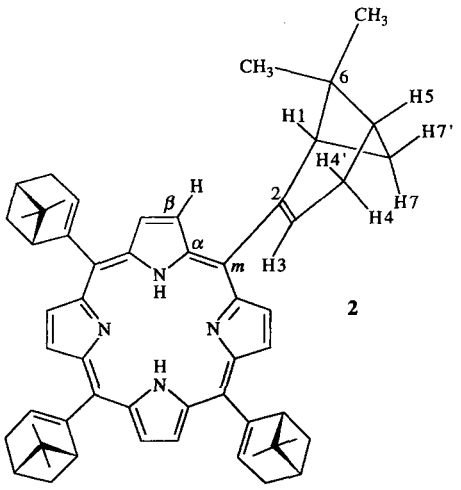
[**] Work at the Centre d'Etudes Nucléaires de Grenoble was supported by the Commissariat à l'Energie Atomique and the Centre National de la Recherche Scientifique, and at Notre Dame by the National Institutes of Health (GM-38401 and RR-06709). We thank P. Dubourdeaux, N. Gon, and B. Soussi for experimental assistance, J. Ulrich and Dr. D. Marion (IBS, Grenoble) for recording mass spectra and a 600 MHz NMR spectrum, Prof. J. P. Collman (Stanford) for providing facilities for separating enantiomers by chiral gas chromatography, C. Kellen-Yuen for help in determining enantiomeric excesses, and Dr. H. Callot and Dr. M. Bardet for helpful discussions. I. T.-T. is on leave from the Department of Chemistry, University of Warsaw (Poland).

 © VCH Verlagsgesellschaft mbH, D-69451 Weinheim, 1994 0570-0833/94/0202-0220 $ 10.00+.25/0



1

metric catalysts in the epoxidation of unfunctionalized aromatic olefins with iodosylbenzene; **1** gives optical yields of up to 70% *ee* for the conversion of dihydronaphthalene to its epoxides.



2

The chiroporphyrin free base **1** was obtained in 4% yield from pyrrole and the bulky (1*R*)-(−)-*cis*-caronaldehydic acid methyl ester[5] under Lindsey condition,[6] and gives one major and two minor spots by thin-layer chromatography. The pyrrole protons of the major product (ca. 50% of total porphyrin) appears as two sharp singlets at $\delta = 9.07$ and 9.18 in the 200 MHz and 400 MHz ^{1}H NMR spectra at room temperature, leading to its unambiguous identification of an $\alpha\beta\alpha\beta$ atropisomer.[4c] The high relative abundance of this D_2-symmetric atropisomer is likely to result from the interaction of the porphyrin with its very bulky *meso* substituents.[7] The moderate upfield shift of the N–H resonance ($\delta = -1.66$) indicates a decreased ring current and a nonplanar conformation of the porphyrin.[8] It is important to note that the coupling constant of the vicinal cyclopropyl protons of **1** ($J' = 8.9$ Hz) is similar to that found in the starting aldehyde ($J' = 8.6$ Hz), indicating a *cis* configuration and the absence of epimerization during acid-catalyzed porphyrin formation.

(1*R*)-(−)-Myrtenal (≥98% *ee*)[9] was allowed to react with pyrrole,[6] and the resulting *meso*-tetrakis[(1*R*)-apopinen-2-yl]porphyrin **2** was isolated in 11% yield after chromatographic purification on alumina. In contrast to **1**, the ^{1}H NMR signal of the pyrrole protons of **2** appears as a broad singlet in [D_8]toluene at 20 °C, turns into a sharp peak at 60 °C, and splits into an asymmetric pair of peaks at −20 °C. This behavior suggests the presence of slowly interconverting atropisomers[4] at room temperature. The chemical shift of the N–H resonance indicates a nonplanar conformation of the porphyrin.[8]

Reaction of **2** with nickel acetate tetrahydrate in chloroform–ethanol afforded the nickel complex **3** in 80% yield. The ^{1}H NMR spectrum of this complex exhibits partially resolved signals at room temperature, even at 400 MHz. Heating **3** to 60 °C in [D_8]toluene induced fast exchange and gave a well-resolved spectrum which could be completely assigned on the basis of selective decoupling and 2D correlation experiments. The stereochemistry found for the *meso* groups is in full agreement with that of the starting myrtenal.[10] A crystalline sample was obtained by slow evaporation to dryness of a solution of **5** in a chloroform/acetone/acetonitrile mixture. Single crystals suitable for X-ray diffraction were selected from this homogeneous crystalline material.

In addition to confirming the nonplanar conformation of the porphyrin ring and the *R* absolute configuration, the structure of the nickel complex **3** determined from diffraction data[11] reveals an unusual feature. Two atropisomers ($\alpha\beta\alpha\beta$ and $\alpha\alpha\beta\beta$) are present in the crystal lattice: they are found as two independent molecules in the asymmetric unit (Fig. 1). The porphyrin macrocycle shows substantial ruffling[12] in both molecules. This deformation results from the severe nonbonding interactions between the very bulky geminal dimethyl groups in the *meso* position and the pyrrole hydrogen atoms.[13] The small size of the nickel atom, which tends to form short Ni–N bonds with a concomitant ruffling of the core, may also be a contributing factor.[14] The saddle distortion bends opposite *meso* substituents towards each other, resulting in a very similar overall shape for the two atropisomers.

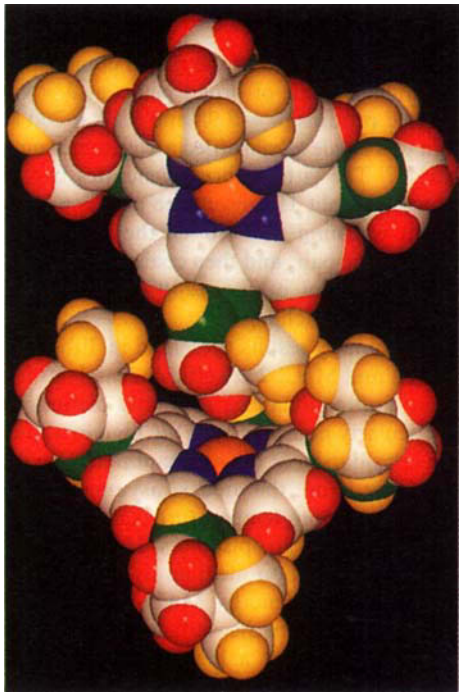


Fig. 1. Structures of the two atropisomers of **3** in the asymmetric unit. The ruffled conformation of the porphyrin is apparent in the side view of the $\alpha\beta\alpha\beta$ atropisomer at the bottom. The $\alpha\alpha\beta\beta$ atropisomer at the top is viewed perpendicular to the plane of the porphyrin ring. Color coding: carbon is white except in double bonds of *meso* substituents in which it is green; hydrogen is red except in vinylic and geminal dimethyl groups of *meso* substituents in which it is yellow; nitrogen is blue; nickel is orange.

 © VCH Verlagsgesellschaft mbH, D-69451 Weinheim, 1994 0570-0833/94/0202-0221 $ 10.00+.25/0

The question obviously arises whether the porphyrin ruffling observed in the crystal is retained in solution. The conformation of **3** was therefore examined in solution by variable-temperature high-resolution ^{1}H NMR spectroscopy (Fig. 2). The 300 MHz

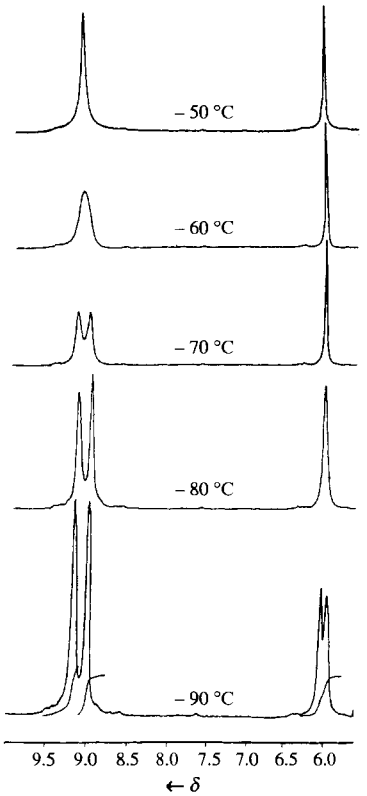


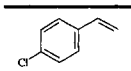
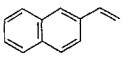
Fig. 2. Variable-temperature 300 MHz ^{1}H NMR spectra of **3** in CD_2Cl_2 showing the evolution of the β-pyrrole H and H3 resonances from −90 to −50 °C.

^{1}H NMR spectrum of the nickel complex **3** at −90 °C exhibits a symmetric pair of broad peaks at $\delta = 9.01$ and 9.19 for the pyrrole protons ($\delta = 8.98$ and 9.17 at 200 MHz), which we assign to a single $\alpha\beta\alpha\beta$ ruffled atropisomer undergoing slow inversion.[15] The latter process generates two distinct conformers, hence the split H3 resonance at $\delta = 6.17$ at this temperature. Upon warming to −80 °C, the pyrrole signals turn into an asymmetric pair, and then coalesce at −60 °C, suggesting gradual population of the $\alpha\alpha\beta\beta$ conformation and concomitant atropisomer exchange.

Preliminary results presented in Table 1 indicate that MnCl-$\alpha\beta\alpha\beta$-**1** and MnCl-**2** are efficient catalysts for the epoxidation of some unfunctionalized aromatic olefins with iodosylbenzene. Particularly noteworthy is the high *ee* value (70%) obtained in the epoxidation of dihydronaphthalene with MnCl-$\alpha\beta\alpha\beta$-**1**. On the other hand, the modest asymmetric induction found with MnCl-**2** at room temperature is not surprising for a mixture of interconverting atropisomers. However, lowering the temperature of the reaction medium to −10 °C for the epoxidation of dihydronaphthalene by MnCl-**2** unambiguously results in an improved asymmetric induction. This encouraging result is assumed to reflect a higher relative abundance of the $\alpha\beta\alpha\beta$ atropisomer of the active Mn complex of **2** at low temperatures, as suggested by the variable-temperature NMR spectra of **3** (see above).

In summary, the chiroporphyrin concept combines several appealing features that are seldom found together among previously described asymmetric epoxidation catalysts. By its inherent simplicity, the synthesis of **1** is comparable to that of asymmetric salen complexes,[16] but it leads to a more chemically robust porphyrin catalyst. Moreover, enantioselectivity can be adjusted by choosing appropriate esters of *cis*-caronaldehydic acid. The open structure of **1** and **2** allows in principle higher turnover rates than most sterically shielded tetraphenylporphyrins with chiral "pickets", "walls", "vaults", or "straps".[1a-h, 17] Compared to the latter, an added bonus is the high relative abundance of the $\alpha\beta\alpha\beta$ atropisomer upon self-assembly of the porphyrin catalyst. Studies are under way on the implications of this concept which we believe will be of wide interest for the design of asymmetric porphyrin catalysts with improved properties.

Table 1. Asymmetric epoxidation of aromatic olefins with MnCl-$\alpha\beta\alpha\beta$-**1** and MnCl-**2** [a].

Substrate	Catalyst	T [°C]	Epoxide yield [%]	*ee* [%] [b]	Configuration [c]	Byproduct yield [%]
	MnCl-$\alpha\beta\alpha\beta$-**1**	25	77	15	*R*(+)	10 [d]
	MnCl-**2**	25	62	8	*R*(+)	35 [d]
	MnCl-$\alpha\beta\alpha\beta$-**1**	25	70	21	(−) [e]	11 [f]
	MnCl-**2**	25	65	6	(−)	–
	MnCl-$\alpha\beta\alpha\beta$-**1**	25	73	29	1*S*,2*R*(+)	16 [g]
	MnCl-**2**	25	71	11	1*R*,2*S*(−)	11 [g], 9 [h]
	MnCl-**2**	−10	67 [i]	15	1*R*,2*S*(−)	7 [g], 19 [h]
	MnCl-$\alpha\beta\alpha\beta$-**1**	25	83	67	1*S*,2*R*(−)	5 [j]
	MnCl-$\alpha\beta\alpha\beta$-**1**	25	75 [k]	70	1*S*,2*R*(−)	4 [j]
	MnCl-**2**	25	90	2	1*S*,2*R*(−)	0

[a] Reactions were generally run for 1 h with 1.0 μmol of catalyst, 100 μmol of iodosylbenzene, 250 μmol of pyridine, 20 μL of nonane, and 1.00 mmol of olefin in 2 mL of CH_2Cl_2. Yields are based upon iodosylbenzene and were determined by GC analysis. [b] Determined by gas chromatography (Cyclodex-B chiral capillary column). [c] Assigned by comparison with results described in ref. [1g]. [d] *p*-Chlorophenylacetaldehyde. [e] The absolute configuration was not determined. [f] 2-Naphthylacetaldehyde. [g] *trans*-β-Methylstyrene epoxide. [h] Benzylmethylketone. [i] Reaction time: 2 h. [j] β-Tetralone. [k] Reaction time: 10 min.

Experimental Procedure

The porphyrins **1** and **2** and the nickel complex **3** were prepared by standard methods. New compounds were characterized by mass spectrometry (VG ZAB-VEQ), UV/VIS (Perkin Elmer Lambda 9), and NMR spectroscopy (Bruker AC 200, AM 300, and AM 400).

1: MS (EI, Fe complex generated in situ): *m/z*: found. 868.810 ($M - 2H + Fe$), calcd. for $C_{48}H_{52}N_4O_8Fe$: 868.808. UV/VIS (CH_2Cl_2), λ_{max} [nm] = 428, 565, 605, 663. ^{1}H NMR (200 MHz, $CDCl_3$, TMS, 20 °C): $\delta = -1.66$ (s, 2H, NH), 0.79 (s, 12H, CH_3), 1.87 (s, 12H, CH_3), 2.69 (d, 4H, $J' = 8.9$ Hz, H_1), 3.07 (s, 12H, CO_2CH_3), 4.75 (d, 4H, $J' = 8.9$ Hz, H_2), 9.07 (s, 4H, pyrrole H), 9.18 (s, 4H, pyrrole H); ^{13}C NMR (50 MHz, $CDCl_3$, TMS, 20 °C): $\delta = 18.2$ (CH_3), 27.7 (C_3), 29.3 (CH_3), 33.2 (CH), 38.3 (CH), 51.0 (OCH_3), 110.1 (*Cm*), 127.2 (*Cβ*), 131.1 (*Cβ*), 143.7 (*Cα*), 148.6 (*Cα*), 170.9 (C = O).

2: FAB$^+$-MS: *m/z* 791.7 (M^+). Correct C,H,N analysis. UV/VIS (CH_2Cl_2), λ_{max} [nm] (lg ε) = 427 (5.52), 528 (4.03), 568 (4.12), 664 (3.82). ^{1}H NMR (200 MHz, $CDCl_3$, TMS, 20 °C): $\delta = -2.70$ (s, 2H, NH), 1.54 (s, 12H, CH_3), 1.68 (s, 12H, CH_3), 2.33 (d, 4H, $J = 8.6$ Hz, H7), 2.58 (m, 4H, H5), 3.06 (m, 12H, H4, H4′, H7′), 3.45 (m, 4H, H1), 6.39 (m, 4H, H3), 9.36 (m, 8H, pyrrole H); ^{1}H NMR (200 MHz, [D_8]toluene, TMS, 20 °C): $\delta = -2.07$ (s, 2H, NH), 1.39 (s, 12H, CH_3), 1.63 (s, 12H, CH_3), 2.29 (d, 4H, $J = 8.6$ Hz, H7), 2.37 (m, 4H, H5), 2.95 (m, 12H, H4, H4′, H7′), 3.44 (t, 4H, H1), 6.35 (m, 4H, H3), 9.53 (m, 8H, pyrrole H); ^{13}C NMR (50 MHz, $CDCl_3$, TMS, 20 °C): $\delta = 22.4$ (CH_3), 26.9 (CH_3), 33.1 (C4), 33.8 (C7), 39.1 (C6), 40.6 (C5), 54.3 (C1), 122.4 (*Cm*), 130.1 (C3), 130.8 (*Cβ*), 146.0 (*Cα*), 149.0 (C2).

3: FAB$^+$-MS: *m/z* 848.4 (M^+). Correct C,H,N,Ni analysis. UV/VIS (CH_2Cl_2), λ_{max} [nm] (lg ε) = 425 (5.34), 541 (4.06), 580 (3.67). ^{1}H NMR (200 MHz, $CDCl_3$, TMS, 20 °C): $\delta = 1.41$ (s, 12H, CH_3), 1.42 (s, 12H, CH_3), 2.14 (d, 4H, $J = 8.6$ Hz, H7), 2.45 (m, 4H, H5), 2.86 (m, 12H, H4, H4′, H7′), 3.03 (m, 4H, H1), 6.17 (m, 4H, H3), 9.17 (m, 8H, pyrrole H); ^{1}H NMR (200 MHz, [D_8]toluene, TMS, 20 °C): $\delta = 1.31$ (s, 12H, CH_3), 1.46 (s, 12H, CH_3), 2.15 (d, 4H, $J = 8.6$ Hz, H7), 2.29 (m, 4H, H5), 2.72 (t, 8H, H4, H4′), 2.77 (m, 4H, H7′), 3.08(t, 4H, H1), 6.18 (m, 4H, H3), 9.35 (m, 8H, pyrrole H); ^{1}H NMR (200 MHz, [D_8]toluene, TMS, 60 °C): $\delta = 1.31$ (s, 12H, CH_3), 1.46 (s, 12H, CH_3), 2.15 (d, 4H, $J = 8.6$ Hz, H7), 2.29 (m, 4H, H5),

 © VCH Verlagsgesellschaft mbH, D-69451 Weinheim, 1994 0570-0833/94/0202-0222 $ 10.00+.25/0

2.74 (t, 8H, H4, H4'), 2.76 (m, 4H, H7'), 3.08 (triplet of doublets, 4H, H1), 6.18 (septet, 4H, H3), 9.35 (s, 8H, pyrrole H); ^{13}C NMR (50 MHz, $CDCl_3$, TMS, 20 °C): δ = 22.0 (CH_3), 26.6 (CH_3), 32.8 (C4), 33.4 (C7), 38.8 (C6), 40.7 (C5), 52.9 (C1), 119.4 (*Cm*), 128.9 (C3), 131.3 (Cβ), 141.1 (Cα), 147.3 (C2).

Received: May 5, 1993
Revised version: August 10, 1993 [Z 6059 IE]
German version: *Angew. Chem.* **1994**, *106*, 200

[1] For leading references on asymmetric porphyrin catalysts, see: a) D. Mansuy, P. Battioni, J. P. Renaud, P. Guérin, *J. Chem. Soc. Chem. Commun.* **1985**, 155–156; b) S. O'Malley, T. Kodadek, *J. Am. Chem. Soc.* **1989**, *111*, 9116–9117; c) J. T. Groves, P. Viski, *J. Org. Chem.* **1990**, *55*, 3628–3634; d) R. L. Halterman, S. T. Jan, *ibid.* **1991**, *56*, 5253–5254; e) K. Konishi, K. I. Oda, K. Nishida, T. Aida, S. Inoue, *J. Am. Chem. Soc.* **1992**,*114*, 1313–1317; f) P. Maillard, J. L. Guerquin-Kern, M. Momenteau, *Tetrahedron Lett.* **1991**, *32*, 4901–4904; g) J. P. Collman, V. J. Lee, X. Zhang, J. A. Ibers, J. I. Brauman, *J. Am. Chem. Soc.* **1993**, *115*, 3834–3835; h) Y. Naruta, N. Ishihara, F. Tani, K. Maruyama, *Bull. Chem. Soc. Jpn.* **1993**, *66*, 158–166; i) G. Proess, L. Hevesi, *J. Mol. Catal.* **1993**, *80*, 395–401; for other properties of chiral porphyrins, see also: j) H. Ogoshi, Y. Aoyama, Y. Okamoto, K. Saita, K. Sakurai, H. Toi, T. Watanabe, *Tetrahedron Lett.* **1986**, *27*, 6365–6368; k) H. P. Pfeiffer, E. Breitmaier, H. Sander, *Liebigs Ann. Chem.* **1987**, 725–726; l) B. Boitrel, A. Lecas, E. Rose, *J. Chem. Soc. Chem. Commun.* **1989**, 349–350; m) Y. Naruta, F. Tani, K. Maruyama, *ibid.* **1990**, 1378–1380; n) S. Licoccia, M. Paci, P. Tagliatesta, R. Paolesse, S. Antonaroli, T. Boschi, *Magn. Reson. Chem.* **1991**, *29*, 1084–1091; o) S. O'Malley, T. Kodadek, *Tetrahedron Lett.* **1991**, *32*, 2445–2448; p) K. Ohkubo, T. Sagawa, H. Ishida, *Inorg. Chem.* **1992**, *31*, 2682–2688; q) N. Nishino, H. Mihara, R. Hasegawa, T. Yanai, T. Fujimoto, *J. Chem. Soc. Chem. Commun.* **1992**, 692–694; r) P. Maillard, C. Huel, M. Momenteau, *Tetrahedron Lett.* **1992**, *33*, 8081–8084; s) P. Le Maux, H. Bahri, G. Simonneaux, *Tetrahedron* **1993**, *49*, 1401–1408; t) K. Konishi, Y. Takahata, T. Aida, S. Inoue, *J. Am. Chem. Soc.* **1993**, *115*, 1169–1170.

[2] A. Pfaltz, *Acc. Chem. Res.* **1993**, *26*, 339–345.

[3] a) J. T. Groves, T. E. Nemo, *J. Am. Chem. Soc.* **1983**, *105*, 5786–5791; b) M. Tavarès, R. Ramasseul, J. C. Marchon, B. Bachet, C. Brassy, J. P. Mornon, *J. Chem. Soc. Perkin Trans.* 2 **1992**, 1321–1329.

[4] a) R. J. Abraham, J. Plant, G. R. Bedford, *Org. Magn. Reson.* **1982**, *19*, 204–210; b) M. J. Crossley, L. D. Field, A. J. Forster, M. M. Harding, S. Sternhell, *J. Am. Chem. Soc.* **1987**, *109*, 341–348; c) The predicted multiplicities of the proton signals, on symmetry grounds [1s], are the following for each atropisomer of a porphyrin tetrasubstituted in the *meso* positions with a chiral substituent. Pyrrolic protons: $\alpha\alpha\beta\beta$, s (2H), s' (2H), dd (4H); $\alpha\alpha\alpha\beta$, s (2H), s' (2H), dd (2H), dd' (2H); $\alpha\beta\alpha\beta$, s (4H), s' (4H); $\alpha\alpha\alpha\alpha$, dd (8H). Protons of the *meso* substituents: $\alpha\alpha\beta\beta$, s (2H), s' (2H); $\alpha\alpha\alpha\beta$, s_1 (1H), s_2 (1H), s_3 (1H), s_4 (1H); $\alpha\beta\alpha\beta$, s (4H); $\alpha\alpha\alpha\alpha$, s (4H).

[5] a) D. Bakshi, V. K. Mahidroo, R. Soman, S. Dev, *Tetrahedron* **1989**, *45*, 767–774; b) This compound was prepared from (1*R*)-*cis*-hemicaronaldehyde (= (1*R*)-*cis*-caronaldehydic acid hemiacetal) (≥ 99.5% *ee*, J. Buendia, personal communication), which was a generous gift from Roussel Uclaf.

[6] a) J. S. Lindsey, I. C. Schreiman, H. C. Hsu, P. C. Kearney, A. M. Marguerettaz, *J. Org. Chem.* **1987**, *52*, 827–836; b) R. W. Wagner, D. S. Lawrence, J. S. Lindsey, *Tetrahedron Lett.* **1987**, *28*, 3069–3070.

[7] Steric effects of *meso* substituents on atropisomer distribution have been noted for several tetraarylporphyrins, see: a) K. Hatano, K. Anzai, T. Kubo, S. Tamai, *Bull. Chem. Soc. Jpn.* **1981**, *54*, 3518–3521; b) T. Fujimoto, H. Umekawa, N. Nishino, *Chem. Lett.* **1992**, 37–40; c) N. Nishino, K. Kobata, H. Mihara, T. Fujimoto, *ibid.* **1992**, 1991–1994.

[8] a) K. M. Barkigia, L. Chantranupong, K. M. Smith, J. Fajer, *J. Am. Chem. Soc.* **1988**, *110*, 7566–7567; b) K. M. Barkigia, M. D. Berber, J. Fajer, C. J. Medforth, M. W. Renner, K. M. Smith, *ibid.* **1990**, *112*, 8851–8857, 9675; c) M. W. Renner, R. J. Cheng, C. K. Chang, J. Fajer, *J. Phys. Chem.* **1990**, *94*, 8508–8511; d) C. J. Medforth, M. D. Berber, K. M. Smith, J. A. Shelnutt, *Tetrahedron Lett.* **1990**, *31*, 3719–3722; e) H. K. Hombrecher, G. Horter, C. Arp, *Tetrahedron* **1992**, *48*, 9451–9460; f) D. Mandon, P. Ochsenbein, J. Fischer, R. Weiss, J. Jayaraj, R. N. Austin, A. Gold, P. S. White, O. Brigaud, P. Battioni, D. Mansuy, *Inorg. Chem.* **1992**, *31*, 2044–2049; g) C. J. Medforth, M. O. Senge, K. M. Smith, L. D. Sparks, J. A. Shelnutt, *J. Am. Chem. Soc.* **1992**, *114*, 9859–9869.

[9] D. Cuvinot, P. Mangeney, A. Alexakis, J. F. Normant, J. P. Lellouche, *J. Org. Chem.* **1989**, *54*, 2420–2425.

[10] a) F. Kaplan, C. O. Schulz, D. Weisleder, C. Klopfenstein, *J. Org. Chem.* **1968**, *33*, 1728–1730; b) R. B. Bates, V. P. Thalacker, *ibid.* **1968**, *33*, 1730–1732.

[11] Crystal data for **3**: $C_{56}H_{60}N_4Ni$; monoclinic, $P2_1$ (No. 4), $Z = 4$, $a = 20.055(4)$, $b = 11.753(1)$, $c = 21.496(3)$ Å, $\beta = 116.267(3)°$, $V = 4543.4$ Å^3, $\rho_{calcd} = 1.24$ g cm^{-3}, $F(000) = 1808$. Data were collected at 293 K on an Enraf–Nonius FAST area detector with $Mo_{K\alpha}$ radiation. The structure was solved by direct methods and refined anisotropically to give $R_1 = 0.051$, $R_2 = 0.061$ for 7396 unique data and 1098 variables. Further details of the crystal structure investigation are available on request from the Director of the Cambridge Crystallographic Data Centre, 12 Union Road, GB-Cambridge CB2 1EZ (UK), on quoting the full journal citation.

[12] a) C. Kratky, R. Waditschatka, C. Angst, J. E. Johansen, J. C. Plaquevent, J. Schreiber, A. Eschenmoser, *Helv. Chim. Acta* **1985**, *68*, 1312–1337; b) W. R. Scheidt, Y. Lee, *Struct. Bonding Berlin* **1987**, *64*, 1–70.

[13] O. Q. Munro, J. C. Bradley, R. D. Hancock, H. M. Marques, F. Marsicano, P. W. Wade, *J. Am. Chem. Soc.* **1992**, *114*, 7218–7230.

[14] Many nickel porphyrins with a four-coordinate metal center adopt a ruffled conformation, see for example: a) L. D. Sparks, C. J. Medforth, M. S. Park, J. R. Chamberlain, M. R. Ondrias, M. O. Senge, K. M. Smith, J. A. Shelnutt, *J. Am. Chem. Soc.* **1993**, *115*, 581–592, and references therein. However, several Ni^{II} porphyrins with a planar structure are also known, see: b) J. C. Gallucci, P. N. Swepston, J. A. Ibers, *Acta Crystallogr. Sect. B* **1982**, *38*, 2134–2139, and references therein.

[15] Inversion of enantiomeric ruffled conformers of nickel(II) *ccccc*-octaethylpyrrocorphinate has been reported, see: R. Waditschatka, C. Kratky, B. Jaun, J. Heinzer, A. Eschenmoser, *J. Chem. Soc. Chem. Comm.* **1985**, 1604–1607.

[16] a) R. Irie, K. Noda, Y. Ito, T. Katsuki, *Tetrahedron Lett.* **1991**, *32*, 1055–1058; b) E. N. Jacobsen, W. Zhang, A. R. Muci, J. R. Ecker, L. Deng, *J. Am. Chem. Soc.* **1991**, *113*, 7063–7064.

[17] J. P. Collman, X. Zhang, V. J. Lee, E. S. Uffelman, J. I. Brauman, *Science* **1993**, *261*, 1404–1411.

Coexistence of Mobile and Localized Electrons in Bis(ethylene)dithiotetrathiafulvalene (BEDT-TTF) Radical Salts with Paramagnetic Polyoxometalates: Synthesis and Physical Properties of $(BEDT\text{-}TTF)_8[CoW_{12}O_{40}] \cdot 5.5H_2O$**

Carlos J. Gómez-García, Lahcène Ouahab,*
Carlos Gimenez-Saiz, Smaïl Triki, Eugenio Coronado,*
and Pierre Delhaès

One of the challenges in materials science is to prepare new molecular compounds with unusual combinations of properties as, for example, compounds coupling magnetic and conducting sublattices. Choosing as molecular building block the π donor bis(ethylene)dithiotetrathiafulvalene (BEDT-TTF or ET), which is the most widely used molecule in the synthesis of molecular superconductors,[1] and polyoxometalate anions,[2] which show a very well-known ability to accommodate magnetic metal ions at specific sites, we have prepared a radical salt in which mobile electrons from the organic component coexist with localized electrons from the magnetic Co^{II}-containing polyoxometalate $[Co^{II}W_{12}O_{40}]^{6-}$, and other related polyanions.

[*] Dr. L. Ouahab, Dr. C. J. Gómez-García [+]
Laboratoire de Chimie du Solide et Inorganique Moléculaire
URA-CNRS 1495, Université de Rennes I
Av. Général Leclerc. F-35042 Rennes Cedex (France)
Telefax: Int. code + (99)383487

Prof. Dr. E. Coronado, C. Gimenez-Saiz, Dr. S. Triki
Departamento de Química Inorgánica
Universidad de Valencia
Dr. Moliner 50, E-46100 Burjasot (Spain)
Telefax: Int. code + (6-)38643322.

Dr. P. Delhaès
Centre de Recherche Paul Pascal
Université de Bordeaux I-CNRS
Av. A. Schweitzer, F-33600 Pessac (France)

[+] Permanent address: Departamento de Química Inorgánica
Universidad de Valencia (Spain)

[**] This work is supported by the Comisión Interministerial de Ciencia y Tecnología (CICYT), the Generalitat de Catalunya (CIRIT) (Grant QFN91-4220), the CNRS, and the EC. C.J.G-G and S.T. thank the Ministerio de Educación y Ciencia for a postdoctoral fellowships. We thank C. Garrigou-Lagrange for her helpful discussions about the IR spectra. We thank H. Noël, J. Amiell, and R. Canet for assistance with the physical measurements.

 © VCH Verlagsgesellschaft mbH, D-69451 Weinheim, 1994 0570-0833/94/0202-0223 $ 10.00+.25/0

Diamagnetic polyoxoanions have been recently used by us[3] and by other groups[4] as inorganic electron acceptor components of charge-transfer salts, with the aim of examining the novel structural and electronic properties in the organic moiety induced by the sizes, shapes, and charges of these inorganic clusters. In some cases the polyoxoanion is reduced by the organic molecule to give a material in which delocalized electrons coexist in both the organic and the inorganic components.[5] However, no structural analyses have been reported for these salts with paramagnetic polyoxoanions.[6] In this communication we report the structure and physical properties of the first example of this kind.

The structure[7] of the title compound shows the presence of alternating layers of the anions and the ET molecules (Fig. 1).

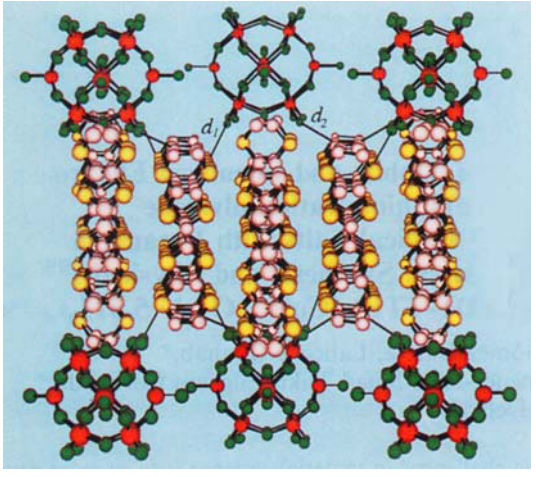


Fig. 1. Perspective view of the organic and inorganic layers showing the chains of eclipsed ET molecules and chains of dimers, as well as the interactions between the anions and the organic C-type molecules [Å]: d_1 (O–S) = 3.04(3), d_2 (O–C) = 3.08(5).

This structure is similar to that found for $ET_8[SiW_{12}O_{40}]$, but in that case the structure is acentric[4a] and the compound does not contain water molecules. In our case the anion displays the well-known Keggin structure containing a Co^{II} ion in its tetrahedral cavity. The anion is disordered (rotation of 90° around the C_2 axis), which makes it appear to be a centrosymmetric unit. This kind of disorder has been unambiguously described by Pope and Evans.[8] The organic layers are formed by three crystallographically independent molecules of ET noted as A, B, and C (Fig. 2a). These molecules are arranged in two different kinds of chains (types I and II, Fig. 2a). Type I chains are formed by alternating B and C type molecules packed eclipsed with S-S distances of 4.04(2) Å. Chains of type II consist of A type molecules packed as dimers with S-S distances within a dimer of 3.86(2) and between dimers of 3.98(1) Å (Fig. 2b). The two types of chains alternate parallel to the direction [$\bar{1}$01] and give rise to an α phase[1a] with a dihedral angle of 46.5° between the ET molecules. The interchain connections (Figure 2a) (ranging from 3.46(2) to 3.52(2) Å), which are much shorter than the intrachain ones, are close to those commonly observed in the quasi 2-D materials based on ET.[1a] Moreover, two kinds of interactions between the organic and inorganic layers can be observed (Fig. 1). The first occurs between the sulphur atoms of the C-type molecules (in the eclipsed chain) and the terminal oxygen atoms of the anion (shortest S–O distance of 3.04(3) Å). The second type of interaction is a hydrogen bond between oxygen atoms of the anion and the carbon atoms of both ethylene groups in the ET molecules of the A type (shortest C–O distance, 3.08(5) Å; Fig. 1). Note that interactions through the ethylene groups have been shown to play an important role in the conducting properties of solid ET.[9] Indeed, this donor arrangement is one of the classical types, called the α phase, in 2-D molecular superconductors.[10]

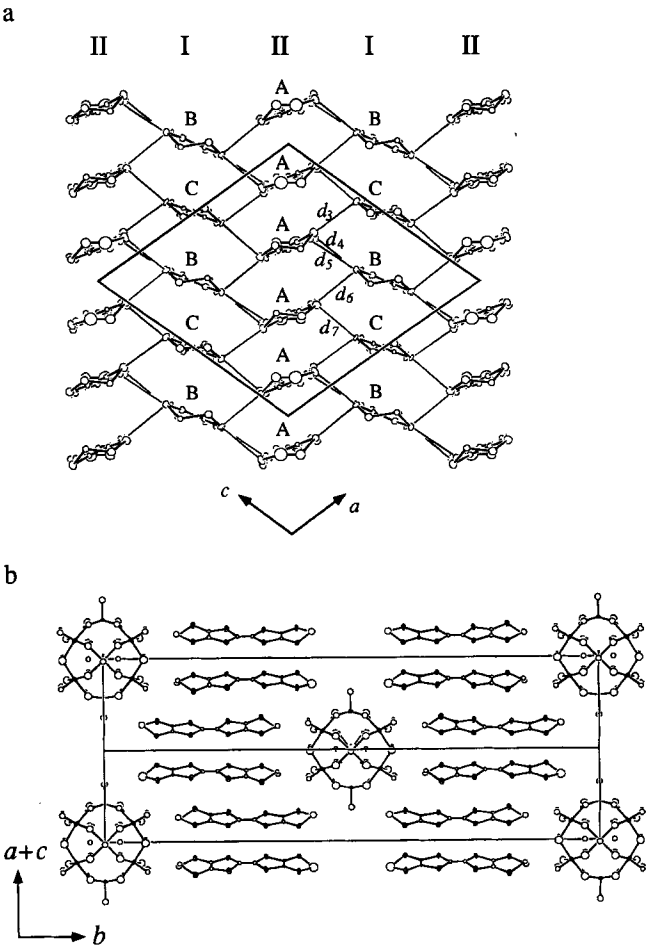


Fig. 2. a) Projection of the organic layer onto the *ac* plane showing the mode of packing of the α phase and the intrachains interactions [Å]: $d_3 = d_4 = 3.51(2)$, $d_5 = d_6 = 3.52(2)$, and $d_7 = 3.46(2)$. b) View of the positions of the anions in the unit cell and the A-type molecules of ET stacked in the chains of dimers (type II) along the [101] direction.

The electrical properties of a single crystal of $ET_8[CoW_{12}O_{40}] \cdot 5.5\,H_2O$ are illustrated through a plot to the normalized resistance versus T in Figure 3. The compound is a semiconductor ($\sigma \leq 0.1\ Scm^{-1}$ at room temperature) showing two different semiconducting behaviors with activation energies of 120 and 27 meV (at high and low temperatures, respectively), and a transition temperature of about 170 K (estimated from the intersection of the two semiconductive regimes).

The IR and visible absorption spectra recorded at room temperature shows the presence of two charge transfer bands and a doublet for the associated vibronic modes. The electronic bands

 © VCH Verlagsgesellschaft mbH, D-69451 Weinheim, 1994 0570-0833/94/0202-0224 $ 10.00+.25/0

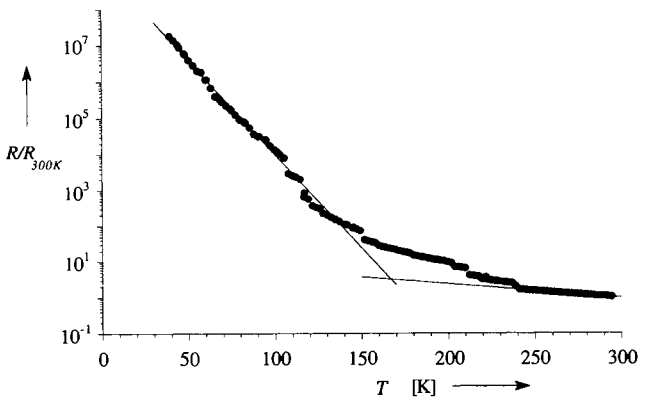


Fig. 3. Plot of the normalized resistance versus T for a single crystal of the title compound. Straight lines represent the fit for the two semiconductive regimes (see text).

are located at 4500 and 9900 cm^{-1}: the first one is associated with a mixed-valence system, whereas the second one accounts for a doubly occupied site.[11] Besides, we observe vibronic lines due to the classical electronic–molecular vibrational coupling with two pairs of lines at 1405 and 1344 cm^{-1} for the $a_g\nu_4$ C=C central stretching mode and at 450 cm^{-1} with a shoulder around 480 cm^{-1} for the $a_g\nu_{10}$ C–S–C stretching mode. In analogy to assignments made for other ET salts[12] we conclude that two different organic stacks are present, as already observed from the X-ray crystal structure data: on one hand, the stack including B- and C-type ET molecules appears to be completely ionized, and on the other, the A-type dimeric molecular arrangement is be a mixed valence system with $+1/2$ charge on each ET molecule (to yield the total anionic charge of -6).

In a wide temperature range (40–300 K), single-crystal EPR measurements show one homogeneous signal at $g \approx 2$ that appears to be mainly related with the organic radical cations. A second signal becomes observable at lower temperatures, which is very sensitive to the orientation of the crystal (the g value of this line varies between 4 and 6 when the static magnetic field is perpendicular or parallel to the long axis of the needle-shaped crystal). This signal is due to the tetrahedral Co^{II} ions. The observation of two signals indicates that the exchange interaction between the two spin sublattices is small. Further indication of magnetic interactions can be obtained from the plot of the dependence of temperature on the spin susceptibility, the g value, and the signal width derived from the radical signal (Fig. 4). Thus, the plot of the χT vs. T decreases continuously on lowering the temperature, and at 4 K reaches a value that is 3% of the room temperature value, which indicates short-range antiferromagnetic interactions in the organic sublattice. On the other hand, both g and line-width parameters do not change, within the experimental error, down to about 80 K, and at lower temperatures a progressive increase of these parameters is observed. This behavior is reminiscent of that previously observed in two other organic/inorganic salts for which magnetic interactions between the localized moments of the inorganic part and the itinerant electrons of the organic moiety have been proposed.[13] However, in our case the presence of a very small organic–inorganic exchange interaction does not seem to be sufficient to justify the strong variability of the experimental parameters. A more plausible explanation arises from the possibility of magnetic interactions between the two kinds of organic chains present in the structure: one probably contains completely ionized ET molecules, and therefore localized spins, while the other is in a delocalized mixed-valence state. In fact, magnetic measurements carried out on the related silicon-containing salt, $ET_8[SiW_{12}O_{40}]$, show a maximum in χ at about 60 K, which indicates the presence of significant antiferromagnetic interactions in the organic sublattice.[14]

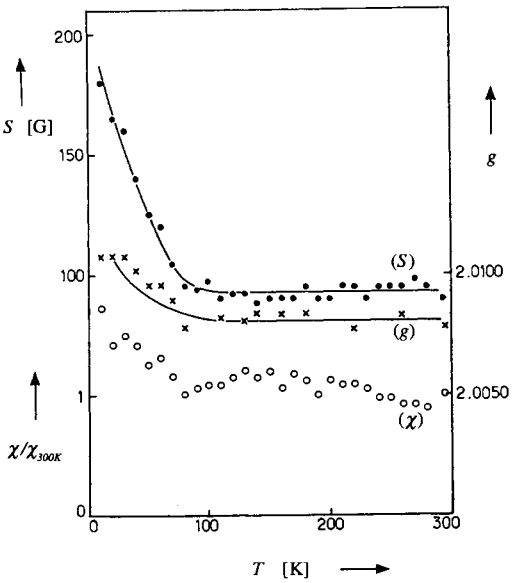


Fig. 4. Temperature dependence of the linewidth S of the ESR signal, the g factor, and the relative spin susceptibility χ for a given position of the single crystal within the resonance cavity.

From the above results we conclude that the two spin sublattices are quasi-isolated. The only significant interaction seems to occur within the organic component. The bulk susceptibility measurements confirm this conclusion: The product χT remains constant in the range 150–300 K and shows a slight decrease from 3 to 2.2 emu mole K^{-1} on lowering the temperature to 4 K. This decrease should arise from the antiferromagnetic interaction in the organic component, while the low temperature value is in good agreement with the presence of isolated Co^{II} ($S = 3/2$ and $g \approx 2.2$).

The material presented here constitutes the first example of organic/inorganic salts made with both magnetic polyoxometalates and π-type organic donors. It opens the possibility of synthesizing new molecular compounds in which the coupling between magnetic and conducting sublattices should lead to new and interesting properties. Radical cation salts containing other polyoxometalates $XW_{12}O_{40}$ are under current investigation in our groups. Preliminary results show that other paramagnetic (X = Co^{III}, Fe^{III}, Cu^{II}, etc.) and diamagnetic (X = H_2^{+2}, Zn^{II}, B^{III}) anions with the Keggin structure present the same α phase. Furthermore, we have also found the existence of two other related phases for almost all the mentioned polyanions.[15] These results now open the possibility of trying other Keggin polyanions having magnetic ions on the surface in order to favor the magnetic interactions with the organic part. Moreover, they show the rich structural polymorphism of this kind of inorganic/organic association and the existence of isostructural series in which different anionic charges (from -4 to -8) and different spins can be accommodated with ease, thus constituting ideal supports for the investigation of systems combining conducting and magnetic behaviors.

 © VCH Verlagsgesellschaft mbH, D-69451 Weinheim, 1994 0570-0833/94/0202-0225 $ 10.00+.25/0

Experimental Procedure

Single crystals of the title compound were obtained from the electrochemical oxidation of ET (3.5×10^{-3} M in a mixture of $CH_2Cl_2/CH_3CN/H_2O$ 10:2:1) in the presence of the tetrabutylammonium salt of the polyoxoanion $[CoW_{12}O_{40}]^{-6}$ [16] (5×10^{-3} M in a mixture of CH_2Cl_2/CH_3CN 1:1) in a U-shaped cell with Pt electrodes (0.5 mm diameter) separated by a sintered-glass frit. The intensity of the current was fixed at 1 μA. After 2 or 3 weeks, amber, platelike single crystals of the title compound were collected carefully and air dried.

Magnetic measurements were carried out on single crystals with a magnetometer (905 VTS, SEH Corporation) equipped with a SQUID sensor (SQUID = *s*uperconducting *q*uantum *i*nterference *d*evice). EPR measurements of the X band at variable temperature were recorded on a Bruker ER 200D spectrometer equipped with a helium cryostat. In the experiment the static magnetic field is perpendicular to the long axis of the needlelike single crystal. Infrared spectra in the range 400–4700 cm^{-1} were made on KBr pellets with a FT-IR interferometer Nicolet MX1. Conductivity measurements were performed using the four-probe method on approximately 4-mm long-needlelike single crystals.

Received: July 14, 1993
Revised version: August 7, 1993 [Z 6139 IE]
German version: *Angew. Chem.* **1994**, *106*, 234

[1] See, for instance: a) J. M. Williams, J. R. Ferraro, R. J. Thorn, K. D. Carlson, U. Geiser, H. H. Wang, A. M. Kini, M. H. Whangbo in *Organic Superconductors. Synthesis, Structure, Properties and Theory* (Ed.: R. N. Grimes), Prentice Hall, Englewood Cliffs, NJ, USA, **1992**; b) *Proc. ICSM'90 (Tübingen): Synth. Met.* **1991**, *41–43* and *Proc. ICSM'92 (Göteborg): ibid.* **1993**, *55–57*.

[2] a) M. T. Pope, *Heteropoly and Isopoly Oxometalates*, Springer, Berlin, **1983**; b) M. T. Pope, A. Müller, *Angew. Chem.* **1991**, *103*, 56; *Angew. Chem. Int. Ed. Engl.* **1991**, *30*, 34; c) *Polyoxometalates: from Platonic Solids to Anti-retroviral activity* (Eds.: M. T. Pope, A. Müller), Kluwer, Dordrecht, in press.

[3] a) L. Ouahab, M. Bencharif, D. Grandjean, *C. R. Aced. Sci. Ser. II.* **1988**, *307*, 749; b) S.Triki, L. Ouahab, J. Padiou, D. Grandjean, *J. Chem. Soc. Chem. Commun.* **1989**, 1068; c) C. J. Gómez-Garcia, E. Coronado, S. Triki, L. Ouahab, P. Delhaès, *Adv. Mater.* **1993**, *4*, 283.

[4] a) A. Davidson, K. Boubekeur, A. Pénicaud, P. Auban, C. Lenoir, P. Batail, G. Hervé, *J. Chem. Soc. Chem. Commun.* **1989**, 1373; b) C. Bellitto, D. Attanasio, M. Bonamico, V. Fares, P. Imperatori, S. Patrizio, *Mater. Res. Soc. Symp. Proc.* **1990**, *173*, 143.

[5] a) A. Mhanni, L. Ouahab, O. Peña, D. Gradjean, C. Garrigou-Lagrange, P. Delhaès, *Synth. Met.* **1991**, *41–43*, 1703, b) L. Ouahab, M. Bencharif, A. Mhanni, D. Pelloquin, J. F. Halet, O. Peña, J. Padiou, D. Grandjean, C. Garrigou-Lagrange, J. Amiell, P. Delhaès, *Chem. Mater.* **1992**, *4*, 666; c) see L. Ouahab in ref. [2c].

[6] Powder materials formed by TTF and paramagnetic polyoxoanions of the type $[Co_4(H_2O)_2(PW_9O_{34})_2]^{-10}$ and $[CrMo_6O_{24}H_6]^{-3}$ have very recently been prepared and magnetically characterized: C. J. Gómez-García, J. J. Borrás-Almenar, E. Coronado, P. Delhaès, C. Garrigou-Lagrange, L. C. W. Baker, *Synth. Met.* **1993**, *55–57*, 2023.

[7] $(BEDT\text{-}TTF)_8[CoW_{12}O_{40}]\cdot5.5$: amber platelike crystal: $0.41\times0.34\times0.01$ mm^3, Enraf-Nonius CAD4 diffractometer, $M = 6081.8$, monoclinic, space group $I2/m$ with $a = 13.971(9)$, $b = 43.117(7)$, $c = 14.042(5)$ Å, $\beta = 107.25(3)$, $V = 8078.5$ $Å^3$, and $Z = 2$ ($\rho_{calcd} = 2.496$ gcm^{-3}; $Mo_{K\alpha}$ radiation, $\lambda = 0.71073$ Å, $\mu = 96.554$ cm^{-1}), structure solved by direct methods and successive Fourier difference synthesis. Refinement of 329 variables with anisotropic thermal parameters (for Co, W and S atoms) gave $R(F) = 0.068$ and $Rw(F) = 0.102$ by using 2614 absorption corrected reflections with $I \geq 6\sigma(I)$. Further details of the crystal structure investigation may be obtained from the Fachinformationszentrum Karlsruhe, D-76344 Eggenstein-Leopoldshafen (FRG), on quoting the depository number CSD-57 908, the authors, and the journal citation.

[8] H. T. Evans, M. T. Pope, *Inorg. Chem.* **1984**, *23*, 501.

[9] J. J. Novoa, F. Mota, M. H. Whangbo, J. M. Williams, *Inorg. Chem.* **1991**, *30*, 54.

[10] H. Mori, S. Tanaka, M. Oshima, G. Saito, T. Mori, Y. Maruyama, H. Inokuchi, *Bull. Chem. Soc. Jpn.* **1990**, *63*, 2183.

[11] J. B. Torrance, *Acc. Chem. Res.* **1979**, *12*, 79.

[12] R. Swietlik, C. Garrigou-Lagrange, C. Sourisseau, G. Pages, P. Delhaes, *J. Mater. Chem.* **1992**, *2*, 857;

[13] a) M. Lequan, R. M. Lequan, C. Hauw, J. Gaultier, G. Maceno, P. Delhaès *Synth. Met.* **1987**, *19*, 409; b) P. Day, M. Kurmoo, T. Mallah, I. R. Marsden, R. H. Friend, F. L. Pratt, W. Hayes, D. Chasseau, J. Gaultier, G. Bravic, L. Ducasse, *J. Am. Chem. Soc.* **1992**, *114*, 10722.

[14] C. Bellitto, M. Bonamico, G. Staulo, *Mol. Cryst. Liq. Cryst.* **1993**, *232*, 155.

[15] A systematic study on the structures and physical properties of these three series is under way in our laboratories and will be published soon.

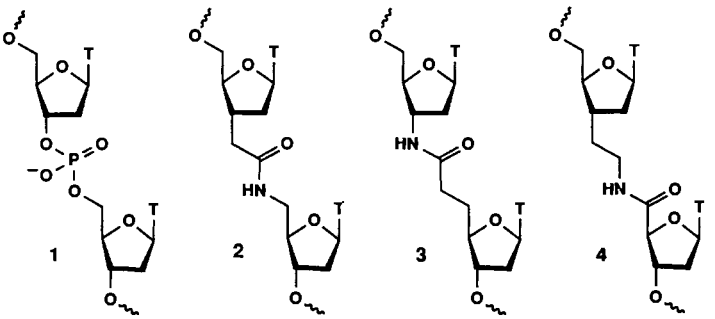
[16] V. E. Simmons, Dissertation, Boston University, **1963**; *Diss. Abstr.* **1963**, *24*, 1391.

Amides as a New Type of Backbone Modification in Oligonucleotides**

Alain De Mesmaeker,* Adrian Waldner, Jacques Lebreton, Pascale Hoffmann, Valérie Fritsch, Romain M. Wolf, and Susan M. Freier

Considerable efforts have been made recently in the structural modification of oligonucleotides.[1] Several properties of the natural 2′-deoxyoligoribonucleotides must be improved for potential therapeutic application of the antisense strategy. For example, the stability of the antisense oligonucleotides towards nucleases must be substantially increased, while the affinity and the specificity for the complementary RNA target is maintained (or even increased). So far, most of the replacements of the phosphodiester linkage that lead to an increased resistance towards nucleases are also connected with a decrease in the affinity for a complementary RNA strand.[1, 2] Two exceptions to this were recently reported in which either an *N*-methylhydroxylamine or a thioformacetal unit was used as a PO_4 replacement.[2a, c]

We proposed to replace the natural phosphodiester linkage in **1** (Scheme 1) by an amide function (as in **2**–**4**), which offers several advantages compared to previously reported modifications.[3] The amide unit is compatible with conditions required



Scheme 1. Structural isomers of oligonucleotide backbones modified by amide linkages.

for solid-phase oligonucleotide synthesis and is also more stable under physiological conditions than the phosphodiester linkage. Furthermore, the lower overall charge of oligonucleotides containing neutral amide groups should facilitate penetration of the negatively charged cell membranes.[4] The amide moiety is readily accessible by simple synthetic methods and is achiral. Thus the formation of diastereomeric mixtures after incorporation into oligonucleotides is avoided.

We disclose here the synthesis of the thymidine dimers **10** (see Scheme 2) having the same substitution pattern in the nucleotide backbone as that in **2**. The incorporation of **10** into oligodeoxynucleotides is described, together with the thermodynamic stability (melting temperatures T_m) of the corresponding duplexes

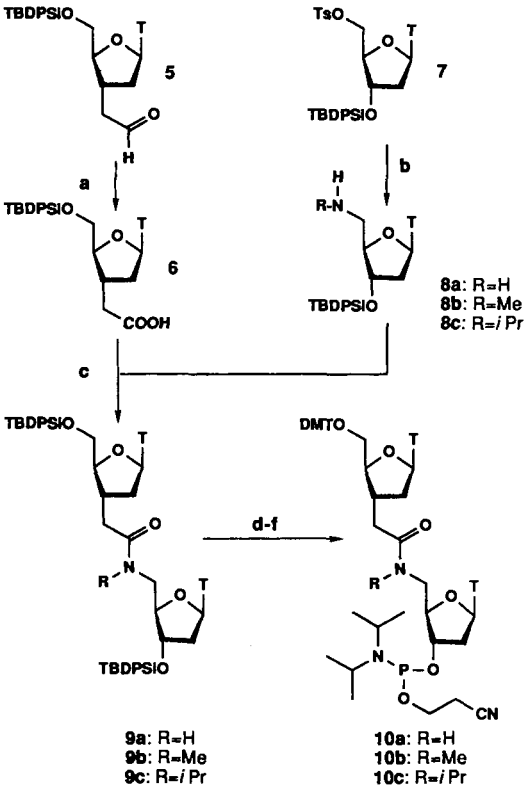
[*] Dr. A. De Mesmaeker, Dr. A. Waldner, Dr. J. Lebreton, P. Hoffmann, Dr. V. Fritsch, Dr. R. M. Wolf
Central Research Laboratories, Ciba-Geigy
CH-4002 Basel (Switzerland)
Telefax: Int. code + (61)679-8252
Dr. S. M. Freier
ISIS Pharmaceuticals
2280 Faraday Avenue, Carlsbad, CA 92008 (USA)

[**] We thank Dr. H. Moser for helpful discussions, and Dr. U. Pieles and Dr. D. Hüsken for the synthesis and the purification of the oligonucleotides.

 © VCH Verlagsgesellschaft mbH, D-69451 Weinheim, 1994 0570-0833/94/0202-0226 $ 10.00+.25/0

formed with the RNA and DNA complements, and the resistance of these oligonucleotides towards 3′-exonucleases.

The synthesis of the amide dimers **10** is depicted in Scheme 2. The oxidation of aldehyde **5**[5] to give the corresponding acid **6** was initially performed in two steps: **5** was oxidized with pyridinium dichromate (PDC) in dimethylformamide (DMF) in the presence of methanol to give the methyl ester in 60% after chromatography;[6] subsequent hydrolysis with sodium hydroxide furnished the desired carboxylic acid **6** in almost quantitative yield. Later on, we found that **5** could be oxidized very efficiently with sodium chlorite to provide **6**.[7] Amines **8a–c** were obtained by treatment of **7** with methyl- or isopropylamine (for **8b, c**) or with lithium azide[8] followed by the reduction of the resulting azide with tin dichloride (for **8a**).[9]



Scheme 2. Synthesis of the phosphoramidites **10a–c**. TBDPSi = *tert*-butyldiphenylsilyl. a) $NaClO_2$, 2-methyl-2-butene, NaH_2PO_4, *t*-BuOH, H_2O, room temperature (RT), 2 h (87%); b) R = H, see [8]; RNH_2, THF, RT, 27 h (R = Me (83%), R = *i*Pr (75%)); c) **6**, *N*-methylmorpholine, TBTU, *N*-hydroxybenzotriazole, MeCN, RT, 0.5 h, then **8**, *N*-methylmorpholine, MeCN, RT, 20 h (R = H (86%), R = Me (80%), R = *i*Pr (85%)); d) nBu_4NF, AcOH, THF, RT, 20 h (85%); e) DMTCl, pyridine, RT, 40 h (85%); f) $(iPr_2N)_2POCH_2CH_2CN$, $iPr_2NH_2^+$ tetrazole$^-$, CH_2Cl_2, RT, 40 h (75%).

Carboxylic acid **6** was activated with *O*-(1*H*-benzotriazol-1-yl)-*N*,*N*,*N*′,*N*′-tetramethyluronium tetrafluoroborate (TBTU) and *N*-hydroxybenzotriazole[10] and then coupled with amines **8a–c**. Only the rotamer depicted in Scheme 2 was detected by ^{1}H NMR spectroscopy in the case of the amide dimer **9a** (R = H). However, both rotamers of the N-disubstituted amides **9b**, **9c** were found in solution and identified by ^{1}H NMR NOE experiments.[11] The major rotamer was, in both cases, the one shown in the Scheme 2 (rotamer ratio ca. 4:1 in $CDCl_3$ at room temperature).

The removal of the silyl protective groups with tetra-*n*-butylammonium fluoride in the presence of acetic acid was followed by the selective introduction of the 4,4′-dimethoxytrityl group (DMT) at the 5′ end and the phosphoramidite function at the 3′ end with standard procedures.[12] The solid-phase synthesis of the oligodeoxynucleotides (Table 1) and their purification were performed by standard methods.[13]

Table 1. Melting temperatures T_m of duplexes of modified oligonucleotides and their RNA and DNA complements [a].

Modified oligodeoxynucleotide (5′ → 3′) [b]	Wild-type T_m [°C]	ΔT_m [K] [b, c] a_1	a_2	a_3
A CTCGTACC**TaT**TCCGGTCC	63.3	+0.9	+1.0	+0.9
B CTCGTAC**TaT TaT**CCGGTCC	61.8	+0.5	−0.2	−0.2
C GCG**TaT TaT TaT TaT TaT**GCG	50.2	−0.3	[d]	−0.7
D TTT**TaT**CTCTCTCTCT	51.6	+0.4	−1.1	−0.4
E GCG**TaT TaT TaT TaT TaT**GCG	54.1	−1.5	[d]	−3.0
F TTT**TaT**CTCTCTCTCT	42.3	−1.7	−2.6	−3.8

[a] **A–D** with RNA complement, **E–F** with DNA complement. [b] **a** = 3′-CH_2–NR–CO–CH_2-4′, (R = H, a_1; R = Me, a_2; R = *i*Pr, a_3). [c] ΔT_m = [T_m(modified oligonucleotide) − T_m(wild-type)]/(number of modifications). [d] Not measured.

The melting temperatures of the duplexes formed between these oligodeoxynucleotides and their RNA and DNA complements are summarized in Table 1.[14] The incorporation of a single amide modification in the middle of the oligonucleotide (**A**) led to an increase in the thermal stability of the duplexes with RNA (+0.9 to +1.0 K). An analogous increase in the affinity for the RNA target is also observed in the case of modification a_1 in the sequences **B** and **D**. A. slight decrease of the stability of the duplex was observed (− 0.3 K per modification) when five a_1 units were introduced in the oligonucleotide (**C**). The same trend was followed by the N-substituted amides a_2 and a_3. However, the destabilization of the duplexes in these cases is rather small, even for the sterically demanding isopropyl group (in a_3). These results indicate that the amide unit a_1 is a good modification in the oligonucleotide backbone and that the introduction of additional substituents on the nitrogen atom does not significantly disturb the structure and the stability of the duplex formed with an RNA complement. The amide modification in **2** also displays a good affinity for a complementary DNA strand (**E** and **F** in Table 1).

These binding data are quite different from the ones we obtained for amides **3**[3b] and **4**:[3c] their incorporation into the same oligonucleotides led to an average drop in the T_m of the duplexes with RNA by −2.9 K per modification for **3** and by −1.6 K per modification for **4**. Molecular dynamics studies (see below) confirmed that the amide modification in **2** adopts a more favorable geometry in the duplex with an RNA complement than those in analogues **3** and **4**. Interestingly, the amide modifications a_1–a_3 destabilize the duplexes formed with the complementary DNA strand (entry **E–F**) more than those with the complementary RNA strand (**A–D**).

Molecular mechanics and molecular dynamics (MD) investigations were undertaken in order to gain insight into the structural features of the modified oligonucleotide backbones.[15] No counterions and solvent molecules were included explicitly at this stage. The permittivity was modulated by the use of a distance-dependent dielectric constant $\varepsilon = 4 \times r_{ij}$, where r_{ij} is the distance separating point charges. In a first step, a hybrid duplex d(CTT**TaT**TTC) · r(GA_6G) composed of an A-form octamer was analyzed with respect to the various possible conformations adopted by the amide linkage 3′-CH_2–CO–NH–CH_2-4′. For this purpose the torsion angles ζ and β (Fig. 1) were changed in 30° increments, and the structure was allowed to relax each time.

 © VCH Verlagsgesellschaft mbH, D-69451 Weinheim, 1994 0570-0833/94/0202-0227 $ 10.00+.25/0

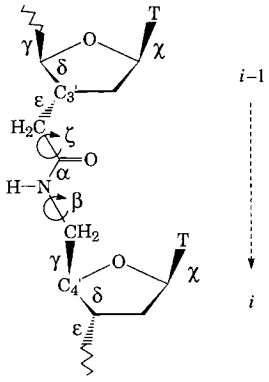


Fig. 1. Definition of torsion angles in a DNA fragment with an amide linkage.

Table 2. Torsion angles [°] at the amide linkage (see also Figs. 1 and 2) [a].

Conformer	Energy [b] [kcal mol^{-1}]	Residue	α	β	γ	δ	ε	ζ	χ
I	0	*i*-1	−75	177	60	77	**178**	**−79**	−157
		i	**170**	**−157**	**166**	85	−155	−62	−169
II	0.5	*i*-1	−74	178	59	75	**171**	**55**	−159
		i	**−172**	**73**	**170**	77	−158	−65	−171
III	2.9	*i*-1	−75	176	58	71	**92**	**81**	−159
		i	**−171**	**157**	**71**	77	−173	−67	−148

[a] Torsion angles in the modified portion C3'-CH_2-CO-NH-CH_2-C4' are in boldface. [b] Relative Amber energy of octamer duplex structure.

Torsion angles ε and γ were left free to adjust during this procedure, the amide bond (torsion angle α) was kept in the *trans* conformation but was allowed to deviate from the default value of 180° from the force field constraints.[16] This approach allowed the identification of several local minima for the conformation of the amide linkage without disrupting the duplex structure at any point during the conformational scanning. Three clearly distinct conformations are shown in Figure 2,[17] and their structural details are listed in Table 2.

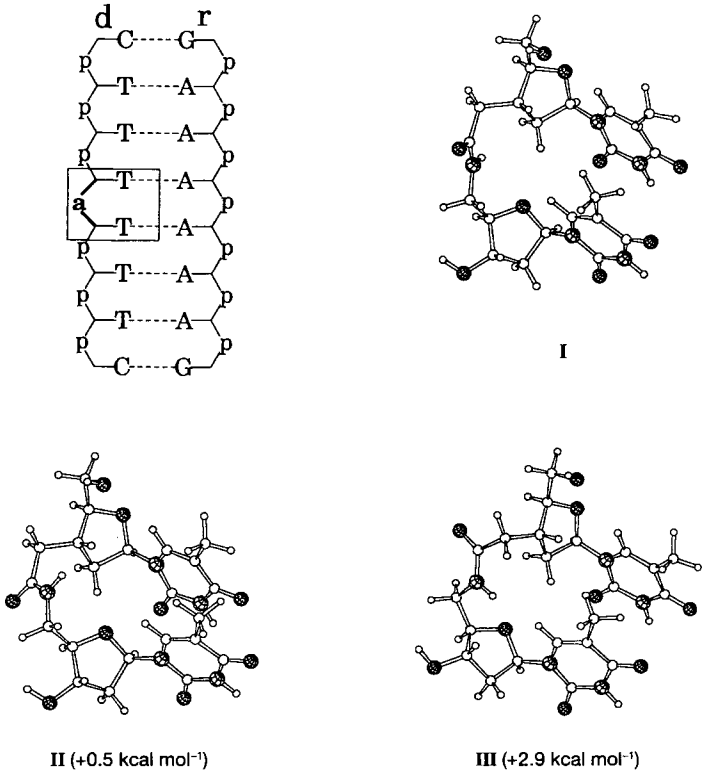


Fig. 2. Structures corresponding to local energy minima for the amide linkage which are cut out of the middle of the octamer duplex (modified DNA) · (RNA) (top left). Energy values are AMBER energies, normalized to the lowest-energy conformer **I**.

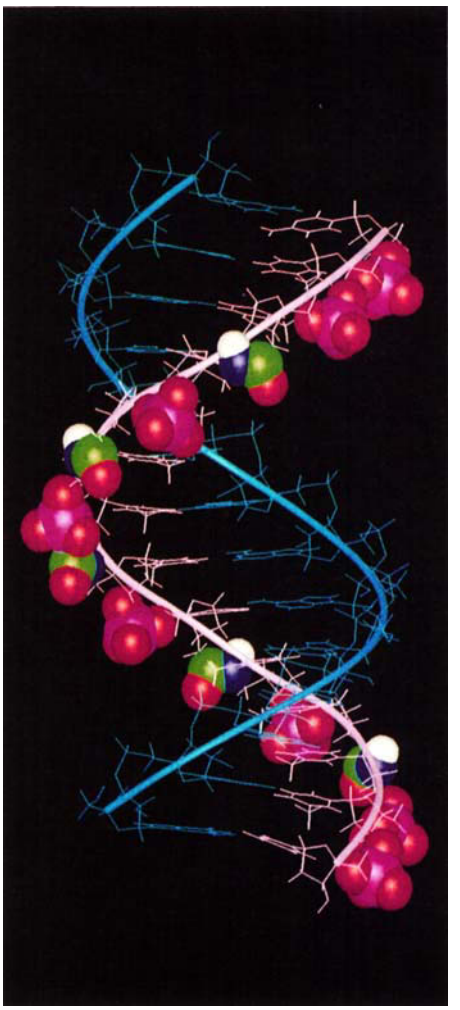


Fig. 3. Fully minimized structure of the 14mer duplex d(CT(**TaT**)$_5$TC)·r(G(A)$_{12}$G). All amide linkages are in the **I** conformation (see Fig. 2 and Table 2 for structural details).

Molecular dynamics studies on 14mer duplex structures with an alternating modified d(CT(**TaT**)$_5$TC) strand and a natural complementary RNA strand (Fig. 3) were carried out for 100 ps at 300 K (progressive heating up to equilibrium in 24 ps). Figure 4 shows the superimposed backbone ribbons of structures spaced by 10 ps for a wild-type d(CT$_{12}$C) · r(GA$_{12}$G) (left) and the duplex depicted in Figure 3, in which all amide linkages are in the conformation **I** at the start of the calculation (right). The dynamic behavior is very similar in both cases, which suggests that the two structures undergo similar oscillations around an equilibrium geometry. Detailed accounts on MD simulations conducted with different starting geometries and the conformational transitions observed will be given in due course.[18]

Compared to the unmodified oligomer, the modified oligonucleotides TCCAGGTGTT**TaT**C exhibit an enhanced resistance

 © VCH Verlagsgesellschaft mbH, D-69451 Weinheim, 1994 0570-0833/94/0202-0228 $ 10.00+.25/0

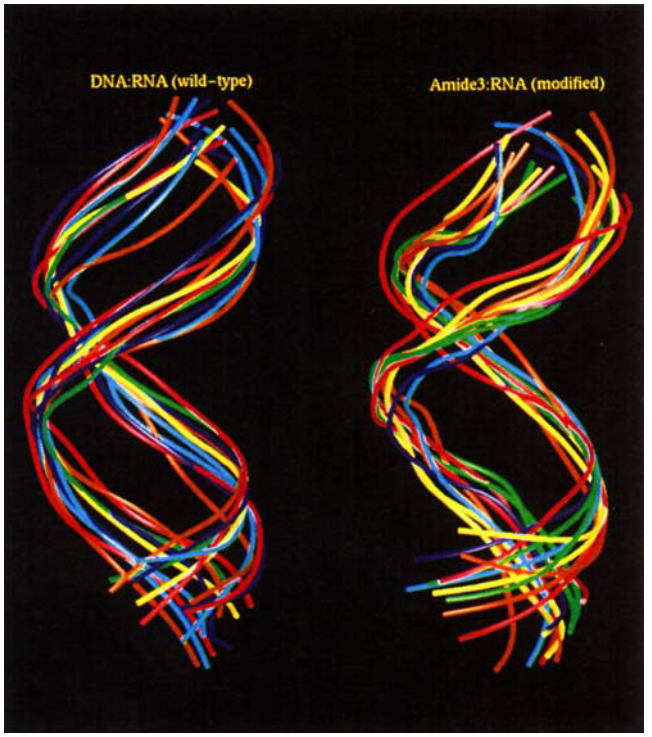


Fig. 4. Superposition of the backbone ribbons of duplex structures. Left: the 14mer DNA · RNA hybrid duplex $d(CT_{12}C) \cdot r(GA_{12}G)$; right: the modified duplex $d(CT(\mathbf{TaT})_5TC) \cdot r(G(A)_{12}G)$ shown in Figure 3. The modified DNA strands start at the upper right.

to hydrolysis by 10% fetal calf serum[19] (predominantly 3′-exonuclease) at 37 °C by factors of 9 and 17 for $\mathbf{a}_2$ and $\mathbf{a}_3$, respectively.

In summary, modified oligonucleotides having the new amide modification in **2** not only display a similar or even slightly higher affinity for an RNA target than the natural analogues, but they are also substantially more stable towards 3′-exonucleases. The introduction of the backbone modification in **2** into biological relevant sequences is under current investigation.

Received: August 13, 1993 [Z 6277 IE]
German version: *Angew. Chem.* **1994**, *106*, 237

[1] a) *Oligodeoxynucleotides. Antisense Inhibitors of Gene Expression* (Ed.: J. S. Cohen), CRC, Boca Raton, FL, USA, **1989**; b) E. Uhlmann, A. Peyman, *Chem. Rev.* **1990**, *90*, 543; c) S. T. Crooke, *Annu. Rev. Pharmacol. Toxicol.* **1992**, *32*, 329; d) P. D. Cook, *Anti-Cancer Drug Des.* **1991**, *6*, 585.

[2] a) J.-J. Vasseur, F. Debart, Y. S. Sanghvi, P. D. Cook, *J. Am. Chem. Soc.* **1992**, *114*, 4006; b) R. C. Reynolds, P. A. Crooks, J. A. Maddry, M. S. Akhtar, J. A. Montgomery, J. A. Secrist, *J. Org. Chem.* **1992**, *57*, 2983; c) R. J. Jones, K. Y. Lin, J. F. Milligan, S. Wadwani, M. D. Matteucci, *ibid.* **1993**, *58*, 2983; d) B. Meng, S. H. Kawai, D. Wang, G. Just, P. A. Giannaris, M. J. Damha, *Angew. Chem.* **1993**, *105*, 733; *Angew. Chem. Int. Ed. Engl.* **1993**, *32*, 729, and references therein.; e) P. J. L. M. Quaedflieg, G. A. Van der Marel, E. Kuyl-Yeheskiely, J. H. van Boom, *Recl. Trav. Chim. Pays-Bas* **1991**, *110*, 435.

[3] a) A. De Mesmaeker, J. Lebreton, A. Waldner, P. D. Cook, WO 92/20823, **1992** (*Backbone Modified Oligonucleotide Analogs*); b) J. Lebreton, A. De Mesmaeker, A. Waldner, V. Fritsch, R. M. Wolf, S. M. Freier, *Tetrahedron Lett.*, in press; c) A. De Mesmaeker, J. Lebreton, A. Waldner, V. Fritsch, R. M. Wolf, S. M. Freier, *Synlett* **1993**, 733. For drastically altered oligonucleotide analogues having mide bonds see: P. E. Nielsen, M. Egholm, R. H. Berg, O. Buchardt, *Science* **1991**, *254*, 1497. After the submission of this manuscript an independent report on the same amide modification appeared using the method we already described in detail in our patent [3a]: I. Idziak, G. Just, M. J. Damha, P. A. Giannaris, *Tetrahedron Lett.* **1993**, *34*, 5417.

[4] J. W. Jaroszewski, J. S. Cohen, *Adv. Drug Delivery Rev.* **1991**, *6*, 235.

[5] a) J. Fiandor, S. Y. Tam, *Tetrahedron Lett.* **1990**, *31*, 597; b) see also ref. [3c].

[6] B. O'Connor, G. Just, *Tetrahedron Lett.* **1987**, *28*, 3235.

[7] E. Dalcanade, *J. Org. Chem.* **1986**, *51*, 567. We thank Dr. P. Chemla (Ciba-Geigy) for bringing this reference to our attention.

[8] T.-S. Lin, W. H. Prusoff, *J. Med. Chem.* **1978**, *21*, 109.

[9] S. N. Maiti, M. P. Singh, R. G. Micetich, *Tetrahedron Lett.* **1986**, *27*, 1423.

[10] R. Knorr, A. Trzeciak, W. Bannwarth, D. Gillessen, *Tetrahedron Lett.* **1989**, *30*, 1927.

[11] We thank Dr. T. Winkler (Ciba-Geigy) for carrying out the ^{1}H NMR NOE experiments.

[12] N. D. Sinha, J. Biernat, J. McManus, H. Köster, *Nucleic Acids Res.* **1984**, *12*, 4539.

[13] The oligonucleotides were prepared on an ABI 390 DNA synthesizer by using standard phosphoramidite chemistry according to M. J. Gait, *Oligonucleotide Synthesis: A Practical Approach*, IRL, Oxford **1984**, but with prolonged coupling times (10 min). DMT oligonucleotides were purified by reversed-phase HPLC (column: Nucleosil RPC_{18}, 10 μm, 10 × 250 mm; eluent A: 50 mM triethylammonium acetate (TEAA), pH 7.0; eluent B: 50 mM TEAA, pH 7.0 in 70% acetonitrile; elution with gradient from A:B = 85:15 to 55:45 in 45 min). After purification by HPLC the oligodeoxynucleotides were checked by capillary gel electrophoresis (concentration: 35 μg oligonucleotide mL^{-1}; injection: 2 kV, 3; separation: 9 kV; capillary: effective length 30 cm, inner diameter 100 μm, polyacrylamide 10% T; buffer: 100 mM H_3PO_4, 100 mM 2-amino-2-hydroxymethyl-1,3-propanediol (Tris), 2 mM ethylenediaminetetraacetate (EDTA), 7 M urea, pH 8.8). The molecular weight of each oligodeoxynucleotide was checked by mass spectrometry (MALDI-TOF: U. Pieles, W. Zürcher, M. Schär, H. Moser, *Nucl. Acids Res.* **1993**, *21*, 3191). The oligodeoxynucleotide was desorbed from a matrix of 2,4,6-trihydroxyacetophenone (detection of megatively charged ions) with diammonium hydrogen citrate as additive (25 mM final concentration).

[14] The thermal denaturation of DNA/RNA hybrids was performed at 260 nm with a Gilford Response II Spectrophotometer (Ciba-Corning Diagnostics, Oberlin, OH, USA) or a Varian Cary 3 UV/Vis spectrophotometer. The extinction vs. temperature profiles were measured for each strand (4 μM) in 10 mM phosphate (pH 7.0, Na salts) with 100 mM total $[Na^+]$ (supplemented as NaCl) and 0.1 mM EDTA). T_m values were obtained from fitting the extinction vs. temperature curves to a two-state model with linear slope baselines (S. M. Freier, D. D. Albergo, D. H. Turner, *Biopolymers* **1982**, *22*, 1107). All values are averages from at least three experiments. The absolute experimental error of the T_m values is ±0.5 K.

[15] AMBER force field (S. J. Weiner, P. A. Kollman, D. T. Nguyen, D. A. Case, *J. Comp. Chem.* **1986**, *7*, 230), as incorporated in the Insight II (version 2.2.0)/DISCOVER (version 2.9) software from BIOSYM Technologies, San Diego, CA 92121 (USA).

[16] The same procedure was applied with the *cis*-configurated amide group. In this case, the local minima were definitely higher in energy than those obtained with the amide in the standard *trans* conformation.

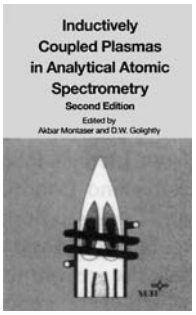
[17] Drawings made with SCHAKAL (E. Keller, Institut für Kristallographie, Universität Freiburg (FRG)).

[18] R. M. Wolf, V. Fritsch, A. De Mesmaeker, J. Lebreton, A. Waldner, unpublished results.

[19] For experimental details see: G. D. Hoke, K. Draper, S. M. Freier, C. Gonzales, V. B. Driver, M. C. Zounes, D. J. Ecker, *Nucleic Acids Res.* **1991**, *19*, 5743.

 © *VCH Verlagsgesellschaft mbH, D-69451 Weinheim, 1994* *0570-0833/94/0202-0229 $ 10.00+.25/0*

Inductively Coupled Plasmas in Analytical Atomic Spectrometry. 2nd Edition. Edited by *A. Montaser* and *D. W. Golightly*. VCH Publishers, New York/VCH Verlagsgesellschaft, Weinheim, 1992. XXII, 1017 pp., hardcover £ 111.00, DM 296.00.—ISBN 1-56081-514-0/3-527-28339-0



Inductively coupled radiofrequency plasmas (ICPs) now play an important role in elemental trace analysis, as radiation sources for optical emission spectrometry and as ion sources for mass spectrometry. This book edited by Montaser and Golightly (which is a revised version of one first published in 1987) gives a comprehensive treatment of the principles and applications of atomic spectrometry using ICP sources. It has been written by a team of 32 authors who have made fundamental contributions to the development and use of ICP atomic spectrometry. The basic principles and different aspects of ICP atomic spectrometry are treated comprehensively, with a wealth of references to the literature on individual topics and applications.

The introduction explains how the ICP, as a source for atomic spectrometry, is related to other types of plasmas. The essential principles and analytical capabilities of direct current (DC) plasmas, microwave plasmas, graphite furnace thermal plasmas, and both DC and radiofrequency glow discharges are all briefly described. The first part of the book is concerned specifically with aspects relevant to atomic spectrometry. The chapter on the fundamentals of atomic emission spectrometry deals mainly with the concepts and methods of plasma physics and plasma diagnostics. Aspects given special attention include the concept of temperature, line-broadening mechanisms, and thermal equilibrium. The chapter on instrumentation for atomic emission spectrometry discusses the principles of spectral dispersion, optical systems, and radiation detection in modern spectrometers. As well as conventional systems some newer developments are discussed, including Fourier transform atomic emission spectrometry and new types of radiation detectors such as charge-coupled (CCD) and charge-injection (CID) devices. The next chapter describes the radiofrequency generators and plasma torch systems used in ICP atomic spectrometry. The chapter on the analytical performance of ICP atomic emission spectrometry gives a clear explanation of optimization procedures, including the simplex method, and of detection limits and interferences. The very important problem of line selection in atomic emission is treated in a separate chapter. High-resolution variants of plasma emission spectrometry and their use in applications such as the analysis of actinides are also discussed as a special topic. This is followed by a chapter on plasma diagnostics and on spectroscopic reference data for ICP atomic emission spectrometry. The first part ends with a chapter describing important applications.

The second part, entitled "Complementary ICP Techniques", begins by describing applications in which an ICP serves as an atomization cell for atomic fluorescence spectrometry. Next comes a detailed description of inductively coupled plasma mass spectrometry (ICP-MS). The importance and performance capabilities of ICP-MS for elemental analysis are discussed, as also are optimization procedures and interferences. Fundamental topics such as the formation of cluster ions and the importance of plasma potentials are then treated. This part ends with a survey of the applications of ICP-MS.

The third part of the book deals with the problems of sample introduction, plasma generation, and mathematical modeling of plasmas. The principles of generating aerosols from liquid samples are treated in detail. A separate chapter then deals with the direct generation of aerosols from solids, including laser vaporization techniques. The injection of gases and vapors, including coupling to chromatography, is also discussed with examples from recently published work. Further chapters deal with the development of plasmas with low gas consumption, the potential for ICPs using gases other than argon, and mathematical modeling of ICPs.

The overall structure of the original edition has essentially been retained, but the part dealing with ICP-MS has been considerably enlarged to take account of recent developments. The authors have also clearly described the current development trends in all the aspects covered. In its updated form this is a standard work that can be recommended to everyone who is either concerned with research on the techniques of plasma spectrometry or uses these methods to solve analytical problems for research or routine purposes.

Jose A. C. Broekaert
Fachbereich Chemie
der Universität Dortmund (FRG)

Sourcebook of Advanced Organic Laboratory Preparations. By *S. R. Sandler* and *W. Karo*. Academic Press/Harcourt Brace Jovanovich, New York, 1992. X, 332 pp., ring-bound $ 59.95—ISBN 0-12-618506-9

Practical laboratory sessions alongside lecture courses are an indispensable part of chemistry training. As well as providing the necessary support to theoretical studies and equipping students with the practical skills that are essential in later professional work, they allow them to experience successes which can keep up their motivation during parts of the course where enthusiasm temporarily wanes. Thus there is a need for a well-chosen and proven collection of preparations. It is satisfying for the student when a preparation works and provides a sudden insight ("aha effect"); if it also affords an opportunity to work on the semi-micro or even micro scale, the satisfaction is still greater. A good collection of student laboratory preparations should include an appropriate amount of introductory theoretical background, information about potential dangers, and brief instructions about the disposal of waste products.

A number of good practical workbooks for the teaching of organic chemistry already exist, and that reviewed here is a useful addition to these. The two authors have already established their reputation with six larger volumes of preparative methods: *Organic Functional Group Preparations I*, **1983**; *II*, **1986**; *III*, **1989** and *Polymer Syntheses I*, 2nd Edition, **1992**; *II*, **1977**; *III*, **1980**. Some well-proven methods have now been taken from these and collected together in a convenient form in a ring-binder. Most of the preparations are also suitable for carrying out on a semi-micro scale. Significantly, some polymerizations have also been included. A short explanation of the theory precedes each one of the 41 sections, arranged by compound classes as follows: Paraffinic/Aromatic Hydrocarbons, Olefins, Acetylenes, Alcohols/Phenols, Ethers/Oxides, Halides, Aldehydes,

This section contains book reviews and a list of new books received by the editor. Book reviews are written by invitation from the editor. Suggestions for books to be reviewed and for book reviewers are welcome. Publishers should send brochures or (better) books to the Book Editor, Dr. Gerhard Karger, Redaktion Angewandte Chemie, Postfach 101161, D-69451 Weinheim, Federal Republic of Germany. The editor reserves the right of selecting which books will be reviewed. Uninvited books not chosen for review will not be returned.

 © *VCH Verlagsgesellschaft mbH, D-69451 Weinheim, 1994* *0570-0833/94/0202-0231 $ 10.00+.25/0*

Ketones, Carboxylic Acids, Esters, Amides, Cyanates/Isocyanates/Thiocyanates/Isothiocyanates, Amines, Hydrazine Derivatives/Hydrazones/Hydrazides, Diazo and Diazonium Compounds, Nitro Compounds, Nitriles, Mercaptans/Sulfides/Disulfides, Sulfoxides, Sulfones, Sulfonic Acids, Allenes, Ortho Esters, Sulfites, Enamines, Ynamines, Ureas/Polyureas, Carbodiimides, *N*-Carbamates, *O*-Carbamates, Imines, Azides, Azo-/Azoxy Compounds, Acetals/Ketals, Anhydrides, Monoalkyl Sulfates, Amidines, Imides, Oximes, Hydroxamic Acids, Polymer Preparations. The 172 preparations for which detailed laboratory recipes are given are based on original papers (with references). Other analogous preparations are also listed in tables together with literature references and data on the conditions. Where appropriate the authors draw attention to special features and/or dangers. However, in a future edition they should, right at the start, substitute safe alternatives for chemicals that carry special risks, for example benzene as substrate or solvent (the carcinogenicity of which is mentioned in the preface).

Measured against the requirements of German university courses, this "Sourcebook of Advanced Organic Laboratory Preparations" should be regarded as a good basis for organic chemistry practical work rather than a book for advanced students. It is mainly suitable for students of chemistry (including those training as teachers) and of pharmacy, and it can also be used to advantage, as the authors suggest, for training people in industrial laboratories. Many of the examples could also be used in practical courses for students of neighboring disciplines, since the authors have evidently taken into consideration the time restrictions that affect many practical classes. Important general working techniques of organic chemistry are explained on the basis of typical examples, and many of the preparations afford opportunities for combining with practice in the use of modern analytical methods. Unfortunately, however, some traditional and well-proven methods are missing (e.g., in the synthesis of mercaptans and ureas), nor are there any examples of natural products syntheses. The Appendix contains very useful advice and explanations regarding standard laboratory practices.

The authors' chosen system of classifying the preparative methods according to compound classes and functional groups is a long proven one. However, in a future edition perhaps more emphasis could be put on the second most practicable method of classification, by reactions of functional groups; this could be done by providing an index on this basis instead of the present "Name Reaction Index". In summary, the book by Sandler and Karo is well suited for organic chemistry practicals in universities and colleges, and departments should add it to their range of teaching resources.

Ralf Miethchen
Lehrstuhl für Organische Chemie II
der Universität Rostock (FRG)

Die Allianz von Wissenschaft und Industrie. August Wilhelm Hofmann (1818–1892). Edited by *C. Meinel* and *H. Scholz*. VCH Verlagsgesellschaft, Weinheim, 1992. X, 375 pp., hardcover DM 148.00.—ISBN 3-527-29009-5

This book was published to mark the centenary of the death of August Wilhelm Hofmann, which coincided with the 125th anniversary of the foundation, through Hofmann's initiative, of the German Chemical Society (Gesellschaft Deutscher Chemiker, GDCh). It contains a loosely structured collection of 22 essays (14 in German and 8 in English) by an international team of authors, in which they discuss the many different aspects of the work of this great patriarch of modern organic chemistry.

In the introductory chapter Heindirk tom Dieck (Frankfurt) gives a brief account of the development and aims of the GDCh, whose early stages were decisively influenced by the personality of A. W. Hofmann. Here one already becomes aware of the close collaboration between academic and industrial chemistry, and this is examined in more detail in the following chapter ("Wissenschaft, Industrie und Kultur zur Zeit A. W. Hofmanns", by Lothar Burchardt, Konstanz). It is sobering to find that many of the problems of concern to university chemists at that time still persist today with only minor shifts of emphasis, even though their dimensions are now quite different: growing student numbers, the degree of autonomy of the universities and of professors, the interplay between research and teaching, the demarcation between the universities and the Technische Hochschulen, the setting up of new faculties, and so on. Even the quite ardently displayed cultural pessimism that is now so fashionable, not only among many intellectuals but also among some politicians, and which is manifested in vaguely expressed criticisms of technology, was already active in that period when scientific societies were being founded and the large-scale chemical industry was becoming established. Despite this, more farsighted minds recognized in good time that the development of culture and civilization is closely related to scientific and technological progress, resulting in a promotion of scientific and cultural studies that was unique throughout the world. It is only against this background that one can appreciate the importance of Hofmann's contribution as a pioneer of new forms of cooperation between universities and industry.

Christoph Meinel (Regensburg) then examines in greater depth the social and political environment within which Hofmann, the reigning "Chief Chemist" of his time, pursued a career which took him from Liebig's laboratory in Gießen on to Bonn and London, back again to Bonn, and finally to Berlin. Hofmann soon came to be recognized as *the* standard-bearer for the revolutionary ideas of Liebig, which were concerned with a teaching based on experimental research that also attracted much attention in England. It was therefore quite consistent when in 1845, at the age of 27, he was appointed as the Principal and first Professor of the Royal College of Chemistry in London, where he was to set up a science-orientated teaching institution. Chemical research too was at that time undergoing a change of emphasis, from analysis towards the development of directed syntheses. In this context Hofmann used the concept of compound classes or substitution and type theory as a sort of template to systematically identify new structures. He became a prominent public figure through his wide-ranging activities in helping to organize world exhibitions, as President for a time of the Chemical Society, and as a lecturer on popular scientific themes. Following his return to Berlin in 1865, Hofmann used his influence, based on the scientific reputation built up while in England, to place chemistry in a key position in the modernization of the universities. Nevertheless, Meinel does not forget to mention that Hofmann's pompous conceit and self-adulation, though perhaps understandable in view of the "zeitgeist" of the time, earned him severe criticism, even from close colleagues.

In the next three chapters British authors discuss the influence of A. W. Hofmann and the Gießen academic tradition on scientific culture in Britain. Colin A. Russell (Milton Keynes) emphasizes the role of Hofmann as cosmopolitan scientist, in his friendships with the top European scientists of the time, and even with the British Royal Family. Through his fluency in the English language he contributed to the Journal of the Chemical

 © VCH Verlagsgesellschaft mbH, D-69451 Weinheim, 1994 0570-0833/94/0202-0232 $ 10.00+.25/0

Society becoming internationally recognized, and later in his homeland he modeled the GDCh on the pattern of the Chemical Society of London. Unfortunately Russell is guilty of an annoying lapse in forgetting to mention Georg Wittig in his gallery of Hofmann's successors; Wittig worked with Hofmann's former student K. von Auwers in Marburg at the same time as Karl Ziegler. Next William A. Brock (Leicester) analyzes several of Hofmann's lectures aimed at popularizing chemistry, in which time and again, in language illuminated by many metaphors, he emphasized the importance of his subject to culture and the standard of living and argued for greater state support. Gerrylynn K. Roberts (Milton Keynes) takes the view that Hofmann's twenty years in England mirror an "uneasy balance between pure and applied science", and that he also felt this in his work at the Royal School of Mines. He persisted in his efforts to replace the practically- and analytically-orientated teaching in these institutions by chemistry studies with a greater scientific content, but it was not until the time of his return to Berlin that these courses were introduced at the then newly founded Royal College of Science in Dublin.

In the first of the strictly science-orientated chapters Michael N. Keas (Norman, USA) discusses Hofmann's work on the nature of organic bases, which led to the development of a theory of the ammonia type. Keas describes how, from 1865 onwards, Hofmann went on from this to propose a "truly natural chemical classification system, a structurally-interpreted type theory consisting of the hydrochloric acid, water, ammonia, and methane types."

Under the title "Science and Technology for an Empire", Anthony S. Travis (Jerusalem) examines the significance of Hofmann's work to the chemistry of the coal-tar and aniline dyes and their commercial development. Important contributions were made in this area by other German chemists who also worked in England at that time (Heinrich Caro, Carl Alexander Martius, Peter Griess, etc.) and, of course, by William H. Perkin, the discoverer of mauveine who was also one of Hofmann's former students. Travis identifies the wide-ranging exchange of ideas between Hofmann and Caro (who was influenced by Hofmann to switch from being a colorist to a chemist) and several British and German dye manufacturers as the starting point for the rise of the first ever science-based industry.

The discussion by Hans-Werner Schütt (Berlin) of the state of chemistry in Prussia before A. W. Hofmann, which comes next, should actually be read immediately after the chapters by Burchardt and Meinel, as this too is concerned with the sociopolitical and educational environment of the times. It deals mainly with Liebig's criticisms against the view taken by the Prussian cultural administration that chemistry was not a fundamental science, and therefore did not justify treatment as an independent area of study. Liebig's arguments seem to have made a considerable impression in Berlin, because after the death of his adversary Eilhard Mitscherlich, A. W. Hofmann was appointed in his place to bring into this region too the new ideas of an inquiring way of teaching. Next is a study by Regine Zott (Berlin) of the ideas that Liebig and Hofmann had in common and those that were unique to each one; like the previous chapter, this really belongs with the introductory essays. The central thesis is that although the two scientists had much in common and both fought with great tactical skill for the independence of their subject, chemistry, they differed quite substantially in their attitudes towards theoretical, philosophical, and political matters. Although the younger of the two, Hofmann was more conventional and bound by the mores of his time than was his more ambitious teacher and friend Liebig.

According to Willem J. Hornix (Nijmegen), the assessment by Hofmann's contemporaries and biographers of his role in the development of the dyestuffs industry has assumed almost mythical dimensions. Hornix then critically analyzes Hofmann's scientific contributions in the dyestuffs field; here again the wider social context and the international ramifications of these studies become apparent. It is interesting to note that Hofmann's influence continued to dominate even when his incorrect ideas regarding the structure of the aniline dyes, based on an ammonia-type analogy, came into conflict with Kekulé's (correct) triphenylmethane structures.

Jeffry A. Johnson (Villanova, USA) contributes another view from abroad on "Hofmann's Role in Reshaping the Academic–Industrial Alliance in German Chemistry", in a detailed and informative discussion including the political background. He deals sympathetically with Hofmann's concerns about the needs for modern teaching establishments with the ability to undertake pure research, for an effective German patents system, and for arranging collaboration between universities and industry through the medium of the scientific learned societies. These efforts eventually won important advantages for Germany's chemists and industry, indicating certain causal connections of which people need to be reminded, especially now.

A quite different topic is addressed by Elisabeth Christine Vaupel (Munich) in her article on Hofmann's role in relation to chemistry at the world exhibitions. We learn how Hofmann, through his brilliant reporting as an adjudicator, systematically worked himself up into a position of authority which gave him a wider forum in which to propagate his views on the balance between pure and applied research. However, these clever tactics were strongly criticized by many of his colleagues, who accused him of seeking prestige, collecting positions of authority, and misusing power ("shameless" patronage, e.g. in the awarding of honors), and viewed these as evidence of serious human weaknesses. From the environmental standpoint it is interesting to learn that even then (about 1855) there were already worries about the toxicity of pigments containing lead and arsenic.

Soná Strbánová (Prague) describes how the influence of Hofmann's work spread into eastern Europe, in her article on the Liebig and Hofmann schools at the Prague universities and the development of chemistry in Bohemia. The Czech University and the independent German Technical University, both in Prague, modeled their chemistry teaching departments directly or indirectly on Hofmann's ideas. Of course, as Hartmut Scholz (Berlin) recounts, Hofmann also took part in the controversial discussions that went on during the latter third of the 19th century regarding the reform of chemistry teaching in the German schools, colleges, and universities. The questions of status that were at issue then were basically similar to those of today, with arguments about the relative merits of the Gymnasium and the Realschule, of the academic and technical universities, of state examinations and the dissertation system, or about the separation of the sciences from the philosophical faculties.

In view of Hofmann's numerous connections with color chemistry and the dyestuffs industry, the next two chapters occupy a key position in this collection of essays. In a historical sketch entitled "Farbstoffe zu Hofmanns Zeiten und heute" (Dyestuffs in Hofmann's Time and Today) Peter Suchanek (Bayer, Leverkusen) discusses the most important discoveries and processes in this field from an industrial standpoint. His account includes the latest developments in color printing inks, laser dyes, color formers,

and ink-jet printers, and highlights the increasing emphasis on environmental aspects in product-orientated research. Siegfried Dähne (Berlin-Adlershof) then considers the theoretical aspects of dyes under the title "Structur-Farbe-Beziehungen im Wandel der Zeit" (Structure-Color Relationships Through the Changing Times). After pointing out that because Hofmann clung to the type theory throughout his life he was unable to arrive at a deeper understanding of the relationship between structure and color, Dähne systematically describes how the different dye color theories developed, from the chromophore theory through the mesomeric school and the polymethine concept to the modern methods based on quantum-chemical calculations. The unavoidable sacrifice of transparency with the latter methods is offset by the following explanation of the heuristically impressive triads principle with its simple color rules.

The reactions that carry Hofmann's name are still used in modern synthetic chemistry, as Hans-Georg Henning (Berlin) shows by describing several examples; unfortunately a slight mix-up has occurred here in the correspondence between text and formulas. But only when we come to the article by Herbert Teichmann (Berlin-Adlershof) with the title "Phosphorchemie bei A. W. Hofmann und heute" (Phosphorus Chemistry in A. W. Hofmann's Time and the Present) are we reminded that Hofmann, in addition to his "great" reactions and investigations, also carried out fundamental studies on phosphorus chemistry which contributed significantly to our present knowledge in this area. In reviewing this work, Teichmann reveals among other facts that in his synthetic studies in this field Hofmann used the Umpolung principle for the first time. Next Günther Wess (Hoechst, Frankfurt) discusses synthetic methods for pharmaceuticals and aspects of medicinal chemistry, and shows that here too there are many fascinating connections with Hofmann's work. This is not only because some of the pharmaceutical compounds known in Hofmann's day were based on the aniline structure; in addition a number of the compounds and reactions that he discovered are still used nowadays in medicinal chemistry. Moreover, the author maintains that in his conceptions of organic chemistry in relation to medicines Hofmann correctly predicted some important later developments.

The chapter entitled "Geschichte der Schering AG—Von der grünen Apotheke zum Chemiekonzern" by Gerd J. Wlasich (Berlin) tells the story of the development of Schering AG from its origins as a small Berlin pharmacy during Hofmann's period in the city, a pattern of development that is typical of many of the major present-day chemical companies. A central theme of the article, and one that again underlines the leitmotif of this book, is the close contacts that existed between the industrialist Ernst Schering and the chemists at Berlin University. Schering also participated in the formation of the GDCh in 1867, and he continued to serve as the Society's treasurer until 1880.

The final essay by Uwe Biethan (Marl) discusses Hofmann's work in relation to modern polymer chemistry. It could well have been entitled "Missed Opportunities", as it shows that on many occasions Hofmann was very close to a breakthrough into polymer chemistry, but failed to follow through the crucial chain of perception. For example, although he described polystyrene he was not the first to discover it, and although he made formaldehyde and oligomerized it he did not follow this up further. Similarly, in his work on (iso)cyanate chemistry he passed within a hair's breadth of stumbling upon the polymer concept, but the polyamine and polyaniline plastics that were later to be derived from his favorite objects of research lay beyond his horizon of experience.

This extensive account of the personality and work of A. W. Hofmann—who is rightly described at several points as the "first Eurochemist"—is in my view an unqualified success. By bringing together the contributions of authors who approach their material from the widely different backgrounds of the academic scientist, the science historian, and the industrial chemist, the book gives us a very complete, though also critical, picture of one of the leading figures in the early development of our science, and of his interactions with the scientific, economic, and sociopolitical network of the time, which already then extended throughout Europe. However, it would have been useful to have some more views about the spread of the influence of Hofmann's work into the cultures of southern and eastern Europe. Also it would have been a good idea to include short biographical notes about the authors, especially as there is in fact enough space for this at the ends of the chapters. I can thoroughly recommend this book to everyone with a serious interest in chemistry. Professional chemists might spend a few contemplative hours away from the hectic activity of their everyday work, and students could well benefit from the relaxation that it offers during the toughest periods of preparing for examinations. The book is suitable for dipping into to read individual chapters to suit one's interests and mood. Readers who appreciate the special appeal of centenaries might like to recall that just a century *before* Hofmann's period of work in England (1845-1865) another great German, the master of baroque music Georg Friedrich Händel, celebrated his triumph there, whereas exactly 100 years *after* Hofmann's arrival in Britain another great innovator of chemistry, Otto Hahn, together with his colleagues from the German atomic research fraternity, became a rather unwilling guest of that nation and there witnessed the end of the war.

Dieter Hellwinkel
Organisch-Chemisches Institut
der Universität Heidelberg (FRG)

Immunosorption Techniques. Fundamentals and Applications. By *P. Mohr, M. Holtzhauer* and *G. Kaiser*. Akademie Verlag, Berlin, 1992. VIII, 173 pp., hardcover DM 112.00.—ISBN 3-05-501350-6

The authors of this book have set out to give a comprehensive review of immunosorption techniques. They describe the basic principles of the methods in an easily understandable way and discuss the various applications. In particular the compilation of examples from the literature makes the book required reading for all who would like to apply this modern methodology but lack experience of their own to draw on.

In the first chapter the authors give a concise and informative explanation of the basic features of the immune system. The structure of antibodies, their interaction with antigens, the concepts of affinity and avidity, and other relevant topics are all treated in adequate depth.

Chapter 2 discusses in considerable detail the choice of substrate and methods of activation and coupling. The extensive tables giving details of the functional groups of the various substrate materials, different methods of activation, and reactive groups in biomolecules that can be used for coupling, together with relevant literature references, provide the beginner with a very useful overview. Ways in which the biological activity of biomolecules can be altered by coupling or modification are also discussed, using antibody binding properties as an example. The favorable impression conveyed by this chapter is reinforced when the authors give details of laboratory procedures for the activation of substrates and for determining the degree of activa-

 © VCH Verlagsgesellschaft mbH, D-69451 Weinheim, 1994 0570-0833/94/0202-0234 $ 10.00+.25/0

tion. The relationship between the pretreatment of an affinity column (for example), the coupling method chosen, and the conditions for adsorption and desorption of the protein to be isolated is clearly explained. The various methods and buffer systems are usefully summarized in tables. Lastly the authors discuss the avidin–biotin system, but their treatment of this standard system is very brief.

Chapter 3 deals with the isolation of antibodies, haptenes, and antigens. Nearly 50 pages are devoted mainly to a very detailed treatment of the isolation of antibodies. As well as immunosorption chromatography the authors discuss precipitation methods and ion exchange chromatography with a degree of detail that seems inappropriate for a book of this kind. Although it is true that antibodies are an important element in immunosorption methods, this book would certainly not be one's only source of help on isolation techniques if the required antibodies were not commercially available and had to be prepared in one's own laboratory.

The final chapter is concerned with immunoassay, immunoblotting, and immunosensors. Immunoassay techniques especially are now very important and widely used, and are based on the principle of immunosorption. It would therefore have been useful to give some guidelines for potential users of these techniques, but unfortunately the various detection systems are only listed in a table, without a more detailed discussion of their advantages and disadvantages. In contrast the second section deals with immunoblotting in considerable detail. The different blotting techniques are compared and general procedures are given. There is a very useful survey, in the form of a table with literature references, of the various membranes, transfer buffers, etc. The authors also discuss important questions such as the sensitivity of different dyeing methods. The last section deals briefly with immunosensors and their classification according to the different detection principles. The depth of treatment here is adequate, since immunosensor techniques have not yet become established in routine use, partly because the detection systems are very complicated.

To summarize, this is a useful book within certain limitions. It can be recommended to everyone who seeks a review of immunosorption techniques. Specialists in the field must decide for themselves whether the information presented in the tables is worth the price.

Uwe Hofmann
Merck, Darmstadt (FRG)

Crown Compounds: Toward Future Applications. Edited by *S. R. Cooper*. VCH Verlagsgesellschaft, Weinheim/VCH Publishers, New York, 1992. 325 pp., hardcover DM 218.00.—ISBN 1-56081-024-6/3-527-28073-1

This book aims to discuss the potential applications of crown ethers and related synthetic macrocycles. As the editor states in the preface, there are now a number of excellent books and reviews on the fundamental aspects of macrocyclic chemistry, or on the broader perspectives of supramolecular chemistry. The book attempts to give a *prospective* view of the field and to answer the question: "Where are these research fields going?". In fact there are two different aspects: future applications and future *developments* which need not necessarily lead to applications. The result of this concept is a mixture of everything, which is not surprising with 16 different (groups of) authors.

Applications, current and future, are clearly addressed in seven of the 16 chapters. In Chapter 2 Chen and Echegoyen briefly discuss the separation of isotopes by redox-switched ligands. An excellent contribution by D. Parker (Chapter 4) gives an overview of the use of macrocycles as ligands for immobilizing radioisotopes with medical applications. He briefly discusses clinical analysis and in more detail diagnostic and therapeutic agents.

Martell describes in Chapter 7 the possibilities of selective complexation (and transport) of molecular oxygen by binuclear macro(bi)cyclic complexes, in the context of a more general overview of this class of compounds. Frabbrizzi et al. include the transport across liquid membranes in their contribution on cyclams (Chapter 9). The same application is dealt with more specifically for enantiomeric recognition by Izatt et al. in Chapter 12. Applications of molecular recognition in sensors are probably the most advanced at present. Sutherland describes one possible application of this kind to chromogenic reagents and chromoionophores. The recognition process is transduced via a light signal in an optical fiber based sensor. The more widely studied potentiometric sensors (ISE and CHEMFET based) are not represented.

In Chapter 16 T. W. Bell describes his planar macrocyclic ligands, the torands, and their possible application in discotic liquid crystalline materials. In Chapter 15 the editor, S. R. Cooper, has succeeded well in his aim to discuss future applications. The coordination chemistry of 99Tc, applied in nuclear medicine, is a good example of the advantages gained by using a specific ligand. Together with Parker he has covered this area very nicely.

Most other chapters review the current status of the authors' individual research topics. Since there are several recent books and review articles, some duplication of existing literature is unavoidable. Gokel and Nakano describe cation complexation, ion channels, and the different chemical structures that introduce selectivity. According to these authors future developments in this field will eliminate artificial barriers between disciplines, such as organic/inorganic or biological/synthetic. In Chapter 3 G. R. Newkome presents a short outline of the development of the research on macrocycles in his group, from the early pyridocrown ethers to the recently described arborols.

Several chapters (5, 6, 8, and 10) deal with different aspects of nitrogen macrocycles. The authors, Adam and Lindoy (Chapter 5), Kimura (Chapter 6), Kaden (Chapter 8), and Hannock (Chapter 10) emphasize the influence of the ligands on the properties of the complexed metal ions. In Chapter 11 Seel and Vögtle describe large tailor-made molecular cavities. The analogy with the natural siderophores, inclusion of neutral guest species, and photophysical properties of complexed ions are the topics discussed. The sulfur analogues of crown ethers have received less attention than the all-oxygen macrocycles. However, in Chapter 14 Kellogg describes how these ligands can be synthesized and their role in the complexation of metal ions such as Ag, Hg, and Pb.

In conclusion, this book offers a random selection of topics in the rapidly growing field of supramolecular chemistry. As a consequence the picture is far from complete. The quality of the individual chapters varies from good to excellent and there is no doubt that the authors are experts in their fields. I would have preferred to have more applications-oriented chapters, in accordance with the expectation raised by the title. This book is a good choice for those entering specific areas of supramolecular chemistry.

David N. Reinhoudt
Department of Organic Chemistry
University of Twente,
Enschede (Netherlands)

 © *VCH Verlagsgesellschaft mbH, D-69451 Weinheim, 1994* *0570-0833/94/0202-0235 $ 10.00+.25/0*

Chemical Communication. The Language of Pheromones. (Scientific American Library Series, Vol. 41.) By *W. C. Agosta*. Scientific American Library, New York/Freeman, Oxford, 1992. IX, 179 pp., hardcover £ 17.95.—ISBN 0-7167-5036-8

The term "semiochemicals" refers to substances that transmit signals and are used by living organisms to exchange information. This book is concerned with the isolation and identification of such substances, their chemical structures, and their biological functions. The seven chapters contain lively and exciting accounts of how chemical communication is achieved in microorganisms, animals, and humans. In each case the author first explains the biological background to the phenomena described, then goes on to the isolation of the biologically active compounds, and lastly the elucidation of their structures and the effects of the corresponding synthetic products. He has taken particular care to emphasize general principles, and has not been afraid to introduce a number of simplifications (and even inaccuracies) in the interests of a unified and rounded overall presentation. For example, the word "pheromone" in the title strictly includes only intraspecific signal transmitting substances, but fortunately this restriction has been relaxed in the text. It was sensible to omit details of the synthesis of the relevant substances in this context, but it would have done no harm to include more information about biosynthesis and sensing mechanisms.

The book begins with a brief introduction to "molecular messengers", which is followed by a chapter on gamete attractants in brown algae and molds and on bacterial pheromones. Chapter 3 describes tracking and alarm substances, and attractants and concealment substances relevant to sea anemones, snails, crabs, mites, and ticks. Chapter 4 is the longest with 40 pages, and describes the various ways in which insects use chemical substances for communication. The topics include the structures and mechanisms of the sexual pheromones of female butterflies. Also included, of course, is the remarkable story of the male butterfly, which feeds on pyrrolizidine alkaloids, firstly to protect itself from enemies, and secondly to ensure successful reproduction and protect the offspring (one really must read this!). Compounds that regulate the aggregation behavior of bark beetles are discussed, as also are the complex systems of bees and ants in the formation of colonies. This chapter also explains the importance of pheromones in selective pest control. Chapter 5 is concerned with fishes and amphibians, and Chapter 6 with pheromones in mammals, a subject which is not yet clearly understood due to the experimental difficulties. Chapter 7 ("Human Attractions") deals with the delicate subject of pheromone communication in humans, covering perfumes as well as odor substances of human origin. (It is interesting that humans wash to remove the individual odors that they undoubtedly possess, then strangely seek to give their "neutralized" bodies a new "individual aura" by the use of a perfume.)

Chapter 7 is followed by a glossary, an important aid for the non-specialist reader. However, if this had been made more comprehensive and had been better integrated into the book by appropriate references in the text, it would have avoided the need to interrupt the latter with explanations (mostly of common chemical terms), thus improving the flow. Also the index could have been made more useful by including a greater number of keywords. The figures vary from good to very good (although some of the drawings seem a little childish). The formula diagrams are (almost) free from errors, although those of brevicomin on page 77 (an aggregation-controlling substance in certain species of bark beetles) and dehydrobrevicomin on page 144 (inactive in itself but a component of an aggression-inducing pheromone complex in mice) both lack the methyl group on the acetal carbon atom. Although *cis–trans* isomerism is explained twice (pp. 7 and 161), it is startling to find that the concept of chirality is neither mentioned nor taken into account, even pictorially, in the formula diagrams of the relevant compounds—this despite the fact that the absolute configuration of chiral natural products is often essential to their biological activity!

However, the author has produced a book which is a pleasure to read and should find friends even at school level. It presents in a small space a great wealth of information, and clearly shows the interdisciplinary nature of research into the fascinating subject of chemical communication. Everyone interested in this field, whether as an expert or an outsider, a biologist or a chemist, should buy this attractive book.

Wittko Francke
Institut für Organische Chemie
der Universität Frankfurt (FRG)

Phthalocyanines. Properties and Applications. Vol. 2. Edited by *C. C. Leznoff* and *A. B. P. Lever*. VCH Verlagsgesellschaft, Weinheim/VCH Publishers, New York, 1993. XI, 305 pp., hardcover DM 268.00.—ISBN 3-527-89544-2/1-56081-544-2

In 1983 Moser and Thomas's two-volume text on phthalocyanines provided an excellent summary of the chemistry, properties, and applications of this remarkable series of macrocycles known up to that time. Attention was drawn to their well established importance as industrial pigments and dyes and their use as oxidation catalysts. Now, ten years on, Leznoff and Lever have produced the second volume of their most welcome series "Phthalocyanines—Properties and Applications", reviewing more recent developments in the field. These have been extensive, stimulated to a considerable degree by the growing interest in the new disciplines of molecular electronics and materials chemistry. Such are the unique properties of the phthalocyanine ring system that there is now world-wide research into its use in gas sensors, displays, data storage systems, fuel cells, solar cells, electrophotography, and photodynamic therapy. This in turn has stimulated a renewed interest in probing the fundamental science of the phthalocyanine ring, in designing new derivatives with particular properties, and in investigating new formulations of phthalocyanines as thin films and mesophases.

The second volume of this new series maintains the high standard set by the first (1989), providing in this case a glimpse of the range of phthalocyanine and phthalocyanine-type structures available, some detailed spectroscopic evaluations, new studies of catalytic function, and investigations of thin film formulations and mesophase behavior. The six chapters are written by authorities in their particular areas, with an interesting mix of general overviews and accounts of work from the authors' own laboratories.

Chapter 1 by Ercolani and Floris ("Metal Phthalocyanine Single-Atom Bridged Dimers", 41 pp., 101 references) surveys derivatives containing five- or six-coordinate metal ions linked via an oxygen, nitrogen, or carbon atom. The review covers aluminum, titanium, manganese, ruthenium, and iron derivatives with particular emphasis given to the complex chemistry of the last of these, unravelling sometimes conflicting information. Mössbauer spectroscopy has been useful in this regard, and the application of this technique to variously substituted iron

 © VCH Verlagsgesellschaft mbH, D-69451 Weinheim, 1994 0570-0833/94/0202-0236 $ 10.00+.25/0

phthalocyanines is dealt with in greater depth by Hanack, Keppeler, Lange, Hirsch, and Dieing in Chapter 2 ("Mössbauer Spectroscopy of Phthalocyaninato-Metal Complexes", 53 pp., 157 references). These authors present extensive data, collected from the standpoint of the organic chemist viewing the method as a means of characterizing materials. As well as work on iron derivatives, the authors also survey the much less extensive data available for tin complexes and iodine-doped complexes.

There are a number of macrocycles related to phthalocyanines by benzofusion, including naphthalocyanines and anthracyanines, and others containing features which help forge a continuum of molecular structures between the phthalocyanines and the porphyrins, eg. the tetraazaporphyrins and the benzporphyrins. These and a host of other ring systems are discussed by Kobayashi in Chapter 3 ("Synthesis and Spectroscopic Properties of Phthalocyanine Analogues", 65 pp., 255 references). Many deserve more extensive investigation but their synthesis requires both skill and patience; a researcher new to the area should heed the author's closing comment to the effect that few, if any, of the systems are synthesized as easily as the parent phthalocyanine ring.

In Chapter 4 ("Thin Film Phthalocyanine Chemistry and Technology", 30 pp., 59 references) Saji gives an account of his group's work on the electrochemical formation of thin films by disruption of micellar aggregates (the MD method). Phthalocyanine particles are released when surfactant molecules adsorbed on them are electrochemically oxidized, allowing the pigment particles to be deposited as an even film on the electrode. Spectra of the films are similar to those of the original particles, indicating that the method provides a means of generating good quality films of different polymorphic forms. Chapter 5 ("Catalytic Functions and Applications of Metallo-Phthalocyanine Polymers", 25 pp., 13 references), by Hanabusa and Shirai, provides another account of research undertaken primarily within the authors' own laboratories and highlights a number of enzyme-like catalytic functions of metallo-phthalocyanines. One of the intriguing potential applications of the chemistry lies in its deodorant action; metallophthalocyanines effectively catalyze the decomposition of offensively smelling gases.

The final chapter by Simon and Bassoul ("Phthalocyanine Based Liquid Crystals: Towards Submicronic Devices", 76 pp., 174 references) gives an overview of those heavily substituted phthalocyanine derivatives that exhibit discotic mesophase behavior and offers a thoughtful analysis of factors controlling mesophase formation. Drawing heavily on their own substantial contributions in this area, including analysis of energy transport and charge transport within columnar mesophases, the authors have provided a chapter which will be of interest to those working on both phthalocyanine and non-phthalocyanine based liquid crystals.

With regard to the production of the present text, purists may regret the move from the typesetting of Volume 1 to the camera-ready copy of Volume 2, a consequence of 'the fiscal realities of the early nineties'. This has resulted in small variations in the typeface between chapters and has favored retention of minor idiosyncracies in style and presentation introduced by the different contributors; at the extreme, one chapter contains structural representations of the phthalocyanine nucleus in which just four of the nitrogens are drawn in. But these are minor quibbles over a text which will certainly be much referred to and cited in years to come. In short, it should prove invaluable to those working directly with this class of compounds, academics and industrialists alike, and will be of interest to those involved more generally in research into advanced materials.

Michael J. Cook
School of Chemical Sciences
University of East Anglia
Norwich (United Kingdom)

The Chemical Bond. Structure and Dynamics. Edited by *A. Zewail.* Academic Press, New York, 1992. XV, 313 pp., hardcover $ 49.94.—ISBN 0-12-779620-7

This book is based on a symposium held on 28 February 1991 at the California Institute of Technology (Caltech) to celebrate the 90th birthday of Linus Pauling. What could be more appropriate than to honor the author of the famous book "The Nature of the Chemical Bond" by publishing a book on the same subject? For this purpose the organizers brought together a number of eminent scientists who have made important contributions to the understanding of the chemical bond. Naturally Linus Pauling himself contributed papers, not only one on the historical aspects but also a report on recent progress with a problem of structural chemistry. There could be no better demonstration that the Linus Pauling era certainly does not yet belong to the past.

The nine articles are arranged under two headings: "Structure" and "Dynamics". The structure group is opened by Linus Pauling with a brief historical survey of the development of crystal structure analysis by X-ray diffraction. As early as 1922, scarcely nine years after the discovery of this method, Pauling began his own researches in this area. During the following years many structural principles were discovered and these have contributed significantly to the understanding of the chemical bond. The discovery of the alpha helix in 1948 was undoubtedly a high point. However, the computation times needed then were enormous, amounting to years for difficult structures. Although many thousands of structures have since been determined, Pauling is rather disappointed that this has revealed few new structural principles. He sees an exception to this in the field of metals and intermetallic compounds.

In the second article Max Perutz reviews structural studies on hemoglobin, myoglobin, and related proteins. He was motivated to begin work in this area by predictions made by Pauling, who postulated that hydrogen bonds had an important influence on the stability of proteins, and suggested that hemoglobin would be a very interesting system for structural analysis. Both these views were to be subsequently confirmed, although the structural analysis was not completed until 30 years later. Experiments with naturally occurring mutants and variants made by genetic engineering methods yielded detailed information about the mechanism whereby oxygen becomes bonded to the heme molecule. This work eventually led to the discovery of a new type of hydrogen bond that could be formed between a heteroatom and a benzene ring.

Hydrogen bonding also plays a key role in the subject of the third article, in this case between DNA and proteins. Certain proteins are apparently able to recognize particular types of sites on the DNA and to bind specifically to these. In his article Alexander Rich first describes the different forms of DNA helices and identifies the parts of the base pairs that are accessible from outside; these lie in different types of depressions in the DNA helix, the minor and major "grooves". From steric considerations one can then predict which amino acid sequences can attach to these sites by hydrogen bonds. The greater the number of possible hydrogen bonds, the more specific are the interactions whereby the DNA and protein can recognize each other. However, the variety of types of

 © *VCH Verlagsgesellschaft mbH, D-69451 Weinheim, 1994* *0570-0833/94/0202-0237 $ 10.00+.25/0*

such recognition interactions is extremely great, and it has not yet been possible to classify these into a simple scheme.

In the fourth article Francis Crick considers the many important initiatives that Linus Pauling has provided for molecular biology, and concludes that he should be regarded as a co-founder of this area of science. The first important initiative was the recognition that weak forms of bonding (hydrogen bonds and dispersive interactions) are extremely important in biology. The second important idea was that biological molecules such as proteins have a definite shape (and are therefore not simply "colloids"), and that this is intimately related to their catalytic function. Another important concept was that attractive interactions are a result of complementarity, and this eventually led to the discovery of the structure of DNA. The interpretation of sickle cell anemia as a "molecular disease", in which the hemoglobin structure has been altered by a mutation, was the first example of a connection between protein chemistry and genetics. Another contribution in this field was the suggestion that the number of mutations that have accumulated in a certain protein can serve as a measure of "evolutionary time".

Pauling himself appears for a second time as the author of the fifth article. Even before he began his formal studies he was interested in minerals, and looked for general relationships between the properties of different substances and their composition. From 1922 onwards he worked on X-ray structural analysis at Caltech, and during this period he also studied theoretical methods of statistical thermodynamics. At that time quantum mechanics was being developed, and the ideas of physicists such as Bohr and Millikan, involving the motion of electrons in circular orbits, seemed to be irreconcilable with those of chemists such as Lewis and Langmuir, who assumed that the electron pairs occupied fixed positions. Pauling tried to find a solution that would unify these views. On the basis of Sommerfeld's work he suggested that the electron pairs in neon or methane moved in highly eccentric elliptical orbits. Thus it came about that he spent a year with Sommerfeld in Munich, and there he was able to become immersed in the new quantum mechanics in its initial phases. After returning to Pasadena he continued, through both experimental and theoretical studies, to seek a better understanding of the chemical bond, and in 1939 he summarized the results of this work in his celebrated book "The Nature of the Chemical Bond".

The part of the book concerned with dynamics is introduced by Sir George Porter, who presents a historical outline, beginning with the Arrhenius equation for the rate of a chemical reaction. The activation energy that appeared in the equation was subsequently assigned to an activated complex (Nernst) or to the transition state (Eyring, Polanyi). In general a chemical reaction proceeds via several stages, and it is therefore necessary to clarify the mechanism before a comparison with theory becomes possible. In order to prove the existence of short-lived species the method of flash photolysis was developed from about 1946 onwards. This led to the detection of a great variety of diatomic and aromatic free radicals and triplet-state molecules. The development of pulsed (Q-switched) lasers improved the time-resolution of this pump-and-probe method to a few nanoseconds. Further advances in laser physics (mode-locking and colliding pulse mode [CPM] ring lasers) mean that one can now achieve a time-resolution of 100 femtoseconds or less.

The progress of a chemical reaction is crucially dependent on the height of the energy barrier and its position on the potential surface. As the barrier height is typically only about 10% of the bond energy, the breaking of the original bond and the formation of the new bond occur simultaneously. Pauling postulated that in this process the sum of the bond orders should remain constant. In the seventh article John C. Polanyi describes how he and his group obtained experimental data on energy barriers from detailed measurements of the rate constants $k(V,R,T)$ for reactions of the type A + B–C $\rightarrow$ A–B + C. Here V, R, and T represent the vibrational, rotational, and translational energies respectively for the product molecules. The populations of the product states were determined by chemiluminescence measurements in the infrared. The distribution of the reaction energy between the different degrees of freedom is clearly indicated by colored triangle diagrams. To obtain even more detailed information it is necessary to impose limits on the initial geometry for the reactive collision. This can be achieved by using photoreactions in which both reacting species are adsorbed at a surface and thus have a fixed orientation. Furthermore, by inducing photodissociation of such adsorbed molecules with different photon energies one can perform a local scattering experiment to probe the potential in the neighborhood of the adsorption site.

In the eighth article Dudley R. Herschbach discusses the important contributions that Pauling made to the development of reaction dynamics. He then turns to some relevant topics in his own field of work. By studying bimolecular reactions between species in crossed molecular beams and measuring the velocity and angular distribution of the product trajectories one obtains a very detailed picture of the reaction dynamics. A highly anisotropic distribution indicates that the reaction has a large degree of "recoil" character, which can be explained in terms of the nodal structure of the frontier orbitals. Further extension of this concept leads to an electronegativity rule, which states that in complexes of the type X–Y–Z the favored structure is that in which Y is the least electronegative element. Scattering experiments of this kind yield results that are averaged over all the collision variables and molecular orientations. By simultaneously measuring and correlating the vector variables the orientational averaging can be partly eliminated. However, a better method is to align the molecules before the collision. Herschbach explains in detail how this can be achieved for cold molecules in strong external fields.

A quite different topic being studied by Herschbach is the calculation of the energies of atoms and molecules with many electrons. If the Schrödinger equation is formally extended to an arbitrary number of dimensions D, exact solutions are possible for the two limiting cases $D \rightarrow 1$ and $D \rightarrow \infty$. If one treats $1/D$ as the expansion parameter in a perturbation calculation and interpolates for $D = 3$, the results are in remarkably good agreement with those from laborious ab initio calculations. The case $1/D = 0$ corresponds to the limiting case where the electrons have an infinitely large mass, which means that the system behaves quasi-classically with the electrons at fixed positions in space. Thus one obtains a higher-dimensional analogue of the "Lewis structures" that were postulated by G. N. Lewis in 1916. Transitions between different Lewis structures can be represented by trajectories along an imaginary time axis, and interpreted as tunneling between different canonical structures.

The methods described in the two preceding articles allow one to determine asymptotic properties of the trajectories that pass through the transition state. The corresponding observable quantities are integrated over the reaction time, and yield only indirect information about the lifetime of the activated complex. For many reactions the lifetimes are in the range from 10 to 1000 femtoseconds. Flash photolysis measurements with this

 © VCH Verlagsgesellschaft mbH, D-69451 Weinheim, 1994 0570-0833/94/0202-0238 $ 10.00+.25/0

order of time resolution ("femtochemistry") are the subject of the ninth article by Ahmed Zewail and Richard Bernstein. The aim here is to observe the passage of the system through the transition state directly as a function of time. After describing the apparatus used in their laboratory at Caltech, the authors discuss the most important results that femtochemistry has yielded up to now. So far the technique has been applied to the study of rapid decomposition reactions and oscillating intermediates (quasi-bound states). A brief update section reporting on progress with the method since about 1988 is also included.

The nine articles are followed by short biographical notes on each of the authors with photographs. The book is completed by an index, which also lists the names of other people mentioned in the text.

The book is equally suitable for specialists and for laypersons with an interest in the subject. It contains a wealth of information for everyone wishing to learn something about the current state of knowledge in this field. Complex topics are clearly explained without too much glossing over of details, and mathematical derivations are avoided completely. Thus the book is primarily concerned with concepts and methods, and should appeal to a wide readership.

Bernhard Dick
Institut für Physikalische und
Theoretische Chemie
der Universität Regensburg (FRG)

Frontier Orbitals and Properties of Organic Molecules. (Ellis Horwood Series in Organic Chemistry. Series editor: *J. Mellor.*) By *V. F. Traven.* Ellis Horwood, Chichester, 1992. XVI, 401 pp., hardcover $ 111.00.—ISBN 0-13-327487-X

I expected to find here an up-to-date book covering the most recent literature in this field. Instead I found an English translation of an obviously older Russian work. It mainly covers work published from the 1950s to the 1970s, with just a few references to 1980s publications. For the subject treated here that is quite inadequate.

The contents are arranged under two broad areas. First is a section of about 60 pages dealing with the various methods of describing the electronic structures of molecules. The main part then begins with an introduction to orbital structure and the properties of organic molecules (30 pp.), which is followed by a systematic treatment of individual classes of organic compounds (250 pp.). The book ends with an appendix listing HMO data for selected molecules (10 pp.) and a bibliography containing 471 references.

The first chapter presents in a very cursory and superficial way some basic principles of physical organic chemistry, and is really of little value. This is followed by an introduction to the methods of quantum chemistry, beginning with the Bohr model of the atom and ending with some concepts of the MO theory. The HMO theory is then introduced, followed by a description of the state of ab initio methods as it was twenty years ago then, as semiempirical methods, the CNDO, NDDO, and PPP approaches. The MNDO, AM1, and PM3 methods appear to be as yet unknown. Next comes a very brief introduction to the experimental methods for investigating the electronic structures of organic molecules: photoelectron spectroscopy (PES), electron transmission spectroscopy (ETS), electron spin resonance (ESR) spectroscopy, UV spectroscopy, polarography. It becomes apparent in this chapter that photoelectron spectroscopy is the author's special field, and one can guess that it is likely to figure prominently in the later chapters. The pleasure of reading this first part is marred by the incomplete and superficial treatment and by the very poor standard of English.

The second part begins with a treatment of orbital structure and reactivity, with special emphasis on frontier orbitals. We read that: "The rules for concerted cycloaddition reactions proposed by Woodward and Hoffmann were a further development of the frontier orbitals concept." In a similarly uncritical vein the author then goes on to consider how the orbital structure is related to biological activity, color, and phototropic behavior.

The treatment of individual compound classes follows the conventional structure of a textbook of organic chemistry. Now we come to the turn of photoelectron spectroscopy, including calculations, some of which are ab initio calculations of the type used in the 1970s. There are many tables listing ionization potentials; however, these are easily available from other sources.

One might expect that the "properties of organic molecules" referred to in the book's title would be limited to structural features, but this turns out not to be so. For example, in the chapter on "Alkenes" certain aspects of the Woodward–Hoffmann rules are discussed. Under "Annulenes" one is disappointed to find that this attractive topic is treated from a completely outdated standpoint.

And so it goes on for one compound class after another. The reader with a special interest in photoelectron spectroscopy will perhaps find something of value here and there, but the average organic chemist will gain little from the book. To summarize, although the title sounds very promising, it would have been better if this book had not been translated into English. The book *Frontier Orbitals and Organic Chemical Reactions* by Fleming (1976), which is not cited by Traven, is more reliable and up-to-date than this book published in 1992.

Reiner Sustmann
Institut für Organische Chemie
der Universität-Gesamthochschule
Essen (FRG)

Supported Reagents. Preparation, Analysis and Applications. By *J. H. Clark, A. P. Kybett* and *D. J. Macquarrie.* VCH, Weinheim, 1992. XI, 152 pp., hardcover DM 108.00.—ISBN 3-527-28043-X

We have probably all at some time read in a publication a sentence claiming that by immobilizing the reagent on a support one can improve the yield and selectivity, facilitate the work-up procedure, etc. These reports often leave some practical questions unanswered: what pretreatment and after-treatment of the support is needed?—how does one get the reagent on to the support? (and which support should be chosen?)—how can the supported reagent be analyzed?—how does one use such supported reagents to perform reactions?—and so on. This book aims to tell the reader how to prepare and use supported reagents, illustrating this by practical examples.

It consists of five chapters as follows. A general introduction to the subject is followed by separate chapters on the preparation of supported reagents and on their analysis. The last two chapters then describe practical examples. One of these discusses in detail, based on a few examples, the factors that need to be optimized for successful work with such reagents. An appendix contains a table listing various types of supported reagents and the reactions that can be carried out using them.

The introduction sets out to stimulate the reader's interest by reviewing the general field of supported reagents and the problems. The importance of the choice of support material is illustrated by a three-page table giving details of some reactions chosen as examples. Unfortunately one becomes aware here of a weakness that

 © *VCH Verlagsgesellschaft mbH, D-69451 Weinheim, 1994* *0570-0833/94/0202-0239 $ 10.00+.25/0*

persists throughout the book: the information in the table is not arranged according to reaction types, nor according to support materials or reagents, and this considerably reduces the usefulness of a book which has been written for the practical user. Also it is unfortunate that the examples in this table are not repeated in the much more detailed table in the appendix; a combined table would have been more useful for quick reference. In the table in the appendix an attempt has been made to arrange the examples according to reaction types, but this has not turned out very successfully: for example, the oxidation of diphenylcarbinol to benzophenone using potassium permanganate appears in three places. A commendable attempt has been made to provide additional notes on the examples in the table, but often these contain no more information than is already evident from the reaction equation. Only rarely is one given information about yields or the compatibility of the reagents with other functional groups, which would have been of interest to every user.

The initial approach to describing the different methods of preparing supported reagents is good. The authors'aim is to outline general procedures for these methods and to explain them by examples. Unfortunately, however, the recipes are too general to be used in practice for the preparation of reagents.

The chapter on techniques for the analysis of supported reagents is well written. The authors describe a wide variety of methods, mainly spectroscopic, illustrated by practical examples. In addition to the conventional spectroscopic methods they describe some recently developed techniques such as electron tunneling microscopy, thermogravimetry, and differential scanning calorimetry.

The "case studies" in Chapter 4 include detailed accounts of the use of supported fluorides, thiocyanates, and catalysts for Friedel–Crafts alkylations and acylations. The section on thiocyanates is especially interesting and comprehensive, with detailed information on the composition of the reagents and a table giving examples of reactions with data on reaction times, yields, etc.

Despite all the above criticisms this is a useful book for readers who wish to gain a general understanding of supported reagents. It is important to take the time to read the whole book, but as it consists of only 152 pages that should not be a problem. In that way the reader will gain a clear impression of the potential of the reagents described and of how they might be applied to his or her own problems. However, as a "comprehensive reference source" (according to the claim on the dustjacket) the book leaves something to be desired, both in form and arrangement of material.

Oliver Reiser
Institut für Organische Chemie
der Universität Göttingen (FRG)

Just what does a referee system achieve?

Regular readers of "Angewandte" are well aware that Dr. Hans-Dieter Daniel has researched this question using *Angewandte Chemie* as example. The preliminary results were presented in a communication on this topic (Issue 2/93). Now the complete analysis by Daniel is available in book form: "The Guardians of Science: Fairness and Reliability in Peer Review" by H.-D. Daniel, foreword by H. Nöth (VCH, Weinheim, 1993, ISBN 3-527-29041-9, DM 78.—).

 © *VCH Verlagsgesellschaft mbH, D-69451 Weinheim, 1994* *0570-0833/94/0202-0240 $ 10.00+.25/0*

New Books

Gas Source Molecular Beam Epitaxy. Growth and Properties of Phosphorus Containing III-V Heterostructures. (Springer Series in Materials Scienc, Vol. 26). By **M. B. Panish, H. Temkin.** Springer, Heidelberg, **1993.** 428 pp., hardcover, DM 98.–.—ISBN 3-540-56540-X

Bioprocessing. (Biotechnology, Vol. 3, Second Revised Edition). Edited by **G. Stephanopoulos.** VCH, Weinheim/New York, **1993.** 816 pp., hardcover, DM 490.–/$ 365.- (subscription price: DM 390.–/$ 295.–).—ISBN 3-527-28313-7/1-56081-153-6

Carbohydrates as Organic Raw Materials II. Edited by G. Descotes. VCH, Weinheim/New York, **1993.** 278 pp., hardcover, DM 148.–/$ 95.–.—ISBN 3-527-30007-4/1-56081-703-8

QSAR: Hansch Analysis and Related Approaches. (Methods in Principles in Medicinal Chemistry, Vol. 1). By **H. Kubinyi.** VCH, Weinheim/New York, **1993.** 240 pp., hardcover, DM 158.–/$ 100.–.—ISBN 3-527-30035-X/1-56081-768-2

Random Walks in Biology. By **H. C. Berg.** Princeton University Press, Princeton, USA, **1993.** 148 pp., paperback, $ 12.95.—ISBN 0-691-00064-6

Lithium. (Die Bibliothek der Wissenschaft, Vol. 2). By **J. Deberitz.** Verlag Moderne Industrie, Landsberg, **1993.** 70 pp., hardcover, DM 16.80.—ISBN 3-478-93093-6

Umwelt. (Römpp Lexikon). Edited by **H. Hulpke, H. A. Koch, R. Wagner.** Thieme, Stuttgart, **1993.** 855 pp., hardcover, DM 298.– (subscription price: 268.–).—ISBN 3-13-736501-5

Catalytic Asymmetric Synthesis. Edited by **I. Ojima.** VCH, Weinheim/New York, **1993.** 476 pp., hardcover, DM 186.–/$ 110.–.—ISBN 3-527-89532-9/1-56081-532-9

Photoinduced Electron Transfer V. (Topics in Current Chemistry, Vol. 168). Edited by **J. Mattay.** Springer, Heidelberg, **1993.** 270 pp., hardcover, DM 248.–.—ISBN 3-540-56746-1

Hagers Handbuch der Pharmazeutischen Chemie, Bd. 7, Stoffe A-D. Edited by **F. Bruchhausen, S. Ebel et al.** Springer, Heidelberg, **1993.** 1451 pp., hardcover, DM 870.–.—ISBN 3-540-52632-3

Peptide Chemistry. A Practical Handbook. By **M. Bodanszky.** Springer, Heidelberg, **1993.** 198 pp., paperback, DM 48.–.—ISBN 3-540-56675-9

Principles of Peptide Synthesis. Edited by **B. Trost.** Springer, Heidelberg, **1993.** 329 pp., paperback, DM 72.–.—ISBN 3-540-56431-4

Mathematik für Chemiker. Eine Einführung. By **N. Rösch.** Springer, Heidelberg, **1993.** 457 pp., paperback, DM 49.80.—ISBN 3-540-56824-7

Flavor Science. Sensible Principles and Techniques. Edited by **T. E. Acree, R. Teranishi.** American Chemical Society, Washington, **1993.** 350 pp., hardcover, $ 79.95.—ISBN 0-8412-2516-8

Reporting Experimental Data. Selected Reprints. Edited by **H. W. White.** American Chemical Society, Washington, **1993.** 360 pp., hardcover, $ 89.95.—ISBN 0-8412-2529-X

The Chemistry of the Atmosphere. Its Impact on Global Change. Edited by **J. W. Birks, J. G. Calvert, R. E. Sievers.** American Chemical Society, Washington, **1993.** 180 pp., hardcover/paperback, $ 34.95/24.95.—ISBN 0-8412-2532-X/0-8412-2533-8

Giftpflanzen - Pflanzengifte. Edited by L. Roth, M. Daunderer, K. Kormann. Ecomed, Landsberg, **1993.** 1250 pp., hardcover, DM 198.–.—ISBN 3-609-64810-4

Life During a Golden Age of Peptide Chemistry. The Concept and Development of Solid-Phase Peptide Synthesis. By **B. Merrifield.** American Chemical Society, Washington, **1993.** 314 pp., hardcover, $ 24.95.—ISBN 0-8412-1842-0

Chronicles of Drug Discovery, Vol. 3. Edited by **D. Lednicer.** American Chemical Society, Washington, **1993.** 350 pp., hardcover/paperback, $ 84.95/34.95.—ISBN 0-8412-2523-0/0-8412-2733-0

Teaching General Chemistry. A Materials Science Companion. By **A. B. Ellis, M. J. Geselbracht, B. J. Johnson et al.** American Chemical Society, Washington, **1993.** 575 pp., hardcover, $ 29.95.—ISBN 0-8412-2725-X

Handbook of Industrial Surfactants. Edited by **M. Ash, I. Ash.** Gower, Hampshire, **1993.** 1006 pp., hardcover, £ 125.–.—ISBN 0-566-07457-5

Processing and Utilization of High-Sulfur Coals V. Edited by **B. K. Parekh, J. G. Groppo.** Elsevier, Amsterdam, **1993.** 638 pp., hardcover, Dfl. 680.–.—ISBN 0-444-81476-0

Photosensitive Metal-Organic Systems. Mechanistic Principles and Applications. (Advances in Chemistry Series No. 238). Edited by **C. Kutal, N. Serpone.** American Chemical Society, Washington, **1993.** 450 pp., hardcover, $ 109.95.—ISBN 0-8412-2527-4

The Language of Colloid and Interface Science. A Dictionary of Terms. By **L. L. Schramm.** American Chemical Society, Washington, **1993.** 196 pp., hardcover/paperback, $ 69.95/39.95.—ISBN 0-8412-2709-8/0-8412-2710-1

Molybdenum Enzymes, Cofactors, and Model Systems. (ACS Symposium Series No. 535). Edited by **E. I. Stiefel, D. Coucouvanis, W. E. Newton.** American Chemical Society, Washington, **1993.** 395 pp., hardcover, $ 94.95.—ISBN 0-8412-2708-X

Kristallographie. Eine Einführung für Naturwissenschaftler. By **W. Borchardt-Ott.** Springer, Heidelberg, **1993.** 310 pp., paperback, DM 36.–.—ISBN 3-540-56678-3

Crystal Pulling from the Melt. By **D. T. J. Hurle.** Springer, Heidelberg, **1993.** 148 pp., hardcover, DM 78.–.—ISBN 3-540-56676-7

Chemical Sciences Graduate School Finder 1992-1993. American Chemical Society, Washington, **1992.** 600 pp., hardcover, $ 44.95.—ISBN 0-8412-2522-2

Intensically Conducting Polymers: An Emerging Technology. Edited by **M. Aldissi.** Kluwer, Dordrecht, the Netherlands, **1993.** 240 pp., hardcover, Dfl. 185.–.—ISBN 0-7923-2456-0

Abbau industrieller Schadstoffe. Edited by **B. Wurster.** Verlag TÜV, Köln, **1993.** 500 pp., unbound, DM 198.–.—ISBN 3-8249-0124-2

Chemistry and Technology of Biodegradable Polymers. Edited by **G. J. L. Griffin.** Chapman & Hall, London, **1993.** 200 pp., hardcover, £ 59.–.—ISBN 0-7514-0003-3

Ionic Polymerization and Living Polymers. By **M. Szware, M. Van Beylen.** Chapman & Hall, London, **1993.** 280 pp., hardcover, £ 35.–.—ISBN 0-412-03661-4

Polymer Technology Dictionary. Edited by **T. Whelan.** Chapman & Hall, London, **1993.** 544 pp., hardcover, £ 85.–.—ISBN 0-412-58180-9

New Gmelin Volumes:
Sn Tin, Vol. 20. Compounds with Bonds between Tin and Main Group IV to Main Group I Elements. Edited by **U. Krüerke.** Springer, Heidelberg, **1993.** 193 pp., hardcover, DM 1170.–.—ISBN 3-540-93667-X

Th Thorium, Vol. C4. Compounds with F, Cl, Br, I. Edited by **R. Keim, C. Keller.** Springer, Heidelberg, **1993.** 175 pp., hardcover, DM 1080.–.—ISBN 3-540-93666-1

Mo Organomolybdenum Compounds Pt 9. Heteronuclear Compounds. Springer, Heidelberg, **1993.** 332 pp., hardcover, DM 1935.–.—ISBN 3-540-93970-X

Compact Handbuch „Chemie". Edited by **H. Gärtner.** Compact Verlag, München, **1993.** 448 pp., hardcover, DM 19.80.—ISBN 3-8174-3560-6

Practical Organic Mass Spectrometry. A Guide for Chemical and Biochemical Analysis, Second Edition. By **J. R. Chapman.** Wiley, Chichester, Great Britain, **1993.** 330 pp., hardcover, £ 39.95.—ISBN 0-471-92753-8

Experimental Techniques in Fracture. Edited by **J. S. Epstein.** VCH, Weinheim/New York, **1993.** 514 pp., hardcover, DM 198.–/$125.–.—ISBN 3-527-89641-4/1-56081-641-4

Shape in Chemistry. An Introduction to Molecular Shape and Topology. By **P. G. Mezey.** VCH, Weinheim/New York, **1993.** 224 pp., hardcover, DM 124.–/$ 75.–.—ISBN 3-527-27932-6/0-89573-727-2

Chlorinate Hydrocarbons - Chloroethanes Phosphoric Acid, Vol. 12. (DECHEMA Corrosion Handbook). Edited by **G. Kreysa, R. Eckermann.** VCH, Weinheim/New York, **1993.** 351 pp., hardcover, DM 775.–/$ 515.– (subscription price: DM 645.–/$ 480.–).—ISBN 3-527-26663-1/0-89573-633-0

Molecular Nonlinear Optics. Materials, Physics, and Devices. Edited by **J. Zyss.** Academic Press, London, **1993.** 478 pp., hardcover, $ 81.–.—ISBN 0-12-784450-3

The Science of Polymer Molecules. (Cambridge Solid State Science Series). Edited by **R. H. Boyd, P. J. Phillips.** Cambridge University Press, Cambridge, **1993.** 410 pp., hardcover, £ 60.–.—ISBN 0-521-32076-3

Concepts in Surface Physics. (Springer Series in Surface Sciences, Vol. 30). Edited by **M. C. Desjonquères, D. Spanjaard.** Springer, Heidelberg, **1993.** 565 pp., hardcover, DM 148.–.—ISBN 3-540-56506-X

Chemical Nomenclatures and the Computer. By **D. J. Polton.** Research Studies Press, Taunton, Great Britain, **1993.** 264 pp., hardcover, £ 52.–.—ISBN 0-86380-156-0

Organic Reactions, Vol. 44. Edited by **L. A. Paquette et al.** Wiley, Chichester, Great Britain, **1993.** 611 pp., hardcover, £ 79.–.—ISBN 0-471-30302-X

Qualitative and Instrumental Analysis. Environmentally Significant Elements. By **T. G. Chasteen.** Wiley, Chichester, Great Britain, **1993.** 131 pp., paperback, £ 15.50.—ISBN 0-471-58649-8

Atomic Transport in Solids. By **A. R. Allnatt, A. B. Lidiard.** Cambridge University Press, Cambridge, **1993.** 527 pp., hardcover, £ 80.–.—ISBN 0-521-37514-2

Thermochemistry and Equilibria of Organic Compounds. Edited by **M. Frenkel.** VCH, Weinheim/New York, **1993.** 584 pp., hardcover, DM 244.–/$ 150.–.—ISBN 3-527-89559-0/1-56081-559-0

Designer Oil Crops. Breeding, Processing and Biotechnology. Edited by **D. J. Murphy.** VCH, Weinheim/New York, **1993.** 317 pp., hardcover, DM 184.–/$ 120.–.—ISBN 3-527-30040-6/1-56081-827-1

Paints, Coatings and Solvents. Edited by **D. Stoye.** VCH, Weinheim/New York, **1993.** 409 pp., hardcover, DM 195.–/$ 125.–.—ISBN 3-527-28623-3/1-56081-809-3

β-Casomorphins and Related Peptides: Recent Developments. Edited by **V. Brantl, H. Teschemacher.** VCH, Weinheim/New York, **1993.** 270 pp., hardcover, DM 176.–/115.–.—ISBN 3-527-30038-4/1-56081-825-5

Einführung in die Theoretische Chemie, Band 2. By **W. Kutzelnigg.** VCH, Weinheim/New York, **1993.** 601 pp., hardcover, DM 118.–.—ISBN 3-527-29210-1

Organizing Principle of Complex Reactions and Theory of Coarctate Transition States

Rainer Herges*

The majority of concerted reactions proceeds by a simultaneous breaking and making of only one bond at each atom involved in the reaction. If this process follows an alternating cyclic sequence, the reactions are called pericyclic. However, there is a hitherto never consistently characterized class of reactions that proceeds by breaking and making two bonds at one or more atoms at a time. The striking relationships that are purely descriptive and formal in the first instance are explained by a common physical principle. Theoretical insight not only permits predictions of mechanisms and stereochemistry; the qualitative theory is also used as an organizing principle for the known reactions and as a tool for predicting unprecedented reactions of this type.

1. Introduction

In principle, any chemical reaction can be described as a sequence of concerted elementary steps. For the theoretical treatment of these elementary processes, molecular orbital (MO) theory has proven to be most fruitful. Among the qualitative descriptions the Woodward–Hoffmann rules[1] are the most prominent example. Quantitative treatment is feasible with smaller systems by using quantum chemical calculations. Particularly geometries and thermodynamic and kinetic energies[2] are predicted with high accuracy.[3]

It is common practice to describe these reactions in a mechanistically simplified manner as a sequence of arrows that indicate the electron shift (that is, the alternating sequence of bond making and breaking). In spite of its lower content of information, the simplistic valence bond (VB) notation has advantages over MO methods because of its higher level of abstraction, and this not only from the aspect of ease of communication.[4] VB theory also forms a suitable basis for organizing principles[5] and for the prediction of unprecedented reactions.[6] The simple structural formula notation in the following is therefore used to demonstrate the formal unity of the "complex reactions". Qualitative MO models explain the striking, descriptive relationships and enable the prediction of mechanisms and stereochemistry. With the aid of quantum chemical calculations (and experimental data if available) the qualitative statements are verified and quantified. The hierarchy of the three levels of abstraction at the same time describes, in correct chronological order, the heuristic that led to the following article.

[*] Priv. Doz. Dr. R. Herges
Institut für Organische Chemie der Universität Erlangen–Nürnberg
Henkestrasse 42, D-91054 Erlangen (FRG)
Telefax: Int. code + (9131)85-9132

Starting point was a systematic classification of about 80000 reactions from the reaction databases ORAC[7] and REACCS[8] and a number of carbene reactions from the literature.[9] According to this study, most of the organic reactions can be described by a linear sequence of electron-pushing arrows; that is, bonds are made and broken in an alternating

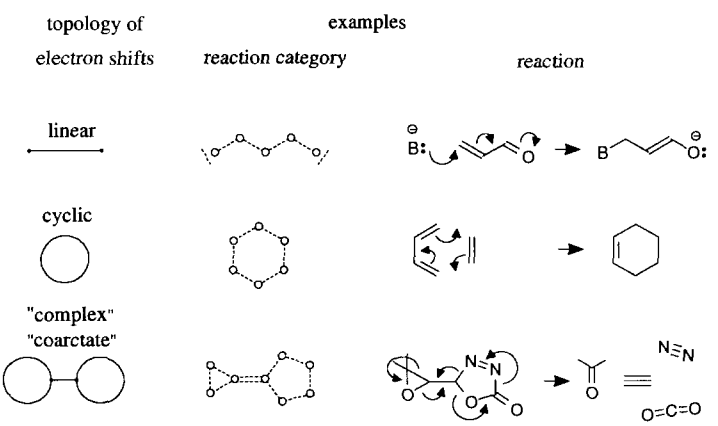


Fig. 1. Topologies of the electron shifts in organic reactions.

sequence (Fig. 1). The linear topology of "electron-pushing" necessarily results in a shift of charges and corresponds to the common way of thinking in organic chemistry (for example, in a nucleophilic or electrophilic attack of a reagent at a substrate that reacts by a double bond shift or by elimination of a leaving group).

The second largest class is formed by reactions that can be described by a cyclic sequence of electron-pushing arrows. They are called pericyclic if the electron shifts are concerted. Within

 © VCH Verlagsgesellschaft mbH, D-69451 Weinheim, 1994 0570-0833/94/0303-0255 $ 10.00+.25/0

the remaining data record, a group of reactions attracts attention that never were described in a coherent context, even though they exibit a number of formal similarities. We class them under the general term "complex reactions" because of their intricate mechanism.

2. Definition and Formal Description of Complex Reactions

Common to these reactions is that at one atom, at least, two bonds at a time are made and broken. The linear succession of bond making and breaking is finished by "terminators" at both ends. Suitable terminators are atoms with a lone pair that is formed or removed in the course of the reaction, or a cyclic shift of electrons over several atoms (Fig. 2). In principle, any combi-

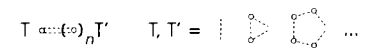


Fig. 2. Formal description of complex reactions. In the terminology used in the following, T and T' are terminators that bound the linear subsystem of length n ($n \geq 1$).

nation of different terminators is possible. The length n of the linear subsystem is variable as well (however, $n \neq 0$). According to this description, complex reactions with $n = 0$ are pericyclic. Most frequent are reactions with $n = 1$, and 2, and with terminators containing lone pairs or three- and five-membered rings.

Figure 3 illustrates the principle by means of examples from important categories of these reactions.

The descriptive treatment disregards mechanistic details and particularly ignores the question whether the reactions are concerted. Nevertheless, the striking formal relationships suggest similarities on the level of physical chemistry as well. In order to find the physical principle that obviously favors these reactions or transition states, we made the following two ad hoc assumptions:

- The reactions are concerted.
- The transiton states are stabilized by conjugation (similar to the pericyclic reactions).

Starting point of our theoretical approach is the traditional qualitative treatment for pericyclic reactions and especially the topological methods of Zimmerman,[27] which therefore should be briefly summarized.

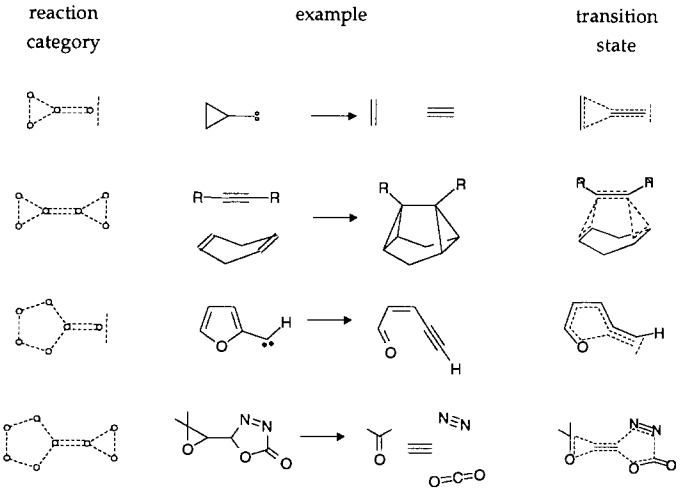


Fig. 3. Examples of complex reactions. The reactions are categorized according to the topology of the electron shift; the transition state is given for a concerted mechanism.

3. The Theory of Coarctate Transition States

3.1. Qualitative Methods for Treating Concerted Reactions

There are three qualitative methods for the theoretical treatment of concerted and, in particular, pericyclic reactions:

1. Conservation of orbital symmetry
   (correlation[10] and state diagrams)
   by Woodward–Hoffmann[1, 11–14] and Longuet-Higgins et al.[15]
2. Frontier orbital method
   (perturbation theory)
   by Oosterhof et al.[16, 17] and Fukui et al.[18–20]
3. Aromaticity of transition states
   (topological methods)
   by Evans and Dewar[21–25] and Zimmerman[26–28]

For the nontheorist, the topological method of the aromaticity of transition states is the easiest to apply. The method was introduced almost concurrently by Dewar as the "Evans principle" and by Zimmerman as the "Hückel–Möbius" method. Notwithstanding the fact that both methods are based on different theoretical grounds, they are almost identical in their formalism. A. C. Day[29] proved later that the general Woodward–Hoffmann rules (based on the number of supra- and antara-



Rainer Herges, born in 1955 in St. Ingbert (Saar), studied Chemistry at the Universität des Saarlandes in Saarbrücken, where he completed his Diplom under the supervision of H. Dürr. He then moved to the research group of I. Ugi at the Technische Universität München and obtained his doctorate there for a dissertation on the systematic, deductive search for new reactions and their experimental realization. As postdoctoral fellow with G. A. Olah in Los Angeles he performed calculations and syntheses for cations and dications (1985). He completed his habilitation on the topic of reaction planning in 1992 at the Universität Erlangen-Nürnberg. He was awarded the prize for doctoral candidates by the TU München for his dissertation, the ADUC-Jahrespreis 1992 for habilitands for the work on rational planning of new chemical reactions, and the CSA Trust Award 1993 (CSA = Chemical Structure Association) for his contributions to the processing by computer of chemical structures and reactions.

facial reacting components) are equivalent to the topological Hückel–Möbius method, because in a certain context the concepts antarafacial and sign inversion imply the same physical meaning. Because of its simple and general applicability and the lack of dependence on explicit knowledge of the MOs of starting materials and products, this "paper-and-pencil method" found favor with most organic chemistry textbooks.

It is evident, but nonetheless very important, to discriminate between the terms "orbital basis" and "molecular orbital".[10b] The basis orbitals that form the orbital basis set are atomic orbitals (for example, atomic functions or hybrid orbitals). Molecular orbitals are formed by mixing the basis orbitals according to the rules of the LCAO method. The resulting number of MOs equals the number of basis orbitals prior to the interaction. (For example, the four π orbitals of butadiene are derived from the four carbon p orbitals perpendicular to the molecular plane.)

In analyzing pericyclic reactions one starts out from the idea that in a first approximation the "mobile" electrons participating in the reaction and the corresponding basis orbitals can be distinguished from the remaining system and treated separately. These basis orbitals are written in arbitrary phase, and a closed curve is drawn (in the following figures in red), which depicts the overlap of neighboring orbitals. Only two aspects are crucial for whether a reaction is allowed: the number of mobile electrons and the topology of the overlap of the basis orbitals. An even number (including 0) of negative overlaps (overlap of orbital phases with opposite sign) indicates a system with Hückel topology that is aromatic with $4n + 2$ electrons and antiaromatic with $4n$ electrons. Möbius systems[30] with an odd number of negative overlaps are aromatic with $4n$ electrons and antiaromatic with $4n + 2$ electrons. Reactions with an aromatic transition state are thermochemically allowed and while those with antiaromatic transition states are forbidden. Fig. 4 illustrates the topological analysis by means of the Diels–Alder reaction and the conrotatory ring opening of cyclohexadiene.

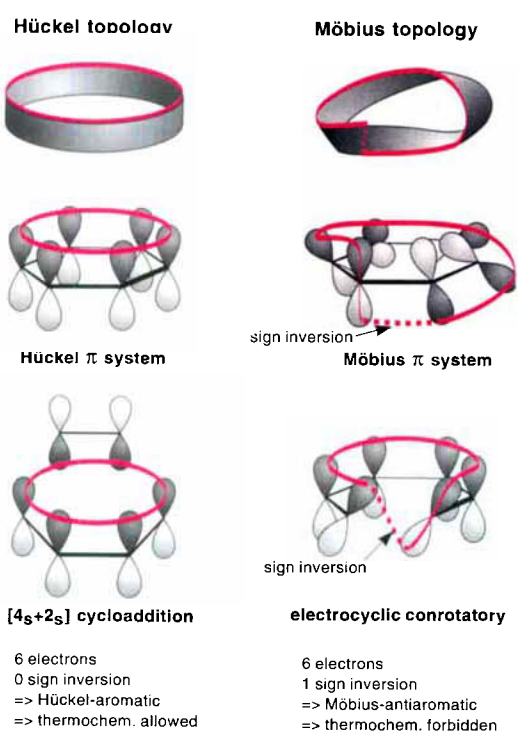


Fig. 4. Topological method for treating pericyclic reactions. The delocalized system of electrons in the transition state of pericyclic reactions is isoconjugate to the π system of aromatic or antiaromatic compounds. Reactions with an "aromatic transition state" are thermochemically allowed, and those with an antiaromatic one are thermochemically forbidden.

3.2. Extension of the Topological Method to Coarctate Transition States

In its original form the topological method, based on the aromaticity of transition states, is solely applicable to pericyclic reactions. Complex reactions, for instance the cyclopropylcarbene fragmentation (first example in Fig. 3), elude this analysis, because in the usual notation there is no cyclic overlap of the basis orbitals. Concerning these reactions Zimmerman and Sousa write in their article about the fragmentation of cycloheptatrienylidene:[31]

> "In analyzing the present reactions, we find that the usual methods do not generally apply. For only one of the reactions is there any symmetry to allow construction of a correlation diagram. The Hückel–Möbius methods presented by us earlier require a cyclic array of orbitals; however, the present reactions consist of linear arrays of orbitals instead."

To solve the problem, Zimmerman et al. proposed a modified version of correlation diagrams that do not rely on symmetry criteria but on the nodal properties of the MOs. Since these correlation diagrams are not suitable for categorizing the diversity of complex reactions and cannot explain the striking relationships, we tried to develop a topological method, which will be presented in this article.

Ad hoc assumption and starting point of our considerations was the claim that the topology of the orbital basis of complex reactions corresponds to the topology of pericyclic reactions: they are both cyclic. Hence the orbital basis of the transition states of complex reactions should be "isoconjugate" to aromatic systems, like the one of pericyclic reactions. In contrast to the situation with pericyclic reactions, the aromaticity of the transition states of complex reactions cannot be directly recognized. However, it can be impressively illustrated by means of topology. Figure 5 shows, as example, the topological transformation[32] of the orbital basis of the π system of the cyclopentadienyl anion into the delocalized system in the transition state of the cyclopropylcarbene fragmentation. (Topological equivalence or homoeomorphism in the following is depicted with the double arrow $\curvearrowleftrightarrow$.[33]) For illustration of the homoeomorphism of the two systems, centers 3 and 5 of the cyclopentadienyl anion are brought together in such a way that their basic orbitals are orthogonal, and the orbital basis of the cyclopropylcarbene fragmentation is thus obtained directly. Neither the topology of the orbital basis nor the number of electrons is changed during the transformation, because the overlap integral of the orthogonal basic orbitals 3 and 5 is zero, and the mutual overlap of all basis orbitals was maintained. As a result both physical preconditions for the topological analysis remain unaltered. This means that the transition state of the cyclopropylcarbene fragmentation is Hückel-aromatic and therefore the

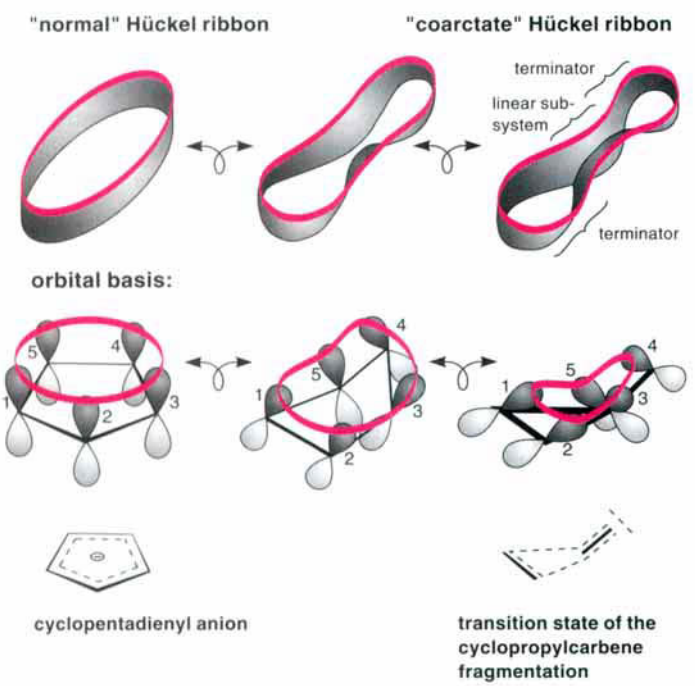


Fig. 5. A topological transformation proves that the delocalized system of electrons in the transiton state of complex reactions is isoconjugate to the π system of arenes. The example shows the topological transformation of the orbital basis of the π system of the cyclopentadienyl anion to the transition state of the complex cyclopropylcarbene fragmentation. The number of electrons as well as the topology of the basis orbital overlap remain unchanged during the operation [38]. In the same way as the topology of the orbital basis in transition states of pericyclic reactions corresponds to a Hückel ribbon (top left) or a Möbius ribbon, the orbital basis in the transition state of complex reactions can be viewed as an intersecting ribbon, the ribbon planes being perpendicular where they intersect (complex, coarctate Hückel ribbon, top right). The two "loops" represent the terminators, and the section where the ribbon intersects forms the linear subsystem.

reaction is thermochemically allowed, which agrees with the experimentally observed facts and with comprehensive theoretical calculations (for the details see Section 4.1). At this point it should be reemphasized that Figure 5 shows the orbital basis and not molecular orbitals. It is therefore not allowed to vectorially sum up the independent basic orbitals 3 and 5 to give one resultant orbital (which would be allowed with molecular orbitals). However, an arbitrary rotation of the orbitals 3 and 5 around the axis that intersects both orbital axes perpendicularly leads to the same physical result, as long as the orbitals remain orthogonal and are pure p functions.

Upon setting up the basis orbitals of complex reactions, it is important to assume a set of two p orbitals at the centers at which two bonds are made and broken simultaneously (which are thus not terminators). They have to be orthogonal to each other but not to the remaining basis.

The same topological transformation that we carried out with the orbital basis (in Fig. 5) can also be applied to the molecular orbitals. Figure 6 shows, on the left, the three occupied π orbitals of the cyclopentadienyl anion (the E_1'' orbitals are degenerate). By topological transformation they are converted into the three corresponding molecular orbitals of the transition state of the cyclopropylcarbene fragmentation (the A'' and A' orbitals are not degenerate). The topology of the overlap including the nodal properties is preserved. Because we are treating molecular orbitals, both components at the central carbon atoms are allowed to be added vectorially.

A comparison of the MOs obtained with this simple paper-and-pencil method and those from a high level ab initio calculation (Fig. 6, right column) demonstrates not only qualitative but also excellent quantitative agreement.

With respect to the topology of the transition state, the complex cyclopropylcarbene fragmentation is, therefore, isoconjugate to the 5-center, 6-electron pericyclic reactions (for example, 1,3 dipolar cycloaddition,[35, 36] 1,5 cyclization,[37] chelotropic reaction of sulfolenes) that are also derived from the cyclopentadienyl anion according to the classical method. Though the mechanisms appear totally different on first inspection, the transition states profit from the same kind of stabilization.

Because the transition states of complex reactions are formally derived from pericyclic reactions by constriction (see Fig. 20) we termed them coarctate.[38] The coarctations correspond to

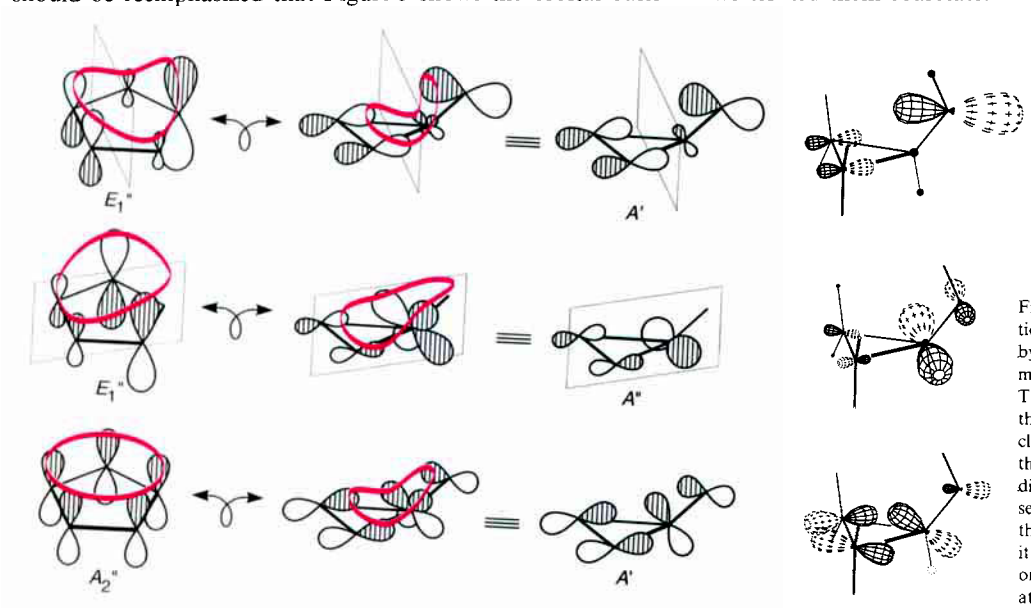


Fig. 6. The molecular orbitals of the transition state of complex reactions are derived by topological transformation from the molecular orbitals of the π system of arenes. The example illustrates the derivation of the three highest occupied π orbitals of the cyclopropylcarbene fragmentation from the three occupied π orbitals of the cyclopentadienyl anion. The nodal properties are preserved during the operation. In contrast to the procedure for deriving the orbital basis, it is now allowed to vectorially add the two orthogonal p orbitals at the central carbon atom. The MOs thus obtained agree well with those of an ab initio calculation (MP2/6-31G*//MP2/6-31G* level, right column).

the atoms where two bonds are broken and made (see formal description, Fig. 2).

In principle, the extended topological method allows the prediction of the stereochemistry and mechanism of complex reactions in a way similar to the traditional method for pericyclic reactions. In the following section the approach is outlined with the aid of a number of known complex reaction types with coarctate transition states.

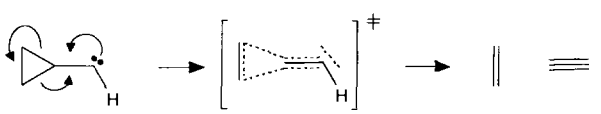
4. Application of the Model to Different Categories of Complex Reactions

4.1. Reactions with Lone-Pair Terminators and Three-Membered Ring Terminators



4.1.1. The Cyclopropylcarbene Fragmentation

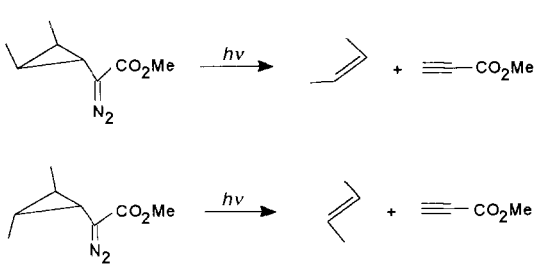
Most thoroughly investigated and the prototype of complex reactions is the cyclopropylcarbene fragmentation (Scheme 1). Formally, two bonds are made between the carbene carbon atom and the three-membered ring. The carbene center with the lone pair and the two cyclopropane carbon atoms 2 and 3 act as terminators.



Scheme 1. Fragmentation of cyclopropylcarbene to acetylene and ethylene.

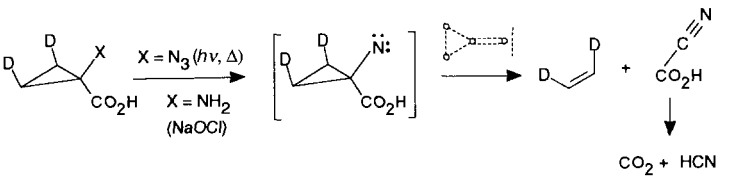
The reaction was discovered in 1960 by Friedman and Shechter.[39] Presumably because of its unusual mechanism it has been thoroughly investigated, both experimentally[40] and theoretically.[31,41,42] The fragmentation of the corresponding cyclopropylnitrenes is also known.[43–49] In both the carbene[50,51] and the nitrene fragmentation[45,46] stereochemistry is preserved (Scheme 2), and for both reaction types a singlet carbene[52] or nitrene[46] intermediate was proposed.

Presumably the biologically important, enzymatic oxidation of the 1-aminocyclopropylcarboxylic acid to ethylene, carbon



Scheme 2. The cyclopropylcarbene fragmentation. The reaction proceeds via the singlet spin state of the carbene and with retention of stereochemistry. (The competing reaction is the likewise allowed ring enlargement affording the four-membered ring.)

dioxide, and cyanide[52] does not pass a cyclopropylnitrene but proceeds via radical intermediates. Oxidation of the acid with sodium hypochlorite[53] and the irradiation of the corresponding azide,[54] however, are stereospecific and share the nitrene as a common intermediate (Scheme 3).



Scheme 3. Fragmentation of derivatives of the 1-aminocyclopropylcarboxylic acid.

With our qualitative topological analysis the stereochemistry of this fragmentation is easily comprehended without any calculation. Additionally, further stereochemical details can be predicted (Fig. 7).

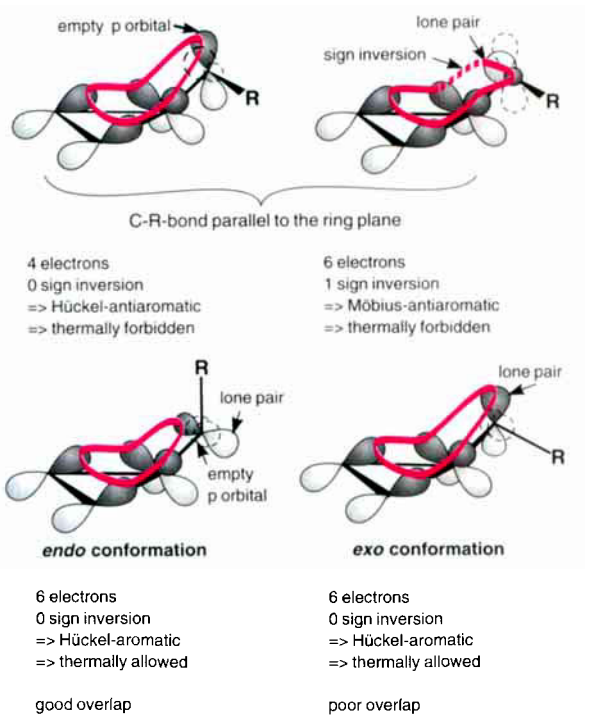
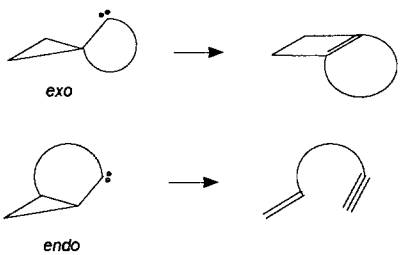


Fig. 7. Topological analysis of the cyclopropylcarbene fragmentation according to Scheme 1. For details, see text.

From the orbital basis of Figure 7, derived in Figure 5, it follows that the overlap is best if the orbital containing the lone pair is parallel to the plane that bisects the plane of the three-membered ring. Under this prerequisite the transition state is aromatic, and the reaction is therefore thermochemically allowed. With the substituent C–R bond parallel to the forming ethylene fragment, the empty lone-pair orbital of the carbene center interacts with the remaining orbital basis, and the transition state with four electrons is Hückel-antiaromatic, which is energetically unfavorable. An alternative view, which, however, yields the same result, is provided by the overlap of the lone-pair orbital at the carbene center with the remaining basis orbitals:

The system includes six electrons; however, because of the sign inversion it is Möbius-antiaromatic and therefore forbidden.

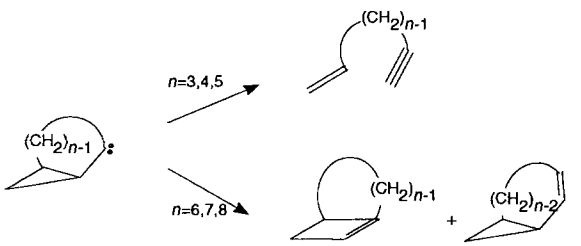
An analysis of the cyclopropylcarbene fragmentation by correlation diagrams leads to the same results. However, the advantage of our method is provided in its ability to discriminate between two or more stereochemically allowed reaction modi. With the substituent either *endo* or *exo* to the cyclopropane ring, C_s symmetry is conserved, and the reaction is thermochemically allowed. As illustrated in Fig. 7, the lone-pair orbital of the carbene overlaps more efficiently with the remaining basis orbitals in *endo* conformation than in *exo* conformation. The fragmentation should therefore proceed preferentially in *endo* systems. Theoretical calculations as well as experiments confirm this prediction. Instructive are investigations of systems in which the carbene is sterically fixed in a particular conformation. Carbenes fixed in *exo* conformation exclusively afford ring enlargement products[55–59] and *endo*-fixed carbenes fragment preferentially.[60–64] (Scheme 4).



Scheme 4. Reactions of *exo*- and *endo*-fixed cyclopropylcarbenes.

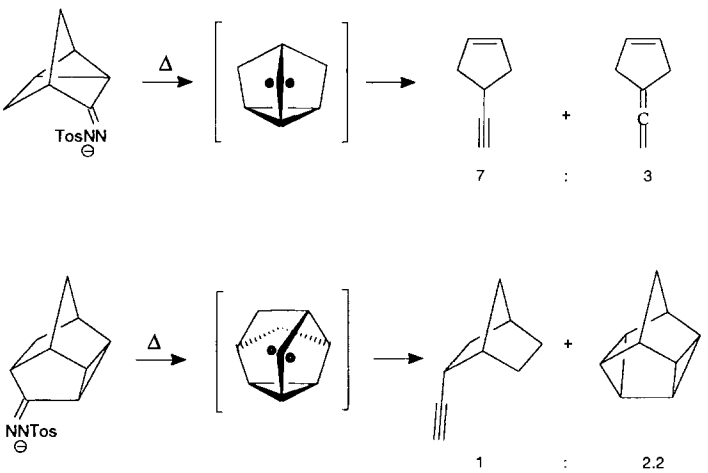
The comparison is unfair for small and medium spiro-annelated rings, because highly strained alkynes would be formed by fragmentation. However, spiro[2.11]tetradec-2-ylidene also does not undergo fragmentation,[65] even though the dodecyne formed as product would be almost unstrained.

Moreover, *endo*-fixed systems do not exclusively afford fragmentation. The yield of fragmentation product critically depends on the alignment of the carbene center relative to the cyclopropane ring. In *endo*-fixed bicyclo[*n*.1.0] systems the larger annelated ring determines the preferred reaction modus. Whereas five-, six, and seven-membered rings steer the reaction in direction of the fragmentation,[60–64] larger ring systems afford 1,2 shifts and ring enlargement[66–68] (Scheme 5). The different reactivity is presumably due to the forcing of the system into *endo* position by small annelated rings; larger rings allow more conformational flexibility.



Scheme 5. Reaction modi of bicyclo[*n*.1.0]alk-2-ylidenes depending on the ring size *n*. Smaller annelated rings force the system into *endo* conformation and favor the fragmentation affording alkynes.

Fragmentations of tricyclo[2.2.1.$0^{2,6}$]-hept-3-ylidene and tetracyclo[4.3.$0^{2,4}$.$0^{3,8}$]non-5-ylidene[69] illustrate the striking effect of small changes in conformation on the product ratio (Scheme 6). In the first system the substituent of the carbene carbon atom is exactly *endo* to the cyclopropane and the orbital of the carbene lone pair lies in the plane that bisects the plane of the three-membered ring. Thus fragmentation dominates.[70, 71] In the second system the lone pair is twisted relative to the bisecting plane by about 30°, and the insertion product prevails.[72]



Scheme 6. Dependence of the proportion of cyclopropylcarbene fragmentation on the conformation in the polycyclic ring system.

Besides these experimental findings, detailed theoretical calculations performed by Shevlin and McKee[73] and also by my group[74] impressively confirm the predictions of the qualitative topological analysis. Figure 8 shows the relative energies of the stationary points on the potential energy surface of the cyclopropylcarbene fragmentation. There are two conformational

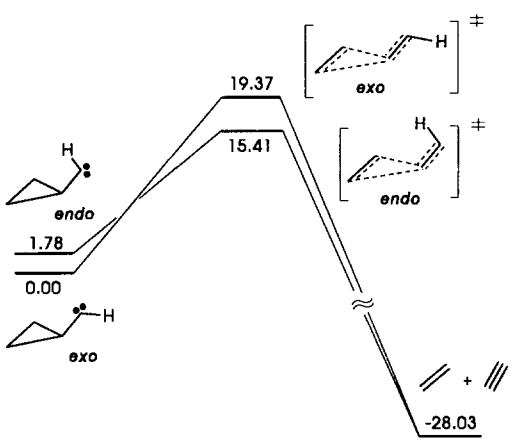


Fig. 8. Relative energies, calculated by ab initio methods, of stationary points on the potential energy surface of the cyclopropylcarbene fragmentation in kcal mol^{-1} [74].

minima of the carbene: in one the carbene H is in *exo* position; in the other it is in *endo* position. In agreement with our qualitative picture, the *endo* transition state of the fragmentation is

almost 4 kcal mol^{-1} lower in energy than the corresponding transition state of the *exo* conformer.

According to the topological analysis in Figure 7, this is due to the better overlap of the carbene lone-pair orbital with the basis orbitals of the neighboring carbon atom. This is also convincingly confirmed by ab initio calculation (Fig. 9).

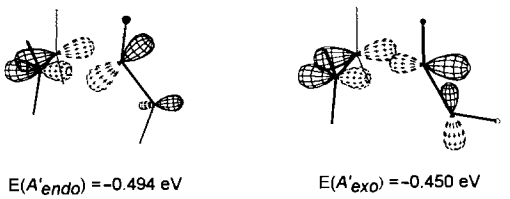


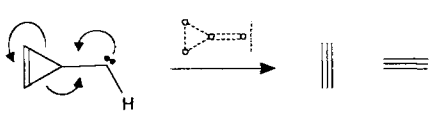
Fig. 9. Comparison of the HOMO-2 orbitals [75] in the transition state of the cyclopropylcarbene fragmentation (ab initio calculation on the MP2/6-31G*// MP2/6-31G* level; orbital plot with PERGRA [76]). The overlap in *endo* conformation is more effective. The other two MOs (HOMO-1 and HOMO) are similar in energy in both conformations because of their nodal properties.

The symmetrical MO of the orbital basis containing no nodes that has the lowest energy (A', HOMO-2,[75] see also Fig. 6) is 0.04 eV more favorable in the *endo* transition state than in the *exo* transition state. The better overlap of the back lobes does not completely compensate for this effect.

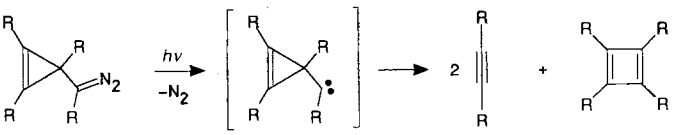
All theoretical considerations presented so far assume that a singlet carbene is the reactive species. The conservation of the stereochemistry in cyclopropylcarbene fragmentations of substituted systems could also be explained by a triplet carbene and a very short-lived, ring-opened, biradical species, whose cleavage to ethylene and acetylene proceeds faster than the isomerization of the double bond. According to our ab initio calculations on QCI level,[77] the cyclopropylcarbene (contrary to conclusions by Shevlin and McKee[73]) definitely has a singlet ground state. The triplet state of lowest energy lies 2.15 kcal mol^{-1} higher. As demonstrated by a comparison of results of ab initio calculations with experimental data of the singlet–triplet splitting in methylene,[78] our level of electron correlation probably still describes the singlet species less adequately than the triplet species. It is reasonable to predict that the singlet state in cyclopropylcarbene lies at least 4 kcal mol^{-1} lower than the triplet state. This explains the experimental findings of Gallucci and Jones,[51] according to which cyclopropylcarbenes generated by triplet-sensitized excitation from diazo compounds fragment stereoselectively (Scheme 2). Presumably the carbene generated in the triplet state changes to the singlet state prior to the elimination and fragments stereoselectively.

4.1.2. Other Fragmentations

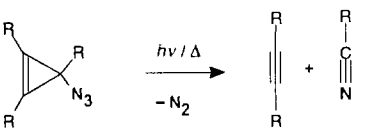
Related to the cyclopropylcarbene fragmentation is the decomposition of cyclopropenylcarbene[79] into two molecules of acetylene[80] (Scheme 7). Cyclopropenylcarbenes have been thoroughly investigated, mainly in the vain hope of gaining access to tetrahedrane by intramolecular carbene addition to the double bond or of generating cyclobutadiene by ring enlargement; for example, see refs. [81,82] (Scheme 8). Apart from some exceptions[83–86] fragmentation was observed in high yields depending on the reaction conditions.[80, 82, 87–91] The fragmentation of cyclopropylnitrenes is also known (Scheme 9).[92–94]



Scheme 7. Fragmentation of the cyclopropenylcarbene into two molecules of acetylene.



Scheme 8. Example of the cyclopropenylcarbene fragmentation (R = *t*Bu). Depending on the experimental conditions, ring enlargement to cyclobutadiene is observed in addition to the fragmentation products.



Scheme 9. Example of the fragmentation of a cyclopropenylnitrene [92]. R = Me.

It would be rash to conclude that the mechanism is concerted and follows a coarctate transition state analogous to the cyclopropylcarbene fragmentation. Our ab initio calculations[95] on the singlet potential energy surface of the cyclopropenylcarbene show at least that the reaction is not synchronous. The transition state is unsymmetrical[96] and has a strong biradical character.[97] The *exo* and *endo* conformations are almost equal in energy (Fig. 10).[98, 99] Since both fragment with low activation energy via the same transition state, the conformation should not have a large effect on the fragmentation of the carbene. (The same is not necessarily true for ring enlargement or the not yet observed, intramolecular carbene addition.)

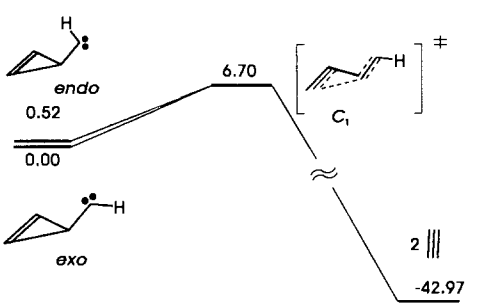
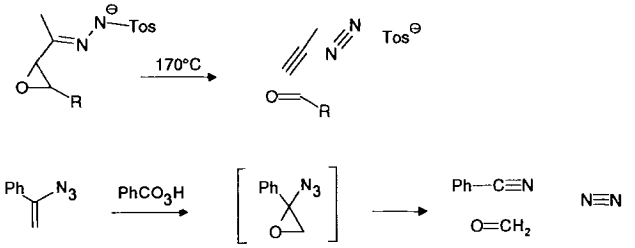


Fig. 10. Relative energies calculated by ab initio methods at the MP4SDTQ/6-31G*//MP2/6-31G* + ZPE level for stationary points on the potential energy surface of the cyclopropenylcarbene fragmentation, in kcal mol^{-1}.

Also related to the cyclopropylcarbene fragmentation are the fragmentation reactions of some oxiranes. The α,β-epoxyhydrazone fragmentation described by Eschenmoser,[100] like the cyclopropylcarbene fragmentation, proceeds preferentially in ster-

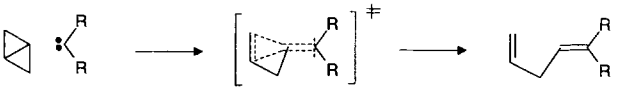
ically *endo*-fixed systems.[101] Based on the reaction conditions (room temperature, acid and base catalysis), a carbene intermediate (and most probably also a diazo compound) can be almost definitely excluded.[102] Presumably, polar intermediates, and thus other mechanisms, determine the stereochemical characteristics. The analogous fragmentations of the sodium salts of tosylhydrazones under Bamford–Stevens conditions[103] and of azidooxirane,[104] however, proceed under pyrolytic or nonpolar conditions. Concerted mechanisms via diazo compounds, carbenes, or nitrenes are therefore plausible (Scheme 10).



Scheme 10. Heteroanalogues of the cyclopropylcarbene fragmentation.

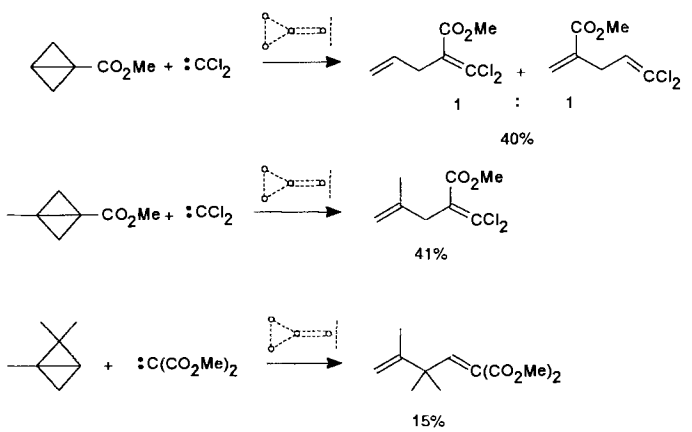
4.1.3. Carbene Additions to Bicyclobutanes

The addition of carbenes to bicyclobutanes to form 1,4-dienes was termed "a pathway without parallel in the chemistry of ... carbenes" by its discoverers (Scheme 11).[105] The parent



Scheme 11. Schematic representation of the addition of carbenes to bicyclobutanes.

compound, bicyclobutane, reacts with methylene affording 1,4-pentadiene in 21% yield.[106] Substituted bicyclobutanes were treated by Wiberg et al.,[106] Applequist et al.,[107] and Jones, Jr. et al.[108] with dichlorocarbene and dimethoxycarbonylcarbene to give the corresponding 1,4-pentadienes (Scheme 12). Doering et al.[105] and Wiberg et al.[106] proposed a diradical mechanism. Detailed experimental investigations and semiempirical calculations of Jones, Jr. et al.[108] suggest a concerted attack of the singlet carbene.



Scheme 12. Examples of carbene addition to bicyclobutanes.

Formally the reaction corresponds to the attack of a carbene at a cyclopropane ring in such a way that two cyclopropane ring bonds are broken simultaneously and two bonds are attached to the carbene center. Besides the least motion process (Fig. 11a), other modes of attack with lower symmetry are conceivable. The point group given in Figure 11 is derived from the symmetry elements that are conserved during the reaction. All the

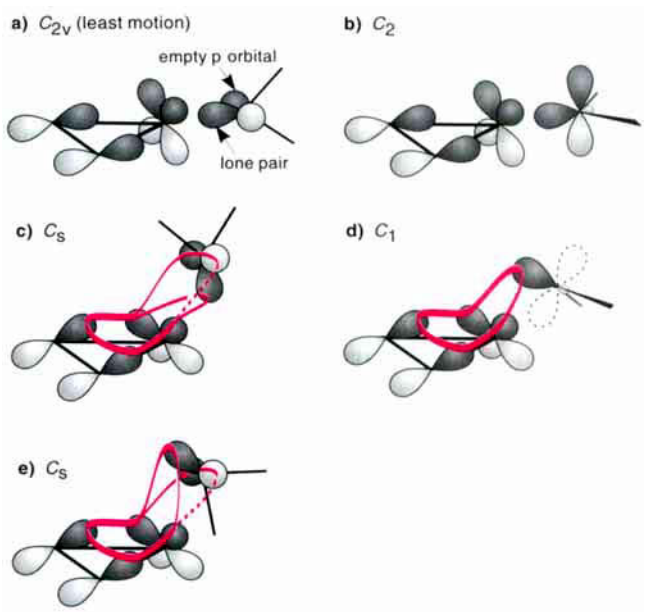


Fig. 11. Topological analysis of the carbene addition to cyclopropanes as given in Scheme 11. For details, see text.

trajectories indicated are allowed according to the rules of the conservation of orbital symmetry. Topological analysis, however, maintains that attacks a) and b) are energetically less favorable than c), d), and e), because there is no way of forming a cyclic topology of the orbital basis. Most favorable are approaches c) and e), since both the lone-pair as well as the empty p orbital at the carbene center form aromatic systems with the remaining orbital basis (a Hückel system with the lone-pair and a Möbius system with the empty p orbital). The attack of the carbene therefore takes place from above the ring plane. This is confirmed by MNDO calculations of Jones, Jr. et al.[108] Examining the addition of methylene to bicyclobutane, they found two transition states of almost equal energy that correspond to the attacks c) and e) in Figure 11. According to the calculations, the angle between the bisector of the three-membered ring and the forming bond of the carbene center with the cyclopropane ring in the transition state is about 30°.[109] This explains why even highly strained cyclpropanes like spiropentane exclusively undergo C–H insertion in contrast to the bicyclobutanes. In cyclopropanes the attacks c) and e) (Fig. 11) are not feasible on steric grounds (because of the impeding H atom), whereas in bicyclobutanes the cyclopropane carbon atom at which the attack occurs is sterically deshielded by the three-membered ring bridge (Fig. 12), and addition is thus possible.

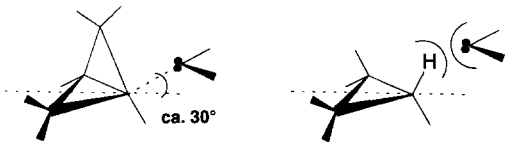
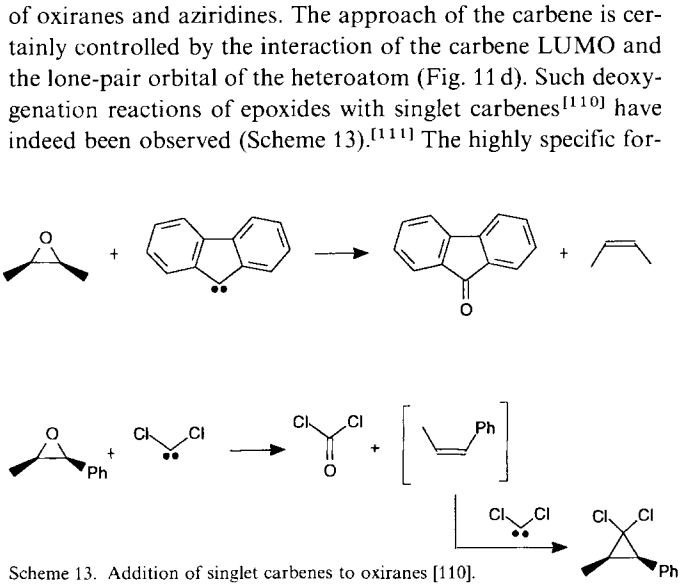
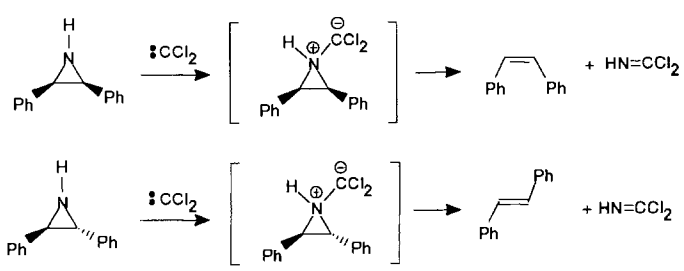


Fig. 12. According to MNDO calculations [108] and in accordance with the topological analysis, the attack of the carbene does not follow the least motion principle (approaches a) or b) in Fig. 11), but starts from above the ring plane with an angle of about 30° and from inside the flap of the bicyclic system. In cyclopropane the corresponding approach is hindered by the cyclopropane H atom.

Similarly there are no steric problems to be expected during the attack of the carbene from above the ring plane in the case of oxiranes and aziridines. The approach of the carbene is certainly controlled by the interaction of the carbene LUMO and the lone-pair orbital of the heteroatom (Fig. 11d). Such deoxygenation reactions of epoxides with singlet carbenes[110] have indeed been observed (Scheme 13).[111] The highly specific formation of the alkene and the small acceleration of the reaction by substituents that stabilize carbenium ions make ring-opened, dipolar intermediates implausible. In principle, an ylide intermediate is conceivable besides the concerted pathway. Most probably, the fragmentation of aziridines found by Hata and Watanabe proceeds via an ylide intermediate and does not follow a complex mechanism[112] (Scheme 14).



Scheme 13. Addition of singlet carbenes to oxiranes [110].



Scheme 14. The carbene addition to aziridines is not concerted but passes an ylide intermediate.

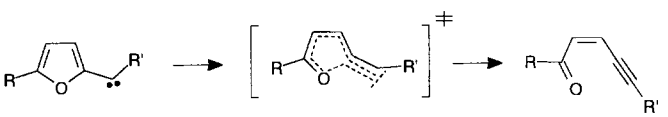
4.2. Reactions with Lone-Pair Terminators and Five-Membered Ring Terminators



The stereochemical relationships in reactions with a five-membered ring and a lone pair as terminators are different to those in which the terminators are three-membered rings and lone pairs. With two more electrons delocalized in the transition state but the same stereochemical constraints, the selection rules are inverted. This is illustrated in this section by the example of the rearrangement of furfurylidene and its heterocyclic analogues.

4.2.1. Rearrangement of Furfurylidene and Its Heterocyclic Analogues

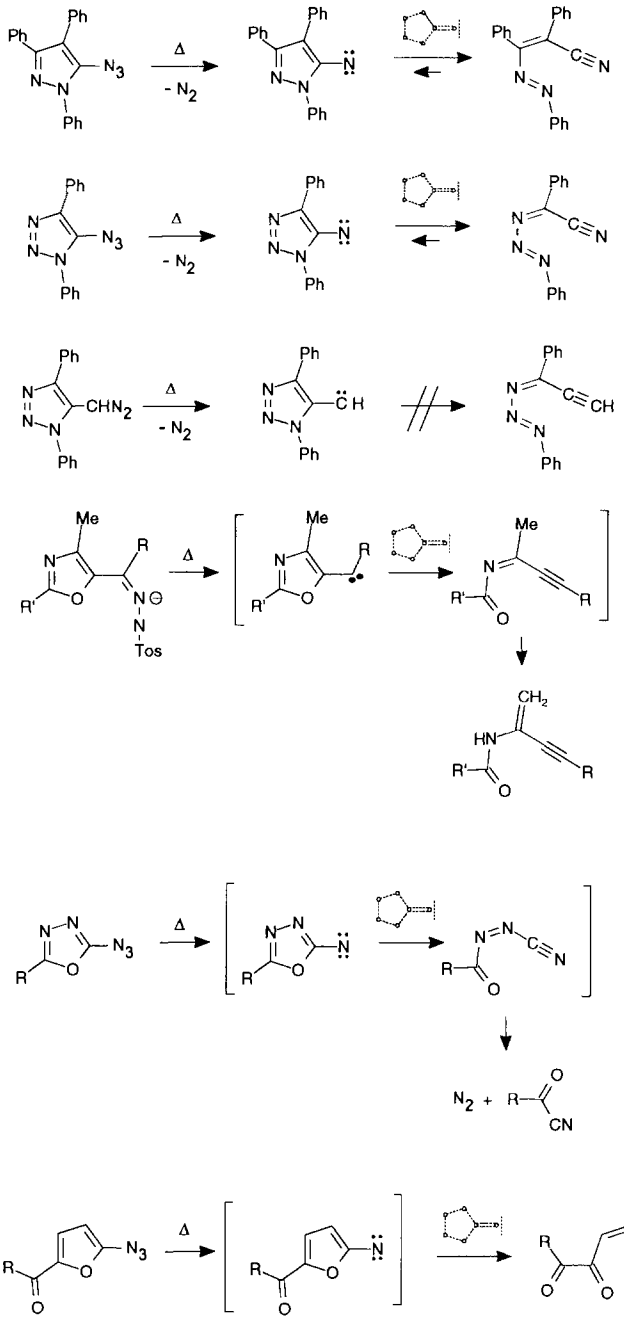
The 2-furfurylcarbene rearrangement was discovered by Hoffman und Shechter.[113-117] In a reaction that seems unusual at the first glance, furfurylidenes rearrange stereoselectively by cleavage of the furan ring to afford *cis*-2-penten-4-ynals (Scheme 15). Dry salts of tosylhydrazones or diazo compounds have served as carbene precursors.[118] Highly interesting are the fragmentations of some heterocyclic analogues of furfurylidene. There are indications that the fragmentation products of both the 5-aminopyrazoles[119] and the 5-azidotriazoles[120, 121] are open-chain nitriles that are in equilibrium with the corresponding cyclic nitrenoid forms; the equilibrium, however, lies for to the side of the nitriles (Scheme 16, first and second examples).[122] The small activation barrier and the consistent stereochemistry is explained by a stabilized coarctate transition state. The cyclic carbenoid form of the analogous 5-triazolylcarbene, however, is so stable that no open-chain alkyne could be detected (Scheme 16, third example).[121]



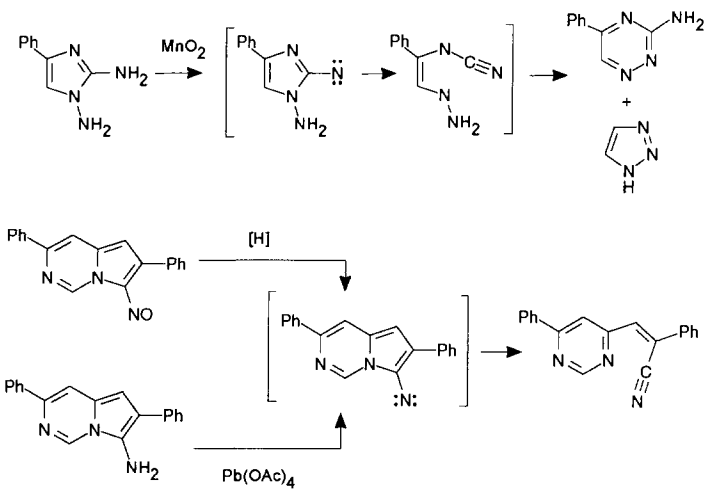
Scheme 15. Schematic representation of the furfurylidene rearrangement.

Similarly analogous to the furfurylidene rearrangement are the reactions of 5-oxazolylcarbenes (Scheme 16, example 4),[123] 5-acyl-2-azidofurans (Scheme 16, example 5),[124-126] and azidooxadiazoles (Scheme 16, example 6).[127]

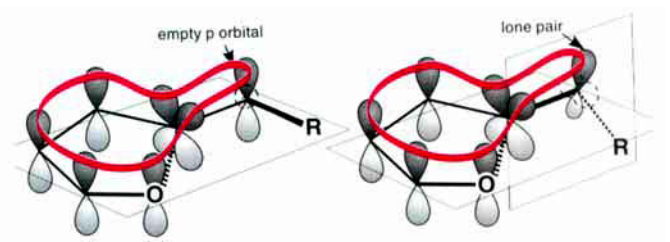
The rearrangements of 1,2-diamino-4-phenylimidazole[128] and 3,6-diphenylpyrrolo[1,2-*c*]pyrimidine derivatives[129] (Scheme 17) most probably proceed via nitrenes or nitrenoide intermediates and therefore are analogous to the furfurylidene rearrangement as well. The ease of the rearrangement despite the annihilation of the aromaticity of the five-membered heterocyclic arenes during the reaction, as well as the *cis*-configuration of the olefinic product, can be explained by topological analysis (Fig. 13). Moreover, the analysis of the coarctate transition state supplies information about the most favorable position of the carbene carbon with respect to the plane of the ring. In contrast to the situations for the three-membered ring in the cyclopropylcarbene fragmentation and the carbene addition to bicyclobutanes, the furan ring makes six electrons available for delocalization in the transition state. Therefore, the empty p orbital of the carbene carbon atom should be included in the orbital basis in the transition state in order to allow Hückel-aromatic topology with six electrons, isoconjugate to the tropylium



Scheme 16. Examples of the rearrangement of heteroanalogues of furfurylidene. In the 4th reaction R′ = H, R = CH_3 or R′ = R = CH_3 or R′ = CH_3, R = Ph; in the 5th reaction R = Ph; in the 6th reaction R = *t*Bu, *i*Pr, H.



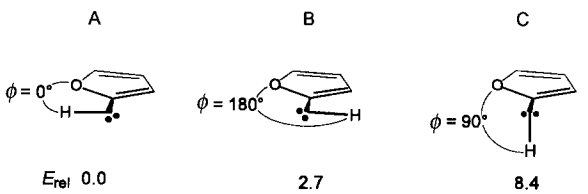
Scheme 17. Rearrangements that presumably proceed via nitrenes or nitrenoid intermediates, which are thus thus analogous to the furfurylidene rearrangement.



6 electrons
0 sign inversion
=> Hückel-aromatic
=> thermally allowed

8 electrons
0 sign inversion
=> Hückel-antiaromatic
=> thermally forbidden

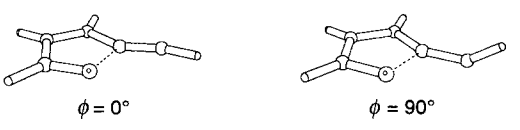
Fig. 13. Topological analysis of the furfurylidene rearrangement according to Scheme 15. For details, see text.



Scheme 18. MNDO calculations of different conformations of furfurylidene. In both conformative minima, the carbene H atom lies within the plane of the furan ring ($\phi = 0$, 180°). The transition state of the rotation around the C–C bond between the carbene and furan is described by C. Relative energies are given in kcal mol^{-1}.

cation. The bond axis between substituent and carbene center has to be parallel to the plane of the furan ring, and C_s symmetry has to be conserved during the reaction. Simple semiempirical calculations show that this is indeed the case. According to our MNDO calculations,[130] furfurylidene has two conformative minimima in C_s symmetry (Scheme 18).[131] The energetically most favorable conformation of the carbene in the starting material at the same time is the most suitable for the rearrangement to proceed.

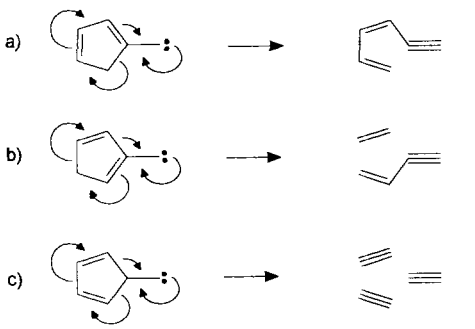
In agreement with the topological analysis, the energy maximum on the reaction path for the rearrangement[132] with a fixed angle of $\phi = 90°$ lies indeed more than 16 kcal mol^{-1} higher in energy than the one with $\phi = 0°$ (Scheme 19). (As to be expected for a forbidden reaction the energy maximum with $\phi = 90°$ is not a true transition state, but a stationary point of higher order.)



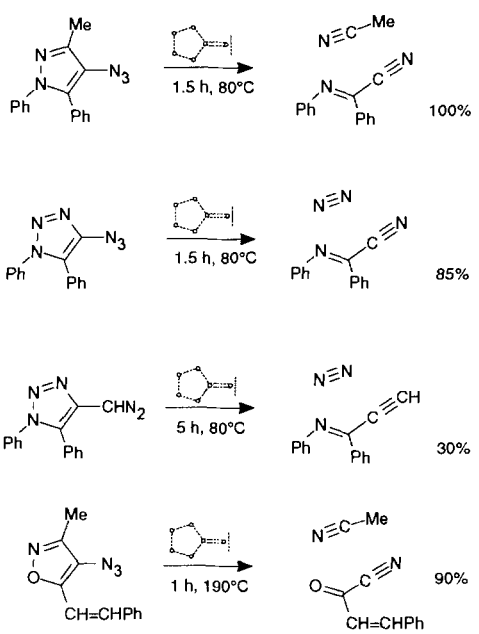
Scheme 19. Energy maxima on the reaction path [132] of the furfurylidene rearrangement, calculated by MNDO. The values E_{rel} [kcal mol^{-1}] are given relative to the energy of furfurylidene with $\phi = 0°$ (Scheme 18).

4.2.2. *Other Reactions*

In principle, three different positional isomers of cyclopentadienyl carbenes or nitrenes that are capable of undergoing complex reactions with five-membered ring and lone-pair terminators are conceivable (Scheme 20). The furfurylidene rearrangement in which the substitutent bearing the lone pair is in 1-position has already been mentioned. Additionally there is an elimination to give two and a fragmentation to afford three unsaturated fragments. In all-carbon systems these reactions have not yet been observed. Examples for nitrenes, however, are known. They derive their driving force mainly from the thermodynamically favorable formation of molecular nitrogen or a CN triple bond. 4-Azidopyrazoles like 4-azido-3-methyl-1,5-diphenylpyrazole react smoothly and in high yields to afford the corresponding nitriles and iminonitriles.[133, 134] Heteroanalogous are the elimination reactions of 4-azido-,[133] 4-diazomethyl-1,2,3-triazoles,[135] and 4-azido-3-methyl-5-styrylisoxazole (Scheme 21).

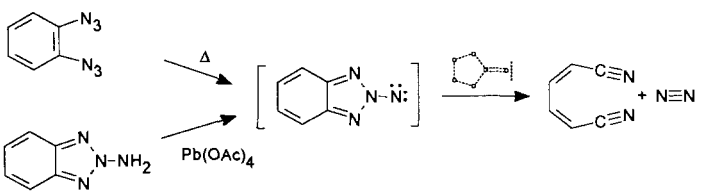


Scheme 20. Three types of complex reaction with five-membered ring and lone-pair terminators. The reactions differ only in the position of the substitutent bearing the lone pair relative to the double bonds in the five-membered ring. a) Furfurylidene rearrangement, b) elimination, c) fragmentation.



Scheme 21. Examples of elimination reactions analogous to mechanism b) in Scheme 20.

The fragmentation c) in Scheme 20 probably occurs in the pyrolysis of *o*-diazides[136] and the oxidation of 1- and 2-aminobenzotriazole[137] (Scheme 22). In agreement with a complex mechanism, *cis,cis*-muconitrile is formed stereoselectively as the product of this unusual fragmentation reaction.



Scheme 22. Example for a fragmentation reaction analogous to mechanism c) in Scheme 20.

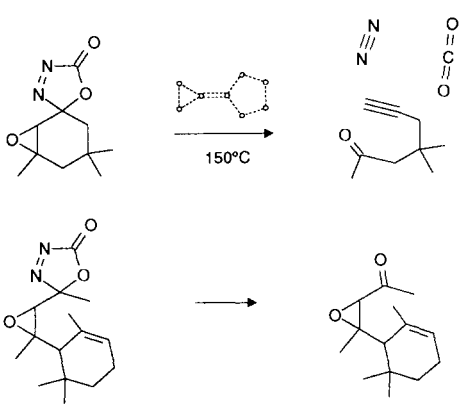
4.3. Reactions of Systems with Three- and Five-Membered Ring Terminators



4.3.1. *Oxirane Fragmentations*

Most of the fragmentation reactions with three-membered ring terminators rely on the principle of the elimination of a ketone from an epoxide. Depending on the length of the linear system of bond-breaking and -making and the size of the other terminator, a number of stereochemical consequences can be derived from a topological analysis of the transition state.

MacAlpine and Warkentin,[138] for instance, found that the fragmentation of oxirane-substituted [5H]-oxadiazolones is observed only if the oxirane and oxadiazolidine rings are fixed in a coplanar conformation by a spiro bridge (Scheme 23). If a concerted mechanism is assumed,[139] this fact can be easily explained by a topological analysis of the transition state (Fig. 14). With ten electrons and Hückel topology the reaction



Scheme 23. The fragmentation of oxirane-substituted oxadiazolones is observed only if the oxadiazol and oxirane rings are fixed in a coplanar orientation by a spiro bridge.

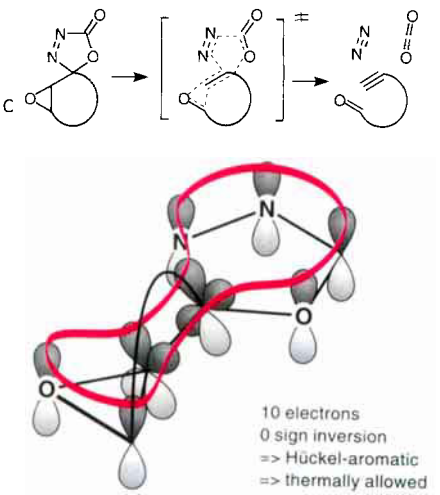
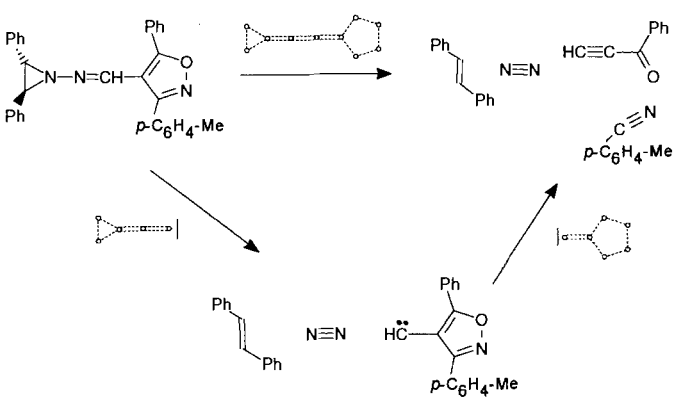


Fig. 14. Schematic representation and topological analysis of the oxirane-substituted oxadiazolone fragmentation.

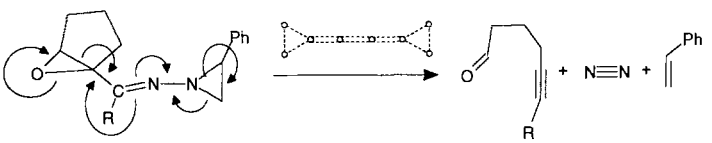
is thermochemically allowed. Oxirane and oxadiazole rings are fixed in a coplanar geometry, and thus the most suitable overlap of the orbital basis and an optimal stabilization of the transition state is attained. The same arguments concerning the stereochemistry are valid for the alternative mechanism via an oxiranyl carbene (see Scheme 26).

Likewise endowed with a three- and a five-membered ring terminator but containing a larger linear system ($n = 4$) is the fragmentation of 4-(aziridine-1-yliminomethyl)isoxazole, discovered by Gilchrist and Pearson.[140] Alternative to a one step mechanism and, considering the size of the system, more probable[141] is a two-step process consisting of two consecutive complex reactions. Both reaction pathways are allowed according to the topological analysis (Scheme 24), and both are favored by a coplanar orientation of the three- and five-membered ring.



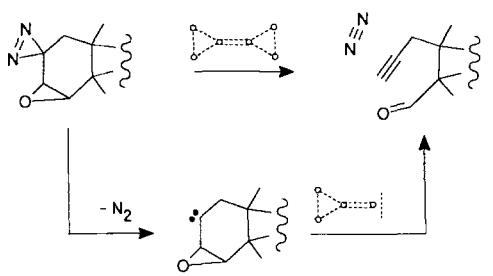
Scheme 24. If formulated as a one step reaction, the fragmentation of 4-(aziridine-1-yliminomethyl)isoxazole proceeds via a complex mechanism with a three- and a five-membered ring terminator and a linear system of $n = 4$. The Hückel aromatic transition state with 14 electrons is favored by a coplanar arrangement of the aziridine and isoxazole ring. Both steps of the alternative two-step mechanism via the 4-isoxazolylcarbene also proceed by complex mechanisms.

Stereochemical relationships should be reversed if a three-membered ring terminator (for example, aziridine ring) replaces the five-membered ring terminator (oxazole ring). Scheme 25 depicts the *N*-aminoaziridine version of the Eschenmoser reaction as example of such a reaction.[142] With 12 electrons and Hückel topology the reaction is thermochemically forbidden. Furthermore, sterically nonfixed systems of such a size rarely react in a concerted way. In some cases diazo compounds have indeed been detected as stable intermediates.[143] Also contradicting a concerted pathway and thus in agreement with the topological analysis is the fact that the reaction occurs in sterically nonfixed systems with high yields.



Scheme 25. The aminoaziridine version of the Eschenmoser reaction with 12 electrons is forbidden as a coarctate Hückel process.

Similarly forbidden according to a toplogical analysis is the fragmentation of the spiro-annelated diazirine shown in Scheme 26. Presumably after elimination of molecular nitrogen a carbene is passed as intermediate. The fragmentation of this intermediate is allowed, since it is an oxirane analogue of the cyclopropylcarbene fragmentation. It is even favored by the imposed *endo* conformation (Scheme 26, bottom).

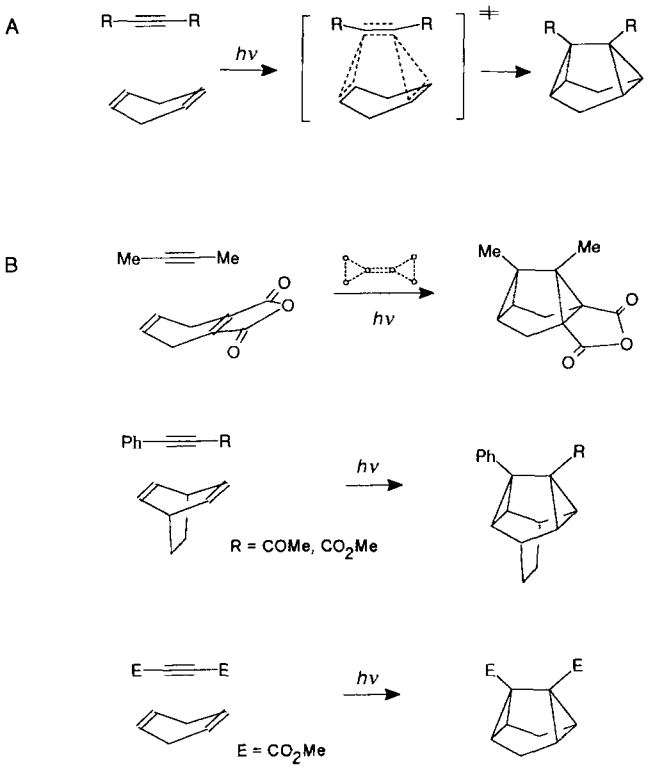


Scheme 26. Fragmentation of a spiro-annelated diazirine. Top: The fragmentation that has been observed in a steroid system is forbidden as concerted process. Bottom: The fragmentation of the diazirine in a two-step mechanism is allowed.

4.3.2. *Cycloadditions of Acetylenes to 1,4-Cyclohexadienes*

Formally the photochemical addition of acetylenes to 1,4-cyclohexadienes can be viewed as a coarctate addition with two three-membered ring terminators (Scheme 27 A). Three experimental investigations have been published (Scheme 27 B).[145–147]

This is one of the few complex reactions that do not need topological transformation to be analyzed with the Hückel–Möbius method. In the linear part of the reaction (acetylene) there are already two orthogonal π systems present. Consequently, this simplifies the choice of the basis orbitals. The reaction was already used as an example for illustrating the application of the Hückel–Möbius method by Zimmerman[27] and treated by Woodward and Hoffmann according to the rules of the conservation of the orbital symmetry.[1] By using the topological approach the reaction can be analyzed without explicitly constructing a correlation diagram (Fig. 15). With eight elec-



Scheme 27. Photochemical addition of acetylenenes to 1,4-cyclohexadienes. A: Schematic representation. B: Examples.

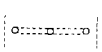
trons and without sign inversion, the orbital basis is Hückel antiaromatic, and the reaction, in agreement with experiment, is photochemically allowed. Topological transformation shows that the transition state is isoconjugate to the antiaromatic cyclooctatetraene.



8 electrons
0 sign inversion
=> Hückel-antiaromatic
=> thermochem. forbidden
photochem. allowed

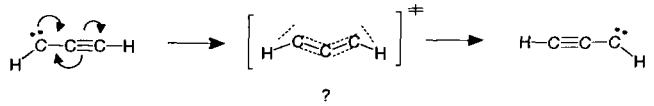
Fig. 15. Topological analysis of the cycloaddition of acetylenes to 1,4-cyclohexadiene according to Scheme 27A.

4.4. Reactions in Systems with Two Lone-Pair Terminators



4.4.1. Bond-Shift Reactions

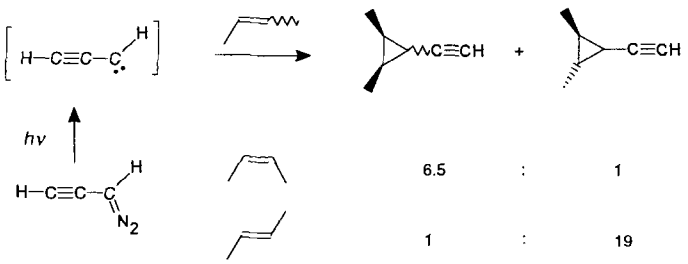
The "bond-shift" reactions in which triple bonds are formally moved, can be considered models for complex reactions. Prototype of these rearrangements is the propynylidene (propargylene") automerization (Scheme 28). Here two bonds are broken and made simultaneously at the central carbon atom. Carbene centers act as lone-pair terminators. Such a 1,3-carbene shift has already been postulated by Skell et al. for propynylidene.[148] In the parent system and in symmetrically substituted



?

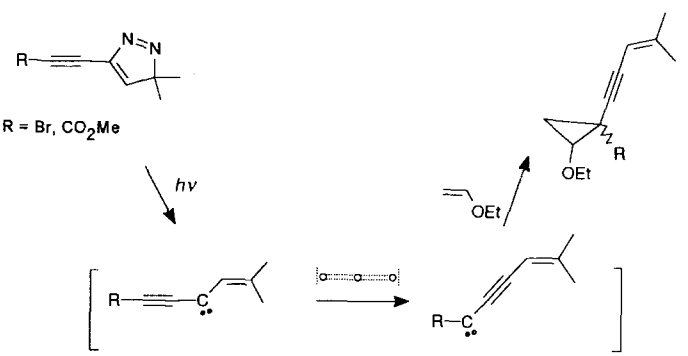
Scheme 28. General schematic representation of the bond-shift reaction of propynylidene.

systems, however, the shift is not detectable. Trapping reactions with *cis*- and *trans*-butene prove that the stereochemistry of the olefin is not completely preserved.[148] Presumably part of the formed propynylidene converts into the more stable triplet state prior to the addition step. The nonstereoselective addition of the triplet then is responsible for the formation of the other stereoisomer (Scheme 29). The work of Franck-Neumann et



Scheme 29. Stereochemistry of the addition of propynylidene to alkenes.

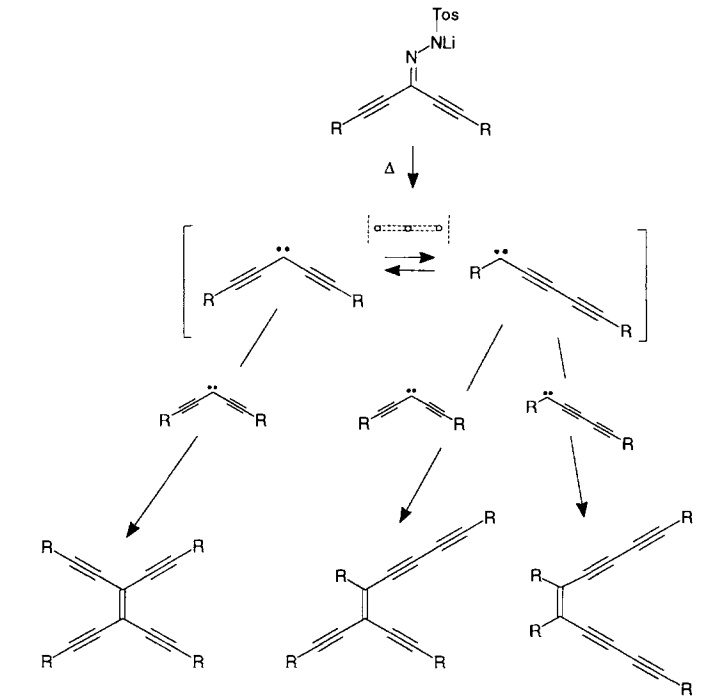
al.,[149, 150] in particular, on vinylsubstituted propynylidenes suggest that a fast bond-shift reaction in the singlet state of the carbene (Scheme 30) takes place. Even though the photolysis was carried out in pure vinyl ether as trapping reagent, the trapped product exclusively derives from the rearranged carbene intermediate.



Scheme 30. Bond-shift reactions of vinylpropynylidenes.

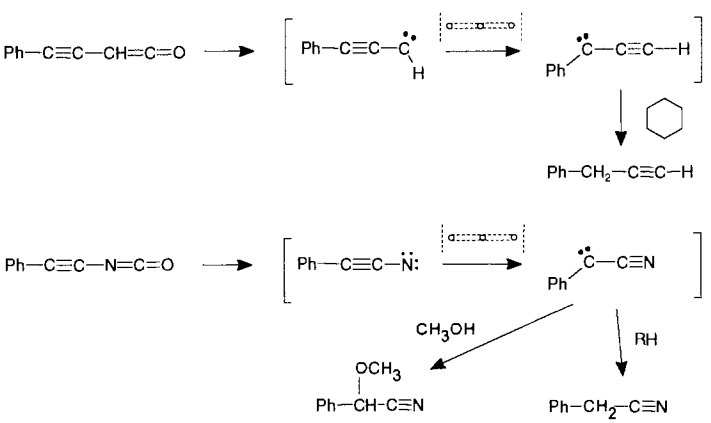
Another bond-shift reaction, though not necessarily in the singlet state, was observed by Hauptmann while generating diethynyl carbenes.[151] All three conceivable dimeric products derived from a 1,3-carbene shift were formed. Because the

dimerization presupposes a long-lived carbene species, the transition to the potential triplet ground state is possible prior to the recombination with another carbene (Scheme 31).



Scheme 31. Bond-shift reactions of diethynylcarbenes.

According to Boyer and Selvarajan the trapped products of phenylpropynylidene[152, 153] and (phenylethynyl)nitrene[154] also derive from a rearranged carbene. In the case of the nitrene, the isomeric carbene species should be favored thermodynamically because of the relative stability of the C≡N bond over the C≡C bond[155] (Scheme 32).



Scheme 32. Bond-shift reactions of phenylpropynylidene and (phenylethynyl)-nitrene.

If the lone-pair orbitals on both potential carbene centers are parallel, the delocalized system of electrons in the transition state of the bond-shift reaction is topologically equivalent to the π system of the cyclobutadiene dianion, according to topological analysis (Fig. 16). With six electrons and Hückel topology, the reaction is thermochemically allowed. An optimal overlap of the orbital basis is attained if the transition state adopts a W shape (C_s symmetry). A transition state with C_2 symmetry, that is, the participation of an empty p orbital and a lone-pair orbital in the delocalized system, would have four electrons and would therefore be forbidden.

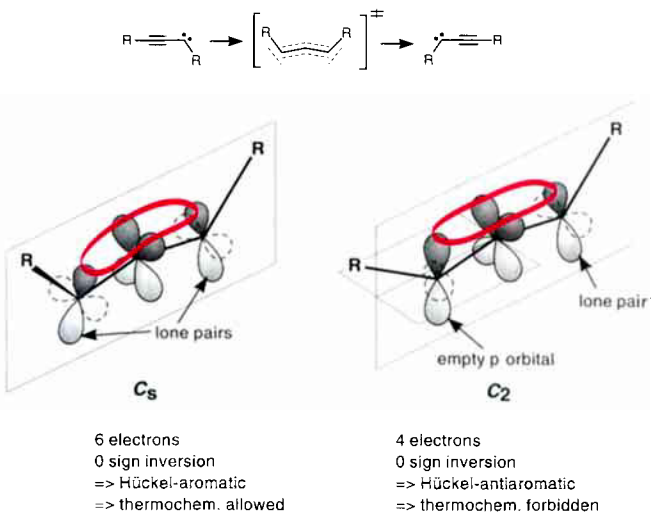


Fig. 16. Schematic representation and topological analysis of the bond-shift reaction of propynylidene.

Ab initio calculations of the singlet propynylidene on a reasonable theoretical level[156] confirm our qualitative predictions (Table 1, Fig. 17).[157] Highly interesting is the fact that on a high level of correlation the postulated "transition state" of the bond-shift reaction is more stable than the carbene species. The C_{2v} symmetrical form thus is not a transition state but an energy minimum on the singlet potential energy surface and accordingly the most stable structure of singlet propynylidene.

Table 1. Calculated relative energies of propynylidene with C_s and C_{2v} symmetry in kcal mol^{-1} (all values with for correction for the zero point energy).

Symmetry	MP2/6-31G*// MP2/6-31G*	MP4/6-31G*// MP4/6-31G*	QCISD/6-31G*// QCISD/6-31G*	QCISD(T)/6-31 + G** QCISD/6-31G*
C_s [a]	0.0	0.0	0.0	0.0
C_{2v} [a]	1.18	−0.24	−0.33	−1.39

[a] See Fig. 17.

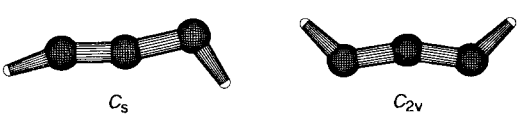


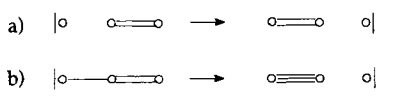
Fig. 17. Structures of propynylidene in C_s and C_{2v} symmetry, calculated with ab initio methods (QCISD/6-31G* level).

The ground state according to matrix investigations[158–162] and ESR studies[163] is the triplet spin state of propynylidene.

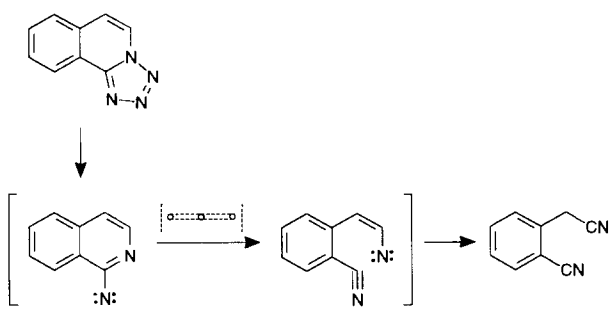
According to calculations[164–169] the triplet is more than 5 kcal mol^{-1} lower in energy than the lowest singlet state. Our calculations, however, suggest that the bond-shift reaction in the singlet state is faster than the spin inversion to the more stable triplet state.

4.4.2. Other Reactions

Theoretically two further complex reactions besides the bond-shift reaction are conceivable with two lone-pair terminators and $n = 1$ (Scheme 33). Reaction a) is rare as a concerted process; most of these abstraction reactions proceed via ylide intermediates.[170] Reaction b) presumably is the crucial step in some nitrene–nitrene and carbene–nitrene rearrangements,[171] such as, for example, those in Scheme 34.[172, 173]

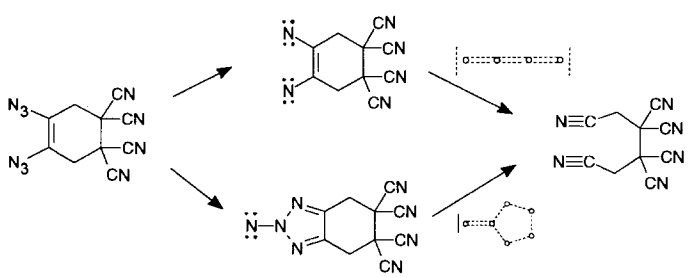


Scheme 33. Formal reaction schemes possible for complex reactions with lone-pair terminators and $n = 1$ (The sign ° represents an arbitrary element and | a lone pair.) Reaction c describes the bond-shift reaction.



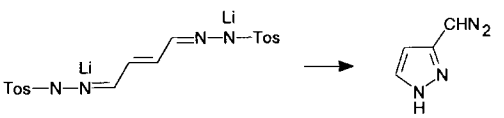
Scheme 34. Rearrangement of the (2-quinolyl)nitrene as an example of a complex nitrene–nitrene rearrangement.

Whereas in reactions with an odd number n (for example, bond-shift reaction $n = 1$) the lone pair of the starting compound is formally pushed to the other end of the linear system, reactions with an even number n imply the occurrence of two lone pairs in the starting compound or product. At least for bis(carbene)s or bis(nitrene)s, such coarctate processes are very unlikely (or only observable under exotic conditions). The fragmentation of *o*-phenylene diazides and vicinal vinyl diazides[174] most probably proceeds (as mentioned in Section 4.2.2) via a triazole intermediate and not a bis(nitrene) (Scheme 35).



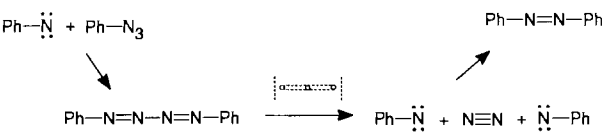
Scheme 35. The thermal and photochemical decomposition of vicinal vinyl azides leads to 1,4-dicyano compounds. Both the reaction path via the bis(azide) as well as that via the triazolylnitrene may be described as coarctate processes.

The fragmentation of the dilithio salt of the *trans*-butenedial ditosylhydrazone, published by Rodewald and Lee,[175] could not be reproduced by Maier and Wolf.[176] In place of the anticipated acetylene via the bis(carbene), 3-pyrazolediazomethane was formed from the intermediates of the Bamford–Stevens reaction (Scheme 36).



Scheme 36.

More probable, however, is an isoelectronic, coarctate process with lone-pair terminators and $n = 2$ for the photolysis of phenyl azide. Waddell et al. found a quantum yield of $\Phi = 300$ for the formation of azobenzene from phenyl azide in acetonitrile.[177–179] The chain mechanism of Scheme 37 was proposed as a conceivable explanation.



Scheme 37. Mechanism of the photolysis of phenyl azide. Phenylnitrene formed by photolysis adds to phenyl azide to afford diphenyltetraazadiene, which decomposes into two molecules of phenyl azide. The chain reaction leads to a quantum yield of $\Phi \gg 1$. Alternatively, the reaction of phenylnitrene with phenyl azide could lead directly to two molecules of phenylnitrene.

5. Back to Theory

5.1. Topology and Symmetry

In all examples shown so far, at those centers where two bonds are broken or made simultaneously, a set of two orthogonal p orbitals, twisted relative to the coordinate system of the remaining basis by 45°, were used for the construction of the orbital basis. The choice of the local coordinate system for the basis orbitals is arbitrary;[180] however, the orientation used in the above cases is neither coincidental nor purely empirical. It can be justified within the scope of qualitative MO theory. In symmetrical systems, the interrelation between qualitative MO theory based on the Hückel approximation and the topological analysis presented in this article can be directly illustrated.

The proper choice and orientation of the basis orbitals at these centers involves creating a set of orthogonal basis orbitals that are interconvertible by symmetry operations within the point group of the molecule, and that are not orthogonal relative to the remaining orbital basis. If one derives the symmetry-adapted MOs from this basis, *all* basis orbitals are included in each MO that is part of the delocalized system.[181] The totally

symmetrical MO without nodes is consequently topologically equivalent to the orbital basis of the topological analysis. Provided that there is a cyclic overlap of the orbital basis, the topology and nodal properties of the π orbitals of the corresponding aromatic or antiaromatic compounds are obtained directly by constructing the symmetry adapted MOs. This will be outlined in the following by means of the hypothetical[182] cycloaddition of two acetylene molecules to form tetrahedrane (Fig. 18).

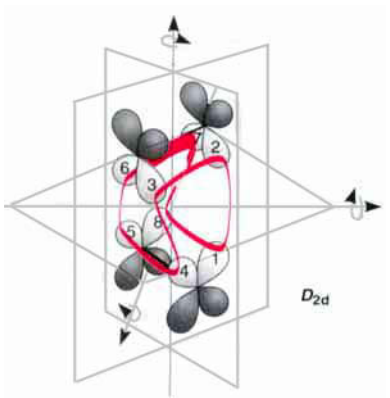


Fig. 18. Orbital basis of the photochemically allowed (hypothetical) addition of two acetylene units to form tetrahedrane. If the orbital axes basis orbitals form an angle of 45° with the corresponding mirror planes, all p functions are interconvertible by symmetry operations within the point group D_{2h}. The symmetry adapted MOs derived from this basis each contain all basis orbitals. Their topology of overlap and nodal properties correspond to those of the antiaromatic cyclooctatetraene (see text).

The point group of the whole system is D_{2d}. By rotating around the C–C bond axis the orientation of each p orbital ϕ is chosen in such a way that all basis orbitals are interconvertible by symmetry operations of the point group D_{2h}.[183] In this way all atomic orbitals that participate in the reaction are used as the basis for the reducible representation Γ of the point group D_{2h}. The reducible representation can be written as a linear combination of irreducible representations [Eq. (a)]. For the sake of simplicity we assume equal resonance integrals between all basis orbitals. The symmetry-adapted molecular orbitals then are derived by applying the projection operator method according to Scheme 38. Their topology and nodal properties exactly correspond to the antiaromatic, hypothetical D_{8h} cyclooctatetraene.[184] The reaction is thus thermochemically forbidden and photochemically allowed.[185]

$$\Gamma = A_1 + A_2 + B_1 + B_2 + 2E \qquad \text{(a)}$$

	Number of Nodes
$\Phi(A_1) = 1/\sqrt{8}\,(\phi_1 + \phi_2 + \phi_3 + \phi_4 + \phi_5 + \phi_6 + \phi_7 + \phi_8)$	0
$\Phi(E) = 1/\sqrt{8}\,(\phi_1 + \phi_2 + \phi_3 - \phi_4 - \phi_5 - \phi_6 - \phi_7 + \phi_8)$	2
$\Phi(E) = 1/\sqrt{8}\,(\phi_1 - \phi_2 - \phi_3 - \phi_4 - \phi_5 + \phi_6 + \phi_7 + \phi_8)$	2
$\Phi(B_1) = 1/\sqrt{8}\,(\phi_1 + \phi_2 - \phi_3 - \phi_4 + \phi_5 + \phi_6 - \phi_7 + \phi_8)$	4
$\Phi(B_2) = 1/\sqrt{8}\,(\phi_1 - \phi_2 - \phi_3 + \phi_4 + \phi_5 - \phi_6 - \phi_7 + \phi_8)$	4
$\Phi(E) = 1/\sqrt{8}\,(\phi_1 + \phi_2 - \phi_3 + \phi_4 - \phi_5 - \phi_6 + \phi_7 - \phi_8)$	6
$\Phi(E) = 1/\sqrt{8}\,(\phi_1 - \phi_2 - \phi_3 + \phi_4 + \phi_5 - \phi_6 - \phi_7 + \phi_8)$	6
$\Phi(A_2) = 1/\sqrt{8}\,(\phi_1 - \phi_2 + \phi_3 - \phi_4 + \phi_5 - \phi_6 + \phi_7 - \phi_8)$	8

Scheme 38. Symmetry-adapted MOs of the (hypothetical) dimerization of acetylene to tetrahedrane (see Fig. 18).

The topological method leads to the same result. It shows directly, and without explicit calculation of the MOs, a cyclic overlap of the basis orbitals (sequence -1-2-3-4-5-6-7-8-) without sign inversion. With eight electrons the transition state is antiaromatic and the reaction is thermochemically forbidden.

5.2. Simplified Rules

Because pericyclic and complex reactions profit from the same kind of stabilization in the transition state, the formal and descriptive relationship (described above in Section 2) has a sound physical foundation. Vice versa, the method of orbital transformation can be reduced to a descriptive level that allows the analysis of complex reactions on a purely formal basis. First the transition state is written in the form given in Figure 2. Each center p and q, at which one bond is broken and made or a lone pair is made or removed, is furnished with one basis orbital. The centers n, at which two bonds are broken or made simultaneously, receive each a set of two orthogonal p orbitals that are twisted by 45° relative to the other orbitals (Fig. 19).

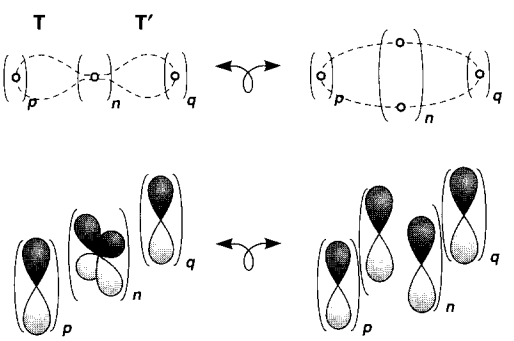


Fig. 19. Formal method to construct and analyze the orbital basis of complex reactions.

Subsequently the transformation to the corresponding cyclic system is performed, which is then analyzed according to the rules of the Hückel–Möbius method:

Complex reactions with $4n + 2$ electrons preferably proceed via Hückel-aromatic transition states and those with $4n$ electrons via Möbius-aromatic transition states.

If there are several stereochemically different, allowed reaction pathways, the following rule is used to select the energetically most favorable:

Of several allowed processes the one with the maximum overlap of the orbital basis is favored.

There is a special rule for carbene reactions:

There is always an allowed reaction path for carbene reactions if the orientation of the carbene center is not stereochemically fixed! If the remaining orbital basis (without the orbitals from the carbene) contains $4n$ electrons, the carbene center replenishes the system to $4n + 2$ electrons with its lone pair. In systems with $4n + 2$ electrons in the remaining orbital basis, the empty p orbital participates at the delocalized sys-

tem in the transition state. Stereochemical and mechanistical consequences only arise if the free orientation of the carbene center is hindered.

5.3. Comparison of the Topological Method with Alternative Methods

As mentioned in Section 3.1, there are three theoretical approaches for the qualitative treatment of pericyclic reactions, namely, correlation and state diagrams, frontier orbital considerations, and topological methods.

Advantages and disadvantages of the different methods have been discussed in detail by Dewar[25] and Zimmerman[27] and should just briefly be mentioned at this point. Being a perturbation method, the frontier orbital theory only is useful for reactions with an "early transition state", since a correct treatment of the interactions is restricted to the beginning of the reaction coordinate. Furthermore, a simple and useful application is limited to interactions between separated components. The extension to intramolecular reactions is rarely used in the literature. It suffers from the fact that first-order perturbations arise that are equal for all MOs (and not relevant exclusively for the frontier orbitals). On the other hand, the energies of the frontier orbitals and the size of the coefficients provide important information on reactivity and regioselectivity.[186] The application of the frontier orbital method presupposes the knowledge of the frontier orbitals, which are accessible only in symmetrical cases with paper-and-pencil methods.

Both the Woodward–Hoffmann rules, which are based on the number of supra- and antarafacial components, as well as the Hückel–Möbius method, are topological methods that are solely applicable to pericyclic reactions, or more precisely to a cyclic arrangement of orbitals. *The extension of the Hückel–Möbius method by topological transformation of the orbital basis, described in this article, offers the advantage that it is applicable to nonpericyclic reactions as well.* This has been illustrated by means of some examples of complex reactions.

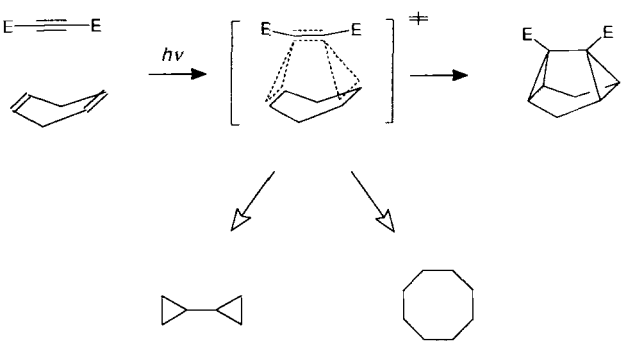
The only feasible alternative in the case of nonpericyclic reactions is the construction of correlation and orbital interaction diagrams. However, the analysis by correlation diagrams is restricted to symmetrical systems[187] and requires the knowledge of the MOs of starting materials and products. Our topological analysis in symmetric and multicomponent reactions is faster than other methods and easier for a nontheorist to apply. In many concerted reactions two or more symmetry-allowed pathways are conceivable. Whereas the rules of the conservation of orbital symmetry provide only yes/no statements,[188] the topological analysis additionally discriminates between several stereochemically allowed pathways (see the cyclopropylcarbene fragmentation, Fig. 7, or carbene addition to bicyclobutanes, Fig. 11).

The most important advantage of the topological method, however, is not provided by its simpler and more general applicability, but by the fact that reaction principles derived from it can be used as organizing principles for known reactions and for the prediction of new reactions. Starting from the principle of topological transformation, new coarctate transition states can thus be derived from cyclic orbital topologies. By combination with the algorithms for the generation of reactions,[189–192] it should be possible to predict a large number of new reactions.

6. Prediction of Reactions

6.1. Create your Own Transition State

Correlation and orbital interaction diagrams allow prediction whether a known reaction is allowed or forbidden; however, there is no way of prediciting an unprecedented symmetry-allowed reaction from a correlation diagram. Innovative achievements in chemistry usually do not rely on abstract, quantum theoretical deliberations but on a topological way of thinking.[4] The topological way of thinking in chemistry manifests itself in its most simple form in the structural formula. The synthetic chemist's customary combinatorial problem of setting up chemical structures, for example to evaluate the products of a reaction, is carried out by manipulation of structural formulas in form of graphs. The same way of thinking is not applicable to designing novel transition states of complex reactions or mechanisms. The reason for this is that the constitutional topology of the participating bonds of a reaction and the topology of the delocalized system of electrons in the transition state are not identical, as the example of the photochemical addition of acetylenes to 1,4-cyclohexadiene illustrates (Scheme 39).



Scheme 39. Comparison of the topology of the newly formed or broken bonds (bottom left) with the topology of the orbital overlap in the delocalized system of the transition state (bottom right) for the addition of methyl acetylenedicarboxylate to 1,4-cyclohexadiene. E = CO_2Me.

However, novel transition states can be predicted by topological transformation of known transition states. Figure 20 shows the derivation of the set of eleven conceivable coarctate transition states from the transition states of pericyclic reactions with six and eight centers (and illustrates the term coarctate). Each transition state again represents a general category of complex reactions comprising a number of specific reactions. They can also be systematically deduced by formal methods.

6.2. Generation of Reactions

By means of graph theory and under defined boundary conditions the complete set of conceivable reactions that proceed via the coarctate transition states can be generated (cf. Fig. 20). For

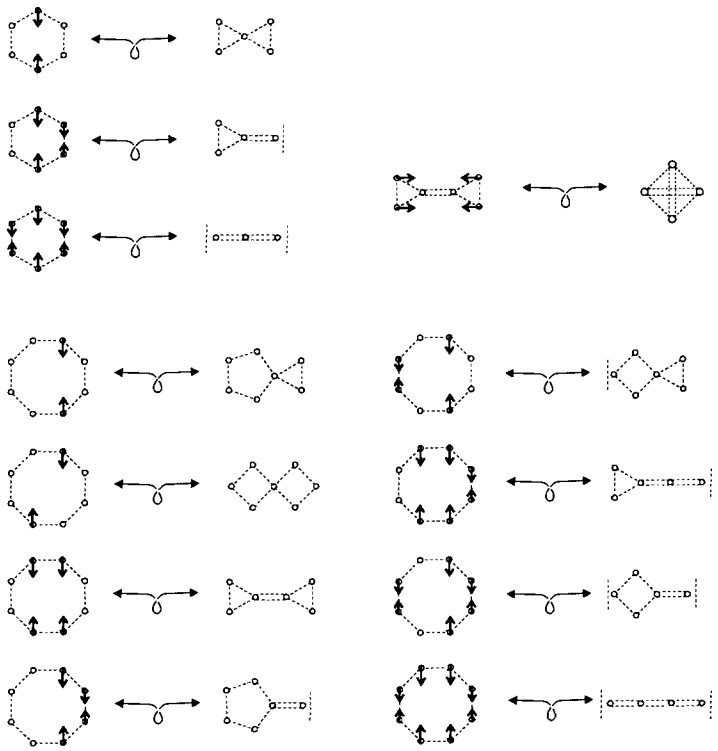


Fig. 20. Derivation of coarctate transition states from pericyclic transition states by topological transformation. The coarctate transition states can be further formally contracted by the same procedure (see last example).

that purpose we used the computer program IGOR[191] and our algorithm for generating subgraphs.[193] A similar approach with the program SYMBEQ was published by Zefirov et al.[194–196] Part of the reactions that are generated on a combinatorial basis should be known. The yet unknown reactions can be predicted as being theoretically conceivable and possibly verified in the laboratory.[5, 190, 197–200]

As an illustrative example we selected the complex reaction category with a three-membered ring terminator, a lone-pair terminator, and $n = 1$. The number of combinatorially possible solutions is restricted, since we are dealing with a small system with only four atoms in the reaction center. Moreover, systems of this size are still conveniently treated even with high-level ab initio methods. Thus the plausibility of the novel reactions can already be theoretically evaluated prior to the experimental verification.

As a boundary condition for the "chemistry" of the four atoms in the reaction center, it is useful to stipulate the "valence schemes" of carbon including carbene structures, because these valence schemes include the coordination properties of the most important heteroatoms. By substituting the not yet specified reaction centers with heteroelements in a second step, heteroanalogues are generated.[201] Structures with allene systems or triple bonds in three-membered rings are excluded as not chemically meaningful. Figure 21 shows the twelve "basic reactions"[202] that are conceivable and comply with these boundary conditions. Four of the twelve reactions are known: reaction 1 corresponds to the cyclopropylcarbene fragmentation, reaction 2 to the cyclopropenylcarbene fragmentation, reaction 3 to the addition of carbenes to bicyclobutanes, and reaction 4 to the known rearrangement of phenylcarbenes to ethynylcyclopentadienes.[171] Reactions 5-12 are unprecedented according to a careful search of the literature.

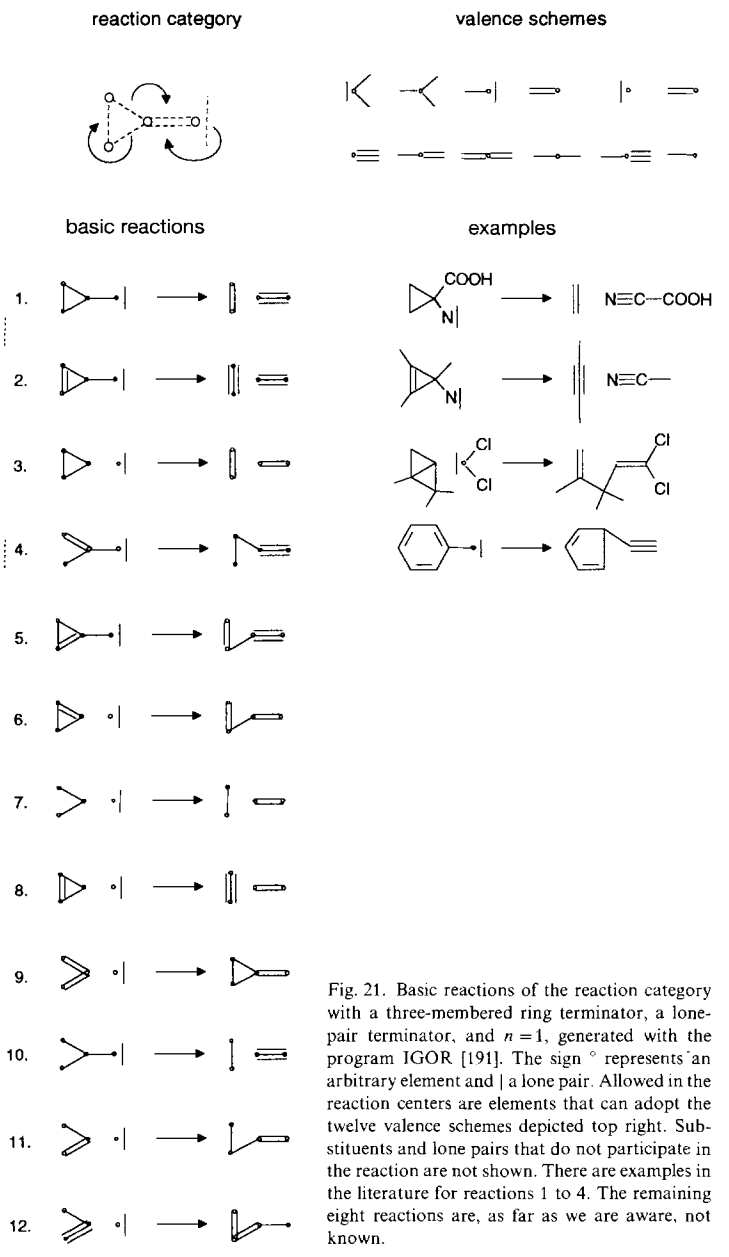


Fig. 21. Basic reactions of the reaction category with a three-membered ring terminator, a lone-pair terminator, and $n = 1$, generated with the program IGOR [191]. The sign ° represents an arbitrary element and | a lone pair. Allowed in the reaction centers are elements that can adopt the twelve valence schemes depicted top right. Substituents and lone pairs that do not participate in the reaction are not shown. There are examples in the literature for reactions 1 to 4. The remaining eight reactions are, as far as we are aware, not known.

The algorithms for the generation of reactions on a pure combinatorial basis do not give an indication for the practical feasibility of the reactions. Plausibility and possible side reactions have to be considered empirically. Thermodynamic and kinetic data in these small systems are predicted by ab initio methods with reasonable reliability. Reactions 6, 8, 9, 11, and 12, for instance, are bimolecular, and the addition of the carbene to the double bond most probably would compete with the coarctate process. In reactions 7 and 10 two sp^3-hybridized centers react with each other, which is unfavorable on sterical grounds. Only reaction 5 remains as a plausible prediction and therefore was selected for further investigations. In the parent

system (with four carbon atoms in the reaction core) the reaction corresponds to a rearrangement of 1-cyclopropenylcarbene to vinylacetylene.

Extensive ab initio calculations on the potential energy surface of C_4H_4[203] revealed only two stationary points with the 1-cyclopropenylcarbene structure (Fig. 22). Neither, however,

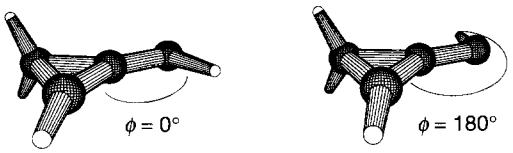


Fig. 22. C_s symmetric structures of 1-cyclopropenylcarbene calculated by ab initio methods (MP2/6-31G*//MP2/6-31G* level).

are minima; instead, according to a harmonic frequency analysis, they are transition states for the rotation around the carbene–cyclopropene C–C bond. If, starting from these two structures, the carbene H-atom is rotated around this bond while all other geometry parameters are optimized, the energy decreases continuously for both cases. At a torsional angle ϕ of $0 \pm 14°$ (or $180 \pm 14°$) the molecule rearranges spontaneously, as predicted, to vinylacetylene. This is likewise in accordance with the topological analysis of the coarctate transition state[204] of the reaction (Fig. 23). At a torsional angle of $\phi = 0°$, the empty

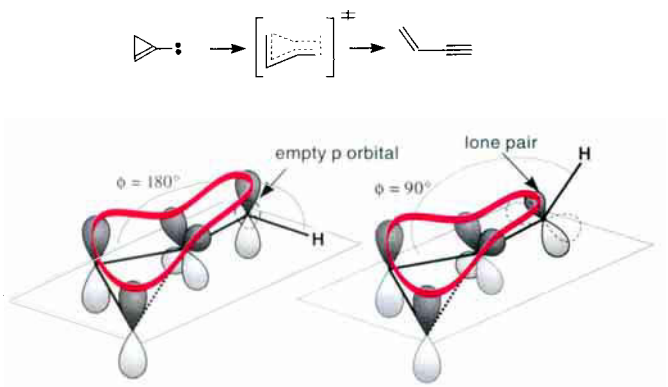


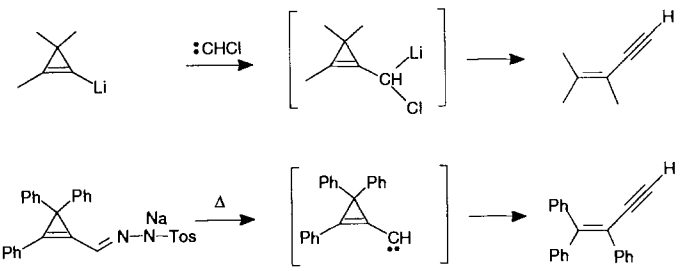
Fig. 23. Schematic representation and topological analysis of the rearrangement of 1-cyclopropenylcarbene to vinylacetylene.

p orbital of the carbene center overlaps with the remaining orbital basis to form a Hückel antiaromatic system; the reaction consequently is forbidden. If the carbene lone pair is turned out of the plane of the three-membered ring, a Hückel system with six electrons is formed, and the reaction therefore is thermochemically allowed.

Because the singlet state of the 1-cyclopropenylcarbene, according to our calculations, does not represent a minimum on the C_4H_4 energy surface but rearranges to vinylacetylene without an activation barrier, no side reactions are anticipated during experimental realization. No obstacles should thus bar the way of a practical verification, apart from potential problems in synthesizing the starting materials.

6.3. Experimental Verification

Trimethylcyclopropenyllithium was synthesized according to the methods of Closs et al.[205–207] and treated with dichloromethane. The intermediate carbenoid[208] formed by insertion of the incipient chlorocarbene into the C–Li bond, indeed rearranges to the corresponding vinylacetylene in 85% yield (Scheme 40). To test the mechanism further, another car-



Scheme 40. Experimental verification of the rearrangement of 1-cyclopropenylcarbene to vinylacetylene.

bene precursor, the tosylhydrazone of triphenylcyclopropene aldehyde,[209] was synthesized. The Bamford–Stevens reaction affords the corresponding vinylacetylene in 85% yield (Scheme 40)[189] in this case as well.

7. Outlook

In contrast to almost any other concerted organic reaction, the constitutional topology of the changing bonds and the overlap of the corresponding basis orbitals in the transition state of complex reactions are not identical[210] (see Scheme 39). This fact complicates not only the analysis of the mechanism, but also in particular, the prediction of unprecedented reactions of this type. Certainly not least for that reason, a large number of complex reactions are still waiting to be discovered. The insight into the formal relationships and physical principles presented here should help to develop this scarcely studied field of organic chemistry.[211, 212] Alongside linear (polar) and cyclic (pericyclic) reactions, the complex reactions form a third, smaller but important and cohesive class of concerted processes.

I would like to thank Professors R. Hoffmann, I. Ugi, and P. von R. Schleyer for helpful comments and discussions, and Molecular Design Ltd., the Fonds der Chemischen Industrie, and the Deutsche Forschungsgemeinschaft for financial support. I am particularly grateful to my wife. In intensive discussions and from the unbiased view of a nonchemist she suggested a number of improvements that contributed to the clearness of the article.

Received: January 22, 1993 [A 924IE]
German version: *Angew. Chem.* **1994**, *106*, ■

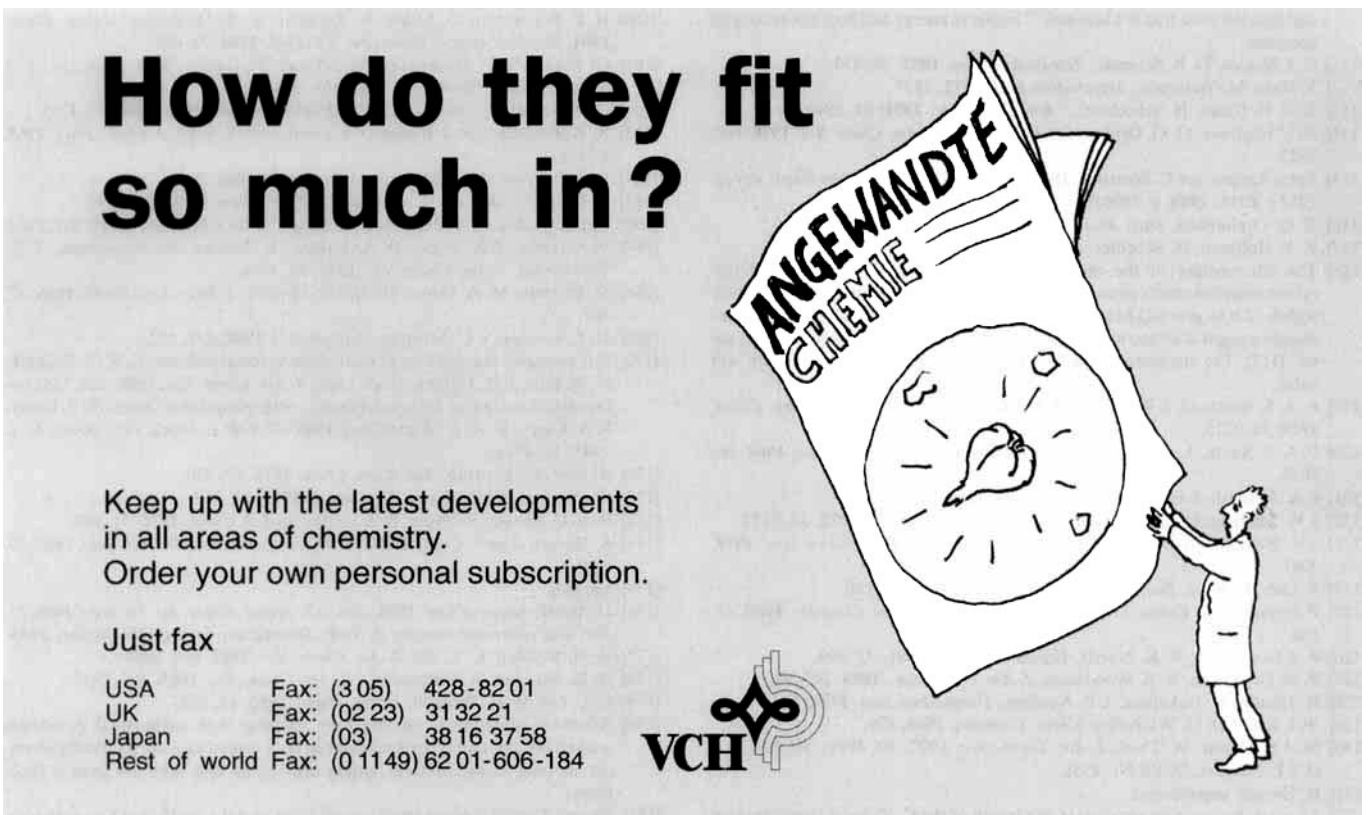
[1] R. B. Woodward, R. Hoffmann, *Angew. Chem.* **1969**, *81*, 797; *Angew. Chem. Int. Ed. Engl.* **1969**, *8*, 781.

[2] In contrast to geometry and energy and parameters derived therefrom, bond order, point charge, and resonance energy, for example, are not quantum theoretical observables and therefore are on principle not unambiguously

quantifiable: that is, the absolute values depend on a more or less arbitrarily defined method for their determination.
[3] See K. N. Houk, Y. Li, J. D. Evanseck, *Angew. Chem.* **1992**, *104*, 711; *Angew. Chem. Int. Ed. Engl.*, **1992**, *31*, 682, and references therein.
[4] N. J. Turro, *Angew. Chem.* **1986**, *98*, 872; *Angew. Chem. Int. Ed. Engl.* **1986**, *25*, 882.
[5] a) A. T. Balaban, *Rev. Roum. Chim.* **1967**, *12*, 875; b) J. B. Hendrickson, *Angew. Chem.* **1974**, *86*, 71; *Angew. Chem. Int. Ed. Engl.* **1974**, *13*, 47.
[6] R. Herges, C. Hoock, *Science*, **1992**, *255*, 711, and references therein.
[7] ORAC Ltd., 18 Lendheim Terrace, Woodhouse Lane, GB-Leeds LS2 9HD (United Kingdom). The data base contains reactions that are most important for organic synthesis, among others those of the "Theilheimer". The investigations were performed in 1988, the data base is now marketed by MDL under REACCS [8].
[8] REACCS, Molecular Design Ltd., 2132 Farallon Drive, San Leandro, CA 94577, USA.
[9] *Methoden Org. Chem. (Houben-Weyl) Vol. E19b, 4th ed. 1952–*, **1989**.
[10] A modified correlation approach, the "MO-following method", developed by Zimmerman, is not based on symmetry criteria but on the analysis of the nodal properties of the MOs: a) H. E. Zimmerman, *Acc. Chem. Res.* **1972**, *5*, 393; b) H. E. Zimmerman, *Org. Chem.* **1977**, *35*, 53.
[11] R. B. Woodward, R. Hoffmann, *J. Am. Chem. Soc.* **1965**, *87*, 395.
[12] R. Hoffmann, R. B. Woodward, *J. Am. Chem. Soc.* **1965**, *87*, 2046.
[13] R. Hoffmann, R. B. Woodward, *J. Am. Chem. soc.* **1965**, *87*, 4389.
[14] R. B. Woodward, R. Hoffmann, *Acc. Chem. Res.* **1968**, *1*, 17.
[15] H. C. Longuet-Higgins, E. W. Abrahamson, *J. Am. Chem. Soc.* **1965**, *87*, 2045.
[16] J. J. C. Mulder, L. J. Oosterhoff, *Chem. Commun.* **1970**, 305.
[17] W. J. van der Hart, J. J. C. Mulder, L. J. Oosterhoff, *J. Am. Chem. Soc.* **1972**, *94*, 5724.
[18] K. Fukui, *Bull. Chem. Soc. Jpn.* **1966**, *39*, 498.
[19] K. Fukui, H. Fujimono, *Bull. Chem. Soc. Jpn.* **1967**, *40*, 2018.
[20] K. Fukui, *Acc. Chem. Res.* **1971**, *4*, 57.
[21] M. G. Evans, E. Warhurst, *Trans. Faraday Soc.* **1938**, *34*, 614.
[22] M. G. Evans, *Trans. Faraday Soc.* **1939**, *35*, 824.
[23] M. G. Evans, M. Polanyi, *Trans. Faraday Soc.* **1938**, *34*, 11.
[24] M. J. S. Dewar, *Tetrahedron Suppl.* **1966**, *8*, 75.
[25] M. J. S. Dewar, *Angew. Chem.* **1971**, *83*, 859; *Angew. Chem. Int. Ed. Engl.* **1971**, *10*, 761.
[26] H. E. Zimmerman, *Science* **1966**, *153*, 837.
[27] H. E. Zimmerman, *Acc. Chem. Res.* **1971**, *4*, 272.
[28] H. E. Zimmerman, *J. Am. Chem. Soc.* **1966**, *88*, 1564.
[29] A. C. Day, *J. Am. Chem. Soc.* **1975**, *97*, 2431.
[30] E. Heilbronner, *Tetrahedron Lett.* **1964**, 1923.
[31] a) H. E. Zimmerman, L. R. Sousa, *J. Am. Chem. Soc.* **1972**, *94*, 834; b) see also ref. [10b].
[32] Topological transformations, according to the mathematical definition, are continuous deformations of figures, whose geometrical properties are not changed thereby, for example, streching, pressing, or turning (not tearing, cutting, or folding). Geometrical figures that can be transformed by topological transformations are called homoeomorphous. Cube and sphere, for instance, are homoeomorphous; however, sphere and torus are not homoeomorphous. The surface of a cube or of a sphere can be divided in two differently colored parts by a closed curve; this is not possible with a torus. A Hückel and a Möbius ribbon (Fig. 5) are not homoeomorphous, because for transformation the ribbon has to be torn (not a topological transformation), twisted by 180°, and pasted.
[33] The symbol for homoeomorphism resembles R. Hoffmann's isolobality symbol (*Angew. Chem.* **1982**, *94*, 725; *Angew. Chem. Int. Ed. Engl.* **1982**, *21*, 711), because there are also similarities in meaning.
[34] The orbital at center 4 in the transition state of the cyclopropylcarbene fragmentation is the orbital that corresponds to the carbene lone pair in the starting material and to a p orbital in the product, acetylene.
[35] R. Huisgen, *J. Org. Chem.* **1976**, *41*, 403.
[36] R. Huisgen, *Angew. Chem.* **1963**, *13*, 604; *Angew. Chem. Int. Ed. Engl.* **1963**, *2*, 565.
[37] R. Huisgen, *Angew. Chem.* **1980**, *92*, 979; *Angew. Chem. Int. Ed. Engl.* **1980**, *19*, 947.
[38] From the Latin coarctare, meaning to compress or contract.
[39] L. Friedman, H. Shechter, *J. Am. Chem. Soc.* **1960**, *82*, 1002.
[40] Reviews: a) J. Arct, U. H. Brinker, *Methoden Org. Chem. (Houben-Weyl) 4th ed 1952*–, Vol. E19b, **1989**, p. 337–375; b) W. Kirmse in *Carbene Chemistry*, 2nd ed. (Ed.: A. T. Blomquist) Academic Press, New York, **1970**, p. 467ff.; c) W. J. Baron, M. R. DeCamp, M. E. Hendrick, M. Jones, Jr., R. H. Levin, M. B. Sohn, *Carbenes 1973-1975* **1973**, *1*; d) T. T. Tidwell in *The Chemistry of the Cyclopropyl Group, Vol. 1* (Eds.: Z. Rappoport), Wiley, New York, **1987**, p. 616.
[41] P. B. Shelvin, M. L. McKee, *J. Am. Chem. Soc.* **1989**, *111*, 519.
[42] W. W. Schoeller, *J. Org. Chem.* **1980**, *45*, 2161.
[43] A. B. Levy, A. Hassner, *J. Am. Chem. Soc.* **1971**, *93*, 2051.
[44] D. S. Wulfman, T. R. Steinheimer, *Tetrahedron Lett.* **1972**, 3933.
[45] G. Szeimies, J. Harnisch, *J. Chem. Soc. Chem. Commun.* **1973**, 739.
[46] A. Hassner, A. B. Levy, E. E. McEntire, J. E. Galle, *J. Org. Chem.* **1974**, *39*, 585.
[47] J. Harnisch, G. Szeimies, *Chem. Ber.* **1979**, *112*, 3914.
[48] R. Jorritsma, H. Steinberg, T. J. de Boer, *Recl. Trav. Chim. Pays-Bas* **1981**, *100*, 307.
[49] G. Szeimies, U. Stiefken, R. Rink, *Angew. Chem.* **1973**, *85*, 173; *Angew. Chem. Int. Ed. Engl.* **1973**, *12*, 161.
[50] A. Guarino, A. P. Wolf, *Tetrahedron Lett.* **1969**, 655.
[51] R. R. Gallucci, M. Jones, Jr., *J. Am. Chem. Soc.* **1976**, *98*, 7704.
[52] Ethylene formed by this process is involved in a number of biological processes as a phytohormone, for example, the ripening of fruit; reviews: a) D. O. Adams, S. F. Yang, *Proc. Natl. Acad. Sci. USA* **1979**, *76*, 17; b) K. Lürssen, *Chem. Unserer Zeit* **1981**, *15*, 122; c) *Nachr. Chem. Tech. Lab.* **1984**, *32*, 697.
[53] R. M. Adlington, J. E. Baldwin, B. J. Rawlings, *J. Chem. Soc. Chem. Commun.* **1983**, 290.
[54] M. C. Pirring, G. M. McGeehan, *J. Org. Chem.* **1983**, *48*, 5144.
[55] K. B. Wiberg, G. J. Burgmaier, R. Warner, *J. Am. Chem. Soc.* **1971**, *93*, 246.
[56] K. B. Wiberg, M. G. Matturro, P. J. Okarma, M. E. Jason, W. P. Dailey, G. J. Burgmaier, W. F. Bailey, P. Warner, *Tetrahedron* **1986**, *42*, 1895.
[57] K. B. Wiberg, J. E. Hiatt, G. J. Burgmaier, *Tetrahedron Lett.* **1968**, 5855.
[58] M. A. Blaustein, J. A. Berson, *J. Am. Chem. Soc.* **1983**, *105*, 6337.
[59] W. Kirmse, K. H. Pook, *Angew. Chem.* **1966**, *78*, 603; *Angew. Chem. Int. Ed. Engl.* **1966**, *5*, 594.
[60] S. S. Olin, R. M. Venable, *J. Chem. Soc. Chem. Commun.* **1974**, 104.
[61] P. K. Freeman, D. G. Kuper, *J. Org. Chem.* **1965**, *30*, 1047.
[62] J. S. Swenton, J. A. Hyatt, T. J. Walker, A. L. Crumrine, *J. Am. Chem. Soc.* **1971**, *93*, 4808.
[63] J. W. Wheeler, R. H. Hung, Y. N. Vaishnav, C. C. Schroff, *J. Org. Chem.* **1969**, *34*, 545.
[64] T. V. Levashova, O. V. Semeikin, *Zh. Org. Khim.* **1980**, *16*, 53.
[65] J. Casanova, B. Waegell, *Bull. Soc. Chim. Fr.* **1975**, 598.
[66] T. V. Levashova, O. V. Semeikin, E. S. Balenkova, *Vestn. Mosk. Univ. Ser. 2 Khim* **1980**, *21*, 401.
[67] T. V. Levashova, O. V. Semeikin, E. S. Balenkova, *Vestn. Mosk. Univ. Ser. 2 Khim.* **1981**, *22*, 485.
[68] T. V. Levashova, O. V. Semeikin, E. S. Balenkova, U. N. Luzikov, *Zh. Org. Khim.* **1978**, *14*, 824.
[69] For other polycyclic systems in which the carbene is sterically fixed in the *endo* position and that undergo cyclopropylcarbene fragmentation as well see: a) tetracyclo[4.3.1.1^{4,8}.0^{2,10}]undec-3-ylidene: R. K. Murray, Jr., T. M. Ford, *J. Org. Chem.* **1977**, *42*, 1806; b) tricyclo[3.3.1.0^{2,8}]nona-3,6-diene-9-ylidene: H. Tsuruta, S. Mori, Y. Nishizawa, T. Mukai, S. Murahashi, K. Hino, K. Bansho, I. Moritani, *Chem. Lett.* **1974**, 1497; c) 2,9-didehydroadamantane-4-ylidene-(tetracyclo[4.3.1.0^{2,4}.0^{3,8}]decane-5-ylidene): R. K. Murray, Jr., T. M. Ford, *J. Org. Chem.* **1977**, *42*, 1806.
[70] S. J. Cristol, J. K. Harrington, *J. Org. Chem.* **1963**, *28*, 1413.
[71] The overall yield of nonpolymeric hydrocarbons was 19%. The allene most probably was formed under the basic conditions of the Bamford-Stevens reaction by rearrangement of the alkyne.
[72] P. K. Freeman, D. M. Balls, *J. Org. Chem.* **1967**, *32*, 2354.
[73] See [41]; calculations on the MP4SDTQ/6-31G*//3-21G level.
[74] R. Herges, unpublished; calculations on the MP4SDTQ/6-31G*//MP2/6-31G* + ZPE level; all stationary points were characterized by harmonic frequency analysis as minima or transition states.
[75] The third highest occupied orbital is termed HOMO-2.
[76] Program PERGRA: R. Sustmann, W. Sicking, Institut für Organische Chemie der Universität Essen, **1991**.
[77] QCISD(T)/6-31G*//MP2/6-31G* level; R. Herges unpublished.
[78] Review: H. F. Schaeffer III, *Science* **1986**, *231*, 1100.
[79] Review: H. Dürr, E.-M. Frühauf, *Methoden Org. Chem. (Houben-Weyl) 4th ed. 1952*–, E19b, **1989**, p. 775.
[80] L. B. Rodewald, H.-K. Lee, *J. Am. Chem. Soc.* **1973**, *95*, 623.
[81] G. Maier, F. Fleischer, *Tetrahedron Lett.* **1991**, *32*, 57.
[82] G. Maier, K. A. Reuter, L. Franz, *Tetrahedron Lett.* **1985**, *26*, 1845.
[83] G. Maier, M. Hoppe, K. Lanz, H. P. Reisenauer, *Tetrahedron Lett.* **1984**, *25*, 5645.
[84] J. Fink, H. Gümbel, P. Eisenbarth, M. Regitz, *Chem. Ber.* **1987**, *120*, 1027.
[85] S. Masamune, N. Nakamura, M. Suda, H. Ona, *J. Am. Chem. Soc.* **1973**, *95*, 848.
[86] G. Maier, R. Wolf, H.-O. Kalinowski, *Angew. Chem.* **1992**, *104*, 764; *Angew. Chem. Int. Ed. Engl.* **1992**, *31*, 738.
[87] E. H. White, R. E. K. Winter, R. Graeve, U. Zirngibl, E. W. Friend, H. Maskill, U. Mende, G. Kreiling, H. P. Reisenauer, G. Maier, *Chem. Ber.* **1981**, *114*, 3906.
[88] G. Maier, M. Hoppe, H. P. Reisenauer, C. Krüger, *Angew. Chem.* **1982**, *94*, 445; *Angew. Chem. Int. Ed. Engl.* **1982**, *21*, 437.
[89] G. Maier, *Angew. Chem.* **1989**, *101*, 1085; *Angew. Chem. Int. Ed. Engl.* **1989**, *28*, 1050.
[90] S. Masamune, M. Kato, *J. Am. Chem. Soc.* **1965**, *87*, 4190.
[91] G. Maier, H. P. Reisenauer, *Chem. Ber.* **1981**, *114*, 3916.
[92] G. L. Closs, A. M. Harrison, *J. Org. Chem.* **1972**, *37*, 1051.

[93] G. Maier, U. Schäfer, *Liebigs Ann. Chem.* **1980**, 798.
[94] U. J. Vogelbacher, M. Regitz, R. Mynott, *Angew. Chem.* **1986**, *98*, 835; *Angew. Chem. Int. Ed. Engl.* **1986**, *25*, 842.
[95] MP4SDTQ/6-31G*//MP2/6-31G* + ZPE level; R. Herges, unpublished; all stationary points were characterized by harmonic frequency analysis as minima or transition states.
[96] On the SCF level and without consideration of correlation (6-31G*//6-31G*), the transition state is calculated to be symmetric (C_s symmetry). The corresponding structure optimized on the MP2/6-31G* level in C_s symmetry, however, yields two imaginary frequencies. It is therefore not a transition state, but a stationary point of second order ("hill top"). Only after removal of the symmetry restrictions does optimization afford a strongly asymmetric structure, which turns out to be a transition state according to frequency analysis. Upon better treatment of the correlation (e.g., MCSCF), the transition state might prove to be more unsymmetrical or even a diradical intermediate might be found. A synchronous reaction can be ruled out on the grounds of these data.
[97] An UHF calculation of the transition state shows a high-spin contamination ($\langle S^2 \rangle = 0.911$).
[98] J. D. Evanseck, J. Mareda, K. N. Houk, *J. Am. Chem. Soc.* **1990**, *112*, 73.
[99] In the tetra-*tert*-butyl derivative (Scheme 8), the *endo* conformation is considerably more stable, pesumably on sterical grounds.
[100] A. Eschenmoser, D. Felix, G. Ohloff, *Helv. Chim. Acta* **1967**, *50*, 708.
[101] J. Schreiber, D. Felix, A. Eschenmoser, M. Winter, F. Gautschi, K. H. Schulte-Elte, E. Sundt, G. Ohloff, J. Kalvoda, H. Kaufmann, P. Wieland, G. Anner, *Helv. Chim. Acta* **1967**, *50*, 2101.
[102] D. Felix, J. Schreiber, G. Ohloff, A. Eschenmoser, *Helv. Chim. Acta* **1971**, *54*, 2896.
[103] R. Joos, Dissertation, ETH Zürich, **1970**.
[104] E. Zbiral, G. Nestler, K. Kischa, *Tetrahedron* **1970**, *26*, 1427.
[105] W. von E. Doering, J. F. Coburn, Jr., *Tetrahedron Lett.* **1965**, 991.
[106] K. B. Wiberg, G. M. Lampman, R. P. Ciula, D. S. Connor, P. Schertler, J. Lavanish, *Tetrahedron* **1965**, *21*, 2749.
[107] D. E. Applequist, J. W. Wheeler, *Tetrahedron Lett.* **1977**, 3411.
[108] J. E. Jackson, G. B. Mock, M. L. Tetef, G.-X. Zheng, M. Jones, Jr., *Tetrahedron* **1985**, *41*, 1453.
[109] Both transition states lead to the same trajectory according to our IRC calculations (IRC = intrinsic reaction coordinate, see K. Fukui, *Acc. Chem. Res.* **1981**, *14*, 363).
[110] The triplet state of fluorenylidene is more stable than the singlet state; the energy difference, however, is only 2 kcal mol^{-1} (P. B. Grasse, B.-E. Brauer, J. J. Zupanic, K. J. Kaufmann, G. B. Schuster, *J. Am. Chem. Soc.* **1983**, *105*, 6833). The two spin species probably are in equilibrium, and the singlet fluorenylidene is the reactive species. Diphenylcarbene has a triplet ground state and a singlet state that is 4 kcal mol^{-1} higher in energy and does not react with epoxides.
[111] C. J. Shields, G. B. Schuster, *Tetrahedron Lett.* **1987**, *28*, 853.
[112] Y. Hata, M. Watanabe, *Tetrahedron Lett.* **1972**, 3827.
[113] R. V. Hoffman, H. Schechter, *J. Am. Chem. Soc.* **1971**, *93*, 5940.
[114] R. V. Hoffman, G. G. Orphanides, H. Shechter, *J. Am. Chem. Soc.* **1978**, *100*, 7927.
[115] For a Review, see C. Wentrup, *Methoden Org. Chem. (Houben-Weyl) 4th ed. 1952–, E19b*, **1989**, p. 1000 ff.
[116] G. G. Orphanides, *Diss. Abstr. B.* **1972**, *33*, 1460.
[117] R. V. Hoffman, H. Schehter, *J. Am. Chem. Soc.* **1978**, *100*, 7934.
[118] The intermediacy of the carbene is not proved in all cases. Ethyl(2-furyl)diazoacetate reacts already at room temperature in solution quantitatively within 12 h to give (*Z*)-hex-4-ene-2-yn-6-al-1-carboxylate. The reaction conditions suggest a concerted elimination of nitrogen and rearrangement; see ref. [117]. The statements from the topological analysis, however, are still valid.
[119] P. A. S. Smith, G. J. W. Breen, M. K. Hajek, D. V. C. Awang, *J. Org. Chem.* **1970**, *35*, 2215.
[120] P. A. S. Smith, L. O. Krbechek, W. Reseman, *J. Am. Chem. Soc.* **1964**, *86*, 2025.
[121] P.A. S. Smith, J. G. Wirth, *J. Org. Chem.* **1968**, *33*, 1145.
[122] J. W. Schilling, C. E. Nordman, *Acta Crystallogr. Sect. B* **1972**, *28*, 2177.
[123] S.-I. Hayashi, M. Nair, D. J. Houser, H. Shechter, *Tetrahedron Lett.* **1979**, 2961.
[124] F. Lieb, K. Eiter, *Justus Liebigs Ann. Chem.* **1972**, *761*, 130.
[125] F. Povazanec, J. Kovac, D. Hesek, *Collect. Czech. Chem. Commun.* **1980**, *45*, 150.
[126] P. J. Newcombe, R. K. Norris, *Tetrahedron Lett.* **1981**, *22*, 699.
[127] P. N. Confalone, R. B. Woodward, *J. Am. Chem. Soc.* **1983**, *105*, 902.
[128] R. Hisada, N. Nakajima, J.-P. Anselme, *Tetrahedron Lett.* **1976**, 903.
[129] W. J. Irwin, D. G. Wibberley, *Chem. Commun.* **1968**, 878.
[130] M. J. S. Dewar, W. Thiel, *J. Am. Chem. Soc.* **1977**, *99*, 4899; MOPAC 6.0 (J. J. P. Stewart, QCPE Nr. 455).
[131] R. Herges, unpublished.
[132] As a suitable reaction coordinate, the length of the C - O bond that is broken during the reaction was chosen. All remaining geometry parameters were optimized.
[133] P. A. S. Smith, H. Dounchis, *J. Org. Chem.* **1973**, *38*, 2958.
[134] The reaction of 3-methyl-4-nitroso-1,5-diphenylpyrazole with triethylphosphite affording phenyl(phenylimino)acetonitrile probably proceeds via a nitrene intermediate as well: J. B. Wright, *J. Org. Chem.* **1969**, *34*, 2474.
[135] See [121].
[136] R. H. Hall, *J. Am. Chem. Soc.* **1965**, *87*, 1147. Analogous to the 2-aminobenzotriazolylbenzene (Scheme 22), a bis(nitrene) could theoretically be postulated as intermediate. Under the reaction conditions this is very unlikely. The reaction would then also be complex, with two lone-pair terminators and $n = 2$.
[137] C. D. Campbell, C. W. Rees, *Chem. Commun.* **1965**, 193.
[138] G. A. MacAlpine, J. Warkentin, *Can. J. Chem.* **1978**, *56*, 308.
[139] Diazo compounds can be excluded as intermediates in this case, because they would also fragment to nonsterically fixed systems in good yields (see *N*-aminoaziridine fragmentation [142].
[140] T. L. Gilchrist, D. P. J. Pearson, *J. Chem. Soc. Perkin Trans. 1* **1976**, 1257.
[141] M. J. S. Dewar, *J. Am. Chem. Soc.* **1984**, *106*, 209.
[142] D. Felix, J. Schreiber, K. Piers, U. Horn, A. Eschenmoser, *Helv. Chim. Acta* **1968**, *51*, 1461.
[143] D. Felix, R. K. Müller, U. Horn, R. Joos, J. Schreiber, A. Eschenmoser, *Helv. Chim. Acta* **1972**, *55*, 1277.
[144] P. Borevang, H. Hjort, R. T. Rapala, R. Edie, *Tetrahedron Lett.* **1968**, 4905.
[145] R. Askani, *Chem. Ber.* **1965**, *98*, 3618.
[146] K. Fujita, K. Matsui, T. Shono, *Nippon Kagaku Kaishi* **1975**, *6*, 1024.
[147] M. Takahashi, *Tetrahedron Lett.* **1968**, 3387.
[148] P. S. Skell, J. Klebe, *J. Am. Chem. Soc.* **1960**, *82*, 247.
[149] M. Franck-Neumann, P. Geoffroy, J. J. Lohmann, *Tetrahedron Lett.* **1983**, *24*, 1775.
[150] M. Franck-Neumann, P. Geoffroy, *Tetahedron Lett.* **1983**, *24*, 1779.
[151] H. Hauptmann, *Tetrahedron* **1976**, *32*, 1293.
[152] R. Selvarajan, J. H. Boyer, *J. Org. Chem.* **1971**, *36*, 1679.
[153] See also: R. F. C. Brown, F. W. Eastwood, K. J. Harrington, G. L. McMullen, *Aust. J. Chem.* **1974**, *27*, 2393.
[154] J. H. Boyer, R. Selvarajan, *J. Am. Chem. Soc.* **1969**, *91*, 6122.
[155] Calculations and experimental studies predict a bent triplet cyano carbene structure for HCCN: E. T. Seidel, H.-F. Schaefer III, *J. Chem. Phys.* **1992**, *96*, 4449 and references therein.
[156] As known from experience the calculation of highly unsaturated carbenes with ab initio methods requires large basis sets and in particular an adequate treatment of the correlation energy.
[157] R. Herges, unpublished.
[158] A. J. Merer, *Can. J. Phys.* **1967**, *45*, 4103.
[159] C. F. Kang, Dissertation, Michigan State University, **1972**.
[160] H. P. Reisenauer, G. Maier, A. Riemann, R. W. Hoffmann, *Angew. Chem.* **1984**, *96*, 596; *Angew. Chem. Int. Ed. Engl.* **1984**, *23*, 641.
[161] G. Maier, H. P. Reisenauer, W. Schwab, P. Carsky, B. A. Hess, Jr., L. J. Schaad, *J. Am. Chem. Soc.* **1987**, *109*, 5183.
[162] G. Maier, H. P. Reisenauer, W. Schwab, *J. Chem. Phys.* **1989**, *91*, 4763.
[163] R. A. Bernheim, R. J. Kempf, J. V. Gramas, P. S. Skell, *J. Chem. Phys.* **1965**, *43*, 196.
[164] D. J. DeFrees, A. D. McLean, *Astrophys. J.* **1986**, *308*, L31.
[165] V. Jonas, M. Böhme, G. Frenking, *J. Phys. Chem.* **1992**, *96*, 1640.
[166] C. E. Dykstra, C. A. Parsons, C. L. Oates, *J. Am. Chem. Soc.* **1979**, *101*, 1962.
[167] W. J. Hehre, J. A. Pople, W. A. Lathan, L. Radom, W. Wasserman, Z. R. Wasserman, *J. Am. Chem. Soc.* **1976**, *98*, 4378.
[168] D. Maynau, M. A. Garcia-Bach, J. P. Malrieu, *J. Phys. Les Ulis Fr.* **1986**, *47*, 207.
[169] D. L. Cooper, S. C. Murphy, *Astrophys. J.* **1988**, *333*, 482.
[170] For example, the addition of methylene to formaldehyde (G. K. S. Prakash, R. W. Ellis, J. D. Felberg, G. A. Olah, *J. Am. Chem. Soc.* **1986**, *108*, 1341) or the desulfuration of thioxocarbonates with phosphorus bases (E. J. Corey, F. A. Carey, R. A. E. Winter, *ibid.* **1965**, *87*, 934; E. Block, *Org. React. N. Y.* **1983**, *30*, 457).
[171] Review: C. Wentrup, *Top. Curr. Chem.* **1976**, *62*, 210.
[172] C. Wentrup, W. D. Crow, *Tetrahedron* **1971**, *27*, 367.
[173] R. F. C. Brown, F. Irvine, R. J. Smith, *Aust. J. Chem.* **1972**, *25*, 607.
[174] K. Banert, *Angew. Chem.* **1987**, *99*, 932; *Angew. Chem. Int. Ed. Engl.* **1987**, *26*, 879.
[175] See [80].
[176] G. Maier, *Angew. Chem.* **1988**, *100*, 317; *Angew. Chem. Int. Ed. Engl.* **1988**, *27*, 309, and references therein; B. Wolf, Disseration, Universität Gießen, **1985**.
[177] W. H. Waddell, C. L. Go, *J. Am. Chem. Soc.* **1982**, *104*, 5804.
[178] W. H. Waddell, N. Feilchenfeld, *J. Am. Chem. Soc.* **1983**, *105*, 2897.
[179] C. L. Go, W. H. Waddell, *J. Org. Chem.* **1983**, *48*, 2897.
[180] Arbitrary orientations obtained by rotating both orthogonal p orbitals around the axis that is perpendicular to both orbital axes are physically identical, as long as the orbitals remain orthogonal and both are pure p functions.
[181] Except if a nodal plane intersects an atom and the coefficient becomes zero.

[182] The reaction has in fact been tried (unsuccessfully, though) in systems where both acetylenic units are fixed in a perpendicular geometry by a molecular frame: a) H. A. Staab, E. Wehinger, W. Thorwart, *Chem. Ber.* **1972**, *105*, 2290, 2310, and 2320; b) E. H. White, A. A. F. Sieber, *Tetrahedron Lett.* **1967**, 2713; c) E. Müller, J. Heiss, M. Sauerbier, *Tetrahedron Lett.* **1968**, 1195; d) R. D. Stephens, C. E. Castro, *J. Org. Chem.* **1963**, *28*, 3313.
[183] When the p orbitals are parallel to the mirror planes, only half of the basis orbitals would be interconvertible by symmetry operations.
[184] MOs with an equal number of nodal planes are here not neccesarily degenerate (in contrast to D_{8h}-cyclooctatetraene). This is only the case in simple ring systems with D_{nh} symmetry.
[185] The reaction failed in the laboratory probably because it is photochemically allowed, but the excitation to the A_2 state that correlates with the product is forbidden and, in addition, lies energetically higher than the allowed transition to the E state.
[186] Review: I. Fleming, "Frontier Orbitals and Organic Chemical Reactions", Wiley, New York, **1976**.
[187] Exception is the MO-following method by Zimmerman, which does not rely on symmetry criteria, but on the nodal properties of the MOs, see [10, 31].
[188] „The orbital symmetry argument proscribes a certain approach geometry. It does not define which reaction path among the myriad other possibilities available will be followed. To establish the favored reaction path we resort to semiempirical molecular orbital calculations" (R. Hoffmann, R. Gleiter, F. B. Mallory, *J. Am. Chem. Soc.* **1970**, *92*, 1460).
[189] R. Herges, *J. Chem. Inf. Comput. Sci.* **1990**, *30*, 377.
[190] I. Ugi, J. Bauer, K. Bley, A. Dengler, A. Dietz, E. Fontain, B. Gruber, R. Herges, M. Knauer, K. Teitsam, N. Stein, *Angew. Chem.* **1993**, *105*, 210; *Angew. Chem. Int. Ed. Eng.* **1993**, *32*, 201.
[191] J. Bauer, R. Herges, E. Fontain, I. Ugi, *Chimia* **1985**, *39*, 43.
[192] N. S. Zefirov, S. S. Trach, *Anal. Chim. Acta* **1990**, *235*, 115.
[193] The combinatorial problem can be reduced to the graph theoretical problem of finding all nonisomorphic, spanning subgraphs of the graph of the transition state, see [189].
[194] S. S. Trach, I. I. Baskin, N. S. Zefirov, *Zh. Org. Khim.* **1988**, *24*, 1121.
[195] S. S. Trach, I. I. Baskin, N. S. Zefirov, *Zh. Org. Khim.* **1989**, *25*, 1585.
[196] See [192].
[197] R. Herges in *Chemical Structures* (Eds.: W. Warr), Springer, Berlin, **1988**, p. 385.
[198] R. Herges, *Tetrahedron Comput. Methodol.* **1988**, *1*, 15.
[199] R. Herges, I. Ugi, *Angew. Chem.* **1985**, *97*, 596; *Angew. Chem. Int. Ed. Engl.* **1985**, *24*, 594.
[200] D. Forstmeyer, J. Bauer, E. Fontain, R. Herges, R. Herrmann, I. Ugi, *Angew. Chem.* **1988**, *100*, 1618; *Angew. Chem. Int. Ed. Engl.* **1988**, *27*, 1558.
[201] The procedure corresponds to the one used by R. Huisgen for generating the 18 1,3-dipolar species with the elements C, O, and N: R. Huisgen, *Angew. Chem.* **1963**, *75*, 604; *Angew. Chem. Int. Ed. Engl.* **1963**, *2*, 565.
[202] For the definition of basis reactions see refs. [197, 198].
[203] R. Herges, unpublished.
[204] Because 1-cyclopropenylcarbene is not a minimum on the potential energy surface of C_4H_4 but rearranges to vinylacetylene with no barrier of activation, there is no transition state structure for this reaction. The topological analysis therefore assumes a hypothetical transition state in which all participating bonds are partly broken or made.
[205] G. L. Closs, L. E. Closs, W. A. Böll, *J. Am. Chem. Soc.* **1963**, *85*, 3796.
[206] G. L. Closs, L. E. Closs, *J. Am. Chem. Soc.* **1963**, *85*, 99.
[207] G. L. Closs, L. E. Closs, W. A. Böll, *J. Am. Chem. Soc.* **1961**, *83*, 2015
[208] For similar reactions of organolithium compounds with dichloromethane and subsequent intramolecular reaction of the carbenoid, see: a) T. J. Katz, E. J. Wang, N. Acton, *J. Am. Chem. Soc.* **1971**, *93*, 3782; b) U. Burger, G. Gandillon, J. Mareda, *Helv. Chim. Acta* **1981**, *64*, 844.
[209] I. N. Domin, E. F. Zhuravleva, V. L. Serebrov, R. R. Bekmukhametov, *Khim. Geterotsikl. Soedin.* **1978**, *8*, 1091.
[210] Another exception is the concerted di-π-methane rearrangement. Only one of the two double bonds is affected by the photorearrangement, even though both of them are involved in the transition state and both are essential for the reaction: a) S. S. Hixson, P. S. Mariano, H. E. Zimmerman, *Chem. Rev.* **1973**, *73*, 531; b) H. E. Zimmerman, *Acc. Chem. Res.* **1982**, *15*, 312.
[211] With the boundary conditions valid in Figure 21, 74 basis reactions are conceivable for the category of complex reactions with lone-pair and five-membered ring terminators and $n = 2$. Most of them are yet unknown.
[212] Some of the most important epoxidation reactions also proceed via coarctate transition states. Prediction of the mechanism and stereochemistry of these reactions would be of practical interest and will be subject of further studies.



Protein Structure Determination with Three- and Four-Dimensional NMR Spectroscopy

Hartmut Oschkinat,* Thomas Müller, and Thorsten Dieckmann

Structural biology has made important contributions to the understanding of biological processes. In recent years an increasing amount of structural information has also been derived from NMR spectroscopic studies, often with special emphasis on dynamic aspects. The introduction of three- and four-dimensional techniques has greatly simplified protein structure determination by NMR spectroscopy, which has in fact become routine. In the past it was more of an art to interpret the complicated NOESY spectra of proteins, but the application of three-dimensional techniques now makes the interpretation of protein spectra straightforward.

In this review we discuss the most important multidimensional NMR techniques along with suitable applications. The emphasis is put less on the discussion of individual pulse sequences than on their application to the structure determination of proteins.

1. Introduction

NMR spectroscopy is now well established as a method for the structure determination of small proteins and DNA fragments.[1] Since it allows the investigation of biological macromolecules in solution and offers additional insight into dynamic phenomena, NMR spectroscopy has proved to be a complementary method to X-ray crystallography. The most important prerequisite for this development was the introduction of two-dimensional (2D) NMR spectroscopy.[2–6] This enabled the interpretation of the complex NMR spectra of proteins and DNA and the determination of the parameters needed for structure calculation, for example, nuclear Overhauser effects (NOEs)[7] and coupling constants.[8, 9] These parameters correlate with distances between nuclei and dihedral angles, which provide the basic data for the calculation of three-dimensional structures using distance geometry[10, 11] and molecular dynamics[12, 13] programs.

The investigation of proteins by NMR spectroscopic methods was first limited to small molecules up to a size of 80 amino acids,[14–20] since the signal overlap in 2D spectra of larger proteins was too extreme. The development of three-dimensional (3D)[21–26] and four-dimensional (4D) NMR techniques[27] overcame this barrier. It is now possible to examine systems with molecular weights of up to 35 kDa when the proteins are uniformly labeled with ^{13}C and ^{15}N. The size of the proteins that can be investigated is still restricted by the transverse relaxation time, which becomes shorter with increasing molecular weight. An additional restriction may be caused by the complexity of the spectra; if a protein is composed of more than 250 amino acids, its 3D spectra will also show strongly overlapping signals. Examples of larger proteins whose structures have been investigated by multidimensional NMR spectroscopy include interleukin-1β,[28] the cyclophilin/cyclosporin complex,[29] and the calmodulin target peptide complex.[30]

The principles applied in 3D and 4D spectroscopy do not differ greatly from those already known from 2D spectroscopy.[6] We will therefore not discuss the pulse sequences here in detail, but rather their application in connection with the structure determination of proteins. After a short introduction to 3D and 4D NMR spectroscopy, a basic set of experiments will be illustrated by studies on interleukin-4 (IL-4)[31, 32] and chicken albumin cystatin (cystatin),[33, 34] whose structures were determined by NMR spectroscopy.

2. Multidimensional NMR Spectroscopy

The basic elements of 3D and 4D NMR spectroscopy are already included in 2D NMR spectroscopy. The general term "multidimensional NMR spectroscopy" applies for all of these techniques. In a typical 2D pulse sequence, given as

preparation – evolution (t_1) – mixing – detection (t_2)

the crucial step is the "coherence transfer".[5] During the evolution time, a nucleus A precesses with its characteristic frequency. A second nucleus B, which interacts with nucleus A by coher-

[*] Dr. H. Oschkinat, Dipl.-Chem. T. Dieckmann
European Laboratory for Molecular Biology
Meyerhofstrasse 1, D-69012 Heidelberg (FRG)
Telefax: Int. code + (6221)387-306
Dipl.-Chem. T. Müller
Institut für Physiologische Chemie
der Universität Würzburg

 © VCH Verlagsgesellschaft mbH, D-69451 Weinheim, 1994 0570-0833/94/0303-0277 $ 10.00+.25/0

ence transfer during the mixing time, is excited, and its frequency is subsequently detected.

A set of experiments can be acquired in which the evolution time is increased for each experiment in suitable steps. Detection in t_2 and Fourier transformation gives a signal of nucleus B that is modulated with the frequency of nucleus A. The signals resulting from different t_1 settings are ordered in a 2D matrix. A second independent Fourier transformation of the orthogonal data vectors provides a signal with two different frequency coordinates, a 2D cross peak. It is obvious that at the end of such a pulse sequence another mixing time can be added before detection. This gives us the general form of a multidimensional NMR experiment:

preparation–(evolution–mixing)$_n$–detection

The individual multidimensional NMR experiments are distinguished by the applied excitation and mixing procedures (Fig. 1). Most of these are the same as those used in 2D spectroscopy and are combined like building blocks to give a 3D or 4D sequence.[6] The COSY (correlated spectroscopy)[3, 35–38] and TOCSY (total correlated spectroscopy)[39–41] sequences give the correlations through chemical bonds, while the NOESY (nuclear Overhauser and exchange spectroscopy)[42] and ROESY (rotating frame Overhauser effect spectroscopy)[43] mixing sequences identify neighboring nuclei through space by means of cross relaxation. The HMQC (heteronuclear multiple quantum coherence)[44, 45] and HSQC (heteronuclear single quantum coherence) sequences[46, 47] are analogous to the COSY sequence but correlate different nuclei (e.g. protons and carbon nuclei). In principle the multidimensional experiments can also be understood as a combination of 2D techniques. For this reason in the nomenclature of the 3D techniques the names of the underlying 2D techniques are combined (e.g. TOCSY-NOESY, NOESY-HMQC) or, as is practiced for most triple-resonance experiments, the participating nuclei are listed. A 3D-HCACO experiment, for example, gives a correlation between the α proton, the α carbon atom, and the carbonyl carbon atom of a single amino acid in the protein. Nuclei given in parentheses are not detected but are involved in coherence transfer (e.g. 3D-HCA(CO)N). A selection of pulse sequences used for structure analysis of proteins is given in Table 1. Figure 2 shows a region of the 3D-TOCSY-NOESY spectrum of interleukin-4.

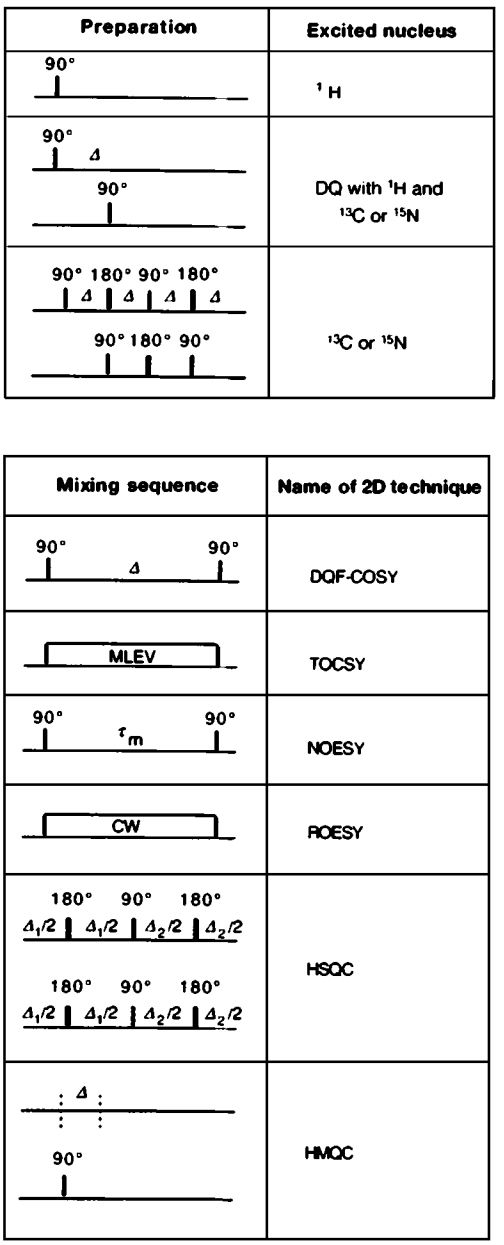


Fig. 1. Some common pulse sequences for excitation and mixing in multidimensional NMR experiments. DQ = double quantum, DQF = double quantum filtered, CW = continuous wave, MLEV = composite pulse mixing sequence. Other abbreviations are explained in the text.



Hartmut Oschkinat, born February 28, 1957, in Frankfurt am Main, studied chemistry in Frankfurt starting in 1975. His studies were interrupted by time spent in community service and with Ray Freeman's research group in Oxford. He earned his Ph.D. in 1985 under the direction of Horst Kessler. Following postdoctoral research with Geoffey Bodenhausen in Lausanne, he worked as an NMR spectroscopist at the Max-Planck-Institut für Biochemie in Martinsried from 1987 to 1991. Has has been a group leader at the EMBL in Heidelberg since 1991. His research interests focus on the determination of protein structures in solution and the study of structures and functions of membrane-bound proteins.

Table 1. A selection of 3D and 4D NMR techniques used in protein structure determination.

Experiment	Information/linkage obtained	Ref.
a) *unlabeled proteins—homonuclear experiments*		
3D-TOCSY-TOCSY	^{1}H spin systems/amino acids	[66]
3D-TOCSY-NOESY	sequential assignment of the spin systems, identification of NOEs	[122]
3D-NOESY-NOESY	identification of NOEs	[82–86]
b) *^{15}N labeled proteins*		
3D-TOCSY-^{1}H-^{15}N-HMQC/HSQC	^{1}H spin systems, ^{15}N shifts	[96–100]
3D-NOESY-^{1}H-^{15}N-HMQC/HSQC	sequential assignment of the spin systems, identification of NOEs with amide protons	[96–100]
3D-HNHB	$H_N(i)$-N(i)-$H_\beta(i)$, stereospecific assignment of methyl protons	[111]
c) *^{13}C-^{15}N labeled proteins*		
3D-TOCSY-^{1}H-^{13}C-HMQC/HSQC	^{1}H spin systems, ^{13}C shifts	[96–100]
3D-NOESY-^{1}H-^{13}C-HMQC/HSQC	sequential assignment of the spin systems, in particular identification of NOEs between side chains	[96–100]
3D-HCCH-COSY	^{1}H spin systems, ^{13}C shifts	[117, 118]
3D-HCCH-TOCSY	^{1}H spin systems, ^{13}C shifts	[119]
3D-HC(C)NH-TOCSY	connection of H_N and side-chain ^{1}H and ^{13}C	[114]
3D-H(CCO)NH	correlation of all side-chain ^{1}H and ^{13}C of amino acid i with $H_N(i+1)$	[112, 113]
H(CA)NH	$H_\alpha(i)$-N(i)-$H_N(i)$	[27]
3D-HCACO	$H_\alpha(i)$-$C_\alpha(i)$-CO(i)	[101]
3D-HNCA	$H_N(i)$-N(i)-$C_\alpha(i)$/$C_\alpha(i-1)$	[101, 102]
3D-HNCACB	$H_N(i)$-N(i)-$C_\alpha(i)$/$C_\alpha(i-1)$/$C_\beta(i)$/$C_\beta(i-1)$	[103]
3D-HN(CA)NNH	$H_N(i)$-N($i+1$)-$H_N(i+1)$	[105]
3D-HA(CA)NNH	$H_\alpha(i)$/$H_\alpha(i-1)$-N(i)-$H_N(i)$	[105]
3D-HN(NCA)NNH	$H_N(i)$-N($i+1$)-$H_N(i+1)$	[104]
3D-HCA(CO)N	$H_\alpha(i)$-$C_\alpha(i)$-N($i+1$)	[101, 106]
3D-HNCO	$H_N(i)$-N(i)-CO($i-1$)	[101]
3D-HN(CA)HA	$H_N(i)$-N(i)-$H_\alpha(i)$/$H_\alpha(i-1$)	[107]
3D-HN(CO)CA	$H_N(i)$-N(i)-$C_\alpha(i-1$)	[108]
3D-HN(COCA)HA	$H_N(i)$-N(i)-$H_\alpha(i-1$)	[109]
3D-H(N)CACO	H_N-$C_\alpha(i)$/$C_\alpha(i-1)$-CO(i)/CO($i-1$)	[110]
3D-H(C)(CO)NH-TOCSY	correlation of side-chain ^{1}H and ^{13}C with $H_N(i,i-1)$ and N($i,i-1$)	[144]
4D-HCANNH	$H_\alpha(i)$-$C_\alpha(i)$-N(i)-$H_N(i)$	[115, 116]
4D-HCA(CO)NNH	$H_\alpha(i)$-$C_\alpha(i)$-N($i+1$)-$H_N(i+1)$	[115, 116]
4D-HNCAHA	$H_N(i)$-N(i)-$C_\alpha(i)$-$H_\alpha(i)$	[115, 116]
4D-HCCH-TOCSY	^{1}H spin systems, ^{13}C shifts	[120]
4D-^{1}H-^{13}C-HMQC-NOESY-^{1}H-^{13}C-HMQC	identification of NOEs between side-chain	[121]
4D-^{1}H-^{15}N-HMQC-NOESY-^{1}H-^{13}C-HMQC	identification of NOEs with amide protons	[27]
$^2J_{CO(H_\alpha)}$-E.COSY	^2J(CO,H_α)	[89]
3D-HNCA	^3J(HN,H_α), ϕ angle	[90]
3D-HMQC-J_{HH}-TOCSY	^3J(HN,H_α), ϕ angle	[88]
3D-H,C-COSY-ct-C,C-COSY-β-INEPT	vicinal ^{1}H-^{1}H couplings	[91]
Soft-HCCH-COSY	^3J(H_β,CO)	[92]
Soft-HCCH-E.COSY	^3J(H_α,H_β)	[92]

Three- and four-dimensional NMR experiments have many qualitative advantages over two-dimensional techniques. At least three dimensions are needed for correlations between heteronuclei in macromolecules, because the magnetization of the protons must be detected for reasons of sensitivity. This technique is indispensable for proteins, as the sequence assignment of the signals can be made independently of the secondary structure analysis. Three dimensions are also needed if the chemical shifts of heteronuclei are used for the resolution of signal overlap in NOESY spectra. This increase in resolution is probably the most important advantage of multidimensional NMR spectroscopy and is shown schematically in Figure 3. Two pairs of

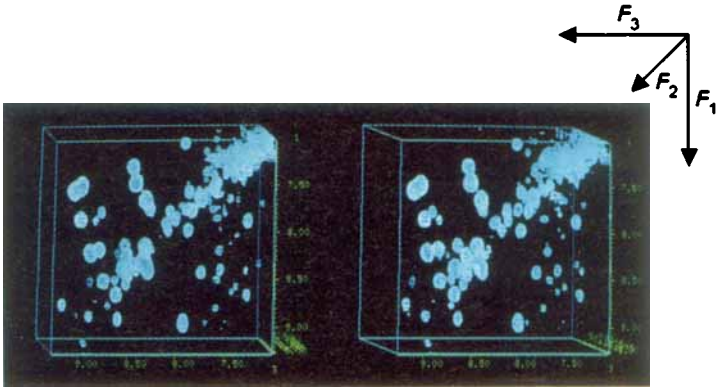


Fig. 2. Section of a 3D-TOCSY-NOESY spectrum of IL-4. In F_1 and F_3 the section with the chemical shifts of the amide protons was chosen, in F_2 the α-proton region.

interacting protons have the same chemical shifts (A), and the NOESY spectrum shows only one signal (B). Application of a third dimension, comprising the different chemical shifts of the ^{13}C nuclei, allows the distribution of the 2D cross peaks into different layers and facilitates the assignment of the blue signals (C).

Despite this increase of resolution, the protons with the "green" frequency in Figure 3 cannot be assigned unambiguously. It is obvious that the introduction of one more frequency dimension, in other words, detection of the carbon atoms connected to those protons, would solve this problem.

2.1. Basics

Owing to the modular construction of multidimensional pulse sequences from units known from 2D spectroscopy (Fig. 1), the events occurring in a higher order pulse sequence are completely analogous. A full description of the individual sequences using the product operator formalism[49] and coherence transfer pathways will therefore not be given here; the reader is referred to articles by Ernst[5] and Kessler et al.[6] for more information. In the following we will discuss some particular problems that arise when switching from two to three or more dimensions.

2.1.1. Sensitivity

The 3D data set is a function of three independent time variables. If the terms describing relaxation during the evolution period are neglected, a single 3D signal can be described by Equation (1).[51] $Z_{(pq,rs,tu)}$ is the amplitude of the coherence transfer [Eq.(2)]. The superoperator element $R^{(n)}_{(pq,rs)}$ describes

$$S_{(pq,rs,tu)}(t_1,t_2,t_3) = Z_{(pq,rs,tu)} \exp(-\omega_{pq} t_3) \exp(-\omega_{rs} t_2) \exp(-\omega_{tu} t_1) \quad (1)$$

$$Z_{(pq,rs,tu)} = D_{pq} R^{(2)}_{(pq,rs)} R^{(1)}_{(rs,tu)} \sigma(0)_{(tu)} \quad (2)$$

the n^{th} coherence transfer between the coherences pq and rs, the operator $D_{(pq)}$ corresponds to the effectiveness of the detection of the transition pq, and $\sigma(0)_{(tu)}$ is the ground state of the density operator for the transition tu. Equation (2) thus describes the integral intensity of the signal.

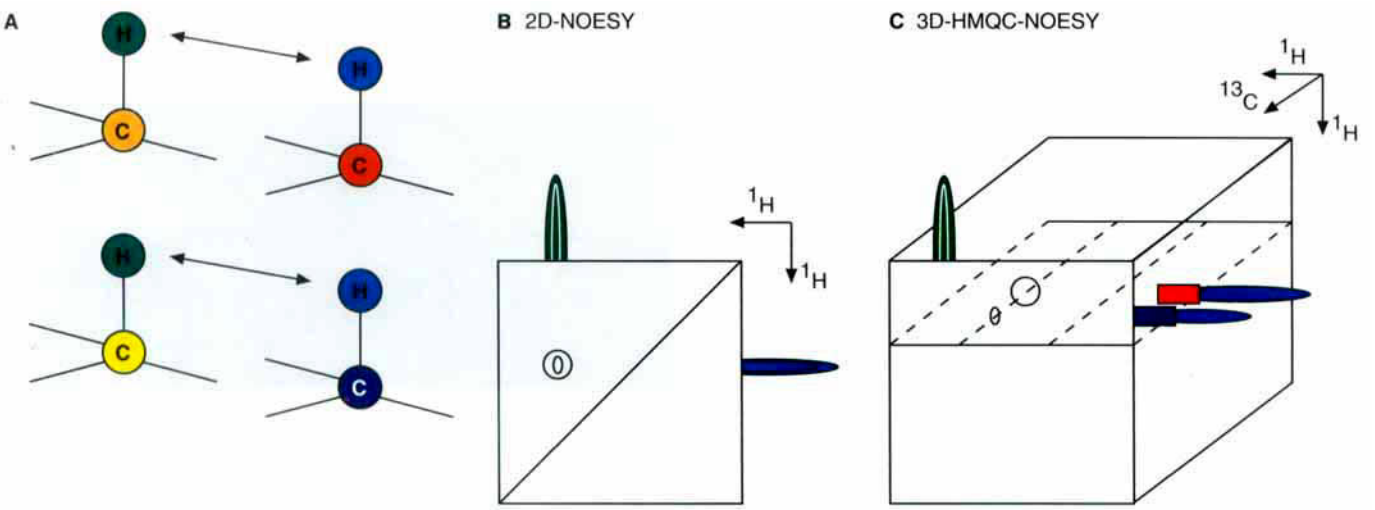


Fig. 3. Schematic representation of the resolution advantages of 3D NMR spectroscopy. Two pairs of protons have the same resonance frequency (same color) (A), which results in an overlap of cross peaks in the 2D NOESY spectrum (B). When the frequency of the carbon atoms is plotted as the third dimension, the problem is solved, since their resonance frequencies are different. The NOESY cross peaks are thus distributed in different planes (C).

Increasing the number of dimensions from two to three may, though not necessarily, result in a much lower signal/noise (S/N) ratio. This can be caused by two main factors: the intensity may be distributed into several multiplet lines occurring in the third dimension, or the coherence transfer steps are not efficient, which results in weak 3D cross peaks. It can be shown that the difference in the signal/noise ratio of a 2D cross peak involving the two protons i and k and that of a 3D cross peak ijk depends on the efficiency of the additional transfer T_{ij} and on the number of multiplet lines of nucleus i, N_i [Eq.(3)]. In the best case, when the signal of nucleus i consists of only one line and

$$\frac{(S/N)^{ijk}_{3D}}{(S/N)^{jk}_{2D}} = T_{ij}/N_i \qquad (3)$$

the transfer is quantitative, no substantial decrease in intensity will be observed compared to the 2D spectrum. This is the basis of techniques that use the chemical shifts of heteronuclei as additional frequency parameters. If there is no relaxation, the signal intensities in a ^{15}N-resolved NOESY spectrum should correspond to those in the 2D-NOESY spectrum. However, if homonuclear 2D techniques are combined, the intensities of the 1D, 2D, and 3D signals is 100:10:1, given a 10% efficiency of each coherence transfer and not taking into account the effect of the increasing number of multiplet lines.

2.1.2. Resolution and Acquisition Time

The advantages of multidimensional NMR spectroscopy can only be made use of if sufficient data points can be accumulated in all dimensions. If the resolution is poor, the spectra are difficult to interpret and will show broad, overlapping signals, which offsets the advantages of higher dimensional NMR experiments. Since the acquisition time increases exponentially with the number of experiments in the indirectly detected dimensions, a compromise must be found between good resolution and acquisition time. The acquisition of a 3D-NOESY-^{1}H-^{15}N-HMQC spectrum, for example, with 196 × 96 × 1024 data points in $F_1(^1H)/F_2(^{15}N)/F_3(^1H_N)$ and accumulation of 16 transients per time increment requires 70–80 hours. Several procedures are therefore applied to obtain sufficient resolution in a reasonable acquisition time, for example backfolding of signals, selective excitation of small spectral regions, use of pulsed field gradients, and the application of mathematical algorithms to enhance the resolution.

Backfolding of Signals: The spectral width of an NMR spectrum is defined by the time increment used in data acquisition. Normally signals lying outside the spectral range are "folded back" after a Fourier transformation of the digitized signal.[4, 52] Carefully planned folding of the spectrum in one frequency domain may make it possible to record a sufficiently resolved spectrum without any loss of information. Multidimensional ^{13}C NMR carbon spectra, in particular, can be improved by this method.[47]

Selective Excitation: A smaller spectral width and hence sufficient resolution in an acceptable time can also be obtained by selective excitation of nuclei, whose signals are found in separate regions of the spectra. Generally, shaped pulses with low power are used.[51, 53, 54] For heteronuclear spectra, multiplicity selection may also be applied.[55–57]

Gradients: The total time required for a multidimensional experiment mainly depends on the phase cycling used to select the desired coherences. In many cases at least 4, 8, or 16 transients are needed for spectra with a minimum of artifacts, which results in long acquisition times. If pulsed field gradients are used, selection of the desired coherence transfer steps is potentially possible in one scan.[58–61] Therefore, no addition of free induction decays (FIDs) is needed as is usually required for selection by phase cycling. As a consequence, more data points can be acquired.[62–64]

Linear Prediction: To improve resolution, the FIDs can be extended by calculating more data points before Fourier transformation by the application of a linear prediction. This is helpful if only a few data points can be acquired in the indirectly detected dimensions. New data points are usually calculated from the measured data by using the Burg algorithm.[65–67]

2.2. What Three-Dimensional Spectra Look Like

In a three-dimensional spectrum the basic 2D spectra of which it is composed appear as diagonal planes. When all three diagonal planes are present, as is the case in homonuclear 3D spectroscopy, the line of intersection of the three diagonal planes is the main diagonal, which is equivalent to the one-dimensional spectrum. The signals are classified according to the number of coherence transfer steps and therefore according to the number of different frequencies contained (Scheme 1).

Diagonal peaks	A → A → A
Cross diagonal peaks	A → A → B
	A → B → B
Back transfer peaks	A → B → A
Cross peaks	A → B → C

Scheme 1. Signal classification in multidimensional NMR spectra.

Diagonal signals containing three identical frequencies correspond to the one-dimensional spectrum, signals with two identical frequencies (cross-diagonal and back transfer signals) represent the 2D spectra. Only from the 3D cross peaks can one extract more information than from the 2D spectra. The type of signal that may appear depends on the kind of 3D experiment. A homonuclear 3D-TOCSY-NOESY spectrum will typically display all three types of signals, whereas 3D-TOCSY or 3D-NOESY-HMQC spectra contain only signals with two or more different frequencies. A triple-resonance experiment such as a 3D-HCACO will give rise exclusively to 3D cross peaks.

2.3. Evaluation of Multidimensional NMR Spectra

The evaluation of a multidimensional NMR spectrum consists of the search for correlations between cross peaks, which have one or more frequencies in common. 3D and 4D NMR spectroscopy has the advantage of yielding cross peaks that have more than one coordinate in common. Thus the combinatory problem is greatly simplified compared to the analysis of the same spin system by 2D cross peaks with only one common frequency. This is illustrated in Figure 4 for six different chemical shifts belonging to one spin system. The frequencies of the spin system in A can be connected only in one way by using 3D cross peaks (B), whereas the 2D cross peaks allow an incorrect assignment (C) as well.

The 3D and 4D spectra are usually evaluated manually by using a set of 2D planes. These planes obtained from various 3D experiments with the same or with a symmetrical frequency in the third dimension are evaluated in parallel; the desired correlation is then given by a second common coordinate.

This procedure is quite time-consuming, since several 3D or 4D data sets must be taken into account simultaneously. Consequently, multidimensional NMR spectra are often analyzed with the help of computer programs.[68-71] Completely automated assignment of spectra, however, is not yet possible, although several steps have already been made in this direction.[72-74] It has proved difficult to transfer the thought processes of an experienced spectroscopist to a computer. The main difficulties are distinguishing artifacts from real cross peaks, and the incomplete information obtained. Despite these problems, automated evaluation seems to be much easier with 3D and 4D techniques, as the data sets are more specific.

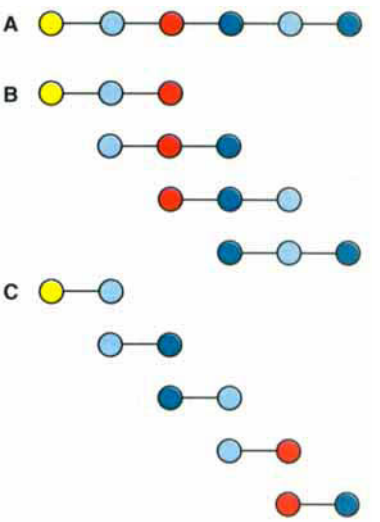


Fig. 4. Assignment of a spin system with six chemical shifts. The system of six nuclei illustrated schematically in A can be linked only in the way shown by using the 3D cross peaks illustrated in B. If only 2D cross peaks are used, an incorrect connection can also result, as shown in C.

2.4. Quantitative Evaluation of Multidimensional NMR Spectra

2.4.1. Determination of Distances

The calculation of protein structures requires estimated distances between proteins which are obtained from quantitative evaluation of NOE- and ROE-dependent cross peaks. The various strategies to quantify distances vary from a general classification of NOEs[1] to a method that treats the problem by using a relaxation matrix formalism.[75-78]

Until now, a classification of the observed NOEs was carried out in most cases, or the distances were calculated after integration of the cross peaks from NOESY spectra with a short mixing time by using a known reference distance.[79,80] In the first method NOESY cross peaks are separated into several classes according to their intensity or their occurrence in NOESY spectra recorded with different mixing times. These classes are assigned an upper distance limit, (e.g. high intensity: distance <2.8 Å; medium intensity: distance <3.5 Å; low intensity: distance <5.0 Å. With the second method the distances r_{ij} are calculated by using Equation (4) from the intensities I_{ij} of the

$$r_{ij} = r_{\mathrm{ref}}\left(\frac{I_{\mathrm{ref}}}{I_{ij}}\right)^{\frac{1}{6}} \qquad (4)$$

signals and a reference distance r_{ref}. The proportionality of Equation (4) holds, however, only if the NOESY spectra are recorded with a sufficiently short mixing time.

Since in 3D and 4D spectra more than one transfer process [see Eq.(2)] contributes to the intensity of a cross peak, there is

no direct correlation between cross peak intensity and interproton distance. The amplitude of a 3D cross peak is determined by the product of the efficiency of each single step. This can be described with a vector diagram, in which the efficiency of the single steps is given by vectors and the amplitude of the 3D cross peak by an extended plane.[81]

The prerequisite for a quantitative evaluation of NOESY-type 3D spectra is that all contributions to the cross peaks are known (except the distance to be determined) or can be considered as constant. The latter can be assumed if one of the contributions is caused by a heteronuclear ^1J coupling, as in NOESY-HMQC or NOESY-HSQC spectra. The range of variation for these couplings is quite small (90–96 Hz for J_{NH}, 125–160 Hz for J_{CH}). The different transverse relaxation times of protons can, however, cause a problem. For biological macromolecules the time of free precession necessary for the evolution of a heteronuclear coupling cannot be ignored and could be quite different for chemically related groups. This means that the signal amplitudes can be distorted by relaxation effects.

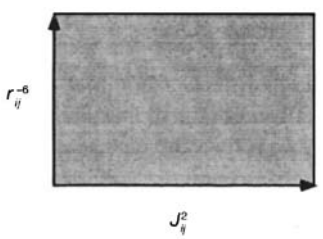


Fig. 5. Vector diagram describing the intensity of TOCSY-NOESY cross peaks. The lengths of the vectors represent the efficiency of the individual coherence transfer steps, the extended plane the intensity of the 3D cross peaks.

The situation becomes more complicated if the efficiency of both coherence transfer steps depends on the conformation of the molecule, as in homonuclear 3D experiments.[81,82] The 3D cross peaks in TOCSY-NOESY spectra, for example, depend to a first approximation on J^2 and r^{-6} (Fig. 5). As $^3J_{NH-H_\alpha}$ is heavily dependent on the backbone angle ϕ, several specific cross peaks can be found in those spectra whose amplitudes are determined by the kind of secondary structure (Fig. 6). It can be seen that for α helices only weak cross peaks are expected with the shifts of H_N and H_α as F_1/F_2 coordinates, whereas β structures lead to very intense signals.

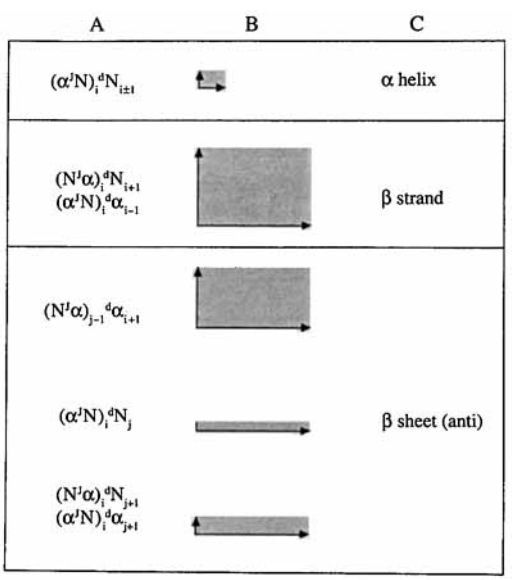


Fig. 6. The dependence of the intensities of cross peaks in TOCSY-NOESY spectra on the secondary structure of a protein (C). A gives the underlying transfer; for example, $(N^J\alpha)_i{}^d N_{i+1}$ is a TOCSY transfer from H_N to H_α in amino acid i followed by a NOESY transfer (distance dependent) to the NH of the next amino acid. B shows vector diagrams of intensities (see Fig. 4) for the various types of cross peaks. Amino acids i and j are adjacent to each other in a β sheet.

The quantitative evaluation of NOESY-NOESY spectra shows some interesting aspects. In a first approximation the amplitude of a cross peak I_{ijk} is influenced by two cross relaxation rates σ [Eq.(5)], where $\tau_m^{(1)}$ and $\tau_m^{(2)}$ are the two applied

$$I_{ijk} \approx \sigma_{ij}\sigma_{jk}\tau_m^{(1)}\tau_m^{(2)} \quad (5)$$

mixing times. If $\tau_m^{(1)} = \tau_m^{(2)}$, then the expression for I_{ijk} corresponds to the second-order terms obtained from a series expansion of the exponential function that describes the magnetization transfer in the NOESY experiment [Eq.(6)].[8] In principle this fact can be used to calculate higher order contributions to 2D and 3D cross peaks.[51,84–86]

$$[e^{-R\tau_m}]_{ij} \approx 1 + \sigma_{ij}\tau_m + \sum_k \sigma_{ij}\sigma_{jk}\tau_m^{(2)} \quad (6)$$

2.4.2. *Determination of Dihedral Angles*

The determination of dihedral angles requires the measurement of coupling constants. For this reason several 3D techniques have been developed that yield multiplets with an e. COSY-type fine structure (e. COSY = exclusive correlation spectroscopy).[87–92] The main problem that must be faced is achieving a sufficiently high resolution. In order to measure small coupling constants with satisfactory accuracy, separate planes of a multidimensional spectrum must usually be calculated with high digital resolution. The coupling constants can then be taken directly from the splitting in the observed e. COSY-type multiplet.

3. Strategies and Experiments for Protein Structure Determination

The choice and combination of multidimensional experiments and the simultaneous decision as to which isotopes should be used depend on various factors such as the size of protein, its secondary structure, the distribution of signals in the ^{1}H NMR spectrum, and availability of labeled protein, which is normally produced by biotechnological methods. These factors must be considered when the isotopic labeling and the NMR experiments are selected so that the information required for structure determination can be obtained. Three tasks must be completed, specifically

- the complete sequence assignment
- the complete assignment of side-chain signals
- the collection of a sufficient number of precisely measured NOEs.

For each labeling strategy a basic set of experiments can be defined (Table 2).

If the protein is not labeled, a conventional concept for the assignment may be chosen which relies on secondary structure analysis by means of ^{1}H techniques (Fig. 7A). The proton sig-

Table 2. NMR experiments and the types of labeling suited for protein structure determination.

	without isotopic labeling	with ^{15}N labeling	with ^{15}N and ^{13}C labeling
assignment of spin systems	TOCSY-TOCSY	TOCSY-HMQC TOCSY-TOCSY	3D/4D-HCCH-TOCSY HCCH-COSY HC(C)NH-TOCSY
sequential assignment	TOCSY-NOESY	NOESY-HMQC TOCSY-NOESY	HCACO HNCA HNCO HCA(CO)N
identification of NOEs	NOESY-NOESY TOCSY-NOESY	NOESY-HMQC NOESY-NOESY TOCSY-NOESY	3D-NOESY-HMQC 4D-HMQC-NOESY-HMQC

nals of the side chains are collected with TOCSY and COSY techniques by utilizing the scalar couplings, and these signal sets are then ordered sequentially by using NOEs between neighboring amino acids. The structure determination is based on distances derived from the 2D-NOESY spectra or from homonuclear 3D spectra.[32, 84, 85, 93–95]

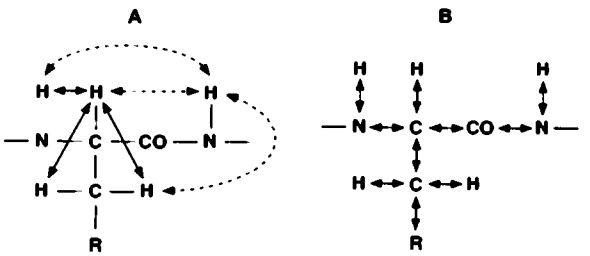


Fig. 7. Identification of spin systems and sequence assignment in proteins. A) For unlabeled proteins the assignment relies on homonuclear spectroscopy utilizing ^3J couplings (solid lines) and NOEs between the protons of neighboring amino acids (broken lines). B) In the case of labeling with ^{15}N and ^{13}C, the assignment is achieved by heteronuclear techniques using the relatively large ^1J couplings ($^1J(H,C) \approx 125$. $^1J(H,N) \approx 90$, $^1J(N,C) \approx 10-17$, $^1J(C,C) \approx 40-60$ Hz).

In ^{15}N-labeled proteins the chemical shifts of the heteronuclei can also be used for the three-dimensional resolution of the NH region of TOCSY and NOESY spectra,[96–100] always relying on the relationships from ^1H NMR experiments (Fig. 7A). The application of ^{15}N labeling and 3D techniques makes the assignment easier, and a larger number of NOEs can also be interpreted. However, the enhancement of resolution resulting from ^{15}N labeling only affects the amide protons. Overlaps in the aliphatic region must therefore be solved by homonuclear 3D techniques,[32] especially for the assignment of NOEs between side-chain protons.

For doubly labeled proteins (^{13}C and ^{15}N) the complete assignment can be carried out without recourse to conformation-dependent parameters (Fig. 7B).[101–116] The assignment of the side chains is achieved with experiments relying on ^1J couplings between ^1H and ^{13}C and between neighboring carbon atoms.[117–120] Two advantages are gained from this procedure. The participating couplings are relatively large and can also be resolved for larger proteins. In addition, the signal overlap always observed in 2D ^1H NMR spectra is largely avoided for some types of amino acids.

The sequence-specific resonance assignment, commonly referred to as the sequential assignment, can now also be carried out with the conformation-independent ^1J couplings (Fig. 7B). A large number of 3D and 4D techniques are available for the correlation of chemical shifts of heteronuclei in the protein main chain. The NOEs needed for structure calculation are extracted from ^{15}N- or ^{13}C-resolved NOESY spectra or may be interpreted from the 2D-NOESY spectrum. In addition, four-dimensional spectra may be recorded[27, 121] to obtain unambiguous assignments of NOEs in analogy to the situation depicted in Figure 3.

Although doubly labeling a protein with ^{15}N and ^{13}C is considered the best approach for NMR spectroscopic structure analysis, good results are often also obtained without complete labeling. However, the size of molecule that can be investigated decreases. Proteins larger than 10 kDa are rarely examined with homonuclear 3D methods, and the investigation of ^{15}N-labeled proteins with a combination of ^{15}N-resolved and homonuclear 3D spectroscopy would be ineffective for proteins with a size greater than 13–15 kD.

3.1. Investigation of Unlabeled Proteins and Peptides

The application of homonuclear 3D techniques for the structure determination of small proteins is particularly useful for proteins that are derived from natural sources and cannot be labeled. Sequential assignments can be made with the TOCSY-NOESY technique,[122] and the NOESY-NOESY technique has mainly been applied in the past to measure a large number of distances and to determine them more precisely.[84, 85] In addition, it has been shown that homonuclear 3D spectra are better suited for the automated assignment of NMR signals than 2D spectra.[72]

In the past heteronuclear methods were only applied to unlabeled biomolecules in cases of smaller proteins or peptides.[55, 56, 123]

3.2. Investigation of a ^{15}N-Labeled Protein: The Structure of Interleukin-4

The complete labeling of a protein is not always practicable, especially if variants are to be examined in addition to the wild-type and not all of them can be labeled with ^{13}C. In such cases ^{15}N labeling and the combined application of ^{15}N-resolved and homonuclear 3D NMR spectroscopy enables the determination of the required parameters. The strategy for investigating a ^{15}N-labeled protein is discussed here with IL-4 as an example.

The structure of IL-4[124–128] consists of four helices which form a four-helix bundle (Fig. 8). The spatial relationship of the four helices can be determined from the NOEs between the side-chain protons in the hydrophobic amino acids that are colored yellow. The sequential assignment is based on the characteristic NOEs between amide protons. Both kinds of interactions are difficult to measure with 2D techniques, as overlapping signals are expected in the region of the signals for NH and the methyl groups. In order to resolve them, the ^{15}N-NOESY-HMQC technique[96] is applied for sequential assignment,

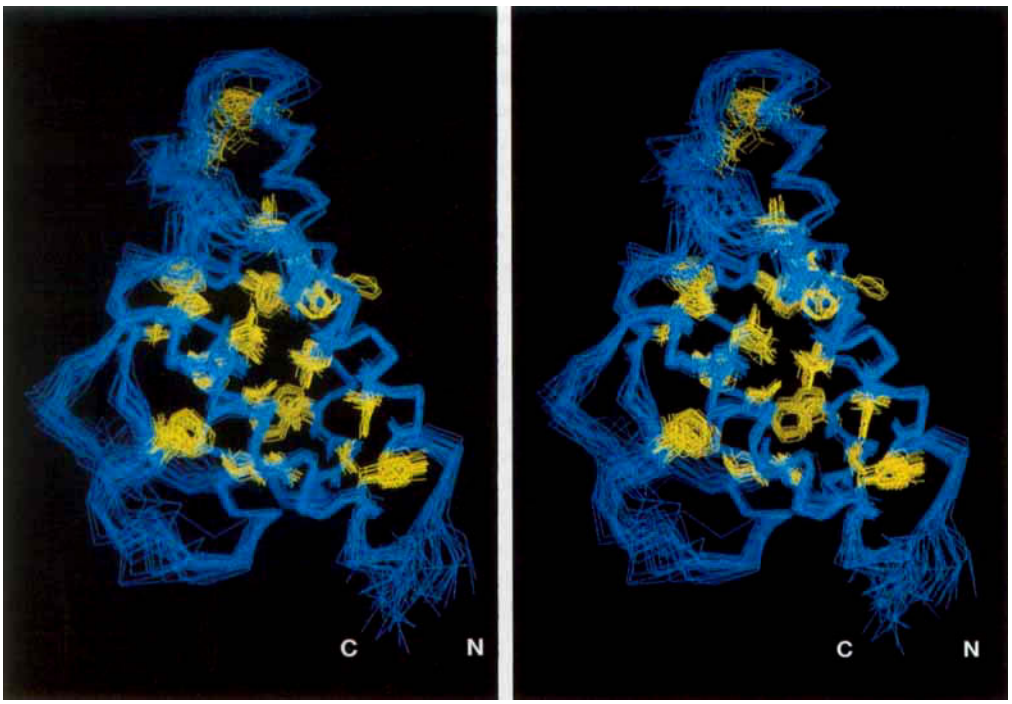


Fig. 8. Superposition of 21 structures of interleukin-4 calculated from NMR data. The atoms of the protein main chain are given in blue, the side chains of the hydrophobic amino acids in yellow.

which gives additional resolution for the amide region. The TOCSY-NOESY technique[32, 122] is used for the detection of NOEs between the side chains. In addition, the H_N, H_α, and H_β resonances of the individual amino acids can be correlated by the ^{15}N-TOCSY-HMQC technique,[96] thus giving the basis for the side-chain assignment.

3.2.1. *Assignment of ^{1}H Signals with ^{15}N-TOCSY-HMQC and ^{15}N-NOESY-HMQC Experiments*

The ^{15}N-TOCSY-HMQC and ^{15}N-NOESY-HMQC techniques (Fig. 9) are among the most useful in 3D NMR spectroscopy. It must be pointed out that HSQC experiments give

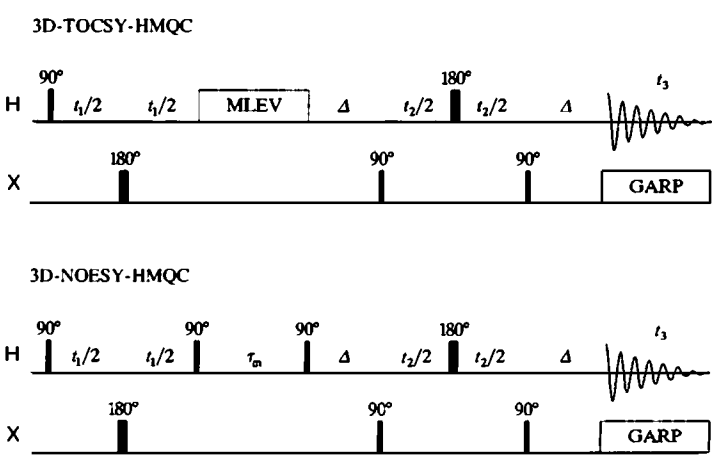


Fig. 9. Pulse sequences for the 3D-^{15}N-TOCSY and -^{15}N-NOESY-HMQC experiments. GARP = composite pulse decoupling sequence.

the same spectra as HMQC experiments. In analogy to the situation shown in Figure 3, degenerate NH signals are distributed onto several planes by the different chemical shifts of the directly connected ^{15}N nuclei. In these 3D spectra a vector is present for each amino acid on the coordinates of the amide proton and amide nitrogen resonances, where all TOCSY or NOESY cross peaks of the amide proton are lined up. The ^{15}N-TOCSY-HMQC technique makes the assignment of the side-chain signals much easier, and ideally all the side-chain protons of an amino acid are given in the corresponding vector.

The sequential assignment of α-helical regions in proteins can be solved very elegantly with only the ^{15}N-NOESY-HMQC technique by finding cross peaks between the NH signals of neighboring amino acids. This is problematic with only a 2D spectrum if, for example, two NH signals from an α helix are degenerate. In this case four cross peaks to other amino acids are expected at this frequency, and an unambiguous assignment is not possible. On the other hand, in the ^{15}N-NOESY-HMQC spectrum the corresponding signals are found on different ^{15}N planes if the ^{15}N nuclei show different chemical shifts. Sequential residues are found by looking for NH–NH cross peaks that are symmetrical to the diagonal in the NOESY spectrum. A successful sequential assignment is usually displayed by showing stripes from the 3D-NOESY-HMQC spectra (Fig. 10). These stripes correspond to the ^{H}N/^{15}N vectors mentioned earlier.

To assign β structures with this technique, a slightly different evaluation strategy should be applied. The superposition of planes with the same ^{15}N frequency from the ^{15}N-NOESY-HMQC and ^{15}N-TOCSY-HMQC spectra makes it possible to locate the corresponding NOESY and TOCSY peaks in the H_α region (Fig. 11). For a particular residue, both 3D cross peaks show the same ^{15}N and H_N chemical shifts and give the connec-

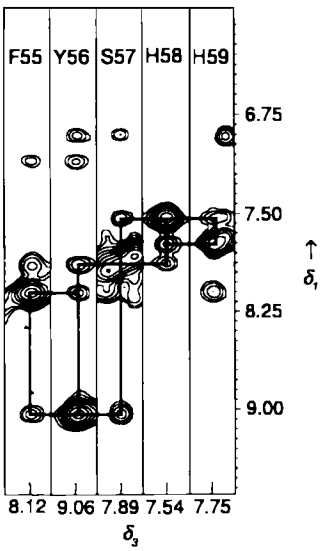


Fig. 10. Example of a sequential assignment for an α-helical region with a 3D-NOESY-HMQC spectrum, shown for the connection between amino acids F55 to H59 in IL-4, by using NOEs of the type $NH_i-NH_{i\pm1}$. The strips are each taken at the frequencies of the amide nitrogen (F_2) and amide protons (F_3).

tion $H_\alpha(i-1) \rightarrow H_\alpha(i)$. For further sequence assignments, planes must be found that contain the corresponding NOESY peak with the appropriate $H_\alpha(i)$ frequency or the TOCSY peak with the frequency of $H_\alpha(i-1)$. In the ideal case only one suitable plane is found, but several H_α signals are usually degenerate. The practicability of the ^{15}N-HMQC-NOESY technique for sequence assignment is therefore restricted to proteins with a large proportion of α helices (see Section 3.2.2).

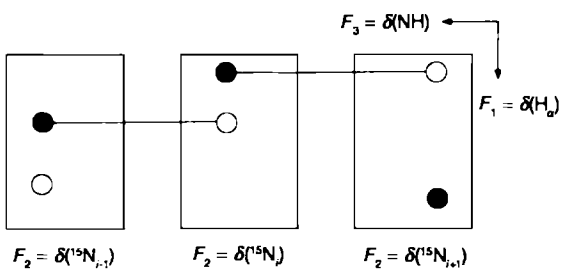


Fig. 11. An example of the sequence assignment in ^{15}N-resolved TOCSY and NOESY spectra based on H_N-H_α correlations. The TOCSY signals (black) and NOESY signals (white) with the coordinates $H_\alpha(i)/H_N(i)$ and $H_\alpha(i-1)/H_N(i)$ belong to the same H_N and are found on the plane with the same ^{15}N frequencies. The neighboring amino acids can be found by searching slices with appropriate TOCSY signals (left) or NOESY signals (right).

3.2.2. *Completing and Checking the Sequence Assignment with TOCSY-NOESY Data*

Overlapping signals in the H_α region also caused problems in the assignment of NOESY and TOCSY spectra of interleukin-4. For example, the H_α signals of some amino acids belonging to the β sheet are degenerate. The 2D spectra and ^{15}N-resolved 3D spectra did not provide unambiguous correlations. 3D-TOCSY-NOESY spectra, however, contain the necessary information. In these spectra signals with the coordinates $H_N(i)/H_\alpha(i)/H_N(i+1)$ and $H_\alpha(i)/H_N(i)/H_N(i+1)$ in $F_1/F_2/F_3$ are observed which contain the desired correlation. This is pointed out in Figure 12, where the region of the 2D-TOCSY and 2D-NOESY spectrum suitable for assignment is shown schematically. The filled circles represent TOCSY signals, the empty ones the NOESY signals. The assignment cannot be made unambiguously, as the chemical shifts of two H_α signals are degenerate. Both possible assignments are indicated, starting from amino acid *i*. The 3D cross peaks mentioned above can be seen as correlation lines between 2D cross peaks, drawing a line between the two NH shifts at the level of the H_α shift (Fig. 12 right). In this way a definite assignment of the 2D cross peaks can be made.

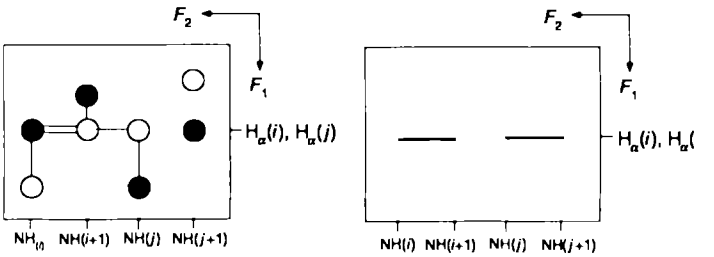


Fig. 12. An example of the use of 3D-TOCSY-NOESY data for the assignment of protein NMR spectra. Left: The assignment procedure with 2D spectra is normally done by connecting cross peaks containing coupling information (black) with those containing distance information (white), which occur, for example, in TOCSY and NOESY spectra. If signals of different α protons occur at the same frequency, several linkages are possible. Right: In a TOCSY-NOESY spectrum the cross peaks with coordinates $H_N(i)/H_\alpha(i)/H_N(i+1)$ or $H_N(i)/H_N(i+1)/H_\alpha(i+1)$ in $F_1/F_2/F_3$ correspond to the correlations depicted in A. In the 2D spectrum they can be depicted as correlation lines at the level of the H_α frequency. The lines connect the frequencies of the amide protons of amino acids *i* and *i* + 1.

In practice the relevant parts of the 3D spectra are calculated separately, then a peak-picking routine gives a list of the signals, and these are entered graphically into the spectrum as described above. This is shown for interleukin-4 in Figure 13. The TOCSY spectrum is shown in turquoise and the NOESY spectrum in red. The correlation lines drawn by the assignment program give horizontal correlations for the sequence assignment. This figure shows correlations that mainly originate from the nonhelical

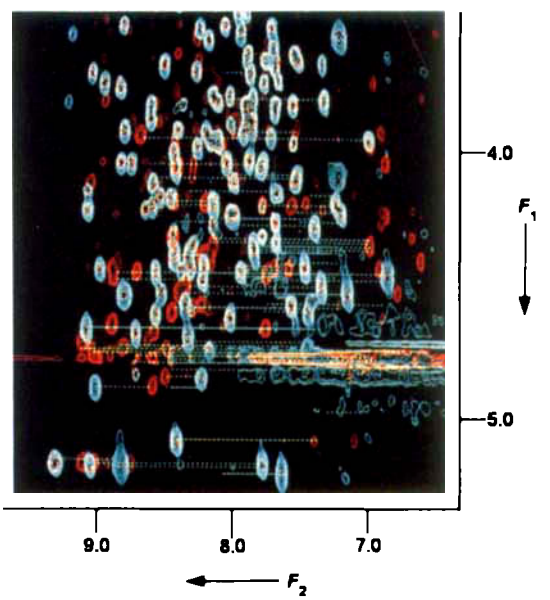


Fig. 13. Superimposed 2D-TOCSY (turquoise) and 2D-NOESY spectra (red) of IL-4 with indicated correlations derived from cross peaks in the 3D-TOCSY-NOESY spectrum (see Fig. 12).

region. Owing to their small couplings between H_N and H_α, amino acids in helices give only very weak cross peaks which were not considered.

3.2.3. *Assignment of Signals in NOESY Spectra*

One of the main problems encountered in the assignment of NOESY spectra is the identification of NOEs between methyl groups or other side-chain atoms. Figure 14 shows an example from the structure determination of IL-4. It is possible to resolve these NOEs based on the couplings of the methyl groups to directly neighboring protons by using a TOCSY-NOESY spectrum. However, it is essential that the cross peaks between the methyl groups of the valine residues and their H_β, as well as those between the methyl groups of the leucine residues and their H_γ, are resolved in the 2D-TOCSY spectrum and are already assigned.

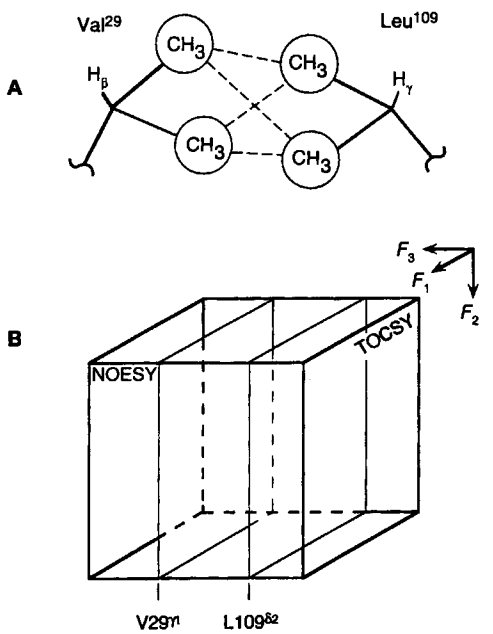


Fig. 14. Identification of NOEs between side-chain protons of IL-4 with the 3D-TOCSY-NOESY technique. The NOEs between the side chains of Val29 and Leu109 in A could be assigned unambiguously by evaluating the TOCSY planes (F_1/F_2) taken at the frequencies of the protons of the methyl groups (F_3) (B; see also Fig. 15).

The 3D spectrum is evaluated conveniently by using TOCSY planes and comparing them with the NOESY spectrum. The NOESY spectrum is investigated in the F_2 direction. The planes with the same F_3 frequencies are taken from the 3D spectrum (Fig. 14B). The F_1 frequencies of the cross peaks in the 2D spectrum can be used to identify the 3D cross peaks necessary for the assignment. They can be found in the TOCSY planes of the 3D spectrum at the same F_2 coordinates as the F_1 coordinate in the NOESY spectrum. The F_1 coordinates of the 3D cross peak give the chemical shift of the coupling partner, and therefore, after comparison to the TOCSY spectrum, also the assignment.

An example is given in Figure 15 showing the assignment of the NOEs between the methyl groups of L109 and V29. The signal of one of the methyl groups of L109 does not overlap with any other signal in the proton spectrum, which makes the problem easier to solve. The F_1/F_2 plane shown here has two cross peaks with the coordinates of V29-H_β in F_1 and the coordinates of the methyl groups of V29 in F_2 (Fig. 15a). This is the proof that the corresponding cross peaks in the NOESY spectra result from NOEs between L109 and V29. If the signal of L109 overlapped with other signals, the interpretation would have to be proved by the symmetrical signals which are found in an F_3

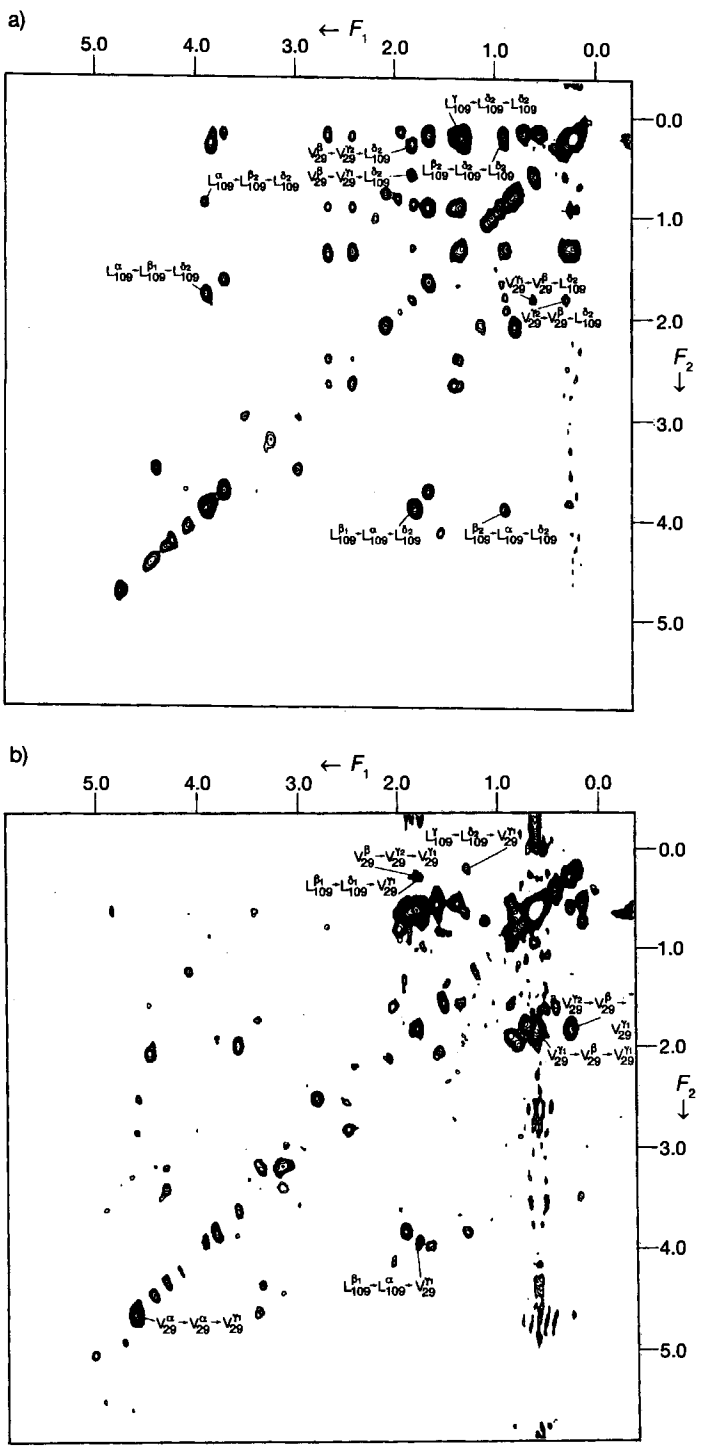


Fig. 15. TOCSY planes (F_1/F_2) from the 3D-TOCSY-NOESY spectrum of IL-4 taken at the positions shown in Figure 14B. a) At $\delta(F_3) = 0.22$, b) at $\delta(F_3) = 0.61$.

plane with the frequency of the methyl group of V29 and which contain the coupling between L109 H_δ and H_γ. These signals are indeed found, as is shown in Figure 15b.

3.2.4. *Measurement of $^3J_{H_\alpha H_N}$ Coupling Constants*

In order to determine the local conformations within the main chain and the conformations of the side chains in proteins, dihedral angles are derived from coupling constants by means of the Karplus equation and used in the structure calculations. The determination of coupling constants for larger proteins is not feasible with 2D experiments, as signal overlap often hides some components of the cross peaks. However, several multidimensional techniques have been developed for the measurement of coupling constants.[88-92]

For IL-4 the 3D-HMQC-J_{HH}-TOCSY technique[88] was used to determine the H_N-H_α couplings, and from that, the ϕ angles of the protein main chain. Small values (<5 Hz) indicate α-helical structures and large values (>9 Hz) suggest stretched conformations. Coupling constants of intermediate values (5 to 9 Hz) indicate conformational averaging from a fast rotation around the $N-C_\alpha$ bond or an unusual conformation of the main chain (e.g. positive ϕ angles). Figure 16 shows a plane from the HMQC-J_{HH}-TOCSY spectrum of IL-4. The H_α-H_N-N cross peaks are split in F_2 by the $^1J_{NH}$ coupling and in F_3 by the $^3J_{H_NH_\alpha}$ coupling.

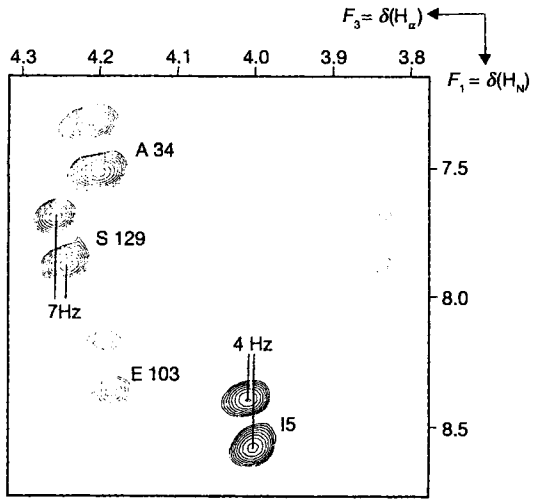


Fig. 16. F_2 section of the 3D-HMQC-J_{HH}-TOCSY spectrum of IL-4. The H_α-H_N-N cross peaks of I5, A34, E103, and S129 are shown. The coupling constants correspond to the separation of cross peak components in the F_3 direction.

3.3. Techniques for the Assignment of ^{15}N,^{13}C-Labeled Proteins; The Structure of Cystatin in Solution

Without ^{13}C labeling, insufficient spectral resolution often hinders the investigation of proteins with more than 100 amino acids. One example is provided by the structures of phosphorylated and nonphosphorylated cystatin.[129-131] The phosphorylated protein was isolated from egg white[132] and could not be isotopically labeled. Its structure is poorly defined in specific regions (Fig. 17 left). The nonphosphorylated form (Fig. 17 right) could be overexpressed in *E. coli*[34] and hence was available for ^{13}C- and ^{15}N-labeling. The structure of the large loop at the lower left of the protein was therefore much better determined by the measurement of a larger number of distances.

The advantages of ^{13}C labeling are manifold. The assignment of the side chains is often simplified because several amino acids are easy to identify by their characteristic chemical shifts in the ^{13}C region. The sequential assignment is additionally simplified by triple-resonance experiments.

In our first investigations of the structure of cystatin we used unlabeled samples, and most of the signals were assigned by

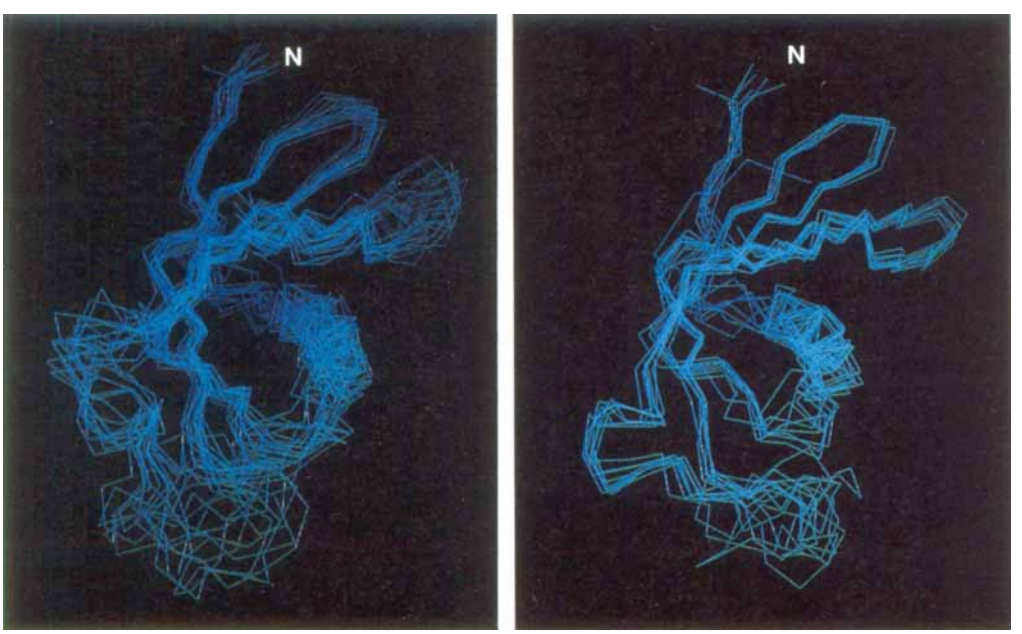


Fig. 17. C_α plot of the calculated structures of phosphorylated albumin cystatin (left) and a recombinant synthesized mutant (right). The structures on the left are based on homonuclear data, those on the right on data from ^{13}C,^{15}N-labeled samples. N denotes the N terminus.

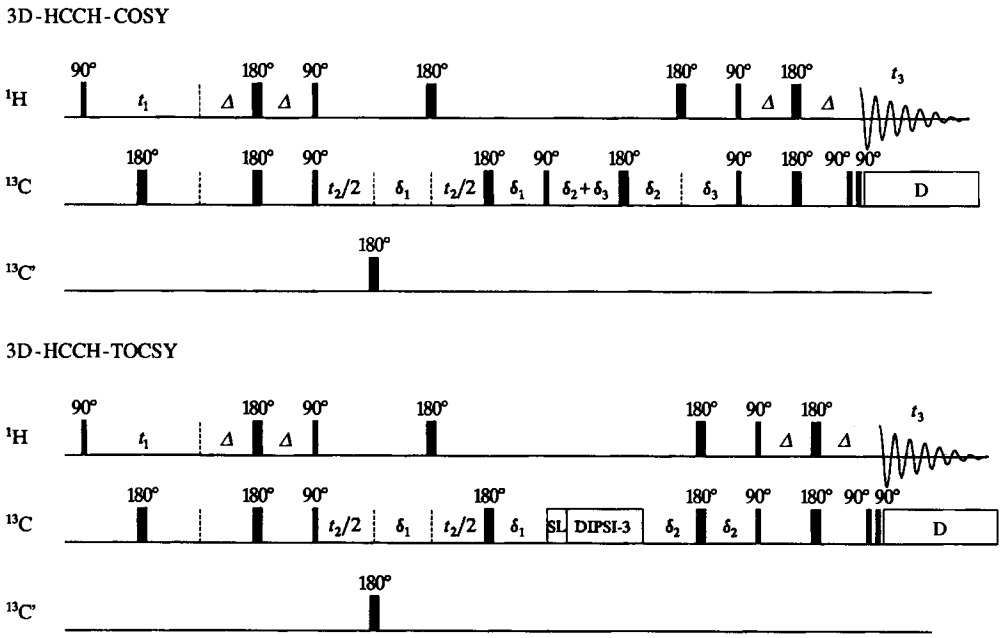


Fig. 18. Pulse sequences for the 3D-HCCH-TOCSY and 3D-HCCH-COSY techniques. D = decoupling.

conventional techniques. For the solution of several problems, however, ^{13}C labeling was absolutely necessary. A major question was whether the N terminus is flexible (up to G9) and also whether there is a large loop (up to residue 10 in the region 69–80), as only poor NOEs were observed for these regions. A complete description of the structure required the measurement of heteronuclear relaxation parameters (especially for ^{15}N), which provided information about the mobility of the peptide chain. For this reason the determination of these parameters will be discussed briefly in Section 4.

3.3.1. Assignment of Side Chains

The assignment of side chains in doubly labeled samples relies mainly on experiments of the HCCH-type, the 3D-HCCH-COSY[117, 118] and 3D-HCCH-TOCSY techniques[119] (Fig. 18).

The latter allows the correlation of all side-chain protons and carbon nuclei with the α proton and α-carbon nucleus of the corresponding amino acid, which is a linking point for the sequential assignment (Fig. 19).[133, 134]

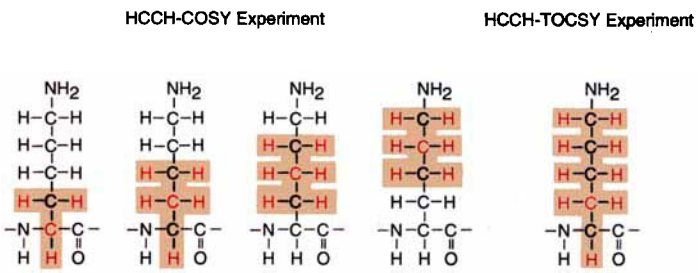


Fig. 19. Schematic view of the "building blocks" obtained in HCCH experiments for assigning side chains, as illustrated for lysine residue. If planes are taken from the HCCH-COSY spectrum at the frequencies of carbons (red), correlations to the directly bound protons and to protons from neighboring carbon atoms (on gray background) can be found. The entire side chain can be assigned by combining the information obtained from the individual planes. In the 3D-HCCH-TOCSY spectrum the plane of one carbon atom contains correlations to all protons of a side chain, in the ideal case.

The pulse sequences generally involve excitation and detection of protons. The excitation of the carbon nuclei proceeds by means of the C–H couplings, such that the $^1J_{CC}$ couplings can be used (see also Fig. 7B). For detection the protons must be excited once more by means of a C–H coupling. As the participating couplings are large (125, 40, 125 Hz), the maximum amplitude for the coherence transfer is reached in a shorter time than when proton–proton couplings are used in homonuclear sequences (TOCSY, COSY). In many cases this helps in finding the side-chain signals, especially of large proteins, for which the transverse relaxation time of the protons is too short for ^1H techniques to be used. The 3D spectra gained from the pulse sequences from Figure 18 have two coordinate axes with ^1H chemical shifts (F_1 and F_3) and one with ^{13}C chemical shifts (F_2). The spectra correspond to a COSY or TOCSY spectrum that is resolved by the ^{13}C chemical shifts.

In the HCCH-COSY spectrum ^{13}C chemical shifts are found in a single F_2 plane, frequencies of the directly bonded protons are found on the F_1 axis, and frequencies of the protons on the adjacent carbon atoms on the F_3 axis. The complete assignment of the side chains is given by the combination of F_2 planes with symmetrical ^1H signals. In the HCCH-TOCSY spectra all protons of a side chain can be found in one F_2 plane ($\delta(^{13}C)$), which makes work much easier (Fig. 19 right).

The HCCH-TOCSY spectrum of cystatin is shown in Figure 20. This plane is defined by the shifts of the α carbons of T70, T96, T94, V99, and the β carbon of S56. The frequency of the directly bonded proton can be found in the F_1 direction, while the frequencies of all protons belonging to the spin system of the relevant amino acid would ideally be found in the F_3 direction. Starting from the C_α/H_α diagonal signal of T96, the 3D cross peaks to H_β as well as to the protons of the γ-methyl group are found.

Both techniques are also suitable for a four-dimensional experiment. In the pulse sequence shown in Figure 18 the excited carbon nucleus is detected first. In principle, the frequency of the second carbon nucleus to which the magnetization is trans-

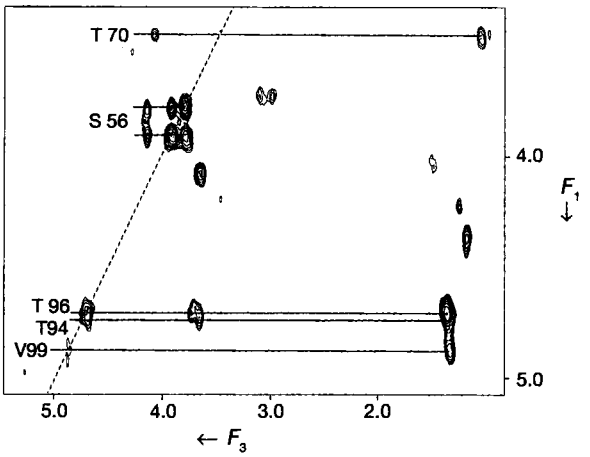


Fig. 20. Plane from a 3D-HCCH spectrum of cystatin. The spin systems of T70, S56, T96, T94, and V99 are indicated.

ferred can also be detected simply by inserting a second evolution time after the COSY or the TOCSY transfer.

3.3.2. *Sequential Assignment with ^1J Couplings between Atoms of the Protein Main Chain*

The sequential assignment of a doubly labeled protein is normally achieved by a combination of so-called triple-resonance experiments,[135-137] which correlate the chemical shifts of the protein main-chain atoms. Each experiment potentially identifies an additional unit of the protein sequence (Fig. 21). These

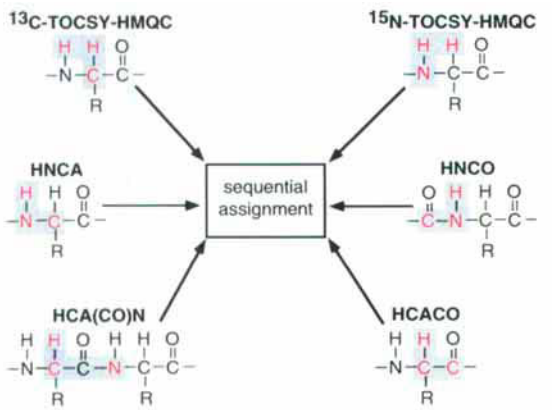


Fig. 21. Schematic representation of units (correlations) in the protein main chain derived from triple-resonance experiments. The spectra show cross peaks with frequencies of the nuclei given in red. A combined evaluation of these spectra gives a sequential assignment.

experiments are characterized by relatively large pulse sequences, which require a well-equipped NMR spectrometer. Two examples that require four frequency channels are shown in Figure 22.

Although a small number of experiments may suffice to obtain a complete sequence-specific resonance assignment, it is helpful to ensure good results by recording all possible kinds of correlations. The sequential assignment is most reliable when it is given by a set of cross peaks always having two frequencies in

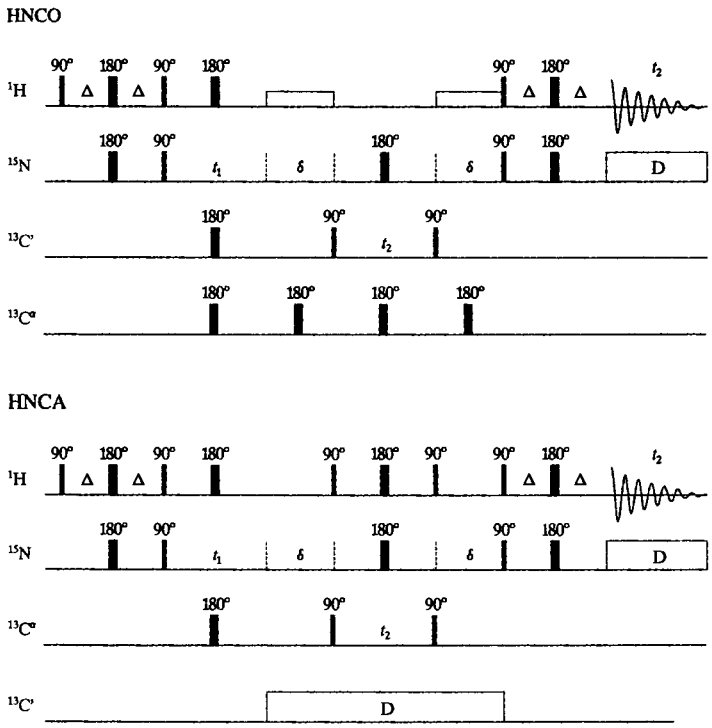


Fig. 22. Pulse sequences for the 3D-HNCO and 3D-HNCA experiments.

common. Such a combination of experiments is shown in Figure 23. HNCA[101,102] and HCACO experiments[101] are used to assign all of the backbone atoms of an amino acid. The connection of the next amino acids in the sequence can be achieved by several correlations. The cross peaks in the HNCO

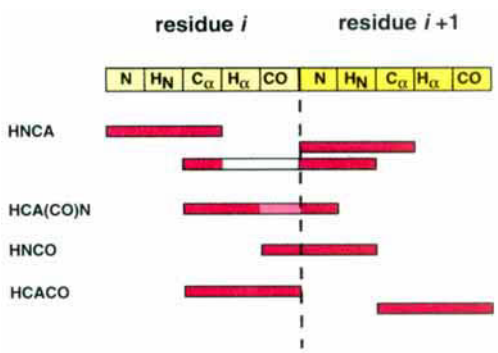


Fig. 23. Correlation of the amino acid i and $i+1$ by means of a basis set of 3D triple-resonance experiments. The red bars give the frequencies that are contained in 3D cross peaks. Nuclei colored pink are not detected but only used for magnetization transfer during the pulse sequence.

spectrum, for example,[101] contain the H_N and ^{15}N frequencies of amino acid i as well as the frequency of the carbonyl carbon atom of amino acid $i-1$. The HCA(CO)N spectrum[101] links H_α and C_α of amino acid i with the amide nitrogen atom of amino acid $i+1$ in an analogous fashion. The sequential assignment can thus be achieved by combining units that partly overlap. Besides the experiments mentioned above, several alternative pulse sequences are available (see Table 1).

The main advantage of this group of experiments is the relatively small number of cross peaks in the spectra; each amino acid shows only one or two cross peaks. This not only simplifies the manual evaluation but also facilitates automated assignment.

Figure 24 shows a three-dimensional view of the 3D-HCACO spectrum of cystatin. Most cross peaks are well resolved in all three frequency dimensions, and about 90% of the expected correlations can be observed.

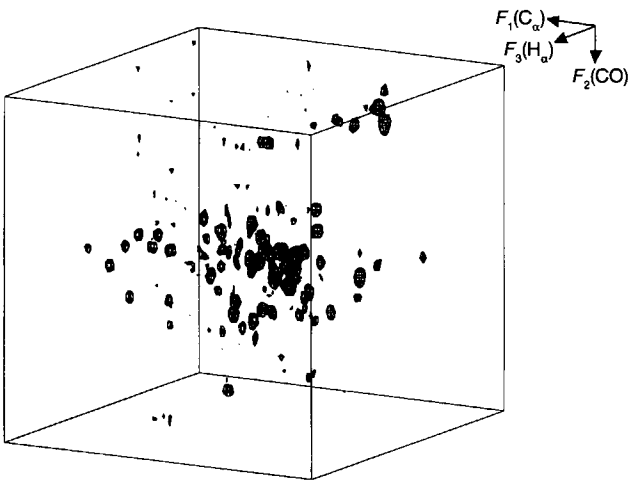


Fig. 24. Three-dimensional representation of the 3D-HCACO spectrum of cystatin.

3.3.3. *Identification of NOEs Using 3D- and 4D-HMQC-NOESY Techniques*

The experiments of the 3D-HMQC/HSQC-NOESY type discussed previously (Section 3.2.1) are especially important for ^{13}C-labeled proteins, as they can be used for the assignment of NOEs between protons in the amino acid side chains. The 3D spectra correspond to 2D-NOESY spectra resolved by means of the frequencies of the directly attached carbons. The NOE signals that occur symmetrically with respect to the diagonal of the 2D spectrum are distributed in two different planes of the 3D spectrum according to the frequencies of the directly bonded carbon atoms. The identification of NOEs is based on the known ^{13}C assignment by using a combination of these planes. This is shown in Figure 25 for the assignment of the NOE between F83-H_α and T69-H_α of cystatin. It is interesting to note that both side chains are clearly identified by their NOE patterns.

The assignment of long-range NOEs to side-chain protons follows the same principle and is shown in Figure 26 for the methyl groups of several alanine, valine, and isoleucine residues. The cross peak identified with a question mark could not be assigned despite the use of a 3D spectrum, because the H_α and C_α signals overlapped with other signals. In cases in which the three-dimensional spreading is not sufficient to make an assignment, a four-dimensional variant of the experiments can be used. Here all protons that contribute to an NOE are correlated with the directly connected heteronuclei, and 4D-HMQC-NOESY-HMQC spectra are obtained.[27, 121] One such experiment (4D-$^1H/^{13}C$-HMQC-NOESY-$^1H/^{13}C$-HMQC [121]) was

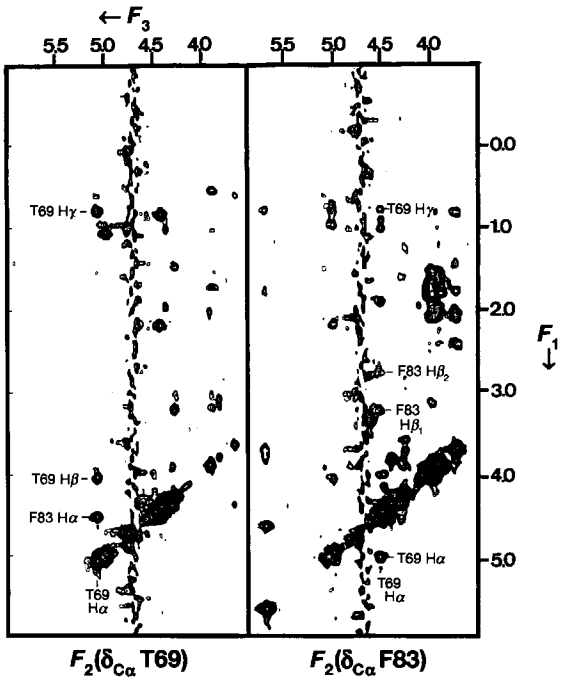


Fig. 25. Sections of two F_3 planes of the 3D-NOESY-^1H-^{13}C-HMQC spectrum of cystatin, which allow the identification of the H_α–H_α NOE between T69 and F83.

used to resolve the ambiguous assignment of the cross peak in Figure 26. The corresponding 4D cross peak appears at the coordinates H_β-(A90)-C_β(A90)-H_α(P87)-C_α(P87), which identifies the NOE as an interaction between the β-methyl group of alanine 90 and the α proton of P87.

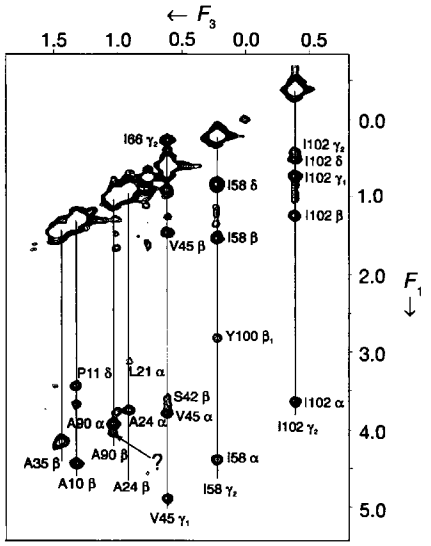


Fig. 26. The plane for $F_2 = 17.5$ (^{13}C) from the 3D-NOESY-^1H-^{13}C-HMQC spectrum of cystatin. The NOE signals of the methyl groups of some valine, isoleucine, and alanine residues are indicated. The signal labeled with a question mark could be assigned only by means of a 4D experiment as an NOE between P87 H_α and A90 H_β.

4. NMR Experiments for the Investigation of Backbone Dynamics of Proteins

The techniques developed for the structure determination of small- and medium-size proteins in solution by NMR spec-

troscopy also enable us to investigate their dynamic properties.[138-142]

The mobility of the peptide chain is reflected in the way protons and heteronuclei relax. As a consequence, the measurement of relaxation parameters (longitudinal relation time T_1, transverse relaxation time T_2, and hetero-NOE) give information concerning the inner dynamics of the protein. For the determination of the relaxation time of heteronuclei and the hetero-NOEs, slightly different H–X correlations of the HSQC-type are used.[143] For each parameter a series of measurements with different relaxation delays must be recorded. The plot of the intensities obtained provides a curve with exponential decay for each heteronucleus and can be used to determine the relaxation time. For the determination of the hetero-NOE, NOESY experiments with and without presaturation of the protons are performed. The NOE results from the relationship between the measured intensities of the cross peaks in both spectra. Figure 27 shows the derived T_1, T_2, and NOE values for cystatin.

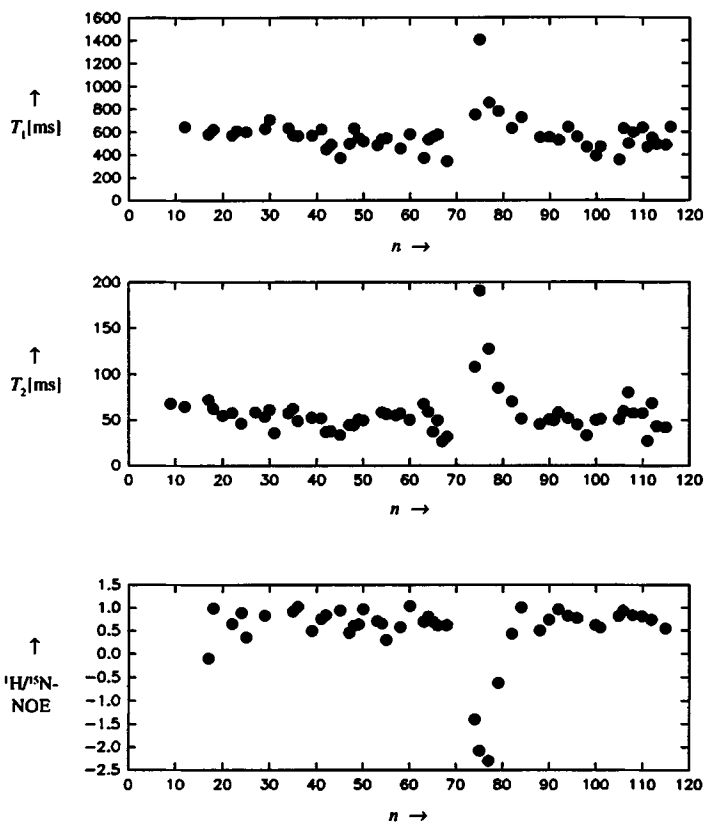


Fig. 27. Values for T_1, T_2, and the $^1H/^{15}N$ NOE of the individual amino acids in cystatin (n = position of the amino acid). There are strikingly different values in the region between C71 and C81, which indicates the higher mobility of the protein main chain in this region.

It clearly demonstrates the very different relaxation times of the ^{15}N nuclei, and as a result, the various mobilities of the protein main chain. In the region of amino acids 72–80, in particular, the relaxation behavior of the amide nitrogen nuclei resembles that of a small peptide more than that of a protein with more than 100 amino acid residues. The high mean variation in this region of the peptide chain (shown in the structures in Figure 17) is therefore no artifact caused by insufficient data but results from the real flexibility of the protein main chain.

5. Summary and Outlook

The introduction of multidimensional NMR techniques together with suitable labeling of recombinant synthesized proteins has made the structure determination of biologically important macromolecules ($M > 10$ kDa) in solution a straightforward matter. The methods described in this article are only a few of the experiments that can be used for the structure determination of proteins by NMR spectroscopy. With these techniques it is now possible to investigate structures of proteins with molecular weights of 20–35 kDa.

The ultimate size limit for proteins studied by NMR spectroscopy may not yet have been reached. Since the transverse relaxation time decreases with increasing molecular size, the applicability of experiments is strongly restricted to proteins with molecular weights < 35 kDa. We therefore assume that, at least with regard to a complete structure determination by NMR spectroscopy, a "natural upper limit" exists.

This work was supported by the Deutsche Forschungsgemeinschaft and the Sonderforschungsbereich 207. The authors thank Dr. E. A. Auerswald, Munich, and Prof. W. Sebald, Würzburg, for the preparation of labeled protein samples, and Dr. P. Neidig for the modification of the program AURELIA. We are also grateful to Bruker for technical support (8-mm probe). Plots of molecules were prepared with the program QUANTA (Molecular Simulations, Inc.).

Received: June 11, 1993 [A3 IE]
German version: *Angew. Chem.* **1994**, *106*, 284
Translated by Drs. M. Hofmann and H. Fry, Heidelberg (FRG)

[1] K. Wüthrich, *NMR of Proteins and Nucleic Acids*, 1st ed., Wiley, New York, **1986**.
[2] J. Jeener, Ampère International Summer School, Basko Polje, Yugoslavia, **1971**, unpublished.
[3] W. P. Aue, E. Bartholdi, R. R. Ernst, *J. Chem. Phys.* **1976**, *64*, 2229.
[4] R. R. Ernst, G. Bodenhausen, A. Wokaun, *Principles of Nuclear Magnetic Resonance in One and Two Dimensions*, 1st ed., Oxford University Press, New York, **1987**.
[5] R. R. Ernst, *Angew. Chem.* **1992**, *104*, 817; *Angew. Chem. Int. Ed. Engl.* **1992**, *31*, 805.
[6] H. Kessler, M. Gehrke, C. Griesinger, *Angew. Chem.* **1988**, *100*, 507; *Angew. Chem. Int. Ed. Engl.* **1988**, *27*, 490.
[7] D. Neuhaus, M. P. Williamson, *The Nuclear Overhauser Effect in Structural and Conformational Analysis*, 1st ed., VCH, Weinheim, **1989**.
[8] M. Karplus, *J. Am. Chem. Soc.* **1963**, *85*, 2870.
[9] V. F. Bystrov, *Prog. Nucl. Magn. Reson. Spectrosc.* **1976**, *10*, 41; V. F. Bystrov, A. S. Arseniev, D. Yu, J. Gavrilov, *J. Magn. Reson.* **1978**, *30*, 151.
[10] T. F. Havel, K. Wüthrich, *J. Mol. Biol.* **1985**, *182*, 281–294; *Bull. Math. Biol.* **1984**, *46*, 673.
[11] W. Braun, N. Go, *J. Mol. Biol.* **1985**, *186*, 611.
[12] W. F. van Gunsteren, H. J. C. Berendsen, *Angew. Chem.* **1990**, *102*, 1020; *Angew. Chem. Int. Ed. Engl.* **1990**, *29*, 992.
[13] A. T. Brünger, G. M. Clore, A. M. Gronenborn, M. Karplus, *Proc. Natl. Acad. Sci. USA* **1986**, *83*, 3801.
[14] W. Braun, G. Wider, K. Wüthrich, *J. Mol. Biol.* **1983**, *169*, 921.
[15] R. Kaptein, E. R. P. Zuiderweg, R. M. Scheek, R. Boelens, W. F. van Gunsteren, *J. Mol. Biol.* **1985**, *182*, 179.
[16] G. Wagner, W. Braun, T. F. Havel, T. Schaumann, T. Go, K. Wüthrich, *J. Mol. Biol.* **1987**, *196*, 611.
[17] A. D. Kline, K. Wüthrich, *J. Mol. Biol.* **1986**, *192*, 869.
[18] M. P. Williamson, T. F. Havel, K. Wüthrich, *J. Mol. Biol.* **1985**, *182*, 295.

[19] G. M. Clore, A. M. Gronenborn, *Protein Eng.* **1987**, *1*, 275.
[20] W. A. Hendrickson, K. Wüthrich (Eds.), *Macromolecular Structures* **1991**, 1.
[21] C. Griesinger, O. W. Sørensen, R. R. Ernst, *J. Am. Chem. Soc.* **1987**, *109*, 7227.
[22] G. W. Vuister, R. Boelens, R. Kaptein, *J. Magn. Reson.* **1988**, *80*, 176.
[23] H. Oschkinat, C. Griesinger, P. J. Kraulis, O. W. Sørensen, R. R. Ernst, A. M. Gronenborn, G. M. Clore, *Nature* **1988**, *332*, 374.
[24] S. W. Fesik, E. R. P. Zuiderweg, *J. Magn. Reson.* **1988**, *78*, 588.
[25] L. E. Kay, D. Marion, A. Bax, *J. Magn. Reson.* **1989**, *84*, 72.
[26] E. R. P. Zuiderweg, S. W. Fesik, *Biochemistry* **1989**, *28*, 2387.
[27] L. E. Kay, G. M. Clore, A. Bax, A. M. Gronenborn, *Science* **1990**, *249*, 411.
[28] G. M. Clore, P. Driscoll, P. T. Wingfield, A. M. Gronenborn, *J. Mol. Biol.* **1990**, *214*, 811.
[29] Y. Theriault, T. M. Logan, R. Meadows, L. Yu, E. T. Olejniczak, T. F. Holzman, R. L. Simmer, S. W. Fesik, *Nature* **1993**, *361*, 88.
[30] M. Ikura, G. M. Clore, A. M. Gronenborn, G. Zhu, C. B. Klee, A. Bax, *Science* **1992**, *256*, 632.
[31] N. Kruse, T. Lehrnbecher, W. Sebald, *FEBS Lett.* **1991**, *286*, 58.
[32] T. Müller, T. Dieckmann, W. Sebald, H. Oschkinat, unpublished.
[33] A. Barret, N. Rawlings, M. Davies, W. Machleidt, G. Salvesen, V. Turk, *Proteinase Inhibitors*, 1st ed., Elsevier, The Netherlands, **1986**.
[34] E. A. Auerwald, G. Genenger, R. Mentele, S. Lenzen, I. Assfalg-Machleidet, L. Mitschang, H. Oschkinat, H. Fritz, *Eur. J. Biochem.* **1991**, *200*, 131.
[35] U. Piantini, O. W. Sørensen, R. R. Ernst, *J. Am. Chem. Soc.* **1982**, *104*, 6800.
[36] M. Rance, O. W. Sørensen, G. Bodenhausen, G. Wagner, R. R. Ernst, K. Wüthrich, *Biochem. Biophys. Res. Commun.* **1983**, *117*, 458.
[37] A. J. Shaka, R. Freeman, *J. Magn. Reson.* **1983**, *51*, 169.
[38] N. Müller, R. R. Ernst, K. Wüthrich, *J. Am. Chem. Soc.* **1986**, *108*, 6482.
[39] L. Braunschweiler, R. R. Ernst, *J. Magn. Reson.* **1983**, *53*, 521.
[40] D. G. Davis, A. Bax, *J. Am. Chem. Soc.* **1985**, *107*, 2821.
[41] C. Giesinger, G. Otting, K. Wüthrich, R. R. Ernst, *J. Am. Chem. Soc.* **1988**, *110*, 7870.
[42] J. Jeener, B. H. Meier, P. Bachmann, R. R. Ernst, *J. Chem. Phys.* **1979**, *71*, 4546.
[43] A. A. Bothner-By, R. L. Stephens, J. Lee, C. D. Warren, R. W. Jeanloz, *J. Am. Chem. Soc.* **1984**, *106*, 811.
[44] A. A. Maudsley, R. R. Ernst, *Chem. Phys. Lett.* **1977**, *50*, 368.
[45] G. Bodenhausen, R. Freeman, *J. Magn. Reson.* **1977**, *28*, 471.
[46] G. Bodenhausen, D. J. Ruben, *Chem. Phys. Lett.* **1980**, *69*, 185.
[47] L. E. Kay, D. Marion, A. Bax, *J. Magn. Reson.* **1989**, *84*, 72.
[48] G. Wagner, *Methods Enzymol.* **1989**, *176*, 93.
[49] O. W. Sørensen, G. W. Eich, M. H. Levitt, G. Bodenhausen, R. R. Ernst, *Prog. Nucl. Magn. Reson. Spectrosc.* **1983**, *6*, 163.
[50] G. Bodenhausen, H. Kogler, R. R. Ernst, *J. Magn. Reson.* **1984**, *58*, 370.
[51] C. Griesinger, O. W. Sørensen, R. R. Ernst, *J. Magn. Reson.* **1989**, *84*, 14.
[52] D. Ziessow, *On Line Rechner in der Chemie, Grundlagen und Anwendungen in der Fourierspektroskopie*, de Gruyter, Berlin, **1976**.
[53] C. Bauer, R. Freeman, T. Frenkiel, J. Keeler, A. J. Shaka, *J. Magn. Reson.* **1984**, *58*, 442.
[54] H. Oschkinat, C. Cieslar, T. A. Holak, G. M. Clore, A. M. Gronenborn, *J. Magn. Reson.* **1989**, *83*, 450.
[55] P. Schmieder, H. Kessler, H. Oschkinat, *Angew. Chem.* **1990**, *102*, 588; *Angew. Chem. Int. Ed. Engl.* **1990**, *29*, 546.
[56] H. Kessler, P. Schmieder, H. Oschkinat, *J. Am. Chem. Soc.* **1990**, *112*, 8599.
[57] J. Schmidt, H. Rüterjans, *J. Am. Chem. Soc.* **1990**, *112*, 1279.
[58] A. Wokaun, R. R. Ernst, *Chem. Phys. Lett.* **1977**, *52*, 407.
[59] A. Bax, P. G. De Jong, A. F. Mehlkopf, J. Smidt, *Chem. Phys. Lett.* **1980**, *69*, 567.
[60] R. E. Hurd, *J. Magn. Reson.* **1990**, *87*, 422.
[61] A. L. Davis, E. D. Laue, J. Keeler, D. Moskau, J. Lohman, *J. Magn. Reson.* **1991**, *94*, 637.
[62] G. W. Vuister, R. Boelens, R. Kaptein, R. E. Hurd, B. John, P. C. M. van Zijl, *J. Am. Chem. Soc.* **1991**, *113*, 9688.
[63] A. L. Davis, R. Boelens, R. Kaptein, *J. Biomol. NMR* **1992**, *2*, 395.
[64] A. Ross, M. Czisch, C. Cieslar, T. A. Holak, *J. Biomol. NMR* **1993**, *3*, 215.
[65] E. T. Olejniczak, H. L. Eaton, *J. Magn. Reson.* **1990**, *87*, 628.
[66] C. Cieslar, T. A. Holak, H. Oschkinat, *J. Magn. Reson.* **1990**, *87*, 400.
[67] G. Zhu, A. Bax, *J. Magn. Reson.* **1990**, *90*, 405.
[68] R. Powers, D. S. Garrett, C. J. March, E. A. Frieden, A. M. Gronenborn, G. M. Clore, *Biochemistry* **1992**, *31*, 4334.
[69] K.-P. Neidig, R. Saffrich, M. Lorenz, H. R. Kalbitzer, *J. Magn. Reson.* **1990**, *89*, 543.
[70] M. Kjaer, K. V. Andersen, H. Shen, S. Ludvigsen, D. Windekilde, B. Sørensen, F. M. Poulsen, *NATO ASI Ser. Ser. A* **1991**, *225*, 291.
[71] C. Eccles, P. Güntert, M. Billeter, K. Wüthrich, *J. Biomol. NMR* **1991**, *2*, 111.
[72] H. Oschkinat, T. A. Holak, C. Cieslar, *Biopolymers* **1991**, *31*, 699.
[73] F. J. M. van de Ven, *J. Magn. Reson.* **1990**, *86*, 633.
[74] R. Bernstein, C. Cieslar, A. Ross, H. Oschkinat, J. Freund, T. A. Holak, *J. Biomol. NMR* **1993**, *3*, 245.
[75] T. L. James, *Curr. Opin. Struct. Biol.* **1991**, *1*, 1042.
[76] R. Boelens, T. M. G. Koning, R. Kaptein, *J. Mol. Struct.* **1988**, *173*, 299.
[77] P. Yip, D. A. Case, *J. Magn. Reson.* **1989**, *83*, 643.
[78] B. A. Borgias, T. L. James, *J. Magn. Reson.* **1988**, *79*, 493.
[79] S. G. Hyberts, M. S. Goldberg, T. F. Havel, G. Wagner, *Protein Sci.* **1992**, *1*, 736.
[80] G. M. Clore, A. M. Gronenborn, *J. Magn. Reson.* **1985**, *61*, 158.
[81] H. Oschkinat, C. Cieslar, C. Griesinger, *J. Magn. Reson.* **1990**, *86*, 453.
[82] R. Boelens, G. Vuister, T. M. G. Koning, R. Kaptein, *J. Am. Chem. Soc.* **1989**, *111*, 8525.
[83] S. Macura, R. R. Ernst, *Mol. Phys.* **1982**, *41*, 95.
[84] A. M. J. J. Bonvin, R. Boelens, R. Kaptein, *J. Magn. Reson.* **1991**, *95*, 626.
[85] T. A. Holak, J. Habazettl, H. Oschkinat, J. Otlewski, *J. Am. Chem. Soc.* **1991**, *113*, 3196.
[86] H. Kessler, S. Seip, J. Saulitis, *J. Biomol. NMR* **1991**, *1*, 83.
[87] O. W. Sørensen, *J. Magn. Reson.* **1990**, *90*, 433.
[88] W. Willker, D. Leibfritz, *J. Magn. Reson.* **1992**, *99*, 421.
[89] G. W. Vuister, A. Bax, *J. Biomol. NMR* **1992**, *2*, 401.
[90] J. C. Madsen, O. W. Sørensen, P. Sørensen, F. Poulsen, *J. Biomol. NMR* **1993**, *3*, 239.
[91] C. Griesinger, U. Eggenberger, *J. Magn. Reson.* **1992**, *97*, 426.
[92] U. Eggenberger, Y. Karimi-Nejad, H. Thürig, H. Rüterjans, C. Griesinger, *J. Biomol. NMR* **1992**, *2*, 583.
[93] J. Habazettl, A. Ross, H. Oschkinat, T. A. Holak, *J. Magn. Reson.* **1992**, *97*, 511.
[94] J. Habazettl, M. Schleicher, J. Otlewski, T. A. Holak, *J. Mol. Biol.* **1992**, *228*, 156.
[95] R. Bernstein, A. Ross, C. Cieslar, T. A. Holak, *J. Magn. Reson. Ser. B* **1993**, *101*, 185.
[96] D. Marion, P. C. Driscoll, L. E. Kay, P. T. Wingfield, A. Bax, A. M. Gronenborn, G. M. Clore, *Biochemistry* **1989**, *28*, 6150.
[97] E. R. P. Zuiderweg, L. P. Mcintosh, F. W. Dahlquist, S. W. Fesik, *J. Magn. Reson.* **1990**, *86*, 210.
[98] M. Wittekind, M. Gorlach, M. Friedrichs, G. Dreyfuss, L. Müller, *Biochemistry* **1992**, *31*, 6254.
[99] K. L. Constantine, V. Goldfarb, M. Wittekind, J. Anthony, S. C. Ng, L. Müller, *Biochemistry* **1992**, *31*, 5033.
[100] W. J. Fairbrother, A. G. Palmer III, M. Rance, J. Seizer, M. H. Saier, P. E. Wright, *Biochemistry* **1992**, *31*, 4413.
[101] L. E. Kay, M. Ikura, R. Tschudin, A. Bax, *J. Magn. Reson.* **1990**, *89*, 496.
[102] B. T. Farmer II, R. A. Venters, L. D. Spicer, M. G. Wittekind, L. Müller, *J. Biomol. NMR* **1992**, *2*, 195.
[103] M. G. Wittekind, L. Müller, *J. Magn. Reson. Ser. B* **1993**, *101*, 201.
[104] R. Weisemann, H. Rüterjans, W. Bermel, *J. Biomol. NMR* **1993**, *3*, 113.
[105] L. E. Kay, M. Ikura, A. Bax, *J. Magn. Reson.* **1991**, *91*, 84.
[106] A. G. Palmer III, J. C. Fairbrother, P. E. Wright, M. Rance, *J. Biomol. NMR* **1992**, *2*, 195.
[107] R. T. Clubb, V. Thanabal, G. Wagner, *J. Biomol. NMR* **1992**, *2*, 203.
[108] A. Bax, M. Ikura, *J. Biomol. NMR* **1991**, *1*, 99.
[109] R. T. Clubb, G. Wagner, *J. Biomol. NMR* **1992**, *2*, 389.
[110] S. Seip, J. Balbach, H. Kessler, *J. Biomol. NMR* **1993**, *3*, 233.
[111] S. J. Archer, M. Ikura, D. A. Torchia, A. Bax, *J. Magn. Reson* **1991**, *95*, 636.
[112] S. Grzesiek, J. Anglister, A. Bax, *J. Magn. Reson. Ser. B* **1993**, *101*, 114.
[113] S. Grzesiek, A. Bax, *J. Am. Chem. Soc.* **1992**, *114*, 6291.
[114] B. Lyons, G. T. Montelione, *J. Magn. Reson. Ser. B* **1993**, *101*, 206.
[115] W. Boucher, E. D. Laue, S. Cambell-Burk, P. J. Domaille, *J. Biomol. NMR* **1992**, *2*, 631.
[116] W. Boucher, E. D. Laue, S. Cambell-Burk, P. J. Domaille, *J. Am. Chem. Soc.* **1992**, *114*, 2262.
[117] L. E. Kay, M. Ikura, A. Bax, *J. Am. Chem. Soc.* **1990**, *112*, 888.
[118] M. Ikura, L. E. Kay, A. Bax, *J. Biomol. NMR* **1991**, *1*, 299.
[119] A. Bax, G. M. Clore, A. M. Gronenborn, *J. Magn. Reson.* **1990**, *88*, 425.
[120] E. T. Olejniczak, R. X. Xu, S. W. Fesik, *J. Biomol. NMR* **1992**, *2*, 655.
[121] G. M. Clore, L. E. Kay, A. Bax, A. M. Gronenborn, *Biochemistry* **1991**, *30*, 12.
[122] H. Oschkinat, C. Cieslar, A. M. Gronenborn, G. M. Clore, *J. Magn. Reson.* **1989**, *81*, 212.
[123] S. W. Fesik, R. T. Gampe, E. R. P. Zuiderweg, *J. Am. Chem. Soc.* **1989**, *111*, 770.
[124] L. Smith, C. Redfield, J. Boyd, G. M. P. Lawrence, R. G. Edwards, R. A. G. Smith, C. M. Dobson, *J. Mol. Biol.* **1992**, *224*, 899.
[125] A. Wlodaver, A. Pavlovsky, A. Gustchina, *FEBS Lett.* **1992**, *309*, 59.
[126] R. Powers, D. S. Garret, C. J. March, E. A. Frieden, A. M. Gronenborn, G. M. Clore, *Science* **1992**, *256*, 1673.
[127] M. R. Walter, W. J. Cook, B. G. Zhao, R. P. Cameron, S. E. Ealick, R. L. Walter, P. Reichert, T. L. Nagabhushan, P. P. Trotta, C. E. Brugg, *J. Biol. Chem.* **1992**, *267*, 20371.
[128] T. Müller, W. Sebald, H. Oschkinat, unpublished.
[129] W. Bode, R. Engh, D. Musil, B. Laber, M. Stubbs, R. Huber, V. Turk, *EMBO J.* **1988**, *7*, 2593.
[130] T. Dieckmann, L. Mitschang, M. Hofmann, J. Kos, V. Turk, E. A. Auerswald, R. Jaenicke, H. Oschkinat, *J. Mol. Biol.*, in press.

[131] R. Engh, T. Dieckmann, W. Bode, E. Auerswald, V. Turk, R. Huber, H. Oschkinat, *J. Mol. Biol.*, in press.
[132] V. Turk, J. Brzin, M. Longer, A. Ritonja, M. Eropkin, U. Borchert, W. Machleidt, *Hoppe-Seyler's Z. Physiol. Chem.* **1983**, *364*, 1487.
[133] G. M. Clore, A. Bax, P. C. Driscoll, P. T. Wingfield, A. M. Gronenborn, *Biochemistry* **1990**, *29*, 8172.
[134] W. J. Fairbrother, A. G. Palmer III, M. Rance, J. Reizer, M. H. Saier, P. E. Wright, *Biochemistry* **1992**, *31*, 4413.
[135] G. T. Montelione, G. Wagner, *J. Magn. Reson.* **1990**, *87*, 183.
[136] M. Ikura, L. E. Kay, A. Bax, *Biochemistry* **1990**, *29*, 4659.
[137] G. M. Clore, A. M. Gronenborn, *Prog. Nucl. Magn. Reson. Spectrosc.* **1991**, *23*, 43.
[138] D. M. Schneider, M. J. Dellwo, A. J. Wand, *Biochemistry* **1992**, *31*, 3645.
[139] G. Barbato, M. Ikura, L. E. Kay, R. W. Pastor, A. Bax, *Biochemistry* **1992**, *31*, 5269.
[140] C. Redfield, J. Boyd, L. J. Smith, R. A. G. Smith, C. M. Dobson, *Biochemistry* **1992**, *31*, 10431.
[141] R. Powers, G. M. Clore, S. J. Stahl, P. T. Wingfield, A. M. Gronenborn, *Biochemistry* **1992**, *31*, 9150.
[142] G. M. Clore, P. C. Driscoll, P. T. Wingfield, A. M. Gronenborn, *Biochemistry* **1990**, *29*, 7387.
[143] L. E. Kay, D. A. Torchia, A. Bax, *Biochemistry* **1989**, *28*, 8972.
[144] T. M. Logan, E. T. Olejniczak, R. X. Xu, S. W. Fesik, *J. Biomol. NMR* **1993**, *3*, 225.

A stop-gap solution?



If the latest library copy of Angewandte spends more time off the shelf than on, stop the gap with a personal subscription.

Just call or fax

VCH

USA: Tel. 1-(800) 422-8824; Fax (305) 428-8201
UK: Tel. (0223) 321111, Fax (0223) 313221

Time-Resolved Photoacoustic Calorimetry: From Carbenes to Proteins

Kevin S. Peters*

Why have molecules only been seen but not heard? For over a century chemists have probed reactions with various spectroscopic methods to learn about structures, dynamics, and reactivities of their molecules. What they have not done is to listen to their molecules react. Although the photoacoustic phenomenon has been known since 1880, it is only in the last twenty years that technology has developed to the point where sound waves produced by reacting molecules can be time resolved and the information contained within the waves deciphered. The information content within the photoacoustic wave is indeed rich, for one can learn about the dynamics and the magnitude of enthalpy changes associated with the reaction as well as the changes in molecular volume. This review article chronicles the development of time-resolved photoacoustic calorimetry and its application to a variety of reactions encountered in organic and organometallic chemistry and biochemistry.

1. Introduction

The realization that molecules produce sound following the absorption of light, the photoacoustic effect, dates back to 1880 when Alexander Graham Bell focused mechanically chopped sunlight upon a sample contained within a cell and listened to the sound by placing his ear against an open tube whose other end made contact with the sample cell.[1] The frequency of the sound that he heard corresponded to the frequency of the mechanical chopping. Today, we can listen to the sound produced by reacting molecules with the time resolution of one nanosecond.

The application of the photoacoustic effect to the study of the dynamics of enthalpy and volume changes originates with the experiments of Callis, Parson, and Gouterman in the early 1970s.[2] The experiment that was used to study *Chromatium vinosum* chromatophores utilized a capacitor microphone that measured the expansion and contraction of the solution caused by a change in the enthalpy and molecular volume upon the evolution of the reactants into the products. The time resolution approached 100 μs.

In 1985 we extended the time resolution of photoacoustic calorimetry onto the 100 ns timescale.[3] The increased time resolution resulted from employing piezoelectric transducers composed of lead zirconate/lead titanate for the detection of acoustic waves and a nanosecond laser for light initiation of the reactions. The photoacoustic calorimetry technology was adapted from the photoacoustic spectroscopic methods developed by Patel and Tam.[4] During this same period Braslavsky et al.[5] independently developed photoacoustic calorimetry. More recently the time resolution of photoacoustic calorimetry has been extended onto the 1 ns timescale by Caldwell, Melton, et al.[6]

In this review article we will discuss the theory, design, and application of time-resolved photoacoustic calorimetry as it has been developed in my laboratory and the laboratories of my former associates. The review is not comprehensive but instead attempts to convey the nature of the problems in organic and organometallic chemistry and biochemistry that can be addressed by this technique. An extensive review of photoacoustic calorimetry and related methodologies has recently appeared.[7]

2. Theory of Photoacoustic Calorimetry

The theory of the photoacoustic effect is well developed and has been thoroughly reviewed.[8] When a chemical reaction in solution is initiated by the absorption of light, the reacting molecules transfer their excess internal energy to the solvent. This sudden increase in the internal energy of the solvent causes its expansion, producing an acoustic wave that propagates through the medium. The amplitude of the acoustic wave is directly proportional to the amount of energy released by the reacting molecules. Acoustic waves are also produced by the increase or decrease in the molecular volume of the reacting molecules. This may be brought about by the cleavage of a covalent bond, (→ increase in the molecular volume) or the creation of charged species leading to electrostriction of the solvent about the charged centers (→ decrease in the molecular volume). Thus both a thermal expansion, ΔV_{th}, and a change in the molecular configuration of the system, ΔV_{con}, contribute to the production

[*] Prof. K. S. Peters
Department of Chemistry and Biochemistry
University of Colorado
Boulder, CO 80309-0215 (USA)
Telefax: Int. code + (303)492-5894

 © VCH Verlagsgesellschaft mbH, D-69451 Weinheim, 1994 0570-0833/94/0303-0294 $ 10.00+.25/0

of the acoustic wave. The amplitude of the acoustic wave, S, measured by the microphone is given by Equation (1), where K is a parameter which is a function of the instrument response.

$$S = K(\Delta V_{th} + \Delta V_{con}) \quad (1)$$

Since the amplitude of the acoustic wave is a measure of contributions of both ΔV_{th} and ΔV_{con}, the problem then arises as to how S is partitioned into the individual components. The volume change attributed to the thermal component is related to the thermal energy, Q, released to the solvent according to Equation (2), where β is the thermal expansion coefficient of the

$$\Delta V_{th} = (\beta/C_p\rho)Q \quad (2)$$

solvent, C_p is the heat capacity, and ρ the density of the solution. Since for aqueous solutions $\beta/C_p\rho$ is highly temperature dependent and approaches 0 at 3.9 °C for water, ΔV_{th} is a function of temperature. By contrast, ΔV_{con} is independent of temperature over a limited interval. Therefore in aqueous media the contributions of ΔV_{th} and ΔV_{con} can be separated by examining the temperature dependence of the acoustic wave amplitude, S. Unfortunately, for organic solvents $\beta/C_p\rho$ is virtually independent of temperature such that the temperature dependence of S cannot be used to separate the contributions of ΔV_{th} and ΔV_{con}. However, one approach to separating these terms is to examine the reaction in a variety of organic solvents with similar solvating abilities but different thermoexpansion coefficients β (see Section 4.1). To date, most photoacoustic studies of reactions in organic solvents have assumed that ΔV_{con} makes only a minor contribution to the overall acoustic wave amplitude and can thus be neglected.

The instrument response function parameter K may be eliminated from the analysis by employing a calibration compound that converts the entire energy of the photon, $E_{h\nu}$, into heat, and undergoes no changes in its molecular structure ($\Delta V_{con} = 0$) on the timescale of the instrument resolution. The acoustic wave amplitude for the calibration compound, S_{cal}, is given by Equation (3). K is eliminated by dividing the acoustic wave amplitude S by S_{cal} [Eq. (4)]. If ΔV_{con} is negligible, then the heat released

$$S_{cal} = K(\beta/C_p\rho)E_{h\nu} \quad (3)$$

$$\phi = S/S_{cal} = (Q/E_{h\nu}) + \{\Delta V_{con}/[(\beta/C_p\rho)E_{h\nu}]\} \quad (4)$$

during the reaction, Q, equals $E_{h\nu}\phi$. For aqueous solutions the correlation of ϕ with $1/(\beta/C_p\rho)$ yields both Q and ΔV.

The transducers used in the detection of acoustic waves are sensitive not only to the amplitude of the acoustic waves but also to their temporal profile. If a reaction involves two sequential decay steps [Eq. (5)], then the observed time-dependent voltage

$$A \xrightarrow{k_1} B \xrightarrow{k_2} C \quad (5)$$

produced by the transducer, $E(t)_{obs}$, will reflect both decay processes, $H(t)$. $E(t)_{obs}$ is produced by the convolution of $H(t)$ with the instrument response function, $T(t)$, which may be independently determined from the calibration compound [Eq. (6)]. For

$$E(t)_{obs} = H(t) * T(t) \quad (6)$$

the two sequential decays in Equation (5), $H(t)$ is expressed according to Equation (7), where ϕ_i is defined by Equation (4).[3] Numerous algorithms have been developed for obtaining the parameters ϕ_i and k_i.[9]

$$H(t) = \phi_1 \exp(-tk_1) + [\phi_2 k_1/(k_2 - k_1)][\exp(-tk_1) - \exp(-tk_2)] \quad (7)$$

3. Photoacoustic Calorimeter

Numerous designs of photoacoustic calorimeters have appeared.[3, 6, 7] Their basic components are a laser for excitation and a transducer for detection of the acoustic waves. The transducers are composed of either polyvinylidene difluoride (PVF_2) thin films or piezoelectric ceramics. PVF_2 thin films have been used as broad-band detectors that directly follow the real time propagation of the acoustic waves. An intrinsically more sensitive detector is the piezoelectric transducer composed of lead zirconate/lead titanate. The output of the transducer is normally passed through a pre-amplifier and then time resolved by a transient digitizer. The arrangement is very sensitive to small temperature changes; for a 10 μJ laser pulse with a beam diameter of 1 mm passed through a 1 cm cuvette, the temperature change along the cylinder defined by the laser beam that generates the acoustic wave is on the order of 10^{-6} °C. The corresponding volume change is 10^{-10} mL.

The plot in Figure 1 illustrates how kinetic phenomena are manifested in the acoustic waves. Irradiation (λ = 365 nm) of



Kevin S. Peters was born in 1949 in Ponca Cita, Oklahoma, USA, received his B. S. in chemistry in 1971 from the University of Oklahoma, and earned his Ph.D. in 1975 for his work with Kenneth Wiberg at Yale. Following postdoctoral research with Fred Richards (Yale), Meredith Applebury (Princeton), and Peter Rentzepis (Bell Laboratories), he accepted a position as professor at Harvard in 1978. He has been a professor of chemistry in the Department of Chemistry and Biochemistry at the University of Colorado at Boulder since 1984. He is a recipient of the Alfred P. Sloan Fellowship and the Henry and Camille Dreyfuss Teacher–Scholar Award. His research focuses on the dynamics and energetics of reactive intermediates in organic and organometallic chemistry and biochemistry.

the calibration compound ferrocene in benzene produces acoustic wave A. This curve represents the response of the piezoelectric transducer to an impulse. Curve B is produced following irradiation ($\lambda = 365$ nm) of benzophenone in benzene. The shift in curve B relative to curve A reflects kinetic phenomena of the reaction of benzophenone on the timescale of the response of the transducer. The first event is the formation of the triplet state of benzophenone from the decay of its singlet state, which occurs in less than 20 ps and thus cannot be temporally resolved. The

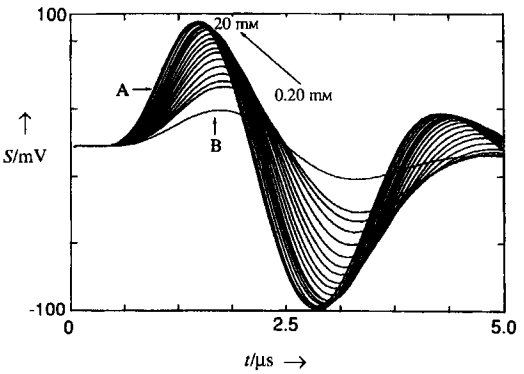


Fig. 1. Acoustic waves generated by the irradiation ($\lambda = 365$ nm) of ferrocene (calibration compound, optical density $OD_{365} = 0.3$, curve A), benzophenone ($OD_{365} = 0.3$, curve B), and benzophenone in the presence of 2,3-dimethyl-2-butene (0.2 mM–20 mM). See text for details.

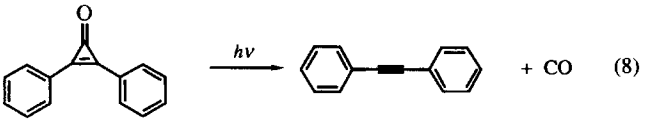
second event is the decay of the triplet state of benzophenone on the 10 μs timescale. The acoustic waves between curve A and curve B are produced when the triplet state of benzophenone is quenched by 2,3-dimethyl-2-butene (0.2 to 20 mM). Analysis of these acoustic waves reveals that the rate constant for the quenching of the triplet state of benzophenone by 2,3-dimethyl-2-butene is $1.30 \pm 0.02 \times 10^9$ L mol^{-1} s^{-1}. These waves are produced by kinetic events within the time range of 38 ns to 3.8 μs.

4. Organic Reactions

Photoacoustic calorimetry allows organic chemists for the first time to directly measure the reaction enthalpies for highly reactive species such as radicals, diradicals, and carbenes in the condensed phase. Prior to this development the energetics for these species could only be estimated. With direct measurements chemists can begin to critically examine the theoretical predictions for the heats of formation and the heats of reaction of highly reactive species.

4.1. Decomposition of Diphenylcyclopropenone

One of the first applications of photoacoustic calorimetry in organic chemistry was an estimation of the resonance energy of diphenylcyclopropenone.[10] The resonance energy was derived from the heat of reaction for the photoinduced decomposition of diphenylcyclopropenone to form diphenylacetylene and carbon monoxide [Eq. (8)], and the heats of formation of the constituent molecules using Benson's group additivity method.



(8)

Irradiation ($\lambda = 337$ nm) of diphenylcyclopropenone in benzene produces diphenylacetylene and CO with quantum yield 1.0. The experimentally derived heat of reaction is -9.9 ± 2.9 kcal mol^{-1}, which leads to an estimate for the resonance energy of -11 kcal mol^{-1}.[10]

In the original study it was assumed that the change in volume due to a change in molecular configuration, ΔV_{con}, was negligible and thus that the resulting acoustic wave was produced only by a release of heat. Recently, Hung and Grabowski have examined the magnitude of the contribution of ΔV_{con} in the decomposition of diphenylcyclopropenone.[11] The contribution of ΔV_{con} was obtained by studying reaction (8) in a homologous series of alkane solvents, whose thermal expansion coefficient, β, varied with chain length. It was implicitly assumed that H_{rxn} and ΔV_{con} are constant in the series of alkane solvents. Their analysis revealed that $H_{rxn} = -6.7 \pm 1.2$ kcal mol^{-1} and $\Delta V_{con} = 23 \pm 4$ mL mol^{-1}. The magnitude of this volume change is that expected for the cleavage of two carbon–carbon bonds; the average volume change associated with the cleavage of one carbon–carbon bond is 10 mL mol^{-1}.[11]

This more recent study reveals that neglecting the contribution of ΔV_{con} led to an overestimation of H_{rxn} by 3 kcal mol^{-1} for reaction (8) in the original study. Clearly for reactions that involve the formation or cleavage of covalent bonds, ΔV_{con} can make a significant contribution to the acoustic wave amplitude in organic solvents.

4.2. Reactions of Carbenes

In recent years there has been a renewed interest, both theoretical and experimental, in the reactivity of carbenes.[12a] Although there have been a variety of methods developed for determining the reactivity of carbenes, until the development of photoacoustic calorimetry there had been little progress in obtaining the energetics for these reactions. Now one is able to measure the enthalpy change for the formation of carbenes and their reactions with a great variety of substrates.

4.2.1. Diphenylcarbene

The dynamics, structural characteristics, and reactivity of the spin states of diphenylcarbene have been well characterized. Eisenthal et al. have shown that the photolysis of diphenyldiazomethane produces singlet carbene within 25 ps which undergoes intersystem crossing to the triplet carbene on the 100 ps timescale [Eq. (9)].[12b] The kinetics of this latter process are de-

$$Ph_2CN_2 \xrightarrow{h\nu} {}^1Ph_2C: + N_2 \xrightarrow{k_{isc}} {}^3Ph_2C: + N_2 \qquad (9)$$

pendent upon solvent polarity. Little is known regarding the energetics for the formation of diphenylcarbene and its associated reactions.

Employing photoacoustic calorimetry we have measured the enthalpy change for the formation of triplet diphenylcarbene from diphenyldiazomethane in benzene [Eq. (10)].[13] The enthalpy change associated with the intersystem crossing of singlet diphenylcarbene to triplet diphenylcarbene was not time resolved, as this process occurs on the 100 ps timescale and the time resolution of the photoacoustic calorimeter was approximately 50 ns. The analysis of the acoustic data to obtain the heat of reaction did not take into account the contribution due to the increase in the molecular volume of the system that accompanied the molecular dissociation. Based upon the experiments of Grabowski,[11] the reported enthalpy change may be in error by as much as 3 kcal mol^{-1}.

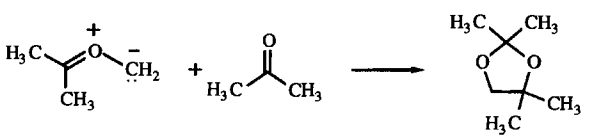
$$Ph_2CN_2 \longrightarrow {}^3Ph_2C: + N_2 \quad \Delta H = 0 \pm 1.7\ \text{kcal mol}^{-1} \qquad (10)$$

Following the formation of triplet diphenylcarbene, a subsequent reaction with molecular oxygen forms benzophenone oxide, the "Criegee intermediate" [Eq. (11)].[13] In oxygen-saturated benzene this reaction occurs within 220 ± 29 ns.

$$^3Ph_2C: + O_2 \rightarrow Ph_2COO \quad \Delta H = -34.7 \pm 2.4\ \text{kcal mol}^{-1} \qquad (11)$$

4.2.2. *Alkylcarbenes*

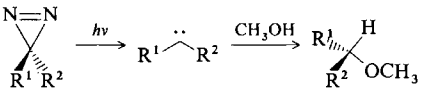
Goodman et al. have developed an extensive research program examining the dynamics and energetics for the reactions of carbenes.[14–20] In one of their first studies they examined the reaction of ylide **1** with acetone to form 2,2,4,4-tetramethyl-1,3-dioxolane (**2**); ylide **1** was produced by the photolysis of diazomethane in acetone.[14] The enthalpy change ΔH is -57.1 ± 13.4 kcal mol^{-1} for the addition reaction giving **2**. From the heat of formation of acetone and the calculated heat of formation of dioxolane **2**, the heat of formation of ylide **1** is derived, $\Delta H_f(\mathbf{1}) = 4.5 \pm 9.9$ kcal mol^{-1}.



1 **2**

One of the proposed reactions of ylide **1** is bond cleavage to form singlet methylene and acetone.[14] From the heats of formation of ylide **1**, methylene (102 kcal mol^{-1}), and acetone (-52.1 kcal mol^{-1}), the enthalpy change for this dissociation is estimated to be 45 kcal mol^{-1}. Given the endothermicity of this reaction it is unlikely that fragmentation of ylide **1** occurs to a significant extent. This value for the enthalpy of fragmentation is in close agreement with the value of 38 kcal mol^{-1} calculated by Houk et al for the fragmentation of formaldehyde *O*-methylide.[21]

In a subsequent study Goodman et al. measured the enthalpy changes associated with the photolysis of diazirines **3a–d** to form the corresponding carbenes **4a–d**, which then insert into the O–H bond of methanol to form the ethers **5a–d**.[15] The enthalpy changes are given in Table 1; the heats of formation for carbenes **4a–d** were deduced from these values. When the experimental heats of formation were compared with the values obtained from MNDO calculations, the experimentally determined values were consistently lower by 10–20 kcal mol^{-1}.[15] The proposed rationale for this discrepancy is that the ΔV_{con} makes a significant contribution to the acoustic wave amplitudes or that the solvation energy for the carbene is high. Alternately, the MNDO calculations may be in error. Clearly, this will be a fruitful area for further investigation.



3 **4** **5**

a, R^1 = Ph, R^2 = F; **b**, R^1 = Ph, R^2 = Cl;
c, R^1 = Ph, R^2 = Br; **d**, R^1 = OMe, R^2 = Cl

Table 1. Enthalpy changes for the reactions **3a–d** → **4a–d** (ΔH_1) and **4a–d** → **5a–d** (ΔH_2), and the heats of formation of **4a–d** (ΔH_f).

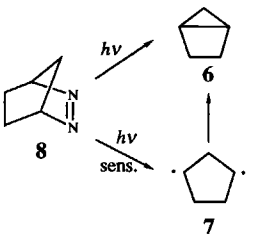
Cmpd.	ΔH_1 [kcal mol^{-1}]	ΔH_2 [kcal mol^{-1}]	ΔH_f [kcal mol^{-1}]
3a	-7.9 ± 2.1	-49.4	27.3
3b	-11.1 ± 1.6	-50.9	67.1
3c	-11.4 ± 2.0	-50.6	79.8
3d	-39.9 ± 2.9	-31.2	-21.6

Goodman and his associates also have used photoacoustic calorimetry to study 1,2 intramolecular hydrogen shifts in halomethylcarbenes, which are produced photochemically from the corresponding diazirines, to form vinyl halides.[17, 19] For chloromethylcarbene the enthalpy change for the 1,2 hydrogen shift is -59.5 kcal mol^{-1}; for bromomethylcarbene this value decreases to -48.9 kcal mol^{-1}. These values are in good agreement with AM1 calculations for the heats of these reactions.

4.3. Reactions of 1,3-Diradicals*

Diradicals are often postulated to be intermediates in thermal rearrangements of cycloalkanes, and thus it is important to be able to estimate their heats of formation.[22] However, there is little direct thermochemical data for diradicals. For example in the thermal isomerization of bicyclopentane (**6**) the heat of formation of the transition state is 76 kcal mol^{-1}. The estimate for the heat of formation of the 1,3-diradical **7** is 67 kcal mol^{-1}. This suggests that the enthalpy of activation for the closure of **7** to form **6** is 9 kcal mol^{-1}. However, the experimental energy of activation for the ring closure is only 2.3 kcal mol^{-1}, which calls into question the validity of the calculated heat of formation for **7**.[23]

Herman and Goodman have determined the heat of formation of **7** by time-resolved photoacoustic calorimetry.[24] The direct irradiation of diazene **8** produces bicyclopentane (**6**) in less than 10 ns; the heat of reaction ΔH_{86} is -20.4 kcal mol^{-1}. Under conditions of triplet sensitization **8** decomposes to form the long-lived triplet state of **7** with a heat of reac-



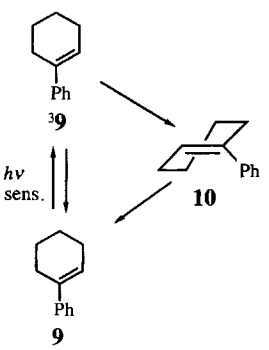
8 **6** **7**

tion of $\Delta H_{87} = 14.1$ kcal mol^{-1}. The heat of formation $\Delta H_f(7)$ is then obtained from relationship $\Delta H_f(7) = \Delta H_f(6) - \Delta H_{86} + \Delta H_{87}$. With $\Delta H_f(6) = 37.0$ kcal mol^{-1}, the value of $\Delta H_f(7)$ is 71.5 ± 2.3 kcal mol^{-1}. This higher value for the heat of formation of **7** is consistent with the experimentally determined energy of activation for the ring closure of **7** and the heat of formation for the transition state for the isomerization of **6**.

These experiments also revealed that the lifetime for the triplet state of **7** is 316 ns, which is significantly shorter that deduced by using oxygen trapping (720 ns).[24] This was the first measurement of the lifetime of a nonconjugated diradical in solution.

4.4. Strain Energy of *trans*-1-Phenyl-cyclohexene

Although there have been numerous attempts to quantify the strain energy in a variety of organic compounds, little is known regarding the magnitude of the torsional strain about double bonds in cyclic systems.[25] One such molecule is *trans*-1-phenylcyclohexene (**10**). Triplet sensitization of *cis*-1-phenylcyclohexene (**9**) with benzophenone produces its triplet state ^{3}**9**, whose lifetime is 65 ns. *trans*-1-Phenylcyclohexene (**10**) is produced from ^{3}**9** with a quantum yield of 0.36, and it in turn rearranges into **9** in 9 μs.



Employing photoacoustic calorimetry we have determined the strain energy of **10**, defined as the difference in the enthalpies of **10** and **9**, to be 44.7 ± 5.0 kcal mol^{-1}.[25] The energy of the triplet state ^{3}**9** is 56.0 ± 3.4 kcal mol^{-1}. This latter value was the first directly measured energy for the relaxed triplet state of an alkene. More recently several photoacoustic calorimetry studies of the relaxed triplet state energies for alkenes and dienes have been published.[26–29]

4.5. O–H Bond Enthalpies

Another application of time-resolved photoacoustic calorimetry has been in the determination of substituent effects upon the enthalpy of the O–H bond in phenols.[13, 30] These bond enthalpies can be derived from the heat of reaction associated with the abstraction of the OH hydrogen atom by *tert*-butoxy radical and the known enthalpy of the O–H bond in *tert*-butyl alcohol as outlined in Equations (12) and (13).

$$t\text{BuO–O}t\text{Bu} \xrightarrow{h\nu} 2\ t\text{BuO}^{\bullet} \quad (12)$$

$$t\text{BuO}^{\bullet} + \text{X–C}_6\text{H}_4\text{OH} \longrightarrow t\text{BuOH} + \text{X–C}_6\text{H}_4\text{O}^{\bullet} \quad (13)$$

The O–H bond enthalpies have been measured for several substituted phenols along with the kinetics for hydrogen atom abstraction (Table 2).[13] The value for phenol, 84.4 ± 1.1 kcal mol^{-1}, is in good agreement with the value determined by gas-phase methods, 86.5 ± 2.0 kcal mol^{-1}.[13] There is a correlation between the kinetics of hydrogen atom abstraction and the bond dissociation energy.

Table 2. Bond dissociation energies (BDE) for hydrogen atom abstraction from substituted phenols (0.06 M in benzene) by *tert*-butoxy radical and the associated half-lives τ.

Phenol	BDE [kcal mol^{-1}]	τ [ns]
4-cyanophenol	88.2 ± 1.1	227
phenol	84.4 ± 1.1	175
4-*tert*-butylphenol	83.2 ± 0.8	213
4-phenylphenol	83.0 ± 1.1	151
4-methoxyphenol	77.9 ± 0.9	128

5. Organometallic Reactions

To develop an understanding of the reactivity and selectivity in organometallic chemistry it is important to have a measure of metal–ligand and metal–metal bond enthalpies. To date there have only been a few thermochemical studies of bond energies for organometallic compounds in solution. With the advent of photoacoustic calorimetry a number of metal–ligand, metal–hydrogen, and metal–metal bond enthalpies have been obtained.

5.1. Metal–Ligand Bond Enthalpies

The first organometallic compound to be studied by photoacoustic calorimetry was $[Cr(CO)_6]$.[31, 32] Upon irradiation ($\lambda = 337$ nm) in heptane, $[Cr(CO)_6]$ undergoes CO dissociation followed by complexation with the solvent within picoseconds. In the presence of a ligand L the coordinated solvent molecule is then displaced [Eq. (14)]. The values for ΔH_1, ΔH_2, and k for a variety of ligands are given in Table 3. From gas-phase stud-

$$[Cr(CO)_6] \xrightarrow[\text{heptane},\ \Delta H_1]{h\nu} [Cr(CO)_5(\text{heptane})] \xrightarrow[\Delta H_2]{k[L]} [Cr(CO)_5L] \quad (14)$$

ies the enthalpy of CO dissociation from $[Cr(CO)_6]$ is 36.8 kcal mol^{-1}.[33] The enthalpy ΔH_1 for the substitution of

Table 3. Reaction enthalpies for the substitution of CO in $[Cr(CO)_6]$ by heptane (ΔH_1) and for the substitution of heptane in $[Cr(CO)_5(\text{heptane})]$ by L (ΔH_2), and the associated rate constants k.

L	ΔH_1 [kcal mol^{-1}]	ΔH_2 [kcal mol^{-1}]	k [10^{-7} L mol^{-1}]
THF	27.2 ± 1.2	-12.4 ± 1.2	11.8
2,5-dimethyltetrahydrofuran	27.1	−10.8	5.3
ethanol	26.5	−13.8	3.6
acetone	27.3	−13.5	15.9
acetonitrile	26.8	−18.2	27.1
N*n*Bu$_3$	27.3	−12.2	1.2
P*n*Bu$_3$	26.3	−21.6	–
1-hexene	27.2	−12.2	3.0
2,3-dimethyl-2-butene	27.2	−9.6	2.6

CO by heptane is 27.0 kcal mol^{-1}. The difference between the two values, 9.8 kcal mol^{-1}, is the enthalpy for the coordination of heptane to [Cr(CO)$_5$]. As expected, the most strongly binding ligands are P*n*Bu$_3$ and acetonitrile. The binding energies for the remainder of the ligands are very similar with the notable exceptions of 2,5-dimethyltetrahydrofuran, which binds 1.6 kcal mol^{-1} less strongly than THF, and tetramethylethylene, whose binding energy is 2.6 kcal mol^{-1} less than that of 1-hexene. These differences are attributed to increased steric interactions.

The kinetics for the displacement of heptane from [Cr(CO)$_5$(heptane)] do not correlate with the reaction enthalpies. The primary factor that governs the rate of substitution would appear to be steric requirements for the incoming ligand. However, there are some notable exceptions; the rate constants for ethanol, for example, appear to be too small based on steric considerations. This anomaly may be a consequence of hydrogen bonding.

In a similar study Klassen and Yang determined the enthalpy change ΔH_2 for the replacement of heptane in [Cr(CO)$_5$(heptane)] by *cis*-cyclooctene to be -14.2 ± 0.9 kcal mol^{-1}, and by *trans*-cyclooctene to be -19.5 kcal mol^{-1}.[34] The greater binding enthalpy of *trans*-cyclooctene relative to *cis*-cyclooctene ($\Delta H_2 = -5$ kcal mol^{-1}) is attributed to the release of the strain energy in *trans*-cyclooctene upon binding to the metal center as a result of a change in hybridization at the olefinic carbon atoms.

Yang et al. have also examined metal–ligand bond dissociation energies for [CpMn(CO)$_2$L] complexes [Eq. (15), Table 4).[35–37]

$$[CpMn(CO)_3] \xrightarrow[\text{heptane, } \Delta H_1]{h\nu} [CpMn(CO)_2(\text{heptane})] \xrightarrow[\Delta H_2]{k[L]} [CpMn(CO)_2L] \quad (15)$$

Table 4. Reaction enthalpies for the substitution of CO in [CpMn(CO)$_3$] by heptane (ΔH_1) and for the substitution of heptane in [CpMn(CO)$_2$(heptane)] by L (ΔH_2), and the associated rate constants *k*.

L	ΔH_1 [kcal mol^{-1}]	ΔH_2 [kcal mol^{-1}]	k [10^{-6} L mol^{-1}]
THF	46.2 ± 1.2	−16.1 ± 1.4	4.4 ± 0.1
acetone	47.8 ± 1.7	−17.4 ± 1.0	3.6 ± 0.4
cis-cyclooctene	47.6 ± 1.4	−24.5 ± 2.3	2.3 ± 0.4
Bu_2S	45.3 ± 1.4	−28.7 ± 2.2	8.2 ± 0.5
Et_3SiH	46.7 ± 2.2	−20.1 ± 2.1	2.5 ± 0.5

In comparisons of the metal–CO bond enthalpies in [Cr(CO)$_6$] and [CpMn(CO)$_3$], the Mn–CO bond enthalpy is 20 kcal mol^{-1} greater than the Cr–CO bond enthalpy. Since the enthalpy of the Mn–CO bond is not known in the gas phase, it is not possible to determine the heptane binding enthalpy in [CpMn(CO)$_2$(heptane)].

5.2. Metal–Metal Bond Enthalpies

A variety of methodologies have been utilized in obtaining the enthalpy of the metal–metal bond in [Mn$_2$(CO)$_{10}$].[38] A wide range of values have been determined: 16 kcal mol^{-1}, 22.5 kcal mol^{-1}, and 34 ± 13 kcal mol^{-1} from thermochemical measurements, values ranging from 19 to 28 kcal mol^{-1} from electron-impact mass spectrometry, 36.8 kcal mol^{-1} from kinetic measurements in solution, and 41 ± 9 kcal mol^{-1} from ICR-photoelectron spectroscopy (ICR = ion cyclotron resonance). This range of values indicates the difficulty of obtaining good thermochemical data for metal–metal bond enthalpies.

In a kinetic study of the photodissociation of [Mn$_2$(CO)$_{10}$] on the picosecond timescale we found that there are two dissociation pathways: cleavage of the metal–metal bond to form two [Mn(CO)$_5$] units and dissociation of CO to give [Mn$_2$(CO)$_9$]. Both reactions occur within 25 ps of excitation.[38] The dominant pathway is cleavage of the metal–metal bond, as the quantum yield for CO dissociation is 0.1. When a previously determined value of 36 kcal mol^{-1} is used for the Mn–CO bond enthalpy,[38] the value obtained for enthalpy of the Mn–Mn bond in [Mn$_2$(CO)$_{10}$] is 38.0 ± 5.0 kcal mol^{-1}.

5.3. Metal–Hydrogen Bond Enthalpies

Reactions involving metal–hydrogen bonds are fundamental in organometallic chemistry and yet little is known about these bond enthalpies. A general approach for obtaining this thermochemical information is by studying the abstraction of the hydrogen atom from a metal hydride by *tert*-butoxy radical [Eq. (16), see also Section 4.5).

$$L_nM{-}H + t\text{BuO}^{\cdot} \longrightarrow L_nM^{\cdot} + t\text{BuOH} \quad (16)$$

We have used this approach to measure the enthalpy of the metal–hydrogen bond in [(η^5-C$_5$Me$_5$)(PMe$_3$)IrH$_2$].[39] The Ir–H bond enthalpy is 72.9 ± 4.3 kcal mol^{-1}, which is in excellent agreement with value of 74 kcal mol^{-1} derived from kinetic measurements.[39] The method should be generally applicable for the determination of metal–hydrogen bond enthalpies.

6. Reactions of Proteins

Understanding the relationship between the molecular motion of a protein and its function is essential for the development of models for enzyme action. Protein structures provided by X-ray crystallography have provided a wealth of information for understanding protein function. However, the picture is incomplete without full characterization of the intermediates that intervene in protein action. One would like to understand how the dynamics and energetics of substrate binding and catalytic function are controlled by protein structure. A number of methodologies have been developed that provide information relating to the intermediates in the reactions of proteins. These techniques include time-resolved absorption spectroscopy, Raman, EPR, NMR, and IR spectroscopy. Information has been notably lacking on the dynamics of the enthalpy changes and the associated molecular motions for protein function on short timescales. Photoacoustic calorimetry is beginning to provide such insights for proteins.

Photoacoustic calorimetry has been used to study the dynamics of photodissociation of carbon monoxide from carboxymyoglobin[40-42] and carboxyhemoglobin,[43] the energetics of the intermediates formed in the bleaching of the visual protein rhodopsin,[44] the dynamics of proton pumping in bacteriorhodopsin,[45] electron transfer in reaction centers, and the photophysics and photochemistry of the plant photosensor pigments phytochrome and chlorophyll.[46,47]

6.1. Myoglobin

One of the most extensively investigated proteins is sperm whale myoglobin, an oxygen storage protein. Although the mechanism of myoglobin function has been addressed by numerous experimental and theoretical studies, two fundamental points are still not understood. The first is the pathway by which a ligand diffuses between the heme pocket and the solvent. The second is how the protein structure modulates the binding energy of the ligand. X-ray studies reveal that there are no channels for ligand diffusion that directly connect the heme pocket with the solvent. Therefore, the protein must undergo significant structural changes to allow ligand diffusion. The dynamics and energetics of these processes are unknown. With the development of photoacoustic calorimetry, we are beginning to gain insight into the nature of these processes.

The photophysics of carboxymyoglobin (MbCO) have been well characterized [Eq. (17)].[48] After MbCO absorbs a photon,

$$\mathrm{MbCO} \xrightarrow{h\nu} (\mathrm{MbCO})^{*} \xrightarrow{350\ \mathrm{fs}} \mathrm{Mg{:}CO} \xrightarrow{180\ \mathrm{ns}} \mathrm{Mb{:}::CO} \xrightarrow{???} \mathrm{Mg} + \mathrm{CO} \quad (17)$$

its excited state decays by cleavage of the Fe–CO bond within 350 fs to create the geminate pair Mb:CO, in which the ligand is located within the heme pocket. Within 180 ns at room temperature CO diffuses out of the heme pocket into the protein matrix (Mb:::CO) and then into the solvent (Mb + CO). The dynamics of this latter process are unknown.

Time-resolved photoacoustic spectra of MbCO in 0.1 M Tris-HCl buffer following irradiation ($\lambda = 510$ nm) are shown in Figure 2. Also displayed is the spectrum of the calibration compound, deoxymyoglobin (Mb), which converts the entire photon energy into heat and undergoes no conformational changes.

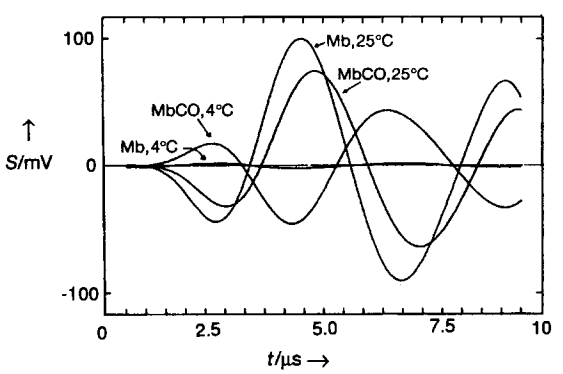
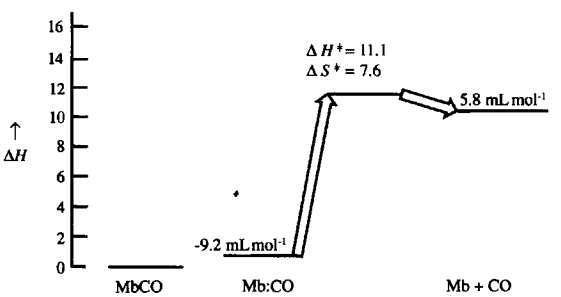


Fig. 2. The temperature dependence of the photoacoustic signal from carboxymyoglobin (MbCO), (1.6×10^{-5} M), and deoxymyoglobin (Mb) (1.6×10^{-5} M) in 0.1 M Tris-HCl, pH 8.0. $T = 25$ and 4 °C, irradiation with $\lambda = 510$ nm.

At 25 °C there is a pronounced shift in the MbCO acoustic wave relative to the Mb acoustic wave, revealing that dynamical processes are occurring on the nanosecond timescale. To probe the dynamics of conformational changes the temperature of the aqueous solution was lowered to 4 °C. At this temperature the thermal expansion coefficient for the system approaches 0, and only changes in the protein structure, ΔV_{con}, will produce acoustic waves. Indeed, at 4 °C the acoustic wave amplitude for Mb is practically 0, since this calibration compound undergoes no structural changes on the nanosecond timescale. However, MbCO has a pronounced acoustic wave at 4 °C with a negative initial amplitude, which results only from structural changes within the protein–solvent system. The analysis of the temperature dependence of the acoustic waves indicated that there are at least two decay processes, and the enthalpy and volume changes for these decay process were resolved.[40] Also, from the temperature dependence of the kinetics for the second decay, the thermodynamic activation parameters were derived.

The results are summarized in Scheme 1. Following the absorption of light, MbCO decays to form the geminate pair Mb:CO in less than 10 ns. The enthalpy change for this process is 0.6 ± 2.2 kcal mol^{-1} and the volume change -9.2 ± 0.5 mL mol^{-1}. At 22 °C a second decay occurs within 700 ns which has an enthalpy change of 10.7 ± 1.8 kcal mol^{-1} and a volume change of 15.0 ± 0.4 mL mol^{-1}. For this second process the enthalpy of activation ΔH^{*} is 11.1 ± 0.3 kcal mol^{-1}, and the entropy of activation ΔS^{*} is 7.6 ± 1.9 cal K^{-1} mol^{-1}.



Scheme 1. Energy diagram for the release of CO from carboxymyoglobin MbCO. ΔH in kcal mol^{-1}, ΔS in cal K^{-1} mol^{-1}.

The most surprising finding is that the enthalpy change for the formation of the geminate pair is 0.6 kcal mol^{-1} and the volume change is -9.2 mL mol^{-1}. Since formation of the geminate pair entails cleavage of the Fe–CO bond, we expected that the enthalpy change would reflect the Fe–CO bond enthalpy, approximately 20 kcal mol^{-1}, and that the volume change would be positive. However, it has recently been proposed, based upon X-ray structural studies, that the pathway by which the ligand diffuses out of the protein entails the breaking of a salt bridge formed between arginine-45 and the propionate side chain.[48] The breaking of a salt bridge and accompanying solvation of the resulting two charged centers releases heat to the solution and causes electrostriction of the water about the charged centers producing a negative volume change for the system.

To probe for the involvement of the arginine-45 salt bridge, this amino acid in sperm whale myoglobin was replaced by

asparagine, which does not form a salt bridge, and the photoacoustic spectrum of this derivative was examined.[41] With the salt bridge deleted, the volume change for the formation of the geminate pair increases from -9.2 to $-4.7\ mL\,mol^{-1}$. The enthalpy change for the formation of the geminate pair increases to $8.7\ kcal\,mol^{-1}$. Clearly, the breaking of the arginine-45 salt bridge is involved in the diffusion of the ligand out of the protein.

These experiments as well as analogous studies of horse carboxymyoglobin[42] and human carboxyhemoglobin[43] are beginning to provide detailed information on the dynamics of enthalpy and volume changes for CO diffusion in heme proteins on the nanosecond timescale.

6.2. Rhodopsin

The visual protein rhodopsin is an integral membrane protein (39 kD) in the disk membranes in the outer segments of the retinal rod cells. Owing to its heterogeneous membrane environment, the study of the dynamics of the enthalpy and volume changes associated with the bleaching of rhodopsin is particularly challenging.[44]

Upon absorption of light, rhodopsin evolves through a series of spectroscopically distinct intermediates that reflect changes in the protein structure important to its function, namely, initiating visual transduction [Eq. (18)]. The intermediate meta-

$$\underset{498\ nm}{\text{rhodopsin}} + h\nu \xrightarrow{<6\ ps} \underset{540\ nm}{\text{batho}} \xrightarrow{50\ ns} \underset{497\ nm}{\text{lumi}} \xrightarrow{0.3\ ms} \underset{478\ nm}{\text{meta I}} \xrightarrow{10\ ms} \underset{380\ nm}{\text{meta II}} \quad (18)$$

rhodopsin II activates the G protein transducin, which initiates the enzyme cascade for visual transduction.

The time resolution of our photoacoustic calorimeter (100 ns) allows the determination of the enthalpy and volume changes associated with the formation of lumirhodopsin, which occurs in 50 ns at ambient temperature.[44] However, it was not possible to resolve the decay of batho- to lumirhodopsin. Also the decay of lumi- to metarhodopsin I (300 μs) is beyond the time resolution of the experiment.

The most difficult aspect of a photoacoustic study of rhodopsin is obtaining a calibration compound. Since the solution is heterogeneous, it must be demonstrated that the protein solution and the calibration compound have the same $\beta/C_p\rho$. Using bleached rhodopsin without the 11-*cis*-retinal chromophore, which undergoes no photochemistry, we were able to demonstrate that the calibration compound bromocresol purple dissolved in a detergent solution of 2% dodecyl-β-D-maltoside has the same $\beta/C_p\rho$ as bleached rhodopsin in this detergent solution. Thus we have examined the photoacoustic spectrum for bovine rhodopsin solubilized in 2% dodecyl-β-D-maltoside solution.[43]

The overall enthalpy and volume change for the formation of lumirhodopsin is $3.9 \pm 5.9\ kcal\,mol^{-1}$ and $29.1 \pm 0.8\ mL\,mol^{-1}$. In a previous low-temperature ($-75\,^{\circ}C$) calorimetric study the enthalpy change for the formation of lumirhodopsin was found to be $26.3 \pm 4.2\ kcal\,mol^{-1}$.[44] A possible explanation for this difference in the values of the enthalpy change for the formation of lumirhodopsin is that the low-temperature matrix perturbs the energetics of lumirhodopsin. When rhodopsin is photoactivated it undergoes a series of conformational changes as evidenced by the changes in the chromophore absorption spectrum. The volume change of $29.1\ mL\,mol^{-1}$ observed in photoacoustic calorimetry may reflect some of these conformational changes. In a low-temperature glycerol–water glass photoactivated rhodopsin may not be able to undergo reorganization of its protein structure which would induce strain within the protein and lead to an increase in enthalpy for the system. Clearly it is important to study the dynamics of enthalpy and volume changes of proteins under conditions that approximate physiological.

7. Summary and Outlook

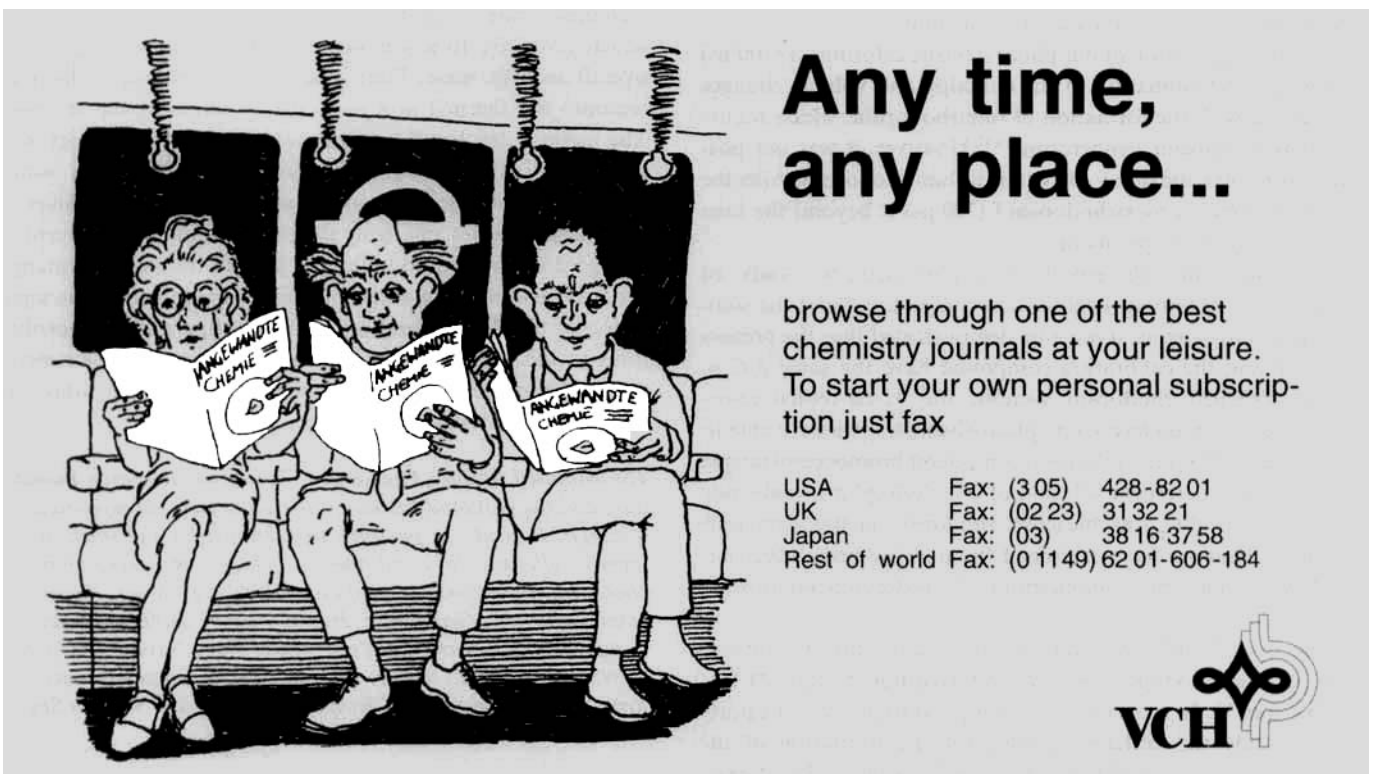
Although time-resolved photoacoustic calorimetry has provided many new insights into organic and organometallic reactions as well as protein dynamics, there is a clear need for the extension of the time resolution into the picosecond time domain. With polyvinylidene difluoride thin film transducers, picosecond lasers, and gigahertz transient digitizers, a time resolution of 100 ps should be possible in the very near future. Increasing the time resolution to the 10 ps timescale is more problematic and will require a different technology. The methods of picosecond optical calorimetry developed by Zimmt et al. are the most promising for this timescale.[49, 50]

Reactions in organic and organometallic chemistry that have been the subject of only a limited number of photoacoustic investigations are those involving the creation or annihilation of charge in nonaqueous solvents. Accompanying the creation of a charged center is electrostriction of the solvent about the ion which gives rise to a significant contribution of ΔV_{con} to the overall acoustic wave. Thus it becomes exceedingly difficult to separate the thermal and molecular configurational changes. The method developed by Grabowski et al.[11] may work well for alkane solvents, but for more polar solvents, in which specific solvation becomes important to the overall stability of the charged species, changing the composition of the solvent to change $\beta/C_p\rho$ would undoubtedly perturb the overall enthalpy for the reaction. Until a new method is developed for the separation of the thermal and molecular configurational contributions to the overall acoustic wave, photoacoustic calorimetry cannot be applied to a very important class of reactions, the creation or annihilation of charged centers.

The National Science Foundation, Petroleum Research Foundation, and the National Institutes of Health have all supported my research. It is also a pleasure to acknowledge the work of my former colleagues who did much to advance the development of photoacoustic calorimetry: Lewis Rothberg, Mark Bernstein, John Simon, Joe Grabowski, Jeanne Rudzki, Josh Goodman, Gil Yang, Judy Westrick, Kathleen Marr, Gary Snyder, and Chris Norris. In addition I wish to acknowledge my collaborations with Professors Veronica Vaida, Richard Caldwell, and Stephen Sligar.

Received: March 8, 1993 [A 930 IE]
German version: *Angew. Chem.* **1994**, *106*, 301

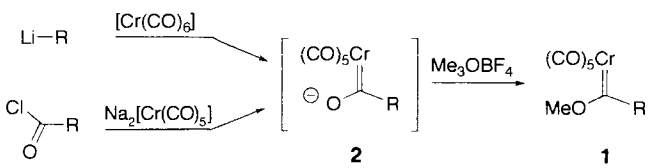
[1] A. G. Bell, *Philos. Mag.* **1881**, *11*, 510.
[2] J. B. Callis, W. W. Parson, M. Gouterman, *Biochem. Biophys. Acta* **1972**, *267*, 348.
[3] J. E. Rudzki, J. L. Goodman, K. S. Peters, *J. Am. Chem. Soc.* **1985**, *107*, 7849.
[4] C. K. N. Patel, A. C. Tam, *Rev. Mod. Phys.* **1981**, *53*, 517.
[5] K. Heihoff, S. E. Braslavsky, *Chem. Phys. Lett.* **1986**, *131*, 183.
[6] L. G. Arnaut, R. A. Caldwell, J. E. Elbert, L. A. Melton, *Rev. Sci. Instrum.* **1992**, *63*, 5381.
[7] S. E. Braslavsky, G. E. Heibel, *Chem. Rev.* **1992**, *92*, 1381.
[8] A. C. Tam, *Rev. Mod. Phys.* **1986**, *58*, 381.
[9] J. Rudzki Small, L. J. Libertini, E. W. Small, *Biophys. Chem.* **1992**, *42*, 29.
[10] J. J. Grabowski, J. D. Simon, K. S. Peters, *J. Am. Chem. Soc.* **1984**, *106*, 4615.
[11] R. R. Hung, J. J. Grabowski, *J. Am. Chem. Soc.* **1992**, *114*, 351.
[12] a) M. S. Platz in Kinetics and Spectroscopy of Carbenes and Biradicals (Ed.: M. S. Platz), Plenum, New York, **1990**, p. 143. b) K. B. Eisenthal, N. J. Turro, M. Aikawa, J. A. Butcher, C. DuPuy, G. Hefferon, W. Hetherington, G. M. Korenowski, M. J. McAuliffe, *J. Am. Chem. Soc.* **1980**, *102*, 6563.
[13] K. S. Peters in *Kinetics and Spectroscopy of Carbenes and Biradicals* (Ed.: M. S. Platz), Plenum, New York, **1990**, pp. 37–49.
[14] J. A. LaVilla, J. L. Goodman, *Tetrahedron Lett.* **1988**, *29*, 2623.
[15] J. A. LaVilla, J. L. Goodman, *J. Am. Chem. Soc.* **1989**, *111*, 712.
[16] M. S. Herman, J. L. Goodman, *J. Am. Chem. Soc.* **1989**, *111*, 1849.
[17] J. A. LaVilla, J. L. Goodman, *J. Am. Chem. Soc.* **1989**, *111*, 6877.
[18] J. A. LaVilla, J. L. Goodman, *Tetrahedron Lett.* **1990**, *31*, 6287.
[19] J. A. LaVilla, J. L. Goodman, *Tetrahedron Lett.* **1990**, *31*, 5109.
[20] X. M. Du, H. Fan, J. L. Goodman, M. A. Kesselmayer, K. Krogh-Jespersen, J. A. LaVille, R. A. Moss, S. Shen, R. S. Sheridan, *J. Am. Chem. Soc.* **1990**, *112*, 1920.
[21] K. N. Houk, N. G. Rondau, C. Santiago, C. J. Gallo, R. W. Gandour, G. W. Griffen, *J. Am. Chem. Soc.* **1980**, *102*, 1504.
[22] W. von E. Doering, *Proc. Natl. Acad. Sci. USA* **1981**, *78*, 5279.
[23] S. L. Buchwalter, G. L. Closs, *J. Am. Chem. Soc.* **1970**, *101*, 4688.
[24] M. S. Herman, J. L. Goodman, *J. Am. Chem. Soc.* **1988**, *110*, 2681.
[25] J. L. Goodman, K. S. Peters, H. Misawa, R. A. Caldwell, *J. Am. Chem. Soc.* **1986**, *108*, 6803; for a discussion of ring strain in a bridgehead imine see G. S. Wayne, G. J. Snyder, D. W. Rogers, *ibid.* **1993**, *115*, 9860.
[26] J. A. LaVilla, J. L. Goodman, *Chem. Phys. Lett.* **1987**, *141*, 149.
[27] D. I. Schuster, G. E. Heibel, R. A. Caldwell, W. Tang, *Photochem. Photobiol.* **1990**, *52*, 645.
[28] T. Ni, R. A. Caldwell, L. A. Melton, *J. Am. Chem. Soc.* **1989**, *111*, 457.
[29] C. M. Brennan, R. A. Caldwell, *Photochem. Photobiol.* **1991**, *53*, 165.
[30] P. Mulder, O. W. Saastad, D. Griller, *J. Am. Chem. Soc.* **1988**, *110*, 4090.
[31] G. K. Yang, K. S. Peters, V. Vaida, *Chem. Phys. Lett.* **1986**, *125*, 566.
[32] G. K. Yang, V. Vaida, K. S. Peters, *Polyhedron* **1988**, *7*, 1619.
[33] K. E. Lewis, D. M. Golden, G. P. Smith, *J. Am. Chem. Soc.* **1984**, *106*, 3905.
[34] J. K. Klassen, G. K. Yang, *Organometallics* **1990**, *9*, 874.
[35] J. K. Klassen, M. Selke, A. A. Sorensen, G. K. Yang, *J. Am. Chem. Soc.* **1990**, *112*, 1267.
[36] A. A. Sorensen, G. K. Yang, *J. Am. Chem. Soc.* **1991**, *113*, 7061.
[37] D. M. Hester, J. Sun, A. W. Harper, G. K. Yang, *J. Am. Chem. Soc.* **1992**, *114*, 5234.
[38] G. L. Goodman, K. S. Peters, V. Vaida, *Organometallics* **1986**, *5*, 815.
[39] S. P. Nolan, C. D. Hoff, P. O. Stoutland, L. J. Newman, J. M. Buchanan, R. G. Bergman, G. K. Yang, K. S. Peters, *J. Am. Chem. Soc.* **1987**, *109*, 3143.
[40] J. A. Westrick, J. L. Goodman, K. S. Peters, *Biochemistry* **1987**, *26*, 8313.
[41] J. A. Westrick, K. S. Peters, J. D. Ropp, S. G. Sligar, *Biochemistry* **1990**, *29*, 6741.
[42] J. A. Westrick, K. S. Peters, *Biophys. Chem.* **1990**, *37*, 73.
[43] K. S. Peters, T. Watson, T. Logan, *J. Am. Chem. Soc.* **1992**, *114*, 4276.
[44] K. Marr, K. S. Peters, *Biochemistry* **1991**, *30*, 1254.
[45] D. R. Ort, W. W. Parson, *Biophys. J.* **1979**, *25*, 355.
[46] H. Arta, W. W. Parson, *Biochim. Biophys. Acta* **1981**, *638*, 201.
[47] K. Jabben, K. Heihoff, S. E. Braslavsky, K. Schaffner, *Photochem. Photobiol.* **1986**, *43*, 127.
[48] K. S. Peters, T. Watson, K. Marr, *Annu. Rev. Biophys. Biophys. Chem.* **1991**, *20*, 243.
[49] M. B. Zimmt, *Proc. SPIE Int. Soc. Opt. Eng.* **1991**, *1599*, 115.
[50] J. Morais, J. Ma, M. B. Zimmt, *J. Phys. Chem.* **1991**, *95*, 3885.



Chromium Carbene Complexes in Organic Synthesis: Recent Developments and Perspectives

Hans-Günther Schmalz*

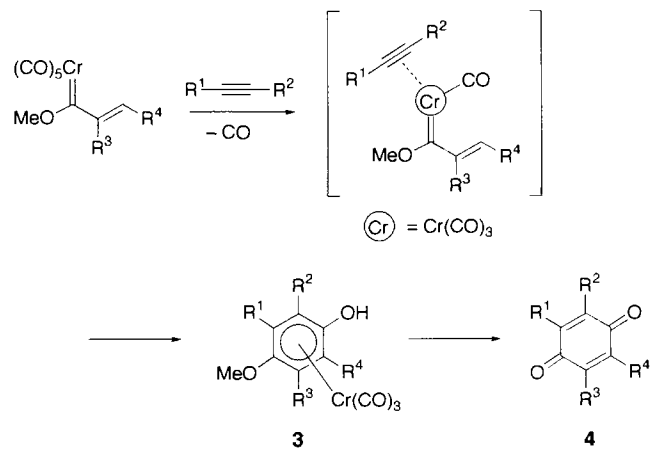
Complexes of the type $[(CO)_5M{=}CR^1R^2]$, M = Cr, Mo, W, which are also known as Fischer carbene complexes, after their discoverer, have found widespread application in organic synthesis in recent years.[1] Heteroatom-stabilized chromium complexes of type **1** have especially played a major role.[2] These compounds can be prepared in good yield by reaction of $[Cr(CO)_6]$ with organolithium reagents followed by O-alkylation. Alternatively, the anionic intermediate **2** can also be generated by reaction of acyl chlorides with $Na_2[Cr(CO)_5]$.[3]



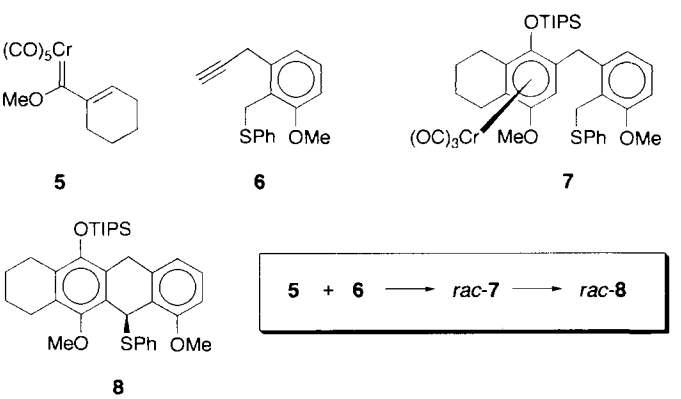
Among the synthetically useful reactions of chromium carbenes, benzannulations certainly are the most prominent.[2] In particular, the so-called Dötz reaction is an efficient synthetic method, which has already proved its worth numerous times within the context of natural product synthesis.[2] In this reaction α,β-unsaturated complexes **1** (R = aryl or alkenyl) are allowed to react with alkynes under thermal conditions to give (in the sense of a formal [3+2+1] cycloaddition) $Cr(CO)_3$-complexed hydroquinone derivatives **3** or, after oxidative workup, *p*-benzoquinone derivatives **4**.

As recently shown by Harrity et al., the typically long reaction times for the Dötz reaction can be drastically reduced by the application of high-intensity ultrasound.[4] Dry-state adsorption of the reaction partners on silica followed by warming to 40–70 °C is an other attractive preparative alternative, which results in markedly improved yields in many cases.[4]

In an effort to further broaden the synthetic scope of the Dötz reaction, S. Chamberlin, W. D. Wulff, and B. Bax succeeded in trapping the free phenol function of the initial products **3** (in situ) as a silyl ether.[5] This in turn allowed them to take advantage of the characteristic reactivity of the resulting arene–$Cr(CO)_3$ complexes, especially towards nucleophiles[6] (tandem



Dötz/Semmelhack reactions). For example, the reaction of the carbene complex **5** with the alkyne **6** in the presence of triisopropylsilyl triflate (TIPS-OTf) and 2,6-lutidine in dichloromethane gave the complex *rac*-**7** (77%), which was then converted to the anthracycline derivative *rac*-**8** in 84% yield by deprotonation with lithium diisopropylamide followed by workup of the reaction mixture with iodine.[5a]

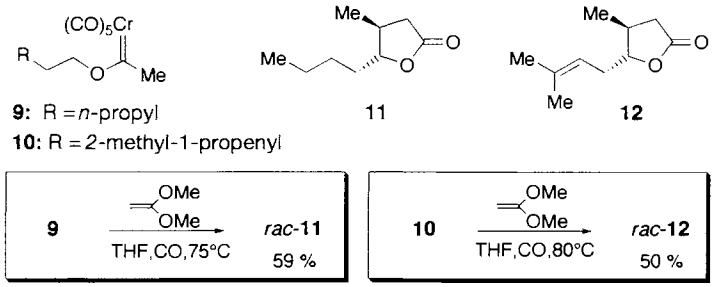


The research group headed by W. D. Wulff also reported on the thermal reaction of chromium carbene complexes with ketene acetals to yield substituted γ-butyrolactones.[7] This reaction, which probably proceeds through insertion of a carbenoid

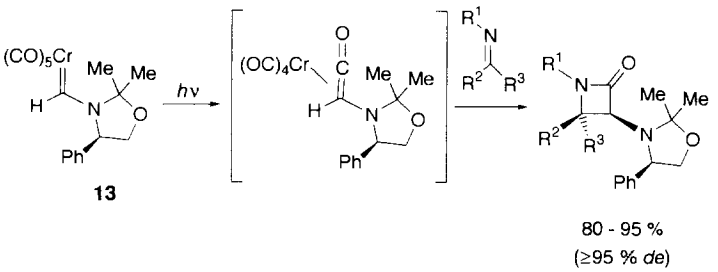
[*] Priv.-Doz. Dr. H.-G. Schmalz
Institut für Organische Chemie der Universität
Marie-Curie-Strasse 11, D-60439 Frankfurt am Main (FRG)
Telefax: Int. code + (69) 5800-9250

 © VCH Verlagsgesellschaft mbH, D-69451 Weinheim, 1994 0570-0833/94/0303-0303 $ 10.00+.25/0

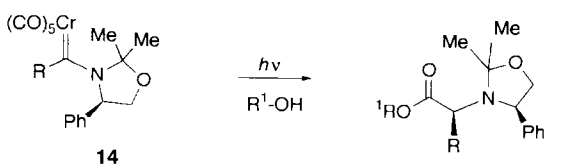
into a C–H bond, was successfully applied to a diastereoselective synthesis of the (albeit racemic) natural products quercuslactone *rac*-**11** and eldanolide *rac*-**12**.[7]



A whole new range of applications of Fischer carbenes in organic synthesis has been developed by L. S. Hegedus et al. after they discovered that the photolysis of chromium carbene complexes produces, under CO insertion, species with a ketene-like reactivity. These intermediates react with nucleophiles to form derivatives of carboxylic acids and with imines (or enol ethers) to form [2+2] cycloaddition products.[8, 9] The introduction of chiral substituents at the carbene carbon atom even allows the control of the absolute configuration of the reaction products. For example, the chiral aminocarbene complex **13** served as the starting point for a quite efficient synthesis of optically active β-lactams.[10]

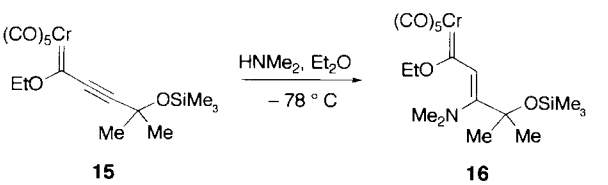


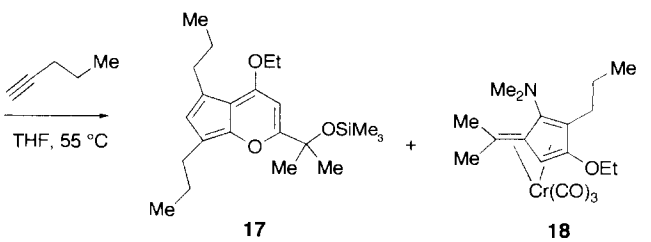
Photolysis of chiral (aminocarbene) complexes of type **14** in the presence of alcohols proceeds with high diastereoselectivity (in the protonation step) and provides an efficient entry to a broad spectrum of optically active, natural and unnatural amino acids,[11] including optically active [2-$^2H_1$]-glycine.[12] A remarkable feature of this chemistry is the possibility of preparing compounds with two neighboring ^{13}C-labeled carbon centers, which are of considerable interest for the investigation of biological problems by NMR spectroscopic methods.[13] For this purpose the starting complexes (e.g. **14**) are prepared from ^{13}C-enriched chromium hexacarbonyl.



Photolysis of (aminocarbene) complexes of type **14** in the presence of carboxyl-protected amino acids allows the (diastereoselective) construction of dipeptides in a one-pot reaction.[14] This process is remarkable for several reasons: firstly, both the peptide bond *and* the new stereogenic center are established in a single preparative operation; secondly, visible light acts as the "coupling agent". This permits the direct incorporation of all kinds of amino acids into peptides without the amino acids themselves having to be presynthesized separately.

The number of publications concerning reactions of Fischer carbene complexes is growing rapidly. Preparative as well as mechanistic aspects of this chemistry are under intense investigation worldwide—and the discovery of unexpected reaction pathways and products does not seem to be a rare exception. In a recent example, A. de Meijere et al. treated complex **16** (which is easily prepared from **15**) with 1-pentyne and obtained considerable amounts of the fulvene–$Cr(CO)_3$ complex *rac*-**18** in addition to the cyclopenta[*b*]pyran **17**.[15]





W. D. Wulff et al. reported the formation of cyclopentenones (by C–H activation) when alkyl chromium carbenes were treated with alkynes.[16] A new entry to cyclopentenones was also discovered by the research group of J. W. Herndon in the reaction of cyclopropyl carbene complexes with alkynes—a reaction which was (rather daringly!) classified by the authors as a [4+2+1–2] cycloaddition[17].

Which of the many new reactions of chromium carbene complexes (only a few have been mentioned here) will stand the test of real-life application in multistep syntheses, is, of course, still uncertain. However, one can certainly expect that Fischer carbene complexes will be good for many more surprises in the future, and that their potential for organic synthesis will be more and more recognized, researched, and utilized. Thus, every synthetic chemist is well advised to follow this fascinating field with appropriate attention.

German version: *Angew. Chem.* **1994**, *106*, 311

[1] The first transition metal carbene complex was reported in 1964 by E. O. Fischer and A. Maasböl: *Angew. Chem.* **1964**, *76*, 645; *Angew. Chem. Int. Ed. Engl.* **1964**, *3*, 580.

[2] Selected reviews: a) K. H. Dötz, *Angew. Chem.* **1984**, *96*, 573; *Angew. Chem. Int. Ed. Engl.* **1984**, *23*, 587; b) K. H. Dötz in *Organometallics in Organic Synthesis* (Eds.: A. de Meijere, H. tom Dieck), Springer, Berlin, **1988**, p. 85; c) W. D. Wulff, *Adv. Met. Org. Chem.* **1989**, *1*, 209; d) W. D. Wulff in *Compre-*

 © VCH Verlagsgesellschaft mbH, D-69451 Weinheim, 1994 0570-0833/94/0303-0304 $ 10.00+.25/0

hensive Organic Synthesis, Vol. 5 (Eds.: B. M. Trost, I. Fleming), Pergamon, Oxford, **1991**, p. 1065.
[3] M. F. Semmelhack, G. R. Lee, *Organometallics* **1987**, *6*, 1839.
[4] J. P. A. Harrity, W. J. Kerr, D. Middlemiss, *Tetrahedron* **1993**, *49*, 5565.
[5] a) S. Chamberlin, W. D. Wulff, *J. Am. Chem. Soc.* **1992**, *114*, 10667; b) S. Chamberlin, W. D. Wulff, B. Bax, *Tetrahedron* **1993**, *49*, 5531.
[6] Review: M. F. Semmelhack in *Comprehensive Organic Synthesis, Vol. 4* (Eds.: B. M. Trost, I. Fleming), Pergamon, Oxford, **1991**, p. 517.
[7] S. L. B. Wang, J. Su, W. D. Wulff, K. Hoogsteen, *J. Am. Chem. Soc.* **1992**, *114*, 10665.
[8] a) L. S. Hegedus, M. A. McGuire, L. M. Schultze, C. Yijun, O. P. Anderson, *J. Am. Chem. Soc.* **1984**, *106*, 2680; b) L. S. Hegedus, G. deWeck, S. D'Andrea, *ibid.* **1988**, *110*, 2122, and references therein.
[9] Review: a) M. A. Schwindt, J. R. Miller, L. S. Hegedus, *J. Organomet. Chem.* **1991**, *413*, 143.
[10] a) L. S. Hegedus, R. Imwinkelried, M. Alarid-Sargent, D. Dvorak, Y. Satoh, *J. Am. Chem. Soc.* **1990**, *112*, 1109; b) Y. Narukawa, K. N. Juneau, D. Snustad, D. B. Miller, L. S. Hegedus, *J. Org. Chem.* **1992**, *57*, 5453; c) B. Roman, L. S. Hegedus, *Tetrahedron* **1993**, *49*, 5549; d) P.-C. Colson, L. S. Hegedus, *J. Org. Chem.* **1993**, *58*, 5918.
[11] a) L. S. Hegedus, M. A. Schwindt, S. DeLombaert, R. Imwinkelried, *J. Am. Chem. Soc.* **1990**, *112*, 2264; b) J. M. Vernier, L. S. Hegedus, D. B. Miller, *J. Org. Chem.* **1992**, *57*, 6914.
[12] L. S. Hegedus, E. Lastra, Y. Narukawa, D. C. Snustad, *J. Am. Chem. Soc.* **1992**, *114*, 2991.
[13] E. Lastra, L. S. Hegedus, *J. Am. Chem. Soc.* **1993**, *115*, 87.
[14] J. R. Miller, S. R. Pulley, L. S. Hegedus, S. DeLombaert, *J. Am. Chem. Soc.* **1992**, *114*, 5602; b) S. R. Pulley, L. S. Hegedus, *ibid.* **1993**, *115*, 9037.
[15] F. Stein, M. Duetsch, M. Noltemeyer, A. de Meijere, *Synlett* **1993**, 486.
[16] C. A. Challener, W. D. Wulff, B. A. Anderson, S. Chamberlin, K. L. Faron, O. K. Kim, C. K. Murray, Y.-C. Xu, D. C. Yang, S. D. Darling, *J. Am. Chem. Soc.* **1993**, *115*, 1359.
[17] S. U. Tumer, J. W. Herndon, L. A. McMullen, *J. Am. Chem. Soc.* **1992**, *114*, 8394.

A New Application of Modified Peptides and Peptidomimetics: Potential Anticancer Agents

Rob M. J. Liskamp*

Wide applications of (unmodified) peptides as drugs are limited by the disadvantages affiliated with their use in biological systems. An unmodified linear peptide is easily degraded by, for example, proteases, it is often too water-soluble to pass through the cell membrane and therefore unable to pass through the blood–brain barrier and is rapidly excreted. In addition, a peptide has a flexible structure and the bioactive conformation is usually only one of several thousand possible conformations.

The desire to remedy these disadvantages and thereby to obtain meaningful pharmaceutical compounds has led to the development of modified peptides and peptidomimetics.[1, 2] All major pharmaceutical companies nowadays are carrying out major research and development in this area, and the number of applications of these substances is steadily increasing. The importance of modified peptides and peptidomimetics is evident from several applications. So far they have been applied for example in the development of drugs regulating blood pressure and blood clotting, in the development of HIV-protease inhibitors and immunosuppressive agents as well as in the development of neuropeptide (ant)agonists.

Two recent reports have described a new promising application of modified peptides and peptidomimetics as potential anticancer agents for the treatment of tumors in which oncogenic Ras proteins (see below) contribute to transformation and abnormal growth.[3, 4] Two aspects of the results presented in these reports are especially noteworthy:
– the inhibition of malignant transformation was achieved on a level other than the DNA level;
– the inhibition originated from inhibition of a post-translational modification process of proteins.

In many conventional chemotherapeutic regimens of cancer, the drug displays its activity on the DNA level. The interference with or damage to the genetic material leads to the arrest of cellular growth and halting of uncontrolled cell division. However, these drugs are often deleterious for other rapidly dividing cells involved in the formation of, for example, bone marrow, gastrointestinal mucosa, and hair follicles, causing the well-known side effects. In addition, interference with the genetic code means that these reagents are inherently carcinogenic and/or mutagenic. Therefore attempts directed towards the development of drugs acting on other cellular levels are especially interesting.

The most direct approach is to employ modified peptides or peptidomimetics for the inhibition of the cleavage of an amide bond in an amino acid sequence, present in a peptide or protein involved in a biological process, which one wants to suppress. For example, HIV-protease inhibitors are supposed to inhibit the cleavage of the amide bond between phenylalanine and proline in a precursor polyprotein of HIV. As a result the formation of proteins necessary for the assemblage of new virus particles is inhibited, and the spread of HIV is diminished. More indirect—perhaps better tunable—approaches focus on the use of modified peptides and peptide mimetics for the inhibition of modification processes which the protein has to undergo once it has been biosynthesized at the ribosome and before it can fully perform its function. These processes are referred to as post-translational modification processes. Since there are many of these processes,[5] often with high selectivity with respect to the protein(s) being modified, interference with a particular post-translational modification process offers a means for very specific intervention in undesired cellular processes. Inhibition of the post-translational modification process by phosphoryla-

[*] Dr. R. M. J. Liskamp
Department of Organic Chemistry, Gorlaeus Laboratories
University of Leiden
P.O. Box 9502, NL-2300 RA Leiden (The Netherlands)
Telefax: Int. code + (71)274537

 © VCH Verlagsgesellschaft mbH, D-69451 Weinheim, 1994 0570-0833/94/0303-0305 $ 10.00+.25/0

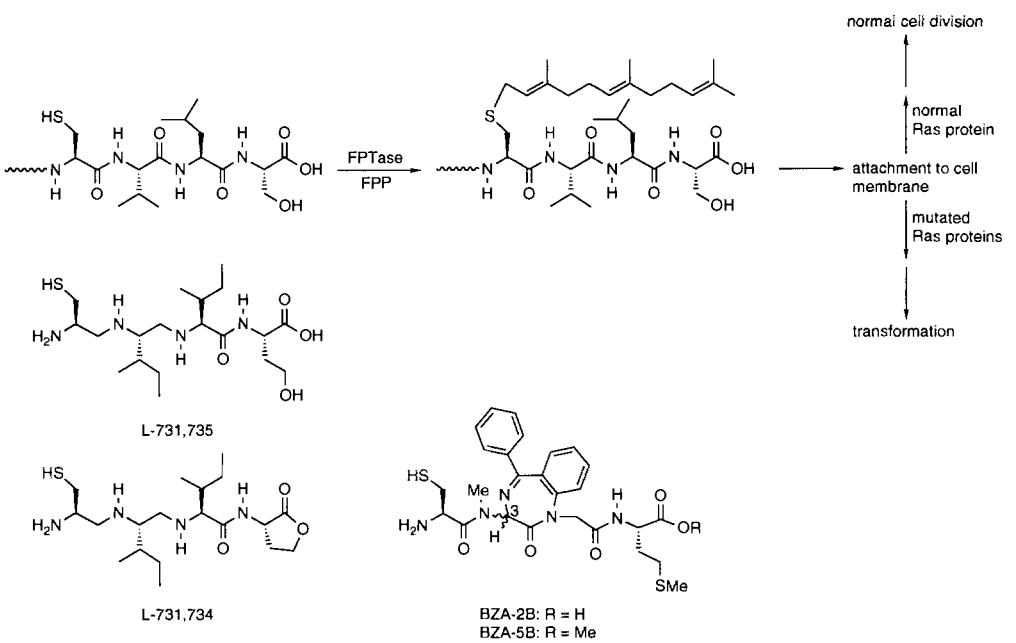
tion catalyzed by protein kinase C (PKC) or tyrosine kinases has been an approach employed to interfere with the carcinogenic process, since, for example, PKC is presumably involved in carcinogenesis.[6] However, inhibition of phosphorylation catalyzed by PKC may also be disastrous for normal cells, since many other proteins are phosphorylated by PKC in addition to those possibly involved in the transformation process. Therefore interference with such a specific post-translational modification process as farnesylation seems a more promising and perhaps an even more viable approach for the development of anticancer drugs.

Eukaryotic polypeptides with a cysteine residue located at the fourth position (counting from the C terminus) are, in principle, candidates for a post-translational modification involving the cysteine-SH. In a reaction catalyzed by farnesyl protein transferase (FPTase), this SH can be alkylated by farnesylpyrophosphate (FPP), an isoprenoid compound also involved in the biosynthesis of cholesterol. This step can be followed by the subsequent post-translational modifications of cleavage of the three C terminal amino acid residues and methyl esterification of the carboxylic acid terminus.[7] The role of farnesylation or geranylgeranylation is not clear at present. The hydrophobic isoprenyl tail may be responsible for membrane association of proteins. Alternatively, the isoprenyl tail and methyl ester may promote binding of the protein to specific membrane associated receptors.[8]

The Ras protein is an intriguing example of an eukaryotic protein which is farnesylated (Scheme 1). Ras is a guanosine triphosphate (GTP) binding protein. When GTP is bound to Ras, cell division is triggered. Normal Ras possesses GTPase activity, this leads to the hydrolysis of the bound GTP to GDP, so that the mitogenic signal is terminated in time. There are, however, mutant forms of Ras, found in about 50% of human colon carcinomas and 90% pancreatic carcinomas, which have an impaired GTPase activity. This impaired GTPase activity has as a consequence that the mutant Ras protein remains constitutively complexed to GTP, leading to unregulated cell proliferation and malignant transformation. Farnesylation of both normal and oncogenic Ras proteins is necessary for attachment to the cell membrane and the resulting biological effects. For the mutant Ras protein farnesylation appears to be required for efficient cell-transforming activity. Therefore a straightforward, albeit elegant, approach to inhibit transformation would be to interfere with Ras membrane localization by preventing farnesylation.[9]

Tetrapeptides with amino acid sequences identical to the COOH terminus of protein substrates for farnesylation by FPTase can compete with Ras for farnesylation. Selectivity of inhibition of farnesylation as opposed to inhibition of the other isoprenylation process of attachment of a geranylgeranyl moiety can be obtained by using peptides of the consensus sequence CAAX in which C is cysteine, A is an aliphatic amino acid, and X is serine or methionine.

In the modified peptides designed by the group at Merck the N-terminal amide bonds were reduced to introduce resistance to hydrolysis by aminopeptidases.[3] In addition, serine or methionine at the C terminus were replaced by homoserine or its lactone. It was also expected that the lactone could penetrate more easily into cells, because of the absence of a charged carboxylic acid moiety. The two compounds L-731,735 and L-731,734 (see Scheme 1) were potent inhibitors of partially purified FPTase, the homoserine compound being the more active in-



Scheme 1. Post-translational modification by farnesylation. The cysteine residue in the consensus sequence CAAX (C, cysteine; A, aliphatic amino acid residue; X, serine or methionine) near the C terminus in the Ras protein is farnesylated by farnesylpyrophosphate (FPP) catalyzed by farnesyl protein transferase (FPTase). The farnesylated protein can then attach itself to the plasma membrane. If mutated Ras proteins are farnesylated and attached to the cell membrane, this leads to transformation. Modified peptides [3] (L-731,735 and L-731,734) based on the consensus sequence CAAX, as well peptidomimetics [4] (BZA-2B and BZA-5B) based on both the consensus sequence and a presumed turn of CAAX act as potent competitive inhibitors of Ras farnesylation.

 © VCH Verlagsgesellschaft mbH, D-69451 Weinheim, 1994 0570-0833/94/0303-0306 $ 10.00+.25/0

hibitor (IC_{50} 18 nM as compared to 282 nM for the lactone derivative). By isolating only soluble—not isoprenylated and therefore not membrane associated—Ras from cells transformed with the *ras* gene, which were treated with L-731,734, it was proven that the modified peptide did in fact interfere with the farnesylation post-translation modification. The cytostatic activity was evident from the inhibition of anchorage-independent growth of Rat1 cells transformed with v-*ras*. At a concentration of 1 mM the modified peptide was capable of inhibiting the growth of these cells in soft agar.

The University of Texas and Genentech groups went a step further.[4] Besides realizing that one needed a tetrapeptide sequence corresponding to the CAAX consensus sequence to obtain alternative substrates, thereby competitively inhibiting the farnesylation of Ras proteins, they hypothesized that the tetrapeptide binds to the FPTase in a turn conformation. This would place the NH_2-terminal cysteine and the COOH-terminal methionine in close proximity to the Zn^{2+} ion that is known to be essential for peptide binding by FPTase. To mimic a turn-like structure of the two middle amino acids in the consensus sequence, they used the benzodiazepine skeleton to which the N-terminal cysteine residue and a C-terminal methionine, serine, or leucine residue were attached.[10] Several structural features in the peptidomimetics (see Scheme 1) were essential for effective inhibition of farnesylation: a) the amino function connecting the cysteine had to be *N*-methylated, b) the configuration at the C-3 atom needed to be the correct one (not determined as yet): only one of the two diastereomers was active, c) methionine at the C terminus was most effective and d) although the free acid (BZA-2B) produced the best results in the in vitro assay (IC_{50} 0.85 nM), the ester (BZA-5B), and to a somewhat lesser extent the amide, were more active in a Chinese hamster ovary cell line, suggesting that the latter compounds may more easily penetrate into cells, because of their reduced polarity. Almost complete inhibition of farnesylation was achieved at a concentration of 25 μM by using the ester, whereas a concentration of 250 μM of the acid was required for the same inhibition.

BZA-2B also displayed selectivity in its inhibition of farnesylation as compared to inhibition of geranylgeranylation and was not itself farnesylated.

Reversal of the transformed phenotype of multilayered clumps to a monolayer system was observed by incubating Rat1 fibroblasts, transformed with an activated mutant of H-Ras, with 200 μM of the peptidomimetic BZA-2B for five days. In the presence of 25 μM of the ester BZA-5B the growth of Ras-transformed Rat1 fibroblasts was inhibited for about 90% after ten days.

The use of modified peptides and peptidomimetics to selectively inhibit Ras farnesylation and thereby transformation and ultimately possible the carcinogenic process is an important and new application of these compounds.[11, 12] It also shows that they can be employed for a finely tuned intervention in complex biochemical and biological processes. It is therefore expected that as the understanding of cellular processes (e.g. protein trafficking, intracellular signal transduction) progresses, it will be possible to intervene in, or selectively inhibit these processes using carefully designed modified peptides and peptidomimetics.

The design, synthesis, and applications of modified peptides and peptidomimetics as well as peptide-like compounds such as peptoids is one of the rapidly growing and increasingly important areas,[13] but it is also important to emphasize that this field can and only will continue to flourish by a close interplay of many disciplines, as was also evident from the research discussed here.

German version: *Angew. Chem.* **1994**, *106*, 313

[1] Modified peptides are defined as peptides in which, in essence, the amino acid sequence is unchanged but the peptide contains, for example, some unnatural amino acids, a modification of a cysteine residue, or a phosphorylated amino acid. Peptidomimetics are compounds which imitate the structure and/or imitate or block the biological effect of a peptide at the receptor level [2]. As a consequence peptidomimetics span the whole range of compounds varying from peptide isosteres to compounds without an identifiable amino acid or peptide moiety.

[2] For a recent review on peptidomimetics see: A. Giannis, T. Kolter, *Angew. Chem.* **1993**, *105*, 1303–1326; *Angew. Chem. Int. Ed. Engl.* **1993**, *32*, 1244–1267.

[3] N. E. Kohl, S. D. Mosser, S. J. deSolms, E. A. Giuliani, D. L. Pompliano, S. L. Graham, R. L. Smith, E. M. Scolnick, A. Oliff, J. B. Gibbs, *Science* **1993**, *260*, 1934–1937.

[4] G. L. James, J. L. Goldstein, M. S. Brown, T. E. Rawson, T. C. Somers, R. S. McDowell, G. W. Crowley, B. K. Lucas, A. D. Levinson, J. C. Masters, *Science* **1993**, *260*, 1937–1942.

[5] Glycosylation see for example: M. A. Kukuruzinska, M. L. E. Bergh, B. J. Jackson, *Annu. Rev. Biochem.* **1987**, *56*, 915–944; acylation: D. A. Towler, J. I. Gordon, S. P. Adams, L. Glaser, *ibid.* **1988**, *57*, 69–99; phosphorylation: E. G. Krebs, J. A. Beavo, *ibid.* **1979**, *48*, 923–959; isoprenylation: ref. [7].

[6] For PKC inhibitors based on modified peptides see for example: T. Eicholtz, D. B. A. de Bont, J. de Widt, R. M. J. Liskamp, H. L. Ploegh, *J. Biol. Chem.* **1993**, *268*, 1982–1986, and references therein.

[7] S. Clarke, *Annu. Rev. Biochem.* **1992**, *61*, 355–386.

[8] J. A. Glomset, M. H. Gelb, C. C. Farnsworth, *Trends Biochem. Sci.* **1990**, *15*, 139–142.

[9] J. B. Gibbs, *Cell* **1990**, *65*, 1–4.

[10] For use of the benzodiazepine skeleton as β-turn mimetic see: W. C. Ripka, G. V. De Lucca, A. C. Bach II, R. S. Pottorf, J. M. Blaney, *Tetrahedron*, **1993**, *49*, 3593–3608.

[11] J. Travis, *Science* **1993**, *260*, 1877–1878.

[12] For a recent review on inhibitors of Ras farnesyltransferases, including microbial products identified as such see: F. Tamanoi, *Trends Biochem. Sci.* **1993**, *18*, 349–353.

[13] Peptoids were recently highlighted by H. Kessler, *Angew. Chem.* **1993**, *105*, 572–573; *Angew. Chem. Int. Ed. Engl.* **1993**, *32*, 543–544.

 © *VCH Verlagsgesellschaft mbH, D-69451 Weinheim, 1994* *0570-0833/94/0303-0307 $ 10.00+.25/0*

Rationally Designed Inorganic Catalysts for Environmentally Compatible Technologies**

John Meurig Thomas* and Kirill Ilyich Zamaraev*

In a recent analysis[1] of the future prospects pertaining to the design of new catalysts and to the improvement of the performance of existing ones, Schlögl viewed the world through the prism of ammonia synthesis. He traced the heroic work that started with Haber, continued with Mittasch, and which has since been the subject of intense study by generations of subsequent investigators, all of whom, in their respective ways, have struggled to understand the behavior of the iron-based catalyst for the large-scale manufacture of ammonia. But Schlögl's assertions must be challenged, especially the following: "All of the catalytic processes vital to industry were developed by purely empirical methods and countless screening experiments". "This heuristic approach has led to the opinion that catalysis research is not a science but rather 'black magic'". Schlögl further asserts that "...industrial chemists tend to be rather sceptical toward inductive-scientific strategies in heterogeneous catalysis, since it is evident that our understanding of *the relationship between structure and reactivity is inadequate*" (our italics). These are strong, strident words with which we disagree for the reasons given below.

Whilst it is true, as Schlögl describes, that the laboratory world of iron single-crystals, cleaned in ultrahigh vacuum and studied under modest pressure, is vastly different from that of the catalyst in the ammonia synthesis reactor, and whilst it is undeniable that, as yet, no new industrially viable ammonia synthesis catalyst (with the possible exception of the recently commissioned, supported ruthenium catalyst) has emerged as a direct consequence of the de novo investigations of single-crystal metal catalysts, his statements cited above are untrue when applied to other important classes of catalysts. There are numerous examples in which causal relationships between crystalline structure and catalytic performance have been incontrovertibly established.

Some examples of the veracity of our claims are contained in a number of recent publications.[2-11] One of these,[2] published in *Angewandte Chemie* five years ago, is entitled "Uniform Heterogeneous Catalysts: The Role of Solid-State Chemistry in their Development and Design". In another,[3] numerous chapters support the view that designed catalysts have already been commercialized and are likely to play a pivotal role in the chemistry of the 21st century. Yet other publications[4, 5] address the timely question of designer catalysts in the quest for cost-effective, environmentally compatible technologies. If Schlögl's claims were true, future employers and boardroom protagonists could well underestimate or misjudge the contributions that the research chemist could make to the future of their industry, and employment prospects for numerous highly trained physical scientists would be bleak.

Examples of intentional design in the genesis and evolution of new catalysts are quite numerous. So relevant and progressive is this sector of solid-state chemical research in devising environmentally acceptable catalysts and processes that we summarize four distinct categories of catalysts:

1) An ever-expanding family of monophasic, microporous, microcrystalline solids, some members of which already function on the industrial scale as essentially shape-selective catalysts.
2) Multiphasic systems embracing supported metals, supported oxides, mixed oxides, and mixed sulfides of "designed" solids nowadays function as robust industrial catalysts.
3) Proven examples where new concepts in the design of molecular and extended (solid-state) catalysts have been demonstrated.
4) Improvements on preexisting industrial catalysts which stemmed from a fundamental reexamination of chemical engineering practice; worthwhile commercial and environmental improvements have already been achieved.

Whilst some amplification of all four theses is given in a recent book,[3] we present here the salient points that constitute our rebuttal of the assertions made by Schlögl.[1]

Shape-selective inorganic catalysts[9] are in extensive commercial use worldwide for the conversion of methanol to gasoline, the isomerization of xylene (maximizing yield of the *para* isomer), the conversion of ethene and benzene to ethyl benzene, the disproportionation of toluene to benzene and paraxylene, and the conversion of phenol to hydroquinone and catechol.[12] Many other processes currently being tested at either the pilot plant or laboratory stage entail the use of shape-selective solid

[*] Sir J. M. Thomas
Davy Faraday Research Laboratory, Royal Institution of Great Britain
21 Albemarle Street, GB-London W1X 4BS (UK)

[*] Prof. Dr. K. I. Zamaraev
Boreskov Institute of Catalysis
5 Prospect Akademika Lavrentyeva, Novosibirsk 630090 (Russia)

[**] J. M. T. and K. I. Z. thank the Science and Engineering Research Council and the Siberian Branch of the Russian Academy, respectively, for their support. This article was written while K. I. Z. was at the Royal Institution with a Kapitza Fellowship from the Royal Society.

catalysts. These include the production of ε-caprolactam by the isomerization of cyclohexanone oxime, the conversion of cyclohexanone into its oxime, the transformation of methanol into light olefins, the selective production of dimethylamine from ammonia and methanol, the isomerization of 1-butene to 2-methylpropene, and the production of diisopropylnaphthalene (DIPN) isomers. The particular monophasic catalysts used for these processes all have well-defined crystal structures possessing channels and cavities lined with active sites of known identity. Typical examples are H-ZSM-5, H-ferrierite, Theta-1, zeolite rho, HZSM-23, acidic clays, mordenite, and the silicoaluminophosphates H-SAPO-34, H-SAPO-11, etc., which, like ZSM-5, are Brönsted solid acids.[5, 8–12] They are all examples of so-called uniform heterogeneous catalysts in which the active sites are distributed in a spatially uniform way throughout their bulk. Another uniform shape-selective catalyst designed for the function it now has industrially (in the selective oxidation of phenol to hydroquinone) is Ti-silicalite, which is nonacidic.

The germ and genesis of the rational concept of shape-selective molecular sieves was the work of Weisz et al.,[9] who demonstrated that by a *controlled* variation of cavity size—exercised by simple application of the principles of crystal engineering—the selectivity of the catalytic dehydration of alkanols could be profoundly changed. In the thirty years that have elapsed since Weisz and his colleagues first reported their results, numerous successful attempts have been made to adapt the structures of naturally occurring molecular sieves (e.g. the well-known zeolite mordenite) and to synthesize a host of new ones. SAPOs and MeAlPOs in which some of the phosphorus or aluminum atoms of the aluminum phosphate microporous framework are replaced by silicon (in SAPO) or divalent ions (in MeALPO), respectively -are now being designed and synthesized for specific catalytic reactions.[4, 10–16] One strong thrust is in the area of large-pore solid acid catalysts, many of which have recently been prepared[14] with the reactions of bulky molecules in mind.

We agree that the statement "No correlation exists between the bulk X-ray diffraction data and catalytic performance" was convincingly demonstrated by Schlögl[1] in the case of ammonia synthesis (iron-based) catalysts. But for the uniform shape-selective catalysts discussed here there is an indisputable link between the powder diffraction pattern, on the one hand, and the catalytic activity, on the other. See, for example, the published correlation between diffraction pattern, crystal structure, and catalytic performance for the Ni^{2+} ion-exchanged zeolite Y catalysts in the cyclotrimerization of acetylene.[17]

Indeed, so well understood is the correlation between crystal structure and selectivity among acidic shape-selective catalysts that computational chemistry has already contributed significantly to the evolution of superior catalysts for a given task. We cite two examples: the acid-catalyzed isomerization of 1-butene into 2-methylpropene, which is calculated[5, 18] to be facilitated better by Theta-1 than by ZSM-5, and the alkylation of naphthalene by propene to yield 2,6-diisopropylnaphthalene as the desired product.[4] Using computational procedures[18–20] that are by now quite routine for evaluating the energetics of docking of reactants and products inside zeolites, and for diffusion of species out of such shape-selective catalysts, Cusumano reports[4] that acidic mordenite is the favored catalyst to replace the environmentally harmful $AlCl_3$ now used for this reaction. (The $AlCl_3$ catalyst yields both the 2,6- and 2,7-disubstituted isomers as well as undesirable tri- and tetrasubstituted products.) DIPN can be selectively oxidized (Fig. 1) to give a number of monomers which may then be copolymerized into speciality high-performance polymers such as polyethylene naphthanate[4] which are of great potential in the liquid crystal and synthetic polymer markets.

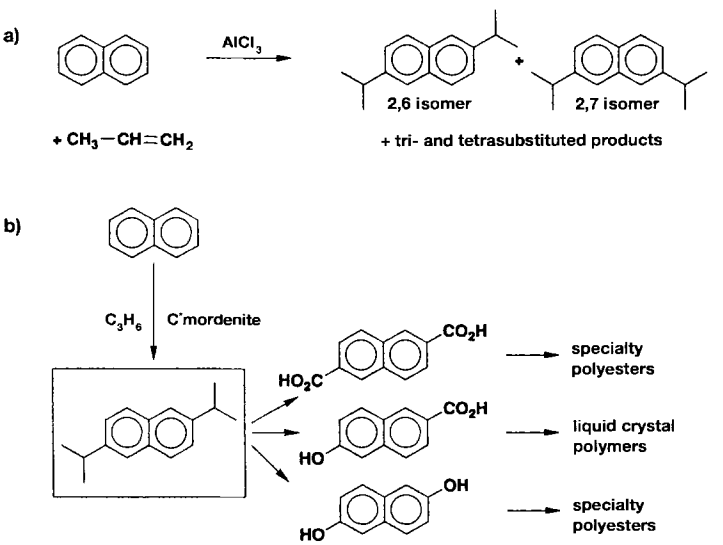


Fig. 1. Alkylation of naphthalene by propene catalyzed by a) $AlCl_3$ to give a mixture of products, b) by mordenite to give 2,6-diisopropylnaphthalene cleanly which can be converted to a number of monomers for specific polymers.

The second category consists of designed multiphasic catalysts. As a typical example, consider a new family of carbon-supported palladium catalysts[21] developed at the Boreskov Institute of Catalysis, Novosibirsk, by Likholobov, Yermakov, et al. These catalysts are prepared by the successive accretion of Pd atoms attached to certain functional groups of the support. A typical procedure is shown schematically in Figure 2. Supported

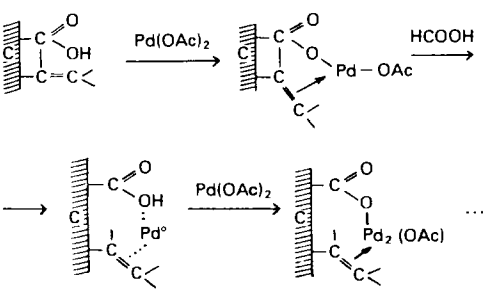


Fig. 2. Accretion of Pd atoms for the production of carbon-supported palladium catalysts.

particles of Pd (crystalline or amorphous) of remarkably uniform size can be obtained in this way. Based on laboratory tests to ascertain the activity of such supported catalysts (for reactions such as the hydrogenation of trifluoromethylnitrobenzene to provide the corresponding aniline), industrial catalysts for large-scale reductions are now in operation with particle sizes in

the range 10 to 30 Å. It is also noteworthy that a new high-strength (ca. 400 kg cm^{-2}) carbon support containing essentially no micropores was especially designed[21] for this catalyst preparation and is already in use industrially.

Designer multiphasic catalysts have also been commercialized to alleviate environmental problems caused by H_2S. This pollutant is found as an impurity in many sources of natural gas, and also in many natural bodies of water, the Black Sea in particular. One popular method of eliminating H_2S has been to use a stoichiometric then a catalytic reaction sequentially [Eq. (a)].

$$H_2S \xrightarrow{+O_2} SO_2 \xrightarrow[\text{cat.}]{+H_2S} S\downarrow + H_2O \qquad \text{(a)}$$

A superior method now on the verge of commercialization for the purification of natural gas[22] is based on a mixed-metal oxide that catalyzes the conversion of H_2S directly into S_2 at such a low temperature that methane remains unoxidized. Natural gas "poisoned" by H_2S may soon by purified efficiently with this designer oxide catalyst.

For removing H_2S from natural bodies of water inorganic photocatalysts that mimic natural bacterial photosynthesis have been designed, prepared, and proven effective.[24] Reaction (b) was demonstrated to proceed quite smoothly in pilot plants upon illumination of semiconductors with visible light.[23]

$$H_2S \xrightarrow{h\nu} H_2 + \tfrac{1}{2}S_2\downarrow \qquad \text{(b)}$$

With the heterojunction arrangement of Figure 3 the whole solar light spectrum is captured, and the efficiency achieved is comparable with that of living organisms.

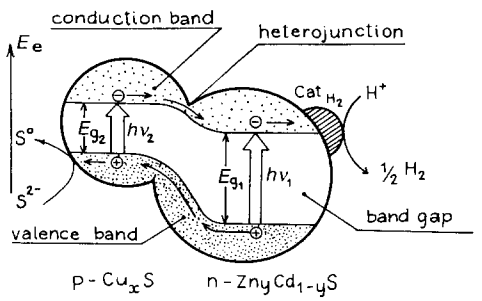


Fig. 3. Energy diagram for the photoseparation of charges and scheme for the catalytic process in a suspended semiconductor particle with the microheterojunction $CuS_x/Zn_yCd_{1-y}S$. E_e is the electrochemical potential of an electron; E_{g1} and E_{g2} are the widths of the band gaps of the semiconductor phases; $h\nu_1$ and $h\nu_2$ are the corresponding quanta of light required to promote an electron into the conduction band.

Another example is the heterogeneous Ziegler–Natta $TiCl_3/MgCl_2$ catalyst for stereoselective polymerization of propene and its copolymerization with other alkenes. Once the mechanism of its mode of action was rationally established, it became possible to tune the catalyst structure and morphology, and the reaction conditions for predominant production of stereoregular polymers with desired physical and mechanical properties.[3] With these carefully designed catalysts one can maximize the yield of the commercially required product and minimize the formation of wastes and consumption of raw material and energy.

A well-known family of inorganic molecular catalysts consists of metal complexes dissolved in liquids (homogeneous) or anchored to solid supports (heterogeneous). Among them, catalysts with chiral ligands for stereocontrolled organic synthesis are particularly noteworthy. The most renowned is the Monsanto rhodium-based catalyst for synthesis of L-dopa, a drug for treating Parkinson's disease (see ref. [4] for further details). Numerous other examples of rationally designed metal complex catalysts are known.[3,4] The active site of one, a bimetallic $(Pd + Co)/SiO_2$ catalyst for hydroformylation of olefins, has been designed by Likholobov and co-workers.[3]

The third category of catalysts includes proven examples in which molecular systems and extended solids have been tailored for a specific catalytic purpose. We cite several noteworthy examples, the first of which relates to the rational development of a system for the photocleavage of water.[23] Here vesicles, microspheres several hundred Å in diameter with walls composed of a bi- or monolayer membrane of amphiphilic molecules, are employed. Aqueous solutions of the appropriate composition are found on either side of this membrane, and the photocatalyst may be "placed" inside the vesicle. The membrane serves to prevent recombination of the photogenerated, energy-rich electron–hole pair. In this way, with the agency of the encapsulated inorganic catalyst—which could be CdS particles of nanoscopic dimension that could serve as a quantum solid with energy levels different from those in the continuous solid—oxidation of water to oxygen and reduction to hydrogen may be smoothly effected.

But inorganic membrane catalysts are already occupying a central role in the development of new catalysts. Palladium-based membranes have been designed by Gryanznov and co-workers[24] at Moscow for numerous selective hydrogenations. In the current industrial production of vitamin K_4[24] a membrane made of a palladium alloy is used that permits facile passage of hydrogen from one compartment to other reactants at the membrane interface. The fundamental principle that governs the mode of operation of a membrane catalyst, be it metal alloy or inorganic (such as a zeolite[25] or a mixed-oxide electrolyte), is that it enables one (or more) crucial reactant(s) to be delivered to an interface in such a manner as to circumvent thermodynamic or other restrictions. Many potentially viable commercial applications, including fuel cells for the direct conversion of chemical into electrical energy in the presence of the appropriate electrocatalyst, are currently being tested.

With the goal of combating the greenhouse effect stemming from the buildup of carbon dioxide in the atmosphere and also exploring new ways of producing alternative feedstocks for C_2-C_3 production, Russian scientists[26] have developed catalytic membranes not based on precious metals for the conversion $CH_4 + CO_2 \longrightarrow 2CO + H_2$; here syn gas is produced with an advantageous $CO:H_2$ ratio.

The fourth category of catalyst research encompasses advances in the application of rationalized new ideas relating to the design and mode of operation of catalytic reactors. The most environmentally useful example to cite here emerged from a recent analysis conducted by Boreskov and Matros of the optimal conditions for the catalytic oxidation of SO_2 to SO_3,[27,28] the basis of sulfuric acid production. Instead of pursuing the traditional practice of operating the catalytic reactor under steady-state conditions, Matros[28] explored the merits of run-

 © VCH Verlagsgesellschaft mbH, D-69451 Weinheim, 1994 0570-0833/94/0303-0310 $ 10.00+.25/0

ning a so-called unsteady-state operation. This entails oxidation of the SO_2 under "forced" conditions for the passage of the reaction mixture through the catalyst bed. The principal advantage of this approach is that, compared with the conventional methods for the production of sulfuric acid, more dilute feedstocks (of SO_2) may be handled, and the size of the plant itself is significantly reduced, thereby limiting the required capital expenditure. Thanks to this work, copper and nickel refining in Russia, which hitherto released its sulfur by-products into the atmosphere as SO_2 leading to acid rain, now produces some 600000 tons of sulfuric acid and processes over 3 billion cubic meters of waste gases per annum.

Numerous other reactor design features have already been implemented commercially. One important example, reactive distillation (otherwise known as catalytic distillation), is the basis of a viable method of etherifying alkenes to produce gasoline additives such as methyl *tert*-butyl ether[29] by the addition of methanol to 2-methylpropene (now readily produced by the isomerization 1-butene[7, 30]).

It is also relevant to note that the pore structure in multiphasic catalysts can be rationally designed to optimize their performance. For example, the new high-strength (ca. 400 $kg\,cm^{-2}$) carbon support, containing predominantly mesopores and almost no micropores and macropores, was especially designed for the Pd catalysts described in Figure 2. Likewise the honeycomb-shaped monolithic catalyst supports for pollution control in power plants and vehicles are the product of rational design.

It is simply not true that the quest for new catalysts is tantamount to black magic. Still less valid is the assertion that all the catalytic processes vital to industry were developed by empirical methods. We concede, however, that although it is already possible, de novo, to compute the rates of diffusion[19] of reactants and products into and out of the pores of shape-selective catalysts, a great deal more must be done before the prospect of computing and accurately predicting catalytic rate coefficients for bond rupture and formation is realized.

[1] R. Schlögl, *Angew. Chem.* **1993**, *105*, 402; *Angew. Chem. Int. Ed. Engl.* **1993**, *32*, 381.
[2] J. M. Thomas, *Angew. Chem.* **1988**, *100*, 1735; *Angew. Chem. Int. Ed. Engl.* **1988**, *27*, 1673. See also *Angew. Chem. Adv. Mater.* **1989**, *101*, 1105; *Angew. Chem. Int. Ed. Engl. Adv. Mater.* **1989**, *28*, 1079.
[3] *Perspectives in Catalysis* (Eds.: J. M. Thomas, K. I. Zamaraev), Blackwell and IUPAC Chemistry for the 21st Century Series, Oxford, **1992**.
[4] J. A. Cusumano, *Chemtech* **1992**, *22*, 482.
[5] J. M. Thomas, *Sci. Am.* **1992**, *266*, 85–88 (UK Edition), 112–118 (US Edition).
[6] A. W. Sleight in *Solid State Chemistry: Compounds* (Eds.: A. K. Cheetham, P. Day), Clarendon, Oxford, **1992**, p. 166.
[7] a) H. H. Mooiweer, K. P. DeJong, B. Braushaar-Czarnatzki, W. H. J. Stork, P. Grondvallet, *Proc. Europacat-1* (Montpellier, 1993), paper A8. b) See also J. Haggin in *Chem. Eng. News* **1993**, *71* (43), 30.
[8] J. M. Thomas, *Philos. Trans. R. Soc. London A* **1990**, *333*, 173.
[9] P. B. Weisz, *Pure Appl. Chem.* **1980**, *52*, 2091.
[10] J. A. Rabo, *Proc. 10th Int. Congr. Catal. (Part A) Budapest 1992*, **1993**, 1.
[11] B. M. Lok, C. A. Messina, R. L. Patton, R. T. Gajek, T. R. Cannan, E. M. Flanigen, US-A 4440871, **1984**.
[12] B. Notari in *Innovation in Zeolite Materials Science* (Eds.: P. J. Grobet, J. A. Martins, P. A. Jacobs), Elsevier, Amsterdam, **1987**, p. 143.
[13] P. A. Wright, J. M. Thomas, J. Chen, S. Natarajan, M. B. Hursthouse, *J. Chem. Soc. Chem. Commun.* **1993**, 633.
[14] M. E. Davies, *Acc. Chem. Res.* **1993**, *26*, 111.
[15] P. A. Wright, J. Chen, S. Natarajan, R. G. Bell, J. M. Thomas, P. L. Gai-Boyes, *Angew. Chem.* **1992**, *104*, 1526; *Angew. Chem. Int. Ed. Engl.* **1992**, *31*, 1472.
[16] P. J. Maddox, J. Stachurski, J. M. Thomas, *Catal. Lett.* **1988**, *1*, 191.
[17] J. W. Couves, R. H. Jones, J. M. Thomas, B. J. Smith, *Adv. Mater.* **1990**, *2*, 181.
[18] C. M. Freeman, C. R. A. Catlow, J. M. Thomas, S. Brode, *Chem. Phys. Lett.* **1991**, *186*, 137.
[19] C. R. A. Catlow, J. M. Thomas, *Philos. Trans. R. Soc. London A* **1992**, *341*, 255.
[20] *Modelling of Structure and Reactivity in Zeolites* (Ed.: C. R. A. Catlow), Academic Press, London, **1992**.
[21] K. I. Zamaraev in ref. [3], p. 35.
[22] Z. R. Ismagilov, K. I. Zamaraev, S. R. Khairulin, US-A 4886649, **1991**.
[23] V. N. Parmon, Z. R. Ismagilov, M. A. Kerzhentsev in ref. [3], p. 337.
[24] V. M. Gryaznov, *Platinum Met. Rev.* **1986**, *30*, 68.
[25] A. J. Burggraaf, K. Keizer, R. S. A. de Lange, Z. A. E. P. Vroon, V. T. Zaspalis, *Proc. Int. Conf. Zeolites 9th*, July **1992**, Montreal (Plenary Lecture).
[26] V. M. Gryaznov, *Proc. Europacat-1* (Montpellier, 1993). See also ref. [7b].
[27] G. K. Boreskov, Y. S. Matros, *Catal. Rev. Sci. Eng.* **1983**, *25*, 551.
[28] Y. S. Matros, *Unsteady Processes in Catalytic Reactors*, Elsevier, Amsterdam, **1985**.
[29] M. Lupieri, E. Picciotto, D. Sanfilippo, *Proc. Europacat-1* (Montpellier, 1993), paper II-262.
[30] S. Natarajan, P. A. Wright, J. M. Thomas, *J. Chem. Soc. Chem. Commun.* in press.

Reply

Robert Schlögl*

In our original highlight article[1] we described the possibilities and limitations of in situ experiments as a modern tool for unraveling the relationships between the structure of a working catalyst and its reactivity. Our conclusion was that although tremendous insight into the complexities of this problem has been gained, our knowledge about the crucial structure–reactivity relationship is, in general, still inadequate for the rational design of a catalyst for a given reaction.

In the immediately preceding correspondence[2] our conclusions are criticized as being only applicable to simple reactions such as the ammonia synthesis (which was not the main subject of the highlight article). Thomas and Zawaraev give an expert description of recent ingenious developments in heterogeneous catalysis; however, proof that these developments are based upon an understanding of the structure–reactivity relationship is lacking.

[*] Prof. Dr. R. Schlögl
Institut für Anorganische Chemie der Universität
Marie-Curie-Strasse 11, D-60439 Frankfurt am Main (FRG)

Their main example of shape-selective, monophasic, zeolite-based catalysts is admittedly a development in which rational ideas about the spatial requirements for diffusion of reactants or transition states in reactions allow the control of reactivity in favorable cases in which the reactant molecules have large structural differences. For any given general case with more subtle structural differences in the desired reactants, the concept of shape selectivity finds its current limits in details such as undisputed "kinetic openings", the influence of the crystallite size on mass transport, and the zeolite lattice dynamics under reaction conditions. A number of empirically derived chemical modifications such as that of the external surface and pore openings were applied, which indicates how chemical intuition can be used to solve problems without a rigorous analysis of the physical background of the application problem.

The second example of "designed multiphasic catalysts" is a further illustration for the general problem. It is simply not feasible to inductively design a catalyst for a reaction, the mechanism of which is not known in detail, and use components with unknown synergetic functions for the catalyst. The important field of selective oxidation catalysis is characterized by the existence of qualitative concepts[3] such as "remote control" which summarize the practical experience of researchers over about 25 years. These concepts are, however, not based on fundamental chemical principles nor can they be used in a quantitative way like a theory.

In view of the formidable complexity of mechanisms for any selective oxidation reactions, such working concepts are of great practical value in guiding the chemical intuition required in developing catalytic processes such as those mentioned by Thomas and Zamaraev. The successful search for such qualitative guiding rules which are commonly used also in other fields of chemistry was inspired by the rational approach of surface physics to the problem of interface reactivity. It is the invaluable contribution of surface science[4] to catalysis that provides guiding ideas and concepts such as that of the active site, geometric reaction control, surface thermodynamics, surface restructuring, and the dynamic nature of reactive systems. The large pool of detailed knowledge about surface reactions under surface-science conditions serves as a source of background information for the development of practical catalyst systems. In this way catalysis has gained a scientific basis in the form of a set of intuitively founded, qualitative working rules. This is, however, not to be mistaken as a quantitative, physically exact, and scientifically proven theory with the predictive power required for the "design approach" in catalysis. The efforts in conducting increasingly complex in situ experiments on existing catalyst systems may find one justification in providing arguments to rationalize the working rules with practical, operating examples.

The "possibilities and limitations of a deductive approach to the development of industrial catalysts" was also analyzed from the viewpoint of a technical chemist.[5] Riekert concludes that it should be in principle impossible to design a catalyst owing to the inherently metastable and kinetically heterogeneous nature of an active catalyst material. This statement may be too restrictive, as we may not require starting catalyst design from first principles and we are also allowed to use some empirical testing in a rational design approach. In his analysis Riekert advocates an evolutionary approach mimicking the controlled "trial-and-error" strategy of nature.

In a recent analysis of the impact of surface science on catalysis[6] it was stated that the direct (rational) impact of surface science in the timeframe of a decade is limited. The indirect impact along the lines of providing working rules and modifying the thinking in catalyst development was, however, estimated as highly important. Catalysis is defined in this analysis as an "interesting mixture of science, engineering, and art". This conclusion is rather similar to that as reached in the initial highlight article.

It is obvious, and I fully agree with Thomas and Zamaraev, that significant progress has been made in selected cases in elucidating a number of aspects of the structure–reactivity relation. We do need, however, a great deal more hard facts about this relation to supplement our set of qualitative rules. There is no need to be pessimistic about an ever-increasing efficiency of catalyst development by the influx of scientific elements, and the semantic polarization of catalyst development strategies into either "scientific" or "intuitive" should also be avoided. Creating unjustified expectations about the potential of rational catalyst design by overestimating the state of our undisputed knowledge about operation principles in catalysis is unproductive and potentially detrimental to the field of catalysis science. Closing the experimental gaps between surface science and catalysis as described in the highlight article is one way to efficiently contribute towards the ideal of a rational approach in catalysis.

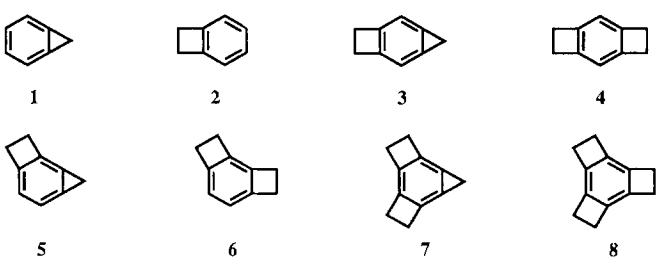
[1] R. Schlögl, *Angew. Chem.* **1993**, *105*, 403; *Angew. Chem. Int. Ed. Engl.* **1993**, *32*, 381.
[2] J. M. Thomas, K. I. Zamaraev, *Angew. Chem.* **1994**, *106*, 316; *Angew. Chem. Int. Ed. Engl.* **1994**, *33*, No. 3.
[3] L. T. Weng, P. Ruiz, B. Delmon in *New Developments in Selective Oxidation by Heterogeneous Catalysis* (Stud. Surf. Sci. Catal. **1992**, *72*, 399).
[4] I. Langmuir, *J. Am. Chem. Soc.* **1916**, *38*, 2221; G. A. Somorjai, *Chemistry in Two Dimensions*, Cornell University Press, **1981**; G. Ertl, *Angew. Chem.* **1990**, *102*, 1258; *Angew. Chem. Int. Ed. Engl.* **1990**, *29*, 1219.
[5] L. Riekert, *Chem. Ing. Tech.* **1981**, *53*, 950.
[6] F. M. Hoffmann, D. J. Dwyer in *Surface Science of Catalysis* (*ACS Symp. Ser.* **1992**, *482*, 1).

The Effect of Fusion of Angular Strained Rings on Benzene: Crystal Structures of 1,2-Dihydrocyclobuta[*a*]cyclopropa[*c*]-, 1,2,3,4-Tetrahydrodicyclobuta[*a*,*c*]-, 1,2,3,4-Tetrahydrodicyclobuta[*a*,*c*]cyclopropa[*e*]-, and 1,2,3,4,5,6-Hexahydrotricyclobuta[*a*,*c*,*e*]benzene**

Roland Boese*, Dieter Bläser, W. Edward Billups*, Michael M. Haley, Andreas H. Maulitz, Debra L. Mohler, and K. Peter C. Vollhardt*

Recent crystallographic studies of arenes that contain fused strained rings have found a marked difference in the structures of cyclopropabenzene ("benzocyclopropene", **1**)[1] and 1,2-dihydrocyclobutabenzene ("benzocyclobutene", **2**)[2]. Although the bond of annelation as well as the bonds adjacent to it are influenced by the effects of strain, the aromatic framework of **2** has undergone a fundamental change from that of **1**. In benzocyclopropenes the annelated bond is always the shortest; in benzocyclobutenes the adjacent bond is the shortest.[3] Incorporating two strained-ring features into a single system, such as **3** and **4**, resulted in structures which reflect a summation of the distortions found in each of the parent systems.[2, 4] The linear [*a*,*d*] annelation did not allow the two effects to influence one another significantly; only the bond angle at C2 was altered noticeably. Combining strained-ring features in a nonlinear [*a*,*c*] fashion (as in **5** and **6**) or [*a*,*c*,*e*] fashion (as in **7** and **8**), however, should result in an overlap of the effects of strain, and thus the structures are expected to be more distorted. In order to determine the extent of structural deformation in **5**–**8**, X-ray analyses were carried out.

While calculations on **5**[5] and **6**[6] are limited and have never been performed on **7**, **8** has been the subject of a burgeoning number of theoretical studies in recent years.[6, 7] This molecule has become the quintessential test case for theoreticians in the long-standing debate over strain-induced bond alternation in benzenoid molecules, now commonly known as the Mills–Nixon effect.[8] Fueled by conflicting theoretical papers, this argument now focuses on two specific approaches: the first postulates control of bond alteration by the σ electron system, the second by the π electron system.[6c, 7c–d] The difference between the alternating interatomic distances in the benzene ring of **8** calculated by different methods varies widely: it is as large as 0.132 Å for the semiempirical AM1 calculations but as little as 0.013 Å at the ab initio 6–31 G* level.[7e] Although syntheses of **8** have been known for some time,[9] the only crystal structure determination was performed on the perfluoro derivative **8**-F_{12}.[10] Fluorine substituents on small rings are known to alter their structures.[11] Therefore, the extrapolation of the data of **8**-F_{12} to **8** is tenuous.[6a] At the end of this paper we will show that only at the highest level of theory can calculations accurately reproduce experimental results.



The arenes were synthesized by published procedures.[9, 12–14] Single crystals of **5** (m.p. −12 °C) and **6** (m.p. 35 °C), prepared by previously described methods,[15] were used for analysis. Suitable crystals of **7** were grown by sublimation directly from the reaction vessel. The structure determinations were performed at 255, 120, and 105 K, respectively, and the molecular structures are presented in Figure 1.[16–18] The structure determination for **8** proved to be suprisingly complex. Crystals were grown from pentane in a computer-controlled device which adjusts the temperature of the solution to optimal crystallization conditions. Most of the crystals were destroyed upon cooling on the diffractometer for low-temperature data collection, which indicated a solid-state phase transition at 205 K.[20] Therefore, the structure of **8** was determined at room temperature, and in the following this "high-temperature" phase is termed **8**-HT.[21] The crystal was then cooled very slowly (1 °C h^{-1} cooling rate) through the transition temperature to 125 K, and a second determination was made (termed the low-temperature phase **8**-LT).[22] As one independent molecule is present in the HT cell and two independent molecules in the LT cell, Figure 2a shows a pair of molecules of **8**-HT, coupled by the inversion centers, and Figure 2b the two independent molecules of **8**-LT.

Common with all benzocyclopropenes,[1, 3] the bond of cyclopropene fusion is found to be the shortest bond in **5** (1.351 Å, see Fig. 1, left)[23] and is in good agreement with that found in **3** (1.349 Å). The bond in **5** between the cyclopropene and cyclobutene rings (C1–C2), however, is significantly shortened because of the added strain of nonlinear fusion (1.363 Å). This additional strain is demonstrated at the bridgehead atom C1; to our knowledge the angle at C1 is the largest yet found at an

[*] Prof. Dr. K. P. C. Vollhardt, Dr. M. M. Haley, [+] D. L. Mohler
Department of Chemistry, University of California at Berkeley
and
Chemical Sciences Division, Lawrence Berkeley Laboratory,
Berkeley, CA 94720 (USA)
Telefax: Int. code + (510)643-5208

Prof. Dr. W. E. Billups
Department of Chemistry, Rice University
PO Box 1892, Houston, TX 77251 (USA)

Priv. Doz. R. Boese, Dipl.-Ing. D. Bläser, Dipl.-Chem. A. H. Maulitz
Institut für Anorganische Chemie der Universität – Gesamthochschule
Universitätsstrasse 5–7, D-45117 Essen (FRG)

[+] New address: Department of Chemistry, University of Oregon
Eugene, OR 97403 (USA)

[**] This work was supported by the Director, Office of Energy Research, Office of Basic Energy Sciences, Chemical Sciences Division of the U.S. Department of Energy (DE-AC03-76SF00098), the National Science Foundation (NSF) (INT-8822541, CHE-9102239, CHE-9202152), the Robert A. Welch Foundation, and the Fonds der Chemischen Industrie. M.M.H. is the recipient of an NSF Postdoctoral Fellowship (1991–93).

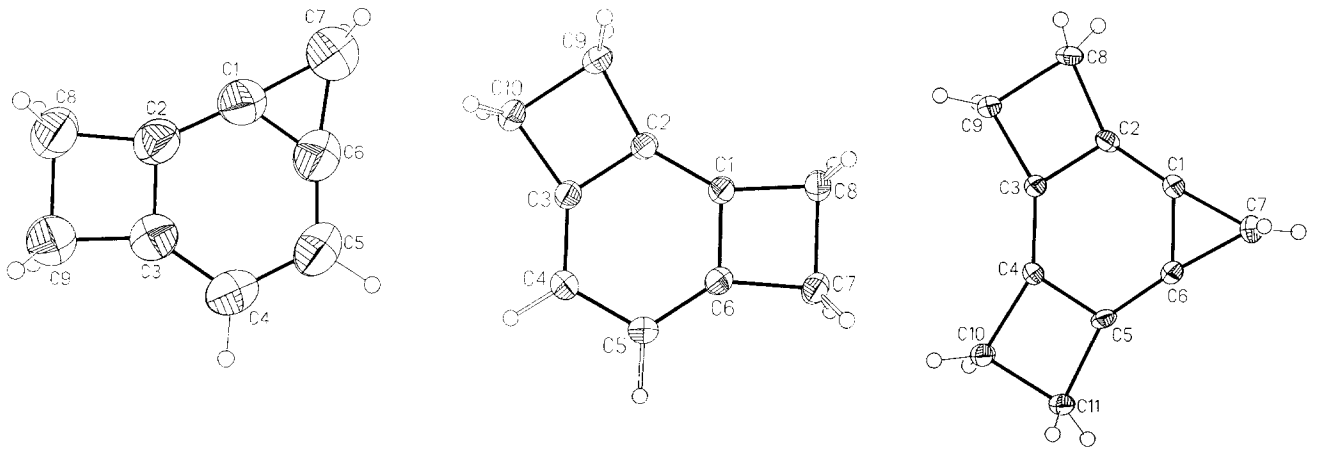


Fig. 1. Molecular structures of **5**–**7** with thermal probability plots of 50%. Distances [Å] and angles [ ] (standard deviations), values after a libration correction [19] in parentheses (mean values for the molecules): Left: **5**: C1-C2 1.363(2) (1.368), C2-C3 1.393(1) (1.401), C3-C4 1.384(2) (1.390), C4-C5 1.401(4) (1.405), C5-C6 1.368(2) (1.376), C1-C6 1.351(3) (1.357), C1-C7 1.507(2) (1.512), C6-C7 1.499(2) (1.508), C2-C8 1.510(3) (1.516), C3-C9 1.516(2) (1.521), C8-C9 1.565(2) (1.574); C1-C2-C3 116.3(2), C1-C2-C8 150.1(1), C1-C6-C5 125.7(2), C1-C7-C6 53.4(1), C2-C1-C6 120.0(1), C2-C1-C7 176.9(1), C2-C3-C4 123.7(2), C2-C8-C9 86.7(1), C3-C4-C5 118.8(1), C3-C9-C8 86.9(1), C4-C3-C9 143.5(2), C4-C5-C6 115.6(2), C5-C6-C7 170.7(2); center: **6**: C1-C2 1.385(1) (1.387), C2-C3 1.402(1) (1.405), C3-C4 1.392(1) (1.395), C4-C5 1.413(1) (1.414), C6-C7 1.522(1) (1.524), C7-C8 1.582(1) (1.585), C1-C8 1.518(1) (1.520); C1-C2-C3 118.1(1), C1-C2-C9 148.4(1), C2-C3-C4 124.3(1), C2-C3-C10 93.2(1), C2-C9-C10 86.5(1), C3-C2-C9 93.8(1), C3-C10-C9 86.8(1), C3-C4-C5 117.7(1), C4-C3-C10 142.5(1); right: **7**: C1-C2 1.372(4) (1.373), C2-C3 1.411(3) (1.412), C3-C4 1.385(4) (1.386), C1-C6 1.363(4) (1.364), C1-C7 1.506(4) (1.507), C2-C8 1.517(3) (1.518), C3-C9 1.521(4) (1.522), C8-C9 1.580(3) (1.581); C1-C2-C3 117.7(2), C1-C2-C8 149.0(3), C1-C6-C5 121.9(3), C1-C7-C6 53.8(2), C2-C1-C7 174.9(3), C2-C3-C4 120.4(2), C2-C8-C9 86.8(2), C3-C9-C8 86.9(2), C4-C3-C9 146.6(3).

sp^2-carbon center—176.9 °C. The remaining bond lengths and angles in **5** are consistent with previously determined structures.

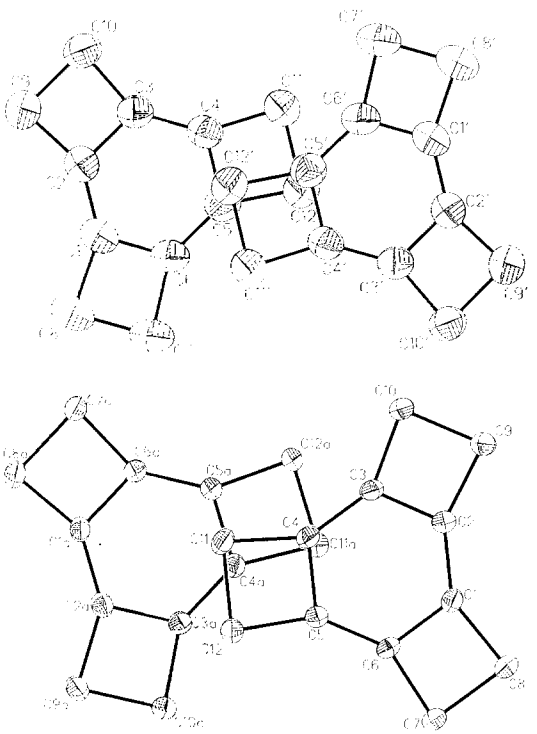


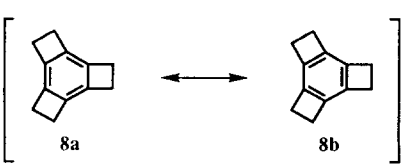
Fig. 2. Molecular structure of a pair of molecules of **8**-HT (top) and of the two independent molecules of **8**-LT (bottom) with thermal probability plots of 50%. Distances [Å] and angles [ ] (maximum standard deviations 0.002 Å and 0.2 , respectively, for **8**-HT: 0.001 Å and 0.1 , respectively, for **8**-LT), values after a libration correction [19] in parentheses (mean values): Top: **8**-HT: C1-C2 1.383 (1.387), C2-C3 1.401 (1.405), C6-C7 1.519 (1.523), C7-C8 1.566 (1.570); C1-C2-C3 120.0, C1-C2-C9 147.0, C2-C9-C10 87.0, C3-C2-C9 93.0; bottom: **8**-LT: C1-C2 1.390 (1.391), C2-C3 1.413 (1.414), C6-C7 1.527 (1.528), C7-C8 1.579 (1.580); C1-C2-C3 120.0, C1-C2-C9 147.0, C2-C9-C10 87.0, C3-C2-C9 93.0.

As in other benzocyclobutenes,[2, 3] the annelated bonds (C1–C6, C2–C3) in **6** (Fig. 1, center) have lengths usual for arenes (1.402 Å and 1.402 Å). The bonds in the benzene ring adjacent to the annelated bonds (C1–C2, C3–C4, C5–C6) are shortened (1.385 Å, 1.392 Å), and the C4–C5 bond is significantly lengthened (1.413 Å). This elongation can be attributed to the strain of nonlinear [*a*,*c*]-fusion of two ring systems. As the sole aromatic bond not connected to a cyclobutene moiety, the strain in the other bonds is imparted to C4–C5, which results in a lengthening of 0.010–0.015 Å.

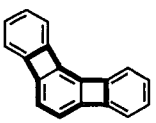
At 1.363 Å, the bond of the three-membered ring annelation in **7** (Fig. 1, right) is the longest of all benzocyclopropenes.[3] The addition of a third strained ring to the system forces a significant lengthening (0.010–0.020 Å) in the otherwise short bond. Similarly, the bonds of four-membered ring annelation are lengthened by 0.010–0.022 Å with respect to benzocyclobutenes.[3] The bridgehead atoms C1 and C6 in **7** also possess unusually large angles (174.9 °) at the sp^2-carbons.

As with **7**, the benzenoid nucleus of **8** (Fig. 2) tries to "breathe" under the "weight" of triangular ring fusion, that is, the ring expands since no bonds can be shortened. The aromatic bond between the cyclobutene rings (e.g., C1–C2) varies between 1.383 (HT) and 1.390 Å (LT), the bond of fusion (e.g., C2–C3) between 1.401 (HT) and 1.413 Å (LT). The resulting differences in bond lengths (0.018 and 0.023 Å, respectively) suggest an approximate difference of 0.026 Å when the data are extrapolated to 0 K. Thus, from the experimentally determined distances, the Kekulé structure **8a** appears to contribute slightly more to the molecule than **8b**.

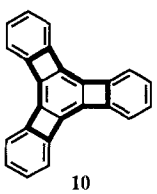
The fusion of equivalent cyclobutene rings induces the minor bond alternation observed in **6** and **8**. [*N*]Phenylenes **9** and **10**,



structural analogues containing the structural units **6** and **8**, have been shown by X-ray crystallography to exhibit pronounced bond alternation in the central six-membered ring.[24] The 0.098–0.159 Å difference in bond lengths within **9** and **10** results in an increased olefinic reactivity of the central ring, as demonstrated by the ease with which **10** can be hydrogenated, epoxidized, and cyclopropanated.[25] The 0.010–0.023 Å difference observed in **6** and **8** (that is, the small preference of **8a** over **8b**) is, however, chemically insignificant, because the central ring in **8** appears to be much less reactive than that of **10**. Hydrogenation required more severe conditions than those employed for **10** and gave a complex mixture of products; attempts at cyclopropanation have failed so far. Although annelation of one additional benzene ring to each cyclobutene moiety alters the structure of the four-membered ring and produces more strain in the molecule, it appears that avoidance of anti-aromatic cyclobutadienoid circuits (π effect) contributes to a much greater degree, thus inducing the larger bond alternation observed in **9** and **10**.



9



10

The ring strain of the cyclobutene moieties of **6** and **8**-LT is clearly evident in Figure 3: the electron-density maxima in the molecular plane (that is, the σ frame) are shifted outside the four-membered ring, and as a consequence the annelated bonds are shifted toward the center of the benzene ring. This results in an outward shift of the electron densities of the neighboring bonds. The outward shift is especially prominent in C1–C2, since this bond is connected to both cyclobutene rings; it results in a shortening of the interatomic distance. The accuracy of the data do not enable the determination of exact amounts of shifts, but they are as depicted qualitatively in Figure 4. These findings are wholly consistent with the concept of bent bonds ("banana" bonds), in which the σ frame dominates the structures of small-ring annelated benzenes, as pointed out by Stanger on the basis of theoretical work.[7c] Structures for **5**–**8** calculated with a variety of methods at different levels are summarized in Tables 1–4, respectively. Although the data also do not allow for estimation of the π contribution to the molecular structure, the detailed study of Baldridge and Siegel[7d] does a splendid job of addressing the issue of σ vs. π control of bond alternation[6, 7] (Mills–Nixon effect). Their work seems at last to bring into line experiment and theory, as illustrated by their calculations for **8**

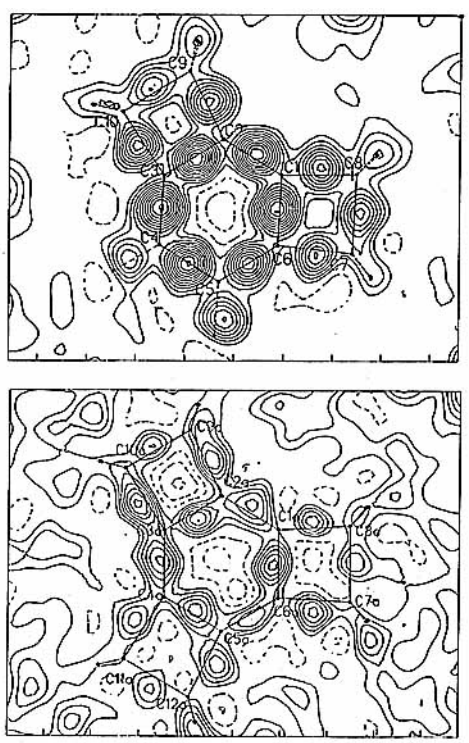


Fig. 3. X–X difference electron densities of **6** (top) and **8**-LT (bottom) in the plane of the molecular framework; distances of 0.05 e Å^{-3} (positive and zero, solid lines) and 0.1 e Å^{-3} (negative, dotted lines).

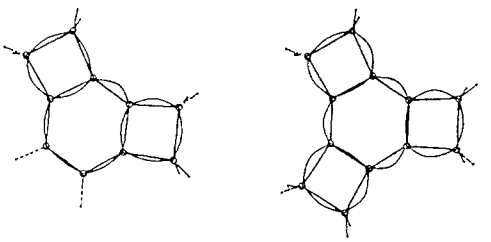


Fig. 4. Shifts of electron-density maxima for **6** (top) and **8**-LT (bottom); the arcs join nucleus to nucleus through the electron density maximum.

Table 1. Calculated and experimental bond lengths [Å] for the arene unit of **5** (C_s-symmetry).

	C1-C2	C2-C3	C3-C4	C4-C5	C5-C6	C1-C6
STO-3G[a]	1.357	1.405	1.379	1.418	1.365	1.352
3-21G[b]	1.354	1.404	1.374	1.419	1.362	1.348
6-31G[a]	1.361	1.403	1.380	1.418	1.369	1.350
6-31G*[a]	1.367	1.390	1.385	1.407	1.374	1.339
6-311G*[a]	1.366	1.389	1.384	1.407	1.373	1.338
MP2(full)/6-31G*[a, c]	1.378	1.403	1.397	1.414	1.368	1.357
exp.[a, d]	1.363(2)	1.393(1)	1.384(2)	1.400(4)	1.368(2)	1.351(3)

[a] This work. [b] Ref. [5]. [c] Calculations performed on a NEC SX-3 computer with the program GAUSSIAN 90. [d] Mean values of the two independent molecules.

Table 2. Calculated and experimental bond lengths [Å] for the arene unit of **6** (C_{2v} symmetry) and, for comparison, experimental values for **9**.

	C1-C2	C2-C3	C3-C4	C4-C5
STO-3G[a]	1.365	1.399	1.375	1.410
3-21G[a, b]	1.361	1.397	1.372	1.408
3-21G(SC)[c]	1.377	1.410	1.387	1.420
6-31G[a]	1.367	1.397	1.378	1.408
6-31G*[d]	1.373	1.386	1.383	1.400
6-311G**[d]	1.373	1.385	1.383	1.399
MP2(fc)/6-31G*[d, e]	1.386	1.402	1.396	1.408
exp.[d, f]	1.385(1)	1.402(1)	1.392(1)	1.413(1)
9[g]	1.345(2)	1.449(2)	1.348(3)	1.446(3)

[a] Ref. [6a]. [b] Ref. [6c]. [c] Ref. [6b]. [d] This work. [e] Calculations performed on an HP 730 computer with the program GAUSSIAN 92. [f] Mean values on C_{2v} symmetry. [g] Ref. [24a].

(Table 4, entries 6 and 9). From the tables, it appears that only the ab initio 6–31G or higher levels accurately reproduce the experimental values. Interestingly, the highest level of theory (MP2/6-31G*) almost duplicates the experimental structures of **6**–**8**, yet it overestimates bond lengths in **5**. Since the structure determination of **5** was conducted at 255 K, the better comparison is with librationally corrected values (Fig. 1, left); with these data the MP2 (full) 6–31G* level gives excellent agreement.

Table 3. Calculated and experimental bond lengths [Å] for the arene unit of **7** (C_{2v} symmetry).

	C1-C2	C2-C3	C3-C4	C1-C6
STO-3G[a]	1.356	1.416	1.367	1.363
3-21G[a]	1.352	1.417	1.361	1.358
6-31G[a]	1.360	1.414	1.369	1.360
6-31G*[a]	1.369	1.397	1.378	1.345
MP2(full)/6-31G*[a, b]	1.380	1.411	1.390	1.364
exp.[a, c]	1.372(4)	1.411(3)	1.385(4)	1.363(4)

[a] This work. [b] Calculations performed on a NEC SX-3 computer with the program GAUSSIAN 90. [c] Mean values on C_{2v} symmetry

Table 4. Calculated and experimental bond lenghts [Å] for the arene unit of **8** (D_{3h} symmetry) and experimental values for **8**-F_{12} and **10**, for comparison.

	C1-C2	C2-C3	Δd[a]
STO-3G[b]	1.388	1.454	0.066
STO-3G[c]	1.365	1.409	0.044
3-21G[b, d, e]	1.361	1.408	0.047
3-21G(SC)[f]	1.377	1.420	0.043
6-31G[b]	1.368	1.406	0.038
6-31G*[g]	1.378	1.391	0.013
6-311G**[c]	1.377	1.391	0.014
MP2(full)/6-31G*[c, h]	1.389	1.406	0.017
LDF[g]	1.382	1.406	0.024
exp. (**8**-HT)[c, i]	1.383(1)	1.401(1)	0.018
exp. (**8**-LT)[c, i]	1.390(1)	1.413(1)	0.023
8-F_{12}[j]	1.392	1.386	−0.006
10[k]	1.335	1.494	0.159

[a] Δd is defined as d(C2–C3) − d(C1–C2). [b] Ref. [6a]. [c] This work. [d] Ref. [7c]. [e] Ref. [6c]. [f] Ref. [7b]. [g] Ref. [7d]. [h] Calculations performed on a NEC SX-3 computer with the program GAUSSIAN 90. [i] Mean values on D_{3h} symmetry. [j] Ref. [10]. [k] Ref. [24b].

The results for the crystal structures of **5**–**8** complete the series of structure determinations for known strained-ring annelated benzenes. From our findings three conclusions can be readily drawn: 1) strained-ring fusion to the benzenoid nucleus leads to the formation of "banana" bonds in the molecule, and thus interatomic distances seem to be somewhat misleading; 2) bond alternation, if present, is very minor (< 0.025 Å) and appears to be chemically insignificant; thus it should not be taken as support for Mills–Nixon arguments; and 3) only the highest level ab initio calculations are able to replicate experimental structures, and of these, the best agreement is found with MP2/6-31G*, therefore, studies at lower levels of theory possibly lead to misleading or erroneous conclusions. Finally, we conclude that benzene, even if distorted in the σ-frame, simply wants to remain "aromatic".

Received: June 7, 1993 [Z 6128/6129IE]
German version: *Angew. Chem.* **1994**, *106*, 321

[1] R. Neidlein, D. Christen, V. Poignée, R. Boese, D. Bläser, A. Gieren, C. Ruiz-Pérez, T. Hübner, *Angew. Chem.* **1988**, *100*, 292; *Angew. Chem. Int. Ed. Engl.* **1988**, *27*, 294.
[2] R. Boese, D. Bläser, *Angew. Chem.* **1988**, *100*, 293; *Angew. Chem. Int. Ed. Engl.* **1988**, *27*, 304.
[3] For a recent review of strained systems, see R. Boese, *Structural Studies of Strained Molecules* (*Adv. Strain Org. Chem.* **1992**, *2*, 191).
[4] D. Bläser, R. Boese, W. A. Brett, P. Rademacher, H. Schwager, A. Stanger, K. P. C. Vollhardt, *Angew. Chem.* **1989**, *101*, 209; *Angew. Chem. Int. Ed. Engl.* **1989**, *28*, 206.
[5] Y. Apeloig, M. Karni, D. Arad at the NATO Advanced Research Workshop on Strain and Its Implication in Organic Chemistry (*NATO ASI Ser. C* **1989**, *273*, 457).
[6] a) M. Eckert-Maksic, D. Kovacek, M. Hodoscek, D. Mitic, K. Poljanec, Z. B. Maksic, *J. Mol. Struct.* **1990**, *206*, 89; b) Z. B. Maksic, M. Eckert-Maksic, D. Kovacek, D. Margetic, *ibid.* **1992**, *260*, 241; c) R. Faust, E. Glendening, A. Streitwieser, K. P. C. Vollhardt, *J. Am. Chem. Soc.* **1992**, *114*, 8263.
[7] a) Z. B. Maksic, M. Eckert-Maksic, M. Hodoscek, W. Koch, D. Kovacek, *Theoretical Studies of the Mills-Nixon Effect* (*Molecules in Natural Science and Medicine: An Encomium for Linus Pauling* (Eds.: Z. B. Maksic, M. Eckert-Maksic), Ellis Horwood, London, **1991**, p. 221); b) Z. B. Maksic, M. Eckert-Maksic, D. Kovacek, M. Hodoscek, K. Poljanek, J. Kudnig, *J. Mol. Struct.* **1991**, *234*, 201; c) A. Stanger, *J. Am. Chem. Soc.* **1991**, *113*, 8277; d) K. K. Baldridge, J. S. Siegel, *ibid.* **1992**, *114*, 9583; e) J. E. Bloor, M. Eckert-Maksic, M. Hodoscek, Z. B. Maksic, K. Poljanec, *New. J. Chem.* **1993**, *17*, 157.
[8] W. H. Mills, I. G. Nixon, *J. Chem. Soc.* **1930**, 2510; see also: L. E. Sutton, L. Pauling, *Trans. Faraday Soc.* **1935**, 939; H. C. Longuet-Higgins, C. A. Coulson, *ibid.* **1946**, *42*, 756; G. M. Q. Badger, *Q. Rev. Chem. Soc.* **1951**, *5*, 147.
[9] E. Heilbronner, B. Kovac, W. Nutakul, A. D. Taggart, R. P. Thummel, *J. Org. Chem.* **1981**, *46*, 5279; see also: C. W. Doecke, P. J. Garrat, H. Shahriari-Zavareh, R. Zahler, *ibid.* **1984**, *49*, 1412. According to IUPAC recommendations, the correct name for **8** is tetracyclo[8.2.0.0^{2,5}.0^{6,9}]dodeca-1,5,9-triene.
[10] R. P. Thummel, J. D. Korp, I. Bernal, R. L. Harlow, R. L. Soulen, *J. Am. Chem. Soc.* **1977**, *99*, 6916; R. E. Cobbledick, F. W. B. Einstein, *Acta Crystallogr. Sect. B* **1976**, *32*, 1908.
[11] D. Cremer, E. Kraka, *J. Am. Chem. Soc.* **1985**, *107*, 3811, and references therein; W. Koch, M. Eckert-Maksić, Z. B. Maksić, *Int. J. Quantum Chem.* **1993**, *48*, 319.
[12] D. Davalian, P. J. Garrat, W. Koller, M. M. Mansuri, *J. Org. Chem.* **1980**, *45*, 4183; see also: W. E. Billups, W. A. Rodin, *ibid.* **1988**, *53*, 1312; W. A. Rodin, Dissertation, Rice University, **1986**. The IUPAC name for **5** is tricyclo[5.2.0.0^{2,4}]nona-1,4,6-triene.
[13] R. P. Thummel, W. Nutakul, *J. Org. Chem.* **1977**, *42*, 300. The IUPAC name for **6** is tricyclo[6.2.0.0^{2,5}]deca-1,5,7-triene.
[14] W. E. Billups, B. E. Arney, Jr., L.-J. Lin, *J. Org. Chem.* **1984**, *49*, 3436. The IUPAC name for **7** is tetracyclo[7.2.0.0^{2,4}.0^{5,8}]undeca-1,4,8-triene.
[15] D. Brodalla, D. Mootz, R. Boese, W. Oßwald, *J. Appl. Crystallogr.* **1985**, *18*, 316; R. Boese, M. Nussbaumer, *In Situ Crystallization Techniques* (*Int. Union Crystallogr. Crystallogr. Symp.* **1993**, *6*, in press).
[16] X-ray structure analysis of **5**: $a = 7.618(2)$, $b = 7.587(3)$, $c = 11.190(3)$ Å, $\alpha = 93.85(2)$, $\beta = 94.14(2)$, $\gamma = 95.32(3)^\circ$, $V = 640.6(3)$ Å^3, 255 K, triclinic, space group $P\bar{1}$, $Z = 4$, $\rho_{calc} = 1.205$ g cm^{-3}, $Mo_{K\alpha}$ radiation, $\mu = 0.06$ mm^{-1}, $2\theta_{max} = 55^\circ$, 3493 unique reflections, 2168 observed ($F_o \geq 4\sigma(F)$), structure refinement (C atoms anisotropic, H atoms isotropic) with SHELXTL-PLUS, 173 parameters, $R = 0.0554$, $R_w = 0.0637$, $w^{-1} = \sigma^2 F_o + 0.0101 F_o^2$ [22b].
[17] X-ray structure analysis of **6**: $a = 5.728(1)$, $b = 7.810(1)$, $c = 8.603(1)$ Å, $\alpha = 79.89(1)$, $\beta = 79.05(1)$, $\gamma = 71.37(1)^\circ$, $V = 352.5(1)$ Å^3, 120 K, triclinic, space group $P\bar{1}$, $Z = 2$, $\rho_{calcd} = 1.217$ g cm^{-3}, $Mo_{K\alpha}$ radiation, $\mu = 0.07$ mm^{-1}, $2\theta_{max} = 80^\circ$, 4495 unique reflections, 3630 observed ($F_o \geq 4\sigma(F)$), structure refinement (C atoms anisotropic, H atoms isotropic) with SHELXTL-PLUS, 131 parameters, $R = 0.0456$, $R_w = 0.0501$, $w^{-1} = \sigma^2 F_o + 0.0032 F_o^2$ [22b].
[18] X-ray structure analysis of **7**: $a = 7.405(2)$, $b = 13.679(4)$, $c = 7.707(3)$ Å, $\beta = 112.43(2)^\circ$, $V = 721.6(4)$ Å^3, 105 K, monoclinic, space group $P2_1/n$, $Z = 4$, $\rho_{calcd} = 1.309$ g cm^{-3}, $Mo_{K\alpha}$ radiation, $\mu = 0.07$ mm^{-1}, $2\theta_{max} = 55^\circ$, 1901 unique reflections, 1154 observed ($F_o \geq 4\sigma(F)$), structure refinement (C atoms anisotropic, H atoms isotropic) with SHELXTL-PLUS, 105 parameters, $R = 0.0597$, $R_w = 0.0629$, $w^{-1} = \sigma^2 F_o + 0.00216 F_o^2$ [22b].
[19] V. Schomaker, K. N. Trueblood *Acta Crystallogr. Sect. B* **1968**, *4*, 63.
[20] Details of the phase transition will be published in a forthcoming full paper.
[21] X-ray structure analysis of **8**-HT: $a = 7.918(1)$, $b = 14.109(2)$, $c = 8.193(1)$ Å, $\beta = 111.46(1)^\circ$, $V = 851.8(2)$ Å^3, 298 K, monoclinic, space group $P2_1/n$, $Z = 4$, $\rho_{calcd} = 1.218$ g cm^{-3}, $Mo_{K\alpha}$ radiation, $\mu = 0.07$ mm^{-1}, $2\theta_{max} = 60^\circ$, 2485 unique reflections, 1695 observed ($F_o \geq 4\sigma(F)$), structure refinement (C atoms anisotropic, H atoms isotropic without constraints) with SHELXTL-PLUS, 157 parameters, $R = 0.0455$, $R_w = 0.0465$, $w^{-1} = \sigma^2 F_o + 0.00039 F_o^2$ [22b].

[22] a) X-ray structure analysis of **8**-LT: $a = 8.784(3)$, $b = 14.304(6)$, $c = 15.711(5)$ Å, $\beta = 122.71(2)°$, $V = 1660.8(9)$ Å^3, 125 K, monoclinic, space group $P2_1/n$, $Z = 8$, $\rho_{calcd} = 1.249$ g cm^{-3}, $Mo_{K\alpha}$ radiation, $\mu = 0.07$ mm^{-1}, $2\theta_{max} = 55°$, 4216 unique reflections, 2894 observed ($F_o \geq 4\sigma(F)$), structure refinement (C atoms anisotropic, H atoms with common isotropic U value, riding groups) with SHELXTL-PLUS, 218 parameters. $R = 0.0479$, $R_w = 0.0544$, $w^{-1} = \sigma^2 F_o + 0.002 F_o^2$. b) Further details of the crystal structure analysis may be obtained from the Fachinformationszentrum Karlsruhe, D-76344 Eggenstein-Leopoldshafen (FRG), on quoting the depository number CSD-57772, and the journal citation.

[23] All bond lengths and angles given are mean values based on the symmetry of the molecule and/or on the number of independent molecules in the unit cell.

[24] a) R. Diercks, K. P. C. Vollhardt, *Angew. Chem.* **1986**, *98*, 268; *Angew. Chem. Int. Ed. Engl.* **1986**, *25*, 266; b) *J. Am. Chem. Soc.* **1986**, *108*, 3150.

[25] a) D. L. Mohler, K. P. C. Vollhardt, S. Wolff, *Angew. Chem.* **1990**, *102*, 1200; *Angew. Chem. Int. Ed. Engl.* **1990**, *29*, 1151; b) D. L. Mohler, K. P. C. Vollhardt, S. Wolff, unpublished results; c) D. L. Mohler, Dissertation, University of California at Berkely, **1992**.

Competitive Generation of C–H and C–Si Bonds by Reductive Elimination: Formation of Silametallacycles by Metalation of Silyl Ligands**

Michael Aizenberg and David Milstein*

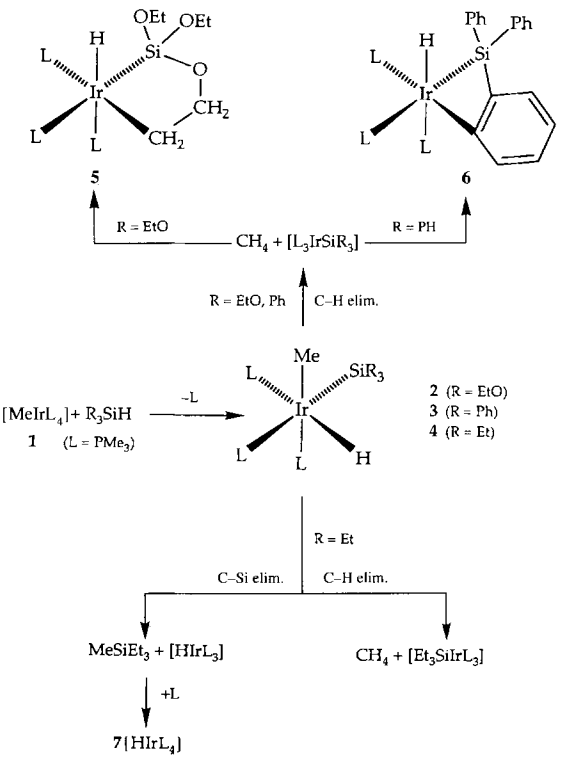
Transition metal catalyzed transformations of organosilicon compounds[1] may sometimes involve either C–Si or C–H bond formation in the product-forming step. For example, the Chalk–Harrod mechanism[2] for the synthetically important hydrosilation of alkenes, in which product formation by C–Si reductive elimination is postulated, has been discussed in many papers.[1, 3] In an alternative mechanism proposed by Wrighton,[4] silyl migration to the coordinated alkene takes place, and the product is released by C–H reductive elimination. A two-silicon cycle for Rh-catalyzed olefin hydrosilation, recently proposed by Perutz,[5] also involves C–H reductive elimination in preference to C–Si elimination. Whereas formation of C–H bonds by reductive elimination is well documented,[6] examples for generation of C–Si bonds that may proceed by this process are very rare.[7–11] Of particular interest is the question of competitive C–H vs. C–Si reductive elimination. Relevant to this is the generation of methane upon reaction of $[MeCo(CO)_4]$ with Me_3SiH[4] and of $[MeRh(PMe)_{3,4}]$ with $HSiPh_3$,[8] although the presumed oxidative addition intermediates have not been observed and the relative disposition of the hydrido, silyl, and methyl ligands in these complexes is not certain. Reactions of $[MPhCl(CO)(PPh_3)_2]$ (M = Ru, Os) with silanes yield benzene,[12] again no intermediates are observed.

We report here for the first time on elimination reactivity of fully characterized complexes which possess the necessary all *cis* arrangement of the hydrido, silyl, and methyl ligands. We find that, depending on the electronic properties of the silyl ligand, C–Si and C–H reductive elimination can be competitive. This study has led to rare examples of metalations of silyl ligands, including the metalation of sp^3-C–H bonds.

[*] Prof. Dr. D. Milstein, Dr. M. Aizenberg
Department of Organic Chemistry
The Weizmann Institute of Science
Rehovot 76100 (Israel)
Telefax: Int. code + (8)344142

[**] This work was supported by the Basic Research Foundation administered by the Israel Academy of Sciences and Humanities. We thank Dr. S. Cohen of the Hebrew University of Jerusalem for performing the X-ray structural analysis.

The facial hydrido-silyl-methyl iridium complexes **2**–**4**[13] are readily formed (in >90% yield) upon addition of one equivalent of the corresponding silane to a solution of $[MeIr(PMe_3)_4]$ (**1**)[14] in benzene at 25 °C (Scheme 1). Although these complexes are stable at 25 °C, quantitative elimination takes place when they are heated for one day at 100 °C in C_6D_6 in a closed vessel; complexes **2** and **3** undergo exclusive quantitative C–H elimination of methane, as detected by ^1H NMR spectroscopy and by gas chromatography (GC). The resulting iridium(I) complexes, which were not observed, undergo unusual intramolecular C–H activation of the silyl ligands, yielding the novel complexes **5** (in >98% yield) and **6** (in >90% yield). Complex **5** is unambiguously characterized by ^1H, ^{31}P, ^{13}C, and ^{13}C DEPT135 NMR spectroscopy. The iridium-bound methylene group appears in the $^{13}C\{^1H\}$ NMR spectrum as a doublet of triplets at $\delta = 3.0$ (^2J(C, P, *trans*) = 59.3 Hz, ^2J(C, P, *cis*) = 5.7 Hz); this signal is negative in the DEPT spectrum, indicating an even number of hydrogen atoms. The second methylene in the iridacycle gives rise to a doublet of triplets at $\delta = 68.7$ (^3J(C, P, *trans*) = 10 Hz, ^3J(C, P, *cis*) = 2.6 Hz), which also appears as a negative signal in the DEPT spectrum. This excludes the possibility of a four-membered iridacycle in which the metal is bound to the carbon atom of the CH_2O group. To our knowledge **5** is the first isolated complex formed by metalation of a silyl ligand not involving an aryl group.[15] This can be contrasted with the several examples known for remote intramolecular metalation by iridium.[16] Interestingly, specific metalation at the δ position takes place, probably as a result of the more stable five-membered ring.



Scheme 1.

Complex **6** was identified spectroscopically and by single-crystal X-ray diffraction[17] (Fig. 1); **6** crystalizes in $P2_1/n$ space group. The iridium atom is surrounded by a distorted octahedron; the silairidacycle is clearly visible. The Ir–Si bond length of 2.404(3) Å lies in the normal range.[18] The bonds Ir–P1 and

Table 1. Selected spectroscopic data of compounds **2**–**6** [a].

2: ^{1}H NMR (C_6D_6): $\delta = -12.12$ (dt, J(H,P, *trans*) = 126 Hz, J(H,P, *cis*) = 17.8 Hz, 1H; Ir-H), 0.3 (m, 3H; Ir-CH_3), 1.13 (d, J(H,P) = 6.9 Hz, 9H; PMe_3), 1.34 (d, J(H,P) = 7.9 Hz, 9H; PMe_3), 1.51 (d, J(H,P) = 8.3 Hz, 9H; PMe_3), 1.4 (t, J = 7 Hz, 9H; CH_3CH_2O), 4.17 (m, 6H; Si-OCH_2); $^{31}P\{^1H\}$ NMR (C_6D_6): $\delta = -63.4$ ("t", J = 21.3 Hz, 1P), −56.6 (m, 1P), −55.4 ("t", J = 17.1 Hz, 1P).

3: ^{1}H NMR (C_6D_6): $\delta = -11.79$ (dt, J (H,P,*trans*) = 123.5 Hz, J (H,P,*cis*) = 15.4 Hz, 1H; Ir-H), 0.15 (m, 3H; Ir-CH_3), 0.72 (d, J(H,P) = 7.3 Hz, 9H; PMe_3), 1.10 (d, J (H,P) = 7.6 Hz, 9H; PMe_3), 1.17 (d, J (H,P) = 7.2 Hz, 9H; PMe_3), [7.1(m), 7.25(t, J = 7.4 Hz), 8.11(m), 15H; SiC_6H_5]; $^{31}P\{^1H\}$ NMR (C_6D_6): $\delta = -63.4$ ("t", J = 15.6 Hz, 1P), −60.1 ("t", J = 17.8 Hz, 1P), −59.2 ("t", J = 17.4 Hz, 1P).

4: ^{1}H NMR (C_6D_6): $\delta = -12.15$ (dt, J (H,P,*trans*) = 135.1 Hz, J (H,P,*cis*) = 19.0 Hz, 1H; Ir-H), 0.20 (m, 3H; Ir-CH_3), 1.09 (d, J(H,P) = 6.8 Hz, 9H; PMe_3), 1.14 (d, J (H,P) = 7.1 Hz, 9H; PMe_3), 1.29 (d, J (H,P) = 7.8 Hz, 9H; PMe_3), 1.08 (m, 6H; $SiCH_2$), 1.43 (t, J = 7.8 Hz, 9H; $SiCH_2CH_3$); $^{31}P\{^1H\}$ NMR (C_6D_6): $\delta = -64.7$ ("t", J = 18.4 Hz, 1P), −59.0 (m, 2P).

5: ^{1}H NMR (C_6D_6): $\delta = -12.54$ (dt, J (H,P,*trans*) = 122.8 Hz, J (H,P,*cis*) = 16.6 Hz, 1H; Ir-H), 1.10 (d, J (H,P) = 6.9 Hz, 9H; PMe_3), 1.30 (d, J (H,P) = 7.8 Hz, 9H; PMe_3), 1.46 (d, J(H,P) = 8.0 Hz, 9H; PMe_3), 1.42 (t, J = 7.0 Hz, 3H; $SiOCH_2CH_3$), 1.48 (t, J = 7.0 Hz, 3H; $SiOCH_2CH_3$), 1.94 (m, 1H; Ir-CH_2; the signal of the second proton is obscured by other signals), 4.0–4.4 (series of m, Ir-$SiOCH_2CH_3$ + Ir-$SiOCH_2CH_2$); $^{31}P\{^1H\}$ NMR: (C_6D_6): $\delta = -61.4$ (dd, J_1 = 19.1 Hz, J_2 = 23.2 Hz, 1P), −57.2 ("t", J = 17.7 Hz, 1P), −56.4 (dd, J_1 = 16.5 Hz, J_2 = 23.0 Hz, 1P); $^{13}C\{^1H\}$ NMR (C_6D_6): δ = 3.0 (dt, J_d = 59.3 Hz, J_t = 5.7 Hz, Ir-CH_2, negative in the DEPT spectrum), [18.8(s), 19.5(s), $Si(OCH_2CH_3)_2$, positive in the DEPT spectrum], [20.5 (dm), 21.4 (dm), 25.1 (dm), $P(CH_3)_3$, positive in the DEPT spectrum], [56.3 (d, J = 1.6 Hz), 57.1 (d, J = 2.5 Hz), $Si(OCH_2CH_3)_2$, negative in the DEPT spectrum], [68.7 (dt, J_d = 10 Hz, J_t = 2.6 Hz, $SiOCH_2CH_3$, negative in the DEPT spectrum)].

6: ^{1}H NMR (C_6D_6): $\delta = -9.8$ (dt, J(H,P,*trans*) = 122.2 Hz, J (H,P,*cis*) = 18.4 Hz, 1H; Ir-H), 0.81 (d, J (H,P) = 7.7 Hz, 9H; PMe_3), 1.27 (d, J (H,P) = 7.7 Hz, 9H; PMe_3), 1.31 (d, J (H,P) = 7.3 Hz, 9H; PMe_3), [7.05–7.40 (several m), 8.01(m, 2H), 8.10 (m, 1H), 8.36 (m, 2H), $Si(C_6H_5)_2$ + $Si(C_6H_4)$-cycle]. $^{31}P\{^1H\}$ NMR (C_6D_6): $\delta = -60.9$ (dd, J_1 = 14.6 Hz, J_2 = 20.7 Hz, 1P), −60.2 (dd, J_1 = 14.4 Hz, J_2 = 18.4 Hz, 1P), −56.7 ("t", J = 19.6 Hz, 1P).

[a] Standards: ^{1}H NMR (400 MHz): C_6D_5H (δ = 7.15); ^{31}P NMR (162 MHz): external 85% H_3PO_4 (δ = 0.00); ^{13}C NMR (100 MHz): C_6D_6 (δ = 128.00).

Ir–P3 are the same length and both longer (by 0.03 Å) than the bond Ir–P2 (P *trans* to C). The strong *trans* influence of silyl ligands has been previously noted;[19] it is expected to be higher than that of hydrido ligands. Apparently, the effect is not fully manifested here because of the large deviation of the Si-Ir-P_3 angle from linearity (157.3°), perhaps as a result of ring constraints.

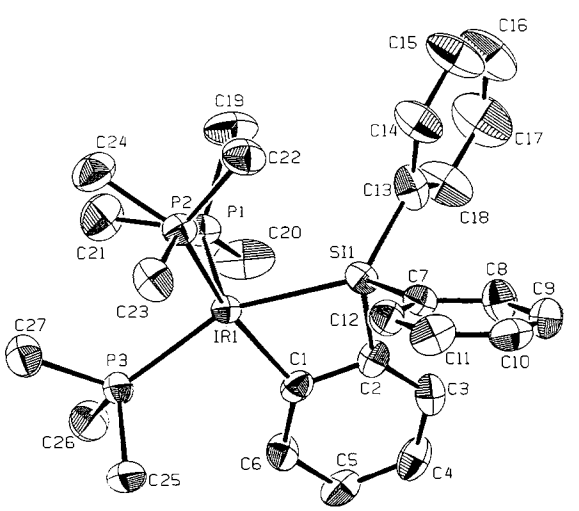


Fig. 1. Crystal structure of **6** (ORTEP: hydrogen atoms are omitted for clarity, thermal ellipsoids drawn at 50% probability level). Selected bond lengths [Å] and angles [°]: Ir1-P1 2.342(3), Ir1-P2 2.314(3), Ir1-P3 2.343(3), Ir1-Si1 2.404(3), Ir1-C1 2.16(1), C1-C2 1.41(1); Si1-C2 1.87(1), P2-Ir1-C1 164.2(3), P3-Ir1-Si1 157.3(1).

To our knowledge, this is the first structural characterization of a complex resulting from metalation of a silyl ligand. Although orthometalation involving arylphosphanes is well documented,[20] we are aware of only one other example of an isolated adduct resulting from the orthometalation of an arylsilyl ligand, namely $[(dcpe)Pt(C_6H_4)Si(SiMe_3)_2]$ (dcpe = 1,2-bis(dicyclohexylphosphano)ethane).[21] As noted in that work, orthometalation may be sterically promoted due to the large substituents on Pt and Si. However steric effects are very unlikely to play a significant role in the formation of the PMe_3 complexes **5** and **6**. It is not clear why metalation of silyl ligands is so rare in comparison with that of phosphane ligands, especially since Si and P have similar covalent radii. Nevertheless, we show here that metalation to form stable silametallacycles can occur readily, not only with aryl groups but even with nonactivated sp^3-C–H bonds in remote positions.

Interestingly, heating a solution of the Et_3Si complex **4** in C_6D_6 at 100 °C for one day in a closed vessel results in both C–H and C–Si reductive elimination. Complex **4** completely disappears, yielding CH_4 (ca. 80% yield, by GC) and $MeSiEt_3$ (ca. 20% yield). Although $[Et_3SiIr(PMe_3)_3]$ and $[HIr(PMe_3)_3]$ could not be detected because of subsequent reactions of these reactive intermediates with the solvent,[22] $[HIr(PMe_3)_4]$[23] was observed when **4** was heated in the presence of PMe_3.[24] Since reductive elimination of CH_4 and $MeSiEt_3$ is very likely irreversible, these processes are probably under kinctic control and a rough estimate of their relative rates is $k_{C-H}/k_{C-Si} \approx 4$.

C–H reductive elimination is generally much more facile than C–C reductive elimination. This has been attributed to kinetic factors, resulting from the need to reorient the direction of p orbitals in the case of C–C elimination, whereas the symmetrical s orbital involved in C–H elimination results in a lower barrier for this process.[25] Our observation that Si–C elimination can be competitive with C–H elimination may be attributed to the notion that the electropositive metal directs a high degree of s character in the silicon contribution to the M–Si bond,[26] as has been discussed also for stannyl derivatives.[27]

The difference in elimination reactivity between complexes **2** and **3**, which undergo only C–H reductive elimination, and **4** may be influenced by the effect of the substituents attached to silicon on the degree of M–Si s character, but the main factor seems to be due to the M–SiR_3 bond strength which increases with the electronegativily of R and follows the order M–$Si(OEt)_3$ > M–$SiPh_3$ > M–$SiEt_3$.[28] This may result not only in a higher kinetic barrier but also in a thermodynamically less favorable C–Si reductive elimination process when groups of higher electronegativity are attached to silicon. Steric factors are probably not important here since $SiEt_3$ is intermediate in size between $Si(OEt)_3$ and $SiPh_3$.

In conclusion, we have unambigously shown that C–H reductive elimination is the most favorable process, especially with electron-withdrawing substituents on Si, whereas C–Si elimination can become competitive when the silyl ligands carry alkyl substituents. The implication of this for the product-forming step in the hydrosilation reaction should be borne in mind. With such a fine balance between C–H and C–Si elimination, generalization of the hydrosilation mechanism is difficult and should take into consideration, among other factors, the particular silane reactant.

Another important aspect of this study is the observation that, although very rare, metalation of silyl ligands, including

sp^3-C–H bonds is possible. This C–H activation process can be regioselective, leading to the specific δ metalations. The synthetic implications of this approach for the generation of novel silametallacycles, like those reported here, are being explored.

Received: August 19, 1993 [Z6297IE]
German version: *Angew. Chem.* **1994**, *106*, 344

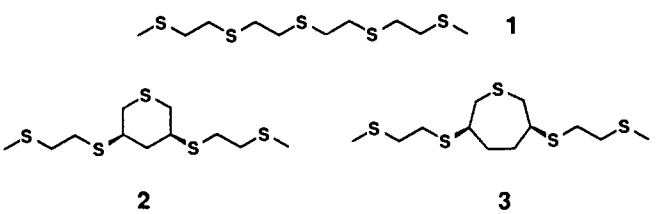
[1] T. D. Tilley, in *The Silicon-Heteroatom Bond*, (Eds.: S. Patai, Z. Rappoport), Wiley, New York, **1991**, p. 288–300, 350–359.
[2] A. J. Chalk, J. F. Harrod, *J. Am. Chem. Soc.* **1965**, *87*, 16.
[3] A recent review: I. Ojima in *The Chemistry of Organic Silicon Compounds* (Eds.: S. Patai, Z. Rappoport), Wiley, New York, **1989**, pp. 1479–1526.
[4] F. Seitz, M. S. Wrighton, *Angew. Chem.* **1988**, *100*, 281; *Angew. Chem. Int. Ed. Engl.* **1988**, *27*, 289.
[5] S. B. Duckett, R. N. Perutz, *Organometallics* **1992**, *11*, 90.
[6] Reviews: a) J. Halpern, *Acc. Chem. Res.* **1982**, *15*, 332; b) D. Milstein, *ibid.* **1984**, *17*, 221.
[7] K. C. Brinkman, A. J. Blakeney, W. Krone-Schmidt, J. A. Gladysz, *Organometallics* **1984**, *3*, 1326.
[8] D. L. Thorn, R. L. Harlow, *Inorg. Chem.* **1990**, *29*, 2017.
[9] a) U. Schubert, C. Müller, *J. Organomet. Chem.* **1989**, *373*, 165; b) U. Shubert, E. Kunz, M. Knorr, J. Müller, *Chem. Ber.* **1987**, *120*, 1079.
[10] Such a process was inferred based on kinetic results: P. Hofmann, H. Heiss, P. Neiteler, G. Müller, J. Lachmann, *Angew. Chem.* **1990**, *102*, 935; *Angew. Chem. Int. Ed. Engl.* **1990**, *29*, 880.
[11] W. Lin, S. R. Wilson, G. S. Girolami, *J. Am. Chem. Soc.* **1993**, *115*, 3022.
[12] G. R. Clark, C. E. F. Rickard, W. R. Roper, D. M. Salter, J. L. Wright, *Pure Appl. Chem.* **1990**, *62*, 1039.
[13] Complex **3** was prepared before [8]. Satisfactory elemental analyses were obtained for complexes **4** and **5**.
[14] D. L. Thorn, *Organometallics* **1982**, *1*, 197.
[15] β-Hydride elimination from silyl ligands in which unobserved metalated complexes are probably involved: a) D. H. Berry, L. J. Procopio, *J. Am. Chem. Soc.* **1989**, *111*, 4099; b) A. A. Zlota, F. Frolow, D. Milstein, *J. Chem. Soc. Chem. Commun.* **1989**, 1826; c) H. Yamashita, N. Kawamoto, M. Tanaka, M. Goto, *Chem. Lett.* **1991**, 2107.
[16] See for example: a) S. Hietkamp, D. J. Stufkens, K. Vrieze, *J. Organomet. Chem.* **1977**, *139*, 189. b) T. H. Tulip, D. L. Thorn, *J. Am. Chem. Soc.* **1981**, *103*, 2448.
[17] Crystal structure analysis of **6**: PW/1100/20 Philips four-circle computer-controlled diffractometer. $Mo_{K\alpha}$ (λ = 0.71069 Å) radiation with a graphite crystal monochromator in the incident beam, T = 20 °C, crystal dimensions 0.17 × 0.20 × 0.26 mm, $C_{27}H_{42}P_3SiIr$, monoclinic, space group $P2_1/n$, a = 12.343(3), b = 19.623(4), c = 12.209(2) Å, β = 97.72(1)°, V = 2930.3(9) Å^3, $\rho_{calcd.}$ = 1.54 g cm^{-3}, $\mu(Mo_{K\alpha})$ = 47.55 cm^{-1}, Z = 4, 4646 unique reflections, 3188 reflections with $I \geq 3\sigma_I$, ω-2θ scan, $2\theta_{max}$ = 46°, $\Delta\omega$ = 1.00 + 0.35 · tanθ, scan speed 3.0 deg min^{-1}, correction for Lorentz and polarization effects. SHELXS-86 direct method for all non-hydrogen atoms, the calculated positions of hydrogen atoms added to the refinement process after two cycles, function minimized $\sum_w(|F_o| - |F_c|)^2$; $R(R_w)$ = 0.042 (0.051). A final Fourier synthesis map showed several peaks less than 2.0 e Å^{-3} scattered about the unit cell without a significant feature. Further details of the crystal structure investigation may be obtained from the Fachinformationszentrum Karlsruhe, D-76344 Eggenstein-Leopoldshafen (FRG), on quoting the depository number CSD-57730, the names of the authors, and their journal citation.
[18] For other examples of structurally characterized iridium silyl complexes, see ref. [1], p. 264 and 343.
[19] a) R. N. Haszeldine, R. V. Parish, J. H. Setchfield, *J. Organomet. Chem.* **1973**, *57*, 279; b) ref. [15b].
[20] G. W. Parshall, *Acc. Chem. Res.* **1970**, *3*, 139.
[21] L. S. Chang, M. P. Johnson, M. J. Fink, *Organometallics* **1991**, *10*, 1219.
[22] These reactions are currently under study and will be reported in the full paper.
[23] D. L. Thorn, T. H. Tulip, *Organometallics* **1982**, *1*, 1580.
[24] Reaction of $[MeRh(PMe_3)_4]$ with $HSiEt_3$ yields CH_4 and $MeSiEt_3$, although the presumed oxidative addition intermediate was not observed: see ref. [8].
[25] J. J. Low, W. A. Goddard III, *Organometallics* **1986**, *5*, 609.
[26] Ref. [1], p. 266
[27] B. Y. K. Ho, J. J. Zuckerman, *J. Organomet. Chem.* **1973**, *49*, 1.
[28] R. N. Haszeldine, R. V. Parish, R. J. Taylor, *J. Chem. Soc. Dalton Trans.* **1974**, 2311.

Strategies for Nonmacrocyclic Polythioether Ligands: New Pentacoordinating Architectures**

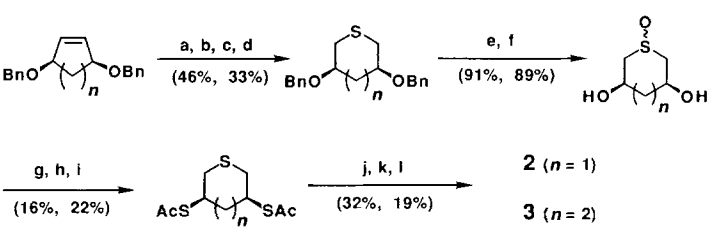
John M. Desper and Samuel H. Gellman*

Polythioethers are of interest as complexing agents for late transition metal ions.[1] Most prior efforts to enhance the chelating efficacy of polythioether arrays have involved construction of a macrocyclic ligand skeleton.[2–5] We have recently demonstrated that peripheral substituents on macrocyclic tetrathioethers can improve metal ion binding.[6] Here we report an approach for preorganization of a nonmacrocyclic pentathioether framework.

Ethylene sulfide oligomers such as, **1** are not well suited for multidentate coordination, because of the strong *anti* conformational preference of SC–CS bonds, the weak preference of the *gauche* conformation about the CS–CC bonds, and the intrinsic flexibility of the acyclic backbone.[7] We reasoned that the latter two problems might be alleviated by incorporation of thiane or thiepane rings into the backbone to generate **2** or **3**. These target



structures require control of configuration at the exocyclic C–S bonds, because the *cis*-disubstituted ring systems are required for pentacoordination. The stereospecific preparations of **2** and **3** from known benzyl-protected *cis*-dihydroxycycloalkenes[8, 9] are outlined in Scheme 1. Construction of the *cis*-dihydroxythiane and -thiepane rings involved ozonolysis of the double bond, activation of the resulting primary hydroxyl groups, and cyclization with Na_2S. Activation of the secondary hydroxyl groups for nucleophilic displacement was not practical with the ring sulfur atom in its reduced form, because of rearrangements



Scheme 1. a) O_3; $NaBH_4$. b) TsCl, Py, CH_2Cl_2. c) nBu$_4$NBr, $NaHCO_3$, 2-butanone, reflux, 4 h. d) Na_2S, aq. EtOH, reflux. e) Na^+, NH_3. f) O_3. g) TsCl, DMAP, CH_2Cl_2. h) AcSK, DMF. i) Me_3SiCl, NaI, CH_3CN. j) NaOEt; $ClCH_2CH_2OH$. k) $SOCl_2$. l) CH_3SNa, EtOH, CH_3CN. The percentages given under each arrow are the yields over the indicated steps in the thiane and thiepane series, respectively. Py = pyridine, Ts = p-$CH_3C_6H_4SO_2$, DMAP = 4-dimethylaminopyridine.

[*] Prof. S. H. Gellman, Dr. J. M. Desper
Department of Chemistry, University of Wisconsin
1101 University Avenue, Madison, WI 53706 (USA)
Telefax: Int. code + (608)265-4534

[**] This research was supported by the U.S. National Science Foundation (Presidential Young Investigator Award to S. H. G), Eastman-Kodak, Procter & Gamble, and Rohm and Haas. J. M. D. was the recipient of a fellowship from the U.S. Department of Education's Graduate Assistance in Areas of National Need Program.

that are known to occur in such systems.[10] "Temporary" oxidation to the sulfoxide decreased intramolecular nucleophilicity sufficiently to allow generation of the required *cis*-ditosylates (as mixtures of compounds epimeric at the sulfur center).[11] Double displacement with thioacetate provided the core with three sulfur atoms and the required configuration. After reduction of the sulfoxide,[12] completion of the syntheses was straightforward.[13]

The structures of **2** and **3**, and their ability to serve as pentadentate ligands, were verified by crystallographic analyses of Ni^{II} and Cu^{II} complexes of each new ligand. Both complexes of **2** and the Ni^{II} complex of **3** were crystallized with perchlorate counterions; the Cu^{II} complex of **3** was crystallized with tetrafluoroborate counterions. The complex $[\mathbf{2}\text{-}Ni^{II}]^{2+}$ (Fig. 1) has five Ni–S bonds of similar length (2.36–2.42 Å); one perchlorate ion serves as a sixth ligand (Ni–O = 2.227(5) Å). In the

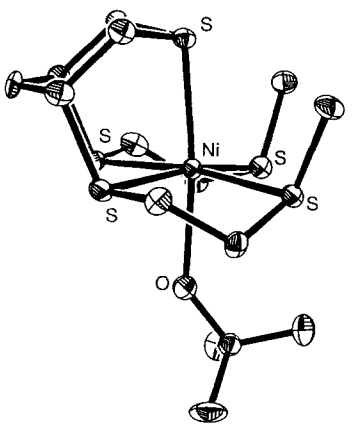


Fig. 1. Crystal structure of $[\mathbf{2}\text{-}Ni^{II}(ClO_4)]^+$; the noncoordinating ClO_4^- counterion is not shown. Hydrogen atoms have been omitted for clarity. Crystals were obtained by vapor diffusion of 1,2-dichloroethane into a solution of the product in nitromethane. Data were collected with $Mo_{K\alpha}$ radiation at 123 K: 1791 unique reflections, 1535 observed reflections. $R = 0.0371$, weighted $R_w = 0.0469$ (observed data); residual electron density minimum = −0.43, maximum = 0.84 e Å^{-3} [16].

analogous Cu^{II} complex (Fig. 2) the thiane sulfur atom forms a distinctly longer bond to the metal ion (2.581(2) Å) than the other four sulfur atoms (Cu–S = 2.32–2.35 Å). The copper ion forms a weak sixth bond to one perchlorate ion (Cu–O = 2.746(6) Å). In both complexes of **2** the thiane ring adopts a chair conformation with the substituents axially disposed, as expected.

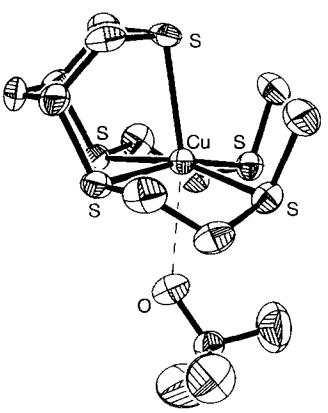


Fig. 2. Crystal structure of $[\mathbf{2}\text{-}Cu^{II}(ClO_4)]^+$; the noncoordinating ClO_4^- counterion is not shown, and the dotted line indicates the long Cu–O bond to the weakly coordinated ClO_4^- anion. Hydrogen atoms have been omitted for clarity. Crystals were obtained by slow evaporation of a solution of the product in methanol–water. Data were collected with $Mo_{K\alpha}$ radiation at 113 K: 3678 unique reflections, 2328 observed reflections, $R = 0.0509$, weighted $R_w = 0.0516$ (observed data); residual electron density minimum = −0.48, maximum = 0.72 e Å^{-3} [16].

The Ni^{II} complex of **3** (Fig. 3) shows octahedral coordination at the metal ion, as observed for $[\mathbf{2}\text{-}Ni^{II}]^{2+}$, but now the sixth ligating atom is an oxygen atom from a water molecule (Ni–O = 2.092(5) Å). The five Ni–S bonds of $[\mathbf{3}\text{-}Ni^{II}]^{2+}$ (2.38–

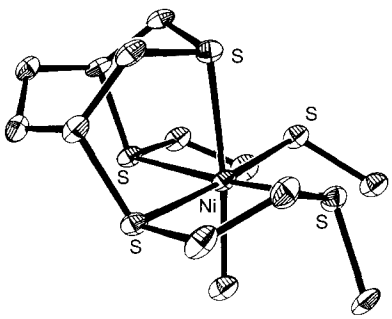


Fig. 3. Crystal structure of $[\mathbf{3}\text{-}Ni^{II}(H_2O)]^{2+}$; the noncoordinating ClO_4^- counterions are not shown. Hydrogen atoms have been omitted for clarity. Crystals were obtained by vapor diffusion of 1,2-dichloroethane into a solution of the product in nitromethane. Data were collected with $Cu_{K\alpha}$ radiation at 113 K: 2895 unique reflections, 2632 observed reflections, $R = 0.0571$, weighted $R_w = 0.0784$ (observed data); residual electron density minimum = −0.85, maximum = 1.09 e Å^{-3} [16].

2.43 Å) are of similar length to one another and to the Ni–S bonds of $[\mathbf{2}\text{-}Ni^{II}]^{2+}$. The $[\mathbf{3}\text{-}Cu^{II}]^{2+}$ complex (Fig. 4) is bisected by a crystallographic mirror plane through the copper and thiepane sulfur atoms. As a result of this symmetry, the conformation about the thiepane C–C bond furthest from the sulfur atom is formally eclipsed, but the high thermal parameters observed for the carbon atoms in the thiepane ring suggest disorder in this part of the structure, which presumably reflects the avoidance of torsional strain in individual molecules. As observed for $[\mathbf{2}\text{-}Cu^{II}]^{2+}$, one of the Cu–S bonds in $[\mathbf{3}\text{-}Cu^{II}]^{2+}$ is longer than the other four: the bond involving the thiepane sulfur atom is 2.510(2) Å in length, while the others are all approximately 2.34 Å. The metal ion forms a weak sixth bond to one of the tetrafluoroborate counterions (Cu–F = 2.735(4) Å).

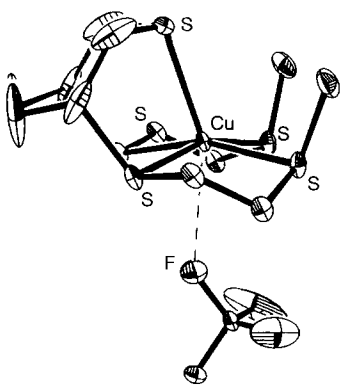
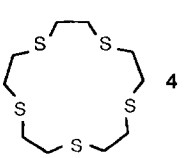


Fig. 4. Crystal structure of $[\mathbf{3}\text{-}Cu^{II}(BF_4)]^+$; the noncoordinating BF_4^- counterion is not shown. Hydrogen atoms have been omitted for clarity. Crystals were obtained by vapor diffusion of 1,2-dichloroethane into a solution of the product in nitromethane. Data were collected with $Cu_{K\alpha}$ radiation at 113 K: 1485 unique reflections, 1368 observed reflections, $R = 0.0456$, weighted $R_w = 0.0646$ (observed data) residual electron density minimum = −0.71, maximum = 0.69 e Å^{-3} [16].

The consistent elongation of one of the Cu–S bonds in the complexes of **2** and **3** is similar to the selective elongation previously observed in the complex between Cu^{II} and pentathia-[15]crown-5 (**4**).[14] In that case, the elongation was less pronounced: four of the Cu–S bonds had lengths in the range 2.29–2.34 Å, and the fifth was 2.40 Å long. Interestingly, the authors of this previous study speculated that the intrinsic preference of Cu^{II} coordinated to five sulfur atoms would be for a greater elongation of the fifth bond than they observed, and that the relatively small elongation with **4** reflected ligand backbone constraints. Our data support this proposition.

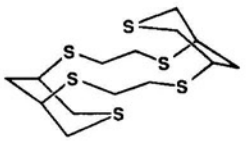


4

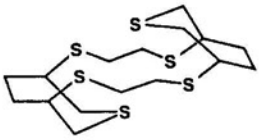
The methodology developed by Rorabacher et al.,[4] in which UV measurements are used to quantify Cu^{II} complexation, is one of the few reliable methods that have been reported for determining stability constants of polythioether–metal complexes. With $CH_3OH:H_2O$ (4:1) containing 0.1 M $HClO_4$ as a solvent, this method gave a stability constant of 88 M^{-1} for $[\mathbf{2}\text{-}Cu^{II}]^{2+}$, which is an order of magnitude lower than that reported for macrocycle **4** in this solvent.[4] We were unable to evaluate the Cu^{II}-binding properties of **3** in $CH_3OH:H_2O$ (4:1)/0.1 M $HClO_4$ because of the low solubility of this thioether. A stability constant of 93 M^{-1} for $[\mathbf{3}\text{-}Cu^{II}]^{2+}$ could, however, be determined in $CH_3OH:H_2O$ (19:1)/0.025 M $HClO_4$. In this solvent system the stability constant for $[\mathbf{2}\text{-}Cu^{II}]^{2+}$ is 55 M^{-1}. Thus, the thiepane-based ligand seems to have a marginally greater affinity for Cu^{II} than the thiane-based ligand.

Attempts to determine a stability constant for the Cu^{II} complex of acyclic pentathioether **1** with the method of Rorabacher et al.[4] were unsuccessful. The data suggested that **1** and Cu^{II} do not form a 1:1 complex; instead, it appeared that higher order complexes were present. This behavior is consistent with the acyclic ligand's expected resistance to wrapping around a single metal ion, a resistance that stems at least in part from the intrinsic conformational preferences of the SC–CS and CS–CC bonds.[7] Thus, the preorganizational strategy underlying the design of **2** and **3** has been successful: the thiane and thiepane ligands enforce 1:1 complexation in solution.

We have developed a stereospecific route to polythioethers containing *cis*-disubstituted thiane and thiepane rings. Our data show that nonmacrocyclic pentathioethers based on these units are predisposed towards pentacoordination with a single metal ion, which represents an improvement in preorganization relative to acyclic ethylene sulfide oligomers. While the new ligands



5



6

do not chelate Cu^{II} as strongly as thiacrown ether **4** does, the synthetic route we have developed for **2** and **3** should provide access to a new type of thiacryptand architecture,[15] exemplified by **5** and **6**, which may lead to very effective complexing agents for late transition metal ions.

Received: August 13, 1993 [Z 6278 IE]
German version: *Angew. Chem.* **1994**, *106*, 335

[1] For leading references, see: S. R. Cooper, S. C. Rawle, *Struct. Bonding (Berlin)* **1990**, *72*, 1; A. J. Blake, M. Schröder, *Adv. Inorg. Chem.* **1990**, *35*, 1; J. J. H. Edema, J. Buter, R. M. Kellogg, A. L. Spek, F. van Bolhuis, *J. Chem. Soc. Chem. Commun.* **1992**, 1558; S. J. Loeb, G. K. H. Shimizu, *ibid.* **1991**, 1119; T. Yoshida, T. Adachi, K. Kawazu, A. Yamamoto, N. Sasaki, *Angew. Chem.* **1991**, *103*, 1025; *Angew. Chem. Int. Ed. Engl.* **1991**, *30*, 982; W. N. Setzer, Y. Tang, G. J. Grant, D. G. VanDerveer, *Inorg. Chem.* **1991**, *30*, 3652.

[2] G. F. Smith, D. W. Margerum, *J. Chem. Soc. Chem. Commun.* **1975**, 807.

[3] T. E. Jones, L. S. W. L. Sokol, D. B. Rorabacher, M. D. Glick, *J. Chem. Soc. Chem. Commun.* **1979**, 140.

[4] L. S. W. L. Sokol, L. A. Ochrymowycz, D. B. Rorabacher, *Inorg. Chem.* **1981**, *20*, 3189.

[5] "Supertripodal" polythioethers: C. M. Thorne, S. C. Rawle, G. A. Admans, S. R. Cooper, *Inorg. Chem.* **1986**, *25*, 3848; *J. Chem. Soc. Chem. Commun.* **1986**, 306.

[6] J. M. Desper, S. H. Gellman, *J. Am. Chem. Soc.* **1990**, *112*, 6732; *ibid.* **1991**, *113*, 704; J. M. Desper, S. H. Gellman, R. E. Wolf, S. R. Cooper, *ibid.* **1991**, *113*, 8663; A. Y. Nazarenko, R. M. Izatt, J. D. Lamb, J. M. Desper, B. E. Matysik, S. H. Gellman, *Inorg. Chem.* **1992**, *31*, 3990; J. M. Desper, J. R. Vyvyan, M. J. Mayer, L. A. Ochrymowycz, S. H. Gellman, *ibid.* **1993**, *32*, 381.

[7] For leading references, see: S. R. Cooper, *Acc. Chem. Res.* **1988**, *21*, 141; J. M. Desper, D. R. Powell, S. H. Gellman, *J. Am. Chem. Soc.* **1990**, *112*, 4321.

[8] J. Fried, C. H. Chin, J. C. Sih, P. Dalven, G. F. Cooper, *J. Am. Chem. Soc.* **1972**, *94*, 4342; B. M. Trost, M. Ochiai, P. G. McDougal, *ibid.* **1978**, *100*, 7113.

[9] J. E. Bäckvall, J. O. Väberg, *J. Org. Chem.* **1988**, *53*, 5695.

[10] S. Ikegami, J.-I. Ohishi, Y. Shimizu, *Tetrahedron Lett.* **1975**, 3923; C. Leroy, M. Martin, L. Bassery, *Bull. Soc. Chim. Fr.* **1974**, 590; S. Ikegami, T. Asai, K. Tsuneoka, S. Matsumura, S. Akaboshi, *Tetrahedron* **1974**, *30*, 2087.

[11] E. Hamanaka, Pfizer, Inc., US-A 4619924; *Chem. Abstr.* **1987**, *107*, 23172z. For a related use of "temporary" sulfur oxidation to minimize side reactions, see: E. Block, E. R. Corey, R. E. Penn, T. L. Renken, P. F. Sherwin, H. Bock, T. Hirabayashi, S. Mohmand, B. Solouki, *J. Am. Chem. Soc.* **1982**, *104*, 3119.

[12] G. A. Olah, S. C. Narang, B. G. B. Gupta, R. Malhotra, *Synthesis* **1979**, 61.

[13] **2**: M.p. (recryst. from EtOH) 69–70 °C; FT-IR (KBr): $\tilde{\nu}$ = 2912, 1420, 1204, 1176, 1136, 722, 683 cm^{-1}; ^1H NMR ($CDCl_3$): δ = 1.35 (dt, J = 13.2, 12.2 Hz, 1H), 2.15 (s, 6H), 2.38 (ddt, J = 13.3, 3.0, 1.5 Hz, 1H), 2.57 (dd, J = 13.6, 11.5 Hz, 2H), 2.7–2.9 (m, 10H), 3.00 (tt, J = 11.9, 3.3 Hz, 2H); ^{13}C NMR ($CDCl_3$): δ = 44.5, 40.3, 34.5, 33.9, 30.1, 15.6; EI-MS: *m/z* 314.0331 (calcd. for $C_{11}H_{22}S_5$ 314.0325). **3**: M.p. (recryst. by vapor diffusion of CH_3OH into $ClCH_2CH_2Cl$) 97–99 °C; FT-IR(KBr): $\tilde{\nu}$ = 2914, 1425, 1204, 1160, 950, 730, 688, 537 cm^{-1}; ^1H NMR ($CDCl_3$): δ = 1.8–2.0 (m, 2H), 2.1–2.3 (m, 2H), 2.14 (s, 6H), 2.5–2.9 (m, 10H), 3.0–3.3 (m, 4H); ^{13}C NMR ($CDCl_3$) δ = 46.6, 40.2, 34.3, 30.7, 30.3, 15.6; EI-MS: *m/z* 328.0477 (calcd. for $C_{12}H_{24}S_5$ 328.0482).

[14] P. W. R. Corfield, C. Ceccarelli, M. D. Glick, I. W.-Y. Moy, L. A. Ochrymowycz, D. B. Rorabacher, *J. Am. Chem. Soc.* **1985**, *107*, 2399.

[15] Previous reports on sulfur-containing cryptands: B. Dietrich, J. M. Lehn, J. P. Sauvage, *J. Chem. Soc. Chem. Commun.* **1970**, 1055; A. H. Alberts, R. Annunziata, J.-M. Lehn, *J. Am. Chem. Soc.* **1977**, *99*, 8502; O. Kahn, I. Morgenstern-Badarau, J. P. Audiere, J. M. Lehn, S. A. Sullivan, *ibid.* **1980**, *102*, 5936; H. L. Ammon, S. K. Bhattacharjee, S. Shinkai, Y. Honda, *ibid.* **1984**, *106*, 262; P. Osvath, A. M. Sargeson, B. W. Skelton, A. H. White, *J. Chem. Soc. Chem. Commun.* **1991**, 1036; P. Osvath, A. M. Sargeson, *ibid.* **1993**, 40.

[16] Further details on the crystallographic analyses are available on request from the Director of the Cambridge Crystallographic Data Centre, 12 Union Road, GB-Cambridge CB2 1EZ (UK), on quoting the full journal citation.

18-, 20-, and 22-Membered Dimetallaortho-, -meta-, and -para[7.7]cyclophanes—The First Typical Metallaphanes**

Ekkehard Lindner,* Walter Wassing, Riad Fawzi, and Manfred Steimann

Dedicated to Professor Helmut Werner on the occasion of his 60th birthday

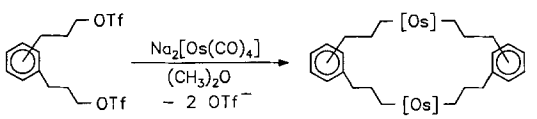
The rapid development of cyclophane chemistry[1] has produced compounds with special cage or niche structures capable of storing extraneous molecules (host–guest compounds).[2, 3] Cyclophane frameworks containing heteroatoms (e.g. N, O, S) have complexation properties which, in cooperation with specific structural parameters, make possible molecular recognition.[3, 4] In contrast to metallocenophanes[5] such as ferrocenophanes, metallaphanes are still unknown, apart from simple benzometallacycloalkanes.[6] The incorporation of transition metal com-

[*] Prof. Dr. E. Lindner, Dipl.-Chem. W. Wassing, Dr. R. Fawzi, M. Steimann
Institut für Anorganische Chemie der Universität
Auf der Morgenstelle 18, D-72076 Tübingen (FRG)
Telefax: Int. code + (7071)29-5246

[**] Preparation and Properties of and Reactions with Metal-Containing Heterocycles. Part 87. This research was supported by the Deutsche Forschungsgemeinschaft and by the Fonds der Chemischen Industrie. We thank BASF Aktiengesellschaft and Degussa AG for gifts of chemicals. Part 86: E. Lindner, T. Schlenker, C. Haase, *J. Organomet. Chem.*, in press.

plex fragments gives rise to new structural elements and reactive centers which form the basis for the synthesis of further cyclophanes.

With the application of the bistriflate method,[7] we have now achieved the synthesis of the first metallacyclophanes **2**, **4**, and **6**, each with four M–C σ bonds. These are formed in good yields by the cationic alkylation of $Na_2[Os(CO)_4]$ with the bis(trifluoromethanesulfonates) **1**, **3**, and **5**, respectively, in dimethyl ether.[7] The clearly favored formation of the "dinuclear" diosma[7.7]cyclophanes, as opposed to oligo- or polymerization, is supported by entropic effects.[8] The latter are also in competition with steric influences. Thus, as a result of the short distance between the terminal C atoms in **5**, its reaction with $Na_2[Os(CO)_4]$ also leads to the "mononuclear" 4,4,4,4-tetracarbonyl-4-osma-[7]orthocyclophane [MS (FD, 8 kV, 34 °C): *m/z* 462.2 (M^+)].



para: **1**
meta: **3**
ortho: **5**

para: **2**
meta: **4**
ortha: **6**

[Os] = $Os(CO)_4$, OTf = OSO_2CF_3

In crystalline form, the diosma[7.7]paracyclophane **2** has C_2 symmetry (Fig. 1).[9] The two phenylene groups give rise to an interplanar angle of 50.3°, and together with the metal centers these mark out the corners of a distorted tetrahedron [Os1–Os1a distance 10.07(2) Å, C13–C13a distance 5.64(3) Å]. The basic cyclophane framework has a bowl-shaped structure, above which the oxygen atoms O3 and O3a are 4.61(2) Å apart.

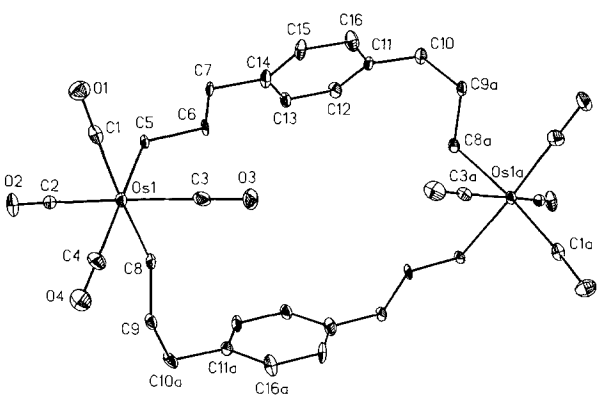


Fig. 1. Crystal structure of **2**. Selected bond lengths [Å] and angles [°]: Os1-C5 2.202(12), Os1-C8 2.182(12), mean Os1-(CO) distance 1.938(14), mean C-O distance 1.152(17); C1-Os1-C2 93.0(4), C1-Os1-C3 96.1(5), C1-Os1-C4 95.9(5), C2-Os1-C3 166.9(5), C5-Os1-C8 84.2(4) (cf. [9]).

Compound **6** is centrosymmetric in the crystal (Fig. 2),[9] and displays two parallel planes (distance 3.2 Å), defined by the phenylene carbon atoms and the chains C10, C9, C8, and Os1 and C10a, C9a, C8a, and Os1a, respectively. The likewise parallel best-fit planes stipulated by the bridging atoms Os1, C5, C6, and C7 and Os1a, C5a, C6a, and C7a (distance 7.3 Å), respectively, are tilted at an angle of 83.6° relative to the arene rings.

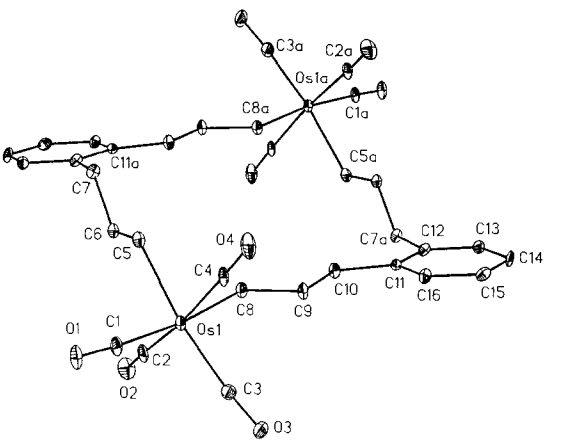


Fig. 2. Crystal structure of **6**. Selected bond lengths[Å] and angles [°]: Os1-C5 2.214(5), Os1-C8 2.218(6), mean Os1-(CO) distance 1.959(7), mean C-O distance 1.122(9), C1-Os1-C2 93.9(3), C1-Os1-C3 99.5(3), C1-Os1-C4 93.2(3), C2-Os1-C4 169.3(2), C5-Os1-C8 85.3(2) (cf. [9]).

In **2** and **6**, the bulky $Os(CO)_4$ groups lead to an angularity at the metal centers of the arene-bridged chains. In **4b** or other metal-free cyclophanes such as 9,12,22,25-tetramethoxy[7.7]-paracyclophane-4,17-dione,[10] the arene is, on the other hand, connected by an "elongated" zigzag chain.

In the $^{13}C\{^1H\}$ NMR spectra of **2**, **4**, and **6**, the ^{13}C signals occurring at highest field correspond to the C atoms adjacent to the metal centers (Table 1). The two, four, and three ^{13}C-resonances of the phenylene groups of **2**, **4**, and **6**, respectively, and the corresponding ^1H NMR signals are comparable to those of the open-chain systems, and are not influenced by cyclization.[7]

Table 1. Selected spectroscopic data of **2**, **4**, **4a**, **4b**, **6**, and **6a** [a]

2: IR (*n*-pentane): ν[cm^{-1}] = 2009, 2039, 2043, 2125 (CO); $^{13}C\{^1H\}$ NMR: δ = –5.71 ($OsCH_2$), 38.71 ($OsCH_2CH_2$), 41.44 ($OsCH_2CH_2CH_2$), 128.30 (CH), 139.01 (C), 170.79 (CO_{eq}), 178.70 (CO_{ax}); MS (FD, 8 kV, 65 °C): *m/z* 925.2 (M^+).

4: IR (*n*-pentane): ν[cm^{-1}] = 2009, 2037, 2040, 2124 (CO); $^{13}C\{^1H\}$ NMR: δ = –4.49 ($OsCH_2$), 39.24 ($OsCH_2CH_2$), 42.42 ($OsCH_2CH_2CH_2$), 125.65, 127.98, 128.85 (CH), 142.04 (C), 170.83 (CO_{eq}), 178.48 (CO_{ax}); MS (FD, 8 kV, 32 °C): *m/z* 925.8 (M^+).

4a: IR (*n*-pentane): ν[cm^{-1}] = 2010, 2020, 2031, 2096 (CO).

4b: IR (CH_2Cl_2): ν[cm^{-1}] = 1710 (>C=O); $^{13}C\{^1H\}$ NMR: δ = 24.74 ($C(O)CH_2CH_2$), 33.99 ($C(O)CH_2$), 42.07 ($C(O)CH_2CH_2CH_2$), 126.08, 128.41, 128.75 (CH), 141.66 (C), 210.20 (>C=O); MS (FD, 8 kV, 70 °C): *m/z* 376.1 (M^+).

6: IR (*n*-pentane): ν[cm^{-1}] = 2010, 2040, 2044, 2125 (CO); $^{13}C\{^1H\}$ NMR: δ = –2.00 ($OsCH_2$), 39.62 ($OsCH_2CH_2$), 40.74 ($OsCH_2CH_2CH_2$), 125.74, 128.92 (CH), 140.34 (C), 170.75 (CO_{eq}), 178.28 (CO_{ax}); MS (FD, 8 kV, 33 °C): *m/z* 925.5 (M^+).

6a: IR (*n*-pentane): ν[cm^{-1}] = 2010, 2020, 2031, 2096 (CO).

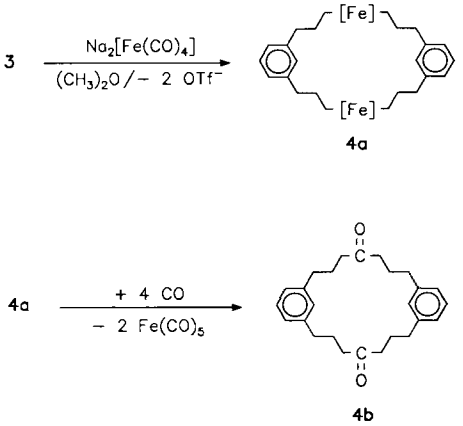
[a] $^{13}C\{^1H\}$ NMR spectra (62.90 MHz, $CDCl_3$, 25 °C, referenced internally to TMS).

The colorless, slightly soluble metallacyclophanes **2**, **4**, and **6** are strikingly stable to heat.[11] In the presence of carbon monoxide, a slow insertion of CO takes place only above 70 °C, leading to the formation of cyclic mono- and diacyl species [IR (*n*-pentane): ν(>C=O) = 1671 cm^{-1}; FD-MS: *m/z* 954 and 982, respectively].[12] A further increase in temperature generates the corresponding [7.7]cyclophanedione in low yield by reductive elimination of $Os(CO)_4$.

The diferracyclophanes **4a** and **6a**, analogous to **4** and **6**, are accessible by a similar route. They are thermally labile (decomp

 © VCH Verlagsgesellschaft mbH, D-69451 Weinheim, 1994 0570-0833/94/0303-0322 $ 10.00+.25/0

> -30 °C), and react with CO, as depicted for **4a** → **4b** (Table 1), to give the cyclic diketones in much higher yield. The molecular structure of **4b** has been confirmed by an X-ray crystal structure analysis.[9]



[Fe] = $Fe(CO)_4$, OTf = OSO_2CF_3

Experimental Procedure

2, **4**, **6**: A solution of **1**, **3**, or **5** (580 mg, 1.27 mmol), respectively in dimethyl ether (20 mL) was added to a suspension of $Na_2[Os(CO)_4]$ (550 mg, 1.58 mmol) in dimethyl ether (30 mL), and the mixture was allowed to react under reflux for 3 d. After removal of the solvent (−70 °C), the residue was taken up in *n*-pentane (70 mL) at 20 °C, and the solution was filtered (P4). Following concentration of the filtrate to 5 mL and cooling to −70 °C, the product was recrystallized twice from *n*-pentane. Yields: **2**: 458 mg (78%), **4**: 417 mg (71%), **6**: 270 mg (46%); correct elemental analyses; m.p. 127, 113, and 122 °C, respectively.

4a and **6a** were synthesized analogously at −70 °C, worked up at −50 °C, and characterized by IR spectroscopy (Table 1).

Thermolysis of **4a**: A solution of $Na_2[Fe(CO)_4]$ (338 mg, 1.58 mmol) and **3** (580 mg, 1.27 mmol) in dimethyl ether (50 mL) was stirred for 2 h at −70 °C, and then CH_2Cl_2 (50 mL) was added. The mixture was warmed to 20 °C with passage of CO, stirred for 2 h, and then concentrated. Purification on a silica gel column, eluting with CH_2Cl_2, followed by acetone gave **4b**. Yield: 90.8 mg **4b** (38% based on **3**); correct elemental analysis; m.p. 79 °C.

Received: September 3, 1993 [Z 6335 IE]
German version: *Angew. Chem.* **1994**, *106*, 363

[1] F. Vögtle in *Cyclophan-Chemie* (Eds.: C. Elschenbroich, F. Hensel, H. Hopf), Teubner, Stuttgart, **1990**.
[2] C. Seel, F. Vögtle, *Angew. Chem.* **1992**, *104*, 542–563; *Angew. Chem. Int. Ed. Engl.* **1992**, *31*, 528–549; J. C. Sherman, D. J. Cram, *J. Am. Chem. Soc.* **1989**, *111*, 4527–4528.
[3] C. J. van Staveren, D. E. Fenton, D. N. Reinhoudt, J. van Eerden, S. Harkema, *J. Am. Chem. Soc.* **1987**, *109*, 3456–3458.
[4] F. C. J. M. Veggel, M. Bos, S. Harkema, W. Verboom, D. N. Reinhoudt, *Angew. Chem.* **1989**, *101*, 800–802; *Angew. Chem. Int. Ed. Engl.* **1989**, *28*, 746–748.
[5] C. Elschenbroich, A. Salzer, *Organometallchemie*, Teubner, Stuttgart, **1988**; *Organometallics*, 2nd edition VCH, Weinheim, **1992**; M. Löwendahl, Ö. Davidson, P. Ahlberg, M. Hadånsson, *Organometallics* **1993**, *12*, 2417–2419.
[6] E. Lindner, *Adv. Heterocycl. Chem.* **1986**, *39*, 237–279.
[7] E. Lindner, W. Wassing, R. Fawzi, M. Steimann, *Z. Naturforsch. B* **1993**, *48*, 1651–1660.
[8] L. Shaw, *J. Organomet. Chem.* **1980**, *200*, 307–318.
[9] Crystal structure analyses [Siemens P4 diffractometer, SHELXTL-PC program, $Mo_{K\alpha}$ radiation, data collected at 173 K; hydrogen atoms for **2**, **6**, and **4b** located geometrically (riding model)]. **2** (Fig. 1) crystallized from chloroform, $C_{33}H_{33}Cl_3O_8Os_2$, $M = 1044.4$, crystal dimensions $0.2 \times 0.2 \times 0.2$ mm^3, monoclinic, space group $P2/n$, $a = 1476(3)$, $b = 589.4(13)$, $c = 2137(4)$ pm, $\beta = 98.75(14)°$, $V = 1837(6) \times 10^6$ pm^3, $\rho_{calcd} = 1.888$ g cm^{-3}, $Z = 2$, $2\theta = 4$–50°, total number of reflections 6435, number of symmetry independent reflections with $I \geq 2\sigma(I)$ 2444, refined parameters 201, absorption correction Ψ scan, $R = 0.049$, $R_w = 0.050$, $S = 0.73$, residual electron density 2.25 eÅ^{-3}. Moderate crystal quality resulted in a high standard deviation: a disordered chloroform molecule is situated within the asymmetric unit, whose location was refined with the occupation factor 0.5.—**6** (Fig. 2) crystallized from chloroform, $C_{32}H_{32}O_8Os_2$, $M = 925.0$, crystal dimensions $0.1 \times 0.1 \times 0.2$ mm^3, monoclinic, space group $P2_1/c$, $a = 1026.3(2)$, $b = 1030.4(1)$, $c = 1544.1(2)$ pm, $\beta = 106.81(1)°$, $V = 1563.2(4) \times 10^6$ pm^3, $\rho_{calcd} = 1.965$ g cm^{-3}, $Z = 2$, $2\theta = 4$–50°, total number of reflections 10641, number of symmetry independent reflections with $I \geq 2\sigma(I)$ 2177, refined parameters 190, absorption correction Ψ scan, $R = 0.024$, $R_w = 0.022$, $S = 0.58$, residual electron density 0.59 eÅ^{-3}. - **4b** crystallized from dichloromethane, $C_{26}H_{32}O_2$, $M = 376.5$, crystal dimensions $0.05 \times 0.25 \times 0.4$ mm^3, orthorhombic, space group $Pna2_1$, $a = 887(2)$, $b = 1296(1)$, $c = 1689(4)$ pm, $V = 1942(6) \times 10^6$ pm^3, $\rho_{calcd} = 1.288$ g cm^{-3}, $Z = 4$, $2\theta = 4$–50°, total number of reflections 12908, number of symmetry independent reflections with $I \geq 2\sigma(I)$ 602, refined parameters 88, $R = 0.0997$, $R_w = 0.0925$, $S = 0.98$ (isotropic refinement), residual electron density 0.51 eÅ^{-3}. The small crystal dimensions resulted in imprecise bond lengths and angles. Further details of the crystal structure determinations of **2** and **6** may be obtained from the Fachinformationszentrum Karlsruhe, D-76344 Eggenstein-Leopoldshafen, on quoting the depository number CSD-57759, the names of the authors and the journal citation.
[10] H. A. Staab, G. Matzke, C. Krieger, *Chem. Ber.* **1987**, *120*, 89–91.
[11] E. Lindner, R.-M. Jansen, W. Hiller, R. Fawzi, *Chem. Ber.* **1989**, *122*, 1403–1409.
[12] W. Fischer, R. T. Hembre, D. R. Sidler, J. R. Norton, *Inorg. Chim. Acta* **1992**, *198–200*, 57–61.

Difluoromethyl Compounds of Chalcogens: A NMR Study of the Reactions of $Cd(CF_3)_2 \cdot 2MeCN$ and $ZnBr(CF_3) \cdot 2MeCN$ with Dialkyl Chalcogenides and Boron Trifluoride**

Dieter Naumann,* Regina Möckel, and Wieland Tyrra

$Zn(CF_3)$ and $Cd(CF_3)$ derivatives have established themselves as polar reagents for the transfer of trifluoromethyl groups.[1, 2] A further possibility for the employment of these derivatives is as difluorocarbene sources at higher temperatures.[3] Products have been identified, however, which indicate a carbenoid or carbene reaction even under extremely mild conditions – in particular in the transfer of CF_3 groups to strong Lewis acid systems.

Based on these findings, we were able to open a simple route to chalcogenides with difluoromethyl groups by optimizing the reaction conditions.[4] Whereas difluoromethyl ethers and difluoromethyl sulfides may already be prepared by base-initiated reactions of chlorodifluoromethane and the corresponding alcohols and thiols[5] or by reactions of difluorodiazirine[6] or fluorosulfonyldifluoroacetic acid[7] with alcohols, the difluoromethyl compounds of the heavier elements—with the exception of aryl(difluoromethyl) compounds[8]—were not known until now.

The alkyl(difluoromethyl) chalcogenides **3a**–**8a** are formed by the BF_3-initiated reaction of **1** or **2** with dialkyl ethers (**3** and **4**), dialkyl sulfides (**5** and **6**), dimethyl selenide (**7**), or dimethyl telluride (**8**), at −30 °C (Eq. (a)). The products were identified by NMR spectroscopic techniques.

$$\underset{\mathbf{1,2}}{M(CF_3)X} + \underset{\mathbf{3-8}}{R_2E} + BF_3 \rightarrow \underset{\mathbf{3a-8a}}{RECF_2H} + [MX]^+ + [BF_4]^- \qquad \text{(a)}$$

$M(CF_3)X$: $Cd(CF_3)_2 \cdot 2MeCN$ **1**, $ZnBr(CF_3) \cdot 2MeCN$ **2**;
R_2E: Me_2O **3**, Et_2O **4**, Me_2S **5**, Et_2S **6**, Me_2Se **7**, Me_2Te **8**

[*] Prof. Dr. D. Naumann, Dr. R. Möckel, Dr. W. Tyrra
Institut für Anorganische Chemie der Universität
Greinstrasse 6, D-50939 Köln (FRG)
Telefax: Int. code + (221)470-5196

[**] Carbenoid Reactions of Trifluormethyl Element Compounds, Part 1. This work was supported by the Fonds der Chemischen Industrie and by the Ministerium für Wissenschaft und Forschung des Landes Nordrhein-Westfalen.

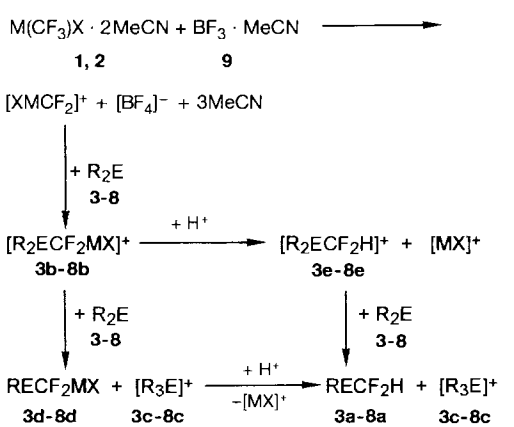
The reactions are selective in dichloromethane between $-78\,^{\circ}C$ and room temperature. The products formed indicate the following reaction mechanism: On the assumption that trifluoromethyl derivatives of cadmium and zinc, analogous to the intensively investigated lithium carbenoids,[10] may be written in the mesomeric forms **1a** and **1b** (see Eq. (b), without MeCN), it would seem apparent that the removal of a fluoride ion by the use of a Lewis acid, such as BF_3, should be possible. The electron deficit that thereby arises on the carbon atom is compensated by a Lewis base, for example, a dialkyl chalcogenide, under formation of an onium intermediate (**3b**–**8b**) (see Scheme 1).

$$\underset{\mathbf{1}}{CF_3CdCF_3} \longleftrightarrow \underset{\mathbf{1a}}{[CF_3Cd]^+[CF_3]^-} \longleftrightarrow \underset{\mathbf{1b}}{[CF_3CdCF_2]^+\,F} \qquad \text{(b)}$$

Intermediates of this type can be identified in the reaction of **1** with cyclic sulfanes by using ^{19}F NMR and ^{113}Cd NMR spectroscopic techniques,[11] and have already been detected by ^{113}Cd NMR spectroscopy in reactions of $Cd(CF_3)_2$ complexes with $I(CF_3)(OCOCF_3)_2$ in the presence of $B(OCOCF_3)_3$.[12]

A two-step reaction involving alkyl group transfer and protolysis can be assumed for the formation of alkyl(difluoromethyl) chalcogenides **3a**–**8a** from **3b**–**8b**. The onium intermediates **3b**–**8b** react with an excess of the dialkyl chalcogenides **3**–**8** to give the trialkylchalcogenium ions **3c**–**8c**, which can be detected by NMR spectroscopy, and the neutral intermediates **3d**–**8d**. The ensuing protolysis of **3d**–**8d** leads to the formation of the alkyl(difluoromethyl) chalcogenides **3a**–**8a**.

The intermediates **3b**–**8b** could initially be protolyzed to give the dialkyl(difluoromethyl)chalcogenium ions **3e**–**8e**. The sulfonium ions **5e** and **6e** were identified. Compounds **3e**–**8e** react with an excess of the chalcogenides **3**–**8** to form **3a**–**8a** and **3c**–**8c** (Scheme 1).



Scheme 1. Suggested course of the title reaction. For M, X, R, E, see Equation (a).

The source of the protons in the reactions of the dialkyl ethers, **3** and **4**, cannot be determined unequivocally. The alkyl cations released in the reaction could further react with the acetonitrile present in the system to form ketenimines under proton abstraction.[13] The possible formation of an intermediate trialkyloxonium ion, which subsequently decomposes to give an ether, an alkene and a proton[14] cannot be ruled out, but appears to be improbable in the system described.

The identification of the alkene and other by-products can be made by the reaction of **1** with $BF_3 \cdot t$BuOMe in *tert*-butylmethyl ether, where $MeOCF_2H$ (**3a**) is formed as the main product. Side-products include hydrogen fluoride, isobutene, *tert*-butylfluoride, and 1,1-difluoro-2,2-dimethylcyclopropane. All products were identified by ^{19}F NMR and $^{13}C\{^1H\}$ NMR spectroscopic techniques. $MeOCF_2H$ (**3a**) is formed according to the mechanism proposed above. The proton needed for the cleavage of the metal–carbon bond originates from reaction of the *tert*-butyl cation yielding isobutene. The formation of *tert*-butylfluoride can be explained by either the decomposition of the intermediate $[t\text{Bu}][BF_4]$, or by a Markovnikov addition of HF to isobutene. The 1,1-difluoro-2,2-dimethylcyclopropane, also identified in the reaction, can be considered as a product of a carbenoid reaction of **1** with isobutene. The absence of tetrafluoroethene or perfluorocyclopropane, the trimer of difluorocarbene, confirms the assumption of a carbenoid reaction pathway and all but completely rules out the formation of the products by a difluorocarbene insertion or [2 + 2] cycloaddition reaction.

In the case of the heavier elements, the complexed acetonitrile functions as a proton source—this was confirmed by deuteration studies.[15] These studies could not ascertain as to how far fluoride ions or tetrafluoroborate ions make the hydrogen abstraction from acetonitrile[16] possible in these systems. However, the ^1H NMR spectra of the reaction mixtures do enable the identification of (*E*)-3-amino-2-butenenitrile as a product of this proton abstraction (cf. [17]).

Table 1. NMR spectroscopic data of the compounds **3a**–**8a**, **5c**–**8c**, **5e** and **6e**. (Measurements made at 21 °C in CH_2Cl_2 unless otherwise stated). Product mixtures were used.

$MeOCF_2H$ **3a**: ^{19}F NMR (188.3 MHz, THF, CCl_3F): $\delta = -86.93$ (d, $^2J(F,H) = 75.4$ Hz, $^1J(F,C) = 259.4$ Hz) [a]

$EtOCF_2H$ **4a**: ^{19}F NMR (188.3 MHz, $MeCN/Et_2O$, CCl_3F): $\delta = -83.86$ (d, $^2J(F,H) = 75.9$ Hz, $^1J(F,C) = 257.9$ Hz) [b]; ^1H NMR (200.1 MHz, $CDCl_3$, TMS): $\delta = 6.15$ (CF_2H, t, $^2J(F,H) = 75.5$ Hz, 1 H), 3.88 (CH_2, q, 2 H), 1.22 (CH_3, t, 3 H); $^{13}C\{^1H\}$ NMR (50.5 MHz, $CDCl_3$, TMS): $\delta = 115.8$ (CF_2H, t, $^1J(F,C) = 260.0$ Hz), 59.0 (CH_2, t, $^3J(F,C) = 5.0$ Hz), 18.5 (CH_3, s)

$MeSCF_2H$ **5a**: ^{19}F NMR (188.3 MHz, CCl_3F): $\delta = -96.38$ (d, $^2J(F,H) = 56.9$ Hz, $^1J(F,C) = 270.6$ Hz); ^1H NMR (200.1 MHz, TMS): $\delta = 6.80$ (CF_2H, t, $^2J(F,H) = 56.6$ Hz, 1 H), 2.23 (CH_3, s, 3 H)

$EtSCF_2H$ **6a**: ^{19}F NMR (188.3 MHz, CCl_3F): $\delta = -93.45$ (d, $^2J(F,H) = 56.3$ Hz, $^1J(F,C) = 271.1$ Hz); ^1H NMR (200.1 MHz, TMS): $\delta = 6.84$ (CF_2H, t, 1 H, $^2J(F,H) = 56.5$ Hz), 2.78 (CH_2, q, 2 H), 1.29 (CH_3, t, 3 H)

$MeSeCF_2H$ **7a**: ^{19}F NMR (282.4 MHz, CCl_3F): $\delta = -94.37$ (d, $^2J(F,H) = 55.1$ Hz, $^2J(Se,F) = 34.2$ Hz); $^{77}Se\{^1H\}$ (57.3 MHz, Me_2Se): $\delta = 289.77$ (t, $^2J(Se,F) = 34.4$ Hz)

$MeTeCF_2H$ **8a**: ^{19}F NMR (282.4 MHz, CCl_3F): $\delta = -91.75$ (d, $^2J(F,H) = 52.5$ Hz, $^2J(Te,F) = 61.0$ Hz); $^{125}Te\{^1H\}$ NMR (94.8 MHz, Me_2Te): $\delta = 534.72$ (t, $^2J(Te,F) = 60.8$ Hz)

$[Me_3S]^+$ **5c**: ^1H NMR (200.1 MHz, TMS): $\delta = 2.89$, s

$[Et_3S]^+$ **6c**: ^1H NMR (200.1 MHz, TMS): $\delta = 3.25$ (CH_2, q, 6 H), 1.43 (CH_3, t, 9 H) [c]

$[Me_3Se]^+$ **7c**: $^{77}Se\{^1H\}$ NMR (57.3 MHz, Me_2Se): $\delta = 255.84$ (s) [d]

$[Me_3Te]^+$ **8c**: $^{125}Te\{^1H\}$ NMR (94.8 MHz, (Me_2Te): $\delta = 446.66$ (s) [e]

$[Me_2SCF_2H]^+$ **5e**: ^{19}F NMR (188.3 MHz, CCl_3F): $\delta = -110.77$ (d, $^2J(F,H) = 52.9$ Hz)

$[Et_2SCF_2H]^+$ **6e**: ^{19}F NMR (188.3 MHz, CCl_3F): $\delta = -104.43$ (d, $^2J(F,H) = 52.5$ Hz, $^1J(F,C) = 291.0$ Hz); ^1H NMR (200.1 MHz, TMS): $\delta = 7.54$ (t, $^2J(F,H) = 52.5$ Hz) [f]

[a] Cf. [6]. [b] Cf. [7]. [c] Cf. [18]. [d] Cf. [19]. [e] Cf. [20]. [f] The signals from the ethyl groups are eclipsed by those from **6c**.

The new reaction type discussed here makes it possible to synthesize alkyl(difluoromethyl) chalcogenides in a very simple manner, and under mild conditions, starting from trifluoromethyl compounds of cadmium and zinc. An elaboration of the reaction principle, using other organometallic and organic derivatives, should open simple routes to the synthesis of both new compounds containing CF_2H groups, and compounds which are otherwise extremely difficult to obtain.

Experimental Procedure

All manipulations were carried out under nitrogen with the careful exclusion of moisture. **1** (1.0 mmol) or **2** (2 mmol) was dissolved (or suspended) in dichloromethane (6 mL) at −78 °C. After addition of **9** (2.0 mmol), the reaction mixture was stirred for several minutes and **3**–**8** (ca. 6 mmol) was added. The mixture was stirred at −78 °C for five hours and then warmed to room temperature. Reactions with $BF_3 \cdot t$BuOMe were carried out in *t*BuOMe. The NMR spectra (Table 1) were recorded at room temperature using the product mixtures. The molar ratios of **5a**–**8a** to **5c**–**8c** were calculated from the NMR spectra and found to be 1:1 in all cases.

Received: July 24, 1993
Revised version: September 20, 1993 [Z 6233 IE]
German version: *Angew. Chem.* **1994**, *106*, 325

[1] For example see D. Naumann, W. Strauss, W. Tyrra, *J. Organomet. Chem.* **1991**, *407*, 1–15.
[2] D. Naumann, M. Finke, H. Lange, W. Dukat, W. Tyrra, *J. Fluorine Chem.* **1992**, *56*, 215–237.
[3] For example see H. Lange, D. Naumann, *J. Fluorine Chem.* **1985**, *27*, 299–308; H. Koroniak, *ibid.* **1984**, *24*, 503–507, and references therein.
[4] D. Naumann, W. Tyrra, R. Möckel, P 4219881.9 (German Patent office), 17. June 1992.
[5] J. Hine, J. J. Porter, *J. Am. Chem. Soc.* **1957**, *79*, 5493–5496; *ibid.* **1960**, *82*, 6118–6120; T. G. Miller, J. W. Thanassi, *J. Org. Chem.* **1960**, *25*, 2009–2012; A. De Cat, R. Van Poucke, R. Pollet, P. Schots, *Bull. Soc. Chim. Belg.* **1965**, *74*, 270–280; G. G. I. Moore, *J. Org. Chem.* **1979**, *44*, 1708–1711.
[6] R. A. Mitsch, J. E. Robertson, *J. Heterocycl. Chem.* **1965**, *2*, 152–156.
[7] Q.-Y. Chen, S.-W. Wu, *J. Fluorine Chem.* **1989**, *44*, 433–440.
[8] H. Suzuki, M. Yishinaga, K. Takaoka, Y. Hiroi, *Synthesis* **1985**, 497–499.
[9] W. Gombler, H. Lange, D. Naumann, *J. Magn. Reson.* **1990**, *89*, 10–20.
[10] H. Siegel, *Top. Curr. Chem.* **1982**, *106*, 55–78; A. Maercker, *Angew. Chem.* **1993**, *105*, 1072–1074; *Angew. Chem. Int. Ed. Engl.* **1993**, *32*, 1023–1025; G. Boche, M. Marsch, A. Müller, K. Harms, *ibid.* **1993**, *105*, 1081–1082 and **1993**, *32*, 1032–1033.
[11] R. Möckel, W. Tyrra, D. Naumann, unpublished results.
[12] W. Tyrra, D. Naumann, *Can. J. Chem.* **1991**, *69*, 327–333.
[13] For example see R. Fuks, D. Baudoux, C. Piccinni-Leopardi, J.-P. Declercq, M. Van Meerssche, *J. Org. Chem.* **1988**, *53*, 18–22.
[14] For example see G. A. Olah, H. Doggweiler, J. D. Felberg, *J. Org. Chem.* **1984**, *49*, 2112–2116; E. J. Munson, J. F. Haw, *J. Am. Chem. Soc.* **1991**, *113*, 6303–6305.
[15] If, instead of $Cd(CF_3)_2 \cdot 2\,CH_3CN$ (**1**) and $BF_3 \cdot CH_3CN$ (**9**), the complexes with CD_3CN are used, the reaction of, for example, Me_2S leads to the formation of $MeSCF_2D$, which can be identified. ^{19}F NMR (188.3 MHz, CH_2Cl_2, 21 °C, CCl_3F): $\delta = -97.15$; $^2J(F,D) = 8.5$ Hz.
[16] K. O. Christe, W. W. Wilson, R. D. Wilson, R. Bau, J. Feng, *J. Am. Chem. Soc.* **1990**, *112*, 7619–7625.
[17] C. Krüger, *J. Organomet. Chem.* **1967**, *9*, 125–134.
[18] G. A. Olah, J. R. DeMember, Y. K. Mo, J. J. Svoboda, P. Schilling, J. A. Olah, *J. Am. Chem. Soc.* **1974**, *96*, 884–892.
[19] W. W. McFarlane, R. J. Wood, *J. Chem. Soc. Dalton Trans.* **1972**, 1397–1402.
[20] H. C. E. McFarlane, W. W. McFarlane, *J. Chem. Soc. Dalton Trans.* **1973**, 2416–2418.

Synthesis and Structure of an Oxovanadium(v)–Organophosphonate Cluster Encapsulating a Chloride Ion: $[ClV_7O_{12}(O_3PC_6H_5)_6]^{2-}$**

Yuan-Da Chang, Jose Salta, and Jon Zubieta*

Recent developments in metal organophosphonate coordination chemistry[1, 2] have received considerable impetus from the applications of such materials as sorbents, catalysts, and catalyst supports.[3, 4] Oxovanadium–organophosphonate chemistry includes numerous new materials such as binuclear coordination compounds,[5] fully oxidized[6] and mixed-valence clusters,[7, 8] and layered compounds.[9, 10] The solid oxovanadium organophosphonates with alternating organic and inorganic layers have been shown to recognize and selectively discriminate between alcohols.[10] The large mixed-valence polyoxovanadium–organophosphonate ions $[(Me_4N)^+ \subset H_6(VO_2)_{16}(CH_3PO_3)_8]^{7-}$,[7] $[(H_2O)_x \subset H_{12}(VO_2)_{12}(PhPO_3)_8]^{4-}$,[8] and $[2\,NH_4^+, 2\,Cl^- \subset V_{14}O_{22}(OH)_4(H_2O)_2(PhPO_3)_8]^{6-}$[11] form inclusion compounds with cationic units, neutral molecules, and even anionic/cationic aggregates, respectively. While an expansive coordination chemistry of organophosphonates with primarily V^{IV}-oxo units is emerging, oxovanadium(v)-organophosphonate chemistry remains relatively unexplored and to date the only example of this class of compound previously reported is the pentanuclear cluster $[V_5O_7(OCH_3)_2(PhPO_3)_5]^-$.[6] We report here the synthesis and structure of a novel oxovanadium(v)–organophosphonate (**1**). This anion exhibits a cage

$(Ph_4P)_2[ClV_7O_{12}(PhPO_3)_6]$ **1**

structure formed by the corner-sharing of V^v/O square pyramids and $PhPO_3$ tetrahedra, in which a Cl^- ion is encapsulated. The anion of **1**, while best described as spherical, shares common structural motifs with the layered phase $VO(C_6H_5PO_3) \cdot H_2O$, and both of these structures may be related in turn to simple binuclear oxovanadium(IV) species such as **2** and **3**.

$(Ph_4P)_2[(VO)_2Cl_4(t\text{-}C_4H_9PO_3H)_2]$ **2**
$[(VO)_2Cl_2(H_2O)_2(RPO_3H)_2]$ **3a**; R = C_6H_5; **3b**; R = CH_3

Red parallelepiped crystals of **1** were prepared by the reaction of $(Ph_4P)VO_2Cl_2$[12] and $PhPO_3H_2$ in acetonitrile. The X-ray structure analysis of **1**[13] revealed the presence of discrete $(Ph_4P)^+$ cations and $[ClV_7O_{12}(O_3PC_6H_5)_6]^{2-}$ anions (Fig. 1 top). The V/P/O framework consists of a spherical shell of corner-sharing vanadium/oxygen square pyramids and organophosphonate tetrahedra. This $[V_7O_{12}(O_3PC_6H_5)_6]^-$ cage acts as a host for the chloride ion, which serves as a template for the organization of the cluster during the condensation process.[14] While the structure of **1** is somewhat reminiscent of that of $[V_{15}O_{36}Cl]^{6-}$,[15, 16] the topological details are quite distinct. The cluster cage of $[V_{15}O_{36}Cl]^{6-}$ is constructed exclusively from vanadium/oxygen square pyramids; this results in the formation of a highly symmetrical spheroid of approximate D_{3h} symmetry. The "facets" of the spheroid consist of two six-membered $\{V_3O_3\}$ rings, three $\{V_4O_4\}$ rings, and eighteen four-membered $\{V_2O_2\}$ rings. In contrast, cluster **1**, which is constructed from vanadium/oxygen square pyramids and phosphorus/oxygen/carbon tetrahedra and displays irregular geometry with approximate C_2 symmetry, exhibits six-membered $\{V_2PO_3\}$ rings, eight-membered $\{V_2P_2O_4\}$ and $\{V_3PO_4\}$ rings, and ten-membered $\{V_3P_2O_5\}$ rings defining four, four, two, and two faces of the cage, respectively.

All illustrated in Figure 1 middle, the cage is constructed from the fusing of a trinuclear $\{V_3O_5(O_3PC_6H_5)_6\}$ unit to a tetranuclear $\{V_4O_7\}$ moiety through bridging organophosphonate groups. While neither unit exists independently in the V/O/organophosphonate system, the trinuclear unit is reminiscent of the $\{V_3O_5(O_3PC_6H_5)_5\}$ unit in $[V_5O_7(OCH_3)_2(O_3PC_6H_5)_5]^-$,[6] and the cage of **1** shares common structural features with the solid phase $VO(O_3PC_6H_5) \cdot H_2O$[9] and with simple binuclear species of the type $[(VO)_2Cl_2(HO_3PR)_2Y_2]^n$ (**2**: R = *t*-C_4H_9, Y = Cl, *n* = 2; **3a** and **3b**: Y = H_2O, *n* = 0, R = C_6H_5 and CH_3, respectively).

The compositions of the binuclear complexes of the V/O/organophosphonate system are dependent on reaction conditions

[*] Prof. J. Zubieta, Y.-D. Chang, J. Salta
Department of Chemistry, Syracuse University
Syracuse, NY 13244-4100 (USA)
Telefax: Int. code + (315)443-4070

[**] This work was supported by the National Science Foundation Grant CHE 9119910.

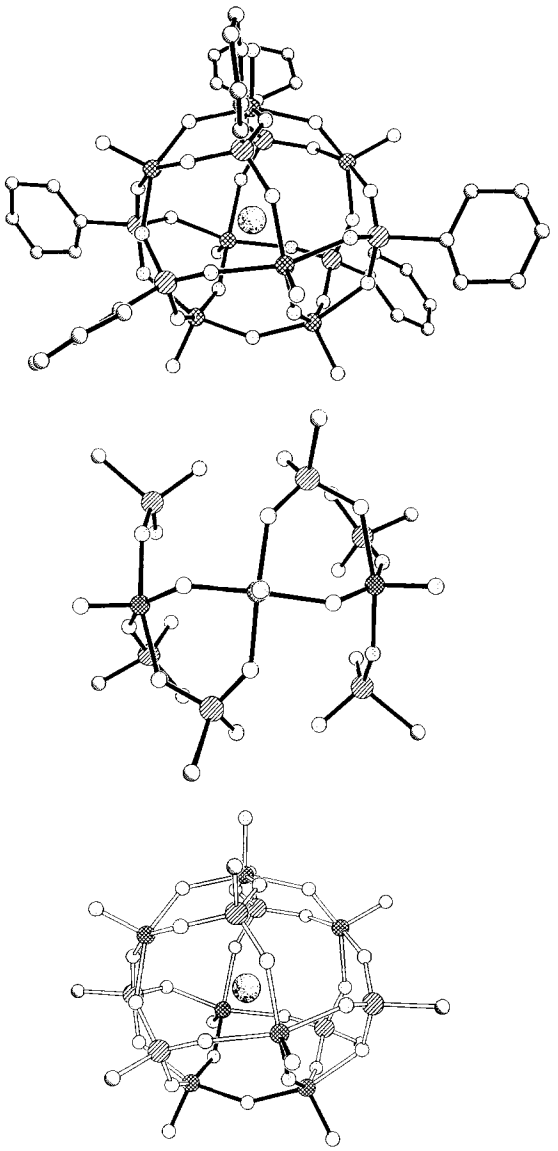


Fig. 1. Top: The structure of the $[V_7O_{12}(O_3PC_6H_5)_6Cl]^{2-}$ anion of **1**. Selected bond lengths [Å] and angles [°]: V-O (terminal) 1.54–1.58, V-O (bridging) 1.70–1.91, V-O (phosphate) 1.88–1.97; V-O-V 140.3–149.9, V-O-P 131.4–149.1, V···Cl 3.133–3.477. Middle: The trinuclear $\{V_3O_5(O_3PC_6H_5)_6\}$ unit which forms a major fragment of the cluster; the phenyl groups have been omitted for clarity. Bottom: View of the anion of **1** with the $\{V_4O_7\}$ fragment highlighted; only the *ipso* C atoms of the phenyl substituents are shown.

and the nature of the organic substituent. The crystal structures[17, 18] of the binuclear species consist of rings of corner-

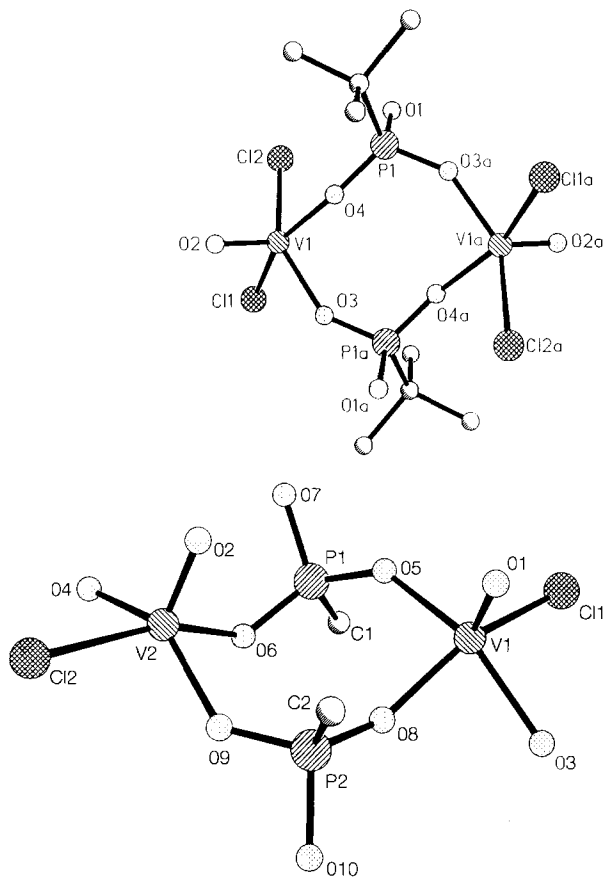


Fig. 2. Top: The structure of the $[(VO)_2Cl_4(t\text{-}C_4H_9PO_3H)_2]^{2-}$ anion of **2**. Selected bond lengths [Å] and angles [°]: V1-Cl1 2.351(2); V1-Cl2 2.371(2); V1-O6 1.571(6); V1-O3 1.980(5); V1-O4 1.974(4); P1-O4 1.504(4); P1-O3 1.497(8); P1-O2(H) 1.585(5); Cl1-V1-O4 155.8(2); Cl2-V1-O3 145.9(2). Bottom: The structure of $[(VO)_2Cl_2(H_2O)_2(CH_3PO_3H)_2]$ (**3b**). Selected bond lengths [Å] and angles [°]: V1-Cl1 2.330(7); V1-O1 1.64(1); V1-O3 1.99(1); V1-O5 1.98(1); V1-O8 1.93(1); V2-Cl2 2.321(6); V2-O2 1.58(1); V2-O4 2.01(1); V2-O6 2.01(1); V2-O9 1.94(1); Cl1-V1-O8 150.6(3); O3-V1-O5 149.2(4); Cl2-V2-O6 155.5(4); O4-V2-O9 144.0(5).

sharing V^V/O square pyramids and organophosphonate tetrahedra. Both orientations of the $\{V{=}O\}$ groups relative to the cyclic $\{V_2P_2O_4\}$ unit have been isolated; **2** and **3a** adopt the *anti* configuration, while **3b** exhibits *syn* geometry (Fig. 2). The structures of **2** and **3a** may be viewed as fragments of the $VO(O_3PR)\cdot H_2O$ layered materials, which may be constructed by linking binuclear units, in such a way that $\{V{-}O\cdots V\}$ interactions with alternating short and long distances are formed along the chains and the pendant {P-OH} groups coordinate to adjacent units. Similarly, **3b** possesses the required *syn* configuration to provide a structural motif for **1**.

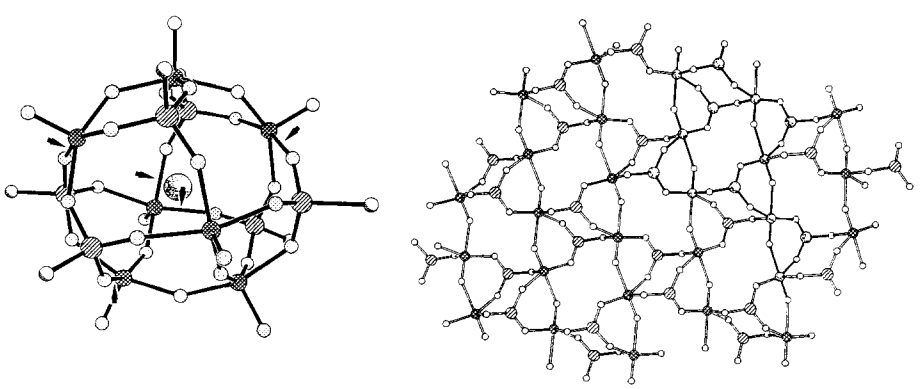


Fig. 3. Left: A view of the anion of **1**. The arrows indicate the V–O(P) bonds that may be broken to provide the $\{V_7O_{12}(O_3PC_6H_5)_6\}$ moiety which is subsequently unfolded and flattened. Right: A view of the *bc* plane of $VO(O_3PC_6H_5)\cdot H_2O$; phenyl carbon atoms and H_2O molecules are omitted for clarity. The unfolded and flattened $\{V_7O_{12}(O_3PC_6H_5)_6\}$ unit derived from **1** is highlighted.

The structure of **1** is also reflected in the layered phase, such that cleavage of V-phosphonate–oxygen bonds, coordination of H_2O to the sixth coordination site on vanadium, and flattening of the cage produces the motif shown in Figure 3 (right). The structural relationships of the cluster **1** to the related binuclear species **2** and **3** and to the layered solid $VO(O_3PR) \cdot H_2O$ are not only striking but extend beyond topological similarities to the chemical behavior of the cluster. Protic degradation and reduction of **1** by alcohol in MeOH/HCl yields the binuclear species **3a**, which in turn serves as a precursor for fragment condensation reactions by mild hydrolysis[5] to give $[V_6O_{10}(PhPO_3)_4(PhPO_3H)_2]^{2-}$, $[(CH_3CN)_2(VO)_{14}O_8(OH)_4(O_3PPh)_8]^{6-}$,[20] and other as yet unidentified oligomers. Under more forcing conditions of hydrolysis/condensation, both **1** and **3a** yield solid phases of composition $VO(O_3PPh) \cdot H_2O$.

The polyvanadate system adopts complex structures based on cage, basket, belt, bowl, and barrel motifs which are topologically and chemically related to the V_2O_5 layer structure.[19] A similar structural diversity may be expected for the V/O/organophosphonate system whose molecular clusters exhibit certain analogous relationships to the solid $VO(O_3PR) \cdot H_2O$ phases. However, the introduction of the organophosphonate tetrahedral unit into the polyhedral backbone clearly expands the structural possibilities as indicated by the $[H_6(VO_2)_{16}(CH_3PO_3)_8]^{8-}$, $[H_{12}(VO_2)_{12}(PhPO_3)_8]^{4-}$, and $[V_{14}O_{22}(OH)_4(H_2O)_2(PhPO_3)_8]^{6-}$[11, 20] frameworks, which exhibit structural motifs related to both V_2O_5 and $VO(O_3PR) \cdot H_2O$ phases.

Experimental Procedure

All reactions were carried out in an atmosphere of N_2.

1: A solution of $PhPO_3H_2$ (1.3 g, 8.2 mmol) in acetonitrile (5 mL) was added to a solution of $(Ph_4P)[VO_2Cl_2]$ (2.0 g, 4.1 mmol) in CH_3CN (15 mL). After stirring for 48 h, the original translucent lime-green color associated with $[VO_2Cl_2]^-$ changed to an intense red-orange. The volume of the reaction mixture was reduced to 10 mL and layered with diethyl ether to give 0.6 g of a fine red precipitate of **1**. Recrystallization was effected by slow evaporation from acetonitrile solution. IR(KBr pellet): $\tilde{\nu}[cm^{-1}] = 1484(m)$, 1438(m), 1178(m), 1132(s), 1039(s), 1019(s), 990(vs), 831(m), 753(m), 722(m), 689(m), 553(m), 526(m), 492(m); $\{PO_3\}$ group vibrations: 1178, 1132, 1039, and 1019.

2: $tBuPO_3H_2$ (0.59 g, 4.27 mmol) was added to a solution of $(Ph_4P)[VO_2Cl_2]$ (2.24 g, 4.54 mmol) in methanol (20 mL). After stirring at room temperature for 48 h, the resultant dark green solution was concentrated to 12 mL and layered with diethyl ether. Blue-green crystals of **2** were recovered after standing at room temperature for 18 days. Yield: 0.40 g. IR(KBr pellet): $\tilde{\nu}[cm^{-1}] = 1585(m)$, 1483(m), 1436(m), 1313(w), 1187(w), 1164(w), 1109(vs), 1013(s), 997(s), 756(s), 722(vs), 688(s), 526(vs); $\{PO_3\}$ group vibrations: 1187, 1164, 1109, 1013.

3b · $2Ph_4PCl$: $(Ph_4P)[VO_2Cl_2]$ (2.51 g, 5.1 mmol) and $CH_3PO_3H_2$ (0.443 g, 4.61 mmol) were allowed to react at room temperature in methanol (20 mL). Conditions and workup were identical to those reported for **2** (yield: 0.56 g of blue crystals). IR(KBr pellet): $\tilde{\nu}[cm^{-1}] = 1609(w)$, 1585(m), 1483(m), 1436(s), 1315(m), 1193(s), 1108(s), 1068(s), 1018(s), 996(s), 949(s), 757(m), 722(s), 688(s), 527(vs). $\{PO_3\}$ group vibrations: 1193, 1108, 1068, 1018. The synthesis of **3a** is reported in reference [5].

Received: August 12, 1993 [Z 6273 IE]
German version: *Angew. Chem.* **1994**, *106*, 347

[1] See for example Y. Zhang, A. Clearfield, *Inorg. Chem.* **1992**, *31*, 2821, and references therein.; G. Cao, T. E. Mallouk, *ibid.* **1991**, *30*, 1434, and references therein.
[2] B. Bujoli, P. Palvadeau, J. Rouxel, *Chem. Mater.* **1990**, *2*, 582.
[3] D. A. Burwell, K. G. Valentine, J. H. Timmermans, M. E. Thompson, *J. Am. Chem. Soc.* **1992**, *114*, 4144.
[4] A. Clearfield, *Chem. Rev.* **1988**, *88*, 125.
[5] Q. Chen, J. Salta, J. Zubieta, *Inorg. Chem.* **1993**, in press.
[6] Q. Chen, J. Zubieta, *Angew. Chem.* **1993**, *105*, 304; *Angew. Chem. Int. Ed. Engl.* **1993**, *32*, 261.
[7] G. Huan, A. J. Jacobson, V. W. Day, *Angew. Chem.* **1991**, *103*, 426; *Angew. Chem. Int. Ed. Engl.* **1991**, *30*, 422.
[8] G. Huan, V. W. Day, A. J. Jacobson, D. P. Goshorn, *J. Am. Chem. Soc.* **1991**, *113*, 3188.
[9] G. Huan, A. J. Jacobson, J. W. Johnson, E. W. Corcoran, Jr., *Chem. Mater.* **1990**, *2*, 2.
[10] J. W. Johnson, A. J. Jacobson, W. M. Butler, S. E. Rosenthal, J. F. Brody, J. T. Lewandowski, *J. Am. Chem. Soc.* **1989**, *111*, 381.
[11] A. Müller, K. Hovemeier, R. Rohlfing, *Angew. Chem.* **1992**, *104*, 1214; *Angew. Chem. Int. Ed. Engl.* **1992**, *31*, 1192.
[12] D. Fenske, A.-F. Shihada, H. Schwab, K. Dehnicke, *Z. Anorg. Allg. Chem.* **1986**, *471*, 140.
[13] **1**: triclinic space group $P\bar{1}$ with $a = 13.949(3)$, $b = 26.027(5)$, $c = 26.251(5)$ Å, $\alpha = 90.41(2)$, $\beta = 91.03(2)$, $\gamma = 92.30(2)$°, $V = 9521(5)$ Å^3, $Z = 4$, $\varrho_{calcd} = 1.643\ g\,cm^{-3}$, $\mu(Mo_{K\alpha}) = 8.98\ cm^{-1}$; $R = 0.0781$ for 10377 reflections with $2\theta < 45°$ and $I \geq 3\sigma(I)$; Rigaku AFC5S diffractometer, graphite monochromated $Mo_{K\alpha}$ radiation. The structure was solved by using direct methods with the SHELXTL program package. Further details of the crystal structure investigation may be obtained from the Fachinformationszentrum Karlsruhe, D-76344 Eggenstein-Leopoldshafen (FRG), on quoting the depository number CSD-57729, the names of the authors, and the journal citation.
[14] H. Reuter, *Angew. Chem.* **1992**, *104*, 1210; *Angew. Chem. Int. Ed. Engl.* **1992**, *31*, 1185.
[15] A. Müller, M. Penk, R. Rohlfing, E. Krickemeyer, J. Döring, *Angew. Chem.* **1990**, *102*, 927; *Angew. Chem. Int. Ed. Engl.* **1990**, *29*, 926.
[16] M. T. Pope, A. Müller, *Angew. Chem.* **1991**, *103*, 34; *Angew. Chem. Int. Ed. Engl.* **1990**, *30*, 34.
[17] **2**: triclinic space group $P\bar{1}$ with $a = 10.179(2)$, $b = 10.668(2)$, $c = 13.874(3)$ Å, $\alpha = 99.74(3)$, $\beta = 92.82(3)$, $\gamma = 99.60(3)$°, $V = 1459.4(7)$ Å^3, $Z = 1$, $\varrho_{calcd} = 1.399\ g\,cm^{-3}$, $\mu(Mo_{K\alpha}) = 6.62\ cm^{-1}$; $R = 0.0599$ for 2750 reflections with $2\theta < 45°$ and $I \geq 3\sigma(I)$. All other conditions and information as for ref. [13].
[18] **3b** · $2Ph_4PCl$: triclinic space group $P\bar{1}$ with $a = 11.137(2)$, $b = 11.892(2)$, $c = 22.105(4)$ Å, $\alpha = 74.91(3)$, $\beta = 76.50(3)$, $\gamma = 77.24(3)$°, $V = 2708(1)$ Å^3, $Z = 2$, $\varrho_{calcd} = 1.448\ g\,cm^{-3}$, $\mu(Mo_{K\alpha}) = 7.13\ cm^{-1}$; $R = 0.0703$ for 2836 reflections with $I \geq 3\sigma(I)$. All other conditions and information as for ref. [13]. The structure of the phenylphosphonate derivative **3a** · $2Ph_4PCl$ is described in ref. [11].
[19] W. G. Klemperer, T. A. Marquart, O. M. Yaghi, *Angew. Chem.* **1992**, *104*, 51; *Angew. Chem. Int. Ed. Engl.* **1992**, *31*, 49.
[20] M. I. Khan, J. Zubieta, unpublished results.

Macrotricyclic Borane–Amine Adducts: The First Uncharged Synthetic Host Compounds Without Lewis Acid Character, for Anionic Guests**

Karin Worm, Franz P. Schmidtchen,* Annette Schier, Andrea Schäfer, and Manfred Hesse*

Two alternative concepts have been used to date for the supramolecular binding of anions in solution to synthetic molecular hosts:[1] A high, positive charge density, such as that found in macrocyclic polyammonium salts, ensures host–guest complexation even when the guest experiences marked protic solvation.[2] The selectivity of molecular recognition certainly suffers from unavoidable competition with the counterions, which are subject to the same electrostatic attraction. In principle, formation of uncharged hosts for anions would be more favorable. Such hosts could be regarded as analogs to the cation-binding crown ethers. Since most anions possess lone electron pairs, the grouping of

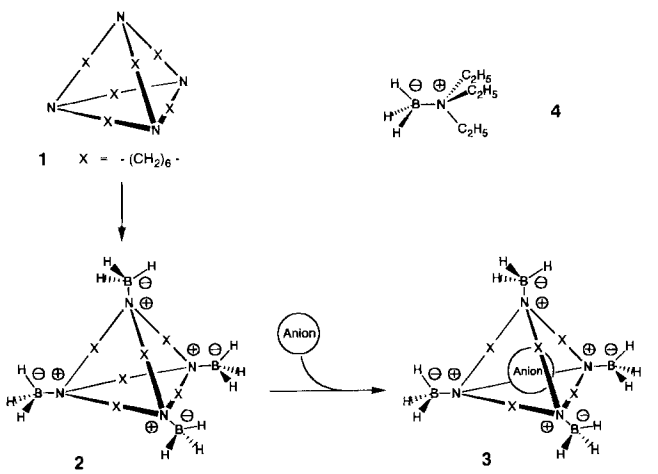
[*] Prof. Dr. F. P. Schmidtchen, Dr. K. Worm
Lehrstuhl für Organische Chemie und Biochemie
der Technischen Universität München
Lichtenbergstrasse 4, D-85747 Garching (FRG)
Telefax: Int. code + (89)3209-3345
Dr. A. Schier
Anorganisch-chemisches Institut der Technischen Universität München
Prof. Dr. M. Hesse, Dr. A. Schäfer,
Organisch-chemisches Institut der Universität
Winterturstrasse 190, CH-8057 Zürich (Switzerland)

[**] This work was supported by the Deutsche Forschungsgemeinschaft and the Fonds der chemischen Industrie.

several Lewis acid centers as complementary binding sites in a preorganized molecular lattice is obvious. A series of successful hosts has already been prepared according to this principle,[3] although they must thereby accept as guests the Lewis base solvent molecules, present in high concentration.

We envisaged a better, third way in the use of anion–dipole interactions, similar to those presumably employed in natural receptors. In numerous crystal structures of enzyme–substrate complexes, protein helices are aligned with the amino terminal directed toward negatively charged groups in the substrate, thereby illustrating the stabilizing effect of this orientation of the macrodipole.[4]

The ion–dipole interaction is nevertheless considerably weaker than the direct ion–ion interaction, decreases more rapidly with increasing distance, and is also dependent on orientation. In order to be able to use the ion–dipole interaction in synthetic hosts, the host must be perfectly preorganized for anion binding. This requirement could be fulfilled by formation of an adduct of the macrotricyclic amine **1**[5] with boron derivatives (cf. **2**). The dipoles of the dative boron–nitrogen bonds converge with the positive dipole terminals towards the center of the molecular cavity. Thus, the highly linked structure guarantees the fixed, unperturbed orientation of the dipoles, whilst the hydrocarbon bridges ensure a nonpolar environment with a low dielectric constant and thus the maximum electrostatic attraction for negatively charged molecular species. As shown by the analogous example of the quaternary ammonium salt,[6] obtained from **1** by Menshutkin alkylation, the molecular cavity is large enough even to bind iodide ions (ionic radius 2.16 Å) as guest in an inclusion complex. In addition, force field calculations in vacuo indicate negative enthalpies of formation for inclusion complexes **3** of the adduct **2** with bromide and cyanide[7] [ΔH ($Br^- \subset$ **2**) = -16 kcal mol^{-1}; ΔH ($CN^- \subset$ **2**) = -26 kcal mol^{-1}].



Preparation of the borane adduct **2** was achieved by reaction of **1** with $BH_3 \cdot THF$ (77%). Crystals from CH_2Cl_2/ether had the molecular structure shown in Figure 1;[8] surprisingly, only two carbon atoms in one of the hydrocarbon bridges are disordered. Unlike the inclusion complexes of tetraalkylated **1** with iodide[6] the borane adduct **2** is distorted from tetrahedral symmetry in the crystal, with the result that the molecular cavity in **2** is markedly smaller than the cavity that the iodide ion occupies in tetracationic hosts.[6] The host **2** must therefore change its equilibrium conformation on migration of a guest into this cavity.

The borane adduct **2** was titrated with a series of quaternary ammonium and phosphonium salts in $CHCl_3/CH_2Cl_2$, during

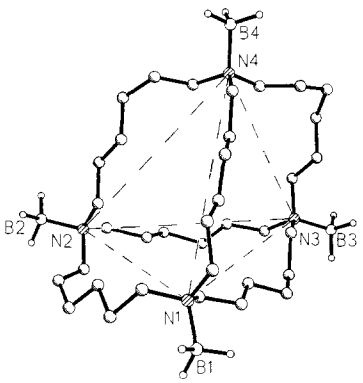


Fig. 1. Crystal structure of the borane–amine adduct **2** [8]; selected distances [Å]: N1–N2 6.92, N1–N3 8.10, N1–N4 7.35, N2–N3 7.08, N3–N4 6.65, N2–N4 7.86.

which procedure the ^{1}H NMR signals of the α-CH_2 group in **2** were observed to be sensitive probes of conformation. The signal pattern of **2** does not change; instead concentration-dependent shifts of the signals appear. These shifts are typical of those found for supramolecular complex formation governed by rapid host–guest exchange kinetics. The change in chemical shift ($\Delta\delta$) is thus a function both of the ratio of free host to host–guest complex and of the maximum value ($\Delta\delta_{max}$), the latter being dependent on the guest anion.[9] For the five anions examined, Figure 2 shows variable but linear dependences for the concentration ratios selected. As absolutely no effect was detected for the analogous triethylamine–borane adduct **4** in titrations under the same conditions, the observed signal shifts cannot be due to unspecified salt effects but must be a result of the macrotricyclic cage structure of **2**. The graduation can therefore be explained without further ado according to the model of an inclusion complex: large anions (PF_6^-, I^-) show no or only very weak shifts, because the concentrations of the host–guest complexes are small. As a result of their size these guests can only be taken up in the molecular cavity with difficulty and therefore have very small binding constants. In contrast, small negatively charged guests (Cl^-, CN^-) migrate easily into the cage of the host and form stable complexes. Since this process, however, requires only a very small adaptation in the conformation of the host, the measured effect is small; for cyanide it is even smaller than for iodide. These counter influences lead to an optimal result for bromide as guest.

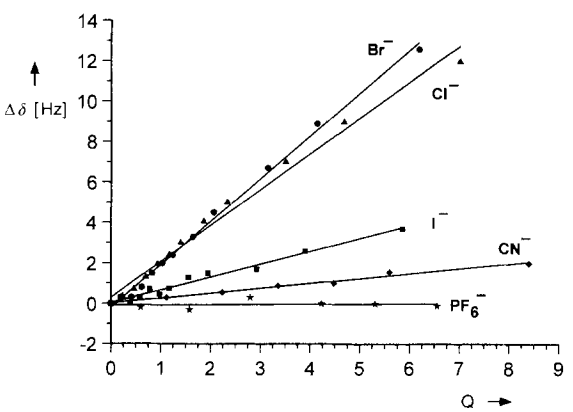


Fig. 2. ^{1}H NMR titrations (360 MHz) of **2** (9.45×10^{-3} M) with five salts at 297 K in 20 vol% $CD_2Cl_2/CDCl_3$; the change in chemical shift $\Delta\delta$ of the α-CH_2 signal in the host is plotted against the host–guest ratio Q. ▲ $(C_6H_5)_4P^+Cl^-$, ● $(C_4H_9)_4N^+Br^-$, ■ $(C_4H_9)_4N^+I^-$, * $(C_4H_9)_4N^+PF_6^-$, ◆ $(C_2H_5)_4N^+CN^-$.

The formation of a host–guest inclusion complex should give a saturation isotherm with 1:1 stoichiometry. The linear dependences in Figure 2 indicate that the dissociation constants of the host–guest complexes must be considerably greater than can be determined from the host and guest concentrations used hitherto in the titrations. The apparent host–guest dissociation constants of **2** with bromide as guest were determined from ^{1}H NMR titrations (360 MHz) with a large excess of bromide (Fig. 3). Under these conditions the unspecific ion-pairing of the salt becomes more important, and the host–guest binding constant is systematically underestimated as a result of this competition. A nonlinear regression function that fits the data well represents a 1:1 binding model with $K_{diss} = 80 \pm 8 \times 10^{-3}$ M (20% CD_2Cl_2/$CDCl_3$; $\Delta\delta_{max} = 80.3 \pm 3$ Hz; complexation range 18–74%) for the bromide complex of the electrically neutral host **2**.

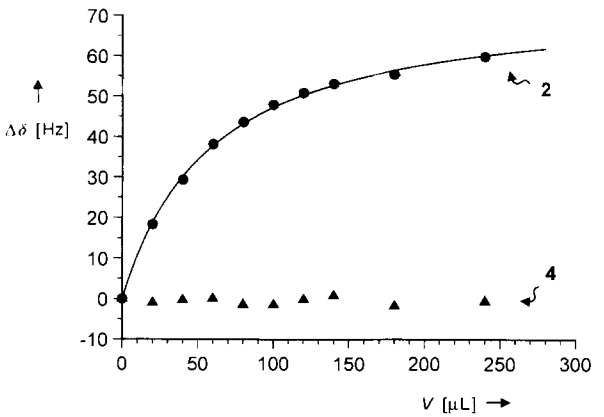


Fig. 3. ^{1}H NMR titration (360 MHz) of **2** (●) (13.6×10^{-3} M) and of triethylamine · BH_3 **4** (▲) with $(C_6H_5)_4P^+Br^-$ (0.78 M) at 297 K in 20 vol% CD_2Cl_2/$CDCl_3$ (500 μL). The change in chemical shift of the α-CH_2 signal is plotted against the volume of the guest solution. The continuous line shows the calculated regression curve. Repeating the titration with [**2**] = 5.8×10^{-3} M gave the same values for K_{diss} and for $\Delta\delta_{max}$ as those found at higher concentration.

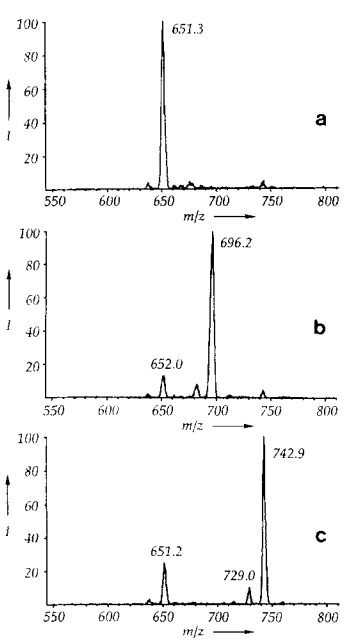


Fig. 4. Electrospray mass spectra of **2** (negative ion mode) in $CHCl_3/CH_3OH$ (1:3, $c = 10^{-4}$ M); a) without additive; b) with addition of $(C_4H_9)_4N^+Br^-$; c) with addition of $(C_4H_9)_4N^+I^-$.

Additional support for the formation of 1:1 host–guest complexes with halide ions in solution is provided by electrospray mass spectra (ESI-MS).[10] Recording the negative ions in $CHCl_3/CH_3OH$ solution yields almost exclusively the chloride complex of **2** (molecular mass 651 = 616 (**2**) + Cl^-;[11] Fig. 4a). The chloride apparently arises from the solvent, which emphasizes the affinity of the host **2** for this anion. On addition of bromide or iodide to the solution (as tetrabutylammonium salt), included Cl^- is replaced by Br^- or I^-, (the extent depends on the concentration of the added halide), and host–guest complexes are recorded at *m/z* 696 (616 (**2**) + Br^-[11]) and 743 (616 (**2**) + I^-)(Figs. 4b and 4c).

The macrotricycle **2** is thereby the first example of a new class of uncharged synthetic host compounds, in which the binding affinity for anions arises essentially from ion–dipole interactions. The success of the host compounds depends on the precise preorganization of the dipole, on the dipole strength, and on the stability and solubility of the abiotic host. Improvements in these properties will provide excellent perspectives for applications.

Received: August 31, 1993 [Z 6324 IE]
German version: *Angew. Chem.* **1994**, *106*, 360

[1] a) F. P. Schmidtchen, *Nachr. Chem. Tech. Lab.* **1988**, *36*, 8–17; b) B. Dietrich, *Pure Appl. Chem.* **1993**, *65*, 1457–1464.

[2] a) B. Dietrich, M. W. Hosseini, J.-M. Lehn, *J. Am. Chem. Soc.* **1981**, *103*, 1282–1283; b) *Helv. Chim. Acta* **1983**, *66*, 1262–1278; c) E. Kimura, Y. Kuramoto, T. Koike, H. Fujioka, M. Kodama, *J. Org. Chem.* **1990**, *55*, 42–46.

[3] a) M. Newcomb, J. H. Horner, M. T. Blanda, P. J. Squattrito, *J. Am. Chem. Soc.* **1989**, *111*, 6294–6301; b) Z. Zheng, X. Yang, C. B. Knobler, M. F. Hawthorne, *ibid.* **1993**, *115*, 5320–5321; c) M. T. Reetz, C. M. Niemeyer, K. Harms, *Angew. Chem.* **1991**, *103*, 1515–1517; *Angew. Chem. Int. Ed. Engl.* **1991**, *30*, 1472–1474.

[4] a) J. Aqvist, H. Luecke, F. A. Quiocho, A. Warshel, *Proc. Natl. Acad. Sci. USA* **1991**, *88*, 2026–2030; b) P. J. Lodi, J. R. Knowles, *Biochemistry* **1993**, *32*, 4338–4343.

[5] a) F. P. Schmidtchen, *Chem. Ber.* **1980**, *113*, 864–874; b) *Angew. Chem.* **1977**, *89*, 751–752; *Angew. Chem. Int. Ed. Engl.* **1977**, *16*, 720–721.

[6] a) F. P. Schmidtchen, G. Müller, *J. Chem. Soc. Chem. Commun.* **1984**, 1115–1116; b) F. P. Schmidtchen, *Pure Appl. Chem.* **1989**, *61*, 1535–1546.

[7] Calculations with the CVFF force field of the Insight/Discover molecular modeling program in vacuo. The partial charges in **2** were taken from a semiempirical MOPAC calculation of a tripropylamine · BH_3 adduct. To overcome kinetic barriers on inclusion of the guest, molecular dynamics calculations were carried out at 500 K, and the total energy of the configuration was minimized every 1 ps. Cyanide was found in the molecular cavity of **2** after only one ps, whereas bromide was found there only after 16 ps. Tetrafluoroborate remained only externally associated with **2**, even after 100 ps at 1000 K.

[8] Crystal structure of **2**: $C_{36}H_{84}B_4N_4$, $M = 616.706$; Enraf–Nonius CAD4 diffractometer; $Mo_{K\alpha}$ radiation ($\lambda = 0.71069$ Å); graphite monochromator; the lattice constants were obtained with 25 reflections; orthorhombic cell, $a = 12.368(1)$, $b = 14.003(1)$, $c = 24.294(2)$ Å, $V = 4208.1$ Å^3, space group $P2_12_12_1$ [no. 19], $Z = 4$, $\rho_{calcd} = 0.974$ g cm^{-3}, $F(000) = 1392$ e, $\mu(Mo_{K\alpha}) = 5.08$ cm^{-1}, ω scan, measured range of reciprocal space: $-14 < h < +14$, $0 < k < 16$, $0 < l < 27$; of 3674 independent reflections, 2608 were regarded as observed [$F_0 > 4\sigma(F_0)$]; structure solution was by direct methods (SHELXS-86), refinement according to the method of full-matrix least squares and difference Fourier synthesis (SHELX-76); all non-hydrogen atoms except the (disordered) atoms C33 and C34 were refined with anisotropic displacement parameters; all hydrogen atoms were placed in calculated positions; $R(R_w) = 0.0778$ (0.0512, with $w = 1/(\sigma^2(F_0) + 3.8103\ F_0^2)$); 411 parameters; maximum residual electron density: + 0.45/−0.46 e Å^{-3}. Refinement of the inverse coordination set produced no changes in the *R* values and geometries. Further details of the crystal structure investigation may be obtained from the Fachinformationszentrum Karlsruhe, D-76344 Eggenstein-Leopoldshafen (FRG) on quoting the depository number CSD-57735 and the journal citation.

[9] C. Wilcox, J. C. Adrian, Jr., T. H. Webb, F. J. Zawacki, *J. Am. Chem. Soc.* **1992**, *114*, 10189–10197.

[10] a) B. Ganem, J. D. Henion, *Chemtracts Org. Chem.* **1993**, *6*, 1–22; b) G. Hopfgartner, C. Piguet, J. D. Henion, A. F. Williams, *Helv. Chim. Acta* **1993**, *76*, 1759–1766.

[11] In Figures 4a and 4b *m/z* 651 is shown with the value of ^{35}Cl and *m/z* 696 with the average values of ^{79}Br and ^{81}Br. The calculated and measured intensities of the signals (from spread and better resolved spectra) are in complete agreement for the three complexes of **2** each containing a different halide ion.

 © VCH Verlagsgesellschaft mbH, D-69451 Weinheim, 1994 0570-0833/94/0303-0329 $ 10.00+.25/0

Complex-Stabilized Alkynyl and Cycloalkenyl Isocyanides**

Rainer Kunz and Wolf P. Fehlhammer*

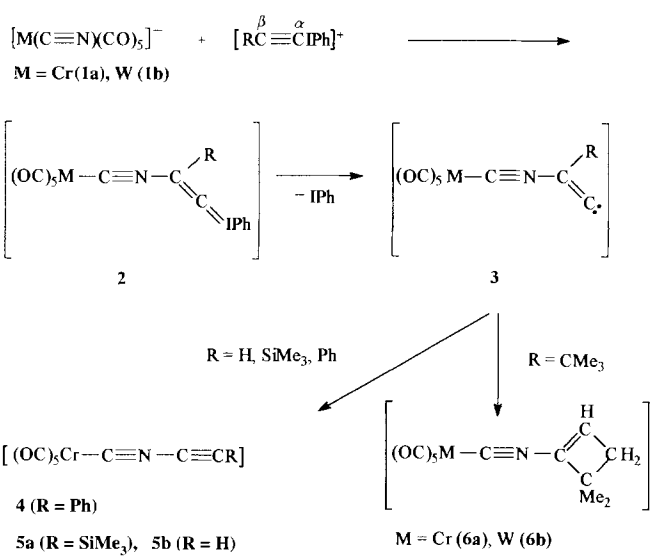
Dedicated to Professor Ernst Otto Fischer on the occasion of his 75th birthday.

For some time now, we have been interested in particularly simple functional isocyanides which – although unstable to various degrees as free molecules—can be readily prepared at the "protecting metal". In this form, these isocyanides are then available as stable molecules. Examples can be found in the proven or postulated interstellar isocyanides CNH,[1] $CNNH_2$,[2] and CNCN.[3, 4] In the meantime, a separate organometallic chemistry has begun to emerge around CNH ("chemistry of hydrogen isocyanide"[4]).

The situation is similar for the poly- and perchloroalkyl isocyanides, for example, $CNCCl_2-CCl_2R$ and $CNCCl_3$,[5, 6] which can be obtained by radical alkylations of cyano complexes. In its coordinated form, $CNCCl_2-CCl_2R$ appears to be a promising precursor for vinyl and also alkynyl isocyanides, a group of compounds which was unknown until recently. However, whereas the 1,2-elimination of two chlorine atoms posed no problem, the complex resisted further elimination to form a C-C triple bond.[7] Recently, Lentz et al. successfully achieved this elimination by flash pyrolysis of $[Cr(CO)_5CNCCl{=}CHCl]$, however, the metal-ligand bond was cleaved in the process as well.[8] The instability and low yield of the free ethynyl isocyanide thus obtained hinder the development of its chemistry.

We have therefore searched for other pathways to alkynyl isocyanide complexes and found one in the reaction of cyano complexes with alkynyl(phenyl)iodonium salts. One should be aware, however, that the advantage of stabilization by complexation carries with it the disadvantage of interference by the metal. Alkynyl(phenyl)iodonium salts are masked acetylene cations and, owing to their electrophilic character, react with cyano complexes according to Scheme 1.

The first step is probably an attack of the cyano complex *N* atom at the β-C atom, yielding the ylide **2**, which readily cleaves off iodobenzene. This reaction sequence has also been observed for other nucleophilic substitutions at alkynyliodonium salts.[9, 10] Depending on the nature of R, the formed isocyanovinylidene complex **3** is stabilized either by migration of the R group, yielding an alkynyl isocyanide complex (**4**, **5a**,**b**), or by insertion into a C–H bond of the alkyl chain, leading to a coordinated cycloalkenyl isocyanide – in this case cyclobutenyl isocyanide (**6a**, **b**). This last reaction step is reminiscent of the tandem Michael carbene insertions, which have been used by Ochiai et al. for elegant and efficient syntheses of cyclopentene derivatives.[9a] Complex **3** can also be used to prepare cyclopentenyl isocyanide complexes.[11]



Scheme 1. Proposed mode of formation of alkynyl and cyclobutenyl isocyanide complexes from cyanometalates and alkynyliodonium salts.

The finding that the use of $MeC{\equiv}ClPh^+$ does not lead to either propynyl or cyclopropenyl isocyanide complexes can serve as further evidence for the proposed mode of reaction, as apparently the primary adduct **2** (M = Cr, R = Me) is isolated. This is indicated by the molecular ion peak and the CO loss pattern in the mass spectrum, as well as by the IR spectrum that exhibits distinctly lower ν(CN) and ν(CO)[E] bands, an observation which is in accordance with the proposed vinyl isocyanide/iodonium ylide structure **7**.[12] A complete characterization has failed so far due to the ready decomposition of this species.

$[(OC)_5Cr{-}C{\equiv}N{-}C(Me){=}\ddot{C}{-}\overset{+}{I}Ph]$ **7**

The reaction of $NEt_4[Cr(CN)(CO)_5]$ with $[HC{\equiv}ClPh]OTf$ (OTf = OSO_2CF_3) leads to **5b**, which contains the simplest complex-bound alkynyl isocyanide. The use of $[Me_3SiC{\equiv}ClPh]BF_4$ allows – after separation by column chromatography—the isolation of two products. According to NMR, IR, and mass spectra, these are the trimethylsilyl derivative **5a** and its hydrolysis product **5b**.

Complex **4** is the first alkynyl isocyanide complex characterized by X-ray crystallography.[13] The C≡N, ≡N–C≡, and C≡C distances along the main molecular axis (Fig. 1) indicate isolated triple bonds, the corresponding bond angles are normal and in agreement with the description of the ligand as a linear isocyanoacetylene. The essentially equal Cr–C(O) bond lengths indicate a *trans* influence of the C≡N–C≡CPh ligand that is similar to that of CO, while it is very much weaker than that of cyano isocyanide C≡N–C≡N, one of the strongest π-acceptor ligands (see below).[3]

The fact that the signals of the axial and equatorial CO carbon atoms are coincident in the ^{13}C NMR spectrum of **5b** also supports the assertion that C≡N–C≡CH acts like a sixth carbonyl ligand.

Ad hoc assignments of the IR vibrational bands in the triple bond region are not feasible due to the various possible couplings between four species with A_1 symmetry ($2\times\nu$(CO), ν(CN), ν(C≡C)). Also ^{13}C labeling of the isocyanide carbon atom in **5b** did not lead to the desired clarity. Surprisingly, none of the original bands shows a truly significant isotopic shift, the only notable difference in the IR spectrum of **5b′** to that of **5b** con-

[*] Prof. Dr. W. P. Fehlhammer
Deutsches Museum
Museumsinsel 1, D-80538 München (FRG)
Telefax: Int. code + (89)2179-425
Dipl.-Chem. R. Kunz
Institut für Anorganische und Analytische Chemie
der Freien Universität Berlin
Fabeckstrasse 34-36, D-14195 Berlin (FRG)

[**] Metal Complexes of Functional Isocyanides. Part 22. This work was supported by the Fonds der Chemischen Industrie and the Bundesministerium für Bildung und Wissenschaft in the context of the Graduiertenkolleg "Synthese und Strukturaufklärung niedermolekularer Verbindungen". We thank Priv.-Doz. Dr. D. Lentz for valuable assistance with the X-ray structure analyses. Part 21: W. P. Fehlhammer, R. Metzner, R. Kunz, *Chem. Ber.*, in press.

cerns the low energy shoulder of the ν(CO)[E] absorption. A previously hidden band was shifted by about $-15\ cm^{-1}$, which indicates a significant ν(CN) component. Interestingly, similar isotope effects have also been observed for pentacarbonylchromium complexes of particularly electron-deficient isocyanides, such as $CNCCl_3$, CNCN, and CNC(O)NC.[4, 5b] In these compounds, the new band appears at even lower wavenumbers, namely 1936, 1929, and 1830 cm^{-1}, respectively.

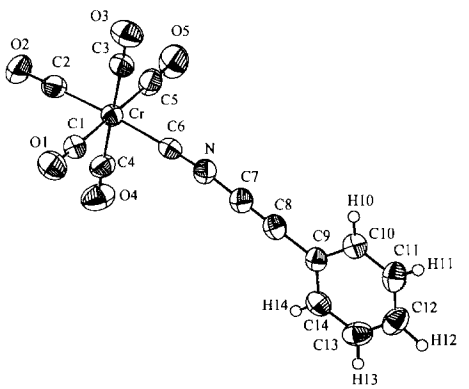


Fig. 1. Crystal structure of **4** (ORTEP, 50% probability ellipsoids), space group $P2_1/n$, $a = 6.044(3)$, $b = 7.403(3)$, $c = 30.667(14)$ Å, $\beta = 91.95(4)°$, $V = 1371.3$ Å^3, $Z = 4$; 2412 measured reflections, 1876 observed ($I > 3\sigma(I)$), 211 refined parameters, $R = 0.039$, ($R_w = 0.039$). Selected bond lengths [Å] and angles [°]: Cr-C2 1.896(4), Cr-C(O)$_{cis}$ (average) 1.891, Cr-C6 1.926(4), C6-N 1.169(5), N-C7 1.314(5), C7-C8 1.179(5); Cr-C6-N 175.7(3), C6-N-C7 175.1(4).

$[(OC)_5Cr\text{-}{}^{13}C{\equiv}N\text{-}C{\equiv}CH]$ **5b′**

The mass and ^{13}C NMR spectra of **4** and **5**, on the other hand, were straightforward. They confirm the formulation as alkynyl isocyanide. The position of the isocyanide carbon atom in **5b′**, which can be unambiguously assigned due to the ^{13}C label, is especially conclusive, but it is still not shifted as far downfield (≈ 200 ppm) as the corresponding C atoms in $[Cr(CO)_5CNCN]$ and $[Cr(CO)_5CNCCl_3]$ (cf. Experimental Procedure).[3, 6]

Preliminary experiments showed that the alkynyl isocyanide synthesis presented here can also be transferred to other cyano complexes ([Fe(CN)Cp(dppe)], [Ru(CN)Cp(dppe)]; dppe = 1,2-bis(diphenylphosphino)ethane). This gives us a very favorable basis for the development of subsequent chemistry, which, according to early results, appears to be primarily a chemistry of functionalized alkynes. For instance, reactions with $[Co_2(CO)_8]$ and $[Pt(\eta\text{-}C_2H_4)(PPh_3)_2]$ lead to the typical μ_2- and η^2-coordination compounds, respectively.

The cyclobutenyl isocyanide complexes **6a, b** also represent a new class of coordinated functional isocyanides. As expected, their IR spectra exhibit bands at 2140 s cm^{-1} (ν(CN)) and 1620 w cm^{-1} (ν(C=C)), and the mass spectra show the appropriate molecular ion peaks. The NMR data permit an unambiguous structure assignment, which is based on the δ values of other vinyl isocyanide complexes synthesized by us.[7]

The X-ray crystal structure analysis of **6a**[13] indicates a Cr-$(CO)_5$ fragment that exhibits a reduced Cr–CO_{trans} distance, when compared to the average value of the Cr–CO_{cis} bonds. This is generally observed for complexes incorporating donor ligands. In general, the geometric parameters reflect the unusual steric conditions at the unsaturated *gem*-disubstituted four-membered ring. Its spontaneous formation is therefore surprising also from this point of view (Fig. 2).

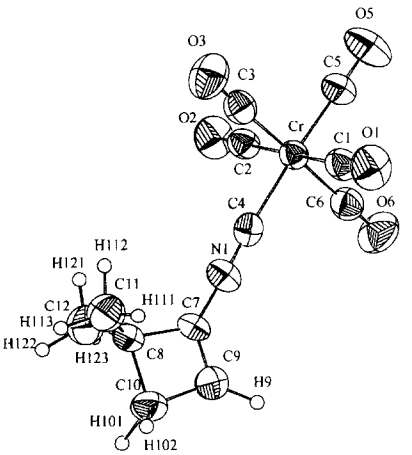


Fig. 2. Crystal structure of **6a** (ORTEP, 50% probability ellipsoids), space group $P2_1/c$, $a = 11.073(3)$, $b = 6.114(2)$, $c = 20.538(5)$ Å, $\beta = 90.60(2)°$, $V = 1390.25$ Å^3, $Z = 4$; 2143 measured reflections, 1547 observed ($I > 3\sigma(I)$), 208 refined parameters, $R = 0.036$, ($R_w = 0.038$). Selected bond lengths [Å] and angles [°]: Cr-C5 1.840(5), Cr-C(O)$_{cis}$ (average) 1.891, Cr-C4 1.968(5), C4-N1 1.165(6), N1-C7 1.371(6), C7-C9 1.316(7), C7-C8 1.496(6), C8-C10 1.587(7), C9-C10 1.500(8); Cr-C4-N1 176.0(4), C4-N1-C7 178.3(4), N1-C7-C8 129.4(4), C8-C7-C9 97.1(4), C7-C9-C10 93.3(4), C9-C10-C8 86.2(4), C10-C8-C7 83.4(3).

Experimental Procedure

4: A solution of $NEt_4[Cr(CN)(CO)_5]$ (3.00 g, 8.62 mmol) and [PhC≡ClPh]OTs (OTs = *p*-$MeC_6H_4OSO_2$) (4.10 g, 8.62 mmol) [14] in dichloromethane (30 mL) was heated to reflux for 60 minutes, after which the solvent was removed and the dark brown residue was extracted with several 50 mL portions of *n*-hexane. The solvent was removed again and the oily residue was separated by column chromatography (10 × 5 cm column, Kieselgel 60 (Merck), solvent *n*-hexane). The product was eluted first as a yellow band. The yellow solid that remained after solvent removal was recrystallized from diethyl ether at 0 °C. This resulted in colorless rod-shaped crystals, which melted under decomposition at about 60 °C. Yield: 0.7 g (25%). Correct elemental analyses for C, H, and N. IR (KBr): ν[cm^{-1}] = 2235 s, 2020 s, 1941 vs, ^1H NMR (250 MHz, $CDCl_3$, 25 °C): δ = 7.45 (m, Ph); $^{13}C\{^1H\}$ NMR (62.9 MHz, $CDCl_3$, 25 °C): δ = 54.7 (α-C), 70.6 (β-C), 119.4, 128.6, 129.9, 132.9 (Ph), 174.4 (C≡N), 213.3 (CO_{eq}), 213.8 (CO_{ax}).

5a, 5b: These compounds were prepared as described for **4** from $NEt_4[Cr(CN)(CO)_5]$ (2.00 g, 5.75 mmol) and $[Me_3SiC{\equiv}ClPh]BF_4$ (2.23 g, 5.75 mmol) [15]. The chromatographic separation (same conditions as for **4**) yielded two fractions. The first fraction contained 0.3 g of **5a** (17% yield, m.p. 42 °C (decomp)). IR (KBr): ν[cm^{-1}] = 2215 s, 2162 s, 2094 s, 2029 s, 1941 s, 1250 s, 850 s; ^1H NMR (250 MHz, $CDCl_3$, 25 °C): δ = 0.25 (s, $SiMe_3$); $^{13}C\{^1H\}$ NMR (62.9 MHz, $CDCl_3$, 25 °C): δ = −1.02 ($SiMe_3$), 30.0, 60.3 (C≡C), 171.6 (C≡N), 213.1 (CO_{eq}), 213.3 (CO_{ax}). The second fraction contained 0.2 g of **5b** (14% yield). Both compounds gave correct elemental analyses for C, H, and N.

5b: This compound was obtained in the same manner as **4** from $NEt_4[Cr(CN)(CO)_5]$ (2.00 g, 5.75 mmol) and [HC≡ClPh]OTf (2.17 g, 5.75 mmol) [16]. After the chromatographic separation (same conditions as for **4**), complex **5b** was obtained in 29% yield; m.p. ≈ 30 °C (decomp). IR (polyoil): ν[cm^{-1}] = 3315 m, 2187 s, 2089 s, 2011 s, 1973 vs. $^{13}C\{^1H\}$ NMR (62.9 MHz, $CDCl_3$, 25 °C): δ = 44.9 (α-C), 63.5 (β-C), 174.2 (C≡N), 213.6 (CO_{ax} + CO_{eq}).

5b′: IR (polyoil): ν[cm^{-1}] = 3314 m, 2087 s, 2011 s, 1975 vs, 1962 vs.

6a: This compound was prepared as described for **4** from $NEt_4[Cr(CN)(CO)_5]$ (2.00 g, 5.75 mmol) and [*t*BuC≡ClPh]BF_4 (2.66 g, 5.75 mmol) [17]. The chromatographic separation (same conditions as for **4**) and subsequent workup afforded 0.4 g (23%) of product. Colorless crystals in the form of platelets were obtained from toluene at room temperature: m.p. 65 °C. IR (KBr): ν[cm^{-1}] = 2137 s, 2060 s, 1921 vs. ^1H NMR (250 MHz, $CDCl_3$, 25 °C): δ = 1.28 (s, 6H, Me), 2.16 (s, 2H, CH_2), 5.8 (s, 1H, CH); ^{13}C NMR (62.9 MHz, $CDCl_3$, 25 °C): δ = 23.5 (Me), 39.8 (CMe_2), 48.9 (CH_2), 125.4 (α-C), 130.2 (β-C), 174.8 (C≡N), 214.3 (CO_{eq}), 216.4 (CO_{ax}).

Received: September 7, 1993 [Z 6347 IE]
German version: *Angew. Chem.* **1994**, *106*, 331

[1] a) R. B. King, *Inorg. Chem.* **1967**, *6*, 25; b) J. F. Guttenberger, *Chem. Ber.* **1968**, *101*, 403; c) G. Winnewisser, *Top. Curr. Chem.* **1989**, *99*, 39.

[2] a) W. P. Fehlhammer, P. Baraças, K. Bartel, *Angew. Chem.* **1977**, *89*, 752; *Angew. Chem. Int. Ed. Engl.* **1977**, *16*, 707; b) B. Weinberger, G. Zinner, W. P. Fehlhammer in *Organometallic Syntheses, Vol. 4* (Eds.: R. B. King, J. J. Eisch), Elsevier, Amsterdam, **1988**, 87.

[3] G. Christian, H. Stolzenberg, W. P. Fehlhammer, *J. Chem. Soc. Chem. Commun.* **1982**, 184.
[4] W. P. Fehlhammer, M. Fritz, *Chem. Rev.* **1993**, *93*, 1243.
[5] a) W. P. Fehlhammer, F. Degel, *Angew. Chem.* **1979**, *91*, 80; *Angew. Chem. Int. Ed. Engl.* **1979**, *18*, 75; b) W. P. Fehlhammer, F. Degel, G. Beck, *Chem. Ber.* **1987**, *120*, 461.
[6] a) W. P. Fehlhammer, G. Beck, *Angew. Chem.* **1988**, *100*, 1391; *Angew. Chem. Int. Ed. Engl.* **1988**, *27*, 1344; b) *J. Organomet. Chem.* **1989**, *369*, 105; c) *Chem. Ber.* **1989**, *122*, 1907; d) *Z. Naturforsch. B* **1989**, *44*, 1414; e) W. P. Fehlhammer, S. Ahn, G. Beck, *J. Organomet. Chem.* **1991**, *411*, 181; f) S. Ahn, G. Beck, W. P. Fehlhammer, *ibid.* **1991**, *418*, 365.
[7] W. P. Fehlhammer, G. Beck, *J. Organomet. Chem.* **1989**, *379*, 97.
[8] M. Krüger, H. Dreizler, D. Preugschat, D. Lentz, *Angew. Chem.* **1991**, *103*, 1674; *Angew. Chem. Int. Ed. Engl.* **1991**, *30*, 1644.
[9] a) P. J. Stang, *Angew. Chem.* **1992**, *104*, 281; *Angew. Chem. Int. Ed. Engl.* **1992**, *31*, 274; b) M. Ochiai, M. Kunishima, Y. Nagao, K. Fuji, M. Shiro, E. Fujita, *J. Am. Chem. Soc.* **1986**, *108*, 8281.
[10] First applications of this reagent in organometallic chemistry have recently been reported by Stang et al.: a) P. J. Stang, C. M. Crittel, *Organometallics* **1990**, *9*, 3191; b) P. J. Stang, R. Tykwinski, *J. Am. Chem. Soc.* **1992**, *114*, 4411.
[11] Alkylethynyliodonium salts with longer chains, such as $[n\mathrm{Pr{-}C{\equiv}ClPh}]^+\ X^-$ and $[n\mathrm{Dec{-}C{\equiv}ClPh}]^+\ X^-$ react with cyanometalates to yield 1-cyclopentenyl isocyanide complexes, that is, in **3** carbene insertion occurs into a γ-C-H bond of the alkyl side chain.
[12] **7**: MS (80 eV): *m/z* 461 [M^+], 433 [$M^+ - \mathrm{CO}$], 405 [$M^+ - 2\mathrm{CO}$], 377 [$M^+ - 3\mathrm{CO}$], 349 [$M^+ - 4\mathrm{CO}$], 321 [$M^+ - 5\mathrm{CO}$], 194 [$M^+ - 5\mathrm{CO} - \mathrm{I}$]; IR(KBr): $\tilde{\nu}$[cm^{-1}] = 2120m (CN), 2055m, 1930vs (CO) [E].
[13] Crystallographic data for **4** (**6a**): STOE four-circle diffractometer, $\lambda(\mathrm{Mo_{K\alpha}}) = 0.71073$ Å, $\mu(\mathrm{Mo_{K\alpha}}) = 8.40$ (8.84) cm^{-1}, $A_{max}/A_{min} = 1.123/0.999$ (1.230/0.858), 2θ range $4 \le 2\theta \le 50°$, temperature -60 (+20) °C, ω scans; structure solution by Patterson method (direct methods). All H atoms were located. Refinement: Method of least squares, H atoms isotropic, maximum residual electron density 0.425 (0.355) eÅ^{-3}. Programs used were XTAL 3.0, SHELX-76, ORTEP, DIFABS. Further details of the crystal structure investigation may be obtained from the Fachinformationszentrum Karlsruhe, D-76344 Eggenstein-Leopoldshafen (FRG) on quoting the depository number CSD-57757, the names of the authors, and the journal citation.
[14] L. Rebrovic, G. F. Koser, *J. Org. Chem.* **1984**, *49*, 4700.
[15] M. Ochiai, T. Ito, Y. Takaoka, Y. Masaki, M. Kunishima, S. Tani, Y. Nagao, *J. Chem. Soc. Chem. Commun.* **1990**, 118.
[16] P. J. Stang, A. M. Arif, C. M. Crittell, *Angew. Chem.* **1990**, *102*, 307; *Angew. Chem. Int. Ed. Engl.* **1990**, *29*, 287.
[17] M. Ochiai, M. Kunishima, Y. Nagao, K. Fuji, E. Fujita, *J. Chem. Soc. Chem. Commun.* **1987**, 1708.

FAST NOESY Experiments— An Approach for Fast Structure Determination**

Matthias Köck and Christian Griesinger*

The determination of cross-relaxation rates by NMR spectroscopic methods[1] provides interproton distances. Two-dimensional experiments like NOESY[2] and ROESY[3] (Fig. 1) are gradually taking the place of classical one-dimensional saturation NOE experiments, since they allow the simultaneous measurement of all interproton distances in a molecule, irrespective of their number. Long longitudinal relaxation times (T_1) often determine the total measurement time. Normally, the relaxation delay between consecutive scans is on the order of two to three times the relaxation time of those protons with the longest T_1 values.[4] For molecules in the extreme narrowing limit (molecular weight below 500 D), in particular, the relaxation delay constitutes the major part of the entire measurement time. In this communication we introduce a post-processing procedure for NOESY and ROESY spectra allowing the acquisition time to be shortened with a marginal loss in the signal-to-noise ratio and the accuracy of the integration of the cross-relaxation peaks. A similar procedure was described for the accelerated measurement of heteronuclear T_1 values in 1975.[4]

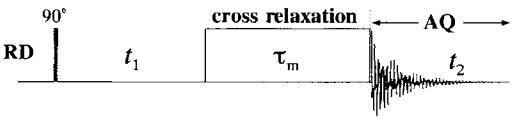
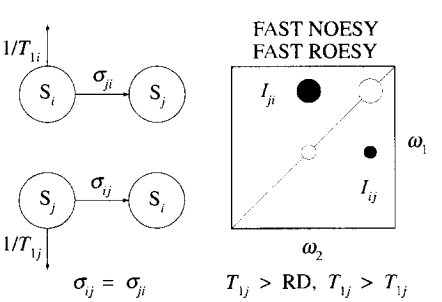


Fig. 1. Pulse sequence of NOESY and ROESY experiments with relaxation delay RD, mixing time τ_m, and acquisition time AQ = t_2(max).

NOESY and ROESY spectra contain cross peaks whose integrals reflect the cross-relaxation rate between magnetically active nuclei in the initial rate approximation.[5] The cross-relaxation rates depend on the correlation time τ_c and the distance r between the interacting nuclei according to r^{-6}. However, this relation only holds if the spin system relaxes back to thermal equilibrium after each scan. An exact solution for incomplete relaxation between scans in a FAST NOESY experiment can be obtained from the Liouville-von-Neumann equation.[1a, 6] The integral of the cross-peak between spin i and j (I_{ij}^F) is dependent on the relaxation delay (RD) between scans, the mixing time τ_m, the acquisition time AQ, and the relaxation matrix $\boldsymbol{\Gamma}$ as given in [Eq. (a)].

$$I_{ij}^F = [\exp(-\boldsymbol{\Gamma}\tau_m)]_{ij} \sum_{k=1}^{N} [\mathbf{1} - \exp(-\boldsymbol{\Gamma}(\mathrm{RD} + \mathrm{AQ})]_{jk} = I_{ij} \sum_{k=1}^{N} [\mathbf{1} - \exp(-\boldsymbol{\Gamma}(\mathrm{RD} + \mathrm{AQ})]_{jk} \quad \text{(a)}$$

The first factor I_{ij} is due to the cross relaxation during the mixing time τ_m, and the second is due to the relaxation to thermal equilibrium during the relaxation delay and the acquisition time. When the T_1 value of a proton is approximately equal or longer than RD + AQ, the integrals in the NOESY are too small owing to incomplete relaxation. The second term in Equation (a) is asymmetric with respect to the permutation of spins i and j, in contrast to the first term I_{ij}. Therefore the cross-peak integrals in NOESY and ROESY spectra above and below the diagonal can be different for short recovery delays (Scheme 1).



Scheme 1. Representation of the cross relaxation σ between spins S_i and S_j. Despite the identity of the cross-relaxation rates σ_{ij} and σ_{ji}, asymmetric NOESY and ROESY spectra result for short recovery delays when the T_1 values of the spins S_i and S_j are different.

This asymmetry is most notable for nuclei with strongly differing T_1 values. This effect has prevented the recording of NOESY spectra with short recovery delays.[7]

[*] Prof. Dr. C. Griesinger, Dr. M. Köck
Institut für Organische Chemie der Universität
Marie-Curie-Strasse 11, D-60439 Frankfurt (FRG)
Telefax: Int. code + (69)5800-9128

[**] This work was supported by the Fonds der Chemischen Industrie. We thank Dr. M. Reggelin for discussion and V. Apelt and O. Schedletzky for support in preparing Figure 3. M. K. thanks the Deutsche Forschungsgemeinschaft and the Fonds der Chemischen Industrie for postdoc grants.

An exact compensation for incomplete relaxation including the effects of spin diffusion by complete relaxation matrix approaches[8] in FAST NOESY will be presented elsewhere.[9] Here we describe a procedure that allows the cross-peak integrals, I_{ij}, of a NOESY spectrum with full relaxation to be obtained from the cross-peak integrals of a FAST NOESY experiment, I_{ij}^{F}. For small molecules the diagonal elements of the relaxation matrix Γ determine the T_1 values. Therefore the multiexponential relaxation $\sum_{k=1}^{N}[\mathbb{1}-\exp(-\Gamma(\mathrm{RD}+\mathrm{AQ})]_{j,k}$ can be simplified to Equation (b).

$$\sum_{k=1}^{N}[\mathbb{1}-\exp(-\Gamma(\mathrm{RD}+\mathrm{AQ})]_{jk}=\mathbb{1}-\exp(-(\mathrm{RD}+\mathrm{AQ})/T_{1j}) \qquad \text{(b)}$$

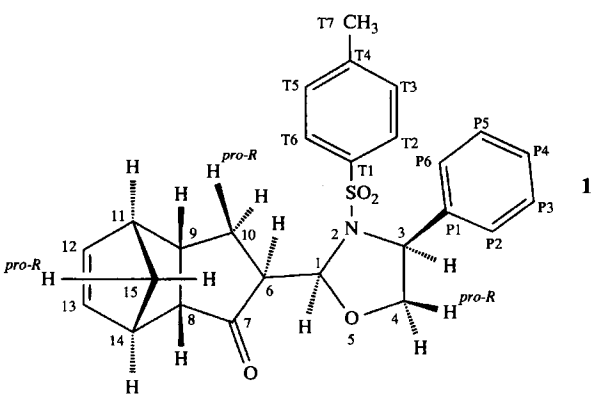
The T_{1j} values of the protons must be determined by Inversion–Recovery before the 2D cross-relaxation experiment is recorded (Table 1). The evaluation of all T_1 values requires a resolved 1D NMR spectrum.

Table 1. T_1 relaxation times for the protons in compound **1** [a].

Proton	T_1	Proton	T_1
1	1.684 (<0.1%)	12	2.533 (<0.1%)
3	1.724 (<0.1%)	13	3.041(<0.1%)
$4^{pro\text{-}R}$	0.782 (0.2%)	14	2.070 (<0.1%)
$4^{pro\text{-}S}$	0.665 (1.6%)	$15^{pro\text{-}R}$	0.758 (0.1%)
6,8	1.593 (0.1%)	$15^{pro\text{-}S}$	0.611 (1.8%)
9	1.064 (0.1%)	P2-P6, T3, T5	3.200 (<0.1%)
$10^{pro\text{-}R}$	0.598 (0.9%)	T2, T6	2.375 (<0.1%)
$10^{pro\text{-}S}$	0.603 (0.8%)	T7	1.184 (0.5%)
11	1.794 (0.2%)		

[a] The assignment of the protons is shown in Scheme 2. The T_1 relaxation times are given in s, the statistical errors in parentheses. The Inversion–Recovery experiment was recorded with 79 different recovery delays and evaluated with the T_1 routine of the Bruker UXNMR program.

We demonstrate this procedure on a complex organic micromolecule (**1**, molecular weight 450 D, Scheme 2) with positive NOEs.[10] A series of NOESY spectra at 400 MHz with relaxation delays of 5.0, 3.0, 1.5, 1.0, 0.75, 0.5, and 0.25 s were recorded. The measurements were performed at a temperature of 300 K in $CDCl_3$ with AQ = 0.53 s and τ_m = 0.5 s.[11] This mixing time is still in the linear region of the NOE build-up (cf. ref. [10]).



Scheme 2. Structure of **1**.

Figure 2 shows sections of NOESY spectra with the cross peaks between H-12/H-13 and H-$15^{pro\text{-}R}$/H-$10^{pro\text{-}S}$. For RD = 5 s (Fig. 2a, b) the cross-peak integrals above and below the diagonal of the NOESY spectrum are almost identical; for RD = 0.25 s (Fig. 2c, d) they differ by up to a factor of 3. Above the diagonal (Fig. 2a, c) the cross-peak integrals remain almost unchanged for RD = 5 s and RD = 0.25 s, because the T_1 values of the protons H-$10^{pro\text{-}S}$ and H-$15^{pro\text{-}R}$ are smaller or equal to RD + AQ (see Table 1).

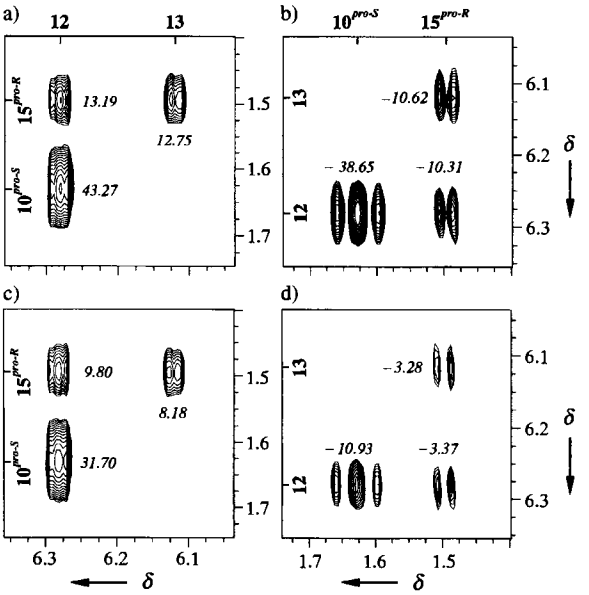


Fig. 2. Cross peaks in NOESY (a and b, RD = 5 s) and FAST NOESY spectra (c and d, RD = 0.25 s) between H-12/H-13 and H-$15^{pro\text{-}R}$/H-$10^{pro\text{-}S}$ above (a and c) and below (b and d) the diagonal. The integrals of the cross peaks are given in italics.

Figure 3a shows a statistical evaluation of the integrals as a function of the relaxation delay RD: $I_{ij}^{F}(\mathrm{RD})/I_{ij}(\mathrm{RD}=5\ \mathrm{s})$. The systematic error of the integrals obtained from the FAST NOESY experiments relative to those obtained from the experiment with RD = 5 s is dramatic, especially for the very short recovery times.

$$I_{ij}=I_{ij}^{F}/[1\text{-}\exp(-(\mathrm{RD}+\mathrm{AQ})/T_{1j})] \qquad \text{(c)}$$

Compensation of the integrals in the FAST NOESY experiment according to Equation (c) provides the integrals, I_{ij}, of an NOESY experiment with full relaxation. This is demonstrated in Figure 3b by a statistical evaluation of the ratio between the compensated integrals from the FAST NOESY and the integrals from the NOESY experiment with RD = 5 s. The ratios are centered around 1 as expected. This is even true for the experiment with RD = 0.25 s, which had a relaxation delay 20 times shorter than the reference experiment (RD = 5 s). The interproton distances obtained from the uncorrected FAST NOESY integrals I_{ij}^{F} deviate from the values obtained from the NOESY spectrum by up to 15%. With compensation for incomplete relaxation, the interproton distances obtained from the FAST NOESY are similar to those obtained from the fully relaxed NOESY to within ±2%.

The acquisition time for NOESY and ROESY experiments can be reduced by a factor of 5 to 10, and the determination of interproton distances is almost as accurate as that based on an NOE spectrum with full relaxation. This allows spectrometer

 © VCH Verlagsgesellschaft mbH, D-69451 Weinheim, 1994 0570-0833/94/0303-0333 $ 10.00+.25/0

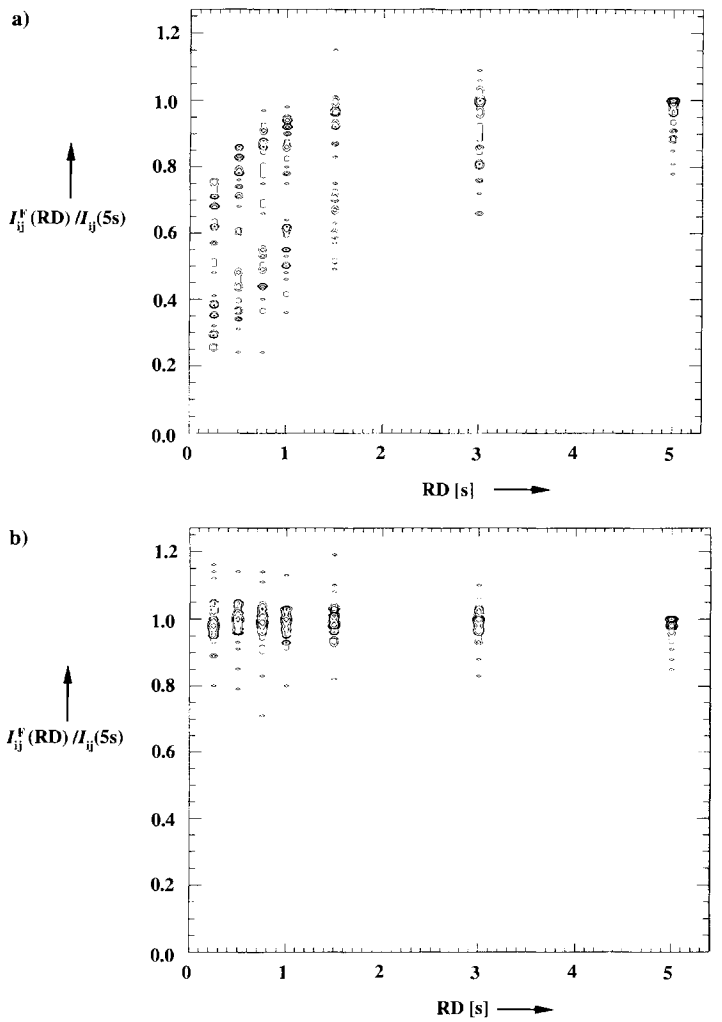


Fig. 3. a) Integral ratios for the cross peaks of **1** obtained from a FAST NOESY, I_{ij}^{I}, (RD) and from a NOESY experiment, I_{ij}, (RD = 5 s) in percent. A contour representation with a factor of 2 for the level spacing was chosen to indicate the number of integral ratios within a given range of percentage. If a value of $I_{ij}^{I}(RD)/I_{ij}(5\ s)$ occurs only once, it is represented by one contour line. If it occurs n times it is represented by trunc($\lg_2 n$) contour lines. Only those 46 cross peaks were evaluated that showed no overlap in the NOESY and whose T_1 values could be determined in the 1D spectrum. The integrals obtained from the FAST NOESY experiments are reduced to 1/5 of those from the fully relaxed NOESY. This corresponds to an error in distance of up to ± 15%. b) Same representation as in a) but with compensation of incomplete relaxation during RD + AQ according to Equation (c). The deviations of the integrals obtained from the FAST NOESY are reduced to ±10%, which corresponds to an error in distances of ±2%.

time to be used much more effectively and reduces the time for the structure determination. If the recovery delay (RD + AQ) approaches or is smaller than the transverse relaxation times T_2, B_0 spoil gradients should be used during the relaxation delay RD.

Received: August 16, 1993 [Z 6287 IE]
German version: *Angew. Chem.* **1994**, *106*, 338

[1] a) R. R. Ernst, G. Bodenhausen, A. Wokaun, *Principles of Nuclear Magnetic Resonance in One and Two Dimensions*, Clarendon, Oxford, **1987**; b) H. Kessler, M. Gehrke, C. Griesinger, *Angew. Chem.* **1988**, *100*, 507–554; *Angew. Chem. Int. Ed. Engl.* **1988**, *27*, 490–536.

[2] a) J. Jeener, B. H. Meier, P. Bachmann, R. R. Ernst, *J. Chem. Phys.* **1979**, *71*, 4546–4553; b) S. Macura, Y. Huang, D. Suter, R. R. Ernst, *J. Magn. Reson.* **1981**, *43*, 259–281.

[3] a) A. A. Bothner-By, R. L. Stephens, J. Lee, C. D. Warren, R. W. Jeanloz, *J. Am. Chem. Soc.* **1984**, *106*, 811–813; b) A. Bax, D. G. Davis, *J. Magn. Reson.* **1985**, *63*, 207–213; c) C. Griesinger, R. R. Ernst, *ibid.* **1987**, *75*, 261–271.

[4] D. Canet, G. C. Levy, I. R. Peat, *J. Magn. Reson.* **1975**, *18*, 199–204.

[5] D. Neuhaus, M. P. Williamson, *The Nuclear Overhauser Effect in Structural and Conformational Analysis*, VCH, New York, **1989**.

[6] J. Bremer, G. L. Mendz, W. J. Moore, *J. Am. Chem. Soc.* **1984**, *106*, 4691–4696.

[7] a) H. L. Eaton, N. H. Andersen, *J. Magn. Reson.* **1987**, *74*, 212–225; b) N. H. Andersen, H. L. Eaton, X. Lai, *Magn. Reson. Chem.* **1989**, *27*, 515–528.

[8] a) R. Boelens, T. M. G. Koning, R. Kaptein, *J. Mol. Struct.* **1988**, *173*, 299–311; b) R. Boelens, T. M. G. Koning, G. A. van der Marel, J. H. van Boom, R. Kaptein, *J. Magn. Reson.* **1989**, *82*, 290–308.

[9] M. Köck, C. Griesinger, lecture at the 5th Chianti Workshop on Magnetic Resonance, 1993, Pisa, Italy; a manuscript is in preparation.

[10] M. Reggelin, H. Hoffmann, M. Köck, D. F. Mierke, *J. Am. Chem. Soc.* **1992**, *114*, 3272–3277.

[11] The spectra were recorded with 16 scans, a spectral width of 3846.15 Hz, 384 real points in t_1 (TPPI) and 4096 points in t_2. TPPI was used in order to obtain pure phase spectra. Processing yielded a matrix of 1024 × 2048 points. Before Fourier transformation a squared cosine function was applied. A baseline correction with a fifth-grade polynomial was applied.

Small Molecules Stabilized in Inorganic Frameworks: NbI_5 Monomers in the Novel Layered Compound $Nb_7S_2I_{19}$**

Gordon J. Miller* and Jianhua Lin

Many types of inorganic extended solids can stabilize and, perhaps, "solubilize" molecular species that may not be thermodynamically stable in either the gaseous state or liquid solution. These extended structures can also serve as reaction templates (heterogeneous catalysts) for reactions that are otherwise kinetically unfeasible. Zeolites and clays are just two examples of a number of interesting materials with such applications, because they exhibit large channels or open layers for insertion of molecular entities.[1] We are presently investigating the possibilities of early transition metal cluster compounds,[2, 3] especially ternary niobium and tantalum chalcogenide halides, for such purposes.

When small molecules are introduced in a solid-state host, often the structure and, in particular, the topology of the host remains unchanged (except for shifts in lattice parameters) or undergoes small displacive transformations. Seldom does one observe major topological changes in the extended solid, although there may certainly be a synergistic relationship between the structures adopted by the extended framework and the enclosed molecule. In $Nb_7S_2I_{19}$ (more precisely $[Nb_3S_2I_7][NbI_5]$), we have found this type of structural synergism.

A (001) projection of the structure of $Nb_7S_2I_{19}$ is shown at the top of Figure 1.[4] This compound forms nearly level sheets composed of Nb_3 triangular clusters, according to the description $[NbS_{1/3}I_{1/3}I_{2/2}I_{2/2}]_3 \triangleq Nb_3SI_7$, which are stacked perpendicular to the monoclinic *ab* plane. In these layers, each Nb atom is octahedrally coordinated by one S and five I atoms, and these coordination polyhedra share faces to form a bicapped Nb_3 triangle with one S and one I atom as the capping atoms. The twofold capping leads to significantly shorter Nb–Nb dis-

[*] Prof. G. J. Miller, Dr. J. Lin
Department of Chemistry, Iowa State University
Ames, IA 50011 (USA)
Telefax: Int. code + (515) 294-0105

[**] This research was supported both by the Chemical Sciences Division, Office of Basic Energy Sciences, U.S. Department of Energy, under Contract D-7405-Eng-82 and the Donors of the Petroleum Research Fund, administered by the American Chemical Society. We thank Dr. L. Miller, Ames, for the resistivity and magnetic susceptibility measurements, and Prof. Dr. U. Müller for several suggestions.

tances (2.776(5) Å) within the cluster than those found in other binary and ternary niobium iodide phases containing monocapped Nb_3 clusters (ca. 3.00 Å).[7] The two-dimensional network forms through two intercluster bridging I atoms; in other words, the coordination polyhedra about each Nb atom in two adjacent clusters share an edge. The Nb–Nb distances between clusters average greater than 4.20 Å. This particular layered framework represents a new structural motif for M_3X_8 compounds[7] but cannot as yet be stabilized in the Nb-S-I system without any inserted species.

The other component in the structure of $Nb_7S_2I_{19}$ is a trigonal-bipyramidal monomer of NbI_5 (Fig. 1 bottom). These NbI_5 molecules pack between the Nb_3SI_7 layers within nearly hexagonal channels along the *c* axis (see Fig. 1 top). In the solid state, brass-colored NbI_5 has been reported to form complex chains of *cis*-vertex-sharing octahedra, $NbI_4I_{2/2}$,[8] which differ from the *trans*-edge-sharing octahedra in $NbCl_5$ and $NbBr_5$.[9, 10] However, since only the I positions and not the Nb positions were determined, another structure involving $(NbI_5)_2$ molecules is also possible.[11]

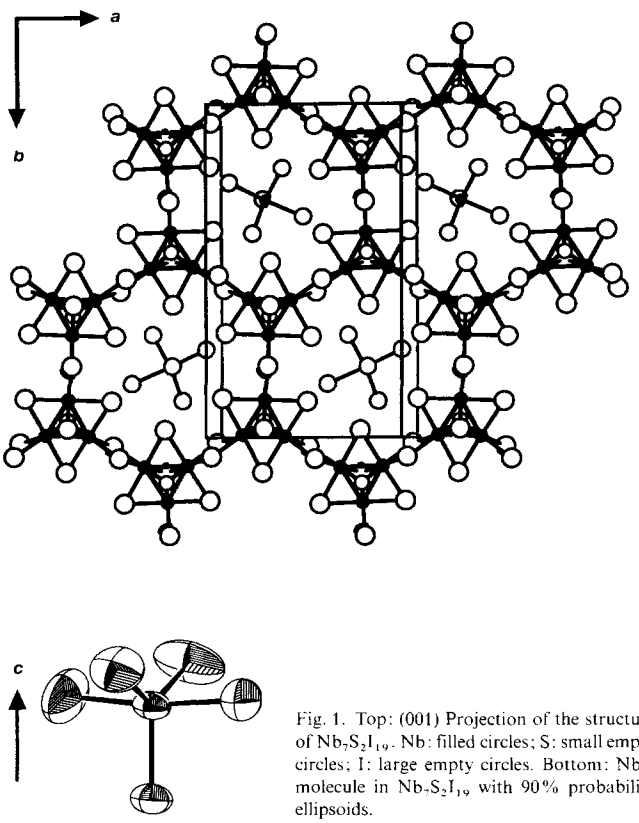


Fig. 1. Top: (001) Projection of the structure of $Nb_7S_2I_{19}$. Nb: filled circles; S: small empty circles; I: large empty circles. Bottom: NbI_5 molecule in $Nb_7S_2I_{19}$ with 90% probability ellipsoids.

Electron diffraction studies on the vapors of $NbCl_5$ and $NbBr_5$ indicate trigonal-bipyramidal structures,[12] but NbI_5 is thermally unstable, and decomposes into reduced niobium iodides.[13] To our knowledge, this is the first example of monomeric NbI_5 molecules in the solid state. The average Nb–I distance of 2.671(6) Å is consistent with a higher formal oxidation state for these Nb atoms than those in the $^2_\infty[Nb_3SI_7]$ framework ($d(Nb-I)_{av}$ = 2.780(5) Å). In addition, there is an excellent correlation between Nb–X distances (X = Cl,[9] Br,[10] I) in NbX_5 and the ionic radii of X^-.[14] A revised value of $r(Nb^{5+})$ based upon these data is 0.51 Å.

As evident in the upper structure in Figure 1, one example of structural synergism between the two-dimensional Nb_3SI_7 layer and the NbI_5 molecules is the formation of a monoclinic lattice, which is only slightly shifted from hexagonal symmetry. In the Nb_3SI_7 partial structure, simple electron counting assigns two valence electrons per Nb atom, which means that the six electrons suffice for three two-center, two-electron bonds in each Nb_3 triangle. Thus, the electronically neutral, two-dimensional layer corresponds to a closed-shell configuration, and adopts a structure that is nearly hexagonal. However, since one equatorial Nb–I bond in the NbI_5 unit is parallel to the stacking axis, the highest rotational symmetry allowed is a twofold axis. Furthermore, minimization of I···I nonbonding repulsions between the NbI_5 molecules and the two-dimensional framework precludes orthorhombic (*mmm*) symmetry and allows at most a monoclinic (2/*m*) lattice.

The structural hierarchy outlined in Scheme 1 gives further insights into the intricacies of the interactions between layer and molecule, and lends support to the twinning mechanism.[15]

Scheme 1.

$P6/m2/m2/m$ ← hypothetical Nb_3I_8
↓ *t*3
$C2/m2/m2/m$
↓ *k*2
$P2_1/m2_1/m2/n$ ← Nb_3SI_7 layer
↓ *k*2, *a*, *b*, 2*c*
$P2_1/c2_1/c2/n$ ← doubled *c* axis
↓ *t*2
$P12_1/c1$ ← $Nb_7S_2I_{19}$

The highest allowed symmetry group for the two-dimensional framework is $P6/mmm$ (a hypothetical Nb_3I_8). If S atoms replace I as the capping atoms of the Nb_3 clusters, an orthorhombic cell with symmetry $Pmmn$ and the metric relations $a_{ortho} = \sqrt{3}a_{hex}$, $b_{ortho} = a_{hex}$, $c_{ortho} = c_{hex}$ is obtained. Doubling along the *c* axis produces the subgroup $Pccn$, and then introducing the NbI_5 monomers such that one Nb–I_{eq} bond lies parallel to *c* lowers the symmetry of the space group to $P2_1/c$ by means of a *t*2 step. The resulting monoclinic cell is given in Scheme 2. Since there are two possible orientations of the trigonal bipyramid with respect to the mirror plane perpendicular to the a_{mono} axis, twinning results.

Scheme 2. The subscripts mono, ortho, and hex denote monoclinic, orthorhombic, and hexagonal, respectively.

$a_{mono} \approx b_{ortho} = a_{2,hex}$
$b_{mono} \approx a_{ortho} = 2a_{1,hex} - a_{2,hex}$
$c_{mono} \approx c_{ortho} = 2c_{hex}$

Calculations of the electronic structure[16] of $Nb_7S_2I_{19}$ reveal that Nb–Nb bonding interactions within each cluster are maximized and that the occupied levels are separated from the unoccupied levels by an energy gap of ca. 0.2 eV (Fig. 2). This result is confirmed by both the diamagnetic and semiconducting behavior of $Nb_7S_2I_{19}$. Nb 4d levels dominate the density of states (DOS) above −11 eV, and the effect of the octahedral ligand field is seen by the separation of Nb 4d orbitals into t_{2g} and e_g sets. Nb–Nb orbital overlap splits these states further, and the nature of this overlap is shown by the Nb–Nb crystal orbital overlap population (COOP) curve. In particular, the t_{2g} levels split into three distinct bands, which correspond to Nb–Nb bonding ($E \approx -10$ eV), nonbonding ($E \approx -9$ eV), and antibonding states ($E \approx -8$ eV). Just above the calculated Fermi level ($E_F = -9.4$ eV) we find Nb 4d levels from the NbI_5 mole-

 © VCH Verlagsgesellschaft mbH, D-69451 Weinheim, 1994 0570-0833/94/0303-0335 $ 10.00+.25/0

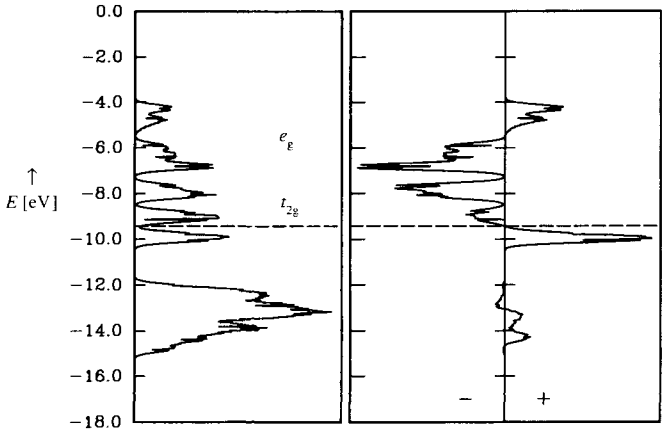


Fig. 2. Total density of states (left) and Nb–Nb overlap population (right) for $Nb_7S_2I_{19}$. (+): bonding Nb–Nb interactions; (−): antibonding Nb–Nb interactions. Dashed line indicates the Fermi level (highest occupied orbital), which occurs at a small energy gap (0.2 eV) in the DOS that is not completely visible on this scale.

cule, which indicates a d^0 configuration for these Nb atoms. If we compare these energies with those for a *trans*-vertex-sharing chain of NbI_6 octahedra,[8] which give rise to a broad Nb 4d band by significant through-bond coupling with the bridging I atoms, this band would overlap with the Nb–Nb bonding band in the Nb_3SI_7 layer. Our calculations strongly suggest, therefore, that the monomers form so as to optimize Nb–Nb interactions within the two-dimensional framework, but with little charge transfer between the two components. Thus, van der Waals and other London dispersion forces are the dominant interactions holding these two structural components together.

Similar calculations on the alternative structure of Nb_3SI_7 expected from earlier work on ternary Nb_3YX_7 compounds in this family[19] reveal that the bicapped Nb_3 cluster is energetically less favorable than the monocapped alternative.[20] All of our attempts to remove the NbI_5 molecules from $Nb_7S_2I_{19}$ have resulted in the formation of NbI_4, I_2, and the Nb_3SI_7 trigonal variant. Thus, a significant structural synergism exists between these two components, each of which is unstable with respect to either another structure (Nb_3SI_7) or towards decomposition (NbI_5), but are stabilized when they "cocondense."

Experimental Procedure

Elemental Nb (foil, Alfa; washed HF/HNO_3 and dried under vacuum), S, and I (sublimed; Alfa) in the molar ratio 7:2:19 were sealed under Ar in a quartz ampule ($\varnothing$ = 10 mm; l = 60 mm) and heated at 1100 K for 2 d. The product forms black, needle-shaped crystals. Chemical analysis with the Volhard method [21] gave I: 75.0% and S: 2.0%. Nb analysis (as Nb_2O_5) gave Nb: 20.2%. X-ray powder diffraction using an Enraf-Nonius Guinier camera indicates the phase $Nb_7S_2I_{19}$ is accompanied by a small amount of a hexagonal phase we identify as Nb_3SI_7 [19]. Magnetic susceptibility measurements show a small Curie–Weiss contribution (0.018 cm^3 K mol^{-1}) from a paramagnetic impurity. Two-probe electrical resistivity measurements indicated ρ(300 K) > 10^4 Ω cm.

Received: August 25, 1993 [Z 6316 IE]
German version: *Angew. Chem.* **1994**, *106*, 357

[1] a) *Inorganic Materials* (Eds.: D. W. Bruce, D. O'Hare), Wiley, Chichester, **1992**; b) D. O'Hare in [1a], p. 165; c) R. W. McCabe in [1a], p. 295.
[2] H. Schäfer, H. G. von Schnering, *Angew. Chem.* **1964**, *76*, 833.
[3] A. Simon, *Angew. Chem.* **1981**, *93*, 23; *Angew. Chem. Int. Ed. Engl.* **1981**, *20*, 1.
[4] Crystals of $Nb_7S_2I_{19}$ were always found as twins; space group $P2_1/c$ (No. 14), Z = 4, a = 1283.0(1), b = 2209.8(2), c = 1465.0(1) pm, β = 94.025(9)° (Siemens P4 diffractometer): $Mo_{K\alpha}$, 6659 unique reflections, 3366 reflections with $F_o^2 \geq 3\sigma(F_o^2)$. The structure was solved with direct methods (SHELXTL PLUS, [5]) and refined with the program SFLS [6] to R(aniso) = 0.054, R_w(aniso) = 0.058. The initial structural model found by direct methods [5] could be refined to $R \approx 0.10$. Systematic deviations occurred for reflections with $h = 6n$, which allowed us to elucidate a twin-law involving planes perpendicular to the monoclinic a axis [6]. The resulting effect produces small but significant shifts in the stacking pattern of the two-dimensional layers along the c direction. Further details of the crystal structure investigation may be obtained from the Fachinformationszentrum Karlsruhe, D-76344 Eggenstein-Leopoldshafen (FRG), on quoting the depository number CSD-57736, the names of the authors, and the journal citation.
[5] SHELXTL-PLUS, Version 4.0, Siemens Industrial Automation, Inc., Madison, WI, USA.
[6] Program SFLS (modification of the program ORFLS): M. Eitel, H. Bärnighausen, Universität Karlsruhe.
[7] A. Simon, H. G. von Schnering, *J. Less-Common Met.* **1966**, *11*, 31.
[8] W. Littke, G. Brauer, *Z. Anorg. Allg. Chem.* **1963**, *325*, 122.
[9] A. Zalkin, D. E. Sands, *Acta Crystallogr.* **1958**, *11*, 615.
[10] α-$NbBr_5$: U. Müller, P. Klingelhöfer, *Z. Naturforsch. B* **1983**, *38*, 559; β-$NbBr_5$: W. Hönle, S. Furuseth, H. G. von Schnering, *ibid.* **1990**, *45*, 952.
[11] U. Müller, *Acta Crystallogr. Sect. A* **1978**, *34*, 256.
[12] H. A. Skinner, L. E. Sutton, *Trans. Faraday Soc.* **1940**, *36*, 668.
[13] J. H. Canterford, R. Colton, *Halides of the Second and Third Row Transition Metals*, Wiley-Interscience, London, **1968**, pp. 154, 161.
[14] L. Pauling, *The Nature of the Chemical Bond*, Cornell University Press, Ithaca, NY, USA, **1960**, p. 514.
[15] H. Bärnighausen, *MATCH* **1980**, *9*, 139; U. Müller, *Inorganic Structural Chemistry*, Wiley, New York, **1993**, p. 235.
[16] Extended-Hückel calculations using the tight-binding approximation: M. H. Whangbo, R. Hoffmann, R. B. Woodward, *Proc. R. Soc. London A* **1979**, *366*, 23. S and I parameters are from standard sources [17, 18], two sets of Nb parameters were obtained by charge iteration. Nb(1-6): ζ(5s) = 1.89, H_{ii}(5s) = −8.96 eV, ζ(5p9) = 1.85, H_{ii}(5p) = −4.99 eV, ζ_1(4d) = 4.08 (c_1 = 0.6401), ζ_2(4d) = 1.64 (c_1 = 0.5516), H_{ii}(4d) = −9.83 eV; Nb(7): same ζ-values as Nb(1-6), H_{ii}(5s) = −9.85 eV, H_{ii}(5p) = −5.68 eV, H_{ii}(4d) = −11.28 eV.
[17] S parameter: M. M. L. Chen, R. Hoffmann, *J. Am. Chem. Soc.* **1976**, *98*, 1647.
[18] I parameter: E. Canadell, O. Eisenstein, *Inorg. Chem.* **1983**, *22*, 2398.
[19] S. Furuseth, W. Hönle, G. Miller, H. G. von Schnering, *9th International Conference of Transition Elements, Abstracts*, The Royal Society of Chemistry, **1988**.
[20] B. E. Bursten, F. A. Cotton, M. B. Hall, R. C. Najjar, *Inorg. Chem.* **1982**, *21*, 302.
[21] *Treatise Analytical Chemistry, Part II, Vol. 7*, Interscience/Wiley, New York, **1961**, p. 401.

Enzymatic Hydrolysis of Hydrophilic Diethyleneglycol and Polyethyleneglycol Esters of Peptides and Glycopeptides by Lipases**

Horst Kunz,* Danuta Kowalczyk, Peter Braun, and Günther Braun

Dedicated to Professor Reinhard W. Hoffmann on the occasion of his 60th birthday

The esters of primary alcohols were used as protective groups for carboxyl groups quite early in peptide synthesis.[1] However, alkaline hydrolysis of these esters bears a high risk of racemization. In glycopeptide synthesis[2] with *O*-glycosyl-serine and -threonine derivatives the β elimination of the carbohydrate constitutes an additional problem.[3]

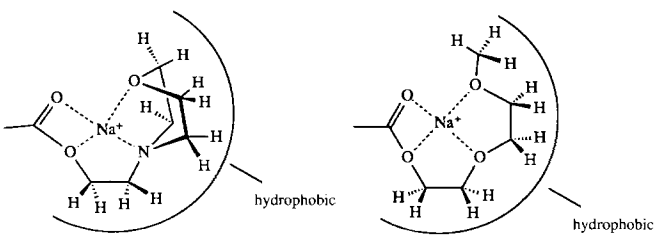
New perspectives open up with enzymatic methods that are carried out in neutral media,[4] as is shown by the selective hydrol-

[*] Prof. Dr. H. Kunz, Dipl.-Ing. D. Kowalczyk, Dipl.-Chem. P. Braun, Dr. G. Braun
Institut für Organische Chemie der Universität
J.-J.-Becher-Weg 18-20
D-55099 Mainz (FRG)
Telefax: Int. code + (6131)39-4786

[**] This work was supported by the Deutsche Forschungsgemeinschaft and the Fonds der Chemischen Industrie. We thank the Amano Pharmaceutical Co. for donating enzymes.

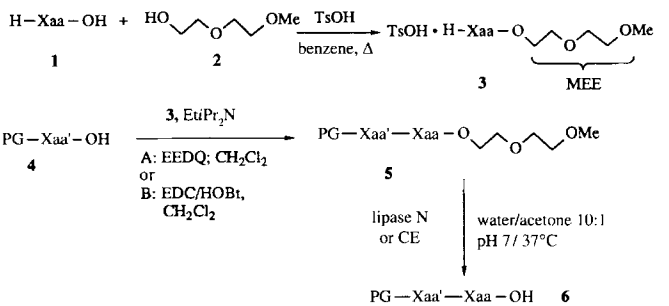
ysis of the heptyl esters of amino acids and peptides by lipases.[5] In peptide synthesis lipases have the advantage that they do not attack the peptide linkage. A limitation is the substrate selectivity of the enzymes; for example, the heptyl esters of hydrophobic dipeptides such as -Val-Phe- are attacked by lipases either very slowly or not at all.[5a] Similarly the heptyl esters of peptides with C-terminal proline,[5a] *O*-azidogalactosyl-threonine, or *O*-galactosaminyl-serine[5b] are not hydrolyzed by either lipase M (Amano) from *Mucor javanicus* or lipase N (Amano) from *Rhizopus niveus*. This lack of reactivity can be explained not only by the fact that the substrate structure is not suited to the active center of the enzyme, but also by simple physical factors such as the poor solubility and water-repelling properties of the heptyl ester in water. Heptyl[5] and similar alkyl esters were originally chosen for the reaction with lipases, since their hydrophobic properties simulate those of the natural substrates for these enzymes.[6] Many researchers have found that lipases incorporate the lipid boundary surface during the catalytic process.[7] Hence, it was generally accepted that compounds containing a polar region and a hydrophobic region provided suitable substrate properties for lipase-catalyzed hydrolysis.

During glycopeptide synthesis, however, we have observed that 2-morpholinoethyl esters (MoEt ester) of peptides, which do not contain any especially hydrophobic regions, are cleanly hydrolyzed by lipases.[8] This surprising result can be interpreted by postulating that complexation of the amphiphilic morpholino ester, for example with Na^+, causes the exposure of a hydrophobic surface which functions as a recognition region for the interaction with the lipase (Scheme 1).



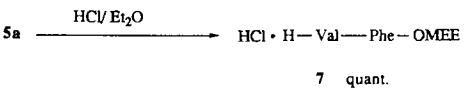
Scheme 1.

By generalizing this interpretation we came to the conclusion that diethyleneglycol esters as well as oligo- and polyethyleneglycol esters of amino acids and peptides ought to be enzymatically cleavable protective groups.[9] To test this hypothesis, the hydrotosylates of esters **3** (2-[2-methoxyethoxy]ethyl ester; MEE) were prepared from amino acids **1** and diethyleneglycol monomethyl ether **2** by azeotropic esterification. Esters **3** were formed almost quantitatively, but the products still contained traces of **2** after drying at 80 °C under high vacuum and washing with diethyl ether. The impure products were therefore converted into the protected dipeptide esters **5** by treatment with N-protected amino acids under the usual peptide condensation conditions. The enzymatic hydrolysis of the dipeptide MEE esters **5** was carried out in water/acetone (10:1) at 37 °C; the reaction mixture was maintained at pH 7 with 0.2 M sodium phosphate buffer solution. Lipase N (Amano) from *Rhizopus niveus* proved to be suitable. Only in the case of alanyl-proline MEE ester **5d** was it necessary to use lipase CE (Amano) from *Humicola lanuginosa* (Scheme 2 and Table 1).



Scheme 2. PG = protective group, EEDQ = ethyl 2-ethoxy-1,2-dihydroquinoline-1-carboxylate, EDC = 1-ethyl-3-(3-dimethylaminopropyl)carbodiimide, HOBt = 1-hydroxybenzotriazole.

The MEE esters are stable under the cleavage conditions for most N-terminal protective groups. For example the Boc group in **5a** can be removed quantitatively with HCl/diethyl ether without the MEE ester bond in **7** being attacked.



In accord with this stability and the favorable solubility of the amino acid and peptide MEE esters, peptide syntheses with these components can be conducted without complications (cf. the total yields of **5** for the two-step sequence in Table 1). In lipase-catalyzed hydrolyses the MEE esters have proved to be superior to all the other esters hitherto investigated.[4, 5, 8] Thus, the completely selective and practically quantitative hydrolysis of the MEE ester **5a** was achieved with lipase N (Amano), whereas the corresponding heptyl ester[5] did not react with any of the lipases investigated. It should be emphasized that even the proline-

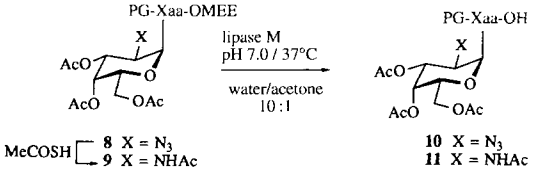
Table 1. Synthesis of amino acid MEE esters **3** from **1** and **2**, conversion of **3** with protected amino acids **4** to provide MEE esters, and the hydrolysis of **4** with lipases to give **6**.

PG	Xaa'	Xaa	Method [a]	5 [b]	Yield [%] [c]	$[\alpha]_D^{22}$ (*c* 1, $CHCl_3$)	Lipase	6	Yield [%] [d]	$[\alpha]_D^{22}$ [d] (*c* 1, MeOH)
Boc	Val	Phe	A	**5a**	71	23.3	N	**6a**	97	−14.3
Boc	Ser	Phe	A	**5b**	64	−6.6	N	**6b**	94	15.4
Tcoc [e]	Ala	Ser	A	**5c**	74	−3.4	N	**6c**	92	−1.0
Z	Ala	Pro	B	**5d**	50	−53.1	CE	**6d**	31	−33.1

[a] For A,B see Scheme 2. [b] Characteristic ^{1}H NMR signals of the MEE group: δ = 4.2 (m, 2H, $COOCH_2$), 3.7–3.4 (m, 6H, OCH_2), 3.3 (s, 3H, OCH_3). [c] Total yield for two steps. [d] The dicyclohexylammonium salt was isolated; its elemental analysis and 200 MHz ^{1}H NMR spectra are consistent with the proposed structure. [e] Tcoc = 2,2,2-trichloroethoxycarbonyl.

terminated MEE ester **5d** was hydrolyzed not with lipase N but with lipase CE (Amano). **5d** is the first proline ester for which a lipase hydrolysis has been found.

To test the MEE esters in glycopeptide syntheses, the *O*-glycosyl amino acid esters **8** were prepared from serine and threonine MEE esters by the introduction of Aloc,[10] Fmoc,[11] or Z protective groups by known literature methods, and subsequent glycosylation with 2-azido-2-deoxy-3,4,6-tri-*O*-acetyl-α-D-galactopyranosyl bromide[12] or ethyl-2-azido-2-deoxy-3,4,6-tri-*O*-acetyl-β-D-1-thiogalactoside.[13] Compounds **8** were converted



into their galactosamine conjugates (T_n-antigen) **9** with thioacetic acid. The MEE esters once again have more favorable properties than the corresponding heptyl and bromoethyl esters[4, 5] in lipase-catalyzed hydrolyses (Table 2).

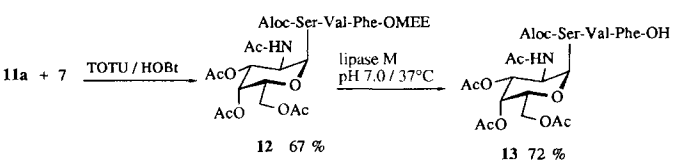
Table 2. Hydrolyses of *O*-glycosyl amino acid MEE esters **8** and **9** catalyzed by lipase M (Amano) from *Mucor javanicus* to give **10** and **11**.

Cmpd.	PG	Xaa	Product [a]	Yield [%]	$[\alpha]_D^{22}$ (*c* 0.5, MeOH)
8a	Aloc	Ser	**10a**	89	132.8
8b	Fmoc	Ser	**10b**	64	101.5
8c	Z	Thr	**10c**	5	–
9a	Aloc	Ser	**11a**	17	113.3 [b]
9b	Z	Thr	**11b**	18	94.4

[a] The products **10a**, **10b**, and **11b** were characterized by their correct elemental analyses and 400 MHz ^{1}H NMR spectra consistent with the proposed structures. [b] (*c* 1, $CHCl_3$).

The differently protected azidogalactosyl-serine MEE esters **8a** and **8b** were hydrolyzed smoothly with lipase M to give **10a** and **10b**, respectively. The corresponding threonine MEE ester **8c** reacted too slowly for preparative purposes. The acetamidogalactosyl-serine and -threonine MEE esters **9a** and **9b**, whose heptyl and bromoethyl ester analogues showed no reactivity with lipases, were hydrolyzed sufficiently fast to be useful. This reaction was not optimized further, since in the meantime it had been shown that glycosyl amino acid MEE esters can be effectively deblocked at the C-terminus with the protease papain.[15]

For glycopeptides whose saccharide side chains are not C-terminally located, and for which deblocking with papain is restricted because of its protease activity, the lipase-catalyzed cleavage of the MEE ester is quite efficient (Scheme 3). The T_n-antigen glycopeptide ester **12** prepared from **11a** and **7** by condensation

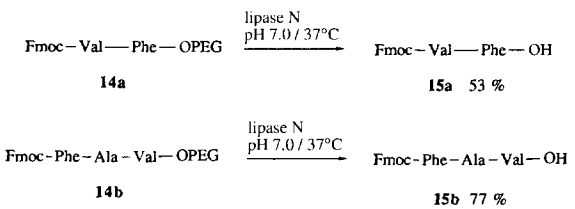


Scheme 3. TOTU = 2-[(ethoxycarbonylcyanomethylene)amino]-1,1,3,3-tetramethyluronium tetrafluoroborate[16].

with TOTU[16] was smoothly and selectively hydrolyzed to **13**.[17] The reaction was quantitative according to thin-layer chromatography. All other protective groups and the glycosidic bond remained untouched.

Encouraged by these results we have prepared the Fmoc-peptide polyethyleneglycol esters (PEG esters) **14** by the method of Mutter and Bayer[18] and hydrolyzed them with lipase N. The loading of the polyethyleneglycol in conjugate **14** was verified by calibration with Fmoc-Phe-OH. According to the first results, the highly hydrophilic peptide PEG esters were hydrolyzed by lipases in practically neutral media. The base-sensitive Fmoc group in **15** remained intact in the polymer-free peptide.

The results obtained in lipase-catalyzed hydrolysis of polar, solubilizing MEE and PEG esters open up new possibilities in both peptide and glycopeptide syntheses as well as syntheses on polymer-bound substrates. The lipases have no protease activity and do not attack peptide linkages. The MEE esters confer wettability and solubility in water and so ensure that the esters of hydrophobic peptide sequences will be hydrolyzable. Some of these polar peptide esters, for example **14a** and **14b**, form clear



solutions in water. Their hydrolysis (see above) brings into question the general validity of the postulate that lipases are only effective on heterogeneous surfaces.[19] The exposed hydrophobic surface resulting from complexation (see Scheme 1) is obviously sufficient for the formation of the enzyme–substrate complexes with lipases. Since the hydrolyses take place in neutral media, sensitive structural elements of the deblocked products, such as protective groups and glycosidic bonds, remain intact.

Experimental Procedure

General method for the hydrolysis of MEE esters: A solution of lipase N or CE (200 mg) in 0.2 M aqueous sodium phosphate buffer (2 mL; pH 7) was stirred with phenylmethylsulfonyl fluoride (PMSF; 3.5 mg) for 1 h at 0 °C to inhibit residual protease activity. After the addition of more sodium phosphate buffer solution (18 mL), the mixture was shaken at 37 °C for another 1 h. (With lipase M this preparatory treatment is not necessary.) A solution of peptide ester **5** (0.5 mmol) in acetone (2 mL) was added dropwise to 20 mL of the lipase solution prepared as above. The mixture was well shaken for 24 h at 37 °C. The solution was saturated with NaCl and extracted five times with ethyl acetate. The combined organic phases were dried over $MgSO_4$ and concentrated. The N-protected peptide **6** was obtained by flash chromatography (petroleum ether/ethyl acetate→ethyl acetate), dissolved in diethyl ether, and converted to its dicyclohexylammonium salt. The precipitated salt was pure according to its elemental analysis and 200 MHz ^{1}H NMR spectra.

Received: August 23, 1993
Revised version: October 26, 1993 [Z 6308 IE]
German version: *Angew. Chem.* **1994**, *106*, 393

[1] a) T. Curtius, F. Goebel, *J. Prakt. Chem. [2]* **1888**, *37*, 150; b) E. Fischer, *Ber. Dtsch. Chem. Ges.* **1906**, *39*, 2893.
[2] H. Kunz, *Pure Appl. Chem.* **1993**, *65*, 1223; *Antibiotics and Antiviral Compounds – Chemical Synthesis and Modifications* (Eds.: K. Krohn, H. Kirst, H. Maas), VCH, Weinheim, **1993**, p. 251.
[3] R. D. Marshall, A. Neuberger, *Adv. Carbohydr. Chem. Biochem.* **1970**, *25*, 407.
[4] A. Reidel, H. Waldmann, *J. Prakt. Chem.* **1993**, *335*, 109.
[5] a) P. Braun, H. Waldmann, W. Vogt, H. Kunz, *Liebigs Ann. Chem.* **1991**, 165; b) P. Braun, H. Waldmann, H. Kunz, *Synlett* **1992**, 39.

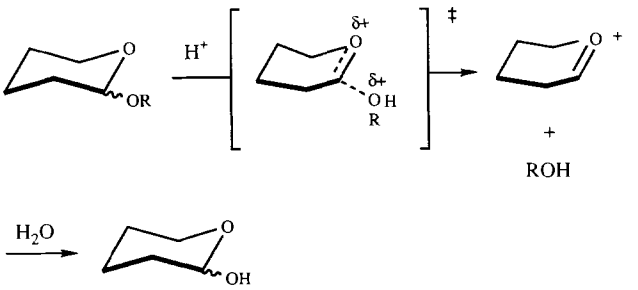
[6] J. B. West, C.-H. Wong, *Tetrahedron Lett.* **1987**, *28*, 1629.
[7] C.-S. Chen, C. J. Sih, *Angew. Chem.* **1989**, *101*, 711; *Angew. Chem. Int. Ed. Engl.* **1989**, *28*, 695, and references therein.
[8] G. Braum, P. Braun, D. Kowalczyk, H. Kunz, *Tetrahedron Lett.* **1993**, *34*, 3111.
[9] H. Kunz, G. Braum, P. Braun, (Hoechst AG), DE-A P 4133139.7 (7 Oct. 1991).
[10] H. Kunz, C. Unverzagt, *Angew. Chem.* **1984**, *96*, 426; *Angew. Chem. Int. Ed. Engl.* **1984**, *23*, 436.
[11] L. A. Carpino, G. Y. Han, *J. Am. Chem. Soc.* **1970**, *92*, 5748.
[12] H. Paulsen, J.-P. Hölck, *Carbohydr. Res.* **1982**, *109*, 89.
[13] H. Paulsen, M. Rauwald, U. Weichert, *Liebigs Ann. Chem.* **1988**, 75.
[14] T. Rosen, J. M. Lico, D. T. W. Chu, *J. Org. Chem.* **1988**, *53*, 1580.
[15] H. Kunz, P. Braun, unpublished.
[16] G. Breipohl, W. König (Hoechst AG), EP-A 0460446, A1 (23 May 1990).
[17] **13**: $[\alpha]_D^{22} = +71.3$ ($c = 1.2$, $CHCl_3$); $R_f = 0.33$ (ethyl acetate/methanol 2:1); ^{1}H NMR (200 MHz, $CDCl_3$, TMS): $\delta = 5.33-5.24$ (m, 2H, H-4, $-CH=CH_{2trans}$), 5.20 (dd, 1H, $J_{gem} = 1.0$ Hz, $J_{cis} = 10.4$ Hz, $-CH=CH_{2cis}$), 5.04 (dd, 1H, $J_{3,2} = 11.5$ Hz, $J_{3,4} = 2.9$ Hz, H-3), 4.80 (m, 1H, α-CH, Phe), 4.72 (d, 1H, $J_{1,2} = 3.2$ Hz, H-1), 0.82 (2d, 6H, CH_3, Val); FAB-MS (3-NOBA): *m/z*: 763.2 $(M-H)^-$ (calc. 763.2).
[18] a) M. Mutter, E. Bayer, *Angew. Chem.* **1974**, *86*, 101; *Angew. Chem. Int. Ed. Engl.* **1974**, *13*, 88; b) V. N. R. Pillai, M. Mutter, E. Bayer, I. Gatfield, *J. Org. Chem.* **1980**, *45*, 5364.
[19] H. L. Brockmann in *Lipases* (Eds.: B. Borgström, H. L. Brockmann), Elsevier, Amsterdam, **1984**, p. 3.

Progress toward an Antibody Glycosidase**

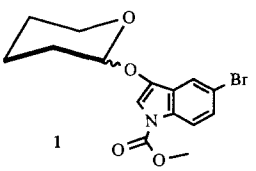
Jaehoon Yu, Linda C. Hsieh, Lynn Kochersperger, Shirlee Yonkovich, James C. Stephans, Mark A. Gallop,* and Peter G. Schultz*

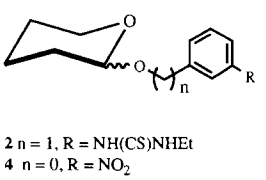
The development of catalysts for sequence-specific oligosaccharide cleavage would have a significant impact on the study of carbohydrate structure and function.[1] Catalytic antibodies may be particularly well-suited for this task, since antibody specificity may be programmed through hapten design. Mechanistic studies of enzymatic oligosaccharide hydrolysis suggest that a catalytic antibody combining site would need to stabilize the delocalized positive charge and/or the half-chair conformation of the high-energy oxocarbenium ion formed by acid-catalyzed leaving group expulsion [Eq. (a)].[2] As part of a program for generating glycosidase antibodies, we have elicited monoclonal antibodies against several transition state analogues for the hydrolysis of model acetal and glycoside substrates (**1**–**4**).

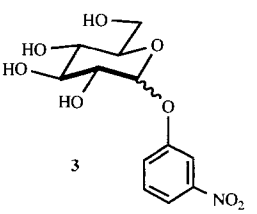
The design of hapten **5** is based on known cyclic amine glycosidase inhibitors such as nojirimycin and castanospermine.[3] The positively charged ammonium ion is expected to induce functional groups in the antibody combining site that stabilize the charge-

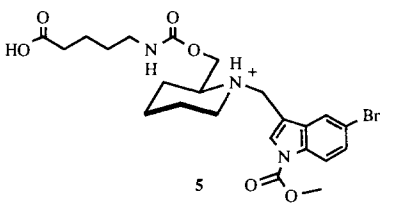


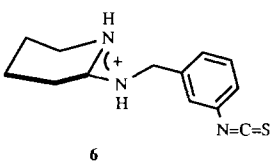
delocalized transition state in the hydrolysis of substrate **1** and/or assist in the acid-catalyzed expulsion of the leaving group. The 5-bromoindolyl leaving group, which is rapidly oxidized in air to form bromoindigo, provides a simple, direct assay of cell culture supernatants for catalytic activity, greatly facilitating the screening process during hybridoma production.[4] In addition, this group serves as a common recognition element between substrate and hapten to ensure substrate binding. Hapten **6** is based on the potent amidine-containing glycosidase inhibitors which are thought to mimic both the half-chair conformation and the positive charge of the high-energy oxocarbenium ion.[5] The less activated benzylic leaving group in substrate **2** ensures protonation of the amidine group in the corresponding hapten and provides the common recognition element. For comparison, antibodies were also raised against the D-galactal derivative **7**, a neutral analogue of the half-chair oxocarbenium ion intermediate formed in the hydrolysis of substrate **3**.[6]

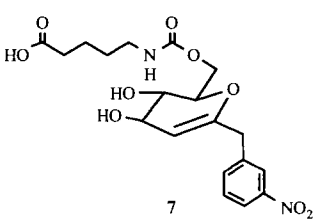












The first step in the synthesis of hapten **5** was formylation of 5-bromoindole with $POCl_3$ in dimethylformamide (DMF), followed by protection of the indole nitrogen with dimethyl pyrocarbonate. The formyl group was then converted to the corresponding primary bromide by sequential treatment with $NaBH_4$ and PPh_3/Br_2, and the resulting bromide was used to alkylate 2-hydroxymethylpiperidine. Derivatization of the primary hy-

[*] Prof. P. G. Schultz, L. C. Hsieh, J. C. Stephans
Department of Chemistry
University of California
and
Lawrence Berkeley Laboratory
Berkeley, CA 94720 (USA)
Telefax: Int. code + (510)642-8369
Dr. M. A. Gallop, Dr. J. Yu,[+1] Dr. L. Kochersperger, S. Yonkovich
Affymax Research Institute
4001 Miranda Avenue, Palo Alto, CA 94304 (USA)
[+] Present address:
Department of Chemistry,
Korea Institute of Technology
Seoul (Korea)

[**] This work was supported by the Office of Naval Research (Grant No. N00014-91-J-1130) and the Assistant Secretary for Conservation and Renewable Energy, Advanced Industrial Concepts Division of the U.S. Department of Energy (Contract No. DE-AC03-76SF00098). L. C. H. is supported by a National Science Foundation Graduate Fellowship. We thank Holly C. Wessling for her assistance.

droxyl group with methyl 5-isocyanovalerate and subsequent saponification afforded hapten **5**. Hapten **5** was linked to carrier proteins keyhole limpet hemocyanin (KLH) and bovine serum albumin (BSA) through an *N*-hydroxysuccinimide (NHS) ester.[7] Hapten **6** was synthesized by treatment of δ-valerothiolactam with *m*-nitrobenzylamine under anhydrous methanolic conditions.[5] After acidification, the nitro group was reduced with $H_2/Pd(OH)_2$ and the resulting amine treated with thiophosgene. Hapten **6** was coupled to KLH and BSA through thiourea linkages.[8] Hapten **7** was synthesized from the coupling reaction of 1-tributylstannyl-3,4,6-tri-*O*-*tert*-butyldimethylsilylglucal with *m*-nitrobenzyl bromide using a Pd^0 catalyst, followed by desilylation with tetrabutylammonium fluoride.[9] Treatment with methyl 5-isocyanovalerate as described above afforded hapten **7**, which was coupled to KLH and BSA.[10]

Balb/c mice were immunized with the KLH conjugates of haptens **5**–**7**, and monoclonal antibodies were obtained by standard protocols.[11] Twenty-eight hybridoma cell lines specific for hapten **5**, twenty-nine specific for hapten **6**, and sixty specific for hapten **7** were isolated.

Cell culture supernatants and crude ascites from cell lines producing antibodies against hapten **5** were directly assayed for hydrolytic activity by using substrate **1**.[12] Ten monoclonal antibodies showed activity in cell culture supernatants, and eight of these antibodies retained activity in ascites fluid. One antibody, AA71.17, was characterized in further detail after purification by protein A affinity chromatography and ion (MONO-S) exchange chromatography.[13] Hydrolysis of substrate **1** by antibody AA71.17 was monitored by reversed-phase high-performance liquid chromatography (RP-HPLC) and assayed in 10 mM 2-(*N*-morpholino)ethanesulfonic acid (MES) or *N*-(2-hydroxyethyl)piperazine-*N'*-3-propanesulfonic acid (EPPS) buffer at pH 5.5, 7.0, or 8.5 with the ionic strength adjusted to 100 mM NaCl.[14] The antibody-catalyzed hydrolysis showed saturation kinetics with $k_{cat} = 0.904\ h^{-1}$ and $K_M = 324\ \mu M$ (pH 5.5), corresponding to an apparent second-order rate constant of $2.3 \times 10^3\ M^{-1}h^{-1}$ (Fig. 1). For comparison, the second-order rate constant for the background hydrolysis of substrate **1** by the general acid, AcOH, was found to be $1.3 \times 10^{-1}\ M^{-1}h^{-1}$. The antibody reaction was competitively inhibited by hapten **5**, which is consistent with the reaction occurring in the antibody combining site. Dixon analysis with hapten **5** afforded a K_i of 35 μM. The k_{cat} and K_M values at pH 7.0 and 8.5 are $k_{cat} = 0.0913\ h^{-1}$, $K_M = 154\ \mu M$ and $k_{cat} = 1.00\ h^{-1}$, $K_M = 178\ \mu M$, respectively, demonstrating that the antibody reaction is both general acid and base catalyzed. The second-order rate constant for the hydrolysis of substrate **1** by AcO^- was determined to be less than $1.6 \times 10^{-2}\ M^{-1}h^{-1}$. Chemical modification of the antibody with diazoacetamide in the absence of hapten **5** showed a 33% reduction in catalytic activity relative to antibody modification in the presence of 2 mM hapten, suggesting some involvement of an active site carboxylate group.[15]

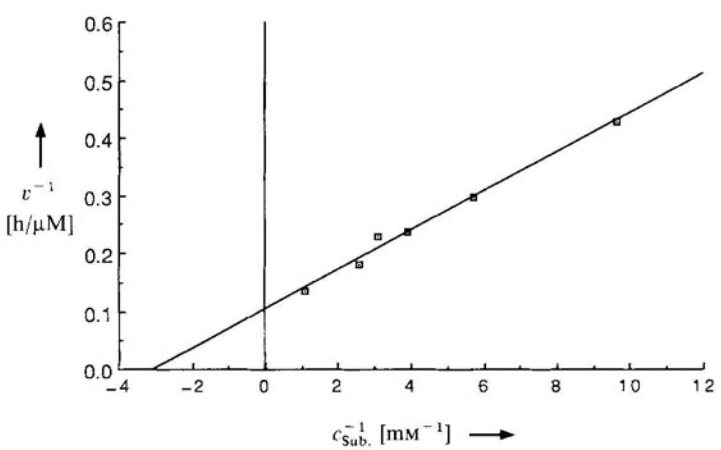


Fig. 1. Lineweaver–Burk plot for the hydrolysis of substrate **1** at pH 5.5 catalyzed by the antibody AA71.17. $c_{Sub.}$ = substrate concentration.

Twenty-nine antibodies specific for hapten **6** were purified to homogeneity as described above[13] and assayed for the ability to catalyze the hydrolysis of substrate **2** both in 50 mM MES, 50 mM NaCl, 0.02% NaN_3 at pH 5.5 and in 10 mM borate, 100 mM NaCl at pH 8.25.[16] These antibodies were also assayed using substrate **4** (pH 5.5 and 8.25), since hapten **6** might represent an "exploded" transition state analogue for the hydrolysis reaction.[16] No activity above the uncatalyzed rate was observed with either substrate. Sixty antibodies specific for hapten **7** were purified to homogeneity[13] and assayed for the ability to catalyze the hydrolysis of the α and β isomers of *m*-nitrophenyl-D-glucoside **3**.[17] Again, no activity above the uncatalyzed rate was observed.[18]

Both this study and recent work by Reymond et al. show that haptens containing a positive charge corresponding to the anomeric center of a cyclic acetal can elicit antibodies with hydrolytic activity.[19] However, two attempts to accommodate the half-chair transition state structure were unsuccessful. The absence of catalytic activity in the antibodies specific for haptens **6** and **7** may result from the fact that the planar structure of these haptens does not permit a favorable axial leaving group geometry in the corresponding substrates. In the case of hapten **7**, the difference in unsaturation compared to the oxocarbenium ion may also be significant.[20] Improvements in hapten design that better accommodate the transition state and leaving group structure should lead to antibody glycosidases. We are currently examining a number of five-membered aza sugars as haptens for oligosaccharide hydrolysis.

Received: September 20, 1993 [Z 6366 IE]
German version: *Angew. Chem.* **1994**, *106*, 327

[1] a) T. Feizi, R. A. Childs, *Trends Biochem. Sci.* **1985**, *10*, 24; b) F. A. Quiocho, *Annu. Rev. Biochem.* **1986**, *55*, 287; c) R. Kornfeld, S. Kornfeld, *ibid.* **1985**, *54*, 631; d) *Structural Glycoproteins in Cell Matrix Interactions* (Eds.: J. Labat-Robert, R. Timpl), Karger, New York, **1986**.

[2] a) M. L. Sinnot, *Chem. Rev.* **1990**, *90*, 1171; b) S. Rosenberg, J. F. Kirsch, *Biochemistry* **1981**, *20*, 3196; c) L. E. H. Smith, L. H. Mohr, M. A. Raftery, *J. Am. Chem. Soc.* **1973**, *95*, 7497; d) B. A. Malcolm, S. Rosenberg, M. J. Corey, J. S. Allen, A. de Baetselier, J. F. Kirsch, *Proc. Natl. Acad. Sci. USA* **1989**, *86*, 133.

[3] a) B. G. Winchester, I. Cenci di Bello, A. C. Richardson, R. J. Nash, L. E. Fellows, N. G. Ramsden, G. Fleet, *Biochem. J.* **1990**, *269*, 227; b) T. Kajimoto, K. K.-C. Liu, R. L. Pedersen, Z. Zhong, Y. Ichikawa, J. A. Porco, C.-H. Wong, *J. Am. Chem. Soc.* **1991**, *113*, 6187; c) G. Legler, *Biochim. Biophys. Acta* **1978**, *524*, 94.

[4] B. Gong, S. A. Lesley, P. G. Schultz, *J. Am. Chem. Soc.* **1992**, *114*, 1486.

[5] a) M. K. Tong, G. Papandreou, B. Ganem, *J. Am. Chem. Soc.* **1990**, *112*, 6137; b) B. Ganem, G. Papandreou, *ibid.* **1991**, *113*, 8964.

[6] Y. C. Lee, *Biochem. Biophys. Res. Commun.* **1969**, *35*, 161.

[7] **5**: ^{1}H NMR (300 MHz, [D$_6$]acetone, 25 °C): δ = 0.7–1.1 (m, 6H), 1.4–1.7 (m, 5H), 1.7–1.8 (m, 1H), 2.1–2.2 (m, 1H), 2.2–2.3 (t, ^3J(H,H) = 7 Hz, 2H), 3.1 (m, 4H), 3.4 (s, 3H), 3.7 (d, ^3J(H,H) = 9 Hz, 1H), 6.8 (m, 1H), 7.0 (s, 1H), 7.4 (m, 2H); ^{13}C NMR (75 MHz, [D$_6$]acetone, 25 °C): δ = 23.1, 24.2, 25.9, 26.0, 30.2, 34.3, 41.3, 49.6, 52.5, 54.4, 63.7, 64.2, 116.4, 117.3, 120.0, 124.0, 126.1, 127.9, 133.0, 135.8, 146.0, 158.9, 180.5; FAB$^+$-MS (high resolution): calcd. 447.1379 (M^+Na$^+$); found 447.1377. Epitope densities (E.D.) of 14 (KLH) and 15 (BSA) were determined by ultraviolet absorption (286 nm); protein concentrations were determined by the method of O. H. Lowry, N. J. Rosebrough, A. L. Farr, R. J. Randall (*J. Biol. Chem.* **1951**, *193*, 265).

[8] **6**: ^{1}H NMR (500 MHz, [D$_6$]dimethylsulfoxide): δ = 1.72 (m, 4H), 2.62 (m, 2H), 3.31 (m, 2H), 4.46 (d, ^3J(H,H) = 5.8 Hz, 2H), 7.36 (d, 1H, ^3J(H,H) = 7.5 Hz), 7.40 (d, ^3J(H,H) = 7.9 Hz, 2H), 7.45 (s, 1H), 7.47 (t, ^3J(H,H) = 7.8 Hz, 1H), 9.45 (br s, 1H), 9.55 (br s, 1H); ^{13}C NMR (125.73 MHz, [D$_6$]dimethylsulfoxide): δ = 17.83, 20.62, 26.26, 41.37, 49.47, 125.39, 130.45,

133.33, 134.47, 137.92, 163.27; IR ($CDCl_3$): $\tilde{\nu}$[cm^{-1}] = 2120 (N=C=S); FAB$^+$-MS (high resolution): calcd. 246.1065 (M^+); found 246.1063. Epitope densities at 276 nm (27 for KLH; 14 for BSA) and protein concentrations were determined as described above.

[9] J. M. Saa, G. Martorell, A. Garcia-Raso, *J. Org. Chem.* **1992**, *57*, 678.

[10] 7: ^{1}H NMR (300 MHz, CD_3OD): δ = 1.5–1.7 (m, 4H), 2.3 (t, ^3J(H,H) = 7 Hz, 2H), 3.1 (t, ^3J(H,H) = 7 Hz, 2H), 3.5 (s, 2H), 3.6 (m, 1H), 3.9–4.0 (m, 1H), 4.1–4.2 (m, 1H), 4.3–4.4 (m, 2H), 4.8 (d, ^3J(H,H) = 2 Hz, 1H), 7.6 (t, ^3J(H,H) = 7 Hz, 1H), 7.7 (d, ^3J(H,H) = 7 Hz, 1H), 8.1–8.2 (m, 2H); ^{13}C NMR (75 MHz, CD_3OD): δ = 24.1, 30.5, 36.7, 40.1, 41.5, 64.3, 70.5, 78.5, 102.1, 122.5, 124.6, 130.5, 136.4, 141.7, 149.7, 154.1, 158.9, 180.5; FAB$^+$-MS (high resolution): calcd. 381.0814 (MH^+); found 381.0819. E.D. (262 nm) = 25 (KLH) and 28 (BSA).

[11] a) B. A. L. Hurn, S. M. Chantler, *Methods Enzymol.* **1980**, *70*, 104; b) R. Sugasawara, C. Prato, J. Sipple, *Infect. Immun.* **1983**, *42*, 863; c) E. Engvall, P. Perlmann, *J. Immunol.* **1972**, *109*, 129.

[12] Substrate **1** was synthesized by coupling 1-acetyl-5-bromoindole with 2-chloropyran under basic conditions followed by deacylation and purification by RP-HPLC. Cell supernatants or ascites fluid were diluted with an equal volume of MES buffer (pH 5.5) containing 2 mM substrate and 20% (v/v) DMF. After incubation at 37 °C for 12 h, indigo color was observable.

[13] a) J. Jacobs, R. Sugasawara, M. Powell, P. G. Schultz, *J. Am. Chem. Soc.* **1987**, *109*, 2174; b) K. M. Shokat, *Dissertation*, University of California, Berkeley, CA, **1991**.

[14] Assays were initiated by adding a stock solution of substrate **1** in DMF to the antibody in the assay buffer at 37 °C (final antibody concentration 6.67 μM; 20% (v/v) DMF). Hydrolysis was monitored with a Microsorb C18 reversed-phase column (4.6 mm × 25 cm) using a 10–60% acetonitrile/water gradient and an internal standard (3-nitrobenzonitrile). Reaction velocities were measured at less than 10% conversion.

[15] A. L. Grossberg, D. Pressman, *J. Am. Chem. Soc.* **1960**, *82*, 5478.

[16] Substrates **2** and **4** were synthesized by condensing 3,4-dihydro-2*H*-pyran with *m*-nitrobenzyl alcohol and *m*-nitrophenol, respectively. Hydrogenation of the former product with palladium on carbon, followed by reaction with thiophosgene in the presence of Hünig's base produced the isothiocyanate. Reaction of the isothiocyanate with ethyl amine afforded substrate **2**. Assay conditions: 6.67 μM antibody, 250 μM substrate, 10% (v/v) CH_3CN in reaction buffer, 22 °C. Product formation was monitored by RP-HPLC as described with 2,4-dimethoxybenzamide as an internal standard.

[17] Substrate **3** was synthesized by condensing α-D-glucose pentaacetate with *m*-nitrophenol in the presence of a catalytic amount of $TiCl_4$ in CH_2Cl_2 at room temperature, followed by deacylation in K_2CO_3/CH_3OH. The ratio of anomers was 3:1 (α:β). Assay conditions: 6.67 μM antibody, 2.5 mM substrate, 10% (v/v) DMF. Product formation was monitored with a Microsorb phenyl column (4.6 mm × 15 cm).

[18] Enzyme-linked immunosorbent assays (ELISAs) with substrate–BSA conjugates indicated that 71 and 63% of the antibodies against haptens **6** and **7**, respectively were capable of binding their substrates.

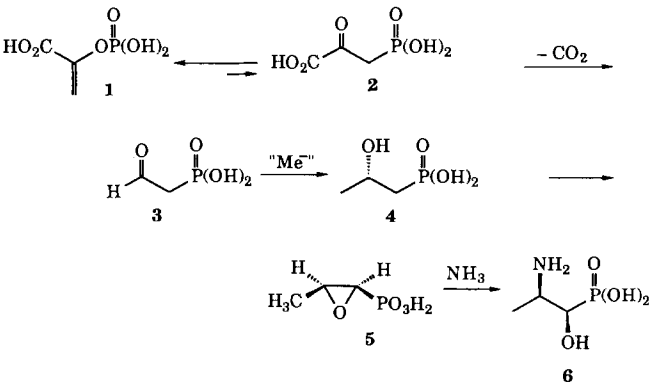
[19] J.-L. Reymond, K. D. Janda, R. A. Lerner, *Angew. Chem.* **1991**, *103*, 1690; *Angew. Chem. Int. Ed. Engl.* **1991**, *30*, 1711.

[20] D. F. Wentworth, R. Wolfenden, *Biochemistry* **1974**, *13*, 4715.

Incorporation of L-[Methyl-$^2H_3$]methionine and 2-[Hydroxy-^{18}O]hydroxyethylphosphonic Acid into Fosfomycin in *Streptomyces fradiae*—An Unusual Methyl Transfer

Friedrich Hammerschmidt*

Fosfomycin (**5**) is a clinically used antibiotic which belongs to the group of natural products with a P–C bond.[1] Its biosynthesis has two most interesting steps: the extension of a P–C_2 unit by a C_1 unit and the formation of an oxirane. The biogenesis of fosfomycin begins with the isomerization[2] of phosphoenolpyruvate (**1**) to give phosphonopyruvic acid (**2**), which presumably decarboxylates to afford phosphonoacetaldehyde (**3**),[3] which in turn is methylated to provide (*S*)-2-hydroxypropylphosphonic acid (**4**).[3–5] The latter is converted into fosfomycin (**5**); the oxirane oxygen originates from the hydroxyl group.[4] This paper provides further experimental evidence for the assumption previously made[6] that in the transformation of **3** into **4** a methyl group, formally CH_3^-, adds to the carbonyl carbon. There is no biosynthetic precedent for this step.[7]



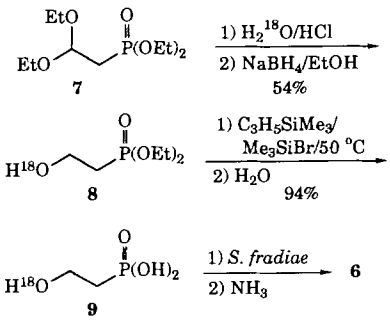
Both the methyl group[3] of [methyl-^{14}C]methionine and the 2-hydroxy[2,2-$^2H_2$]ethylphosphonic acid (cf. **9**)[6, 8] are incorporated into fosfomycin. The latter is incorporated with retention of one of the deuteriums via a postulated aldehyde intermediate,[5, 6, 8] which is indeed plausible in the general context of biosynthesis of natural products with a P–C bond. Umpolung of the C=O functionality via a thiamine pyrophosphate adduct must be ruled out. Hence, a feeding experiment with L-[methyl-$^2H_3$]methionine (300 mg L^{-1}) with *Streptomyces fradiae* was undertaken to determine whether the methyl group was transferred intact, that is, without replacement of any of the deuteriums by protium. The fosfomycin produced (8 mg L^{-1}) was transformed into the labeled 2-amino-1-hydroxypropylphosphonic acid (**6**),[9] which was easily isolated and analyzed by NMR spectroscopy. In the ^{1}H NMR spectrum (400.1 MHz, D_2O) the pattern of signals and their integration show that **6** consists of 19% unlabeled and 81% trideuteriated compound. This can be deduced from the sharp doublet (^3J(H,H) = 7.0 Hz) at δ = 1.54 for 3-H and from the triplet (^3J(P,H) = ^3J(H,H) = 5.0 Hz) at δ = 3.72 for 2-H. In the ^{13}C{^{1}H} NMR spectrum (100.6 MHz, D_2O, sodium 4,4-dimethyl-4-silapentanesulfonate (DSS)) this result is supported by satellite doublets (isotope-induced β and γ shifts)[10] upfield for C-1 (δ = 72.917, ^1J(P,C) = 155.0 Hz, $\Delta\delta$ = 0.04) and C-2 (δ = 53.314, ^2J(P,C) = 4.5 Hz, $\Delta\delta$ = 0.16) for the labeled compound. The presence of a mono- or a dideuteriated species must be ruled out, as in the ^{1}H NMR spectrum these would give rise to additional doublets for 3-H, which would be considerably broadened through coupling with either one or two deuterium atoms. Additional satellite doublets for C-2 in the ^{13}C NMR spectrum would also be expected. Thus, the methyl group is transferred intact.

In order to determine whether phosphonoacetaldehyde (**3**) itself or another, as yet unknown, compound serves as the acceptor for the methyl group, 2-[hydroxy-^{18}O]hydroxyethylphosphonic acid (**9**) was synthesized from acetal **7** and added to the growth medium (470 mg L^{-1}). **9** is dehydrogenated by a dehydrogenase to give the aldehyde and is then taken up into the biosynthetic pathway. The ease with which oxygen exchanges in aldehydes appears to render [formyl-^{18}O]phosphonoacetaldehyde (cf. **3**) an unsuitable substrate. The half-life for the exchange of oxygen

[*] Dr. F. Hammerschmidt
Institut für Organische Chemie der Universität
Währingerstrasse 38, A-1090 Wien (Austria)
Telefax: Int. code + (1)3196-312

[**] Biosynthesis of Natural Products with a P–C Bond, Part 11. This work was supported by the Fonds zur Förderung der wissenschaftlichen Forschung (Projects 8671 and 6537C). – Part 10: F. Hammerschmidt, H. Kählig, *Liebigs Ann. Chem.* **1992**, 1201–1203.

in acetaldehyde is approximately 1 min in neutral aqueous solution.[11] In the cell the [formyl-^{18}O]phosphonoacetaldehyde generated in situ should be methylated quickly before ^{18}O is completely exchanged. For the synthesis of **9**, diethyl 2,2-diethoxyethylphosphonate (**7**)[12] was hydrolyzed in $H_2{}^{18}O$ (95% ^{18}O) with HCl formed by addition of chlorotrimethylsilane. After three days the mixture (molar ratio of aldehyde **3**/acetal **7** = 1:1 after two days; ^{1}H NMR) was reduced with sodium borohydride in anhydrous ethanol. The ^{18}O-labeled hydroxyphosphonate **8** corresponded to the unlabeled compound (thin-layer chromatography (TLC), boiling point, ^{1}H NMR and IR spectra) which was obtained by the same procedure, except that H_2O was employed for the hydrolysis of **7** instead of $H_2{}^{18}O$. The electron impact (EI) mass spectrum of **7** showed that ^{16}O of the P=O bond had not been exchanged for ^{18}O.



According to the field desorption (FD) mass spectrum, the extent of labeling was at least 92%. The $^{13}C\{^1H\}$ NMR spectrum (100.6 Hz, $CDCl_3$) of the labeled compound **8** shows the C-2 doublet to be upfield (δ = 56.417, ^2J(C,P) = 4.6 Hz, $\Delta\delta$ = 0.018). **8** was treated with bromotrimethylsilane/allytrimethylsilane[9, 13] and finally hydrolyzed to give the free phosphonic acid **9**, which was added to the growth medium (470 mg L^{-1}). The labeled fosfomycin that formed (10 mg L^{-1}) was once again transformed into 2-amino-1-hydroxypropylphosphonic acid and isolated. The ^{1}H NMR spectrum (400.1 MHz, D_2O) of this material is identical to that of the unlabeled compound **6**. The $^{13}C\{^1H\}$ spectrum obtained after the addition of NaOD (30%) in D_2O[9] showed that adjacent to the doublet (δ = 78.885, ^1J(P,C = 144.7 Hz) for C-1 is a satellite doublet with the same intensity as for ^{18}O-labeled **6** which is shifted upfield by $\Delta\delta$ = 0.025. This corresponds to 50% labeling. It is evident, therefore, that the labeled phosphonoacetaldehyde has a short lifetime in the cell. According to these two experiments the methyl group is probably transferred formally as CH_3^- which, however, rules out L-methionine and (*S*)-adenosylmethionine (which deliver the methyl group formally as CH_3^+ in biological systems) as direct donors for the CH_3^- unit.[14] It is, however, assumed that the methyl group of L-methionine is transferred possibly with a corrin as an intermediate carrier (reverse formation[15] of L-methionine from methylcobalamin and homocysteine?) and from there as CH_3^- to phosphonoacetaldehyde (**3**). Seto et al. showed that the methyl group of [^{14}C-methyl]methylcobalamin is incorporated into fosfomycin by a growing culture of *Streptomyces wedmorensis*.[5] It is, however, in no way shown that this is the direct donor for the methyl group.

The two experiments described add further support to the assumption that in the biosynthesis of fosfomycin a methyl group originating from L-methionine adds to the carbonyl group of phosphonoacetaldehyde as CH_3^- by means of an umpolung step which has, until recently, been unknown. Experiments are currently underway to ascertain whether a chiral methyl group is transferred with retention or inversion of configuration.

Experimental Procedure

8: To a solution of 7 (5.08 g, 20 mmol) in $H_2{}^{18}O$ (95% ^{18}O; 1.0 g, 50 mol) was added chlorotrimethylsilane (0.51 mL, 4 mmol), and the solution was stirred for 72 h at room temperature. The mixture was then taken up in 40 mL anhydrous ethanol (pretreated with sodium) to which $NaBH_4$ (0.756 g, 20 mmol) was added in portions (exothermic reaction). After one hour glacial acetic acid (0.57 mL, 10 mmol) was added. The solution was concentrated and the residue dissolved in 30 mL water. Mannitol (4.0 g) was added and the solution was continuously extracted with ethyl acetate for 2 h. Purification by flash chromatography (eluting first with ethyl acetate, then ethyl acetate/ethanol 10/1; R_f **8** = 0.49 (in ethyl acetate/ethanol 10/1), visualized with I_2) and Kugelrohr distillation (90–100 °C/8 Torr) gave 2.0 g (54% yield) of **8** as a colorless oil. IR (film) [cm^{-1}]: ν = 3374 (OH); ^{1}H NMR (400.1 MHz, $CDCl_3$, TMS): δ = 4.12 (m, 4H; 2 × $POCH_2$), 3.88 (dt, ^3J(P,H) = 18.7 Hz, ^3J(H,H) = 6.4 Hz, 2H; CH_2OH), 3.48 (br. s, 1H, OH), 2.07 (dd, ^2J(P,H) = 17.7 Hz, ^3J(H,H) = 6.4 Hz, 2H; PCH_2), 1.34 (t, ^3J(H,H) = 6.9 Hz, 6H; 2 × CH_3); $^{13}C\{^1H\}$ NMR (100.6 MHz, $CDCl_3$): δ = 61.694 (d, ^2J(P,C) = 6.5 Hz; $POCH_2$), 56.435 (d, ^2J(P,C) = 4.6 Hz, C-^{16}O; d for C-^{18}O shifted upfield by $\Delta\delta$ = 0.018), 29.069 (d, ^1J(P,C) = 138.0 Hz; PCH_2), 16.259 (d, ^3J(P,C) = 3.0 Hz; CH_3).

9: A solution of **8** (1.83 g, 10 mmol), bromotrimethylsilane (5.2 mL, 40 mmol), and allyltrimethylsilane (3.2 mL, 20 mmol) in anhydrous CCl_4 (20 mL) was heated for 3 h at 50 °C with exclusion of moisture. Volatile components were removed in vacuo (0.2 Torr, up to 40 °C). The residue was dissolved in 15 mL ethanol and 15 mL water and concentrated after 10 min. Water was added again twice and the solution concentrated. Finally the residue was dissolved in 30 mL water and lyophilized; 1.2 g (94% yield). The viscous oil was used directly for the feeding experiments. ^{1}H NMR (400.1 MHz, D_2O): δ = 3.95 (dt, ^3J(P,H) = 12.3 Hz, ^3J(H,H) = 7.4 Hz, 2H; CH_2OH), 2.20 (dt, ^3J(P,H) = 18.2 Hz, ^3J(P,H) = 7.4 Hz, 2H; PCH_2).

The feeding experiment with L-[methyl-$^2H_3$]methionine (300 mg L^{-1}, 99% D) and the isolation of labeled **6** were carried out according to literature procedures [9]. Six 1 L Erlenmeyer flasks, each with 220 mL medium were used. **6** was isolated by ion-exchange chromatography (Dowex 50, H^+; Dowex 50, H^+; Dowex 1, OAc; Dowex 50 H^+, 1 N HCO_2H). Yield after crystallization: 5.5 mg.

Feeding experiment with **9**: The free acid was added to the main culture before autoclaving (470 mg L^{-1}); 2 × 6 Erlenmeyer flasks. The eluates of the first Dowex-50 H^+ column were combined for further workup. Yield: 8 mg labeled **6**.

Received: July 5, 1993
Revised: August 9, 1993 [Z 6189 IE]
German version: *Angew. Chem.* **1994**, *106*, 334

[1] T. Hori, M. Horiguchi, A. Hayashi, *Biochemistry of Natural C-P Compounds*, Maruzen, Kyoto Branch Publishing Service, **1984**.
[2] W. A. Warren, *Biochim. Biophys. Acta* **1968**, *156*, 340–346; E. Bowman, M. McQueney, R. J. Barry, D. Dunaway-Mariano, *J. Am. Chem. Soc.* **1988**, *110*, 5575–5576; H. M. Seidel, S. Freeman, C. H. Schwalbe, J. R. Knowles, *ibid.* **1990**, *112*, 8149–8155; T. Hidaka, H. Iwakura, S. Imai, H. Seto, *J. Antibiot.* **1992**, *45*, 1008–1010.
[3] T. O. Rogers, J. Birnbaum, *Antimicrob. Agents Chemother.* **1974**, *5*, 121–132.
[4] F. Hammerschmidt, *J. Chem. Soc. Perkin Trans. 1* **1991**, 1993–1996.
[5] T. Kuzuyama, T. Hidaka, K. Kamigiri, S. Imai, H. Seto, *J. Antibiot.* **1992**, *45*, 1812–1814.
[6] F. Hammerschmidt, H. Kählig, *J. Org. Chem.* **1991**, *56*, 2364–2370.
[7] In the biosynthesis of thienamycin a chiral methyl group in methionine was added, possibly as $CHDT^-$ formed by umpolung, to an intermediate of an unknown structure with retention of configuration [17].
[8] S. Imai, H. Seto, H. Ogawa, A. Satoh, N. Otake, *Agric. Biol. Chem.* **1985**, *49*, 873–874.
[9] F. Hammerschmidt, G. Bowermann, K. Bayer, *Liebigs Ann. Chem.* **1990**, 1055–1061.
[10] J. C. Vederas, *Nat. Prod. Rep.* **1987**, *4*, 277–337.
[11] P. Greenzaid, Z. Luz, D. Samuel, *J. Am. Chem. Soc.* **1967**, *89*, 756–759.
[12] J. M. Varlet, G. Fabre, F. Sauveur, N. Collignon, *Tetrahedron* **1981**, *37*, 1377–1384.
[13] A. H. Schmidt, *Aldrichimica Acta* **1981**, *14*, 31–38.
[14] The direct replacement of a hydrogen atom at C-2 of 2-hydroxyethylphosphonic acid by a methyl group can not be excluded, although this is more difficult to conceive of mechanistically than the addition of a methyl group to the carbonyl carbon of phosphonoacetaldehyde (**3**).
[15] R. G. Metthews in *Folates and Pterins, Vol. 1* (Eds.: R. L. Blakley, S. J. Benkovic), Wiley, New York, **1984**, p. 497.
[16] A. N. Pudovik, B. E. Ivanov, *Izv. Akad. Nauk SSSR Otd. Khim. Nauk* **1952**, 947–955 [*Chem. Abstr.* **1953**, *47*, 10464c].
[17] D. R. Houck, K. Kobayashi, J. M. Williamson, H. G. Floss, *J. Am. Chem. Soc.* **1986**, 108, 5365–5366.

Selective Measurement of the Time-Dependence of Transient Overhauser Effects in Magnetic Resonance: Applications to Oligonucleotides**

Sébastien J. F. Vincent, Catherine Zwahlen, and Geoffrey Bodenhausen*

Ever since Anil Kumar, Wagner, Ernst, and Wüthrich[1] recorded "build-up plots" by two-dimensional nuclear Overhauser effect spectroscopy (NOESY)[2] to monitor cross-peak amplitudes a_{AX} as a function of the mixing time τ_m, it has been known that cross relaxation in macromolecules can be misleading and that the correct interpretation of NOESY experiments must take spin-diffusion effects into account.[3-6] Spin diffusion can be avoided for very short mixing times τ_m, but in this case the long-range Overhauser effects—which are crucial in order to derive structural information—are too weak to be observed. If the mixing time is increased to reveal weaker interactions, the strongest dipole–dipole couplings become so dominant that the magnetization is immediately transmitted to near neighbors through spin diffusion. A correct interpretation is possible if one considers the simultaneous effect of all cross-relaxation rates σ_{ij}, so that all transfer processes of longitudinal magnetization, both direct and indirect, are properly accounted for. This approach has come to be known as the "full relaxation matrix" method.[7] Although some authors[8-10] believe that a single high-quality NOESY spectrum obtained with a suitably chosen mixing time is sufficient, the majority of researchers appear to be convinced that extensive build-up plots hold the key to meaningful comparisons between molecular models and experiment. With the help of linear prediction and singular value decomposition methods,[11] it is possible to analyze a build-up curve corresponding to a single cross peak and decompose the envelope into its constituent exponential components.[12] This promising approach requires a good signal-to-noise ratio and a large number of τ_m increments. Unfortunately, extensive series of two-dimensional NOESY experiments are very time consuming and set stringent demands on the stability of both sample and instrument. The recording of extensive build-up curves may also tend to be neglected because various other forms of 3D spectroscopy[13] seem to be more attractive. This is why we propose to use 1D methods that can supplement the information provided by 2D NOESY spectra and give insight into the build-up behavior of a few strategically chosen cross peaks.

Figure 1 shows the pulse sequence of a one-dimensional experiment that is designed for the selective measurement of the time dependence of transient Overhauser effects, which can be adapted for the selective measurement of the decay of longitudinal magnetization (see below). The pulse sequence starts with a selective inversion of the longitudinal magnetization of a chosen source spin A, that is, $\langle I_z^A \rangle \rightarrow -\langle I_z^A \rangle$. This inversion can be achieved by using a Gaussian Q^3 cascade,[14] which must be applied at the chemical shift Ω_A of spin A. The longitudinal magnetization of A (more accurately, its deviation from thermal equilibrium) is allowed to migrate freely through cross relaxation during the interval τ_m. The cross-relaxation behavior

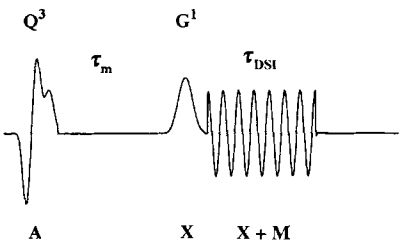


Fig. 1. Pulse sequence for selective build-up measurements of transient Overhauser effects. For details, see text. The method can be readily adapted for measuring the τ_m dependence of the amplitude a_{AA} of a diagonal peak by applying the G^1 pulse to A and transferring the magnetization from A to M′ with $\tau_{DSI} \approx 1/J_{AM'}$.

observed by our method is *exactly the same* as in a NOESY experiments.[2] A fraction of the magnetization migrates from the source spin A to a target spin X, that is, $\langle I_z^A \rangle \rightsquigarrow \langle I_z^X \rangle$. In principle, if there is no overlap between cross peaks in the NOESY spectrum, it should be possible to observe the magnetization of the X spin directly. In practice, however, limitations in the accuracy of difference spectroscopy make this difficult. Therefore, we resort to a more sophisticated scheme that is related to three-dimensional spectroscopy in the sense that there are two consecutive mixing events. At the end of the mixing period, the longitudinal component $\langle I_z^X \rangle$ of the target spin X is converted into $\langle I_x^X \rangle$ by a selective 270° Gaussian G^1 pulse,[15] and then transferred to a scalar-coupled "spy" nucleus M, that is, $\langle I_x^X \rangle \rightarrow \langle I_x^M \rangle$. This transfer can be achieved through a doubly selective homonuclear Hartmann–Hahn effect[16] during a *d*oubly *s*elective *i*rradiation period τ_{DSI}. The audio modulation of the radiofrequency field required for the transfer can be readily set up,[17] and the duration of the double irradiation can be optimized empirically in the vicinity of $\tau_{DSI} \approx 1/J_{MX}$ (shorter values of τ_{DSI} are advisable if relaxation is rapid). If the transfer efficiency is less than 100%, only the sensitivity of the experiments is affected, but not the accuracy of the build-up and decay curves. Two complementary experiments are performed, one with and one without the initial inversion pulse, and the difference spectrum is calculated. For longer τ_m values, the signals therefore tend to decay to zero like in NOESY, but in contrast to the selective inversion–recovery method[18] in which the signals asymptotically approach a nonvanishing equilibrium value. Unlike the usual NOESY technique, this method does not suffer from artifacts due to zero-quantum coherences (so-called *J* cross peaks),[19] nor can it be affected by longitudinal two-spin order.[20]

Many commentators of exchange and relaxation effects in multi-dimensional NMR spectroscopy have emphasized the fact that it would be useful to monitor the amplitudes of diagonal peaks.[5, 9, 21] In particular, Mirau[9] has pointed out that it would be possible to normalize the amplitudes of all cross peaks in a spectrum if the decay of one or several diagonal peaks could be measured accurately. Unfortunately, in most NOESY and other 2D spectra it is difficult to measure the amplitudes of crowded diagonal peaks quantitatively.[22] Although 3D spectroscopy[13] can be helpful in principle, limited digital resolution makes integration of peak volumes hazardous. Our 1D techniques can help to overcome this restriction. It is sufficient to apply, at the end of the τ_m interval, the 270° Gaussian G^1 pulse to the A spin, and then to transfer the A magnetization to a spy spin M′ through a scalar coupling $J_{AM'}$, that is, $\langle I_x^A \rangle \rightarrow \langle I_x^{M'} \rangle$. A difference spectrum is again obtained by subtracting a signal recorded without initial inversion.

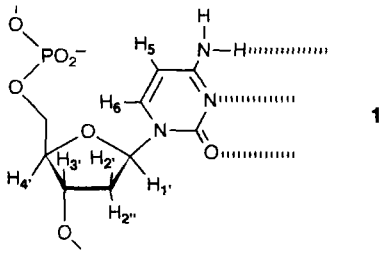
We have tested our methods on oligonucleotides, because spin-diffusion effects are known to be severe in these systems,[4]

[*] Prof. Dr. G. Bodenhausen, S. J. F. Vincent, C. Zwahlen
Section de Chimie, Université de Lausanne
Rue de la Barre 2, CH-1005 Lausanne (Switzerland)

[**] We gratefully acknowledge Dr. Philip Bolton (Wesleyan, Connecticut) and Dr. Jane Withka (Pfizer, New London, Connecticut) for a DNA sample and for calculations and stimulating discussions. This research was supported by the Fonds National de la Recherche Scientifique (FNRS) and by the Commission pour L'Encouragement de la Recherche Scientifique (CERS).

 © VCH Verlagsgesellschaft mbH, D-69451 Weinheim, 1994 0570-0833/94/0303-0343 $ 10.00+.25/0

and build-up curves are therefore of particular interest.[23] Here we report measurements on the cytosine-9 residue (**1**) in the dimer of the self-complementary palindromic DNA dodecamer d(CGCGAATTCGCG). This system, which is often referred to as Dickerson's dodecamer, has been the object of extensive X-ray diffraction[24] and NMR[25, 26] studies, and has been investigated in detail by molecular dynamics.[10, 26–28]



1

Figure 2 shows build-up measurements for selected pairs of protons in **1**. The spins of C9-H1′ and C9-H3′ of the deoxyribose ring of the cytosine-9 residue **1**, as well as the proton C9-H5 of the corresponding pyrimidine base were inverted in turn. Each

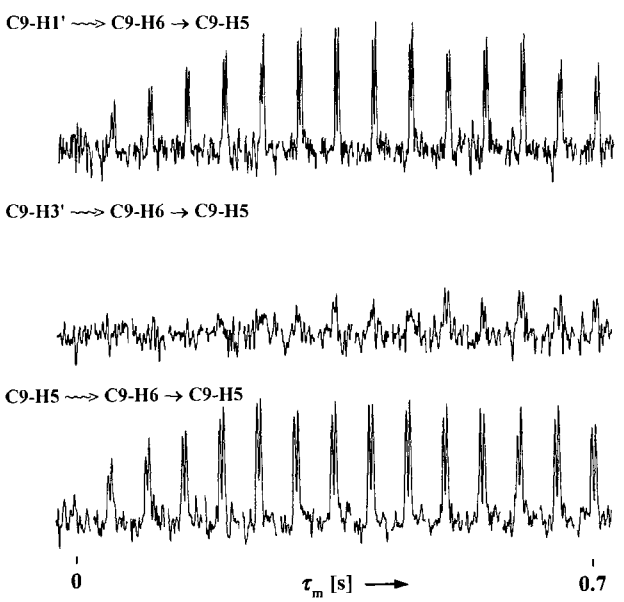


Fig. 2. Examples of selective build-up measurements of NOEs in d(CGCGAATTCGCG)$_2$, dissolved in D_2O. Conditions: $T = 303$ K, pH = 7.0, 3 mM d(CGCGAATTCGCG) monomer, 100 mM sodium chloride and 10 mM phosphate buffer, $\tau_{DSI} = 131.7$ ms. The mixing time τ_m was incremented in 50 ms steps from 0 to 0.7 s. The experiments were performed on a Bruker MSL 300 spectrometer equipped with an Oxford Research Systems selective excitation unit. For further details, see text.

of these three protons thus fulfilled the role of source spin. We then monitored cross-relaxation processes (NOE's) to the C9-H6 proton of the pyrimidine base of the same cytosine-9; the spin of this proton was the target in each case. The magnetization of the C9-H6 proton was transferred for observation through a doubly selective homonuclear Hartmann–Hahn effect to the C9-H5 proton; this pyrimidine proton acted as spy in these experiments. This latter transfer can only be used for cytosine, which has two scalar-coupled aromatic protons. Purine and thymine residues containing only one aromatic proton cannot be handled in the same manner. In these cases the same information can be obtained by observing cross relaxation in the reverse direction, that is, from the aromatic base to the deoxyribose.

It is known that symmetrically related cross peaks in NOESY spectra should have equal amplitudes.[29] This rule applies to 2D experiments that begin with a nonselective excitation pulse and involve a mixing period that is symmetrical with respect to time- and phase-reversal. At first sight, it would appear that our selective one-dimensional experiments, which are inherently asymmetrical in the time domain, need not necessarily obey this symmetry rule. In fact, the symmetry is preserved, because the physical processes taking place during the mixing period are the same as in conventional NOESY. Figure 3 shows two build-up curves resulting from cross relaxation between C9-H2′ and C9-H6 in **1**, which represent transfer processes in opposite directions. Since

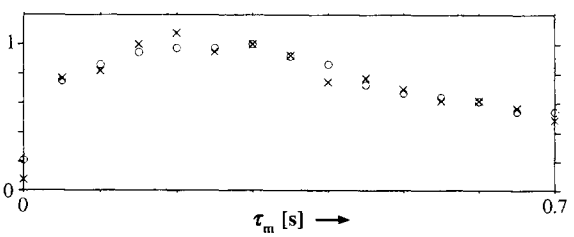


Fig. 3. Selective measurements of symmetrically related transient Overhauser effects between the C9-H6 and C9-H2′ protons of **1** in duplex d(CGCGAATTCGCG)$_2$. Circles: NOE from C9-H2′ to C9-H6 with a magnetization transfer to C9-H5 ($\tau_{DSI} = 131.7$ ms). Crosses: NOE from C9-H6 to C9-H2′ with transfer to C9-H1′ ($\tau_{DSI} = 64.8$ ms). The two series of experiments yield similar build-up curves after normalization of the vertical scale ($I_{rel} = 1$ for $\tau_m = 300$ ms). All other experimental parameters were as for Figure 2.

we observed two different protons with different multiplet structures, and since the Hartmann–Hahn transfer processes may have unequal efficiencies, the vertical scales of the two build-up curves were normalized to illustrate the equivalence of the two symmetrically related cross-relaxation processes.

It is also possible to measure NOEs between protons belonging to the same sugar residue. Figure 4 shows a build-up measurement revealing the cross-relaxation process between two geminal protons of the deoxyribose ring of **1**. The C9-H2″ proton

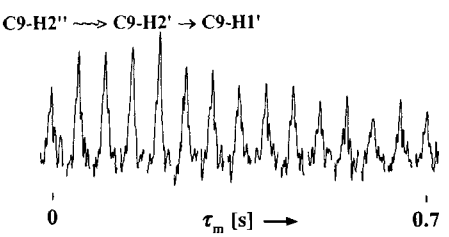


Fig. 4. Selective measurement of a transient Overhauser effect similar to Figure 2. The spin of the source proton C9-H2″ of **1** was selectively inverted, and the NOE to the neighboring target C9-H2′ proton was monitored by transferring the magnetization to the spy spin C9-H1′ ($\tau_{DSI} = 64.8$ ms). All other parameters were as for Figure 2.

played the role of source spin, while the C9-H2′ proton was the target spin, and the C9-H1′ proton the spy. The success of these procedures depends on the spread in chemical shifts of the protons under investigation. Barring near-degeneracies, we have found that it is not particularly difficult to use protons in the

same deoxyribose ring. Figure 5 shows two examples of "diagonal peak measurements" in duplex d(CGCGAATTCGCG)$_2$, obtained with the modified pulse sequence of Figure 1, described above. The magnetization was transferred from the aromatic C9-H6 proton to C9-H5 in Figure 5a, and from the C9-H2′ proton of deoxyribose to C9-H1′ in Figure 5b.

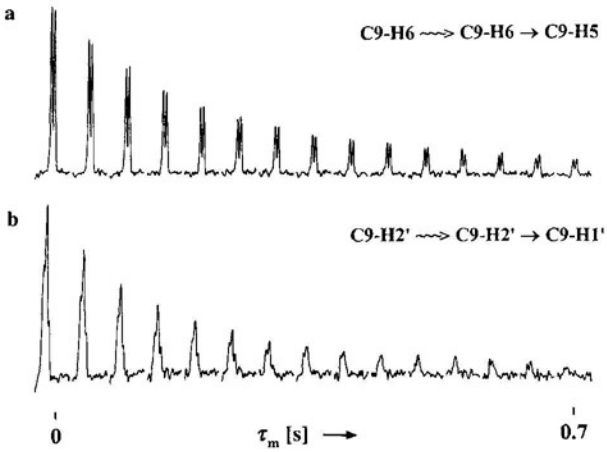


Fig. 5. Selective measurements of the τ_m dependence of the diagonal peak intensity of a) C9-H6 and b) C9-H2′ in duplex d(CGCGAATTCGCG)$_2$. The magnetization was transferred for observation in a) from C9-H6 to C9-H5 (τ_{DSI} = 131.7 ms) and in b) from C9-H2′ to C9-H1′ (τ_{DSI} = 64.8 ms). All other parameters were as for Figure 2.

The amplitudes of build-up plots such as those in Figure 2 can be compared directly with those of the molecular dynamics (MD) simulations of Withka et al.[28] The build-up curves of Figure 6a allowed us to rank the six proposed models. The "electrostatic simulation" based on the standard potential energy function of GROMOS86[30] is not satisfactory. A much better agreement can be obtained by adding harmonic constraints for the hydrogen bonds involved in Watson–Crick pairing.[28] The hypothesis of isotropic tumbling with a single correlation time τ_c of 6 ns can also be discarded on the grounds of our experiments. However, it remains difficult to distinguish between the two models of Withka et al.[28] that both consider the overall motion to be anisotropic, but in which internal motion is either excluded or included. The build-up curves for the most sophisticated model of Withka et al.[28] are reproduced in Figure 6b. With respect to our experimental observations (Fig. 6a), one significant divergence remains for the process C9-H1′ ⇝ C9-H6, which though predicted to be nearly as weak as the C9-H3′ ⇝ C9-H6 conversion, appears to be much stronger in our experiments.

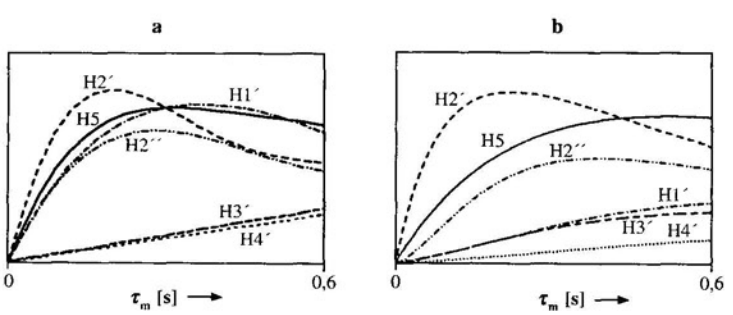


Fig. 6. a) Selective build-up measurements of NOEs to the C9-H6 proton of **1** in duplex d(CGCGAATTCGCG)$_2$. The source protons C9-H1′, C9-H2′, C9-H2″, C9-H3′, and C9-H5 of **1** were inverted in turn. Experimental conditions as for Figure 2. b) Corresponding curves, reproduced from Withka et al. [28], and obtained for the most sophisticated MD model, which includes overall anisotropy and internal motion as described in the text.

As shown in the last example of Figure 2, it is possible to set up experiments where the source and spy spins are identical. At first sight, this may appear paradoxical, but, thanks to the combination of difference spectroscopy and phase alternation, there is in fact no contradiction in this dual function. The absence of zero-quantum interference makes it possible to use nominal values of zero for τ_m. If cross relaxation is very rapid, however, (as between the geminal protons illustrated in Figure 4), and if the spectrum is so crowded that the inversion pulse must be fairly long to be selective enough, some cross relaxation will occur *during* this inversion pulse. In this case one observes a nonvanishing signal at $\tau_m = 0$. In order to ensure that even the weakest Overhauser effects emerge from the noise, all signals shown were obtained with 512 transients at 1.5 s intervals; thus, each multiplet required 13 minutes, and each of the complete build-up curves, which consist of 15 increments extending from $\tau_m = 0$ to 0.7 s, required 3.2 h. To extract similar information from conventional two-dimensional exchange NOESY experiments, one would have to run a series of 15 high-resolution NOESY spectra, taking suitable precautions to suppress J cross peaks, which would require about a week of spectrometer time. In the same time, one could record more than 50 build-up plots of the type shown in Figure 3. Of course, our one-dimensional methods are in essence selective, and only provide information on the interaction between one particular pair of protons, while a set of NOESY spectra provides information on all pairs. Yet we believe that a few strategically chosen pairs of resonances would provide sufficient evidence to test some crucial predictions made by molecular dynamics calculations.[10, 26–28]

The one-dimensional techniques presented in this paper allow one to measure the build-up and decay curves corresponding to selected peaks in NOESY. The methods can be used to refine measurements obtained by the standard 2D NOESY method and have a resolving power that is similar to 3D techniques. It is possible to monitor the build-up of Overhauser effects under conditions that are identical to those prevailing in 2D NOESY, but without the inconvenience of J cross peaks and longitudinal two-spin order. In general, one can choose the nuclei at will, subject only to the conditions that the coupling J_{MX} between the target X and the spy M should be nonvanishing, and that these two spins should have nondegenerate chemical shifts. The time-efficient manner in which the amplitudes of individual cross peaks in a NOESY survey spectrum can be quantitated lead us to dub our experiment *q*uantitative *u*nraveling of *i*ntensities for *c*orroborating *k*nowledge in *n*uclear *O*verhauser *e*ffect *s*pectroscop*y* (QUICK-NOESY). The experiment is equally applicable to proteins and other macromolecular systems including protein/DNA complexes, and to small molecules, either in isolation or bound to large receptors.

Received: August 13, 1993
Revised version: October 11, 1993 [Z 6280 IE]
German version: *Angew. Chem.* **1994**, *106*, 340

[1] Anil Kumar, G. Wagner, R. R. Ernst, K. Wüthrich, *J. Am. Chem. Soc.* **1981**, *103*, 3654.
[2] Anil Kumar, R. R. Ernst, K. Wüthrich, *Biochem. Biophys. Res. Commun.* **1980**, *95*, 1; S. Macura, R. R. Ernst, *Mol. Phys.* **1980**, *41*, 95; K. Wüthrich, *NMR of Proteins and Nucleic Acids*, Wiley, Chichester, **1986**; D. Neuhaus, M. P. Williamson, *The Nuclear Overhauser Effect in Structural and Conformational Analysis*, VCH, Weinheim, **1989**.
[3] A. Kalk, H. J. C. Berendsen, *J. Magn. Reson.* **1976**, *24*, 343; E. T. Olejniczak, R. T. Gampe, Jr., S. W. Fesik, *ibid.* **1986**, *67*, 28; A. N. Lane, *ibid.* **1988**, *78*, 425.
[4] W. Massefski, Jr., A. G. Redfield, *J. Magn. Reson.* **1988**, *78*, 150.
[5] J. W. Keepers, T. L. James, *J. Magn. Reson.* **1984**, *57*, 404.
[6] S. G. Hyberts, G. Wagner, *J. Magn. Reson.* **1989**, *81*, 418; J. D. Baleja, J. Moult, B. D. Sykes, *ibid.* **1990**, *87*, 375.

 © VCH Verlagsgesellschaft mbH, D-69451 Weinheim, 1994 0570-0833/94/0303-0345 $ 10.00+.25/0

[7] B. A. Borgias, M. Gochin, D. J. Kerwood, T. L. James, *J. Magn. Reson.* **1986**, *67*, 28; R. Boelens, T. M. G. Koning, R. Kaptein, *J. Mol. Struct.* **1988**, *173*, 299; B. A. Borgias, T. L. James, *J. Magn. Reson.* **1988**, *79*, 493; R. Boelens, T. M. G. Koning, G. A. van der Marel, J. H. van Boom, R. Kaptein, *ibid.* **1989**, *82*, 290; B. A. Borgias, M. Gochin, D. J. Kerwood, T. L. James, *Prog. Nucl. Magn. Reson. Spectrosc.* **1990**, *22*, 83.
[8] J. E. Mertz, P. Güntert, K. Wüthrich, W. Braun, *J. Biomol. NMR* **1991**, *1*, 257.
[9] P. A. Mirau, *J. Magn. Reson.* **1988**, *80*, 439.
[10] K. Kaluarachchi, R. P. Meadows, D. G. Gorenstein, *Biochemistry* **1991**, *30*, 8785.
[11] H. Barkhuijsen, R. de Beer, W. M. M. J. Bovée, D. van Ormondt, *J. Magn. Reson.* **1985**, *61*, 465.
[12] T. E. Malliavin, M. A. Delsuc, J. Y. Lallemand, *J. Biomol. NMR* **1992**, *2*, 349; C. Reisdorf, T. E. Malliavin, M. A. Delsuc, *Biochimie* **1990**, *87*, 375.
[13] C. Griesinger, O. W. Sørensen, R. R. Ernst, *J. Am. Chem. Soc.* **1987**, *109*, 7227; S. W. Fesik, E. R. P. Zuiderweg, *J. Magn. Reson.* **1988**, *78*, 588; G. W. Vuister, P. de Waard, R. Boelens, J. F. G. Vliegenthart, R. Kaptein, *J. Am. Chem. Soc.* **1989**, *111*, 772; D. Marion, L. E. Kay, S. W. Sparks, D. A. Torchia, A. Bax, *ibid.* **1989**, *111*, 1515.
[14] L. Emsley, G. Bodenhausen, *J. Magn. Reson.* **1992**, *97*, 135.
[15] L. Emsley, G. Bodenhausen, *J. Magn. Reson.* **1989**, *82*, 211.
[16] R. Konrat, I. Burghardt, G. Bodenhausen, *J. Am. Chem. Soc.* **1991**, *113*, 9135; C. Zwahlen, S. J. F. Vincent, G. Bodenhausen, *Proc. Int. Sch. Phys. Enrico Fermi* **1992**, in press.
[17] L. Emsley, I. Burghardt, G. Bodenhausen, *J. Magn. Reson.* **1990**, *90*, 214; corrigendum: *ibid.* **1991**, *94*, 448.
[18] B. Boulat, R. Konrat, I. Burghardt, G. Bodenhausen, *J. Am. Chem. Soc.* **1992**, *114*, 5412; B. Boulat, G. Bodenhausen, *J. Biomol. NMR* **1993**, *3*, 335.
[19] S. Macura, Y. Huang, D. Suter, R. R. Ernst, *J. Magn. Reson.* **1981**, *43*, 259.
[20] G. Bodenhausen, G. Wagner, M. Rance, O. W. Sørensen, K. Wüthrich, R. R. Ernst, *J. Magn. Reson.* **1984**, *59*, 542.
[21] C. L. Perrin, R. K. Gipe, *J. Am. Chem. Soc.* **1984**, *106*, 4036.
[22] H. Kessler, H. Oschkinat, C. Griesinger, W. Bermel, *J. Magn. Reson.* **1986**, *70*, 106.
[23] C. Zwahlen, S. J. F. Vincent, L. Di Bari, M. H. Levitt, G. Bodenhausen, *J. Am. Chem. Soc.*, in press.
[24] H. R. Drew, R. M. Wing, T. Takano, C. Broka, S. Tanaka, K. Itakura, R. E. Dickerson, *Proc. Natl. Acad. Sci. USA* **1981**, *78*, 2179; P. E. Pjura, K. Grzeskowiak, R. E. Dickerson, *J. Mol. Biol.* **1987**, *197*, 257; M. Teng, N. Usman, C. A. Frederick, A. H.-J. Wang, *Nucleic Acids Res.* **1988**, *16*, 2671.
[25] D. J. Patel, A. Pardi, K. Itakura, *Science* **1982**, *216*, 581; D. R. Hare, D. E. Wemmer, S.-H. Chou, G. P. Drobny, B. R. Reid, *J. Mol. Biol.* **1983**, *171*, 319; J. M. Withka, S. Swaminathan, J. Srinivasan, D. L. Beveridge, P. H. Bolton, *Science* **1992**, *255*, 597.
[26] W. Nerdal, D. R. Hare, B. R. Reid, *Biochemistry* **1989**, *28*, 10008; J. A. Parkinson, J. Barber, B. A. Buckingham, K. T. Douglas, G. A. Morris, *Magn. Reson. Chem.* **1992**, *30*, 1064.
[27] G. Ravishankar, S. Swaminathan, D. L. Beveridge, R. Lavery, H. Sklenar, *J. Biomol. Struct. Dyn.* **1989**, *6*, 669; J. Srinivasan, J. M. Withka, D. L. Beveridge, *Biophys. J.* **1990**, *58*, 533; S. Swaminathan, G. Ravishankar, D. L. Beveridge, *J. Am. Chem. Soc.* **1991** *113*, 5027.
[28] J. M. Withka, S. Swaminathan, D. L. Beveridge, P. H. Bolton, *J. Am. Chem. Soc.* **1991**, *113*, 5041.
[29] C. Griesinger, C. Gemperle, O. W. Sørensen, R. R. Ernst, *Mol. Phys.* **1987**, *62*, 295.
[30] W. F. van Gunsteren, H. J. C. Berendsen, GROMOS86: Groningen Molecular Simulation System, University of Groningen, The Netherlands, **1986**.

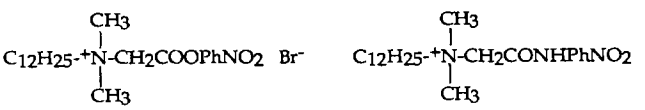
Fast Amide Cleavage under Mild Conditions: An Evolutionary Approach to Bioorganic Catalysis**

Fredric M. Menger* and Zheng X. Fei

F. Monod has written that "Nature is a tinkerer".[1] This statement might be amended to read, "Nature is a tinkerer with no time constraints." Thus, Nature has had 4.5 billion years in which to synthesize and examine, unhurredly, innumerable compounds while progressively selecting the most serviceable ones. This random search for improvement has led to a family of catalytic proteins called enzymes. Chemists attempting to imitate enzymes face, unfortunately, a seemingly unsolvable problem: the finite lifetime of human beings. Synthesizing complicated molecules with potential enzyme-like activity is a time-consuming business and, through no personal fault, chemists can survey only a limited number in the years allowed them. The evolutionary approach that has served Nature so well seems hopeless in the organic laboratory.

It occurred to us that the problem facing mortal chemists could, in small measure, be alleviated by avoidance of the covalent bond. Formation of covalent bonds is, after all, the major consumer of time when enzyme mimics are constructed. If, alternatively, mimics were assembled through noncovalent bonds, then one could test large numbers of them because noncovalent bonds establish themselves, to all intents and purposes, instantaneously.

The original idea was, therefore, to mix in water various proportions of long-chained compounds bearing at their termini an imidazole, carboxylic acid, hydroxyl, or amine functionality. Owing to hydrophobic association, the compounds would assemble into species we call "clumps". A clump is defined as a multicomponent mixture of weakly associated species, each possessing a potentially catalytic group that can function in concert with its neighbors. Literally hundreds of clumps have recently been screened, in two-minute spectrophotometric assays, for their ability to accelerate the hydrolysis of ester **1**. In this manner, we discovered systems that catalyze the hydrolysis of **1** at rates too fast to measure conventionally. Among these systems, the fastest turned out to be, to our surprise, pure hexadecanoate. Although multicomponent clumps might likely be more effective for various other reaction types (a point being tested),[2] we were so intrigued by the fast hexadecanoate-induced hydrolyses that we continued their study using a less reactive substrate, amide **2**. Before the kinetic details are given, a word should be said about amide hydrolyses.



1 **2**

Amide hydrolysis is widespread in biological systems, but that is not the only reason the reaction has, over the years, attracted the attention of bioorganic chemists.[3–8] Amides are resonance-stabilized entities and difficult to hydrolyze. For example, a typical chemical procedure for hydrolyzing aliphatic amides calls for heating in 8 N HCl at reflux for ten hours.[9] Thus, amides present a special challenge to those interested in catalyzing reactions of recalcitrant functionalities. Until now the challenge has been met mainly by intramolecular catalysis[3–8] including an example of our own (i.e. an amide of Kemp's triacid that hydrolyzes with a $\geq 10^{12}$ acceleration).[10] But these enzyme mimics rely on the juxaposition between amide and catalytic group that is enforced by covalent bonds and is imparted to the molecule during its synthesis.[11] Enzymes, of course, do not have this advantage; they must operate by means of noncovalent association at their active sites. Thus, it would be desirable to find an enzyme mimic that splits amides under biological conditions in the absence of "covalent assistance". The hydrophobic clumping of **2** with hexadecanoate, and the subsequent fast reaction, provides an example of such enzyme-like behavior.

[*] Prof. F. M. Menger, Dr. Z. X. Fei
Department of Chemistry, Emory University
Atlanta, GA 30322 (USA)
Telefax: Int. code + (404)727-6586

[**] This work was supported by the National Science Foundation.

Hydrophobic association of a substrate to a catalyst, leading to enhanced rates, has been known for a long time. Three old but classical studies can be mentioned as examples. Wagner et al.[12] reported that a long-chained *p*-nitrophenyl carbonate ester is hydrolyzed by *N*-stearoylhistidine about 2000 times faster than by *N*-acetylhistidine. Gitler and Ochoa-Solano[13] found that micellar *N*-myristoylhistidine hydrolyzes *p*-nitrophenyl hexanoate about 20 times faster than *p*-nitrophenyl acetate. And Moss et al.[14] observed that a long-chained imidazole derivative is a 200-fold better catalyst than imidazole in the hydrolysis of *p*-nitrophenyl hexanoate. It is now known that *p*-nitrophenyl esters are not realistic surrogates for amides.[15]

Lerner et al.,[16] in an effort to "develop catalytic antibodies that can catalyze reactions that are energetically more demanding", studied, as we did, the hydrolysis of a *p*-nitrophenyl amide. The success of their biological screening as compared to our chemical screening will be discussed momentarily.

Amide **2** is an inherently stable molecule. It was unchanged after 27 days at pH 8.0 and 25.0 °C (as indicated by a flat curve in a plot of absorbance (at 390 nm) vs. time). If a finite rate was created by deliberately imparting a small slope to the plot, then a reaction half-life of about a year could be obtained (Table 1). In reality, of course, the half-life must be even longer. When amide **2** (2×10^{-5} M) was dissolved in a buffer solution at pH 8 and 25.0 °C containing 0.2 M sodium acetate, no reaction was observed after 45 h. Acetate is worthless as a catalyst even at high concentrations.

Table 1. Kinetic data[a] on the amide cleavage of amide **2** (2×10^{-5} M) in water at 25.0 °C.

Catalyst	[Catalyst] [M]	pH [b]	k_{obs} [min^{-1}]	Half-life
–		8.0		> 1 year
acetate	0.20	7.0		> 450 h
hexadecanoate	2×10^{-5}	8.0	0.22	3.1 min
hexadecanoate	1×10^{-5}	8.0	0.12	5.8 min
hexadecanoate	5×10^{-6}	8.0	0.067	10 min
hexadecanoate	2×10^{-5}	5.0	0.11	6.3 min
hexadecanoate	2×10^{-5}	9.0	0.22	3.1 min
dodecanoate	2×10^{-5}	8.0	0.00082	840 min

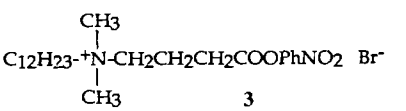
[a] Rate constants represent the average of at least two runs and are accurate to ±6%. The kinetics were cleanly first order for two half-lives, indicative of "pseudo-intramolecular" reactivity within the clumps to which the reactants remain totally bound. [b] System is insoluble at pH 4.0. Solutions at pH 7.0 and 8.0 were prepared with 0.05 M phosphate. Solutions at pH 5.0 and 9.0 were prepared with 0.05 M phthalate and 0.1 M borate, respectively.

When 2×10^{-5} M amide **2** was mixed with 2×10^{-5} M hexadecanoate (pH 8.0, 25.0 °C), the observed rate constant k_{obs} was found to equal 0.22 min^{-1}, corresponding to a half-life of 3 min (Table 1). In order to estimate the acceleration induced by hexadecanoate, we assumed (conservatively) that the half-life of the 0.2 M acetate system is 450 h. Thus, when concentration differences are taken into consideration, hexadecanoate is seen to be at least 10^8 times more effective than acetate (a number obtained from $[450 \times 60]/3$ multiplied by $0.2/2 \times 10^{-5}$). The acceleration by hexadecanoate relative to acetate-free buffer is an incalculably large number. Clearly, hexadecanoate catalysis at enzyme-like concentrations rivals or exceeds that found in many of the better covalently enforced intramolecular catalysts.[11]

A pH–rate profile of amide **2** and hexadecanoate (2×10^{-5} M of each) (not shown) revealed only a twofold variation between pH 5 and 9. Hexadecanoic acid must function primarily in the carboxylate form. Importantly, the rate constant diminished to 8.2×10^{-4} min^{-1} (a 256-fold decrease) when 2×10^{-5} M dodecanoate was used in place of 2×10^{-5} M hexadecanoate (Table 1). The simplest explanation is that catalysis proceeds in hexadecanoate clumps induced, very likely, by the presence of cationic **2**. Dodecanoate has, presumably, too short a chain to aggregate at the extremely low concentration used in the experiments. Mixed clumps of **2** and hexadecanoate were undetectable by dynamic light scattering under kinetic conditions owing to the low concentrations of the components. It is known, however, that mixtures of oppositely charged amphiphiles form tight complexes that often develop into vesicles[17] or coacervates[18] at higher concentrations.

A precipitate forms when 2×10^{-5} M amide **2** is mixed with $> 3 \times 10^{-5}$ M hexadecanoate, reaffirming our contention that catalysis arises from complex formation. Although solubility problems prevented an examination of reaction molecularity and kinetics over a wide concentration range, we were able to ascertain that the rate constants decrease proportionally to the concentration of hexadecanoate as the latter is reduced from 2×10^{-5} to 5×10^{-6} M (Table 1). The infinity absorbance also decreased proportionally, indicating that the reaction between amide **2** and hexadecanoate is stoichiometric. Apparently, formation of a mixed anhydride intermediate prevents turnover. In other words, amide cleavage is so fast within the clump that anhydride hydrolysis is actually rate-limiting in the overall amide hydrolysis.[19]

The hexadecanoate catalyst also possesses a degree of substrate specificity. Thus, no amide cleavage was observed with amide **3**, a close analogue of amide **2**. Lack of reaction could arise from a diminished inductive activation of the carbonyl group in **3** as well as from improper positioning of the amide group, relative to the carboxylate function, within the clump.



3

How does our system compare with an antibody-catalyzed hydrolysis of a *p*-nitrophenyl amide?[16] The k_{cat} for the antibody reaction is 0.05 min^{-1}, decidedly smaller that our k_{obs} of 0.2 min^{-1}. Moreover, the antibody experiments were carried out under more severe conditions (pH 9.0, 37 °C) than ours (pH 7–8, 25 °C). On the other hand, amide **2** is activated by an ammonium group, unlike the substrate used in the antibody work. On balance, one might tentatively conclude that the two rates are comparable, and that a "hopeful search" through a random collection of clumps is no less profitable than a "hopeful search" through a random collection of antibodies.

In summary, a peptidase "model" has been developed in which low concentrations of catalyst (ca. 10^{-5} M) induce large rate enhancements (ca. 10^8) in an amide substrate. Reaction rates are highly sensitive to the structure of both the substrate and catalyst. We surmise that hydrophobic binding, in cooperation with electrostatic attraction between the carboxylate group and cationic nitrogen center, enforces an intimate contact between the carboxylate function and the amide's carbonyl group prior to actual reaction. This is totally consistent with the observed first-order kinetics (Table 1), the structural specificity, and the known tendency for oppositely charged amphiphiles to complex tightly with each other.[17, 18] Note that we have al-

ready expressed our view that prolonged contact at close distances holds the key to the reactivity of both enzymes and enzyme models.[20, 21]

Multicomponent clumps are being investigated as catalysts for diverse organic reactions by using the same screening procedure that uncovered the fast amide hydrolysis.[2] There is an amusing parallel here to biological evolution: The randomly created clumps correspond to random mutations; our selecting clumps with the fastest rates corresponds to natural selection of the fittest; and (to push the analogy to its limits) the publishing of our best clumps corresponds to the passing on of the most advantageous traits to future generations.

Experimental Procedure

Amide **2** was synthesized following the reaction $C_{12}H_{25}N(CH_3)_2 + BrCH_2COOCH_3 \rightarrow C_{12}H_{25}\overset{+}{N}(CH_3)_2CH_2COOCH_3Br^- = RCOOCH_3 \rightarrow RCOOH \rightarrow RCOBr \rightarrow RCONHPhNO_2$ (*para* isomer). After three recrystallizations amide **2** had a m.p. of 213–214 °C; the spectroscopic data (^1H NMR, FAB-MS, IR) and elemental analysis were consistent with the given structure. Reactions were monitored at 390 nm by using a Varian DMS 200 spectrophotometer with a cell chamber thermostated at 25.0 ± 0.1 °C. The solvent consisted of 3% CH_3CN in an aqueous phosphate buffer.

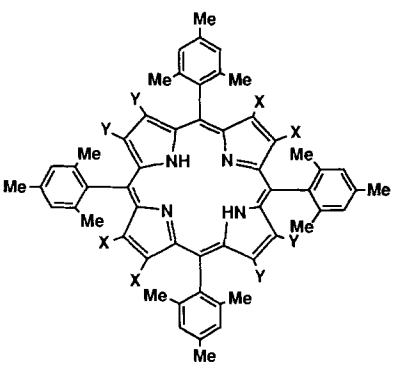
Received: July 28, 1993
Revised: September 2, 1993 [Z 6241 IE]
German version: *Angew. Chem.* **1994**, *106*, 329

[1] F. Monod, *Science* **1977**, *196*, 1161.
[2] Typical clump components (hexadecanoate, *N,N*-dimethyldodecylamine, dodecanol, the copper complex of $C_{14}H_{29}N(CH_3)CH_2CH_2N(CH_3)_2$ etc.) were combined in concentrations of $< 10^{-5}$ M each. Details will be described when the work is completed.
[3] M. L. Bender, *J. Am. Chem. Soc.* **1957**, *79*, 1258.
[4] R. Kluger, J. Chin, W.-W. Choy, *J. Am. Chem. Soc.* **1979**, *101*, 6976.
[5] J. T. Groves, R. M. Dias, *J. Am. Chem. Soc.* **1979**, *101*, 1033.
[6] I. B. Blagoeva, A. J. Kirby, *J. Chem. Soc. Perkin Trans. 2* **1985**, 1017.
[7] J. Suh, M. J. Kim, N. J. Seong, *J. Org. Chem.* **1981**, *46*, 4354.
[8] A. J. Kirby, R. S. McDonald, C. R. Smith, *J. Chem. Soc. Perkin Trans. 2* **1974**, 1495.
[9] J. C. Eck, C. S. Marvel, *Organic Synthesis, Collect. Vol. II*, Wiley, New York, **1943**, p. 374.
[10] F. M. Menger, M. Ladika, *J. Am. Chem. Soc.* **1988**, *110*, 6794.
[11] A. J. Kirby, *Adv. Phys. Org. Chem.* **1980**, *17*, 183.
[12] R. G. Shorenstein, C. S. Pratt, C. J. Hsu, T. E. Wagner, *J. Am. Chem. Soc.* **1968**, *90*, 6199.
[13] C. Gitler, A. Ochoa-Solano, *J. Am. Chem. Soc.* **1968**, *90*, 5004.
[14] R. A. Moss, R. C. Nahas, S. Ramaswani, W. J. Sanders, *Tetrahedron Lett.* **1975**, 3379.
[15] F. M. Menger, M. Ladika, *J. Am. Chem. Soc.* **1987**, *109*, 3145.
[16] K. D. Janda, D. Schloeder, S. J. Benkovic, R. A. Lerner, *Science* **1988**, *241*, 1188.
[17] E. W. Kaler, A. K. Murthy, B. E. Rodriguez, J. A. Zasadzinski, *Science* **1989**, *245*, 1371; H. Fukuda, K. Kawata, H. Okuda, S. L. Regen, *J. Am. Chem. Soc.* **1990**, *112*, 1635.
[18] H. W. Hoyer, A. Marmo, M. Zoellner, *J. Phys. Chem.* **1961**, *65*, 1804.
[19] See ref.[10] for a related intramolecular case in which amide cleavage can be slower than hydrolysis of an anhydride.
[20] F. M. Menger; *Acc. Chem. Res.* **1993**, *26*, 206.
[21] For a review of catalysis in organic "systems", see F. M. Menger, *Angew. Chem.* **1991**, *103*, 1104; *Angew. Chem. Int. Ed. Engl.* **1991**, *30*, 1086.

Conformational Effects on the Redox Potentials of Tetraarylporphyrins Halogenated at the β-Pyrrole Positions**

Philippe Ochsenbein, Khadija Ayougou, Dominique Mandon, Jean Fischer, Raymond Weiss,* Rachel N. Austin, Karupiah Jayaraj, Avram Gold, James Terner, and Jack Fajer

Porphyrins with alkyl substituents in the β-positions of the pyrroles are easier to oxidize and harder to reduce than porphyrins bearing phenyl substituents at the *meso* positions.[1] Nickel(II) and zinc(II) derivatives of β-alkyl-substituted tetraphenylporphyrins, which are hybrids of these two major types, adopt saddle conformations and are more easily oxidized than the corresponding octaethyl- or tetraphenylporphyrins, in accord with the theoretically predicted destabilization of the π system resulting from the saddle distortion.[2, 3] In contrast, tetraphenylporphyrins that are partially halogenated at the pyrrole β-positions are easier to reduce and harder to oxidize than the nonhalogenated parent macrocycle.[4] To gain insights into the relationship between the redox potentials of tetraarylporphyrins halogenated at the β-positions of the pyrroles and substituent-induced changes in macrocycle conformation, we have investigated the electrochemical properties and crystal structures of 5,10,15,20-tetramesitylporphyrin **1**,[5] derivatives **2** and **3**[6] halogenated at antipodal pyrrole β-positions (7,8,17,18), and derivatives **4** and **5**[7] halogenated at *all* β-pyrrole positions (2,3,7,8,12,13,17,18). The observation that the octahalogenated macrocycles are easier to oxidize than the te-



1: X = H, Y = H
2: X = Cl, Y = H
3: X = Br, Y = H
4: X = Cl, Y = Cl
5: X = Br, Y = Br

[*] Prof. Dr. R. Weiss, P. Ochsenbein, K. Ayougou, Dr. D. Mandon, Prof. Dr. J. Fischer, Dr. J. Fajer[+]
Laboratoire de Cristallochimie et de Chimie Structurale (UA 424)
Université Louis Pasteur, Institut Le Bel
4, rue B. Pascal, F-67070 Strasbourg (France)
Telefax: Int. code + (33)88415363

R. N. Austin, Dr. K. Jayaraj, Prof. Dr. A. Gold
Department of Environmental Science and Engineering
University of North Carolina
Chapel Hill, NC 27599-7400 (USA)

Prof. Dr. J. Terner
Department of Chemistry, Virginia Commonwealth University
Richmond, VA 23284-2006 (USA)

[+] Permanent address:
Department of Applied Science
Brookhaven National Laboratory, Upton, NY 11973 (USA)

[**] This work was supported by the Centre National de la Recherche Scientifique (UA-424), the U.S. Public Health Service (Grants ES03433 for A. G. and GM34442 for J. T.), the U.S. Department of Energy (Contract DE-AC02-76CH00016 for J. F.), and NATO (collaborative research grant for R. W. and A. G.). J. Fajer thanks the Department of Chemistry of the Université Louis Pasteur de Strasbourg for a visiting professorship.

trahalogenated derivatives is rationalized by the effects of distortion of the porphyrin framework.

The crystal structures of **2** and **3** have a center of symmetry and hence at least C_i symmetry.[8] As a consequence, they are not saddle-shaped but show a slightly distorted chairlike conformation (Fig. 1). The two opposite halogenated pyrrole rings are tilted up and down with respect to the mean plane of the porphyrin framework and are also twisted around their median lines, whereas the nonhalogenated rings are only twisted. Both β-carbon atoms of the halogenated pyrrole rings lie above or below the porphyrin mean plane; their average displacements are 0.03(1) Å in **2** and 0.105(6) Å in **3**. The β-carbon atoms of the nonhalogenated rings have corresponding average displacements of 0.02(2) Å in **2** and 0.050(6) Å in **3**. Difference electron density maps of **3** and ^{1}H NMR studies of **2** and **3** in CD_2Cl_2 show that the two NH protons are located on the nonhalogenated pyrrole rings, in agreement with a previous study of β-tetrabrominated tetraarylporphyrins.[6]

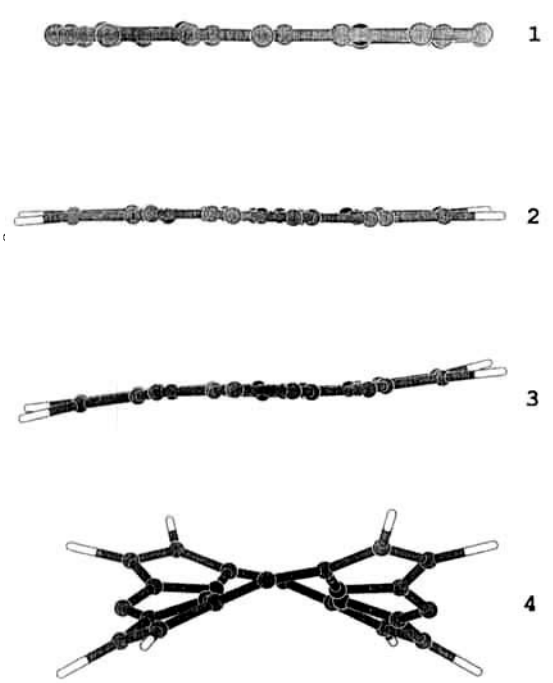


Fig. 1. Edge-on views of the skeletons of tetramesitylporphyrin **1**, the antipodal tetrasubstituted derivatives **2** and **3**, and the octachloro derivative **4** (the *meso*-mesityl groups are omitted for clarity).

As in the crystal structure of **5**,[7] the macrocycle **4** lies on a crystallographic fourfold inversion axis and hence has S_4 symmetry.[8] Since the two NH groups preclude symmetry higher than C_2, two tautomeric forms must be disordered around the S_4 axis. Porphyrin **4** is also clearly saddle-shaped;[8] alternate pyrrole rings are tilted severely up or down relative to the porphyrin mean plane and are also twisted about their median lines (Fig. 1). The average displacement of the β-carbon atoms of one pyrrole ring relative to the porphyrin mean plane is 0.905(5) Å in **4**, compared to 0.95(2) Å in **5**.[7] The mesityl rings are twisted into the porphyrin mean plane to minimize unfavorable contacts with the β-pyrrole substituents. The average dihedral angle between the two planes is 58.1(1)° in **4** and 58.6(6)° in **5**. The corresponding values of 83.6(3)° in **2** and 84.9(1)° in **3** are close to the angle of 83.6(1)° found in **1**. Unfavorable contacts are minimized in the tetrahalogenated macrocycles by increasing the $(X\text{-}C_\beta)C_z\text{-}C_m\text{-}C_{Ph}$ angle relative to the $(H\text{-}C_\beta)C_z\text{-}C_m\text{-}C_{Ph}$ complement. The mean values of these angles are 120.8(4)° and 113.9(4)° in **2** and 122.2(2)° and 112.4(2)° in **3**, respectively.

The smallest ruffling of the porphyrin ring occurs in **1**, where the average displacement of the C_m carbon atoms with respect to the porphyrin mean plane is only 0.015(4) Å (Fig. 1).[8] The tetrahalogenated tetramesitylporphyrins are slightly more ruffled; the *meso*-carbon atoms lie 0.04(1) Å above (and below) the porphyrin mean plane in **2** and 0.087(6) Å in **3**. Ruffling is most pronounced in the octahalogenated porphyrins **4** and **5**, where the displacement of the *meso*-carbon atoms relative to the porphyrin mean plane is 0.322(5) Å and 0.30(2) Å, respectively.

The experimental one-electron redox potentials $E_{ox}^{1/2}$ and $E_{red}^{1/2}$ were determined by cyclic voltammetry for **1**–**5** (Table 1). Substitution at the pyrrole β-positions with electron-withdrawing groups makes the porphyrins easier to reduce and harder to oxidize than the parent tetramesitylporphyrin. The differences in the reduction potentials $\Delta E_{red}^{1/2}$ for **1**/**2**, **1**/**3**, **2**/**4**, and **3**/**5** range from +0.25 to +0.32 V. While the difference in the oxidation potentials $\Delta E_{ox}^{1/2}$ for **1**/**2** and **1**/**3** are positive (though somewhat smaller than the values of $\Delta E_{red}^{1/2}$), the $\Delta E_{ox}^{1/2}$ values are negative for **2**/**4** (−0.10 V) and **3**/**5** (−0.13 V) indicating that the octahalogenated porphyrins **4** and **5** are easier to oxidize than the tetrahalogenated derivatives **2** and **3**, in spite of the additional β-halogen substituents.

Table 1. Redox potentials determined by cyclic voltammetry [a].

Porphyrin	Halogen substituents	$E_{red}^{1/2}$	$\Delta E_{red}^{1/2}$	$E_{ox}^{1/2}$	$\Delta E_{ox}^{1/2}$
1	–	−1.41		+0.91	
			+0.29		+0.24
2	4 Cl	−1.12		+1.15	
			+0.27		−0.10
4	8 Cl	−0.85		+1.05	
1	–	−1.41		+0.91	
			+0.32		+0.21
3	4 Br	−1.09		+1.12	
			+0.25		−0.13
5	8 Br	−0.84		+0.99	

[a] $E^{1/2}$ in V; solvent CH_2Cl_2, electrolyte NBu_4PF_6 (0.1 mol L^{-1}) vs. SCE, scan rate 200 mV s^{-1}, T = 25 °C.

The one-electron redox potentials of porphyrins reflect the energy levels of their HOMOs and LUMOs.[3] INDO calculations on tetraphenylporphyrins octaalkyl-substituted at the pyrrole β-positions have shown that saddle distortions of the macrocycle decrease the energy gap between the HOMOs and LUMOs by raising the energy of the HOMOs.[2] Thus, β-alkyl substitution decreases $E_{ox}^{1/2}$, while $E_{red}^{1/2}$ is almost unchanged.[3] The data in Table 1 shows that the electron-withdrawing β-halogen substituents stabilize the LUMOs and, to a slightly lesser degree, the HOMOs. The negative values of $\Delta E_{ox}^{1/2}$ for **2**/**4** and **3**/**5** can be explained if the energy decrease in the HOMOs of **4** and **5** expected from substitution with additional electron-withdrawing halogens is offset by the saddle distortion. That the saddle distortions observed in the solid state are maintained in solution is evidenced by the strongly red-shifted Soret and Q absorption bands of **4** and **5** and shifts of the ν_2 marker bands in the resonance Raman spectra of the molecules.[9, 10]

Experimental Procedure

1 was prepared according to a published procedure [5]. Single crystals of **1** · $2CHCl_3$ were obtained by slow diffusion of hexane into a solution of the porphyrin in

chloroform. Crystal data (−100 °C, dark blue crystal of dimensions $0.30 \times 0.30 \times 0.22$ mm): $C_{58}H_{36}N_4Cl_6$, $M = 1021.8$, tetragonal, space group $I4_1/a$, $a = 27.093(8)$, $c = 14.876(6)$ Å, $V = 10919.4$ Å^3, $Z = 8$, $\varrho_{calcd} = 1.246$ g cm^{-3}, $\lambda(CuK_\alpha) = 1.5418$ Å, 4269 reflections ($3° < \theta < 52°$) were collected; empirical absorption corrections were applied, 2337 reflections with $I > 3\,\sigma(I)$ were used in the refinements; number of parameters 337, $R = 0.064$, $R_w = 0.089$, GOF = 1.45, final residual electron density = 0.21 e Å^{-3}.

2: **1** (100 mg) was treated with 5.4 equiv of *N*-chlorosuccinimide in boiling 1,1,2,2-tetrachloroethane (30 mL) for 60 h. The crude reaction product was purified twice by chromatography on a SiO_2 column, first eluting with toluene and then with toluene/hexane (1:1). The product was recrystallized by slow addition of methanol to solution of the compound in chloroform. Yield: 59%. UV/VIS (CH_2Cl_2, 25 °C): λ_{max} (ε [mol^{-1} L cm^{-1}]) = 426 (231), 522 (19.5), 598.5 (6.8), 654.5 nm (8.0). Single crystals of **2** · $4CHCl_3$ were obtained by slow diffusion of methanol into a solution of the porphyrin in chloroform. Crystal data (−100 °C, red-purple crystal of dimensions $0.15 \times 0.20 \times 0.32$ mm): $C_{60}H_{54}N_4Cl_{16}$, $M = 1398.4$, triclinic, space group $P\bar{1}$, $a = 11.182(3)$, $b = 12.078(3)$, $c = 13.501(4)$ Å, $\alpha = 74.57(2)$, $\beta = 67.59(2)$, $\gamma = 87.87(2)$, $V = 1620.8$ Å^3, $Z = 1$, $\varrho_{calcd} = 1.433$ g cm^{-3}, $\lambda(Mo_{K\alpha}) = 0.7107$ Å, 4475 reflections ($2° < \theta < 23°$) were collected; empirical absorption corrections were applied, 1712 reflections with $I > 3\,\sigma(I)$ were used in the refinements; number of parameters 266, $R = 0.093$, $R_w = 0.116$, GOF = 2.02, final residual electron density = 0.81 e Å^{-3}.

3 was obtained according to a published procedure for tetraarylporphyrins [6]. UV/VIS (CH_2Cl_2, 25 °C): λ_{max} (ε [mol^{-1} L cm^{-1}]) = 430 (214), 525.5 (20.3), 604 (8.0), 660.5 nm (9.0). Single crystals of [**3** · $2Cl_2CH_2$] were obtained by slow diffusion of pentane into solution of the porphyrin in dichloromethane. Crystal data (−100 °C, black crystal of dimensions $0.13 \times 0.20 \times 0.38$ mm): $C_{58}H_{54}N_4Br_4Cl_4$, $M = 1268.5$, monoclinic, space group $P2_1/n$, $a = 11.413(3)$, $b = 17.856(5)$, $c = 13.736(4)$ Å, $\beta = 102.40(2)$°, $V = 2731.1$ Å^3, $Z = 2$, $\varrho_{calcd} = 1.436$ g cm^{-3}, $\lambda(Mo_{K\alpha}) = 0.7107$ Å; 5189 reflections ($2° < \theta < 25°$) were collected; empirical absorption corrections were applied, 3030 reflections with $I > 3\,\sigma(I)$ were used in the refinements; number of parameters 319, $R = 0.052$, $R_w = 0.075$, GOF = 1.58, final residual electron density = 0.31 e Å^{-3}.

4: The zinc salt of **1** (200 mg) was treated with 70 equiv of *N*-chlorosuccinimide in refluxing tetrachloroethylene (200 mL) for 17 h. The crude product was purified by chromatography on a SiO_2 column eluting with dichloromethane/hexane (1:1). The complex was demetalated by stirring in 10% v/v trifluoroacetic acid in dichloromethane for 23 h. Yield: 34%. Single crystals of **4** · $2CH_3OH$ were obtained by slow diffusion of hexane into a solution of the porphyrin in dichloromethane/methanol. Crystal data (−100 °C, black crystal of dimensions $0.15 \times 0.25 \times 0.40$ mm): $C_{58}H_{54}N_4Cl_8O_2$, $M = 1122.7$, tetragonal, space group $P\bar{4}2_1c$, $a = 15.011(4)$, $c = 13.289(3)$ Å, $V = 2994.4$ Å^3, $Z = 2$, $\varrho_{calcd} = 1.206$ g cm^{-3}, $\lambda(Mo_{K\alpha}) = 0.7107$ Å, 4851 reflections ($2° < \theta < 29°$) were collected; empirical absorption corrections were applied, 1257 reflections with $I > 3\,\sigma(I)$ were used in the refinements; number of parameters 172, $R = 0.044$, $R_w = 0.058$, GOF = 1.12, final residual electron density = 0.43 e Å^{-3}.

Received: August 26, 1993 [Z 6317 IE]
German version: *Angew. Chem.* **1994**, *106*, 355

[1] R. H. Felton in *The Porphyrins, Vol. 5* (Ed.: D. Dolphin), Academic Press, New York, **1978**, p. 53.
[2] K. M. Barkigia, L. Chantranupong, K. M. Smith, J. Fajer, *J. Am. Chem. Soc.* **1988**, *110*, 7566.
[3] K. M. Barkigia, M. W. Renner, L. R. Furenlid, C. J. Medforth, K. M. Smith, J. Fajer, *J. Am. Chem. Soc.* **1993**, *115*, 3627.
[4] A. Giraudeau, H. J. Callot, M. Gross, *Inorg. Chem.* **1979**, *18*, 201.
[5] M. Kihn-Botulinski, B. Meunier, *Inorg. Chem.* **1988**, *27*, 209.
[6] M. J. Crossley, P. L. Burn, S. S. Chew, F. B. Cuttance, I. A. Newsom, *J. Chem. Soc. Chem. Commun.* **1991**, 1564.
[7] D. Mandon, P. Ochsenbein, J. Fischer, R. Weiss, K. Jayaraj, R. N. Austin, A. Gold, P. S. White, O. Brigaud, P. Battioni, D. Mansuy, *Inorg. Chem.* **1992**, *31*, 2044.
[8] Further details of the crystal structure investigations may be obtained from the Fachinformationszentrum Karlsruhe, D-76344 Eggenstein-Leopoldshafen 2 (FRG), on quoting the depository number CSD-57734, the names of the authors, and the journal citation.
[9] UV/VIS (CH_2Cl_2, 25 °C): **4**: λ_{max} (ε[mol^{-1} L cm^{-1}]) = 453.5(211), 548.5(17), 592.5(11), 702.5 nm(8); **5**: λ_{max} (ε[mol^{-1} L cm^{-1}]) = 463(177), 559(14), 606(9), 717 nm(7).
[10] Resonance Raman spectrum (CH_2Cl_2, 4067-Å excitation, based on polarization studies): **4**: $\nu_2 = 1537$ cm^{-1}; **5**: $\nu_2 = 1513$ cm^{-1}.

The Effect of Chiral Bilayers: Wax Tubes Made of (*S*)-Nonacosan-10-ol**

Jürgen-Hinrich Fuhrhop,* Thomas Bedurke, Airan Hahn, Siegfried Grund, Jürgen Gatzmann, and Markus Riederer

The CO_2/O_2 gaseous exchange in pine needles and similar lipophilic leaf structures occurs through stomata which are covered by a dense mesh of lipid tubes.[1] These tubes have internal diameters of 0.1–0.5 μm and consist of hydrophobic wax with an extremely high content of hydrocarbon units.[2, 3] The function of these tubes is presumably to filter off suspended particles from the air, which —if they have accumulated despite this— may be washed off the smooth, hydrophobic surface by rain. Whereas pine needles from healthy trees keep their tube system intact for six years, the tube system of diseased trees breaks down within months.[4] The stomata become blocked by the lipids of the tubes. We are interested in whether the curvature of the tubes is related to the chirality of their constituents.[5]

The main component of the lipid tubes that are pressed out through the wax cuticle (Fig. 1a) is the secondary alcohol nona-

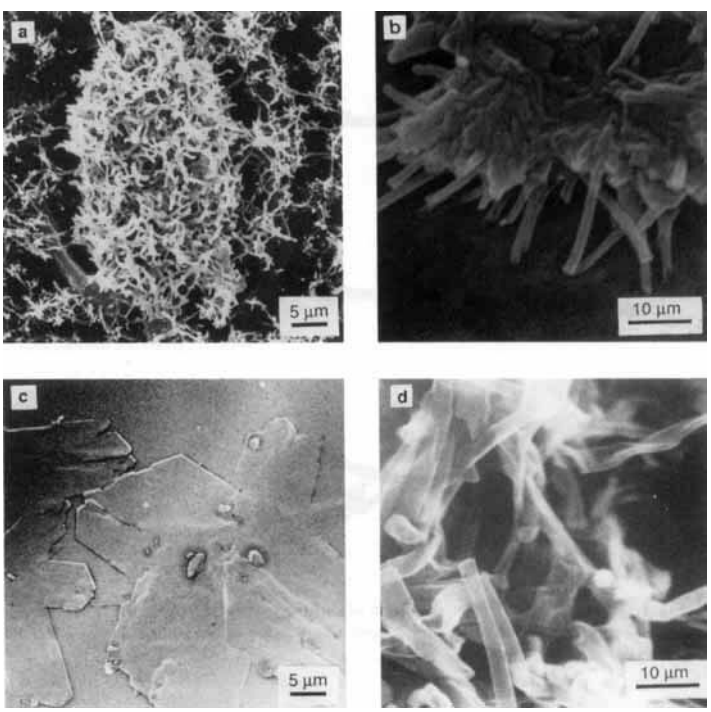


Fig. 1. Scanning electron microscopy images of a) wax tubes in their natural environment in pine needle stomata, b) wax tubes made from natural nonacosan-10-ol, c) platelets made from synthesized (*S,R*)-nonacosan-10-ol, and d) tubes made from synthesized (*S*)-nonacosan-10-ol. The tubes in Fig. 1b, d and the platelets in Fig. 1c were obtained from chloroform.

[*] Prof. Dr. J.-H. Fuhrhop, T. Bedurke, A. Hahn
Institut für Organische Chemie der Freien Universität
Takustraße 3, D-14195 Berlin (FRG)
Prof. Dr. S. Grund, J. Gatzmann
Laboratorium für Elektronenmikroskopie der Freien Universität Berlin und der Humboldt-Universität (FRG)
Prof. Dr. M. Riederer
Institut für Physiologische Ökologie der Universität Kaiserslautern (FRG)

[**] This work was supported by the Bundesministerium für Forschung und Technologie (Supramolecular chemistry pilot project), the Deutsche Forschungsgemeinschaft (SFB 312 directional membrane processes), the FNK der Freien Universität Berlin, and the Fonds der Chemischen Industrie. We thank Dr. A. Schäfer for NMR measurements.

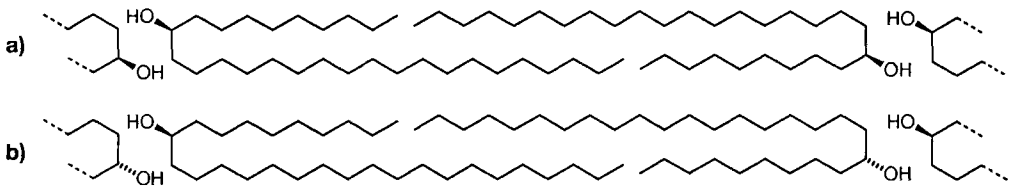


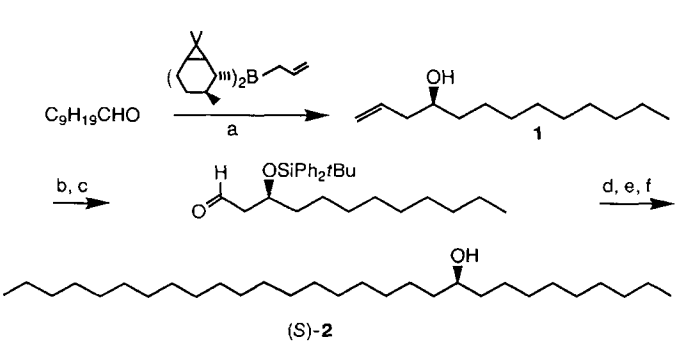
Fig. 2. Model of the molecular bilayer made of (*S*)-nonacosan-10-ol (a) and racemic (*R,S*)-nonacosan-10-ol (b). Curved bilayers are formed from (*S*)-**2** and planar bilayers from *rac*-**2**.

cosan-10-ol (**2**).[6] It is not known whether the natural substance nonacosanol is a pure enantiomer.[7] Attempts to separate a synthesized racemate chromatographically by means of diastereomeric derivatives such as (1-naphthylethyl)carbamate failed, as did attempts at differentiation by NMR spectroscopy. The carbon chains at the asymmetric center, of **2** with nine and nineteen neighboring methylene groups are too similar to be able to be differentiated chemically or spectroscopically.[7] We could repeat the experiment already described[8] to produce thin lipid tubes from the natural product nonacosanol by evaporating solutions of the natural material in chloroform (Fig. 1 b). However, use of the racemate obtained by a Grignard reaction (Fig. 1 c) produced only interlocked platelets without curvature. The same result was obtained with many other racemic alcohols of different chain lengths.

In order to provide evidence that the curvature of the tubes depends on the chirality of the alcohol component we finally carried out a moderately stereoselective synthesis of **2** by an allylboration as described by Brown (Scheme 1).[9] The enantiomeric excess of 76% could not be increased despite many attempts because the long chain starting material did not react at the low reaction temperatures (3 h at $-78\,^{\circ}C$) in the original procedure. Within 17 hours the desired tridecanol **1** formed with a yield of only 22% at $-50\,^{\circ}C$ with an enantiomeric excess of 76% (S:R = 8:1). The impure (*S*)-nonacosan-10-ol (*S*)-**2** that was finally obtained was, however, completely sufficient for our purposes.[7, 10] This was then "crystallized" from chloroform under identical conditions to the racemate, and tubes did in fact form (Fig. 1 d).

How does the curvature of the tubes of this extremely simple chiral compound arise and why is it not found in the crystallized racemate *rac*-**2**? As the structure of **2** is so simple, the explanation of these questions may also be readily deduced despite the lack of knowledge of diffraction data which can not be obtained from the wax: The hydroxy groups and the short and long chains of **2** will, of course, be located together (Fig. 2). The resulting bilayer of (*S*)-**2** has all OH groups on one side, and methine protons on the other. The bilayer curves in this case because of unsymmetrical molecular interactions. In the racemate of **2** one hydroxy group is located on each side of the bilayer in a uniform molecular arrangement.

To our knowledge, this case is the simplest curvature-producing effect of chiral bilayers for amphiphiles.[5] It is characteristic that it is produced by the interaction of hydroxy groups in an apolar medium in which the intermolecular association at the center of chirality is less influenced by solvation than it is in water. This case is similar to the helices of 11-hydroxystearates produced by Tachibana et al. in toluene.[11] Kunitake et al. have converted glutamate ester with cationic head groups into helical fibers in water,[12] and we could prepare not only helices from gluconamides in aqueous media[5, 13] but also tubes in xylene.[14] In all four cases the racemates formed crystalline platelets under identical conditions. The spontaneous curvature of molecular bilayers and the chirality of their amphilic building blocks are therefore closely related to each other. There is incidentally also a quantitative physical description of this in the form of an equation for the energy of curvature.[15] The case described here is particularly noteworthy because, firstly, the tube structure occurs in nature, and secondly, it may be attributed to a molecular asymmetry which only becomes effective at a great distance from the center of chirality. In solution it is hardly detectable; however, it determines the structure in the case of molecular assemblies.



Scheme 1. a) Et_2O, 17 h, $-50\,^{\circ}C$ (instead of $-78\,^{\circ}C$), 22% yields based on decanal; b) THF, imidazole, *t*BuPh$_2$SiCl, 48 h, 40 °C (73%); c) 1. THF, O_3, Me_2S, 15 min, $-70\,^{\circ}C$; 2. heat to room temperature, H_2O, 16 h, 50 °C (50%); d) Et_2O, $C_{17}H_{35}PPh_3Br$, BuLi, 17 h, heat from $-80\,^{\circ}C$ to room temperature (42%); e) THF, H_2(Pd/C), 3 bar, 16 h, room temperature (71%); f) THF, (nBu$_4$N)BF$_4$, 48 h, 50 °C (52%).

Received: August 20, 1993 [Z 6304 IE]
German version: *Angew. Chem.* **1994**, *106*, 351

[1] P. Wettstein-Knowles, *J. Ultrastruct. Res.* **1974**, *46*, 483–498.
[2] M. Riederer, *Ecol. Stud.* **1989**, *77*, 157–192.
[3] H. J. Schuck, *Flora* **1976**, *165*, 303–314.
[4] J. J. Santo, J.-U. Voß, *Eur. J. For. Pathol.* **1986**, *16*, 408–423.
[5] J.-H. Fuhrhop, P. Schnieder, J. Rosenberg, E. Boekema, *J. Am. Chem. Soc.* **1987**, *109*, 3387–3390.
[6] M. S. Günthardt, *Bull. Soc. Bot. Suisse* **1985**, *95*, 5–12.
[7] Tris[3-(2,2,2-trifluoro-1-hydroxyethylidene)-D-camphorato]europium was used as shift reagent in chloroform. The signals for the terminal allyl alcohol reproduced in Scheme 1 occurred at $\delta = 5.5-6.0$ and split into four doublets of equal intensities in the racemate. In the synthesized *S* isomer we found two similar signal groups in a ratio of 8:1. Racemic (*S,R*)-**2**, on the other hand, produced no such splitting of the signals.
[8] G. R. Lister, B. W. Thair, *Can. J. Bot.* **1981**, *59*, 640–648.
[9] H. C. Brown, R. S. Randad, K. S. Bhat, M. Zaidlewicz, U. S. Racherla, *J. Am. Chem. Soc.* **1990**, *112*, 2389–2392.
[10] The *S* configuration was established by comparison of the angles of optical rotation ($[\alpha]_D^{25} = -8.5$ (benzene)) with a corresponding literature value (H. Riediker, R. D. Duthaler, *Angew. Chem.* **1989**, *101*, 488–490; *Angew. Chem. Int. Ed. Engl.* **1989**, *28*, 494–495) and following predictions of H. C. Brown [9]. For natural 10-nonacosanol and $[\alpha]_D^{25}$ (chloroform) values of 1.9 and 2.2 were reported (S. Beckmann, H. Schinkle, *Z. Naturforsch. B* **1968**, *23*, 471). We found values of 0.33 and 0.30 for the synthetic (*S*)-nonacosanol. The common positive sign of the rotation angles for the natural and synthetic alcohols suggest an *S* configuration also for the natural compound. Since the angle of rotation is so small, the conclusion is uncertain. Attempts to crystallize diastereomeric derivatives failed. Only a molecular structure determination of such a diastereomer could establish the chirality of the natural product.
[11] T. Tachibana, H. Kambara, *Bull. Chem. Soc. Jpn.* **1969**, *42*, 3422–3424.
[12] N. Nakashima, S. Asakuma, T. Kunitake, *J. Am. Chem. Soc.* **1985**, *107*, 509–510.
[13] J. Köning, C. Boettcher, H. Winkler, E. Zeitler, Y. Talmon, J.-H. Fuhrhop, *J. Am. Chem. Soc.* **1993**, *115*, 693–700.
[14] J.-H. Fuhrhop, P. Schnieder, E. Boekema, W. Helfrich, *J. Am. Chem. Soc.* **1988**, *110*, 2861–2867.
[15] W. Helfrich, J. Prost, *Phys. Rev. A* **1988**, *38*, 3065.

The Biosynthesis of Nitro Compounds: The Enzymatic Oxidation to Pyrrolnitrin of Its Amino-Substituted Precursor**

Sabine Kirner and Karl-Heinz van Pée*

Several of the naturally occurring nitro compounds are biologically active, and the nitro group plays an important role in their activity. In the biosynthesis of the antibiotics chloramphenicol[1] and pyrrolnitrin **5**,[2] the nitro group is formed in the final step, by oxidation of an amino group, but till now nothing has been reported about the enzymes that catalyze this oxidation. Here we describe the oxidation of the precursor **4** to pyrrolnitrin **5** by chloroperoxidase (CPO-P) from *Pseudomonas pyrrocinia*.[3]

Compound **5** is an antifungal agent which is produced by several species of soil bacteria. The biosynthesis of **5** has not yet been fully elucidated (Fig. 1), but contains two chlorination steps and the oxidation of an amino group to a nitro group.

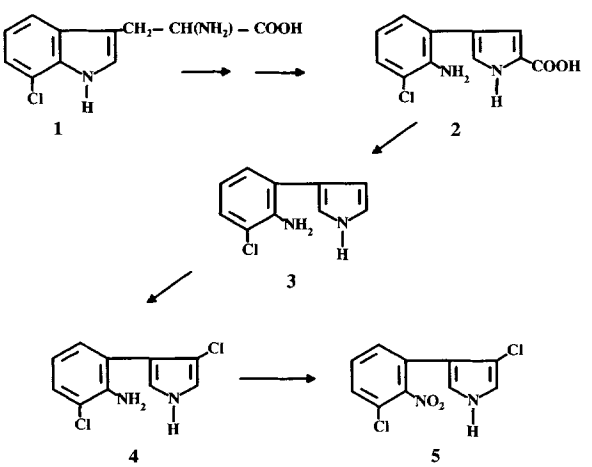


Fig. 1. Hypothetical biosynthetic pathway according to van Pée et al. [2]. **1**, 7-chlorotryptophan; **2**, 4-(2-amino-3-chlorophenyl)pyrrole-2-carboxylic acid; **3**, 3-(2-amino-3-chlorophenyl)pyrrole; **4**, 3-(2-amino-3-chlorophenyl)-4-chloropyrrole; **5**, pyrrolnitrin.

Investigations by the research group of Itoh[4] on a partially purified bromoperoxidase from a *Pseudomonas putida* strain have demonstrated that this enzyme can oxidize aniline to nitrobenzene. Attempts to use the enriched extract to transform other arylamines, such as *o*-chloroaniline, *p*-toluidine and **4**, to their nitro derivatives were unsuccessful.

A chloroperoxidase (CPO-P) which could perform the chlorination reaction **3** → **4** was isolated from the pyrrolnitrin producer *Pseudomonas pyrrocinia*.[3] It seemed logical to test whether this enzyme, in contrast to that studied by Itoh et al.,[4] can catalyze the oxidation of **4** to **5**. Since the chloroperoxidase gene has been cloned and overexpressed,[5] large amounts and high concentrations of the highly purified enzyme were available (340 Units g^{-1} cell material). The enzyme could therefore be added at higher concentrations (1.8 Units mL^{-1}) than in the experiments of Itoh et al. (3 mUnits mL^{-1}).[4]

In analogy to the halogenation reaction with CPO-P, we chose a tenfold higher acetate concentration and a lower pH value for the oxidation than were used by Itoh et al. The reaction product was isolated by preparative TLC and compared with authentic **5** by GC and HPLC. The retention times of the isolated product, and its mass spectrum, were identical to those of **5**. In the absence of the enzyme, no disappearance of **4** was observed.

In contrast to the halogenation reaction catalyzed by this metal- and cofactor-free haloperoxidase, nothing is known about the mechanism of the oxidation reaction.[6] No intermediates have yet been identified in the oxidation of **4**.

The fact that two separate steps in the biosynthesis of pyrrolnitrin are catalyzed in vitro by the same enzyme makes it very probable that the CPO-P of *Pseudomonas pyrrocinia* also participates in the biosynthetic pathway in vivo. This will be further investigated at the genetic level by inactivation of the gene.

H_2O_2 also presumably serves as cosubstrate in vivo, although the intracellular concentration is certainly much lower than that used here. The role of acetate, which is absolutely required for the reaction, is still unclear. It is possible that another substance assumes its function in vivo, since the concentrations required for optimum activity in vitro are too high to be considered physiological.

It remains to be seen whether similar enzymes participate in the biosynthesis of other nitro compounds such as chloramphenicol, and whether other bacterial haloperoxidases, either of heme or non-heme type, can also catalyze the described reaction.

Experimental Procedure

4 was synthesized from **5** by reduction with sodium dithionite [7]. Experiments on the in vitro oxidation of **4** were carried out in 1 M sodium acetate buffer, pH 4.5, 40 mM H_2O_2, and 1 mM **4** (500 μL total volume). The reaction was started by the addition of 300 mUnits CPO-P (100 Units mL^{-1} in 5 mM ammonium acetate, pH 6.8; specific activity 63 Units mg^{-1}). The mixture was incubated at 30 °C with shaking, and additional enzyme (300 mUnits) was added after 2 and 4 h. Control experiments contained no enzyme. After a total of 6 h incubation, the samples were extracted with 800 μL ethyl acetate and dried under vacuum. The residue was dissolved in ethanol and chromatographed over silica gel (with fluorescence indicator), with toluene as eluent. **4** and **5** have R_f values of 0.29 and 0.62. The compounds were located by spraying with van Urks reagent [8], which leads to a characteristic purple color in the presence of **5**. The reaction product was purified for HPLC and MS by preparative TLC. The region which fluoresced under UV (254 nm) was scraped off the plate, extracted with ethyl acetate, and dried under vacuum. The residue was dissolved in a suitable solvent and compared directly with authentic **5**, using HPLC [9], GC [10], and MS.

Received: 20 August, 1993 [Z6302IE]
German version: *Angew. Chem.* **1994**, *106*, 346

[*] Priv.-Doz. Dr. K.-H. van Pée, Dipl.-Biol. S. Kirner
Institut für Mikrobiologie der Universität Hohenheim
Garbenstrasse 30, D-70593 Stuttgart (FRG)
Telefax: Int. code + (711)459-2238

[**] This study was supported by the Deutsche Forschungsgemeinschaft and the Fonds der Chemischen Industrie. We thank the Ciba-Geigy corporation, Basel (Switzerland) for pyrrolnitrin **5**.

[1] S. Vats, C. Stuttard, L. C. Vining, *J. Bacteriol.* **1987**, *169*, 3809–3813.
[2] K.-H. van Pée, O. Salcher, F. Lingens, *Angew. Chem.* **1980**, *92*, 855–856; *Angew. Chem. Int. Ed. Engl.* **1980**, *19*, 828–829.
[3] W. Wiesner, K.-H. van Pée, F. Lingens, *J. Biol. Chem.* **1988**, *263*, 13725–13732.
[4] N. Itoh, N. Morinaga, T. Kouzai, *Biochem. Mol. Biol. Int.* **1993**, *29*, 785–791.
[5] C. Wolfframm, F. Lingens, R. Mutzel, K.-H. van Pée, *Gene* **1993**, *130*, 131–135.
[6] T. Haag, F. Lingens, K.-H. van Pée, *Angew. Chem.* **1991**, *103*, 1550–1552; *Angew. Chem. Int. Ed. Engl.* **1991**, *30*, 1487–1488.
[7] K.-H. van Pée, O. Salcher, P. Fischer, M. Bokel, F. Lingens, *J. Antibiot.* **1983**, *36*, 1735–1742.
[8] E. Stahl, H. Kaldewey, *Hoppe-Seyler's Z. Physiol. Chem.* **1961**, *323*, 182.
[9] HPLC: Lichrospher RP 18, 5 μm, 250 mm × 4.6 mm, MeOH:H_2O 65:35, 1.0 mL min^{-1}, UV 252 nm, retention time of product and **5**: 12.9 min.
[10] GC: capillary column SE 30, 25 m × 0.32 mm, isothermal 200 °C, detector 300 °C, injection port 250 °C, retention time of product and **5**: 9.1 min.

Phosphindolyl Anions by Elimination from 1-Phosphoallyllithium Complexes–η^5 and η^3 Coordination of a Phospholyl Fragment**

Edgar Niecke,* Martin Nieger, and Peter Wenderoth

Lithium complexes of hydrocarbons with delocalized π bonding systems are a major research area in organoelement chemistry because of their synthetic potential and their unique bonding.[1] It is therefore not surprising that recently similar anionic P/C-pπ bonding systems have also aroused increasing interest. One priority in this research is the phospholyl system, and many transition metal complexes with this system in the coordination sphere have been synthesized.[2] However, knowledge about the phospholyl anions is rare and has until now been limited to NMR studies[3] and to the crystal structure of the phospholyl derivative [Li(tmeda)PC_4Me_4] **I**.[4] Here we report on a simple route to phoshindolyl lithium complexes of type **II** and their structure in the solid state.



I **II**

As we could show recently, lithium alkyl- and arylphosphides (**1**) react with tolane (**2**) in the presence of the strong donor dimethoxyethane (DME) to form isolated 1-phosphoallyl anions **3**.[6, 7] The attempt in the presence of a weak donor (ether) to realize π coordination between lithium and the phosphoallyl system, as in **4**, led surprisingly in the case of lithium arylphosphides **1a** (R = C_6H_5) and **1b** (R = 2,4,6-tBu$_3$-C_6H_2) to the formation of the phosphindolyl lithium complexes **5a** and **5b**[10] through elimination of hydrogen (**a**) or hydrogen and 2-methylpropene (**b**),[8] respectively.

Crystals suitable for an X-ray structural analysis[11] could be obtained from **5b**. The unit cell contains two independent molecules (**A** and **B**), which differ essentially in the coordination of the lithium (Fig. 1). Thus lithium is η^5-coordinated with respect

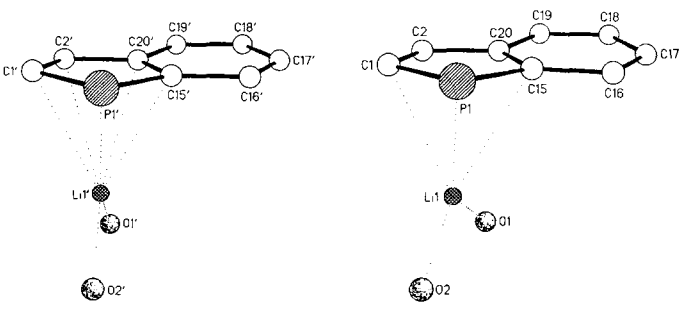
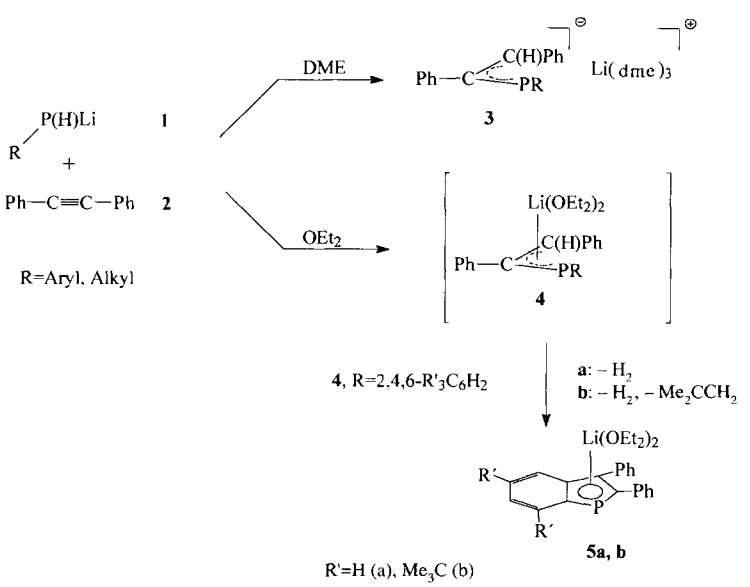
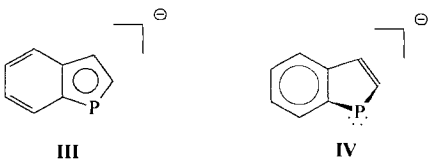


Fig. 1. Reduced representation of the two independent molecules of **5b**. Selected distances [Å] and angles [°] (molecules **A** and [**B**]): P1-C1 177.4(2) [177.0(2)], P1-C15 178.5(3) [178.9(3)], C1-C2 140.4(4) [139.4(4)], C2-C20 143.5(4) [144.3(4)], C15-C20 143.5(3) [143.1(3)], C15-C16 144.0(4) [143.4(4)], C16-C17 136.1(4) [137.1(4)], C17-C18 141.6(3) [142.2(3)], C18-C19 137.3(4) [137.9(4)], P1-Li1 258.4(5) [252.1(5)], Li1-C1 262.9(6) [261.9(6)], Li1-C15 260.1(6) [270.8(6)], Li1-C2 276.6(5) [291.9(6)], Li1-C20 276.2(6) [298.2(6)], Li1-O1 197.0(6) [189.6(7)], Li1-O2 199.2(6) [195.4(7)]; C1-P1-C15 90.6(1) [90.4(1)], O1-Li1-O2 100.8(2) [110.1(3)].

to the planar PC_4 fragment in molecule **A**, as is also observed for the phospholyl lithium complex [Li(tmeda)$P(CMe)_4$] (type **I**).[4] Longer Li-C distances are observed, however, for the fused benzene (Li1'–C1'[C15', C2',C20'] 260–277 pm) than are found for the monocycle (about 240 pm).

In molecule **B** two Li–C distances (Li1–C1[C15] 262, 271 pm) are comparable to those found in **A**, whilst two (Li1–C2[C20] 292, 298 pm) are significantly longer. This corresponds to a η^3 coordination of the metal to the ring fragment C1-P1-C15. Even though the P–C[C'] (177–179 pm) and C–C[C'] distances (139–144 pm) in the five-membered ring of both molecules can be taken as evidence for a delocalized π system as in **III**, a preferential localization of the negative charge on the hetero atom as in **IV** is already indicated in the observed structure change in the transition from **A** to **B**. Thus the PC_4 fragment in **B** is significantly distorted toward an envelope conformation (deviation of the P1 atom of the ring plane C15-C20-C2-C1 = 5 pm), and the Li–P1 distance is reduced to 252 pm (258 pm in **A**). The slight shortening of the C1–C2 bond to 139.4 pm (140.4 pm in **A**) is in agreement with these findings. The O1-P1-O2 plane in **5** is orthogonal to the PC_4 ring plane; the Li···O distances (190–199 pm) correspond to typical values for ether-coordinated lithium salts.





III **IV**

The ^{7}Li NMR spectrum of **5b** (–75 °C, Et_2O; LiBr/H_2O ext.) shows a signal at δ = –4.6 (W = 40 Hz), whose high-field position at least indicates a contribution from a π complex in solution. The determination of the constitution of **5a** was achieved by interpretation of the NMR spectra. The ^{7}Li NMR spectrum of **5a** resembles that of **5b**; whereas the ^{31}P NMR spectrum shows a resonance shifted upfield (δ = 19.7(d), $^3J_{PP}$ = 6.0 Hz) compared to that of **5b** (δ = 30.0(s)). The ^{13}C NMR spectrum of **5a** shows the expected number of signals for a 2,3-diphenylphosphindolyl system.[13]

Received: 28 August, 1993, [Z6322IE]
German version: *Angew. Chem.* **1994**, *106*, 362

[*] Prof. Dr. E. Niecke, Dr. M. Nieger, P. Wenderoth
Anorganisch-chemisches Institut der Universität
Gerhard-Domagk-Strasse 1, D-53121 Bonn (FRG)
Telefax: Int. code + (228) 735-327

[**] This work was supported by the Deutsche Forschungsgemeinschaft and the Fonds der Chemischen Industrie.

[1] Allyl- und Cyclopentadienidlithium-Komplexe: P. von R. Schleyer, T. Clark, E. D. Jammic, *J. Organomet. Chem.* **1978**, *150*, 1–6; S. Alexandratos, A. Streitwieser, Jr., H. F. Schaefer, *J. Am. Chem. Soc.* **1976**, *98*, 7959–7962; P. Jutzi, E. Schlüter, C. Krüger, S. Pohl, *Angew. Chem.* **1983**, *95*, 1015–1016; *Angew. Chem. Int. Ed. Engl.* **1983**, *22*, 994; M. F. Lappert, A. Singh, L. M. Engelhardt, A. H. White, *J. Organomet. Chem.* **1984**, *262*, 271–278; L. A. Paquette, W. Bauer, M. R. Sivik, M. Bühl, M. Feigel, P. von R. Schleyer, *J. Am. Chem. Soc.* **1990**, *112*, 8776–8789.

[2] J. F. Nixon, *Chem. Rev.* **1988**, *88*, 1327–1962; B. Deschamps, F. Mathey, *Organometallics* **1992**, *11*, 1411–1413, and references therein.

[3] F. Mathey, *Chem. Rev.* **1988**, *88*, 429–453, and references therein.

[4] T. Douglas, K. H. Theopold, *Angew. Chem.* **1989**, *101*, 1394–1395; *Angew. Chem. Int. Ed. Engl.* **1989**, *28*, 1367–1368.

[5] A phosphindolyl anion was obtained by reaction of phosphindol with lithium and was characterized by ^{31}P NMR spectroscopy: F. Nief, C. Charrier, F. Mathey, M. Simalty, *Phosphorus Sulfur Relat. Elem.* **1982**, *13*, 259–267.

[6] E. Niecke, M. Nieger, P. Wenderoth, *J. Am. Chem. Soc.* **1993**, *115*, 6989–6990; E. Niecke, M. Nieger, P. Wenderoth, unpublished results; see also [7].

[7] 1-Phosphoallyl anions were prepared for the first time by metalation of secondary vinyl phosphane and characterized by ^{31}P NMR spectroscopy: A. C. Gaumont, X. Morise, J. M. Denis, *J. Org. Chem.* **1992**, *57*, 4292–4295.

[8] The formation of 2-methylpropene was detected by GC–MS analysis. The extent to which the reaction is induced by the formation of a lithium hydride intermediate [9] requires further investigations.

[9] T. Kauffmann, A. Busch, K. Habersaat, E. Köppelmann, *Angew. Chem.* **1973**, *85*, 584–585; *Angew. Chem. Int. Ed. Engl.* **1973**, *12*, 569–570.

[10] Experimental details for **5a** (details for **5b** in parentheses): 1 mL of a 1.6 *M* solution of butyl lithium is added to a solution of 1.6 mmol of phenylphosphane (2,4,6-tri-*tert*-butylphenylphosphane) in ether. After 30 min. stirring, an equimolar quantity of tolane (**2**) is added in 3 mL ether. The reaction solution is stirred for about 2 days at 30 °C until the reaction is complete (monitored by ^{31}P NMR). During this time the solution changes color from orange to deep red. Crystalline **5a** (75%) or **5b** (82%) is obtained on crystallization from a little ether.

[11] Crystal structure analysis of **5b** ($[C_{28}H_{30}P][Li(C_4H_{10}O)_2]$): orange crystals, crystal dimensions: $0.35 \times 0.40 \times 0.50$ mm; $M_r = 552.7$; space group $P2_1/n$ (no. 14), $a = 20.966(5)$, $b = 15.888(5)$, $c = 21.845(3)$ Å, $\beta = 109.44(2)°$, $V = 6.862$ nm^3, $Z = 8$, $\rho_{calcd} = 1.07$ g cm^{-3}, $\mu = 0.91$ mm^{-1}, 10176 symmetry independent reflections ($2\theta_{max.} = 120°$, $T = 193$ K) of which 8472 reflections with $F > 4\sigma(F)$ were used for structure solution (direct method) and refinement (741 parameters), non-hydrogen atoms anisotropic; H atoms refined with a "riding" model: $R = 0.061$ ($Rw = 0.070$, $w^{-1} = \sigma^2(F) + 0.0003F^2$). An empirical absorption correction was carried out with the program DIFABS [12]. Two ether groups are disordered. Further details of the crystal structure investigation may be obtained from the Fachinformationszentrum Karlsruhe, D-76344 Eggenstein-Leopoldshafen (FRG) on quoting the depository number CSD-57728 and the journal citation.

[12] N. Walter, D. Stuart, *Acta Crystallogr. Sect. A* **1983**, *39*, 158–166.

[13] ^{13}C NMR (C_6D_6, 25 °C): δ[J_{CH}] = 140.86(d) [5.4 Hz], 140.84(d) [46.6 Hz], 139.34(d) [15.2 Hz (CH)], 137.68(s), 135.46(d) [20.6 Hz (CH)], 135.11(d) [15.6 Hz], 129.95(d) [3.1 Hz (CH)], 129.92(d) [5.0 Hz (CH)], 129.08(d), [7.3 Hz (CH)], 128.70(s) [(CH)], 128.89(s) [(CH)], 128.58(s) [(CH)], 127.87(s) [(CH)], 127.61(d) [1.5 Hz (CH)], 124.12(s), 90.45(s). The C(H) resonances were determined by a dept-90 experiment.

Synthesis of Benzylated Cycloisomaltotri- and -hexaoside**

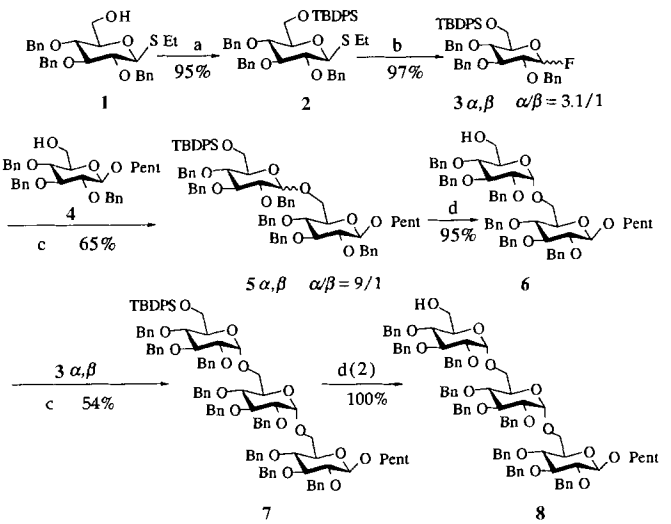
Stéphan Houdier and Philippe J. A. Vottéro*

Cyclomaltooligosaccharides known as α-, β- and γ-cyclodextrins are obtained in large quantities by enzymic synthesis with cyclodextrin glycosyl transferase.[1] The well-known ability of cyclodextrins to include apolar molecules and their solubility in water can be improved by chemical modifications.[2] Very promising modifications are the per-3,6-anhydro-α- and -β-cyclodextrins,[3] and the per-2,3-anhydro-β-cyclodextrins[4] previously synthesized.

Besides these "derivatizations" of natural cyclodextrins, a parallel route based on chemical synthesis was developed by Ogawa et al.[5] and Vignon et al.[6] The strategy centers around the preparation of a linear precursor with the suitable number of sugar residues activated in such a way that the cyclization may be achieved. Beyond the inherent difficulties of glycosylation, chemical synthesis of cyclooligosaccharides as hosts for predefined guests is a challenge.[7]

It is in this context that we synthesized cyclooligosaccharides in the isomaltose series that may have new or optimized inclusion properties with respect to natural or modified cyclodextrins. The α-1,6-glucosidic linkage can be considered as a highly flexible bridge between two D-glucopyranosyl residues. Starting from this idea we designed the synthesis of oligocycloisomaltosides consisting of two, three, four, and six monomer units. We recently reported the first synthesis of benzylated cycloisomaltotetraoside[8] using a modification of the Mukaiyama method for the cycloglycosylation step.[9]

We report here on the synthesis of benzylated cycloisomaltotrioside **9** and benzylated cycloisomaltohexaoside **10**. The glycosylation method proposed by Fraser-Reid based on activation of pentenyl glycosides with I^+[10] was used for the cyclization of the linear precursor **8** (Scheme 1). Along with the cyclic trimer **9** a small amount of the hexamer **10** and a nonsymmetric trimer **11** were also obtained (Scheme 2). These new compounds were characterized by NMR spectroscopy and mass spectrometry. Because of the symmetry of **9** and **10**, their NMR spectra, which exhibit the signals of a benzylated α-D-glucopyranoside, give no information about the number of monomers. The FAB$^+$ and DCI mass spectra clearly show molecular peaks consistent with the proposed structures of **9** and **10**. The NMR spectrum of **11** indicates three anomeric protons, two of which are α-configurated and one β-configurated according to the coupling constants. The molecular peak in the mass spectrum con-



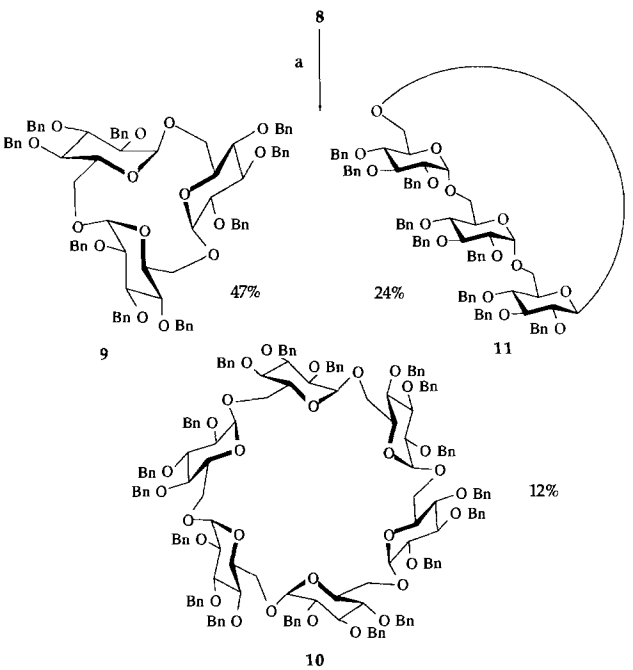
Scheme 1. Synthesis of the linear precursor **8** of the title compounds **9**, **10**, and **11**. Abbreviations: TBDPS = *tert*-butyldiphenylsilyl, Pent = pent-4-enyl. **a**: TBDPSCl, imidazole, DMF. **b**: diethylammonium sulfur trifluoride (1.5 equiv), *N*-bromosuccinimide, 1,2-dichloroethane, −15 °C. **c**: $AgClO_4$ (3 equiv)/$SnCl_2$ (3 equiv), Et_2O. **c'**: as in **c** but with 3 equiv reagents and 2.3 equiv **3**. **d**(1): HPLC; (2): tetrabutylammonium fluoride/THF (1 M), THF.

[*] Prof. Dr. P. J. A. Vottéro, Dr. S. Houdier
CEA/Département de Recherche Fondamentale sur la Matière Condensée
SESAM/MV, 85X, F-38041 Grenoble (France)

[**] We thank C. Lebrun and V. Chardin for technical assistance with column chromatography and HPLC separations.

firmed the trimeric structure of **11**. Studies of conformational and inclusion properties of **9**–**11** are in progress.

Scheme 2 outlines the cycloglycosylation of the linear precursor **8**. The cyclization was carried out unter high-dilution conditions to favor the intramolecular glycosylation over intermolecular reaction; the yield is quite good (83%). A compromise was found



Scheme 2. Cycloglycosylation of the linear precursor **8** by the Fraser-Reid method giving the title compounds **9**, **10**, and **11**. **a**: iodonium dicollidine perchlorate (2 equiv), 1,2-dichloroethane/Et_2O (1:1).

between rate and stereoselectivity by using a 1:1 mixture of 1,2-dichloroethane and diethyl ether as solvent for the reaction. Our experience has shown that a higher proportion of the α-configurated product (1,2-*cis*-glycosylation) is obtained with this solvent system, but the rate is generally slowed dramatically.[10] In the typical experiment described here, all traces of the linear precursor **8** disappeared within approximately 30 minutes. As a result of the solvent system, but probably also because of the strained molecular structure of **9**, a significant amount (24%) of the nonsymmetric benzylated cycloisomaltotrioside **11** with one β-1,6- and two α-1,6-linkages was produced by 1,2-*trans*-glycosylation. It is very interesting to note that no trace of nonsymmetric cycloisomaltohexaoside (one β-1,6- and five α-1,6-glucosidic linkages) was detected. This is probably due to the fact that practically no strain develops during the cyclization step leading to **10**, in contrast to the formation of **9** which is stereoselective. A molecular mechanics simulation will be undertaken to confirm or reject this hypothesis. NMR data are given in Tables 1 and 2 for compounds **9**–**11**.

Table 1. ^1H and ^{13}C NMR data for **9** and **10** ($CDCl_3$, 400 MHz, 100 MHz, δ values, *J* [Hz]).

δ	H-1	H-2	H-3	H-4	H-5	H-6a	H-6b
9	4.82	3.40	3.84	3.11	4.15	3.51	4.06
10	4.94	3.30	3.93	3.65	3.77	3.65	3.71
J	1,2	2,3	3,4	4,5	5,6a	5,6b	6a, 6b
9	3.54	9.77	9–10	10.44	6.96	4.15	11.72
10	3.48	9.58	9–10	7.86	4.00	1.90	8.33
δ	C-1	C-2	C-3	C-4	C-5	C-6	
9	97.94	80.37	81.38	80.56	71.39	71.58	
10	97.46	80.51	81.56 [a]		71.26	66.57	

[a] Signal overlaps with that of the solvent.

Table 2. ^1H and ^{13}C NMR data for **11** ($CDCl_3$, 400 and 100 MHz, respectively, δ values, *J* [Hz]).

δ	H-1	H-1′	H-1″	C-1	C-1′	C-1″
11	4.25	4.59	4.77	104.55	97.88	97.24
J	1,2	1′,2′	1″,2″			
11	7.01	3.71	3.69			

Experimental Procedure

General: Thin-layer chromatograms (Riedel de Haen 37332) developed by charring. Column chromatography (SiO_2 Merck 7734). NMR spectroscopy (Bruker AM400 or Varian Unity-400). Mass spectrometry (ZAB-SEQ(VG) for FAB^- or DCI modes; NERMAG R10-10 for DCI).

Compound **1** was prepared from the 6-*O*-trityl compound [8] by detritylation [11] (BF_3, Et_2O). Subsequent treatment with *tert*-butyldiphenylsilyl chloride [12] afforded **2**, which was fluorinated following the method of Nicolaou et al. [13] to give **3**. Compound **4** was prepared from the 6-*O*-trityl compound previously described [11].

5: **4** and **3**α, β (1.46 equiv) were dissolved in diethyl ether, and molecular sieves 4 Å were added. A mixture of silver perchlorate (3 equiv) and molecular sieves 4 Å in diethyl ether/THF (2:1) was prepared separately. The two solutions were stirred for 24 h before mixing. Tin(II) chloride (3 equiv) was finally added. After 4 d at room temperature the reaction mixture was diluted with dichloromethane, filtered on celite, and washed (saturated NaCl solution). The crude product was directly purified by HPLC (Merck L-6200 pump; IOTA refractometer; commercial column: Si-60/5 μm, LiChroCART 250-4; toluene/ethyl acetate 98:2). **5**α 59%, R_f 0.51 (toluene/ethyl acetate 95:5); **5**β 6%, R_f 0.41 (same solvent). MS (FAB^-) *m/z* (%): 1321.8(43) [$(M+Cs)^+$]. **5**α ^1H NMR ($CDCl_3$, 400 MHz): δ = 4.40 (d, 1H, H-1, $J_{1,2}$ = 7.82 Hz), 5.08 (d, 1H, H-1′, $J_{1',2'}$ = 3.51 Hz). ^{13}C NMR ($CDCl_3$, 100 MHz): δ = 26.70 (*t*Bu), 28.88(2), 30.13(3), 62.82 (C-6′), 65.13 (C-6), 68.95(1), 96.62 (C-1′), 103.28 (C-1), 114.76(5), 137.91(4), 127.32–138.86 (C arom.). **5**β ^1H NMR ($CDCl_3$, 400 MHz): δ = 4.42 (d, 1H, H-1, $J_{1,2}$ = 7.98 Hz), 4.52 (d, 1H, H-1′, $J_{1',2'}$ = 7.77 Hz). ^{13}C NMR ($CDCl_3$, 100 MHz): δ = 26.96 (*t*Bu), 29.06(2), 30.32(3), 62.83 (C-6′), 66.50 (C-6), 69.61(1), 74.78, 75.30, 75.80, 76.06 (6 × CH_2Ph), 103.80 (C-1 or C-1′), 104.16 (C-1 or C-1′), 115.01(5), 127.9–136.06 (C arom.), 138.15(4).

6: To a solution of **5**α in THF was added a 1 M solution (2 equiv) of tetrabutylammonium fluoride in THF. After 2 d the reaction mixture was diluted with 1,2-dichloroethane, washed with saturated NaCl solution, concentrated, and purified by column chromatography (SiO_2, petroleum ether/ether 4:1) to give **6** in 95% yield. R_f 0.36 (hexane/ethyl acetate, 7:3). ^1H NMR ($CDCl_3$, 400 MHz): δ = 4.36 (d, 1H, H-1, $J_{1,2}$ = 7.83 Hz), 4.96 (d, 1H, H-1′, $J_{1',2'}$ = 3.39 Hz); ^{13}C NMR ($CDCl_3$, 100 MHz): δ = 28.91(2), 30.13(3), 61.79 (C-6′), 96.87 (C-1′), 103.39 (C-1), 114.81(5), 127.44–128.31 (C arom.).

7 was prepared in analogy to **5**, except 2.3 equiv 3α, β (3.1/1) were employed. Yield: 54%; R_f 0.75 (hexane/ethyl acetate 7:3). MS (FAB^+): *m/z* (%): 1754.7 (63) [$(M+Cs)^+$]. ^1H NMR ($CDCl_3$, 400 MHz): δ = 4.42 (d, 1H, H-1, $J_{1,2}$ = 7.84 Hz), 5.04 (d, 1H, H-1″, $J_{1'',2''}$ = 3.51 Hz), 5.10 (d, 1H, H-1′, $J_{1',2'}$ = 3.51 Hz). ^{13}C NMR ($CDCl_3$, 100 MHz): δ = 26.68 (*t*Bu), 28.87(2), 30.10(3), 62.62 (C-6″), 65.36, 65.49 (C-6 or C-6′), 68.98(1), 72.01, 72.20, 74.73, 74.85, 75.42, 75.59 (9 × CH_2Ph), 80.20 (C-2″), 81.68 (C-3′), 82.24 (C-2), 96.82 (C-1′, C-1″), 103.30 (C-1), 114.78(5), 127.3–135.7 (C arom.), 137.85(4).

8 was prepared in analogy to **6**. Yield: 100%; R_f 0.46 (hexane/ethyl acetate 6:4). MS (FAB^-): *m/z* (%): 1515.6 (65.5) [$(M+Cs)^+$].

9–**11**: **13**, **14**, **15**: After dissolution of **8** (26 mg, 1.85×10^{-2} mmol) in 1,2-dichloroethane/diethyl ether (3 mL, 1:1) iodonium dicollidine perchlorate (2 equiv) was added. Although **8** disappeared totally within 30 minutes, the reaction mixture was left under stirring for another 12 h. The reaction mixture was then diluted with dichloromethane, washed (saturated $Na_2S_2O_3$ solution), and dried (Na_2SO_4). The crude product mixture was separated in two steps by HPLC (Merck L-6200 pump; IOTA refractometer; commercial Si-60/5 mm, LiChroCART 250-4); first step:

(hexane/ethyl acetate 83:17; flow rate: 2 mL min^{-1}), **9**: 47%; t_r (retention time) 24.17 min; R_f 0.6 (hexane/ethyl acetate 7:3), MS (FAB$^+$): *m/z* (%): 865(62) [(2*M*/3+H)$^+$], 1297(42) [(*M*+H)$^+$], 1319(100) [(*M*+Na)$^+$], 2616(5) [(2*M*+Na)$^+$]; MS (DCI): *m/z* (%): 1313.6(100), [(*M*+NH$_3$)$^+$], and (**10**+**11**) t_r 42.42 min; second step: (toluene/ethyl acetate 75:25; flow rate: 2 mL min^{-1}), **10**: 12%; t_r 5.58 min; R_f 0.48 (toluene/ethyl acetate 9:1), MS (FAB$^+$): *m/z* (%): 431.2(100) [*M*/6+H)$^+$], 865.3(10) [(*M*/3+H)$^+$], 2727.5(80) [(*M*+Cs)$^+$], MS (DCI): *m/z* (%): 2610.4(100) [(*M*+NH$_3$)$^+$], **11**: 24%; t_r 8.49 min; R_f 0.26 (toluene/ethyl acetate 9:1), MS (FAB$^+$): *m/z* (%): 865(12) [(2*M*/3+H)$^+$], 1429.3(100) [(*M*+Cs)$^+$], MS (DCI): *m/z* (%): 1314.6(100) [(*M*+NH$_3$)$^+$].

Received: August 7, 1993 [Z 6265 IE]
German version: *Angew. Chem.* **1994**, *106*, 365

[1] a) *New Trends in Cyclodextrins and Derivatives* (Ed.: D. Duchêne), Editions de Santé, Paris, **1991**; b) G. Schmid in [1a], p. 25; c) P. J. Sicard, M. H. de Santé in [1a], p. 75; S. Vaisman, *Biofutur* **1988**, *66*, 47–48.
[2] K. Takeo, K. Uemura, H. Mitoh, *J. Carbohydr. Chem.* **1988**, *7*, 293–308; P. Fügedi, P. Nanasi, P. Szejtli, *Carbohydr. Res.* **1988**, *175*, 173–181; S. Cottaz, H. Driguez, *Synthesis* **1989**, 755–758; J. Defaye, A. Gadelle, A. Guiller, R. Darcy, T. O'Sullivan, *Carbohydr. Res.* **1989**, *192*, 251–258.
[3] A. Gadelle, J. Defaye, *Angew. Chem.* **1991**, *103*, 94–95; *Angew. Chem. Int. Ed. Engl.* **1991**, *30*, 78–80; P. R. Ashton, P. Ellwood, I. Staton, J. F. Stoddart, *ibid.* **1991**, *103*, 96–97 and **1991**, *30*, 80–81.
[4] A. R. Khan, L. Barton, V. T. D'Souza, *J. Chem. Soc. Chem. Commun.* **1992**, 1112.
[5] T. Ogawa, Y. Takahashi, *Carbohydr. Res.* **1985**, *138*, C5–C9; Y. Takahashi, T. Ogawa, *ibid.* **1987**, *164*, 277–296; *ibid.* **1987**, *169*, 127–149; *Trends in Synthetic Carbohydrate Chemistry* (*ACS Symp. Ser.* **1989**, *386*, 150–158).
[6] D. Gagnaire, V. Tran, M. Vignon, *J. Chem. Soc. Chem. Commun.* **1976**, 6–7; D. Gagnaire, M. Vignon, *Carbohydr. Res.* **1976**, *51*, 140–144.
[7] M. Mori, Y. Ito, T. Ogawa, *Tetrahedron Lett.* **1990**, *31*, 3029–3030; P. M. Collins, M. H. Ali, *ibid.* **1990**, *31*, 4517–4520.
[8] S. Houdier, P. J. A. Vottéro, *Carbohydr. Res.* **1993**, in press.
[9] S. Houdier, P. J. A. Vottéro, *Tetrahedron Lett.* **1993**, *34*, 3283–3284.
[10] S. Houdier, P. J. A. Vottéro, *Carbohydr. Res.* **1992**, *232*, 349–352, and references therein on the Fraser-Reid glycosylation procedure.
[11] D. R. Mootoo, P. Konradson, U. Udodong, B. Fraser-Reid, *J. Am. Chem. Soc.* **1988**, *110*, 5583–5584.
[12] S. Hannessian, P. Lavallée, *Can. J. Chem.* **1975**, *53*, 2975–2977.
[13] K. C. Nicolaou, R. E. Dolle, D. P. Papahatjis, J. L. Randall, *J. Am. Chem. Soc.* **1984**, *106*, 4189–4192.

Synthesis and Structure of the Magnesium Imide [(thf)MgNPh]$_6$**

Tony Hascall, Karin Ruhlandt-Senge, and Philip P. Power*

Metal imides[1] may, most simply, be represented by the monomeric formula MNR (M = divalent metal, R = H, alkyl, or aryl group). In reality, however, monomeric structures are not observed in condensed phases owing to the tendency of the MNR units to associate strongly. In main group chemistry this behavior is exemplified by the polyiminoalanes (R'AlNR)$_n$[2] and compounds of the composition (MNR)$_n$ (where M is a main group 4 metal (Ge, Sn, or Pb) in a lower oxidation state).[3–5] Usually, association numbers of $n \geq 4$, are observed for these compounds, and the resulting structures are three-dimensional cages. At present, however, no well-characterized homometallic imido derivatives of the neighboring main group 2 elements have been reported.[6] In this paper, the first X-ray crystal structure of such a species is now described.

[*] Prof. P. P. Power, T. Hascall, Dr. K. Ruhlandt-Senge
Department of Chemistry, University of California
Davis, CA 95616 (USA)
Telefax: Int. code + (916)752-8995

[**] This work was supported by the National Science Foundation and the Petroleum Research Fund.

The title compound **1** · THF was synthesized as a colorless

[(thf)MgNPh]$_6$ **1**

crystalline material by the straightforward reaction of Et_2Mg with H_2NPh in ether and crystallization from hexane/THF. The ^1H and ^{13}C NMR spectra are consistent with a 1:1 stoichiometry of THF and Ph ligands in **1**. The X-ray crystal structure analysis of **1**[7] reveals a slightly distorted hexagonal-prismatic framework of magnesium and nitrogen atoms arranged in an alternating manner at the apices (Fig. 1). Each nitrogen atom

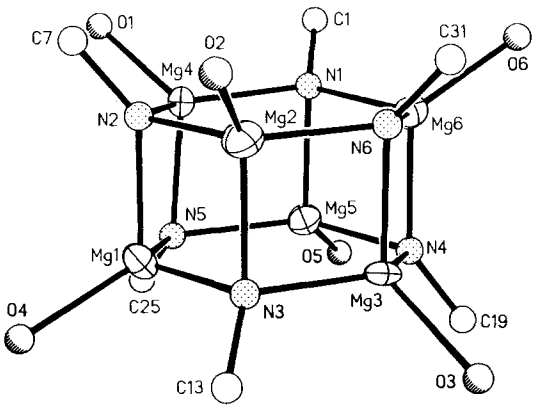


Fig. 1. Molecular structure of **1** (computer-generated). For clarity, only the oxygen atoms of the THF molecules, *ipso*-carbon atoms of the Ph substituents, and the Mg_6N_6 framework are shown.

bears a phenyl substituent, whereas the magnesium atoms are each solvated by a single THF donor molecule. The N and Mg atoms are thus tetracoordinated in a distorted-tetrahedral fashion. The average Mg–N distance between the six-membered rings (2.08 Å) is slightly longer than the average Mg–N bond length (2.05 Å) within the six-membered rings. In addition, the parallel, hexagonal Mg_3N_3 arrays are almost planar with a slight distortion toward chair configurations. The maximum deviation of Mg or N atoms from the best-fit plane is no greater than 0.08 Å. The average internal angle at the Mg atoms (122.7°) in the six-membered ring is greater than that at the N atoms (116.5°). The average Mg–O bond length is 2.04 Å and the average N–C distance is 1.37 Å.

The structure observed for **1** closely resembles those found for the related iminoalanes (R'AlNR')$_6$,[8, 9] which also possess hexagonal prismatic frameworks with slightly puckered Al_3N_3 ring planes. As in **1** the Al–N distances between the six-membered rings are longer (e.g. 1.956 vs. 1.898 Å in [HAlN(*i*Pr)]$_6$[8]) than those within the rings. The Mg–N bonds in **1** are, of course, longer than these distances owing to the larger radius of magnesium (1.45[10] vs. 1.3 Å[10] for Al). The Mg–N bond lengths in **1** are, in fact, very close to those observed (Mg–N = 2.09 Å) in the cubane species **2**[11] in which one of the Al–H corners is

[(HAlN*t*Bu)$_3${MgN*t*Bu(thf)}] **2**

replaced by a Mg(thf) moiety. Compound **2** appears to be the only other instance of the involvement of a magnesium atom in a metal-imide cage structure.[6, 12] The Mg–N distances in cage species **1** and **2** can be regarded as being relatively short, since they involve λ^4-Mg-λ^4-N type bonds (cf. 2.055 for λ^4-Mg-λ^3-N connectivity in [(thf)$_2$Mg(N*t*Bu)$_2$(SiMeN*t*Bu)$_2$],[13] 2.118 Å for

λ^3-Mg-λ^4-N bonds in $[\{s\text{BuMgN(SiMe}_3)_2\}_2]$,[14] 2.082 Å for λ^4-Mg-λ^4-N bonds in $[\{(Et_2O)Mg(NSiMe_3)_2C_6H_4\}_2]$[15]). The average Mg–O distances in **1** and **2** are also very similar (2.04 and 2.002 Å, respectively).[11]

In summary, it has been shown that a magnesium imide $[(thf)MgNPh]_6$ (**1**) can be readily synthesized and crystallized in a facile manner. Its structure is similar to that observed for the related $(R'AlNR)_6$ hexamers. It remains to be seen whether the reactivity pattern of **1** will have widespread synthetic applicability. An investigation of the chemistry and the potential structural diversity of these novel species is now in progress.

Experimental Procedure

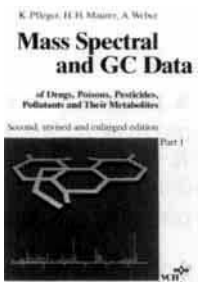
All manipulations were carried out under anaerobic and anhydrous conditions. Diethyl magnesium was prepared by the dioxane precipitation method [16] from the corresponding Grignard reagent. After evaporating the solvent, coordinated ethers were removed by heating at 170 °C under high vacuum for 2 h [17].

Freshly distilled (over $LiAlH_4$) aniline (0.66 g, 7.1 mmol) was dissolved in diethyl ether (30 mL) and added with cannula to a solution of Et_2Mg (0.71 g, 8.7 mmol) in Et_2O (30 mL). This resulted in a slight warming of the mixture and gas evolution. The solution was stirred for a further 1 h whereupon the volume of Et_2O was reduced to 30 mL. Addition of hexane (5 mL) afforded a white precipitate which was dissolved in THF (45 mL). Filtration over a bed of Celite followed by cooling the solution in a −20 °C freezer gave white crystals of **1** · THF. Yield 0.50 g, 38%. The crystals rapidly turned brown on exposure to air and did not melt on heating to 320 °C but showed evidence of desolvation. The IR spectrum (nujol mull) displays several bands in the metal–ligand region (< 600 cm^{-1}) that are presumably due to Mg–O and Mg–N stretching bands: 580, 550, 510, 480, 320 cm^{-1}; ^1H NMR: (300 MHz, C_7D_8) δ = 1.203 (s, 4H, THF), 3.58 (m, 4H, THF), 6.45 (m, 1H, *p*-H), 6.83 (m, 2H, *m*-H), 7.013 (m, 2H, *o*-H). $^{13}C\{^1H\}$ NMR: (75.47 MHz, C_7D_8) δ = 24.64 (s, THF), 69.38 (s, THF) 109.76 (s, *o*-C), 128.96 (s, *m*-C), 167.82 (s, *ipso*-C).

Received: August 23, 1993 [Z 6310 IE]
German version: *Angew. Chem.* **1994**, *106*, 350

[1] There appears to be some controversy with regard to the nomenclature of these species in the literature. This arises from the fact that the description "metal imide" has also been applied to species of formula $M(N{=}CR_2)_n$.
[2] M. Cesari, S. Cucinella in *The Chemistry of Inorganic Homo- and Heterocycles, Vol. 1* (Eds.: I. Haiduc, D. B. Sowerby), Academic Press, London, **1987**, Ch. 6, p. 167.
[3] M. Veith, *Angew. Chem.* **1987**, *99*, 1; *Angew. Chem. Int. Ed. Engl.* **1987**, *26*, 1; *Chem. Rev.* **1990**, *90*, 1.
[4] R. A. Bartlett, P. P. Power, *J. Am. Chem. Soc.* **1990**, *112*, 3660; H. Chen, R. A. Bartlett, H. V. R. Dias, M. M. Olmstead, P. P. Power, *Inorg. Chem.* **1991**, *30*, 3390.
[5] P. B. Hitchcock, M. F. Lappert, A. J. Thorne, *J. Chem. Soc. Chem. Commun.* **1990**, 1587.
[6] Species which have elemental analyses corresponding to the formula $(MNR)_x$ (M = Mg or Zn; R = alkyl or aryl group) have been obtained from the thermal decomposition of $R'MNR_2$ precursors: E. C. Ashby, G. F. Willard, *J. Org. Chem.* **1978**, *43*, 4750.
[7] Crystal data at 130 K with $Mo_{K\alpha}$ (λ = 0.71073 Å radiation: a = 34.574(5), c = 11.474(3) Å, tetragonal, space group $P\bar{4}2_1c$, Z = 8, 2268 ($I > 3\sigma(I)$) data, R = 0.093. Further details of the structure may be obtained from the Fachinformationszentrum Karlsruhe, D-76344 Eggenstein-Leopoldshafen (FRG), on quoting the depository number CSD-57888, the names of the authors and journal citation.
[8] M. Cesari, G. Perego, G. Del Piero, S. Cucinella, E. Cernia, *J. Organomet. Chem.* **1974**, *78*, 203.
[9] G. Del Piero, G. Perego, S. Cucinella, M. Cesari, A. Mazzei, *J. Organomet. Chem.* **1977**, *136*, 13.
[10] J. Huheey, *Inorganic Chemistry*, 3rd edition, Harper-Row, New York, **1983**, p. 258.
[11] G. Del Piero, M. Cesari, S. Cucinella, A. Mazzei, *J. Organomet. Chem.* **1977**, *137*, 265.
[12] The structure of one other cluster related to **1**, has been published. This is the the nitrido/amido species $[Mg_6N(NHtBu)_9]$ which has a trigonal prismatic arrangement of Mg^{2+} ions surrounding N^{3-} ions: G. Dozzi, G. Del Piero, M. Cesari, C. Cucinella, *J. Organomet. Chem.* **1980**, *190*, 229.
[13] M. Veith, F. Goffing, V. Huch, *Z. Naturforsch. B* **1988**, *43*, 846.
[14] L. M. Engelhardt, B. S. Jolly, P. C. Junk, C. L. Raston, B. W. Skelton, A. H. White, *Aust. J. Chem.* **1986**, *39*, 1337.
[15] A. W. Duff, P. B. Hitchcock, M. F. Lappert, R. G. Taylor, J. A. Segal, *J. Organomet. Chem.* **1985**, *293*, 271.
[16] W. Schlenk, W. Schlenk, *Chem. Ber.* **1929**, *62*, 290.
[17] W. Strohmeier, F. Seifert, *Chem. Ber.* **1961**, *94*, 2356.

Mass Spectral and GC Data of Drugs, Poisons, Pesticides, Pollutants and Their Metabolites. Volumes 1–3. 2nd edition. By *K. Pfleger, H. H. Maurer* and *A. Weber*. VCH Verlagsgesellschaft, Weinheim/VCH Publishers, New York, 1992. XXIX, 4224 pp., hardcover DM 1290.00.—ISBN 3-527-26989-4/0-89573-855-4



In clinical toxicology the diagnosis of toxic symptoms requires that a poison must be definitely identified from the various possibilities in a very short time, so that remedial treatment can begin as soon as possible. Mass spectrometry in combination with gas chromatography (GC–MS) has become established as the analytical method of choice for this application. The mass spectra obtained by electron impact ionization in the full scan mode yield detailed structural information which can be verified by comparing with reference spectra. For this purpose, in 1985 the authors of this work published the first (two-volume) version, a compilation of over 1500 mass spectra of drugs, poisons, and their metabolites. In this second, three-volume edition the collection has been enlarged to include data from further toxicological studies. Of the 4370 spectra about 1500 are of drugs and poisons, 800 of pesticides and environmental pollutants, and 2000 of metabolites.

In addition to giving mass spectra (measured in their own laboratory) of all these biologically active substances and metabolites, with details of artefacts resulting from the sample preparation or from the gas chromatographic separation, the authors also relate these directly to the corresponding sample matrix (e.g., plasma, intestine contents, urine, or the pure compound). Volume 1 describes the analytical procedures used, including extraction, derivatization, concentration, and measurement of retention time (RT) index. Computer monitoring programs for rapid detection of individual suspected compounds are also given; with these one searches for specific substances in defined retention time windows using the ion-specific mass chromatogram. To complete this volume there are tables in which the substances are indexed according to compound name (or common name), active groups, RT index, exact molar mass, and CAS Registry number.

All this information, coded by means of a set of abbreviations, as well as molecular and structural formulas, is given along with the individual mass spectra. One is also told whether or not background subtraction has been applied to the spectrum shown, since this can affect the intensity ratios of the ions. Also important are the indications given in cases where the analysis of standard solutions is essential for unambiguous identification, and especially for quantification.

With electron impact ionization the molecular ion peak, whose mass is the most important piece of structural information, is not always strong enough to be measured satisfactorily. Consequently the arrangement of the mass spectra in Volume 2 ($m/z = 4$ to 221 amu) and Volume 3 ($m/z = 222$ to 777 amu) is not wholly consistent, being in order of increasing mass of a characteristic fragment ion or of the molecular ion itself. Thus, for example, in the mass spectra of the morpholine fungicides one finds tridemorph (p. 491) listed under the base peak $m/z = 128$, whereas fenpropimorph (p. 1502) appears under the molecular ion $m/z = 303$, despite the fact that the base peak is at $m/z = 128$. Consequently, when searching for compounds according to their molar mass one must first refer to Table 4 in Volume 1 to find the page numbers of the corresponding spectra in Volumes 2 or 3. In cases where there are two further ion peaks with intensities greater than 80% of the base peak, variations in measurement conditions affecting the intensities can result in the mass spectrum appearing twice. Thus, the metabolites of the neuroleptic agent promethazine-M (Nor-sulfoxide) after acetylation give as the strongest ion peaks $m/z = 58$ and $m/z = 212$ (base peak). However, following the entry under $m/z = 58$ (p. 104), the second entry appears not under the base peak but under the molecular ion $m/z = 328$ (p. 1634). The system whereby an individual mass spectrum can appear twice therefore seems to be rather unhelpful, especially since in this example only the mass spectrum on page 1634 is listed in the volume containing the tables (Vol. 1).

The data systems of modern mass spectrometers include commercially available libraries of spectra such as the NIST or Wiley collections, containing as many as 130000 entries, which can be augmented by users' own spectra libraries. One therefore has to question the justification for producing this present spectra collection in book form. However, a comparison of the spectra entries reveals that the standard collections only partly cover the range of compounds included in this Pfleger/Maurer/Weber library, which is expressly intended for use in systematic clinical and toxicological analysis, and is also an important resource for toxicological work in the fields of legal medicine, the workplace, food analysis, and the environment, as well as the control of doping. Whereas computerized spectra libraries often consist only of reduced mass spectra, those reproduced in these volumes are complete spectra with much useful additional information.

On-line library searching allows one to apply different search criteria and thus offers greater flexibility, and therefore for routine analysis it is desirable to be able to use the Pfleger/Maurer/Weber library in computerized form. However, it is not available from all mass spectrometer manufacturers, as licensing arrangements do not exist in all cases. Moreover, for some mass spectrometers, especially older ones, compatible data storage media are not available, and thus the three-volume work should prove a valuable resource in these cases.

Robert Kreuzig, Müfit Bahadir
Institut für Ökologische Chemie
und Abfallanalytik
der Technischen
Universität Braunschweig (FRG)

Relationships between Structure and Function of Cytochrome P-450—Experiments, Calculations, Models. (Series: Frontiers in Biotransformation, Vol. 7.) Edited by *K. Ruckpaul* and *H. Rein*. Akademie-Verlag, Berlin, 1992. VIII, 370 pp., hardcover DM 224.00. —ISBN 3-05-501 329-8

Researchers in the field of cytochrome P-450 are currently investigating possible ways around the unsolved problem of the three-dimensional structure of the isoforms of membrane-bound eukaryontic P-450. Of the three prokaryontic soluble forms of cytochrome P-450 that have so far been crystallized, a detailed structural characterization has up to now been achieved for only one of these (P-450-cam). Therefore, in order to get the information about structure–function relationships that is so essential for understanding the many reactions of biosynthesis, toxicity, and

This section contains book reviews and a list of new books received by the editor. Book reviews are written by invitation from the editor. Suggestions for books to be reviewed and for book reviewers are welcome. Publishers should send brochures or (better) books to the Book Editor, Dr. Gerhard Karger, Redaktion Angewandte Chemie, Postfach 101161, D-69451 Weinheim, Federal Republic of Germany. The editor reserves the right of selecting which books will be reviewed. Uninvited books not chosen for review will not be returned.

detoxification that are catalyzed by P-450, there is no alternative to the approaches based on modeling of proteins, directed mutagenesis, matching of ligands, comparisons with analogous (or supposedly analogous) model systems, more sophisticated methods of spectroscopic analysis, etc. This volume collects together some of the results obtained by such strategies.

The editors have recruited a team of competent authors to prepare the ten chapters. The book begins with a chapter on that same P-450-cam (one is tempted to add, in accordance with tradition), in which Raag and Poulos emphasize the importance of matching the substrate to the enzyme used for the catalysis. This is followed by a shorter contribution by Strobel summarizing current ideas about the likely topology of eukaryontic cytochrome P-450 variants in membranes of the endoplasmic reticulum. An excellent review by Woggon and Matile provides an introduction to the 'P-450 mimics', metalloporphyrin models that can simulate the bonding to and activation of substrates, the role of the thiolate group, and the embedding of cytochrome P-450 in lipid membranes. Lewis discusses, with an appropriate degree of reserve and critical caution, the possibilities of using computer modeling as an aid to rationalization in making predictions about carcinogenicity, in the context of known metabolic reactions and known structural characteristics of P-450 variants. In another highly informative contribution Loew and Collins give an impressive account of the interesting results (predictions of regio- and stereoselectivities) that can be obtained by integrating together a number of different experimental and modeling strategies. Hildebrandt contributes an article on studies of P-450 by resonance Raman spectroscopy.

The articles that follow are concerned with the characterization of enzyme systems, which one can expect to lead indirectly to further insights into the structure and function of P-450. Hawkins and Dawson discuss the only monooxygenase that is not a P-450 (which catalyzes the oxidative *N*-dealkylation of secondary amines in certain bacteria), mainly from the viewpoint of the iron–oxygen interaction, while Veitch and Williams give a general overview of electron transfer systems, including cytochromes c and b_5 and iron–sulfur clusters. After this digression the two concluding chapters revert to concentrating solely on P-450. Gray summarizes current knowledge regarding electron transfer in P-450 monooxygenase systems, and discusses the importance of each individual component, which involves some overlapping with the subject matter of the preceding chapter. In the final article Lu gives a lucid introduction to the interpretation of the deuterium isotope effect and the contribution that this brings to understanding the P-450 catalyzed cleavage of C–H bonds.

This book appears at a rather turbulent time in the progress of such research. In the first place, work is proceeding on the three-dimensional structure of bacterial $P\text{-}450_{BM-3}$, which shows promise as a model for most eukaryontic cytochrome P-450 variants, but it has not been possible to include that work in this volume. Secondly, there is active competition in books on this theme: the past year saw the appearance of Volume 206, *Cytochrome P-450*, in the *Methods in Enzymology* series, which contains not only detailed procedures for the analysis of P-450 enzymic activities, for purification, and for heterologous expression, but also some limited information about P-450 structures. And now Volume 105 of the *Handbook of Experimental Pharmacology*, also entitled *Cytochrome P-450*, has been published, containing a greater number of individual contributions which make up a survey that is nearly exhaustive, although orientated mainly towards P-450 function.

In this area of research the volume reviewed here suffers from the disadvantage that, although the chosen topics are certainly interesting and are competently reviewed (covering publications up to mid-1991 in most cases), such a selection does not provide a consistent overview of the current state of knowledge on P-450 structural characteristics, nor is it claimed by the editors to do so. It seems to this reviewer that the work could have been improved if the editors had exercised firmer control to impose some order; in particular it would have made life easier for the reader seeking information if the contents of the individual volumes of the series were more clearly coordinated with each other, at least by cross-referencing and perhaps also by a cumulative index. For example, important information relating to the structure of P-450-cam (corresponding to Ch. 1 of this volume) also appears in Volume 4 of the series (*Microbial and Plant Cytochromes P-450*), information on P-450 insertion into membranes (corresponding to Ch. 2) also appears in Volume 5 (*Membrane Organization and Phospholipid Interaction of Cytochrome P-450*), and information on metalloporphyrin models (corresponding to Ch. 3) can also be found in Volume 1 (*Basis and Mechanisms of Regulation of Cytochrome P-450*).

Nevertheless, this volume forms an appropriate extension to and advance on the earlier volumes that appeared in the *Frontiers in Biotransformation* series from 1989 onwards. As a comprehensive work on this field the series is almost unrivalled, and it should be in the departmental library of every laboratory with ambitions in this area, whether concerned primarily with biochemistry, microbiology, pharmacology, endocrinology, or protein structure.

W. Nikolaus Kühn-Velten
Institut für Physiologische Chemie
der Universität Düsseldorf (FRG)

A Dictionary of Concepts in NMR. (Biophysical Techniques Series. Series editor: *R. A. Dwek.*) By *S. W. Homans.* Clarendon Press, Oxford, 1992. VI, 372 pp., paperback £ 17.50.—ISBN 0-19-854765-X

This book is an introduction to the basic concepts of NMR spectroscopy. The theoretical fundamentals are explained under subject headings arranged alphabetically, together with a brief mathematical appendix on the properties of cartesian product operators, trigonometric identities, matrix algebra, and rotation operators. As the author explains in his preface, the book is intended to help the reader with a basic knowledge of NMR spectroscopy to deal with the confusing plethora of acronyms and technical jargon. He believes that this form of presentation enables the reader to get a quick overview of a particular topic in NMR spectroscopy without a laborious study of the original literature. The book is intended especially for chemists and biochemists concerned with applications, so that they can remedy gaps in their understanding of the methods that they are using to an ever greater extent.

The subject headings have been well chosen. There is a definite emphasis on the description of multidimensional NMR experiments on solutions, and nearly all the applications described are taken from the armory of methods used for determining the structures of biochemical macromolecules. At least of equal importance to this is the quality of the information given. In this respect we find that there are peaks and troughs. Apart from a few small errors the most important standard procedures such as COSY and NOESY (each occupying about ten pages) are explained clearly and in considerable detail, with the help of the product operator formalism. The liberal use of the latter concept for describing NMR experiments, combined with a good introduction under the relevant subject heading, is undoubtedly an important

 © VCH Verlagsgesellschaft mbH, D-69451 Weinheim, 1994 0570-0833/94/0303-0360 $ 10.00+.25/0

positive aspect of the book. Based on this foundation the book provides clear explanations of even those methods that have been most recently adopted into biological NMR spectroscopy, the 3D and 4D techniques (HCACO, HCA[CO]N, HNCA, and HNCO). The pulse sequences shown here have already been superseded by new ones, but this can hardly be avoided in a field that is undergoing such rapid development. The descriptions of the basic principles of NMR spectroscopy also leave one with a positive impression. This applies to the quantum-mechanical aspects as well as to the terminology of Fourier analysis. Regrettably, however, there is no quantum-mechanical discussion of relaxation phenomena, despite their great importance in structure determination. One searches in vain for the heading "heteronuclear T_1 values", even though these are essential parameters for describing internal mobilities in systems such as proteins. The absence of a more thorough introduction to relaxation theory is all the more surprising when one notes that the author does not shrink elsewhere from explaining relationships that are more difficult than these. The explanations under the headings "Average Hamiltonian theory" and "Dyson time ordering parameter" could easily have been omitted in favor of relaxation, especially since one is none the wiser after reading them.

In the descriptions of the NOESY and ROESY procedures it is always assumed that one is dealing with large molecules for which the extreme narrowing condition does not apply, which is perhaps reasonable from a biochemical standpoint. However, this leads the author to the erroneous conclusion that one can never distinguish between exchange effects and nuclear Overhauser effects in NOESY spectra. The discussion of the ROESY experiment is also not very satisfactory. The statements regarding the possibility of integrating ROESY cross-peaks, and in particular the view that the transmitter frequency should be positioned on the low-field side of the spectrum to avoid TOCSY peaks, do not reflect the state of the art in 1992 when the book was published. Also the description of the *z*-filter technique as one whose use is restricted to generating pure phases in 2D spectra does not convey the true importance of the device.

In our view one of the book's most serious shortcomings is that the literature references given at the ends of the articles are often not up-to-date and not very relevant. This is especially obvious under the important heading "Cross relaxation". The references begin (correctly) with the historically important paper by I. Solomon in *Physical Reviews* (1955), but then there is only one reference to the special problems of cross-relaxation in proteins from a 1976 paper! On following up the cross-references (e.g., to "Spin-lattice relaxation" and "Nuclear Overhauser effect") one at last finds the classical 1971 book on the nuclear Overhauser effect by Noggle and Schirmer. The modern treatment of the subject in the excellent monograph by Williamson and Neuhaus (1989) is, unfortunately, not listed. A more extensive and up-to-date listing of carefully chosen literature references would have made this a valuable resource for the reader!

It also seems quite incomprehensible that the author has failed to include methods for determining coupling constants. The important E.COSY experiments for this purpose are not mentioned. The book seriously undervalues the importance of this NMR parameter, which is so relevant to conformation, especially in biopolymers. The treatment of the Karplus relationship is very short on detail, which is consistent with the above undervaluation. The uninitiated reader would get the impression that coupling constants are of a similar nature to house numbers, with little relevance to structure. Here, as also in the descriptions of the NOESY and ROESY experiments, the reader interested specifically in obtaining structural information is offered no help whatsoever.

In addition to these shortcomings in the contents, it also becomes apparent that this paperback version is not very successful in its external appearance and in the author's lack of care in adopting illustrations from the original papers. Figures and legends that do not belong together have been copied uncritically from the original literature (see HMQC, HMBC). On page 189 (at least in this reviewer's copy), the reader encounters total chaos, for which the author is, of course, not responsible. Here, in order to follow the discussion, one needs to make a tremendous mental leap, since the explanation of "Magnetogyric ratio" begins at the foot of this page, whereas the top of the next page unexpectedly continues in the middle of "Multiple quantum filter", followed by an equally abrupt switch to an explanation of "Matrix representation". The beginning of the latter and the equations M4 to M16 that belong with it are missing altogether. Instead one finds on pages 203 and 204 a repeat of pages 190 and 191! A survey of the findings of colleagues who also possessed copies of Homan's book showed that anyone buying it has about a 50% chance of enjoying this "random reading".

However, although this review has up to now emphasized the negative aspects of the book, it must be said in conclusion that it affords the interested user of modern NMR methods quick access to basic information on many important topics. Despite its faults it can be recommended for the readership mentioned in the preface (biologists and chemists with biological interests), especially in view of the affordable price. But it certainly does not live up to the author's claim of eliminating the need to study more advanced texts, nor of giving easy access to relevant literature.

Michael Reggelin, Harald Schwalbe
Institut für Organische Chemie
der Universität
Frankfurt am Main (FRG)

Fourier Transform Raman Spectroscopy. Instrumentation and Chemical Applications. By *P. Hendra, C. Jones* and *G. Warnes*. Ellis Horwood, Chichester, 1991. 311 pp., hardcover $ 90.50.—ISBN 0-13-327032-7

To state the most important fact first: this book is a must for anybody considering the purchase of a Raman spectrometer for almost any conceivable application or contemplating the addition of Raman spectroscopy to an analytical laboratory already operating a Fourier Transform infrared spectrometer. It is a recommended text for researchers and students alike interested in an up-to-date introduction to vibrational spectroscopy focussing on instrumentation and applications.

After a brief historical background of Raman spectroscopy in the first section, the second chapter outlines the vibrational behavior of molecules and their absorption and scattering of electromagnetic radiation. Conventional Raman spectrometers and their components are discussed in the third chapter; this section contains much information that is difficult to get from manufacturers' instructions supplied with some conventional instruments. Vibrational Fourier transform (FT) spectroscopy is discussed next; after dealing with technical aspects the authors clearly explain the principal advantages of interferometry (the Jacquinot, Fellgett, and Connes advantages). The development of practical FT Raman spectroscopy, sampling, safety, and criteria for instrument purchasing are discussed in Chapter 6.

 © VCH Verlagsgesellschaft mbH, D-69451 Weinheim, 1994 0570-0833/94/0303-0361 $ 10.00+.25/0

The determination of Raman intensities for quantitative measurements is discussed in the next section. Advantages compared with dispersive spectrometers, where these calculations are rather difficult, are clearly indicated. The remaining chapters are devoted to a broad survey of applications of FT Raman spectroscopy in organic, inorganic, surface, and polymer chemistry, and biology. Numerous examples illustrating the advantages are provided. The lack of fluorescence that results from sample excitation with near-infrared laser light in a region of the spectrum where few absorptions occur is the most obvious argument in favor of FT Raman spectroscopy. In addition the ease of data manipulation and the capability for quantitative analysis even of complicated samples indicate a bright future for FT Raman spectroscopy. A brief outlook to further instrumental developments and an appendix explaining data processing in FT spectrometers in a very lucid and understandable manner are presented in the last chapters. The index is brief, but it seems to contain enough keywords to facilitate using the book.

There are only a few minor weak points and errors. The trace for the ideal output function of a monochromator in Figure 3.8 has been omitted, and presumably trace d is meant when reference is made in the text to trace b. When discussing the advantages of charge-coupled devices as detectors, a word about the smaller dynamic range of these devices as compared to photomultipliers might have been appropriate. The authors use the term "Jacquinot stops" for the interferometer components usually referred to by instrument manufacturers as apertures; unfortunately this is not explained anywhere in the book. The width of vibrational bands is generally described by giving the full width at half maximum, commonly abbreviated as FWHM; in this book it is called FWHH (H = height). In the chapter on surface enhanced Raman spectroscopy (SERS) the enhancement mechanism discussed is confined to electromagnetic contributions; considering the wealth of review papers a more balanced view including other explanations should have been possible.

Anybody wondering about the plastic duck on the book's front cover will find on page 179 the experimental arrangement used in measuring the FT Raman spectrum of the plastic material whose spectrum is also displayed on the cover. Better than any words this illustrates the ease of using FT Raman spectroscopy to study real world samples.

All the chapters contain short lists of references and an additional bibliography of pertinent books, enabling the reader to easily locate the original papers discussed and to find additional literature for further reading. The many figures and photographs are carefully reproduced, and they support the text in a very eye-opening way. Considering the size and quality of the book the price seems to be appropriate both for libraries operating on a tight budget and for interested researchers.

Rudolf Holze
Fachbereich Chemie
der Technischen Universität
Chemnitz-Zwickau (FRG)

Electron Paramagnetic Resonance of d Transition Metal Compounds. (Series: Studies in Inorganic Chemistry, Vol. 16.) By *F. E. Mabbs* and *D. Collison*. Elsevier, Amsterdam, 1992. XX, 1326 pp., hardcover HFl 995.00, $ 622.00.—ISBN 0-444-89852-2

This book of 18 chapters and 13 appendices gives a very comprehensive and detailed description of the application of continuous-wave (CW) EPR spectroscopy to transition metal complexes. It is intended mainly for all chemistry undergraduate and graduate students, as well as interested readers from neighboring disciplines. Beginners are recommended to start by reading Chapters 1, 2, and 4.

Eight of the chapters are devoted to a description of the EPR of systems with spin $S = 1/2$ and of complex molecules with $S > 1/2$, which is well-balanced and of gradually advancing difficulty. The authors explain thoroughly all the relevant magnetic interactions ($\boldsymbol{B}_0.\boldsymbol{S}$, $\boldsymbol{S}.\boldsymbol{I}$, $\boldsymbol{S}.\boldsymbol{S}$, $\boldsymbol{B}_0.\boldsymbol{I}$) and electric (quadrupole) interactions, and the effects of symmetry on these interactions (based on ligand field theory), extending even to cases of non-coincident tensor principal axes in ligand hyperfine structure interactions. However, although the material is skillfully presented, CW-EPR is not the most appropriate experimental technique for studying the last-named interactions, nor for the majority of small quadrupolar effects, and even simulations are not very helpful.

In contrast to most treatments by other authors, the mathematical derivations of the relationships that make up the essential 'toolkit' of formulas for EPR spectroscopy are here given in full and explicit detail. One's first reaction is that this will probably cause the uninitiated reader just as much 'pain' as it would to read up these matters in the more usual compact form of presentation. On second thought, however, the reader will come to appreciate the value of this approach, as it clearly explains the intermediate steps leading to the final result. Moreover, there are practically no errors in the equations and formulas! The explanations presented are especially valuable for users who rely exclusively on standard EPR software (Ch. 16), as they will learn the basic principles on which their work depends. Equally useful are the many simulated spectra, which occupy more than 500 pages distributed throughout the chapters; these show very clearly the effects of altering the various spectral parameters for paramagnetic species with different symmetry properties. These enable even a chemist with only a basic knowledge of EPR to become aware of the more detailed aspects of the problem in hand and to assess their relative importance.

It is unfortunate that in such a detailed treatment of the EPR of transition metal complexes there is little or no discussion of ligand exchange reactions in complexes and their thermodynamics and kinetics, nor of short-lived complexes. Dynamic effects have been excluded so far as possible, and the Jahn–Teller effect receives only a bare mention. Relaxation effects are briefly discussed in Chapter 18. However, the authors explain in the preface that they make no claim to completeness.

To summarize, the book offers a very comprehensive description of CW-EPR, treating in particular detail the mathematical armory needed, with simulated spectra to illustrate the discussion, and useful additional information in the appendices. Newcomers to EPR spectroscopy need not be deterred, but must have a sound mathematical background knowledge; Chapters 1, 2, and 4 are recommended for beginners, and can be read in a short time. However, the price is very high for newcomers to the field. On the other hand, the book will prove indispensable for departments that have already installed equipment for EPR spectroscopy.

Reinhard Kirmse
Institut für Anorganische Chemie
der Universität Leipzig (FRG)

 © VCH Verlagsgesellschaft mbH, D-69451 Weinheim, 1994 0570-0833/94/0303-0362 $ 10.00+.25/0

New Books

Bioconversion of Cereal Products. Edited by **B. Godon.** VCH, Weinheim/New York, **1993.** 219 pp., hardcover, DM 168.–/$ 100.– –ISBN 3-527-89600-7/1-56081-600-7

Wörterbuch: Umweltschutz/Protection de l'Environnement. By **D. Lukhaup.** VCH, Weinheim, **1993.** 527 pp., hardcover, DM 178. .—ISBN 3-527-28243-2

Vom Wasser, Band 81. By **Fachgruppe Wasserchemie of the Gesellschaft Deutscher Chemiker.** VCH, Weinheim, **1993.** 413 pp., hardcover, DM 268.– (GDCh-Mitgliedspreis: DM 210.–).— ISBN 3-527-28566-0

Cumulative Index for Volumes 1 to 12. Corrosive Agents and Their Interaction with Materials. (DECHEMA Corrosion Handbook). Edited by **D. Behrens, G. Kreysa, R. Eckermann.** VCH, Weinheim/New York, **1993.** 256 pp., hardcover, DM 295.–/$ 190.–.—ISBN 3-527-28640-3/1-56081-856-5

Bioreaktionen. Prinzipien, Verfahren, Produkte. By **O. P. Ward.** Springer, Heidelberg, **1993.** 259 pp., paperback, DM 68.– . –ISBN 3-540-56723-2

Ullmanns Encyclopedia of Industrial Chemistry. Index to Volumes A1 to A21, B1 to B4. Edited by **W. Gerhartz, M. Pikart-Müller, C. Thümmler.** VCH, Weinheim/New York, **1993.** 544 pp., paperback, DM 168. / $ 82.50. ISBN 3-527-20147-5/0-89573-187-8

Organic Electronic Spectral Data, Vol. XXIX. Edited by **J. P. Phillips, D. Bates, H. Feuer, B. S. Thyagarajan.** Wiley, Chichester, Great Britain, **1993.** 916 pp., hardcover, £ 136.–.— ISBN 0-471-31121-9

New Gmelin Volumes:

Be Beryllium. Suppl. Vol. A, Part 3. Edited by **L. Berg et al.** Springer, Heidelberg, **1993.** 277 pp., hardcover, DM 1670. . —ISBN 3-540-93674-2

Formula Index. Vol. 1, Suppl. 3, Ag-B5. By **R. Bohrer et al.** Springer, Heidelberg, **1993.** 277 pp., hardcover, DM 1495. . ISBN 3-540-93668-8

Formula Index. Vol. 2, Suppl. 3, B6-C7,5. Edited by **U. Nohl, G. Olbrich.** Springer, Heidelberg, **1993.** 299 pp., hardcover, DM 1595.–. ISBN 3-540-93669-6

Advances in the Use in Synthons in Organic Chemistry, Vol. 1. Edited by **A. Dondoni.** JAI Press, London, **1993.** Ca. 300 pp., hardcover, £ 53.–.—ISBN 1-55938-183-3

Human Medicinal Agents from Plants. (ACS Symposium Series No. 534). Edited by **A. Douglas Kinghorn, M. F. Balandrin.** American Chemical Society, Washington (USA), **1993.** 359 pp., hardcover, $ 89.95.—ISBN 0-8412-2705-5

Polymers of Biological and Biomedical Significance. (ACS Symposium Series No. 540). Edited by **S. W. Shalaby et al.** American Chemical Society, Washington (USA), **1993.** 390 pp., hardcover, $ 89.95. –ISBN 0-8412-2732-2

Mass Spectrometry for the Characterization of Microorganisms. (ACS Symposium Series No. 541). Edited by **C. Fenselau.** American Chemical Society, Washington (USA), **1993.** 238 pp., hardcover, $ 64.95.— ISBN 0-8412-2737-3

Relativistic Theory of Atoms and Molecules II. A Bibliography 1986-1992. (Lecture Notes in Chemistry, Vol. 60). By **P. Pyykkö.** Springer, Heidelberg, **1993.** 479 pp., paperback, DM 130.–.—ISBN 3-540-57219-8

Catalyzed Direct Reactions of Silicon. (Studies in Organic Chemistry, Vol. 49). Edited by **K. M. Lewis, D. G. Rethwisch.** Elsevier, Amsterdam, **1993.** 664 pp., hardcover, Dfl. 465.–.– ISBN 0-444-81715-8

Catalysis of Organic Reactions. (Chemical Industries Series 53). Edited by **J. R. Kosak, T. A. Johnson.** Marcel Dekker, New York, **1993.** 608 pp., hardcover, $ 185.–. —ISBN 0-8247-9140-1

Dictionary of Natural Products. Chapman & Hall, London, **1993.** 9500 pp. in seven volumes, hardcover, £ 3250.–.—ISBN 0-412-46620-1

Organic Syntheses, Vol. 71. Edited by **L. E. Overman.** Wiley, Chichester, Great Britain, **1993.** 285 pp., hardcover. –ISBN 0-471-30531-6

Applications of Artificial Intelligence in Chemistry. By **H. M. Cartwright.** Oxford University Press, Oxford, **1993.** 92 pp., paperback, £ 4.99. –ISBN 0-19-855736-1

The Mechanisms of Reactions at Transition Metal Sites. By **R. A. Henderson.** Oxford University Press, Oxford, **1993.** 87 pp., paperback, £ 4.99.—ISBN 0-19-855746-9

Chemie und Umwelt. Ein Studienbuch für Chemiker, Physiker, Biologen und Geologen. By **A. Heintz, G. A. Reinhardt.** Vieweg, Wiesbaden, **1993.** 282 pp., hardcover, DM 49.50.—ISBN 3-528-26349-0

Chemie - Basis des Lebens. Forschung und Praxis im Wandel der Zeit. By **G. Hansen.** Autorenkreis Sachdialog, Weißenhorn, **1993.** 199 pp., hardcover, DM 28.–. –ISBN 3-925467-07-6

Liquid-Phase Oxidation of Unsaturated Compounds. By **V. L. Rubajlo, S. A. Maslov, G. E. Zaikov.** Nova Science Publishers, Commack, USA, **1993.** 227 pp., hardcover, $ 83.–.—ISBN 1-56072-119-7

Bioactive Compounds: Biotransformation and Biological Action. Edited by **I. N. Todorov, G. E. Zaikov, I. A. Degterev.** Nova Science Publishers, Commack, USA, **1992.** 378 pp., hardcover, $ 87.–.—ISBN 1-56072-075-1

Chemical Nomenclatures and the Computer. By **D. J. Polton.** Research Studies Press, Taunton, Great Britain, **1993.** 264 pp., hardcover, £ 52.–.– ISBN 0-86380-156-0

Gesundheitsschädliche Arbeitsstoffe. MAK-Werte. Edited by **Deutsche Forschungsgemeinschaft.** VCH, Weinheim, **1993.** pp., loose-leaf edition, DM 228.–. –ISBN 3-527-27635-1

List of MAK and BAT Values 1993. Edited by **Deutsche Forschungsgemeinschaft.** VCH, Weinheim/New York, **1993.** 152 pp., paperback, DM 48.–. –ISBN 3-527-27558-4

Occupational Toxicants, Vol. 6. Critical Data Evaluation for MAK Values and Classification of Carcinogens. Edited by **Deutsche Forschungsgemeinschaft.** VCH, Weinheim/New York, **1993.** 368 pp., hardcover, DM 168. /$ 110.– (series price: DM 115. /$ 75.–). ISBN 3-527-27031-0/1-56081-865-4

Linear and Nonlinear Optical Properties of Molecules. By **G. H. Wagnière.** VCH, Weinheim/New York; VHCA, Basel, **1993.** 195 pp., hardcover, DM 88. / $ 55.–/SFr 86.–.—ISBN 3-527-29045-1/1-56081-757-7/ 3-906390-07-1

Extremophile. Mikroorganismen in ausgefallenen Lebensräumen. Edited by **K. Hausmann, B. P. Kremer.** VCH, Weinheim, **1994.** 419 pp., hardcover, DM 49.–.—ISBN 3-527-30026-0

Advances in Electrochemical Science and Engineering, Vol. 3. Edited by **H. Gerischer, C. W. Tobias.** VCH, Weinheim/New York, **1994.** 331 pp., hardcover, DM 188.–/$ 120.– (series price: DM 148.–/$ 95.–).– ISBN 3-527-29002-8/1-56081-282-8

Organosilicon Chemistry. From Molecules to Materials. Edited by **N. Auner, J. Weis.** VCH, Weinheim/New York, **1994.** 349 pp., hardcover, DM 128.–/$ 85.–.– ISBN 3-527-29061-3/1-56081-869-7

Advances in Electrophoresis. Edited by **A. Chrambach, M. J. Dunn, B. J. Radola.** VCH, Weinheim/New York, **1993.** 382 pp, hardcover, DM 278.–/$ 180.–.—ISBN 3-527-30034-1/0-56081-776-3

Human Protein Data, 2nd Installment. Edited by **A. Haeberli.** VCH, Weinheim, New York, **1993.** 180 pp., looseleaf edition, DM 185.–/$ 115.– (subscription price: DM 155. /95.–).—ISBN 3-527-30015-5/ 1-56081-709-7

Template Syntheses

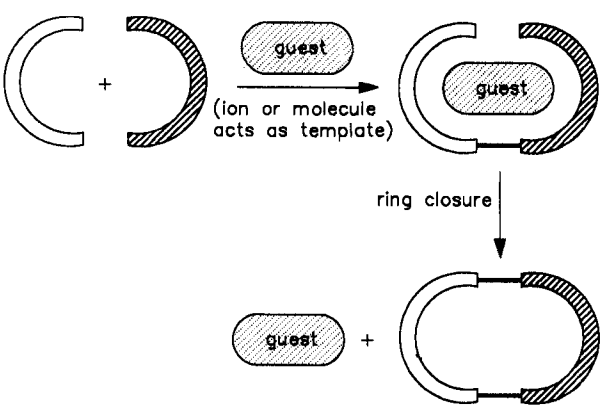
Ralf Hoss and Fritz Vögtle*

Although the principle of template synthesis has been known since the sixties, surprising discoveries and new applications in the field of supramolecular chemistry over the last decade have provoked a boom in the subject. The synthesis of supramolecular species has been made much more efficient, or even in some cases possible, by the introduction of template ions or molecules. It is not just metal ions that can act as templates. Neutral molecules, electrostatic interactions, and hydrogen bonds also support the formation of binary and tertiary complexes. Energetically favorable conformations then lead to the formation of a specific desired product in high yield. In addition to the discussion of metal ions and neutral molecules as templates, covalent, positive, and negative templates are differentiated. Kinetic and thermodynamic aspects will also be considered in this review, together with the influence of templates on the phenomenon of self-organization. Further developments and applications include the synthesis of oligonucleotides, peptide blocks capable of forming secondary structure, and template polymers. Template synthesis of defined molecular cavities ultimately leads to "inclusion chemistry on a nanometer scale."

1. Introduction

That metal ions can affect the course of "organic" reactions has been known for decades.[1] In the preparation of large ring compounds containing donor atoms by condensation reactions, such an effect is used intentionally by the addition of suitable cations and has achieved considerable importance.[2] As guest the metal ion or—as first found in the 1980s (see Section 3)—the neutral molecule as guest "coordinates" a ligand or host molecule, which is thereby generally brought into a suitable conformation for the formation of a specific (most often cyclic) product. This phenomenon is generally described as the "template effect" (Scheme 1). In this and the following schemes the template is marked by shading. In later Schemes, in addition, the strategic bond formed in the template synthesis is indicated by a dotted circle.

The term template effect was first used and defined at the beginning of the sixties.[3] (In this review the term matrix is used as a synonym for template.) Generally, all intermolecular forces that play a role in host–guest complexes effect a stabilization of the necessary binary or tertiary complexes. The countless examples found in the literature cover the relevance of the template effect under the heading of rational synthesis on the one hand, and on the other differentiate the individual template effects necessary. A selection has necessarily been made, and the latest examples have been given prominence here.



Scheme 1. Principle of the template effect: The guest (ion or molecule, indicated by shading) acts as a template, favoring connection of the decisive ("strategic") bond.

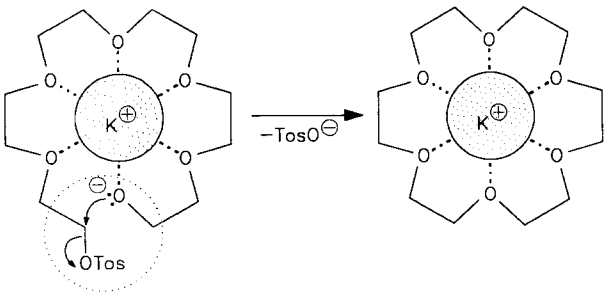
2. Template Syntheses with Metal Cations

The longest known and most frequently employed template syntheses are those based on metal ion chelates—either temporary or permanent.[4] The formation of copper phthalocyanines[5] and crown ethers,[6] now textbook examples, were among the first ligand syntheses in which metal ions acted as templates and ensured good yields: The ligand building blocks wrap themselves around the metal ion (Scheme 2), thereby favoring ring closure to the macrocycle.

The synthesis of catenanes,[7] among the highlights of supramolecular chemistry, is based (for example, for those of Sauvage et al.[8]) on the tetrahedral coordination of Cu^{I} ions by functional-

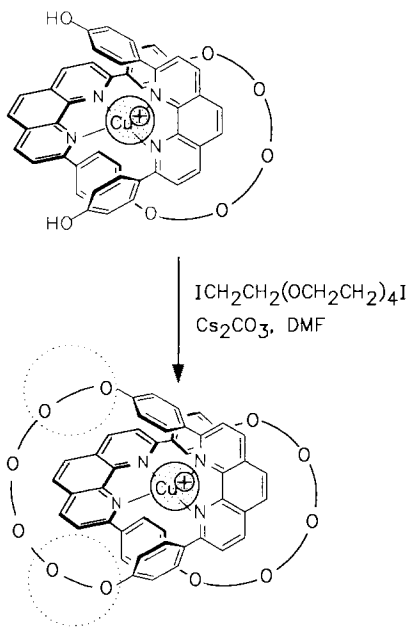
[*] Prof. Dr. F. Vögtle, Dr. R. Hoss
Institut für Organische Chemie und Biochemie der Universität
Gerhard-Domagk-Strasse 1, D-53121 Bonn (FRG)
Telefax: Int. code + (228)73-5662

 © *VCH Verlagsgesellschaft mbH, D-69451 Weinheim, 1994* *0570-0833/94/0404-0375 $ 10.00+.25/0*



Scheme 2. Template synthesis of [18]crown-6. The potassium ion acts as a convex template.

ized phenanthroline ligands. In the synthesis these ligands become rigidly but reversibly and orthogonally arranged (Scheme 3).

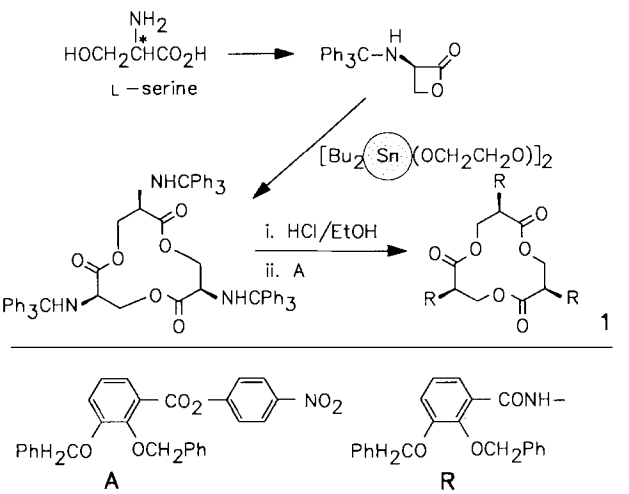


Scheme 3. Synthesis of [2]catenanes with Cu^{I} as convex template (from Sauvage [8]). DMF = dimethylformamide.

The total synthesis of protected enterobactin **1**, developed by Shanzer and Libman,[9a] involves the use of tin compounds as templates in the cyclooligomerization of β-lactones to macrocyclic polylactones (Scheme 4).[9b]

3. Neutral Molecules as (Supramolecular) Templates

An example of π-stacking as the driving force in a template synthesis is that by Hünig et al.[10] of the cationic host molecule **2**. The latter displays π-acceptor properties. In this case an increase in yield from 3–5% to 16% was observed when an excess



Scheme 4. The template-controlled total synthesis of the protected enterobactin **1**, which makes use of the potential of optically active natural products (L-serine).

of phenanthrene (as π-donor guest) was added to the reaction mixture. This example could even be considered as the first template effect of a hydrocarbon guest. Simultaneously the authors cast doubt on an earlier[11] template effect postulated as a result



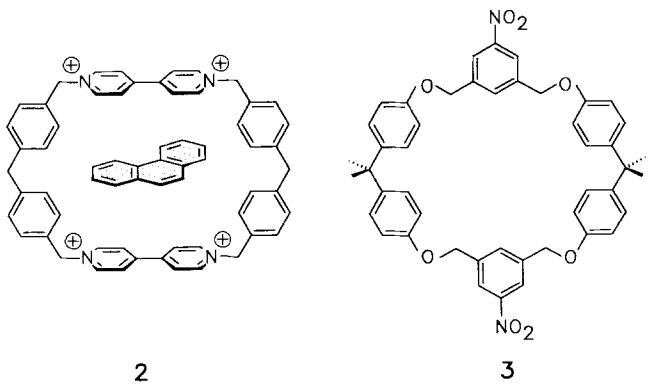
F. Vögtle



R. Hoss

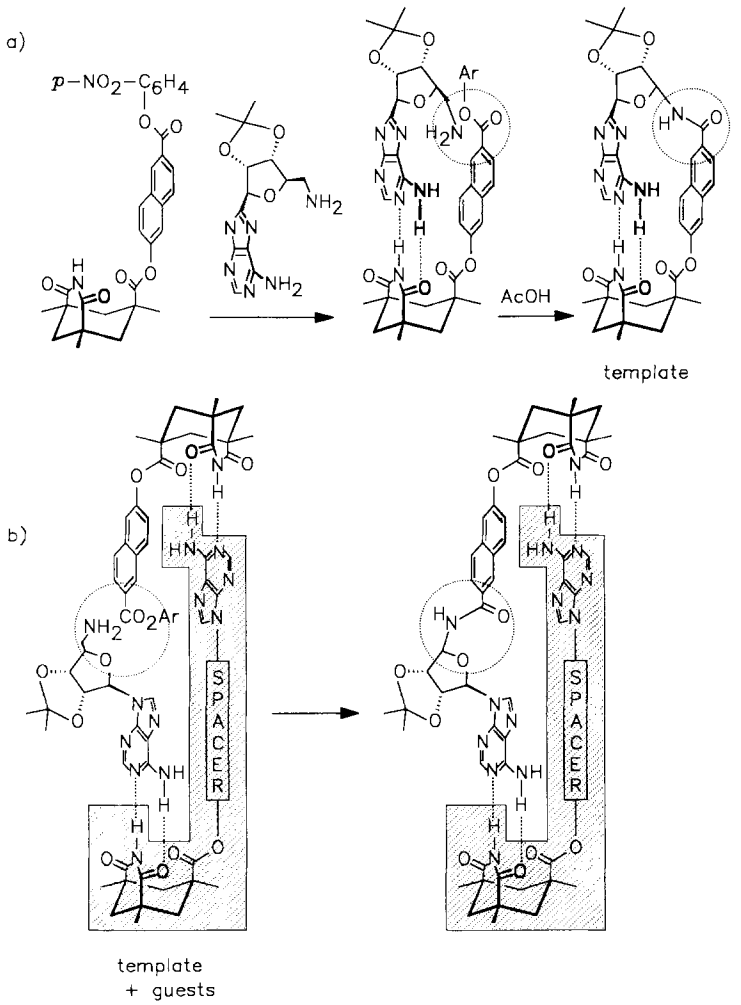
Fritz Vögtle, born in 1939 in Ehingen/Donau, studied chemistry in Freiburg as well as chemistry and medicine in Heidelberg. There he received his Ph.D. for research with H. A. Staab on the valence isomerization of double Schiff bases. After his habilitation on steric interactions inside cyclic compounds, he was H2/H3 professor in Würzburg from 1969 to 1975. He then accepted a position as full professor and director of the Institut für Organische Chemie und Biochemie in Bonn. He is interested in the fields of supramolecular chemistry and molecular recognition, and after working on topics concerning crown ethers, podands, and siderophores, he has concentrated on compounds with large intramolecular cavities, ligands for supramolecular photochemistry, concave dyes, molecular tweezers, and spherical and tubular molecules. His further areas of research are deformed, strained and helical molecules, cyclophanes, and compounds with appealing architecture.

Ralf Hoss was born in 1963 in Mechernich/Eifel and studied in Bonn from 1983–1989. In 1993 he completed his Ph.D. under the supervision of F. Vögtle on macromonocyclic hosts to complex organic guest molecules. Currently he holds a postdoctoral position at the University of Bern in the group of J. Hulliger, working in the field of crystal growth and solid state properties of inorganic and organic materials.



2 3

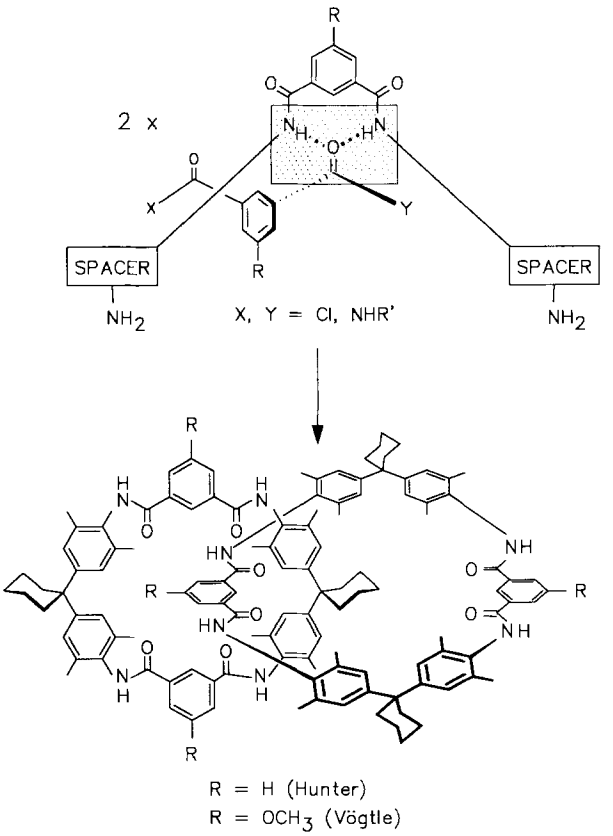
Scheme 5. Template synthesis of the cationic host molecule **2**, governed by π-stacking interactions. Addition of phenanthrene increases the yield from 4% to 16% [10]. In the synthesis of **3** [11], there is probably no template effect operative (see text).



Scheme 6. Replication experiment of Rebek et al. a) π-Stacking and hydrogen bonding support formation of the concave template molecule; b) the supramolecular (tertiary) complex promotes reaction between the amine and the carboxylic acid ester guest. The overall process is autocatalytic.

of an increased yield, because the macrocycle **3** binds benzene as guest only in the crystal lattice, not in solution (Scheme 5).

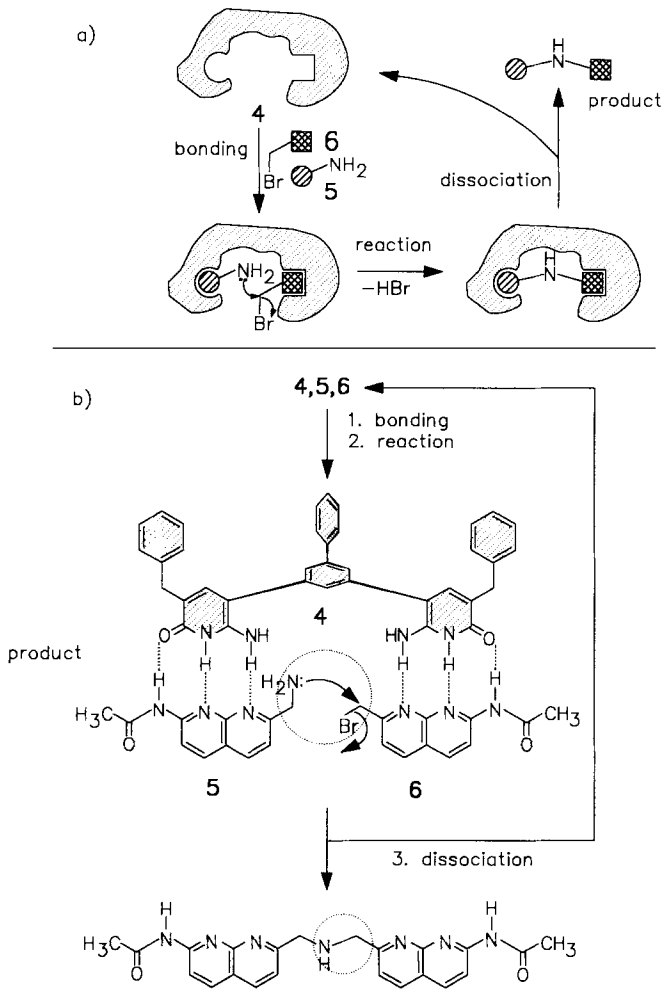
The phenomenon of π-stacking, supported by additional hydrogen bonds, leads in Rebek et al.'s replication experiments to aggregation (Scheme 6),[12] and in the productive two- and one-step catenane syntheses of Hunter (34% yield)[13] and Vögtle et al. (8.4% yield),[14] respectively, to orthogonalization of the intertwined macrocyclic molecular chains (Scheme 7).



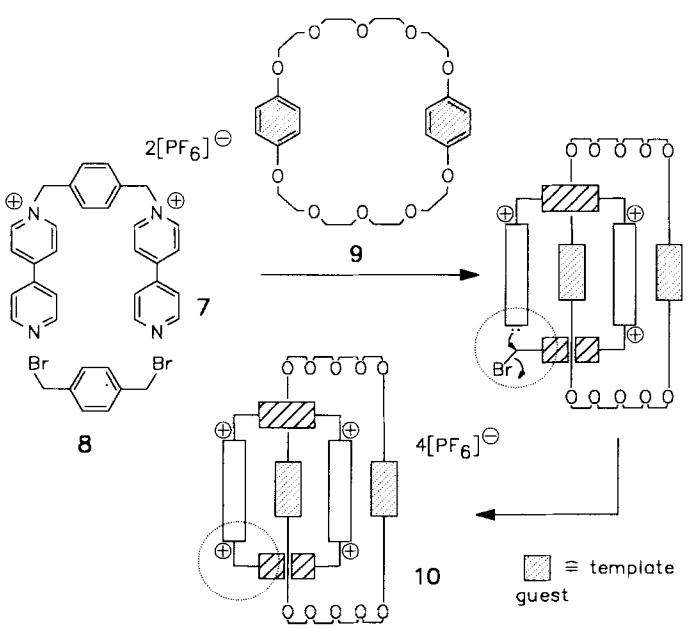
Scheme 7. [2]Catenane syntheses by Hunter and by Vögtle et al. with a concave template.

In 1989 Kelly et al. carried out a template-promoted reaction between two substrates (Scheme 8).[15] As a result of its architecture the completely synthetic molecule **4** possesses two binding centers and is able to temporarily bind two organic substrates at the same time. Analogously to natural enzymes it is thereby able to convert an intermolecular reaction into an "intramolecular" process. Kinetic measurements show that **4** accelerates the S_N2 reaction between the amine **5** and the bromide **6**. Results of molecular calculations and kinetic experiments are in agreement with the assumption of a ternary complex (**4**···**5**···**6**) as intermediate.

Stoddart et al. developed the efficient template-directed one-pot synthesis of the [2]catenane **10** from the bispyridinium salt **7**·2PF_6^-, the bis(bromomethyl)benzene **8**, and the paracyclophane crown ether **9** (Scheme 9).[16] The dominant, noncovalent interactions involved are based on electrostatic and dispersive forces—brought about by the reciprocal formation of a sandwich a) of a hydroquinone ether unit (guest) between parallel bipyridinium units (host) and b) of a bipyridinium unit (guest) between parallel hydroquinone ether units. The π-donor–π-acceptor stacking of the electron-rich and electron-poor arene groups leads to an orthogonal arrangement of the building blocks, the logical consequence of which is the formation of [2]catenanes in yields that were previously not held to be possible.

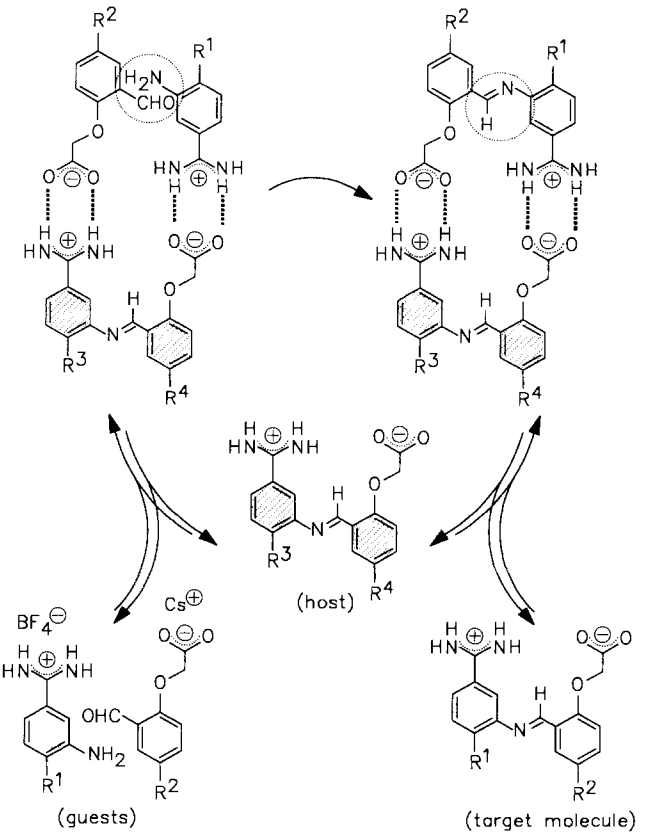


Scheme 8. Reaction between **5** and **6** in $CDCl_3$ in the presence of the concave template **4**. a) Schematic representation, b) specific template synthesis. Concentrations: **4**, **5**, **6** 4×10^{-3} M. The addition of the template accelerates the reaction by a factor of 6.



Scheme 9. Template-supported macrocyclization to give [2]catenane **10**, according to Stoddart et al. The unexpectedly high yield of **10** is 70% based on **7** [16], whereas without template support the macrocycle from **7** and **8** is formed with a yield of only 12% (ambient pressure) [16].

An interesting aspect of the template effect also dependent on electrostatic interactions is the parabolic self-multiplication-replication—with the aid of amidinium carboxylate bridges (Scheme 10).[17a] Replication generally takes place by way of



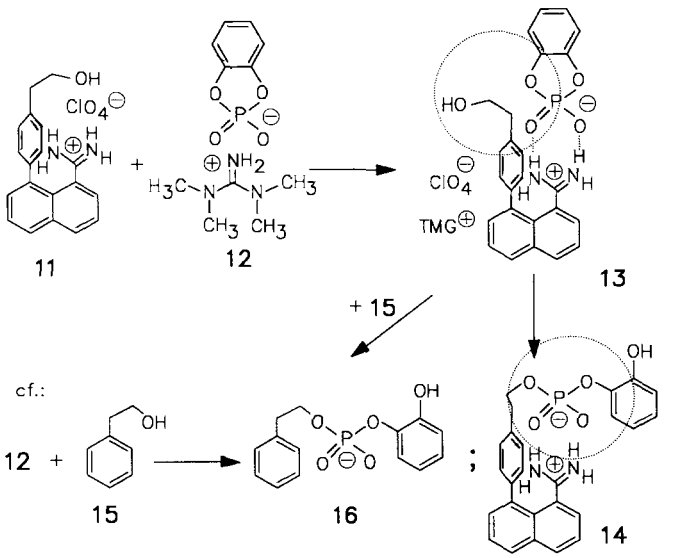
Scheme 10. Formation of the target molecule (R^1 = Me, R^2 = NO_2) in [D_6]dimethylsulfoxide ([D_6]DMSO). The reaction was monitored at 27 °C to a conversion of 25% with ^{1}H NMR spectroscopy. In the presence of the (host) template molecule (R^3 = *t*Bu, R^4 = H), the synthesis of the target molecule, a Schiff's base, is accelerated by a factor of about 370 M^{-1}.

(+)- or (−)-strands: The (+)-strand, as matrix, catalyzes formation of the (−)-strand and vice versa. In the self-complementary (palindromic) sequences the (+)- and (−)-strands are not distinguishable. A chemical "ligature" with a palindromic matrix is potentially a self-replicating system, or, in other words, the simplest model of self-replication is the autocatalytic synthesis of a self-complementary template molecule.[17b]

Göbel et al.[18] attempted to devise simple synthetic phosphordiesterases based on the strategy of formation of amidinium phosphate ion pairs. The rate of reaction of the amidinium alcohol **11** with **12** to give **14**, via the ion pair **13**, was considerably higher than that of the control reaction of **12** with **15** (Scheme 11). The phosphorylation of **11** took place as a supramolecular (quasi-intramolecular) process within the ion pair **13** rather than as an intermolecular process.

4. Template Syntheses with Covalent Molecules

Apart from the cyclization around a metal ion, specific atoms or molecular groups can be construed as temporary, covalently



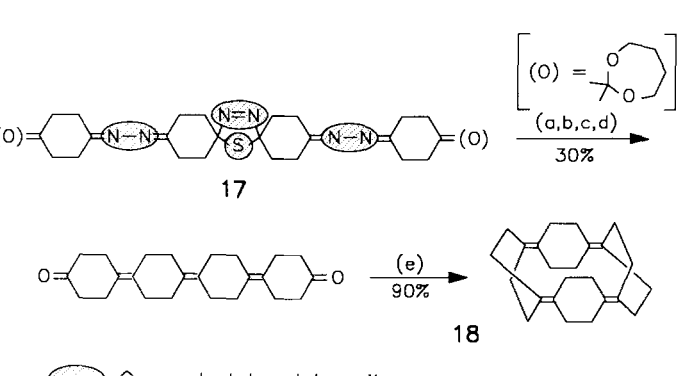
Scheme 11. Condensation of the alcohol **11** that functions as template with the tetramethylguanidinium (TMG) salt **12**. The conversion takes place 9000 times faster than the reaction of **12** with the neutral phenylethanol **15**.

bound templates. There is a fundamental difference between these and supramolecular host–guest systems, in that molecular recognition is not necessary, rather "host" and "guest" (here, of course, not functioning as such) are joined together by one or more covalent bonds from the outset.

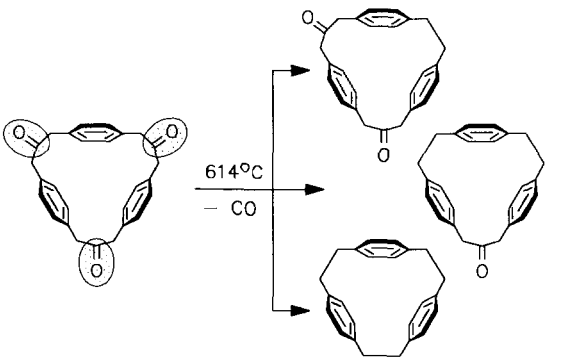
4.1. Temporary, Covalently Bound ("External") Templates

A template is described as temporary or external if it is eliminated at the end of a synthesis and is therefore not incorporated into the end product.[19] Sulfur or nitrogen, which can be eliminated by pyrolysis from the product after a successful reaction, can be regarded as the best known *exo*-templates. For example, McMurry et al.[20] used extrusion of N_2 and S (Barton method) from the thiadiazolines **17** in the preparation of the 16-membered hydrocarbon macrocycle **18** (Scheme 12).

The stereoselective synthesis of sterically unhindered alkenes takes place according to this principle.[21] Similarly, the carbocyclic [2.2]cyclophanes are easily accessible by extrusion of sulfur from dithia[3.3]metacyclophanes.[22] The synthesis of unsymmetrical [*m.n*]paracyclophanes (*m* and *n* are the number of bridging atoms) was hitherto only possible by multistep reactions. Selective ketone pyrolysis—the carbonyl group was introduced as temporary template by reaction of the corresponding benzyl halides with tosylmethyl isocyanide—allowed a new entry to hydrocarbon structures of this type (Scheme 13).[23, 24]

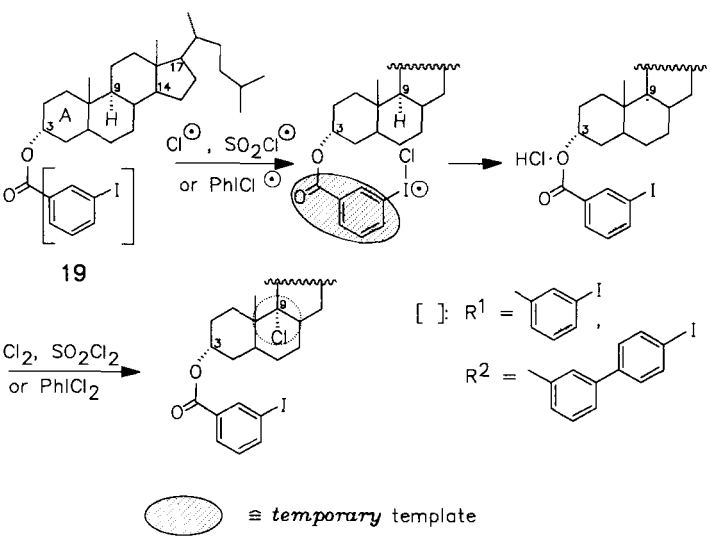


Scheme 12. Use of a covalently bound template for bond formation. a) H_2S, H_3CCN; b) $Pb(OAc)_4$, H_2CCl_2; c) HCl, H_2O, H_2CCl_2; d) toluene, Δ; e) $TiCl_3/Zn/Cu$, dimethoxyethane, 48 h, Δ.



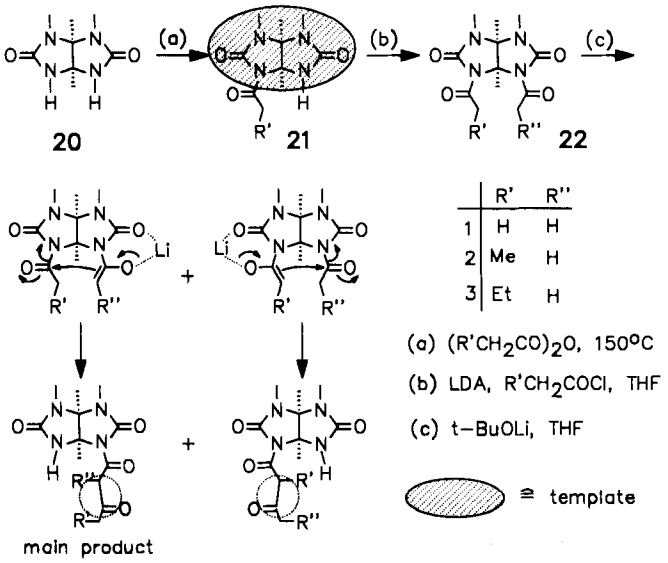
Scheme 13. Carbonyl groups as temporary covalently bound templates in the preparation of [*m.n*]paracyclophanes.

Radical chlorination of the steroid backbone was achieved by R. Breslow et al.[25] by introduction of a *m*-iodobenzoate template (see **19**, Scheme 14); the latter is easily removed by hydrolysis. With chlorinating agents such as $PhICl_2$, SO_2Cl_2, or Cl_2, attack of the free radical takes place not directly at the steroid H-atom as expected, but preferentially at the iodine atom. As a consequence, even such unselective radicals as Cl· or SO_2Cl· can be controlled and spatially directed by means of a template. The remarkable advantage of this process is that functional groups attached to the A ring are unaffected, and the unactivated position at C9 is attacked selectively (remote control of reactions).



Scheme 14. The selectivity of biochemical reactions can be traced back to the geometry of the enzyme/substrate complex. Breslow et al. attempted to obtain such geometric control by using the reagent/substrate complex [25]. The reagent (e.g., Cl·) is attached to a covalently bound template and thereby permits regioselective attack on the substrate at C9.

Acylation of the 3,4,7,8-tetramethylglycoluril (**20**) by the method of Sun and Harrison[26] leads to the monoacyl derivative **21**, which can be further selectively acylated with lithium diisopropylamide (LDA) and acyl chlorides. The resulting symmetrical or asymmetrical diacyl compounds **22** undergo a base-catalyzed acyl transfer reaction (Scheme 15). Consequently, **20** acts

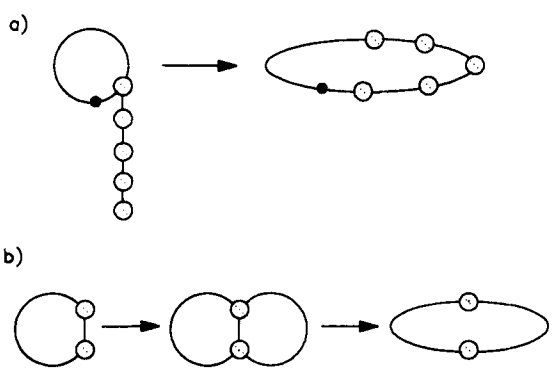


Scheme 15. The tetramethylglycoluril **20** acts as a temporary, covalently bound template in a base-catalyzed acyl transfer. R' = H, Me, Et; R'' = H. a) $(R'CH_2CO)_2O$, 150 °C; b) LDA, $R''CH_2COCl$, THF; c) *t*BuOLi, THF.

as a temporary template that facilitates a simple condensation between acyl units. The absence of O-acylation products is explained by chelation of the lithium by the intermediate enolate.

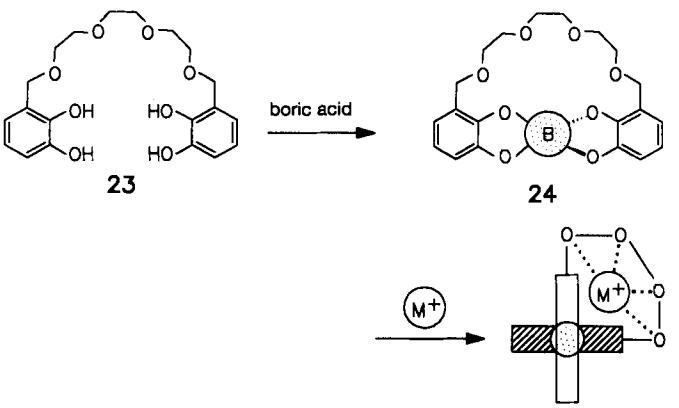
4.2. Permanent, Covalently Bound ("Internal") Templates

If the formation of a macrocycle is effected, for example, by expansion of a smaller ring by the insertion of a side chain already present, the smaller ring is designated as a permanent template or *endo*-template, because all the molecular components originally present are also found in the end product (Scheme 16a). The most common example is probably the "zip" reaction (transamidation).[27] In addition, selected bond cleavage (C–N,[28] N–N,[29] C–C,[30] or C=C bonds[31]) of an initially synthesized bicyclic molecule can lead to macrocycles that contain all the original atoms. Thus, this method of ring formation can also be regarded as involving a permanent template (Scheme 16b).



Scheme 16. Template syntheses with permanently bound templates. a) Ring extension by insertion and b) ring expansion by selected bond cleavage.

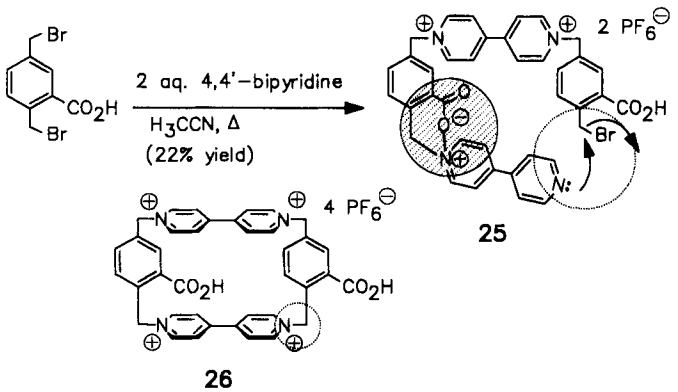
Kobuke et al.[32] demonstrated that the podand **23** only forms weak complexes with alkali metal ions. However, when a chiral macrocyclic crown ether structure is formed by complexation with boric acid, alkali metal ions are bound much more strongly (Scheme 17). A certain amount of stiffening, provided by a covalent B–O bond, improves the preorganization of the ligands that is required for the complexation of metal ions.



Scheme 17. The podand **23** displays more marked concave preorganization on esterification with boric acid (conversion to the crown **24**).

The functionalized cyclophane **26** was synthesized by Harriman et al.[33] in a one-step cyclization (Scheme 18). The crucial step in this synthesis is the postulated formation of the zwitterionic open-chain intermediate **25**, in which the degree of rotational freedom is restricted by interaction between the carboxylate group and the pyridinium nitrogen atom, thereby leading to the correct geometry for the formation of the macrocycle. The zwitterionic structure element in **25** can be regarded as both an internal and a permanent, ionic template.

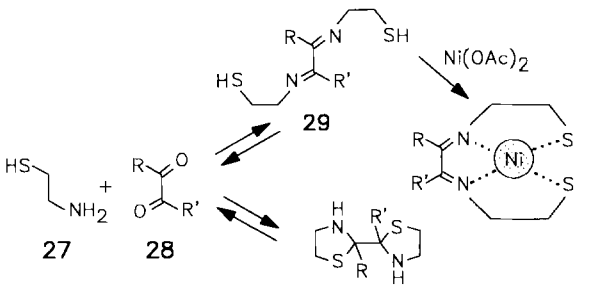
From the last two examples it can be seen that the distinction between covalent and noncovalent (supramolecular, weakly bound) templates is not rigid.



Scheme 18. The carboxylate group in **25** provides an "internal template effect" by ion association and facilitates the intramolecular ring closure to **26**.

5. Kinetic and Thermodynamic Template Effects

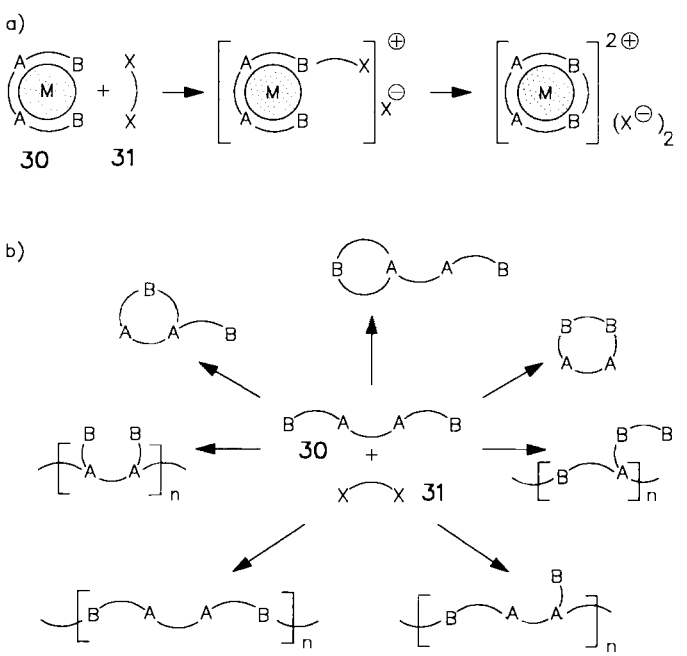
The thermodynamic or "equilibrium" template effect is based on the fact that in the absence of the template the desired product is indeed formed, but with one or more (undesired) compounds that are in equilibrium with each other.[34] A marked tendency of the product to form chelates enables a template to displace the product equilibrium in the desired direction. The first example of an equilibrium template effect was the formation of a nickel(II) complex of the Schiff base **29** formed from β-aminoethanethiol (**27**) and the α-diketone **28** (Scheme 19).[35]



Scheme 19. Example of a thermodynamic template effect.

As the equilibria are frequently complex, it is often difficult to recognize a thermodynamic template effect unequivocally. Not infrequently, the best indication is the formation of an unexpected product in high yield. The principle of complementarity must be emphasized here: if a ligand (host) in a product mixture is complementary to an available metal ion or neutral (guest) molecule, then this will be bound selectively, and the equilibrium shifted in its favor.

The kinetic template effect exploits the advantage of molecular organization ("self-organization") of ligands around a template.

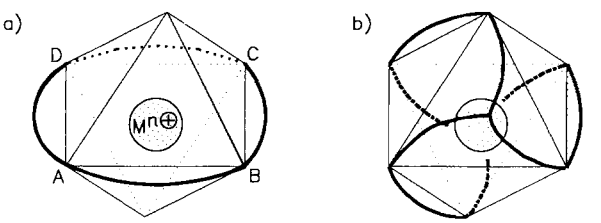


Scheme 20. Kinetic template effects. a) Function of a template molecule M as coordination center; b) in the absence of M numerous equilibria often occur.

The formation of oligo- or polycondensation products is largely suppressed by the action of the template as a coordination center. A simplification of the possible reactions between a linear ligand **30** and a bifunctional, electrophilic reagent **31** in the presence and absence of a template species is shown in Scheme 20.

If no guest molecule is present then the two reagents can react to give a series of polymeric and cyclic products (Scheme 20b). The presence of a template M can steer the reaction. If the template binds the linear ligand selectively in a planar arrangement, the two terminal functional groups (B) will be held adjacent to each other within the "coordination sphere" of the template (Scheme 20a). Then the terminal donor atoms (B), if still able to react as nucleophiles in spite of interaction with the template (M), are correctly positioned to react with the bifunctional electrophile.

A metal ion in a template reaction usually organizes two or three reactive centers (A, B, C) at the corners or faces of its idealized coordination polyhedron. If one of the corners is included (e.g. with Ni^{2+}), a chelate ring is formed, and the product is usually a large monocyclic ligand (Scheme 21a). If a face is involved (e.g.

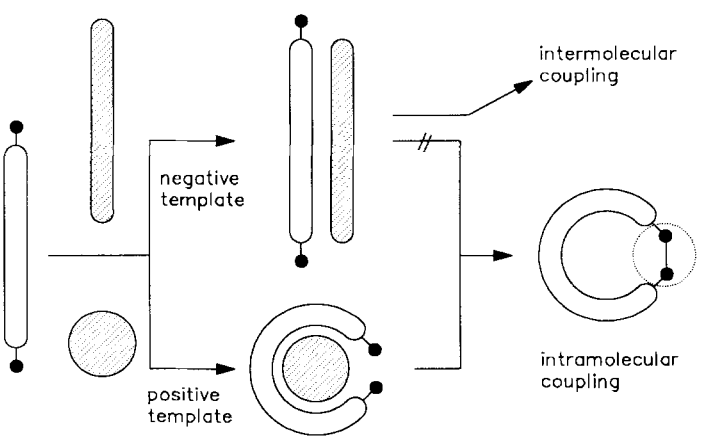


Scheme 21. The corners or faces of an idealized coordination polyhedron act as reactive centers in a template reaction.

with Co^{3+}), then the product can be a cage compound (Scheme 21b). This synthetic strategy has been used successfully for the construction of numerous polydentate ligands.[36–38]

6. Positive and Negative Templates

In the use of templates, Sanders et al.[39] differentiate between two modes of action that are complementary (Scheme 22): A



Scheme 22. Only the positive template leads by intramolecular ring closure to the desired result (discrete target molecule). In contrast, the negative template leads to less uniform, higher molecular mass products, most of which cannot be aspired to. Both cases involve convex templates.

"positive" template directs the approach of two reactive end groups in a molecule, thereby generally supporting the desired intramolecular cyclization. In contrast, a "negative" template effect holds the reactive groups apart, thereby suppressing the intramolecular cyclization and leading preferentially to the—undesired—intermolecular reaction.

7. Self-Organization

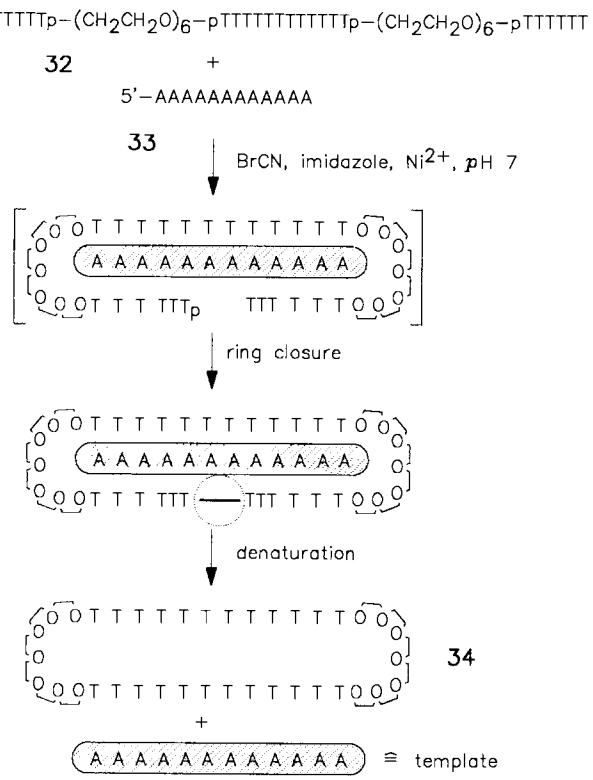
From template effect to self-organization (self-assembly) is only a small jump, if even that. It follows from the view that an arbitrary number of subunits with corresponding molecular recognition properties can not only congregate by self-recognition to form a superstructure, but that substrate–template recognition can also lead to the organization of a defined supramolecule and that the features of natural self-assembling systems, classified by Stoddart et al.,[40] can be transfered to the supramolecular template-substrate complex. If subunits have corresponding molecular recognition properties, the template effect will underly the self-examination prior to assembly. On the grounds of exact recognition characteristics, specific for every subunit, it is improbable that defective subunits would be used in the construction of a superstructure. Defective subunits would be rejected by the growing supramolecular structure. Thus, absolute accuracy in the construction of a subunit is not necessary, as mistakes will be removed in the aggregating step. The high synthetic efficiency, a direct result of self-examination, is convincing. The use of specially synthesized templates is becoming more common, for example in the synthesis of polypeptides.[41–44]

8. Further Developments and Applications

Kool et al.[45] have reported on the construction of the cyclic hybrid molecule **34**, which contains two oligonucleotide sections bridged by two oligo(ethylene glycol) chains (Scheme 23). The oligomer **33** is employed as (guest) template in the cyclization, in order to bring the reactive phosphate and hydroxy end groups into the appropriate orientation for intramolecular esterification in the presence of BrCN, imidazole, and $NiCl_2$.

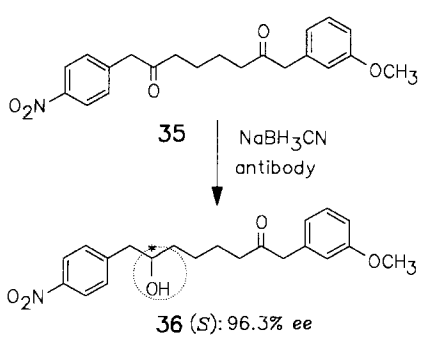
The sequence-specific binding of synthetic oligonucleotides and analogs to RNA and DNA is being studied intensively in the examination of natural polynucleotides and for the development of potential therapeutics.[46]

Natural proteins undergo a folding process that leads to a spatially defined tertiary structure. With synthetic polypeptides folding to a globular structure is not a matter of course. The situation in vivo is not always comparable with that in a test tube. A concept introduced by Mutter et al.[47] represents a step toward achieving the folding of artificial proteins. According to this concept, peptide blocks leading to formation of secondary structure are covalently attached to a topologically tailor-made template. The template serves to direct the peptide chains into a characteristic three-dimensional structure, as in proteins. The resulting macromolecules are described by Mutter et al., in accord with the method used in their formation, as template-associated synthetic proteins (TASPs). In contrast to the other template molecules discussed here, in this case the template results in the stabilization of a specific conformation rather than in supporting the formation of a covalent link.



Scheme 23. Preparation of the cyclic hybrid molecule **34** with the aid of oligonucleotide **33** as (guest) template. T = thymidine, A = adenosine.

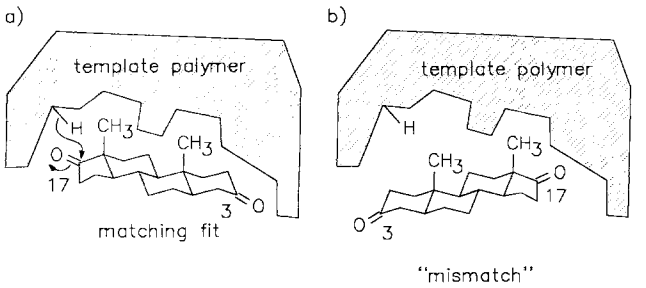
The remarkable specificity of a monoclonal antibody has been used by P. G. Schultz et al.[48] to control the selective reduction of the carbonyl compound **35** with $NaBH_3CN$ (Scheme 24). The observed enantiomeric excess of 96% (*S*)-**36** cannot be obtained with conventional chemical methods.



Scheme 24. Stereoselective reduction of diketone **35** with $NaBH_3CN$ in the presence of a monoclonal antibody (*ee* = 96%) [48].

Use of polymers in place of discrete metal ions or neutral molecules gave rise to the template polymers[49] of Byström et al. If the term "template" is taken in its original meaning borrowed from photography, the template polymers are actually templates in the true sense. In a process similar to that used in photography, impressions (macromolecular niches) are initially generated on

the surface (or in the interior) of the polymer by so-called "imprint molecules". If the molecular imprint contains appropriate functional groups, molecules can be adsorbed and chemically converted with regio- and stereoselectivity (Scheme 25). The selective reduction of steroid ketones by means of $LiAlH_4$-activated template polymers can be carried out following the principle of an ion exchanger. Although the application of polymers in template syntheses is currently limited, and the reactions do not always run satisfactorily, this method appears to be a landmark for future rational syntheses.



Scheme 25. Niches, which allow regio- and stereoselective conversion of the substrate, are produced on the surface of the polymer by "imprint" molecules. For the steroidal ketone selected here only a specific polymer/substrate binding leads to optical transfer of the hydride from the concave template to the carbonyl group of the guest (a). All other polymer/substrate bindings are unsuitable on steric grounds (b) and do not lead to the desired reaction (at the carbonyl group).

Microporous phases with three-dimensional lattice networks and defined pore structures and sizes can be obtained by the use of molecules or hydrated ions of alkali metals or alkaline earth metals as templates.[50] A concept developed by the Mobil Oil Company for the synthesis of porous materials employs a regular arrangement of molecules formed by self-assembly rather than a single, solvated, organic molecule or metal ion as template. Three-dimensional porous media can be used in their turn for molecular recognition and as templates. Defined cavity structures could lead to "inclusion chemistry on the nanoscale" and are termed "reaction vessels of nanometer dimensions".

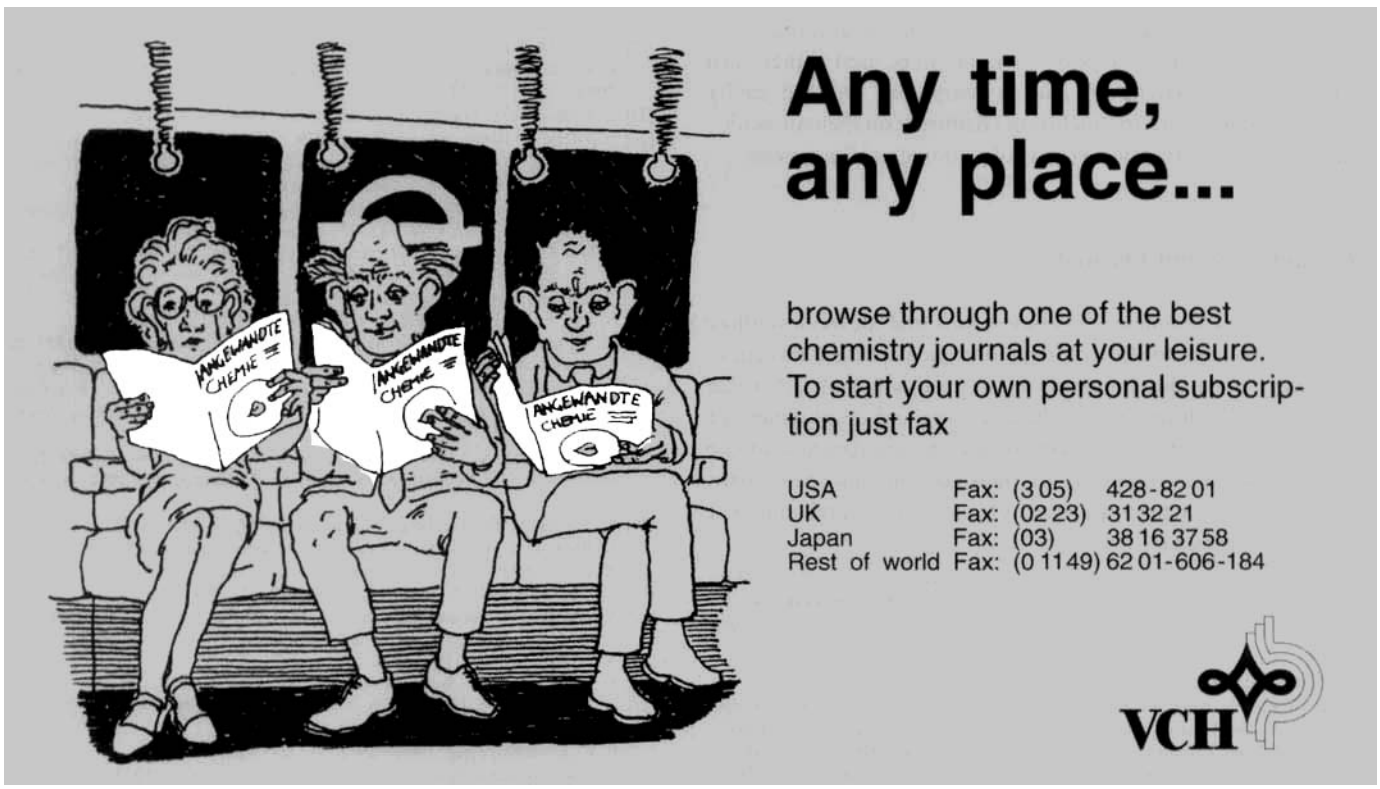
9. Summary and Outlook

Tailor-made template units (guest ions and molecules) allow acceleration and control of reactions in a defined direction, frequently even the preparation of products that otherwise would be difficult to obtain. The discovery and development of new template-controlled reactions and the clarification of the basic mechanisms involved in intermediate and permanent host–guest interactions are worthy targets of research aimed at effective syntheses.

Received: April 26, 1993 [A 931 IE]
German version: *Angew. Chem.* **1994**, *106*, 389
Translated by Dr. M. D. Ravenscroft, Bischwiller (France)

[1] N. F. Curtis, *J. Chem. Soc.* **1960**, 4409–4413; M. M. Jones, *Ligand Reactivity and Catalysis*, Academic Press, New York, **1968**; P. A. Chaloner, *Handbook of Coordination Catalysis in Organic Chemistry*, Butterworths, London, **1986**.
[2] *Coordination Chemistry of Macrocyclic Compounds* (Ed.: G. A. Melson), Plenum, New York, **1979**; S. M. Nelson, F. S. Esho, M. G. B. Drew, *J. Chem. Soc. Dalton Trans.* **1982**, 407–415; D. K. Mitchell, J.-P. Sauvage, *Angew. Chem.* **1988**, *100*, 985–987; *Angew. Chem. Int. Ed. Engl.* **1988**, *27*, 930–932; C. O. Dietrich-Buchecker, J.-P. Sauvage, *Chem. Rev.* **1987**, *87*, 795–810.
[3] M. C. Thompson, D. H. Busch, *J. Am. Chem. Soc.* **1962**, *84*, 1762.
[4] Critical considerations on the "cesium effect" in macrocyclization, which is not generally regarded as a template effect: C. Galli, *Org. Prep. Proced. Int.* **1992**, *24*, 285–307. The term cesium effect is thus misleading, as the cesium atom itself is not responsible for the rate acceleration, the higher yield, or the cyclooligomer selectivity. The effect is caused, for example, by aggregation of cesium carbonate (often added as auxiliary base), which sets up a specific basicity/nucleophilicity of the reaction medium. See also A. Osbrowicki, E. Koepp, F. Vögtle, *The Cesium Effect* (*Top. Curr. Chem.* **1991**, *161*, 37–67).
[5] D. Wöhrle, G. Meyer, *Kontakte Darmstadt* **1985**, *3*, 38.
[6] F. Vögtle, *Supramolekulare Chemie*, 2nd. ed., Teubner, Stuttgart, **1992**. Chap. 2.2 (English translation: *Supramolecular Chemistry*, Wiley, Chichester, England, **1991**, **1993**.
[7] Editorial comment: in this issue is a report on [4]- and [5]-catenanes: D. B. Amabilini, P. R. Ashton, A. S. Reder, N. Spencer, J. F. Stoddardt, *Angew. Chem.* **1994**, *106*, 450; *Angew. Chem. Int. Ed. Engl.* **1994**, *33*, 433.
[8] J.-P. Sauvage, C. O. Dietrich-Buchecker, J. Guilhem, C. Pascard, *Angew. Chem.* **1990**, *102*, 1202–1204; *Angew. Chem. Int. Ed. Engl.* **1990**, *29*, 1154–56; J.-C. Chambron, V. Heitz, J.-P. Sauvage, *J. Chem. Soc. Chem. Commun.* **1992**, 1131–1133.
[9] a) A. Shanzer, J. Libman, *J. Chem. Soc. Chem. Commun.* **1983**, 846–847; b) A. Shanzer, J. Libman, F. Frolow, *J. Am. Chem. Soc.* **1981**, *103*, 7339.
[10] M. Bühner, W. Geuder, W.-K. Gries, S. Hünig, M. Koch, T. Poll, *Angew. Chem.* **1988**, *100*, 1611–1614; *Angew. Chem. Int. Ed. Engl.* **1988**, *27*, 1553–1556.
[11] K. Saigo, R.-J. Lin, M. Kubo, A. Youda, M. Hasegawa, *J. Am. Chem. Soc.* **1986**, *108*, 1996–2000.
[12] T. Tjivikua, P. Ballester, J. Rebek, Jr., *J. Am. Chem. Soc.* **1990**, *112*, 1249–1250; J. S. Nowick, Q. Feng, T. Tjivikua, P. Ballester, J. Rebek, Jr., *ibid.* **1991**, *113*, 8831–8839.
[13] C. A. Hunter, *J. Am. Chem. Soc.* **1992**, *114*, 5303–5311.
[14] F. Vögtle, S. Meier, R. Hoss, *Angew. Chem.* **1992**, *104*, 1628–1631; *Angew. Chem. Int. Ed. Engl.* **1992**, *31*, 1619–1622.
[15] T. R. Kelly, C. Zhao, G. J. Bridger, *J. Am. Chem. Soc.* **1989**, *111*, 3744–3745.
[16] a) C. L. Brown, D. Philp, J. R. Stoddart, *Synlett* **1991**, 462–464; b) B. Odell, M. V. Reddington, A. M. Z. Slawin, N. Spencer, J. F. Stoddart, D. J. Williams, *Angew. Chem.* **1988**, *100*, 1605–1608; *Angew. Chem. Int. Ed. Engl.* **1988**, *27*, 1547–1550.
[17] a) G. von Kiedrowski, *Angew. Chem.* **1986**, *98*, 932–934; *Angew. Chem. Int. Ed. Engl.* **1986**, *25*, 932–935; b) G. von Kiedrowski, B. Wlotzka, J. Helbing, M. Matzen, S. Jordan, *ibid.* **1991**, *103*, 456–459 and **1991**, *30*, 423–426.
[18] M. W. Göbel, J. W. Bats, G. Dürner, *Angew. Chem.* **1992**, *104*, 217–218; *Angew. Chem. Int. Ed. Engl.* **1992**, *31*, 207–208.
[19] B. Dietrich, V. Viout, J.-M. Lehn, *Macrocyclic Chemistry*, VCH, Weinheim, **1993**, Chap. 3.3.
[20] a) J. E. McMurry, G. J. Harley, J. R. Matz, J. C. Clardy, J. Mitchell, *J. Am. Chem. Soc.* **1986**, *108*, 515; b) R. Friederich, M. Nieger, F. Vögtle, *Chem. Ber.* **1993**, *126*, 1723–1732.
[21] L. Collazo, F. S. Guziec, Jr., *J. Org. Chem.* **1993**, *58*, 43–46.
[22] F. Vögtle, L. Rossa, *Angew. Chem.* **1979**, *91*, 534–549; *Angew. Chem. Int. Ed. Engl.* **1979**, *18*, 514–529; A. Dohm, F. Vögtle, *Synthesis of (Strained) Macrocycles by Sulfone Pyrolysis* (*Top. Curr. Chem.* **1991**, *161*, 69–106).
[23] J. Breitenbach, F. Ott, F. Vögtle, *Angew. Chem.* **1992**, *104*, 360–362; *Angew. Chem. Int. Ed. Engl.* **1992**, *31*, 307–310.
[24] F. Ott, J. Breitenbach, M. Nieger, F. Vögtle, *Chem. Ber.* **1993**, *126*, 97–101.
[25] R. Breslow, *Acc. Chem. Res.* **1980**, *13*, 170–177; see also R. Breslow, D. Wiedenfeld, *Tetrahedron Lett.* **1993**, *34*, 1107.
[26] S. Sun, P. Harrison, *Tetrahedron Lett.* **1992**, *33*, 7715–7718.
[27] U. Kramer, A. Guggisberg, M. Hesse, H. Schmidt, *Angew. Chem.* **1977**, *89*, 899–900; *Angew. Chem. Int. Ed. Engl.* **1977**, *16*, 861; A. Guggisberg, B. Dabrowski, U. Kramer, C. Heidelberger, M. Hesse, H. Schmidt, *Helv. Chim. Acta* **1978**, *61*, 1039–1049. See also: M. Hesse, *Ring Enlargement in Organic Chemistry*, VCH, Weinheim, **1991**.
[28] N. J. Leonard, S. Swann, Jr., J. Figueras, Jr., *J. Am. Chem. Soc.* **1952**, *74*, 4620–4624; N. J. Leonard, S. Swann, Jr., E. H. Mottus, *ibid.* **1952**, *74*, 6251–6253.
[29] H. Stetter, H. Spangenberger, *Chem. Ber.* **1958**, *91*, 1982–1988.
[30] V. Bhat, R. C. Cookson, *J. Chem. Soc. Chem. Commun.* **1981**, 1123–1124; R. C. Cookson, P. S. Ray, *Tetrahedron Lett.* **1982**, *23*, 3521–3524.
[31] J. R. Mahajan, H. C. Araujo, *Synthesis* **1976**, *54*, 111–112.
[32] Y. Kobuke, Y. Sumida, M. Hayashi, H. Ogoshi, *Angew. Chem.* **1991**, *103*, 1513–1514; *Angew. Chem. Int. Ed. Engl.* **1991**, *30*, 1496–1497.
[33] A. C. Benniston, A. Harriman, *Synlett* **1993**, 223–226.
[34] D. H. Busch, N. A. Stephenson, *Coord. Chem. Rev.* **1990**, *100*, 119–154.
[35] M. C. Thompson, D. H. Busch, *J. Am. Chem. Soc.* **1962**, *84*, 3744–3745.
[36] A. Eschenmoser, *Pure Appl. Chem.* **1963**, *7*, 297.
[37] E. K. Barefield, *Inorg. Chem.* **1972**, *11*, 2273–2274.
[38] *Crown Compounds* (Ed.: S. R. Cooper), VCH, Weinheim, **1992**.

[39] S. Anderson, H. L. Anderson, J. K. L. Sanders, *Angew. Chem.* **1992**, *104*, 921–924; *Angew. Chem. Int. Ed. Engl.* **1992**, *31*, 907–910; see also *Acc. Chem. Res.* **1993**, *26*, 469–475.
[40] D. Philp, J. F. Stoddart, *Synlett* **1991**, 445–458.
[41] N. Nishino, H. Mihara, H. Koyota, K. Kobata, T. Fujimoto, *J. Chem. Soc. Chem. Commun.* **1993**, 162–163.
[42] J.-L. Mascarenas, K. C. Hayashibara, G. L. Verdine, *J. Am. Chem. Soc.* **1993**, *115*, 373–374.
[43] Y. Jenkins, J. Barton, *J. Am. Chem. Soc.* **1992**, *114*, 8736–8738.
[44] R. Rubin, T. L. McKee, E. T. Kool, *J. Am. Chem. Soc.* **1993**, *115*, 360–361.
[45] S. Rumney IV, E. T. Kool, *Angew. Chem.* **1992**, *104*, 1686–1689; *Angew. Chem. Int. Ed. Engl.* **1992**, *31*, 1617–1619.
[46] J. S. Cohen, *Oligodeoxynucleotides: Antisense Inhibitors of Gene Expression*, CRC Boca Raton, FL, USA, **1989**.
[47] M. Mutter, S. Vuilleumier, *Angew. Chem.* **1989**, *101*, 551–692; *Angew. Chem. Int. Ed. Engl.* **1989**, *28*, 535–554; I. Ernest, J. Kalvoda, C. Sigel, G. Rihs, H. Fritz, M. J. J. Blommers, F. Raschdorf, E. Francotte, M. Mutter, *Helv. Chim. Acta* **1993**, *76*, 1539.
[48] L. C. Hsieh, S. Yonkovich, L. Kochersperger, P. G. Schultz, *Science* **1993**, *260*, 337–339.
[49] S. E. Byström, A. Börje, B. Akermark, *J. Am. Chem. Soc.* **1993**, *115*, 2081–2083.
[50] P. Behrens, G. D. Stucky, *Angew. Chem.* **1993**, *105*, 729–732; *Angew. Chem. Int. Ed. Engl.* **1993**, *32*, 696–699.



Organic and Organometallic Molecular Magnetic Materials—Designer Magnets

Joel S. Miller* and Arthur J. Epstein*

Magnets composed of molecular species or polymers and prepared by relatively low-temperature organic synthetic methodologies are a focus of contemporary materials science research. The anticipated properties of such molecular-species-based magnetic materials, particularly in combination with other properties associated with molecules and polymers, may enable their use in future generations of electronic, magnetic, and/or photonic/photronic devices ranging from information storage and magnetic imaging to static and low-frequency magnetic shielding. A tutorial of typical magnetic behavior of molecular materials is presented. The three distinct models (intramolecular spin coupling through orthogonal orbitals in the same spatial region within a molecule/ion, intermolecular spin coupling through pairwise "configuration interaction" between spin-containing moieties, and dipole–dipole, through-space interactions) which enable the design of new molecular-based magnetic materials are discussed. To achieve the required spin couplings for bulk ferro- or ferrimagnetic behavior it is crucial to prepare materials with the necessary primary, secondary, and tertiary structures akin to proteins. Selected results from the worldwide effort aimed at preparing molecular-based magnetic materials by these mechanisms are described. Some organometallic solids comprised of linear chains of alternating metallocenium donors (D) and cyanocarbon acceptors (A) that is, $\cdots D^{\bullet+}A^{\bullet-}D^{\bullet+}A^{\bullet-}\cdots$, exhibit cooperative magnetic phenomena. Bulk ferromagnetic behavior was first observed below the critical (Curie) temperature T_c of 4.8 K for $[Fe^{III}(C_5Me_5)_2]^{\bullet+}[TCNE]^{\bullet-}$ (Me = methyl; TCNE = tetracyanoethylene). Replacement of Fe^{III} with Mn^{III} leads to a ferromagnet with a T_c of 8.8 K in agreement with mean-field models developed for this class of materials. Replacement with Cr^{III}, however, leads to a ferromagnet with a T_c lowered to 3.65 K which is at variance with this model. Extension to the reaction of a vanadium(0) complex with TCNE leads to the isolation of a magnet with a $T_c \approx 400$ K, which exceeds the thermal decomposition temperature of the material. This demonstrates that a magnetic material with a T_c substantially above room temperature is achievable in a molecule/organic/polymeric material. Finally, a new class of one-dimensional ferrimagnetic materials based on metalloporphins is discussed.

1. Introduction

Magnets have captivated mankind from time immemorial and have played a prominent role in the development of both science and technology as well as in the evolution of society.[1] In perhaps the earliest example of technology transfer involving condensed matter science, Chinese workers exploited the fundamental observation of magnetic behavior that had been discovered by ancient Grecians by invention of the "south-pointing" compass.[1b] The development of present day experimental[1c] and theoretical condensed matter physics as well as quantum mechanics and molecular chemistry are also deeply indebted to magnetism. Magnets have become ubiquitously woven into the fabric of everyday life and are indispensable in our present world. This is reflected by the annual sales of magnets in the western-world which reached $\$2 \times 10^9$[2] in 1990. Applications of magnets span from magneto-mechanical machines (frictionless bearings, medical implants, magnetic separators, etc.) to magnetic shielding and electromagnetic radiation absorption (deflection of static and low-frequency magnetic fields), to acoustic devices (loudspeakers, microphones, etc.), to telecommunication/information technology (switches, sensors, magnetic resonance imaging, as well as magnetic and optical disks, etc.), and to motors and generators.[3] Futuristic "smart" materials and systems will rely upon "smart" switches, sensors, and transducers that undoubtedly will be comprised in part by mag-

[*] Dr. J. S. Miller[+]
Central Research & Development
Experimental Station E328
Du Pont, P.O. Box 80328, Wilmington, DE 19880-0328 (USA)
Dr. A. J. Epstein
Department of Physics and Department of Chemistry
The Ohio State University
Columbus, OH 43210-1106 (USA)
Telefax: Int. code + (614)292-3706
[+] New Address:
Department of Chemistry
University of Utah
Salt Lake City, UT 84112 (USA)
Telefax: Int. code + (801)581-8433

 © VCH Verlagsgesellschaft mbH, D-69451 Weinheim, 1994 0570-0833/94/0404-0385 $ 10.00+.25/0

netic materials. Magnets consequently are an important focus of modern materials research programs, with emphasis on improvement of their technologically useful properties.

Current magnetic materials share the generic attributes of a) being atom-based, b) having d or f orbital transition- or lanthanide-metal-based spin sites, and c) possessing extended network bonding in at least two dimensions. Furthermore, they d) are prepared by high-temperature metallurgical methodologies. Metamorphosis from such atom-based inorganic materials to molecule-based organic/polymeric materials should enable the a) specific alteration of the magnetic properties by established organic chemistry methodologies, b) combination of magnetic properties with other mechanical, electrical, and/or optical properties, and c) simplicity of fabrication often enjoyed by organic materials, that is, low-temperature synthesis as opposed to the high-temperature metallurgical methods currently utilized. These qualities may herald the use of organic materials in future generations of electronic, magnetic, photonic and/or photronic devices. The discovery of molecule-based magnets parallels the discovery of cooperative electrical phenomena in organic/molecular superconductors with the advent of cooperative magnetic phenomena in organic/molecular materials.

The issue of what constitutes a molecule-based magnet frequently arises. As noted previously classical magnets are comprised solely of a high density of d or f orbital metal spin sites and are prepared by metallurgy. An organic magnetic material, in contrast, must possess at least one type of spin site that is based on s and p orbitals and be prepared by organic chemistry methodology; that is, an organic component of the material plays an active role in the resultant magnetic behavior. Intermediate between these extremes lie solely metal-spin-site-based magnetic materials prepared and modified by organic chemistry methodologies (i.e., an organic component of the material plays a passive role in the resultant magnetic behavior). In principle, organic-based materials prepared by metallurgy (i.e., high-temperature pyrolysis of organic compounds[7]) lie between these extremes. Although various specific criteria for a molecule/organic magnetic material have been applied, we define organic/polymeric magnetic materials as those materials prepared through the established low-temperature synthetic procedure of organic, organometallic, and coordination metal synthetic chemistry. We use the term "molecular species" to refer to any of the above be it a molecule, ion, or polymer. This feature is common to all the materials studied by the majority of the scientists that have participated at conferences on this topic.[4] It should be noted that the ferromagnetic Zintl phase $Ca_{14}MnBi_{11}$ composed of isolated ions,[5] the ferromagnet Rb_2CrCl_4 composed of a covalently bonded two-dimensional



Joel S. Miller was born in Detroit, Michigan and received his Bachelor of Science in Chemistry from Wayne State University (1967) and Ph. D. from UCLA (1971). After a postdoctoral fellowship at Stanford University he joined the Xerox Webster Research Center in 1972 and later he joined the late Occidental Research Corporation (1978). He was Visiting Professor of Chemistry at the University of California, Irvine, CA and Chairman of the Southern California Section of the American Chemical Society (1981). He joined the Central Research & Development Department at the Du Pont Company in 1983 where he was a Research Supervisor for solid-state science. He has been a Visiting Scientist at the Weizmann Institute (1985) and a Visiting Professor of Chemistry at the University of Pennsylvania (1988). Recently he joined the faculty of department of chemistry at the University of Utah. He is on the advisory board of Advanced Materials, Chemistry of Materials, and Journal of Materials Chemistry, and a member of the Inorganic Synthesis Corporation. His research interests focus on the solid-state magnetic, electrical, and optical properties of molecular (organic, organometallic, and inorganic coordination) compounds and electron transfer complexes as well as the surface modification of solids. Currently he is actively involved in synthesis and characterization of molecular/organic-based ferromagnets. In addition to patents he has edited eight monographs and published over 240 papers in these and other areas.



Arthur J. Epstein was born in Brooklyn, New York and received his B. S. in Physics from the Polytechnic Institute of Brooklyn in 1966 and his Ph. D. in Physics from the University of Pennsylvania in 1971. After thirteen years at the Xerox Webster Research Center, where he was Principal Scientist, he joined The Ohio State University in 1985 as Professor of Physics and Professor of Chemistry. He has been The Director of the Ohio State University Center for Materials Research since 1989. He also has been adjunct Professor of Physics at the University of Florida and was a Visiting Professor at Université Paris-Sud and The Technion-Israel Institute of Technology. He is a Regional Editor for Synthetic Metals. His current research interests include experimental and theoretical study of magnetic, electronic/optical, and transport phenomena of synthetic magnets (molecular, organic and polymeric magnets) and synthetic metals (conducting polymers, organic and molecular materials), including the study of excitations and their dynamics. He also is active in the exploration of potential applications of unconventional magnetic, electronic, and optical materials for which he consults with several companies. In addition to having originated twenty patents and editing three conference proceedings, he has published over 350 papers in these and other areas.

network structure,[6] as well as several examples of magnetic materials prepared by the pyrolysis of organic molecules[7] are typically prepared at high temperatures and as such are not within the direct focus of this review.

Molecular-species-based ferromagnetic compounds although postulated in the 1960s have been realized only within the past decade.[4, 8, 9] In this review we will briefly summarize the essence of the magnetic behavior important for understanding the physical properties of this class of materials[9, 10] and review some of the research results achieved worldwide in this rapidly developing area of contemporary inquiry.

2. Magnetic Behavior—A Tutorial

Magnetic behavior is typically detected by a material's attraction (or repulsion) to a magnet. It arises from the intrinsic spin of an electron and how the electron spins on adjacent atoms (or molecules) couple with each other. Every electron has a minute magnetic moment associated with the quantum-mechanical "spin". The electrons reside in orbitals and each orbital may have two electrons—one "spin-up", that is, spin aligned with an applied magnetic field (↑), and one "spin-down", that is, spin aligned opposing an applied magnetic field (↓)—such that the spins cancel. A radical is an atom, ion, or molecule with an odd number of electrons (or an even number of electrons n in more than $n/2$ orbitals. Thus, a radical must have at least one orbital with an unpaired electron and hence have a net spin.

The unpaired electron has a spatial distribution, termed spin density, which can be distinct from the charge and electron densities of a molecular species. For a radical anion such as the tetracyanoethenide radical, $[TCNE]^{\cdot -}$, the additional electron is added to the lowest unoccupied molecular orbital (LUMO) of the closed shell TCNE. The original LUMO of TCNE is now a partially occupied molecular orbital (POMO), if we follow a restricted open-shell Hartree–Fock (ROHF) formalism in which all of the orbitals are doubly occupied except for the POMO. (Note that POMO refers to orbital occupancies that may lead to states that can be different.) For $[TCNE]^{\cdot -}$ the POMO is a π^* orbital of b_{2g} symmetry,[11] and there are several nodes in this orbital which are dominated by a large node between the central carbon atoms participating in the TCNE double bond (Fig. 1 top). In the ROHF formalism, the spin density of the POMO represents the excess spin density in the molecular species, and this spin density must be in one direction (positive) and is termed α spin. Furthermore, for $[TCNE]^{\cdot -}$ this excess spin density can only reside in the p orbitals, and it should not have EPR hyperfine splittings because there is no mechanism for the spin to interact with the s orbitals which have the proper symmetry to interact with the nuclear spins. The simplest way to couple all of the orbitals is to use the unrestricted Hartree–Fock (UHF) model in which the restriction of double occupancy in an orbital is relaxed. In the UHF model each orbital is singly occupied and one thus solves for positive (α) or negative (β) spin densities.[13a] (By convention for a radical, the positive spin density (α spin) is greater than the negative spin density (β spin)). Because the α- and β-spin densities are calculated individually, coupling of all of the orbitals is possible so that regions exist with excess α and β spins. The amount of unpaired spin density on an atom within the molecular species need not, however, correspond to the atom contributions in the POMO (Fig. 1 middle). Furthermore, the regions of excess spin are now no longer determined by the ROHF POMO; thus mixing with s orbitals leads to the observation of EPR hyperfine splittings.

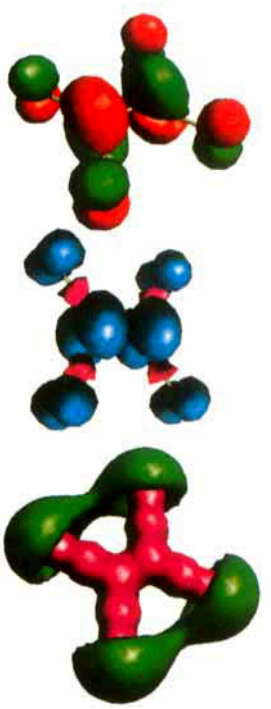


Fig. 1. Electron structure information for $[TCNE]^{\cdot -}$. All calculations were done on $[TCNE]^{\cdot -}$ with the local density functional method using the optimum calculated geometry [11] and the unrestricted spin formalism with the program DGauss and visualizations with UniChem [14a]. Highest occupied α-spin orbital (top); spin density (middle); electrostatic potential (ESP) energy surface at ± 90 kcal mol^{-1} (3.9 eV) (bottom). ESP surface was obtained by the interaction of a particle of 1+ charge with the unrelaxed molecular electron density. Positive regions (violet) correspond to repulsive interactions and negative regions (green) correspond to attractive regions (from ref. [14b]). (Figures kindly provided by D. A. Dixon and S. C. Walker).

Spin polarization can be described by either valence bond (Fig. 2) or molecular orbital approaches. Spin polarization arises because there are different exchange interactions between the unpaired α-spin electrons in the POMO and the other α-spin electrons as compared to no exchange with the β-spin electrons. For example, for the Li atom the 2s electron polarizes the 1s electrons because there are different effective potentials for the α- and β-spin 1s electrons. Relaxing the double occupancy for the 1s orbital will lead to a lower energy. Another way to consider such spin polarizations, which has been used to explain the spin density in the $CH_3^{\bullet}$ radical[13b] (positive (α) spin density on C and negative (β) spin density on H), is the use of two simple rules: 1) an intraatomic Hund's rule in which electrons on an atom tend to have parallel spins and 2) electrons that form a chemical bond tend to have antiparallel spins. Because the α- and β-spin densities can interact, spin polarization can occur, by which an unpaired electron can polarize the paired spins in an adjacent σ or π bond in such a way that one of the paired electrons in the bond is closer to one atom than another (Fig. 2).

A way to view the charge distribution in a molecular species, in addition to the use of Mulliken charges,[13c] is to calculate the electrostatic surface potential (ESP). The interaction energy (attractive or repulsive) of a test charge (in this case 1+) with the unrelaxed electron density is thus calculated as illustrated for $[TCNE]^{\cdot -}$ in Figure 1 bottom. The ESP surface shows that there is significant negative charge on the nitrogen atoms even though one formally would place most of the negative charge on the two carbon atoms of the double bond.

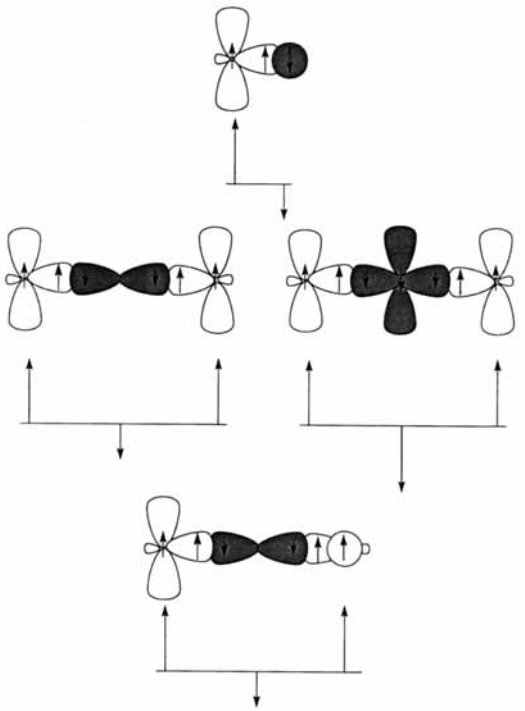


Fig. 2. Illustration of the orbital interactions for spin polarization in a σ bond (top), between π orbitals through two σ bonds (center left), between π orbitals through σ bonds and π orbitals (center right), and between π orbitals rotated by 90° through σ bonds (bottom).

The net $S = 1/2$ spin density (positive or negative) on each atomic site of a molecular species is determined by adding up separately the contribution to each atomic site of every "up-spin" and "down-spin" filled electron orbital, that is, the sum of all α-spin electron densities minus the sum of all β-spin electron densities. The POMO electron and spin densities differ from the molecular/ion charge densities. The total charge density is a sum of the charge density associated with each occupied energy level (both α and β spin) at each atomic site less the positive nuclear charge, and is illustrated by the electrostatic surface generated when a point charge is brought toward a molecular species (Fig. 1 bottom). The POMO electron density, the unpaired spin density, and the total charge density of a molecule will therefore differ from each other as shown in Figure 1 for $[TCNE]^{\cdot -}$.

The wavefunction and therefore the POMO valence-electron density is determined computationally, however, electron and spin densities can be determined experimentally by diffraction methods. The valence-electron density can be determined from the low-angle scattering in a high-resolution single-crystal structural determination[12e] or preferably from the difference between results obtained by using single-crystal X-ray and neutron diffraction studies at the same temperature. The absolute spin density can be directly determined from single-crystal polarized-neutron diffraction studies at low temperature. Absolute spin densities may also be obtained experimentally from analysis of either the NMR contact shifts[12b] or detailed analysis of the EPR hyperfine couplings constants;[15] however, the relaxation time of the species must be amenable for these resonance measurements to be applicable.

Radicals are usually far enough apart that their magnetic coupling energy is small compared to the coupling-breaking thermal energy. Such spins do not couple (that is, align cooperatively), instead they form a weak magnet (paramagnet Fig. 3a). When the radicals come sufficiently close to each other, the coupling energies increase, ultimately influencing the alignment of the neighboring spins. If this alignment occurs in such a manner that the spins oppose each other, this leads to antiferromagnetic behavior (Fig. 3b). Bulk ferromagnetic behavior, albeit rare, occurs when the spins in a solid align in the same direction (Fig. 3c), resulting in a net magnetic moment. Thus, ferromagnetism requires that the individual unpaired spins interact collectively with each other aligning themselves. Ferrimagnets can occur when there are different moments (essentially a different number of spins) on neighboring sites which align antiferromagnetically but do not cancel; this leads to a net moment for the solid (Fig. 3d). It is vital to note that this commercially useful highly magnetic behavior is not a property of a molecular species; it is a cooperative solid-state (bulk) property. Three-dimensional (3D) interactions are typically necessary to achieve long-range magnetic order and bulk ferromagnetic behavior; however, two-dimensional (2D) interactions in some circumstances suffice, as is probably the situation for Rb_2CrCl_4[6a] in which interlayer spacings can be increased by replacing Rb^+ with bulky alkylammonium counterions (vide infra), but the T_c is not significantly altered. For strictly one-dimensional (1D) nearest neighbor interactions, long-range order can only occur at 0 K. However, for the special case when a chain has anisotropic interactions with randomness in the anisotropy, hysteretic effects mimicking three-dimensional order may occur (vide infra). For ferrigmagnets (e.g., chain systems comprised of alternating quantum ($S = 1/2$) and classical ($S > 1/2$) spins) the net magnetization may reverse direction as a function of increasing temperature (i.e., compensation may occur).

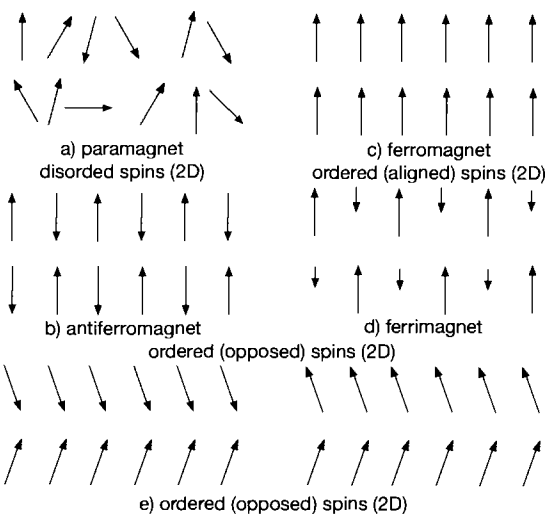


Fig. 3. Two-dimensional spin alignment for a) paramagnet, b) antiferromagnet, c) ferromagnet, d) ferrimagnet, and e) canted ferromagnet behavior.

As noted previously, magnets are characterized by their response to a nearby magnet, or more specifically to an applied magnetic field, H. For ideal, noninteracting spins a net magnetic moment or magnetization, M, is induced in the solid when ex-

posed to an applied magnetic field, H; where M is proportional to H [Eq. (1)]. The proportionality constant is termed the molar

$$M = \chi H \tag{1}$$

magnetic susceptibility χ, and it has a temperature dependence that is characterized by the Curie expression [Eq. (2)]. The Curie

$$\chi = \frac{C}{T} \tag{2}$$

constant C in emu K mol^{-1}, is defined according to [Eq. (3)], in

$$C = \frac{Ng^2\mu_B^2 S(S+1)}{3k_B} \tag{3}$$

which S is the spin quantum number (one-half of the number of unpaired electrons per radical), N is Avogadro's number, g is the Lande factor, μ_B is the Bohr Magneton, and k_B is the Boltzmann constant. Sometimes the spins experience an effective parallel (or antiparallel) exchange field due to cooperative interactions with the neighboring spins which increases (or decreases) the measured susceptibility from that predicted for independent spins by the Curie law. The high-temperature susceptibility data often can be fit to the Curie–Weiss law [Eq. (4)]; where for

$$\chi = \frac{C}{T-\theta} \tag{4}$$

parallel (ferromagnetic) and antiparallel (antiferromagnetic) interactions, θ is greater or less than zero, respectively. The value of θ can be determined from the $\chi^{-1} = 0$ intercept obtained in the linear extrapolation of the plot of χ^{-1} versus T at high temperature; note the value of χ is temperature-dependent. Chemists frequently report the effective moment μ_{eff} or sometimes simply χT. The effective moment is defined in Equation (5).[16a]

$$\mu_{eff} = \sqrt{\frac{3\chi k_B T}{N}} = 2.83\sqrt{\chi T} \tag{5}$$

For a simple system comprising one mole of noninteracting spins (i.e., $\theta = 0$), and where S is a valid spin quantum number, μ_{eff} is temperature-independent [Eq. (6)].

$$\mu_{eff} = \mu_B\sqrt{g^2 S(S+1)} \tag{6}$$

The magnetization M also has a characteristic applied magnetic field dependency that enables the rapid qualitative determination of the magnetic behavior. At low temperatures and high magnetic fields (conditions under which the magnetic energy ($gS\mu_B H$)[16b] is comparable in magnitude to the thermal energy ($k_B T$)), the magnetization no longer obeys Equation (1), but approaches the limiting value or saturation magnetization M_s [Eq. (7)]. M_s has the units of emuG mol^{-1}, though it sometimes

$$M_s = \mu_B NSg \tag{7}$$

is reported in units of μ_B molecule^{-1}. For independent spins the temperature dependence of M is described by the Brillouin function [Eq. (8)]

$$M = \mu_B NSgB \tag{8}$$

where

$$B = \frac{2S+1}{2S}\coth\left(\frac{2S+1}{2S}x\right) - \frac{1}{2S}\coth\left(\frac{x}{2S}\right)$$

and

$$x = \frac{gS\mu_B B}{k_B T}.$$

The Brillouin function no longer applies when there are significant ferromagnetic or antiferromagnetic interactions among the spins. However, for $T \gg \theta$ an effective temperature given by $T_{eff} = T - \theta$ may be used in the argument of the Brillouin function to obtain a "fitting" of the data.[38] Table 1 summarizes typical expected values for χT, μ_{eff}, and M_s as a function of S.

Table 1. Representative values of χT, μ_{eff}, and M_s as a function of S and the Lande g value.

S	g	χT [emu K mol^{-1}]	μ_{eff} [μ_B mol^{-1}]	μ_{eff}^2 [μ_B^2 mol^{-2}]	M_s [emuG mol^{-1}]	gS [μ_B per molecule]
1/2	2	0.375	1.73	3	5585	1
2 × 1/2	2	0.750	2.45	6	11170	2
1	2	1.000	2.83	8	11170	2
3 × 1/2	2	1.125	3.00	9	16755	3
1/2 + 1	2	1.375	3.32	11	16755	3
3/2	2	1.875	3.87	15	16755	3
4 × 1/2	2	1.500	3.46	12	22340	4
2 × 1	2	2.000	4.00	16	22340	4
1/2 + 3/2	2	2.250	4.24	18	22340	4
1/2 + 2	2	3.375	5.20	27	27925	5

The temperature dependencies of χ, χ^{-1}, and μ_{eff} are illustrated for independent spins (Curie), and spins with ferro-, and antiferromagnetic interactions in Figure 4. A schematic illustration of a number of field-dependent magnetization behaviors is shown in Figure 5.

At sufficiently low temperature the spins may order. This temperature is the critical temperature T_c. If the spins align parallel to each other (ferromagnet, Fig. 3c), a macroscopic spontaneous magnetization in zero applied field (i.e., $M(H_{applied} = 0) > 0$) is present, and the critical temperature in this case is sometimes referred to as the Curie temperature T_C. If neighboring spins are aligned antiparallel (antiferromagnet, Fig. 3b), there is no net macroscopic moment and the susceptibility is anisotropic. Here the critical temperature is sometimes referred to as the Néel temperature T_N. As noted earlier, ferrimagnetism can occur when the antiferromagnetically aligned spins have differing local moments, resulting in the incomplete cancellation of the parallel and antiparallel spin sublattices which leads to a reduced, but nonzero, moment (Fig. 3d). In this case the critical temperature is also sometimes referred to as the Néel temperature T_N.

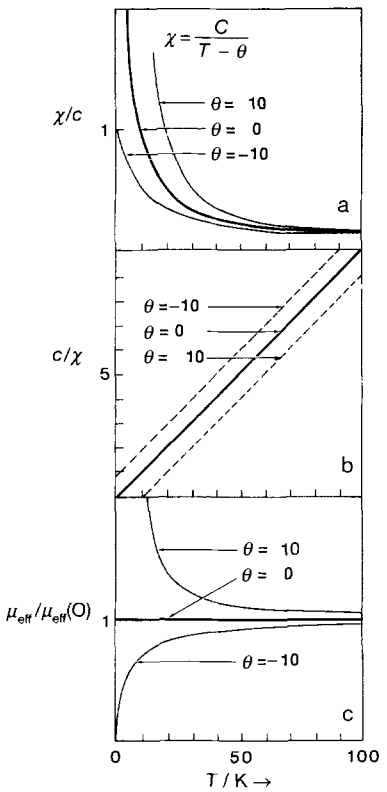


Fig. 4. The susceptibility χ (a), the reciprocal susceptibility χ^{-1} extrapolated from the high-temperature region (b), and the effective moment μ_{eff} (c) as a function of temperature for independent $g = 2$, $S = 1/2$ spins as well as ferromagnetically coupled ($\theta = 10$ K) and antiferromagnetically coupled ($\theta = -10$ K) spins. The Curie–Weiss law. (Taken from ref. [9]).

For ferro- and ferrimagnets well below the critical temperature, the atomic or molecular magnetic moments are essentially all aligned on a microscopic scale. Actual samples, however, are composed of small regions termed domains, within which the local magnetization is essentially saturated. The relative direction of the magnetic moment in adjacent domains is not parallel. This phenomenon has its origin in the lowering of the total energy of the magnet by transformation from a configuration of all parallel moments (resulting in a high energy stored in the magnetic field generated by these moments) to an array of domains that point in various directions (resulting in little energy stored in magnetic fields but at an energy cost of forming "domain walls" between the domains). The coercive field H_c is the reverse magnetic field necessary to reduce the magnetization of a sample to zero starting in a saturation condition magnetization. "Hard" magnets have large values of H_c (>100 Oe), whereas "soft" magnets have low, sometimes unobservable values of H_c (<10 Oe). Large values (hundreds of Gauss) of H_c are necessary for magnetic storage of data, while low values (milliGauss) are necessary for ac motors. An example of a molecular-species-based soft ferromagnet is the complex $[Fe^{III}(S_2CNEt_2)_2]Cl$, which has been characterized by magnetic susceptibility, heat capacity, and ^{57}Fe Mössbauer spectroscopy. It exhibits a T_c of 2.46 K, but does not exhibit hysteretic effects.[17] Magnetic materials that are subdomain in size exhibit superparamagnetic (high-spin) behavior, for example, naturally occurring ferritin.[18a] The magnetization and coercivity are important parameters in ascertaining the commercial utility of a magnet. Table 2 summarizes values for some of the more common magnetic materials and new molecular-species-based magnets.

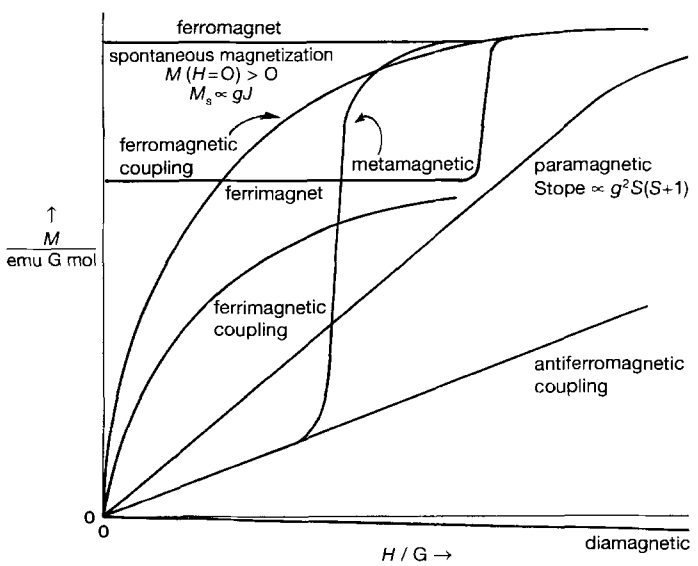


Fig. 5. Schematic illustration of the magnetization M as a function of applied magnetic field H for several types of commonly observed magnetic behavior (from ref. [9]).

It is interesting to ponder the limiting size of a molecule beyond which its spins will no longer remain aligned within a single magnetic domain. Calculations of the size of a single magnetic domain are very complex due to dependencies on the geometry, magnetic anisotropy etc.,[18b,d] and to the best of our knowledge this question has not been experimentally or theoretically addressed for a molecular-species-based system. As a preliminary model one may consider typical spin magnitudes in a known single-domain magnetic material. The single domain of magnetite, Fe_3O_4, which is present in magnetotactic bacteria,[19] has a volume of about 1×10^8 Å^3,[19] and thus contains 1.2×10^6 Fe_3O_4 units with four net spins each or about 5×10^6 total spins (i.e., 0.05 spin per Å^3). For iron, if one assumes an effective critical domain radius of 75 Å for a spherical single domain,[18e] each single-domain particle has 1.5×10^4 iron atoms and about 3.3×10^4 spins (0.2 spin per Å^3). Likewise, for $Nd_2Fe_{14}B$, if one assumes a conservative single-domain radius of 150 Å,[18f] 2×10^6 spins (0.1 spin per Å^3) are present per domain. Assuming that the single domain contains at least 10^6 spins, it is feasible that a molecular-species-based material, containing a single spin per repeat unit with an equivalent weight of 100 daltons, and with about 10^6 repeat units (thus a molecular weight of 10^8 daltons), might also be a single domain. The spatial dimensions of such a domain would be quite large and its spin density would be relatively low. Note that the domain size also depends strongly on the shape of the particle; for example, altering the shape of an iron particle from a sphere to a prolate ellipsoid with an aspect ratio of ten increases the domain size from 1.5×10^5 to 9.6×10^7 Fe atoms.[18e] Thus, materials with a high aspect ratio such as linear and minimally branched polymers may have a substantially greater number of spins and larger dimensions and still remain single magnetic domains.

If the relatively large single-domain molecular species remain far apart from each other so that the interaction among these molecules is very weak, the temperature and magnetic field dependence of the measured magnetization would reflect the behavior of single-domain particles. In this case, the magnetization of the single-domain molecule follows the direction of the applied magnetic field by rotation of the magnetic moment. If an uniaxial anisotropy is present, there will be a barrier to the rotation of the magnetic moment in response to the changes in the magnetic field. The "supermagnetic" behavior of single-domain magnets differs in time dynamics from that of the reversal of magnetization within a multimagnetic domain particle due to domain wall motion.[10, 20]

orientation at neighboring sites in the ordered state may be canted with respect to each other.

Metamagnetism is a magnetic-field-dependent transformation from an antiferromagnetic state to a high-moment ferromagnetic state; that is, the spin alignment depicted in Figure 3b is transformed to that depicted in Figure 3c by application of an applied magnetic field. Decamethylferrocenium 7,7,8,8-tetracyano-*p*-quinodimethanide, $[Fe(C_5Me_5)_2][TCNQ]$, is a molecular-species-based metamagnet (see Section 5). A spin glass occurs when there are local spatial correlations in the directions of neighboring spins, but no long-range order. For a spin glass the spin alignment is as described for a paramagnet (Fig. 3a). However, unlike a paramagnet where the directions of the spins vary

Table 2. Selected magnetic properties of representative magnetic materials.

Material	θ [K]	Magnetism [a]	M [g mol^{-1}]	T_c [K]	Density [g cm^{-3}]	Saturation Magnetization [emuG] [mol^{-1}]	[M^{-1}]	[g^{-1}]	[cm^{-3}]	Coercivity [b] H_c [G] (T [K])	X-ray [b]
iron	1101	FO	55.8	1043	7.86	12175	12175	218	1715	1	SC
cobalt	1408	FO	58.9	1394	8.89	9500	9500	161	1434		SC
nickel	650	FO	58.7	627	8.91	3200	3200	54.5	486	≈7	SC
Fe_3O_4	673	FI	232	858	5.1	21300	7100	91.8	468	213	SC
$SmCo_5$		FO	445	993	8.59	66050	11000	148	1275	56000	P
$Nd_2Fe_{14}B$		FO	1081	585	7.6	181100	11300	168	1273	25000	
$Cr^{IV}O_2$		FO	84	387	4.89	8800	8800	105	512	650	SC
Rb_2CrCl_4	92	FO	365	52.4	2.91	22700	22700	62.2	181		SCn
Rb_2CrCl_3Br		FO	409	55	3.26	22500	22500	55	179		Pn
$[Fe^{III}Cl(S_2CNEt_2)_2]$	3.6	FO	388	2.46	1.5	14500	14500	37.4	56.1	none	SC
β-[Mn^{II}Pc] [c]	23	C/W	567	8.3	1.63	12000	12000	21.1	34.4		SC
$[Mn^{II}Cu^{II}(obbz)] \cdot H_2O$ **13**		FI	465	14	1.8	22300	11150	48	86.3	60 (4.2)	-
$[Mn^{II}Cu^{II}(obbz)] \cdot 2H_2O$		FI	417	4.6	1.8	22300	11150	53.5	96.3	10 (2)	-
$[Cu^{II}$(terephtalato)MeOH$] \cdot 1/2\,H_2O$		FO	269	13	1.65	6400	6400	23.8	39.3	80 (4.2)	-
$[Mn^{II}Cu^{II}(pbaOH)] \cdot 2H_2O$		FI	385	30	2	22300	11150	58	116	60 (4.2)	-
$[Mn^{II}Cu^{II}(pbaOH)] \cdot 3H_2O$ **14**		FI	403	4.6	2.02	22300	11150	55.4	112	50 (1.3)	SC
$[Mn^{II}(hfac)_2NITEt]$		FI	654	8.1	1.61	22000	22000	33.6	54.1	320 (1.2)	SC
$[Mn^{II}(hfac)_2NITiPr]$ **15**		FI	668	7.6	1.61	22000	22000	32.9	53	< 5 (1.2)	SC
$[Fe^{II}$(4-imidazoleacetate)$_2] \cdot 2$MeOH		C/W	370	15	1.57	3900	3900	10.5	16.5	6200 (4.2)	
$[(NBu_4)Ni^{II}\{Cr^{III}(ox)_3\}]$	19	FO	617	14	1.49	27590	13795	44.7	66.6	160 (5)	
$[Fe^{III}Cp_2^*]^{+} [TCNE]^{\cdot -}$	30	FO	454	4.8	1.31	16300	16300	35.9	47	1000 (2)	
$[Fe^{III}Cp_2^*]^{+} [TCNQ]^{\cdot -}$	3	MM	531	2.55	1.26	18000	18000	33.9	42.7	H_{cr} 1.6 kG	SC
$[Fe^{III}Cp_2^*]^{+} [C_4(CN)_6]^{\cdot -}$	35	FO	502		1.31	17700	17700	35.2	46.1	none	SC
$[Cr^{III}Cp_2^*]^{+} [TCNE]^{\cdot -}$	22.2	FO	527	3.65	1.21					none	UC
$[Cr^{III}Cp_2^*]^{+} [TCNQ]^{\cdot -}$	11.6	FO	527	3.1	1.25	22500	22500	42.7	53.4	none	UC
$[Mn^{III}Cp_2^*]^{+} [TCNQ]^{\cdot -}$	10.5	FO	530	6.2	1.26	13500	13500	25.5	32.1	3600	SC
$[Mn^{III}Cp_2^*]^{+} [TCNE]^{\cdot -}$	22.6	FO	453	8.8	1.31	20000	20000	44.2	57.8	1200 (2)	UC
$[Mn^{III}Cp_2^*]^{+} [DDQ]^{\cdot -}$	27.8	MM	552	8.5	1.39	24200	24200	43.8	60.9		P
$[Mn^{III}Cp_2^*]^{+} [Pd\{S_2C_2(CF_3)_2\}_2]^{\cdot -}$	3.7	MM	896	2.8		12500	6250			H_{cr} 800 G	
$[MnTPP]^{+} [TCNE]^{\cdot -}$	61	FO	980	18	1.33	30000	30000	30.6	40.7	375 (5)	SC
β-p-$O_2NC_6H_4NIT$ **17**	1	FO	278	0.6	1.41	2800	2800	10.1	14.2	≈1 (0.44)	SC
tanol suberate **18**	0.7	MM	483	0.38	1.12	11125	11125	23	25.8	H_{cr} 100 G	P
$[V(TCNE)_2] \cdot 1/2CH_2Cl_2$	>350	FI	350	>350		6000	6000	17.1		60 (300)	D

[a] FO = ferromagnetic, FI = ferrimagnet, MM = metamagnet, C/W = canted/weak ferromagnet. [b] D = disordered, P = powder diffraction, Pn = neutron powder diffraction, SC = single crystal, SCn = neutron single crystal, UC = unit cell, H_{cr} = metamagnet critical field. [c] Abbreviations H_2Pc = phthalocyanine.

Many other magnetic phenomena are possible. Canted ferromagnetism, metamagnetism, and spin-glass behaviors are examples. A canted ferromagnet can result from the relative tilting of ferromagnetically coupled chains such that, though the material is ferromagnetic, there is a reduction of the moment (see Fig. 3e). Sometimes a canted ferromagnet is referred to as a weak ferromagnet. A molecular-species-based example is phthalocyaninatomanganese(II) (MnPc). This complex has a T_c of 8.3 K, but a saturation magnetization corresponding to only 72% of the fully aligned spins due to the canting arising from the herringbone structural motif.[21] In other cases, the spin with time, the spins remain fixed in their orientations for a spin glass. A correlated spin glass has spins pointing in similar directions for short distances, but no long-range order. $[V(TCNE)_x] \cdot y(MeCN)$ at low temperature is an example of a correlated spin glass (see Section 9).

Like the familiar gas/liquid critical behavior, critical behavior occurs at the onset of cooperative magnetic ordering near the critical temperature T_c. The critical exponents can be compared to theoretical expectations to elucidate the dimensionality and anisotropy of the spin interactions which dominate the formation of the ordered spin state.

3. Origin of Cooperative Magnetic Behavior in Molecular-Based Magnetic Materials

Creating a magnetic molecular material demands the alignment of the spins in all three directions of the solid material.[22] The "exchange interaction" J describes the type (ferro- or antiferromagnetic) and degree of coupling between pairs of spins and is to first order a two-body interaction. It is thus essential to have magnetic exchange interactions in all three directions and any de novo design of new materials must include an exchange interaction between neighboring spins in all directions.[22] In order to accomplish this, it is, of course, necessary to examine the sign and magnitude of the exchange between pairs of molecular-species-based spins.

The magnetic exchange interaction is a direct consequence of quantum mechanics. The total electronic wavefunction can be factored into spatial and spin terms. Because electrons are fermions, the total electronic wavefunction must be antisymmetric. The spin (magnetic) exchange has its origin in the requirement that the total electronic wavefunction must change sign under the interchange of two electrons. For example, consider bringing two H atoms together to form H_2. If the two electron spins are antiparallel ($\uparrow\downarrow$: $S_1 + S_2 = 0$), the real-space wavefunction is symmetric or bonding. On the other hand if the two electron spins are parallel ($\uparrow\uparrow$: $S_1 + S_2 = 1$), the real-space wavefunction is antisymmetric or antibonding. The difference in energy of the symmetric and antisymmetric wavefunctions is related to the exchange energy. The lower energy of the real-space bonding wavefunction for H_2 results in an antiferromagnetic exchange, since the pair of electron spins are antiparallel.

The close approach of two spin-containing molecular species ($\boldsymbol{A}$ and $\boldsymbol{B}$) leads to a similar interaction. The new total wavefunction is often calculated in a configuration interaction (CI) (i.e., perturbation theory) approach. That is, the total wavefunction for the combined pair of molecules is approximated by admixing the ground state with an excited state arising from the promotion of an electron from the partly filled (spin-containing) orbital of $\boldsymbol{A}$ to a virtual (empty) orbital of $\boldsymbol{B}$ as well as the opposite case for partially occupied orbitals of $\boldsymbol{B}$ and virtual orbitals of $\boldsymbol{A}$. This leads to a new set of energies for each spin-symmetry state. The spin state of the lowest energy configuration determines whether the pair of molecular species are coupled antiferromagnetically (antiparallel spins on the adjacent molecules) or ferromagnetically (parallel spins on the adjacent molecules). The difference in energy between this lowest energy configuration and the lowest energy configuration of the opposite spin state is related to the exchange energy.[23, 24] The relative energies of the differing configurations depend strongly upon the charge transfer integrals between the selected orbitals of $\boldsymbol{A}$ and $\boldsymbol{B}$ (i.e., i and j, respectively) ($\beta^{ij}_{\boldsymbol{AB}}$), and also upon the difference in energy between the ground state of isolated **A** and **B** and the various excited state configurations ($\Delta E^{ij}_{\boldsymbol{AB}}$). The magnitude of each contribution to the total pairwise-exchange interaction is proportional to $(\beta^{ij}_{\boldsymbol{AB}})^2/\Delta E^{ij}_{\boldsymbol{AB}}$; the sign is determined by the total spin of the excited state.[25, 26] (The formation of this "incipient" chemical bond is sometimes termed "kinetic" exchange.) If the charge transfer integral between $\boldsymbol{A}$ and $\boldsymbol{B}$ is zero (i.e., orthogonal orbitals), the antisymmetrized real-space total wavefunction and symmetrized spin-space wavefunction (high-spin state) is lower in energy than the symmetrized real-space total wavefunction and antisymmetrized spin-space total (low-spin state), that is, Hund's rule applies. (Of course, if $\boldsymbol{A}$ and $\boldsymbol{B}$ approach close enough to form a covalent bond, the perturbation approach of CI must be replaced by calculating the full wavefunction of the new molecule derived from $\boldsymbol{A}$ and $\boldsymbol{B}$.)

It is not possible to calculate accurately the total energies and transfer integrals for pairs of molecular species each containing hundreds of electrons. Therefore a number of simplifying special cases of the configuration interaction concept have been emphasized by several research groups as a practical guide to enable the synthetic design of molecular-species-based magnets. These simplifying approximations differ in complexity and in their usefulness to the synthetic chemist. The simplest intramolecular approach is to consider molecular species with spins in orthogonal orbitals. The next simplest would involve spin polarization through bridging groups with filled orbitals connecting two spin-containing species. The next level of interaction involves the partial transfer of electrons between different molecular species. The simplest intermolecular approach utilizes the CI of the spin-containing molecular species, each considered as a whole unit, and where only interactions between the POMO of one molecular species and the POMO of its neighbor are examined. Other still more complex cases include the CI between the next highest HOMO (NHOMO) and/or the next lowest LUMO (NLUMO) of a pair of molecular species. An even more complex variant is to consider the excitations of occupied $\boldsymbol{A}$ orbitals to virtual orbitals on $\boldsymbol{A}$ as well as to virtual orbitals of $\boldsymbol{B}$. Again, it is important to emphasize that the CI models give two-body (pairwise coupling) terms. This is insufficient to account for three-dimensional magnetic behavior, for which configuration interactions in all three directions are crucial.

Increasing the complexity of CI calculations more accurately describes the system, however, it makes the model less useful to the practicing synthetic chemist. As a practical guide to the synthetic chemist we have classified the three distinct mechanisms for spin coupling (Scheme 1).

1. Ferromagnetic exchange resulting from orthogonal orbitals (no CI)—Hund's rule (intramolecular spin coupling)
2. Configuration interaction (CI) to determine dominant ferro- or antiferromagnetic exchange
   - 2.1. Intramolecular species excitations (spin polarization)
   - 2.2. Intermolecular species excitations
     - 2.2.1. Involving only the POMOs on adjacent molecular species
       - 2.2.1.1. Without spatial constraints
       - 2.2.1.2. With spatial constraints
     - 2.2.2. Involving NHOMOs and/or NLUMOs on adjacent molecular species
       - 2.2.2.1. Intermolecular species excitations
       - 2.2.2.2. Intramolecular species excitations
     - 2.2.3. Excitations between localized and delocalized (metallic) states (intramolecular spin coupling)
3. Dipole–dipole (through-space) exchange (intermolecular spin coupling)

Scheme 1. Classification of three mechanisms of spin coupling.

Often in discussions of the exchange mechanisms emphasis is given to the chemical stabilization of a spin state capable of exchange. This leads to identification of exchange mechanisms by their chemical or physical nomenclature. An example of this

is ferromagnetic exchange between polarons created in conjugated segments of block copolymers. In this case, polarons are the means of creating spin-containing units. The exchange between these polarons comes from CI through the intervening moieties (vide infra). The above is a classification of operative spin-exchange mechanisms, not the means to achieve spins.

Frequently it is unclear which mechanism is the primary exchange mechanism in a particular chemical system. Particularly for molecular-species-based systems with complex compositions and structures, it is probable that more than one mechanism plays a significant role (e.g., ferromagnetic coupling of spins within a one-dimensional chain due to orthogonal orbitals (mechanism 1) and ferromagnetic or antiferromagnetic coupling between chains due to configuration interaction (mechanism 2) or possibly dipole–dipole interactions between chains (mechanism 3)). Furthermore, since there are many levels of complexity of the CI model (mechanism 2), there are many ways to describe this exchange mechanism and properly truncated exhaustive calculations are required to provide a detailed understanding.

Examples of these models elaborated in terms of their chemical embodiments are described below. Note that the suggested mechanisms may not stand the test of time, but evolve with increased understanding of the structures and properties. Each of the mechanisms given in Scheme 1 is discussed below.

3.1. Intramolecular Ferromagnetic Exchange Resulting from Orthogonal Orbitals (No CI)—Hund's Rule

The essence of achieving high-spin behavior by using this approach is the presence of unpaired electrons in orthogonal orbitals (zero quantum mechanical overlap), which, however, reside in the same spatial region. The greater the latter condition is fulfilled, the stronger the ferromagnetic exchange. In this case the antibonding real-space total electron wavefunction is lower in energy than the bonding real-space total electron wavefunction so that the high-spin state is stabilized. This has been demonstrated for orthogonal orbitals on the same site, for example, carbene, $:CH_2$ ($S = 1$) and Mn^{II} ($S = 5/2$), and multiple sites in the same spatial region, for example, trimethylenemethane, $:C(CH_2)_3$ ($S = 1$) and O_2 ($S = 1$). This essence of Hund's rule is schematically illustrated in Figure 6.

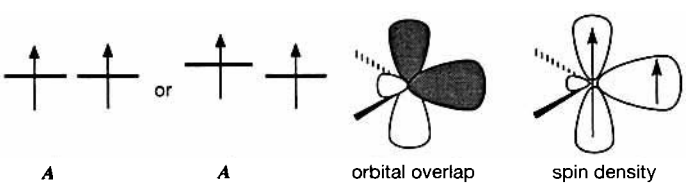


Fig. 6. Schematic illustration of the relative energy, orbital overlap, and spin density for orthogonal POMOs on *A*.

The concept of having a large number of unpaired electrons residing in orthogonal orbitals that are ferromagnetically coupled by CI through-bond coupling or superexchange (vide infra) through a spinless bridging halide has been exploited by P. Day et al. in their studies of Rb_2CrCl_4 and related materials which have an extended-network structure in two dimensions.[6a] These materials are not normally attributed to molecular-species-based chemistry and thus might be considered by some to be inappropriate to be discussed in this review. Nonetheless, ferromagnetic materials can be also prepared by substitution of the alkali metal cation with a quaternary ammonium ion, $[RNH_3]^+$ (R = Me, Et, $PhCH_2$ etc.). These fascinating ferromagnets have relatively high T_c values (> 50 K) which are essentially independent of interlayer separation and are reasonably transparent.[6] These layered compounds, in principle, lend themselves to form Langmuir–Blodgett-like monolayer films which would be suitable to test concepts of two-dimensional magnetic behavior.

The general idea of designing a material with spins residing in orthogonal orbitals on adjacent sites has also been pursued by O. Kahn et al. as well as others; however, only intriguing high-spin small molecules have been reported.[27] Recently extended-network solids of $[Bu_4N][MCr(ox)_3]$ (ox = oxalato; M = Fe, Co, Ni, Mn, Cu) have been reported to exhibit ferromagnetic behavior.[28]

It is important to reemphasize that highly magnetic behavior is not a property of a molecular species; it is a cooperative solid-state (bulk) property. Thus, to achieve bulk ferromagnetic behavior in the context of the aforementioned high-spin molecular species, intermolecular interactions, perhaps as described below, must be operative or the molecular species need to be sufficiently large to be considered a magnetic domain (vide supra).

3.2. Configuration Interaction to Determine Dominant Ferro- or Antiferromagnetic Exchange

The orthogonal-orbital mechanism (see Section 3.1) provides a means to achieve a high-spin ferromagnetically coupled molecular species in which the spins reside in the same spatial region. In order to magnetically couple spins residing in distant spatial regions within a molecular species, the total wavefunction of the system must be considered, and it is typically evaluated by configurational interactions. Additionally, the CI can be applied between molecular species within a solid to achieve the ferromagnetic coupling between these species needed to induce bulk ferromagnetic behavior. These are complex, time-consuming computations that are often simplified by limiting the number of CIs considered. The details of the CI, of course, depend on how the problem is formulated, that is, what is given for the ground state and excited state wavefunctions. The simplest approximation employs only the POMOs on adjacent molecular species.

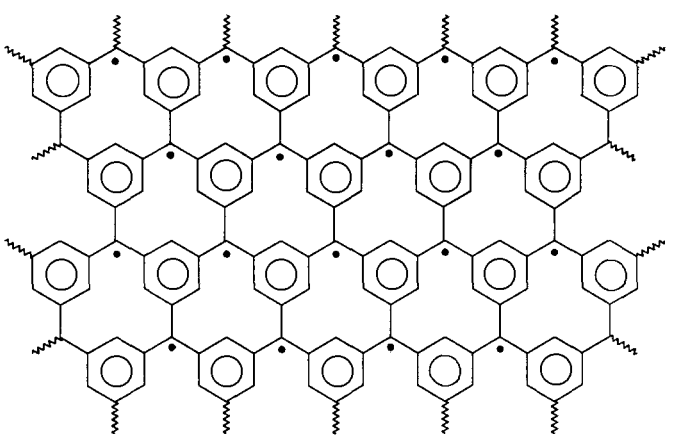
3.2.1. Intramolecular Excitations (Spin Polarization)

As discussed above, an unpaired electron spin in a POMO can polarize the paired electron spins in an orthogonal bond connecting it to another moiety with a POMO. This polarization is illustrated by the coupling between a carbon π electron and a proton nucleus through the hyperfine interactions. Although a valence bond-like picture is usually utilized (see Fig. 2 top), a full molecular orbital calculations reveals that the proper description of the spin polarization requires the admixture (config-

uration interaction) of a small amount of an antibonding excited state into the ground state to obtain the spin polarization.[12a] Hence the spin polarization mechanism is an intramolecular configuration interaction mechanism.

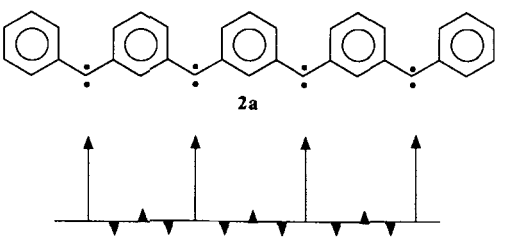
Spin polarization is an intramolecular effect that is used extensively to interpret EPR hyperfine coupling constants.[12, 30, 31] Hyperfine splittings are observed for unpaired electrons in proximity to ring hydrogens in aromatic compounds, and although unpaired spin density is not delocalized directly onto the hydrogen atom, unpaired spin density is induced at the hydrogen nucleus and observed (through the hyperfine splitting) by spin polarization (i.e., an unpaired electron in a C-based p orbital polarizes the paired spins in an orthogonal C–H σ bond so that one of the paired electrons is more in the vicinity of the C atom than another, even though there is no unpaired spin density delocalized onto it; Fig. 2 top).[12c, d]

With the knowledge of the spin-polarization mechanism and that the ground states of dioxygen and some carbenes were high-spin triplets due to spins residing in orthogonal orbitals, K. Itoh and N. Mataga in 1968 suggested[29] that large planar alternate hydrocarbons comprised of *meta*-substituted triplet diphenylcarbene moieties would have a high-spin (ferromagnetically coupled) ground state in accord with Hund's rule and spin polarization. Proposed examples of high-spin multiplicity polymers[29b] include **1**.

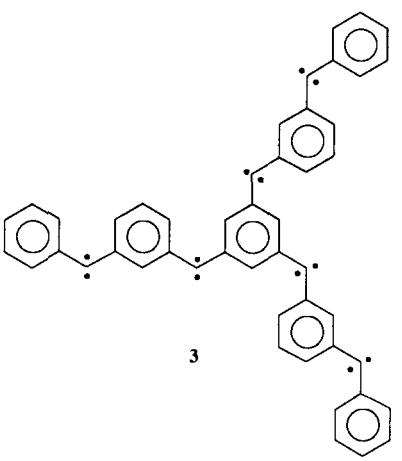


1

H. Iwamura et al.[32] have prepared several high-spin polycarbene radicals including **2a** ($S = 4$). The largest compounds characterized, albeit in situ, are the hexacarbene **3** ($S = 6$)[32b] and a nonacarbene ($S = 9$).[32c] The magnetization of **3** confirms the $S = 6$ ground state, however, the temperature dependence of the susceptibility demonstrates only antiferromagnetic coupling between the $S = 6$ radicals.[32b] The high-spin ($S = 4$) ground state in **2** has been attributed to four $S = 1$ carbene sites (arising from spins in orthogonal orbitals in the same spatial region, Fig. 6 right) (vide supra) coupled by spin polarization as illustrated in **2a** with arrows denoting the direction of the polarized spins.[33] (Note that for *ortho*- or *para*-substituted analogues spin polarization results in antiferromagnetic coupling and diamagnetic behavior.) The spin polarization in an idealized poly(*m*-diphenylcarbene) was evaluated by K. Nasu by using a CI approach (tight-binding calculation of energy bands) that includes the effects of on-site Coulomb repulsions (Hubbard model) to describe the antiferromagnetic coupling between adjacent π electrons within the C_6 ring and the bridging carbene moieties, resulting in a net ferromagnetic coupling. Nasu accounts for the ferromagnetic coupling between the nonbonding and π electrons of the carbene by using a periodic Kondo model (i.e., Hund's rule for orthogonal orbitals).[34a] K. Tanaka et al. similarly calculated spin polarization by which long-range magnetic coupling is possible in poly(phenylnitrenes) using a tight-binding calculation of energy bands (CI).[34b] The efficacy of the polyene bridges in pairs of spins has been recently demonstrated by using bipyridylpolyene-bridged bimetallic complexes.[34c]



2a

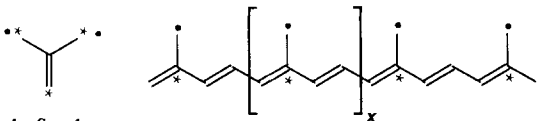


3

A. A. Ovchinnikov[35] has developed a simple approach to account for the CI between spins on arrays of adjacent carbon atoms each with a single p_z electron. He noted that the net S for planar alternate hydrocarbons (e.g., **2**–**6**) can be calculated by Equation (9), where n is the number of nonstarred atoms and n^*

$$S = \frac{|n^* - n|}{2} \tag{9}$$

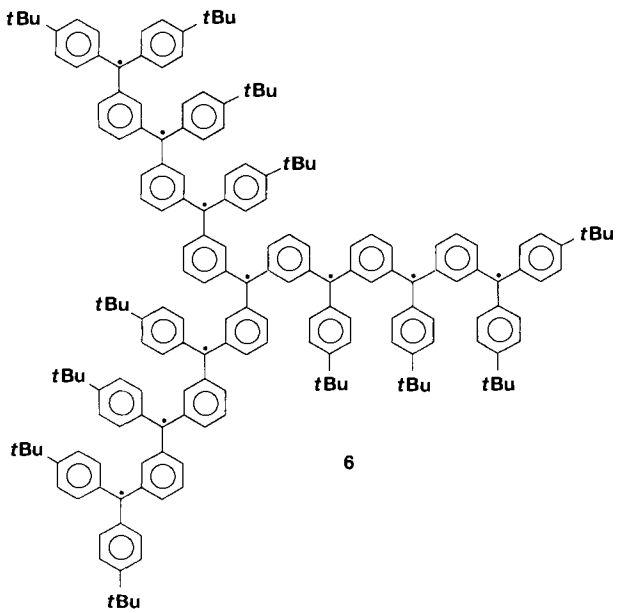
is the number of starred atoms (adjacent atoms are alternately starred (*) and nonstarred and identically denoted atoms are not adjacent to each other). For example, trimethylenemethane (**4**) has an $S = 1$ ground state, and larger molecules could have large values of S. Polymers such as **5** are predicted to have a large value for S ($S = x/2$, where x is the number of repeat units within the polymer).[35, 36] Chemical reactivity arising from the strong tendency of unpaired electrons to form covalent bonds suggests that stable high-spin materials are difficult to prepare following this methodology. Bond distortions as well as inter-



4 $S = 1$ 5 $S = x/2$

molecular coupling which pair-up electrons must also be avoided.

High-spin radicals based upon several triarylmethyl radical sites are under investigation by several research groups worldwide. An $S = 5$ radical, **6**, has been prepared.[37] Perchloropoly-



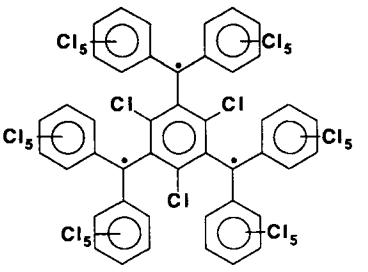
6

triarylmethyl radicals have also been studied; the largest example characterized is **7** ($S = 3/2$), which has been isolated in two stereoisomeric forms.[38] Polymers based on triarylmethyl radicals have been reported to exhibit saturation magnetizations of the order of 1 % of bulk.[7, 39] These materials are poorly characterized.

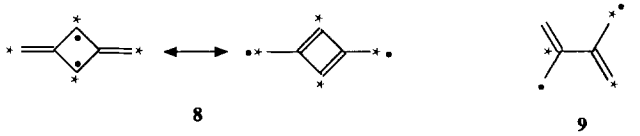
Another example of a high-spin moiety sought as a building block for an s/p orbital-based magnet is 1,3-cyclobutanediyl (**8**), which has spins residing in different regions within the radical and, like trimethylenemethane (**4**) has a strong triplet preference.[40]

Equation (9) is not sacrosanct and may fail for the prediction of $S = 0$ compounds; thus it may not reliably guide the synthetic chemist toward high-spin molecules. This is clear as tetramethyleneethane (**9**) is an unsolved puzzle. Equation (9) as well as more sophisticated molecular orbital calculations lead to the expectation that **9** has a singlet ground state; however, a triplet ground state has been reported for **9** in its twisted as well as its planar analogues.[41] Thus, Equation (9) appears valid for $n^* \neq n$, but may not properly describe a system for $n = n^*$, if they are non-Kekulé or cross-conjugated.[43b]

H. Fukutome et al. suggested that block copolymers comprised of conjugated conducting oligomers and ferromagnetic spin-coupling segments (for configuration interaction, e.g., *meta*-substituted benzene unit) will upon doping have ferromag-

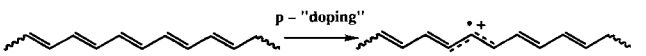


7



8 9

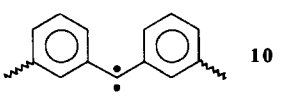
netically coupled polarons.[42a] Conducting oligomers based upon poly(*trans*-acetylene), poly(pyrrole) or similar polymers were identified as candidates to test this approach. Upon, for example, p-"doping", a cation radical (positive polaron) segment is formed, which may be schematically represented as shown in Scheme 2. Ferromagnetic coupling of these radicals is



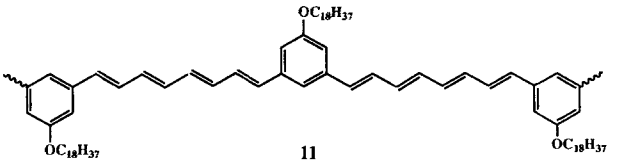
Scheme 2.

proposed[34, 42] to be stabilized by a *meta*-substituted diphenylcarbene moiety such as **10** (vide supra).

Synthetic chemists have just started to prepare suitable examples of these block copolymers to test this model. D. A. Dougherty et al. reported[43a] that partial oxidation of **11** with either I_2 or AsF_5 leads to a material for which the magnetization is best described by the presence of spins with an $S > 2$ behavior, not an independent spin ($S = 1/2$) behavior; however, antiferromagnetic coupling among these spins and the low density of spins need to be circumvented.[43b]



10



11

3.2.2. *Intermolecular Species Excitations*

Configuration interaction can be applied between molecular species within a solid to provide a means for magnetic coupling among these species that is needed to achieve bulk magnetic behavior. In the simplest case this can be done by considering only the POMOs. It can also be done by considering the next highest occupied (NHOMO) and/or next lowest unoccupied molecular orbitals (NLUMO) or between a localized state and a delocalized (metallic) state.

3.2.2.1. Involving the POMOs on Adjacent Molecular Species

Dominant ferromagnetic or antiferromagnetic exchange determined by configuration interaction (CI) between POMOs on adjacent molecular species can be enhanced by the spatial relationship of the atoms on adjacent molecules and their pairwise contribution to the total exchange (i.e., Heisenberg exchange).

3.2.2.1.1. Without Spatial Constraints

The application of configuration mixing of a virtual triplet charge-transfer excited state of a whole molecular species with the ground state, in order to stabilize ferromagnetic exchange coupling (kinetic exchange) for $\cdots[A]^{\bullet+}[B]^{\bullet-}[A]^{\bullet+}[B]^{\bullet-}\cdots$ (A = donor, B = acceptor) chains, was introduced by H. M. McConnell.[44a] The large separations and energy differences between ions on adjacent sites lead to small overlaps of the frontier orbitals ("incipient" bonding) and prevent the formation of metallic energy bands for mixed-stack electron-transfer salts.[26a, 45] In contrast, the spins of the $[A]^{\bullet+}[B]^{\bullet-}$ repeat units with half-occupied nondegenerate POMOs can couple antiferromagnetically (Fig. 7a). Admixture of the higher energy charge-transfer states (Fig. 7a, right) with the ground state (Fig. 7a, left) lowers the total electronic energy and stabilizes antiferromagnetic coupling ($\uparrow\downarrow$) which, if the number of spins on the two moieties are different, leads to ferrimagnetic behavior.

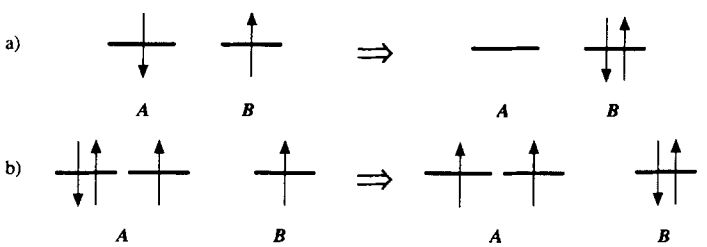


Fig. 7. Schematic illustration of the stabilization of ferro- or antiferromagnetic coupling by configurational interaction (CI) only involving POMOs on adjacent sites (A and B). If both A and B have a half-filled nondegenerate POMO (s^1), the $B \leftarrow A$ (or $A \leftarrow B$) virtual charge-transfer excited state stabilizes antiferromagnetic coupling (a). If B (or A) has a nonhalf-filled degenerate POMO (e.g., d^3, assumed here to be A), the $B \leftarrow A$ charge-transfer excited state formed (b) will stabilize ferromagnetic coupling (or $A \leftarrow B$ charge-transfer excited states formed through excitation of a "spin-up" B electron will stabilize antiferromagnetic coupling).

This energy reduction and spin delocalization does not occur when the two electron spins are parallel ($\uparrow\uparrow$; ferromagnetically aligned) in accord with the Pauli exclusion principle. Thus, antiferromagnetic coupling ($\theta = -18$ K) has been reported for the salt $[TTF]^{\bullet+}[Ni\{S_2C_2(CF_3)_2\}_2]^{\bullet-}$ (TTF = tetrathiafuvalene)[46a] which has the $\cdots[A]^{\bullet+}[B]^{\bullet-}[A]^{\bullet+}[B]^{\bullet-}\cdots$ structure in all three directions.[46b] (Note, however, ferromagnetic coupling ($\theta = +16$ K) has been reported (vide infra) for the isoelectronic $[TTF]^{\bullet+}[Pt\{S_2C_2(CF_3)_2\}_2]^{\bullet-}$ salt[46a, c] which has a similar structure, but is not isomorphous.[46d])

For other electron configurations involving partially occupied degenerate orbitals pairwise (AB) ferromagnetic coupling may be achieved (see Fig. 7b). Magnetic couplings predicted by this model for representative electronic configurations are summarized in Table 3. To achieve ferromagnetic coupling with this model requires that at least A or B possesses a degenerate (accidental or intrinsic) orbital that is not half-filled, empty, or filled. The magnetic properties of several electron-transfer salts based on metallocenes and cyanohydrocarbons have been discussed within this model.[8i, 9, 44b] The configurational interaction model for the degenerate (d, t ...) and nondegenerate (s) cases (see Table 3 for abbreviations) can be represented by using forms for the nearest neighbor Hubbard model.[25, 26]

Table 3. Representative magnetic couplings for homo- and heterospin systems with singly, doubly, and triply degenerate POMOs [a].

	A (or B)	B (or A)	$B \leftarrow A$	$A \leftarrow B$	Example
$S = 1/2$	s^1	s^1	AF	AF	[TMPD][TCNQ], $[TTF]\{Ni[S_2C_2(CF_3)_2]_2\}$
	d^1	s^1	AF	FO	$[Ni^{III}Cp_2^*]^{\bullet+}[TCNE]^{\bullet-}$
	d^3	s^1	FO	AF	$[Fe^{III}Cp_2^*]^{\bullet+}[TCNE]^{\bullet-}$
	d^3	d^1	AF	AF	
	t^1	d^1	FO	FO	
	t^5	d^1	AF	AF	
	d^3	d^3	FO	FO	$[\{Fe^{III}Cp_2^*\}^{\bullet+}]_2[C_4(CN)_6]^{2-}$
	t^1	d^3	AF	AF	
	t^1	t^1	FO	FO	$[C_{60}]^{\bullet-}$?
$S = 1$	d^2	d^2	AF	AF	O_2, $[Ru(OEP)]_2$
	d^2	t^2	FO	AF	
	t^2	t^2	FO	FO	$[C_{60}]^{2-}$?
$S = 1/2/1$	d^2	s^1	FI	FI	
	t^2	s^1	FI	FO	
	t^4	s^1	FO	FI	$[Mn^{III}Cp_2^*]^{\bullet+}[TCNE]^{\bullet-}$
	d^2	d^1	FO	FI	
$S = 1/2/3/2$	t^3	s^1	FI	FI	$[Cr^{III}Cp_2^*]^{\bullet+}[TCNE]^{\bullet-}$, $[V(TCNE)_x]$
	t^3	d^1	FO	FI	
	t^3	d^3	FI	FO	

[a] AF = antiferromagnetic coupling; FI = ferrimagnetic coupling; FO = ferromagnetic coupling. Intrinsic or accidental orbital degeneracies: s = singly (a or b), d = doubly (e), t = triply (t).

Configurational mixing of a virtual singlet excited state with the ground state for $[A]^+[B]^-$ systems, which stabilizes antiferromagnetic coupling when the spin on the donor and that on the acceptor are unequal and produces ferrimagnetic order,[44b] has been applied[8j, 47-51] to the high-temperature molecular-species-based magnet $[V(TCNE)_x] \cdot y$ (solvent) (t^3/s^1) (vide infra). Application of the model to $[Cr^{III}Cp_2^*]^{\bullet+}[TCNQ]^{\bullet-}$ or $[Cr^{III}Cp_2^*]^{\bullet+}[TCNE]^{\bullet-}$ (t^3/s^1) leads to the expectation of antiferromagnetic coupling leading to ferrimagnetic behavior; however, ferromagnetic order is observed (vide infra). Other subsets of this model have been the specific research focus of several groups.[52]

Key to achieving pairwise bulk magnetic ordering is the extension of the model beyond pairwise (AB) interactions in one-dimension. Figure 8 illustrates how the energy of the ferromagnetically coupled system depicted in Figure 7b is lowered upon the admixture of the ground state of energy E_{gs} with one or two intrachain (a and a, b, respectively) virtual charge-transfer excited states of energy E_{es} and additionally with a second interchain excited state (a, b, c).[8g-i, 9]

3.2.2.1.2. With Spatial Constraints

In 1963 McConnell suggested a mechanism for ferromagnetic exchange that involved a spatial arrangement of neighboring

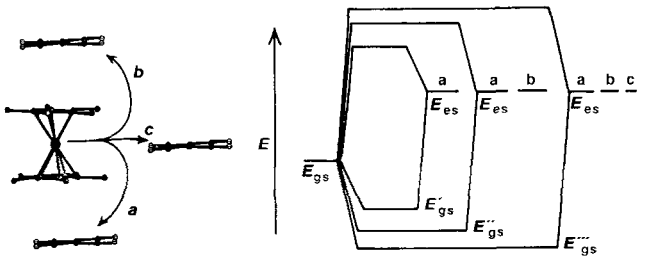


Fig. 8. Schematic state diagram depicting the relative energy of the ground E_{gs} and excited states E_{es} before and after admixing (virtual $[A]^{+}[B]^{-}$ charge transfer) with a single excited state a), an intrachain pair of excited states a) and b), and with a third interchain excited state arising from admixture with an out-of-registry acceptor to stabilize ferromagnetic coupling (from ref. [8g]).

radicals, which possessed both positive and negative spin densities.[53] He claimed that radicals with "... large positive and negative atomic π-spin densities... [that] pancake... so that atoms of positive spin density are exchanged coupled... to atoms of negative spin density in neighboring molecules... gives a ferromagnetic exchange interaction." This is illustrated in Figure 9 for a pair of identical allyl radicals, *A* and *A'* which have positive spin densities on the terminal carbon atoms and negative spin density on the central carbon atom.[12b] For large separations between *A* and *A'* spin interactions do not occur (Fig. 9a). As *A* and *A'* approach each other in such a way that regions of positive and negative atomic π-spin densities can "pancake", net ferromagnetic exchange resulting from the incomplete cancellation of antiferromagnetic coupled spin components arising from pairwise (CI-like) interactions of atomic components of the radicals increasingly occurs (Figs. 9b, c). To achieve ferromagnetic exchange by this mechanism, routes to spin pairing, for example bond formation, arising from the close approach of the *A* and *A'*, (see Fig. 9d) must be avoided. (Note that the molecule in Fig. 9d may be a triplet.) Like the mechanism 2.2.1.1 in Scheme 1, this is a mechanism for ferromagnetic exchange between adjacent radicals, not bulk ferromagnetism. Ferromagnetic exchange in three dimensions is necessary for bulk ferromagnetic behavior.

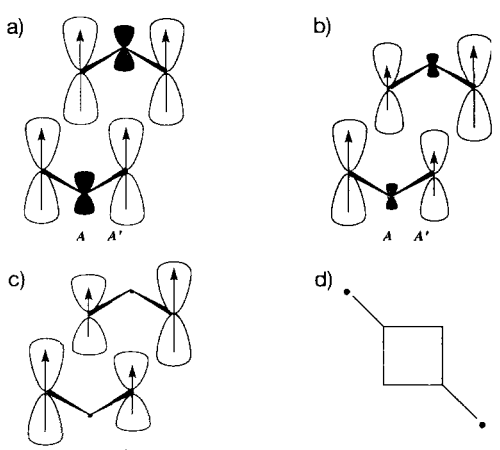
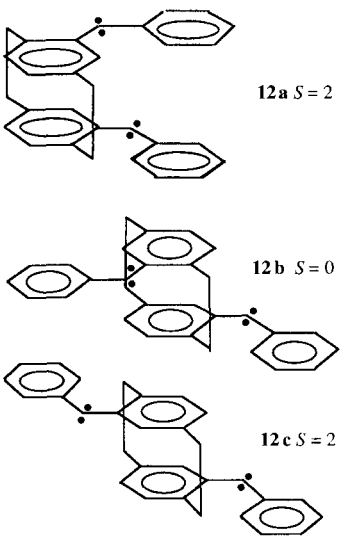
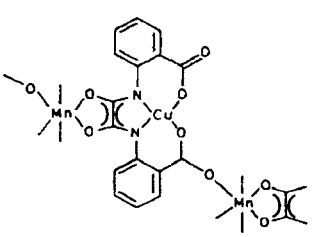


Fig. 9. Schematic illustration using the spin density of a pair of allyl radicals (*A* and *A'*) for the stabilization of ferromagnetic coupling by configurational interaction (CI) involving spin-exchange which results from regions of positive spin density (not of the entire POMOs) of *A* interacting with regions of negative spin density on *A'* as these exemplary $S = 1/2$ radicals as they are brought closer together. Minimal interactions occur at large separations (a), which increase as the separation decreases (b) and (c), until bonding occurs at short separations (d).

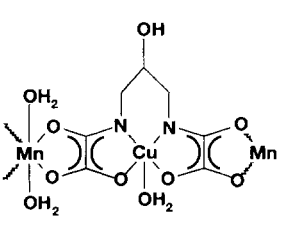
Cleverly designed stable radicals were sought to test this model. The spin multiplicity of dicarbenes incorporated into rigid [2.2]cyclophanes have been shown to be controlled by the overlapping of the spin-containing orbitals in the aromatic C_6 rings.[54] McConnell's model[53] suggests that the pseudo-*meta* isomer **12b** should possess a singlet ground state. This is in contrast to the behavior of the pseudo-*ortho* **12a** and pseudo-*para* **12c** isomers of the bis(phenylmethylenyl)[2.2]cyclophanes, which both have a quintet ground state. ESR data on this system are consistent with these results, suggesting that ferromagnetic exchange can be achieved by this McConnell model.[54] Note that the ground state spin multiplicity of these isomers has been described by CI by K. Yamaguchi et al.[55a] Tanaka et al. used CI incorporating the spatial distribution of the spin to calculate the favorable orientations for ferromagnetic exchange between diphenylcarbenes as a function of relative rotation and tilt angles of the molecules.[55b] Achievement of bulk ferromagnetic behavior in these materials has yet to be reported.



Similar to this McConnell approach using molecules with registered spin distributions, the antiferromagnetic coupling of alternating spin sites with different metal atoms with a different number of spins per site leading to ferrimagnetic behavior has been promoted by O. Kahn.[8b] Likewise, D. Gatteschi and P. Rey[8c] have focused on the same paradigm by utilizing extended network structures comprised of metal ions and nitroxide radicals. Due to configuration interaction, adjacent spin sites couple antiferromagnetically (↑↓), whereas next-adjacent spin sites couple ferromagnetically (↑↓↑). Thus, through alternating sites with a larger number of spins (e.g., 5 for ($S = 5/2$) Mn^{II}) with sites with fewer spins (e.g., 1 for ($S = 1/2$) Cu^{II} or nitroxide ligands) (i.e., ↑↓), the *S*s cannot cancel, thereby leading to a ferrimagnetic system (see Fig. 3d). Kahn et al. have reported several examples of highly magnetic systems developed by this strategy using Mn^{II}/Cu^{II}; for example, $[Cu^{II}Mn^{II}$ (obbz)] · H_2O[56a] (**13**) (obbz = *N,N'*-bis(2-carboxyphenyl)oxamidato) has a T_c of 14 K. This group also reported that the



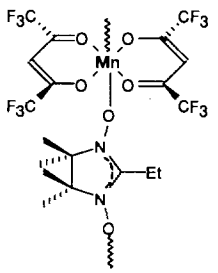
13



14

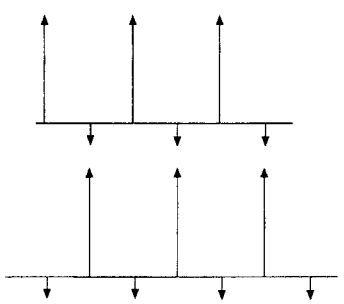
structurally characterized $[Mn^{II}Cu^{II}(pbaOH)] \cdot 3H_2O$ (**14**) (pbaOH = 2-hydroxy-1,3-propanediylbis(oxamato)) has a T_c of 4.6 K,[56b] and upon dehydration and concomitant structural alteration to $[Mn^{II}Cu^{II}(pbaOH)] \cdot 2H_2O$ the T_c is increased to 30 K.[56c]

The Gatteschi and Rey collaboration has focused on Mn^{II}/nitroxide systems, such as the ferrimagnetic complex **15** with a T_c of 8.1 K.[57a] They have also reported on a nonstructurally characterized $[\{Mn(O_2CC_6F_5)_2\}_2$-NITEt] (NITEt = ethyl nitronyl nitroxide) compound with a θ-value of about 25 K and a T_c of 20.5 K.[57b] The rare-earth-containing analogue $[\{Dy^{III}$-$(hfac)_3NITEt\}]$ (hfac = hexafluoroacetylacetonate), in contrast, exhibits antiferromagnetic ordering at 4.4 K ($\theta = -6.1$ K).[57c]



15

For **13**–**15** the interchain interactions may well involve the spin-exchange mechanism illustrated in Scheme 3; here each horizontal line depicts a chain of alternating $S = 5/2$ (↑) and antiferromagnetically coupled $S = 1/2$ (↓) spins, and the adjacent out-of-registry chains are arranged so that the $S = 5/2$ spins (↑) are close to the antiferromagnetically coupled $S = 1/2$ (↓) spins, which leads to ferromagnetic coupling of antiferromagnetically coupled spins.



Scheme 3.

Note that these ferrimagnetic systems possess a few common features; namely, they do not obey the Curie–Weiss expression, as $\chi^{-1}(T)$ is not linear, but a fit to the higher temperature susceptibility has $\theta < 0$. Also plots of χT and moment vs. temperature have a minimum value. A mathematical model describing isolated linear chains of alternating $S = 1/2$ quantum spins and $S > 1/2$ classical spins has been derived by J. Seiden and has been used for some of the aforementioned ferrimagnetic systems.[57d]

3.2.2.2. Excitations Involving NHOMO and/or NLUMO

Configuration interactions can be more complex by inclusion of either the NHOMO and/or NLUMO in addition to the POMO on one or more of the molecular species. In this case the CI can be considered within each molecular species (e.g., excitations from occupied *A* orbitals to virtual orbitals on *A*) as well as between species (e.g., excitations from occupied orbitals on *A* to virtual orbitals of *B*).

3.2.2.2.1. Intermolecular Species Excitations

Configuration interactions involving intermolecular excitations from a POMO to NLUMO or NHOMO to POMO are illustrated in Figure 10. As pointed out in the discussion of mechanism 2.2.1.1 (Section 3.2.2.1.1), the simplest application of the CI model between partially occupied molecular orbitals on adjacent molecules does not produce the correct sign of the exchange interaction for $[CrCp_2^*][TCNE]$[58a, b] (t^3/s^1) ($Cp^* = C_5Me_5$) as well as for $[CrCp_2^*][TCNQ]$ (t^3/s^1),[59] $[Cr(C_6Me_xH_{6-x})_2]^{\cdot+}[TCNE]^{\cdot-}$ ($x = 3,6$) ($\theta > 10$ K) (s^1/s^1),[58c] and $[TTF]^{\cdot+}[Pt\{S_2C_2(CF_3)_2\}_2]^{\cdot-}$ ($\theta = 18$ K) (s^1/s^1).[46c, 58c] For these materials the CI between POMOs predicts antiferromagnetic exchange (resulting in ferrimagnetism for the former pair of examples), yet ferromagnetic exchange and, for the former pair of compounds, ferromagnetic order was observed. Instead

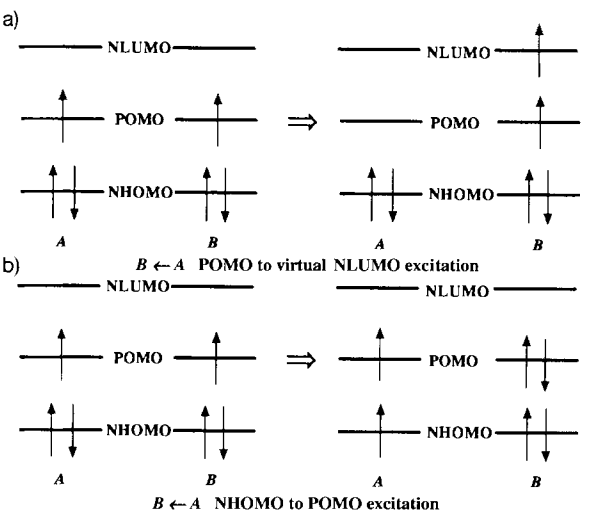


Fig. 10. Schematic illustration of the stabilization of ferromagnetic coupling by configurational interaction (CI), involving only virtual excitation from a POMO on *A* to a virtual NLUMO on *B* (a) or NHOMO on *A* to a POMO on *B* (b).

of considering an excitation between POMOs, an excitation from the POMO of $[CrCp_2^*]^{\cdot+}$ to the NLUMO of $[TCNE]^{\cdot-}$ (or alternatively an excitation from the POMO of $[TCNE]^{\cdot-}$ to the NLUMO of $[CrCp_2^*]^{\cdot+}$) results in the expectation of ferromagnetic exchange. (Similarly, an excitation from the NHOMO of $[CrCp_2^*]^{\cdot+}$ to the POMO of $[TCNE]^{\cdot-}$ as well as the reverse from the NHOMO of $[TCNE]^{\cdot-}$ to the POMO of $[CrCp_2^*]^{\cdot+}$ results in the expectation of ferromagnetic exchange.) The importance of "subjacent" orbitals has also been invoked to explain the observation of reactions forbidden by the Woodward–Hoffmann rules.[60] Thus, the extended configurational admixing model can account for the ferromagnetic coupling observed for a pair of $[CrCp_2^*]^{\cdot+}$ salts. Because of the large number of electrons involved, an ab initio calculation to determine the primary exchange mechanism is beyond current computational capabilities. The necessity to invoke NHOMO → POMO excitation to stabilize ferromagnetic coupling was originally used to explain the ferromagnetic coupling ($\theta > 10$ K) observed for $[Cr(C_6Me_xH_{6-x})_2]^{\cdot+}[TCNE]^{\cdot-}$ ($x = 3,6$).[58c]

3.2.2.2.2. Intramolecular Species Excitations

As discussed previously one may consider CI by intramolecular excitations as well as intermolecular excitations. This special

case is sometimes described as spin polarization (or spin delocalization) or superexchange.[122, 123] It depends upon which energy levels are admixed with the chosen ground state wavefunction and it is closely related to the previous discussion. For example, Figure 11 a illustrates an intramolecular species virtual excitation from the POMO to the NLUMO on *A* followed by a virtual excitation from the POMO on ***B*** to the NLUMO on *A* and is referred to as spin delocalization, while Figure 11 b illustrates intramolecular species virtual excitation from the NHOMO to the POMO on *A* followed by a virtual excitation from the POMO on ***B*** to the NLUMO on *A* and is referred to as superexchange. It is important to note that these mechanisms can give rise to either ferromagnetic or antiferromagnetic coupling.

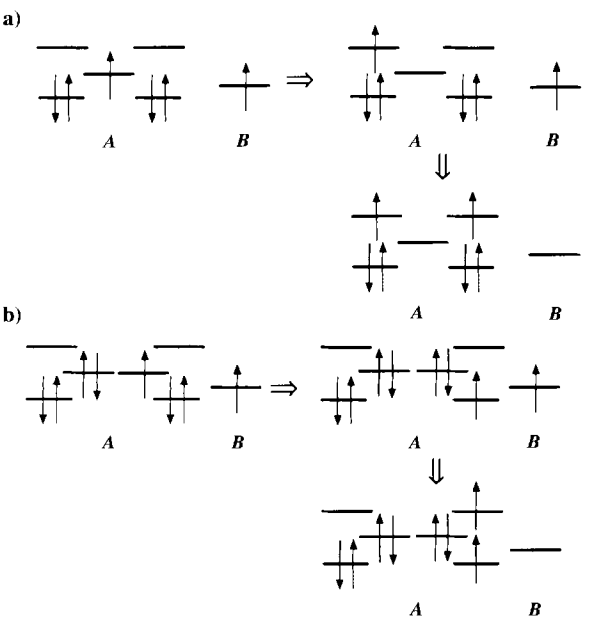


Fig. 11. Schematic illustration of the stabilization of ferromagnetic coupling by configurational interaction (CI), involving the virtual excitation of an electron from a POMO to a NLUMO on *A* followed by a virtual excitation from the POMO on ***B*** to the NLUMO on *A* (spin delocalization) (a), or from a NHOMO to the POMO on *A* followed by a virtual excitation of an electron from the POMO on ***B*** to the NLUMO on *A* (superexchange) (b).

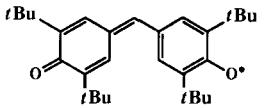
Intramolecular species spin polarization was discussed under mechanism 2.1 (Section 3.2.1) and can also be considered as an intramolecular species effect. For $[FeCp_2^*]^{\bullet+}[TCNE]^{\bullet-}$ A. L. Buchachenko suggested that intramolecular spin polarization of the Cp* five-membered rings by the spin(s) of the transition metal ions (e.g., Fe^{III}) should induce a small negative spin on Cp* ring carbon atoms and result in net ferromagnetic coupling to the adjacent $[TCNE]^{\bullet-}$.[33] This was later quantified by Kahn et al.[61a, b] They suggest a polarization (by CI arising from an intra-ion excitation of electrons from the Cp* ligand to the metal-ion) of the bonds between the ring C atoms of the Cp* ligand, leading to a negative spin density on the carbon atoms of the Cp* five-membered ring, the magnitude of which increases with the spin on the metal ($S = 1/2$, 1, and 3/2 for $[FeCp_2^*]^{\bullet+}$, $[MnCp_2^*]^{+}$, and $[CrCp_2^*]^{\bullet+}$, respectively). In contrast, for $[NiCp_2^*]^{+}$, a direct delocalization of spin density from the Ni^{III} to the Cp* ring, resulting in positive spin density on the ring carbon atoms is suggested. The ferromagnetic (for $[FeCp_2^*]^{\bullet+}$, $[MnCp_2^*]^{+}$, and $[CrCp_2^*]^{\bullet+}$) or antiferromagnetic (for $[NiCp_2^*]^{\bullet+}$) exchange with $[TCNE]^{\bullet-}$ or $[TCNQ]^{\bullet-}$ then results from interaction of the spin on the Cp* ring carbon atoms with that of the anion radical.[61a, b] Recent NMR studies of $[M(C_5EtMe_4)_2]^{+}$ support the presence of negative spin densities on the carbon atoms of the five-membered ring for M = Fe, Mn, and Cr and positive spin density on the carbon atoms of the five-membered ring for M = Ni, consistent with the hypothesis.[62] Polarized single-crystal neutron diffraction studies are in progress to directly determine the spin density of the $[FeCp_2^*]^{\bullet+}$ cation. Configuration interaction involving excitation from the POMO of the nitroxyl radical to the higher occupied Cu^{II}-based orbitals has been suggested as the origin of the ferromagnetic exchange for bischelated Cu^{II} complexes with axially coordinated nitroxyl ligands. In contrast the CI between the POMO of the nitroxyl ligand and the Cu^{II} POMO gives rise to antiferromagnetic exchange for similar complexes with equatorially coordinated nitroxyl ligands.[63]

Soos and McWilliams,[61d] as well as more recently Kollmar and Kahn[61c] pointed out that many additional competing excitations need to be considered by CI than those described under mechanism 2.2.1.1. Furthermore, due to the almost-orthogonal nature of the POMOs on the donor and acceptor for $[FeCp_2^*][TCNE]$, the simplest POMO/POMO-based CI is less likely than the many competing excitations; thus, the Cp* ligand can provide a pathway for superexchange or spin delocalization. Yamaguchi et al.[64] describes an intramolecular spin polarization of the Cp* ring by the spin(s) of the transition metal ions as partial charge transfer from the Cp* of an electron (with spin parallel to that of the metal) to the metal atom followed by the CI between the Cp* and the acceptor ($[TCNE]^{\bullet-}$). The net effect is usually ferromagnetic: $M^{+}(\uparrow)Cp^{*}(\downarrow)A(\uparrow)$. The sign of the net exchange then depends upon the sign of the exchange between Cp* and $[TCNE]^{\bullet-}$.

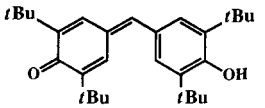
It is noted, however, that the T_c values increase as $[MnCp_2^*]^{+} > [FeCp_2^*]^{\bullet+} > [CrCp_2^*]^{\bullet+}$, and do not increase monotonically with S as expected (see Section 6). This suggests that for the $[CrCp_2^*]^{\bullet+}$ salts, which are predicted to have antiferromagnetic coupling by the simplest POMO/POMO-based CI model, the POMO/POMO CI does not dominate, and ferromagnetic coupling by the more complex POMO/NHOMO/NLUMO-based CI model or an intramolecular CI spin polarization model may be more appropriate.[58a, 59, 61c] Thus, further studies are necessary to firmly establish which specific exchange mechanisms dominate in this series of electron-transfer salts.

The combination of CI using POMO/NHOMO/NLUMOs as well as spin polarization have been used to explain the ferromagnetic coupling reported for galvinoxyl (**16a**). Galvinoxyl has received substantial attention because it exhibits relatively strong ferromagnetic coupling ($\theta = 19$ K) in the solid state. The θ value is too large for dipole interactions (vide infra) alone to be operative. Below 85 K it undergoes a first-order phase transition to a weakly magnetic state.[65a] The details of this structural transformation are unknown. A solid solution of **16a** and hydroxygalvinoxyl (**16b**) has been reported to exhibit ferromagnetic coupling ($10 < \theta < 19$ K), since the high-temperature

structure is maintained.[65b] Hysteresis curves characteristic of a bulk ferromagnet were not observed for either of these materials.[65a]

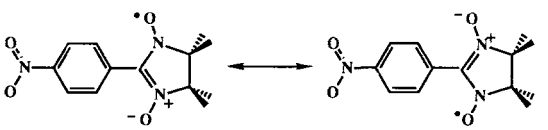


16a



16b

More recently, the ferromagnetic ordering reported for β-*p*-$O_2NC_6H_4NIT$ (NIT = nitronyl nitroxide) (**17**) has been ascribed to a CI between the POMO on one site and a NHOMO on another site.[66] It, however, is plausible that nonbonding,



17

through-space dipole–dipole interactions may be important, and this system is described in greater detail under mechanism 3 (see Section 3.3).

3.2.2.3. Excitations between Localized and Delocalized (Metallic) States (Intramolecular Spin Coupling)

A model of antiferromagnetic exchange (by configuration interaction) between localized d electron spins of the organometallic radicals and a proposed band of delocalized organic moiety based π electrons has been proposed by Tchougreeff and Misurkin and applied to [$FeCp_2^*$][TCNE].[67] This picture resembles those which arise in the Kondo problem[68] and in the Ruderman, Kittel, Kasuda, and Yoshida (RKKY) model for the interaction of magnetic impurities in metals.[23f] They proposed that the POMO b_{2g} $[TCNE]^{\cdot -}$ π^* orbital hybridizes with the delocalized π orbitals of the Cp* ligands and the overlapping 4s and 4p orbitals of Fe^{III} to form a partially filled band of states. They showed that antiferromagnetic exchange between the localized d electrons of $[FeCp_2^*]^{\cdot +}$ and the delocalized π electrons of the organic system could lead to ferromagnetic order in the system of localized Fe d-orbital-based spins. This does not, however, produce the correct saturation magnetization for [$FeCp_2^*$][TCNE], because the delocalized π electrons would have a reduced net spin, part of which would order antiferromagnetically with respect to the Fe d-orbital-based spins. Furthermore, the insulating nature of [$FeCp_2^*$][TCNE] indicates that a delocalized π electron band model is inappropriate. However, a similar approach of interaction of localized metal-based spins with delocalized π electrons was used to account for phenomena in selected phthalocyanine-based salts.[69]

Recent work on the ferromagnetic Zintl phase $A_{14}MnBi_{11}$ (A = Ca and Sr) with critical temperatures of 55 and 33 K, respectively, attributes the magnetic properties to the ferromagnetic coupling of spins between the localized Mn^{III} centers by the conduction electrons (the RKKY model).[5]

3.3. Dipole–Dipole (Through-Space) Exchange

Dipole–dipole, through-space spin-spin interactions not involving the overlap of orbitals have not been formally discussed as a mechanism to achieve bulk ferromagnetic behavior; however, the results of several studies show that through-space spin-spin interactions can lead to cooperative magnetic behavior below about 1 K.[70] This weak magnetic interaction is due to magnetic fields generated by the magnetic moment associated with each spin. It does not involve overlap of orbitals or spin density as illustrated in Figure 12.

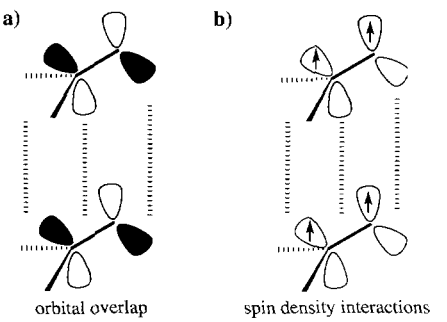
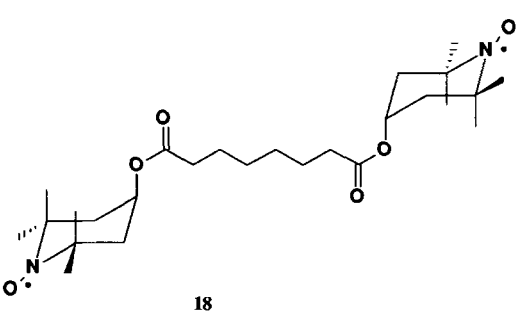
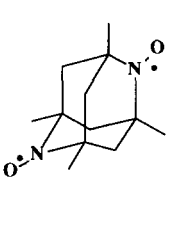


Fig. 12. Schematic illustration of the orbitals (a) and spin densities (b) for nonbonding dipole–dipole, through-space interactions involving a POMO on *A*.

Tanol suberate (**18**), which has a sheetlike crystal structure, and exhibits Curie–Weiss behavior at higher temperature (θ = 0.7 K) and metamagnetic behavior below a T_c of 0.38 K, is a candidate for this mechanism. Below the critical field (H_{cr}) of 100 G **18** is an antiferromagnet, while above 100 G **18** has a high-moment state.[71] Polarized-neutron studies were utilized to determine that the spin density is solely located on the NO moiety, equally between the O and N.[72a] Neutron scattering has also determined that the NO groups couple ferromagnetically within layers separated by 5.9, 6.4, and 6.9 Å, and couple antiferromagnetically between the layers separated by 10.8 Å. Very recently 1,3,5,7-tetramethyl-2,6-diazaadamantane-2,6-dioxyl (**19**) was reported to exhibit ferromagnetic interactions in the solid as evidenced by a θ of 10 K and a fit of the $M(H)$ data to $S = 6$.[73a] The relatively large value of θ suggests that through-space dipole–dipole interaction is not the only mechanism operative. Compound **19** recently has been reported to order at 1.48 K.[73b]



18



19

Crystals of **17** fit the Curie–Weiss expression ($\theta \approx 1$ K) at higher temperatures and have been reported to have a ferromag-

netic state for a T_c at 0.60 K.[66] In contrast γ-p-$O_2NC_6H_4NIT$ is an antiferromagnet.[66b] The origin of the exchange has been ascribed to a CI between the POMO on one site and a NHOMO on another site (vide supra).[66d] However, due to the nonbonding interactions, dipole–dipole interactions may be important. Under hydrostatic pressure the ferromagnetic coupling, as evidenced by an increase of θ, is increased by 40% at 9 kbar pressure.[66c] The large pressure-dependence suggests that through-space dipole–dipole interaction is insufficient to account for the three-dimensional ordering. Zero-field muon spin resonance, which detects the spontaneous static local magnetic fields in ordered states, clearly shows a precession signal comparable to that expected from a three-dimensional Heisenberg model and a T_c of about 0.67 K.[74] Antiferromagnetic coupling has been observed for several other nitronyl nitroxides.[75]

4. Progress in the Discovery of Magnetic Materials Based on Molecular Species

Worldwide interest in molecular-species-based ferromagnets is growing at the present time.[4] Experimental evidence for bulk ferromagnetic behavior in molecular-species-based compounds has been limited to the electron-transfer salts comprised of decamethylmetallocenes and tetracyanoethylene (TCNE) and/or 7,7,8,8-tetracyano-p-quinodimethane (TCNQ), and β-p-$NO_2C_6H_4NIT$ (**17**). Ferromagnetic coupling has been reported for $[(Me_2N)_2CC(NMe_2)_2](C_{60})$, though no hysteresis curves were reported below a transition temperature of $\approx$16 K, and the saturation moment at 5 K corresponds to about 10% of the expected value for only one spin per C_{60}.[76] Recent studies ascribe the high-temperature antiferromagnetic behavior ($\theta = -58$ K) to a superparamagnetic state above $\approx$16 K.[76c] Preliminary zero-field muon spin resonance, however, does not show a change in the spectra as the temperature is reduced to below T_c.[74] There is a rapid suppression of the T_c with pressure by about 10 K per kbar.[76d] The unusually strong pressure-dependence combined with the relatively high conductivity ($\approx 10^{-2}$ S cm^{-1}) of $[(Me_2N)_2CC(NMe_2)_2](C_{60})$ led to the suggestion[76d] that the transition at 16.1 K may be due to an itinerant ferromagnetic state. In contrast, ESR studies suggested[76b,c] that the radical spins in the magnetically ordered state localize on the C_{60} moiety and are ferromagnetically correlated. Further study is necessary to establish the low-temperature magnetic state of this system and determine the origin of the exchange interaction. Cooperative magnetic behavior is not observed for $[(Me_2N)_2CC(NMe_2)_2](C_{70})$.[76b,c]

Evidence for ferrimagnetic ordering has been demonstrated for several $Mn^{II}Cu^{II}$ and Mn^{II} (nitroxide) extended chain structures discussed previously as well as the room-temperature magnet $[V(TCNE)_x] \cdot y(CH_2Cl_2)$ and the recently reported manganese(III) prophyrin-TCNE electron-transfer salt (vide infra).

Numerous attempts to prepare ferromagnetic polymers by the topochemical polymerization of a dinitroxyldiacetylene, oxidation of 1,3,5-triaminobenzene or an indigo polymer, thermolysis of numerous hydrocarbons and polymers, hydrogen abstraction from polymers based upon triphenylmethyl fragments, and electrodeposited polyaniline have been reported. The stated magnetizations correspond to only a few percent of the maximum theoretical magnetization. The poor chemical characterization, low values of the saturation magnetization, and marked variation between samples suggest that the ferromagnetic behavior in these infusible, intractable polymers may not be intrinsic. This area has been recently reviewed.[7] In the remainder of this review we focus on research primarily, but not exclusively, carried out in our laboratories which was initiated with the discovery of cooperative magnetic behavior in a metallocene-based electron-transfer salt.

5. Structure and Magnetic Properties of Electron-Transfer Donor/Acceptor Salts

In 1979 $[Fe^{III}Cp^*_2]^{\bullet+}[TCNQ]^{\bullet-}$ was shown to exhibit a high-moment ferromagnetic state above 1600 Oe (i.e., cooperative metamagnetic properties).[77a] The linear chain structure was established for the kinetic phase of $[Fe^{III}Cp^*_2]^{\bullet+}[TCNQ]^{\bullet-}$[77b] (Fig. 13). The moment μ significantly deviates to positive values

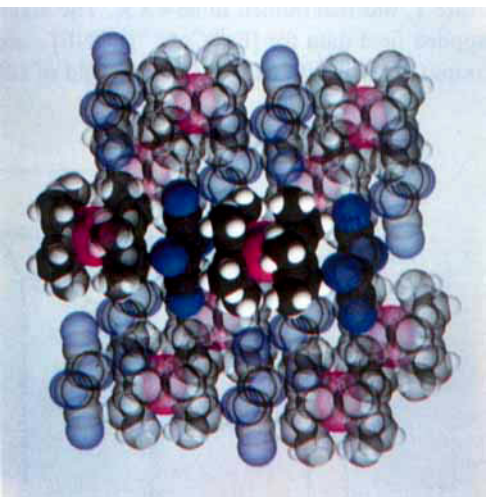
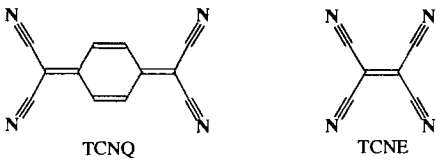


Fig. 13. Alternating donor/acceptor $\cdots D^{\bullet+}A^{\bullet-}D^{\bullet+}A^{\bullet-}\cdots$ linear chain structure of $[Fe^{III}Cp^*_2]^{\bullet+}[A]^{\bullet-}$ [A = TCNQ, TCNE, $DDQCl_2$, $C_4(CN)_6$], $[Fe^{II}Cp_2][TCNE]$, and $[Fe^{III}Cp^*_2]^{\bullet+}[C_3(CN)_5]^-$. The structure shows views of adjacent in-registry and out-of-registry chains for A = TCNE.

at low temperature from the temperature-independent Curie behavior characteristic of ferrocenium salts with spinless anions.[9, 77a] The field-dependent magnetization $M(H)$ reveals metamagnetic behavior, that is, for an applied field of less than 1600 Oe the magnetization is characteristic of an antiferromagnet; whereas above 1600 Oe a sharp rise and approach to magnetization saturation characteristic of a ferromagnet is observed (cf. Fig. 5).[77a] While several metamagnets, for example, $FeCl_2$, had been characterized,[78] this was the initial example in which neither a one-, two- nor a three-dimensional covalently bonded network structure is present. Subsequently, we sought to elucidate the structure–function relationship by the systematic modification of the acceptor A, the substituents on the C_5Me_5 ring, and the metal ion to identify the steric/electronic features necessary to stabilize ferromagnetism and ultimately design a molecular-species-based ferromagnet.

On the supposition that a smaller radical anion would have a greater spin density which could lead to increased spin-spin interactions, we sought to identify stable radical anions smaller than $[TCNQ]^{\bullet -}$, and thus selected $[TCNE]^{\bullet -}$. $[Fe^{III}Cp_2^*]^{\bullet +}[TCNE]^{\bullet -}$ was prepared and found to possess the same $\cdots D^{\bullet +}A^{\bullet -}D^{\bullet +}A^{\bullet -}\cdots$ motif (Fig. 13).[79] With application of only the Earth's magnetic field a spontaneous magnetization is observed.[25] The saturation magnetization for single



crystals aligned parallel to the $\cdots D^{\bullet +}A^{\bullet -}D^{\bullet +}A^{\bullet -}\cdots$ stacking axis is 36% greater than iron on a g-atom basis, and agrees with the calculated saturation moment for ferromagnetic alignment of the donor and the acceptor.[8g-j] The critical (Curie) temperature T_c was determined to be 4.8 K. The magnetization versus applied field data for $[Fe^{III}Cp_2^*]^{\bullet +}[TCNE]^{\bullet -}$ exhibits hysteresis loops (Fig. 14) with a large coercive field of 1000 Oe at 2 K.[25]

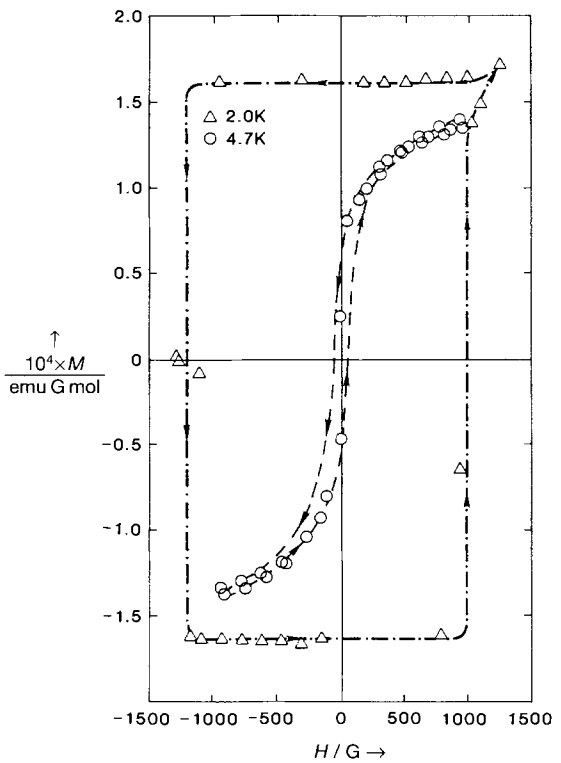


Fig. 14. The magnetization M as a function of applied field H for $[Fe^{III}Cp_2^*]^{\bullet +}[TCNE]^{\bullet -}$ shows hysteresis loops at 2 K.

It is sufficiently magnetic at low temperatures to be attracted to a Co_5Sm magnet (Fig. 15).

Fitting the single-crystal magnetic susceptibility data taken for the applied magnetic field parallel to the C_5 axis of the donor

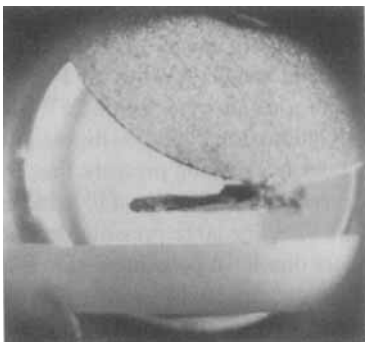


Fig. 15. Photograph of a compacted powder sample of $[Fe^{III}Cp_2^*]^{\bullet +}[TCNE]^{\bullet -}$ being attracted to a Co_5Sm magnet at low temperature in a liquid helium dewar. (Photograph by J. V. Caspar and R. S. McLean.)

to different physical models aids in the understanding of the microscopic spin interactions. Above 16 K interactions among the nearest neighbor spins within individual one-dimensional chains are sufficient to understand the magnetic behavior. The Curie–Weiss Law is sufficient to model the higher temperature ($T > 130$ K) data with $\theta = 30$ K.[25, 79] A one-dimensional Heisenberg model with a ferromagnetic exchange coupling (J) of 19 cm^{-1} (27 K), however, better accounts for the data down to 16 K.[25] These models are insufficient to account for the magnetic behavior below 16 K as long-range spin correlations and three-dimensional spin interactions become increasingly important. This continues until permanent long-range (three-dimensional) ferromagnetic order occurs at 4.8 K. Preliminary studies of the pressure dependence of T_c reveals that T_c increases with applied pressure by 0.21 K $kbar^{-1}$ and reaches 7.8 K at 14 kbar applied pressure.[80a] (This is in marked contrast to decreasing T_c with increasing pressure of the organic superconductors.[80b]) Variation of the low-field magnetic susceptibility with temperature above T_c, magnetization with temperature below T_c, and the magnetization with magnetic field at T_c enabled a measurement of three critical exponents (Table 4) for the magnetic field parallel to the chain axis. The observed values are in accord with a transition to a three-dimensional ordered magnetic state.

The configuration admixing of a virtual-triplet excited state with the ground state model (mechanism 2.2.1.1 in Scheme 1) provides a mechanism to stabilize ferromagnetic interactions within donor/acceptor (D/A) complexes and a simple, preliminary framework to view this class of materials and make some predictions as to the magnetic coupling of new materials. The paradigm of this model is realized by this series of electron-transfer salts possessing a linear chain (one-dimensional) structure comprised of alternating cation donors (D) and anion acceptors (A) that is, $\cdots D^{\bullet +}A^{\bullet -}D^{\bullet +}A^{\bullet -}\cdots$ (Fig. 13).[8g, 9] This model is described in further detail under the mechanism 2.2.1.1 (Scheme 1; Section 3.2.2.1.1). More complex models have been invoked to describe this system and are described under the mechanism 2.2.2 (Scheme 1; Section 3.2.2.2).

To identify the structure–function relationship with the goal of preparing a molecular-species-based ferromagnet with a higher critical temperature, the properties of $\cdots$DADA$\cdots$ structured compounds based on $[M(C_5R_5)_2]^+$ were studied. Three modifiable entities are: replacement of the Me groups with H and Et, use of alternate open and closed-shell anions, and replacement of Fe^{III} with other metal ions.

Table 4. Summary of the critical temperatures T_c and data for the coercive fields of compunds of the $[MCp^*_2]$ [A].

Compound $[MCp^*_2]$	[A]	S_D	S_A	T_c [K]	θ [K] [d]	H_c [G] (T [K])	α [h]	β [h]	γ [h]	δ [h]	Ref.
$[FeCp^*_2]^{+\cdot}$	$[TCNE]^{-\cdot}$	1/2	1/2	4.8	+16.9 [e]	1000(2)	0.09	≈ 0.5	1.21	4.42	[25, 79]
$[MnCp^*_2]^{+\cdot}$	$[TCNE]^{-\cdot}$	1	1/2	8.8	+22.6	1200(4.2)					[81]
$[CrCp^*_2]^{+\cdot}$	$[TCNE]^{-\cdot}$	3/2	1/2	3.65 [j]	+22.2	[g]		0.5	1.1		[58]
$[FeCp^*_2]^{+\cdot}$	$[TCNQ]^{-\cdot}$	1/2	1/2	2.55 [a]	+12.3						[77a]
$[MnCp^*_2]^{+\cdot}$	$[TCNQ]^{-\cdot}$	1	1/2	6.3 [b]	+10.5 [i]	3600(3)					[82]
$[CrCp^*_2]^{+\cdot}$	$[TCNQ]^{-\cdot}$	3/2	1/2	3.3 [c]	+11.6 [f]	[k]					[59]

[a] Metamagnetic with a 1600 G critical field. [b] 50 G, T_c from the maximum slope of dM/dT is reported as 6.2 K. [c] 15 G, T_c from the maximum slope of dM/dT is reported as 3.1 K. [d] For polycrystalline samples. [e] For crystals aligned parallel and perpendicular to the applied magnetic field: $\theta_{\parallel} = 30$ K and $\theta_{\perp} = 10$ K [25]. [f] 12.8 K (R. S. McLean, J. S. Miller unpublished results). [g] Not observed. [h] Critical constants. [i] 9.0 K (R. S. McLean, J. S. Miller unpublished results). [j] 0.15 G. [k] Not observed; <0.15 Oe.

Substituted C_5 rings may maintain the fivefold symmetry necessary to form a cation with degenerate partially occupied molecular orbitals and a Kramers doublet (^2E) ground state as reported for decamethylferrocenium. Three other such ferrocenes have been studied: ferrocene, 1,2,3,4,5-pentamethylferrocene, and decaethylferrocene. Ferrocene is significantly more difficult to oxidize than decamethylferrocene, and is not oxidized by TCNE.[83] Nonetheles, $[Fe^{II}Cp_2][TCNE]$ forms and belongs to the same structure type[84] (Fig. 13) and is diamagnetic.[84b] [FeCpCp*] (Cp = cyclopentadienide, C_5H_5) is a sufficiently strong donor to reduce TCNE, and the simple (1:1) one-dimensional salt as well as three other phases were prepared.[85] This 1:1 phase exhibits weak ferromagnetic coupling as evidenced from the fit of its susceptibility to the Curie–Weiss expression with $\theta = 3.2$ K, but cooperative three-dimensional magnetic ordering is not observed to the lowest temperature studied (≈2 K).[85] A linear chain structure is proposed for $[Fe^{III}(C_5Et_5)_2]^{+\cdot}[TCNE]^{-\cdot}$, which also exhibits ferromagnetic coupling as evidenced from the fit of its susceptibility to the Curie–Weiss expression with $\theta = 7.5$ K. It also did not exhibit cooperative three-dimensional magnetic ordering.[86]

To test the necessity of a ^2E ground state, the TCNE electron-transfer salt with the lower symmetry $[Fe(C_5Me_4H)_2]$ donor was prepared.[87] The magnetic susceptibility can be fit by the Curie–Weiss expression with $\theta \approx 0$ K. The absence of either three-dimensional ferro- or antiferromagnetic ordering above 2.2 K in $[Fe(C_5Me_4H)_2]^{+\cdot}[TCNE]^{-\cdot}$ contrasts with the behavior of $[FeCp^*_2]^{+\cdot}[TCNE]^{-\cdot}$. The ^{57}Fe Mössbauer data are in accord with the absence of significant magnetic coupling among the radical ions, and show only nuclear quadrupole splitting for the $[Fe(C_5Me_4H)_2]^{+\cdot}$ salts and not the zero-field Zeeman splitting observed for $[FeCp^*_2]^{+\cdot}[TCNE]^{-\cdot}$,[79] $[FeCp^*_2]^{+\cdot}[TCNQ]^{-\cdot}$,[77b] $[FeCp^*_2]^{+\cdot}[C_4(CN)_6]^{-\cdot}$,[88] and $[FeCp^*_2]^{+\cdot}[DDQCl_2]^{-\cdot}$ ($DDQCl_2$ = 2,3-dichloro-5,6-dicyanobenzoquinone).[89] The lack of magnetic ordering apparently arises from poorer intra- and intermolecular overlap within and between the chains leading to substantially weaker magnetic coupling for $[Fe(C_5Me_5H)_2]^{+\cdot}[TCNE]^{-\cdot}$. This suppresses the spin-ordering temperature. Alternatively, due to the overall C_{2v} symmetry the $[Fe(C_5Me_4H)_2]^{2+}$ charge-transfer excited state may be a singlet, not a triplet as expected for $[FeCp^*_2]^{2+}$, and the admixture of a singlet, not a triplet charge-transfer excited state should lead to antiferromagnetic, not ferromagnetic, coupling.[8g, 87] Since significant antiferromagnetic coupling was also absent for $[Fe(C_5Me_4H)_2]^{+\cdot}[TCNE]^{-\cdot}$, perhaps a reduced overlap with neighboring radicals is the more important effect of modification of the cation.

Substitution of TCNE with either TCNQ,[90] $C_4(CN)_6$,[88] $TCNQI_2$,[91] ($TCNQI_2$ = 2,5-diiodo-TCNQ), $DDQCl_2$,[89] or $[M\{S_2C_2(CF_3)_2\}_n]^{-\cdot}$ {$n = 2$, M = Ni,[92a] Pt[92b]; $n = 3$, M = Mo[92c]} acceptors leads to $\cdots D^{+\cdot}A^{-\cdot}D^{+\cdot}A^{-\cdot}\cdots$ structured complexes with dominant ferromagnetic coupling (see Tables 5 and 6).

Replacement of $[TCNE]^{-\cdot}$ with diamagnetic $[C_3(CN)_5]^-$ also leads to the formation of a $\cdots D^{+\cdot}A^{-}D^{+\cdot}A^{-}\cdots$ structured phase; it exhibits only Curie susceptibility ($\theta = -1$ K).[79] The $[Co^{III}Cp^*_2]^+[TCNE]^{-\cdot}$ complex with a diamagnetic donor has been prepared and exhibits essentially the Curie susceptibility anticipated for $[TCNE]^{-\cdot}$.[79] This demonstrates the necessity of having both the D and A radicals for stabilizing ferromagnetic coupling in the linear chain alternating $\cdots D^{+\cdot}A^{-\cdot}D^{+\cdot}A^{-\cdot}\cdots$ motif.

Attempts to prepare $[M^{III}Cp^*_2]^+$ (M = Ru, Os) salts of $[TCNE]^{-\cdot}$ have yet to lead to compounds suitable for comparison with the highly magnetic Fe^{III} phase.[93] Replacement of Fe^{III} in $[Fe^{III}Cp^*_2]^{+\cdot}[A]^{-\cdot}$ (A = TCNE, TCNQ, $C_4(CN)_6$) with doublet Ni^{III}, triplet Mn^{III}, and quartet Cr^{III} leads to compounds exhibiting antiferro-, ferro-, and ferromagnetic coupling, respectively (see Tables 4 and 5). This series enables the direct testing of several models. The simplest POMO/POMO-based CI model predicts antiferro-, ferro-, and antiferromagnetic coupling, respectively; whereas invoking the more complex NHOMO/NLUMO excitation CI model predicts the observed antiferro-, ferro-, and ferromagnetic coupling, respectively. More importantly, the anomalous behavior of $[Cr^{III}Cp^*_2]^{+\cdot}[TCNE]^{-\cdot}$ is striking since its T_c is less than that observed for $[Fe^{III}Cp^*_2]^{+\cdot}[TCNE]^{-\cdot}$ and $[Mn^{III}Cp^*_2]^{+\cdot}[TCNE]^{-\cdot}$, and fails to follow $T_c \propto S(S+1)$, which suggests the competition of more than one mechanism (vide infra).

Magnetic ordering is not observed for bis(dithiolato)metallate salts of decamethylferrocenium; however, ferromagnetic coupling as evidenced by Curie–Weiss θ constants which range from 0 to 27 K is observed (Table 6). This provides an insight into a structure–function relationship. Of the compounds studied only $[MCp^*_2][M'\{S_2C_2(CF_3)_2\}_2]$ (M' = Ni, Pt; M = Fe,[92b] Mn[97]) and $[FeCp^*_2][Mo\{S_2C_2(CF_3)_2\}_3]$[92c] have a one-dimensional chain structure. The M = Fe complexes have the largest θ values, the largest effective moments, and the most pronounced magnetic field dependencies of the susceptibility. The Pt analogue ($\theta = 27$ K) possesses one-dimensional

Table 5. Summary of the Curie–Weiss θ values and critical temperatures (T_c) for $\cdots D^+A^-D^+A^- \cdots$ structures.

Salt with $\cdots D^+A^-D^+A^- \cdots$ structure	θ [K]	T_c [K] [a]	[Ref.]
$[FeCp_2^*]^{\bullet+}[C_4(CN)_6]^{\bullet-}$	35		[88]
$[FeCp_2^*]^{\bullet+}[Pt\{S_2C_2(CF_3)_2\}_2]^{\bullet-}$	27		[92b]
$[MnCp_2^*]^{+}[DDQCl_2]^{\bullet-}$	27		[94]
$[MnCp_2^*]^{+}[TCNE]^{\bullet-}$	22.6	8.8	[81]
$[CrCp_2^*]^{\bullet+}[TCNE]^{\bullet-}$	22.2	3.65	[58]
$[MnCp_2^*]^{+}[DDQBr_2]^{\bullet-}$	20		[b]
$[MnCp_2^*]^{+}[DDQI_2]^{\bullet-}$	19		[b]
$[FeCp_2^*]^{\bullet+}$[bromanil]$^{\bullet-}$	19		[b]
$[FeCp_2^*]^{\bullet+}[DDQBr_2]^{\bullet-}$	19		[b]
$[MnCp_2^*]^{+}[C_4(CN)_6]^{\bullet-}$	18		[b]
$[FeCp_2^*]^{\bullet+}[TCNE]^{\bullet-}$	16.8 [g]	4.8 [h]	[25, 79]
$[FeCp_2^*]_{0.955}^{+}[CoCp_2^*]_{0.045}^{+}[TCNE]^{\bullet-}$		4.4	[95]
$[FeCp_2^*]_{0.923}^{+}[CoCp_2^*]_{0.077}^{+}[TCNE]^{\bullet-}$		3.8	[95]
$[FeCp_2^*]_{0.915}^{+}[CoCp_2^*]_{0.085}^{+}[TCNE]^{\bullet-}$		2.75	[95]
$[FeCp_2^*]_{0.855}^{+}[CoCp_2^*]_{0.145}^{+}[TCNE]^{\bullet-}$		0.75 [c]	[95]
$[FeCp_2^*]^{\bullet+}[C_5(CF_3)_4O]^{\bullet-}$	15.1		[96]
$[FeCp_2^*]^{\bullet+}[Ni\{S_2C_2(CF_3)_2\}_2]^{\bullet-}$	15		[92a]
$[MnCp_2^*]^{+}[Me_2DCNQI]^{\bullet-}$	15		[k]
$[CrCp_2^*]^{\bullet+}[C_4(CN)_6]^{\bullet-}$	13.8		[b]
$[FeCp_2^*]^{\bullet+}$[chloranil]$^{\bullet-}$	13.5		[b]
$[CrCp_2^*]^{\bullet+}[TCNQ]^{\bullet-}$	12.8	3.5 [f]	[59]
$[FeCp_2^*]^{\bullet+}[TCNQ]^{\bullet-}$	12.3	2.55 [d]	[77a, b]
$[MnCp_2^*]^{+}[TCNQ]^{\bullet-}$	10.5	6.5 [e]	[81]
$[FeCp_2^*]^{\bullet+}[DDQI_2]^{\bullet-}$	12		[b]
$[Cr(C_6Me_6)_2]^{\bullet+}[TCNE]^{\bullet-}$	11.8		[60]
$[Cr(C_6Me_3H_3)_2]^{\bullet+}[TCNE]^{\bullet-}$	11.0		[60]
$[FeCp_2^*]^{\bullet+}[Me_2DCNQI]^{\bullet-}$	10.8		[k]
$[TTF]^{\bullet+}[Pt\{S_2C_2(CF_3)_2\}_2]^{\bullet-}$	10.8 [j]		[b] [46c]
$[FeCp_2^*]^{\bullet+}[DDQCl_2]^{\bullet-}$	10.3		[89, b]
$[FeCp_2^*]^{\bullet+}[TCNQI_2]^{\bullet-}$	9.5		[91]
$[FeCp_2^*]^{\bullet+}\{Mo[S_2C_2(CF_3)_2]_3\}^{\bullet-}$	8.4		[92c]
$[Fe(C_5Et_5)_2]^{\bullet+}[TCNE]^{\bullet-}$	7.5		[86]
$[Fe(C_5Et_5)_2]^{\bullet+}[TCNQ]^{\bullet-}$	6.1		[86]
$[FeCpCp^*]^{\bullet+}[TCNE]^{\bullet-}$	3.3		[85]
$[MnCp_2^*]^{+}[Pd\{S_2C_2(CF_3)_2\}_2]^{\bullet-}$	3.7	2.8 [d]	[97]
$[MnCp_2^*]^{+}[Ni\{S_2C_2(CF_3)_2\}_2]^{\bullet-}$	2.6	2.4 [d]	[97]
$[MnCp_2^*]^{+}[Pt\{S_2C_2(CF_3)_2\}_2]^{\bullet-}$	1.9	2.3 [d]	[97]
$[Fe(C_5Me_4H)_2]^{\bullet+}[TCNQ]^{\bullet-}$	0.8		[87]
$[Fe(C_5Me_4H)_2]^{\bullet+}[TCNE]^{\bullet-}$	−0.3		[87]
$[FeCp_2^*]^{\bullet+}$[cyanil]$^{-}$ [l]	−0.6		[98]
$[CoCp_2^*]^{+}[TCNE]^{\bullet-}$	−1		[79]
$[FeCp_2^*]^{\bullet+}[C_5(CN)_4Cl]^{-}$	−1		[b]
$[FeCp_2^*]^{\bullet+}[C_5(CN)_5]^{-}$	−1.2		[79]
$[NiCp_2^*]^{\bullet+}[C_4(CN)_6]^{\bullet-}$	−6		[b]
$[NiCp_2^*]^{\bullet+}[TCNE]^{\bullet-}$	−11.5		[b]
$[TTF]^{\bullet+}[Ni\{S_2C_2(CF_3)_2\}_2]^{\bullet-}$	−34 [i]		[b] [46a]

[a] T_c determined from a linear extrapolation of the steepest slope of the $M(T)$ data to the temperature at which $M = 0$. [b] Unpublished data. [c] ac (100 Hz) measurement. [d] Metamagnetic. [e] 50 G, T_c from the maximum slope of dM/dT is reported as 6.2 K. [f] 15 G, T_c from the maximum slope of dM/dT is reported as 3.1 K. [g] For crystals aligned parallel and perpendicular to the applied magnetic field: $\theta_{\parallel} = 30$ K and $\theta_{\perp} = 10$ K [25]. [h] 7.8 K at 14 kbar [80]. [i] −18 K reported [46a]. [j] 16 K reported [46c]. [k] Me_2DCNQI = 2,5-dimethyl-*N*,*N*′-dicyanoquinonediimine: J. S. Miller, C. Vazquez, R. S. McLean, W. M. Reiff, S. Hünig, *Adv. Mater.* **1993**, *5*, 448.

Table 6. Summary of the Curie–Weiss θ values and μ_{eff} values for $[FeCp_2^*][M\{S_2C_2(CN)_2\}_n]$.

Anion	Structural arrrangement	Spin repeat unit	Susceptibility θ [K]	μ_{eff} [μ_B]
$[Ni\{S_2C_2(CN)_2\}_2]^{\bullet-}$	$D^{\bullet+}[A]_2^{2-}D^{\bullet+}$ dimer [a]	$D^{\bullet+}$	0	2.83
α-$[Pt\{S_2C_2(CN)_2\}_2]^{\bullet-}$	$\cdots D^{\bullet+}A^{\bullet-}D^{\bullet+}\cdots$ sheets $1D\cdots D^{\bullet+}[A]_2^{2-}\cdots$ chains [a]	$D^{\bullet+}$ +1/3 $A^{\bullet-}$	6.6	3.05
β-$[Pt\{S_2C_2(CN)_2\}_2]^{\bullet-}$	$1D\cdots D^{\bullet+}A^{\bullet-}\cdots$ chains $D^{\bullet+}[A]_2^{2-}D^{\bullet+}$ dimer [a]	$D^{\bullet+}$ +1/3 $A^{\bullet-}$	9.8	3.10
$[Ni\{S_2C_2(CF_3)_2\}_2]^{\bullet-}$	$1D\cdots D^{\bullet+}A^{\bullet-}\cdots$ [b]	$D^{\bullet+}$ + $A^{\bullet-}$	15	3.73
$[Pt\{S_2C_2(CF_3)_2\}_2]^{\bullet-}$	$1D\cdots D^{\bullet+}A^{\bullet-}\cdots$ chains	$D^{\bullet+}$ + $A^{\bullet-}$	27	3.76
$[Mo\{S_2C_2(CF_3)_2\}_3]^{\bullet-}$	$1D\cdots D^{\bullet+}A^{\bullet-}\cdots$ chains	$D^{\bullet+}$ + $A^{\bullet-}$	8.4	3.85

[a] $[A]_2^{2-}$ = isolated $S = 0$ $[M\{S_2C_2(CN)_2\}_2]_2^{2-}$ dimer. [b] Zigzag chains.

$\cdots D^{\bullet+}A^{\bullet-}D^{\bullet+}A^{\bullet-}\cdots$ chains, whereas the Ni analogue (θ = 15 K) possesses zigzag one-dimensional $\cdots D^{\bullet+}A^{\bullet-}D^{\bullet+}A^{\bullet-}\cdots$ chains and longer M···M separations (11.19 Å vs. 10.94 Å for the Pt analogue). Thus, the enhanced magnetic coupling the Pt compound compared with that of the Ni compound presumably arises from the stronger intrachain coupling. In contrast, for $[MnCp_2^*][M'\{S_2C_2(CF_3)_2\}_2]$ (M′ = Ni, Pd, Pt) weak ferromagnetic coupling is observed ($\theta = 2.8 \pm 0.8$ K), and metamagnetic behavior with a T_c of 2.5 ± 0.3 K was reported.[97] This is comparable to the T_c reported for metamagnetic $[FeCp_2^*]^{\bullet+}[TCNQ]^{\bullet-}$.[77a]

It is curious to note that, whereas replacement of $[FeCp_2^*]^{\bullet+}$ ($S = 1/2$) in $[FeCp_2^*]^{\bullet+}[TCNE]^{\bullet-}$ with $[MnCp_2^*]^{+}$ ($S = 1$) increases T_c nominally in accord with theory (i.e., $T_c \propto S(S+1)$, vide infra),[81] and replacement of $[FeCp_2^*]^{\bullet+}$ in $[FeCp_2^*]^{\bullet+}[TCNQ]^{\bullet-}$ with $[MnCp_2^*]^{+}$ destabilizes the metamagnetic behavior and stabilizes ferromagnetic ordering, however, replacement of $[FeCp_2^*]^{\bullet+}$ in $[FeCp_2^*][M'\{S_2C_2(CF_3)_2\}_2]$ with $[MnCp_2^*]^{+}$ stabilizes metamagnetic behavior.[97] The absence of simple trends emphasizes the important role of interchain as well as intrachain interactions (vide infra).

In the opposite extreme $[FeCp_2^*][Ni\{S_2C_2(CN)_2\}_2]$ possesses isolated $D^{\bullet+}A_2^{2-}D^{\bullet+}$ dimers and has a zero θ, the lowest μ_{eff}, and has no field dependence of the susceptibility.[92a] The observed high moment is consistent with one spin possessing a highly anisotropic *g* value per repeat unit. Intermediate between the one-dimensional chain and dimerized chains structures are the α- and β-phases of $[FeCp_2^*][Pt\{S_2C_2(CN)_2\}_2]$ which have one-dimensional $\cdots D^{\bullet+}A^{\bullet-}D^{\bullet+}A^{\bullet-}\cdots$ strands in one direction and $\cdots$ DAAD $\cdots$ dimer units in another direction. Their θ and μ_{eff} are intermediate in value (Table 6). This is consistent with one-third of the anions having a singlet ground state. Thus a correlation exists between the presence of one-dimensional $\cdots D^{\bullet+}A^{\bullet-}D^{\bullet+}A^{\bullet-}\cdots$ chains and the presence and magnitude of ferromagnetic coupling as evidenced by a positive θ value.

Insight into the effect of increasing the intrachain separation was obtained through the study of a tris(dithiolato)metallate salt of $[FeCp_2^*]^{\bullet+}$, namely $[FeCp_2^*]^{\bullet+}[Mo\{S_2C_2(CF_3)_2\}_3]^{\bullet-}$.[92c] The salt possesses only parallel out-of-registry one-dimensional $\cdots D^{\bullet+}A^{\bullet-}D^{\bullet+}A^{\bullet-}\cdots$ chains with intrachain Mo···Mo separations of 14.24 Å. The θ value is only 8.4 K, which probably reflects the enhanced shielding of the spin and reducing of the spin-spin interactions due to the bulky CF_3 groups. $[FeCp_2^*]^{\bullet+}[Mo\{S_2C_2(CF_3)_2\}_3]^{\bullet-}$ and $[TTF]^{\bullet+}[Mn\{S_2C_2(CF_3)_2\}_2]^{\bullet-}$ (M = Ni, Pt) are the sole structures reported to date that only possess out-of-registry parallel chains and do not have parallel chains in-registry. Thus, the antiferromagnetic s^1/s^1 $A^{\bullet-}/A^{\bullet-}$ interchain interactions are eliminated; however, for the latter pair of electron-transfer salts antiferromagnetic s^1/s^1 $D^{\bullet+}/A^{\bullet-}$ interchain interactions are present.

These results support the utility of one-dimensional $\cdots D^{\bullet+}A^{\bullet-}D^{\bullet+}A^{\bullet-}\cdots$ chain structures for achieving significant ferromagnetic coupling and ultimately bulk ferromagnetic behavior as observed for $[FeCp_2^*]^{\bullet+}[TCNE]^{\bullet-}$.[79] With the wide variation of bis- and tris-dithiolates available other salts may exhibit stronger ferromagnetic coupling and possibly bulk ferromagnetic behavior. Furthermore, many polymorphs with differing physical properties can easily, albeit sometimes irreproducibly, be prepared and the specific design of structure types,

for example, one-dimensional $\cdots$ DADA $\cdots$ chains, continues to be an art.

6. Calculation of the Critical (Curie) Temperature T_c

Heisenberg along with Dirac[99] solved expressions that relate T_c to the exchange integral (J) between sites i and j for the general spin case assuming that only the number of equivalent nearest neighbor sites (z) is important. This simplest mean-field model leads to Equation (10).[23]

$$T_c = \frac{2JzS(S+1)}{3k_B} \tag{10}$$

Equation (10) is constrained to have only one spin site S and a unique J. These are poor assumptions for the $[MCp_2^*]^+[TCNE]^{\bullet -}$ system since the distinct spin sites may have different values of S, and the crystal structure implies four distinctly different nearest neighbor exchange integrals, that is, J_z, J_{AA}, J_{DD}, and J_{OR}^{DA} (Fig. 16). A more appropriate mean-field expression for T_c was therefore developed.[24] In the simplest form, since the values for the four exchange integrals are unknown, a single effective J, J_{eff}, is utilized. In this simplified description, which may be inadequate for highly anisotropic materials, there are two distinct spin averages (S_D and S_A corresponding to the D^+ and $A^{\bullet -}$ sites, respectively). The Hamiltonian per molecule ($\mathscr{H}$) takes the form of Equation (11): The directions of the vectors $\langle \boldsymbol{S}_A \rangle$ and $\langle \boldsymbol{S}_D \rangle$ are along their respective effective magnetic fields. A state of spontaneous spin polarization in the absence of an external field exists in the mean-field model whenever the Equations (12) have nonzero solutions. The transition temperature T_c is the highest temperature for which this is valid. Near the T_c the self-consistent spin averages are small and a Taylor series expansion of the equations reduces them to the coupled linear Equations (12a and 12b).

$$\mathscr{H} \approx -\mu_B H \cdot g_A S_A - \mu_B H \cdot g_D S_D - 4\{S_A \cdot [J_{eff}\langle \boldsymbol{S}_A \rangle + 3J_{eff}\langle \boldsymbol{S}_D \rangle] - S_D \cdot [J_{eff}\langle \boldsymbol{S}_D \rangle + 3J_{eff}\langle \boldsymbol{S}_A \rangle]\} \tag{11}$$

$$\langle \boldsymbol{S}_A \rangle = \frac{2S_A(S_A+1)[2J_{eff}\langle \boldsymbol{S}_A \rangle + 6J_{eff}\langle \boldsymbol{S}_D \rangle]}{3k_BT} \tag{12a}$$

$$\langle \boldsymbol{S}_D \rangle = \frac{2S_D(S_D+1)[2J_{eff}\langle \boldsymbol{S}_D \rangle + 6J_{eff}\langle \boldsymbol{S}_A \rangle]}{3k_BT} \tag{12b}$$

Equations (12) have a solution only if the determinant of the coefficients vanishes; a condition which leads to a quadratic equation for $1/T = 1/T_c$, and only one of the roots gives a positive T_c. This formalism breaks down as J in one direction becomes large compared to the other interactions because a one-dimensional system is formed in this limit and T_c must approach zero Kelvin. The prediction of a finite transition temperature for a one-dimensional system is a well-known fundamental deficiency of mean-field models, and a more sophisticated method is probably required to fully treat the strongly anisotropic case. Nonetheless, the general solution for a single effective J, J_{eff}, for Equation (12) is Equation (13).

$$T_c = \frac{64J_{eff}(S_AS_D + S_A^2S_D + S_AS_D^2 + S_A^2S_D^2)}{3\left[\sqrt{S_A^2 + 2S_D^3 + S_A^4 + S_D^2 + 2S_D^3 + D_D^4 + 34(S_AS_D + S_A^2S_D + S_AS_D^2 + S_A^2S_D^2)} - (S_A + S_A^2 + S_D + S_D^2)\right]} \tag{13}$$

Assuming that the intra- and interchain interactions remain unchanged as the donor is varied, J_{eff} will remain constant and consequently the relative T_c can be calculated for different values of S_A and S_D (Table 7). For $[Fe^{III}Cp_2^*]^{\bullet +}[TCNE]^{\bullet -}$, T_c is $4J_{eff}$ within this mean-field model. Since the observed T_c is 4.8 K, J_{eff} is 1.2 K (0.83 cm^{-1}, 0.1 meV). This result points out that though the value of J_{eff} is indeed small, it is sufficient to enable a T_c at experimentally accessible temperatures due to the large number of nearest neighbors.

The major advantage of the above equation is that T_c can be scaled for different S_D values (Table 7). Thus, T_c for a donor ($S_D = 1$) (with an $S_A = 1/2$ acceptor) is 6.8 J or 1.7 times greater than that for a $S_D = 1/2$ donor (with an $S_A = 1/2$ acceptor) system. Hence, since T_c is 4.8 K for $[Fe^{III}Cp_2^*]^{\bullet +}[TCNE]^{\bullet -}$, and all else being equal, T_c would be expected to be 8.2 K for the isostructural $[Mn^{III}Cp_2^*]^{\bullet +}[TCNE]^{\bullet -}$. This is in good agreement with the reported value of 8.8 K for $[Mn^{III}Cp_2^*]^{\bullet +}[TCNE]^{\bullet -}$.[81] (More complex equations utilizing four different J values lead to

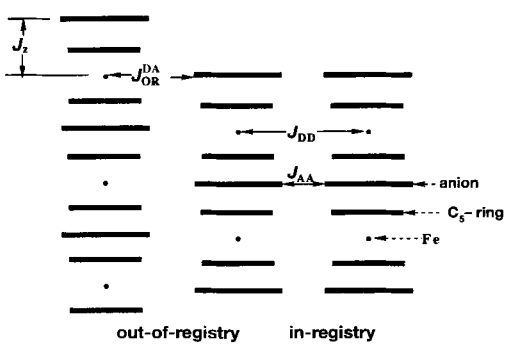


Fig. 16. Schematic illustration of the structure of orthorhombic $[Fe^{III}Cp_2^*]^{\bullet +}[TCNE]^{\bullet -}$ showing intrachain, pairwise out-of-registry and in-registry interactions.

Table 7. Calculated mean-field T_c as a function of S_D for $S_A = 1/2$ systems.

S_D	T_c	scaled T_c [a]
1/2	4 J	1.00
1	6.8 J	1.70
3/2	10 J	2.50
2	13.7 J	3.43

[a] Scaled: $T_c = T_c/T_c$ ($S_D = 1/2$).

an improved scaling of T_c as a function of S_D.[24, 81]) Thus, the observed T_c is in excellent agreement with the experimental values and suggests that if this mean-field model is correct, similar exchange interactions operate for both $[Fe^{III}Cp_2^*]^{\cdot+}[TCNE]^{\cdot-}$ and $[Mn^{III}Cp_2^*]^{+}[TCNE]^{\cdot-}$.[100]

The $S_D = 3/2/S_A = 1/2$ case (i.e., $[Cr^{III}Cp_2^*]^{\cdot+}[TCNE]^{\cdot-}$) was also theoretically treated and a predicted scaled value for the T_c of 12 K was obtained. Experimental study of the magnetic susceptibility of $[Cr^{III}Cp_2^*]^{\cdot+}[TCNE]^{\cdot-}$ shows a ferromagnetic transition at 3.65 K substantially lower than that of either $[Fe^{III}Cp_2^*]^{\cdot+}[TCNE]^{\cdot-}$ or $[Mn^{III}Cp_2^*]^{+}[TCNE]^{\cdot-}$.[58] This trend is also observed for $[Mn^{III}Cp_2^*]^{+}[TCNQ]^{\cdot-}$ ($T_c = 6.2$ K)[82] and $[Cr^{III}Cp_2^*]^{\cdot+}[TCNQ]^{\cdot-}$ ($T_c = 3.1$ K)[59] and may arise from the Cr^{III} salts having significantly lower values of J than the Mn^{III} and Fe^{III} salts.[101] The anomalously low value of T_c is further compounded by the observed ferromagnetic exchange, in contrast to the prediction of antiferromagnetic exchange and a ferrimagnetic ground state for the configuration mixing model described previously. (This model successfully yields the sign of the magnetic exchange of all other linear chain metallocene cases studied so far.) Experimental study of $[CrCp_2^*][TCNE]$ is complicated by its extreme sensitivity to the presence of oxygen which modifies the observed exchange interactions.[58]

7. Dimensionality of the Electron-Transfer Donor/Acceptor Salt System

The mean-field models described previously emphasize a three-dimensional approach to magnetic ordering. The low value of the three-dimensional ordering temperature ($T_c = 4.8$ K) compared to the one-dimensional exchange interaction (as indicated by $J = 19$ cm^{-1} (27 K)) for $[FeCp_2^*]^{\cdot+}[TCNE]^{\cdot-}$, suggests the applicability of quasi-one-dimensional models for the onset of three-dimensional cooperative ordering. For example, for a tetragonal lattice with interacting nearest neighbor chains [(Eq. (14)].[102]

$$T_c = \frac{1.556\sqrt{J_{intra}J_{inter}}}{k_B} \qquad (14)$$

Using a value of $J = 27$ K for the intrachain exchange and the experimental value of T_c, a ratio of $J_{intra}/J_{inter} = 77$ is obtained. Thus, $[FeCp_2^*]^{\cdot+}[TCNE]^{\cdot-}$ and most of the other metallocene electron-transfer salts are in the one-dimensional limit.

To test the critical importance of the one-dimensionality, spinless $S = 0$ $[CoCp_2^*]^{+}$ cations were randomly substituted for the cation in the $[FeCp_2^*]^{\cdot+}[TCNE]^{\cdot-}$ structure. This resulted in the formation of random finite magnetic chain segments embedded into the linear chains.[95] The dramatic, precipitous reduction of T_c with increasing $[CoCp_2^*]^{+}$ content is in excellent agreement with theoretical concepts[103] (Fig. 17, Table 5) for highly anisotropic systems. With a 14.5% replacement of Co^{III} for Fe^{III}, T_c dropped from 4.8 to 0.75 K. The extreme sensitivity of the three-dimensional ordering temperature T_c stands as a cautionary note in attempts to observe a high T_c for solids comprised of high-spin oligomers. For such systems the ratio of the intra- to the interoligomer exchange may be very large. Given the finite length of oligomers, the results of the aforementioned doping

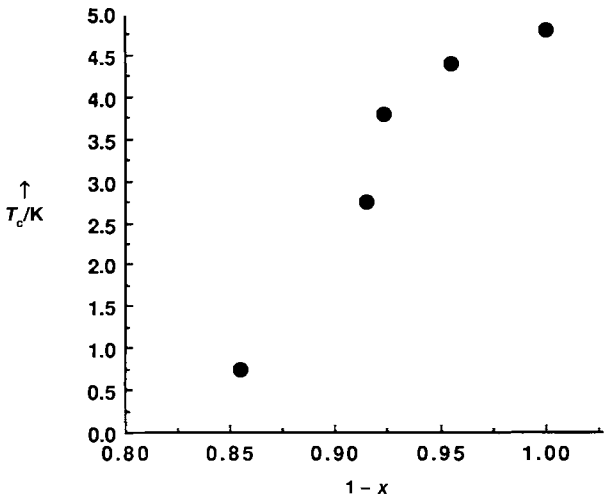


Fig. 17. Variation of T_c with the amount of $[CoCp_2^*]^{+}$ introduced into the structure of $[FeCp_2^*]^{\cdot+}[TCNE]^{\cdot-}$, $[\{FeCp_2^*\}^{\cdot+}]_{1-x}[\{CoCp_2^*\}^{+}]_x[TCNE]^{\cdot-}$.

experiments suggest a significant suppression of three-dimensional ordering.

8. Unusual Magnetic Properties of $[MnCp_2^*]^{+}[DDQCl_2]^{\cdot-}$

With the goal of preparing additional molecular-species-based ferromagnets, the ferromagnetically coupled $[FeCp_2^*]^{\cdot+}[DDQCl_2]^{\cdot-}$ electron-transfer salt was characterized ($\theta = 10$ K).[89] As T_c is proportional to the spin magnitude (Eqs. (10) and (13)), $[MnCp_2^*]^{+}[DDQ]^{\cdot-}$ was prepared anticipating that T_c might occur at temperatures accessible in our laboratories.[94] The high-temperature magnetic susceptibility of $[MnCp_2^*]^{+}[DDQCl_2]^{\cdot-}$ can be fit by the Curie–Weiss expression with a θ value of 26.8 K, which suggests that the strongest exchange interactions (the interactions within individual chains) are ferromagnetic. Hysteretic magnetic field dependent behavior, albeit complex, was observed below ≈ 7 K. The 150 to 2000 G magnetic field dependencies of the magnetization for a sample previously aligned in zero field or in high field (19.5 kG) is presented in Figure 18 for increasing and decreasing magnetic fields. Above ≈ 3.8 K the magnetization exceeds the expected value calculated from the Brillouin function [Eq. (8)] for fully aligned $S = 1$ and $S = 1/2$ spins, whereas dramatically different behavior is observed below this temperature. Thus, the data imply a complex magnetic phase diagram at low temperature (Fig. 19). If one assumes complete alignment of the crystals with magnetic field parallel to the C_5 molecular axis, a sample-history dependent saturation magnetization (M_s) is observed with values up to 24200 emuG mol^{-1}. The data are consistent with strong ferromagnetic coupling between adjacent radicals within each chain and a net weak antiferromagnetic coupling between the chains.[104] This leads to metamagnetic behavior. Thus, when an applied magnetic field is large enough, it becomes energetically favorable for the spins in all the chains to align ferromagnetically. Below ≈ 4 K there is an anomalous behavior with large hysteresis and remnant magnetization.[104] For example, at ≈ 4 K the magnetization abruptly drops by

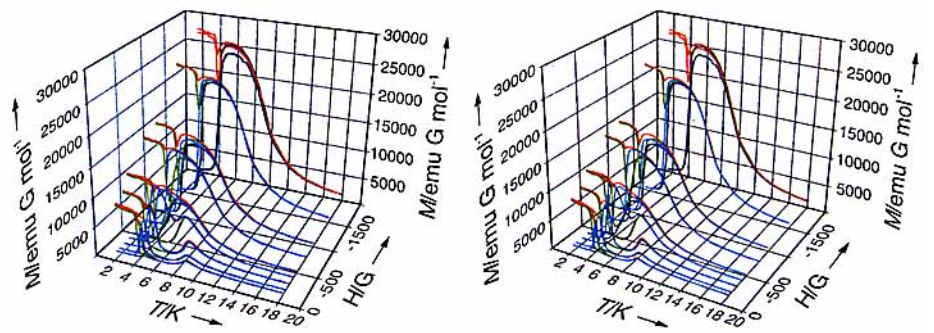


Fig. 18. Stereoview of the molar magnetization M as a function of temperature for a zero-field (blue and cyan) and high-field (red and green) cooled (previously aligned in 19.5 kG) polycrystalline sample of $[MnCp_2^*]^+[DDQCl_2]^-$. The cyan and green data were taken from decreasing applied fields, while the red and blue data were taken from increasing applied fields. (The actual field application sequence was 150, 300, 500, 1000, 2000, 1500, 750, 400, and 200 G prior to annealing at 25 K in zero field for 30 min and then applying 200, 400, 750, 1500, 2000, 1000, 500, 300, and 150 G fields.) The pair of similar curves at 2000 G arises from the two independent times the data was acquired.

more than an order of magnitude depending on the applied field to a value lower than that calculated from the Brillouin function. At high temperature there is a field-dependent crossover from a low-magnetization to a high-magnetization state. This is suggestive of the presence of perhaps both metamagnetic and possible lattice distortion (spin-Peierls-like) transitions. However, since spin-Peierls transitions occur only in antiferromagnetic states, complex magnetic behaviors must be operative in the material. Simple metamagnetic behavior has been reported for $[FeCp_2^*]^{\bullet+}[TCNQ]^{\bullet-}$[77a] and $[MnCp_2^*]^+[M\{S_2C_2(CF_3)_2\}_2]^{\bullet-}$ (M = Ni, Pd, Pt).[97]

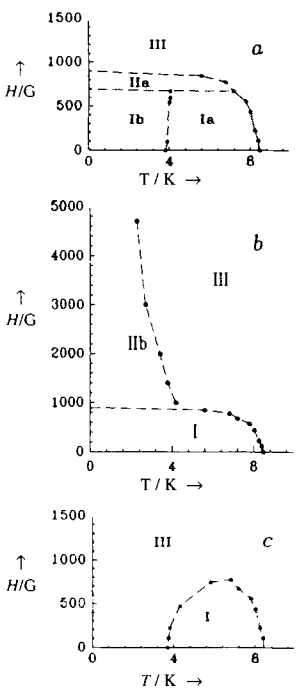


Fig. 19. Magnetic phase diagram (see text) for $[MnCp_2^*]^+[DDQCl_2]^-$ (from ref. [104]).

On the basis of the experimental results three phase diagrams were derived to describe the various transitions. The equilibrium phase diagram for decreasing and increasing temperatures in which the value of applied magnetic field is changed above a three-dimensional antiferromagnetic ordering temperature of 8.5 K and is kept constant during the temperature scan is presented in Figure 19a. There are three distinct regions: antiferromagnetic phase I, mixed phase II, and the coexisting ferromagnetic-paramagnetic phase III. A nonequilibrium phase diagram was derived by cooling the sample in a zero applied field above 8 K, followed by increasing the applied magnetic fields at constant temperatures (Fig. 19b). This diagram shows the first-order boundary separating the different phases: the antiferromagnetic phase I, the intermediate phase IIb, and the ferromagnetic–paramagnetic phase III. A nonequilibrium phase diagram can be generated for the metastable ferromagnetic state, which appears after the system is cooled from 10 K (in an applied field exceeding 1500 Oe) to the desired temperature and the field is decreased to the selected value and the temperature is subsequently reduced. This phase diagram is also achieved if a zero-field cooled sample is exposed to a sufficiently large external field (Fig. 19c). The field is then decreased to the desired value and the temperatureis subsequently raised. The ferromagnetic state is stabilized at low fields (<650 G) below 4 K by using this procedure.[104]

9. Room Temperature Polymeric Magnet $[V(TCNE)_x] \cdot y(CH_2Cl_2)$

Following the observation of bulk ferromagnetic behavior for $[MnCp_2^*]^+[TCNE]^-$ we targeted the preparation of the electron-transfer salt of $[V(C_6H_6)_2]^{\bullet}$ and TCNE.[47–50] $[V^I(C_6H_6)_2]^+$, like $[Mn^{III}Cp_2^*]^+$, is an $S = 1$ cation possessing a $^3E_{2g}$ ground state $[a_{1g}^1 e_{2g}^3 (\approx d_{z^2}^1 d_{xy}^2 d_{x^2-y^2}^1)]$ (Fig. 20).[105] The addition of $[V(C_6H_6)_2]^{\bullet}$ to an excess of TCNE in dichloromethane results in an immediate black precipitate. The empirical composition of this material is $[V(TCNE)_x] \cdot y(CH_2Cl_2)$ ($x \approx 2$; $y \approx 1/2$).[106] However, due to the extreme insolubility of the precipitate, reactivity of the solvent, and extreme air and water sensi-

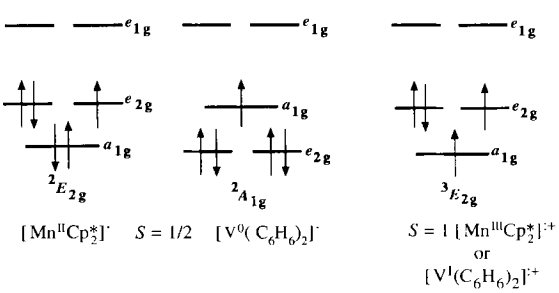


Fig. 20. Schematic illustration of the electronic configurations of $[Mn^{II}Cp_2^*]^{\bullet}$, $[Mn^{III}Cp_2^*]^+$, $[V^0(C_6H_6)_2]^{\bullet}$, and $[V^I(C_6H_6)_2]^+$.

tivities, variations in composition as a function of preparation conditions have been observed. The first step in the reaction is electron transfer from $[V(C_6H_6)_2]^*$ to TCNE followed, unexpectedly, by loss of the benzene ligands, as is evident from the IR spectra which lack ν_{C-H} absorption bands in the 3060 to 3100 cm^{-1} region.[47, 49, 50] The mass spectrum of the magnetic material has peaks assignable to CH_2Cl_2 and TCNE; however, a peak at m/z 78 assignable to $C_6H_6^+$ was not observed. All of the materials exhibit strong, broad absorption bands at 2099 and 2188 cm^{-1} which can be assigned to $\nu_{C\equiv N}$ or perhaps $\nu_{N=C=C}$. The breadth of the $\nu_{C\equiv N}$ absorption bands and their relatively low energy are consistent with the presence of reduced TCNE, with its nitrogen atoms coordinated to vanadium. The oxidation state of the vanadium or TCNE (Table 8) has yet to be determined.[47, 49, 50]

Table 8. Charge and spin states for V and TCNE as a function of oxidation states.

Species	Oxidation state	Charge z	Spin State S
V^0	0	0	1/2
V^I	I	1+	1
V^{II}	II	2+	3/2
V^{III}	III	3+	1
V^{IV}	IV	4+	1/2
V^V	V	5+	0
$[TCNE]^0$	0	0	0
$[TCNE]^{\cdot -}$	−I	1−	1/2
$[TCNE]^{2-}$	−II	2−	0

$[V(TCNE)_x] \cdot y(CH_2Cl_2)$ has a field-dependent magnetization (M) between 1.4 and 350 K (Fig. 21). The nearly linear increase

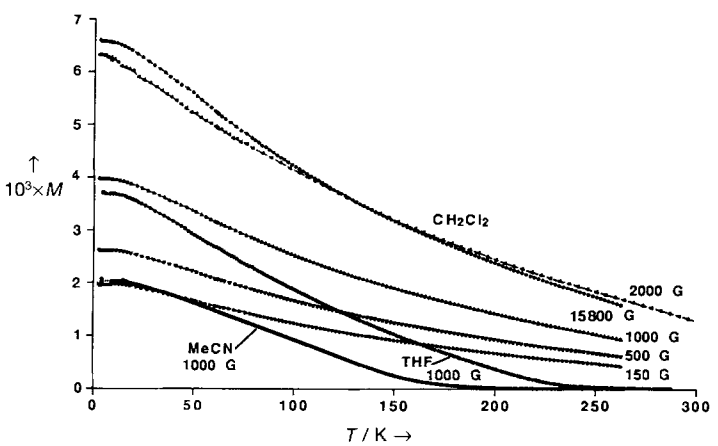


Fig. 21. Typical magnetization (M) [emuG mol^{-1}] as a function of temperature (T) at 15.8 (◂), 2.0 (♦), 1.0 (▲), 0.5 (▾), and 0.15 (▸) kG for $[V(TCNE)_x] \cdot y(CH_2Cl_2)$, 1.0 kG (●) for $[V(TCNE)_x] \cdot y(MeCN)$, and 1.0 kG (○) for $[V(TCNE)_x] \cdot y(THF)$.

of M with decreasing temperature is unusual and may reflect the contribution of the two spin sublattices (V and TCNE) and/or the effects of disorder. Hysteresis with a coercive field of 60 G is observed at room temperature (Fig. 22). The strong magnetic behavior of this material is readily observed by its attraction to a permanent magnet at room temperature (Fig. 23). Thus, this system is the first and only example to date of a molecular/organic-based material with a critical temperature above room temperature. The critical temperature exceeds 350 K, the thermal decomposition temperature of the sample. A linear extrapolation of the magnetization to a temperature at which it would vanish leads to an estimate of a $T_c \approx 400$ K. An independent estimate to T_c was obtained[48] by using the empirical correlation between the spin-wave coefficient and T_c for amorphous magnets.[107] From spin-wave theory and data taken below 60 K a spin-wave dispersion coefficient has been estimated for the V-based magnet,[8j, 48, 108] and T_c is estimated to be ≈ 400 K in agreement with the linear extrapolation of $M(T)$.

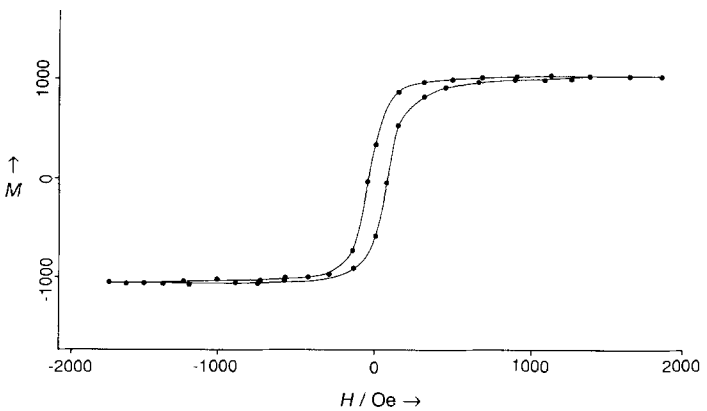


Fig. 22. Hysteresis ($M(H)$) of $[V(TCNE)_x] \cdot y(CH_2Cl_2)$ at room temperature. (The data was taken on a vibrating sample magnetometer: $T = 300$ K, $H_c = 60$ G (From ref. [47]).

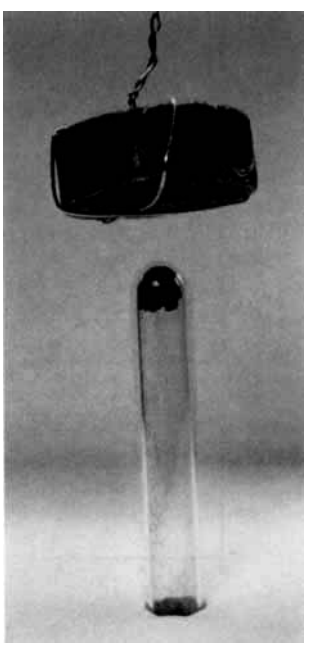


Fig. 23. Photograph of a powdered sample of the $[V(TCNE)_x] \cdot y(CH_2Cl_2)$ magnet being attracted to a Co_5Sm magnet.

$[V(TCNE)_x] \cdot y$(solvent) has been prepared with a variety of $S = 0$ solvents including THF, acetonitrile (MeCN), diethyl ether, benzene, 1,2-dichloroethane, and hexane; CH_2Cl_2, THF, and MeCN have been most extensively studied. The magnetization varies dramatically with the choice of solvent, and T_c sys-

tematically decreases with the ability of the solvent to coordinate with the vanadium center (vide infra).

Due to the structural disorder and variable composition of the magnetic material, the detailed structure has yet to be elucidated (vide infra). TCNE may bond to metals in many ways. For early transition metals linear or bent V–N σ bonds are anticipated. Presently we formulate each vanadium center as being surrounded by up to six ligands which are primarily nitrogen atoms from different TCNE moieties. Chlorine atoms from the weak CH_2Cl_2 ligand or from oxidative addition of CH_2Cl_2 may also coordinate (Fig. 24). Any trace oxygen that is present will strongly bond to the vanadium. The TCNE ligands may bind up to four different vanadium centers through σ N bonds. This fragment may be planar or twisted (Fig. 24). Nonetheless, its ability to bind to more than one vanadium atom enables the construction of a three-dimensional network structure that supports the strong three-dimensional spin-spin coupling necessary for a T_c of 400 K. By using THF or MeCN as alternative solvents, materials with a $T_c < 350$ K can be isolated and characterized. Given the geometrical constraints imposed by the coordination of TCNE to a metal, an open structure with unfilled vanadium coordination sites is unexpected, and thus would be consistent with the observed high surface area of $\approx 100\ m^2\,g^{-1}$, which suggests internal porosity on the molecular level.

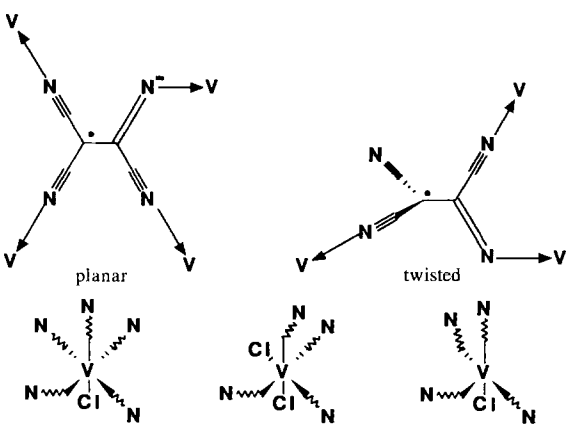


Fig. 24. Proposed local bonding about each TCNE and V center in $[V(TCNE)_x] \cdot y(CH_2Cl_2)$.

Attempts to prepare magnetic materials from the reaction of $[V^0(C_5H_5)(C_7H_7)]$[109] or $[V^{II}(C_5H_5)_2]$ and TCNE or with $[V^0(C_6H_6)_2]$ and other acceptors such as perfluoro-TCNQ ($TCNQF_4$), $C_4(CN)_6$, $C_3[C(CN)_2]_3$, 2,3,5,6-tetrachlorobenzoquinone (chloranil), $DDQCl_2$, and 2,3,5,6-tetracyanobenzoquinone (cyanil)[98] lead to the isolation of insoluble precipitates of unknown composition. These materials do not exhibit field-dependent magnetic susceptibilities and their high-temperature susceptibilities can be fit to the Curie–Weiss expression with $\theta \approx -1$ K characteristic of weak antiferromagnetic coupling between spins. Likewise, in an attempt to prepare the Nb analogue of the V-based magnet, TCNE was allowed to react with $[Nb(C_6H_3Me_3)_2]$; the rapidly formed precipitate exhibited weak antiferromagnetic coupling.

Although the structure is as yet unknown, it is interesting to speculate as to the type of magnetic coupling present in this system. Based upon the IR data and elemental analysis, the composition of the precipitate is presently best formulated as $[V^{II}(TCNE)_2] \cdot 1/2(CH_2Cl_2)$ with $S = 3/2$ V^{II} and two $S = 1/2$ $[TCNE]^{\bullet -}$ ligands. Ferromagnetic coupling gives a total spin S_{total} of 5/2, and if one assumes that g is 2, the saturation magnetization (M_s) is expected to be 28×10^3 emuG mol^{-1}. For antiferromagnetic coupling between V^{II} and the two $[TCNE]^{\bullet -}$ ligands, and hence ferrimagnetic behavior, the S_{total} is 1/2 and M_s is expected to be 5.6×10^3 emuG mol^{-1}; the latter is in good agreement with the value of 6×10^3 emuG mol^{-1} observed at 2 K and 19.5 kG.[47]

The origin of the antiferromagnetic exchange between the spins is important for the design of future high-temperature molecular-based magnets. A variation of the CI mixing of virtual triplet excited states with the ground state to produce a ferromagnetic coupling model (mechanism 2.2.1.1 (Scheme 1; Section 3.2.2.1.1), proposed to account for the ferromagnetic exchange in $[FeCp_2^*][TCNE]$,[44b] can account for the antiferromagnetic exchange of $[V(TCNE)_x] \cdot y$(solvent) and the resulting ferrimagnetic state with a high T_c. The configurational mixing suggested is that of a virtual singlet excited state with the ground state for the $V[TCNE]_2$ system, in which the spin on the V^{II} center ($S = 3/2$) and that on the acceptor ($S = 1/2$) are unequal and produce ferrimagnetic order.[8j, 47, 51] The proposed bonding of the TCNE nitrogen atoms to the vanadium center leads to a sizable orbital overlap; thus, this mechanism should produce a sizable exchange.

The degree of randomness in $[V(TCNE)_x] \cdot y$(solvent) appears to increase for the CH_2Cl_2 < THF < MeCN prepared materials, respectively.[110] This is probably due to the increasing ability of the solvents to coordinate with the vanadium center which in turn displaces some of the TCNE-based radicals and limits the connectivity between vanadium sites. The random anisotropy then leads to the formation of a wandering axis ferrimagnet or even a correlated spin-glass (vide infra).[111] These types of local order are shown schematically in Figure 25 and may be contrasted with the more rigid ordering indicated in

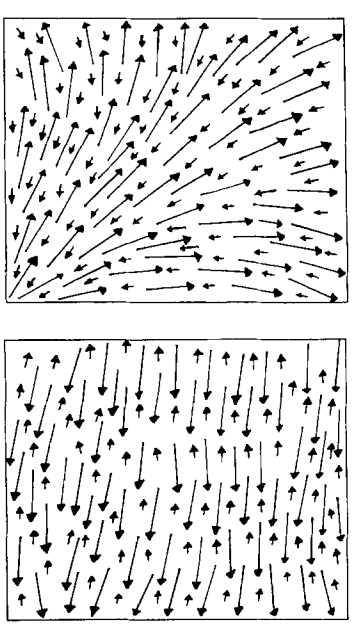


Fig. 25. Schematic illustration of wandering axis ferrimagnet (top) and correlated (ferrimagnetic) spin-glass (bottom).

Figure 3d for a classical ferrimagnet. For the case where the randomness is small compared to the uniaxial anisotropy, a wandering axis ferrimagnet is obtained. This differs from the usual ferrimagnet as the spins do not completely align even at relatively large applied fields. However, when the random anisotropy is larger than the uniaxial anisotropy the average direction the spins point in varies over a spatial correlation length.

Extensive physical studies have now been carried out on the $[V(TCNE)_x] \cdot y(CH_2Cl_2)$ system as well as on similar materials prepared from THF and MeCN solvents. The results of temperature- and magnetic-field-dependent magnetization,[108, 112] ac susceptibility,[113] electron paramagnetic resonance,[112b, 114] dc and audio frequency (10^1 through 10^5 Hz) conductivity and dielectric constant,[115] and microwave frequency conductivity, dielectric constant, and permeability[115, 116] lead to a self-consistent picture of the $[V(TCNE)_x] \cdot y$(solvent) systems as being dominated by the presence of weak random anisotropy.[111a] That is, the magnetic phenomena are dominated by the effects of variation of magnetic interactions from site to site due to the solvent and disorder in the system.

Extensive $M(H,T)$ studies of $[V(TCNE)_x] \cdot y$(THF) and $[V(TCNE)_x] \cdot y$(MeCN), in addition to studies of $[V(TCNE)_x] \cdot y(CH_2Cl_2)$ provide strong support for the key role of random anisotropy. The $[V(TCNE)_x] \cdot y(CH_2Cl_2)$ system has a T_c in excess of room temperature. The T_c for the materials prepared in THF and MeCN are ≈ 200 and ≈ 140 K, respectively (Fig. 21), although this transition temperature is sample-dependent and varies with solvent content and structural order. The ac susceptibility studies suggest that the most disordered of these materials $[V(TCNE)_x] \cdot y$(MeCN) is a reentrant spin-glass with a spin-glass freezing temperature (T_f) of ≈ 10 K (again the transition temperature varies with solvent content and structural order). The materials prepared in THF and MeCN have only weak or absent coercive fields in accord with the greater randomness.

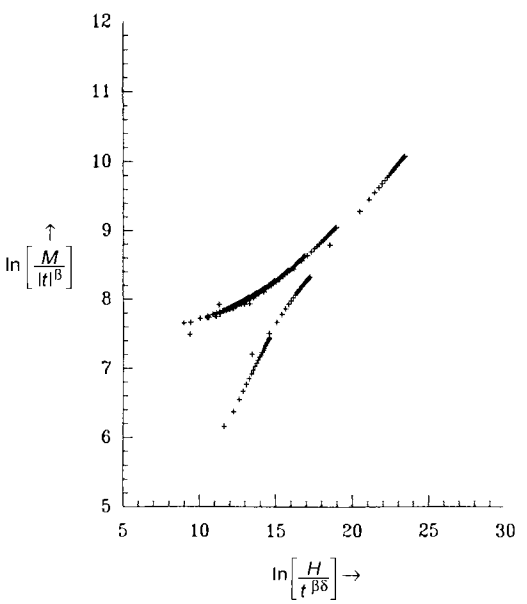


Fig. 26. Scaling plot of $M(T,H)$ for $[V(TCNE)_x] \cdot y$(MeCN). The ordinate is the natural log of M divided by the reduced temperature $t\,[\equiv (|t| = |(T - T_c)/T_c|]$ raised to the β power; the abscissa is H divided by $t^{\beta\delta}$, where β and δ are critical exponents. Note that the data collapse onto the universal curves, the upper one for $T < T_c$ and the lower one of $T > T_c$ (ref. [112a]).

The results of an equation-of-state analysis for the materials prepared in MeCN in the vicinity of the three-dimensional ordering temperature $T_c \approx 138$ K are shown in Figure 26. Here the magnetization data for all H and T studied in the vicinity of T_c collapses to universal curves for $T > T_c$ and $T < T_c$. The values of the effective critical exponents are in accord with the random anisotropy model.[112]

The EPR spectra of $[V(TCNE)_x] \cdot y$(solvent) have been recorded for CH_2Cl_2, THF, and MeCN solvents.[114] The rich set of temperature-dependent spectra obtained provide an insight into the magnetism. A typical derivative spectrum at room temperature for $[V(TCNE)_x] \cdot y(CH_2Cl_2)$ is shown in Figure 27.

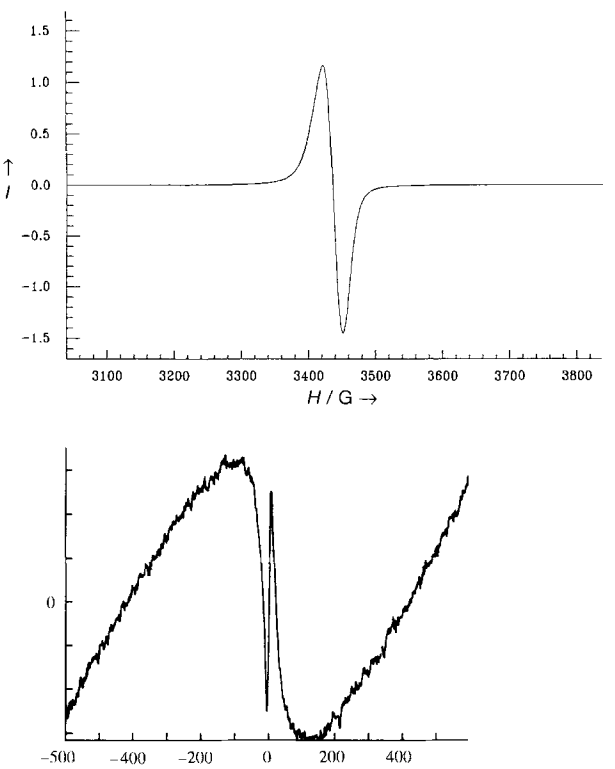


Fig. 27. Top: Derivative EPR signal vs. H for $[V(TCNE)_x] \cdot y(CH_2Cl_2)$ at 295 K. I = intensity (arbitrary units). Bottom: Near zero-field EPR signal of $[V(TCNE)_x] \cdot y(CH_2Cl_2)$ at 200 K (from ref. [114]). Note the greatly expanded vertical scale. The abcissa is in units of Gauss; the ordinate is the derivative of EPR intensity in arbitrary units.

Four distinct resonance signals are observed: 1) the main resonance with $g \approx 1.92$, 2) an approximately half-field resonance, 3) a broad near-zero-field resonance, and 4) a narrow zero-field antiresonance.[114] These resonance signals vary systematically with the composition of the sample (including differing solvents) and the temperature. The latter two signals at 200 K are more clearly shown in Figure 27b. The integrated intensity of the main resonance for each of the compositions studied is proportional to the measured temperature-dependent dc magnetization, hence it is associated with the ferrimagnetic resonance. Contrary to the usual magnetic systems, the linewidth reaches a minimum at T_c, with a critical behavior mimicking the critical behavior of $M(T)$, as expected for a material with "sloppy" waves (spin waves with wavevector $q > \zeta$, where ζ is the correla-

tion length).[117] The shift of the g value of the main resonance correlates with the magnetization and agrees in magnitude with the expected values for demagnetization effects.

The broader low-field signal is largest in the materials prepared in CH_2Cl_2, weak in the systems prepared in THF, and virtually nonexistent in the materials prepared in MeCN. The peak-to-peak width and its sample variation suggest that this low-field signal is similar to that observed for a domain wall like resonance. The sharp zero-field signal is unusual. It is present in each of the compositions below T_c, though for the samples prepared in MeCN it evolves into a resonance signal from an antiresonance below ≈ 15 K, a temperature associated with freezing out of the spins into a spin-glass phase.[113] Based on this temperature dependence, this antiresonance may be caused by a low-field magnetoresistance which makes it more difficult for electrons to hop among charge carrier sites (presumably TCNE), thereby reducing the sample absorbance of microwaves at higher magnetic fields.

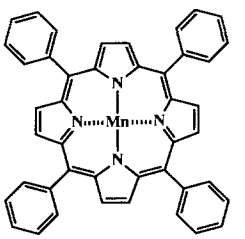
The $[V(TCNE)_x] \cdot y$(solvent) materials are semiconductors which have moderate conductivities of the order 10^{-5} to 10^{-3} S cm^{-1} at room temperature depending upon the solvent.[115, 116] In general, the dc conductivity varies as $\exp[-(T_0/T)^{1/4}]$, which is reminiscent of Mott variable-range hopping.[118] However, the strongly temperature-dependent frequency dependence suggests that the behavior is more complex. This effect was suggested to be a ramification of the correlated spin-glass behavior of the $[V(TCNE)_x] \cdot y$(solvent) materials.[115, 116] The charge transport probably involves charge hopping among anionic $[TCNE]^{\bullet -}$ sites.

The results of the physical studies reinforce the importance of three-dimensional coupling in the $[V(TCNE)_x] \cdot y$(solvent) system. Because of the three-dimensional network structure present, Equation (10) (Table 7) may be used to provide an estimate of the effective exchange interaction J_{eff} operative in the room temperature magnet system (solvent = CH_2Cl_2). If one assumes a T_c of 400 K, an average of five nearest neighbors, and for $S(S+1)$ the root-mean square of $S_A = 1/2$, and $S_D = 3/2$ (i.e., $[(1/2)(1/2+1)(3/2)(3/2+1)]^{1/2}$), a value of J_{eff} of 70 K (50 cm^{-1}) is obtained. This is less than a factor of three larger than the intrachain exchange (Section 5) in $[FeCp_2^*][TCNE]$ for which $T_c = 4.8$ K; yet T_c is nearly one hundred times larger. The differences in transition temperatures do not correlate with the difference in J_{eff} alone, but also with the change in dimensionality from a quasi one-dimensional (for which Equation (14) is operative) to essentially a three-dimensional system (for which Equation (13) is operative). Hence, we conclude that to achieve a high T_c in a molecular-species-based system it is a significant advantage to increase the dimensionality and connectivity of the spin network as well as J.

The solvents are suggested to effect the magnetic state through several mechanisms. These mechanisms include 1) reducing the number of nearest neighbor spins surrounding the vanadium ion, 2) reducing the connectiveness among the vanadium ions by the multicoordinating molecular unit (thereby effectively reducing the dimensionality of the magnetic state), and 3) effecting the degree of crystalline order around each of the vanadium ion sites (thus introducing random anisotropy and also random exchange).

10. Metalloporphyrin-Based Magnets

We recently reported[119] that $[MnTPP]^{\bullet +}[TCNE]^{\bullet -} \cdot 2PhMe$ (TPP = *meso*-tetraphenylporphinato) represents a new structural class of molecular magnets. $[MnTPP]^{\bullet +}[TCNE]^{\bullet -} \cdot 2PhMe$ crystallizes as parallel one-dimensional $\cdots [D]^{\bullet +}[A]^{\bullet -}[D]^{\bullet +}[A]^{\bullet -} \cdots$ chains in which the $[TCNE]^{\bullet -}$ binds identically to two $[MnTPP]^{\bullet +}$ (**20**) moieties in a *trans*-μ_2-N-σ-bound fashion (Fig. 28a). The solid-state motif is distinctly different than that for the $[MCp_2^*]^+[A]^{\bullet -}$ electron-transfer salts (Fig. 13), since $[A]^{\bullet -}$ does not coordinate to the M in the latter system. Thus, the bonding of reduced TCNE to Mn is a model for the bonding of reduced TCNE to V in the $[V(TCNE)_x] \cdot y$(solvent) magnet.



20 MnTPP

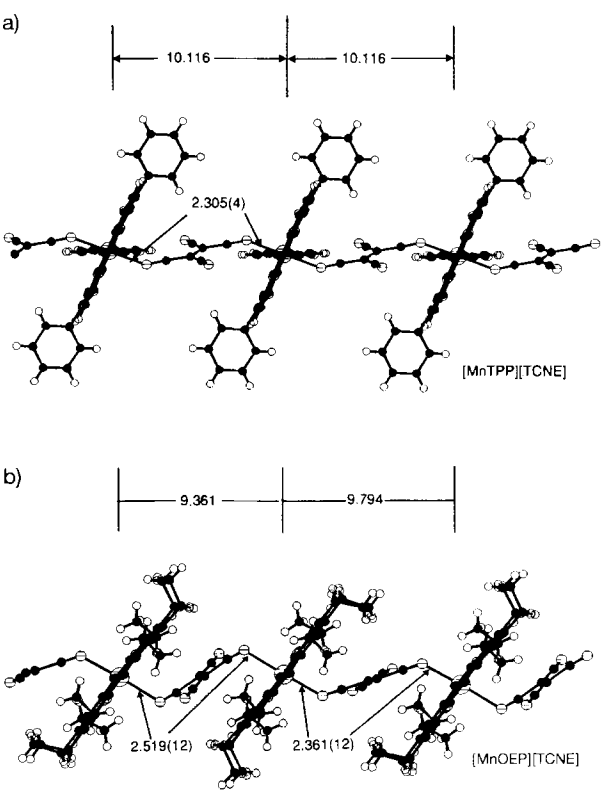


Fig. 28. Segment of a one-dimensional $\cdots D^{\bullet +}A^{\bullet -}D^{\bullet +}A^{\bullet -} \cdots$ chain showing $[TCNE]^{\bullet -}$ *trans*-μ_2-N-σ-bonding to (a) $[MnTPP]^{\bullet +}$ (the toluene molecules of solvation are not shown for clarity) and (b) $[MnOEP]^{\bullet +}$. Distances in Å.

The susceptibility for $[MnTPP]^{\bullet +}[TCNE]^{\bullet -} \cdot 2PhMe$ can be fit by the Curie–Weiss expression between 115 and 250 K ($\theta = 61$ K) and above 280 K ($\theta \approx -15$ K). A minimum in the value of χT characteristic of one-dimensional ferrimagnetic behavior (vide supra)[27a, 120] is observed at ≈ 310 K, and field-dependent susceptibility is observed below 50 K. The saturation magnetization M_s of 30 000 emu G mol^{-1} is in good agreement with the expected saturation magnetization of

29900 emuG mol^{-1} if one assumes ferromagnetic ordering of the $S = 1/2$ [TCNE]$^{\bullet -}$ spin and $S = 2$ [MnTPP]$^{\bullet +}$ spins. A hysteresis curve with a coercive field of 375 G was obtained at 5 K (Fig. 29), which demonstrates that [MnTPP][TCNE] is a magnet at low temperature. Extrapolation of the steepest slope of

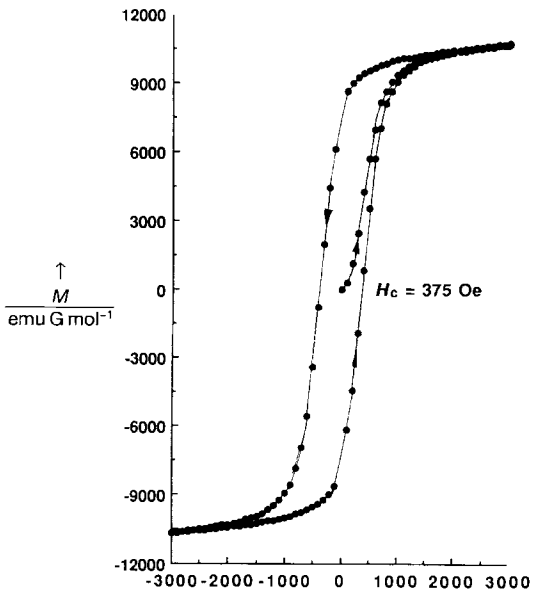
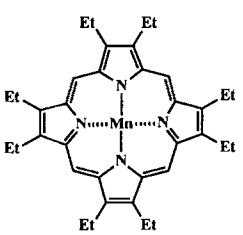


Fig. 29. Hysteresis data at 5 K for polycrystalline [Mn^{III}TPP]$^{+}$[TCNE]$^{\bullet -}$ · 2 MePh. (Recorded with a SQUID magnetometer; SQUID = superconducting quantum interference device).

the 3 G $M(T)$ data to zero yields an estimate of a magnetic ordering temperature of 18 K. A much weaker second transition is observed at 40 K which may reflect ordering to a canted spin state or other complex magnetic behavior. Thus, [MnTPP][TCNE] with the *trans*-μ_2-N-σ-bonded [TCNE]$^{\bullet -}$ is an example of a new structure type of molecular-species-based magnetic material. The presence of magnetic hysteresis and a relatively high T_c value for such a structurally (and probably magnetically) one-dimensional material suggests the possible role of random anisotropy or other disorder in the production of these "ordering" effects.[121a]

As a consequence of the alternating $S = 2$ and $S = 1/2$ chain structure, the [MnTPP]$^{\bullet +}$[TCNE]$^{\bullet -}$ · 2 PhMe one-dimensional chain is an excellent model system for studying a number of unusual magnetic phenomena, for example, the magnetic behavior of mixed quantum/classical spin systems.[122] Thus, for example, [MnTPP]$^{\bullet +}$[TCNE]$^{\bullet -}$ · 2 PhMe may reveal a compensation phenomenon upon further study.[123]



21 MnOEP

To extend this system the analogous TCNE electron-transfer complex was prepared with the easier to oxidize MnOEP (OEP = octaethylporphine), **21**. [MnOEP]$^{\bullet +}$[TCNE]$^{\bullet -}$ exhibits weak ferromagnetic coupling as evidenced by the fit of the susceptibility to the Curie–Weiss expression with a θ of 7 K. However, this material does not exhibit any evidence for cooperative magnetic ordering down to 2 K. The differences in the magnetic properties lie in the structural differences. Although both [MnTPP]$^{\bullet +}$[TCNE]$^{\bullet -}$ and [MnOEP]$^{\bullet +}$[TCNE]$^{\bullet -}$ form parallel one-dimensional $\cdots$[D]$^{\bullet +}$[A]$^{\bullet -}$[D]$^{\bullet +}$[A]$^{\bullet -}\cdots$ chains as noted in Figure 28, they are dimeric instead of uniform for [MnOEP]$^{\bullet +}$[TCNE]$^{\bullet -}$. Also the π^*[TCNE]$^{\bullet -}$ orbitals interact differently with the Mn^{III} centers. Thus, uniform chains appear to be important to achieve long-range magnetic order. This necessity has also been identified to achieve high, metallike dc electrical conductivity for one-dimensional molecule-based metals such as those based on TCNQ.[45]

11. Epilogue

Since the initial reports of three-dimensional cooperative metamagnetism in [FeCp$_2^*$][TCNQ][77a] and ferromagnetism in [FeCp$_2^*$][TCNE],[124] there has been very rapid progress in the development of materials, models for the origin and control of the spin-exchange interaction, theories for the origin, and details of the observed magnetic behavior such as T_c and saturation magnetization (M_s). The chronology of increases in T_c is compared to that of the organic and ceramic superconductors in Figure 30. From these first examples of materials exhibiting

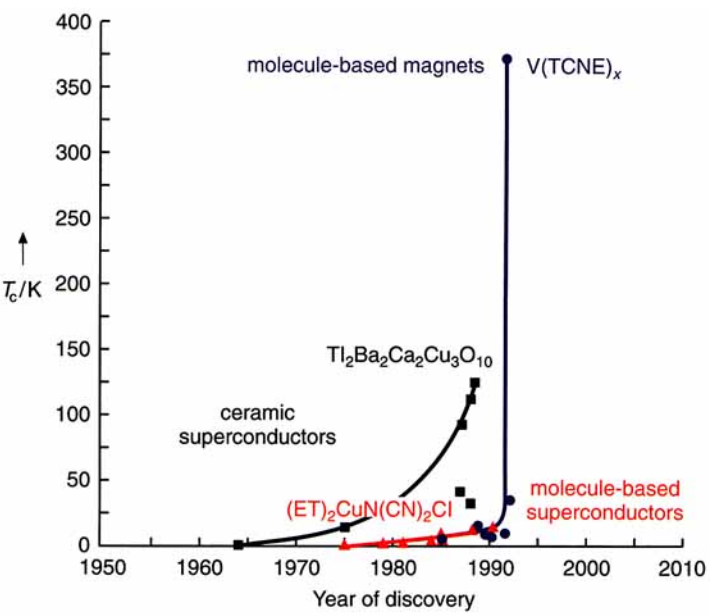


Fig. 30. Time evolution of the discovery of increasing critical temperatures, T_c, for molecular-based magnetic materials as well as organic and oxide superconductors. ET = bis(ethylenedithio)tetrathiafulvalene.

cooperative magnetic ordering, the field of molecular-species-based magnets has evolved. It now includes a wide range of phenomena such as magnetism in molecular-species-based materials at temperatures significantly in excess of room temperature. As this research area has evolved, based upon the models of spins in orthogonal orbitals in the same spatial region within a molecular species in order to achieve intramolecular spin coupling and high-spin behavior, the pairwise configuration inter-

action between molecular species and/or dipole–dipole, through-space interactions to achieve intermolecular spin coupling, several chemical features have emerged as important considerations in designing new magnetic materials. Clearly, to prepare a molecular-species-based magnet, both the donor and acceptor, if present, must be radicals. Such radicals need only have one spin per site; however, a greater number of spins per site is expected to lead to materials with a higher T_c. For donor/acceptor-based systems the competition between ferromagnetic and antiferromagnetic interactions arises from D···D, D···A, as well as A···A interactions. Subtle changes in the orbital overlaps presumably lead to substantial changes in magnetic coupling. Thus, as is the case with proteins, the primary, secondary, and tertiary structures are crucial for achieving the desired cooperative magnetic properties. Currently the discovery of new molecular-species-based magnets is limited by the rational design of solid-state structures which remains an art. This is due to the formation of numerous polymorphs, complex and solvated compositions, as well as undesired structure types. The growth of crystals enabling the study of the single-crystal structure and magnetic properties is also an important limitation. New radicals, donors, and acceptors as well as new structure types are necessary for this area of research to develop further. Finally, one needs to understand the frontier orbital overlaps as they contribute to the interchain and intrachain coupling. Given the present rapid growth in this field it is clear that major advances will be occurring over the next decade in this new multidisciplinary branch of solid-state science.

We have benefited greatly from the stimulating interactions and continued collaborations with our colleagues, postdoctoral fellows, and students for they have made important contributions enabling the rapid progress of the work reported herein. Special thanks are extended to L. Abrams, A. Böhm, M. J. Burk, J. C. Calabrese, F. Chen (Houston), C. W. Chu (Houston), K. R. Cromack, D. A. Dixon, G. Du, A. Grand (Grenoble), R. Hoffmann (Cornell), Z. J. Huang (Houston), G. A. Jones, J. Joo, N. J. Jones, M. Laridjani (Orsay), L. Lardear, S. Long, W. Marshall, R. S. McLean, B. G. Morin, K. S. Narayan, Z. Oblakowski, J. P. Pouget (Orsay), Y. T. Ren (Houston), E. Ressouche (Grenoble), J. Schweizer (Grenoble), A. Suna, A. L. Tchougreeff (Cornell), C. Vazquez, Y. Y. Xue (Houston), S. Zane (Miami), A. Zheludev (Grenoble), P. Zhou, and F. Zuo (Miami) for allowing us to report work in progress. The authors furthermore gratefully acknowledge the support that the Department of Energy, Division of Materials Sciences (Grant Nos. DE-FG02-86BR45271 and DE-FG03-93ER45504) has given for these studies.

Received: December 2, 1992 [A 929 IE]
German version: *Angew. Chem.* **1994**, *106*, 399

[1] a) A. Hellemans, B. Bunch, *Timetables of Science*, Simon and Schuster, New York, **1988**; b) [1a], p. 19; c) [1a], p. 61.

[2] *Magnets in Your Future* **1991**, *5* (6), 22; W. G. Hart, *Intertech Conference on Polymer-Bonded Magnets '92*, Rosemont, IL, USA, unpublished, and W. G. Hart, personal communication.

[3] R. Wood, *Understanding Magnetism*, Tab Books, Blue Ridge Summit, PA, USA, **1988**, Chapter 2; D. C. Mattis, *The Theory of Magnetism*, Springer, New York, **1981**, Chapter 1; A. L. Robinson, *Science* **1984**, *223*, 920; K. H. J. Buschow, *Mater. Sci. Rep.* **1986**, *1*, 1; M. Cohen, *Advancing Materials Research* (Eds.: P. A. Psaras, H. D. Langford), National Academy Press, Washington, DC, USA, **1987**, p. 91; J. J. Croat, J. F. Herbst, *MRS Bull.* **1988**, *13* (6), 37; R. M. White, *Science* **1985**, *229*, 4807; W. E. Wallace, *J. Less-Common Met.* **1984**, *100*, *85*; P. Chaudhari, M. Flemings, *Materials Science and Engineering for the 1990s*, National Research Council, National Academy Press, Washington, DC, USA, **1989**, p. 94.

[4] a) *Proc. Conf. Ferromagnetic and High Spin Molecular Based Materials* (Eds.: J. S. Miller, D. A. Dougherty) (*Mol. Cryst. Liq. Cryst.* **1989**, *176*); b) *Proc. Conf. Molecular Magnetic Materials: NATO ARW Molecular Magnetic Materials* (Eds.: O. Kahn, D. Gatteschi, J. S. Miller, F. Palacio), Kluwer, London, **1991**, *E198*; c) *Proc. Int. Symp. on Chemistry and Physics of Molecular Based Magnetic Materials* (Eds.: H. Iwamura, J. S. Miller) (*Mol. Cryst. Liq. Cryst.* **1993**, *232*, *233*).

[5] T. Y. Kuromoto, S. M. Kauzlarich, D. J. Webb, *Chem. Mater.* **1992**, *4*, 435.

[6] a) P. Day, *Acc. Chem. Res.* **1979**, *14*, 236; C. Bellito, P. Day, *J. Mater. Chem.* **1992**, *2*, 265. b) Some A_2CrX_4 materials have been prepared by low-temperature solution chemistry.

[7] J. S. Miller, *Adv. Mater.* **1992**, *4*, 298, 435.

[8] Reviews: a) A. L. Buchachenko, *Russ. Chem. Rev.* **1990**, *59*, 307; *Usp. Khim.* **1990**, *59*, 529; b) O. Kahn, *Struct. Bonding Berlin* **1987**, *68*, 89; O. Kahn, Y. Journaux, in *Inorganic Materials* (Eds.: D. W. Bruce, D. M. O'Hare), Wiley, New York, **1993**, p. 59; c) A. Caneschi, D. Gatteschi, R. Sessoli, P. Rey, *Acc. Chem. Res.* **1989**, *22*, 392; d) L. Dulog, *Nachr. Chem. Tech. Lab.* **1990**, *38*, 448; e) H. Ishida, *Encyl. Polym. Sci. Eng.* **1985–1989**, p. 446; f) T. Sugawara, *Yuki Gosei Kagaku Kyokaishi* **1989**, *47*, 306; g) J. S. Miller, A. J. Epstein, W. M. Reiff, *Acc. Chem. Res.* **1988**, *21*, 114; h) J. S. Miller, A. J. Epstein, W. M. Reiff, *Science* **1988**, *240*, 40; i) J. S. Miller, A. J. Epstein in *New Aspects of Organic Chemistry* (Eds.: Z. Yoshida, T. Shiba, Y. Ohsiro), VCH, New York, **1989**, p. 237; j) A. J. Epstein, J. S. Miller, *Mol. Cryst. Liq. Cryst.* **1993**, *228*, 99.

[9] J. S. Miller, A. J. Epstein, W. M. Reiff, *Chem. Rev.* **1988**, *88*, 201.

[10] F. Palacio, F. J. Lazaro, A. J. Van Duyneveldt, *Mol. Cryst. Liq. Cryst.* **1989** *176*, 289; F. Palaeio in [4b] p. 1; F. Palacio, J. Ramos, C. Castro, *Mol. Cryst. Liq. Cryst.* **1993**, *232*, 179.

[11] D. A. Dixon, J. S. Miller, *J. Am. Chem. Soc.* **1987**, *109*, 3656.

[12] a) A. Carrington, A. D. McLachlan, *Introduction to Magnetic Resonance*, Harper & Row, New York, **1967**; b) [12a], p. 223ff; c) [12a], p. 81–83; d) R. S. Drago, *Physical Methods of Chemistry*, Saunders, Philadelphia, PA, USA, **1977**, p. 329ff; e) P. Coppins, *Annu. Rev. Phys. Chem.* **1993**, *43*, 663.

[13] a) Note that by allowing more freedom of the orbitals, a lower energy can be reached with more relaxation of the positions of the electrons. Although $\langle S^2 \rangle$ is a good quantum number for the ROHF wavefunction, it is not for the UHF formalism; so the latter formalism must be used with caution. b) A. Szabo, N. S. Ostlund, *Modern Quantum Chemistry: Introduction to Advanced Electronic Structure Theory*, MacMillan, New York, **1982**; c) W. J. Hehre, L. Radom, P. von R. Schleyer, J. A. Pople, *Ab Initio Molecular Orbital Theory*, Wiley, New York, **1986**.

[14] a) J. W. Andzelm in *Density Functional Methods in Chemistry* (Eds.: J. Labanowski, J. Andzelm), Springer, New York, **1991**, p. 101; J. W. Andzelm, E. J. Wimmer, *Chem. Phys.* **1992**, *96*, 1280; *Physica B* **1991**, *172*, 307. DGauss is a local density functional program available from the Cray Unichem Project. b) A. Zheludev, A. Grand, E. Ressouche, J. Schweitzer, B. G. Morin, A. J. Epstein, D. A. Dixon, J. S. Miller, *Angew. Chem.* **1994**, *106*, *Angew. Chem. Int. Ed. Engl.* **1994**, *33*, in press.

[15] M. S. Davis, K. Morokuma, R. W. Kreilick, *J. Am. Chem. Soc.* **1972**, *94*, 5588.

[16] a) χ is in units of emu mol^{-1} and T is in K. b) For a system with $S = 1/2$, $g = 2$ the magnetic energy at 10^4 G (1 T) is 0.7 K 0.5 cm^{-1}, 62 μeV.

[17] H. H. Wickman, A. M. Trozzolo, H. J. Williams, G. W. Hull, F. R. Merritt, *Phys. Rev.* **1967**, *155*, 563; H. H. Wickman, *J. Chem. Phys.* **1972**, *56*, 976; G. C. DeFotis, F. Palacio, C. J. O'Connor, S. N. Bhaatia, R. L. Carlin, *J. Am. Chem. Soc.* **1977**, *99*, 8314; N. Arai, M. Sorai, H. Suga, S. Seki, *J. Phys. Chem. Solids* **1977**, *36*, 1231.

[18] a) S. M. Heald, E. A. Stern, B. Bunker, E. M. Holt, S. L. Holt, *J. Am. Chem. Soc.* **1979**, *101*, 67; b) S. Chikazumi, *Physics of Magnetism*, Part 3, Wiley, New York, **1964**; c) A. H. Morrish, *The Physical Principles of Magnetism*, Wiley, New York, **1965**; d) [18c], Chapter 7; e) [18c], p. 341; f) J. S. Cook, P. L. Rossiter, *Crit. Rev. Solid State Mater. Sci.* **1989**, *15*, 509.

[19] R. B. Frankel, R. B. Blakemore, *J. Magn. Magn. Mater.* **1980**, *15–18*, 1562; R. B. Frankel, G. C. Papaefthymiou, R. B. Blakemore, W. O'Brian, *Biochim. Biophys. Acta* **1983**, *763*, 147.

[20] D. B. Awschalom, D. P. DiVincenzo, J. F. Smyth, *Science* **1992**, *258*, 414.

[21] S. Mitra, A. K. Gregson, W. E. Hatfield, R. R. Weller, *Inorg. Chem.* **1983**, *22*, 1729.

[22] Generally three-dimensional interactions are necessary; however, in some circumstances two-dimensional and even one-dimensional interactions for alternating quantum ($S = 1/2$) and classical ($S > 1/2$) spins, hysteretic effects can occur. See for example, R. A. Serota, P. A. Lee, *Phys. Rev. B* **1986**, *34*, 1806; R. Dickman, E. M. Chudnovsky, *ibid.* **1991**, *44*, 4397.

[23] a) J. H. Van Vleck, *The Theory of Electric and Magnetic Susceptibilities*, Oxford University Press, London, **1932**; b) J. H. Van Vleck, *Rev. Mod. Phys.* **1945**, *17*, 7; c) J. H. Van Vleck, *ibid.* **1953**, *25*, 220; d) J. B. Goodenough, *Magnetism and the Chemical Bond*, Wiley, New York, **1963**; e) R. L. Carlin, *Magnetochemistry*, Springer, Berlin, **1986**; f) C. Kittel, *Introduction to Solid State Physics*, 5th. edition, Wiley, New York, **1976**.

[24] D. A. Dixon, A. Suna, J. S. Miller, A. J. Epstein in [4b] p. 171.

[25] S. Chittapeddi, K. R. Cromack, J. S. Miller, A. J. Epstein, *Phys. Rev. Lett.* **1987**, *58*, 2695.

[26] Z. G. Soos in *Physics and Chemistry of Low-Dimensional Solids* (Ed.: L. Alcacer), Reidel, Dordrecht, **1980**, p. 143; G. Beni, P. Pincus, D. Hone, *Phys. Rev. B* **1973**, *8*, 3389; C. Lyon-Caen, M. Cyrot, *J. Phys. C* **1975**, *8*, 2091.
[27] a) O. Kahn, *Struct. Bonding* **1987**, *68*, 89; b) O. Kahn, *Angew. Chem.* **1985**, *97*, 837; *Angew. Chem. Int. Ed. Engl.* **1985**, *24*, 834.
[28] H. Tamaki, Z. J. Zhong, N. Matsumoto, S. Kida, M. Koikawa, N. Achiwa, H. Okawa, *J. Am. Chem. Soc.* **1992**, *114*, 6974.
[29] a) S. Morimoto, K. Itoh, F. Tanaka, N. Mataga, *Preprints of the Symposium on Molecular Structure*, Tokyo, **1968**, p. 6; b) N. Mataga, *Theor. Chim. Acta* **1968**, *10*, 372.
[30] R. L. Carlin, *Magnetochemistry*, Springer, New York, **1986**, p. 70–71.
[31] W. E. Hatfield in *Theory and Applications of Molecular Paramagnetism* (Eds.: E. A. Boudreaux, L. N. Mulay), Wiley, New York, **1976**, Chapter 7.
[32] a) H. Iwamura, *Pure Appl. Chem.* **1986**, *58*, 187; T. Sugawara, S. Murata, K. Kimura, H. Iwamura, *J. Am. Chem. Soc.* **1985**, *107*, 5293; T. Sugawara, S. Bandow, K. Kimura, H. Iwamura, *ibid.* **1984**, *106*, 6449; T. Sugawara, S. Bandow, K. Kimura, H. Iwamura, K. Itoh, *ibid.* **1986**, *108*, 368; b) N. Nakamura, K. Inoue, H. Iwamura, T. Fujioka, Y. Sawaki, *ibid.* **1992**, *114*, 1484; c) H. Iwamura, N. Nakamura, N. Koga, S. Sasaki, *Mol. Cryst. Liq. Cryst.* **1992**, *218*, 207; H. Iwamura, *Pure Appl. Chem.* **1993**, *65*, 57; N. Nakamura, K. Inoue, A. Iwamura, *Angew. Chem.* **1993**, *105*, 900; *Angew. Chem. Int. Ed. Engl.* **1993**, *32*, 871.
[33] A. L. Buchachenko, *Mol. Cryst. Liq. Cryst.* **1989**, *176*, 307.
[34] a) K. Nasu, *Phys. Rev. B* **1986**, *33*, 330; b) K. Yoshizawa, A. Chano, A. Ito, K. Tanaka, T. Yamabe, *Synth. Met.* **1992**, *52*, 377; c) J. A. Thomas, C. J. Jones, J. A. McCleverty, D. Collison, F. E. Mabbs, C. J. Harding, M. G. Hutching, *J. Chem. Soc. Chem. Commun.* **1992**, 1796.
[35] A. A. Ovchinnikov, *Theor. Chim. Acta* **1978**, *47*, 297.
[36] D. J. Klein, C. J. Nelin, S. Alexander, F. A. Matsen, *J. Chem. Phys.* **1982**, *77*, 3101.
[37] A. Rajca, S. Utamapanya, S. Thayumanavan, *J. Am. Chem. Soc.* **1992**, *114*, 1884; S. Utamapanya, A. Rajca, *ibid.* **1991**, *113*, 9294.
[38] a) J. Veciana, C. Rovira, N. Ventosa, M. I. Crespo, F. Palacio, *J. Am. Chem. Soc.* **1993**, 115, 57; b) J. Veciana, C. Rovira, M. I. Crespo, O. Armet, V. M. Domingo, F. Palacio, *J. Am. Chem. Soc.* **1991**, *113*, 2552.
[39] M. Ota, S. Otani, *Chem. Lett.* **1989**, 1179; M. Ota, S. Otani, M. Igartashi, *ibid.* **1989**, 1183; M. Ota, S. Otani, K. Kobayashi, M. Igarashi, *Mol. Cryst. Liq. Cryst.* **1989**, *176*, 99; M. Ota, S. Otani, *Mater. Res. Soc. Symp.* **1990**, *173*, 71.
[40] D. A. Dougherty, *Acc. Chem. Res.* **1991**, *24*, 88.
[41] P. Nachtigall, K. D. Jordan, *J. Am. Chem. Soc.* **1992**, *114*, 4743; *ibid.* **1993**, *115*, 270.
[42] a) H. Fukutome, A. Takahashi, M. Ozaki, *Chem. Phys. Lett.* **1987**, *133*, 34; b) K. Yamaguchi, Y. Toyoda, T. Fueno, *Synth. Met.* **1987**, *19*, 81.
[43] a) D. A. Kaisaki, W. Chang, D. A. Dougherty, *J. Am. Chem. Soc.* **1991**, *113*, 2764; b) D. A. Dougherty, California Institute of Technology (Pasadena, CA), personal communication.
[44] a) H. M. McConnell, *Proc. Robert A. Welch Found. Conf. Chem. Res.* **1967**, *11*, 144; b) J. S. Miller, A. J. Epstein, *J. Am. Chem. Soc.* **1987**, *109*, 3850.
[45] J. S. Miller, *Ann. N. Y. Acad. Sci.* **1978**, *313*, 25.
[46] a) I. S. Jacobs, L. V. Interrante, H. R. Hart, Jr., *AIP Conf. Proc.* **1975**, *24*, 355; I. S. Jacobs, H. R. Hart, Jr., L. V. Interrante, J. W. Bray, J. S. Kasper, G. D. Watkins, D. E. Prober, W. P. Wolf, J. C. Bonner, *Physica B (Amsterdam)* **1977**, *86–88*, 655; b) J. S. Miller, J. C. Calabrese, unpublished results; c) J. C. Bonner, T. S. Wei, G. D. Watkins, H. W. J. Blöte, *J. Appl. Phys.* **1978**, *49*, 1321; d) J. S. Kasper, L. V. Interrante, *Acta Crystallogr. Sect. B* **1976**, *32*, 2914.
[47] J. M. Manriquez, G. T. Yee, R. S. McLean, A. J. Epstein, J. S. Miller, *Science* **1991**, *252*, 1415.
[48] A. J. Epstein, J. S. Miller in *Conjugated Polymers and Related Materials: The Interconnection of Chemical and Electronic Structure* (Eds.: W. R. Salaneck, I. Lündstrom, B. Rånby) (*Proc. Nobel Symp. No. NS-81*), Oxford University Press, Oxford, **1993**, p. 475.
[49] J. S. Miller, G. T. Yee, J. M. Manriquez, A. J. Epstein, in ref. [48], p. 461.
[50] J. S. Miller, A. J. Epstein, *Mol. Cryst. Liq. Cryst.* **1993**, *233*, 133.
[51] A. L. Tchougreeff, R. Hoffmann, *J. Phys. Chem.* **1993**, *97*, 350.
[52] a) T. P. Radhakrishnan, Z. Soos, H. Endres, L. J. Azevedo, *J. Chem. Phys.* **1986**, *85*, 1126; b) E. Dormann, M. J. Nowak, K. A. Williams, R. O. Angus, Jr., F. Wudl, *J. Am. Chem. Soc.* **1987**, *109*, 2594.
[53] H. M. McConnell, *J. Chem. Phys.* **1963**, *39*, 1910.
[54] A. Izoka, S. Murata, T. Sugawara, H. Iwamura, *J. Am. Chem. Soc.* **1985**, *107*, 1786; *ibid.* **1987**, *109*, 2631.
[55] a) K. Yamaguchi, T. Fueno, K. Nakasuji, I. Murata, *Chem. Lett.* **1986**, 629; b) K. Tanaka, T. Takeuchi, K. Yoshizawa, M. Toriumi, T. Yamabe, *Synth. Met.* **1991**, *44*, 1.
[56] a) F. Nakatani, J. Y. Carriat, Y. Journaux, O. Kahn, F. Lloret, J. P. Renard, Y. Pei, J. Sletten, M. Verdaguer, *J. Am. Chem. Soc.* **1989**, *111*, 5739; b) O. Kahn, Y. Pei, M. Verdaguer, J. P. Renard, J. Sletten, *ibid.* **1988**, *110*, 782; c) F. Nakatani, P. Bergerat, E. Codjovi, C. Mathoniere, Y. Pei, O. Kahn, *Inorg. Chem.* **1991**, *30*, 3977.
[57] a) A. Caneschi, D. Gatteschi, J. P. Renard, P. Rey, R. Sessoli, *Inorg. Chem.* **1989**, *28*, 3314; b) A. Caneschi, D. Gatteschi, J. P. Renard, P. Rey, R. Sessoli, *J. Am. Chem. Soc.* **1989**, *111*, 785; c) C. Bellini, A. Caneschi, D. Gatteschi, R. Sessoli, *Adv. Mater.* **1992**, *4*, 504; d) J. Seiden, *J. Physique Lett.* **1983**, *44*, L947.
[58] a) F. Zuo, A. J. Epstein, C. Vazquez, R. S. McLean, J. S. Miller, *J. Mater. Chem.* **1993**, *3*, 215; b) F. Zuo, S. Zane, P. Zhou, A. J. Epstein, R. S. McLean, J. S. Miller, *J. Appl. Phys.* **1993**, *73*, 5476; P. Zhou, M. Makivic, F. Zuo, S. Zane, J. S. Miller, A. J. Epstein, *Phys. Rev. B.* **1994**, *49*; c) J. S. Miller, D. M. O'Hare, A. Chackraborty, A. J. Epstein, *J. Am. Chem. Soc.* **1989**, *111*, 7853.
[59] W. E. Broderick, B. M. Hoffman, *J. Am. Chem. Soc.* **1991**, *113*, 6334.
[60] J. A. Berson, L. Salem, *J. Am. Chem. Soc.* **1972**, *94*, 8917; H. E. Zimmerman, *Acc. Chem. Res.* **1971**, *4*, 272.
[61] a) C. Kollmar, M. Couty, O. Kahn, *J. Am. Chem. Soc.* **1991**, *113*, 7994; b) C. Kollmar, O. Kahn, *J. Chem. Phys.* **1992**, *96*, 2988; c) C. Kollmar, O. Kahn, *J. Am. Chem. Soc.* **1991**, *113*, 7987; d) Z. G. Soos, P. C. M. McWilliams, *Mol. Cryst. Liq. Cryst.* **1989**, *176*, 369.
[62] J. Blümel, N. Hebendanz, P. Hudeczek, F. H. Köhler, W. Strauss, *J. Am. Chem. Soc.* **1992**, *114*, 4223.
[63] R. N. Musin, P. V. Schastnev, S. A. Malinovskaya, *Inorg. Chem.* **1992**, *31*, 4118.
[64] K. Yamaguchi, M. Okumura, T. Kawamura, T. Noro, K. Nakasuji, *Mol. Cryst. Liq. Cryst.* **1992**, *218*, 229.
[65] a) M. Kinoshita, *Mol. Cryst. Liq. Cryst.* **1989**, *176*, 163; K. Awaga, T. Sugano, M. Kinoshita, *Chem. Phys. Lett.* **1987**, *141*, 540; b) K.-M. Chi, J. C. Calabrese, J. S. Miller, S. I. Khan, *Mol. Cryst. Liq. Cryst.* **1989**, *176*, 185.
[66] a) M. Tamura, Y. Nakazawa, D. Shiomi, K. Nozawa, Y. Hosokoshi, M. Ishikawa, M. Takahashi, M. Kinoshita, *Chem. Phys. Lett.* **1991**, *186*, 401; b) M. Kinoshita, Tokyo, Japan, personal communication; c) K. Awaga, Y. Maruyama, *Chem. Mater.* **1990**, *2*, 535; d) K. Awaga, Y. Maruyama, *J. Chem. Phys.* **1990**, *173*, 33.
[67] A. L. Tchougreeff, I. A. Misurkin, *Chem. Phys.* **1991**, *153*, 371; A. L. Tchougreeff, I. A. Misurkin, *Phys. Rev. B* **1992**, *46*, 5357.
[68] J. Kondo, *Solid State Phys.* **1969**, *23*, 183.
[69] M. Y. Ogawa, B. M. Hoffman, S. Lee, M. Yudkowsky, W. P. Halperin, *Phys. Rev. Lett.* **1986**, *57*, 1177; M. Y. Ogawa, J. Martinsen, S. M. Palmer, J. L. Stanton, J. Tanaka, R. L. Greene, B. M. Hoffman, J. A. Ibers, *J. Am. Chem. Soc.* **1987**, *109*, 1115.
[70] J. S. Miller, D. T. Glatzhofer, R. Laversanne, S. Chittipeddi, P. Vaca, T. B. Brill, M. D. Timken, C. J. O'Connor, J. H. Zhang, J. C. Calabrese, A. J. Epstein, *Chem. Mater.* **1990**, *2*, 60.
[71] G. Chouteau, C. Veyret-Jeandey, *J. Phys. (Paris)* **1981**, *42*, 1441.
[72] a) P. J. Brown, A. Capiomont, B. Gillon, J. Schweizer, *J. Magn. Magn. Mater.* **1979**, *14*, 289; b) A. Benoit, J. Flouquet, B. Gillon, J. Schweizer, *ibid.* **1983**, *31–33*, 1155.
[73] a) R. Chiarelli, A. Rassat, P. Rey, *J. Chem. Soc. Chem. Commun.* **1992**, 1081; b) R. Chiarelli, M. A. Novak, A. Rassat, J. L. Tholence, *Nature* **1993**, *363*, 147.
[74] Y. J. Uemura, L. P. Le, G. M. Luke, *Synth. Met.* **1993**, *56*, 2845.
[75] T. Sugano, T. Goto, M. Kinoshita, *Solid State Commun.* **1991**, *80*, 1021; K. Awaga, T. Inabe, Y. Maruyama, *Chem. Phys. Lett.* **1992**, *190*, 349; K. Awaga, T. Inabe, U. Nagashima, T. Nakamura, M. Matsumoto, Y. Kawabata, Y. Maruyama, *ibid.* **1992**, 1777.
[76] a) P. Allemand, K. Khemani, A. Koch, F. Wudl, K. Holczer, S. Donovan, G. Grüner, J. D. Thompson, *Science* **1991**, *253*, 301; P. W. Stephen, D. Cox, J. W. Lauher, L. Mihary, J. B. Wiley, P. Allemand, A. Hirsch, K. Holczer, Q. Li, J. D. Thompson, F. Wudl, *Nature* **1992**, *355*, 331; b) K. Tanaka, A. A. Zakhidov, K. Yoshizawa, K. Okahara, T. Yamabe, K. Yakushi, K. Kikuchi, S. Suzuki, I. Ikemoto, Y. Achiba, *Phys. Lett. A* **1992**, *164*, 221; c) K. Tanaka, A. A. Zakhidov, K. Yoshizawa, K. Okahara, T. Yamabe, K. Yakushi, K. Kikuchi, S. Suzuki, I. Ikemoto, Y. Achiba, submitted; d) J. D. Thompson, G. Sparn, F. Diederich, G. Grüner, K. Holczer, R. B. Kaner, R. L. Whetten, P. Allemand, Q. Chen, F. Wudl, *Mater. Res. Soc. Symp. Ser. Proc.* **1992**, *247*, 315.
[77] a) G. A. Candela, L. Swartzendruber, J. S. Miller, M. J. Rice, *J. Am. Chem. Soc.* **1979**, *101*, 2755; b) J. S. Miller, J. H. Zhang, W. M. Reiff, L. D. Preston, A. H. Reis, Jr., E. Gerbert, M. Extine, J. Troup, M. D. Ward, *J. Phys. Chem.* **1987**, *91*, 4344.
[78] E. Stryjewski, N. Giordano, *Adv. Phys.* **1977**, *26*, 487.
[79] J. S. Miller, J. C. Calabrese, H. Rommelmann, S. Chittapeddi, J. H. Zhang, W. M. Reiff, A. J. Epstein, *J. Am. Chem. Soc.* **1987**, *109*, 769.
[80] a) Z. J. Huang, F. Chen, Y. T. Ren, Y. Y. Xue, C. W. Chu, J. S. Miller, *J. Appl. Phys.* **1993**, *73*, 6563; b) J. M. Williams, A. J. Schultz, U. Geiser, K. D. Carlson, A. M. Kini, H. H. Wang, W.-K. Kwok, M.-H. Whangbo, J. E. Schirber, *Science* **1991**, *252*, 1501; G. Sparn, J. D. Thompson, R. L. Whetten, S.-M. Huang, R. B. Kaner, F. Diederich, G. Grüner, K. Holczer, *Phys. Rev. Lett.* **1992**, *68*, 1228; J. E. Schirber, D. L. Overmeyer, H. H. Wang, J. M. Williams, K. D. Carlson, A. M. Kini, U. Welp, W.-K. Kwok *Physica C (Amsterdam)* **1991**, *178*, 137; G. Sparn, J. D. Thompson, S.-M. Huang, R. B. Kaner, F. Diederich, G. Grüner, K. Holczer, *Science*, **1991**, *252*, 1829.
[81] G. T. Yee, J. M. Manriquez, D. A. Dixon, R. S. McLean, D. M. Groski, R. B. Flippen, K. S. Narayan, A. J. Epstein, J. S. Miller, *Adv. Mater.* **1991**, *3*, 309.
[82] W. E. Broderick, J. A. Thompson, E. P. Day, B. M. Hoffman, *Science* **1990**, *249*, 410.

[83] J. L. Robbins, N. Edelstein, B. Spencer, J. C. Smart, *J. Am. Chem. Soc.* **1982**, *104*, 1882.

[84] a) O. W. Webster, W. Mahler, R. E. Benson, *J. Am. Chem. Soc.* **1962**, *84*, 3678; M. Rosenblum, R. W. Fish, C. Bennett, *ibid.* **1964**, *86*, 5166; R. L. Brandon, J. H. Osipcki, A. Ottenberg, *J. Org. Chem.* **1966**, *31*, 1214; E. Adman, M. Rosenblum, S. Sullivan, T. N. Margulis, *J. Am. Chem. Soc.* **1967**, *89*, 4540; B. Foxman, Brandeis University, Watham, MA, USA, personal communication; B. W. Sullivan, B. Foxman, *Organometallics* **1983**, *2*, 187; b) J. S. Miller, J. C. Calabrese, W. M. Reiff, D. T. Glatzhofer, unpublished results.

[85] J. S. Miller, J. C. Calabrese, D. T. Glatzhofer, unpublished results.

[86] K. M. Chi, J. C. Calabrese, W. M. Reiff, J. S. Miller, *Organometallics* **1991**, *10*, 688.

[87] J. S. Miller, D. T. Glatzhofer, D. M. O'Hare, W. M. Reiff, A. Chackraborty, A. J. Epstein, *Inorg. Chem.* **1989**, *27*, 2930.

[88] J. S. Miller, J. H. Zhang, W. M. Reiff, *J. Am. Chem. Soc.* **1987**, *109*, 4584.

[89] E. Gerbert, A. H. Reis, J. S. Miller, H. Rommelmann, A. J. Epstein, *J. Am. Chem. Soc.* **1982**, *104*, 4403; J. S. Miller, P. J. Krusic, D. A. Dixon, W. M. Reiff, J. H. Zhang, E. C. Anderson, A. J. Epstein, *ibid.* **1986**, *108*, 4459.

[90] A. H. Reis, Jr., L. D. Preston, J. M. Williams, S. W. Peterson, G. A. Candela, L. J. Swartzendruber, J. S. Miller, *J. Am. Chem. Soc.* **1979**, *101*, 2756.

[91] J. S. Miller, D. A. Dixon, J. C. Calabrese, R. L. Harlow, J. H. Zhang, W. M. Reiff, S. Chittappeddi, M. A. Selover, A. J. Epstein, *J. Am. Chem. Soc.* **1990**, *112*, 5496.

[92] a) J. S. Miller, J. C. Calabrese, A. J. Epstein, *Inorg. Chem.* **1989**, *27*, 4230; b) J. S. Miller, J. C. Calabrese, A. J. Epstein, unpublished results; c) W. B. Heuer, D. O'Hare, M. L. H. Green, J. S. Miller, *Chem. Mater.* **1990**, *2*, 764.

[93] D. O'Hare, J. S. Miller, J. C. Green, J. C. Chadwick, *Organometallics* **1988**, *7*, 1335.

[94] J. S. Miller, R. S. McLean, C. Vazquez, G. T. Yee, K. S. Narayan, A. J. Epstein, *J. Mater. Chem.* **1991**, *1*, 479.

[95] K. S. Narayan, K. M. Kai, A. J. Epstein, J. S. Miller, *J. Appl. Phys.* **1991**, *69*, 5953; K. S. Narayan, B. G. Morin, J. S. Miller, A. J. Epstein, *Phys. Rev. B* **1992**, *46*, 6195.

[96] M. D. Burk, J. C. Calabrese, J. S. Miller, unpublished results.

[97] W. E. Broderick, J. A. Thompson, B. M. Hoffman, *Inorg. Chem.* **1991**, *30*, 2960.

[98] C. Vazquez, D. A. Dixon, J. C. Calabrese, J. S. Miller, *J. Org. Chem.* **1993**, *58*, 65.

[99] a) P. A. M. Dirac, *The Principles of Quantum Mechanics*, 2nd edition, Oxford University Press, Oxford, **1935**; b) P. A. M. Dirac, *Proc. R. Soc. London A* **1926**, *112*, 661.

[100] Though the observed T_c is in excellent agreement with this mean-field model prediction, and suggests similar exchange interactions are operating for both the $[MCp^*_2]^+[TCNE]^{\cdot-}$ M = Fe, Mn) systems, the Curie–Weiss θ value of 22.6 K observed for the $[MnCp^*_2]^{\cdot+}[TCNE]^{\cdot-}$ in the high-temperature regime does not scale with the increased magnitude of the spin (S) on the metallocene. Instead it is slightly less than the value of θ recorded for $[FeCp^*_2]^{\cdot+}[TCNE]^{\cdot-}$; hence these mean-field scaling models must be used with caution.

[101] Since as described earlier $J \propto 1/\Delta E^2_{AB}$ and since instead of the POMOs being involved in the charge-transfer excitation, the excitation involves the NHOMO and/or NLUMO; thus, the ΔE will be greater and J will be smaller.

[102] S. H. Liu, *J. Magn. Magn. Mater.* **1988**, *82*, B417.

[103] R. B. Stinchcombe in *Phase Transitions and Critical Phenomena* (Eds.: C. Domb, J. L. Lebowitz), Academic Press, London, **1983**, *7*, 152.

[104] K. S. Narayan, O. Heres, A. J. Epstein, J. S. Miller, *J. Magn. Magn. Mater.* **1992**, *110*, L6.

[105] a) J. L. Robbins, N. Edelstein, B. Spencer, J. C. Smart, *J. Am. Chem. Soc.* **1982**, *104*, 1882; b) F. G. N. Cloak, A. N. Dix, J. C. Green, R. N. Perutz, E. A. Seddon, *Organometallics*, **1983**, *2*, 1150.

[106] For $[V\{TCNE\}_x] \cdot y(CH_2Cl_2)$ a range of x and y is observed for preparations in different solvents and with different mole ratios of the starting materials; benzene in small amounts is present in some cases. For the material discussed herein $x \approx 2$; $y \approx 1/2$. Trace elements were determined by ICP: Fe 41 ppm), Co [none detected < 25 ppm)], Ni [none detected < 50 ppm)]. Cr 34 ppm).

[107] F. E. Luborsky, in *Ferromagnetic Materials Vol. 1* (Ed.: E. P. Woblfarth), North Holland, Amsterdam, **1980**, p. 452.

[108] A. J. Epstein, J. S. Miller, *Mol. Cryst. Liq. Cryst.* **1993**, *233*, 171; P. Zhou, J. S. Miller, A. J. Epstein, unpublished results.

[109] G. Engebretson, R. E. Rundle, *J. Am. Chem. Soc.* **1963**, *85*, 481.

[110] Z. Oblakowski, A. J. Epstein, M. Laridjani, J.-P. Pouget, J. S. Miller, unpublished results.

[111] a) E. Chudnovsky, *J. Magn. Magn. Mater.* **1988**, *64*, 5770; E. Chudnovsky, *ibid.* **1989**, *79*, 127 and references therein; b) P. Gebring, M. Salamon, A. Moral, J. Arnaudas, *Phys. Rev. B Condens. Matter* **1990**, *41*, 9134, and references therein

[112] a) P. Zhou, B. G. Morin, J. S. Miller, A. J. Epstein, *Phys. Rev. B* **1993**, *48*, 1325; b) P. Zhou, J. S. Miller, A. J. Epstein, *Phys. Lett. A* **1993**, *181*, 71.

[113] B. G. Morin, P. Zhou, C. Hahm, A. J. Epstein, J. S. Miller, *J. Appl. Phys.* **1993**, *73*, 5648.

[114] S. Long, J. S. Miller, A. J. Epstein, unpublished results.

[115] G. Du, J. Joo, A. J. Epstein, J. S. Miller, *J. Appl. Phys.* **1993**, *73*, 6566.

[116] J. Joo, J. S. Miller, A. J. Epstein, unpublished results.

[117] D. L. Huber, *Phys. Lett. A* **1971**, *37*, 285.

[118] N. F. Mott, E. Davis, *Electronic Processes in Noncrystalline Solids*, Clarendon, Oxford, **1979**.

[119] J. S. Miller, J. C. Calabrese, R. S. McLean, A. J. Epstein, *Adv. Mater.* **1992**, *4*, 498.

[120] See for example: M. Verdauger, M. Julve, A. Michalowicz, O. Kahn, *Inorg. Chem.* **1983**, *22*, 2624; M. Drillon, J. C. Gianduzzo, R. Georges, *Phys. Lett. A* **1983**, *96*, 413.

[121] a) R. A. Serota, P. A. Lee, *Phys. Rev. B Condens Matter* **1986**, *34*, 1806; R. Dickman, E. Chudnovsky, *ibid.* **1991**, *44*, 4397; b) J. Curely, R. Georges, M. Drillon, *ibid.* **1986**, *33*, 6243.

[122] P. Zhou, B. G. Morin, A. J. Epstein, R. S. McLean, J. S. Miller, *J. Appl. Phys.* **1993**, *73*, 6569.

[123] J. Curely, R. Georges, M. Drillion, *Phys. Rev. B Condens. Matter* **1986**, *33*, 6243.

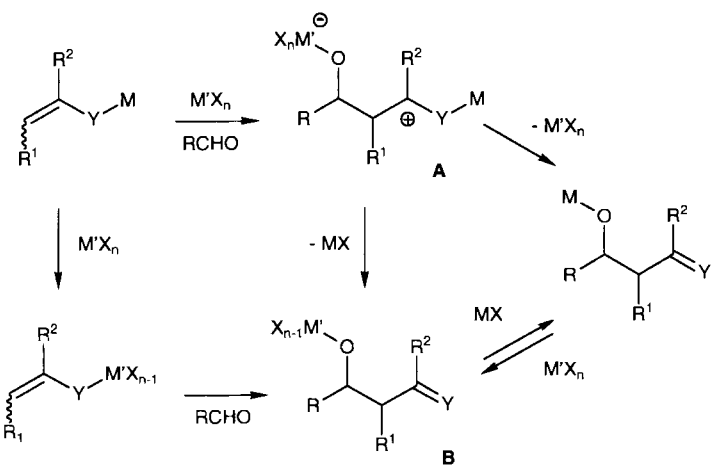
[124] J. S. Miller, A. J. Epstein, W. M. Reiff, *Mol. Cryst. Liq. Cryst.* **1986**, *120*, 27.

Catalytic Enantioselective C–C Coupling— Allyl Transfer and Mukaiyama Aldol Reaction

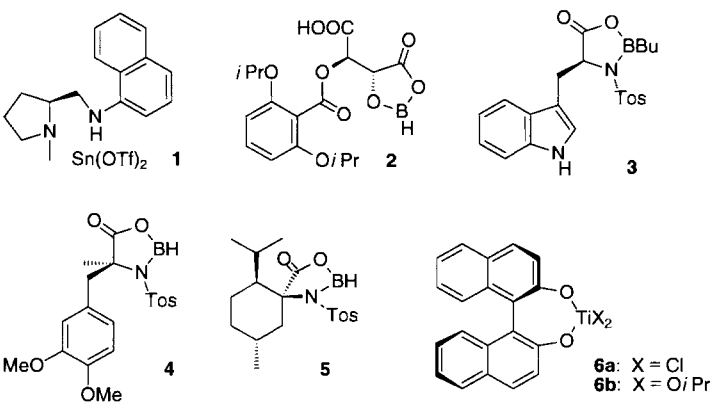
Thorsten Bach*

The search for a synthetic access to enantiomerically pure, naturally occurring products derived from polyketides has in the past years repeatedly pushed back the frontiers of organic chemistry. The allyl transfer[1] and aldol reaction[2] have been developed from these endeavors as the most elegant methods of extending the carbon framework. By now the relative and absolute configuration of the target molecule can be skillfully controlled in almost every case. Nevertheless, for enantioselective reaction courses, the stoichiometric use of chiral reagents can hardly be relinquished. A catalytic modification should remove this drawback. The strategy would be to employ a reagent that under normal conditions does not react with the substrate, but that undergoes a selective reaction under the influence of catalytic amounts of a chiral substance.

Certain metal compounds like silyl enol ethers[3] (Y = O, M = SiR_3), allyl silanes[1,4] (Y = CH_2, M = SiR_3), and allyl stannanes[1,4,5] (Y = CH_2, M = SnR_3) can indeed react specifically with carbonyl compounds in the presence of Lewis acids $M'X_n$, that is, they offer a catalytic alternative to conventional allyl transfer and aldol reactions (Scheme 1). The tiresome snag to this method is the choice of the suitable chiral Lewis acid catalyst. The demands made on such a miracle reagent are considerable. Under no circumstances may the catalyst react irreversibly with the products and substrates, because then it would be anchored to the oxygen atom of alcoholate **B** and would have to be used in stoichiometric amounts. During the reaction either an even stronger oxophile (MX) must form to procure the cleavage of the catalyst, or ideally, $M'X_n$ must activate only the carbonyl component. In the latter scenario, the metal transfer must proceed rapidly after the formation of a cationic intermediate **A**. Moreover, the catalytic activation of other nonchiral species like MX must be excluded. An additional requirement, and most often a more difficult task to solve, is the distinction between the two faces of the carbonyl compound, which must be as close to perfect as possible to guarantee high *ee* values; that is, one side of the prochiral carbonyl compound must be efficiently shielded. In fact, almost all the procedures with Lewis acids employed today (Scheme 2) fulfill the last demand; a lower priority was assigned to the attempt to introduce suitable modifications so that a catalytic enantioselective method may be developed. For this reason the often relatively large amounts of catalyst required reflect a compromise that is justifiably eyed critically, and that is dominated by the desire for a sufficiently fast, enantioselective reaction.



Scheme 1. Catalysis of the allyl transfer and the Mukaiyama aldol reaction by a Lewis acid $M'X_n$.



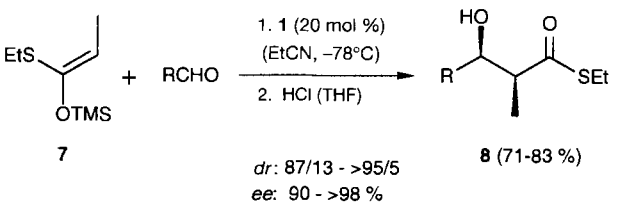
Scheme 2. Common chiral catalysts for enantioselective C–C coupling (Tos: toluenesulfonate; Tf: trifluoromethanesulfonate).

For a long time the enantiomeric excesses achieved with Mukaiyama aldol reactions were not particularly high. At the beginning of the 90s, however, two communications simultaneously heralded good news. Mukaiyama et al. had succeeded in

[*] Dr. T. Bach
Organisch-chemisches Institut der Universität
Orléansring 23, D-48149 Münster (FRG)
Telefax: Int. code + (251)83-9772

 © VCH Verlagsgesellschaft mbH, D-69451 Weinheim, 1994 0570-0833/94/0404-0417 $ 10.00+.25/0

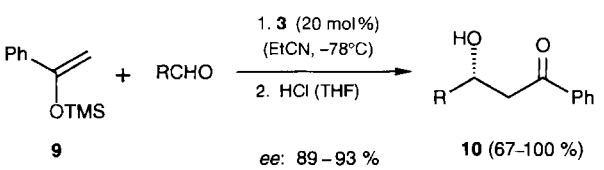
achieving the catalytic Sn^{II}-initiated transformation of the thioketal **7** (TMS = Me_3Si) by the use of propionitrile as solvent and slow addition of the electrophile.[6] The choice of solvent seems to be crucial for a successful catalytic cycle. In the reaction **7** → **8**, an intermediate analogous to **B** is probably formed, which reacts with TMSOTf (MX) to regenerate the Lewis acid **1**. Propionitrile appears to influence this process positively and prevents—together with the dosage of the reagent—too high a concentration of the likewise catalytic TMSOTf. This solvent was used in almost all subsequent investigations. The control of the simple diastereoselectivity is good, and after desilylation the corresponding *syn* products **8** are furnished in excellent enantiomeric excesses. The ketene acetal stereoisomeric to **7** yields poorer results.



7 *dr*: 87/13 - >95/5 *ee*: 90 - >98 % **8** (71-83 %)

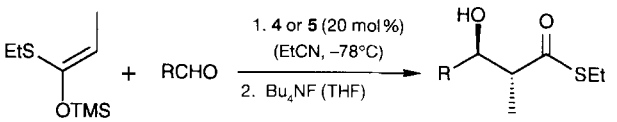
A little later H. Yamamoto et al. reported the reaction of silyl enol ethers with aldehydes in the presence of the previously known chiral acyloxyborane complex **2** (CAB).[7] The β-hydroxy-α-methylcarbonyl compounds are also obtained predominantly in the *syn* configuration (diastereomeric ratio *dr*: 80/20–95/5; *ee*: 80–96%). The *E*/*Z* configuration of the olefin is immaterial for the relative configuration of the products, and this stereoconvergent course of reaction probably proceeds via open-chain transition states. Unsubstituted silyl enol ethers and ketene acetals were tested with slightly smaller success (*ee*: 80–85%). The methyl-substituted ketene acetal prepared from phenyl propionate afforded the best results with α,β-unsaturated aldehydes (*dr*: >95/5; *ee* 94–97%).

A series of recent papers make use of chiral oxazaborolidine catalysts.[8, 9] The stoichiometric conversions of Kiyooka et al.[10] were followed by the first substoichiometric process of Masamune et al.[11] and other catalytic variants of Corey et al.[12] and Kiyooka et al.[13] Corey et al.[12] used mainly unsubstituted silyl enol ethers **9** and from them they obtained **10** in good enantiomeric excesses.[12a]



9 *ee*: 89–93 % **10** (67–100 %)

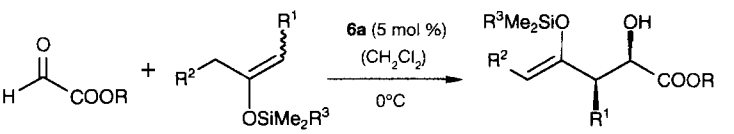
Ketene acetals are too reactive and afford only unsatisfactory *ee* values. In accord with results of prior studies on the asymmetric Diels–Alder reaction, the electrophile attacks from the *re* side.[12b] Masamune et al. achieved good results with **5** as catalyst also for unsubstituted ketene acetals (81–93% *ee*).[11b] Interestingly, from ketene acetals with the (*O*)-*E* configuration predominantly *anti* products like **11** are isolated, which, however, arise in only average enantiomeric excesses.[11, 13] Nevertheless, for the first time this system offers an acceptable enan-



7 *dr*: 66/33 - 91/9 *ee*: 60 - 89 % **11** (78-94 %)

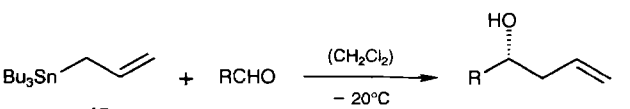
tioselective solution of the *anti* configuration problem, whereas—as we have seen—a few synthesis paths had already been opened up for *syn*-β-hydroxy-α-methylcarbonyl compounds and their α-unsubstituted counterparts. With respect to the direction of the asymmetric induction, the surprising reversal of the side differentiation on use of **4** and **5** as opposed to **3** may be explained by a rotation of the aldehyde about the coordinate O–B bond.[12b, 14] Other transition states were also discussed in this context.[13]

A reaction path that is different from a mechanistic point of view can also lead to β-hydroxycarbonyl compounds, as Mikami et al. recently reported.[15] The reaction of glyoxylate **12** with the silyl enol ethers **13** yields, in the presence of **6a**, aldol products that can be isolated on careful workup as silyl enol ethers **14**. The reaction is stereoconvergent and yields *syn* adducts. The absolute configurations of **14** are the same as those of the products of conventional ene reactions catalyzed with **6a**.[16] An alternative mechanistic interpretation to a pericyclic process is an intramolecular proton abstraction from the intermediate **A**.[17]



12 R = Me, Bu **13** R^1 = H, Me R^3 = Me, *t*Bu *dr*: 73/27 - 99/1 *ee*: 77 - >99 % **14** (54-73 %)

A crucial breakthrough in the area of allyl transfer was achieved with catalyst **6**. After the CAB complex **2** developed by Yamamoto et al. already had given respectable enantiomeric excesses for some transformations of allyl silanes and stannanes,[18] Keck et al.[19] and Tagliavini, Umani-Ronchi et al.[20] discovered almost simultaneously that the allyl stannane **15** undergoes highly selective reactions with diverse aldehydes. Keck et al.'s catalyst was the diisopropoxide **6b**, whereas the Italian group employed the dichloride **6a**.



15 **16**

6b (10 mol%): *ee*: 77 - 96 % **16** (78-99 %)
ent-**6a** (20 mol%): *ee*: 80 - 98 % *ent*-**16** (75-96 %)

 © VCH Verlagsgesellschaft mbH, D-69451 Weinheim, 1994 0570-0833/94/0404-0418 $ 10.00+.25/0

Interestingly, the direction of the asymmetric induction is in accord with results of Mikami et al.[15,16] In contrast to the ene reaction, the 4 Å molecular sieve used in the preparation of the catalyst has some significance for the selectivity and rate of this reaction.[20] This new process appears to be suitable for many applications because of the really broad range of substrates that it can convert, and it is likely to stimulate several new impulses both in methodology and in synthesis.

German version: *Angew. Chem.* **1994**, *106*, 433

[1] Y. Yamamoto, N. Asao, *Chem. Rev.* **1993**, *93*, 2207–2293.

[2] C. H. Heathcock, B. M. Kim, S. F. Williams, S. Masamune, M. W. Rathke, P. Weipert, I. Paterson in *Comprehensive Organic Synthesis, Vol. 2* (Ed.: B. M. Trost). Pergamon, Oxford, **1991**, p. 133–319.

[3] C. Gennari in *Comprehensive Organic Synthesis, Vol. 2* (Ed.: B. M. Trost), Pergamon, Oxford, **1991**, p. 629–660.

[4] I. Fleming in *Comprehensive Organic Synthesis, Vol. 2* (Ed.: B. M. Trost), Pergamon, Oxford, **1991**, p. 563–593.

[5] Y. Nishigaichi, A. Takuwa, Y. Naruta, K. Maruyama, *Tetrahedron* **1993**, *49*, 7395–7426.

[6] a) S. Kobayashi, Y. Fujishita, T. Mukaiyama, *Chem. Lett.* **1990**, 1455–1458; b) S. Kobayashi, H. Uchiro, I. Shiina, T. Mukaiyama, *Tetrahedron* **1993**, *49*, 1761–1772, and references therein.

[7] a) K. Furuta, T. Maruyama, H. Yamamoto, *J. Am. Chem. Soc.* **1991**, *113*, 1041–1042; b) *Synlett* **1991**, 439–440; c) After this overview had been completed, a mechanistic investigation on CAB-catalyzed transformations appeared: K. Ishihara, Q. Gao, H. Yamamoto, *J. Am. Chem. Soc.* **1993**, *115*, 10412–10413.

[8] B. B. Lohray, V. Bhushan, *Angew. Chem.* **1992**, *104*, 740–741; *Angew. Chem. Int. Ed. Engl.* **1992**, *31*, 729–730.

[9] a) L. Deloux, M. Srebnik, *Chem. Rev.* **1993**, *93*, 763–784; b) S. Wallbaum, J. Martens, *Tetrahedron: Asymmetry* **1992**, *3*, 1475–1504.

[10] S. Kiyooka, Y. Kaneko, M. Komura, H. Matsuo, M. Nakano, *J. Org. Chem.* **1991**, *56*, 2276–2278.

[11] a) E. R. Parmee, O. Tempkin, S. Masamune, A. Abiko, *J. Am. Chem. Soc.* **1991**, *113*, 9365–9366; b) E. R. Parmee, Y. Hong, O. Tempkin, S. Masamune, *Tetrahedron Lett.* **1992**, *33*, 1729–1732.

[12] a) E. J. Corey, C. L. Cywin, T. D. Roper, *Tetrahedron Lett.* **1992**, *33*, 6907–6910; b) E. J. Corey, T.-P. Loh, T. D. Roper, M. D. Azimioara, M. C. Noe, *J. Am. Chem. Soc.* **1992**, *114*, 8290–8292.

[13] S. Kiyooka, Y. Kaneko, K. Kume, *Tetrahedron Lett.* **1992**, *33*, 4927–4930.

[14] D. Sartor, J. Saffrich, G. Helmchen, C. J. Richards, H. Lambert, *Tetrahedron: Asymmetry* **1991**, *2*, 639–642.

[15] K. Mikami, S. Matsukawa, *J. Am. Chem. Soc.* **1993**, *115*, 7039–7040.

[16] K. Mikami, M. Tereda, S. Narisawa, T. Nakai, *Synlett* **1992**, 255–265.

[17] H. Shoda, T. Nakamura, K. Tanino, I. Kuwajima, *Tetrahedron Lett.* **1993**, *34*, 6281–6284.

[18] a) K. Furuta, M. Mouri, H. Yamamoto, *Synlett* **1991**, 561–562; b) J. A. Marshall, Y. Tang, *ibid.* **1992**, 653–654.

[19] a) G. E. Keck, K. H. Tarbet, L. S. Geraci, *J. Am. Chem. Soc.* **1993**, *115*, 8467–8468; b) extension to methallylstannanes: G. E. Keck, D. Krishnamurthy, M. C. Grier, *J. Org. Chem.* **1993**, *58*, 6543–6544.

[20] A. L. Costa, M. G. Piazza, E. Tagliavini, C. Trombini, A. Umani-Ronchi, *J. Am. Chem. Soc.* **1993**, *115*, 7001–7002. The complex enantiomeric to **6a** was used with the result that the products have the opposite configuration.

Making and Breaking of Si–E (E = C, Si) Bonds by Oxidative Addition and Reductive Elimination Reactions

Ulrich Schubert*

The making and breaking of silicon–element bonds in the coordination sphere of transition metals is a preparative tool which is becoming increasingly interesting for transformations of organosilicon compounds. While metal-catalyzed addition of Si–H bonds to unsaturated organic groups ("hydrosilylation") is well established, other metal-mediated stoichiometric or catalytic reactions of organosilicon compounds are becoming more and more important. This is particularly true for reactions involving Si–E bonds, where E is a group IV element (mainly C or Si), because of the growing interest in making or modifying polymers containing Si–E bonds.

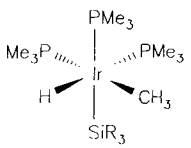
There are mainly two ways in which silicon–element bonds can be formed or broken in catalytic reactions: σ-bond metathesis[1] and oxidative addition/reductive elimination. The latter type of reaction has received much attention for C–C, C–H, and C–halogen bonds in organometallic chemistry, because it constitutes a key step in many catalytic reactions. In comparison, surprisingly little is known about the oxidative addition and reductive elimination of silicon–element bonds, with the exception of Si–H bonds.

[*] Prof. Dr. U. Schubert
Institut für Anorganische Chemie der Universität
Am Hubland, D-97074 Würzburg (FRG)
Telefax: Int. code + (931)888-4605

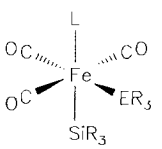
There are very few examples for the reductive elimination of Si–C or Si–Si bonds from isolated complexes. A very recent article by Milstein et al.[2] and prior results on a related system[3] provide new evidence for answering the still unresolved question: What conditions are required to make these elimination reactions occur in a particular complex? The complexes **1** are a particularly interesting class of compounds, because, in principle, H–CH_3, H–SiR_3, or H_3C–SiR_3 could be eliminated. The elimination behavior was found to depend very much on the electronic properties of the SiR_3 ligand. While both the $Si(OEt)_3$ and the $SiPh_3$ derivatives exclusively liberate CH_4 on heating, the $SiEt_3$ derivative gives CH_4 *and* $MeSiEt_3$ in a 4:1 ratio.[2] The Rh analogue (only formed as an intermediate) behaves similarly.[3] The different behavior of the SiR_3 complexes was attributed to the different M–Si bond (M = metal) strengths. Electron-donating groups at the silicon atom weaken the M–Si bond and make Si–C elimination competitive with C–H elimination. It should be noted that no H–SiR_3 elimination is observed.

A related problem was encountered when the reductive elimination of R_3E–SiR'_3 from the complexes **2** (E = C, Si, Sn; L = CO, PPh_3) was studied.[4] The ER_3 groups had a pronounced influence on the kind of products formed. Reductive elimination was only observed for the alkyl(silyl) derivatives

mer-$[(CO)_3LFe(CH_3)ER_3]$ (E = Si). The reactivity of the corresponding bis(silyl) (E = Si) or silyl(stannyl) complexes (E = Sn) is much more complicated. Depending on the substituents at the silicon atom and the ligand L, a variety of products was formed; however, reductive elimination was never observed. Disiloxanes or siloxystannanes were the only organosilicon products formed besides various metal complexes; the oxygen atom stems from one of the CO ligands.



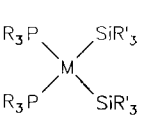
1



2

A recent ab initio MO study, in which the oxidative addition reactions (the reversal of the reductive eliminations) of C–H, C–C, and Si–E bonds (E = H, C, Si) to $Pt(PH_3)_2$ were compared,[5] sheds light on the energetics of such reactions and may lead to an understanding of some of these observations. The exothermicity, which can be predicted from the bond energies, decreases in the order Si–Si > Si–H > Si–C > C–C > C–H (for the hydrogen-substituted compounds), while the activation barrier was found to increase in the order Si–H < Si–Si < C–H ≈ Si–C ≪ C–C. In the Si–H oxidative addition the Pt–H bond can be formed without having to completely break the Si–H bond, due to the spherical valence orbital of the H atom. The reaction therefore proceeds with a small activation barrier. Although the Si–Si oxidative addition is much more exothermic, the activation barrier is much higher; this mainly results from the distortion of $H_3Si–SiH_3$ at the transition state. The SiH_3 group must shift the direction of the highly directional sp^3 valence orbital of SiH_3 to form the bond with the metal atom.

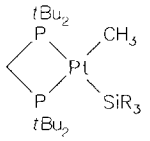
From these results it is clear that to get disilane eliminations, alternative reactions with lower activation barriers or thermodynamically more favorable products must be avoided. It is apparent that the reaction channel leading to oxygen-containing products can be switched off if complexes without CO ligands are used. Reductive elimination of disilanes was indeed observed for a few CO-free complexes. In complexes of the type **3** (M = Pd, Pt) the kind of metal center and ligands influenced the elimination reactions as predicted: more electron-donating and/or less sterically demanding ligands in *cis*-$[(R_3P)_2Pt(SiMe_2Ph)_2]$ resulted in thermally more stable bis(silyl) complexes, that is, complexes less prone to the reductive elimination of the disilane.[6] The corresponding palladium complexes, for example, *cis*-$[(MePh_2P)_2Pd(SiHPh_2)_2]$ were much more labile than the platinum complexes, as expected, and readily decomposed by elimination of the disilane $HPh_2Si–SiPh_2H$.[7] The elimination of $MeSiPh_2H$ from $[(MePh_2P)_2Pd(Me)SiHPh_2]$ was also observed.[7]



3

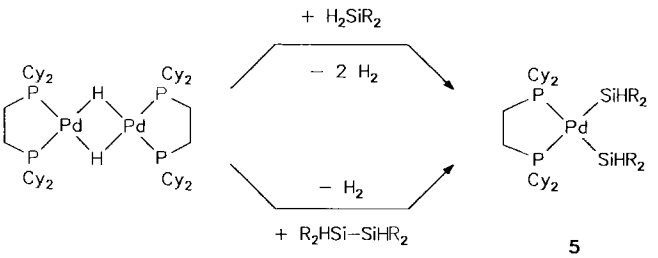
There are only a few examples in which the oxidative addition of Si–C or Si–Si bonds has resulted in stable metal complexes. The preparation of bis(silyl) or alkyl(silyl) complexes by such reactions is not only a question of bond activation, but also of stabilizing the obtained complexes with regard to reductive elimination. Electronic and steric factors favoring reductive eliminations disfavor oxidative additions, and vice versa. Oxidative additions are facilitated by heavy transition metals (which are easier to oxidize), by a high electron density at the metal center, and by small ancillary ligands. Furthermore, oxidative additions of organosilicon compounds are also promoted by electronegative substituents at the silicon atom. It is therefore not surprising that halogenated disilanes were employed in nearly all examples for the formation of stable bis(silyl) complexes by oxidative addition of disilanes.[8]

However, there are additional possibilities to make oxidative additions of Si–E bonds easier. Hofmann et al. generated the 14-electron species [(dtbpm)Pt] (dtbpm = $tBu_2PCH_2PtBu_2$), in which the small P-Pt-P angle both raises the total energy and changes the frontier orbitals relative to the corresponding complexes with linear phosphane ligands $[(R_3P)_2Pt]$. With the "hot" (dtbpm)Pt species the activation of Si–C bonds is possible under mild conditions. The complexes **4** (SiR_3 = $SiMe_3$, Si_2Me_5, $SiMe_2OSiMe_3$) were obtained at room temperature from the corresponding methylsilanes.[9] In the light of the above-mentioned energetics, it is rather surprising that in the reaction with Si_2Me_6 the Si–C bond was exclusively added to the metal, but not the Si–Si bond.



4

Distortion of the structure of the metal fragment also stabilized the bis(silyl) palladium complexes with regard to reductive elimination. Unlike the $[(MePh_2P)_2Pd(SiHPh_2)_2]$ complexes with nonchelating phosphane ligands, the bis(silyl) complexes $[(dcpe)Pd(SiHR_2)_2]$ (**5**) (dcpe = $Cy_2PCH_2CH_2PCy_2$) were very stable and could even be prepared by oxidative addition of $HR_2Si–SiR_2H$ to $[\{(dcpe)Pd\}_2(\mu\text{-}H)_2]$.[10]



5

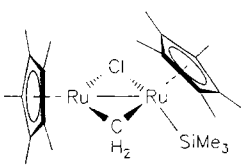
In the 1970s Lappert et al.[11] and Sakurai et al.[12] obtained 1-sila-2-ferracyclopentanes and 1,3-disila-2-ferracyclopentenes, respectively, by insertion of $[Fe(CO)_4]$ into the Si–C bond of silacyclobutanes or the Si–Si bond of 1,2-disilacyclobutenes, respectively. C. S. Liu et al. developed a rich chemistry by reacting 1,1,2,2-tetrafluoro-3-*tert*-butyl-1,2-disilacyclobutene with a variety of transition metal complexes.[13] Oxidative addition of the Si–Si bond is often the primary step in these reactions. The reactivity of the Si–C or Si–Si bond in the four-membered rings is increased by the ring strain, and the stability of the oxidative addition products is high, because reductive elimination is very unfavorable.

A final possibility to promote oxidative addition is to use the chelate effect (chelate-assistance). For example, oxidative addition of the Si–H bond of $Ph_2PCH_2CH_2SiR_2H$ results in com-

plexes with the chelating phosphinoalkylsilyl ligands, in which the reductive elimination of the R_3Si-H bond is not favored by entropy, as in the corresponding nonchelated complexes.[14] "Chelate-assistance" could certainly also make the oxidative addition of other bonds to transition metal center easier. This was recently demonstrated for Sn–C bonds;[15] however, there is no example for Si–C or Si–Si bonds yet.

The tools to tune the ability of a metal complex fragment to undergo oxidative addition reactions with Si–E bonds (or to influence the stability of metal complexes with regard to reductive elimination, respectively) are in principle known. However, most of these parameters also influence the oxidative addition behavior of other groups present in the reactants (for instance, C–C or C–H bonds). The challenge ahead is to control the selectivity and thus make oxidative addition (reductive elimination) of Si–E bonds more predictable. In most of the known examples the reaction proceeds in only one direction, that is, oxidative addition *or* reductive elimination of the Si–E unit. For the better understanding of Si–H oxidative additions and reductive eliminations the investigation of reversible reactions was very beneficial. It might be also helpful in finding such reactions for Si–E bonds.

In this context the recent observation of a reversible C–Si bond cleavage in a dinuclear complex is remarkable. Treatment of $[\{Cp^*RuCl\}_4]$ ($Cp^* = C_5Me_5$) with $Mg(CH_2SiMe_3)_2$ resulted in the complex **6**. There was NMR spectroscopic evidence for a reversible migration of the $SiMe_3$ group to the methylene carbon atom, leading to the reformation of the Si–C bond. Reformation of the Si–C bond was also achieved by reaction with PMe_3, CO, or F_3CCOOH.[16]



6

Intramolecular activation of Si–E bonds in metal complexes is still an underdeveloped area. Rapid progress is predicted for the near future, because the known examples spectacularly show that these reactions may be very relevant to catalytic processes. While the above example is the only one for an intramolecular Si–C activation, there is now convincing evidence that Si–Si bonds both in α and β positions with respect to the metal center are activated. Several groups have shown that disilanyl complexes $[L_nM-SiR_2SiR_3]$ may rearrange via intermediate silyl(silylene) complexes $[L_nM(=SiR_2)SiR_3]$, if L_nM is an electron-deficient fragment.[17] The cleavage of the β-Si–Si bond was similarly postulated for the rearrangement of complexes of the type $[L_nM\text{-}CH_2SiR_2SiR_3]$.[18] It is assumed that intermediate silyl(silene) complexes $[L_nM(SiR_3)(\eta^2\text{-}SiR_2CH_2)]$ are formed by SiR_3 migration. From the available evidence, α-Si–Si bonds seem to be more active than β-Si–Si bonds and β-Si–Si bonds more active than α-Si–C bonds.

German version: *Angew. Chem.* **1994**, *106*, 435

[1] H.-G. Woo, J. F. Walzer, T. D. Tilley, *J. Am. Chem. Soc.* **1992**, *114*, 7047.
[2] M. Aizenberg, D. Milstein, *Angew. Chem.* **1994**, *106*, 344; *Angew. Chem. Int. Ed. Engl.* **1994**, *33*, 317.
[3] D. L. Thorn, R. L. Harlow, *Inorg. Chem.* **1990**, *29*, 2017.
[4] K. C. Brinkman, A. J. Blakeney, W. Krone-Schmidt, J. A. Gladysz, *Organometallics* **1984**, *3*, 1325; U. Schubert, E. Kunz, M. Knorr, J. Müller, *Chem. Ber.* **1987**, *120*, 1079; U. Schubert, M. Knorr, C. Strasser, *J. Organomet. Chem.* **1991**, *411*, 75.
[5] S. Sakaki, M. Ieki, *J. Am. Chem. Soc.* **1993**, *115*, 2373.
[6] T. Kobayashi, T. Hayashi, H. Yamashita, M. Tanaka, *Chem. Lett.* **1988**, 1411.
[7] U. Schubert, C. Müller, *J. Organomet. Chem.* **1989**, *383*, 165.
[8] For instance: T. J. Groshens, K. J. Klabunde, *Organometallics* **1982**, *1*, 564; T. R. Bierschenk, M. A. Guerra, T. J. Juhlke, S. B. Larson, R. J. Lagon, *J. Am. Chem. Soc.* **1987**, *109*, 4855.
[9] P. Hofmann, H. Heiss, P. Neiteler, G. Müller, J. Lachmann, *Angew. Chem.* **1990**, *102*, 935; *Angew. Chem. Int. Ed. Engl.* **1990**, *29*, 880.
[10] Y. Pan, J. T. Mague, M. J. Fink, *Organometallics* **1992**, *11*, 3495.
[11] C. S. Cundy, M. F. Lappert, J. Dubac, P. Mazerolles, *J. Chem. Soc. Dalton Trans.* **1976**, 910; C. S. Cundy, M. F. Lappert, *ibid.* **1976**, 665.
[12] H. Sakurai, T. Kobayashi, Y. Nakadaira, *J. Organomet. Chem.* **1978**, *162*, C43.
[13] For instance: C. Y. Huang, C. S. Liu, *J. Organomet. Chem.* **1989**, *373*, 353; K. M. Horng, S. L. Wang, C. S. Liu, *Organometallics* **1991**, *10*, 631.
[14] S. L. Grundy, R. D. Holmes-Smith, S. R. Stobart, M. A. Williams, *Inorg. Chem.* **1991**, *30*, 3333.
[15] C. Müller, U. Schubert, *Chem. Ber.* **1991**, *124*, 2181; U. Schubert, S. Grubert, U. Schulz, S. Mock, *Organometallics* **1992**, *11*, 3165.
[16] W. Lin, S. R. Wilson, G. S. Girolami, *J. Am. Chem. Soc.* **1993**, *115*, 3022.
[17] K. H. Pannell, J. Cervantes, C. Hernandez, J. Cassias, S. Vincenti, *Organometallics* **1986**, *5*, 1056; H. Tobita, K. Ueno, M. Shimoi, H. Ogino, *J. Am. Chem. Soc.* **1990**, *112*, 315; A. Haynes, M. W. George, M. T. Haward, M. Poliakoff, J. J. Turner, N. M. Boag, M. Green, *ibid.* **1991**, *113*, 2011; H. Yamashita, M. Tanaka, M. Goto, *Organometallics* **1992**, *11*, 3227; M. J. Michalczyk, C. A. Recatto, J. C. Calabrese, M. J. Fink, *J. Am. Chem. Soc.* **1992**, *114*, 7955.
[18] K. H. Pannell, T. Kobayashi, R. N. Kapoor, *Organometallics* **1992**, *11*, 2229.

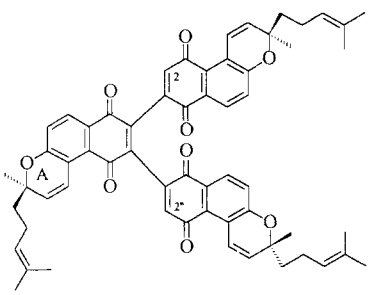
 © VCH Verlagsgesellschaft mbH, D-69451 Weinheim, 1994 0570-0833/94/0404-0421 $ 10.00+.25/0

Conocurvone—Prototype of a New Class of Anti-HIV Active Compounds?**

Hartmut Laatsch*

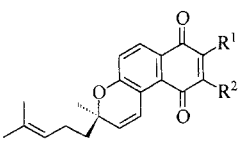
Workers at the National Cancer Institute recently achieved a remarkable success in their search for active plant metabolites. During routine screening, extracts of a shrub indigenous to Australia were noted for their exceptionally high, and, more importantly, selective anti-HIV activity in a variety of cellular in vitro tests. The substance responsible for this effect was the naphthoquinone conocurvone **1a**, which was isolated after an elaborate purification procedure in a yield of 22 mg per kg plant material (*Conospermum sp. Proteaceae*).[1]

As fluorescence tests with BCECF (2',7'-bis-2(2-carboxyethyl)-4(5)-carboxyfluorescein), the XTT–tetrazolium test, and a test with the intercalating dye DAPI (4',6-diamidino-2-phenylindole dihydrochloride) showed, the presence of conocurvone **1a** at a concentration of $EC_{50} \leq 0.02$ μM completely averted the death of HIV1-infected human lymphoblastoid cells (CEM–SS). Measurements of viral reverse transcriptase, the viral P24 antigen, and the syncytium forming units (SFU) revealed that virus replication came to a standstill at the same time. Since conocurvone **1a** is cytotoxic and inhibits growth only at or above a concentration of 50 μM, the therapeutic index has the unusually high value for a virostatic of 2500. Whether this value also holds for other viruses, or is limited to HIV-1 viruses, was not reported.



1a

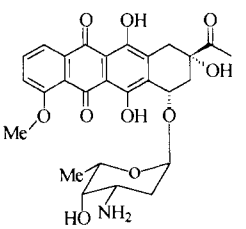
1b: Hydrogen instead of ring A



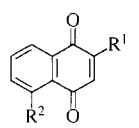
2a: R^1 = OH, R^2 = H
2b: $R^1 = R^2$ = H
2c: R^1 = H, R^2 = *p*-$O_2CC_6H_4Br$
2d: $R^1 = R^2 = SC_6H_5$

Conocurvone **1a** is a deoxy-trimer of teretifolion B (**2a**), a compound that has been known for longer and was first isolated from *Conospermum teretifolium*. The fast atom bombardment (FAB) mass spectrum of the trimeric quinone revealed a molecular ion corresponding to the formula $C_{60}H_{56}O_{11}$, but the structure of **1a** was in the end only fully elucidated by synthesis. The reason for this was that atropoisomeric equilibria were formed and led to more or less complex ^1H NMR spectra that varied with solvent and with temperature. The compound therefore appeared to be a complex mixture. However, the synthetic product was identical to the natural material, even in its chiroptical parameters, thus confirming the structure and also the low rotation barrier around the quinone–quinone axis, a property which has also been found for other quinonoid-quinonoid-coupled oligomers.

Quinones constitute an extremely important group of natural products. They are one of the oldest known classes of compounds, have achieved importance as dyestuffs, and in addition possess many different biological activities: many quinones are active as antibiotics, are cytotoxic (like daunomycin (**3**), or are (weakly) antiviral. Even simple compounds such as plumbagin (**4a**) prove to be highly effective and selective as enzyme inhibitors. For other quinones the activity derives from interaction with physiological redox systems, or—at least for unsubstituted quinonoid double bonds—from the reaction with nucleophiles.[2]



3



4a: R^1 = Me, R^2 = OH
4b: R^1 = H, R^2 = OH
4c: R^1 = OH, R^2 = H

In the case of conocurvone (**1a**) a physiological effect has once again been found for an oligomeric quinone, which is completely absent for the monomer **2a**. This must therefore be a new property that arises from the *oligomerization*, and should thus stimulate renewed interest in oligonaphthoquinone synthesis. A brief outline of the current state of knowledge about this class of substances is hence justified.

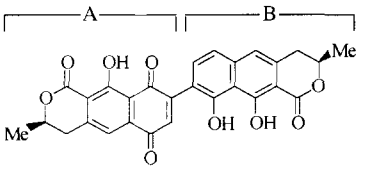
In all but a few cases (one of which is **1a**), the over seventy naturally occurring dimeric, trimeric, *cyclo*-trimeric, and higher oligomers are all constructed of identical units derived from juglone (**4b**, 5-hydroxynaphthoquinone). These units are linked together in various ways, symmetrically or asymmetrically with respect to the C–C framework. With the exception of crisamicin A, all these compounds have an oxygen atom in the *ortho* position to the linkage site.

The reason for this variety lies in the mechanism of formation of dimeric quinones, which may be regarded as a phenol oxidation. The synthesis starts from substituted naphthols, such as **5b**, and leads, depending on the initial substrate and the enzymes of the organism concerned, not only to the monomeric quinone but via binaphthols (e.g. vioxanthin (**5c**)) also to dimeric (e.g. xanthomegnin (**5d**)) or oligomeric quinones. It also yields the polymeric, black allomelanin, which gives ebony, for instance, its characteristic color. This pathway is confirmed by the presence—often in the same organism—of dimers with lower oxidation states, which are formal intermediates in diquinone

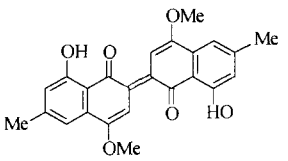
[*] Prof. Dr. H. Laatsch
Institute of Organic Chemistry
Tammannstrasse 2, D-37077 Göttingen (FRG)
Telefax: Int. code + (551)39-9660

 © VCH Verlagsgesellschaft mbH, D-69451 Weinheim, 1994 0570-0833/94/0404-0422 $ 10.00+.25/0

biosynthesis: examples are the monoquinone viomellein **5a** and the binaphthylidenedione (**6**, diosindigo A).



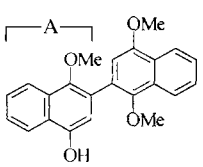
5a ≙ A–B
5b: only component B
5c: B instead of A in **5a**
5d: A instead of B in **5a**



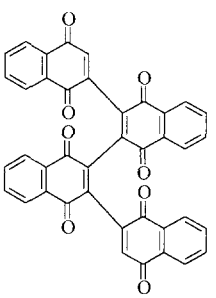
6

In nature, the oxidative dimerization of phenols is controlled by enzymes, as is demonstrated by the axial chirality of the 6,8′-coupled juglone derivative isodiospyrin. In synthesis, however, phenol oxidation only proceeds in high yields when the enzymatic reaction control is replaced by substituent control, that is, if all but one of the positions with high spin density in the radical (*ortho* and *para* positions) are blocked.

The synthetic usefulness of this principle is well documented by numerous examples, even under biomimetic conditions.[3] In this way, using a similar synthetic sequence by co-oxidation of **7a** and **7b**, we have obtained not only the dimers, but also quinones **8a** and **8b**. These are related to conocurvone **1a**, but their antiviral properties have not yet been studied.



7a
7b: only component A

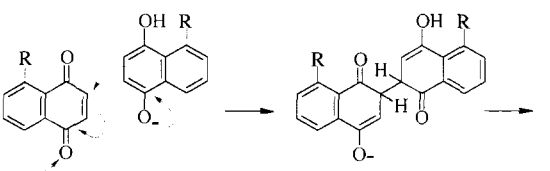


8a
8b: trimer instead of tetramer

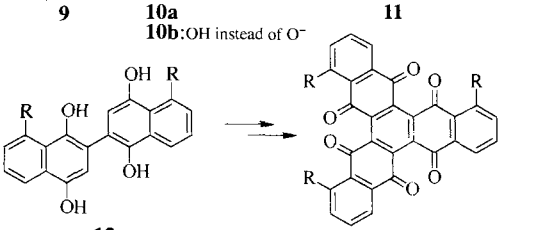
Unlike in the case of phenols, direct oxidative dimerization of quinones only takes place under drastic conditions and requires a hydroxy or amino group on the quinonoid double bond, as in Lawson **4c**, the dye in Arabian henna. Since the work of Pummerer (1937), however, it has been known that monomeric 1,4-quinones can be oligomerized much more easily under acidic or basic conditions.[5] In pyridine/ethanol, or by warming in glacial acetic acid, we have converted naphthoquinone, 1,4-anthraquinone, and numerous derivatives—though not benzoquinones—smoothly into dimers and *cyclo*-trimers. In this highly regioselective reaction, juglone (**4b**) and several of its derivatives afford exclusively the symmetrical 3,3′-linked dimers, several of which were already known as natural products.[6] It was only recently discovered that *o*-quinones may also be dimerized by this principle.[7]

According to Brockmann, this process is an autocatalytic one, in which traces of hydroquinone, which are always present, undergo a Michael addition to the excess of quinone to form a biaryltetrol (**12**),[8] an intermediate which also occurs during phenol oxidation. Dehydrogenation of this intermediate by the monomeric quinone yields the biaryldiquinone and further hydroquinone, until all the monomeric quinone has been transformed ($3\,\mathbf{9} + x\,\mathbf{10c} \rightarrow \mathbf{12c} + \mathbf{10b}$). When air is excluded, conversions of naphthoquinone reach 90%; when air is present, or when nitrobenzene is used as solvent, the yield of dimer can be increased even more through reoxidation of the hydroquinone.

Under suitable reaction conditions, the dimer that is initially formed can react further to yield trimers of type **8b**. It has not yet been possible to isolate these compounds, since they are always converted into the trimeric cyclic quinones **13a**. Indeed, **8b** is also converted into **13a** by phenol oxidation under weakly basic conditions. The stability of conocurvone **1a** is therefore due to the presence of hydroxy groups at position 2 of the monomer, which prevent cyclization. This cyclization via a symmetrical dimer of type **12b** explains why none of the known hydroxylated *cyclo*-trimers (e.g. *cyclo*-trijuglone **13b**) display C_3-symmetry with respect to the *peri*-hydroxy groups.



9 **10a** **11**
10b: OH instead of O^-



12a: R = H
12b: R = OH
12c: R = H, quinone instead of hydroquinone

13a: R = H
13b: R = OH

The synthesis of conocurvone (**1a**) also makes use of the well established principle of phenol/quinone addition, even though the term was inspired by the reaction of quinones with hydroxy-2*H*-1-benzopyran-2-ones, a reaction that was discovered later but proceeds in a similar manner. Brief warming of two equivalents of teretifolion B (**2a**) with naphthoquinone in glacial acetic acid afforded the predicted **1b** in 9% yield. For the synthesis of conocurvone (**1a**), 2-deoxyteretifolione (**2b**) was warmed with two equivalents of **2a** in pyridine, analogously to the synthesis of 2,2′-binaphthyldiquinone. All the spectroscopic and pharmacological properties of the synthetic material agreed with those of the natural product.

The main difficulty in the synthesis of **1a** lay in the deoxygenation of **2a** to **2b**. This was eventually carried out by transforming

the *p*-bromobenzoate **2c** to **2d** with thiophenol, with subsequent catalytic reduction with Raney nickel.

Nothing is yet known about the site of action or structure–function relationships for derivatives of **1a** (as, for example, **1b**), and any discussion is therefore very speculative in nature. However, it is conceivable that **1a** assumes a helical conformation which winds into the groove of the DNA strand. Similar conformations are also expected for **8a**, and in particular for **8b** and higher oligomers. As we have shown, partial reduction of these compounds leads to deep blue, intramolecular quinhydrones, which are also stable in solution and can be shown by molecular modeling to be stabilized in a helical conformation. For **1a**, additional interactions may be expected between the quinonoid hydroxy groups and petides, like those that play a role in coloring hair and skin with henna (**4c**). It will be fascinating to see whether these hypotheses are confirmed.

German version: *Angew. Chem.* **1994**, 106, 438

[1] L. A. Decosterd, I. C. Parsons, K. R. Gustafson, J. H. Cardellina II, J. B. McMahon, G. M. Cragg, Y. Murata, L. K. Pannell, J. R. Steiner, J. Clardy, M. R. Boyd, *J. Am. Chem. Soc.* **1993**, *115*, 6673–6679.
[2] R. H. Thomson, *Naturally Occurring Quinones, Vol. 2*, Academic Press, London, **1971**; *Naturally Occurring Quinones, Vol. 3*, Chapman and Hall, London, **1987**.
[3] H. Laatsch, Liebigs Ann. Chem. 1987, 297-304, and preceding publications on the same theme.
[4] H. Laatsch, *Liebigs Ann. Chem.* **1990**, 433–440.
[5] E. Rosenhauer, F. Braun, R. Pummerer, G. Riegelbauer, *Ber. Dtsch. Chem. Ges.* **1937**, *70*, 2281-2295.
[6] H. Brockmann, H. Laatsch, *Liebigs Ann. Chem.* **1983**, 433–447.
[7] K. Krohn, K. Khanbabaee, *Liebigs Ann. Chem.* **1993**, 905–909.
[8] H. Brockmann, *Liebigs Ann. Chem.* **1988**, 1–7.

A stop-gap solution?



If the latest library copy of Angewandte spends more time off the shelf than on, stop the gap with a personal subscription.

Just call or fax

VCH

USA: Tel. 1-(800) 422-8824; Fax (305) 428-8201
UK: Tel. (0223) 321111, Fax (0223) 313221

 © VCH Verlagsgesellschaft mbH, D-69451 Weinheim, 1994 0570-0833/94/0404-0424 $ 10.00+.25/0

Bond-Stretch Isomers: Fact not Fiction

Philipp Gütlich,* Harold A. Goodwin, and David N. Hendrickson

The concept of bond-stretch isomerism was introduced by Stohrer and Hoffmann in 1972.[1] In the simplest terms, two molecules are bond-stretch isomers if they differ only in the length of one or more bonds. During the last two decades several transition metal complexes have been reported to exhibit bond-stretch isomerism.[2–11] Interest in this new form of isomerism has recently been revived,[12] and a lively debate on its actual existence has ensued.[13]

We wish to draw attention to the long known and now well-characterized phenomenon of thermal spin-crossover, which indeed leads to genuine bond-stretch isomers. In certain transition metal complexes with thermal spin-crossover the energy difference between the high-spin (HS) and low-spin (LS) states is on the order of thermal energy kT, such that the two spin states may coexist in thermal equilibrium. The most thoroughly studied spin-crossover systems are Fe^{II} complexes in which the Fe center is coordinated to six nitrogen atoms.[14]

The criteria for thermal spin-crossover leading to coexisting bond-stretch isomers can best be illustrated by means of the one-dimensional potential energy diagram shown in Figure 1. If a molecule exists in two bond-stretch isomeric forms, then, as pointed out previously,[1] there must be two electronic states that are close in energy and separated by a potential energy barrier ΔE_{pot}. In Figure 1 the potential energy of an Fe^{II} complex is plotted as a function of some nuclear coordinate, for example, the totally symmetric Fe–ligand stretch. The two minima correspond to the LS($^1A_{1g}$) and HS($^5T_{2g}$) electronic states of an octahedral Fe^{II} complex, which arise from the t_{2g}^6 and the $t_{2g}^4e_g^2$ electronic configurations, respectively. The two states coexist in thermal equilibrium if $\Delta E_{HL}^{o} \approx kT$. These two isomeric forms have long been known as spin-state isomers (in other words, isomers that differ only in their total spin), and there is no doubt that they can also be considered bond-stretch isomers for the following reason: In the conversion from the LS state to the HS state, two electrons are moved from the bonding t_{2g} orbitals to the antibonding e_g orbitals. As a consequence, the length of the Fe–ligand bond Δr_{HL} is roughly 10% greater in the HS state than in the LS state.[15] The potential energy minima shift further apart by Δr_{HL}, and the increased energy barrier leads to a stabilization of the two electronic states. For example, in single-crystal X-ray structure determinations of the spin-crossover complex $[Fe(2\text{-pic})_3]Cl_2 \cdot EtOH$ (2-pic = 2-picolylamine)[16] it was found that the Fe–N(amine) bond length changes from 2.199 Å in the HS state (227 K) to 2.032 Å in the LS state (115 K); the Fe–N(pyridine) bond length changes from 2.197 to 2.000 Å in the same temperature range.

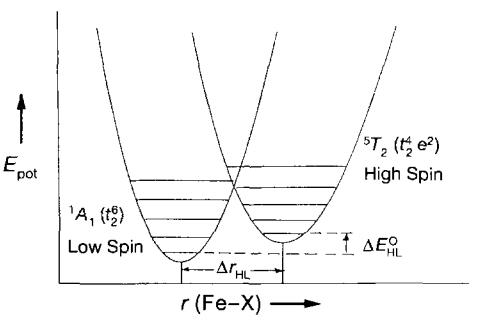


Fig. 1. One-dimensional potential energy diagram for an octahedral Fe^{II} spin-crossover complex. The potential energy E_{pot} is plotted as a function of distance between the iron center and the coordinating ligand atom X. The low-spin ($^1A_{1g}$) and high-spin ($^5T_{2g}$) electronic states are separated in energy by ΔE_{HL}^{o}.

The distance between the metal center and the coordinating ligand atom is always greater in the HS bond-stretch isomer than in the LS isomer.[15] The largest value of Δr_{HL} is 0.28 Å for the average Fe–P distance in $[Fe(dppen)_2Cl_2] \cdot 2(CH_3)_2CO$[17] (dppen = $Ph_2PCH{=}CHPPh_2$), and the smallest value is 0.04 to 0.05 Å for the Co–N bonds in $[Co(terpy)_2]I_2 \cdot 2H_2O$[18] (terpy = 2,2′,2″-terpyridine). The inescapable conclusion is that each complex exhibiting thermal spin-crossover has two bond-stretch isomers that coexist if $\Delta E \approx kT$. The magnitude of the potential energy barrier between them dictates the rate at which the two bond-stretch isomers interconvert.

The difference in the Gibbs free energy of the HS and LS states ($\Delta G_{HL} = \Delta H_{HL} - T\Delta S_{HL}$) is a measure of the thermodynamic energy difference between the two isomers; $\Delta H_{HL} = H_{HS} - H_{LS}$ and $\Delta S_{HS} = S_{HS} - S_{LS}$ are the differences in enthalpy and entropy, respectively. Since ΔH_{HL} (enthalpy difference of the electronic states) is rather small (between 5 and 10 kJ mol^{-1}), the entropy change, which is on the order of 50 to 80 J K mol^{-1}, is the essential driving force for thermal spin-crossover.[19] Con-

[*] Prof. Dr. P. Gütlich
Institut für Anorganische Chemie und Analytische Chemie der Universität
Staudinger Weg 9, D-55099 Mainz (FRG)
Telefax: Int. code + (6131)39-2990
Prof. Dr. H. A. Goodwin
School of Chemistry, University of New South Wales
N. Kensington, N.S.W. 203 (Australia)
Prof. Dr. D. N. Hendrickson
Department of Chemistry 0358, University of California at San Diego
La Jolla, CA 92093-0358 (USA)

 © VCH Verlagsgesellschaft mbH, D-69451 Weinheim, 1994 0570-0833/94/0404-0425 $ 10.00+.25/0

tributions to ΔS_{HL} arise from differences in the numbers of unpaired electrons, in other words spin multiplicities, as well as from differences in the vibrational degrees of freedom between the two isomeric forms.

Bond-stretch isomers are conveniently detected by their different magnetic properties, optical spectra, vibrational spectra, Mössbauer spectra, and by their crystal structures.[14] ^{57}Fe Mössbauer spectroscopy is particularly sensitive for the detection of bond-stretch isomers in Fe^{II} spin-crossover complexes. As an example, Figure 2 shows Mössbauer spectra of $[Fe(mtz)_6](BF_4)_2$ (mtz = 1-methyltetrazole) recorded at 120, 75, and 20 K.[20] The

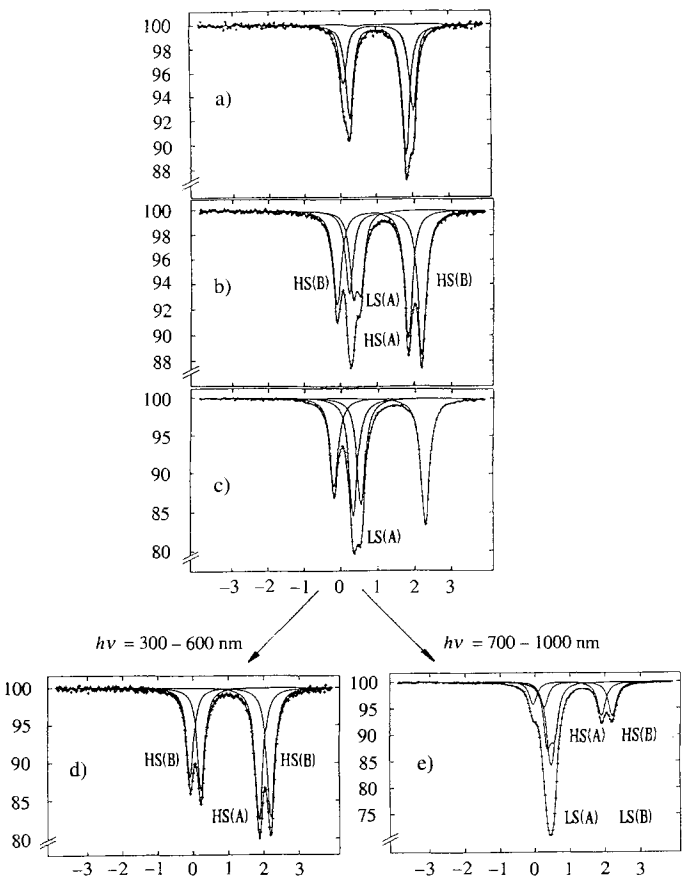


Fig. 2. The ^{57}Fe Mössbauer spectra of $[Fe(mtz)_6](BF_4)_2$ a) at 120 K, b) at 75 K, c) at 20 K, d) at 20 K after irradiation with green light, e) after irradiation with red light. The relative velocity between the Mössbauer source and the absorber v [mm s^{-1}] is plotted on the x axis, the relative transmission [%] on the y axis.

spectrum at 120 K is composed of two quadrupole-split doublets characteristic of Fe^{II} ions in the HS state. This result is consistent with the two crystallographically nonequivalent cation sites (A and B in Fig. 2) seen in the X-ray structure at room temperature.[21] As the temperature is decreased below 120 K, the doublet HS(A) disappears gradually in favor of a new doublet (LS(A)), which has a smaller splitting characteristic of a LS Fe^{II} complex. At 20 K the spectrum shows clearly that the cations in site A have converted totally to the LS state, whereas those in site B remain in the HS state at all temperatures. Thus, at this temperature the bond-stretch isomers A and B coexist.

At 75 K equal amounts of the LS and HS complexes are found in crystal site A,[20] and the Gibbs free energy difference ΔG is 0. The Mössbauer spectrum recorded at this temperature (Fig. 2b) reveals the coexistence of three bond-stretch isomers, LS(A), HS(A), and HS(B). Admittedly, the differences in the bond lengths of HS(A) and HS(B) are small.[21]

In 1984 the remarkable observation was made that the spin-crossover complex $[Fe(ptz)_6](BF_4)_2$ (ptz = 1-propyltetrazole) can be converted at low temperatures from the LS state to the HS state by irradiation with green light.[22] The crystalline sample remains in the HS state practically indefinitely. This phenomenon, the mechanism of which has been elucidated,[23] is called the LIESST effect (light-induced excited spin state trapping) and has since been observed in many other Fe^{II} spin-crossover compounds. Furthermore, the metastable HS state can be converted back to the stable LS state by irradiation with red light (reverse LIESST effect).[24] The LIESST effect in $[Fe(ptz)_6](BF_4)_2$ is illustrated in Figure 2; at 20 K green light ($300 \leq \lambda \leq 600$ nm) converts the stable LS(A) state to the metastable HS(A) state. The back-conversion with red light has also been demonstrated for this complex.[20] Since the lifetime of the metastable HS(A) state is at least a few days, we may consider HS(A) and its precursor LS(A) to be two bond-stretch isomers that are interconvertible by light. It is interesting to note that spectrum d confirms the coexistence of HS(A) and HS(B) at 20 K, which is also seen at higher temperatures, for example at 120 K (spectrum a), for two stable HS states.

Finally, upon irradiation of a sample of the mtz complex at 20 K with red light ($700 \leq \lambda \leq 1000$ nm) the intensity of the HS(B) signal is reduced considerably in favor of a new signal arising from a metastable LS(B) state (spectrum e). Since the light-induced conversion in this experiment was not complete (owing to broad-band irradiation), the Mössbauer spectrum shows the presence of four isomers, actually two pairs of bond-stretch isomers, one pair for each lattice site.

In conclusion, we are not responsible for the birth of the concept of bond-stretch isomerism[1] or its apparent demise;[13] however, we have definitively shown that bond-stretch isomerism is a reality in spin-crossover complexes.

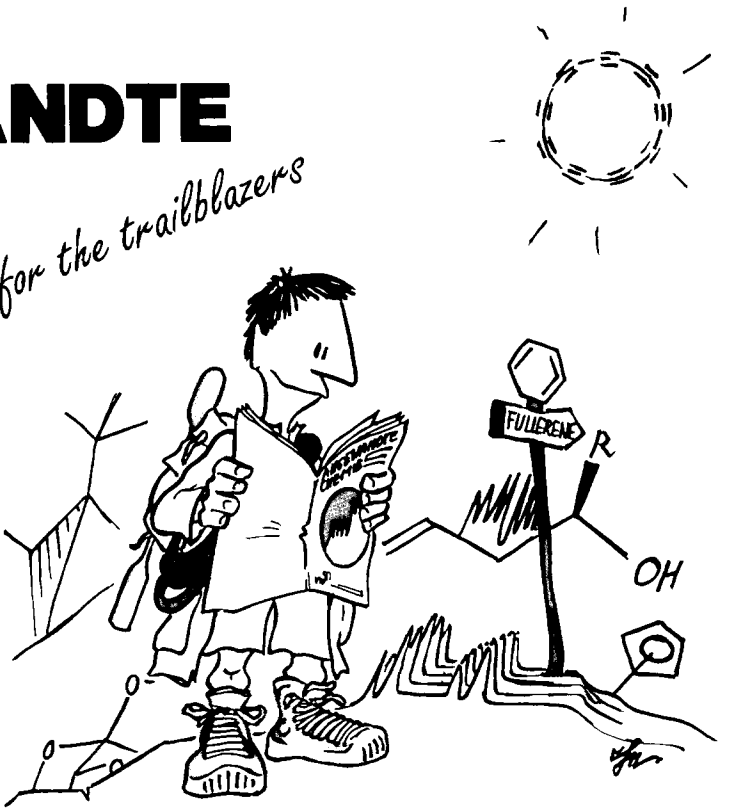
German version: *Angew. Chem.* **1994**, *106*, 441

[1] W.-D. Stohrer, R. Hoffmann, *J. Am. Chem. Soc.* **1972**, *94*, 1661.
[2] A. V. Butcher, J. Chatt, *J. Chem. Soc. A* **1970**, 2652.
[3] L. Manojlovic-Muir, *J. Chem. Soc. A* **1971**, 2796.
[4] L. Manojlovic-Muir, K. W. Muir, *J. Chem. Soc. Dalton Trans.* **1972**, 686.
[5] B. L. Haymore, W. A. Goddard III, J. N. Allison, *Proc. Int. Conf. Coord. Chem. 23rd* **1984**, 535.
[6] J. M. Mayer, *Inorg. Chem.* **1988**, *27*, 3899.
[7] K. Wieghardt, G. Backes-Dahmann, B. Nuber, J. Weiss, *Angew. Chem.* **1985**, *97*, 773; *Angew. Chem. Int. Ed. Engl.* **1985**, *24*, 777; K. Wieghardt, G. Backes-Dahmann, W. Holzbach, W. J. Swiridoff, J. Weiss, *Z. Anorg. Allg. Chem.* **1983**, *499*, 44.
[8] Y. Jean, A. Lledos, J. K. Burdett, R. Hoffmann, *J. Am. Chem. Soc.* **1988**, *110*, 4506.
[9] S. Lincoln, S. A. Koch, *Inorg. Chem.* **1986**, *25*, 1594.
[10] A. Bashall, V. C. Gibson, T. P. Kee, M. McPartlin, O. B. Robinson, A. Shaw, *Angew. Chem.* **1991**, *103*, 1021; *Angew. Chem. Int. Ed. Engl.* **1991**, *30*, 980.
[11] W. M. Nugent J. M. Mayer, *Metal-Ligand Multiple Bonds*, Wiley, New York, **1988**, pp. 152–154.
[12] J. M. Mayer, *Angew. Chem.* **1992**, *104*, 293; *Angew. Chem. Int. Ed. Engl.* **1992**, *31*, 286.

[13] G. Parkin, *Acc. Chem. Res.* **1992**, *25*, 455.
[14] H. A. Goodwin, *Coord. Chem. Rev.* **1976**, *18*, 293; P. Gütlich, *Struct. Bonding* **1981**, *44*, 83; P. Gütlich, A. Hauser, H. Spiering, *Angew. Chem.*, submitted.
[15] E. König, *Prog. Inorg. Chem.* **1987**, *35*, 527.
[16] B. A. Katz, C. E. Strouse, *J. Am. Chem. Soc.* **1979**, *101*, 6214; M. Mikami, M. Konno, Y. Saito, *Acta Crystallogr. Sect. B* **1980**, *36*, 275; *Chem. Phys. Lett.* **1979**, *63*, 566.
[17] F. Cecconi, M. Di Vaira, S. Midollini, A. Orlandini, L. Sacconi, *Inorg. Chem.* **1981**, *20*, 3423.
[18] B. N. Figgis, E. S. Kucharski, A. H. White, *Aust. J. Chem.* **1983**, *36*, 1527.
[19] E. König, G. Ritter, S. K. Kulshreshtha, *Chem. Rev.* **1985**, *85*, 219.
[20] P. Poganiuch, S. Decurtins, P. Gütlich, *J. Am. Chem. Soc.* **1990**, *112*, 3270.
[21] L. Wiehl, *Acta Crystallogr. Sect. B* **1993**, *49*, 289.
[22] S. Decurtins, P. Gütlich, C. P. Köhler, H. Spiering, A. Hauser, *Chem. Phys. Lett.* **1984**, *105*, 1; S. Decurtins, P. Gütlich, K. M. Hasselbach, A. Hauser, H. Spiering, *Inorg. Chem.* **1985**, *24*, 2174.
[23] A. Hauser, *Coord. Chem. Rev.* **1991**, *111*, 275.
[24] A. Hauser, *Chem. Phys. Lett.* **1986**, *124*, 543.

ANGEWANDTE
CHEMIE
International Edition in English

for the trailblazers



Twice a month in 1994

To start your personal subscription please contact:

VCH, Reader Service
P.O. Box 10 11 61, D-69451 Weinheim
Federal Republic of Germany
Telephone: +49 (6201) 60 64 27
Fax: +49 (6201) 60 61 17

VCH
8 Wellington Court
Cambridge CB1 1HZ, UK
Fax: (0223) 31 33 21
(for customers in the UK)

VCH
220 East 23rd Street
New York, NY 10010-4606, USA
Fax: (212) 481 0897
(for customers in the USA and Canada)

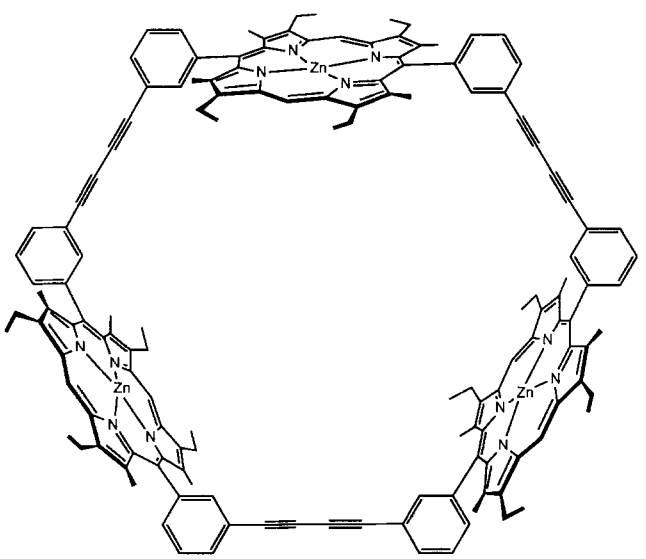
VCH
Hardstrasse 10, Postfach
CH-4020 Basel, Switzerland
Fax: (061) 2 71 06 18
(for customers in Switzerland)

VCH

Crystal Structure of a Supramolecular Dimer Formed by $\pi-\pi$ Interactions between Two Interlocked Cyclic Zinc Porphyrin Trimers**

Harry L. Anderson, Alan Bashall, Kim Henrick, Mary McPartlin,* and Jeremy K. M. Sanders*

One of the key features of many natural enzymes is the ability to bind two substrate molecules in a close and well-defined spatial relationship; model systems that are intended to mimic this property will therefore need to possess two or more convergent binding sites for organic guest molecules.[1, 2] Previously, as part of a project to design catalytic systems, the synthesis[2, 3] and some binding properties[3, 4] of the zinc porphyrin trimer **1** were reported, and very recent results show that **1** can stereoselectively accelerate the Diels–Alder reaction between appropriate ligands.[5] Successful molecular design in this system has so far been based on the structures deduced from space-filling models and molecular mechanics calculations. We now report the details of a full single-crystal analysis[6] of **1**·py_3, a tris(pyridine) adduct of **1**, which provides an insight into the sources of flexibility and distortion within the porphyrin trimer and will facilitate further progress in planned molecular assembly. Furthermore, we present evidence that $\pi-\pi$ interactions between guest pyridines and between pyridines and porphyrins provide the driving force for the formation of a remarkable interlocking dimer of trimers.



1



pyridine



quinuclidine

The molecular structure of **1**·py_3 shown in Figure 1 provides proof that the host can indeed accommodate three independent ligands, as had been deduced previously.[2] The mean distances from the zinc atom to the porphyrin and pyridine nitrogen atoms, 2.05 and 2.16 Å, respectively, are similar to those observed in other zinc porphyrins (2.06–2.08 and 2.15–2.20 Å, respectively).[7] The nitrogen atoms of each porphyrin ring are nearly coplanar [maximum deviations 0.01 (ring a), 0.07 (b), and 0.05 Å (c)]; the zinc atoms lie at a mean distance of 0.32 Å above the N_4 planes towards the pyridine group [Zn(1a) 0.32, Zn(1b) 0.33, Zn(1c) 0.30 Å], which is within the range observed for this displacement in mononuclear zinc porphyrins (0.31–0.37 Å).[7]

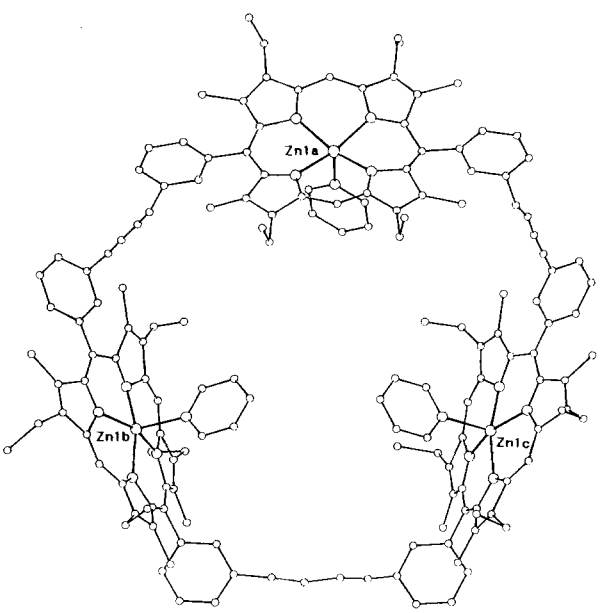


Fig. 1. The molecular structure of the pyridine adduct **1**·py_3 of the zinc porphyrin trimer **1**.

The trimer does not have an idealized D_{3h}-symmetric structure in which all aryl and butadiyne groups lie in a plane perpendicular to the porphyrin rings, as might have been expected from the known geometric properties of aryl and alkyne groups. Inspection of models and molecular mechanics calculations on the isolated molecule show that the zinc atoms form an approximately equilateral triangle with three Zn···Zn separations of

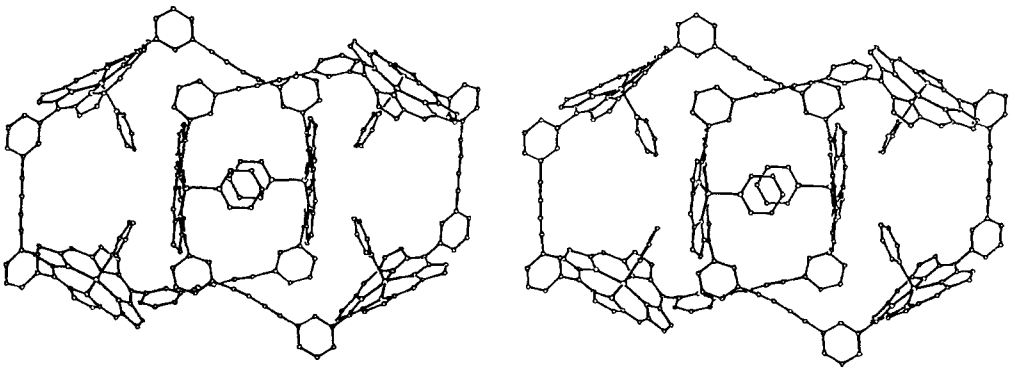
[*] Prof. M. McPartlin, A. Bashall
School of Chemistry, University of North London,
Holloway Road, GB-London N7 8DB (UK)
Telefax: Int. cod + (71) 753-5029

[*] Dr. J. K. M. Sanders, Dr. H. L. Anderson
Cambridge Centre for Molecular Recognition
University Chemical Laboratory
Lensfield Road, GB-Cambridge CB2 1EW (UK)

Dr. K. Henrick
Centre for Protein Engineering, Medical Research Centre
Hills Road, GB-Cambridge CB2 2QH (UK)

[**] This work was supported by the British Science and Engineering Research Council and Magdalene College Cambridge. We thank Dr. C. A. Hunter (Sheffield University) for valuable discussions.

 © VCH Verlagsgesellschaft mbH, D-69451 Weinheim, 1994 0570-0833/94/0404-0429 $ 10.00+.25/0



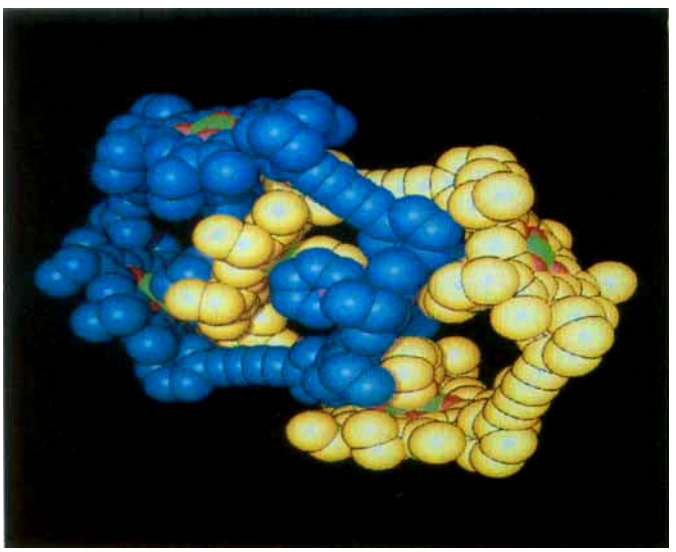


Fig. 2. Top: A stereoview showing the dimer of trimers formed by interpenetration of two centrosymmetrically related molecules of $1 \cdot py_3$. Left: A computed space-filling model of the dimeric supramolecule showing the interpenetration of two trimers.

around 16 Å. However, in the crystal there is considerable molecular distortion such that only two Zn $\cdots$ Zn separations are of about this length [Zn(1a)–Zn(1b) 15.899, and Zn(1a)–Zn(1c) 15.255 Å), whereas the third is considerably shorter [Zn(1b)–Zn(1c) 13.941 Å]. Overall the molecule has only virtual C_s symmetry; the approximate mirror plane passes through Zn(1a), N(5a), and the *para* carbon atom C(52a) of the pyridine ring, bisecting porphyrin ring a and its associated pyridine ring and lying between the two remaining porphyrins.

The flexibility of the framework, demonstrated by the marked deviation from threefold symmetry, is clearly seen in the different orientations of the porphyrin planes in Figure 1: none are perpendicular to the Zn_3 plane. Two porphyrin planes (b and c) tilt towards each other (dihedral angle between N_4 and Zn_3, 104 and 101°, respectively], and porphyrin a tilts in the opposite direction (dihedral angle 76°). The molecular distortion results from a remarkable interpenetration of pairs of the trimer molecules giving a strongly interlocked centrosymmetric "dimers of trimers" in the solid state, in which one porphyrin of each trimer is a guest in the cavity of the second. One side of porphyrin ring a of the first trimer is tightly wedged between the three pyridine rings of the second trimer and vice versa to give the supramolecular dimeric unit shown in Figure 2. The pyridine ligand of Zn(1a) of the first trimer lies parallel to that of the second trimer, at a separation (3.8 Å) slightly larger than the sum of the van der Waals distances. The remaining two pyridine ligands (b anc c) of the first trimer are right round on the opposite side of the unique porphyrin ring a of the second trimer with closest contact distances of 3.4 (Zn(1a)–H(52b′) and 3.3 Å (Zn(1a)–H(52c′). Thus the unique porphyrin a of each trimer is effectively trapped in the central cavity of the other.

The overall crystal structure is composed of layers of interlocked dimers of trimers parallel to a plane defined by the *b* axis and the *ac* diagonal of the unit cell. Large channels run between the layers throughout the crystal parallel to the *b* axis (Fig. 3), which accommodate the many solvent molecules trapped in the lattice. There is a marked resemblance to the structure of many

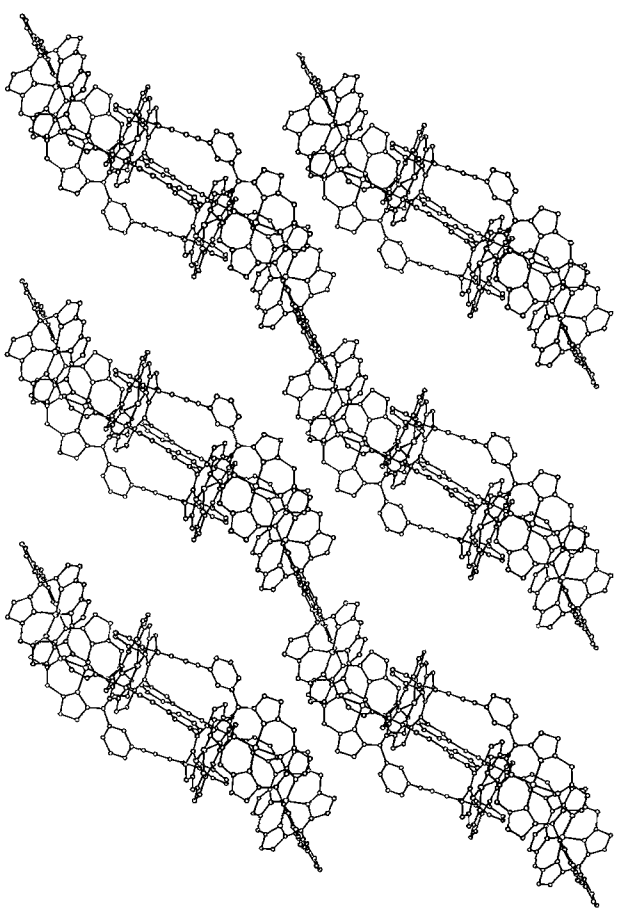


Fig. 3. The crystal structure of the porphyrin trimer $1 \cdot py_3$ viewed down the *b* axis showing the large diamond-shaped channels that run right through the crystal parallel to *b* (pyridine ligands and alkyl substituents removed for clarity).

 © VCH Verlagsgesellschaft mbH, D-69451 Weinheim, 1994 0570-0833/94/0404-0430 $ 10.00+.25/0

tetraarylporphyrins, which have been described as "porphyrin sponges" because they contain many solvent molecules trapped in the cavities in their solid-state structures. These channels are known to persist even in the absence of the solvent.[8] The crystal of **1**·py_3 has a similar spongelike structure giving a clathrate with eleven molecules of solvent per dimer unit.

Remarkably, the adduct of **1** with quinuclidine, **1**·qn_3, has quite a different structure even when crystallized from precisely the same solvent mixture as the pyridine adduct. Preliminary X-ray structural studies show that the trimeric molecule of **1**·qn_3 forms discrete monomeric units and has significantly less molecular distortion than in **1**·py_3; the Zn···Zn distances are nearly equal (14.2–14.8 Å).[9] Given the very similar size of pyridine and quinuclidine we must find another cause of the different structure, and the most likely is the pyridine π-system. Inspection of the crystal structure of the pyridine adduct reveals at least three sets of arrangements favorable for π–π interactions:[10, 11] 1) the pyridine ligands of the two unique a porphyrins are in near van der Waals contact, parallel and offset by 1.1 Å in the now-classic arrangement identified by Hunter and Sanders.[10] 2) The b and c pyridines are each in van der Waals contact with a pyrrole unit of porphyrin a of the other trimer unit; the angle between each pyridine and pyrrole is approximately 34°. This favorable arrangement is often found in hydrophobic protein cores[11] (four of these interactions are found in each dimer of trimers). 3) Protons of the aryl linking groups attached to porphyrin a point directly at pyridines b and c to give the T-shaped arrangement found in the crystal structures of many arenes (again four of these interactions are found in each dimer of trimers). It is difficult to assess the energies of these π–π interactions, but each could be as large as 4–6 kJ mol^{-1}.[11] This gives a maximum of less than 60 kJ mol^{-1} of stability to the dimer, which corresponds roughly to the entropy required to bring the two ligated trimer arrays together in solution. The equilibrium constant for dimerization will therefore be too small to observe experimentally in solution at accessible concentrations but is more than large enough to control the mode of crystallization.

The results presented here show that trimer **1** is rather flexible and able to respond to weak interactions and differing substrates by distorting the porphyrin framework and by torsion around the bond connecting the porphyrin to its aryl linker. Whether this flexibility confers the disadvantage of dissipating catalytic potential, or the advantage of allowing it to reach an optimum binding geometry, remains to be tested by synthesis of both less flexible and more flexible analogues.

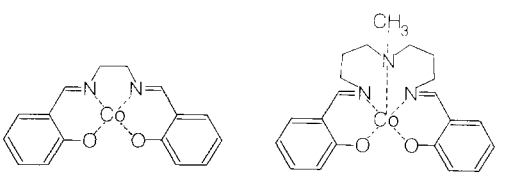
Recieved: June 22, 1993
Revised version: September 13, 1993 [Z 6159 IE]
German version: *Angew. Chem.* **1994**, *106*, 445

[1] F. Vögtle, I. Lüer, V. Balzani, N. Armaroli, *Angew. Chem.* **1991**, *103*, 1367; *Angew. Chem. Int. Ed. Engl.* **1991**, *30*, 1333.
[2] H. L. Anderson, J. K. M. Sanders, *J. Chem. Soc. Chem. Commun.* **1990**, 1714.
[3] H. L. Anderson, J. K. M. Sanders, *Angew. Chem.* **1990**, *102*, 1478; *Angew. Chem. Int. Ed. Engl.* **1990**, *29*, 1400.
[4] H. L. Anderson, J. K. M. Sanders, *J. Chem. Soc. Chem. Commun.* **1992**, 946.
[5] C. J. Walter, H. L. Anderson, J. K. M. Sanders, *J. Chem. Soc. Chem. Commun.* **1993**, 458.
[6] Crystal data for **1**·py_3·(4.5C_6H_{12})·C_6H_5Cl: $C_{195}H_{200}ClN_{15}Zn_3$, M_r = 2985.45, triclinic, space group $P\bar{1}$ (No. 2) a = 21.883(6), b = 22.325(6), c = 20.746(5) Å, α = 99.40(3), β = 98.84(4), γ = 82.32(3)°, Z = 2, V = 9818.90 Å^3, ρ_{calc} = 1.010 g cm^{-3}, $F(000)$ = 3116, $\mu(Mo_{K\alpha})$ = 4.1 cm^{-1}, R = 0.1087 for 4550 reflections with $I \geq 3.0\sigma(I)$. Crystals of **1**·py_3 were extremely fragile and lost solvent rapidly in air, so X-ray data were collected, with considerable difficulty, using a crystal sealed with mother liquor in a Lindemann tube. 13437 Data were scanned in the σ-range 2–18° using a Phillips PW1100 diffractometer. The three metal atoms were located by direct methods, and all non-hydrogen atoms of **1**·py_3 were located from very many subsequent difference-Fourier syntheses. No recognizable solvent fragments could be identified, but nine separate rings of extended electron density were apparent in difference-Fourier syntheses. Satisfactory refinement was achieved by including all peaks greater than ca. 1.5 e Å^{-3} as partial atoms in structure factor calculations (population parameters of these atoms were adjusted to correspond to the total of ca. 1.0 chlorobenzene and 4.5 cyclohexane molecules indicated from analysis of the ^{1}H NMR spectrum), but only their thermal parameters were refined. The phenylene and pyridine rings were treated as rigid groups in blocked full-matrix refinement. Further details of the crystal structure investigation are available on request from the Director of the Cambridge Crystallographic Data Centre, 12 Union Road, GB-Cambridge CB12 1EZ (UK), on quoting the full journal citation.
[7] K. Hatana, K. Kawasaki, S. Munakata, Y. Iitaka, *Bull. Chem. Soc. Jpn.* **1987**, *60*, 1985, and references therein.
[8] M. P. Byrn, C. J. Curtis, I. Goldberg, Yu Hsiou, S. I. Khan, P. A. Sawin, S. K. Tendick, C. E. Strouse, *J. Am. Chem. Soc.* **1991**, *113*, 6549.
[9] K. Henrick, unpublished results.
[10] C. A. Hunter, J. K. M. Sanders, *J. Am. Chem. Soc.* **1990**, *112*, 5525.
[11] C. A. Hunter, J. Singh, J. M. Thornton, *J. Mol. Biol.* **1991**, *218*, 837.

Schiff Base Complexes with Five-Coordinate Cobalt as Dioxygen Activating Sites in Zeolites**

Dirk E. De Vos, Frédéric Thibault-Starzyk, and Peter A. Jacobs*

Metal complexes have been heterogenized on microporous inorganic materials like zeolites in view of applications in photochemistry, the separation of gases, and catalysis. Several classes of dioxygen-binding Co^{2+} compounds, such as the polyamine and cyanide complexes, were prepared in the intracrystalline cages of zeolite Y and characterized.[1] The synthesis of [Co(salen)] (**1**) (H_2salen = bis(salicylidene)ethylenediamine) in zeolite Y has also been claimed, but the spectroscopic and electrochemical features of the resulting material deviate from those of **1** in the solid state or in solution.[2] Schiff base complexes like **1** and the related [Co(smdpt)] (**2**) (H_2smdpt = bis[3-(salicylidenamino)propyl]methylamine) catalyze homogeneous oxidations with dioxygen.[3] In view of heterogenization of these catalysts, we have



1 **2**

reexamined the synthesis of Co^{2+} Schiff base complexes in faujasite-type zeolites. The newly proposed use of the smdpt ligand in a zeolitic environment leads to a much simplified synthesis method and results in the formation of many sites for the reversible binding of dioxygen, whereas with salen only small

[*] Prof. Dr. P. A. Jacobs, D. E. De Vos, Dr. F. Thibault-Starzyk
Center for Surface Chemistry and Catalysis, Katholieke Universiteit Leuven
Kardinaal Mercierlaan 92, B-3001 Heverlee (Belgium)
Telefax: Int. code + (16)295126

[**] This work was supported by the Belgian government under the auspices of an Interuniversitary Attraction Pole (IUAP). D. De V. thanks the Belgian National Fund for Scientific Research for a fellowship. F. T.-S. thanks the European Community for a postdoctoral fellowship administered by the Human Capital and Mobility Program.

amounts of atypical species can be detected; no reversible oxygen binding is observed in salen-loaded zeolites.

Herron first proposed the use of salen on zeolite Y exchanged with Co^{2+} to mimic the oxygen-binding function of hemoglobin.[2] However, since the material was EPR-inactive even after the adsorption of pyridine, it is doubtful that square-planar **1** or its square-pyramidal pyridine adduct were indeed formed.[4] The pyridine adduct of **1** may even be too large to fit in a NaY supercage, and the role of pyridine in the observed oxygen sorption is hence unclear. In order to enhance the interaction between Co^{2+}, salen, and the axial base, Putyera et al. used an isonicotinate-exchanged hydrotalcite as a support.[5]

We now propose the use of the pentadentate ligand smdpt as an alternative for the tetradentate salen; in this case the supplementary axial base ligand is no longer needed. Though it is generally accepted that square-planar **1** can be accommodated easily inside the supercage of a cubic faujasite (FAU), it is less clear whether the more voluminous, trigonal-bipyramidal **2** can be placed in a NaY supercage. Therefore the steric interactions of the guest complex **2** with the host structures were simulated with a molecular graphics program.[6] This simulation indicated that the fit of **2** in a supercage of NaY is tight (Fig. 1): the aromatic moieties pass through the twelve-membered rings of the zeolite cage and almost inhibit motion of the complex.

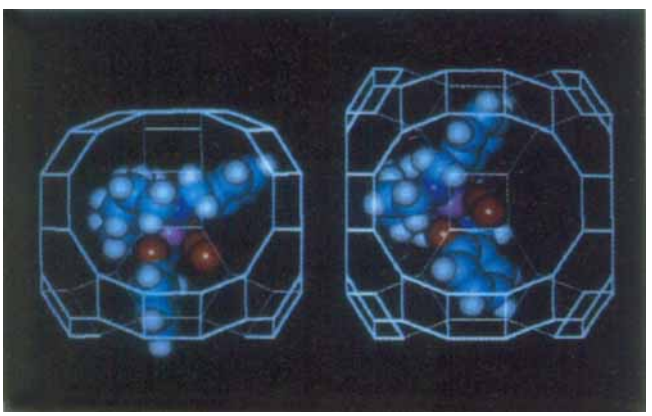


Fig. 1. Computer-generated model (Hyperchem) of [Co(smdpt)] (**2**) in the hypercage of EMT (right) and in the smaller supercage of FAU (left).

Therefore the new, hexagonal polymorph of faujasite, a zeolite with EMT topology, was also used.[7] As in the case of NaY, the cages of EMT are accessible through twelve-membered rings with an inner diameter of about 0.74 nm; some cages in EMT, however, the so-called hypercages, have five of these windows instead of four and are thus considerably more spacious than the FAU supercages of NaY, which are limited by just four windows. A new calculation revealed that **2** can assume a variety of positions in an EMT hypercage but is too large to pass through the twelve-membered rings of the cage; hence, the complex should be truly entrapped (Fig. 1).

The EPR spectrum of [salen]-CoNaY (i.e. CoNaY loaded with salen, see Experimental Procedure) recorded at room temperature shows only the background signal of the NaY zeolite,[2] which is due to Fe impurities in the zeolite. Upon cooling, however, spectral features appear which indicate that some of the Co^{2+} ions experience a higher ligand field through interaction with salen; the typical spectra of low-spin **1** (with an unpaired electron in the $d_{x^2-y^2}$ or the d_{z^2} orbital) are not observed (Fig. 2).[4]

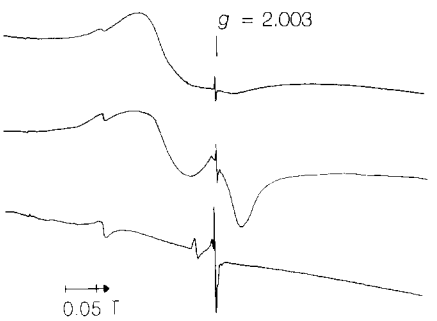


Fig. 2. EPR spectra of [salen]-CoNaY (X-band, gain 10^5) before soxhlet extraction at 293 K (top) and at 130 K (middle), and after pyridine extraction, 130 K (bottom).

The synthesis product [salen]-CoNaY was extracted not only to remove the excess ligand and thus restore the diffusion in the material, but also to bring a solvent molecule as a fifth ligand onto the complex. Extractions drastically changed the [salen]-CoNaY EPR spectra. Both strongly and weakly coordinating solvents (pyridine, dimethylformamide, and CH_2Cl_2) were employed. After extraction the signals possibly arising from square-planar Co^{2+} or from superoxo adducts (around $g = 2$) were still very weak (Fig. 2). The signals observed at $g = 2.20$ and $g = 1.94$ may arise from low-spin Co^{2+}, but the values do not correspond to those of low-spin **1**, and the typical hyperfine structure on the parallel component is lacking.[4] Apparently, formation of square-planar **1** by simple adsorption of salen on CoNaY is very limited. All extraction solvents yielded similar results, which proves that the simple liquid-phase technique for the axial coordination of a base on **1** cannot be used in this zeolitic environment because of steric interactions or adsorption effects.

In contrast, **2** is a high-spin Co^{2+} complex and should hence be EPR-inactive.[8] A strong EPR signal is observed, however, even before extraction of the [smdpt]-CoNaY and [smdpt]-CoNaEMT samples (Fig. 3). In the spectrum of NaY, in particular, the

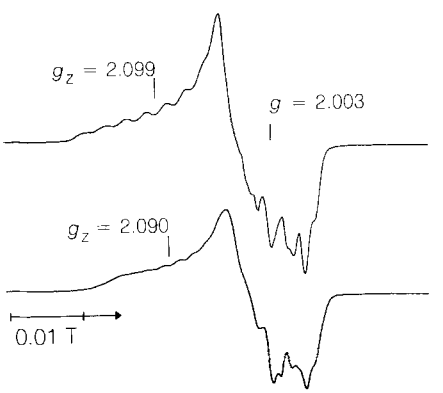


Fig. 3. EPR spectra of Co^{2+} faujasite loaded with smdpt (X-band, 130 K): FAU before soxhlet extraction (top), $g_z = 2.099$, $A_z = 27$ G (gain 2.5×10^4); EMT extracted with CH_2Cl_2 (bottom), $g_z = 2.090$, $A_z = 20$ G (gain 3.2×10^3).

eight-line hyperfine structure of the signal is clearly resolved. Due to the immobilization of the guest complex in the zeolite, the signal is anisotropic even at room temperature. An estimation of the EPR parameters by spectral simulation yielded $g_z = 2.099 \pm 0.003$, $A_z = 27.0 \pm 0.5$ G, $g_y = 2.00 \pm 0.01$, $A_y = 15 \pm 2$ G, $g_x = 2.00 \pm 0.01$, $A_x = 15 \pm 2$ G, a parameter set typical for

 © VCH Verlagsgesellschaft mbH, D-69451 Weinheim, 1994 0570-0833/94/0404-0432 $ 10.00+.25/0 Angew. Chem. Int. Ed. Engl. 1994, 33, No. 4

Co^{2+} superoxo adducts. The binding of dioxygen to this complex requires a roughly square-pyramidal disposition of the five ligand donor atoms around the Co^{2+} ion; hence, at least some of the Co^{2+} cations can no longer be coordinated by the zeolite. The EPR parameters (especially the rather large A_z value) do not exactly match those of [Co(smdpt) · O_2] in frozen solution. Nevertheless, they are reminiscent of those of some related Schiff base chelates in which the tertiary nitrogen base is replaced by a noncoordinating sulfur or oxygen linkage.[9] An imposed distortion of the complex and a weakened ligand field around Co^{2+} may thus result in a smaller electron transfer to O_2 and a larger A_z value. The occurrence of isomers with a different stereochemistry at the Co^{2+} ion may be an alternative explanation for the anomalous EPR parameters. A similar superoxo species is observed on the NaEMT zeolite, though the spectral resolution is somewhat less than on NaY. In both cases the molar ratio (bound O_2: total Co^{2+}) is less than 0.05 before soxhlet extraction.

The extraction with CH_2Cl_2 weakened the signal for [Co(smdpt) · O_2] in NaY, but increased its intensity in NaEMT. More strikingly, the EPR parameters were unaffected in the case of NaY but assumed new values ($g_z = 2.090$, $A_z = 20$ G) in the case of NaEMT (see Fig. 3). Since the new parameters are quite close to those observed for the frozen solution,[9] it can be safely stated that the electronic structures of the EMT and the solution species are very similar. The reorganization of the first type of [Co(smdpt) · O_2] (most clearly observed in NaY before extraction) into the second, more common type (observed in NaEMT after extraction) is apparently impossible in NaY; the only reasonable explanation for this is a distortion of the complex imposed by the NaY supercage. The larger NaEMT hypercage allows a more relaxed and normal complex conformation.

Evacuation of CH_2Cl_2-extracted [Co(smdpt)]-NaEMT and subsequent reexposure to oxygen results in removal and reappearance of the superoxo signal; the evacuation and oxygenation cycle can be repeated at room temperature several times without a noticeable loss in signal intensity. This proves that the dispersion of the complexes over the zeolite cages effectively protects the active sites against dimerization and irreversible oxidation. The maximal amount of [Co(smdpt) · O_2] in NaEMT, which was measured at 130 K and determined by double integration of the EPR spectrum, corresponds to about 25% of the total Co^{2+} content.

The present results demonstrate that formation of the square-planar complex **1** with four-coordinate cobalt is very difficult in faujasite, while complex **2** with five-coordinate cobalt is easily formed. This strongly suggests that the additional tertiary nitrogen in the ligand provides the donor strength required to remove Co^{2+} from the zeolite coordination environment, while the softer salen donor atoms are not capable of this. Simultaneously, the problem of the addition of an axial base is circumvented by use of pentadentate smdpt: the consecutive coordination by four equatorial donors (of the tetradentate salen ligand) and one axial base ligand (pyridine), which is hardly controllable in heterogeneous media, is replaced by a concerted equatorial and axial coordination by smdpt. This system provides one of the first examples of chelation by a multidentate ligand inside a zeolite cavity and the first example of a single coordination compound that displays structural differences when encaged in two different zeolite cages.

Experimental Procedure

FAU was obtained as a commercial NaY zeolite from the PQ Corporation. EMT was synthesized by using [18]crown-6 (Janssen Chimica) as a template, according to the procedure of Delprato et al. [7]. The X-ray powder diffraction pattern of the calcined sample was consistent with a purely hexagonal phase. The salen ligand was from Strem, smdpt was crystallized by condensation of 2 equiv of salicylaldehyde (Merck) with 1 equiv of bis(3-aminopropyl)methylamine (Aldrich) in the absence of a solvent. The Na^+ ions of both zeolites were exchanged for Co^{2+} (up to 0.9 wt.% Co). The samples were dried under an oxygen flow at 473 K, flushed with nitrogen, and mixed with an excess of crystalline ligand (ligand: Co ratio 2:1). The synthesis mixture was heated in a dry atmosphere at 373 K (smdpt) or 413 K (salen) for 10 h; soxhlet extractions were performed with pyridine, dimethylformamide, or dichloromethane (salen), or with dichloromethane (smdpt). After 10 h the extraction solvent was colorless.

Received: June 21, 1993
Revised version: September 3, 1993 [Z 6152 IE]
German version: *Angew. Chem.* **1994**, *106*, 447

[1] E. F. Vansant, J. H. Lunsford, *Adv. Chem. Ser.* **1973**, *121*, 441–447; K. Mizuno, S. Imamura, J. H. Lunsford, *Inorg. Chem.* **1984**, *23*, 3510–3514; R. J. Taylor, R. S. Drago, J. E. George, *J. Am. Chem. Soc.* **1989**, *111*, 6610–6615.
[2] N. Herron, *Inorg. Chem.* **1986**, *25*, 4714–4717.
[3] A. Zombeck, R. S. Drago, B. Corden, J. Gaul, *J. Am. Chem. Soc.* **1981**, *103*, 7580–7585; D. E. Hamilton, R. S. Drago, A. Zombeck, *ibid.* **1987**, *109*, 374–379.
[4] A. Earnshaw, P. C. Hewlett, E. A. King, L. F. Larkworthy, *J. Chem. Soc. A* **1968**, 241–246; E. Ochiai, *J. Inorg. Nucl. Chem.* **1973**, *35*, 1727–1739.
[5] K. Putyera, G. Plesch, M. Vanickova, M. Valko, M. Zikmund, *Proc. XIII Conf. Coord. Chem. (Smolenice)* **1991**, 239–242.
[6] Overlaps between the zeolite cage and the guest complex were estimated with the programs ChemX (Chemical Design Ltd.) and Hyperchem V. 3.0 (Autodesk Inc.), using the MM+ force field (a completed version of Allinger's MM2(91) force field (N. L. Allinger, *J. Am. Chem. Soc.* **1977**, *99*, 8127). The starting structures of the complexes determined by X-ray crystallography were from R. Cini, P. Orioli, *J. Chem. Soc. Dalton Trans.* **1983**, 2563–2566; M. Calligaris, G. Nardin, L. Randaccio, A. Ripamonti, *J. Chem. Soc. A* **1970**, 1069–1074.
[7] J. Newsam, M. Treacy, D. Vaughan, K. Strohmaier, W. Mortier, *J. Chem. Soc. Chem. Commun.* **1989**, 493–494; F. Delprato, L. Delmotte, J. Guth, L. Huve, *Zeolites* **1990**, *10*, 546–552.
[8] B. Tovrog, R. S. Drago, *J. Am. Chem. Soc.* **1974**, *96*, 6765–6766.
[9] B. Tovrog, D. Ktiko, R. S. Drago, *J. Am. Chem. Soc.* **1976**, *98*, 5144–5153; R. Niswander, L. Taylor, *J. Magn. Reson.* **1977**, *26*, 491–503.

The Two-Step Self-Assembly of [4]- and [5]Catenanes**

David B. Amabilino, Peter R. Ashton, Anatoli S. Reder, Neil Spencer, and J. Fraser Stoddart*

Although polyrotaxanes[1] have already received considerable attention,[2] no convincing strategy for the synthesis of polycatenanes[3] has yet been proposed. Polycatenanes embody one of the ultimate goals of polymer chemists—namely, the construction of polymer chains in which the components are a series of interlinked rings, reminiscent of our familiar mechanical chains.

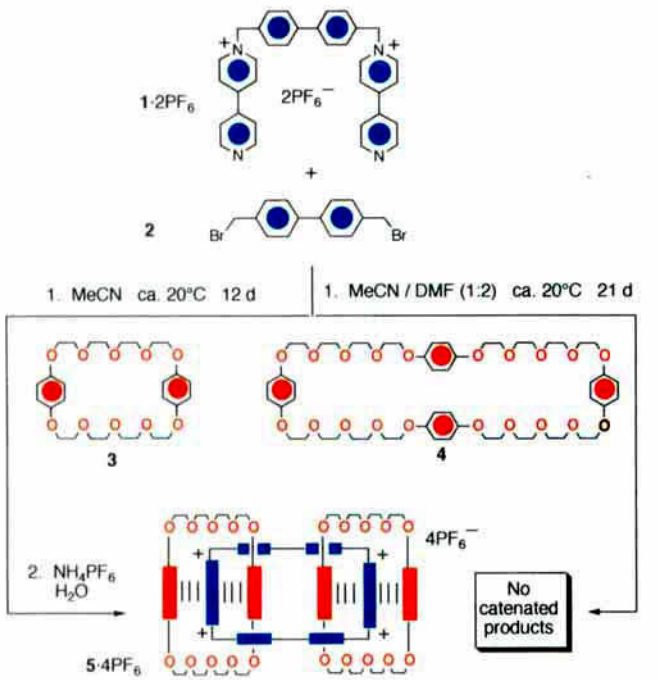
Our recent demonstrations[4, 5] that [3]catenanes, such as **5** · $4PF_6$, can be self-assembled[6, 7] from appropriate building blocks (**1** · $2PF_6$, **2**, and **3** in Scheme 1) with remarkable efficiencies appeared, at first sight, to open up the possibility of a template-directed approach to the synthesis of polycatenanes. However, even although **4** serves readily[5] as a template around which to construct either one or two cyclobis(paraquat-*p*-phenylene) macrocycles, all our numerous attempts to catenate **4** with cyclobis(paraquat-4,4'-biphenylene) rings—starting

[*] Prof. J. F. Stoddart, Dr. D. B. Amabilino, P. R. Ashton, A. S. Reder, Dr. N. Spencer
School of Chemistry, The University of Birmingham
Edgbaston, Birmingham B15 2TT (UK)

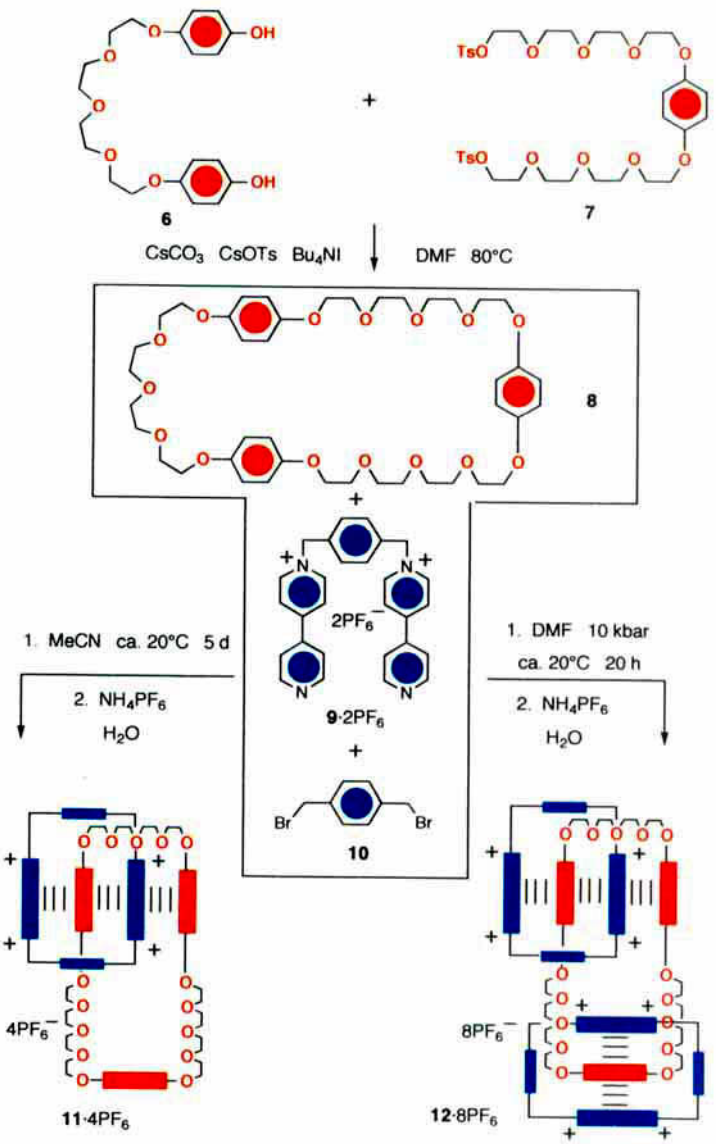
[**] This work was supported by the Science and Engineering Research Council.

from, for example, $1 \cdot 2PF_6$ and **2**—have so far met with no success. We attribute these failures to the large dimensions of the two macrocycles involved and to the flexibility of **4**. Presumably, the molecular recognition between intermediates formed when $1 \cdot 2PF_6$, **2**, and **4** are mixed together in solution in the required molar proportions does not attain that critical level which is essential to sustain an efficient self-assembly process. With these thoughts in mind, we decided to find out whether tris-*p*-phenylene-[51]crown-15 (**8**)—intermediate in constitution between the successful building block bis-*p*-phenylene-[34]crown-10 (**3**) and the failed unit, tetrakis-*para*-phenylene-[68]crown-20 (**4**)—would participate in the template-directed syntheses of catenanes. The answer is that it does! Here we report: 1) the one-step self-assembly (Scheme 2) of the [2]catenane $\mathbf{11} \cdot 4PF_6$ and the [3]catenane $\mathbf{12} \cdot 8PF_6$ and 2) the two-step self-assembly (Scheme 3) of the [4]catenane $\mathbf{14} \cdot 8PF_6$ and the [5]catenane $\mathbf{15} \cdot 12PF_6$ via the intermediate [3]catenane $\mathbf{13} \cdot 4PF_6$, following 3) the cesium-ion-promoted, phase-transfer-catalyzed synthesis (Scheme 2) of tris-*p*-phenylene-[51]crown-15 (**8**) from its immediate precursors, the diphenol **6** and the ditosylate **7**. We describe 4) the characterization of these new catenanes by FAB-MS (FAB-MS = Fast Atom Bombardment Mass Spectrometry),[8] LSI-MS (LSI-MS = Liquid Secondary Ion Mass Spectrometry),[9] and NMR spectroscopy[10] and draw attention to 5) the temperature dependences of the ^1H NMR spectra of $\mathbf{11} \cdot 4PF_6$, $\mathbf{12} \cdot 8PF_6$, $\mathbf{13} \cdot 4PF_6$, $\mathbf{14} \cdot 8PF_6$, and $\mathbf{15} \cdot 12PF_6$.

The macrocyclic polyether **8** was obtained (Scheme 2) in 14% yield from the readily available starting materials **6** and **7** by using a procedure similar to that described[5] for the preparation of tetrakis-*p*-phenylene-[68]crown-20. In the knowledge that it was possible with this macrocyclic polyether to isolate a [2]catenane on reaction of $\mathbf{9} \cdot 2PF_6$ with **10** at normal pressure and a [3]catenane when the same 'clipping' reaction was carried out at ultrahigh pressure, we employed a similar approach to the catenation of **8**. As anticipated, the [2]catenane $\mathbf{11} \cdot 4PF_6$ can be assembled from $\mathbf{9} \cdot 2PF_6$ and **10** in the presence of an excess of **8** in 48% yield at normal pressure. The [3]catenane $\mathbf{12} \cdot 8PF_6$ can be isolated (in 15% yield) *only* under ultrahigh pressure conditions (10 kbar) when $\mathbf{9} \cdot 2PF_6$ and **10** are employed in excess relative to **8**. Encouraged by this result, we carried out a reaction at normal pressure and room temperature in acetonitrile between $\mathbf{1} \cdot 2PF_6$, **2**, and an excess of **8** (Scheme 3), and managed to isolate,[11] albeit in low yield, the [3]catenane $\mathbf{13} \cdot 4PF_6$, a key intermediate in the construction of the [4]catenane $\mathbf{14} \cdot 8PF_6$ and the [5]catenane $\mathbf{15} \cdot 12PF_6$: a subsequent ultrahigh pressure reaction in the range 11–14 kbar between $\mathbf{13} \cdot 4PF_6$ and an excess of $\mathbf{9} \cdot 2PF_6$ and **10** in DMF at room temperature for 8 days afforded $\mathbf{14} \cdot 8PF_6$ in 22% yield and a trace[12] of $\mathbf{15} \cdot 12PF_6$.

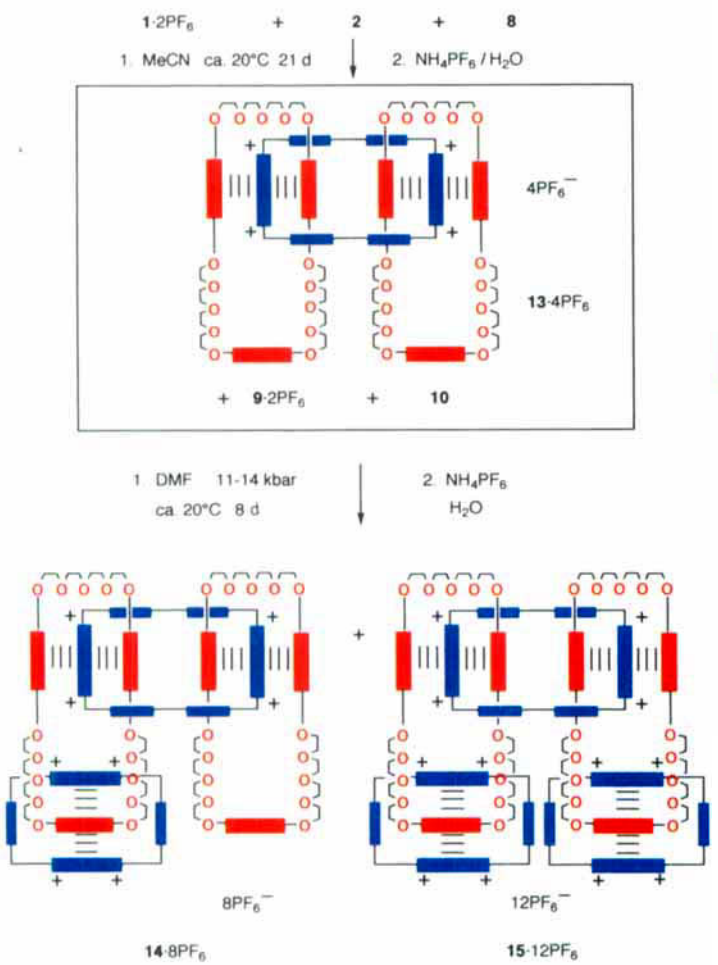


Scheme 1. The template-directed synthesis of the [3]catenane $\mathbf{5} \cdot 4PF_6$ [5] and the failure to catenate **4**. The chemical cartoons are defined as follows: *para*-phenylene rings ≡ small blue rectangles, bipyridinium units ≡ large blue rectangles, hydroquinol rings ≡ red rectangles.



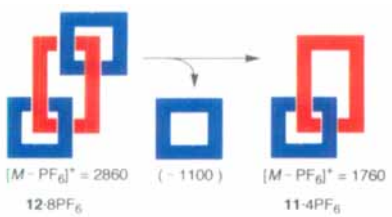
Scheme 2. The cesium template-directed synthesis of **8** from the diphenol **6** and ditosylate **7**, and the subsequent template-directed synthesis of the [2]catenane $\mathbf{11} \cdot 4PF_6$ and the [3]catenane $\mathbf{12} \cdot 8PF_6$ from **8**, $\mathbf{9} \cdot 2PF_6$, and **10**.

 © VCH Verlagsgesellschaft mbH, D-69451 Weinheim, 1994 0570-0833/94/0404-0434 $ 10.00+.25/0



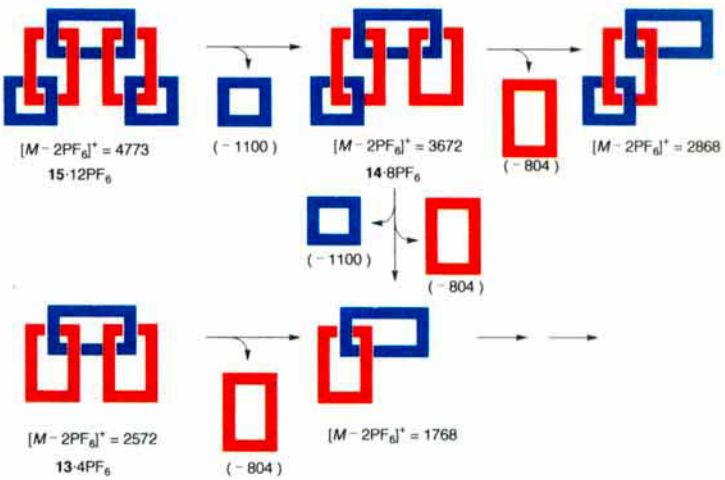
Scheme 3. The two-step template-directed synthesis in which the [3]catenane $\mathbf{13} \cdot 4PF_6$ is prepared first at normal pressure from $\mathbf{1} \cdot 2PF_6$, **2**, and **8**, and then used with $\mathbf{9} \cdot 2PF_6$ and **10** to form the [4]catenane $\mathbf{14} \cdot 8PF_6$ and the [5]catenane $\mathbf{15} \cdot 12PF_6$.

The techniques of FAB-MS and LSI-MS allowed us to identify and interrelate $\mathbf{11} \cdot 4PF_6$ and $\mathbf{12} \cdot 8PF_6$, and $\mathbf{13} \cdot 4PF_6$, $\mathbf{14} \cdot 8PF_6$, and $\mathbf{15} \cdot 12PF_6$. The combined mass spectrometry data is summarized in Table 1: comparisons of m/z values are made in the horizontal direction. The relationships between the various catenanes in terms of the stepwise losses of rings during FAB-MS and LSI-MS are highlighted in Schemes 4 and 5. The fragmentation patterns listed in Table 1 are highly characteristic[13, 14] of catenanes and establish the identities of all the [2]-, [3]-, [4]-, and [5]catenanes beyond any doubt.



Scheme 4. The initial fragmentation experienced by $\mathbf{12} \cdot 8PF_6$ to afford $\mathbf{11} \cdot 4PF_6$ (see Scheme 2). The large red rectangle represents tris-*p*-phenylene-[51]crown-5 (**8**), and the small blue rectangle cyclobis(paraquat-*p*-phenylene) tetrakis(hexafluorophosphate).

All the catenanes of Table 1 exhibit multiple temperature dependencies in their ^1H NMR spectra above and below room temperature that are commensurate with site exchange processes involving different kinds of movements (for example, circumrotation and pirouetting, as well as rocking and rattling)[15] of the interlocked rings relative to each other.



Scheme 5. The sequence of fragmentations in FAB and LSI mass spectra experienced by $\mathbf{13} \cdot 4PF_6$, $\mathbf{14} \cdot 8PF_6$, and $\mathbf{15} \cdot 12PF_6$. The large blue rectangle represents cyclobis(paraquat-4,4′-biphenylene) tetrakis(hexafluorophosphate). The nature of the other rectangles is defined in the caption to Scheme 4. The values for $[M - 2PF_6]^+$ are calculated ones. Any arithmetic anomaly reflects the fact that no more than four significant figures are quoted.

We have demonstrated that, by subtle and appropriate modification of 'intelligent' components, the efficient molecular recognition and assembly processes that have spawned [2]- and [3]catenanes incorporating hydroquinol rings as π-donors and bipyridinium units as π-acceptors[4–7, 15] can be applied successfully to the construction of more highly catenated molecules. We trust that constitutional amendments that increase the information[16] content of the compounds are both possible and practical; this confidence leads us to believe that polycatenanes will soon be commonplace.

Experimental Procedure

8: A solution of the diphenol **6** [15] (1.9 g, 5.0 mmol) in dry DMF (70 mL) was added to a stirred suspension of Cs_2CO_3 (16.3 g, 50 mmol) in dry DMF (50 mL) under nitrogen, and the mixture was heated to 60 °C. After an additional 30 min, CsOTs (3.0 g, 10.0 mmol) and Bu_4NI (0.2 g, 0.5 mmol) were added as solids. A solution of the ditosylate **7** [5] (3.9 g, 5.0 mmol) in dry DMF (80 mL) was added over 2 h, and the temperature was then raised to 80 °C. Stirring and heating at 80 °C were continued for 3 days. The reaction mixture was then filtered, and the precipitate washed with DMF (30 mL). The solvent was removed under vacuum, and the residue was partitioned between toluene (250 mL) and water (50 mL). The toluene fraction was dried and concentrated under vacuum to afford a residue that was purified by column chromatography [SiO_2, Me_2CO/C_6H_{14} (2.5:3)] to yield **8** as a white solid (0.55 g, 14%, m.p. 49–51 °C); positive-ion FAB-MS: m/z 804 (M^+); ^1H NMR ($CDCl_3$): δ = 3.64–3.72 (m, 24H), 3.78–3.84 (m, 12H), 4.02–4.09 (m, 12H), 6.82 (s, 12H); ^{13}C NMR ($CDCl_3$): δ = 68.2, 69.8, 70.7, 70.8, 115.7, 153.1. Subsequently, when the same reaction procedure was repeated with 1,4-bis[2-[2-[2-[2-(4-hydroxyphenoxy)ethoxy]ethoxy]ethoxy]ethoxy]benzene [5] and tetraethyleneglycol bistosylate as starting materials, a 30% yield of **8** was obtained.

$\mathbf{11} \cdot 4PF_6$: **10** (38 mg, 0.14 mmol) in dry MeCN (2 mL) was added to a solution of $\mathbf{9} \cdot 2PF_6$ (88 mg, 0.12 mmol) and **8** (200 mg, 0.25 mmol) in dry MeCN (5 mL). After the reaction mixture had been stirred at room temperature for 5 days, the solvent was removed under vacuum to afford a red solid which was subjected to column chromatography [SiO_2, MeOH:2 N aqueous NH_4Cl:$MeNO_2$ (7:2:1)]. The solvents were evaporated off under vacuum from the crude product, which was dissolved in

 © VCH Verlagsgesellschaft mbH, D-69451 Weinheim, 1994 0570-0833/94/0404-0435 $ 10.00+.25/0

Table 1. Comparison of *m/z* values obtained from FAB-MS or LSI-MS for **11** · $4PF_6$, **12** · $8PF_6$, **13** · $4PF_6$, **14** · $8PF_6$, and **15** · $12PF_6$ [a].

m/z Values [Ion]				
11 · $4PF_6$ [b]	**12** · $8PF_6$ [b]	**13** · $4PF_6$ [b]	**14** · $8PF_6$ [c]	**15** · $12PF_6$ [c]
	2860 $[M - PF_6]^+$			4774 $[M - 2PF_6]^+$
	2715 $[M - 2PF_6]^+$			4629 $[M - 3PF_6]^+$
	2570 $[M - 3PF_6]^+$			4483 $[M - 4PF_6]^+$
	2425 $[M - 4PF_6]^+$			4338 $[M - 5PF_6]^+$
1904 $[M]^+$			3818 $[M - PF_6]^+$	3818 [h]
1759 $[M - PF_6]^+$	1760 [d]		3672 $[M - 2PF_6]^+$	3673 [h]
1613 $[M - 2PF_6]^+$	1615 [d]		3527 $[M - 3PF_6]^+$	3528 [h]
1469 $[M - 3PF_6]^+$			3382 $[M - 4PF_6]^+$	
				3013 [i]
			2868 [f]	2868 [i]
			2723 [f]	2723 [i]
			2578 [f]	2577 [i]
		2861 $[M]^+$		
		2716 $[M - PF_6]^+$		
		2571 $[M - 2PF_6]^+$		
		2425 $[M - 3PF_6]^+$		
		2056 [e]		
		1911 [e]	1912 [g]	
		1767 [e]	1767 [g]	
		1620 [e]	1622 [g]	

[a] The fragmentation patterns for the catenanes should be compared with the diagrams of Schemes 4 and 5. [b] See ref. [8] for details of how the FAB-MS were obtained. [c] See ref. [9] for details of how the LSI-MS were obtained. [d] Peaks indicating the generation of the [2]catenane **11** · $4PF_6$ by loss of the cyclobis(paraquat-*p*-phenylene) macrocycle from the [3]catenane **12** · $8PF_6$. [e] Peaks indicating the generation of a [2]catenane by loss of **8** from the [3]catenane **13** · $4PF_6$. This [2]catenane has indeed been isolated and characterized. The positive-ion FAB-MS of this catenane yields a very similar series of peaks. The peaks reported represent the ion corresponding to this fragment, followed by the loss of one, two, and three PF_6 ions. See ref. [11]. [f] Peaks indicating the generation of a [3]catenane by loss of **8** from the [4]catenane **14** · $8PF_6$. The peaks reported correspond to the loss of two, three, and four PF_6 ions from the fragment. [g] Peaks indicating the generation of a [2]catenane by loss of **8** and the cyclobis(paraquat-*p*-phenylene) macrocycle from the [4]catenane **14** · $8PF_6$. This [2]catenane has indeed been isolated and characterized. The positive-ion FAB-MS of this catenane yields a very similar series of peaks. The peaks reported correspond to the loss of one, two, and three PF_6^- ions from the fragment. See ref. [11]. [h] Peaks indicating the generation of the [4]catenane **14** · $8PF_6$ by loss of the cyclobis(paraquat-*p*-phenylene) macrocycle from the [5]catenane **15** · $12PF_6$. The peaks reported correspond to the loss of one, two, and three PF_6^- ions from the fragment. [i] Peaks indicating the generation of a [3]catenane by loss of **8** and the cyclobis(paraquat-*p*-phenylene) macrocycle from the [5]catenane **15** · $12PF_6$. The peaks reported correspond to the loss of one, two, three, and four PF_6^- ions from the fragment.

water (10 mL). A saturated aqueous NH_4PF_6 solution was added to this solution until precipitation was complete. The precipitate was filtered off, washed with H_2O (10 mL), and dried under vacuum to give **11** · $4PF_6$ as a red solid (110 mg, 48%, m.p. >250 °C); positive-ion FAB-MS: *m/z* 1904 (M^+), 1759 ([M − PF_6]$^+$), 1613 ([$M - 2PF_6$]$^+$), 1469 ([$M - 3PF_6$]$^+$); ^{1}H NMR (CD_3COCD_3): δ = 3.50–4.10 (m, 52H), 6.01 (s, 8H), 6.60 (br s, 8H), 7.96 (s, 8H), 8.15 (d, J = 7 Hz, 8H), 9.30 (d, J = 7 Hz, 8H); ^{13}C NMR (CD_3COCD_3): δ = 65.7, 70.6, 71.3, 115.9, 126.6, 128.5, 128.6, 130.5, 130.7, 131.3, 131.8, 137.7, 145.7, 147.2, 151.5.

12 · $8PF_6$: **10** (300 mg, 1.16 mmol), **9** · $2PF_6$ (750 mg, 1.06 mmol), and **8** (170 mg, 0.21 mmol) were dissolved in dry DMF (10 mL), and the solution was subjected to pressure (10 kbar) for 20 h at room temperature. After evaporation of the solvent, the residue was purified by column chromatography [SiO_2, MeOH:2 N aqueous NH_4Cl:DMF (4:5:2)]. After counterion exchange, as described for **11** · $4PF_6$, pure **12** · $8PF_6$ was isolated as a red solid (92 mg, 15%, m.p. >250 °C); positive-ion FAB-MS: *m/z* 2860 ([$M - PF_6$]$^+$), 2715 ([$M - 2PF_6$]$^+$), 2570 ([$M - 3PF_6$]$^+$), 2425 ([$M - 4PF_6$]$^+$); ^{1}H NMR (CD_3COCD_3, 53 °C): δ = 3.64–4.03 (m, 48H), 4.74 (br s, 12H), 6.05 (s, 16H), 8.03 (s, 16H), 8.22 (d, J = 7 Hz, 16H), 9.32 (d, J = 7 Hz, 16H); ^{13}C NMR (CD_3COCD_3): δ = 65.8, 67.9, 70.7, 71.2, 71.5, 114.5, 126.9, 131.9, 137.8, 145.8, 147.7, 152.1.

13 · $4PF_6$: **2** (0.31 g, 0.91 mmol) in dry MeCN (5 mL) was added to a solution of **1** · $2PF_6$ (0.65 g, 0.83 mmol) and **8** (2.0 g, 2.5 mmol) in dry MeCN (20 mL). Following a procedure identical to that described for the preparation of **11** · $4PF_6$, apart from the reaction time (in this case, 21 days), **13** · $4PF_6$ was isolated as a red solid (83 mg, 3.5%, m.p. <250 °C); positive-ion FAB-MS: *m/z* = 2861 (M^+), 2716 ([$M - PF_6$]$^+$), 2571 ([$M - 2PF_6$]$^+$), 2425 ([$M - 3PF_6$]$^+$); ^{1}H NMR (CD_3COCD_3): δ = 3.57–3.78 (m, 96H), 5.99 (s, 24H), 6.02 (s, 8H), 7.83–7.90 (AB system, J_{AB} = 8 Hz, 16H), 8.13 (d, J = 7 Hz, 8H), 9.31 (d, J = 7 Hz, 8H); ^{13}C NMR (CD_3COCD_3): δ = 65.8, 68.5, 70.5, 71.3, 71.3, 115.7, 127.3, 128.8, 131.1, 135.3, 141.6, 146.0, 148.1, 153.2. See also ref. [11].

14 · $8PF_6$: **10** (21.1 mg, 0.080 mmol), **9** · $2PF_6$ (51.2 mg, 0.073 mmol), and **13** · $4PF_6$ (41.5 mg, 0.015 mmol) were dissolved in dry DMF (7 mL), and the solution was subjected to 11 kbar for 5 days at room temperature. Then further quantities of **10** (21.1 mg, 0.080 mmol) and **9** · $2PF_6$ (51.2 mg, 0.073 mmol) were added, and the reaction was continued under pressure (14 kbar) for 3 days. The reaction was worked up as described for **12** · $8PF_6$. Pure **14** · $8PF_6$ was isolated as a red solid (12.9 mg, 22%, m.p. >250 C); LSI-MS: *m/z* 3818 ([$M - PF_6$]$^+$), 3672 ([$M - 2PF_6$]$^+$), 3527 ([$M - 3PF_6$]$^+$), 3382 ([$M - 4PF_6$]$^+$); ^{1}H NMR (CD_3COCD_3): δ = 3.50–3.95 (m, 100H), 5.97 (s, 20H), 5.99 (s, 8H), 6.07 (s, 8H), 7.82–7.88 (m, 16H), 8.07, (s, 8H), 8.10 (d, J = 7 Hz, 8H), 8.29 (d, J = 7 Hz, 8H), 9.28 (d, J = 7 Hz, 8H), 9.39 (d, J = 7 Hz, 8H); ^{13}C NMR (CD_3COCD_3): δ = 65.7, 67.8, 68.4, 70.5, 71.1, 71.3, 71.4, 114.9, 115.7, 127.0, 127.4, 128.7, 131.0, 132.0, 135.4, 137.9, 141.6, 146.0, 147.8, 148.2, 153.2. See also ref. [12].

Received: September 3, 1993 [Z 6333 IE]
German version: *Angew. Chem.* **1994**, *106*, 450

[1] A. Harada, M. Kamachi, *J. Chem. Soc. Chem. Commun.* **1990**, 1322; *Macromolecules* **1990**, *23*, 2821; A. Harada, J. Li, M. Kamachi, *Nature* **1992**, *356*, 325; G. Wenz, B. Keller, *Angew. Chem.* **1992**, *104*, 201; *Angew. Chem. Int. Ed. Engl.* **1992**, *31*, 197; M. Born, H. Ritter, *Makromol. Chem. Rapid Commun.* **1991**, *121*, 471; Y. X. Shen, H. W. Gibson, *Macromolecules* **1992**, *25*, 2058; H. W. Gibson, H. Marand, *Adv. Mater.* **1993**, *5*, 11.

[2] J. F. Stoddart, *Angew. Chem.* **1992**, *104*, 860; *Angew. Chem. Int. Ed. Engl.* **1992**, *31*, 846.

[3] Higher nonlinear catenanes containing three, four, five, six, and seven rings have been prepared in a single macrocyclization. See C. O. Dietrich-Buchecker, J. Guilhem, A.-K. Khémiss, J.-P. Kintzinger, C. Pascard, J.-P. Sauvage, *Angew. Chem.* **1987**, *99*, 711; *Angew. Chem. Int. Ed. Engl.* **1987**, *26*, 661; F. Bitsch, C. O. Dietrich-Buchecker, A.-K. Khémiss, J.-P. Sauvage, A. Van Dorsselaer, *J. Am. Chem. Soc.* **1991**, *113*, 4023; C. Dietrich-Buchecker, J.-P. Sauvage, *Bull. Soc. Chim. Fr.* **1992**, *129*, 113. Most recently, three rings have been constructed around a bicyclic molecule bearing three template sites. See C. O. Dietrich-Buchecker, B. Frommberger, I. Lüer, J.-P. Sauvage, F. Vögtle, *Angew. Chem.* **1993**, *105*, 1526; *Angew. Chem. Int. Ed. Engl.* **1993**, *32*, 1434.

[4] P. R. Ashton, C. L. Brown, E. J. T. Chrystal, T. T. Goodnow, A. E. Kaifer, K. P. Parry, A. M. Z. Slawin, N. Spencer, J. F. Stoddart, D. J. Williams, *Angew. Chem.* **1991**, *103*, *1055*; *Angew. Chem. Int. Ed. Engl.* **1991**, *30*, 1039.

[5] P. R. Ashton, C. L. Brown, E. J. T. Chrystal, K. P. Parry, M. Pietraszkiewicz, N. Spencer, J. F. Stoddart, *Angew. Chem.* **1991**, *103*, 1058; *Angew. Chem. Int. Ed. Engl.* **1991**, *30*, 1042.

[6] J. F. Stoddart in *Host-Guest Molecular Interactions: From Chemistry to Biology* (Ciba Found. Symp. *158*), Wiley, Chichester, **1991**, p. 5–22; J. S. Lindsey, *New J. Chem.* **1991**, *15*, 153; G. M. Whitesides, J. P. Mathias, C. T. Seto, *Science* **1991**, *254*, 1312; J. Rebek, Jr. in *Molecular Recognition: Chemical and Biochemical Problems II* (Ed.: S. M. Roberts), RSC Special Publ. No. 111, Cambridge, **1992**, p. 65–73. Editorial comment: See also the review on template syntheses in this issue: F. Vögtle, R. Hoss, *Angew. Chem.* **1994**, *106*, 389; *Angew. Chem. Int. Ed. Engl.* **1994**, *33*, 375.

[7] D. Philp, J. F. Stoddart, *Synlett* **1991**, 445; P. R. Ashton, C. L. Brown, E. J. T. Chrystal, T. T. Goodnow, A. E. Kaifer, K. P. Parry, D. Philp, A. M. Z. Slawin, N. Spencer, J. F. Stoddart, D. J. Williams, *J. Chem. Soc. Chem. Commun.* **1991**, 634; P. L. Anelli, N. Spencer, J. F. Stoddart, *J. Am. Chem. Soc.* **1991**, *113*, 5131; J. F. Stoddart, *Chem. Aust.* **1992**, *59*, 576; C. L. Brown, D. Philp, N. Spencer, J. F. Stoddart, *Isr. J. Chem.* **1992**, *32*, 61; J. F. Stoddart, *An. Quím.* **1993**, *89*, 51.

[8] FAB-MS for samples **11** · $4PF_6$, **12** · $8PF_6$, and **13** · $4PF_6$ was carried out on a Kratos MS80RF mass spectrometer (accelerating voltage, 3 kV; resolution, 1000) coupled to a DS90 data system and off-line Sun Workstation for processing the raw data experiments. The atom gun was an adapted saddle field source (Ion Tech Ltd.) operated at about 8 keV and a tube current of about 2 mA. Krypton was used to provide a primary beam of atoms, and the samples were dissolved in a small volume of 3-nitrobenzyl alcohol that had previously been coated onto a stainless steel probe tip. Spectra were recorded in the positive-ion mode at a scan speed of 30 seconds per decade.

[9] For samples **14** · $8PF_6$ and **15** · $12PF_6$, LSI-MS was carried out on a Kratos Concept 1H mass spectrometer (accelerating voltage, 8 kV; resolution, 1000) coupled to a Sun Sparc Station with Mach3 Software. The samples were dissolved in acetone, and a small volume (1–2 μL) was added to the 3-nitrobenzyl alcohol matrix. Spectra were recorded in the positive-ion mode at a scan speed of 5 seconds per decade. We gratefully acknowledge the assistance of Kratos

Analytical, and in particular Dr. M. Kimber, Dr. H. Wight, and Dr. J. Moncur, in the collection of the mass spectra for these compounds.

[10] The ^1H and ^{13}C NMR spectra were recorded on a Bruker AMX400 spectrometer operating at 400.13 MHz and at 100.63 MHz, respectively. All chemical shifts are referenced by means of the residual CHD_2COCHD_2 or CHD_2CN signals to Me_4Si.

[11] A minor product of this reaction was the [2]catenane comprising a cyclobis(paraquat-4,4'-biphenylene) macrocycle and a tris-*p*-phenylene-[51]crown-15 ring. It was isolated as a red solid (0.7%, m.p. > 250°C); positive-ion FAB-MS: *m/z* 2056 (M^+), 1911 ($[M - PF_6]^+$), 1766 ($[M - 2PF_6]^+$), 1621 ($[M - 3PF_6]^+$), 1476 ($[M - 4PF_6]^+$); ^1H NMR (CD_3COCD_3): δ = 3.68–3.79 (m, 48H), 6.05 (s, 12H), 6.10 (s, 8H), 7.70–7.80 (AA'BB' system, J_{AB} = 8.5 Hz, 16H), 8.49 (d, J = 6 Hz, 8H), 9.49 (d, J = 6 Hz, 8H); ^{13}C NMR (CD_3COCD_3): δ = 65.8, 68.6, 70.4, 71.2, 71.3, 115.9, 127.9, 128.7, 130.8, 135.3, 141.5, 146.2, 149.2, 153.4.

[12] A very small quantity (< 1 mg) of the [5]catenane **15** · $12PF_6$ was isolated from the reaction yielding the [4]catenane **14** · $8PF_6$. The identification of **15** · $12PF_6$ rests solely on its LSI-MS (Table 1) at present. The sluggishness of the [4]catenane to go on and afford the [5]catenane perplexes us. We speculate that a negative allosteric effect is operating in so far as the first catenation of **13** · $4PF_6$ by a cyclobis(paraquat-*p*-phenylene) macrocycle to give **14** · $4PF_6$ inhibits the second catenation to give **15** · $12PF_6$.

[13] W. Welter, E. Logemann, G. Schill, *Org. Mass. Spectrom.* **1977**, *12*, 351.

[14] J.-P. Sauvage, *Acc. Chem. Res.* **1990**, *23*, 319.

[15] P. L. Anelli, P. R. Ashton, R. Ballardini, V. Balzani, M. Delgado, M. T. Gandolfi, T. T. Goodnow, A. E. Kaifer, D. Philp, M. Pietraszkiewicz, L. Prodi, M. V. Reddington, A. M. Z. Slawin, N. Spencer, J. F. Stoddart, C. Vicent, D. J. Williams, *J. Am. Chem. Soc.* **1992**, *114*, 193.

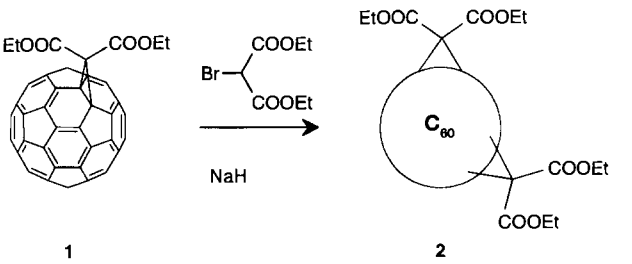
[16] J.-M. Lehn, *Angew. Chem.* **1990**, *102*, 1347; *Angew. Chem. Int. Ed. Engl.* **1990**, *29*, 1304; *Science* **1993**, *260*, 1762.

Fullerene Chemistry in Three Dimensions: Isolation of Seven Regioisomeric Bisadducts and Chiral Trisadducts of C_{60} and Di(ethoxycarbonyl)methylene**

Andreas Hirsch,* Iris Lamparth, and Heinrich R. Karfunkel

The exohedral chemistry of C_{60} has been dominated thus far by investigations of its reactivity and the isolation and characterization of monoaddition products.[1] Up to this point the regiochemistry of polyadducts has hardly been examined systematically.[2] The synthesis of polyadducts with defined three-dimensional structure is also topical in view of fullerene derivatives with interesting biological[3] or material properties.[4] We describe here the systematic investigation of the regiochemistry of C_{60} derivatives with two and three methano bridges; of the eight possible products, the seven stable regioisomeric bisadducts and chiral trisadducts formed in a stepwise fashion and were isolated.

The cyclopropanation of C_{60} with diethyl bromomalonate was chosen as a model reaction.[5] This reaction proceeds very uniformly, and only the bonds common to two six-membered rings in the fullerene framework (6-6 bonds) are attacked. We first isolated the monoaddition product $C_{61}(COOEt)_2$ **1** by chromatography, and subjected it to the same reaction conditions to synthesize $C_{62}(COOEt)_4$ **2**.



1 **2**

For a description of the spatial arrangement of the added groups, the C_{60} molecule is divided into three sections with regard to the location of the second attack (Fig. 1). This second addition can take place on the same hemisphere (*cis*), at the equator (*e*), or on the opposite hemisphere (*trans*). Three different sets of double bonds can be attacked within the same hemisphere (*cis*-1, *cis*-2, *cis*-3), and four different sets of double bonds are available on the opposite hemisphere (*trans*-1, *trans*-2, *trans*-3).[6]

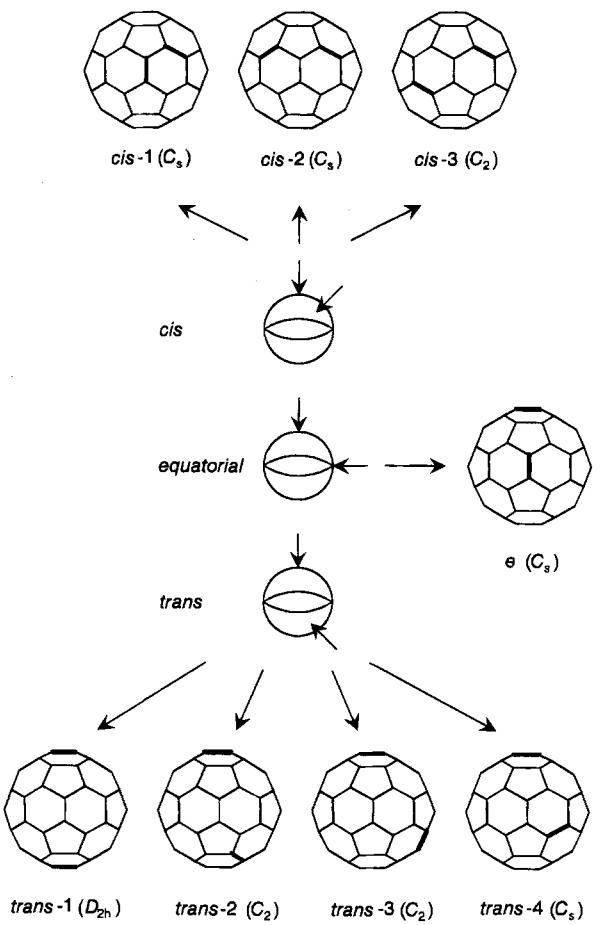


Fig. 1. Positional relationships between the 6-6 bonds in C_{60} and the symmetry of the corresponding bisadducts.

Chromatographic separation of the reaction mixture gave (in order of elution following **1**) a fraction of five different bisadducts **2a–e** and a mixed fraction consisting of two further bisadducts **2f, g** (Table 1) as well as trisadducts **3**. Further separation with preparative HPLC provided the bisadducts **2a–e** (on SiO_2) and **2f, g** (on a nitrophenyl phase with toluene as eluent). Compounds **2a–g** were characterized by UV/VIS, IR, ^1H NMR, and ^{13}C NMR spectroscopy (Table 2) as well as by mass spectrometry.[7]

[*] Dr. A. Hirsch, I. Lamparth
Institut für Organische Chemie der Universität
Auf der Morgenstelle 18, D-72076 Tübingen (FRG)
Telefax: Int. code + (7071) 29-5244
Priv.-Doz. H. R. Karfunkel
Ciba Geigy AG, Basel (Switzerland)

[**] This research was supported by the Deutsche Forschungsgemeinschaft, the Bundesministerium für Forschung und Technologie, and Hoechst AG.

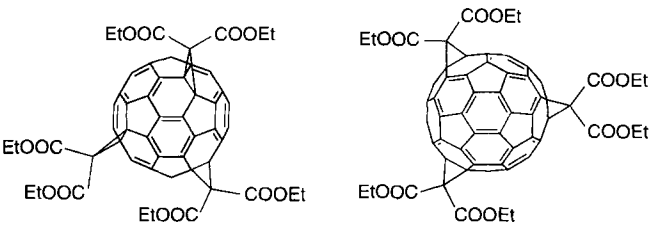
Table 1. Order of elution (Elution no.), symmetry, number of the possible modes of construction (No.), yield [%], and assignment of the isolated bisadducts **2a–g**, along with the calculated relative AM1 heats of formation ($AM1_F$) in kcal mol^{-1} and AM1 dipole moments ($AM1_D$) in Debye for all eight regioisomers (the *cis*-1 isomer was not isolated).

Elution no.	Cmpd.	Sym. [a]	No.	Yield	Assign. [b]	$AM1_F$ [c]	$AM1_D$ [c]
1	**2a**	D_{2h}	1	0.8	*trans*-1*	0.2	0.1
2	**2b**	C_2	4	5.3	*trans*-2* (*cis*-3)	0.2	1.2
3	**2c**	C_2	4	12.0	*trans*-3*	0.1	2.0
4	**2d**	C_s	4	3.7	*trans*-4* (*cis*-2) (*cis*-1)	0.0	2.3
5	**2e**	C_s	4	15.5	*e** (*trans*-2)	0.0	2.6
6	**2f**	C_2	4	2.5	*cis*-3* (*trans*-4)	1.3 [d]	3.0 [d]
7	**2g**	C_s	4	0.9	*cis*-2* (*cis*-1)	1.8	3.5
–	–	C_s	4	0.0	*cis*-1	17.7 [e]	3.8 [e]

[a] Determined from the ^{1}H and ^{13}C NMR spectra. [b] The assignments marked with * are based on the order of elution. The isomers with the same symmetry are listed in parentheses. [c] To simplify the calculation the methyl esters $C_{62}(COOMe)_4$ were examined. [d] Value for one of the two optimized conformers. [e] Value for one of the three optimized conformers.

The symmetry of **2a–g** is evident from their NMR spectra (Table 1). The least polar isomer **2a** could thus be assigned as the *trans*-1 product with D_{2h} symmetry and **2e** as the *e* isomer with C_s symmetry.[8] The order of elution of these isomers corresponds to the calculated polarities (Table 1). The other isomers are either C_s-symmetric with 32 NMR sigals for the fullerene C atoms, of which four are half as intense as the others, or they are chiral and C_2-symmetric giving rise to 30 NMR signals for the fullerene C atoms. The red to copper-colored compounds **2b–g** are readily soluble in toluene and $CHCl_3$, whereas the least polar orange isomer **2a** (*trans*-1) is only marginally soluble. Compound **2a** can arise from **1** by attack at only a single double bond; in the formation of the other isomers four bonds are available in each case. These relations are reflected in the low yield of **2a** especially relative to the yields of **2b**,**e** (see Table 1). The uncertainty in the structure assignments can be further reduced by comparison of the order of elution, the yields, and the symmetries of the regioisomers of **2** with their calculated stabilities and dipole moments (Table 1). The calculations also show that the formation of a *cis*-1 isomer is considerably disfavored. Indeed, a yet more polar eighth regioisomer of **2** could not be detected in the reaction mixture.

The isomerically pure compounds **2b–e** were cyclopropanated to give the trisadducts **3**. Each crude product was separated into at least three fractions of trisadducts **3** by preparative HPLC. Remarkably, the bisadduct **2e** with the methano bridge in position *e* gave the intensely orange-red trisadduct **3a** preferentially; **2c** gave primarily the red trisadduct **3b**. In each case the yield



3a **3b**

was 40%. Both regioisomers are chiral; the ^{1}H and ^{13}C NMR spectra (Table 2) demonstrate unequivocally that **3a** has C_3 symmetry and **3b** D_3 symmetry. In **3a** all methano bridges are in *e* positions relative to each other (*e*,*e*,*e*) and in **3b** in *trans*-3 positions (*trans*-3,*trans*-3,*trans*-3). In **3b** the methano bridges lie on a belt along the equator about the threefold axis of the C_{60} framework. For each enantiomer the 6-6 bonds point either up or down. The spectroscopic characterization of **3b** also indicates that **2c** can be conclusively assigned as the *trans*-3 isomer (see Table 2). The apparently preferred formation of **3a** and **3b** (additions in *trans*-3 and *e* positions) can be correlated with the relatively high yields of **2c** and **2e** (see Table 1). In the cyclopropanation of **2b** and **2d** the main reactions are *trans*-3 and *e* additions.

The regioselective assembly of tetra- and hexaadducts with higher symmetry by *e* additions to **2a** and **2e** is a topic of further investigations.

Received: October 1, 1993 [Z 6384 IE]
German version: *Angew. Chem.* **1994**, *106*, 453

Table 2. Selected data from the NMR spectra of the bisadducts **2a**, **e** and trisadducts **3a**, **b**. All samples were measured in $CDCl_3$ at 25 °C.

2a: ^{1}H NMR (400 MHz): $\delta = 4.65$ (q, $J = 7.1$ Hz, 4H; CH_2), 1.55 (t, $J = 7.1$ Hz, 6H; CH_3); ^{13}C NMR (100 MHz): $\delta = 164.08$, 145.25 (8C), 144.84 (8C), 143.66 (8C), 143.61 (8C), 143.48 (8C), 141.23 (8C), 139.17 (8C), 70.24 (4C), 63.40, 45.89, 14.30

2e: ^{1}H NMR (400 MHz): $\delta = 4.47$, 4.46, 4.42 (3 q, $J = 7.1$ Hz, 8H; CH_2), 1.41, 1.40, 1.38 (3 t, $J = 7.1$ Hz, 12H; CH_3); ^{13}C NMR (100 MHz): $\delta = 163.51$, 163.48, 163.38, 147.61 (2C), 147.22 (2C), 146.44 (3C), 146.16 (2C), 146.03 (2C), 145.54 (2C), 145.36 (2C), 145.13 (2C), 144.98 (1C), 144.68 (4C), 144.57 (2C), 144.43 (2C), 144.35 (2C), 144.08 (2C), 144.01 (2C), 143.72 (4C), 143.36 (2C), 143.25 (2C), 143.16 (2C), 142.86 (2C), 142.33 (2C), 141.83 (2C), 141.64 (2C), 141.54 (2C), 138.76 (2C), 138.66 (2C), 71.61 (2C), 70.35 (1C), 64.82 (1C), 63.19, 53.48, 51.29, 14.15, 14.08

3a: ^{1}H NMR (400 MHz): $\delta = 4.39$ (dq, $J = 7.1$ Hz, 6H; CH_2), 4.32 (q, $J = 7.1$ Hz, 6H; CH_2), 1.35 (t, $J = 7.1$ Hz, 9H; CH_3), 1.32 (t, $J = 7.1$ Hz, 9H; CH_3); ^{13}C NMR (100 MHz): $\delta = 163.32$, 147.36 (3C), 146.81 (3C), 146.74 (3C), 146.57 (6C), 146.46 (3C), 146.26 (3C), 145.57 (6C), 145.05 (3C), 144.99 (3C), 144.25 (3C), 143.43 (3C), 143.01 (3C), 142.28 (3C), 141.71 (6C), 140.89 (3C), 70.93 (3C), 70.10 (3C), 63.00, 52.90, 14.10, 14.02

3b: ^{1}H NMR (250 MHz): $\delta = 4.46$ (q, $J = 7.0$ Hz, 12H; CH_2), 1.41 (t, $J = 7.0$ Hz, 18H; CH_3); ^{13}C NMR (62.9 MHz): $\delta = 163.42$, 148.51 (6C), 147.51 (6C), 146.93 (6C), 146.68 (6C), 146.42 (6C), 145.48 (6C), 143.14 (6C), 142.33 (6C), 141.76 (6C), 71.04 (6C), 63.20, 51.10, 14.16

[1] Reviews: a) R. Taylor, D. R. M. Walton, *Nature* **1993**, *363*, 685; b) A. Hirsch, *Angew. Chem.* **1993**, *105*, 1189; *Angew. Chem. Int. Ed. Engl.* **1993**, *32*, 1138, and references therein.

[2] J. M. Hawkins, A. Meyer, T. A. Lewis, U. Bunz, R. Nunlist, G. E. Ball, T. W. Ebbesen, K. Tanigaki, *J. Am. Chem. Soc.* **1992**, *114*, 7954.

[3] a) S. H. Friedman, D. L. DeCamp, R. P. Sijbesma, G. Srdanov, F. Wudl, G. L. Kenyon, *J. Am. Chem. Soc.* **1993**, *115*, 6506; b) R. Sijbesma, G. Srdanov, F. Wudl, J. A. Castoro, C. Wilkins, S. H. Friedman, D. L. DeCamp, G. L. Kenyon, *ibid.* **1993**, *115*, 6510.

[4] A. Hirsch, *Adv. Mater.* **1993**, *5*, 859.

[5] C. Bingel, *Chem. Ber.* **1993**, *126*, 1957.

[6] The individual derivatives can be named according to the nomenclature suggested by Chemical Abstracts in which all C atoms are numbered in a spiral pattern starting from a five-membered ring; however, this does not provide a clear description of the spatial relationships (like *ortho*, *meta*, and *para* in benzene chemistry) necessary for a discussion of the regiochemistry of fullerene derivatives.

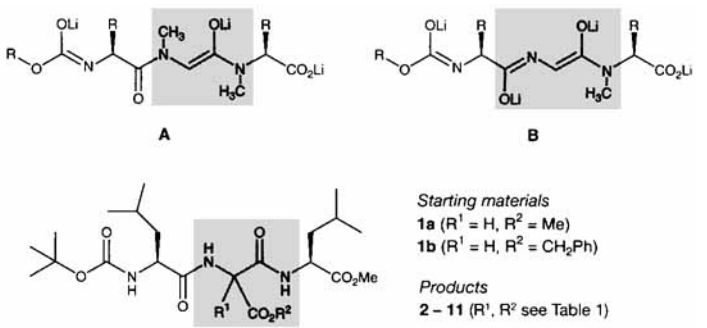
[7] The FD mass spectra of **2a–g** display an M^+ peak at $m/z = 1036$ as the only peak. The UV/VIS spectra (CH_2Cl_2) resemble that of **1** [5], although significant differences are observed in the region between 400 and 600 nm. The FT-IR spectra (KBr) show typical C_{60} bands at 1427 and 580–514 cm^{-1} in addition to ester bands.

[8] Two sp^3 C_{60} atoms lie in the mirror plane in **2e**. Thus three signals are observed for sp^3 C_{60} C atoms, two signals for the C atoms of the methylene bridge and three signals each for the ester groups.

Preparation and C-Alkylation of Peptides with Aminomalonate Building Blocks**

Hans G. Bossler, Pius Waldmeier, and Dieter Seebach*

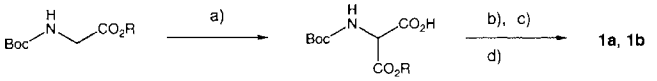
As was shown in previous papers,[1, 2] oligopeptides that may contain more than ten amino acids can be alkylated at sarcosine or glycine residues through polylithiated derivatives. This method is suitable for the preparation of numerous analogous peptides with various side chains from a single precursor. Yet this procedure can be used only if an N-methylated amino acid is incorporated next to the peptide enolate unit in the direction of the C terminus. The method is based upon the following principle: all relatively acidic HX protons are first removed and then the CH_2 group can be deprotonated to form an enolate (see Li_3[1] and Li_4 derivatives[2] **A** and **B** in Scheme 1). In order to alkylate oligopeptides that are not N-alkylated we have now reversed this principle so that the position to be substituted is the most acidic one of the molecule.[3]



Scheme 1. Polylithiated peptides **A** and **B** (geometry of C=C and C=N double bonds drawn arbitrarily), containing enolate moieties, and C-alkoxycarbonylated tripeptides **1** – **11**.

As a first example the aminomalonate-containing tripeptides **1a** and **1b** have been prepared (with Boc and methyl ester protecting groups at the *N* and C termini, respectively). In these peptides the hydrogen atom in the R^1 position can be removed with an alkoxide base. The synthesis of the methyl and benzyl esters **1a** and **1b**, respectively, is straightforward: The Boc-protected glycine esters were doubly deprotonated and carboxylated with CO_2 to the aminomalonic acid mono esters.[4] These were then coupled with the appropriate leucine derivative at the acid and amino groups, following standard procedures (see specifications in Scheme 2). To the best of our knowledge, only a diketopiperazine,[5a] a tripeptide,[5b] and some peptide isosteres[5c] containing one or two aminomalonic acid building blocks have been reported.

For the reaction of the new Boc-tripeptide diester **1** with electrophiles we chose MeONa or *t*BuOK as bases. They were employed stoichiometrically (1.3 equiv) in tetrahydrofuran for alkylations with halides, and catalytically (0.3 equiv) in methanol for Michael additions to acrylic acid derivatives and nitrostyrene. The yields of products **2**–**11** consisting of mixtures of diastereo-



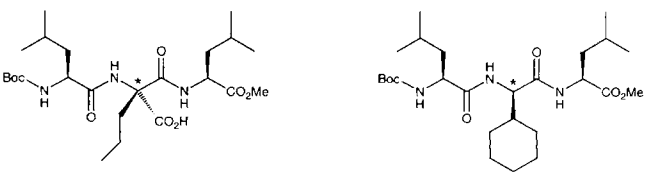
Scheme 2. Preparation of tripeptide derivatives **1**. a) LDA and TMEDA, each 2 equiv, THF, −75 °C, then CO_2 bubbled in; workup with dilute H_2SO_4; quantitative yields. b) Leucine methyl ester · HOTos, DCC, HOBt, NMM, THF, 0 °C to 20 °C; yields 50–70%, 10 g starting material. c) Et_2O saturated with HCl, about 95% yield. d) Boc-Leu-OH, conditions as in b), yields for **1a** 66%, for **1b** 83%; both compounds are powders and are produced as 1:1 mixtures of products epimeric at the amino acid residue in the middle.

isomers (ca. 1:1) range from 70 to 90% (see Table 1). So far, we have not been able to saponify and decarboxylate the malonate group of the dimethyl esters **2**–**7**, whereas the benzyl ester groups of the benzyl methyl esters **8**–**11** could be smoothly cleaved by hydrogenolysis (H_2/Pd-C/MeOH). Depending on

Table 1. Products **2** – **7** and **8** – **11** from the reaction of **1a** and **1b**, respectively, with alkyl halides and with Michael acceptors. Solvent THF (for **2** – **4** and **8** – **11**) or methanol (for **5**–**7**), base (quantity see text) MeONa (for **3** – **7**) or *t*BuOK (for **2**, **8**–**11**), temperature 0 °C, reaction times 10 min to 4 h. Yield of **2** with MeONa only 74%. The yields given are those of chromatographically purified products. The epimers were not separated. The structures of **2** – **11** follow unequivocally from ^1H, ^{13}C NMR, and FAB mass spectra.

Starting material no.	Electrophile	Product no.	R^1	R^2	yield [%]
1a	methyl iodide	**2**	Me	Me	91
1a	allyl bromide	**3**	CH_2–CH=CH_2	Me	58
1a	benzyl bromide	**4**	CH_2Ph	Me	87
1a	methyl acrylate	**5**	CH_2–CH_2–CO_2Me	Me	93
1a	acrylonitrile	**6**	CH_2–CH_2–CN	Me	80
1a	*β*-nitrostyrene	**7**	CH(Ph)CH_2NO_2	Me	67
1b	methyl iodide	**8**	Me	CH_2Ph	88
1b	allyl bromide	**9**	CH_2–CH=CH_2	CH_2Ph	72
1b	cyclohex-2-enyl bromide	**10**	2-cyclohexene-1-yl	CH_2Ph	73
1b	benzyl bromide	**11**	CH_2Ph	CH_2Ph	75

the reaction times, the free acids or the decarboxylated products were isolated. The double bond of the allyl and of the cyclohexenyl derivatives **9** and **10** was simultaneously hydrogenated (see examples in Scheme 3). The diastereoisomeric acids (e.g. **12** from **9**) as well as the decarboxylated products (e.g. **13** from **10**) were separated by chromatography (Scheme 3).



Boc-Leu-(2-HO_2C)Nva-Leu-OMe (**12** + *epi*-**12**) Boc-Leu-(2-cyclohexyl)Gly-Leu-OMe (**13** + *epi*-**13**)

Scheme 3. Two products **12** and **13** from the debenzylation and decarboxylation of the malonate units in **9** and **10**, respectively. The allylic substituents in **9** and **10** were hydrogenated under the debenzylation conditions (H_2/Pd-C/MeOH). Yields of carboxylic acids 74 and 89% from **9** and **11**, of Boc-tripeptide methyl ester quantitative (from **8** and **10**), see also text. The pairs of diastereoisomers at the stage of the carboxylic acids and of the decarboxylated products were separated by chromatography (thick layer, SiO_2, H_2O-sat. EtOAc or – for the products from **11** – EtOAc/MeOH 9:1). The tripeptide derivates from the debenzylation were cleaved as usual for peptides (HCl/H_2O) and derivatized following the method of Bayer [6] [a) *i*PrOH/HCl, b) $(C_2F_5CO)_2O$] and analyzed on a Chirasil-Val GC column. Hereby the racemic amino acids H-Ala-OH, H-Phe-OH, H-Nva-OH, and cyclohexylglycine were identified, as well as the non-racemic H-Leu-OH.

[*] Prof. Dr. D. Seebach, Dr. H. G. Bossler, Dipl.-Chem. P. Waldmeier
Laboratorium für Organische Chemie der
Eidgenössischen Technischen Hochschule
ETH-Zentrum, Universitätstrasse 16, CH-8092 Zürich (Switzerland)
Telefax: Int. code + (1) 262-0529

[**] From the Ph.D. thesis (dissertation no. 10254) of H. G. Bossler and from the diploma thesis of P. Waldmeier, both ETH Zürich, 1993.

 © VCH Verlagsgesellschaft mbH, D-69451 Weinheim, 1994 0570-0833/94/0404-0439 $ 10.00+.25/0

Nothing can be said about the diastereoselectivities of the three steps (enolate formation, alkylation, and decarboxylation), since all reactions have so far been carried out only with 1:1 mixtures of diastereoisomers (to obtain both separable epimers may be an advantage rather than a disadvantage for medicinal chemists!). It appears certain that this way of modifying peptides[7] is more suitable for larger oligopeptides than is polylithiation. Corresponding experiments are in progress, and these might lead to an attractive general method of preparing entire series of peptides from a single precursor, a process of much current interest in connection with establishing peptide libraries.[8]

Received: July 26, 1993 [Z 6235 IE]
German version: *Angew. Chem.* **1994**, *106*, 455

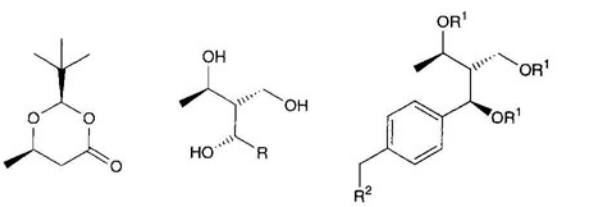
[1] Review: D. Seebach, *Aldrichimica Acta* **1992**, *25*, 59; most recent papers: S. A. Miller, S. L. Griffiths, D. Seebach, *Helv. Chim. Acta* **1993**, *76*, 563; D. Seebach, A. K. Beck, H. G. Bossler, C. Gerber, S. Y. Ko, C. W. Murtiashaw, R. Naef, S.-I. Shoda, A. Thaler, M. Krieger, R. Wenger, *ibid.* **1993**, *76*, 1564.
[2] H. G. Bossler, D. Seebach, *Helv. Chim. Acta*, **1994**, *77*, in press.
[3] Another strategy is to use poly-Li derivates of the type **B** with N-CH_2Ph instead of N-Me [2].
[4] Another method for the preparation of this half ester has been described: U. Schmidt, V. Leitenberger, H. Griesser, J. Schmidt, R. Meyer, *Synthesis* **1992**, 1248.
[5] a) H. E. Zaugg, M. Freifelder, H. J. Glenn, B. W. Horrom, G. R. Stone, M. R. Vernsten, *J. Am. Chem. Soc.* **1956**, *78*, 2626; b) P. Wheelan, W. M. Kirsch, T. H. Koch, *J. Org. Chem.* **1989**, *54*, 1364; c) J. T. Repine, R. J. Himmelsbach, J. C. Hodges, J. S. Kaltenbronn, I. Sircar, R. W. Skeean, S. T. Brennan, T. R. Hurley, E. Lunney, C. C. Humblet, R. E. Weishaar, S. Rapundalo, M. J. Ryan, D. G. Taylor, Jr., S. C. Olson, B. M. Michniewicz, B. E. Kornberg, D. T. Belmont, M. D. Taylor, *J. Med. Chem.* **1991**, *34*, 1935.
[6] S. Abdalla, E. Bayer, *Chromatographia* **1987**, *23*, 83.
[7] As far as we know, only the diketopiperazine from glycine and aminomalonic acid half ester (cited in [5a]), has been alkylated in such a way. On the other hand, *rac*-tryptophan is prepared by alkylation of acetamidomalonate with gramine, see J. P. Greenstein, M. Winitz, *Chemistry of Amino Acids*, Wiley, New York, **1961**, p. 2330, and references therein.
[8] Recent review article with a discussion of peptide libraries: G. Jung, A. G. Beck-Sickinger, *Angew. Chem.* **1992**, *104*, 375–391; *Angew. Chem. Int. Ed. Engl.* **1992**, *31*, 367–383.

Chiral Dendrimers from Tris(hydroxymethyl)-methane Derivatives**

Dieter Seebach,* Jean-Marc Lapierre, Konstantinos Skobridis, and Guy Greiveldinger

Dendrimers are molecules in the no-man's land between the conventional target molecules of organic synthesis and those of polymer chemistry,[1] which may have interesting properties and applications.[1, 2] As far as we know, there is only one report[3] on chiral starburst[1–4] dendrimers which were obtained by attaching tryptophan units to the end groups of a second generation dendrimer with a four-branch center piece or core. We report here on the first synthesis of starburst dendrimers with chiral core units and, in one case, also chiral branch units. We hope that this work will provide information about questions such as: a) Will a chiral core in a dendrimer with otherwise achiral building blocks cause the dendrimer to have a chiral shape or to be optically active? b) Will there be enantioselective clathration or host–guest interaction near the core of such a dendrimer? c) Will a dendrimer containing chiral, unsymmetrical branching units really have the predicted surface with fractal dimensions[5] and thus a pronounced capability for chiral recognition?

Our trifunctional chiral building blocks were prepared, as described previously,[6] from the dioxanone **1**, which is accessible from poly (*R*)-3-hydroxybutanoate (PHB).[7] The aldol adducts of the dioxanone **1** to aldehydes can be reduced to the chiral tris(hydroxymethyl)methane derivatives **2**–**4a**. By using the Fréchet

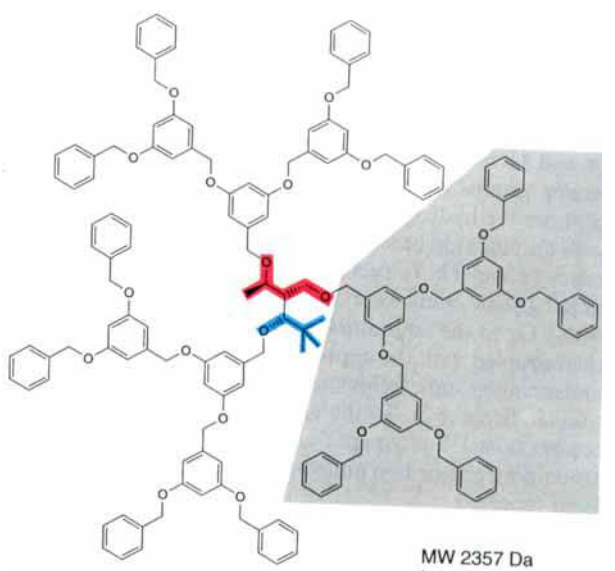


1

2 R = *iso*-Pr
3 R = *tert*-Bu

4a R^1 = H, R^2 = OSi*tert*-BuPh_2
4b R^1 = Me, R^2 = OSi*tert*-BuPh_2
4c R^1 = Me, R^2 = OH
4d R^1 = Me, R^2 = Br

method,[8] the triol **3**, either prior to or after attachment[6c] of spacer groups, was converted into the products **5** and **6**, **7**, respectively. In these formulae, the 3-hydroxybutanoic acid skeleton is marked in red, and the aldehyde part (from **3**) in blue. For

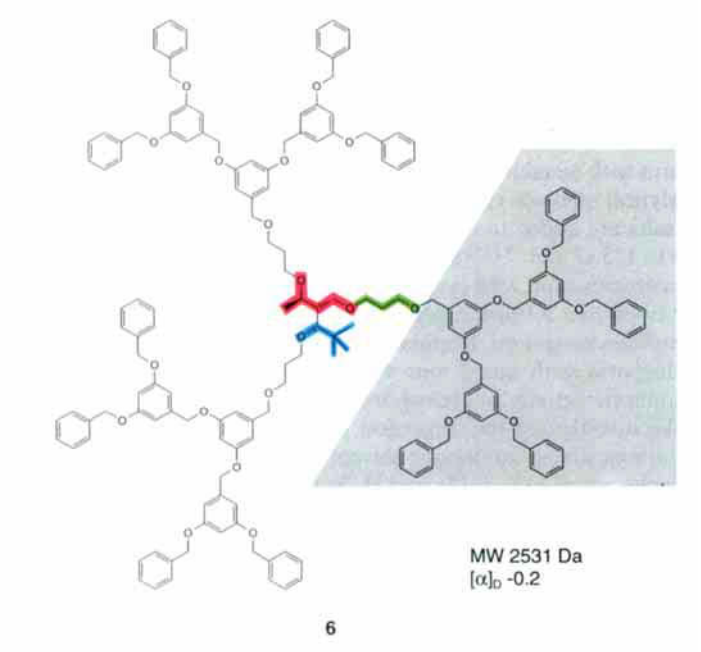


5

one branch, the spacer is marked in green, and the dendron, introduced by etherification of the triol **3** with the corresponding benzylic bromide, is marked in gray. The compounds **5**–**7** with twelve terminal phenyl groups may be classified as third generation dendrimers.[1] The second generation dendrimer **8** with twelve peripheral nitro groups was synthesized from the triol **2** by esterification with 3,5-dinitrobenzoyl chloride in pyri-

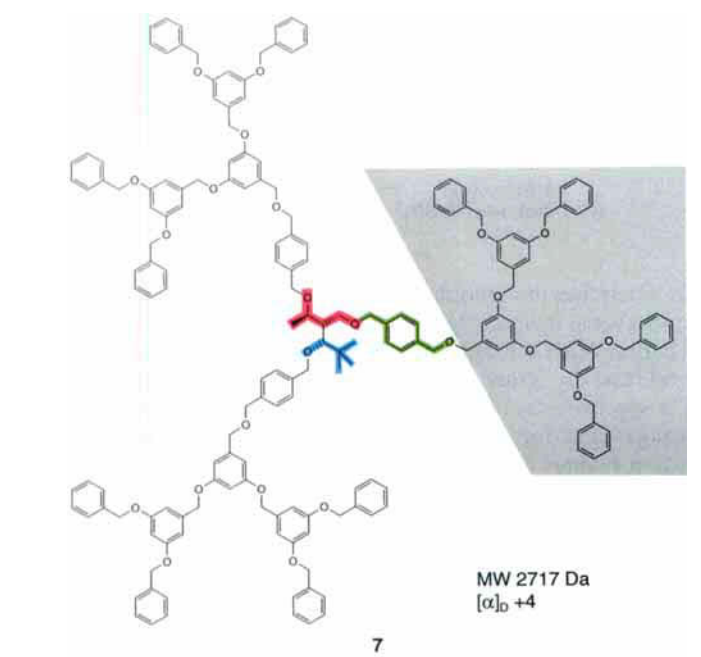
[*] Prof. Dr. D. Seebach, Dr. J.-M. Lapierre, Dr. K. Skobridis, Dipl.-Chem. G. Greiveldinger
Laboratorium für Organische Chemie der
Eidgenössischen Technischen Hochschule
ETH-Zentrum, Universitätstrasse 16, CH-8092 Zürich (Switzerland)
Telefax: Int. code + (1)262-0529

[**] J.-M. L. was recipient of a fellowship from the Natural Sciences and Engineering Research Council of Canada (1991–1993), K. S. from the Deutsche Forschungsgemeinschaft (1992/1993); part of the Diplomarbeit of G. G., ETH Zürich, 1993.



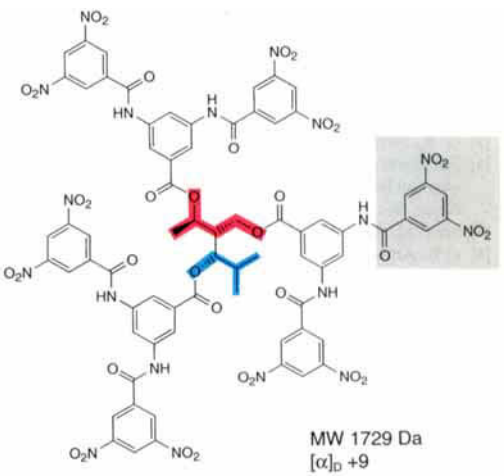
6

dine (>95%). The six nitro groups of the product were reduced to amino groups (>95%), which were acylated with the same acid cloride (83%). The dendrimer **9** (generation 1), in which both the core and the branches are chiral, was prepared from the triols **3** and **4a**.[9] After the triol **4a** was O-methylated (→ **4b**), the *tert*-butyldiphenylsilyl (OTBDPS) group was cleaved (→ **4c**), and the benzylic alcohol was converted into a benzyl bromide (→ **4d**, overall yield of 70%). This in turn was used for etherification of the triol **3**. Compound **9** is *one* out of 4096 possible stereoisomers!



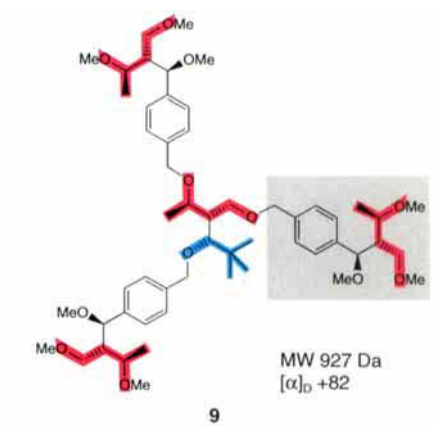
7

After the etherification step with the corresponding benzylic bromides, the dendrimers **5**, **6**, **7**, and **9** were isolated in yields of between 55 and 75% from reactions carried out on a 0.5–1.0 g scale. The dendrimers were purified by flash chromatography and fully characterized by IR, ^{1}H, and ^{13}C NMR spectroscopy, FAB mass spectrometry, and elemental analysis. In the ^{1}H NMR spectra of the dendrimers **5**–**7** we noticed that nonequivalent benzylic and aromatic protons gave rise to complex signals when they are found near the core and to singlets when they are found near the periphery of the dendrimer molecule. In the formulae shown the molecular weights and the specific rotations[10] of the compounds **5**–**9** are also given. It turns out that



8

the optical activity decreases as the dendrimers of type **5**, **6** and **7** increase in size;[11] in contrast, for the "fully chiral" dendrimer **9**, the rotation is approximatively the same as that of the building block ([α]$_D$ of **4c** and **4d**: +88 and +78). The transition



9

from the first to the second generation of the nitro-substituted dendrimers leads to a change of sign for the optical activity (dendrimer of first generation with six NO_2 groups: $[\alpha]_D = -17$; Dendrimer **8** with twelve NO_2 groups: $[\alpha]_D = +9$).

With several of the starburst dendrimers we observed the formation of very stable clathrates. Thus, compound **5** could be freed from CCl_4 only by heating at 100 °C/0.5 Torr for several hours. Moreover, the dodecanitro derivative **8** was isolated and characterized as a complex of composition [(2 · **8**) · EtOAc · (8 H_2O)], and for its hexaamine precursor we have identified 1:1, 2:1, and 6:1 complexes with 1,4-dioxane.[6c]

The preliminary results obtained so far lead us to believe that the synthesis of higher generation chiral dendrimers[12] will provide answers to the questions posed in the introduction and

thus deepen our understanding of organized complex molecules and their interactions with small molecules.[13]

Received: August 12, 1993 [Z 6276 IE]
German version: *Angew. Chem.* **1994**, *106*, 457

[1] a) D. A. Tomalia, A. M. Naylor, W. A. Goddard III, *Angew. Chem.* **1990**, *102*, 119; *Angew. Chem. Int. Ed. Engl.* **1990**, *29*, 138; b) *Genealogically Directed Synthesis: Starburst/Cascade Dendrimers and Hyperbranched Structures* (Eds.: D. A. Tomalia, H. D. Durst), *Top. Curr. Chem.* **1993**, *165*, 193; c) H.-B. Mekelburger, W. Jaworek, F. Vögtle, *Angew. Chem.* **1992**, *104*, 1609; *Angew. Chem. Int. Ed. Engl.* **1992**, *31*, 1571.

[2] See the report on dendrimer synthesis by the Dutch DSM company (*Chem. Rundsch.* **1993**, *46* (15), 3) and the article on Ru-containing dendrimers (*Chem. Eng. News* **1993**, *71* (5), 28) and on possible applications of dendrimers (*ibid.* **1992**, *70* (51), 16).

[3] G. R. Newkome, X. Lin, C. D. Weis, *Tetrahedron: Asymmetry* **1991**, *2*, 957.

[4] For chiral one- and two-directional cascade molecules starting from lysine and oligonucleotides, see [1a], there [73, 74]; R. H. E. Hudson, M. J. Damha, *J. Am. Chem. Soc.* **1993**, *115*, 2119.

[5] See [1a], there [80–82, 84].

[6] a) W. Amberg, D. Seebach, *Chem. Ber.* **1990**, *123*, 2413; b) D. Seebach, J.-M. Lapierre, W. Jaworek, P. Seiler, *Helv. Chim. Acta* **1993**, *76*, 459; c) J.-M. Lapierre, K. Skobridis, D. Seebach, *ibid.* **1993**, *76*, 2419 (includes experimental details for the preparation of chiral cores with spacer of **6** and **7**).

[7] H.-M. Müller, D. Seebach, *Angew. Chem.* **1993**, *105*, 483–509; *Angew. Chem. Int. Ed. Engl.* **1993**, *32*, 477–501.

[8] C.-J. Hawker, J. M. J. Fréchet, *J. Am. Chem. Soc.* **1990**, *112*, 7638; K. L. Wooley, C. J. Hawker, J. M. J. Fréchet, *J. Chem. Soc. Perkin Trans. 1* **1991**, 1059.

[9] Compound **4a** was obtained as the minor diastereomeric product from **1** and 4-(*tert*-butyldiphenylsiloxymethyl)benzaldehyde, see [6c]. The epimer at the benzylic position of **4a** was also used for preparing the corresponding diastereomer of **9**.

[10] **5**, **6**, **7**, **9** in $CHCl_3$ ($c = 1$ 2 g/100 mL), **8** in dioxane ($c = 1.05$ g/100 mL).

[11] The $[\alpha]_D$ values in generation 1 (three peripheral OBn), 2 (six OBn), and 3 (twelve OBn) of the dendrimer without spacer (type **5**), with aliphatic spacer (type **6**), and with aromatic spacer (type **7**) are: $+15/+8/+4$, $-1/-2/-0.2$, and $+12/+7/+4$, respectively; for simple presentation of the generations of such Fréchet dendrimers, see [1c].

[12] There are five principle methods of assembling chiral dendritic structures: 1) chiral core with achiral branch units, 2) achiral core with chiral branch units, 3) both the core and the building blocks for the branches are chiral, 4) constitutionally different branches attached to an achiral core (see discussion in: J. Ehrler, D. Seebach, *Liebigs Ann. Chem.* **1990**, 379; G. Guanti, L. Banfi, E. Narisano, *J. Org. Chem.* **1992**, *57*, 1540), and 5) constitutionally different branches attached to a chiral core.

[13] *Supramolekulare Chemie* (Ed.: F. Vögtle), Teubner, Stuttgart, **1992**; *Macrocyclic Chemistry* (Eds.: B. Dietrich, P. Viout, J.-M. Lehn), VCH, Weinheim, **1993**.

Cyclosporin: A Li- and Ca-Specific Ionophore!**

H. Michael Bürger and Dieter Seebach*

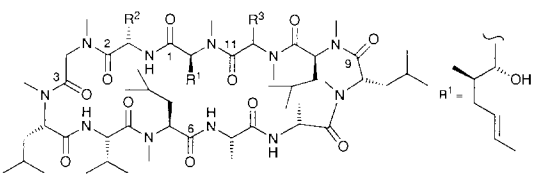
The cyclic undecapeptide cyclosporin A (**1**) is an immunosuppressive agent that has revolutionized the field of organ transplantation.[1] Although its biological activity is subject to intensive research, the detailed mode of interaction in the complex immune reaction of mammals is far from being completely understood.[2, 3] It has been established that an initial step of the immunosuppressive action of cyclosporin and FK 506 (another, although nonpeptidic immunosuppressive agent) is the inhibition of Ca^{2+}-dependent signaling pathways in T and mast cells.

[*] Prof. Dr. D. Seebach, Dr. H. M. Bürger
Laboratorium für Organische Chemie der
Eidgenössischen Technischen Hochschule
ETH-Zentrum, Universitätstrasse 16, CH-8092 Zürich (Switzerland)
Telefax: Int. code + (1) 262-0529

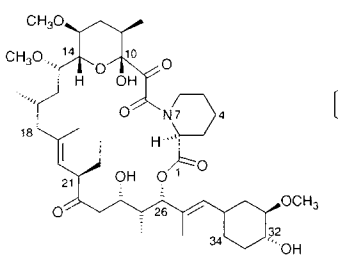
[**] Part of the Ph.D. Thesis of H. M. Bürger, dissertation no. 10436, ETH, Zürich, **1993**.

The structure of cyclosporin in organic solvents,[4] in the solid state,[5] and in a complex with its cytoplasmatic binding protein cyclophilin[6, 7] is well known from NMR spectroscopy[4, 6] and X-ray structure determinations,[5, 7] but its structure in an aqueous environment is still uncertain. Interactions of cyclosporin with metal ions are known;[8, 9] it was shown by thermoanalytical methods that surprisingly high enthalpies result when Li salts are added to cyclosporin solutions in tetrahydrofuran (up to 125 kJ mol^{-1}).[9] Similar conformational changes[10] as in the complexation with cyclophilin[6, 7] (e.g. the isomerization of a 9,10-*cis* to a 9,10-*trans* peptide bond) occur when cyclosporin complexes metal ions. Inspired by the pronounced interaction of cyclosporin with metal ions we set out to look for possible ionophoric activity of cyclosporin.

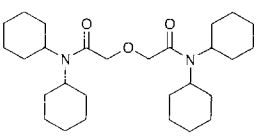
We investigated the migration of alkali and alkaline-earth metal ions across an organic solvent phase under the influence of cyclosporin A (**1**), C (**2**), and H (**3**) as well as of ascomycin (**4**) and the Ca-ionophore ETH 129 (**5**), by using the U-tube technique we recently employed for studying ion transport by derivatives of 3-hydroxybutanoic acid.[11, 12]



1 Cyclosporin A (CS), R^2 = Et, R^3 = (*S*)-*i* Pr
2 Cyclosporin C ([Thr^2]CS), R^2 = CH(OH)CH_3, R^3 = (*S*)-*i* Pr
3 Cyclosporin H ([D-MeVal^{11}]CS), R^2 = Et, R^3 = (*R*)-*i* Pr



4 Ascomycin
(21-Dihydro-*nor*-FK506)



5 ETH 129

To determine the ionophoric properties of compounds **1**–**5** we overlayered their dichloromethane solutions in a U tube with two buffered (pH 8.1) aqueous phases, one containing the metal chloride and its picrate. The extent of migration was monitored by UV spectrometry (356 nm; see *Experimental Procedure*). The transport rates for the alkali and alkaline-earth metal salts shown in Figures 1a and b were measured with a 0.005 M solution of cyclosporin A (**1**). The rates follow the Hofmeister or lyotropic sequence (increasing ionic radius – decreasing heat of hydration – increasing transport rate)[13] in both series – with two remarkable exceptions: first Li^+ migrates faster than Na^+, K^+, and Rb^+ and second Ca^{2+} migrates faster than the other alkaline-earth metal ions, even significantly faster than Ba^{2+}! The Ca^{2+} transport is strongly dependent on the cyclosporin A concentration,[14] as evident from the data collected in Table 1.

Like the physiological activity,[15] the Ca^{2+} migration through the organic phase depends upon the substituents on the cyclosporin skeleton: a comparison of compounds **1**–**5** shows (Fig. 1c) that cyclosporin H (**3**) is slightly more and cyclosporin C (**2**) distinctly less efficient[16] than cyclosporin A (**1**)

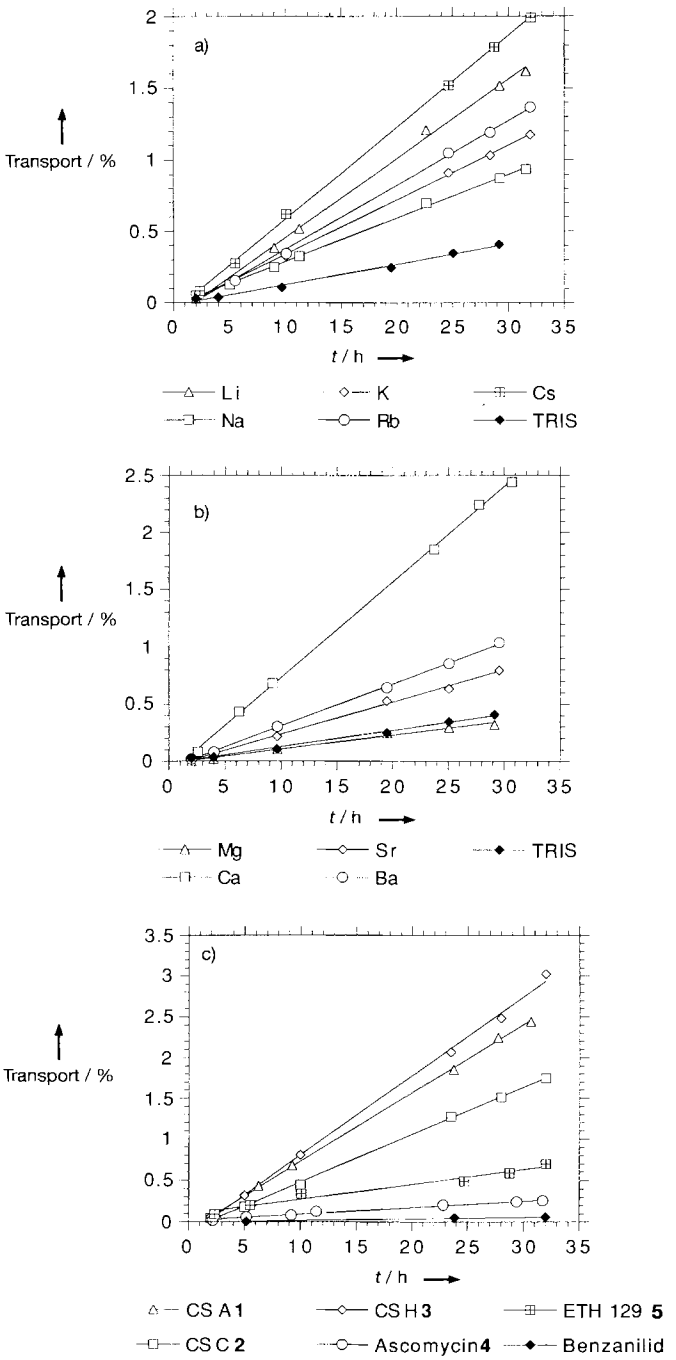


Fig. 1. Transport rates of the alkali and alkaline-earth metal picrates across a bulk liquid CH_2Cl_2 membrane. No metal ions were added to the donating solution in the control experiment (TRIS). a) Transport of the alkali metal ions with cyclosporin A (**1**) as ionophore. b) Transport of the alkaline-earth metal ions with cyclosporin A (**1**) as ionophore. c) Transport of calcium ions with the cyclosporins (CS) A (**1**), C (**2**), H (**3**), as well as ascomycin (**5**), and the ETH ligand **5** as ionophores. An experiment with benzanilid, employing the same amount of amide groups as in the cyclosporin experiments, was done as a reference.

(the order of immunosuppressive activity is: **1** ≥ **2** ≫ **3**).[15] Furthermore, ascomycin (**4**) and the ETH ligand **5**[17] are much poorer Ca^{2+} ionophores under these conditions.

The following comments concerning the preferred transport of Li^+ and Ca^{2+} ions by cyclosporin appear appropriate to us: a) Although the immunosuppressive agents **1**–**4** change intracellular Ca^{2+} levels in T cells,[12] only the cyclosporins **1**–**3** show pronounced ionophoric activity in our experiments. b) The Ca^{2+}-binding serin-threonin-phosphatase calcineurin and the ubiquitous Ca^{2+}-modulator calmodulin are involved in the cascade of the immune response.[1–3, 18] c) The results described herein shed new light on the role of cyclosporin in immunosuppression and should encourage new biochemical, physiological, and medical investigations.[19]

Table 1. Comparison of the transport rates of the alkali and alkaline-earth metal picrates with cyclosporin A (**1**) as ionophore. The error in the transport rates is aproximately ±10%.

Metal ion	Concentration [mM]	Transport rate [% transported in 100 h]
Li^+	5	5.5
Na^+	5	3.1
K^+	5	3.8
Rb^+	5	4.5
Cs^+	5	6.4
Mg^{2+}	5	1.2
Ca^{2+}	1	2.5
	5	8.4
	50	39.4
Sr^{2+}	5	2.8
Ba^{2+}	5	3.7
(TRIS)	5	1.4

Experimental Procedure

The transport experiments were done in a similar way as described for the derivatives of 3-hydroxybutanoic acid [12] (see also [11]). The ion-donating solutions were 0.101 M alkali metal chloride and 1 mM picric acid or 0.101 M alkaline-earth metal chloride and 2 mM picric acid in 0.1 M tris-(hydroxymethyl)-aminomethane (TRIS)/HCl buffer (final pH 8.1). The pure buffer solution served as acceptor solution. For the determination of the ionophoric behavior, 15 mL of a CH_2Cl_2 solution of the compounds **1**–**5** (0.005 M) was placed in a U-shaped tube (internal diameter 15 mm) made of quartz glass and overlayered with 7.5 mL of the donor and 7.5 mL of the acceptor solutions in the two legs. The organic phase was stirred magnetically (ca. 200 rpm) at room temperature, and the extent of transport was measured UV spectrometrically by recording the migration of picrate (λ_{max} 356 mm).

Received: August 20, 1993 [Z 6305 IE]
German version: *Angew. Chem.* **1994**, *106*, 459

[1] J. F. Borel, F. D. Padova, J. Mason, V. Quesinaux, B. Ryffel, R. Wenger, *Pharmacol. Rev.* **1989**, *41*, 239 and the following articles in issue 3.
[2] M. K. Rosen, S. L. Schreiber, *Angew. Chem.* **1992**, *104*, 413; *Angew. Chem. Int. Ed. Engl.* **1992**, *31*, 384; S. L. Schreiber, M. W. Albers, E. J. Brown, *Acc. Chem. Res.* **1993**, *26*, 412.
[3] "Immunophilins as Drug Targets": A. Stütz, M. A. Grassberger, K. Baumann, A. J. F. Edmunds, P. Hiestand, J. F. Meingassner, P. Nussbaumer, W. Schuler, G. Zenke in *Perspectives in Medicinal Chemistry* (Eds.: B. Testa, E. Kyburz, W. Fuhrer, R. Giger), Verlag Helv. Chim. Acta, Basel/VCH, Weinheim, **1993**, Chapter 27, p. 427.
[4] "Investigations of peptides by two-dimensional NMR spectroscopy—The conformation of cyclosporin A in solution": H. Kessler, H. R. Loosli, H. Oschkinat in *Peptides* (Ed.: U. Ragnarsson), Almqvist & Wiksell International, Stockholm, **1984**, p. 65.
[5] D. Seebach, S. Y. Ko, H. Kessler, M. Köck, M. Reggelin, P. Schmieder, M. D. Walkinshaw, J. J. Balsterli, *Helv. Chim. Acta* **1991**, *74*, 1953, and references therein.
[6] C. Spitzfaden, H. P. Weber, W. Braun, J. Kallen, G. Wider, H. Widmer, M. D. Walkinshaw, K. Wüthrich, *FEBS Lett.* **1992**, *300*, 291.
[7] G. Pflügl, J. Kallen, T. Schirmer, J. N. Jansonius, M. G. M. Zurini, M. D. Walkinshaw, *Nature* **1993**, *361*, 91.
[8] H. Kessler, M. Gehrke, J. Lautz, M. Köck, D. Seebach, A. Thaler, *Biochem. Pharmacol.* **1990**, *40*, 169, erratum, p. 2185.
[9] D. Seebach, H. G. Bossler, R. Flowers, E. M. Arnett, *Helv. Chim. Acta* **1994**, *77*, in press; NMR papers describing the effect of various ions on the spectrum of **1** are cited therein.
[10] M. Köck, H. Kessler, D. Seebach, A. Thaler, *J. Am. Chem. Soc.* **1992**, *114*, 2676.
[11] H.-M. Müller, D. Seebach, *Angew. Chem.* **1993**, *105*, 483; *Angew. Chem. Int. Ed. Engl.* **1993**, *32*, 477.
[12] H. M. Bürger, D. Seebach, *Helv. Chim. Acta*, **1993**, *76*, 2570, and references therein.

[13] S. G. A. McLaughlin, G. Szabo, S. Ciani, G. Eisenman, *J. Membr. Biol.* **1972**, *9*, 3; F. Hofmeister, *Arch. Exp. Pathol. Pharmakol.* **1888**, *24*, 247.
[14] R. M. Izatt, G. A. Clark, J. S. Bradshaw, J. D. Lamb, J. J. Christensen, *Sep. Purif. Methods* **1986**, *15*, 21.
[15] A. von Wartburg, R. Traber, *Prog. Med. Chem.* **1988**, *25*, 1; R. M. Wenger, *Angew. Chem.* **1985**, *97*, 88; *Angew. Chem. Int. Ed. Engl.* **1985**, *24*, 77.
[16] Quite surprisingly **2**, despite having an additional hydroxy group in the side chain of amino acid no. 2, transports less efficiently than the more lipophilic **1**.
[17] The Ca-ionophore ETH 129 **5** forms strong complexes with Ca^{2+} (E. Bakker, M. Willer, M. Lerchi, K. Seiler, E. Pretsch, *Anal. Chem.* **1994**, *66*, (4), in press). Strong complexing agents are not well suited for transport experiments, since the release of ions into the receiving solution is slow and may determine the overall transport rate (M. Kirch, J.-M. Lehn, *Angew. Chem.* **1975**, *87*, 542; *Angew. Chem. Int. Ed. Engl.* **1975**, *14*, 555). In a separate extraction experiment with equal volumes of the described donor and organic solutions the picrate extraction by **5** into the organic layer was almost complete, an effect not observed with the immunosuppressive compounds **1**–**4**.
[18] With regard to the Li^+ selectivity in the interaction [9] between alkali metal ions and cyclosporin **1** it should be noted that the physiological activity of Li^+ as an antidepressive drug is related to the inhibition of a Mg^{2+}-dependent inositol phosphatase in the neurotransmitter system: A. J. Wood, G. M. Goodwin, *Psychological Medicine* **1987**, *17*, 579.
[19] The use of cyclosporin as an ionophore in ion-sensitive electrodes is currently being investigated by Prof. E. Pretsch, Laboratorium für Organische Chemie, ETH Zürich. Quite some time ago the Mg^{2+} selectivity of several cyclic octa- and dodecapeptides was described: F. Behm, D. Ammann, W. Simon, K. Brunfeldt, J. Halstrøm, *Helv. Chim. Acta* **1985**, *68*, 110. Synthetic Li-selective ionophores for application in ion-sensitive electrodes have been investigated by the same group (E. Metzger, D. Ammann, R. Asper, W. Simon, *Anal. Chem.* **1986**, *58*, 132; E. Metzger, R. Aeschimann, M. Egli, G. Suter, R. Dohner, D. Ammann, M. Dobler, W. Simon, *Helv. Chim. Acta* **1986**, *69*, 1821) and by other groups as well (R. Kataky, P. E. Nicholson, D. Parker, *J. Chem. Soc. Perkin Trans. II* **1990**, 321; R. Kataky, P. E. Nicholson, D. Parker, A. K. Covington, *Analyst* **1991**, *116*, 135; M. Bocheńska, J. E. Biernat, J. S. Bradshaw, *J. Inclusion Phenom. Mol. Recognit. Chem.* **1991**, *10*, 19).

Diastereoselective Hydroxyalkylation of Enantiomerically Pure 2-Alkenylsulfoximides**

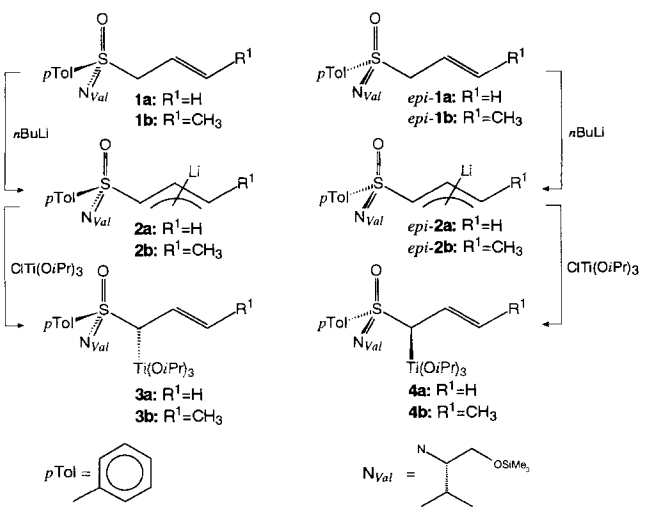
Michael Reggelin* and Heinz Weinberger

For a new asymmetric reaction the direction and extent of the attainable asymmetric induction must be predictable. In addition the reagent should be invariant with respect to stereogenic elements already present in the substrate. For the practical implementation of such reagent-controlled asymmetric conversions electrophilic substitutions, enantiomerically pure and configurationally stable organometallic compounds are available. In these reactions the stereocontrol achieved is usually directly correlated with the specificity associated with electrophilic substitution. Prime examples of this strategy are the chiral, dipole-stabilized[1] α-oxyalkanides introduced by D. Hoppe et al.[2] and an analogous pyrrolidine derivative prepared by P. Beak et al.[3] For the synthesis of such uniformly configurated, enantiomerically pure organometallic compounds, which are usually lithium compounds, three general methods are available:

1) tin–lithium exchange in uniformly configurated stannanes, which are in turn obtained from the resolution of racemates,[4, 5]
2) diastereotopos-differentiating[*] deprotonation,[6]
3) enantiotopos-differentiating[*] deprotonation with chiral, nonracemic base systems.[2, 3]

The diastereotopos-differentiating bromine–lithium exchange on substituted α-dibromoalkanes introduced by R. W. Hoffmann, which is stereochemically related to 2), also leads to configurationally uniform, though till now only racemic, organometallic compounds.[7]

Most important for the success of the reaction is the configurational stability of the organometallic compound under the conditions required for its generation. This requirement necessarily restricts the choice of possible reagents, since resonance-stabilized "carbanions" are configurationally stable only to a certain extent[8] and α-acceptor-substituted, polar organometallic compounds with uniform absolute configuration at the metalated carbon are, as yet, not available in enantiomerically pure form.[9] We describe here one solution, the diastereoface-differentiating transmetalation of configurationally labile, enantiomerically pure, lithiated 2-alkenylsulfoximides **2** to give the enantiomerically pure, configurationally stable (?) 2-alkenyltitanium compounds **3** and **4** (Scheme 1).



Scheme 1. Deprotonation and transmetalation of 2-alkenylsulfoximides.

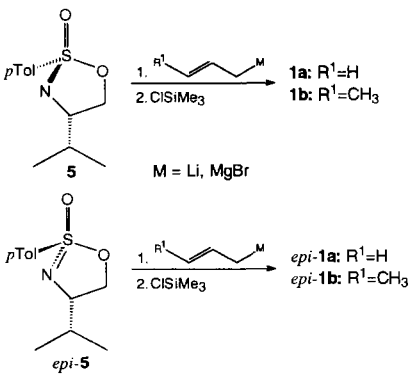
The required starting material, enantiomerically pure allylsulfoximides **1**, can be prepared in high yield from 4,5-dihydro-1,2λ⁶,3-oxathiazol-2-oxides **5** and *epi*-**5** recently described by us, which itself is available in 70% yield from *O*-trimethylsilylvalinol and *p*-toluenesulfinic chloride (Scheme 2).[10]

Deprotonation of sulfoximides **1** at −78 °C with *n*BuLi generates the configurationally labile lithium compounds **2**, which react with high diastereoselectivity at 0 °C with chlorotris(isopropoxy)titanium[11] to form **3** and **4**. Reaction of **3** and **4** with aldehydes yield the diastereomerically pure γ-hydroxyvinylsulfoximides **6** and **7**, respectively (Scheme 3, Table 1). Workup of the titanium-containing reaction mixture with saturated ammonium carbonate as indicated in Scheme 3 is essential for the successful termination of the reaction. This workup protocol is superior to the alternative method with potassium fluoride solution[12] and is the method of choice for cases in which the usual acidic workup cannot be used because of insufficient product

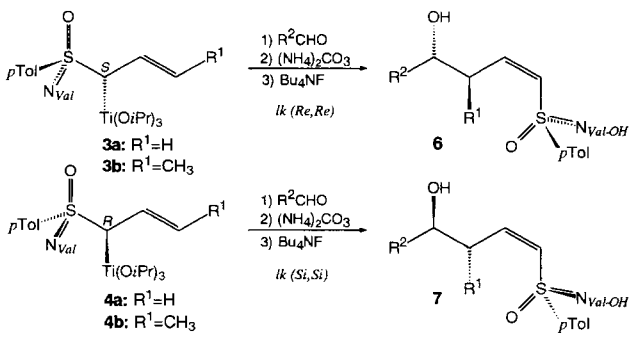
[*] Dr. M. Reggelin, Dipl.-Chem. H. Weinberger
Institut für Organische Chemie der Universität
Marie-Curie-Strasse 11, D-60439 Frankfurt (FRG)
Telefax: Int. code + (69) 5800-9128

[**] This work was supported by the Deutsche Forschungsgemeinschaft (DFG) and the Fonds der Chemischen Industrie. M. R. thanks the DFG for a "Habilitationsstipendium". H. W. thanks the Graduiertenkolleg der Universität Frankfurt for a predoctoral fellowship. We wish to thank Prof. Dr. C. Griesinger for his generous support.

[*] The descriptors "diastereotopos-differentiating" and "enantiotopos-differentiating" denote the differentiation of two stereoheterotopic positions in a molecule in contrast to the differentiation of two stereoheterotopic faces.



Scheme 2. Synthesis of 2-alkenylsulfoximides.



Scheme 3. γ-Hydroxyalkylation of titanated 2-alkenylsulfoximides.

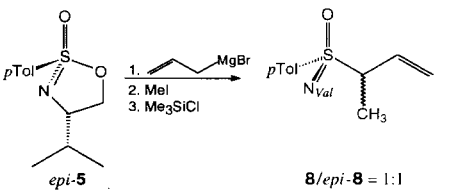
stability. The relative and absolute configurations of the aldehyde adducts have been established by an X-ray structure analysis of **6k**.[13]

Table 1. γ-Hydroxyalkylation of metalated 2-alkenylsulfoximides.

Cmpd.	R^1	R^2	*ds* [%][a]	$[\alpha]_D^{20}$ [b]	Yield [%]
6a	H	CH_3	≥97	−125.9	51
6b	H	$(CH_3)_2CH$	≥97	−163.9	68
6c	H	*c*-C_6H_{11}	96	−130.1	54
6d	H	(*E*)-C_3H_5	≥97	−99.1	44
6e	H	C_6H_5	≥97	−73.7	66
6f	CH_3	CH_3	96	−123.7	74
6g	CH_3	$(CH_3)_2CH$	≥97	−158.7	72
6h	CH_3	*c*-C_6H_{11}	≥97	−155.5	78
6i	CH_3	(*E*)-C_3H_5	≥97	−142.6	72
6k	CH_3	C_6H_5	≥97	−93.0	82
7a	H	CH_3	≥97	−1.9	81
7b	H	$(CH_3)_2CH$	98	28.8	86
7c	H	*c*-C_6H_{11}	98	29.1	71
7d	H	(*E*)-C_3H_5	≥97	−20.2	74
7e	H	C_6H_5	≥97	−48.9	75
7f	CH_3	CH_3	≥97	9.9	57
7g	CH_3	$(CH_3)_2CH$	≥97	49.9	50
7h	CH_3	*c*-C_6H_{11}	≥97	60.4	44
7i	CH_3	(*E*)-C_3H_5	96	20.1	55
7k	CH_3	C_6H_5	≥97	−21.7	50

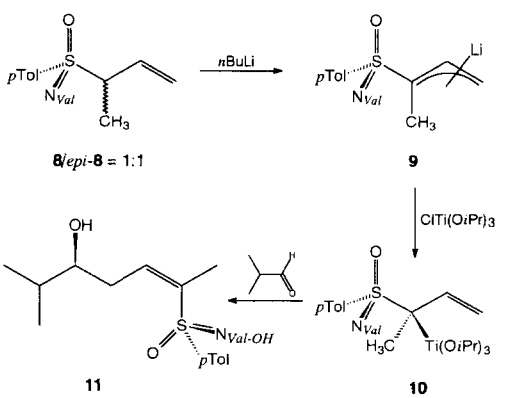
[a] Determined from the ^{1}H NMR spectrum of the crude product. When no other diastereoisomers could be detected a detection limit of 3% was assumed and the diastereoselectivity *ds* is given as ≥97%. [b] After chromatography on silica gel; pure by ^{1}H NMR spectroscopy.

In order to verify our working hypothesis that the configuration of the products is controlled by diastereoface-differentiating transmetalation of a configurationally labile organolithium compound, the epimeric 1-methallylsulfoximides **8** and *epi*-**8** were prepared as a 50:50 epimeric mixture (determined by ^{1}H NMR spectroscopy) (Scheme 4).



Scheme 4. Allylation and C-methylation of *epi*-**5**.

Remarkably, the opening and C-methylation of the sulfonimidate *epi*-**5** occurs in one step. The lithium compound generated after deprotonation of the allyl derivative reacts exclusively at C1. O-methylated products could not be detected. If the Li compounds generated from **8** or *epi*-**8** are configurationally labile, a stereoconvergent course for the γ-hydroxyalkylation is expected, since after deprotonation the stereogenic center at C1 is destroyed and the same anion is formed from both epimers (Scheme 5).



Scheme 5. Stereoconvergent γ-hydroxyalkylation of methallylsulfoximides **8**/*epi*-**8**.

In accord with this configurational behavior, the expected product **11** was isolated as a single enantiomerically pure diastereoisomer. This result is important not only for our investigations but is also instructive, since quantitative studies of metalated secondary sulfones (i.e. the oxa analogues of the sulfoximides) verify their configurational stability.[9]

Conclusive experimental confirmation of our working hypothesis with respect to the configurational stability of the titanated intermediate is not yet available. However, we assume a configurationally stable titanium compound, since the observed substrate independence of the γ-hydroxyalkylation (see Table 1) is characteristic for a 1,3-chirality transfer. Here the degree of stereocontrol achieved correlates directly with the absolute configuration at C1. If configurational lability were present, then both the imides **1a** and **1b** and their S epimers must be assumed to have an equally high induction for all the chosen aldehydes. This seems hardly likely, as in this case (substrate control) a combination of the C and S chiral centers should determine the stereochemical result of the reaction, and the existence of a "matched" and a "mismatched" combination of these two stereogenic elements would be expected. This, in turn, should lead to higher induction for one series of diastereo-

 © VCH Verlagsgesellschaft mbH, D-69451 Weinheim, 1994 0570-0833/94/0404-0445 $ 10.00+.25/0

isomers and lower induction for the other series; however, this is not observed.

On account of the combination of properties of the sulfoximides **1** which at first sight seem incompatible – acidification of protons in the α position by means of an electron acceptor and stereocontrol by electrophilic substitution at a metalated carbon atom of stable configuration – 1,3-chirality transfer to homoallylic alcohols with acceptor-substituted double bonds can be achieved. A series of subsequent reactions are then possible which rely on the one hand on the electron deficiency of the acceptor-substituted double bond (e.g. Diels–Alder reactions) and on the other hand on the carbanion-stabilizing effect of the sulfoximide group (e.g. "Michael" additions at C2).

The titanated sulfoximides **3** and **4** may serve as asymmetric allyl transfer agents which, on account of their structure, allow functionalizations of the initial product of their addition to aldehydes, which are not necessarily possible with alternative allyl transfer agents.[14]

We are conducting NMR experiments to obtain detailed information about the structure and dynamics of the metalated intermediates.[15] We are interested most of all in the configurational behavior of the organometallic compounds so that the stereochemical course of the reaction can be explained even without a model of the transition state. Preliminary results of the NMR determination of relative configurations, which were made without prior assumptions about the conformational preferences of the system under study, will be reported in one of the next issues of this journal.

Experimental Procedure

A solution of 0.267 g (0.755 mmol) *epi*-**1a** in 3 mL of dry THF was cooled to −78 °C under argon and allowed to react with 1.1 equiv *n*BuLi (1.6 M in hexane). After 15 min, 1.2 equiv $ClTi(OiPr)_3$ was added. After 5 min the mixture was warmed to 0 °C, stirred for 55 min, and finally cooled again to −78 °C at which point 2.0 equiv of 2-methylpropanal was added dropwise over 15 min. The reaction mixture was then poured, with vigorous stirring, into a saturated solution of $(NH_4)_2CO_3$ (20 mL). After 30 min the mixture was extracted with ether, and the organic phase was dried over $MgSO_4$. The crude product was dissolved in 4 mL of THF, and 1.2 equiv of nBu_4NF (1.1 M in THF) was added dropwise at 0 °C. After 15 min the mixture was poured onto ice and extracted with ethyl acetate. The organic phase was dried over $MgSO_4$, and flash chromatographed on silica gel (eluent: ethyl acetate/hexane) to provide 0.299 g (0.648 mmol, 86%) **7b** as a colorless oil.

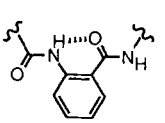
Received: September 6, 1993 [Z 6343 IE]
German version: *Angew. Chem.* **1994**, *106*, 489

[1] a) P. Beak, D. B. Reitz, *Chem. Rev.* **1978**, *78*, 275–316; b) N. G. Rondan, K. N. Houk, P. Beak, W. J. Zajdel, J. Chandrasekhar, P. von R. Schleyer, *J. Org. Chem.* **1981**, *46*, 4108–4110.
[2] a) D. Hoppe, F. Hintze, P. Tebben, *Angew. Chem.* **1990**, *102*, 1457–1458; *Angew. Chem. Int. Ed. Engl.* **1990**, *29*, 1422–1424.
[3] S. T. Kerrick, P. Beak, *J. Am. Chem. Soc.* **1991**, *113*, 9708–9710.
[4] a) W. C. Still, A. Mitra, *J. Am. Chem. Soc.* **1978**, *100*, 1927–1928; b) J. S. Sawyer, A. Kucerovy, T. L. Macdonald, G. J. McGarvey, *ibid.* **1988**, *110*, 842–853.
[5] W. H. Pearson, A. C. Lindbeck, *J. Am. Chem. Soc.* **1991**, *113*, 8546–8548.
[6] a) K. Rein, M. Goicoechea-Pappas, T. V. Anklekar, G. C. Hart, G. A. Smith, R. E. Gawley, *J. Am. Chem. Soc.* **1989**, *111*, 2211–2217; b) R. E. Gawley, G. C. Hart, L. J. Bartolotti, *J. Org. Chem.* **1989**, *54*, 175–181.
[7] a) R. W. Hoffmann, M. Bewersdorf, M. Krüger, W. Mikolaiski, R. Stürmer, *Chem. Ber.* **1991**, *124*, 1243–1252; b) R. W. Hoffmann, M. Bewersdorf, *ibid.* **1991**, *124*, 1259–1264.
[8] a) D. Hoppe, O. Zschage, *Angew. Chem.* **1988**, *101*, 67–69; *Angew. Chem. Int. Ed. Engl.* **1989**, *28*, 69–71; b) D. Hoppe, T. Krämer, *ibid.* **1986**, *98*, 171–173 and **1986**, *25*, 160–162; c) O. Zschage, D. Hoppe, *Tetrahedron* **1992**, *48*, 5657–5666; d) R. W. Hoffmann, T. Rühl, F. Chemla, T. Zahneisen, *Liebigs Ann. Chem.* **1992**, 719–724.
[9] Lithiosulfones, which are configurationally stable for a short while at low temperatures, are an exception; a) H.-J. Gais, G. Hellmann, *J. Am. Chem. Soc.* **1992**, *114*, 4439–4440, in particular lithiotrifluoromethylsulfones (Li-triflones); b) H.-J. Gais, G. Hellmann, H. Günther, F. Lopez, H. J. Lindner, S. Braun, *Angew. Chem.* **1989**, *101*, 1061–1063; *Angew. Chem. Int. Ed. Engl.* **1989**, *28*, 1025–1027; c) H.-J. Gais, G. Hellmann, H. J. Lindner, *ibid.* **1990**, *102*, 96–99 and **1990**, *29*, 100.
[10] M. Reggelin, H. Weinberger, *Tetrahedron Lett.* **1992**, *33*, 6959–6962.
[11] a) C. Dijkgraaf, J. P. G. Rousseau, *Spectrochim. Acta Part A* **1968**, *24*, 1213; b) M. T. Reetz, *Organotitanium Reagents in Organic Synthesis*, Springer, Berlin, **1986**.
[12] D. Seebach, B. Weidmann, L. Widler in *Modern Synthetic Methods Vol. 3* (Ed.: R. Scheffold), Salle, Sauerländer, **1983**, pp. 217–353.
[13] a) Further details of the crystal structure investigation may be obtained from the Fachinformationszentrum Karlsruhe, D-76344 Eggenstein-Leopoldshafen (FRG) on quoting the depository number CSD-57981, the names of the authors, and the journal citation.; b) B. Berger, M. Bolte, *Acta Crystallogr. Sect. C*, submitted.
[14] W. R. Roush in *Comprehensive Organic Synthesis Vol. 2* (Ed.: B. M. Trost), Pergamon Press, Oxford, **1991**, pp. 1–49.
[15] The first chemical and NMR spectrographic results concerning the configurational behavior of lithiosulfoximides are found in ref. [9].

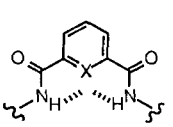
Novel Molecular Scaffolds: Formation of Helical Secondary Structure in a Family of Oligoanthranilamides**

Yoshitomo Hamuro, Steven J. Geib, and Andrew D. Hamilton*

The two most important secondary structural features in polypeptides are α helices and β sheets.[1] These form the ordered molecular scaffolding in proteins to which less repetitive catalytic or recognition elements are linked. A critical role in stabilizing both α helices and β sheets is played by intramolecular hydrogen bonds from one amide group to others further along the chain. As part of our work on molecular recognition, we wondered if a biomimetic approach might be applied to the design of novel scaffolds with well-defined and compact conformations.[2, 3] In this paper we report that a simple combination of anthranilamide[4] and 2,6-pyridinedicarboxamide derivatives (shown in **1** and **2**, respectively) can lead to molecules that take up a helical secondary structure stabilized, in part, by hydrogen bonding between the components.[5]



1

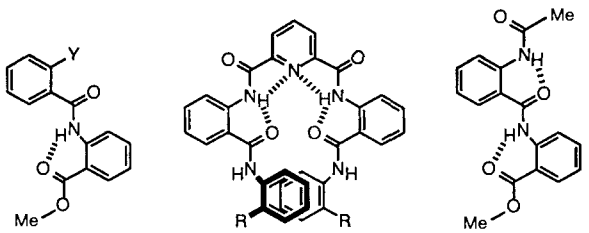


2, X = N, $N^- — O^+$

These individual subunits can be readily linked by a series of simple synthetic transformations. Treatment of 2-nitrobenzoyl chloride with methyl anthranilate gave **3**, which was converted by catalytic hydrogenation to aminoamide **4** and then treated with 2,6-bis(chloroformyl)pyridine to give **5a**.[6] Our expectation was that **5a** would take up a helical structure, as depicted in **5a** and **7** (≡ **5a**), in which the terminal anthranilamide rings overlap each other in a face-to-face arrangement.[7, 8] This struc-

[*] Prof. A. D. Hamilton, Y. Hamuro, Dr. S. J. Geib
Department of Chemistry, University of Pittsburgh
Pittsburgh, PA 15260 (USA)
Telefax: Int. code + (412)624-8552

[**] We thank the National Science Foundation (CHE 9213937) for partial support of this work, the Kurcha Chemical Industry for a fellowship to Y. H., and Professor George Newkome for helpful comments.

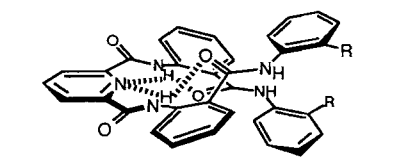


3, Y = NO_2
4, Y = NH_2

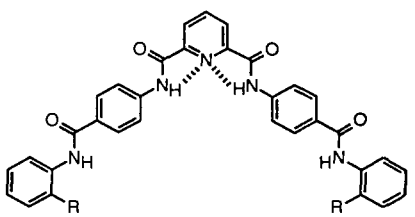
5a, R = CO_2Me
5b, R = H

6

ture should be stabilized by intramolecular hydrogen bonding[9] and $\pi-\pi$ stacking between the subunits as well as the normal preference for secondary benzamides to take up a *trans* conformation with only a small deviation from planarity.[11]



7, R = CO_2Me (≡ **5a**)



8, R = CO_2Me

The ^1H NMR of **5a** in $CDCl_3$ shows several features consistent with a helical structure in solution, and these are collected in Table 1 together with data from model compounds **6** and **8**.

Table 1. Selected ^1H NMR chemical shifts [δ] of oligoanthranilamides **5a**, **6**, **8**, and **9** in $CDCl_3$ (all spectra measured for 2 mM solutions except that of **8** which reached saturation at <1 mM). Ph_a and NH_a refer to those groups adjacent to the pyridine, and Ph_b and NH_b to the terminal anthranilamides.

Cmpd.	NH_a	NH_b	Ph_a6H	Ph_a5H	Ph_a4H	Ph_a3H	Ph_b6H	Ph_b5H	Ph_b4H	Ph_b3H
5a	13.08	11.60	7.58	7.22	7.63	8.88	7.90	6.89	6.70	8.50
6	11.17	12.05	7.87	7.24	7.54	8.67	8.11	7.18	7.64	8.78
8	9.72	12.12	8.18	8.18	8.00	8.00	8.11	7.14	7.63	8.95
9	13.80	11.78	7.86	7.35	7.58	8.60	7.91	6.92	7.27	8.88

The large downfield shift of the pyridinecarboxamide proton NH_a in **5a** compared to the equivalent resonances in **6** and **8** indicates bifurcated intramolecular hydrogen bonds involving both pyridine N and carbonyl O atoms as acceptors. In contrast, the signal for NH_b as well as those for the protons in the 6-, 5-, 4-, and 3-positions of the terminal anthranilamides are shifted upfield ($\Delta\delta$ = 0.45, 0.21, 0.29, 0.94, and 0.28, respectively) compared to the corresponding signals in **6**, consistent with their position above the ring current of the opposing anthranilamides in a helical conformation (see **5a**/**7**).[12] Further support for the role of intramolecular hydrogen bonds in stabilizing this conformation comes from the temperature dependence of the amide NH resonances in 20% [D_6]DMSO/$CDCl_3$ (DMSO = dimethyl sulfoxide). Both the NH_a and the NH_b signals in **5a** show a small variation with temperature (3.0×10^{-3} and 1.5×10^{-3} ppm K^{-1}, respectively), as expected for amide NH groups forming intramolecular H bonds in a polar solvent.[13] As a comparison, the signal for the anilide NH proton in **5b**, which is incapable of intramolecular hydrogen bonding, shows a large upfield shift with increasing temperature (7.1×10^{-3} ppm K^{-1}), while the NH_a resonance undergoes little change (2.1×10^{-3} ppm K^{-1}).

Tetraamide **5a** maintains its helical conformation in the solid state. X-ray analysis of a crystal of **5a** (grown from $CHCl_3$/hexane) shows a distinct helical arrangement of the five rings stabilized by six intramolecular hydrogen bonds (Fig. 1; $NH_a\cdots N$, 2.20 and 2.22 Å;[9] $NH_a\cdots OC$, 2.00 and 1.62 Å; $NH_b\cdots OC$, 1.64 and 1.67 Å). The pitch of the helix is narrow with close contact between the terminal anthranilamide rings and a distance of only 3.69 Å from Ph_bC2 to $Ph_b'C2$. As a result Ph_b4H is positioned above the first anthranilamide ring (Ph_a), suggesting an explanation for the large upfield shift of its ^1H NMR resonance in solution (Table 1).[14] Figure 1 shows the right-handed helix; however, the crystal is racemic with both right- and left-handed forms present in the unit cell.

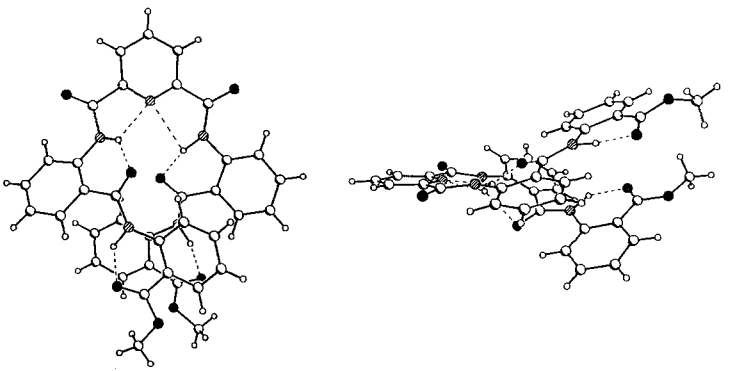
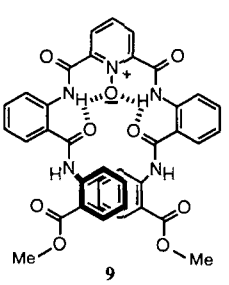


Fig. 1. X-ray structure of the helical oligoanthranilamide **5**. Left: front view; right: side view.

Subtle modifications can be made to the secondary structure by converting pyridinedicarboxamide (**5a**) to its *N*-oxide derivative as in **9**.[15] This leads to strong intramolecular hydrogen bonds completing six-membered rings in the turn region with a resultant expansion of the helix. Figure 2 shows the X-ray structure of **9** and confirms the persistence of the intramolecular hydrogen bonding motif despite changes in the components. Two short ($NH_a\cdots ON$, both 1.83 Å) and two long ($NH_a\cdots OC$, both 2.13 Å) hydrogen bonds enforce the helical conformation in the turn region, with two additional interactions ($NH_b\cdots OC$, both 1.81 Å) in the terminal rings. However, the increased steric bulk of the pyridine *N*-oxide unit relative to that of the simple pyridine in **5a** leads to a wider separation of the two terminal anthranilamide rings (Ph_bC2 to $Ph_b'C2$ distance 9.24 Å in **9**) and an increase in the pitch of the helix.[14] The expanded helical structure of **9** is also reflected in its ^1H NMR spectrum in $CDCl_3$ which shows (Table 1) large downfield shifts of the NH_a and NH_b resonances, similar to **5a** and consistent



9

 © VCH Verlagsgesellschaft mbH, D-69451 Weinheim, 1994 0570-0833/94/0404-0447 $ 10.00+.25/0

with strong intramolecular hydrogen bonding, but much smaller upfield shifts of Ph_b4H and Ph_b5H due to reduced ring current effects.

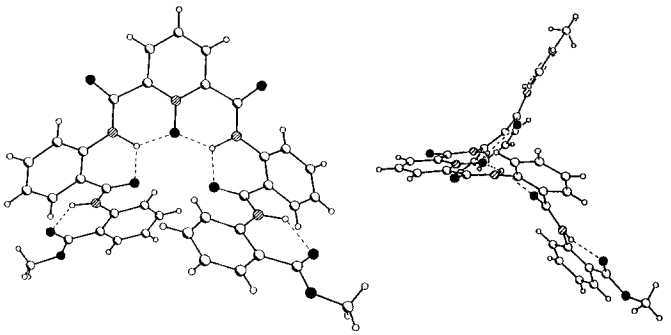


Fig. 2. X-ray structure of **9**. Left: front view; right: side view.

In summary, we have shown that a very simple series of anthranilic acid based subunits can be induced to take up, in both the solution and solid state, a helical secondary structure stabilized in part by intramolecular hydrogen bonding. We are currently preparing extended and substituted versions of these scaffolds to test the generality of the approach.

Received: August 24, 1993 [Z 6312 IE]
German version: *Angew. Chem.* **1994**, *106*, 465

[1] C. Brandon, J. Tooze, *Introduction to Protein Structure*, Garland, New York, **1991**.

[2] A family of novel polypeptide-like structures based on vinylogous amino acids has recently been reported: M. Hagihara, N. J. Anthony, T. J. Stout, J. Clardy, S. L. Schreiber, *J. Am. Chem. Soc.* **1992**, *114*, 6568–6570.

[3] Intramolecular hydrogen bonds have recently been used to control the structure of oligourea scaffolds: J. S. Nowick, N. A. Powell, E. J. Martinez, E. M. Smith, G. Noronha, *J. Org. Chem.* **1992**, *57*, 3763–3765. Bisacylguanidinium receptors: R. P. Dixon, S. Geib, A. D. Hamilton, *J. Am. Chem. Soc.* **1992**, *114*, 365–367.

[4] M. Feigel, G. Lugert, J. Manero, M. Bremer, *Z. Naturforsch. B* **1989**, *44*, 1109–1116; *ibid.* **1990**, *45*, 258–266.

[5] For a recent discussion of the role of intramolecular hydrogen bonding in a family of simple diamides see: G. P. Dado, S. H. Gellman, *J. Am. Chem. Soc.* **1993**, *115*, 4228–4245.

[6] A related approach has been used to prepare cyclic anthranilamide oligomers: a) A. Hoorfar, W. D. Ollis, J. F. Stoddart, *Tetrahedron Lett.* **1980**, 4211–4214; b) M. Feigel, G. Lugert, *Liebigs Ann. Chem.* **1989**, 1089–1092.

[7] Several helical structures stabilized by metal template effects have been reported: E. C. Constable, *Angew. Chem.* **1991**, *103*, 1530; *Angew. Chem. Int. Ed. Engl.* **1991**, *30*, 1490; U. Koert, M. M. Harding, J. M. Lehn, *Nature* **1990**, *346*, 339; C. O. Dietich-Buchecker, J. Guilhem, C. Pascard, J.-P. Sauvage, *Angew. Chem.* **1990**, *102*, 1202; *Angew. Chem. Int. Ed. Engl.* **1990**, *29*, 1154; E. C. Constable, M. D. Ward, D. A. Tocher, *J. Chem. Soc. Dalton Trans.* **1991**, 1675; D. A. Evans, K. A. Woerpel, M. J. Scott, *Angew. Chem.* **1992**, *104*, 439; *Angew. Chem. Int. Ed. Engl.* **1992**, *31*, 430.

[8] For examples of helical molecules stabilized by covalent interactions see: K. Deshayes, R. D. Broene, I. Chao, C. B. Knobler, F. Diederich, *J. Org. Chem.* **1991**, *56*, 6787, and references therein; R. Fritsch, E. Hartmann, D. Andert, A. Mannschreck, *Chem. Ber.* **1992**, *125*, 849; D. Gange, P. Magnus, L. Bass, E. V. Arnold, J. Clardy, *J. Am. Chem. Soc.* **1980**, *102*, 2134.

[9] The intramolecular hydrogen bonds of the simple 2,6-pyridinedicarboxamide forming five-membered rings are expected to be weak due to the reduced basicity of the pyridine [10]. However, the conformation shown in **5a** is still expected to be favored, since the alternative (nearly planar) conformations, involving $\approx 180^\circ$ rotation about one or both pyridine–CO bonds, should be destabilized by electrostatic repulsion between the pyridine N and carbonyl O atoms.

[10] G. R. Newkome, F. Fronczek, D. K. Kohli, *Acta Crystallogr. Sect. B* **1981**, *37*, 2114; E. Weber, G. R. Newkome, F. Fronczek, S. Franken, *J. Inclusion Phenom.* **1988**, *6*, 1.

[11] See, for example: F. Garcia-Tellado, S. Goswami, S. K. Chang, S. J. Geib, A. D. Hamilton, *J. Am. Chem. Soc.* **1990**, *112*, 7393; S. Harema, R. J. Gaymans, *Acta Crystallogr. Sect. B* **1977**, *33*, 3609.

[12] Repeated attempts to confirm helix formation in solution by adding chiral shift reagents were unsuccessful, even at low temperature, presumably due to the fast exchange between right- and left-handed helical forms.

[13] H. Kessler, *Angew. Chem.* **1982**, *94*, 509–520; *Angew. Chem. Int. Ed. Engl.* **1982**, *21*, 512–523.

[14] Further details of the crystal structure investigations are vailable on request from the Director of the Cambridge Crystallographic Data Centre, 12 Union Road, GB-Cambridge CB2 1EZ (UK), on quoting full journal citation.

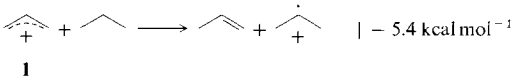
[15] U. Rychlewska, M. Gdaniec, *Acta Crystallogr. Sect. B* **1977**, *33*, 3555–3558; B. Brzezinski, G. Zundel, R. Krämer, *Chem. Phys. Lett.* **1986**, *124*, 395–400.

Generation of the Parent Allyl Cation in a Superacid Cryogenic Matrix**

Peter Buzek, Paul von R. Schleyer,* Hrvoj Vančik, Zlatko Mihalic, and Jürgen Gauss

Although many substituted allyl cations have been observed as persistent species in superacid media,[1] the parent allyl cation (**1**) has remained elusive. The putative ^{1}H NMR spectrum was reported in the early days of superacid chemistry,[2] but this observation has not been cofirmed. Numerous subsequent attempts to obtain ^{1}H and ^{13}C spectra of **1** failed.[3] Evidently, the allyl precursors polymerized instead.

The direct observation of **1** in condensed phases is quite challenging, as this allyl cation is about 6 kcal mol^{-1} less stable thermodynamically[5] than the isopropyl cation, 2-$C_3H_7^+$, the smallest carbocation persistent in superacid media (Scheme 1).



1

Scheme 1.

While there were earlier indications of the formation of allyl cation intermediates in zeolites,[6] the first direct CP-MAS NMR spectroscopic observation (CP-MAS = *c*ross *p*olarization *m*agic *a*ngle *s*pinning) of **1** adsorbed on H-ZSM-5 zeolite has only just been claimed by Biaglow, Gorte, and White (BGW).[7] They employed allyl alcohol enriched at the hydroxylated carbon with ^{13}C as the precursor and low surface coverage to minimize polymerization. Upon heating, a ^{13}C NMR

[*] Prof. P. von R. Schleyer, Dr. P. Buzek
Institut für Organische Chemie I der
Universität Erlangen-Nürnberg
D-91054 Erlangen (FRG)
Telefax: Int. code + (9131)859132
Dr. H. Vančik, Dr. Z. Mihalic
Laboratory of Organic Chemistry and Biochemistry
University of Zagreb
Strossmayerov trg. 14, 41000 Zagreb (Croatia)
Dr. J. Gauss
Institut für Physikalische Chemie der Universität Karlsruhe
D-76128 Karlsruhe (FRG)

[**] The work at Erlangen was supported by the Fonds der Chemischen Industrie, the Stiftung Volkswagenwerk, the Deutsche Forschungsgemeinschaft, and the Convex Computer Corporation, at Zagreb by the Research Council of Croatia (project: 1-07-226), and at Karlsruhe by the Fonds der Chemischen Industrie. We appreciate the special efforts of Prof. H.-U. Siehl, Martin Fuss, and Bernhard Müller to observe the allyl cation by NMR. Bernd Reindl performed the geometry optimizations for several of the allyl cations in Table 1. In addition, J. G. thanks Prof. Ahlrichs for his generosity and encouragement.

signal at $\delta = 218$ appeared; this was assigned to C1 and C3 in **1**, although other possibilities were discussed. However, this chemical shift does not agree with $\delta(^{13}C) = 245.7$ predicted by Schindler from IGLO chemical shift computations (Basis III level) for carbocations.[8] The chemical shift of $\delta = 218$ is also lower than a rough estimate ($\delta = 236$) based on an extrapolation of the experimental ^{13}C data for the methylene carbons in the 1,1-dimethylallyl ($\delta = 274.3$) and 1-methylallyl ($\delta = 255.1$) cations.[1]

This paper has several objectives. We first analyze BGW's data in light of new theoretical results for the ^{13}C chemical shifts obtained with the recently developed GIAO–MP2[9] method for calculating chemical shifts as a correlated level. These calculations, which are more accurate and reliable than the previous SCF based calculations (IGLO[8] or GIAO–SCF[10]), cast some doubt on BGW's suggestion that the zeolite species was a free allyl cation. We then report our own direct observation of the allyl cation (**1**) by infrared spectroscopy in a cryogenic superacid matrix.

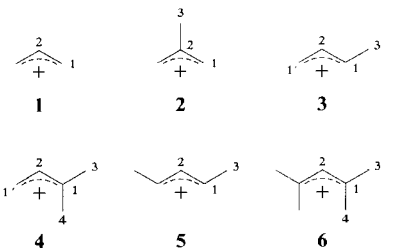
Schindler's IGLO ^{13}C shifts for alkyl-substituted allyl cations[8] deviated significantly from the available experimental values. (The IGLO data in Table 1 have been refined by using the MP2/6-31G* geometries, but do not differ appreciably from Schindler's.) Similar errors in ^{13}C chemical shifts calculated at

Table 1. Calculated ^{13}C NMR chemical shifts of allyl cations.

Cmpd.	C Atom	IGLO [a] DZ	IGLO [a] BasII	GIAO-MBPT(2) [a] dzp/dz SCF	dzp/dz MP2	tzp/dz SCF	tzp/dz MP2	Exp. [b]
1	C1	232.4	241.0	234.1	219.5	236.5	227.4	218 (?)
	C2	140.2	148.2	139.1	145.3	142.8	152.8	–
2	C1	233.9	241.0	234.4	218.4	236.5	226.0	–
	C2	149.0	162.4	153.3	160.9	156.7	168.3	–
	C3	15.3	18.4	16.0	19.5	16.3	20.5	–
3	C1	257.6	267.2	258.6	245.5	261.4	257.0	255.1
	C2	140.6	146.9	137.8	143.7	141.3	151.0	149.8
	C1′	216.4	222.0	215.4	198.3	217.6	205.8	201.5
	C3	31.8	33.9	29.9	36.0	31.1	38.2	36.3
4	C1	274.3	285.7	276.4	264.1	279.9	274.9	274.3
	C2	137.1	142.3	134.1	139.9	137.2	147.0	146.0
	C1′	192.8	198.8	193.1	174.4	195.3	181.1	175.0
	C3	37.4	39.0	35.4	41.0	35.9	42.5	41.4
	C4	29.7	31.7	27.6	31.4	28.7	33.7	33.1
5	C1	239.0	249.2	241.3	226.0	244.5	233.9	231.3
	C2	139.4	144.4	135.8	142.5	139.5	150.3	147.0
	C3	28.1	30.6	27.0	31.9	27.9	33.7	29.8
6	C1	240.8	254.5	245.8	228.7	249.7	239.0	233.7
	C2	133.6	135.8	129.4	138.7	132.1	145.3	141.1
	C3	36.6	38.9	35.9	40.6	36.2	42.0	–
	C4	29.6	32.4	29.3	33.8	29.0	34.5	–
mean deviation		±6.9	±9.1	±9.1	±4.1	±9.2	±2.7	
largest deviation		+17.8	+23.8	+18.1	−10.2	+20.3	+6.1	

[a] All allyl cations were optimized at MP2(FULL)/6-31G*: **4**, **5**, **6** by Bernd Reindl; for numbering of C atoms, see Scheme 2. [b] **1**: [7], **3**: [1g]; **4**: [1f], **5**: [1c]; **6**: [1b]. [c] Averaged values for C1 and C1′ (C_s symmetry).

SCF levels (e.g., IGLO or GIAO) for unsaturated organic compounds are corrected at GIAO–MP2,[9] which includes electron correlation in a practical method for the computation of magnetic properties for the first time. Our recent application to the benzenonium and the phenonium ions demonstrates the decisive improvements that are possible in unsaturated carbocations.[11] The agreement with the experimental data for the set of four methyl-substituted allyl cations included in Table 1 is improved similarly. The ^{13}C chemical shifts at the IGLO–SCF and GIAO–SCF levels differ by an average of $\Delta\delta = 9.2$, and the largest discrepancy is $\Delta\delta = 24$. The GIAO–MP2 performance is superior. With the larger tzp/dz basis set (tzp = triple zeta + polarization, dz = double zeta), the average deviation is reduced to $\Delta\delta = 2.7$, and the largest discrepancy drops to $\Delta\delta = 6$.



Scheme 2. Structures of the allyl cations in Table 1, showing the numbering of the C atoms.

At the higher tzp/dz level, GIAO–MP2 predicts $\delta = 227.4$ for C1 and C3 of the allyl cation. BGW observed a signal at $\delta = 218$ in their solid-state zeolite NMR spectrum.[7] While the difference is not large it is outside the error range found for the other cations in Table 1. The experimental signal may be due to another species, or it may be displaced in the solid state, for example, by complexation of the allyl cation with the zeolite (cf. ref. [15d] for a more extreme example of the effects of complexation on NMR spectra).

The recent development of cryogenic techniques for the determination of the vibrational spectra of carbocations under matrix conditions[12] prompted our reexamination of the problem. Allyl cation formation, rather than polymerization, might be favored under the codeposition conditions, which ensure lower concentrations, and the controlled gradual increase in temperature.

Moreover, computed ab initio IR spectra[13] (see, for example, Table 2 and the simulation in Figure 1 for **1** at CISD/6-31G**) provide a reliable basis for interpreting experimental results. Such theoretical spectra predict that allyl cations have a

Table 2. Experimental and calculated (CISD/6-31G**) vibrational frequencies [cm^{-1}] of the allyl cation **1**.

Experiment Freq. [cm^{-1}]	Int. [a]	Calculation Freq. [cm^{-1}] [b]	Int. [$km\,mol^{-1}$]	Ass. [c]
3117	w	3121, 3120	19.4, 9.2	*A1*, *B2*
–		3083	5.5	*A1*
3033	w	3017, 3016	4.8, 1.6	*B2*, *A1*
1578	s	1558	280.2	*B2*
–		1505	10.8	*A1*
1418	vs	1391	153.1	*B2*
1267	vs	1265	4.2	*A1*
1249	s	1240	72.5	*B2*
–		1120	0.0	*A2*
1195	m	–		
1074	m	1112	24.2	*B1*
1061	m	–		
1043	m	1013	1.6	*A1*
957	m	986	40.2	*B1*
928	m	915	1.7	*B2*
845	m	–		
814	m	–		
		613	0.0	*A2*
		425	0.3	*A1*
		298	16.5	*B1*

[a] Intensities: vs (very strong), s (strong), m (medium), w (weak). [b] Calculated frequencies scaled by 0.92. [c] Assignment of the vibrations (C_{2v} symmetry).

characteristic feature: an intense IR absorption near 1580 cm^{-1} attributable to the asymmetric allyl C-C-C stretching vibration. We have reported an intense peak at 1581 cm^{-1} for the *trans*-1-methylallyl cation generated from crotyl chloride under cryogenic conditions.[14a] The MP2/6-31G* computed frequency,[14b] when scaled by 0.94, was 1604 cm^{-1}. Since the harmonic approximation is employed,[13] ab initio frequencies are systematically too high and are scaled to correspond with the anharmonic experimental values (see Table 2). The asymmetric C-C-C stretching vibration of **1** is predicted to be 1592 cm^{-1} (MP2/6-31G*, scaled by 0.94) and 1558 cm^{-1} (CISD/6-31G**, scaled by 0.92).

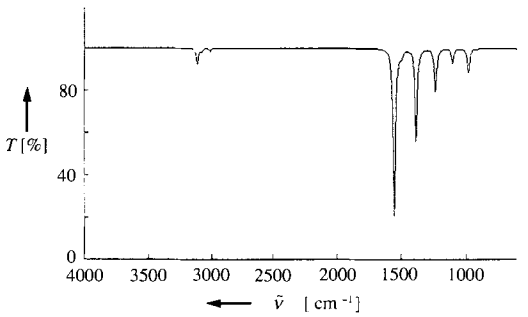


Fig. 1. Simulated IR spectrum of the allyl cation (CISD/6-31G** level).

Different procedures and precursors were employed in attempts to prepare the parent allyl cation (**1**). The most obvious way is to ionize allyl halides directly. In Erlangen, allyl chloride was codeposited with SbF_5 in vacuo on a sodium chloride window at 130 K. Even at that temperature, new signals accompanied the allyl chloride spectrum, which was characterized by the C=C stretching vibration at 1641 cm^{-1}. Further changes occurred on warming to 170 K (Fig. 2a). In particular, two signals at 1577 (the more intense signal) and 1547 cm^{-1} became stronger as the 1641 cm^{-1} peak first diminished and then disappeared. Other changes in the spectrum occurred on further warming, and at 230 K both the 1547 cm^{-1} and the 1577 cm^{-1} peaks are prominent (Fig. 2b). This suggests that the allyl cation formed first (1577 cm^{-1} peak) but then converted to undefined products (1547 cm^{-1}; perhaps polymer) at the higher temperatures. However, since the observed spectra (Fig. 2) have many more peaks than are computed for the allyl cation (Fig. 1), oligomerization or other side reactions must have occurred even at the low temperatures.

Allyl bromide gave analogous results in Zagreb. There was also some evidence for the formation of the allyl cation indirectly from trimethylsilyl propyne codeposited with a HBr/SbF_5 protonation medium. The initial IR spectrum at 77 K (displaying the C≡C stretching frequency of the precursor at 2184 cm^{-1}), underwent a number of changes on warming (details will be reported elsewhere). A transient signal at 2017 cm^{-1} was assigned to the Si–C hyperconjugatively stabilized[15] vinyl cation, $(CH_3)_3SiCH{=}C^+CH_3$. Above 180 K this peak disappeared, but the spectrum, while still indicating some starting material, resembled Figure 2b rather closely. Evidently, β-elimination of the $SiMe_3$ group (presumably as $FSiMe_3$) from the starting material gave propyne, which, at least in part, was protonated immediately in situ, and rearranged to the allyl cation **1**. Nevertheless, attempts to prepare **1** directly by protonating propyne failed to give any promising IR spectra.

In contrast to all these experiments, clean spectra were obtained in Erlangen by using cyclopropyl bromide as a precursor for **1**. Schleyer et al. had shown in 1969 that 1,3-dimethylallyl cations could be generated stereospecifically from the 2,3-dimethylcyclopropyl chloride isomers.[16] Codeposition with SbF_5 at 110 K results in an IR spectrum (Fig. 3a) completely different from the starting material. The prominant signal at 1578 cm^{-1} already had been observed (at 1577 cm^{-1}, Fig. 2) from the reaction of allyl chloride (and allyl bromide) with SbF_5. The intensity of the signals at 1578, 1418, and 1267 cm^{-1} increased when warmed to 140 K (cf. Fig. 3b), but additional peaks at 966 and 901 cm^{-1}, due to some side product also arise. At 250 K, the peak attributable to the asymmetric C-C-C stretching vibration of **1** (1578 cm^{-1}) is almost completely replaced by a peak at 1535 cm^{-1}.

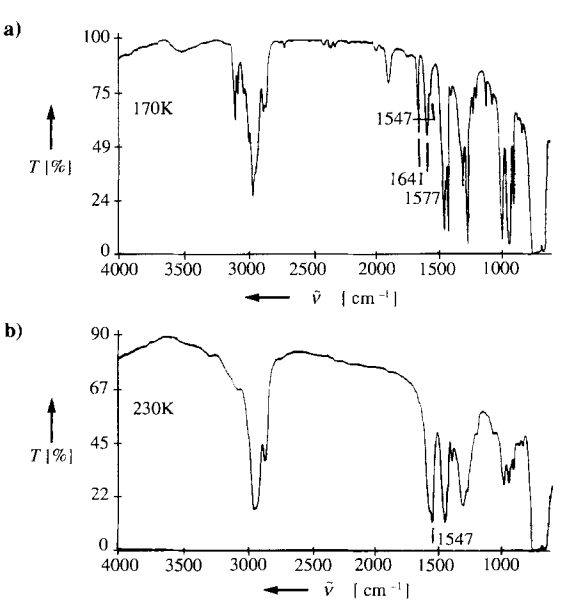


Fig. 2. a) Experimental IR spectrum from allyl chloride in an SbF_5 matrix at 170 K. Note the peak for the allyl cation (**1**) at 1577 cm^{-1}. Some "polymer" is present (e.g. band at 1547 cm^{-1}). b) Final spectrum at 230 K, attributed to "polymer".

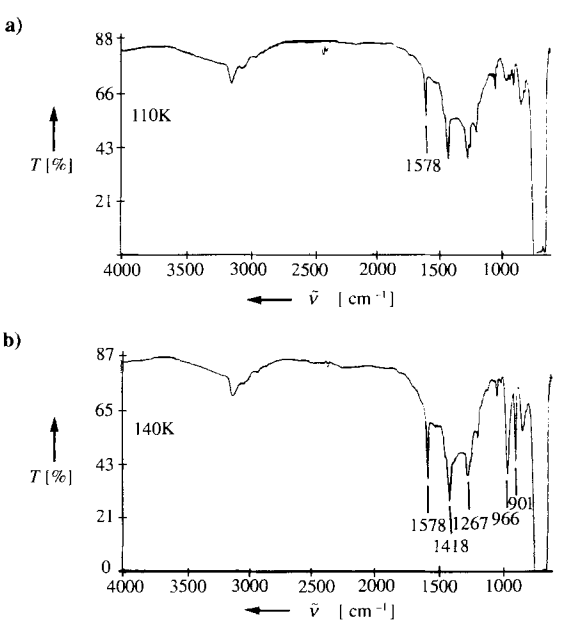


Fig. 3. a) Experimental IR spectrum of the allyl cation (**1**) generated from cyclopropyl bromide in SbF_5 matrix at 110 K. b) The spectrum at 140 K; the new signals at 966 and 901 cm^{-1} are due to side products.

Very good agreement is found between the calculated and experimental frequencies for **1** (Table 2). The graphical comparison (Fig. 4) demonstrates that the experimental frequencies correspond excellently to the calculated values.

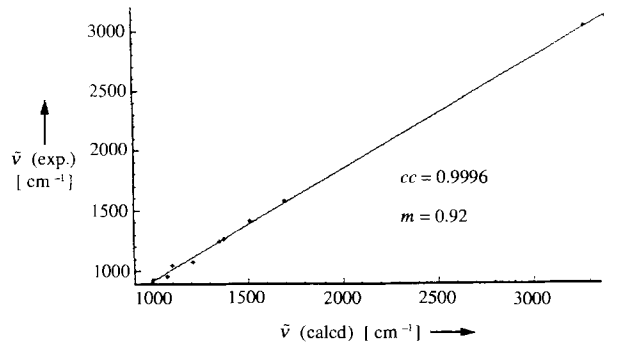


Fig. 4. Correlation of the experimental and calculated (CISD/6-31G**) IR frequencies of the allyl cation **1**. *cc* = correlation coefficient, *m* = slope.

The allyl cation **1** is now the smallest long-lived carbocation observable in a solid SbF_5 matrix. Our findings provide solid evidence that the allyl cation was formed under cryogenic conditions by ionizing cyclopropyl bromide. Unlike the unsaturated precursors of **1**, cyclopropyl bromide evidently does not react with **1** during generation. The IR asymmetic stretching vibration at about 1575 cm^{-1} characterizes **1** as well as allyl cations in general. Although accompanied by side reactions, **1** apparently also formed from allyl chloride and bromide, and possibly from trimethylsilylpropyne as well.[17] BGW's NMR evidence for **1** is equivocal. In light of the difference of $\Delta\delta \approx 10$ in the ^{13}C chemical shifts of the zeolite and the GIAO–MP2 ^{13}C chemical shifts, confirmation is desirable.

Received: April 14, 1992
Revised: August 31, 1993 [Z 5303 IE]
German version: *Angew. Chem.* **1994**, *106*, 470

[1] a) N. C. Deno in *Carbonium Ions, Vol. 2* (Ed.: G. A. Olah, P. von R. Schleyer), Wiley-Interscience, New York, **1970**, Chapter 2; b) G. A. Olah, P. R. Clifford, Y. Halpern, R. G. Johanson, *J. Am. Chem. Soc.* **1971**, *93*, 4219; c) G. A. Olah, R. J. Spear, *ibid.* **1975**, *97*, 1539, 1845; d) G. A. Olah, J. S. Staral, R. J. Spear, G. Liang, *ibid.* **1975**, *97*, 5489; e) G. A. Olah, H. Mayr, *ibid.* **1976**, *98*, 7333; *ibid.* **1978**, *100*, 6544; f) H. Mayr, G. A. Olah, *ibid.* **1977**, *99*, 510; g) *Methoden Org. Chem. (Houben-Weyl) 4th ed. 1952–*, Bd. E19c, **1990**.
[2] G. A. Olah, M. B. Comisarow, *J. Am. Chem. Soc.* **1964**, *86*, 5682.
[3] a) H.-U. Siehl, C. S. Yannoni, G. A. Olah, personal communication; b) P. Vogel, *Carbocation Chemistry*, Elsevier, Amsterdam, **1985**, p. 173.
[4] a) G. A. Olah, E. B. Baker, J. C. Evans, W. S. Tolgyesi, J. S. McIntyre, I. J. Bastien, *J. Am. Chem. Soc.* **1964**, *86*, 1360; b) W. Koch, P. von R. Schleyer, P. Buzek, B. Liu, *Croat. Chem. Acta* **1992**, *65*, 655.
[5] S. G. Lias, J. E. Bartmess, J. F. Liebman, J. L. Holmes, R. D. Levin, G. Hallard, *J. Phys. Chem. Ref. Data Suppl.* **1988**, *17*, 1.
[6] a) G. I. Hutchings, D. F. Lee, C. D. Williams, *J. Chem. Soc. Chem. Commun.* **1990**, 1475; b) E. J. Munson, T. Xu, J. F. Haw, *ibid.* **1973**, 75.
[7] A. I. Biaglow, R. J. Gorte, D. White, *J. Chem. Soc. Chem. Commun.* **1993**, 1164.
[8] M. Schindler, *J. Am. Chem. Soc.* **1987**, *109*, 1020. IGLO = Individual Gauges for Localized Orbitals.
[9] a) J. Gauss, J. F. Stanton, R. J. Bartlett, *Chem. Phys. Lett.* **1992**, *191*, 614; *J. Chem. Phys.* **1993**, *99*, 3629. The (GIAO)-Gauge-Including Atomic Orbital MP2-Programm has been implemented into the ACES II program system (J. F. Stanton, J. Gauss, J. D. Watts, W. J. Lauderdale, R. J. Bartlett, Quantum Theory Project, University of Florida, Gainsville, **1992**). b) Basis sets are given in: A. Schäfer, H. Horn, R. Ahlrichs, *J. Chem. Phys.* **1992**, *97*, 2571.
[10] a) R. Ditchfield, *Mol. Phys.* **1974**, *27*, 789; b) K. Wolinksi, J. F. Hinton, P. Pulay, *J. Am. Chem. Soc.* **1990**, *112*, 8251; c) M. Häser, R. Ahlrichs, H. P. Baron, P. Weis, H. Horn, *Theor. Chim. Acta* **1992**, *83*, 455.
[11] S. Sieber, P. von R. Schleyer, J. Gauss, *J. Am. Chem. Soc.* **1993**, *115*, 6987.
[12] a) H. Vančik, D. E. Sunko, *J. Am. Chem. Soc.* **1989**, *111*, 3742; b) W. Koch, B. Liu, D. J. DeFrees, D. E. Sunko, H. Vančik, *Angew. Chem.* **1990**, *102*, 198; *Angew. Chem. Int. Ed. Engl.* **1990**, *29*, 183; c) P. Buzek, P. von R. Schleyer, S. Sieber, W. Koch, J. W. de M. Carneiro, H. Vančik, D. E. Sunko, *J. Chem. Soc. Chem. Commun.* **1991**, 671; d) P. Buzek, P. von R. Schleyer, H. Vančik, D. E. Sunko, *ibid.* **1991**, 1538.
[13] a) W. Hehre, L. Radom, P. von R. Schleyer, J. A. Pople, *Ab Initio Molecular Orbital Theory*, Wiley, New York, **1986**; b) B. A. Hess, Jr., L. J. Schaad, P. Carsky, R. Zahradnik, *Chem. Rev.* **1986**, *86*, 709.
[14] a) H. Vančik, V. Gabelica, D. E. Sunko, P. Buzek, P. von R. Schleyer, *J. Phys. Org. Chem.* **1993**, *6*, 421; b) W. Koch, B. Liu, D. J. De Frees, *J. Am. Chem. Soc.* **1988**, *110*, 7325.
[15] a) H.-U. Siehl, F. P. Kaufmann, Y. Apeloig, V. Braude, D. Danovich, A. Berndt, N. Stamatis, *Angew. Chem.* **1991**, *103*, 1546; *Angew. Chem. Int. Ed. Engl.* **1991**, *30*, 1479; b) G. A. McGibbon, M. A. Brook, J. K. Terlouw, *J. Chem. Soc. Chem. Commun.* **1992**, 360; c) Y. Apeloig in *The Chemistry of Organic Silicon Compounds* (Eds.: S. Patai, Z. Rappaport); Wiley, Chichester, **1989**; d) P. von R. Schleyer, P. Buzek, T. Müller, Y. Apeloig, H.-U. Siehl, *Angew. Chem.* **1993**, *105*, 1558; *Angew. Chem. Int. Ed. Engl.* **1993**, *32*, 1471.
[16] P. von R. Schleyer, T. M. Su, M. Saunders, J. C. Rosenfeld, *J. Am. Chem. Soc.* **1969**, *91*, 5174.
[17] It has not been possible to observe the allyl cation by NMR starting with cyclopropyl bromide. New experiments carried out at Tübingen by Prof. H.-U. Siehl, Martin Fuss, and Bernhard Müller using the matrix cocondensation technique (ref. [1g] p. 31) only gave the broad, featureless spectra characteristic of polymers. The ^1H NMR spectra were not clean enough to allow identification of signals expected for the allyl cation. No peak near $\delta = 227$ in the ^{13}C NMR spectrum, as predicted from GIAO-MP2 calculations for **1**, could be detected.

Novel Conjunction of Hetero(macro)cycles and a Pentamolybdodiphosphonate Cage**

Mark P. Lowe, Joyce C. Lockhart,* William Clegg, and Kelly A. Fraser

Macrocycles having separate additional functionality are much sought after for the development of supramolecular chemistry.[1] Polyoxometalates with separate, additional functionality are also in demand in materials sciences for the development of difunctional catalysts[2] and a whole gamut of other applications.[3] The conjunction of these two major areas of current research has been achieved with the synthesis of the first examples of polyoxomolybdate cages derivatized with hetero(macro)cycles. The potential of these novel conjugates for a variety of applications from catalysis to nuclear medicine is under investigation.

Incorporation of the heterocycles as their methylphosphonates was achieved by mixing phosphonate (**1** or **2**) and molybdate according to Equation (a) at pH 2–5. The mixture was

$$2\,[C(NH_2)_3]^+ + 2\,ZPO_3H + 5\,MoO_4^{2-} + 8\,H^+ \rightleftharpoons [C(NH_2)_3]_2[Mo_5(ZP)_2O_{21}] + 5\,H_2O \quad \text{(a)}$$

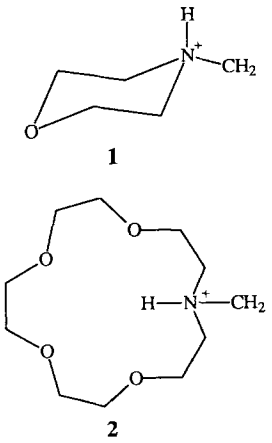
$Z^+ = \mathbf{1}, \mathbf{2}$

heated to nearly boiling and allowed to cool slowly to give colorless crystals suitable for X-ray crystallography.[4]

Since heterocycle Z has a protonated nitrogen atom, ZPO_3H is a zwitterion. The structure of $[C(NH_2)_3]_2$[**3**] · 3 H_2O consists

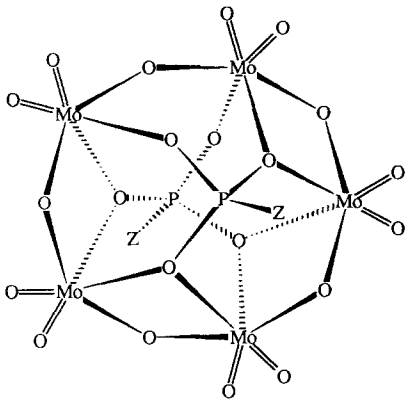
[*] Dr. J. C. Lockhart, M. P. Lowe, Prof. W. Clegg, K. A. Fraser
Department of Chemistry, University of Newcastle
Newcastle-upon-Tyne, NE1 7RU (UK)
Telefax: Int. code + (91)261-1182

[**] This work was supported by the Science and Engineering Research Council and Courtaulds Coatings PLC. We thank C. J. Matthews for preliminary ^{31}P NMR measurements and a particularly careful referee for his helpful comments.



1

2



ligand **1**: ZPO_3H (Z=**1**)
ligand **2**: ZPO_3H (Z=**2**)

anion **3**: Z^+ = **1**
anion **4**: Z^+ = **2**

of guanidinium cations, water molecules of crystallization and $[(ZP)_2Mo_5O_{21}]^{2-}$ anions **3** (the protonated nitrogen atoms of Z provide two additional internal counterions). Anion **3** lies on a crystallographic C_2 axis passing through Mo3 and O7. Its structure (Fig. 1 and Table 1) is similar to that well known for the $[P_2Mo_5O_{23}]^{6-}$ anion[5] in that it consists of a ring of five distorted MoO_6 octahedra. Four of the octahedra are joined by edge-

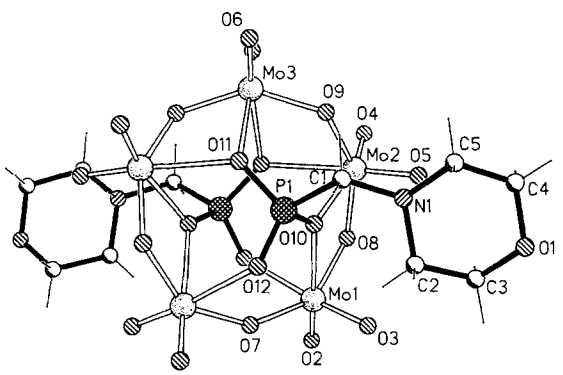


Fig. 1. Structure of the anion **3** in a crystal of $[C(NH_2)_3]_2$[**3**] · 3 H_2O.

sharing oxygen atoms; the ring is completed and the symmetry broken by one corner-sharing oxygen atom between two molybdenum atoms. Two ZPO_3 tetrahedra cap the top and bottom of the ring; one oxygen atom is shared with only one MoO_6 octahedron (the corner-sharing one) and the other two shared with two MoO_6 octahedra each. As a result the ten-membered $(Mo-O)_5$ ring has an envelope-type conformation, whereby one molybdenum atom is bent out of the plane formed by the other four. This is reflected in the Mo-O-Mo bond angles. The angles at the four edge-sharing linkages are roughly 123°, whereas the angle at the shared corner is 148°. Extensive intra- and intermolecular hydrogen bonding is evident throughout the crystal. The morpholine ring bends over the molybdenum cage and its protonated nitrogen atom forms an intramolecular hydrogen bond to a terminal molybdenum oxygen atom (N–H···O = 2.043 Å, angle = 106.4°). This is reflected in the terminal Mo=O bond lengths: Mo–O groups not involved in hydrogen bonding have a Mo=O bond length of 1.700 Å; however, the

Table 1. Selected bond lengths [Å] and angles [°] of the anion **3** in a crystal of $[C(NH_2)_3]_2$ [**3**] · 3 H_2O [a].

Mo1-O2	1.701(3)	Mo1-O3	1.709(3)
Mo1-O7	1.947(2)	Mo1-O8	1.922(3)
Mo1-O10	2.380(3)	Mo1-O12′	2.343(3)
Mo2-O4	1.702(3)	Mo2-O5	1.715(3)
Mo2-O8	1.919(3)	Mo2-O9	1.950(3)
Mo2-O10	2.251(3)	Mo2-O11′	2.349(3)
Mo3-O6	1.723(3)	Mo3-O9	1.891(3)
Mo3-O11	2.366(3)	P1-O10	1.543(3)
P1-O11	1.539(3)	P1-O12	1.506(3)
P1-C1	1.826(4)	C1-N1	1.498(5)
O2-Mo1-O3	102.1(2)	O2-Mo1-O8	100.44(14)
O3-Mo1-O8	100.13(14)	O2-Mo1-O7	102.66(14)
O3-Mo1-O7	100.88(12)	O8-Mo1-O7	144.52(14)
O2-Mo1-O12′	83.27(13)	O3-Mo1-O12′	174.34(13)
O8-Mo1-O12′	77.10(11)	O7-Mo1-O12′	79.28(9)
O2-Mo1-O10	169.20(12)	O3-Mo1-O10	85.51(13)
O8-Mo1-O10	70.44(11)	O7-Mo1-O10	83.07(12)
O12′-Mo1-O10	88.90(10)	O4-Mo2-O5	106.4(2)
O4-Mo2-O8	99.93(14)	O5-Mo2-O8	100.58(14)
O4-Mo2-O9	100.22(14)	O5-Mo2-O9	95.96(14)
O8-Mo2-O9	149.07(12)	O4-Mo2-O10	162.28(13)
O5-Mo2-O10	91.15(13)	O8-Mo2-O10	73.53(11)
O9-Mo2-O10	80.23(12)	O4-Mo2-O11′	90.10(13)
O5-Mo2-O11′	161.45(12)	O8-Mo2-O11′	84.53(11)
O9-Mo2-O11′	72.22(11)	O10-Mo2-O11′	73.07(11)
O6-Mo3-O6′	104.2(2)	O6-Mo3-O9	99.15(14)
O6′-Mo3-O9	102.21(14)	O9-Mo3-O9′	144.9(2)
O6-Mo3-O11	87.02(13)	O6′-Mo3-O11	167.55(13)
O9-Mo3-O11	80.92(12)	O9′-Mo3-O11	72.78(12)
O11-Mo3-O11′	82.39(14)	Mo1′-O7-Mo1	147.7(2)
Mo2-O8-Mo1	122.6(2)	Mo3-O9-Mo2	123.1(2)
P1-O10-Mo2	130.6(2)	P1-O10-Mo1	134.7(2)
Mo2-O10-Mo1	93.35(10)	P1-O11-Mo2′	129.2(2)
P1-O11-Mo3	123.7(2)	Mo2′-O11-Mo3	91.55(10)
P1-O12-Mo1′	115.8(2)	O12-P1-O11	113.1(2)
O12-P1-O10	109.2(2)	O11-P1-O10	112.6(2)
O12-P1-C1	110.3(2)	O11-P1-C1	104.5(2)
O10-P1-C1	106.9(2)	N1-C1-P1	113.1(3)

[a] Symmetry transformation for primed atoms: $-x+1, y, -z+3/2$.

group forming a hydrogen bond has one of 1.715 Å. Although this difference is hardly significant, the overall pattern of bond lengths for terminal Mo=O bonds in the anion (see below) does show a real correlation with the hydrogen bonding.

The C–H protons of the morpholine ring and of the NCH_2P group are extremely close to the terminal (Mo=O) and bridging (Mo–O–P) oxygen atoms on the adjacent molecule. The O···H–C distances are in the range 2.3–2.5 Å. The guanidinium counterions form hydrogen bonds to the oxygen atoms in the molybdenum cage, the morpholine oxygen atoms, and the water molecules with O···H–N distances of 2.2–2.3 Å. The water molecule, as well as being involved in hydrogen bonding with the previously mentioned guanidinium ions, is also hydrogen bonded to just one terminal molybdenum oxygen atom (Mo3-O6) with O–H···O distances of approximately 2.3 Å. The combination of two water molecules forming hydrogen bonds to this oxygen atom results in an increase in the Mo=O bond length from roughly 1.700 Å to 1.723 Å.

The cage anions were characterized in solution by ^{31}P NMR spectroscopy. Individual species have been assigned in systems of pentamolybdodiphosphonates (and other systems) by Pettersson et al.[6] by using electromotive force (EMF) and spectroscopic methods including ^{31}P NMR. These studies indicate that at defined ratios of P:Mo in defined pH ranges, signals maximize in sequence according with species postulated based on the results of EMF and crystallographic studies.

A selection of ^{31}P NMR spectra at a P:Mo ratio of 2:5 and pH 1–6 (for phosphonates **1** and **2**) is shown in Figure 2. In

 © VCH Verlagsgesellschaft mbH, D-69451 Weinheim, 1994 0570-0833/94/0404-0452 $ 10.00+.25/0

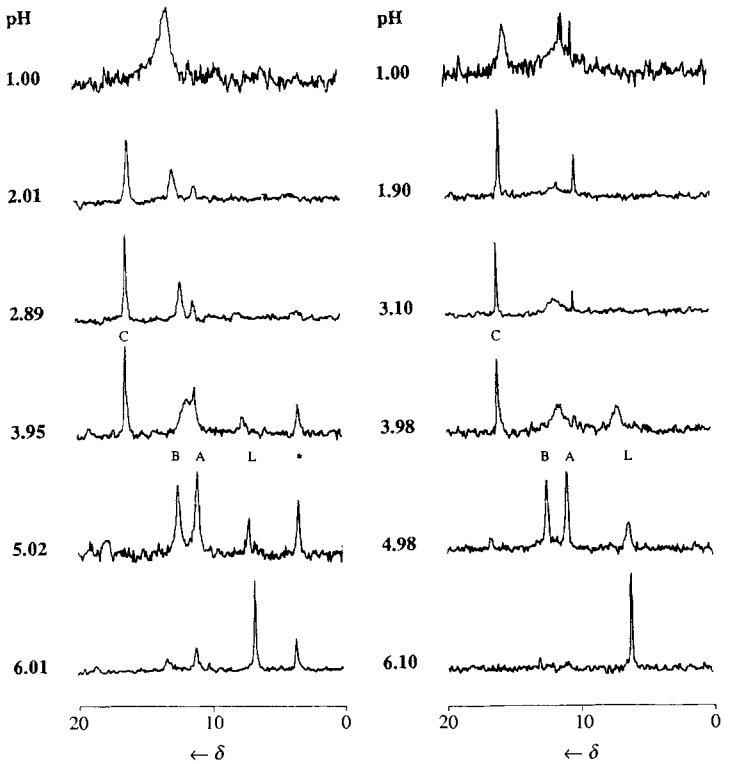


Fig. 2. Change in the ^{31}P NMR signals with pH in mixtures of [**2**] and $[MoO_4]^{2-}$ (left), and [**1**] and $[MoO_4]^{2-}$ (right), in both cases at a ratio of 2:5. Chemical shifts: free ligand L: $\delta = 6.50-7.60$, A: $\delta = 10.95-11.10$, B: $\delta = 11.80-12.80$, C: $\delta = 15.60-17.70$, H_3PO_3 (impurity marked with *): $\delta = 3.30-3.50$.

addition to signal L of the phosphonate reagent, which disappeared around pH 3, three prominent signals marked A, B, and C were observed for both phosphonates in the range $\delta = 10.9-11.1$ (A), 11.8–12.8 (B) and 15.6–17.7 (C) within the pH range 1.5–4.5. That signal C pertains to the cage is confirmed for phosphonate **1**: upon addition of guanidinium chloride the salt of anion **3** precipitates and concomitantly signal C disappears

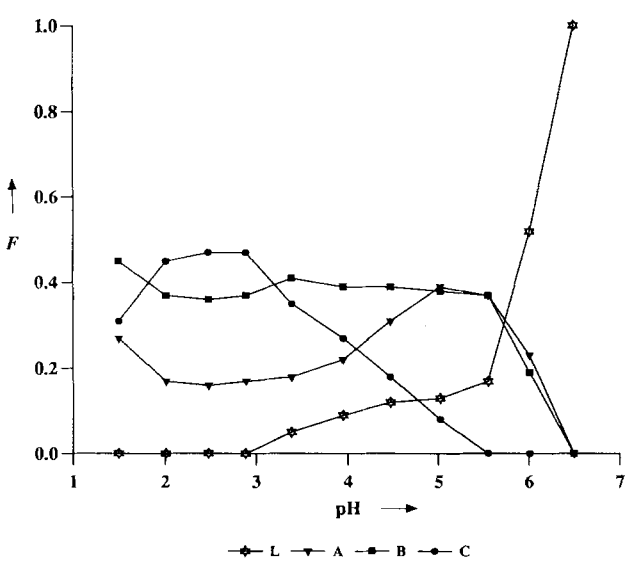


Fig. 3. Mole fraction of phosphorus F (derived from the ^{31}P NMR spectra of ligand **2** by using the relation F = (integral of one P signal)/(total integral of all P signals) for each of the species A, B, C, and L for L = **2** at different pH values.

from the spectrum of the filtrate; however, no attempt was made to observe the reestablishment of the equilibrium. The signals broadened at lower pH values indicating fast exchange processes not quite at the fast-exchange limit on the NMR timescale. Cage rearrangements are a recognized phenomenon in polyoxometalate chemistry and have been studied in much detail by NMR spectroscopic methods.[7]

The plot of signal intensities in Figure 3 indicates that the concentration of the $[(ZP)_2Mo_5O_{21}]^{2-}$ anion should be maximized at pH = 2–3. The plot also indicates (as noted by other workers[8]) that the most abundant species in solution is not necessarily the one that precipitates. Indeed the 2:5 compound is never the most abundant species here. Also clear from the plot is the total incorporation of the macrocycle into some form of molybdenum cluster at pH < 3.

Intramolecular hydrogen bonding between the protonated nitrogen atom of the hetero(macro)cycle and the terminal Mo–O oxygen atom of the MoO_6 octahedra is an integral part of these structures, and the bending of the hetero(macro)cycle to form this hydrogen bond can clearly bring an attached macrocyclic ring and associated metal ions into close proximity to the MoOP cage. Since analogous phosphonomolybdates with rings containing N, S, and O donors have been successfully synthesized in this work, an entire range of metal ions from hard alkali metals to soft thiophiles could be incorporated. In view of the great potential of these conjugates at the interface of two burgeoning fields, we are seeking to extend the range of cages and macrocycles that may be joined, especially by using organic solvents.

Experimental Procedure

All chemicals were obtained from Aldrich except the phosphonic acids, which were synthesized by using modifications to the Moedritzer–Irani reaction [9].

$[C(NH_2)_3]_2$[**3**] · 3 H_2O: $Na_2MoO_4 \cdot 2\ H_2O$ (3.00 g, 12.40 mmol) and the hydrate of ligand **1** (1.00 g, 5.02 mmol) were dissolved with stirring in H_2O (50 mL). Guanidine carbonate (0.70 g, 3.89 mmol) was neutralized with HCl (11.34 M) and added dropwise to the stirred solution. The pH was lowered to 3.5 with HCl (3 M). The white precipitate that formed was redissolved by heating the solution to 90 °C. On slow cooling large colorless crystals formed (yield: 1.1 g, 35%); IR (KBr): $\tilde{\nu}$[cm^{-1}] = 925, 897 [Mo-O(terminal)]; 690 [Mo-O(bridging)], 1151, 1067, 978 (P–O); 1296, 1263 (P–C); correct C,H,N analysis.

NMR Titration of ligand **2** with the molybdate anion: A solution containing $Na_2MoO_4 \cdot 2\ H_2O$ (0.095 g, 0.39 mmol) and the sodium salt of ligand **2** (0.054 g, 0.16 mmol) in H_2O (1 mL) was titrated with HCl (11.34 M). No correction was made for the 7% volume increase during the titration. The ^{31}P NMR spectra of samples were recorded at regular intervals of pH [10]. The resultant spectra are shown in Figure 2, and a plot of the relative intensities of the signals is shown in Figure 3. Corresponding spectra for ligand **1**, shown in Figure 2 for comparison, were obtained similarly by using a solution in H_2O (10 mL) containing $Na_2MoO_4 \cdot 2\ H_2O$ (0.45 g, 1.88 mmol) and the hydrate of ligand **1** (0.15 g, 0.75 mmol).

Received: August 18, 1993 [Z 6296 IE]
German version: *Angew. Chem.* **1994**, *106*, 463

[1] a) C. Seel, F. Vögtle, *Angew. Chem.* **1992**, *104*, 542; *Angew. Chem. Int. Ed. Engl.* **1992**, *31*, 528; b) *Frontiers in Supramolecular Organic Chemistry and Photochemistry* (Eds.: H.-J. Schneider, H. Dürr), VCH, Weinheim, **1990**; c) J.-M. Lehn, *Angew. Chem.* **1990**, *102*, 1347; *Angew. Chem. Int. Ed. Engl.* **1990**, *29*, 1304.

[2] A. Proust, P. Gouzerh, F. Robert, *Angew. Chem.* **1993**, *105*, 81; *Angew. Chem. Int. Ed. Engl.* **1993**, *32*, 115.

[3] a) V. W. Day, W. G. Klemperer, *Science* **1985**, *228*, 533; b) M. T. Pope, A. Müller, *Angew. Chem.* **1991**, *103*, 56; *Angew. Chem. Int. Ed. Engl.* **1991**, *30*, 34.

[4] $[C(NH_2)_3]_2$[**3**] · 3 H_2O: $M_r = 1254.16$, monoclinic, $C2/c$, $a = 16.347(5)$, $b = 13.776(5)$, $c = 16.132(5)$ Å, $\beta = 102.71(4)°$, $V = 3544(2)$ Å^3, $Z = 4$, $\varrho_{calcd} = 2.351$ g cm^{-3}, $F(000) = 2464$, $Mo_{K\alpha}$ radiation, $\lambda = 0.71073$ Å, $\mu = 1.92$ mm^{-1}. The structure was determined by direct methods and refined on F^2 for all 3095 independent reflections measured at 160 K with a Stoe-Siemens diffractometer ($2\theta_{max} = 50°$), with anisotropic atomic displacement parameters and with isotropic hydrogen atoms: $R' = [\Sigma w(F_o^2 - F_c^2)^2/\Sigma w(F_o^2)^2]^{1/2} = 0.0762$ for all

data, conventional R [on F values for 2999 reflections with $F_o^2 > 2\sigma(F_o^2)$] = 0.0266, goodness of fit on $F^2 = 1.199$ for 272 parameters. Programs: SHELXTL/PC and SHELXL-93, G. M. Sheldrick, Universität Göttingen. Further details of the crystal structure investigation are available on request from the Director of the Cambridge Crystallographic Data Centre, 12 Union Road, GB-Cambridge CB21EZ (UK), on quoting the full journal citation.

[5] a) R. Strandberg, *Acta Chem. Scand. Ser. A* **1973**, *27*, 1004; b) W. Kwak, M. T. Pope, T. F. Scully, *J. Am. Chem. Soc.* **1975**, *97*, 5735; c) J. K. Stalick, C. O. Quicksall, *Inorg. Chem.* **1976**, *15*, 1577; d) D.-G. Lyxell, R. Strandberg, *Acta Crystallogr. Sect. C* **1988**, *44*, 1535.

[6] a) A. Yagasaki, I. Andersson, L. Pettersson, *Inorg. Chem.* **1987**, *26* 3926; b) L. Pettersson, I. Andersson, L.-O. Öhman, *ibid.* **1986**, *25*, 4726; c) *Acta Chem. Scand. Ser. A* **1985**, *39*, 53.

[7] W. G. Klemperer, C. Schwartz, D. A. Wright, *J. Am. Chem. Soc.* **1985**, *107*, 6941.

[8] D.-G. Lyxell, R. Strandberg, D. Boström, L. Pettersson, *Acta Chem. Scand. Ser. A* **1991**, *45*, 681.

[9] K. Moedritzer, R. Irani, *J. Org. Chem.* **1966**, *31*, 1603.

[10] The ^{31}P NMR spectra were recorded on a JEOL 90-FXQ spectrometer at 36.2 MHz with proton decoupling and referenced to external 85% H_3PO_4.

Enantioselective Reactions in a Static Magnetic Field

Guido Zadel, Catia Eisenbraun, Gerd-Joachim Wolff, and Eberhard Breitmaier*

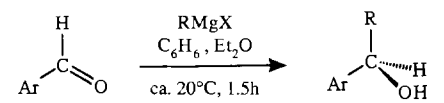
Absolute asymmetric synthesis (AAS)[1] denotes an enantioselective synthesis from achiral starting materials without the help of chiral reagents. An example is the synthesis of hepta- and octahelicenes in circular polarized light with enantiomeric excesses up to 7.3%.[2, 3] Absolute asymmetric synthesis has been discussed as the origin of optical activity in evolution.[4–11]

In 1975 P. Gerike introduced a new absolute asymmetric synthesis.[12] He carried out reactions in electric fields (15–8100 Vcm^{-1}) to which parallel, antiparallel, or orthogonal constant or alternating magnetic fields (8×10^3–1.17×10^5 Am^{-1}, 0–50 Hz) were superimposed. The formation of oxiranes, the addition of bromine to C–C double bonds, and the alkylation of prochiral ketones with Grignard reagents to form secondary alcohols were studied. The enantiomeric excesses amounted to at most 0.94% without preference for either (*R*) or (*S*) isomer. However, the level of enantiomeric excesses contradicts the theoretical prediction of W. Rhodes and R. C. Dougherty[13] that enantiomeric excesses of no more than 3×10^{-5}% should be achievable with magnetic flux densities of up to 1 T. R. C. Dougherty et al. later studied the formation of oxiranes and cyclopropanes at flux densities of "about 1.1 T"[14, 15] without, however, the simultaneous application of an electric field. Instead, they spun the reaction vessel at high speeds (6000–14000 rpm) in order to achieve the desired selectivity with the additional gravitational field.[14] As Gerike had reported, they found an irregular preference for the (*R*) or (*S*) enantiomer (*ee* < 1%), which they traced back to photochemical side-effects (daylight, artificial light), after the influence of the earth's magnetic field had been eliminated by aligning the apparatus with the compass.

[*] Prof. Dr. E. Breitmaier, Dr. G. Zadel, Dipl.-Chem. C. Eisenbraun
Institut für Organische Chemie und Biochemie der Universität
Gerhard-Domagk-Strasse 1, D-53121 Bonn (FRG)
Telefax: Int. code + (228)73-5683
Dr. G.-J. Wolff
Bruker Analytische Messtechnik
D-76287 Rheinstetten (FRG)

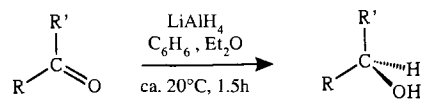
Before we were aware of this work we investigated two preparatively versatile reactions in static magnetic fields of varying flux densities. These were the alkylation of aldehydes **1** with alkyl magnesium halides and the reduction of prochiral ketones **2** with complex metal hydrides. The dependence of the enantioselectivity of these reactions on the magnetic flux density was studied.

It was found that a static magnetic field of flux density 0.2–2.1 T was sufficient to achieve considerable enantiomeric excesses in these reactions.[16] Thus the addition of dimethylmagnesium, methyl magnesium iodide, or ethylmagnesium *t*-butylalcoholate to benzaldehyde (**1a**) or naphthalene-2-carbaldehyde (**1b**) in a static magnetic field of flux density 1.2 T leads to (*R*)- or (*S*)-1-phenylethanol (**3a**), -1-(2-naphthyl)ethanol (**3b**), or -1-phenylpropanol (**3c**), respectively, with enantiomeric excesses of 65, 98, and 57%, respectively. The reduction of phenones **2a–c** with lithium aluminum hydride at 1.2 T yielded the (*R*)- or (*S*)-1-arylethanols **3a–c** with similar selectivity (55–98% *ee*). Significantly lower enantiomeric excesses (11%, 2.1 T) were achieved in the reduction of butanone **2d** to give (*R*)- or (*S*)-2-butanol **3d**.



1 **3**

	R	Ar	X	B_0 [T]	*ee* [%]
3a	Me	Ph	I/Me	1.2	65
3b	Me	2-naphthyl	I	1.2	98
3c	Et	Ph	O*t*Bu	1.2	57



2 **3**

	R	R'	B_0 [T]	*ee* [%]
3a	Ph	Me	1.2	67
3b	2-naphthyl	Me	0.4	68
3c	Ph	Et	2.1	55
3d	Et	Me	2.1	11

When the reactions were repeated under the same flux density the enantiomeric excesses were always reproducible, although which enantiomer dominated was unpredictable. However, in the case of the crystalline 1-(2-naphthyl)ethanol (**3b**), we could repeatably demonstrate that by seeding the reaction mixture of **2b** in the magnetic field with the desired isomer of **3b** before the start of the reaction, it was possible to produce the desired isomer. Without the magnetic field the observed enantiomeric excess corresponded to the amount of seed crystals added.[16]

The enantiomeric excesses were determined by specific rotation and also by ^1H and ^{13}C NMR measurements in the presence of tris(3-heptafluoropropylhydroxymethylene)-D-camphoratoeuropium(III) or -praseodymium(III) as chiral shift reagent (Fig. 1). The absolute configurations of the products were determined by comparison with the known, published directions of rotation. As shown in Figure 2 the enantiomeric excess increases steadily with the magnetic flux density B_0 within the field range investigated so far.

No Enantioselective Reactions in a Static Magnetic Field

Based on part of the PhD thesis by G. Zadel (completed 1993) and parallel investigations by Catja Eisenbraun the communication "Enantioselective Reactions in a Static Magnetic Field" appeared under my auspices together with G. Zadel, C. Eisenbraun, and G. J. Wolff in this journal (*Angew. Chem.* **1994**, *106*, 460; *Angew. Chem. Int. Ed. Engl.* **1994**, *33*, 454). Several independent research groups have informed me since that the experiments reported (1,2-addition of Grignard compounds to aldehydes; reduction of prochiral ketones with lithium aluminum hydride), contrary to the results published by us gave no enantiomeric excesses. In light of this I instructed three experienced co-workers from my research group (F. Keller, K. Berlin, and T. Marx) to repeat the most important experiments [reduction of 2-acetylnaphthalene with lithium aluminum hydride to (*R*)- or (*S*)-1-(2-naphthyl)ethanol; 1,2-addition of methylmagnesium iodide to benzaldehyde to give (*R*)- or (*S*)-1-phenylethanol] completely independently from the chief experimentalist (G. Zadel). These co-workers carried out several experiments in Bonn and Karlsruhe, some in my presence but all in the absence of G. Zadel, and could detect no measureable enantiomeric excesses (NMR with $[Eu(hfc)_3]$, GC with β-cyclodextrin, polarimetry). In one case, we were able to prove quite clearly (GC-MS, polarimetry) that the starting solution prepared by G. Zadel for the reduction of propiophenone with lithium aluminum hydride also contained considerable amounts of (+)-1-phenylpropanol in addition to propiophenone. G. Zadel admitted this deception and two other manipulations in front of witnesses. Therefore we must assume that the data in the publication as well as "successful" attempts at reproducing the results by other co-workers in my research group and guest scientists in the presence of G. Zadel came about because of consistent and particularly cleverly disguised manipulations. I therefore wish to disassociate myself and the coauthors C. Eisenbraun and G. J. Wolff from all the experimental results in this publication.

E. Breitmaier
Institut für Organische Chemie und Biochemie der Universität
Gerhard-Domagk-Strasse 1, D-53121 Bonn (FRG)
Received: June 21, 1994

data, conventional R [on F values for 2999 reflections with $F_o^2 > 2\sigma(F_o^2)$] = 0.0266, goodness of fit on $F^2 = 1.199$ for 272 parameters. Programs: SHELXTL/PC and SHELXL-93, G. M. Sheldrick, Universität Göttingen. Further details of the crystal structure investigation are available on request from the Director of the Cambridge Crystallographic Data Centre, 12 Union Road, GB-Cambridge CB21EZ (UK), on quoting the full journal citation.

[5] a) R. Strandberg, *Acta Chem. Scand. Ser. A* **1973**, *27*, 1004; b) W. Kwak, M. T. Pope, T. F. Scully, *J. Am. Chem. Soc.* **1975**, *97*, 5735; c) J. K. Stalick, C. O. Quicksall, *Inorg. Chem.* **1976**, *15*, 1577; d) D.-G. Lyxell, R. Strandberg, *Acta Crystallogr. Sect. C* **1988**, *44*, 1535.

[6] a) A. Yagasaki, I. Andersson, L. Pettersson, *Inorg. Chem.* **1987**, *26* 3926; b) L. Pettersson, I. Andersson, L.-O. Öhman, *ibid.* **1986**, *25*, 4726; c) *Acta Chem. Scand. Ser. A* **1985**, *39*, 53.

[7] W. G. Klemperer, C. Schwartz, D. A. Wright, *J. Am. Chem. Soc.* **1985**, *107*, 6941.

[8] D.-G. Lyxell, R. Strandberg, D. Boström, L. Pettersson, *Acta Chem. Scand. Ser. A* **1991**, *45*, 681.

[9] K. Moedritzer, R. Irani, *J. Org. Chem.* **1966**, *31*, 1603.

[10] The ^{31}P NMR spectra were recorded on a JEOL 90-FXQ spectrometer at 36.2 MHz with proton decoupling and referenced to external 85% H_3PO_4.

Enantioselective Reactions in a Static Magnetic Field

Guido Zadel, Catia Eisenbraun, Gerd-Joachim Wolff, and Eberhard Breitmaier*

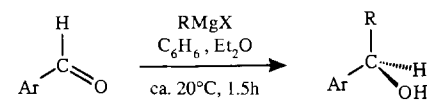
Absolute asymmetric synthesis (AAS)[1] denotes an enantioselective synthesis from achiral starting materials without the help of chiral reagents. An example is the synthesis of hepta- and octahelicenes in circular polarized light with enantiomeric excesses up to 7.3%.[2, 3] Absolute asymmetric synthesis has been discussed as the origin of optical activity in evolution.[4–11]

In 1975 P. Gerike introduced a new absolute asymmetric synthesis.[12] He carried out reactions in electric fields (15–8100 Vcm^{-1}) to which parallel, antiparallel, or orthogonal constant or alternating magnetic fields (8×10^3–1.17×10^5 Am^{-1}, 0–50 Hz) were superimposed. The formation of oxiranes, the addition of bromine to C–C double bonds, and the alkylation of prochiral ketones with Grignard reagents to form secondary alcohols were studied. The enantiomeric excesses amounted to at most 0.94% without preference for either (*R*) or (*S*) isomer. However, the level of enantiomeric excesses contradicts the theoretical prediction of W. Rhodes and R. C. Dougherty[13] that enantiomeric excesses of no more than 3×10^{-5}% should be achievable with magnetic flux densities of up to 1 T. R. C. Dougherty et al. later studied the formation of oxiranes and cyclopropanes at flux densities of "about 1.1 T"[14, 15] without, however, the simultaneous application of an electric field. Instead, they spun the reaction vessel at high speeds (6000–14000 rpm) in order to achieve the desired selectivity with the additional gravitational field.[14] As Gerike had reported, they found an irregular preference for the (*R*) or (*S*) enantiomer (*ee* < 1%), which they traced back to photochemical side-effects (daylight, artificial light), after the influence of the earth's magnetic field had been eliminated by aligning the apparatus with the compass.

[*] Prof. Dr. E. Breitmaier, Dr. G. Zadel, Dipl.-Chem. C. Eisenbraun
Institut für Organische Chemie und Biochemie der Universität
Gerhard-Domagk-Strasse 1, D-53121 Bonn (FRG)
Telefax: Int. code + (228)73-5683
Dr. G.-J. Wolff
Bruker Analytische Messtechnik
D-76287 Rheinstetten (FRG)

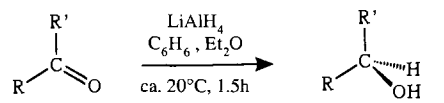
Before we were aware of this work we investigated two preparatively versatile reactions in static magnetic fields of varying flux densities. These were the alkylation of aldehydes **1** with alkyl magnesium halides and the reduction of prochiral ketones **2** with complex metal hydrides. The dependence of the enantioselectivity of these reactions on the magnetic flux density was studied.

It was found that a static magnetic field of flux density 0.2–2.1 T was sufficient to achieve considerable enantiomeric excesses in these reactions.[16] Thus the addition of dimethylmagnesium, methyl magnesium iodide, or ethylmagnesium *t*-butylalcoholate to benzaldehyde (**1a**) or naphthalene-2-carbaldehyde (**1b**) in a static magnetic field of flux density 1.2 T leads to (*R*)- or (*S*)-1-phenylethanol (**3a**), -1-(2-naphthyl)ethanol (**3b**), or -1-phenylpropanol (**3c**), respectively, with enantiomeric excesses of 65, 98, and 57%, respectively. The reduction of phenones **2a–c** with lithium aluminum hydride at 1.2 T yielded the (*R*)- or (*S*)-1-arylethanols **3a–c** with similar selectivity (55–98% *ee*). Significantly lower enantiomeric excesses (11%, 2.1 T) were achieved in the reduction of butanone **2d** to give (*R*)- or (*S*)-2-butanol **3d**.



1 **3**

	R	Ar	X	B_0 [T]	*ee* [%]
3a	Me	Ph	I/Me	1.2	65
3b	Me	2-naphthyl	I	1.2	98
3c	Et	Ph	O*t*Bu	1.2	57



2 **3**

	R	R'	B_0 [T]	*ee* [%]
3a	Ph	Me	1.2	67
3b	2-naphthyl	Me	0.4	68
3c	Ph	Et	2.1	55
3d	Et	Me	2.1	11

When the reactions were repeated under the same flux density the enantiomeric excesses were always reproducible, although which enantiomer dominated was unpredictable. However, in the case of the crystalline 1-(2-naphthyl)ethanol (**3b**), we could repeatably demonstrate that by seeding the reaction mixture of **2b** in the magnetic field with the desired isomer of **3b** before the start of the reaction, it was possible to produce the desired isomer. Without the magnetic field the observed enantiomeric excess corresponded to the amount of seed crystals added.[16]

The enantiomeric excesses were determined by specific rotation and also by ^1H and ^{13}C NMR measurements in the presence of tris(3-heptafluoropropylhydroxymethylene)-D-camphoratoeuropium(III) or -praseodymium(III) as chiral shift reagent (Fig. 1). The absolute configurations of the products were determined by comparison with the known, published directions of rotation. As shown in Figure 2 the enantiomeric excess increases steadily with the magnetic flux density B_0 within the field range investigated so far.

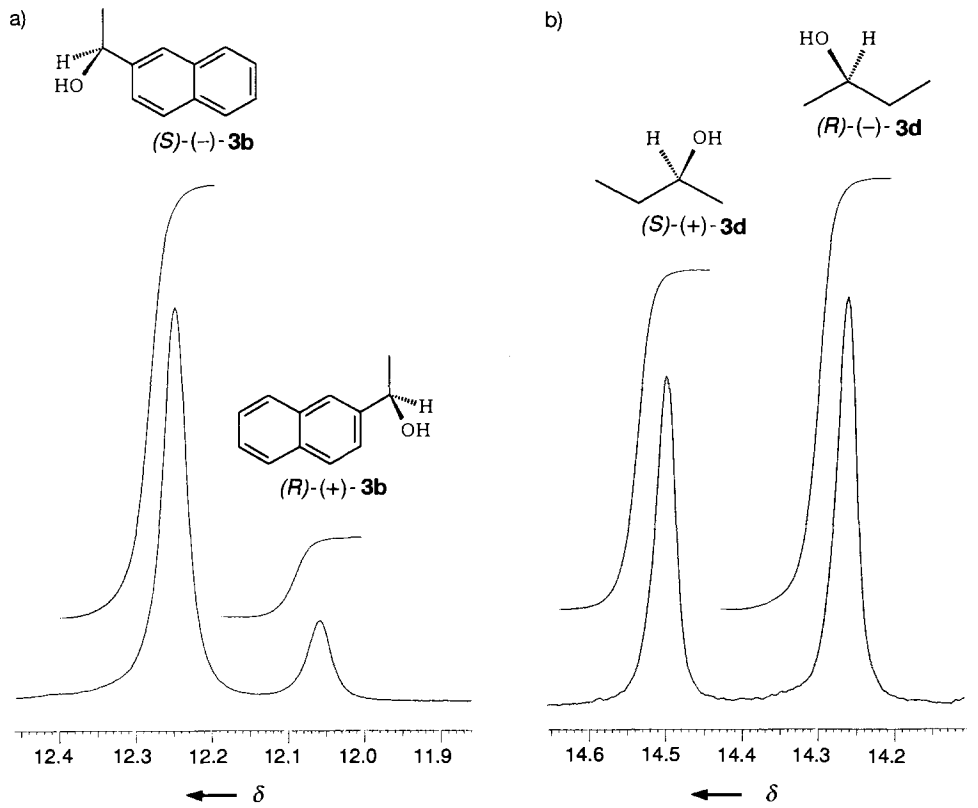


Fig. 1. *ee* Determination with $[Eu(hfc)_3]$. Extreme cases: a) (*R*)- and (*S*)-**3b** from **1b** and methylmagnesium iodide at 0.4 T; ^{1}H NMR signal for the methyl protons (400 MHz): 68% *ee*. b) (*R*)- and (*S*)-**3d** from reduction of **2d** with lithium aluminum hydride at 2.1 T; ^{1}H NMR signal for the C-1 methyl protons (400 MHz): 11% *ee*.

The enantiomeric excesses obtained for 1-arylethanols **3a–c** in the magnetic fields available to us (flux density up to 2.1 T) are comparable to those achieved with other methods of enantioselective synthesis, such as the use of chiral auxiliaries.[17] Substantially less preparative effort, good reproducibility, low cost, and minimal environmental impact make enantioselective reactions in static magnetic fields rather attractive within the preparative scales limited by the size of commercial electro- and cryomagnets.

From the study of further reactions[16] it appears that particularly those reactions between compounds with prochiral polar double bonds and organometallic reagents can proceed enantioselectively in a static magnetic field. On the other hand, the addition of *m*-chloroperbenzoic acid to the nonpolar C–C double bond of styrene (which contains a prochiral C atom) in a magnetic field (up to 2.1 T) yields racemic styrene oxide; similarly the [4 + 2] cycloaddition of methyl acrylate to cyclopentadiene in a magnetic field gives racemic *endo* and *exo* isomers.[16]

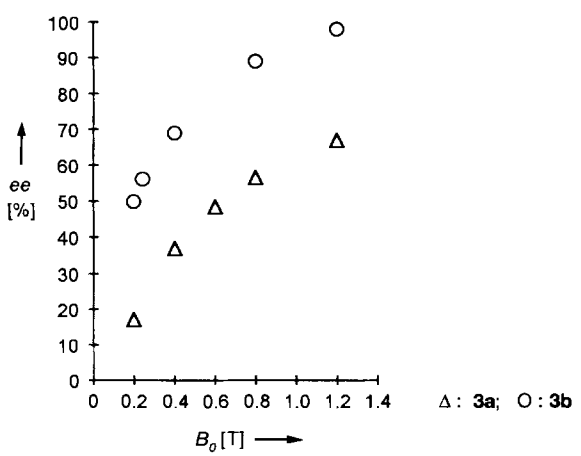


Fig. 2. Enantiomeric excess of **3a** by reduction of **2a** with $LiAlH_4$ and of **3b** by Grignard methylation of **1b** as a function of the magnetic flux density B_0 of the static magnetic field.

The limits of applicability and the elucidation of the mechanism of this asymmetric induction by a static magnetic field requires numerous further experiments. It is unlikely that the precession of polar, prochiral double bonds in a static magnetic field is the (sole) source of the enantioselectivity. The somewhat greater population of the lower energy (and therefore preferred) direction of dipole precession (along and not opposed to the B_0 direction) could indeed cause the *Re–Si* face differentiation necessary for the observed enantioselectivity (accessible side outside, protected side inside the precession cone); however, the difference in populations would fall far short of that required to explain the enantiomeric excesses obtained.[13] Particularly striking are the high enantiomeric excesses of the 1-arylalkanols. The constant dependence of the enantiomeric excesses on the magnetic flux density (Fig. 2) suggests a regularity; understanding this should further promote the development of the method.

Experimental Procedure

1. Arylethanols by addition of organometallic compounds to prochiral carbonyl compounds

A solution of the aromatic aldehyde (**1a,b,c**, 1 mmol) in benzene (0.2 mL) was diluted to a total volume of 4 mL with isoamyl ether at room temperature and transferred to a 50 mL three-neck flask fitted with an inert gas inlet (glass capillary) and reflux condenser. The reaction flask was held in position in the homogeneous region of a regulated electromagnet (7 cm bore). After 5 min a solution of methylmagnesium iodide (1.27 M) in isoamyl ether (1 mL ampule, Merck, was added dropwise over 1 h (for the formation of **3a** and **3b**). For the preparation of **3a** a solution of dimethylmagnesium (1 M) in 1,4-dioxane:tetrahydrofuran (1:1, 1.27 mL) was

 © VCH Verlagsgesellschaft mbH, D-69451 Weinheim, 1994 0570-0833/94/0404-0455 $ 10.00+.25/0

also used. The preparation of **3c** was carried out in the same manner with 1.27 mL of a solution of ethylmagnesium *tert*-butylalcoholate in 1,4-dioxane (1 M). To ensure mixing a slow stream of nitrogen was bubbled through the solution. The reaction was quenched by addition of water (5 mL) and worked up by pouring the resulting mixture into saturated ammonium chloride solution (10 mL). After separation of the organic phase, the aqueous phase was extracted with diethyl ether (3 × 10 mL). The combined organic phases were washed with saturated aqueous sodium bisulfite solution (5 mL) and dried with magnesium sulfate; the solvent was removed under vacuum (18 hPa, 13 Torr).

1-Phenylethanol (**3a**): Yield 56%; b.p. 83 °C (18 hPa); 65% *ee* (NMR) at 1.2 T; $[\alpha]_D^{20} = +29.9$ ($c = 1.08$ in toluene); pure enantiomer: $[\alpha]_D^{20} = \pm 46.3$ ($c = 1$ in toluene).

1-(2-Naphthyl)ethanol (**3b**): Yield 40%; m.p. 68–70 °C; 98% *ee* (NMR) at 1.2 T; $[\alpha]_D^{20} = -36.8$ ($c = 1.24$ in methanol); pure enantiomer: $[\alpha]_D^{20} = \pm 38$ (± 0.5) ($c = 1$ in methanol); for further ee/B_0 pairs see Figure 2.

1-Phenylpropanol (**3c**): Yield 60%; b.p. 96 °C (18 hPa); 57% *ee* (NMR) at 1.2 T; $[\alpha]_D^{20} = +26.8$ ($c = 1.8$ in hexane): pure enantiomer: $[\alpha]_D^{20} = \pm 46$–48 ($c = 2.2$ in hexane).

2. Secondary alcohols by reduction of prochiral carbonyl compounds with complex metal hydrides

Lithium aluminium hydride (0.08 g, 2 mmol) was covered with anhydrous THF (ca. 2 mL). Anhydrous benzene was then added to give a total volume of 6 mL. The apparatus was inserted in the magnetic field; 5 min later the carbonyl compound (**2a–d**, 1.7 mmol in the same volume of benzene) was added dropwise over 1 h. After an additional 15–30 min the reaction mixture was removed from the magnetic field and carefully quenched with water (5 mL). The workup consisted of pouring the reaction mixture into saturated ammonium chloride solution (10 mL), extracting the alcohol with diethyl ether, and drying the solution over $MgSO_4$, and removing the solvent by distillation. For the production of a particular enantiomer of **3b** the reaction mixture was seeded in the magnetic field with 0.04 mmol (7 mg) of the desired isomer before the addition of the carbonyl compound **2b**[16].

3a: Yield 98%; b.p. 83 °C (18 hPa); 67% *ee* (NMR) at 1.2 T; $[\alpha]_D^{20} = +31.4$ ($c = 1.3$ in toluene); pure enantiomer $[\alpha]_D^{20} = \pm 46.3$ ($c = 1$ in toluene); for further ee/B_0 pairs see Figure 2.

3b: Yield 98%; m.p. 68–70 °C; 68% *ee* (NMR) at 0.4 T; $[\alpha]_D^{20} = -25.8$ ($c = 1.3$ in methanol); 52% *ee* at 0.25 T (average of 5 seeding experiments); $[\alpha]_D^{20} = -19.3$ ($c = 1.3$ in methanol); pure enantiomer: $[\alpha]_D^{20} = \pm 38$ (± 0.5) ($c = 1$ in methanol).

3c: Yield 88%; b.p. 96 °C (18 hPa), 55% *ee* (NMR) at 2.1 T $[\alpha]_D^{20} = +25.4$ ($c = 2.1$ in hexane); pure enantiomer $[\alpha]_D^{20} = \pm 46$–48 ($c = 2.2$ in hexane).

3d: Yield 98% (GC); b.p. 99–100 °C, 11% *ee* (NMR) at 2.1 T (average of nine experiments); $[\alpha]_D^{20} = -1.09$ (neat); pure enantiomer $[\alpha]_D^{20} = \pm 10$–12.5 (neat).

Received: August 20, 1993
Revised: December 8, 1993 [Z 6306 IE]
German version: *Angew. Chem.* **1994**, *106*, 460

[1] B. Bredig, P. Mangold, T. G. Williams, *Angew. Chem.* **1923**, *36*, 456.
[2] W. J. Bernstein, M. Calvin, O. Buchardt, *J. Am. Chem. Soc.* **1972**, *94*, 494; *ibid.* **1973**, *95*, 527; *Tetrahedron Lett.* **1972**, 2195.
[3] H. Kagan, A. Moradpour, J. F. Nicoud, G. Balavoine, R. H. Martin, J. P. Cosyn, *Tetrahedron Lett.* **1971**, 2479.
[4] A. I. Oparin, *Origin of Life*, 3rd ed., Academic Press, New York, **1957**.
[5] I. Keosian, *The Origin Of Life*, 2nd ed., Rheinhold, New York, **1968**.
[6] G. Wald, *Ann. N. Y. Acad. Sci.* **1967**, *69*, 352; *Chem. Abstr.* **1966**, *66*, 14093g.
[7] A. S. Garay, *Nature (London)* **1968**, *219*, 338.
[8] J. D. Morrison, H. S. Mosher, *Asymmetric Organic Reactions*, Prentice Hall, London, **1971**.
[9] P. Curie, *J. Phys. Radium* **1894**, *3*, 409.
[10] A. Gupta, G. S. Hammond, *J. Chem. Phys.* **1972**, *57*, 1789; *Chem. Abstr.* **1972**, *77*, 953191.
[11] T. L. V. Ulbricht, *Q. Rev. Chem. Soc.* **1959**, *13*, 48; *Chem. Abstr.* **1959**, *53*, 11189a.
[12] P. Gerike, *Naturwissenschaften* **1975**, *62*, 38.
[13] W. Rhodes, R. C. Dougherty, *J. Am. Chem. Soc.* **1978**, *100*, 6247.
[14] R. C. Dougherty, *J. Am. Chem. Soc.* **1980**, *102*, 380, 382.
[15] K. Piotrowska, D. Edwards, A. Mitch, R. C. Dougherty, *Naturwissenschaften* **1980**, *67*, 442.
[16] G. Zadel, Dissertation, Universität Bonn, **1993**; Patent application June 1 with Bruker Analytische Meßtechnik; C. Eisenbraun, Dissertation, Universität Bonn, in preparation.
[17] B. Weber, D. Seebach, *Angew. Chem.* **1992**, *103*, 96; *Angew. Chem. Int. Ed. Engl.* **1992**, *31*, 84.

A Stannanediyl with a Tin–Carbon Multiple Bond**

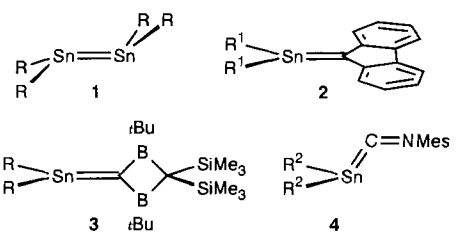
Hansjörg Grützmacher,* Werner Deck, Hans Pritzkow, and Michael Sander

Dedicated to Professor Wolfgang Sundermeyer on the occasion of his 65th birthday

According to a model from Trinquier and Malrieu, the structures of compounds with the formula $R_2X{=}YR_2$ can be correlated with the singlet–triplet excitation energy $\Delta E_{(S\rightarrow T)}$ of diylene, R_2X: (X, Y = C, Si, Ge, Sn).[1] When the relationship $\Sigma\Delta E_{(S\rightarrow T)} < 1/2\,E_{\sigma+\pi}$ ($E_{\sigma+\pi}$ = total bond energy) is fulfilled, "classical" planar molecular structures, such as ethylene, are formed ($\Sigma\Delta E_{(S\rightarrow T)} \approx -20$ kcal mol^{-1}; $1/2\,E_{\sigma+\pi} = 86.6$ kcal mol^{-1}). If, on the other hand, $\Sigma\Delta E_{(S\rightarrow T)} > 1/2\,E_{\sigma+\pi}$, "non-classical" double bond systems are predicted, with the molecular fragments occupying *trans* positions being bent with respect to the plane of the X=Y double bond.[2] The best known example is the distannene **1**, which was investigated by Lappert et al. The R_2Sn molecular fragments in this molecule are bent to the extent of 41°[3] ($\Sigma\Delta E_{(S\rightarrow T)} \approx 45$ kcal mol^{-1}; $1/2\,E_{\sigma+\pi} < 35$ kcal mol^{-1}, calculated values for $H_2Sn{=}SnH_2$[1]).

Investigations on borderline cases, such as compounds with tin–carbon multiple bonds, are particularly interesting. Depending on the substituents, these compounds can belong to either the one double bond type, or the other, due to the weak nature of the tin–carbon bond in stannaethenes, $R_2Sn{=}CR'_2$ (ca. $E_{\sigma+\pi} < 70$ kcal mol^{-1}). These compounds may also, therefore, be considered as carbene-fragment transfer reagents.

The intermediate behavior of stannaethenes has been discussed;[4] however, only a few compounds, such as **2** and **3**, have been isolated, of which the latter was structurally characterized.[4e] The tin–carbon bond in **3** is short, in spite of the severe twisting of the molecular fragments, and has essentially been attributed to electrostatic interactions. We recently described the stannaketenimine **4**, with its considerably bent Sn–C–N arrangement, as being a weakly bonded adduct formed from an isonitrile and a stannanediyl.[5] Both fragments have singlet



R = $CH(SiMe_3)_2$ R^1 = 2,4,6-$iPr_3C_6H_2$ R^2 = 2,4,6-$CF_3C_6H_2$

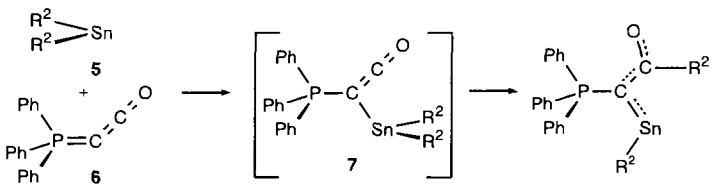
ground states, so the relationship $\Sigma\Delta E_{(S\rightarrow T)} > 1/2\,E_{\sigma+\pi}$ is satisfied. We have now investigated the reaction of the stannanediyl **5**[6] with the ketene ylide **6**,[7] and are able to report on a new

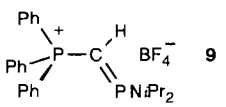
[*] Prof. Dr. H. Grützmacher, Dr. W. Deck
Institut für Anorganische und Analytische Chemie der Universität
Albertstrasse 21, D-79104 Freiburg (FRG)
Telefax: Int. code + (761)203-5987
Dr. H. Pritzkow, Dipl.-Chem. M. Sander
Anorganisch-chemisches Institut der Universität
Im Neuenheimer Feld 270, D-69120 Heidelberg (FRG)

[**] This work was supported by the Deutsche Forschungsgemeinschaft (SFB 247) and the Fonds der Chemischen Industrie.

reaction, leading to a product in which a tin–carbon multiple bond can be discussed.

In the reaction of the stannanediyl **5** with the cumulene **6** in toluene, the adduct **7** is formed, in which the ylidic α-carbon atom in **6** is coordinated to the low-coordinate tin atom in **5** (cf. [4b]). In addition, a further product can be detected by NMR spectroscopy, which, after reaction at 25 °C for about 6 h, becomes the main product together with small amounts of various hydrolysis products.[8] In contrast to **7** [$\delta(^{119}Sn) = 121$], **8** is characterized by a ^{119}Sn resonance signal which is strongly shifted down field to $\delta = 932$. This signal is shifted approxi-





mately 250 ppm down field from the signal of the stannanediyl **5**. The molecular peak for *m/z* (**5** + **6**) in the field-desorption (FD) mass spectrum is observed with the correct isotopic distribution. Attempts to crystallize the products were difficult, as very small amounts of impurities, such as those arising from hydrolysis due to the water contained in the glass walls of the reaction vessels,[9] prevented the formation of crystals suitable for X-ray structure analysis. Only after the glass vessels had been treated with hexamethyldisilazane, $HN(SiMe_3)_2$,[10] was it possible to grow crystals of suitable quality. The data set for the determination of the molecular structure of **8** was collected at 173 K in an attempt to limit the disorder of the *para* CF_3 groups.[11] The molecular structure of one of the two crystallographically independent molecules in the unit cell of **8** is shown in Figure 1, and confirms the structure previously assumed. Compound **8** contains a tin atom with coordination number 2 and is formed by a new type of ligand coupling reaction on a tin atom with coordination number 3, in which an aryl substituent, R^2, on the tin atom is transferred to the activated CO group of the ketene **7**.

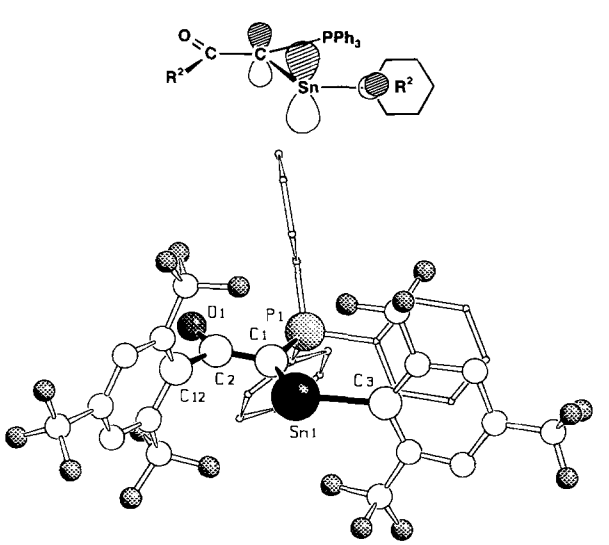
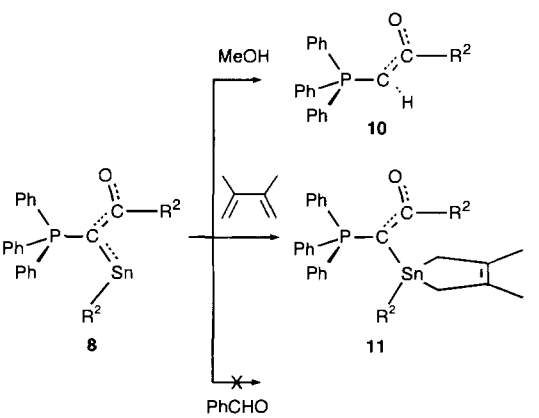


Fig. 1. Molecular structure of one of the independent molecules in **8** (SCHAKAL). Selected distances [Å] and angles [°]: Sn1-C1 2.12(2), Sn1-C3 2.25(2), P1-C1 1.76(2), C1-C2 1.41(2), C2-O1 1.29(2), C2-C12 1.54(2), P1-*ipso*-C(Ph) 1.796–1.835(9), R^2 to Sn1 (C3-C8) 1.37–1.42(3), R^2 to C2 (C12-C17) 1.38–1.45(2); C1-Sn1-C3 108.4(5), P1-C1-Sn1 135.2(8), P1-C1-C2 110.7(11), C2-C1-Sn1 113.3(10), O1-C2-C1 125.3(14), O1-C2-C12 111.5(13), C12-C2-C1 123.1(14).

The tin center in **8** is bonded to two sp^2-hybridized carbon atoms, each of which is part of a conjugated multiple bond system. The atoms C3, Sn1, C1, C2, and P1 all lie approximately in a plane (max. deviations: C3 0.010, Sn1 0.007, C1 −0.068, C2 0.033, P1 −0.010 Å), so that the p orbital functions on Sn1 and C1 have maximum overlap. The aryl ring containing C3 as a ring member, in contrast, is arranged almost perpendicular (96.5°) to this plane. The Sn1–C3 distance [2.25(2) Å] is somewhat shorter than the corresponding distance in the stannanediyl **5** [2.278(5) Å] and lies within the range that we determined for ($R^2_2Sn^{IV}$ compounds [R^2 = 2,4,6-$(CF_3)_3C_6H_2$].[12] The Sn1–C1 bond is only 2.12(2) Å long, however. For the undisturbed Sn=C bond in $H_2Sn{=}CH_2$, a bond length of 1.982 Å was calculated [experimentally determined in **3**: 2.025(4) Å]. The value found in **8** therefore lies between that of a single bond (ca. 2.23 Å) and a double bond. Compound **8** can be compared with the isosteric phosphonio-substituted methylenephosphane **9**, the P–C double bond character of which has been proven.[13] As is the case in **9**, an elongated P1–C1 bond, as compared to that in phosphorus ylides, is also observed in **8** [**9**: 1.788(14); **8**: 1.76(2); ylide: 1.65–1.70 Å[14]]. The P1–C1 bond in **8** is, however, only insignificantly longer than the corresponding distances in stabilized ylides such as **10** (1.73–1.76 Å),[15] and is in this case, therefore, not a suitable indicator for the presence of a Sn=C bond in **8**.



Admittedly, the ^{31}P NMR signal in **8** (22.3 ppm) is observed in a resonance area typical for triphenylphosphonium salts and is clearly shifted down field in comparison to the signal in **10** (δ = 13.9). The C1–C2 distance [1.41(2) Å] and distances within the aryl rings [1.35–1.41 Å] all correspond with the expected values. The C2–O1 bond length [1.29(2) Å] of the carbonyl group is, as expected, significantly longer than the C=O distance found in $H_2C{=}O$ [1.209 Å] and also somewhat longer than that found in stabilized ylides (1.23–1.25 Å).[15] The frequency ν(C=O) in **8** (1525 cm^{-1}) is shifted 30 cm^{-1} to lower wavenumbers than in **10** [ν(C=O) = 1555 cm^{-1}].[16] This observation is in agreement with the formulation of a Sn=C–C=O bonding system, but can also be simply explained, however, by the σ-donor effect of the electropositive tin atom.

The reactivity of compound **8** is similar to that of the stannanediyl **5**: reaction with MeOH leads to cleavage of the

tin–carbon bond, formation of $Sn(OMe)_2$, R^2H, and the ylide **10** in almost quantitative yield.[16] The reaction with 2,3-dimethylbutadiene (DMB) occurs by [1 + 4]cycloaddition to give **11**; a [2 + 4]cycloaddition does not occur (cf. [5]). Compound **8** does not react with aldehydes even at elevated temperatures. Our assumption that there is a tin–carbon multiple bond in the *planar* molecular framework of **8** (P1, C1, C2, Sn1, C12) is largely based on the significant shortening of the Sn1–C1 bond. A shortening of about 0.1 Å for a Sn=N bond in the stannanimine $[(Me_3Si)_2N]_2Sn{=}N(2,6\text{-}iPr_2C_6H_3)$ (**12**) was recently reported by Meller et al, the tin atom having a trigonal-planar coordination.[17] Together with the observations on **3** and **12**, this would seem to indicate that planar multiple bonding systems between the main group *metal* elements of the higher periods and the *nonmetal* elements of the second period may be accessible. In addition, an interesting ligand coupling reaction on a low-coordinate tin atom was observed, which extends still further the synthetic potential of organotin compounds.

Experimental Procedure

8: **5** (2.25 g, 3.3 mmol) and **6** (1 g, 3.3 mmol) were placed in an apparatus consisting of two 100 mL round-bottomed flasks fitted with taps, and connected to each other by a glass frit (GIII). The apparatus was treated with hot $HN(SiMe_3)_2$ prior to use. Subsequently, toluene (20 mL) was condensed into the apparatus and the solution stirred for about 24 h at 25 °C. All volatile components were then removed under vacuum, and *n*-hexane (20 mL) was condensed on to the oily yellow residue. A homogeneous solution resulted temporarily on stirring. Compound **8** precipitated as a finely crystalline product after a short period of time. Further product could be crystallized from the mother liquor at 0 °C. Yield 70–85 %; m.p. 99–103 °C.

10: **8** (1 g, 1 mmol) in toluene (5 mL) was treated with a few drops of MeOH. The reaction solution immediately became colorless and a colorless, finely crystalline precipitate was formed. All volatile components were removed under vacuum and the residue partially redissolved in a small amount of toluene. Insoluble components were filtered off and the filtrate concentrated by evaporation of solvent under reduced pressure. The ensuing oil crystallized over a period of several hours to give beige colored crystals. Yield 85–92%; m.p. 148–150 °C.

Received: August 27, 1993
Revised version: October 18, 1993 [Z 6321 IE]
German version: *Angew. Chem.* **1994**, *106*, 467

[1] a) G. Trinquir, J.-P. Malrieu, *J. Am. Chem. Soc.* **1987**, *109*, 5303; b) G. Trinquier, J.-P. Malrieu in *The chemistry of functional groups, Suppl. A: The Chemistry of double-bonded functional groups, Vol. 2, Part 1* (Ed.: S. Patai), Wiley, Chichester, **1989**, pp. 1–52.

[2] H. Grützmacher, *GIT Fachz. Lab.* **1993**, *37*, 203.

[3] D. E. Goldberg, P. B. Hitchcock, M. F. Lappert, K. M. Thomas, A. J. Thorne, T. Fjeldberg, A. Haaland, B. E. R. Schilling, *J. Chem. Soc. Dalton Trans.* **1986**, 2387.

[4] a) D. Seyferth, J. L. Lefferts, *J. Am. Chem. Soc.* **1974**, *96*, 6237; b) M. Veith, V. Huch, *J. Oganomet. Chem.* **1986**, *306*, 263; c) H. Grützmacher, H. Pritzkow, *Organometallics* **1991**, *10*, 938; d) N. Wiberg, K. S. Vasisht, *Angew. Chem.* **1991**, *103*, 105; *Angew. Chem. Int. Ed. Engl.* **1991**, *30*, 93; e) H. Meyer, G. Baum, W. Massa, S. Berger, A. Berndt, *ibid.* **1987**, *99*, 559 and **1987**, *26*, 547.

[5] H. Grützmacher, S. Freitag, R. Herbst-Irmer, G. M. Sheldrick, *Angew. Chem.* **1992**, *104*, 459; *Angew. Chem. Int. Ed. Engl.* **1992**, *31*, 437.

[6] H. Grützmacher, H. Pritzkow, F. T. Edelmann, *Organometallics* **1991**, *10*, 23.

[7] H. J. Bestmann, D. Sandmeier, *Chem. Ber.* **1980**, *113*, 274.

[8] **8**: [R^2 = 2,4,6-$(CF_3)_3C_6H_2$]: ^{1}H NMR (C_6D_6, 200.132 MHz): δ = 6.83–6.88 [m, 9H, aromat. CH, PPh_3]; 7.38 [s, 2H, aromat. CH, R^2-CO]; 7.58–7.69 [m, 6H, aromat. CH, PPh_3]; 7.87 [s, 2H, aromat. CH, R^2-Sn]. – ^{19}F NMR (C_6D_6, 188.313 MHz): δ = – 57.3 [s, 6F, *o*-CF_3, R^2-CO, satellites: $J(^{119}Sn,^{19}F)$ = 71 Hz]; –60.3 [s, 6F, *o*-CF_3, R^2-Sn, satellites: $J(^{119}Sn, ^{19}F)$ = 176 Hz]; –63.3 [s, 3F, *p*-CF_3]; –63.5 [s, 3F, *p*-CF_3]. – ^{31}P NMR (C_6D_6, 81.015 MHz): δ = 22.3 [s, satellites: $^2J(^{119}Sn,^{31}P)$ = 179 Hz]. – ^{119}Sn NMR (C_6D_6, 74.544 MHz): δ = 932 [s, $\nu(\frac{1}{2}) \approx$ 1200 Hz]. – IR (Nujol): ν(C=O) = 1525 cm^{-1}. – FD-MS (3 kV): 982 [M^+(^{118}Sn), 100%].

[9] W. P. Neumann, H. Sakurai, G. Billeb, H. Brauer, J. Köcher, S. Viebahn, *Angew. Chem.* **1989**, *101*, 1074; *Angew. Chem. Int. Ed. Engl.* **1989**, *28*, 1028.

[10] $HN(SiMe_3)_2$ silanizes glass vessels more effectively than Me_3SiCl. We thank Prof. Dr. M. J. Hambden-Smith, University of New Mexico for this valuable piece of advice.

[11] a) Crystal structure analysis of **8**: $C_{38}H_{25}F_{18}OPSn$, M_r = 989.3, triclinic, space group $P\bar{1}$ (no. 2), a = 9.466(4), b = 18.935(5), c = 24.401(8) Å, α = 110.00(3), β = 91.73(3), γ = 92.55(3)°, V = 4101(2) Å^3, Z = 4, ρ_{calcd} = 1.602 g cm^{-3}, absorption coefficient 0.777 mm^{-1}, Enraf-Nonius Turbo CAD4 diffractometer ($Mo_{K\alpha}$ radiation, λ = 0.71073 Å, graphite monochromator, T = 173 K) ω-2θ scan, 2θ = 4.58–46.94°, ($-9 \le h \le 0$; $-21 \le k \le 19$; $-24 \le l \le 24$). 9961 reflections were measured, of which 9276 were independent reflections, and 9253 of these were used for the structure analysis [12b] by using direct methods and for the structure refinement [12c]. The structure was refined by using the least squares method on F^2 with 963 independent parameters to an R_1 value ($I > 2\sigma I$) of 0.0783. Residual electron density = + 0.90 and –2.53 eÅ^{-3}. The program SCHAKAL-92 [12d] was used for the graphical depiction of the structure. Further details of the crystal structure investigation may be obtained from the Fachinformationszentrum Karlsruhe, D-76344 Eggenstein-Leopoldshafen (FRG) on quoting the depository number CSD-57785, the names of the authors, and the journal citation. The bond lengths of the second molecule in the unit cell of **8** differ only slightly from those discussed in the text: Sn2–C39 2.14(2), Sn2–C41 2.27(2), P2–C39 1.76(2), C39–C40 1.39(2) (corresponding to Sn1–C1, Sn1–C3, P1–C1, C1–C2 in Fig. 1). In addition, an X-ray structure analysis was performed on a second crystal of **8** at room temperature. The distances and angles determined agreed with those described here; b) PC version of the SHELX-86 program: G. M. Sheldrick, *Acta Crystallogr. Sect. A*, **1990**, *46*, 467; c) SHELXL-93: G. M. Sheldrick, Universität Göttingen, 1993; d) SCHAKAL 92—A Computer Program for the Graphic Representation of Molecular and Crystallographic Models: E. Keller, Universität Freiburg, **1992**.

[12] For example: $R^2_2Sn(CH_2Ph)Mes$: Sn–C 2.23 and 2.25 Å; $R^2_2Sn(SPh)_2$: Sn–C 2.23 and 2.22 Å; $R^2_2Sn(OOCCF_3)_2$: Sn–C 2.18 Å (H. Grützmacher, H. Pritzkow, unpublished results).

[13] H. Grützmacher, H. Pritzkow, *Angew. Chem.* **1980**, *101*, 768; *Angew. Chem. Int. Ed. Engl.* **1989**, *28*, 740.

[14] H. Schmidbaur, J. Jeong, A. Schier, W. Graf, D. L. Wilkinson, G. Müller, G. Krüger, *New. J. Chem.* **1989**, *13*, 341, and references therein.

[15] U. Linger, H. Burzlaff, *Acta Crystallogr. Sect. B* **1974**, *30*, 1715, and references therein

[16] **10**: m.p. 148–150 °C. – ^{1}H NMR ($CDCl_3$, 200.132 MHz): δ = 3.91 [d, $^2J(^{31}P,^1H)$ = 22 Hz, 1H, PCH]; 7.45–7.57 [m, 9H, aromat. CH, PPh_3]; 7.69–7.79 [m, 6H, aromat. CH, PPh_3]; 8.08 [s, 2H, aromat. CH, R^2-CO]. – ^{19}F NMR ($CDCl_3$, 188.313 MHz): δ = – 58.1 [s, 6F, *o*-CF_3]; –63.4 [s, 3F, *p*-CF_3]. – ^{31}P NMR ($CDCl_3$, 81.015 MHz): δ = 13.9. – ^{13}C NMR ($CDCl_3$, 50.323 MHz): δ = 57.8 [d, $^1J(^{31}P,^1H)$ = 106.6 Hz, C_{ylide}]. – IR (Nujol): ν(C=O) = 1555 cm^{-1}. – EI-MS (70 kV): 584 (M^+, 85%), 583 ((M –1)$^+$, 100%).

[17] a) G. Ossig, A. Meller, S. Freitag, R. Herbst-Irmer, *J. Chem. Soc. Chem. Commun.* **1993**, 497; b) G. Ossig, A. Meller, S. Freitag, R. Herbst-Irmer, G. M. Sheldrick, *Chem. Ber.* **1993**, *126*, 2247.

Diastereoselective Synthesis of Amino-Substituted Indolizidines and Quinolizidines by the Intramolecular Hetero-Ene Reaction of Prolinal Imine and 2-Piperidine Carbaldimine**

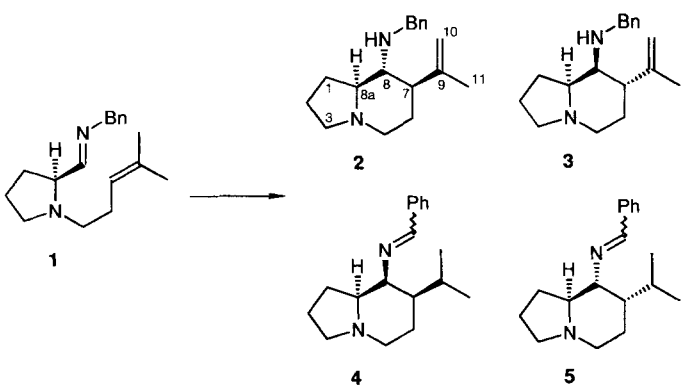
Sabine Laschat* and Matthias Grehl

Despite its great synthetic potential the hetero-ene reaction of unactivated imines[1–3] has remained relatively unexplored in comparison to the carbonyl–ene reaction[4] which has been investigated intensively for years. In addition, the intramolecular type I imino–ene reaction [5] seems particularly suitable for the synthesis of alkaloids, since in this reaction a ring is formed in one step stereoselectively, and simultaneously two neighboring stereocenters are constructed, to one of which an N atom is bound. We have thus concerned ourselves with the question of the extent to which diastereoselectively substituted indolizidines and quinolizi-

[*] Dr. S. Laschat, Dr. M. Grehl
Organisch-chemisches Institut der Universität
Corrensstrasse 40, D-48149 Münster (FRG)
Telefax: Int. code + (251)839-772

[**] This work was supported by the Alfried-Krupp-von-Bohlen-und-Halbach-Stiftung and the Wissenschaftsministerium Nordrhein-Westfalen (Lise-Meitner-Stipendium for S. L). We thank Dr. Andreas Ruchmann and Karin Busse for their help with the NMR spectroscopic structure investigation.

dines can be constructed with such hetero-ene reactions[6] particularly in view of the fact that a range of these alkaloid derivatives are effective glucosidase inhibitors[7] and are thus of increasing interest because of their Anti-HIV activity.[8] In the following we report on a new intramolecular Lewis acid catalyzed imino–ene reaction for the diastereoselective construction of 7-alkenyl-8-amino-substituted indolizidines and 2-alkyl-1-amino-substituted quinolizidines. In this reaction the relative configuration of the two newly formed stereocenters can be controlled by the choice of Lewis acid. The reaction of (−)-(*S*)-*N*-[*N*-(4-methyl-3-pentenyl)pyrrolidine-2-methylidene]benzylamine (**1**) with $FeCl_3$ affords three stereoisomeric indolizidines in a ratio of 90.3:7.0:2.7 (Scheme 1, Table 1). After chromatographic purification the main



Scheme 1. Cyclization of **1**. Reaction conditions: 2.5 equiv Lewis acid, CH_2Cl_2, room temperature.

Table 1. Reaction of **1** with Lewis acids [a,b].

Lewis acid	*t*[h]	Product ratio [c] 2	3	4	5	Yield [%]
$FeCl_3$	48	90.3	7.0	2.7	–	62 (**2**)
$TiCl_4$	21.5	1.2	3.7	94.7	0.3	45 (**4**)

[a] The reactions were carried out with 2.5 equiv Lewis acid in CH_2Cl_2 at room temperature. [b] Enantiomeric purity of the isolated products **2** and **4**: > 98% *ee*. For the determination of the *ee* values see ref. [9]. [c] Isomeric ratios were determined from the crude products by capillary GC.

product **2** was isolated with an enantiomeric excess of > 98 %.[9] If, however, $TiCl_4$ is used as Lewis acid, the isomeric ratio was altered completely (Table 1), and an additional indolizidine **5** was also formed.[10] As a result of the X-ray structure analysis,[11] product **2** can be assigned unambiguously to the all-*trans* configuration shown in Scheme 1. NMR spectroscopic investigations showed that one benzylideneamino group is bound to the indolizidine framework of **4** at position 8 and one isopropyl group at position 7; however, the unequivocal stereochemical assignment of **4** was only achieved after its transformation into the *N*-acetyl derivative **6** (Scheme 2). For this, first a hydrogenolysis in the presence of $PdCl_2$ was carried out on the imine **4**,[12] the resulting product was then acetylated with acetic anhydride. The vicinal coupling constants for H-8 obtained from the ^1H NMR spectrum of **6** (Table 2) clearly show the all-*cis* arrangement of H-8a, H-8, and H-7. This arrangement was confirmed by a NOESY experiment, in which a nuclear Overhauser effect (NOE) was observed between H-8a and H-8 and also between H-8 and H-7. The application of the same hydrogenation/hydrogenolysis/acetylation sequence on **2** yielded the diastereomeric *N*-acetyl product **7**, whose vicinal coupling constants of H-8 confirm the all-*trans* configuration of **4**. Although, the stereochemical configuration of the two by-products **3** and **5** could not be elucidated unambiguously, the assignment made according to Scheme 1 is supported by the mass spectra of **3** and **5**. The mass spectrum of **3** shows an almost identical fragmentation pattern and comparable intensities to that of **2**; accordingly, the spectrum of **5** is extremely similar to that of **4**. The formation of the products **2** and **3** can

Table 2. Selected spectroscopic and analytical data of the indolizidines.

2: ^1H NMR (200 MHz, $CDCl_3$): δ = 7.26–7.16 (m, 5H; Ph), 4.80 (br. s, 2H; H-10), 3.84 (d, J = 12.7 Hz, 1H; H-12a), 3.63 (d, J = 12.7 Hz, 1H; H-12b), 3.08–3.00 (m, 3H; H-8, H-8a, NH), 2.34 (dd, J = 10.2, 8.4 Hz, 2H; H-3eq, H-5eq), 2.12–1.87 (m, 3H), 1.86–1.50 (m, 5H), 1.50 (s, 3H; H-12), 0.81 (dd, J = 11.2, 6.5 Hz, 1H; H-7); ^{13}C NMR (50 MHz, $CDCl_3$): δ = 146.3 (s, C-9), 140.6 (C-*i*), 128.3 (d, J = 160 Hz, C-*o*, C-*p*), 126.8 (C-*m*), 113.5 (t, J = 155 Hz, C-10), 70.5 (d, J = 134 Hz, C-8a), 60.3 (d, J = 131 Hz, C-8), 53.7 (CH_2Ph), 53.1 (C-3), 51.9 (C-5), 51.1 (C-7), 30.4 (t, J = 134 Hz, C-6), 30.1 (C-1), 21.1 (C-2), 18.3 (C-11); GC-MS (EI, 70 eV): *m/z* (%): 270 (7) [M^+], 201 (3), 186 (13), 173 (75), 158 (66), 122 (2), 110 (33), 98 (38), 91 (100), 84 (64)

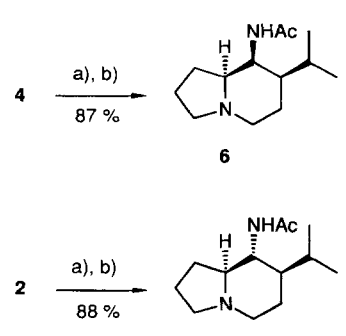
3: GC-MS (EI, 70 eV): *m/z* (%): 270(9) [M^+], 201 (3), 186 (14), 173 (78), 158 (85), 122 (10), 110 (35), 98 (38), 91 (100), 84 (68)

4: ^1H NMR (300 MHz, C_6D_6): δ = 8.21 (br. s, 1H; HC = N), 7.91–7.88 (m, 2H; H-*o*), 7.35–7.18 (m, 3H, H-*m*, H-*p*), 3.50 (br. s, 1H; H-8), 3.39 (ddd, J = 10.6, 4.1, 2.6 Hz, 1H), 3.13 (ddd, J = 10.6, 10.6, 2.3 Hz, 1H), 2.42 (dddd, J = 12.2, 12.2, 12.2, 4.0 Hz, 1H), 2.24–2.15 (m, 2H), 2.06 (dd, J = 8.7, 8.7 Hz, 1H), 1.97–1.36 (m, 6H), 1.29–1.20 (m, 1H), 0.99 (d, J = 6.8 Hz, 3H; H-10), 0.93 (d, J = 6.4 Hz, 3H; H-11); ^{13}C NMR (75 MHz, C_6D_6): δ = 160.4 (HC = N), 137.0 (C-*i*), 130.4 (C-*m*), 128.6 (C-*o*, C-*p*), 69.3 (C-8), 68.9 (C-8a), 54.4 (C-3), 53.5 (C-5), 49.2 (C-7), 29.2 (C-9), 26.2 (C-1), 25.7 (C-6), 21.3 (C-2), 21.0 (C-11), 20.3 (C-12); GC-MS (EI, 70 eV): *m/z* (%): 270 (9) [M^+], 227 (23), 201 (5), 186 (3), 173 (10), 167 (22), 158 (100), 122 (39), 110 (9), 91 (19), 84 (16)

5: GC-MS (EI, 70 eV): *m/z* (%): 270 (11) [M^+], 227 (21), 201 (4), 186 (2), 173 (12), 167 (22), 158 (100), 122 (38), 110 (10), 91 (21), 84 (28)

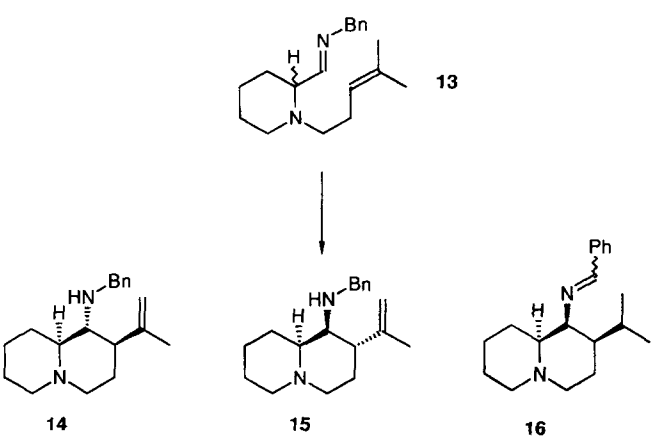
6: ^1H NMR (360 MHz, $CDCl_3$): δ = 7.75 (d, $J_{8,NH}$ = 10.6 Hz, 1H; NH), 4.63 (ddd, $J_{8,NH}$ = 10.6 Hz, $J_{8,8a}$ = 2.6, $J_{7,8}$ = 2.6 Hz, 1H; H-8), 3.54–3.44 (m, 2H; H-3eq, H-5eq), 2.92 (ddd, $J_{1ax,8a}$ = 11.9, $J_{1eq,8a}$ = 6.1, $J_{8,8a}$ = 2.6 Hz, 1H; H-8a), 2.62 (ddd, $J_{2eq,3ax}$ = 11.2, $J_{3ax,3eq}$ = 9.3, $J_{2ax,3eq}$ = 8.8 Hz, 1H; H-3ax), 2.58 (ddd, $J_{5ax,6ax}$ = 12.0, $J_{5ax,5eq}$ = 11.8, $J_{5ax,6eq}$ = 4.2 Hz, 1H; H-5ax), 1.97 (s, 3H; $COCH_3$), 2.04–1.77 (m, 5H; H-1eq, H-2, H-6), 1.68 (dddd, $J_{1ax,8a}$ = 11.8, $J_{1ax,2eq}$ = 11.8, $J_{1ax,1eq}$ = 10.6, $J_{1ax,2ax}$ = 5.3 Hz, 1H; H-1ax), 1.39 (dddd, $J_{7,9}$ = 6.7, $J_{9,10}$ = 6.7, $J_{9,11}$ = 6.7, $J_{8,9}$ = 2.9 Hz, 1H; H-9), 1.27–1.15 (m, 1H; H-7), 0.81 (d, J = 6.6 Hz, 3H; H-10), 0.78 (d, J = 6.6 Hz, 3H; H-11); ^{13}C NMR (50 MHz, $CDCl_3$): δ = 171.2 (CO), 69.4 (C-8a), 52.0 (C-3), 51.5 (C-5), 45.4 (C-7), 45.0(C-8), 28.6 (C-9), 24.0 (C-1), 23.0 (C-6), 22.7 ($COCH_3$), 20.5 (C-10, C-11), 19.7 (C-2)

7: ^1H NMR (360 MHz, $CDCl_3$): δ = 6.18 (d, $J_{8,NH}$ = 10.7 Hz, 1H; NH), 3.66 (ddd, $J_{8,NH}$ = 10.7, $J_{8,8a}$ = 10.7, $J_{7,8}$ = 10.7 Hz, 1H; H-8), 3.09–2.92 (m, 2H; H-5eq, H-3eq), 2.12 (ddd, $J_{2ax,3ax}$ = 8.7, $J_{2eq,3ax}$ = 8.7, J_{3a}Tx,3eq = 8.7 Hz, 1H; H-3ax), 1.95 (ddd, $J_{5ax,6ax}$ = 11.7, $J_{5ax,5eq}$ = 11.4, $J_{5ax,6eq}$ = 2.8 Hz, 1H; H-5ax), 1.86 (s, 3H; $COCH_3$), 1.85–1.47 (m, 7H), 1.39 (dddd, $J_{6ax,6eq}$ = 12.3, $J_{6ax,7}$ = 12.3, $J_{5ax,6ax}$ = 11.8, $J_{5eq,6ax}$ = 4.4 Hz, 1H; H-6ax), 1.19–1.11 (m, 1H; H-7), 0.79 (d, J = 6.9 Hz, 3H; H-10), 0.71 (d, J = 6.9 Hz, 3H; H-11); ^{13}C NMR (50 MHz, $CDCl_3$): δ1 = 169.6 (CO), 69.3 (C-8a), 54.0 (C-3), 52.0 (C-8), 51.5 (C-5), 47.0 (C-7), 28.4 (C-1), 26.2 (C-9), 23.4 (C-6), 23.2 ($COCH_3$), 21.1 (C-10), 20.6 (C-2), 16.2 (C-11)



Scheme 2. Synthesis of *N*-acetylindolizidines **6** and **7**. Reaction conditions: a) 1 equiv $PdCl_2$, MeOH, 1 atm H_2, 20 °C, 4 h; b) 1.1 equiv Ac_2O, 3 equiv NEt_3, CH_2Cl_2, reflux, 12 h.

be explained by an intramolecular type I hetero-ene reaction (Scheme 3). An alternative multistep mechanism is also conceivable, in which at first the alkene attacks the initially formed iminium ion **9** leading to the formation of the carbenium ions **10**.[14, 15] Starting from **10** either a reprotonation via **11**, leading to the benzylamines **2** and **3**, or a hydride shift takes place to give the benzyl cation **12**, from which the imines **4** and **5** are formed after the elimination of the Lewis acid. The stereochemistry of the cyclization products **2**–**5** indicates that the competing pathways of reprotonation or hydride shift depend on the relative configuration at C-7/C-8 of the carbenium ion **10**, that is, a hydride shift is only favored when the benzyl and the isopropyl group (C-7/C-8-*cis*) lie in close proximity to each other. However, so far we have not found a reasonable explanation for why the two Lewis acids $FeCl_3$ and $TiCl_4$ react so differently with regard to the stereochemistry of the ring closure. The different coordination geometry of the two Lewis acids cannot be the reason, since other Lewis acids, for example $SnCl_4$, show isomeric ratios comparable to the $FeCl_3$ case. A similar dependence of the diastereoselectivity on the Lewis acid used is also observed for the analogous reaction of racemic piperidine carbaldimine **13** to give the quinolizidines **14**–**16** (Scheme 4). Other products were not observed, and the diastereoselectivities are significantly lower than those for the corresponding indolizidines (Table 3).



Scheme 4. Cyclization of *rac*-**13**. For clarity only one enantiomer of **14**–**16** is shown in each case. Reaction conditions: 2.5 equiv Lewis acid, CH_2Cl_2, room temperature.

Table 3. Reaction of **13** with Lewis acids [a].

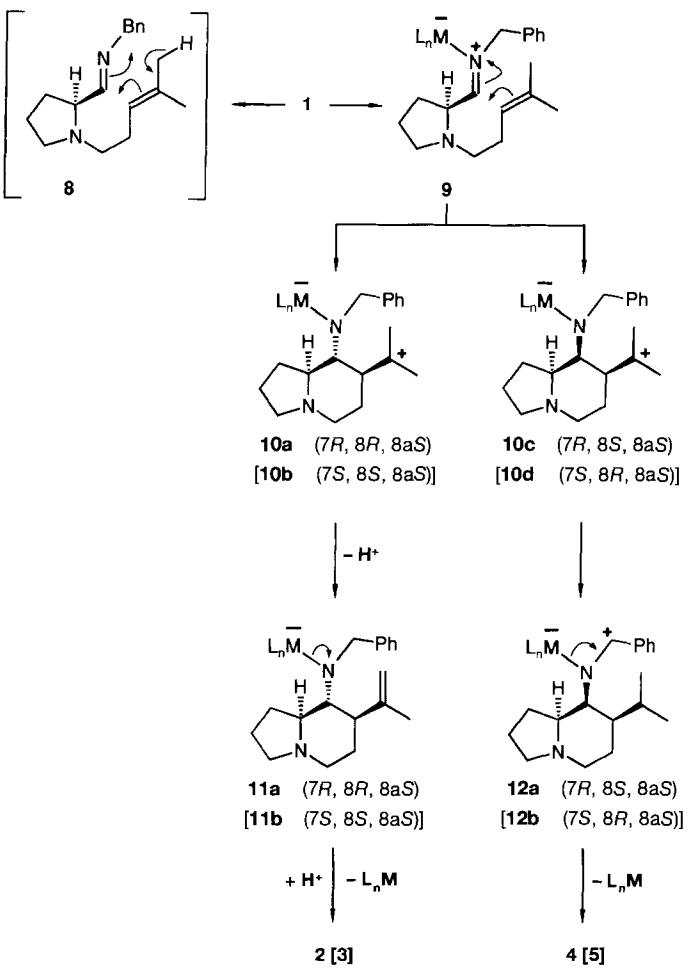
Lewis-acid	*t* [h]	Product ratio [b]			Yield [%]
		14	**15**	**16**	
$FeCl_3$	48	71.6	14.8	13.6	68 (**14**)
$TiCl_4$	48	2.0	1.4	96.6	50 (**16**)

[a] Reaction conditions see Table 1, footnote [a]. [b] Compare Table 1, footnote [c].

Regardless of the mechanisms discussed above, the hetero-ene reactions of **1** and **13** described here provide a simple and diastereoselective access to α-amino-functionalized indolizidines and quinolizidines, respectively, which opens new perspectives in natural product chemistry.

Experimental Procedure

To an ice-cooled solution of imine **1** or **13** (1.00 mmol) in dry CH_2Cl_2 (28 mL), Lewis acid (2.5 mmol; $FeCl_3$: 1.0 M solution in Et_2O; $TiCl_4$: 1.0 M solution in CH_2Cl_2) was added dropwise over 30 min, and the resulting mixture was stirred at room temperature. Following complete conversion (GC control) the mixture was hydrolyzed by addition of 2 N NaOH and extracted three times with CH_2Cl_2 (100 mL). After the organic phase had been dried over $MgSO_4$ and concentrated, the crude product was purified by flash chromatography (silica gel, hexane/ethyl acetate/triethylamine 79:16:5).



Scheme 3. Possible reaction mechanisms for the formation of the products **2**–**5**.

Received: August 28, 1993
Revised version: November 5, 1993 [Z 6323 IE]
German version: *Angew. Chem.* **1994**, *106*, 475

[1] Reviews on the ene reaction: a) H. M. R. Hoffmann, *Angew. Chem.* **1969**, *81*, 597; *Angew. Chem. Int. Ed. Engl.* **1969**, *8*, 556; b) W. Oppolzer, V. Snieckus, *ibid.* **1978**, *90*, 506 and **1978**, *17*, 476; c) B. B. Snider in *Comprehensive Organic Synthesis, Vol. 5* (Ed.: B. M. Trost), Pergamon, Oxford, **1991**, pp. 1–27.

[2] Activated, =M-substituted imines: a) J. M. Liu, K. Koch, F. W. Fowler, *J. Org. Chem.* **1986**, *51*, 167; b) K. Koch, J. M. Liu, F. W. Fowler, *Tetrahedron Lett.* **1983**, *24*, 1581; G. E. Keck, R. R. Webb, J. B. Yates, *Tetrahedron* **1981**, *37*, 4007; d) D. M. Tschaen, E. Turos, S. M. Weinreb, *J. Org. Chem.* **1984**, *49*, 5058; e) K. Mikami, M. Kaneko, T. Yajima, *Tetrahedron Lett.* **1993**, *34*, 4841; f) L. F. Tietze, M. Bratz, *Chem. Ber.* **1989**, *122*, 997; g) L. F. Tietze, M. Bratz, M. Praetor, *ibid.* **1989**, *122*, 1955; h) L. F. Tietze, M. Bratz, *Synthesis* **1989**, 439; i) *Liebigs Ann. Chem.* **1989**, 559.

[3] Unactivated imines: a) G. Demailly, G. Solladie, *Tetrahedron Lett.* **1977**, 1885; b) *J. Org. Chem.* **1981**, *46*, 3102; c) J. Cossy, A. Bouzide, M. Pfau, *Tetrahedron Lett.* **1992**, *33*, 4883.

[4] Reviews: a) K. Mikami, M. Terada, S. Narisawa, T. Nakai, *Synlett* **1992**, 255; b) K. Mikami, M. Shimizu, *Chem. Rev.* **1992**, *92*, 1021; c) B. B. Snider in *Comprehensive Organic Synthesis, Vol. 2* (Ed.: B. M. Trost), Pergamon, Oxford, **1991**, pp. 527–561.

[5] Classification of ene reactions (type I–IV) according to D. F. Tauber, *Intramolecular Diels–Alder and Alder Ene Reactions*, Springer, Berlin, **1984**, pp. 61-94.

[6] To date very little has been reported on the synthesis of indolizidines by in-

tramolecular carbonyl–ene reactions: S. Y. Dike, M. Mahalingam, A. Kumar, *Tetrahedron Lett.* **1990**, *31*, 4641.
[7] Reviews: a) L. E. Fellows, G. W. J. Fleet in *Natural Products Isolation* (Eds.: G. H. Wafman, R. Cooper), Elsevier, Amsterdam, **1989**, pp. 539–559; b) A. D. Elbein, R. J. Molyneux, *Alkaloids: Chem. Biol. Perspect.* **1987**, *5*, 1.
[8] a) B. D. Walker, M. Kowalski, W. C. Goh, K. Kozarsky, M. Krieger, C. Rosen, L. Rohrschneider, W. A. Haseltine, J. Sodroski, *Proc. Natl. Acad. Sci. USA* **1987**, *84*, 8120; b) A. Karpas, G. W. J. Fleet, R. A. Dwek, S. Petursson, S. K. Namgoong, N. G. Ramsden, G. S. Jacob, T. W. Rademacher, *ibid.* **1988**, *85*, 9229; c) D. C. Montefiori, W. E. Robinson, W. M. Mitchel, *ibid.* **1988**, *85*, 9248; d) P. S. Sunkara, D. L. Taylor, M. S. Kang, T. L. Bowlin, P. S. Liu, A. S. Tyms, A. Sjoerdsma, *Lancet* **1989**, 1206; A. S. Tyms, E. M. Berri, T. A. Ryder, R. J. Nash, M. P. Hegarty, D. L. Taylor, M. A. Mobberley, J. M. Davis, E. A. Bell, D. J. Jeffries, D. Taylor-Robinson, L. E. Fellows, *ibid.* **1987**, 1025.
[9] The enantiomeric purity of the products **2** and **4** (each > 98% *ee*) was determined by using one molar equivalent of (−)-(*R*)-1-(9-anthryl)-2,2,2-trifluoroethanol in the 200 MHz ^{1}H NMR spectrum see: W. Pirkle, D. L. Sikkenga, M. S. Pavlin, *J. Org. Chem.* **1977**, *42*, 384.
[10] The isolated products **2** or **4** do not epimerize on renewed reaction with 2.5 equiv Lewis acid in CH_2Cl_2 at room temperature. After a reaction time of more than 4 h, however, increasing decomposition leading to the formation of benzylamine is observed in the gas chromatogram. The same effect occurs on much longer reaction times for the benzylimine **1**.
[11] X-ray structure analysis of **2**: $C_{18}H_{26}N_2$, colorless, orthorhombic, space group $P2_12_12_1$, no. 19, $a = 5.566(2)$, $b = 32.751(14)$, $c = 8.948(4)$ Å, $V = 1631(1)$ Å^3, $Z = 4$, $\rho_{calcd} = 1.101$ g cm^{-3}, $\mu = 0.6$ cm^{-3}, $Mo_{K\alpha}$ radiation (graphite monochromator); 2773 independent reflections, observed 1387, $R = 0.065$, $wR^2 = 0.1724$; structure solution with direct methods (SHELXS-86 [13]); refinement of 181 parameters according to F^2 (SHELXL-93). Further details of the crystal structure investigation may be obtained from the Fachinformationszentrum Karlsruhe, D-76344 Eggenstein-Leopoldshafen (FRG) on quoting the depository number CSD-57921, the names of the authors, and the journal citation.
[12] T. Kaseda, T. Kikuchi, C. Kibayashi, *Tetrahedron Lett.* **1989**, *30*, 4539.
[13] G. M. Sheldrick in *Crystallographic Computing 3* (Eds.: G. M. Sheldrick, C. Krüger, R. Goddard), Clarendon, Oxford, **1985**, p. 175.
[14] In comparable imino–ene reactions a cationic process was detected by Tietze et al. (cf. refs. [2f–i]).
[15] Compare cyclization reactions of acyliminium ions with allyl/vinyl silanes: a) W. N. Speckamp, H. Hiemstra, *Tetrahedron* **1985**, *41*, 4367; b) H. Hiemstra, H. P. Fortgens, W. N. Speckamp, *Tetrahedron Lett.* **1985**, *26*, 3155; c) C. Flann, T. C. Malone, L. E. Overman, *J. Am. Chem. Soc.* **1987**, *109*, 6097; d) P. A. Grieco, W. F. Fobare, *Tetrahedron Lett.* **1986**, *27*, 5067; e) S. D. Larsen, P. A. Grieco, W. F. Fobare, *J. Am. Chem. Soc.* **1986**, *108*, 3512; f) L. F. Tietze, J. R. Wünsch, *Angew. Chem.* **1991**, *103*, 1665; *Angew. Chem. Int. Ed. Engl.* **1991**, *30*, 1697; g) L. F. Tietze, J. R. Wünsch, M. Noltemeyer, *Tetrahedron* **1992**, *48*, 2081.

Structural Principles in Seven-Coordinate Subgroup Compounds: The Complex Anions MoF_7^-, WF_7^-, and $ReOF_6^-$ **

Steffi Giese and Konrad Seppelt*

It was recently shown that main group molecules or molecular anions like IF_7, TeF_7^-, $ROTeF_6^-$, $(RO)_2TeF_5^-$, and IOF_6^- always form as pentagonal bipyramids.[1–6] This is remarkable considering that the interligand repulsions that result from this special geometry are greater, albeit only slightly, than those arising from the competing capped octahedral and capped trigonal-prismatic geometries.[7] It thus appears that as long as lattice forces or special electronic effects do not influence the structure in some other way, molecules of this type having the coordination numbers (CN) five, seven, and eight will always form the highest symmetry coordination polyhedra of the possible structural alternatives (trigonal bipyramid vs. square pyramid; pentagonal bipyramid vs. capped octahedron; square antiprism vs. trigonal dodecahedron).[8] The highest symmetry may be defined as that which requires the smallest number of parameters for its complete description. In the case of CN = 7 this principle of the highest possible symmetry clearly dominates, and the greater ligand–ligand repulsions of this coordination polyhedron are alleviated through small systematic deviations from the ideal D_{5h} structure ("ring puckering"). As yet, there has been no attempt to transcribe this principle of highest possible symmetry into a unified bonding model.

Is this structure principle also valid for subgroup compounds? Ideally, an accurate structural investigation of a homoleptic neutral compound should be used to approach this problem; the only molecule that comes into consideration here is ReF_7. However, just as with IF_7,[2, 9] the structure of ReF_7 is very difficult to determine experimentally. Electron diffraction investigations suggest a distorted D_{5h} structure.[10] Since the thermal fluctuations of the ligands in molecules with CN = 7 are expected to cause large-amplitude vibrations, no definitive structural information is possible with electron diffraction alone.[9] Because of the existence of several solid phases, including one that is plastic, the crystal structure of ReF_7 has not yet been determined with certainty.[11]

To clarify this problem we have investigated the structures of the anions MoF_7^- and WF_7^-. The influence of the lattice energy on the structures of these anions should be precluded by variation of the countercations. MoF_6 and WF_6 are known to form complexes with fluorides which, according to their elemental analyses, have the compositions MF_7^- and MF_8^{2-} (M = Mo, W).[12] Reliable structure information on these, however, does not exist.

The complexes $Cs^+MoF_7^-$ and $Cs^+WF_7^-$ are formed from the reaction of CsF with an excess of MoF_6 and WF_6, respectively. The colorless salts recrystallize well from acetonitrile. Crystal structure analyses showed that both salts have isotypic structures in which the anions take the form of capped octahedra (Fig. 1). Each anion lies on a threefold axis of the cubic crystal

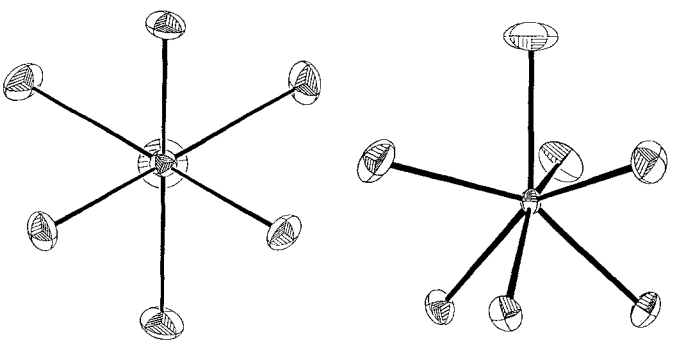


Fig. 1. The structure of the MoF_7^- ion in $Cs^+MoF_7^-$. Left: view along the threefold axis; right: view perpendicular to the C_3 axis (ORTEP representation with thermal ellipsoids at the 50% probability level). The structure of the anions in $Cs^+WF_7^-$ and in the other hexafluoromolybdates(IV) are qualitatively the same.

system which coincides with the symmetry axis of the anion. Thus, the structure of the anion could be dictated by the crystal system itself. To clarify this we synthesized $NO_2^+MoF_7^-$ from the reaction between NO_2F and MoF_6, obtained single crystals, and examined the salt by X-ray crystallography.[13] The compound crystallizes as $NO_2^+MoF_7^- \cdot CH_3CN$. The MoF_7^- ion has

[*] Prof. Dr. K. Seppelt, Dipl.-Chem. S. Giese
Institut für Anorganische und Analytische Chemie der Freien Universität
Fabeckstrasse 34–36, D-14195 Berlin (FRG)
Telefax: Int. code + (30)838-2424

[**] This work was supported by the Deutsche Forschungsgemeinschaft and the Fonds der Chemischen Industrie.

a capped octahedral structure here as well as in $C_{11}H_{24}N^+MoF_7^-$ ($C_{11}H_{24}N^+$ = 1,1,3,3,5,5-hexamethylpiperidinium).[14] Finally, $(CH_3)_4N^+MoF_7^-$ was prepared from $(CH_3)_4N^+F^-$[15] and MoF_6, and its crystal structure determined. Its anion also exhibits a capped octahedral structure, but, as a result of the tetragonal crystal symmetry, a fourfold disorder is observed for the anion. This result is meaningful, since both $(CH_3)_4N^+TeF_7^-$[1] and $(CH_3)_4N^+MoF_7^-$ crystallize in the same space group (*P4/nmm*). The coordinates of the atoms of the cations as well as those of the Te and Mo atoms are identical, but the coordinates of the fluorine atoms differ such that different types of disorder are exhibited; TeF_7^- forms a pentagonal bipyramid and MoF_7^- a capped octahedron. It can therefore be concluded here that neither the lattice type nor the crystal packing have an influence on the different structures of the anions.

Three types of bonds can be distinguished in the capped octahedron: one apical, three equatorial, and three basal bonds. The bonds from the metal center to the equatorial fluorine atoms are always observed to be shorter than those to the other four fluorine atoms (Table 1). If the valence shell electron pair repulsion model is used, the larger ligands in capped octahedral complexes containing different types of ligands in ratios of 3:4 or 1:3:3 should occupy equatorial sites preferentially. Two of the few known examples are the compounds $[MoCl_4\{(CH_3)_2C_6H_5P\}_3]$[16] and $[WBr_3(CO)_4]^-$,[17] assuming that the phosphane and carbonyl ligands require more space owing to the π-bonding part of their M–P and M–CO bonds.

Table 1. Interatomic M–F distances (M = Mo, W) [pm] and F-M-F bond angles [°] in the capped octahedral structures of the MoF_7^- and WF_7^- anions (ap = apical, eq = equatorial, ba = basal).

Cmpd.	M-F_{ap}	M-F_{eq}	M-F_{ba}	F_{ap}-M-F_{eq}	F_{ap}-M-F_{ba}
$Cs^+MoF_7^-$	189.4(9)	185.3(5)	189.8(5)	75.5(2)	131.8(2)
$NO_2^+MoF_7^-$	185.2(2)	183.5(2) [a]	187.3(2) [a]	76.8(1) [a]	132.4(1) [a]
$C_{11}H_{24}N^+MoF_7^-$	184.4(3)	183.3(3) [a]	184.4(4) [a]	75.7(2) [a]	130.0(2) [a]
$Cs^+WF_7^-$	191.0(10)	186.4(5)	189.8(5)	75.5(2)	131.8(2)

[a] Averaged value.

Of course the capped octahedral coordination polyhedron is not rigid. In both compounds the MoF_7^- and WF_7^- anions show a sharp singlet in their solution ^{19}F NMR spectra.

Already when just one bulkier ligand is introduced, the structure principle of a capped octahedron no longer holds; the pentagonal-bipyramidal structure results, since the larger ligand(s) can now coordinate at one (or two) of the axial positions. Exactly this is found in the anion $ReOF_6^-$, as first prepared by us with the complexes $Cs^+ReOF_6^-$ and $NO_2^+ReOF_6^-$. In these salts the anions have a pentagonal-bipyramidal structure, in which the oxygen atom occupies an axial position (Fig. 2). In principle these complexes are similar to the recently prepared IOF_6^- anion; however, the two pentagonal-bipyramidal structures differ upon closer examination. Whereas the axial Re–O bond is considerably shorter in $ReOF_6^-$, the axial and equatorial Re–F bonds are almost of equal length. In addition, the equatorial fluorine atoms are coplanar, in other words the "ring puckering" observed for the pentagonal bipyramids of the main group compounds is not found here (Table 2). These differences can be explained by the size of the rhenium atom. Owing to the longer Re–F bonds, the repulsive forces between the fluorine atoms are so small that an undistorted structure forms in which all the bonds are equivalent. Both IOF_6^- and $ReOF_6^-$ are rigid molecules; a well-resolved AB_6 system is observed in their ^{19}F NMR spectra (Fig. 3), which provides additional qualitative evidence for the correctness of the structure model. The space requirements of the oxygen atom is apparently so large that intramolecular exchange processes are suppressed. The Raman spectrum of the $ReOF_6^-$ anion can also be interpreted based on C_{5v} symmetry in analogy to the spectrum of IOF_6^-.[5]

Table 2. Interatomic distances [pm] and bond angles [°] in the pentagonal-bipyramidal $ReOF_6^-$ anions of the complexes $Cs^+ReOF_6^-$ and $NO_2^+ReOF_6^-$. Two crystallographically distinct anions I and II are found in the latter (ax = axial, eq = equatorial).

	Re-O	Re-F_{ax}	Re-F_{eq}	O-Re-F_{ax}	O-Re-F_{eq}
$Cs^+ReOF_6^-$	167.1(7)	192.3(6)	186.6–190.8(7)	178.0(3)	93.2–94.7(3)
$NO_2^+ReOF_6^-$(I)	165.9(13)	192.7(10)	189.9–191.4(7)	178.0(3)	91.7–94.6(4)
$NO_2^+ReOF_6^-$(II)	162.9(14)	189.4(11)	186.2–191.7(7)	178.4(4)	91.5–95.7(5)

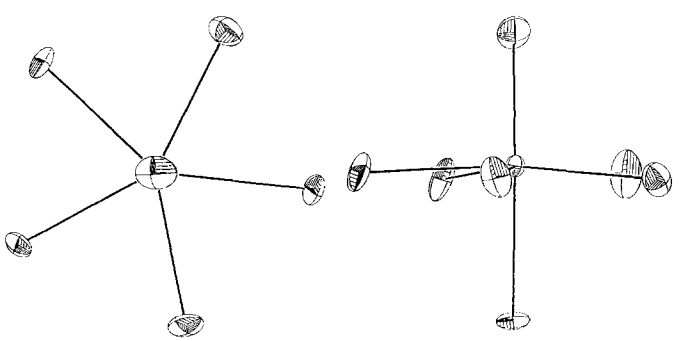


Fig. 2. The structure of the crystallographically distinct $ReOF_6^-$ anion II in $NO_2^+ReOF_6^-$. Left: view along the fivefold axis; right: view perpendicular to the C_5 axis (ORTEP representation with thermal ellipsoids at the 50% probability level). The structure of the $ReOF_6^-$ anion I and that of the anion in $Cs^+ReOF_6^-$ are qualitatively the same.

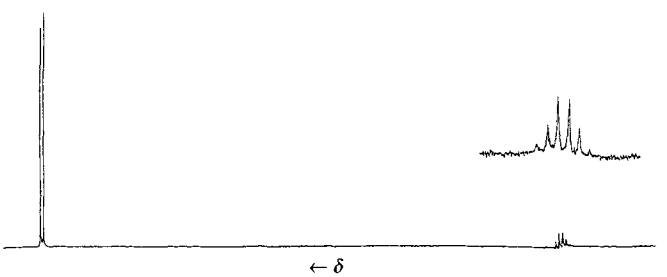


Fig. 3. ^{19}F NMR spectrum of $NO_2^+ReOF_6^-$ in CH_3CN. The signals for the axial and equatorial ligands are observed at δ = 68.44 and δ = −53.35 (J_{FF} = 65.9 Hz), respectively.

Surprisingly, if one introduces a more weakly binding ligand in addition to the six fluorine atoms, as in 2-fluoropyridine·WF_6, a capped trigonal prism is formed in which the nitrogen atom occupies the capping position.[18] This structure is also found in K_2NbF_7 and K_2TaF_7, but strong interionic interactions dominate in these structures.[19]

Experimental Procedure

$Cs^+MoF_7^-$: Powdered anhydrous CsF was treated with a fivefold excess of MoF_6 at 50–60 °C in a perfluoropoly(ethylene propylene) (FEP) reaction tube to give a colorless microcrystalline solid. Unreacted hexafluoride was sublimed off under

 © VCH Verlagsgesellschaft mbH, D-69451 Weinheim, 1994 0570-0833/94/0404-0462 $ 10.00+.25/0

vacuum. Cubic crystals of $Cs^+MoF_7^-$ were obtained from CH_3CN at -40 °C. Raman (solid): $\tilde{\nu}$[cm^{-1}] = 1020.5 (s), 976 (m), 915 (m), 841.5 (s), 682.5 (sst), 427.5 (s, br), 317.5 (s, br). ^{19}F NMR (CH_3CN): δ = 193.1. Correct Cs, Mo, F analyses. Here, and in all further cases, a single crystal was mounted with a special apparatus under nitrogen atmosphere on a CAD-4 diffractometer ($Mo_{K\alpha}$, graphite monochromator) and measured at -145 °C. Crystal structure: a = 102.8(2) pm, $Pa3$ (No. 205), $V = 1167.4(4) \times 10^6$ pm^3, 524 independent reflections with $F \geq 3\sigma(F)$, 29 parameters, R = 0.037, Rw = 0.037.

$Cs^+WF_7^-$ was prepared in analogy to $Cs^+MoF_7^-$. Raman (solid): $\tilde{\nu}$[cm^{-1}] = 984.5 (m), 712 (sst), 439 (s, br), 323 (s, br). ^{19}F NMR (CH_3CN): δ = 143.9. Correct Cs, W, F analyses. Crystal structure: a = 1056.5(4) pm, $Pa3$ (No. 205), $V = 1179(1) \times 10^6$ pm^3, 458 independent reflections with $F \geq 3\sigma(F)$, 29 parameters, R = 0.027, Rw = 0.022.

$NO_2^+MoF_7^- \cdot CH_3CN$: MoF_6 and NO_2F were allowed to react in a 1:1 stoichiometric ratio at -78 °C to yield a colorless crystalline solid. Colorless needle-shaped single crystals were obtained from CH_3CN. Raman (solid): $\tilde{\nu}$[cm^{-1}] = 1022, 686.5 (sst), 662 (ss), 630.5 (s), 514.5 (s), 422.5 (m), 335.5 (s). ^{19}F NMR (CH_3CN): δ = 269.67. Crystal structure $C2/c$: a = 2592.1(3), b = 521.6(2), c = 1420.4(2) pm, β = 116.79(5)°, $V = 1714.4 \times 10^6$ pm^3, 2112 independent reflections with $F \geq 3\sigma(F)$, 136 parameters, R = 0.025, Rw = 0.021.

$(CH_3)_4N^+MoF_7^-$: MoF_6 was condensed into a FEP tube containing a partially dissolved mixture of $(CH_3)_4N^+F^-$ [13] in acetonitrile. After the reaction mixture was allowed to warm to room temperature and the excess unreacted MoF_6 was removed by vacuum sublimation, colorless needle-shaped crystals were obtained by slowly cooling the solution to -18 °C. Raman (solid): $\tilde{\nu}$[cm^{-1}] = 949 (m), 753.5 (m), 679 (sst), 459.5 (s), 429.5 (s), 320 (s, br). ^{19}F NMR (CH_3CN): δ = 204.1. Correct C,H,N,Mo,F analyses. Crystal structure: a = 831.3(2), c = 704.8(2) pm, $P4/mmn$ (No. 129), $V = 487.1(3) \times 10^6$ pm^3, 524 independent reflections with $F \geq 3\sigma(F)$, 33 parameters, R = 0.049, Rw = 0.044.

$(CH_3)_4N^+WF_7^-$ was prepared in analogy to $(CH_3)_4N^+MoF_7^-$. Raman (solid): $\tilde{\nu}$[cm^{-1}] = 983.5(s), 948.5 (m), 753.5 (m), 707.5 (sst), 683.5 (s), 459.5 (s), 322 (s, br). ^{19}F NMR (CH_3CN): δ = 147.6. Correct C,H,N,W,F analyses. Crystal structure: a = 835.1(5), c = 703.6(5) pm, $V = 490.8(4) \times 10^6$ pm^3, $P4/nmm$ (No. 129).

$C_{11}H_{24}N^+MoF_7^-$: 1,1,3,3,5,5-hexamethylpiperidinium fluoride[14] was treated with a twofold excess of MoF_6 in acetonitrile at room temperature. Unreacted hexafluoride was sublimed off under vacuum. The colorless salt crystallized out at -40 °C. ^{19}F NMR (CH_3CN): δ = 272.05. Raman (solid): $\tilde{\nu}$ = 427.5 (s), 570 (m), 676.5 (sst), 785 (m), 902 (m), 964 (m), 1253.5 (s), 1294 (s), 1377.8 (s), 1466 (s). Correct C,H,N,Mo,F analyses. Crystal structure: a = 764.5(3), b = 878.4(2), c = 1234.1(3) pm, α = 89.47(2), β = 75.27(2), γ = 79.83(2)°, $V = 791.0(4) \times 10^6$ pm^3, $P\bar{1}$, 2552 independent reflections with $F \geq 3\sigma(F)$, 253 parameters, R = 0.044, Rw = 0.034.

$Cs^+ReOF_6^-$: $ReOF_5$ (obtained according to the reaction $2ReF_7 + SiO_2 \rightarrow 2ReOF_5 + SiF_4$) was allowed to react with CsF in a 1:1 stoichiometric ratio over 20 h in a FEP tube at 60 °C. Recrystallization from acetonitrile at -40 °C gave pale yellow, single crystals. $Cs^+ReOF_6^-$ also crystallized out of an acetonitrile solution of $Cs^+ReF_8^-$; traces of moisture account for the slow hydrolysis. Raman (solid): $\tilde{\nu}$[cm^{-1}] = 999.5 (m, ν_{ReO}), 697 (m), 683 (sst), 659 (m), 445 (m), 341.5 (s, br). ^{19}F NMR (CH_3CN): δ = 68.80 (d), -53 (st, J_{FF} = 68.4 Hz). Correct Cs,F analyses. Crystal structure: a = 797.1(1), b = 702.2(2), c = 1063.9(3) pm, β = 93.04(2)°, $V = 594.6(3) \times 10^6$ pm^3, $P2_1/c$, 2220 independent reflections with $F \geq 3\sigma(F)$, 82 parameters, R = 0.041, Rw = 0.038.

$NO_2^+ReOF_6^-$: ReF$_5$ was treated with a 2.5-fold excess of NO_2F at -78 °C to give a light yellow salt. After the excess NO_2F was removed under vacuum, the salt was dissolved in a minimal amount of CH_3CN. The solution was cooled to -40 °C, and slow hydrolysis produced single crystals. Raman (solid): $\tilde{\nu}$[cm^{-1}] = 1001 (m), 988 (s, ν_{ReO}), 702.5 (s), 688 (st), 659.5 (m), 644.5 (m), 450 (m), 419 (s), 342 (s, br). ^{19}F NMR (CH_3CN): δ = 68.44 (d), -53.35 (st, J_{FF} = 65.9 Hz). Crystal structure: a = 1210.8(1), b = 1007.9(1), c = 1045.9(1) pm, β = 115.56 (6)°, $V = 1152.7(3) \times 10^6$ pm^3, $P2_1/c$, 2220 independent reflections with $F \geq 3\sigma(F)$, 202 parameters, R = 0.035, Rw = 0.036. Further details of the crystal structure investigations may be obtained from the Fachinformationszentrum Karlsruhe, D-76344 Eggenstein-Leopoldshafen (FRG) on quoting the depository number CSD-57737.

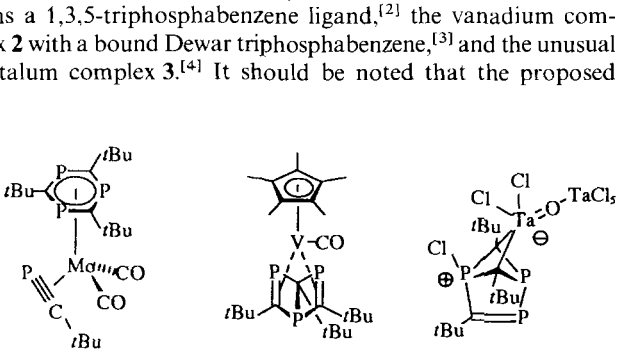
Received: September 1, 1993
Revised: October 8, 1993 [Z 6330 IE]
German version: *Angew. Chem.* **1994**, *106*, 473

[1] K. O. Christe, E. C. Curtis, D. A. Dixon, *J. Am. Chem. Soc.* **1993**, *115*, 1520–1526.
[2] T. Vogt, A. N. Futch, J. K. Cockcroft, *J. Solid State Chem.* **1993**, *103*, 275–279.
[3] A.-R. Mahjoub, T. Drews, H. Seppelt, *Angew. Chem.* **1992**, *104*, 1047–1050; *Angew. Chem. Int. Ed. Engl.* **1992**, *31*, 1036–1039.
[4] K. O. Christe, J. C. P. Sanders, G. J. Schrobilgen, W. W. Wilson, *J. Chem. Soc. Chem. Commun.* **1991**, 837–840.
[5] A.-R. Mahjoub, K. Seppelt, *J. Chem. Soc. Chem. Commun.* **1991**, 840–841.
[6] K. O. Christe, D. A. Dixon, A.-R. Mahjoub, H. P. A. Mercier, J. C. P. Sanders, K. Seppelt, G. J. Schrobilgen, W. W. Wilson, *J. Am. Chem. Soc.* **1993**, *115*, 2696–2706.
[7] D. L. Kepert, *Inorganic Stereochemistry* in *Inorganic Chemistry Concepts, Vol. 6*, Springer, Berlin, **1982**.
[8] A.-R. Mahjoub, K. Seppelt, *Angew. Chem.* **1991**, *103*, 844–845; *Angew. Chem. Int. Ed. Engl.* **1991**, *30*, 876–878.
[9] K. O. Christe, E. C. Curtis, D. A. Dixon, *J. Am. Chem. Soc.* **1993**, *115*, 1520–1526.
[10] E. J. Jacob, L. S. Bartell, *J. Chem. Phys.* **1970**, *53*, 2235–2242.
[11] S. Siegel, D. A. Northrop, *Inorg. Chem.* **1966**, *5*, 2187–2188.
[12] G. B. Hargreaves, R. D. Peacock, *J. Chem. Soc.* **1958**, 2170–2175; W. A. Sunder, A. L. Wayda, D. Distefano, W. E. Falconer, J. E. Griffiths, *J. Fluorine Chem.* **1979**, *14*, 299–325.
[13] The existence of $NO_2^+MoF_7^-$ has been suggested based on vibrational spectroscopy and analytical data: J. R. Geichman, E. A. Smith, P. R. Ogle, *Inorg. Chem.* **1963**, *2*, 1012–1015.
[14] The synthesis of solvent-free 1,1,3,3,5,5-hexamethylpiperidinium fluoride will be described elsewhere: H. Zhang, K. Seppelt, unpublished results.
[15] K. O. Christe, W. W. Wilson, R. D. Wilson, R. Bau, J. Feng, *J. Am. Chem. Soc.* **1990**, *112*, 7619–7625.
[16] L. Manojlovic-Muir, *J. Chem. Soc. Dalton Trans.* **1976**, 192–195.
[17] M. G. B. Drews, A. P. Wolters, *J. Chem. Soc. Chem. Commun.* **1972**, 457–458.
[18] L. Amaudet, R. Bougon, B. Buu, M. Lance, M. Nierlich, J. Vignier, *Inorg. Chem.* **1993**, *32*, 1142–1146.
[19] J. L. Hoard, *J. Am. Chem. Soc.* **1993**, *61*, 1252–1259; G. M. Brown, L. A. Walker, *Acta Crystallogr.* **1966**, *20*, 220–229. The same restrictions also hold for the structure of $(NH_4)_3ZrF_7$: G. C. Hampson, L. Pauling, *J. Am. Chem. Soc.* **1938**, *60*, 2707; H. J. Hurst, J. C. Taylor, *Acta Crystallogr. Sect. B* **1970**, *26*, 417–421, 2136–2137.

Novel Trimerization of Phosphaalkynes in the Coordination Sphere of Ruthenium Complexes**

Peter B. Hitchcock, Cameron Jones, and John F. Nixon*

Despite the current interest in the oligomerization of phosphaalkynes at transition metal centers,[1] only a few complexes possessing a coordinated trimeric phosphaalkyne unit have been reported. These include the molybdenum complex **1**, which contains a 1,3,5-triphosphabenzene ligand,[2] the vanadium complex **2** with a bound Dewar triphosphabenzene,[3] and the unusual tantalum complex **3**.[4] It should be noted that the proposed



1 **2** **3**

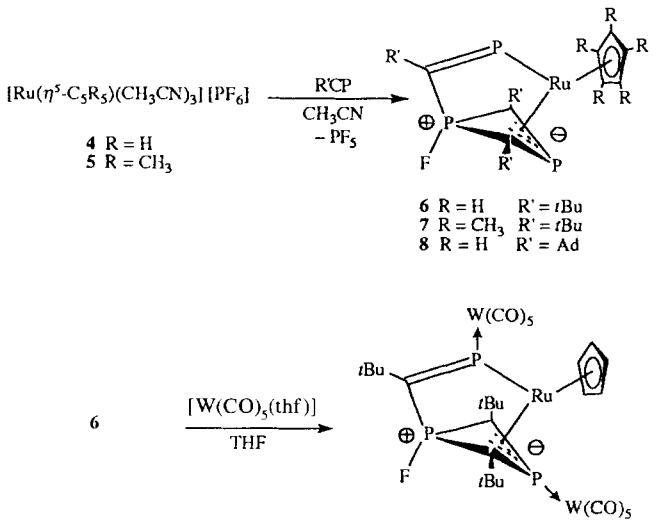
structure of **1** could not be confirmed by independent investigators and therefore must remain tentative. Herein we report a new structural type for trimers of phosphaalkynes, which incorporates the first example of a 2-phosphaallyl fragment that can coordinate η^3 and η^1 to two different metal centers.

Treatment of the ionic ruthenium complexes **4** and **5**[5] with $R'C{\equiv}P$[6] [R' = *t*Bu or adamantyl (Ad)] afforded the neutral

[*] Prof. J. F. Nixon, Dr. P. B. Hitchcock, Dr. C. Jones
School of Chemistry and Molecular Sciences
University of Sussex
GB-Brighton, BN1 9QJ (UK)
Telefax: Int. code + (273)677196

[**] We acknowledge financial support from the Science and Engineering Research Council (SERC).

yellow complexes **6**–**8** (Scheme 1) which were purified by recrystallization, or by sublimation (10^{-3} mbar) in the case of **6** and **7** (100 and 130 °C, respectively). At room temperature **6** readily reacts with two equivalents of $[W(CO)_5(thf)]$ yielding **9** as orange crystals.



Scheme 1. Synthesis of compounds **6**–**9**.

From the results of the X-ray crystal structure analysis[7] (Fig. 1), compound **6** can be formulated as possessing a metallophosphaalkene fragment (Ru-P3-C11) which is bound through a fluoro-substituted phosphonium center (P2) to a four-membered P_2C_2 ring. The positive charge on the phosphonium center is balanced by the negative charge delocalized over the atoms C1-P1-C2. This novel 2-phosphaallylic unit can be considered to act as a four-electron donor to the ruthenium(II) center.

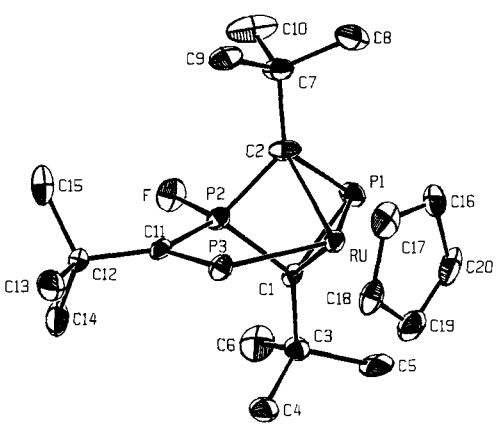


Fig. 1. Molecular structure (ORTEP, 50% thermal ellipsoids) of **6**. Important bond lengths [Å] and angles [°]: Ru-P1 2.323(2), Ru-P3 2.348(2), Ru-C1 2.170(8), Ru-C2 2.187(8), P2-F 1.601(5), P1-C1 1.816(9), P1-C2 1.811(8), P2-C2 1.758(9), P2-C11 1.716(8), P2-C1 1.753(8), P3-C11 1.692(8); P1-Ru-P3 125.0(1), C2-P1-C1 82.1(4), C2-P2-C1 85.5(4), Ru-P3-C11 104.4(3), P2-C1-P1 92.6(4), P2-C2-P1 92.6(4), P2-C11-P3 100.1(4).

Although **6** crystallizes with five independent molecules in the asymmetric unit, there are no significant geometric differences found between them. As a result of the allylic nature of the C1-P1-C2 unit, the four-membered ring is considerably bent, forming a dihedral angle of 25.7(7)° between the two PC_2 planes. This angle compares well with that between the corresponding planes in $[Mo(\eta^5\text{-}C_9H_7)(CO)_2(\eta^3\text{-}t\text{BuCPC}t\text{BuPFBF}_3)]$ (**10**),[8] the only other example of a complex containing a 2-phosphaallylic unit within a P_2C_2 ring. It is noteworthy that uncomplexed 2-phosphaallyl anions are unknown, however, a related 1-phosphaallyl anion was reported very recently.[9] The P3–C11 double bond length in **6** (1.692(8) Å) is close to those in related metallophosphaalkenes.[10] Both Ru–P bonds (Fig. 1) are slightly shorter than the mean Ru–P distance (2.44 Å) in the sandwich complex $[Ru(\eta^5\text{-}C_2t\text{Bu}_2P_3)_2]$.[11]

The solid-state molecular structure of **9**[7] (Fig. 2) retains the same structural features as that of **6**. A crystallographic mirror

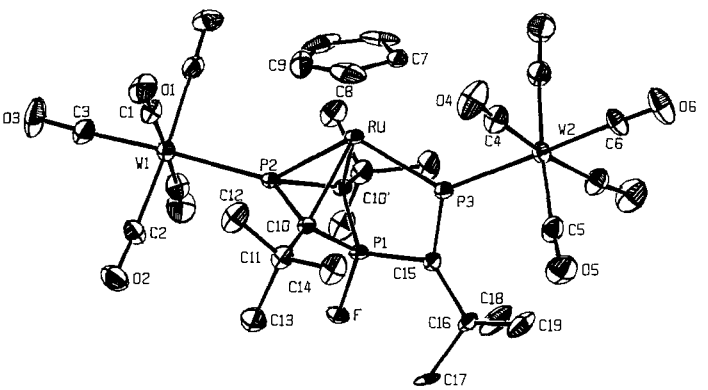


Fig. 2. Molecular structure (ORTEP, 20% thermal ellipsoids) of **9**. Important bond lengths [Å] and angles [°]: Ru-P2 2.310(1), Ru-P3 2.388(4), Ru-C10 2.20(1), W1-P2 2.502(2), W2-P3 2.587(1), F-P1 1.582(5), P1-C15 1.77(2), P1-C10 1.76(2), P2-C10 1.81(2), P3-C15 1.70(1); P2-Ru-P3 123.1(1), P2-Ru-C10 47.3(3), C10-P1-C10' 87(1), C10-P2-C10' 84.0(8), Ru-P3-C15 105.7(8), P2-C10-P1 90.5(4).

plane containing all three phosphorus atoms bisects the molecule. The P3–W2 distance (2.587(1) Å) is significantly longer than the P2–W1 distance (2.502(2) Å), and lies close to the P–W distance known for $[W(CO)_5]$ fragments η^2-bonded to P=C double bonds.[12] The lengthening of the P3–W2 bond probably results from the steric constraints imposed by the proximity of the *t*Bu group at C10′ and the cyclopentadienyl ring.

The results of NMR spectroscopic studies of **6**–**8** are consistent with each having a similar structure in solution as **6** in the solid state. Three inequivalent phosphorus signals are observed in the ^{31}P NMR spectrum of **6** (Table 1). The signal of P3 lies at low field (δ = 559.3) in the region characteristic of metallophosphaalkenes.[10] Similarly, the signal for the P1 atom occurs, as expected, at high-field (δ = −72.6), in the chemical shift range known for η^3-1-phosphaallyls.[13] The multiplet centered at δ = − 50.4 (P2) is, however, upfield of usual monofluorophosphonium ion δ values.[14]

The ^{31}P and ^{19}F NMR spectra provide supporting evidence for the proposed charge-separated structure of **6**. Surprisingly, the $^1J(P,F)$ coupling (1250 Hz) is considerably greater than the expected value (900–1000 Hz) for ions of the type $(R_3PF)^+$ (R = alkyl, aryl).[14] However, the high value in **6** can be explained by the proximity of the electron-withdrawing allylic group to the phosphonium center. Indeed, this coupling constant is nearer to that normally found for halogeno-substituted phosphonium ions (e.g. $[Cl_3PF]^+$ $^1J(P,F)$ = 1296 Hz).[14] Also, the eight line pattern in the ^{19}F NMR spectrum is centered at δ = 0.4, downfield from that normally seen for $[R_3PF]^+$ but close to the region of its halo-analogues (e.g. $[Cl_3PF]^+$ δ = 8.8).[14]

Several changes are seen in the ^{31}P NMR spectral pattern when **6** is complexed to two $[W(CO)_5]$ fragments to yield complex **9**. Significant differences occur in the chemical shifts of all three phosphorus centers, most notably a 115 ppm upfield shift for the metallophosphaalkene phosphorus atom (P3). In addi-

Table 1. Selected physical data for compounds **6**–**9** [a]

6: ^{1}H NMR: $\delta = 0.68$ (s, 18H, *t*Bu), 1.36 (s, 9H, *t*Bu), 5.29 (s, 5H, C_5H_5); ^{31}P NMR: $\delta = -72.6$ (pseudo-t, ^2J(P,P) = 6 Hz, ^3J(P,F) = 6 Hz, P1), −50.4 (ddd, ^1J(P,F) = 1250 Hz, ^2J(P,P) = 43, 6 Hz, P2), 559.3 (dd, ^2J(P,P) = 43 Hz, ^3J(P,F) = 37 Hz, P3); ^{19}F NMR: $\delta = 0.4$ (ddd, PF); MS (70 eV) *m/z* (%): 486 (28) [M^+], 471 (9) [$M^+ - CH_3$], 429 (60) [$M^+ - t$Bu], 167 (16) [$C_5H_5Ru^+$], 57 (100) [*t*Bu].

7: ^{1}H NMR: $\delta = 0.63$ (s, 18H, *t*Bu), 1.36 (s, 9H, *t*Bu), 1.92 (s, 15H, CH_3); ^{31}P NMR: $\delta = 52.1$ (ddd, ^1J(P,F) = 1238 Hz, ^2J(P,P) 46, 7 Hz, P2), −49.9 (pseudo-t, ^2J(P,P) = 7 Hz, ^3J(P,F) = 6 Hz, P1), 597.0 (dd, ^2J(P,P) = 46 Hz, ^3J(P,F) = 34 Hz, P3); ^{19}F NMR: $\delta = 0.7$ (ddd, PF).

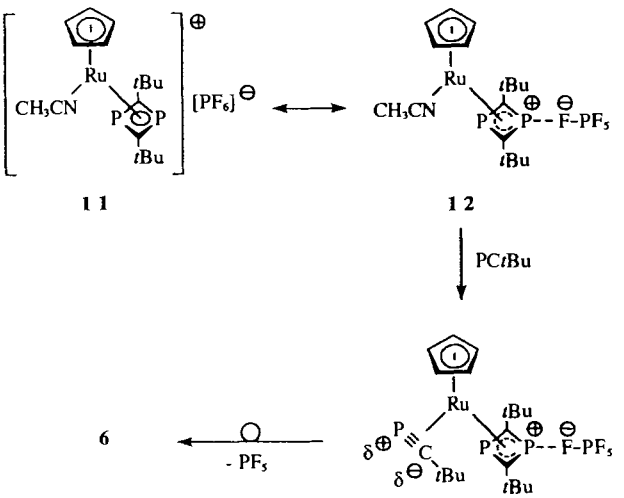
8: ^{1}H NMR: $\delta = 0.9$–2.4 (m, 45H, Ad), 5.11 (s, 5H, C_5H_5); ^{31}P NMR: $\delta = -76.4$ (dd, ^2J(P,P) = 6 Hz, ^3J(P,F) = 8 Hz, P1), −49.7 (ddd, ^1J(P,F) = 1251 Hz, ^2J(P,P) = 42, 6 Hz, P2), 567.2 (dd, ^2J(P,P) = 42 Hz, ^3J(P,F) = 40 Hz, P3); ^{19}F NMR: $\delta = 4.8$ (ddd, PF).

9: ^{1}H NMR: $\delta = 0.95$ (s, 18H, *t*Bu), 1.50 (s, 9H, *t*Bu), 5.47 (s, 5H, C_5H_5); ^{31}P NMR: $\delta = -39.9$ (ddd, ^2J(P,P) = 5, 14 Hz, ^3J(P,F) = 8 Hz, ^1J(P,W) = 248 Hz, P2), −15.4 (ddd, ^1J(P,F) = 1242 Hz, ^2J(P,P) = 122, 5 Hz, P1), 445.6 (ddd, ^2J(P,P) = 122, 14 Hz, ^3J(P,F) = 22 Hz, ^1J(P,W) = 195 Hz, P3); ^{19}F NMR: $\delta = -15.7$ (ddd, PF); IR(nujol): $\tilde{\nu} = 2078$, 2066, 1952, 1915 cm^{-1} (CO).

[a] ^{1}H (250 MHz, TMS), ^{31}P (101.3 MHz, 85% H_3PO_4) and ^{19}F NMR spectra (75.4 MHz, $CFCl_3$) in $CDCl_3$. The numbering of the atoms corresponds to that in Fig 1 for **6**–**8** and to that in Fig. 2 for **9**.

tion, the P3 center displays a ^2J(P,P) coupling to the allylic phosphorus atom of 14 Hz, whereas the same coupling was not detected in **6**. Both ^1J(W,P) couplings in **9** are unexceptional.

At present we have little evidence to propose a mechanism of formation of **6**. However, it seems likely[15] that in the initial stages of the reaction two molecules of acetonitrile are displaced from **4** followed by a head-to-tail coupling of the coordinated phosphaalkyne molecules to give the cationic η^4-diphosphacyclobutadiene complex **11** (Scheme 2). It is conceivable that a



Scheme 2. Proposed mechanism for the formation of **6**.

shift in the positive charge from the metal center to one phosphorus atom in the C_2P_2 ring would give rise to **12**, which can be considered as containing a phosphenium ion in contact with a $[PF_6]^-$ ion. Precedent for this structure lies with the recently crystallographically characterized complex **10**.[8] Displacement of the remaining acetonitrile ligand from **12** could then promote an attack on the electrophilic phosphenium center by the nucleophilic phosphaalkyne carbon atom, subsequently yielding **6** by abstraction of F^- from the $[PF_6]^-$ ion.

Experimental Procedure

6: To a solution of **4** (0.26 g, 0.6 mmol) in acetonitrile (25 mL) at 0 °C was added *tert*-butylphosphaacetylene (0.5 g, 5 mmol). After 10 h at 20 °C the yellow solution was concentrated under vacuum (10^{-3} mbar) to about 6 mL. Cooling to −30 °C overnight yielded **6** as yellow crystals. Yield: 0.14 g (48%); m.p. 95 °C. Compounds **7** and **8** were prepared by similar procedures; **7**: M.p. 126 °C; **8**: M.p. 143 °C.

9: To a solution of [W(CO)$_5$(thf)] (0.28 g, 0.7 mmol) in THF (50 mL) was added **6** (0.10 g, 0.2 mmol) in THF (8 mL). After 10 h volatiles were removed under vacuum 25 °C/10^{-3} mbar and the brown residue was eluted on a silica gel column (hexane). Concentration of the yellow band under vacuum 25 °C/10^{-3} mbar to about 10 mL gave orange crystals of **9** overnight at −30 °C. Yield: 0.17 g (74%); m.p. 168 °C (decomp).

Received: September 6, 1993 [Z 6342 IE]
German version: *Angew. Chem.* **1994**, *106*, 478

[1] J. F. Nixon, *Chem. Rev.* **1988**, *88*, 1327.
[2] A. R. Barron, A. H. Cowley, *Angew. Chem.* **1987**, *99*, 956; *Angew. Chem. Int. Ed. Engl.* **1987**, *26*, 907.
[3] R. Milczarek, W. Rüsseler, P. Binger, K. Jonas, K. Angermund, C. Krüger, M. Regitz, *Angew. Chem.* **1987**, *99*, 957; *Angew. Chem. Int. Ed. Engl.* **1987**, *26*, 908.
[4] G. Becker, W. Becker, R. Knebl, H. Schmidt, M. Mildenbrand, M. Westerhausen, *Phosphorus Sulfur Relat. Elem.* **1987**, *30*, 349.
[5] T. P. Gill, K. R. Mann, *Organometallics* **1982**, *1*, 485.
[6] G. Becker, H. Schmidt, G. Uhl, W. Uhl, *Inorg. Synth.* **1990**, *27*, 249.
[7] a) Crystal structure analysis of **6** at 173 K: $C_{20}H_{32}FP_3Ru$, space group $P\bar{1}$, $a = 9.473(2)$, $b = 16.176(2)$, $c = 37.32(1)$ Å, $\alpha = 78.41(2)$, $\beta = 89.32(2)$, $\gamma = 87.41(2)°$, $Z = 10$, $\varrho_{calcd} = 1.44$ g cm^{-3}, $\mu(Mo_{K\alpha}) = 9.08$ cm^{-1}, CAD4: 10413 measured reflections, 8489 observed ($I > 2\sigma(I)$), $R = 0.037$, $R_w = 0.043$, ($w = 1/\sigma^2(F_0)$) for 451 parameters; b) crystal structure analysis of **9** at 293 K: $C_{30}H_{32}FO_{10}P_3RuW_2$, space group $C2/m$, $a = 16.894(5)$, $b = 13.855(3)$, $c = 17.691(4)$ Å, $\beta = 115.86(2)°$, $Z = 4$, $\varrho_{calcd} = 2.02$ g cm^{-3}, $\mu(Mo_{K\alpha}) = 68.7$ cm^{-1}, CAD4; 3409 measured reflections, 2403 observed ($I > 2\sigma(I)$) $R = 0.037$, $R_w = 0.044$ ($w = 1/\sigma^2(F_0)$) for 247 parameters; c) Further details of the crystal structure investigations are available on request from the Director of the Cambridge Crystallographic Data Centre, 12 Union Road, GB-Cambridge CB2 1EZ (UK), on quoting the full journal citation.
[8] P. B. Hitchcock, M. J. Maah, J. F. Nixon, M. Green, *J. Organomet. Chem.* **1993**, in press.
[9] E. Niecke, M. Nieger, P. Wenderoth, *J. Am. Chem. Soc.* **1993**, *115*, 6989.
[10] a) D. Gudat, E. Niecke, W. Malisch, U. Hofmockel, S. Quashie, A. H. Cowley, A. M. Arif, B. Krebs, M. Dartmann, *J. Chem. Soc. Chem. Commun.* **1985**, 1687; b) P. Binger, J. Haas, A. T. Herrmann, F. Langhauser, C. Krüger, *Angew. Chem.* **1991**, *103*, 316; *Angew. Chem. Int. Ed. Engl.* **1991**, *30*, 310.
[11] R. M. Matos, D. Phil Thesis, University of Sussex, **1993**.
[12] S. Holand, C. Charrier, F. Mathey, J. Fischer, A. Mitschieler, *J. Am. Chem. Soc.* **1984**, *106*, 826.
[13] F. Mercier, J. Fischer, F. Mathey, *Angew. Chem.* **1986**, *98*, 347; *Angew. Chem. Int. Ed. Engl.* **1986**, *25*, 357.
[14] a) V. F. Seel, H. J. Bassler, *Z. Anorg. Allg. Chem.* **1975**, *418*, 263; b) R. Bartsch, O. Stelzer, R. Schmutzler, *Z. Naturforsch. B* **1981**, *36*, 1349.
[15] a) P. B. Hitchcock, M. J. Maah, J. F. Nixon, *J. Chem. Soc. Chem. Commun.* **1986**, 737; b) P. Binger, B. Biedenbach, R. Mynott, P. Betz, C. Krüger, *J. Chem. Soc. Dalton Trans.* **1990**, 1771.

2*H*,5*H*-Benzo[1,2-*b*:4,5-*b'*]bisthiete—A Highly Reactive Bisdiene System**

Herbert Meier* and Axel Mayer

Rigid molecules with two or more 1,3-diene units are of particular interest for the construction of molecular band- and starlike structures by repetitive cycloadditions.[1] The selection of suitable compounds for these reactions, however, is small and is limited still further because of unsatisfactory yields of the pure compounds or because of their low reactivity.

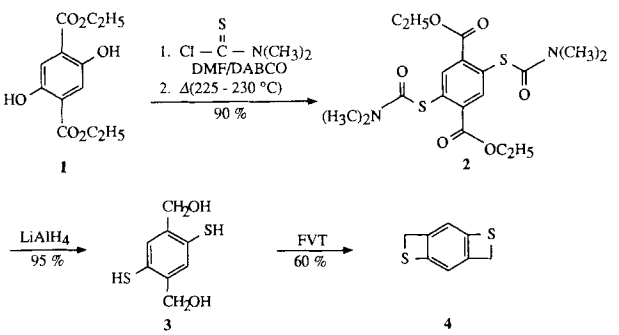
Encouraged by the high reactivity of 2*H*-benzo[*b*]thiete towards a large number of dienophiles and heterodienophiles,[2] we

[*] Prof. Dr. H. Meier, Dipl.-Chem. A. Mayer
Institut für Organische Chemie der Universität
J.-J.-Becher-Weg 18–22, D-55099 Mainz (FRG)
Telefax: Int. code + (6131)395396

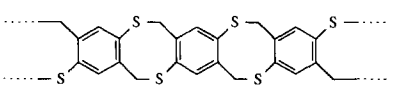
[**] This work was supported by the Deutsche Forschungsgemeinschaft and the Fonds der Chemischen Industrie.

set about the synthesis of 2*H*,5*H*-benzo[1,2-*b*:4,5-*b*']bisthiete(4,9-dithiatricyclo[6.2.0.0^{3,6}]deca-1,3(6),7-triene) (**4**).

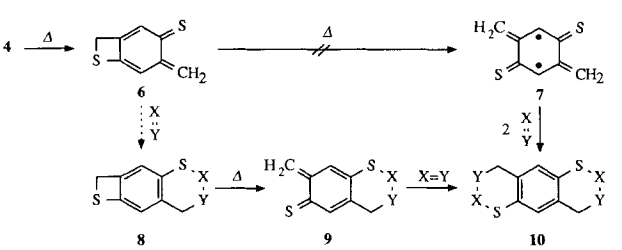
Diethyl 2,5-dihydroxyterephthalate (**1**) was treated with *N*,*N*-dimethylthiocarbamoyl chloride in the presence of DMF/DABCO at room temperature.[3,4] The resulting double *O*-thiocarbamate was formed in quantitative yield and rearranges by way of a Newman–Kwart reaction[5] into the double *S*-thiocarbamate **2** on heating in diphenyl ether. The reduction of **2** with $LiAlH_4$ affects all four functional groups, and 2,5-dimercapto-1,4-phenylenedimethanol (**3**) is obtained in 95% yield. The desired compound **4** is obtained from this by flash vacuum thermolysis (FVT);[6] **4** is a colorless solid that decomposes above 160 °C with deflagration.[7]



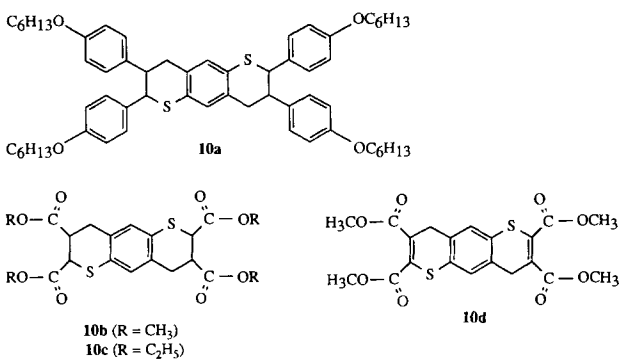
The four-membered ring of the 2*H*-benzo[*b*]thiete can be readily opened thermally or photochemically. This leads to a highly reactive 8π-electron system. In the absence of reaction partners the thermal reaction results in a dimerization ([8π + 8π] cycloaddition) to give 6*H*,12*H*-dibenzo[*b*,*f*][1,5]dithiocin.[2] Under these circumstances a polymer is formed from **4** which has the band structure **5**. Disulfide bridges can be excluded. The IR spectrum (in KBr) reveals a saturation of the chain ends by the trace amounts of water present. Small quantities of higher cyclooligomers can also form from benzo[*b*]thiete[2]—a variant which will be investigated for **4** in more detail.



With 2π components X=Y compound **4** undergoes the reaction sequence **4** → **6** → **8** → **9** → **10** which is composed of alternating ring-openings and [8π + 2π] cycloadditions. A double ring opening **4** → **6** → **7** can be excluded for the thermal reaction (toluene, 90 °C). (However, the high-energy diradical **7** or the corresponding bicycle 3,6-dimethylenebicyclo[2.2.0]hexane-2,5-dithione might be realizable by photochemical ring-opening with intensive laser light).



Even fairly unreactive components X=Y such as (*E*)-stilbenes add smoothly to **6** and **9**. The 2:1 adduct **10a**[8] is formed from **4** and (*E*)-1,2-bis(4-hexyloxyphenyl)ethene in 40% yield. Similar reactions of **4** with dimethyl fumarate and diethyl maleate lead to **10b**[9] (≥ 90%) and **10c**[10] (68%), respectively. The investigation of the stereochemistry of **10a–c** always reveals a *trans* position of the substituents on the thiopyran rings; that is, cycloadducts with *trans* configuration are formed from the (*E*)-configurated olefins as expected; however, from the (Z)-configurated dimaleate, the di-*trans* adduct with high stereoselectivity is formed in addition.[11] The stereogenic centers of **10a–c** do not show any observable interaction over the benzene ring, that is, the di-*trans* products are composed of 1:1 distributions of one chiral C_2 and one achiral C_i configuration each.[12]



The 2:1 adduct **10d**[13] (68%) is isolated with dimethyl acetylenedicarboxylate. Furthermore, the crude product of this reaction contains cycloadducts, whose compositions correspond to alkyne:benzobisthiete ratios of 2:2, 2:3, and 3:3, which confirms the construction of band structures.

Moreover, as a result of the extremely high reactivity of benzothiete with almost all double bond systems (C=C, C=N, C=O, N=N, N=O, etc.),[2] the bisthiete **4** is of interest for thermal and photochemical cross-linking of polymers.

The carbocyclic system analogous to **4**, tricyclo[6.2.0.0^{3,6}]deca-1,3(6),7-triene, synthesized for the first time by Cava et al.,[14] has a very much higher activation energy for opening the four-membered ring and is hardly suitable for repetitive cycloadditions. From the pyrolysis under optimized conditions[15] it forms "belt structures", whose occurrence has so far not been confirmed for **4**.

Received: September 6, 1993 [Z 6340 IE]
German version: *Angew. Chem.* **1994**, *106*, 493

[1] A.-D. Schlüter, *Nachr. Chem. Techn. Lab.* **1990**, *38*, 8, and references therein.; F. H. Kohnke, J. P. Mathias, J. F. Stoddart, *Angew. Chem. Adv. Mater.* **1989**, *101*, 1129; *Angew. Chem. Int. Ed. Engl. Adv. Mater.* **1989**, *28*, 1103, and references therein.

[2] H. Meier, K. Saul, D. Jacob, *Liebigs Ann. Chem.* **1993**, 313; K. Saul, H.-L. Eckes, D. Jacob, H. Meier, *Chem. Ber.* **1993**, *126*, 775; H. Meier, K. Saul, R. Mengel, H.-P. Niedermann, *J. Heterocycl. Chem.* **1991**, *28*, 843; M. Schmidt, H. Meier, S. A. Saleh, *ibid.* **1991**, *28*, 573; M. Schmidt, H. Meier, H.-P. Niedermann, R. Mengel, *Chem. Ber.* **1990**, *123*, 1143 and references therein.

[3] H.-J. Kurth, U. Kraatz, F. Korte, *Chem. Ber.* **1973**, *106*, 2419.

[4] L. Field, P. R. Engelhardt, *J. Org. Chem.* **1970**, *35*, 3647.

[5] M. S. Newman, H. A. Karnes, *J. Org. Chem.* **1966**, *31*, 3980; H. Kwart, E. R. Evans, *ibid.* **1966**, *31*, 410; see also A. Schönberg, L. von Vargha, *Ber. Dtsch. Chem. Ges.* **1930**, *63*, 178.

[6] 750 °C/10^{-3} Torr. At the end of the pyrolysis zone small quantities of **5** may form when the route to the cold trap is not heated.

[7] **4**: ^{1}H NMR (400 MHz, $CDCl_3$): δ = 4.22 (s, 4H, CH_2), 6.57 (s, 2H, aryl-H); ^{13}C NMR (100 MHz, $CDCl_3$): δ = 36.1 (CH_2), 116.6 (CH), 137.0/138.6 (C_q).

[8] **10a**: M.p. 121 °C; ^{1}H NMR (400 MHz, $CDCl_3$): δ = 0.91 (t, 12H, CH_3), 1.30 (m, 24H, CH_2), 1.72 (m, 8H, CH_2), 2.97 (m, 2H, 4-H, 9-H), 3.11 (m, 2H, 4-H,

 © VCH Verlagsgesellschaft mbH, D-69451 Weinheim, 1994 0570-0833/94/0404-0466 $ 10.00+.25/0

9-H), 3.22 (m, 2H, 3-H, 8-H), 3.84 (t, 8H, OCH_2), 4.46 (d, ^3J = 9.9 Hz, 2H, 2-H, 7-H), 6.68 (m, 8H, aryl-H), 6.91 (m, 4H, aryl-H), 6.93 (s, 2H, 5-H, 10-H), 7.08 (m, 4H, aryl-H); ^{13}C NMR (100 MHz, $CDCl_3$), δ = 14.0 (CH_3), 22.6/25.7/29.2/31.6 (CH_2), 39.0 (C-4, C-9), 47.0 (C-3, C-8), 52.0 (C-2, C-7), 67.9 (OCH_2), 114.2/114.4/125.9/128.4/129.4/(aryl-CH), 130.3/132.3/133.8/135.0/157.7/158.2 (C_q). Several signals are doubled, which confirms the formation of diastereoisomers.

[9] **10b**: M.p. 137 °C; ^1H NMR (400 MHz, $CDCl_3$): δ = 2.81 (m, 2H, 4-H, 9-H), 3.05 (m, 2H, 4-H, 9-H), 3.20 (m, 2H, 3-H, 8-H), 3.72 (4s, 12H, OCH_3), 4.316 (d, ^3J = 8.35 Hz, 2H, 2-H, 7-H)/4.318 (d, ^3J = 8.37 Hz, 2H, 2-H, 7-H), 6.98 (s, 2H, 5-H, 10-H)/6.99 (s, 2H, 5-H, 10-H); ^{13}C NMR (100 MHz, $CDCl_3$): δ = 31.69 (C-4, C-9)/31.74 (C-4, C-9), 42.4 (C-3, C-8)/42.5 (C-3, C-8), 43.6 (C-2, C-7)/43.7 (C-2, C-7), 52.5/52.9 (OCH_3), 127.2 (aryl-CH), 128.8/128.8/133.7/134.0 (C_q), 171.2/171.3/172.8/172.8 (CO).

[10] **10c**: M.p. 94 °C; ^1H NMR (400 MHz, $CDCl_3$): δ = 1.23 (m, 12H, CH_3), 2.81 (m, 2H, 4-H, 9-H), 3.04 (m, 2H, 4-H, 9-H), 3.15 (m, 2H, 3-H, 8-H), 4.10 (m, 8H, OCH_2), 4.29 (d, ^3J = 8.4 Hz, 2H, 2-H, 7-H), 6.98 (s, 2H, 5-H, 10-H); ^{13}C NMR (100 MHz, $CDCl_3$): δ = 14.0 (CH_3), 31.8 (C-4, C-9), 42.5 (C-3, C-8), 43.9 (C-2, C-7), 61.4/61.9 (OCH_2), 127.1 (aryl-CH), 128.8/133.9 (C_q), 172.4/172.4 (CO). Several signals are doubled.

[11] Cf. dazu H. Meier, H.-L. Eckes, H.-P. Niedermann, H. Kolshorn, *Angew. Chem.* **1987**, *99*, 1040; *Angew. Chem. Int. Ed. Engl.* **1987**, *26*, 1046.

[12] These symmetries require a rapid inversion of the thiopyran rings, as observed at room temperature in the NMR spectra.

[13] **10d**: M.p. 179 °C; ^1H NMR (400 MHz, $CDCl_3$): δ = 3.62 (s, 4H, 4-H), 3.79 (s, 6H, OCH_3), 3.84 (s, 6H, OCH_3), 7.23 (s, 2H, 5-H, 10-H); ^{13}C NMR (100 MHz, $CDCl_3$): δ = 33.2 (C-4, C-9), 52.7/53.2 (OCH_3), 125.9 (C-5, C-10), 127.5/130.5/131.7/131.7 (C-2, C-3, C-4a, C-5a, C-7, C-8, C-9a, C-10a), 164.8/165.0 (CO).

[14] M. P. Cava, A. A. Deana, K. Muth, *J. Am. Chem. Soc.* **1960**, *82*, 2524.

[15] H. C. Kang, A. W. Hanson, B. Eaton, V. Boekelheide, *J. Am. Chem. Soc.* **1985**, *107*, 1979.

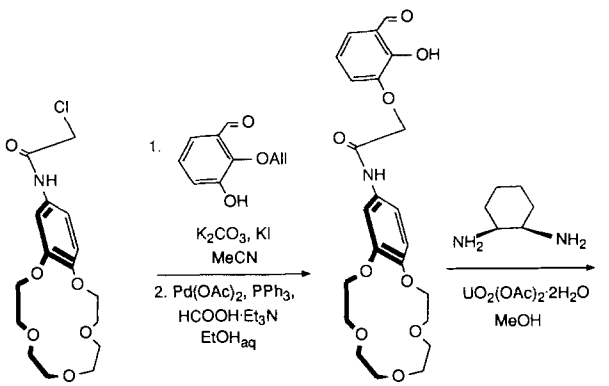
A Difunctional Receptor for the Simultaneous Complexation of Anions and Cations; Recognition of KH_2PO_4

Dmitry M. Rudkevich, Zbigniew Brzozka, Marcin Palys, Herman C. Visser, Willem Verboom, and David N. Reinhoudt*

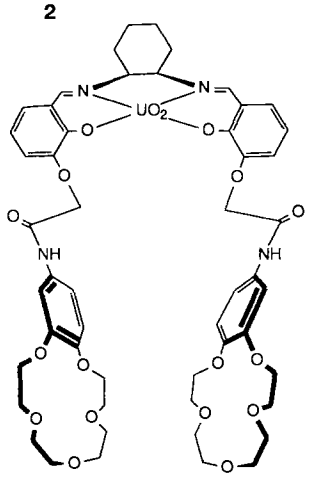
The design and synthesis of neutral macrocyclic receptors that selectively complex cations in apolar solvents rests on their ability to arrange their nucleophilic binding sites (Lewis-basic oxygen atoms of crown ethers etc.) in an array complementary to the cation.[1] Similarly macrocyclic and acyclic ligands that contain Lewis-acidic binding sites like boron, silicon, tin, and mercury centers complex anions, but the selectivity is not simply introduced.[2] Recently Reetz et al.[3] reported on a heterotopic receptor which, in addition to a crown ether moiety for complexation of K^+ ions, contains a σ-bonded Lewis-acidic boron center that is able to form a tetracoordinated adduct with anions and binds F^- ions selectively.

Recently we showed that neutral metalloclefts and metallomacrocycles containing both immobilized Lewis-acidic UO_2^+ centers and amido units as additional binding sites are excellent receptors for anions with a high selectivity for dihydrogen phosphate $H_2PO_4^-$.[4] We now describe the synthesis and complexation properties of a difunctional neutral receptor which contains binding sites for both *cations* and *anions* is therefore able to complex both species simultaneously in apolar solvents.[5]

The synthesis of the difunctional receptor **3** is summarized in Scheme 1. Reaction of (4-aminobenzo)[15]crown-5[6] with chloroacetyl chloride and K_2CO_3 in EtOAc/H_2O gave the corresponding [4-(chloroacetamido)benzo][15]crown-5 (**1**) in 85% yield. Aldehyde **2** was obtained by alkylation of 2-(2-allyloxy)-3-hydroxybenzaldehyde[7] with **1**, followed by palladium-catalyzed deallylation in 69% overall yield. Subsequent reaction of **2** with *cis*-1,2-diaminocyclohexane and $UO_2(OAc)_2 \cdot 2H_2O$ afforded the difunctional receptor **3** in 76% yield.



1 **2**



3

Scheme 1. All = allyl.

The complexation of the difunctional receptor **3** with cations and with anions was investigated by ^1H NMR spectroscopy, cyclic voltammetry, fast atom bombardment mass spectrometry (FAB-MS), and liquid–liquid extraction experiments. We first studied the complexation of tetrabutylammonium dihydrogen phosphate and potassium picrate, because UO_2-containing clefts complex $H_2PO_4^-$ [4] and bis(benzo[15]crown-5) ethers bind K^+ with a high degree of selectivity.[8]

In dilution experiments[9] with solutions of **3** and $Bu_4N^+H_2PO_4^-$ in [D_6]DMSO the ^1H NMR signals of the HC=N groups of both the free and complexed ligand were observed at δ = 9.51 and 9.46, respectively. From this experiment an association constant K_{ass} of $1.1 \times 10^3\ M^{-1}$ was calculated. The contribution of the C(O)NH $\cdots$ $H_2PO_4^-$ hydrogen bond to the overall anion complexation can clearly be observed in the

[*] Prof. Dr. Ir. D. N. Reinhoudt, Dr. Ir. D. M. Rudkevich, Dr. Ir. Z. Brzozka,[+] Dr. M. Palys,[++] Dr. H. C. Visser, Dr. W. Verboom
Laboratory of Organic Chemistry, University of Twente
P. O. Box 217, NL-7500 AE Enschede (The Netherlands)
Telefax: Int. code + (53)356024

[+] Permanent address:
Department of Analytical Chemistry,
Technical University of Warsaw (Poland)

[++] Permanent address:
Department of Chemistry, University of Warsaw (Poland)

 © VCH Verlagsgesellschaft mbH, D-69451 Weinheim, 1994 0570-0833/94/0404-0467 $ 10.00+.25/0

^{1}H NMR spectrum even in [D$_6$]DMSO as a solvent, since the N–H signals of the free and complexed **3** appear at $\delta = 10.47$ and 11.21, respectively.

Complexation of K^+ ions by receptor **3** was studied by picrate (Pic) extraction[8] experiments. For the 1:1 complex **3** · K^+Pic^- a value of lg $K_{ex} = 5.3$ was obtained in chloroform.[10]

The complexation of K^+ and $H_2PO_4^-$ ions by **3** was also investigated by cyclic voltammetry in DMSO with 2% H_2O and with tetrabutylammonium tetraphenylborate as a supporting electrolyte. Addition of Bu_4N^+ $H_2PO_4^-$ to a solution of **3** causes a clear shift of both cathodic and anodic peaks toward more negative potentials. This effect is accompanied by a systematic increase in the peak separation, from 85 to 100 mV, and by a decrease of the normalized peak heights. These results suggest that a labile, redox-inactive complex is formed with $H_2PO_4^-$. Assuming the formation of a 1:1 complex, a K_{ass} value of 1.3×10^3 M^{-1} for $H_2PO_4^-$ is obtained, which is in a good agreement with the ^{1}H NMR measurements.

Upon addition of potassium tetraphenylborate to a solution of receptor **3** in DMSO the electrochemical behavior did not change, probably since the crown ether moieties in **3** are situated rather far from the redox-active UO_2 center. However, an indirect procedure for the determination of complexation constants[11] based on competition between Tl^+ and K^+ ions gave a K_{ass} value of 1.0×10^2 M^{-1} for K^+.

Finally, we used FAB-MS, an established technique for investigation of complexes in which cations[12] and anions are bound noncovalently.[4, 13] In the FAB$^+$ mass spectrum (*m*-nitrobenzyl alcohol as matrix) of the 1:1 complex[14] of receptor **3** and KH_2PO_4, prepared by mixing the host and guest in acetonitrile with 10% water and evaporating the solvent, an intense peak corresponding to $[\mathbf{3} + K^+]^+$ was observed. The corresponding FAB$^-$ mass spectrum of the same sample yielded an intense peak for $[\mathbf{3} + H_2PO_4^-]^-$, while a signal for $[\mathbf{3} + H_2PO_4^- + K^+]^-$ is also present, which clearly proves the complexation of the salt.

Previously in our laboratory cation carrier assisted transport of *lipophilic* potassium salts was studied.[15] Now preliminary investigations have shown a significant transport of KH_2PO_4 as a *hydrophilic* potassium salt through a supported liquid membrane with receptor **3**.

In conclusion, we have demonstrated that the combination of binding sites for both cations and anions in a neutral receptor molecule leads to hosts with unique, multifunctional complexation behavior.

Experimental Procedure

A solution of aldehyde **2** (1.3 mmol) and *cis*-1,2-cyclohexanediamine [16] (0.65 mmol) in MeOH (100 mL) was refluxed for 1 h. Subsequently a solution of $UO_2(OAc)_2 \cdot 2H_2O$ (0.65 mmol) in MeOH (10 mL) was added and refluxing was continued for 1 h. After cooling, the precipitate that formed was filtered off and washed with MeOH (2 × 10 mL) to give **3** as a red solid in 76% yield. M.p. 185–187 °C; IR (KBr) $\tilde{\nu} = 1685$, 1617, 904 cm^{-1}; ^{1}H NMR ([D$_6$]DMSO): $\delta = 10.47$ (s, 2H, NH), 9.51 (s, 2H, HC=N), 7.47, 7.31 (2 d, $^3J_{HH} = 7.8$ Hz, 4H, arom.), 7.20–6.70 (m, 8H, arom.), 4.95 (s, 4H, $CH_2C(O)$), 4.75–4.65 (m, 2H, cyclohexylene), 4.70–4.00 (m, 32H, OCH_2), 2.40–1.70 (m, 8H, cyclohexylene); ^{13}C NMR ([D$_6$]DMSO): $\delta = 167.8$ (d, HC=N), 167.3 (s, C=O), 159.7, 149.5, 148.4, 144.7, 132.1 (5 s, arom.), 128.6 (d, arom.), 124.5 (s, arom.), 122.0, 116.2, 114.0, 112.0, 106.3 (5 d, arom.), 71.0 (t, $CH_2C(O)$), 70.5 (d, cyclohexylene), 69.8, 69.6, 68.7, 68.1 (4 t, OCH_2), 27.3, 21.5 (2 t, cyclohexylene); FAB-MS (NBA matrix): *m/z* 947.0 [(*M* + H)$^+$, calcd. 947.3]; correct C,H,N analysis.

Received: September 16, 1993 [Z 6361 IE]
German version: *Angew. Chem.* **1994**, *106*, 480

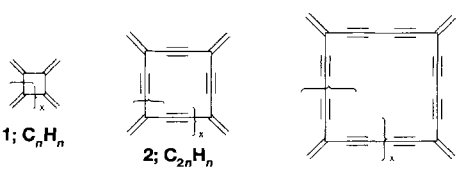
[1] a) D. J. Cram, *Angew. Chem.* **1988**, *100*, 1041; *Angew. Chem. Int. Ed. Engl.* **1988**, *27*, 1009; b) J.-M. Lehn, *ibid.* **1988**, *100*, 91 and **1988**, *27*, 89; c) C. J. Pedersen, *ibid.* **1988**, *100*, 1053 and **1988**, *27*, 1021.
[2] a) H. E. Katz, *J. Org. Chem.* **1989**, *54*, 2179; b) M. E. Jung, H. Xia, *Tetrahedron Lett.* **1988**, *29*, 297; c) M. T. Blanda, J. N. Horner, M. Newcomb, *J. Org. Chem.* **1989**, *54*, 4626; d) J. D. Wuest, B. Zacharie, *J. Am. Chem. Soc.* **1987**, *109*, 4714; e) X. Yang, C. B. Knobler, M. F. Hawthorne, *ibid.* **1992**, *114*, 380.
[3] M. T. Reetz, C. M. Niemeyer, K. Harms, *Angew. Chem.* **1991**, *103*, 1515; *Angew. Chem. Int. Ed. Engl.* **1991**, *30*, 1472.
[4] D. M. Rudkevich, W. P. R. V. Stauthamer, W. Verboom, J. F. J. Engbersen, S. Harkema, D. N. Reinhoudt, *J. Am. Chem. Soc.* **1992**, *114*, 9671.
[5] Recently, Lockhart et al. reported on a multifunctional receptor containing two crown ether units for cation complexation and polyamine linkers which after protonation are able to bind chloride anions: E. A. Arafa, K. I. Kinnear, J. C. Lockhart, *J. Chem. Soc. Chem. Commun.* **1992**, 61. Schmidtchen prepared a novel artificial polytopic receptor for binding zwitterionic ω-amino carboxylates: F. P. Schmidtchen, *J. Org. Chem.* **1986**, *51*, 5161.
[6] R. Ungaro, B. El Haj, J. Smid, *J. Am. Chem. Soc.* **1976**, *98*, 5198.
[7] C. J. van Staveren, J. van Eerden, F. C. J. M. van Veggel, S. Harkema, D. N. Reinhoudt, *J. Am. Chem. Soc.* **1988**, *110*, 4994.
[8] F. de Jong, D. N. Reinhoudt, *Stability and Reactivity of Crown-ether Complexes*, Academic Press, London, **1981**.
[9] The K_{ass} value was determined by integration of the individual signals of the imine and amide protons of both free ligand and complex upon dilution of a receptor solution (10^{-3}–10^{-2} M) with a stock solution of the free salt.
[10] Liquid–liquid extraction ($CHCl_3$/H_2O) of KH_2PO_4 with difunctional receptor **3** resulted in 15–20% complex formation (**3** · KH_2PO_4) in the organic phase (according to ^{1}H NMR spectroscopy). At the same time no extraction of KH_2PO_4 was observed with functionalized UO_2-containing clefts [4] that do not contain cationic binding sites.
[11] E. L. Yee, J. Tabib, M. J. Weaver, *J. Electroanal. Chem. Interfacial Electrochem.* **1979**, *96*, 241.
[12] a) R. A. W. Johnstone, I. A. S. Lewis, M. E. Rose, *Tetrahedron* **1983**, *39*, 1597; b) R. A. W. Johnstone, M. E. Rose, *J. Chem. Soc. Chem. Commun.* **1983**, 1268.
[13] a) S. S. Flack, J.-L. Chaumette, J. D. Kilburn, G. J. Langley, M. Webster, *J. Chem. Soc. Chem. Commun.* **1993**, 399; b) G. J. Langley, J. D. Kilburn, S. S. Flack, *Org. Mass Spectrom.* **1993**, *28*, 478.
[14] Selected ^{1}H NMR data for **3** · KH_2PO_4 in [D$_6$]DMSO: $\delta = 11.20$ (br. s, 2H, NH), 9.46 (s, 2H, HC=N), 5.35 (s, 4H, $CH_2C(O)$).
[15] a) T. B. Stolwijk, E. J. R. Sudhölter, D. N. Reinhoudt, *J. Am. Chem. Soc.* **1987**, *109*, 7042; b) M. M. Wienk, T. B. Stolwijk, E. J. R. Sudhölter, D. N. Reinhoudt, *ibid.* **1990**, *112*, 797; c) W. F. Nijenhuis, E. G. Buitenhuis, F. de Jong, E. J. R. Sudhölter, D. N. Reinhoudt, *ibid.* **1991**, *113*, 7963.
[16] For solubility reasons *cis*-1,2-cyclohexanediamine was used instead of 1,2-benzenediamine.

Expanded Radialenes: A Novel Class of Cross-Conjugated Macrocycles**

Armen M. Boldi and François Diederich*

Dedicated to Professor Donald J. Cram on the occasion of his 75th birthday

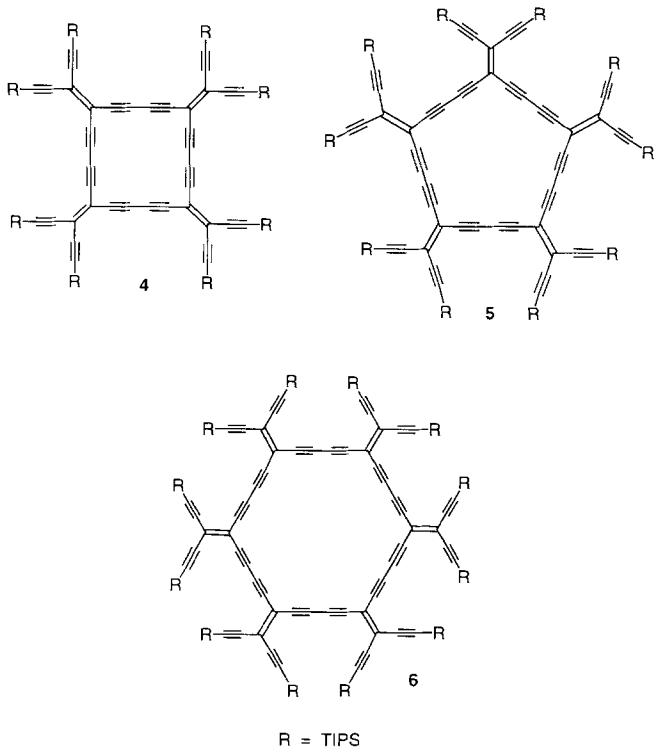
Radialenes (**1**) are a homologous series of all-*exo*-methylenecycloalkanes of molecular formula C_nH_n (for a recent review see ref. [1]). Upon insertion of acetylene or diacetylene moieties between each pair of vicinal *exo*-methylene units in the cyclic framework, the carbon-rich, hitherto unknown homologous se-



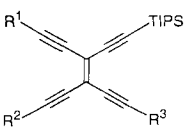
[*] Prof. Dr. F. Diederich, A. M. Boldi
Laboratorium für Organische Chemie
der Eidgenössischen Technischen Hochschule
ETH-Zentrum, Universitätstrasse 16, CH-8092 Zürich (Switzerland)
Telefax: Int. code + (1)261 3524

[**] This work was supported by the Schweizerischen Nationalfonds zur Förderung der wissenschaftlichen Forschung. We thank ETH Zürich for the purchase of the MALDI-TOF mass spectrometer.

ries of *expanded radialenes* **2** and **3** with the molecular formulae $C_{2n}H_n$ and $C_{3n}H_n$, respectively, are obtained. Here we report on the synthesis and electronic properties of the perethynylated derivatives **4**–**6**, the first representatives of the expanded radialenes, which can also be viewed as persilylated C_{40} (**4**), C_{50} (**5**), and C_{60} (**6**) isomers. With their extended π-electron perimeters, these compounds could potentially show interesting conducting and nonlinear optical properties.[2]



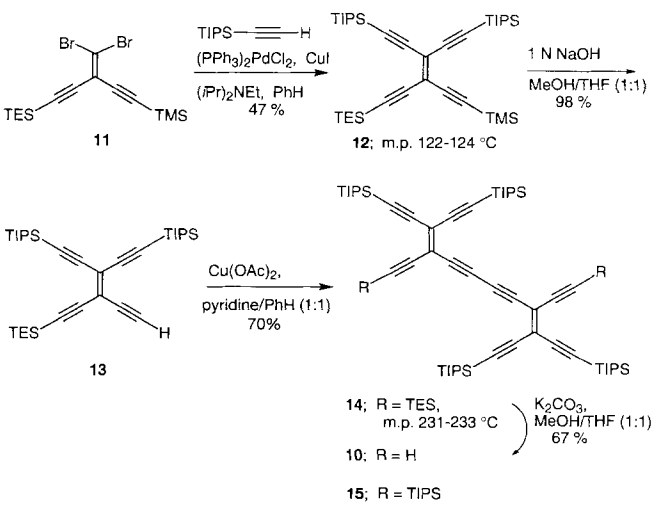
Initial attempts to prepare **4**–**6** by means of Eglinton–Glaser cyclization of **7**[3] did not afford any isolable quantities of the macrocycles but led to acyclic oligomeric material. To favor the cyclization providing **4**–**6** over competing polymerization reactions, the dimeric compound **10** was prepared as the cyclization component.[4, 5]



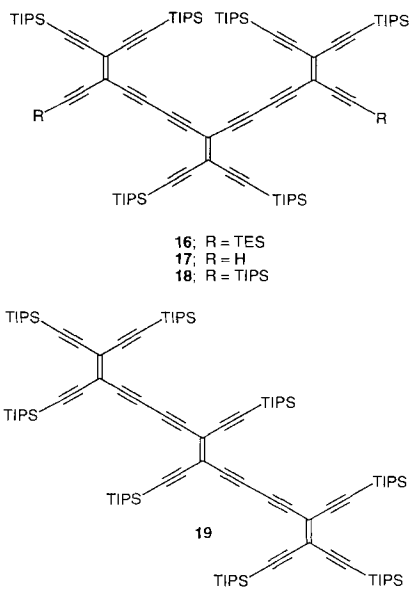
	R^1	R^2	R^3
7	TIPS	H	H
8	TIPS	TIPS	H
9	H	TIPS	H

Sequential, kinetically controlled deprotection of trimethylsilyl (TMS)- and triethylsilyl (TES)-protected acetylenes in the presence of the analogous triisopropylsilyl (TIPS)-protected groups was the key to the successful preparation of **10**.[6] We removed the TMS group in **12** selectively in 98% yield by stirring the compound for 2–5 min in MeOH/THF (1:1) containing a few drops of 1 N NaOH. Stirring the mixture for longer periods of time also led to the cleavage of the TES group to give **7**. Removal of the TES groups in **14** with K_2CO_3 in MeOH/THF (1:1) gave **10** as an unstable oil in 67% yield.

When **10** (0.02 mmol) was added under N_2 dropwise by syringe over several hours to a solution of anhydrous $Cu(OAc)_2$



(0.19 mmol) in pyridine/benzene (3:2, 10 mL), the expanded radialenes **4** and **6** were formed in 15% and 20% yield, respectively.[7] For the synthesis of the pentagonal macrocycle **5**, the cyclization component **17** was prepared by coupling **7** with **13** (2 equiv) [$Cu(OAc)_2$, pyridine/benzene (1:1), 9%] to give **16** followed by deprotection of the TES-alkynyl residues [K_2CO_3, MeOH/THF (1:1), 60%]. Oxidative cyclization of **17** (0.003 mmol) with **10** (0.003 mmol) in pyridine/benzene (3:2, 10 mL) in the presence of $Cu(OAc)_2$ (0.055 mmol) afforded **5** (15%) as the major product besides very small amounts of **4** and **6**.



All three expanded radialenes **4**–**6** are readily soluble, highly stable compounds with melting points above 260 °C. The remarkable stability indicates the absence of free terminal alkyne groups which generally destabilize polyacetylenic chromophores. The proposed cyclic structures are also supported by the absence of signals for terminal acetylenic protons in the ^1H NMR spectra (Table 1). Similarly, the IR spectra did not show any ≡C–H stretches; only weak C≡C stretches at 2125 (**4**), 2122 (**5**), and 2124 cm^{-1} (**6**) were visible. No C=C stretching

 © VCH Verlagsgesellschaft mbH, D-69451 Weinheim, 1994 0570-0833/94/0404-0469 $ 10.00+.25/0

bands were observed, which is in agreement with the IR spectra of other weakly polar tetraethynylethene derivatives. In the ^{13}C NMR spectra four acetylenic and two characteristic olefinic carbon resonances are observed (Table 1). The molecular weight

Table 1. Selected physical data of compounds **4**, **5**, **6**, **18**, and **19** [a, b].

4: Yellow microcrystals. $R_f = 0.31$ (CH_3CN/CH_2Cl_2, 1:3) [c]. M.p. >260 °C. FT-IR (CCl_4): $\nu = 2125$ (C≡C) cm^{-1}. ^1H NMR (400 MHz): $\delta = 1.09$ (s). ^{13}C NMR (100.6 MHz): $\delta = 11.2$, 18.6, 84.1, 85.7, 103.4, 106.6, 115.0, 118.4. UV/VIS (hexane): λ_{max} [nm] = 212 sh (ε 90000), 227 sh (51800), 247 sh (25500), 292 (31200), 308 (32700), 357 sh (28700), 385 sh (55300), 418 (115300), 438 (72700), 451 (77200). LD-TOF-MS: m/z 1739 (M^-); $C_{112}H_{168}Si_8$ (1739.27).

5: Yellow microcrystals. $R_f = 0.25$ (CH_3CN/CH_2Cl_2, 1:3) [c]. M.p. >260 °C. FT-IR (CCl_4): $\nu = 2122$ (C≡C) cm^{-1}. ^1H NMR (500 MHz): $\delta = 1.10$ (s). ^{13}C NMR (125.8 MHz): $\delta = 11.2$, 18.6, 83.2, 83.5, 103.3, 106.4, 114.8, 120.7. UV/VIS (hexane): λ_{max} [nm] = 216 (ε 110500), 225 sh (103500), 245 sh (58700), 309 (61600), 351 sh (70200), 376 sh (108700), 393 (116800), 407 (143300), 428 (106200), 441 (107800). LD-TOF-MS: m/z 2174 (M^-); $C_{140}H_{210}Si_{10}$ (2174.09).

6: Yellow microcrystals. $R_f = 0.19$ (CH_3CN/CH_2Cl_2, 1:3) [c]. M.p. >260 °C. FT-IR (film): $\nu = 2124$ (C≡C) cm^{-1}. ^1H NMR (300 MHz): $\delta = 1.10$ (s). ^{13}C NMR (75.5 MHz): $\delta = 11.2$, 18.6, 82.3, 83.2, 103.0, 106.1, 115.1, 121.8. UV/VIS (hexane): λ_{max} [nm] = 215 sh (ε 120600), 225 (122000), 246 (106400), 258 (93100), 275 (81200), 307 (78700), 349 sh (116800), 373 (186900), 392 (183300), 408 sh (119000) 422 sh (96800), 446 (77700). LD-TOF-MS: m/z 2608 (M^-); $C_{168}H_{252}Si_{12}$ (2608.91).

18: Yellow microcrystals. M.p. 116–118 °C. FT-IR (film): $\nu = 2153$, 2127 (C≡C) cm^{-1}. ^1H NMR (500 MHz): $\delta = 1.087$ (s), 1.091 (s). ^{13}C NMR (125.8 MHz): $\delta = 11.19$, 11.20, 11.23, 11.25, 18.54, 18.55, 18.63, 18.67, 81.33, 81.95, 83.54, 83.78, 101.51, 103.09, 103.36, 103.53, 103.68, 103.72, 105.19, 106.02, 115.68, 115.72, 121.10, 122.83. UV/VS (hexane): λ_{max} [nm] = 213 sh (ε 48400), 227 (52800), 236 sh (51400), 287 sh (38300), 302 (43000), 324 sh (35800), 347 sh (40900), 361 sh (40200), 375 (49200), 406 (45600) 418 (41500), 444 (58900). LD-TOF-MS: m/z 1619 (M^-); $C_{102}H_{168}Si_8$ (1619.16).

19: Orange microcrystals. M.p. 257–258 °C. FT-IR (film): $\nu = 2155$, 2116 (C≡C) cm^{-1}. ^1H NMR (300 MHz): $\delta = 1.09$ (s, 24H), 1.10 (s, 144H). ^{13}C NMR (75.5 MHz): $\delta = 11.17$, 11.24, 18.55, 18.60, 82.21, 82.66, 84.51, 84.70, 101.32, 101.51, 103.34, 103.65 (2 ×), 103.70, 104.81, 105.47, 115.71, 119.89, 121.31. UV/VIS (hexane): λ_{max} [nm] = 207 sh (ε 91500), 225 (58000), 235 sh (54700), 308 sh (41000), 328 sh (37100), 344 sh (34100), 368 (30500), 390 sh (26900), 417 sh (40100), 431 sh (46900), 455 sh (56900), 475 (42400), 479 (39600). LD-TOF-MS: m/z 1619 (M^-); $C_{102}H_{168}Si_8$ (1619.16).

[a] All NMR spectra were recorded in $CDCl_3$. [b] All new compounds were fully characterized by ^1H and ^{13}C NMR, FT-IR, and UV/VIS spectroscopy, EI or LD-TOF mass spectrometry, and correct elemental analysis. [c] C18 reversed-phase.

of the three macrocyles was confirmed by laser desorption time-of-flight (LD-TOF) mass spectrometry in the negative ion mode. The spectra, obtained without matrix assistance, showed strong molecular ions in the expected m/z range as well as a complete absence of any fragmentation or impurity peaks (Fig. 1). LD-TOF mass spectrometric techniques, which previously had been successfully applied to the analysis of fullerenes and their covalent derivatives,[8] clearly provide a powerful analytical tool for the detection and characterization of all-carbon and carbon-rich materials.[9] The formation and detection of anions in the gas phase suggests that the expanded radialenes can be electrochemically reduced, and an examination of the redox properties of **4**–**6** is under way.

Despite their high degree of unsaturation, **4**–**6** are yellow colored, which indicates the existence of only a weak macrocyclic π-electron conjugation. This assumption is clearly supported by a comparison between the electronic absorption spectra of **4**–**6** and **15** (Fig. 2). Compound **15** contains the 3,4,9,10-tetraalkynyl-substituted dodeca-3,9-diene-1,5,7,11-tetrayne chromophore[4] in a preferred *anti* array; in the enforced *syn* array this is also the longest linearly conjugated π-electron fragment in the macrocycles. The spectral end absorption does not change much between **15** and **4**–**6** and, within the macrocyclic sequence, it even remains almost constant. Hence, π-electron delocalization in **4**–**6** seems to extend efficiently only through the longest linearly conjugated fragment, and the measured linear increase in the extinction coefficient of the strongest absorption band with increasing ring size presumably results from the increasing number of such fragments in the macrocycles. The low extent of π-electron delocalization in **4**–**6** could be due to inefficient macrocyclic cross-conjugation[10] and/or the nonplanarity of the rings.[11] Preliminary AM1 calculations[12] show that the steric repulsion between the bulky peripheral TIPS groups distorts all three expanded radialenes significantly

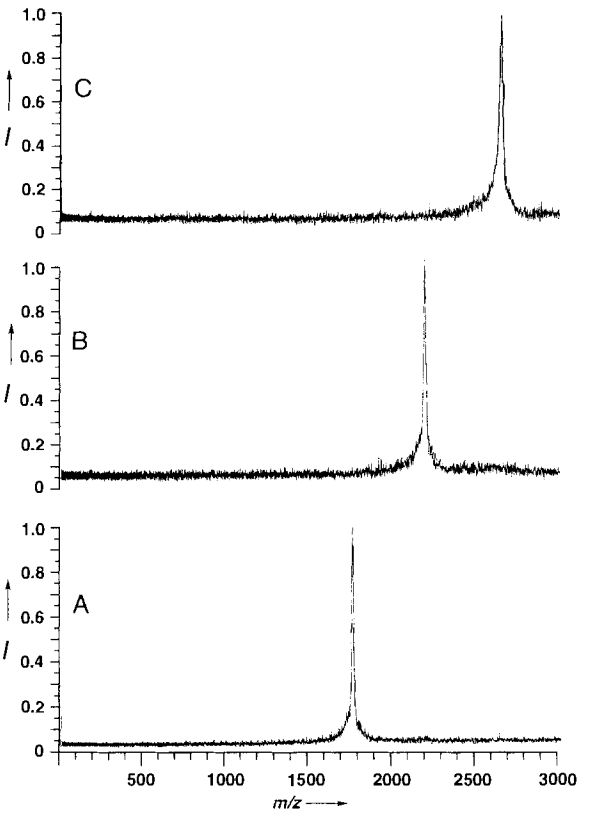


Fig. 1. Laser desorption time-of-flight mass spectra of **4** (A), **5** (B), and **6** (C) recorded in the linear mode at −15 kV.

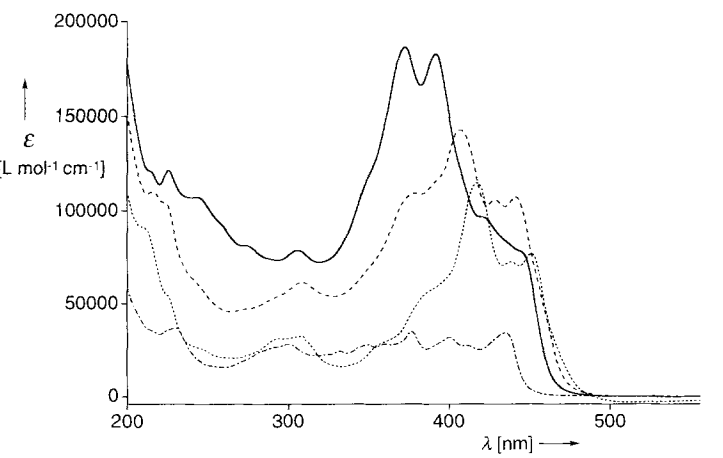


Fig. 2. Electronic absorption spectra of **15** (— · · —), **4** (· · ·), **5** (— — —), and **6** (— · —) recorded in hexane. $T = 298$ K.

out of planarity. However, the pronounced vibrational fine structure of the electronic absorption spectra also suggests that the macrocycles have strong conformational preferences and are not very flexible.

We compared these electronic properties to those of the acyclic isomeric chromophores **18** and **19**. The dendralene-type[13] isomer **18** was prepared in 6% yield by mixed coupling [$Cu(OAc)_2$, pyridine/benzene (1:1)] of **7** with **8** (2 equiv), and the linear isomer **19** of the poly(enebutadiyne) type[14] was obtained in 5% yield by coupling **9** with **8** (2 equiv). The UV/VIS spectra show that the extension of the linear π-electron conjugation in **19** leads to a significant bathochromic shift ($\approx$ 30 nm) in the end absorption as compared to **15** (Fig. 3). In sharp contrast, isomer **18** does not give a significant red shift but rather shows a spectrum nearly identical to that of the smaller π system **15**. Since **18** contains twice the chromophore of **15**, the extinction coefficients of its absorption bands are nearly doubled. Similar to the macrocycles **4**–**6**, π-electron delocalization in **18** is limited to the longest linearly conjugated fragment. The origin of this limited π-electron delocalization, owing to inefficient cross-conjugation or nonplanarity because of TIPS group repulsion, as well as the chemical reactivity of the new π systems are now under further investigation.

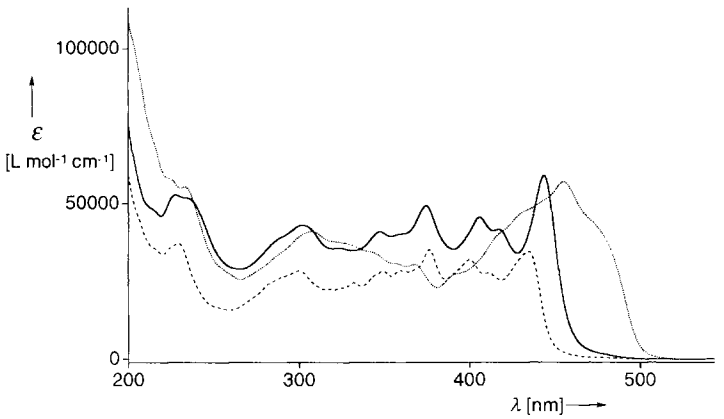


Fig. 3. Electronic absorption spectra of **15** (----), **18** (—), and **19** (···) recorded in hexane, T = 298 K.

Received: October 5, 1993 [Z 6393 IE]
German version: *Angew. Chem.* **1994**, *106*, 482

[1] H. Hopf, G. Maas, *Angew. Chem.* **1992**, *104*, 953–977; *Angew. Chem. Int. Ed. Engl.* **1992**, *31*, 931–954.
[2] H. S. Nalwa, *Adv. Mater.* **1993**, *5*, 341–358.
[3] Y. Rubin, C. B. Kobler, F. Diederich, *Angew. Chem.* **1991**, *103*, 708–710; *Angew. Chem. Int. Ed. Engl.* **1991**, *30*, 698–700.
[4] A. M. Boldi, J. Anthony, C. B. Knobler, F. Diederich, *Angew. Chem.* **1992**, *104*, 1270–1273; *Angew. Chem. Int. Ed. Engl.* **1992**, *31*, 1240–1242.
[5] Dibromide **11** was prepared from 1-triethylsilyl-5-trimethylsilyl-penta-1,4-diyne-3-ol (obtained in 46% yield by addition of $Et_3SiC{\equiv}CLi$ to $Me_3SiC{\equiv}CCHO$ in THF) by oxidation with pyridinium chlorochromate in CH_2Cl_2 (97%) and dibromoolefination (CBr_4, PPh_3, benzene, 52%).
[6] R. Eastmond, T. R. Johnson, D. R. M. Walton, *Tetrahedron* **1972**, *28*, 4601–4616.
[7] After workup as described for **15** [4], compounds **4**–**6**, **16**, and **18** were purified by chromatography on a C18 reversed-phase column [CH_3CN/CH_2Cl_2 (1:2)]. Compound **19** was purified by flash chromatography (SiO_2, hexane).
[8] a) F. Diederich, R. Ettl, Y. Rubin, R. L. Whetten, R. Beck, M. Alvarez, S. Anz, D. Sensharma, F. Wudl, K. C. Khemani, A. Koch, *Science* **1991**, *252*, 548–551; b) F. Diederich, R. L. Whetten, C. Thilgen, R. Ettl, I. Chao, M. M. Alvarez, *ibid.* **1991**, *254*, 1768–1770; c) F. Diederich, U. Jonas, V. Gramlich, A. Herrmann, H. Ringsdorf, C. Thilgen, *Helv. Chim. Acta* **1993**, *76*, 2445–2453.
[9] F. Diederich, Y. Rubin, C. B. Knobler, R. L. Whetten, K. E. Schriver, K. N. Houk, Y. Li, *Science* **1989**, *245*, 1088–1090.
[10] a) M. J. S. Dewar, *J. Chem. Soc.* **1952**, 3544–3550; b) N. F. Phelan, M. Orchin, *J. Chem. Educ.* **1968**, *45*, 633–637; c) M. Traetteberg, P. Bakken, A. Almenningen, W. Lüttke, J. Janssen, *J. Mol. Struct.* **1982**, *81*, 87–103; d) H. Berneth, B. Hagenbruch, S. Hünig, B. Ort, *Liebigs Ann. Chem.* **1984**, 354–369; e) W. Hutter, H.-K. Bodensch, *J. Mol. Struct.* **1993**, *291*, 151–158.
[11] a) F. Bohlmann, *Chem. Ber.* **1956**, *89*, 2191–2197; b) Y. Hori, K. Noda, S. Kabayashi, H. Taniguchi, *Tetrahedron Lett.* **1969**, 3563–3566.
[12] M. J. S. Dewar, E. G. Zoebisch, E. F. Healy, J. J. P. Stewart, *J. Am. Chem. Soc.* **1985**, *107*, 3902–3909.
[13] H. Hopf, *Angew. Chem.* **1984**, *96*, 947–958; *Angew. Chem. Int. Ed. Engl.* **1984**, *23*, 948–959.
[14] J. Anthony, C. Boudon, F. Diederich, J.-P. Gisselbrecht, V. Gramlich, M. Gross, H. Hobi, P. Seiler, *Angew. Chem.* and *Angew. Chem. Int. Ed. Engl.*, in press.

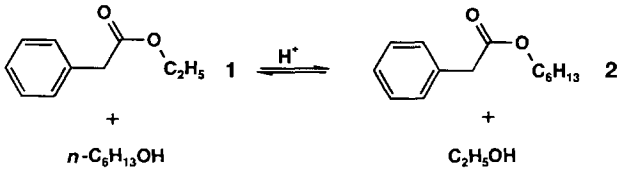
Selective Catalysis on Silicon Dioxide with Substrate-Specific Cavities**

Jens Heilmann and Wilhelm F. Maier*

Many properties (thermal, chemical and mechanical stability, activity, space–time yields, regenerability, long term stability, applicability) make technically important heterogeneous catalysts superior to biocatalysts. As yet unattainable, however, is the selectivity of enzymes, which is attributable to the substrate-specific clefts at the binding site of the enzyme. The limited availability of enzymes recently led to the preparation of antibodies that can bind transition state analogues of reactions for which no natural enzymes are known. These antibodies show an enzyme-like, highly selective catalytic activity.[1, 2] The cavity in enzymes and antibodies is not rigid, but during the interaction with the substrate it is complementary to the structure of the transition state (lock-and-key principle).

Substrate-selective cavities can also be generated in nonbiological systems, for example, in organic polymers, which can then be employed for selective chromatographic separation[3] and molecular recognition.[4] A desired goal for heterogeneous catalysis is the combination of the particular catalytic properties of two systems: the high activity and stability of the technical catalysts and the high selectivity of enzymes. Such a combination could be achieved if it were possible to fix a rigid cavity complementary to a transition state in an inorganic matrix.

Morihara et al.[5] reported in 1988 on the first generation of specific imprints of transition state analogues in the surface of alumina-containing silica gels. Such catalysts were used in the butanolysis of benzoic anhydride and showed substrate inhibition as well as a reduced Michaelis constant k_M, but a reduced rate of reaction relative to control catalysts containing no imprint. Chemoselective and enantioselective effects have also

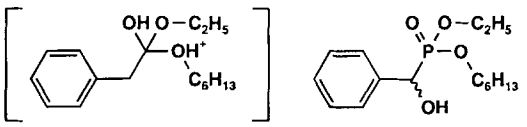


[*] Prof. Dr. W. F. Maier, Dipl.-Chem. J. Heilmann
Max-Planck-Institut für Kohlenforschung
Kaiser-Wilhelm-Platz 1, D-45466 Mülheim an der Ruhr (FRG)
Telefax: Int. code + (208)306-2980

[**] We thank H. Grondey for the solid-state NMR investigations.

been shown.[6] We report here on the preparation of catalytically selective, amorphous silicon dioxide catalysts by a modified sol–gel process[7] involving a transition state analogue. The transesterification of ethyl phenylacetate (**1**) with *n*-hexanol to form hexyl phenylacetate (**2**) served as the reaction to be catalyzed.

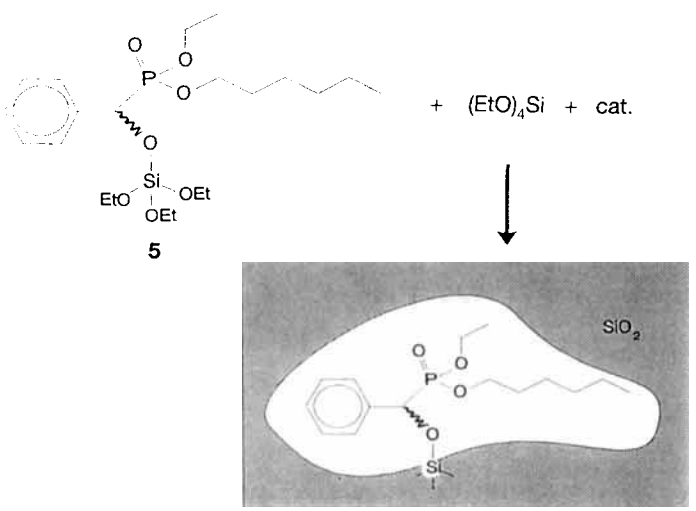
This transesterification of **1** proceeds at measurable rates only with acid or base catalysis; the transition state **3** with a C atom in a tetrahedral environment can be formulated for the acid catalyzed reaction. As transition state analogue, the phosphonate **4** with tetrahedrally surrounded phosphorus atom was synthesized, and coupled to a triethoxysilyloxy group as monomer unit to form **5**. The synthesis of **4** started with commercially



3 **4**

available diethyl phosphite that was transformed into the monosodium salt with NaOH.[8] Exchange of the Na^+ ion for the tetrabutylammonium ion and treatment with *n*-hexyl iodide, analogous to the method of Kluba and Zwierzak[9] afforded the mixed ethyl hexyl phosphite, which was coupled with benzaldehyde according to the method of Texier-Boullet and Foucaud in the presence of CsF to form ethyl hexyl 1-hydroxyphenylmethanephosphonate (**4**).[10] This transition state analogue was coupled to chlorotriethoxysilane with pyridine to give the copolymerizable **5**. Compound **5** was subjected to the HCl catalyzed sol–gel process together with a 100-fold molar excess of $Si(OEt)_4$ (Scheme 1).

The finished gel was dried for several days at room temperature and crushed finely in a mortar. With the aim of creating cavities, the powder was slowly heated to 250 °C, maintained at this temperature for 5 h, and then cooled. The container was evacuated and refilled with Ar for storage (selective catalyst **A**). In the mass spectrum of this heat-treated material, none of the transition state analogue **4** was detected. To confirm that before the heat treatment there was still **4** in the pulverized silicon dioxide, the powder was examined by mass spectrometry. In the mass spectrum the characteristic mass of **4** could be clearly

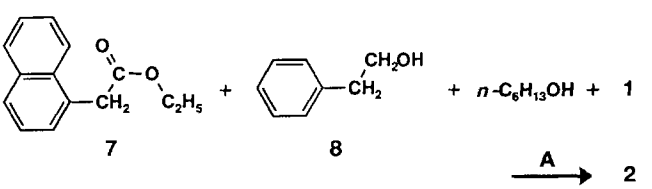


5 **6**

Scheme 1.

detected as major decomposition product at temperatures above 200 °C, which shows that at least a part of the transition state analogue **4** leaves the solid without decomposition. Thus, cavities possibly complementary to **4** might be left behind. Parallel to this procedure, silicon dioxide was prepared under identical conditions but without addition of **5** to act as control catalyst **B**. A comparison by means of ^1H and ^{29}Si solid state NMR spectroscopy and crossover polarization experiments of **A** before heat treatment with **B** and with **B** containing physically adsorbed **5** confirms the chemical incorporation of **5** in the SiO_2 matrix of the untreated **A**, as formulated in **6**. N_2 and Ar adsorption isotherms of all synthesized materials were recorded routinely. The silica gels **A** and **B** were shown to be not only highly porous but also entirely microporous; they do not differ significantly in either the pore distribution or in the BET overall surface (800–900 m^2g^{-1}). Interpretation of the isotherms by the method of Horvath–Kawazoe gave a pore distribution with a maximum at a pore diameter of 10 Å. The anticipated cavities in **A** cannot be recognized in the adsorption isotherms, which is probably due to the small proportion of cavities relative to the total porosity of 0.2 cm^3g^{-1}. Studies on **A** with transmission electron microscopy revealed that the silica gel is completely amorphous. The elemental distribution in dried, but not heat-treated **A** (which still contained **6**) determined with nm resolution by X-ray back-scattering analysis (EDX) showed, however, that the proportion of carbon in the material varied over a wide range, which suggests a partial association of the transition state analogue in the gel process and refutes the desired uniform molecular distribution of **6** in the glass.

The transesterification of **1** was performed under argon at 130–140 °C. The catalyst was pulverized, and the rate of stirring was increased until the reaction rate no longer increased. A mixture, free of traces of acid or base, containing 10 mmol of **1**, 100 mmol of *n*-hexanol, 100 mmol of *n*-octanol, and 100 mmol of phenylethanol (**8**), to which no catalyst had been added, underwent no detectable reaction within 2 h; after 2 h incipient autocatalysis was detectable. In the presence of the control catalyst **B** no reaction was detectable within 48 h. With catalyst **A** an immediate turnover to a 1:1 mixture of hexyl and octyl phenylacetate at a rate of 7 $mmol\,h^{-1}\,g^{-1}$ was observed. At the beginning of the reaction the formation of phenylethyl ester could not be detected. This showed that the reaction which does not take place in the presence of control SiO_2 **B** under these conditions is catalyzed by **A**. To monitor the selectivity, **1** was subjected to the analogous reaction in the presence of sulfuric acid. The rate of transesterification was the same for all three alcohols in the mixture. This experiment, repeated without sulfuric acid with the control material **B**, showed no conversion within 24 h. Addition of **A** immediately initiated the reaction,



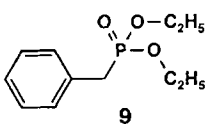
7 **8**

but the reaction with phenylethanol **8** was distinctly delayed. Repetition and long-time experiments demonstrated that the two alkyl esters formed 8–10 times faster than the phenylethyl ester. The extent to which the formation of the undesired phenylethyl ester, detectable after 2 h, is caused by unavoidable autocatalysis or is an indication of the intrinsic selectivity of **A** could not be clarified. These experiments confirmed the high

substrate selectivity of the catalyst **A**. A further pointer to the high selectivity of the catalyst was obtained with **7** and **8**, whose transesterification was not measurably catalyzed by **A** within 12 h. Addition of **1** and *n*-hexanol to this mixture again yielded **2** immediately and selectively.

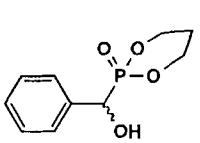
Kinetic investigations showed that the reaction is first order with respect to ester, alcohol, and catalyst. Michaelis-Menten kinetics with $V_{max} = 3.75$ μmol and $k_M = 3.6$ mmol was observed for the conversion of **1** with hexanol and 400 mg of **A** from 0 to 30% conversion. At higher conversions, however, the reaction begins to deviate slightly from this model, which suggests deactivation. In fact, in further experiments and also on reuse of the catalyst, a distinct, irreversible deactivation affecting not only the loss of activity, but also the selectivity was observed. This decrease in selectivity was also noticeable at higher conversion (> 50%). The long reaction time of several days at 130 °C presumably causes a slow, but irreversible sintering of the original cavity structure.

It remained to be proved whether the observed activity and selectivity of **A** was perhaps attributable to a combination of adsorption and diffusion effects or to some acidic decomposition product of **4** deposited on the inner SiO_2 surface. Half a gram of **B** was impregnated with 30 mg of phosphorous acid, tempered at 100 °C, and used as catalyst in the transesterification with the mixture of three alcohols. The material was catalytically active, but the selectivity of the alkyl ester formation over the phenylethyl ester formation of a factor of 1.5 was distinctly less than that of **A**. The presence of catalytic amounts of Brønsted acid centers in **A** was demonstrated by the selective formation of *tert*-butyl ethers catalyzed by **A** in the absence of phenylacetate from a mixture of *tert*-butanol, *n*-hexanol, *n*-octanol, and 2-phenylethanol (140 °C in a closed vessel). It must therefore be assumed that phosphoric acid centers arise during the calcination of **A** at 250 °C, and that these are probably responsible for the catalytic activity of **A**. This assumption was also supported by the observation that neither **4** (decomposes at higher temperatures in benzaldehyde and hexyl ethyl phosphite) nor the thermally stable, specifically synthesized compound **9** could influence the catalytic transesterification (no inibition). Extraction of **A** in a Soxhlet apparatus with THF, acetic acid, and water resulted in complete deactivation.



9

Because of the high porosity of these silica gels, it must be determined whether the observed selectivity is caused by transport phenomena (different diffusion rates, different adsorption) of the alcohols through the micropores. If transport phenomena are responsible for the selectivity, an increase in the particle size should not only decrease the reaction rate, but also increase the catalytic selectivity, or at least change it. Although an experiment with very large catalyst particles (> 500 μ) gave the expected reduction in the reaction rate of a factor of 10, the selectivity (alkyl ester formation 8–9 times faster than phenylethyl ester formation) remained of the same order as that with the finely pulverized catalyst. In the meanwhile, a catalyst, analogous to **A** but containing another transition state analogue (**10**) for a lactonization reaction, was prepared in the same way.[11] This catalyst, which is just as microporous as **A** (pore distribution maximum 10 Å), was tested in the transesterification reaction. Its activity is comparable with that of **A**, but the attained selectivity of a factor of 1.5 lay in the same range as that of **B** impregnated with phosphoric acid. Apparently the observed selectivity of the transesterification reaction is only achievable with a silica gel with cavities, structure-complementary to **4**.



10

The investigations indicate that we have prepared a selective silicon dioxide catalyst that in its action—combination of active Brønsted acid centers and discriminating cavities ("footprint")—resembles the catalysts of Morihara, but shows a higher selectivity. We have thereby shown that this type of catalyst is not unique, but can be prepared by other routes. How the cavities in silicon dioxide responsible for the selectivity are constructed, where the active centers are, where the limits of applicability, selectivity, activity, and maximum capacity lie, and what can be improved in these materials must still be studied. The thermal and long-term stability of these cavities must be significantly improved for practical applications. It is remarkable that even in such a simple compound like silicon dioxide the spatial requirements of an organic molecule can be so precisely imprinted on it that the material can distinguish between phenyl and naphthyl, or octyl and phenylethyl groups, and that this imprint is retained also at temperatures up to 250 °C. This demonstrates that glassy cavity structures can be generated with molecular resolution.

Received: April 2, 1993
Revised: November 9, 1993 [Z5974IE]
German version: *Angew. Chem.* **1994**, *106*, 491

[1] P. G. Schultz, *Angew. Chem.* **1989**, *101*, 1336; *Angew. Chem. Int. Ed. Engl.* **1989**, *28*, 1283; R. A. Lerner, S. J. Benkovic, P. G. Schultz, *Science* **1991**, *252*, 659; P. G. Schultz, K. Shokat, *Welch Symp. Proc.* **1991**, 19.
[2] K. M. Shokat, M. K. Koo, T. S. Scalan, L. Kochersperger, S. Yonkovich, S. Thaisrivongs, P. G. Schultz, *Angew. Chem.* **1990**, *102*, 1339; *Angew. Chem. Int. Ed. Engl.* **1990**, *29*, 1296.
[3] G. Wulff, M. Minarik, S. Schauhoff, *GIT* **1991**, 10; G. Wulff, G. Kirstein, *Angew. Chem.* **1990**, *102*, 706; *Angew. Chem. Int. Ed. Engl.* **1990**, *29*, 684.
[4] G. Vlatakis, L. I. Anderson, R. Müller, K. Mosbach, *Science* **1993**, *361*, 645.
[5] K. Morihara, S. Kurihara, J. Suzuki, *Bull. Chem. Soc. Jpn.* **1988**, *61*, 3991.
[6] K. Morihara, M. Kurokawa, Y. Kamata, T. Shimada, *J. Chem. Soc. Chem. Commun.* **1992**, 358.
[7] C. J. Brinker, G. W. Scherer, *Sol-Gel-Science*, Academic Press, New York, **1990**; H. Dislich, *Angew. Chem.* **1971**, *83*, 428; *Angew. Chem. Int. Ed. Engl.* **1971**, *10*, 363.
[8] P. Nylen, *Sven. Kem. Tidskr.* **1936**, *48*, 2.
[9] M. Kluba, A. Zwierzak, *Synthesis* **1978**, 134.
[10] F. Texier-Boullet, A. Foucaud, *Synthesis* **1982**, 165.
[11] J. Heilmann, W. F. Maier, unpublished results.

Silane Nitrile: Matrix Isolation, Adduct with Hydrogen**

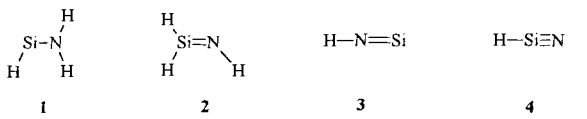
Günther Maier* and Jörg Glatthaar

Divalent silicon compounds (silylenes, silanediyls)[1] and compounds with Si–element multiple bonds[2] are still of great interest to theoreticians and preparative chemists. Our attention has been directed particularly toward the unsubstituted parent compounds. Of the nitrogen-containing derivatives **1**–**4**, aminosilylene (**1**)[3] and iminosilylene (silaisonitrile) (**3**)[4] were previously trapped in an argon matrix and identified. We report here on the identification of the two compounds still missing, **2** and

[*] Prof. Dr. G. Maier, Dipl.-Chem. J. Glatthaar
Institut für Organische Chemie der Universität
Heinrich-Buff-Ring 58, D-35392 Giessen (FRG)
Telefax: Int. code + (641)702-5712

[**] Hetero π Systems, Part 19; lecture (G. M.) given at the Silicon conference (August 3, 1992) in München. This work was supported by the Fonds der Chemischen Industrie. Part 18: G. Maier, H.-J. Wolf, R. Boese, *Chem. Ber.* **1990**, *123*, 505-511.

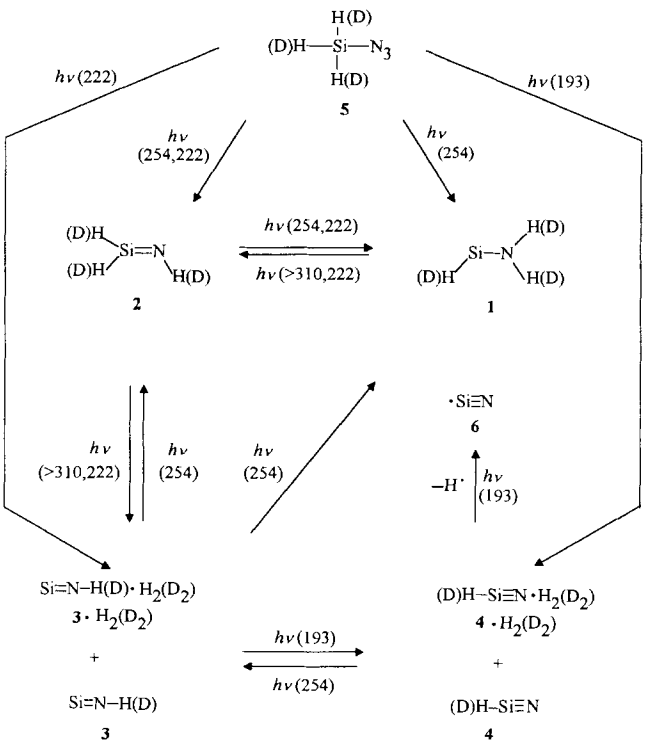
4. Silane nitrile (**4**) is of particular interest since, whereas in the equilibrium RCN⇌RNC[5] the nitrile form is preferred, the opposite is expected in the sila series. According to ab initio calculations[6] silane nitrile (**4**) is—depending of the basis set used—50–100 kcal mol^{-1} higher in energy than the isomer **3**.



The ideal experimental access to the H_3SiN and HSiN hypersurface is offered by silyl azide (**5**).[3,4] As previously described by us,[3] after irradiation of **5** in argon at 10 K with light of wavelength 254 nm, aminosilylene (**1**) is detected [UV: λ_{max} = 348, 220, 208 nm; IR: $\tilde{\nu}$ = 866(ν_{Si-N}) cm^{-1}; calcd[7]: 948 cm^{-1}]. If light of shorter wavelength (222 nm; KrCl excimer laser) is applied, the main product is iminosilylene (**3**) [UV: λ_{max} = 250 nm (weak); IR: $\tilde{\nu}$ = 3585, 3580(ν_{N-H}), 1202, 1200($\nu_{Si=N}$), 522(δ_{N-H}) cm^{-1}; calcd[8]: 3613, 1216.5, 518.4 cm^{-1}]. Aminosilylene (**1**) is not directly transformed into the iminosilylene (**3**). In accordance with theory[7] it can be assumed that initially a H shift **1** → **2** (calculated barrier: 74 kcal mol^{-1}) occurs followed by a dehydrogenation of **2** to give **3**.[9a] Indeed, an intermediate can be detected along the pathway **1** → **3**, which can be interpreted as the unsubstituted silane imine (**2**) [UV: λ_{max} = 240 nm; calcd[9b]: 238 nm; IR: $\tilde{\nu}$ = 2253, 2175 (ν_{Si-H}), 1097 ($\nu_{Si=N}$) cm^{-1}; calcd[7]: 1247 cm^{-1}].

The reaction proceeds differently for the matrix irradiation of silyl azide (**5**) with an ArF excimer laser (193 nm). The IR spectrum of a new species is recorded, which according to the spectral data must be silane nitrile (**4**) [UV: λ_{max} = 238, 258, 266, 350 nm; IR: $\tilde{\nu}$ = 2151, 2149 (ν_{Si-H}); 1163, 1161 ($\nu_{Si\equiv N}$) cm^{-1}]. Thus, to our knowledge, this is the first compound with a formal Si≡N triple bond of the nitrile type to be identified spectroscopically.[10] Additional structural evidence for **4** is derived from the fact that it loses its hydrogen atom on prolonged irradiation at 193 nm, and is transferred into the well-known[11] SiN radical **6** [UV: particularly strong band at 410 nm; IR: $\tilde{\nu}$ = 1144 ($\nu_{Si\equiv N}$) cm^{-1}].

The genetic relationships between the species **1**–**6** are given in Scheme 1. They result from the increase or decrease of the corresponding bands when different light sources are applied. The crucial intermediate is silane imine (**2**). This is formed from silyl azide (**5**) via the silyl nitrene H_3SiN:, which cannot be trapped.[3] Silane imine (**2**) forms a photoequilibrium with aminosilylene (**1**), but yields mainly iminosilylene (**3**) by H_2 elimination. The eliminated hydrogen remains in the matrix cage. This is not only supported by the fact that the hydrogen elimination is reversible (!), at least as long as the hydrogen occurs in the same matrix cage as **3**, but there is also spectroscopic evidence: First the stretching vibrational bands of **3** are doubled. This is probably the result of the occurrence of a mixture of free **3** (ca. 10%; $\tilde{\nu}$ = 3585, 1202 cm^{-1}) and a H_2 adduct **3**·H_2 (ca. 90%; $\tilde{\nu}$ = 3580, 1200 cm^{-1}). Second, and this finding is particularly informative, the hydrogen molecule associated with **3** can be observed directly. Because of its proximity to **3** the H_2 molecule eliminated from **2** becomes IR "active", and a band is registered at 4178 cm^{-1}.[12] This absorption band disappears together with the bands of **3**·H_2 on thawing of the matrix to 30 K. Simultaneously, an increase in pressure is noted, which indicates that the hydrogen eliminated does not remain in the matrix but escapes under these conditions into the gas phase. The absorption bands of free **3** (higher wavenumbers) increase in intensity. At



Scheme 1.

the same time the possibility of retrapping the hydrogen by irradiation (254 nm) of iminosilylene (**3**) and reforming the aminosilylene (**1**) via silane imine (**2**) disappears. The phenomenon of adduct formation with hydrogen is also observed for silane nitrile (**4**). As mentioned previously, irradiation of **5** at 193 nm affords double bands with two almost equally intensive peaks. This means that a mixture of fortuitously equal fractions of H_2 adduct **4**·H_2 ($\tilde{\nu}$ = 2149, 1161 cm^{-1}) and free **4** ($\tilde{\nu}$ = 2151, 1163 cm^{-1}) can be assumed. The hydrogen stretch for **4**·H_2 appears at 4164 cm^{-1}. Again, on thawing to 30 K the band for free **4** becomes more intensive, that for **4**·H_2 weaker.

As long as the H_2 adduct **4**·H_2 occurs, irradiation at 254 nm leads back to aminosilylene (**1**) via **3**·H_2 and **2**. This reaction is

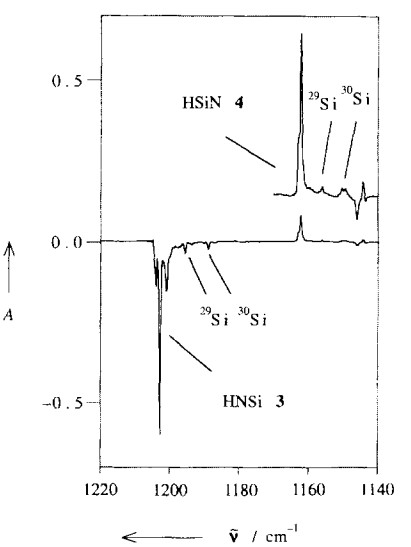


Fig. 1. IR spectra (difference spectrum of the photoreaction **3** → **4** at 193 nm) of HSiN (**4**) and HNSi (**3**) in argon at 10 K. A = absorbance.

no longer possible after annealing at 30 K when only free silane nitrile (**4**) is still present. In this case only the rearrangement **4** → **3** is observed on irradiation at 254 nm. By changing to 193 nm light the corresponding backreaction **3** → **4** occurs (Fig. 1). These mutual relationships are additional proof that the two participating species **3** and **4** must be isomers.

The complete reaction process can be confirmed from the corresponding spectra of the deuterated isotopomers ([D_3]**2**: $\tilde{\nu}$ = 1638, 1585 (ν_{Si-D}); 1063 ($\nu_{Si=N}$) cm^{-1}; calcd 1754, 1704, 1200 cm^{-1}; [D]**4**: $\tilde{\nu}$ = 1580, 1578 (ν_{Si-D}), 1145, 1144 ($\nu_{Si\equiv N}$) cm^{-1}. The absorption band of the "associated" deuterium for [D]**3**·D_2 appears at 2994, that of [D]**4**·D_2 at 3010/3005 cm^{-1}.[12]

The structure of silane nitrile (**4**) is derived from the analysis of the IR spectra; the isotopic shifts provide additional proof. Three fundamental vibrations are expected for **4**. The two valence stretches can be proven experimentally, but not the bending mode. The latter is either very weak or lies outside the range possible for us to measure (up to 220 cm^{-1}). The calculations (Table 1)[13] show an unusually strong deviation of the band positions for the SiN valence stretches (ν_3) depending on the basis set used. Contrary to our expectations, calculation at the MP2 level gives a lower value than that observed. Our experience indicates that this result is typical for systems containing SiN multiple bonds. Nonetheless, the calculated isotopic shifts are consistent with those obtained from the experiment. The following force constants are calculated from the four IR bands measured (see Table 1): f_{SiH} = 2.59, f_{SiN} = 7.08, $f_{SiH/SiN}$ = − 0.45 N cm^{-1}. According to Siebert[14] this results in a bond order of 2.0. An analogous analysis for HNSi (**3**) (f_{SiN} = 8.85) gives a value of 2.3.

Table 1. Observed (Ar matrix) and calculated IR spectra of HSiN (**4**) and DSiN [D]**4**; wavenumbers in cm^{-1}. Integrated intensities (relative to the strongest band) in parentheses.

Band			exp.	MP2/6-31G*	MP2/D95**
ν_1	σ	ν_{SiH}	2152.2 (0.59)	2249.1 (0.76)	2261.8 (0.45)
		ν_{SiD}	1580.5 (0.31)	1629.2 (0.22)	1637.7 (0.11)
ν_2	π	δ_{SiH}	–	444.4 (0.10)	466.7 (0.18)
		δ_{SiD}	–	338.7 (0.14)	355.5 (0.22)
ν_3	σ	ν_{SiN} [a]	1162.2 (1.00)	990.2 (1.00)	1004.9 (1.00)
		^{29}Si	−6.1	−5.3	−5.3
		^{30}Si	−11.8	−10.2	−10.3
		ν_{SiN} [b]	1145.4 (1.00)	978.2 (1.00)	993.2 (1.00)
		^{29}Si	−5.0	−4.6	−4.6
		^{30}Si	−9.5	−8.8	−9.0

[a] HSiN **4**. [b] DSiN [D]**4**.

Conclusion: Matrix isolation spectroscopy not only provides proof of silane nitrile (**4**) (and silane imine (**2**)), even the photochemically eliminated hydrogen can be directly detected spectroscopically. Furthermore, experiment and theory[6] agree perfectly in at least five points: 1. The stability within the series of H_3NSi isomers increases in the series silyl nitrene/silane imine (**2**)/aminosilylene (**1**). Thus, it is not surprising that silyl nitrene cannot be observed. 2. A considerable barrier exists between **1** and **2**, which can be overcome by photoexcitation. 3. The predicted small barrier (calcd 4–13[6e] or 7.8 kcal mol^{-1}[6i]) for the isomerization **4** → **3** is sufficient for the spectroscopic detection of **4** in an argon matrix. 4. α-Elimination of two hydrogen atoms at one silicon atom is preferred over β-elimination, for which the second H atom is situated at a neighboring C or N atom. 5. HSiN (**4**) is a better source of the SiN radical **6** than HNSi (**3**).

Received: September 17, 1993 [Z 6364 IE]
German version: *Angew. Chem.* **1994**, *106*, 486

[1] Summaries on silylenes: P. P. Gaspar, *React. Intermed., Wiley*, **1978**, *1*, 229–277; *ibid.* **1981**, *2*, 335–385; *ibid.* **1985**, *3*, 333–427; L. Fabry, *Chem. Ztg.* **1985**, *109*, 281–289.
[2] Review on Si-element multiple bonds: a) G. Raabe, J. Michl, *Chem. Rev.* **1985**, *85*, 419–509; b) G. Raabe, J. Michl in *The Chemistry of Organic Silicon Compounds, Part 2* (Eds.: S. Patai, Z. Rappoport), Wiley, Chichester, **1989**, pp. 1015–1142.
[3] G. Maier, J. Glatthaar, H. P. Reisenauer, *Chem. Ber.* **1989**, *122*, 2403–2405.
[4] a) J. F. Ogilvie, S. Cradock, *J. Chem. Soc. Chem. Commun.* **1966**, 364–365; b) M. Bogey, C. Demuynck, J. L. Destombes, A. Walters, *Astron. Astrophys.* **1991**, *244*, L47; c) M. Elhanine, R. Farren, G. Guelachvili, *J. Chem. Phys.* **1991**, *94*, 2529–2531.
[5] C. Rüchardt, K. Meier, K. Haaf, J. Pakusch, E. K. A. Wolber, B. Müller, *Angew. Chem.* **1991**, *103*, 907–915; *Angew. Chem. Int. Ed. Engl.* **1991**, *30*, 893–901.
[6] Summaries on quantum chemical calculations of the H_3SiN and HNSi hypersurfaces: a) see ref. [2]; b) Y. Apeloig in *The Chemistry of Organic Silicon Compounds, Part 1* (Eds.: S. Patai, Z. Rappoport), Wiley, Chichester, **1989**, pp. 57–225; c) *Gmelin Handbook of Inorg. and Organomet. Compounds, Silicon-Nitrogen Compounds, Suppl. Vol. B4*, **1989**, pp. 17–37, 64–83; more recent calculations (apart from ref. [7, 8]): d) J. N. Murrell, H. W. Kroto, M. F. Guest, *J. Chem. Soc. Chem. Commun.* **1977**, 619–620; H. W. Kroto, J. N. Murrell, A. Al-Derzi, M. F. Guest, *Astrophys. J.* **1978**, *219*, 886–890; J. N. Murrell, S. Carter, A. J. Varandas, *J. Mol. Phys.* **1978**, *35*, 1325–1326; e) R. Preuss, R. J. Buenker, S. D. Peyerimhoff, *J. Mol. Struct.* **1978**, *49*, 171–179; *Chem. Phys. Lett.* **1979**, *62*, 21; f) B. T. Luke, J. A. Pople, M.-B. Krogh-Jespersen, Y. Apeloig, M. Karni, J. Chandrasekhar, P. von R. Schleyer, *J. Am. Chem. Soc.* **1986**, *108*, 270–284; g) M. T. Nguyen, M. Paul, N. J. Fitzpatrick, *J. Chem. Soc. Perkin Trans. II* **1987**, 1289–1292; h) P. Botschwina, M. Tommek, P. Sebald, M. Bogey, C. Demuynck, J. L. Destombes, A. Walters, *J. Chem. Phys.* **1991**, *95*, 7769–7770; i) N. Goldberg, M. Iraqi, J. Hrušák, H. Schwarz, *Int. J. Mass Spectrom. Ion Processes* **1993**, *125*, 267–270.
[7] T. N. Truong, M. S. Gordon, *J. Am. Chem. Soc.* **1986**, *108*, 1775–1778.
[8] P. Botschwina and M. Oswald cited in: D. P. Chong, D. Papoušek, Y. I. Chen, P. Jensen, *J. Chem. Phys.* **1993**, *98*, 1352–1357.
[9] a) C. F. Melius, P. Ho, *J. Phys. Chem.* **1991**, *95*, 1410–1419; b) P. J. Bruna, V. Krumbach, S. D. Peyerimhoff, *Can J. Chem.* **1985**, *63*, 1594–1608.
[10] With regard to an indirect detection of phenylsilane nitrile by a trapping experiment with *tert*-butyl alcohol compare C. Cross, J. Michl, R. West, citation 406 in ref. [2b].
[11] R. S. Mullikan, *Phys. Rev.* **1925**, *26*, 319–338.
[12] Complexes of this kind produced by cocondensation are known for hydrogen fluoride; H_2·HF absorbs in a neon matrix at 4155, D_2·DF at 2988 cm^{-1}: R. D. Hunt, L. Andrews, *J. Chem. Phys.* **1987**, *86*, 3781–3786.
[13] Gaussian 92, Revision B: M. J. Frisch, G. W. Trucks, M. Head-Gordon, P. M. W. Gill, M. W. Wong, J. B. Foresman, B. G. Johnson, H. B. Schlegel, M. A. Robb, E. S. Repogle, R. Gomperts, J. L. Andres, K. Raghavachari, J. S. Binkley, C. Gonzalez, R. L. Martin, D. J. Fox, D. J. Defrees, J. Baker, J. J. P. Stewart, J. A. Pople, Gaussian, Inc., Pittsburgh, PA, **1992**.
[14] H. Siebert, *Anwendungen der Schwingungsspektroskopie in der Anorganischen Chemie*, Springer, Berlin, **1966**.

Enantioselective, Multigram-Scale Synthesis with a Catalytic Antibody**

Jean-Louis Reymond,* Jean-Louis Reber, and Richard A. Lerner*

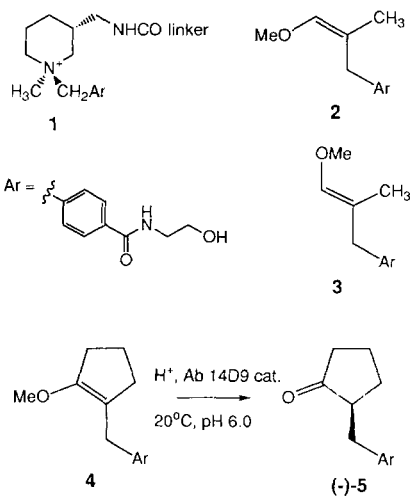
The scope of antibody catalysis now encompasses many reactions of interest to synthetic chemists including enantioselective and disfavored processes.[1] These reactions can be carried out under very mild aqueous conditions, which would make them

[*] Prof. Dr. R. A. Lerner, Dr. J.-L. Reymond, Dr. J.-L. Reber [+]
Department of Molecular Biology
The Scripps Research Institute
10666 North Torrey Pines Road, La Jolla, CA 92037 (USA)
Telefax: Int. code + (619)554-9899
[+] Present address:
Sandoz Pharma, Chemical Process R + D
CH-Basel (Switzerland)

[**] We would like to thank Prof. L. Ghosez, Belgium, for pointing out the importance of a preparative-scale experiment with a catalytic antibody. We thank Sandoz, Basel, for sabbatical support to J.-L. Reber.

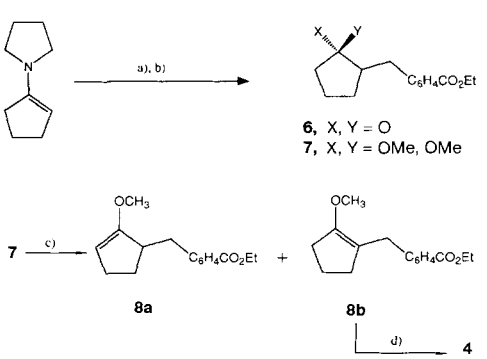
very attractive for preparative chemistry provided that they can be carried out on a large scale. We now report the preparation of gram quantities of product using a catalytic antibody and a very simple laboratory procedure. This demonstrates that catalytic antibodies should be considered as practical tools for organic synthesis in the laboratory.

We recently reported that antibodies raised against hapten **1** catalyzed the hydrolysis of enol ethers **2** and **3** (Scheme 1) with very high enantioselectivity for proton delivery.[2] In the course of our investigation into alternative substrates, we discovered that antibody 14D9 was particularly effective for the hydrolysis of the cyclic enol ether **4** to produce enantiomerically pure ketone (−)-**5** with a turnover $k_{cat.}$ of 0.4 s^{-1} at pH 6.0 and a rate enhancement $k_{cat.}/k_{uncat.}$ of 10^4.[3] Furthermore, when a 1 mM solution of substrate **4** was incubated at pH 7.0 and 20 °C with a 10 μM solution of antibody 14D9, complete conversion to product was observed within one hour with no apparent product inhibition. Without antibody less than 5% of the substrate was converted to product. Encouraged by these preliminary results, we set out to scale up this reaction.



Scheme 1. Hapten, substrates, and catalytic reaction of antibody 14D9.

Substrate **4** was synthesized as follows (Scheme 2): alkylation of pyrrolidino-1-cyclopentene with ethyl (4-chloromethyl)benzoate and ketalization of the resulting ketone **6** gave **7**. Ketal **7** was converted in high yield to a 1:1 mixture of enol ethers **8a** and **8b** upon heating in trimethylorthoformate with ammonium camphorsulfonate (NH_4^+CSA) catalyst.[4] Isomer **8b** was purified by column chromatography and converted into **4** by treatment with ethanolamine.[5]



Scheme 2. Synthesis of **4**: a) $ClCH_2C_6H_4CO_2Et$ (0.5 equiv.), CH_3CN, reflux, 10 min, 58%; b) $(MeO)_3CH$, MeOH, CSA cat., room temperature, 15 min, 100%; c) $(MeO)_3CH$, NH_4^+CSA cat., reflux, 30 min, 85%; d) ethanolamine, ethanol, K_2CO_3, 50 °C, 17 h, 94%.

Monoclonal antibody 14D9 was prepared and purified as previously described.[6] For the antibody-catalyzed reaction we wanted a procedure that required only conventional laboratory glassware and allowed efficient recovery of the antibody catalyst. Our procedure[7] is based on the use of dialysis for the separation of product and unreacted substrate from the catalyst and relies on the significant solubility of both **4** and **5** in water. Thus, a solution of substrate **4** (500 mg, 1.83 mmol) in 1 mL of methanol is added to a solution of antibody (57 mL, 7 mg mL^{-1}, 400 mg) in buffer[8] and magnetically stirred at room temperature in a 250 mL glass round-bottom flask. The reaction proceeds to 80% conversion in 5 h giving **5** with 89–91% *ee*.[9] The solution is then transferred to a dialysis bag and dialyzed into 1 L of the same buffer at pH 7, which effectively separates 95% of the products from the antibody catalyst by dilution.[10] Unreacted starting material and product are recovered from the dialysis buffer by extraction.[11] The pure ketone (−)-**5**[12] is obtained by recrystallization[13] in 60–65% yield (based on starting material) and with an optical purity of 86% *ee*.[14] The antibody contained in the dialysis bag is dialyzed again with 1 L of buffer at pH 6, which returns it to the original conditions while removing the remaining product by dilution. The antibody solution is then returned to the original flask for another reaction cycle.

The procedure was repeated five times to consume a total of 2.55 g of substrate **4**. The total yield of (−)-**5** was 1.50 g (62% based on invested substrate) with 86% *ee* after recrystallization. The activity of the antibody sample dropped by 5% after each run, which probably reflects loss upon transfer of the solutions. Each catalytic site invested in this experiment carried out 4700 turnovers (940 in each run).[15]

Although we used purified antibody in the experiment described above, all preliminary experiments were carried out with the crude ammonium sulfate precipitate. In both cases all the catalytic activity observed for the hydrolysis of **4** was completely inhibited by the hapten and was thus specific to the antibody combining site. In fact, the catalytic activity of the purified antibody per weight unit turned out to be lower than for the ammonium sulfate precipitate, which suggests that purification was accompanied by partial, irreversible denaturation of the protein. In both cases the activity corresponds to 20–40% of the activity expected for a pure protein. The use of the crude antibody preparation provides significant labor and cost advantages, as subsequent prufications consume time and material.

In summary, we have shown that antibody-catalyzed reactions can be carried out on a gram scale with conventional laboratory techniques. The antibody catalyst is recovered and can be reused. The reaction chosen in this study is examplary, as it cannot be carried out enantioselectively by any other known catalytic system, and it illustrates the contribution that antibodies can make as catalysts in synthetic organic chemistry.

Received: September 28, 1993 [Z 6380 IE]
German version: *Angew. Chem.* **1994**, *106*, 485

[1] a) R. A. Lerner, S. G. Benkovic, P. G. Schultz, *Science* **1991**, *252*, 659; b) P. G. Schultz, R. A. Lerner, *Acc. Chem. Res.* **1993**, *26*, 391–395.
[2] a) J.-L. Reymond, K. D. Janda, R. A. Lerner, *Angew. Chem.* **1991**, *103*, 1690; *Angew. Chem. Int. Ed. Engl.* **1991**, *30*, 1711; b) *J. Am. Chem. Soc.* **1992**, *114*, 2257.
[3] J.-L. Reymond, G. K. Jahanghiri, R. A. Lerner, *J. Am. Chem. Soc.* **1993**, *115*, 3909.

[4] This procedure is simpler than other published procedures. Its generality is under current investigation.

[5] Selected physical properties of **4**. Colorless crystals, m.p. 74–75 °C; ^{1}H NMR (500 MHz, $CDCl_3$): δ = 7.67, 7.22 (2 m, 2 × 2 H), 6.69 (br. t, 1 H), 3.82 (td, 2 H, J = 5, 4.5), 3.61 (dt, 2 H, J = 8, 4), 3.40 (br. s, 2 H), 2.48 (m, 2 H), 2.10 (m, 2 H), 1.81 (m, 2 H); ^{13}C NMR (125 MHz, $CDCl_3$): δ = 168.7, 152.3, 145.1, 131.4, 128.8, 126.9, 112.9, 62.5, 56.8, 42.8, 32.4, 31.0, 28.8, 19.5; IR (KBr): $\tilde{\nu}$ = 3287, 2937, 2850, 1689, 1639, 1546, 1339, 1292, 1163, 1108, 1060, 1033, 860, 704 cm^{-1}.

[6] 14D9 is a murine hybridoma cell line obtained by fusion of a 129G1X$^+$ spleen cell (from a mouse immunized with hapten **1**) with a balb/c myeloma cell, and it produces a $\kappa\gamma_1$ antibody. Antibody 14D9 was produced by growing ascites from this cell line. Purification of the ascites fluid involved ammonium sulfate precipitation, anion exchange, and protein G chromatography. a) G. Köhler, C. Milstein, *Nature* **1975**, *256*, 495; b) E. Enguall, *Methods Enzymol.* **1980**, *70*, 419.

[7] All reactions were monitored by HPLC (Chiralpak AS column, 0.45 × 22 cm; hexane/isopropanol 7:3; 1 mL min^{-1}): t_R(**4**) = 5.3 min, t_R((+)-**5**) = 9.2 min, t_R((−)-**5**) = 12.5 min. Detection by UV at 240 nm.

[8] The buffer is 50 mM bistris (*N,N*-bis(hydroxyethyl)tris(hydroxymethyl)aminomethane), 100 mM NaCl, pH 6.0.

[9] The antibody-catalyzed reaction is 100% enantioselective. Under the present conditions, 10% of the product is formed by the hydrolysis of **4** catalyzed by H_3O^+ to give racemic **5**.

[10] We used cellulose dialysis tubes that allow the diffusion of proteins up to 12–14 kDa. The antibody has a molecular weight of 150 kDa and is retained inside the bags, while molecules smaller than 12–14 kDa diffuse through the membrane. Equilibration was reached after 17 h at 20 °C. Dialysis bags are also used with enzymes. See C.-H. Wong, *Science* **1989**, *244*, 1145.

[11] Extraction with toluene (4 × 50 mL) selectively removes the unreacted **4**. The buffer is then saturated with NaCl, and **5** extracted with ethyl acetate (4 × 200 mL).

[12] The absolute configuration of (−)-**5** was shown as (*S*) by comparison with (+)-(*R*)-2-benzylcyclopentanone. K. Matsumoto, H. Ohta, *Tetrahedron Lett.* **1991**, *32*, 4729.

[13] The crude product (370 mg) was dissolved in 2 mL of hot ethyl acetate and recrystallized by dropwise addition of 1.5 mL hexane, yielding 310 mg (65%) of (−)-**5**. Colorless crystals, m.p. 88–90 °C. $[\alpha]_D^{25} = -134$ (c = 0.9 in EtOH); ^{1}H NMR (500 MHz, $CDCl_3$): δ = 7.69, 7.21 (2 m, 2 × 2 H), 6.78 (br. t, 1 H), 3.81 (br. m, 2 H), 3.61 (q, 2 H, J = 5), 3.15 (dd, 1 H, J = 14, 4), 3.04 (br. m, 1 H), 2.60 (dd, 1 H, J = 14, 9), 2.36 (m, 2 H), 2.08 (m, 2 H), 1.96 (m, 1 H), 1.81 (br. s, 1 H), 1.74 (m, 1 H), 1.53 (ddd, 1 H, J = 23, 11, 7); ^{13}C NMR (125 MHz, $CDCl_3$): δ = 220.0, 168.4, 144.0, 132.1, 129.1, 127.2, 62.1, 50.7, 42.8, 38.1, 35.3, 29.0, 20.5; IR (KBr): $\tilde{\nu}$ = 3296, 2936, 2874, 1731, 1637, 1557, 1503, 1441, 1404, 1055, 805, 682 cm^{-1}.

[14] The drop in optical purity is due to partial hydrolysis of the remaining enol ether **4** during dialysis. When dialysis was attempted at pH 8, hydrolysis of **4** was stopped but racemization of **5** was then observed.

[15] The concentration of catalytic sites before and after each run was measured by quantitative titration of the catalytic activity with the hapten as described before (see ref. [3]). The total amount of active catalyst in the experiment was 1.3 μm at the start and gradually dropped to 0.97 μm after five runs. Thus, only approximately 0.06 mol% catalyst was present in each run.

How do they fit so much in?



Keep up with the latest developments in all areas of chemistry.
Order your own personal subscription.

Just fax

USA	Fax: (305)	428-8201
UK	Fax: (0223)	313221
Japan	Fax: (03)	3816 3758
Rest of world	Fax: (0 1149)	62 01-606-184

VCH

Inorganic Structural Chemistry. By *U. Müller*. Wiley, Chichester, 1993. 246 pp., paperback £ 14.95.—ISBN 0-471-93717-7

The significance of this book is well summed up by the following extract: "Chemical and physical properties of a substance can only be understood when its structure is known." Thus, an integrated course on *structural chemistry* which extends beyond organic stereochemistry is a highly appropriate topic for any college chemistry curriculum. This text has been developed from a lecture course given by H. Bärnighausen at the University of Karlsruhe, Germany. With respect to the United States, the level of this book would probably be suitable for advanced undergraduates, or perhaps as a starting graduate text. In Britain, it might well serve as a second-year or third-year coursebook. As in any good teaching text, there are exercise problems, both numerical and descriptive, at the end of each chapter; answers are also provided to many of these. Basic knowledge of atomic theory and bonding are a prerequisite, and some background knowledge of structure determination techniques will be useful. Some familiarity with calculus is helpful, although the mathematics in the text is largely descriptive.

The subject is developed over 19 well-illustrated chapters, which fall into two broad categories. Firstly, there are several general sections which range from *how to describe structures* (either empirically or by a more formal symmetry/crystallographic description), to *what factors are responsible for particular structures* (thermodynamics, atomic/ionic sizes, ligand field theory, simple molecular orbital theory). These are nicely set out, and concepts such as Pauling's rules, VSEPR theory, the Jahn–Teller effect, and simple band theory are covered.

Secondly, there are several chapters detailing the actual structures of non-metals (nice treatment of S, Se, P, As, etc.), continuous structures (diamond-like, etc.), clusters, metals (sphere packing), and polyhedral networks. Some of the more complex structures discussed include zintl phases, chevrel phases, perovskites, and silicate networks. The treatment is up-to-date and well referenced with some 65 primary literature citations: the ubiquitous $YBa_2Cu_3O_{7-\delta}$ high-T_c superconductor phase and C_{60} "buckyballs" are described in the appropriate sections. The treatment of structure in these chapters is descriptive rather than crystallographic.

There is a tantalizingly brief section on the physical properties of solids, which provides an overview of bulk mechanical, electrical, and magnetic properties and their relationship to the structures of solid materials. However, the reader is referred elsewhere for more detailed treatments. It would have useful to include some more examples of real materials here.

There are no details provided on structure determination in this volume, and the two sections on crystallographic descriptions are brief: the first describes the basis of symmetry in three dimensions, and the second largely discusses crystallographic group–subgroup relationships, which may prove to be heavy going for some. I would have liked to see some straightforward descriptions of the crystallographic representation of real structures, perhaps akin to the treatment provided in H. D. Megaw's classic *Crystal Structures: A Working Approach*.

Overall, this book reminded me somewhat of *Structural Inorganic Chemistry* by A. F. Wells, but at a somewhat simplified level, and at a greatly reduced price. It is nicely produced and well set out with the TEX typesetting system, and largely illustrated by means of the ATOMS molecular graphics program. I recommend this book for courses teaching structural chemistry and also for those who wish to obtain a clear and up-to-date overview of this important area of solid-state science.

Bill Harrison
Department of Chemistry
University of Houston
Houston, Texas (USA)

This section contains book reviews and a list of new books received by the editor. Book reviews are written by invitation from the editor. Suggestions for books to be reviewed and for book reviewers are welcome. Publishers should send brochures or (better) books to the Book Editor, Dr. Gerhard Karger, Redaktion Angewandte Chemie, Postfach 101161, D-69451 Weinheim, Federal Republic of Germany. The editor reserves the right of selecting which books will be reviewed. Uninvited books not chosen for review will not be returned.

Gaseous Molecular Ions. An Introduction to Elementary Processes Induced by Ionization. (Series: Topics in Physical Chemistry, Vol. 2. Series editor: Deutsche Bunsen-Gesellschaft für Physikalische Chemie.) By *E. Illenberger* and *J. Momigny*. Steinkopf, Darmstadt/Springer, New York, 1992. XIV, 344 pp., hardcover DM 64.00.—ISBN 3-7985-0870-4/0-387-91401-3

This book is concerned with elementary processes in the ionization of molecular systems. As the title of the series indicates, the emphasis expected from the authors is not so much on giving a comprehensive treatment of the subject as on introducing the reader to a topical area of research from a chemical perspective. Here the authors have sensibly limited their treatment to research topics with which the chemist is likely to be already familiar from a number of aspects, and have reported on the latest state of progress in these areas. The book is of outstanding interest for the chemist, providing not only a survey of well-established experimental techniques such as photoelectron spectroscopy and electron capture but also an up-to-date description of the dynamics of unimolecular breakdown, which is also of interest for teaching purposes. The latest high-resolution laser techniques such as resonance-enhanced multiphoton ionization (REMPI), ZEKE (zero kinetic energy) photoelectron spectroscopy, and photodetachment receive only marginal coverage—these topics could have been treated more effectively in a separate volume.

The book is divided into three parts. The first part deals with experimental techniques for generating molecular ions, the second with the breakdown of electronically excited molecular ions, and the third with electron capture by molecules and clusters. The book certainly lives up to the claim of providing a survey of a large part of this rapidly developing field. The literature coverage is extensive and up-to-date, even including most of the work published in 1991.

In the experimental part, methods such as photoelectron spectroscopy and photoionization mass spectrometry for studying molecular ions are described in detail. Light sources, analyzers, and the important coincidence techniques are described in such a way that the reader will gain a good understanding of the experimental aspects without needing to consult the original literature. Here the authors concentrate on results obtained by single-photon ionization using vacuum-UV sources;

they describe examples of different types of mass spectrometric systems, as well as the most important types of photoelectron analyzers and detectors. This survey is quite comprehensive and reasonably up-to-date, although it would have been useful to draw attention to the laser ionization methods that have recently become so important, by including references to relevant review articles. Also the book does not cover methods for studying free radicals, such as the important photoelectron spectroscopic techniques reported during the last ten years, and the use of photodetachment spectroscopy for studying negative ions is only treated sketchily. Despite these reservations (concerning topics that could only be treated properly in a separate volume), this review of experimental aspects is very useful, as it provides a degree of detail and up-to-dateness that was hitherto only accessible by reading the original literature.

The second part of the book deals with unimolecular breakdown processes in electronically excited molecular ions. As well as describing the most important ionization processes and showing how these can be understood on the basis of molecular orbital theory, the authors give special attention to the energetic aspects (breakdown curves) that are so important to the chemist, and to ionization mechanisms. A digression to consider the possible types of transitions between electronic states of molecular ions is followed by a discussion of the energy distribution in dissociation. Here the authors include a chapter on the application of statistical theories of breakdown (RRKM and QET). Although these methods are also described in other books and in the original literature, this chapter is very useful, even for advanced students. In it the authors discuss the most important points that must be considered when using the RRKM theory, including the choice of the transition state, effects of nonadiabatic interactions, and numerical methods for performing the calculations. However, the effects of rotation and angular momentum on the reaction rate are only treated marginally. Altogether this chapter gives the reader a good introduction to the complexities of the theoretical approaches that are currently available, such as the use of potential surfaces derived by ab initio methods to support RRKM calculations.

The third part of the book is concerned with the 'classical' experimental methods of electron capture in thermal gases. The difficulty with these methods is the poor resolution due to the broad thermal energy distribution, which prevents one from obtaining state-selective information. Here it would have been useful to give a survey of modern techniques, such as the generation of very low temperature negative ions using an ultrasonic beam. The authors also neglect to include the important recent work on the photodetachment of molecular and cluster anions, which yields much more detailed information than the classical electron capture methods. Nevertheless, this part of the book summarizes the most important mechanisms of the formation, stabilization, and energetics of negative ions in a form that will make it much easier for the chemist to get a grasp of this subject.

In this book the authors have succeeded in presenting the subject of molecular ions, which is extremely important to chemists, in such a way that not only physical chemists but also inorganic and organic chemists should have sufficient background knowledge to understand it. The reader is given a very good introduction to the problems of this very active field of research. The book belongs in the library of every chemist who is concerned with matters such as the formation, reactivity, energetics, and kinetics of ions. It is also attractively priced.

Klaus Müller-Dethlefs
Institut für Physikalische und
Theoretische Chemie
der Technischen Universität München
Garching (FRG)

The Organic Chemistry of β-Lactams. Edited by *G. I. Georg*. VCH Verlagsgesellschaft, Weinheim/VCH Publishers, New York, 1993. XI, 381 pp., hardcover DM 189.00.—ISBN 3-527-38188-6/1-56081-083-1

Although it is 65 years since Fleming's momentous discovery of penicillin, research on the chemistry of the 'enchanted ring' (J. C. Sheehan) is still active and flourishing. It is therefore difficult to get a comprehensive overview of all the recent developments in the chemistry of β-lactams. This book aims to remedy that situation by collecting together all the most important results achieved during the 1980s, with a few references to work published up to 1991. Instead of treating individual types of antibiotics in turn, as in similar books on the subject, the authors discuss methods that are of general importance.

The first chapter, "Protective Groups in β-Lactam Chemistry" (H. Wild, 48 pp.) goes straight into practical matters with a survey of the special protecting group methods used, supported by numerous tables. The next chapter, "Introduction and Transformation of Functional Groups in β-Lactam Chemistry" (H. Wild, 71 pp.), well illustrates the extent to which the lability often encountered with the four-membered ring forces one to adapt the reactions and methods to suit special situations. In "Strategies for the Synthesis of Bicyclic β-Lactams" (76 pp.) J. Kant and D. G. Walker describe methods for anellating an additional ring on to the existing β-lactam system. In the chapter entitled "β-Lactam Synthon Method: Enantiomerically Pure β-Lactams as Synthetic Intermediates" (I. Ojima, 59 pp.), we are taken outside the usual area of antibiotics for a description of the use of β-lactams as intermediates for the synthesis of aminoacids, especially optically active products, and of oligopeptides. In "Novel Methods for the Construction of the β-Lactam Ring" (37 pp.) R. J. Ternansky and J. M. Morin Jr. collect together various ring closure reactions for synthesizing β-lactams; however, the information content of this chapter falls well short of that in other treatments of β-lactam antibiotics. Lastly, the editor and V. T. Ravikumar together report on "Stereocontrolled Ketene–Imine Cycloaddition Reactions" as applied to the synthesis of β-lactams (74 pp.). Two topics not covered in the book are syntheses of β-lactams by cyclocondensation of ester-enolates with imines, and reactions of imines with carbene complexes.

The chapters are well furnished with literature references and appear to have been carefully checked; one error that has slipped through appears in the formula of Dane's salt (p. 346). The formula diagrams have evidently been drawn by the individual authors, and consequently they differ in style from chapter to chapter; however, this does not detract from the very good visual impression given by the book. Altogether this is a work which contains much interesting and valuable information for β-lactam chemists, and it can be recommended unreservedly to everyone working in this field.

Jens Nieschalk, Ernst Schaumann
Institut für Organische Chemie
der Technischen Universität
Clausthal (FRG)

Multiple Bonds Between Metal Atoms. 2nd edition. By *F. A. Cotton* and *R. A. Walton*. Oxford University Press, Oxford, 1993. 787 pp., hardcover £ 70.00.—ISBN 0-19-855649-7

In 1994 it will be thirty years since the crystal structure of $K_2Re_2Cl_8 \cdot 2H_2O$ was

determined, and the term quadruple bond was introduced into the literature, together with the recognition that multiple bonds between metals were experimentally accessible. In retrospect it is clear that the occurrence of multiple bonds between metal atoms was discovered in the most favorable circumstances. The previous decade had seen great advances in the understanding of the electronic structure of transition metal compounds, the physical methods necessary for the characterization and study of inorganic materials had largely been developed, and finally, the quadruple bond was first established in the laboratory of one of the most dynamic of modern inorganic chemists, Professor F. A. Cotton. The model of the bonding that was proposed in the very first publications served as a guide for further synthetic efforts, and the increasing availability of X-ray crystal structure determination as a routine tool allowed rapid and unambiguous characterization of the compounds. The subject has developed rapidly, but coherently, to become a paradigm of modern descriptive chemistry. Many high yield syntheses of these multiply bonded compounds are now available, and the bonding exotica of twenty-five years ago have become the readily available starting materials of today. There have, of course, been many surprises in this development, not least in the number of multiply bonded species that may be prepared for a wide variety of transition metals. The extraordinary reactivity of the metal–metal multiple bond (shown for example by the rapid breaking of the carbon–carbon triple bond on reaction of alkynes with $W_2(OR)_6$, or the dissociation of the chromium–chromium quadrupole bond of $[Cr_2(O_2CCH_3)_4]$ in aqueous solution) was hardly predictable.

The continuing interest in this remarkable chemistry has led the authors to produce a second edition of the book they originally published in 1982. The activity during the ten years following its publication was such that the second edition is 70% longer than the first. It comprehensively covers the literature up to 1990, with most of 1991 and some papers of early 1992. After a brief historical introduction, the greater part of the book discusses the compounds according to the metals involved: dirhenium and ditechnetium compounds (111 pp.), dimolybdenum and ditungsten compounds (119 pp.), excluding the $L_3M{\equiv}ML_3$ compounds which are treated in a separate chapter (96 pp.), dichromium compounds (45 pp.), diruthenium and diosmium compounds (32 pp.), dirhodium compounds (71 pp.), other dimetal compounds (31 pp.), and metal–metal multiple bonds in other contexts (97 pp.). Each chapter is logically subdivided according to metal type, metal oxidation state, and ligand type. The text is extremely well presented, with abundant use of tables, figures, and structural formulas. In contrast to this element by element approach, Chapter 10 discusses physical, spectroscopic, and theoretical results for all compounds, and thereby gives a more comparative view. It shows not only the power of modern physical methods, but also the limitations and difficulties of interpretation associated with the methods, be they experimental or theoretical. It is piquant to note that it is easier to measure the metal–metal vibrational frequencies in the first excited state than to make a reasonably accurate ($\pm 10\%$) estimate of the metal–metal bond energy. Finally, Chapter 11 gives a brief coverage of the literature of late 1991 and early 1992. The chapter lengths given above show clearly how metals of Groups 6 and 7 still occupy a dominating position in this field, quite logically since they are most easily obtained in the d^3 and d^4 configurations so well suited for metal–metal multiple bonding. This reviewer was, however, struck by the relative paucity of mechanistic studies involving the classical L_4MML_4 systems in comparison with the abundance of reactivity studies for $L_3M{\equiv}ML_3$ compounds.

The authors are to be thanked for undertaking the arduous task of assembling the data from over 2000 research papers into a critical and comprehensive book, and should be congratulated on their success. As in the case of the first edition, this book will become the standard reference and an essential tool for anyone working in the field. However, this book is too good to leave to specialists alone. The introductory chapter could be read with pleasure and profit by any advanced undergraduate, and the chapter on physical, spectroscopic, and theoretical results, while it may require some cross-references to earlier chapters, is a model of clear exposition and critical examination of results which should interest all inorganic chemists. This book gives a masterly description of one of the most active areas of modern inorganic chemistry, and will serve not only as a reference, but as a stimulus for further research.

Alan F. Williams
Department of Inorganic, Applied and Analytical Chemistry
University of Geneva (Switzerland)

Kinetic Theory and Irreversible Thermodynamics. By *B. C. Eu.* Wiley, Chichester, 1992. 732 pp., hardcover £ 67.00. ISBN 0-471-61 524-2

The thermodynamics of irreversible processes close to equilibrium is now a well-established area of physics and physical chemistry. In order to calculate the increase in entropy resulting from an irreversible process, one assumes that a local thermodynamic equilibrium is established. The flows and the thermodynamic forces driving them are related by appropriately chosen linear equations, in which the reciprocity condition of Onsager and the Curie principle play an important role. The range over which the linear equations are valid must be determined experimentally.

However, irreversible processes also take place under conditions such that the system under observation is far removed from equilibrium and the linear equations are no longer applicable. The theoretical treatment of such processes raises a number of fundamental questions which must be answered before one can attempt to formulate a consistent theory of irreversible processes remote from equilibrium. This monograph is a contribution towards the development of an appropriately extended form of irreversible thermodynamics. The author considers irreversible kinetic equations such as the Boltzmann equation as fundamental relationships that are based on the microscopic equations of motion of particles. The irreversible kinetic equations are used to describe the behavior of macroscopic systems (gases, liquids, etc.). Based on the theory of irreversible processes, methods of solution are developed which are consistent with the laws of thermodynamics.

The book is divided into fifteen chapters. The continuum theory and the thermodynamics of irreversible processes (including a chapter on irreversible processes in electromagnetic fields) are treated in Chapters 2 to 9, then the kinetic theory and the statistical-mechanical basis of irreversible thermodynamics remote from equilibrium are treated in Chapters 10 to 15.

The book is intended for physicists and chemists with interests in this area of theory, and can be recommended for reading by everyone who wishes to learn about the current situation in the development of an extended thermodynamic theory of irreversible processes.

Dietrich Woermann
Institut für Physikalische Chemie der Universität Köln (FRG)

Super-Acids and Acidic Melts as Inorganic Chemical Reaction Media. By *T. A. O'Donnell*. VCH Verlagsgesellschaft, Weinheim/VCH Publishers, New York, 1993. XI, 243 pp., hardcover DM 184.00.—ISBN 3-527-28092-8/1-56081-035-1

There have been a number of monographs on this subject area, most recently the book *Superacids*, by Olah, Surga Prakash, and Sommer, which appeared in 1985 and dealt mainly with the protonation of organic molecules. The latter topic is therefore not treated in the book reviewed here.

After giving the essential definitions of acids and bases and an introduction to the chemistry of aqueous solvent media, the author compares different methods for investigating dissociation in superacids and establishing a scale of acidity. This is followed by a description of the most commonly used acidic solvents, H_2SO_4, CF_3SO_3H, and FSO_3H; in accordance with their importance, considerable space is devoted to hydrogen fluoride and its mixtures with Lewis acids. The part on specific substances covers a wide range, extending from the homonuclear cations of halogens, chalcogens, and metals, through transition element cations in both normal and lower oxidation states, to zintl, polychalcogen, and polyhalogen anions.

The author points out that the various ions described have certain common properties, insofar as polycations can only exist in superacids and acidic melts, whereas polyanions can be formed in basic solvents. This general ordering principle accounts for various observations. Since Br_2^+ and Br_3^+ are only formed in extremely strong superacids with H_0 values of about -19 and -15 respectively, the still significantly electrophilic species Cl_2^+ cannot be isolated as a substance. The example of I_3^+ discussed on pages 109 and 219 provides impressive confirmation that, in addition to the absolute acidity, the individual properties of the solvent play an important role in stabilization. The fact that bases catalyze the disproportionation of polycations is regarded as highly significant. The author cites many examples of this behavior, which is observed both in superacids and in chloroaluminate melts when their basicity is increased. Aspects of the chemistry in salt melts are also discussed at length, with special attention to the similarities and differences compared with superacids.

This book is well worth reading, not only for its systematic treatment but also for the valuable practical hints on working with these very difficult solvents. For example, how many chemists already know all the factors that must be observed in order to achieve the record value $H_0 = -21$ in HF/SbF_5?

The subject matter is clearly arranged, and the individual chapters can be read independently of each other. Many cross-references are given, so that one can work through the material quite rapidly. A less satisfactory aspect is that, apart from his own publications, the author relies mainly on the reviews by Gillespie, Passmore, Corbett, Mamantov, and others, while neglecting the primary literature, especially the most recent work. Consequently the book is not very up-to-date. However, despite some shortcomings in matters of detail it can be recommended unreservedly for advanced students.

Rolf Minkwitz
Fachbereich Anorganische Chemie
der Universität Dortmund (FRG)

Icons and Symmetries. By *S. L. Altmann*. Oxford University Press, Oxford, 1992. VIII, 104 pp., hardcover £ 14.95.—ISBN 0-19-855 599-7

The subject of symmetries and their mathematical description using group theory is a popular one for book authors. It has become difficult even to keep track of the number of textbooks written specifically for chemists. Simon Altmann has already published several monographs and textbooks on the subject, all of which introduce novel aspects, both in content and form of presentation.

Thus, one opens this slim book with great curiosity, and is not disappointed. Treating the subject at a mathematical level accessible to most readers, Altmann uses three case studies, taken from his lectures in the Science Faculty of the Catholic University of Leuven, to explore the relationships between physical objects, models, and symbols ("icons"). Although he cites Hermann Weyl's well-known book *Symmetry* as the model for these lectures, Altmann wisely decides on a different, quite original, approach. He discusses the formulation of the physical problem hand-in-hand with the historical and philosophical aspects, with the aim of showing how ideas of symmetry have entered into our scientific thinking. Thus, the book is concerned with discussing symmetry in a general way rather than with formally describing it by group theory, and accordingly the term "group" is not even mentioned.

The three examples can be roughly classified as belonging respectively to physics, mathematics, and chemistry. In the first the author discusses the concept of symmetry from the standpoint of Oersted's paradox concerning the interaction between a compass needle and an electric current. This involves mirror image symmetry—to be more precise, the transformation properties of vectors on reflection. Altmann compares different formulations of the symmetry principle by Archimedes, Thomas Aquinas, and Pierre Curie ("Lorsque certaines causes produisent certains effets, les éléments de symmetrie doivent se retrouver dans les effets produits"). [Since definite causes produce definite effects, the elements of symmetry must be deduced from the effects that they produce.] He shows very convincingly the sort of confusion that can arise if one applies symmetry uncritically to analyze a physical problem and equates the properties of a symbol such as a vector arrow with those of the physical entity that it represents. Nowadays we are all familiar with the need to distinguish between polar and axial vectors.

In the second example Altmann discusses the relationship between quaternions and rotations, which he treated in detail a few years ago in a monograph devoted to the topic. He relates the fascinating history of quaternions as an example of how even such a clever intellect as that of Hamilton, the inventor of quaternions, could be led astray through a wrong choice of an "εικών". In a conclusive analysis Altmann shows how this error, which influenced later developments over a long period, was related to Hamilton's particular philosophical view of nature. Hamilton arrived at the idea of quaternions by an algebraic route while attempting to further generalize complex numbers. Altmann contrasts Hamilton's approach with that of Rodrigues, who, independently and at almost the same time, developed a theory of rotations from a geometrical standpoint. The chapter ends with a rigorous and detailed consideration of the transformation properties of vectors, with a look also at tensors and spinors and their symmetry properties.

In the third chapter the author discusses the use of symmetry considerations to classify the energy levels of atoms and solids. He bases the latter on a version of the band structure theory of solids reduced to its minimum essentials, that of a linear chain. Next he discusses the problem of symmetry breaking, taking as an example the Peierls instability of polyacetylene. Here again a paradox only arises if one too hastily equates the symmetry of the model with that of the real physical situation. However, as the author himself

 © VCH Verlagsgesellschaft mbH, D-69451 Weinheim, 1994 0570-0833/94/0404-0482 $ 10.00+.25/0

points out, the reader needs to be more adept at formal reasoning here than in the rest of the book, in order to follow the proof given here for the degeneracy of states at the boundaries of the Brillouin zone in a quasilinear chain as a consequence of the presence of a glide plane. Nevertheless, it is difficult to see why the author, despite his insistence on care in the choice of symbols, does not use two orbital representations of the corresponding Bloch functions, which would have immediately convinced any chemist that a degeneracy exists.

This book contains many ideas to stimulate the reader to think about symmetry and its effects as they relate to describing nature. The historical perspectives undoubtedly help here, although occasionally these are presented in a way that the reader may find trying. Sometimes one has the impression that extra details are included not so much to illuminate the problem as to show off the author's historical knowledge. At one point (p. 44) it seems that he is conscious of this himself: "...and thus you will feel like closing the book. If this is so, please listen to my entirely disinterested advice (my royalties are paid to me even if you burn this book) and go on reading...". This style is perhaps not to everyone's taste. It also seems a little surprising when the author, in the preface, expresses a wish that young people might read this book before coming to university. Despite these comments, the book can be thoroughly recommended to everyone who wishes to become involved with symmetry and its role in science.

Notker Rösch
Lehrstuhl für Theoretische Chemie
der Technischen Universität München
Garching (FRG)

Charge Transfer Photochemistry of Coordination Compounds. By *O. Horváth* and *K. L. Stevenson*. VCH Publishers, New York/VCH Verlagsgesellschaft, Weinheim, 1993. XVIII, 380 pp., hardcover $ 98.00, DM 238.00.—ISBN 1-56081-564-7/3-527-89564-7

It is now almost a quarter of a century since Balzani and Carassiti, in their classic work *Photochemistry of Coordination Compounds* (Academic Press, 1970), presented the last comprehensive picture of the subject. In the monograph reviewed here, O. Horváth and K. L. Stevenson set out to bridge this gap in time for an important part of that subject, namely charge transfer photochemistry. Their treatment is mainly concerned with photoreactions in which the primary step is a charge transfer process involving light excitation of a Werner type metal complex in homogeneous solution. The book also briefly covers some photoredox reactions of such complexes in the solid state or in microheterogeneous systems. The restriction of the coverage of the photochemistry of organometallic compounds, which is stated in the preface, is only departed from significantly in the treatment of rhenium complexes.

The book is divided into two parts, with thirteen chapters altogether. The first part consists of three chapters which deal, mainly in a condensed form, with the basic principles of the spectroscopy, photochemistry, and photophysics of coordination compounds. The second part covers in detail the results published up to the beginning of 1991 on the charge transfer photochemistry of the complexes, arranged according to the group of the Periodic Table to which the central atom belongs. Here the authors have sensibly devoted most attention to the photochemistry of the Main Group metals, previously only rather scantily covered in monographs, while presenting in condensed form the photochemistry of ruthenium(II)-polypyridyl complexes, which has already been very adequately reviewed elsewhere. To make the work as up-to-date as possible there is a bibliographic appendix listing publications that appeared in the period 1990–1992 and could not be reviewed in the individual chapters. A further appendix explains the abbreviations and symbols used, and the volume is completed by formula and keyword indexes.

The exhaustive coverage of experimental results makes this book a mine of information for the professional photochemist. On the other hand, it is doubtful whether the authors have succeeded in their declared aim of presenting the subject in an attractive way to many potential newcomers. There are three main reasons for this. Firstly, the concentration on experimental results has meant that many fascinating applications of charge transfer photochemistry, such as solar energy conversion, information processing, or the generation of catalytically active species for organic synthesis, have had to be virtually ignored. Secondly, the arrangement of the complexes according to which group of the Periodic Table the central atom belongs to creates a problem, as it means that generalizations within individual chapters are rarely possible, since the direction of the photoinduced charge transfer, and therefore the subsequent reaction steps, are greatly dependent on the oxidation state of the central atom and the nature of the ligands. The authors have tried to take this into account by dividing the chapters into subsections for different oxidation states of the central atom and by including many cross-references. However, it is hard to understand why the further subdivision according to coordination pattern that has been used in the text is not indicated in the list of contents. Thirdly, it would have been desirable to have a summary classifying the reactions according to broad types.

Regrettably, the reader is often confused by the inconsistent use of terms and symbols, and by the many printing errors which in some cases alter the meaning. For example, the quantum yield is represented by the symbol Π in the introduction and in the list of abbreviations and symbols, whereas in the main text the more usual symbol Φ is used. The neutral complex $[Co(gly)_3]$ is shown in the formula index, and sometimes also in the text, with a triple positive charge. The acetate ion in Equation 9.123 is shown as retaining its negative charge even after oxidation. In the text accompanying Equation 12.29 reference is made to a ring-opening with cleavage of a Co–C bond, whereas the formula diagram shows cleavage of the Co–N bond. In the classification of charge transfer transitions in Chapter 3 the expression 'ion pair charge transfer' (IPCT) is not mentioned, despite the fact that it is used frequently, even incorrectly in a few cases (pp. 94, 163). Lastly a word about the presentation: in the illustrations to the chapters of the second part the authors have gone to the trouble of converting the formula diagrams and spectra copied from the original papers into a uniform style; however, the result is not altogether convincing when compared with the quality of the figures in the first part.

Notwithstanding these critical comments, the book is likely to be very well received by both coordination chemists and photochemists. The former will learn how light can serve as a reagent by interacting with their compounds in ways that may be new to them, while the latter will appreciate having easy access to a large collection of factual material. Therefore, despite the high price it deserves a place in every chemical library.

Roland Billing
Fachbereich Chemie
der Universität Leipzig (FRG)

Organic Photochemistry: A Visual Approach. By *J. Kopecký*. VCH Publishers, New York/VCH Verlagsgesellschaft,

 © VCH Verlagsgesellschaft mbH, D-69451 Weinheim, 1994 0570-0833/94/0404-0483 $ 10.00+.25/0

Weinheim, 1992. IX, 285 pp., hardcover DM 98.00.—ISBN 0-89573-296-3/3-527-26952-6

This book is an introduction to organic photochemistry for students who have already assimilated "regular" organic chemistry, and for mature synthetic organic chemists. Nothing new there, one might think. Not so, because the book is based on a brilliant teaching concept. Many chemists would rather listen to lectures than read books, as the former are illustrated by slides which present scientific information in a remarkably concentrated and striking form which is well suited to the strongly visual nature of the scientist's thinking, especially that of the organic chemist. Thus one should write a book in the style of a slide presentation, with the "slides" arranged one after another on the left-hand side and the explanations on the right. The book consists of 16 such "slide talks": an introduction; electronically excited states; photophysical processes; theoretical concepts; eight chapters on individual compound classes; photochemical oxidations and singlet oxygen; preparative techniques; factors influencing the progress of photochemical reactions; applications (including a last example from outside the research laboratory, concerning what happens to beer in sunlight and why it is better kept in brown bottles than green ones). The book is illustrated by 597 "slides", representing an enormous amount of work by the author and his colleagues. These are intended to be mainly self-explanatory, so that the accompanying text should be almost superfluous. This works very well in the chapters dealing with the photochemical behavior of the individual compound classes, but is less well suited for the first four chapters which are more theoretical. For the novice meeting these ideas for the first time, much of the content of these first four chapters will probably remain enigmatic, despite the explanatory text, which needs to be expanded in some parts to remedy this; space for this could be made by eliminating some of the repetitions. However, for the reader who has failed to understand some points, the many literature references on particular matters in the theoretical chapters and the detailed lists of material for further reading should help considerably. Throughout the book generally, the original literature is thoroughly covered; for example, there are 776 references just in the chapters on photochemical reactions. It is unfortunate, though, that the CIEEL (chemically induced electron excitation luminescence) mechanism receives only one brief mention (in 13.26), with neither an explanation nor a literature reference. The chapter on applications is excellent, not only describing industrial and analytical applications but also emphasizing the importance of photochemical reactions in biology, medicine, and the environment.

In a work of this kind one inevitably finds that a few errors have crept in. The incidence of errors in the physical and theoretical sections is somewhat higher than elsewhere. This begins with Figure 1.3, where the vibrational energy in the electromagnetic spectrum should correspond approximately to the range 2500–15000 nm rather than 700–1100 nm, and the values of the λ(cm)-scale should be reduced by about a factor of ten. The symmetry symbols contain a number of errors: for example, in 2.30 (explanatory text) the subscripts 2 and 1 relate not to σ_v but to C_2' (through the atoms). Similarly in 2.29 (the figure), it should be mentioned that, depending on symmetry group, these same two subscripts may relate not to σ_v but to C_2'. Also, in the same figure, the symbols A, B do not have the absolute significance for certain groups (D_{nd} and S_n) that is given here. The direct product $E_{1g} \times E_{2u}$ is incorrectly written in 2.31 (figure) and in 2.33 (text) on the left-hand side of each equation. In 2.31 (figure), where the point group is given as $D_{6\infty}$ instead of $D_{\infty h}$, the error is innocuous and immediately obvious, but a more serious error appears in 5.3 (figure), where the T_1 and T_2 states of the planar ethylene molecule are wrongly denoted as $^3B_{2g}$ and $^3B_{2u}$ (instead of $^3B_{1u}$ and $^3B_{3u}$). In 3.11 (text) it appears that the first two arrows should be reversed. In the equations given in 3.44 and 3.45 $\Sigma_i k_1$ should be replaced by $\Sigma_i k_i$, $1/k_i$ by $1/\Sigma_i k_i$, and $k_q + k_q$ [Q] by $k_d + k_q$ [Q]. In 4.13 (figure) under (c), "adiabatic" should be "nonadiabatic". In 4.23 (figure) the "bonding interactions" for $A^{\bullet +}$ are wrongly stated to be always weakened compared with those for A; if the outermost electron of A is in an antibonding molecular orbital (MO), the bonding interactions are instead increased ($N_2H_4 \rightarrow (N_2H_4)^{\bullet +}$, $O_2 \rightarrow (O_2)^{\bullet +}$). The entire analysis in Figure 13.9 is incorrect, since both the highest occupied MO and the lowest unoccupied MO of $^1\Delta_g - O_2$ are not symmetric but antisymmetric with regard to a reflection through the plane perpendicular to the axis of the molecule. The "organic" chapters contain a number of incorrect formula diagrams (in 5.29, 6.31, 6.42, 9.11, 15.3, two in 15.30, and 15.43); these are innocuous, since even the novice reader will notice that something is wrong and can look it up if necessary. In 5.17 cyclohexene is a badly chosen example to illustrate the text, since in this particular case dimerization occurs via *cis–trans* isomerization. In 5.18 the value of E_T for acetone should be 79–82 instead of 75. In 6.10 the middle arrow should be a two-way one (mesomerism, not reaction). In 2.86 (text) the descriptions "in the plane of the molecule" and "perpendicular to the molecular plane" should be interchanged, as also should "electron deficient" and "electron rich" in 8.27 (text). In 13.43 (figure) CP$^\bullet$ should be CP$^{\bullet +}$ in both cases.

There are also some explanations that could be misunderstood. In 2.10 (text, fifth sentence) the impression is given that no molecular π-orbitals are present in molecules such as O_2, N_2, and acetylene. (Although these molecules have no low-lying Π-states they do have π-MOs.) In 2.23 (fourth sentence), 2.38 (first sentence), and 6.40 (first sentence) some readers may have difficulty in understanding the author's meaning, even though the facts themselves are simple. In 3.7 the reasoning would be much clearer if the words "thermally equilibrated" appeared before S_1 and T_1 in the statement of Kasha's rule. In any case, Ermolaev's rule is not a consequence of Kasha's rule, and to emphasize it in 3.7 is misleading, as it is so seldom valid for solutions. In 4.3 (figure), the explanation could be expressed more simply as follows: "The total number of electrons involved, divided by two, plus the total number of antarafacial interactions is even." In 8.28, the *cis–trans* isomerization of 1,2-dicyanoethylene is, of course, not "stereospecific", as is stated in the text and suggested by the figure; instead it always yields a *cis–trans* mixture.

However, these shortcomings (and others that have no doubt passed unnoticed) can be remedied, though the reader should be aware of them. They are of relatively little importance compared with the great service to organic photochemistry that is achieved in this book. It is a great pity that Professor Kopecký is no longer here to witness the favorable reception of his book. One certainly wishes it great success!

Johannes Leitich
Max-Planck-Institut für Strahlenchemie
Mülheim an der Ruhr (FRG)

Nitrogen Donors in Organometallic Chemistry and Homogeneous Catalysis

Antonio Togni* and Luigi M. Venanzi

Homogeneous catalysis has been responsible for many major recent developments in synthetic organic chemistry. The combined use of organometallic and coordination chemistry has produced a number of new and powerful synthetic methods for important classes of compounds in general and for optically active substances in particular. For this purpose, complexes with optically active ligands have been used, most of them coordinating through phosphorus. More recent developments have highlighted the use of "nitrogen-donors", particularly as they are easily obtained from the "chiral pool". However, the remarkable achievements in this area have been based on an empirical approach. This article attempts to bridge the gap between the synthetic and the coordination chemist. The first section discusses the rates of formation and dissociation of complexes with nitrogen donors, their relationship to the rates of product formation, and presents the factors which induce homolytic cleavage of M–C bonds. It also provides a summary of the main types of organometallic complexes formed by metal centers coordinated to nitrogen donors and their reactivity patterns. The second section highlights the most significant, homogeneously catalyzed reactions involving complexes with nitrogen ligands. Foremost among them are the asymmetric aspects of hydrogenation (particularly those involving boranes as reducing agents), hydrosilylation, cyclopropanations, Diels–Alder reactions, aldol condensations, alkylation of aldehydes, conjugate addition reactions, Grignard cross-coupling reactions, allylic alkylations, oxidation reactions, olefin epoxidations, and dihydroxylation of olefins.

1. Introductory Remarks

The development of organometallic chemistry and homogeneous catalysis during the last forty years, and particularly that involving transition metals, has been closely associated with the realization that their formation, stability, and reactivity are governed by the fundamental rules of coordination chemistry.[1] Thus, an awareness of these rules is essential for any rational discussion of organometallic reactions.

When applying these rules to carbon donors one must take into account the fact that the great majority of compounds containing M–C bonds also contain coligands (often referred to as "spectator ligands", although their real role is far from that of being mere spectators) which have donor atoms other than carbon. Foremost among these are the P-donors. Two other essential coligands in organometallic chemistry are the hydride ion and CO, itself a C-donor. Indeed these two ligands played a central role in the early developments of the synthetic applications of organometallic chemistry, particularly because of their dual role as "reagents" and coligands.

Textbooks of organometallic chemistry and homogeneous catalysis[2] make sporadic reference to the use of N-donors, but hitherto no attempt has been made to systematize their role, as has been done for P-donors. Furthermore, although phosphorus donors and their higher homologues have received much attention, and numerous books and reviews describing their coordination chemistry have been published,[3] nothing of the kind has occurred for the organic nitrogen donors, possibly because their complexes have not been extensively used for synthetic organic applications. Therefore, this article will discuss the role of the N-donors in the above areas, often by comparing and contrasting them mainly with P-donors.

[*] Prof. Dr. A. Togni, Prof. Dr. L. M. Venanzi
Laboratorium für Anorganische Chemie der Eidgenössischen
Technischen Hochschule
ETH-Zentrum
Universitätstrasse 6, CH-8092 Zürich (Switzerland)
Telefax: Int. code + (1)252-8935

2. Fundamental Concepts of Organometallic Chemistry

The organometallic chemistry discussed here is concerned with the formation, transformation, and rupture of M–C bonds. Nevertheless, as this review emphasizes the role of complexes with nitrogen donors in organic synthesis, reactions that are not organometallic in the sense defined above will also be included in the section dealing with catalytic processes.

The metal centers which will feature prominently are those of the transition and post-transition series, although the organometallic chemistry of the lanthanides and actinides is being actively investigated.[4] Organometallic compounds of some of the alkali and alkaline earth elements, as well as those of boron

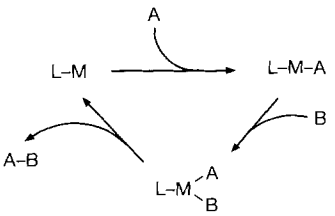
and aluminum, are frequently used as reagents or catalysts in the reactions described later. Furthermore, there is no fundamental difference between their chemistry and that of the transition and post-transition elements: They share an essential and common feature in their "coordination behavior", even though boron and aluminum frequently form compounds having three-center, two-electron bonds.[5]

As its title implies, this review will be mainly concerned with compounds containing nitrogen donors as coligands and their organometallic chemistry. For this purpose it will be useful to summarize briefly the main features of coordination behavior, of the carbon donors and their properties, and of the nitrogen donors.

2.1. Coordination Behavior

Any atom, generally referred to as the "central atom", which possesses low energy orbitals containing fewer electrons than required for the formation of the maximum possible number of conventional, two-electron covalent bonds, can easily form more bonds than its "classical" covalency implies. In other words, a molecule containing such a central atom is a Lewis acid. Conversely, a Lewis acid is a molecule containing such a central atom and is said to be "coordinatively unsaturated". This is a major feature in the context of this article, as many Lewis acidic complexes containing nitrogen donors play a role in catalytic processes (see, for example, Sections 5.6 and 5.7).

As will become apparent later, the most prominent application of complexes containing nitrogen donors is the synthesis of optically active organic molecules. For most organometallic reactions of interest here, one can envisage a pathway of the type shown in Scheme 1.



Scheme 1. A general description of organometallic or related reactions. L = coligand or ligands; M = central atom; A, B = organometallic or other reagent.

The ligand or ligands denoted by L in this Scheme may fulfill a variety of functions:

1. modulation of the electron density at the central atom M and, therefore, its reactivity;
2. blocking of a number of coordination sites at M and, consequently, control of the multiplicity and symmetry of the valence orbitals available for the organometallic reaction;
3. provision of the environment within which the organometallic reaction will take place.

Furthermore, the dynamics of the M–L interactions play a crucial role in successful organometallic reactions. This is obviously connected with the dissociation rate of the M–L fragment: if it is much faster than the rate-determining step for the formation of A–B, the ligand L will not exert a significant influence on the organometallic reaction. Important exceptions to this simplified behavior are those catalytic systems in which ligand-induced acceleration is observed (see Section 5.12.2). It follows that, when considering the role of a coligand L (a nitrogen donor in our case), not only the thermodynamics[6] but also the kinetics of complex formation between M and L must be considered.

Before discussing these factors it is appropriate to say a few words about the organometallic steps of a reaction sequence. An essential feature of a catalytic reaction is that it includes one step that is either irreversible or virtually irreversible. Most frequent-



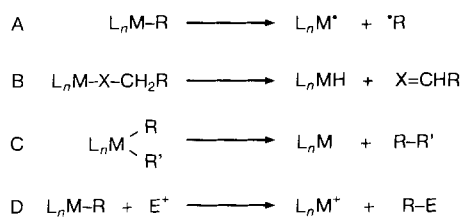
Antonio Togni, born in 1956 in Roveredo, Switzerland, studied chemistry at the Eidgenössische Technische Hochschule (ETH) Zurich, where he completed his Diploma in 1979, and his Ph.D. in 1983, working with Luigi M. Venanzi. After a postdoctoral year at the California Institute of Technology in John E. Bercaw's group and a short stay with Alberto Albinati at the University of Milan, he returned to the ETH as a research associate. In 1985 he joined the Central Research Laboratories of CIBA-GEIGY Ltd., where he spent seven years as a research scientist in the field of asymmetric catalysis. He is currently Assistant Professor of Organometallic Chemistry at the Laboratory of Inorganic Chemistry at ETH. His research interests are in the field of homogeneous catalysis and molecular materials.



Luigi M. Venanzi was born in Rome in 1927 and received his Diplom in Chemistry at the University of Kiel in 1952. He then joined the Butterwick Research Laboratories of ICI Ltd., working in the group of J. Chatt. In 1956 he was appointed ICI Research Fellow at the University of Oxford. After attaining the degree of D. Phil. in 1958, he became a Lecturer at the Inorganic Chemistry Laboratory and a Fellow of Magdalen College, Oxford, positions he held until 1968 when he joined the State University of New York at Albany as Professor of Chemistry. In 1971 he became E.I. du Pont Professor and Chairman of the Chemistry Department at the University of Delaware. He has been Professor of Inorganic Chemistry at the ETH in Zürich since 1973. His research interests range from homogeneous catalysistro cluster chemistry, with a strong bias for the coordination chemistry of the platinum-group metals and polydentate phosphanes.

ly, this is a reductive elimination reaction,[2] as shown in the last step of Scheme 1, where either a C–H or a C–C bond is formed. Furthermore, in principle, one can envision the same organometallic reaction with a variety of coligands coordinating through different donor atoms; their electronic nature and geometry will favor, or disfavor, one or more steps of the same reaction. Thus for the same metal, a given catalytic cycle may be more or less disfavored by the use of a particular ligand, or, for the same ligand, by a suitable choice of metal.

At this point it is necessary to discuss *undesirable* organometallic reactions. Foremost among them are those leading to the homolytic cleavage of M–C bonds and, consequently, to loss of regiochemical or stereochemical selectivity (Scheme 2).



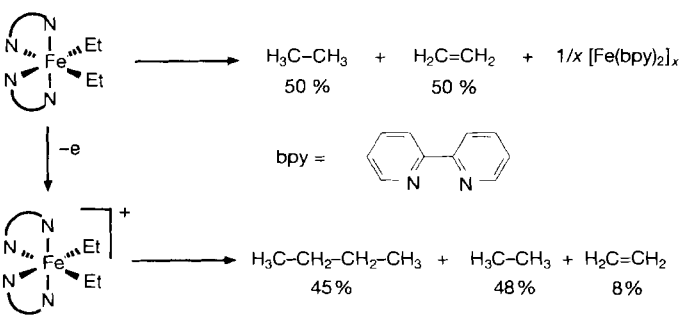
Scheme 2. Processes leading to the cleavage of an M–C bond: A) homolytic cleavage [7]; B) β-hydrogen abstraction [8]; C) reductive elimination [9]; D) electrophilic attack at a coordinated carbon atom [10].

Nucleophilic displacement of a coordinated C-σ-donor is generally associated with its transformation into a π-donor and will not be considered here.

While reactions B–D in Scheme 2 can constitute integral parts of desirable catalytic cycles, reaction A is generally to be suppressed, and therefore metal complexes in which homolytic cleavage can easily take place should be avoided.

The ease of cleavage A is related to the stability of the resulting fragments $L_mM^{\bullet}$ and $^{\bullet}$R. However, the role of the metal-containing fragment is the more complex given the variety of metal centers, their spin states, and the number and nature of the accompanying ligands. The foremost consideration is that the unpaired electron, associated with the metal fragment produced after the homolytic cleavage, will be localized on the metal center, thereby lowering its oxidation state by one unit.

A good example of this effect is shown in Scheme 3.[11] The "normal" mode of Fe–C cleavage of the d^6 Fe^{II} compound, a β-H abstraction reaction, changes to a radical decomposition



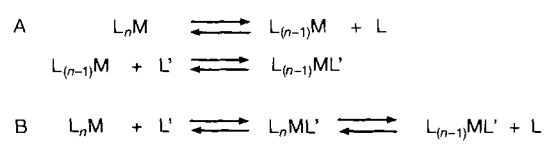
Scheme 3. Different decomposition pathways of dialkyl Fe^{II} and Fe^{III} complexes (β-hydrogen elimination vs. homolytic cleavage) [11].

after the corresponding d^5 Fe^{III} complex is formed. In general, whenever the metal complex can give another stable species with the metal center in an oxidation state one unit lower, homolytic cleavage will be favored. Complexes of the metal centers d^7 Co^{II} and d^9 Cu^{II} provide good illustration of this behavior. On the other hand, homolytic cleavage in d^8 Ni^{II} complexes is uncommon.[12]

Thus the *preferred* metal centers for organometallic reactions should have even-numbered electron configurations, particularly d^0, d^6 (low spin), d^8 (low spin), and d^{10}. However, numerous exceptions are known (e.g., d^7 Rh^{II} in Section 5.5.3, or d^5 Fe^{III} in Section 5.6).

These redox reactions do not prevent the use of catalyst precursors containing metal centers with electron configurations such as d^7 and d^9, as, upon addition of an organometallic reagent, reduction will take place, and the metal center of the resulting complex will be in the oxidation state best suited for catalysis (see, for example, the cobalt catalyst in Section 5.2.2). However, the use of a catalyst precursor containing the metal center in the appropriate oxidation state is usually preferable, as fewer side-reactions are then likely.

Any discussion of ligand exchange processes must be approached from their reaction mechanisms. These can be conveniently described in terms of the two extreme models illustrated in Scheme 4.[13] In the absence of specific information about a



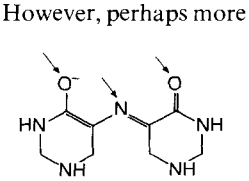
Scheme 4. The limiting models for the mechanism of a ligand exchange process. A: dissociative, B: associative.

given ligand-exchange reaction in organometallic chemistry, one can judiciously use the following generalizations:

1. Coordinatively saturated complexes, particularly those in which the central atom has either an effective atomic number (EAN) of 18, or a half-filled d shell, are likely to undergo ligand exchange by a dissociative process.
2. Coordinatively unsaturated complexes, that is, those with EAN < 18, *may* undergo ligand exchange by an associative mechanism.

It is apparent from these generalizations that one cannot always expect a direct correlation between velocity of a ligand exchange and thermodynamic stability of a given ML_n complex. However, for dissociative ligand-exchange processes their rates are presumably closely related to the strengths of the M–L interactions in the ML_n complexes.

Before discussing the factors influencing ligand exchange rates, it is useful to have an idea of their range. The most complete set of data relates to water exchange in most metal cations, which extends from 10^{-7} to 10^9 s^{-1}.[14] However, perhaps more relevant to the chemistry discussed here are the dissociation rates in complexes with polydentate ligands. Some data for murexide [valid for reaction (a)], which, under the experi-



1

mental conditions used, acts as a uninegative, terdentate ligand coordinating through the donor atoms indicated by the arrows in the structure sketched below, are listed in Table 1.[15]

Table 1. Some rate constants for reaction (a) in 0.1 M KNO_3 at pH 4.0 and 10 °C.

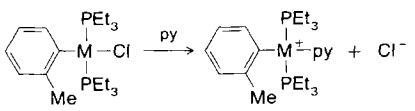
M^{z+}	k_1 [$M^{-1}s^{-1}$]	k_{-1} [s^{-1}]	M^{z+}	k_1 [$M^{-1}s^{-1}$]	k_{-1} [s^{-1}]
Ca^{2+}	$\geq 6\times10^7$	$\geq 1.6\times10^5$	In^{3+}	2.0×10^6	50
Sr^{2+}	$>6\times10^7$	$>6\times10^5$	Sc^{3+} [a]	4.8×10^7	1.5×10^3
Mn^{2+}	ca. 9×10^6	ca. 7.5×10^4	Y^{3+} [b]	1.7×10^7	5.5×10^3
Co^{2+}	1.5×10^5	5.1×10^2	La^{3+} [b]	8.6×10^7	3.2×10^4
Ni^{2+}	1.0×10^3	0.41	Gd^{3+} [b]	5.2×10^7	4.3×10^3
Cu^{2+}	1.2×10^8	5.2×10^3	Tb^{3+} [b]	3.0×10^7	3.3×10^3
Zn^{2+}	2.0×10^7	2.0×10^4	Lu^{3+} [b]	1.3×10^7	4.5×10^3
Cd^{2+}	1.1×10^8	7.8×10^3			

[a] At pH 3.0 and 12 °C. [b] At 12 °C.

$$M^{z+}_{aq} + \mathbf{1} \underset{k_{-1}}{\overset{k_1}{\rightleftharpoons}} [M(\mathbf{1})]^{(z-1)+} \qquad \text{(a)}$$

As can be seen, even these rates span a very wide range, which is comparable to that of water exchange if the same metal ion is used. Several factors influence these rates. Foremost among them are the electron configuration, ionic charge, size, spin-state, coordination number, and geometry of the metal center, the ionic charge of the complex, the nature of the coligands, and the nature of the chemical reaction.

One further general point is that the kinetics of substitution reactions for transition metal complexes with the same outer electron configuration are faster for metal centers of the first transition series than for the corresponding centers of the second and third transition series, as can be seen for the examples shown in Scheme 5.[16]



M	T [°C]	k_{obs} [s^{-1}]
Pt	25	1.7×10^{-5}
Pd	−40	5.8×10^{-3}
Ni	−65	1.6×10^{-2}

Scheme 5. Ligand exchange reactions for Ni^{II}, Pd^{II}, and Pt^{II} complexes with pyridine ([py] = 6.2×10^3 M) [16].

Another consideration should be kept in mind: ligand-disproportionation reactions [Eq. (b)] can easily occur. Obviously,

$$2MLX \rightleftharpoons MX_2 + ML_2 \qquad \text{(b)}$$

processes of this type are to be avoided as, in such cases, the organometallic reaction at one center is not influenced by the nitrogen ligand, while the second center, being strongly coordinated to two L moieties, may not be available for the organometallic reactions. This disproportionation can be prevented by the use of nitrogen ligands with bulky substituents.

Useful reactivity is likely to be found for metal ions that show intermediate exchange rates (10^{-2} to 10^2 s^{-1}). The lower boundary is fixed by the need to have a reasonably fast catalytic reaction, while the higher boundary is coupled to the speed of the organometallic transformation leading to the product, as this must clearly be faster than the ligand-exchange rate. This is merely a guideline, and significant deviations can be found in practice as the intrinsic lability of a given metal center can be decreased or increased in a variety of ways. Therefore, the range of "useful" metal centers can be considerably extended.

When nitrogen donors are used as coligands one has to solve a problem which does not arise with Lewis bases coordinating through phosphorus atoms. As has been pointed out when discussing Scheme 1, the influence of the ligand L will be felt if the M–L exchange rate is significantly slower than the rate of the organometallic reaction, as is the case of a phosphorus donor, which has the great advantage of labilizing the ligand *trans* to it. The labilizing effect of a given ligand upon the rates of substitution of other ligands present in the same complex has been extensively studied. In the present context one only needs to consider the *trans* effect, that is, the labilizing effect of one ligand upon another situated in *trans* position.[17] Some data on this effect are summarized in Table 2.

Table 2. The more common donors arranged in order of decreasing *trans* effect, and approximate values of the exchange rates of the *trans* ligands in a Pt^{II} complex [13a].

trans effect	Donor ligand	$k_{rel.}$
very large	CO, CH^-, C_2H_4, $PR_3 \approx H$	ca. 10^5
large	$SC(NH_2)_2$, NO_2^-, I^-, SCN^-, CH_3^-, $C_6H_5^-$	ca. 10^2
moderate	Br^-, Cl^-	ca. 1
weak	py, NH_3, OH^-	ca. 10^{-1}

As can be seen, in a given complex one can have a substitutionally inert, coordinated phosphane ligand and *trans* to this P-donor, a kinetically very labile ligand. This, unfortunately, is not the case for nitrogen donors, because they are among the ligands that exert the weakest *trans* effect. Nevertheless, coordinated amines do impart a smaller labilizing effect on the residual ligands, as can be seen from the data shown in Table 3.[14] However, generally, in order to have reasonable reaction rates in the case of complexes containing nitrogen coligands one must choose labile metal centers and find a way of reducing the lability of the metal–nitrogen bond(s).

Table 3. The labilizing effect on M-OH_2 bonds of coordinated aliphatic amines, as expressed by the water exchange reaction.

$$[Ni(H_2O)_{6-n}L_n]^{2+} + H_2O \overset{k_{H_2O}}{\rightleftharpoons} [Ni(H_2O)_{6-n-1}L_n]^{2+} + H_2O$$

Complex [a]	k_{H_2O} [b]
$[Ni(H_2O)_6]^{2+}$	3×10^4
$[Ni(H_2O)_5(NH_3)]^{2+}$	2.5×10^5
$[Ni(H_2O)_4(NH_3)_2]^{2+}$	6.1×10^5
$[Ni(H_2O)_4(en)]^{2+}$	4.4×10^5
$[Ni(H_2O)_3(dien)]^{2+}$	1.2×10^6
$[Ni(H_2O)_2(trien)]^{2+}$	2.9×10^6
$[Ni(H_2O)_3(tach)]^{2+}$	3.8×10^6

[a] en = ethylenediamine, dien = diethylenetriamine, trien = triethylenetetramine, tach = 1,3,5-triaminocyclohexane. [b] At 25 °C; k_{H_2O} is defined as $k_f(6)/k_{obs}(6-n)$, where n is the number of bound nitrogen ligands; k_f = rate constant for the formation reaction.

This can be achieved by the use of polydentate or anionic ligands of rigid structure optimally designed to fit the size of the metal center (see, for example, the polydentate ligands in Section 5.12.1). The lower lability of chelating systems has been amply demonstrated in classical coordination compounds. As can be seen from Table 4,[18] monodentate ligands are much

Table 4. Rate constants [s^{-1}] for the dissociation of mono- and bidentate nitrogen heterocycles [s^{-1}] from Ni^{II} and Co^{II} complexes: $T = 25\,^{\circ}C$, pH ≈ 6.0.

Complex [a]	M = Ni	M = Co
$[M(H_2O)_5(py)]^{2+}$	40	8×10^{-2}
$[M(H_2O)_4(bpy)]^{2+}$	5×10^{-5}	6×10^{-2}
$[M(H_2O)(phen)]^{2+}$	1×10^{-5}	1×10^{-2}

[a] py = pyridine, bpy = bipyridine, phen = phenanthroline.

more labile than the corresponding bidentate ligands. Indeed, with ter- and tetradentate ligands measurable dissociation rates can only be measured in acidic solution.[14] However, as acidic media are only used for workup of organometallic reactions, it is useful to have an idea of the inertness of a chelating nitrogen ligand in neutral solution. Thus, the bpy dissociation rate constant for the complex $[Ni(H_2O)_4(bpy)]^{2+}$ is $5 \times 10^{-5}\ s^{-1}$, in contrast to $40\ s^{-1}$ for the corresponding monopyridine complex.[18]

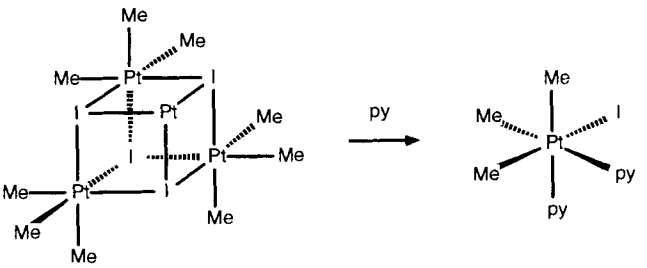
Particularly relevant for the transfer of chiral information from a metal complex to a product is the rigidity of the coligand(s). Thus, as can be seen in the data of Table 4, the rigid phenanthroline exchanges at a slower rate than the more flexible 2,2′-bipyridine ligand.

Finally, ligand-exchange rates in polydentate ligands do not necessarily give a complete picture as far as transfer of chirality is concerned, as a facile process involving the opening and closing of one arm of a polydentate ligand could lead to a decrease in transfer of chirality without complete detachment of the ligand from the metal. Thus, macrocyclic and related ligands prove to be particularly valuable as "spectator" ligands.

2.2. Characteristics of Coordination Compounds with M–C Bonds

Because there are many types of C-donors it should be noted that even those classified as "one-carbon centers" may bind to more than one metal center and, if available, may use more than one electron pair for bonding; furthermore, while most C-donor ligands also act as reagents in organometallic reactions, some of them, particularly six-electron donors such as the cyclopentadienyl anion and benzene, mainly function as coligands ("protecting groups"), that is, they block a number of coordination sites at a metal center, leaving available for further reaction a given number of free coordination sites in well-defined spatial relationships. Furthermore, they can direct incoming reagents and leaving groups along specific pathways and also strongly influence the electronic properties of the reacting fragment, L_nM.

The most stable organometallic compounds of a given metal center are those in which all low-energy orbitals are involved in bonding (preferably two-electron bonding). For instance, $PtIMe_3$ is tetrameric with the structure shown in Scheme 6, but



Scheme 6. The reaction of $[PtIMe_3]_4$ with pyridine (the methyl groups at one Pt atom are omitted for clarity) [19].

mononuclear complexes are readily obtained by reaction with additional ligands, for example pyridine, which gives the complex $[PtIMe_3(py)_2]$.[19] The platinum centers in both complexes are 18-electron systems with octahedral coordination geometry. Catalyst precursors are often di- or oligomeric and can become monomeric under the reaction conditions used (see, for example, the aluminum Lewis acid in Scheme 36, Section 5.6).

The absence of unpaired electrons on a metal centers of coordination compounds implies first that the metal center should have an even number of electrons and second that the complex should be of the low-spin type, that is, one where there is maximum pairing of all the available metal d electrons. This second requirement dictates the choice of the metal center and of its ligands. Thus, all metal centers of the second and third transition series give virtually only low-spin complexes. Furthermore, their metal centers in oxidation states having an odd number of electrons (generally only one) are relatively unstable and easily reduced. As C-donors are good reducing agents, paramagnetic organometallic compounds of these elements are rare.

Mention has been made earlier that the complexes of metal centers of the second and third transition series, in their stable oxidation states, are intrinsically kinetically inert (see Scheme 5). Thus, their use as catalysts generally requires coligands other than nitrogen (*trans* effect). An important exception is the $[Os^{II}(NH_3)_5]$ system discussed in Section 5.13.

A metal center from the first transition series can be chosen by taking into account that the tendency of a given metal ion to form low-spin complexes is generally expressed in terms of two parameters. The first, the spin-pairing energy P_T, expresses the metal-based, unfavorable energy change upon spin-pairing, while the second, the ligand field stabilization energy Δ, expresses the ligand-based, favorable energy change upon spin-pairing. Values for these parameters for some metal centers and ligands are listed in Table 5.[20]

The data confirm that the metal ions of the first transition series show a lower tendency to give low-spin complexes and thus require coligands such as phosphanes to be formed.

However, all the d^6 low-spin complexes, particularly if in an octahedral coordination environment, give slow substitution rates. Thus their complexes with nitrogen donors are seldom useful in homogeneous catalysis. This leaves the important class of low-spin complexes with coordination numbers four and a square-planar structure, or five and structures which can range from square-pyramidal to trigonal-bipyramidal.

Another group of metal centers deserves special mention, namely those with a d^5 electron configuration such as Mn^{II}. This

Table 5. Spin-pairing (P_r) and ligand field (Δ or f) parameters for some metal ions in hexaaqua complexes, and for various ligands [a].

M^{z+}	Electron config.	P_r [kJ mol^{-1}]	Δ (H_2O) [kJ mol^{-1}] [a]	X or L [b]	f
Cr^{2+}	d^4	244.3	100.3	Br	0.72
Mn^{3+}		301.6	150.1	Cl	0.78
Mn^{2+}	d^5	285.0	0	F	0.9
Fe^{3+}		357.4	0	dmf	0.98
Fe^{2+}	d^6	229.1	47.6	H_2O	1.00
Co^{3+}		282.6	188	$MeNH_2$	1.17
Co^{2+}	d^7	250	71.5	MeCN	1.22
				NH_3	1.25
				bipy	1.33
				phen	1.34
				CN	ca. 1.7

[a] $\Delta = f$ (ligands) $\cdot g$ (central ion); g: see ref. [20]. [b] X = anionic ligand, L = neutral ligand.

electron configuration is particularly stable and, although very labile, the complexes of these metal centers exibit useful reactivity for homogeneously catalyzed reactions.

Finally, another group of metal centers particularly useful for organometallic reactions is that with d^{10} electron configuration: Cu^{I}, Ag^{I}, Au^{I}; Zn^{II}, Cd^{II}, Hg^{II}; Ga^{III}, In^{III}, Tl^{III}; Sn^{IV}.

Summing up, complexes with nitrogen donors displaying useful reactivity for organometallic reactions will be found mainly among low-spin complexes of transition elements having coordination numbers four and five or having metal centers with d^5 configuration, or even among complexes of the post-transition elements. The considerably oxophilic character of the early transition elements will severely restrict their use.

3. Characteristics of Nitrogen-Donors

Before discussing in detail the coordination chemistry of nitrogen donors it is appropriate to mention the relative strength of M–C, M–N, and M–O bonds. (The M–O bond is included, because many of the ligands used for the reactions to be discussed later also contain this atom as donor.)

Some representative values of the M–Y bond energies are listed in Table 6.[121] The M–C bonds are weaker than the M–N

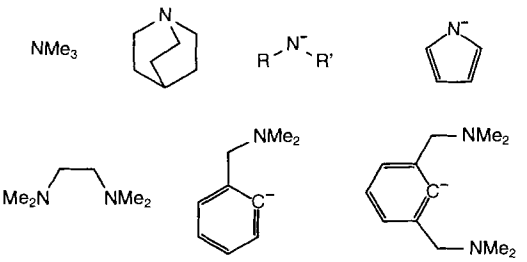
Table 6. Mean M–L bond dissociation enthalpies $\bar{D}$ [kJ mol^{-1}] for homoleptic metal compounds ML_4 as well as M–X bond dissociation enthalpies for X = H, C, N [kcal mol^{-1}].

	ML_4			$X-M^+$			
L	Ti	Zr	Hf	M	H	CH_3	NH_2
CH_2tBu	188	227	224	Sc	57(2)	59(3)	85(2)
NEt_2	309	340	367	Ti	54(3)	54(2)	85(3)
O*i*Pr	444	518	534	V	48(2)	50(2)	73(2)
F	586	648	665	Fe	50(2)	58(2)	67(12)
				Co	47(2)	49(4)	62(2)
				Ni	40(2)	45(2)	56(5)

bonds, which in turn are weaker than the M–O bonds.[122] Although different types of complexes may show significant deviations from the data in Table 6, the values quoted can be taken as a guideline.

The range of nitrogen donors is more extensive than that of any other atom: It is enough to recall how varied the organic chemistry of nitrogen is and that most of these compounds are potential donors. By comparison, in inorganic chemistry only very few molecules or ions bind to metals through a nitrogen atom. Thus, only ligands of the former group will be discussed here.

An appropriate classification of nitrogen donors can be based on the hybridization of this atom, sp^3, sp^2, and sp. The types of compounds containing sp^3-hybridized nitrogen atoms are summarized in Scheme 7. Complexes with nitrogen donors containing N–H bonds are generally not suitable for most organometallic reactions as the H atom (or atoms) on coordinated nitrogen are sufficiently acidic to react with a nucleophile. Therefore, the common nitrogen donors having N–H bonds have not been included in Scheme 7. Furthermore, coordinated nitrogen atoms containing nonbonding pairs of electrons are susceptible to electrophilic attack by suitable reagents. However, coordinated "nitrogen anions", also listed in Scheme 7, show an extensive and useful coordination chemistry, particularly when associated with sp^2-hybridized carbon atoms.



Scheme 7. Some nitrogen-donors with tertiary sp^3-hybridized N atoms.

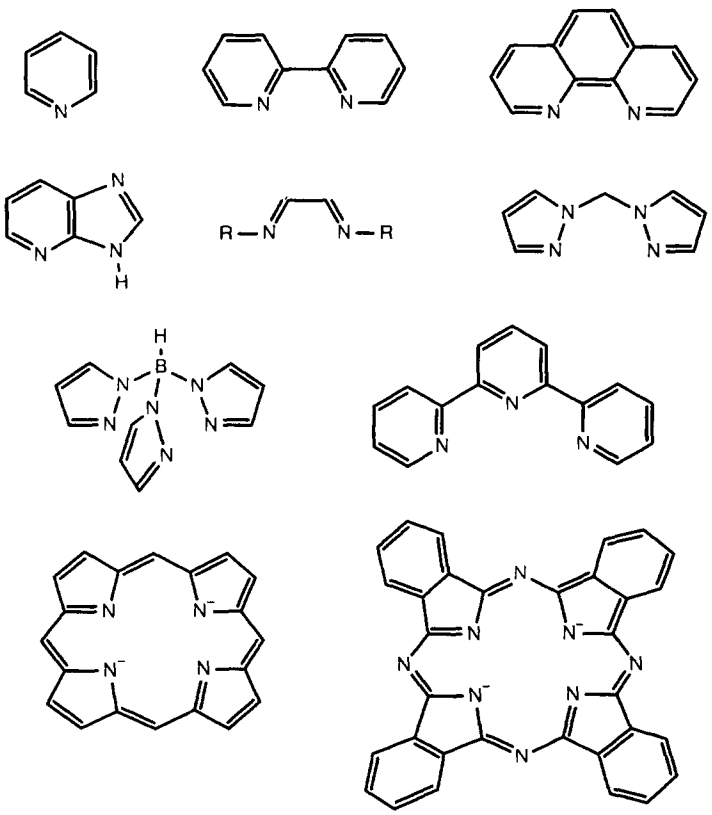
Of special interest in the present context are many natural products containing ternary nitrogen atoms, for example the alkaloids. A number of them have been successfully used for the enantioselective synthesis of organic compounds (see, for example, Sections 5.11 and 5.12.2).

Ligands containing sp^2-hybridized nitrogen atoms, particularly when the N-atom is part of an aromatic system (see, for example, Scheme 8), have a very extensive coordination chemistry. Also for donors of this type, a much more extensive and useful coordination chemistry is possible when they are bi- or terdentate ligands. However, the use of such ligands in asymmetric catalysis requires the presence of a stereogenic substituent.

The presence of C–N and C–C double bonds in these molecules renders them susceptible to further reactions, such as nucleophilic attack or, under appropriate conditions, hydrogenation. This is particularly true of Schiff's bases.

The only class of organic nitrogen donors with sp hybridization are the nitriles. Their main function is as labile ligands that are replaced by appropriate reagents. Furthermore, once coordinated, nitriles are quite susceptible towards nucleophilic attack.

As might be expected, the donor properties of nitrogen ligands differ significantly from those of phosphorus. However, an accurate assessment of their relative donor properties and of



Scheme 8. Some nitrogen-donors with sp^2-hybridized N atoms.

related ligands with other donor atoms is difficult. The most commonly used criterion to compare donor properties of nitrogen compounds is their pK value. However, these values refer to aqueous solutions and meaningful comparisons are seldom possible, because solvation effects may mask true electronic contributions. Furthermore, for compounds sparingly soluble in water, the pK values are not available.

Another useful criterion for the comparison of the donor ability of various ligands is the first ionization potential of the donor atoms. Also in this case the values can only be used qualitatively, as removal of an electron to infinity is conceptually and quantitatively different from the formation of a dative bond, particularly as the former process is not influenced by steric effects whereas the latter is. Therefore, any consideration of relative stability of metal–ligand bonds in general and metal–nitrogen bonds in particular must take into account steric interactions. These have been successfully parametrized for the phosphorus donors by means of Tolman's "cone-angle" values, θ_P. Some of these values are shown in Table 7.[23] The corresponding values for nitrogen donors, θ_N, have only been reported, recently.[23b] They are in general larger than for the corresponding P-donors, the difference being greater for the larger ligands.

Table 7. Tolman's cone angle values for phosphorus-donors (θ_P [23a]) and the corresponding values θ_N for nitrogen-donors [23b].

Ligand	θ_P [°]	θ_N [°]
EH_3	87	94
EMe_3	118	132
EEt_3	132	150
EPh_3	145	166

Tolman has also obtained a set of values for an "electronic parameter", v_p, which expresses the relative donor capacity of a phosphane ligand in the absence of distortions caused by steric effects.[23] Once again, a similar set of data does not appear to have been obtained for nitrogen ligands. However, in this case the corresponding nitrogen values cannot be estimated from the phosphorus data because the nature of the M–L bonds in the two cases are different. M–N bonds are mainly of σ type and M–P bonds of σ and π type.

Finally, H. C. Brown et al. obtained data useful in the context of the stability of metal–nitrogen bonds and their relation to steric effects (relevant in the context of reactions catalyzed by oxazaborolidines; see Sections 5.2.2, 5.6, and 5.7).[24] This is summarized in Table 8.

Table 8. Bond dissociation energies [kcal mol^{-1}] for trimethylborane adducts of amines at 100 °C.

Compound	ΔG	ΔH	ΔS
Me_3B-NH_3	−1.134	13.75	0.040
Me_3B-NH_2Me	2.472	17.64	0.041
$Me_3B-NHMe_2$	2.885	19.26	0.044
Me_3B-NMe_3	0.557	17.62	0.046
Me_3B-NEt_3		ca. 10.0	
Me_3B–quinuclidine	2.916	19.94	0.046

In conclusion, if one considers only the nitrogen ligands relevant for organometallic chemistry, one reaches the conclusion that nitrogen atoms in donor molecules in coordination chemistry, as well as in other branches of chemistry, can form strong bonds to metal centers; the strength of the bonds depends largely on their σ covalency with a potentially significant contribution from the ionic character of the bond itself.

Nevertheless, π interactions are possible with ligands containing sp^2-hybridized nitrogen donors, and π back-bonding effects, particularly between nitrogen heterocycles and metal centers, have been frequently invoked to explain a variety of observations. However, while their occurrence may be beyond dispute, the extent to which they determine the chemical properties of any given compound is controversial, because ground-state effects are likely to be small.

Thus the following gneralizations, which typically must be used in this case probably with a rather large grain of salt(!), can be made:

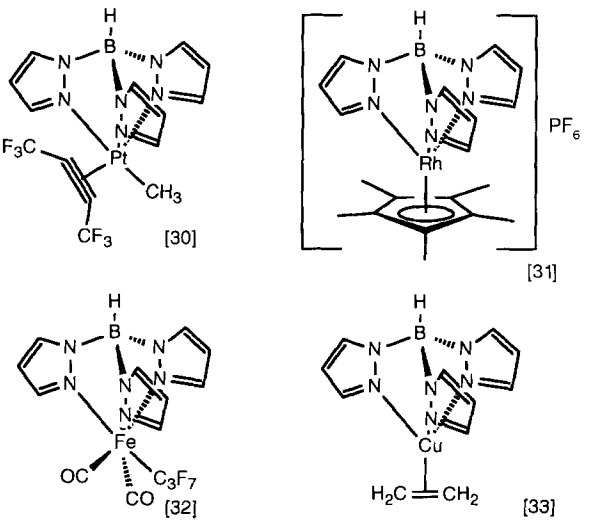
1. Donor–acceptor bonds formed by nitrogen donors are generally fairly strong and, in contrast to those formed by phosphorus donors, their strength is unlikely to show drastic changes if the metal center, but not the ionic charge, is changed. As a consequence, bonds of nitrogen donors to the transition elements of the first transition series and the inner transition series as well as some of the post-transition metals will be stronger than those of the related phosphorus donors ("A" vs. "B" character, "hard" vs. "soft" donors).
2. The strength of the M–N bonds will be affected much more by steric effects than that of the corresponding M–P bonds.
3. The nitrogen donors, generally, will not be as effective in producing low-spin complexes with the consequence that the species produced are less thermodynamically stable and more kinetically labile than their low-spin analogues with P-donors.

The consequences of these "boundary conditions" are that nitrogen-donor ligands forming robust complexes are, in general, di-, ter-, or multidentate ligands, often macrocyclic, and contain ligands with sp^2-hybridized N-atoms. Thus, the organometallic complexes with nitrogen donors as coligands described in the next section are likely to contain the above-mentioned types of compounds.

4. Organometallic Complexes Containing Nitrogen-Donors

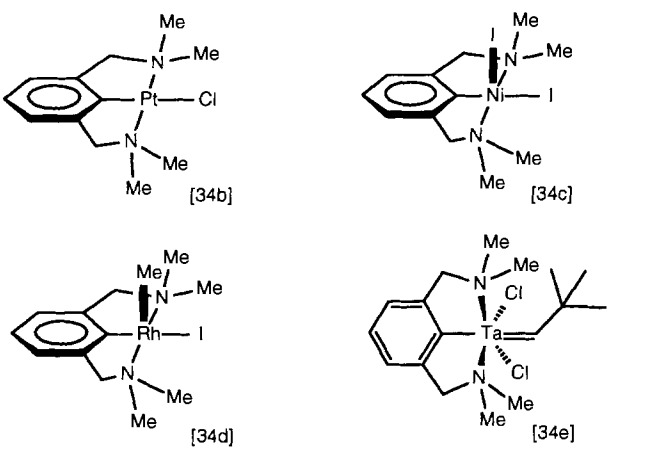
Many ligands of organometallic complexes contain double (C=X) or triple (C≡Y) bonds (X and Y are atoms other than nitrogen), and it is now well established that a significant contribution to their total M–L bond strength is provided by the formation of π back bonds. However, nitrogen donors do not form π bonds to any significant extent, and thus, the strength of the M–C bonds in the presence of these ligands is directly related to the electron density at the metal center. Thus the isolated occurrence of organometallic compounds containing nitrogen coligands is not surprising. There is, however, an increasing body of evidence showing that organometallic complexes of the type $[MR_n(L^N)_m]$ (L^N = nitrogen donor ligand) are readily formed and, in many cases, can be isolated, even if the metal center belongs to the second or third transition series. Particularly instructive examples are provided by the complex $[PdX(Me)_3(NN)]$ (X = halide; NN = *N,N,N′,N′*-tetramethylethylenediamine, or 2,2′-bipyridine),[25] and by the $[Os^{II}(NH_3)_5]$ system described in Section 5.13. Furthermore, nitrogen donors are frequently used as part of chelating systems together with phosphorus- or carbon-donors. The organometallic chemistry of the P,N-donors does not significantly differ from that of the P,P-ligands, but several interesting differences in organometallic reactivity, including catalysis, have been reported.[26] On the other hand the C,N-donors have played a significant role in organometallic chemistry because of their ready formation through a cyclometalation reaction,[27] and because an optically active cyclometalated compound is useful for the separation of racemic mixtures, generally of phosphanes (see Scheme 9).[28]

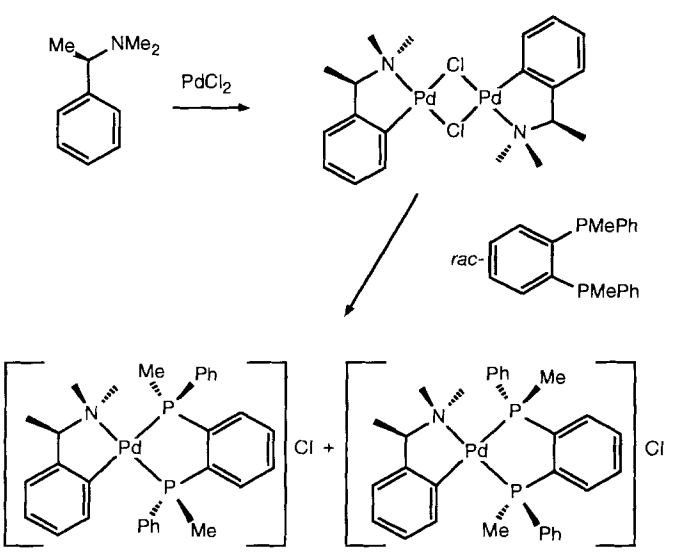
Many organometallic compounds containing nitrogen donors have been obtained by using polypyrazolylborate ligands.[29] A representative selection of compounds of this type is shown in Scheme 10.[30–33]



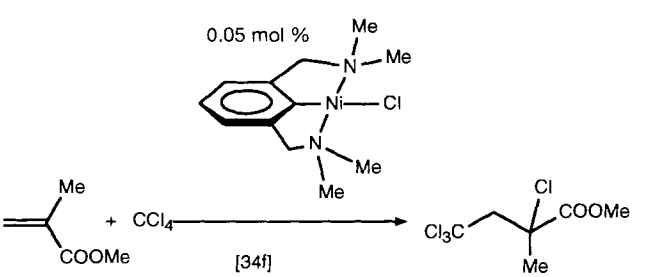
Scheme 10. Examples of organometallic complexes containing the tris(pyrazolyl)borato ligand [30–33].

Noteworthy is also the organometallic chemistry based on complexes of the N,C,N-terdentate ligand shown in Scheme 11,[34] and that of complexes containing 1,4-diaza-1,3-dienes, some of which are given in Scheme 12.[35]





Scheme 9. The formation of optically active Pd^{II} complexes with C,N-donors and their use in the separation of racemic mixtures via diasteromeric complexes [28a].



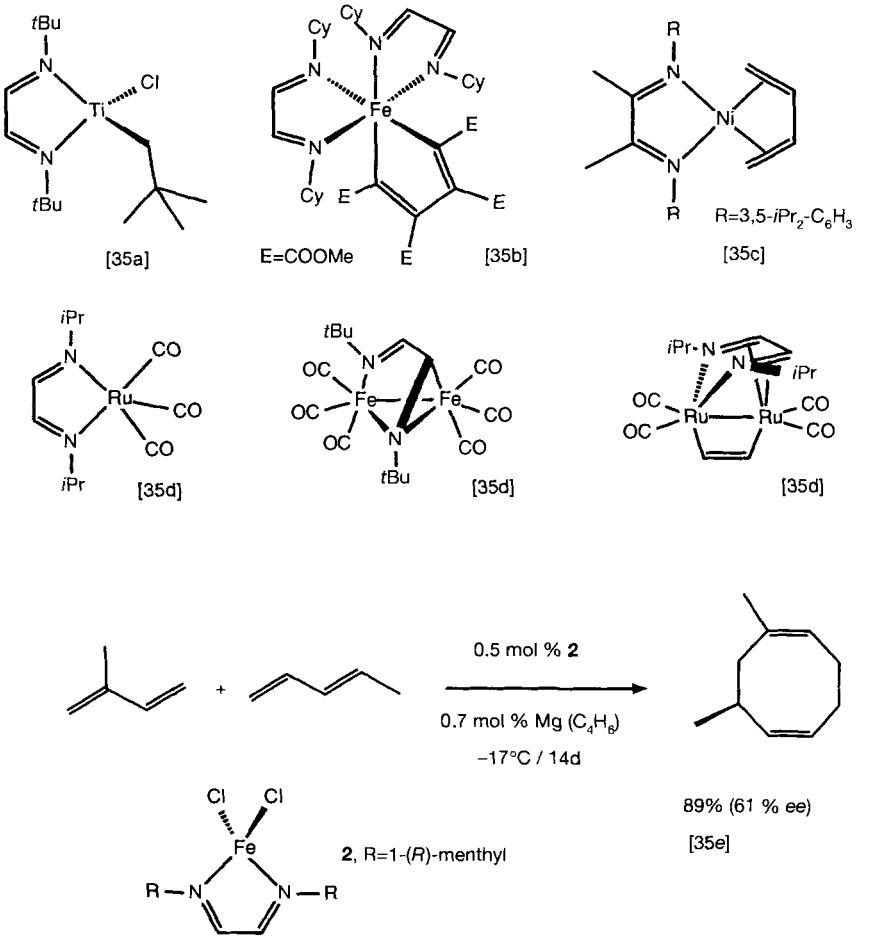
Scheme 11. Some complexes with van Koten's "pincer" ligand, and a reaction catalyzed by it [34].

However, a common feature of organometallic compounds containing nitrogen ligands is apparent: they usually exhibit high reactivity. Examples of this type of behavior are shown in Scheme 13.[36]

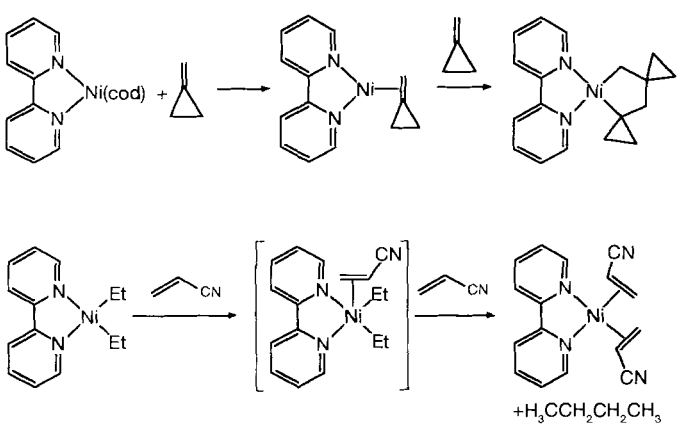
The electron-withdrawing effect of coordinated alkenes is well illustrated by the reaction of the complex $[Ni(Et)_2(bpy)]$. Upon addition of acrylonitrile, this complex gives a relatively stable adduct with pentacoordinated Ni atoms, but exposure to excess acrylonitrile leads to clean reductive elimination of butane to afford the corresponding bis(olefin)-Ni^0 complex.[36b]

Finally, even a very brief survey of the organometallic chemistry with nitrogen-donors would be grossly incomplete without a mention of the extensive and fascinating chemistry of Vitamin B_{12}, its coenzyme (Scheme 14), and the cobalamines. While reference to more specialized reviews[37a] will give for a deeper understanding of the chemistry of systems of this type, two general points of coordination chemistry emerge from published work, which may be relevant in some catalytic systems used for organic synthesis.[37b] The first of them concerns the mode of cleavage of Co-R bonds in compounds of this type (Scheme 15).[38] All the cleavage modes described in Section 2.1 are found to occur with comparable activation energies in the presence of the appropriate reagents. The second point concerns the oxidation state at the cobalt atom. A summary of the electron-transfer processes are shown in Scheme 16.[38]

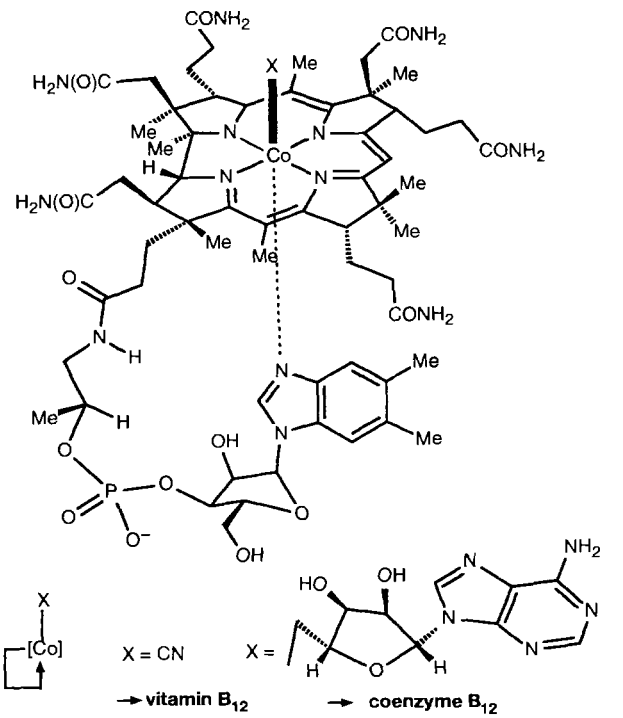
Given the complex chemical nature of vitamin B_{12} and its coenzyme, coordination chemists have invested much time in developing and studying model systems. The simplest (and not the least effective) models for B_{12} systems are the cobalamines, shown schematically in Scheme 17.[38]



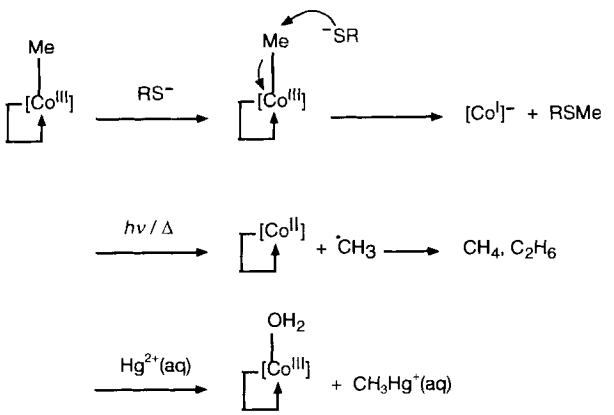
Scheme 12. Some transition metal complexes with 1,4-diaza-1,3-dienes and a reaction catalyzed by them [35].



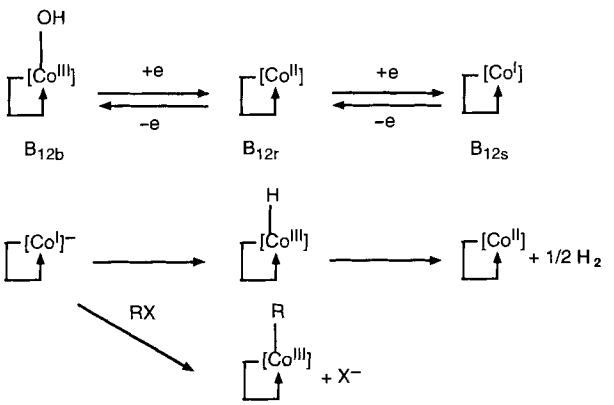
Scheme 13. Reactions of organometallic (bpy)Ni^{II} complexes with olefins [36].



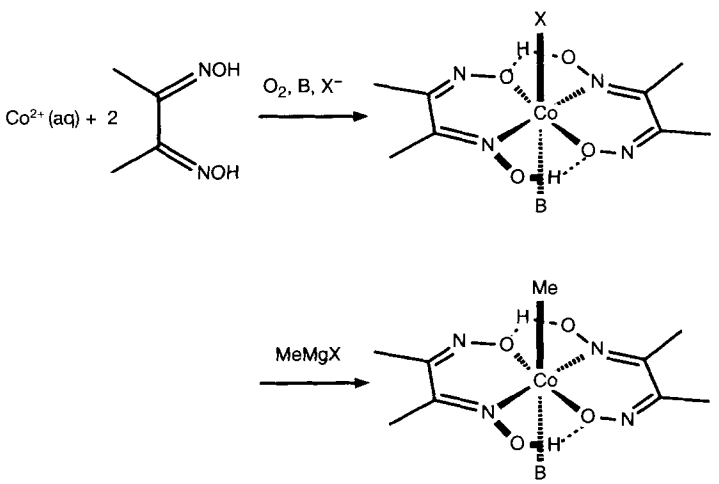
Scheme 14. Vitamin B_{12} and its coenzyme.



Scheme 15. Course of the cleavage of Co–C bonds in the B_{12} system by nucleophilic attack, heating or irradiation, and electrophilic attack.



Scheme 16. Changes of Co oxidation state in the B_{12} system.



Scheme 17. Cobaloximes, models for the B_{12} system (B is, for example, pyridine).

5. Homogeneous Catalysis with Nitrogen Ligands

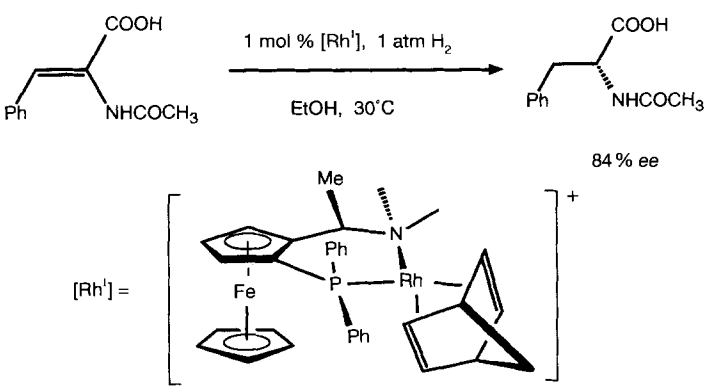
5.1. Introductory Note

Nitrogen ligands in homogeneous catalysis have received increasing attention in recent years. In particular, the use of optically active, chelating, nitrogen-containing ligands made many significant contributions to the field of asymmetric catalysis. Very often in such cases the N-ligands are derivatives of amino acids and thus obtainable from the chiral pool.[39] The following discussion will focus on the type of reaction that is catalyzed by complexes containing N-ligands, because a reaction-oriented section should enable comparisons (for example, with phosphane ligands used in the same reaction), as well as the identification of new possibilities and trends. Since systematic studies of the significance of N-ligands, for example, as opposed to P-ligands, for a given reaction do not exist, and coordination-chemical rationalizations for the choice of such ligands have not been reported, the N-ligands have been used on an ad hoc basis. Studies concerning the influence of basicity, steric hindrance, and electronic properties of a certain class of nitrogen ligands on the catalytic properties of the corresponding complexes do not exist either. Such theoretical viewpoints are well established for phosphane ligands (for example, the concept of cone-angle,[23] or the well-defined electronic influence of the substituents on the phosphorus atoms upon reactivity) and are often applied in the discussion of catalytic effects. Despite the relative infancy of nitrogen ligands in homogeneous catalysis, the amount of published work is considerable. Therefore, this review cannot present a comprehensive account, and only the most significant or recent examples will be discussed.

5.2. Asymmetric Hydrogenation and Reduction

5.2.1. Hydrogen as Reducing Agent

Asymmetric hydrogenation reactions, catalyzed by rhodium complexes containing chiral chelating diphosphanes, have been very successful and constitute classic examples of well-established catalytic methodologies.[40] Probably for this reason nitrogen ligands have been rather neglected. However, mixed P,N-ferrocenyl ligands have been shown by Cullen et al. to give enantioselectivities as high as 84% in the rhodium-catalyzed hydrogenation of acetamidocinnamic acid[41] (Scheme 18). An

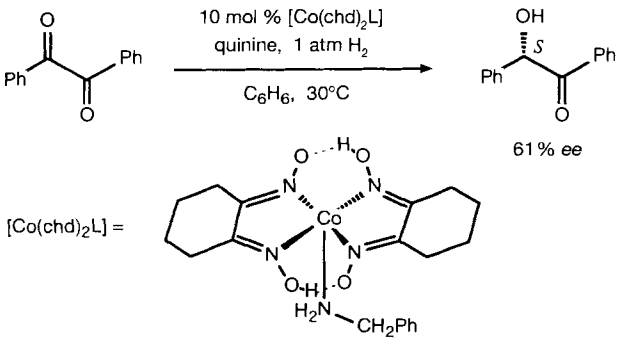


Scheme 18. Asymmetric hydrogenation catalyzed by a Rh^I complex [41].

X-ray crystal structure determination of the catalyst precursor $[Rh^I]$ as PF_6 salt shows that the ligand coordinates as a chelate to the rhodium atom.[41a] However, selectivity and activity seem to be dominated by the phosphorus ligand. Thus, replacement of the PPh_2 group by a $P(t\text{Bu})_2$ fragment leads to a more active

catalyst, which gives products of the opposite absolute configuration.[41b] These catalysts are less active than those containing chelating diphosphanes.

A completely different catalyst system for the hydrogenation of benzil to benzoin has been reported by Ohgo, Takeuchi et al.[42] Chiral bis(glyoximato)Co^{II} complexes in the presence of an optically active amino alcohol as cocatalyst (e.g., quinine) were found to afford enantioselectivities up to 61% *ee* (Scheme 19). The same system also hydrogenates acetamido

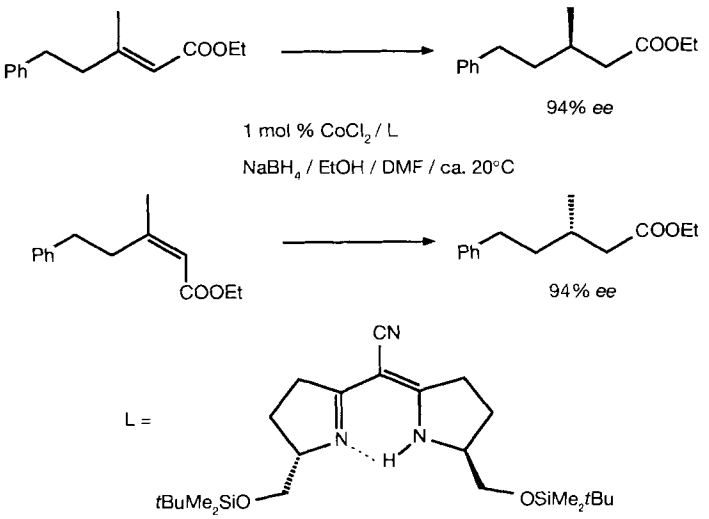


Scheme 19. Asymmetric hydrogenation catalyzed by bis(glyoximato) Co^{II} complexes, with quinine as cocatalyst [42].

acrylic acid derivatives, but with a much lower enantioselectivity (up to 20% *ee*). The axial ligand in the catalyst precursor (typically an amine or a tertiary phosphane) has only a minor influence on the efficiency of the catalyst, but increasing the hydrogen pressure had a beneficial effect on the reaction rate. Although its details still remain obscure, this reaction raises several interesting mechanistic aspects: The chiral cocatalyst quinine does not appear to be directly bonded to cobalt; a second-sphere interaction between the chiral amino alcohol and the coordinated substrate has been invoked in the stereodifferentiating step; an electron-transfer step seems to be involved in the course of substrate hydrogenation.[42a] The possibility that the actual catalyst is a Co^{I} complex does not appear to have been considered.

5.2.2. *Boranes as Reducing Agents*

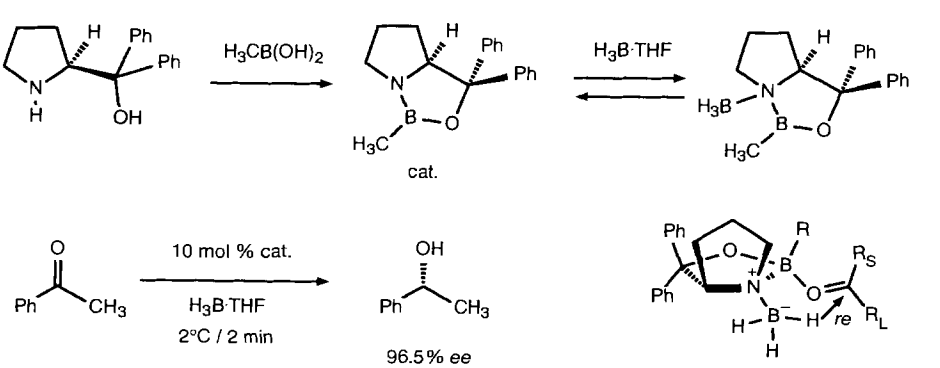
In recent years, Pfaltz et al.[43] have developed chiral chelating semicorrin ligands and used them for several asymmetric, homogeneously catalyzed reactions (see also Sections 5.5 and 5.11). Such monoanionic ligands are easily prepared from pyroglutamic acid and form six-membered conjugated chelate rings which are C_2-symmetric.[43] The reduction of α,β-unsaturated esters with $NaBH_4$ in ethanol/dimethylformamide (DMF) is efficiently catalyzed by Co^{II} salts in the presence of the ligand shown in Scheme 20. The enantioselectivities reach 94%. Iso-



Scheme 20. (Semicorrinato)Co^{I}-catalyzed asymmetric reduction of α,β-unsaturated esters with $NaBH_4$ [44].

meric configurations at the double bonds yield products of opposite absolute configurations, and nonactivated olefins are not reduced.[44] The active catalyst, formed in situ from $CoCl_2$ and the ligand, is thought to be a Co^{I} species.

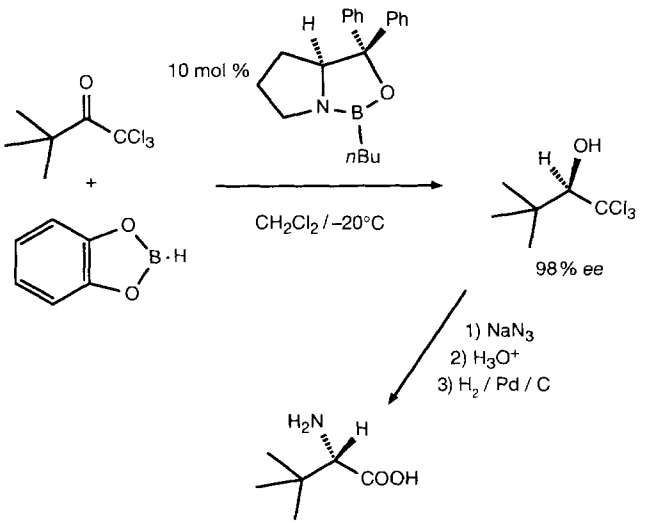
Chiral β-amino alcohols, mainly derived from α-amino acids, react with BH_3 (mostly used as its THF adduct) to form 1,3,2-oxazaborolidines.[45] These compounds are also efficient and highly selective catalysts for the reduction of ketones with $H_3B \cdot L$ (L = THF, or $S(CH_3)_2$). Itsuno et al. were the first to report, in 1981,[46] the use of such borolidines as stoichiometric reductants. Catalytic applications of oxazaborolidines were also initiated by the Itsuno group,[47] and the methodology has been exploited more recently by several other groups.[48–53] Scheme 21 shows one specific example; a more detailed collection of data is found in a recent review by Wallbaum and Martens.[45]



Scheme 21. Formation of a 1,3,2-oxazaborolidine and its use as catalyst for the enantioselective reduction of ketones with $BH_3 \cdot THF$ [54]. Bottom right: result of the X-ray structure analysis.

Oxazaborolidines are unique in that they contain a Lewis acidic and a Lewis basic center next to each other, and, according to the model developed by Corey,[54] are able to activate both the carbonyl functionality of the substrate and the borane. This model, which allows a prediction of the absolute configuration of the secondary alcohol formed, has recently been corroborated by the X-ray crystal structure of the BH_3 adduct shown in Scheme 21,[54] as well as by quantum mechanical calculations.[55]

The reduction of trichloromethyl ketones with catecholborane offers a general and highly selective method for the synthesis of α-amino acids[56] (Scheme 22). Finally, the oxazaborolidine methodology has recently been extended to the reduction of ketimines.[57] The optical yields are generally lower than those obtained for the reduction of ketones and also lower than those of the corresponding stoichiometric reactions.

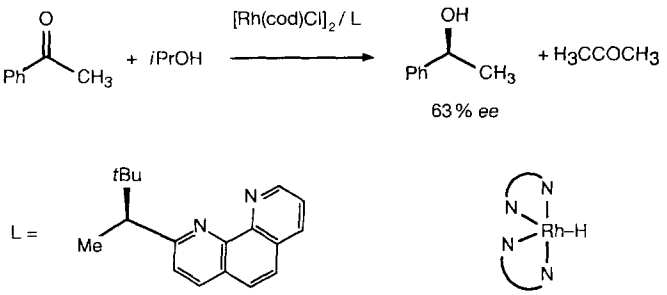


Scheme 22. Synthesis of α-amino acids by asymmetric reduction of trichloromethyl ketones [56].

5.3. Asymmetric Transfer Hydrogenation

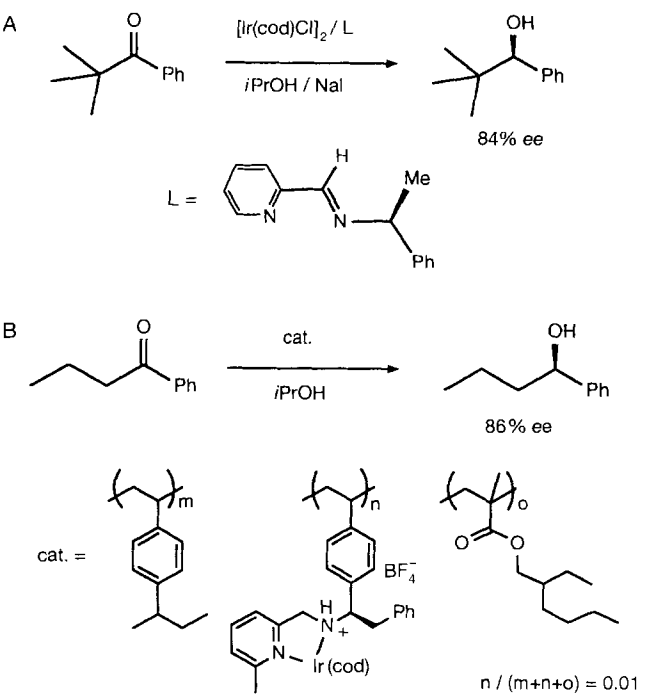
Chiral nitrogen ligands have been used in the asymmetric hydrogen transfer more frequently and more successfully[58] than in hydrogenation reactions with H_2. This reflects the compatibility of nitrogen donor atoms with the mechanistic peculiarities of this reaction. In the typical hydrogen-transfer reaction, the coordination sphere of the metal comprises hard donor ligands (e.g., nitrogen and alkoxy), and no change in the formal metal oxidation state need be invoked.[58]

Rhodium catalysts containing chiral bipyridine or phenanthroline derivatives have been used by Mestroni et al.[59] Because such ligands are planar, stereogenic groups can only be introduced in peripheral regions of the molecule, where their influence is rather modest. Accordingly, the selectivities obtained are rather low. The nature of the rhodium-containing catalyst precursors ([Rh_2(1,5-cyclooctadiene)$_2Cl_2$] or [Rh_2(1,3-cylohexadiene)$_2Cl_2$]), as well as the rhodium-to-ligand ratio, seem to influence the selectivity significantly. A pentacoordinated hydridorhodium complex is postulated as an intermediate in the catalytic cycle[60] (Scheme 23).



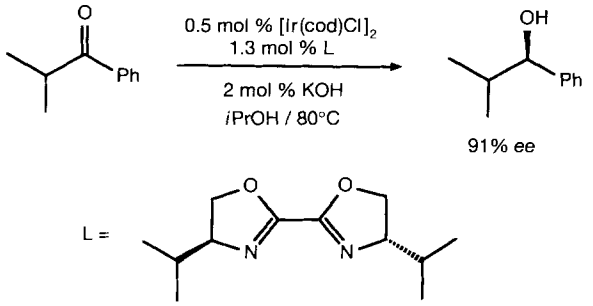
Scheme 23. Rh-catalyzed asymmetric transfer hydrogenation of acetophenone in the presence of a chiral phenanthroline derivative [59] and the postulated Rh-hydrido intermediate [60].

Alkylaminomethyl- and alkyliminomethylpyridines have been used as ligands in the Ir-catalyzed hydrogenation reaction. Selectivities are generally low, and only the bulky *tert*-butyl phenyl ketone can be reduced according to Scheme 24 A in 84% *ee*.[61] The same type of ligand in a polymer-bound form yields enantioselectivities up to 86% (Scheme 24 B).[62]



Scheme 24. Ir-catalyzed transfer hydrogenation in the presence of an alkyliminopyridine (A) [61] and an immobilized alkylaminomethylpyridine (B) [62] as ligands. For B the composition of the polymer is also given.

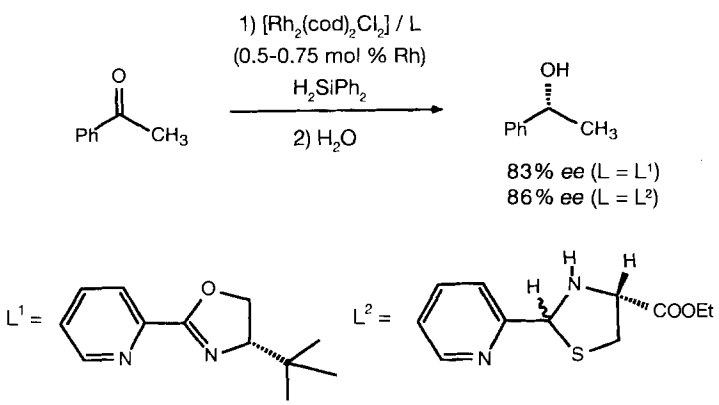
Pfaltz et al. have recently shown that C_2-symmetric tetrahydrobioxazoles are effective ligands for this type of reaction and reported that enantiomeric excesses reach 91% (Scheme 25).[63]



Scheme 25. Tetrahydrobisoxazole–Ir complexes in the asymmetric transfer hydrogenation of alkyl aryl ketones [63].

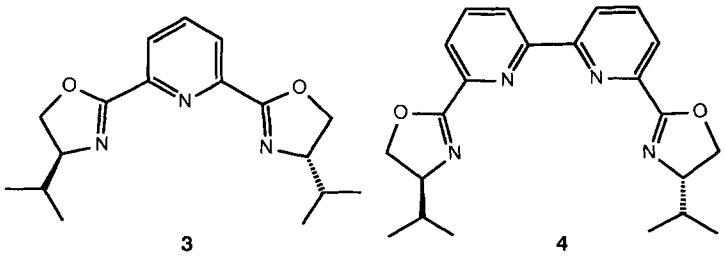
5.4. Asymmetric Hydrosilylation

Brunner et al. have demonstrated that chelating nitrogen ligands containing a stereogenic fragment in a peripheral region of the molecule are superior to conventional C_2-symmetric chiral diphosphanes in the Rh-catalyzed asymmetric hydrosilylation of ketones.[64] The diphosphanes are characterized by the rather rigid chiral array of the phenyl substituents on the phosphorus atoms. This feature is one of the dominant selectivity-determining factors and was already recognized in the early days of asymmetric Rh-catalyzed hydrogenation.[65] However, for hydrosilylation the key factor appears to be a stereogenic group close to the free coordination sites at the metal center. This is achieved by using pyridine derivatives such as those shown in Scheme 26. The hydrosilylation of acetophenone with diphenylsilane affords 1-phenylethanol with a maximum enantiomeric excess of 86%.[66]

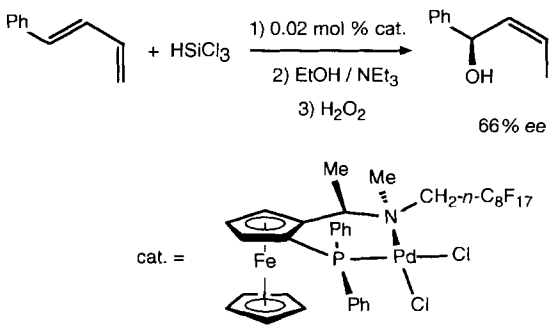


Scheme 26. Asymmetric hydrosilylation of acetophenone with diphenylsilane catalyzed by Rh in the presence of pyridyldihydrooxazoles and pyridylthiazolidines [66].

Much higher enantioselectivities for the same reaction (up to 94%) have been reported by Nishiyama et al., who used terdentate ligands like **3**.[67] The corresponding trichlororhodium complex, characterized by X-ray diffraction,[67b] was used as a catalyst precursor. For the catalytic reaction to take place, the addition of a Ag^I salt was required. This led to the formation of a Rh^{III} cationic complex, which was then reduced by the silane to the catalytically active Rh^I species. A tetraaza ligand (**4**), related to **3**, which was recently reported by the same group, gave slightly lower enantioselectivities.[67d]



A completely different system for the hydrosilylation of 1,3-dienes with $HSiCl_3$ was reported by Hayashi et al.[68] (Scheme 27). The catalyst precursor was a $PdCl_2$ complex containing a chiral P,N-ferrocenyl ligand. Good regioselectivities



Scheme 27. Pd-catalyzed asymmetric hydrosilylation of a 1,3-diene [68].

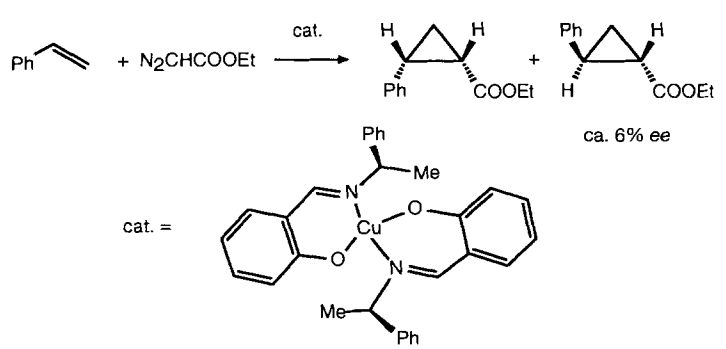
(up to 93%) as well as moderate enantioselectivities (up to 66% *ee*) were obtained. The ligand contains a perfluorinated alkyl substituent on the nitrogen atom, which ensures catalyst solubility in the solvent-free mixture of reactants.

5.5. Asymmetric Cyclopropanation

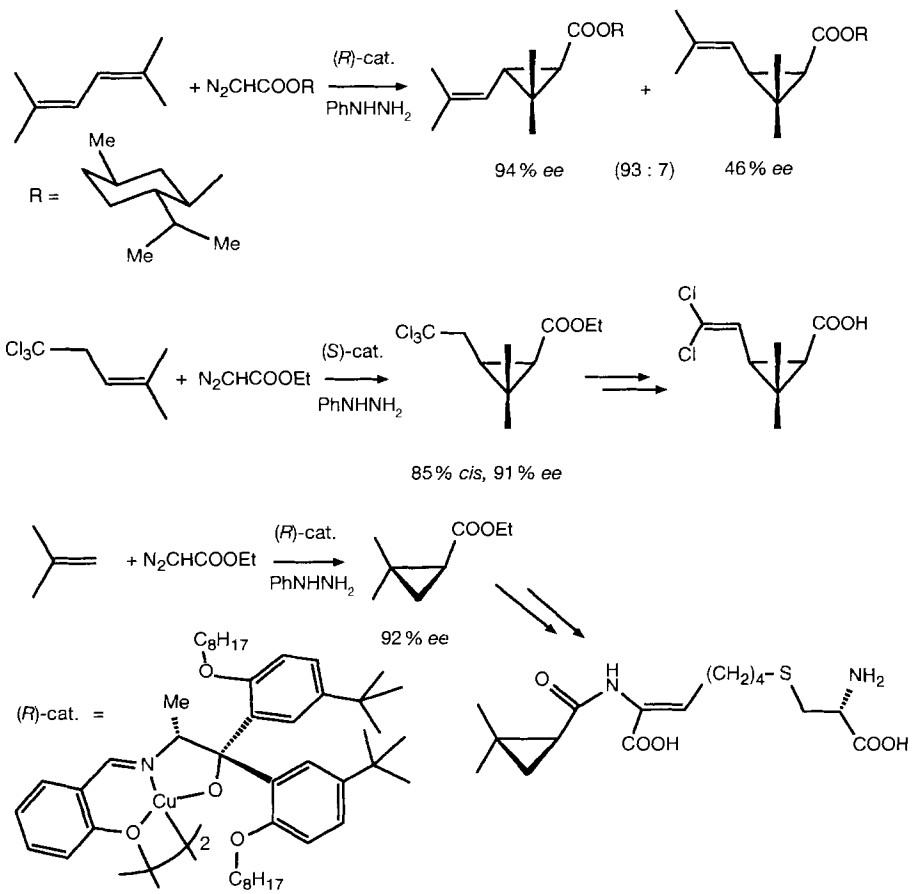
5.5.1. Copper Catalysts

The synthesis of optically active cyclopropane derivatives[69] by the stereoselective addition of a carbenoid reagent to an olefin is a most important reaction from both a historical as well as from a practical point of view.[70] The vast majority of the known and successful catalysts for this reaction are complexes of the late transition metals (Cu, Co, Rh) with nitrogen ligands.

Apparently the very first example of asymmetric catalysis by a soluble metal complex is a cyclopropanation reaction reported by Nozaki et al. in 1966. The Cu^{II} complex shown in Scheme 28



Scheme 28. The first asymmetric reaction catalyzed by a soluble transition metal complex [71a].



Scheme 29. Industrially important applications of the Cu-catalyzed asymmetric cyclopropanation. Synthesis of chrysanthemic acid esters (R = D-menthyl), permethrinic acid, and cilastatin [72]. Bottom left: the catalyst precursor in its *R* configuration.

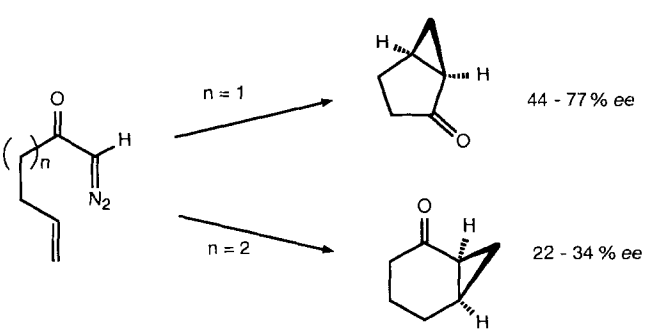
contains a Schiff base ligand derived from salicylaldehyde and optically pure 1-phenylethylamine and served as catalyst precursor for the "decomposition of diazoacetates in the presence of olefins".[71] The stereoselectivities were rather modest, but intensive screening and improvement of the ligand system by the Aratani group finally led to the commercialization of the copper-catalyzed cyclopropanation.[72] Industrially important applications of this reaction are the synthesis of intermediates of pyrethroid insecticides and cilastatin. Some relevant examples with *ee*'s higher than 90% are summarized in Scheme 29. The best ligands are terdentate dihydroxyl Schiff bases with two hydroxyl groups (O,N,O) derived from amino alcohols bearing bulky *ortho*-alkoxyphenyl substituents. The dimeric, μ-O-Cu^{II} complexes formed by such ligands are used as catalyst precursors. The catalytically active Cu^{I} species is generated in situ with phenylhydrazine as a reducing agent.

Dauben et al. have shown the Aratani catalyst to be effective in the intramolecular version of the cyclopropanation reactions too, although the resulting enantioselectivities were only moderate (up to 77% *ee*)[73] (Scheme 30).

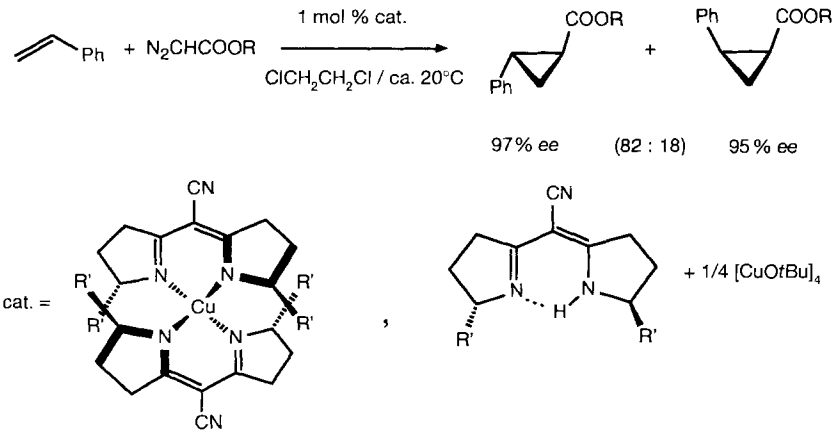
Whereas nowadays high enantioselectivities can be obtained with several catalysts (see Sections 5.5.2–5.5.4), relatively modest diastereoselectivities (*cis*/*trans* cyclopropane derivatives) still constitute the major stereochemical problem of catalytic cyclopropanation. This problem has not been completely solved as yet, even by using catalysts bearing C_2-symmetric semicorrinato ligands propanation. This problem has not been completely solved as yet, even by using catalysts bearing C_2-symmetric semicorrinato ligands, first reported by Pfaltz et al. in 1986,[74] or by employing bis(dihydrooxazole) ligands, described in more recent years (Scheme 31).

Enantioselectivities up to 97% are obtained in the cyclopropanation of styrene with methyl diazoacetate (Scheme 31). A slight effect of double stereodifferentiation is observed by using the two enantiomeric menthyl esters. Selectivity does not depend upon the method of generation of the catalyst. Thus, either the bis(semicorrinato)Cu^{II} complex as catalyst precursor, or the catalyst generated in situ from equivalent amounts of the ligand and $[CuO\mathit{t}Bu]_4$ give identical stereochemical results.

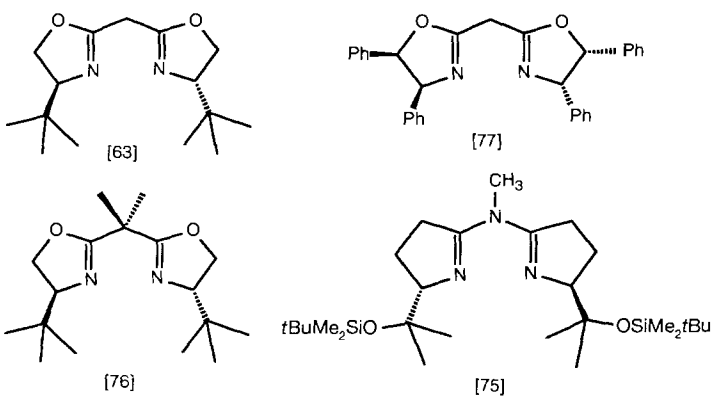
More recently the Pfaltz group showed that very high enantioselectivities can be obtained by using the conceptually similar (from a stereochemical and electronic point of view), but synthetically more easily accessible bis(dihydrooxazole)[63] and 5-azasemicorrins.[75] Both the Evans and Masamune groups have developed analogous systems.[76, 77] Representative bis(dihydrooxazole) ligands are shown in Scheme 32. With these ligands extremely high optical yields (up to 99% *ee*) can be obtained in the reaction of styrene with ethyl diazoacetate.[76] However, high *trans*/*cis* ratios of the diastereomeric cyclopropanes are achieved only when the diazo ester bears a very bulky group (e.g., 2,6 di-*tert*-butyl-4-tolyl). The catalysts are best generated in situ from soluble Cu^{I} salts containing weakly coordinating anions (triflate, ClO_4^-); $[CuO\mathit{t}Bu]_4$ seems to give erratic results.[75] Evans et al. have shown that the catalyst formed from the CMe_2-bridged bis(dihydrooxazole) of Scheme 32 and CuOTf is polymeric in the solid state.[76b] An interesting helical structure results from the nearly linear coordination of two oxazole nitrogen atoms to



Scheme 30. Intramolecular cyclopropanation of diazoketones catalyzed by Aratani's complex (see Scheme 29) [73].



Scheme 31. Pfaltz's semicorrinato ligands in the Cu-catalyzed cyclopropanation [74]. R = D-menthyl, R' = CMe_2OH.

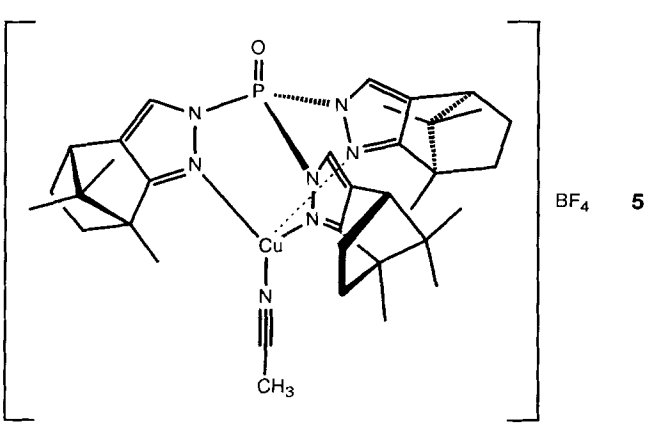


Scheme 32. The novel methylenebis(dihydrooxazole) and 5-aza-semicorrin ligands used in the Cu^I-catalyzed asymmetric cyclopropanation.

each Cu^I center, in which the ligands act as bridging units. The triflate anions are not coordinated.

The CMe_2-bridged bis(dihydrooxazole)s and the 5-azasemicorrins behave strictly as neutral ligands, whereas their methylene-bridged counterparts, like the semicorrins, can be deprotonated, thus forming anionic ligands. This is an interesting feature which shows the flexibility of the copper catalysts, because all classical ligands are anionic.

Finally, a C_3-symmetric optically active ligand containing stereogenic pyrazolyl units, recently described by Tolman et al.,[78] was found to bind in a terdentate manner to Cu^I to form complexes like **5**. This complex is a cyclopropanation catalyst, but the reported enantioselectivities are modest to moderate (up to 60% *ee*).

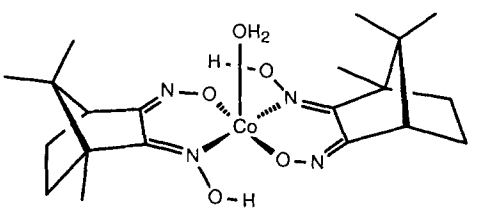


5

5.5.2. Cobalt Catalysts

Parallel to the development of efficient copper catalysts by Aratani et al., the Nakamura and Otsuka groups reported in the seventies the use of Co^{II} complexes of type **6** bearing α-camphorquinonedioximato ligands.[79]

These catalysts are somewhat unusual in that they show good activity only for the conversion of conjugated olefins. Enantiomeric excesses up to 88% were obtained in the reaction of styrene with neopentyl diazoacetate. Despite the relatively high selectivity reported, no further development of these catalysts has appeared in the literature.



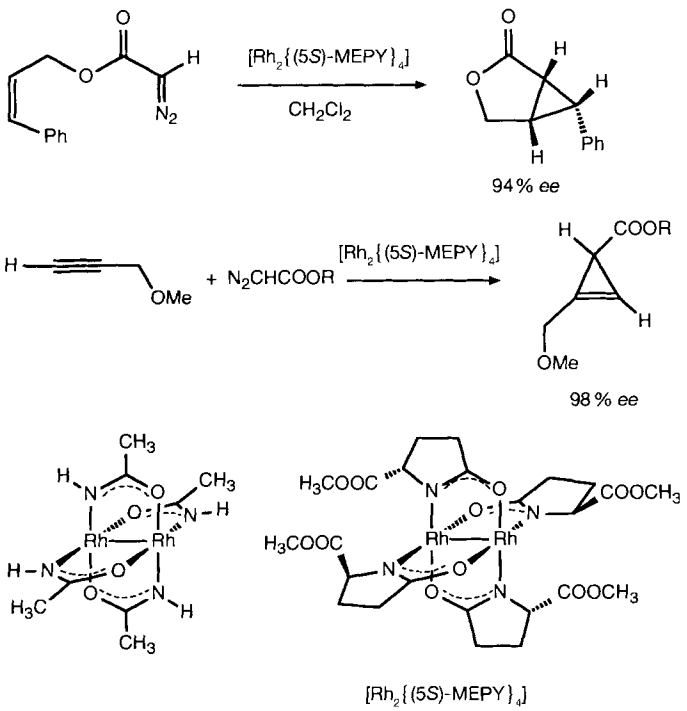
6

5.5.3. Rhodium Catalysts

The prototype of a catalyst for carbenoid reactions of diazocarbonyl compounds is $[Rh_2(OAc)_4]$. Not only cyclopropanations, but also insertions into C–H and N–H bonds are effectively catalyzed by a number of tetracarboxylato dirhodium complexes.[80] Attempts to achieve stereoselectivity by using optically active amino acids in such complexes were not very successful.[81] Doyle et al. used carboxamido complexes of the type shown in Scheme 33[82] after it was reported that acetamide can displace acetate in $[Rh_2(OAc)_4]$.[83] This discovery was the underlying idea for the development of, in part, highly enantioselective Rh^{II} cyclopropanation catalysts, containing optically active, bidentate N,O ligands of this type. The most efficient of them appears to be methyl 2-pyrrolidone-5-carboxylate (5-HMEPY). Its Rh^{II} complex gives up to 86% *ee* in the cyclopropanation of styrene with menthyl diazoacetate,[84a] and up to 94% *ee* in the intramolecular reaction of allylic diazoacetates.[84b,c] Furthermore, $[Rh_2(5\text{-MEPY})_4]$ is a very effective catalyst for the cyclopropenation of alkynes[85] (see Scheme 33).

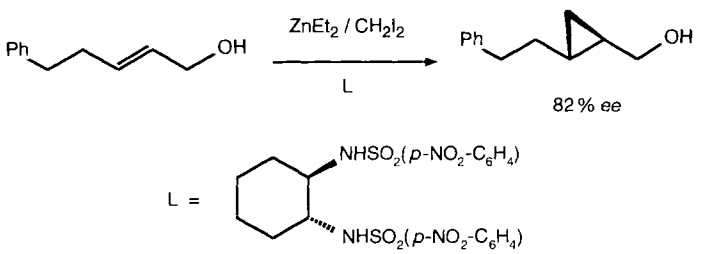
5.5.4. Miscellaneous

A procedure that does not employ diazo reagents for the synthesis of cyclopropane derivatives from olefins is the Simmons–Smith cyclopropanation.[86] The carbene is typically generated from CH_2I_2 and mediated by a Zn–Cu couple. Kobayashi et al. recently reported the first catalytic, enantioselective Simmons–Smith cyclopropanation of disubstituted allylic alcohols by a $ZnEt_2/CH_2I_2$ system. Chiral disulfonamide



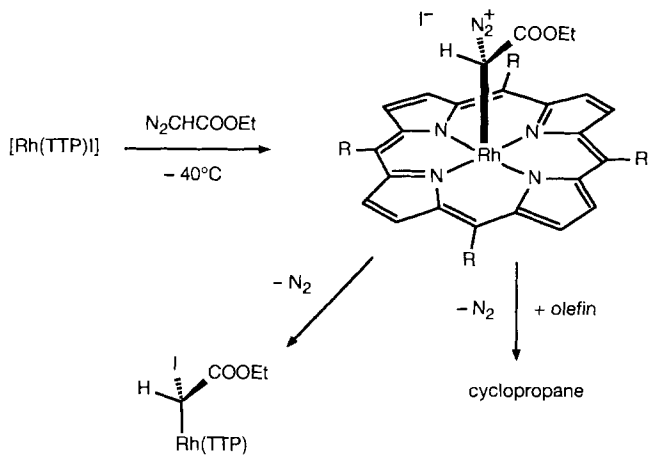
Scheme 33. Asymmetric intramolecular cyclopropanation of an allylic diazoacetate [84b, c] and cyclopropenation of an acetylene (R = D-menthyl) [85] catalyzed by a carboxamidato-Rh^{II} complex.

ligands were used as catalysts, and optical yields up to 82% were obtained.[87] An example is given in Scheme 34.



Scheme 34. The first example of asymmetric Simmons–Smith cyclopropanation with a catalyst containing a chiral disulfonamide ligand [87].

For the vast majority of the known cyclopropanation reactions no reliable experimental details on the mechanism are available. The formation of carbene complexes is obviously the most probable route, but such complexes have never been observed in catalytic systems. The formation of the cyclopropane ring can occur either by a concerted addition of the olefin, or via a metallacyclobutane intermediate.[88] A recent spectroscopic study addressed these questions for the iodo(tetra-*p*-tolylporphyrin)-rhodium system.[89] The 1-diazoalkyl complex resulting from the addition of ethyl diazoacetate to the catalyst could be detected at low temperatures (Scheme 35). At temperatures higher than $-20\,^{\circ}C$ this complex decomposed in the presence of olefins to afford cyclopropanes. If no olefins were added, the corresponding 1-iodoalkyl complex formed. Both reactions are taken as indicative of the generation of a highly reactive carbene intermediate.

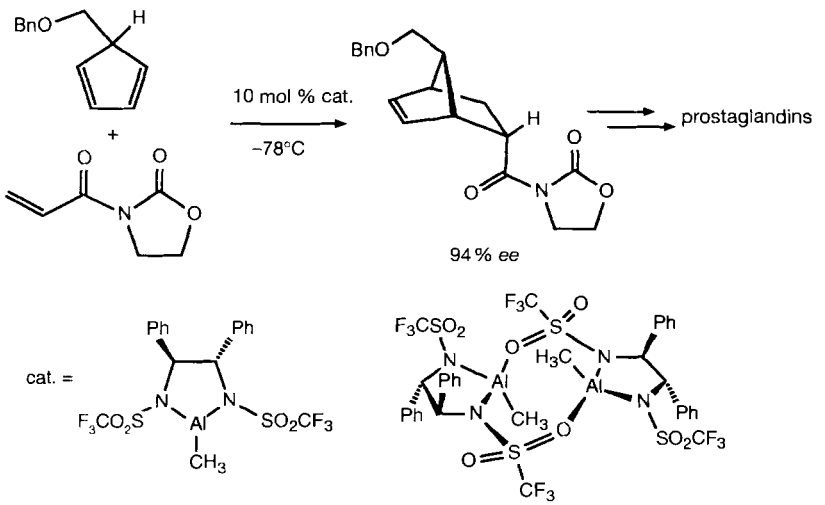


Scheme 35. Identification of intermediates in the addition of ethyl diazoacetate to a Rh–porphyrin cyclopropanation catalyst [89]. TTP = tetra-*p*-tolylporphyrin, i.e. R = *p*-tolyl.

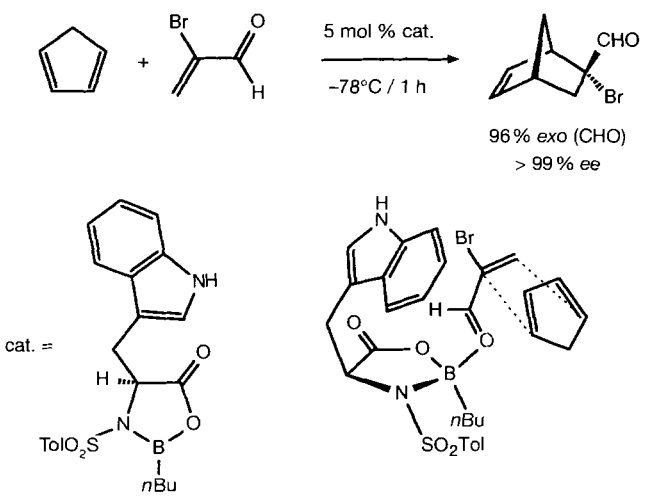
5.6. Asymmetric Diels–Alder Reactions

Chiral Lewis acids effectively catalyze [4 + 2] cycloaddition reactions of various dienes and dienophiles.[90] In recent years several boron and aluminum catalysts bearing optically active nitrogen ligands have been shown to impart very high enantioselectivities to Diels–Alder reactions. Whereas the vast majority of the successful catalysts contain chelating oxygen ligands, recent developments have shown that optically active nitrogen-ligands can give superior results. In particular, with the nitrogen-ligands, fine-tuning the electronic and steric properties seems to be much more flexible. Corey et al. have demonstrated that the diazaaluminolidine represented in Scheme 36 is an effective catalyst for the cycloaddition of cyclopentadiene derivatives to activated dienophiles.[91] The specific product shown in the example was used as an intermediate for the synthesis of prostaglandins. The ligand is a C_2-symmetric bis(sulfonamide), derived from 1,2-diamino-1,2-diphenylethane. The catalyst, which is easily formed in situ from the bis(sulfonamide) and, for example, $AlMe_3$, displays an interesting dimeric structure in the solid state (Scheme 36, bottom right).[91c] One of the two sulfonyl groups of each monomeric unit acts as a bridge through one oxygen atom, to give a tetrahedral coordination environment at the aluminum centers.

An oxazaborolidine derived from tryptophane has recently been shown by Corey et al. to impart extremely high enantioselectivity (>99% *ee* according to NMR) to the cycloaddition of 2-bromoacrolein and cyclopentadiene (see Scheme 37).[92] The high stereoselectivity is ascribed to an attractive interaction between the π-acidic dienophile and the π-basic indole moiety in the transition state, which leads to a highly preferential exposure of one enantioface of the dienophile to the attack by the diene. Such an attractive interaction is similar in concept to secondary interactions between ligands and substrates, which were postulated, for example, for several reactions catalyzed by functionalized ferrocenylphosphane complexes.[93] Very similar oxazaborolidines, also derived from amino acids but not able to display such crucial interactions, were found to afford lower optical yields (up to 86% *ee*).[94]



Scheme 36. Al-catalyzed asymmetric Diels–Alder reaction of a functionalized cyclopentadiene and (bottom right) a schematic representation of the dimeric structure of the catalyst in the solid state [91].

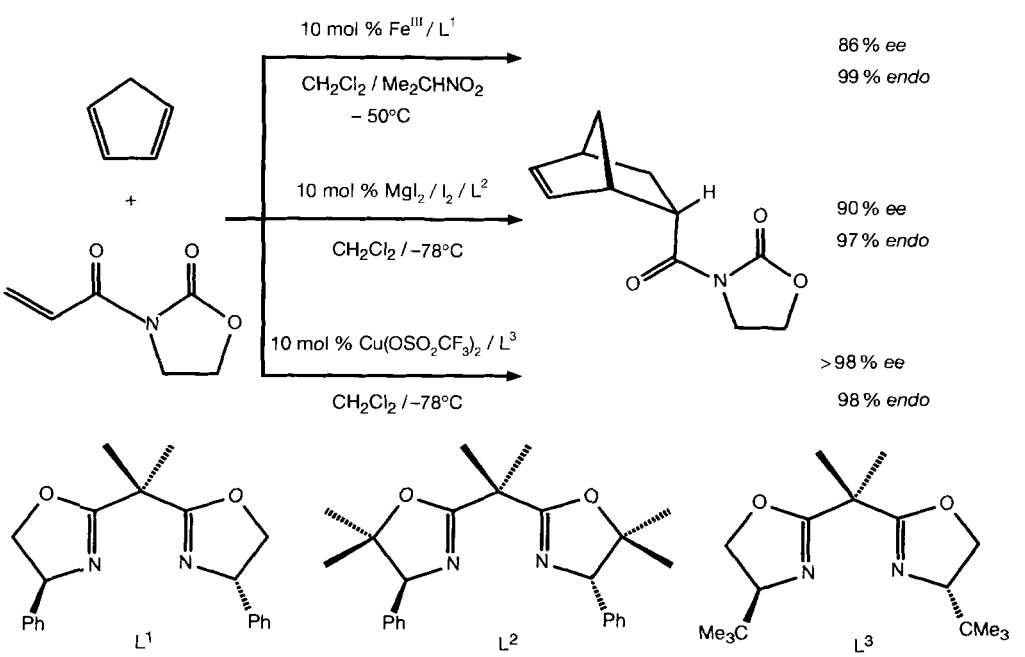


Scheme 37. Asymmetric Diels–Alder reaction of 2-bromoacrolein with cyclopentadiene catalyzed by an oxazaborolidine derived from tryptophan, and the proposed transition-state assembly [92].

Bis(dihydrooxazole) complexes of Fe^{III}, Mg^{II}, and Cu^{II} have also been successfully employed as catalysts for the Diels–Alder reaction.[95] The exact nature of the iron catalyst, which is generated in situ from the ligand L^1 in Scheme 38 and $FeCl_2$, FeI_2, or Fe powder and I_2, is rather obscure. This catalyst affords enantiomeric excesses of up to 86% in the Diels–Alder condensation illustrated in Scheme 38. It is also one of the still rare examples of non-d^0 transition metal Lewis acids used as catalysts in asymmetric cycloaddition reactions.[96] Slightly higher optical yields (90% *ee*) were reported for the same reaction when MgI_2 and the more bulky ligand L^2 formed the catalyst, whereas enantiomeric excesses of exceeding 98% were obtained in the case of the Cu catalyst in combination with ligand L^3, which demonstrates that the choice of metal *and* ligand plays a very important role.[95c] In all systems, cationic or dicationic complexes are assumed to be the catalytically active species.

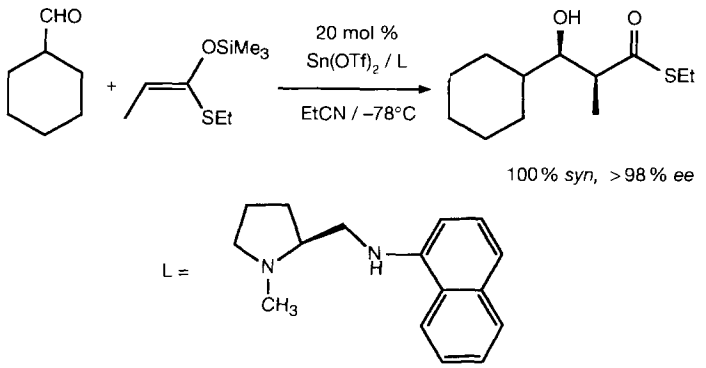
5.7. Asymmetric Aldol Condensations

The addition of silyl enol ethers to carbonyl compounds, the Mukaiyama aldol reaction,[97] is promoted by several Lewis acids. Studies by Mukaiyama et al. have in recent years shown that the combination of Sn^{II} triflate and a chiral diamine impart very high stereoselectivities to this reaction.[98] This system is commonly best used in a stoichiometric fashion with addition of tributyltin fluoride or dibutyltin diacetate as promoters. However, a judicious choice of solvent and reaction conditions turns this reaction into a catalytic process, albeit with modest turnover numbers. Thus, slow addition of the reactants to a solution of the catalyst (20 mol%) in propionitrile at low tem-



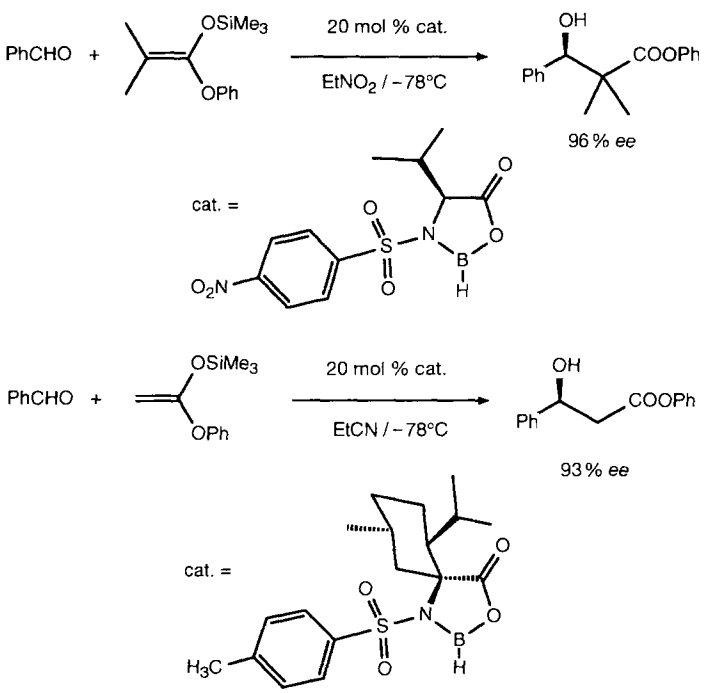
Scheme 38. Asymmetric Diels–Alder reactions catalyzed by Fe^{III} and Mg^{II} halide as well as by Cu^{II} triflate complexes containing bis(dihydrooxazole) ligands [95].

perature affords the aldol products in good yields and high stereoselectivities. The condensation of cyclohexylcarbaldehyde with (*Z*)-1-trimethylsilyloxy-1-(ethylthio)propene is shown in Scheme 39. The *syn*-configurated aldol product is exclusively formed with an optical yield that is higher than 98% *ee*.



Scheme 39. Asymmetric Mukaiyama aldol condensation catalyzed by a Sn^{II} complex containing a chiral chelating diamine [98].

More recently, the Kiyooka[99] and Masamune[100] groups have shown that chiral oxazaborolidines similar to those described in Section 5.6 (Diels–Alder reactions) are very effective catalysts for the Mukaiyama reaction. Optical yields up to 99% *ee* were reported. The catalysts are formed in situ from $BH_3 \cdot THF$ and an arenesulfonamide of an α-amino acid. Two examples are illustrated in Scheme 40. As was the case for the Sn-catalyzed reactions, the choice of solvent and reaction conditions plays a crucial role; best results are obtained in nitroethane, or propionitrile, and by slow addition of the aldehyde compound to the reaction mixture.



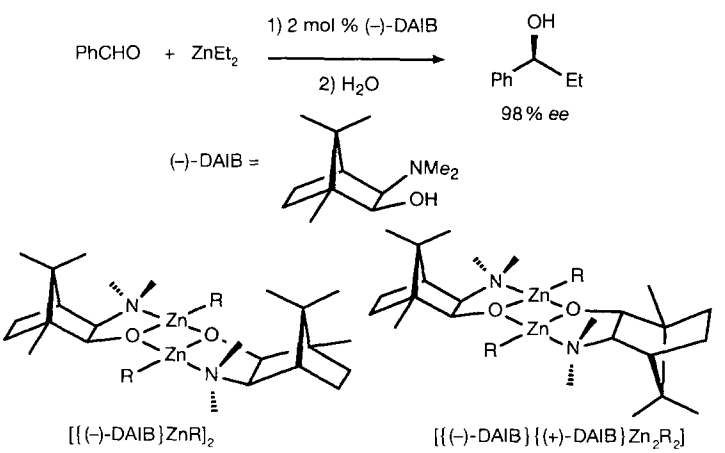
Scheme 40. Asymmetric Mukaiyama aldol condensations catalyzed by chiral oxazaborolidinones derived from *N*-sulfonylamino acids [99, 100].

Future developments of this important reaction will probably focus on the improvement of the catalytic activity of the already successful systems described above.

5.8. Asymmetric Alkylation of Aldehydes

The enantioselective nucleophilic addition of dialkylzinc reagents to aldehydes, in the presence of catalytic amounts of a chiral ligand (typically an amino alcohol), has been extensively studied by several groups. Excellent review articles on this topic have appeared in recent years.[101]

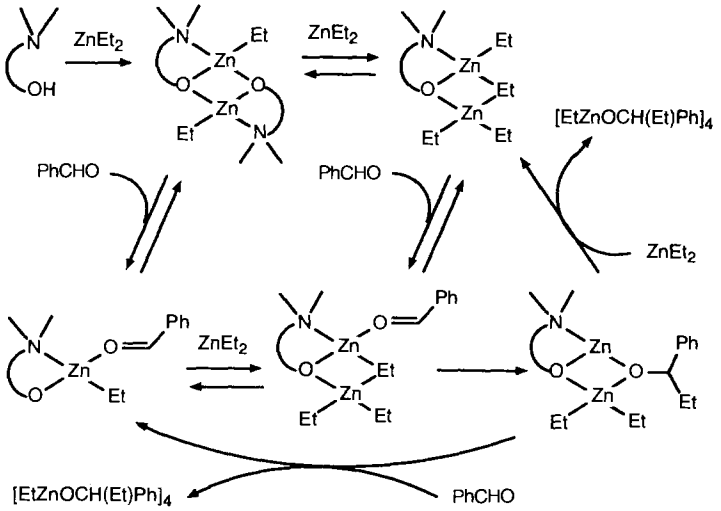
Oguni and Omi first showed that the reaction of $ZnEt_2$ with benzaldehyde is effectively catalyzed by chiral 2-amino-1-alcohols derived from simple amino acids.[102] Since then, this reaction has served as a standard test reaction in the development of new catalysts. One of the best understood systems has been described by Noyori et al.[103] The main conclusions from that study will be briefly discussed here, as they can be applied to other systems. There, 3-*exo*-(dimethylamino)isoborneol (DAIB) is used as catalyst in 1–5 mol% (to aldehyde). A virtually quantitative yield of the secondary alcohol is obtained if one equivalent of the $ZnEt_2$ reagent is employed (Scheme 41). Only one



Scheme 41. The DAIB-catalyzed asymmetric addition of $ZnEt_2$ to benzaldehyde and the two diastereomeric dimers $[(DAIB)ZnR]_2$, involved in chiral amplification (characterized by X-ray crystallography for R = Me): The less stable and more reactive homochiral form, and the more stable and less reactive *meso* form [103].

ethyl group is transferred to the electrophile, and the actual alkylation takes place via a dinuclear zinc species as illustrated in Scheme 42.

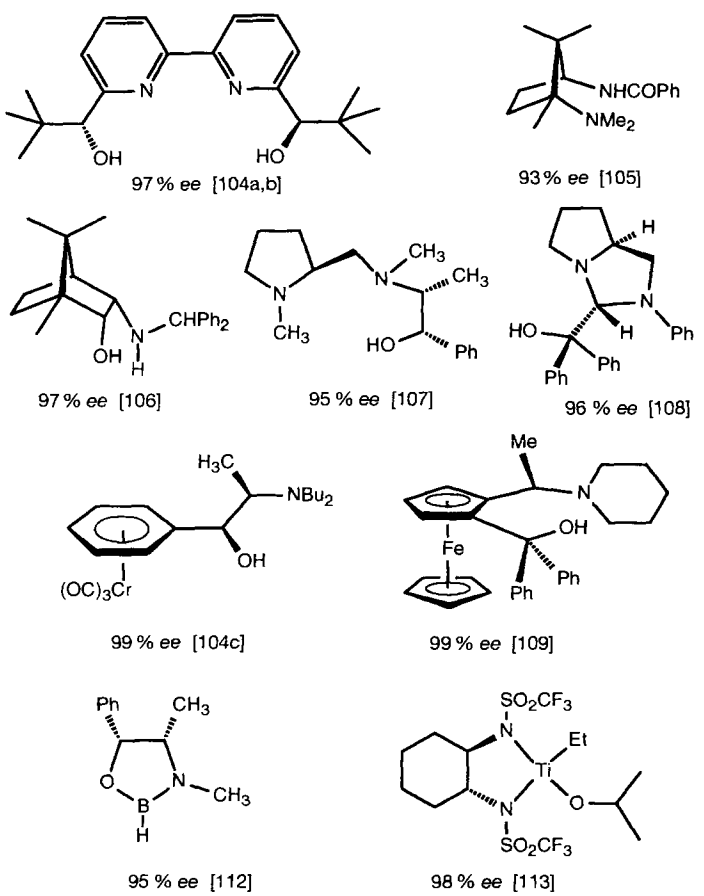
One of the most interesting features of this reaction are the nonlinear effects in the enantioselectivity. Thus, maximum enantioface discriminations (95–98% *ee*) in the ethylation of benzaldehyde are still obtained when scalemic mixtures of DAIB, for instance, in an optical purity as low as 15%, are used. This has been explained by the formation of two diastereomeric dimeric complexes (both characterized by X-ray diffraction), one of them a homochiral and the other a centrosymmetric *meso* form (see Scheme 41). The former is both thermodynamically and kinetically less stable and therefore exhibits much higher turnover frequencies than the achiral counterpart. The possibil-



Scheme 42. The mechanism of the DAIB-catalyzed addition of $ZnEt_2$ to benzaldehyde [103].

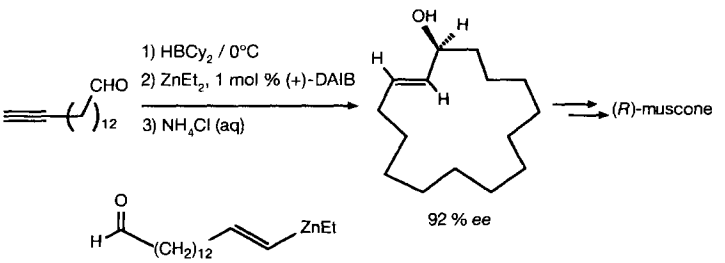
ity of obtaining high enantioselectivities despite the relatively low optical purity of the inducing ligand has been named *asymmetric amplification*, and was first observed by Kagan et al.,[104d] as well as by other groups more recently.[104a-c]

Several other N,O-ligands catalyze the addition of dialkylzinc to aldehydes in high optical yields. Scheme 43 illustrates the structural variety of such ligands.[105-109]



Scheme 43. A selection of ligands and complexes used as catalysts in the addition of $ZnEt_2$ to benzaldehyde (the *ee* values of the product 1-phenylpropanol are indicated).

In recent years efforts have been made to extend the range of zinc reagents from simple to functionalized alkyls.[110] Progress in this area is exemplified by the work of Knochel et al.[110a] and Oppolzer et al.[110b-d] For example, alkenylzinc reagents are generated in situ by transmetalation from ZnR_2 (R = Me, Et) and a vinylborane, the latter being obtained by hydroboration of the corresponding terminal alkyne. The addition of such nucleophiles is catalyzed, for example, by DAIB, which gives excellent enantioselectivities. This methodology was very recently applied, in an intramolecular variation, to the total synthesis of (*R*)-muscone[110d] (Scheme 44). Finally, dialkynylzinc and alkynylbromozinc reagents can also be used in this type of reaction (catalyzed by, for instance, ephedrine derivatives) and give moderate to good stereoselectivities.[111]

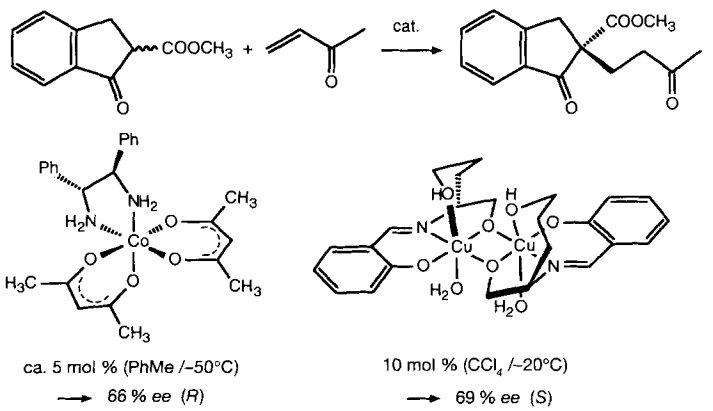


Scheme 44. Oppolzer's synthesis of muscone by the intramolecular reaction of the alkenylzinc reagent (shown at the bottom) that arises in situ from $ZnEt_2$ and the hydroborated ω-pentadecinal [110d].

Scattered reports have appeared on the use of boron and titanium catalysts containing nitrogen-ligands. Thus, the oxazaborolidine, formed in situ from (−)-ephedrine and $H_3B \cdot S(CH_3)_2$, catalyzes the standard formation of 1-phenylpropanol with an enantiomeric excess of 95%.[112] The same reaction is very efficiently catalyzed by the bistrifluoromethanesulfonamide of *trans*-1,2-diaminocyclohexane in the presence of equivalent amounts of titanium tetraisopropoxide, and affords the product in 98% *ee*.[113] The actual catalyst is considered to be the ethyltitanium complex shown in Scheme 43.

5.9. Asymmetric Conjugate Addition Reactions

The conjugate addition reaction (this term includes any nucleophilic 1,4-addition to an α,β-unsaturated system) is an extremely important transformation which finds wide application in organic synthesis.[114] The number of recent publications dealing with the asymmetric version of this reaction testifies to the worldwide interest.[115] However, asymmetric catalysis still plays a minor role in conjugate addition, since most studies have employed chiral ligands (or complexes) in stoichiometric amounts.[116] One of the first studies, carried out by Brunner et al.,[117] was the cobalt-catalyzed 1,4 addition of methyl 1-oxo-2-indanate to vinyl methyl ketone. By using 1,2-diphenyl-1,2-ethanediamine as the chiral ligand, optical yields up to 66% *ee* were obtained (Scheme 45). The catalyst precursor is the octahedral Co^{II} complex $[Co(acac)_2(diamine)]$, formed in situ from $[Co(acac)_2]$. The same reaction is also catalyzed by a

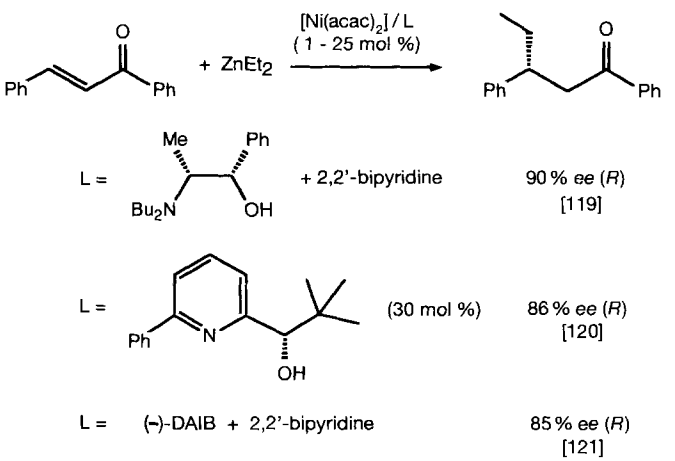


Scheme 45. Asymmetric Michael addition catalyzed by Co^{II} [117] and Cu^{II} complexes [118].

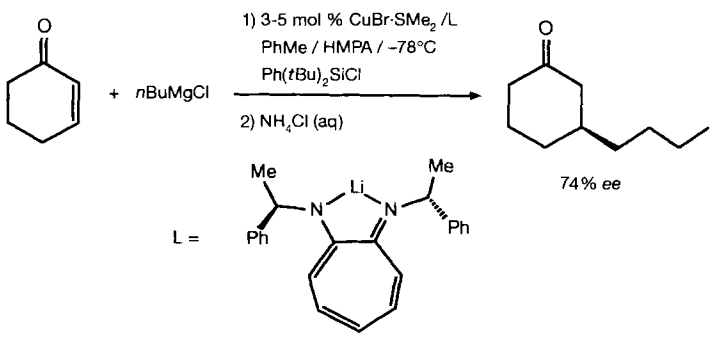
dimeric Cu^{II} complex bearing a tetradentate Schiff base as ligand) (Scheme 45). A slightly higher enantioselectivity (69% *ee*) was observed by Desimoni et al. with this complex.[118]

The use of $[Ni(acac)_2]$ as a catalyst precursor in the addition of diethylzinc to chalcone in the presence of various chelating, optically active N,O-ligands has been reported by Soai et al.,[119] Bolm et al.,[120] and Feringa et al.[121] Simple ephedrine derivatives, novel pyridyl (or 2,2'-bipyridyl) alcohols, or the well-known DAIB afforded enantiomeric excesses of up to 90%. Relevant examples are shown in Scheme 46. An interesting aspect of this reaction is the beneficial effect that the presence of a second, achiral nitrogen ligand has on the enantioselectivity. Thus, a variety of chelating diamines such as 2,2'-bipyridine, 1,10-phenanthroline, and 2,2'-biquinoline were found to improve selectivity significantly.[119, 121]

Finally, Lippard et al. have shown that chiral aminotropone imidates are effective ligands in the Cu-catalyzed conjugate addition of Grignard reagents to cylohexenone.[122] This virtually unique ligand system afforded enantiomeric excesses as high as 74% (Scheme 47).



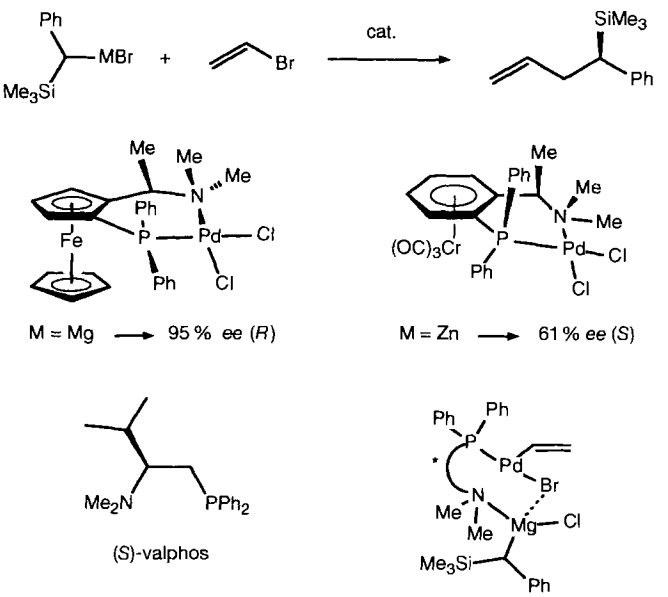
Scheme 46. Enantioselective 1,4 addition of $ZnEt_2$ to chalcone catalyzed by Ni^{II} in the presence of chelating N,O-ligands [119–121].



Scheme 47. A chiral *N,N'*-dialkylaminotropone imidate ligand in the Cu^{I}-catalyzed 1,4 addition of Grignard reagents to cyclohexenone [122].

5.10. Asymmetric Grignard Coupling

The use of nitrogen-containing ligands in the Ni- and Pd-catalyzed coupling of secondary Grignard reagents with alkenyl halides has been pioneered by Hayashi and Kumada.[123] The most successful ligands used for this reaction are chelating P,N-systems, derived either from amino acids[124] or from chiral ferrocenyl systems.[125] The best characterized catalysts are the $NiCl_2$, or $PdCl_2$ complexes with ppfa ((*S**)-*N,N*-dimethyl-1-[(*R**)-2-diphenylphosphino)ferrocenyl]ethylamine). Enantiomeric excesses exceeding 90% were obtained in the reaction of [α-(trimethylsilyl)benzyl]magnesium bromide with vinyl bromide, which afforded an optically active allylsilane (Scheme 48). It



Scheme 48. Synthesis of β,γ-unsaturated allylsilanes by asymmetric Pd-catalyzed Grignard coupling. Examples of catalysts with ferrocenyl [125], (η^6-arene)Cr [126], and amino acid derived P,N-ligands [124], and the postulated transition-state assembly.

has been proposed that the dimethylamino group on the ligands fulfills an important role in the transition state of the reaction. Its dissociation from palladium (or nickel) and temporary coordination to magnesium enables one of the enantiomers of the Grignard reagent to be selected, which leads to the formation of the preferred diastereomeric transition-state assembly, as illustrated in Scheme 48.[125c] Such an assembly immediately

precedes the key transmetalation step of the alkyl fragment from magnesium to palladium (or nickel). However, this model postulates a coordinatively unsaturated palladium (or nickel) center, which seems rather unlikely.

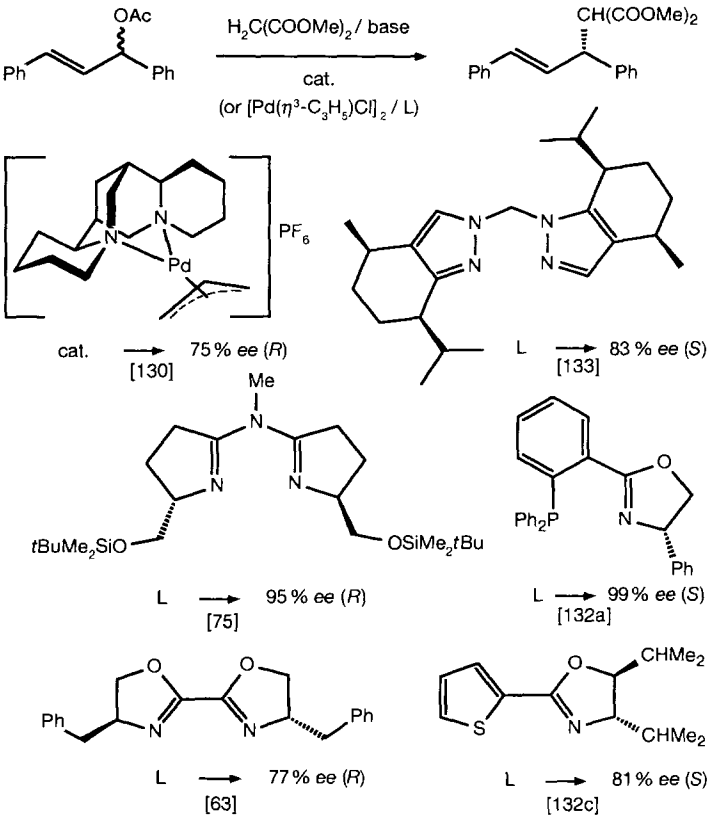
Of the two elements of chirality contained in ferrocenyl ligands of the ppfa type, the planar chirality due to the 1,2-disubstitution of the ferrocene moiety plays the dominant role in determining stereoselectivity in Grignard cross-coupling reactions.[125c] Hayashi and Uemura recently reported the synthesis of a chromium complex containing an analogous P,N-ligand system in which the planar-chirality is part of a η^6-coordinated arene.[126] The novel ligand provided enantioselectivities up to 61% *ee* (Scheme 48).

5.11. Asymmetric Allylic Alkylation

The allylic alkylation reaction consists of the substitution of a suitable leaving group in allylic position by a carbon nucleophile.[127] This transformation is typically catalyzed by phosphane–Pd complexes, and high degrees of enantioselection have been obtained by using a variety of chiral chelating diphosphanes.[128] Reports on the use of optically active nitrogen-ligands did not appear until 1990 and are still very rare.[129] In fact, it is commonly accepted that Pd(0) species that are stabilized by phosphane ligands are involved in the catalytic cycle.[127] It is also well-known that nitrogen-donors are generally rather poor ligands for the stabilization of low oxidation states of late transition metals. A combination of these factors may have generated a prejudice against nitrogen-ligands as alternatives to phosphorus-ligands.

One of us has recently shown that the alkaloid (−)-sparteine is an effective inducing ligand for aymmetric allylic alkylation.[130, 131] Optical yields of up to 85% *ee* were obtained in the alkylation of simple 1,3-disubstituted allylic acetates with the anion of dimethyl malonate as a nucleophile. The Pd^{II} complex $[Pd(\eta^3\text{-}C_3H_5)(\text{sparteine})]PF_6$ was used as catalyst precursor (Scheme 49). The corresponding η^3-cyclohexenyl and η^3-1,1,3-triphenylallyl complexes, postulated as intermediates in the catalytic alkylation of cyclohexenyl acetate and 1,1,3-triphenylallylacetate, respectively, were prepared and characterized by X-ray crystallography.[130b] The catalytic activity of such sparteine–Pd complexes was qualitatively estimated to be one to two orders of magnitude lower than that of phosphane–Pd systems[130a] (this rule of thumb seems to apply to other nitrogen-containing systems; see below).

Highly enantioselective catalysts containing bis(dihydrooxazole), or 5-azasemicorrin ligands were used by Pfaltz et al.[63, 75] Under conditions where the nucleophile is generated in situ from dimethylmalonate, *N,O*-bis(trimethylsilyl)acetamide, and a cocatalytic amount of KOAc in CH_2Cl_2, alkylation products were obtained in very high optical yields (up to 95% *ee*). Recently Pfaltz and von Matt[132a] and Helmchen and Sprinz,[132b] independently, developed (phosphinoaryl)dihydrooxazoles as P,N-ligands, which were shown to give more active and highly selective catalysts in this reaction. Thienyl dihydrooxazoline ligands were used by Frost and Williams,[132c] but were inferior, both in terms of activity and selectivity, when compared to the abovementioned P,N-systems (Scheme 49).



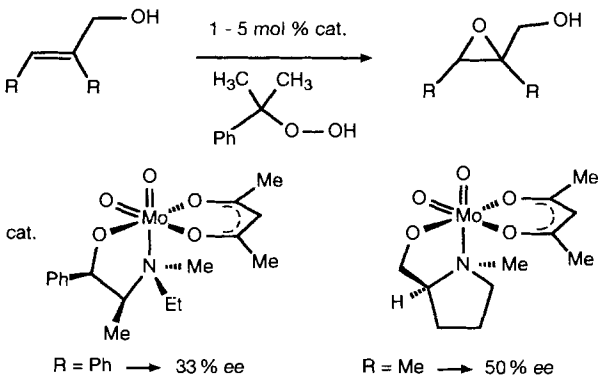
Scheme 49. Asymmetric allylic alkylation catalyzed by Pd complexes containing chelating nitrogen-ligands.

A novel asymmetric bis(pyrazolyl)methane ligand derived from menthone was recently prepared in these laboratories.[133] Good enantioselectivities (up to 83% *ee*) were obtained in the standard alkylation reaction of 1,3-diphenylallylacetate (Scheme 49). It was found that one equivalent of chloride, for example, present in solution when the catalyst was prepared in situ from the binuclear complex $[Pd_2(\eta^3\text{-}C_3H_5)_2Cl_2]$ and the ligand, had a beneficial effect on stereoselectivity. A halide effect of this type, which possibly also plays an important role in the systems of Pfaltz et al., is not yet understood, and holds out the hope that future mechanistic studies may lead to further improvements of this "old" reaction.

5.12. Asymmetric Oxidation Reactions

Before the advent of the Sharpless epoxidation of allylic alcohols with *tert*-butylhydroperoxide (TBHP) catalyzed by titanium tartrate systems,[134] several reports of molybdenum[135] and vanadium[136] catalysts had appeared. These systems contain chiral auxiliaries such as ephedrine and proline derivatives. The cases where the nitrogen-donors interact directly with the metal are illustrated in Scheme 50. Modest to good enantioselectivities were obtained (up to 50% *ee*). It should be noted that the dioxomolybdenum complexes shown there can give rise to diastereomeric mixtures, because the metal atom becomes a stereogenic center.

After the spectacular success of the Sharpless epoxidation reaction, progress in this field followed very slowly, and effec-



Scheme 50. Early example of asymmetric epoxidation of an allylic alcohol with cumene hydroperoxide catalyzed by Mo^{VI} complexes [135].

tive chiral catalysts capable of epoxidizing nonfunctionalized olefins have been discovered only in recent years.

5.12.1. Asymmetric Expoxidation of Simple Olefins

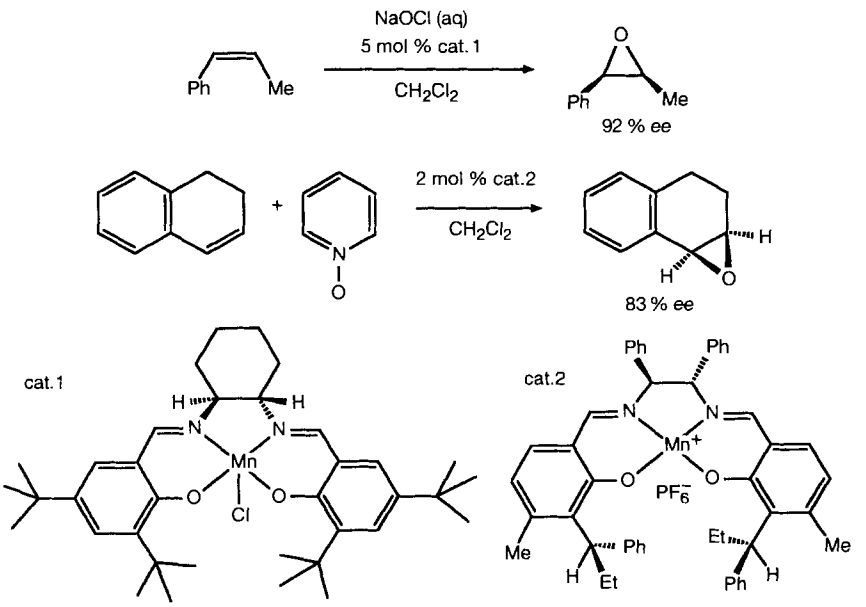
Kochi et al. have shown that achiral Mn^{III} and Cr^{III} complexes containing salen type ligands (salen = *N*,*N*′-bis(salicylidene)-ethylenediamine) are active catalysts for the epoxidation of nonfunctionalized olefins with, for example, iodosylbenzene as oxidant.[137] In the case of chromium, an oxochromium(v) species is an intermediate in the catalytic cycle. An analogous oxomanganese(v) could not be isolated and characterized, but sound indirect evidence for its existence has been reported.[137a] The formation of such oxo species implies the successive oxygen atom transfer from the oxidant to the metal and hence to the substrate, the "oxygen rebound".[138] This mechanism is fundamentally different from that operating with Sharpless's titanium catalysts.

Following up Kochi's pioneering work, Jacobsen et al.[139] and, independently, Katsuki et al.[140] prepared chiral derivatives of the $[Mn(salen)]^+$ complexes and, using oxidants such as PhIO, or more elegantly, aqueous NaOCl (commercial bleach) under phase-transfer conditions, achieved the catalytic epoxidation of simple olefins with enantiomeric excesses exceeding 90%. Some examples are shown in Scheme 51. Chirality is introduced in the essentially planar salen–manganese system by replacing the ethylenediamine backbone by optically active 1,2-diphenylethylene diamine or *trans*-1,2-diaminocylohexane. Furthermore, it is crucial that the ligand bears bulky substituents adjacent to the phenoxy oxygen atoms. Whereas Jacobsen et al. showed that a *tert*-butyl group is sufficient to achieve high selectivities in the phase-transfer process (using NaOCl as oxidant), Katsuki et al. obtained better results (with PhIO as oxidant) by introducing a stereogenic 1-phenylprop-1-yl group. These systems seem to be particularly well suited for the epoxidation of *Z*-configurated, 1,2-disubstituted and cyclic olefins. Thus, enantioface discriminations of up to 98% *ee* were obtained with chromene derivatives as substrates.[139c,d] Mukaiyama et al. recently demonstrated that chiral salen–manganese complexes are also suitable catalysts for the epoxidation of nonfunctionalized olefins with molecular oxygen.[141] Since the system additionally requires pivalaldehyde as reductant, the actual oxidant is possibly a hydroperoxide (peroxopivalic acid). These findings show the versatility of the manganese catalysts and their potential for future developments and applications.

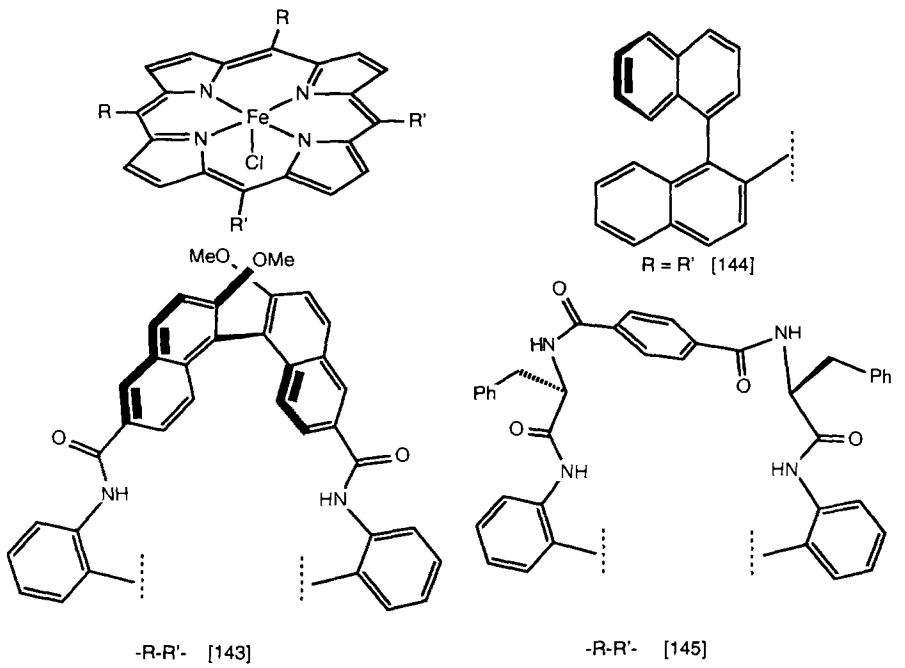
Moderate enantioselectivities (up to 62% *ee*) were recently reported by Thornton et al. for the oxidation of silyl enol ethers to α-hydroxy ketones with PhIO, catalyzed by another salen–manganese complex.[142] Finally, efforts to develop chirally modified porphyrin ligands are worth mentioning. The groups of Groves,[143] Kodadek,[144] Mansuy,[145] and Collman[146] prepared peripherally functionalized porphyrins bearing stereogenic binaphthyl, amino acid, or threitol units, as illustrated in Scheme 52. Fe^{III} as well as Mn^{III} complexes of porphyrins of the above type were shown to be efficient catalysts for the epoxidation of simple olefins in combination with either NaOCl or PhIO as oxidants, and afforded enantioselectivities in the range of 15–88% *ee*. The strategy common to the different approaches is apparent: Introduction of stereogenic substituents onto the porphyrin moiety, either with bulky and conformationally rigid groups or by bridging the *meso* positions, generates a "chiral pocket" around the metal. The results obtained so far are encouraging and show scope for further developments.

5.12.2. Osmium-Catalyzed Dihydroxylations

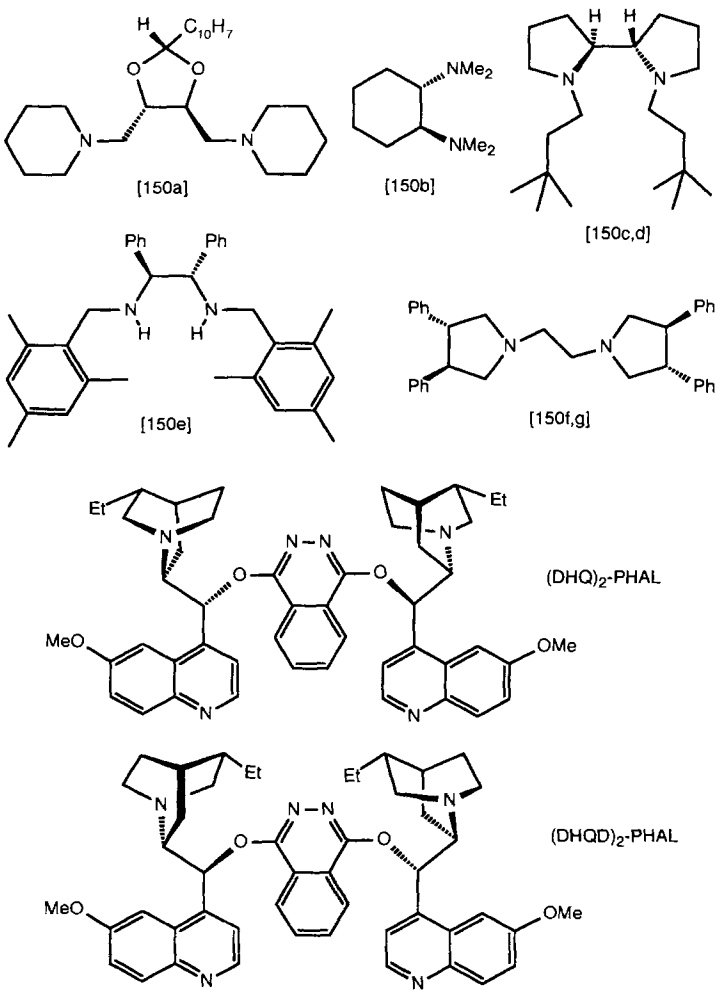
The development of the asymmetric Os-catalyzed dihydroxylation of olefins by Sharpless et al. is recognized to be one of the most significant advances in homogeneous catalysis in recent years. Scope, applications, and mechanistic aspects of this reaction have been studied in detail and excellent reviews have ap-



Scheme 51. Asymmetric epoxidation of unfunctionalized olefins catalyzed by Mn^{III}–salen complexes [139, 140].



Scheme 52. Partial structures of some chiral porphyrins that in Fe^{III} complexes are used as catalysts in asymmetric tion of simple olefins [143–145].



Scheme 53. A selection of chiral chelating diamines used in the stoichiometric osmylation of olefins [150] and the state-of-the-art dihydroquinine and dihydroquinidine ligands for the catalytic dihydroxylation [152]. $C_{10}H_7$ = naphthyl.

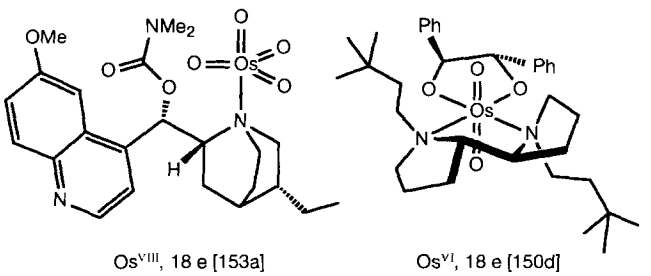
peared.[147] Therefore, just the relevant aspects related to the use of chiral nitrogen ligands will be highlighted.

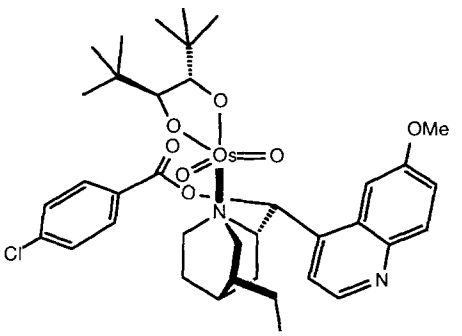
It has been known for decades that pyridines or tertiary amines accelerate the addition of OsO_4 to olefins.[148] Sharpless et al. introduced cinchona alkaloids as inducing agents in the stoichiometric osmylation of olefins in 1980.[149] In succeeding years several authors reported the use of chelating diamines as chiral auxiliares in this reaction.[150] Some are shown in Scheme 53. Enantiomeric excesses approaching 100% were obtained, but none of these diamine systems could be turned into a catalytic process. The fundamental breakthrough came in 1988 when Sharpless reported the catalytic version of the dihydroxylation with the OsO_4/cinchona system and *N*-methylmorpholine-*N*-oxide as a cooxidant.[151] During the following years, they further developed and optimized the process.[152] In particular, the use of $K_3[Fe(CN)_6]$ as a co-oxidant in a biphasic system and a broad screening of cinchona alkaloid derivatives impressively extended the scope of the catalytic reaction. Thus, for a wide variety of olefins, excellent enantioselectivities were obtained (>95% *ee*). The new class of phthalazine ligands, $(DHQD)_2$-PHAL and $(DHQ)_2$-PHAL, incorporating two alkaloid units into the same molecule, are derivatives of dihydroquinidine (DHQD) and dihydroquinine (DHQ). As DHQD and DHQ are a pseudoenantiomeric pair, both optical isomers of the dihydroxylation products are accessible in remarkably similar stereoselectivities.[152a]

A very important aspect of cinchona alkaloid derivatives (with respect to catalysis) is that they behave as monodentate ligands, that is, only the quinuclidine nitrogen atom coordinates to the metal. The complexes characterized by X-ray diffraction are shown in Scheme 54 (top left).[153]

The dioxoosmium(VI)diolato complexes (osmate esters), resulting from the reaction of [OsO_4 · amine] with an olefin during the catalytic cycle are coordinatively unsaturated species (16 e) only when monodentate amine ligands are used (Scheme 54, bottom). As pointed out by Sharpless et al.,[154] coordinative unsaturation at this stage is required to achieve reoxidation of the osmate ester and its hydrolysis. A coordinatively saturated system (for example, when a chelating diamine is used) or one formed in the presence of an excess of amine, is not susceptible to fast reoxidation/hydrolysis. This offers an explanation why chelating diamines, despite the excellent stereochemical results obtained in stoichiometric reactions, cannot be employed in catalytic processes.

A speculative, postulated mechanism for the Os-catalyzed dihydroxylation has been reported by Corey et al.[155a,b] They suggested that the cinchona ligands, which contain two alkaloid moieties, are able to accommodate two OsO_4 units coordinated to the quinuclidine nitrogen atoms. These complexes can exist as an equilibrium mixture (Scheme 55). Whereas the open form in which the OsO_4 fragments do not interact with each other was



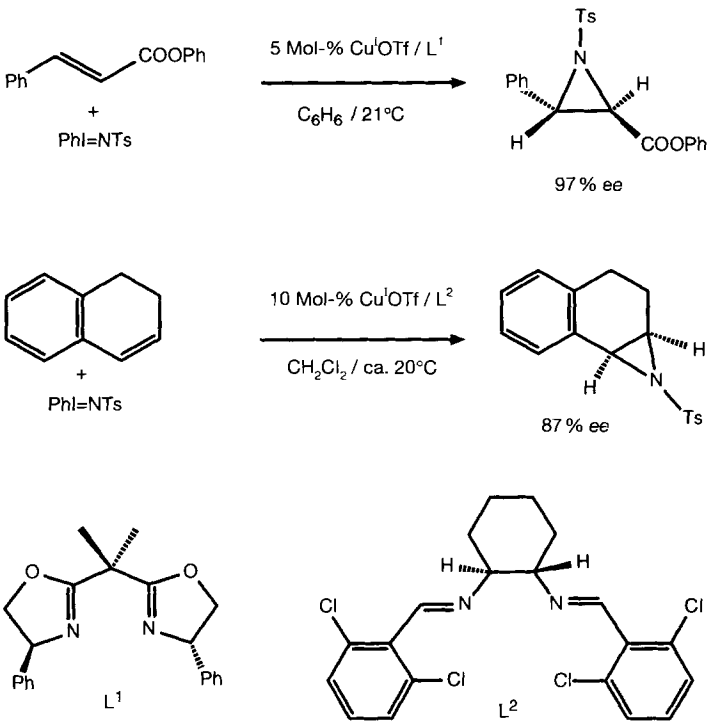


Scheme 54. Schematic representation of results of X-ray structural analyses of oxo-osmium complexes with dihydroquinine derivatives as monodentate ligands [153] and with a chelating diamine [150d].

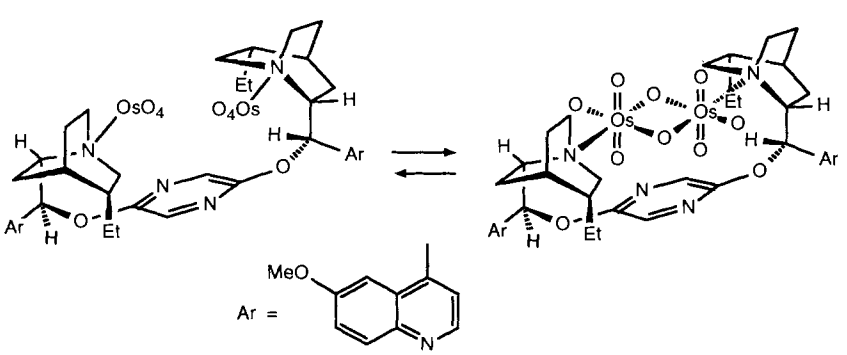
isolated and characterized by X-ray diffraction, the more reactive oxo-bridged form is proposed to be involved in the catalytic cycle. Recently, however, Sharpless et al.[155c] have shown that the kinetics of catalytic dehydroxylation is first order in osmium. This throuws doubt on the relevance of Corey's postulate.

5.12.3. *Asymmetric Aziridination*

A topic closely related to epoxidation is aziridination (the formation of an aziridine from an olefin and a suitable nitrene-delivering reagent).[156] An important discovery was made by the Evans group in 1991,[157a] when the catalytic activity of Cu^I salts was demonstrated. The simple compound $[Cu(NCMe)_4]ClO_4$ effectively catalyzed the aziridination of various olefins with (*N*-(*p*-toluenesulfonyl)imino)phenyliodinane (PhI=NTs). More recently, other groups have shown that several salen–metal complexes are able to catalyze this reaction,[158] but only very recently were highly enantioselective Cu^I catalysts disclosed. Using CuOTf with bis(dihydrooxazole) ligands (these catalysts are also very successful in cyclopropanation reactions; see Section 5.5.1), Evans et al. obtained optical yields of up to 97% *ee* for the aziridination of α,β-unsaturated esters (Scheme 56). The aziridines themselves are suitable precursors for the synthesis of α-amino acid derivatives.[157b] A further, remarkably simple, chiral, bidentate ligand has been reported by Jacobsen et al. (L^2 in Scheme 56).[159] A common feature of these first two successful approaches is the use of neutral, C_2-symmetric N,N-ligands. In analogy to cyclopropanation and to Mn-catalyzed epoxidation, the transfer of the nitrene fragment could occur via intermediate imido–metal complexes. Although such complexes are known for several transition metals,[160] and play an important role in ROMP catalysis (see Section 5.13), whether they are involved in catalytic aziridination remains the subject of speculation.



Scheme 56. Asymmetric aziridination of olefins catalyzed by Cu^I complexes [157b, 159].



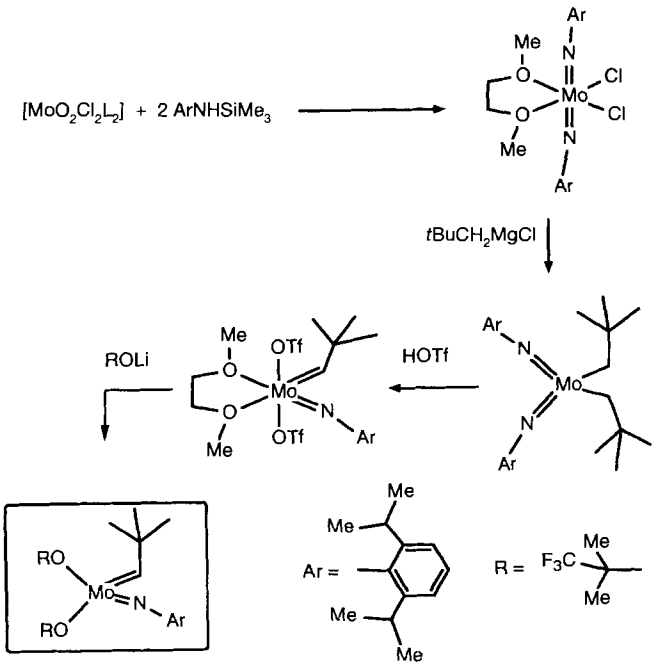
Scheme 55. Structure of a binuclear oxoosmium complex (characterized by X-ray analysis) and its postulated more reactive, dioxo-bridged form [155].

5.13. Miscellanous Reactions

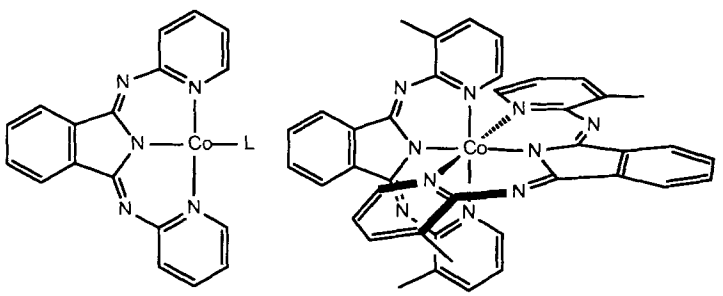
The oxidation of cyclohexane by air, which gives a mixture of cyclohexanol and cyclohexanone, is a fundamentally important industrial process.[161] The reaction, in which cyclohexyl hydroperoxide is an intermediate, is catalyzed by a hydrocarbon-soluble Co^{II} carboxylate, whose role is to decompose the hydroperoxide. Tolman, Ittel, et al. reported in 1988 that bis(2-pyridylimino)dihydroindolatocobalt complexes (Scheme 57) are very active and long-lived catalysts for this

oxidation process.[162] The advantage of such complexes is that they are active at lower temperatures and higher peroxide concentrations (higher conversions) than conventional catalysts. Cobalt porphyrins and phthalocyanins were also found to be efficient catalysts.[162]

In recent years well-defined catalysts for the ring-opening metathesis polymerization (ROMP) reaction have been developed. Starting from (usually) strained cyclic olefins and using ROMP it is now possible to prepare homopolymers and block copolymers with a very narrow molecular weight distribution.[163] The best catalysts are pseudo-tetrahedral alkylidene complexes of molybdenum and tungsten in the formal oxidation state +VI. The coordination sphere of the metal in these complexes contains two bulky alkoxide ligands and one sterically demanding imido ligand. This combination of ligands ensures sufficient stability of the alkylidene complex by preventing, for example, intermolecular ligand scrambling or other decomposition reactions. At the same time it still allows the coordination of the substrate with formation of a five-coordinate complex, and thus its transformation into the intermediate metallacyclobutane complex.[164a] One of two imido ligands also plays the role of a protecting group in a precursor of the catalyst, allowing the selective introduction of two alkyl ligands.[164] The synthesis and reactivity of such imido complexes are illustrated in Scheme 58. Several of these complexes have been characterized by X-ray diffraction and show the peculiarity of the NAr ligand: Because of the relative electron-deficiency of the metal center, a strong donation of the nitrogen lone pair takes place. This causes an apparent sp hybridization at the nitrogen atom, resulting in an M-N-C angle approaching 180°. Correspondingly, the M–N distance in the range of 1.70–1.75 Å is very short—indeed shorter than the M–C distance of the alkylidene ligands (1.85–1.95 Å).[164]



Scheme 58. Synthesis of a Mo ROMP catalyst containing imido ligands [164a]. L = thf.



Scheme 57. Cobalt catalysts containing bis(pyridylimino)dihydroisoindolato ligands for cyclohexane oxidation (L = $RCOO^-$ or second ligand) [162].

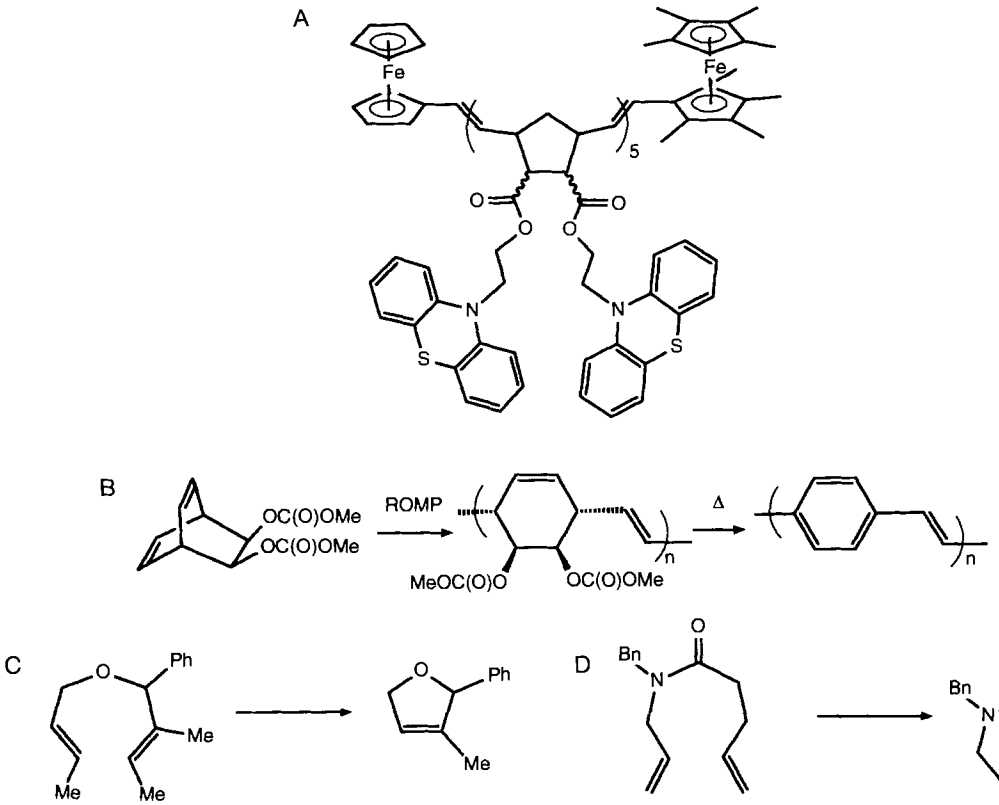
With ROMP catalysts the synthesis of, for example, small block copolymers containing redox-active groups was recently achieved (Scheme 59A). The well-behaved solution electrochemistry of such copolymers has been reported by Schrock, Wrighton, et al.[165]

Grubbs et al. have shown that the interesting polymer poly(1,4-phenylenevinylene) is readily accessible by ROMP (Scheme 59B)[166] and that the catalysts shown in Scheme 57 can be employed in the ring-*closing* olefin metathesis of diolefins for the synthesis of oxygen- and nitrogen-heterocycles (Scheme 59C and D).[167]

An alkylideneoxotungsten(VI) complex containing a tris(pyrazolyl)borato ligand has been reported by Boncella et al.[168] as an exceptionally stable ROMP catalyst. Its synthesis is achieved from an alkylidynetrichloro complex by ligand exchange and treatment with neutral alumina, as shown in Scheme 60. It is found to be a very active ROMP catalyst, in the presence of $AlCl_3$ as a cocatalyst, for example, for cyclooctene and norbornene polymerization. The role of the Lewis acid $AlCl_3$ is thought to involve abstraction of the chloride ligand, thus generating a coordinatively unsaturated cationic alkylidene species which acts as the actual catalyst.[168]

Although not directly relevant to homogeneous catalysis, the unique reactivity patterns imparted to arenes by the fragment $[Os(NH_3)_5]^{n+}$, $n = 2, 3$, discovered by Harman and Taube[169] should be mentioned. When Os^{III} but also Ru^{III} pentaammine salts are reduced in the presence of benzene, exceptionally stable $[M^{II}(NH_3)_5(\eta^2\text{-}C_6H_6)]^{2+}$ complexes are formed. This behavior is unprecedented in the coordination chemistry of such ammine complexes. The arene derivatives undergo smooth arene substitution reactions, but most important, they are susceptible to selective hydrogenation reactions and electrophilic substitution processes. Thus, a coordinated, substituted arene can be stereospecifically hydrogenated (for example, in the presence of a heterogeneous catalyst) to the corresponding η^2-cyclohexene derivative (Scheme 61A). Furthermore, the electrophilic substitution at a coordinated phenol derivative by, for example, maleic anhydride (a potentially acylating reagent) can be mechanistically viewed as a 1,4 addition (Scheme 61B). This reaction has been shown to be useful in the dearomatization of β-estradiol by direct stereospecific 1,4 alkylation (Scheme 61C).

Finally, to return to asymmetric reactions, a recent report by Inoue et al.[170] about the Ti-catalyzed formation of cyanohy-

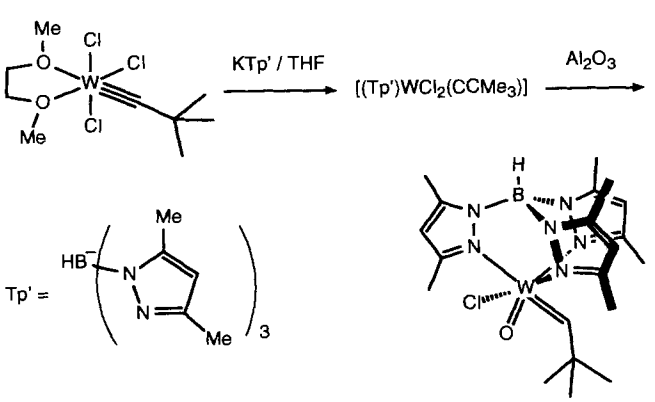


Scheme 59. Examples of recent applications of the imidomolybdenum ROMP catalysts.

drins is worth mentioning. Enantiomeric excesses up to 97% have been obtained for the addition of HCN to aldehydes in the presence of 10 mol% of ethyl or isopropyl orthotitanate and a Schiff base of a peptide as chiral ligand (Scheme 62). MM2 calculations indicate that such compounds behave as terdentate O,N,O ligands; the oxygen atom of the peptide linkage coordinates to the metal. A judicious construction of the ligand system utilizing only natural amino acids allows the preparation of both enantiomers of the products in high *ee*'s.

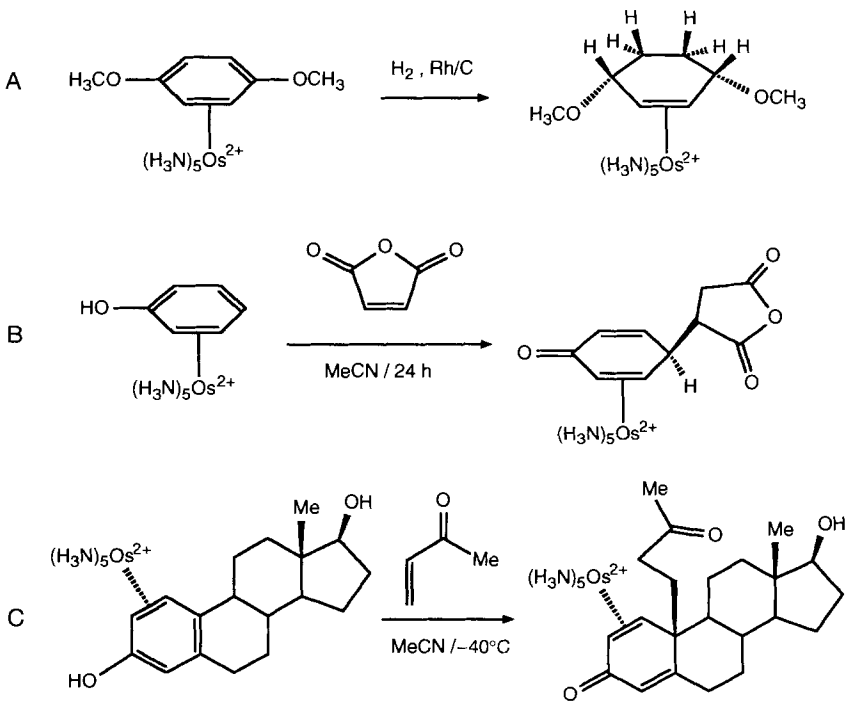
6. Conclusions

Nitrogen-ligands play an important role in modern organometallic chemistry and homogeneous catalysis. The properties and reactivities of the many complexes reported in the literature that contain such donors can be understood if one takes into consideration the general rules of coordination chemistry. Thus, in terms of their coordination behavior, it is fundamental to recognize the most important differences between nitrogen- and phosphorus-ligands: 1. the π backbonding ability of N-donors is insignificant, thus making them generally unsuited for the stabilization of low oxidation states of the transition metal center. 2. The *trans* effect exerted by N-donors is negligible, when compared to that of most other ligands encountered in organometallic chemistry, and thus their own rates of substitution reactions are usually high. 3. The reactivity of, for example, alkyl complexes of transition metals containing N-donors is usually high.

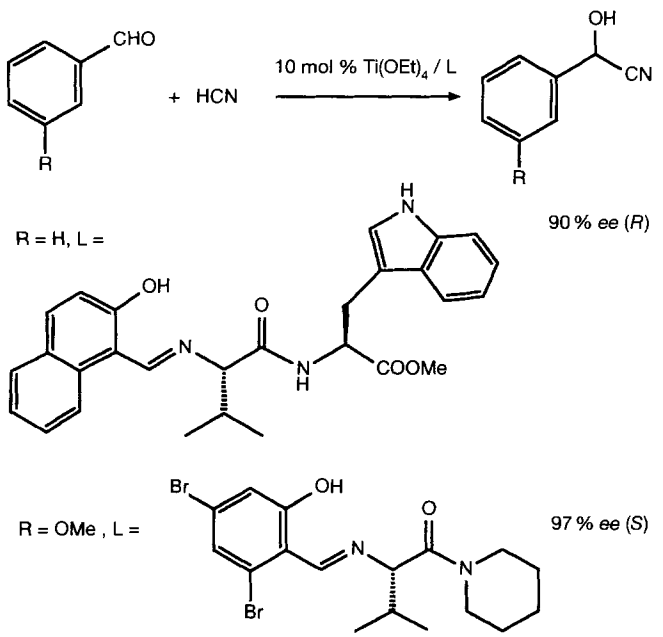


Scheme 60. Synthesis of an exceptionally stable W–alkylidene complex for applications as a ROMP catalyst [168].

For the vast majority of the reported cases nitrogen-ligands have been used as part of a chelating system that also involves other donor atoms such as C, O, P, and S. This is particularly true for the many applications in homogeneous catalysis described in Section 5, where nitrogen-ligands are responsible for various important developments in the field of asymmetric synthesis. Progress in this field in recent years has been achieved in a very empirical manner, mainly by synthetically oriented research groups, because chiral nitrogen ligands are often easily accessible from the "chiral pool". Thus, one is tempted to attribute the success of such ligands to organic chemists. At the same time, the wealth of applications of nitrogen-ligands in a variety of catalytic homogeneous reactions should be an incentive for systematic studies from the point of view of coordination chemistry in the near future.



Scheme 61. Catalytic reactions involving the $[Os(NH_3)_5]$ system of Harman, Taube et al. [169].



Scheme 62. Asymmetric addition of HCN to aldehydes catalzyed by Ti–peptide complexes [170].

The authors are particularly indebted to the late Prof. G. Geier for his valuable assistance with the selection and critical evaluation of the kinetic data as well as the thorough discussion of the section on equilibria in solution.

Received: June 18, 1993 [A 5]
German version: *Angew. Chem.* **1994**, *106*, 517

[1] J. E. Huheey, E. A. Keiter, R. L. Keiter, *Inorganic Chemistry: Principles of Structure and Reactivity*, Harper Collins, New York, **1993**, Chapter 11–13.
[2] a) J. P. Collman, L. S. Hegedus, J. R. Norton, R. G. Finke, *Principles and Applications of Organotransition Metal Chemistry*, University Science Books, Mill Valley, CA, USA, **1987**; b) A. Yamamoto, *Organotransition Metal Chemistry*, Wiley, New York, **1986**; c) R. H. Crabtree, *The Organometallic Chemistry of the Transition Metals*, Wiley, New York, **1988**; d) C. Elschenbroich, A. Salzer, *Organometallics*, 2nd ed., VCH, Weinheim, **1992**; *Organometallchemie*, Teubner, Stuttgart, **1988**; e) G. W. Parshall, S. D. Ittel, *Homogeneous Catalysis*, Wiley, New York, **1992**.
[3] a) C. A. McAuliffe, W. Levason, *Phosphine, Arsine and Stibine Complexes of the Transition Elements*, Elsevier, Amsterdam, **1979**; b) E. C. Alyea, *Catalytic Aspects of Metal Phosphine Complexes* (*Adv. Chem. Ser.* **1982**, *196*); c) *Homogeneous Catalysis with Metal Phosphine Complexes* (Ed.: L. H. Pignolet), Plenum, New York, **1983**; d) C. A. McAuliffe in *Comprehensive Coordination Chemistry, Vol. 2* (Eds.: G. Wilkinson, R. D. Gillard, J. A. McCleverty), Pergamon, Oxford, **1987**, p. 989–1066.
[4] See, for example, a) W. J. Evans, S. E. Foster, *J. Organomet. Chem.* **1992**, *433*, 79–94; b) W. J. Evans, *Adv. Organomet. Chem.* **1985**, *24*, 131–177; c) T. J. Marks, R. D. Ernst in *Comprehensive Organometallic Chemistry, Vol. 3* (Ed.: G. Wilkinson, F. G. A. Stone, E. W. Abel), Pergamon, Oxford, **1982**, pp. 173–279.
[5] N. N. Greenwood, A. Earnshaw, *Chemie der Elemente*, VCH, Weinheim, **1990**.
[6] See, for example, a) S. J. Ashcroft, C. T. Mortimer, *Thermochemistry of Transition Metal Complexes*, Academic Press, London, **1970**; b) *Bonding Energetics in Organometallics Chemistry* (Ed.: T. J. Marks) (*ACS Symp. Ser.* **1990**, *428*).
[7] J. K. Kochi, *Organometallic Mechanisms and Catalysis*, Academic Press, New York, **1978**.
[8] See, for example, ref. [2c], pp. 154–159.
[9] See, for example, ref. [2a], pp. 322–343.
[10] See, for example, ref. [7], pp. 293–310.
[11] W. Lau, J. C. Huffman, J. K. Kochi, *Organometallics* **1982**, *1*, 155–169.
[12] See, for example, ref. [7], Chapter 14.
[13] a) C. M. Langford, H. B. Gray, *Ligand Substitution Processes*, Benjamin, New York, **1965**; b) F. Basolo, R. G. Pearson, *Mechanism of Inorganic Reactions*, Wiley, New York, **1967**; c) R. G. Wilkins, *Kinetics and Mechanism of Reactions of Transition Metal Complexes*, 2nd ed., VCH, Weinheim, **1991**.
[14] D. W. Margerum, G. R. Cayley, D. C. Weatherburn, G. K. Pagenkopf, *Coordination Chemistry* (*ACS Monogr.* **1978**, *174*).
[15] G. Geier, *Helv. Chim. Acta* **1968**, *51*, 94–105.
[16] F. Basolo, J. Chatt, H. B. Gray, R. G. Pearson, B. L. Shaw, *J. Chem. Soc.* **1961**, 2207–2215.
[17] J. K. Burdett, *Molecular Shapes. Theoretical Models in Inorganic Stereochemistry*, Wiley, New York, **1980**, Chapter 9, and references therein.
[18] R. H. Holyer, C. D. Hubbard, S. F. A. Kettle, R. G. Wilkins, *Inorg. Chem.* **1965**, *4*, 929–935.
[19] H. Hagnauer, G. C. Stocco, R. S. Tobias, *J. Organomet. Chem.* **1972**, *46*, 179–191.
[20] See ref. [1], p. 394–413.
[21] P. B. Armentrout, *Periodic Trends in Transition Metal Bonds to Hydrogen, Carbon and Nitrogen* (*ACS Symp. Ser.* **1990**, *428*, 18–23).
[22] J. A. Connor, *Thermochemical Studies of Organo-Transition Metal Carbonyls and Related Compounds* (*Top. Curr. Chem.* **1977**, *71*, 71–110).
[23] a) C. A. Tolman, *Chem. Rev.* **1977**, *77*, 313–348; see also H. C. Clark, *Isr. J. Chem.* **1976/1977**, *15*, 210–213; T. L. Brown, K. J. Lee, *Coord. Chem. Rev.* **1993**, *128*, 89–116; b) A. L. Seligson, W. C. Trogler, *J. Am. Chem. Soc.* **1991**, *113*, 2520–2527.
[24] a) H. C. Brown, H. Bartholomay, Jr., M. D. Taylor, *J. Am. Chem. Soc.* **1944**, *66*, 435–442; b) H. C. Brown, S. Sujishi, *ibid.* **1948**, *70*, 2878–2881; c) H. C. Brown, *J. Chem. Educ.* **1959**, *36*, 424–431.
[25] a) K. P. Byers, A. J. Canty, B. W. Skelton, H. A. White, *J. Chem. Soc. Chem. Commun.* **1986**, 1722–1724; b) T. G. Appleton, J. R. Hall, M. Williams, *J. Organomet. Chem.* **1986**, *303*, 139–149.
[26] See, for example, R. Crabtree, *Acc. Chem. Res.* **1979**, *12*, 331–338, and references therein
[27] For Reviews see, for example, a) J. Dehand, M. Pfeffer, *Coord. Chem. Rev.* **1976**, *18*, 327–352; b) M. I. Bruce, *Angew. Chem.* **1977**, *89*, 75–89; *Angew. Chem. Int. Ed. Engl.* **1977**, *16*, 73–87; c) E. C. Constable, *Polyhedron*, **1984**, *3*, 1037–1057; d) A. D. Ryabov, *Synthesis* **1985**, 233–252.

[28] See, for example, a) N. K. Roberts, S. B. Wild, *J. Am. Chem. Soc.* **1979**, *101*, 6254–6260; b) K. Tani, L. D. Brown, J. Ahmed, J. A. Ibers, M. Yokota, A. Nakamura, S. Otsuka, *ibid.* **1977**, *99*, 7878–7886.

[29] For reviews see, for example, a) S. Trofimenko, *Prog. Inorg. Chem.* **1986**, *34*, 115–210; b) P. K. Buyers, A. J. Canty, R. T. Honeyman, *Adv. Organomet. Chem.* **1992**, *34*, 1–65.

[30] B. W. Davies, N. C. Payne, *Inorg. Chem.* **1974**, *13*, 1843–1848.

[31] R. J. Restivo, G. Ferguson, D. J. O'Sullivan, F. J. Lalor, *Inorg. Chem.* **1975**, *14*, 3046–3052.

[32] R. B. King, A. Bond, *J. Am. Chem. Soc.* **1974**, *96*, 1334–1338.

[33] J. S. Thompson, R. L. Harlow, J. F. Whitney, *J. Am. Chem. Soc.* **1983**, *105*, 3522–3527.

[34] a) G. van Koten, *Pure Appl. Chem.* **1989**, *61*, 1681–1694; b) J. Terheijden, G. van Koten, J. L. de Booys, H. J. C. Ubbels, C. H. Stam, *Organometallics* **1983**, *2*, 1882–1884; c) D. M. Grove, G. van Koten, W. P. Mul, R. Zoet, J. G. M. van der Linden, J. Legters, J. E. J. Schmitz, N. W. Murrall, A. J. Welch, *Inorg. Chem.* **1988**, *27*, 2466–2473, and references therein; d) A. A. H. van der Zeijden, G. van Koten, J. M. Ernsting, C. J. Elsevier, B. Krijen, C. H. Stam, *J. Chem. Soc. Dalton Trans.* **1989**, 317–324; e) H. C. L. Abbenhuis, N. Feiken, D. M. Grove, J. T. B. H. Jastrzebski, H. Kooijman, P. van der Sluis, W. J. J. Smeets, A. L. Spek, G. van Koten, *J. Am. Chem. Soc.* **1992**, *114*, 9773–9781; f) D. M. Grove, G. van Koten, A. H. M. Verschuuren, *J. Mol. Catal.* **1988**, *45*, 169–174.

[35] a) H. tom Dieck, H. J. Rieger, G. Fendesak, *Inorg. Chim. Acta* **1990**, *177*, 191–197; b) H. tom Dieck, R. Diercks, L. Stamp, H. Bruder, T. Schuld, *Chem. Ber.* **1987**, *120*, 1943–1950; c) J. C. M. Sinnema, G. B. H. Fendesak, H. tom Dieck, *J. Organomet. Chem.* **1990**, *390*, 237–250; d) K. Vrieze, *ibid.* **1986**, *300*, 307–326; e) K.-U. Baldenius, H. tom Dieck, W. A. König, D. Icheln, T. Runge, *Angew. Chem.* **1992**, *104*, 338–340; *Angew. Chem. Int. Ed. Engl.* **1992**, *31*, 305–307.

[36] a) P. Binger, M. J. Doyle, R. Benn, *Chem. Ber.* **1983**, *116*, 1–10; b) T. Yamamoto, A. Yamamoto, S. Ikeda, *J. Am. Chem. Soc.* **1971**, *93*, 3350–3359, 3360–3364; see also P. Binger, M. J. Doyle, C. Krüger, Y.-H. Tsay, *Z. Naturforsch. B* **1979**, *34*, 1289–1292.

[37] a) B. Kräutler, *Chimia* **1987**, *41*, 277–292; b) R. Scheffold, G. Rytz, L. Walder in *Modern Synthetic Methods, Vol. 3* (Ed.: R. Scheffold), Salle + Sauerländer, Frankfurt, **1983**, pp. 355–440.

[38] See ref. [2b], p. 201.

[39] See, for example, J. W. Scott in *Asymmetric Synthesis, Vol. 4* (Ed.: J. D. Morrison), Academic Press, Orlando, FL, USA, **1984**, pp. 1–226.

[40] K. E. Koenig in *Asymmetric Synthesis, Vol. 5* (Ed.: J. D. Morrison), Academic Press, Orlando, FL, USA, **1985**, pp. 71–101.

[41] a) W. R. Cullen, F. W. B. Einstein, C.-H. Huang, A. C. Willis, E.-S. Yeh, *J. Am. Chem. Soc.* **1980**, *102*, 988–993; b) W. R. Cullen, J. D. Woollins, *Can. J. Chem.* **1982**, *60*, 1793–1799; c) T. D. Appleton, W. R. Cullen, S. V. Evans, T.-J. Kim, J. Trotter, *J. Organomet. Chem.* **1985**, *279*, 5–21.

[42] a) Y. Ohgo, S. Takeuchi, Y. Natori, J. Yoshimura, *Bull. Chem. Soc. Jpn.* **1981**, *54*, 2124–2135; b) S. Takeuchi, Y. Ohgo, *ibid.* **1981**, *54*, 2136–2141; c) *ibid.* **1984**, *57*, 1920–1928; d) Y. Ohgo, Y. Tashiro, S. Takeuchi, *ibid.* **1987**, *69*, 1549–1551.

[43] a) A. Pfaltz, *Acc. Chem. Res.* **1993**, *26*, 339–345; b) *Mod. Synth. Methods* **1989**, *5*, 199–248.

[44] U. Leutenegger, A. Madin, A. Pfaltz, *Angew. Chem.* **1989**, *101*, 61–62; *Angew. Chem. Int. Ed. Engl.* **1989**, *28*, 60–61. Under the same conditions α,β-unsaturated carboxamides are reduced affording slightly higher enantioselectivities: P. von Matt, A. Pfaltz, *Tetrahedron Asymmetry* **1991**, *2*, 691–700.

[45] S. Wallbaum, J. Martens, *Tetrahedron Asymmetry* **1992**, *3*, 1475–1504.

[46] a) A. Hirao, S. Itsuno, S. Nakahama, N. Yamazaki, *J. Chem. Soc. Chem. Commun.* **1981**, 315–317; b) S. Itsuno, A. Hirao, S. Nakahama, N. Yamazaki, *J. Chem. Soc. Perkin Trans. 1* **1983**, 1673–1675.

[47] S. Itsuno, Y. Sakurai, K. Ito, A. Hirao, S. Nakahama, *Bull. Chem. Soc. Jpn.* **1987**, *60*, 395–396.

[48] a) E. J. Corey, R. K. Bakshi, S. Shibata, *J. Am. Chem. Soc.* **1987**, *109*, 5551–553, b) E. J. Corey, R. K. Bakshi, S. Shibata, C.-P. Chen, V. K. Singh, *ibid.* **1987**, *109*, 7925–7926; c) E. J. Corey, J. O. Link, *Tetrahedron Lett.* **1989**, *30*, 6275–6278; d) E. J. Corey, C.-P. Chen, G. A. Reichard, *ibid.* **1989**, *30*, 5547–5550.

[49] G. Bringmann, T. Hartung, *Angew. Chem.* **1992**, *104*, 782–783; *Angew. Chem. Int. Ed. Engl.* **1992**, *31*, 761–762.

[50] a) A. V. R. Rao, M. K. Gurjar, P. A. Sharma, V. Kaiwar, *Tetrahedron Lett.* **1990**, *31*, 2341–2344; b) A. V. R. Rao, M. K. Gurjar, V. Kaiwar, *Tetrahedron Asymmetry* **1992**, *3*, 859–862.

[51] a) W. Behnen, C. Dauelsberg, S. Wallbaum, J. Martens, *Synth. Commun.* **1992**, *22*, 2143–2155; b) J. Martens, C. Dauelsberg, W. Behnen, S. Wallbaum, *Tetrahedron Asymmetry* **1992**, *3*, 347–350; c) S. Wallbaum, J. Martens, *ibid.* **1991**, *2*, 1093–1096; K. Stingl, J. Martens, S. Wallbaum, *ibid.* **1992**, *3*, 223–226.

[52] I. K. Youn, S. Lee, C. S. Pak, *Tetrahedron Lett.* **1988**, *29*, 4453–4456.

[53] K. Tanaka, J. Matsui, H. Suzuki, *J. Chem. Soc. Chem. Commun.* **1991**, 1311–1312.

[54] E. J. Corey, M. Azimioara, S. Sarshar, *Tetrahedron Lett.* **1992**, *33*, 3429–3430.

[55] a) V. Nevalainen, *Tetrahedron Asymmetry* **1992**, *3*, 1563–1572; b) D. K. Jones, D. C. Liotta, I. Shinkai, D. J. Mathre, *J. Org. Chem.* **1993**, *58*, 799–801.

[56] a) E. J. Corey, J. O. Link, *Tetrahedron Lett.* **1992**, *33*, 3431–3434; b) *J. Am. Chem. Soc.* **1992**, *114*, 1906–1908.

[57] B. T. Cho, Y. S. Chun, *Tetrahedron Asymmetry* **1992**, *3*, 1583–1590.

[58] The subject has recently been reviewed: G. Zassinovich, G. Mestroni, S. Gladiali, *Chem. Rev.* **1992**, *92*, 1051–1069.

[59] See, for example S. Gladiali, L. Pinna, G. Delogu, S. De Martin, G. Zassinovich, G. Mestroni, *Tetrahedron Asymmetry* **1990**, *1*, 635–648.

[60] a) M. Chou, C. Creutz, D. Mahajan, N. Sutin, A. P. Zipp, *Inorg. Chem.* **1982**, *21*, 3989–3997; b) D. Mahajan, C. Creutz, N. Sutin, *ibid.* **1985**, *24*, 2063–2067.

[61] a) G. Zassinovich, R. Bettella, G. Mestroni, N. Bresciani-Pahor, S. Geremia, L. Randaccio, *J. Organomet. Chem.* **1989**, *370*, 187–202; b) S. De Martin, G. Zassinovich, G. Mestroni, *Inorg. Chim. Acta* **1990**, *174*, 9–11.

[62] J. Kaschig (CIBA-GEIGY), EP-B 0246 194 A2, **1985**; EP-B 0 246 195 A1, **1985**; EP-B 0 246 196 A1, **1985**; EP-B 0 251 994 A1, **1986**.

[63] D. Müller, G. Umbricht, B. Weber, A. Pfaltz, *Helv. Chim. Acta* **1991**, *74*, 232–240.

[64] For a review see H. Brunner, *Angew. Chem.* **1983**, *95*, 921–931; *Angew. Chem. Int. Ed. Engl.* **1983**, *22*, 897–907, and references therein.

[65] B. D. Vineyard, W. S. Knowles, M. J. Sabacky, G. L. Bachman, D. J. Weinkauff, *J. Am. Chem. Soc.* **1977**, *99*, 5946–5952.

[66] a) H. Brunner, U. Obermann, *Chem. Ber.* **1989**, *122*, 499–507; b) H. Brunner, A. Kürzinger, *J. Organomet. Chem.* **1988**, *346*, 413–424; see also c) C. Botteghi, A. Schionato, G. Chelucci, H. Brunner, A. Kürzinger, U. Obermann, *ibid.* **1989**, *370*, 17–31; d) H. Brunner, R. Becker, G. Riepl, *Organometallics* **1984**, *3*, 1354–1359; e) H. Brunner, B. Reiter, G. Riepl, *Chem. Ber.* **1984**, *117*, 1330–1354.

[67] a) H. Nishiyama, S. Yamaguchi, M. Kondo, K. Itoh, *J. Org. Chem.* **1992**, *57*, 4306–4309; b) H. Nishiyama, M. Kondo, T. Nakamura, K. Itoh, *Organometallics* **1991**, *10*, 500–508; c) H. Nishiyama, H. Sakaguchi, T. Nakamura, M. Horihata, M. Kondo, K. Itoh, *ibid.* **1989**, *8*, 846–848; d) H. Nishiyama, S. Yamaguchi, S.-B. Park, K. Itoh, *Tetrahedron Asymmetry* **1993**, *4*, 143–150.

[68] T. Hayashi, Y. Matsumoto, I. Morikawa, Y. Ito, *Tetrahedron Asymmetry* **1990**, *1*, 151–154; see also T. Hayashi, S. Hengrasmee, Y. Matsumoto, *Chem. Lett.* **1990**, 1377–1380.

[69] J. Salaün, *Chem. Rev.* **1989**, *89*, 1247–1270.

[70] For reviews see a) M. P. Doyle, *Recl. Trav. Chim. Pays-Bas* **1991**, *110*, 305–316; b) *Chem. Rev.* **1986**, *86*, 919–939; c) G. Maas, *Top. Curr. Chem.* **1987**, *137*, 75–253; d) M. Brookhart, W. B. Studabaker, *Chem. Rev.* **1987**, *87*, 411–432; e) M. P. Doyle, *Acc. Chem. Res.* **1986**, *19*, 348.

[71] a) H. Nozaki, H. Takaya, S. Moriuti, R. Noyori, *Tetrahedron Lett.* **1966**, 5239–5242; b) *Tetrahedron* **1968**, *24*, 3655–3669; c) R. Noyori, H. Takaya, Y. Nakanishi, H. Nozaki, *Can. J. Chem.* **1969**, *47*, 1242–1245.

[72] a) T. Aratani, *Pure Appl. Chem.* **1985**, *57*, 1839–1844; b) T. Aratani, Y. Yoneyoshi, T. Nagase, *Tetrahedron Lett.* **1982**, *23*, 685–688; c) *ibid.* **1977**, 2599–2602; d) *ibid.* **1975**, 1707–1710.

[73] W. G. Dauben, R. T. Hendricks, M. J. Luzzio, H. P. Ng, *Tetrahedron Lett.* **1990**, *31*, 6969–6972.

[74] a) H. Fritschi, U. Leutenegger, A. Pfaltz, *Angew. Chem.* **1986**, *98*, 1028–1029; *Angew. Chem. Int. Ed. Engl.* **1986**, *25*, 1005–1006; b) H. Fritschi, U. Leutenegger, K. Siegmann, A. Pfaltz, W. Keller, C. Kratky, *Helv. Chim. Acta* **1988**, *71*, 1541–1542; c) H. Fritschi, U. Leutenegger, A. Pfaltz, *ibid.* **1988**, *71*, 1553–1565; d) see also ref. [44] and A. Pfaltz, *Chimia* **1990**, *44*, 202–213.

[75] U. Leutenegger, G. Umbricht, C. Fahrni, P. von Matt, A. Pfaltz, *Tetrahedron* **1992**, *48*, 2143–2156.

[76] a) D. A. Evans, K. A. Woerpel, M. M. Hinman, M. M. Faul, *J. Am. Chem. Soc.* **1991**, *113*, 726–728; b) D. A. Evans, K. A. Woerpel, M. J. Scott, *Angew. Chem.* **1992**, *104*, 439–441; *Angew. Chem. Int. Ed. Engl.* **1992**, *31*, 430–432.

[77] R. E. Lowenthal, S. Masamune, *Tetrahedron Lett.* **1991**, *32*, 7373–7376.

[78] a) C. J. Tokar, P. B. Kettler, W. V. Tolman, *Organometallics* **1992**, *11*, 2737–2739; for similar ligands see b) D. D. LeCloux, W. B. Tolman, *J. Am. Chem. Soc.* **1993**, *115*, 1153–1154; c) P. J. Pérez, M. Brookhart, J. L. Templeton, *Organometallics* **1993**, *12*, 261–262.

[79] a) Y. Tatsumo, A. Konishi, A. Nakamura, S. Otsuka, *J. Chem. Soc. Chem. Commun.* **1974**, 588–589; b) A. Nakamura, A. Konishi, R. Tsujitani, M. Kudo, S. Otsuka, *J. Am. Chem. Soc.* **1978**, *100*, 3449–3461; c) A. Nakamura, A. Konishi, Y. Tatsuno, S. Otsuka, *ibid.* **1978**, *100*, 3443–3449, 6544.

[80] a) For a new review see J. Adams, D. M. Spero, *Tetrahedron* **1991**, *47*, 1765–1808; b) for applications in β-lactam chemistry see, for example, A. G. M. Barrett, M. A. Sturgess, *ibid.* **1988**, *44*, 5615–5652.

[81] In the enantioselective C-H insertion reaction of α-diazo-β-ketoesters catalyzed by carboxylato Rh^{II} complexes containing amino acid derivatives as ligands, selectivities up to 46% obtained; see S. Hashimoto, N. Watanabe, S. Ikegami, *Tetrahedron Lett.* **1990**, *31*, 5173–5174.

[82] a) M. P. Doyle, K.-L. Loh, K. M. DeVries, M. S. Chinn, *Tetrahedron Lett.* **1987**, *28*, 833–836; b) M. P. Doyle, V. Bagheri, T. J. Wandless, N. K. Harn, D. A. Brinker, C. T. Eagle, K.-L. Loh, *J. Am. Chem. Soc.* **1990**, *112*, 1906–1912; c) A. Pawda, D. J. Austin, S. F. Hornbuckle, M. A. Semones, M. P. Doyle, M. N. Protopopova, *ibid.* **1992**, *114*, 1874–1876.

[83] M. O. Ahsan, I. Bernal, J. L. Bear, *Inorg. Chem.* **1986**, *25*, 260–265.

[84] a) M. P. Doyle, B. D. Brandes, A. P. Kazala, R. J. Pieters, M. B. Jarstfer, L. M. Watkins, C. I. Eagle, *Tetrahedron Lett.* **1990**, *31*, 6613–6616; b) M. P. Doyle, R. J. Pieters, S. F. Martin, R. E. Austin, C. J. Oalmann, P. Müller, *J. Am. Chem. Soc.* **1991**, *113*, 1423–1424; c) S. F. Martin, C. J. Oalmann, S. Liras, *Tetrahedron Lett.* **1992**, *33*, 6727–6730.

[85] M. N. Protopopova, M. P. Doyle, P. Müller, D. Ene, *J. Am. Chem. Soc.* **1992**, *114*, 2755–2757.

[86] H. E. Simmons, T. L. Cairns, S. A. Vladuchick, C. M. Hoiness, *Org. React.* **1973**, *20*, 1–131.

[87] H. Takahashi, M. Yoshioka, M. Ohno, S. Kobayashi, *Tetrahedron Lett.* **1992**, *33*, 2575–2578.

[88] The role of olefin coordination to Cu^{I} catalysts has been discussed as early as 1973: R. G. Salomon, J. K. Kochi, *J. Am. Chem. Soc.* **1973**, *95*, 3300–3310.

[89] a) J. L. Maxwell, K. C. Brown, D. W. Bartley, T. Kodadek, *Science* **1992**, *256*, 1544–1547; b) D. W. Bartley, T. Kodadek, *J. Am. Chem. Soc.* **1993**, *115*, 1656–1660.

[90] For reviews see a) H. B. Kagan, O. Riant, *Chem. Rev.* **1992**, *92*, 1007–1019; b) M. J. Taschner, *Org. Synth. Theory Appl.* **1989**, *1*, 1–101.

[91] a) E. J. Corey, R. Imwinkelried, S. Pikul, X. B. Xiang, *J. Am. Chem. Soc.* **1989**, *111*, 5493–5495; b) E. J. Corey, N. Imai, S. Pikul, *Tetrahedron Lett.* **1991**, *32*, 7517–7520; c) E. J. Corey, S. Sarshar, J. Bordner, *J. Am. Chem. Soc.* **1992**, *114*, 7938–7939.

[92] a) E. J. Corey, T.-P. Loh, *J. Am. Chem. Soc.* **1991**, *113*, 8966–8967; b) E. J. Corey, T.-P. Loh, T. D. Roper, M. D. Azimioara, M. C. Noe, *ibid.* **1992**, *114*, 8290–8992.

[93] For a review see M. Sawamura, Y. Ito, *Chem. Rev.* **1992**, *92*, 857–871.

[94] a) M. Takasu, H. Yamamoto, *Synlett* **1990**, 194–196; b) D. Sartor, J. Saffrich, G. Helmchen, *ibid.* **1990**, 197–198; c) D. Sartor, J. Saffrich, G. Helmchen, C. J. Richards, H. Lambert, *Tetrahedron Asymmetry* **1991**, *2*, 639–642.

[95] a) E. J. Corey, N. Imai, H.-Y. Zhang, *J. Am. Chem. Soc.* **1991**, *113*, 728–729; b) E. J. Corey, K. Ishihara, *Tetrahedron Lett.* **1992**, *33*, 6807–6810; c) D. A. Evans, S. J. Miller, T. Lectka, *J. Am. Chem. Soc.* **1993**, *115*, 6460–6461.

[96] Bosnich et al. have recently shown that the complex [Ru(salen)(NO)Cl] is a precursor for an achiral Diels–Alder catalyst: W. Odenkirk, A. L. Rheingold, B. Bosnich, *J. Am. Chem. Soc.* **1992**, *114*, 6293–6398; for a discussion of transition metal Lewis acidity in Diels–Alder reactions, see P. V. Bonnesen, C. L. Puckett, R. V. Honeychuck, W. H. Hersh, *J. Am. Chem. Soc.* **1989**, *111*, 6070–6081. For an example of a V^{IV} complex (not containing nitrogen ligands) highly active in the hetero Diels–Alder reaction, see A. Togni, *Organometallics* **1990**, *9*, 3106–3113; A. Togni, G. Rist, G. Rihs, A. Schweiger, *J. Am. Chem. Soc.* **1993**, *115*, 1908–1915.

[97] a) T. Mukaiyama, K. Banno, K. Narasaka, *Chem. Lett.* **1973**, 1011–1014; b) *J. Am. Chem. Soc.* **1974**, *96*, 7503–7509.

[98] a) S. Kobayashi, H. Uchiro, Y. Fujishita, I. Shiina, T. Mukaiyama, *J. Am. Chem. Soc.* **1991**, *113*, 4247–4252; b) S. Kobayashi, I. Shiina, J. Izumi, T. Mukaiyama, *Chem. Lett.* **1992**, 373–376; c) T. Mukaiyama, I. Shiina, S. Kobayashi, *ibid.* **1991**, 1901–1904; d) T. Mukaiyama, H. Asanuma, I. Hachiya, T. Marada, S. Kobayashi, *ibid.* **1991**, 1209–1212; e) T. Mukaiyama, M. Furuya, A. Ohtsubo, S. Kobayashi, *ibid.* **1991**, 989–992; f) S. Kobayashi, A. Ohtsubo, T. Mukaiyama, *ibid.* **1991**, 831–834; g) S. Kobayashi, Y. Fujishita, *ibid.* **1990**, 1455–1458.

[99] S. Kiyooka, Y. Kaneko, K. Kume, *Tetrahedron Lett.* **1992**, *33*, 4927–4930.

[100] a) E. R. Parmee, O. Tempkin, S. Masamune, A. Abiko, *J. Am. Chem. Soc.* **1991**, *113*, 9365–9366; b) E. R. Parmee, Y. Hong, O. Tempkin, S. Masamune, *Tetrahedron Lett.* **1992**, *33*, 1729–1732.

[101] a) K. Soai, S. Niwa, *Chem. Rev.* **1992**, *92*, 833–856; b) R. Noyori, M. Kitamura, *Angew. Chem.* **1991**, *103*, 34–55; *Angew. Chem. Int. Ed. Engl.* **1991**, *30*, 49–69; c) R. Noyori, S. Suga, K. Kawai, S. Okada, M. Kitamura, *Pure Appl. Chem.* **1988**, *60*, 1597–1606.

[102] N. Oguni, T. Omi, *Tetrahedron Lett.* **1984**, *25*, 2823–2824.

[103] M. Kitamura, S. Okada, S. Suga, R. Noyori, *J. Am. Chem. Soc.* **1989**, *111*, 4028–4036, and references therein

[104] a) C. Bolm, G. Schlingloff, K. Harms, *Chem. Ber.* **1992**, *125*, 1191–1203, and references therein; b) C. Bolm, M. Zehnder, D. Bur, *Angew. Chem.* **1990**, *102*, 206–208; *Angew. Chem. Int. Ed. Engl.* **1990**, *29*, 205–207; c) G. B. Jones, S. B. Eaton, *Tetrahedron Asymmetry* **1993**, *4*, 261–272; d) C. Puchot, O. Samuel, E. Duñach, S. Zhao, C. Agami, H. B. Kagan, *J. Am. Chem. Soc.* **1986**, *108*, 2353–2357.

[105] H. Urabe, T. Yamakawa, F. Sato, *Tetrahedron Asymmetry* **1992**, *3*, 5–8.

[106] K. Tanaka, H. Ushio, H. Suzuki, *J. Chem. Soc. Chem. Commun.* **1989**, 1700–1701.

[107] E. J. Corey, F. J. Hannon, *Tetrahedron Lett.* **1987**, *28*, 5233–5236, 5237–5240.

[108] M. Asami, S. Inoue, *Chem. Lett.* **1991**, 685–688.

[109] a) M. Watanabe, S. Araki, Y. Butsugan, M. Uemura, *J. Org. Chem.* **1991**, *56*, 2218–2224; b) M. Watanabe, N. Hashimoto, S. Araki, Y. Butsugan, *ibid.* **1992**, *57*, 742–744.

[110] See, for example, a) M. J. Rozema, A. Sidduri, P. Knochel, *J. Org. Chem.* **1992**, *57*, 1956–1958; b) W. Oppolzer, R. N. Radinov, *Tetrahedron Lett.* **1991**, *32*, 5777–5780; c) *Helv. Chim. Acta* **1992**, *75*, 170–173; d) *J. Am. Chem. Soc.* **1993**, *115*, 1593–1594.

[111] See, for example, a) S. Niwa, K. Soai, *J. Chem. Soc. Perkin Trans. 1* **1990**, 937–948; b) G. M. Ramos Tombo, E. Didier, B. Loubinoux, *Synlett* **1990**, 547–548.

[112] N. N. Joshi, M. Srebnik, H. C. Brown, *Tetrahedron Lett.* **1989**, *30*, 5551–5554.

[113] a) M. Yoshioka, T. Kawakita, M. Ohno, *Tetrahedron Lett.* **1989**, *30*, 1657–1660; b) H. Takahashi, T. Kawakita, M. Yoshioka, S. Kobayashi, M. Ohno, *ibid.* **1989**, *30*, 7095–7098.

[114] a) P. Perlmutter, *Conjugate Addition Reactions in Organic Synthesis* (*Tetrahedron Org. Chem. Ser. Vol 9*, Pergamon, Oxford, **1992**); b) for the 1,4 addition of organocopper reagents see B. H. Lipshutz, S. Sengupta, *Org. React. N. Y.* **1992**, *41*, 138–631.

[115] For an up-to-date review see B. E. Rossiter, N. M. Swingle, *Chem. Rev.* **1992**, *92*, 771–806.

[116] For recent examples of stoichiometric 1,4 addition reactions of organocuprates bearing nitrogen ligands, see B. E. Rossiter, M. Eguchi, G. Miao, N. M. Swingle, A. E. Hernández, D. Vickers, E. Fluckinger, R. G. Patterson, K. V. Reddy, *Tetrahedron* **1993**, *49*, 965–986, and references therein.

[117] H. Brunner, B. Hammer, *Angew. Chem.* **1984**, *96*, 305–306; *Angew. Chem. Int. Ed. Engl.* **1984**, *23*, 312–313.

[118] G. Desimoni, P. Quadrelli, P. P. Righetti, *Tetrahedron* **1990**, *46*, 2927–2934.

[119] a) K. Soai, T. Hayasaka, S. Ugajin, *J. Chem. Soc. Chem. Commun.* **1989**, 516–517; b) K. Soai, S. Yokoyama, T. Hayasaka, K. Ebihara, *J. Org. Chem.* **1988**, *53*, 4148–4149; c) K. Soai, T. Hayasaka, S. Ugajin, S. Yokoyama, *Chem. Lett.* **1988**, 1571–1572; d) K. Soai, M. Okuda, M. Okamoto, *Tetrahedron Lett.* **1991**, *32*, 95–96.

[120] a) C. Bolm, M. Ewald, M. Felder, *Chem. Ber.* **1992**, *125*, 1205–1215; b) C. Bolm, M. Ewald, *Tetrahedron Lett.* **1990**, *31*, 5011–5012; c) C. Bolm, *Tetrahedron Asymmetry* **1991**, *2*, 701–704.

[121] a) J. F. G. A. Jansen, B. L. Feringa, *Tetrahedron Asymmetry* **1992**, *3*, 581–582; b) *J. Org. Chem.* **1990**, *55*, 4168–4175; c) *J. Chem. Soc. Chem. Commun.* **1989**, 741–742.

[122] a) K.-H. Ahn, R. B. Klassen, S. J. Lippard, *Organometallics* **1990**, *9*, 3178–3181; b) G. M. Villacorta, C. P. Rao, S. J. Lippard, *J. Am. Chem. Soc.* **1988**, *110*, 3175–3182.

[123] T. Hayashi, M. Kumada in *Asymmetric Synthesis, Vol. 5* (Ed.: J. D. Morrison), Academic Press, Orlando, FL, USA, **1985**, pp. 147–169, and references therein.

[124] a) T. Hayashi, M. Konishi, M. Fukushima, K. Kanehira, T. Hioki, M. Kumada, *J. Org. Chem.* **1983**, *48*, 2195–2202; b) T. Hayashi, M. Fukushima, M. Konishi, M. Kumada, *Tetrahedron Lett.* **1980**, *21*, 79–82.

[125] a) T. Hayashi, M. Konishi, Y. Okamoto, K. Kabeta, M. Kumada, *J. Org. Chem.* **1986**, *51*, 3772–3781; b) T. Hayashi, T. Hagihara, Y. Katsuro, M. Kumada, *Bull. Chem. Soc. Jpn.* **1983**, *56*, 363–364; c) T. Hayashi, M. Konishi, M. Fukushima, T. Mise, M. Kagotani, M. Tajika, M. Kumada, *J. Am. Chem. Soc.* **1982**, *104*, 180–186; d) T. Hayashi, M. Konishi, H. Ito, M. Kumada, *ibid.* **1982**, *104*, 4962–4963.

[126] M. Uemura, R. Miyake, H. Nishimura, Y. Matsumoto, T. Hayashi, *Tetrahedron Asymmetry* **1992**, *3*, 213–216.

[127] Significant reviews: a) B. M. Trost, T. R. Verhoeven in *Comprehensive Organometallic Chemistry*, *Vol. 8* (Eds.: G. Wilkinson, F. G. A. Stone, E. W. Abel), Pergamon, London, **1984**, pp. 799–938; b) J. Tsuji, *Tetrahedron* **1986**, *42*, 4361–4401.

[128] For a review see G. Consiglio, R. M. Waymouth, *Chem. Rev.* **1989**, *89*, 257–276; for a more recent application see B. M. Trost, D. L. Van Vranken, C. Bingel, *J. Am. Chem. Soc.* **1992**, *114*, 9327–9343, and references therein

[129] For the use of achiral nitrogen ligands in Pd-catalyzed allyl reactions see, for example, B. M. Trost, D. J. Jebaratnam, *Tetrahedron Lett.* **1987**, *28*, 1611–1614.

[130] a) A. Togni, *Tetrahedron Asymmetry* **1991**, *2*, 683–690; b) A. Togni, G. Rihs, P. S. Pregosin, C. Ammann, *Helv. Chim. Acta* **1990**, *73*, 723–732.

[131] Sparteine was employed as an inducing agent in stoichiometric amounts by Trost et al. as early as 1973: B. M. Trost, T. J. Dietsche, *J. Am. Chem. Soc.* **1973**, *95*, 8200–8201.

[132] a) P. von Matt, A. Pfaltz, *Angew. Chem.* **1993**, *105*, 614–616; *Angew. Chem. Int. Ed. Engl.* **1993**, *32*, 566–568; b) J. Sprinz, G. Helmchen, *Tetrahedron Lett.* **1993**, *34*, 1769–1772; c) C. G. Frost, J. M. J. Williams, *ibid.* **1993**, *34*, 2015–2018.

[133] M. Bovens, A. Togni, L. M. Venanzi, *J. Organomet. Chem.* **1993**, *451*, C28–C31; for an application of this pyrazole derivative for the synthesis of a tridentate ligand, see D. D. Le Cloux, W. B. Tolman, *J. Am. Chem. Soc.* **1993**, *115*, 1153–1154.

[134] For reviews see, for example, M. G. Finn, K. B. Sharpless and B. E. Rossiter in *Asymmetric Synthesis, Vol. 5* (Ed.: J. D. Morrison), Academic Press, Orlando, FL, USA, **1985**, p. 247–308 or 194–246.

[135] a) S. Yamada, T. Mashiko, S. Terashima, *J. Am. Chem. Soc.* **1977**, *99*, 1988–1990; b) S. Coleman Kammula, E. T. Duim-Koolstra, *J. Organomet. Chem.* **1983**, *246*, 53–56.

[136] a) R. C. Michaelson, R. E. Palermo, K. B. Sharpless, *J. Am. Chem. Soc.* **1977**, *99*, 1990–1992; b) K. B. Sharpless, T. R. Verhoeven, *Aldrichmica Acta* **1979**,

12, 63–74. Sharpless et al. used hydroxamic acids as ligands. Strictly speaking, these are not nitrogen ligands.

[137] a) Mn: K. Srinivasan, P. Michaud, J. K. Kochi, *J. Am. Chem. Soc.* **1986**, *108*, 2309–2320; Cr: b) E. G. Samsel, K. Srinivasan, J. K. Kochi, *ibid.* **1985**, *107*, 7606–7617; c) K. Srinivasan, S. Perrier, J. K. Kochi, *J. Mol. Catal.* **1986**, *36*, 297–317, and references therein.

[138] a) J. T. Goves, G. A. McClujsky, *J. Am. Chem. Soc.* **1976**, *98*, 859–861; b) J. T. Groves, T. E. Nemo, R. S. Myers, *ibid.* **1979**, *101*, 1032–1033.

[139] a) W. Zhang, J. L. Loebach, S. R. Wilson, E. N. Jacobsen, *J. Am. Chem. Soc.* **1990**, *112*, 2801–2803; b) W. Zhang, E. N. Jacobsen, *J. Org. Chem.* **1991**, *56*, 2296–2298; c) E. N. Jacobsen, W. Zhang, A. R. Muci, J. R. Ecker, L. Deng, *J. Am. Chem. Soc.* **1991**, *113*, 7063–7064; d) N. H. Lee, A. R. Muci, E. N. Jacobsen, *Terahedron Lett.* **1991**, *32*, 5055–5058; e) L. Deng, E. N. Jacobsen, *J. Org. Chem.* **1992**, *57*, 4320–4323.

[140] a) R. Irie, K. Noda, Y. Ito, N. Matsumoto, T. Katsuki, *Tetrahedron Lett.* **1990**, *31*, 7345–7348; b) R. Irie, K. Noda, Y. Ito, T. Katsuki, *ibid.* **1991**, *32*, 1055–1058; c) R. Irie, Y. Ito, T. Katsuki, *Synlett* **1991**, 265–266; d) R. Irie, K. Noda, N. Matsumoto, T. Katsuki, *Tetrahedron Asymmetry* **1991**, *2*, 481–494.

[141] a) T. Yamada, K. Imagawa, T. Nagata, T. Mukaiyama, *Chem. Lett.* **1992**, 2231–2234; b) T. Mukaiyama, T. Yamada, T. Nagata, K. Imagawa, *ibid.* **1993**, 327–330.

[142] D. R. Reddy, E. R. Thornton, *J. Chem. Soc. Chem. Commun.* **1992**, 172–173.

[143] J. T. Groves, P. Viski, *J. Org. Chem.* **1990**, *55*, 3628–3634, and references therein.

[144] S. O'Malley, T. Kodadek, *J. Am. Chem. Soc.* **1989**, 111, 9116–9117.

[145] a) D. Mansuy, P. Battioni, J.-P. Renaud, P. Guerin, *J. Chem. Soc. Chem. Commun.* **1985**, 155–156; b) J.-P. Renaud, P. Battioni, D. Mansuy, *New J. Chem.* **1987**, *11*, 270–290.

[146] J. P. Collman, V. J. Lee, X. Zhang, J. A. Ibers, J. I. Brauman, *J. Am. Chem. Soc.* **1993**, *115*, 3834–3835.

[147] For reviews see a) R. A. Johnson, K. B. Sharpless in *Catalytic Asymmetric Synthesis* (Ed.: I. Ojima), VCH, Weinheim, **1993**, in press. A. T. thanks Professor Sharpless for a copy of the manuscript; b) B. B. Lohray, *Tetrahedron Asymmetry* **1992**, *3*, 1317–1349.

[148] R. Criegee, B. Marchand, H. Wannowius, *Justus Liebigs Ann. Chem.* **1942**, *550*, 99–133.

[149] S. G. Hentges, K. B. Sharpless, *J. Am. Chem. Soc.* **1980**, *102*, 4264–4265.

[150] See, for example, a) T. Yamada, K. Narasaka, *Chem. Lett.* **1986**, 131–134; b) M. Tokles, J. K. Snyder, *Tetrahedron Lett.* **1986**, *27*, 3951–3954; c) M. Hirama, T. Oishi, S. Ito, *J. Chem. Soc. Chem. Commun.* **1989**, 665–666; d) T. Oishi, M. Hirama, *J. Org. Chem.* **1989**, *54*, 5834–5835; e) E. J. Corey, P. DaSilva Jardine, S. Virgil, P.-W. Yven, R. D. Connell, *J. Am. Chem. Soc.* **1989**, *111*, 9243–9244; f) K. Tomioka, M. Nakajima, K. Koga, *ibid.* **1987**, *109*, 6213–6215; g) *Tetrahedron Lett.* **1990**, *31*, 1741–1744.

[151] E. N. Jacobsen, I. Markó, W. S. Mungall, G. Schröder, K. B. Sharpless, *J. Am. Chem. Soc.* **1988**, *110*, 1968–1970.

[152] For improvements and applications of the Sharpless dihydroxylation see a) K. B. Sharpless, W. Amberg, Y. L. Bennani, G. A. Crispino, J. Martung, K.-S. Jeong, H.-L. Kwong, K. Morikawa, Z.-M. Wang, D. Xu, X.-L. Zhang, *J. Org. Chem.* **1992**, *57*, 2768–2771; b) G. A. Crispino, K. B. Sharpless, *Tetrahedron Lett.* **1992**, *33*, 4273–4274; c) R. Oi, K. B. Sharpless, *ibid.* **1992**, *33*, 2095–2098; d) K. B. Sharpless, W. Amberg, M. Beller, H. Chen, J. Hartung, Y. Kawanami, D. Lübben, E. Manoury, Y. Ogino, T. Shibata, T. Ukita, *J. Org. Chem.* **1991**, *56*, 4585–4588; e) Y. Ogino, H. Chen, E. Manoury, T. Shibata, M. Beller, D. Lübben, K. B. Sharpless, *Tetrahedron Lett.* **1991**, *32*, 5761–5764; f) Y. Ogino, H. Chen, H.-L. Kwong, K. B. Sharpless, *ibid.* **1991**, *32*, 3965–3968; g) B. M. Kim, K. B. Sharpless, *ibid.* **1990**, *31*, 3003–3006; h) C. Y. Park, B. M. Kim, K. B. Sharpless, *ibid.* **1991**, *32*, 1003–1006; i) B. B. Lohray, T. H. Kalantar, B. M. Kim, C. Y. Park, T. Shibata, J. S. M. Wai, K. B. Sharpless, *ibid.* **1989**, *30*, 2041–2044.

[153] a) J. S. Svendsen, I. Markó, E. J. Jacobsen, C. P. Rao, S. Bott, K. B. Sharpless, *J. Org. Chem.* **1989**, *54*, 2263–2264; b) R. M. Pearlstein, B. K. Blackburn, W. M. Davis, K. B. Sharpless, *Angew. Chem.* **1990**, *102*, 710–712; *Angew. Chem. Int. Ed. Engl.* **1990**, *29*, 639–641.

[154] E. N. Jacobsen, I. Markó, M. B. France, J. S. Svendsen, K. B. Sharpless, *J. Am. Chem. Soc.* **1989**, *111*, 737–739.

[155] a) E. J. Corey, M. C. Noe, S. Sarshar, *J. Am. Chem. Soc.* **1993**, *115*, 3828–3829; see also b) E. J. Corey, G. I. Lotto, *Tetrahedron Lett.* **1990**, *31*, 2665–2668; c) H. C. Kolb, P. G. Andersson, Y. L. Bennani, G. A. Crispino, K.-S. Jeong, H.-L. Kwong, K. B. Sharpless, *J. Am. Chem. Soc.* **1993**, *115*, 12226–12227.

[156] For earlier reports see, for example, a) H. Kwart, A. A. Kahn, *J. Am. Chem. Soc.* **1967**, *89*, 1951–1953; b) J.-P. Mahy, G. Bedi, P. Battioni, D. Mansuy, *J. Chem. Soc. Perkin Trans. 2* **1988**, 1517–1524, and references therein.

[157] a) D. A. Evans, M. M. Faul, M. T. Bilodeau, *J. Org. Chem.* **1991**, *56*, 6744–6746; b) D. A. Evans, M. M. Faul, M. T. Bilodeau, B. A. Anderson, D. M. Barnes, *J. Am. Chem. Soc.* **1993**, *115*, 5328–5329.

[158] See, for example, K. J. O'Connor, S.-J. Wey, C. J. Burrows, *Tetrahedron Lett.* **1992**, *33*, 1001–1004.

[159] Z. Li, K. R. Conser, E. N. Jacobsen, *J. Am. Chem. Soc.* **1993**, *115*, 5326–5327.

[160] For a review see W. A. Nugent, B. L. Haymore, *Coord. Chem. Rev.* **1980**, *31*, 123–175.

[161] G. W. Parshall, S. D. Ittel, *Homogeneous Catalysis*, Wiley, New York, **1992**, pp. 237–268.

[162] C. A. Tolman, J. D. Druliner, P. J. Krusic, M. J. Nappa, W. C. Seidel, I. D. Williams, S. D. Ittel, *J. Mol. Catal.* **1988**, *48*, 129–148.

[163] The major breakthrough came from Grubbs's and Schrock's groups. The topic has been extensively reviewed by R. R. Schrock a) in *Ring-Opening Polymerization* (Ed.: D. J. Brunelle), Hauser, München, **1993**, S. 129–156; b) *Acc. Chem. Res.* **1990**, *23*, 158–165; c) *J. Organomet. Chem.* **1986**, *300*, 249–262; d) R. H. Grubbs, W. Tomas, *Science* **1989**, *243*, 907–915.

[164] a) R. R. Schrock, R. T. DePue, J. Feldman, C. J. Schaverien, J. C. Dewan, A. M. Liu, *J. Am. Chem. Soc.* **1988**, *110*, 1423–1435; b) R. R. Schrock, J. S. Murdzek, G. C. Bazan, J. Robbins, M. DiMare, M. O'Regan, *ibid.* **1990**, *112*, 3875–3886; c) R. R. Schrock, R. T. DePue, J. Feldman, K. B. Yap, D. C. Yang, W. M. Davis, L. Park, M. DiMare, M. Schofield, J. Anhaus, E. Walborsky, E. Evitt, C. Krüger, P. Betz, *Organometallics* **1990**, *9*, 2262–2275; e) D. S. Williams, M. H. Schofield, J. T. Anhaus, R. R. Schrock, *J. Am. Chem. Soc.* **1990**, *112*, 6728–6729.

[165] D. Albagli, G. Bazan, M. S. Wrighton, R. R. Schrock, *J. Am. Chem. Soc.* **1992**, *114*, 4150–4158.

[166] V. P. Ponticello, D. L. Gin, R. H. Grubbs, *J. Am. Chem. Soc.* **1992**, *114*, 9708–9710.

[167] G. C. Fu, R. H. Grubbs, *J. Am. Chem. Soc.* **1992**, *114*, 5426–5427, 7324–7325.

[168] L. L. Blosch, K. Abboud, J. M. Boncella, *J. Am. Chem. Soc.* **1991**, *113*, 7066–7068.

[169] a) W. D. Harman, H. Taube, *J. Am. Chem. Soc.* **1987**, *109*, 1883–1885; b) W. D. Harman, M. Sekine, H. Taube, *ibid.* **1988**, *110*, 5725–5731; c) W. D. Harman, H. Taube, *ibid.* **1988**, *110*, 7555–7557; d) W. D. Harman, W. P. Schaefer, H. Taube, *ibid.* **1990**, *112*, 2682–2685; e) M. E. Kopach, J. Gonzalez, W. D. Harman, *ibid.* **1991**, *113*, 8972–8973; f) M. E. Kopach, L. P. Kelsh, K. C. Stork, W. D. Harman, *ibid.* **1993**, *115*, 5322–5323.

[170] H. Nitta, D. Yu, M. Kudo, A. Mori, S. Inoue, *J. Am. Chem. Soc.* **1992**, *114*, 7969–7975.

Nitrile Imines: From Matrix Characterization to Stable Compounds

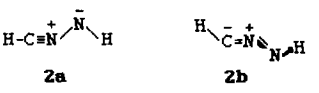
Guy Bertrand* and Curt Wentrup*

The concept of 1,3-dipolar cycloaddition was developed, starting in the late 1950s, largely by Rolf Huisgen and his students in Munich, and it has led to one of the most versatile methods for the construction of five-membered ring heterocycles. Although first known only as transient intermediates, nitrile imines have been at the heart of mechanistic studies of this type of cycloaddition reactions. Hundreds of mechanistic papers appeared in 1960s and 1970s; reliable spectroscopic observations were achieved in the early 1980s both at low temperatures and in the gas phase; finally, the first crystalline nitrile imine was reported in 1988. The unusual structures found by X-ray analyses as well as the facile rearrangements observed experimentally have fostered a new interplay between experiment and theory. The story of nitrile imines, from matrix characterization to stable compounds, nicely illustrates the role that main group elements can play in organic chemistry.

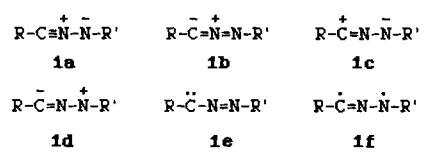
1. Introduction

Until recently, nitrile imines **1**,[1-6] like several other 1,3-dipoles, were considered reactive intermediates. Since their discovery by Huisgen at al. in 1959,[1a] nitrile imines have been generated in situ and used in numerous 1,3-dipolar cycloaddition reactions leading to pyrazoles, pyrazolines, and other heterocyclic compounds.[6, 7] Furthermore, nitrile imines have been at the heart of mechanistic studies of the 1,3-dipolar cycloaddition reaction and of the controversy over Firestone's diradical pathway.[8]

Nevertheless, because of their character as reactive intermediates, there has been very little direct experimental evidence on the structures of nitrile imines. The most important canonical structures[6] are indicated in formulas **1a**–**f** (Scheme 1). These do not say anything about the actual structures, not even whether the nitrile imines are linear or bent. Ab initio calculations by Houk et al.[9, 10] reveal that the parent compound formonitrile imine **2n**[**] may exist in either a planar (propargylic, **2a**) or a nonplanar, bent (allenic, **2b**) form; **2b** is favored by 2.2 kcal mol^{-1} when the STO-3G basic set is employed, but the progargylic form **2a** is favored by 3.9 kcal mol^{-1} at the 4-31G level. Thus, the unsubstituted nitrile imine is described as a "floppy" molecule,[9] which may be able to adapt its geometry easily in response to substituents. Similar calculations[9] for nitrile ylides ($R-C\equiv\overset{+}{N}-\overset{-}{C}R_2$) indicate that these prefer bent, nonplanar structures, whereas in nitrile oxides ($R-C\equiv\overset{+}{N}-O^-$) the linear form is theoretically favored, in agreement with experiment. For both nitrile imines and nitrile ylides, electron-withdrawing substituents, particularly at the N or CR_2 termini, are expected to promote the planar, propargylic forms.[9, 11]



2a **2b**



1a **1b** **1c**

1d **1e** **1f**

Scheme 1. Canonical structures of nitrile imines.

The situation has changed recently. Nitrile imines have become accessible as stable, sometimes crystalline solids or distillable liquids. Accordingly, their structures and properties can now be probed in a much more direct manner. It has been found, as described in Section 5.1, that all stable nitrile imines examined by X-ray crystallography to date definitely possess bent, helical backbones, more of the "allenic" type **2b**. Furthermore, high-level calculations[11,2] also predict that the bent, helical structure represents the lowest energy form of nitrile imines (see Section 5.1).

Another problem concerns the rearrangements of nitrile imines and of 1,3-dipoles in general. Rearrangements to diazo compounds ($R_2C=\overset{+}{N}=N^-$) have been postulated several times

[*] Dr. G. Bertrand
Laboratoire de Chimie de Coordination du CNRS
205, route de Narbonne, 31077 Toulouse Cédex (France)
Telefax: Int. code + (61)55-3003
Prof. Dr. C. Wentrup
Department of Chemistry
The University of Queensland
Brisbane, Qld. 4072 (Australia)
Telefax: Int. code + 7365 4580

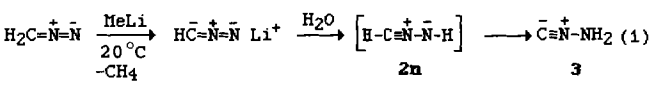
[**] In this review formula numbers with the letter **n** refer to nitrile imines, and those with the letter **d** refer to diazomethane derivatives.

 © VCH Verlagsgesellschaft mbH, D-69451 Weinheim, 1994 0570-0833/94/0505-0527 $ 10.00+.25/0

(see Section 7). If this is a concerted process, it constitutes a highly interesting and formally "forbidden" 1,3-shift. Likewise, both thermal and photochemical rearrangements to carbodiimides (RN=C=NR) have been reported (Section 7). With the emergence of stable, isolable nitrile imines, it has become possible to probe such rearrangements directly.

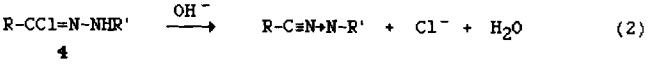
2. History

The parent formonitrile imine **2n** is still unknown. It was once thought to be formed on deprotonation of diazomethane with methyllithium at room temperature, followed by hydrolysis [Eq. (1)].[13] However, 34 years later, it was established, largely

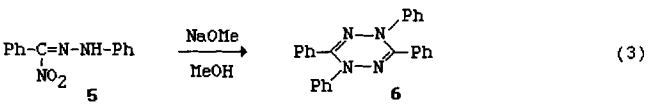


on the basis of the NMR and infrared spectra, that this "isodiazomethane" was in fact isocyanoamine **3**.[14–16] It is not known whether nitrile imine **2n** is actually an intermediate in this reaction.[17] Isocyanoamine **3** is rapidly converted to diazomethane under the influence of alkali metal hydroxides. It is interesting to note that E. Müller called **3** "Knallsäureamid", that is, fulminic acid amide. However, W. Beck later established that fulminic acid has the structure HCNO, not HONC as had been believed until then.[18] H_2N-NC (**3**) may thus be considered as an amide of HONC (isofulminic acid) but not of fulminic acid.

In the 1930s and 1940s Fusco and his students in Italy carried out work on hydrazonoyl chlorides **4**.[19] It is now known that these compounds generate nitrile imines, which undergo cycloaddition reactions to furnish pyrazoles. The possibility of formation of disubstituted isodiazomethanes ("isodiazometani bisostituiti") was mentioned in 1946 and 1948 by Fusco and Romani, who also considered other isomers of diazomethane [Eq. (2)].[20]



Even earlier, a compound had been postulated which would nowadays be called diphenylnitrile imine. In 1901 Bamberger and Grob treated α-nitrobenzylidenephenylhydrazine (**5**) with sodium methoxide in methanol and obtained tetraphenyldihydrotetrazine (**6**) in 39% yield [Eq. (3)].[21, 22] This was explained

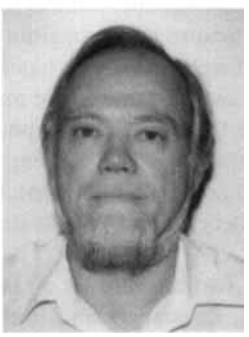


with the words: "Das Natriumsalz des Isonitrokörpers zerfällt in Nitrit und den Molekularrest $C_6H_5-\ddot{C}-N=N-C_6H_5$, welcher sofort zum Tetrazolinderivat polymerisiert".[21b] As Huisgen et al. later pointed out,[22] this "molecular residue" corresponds to the canonical structure **1e** of a nitrile imine.

Nitro compounds such as **5** are versatile precursors of nitrile imines, in particular in cases where the corresponding hydrazonoyl halides are inaccessible. It is also known that the "nitrohydrazone route" gives particularly high yields of dihydrotetrazines; this cannot be due to direct dimerization of the nitrile imines but rather to a reaction between one molecule of nitrile



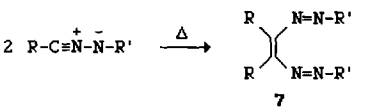
Guy Bertrand was born in Limoges, France, on July 17, 1952. He graduated (ingénieur ENSCM) from the University of Montpellier and moved to Toulouse as an "Attaché de Recherche CNRS" in 1975. He defended his "Thèse d'Etat" at the University of Toulouse in 1979. After one year at Sanofi Recherche Company, he came back to the University Paul Sabatier as a "Chargé de Recherche". In 1988 he went to the Laboratoire de Chimie de Coordination du CNRS where he is now "Directeur de Recherche CNRS". By employing main group elements, his group is trying to isolate at room temperature species hitherto believed to be only transient intermediates. They use these species in organic synthesis, as ligands for transition metal complexes, and as precursors for new materials.



Curt Wentrup was born in Holtug, Denmark, on July 11, 1942. He received his "Diplom (cand. scient.)" in chemistry in 1966 from the University of Copenhagen for work with K. A. Jensen on alkyl cyanates, his Ph.D. in 1969 from the Australian National University, Canberra, and his Dr. scient. in 1977 from the University of Copenhagen for work on carbene and nitrene rearrangements. After a period as a postdoctoral associate and later "Privatdozent" with Hans Dahn at the University of Lausanne, Switzerland (1969–1976), he joined the chemistry faculty at the University of Marburg, Germany (1976–1985). In 1985 he returned to Australia as professor of organic chemistry and head of the Organic Chemistry Section, Department of Chemistry, University of Queensland, Brisbane. His research interests include reactive intermediates and unusual molecules often generated by flash vacuum pyrolysis and studied by matrix isolation techniques.

imine with the long-lived anion of the starting material **5**.[22] In general, it appears that the formation of dihydrotetrazines in substantial yields is indicative of reaction between the nitrile imine and its precursor.[22-25]

The true dimerization of nitrile imines in the absence of other reaction partners leads to bis(azo)ethylenes of the type **7**, which can be isolated in certain cases[26-28] [Eq. (4)] (see also Section 3.2).

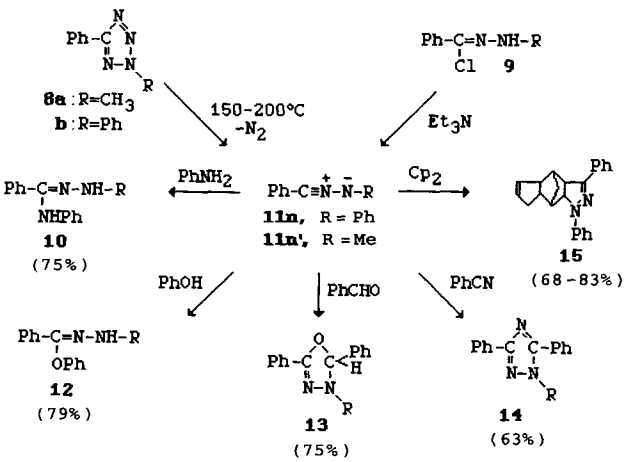


(4)

3. Nitrile Imines as Reactive Intermediates

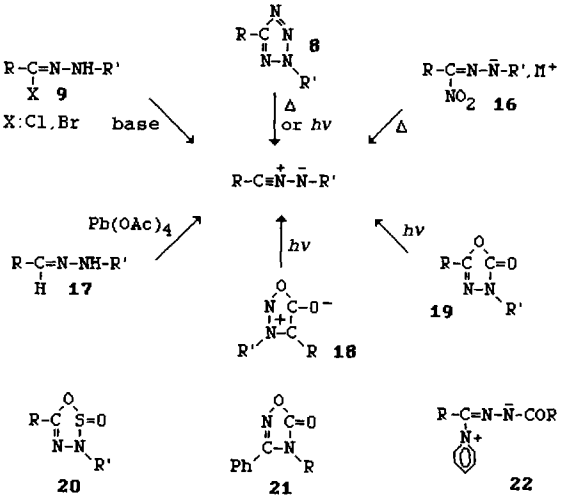
3.1. Generation

Since very authoritative reviews of the classical chemistry of nitrile imines and other 1,3-dipoles exist,[2-7] only a brief sketch will be provided here. In the first deliberate generation and trapping of nitrile imines in 1959,[1a] both the thermal decomposition of 2,5-disubstituted tetrazoles **8** at 150–200 °C and the base-induced dehydrochlorination of the hydrazonoyl chloride **9** were examined. Diphenylnitrile imine **11n** was trapped in situ in nucleophilic additions of aniline and phenol (giving compounds **10** and **12**, respectively) and in 1,3-dipolar cycloaddition reactions with benzaldehyde, benzonitrile, and dicyclopentadiene to produce **13**, **14** and **15**, respectively (Scheme 2).



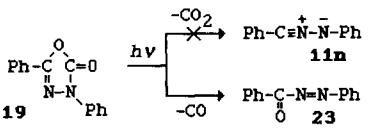
Scheme 2. First generation and trapping of a transient nitrile imine. Here and in subsequent schemes the percentages in parentheses refer to the yields.

The generation of nitrile imines by photolytic decomposition of tetrazoles **8** was reported soon afterwards.[1b] These methods, as well as the use of salts of *aci*-nitro-azo compounds (α-nitrohydrazones) **16**,[22,29] have become standard procedures for nitrile imine production. In addition, the oxidation of hydrazones **17** with lead tetraacetate,[30] the photolysis of sydnones **18**,[26,31] and the photolysis of 1,3,4-oxadiazol-5(4*H*)-ones **19**[32] also provide nitrile imines (Scheme 3). Whether the latter reaction,



Scheme 3. Methods used for the generation of transient nitrile imines.

photolysis of **19**, actually generates nitrile imines is disputed.[26] Although the same products and the same orientations of cycloaddition are obtained with **19** (R = R′ = Ph) as with diphenylnitrile imine (**11n**) generated from 2,5-diphenyltetrazole (**8b**),[32a] the photolysis of **19** in the absence of a dipolarophile was found to be extremely sluggish, and it was postulated that CO and benzoylazobenzene **23** formed rather than the nitrile imine (Scheme 4).[26]



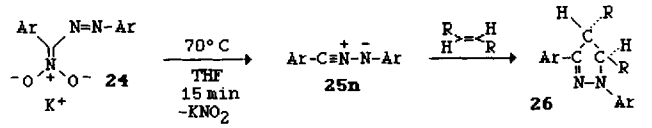
Scheme 4. Photolysis of 1,3,4-oxadiazol-5(4*H*)-ones **19**.

Thus, the cycloadditions starting with **19**, which mimic nitrile imine cycloadditions, may involve direct reaction between an excited state of **19** and the dipolarophile. Interestingly, it was reported that no nitrile imine dimers were formed in the photolysis of **19**.[32a] Although the yields of dimers are often low, their total absence may be a telltale sign that no nitrile imine was formed.

Less common precursors for nitrile imines are 1,2,3,4-oxathiadiazole-2-oxides **20**,[33] 1,2,4-oxadiazol-5(4*H*)-ones **21**,[34] and pyridinium betaines **22**.[35]

3.2. Methods for the Direct Observation of Transient Nitrile Imines

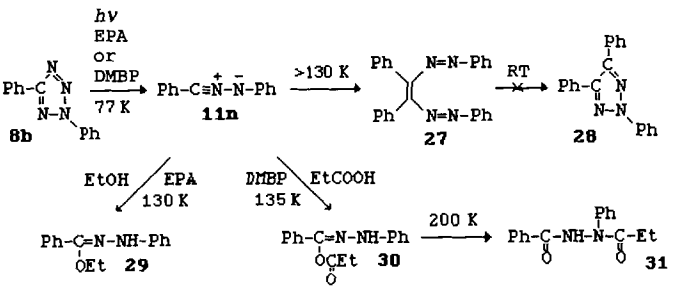
Surprisingly, before 1988, there was only one report on the direct observation of a nitrile imine in solution. Grundmann and Flory[29] used the thermal decomposition of the *aci*-nitro-azo compound **24** to prepare dimesitylnitrile imine **25n** in solvents such as THF and benzene (Scheme 5). Potassium nitrite formed quantitatively in 10–20 minutes, and the solution turned orange, presumably because of the formation of **25n**. When the reaction was carried out in the presence of dimethyl fumarate, cycloadduct **26** was formed in over 90% yield. When



Scheme 5. Generation and trapping of dimesitylnitrile imine **25n**. Ar = 2,4,6-trimethylphenyl (mesityl); R = CO_2Me.

the reaction was repeated in the absence of the trapping agent and the solution filtered to remove KNO_2 before dimethyl fumarate was added, **26** was still isolated in 18% yield. The IR spectrum of the orange solution featured a band at 2200 cm^{-1}, which disappeared in the course of 24 h. In the spectra of reaction mixtures containing dimethyl fumarate, the same band disappeared in 1–2 h (surprisingly slowly). This experiment constitutes the first direct observation of a nitrile imine.

2,5-Disubstituted tetrazoles **8** have been used to generate nitrile imines both photochemically and thermally (flash vacuum pyrolysis) for direct UV and IR spectroscopic observation. Heimgartner et al.[36] photolyzed 2,5-diphenyltetrazole (**8b**) at 77 K in organic glasses (ether/pentane/ethanol (EPA), 2-methylpentane (2MP), or 2,3-dimethylbutane-pentane (DMBP)). Upon irradiation with light of wavelength 280–290 nm, a new species was observed (λ_{max} = 378 nm) which, on the basis of its behavior, was identified as diphenylnitrile imine **11n** (Scheme 6).

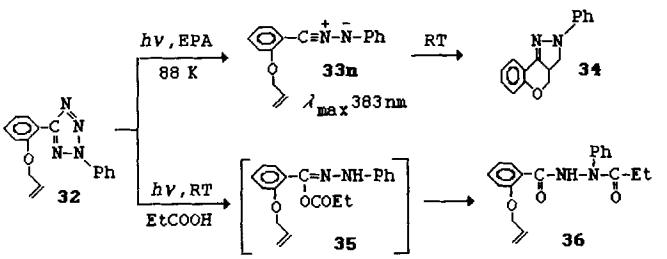


Scheme 6. Synthesis and characterization of diphenylnitrile imine **11n**. RT = room temperature.

Toubro and Holm[37] carried out similar photolyses (λ = 250 nm) of **8b** in EPA or poly(vinyl chloride) (PVC) at 85 K and observed the UV spectrum of **11n** at 377 nm. Moreover, they observed a major IR band at 2228 cm^{-1} (PVC, 85 K), which was ascribed to the C≡N stretch in **11n**. This assignment was corroborated by generation of ^{15}N isotopomers by photolysis of suitably labeled tetrazoles. Nitrile imine **11n** is stable in the glass at temperatures below roughly 130 K. In the absence of trapping agents, it dimerizes above 130 K, in all likelihood forming bis(azo)ethylene **27**. The latter compound decomposes at room temperature, but 1,2,3-triazole **28** is not formed in the process (**28** is formed on room-temperature photolysis of **8b**).[36]

Nitrile imine **11n** is trapped by ethanol above the softening point of the EPA matrix, giving hydrazone **29** at 130 K.[28] With propionic acid in DMBP glass at 135 K, **11n** was trapped to give initially **30**, which on warming to 200 K isomerized to hydrazide **31** (Scheme 6). The reaction **30** → **31** was monitored by UV spectroscopy.[28]

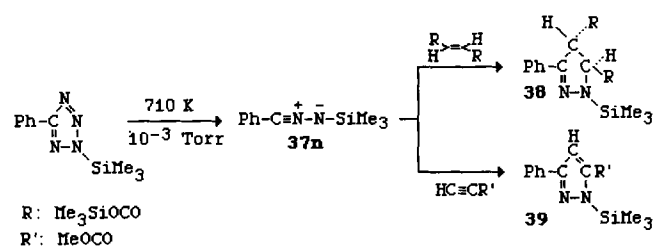
Nitrile imine **33n** was generated analogously by photolysis of tetrazole **32** and observed by UV spectroscopy (Scheme 7).[28]



Scheme 7. Photolysis of tetrazole **32**.

Warming nitrile imine **33n** to room temperature resulted in an intramolecular[38] 1,3-dipolar cycloaddition reaction giving **34**. This compound was also obtained in 84% yield in the preparative photolysis of **32** at room temperature. Preparative photolysis in the presence of a 1000-fold excess of propionic acid gave hydrazide **36** in 83% isolated yield, presumably via an initial adduct **35**. Thus, carboxylic acids were found to be extremely efficient traps for nitrile imines, and the corresponding reactions compete with the intramolecular 1,3-dipolar cycloaddition reaction (Scheme 7).[28]

The direct detection of thermally generated nitrile imines is more difficult because of rapid rearrangement reactions[39–42] (see Section 7). However, *N*-trimethylsilyl-*C*-phenylnitrile imine (**37n**) turned out to be quite stable under flash vacuum pyrolysis (FVP) conditions (Scheme 8). It was directly observed



Scheme 8. Thermal generation and trapping of nitrile imine **37n**.

in the gas phase by mass spectrometry and distinguished from the isomeric carbodiimide and diazo compound by collisional activation mass spectrometry.[43] Deposition of **37n** at 77 K permitted the recording of the IR spectrum, which featured a strong absorption at 2230 cm^{-1}. The IR spectrum was also distinct from those of the isomeric diazo compound and carbodiimide.

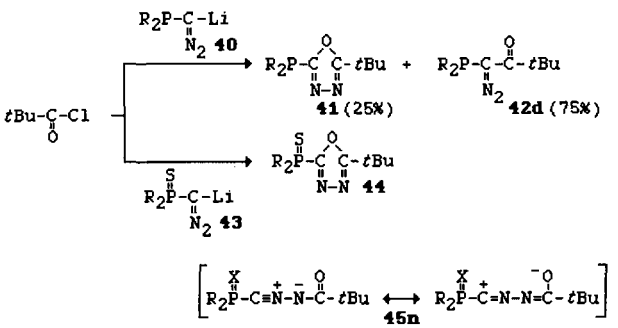
Nitrile imine **37n** was trapped in high yields in 1,3-dipolar cycloadditions in the gas phase. More importantly, it could also be cocondensed with the trapping reagent at 77 K and observed by IR spectroscopy (absorption band at 2230 cm^{-1}). Warming to 170 K resulted in cycloaddition reaction, giving the products **38** and **39** (Scheme 8) in almost quantitative yields. Trapping **37n** with methyl propiolate gave **39** regiospecifically; the product was identical to the compound obtained on silylation of methyl 5-phenylpyrazole-3-carboxylate, and the latter compound was also obtained on hydrolysis of **39** in 90% ethanol.

This work made it possible also to obtain the first photoelectron spectra of nitrile imines by directly monitoring the FVP reactions. The first ionization potential was 7.85 eV for $Ph-C\equiv\overset{+}{N}-\overset{-}{N}-SiMe_3$ (**37n**), and 8.14 eV for $CH_3-C\equiv\overset{+}{N}-\overset{-}{N}SiMe_3$.[44]

4. Synthesis of Stable Nitrile Imines

4.1. Starting from Lithium Salts of Diazo Compounds

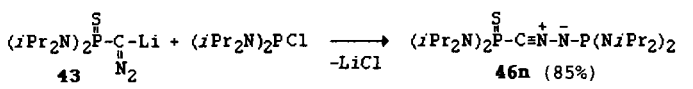
As often happens, the discovery of the synthetic route later used to prepare most of the stable nitrile imines was unexpected. In one attempt to synthesize *C*-acylated phosphinodiazomethane **42d** by reacting pivaloyl chloride with the lithium salt **40** of bis(diisopropylamino)phosphinodiazomethane, the formation of 1,3,4-oxadiazole **41** was observed in addition to the expected diazoketone **42d**.[45] Moreover, the reaction of pivaloyl chloride and the thiophosphinoyldiazo analogue **43** quantitatively afforded the five-membered ring heterocycle **44**.[46] These results strongly suggested that *N*-acylation could compete with *C*-acylation in the case of phosphorus-substituted diazo lithium salts, since the simplest explanation for the formation of oxadiazoles **41** and **44** was a 1,5-electrocyclization[47] of the initially formed carbonylnitrile imine **45n** (Scheme 9).



Scheme 9. *N*- and *C*-acylations of phosphorus-substituted diazo lithium salts. R = iPr_2N; X = lone pair or S.

However, although salts of diazo compounds possess two nucleophilic centers, it was generally believed that electrophiles only react at carbon giving the corresponding substituted diazo compound.[48] Since diazo compounds and nitrile imines both react with dipolarophiles,[6] the best way to prove the hypothesis was to try to prepare a stable nitrile imine. A good approach to forcing the attack of the electrophiles at the nitrogen nucleophilic center is to try to prevent the attack at carbon: the use of sterically hindered salts of diazo compounds and electrophiles was the obvious answer. Moreover, push–pull substituents could decrease the polarity of the nitrile imine skeleton and therefore increase its kinetic stability.

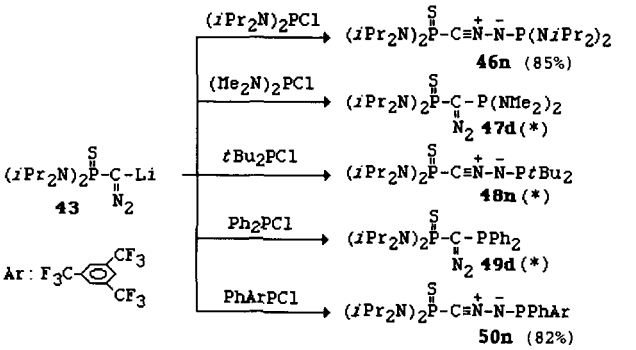
The first stable nitrile imine **46n** was obtained in 85% yield from the reaction of the lithium salt **43** of bis(diisopropylamino)thiophosphinoyldiazomethane with chlorobis(diisopropylamino)phosphane (Scheme 10).[46,49] Nitrile imine **46n**, which was fully characterized (including an X-ray crystal study



Scheme 10. Synthesis of the first stable nitrile imine **46n**.

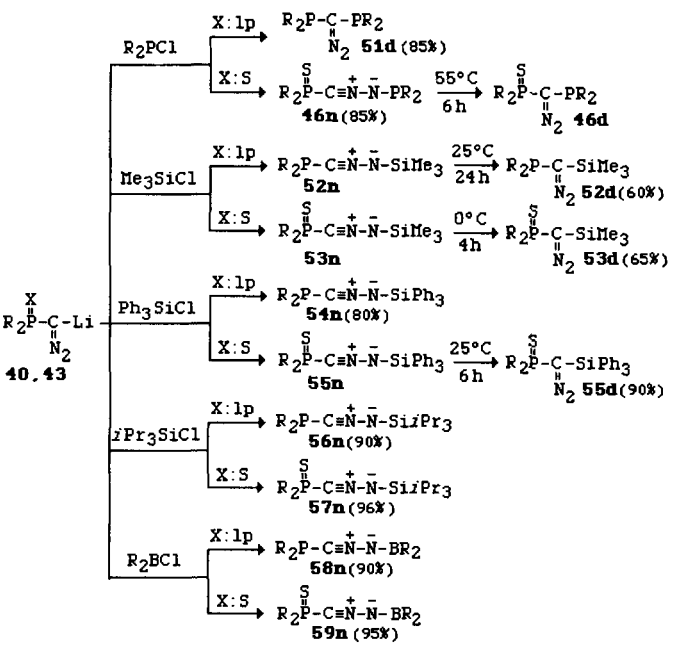
(see Fig. 2)), is not air sensitive, and since it melts at 100 °C without decomposition, the compound is quite stable thermally.

The influence of both the lithium salt and the electrophile on the reaction has been studied. The reactions of the thiophosphinoyl diazo lithium salt **43** with chlorophosphanes as electrophiles were unequivocal.[46,49–53] When electronic factors are constant, reactions with bulky and less hindered chlorophosphanes lead to nitrile imines and diazo compounds, respectively (Scheme 11).



Scheme 11. Influence of the chlorophosphanes in the reactions with thiophosphinoyl diazo lithium salt **43**. (*): High yield according to ^{31}P NMR spectrum; the compound was not isolated.

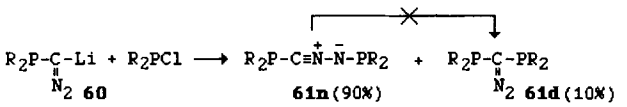
Comparison of the results of the reaction of diazo lithium salts **40** and **43** with various electrophiles (Scheme 12) poses a second problem. The nitrile imines resulting from the N-attack of the electrophiles can isomerize into the thermodynamically favored diazo compounds. Scheme 12 gives four examples of



Scheme 12. Reactivity of diazo lithium salts **40** and **43** with various electrophiles. R = iPr_2N; lp = lone pair.

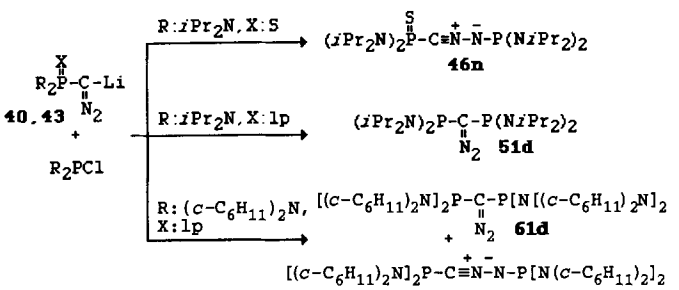
this rearrangement, which takes place, depending on the substituents, between 0 and 55 °C.[49, 50, 54] Therefore, one possible way to rationalize the formation of diazo compounds in cases in which no nitrile imines were observed was to postulate that the nitrile imines were always the kinetic products of the electrophilic attack on the diazo lithium salts, but that they rearranged into the thermodynamically favored diazo compounds (see Section 7). This hypothesis was reinforced by the formation of diazo compound **51d**[45, 55] in the reaction of the phosphinoyldiazo lithium salt **40** with chlorobis(diisopropylamino)-phosphane, and the formation of nitrile imine **46n** in the analogous reaction of the thiophosphinonyl analogue **43**.[46, 49] Indeed, since lithium salts **40** and **43** are sterically quite similar, the opposite regioselectivity of the reactions was difficult to explain. The results observed are apparently best attributed to electronic factors: the presence of two electron-donating groups destabilizes nitrile imine **51n** ($R_2P-CNN-PR_2$, $R = iPr_2N$) thus favoring the rearrangement to the thermodynamically preferred isomer **51d**.

Finally, the concomitant formation of both isomers **61n** and **61d** in the reaction of the lithium salt **60** of bis(dicyclohexylamino)phosphinoyldiazomethane and chlorobis(dicyclohexylamino)phosphane, and the absence of isomerization of **61n** into **61d**, demonstrated that the C- and N-attacks of electrophiles on salts of phosphorus-substituted diazo compounds are competitive processes (Scheme 13).[56]



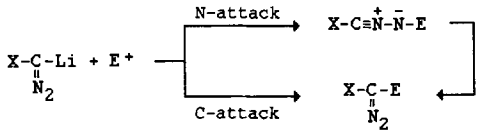
Scheme 13. Concomitant formation of diazo derivative **61d** and nitrile imine **61n**.

A very small change in the steric factors, such as replacing a lone pair by a sulfur atom, or exchanging diisopropylamino by dicyclohexylamino groups, can totally reverse the ratio of nitrile imine to diazo compound (Scheme 14).



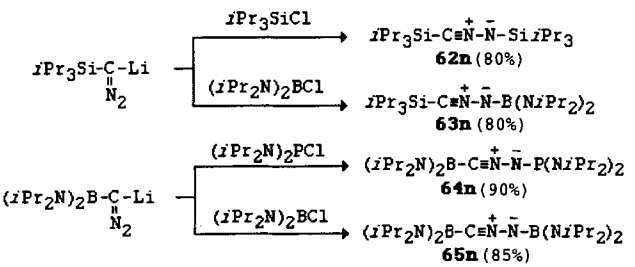
Scheme 14. Influence of the diazo lithium salt on the formation of the nitrile imine and diazo derivative.

Although electronic factors are not totally negligible, steric factors are of primary importance for the kinetic stabilization of nitrile imines that can isomerize into the thermodynamically preferred diazo compounds. Thus, the formation of diazo compounds can result either from C-attack of the electrophile or from N-attack followed by rearrangement of the initially formed nitrile imine (Scheme 15).



Scheme 15. The two pathways for the formation of diazo compounds.

In any case, the route employing diazo lithium salts appeared to be a very general method for synthesizing stable nitrile imines, as two further examples demonstrate. The two *C*-silylated nitrile imines **62n**[54, 57] and **63n**[58] were prepared, and more recently the two *C*-borylated nitrile imines **64n** and **65n** were synthesized from the first stable boryldiazomethane (Scheme 16).[58, 59]



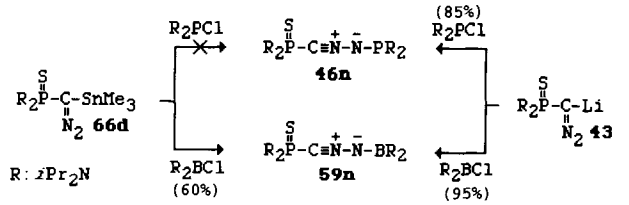
Scheme 16. Synthesis of *C*-silyl- and *C*-borylnitrile imines.

Phosphorus–carbon bonds are not easily cleaved, thereby limiting application of the *C*-phosphorus-substituted nitrile imines in organic synthesis. In contrast, silicon–carbon and boron–carbon bonds are easily cleaved. Thus, nitrile imines **62n**–**65n** are not only laboratory curiosities but potential building blocks for the facile synthesis of a variety of heterocycles.

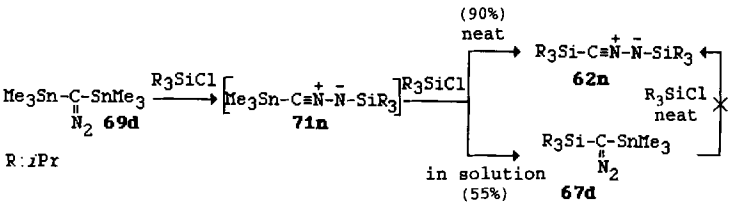
4.2. Starting from Stannyldiazo Compounds

Since the regioselectivity of the attack of electrophiles on the lithium salts of diazo compounds depends almost entirely on steric factors, it was logical to think that the use of diazo precursors bearing a metal atom larger than lithium would favor the formation of nitrile imines over diazo compounds; stannyl diazo compounds were potentially good candidates. In contrast to lithium diazo compounds, their structures are well established;[60] the tin atom is bound to carbon. The reaction of stannyl(thiophosphinoyl)diazomethane **66d** with chlorobis(diisopropylamino)borane was examined first. Indeed, the corresponding nitrile imine **59n**, already prepared by the diazolithium salt method, was obtained.[56] However, no reaction occurs between stannyldiazomethane **66d** and chlorobis(diisopropylamino)phosphane, thus proving that **66d** is less reactive than its lithium analogue **43** (Scheme 17).[56]

In the same way, triisopropylsilyl(trimethylstannyl)diazomethane (**67d**) does not react with triisopropylchlorosilane, but a clean reaction occurs with chlorobis(diisopropylamino)-

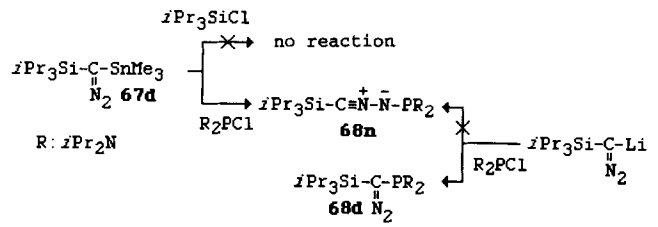


Scheme 17. Comparison of the reactivity of stannyl- and lithiodiazo compounds **66d** and **43**.



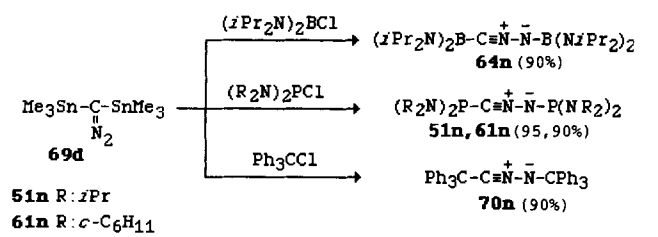
Scheme 20. Reactivity of **69d** with chlorotriisopropylsilane.

phosphane leading to nitrile imine **68n**.[56] This result is of special interest since nitrile imine **68n** was not available by the diazolithium salt method, which instead gave the diazo isomer **68d**[54] (Scheme 18).



Scheme 18. Comparison of the reactivity of stannyldiazo derivative **67d** with that of its lithio analogue.

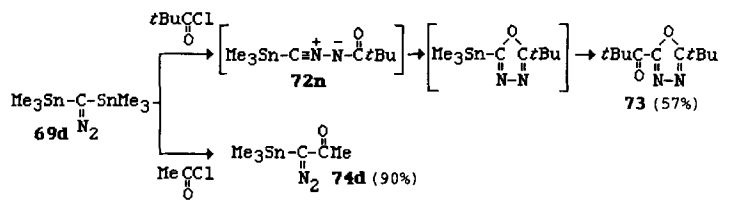
The question then arises whether bis(trimethylstannyl)-diazomethane (**69d**)[61] would act as a CNN^{2-} transfer agent and thus allow the one-step synthesis of nitrile imines, especially those not accessible by the diazo lithium salt method. The results summarized in Scheme 19 clearly demonstrate that this is possible. The formation of the bis(boryl)nitrile imine **64n** in high yield shows the efficiency of the method.[56] By the diazo lithium salt method, diphosphinonitrile imine **51n** was not available,[45] while **61n** was obtained as a mixture with its diazo isomer **61d**.[56] The stannyldiazomethane starting material unequivocally leads to nitrile imines **51n** and **61n**, demonstrating the high selectivity of the method.[56] The most striking result is certainly the preparation of the first stable, purely organic nitrile imine **70n**[56, 62] (Scheme 19).



Scheme 19. Synthesis of nitrile imines from bis(stannyl)diazomethane **69d**.

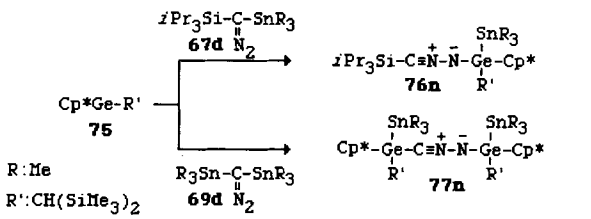
The dramatic differences observed in the reaction of **69d** with triisopropylchlorosilane, with and without solvent, are of primary interest (Scheme 20).[56] Since silyl(stannyl)diazomethane **67d** does not react with chlorotriisopropylsilane, it is obvious that **67d** is not the intermediate leading to nitrile imine **62n**. Thus, under both sets of experimental conditions the first step is certainly *N*-silylation giving rise to the *N*-silyl-*C*-stannylnitrile imine **71n**. In the absence of solvent, **71n** undergoes a substitution reaction by another molecule of chlorosilane affording bis-(silyl)nitrile imine **62n**, whereas in the presence of a solvent, the nitrile imine isomerizes to the diazo compound **67d** (Scheme 20).

These results seemed to show that, in contrast to lithiodiazomethanes, stannyldiazomethanes always react with electrophiles at the nitrogen terminus. However, it has been proven that they also undergo substitution at the carbon atom. Diazo compound **69d** reacts with the bulky pivaloyl chloride giving oxadiazole **73**, thus implying the primary formation of *N*-acyl-*C*-stannylnitrile imine **72n**; in contrast, with the sterically less demanding acetyl chloride, acyl(stannyl)diazomethane **74d** is formed (Scheme 21).[56]



Scheme 21. Reactivity of **69d** with acyl chlorides.

Stannyldiazo compounds **67d** and **69d** have also been treated with germanediyl **75** to prepare germyl-substituted nitrile imines **76n** and **77n**.[63] However, these reactions proceed by a completely different mechanism, since no trimethylchlorostannane is eliminated; so far this mechanism has not been investigated in more detail (Scheme 22).



Scheme 22. Synthesis of nitrile imines starting from germanediyl **75**. Cp* = C_5Me_5.

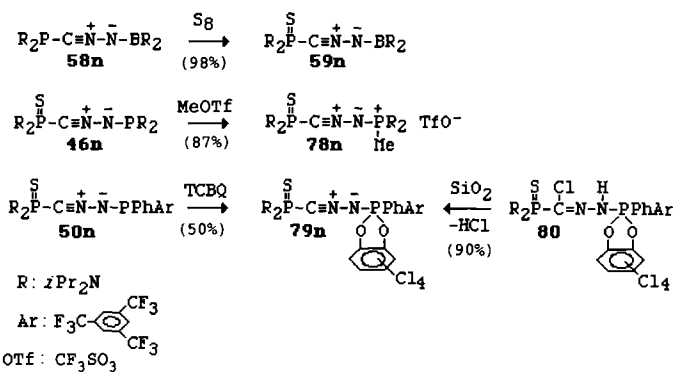
Stannyldiazo compounds allow the straightforward synthesis of a variety of symmetrically and unsymmetrically substituted nitrile imines. The experimental conditions are very mild, and the trimethylstannyl chloride formed is easily removed by sublimation (10^{-2} mm Hg, room temperature). Moreover,

bis(trimethylstannyl)diazomethane (**69d**) can be easily prepared in multigram quantities and acts as a safe CNN^{2-} transfer reagent, in contrast to analogues such as the dimercury, disilver, and dilithium diazomethane salts, which are explosive.[48]

4.3. Starting from Stable Nitrile Imines

Since stable nitrile imines were available, the question arose as to whether it was possible to use the heteroatom bound to the 1,3-dipole as a second center of functionality in the molecule. In other words, was it possible to do chemistry at the periphery of the nitrile imine without destruction of the CNN skeleton?

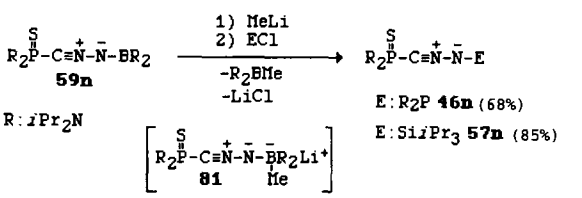
Three examples have been reported with phosphinonitrile imines. Addition of elemental sulfur to the *N*-boryl-*C*-phosphinonitrile imine **58n** led quantitatively to the *C*-thiophosphinoyl analogue **59n**,[58] already obtained by the lithiodiazomethane and the stannyldiazomethane methods (Scheme 23). More interestingly, addition of methyl trifluoromethanesulfonate to the *N*-phosphinoylnitrile imine **46n** afforded the corresponding *N*-phosphonio-substituted nitrilium betaine **78n**.[64] Since it is rather difficult to imagine another route to compound **78n**, this approach is of real synthetic interest. Lastly, *N*-phosphinonitrile imine **50n**, which has a phenyl and a 2,4,6-trifluoromethylphenyl group at phosphorus, reacted with tetrachloro-*o*-benzoquinone (TCBQ) to afford the only known $\lambda^5\sigma^5$-phosphorus-substituted nitrile imine **79n**.[65] However, this reaction is not general (see Section 7).



Scheme 23. Synthesis of stable nitrile imines starting from nitrile imines.

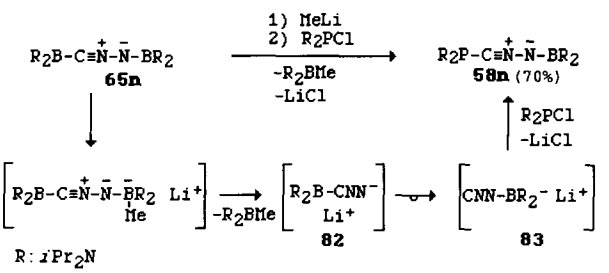
Surprisingly, **79n** can also be obtained by simply filtering a solution of the corresponding hydrazonoyl chloride **80** on silica gel. The ready elimination of HCl has been explained by the structure of compound **80** and the fact that the proton and the chlorine atom are only 2.45 Å apart (according to a single-crystal X-ray analysis).[65] So far, **79n** is the only example of a stable nitrile imine prepared by this classical method.

The high reactivity of boron–nitrogen bonds has been exploited in substitution reactions of boryl-substituted nitrile imines.[66] Addition of methyllithium to *N*-boryl-*C*-thiophosphononitrile imine **59n**, followed by addition of chlorobis(diisopropylamino)phosphane (or chlorotriisopropylsilane) led to the corresponding *N*-phosphinoylnitrile imine **46n** (or *N*-silylnitrile imine **57n**) in reasonable yields (Scheme 24). The first step of the reaction must be electrophilic attack by the boron atom, leading to a transient borate **81**, which after elimination of bis(diisopropylamino)methylborane gives rise to diazo lithium salt **43** (cf. Scheme 9).



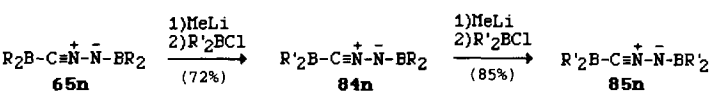
Scheme 24. N-substitutions on a nitrile imine.

Interestingly, formal C-substitution can also be performed with C,N-disubstituted nitrile imines.[66] Indeed, addition of methyllithium to a THF solution of *C,N*-[bis(diisopropylamino)boryl]nitrile imine (**65n**), followed by addition of chlorophosphane, afforded *C*-phosphinoylnitrile imine **58n** in 70% yield. It has been shown that **58n** does not result from substitution at the carbon end of the nitrile imine but from rearrangement of the first-formed boryllithiodiazomethane **82** into the isomeric "boryllithioisodiazomethane" **83**[59] (Scheme 25).



Scheme 25. Formal C-substitutions on a nitrile imine.

By using these properties, it has been possible to substitute nitrile imines at both carbon and nitrogen in a two-step sequence. *C,N*-[Bis(diisopropylamino)boryl]nitrile imine (**65n**) was first treated with methyllithium and then with chlorobis(dicyclohexylamino)borane. This led to *C*-[bis(dicyclohexylamino)boryl]-*N*-[bis(diisopropylamino)boryl]nitrile imine (**84n**). The reaction sequence was repeated with **84n** to give *C,N*-[bis(dicyclohexylamino)boryl]nitrile imine (**85n**) in fair yield (Scheme 26).[66] This method could be of special interest when the diazo compounds are not stable, since preparation of the corresponding lithium salts would not be required. In summary, a large variety of stable nitrile imines is now available (Table 1). Their stability is essentially due to steric factors.



Scheme 26. Formal C- and N-substitutions on a nitrile imine.

Table 1. Selected data of some nitrile imines L_nX-C-N-N-$YL_{n'}$.

No.	L_nX	$YL_{n'}$	Cmpd.	Physical data	$\tilde{\nu}$ [cm^{-1}]	δ (^{13}C) [a] (J_{PC})	δ (^{14}N) [a] ($\nu_{1/2}$)	δ (X) [a] (J_{PX})	δ (Y) [a]	Method [b]	Yield [%] [c]	Ref.
1	$(i\mathrm{Pr}_2\mathrm{N})_2\mathrm{P(S)}$	$\mathrm{P}(\mathrm{N}i\mathrm{Pr}_2)_2$	**46n**	m.p. 100 °C	2040	61.04 (99.4)	−173.6 (107)	+35.4 (5.2)	+99.9	A C	85 68	[49] [66]
2	$(i\mathrm{Pr}_2\mathrm{N})_2\mathrm{P(S)}$	$\mathrm{P}t\mathrm{Bu}_2$	**48n**	solution [d]	2060			+31.6 (<1)	+119.0	A		[49]
3	$(i\mathrm{Pr}_2\mathrm{N})_2\mathrm{P(S)}$	PPhAr [e]	**50n**	oil	2138			+27.9 (<1)	+70.6	A	82	[52]
4	$(i\mathrm{Pr}_2\mathrm{N})_2\mathrm{P(S)}$	$\mathrm{P}(\mathrm{N}i\mathrm{Pr}_2)_2$TCBQ [e]	**79n**	m.p. 166 °C	2162	65.53 (133.7)		+27.8 (8.6)	−24.3	C C	50 90	[65] [65]
5	$(i\mathrm{Pr}_2\mathrm{N})_2\mathrm{P(S)}$	$\mathrm{P}(\mathrm{N}i\mathrm{Pr}_2)_2\mathrm{Me}^+$	**78n**	m.p. 100 °C	2170	69.83 (90.3, 17.7)	−215.0 (200)	+28.7 (6.7)	+52.7	C	87	[64]
6	$(i\mathrm{Pr}_2\mathrm{N})_2\mathrm{P(S)}$	SiMe_3	**53n**	solution [d]	2010			+32.5		A		[54]
7	$(i\mathrm{Pr}_2\mathrm{N})_2\mathrm{P(S)}$	SiPh_3	**55n**	solution [d]	2120			+31.1		A		[54]
8	$(i\mathrm{Pr}_2\mathrm{N})_2\mathrm{P(S)}$	$\mathrm{Si}i\mathrm{Pr}_3$	**57n**	m.p. 54 °C	2050			+33.1	+12.8	A C	96 85	[54] [66]
9	$(i\mathrm{Pr}_2\mathrm{N})_2\mathrm{P(S)}$	$\mathrm{B}(\mathrm{N}i\mathrm{Pr}_2)_2$	**59n**	oil	2095	55.67 (132.2)		+31.8	+27	A B C	95 60 98	[58] [56] [58]
10	$(i\mathrm{Pr}_2\mathrm{N})_2\mathrm{P(S)}$	BMes_2 [e]		m.p. 84 °C	2144	71.48 (131.2)		+27.1		A	65	[67]
11	$(i\mathrm{Pr}_2\mathrm{N})_2\mathrm{P}$	$\mathrm{P}(\mathrm{N}i\mathrm{Pr}_2)_2$	**51n**	oil	2047	63.28 (62.5)	−191.9 (250)	+45.5 (9.0)	+96.0	B	95	[56]
12	$[(c\text{-}\mathrm{C}_6\mathrm{H}_{11})_2\mathrm{N})]_2\mathrm{P}$	$\mathrm{P}[\mathrm{N}(c\text{-}\mathrm{C}_6\mathrm{H}_{11})_2]_2$	**61n**	oil	2047	64.40 (72.8)		+52.0 (9.1)	+100.0	B	90	[56]
13	$\mathrm{P}(\mathrm{N}i\mathrm{Pr}_2)_2$	SiMe_3	**52n**	solution [d]	2100			+44.1		A		[54]
14	$\mathrm{P}(\mathrm{N}i\mathrm{Pr}_2)_2$	SiPh_3	**54n**	oil	2140			+42.4	−10.4	A	80	[54]
15	$\mathrm{P}(\mathrm{N}i\mathrm{Pr}_2)_2$	$\mathrm{Si}i\mathrm{Pr}_3$	**56n**	oil	2110			+45.7	+6.6 (3.6)	A	90	[54]
16	$\mathrm{P}(\mathrm{N}i\mathrm{Pr}_2)_2$	$\mathrm{B}(\mathrm{N}i\mathrm{Pr}_2)_2$	**58n**	b.p. 110 °C (0.2 Torr)	2113	61.87 (48.3)		+45.1	+29	A C	90 70	[58] [66]
17	$i\mathrm{Pr}_3\mathrm{Si}$	$\mathrm{P}(\mathrm{N}i\mathrm{Pr}_2)_2$	**68n**	solution [d]	2099				+101.4	B		[56]
18	$i\mathrm{Pr}_3\mathrm{Si}$	$\mathrm{Si}i\mathrm{Pr}_3$	**62n**	b.p. 90 °C (0.05 Torr)	2120	46.73	−189.0 (78)	+0.71	+6.4	A B	80 90	[54] [56]
19	$i\mathrm{Pr}_3\mathrm{Si}$	$\mathrm{B}(\mathrm{N}i\mathrm{Pr}_2)_2$	**63n**	m.p. < 20 °C	2164	45.10		+8.35	+22	A	80	[58]
20	$i\mathrm{Pr}_3\mathrm{Si}$	GeRR′R″ [e]	**76n**	oil	2076	49.83	−182.9			B	60	[63]
21	RR′R″Ge [e]	GeRR′R″ [e]	**77n**	m.p. 136 °C	2052	63.71	−173.0			B	48	[63]
22	$(i\mathrm{Pr}_2\mathrm{N})_2\mathrm{B}$	$\mathrm{P}(\mathrm{N}i\mathrm{Pr}_2)_2$	**64n**	b.p. 105 °C (0.001 Torr)	2145	67.00	−184.4 (220)	+22	+96.6	A	90	[59]
23	$(i\mathrm{Pr}_2\mathrm{N})_2\mathrm{B}$	$\mathrm{B}(\mathrm{N}i\mathrm{Pr}_2)_2$	**65n**	b.p. 110 °C (0.001 Torr)	2160	65.80	−186.4 (140)	+23	+28	A B	85 90	[58] [56]
24	$[(c\text{-}\mathrm{C}_6\mathrm{H}_{11})_2\mathrm{N})_2\mathrm{B}]$	$\mathrm{B}(\mathrm{N}i\mathrm{Pr}_2)_2$	**84n**	m.p. 115 °C [f]	2155	68.01 (175)	−188.0	+27	+27	C	72	[66]
25	$[(c\text{-}\mathrm{C}_6\mathrm{H}_{11})_2\mathrm{N})_2\mathrm{B}]$	$\mathrm{B}[\mathrm{N}(c\text{-}\mathrm{C}_6\mathrm{H}_{11})_2]_2$	**85n**	m.p. 121 °C [f]	2152	66.50 (550)	−191.0	+25	+25	C	85	[66]
26	$\mathrm{Ph}_3\mathrm{C}$	CPh_3	**70n**	m.p. 60 °C [f]	2052	85.5 (280)	−182.1	60.71	76.26	B	90	[56]

[a] External standards ^{13}C and ^{29}Si NMR: Me_4Si; ^{11}B, ^{14}N, and ^{31}P NMR: $BF_3 \cdot OEt_2$, $MeNO_2$, and H_3PO_4, respectively. J_{PC} and J_{PX} coupling constants in Hz; $\nu_{1/2}$ in Hz. [b] A, B, C refer to the synthetic methods described in Sections 4.1, 4.2, and 4.3, respectively. [c] Isolated yield. [d] Compounds characterized in solution but not isolated. [e] Ar: 2,4,6-tris(trifluoromethyl)phenyl; TCBQ: tetrachloro-*o*-benzoquinone; Mes: 2,4,6-trimethylphenyl; R,R′,R″: pentamethylcyclopentadienyl, trimethylstannyl, bis(trimethylsilyl)methyl. [f] Decomposition.

5. Characterization of Nitrile Imines

5.1. X-ray Data and Ab Initio Calculations

The key angles and bond lengths in those nitrile imines for which X-ray crystallographic structures have been determined are listed in Table 2. Selected X-ray structures are shown in Figures 1–3. Inspection of the data immediately reveals the large variability of structures, which range from close to propargylic (cf. **2a**) to allenic (cf. **2b**).

The X-ray data in Table 2 may be compared with the results of high-level ab initio calculations[12] on model compounds (Table 3). On the basis of STO-3G and HF/4-31G calculations Houk et al.[9, 11] found two minima for the unsubstituted nitrile imine HCNNH **2n** at the STO-3G level. These correspond to **2a** and **2b**. However, at the MP2/6-31G* level, there is only one stable form, which is bent and nonplanar and thus resembles the allenic structure **2b** more than the propargylic **2a**. This preference for the allenic form is further supported by higher level geometry optimization at the MP2/6-311 + G(2df,2p) and QCISD/6-311G** levels (Table 4).[12]

Table 2. Selected X-ray data for nitrile imines $X-C\equiv\overset{+}{N}-\overset{-}{N}-Y$ [a].

Parameter [a]	**70n**	**46n**	**78n**	**85n**	**77n**
r(C-N)	1.173	1.177	1.143	1.171	1.183
r(N-N)	1.262	1.240	1.285	1.268	1.264
r(X-C)	1.503	1.771	1.815	1.559	1.935
r(N-Y)	1.530	1.777	1.623	1.452	1.833
∢(XCN)	137.3	138.2	163.5	165.1	150.1
∢(CNN)	169.4	173.6	169.6	169.4	174.2
∢(NNY)	115.2	115.0	123.6	122.4	129.9
τ(XCNN)	135.7	121	84.1	52.48	68.2
τ(CNNY)	134	152	177.7	-178.9	148.7
$\tilde{\nu}$ [b]	2052	2040	2170	2160	2052
ref.	[62]	[49]	[64b]	[66]	[63]

[a] Angles in degrees, bond lengths in Å. [b] Frequencies [cm^{-1}] of the IR absorption band of the CNN unit for comparison.

Table 3. Calculated structural parameters (MP2/6-31G*) for C- and N-substituted nitrile imines XCNNH and HCNNY [12].

Parameter [a]	H	PH_2	PH_3^+	BH_2	SiH_3	CH_3	C_6H_5
			Substituent X				
r(C-N)	1.192	1.194	1.199	1.190	1.194	1.193	1.195
r(N-N)	1.267	1.268	1.227	1.263	1.263	1.273	1.270
r(X-C)	1.073	1.777	1.705	1.485	1.825	1.476	1.436
r(N-H)	1.027	1.028	1.029	1.030	1.026	1.028	1.028
∢(CNN)	169.2	169.6	170.0	172.3	171.5	169.1	169.4
∢(XCN)	140.6	148.6	149.0	178.7	175.1	145.4	150.3
∢(HNN)	108.0	108.0	116.2	107.8	109.2	107.6	108.1
τ(XCNN)	138.1	134.4	112.4	179.9	108.6	134.3	127.5
τ(HNNC)	131.8	150.3	148.2	179.7	162.1	135.9	137.0
$\tilde{\nu}$(CN) [b]	2383	2442	2399	2485	2431	2460	[c]
Parameter [a]	H	PH_2	PH_3^+	BH_2	SiH_3	CH_3	C_6H_5
			Substituent Y				
r(C-N)	1.192	1.196	1.172	1.197	1.197	1.196	1.195
r(N-N)	1.267	1.258	1.289	1.257	1.250	1.260	1.262
r(H-C)	1.073	1.072	1.074	1.068	1.070	1.075	1.076
r(N-Y)	1.027	1.757	1.641	1.422	1.755	1.474	1.419
∢(CNN)	169.2	170.9	170.8	166.3	171.1	169.8	169.7
∢(HCN)	140.6	144.8	179.9	151.5	147.0	138.1	140.1
∢(YNN)	108.0	115.6	119.4	121.8	120.4	111.8	115.2
τ(HCNN)	138.1	151.2	171.0	180.0	145.2	153.2	148.8
τ(YNNC)	131.8	114.0	179.9	180.0	120.1	114.6	118.1
$\tilde{\nu}$(CN) [b]	2383	2319	2217	2146	2315	2351	[c]

[a] Angles in degrees, bond lengths in Å. [b] CNN stretching frequency in cm^{-1} (uncorrected MP2/6-31G* values). Note: these vibrations are coupled with the N–H or C–H stretching modes and therefore cannot be compared with experimental values for differently substituted compounds. [c] Beyond the computational power of current supercomputers.

Table 4. Calculated structural parameters of formonitrile imine **2n** (allenic form $HC^{-}=N^{+}=N-H$ **2a**) [12].

Parameter	HF/6-31G*	MP2/6-31G*	Level MP2/6-311 + G(2df,2p)	QCISD/6-311G** [a]
r(C-H)	1.069	1.073	1.065	1.082
r(C-N)	1.179	1.192	1.181	1.207
r(N-N)	1.223	1.267	1.253	1.254
r(N-H)	1.009	1.027	1.018	1.028
∢(HCN)	127.5	140.6	145.5	128.2
∢(CNN)	171.7	169.2	170.6	168.5
∢(HNN)	108.7	108.3	108.8	107.1
τ(HCNN)	140.2	138.1	132.6	140.8
τ(HNNC)	130.1	131.8	137.2	130.6

[a] QCISD = Quadratic configuration interaction with single and double excitations.

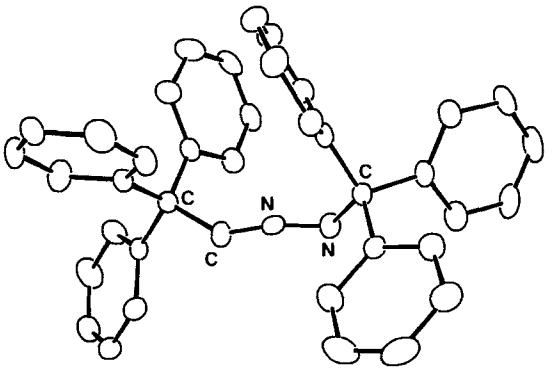


Fig. 1. Crystal structure of **70n** [62].

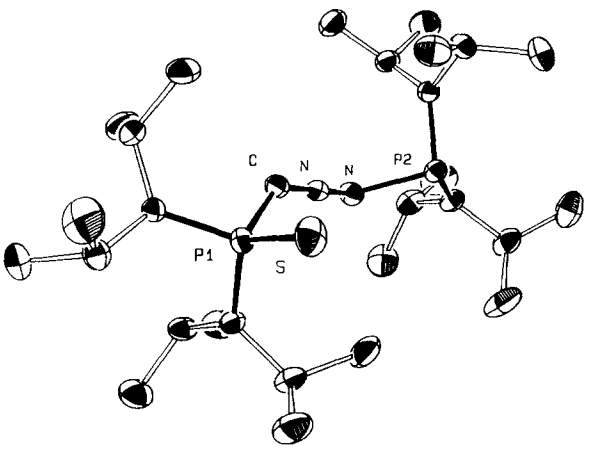


Fig. 2. Crystal structure of **46n** [49].

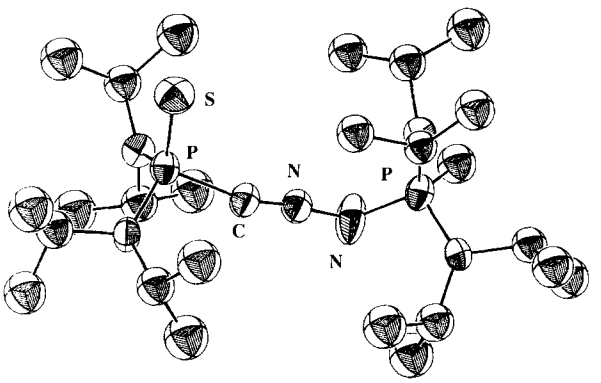


Fig. 3. Structure of the cation of **78n** in the crystal [64b].

The MP2/6-311G**(2df,2p)-level geometry of HCNNH (Tables 3 and 4) is in excellent agreement with the experimental data for bis(triphenylmethyl)nitrile imine (**70n**) given in Table 2 and Figure 1. Thus, this compound may be considered typically allenic and perturbed minimally by steric or electronic effects.

The *N*-phosphino-*C*-thiophosphinoylnitrile imine **46n** (Fig. 2) also has an allenic structure very similar to that of **70n**; however, the structure of the phosphonio-substituted compound **78n** is dramatically different (Fig. 3). The P-C-N angle is much flatter (163.5°); the C–N bond is particularly short (1.14 Å), and the N–N bond correspondingly long (1.285 Å). This change in geometry is nicely corroborated by the results of calculations for $HCNNPH_3^+$ (Table 3), which was shown to be a planar and "propargylic" compound with a linear HCN moiety, a short C–N bond, and a long N–N bond. The main difference between the actual structure of **78n** and that calculated for the model compound is the dihedral angle of 84° between the PCN and CNN planes in the former. However, the CNNP moiety in **78n** is nearly planar, and the CNN backbone nearly linear, so that the deviation from the calculated structure is not so dramatic, and it may well be caused by steric and/or crystal lattice effects.

According to calculations the boryl compound $H_2B-CNN-H$ also tends toward linearity and planarity, although the C–N bond is not quite so short and the compound thus less "propargylic" (Table 3). The bis(boryl) compound $H_2B-CNN-BH_2$ has a similar structure.[12] These trends are

in accord with the X-ray structure of **85n**, which is similar to that of the phosphonio compound **78n** but not quite as clearly propargylic as judged by the lengths of the C–N and N–N bonds (Table 2). The BCNN skeleton is close to linear (BCN = 165.1°), and the B–C bond is quite short (1.559 Å).

In the propargylic forms of these molecules with partial C≡N triple bonds the negative charge on the terminal nitrogen atom is increased as in **2a**, and the electronegative *N*-phosphonio and *N*-boryl substituents are thus stabilized. Accordingly, the N–P bond in **78n** is rather short (1.623 Å in **78n** vs 1.777 Å in **46n**).[64b] The calculations indicate, however, that a BH_2 group on carbon has a greater "linearizing" effect than one on nitrogen (Table 3).[12]

5.2. Infrared Spectra

The frequencies of the asymmetric CNN stretching vibrations of all the stable nitrile imines are given in Table 1, and the calculated IR spectrum of HCNNH is in Table 5. By applying the usual correction factor[68] of 0.93 to the calculated frequency, it is seen that the absorption band of the still unknown[17] parent formonitrile imine may be expected in the range 2100–2200 cm^{-1}.

Table 5. Calculated harmonic vibrational frequencies and IR intensities for formonitrile imine **2n** (MP2/6-311G (2df, 2p)) [12].

No.	$\tilde{\nu}$[cm^{-1}]	Int. [km mol^{-1}]	Assignment
ω_1	503	6	CNN bend
ω_2	527	36	CNN bend
ω_3	620	191	CH bend
ω_4	696	46	CH + NH rock
ω_5	1158	133	CNN antisymmetric stretch
ω_6	1253	28	NH bend
ω_7	2228	194	CNN symmetric stretch
ω_8	3236	95	CH stretch
ω_9	3296	34	NH stretch

The experimental data in Table 1 indicates that stabilized nitrile imines fall in two classes: 1) those absorbing in the range 2010–2100 cm^{-1}, and 2) those absorbing from 2140 to 2170 cm^{-1}. According to a valence bond description, the propargylic structure -C≡N–N- is expected to have a high C≡N stretching frequency approaching the nitrile region (≥2200 cm^{-1}), whereas the frequency for the allenic structure -C=N=N- should be lower. The data agrees with the results of the X-ray determinations described previously. Thus, the compounds listed as entries 3–5, 11, 14, 19, and 22–25 in Table 1 may be described as partially propargylic. For compounds **78n** and **85n** (entries 5 and 25) this has been discussed already. The electron-withdrawing tris(trifluoromethyl)phenyl substituent on phosphorus in **50n** (entry 3) is seen to have a large effect and increases the CNN stretching frequency into the "propargylic" range. Even phenyl groups on silicon have this effect in compounds **55n** and **54n** (entries 7 and 14). Boron has a large effect in the same direction both in *C*-boryl (**64n**, entry 22) and *C,N*-bis(boryl) compounds (**65n**, **84n**, **85n**, entries 23–25). The diaminoboryl substituent on nitrogen alone has little effect (**59n**, entry 9), but the more electrophilic dimesitylboryl substituent in entry 10 has a large effect.

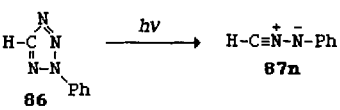
None of the stable nitrile imines for which X-ray structures have been determined so far are truly "propargylic": none have a linear X–C≡N- backbone, and none absorb in the actual nitrile region of the IR spectrum. It appears that the *C*-arylnitrile imines examined in low-temperature matrices constitute a separate class with nitrile-like Ar–C≡N- moieties, which absorb above 2200 cm^{-1} in the IR spectrum.

Diphenylnitrile imine (**11n**) absorbs at 2228 cm^{-1} in PVC matrix[37] and at 2242 in Ar matrix.[69] ^{15}N labeling of the central nitrogen atom causes, as expected, a large isotopic shift (to 2195 cm^{-1}), whereas labeling of the terminal nitrogen atom has a miniscule effect (2227 cm^{-1} in PVC matrix).[37] This is in line with the nitrile-type Ar–C≡$\overset{+}{N}$–$\overset{-}{N}$–Ar structure. The corresponding ^{15}N isotope shift in benzonitrile itself is 27 cm^{-1} (PhC≡N 2228 cm^{-1}; PhC≡^{15}N 2201 cm^{-1} in PVC).[37] Evidence that the compound observed was in fact diphenylnitrile imine was given by its photochemical rearrangement to diphenylcarbodiimide and cleavage to benzonitrile and phenylnitrene (see Section 7).[37]

Similarly, *C*-phenyl-*N*-trimethylsilylnitrile imine absorbs at 2230 cm^{-1} (film, 77 K), and its structure was confirmed by mass spectrometry, photoelectron spectroscopy, and trapping reactions,[43, 44] as well as by its photochemical rearrangement to *N*-phenyl-*N'*-trimethylsilylcarbodiimide.[69]

Dimesitylnitrile imine (**25n**) (Scheme 5) absorbs in solution at 2200 cm^{-1}, as Grundmann and Flory observed.[29]. However, *N*-methyl-*C*-phenylnitrile imine, generated by Ar matrix photolysis of 2-methyl-5-phenyltetrazole at 12 K, absorbs at 2032 and 1361 cm^{-1} and is photochemically converted to *N*-phenyl-*N'*-methyl-carbodiimide.[69] It would be highly interesting to synthesize a stable *C,N*-diarylnitrile imine to further investigate the structure.

N-Phenylnitrile imine (**87n**), generated in PVC matrix by photolysis of 2-phenyltetrazole (**86**) [Eq. (5)], was reported to

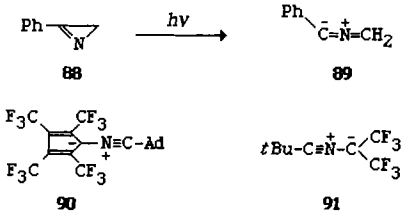


(5)

absorb at the low frequency of 2014 cm^{-1}.[37] This compound is a derivative of HCN, which absorbs near 2100 cm^{-1}.[70] Nitrile imine **87n**, which lacks a *C*-aryl substituent, may be more of the allenic type. ^{15}N labeling could give more information, but at any rate a low-frequency absorption band for **87n** is not unexpected. The nitrile oxides R–C≡$\overset{+}{N}$–$\overset{-}{O}$, which are linear or nearly linear,[71] absorb at very high frequencies near 2300 cm^{-1}, except for the parent member, fulminic acid, H–C≡$\overset{+}{N}$–$\overset{-}{O}$, which has a strong band at 2198 cm^{-1} (gas)[18] or 2193 cm^{-1} (Ar matrix).[72]

It is instructive to note that the C≡N–C absorption frequencies of nitrile ylides span almost 400 cm^{-1}. Benzonitrile methylide **89**, generated in Ar matrix by photolysis of 2*H*-azirine **88**, was reported to absorb strongly at a relatively low frequency, 1930 cm^{-1}.[73] The only stable nitrile ylide known was prepared and characterized by Arduengo et al.:[74] in com-

pound **90** an essentially linear C–N≡C- moiety was established by X-ray crystallography. The IR spectrum of this compound features a C–N stretching vibration at extremely high frequencies: a doublet at 2210, 2323 cm^{-1}.[75] Electron-withdrawing substituents on the ylidic carbon atom are expected[11] to stabilize the linear structure as in **90** and **91**. Ylide **91** has been isolated in matrix and absorbs in the nitrile region at 2250 cm^{-1}[76] (Scheme 27).



Scheme 27. Nitrile ylides characterized by IR spectroscopy. Ad = adamantyl.

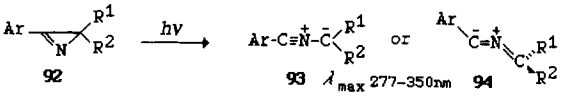
The span of approximately 200 cm^{-1} in the symmetric stretching vibration ν_{CNN} in nitrile imines is thus perhaps not so surprising. Unfortunately, the calculated IR frequencies (Table 3) cannot be compared directly with experimental values for differently substituted compounds, because the ν_{CNN} vibrations in the monosubstituted nitrile imines are found computationally to be strongly coupled with either the C–H or N–H stretching modes. The existence of coupled vibrations could explain all the variations observed in the IR spectra. More work is needed to understand the relationship between structure and vibrational frequencies in nitrile imines.

5.3. UV Spectra

Selected UV spectral data for nitrile imines are given in Table 6. While less structural information can be gleaned from these data, it is instructive to compare the UV spectrum of diphenylnitrile imine (**11n**; λ_{max} = 378 nm) with that of the corresponding benzonitrile benzylide PhC≡$\overset{+}{N}$–$\overset{-}{C}$HPh.[77] In their discussion whether nitrile ylide **93** or **94** is generated by photolysis of 2*H*-azirines **92** in 2MP or DMBP glasses at 77 K (Scheme 28), Hansen and Heimgartner[77] argue in favor of the bent allene-type structure **94**, because the changes in the UV spectra are more in line with those observed for benzylideneamines than for benzonitriles. In the same vein, one can argue that diphenylnitrile imine is linear because of the bathochromic shift of the UV absorption maximum relative to that of benzonitrile benzylide (PhC≡$\overset{+}{N}$–$\overset{-}{C}$HPh; λ_{max} = 344 nm). If **11n** were bent like **94**, a hypsochromic shift would be expected. Nevertheless, the high-level ab initio calculations given in Table 3 predict that nitrile imines with aromatic substituents will be nonlinear and allenic.

Table 6. UV spectroscopic data of nitrile imines.

Cmpd.	λ_{max} [nm]	Phase	Ref.
26n	378	EPA or PVC	[36, 37]
33n	383	EPA	[28]
54n	256, 292	pentane	[54]
56n	244, 273	pentane	[54]
57n	275	pentane	[54]
62n	272	pentane	[54]
87n	310	PVA	[37]



Scheme 28. Photolysis of 2*H*-azirine **92**.

5.4. NMR Spectra

In contrast to X-ray analyses and IR spectroscopy, NMR spectroscopy does not really allow a differentiation between the allenic and propargylic structures. For illustration, we can compare the NMR data for the best representative of each structure type, namely the allenic *N*-phosphino-*C*-thiophosphinoylnitrile imine **46n** and the propargylic *N*-phosphonio-*C*-thiophosphinoylnitrile imine **78n**. The ^{13}C NMR signal for the quaternary carbon atom of **46n** and **78n** appears at δ = 61.04 and 69.83, respectively; the difference is not significant. The ^{14}N NMR signals of **46n** and **76n**, δ = −173.6 and −215, respectively, are possibly more informative. It is, however, surprising to find a δ value of only −191.0 for the *C*,*N*-bis(boryl)nitrile imine **85n**.

However, NMR spectroscopy is a very valuable tool for the identification of nitrile imines. In studies of reactions in which a nitrile imine and/or a diazo compound can be formed, a rapid and reliable method is needed for distinguishing these two structural isomers. The IR absorptions for both types of compounds are very similar.

The ^{13}C NMR chemical shift of the quaternary carbon atom of nitrile imines is generally in the range δ = 45–70; ditritylnitrile imine with a signal for the corresponding carbon atom at δ = 85.5 is an exception. This chemical shift range can serve as a criterion for differentiation of nitrile imines and diazo compounds, since the signal of the diazo carbon atom appears at higher field (δ < 40). However, observation of these ^{13}C NMR resonances is hampered owing to the fairly long longitudinal relaxation time T_1 (^{13}C). In addition, the transverse relaxation time T_2 (^{13}C) is considerably shortened by second-order scalar relaxation caused by the adjacent ^{14}N nucleus. Further difficulties arise when nuclei such as ^{11}B or ^{31}P are attached to the carbon atom, giving rise to additional broadening or splitting, respectively.

So far, all attempts to obtain a ^{15}N NMR spectrum of nitrile imines have failed. In contrast, ^{14}N NMR spectroscopy provides a simple and quick way to identify nitrile imines and differentiate them from diazo isomers.[78] The $^{14}N_\alpha$ nuclei ($CN_\alpha N_\beta$) give rise to comparatively narrow ^{14}N NMR signals, which are easily observed at room temperature. The chemical shifts of the N_α atoms of nitrile imines are between δ = −170 and −215, while for diazo compounds the analogous signals are between δ = −110 and −130; this difference is sufficient for a definitive structure assignment. Note that, as expected, the $^{14}N_\alpha$ chemical

shifts for the nitrile imines are found in a range similar to those of nitrile oxides.[79] The $^{14}N_\beta$ resonance has never been observed even at high temperature (80 °C), probably because the electric field gradient at the site of the $^{14}N_\beta$ nucleus is very large, thus causing the $^{14}N_\beta$ relaxation time T_Q to be very short.

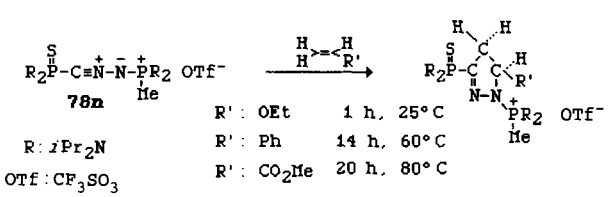
Since many of the known, stable nitrile imines have heteroatom substitutents, NMR data from heteronuclei have been widely used for structure determination. In the case of *C*-phosphorus-substituted nitrile imines, the ^{31}P chemical shift was always at higher field than that of the diazo isomer; this is particularly dramatic with thiophosphinoyl substituents ($\Delta\delta = 27-43$) but also evident with phosphino substituents ($\Delta\delta = 9-12$). Moreover, the presence of a phosphorus atom at the carbon terminus induces couplings with the nitrile imine carbon ($^1J_{PC} = 48-133$ Hz) and also sometimes with the *N*-nitrile imine substituent ($^4J_{PP} = 0-9$ Hz; $^4J_{PSi} = 0-4$ Hz). The ^{29}Si NMR signals are somewhat difficult to observe and are not indicative of the structure. In the same way, ^{11}B NMR spectra are not very helpful, since the signals are very broad and the range very narrow. For instance, in the case of *C,N*-bis(boryl)nitrile imine **65n**, the boron atoms can only be differentiated at 348 K ($\delta = +23$ and $+28$).[58]

6. Reactivity of Nitrile Imines

6.1. 1,3-Dipolar Cycloaddition Reactions

The general features of 1,3-dipolar cycloaddition reactions are well known.[2-6, 11, 38c, 77] In this section we briefly compare the results obtained with transient and stable nitrile imines, emphasizing the differences between these to types of compounds.

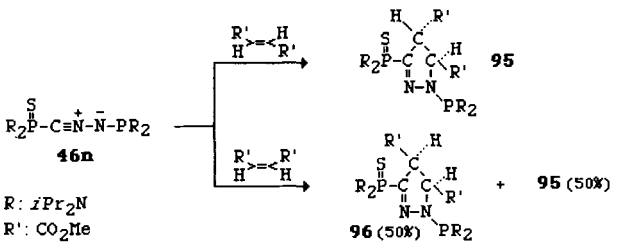
Nitrile imines are Class II dipoles in the classification of Sustmann;[80] in other words, HOMO(dipole)/LUMO(dipolarophile) and HOMO(dipolarophile)/LUMO(dipole) interactions are about equally important. Consequently, nitrile imines can behave as both nucleophiles and electrophiles toward the dipolarophile; that is, the nitrile imines are ambiphilic. This statement fits well with the experimental results for transient nitrile imines. Most of the known stable nitrile imines do not react with styrene, butadiene, or phenylacetylene but react with electron-poor dipolarophiles (note that even the transient diphenylnitrile imine adds to dimethyl fumarate 177 times faster than to styrene).[81] The only real exception is the *N*-phosphonio-substituted nitrile imine **78n**, which is strongly electrophilic.[64b] It reacts with electron-rich olefins such as ethyl vinyl ether at room temperature, whereas the reaction with styrene requires 14 h at 60 °C. Reaction with the electron-poor olefin methyl acrylate needs 20 h at 80 °C (Scheme 29). This order of reactivity of **78n** with dipolarophiles was confirmed by competition experiments.



Scheme 29. Reactivity of nitrile imine **78n** to dipolarophiles.

Lastly, it should be noted that the reactivity of the *N*-borylnitrile imines (**58n**, **59n**, **63n**) is quite usual but, surprisingly, the *C*-borylnitrile imines (**64n**, **65n**, **84n**, **85n**) are rather unreactive.[58]

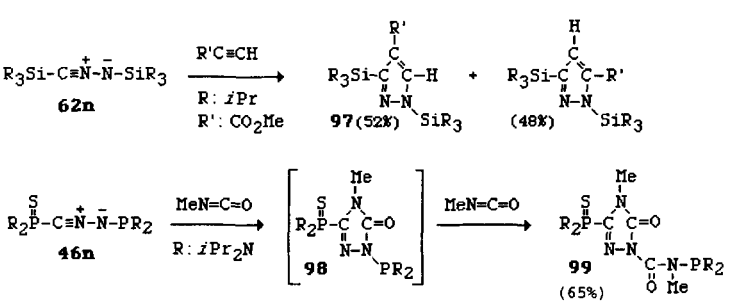
1,3-Dipolar cycloaddition reactions are usually stereospecific, and it was long assumed that any exception was due to prior isomerization of the dipolarophile or subsequent isomerization of the product.[4, 5] Surprisingly, nitrile imine **46n** reacted stereospecifically with dimethyl fumarate affording the *trans* adduct **95**, while with dimethyl maleate a mixture of *cis*-**96** and *trans* adducts **95** was obtained. Since attempted epimerization of **96** failed, and NMR spectroscopy revealed that the unconsumed dipolarophile was not isomerized when the reaction was run with 1.2 equivalent of maleic ester, it was concluded that the lack of stereoselectivity observed was due to a "nonconcerted addition" process[49] (Scheme 30). Two previous examples of



Scheme 30. An example of nonstereoselectivity in [2 + 3] cycloaddition reactions.

nonconcerted [2 + 3] cycloaddition reactions have been reported; the first was described by Huisgen et al. for the reaction of strongly nucleophilic thiocarbonyl ylides with particularly electrophilic alkenes,[82] and the second by Quast et al. for the reaction of electrophilic azides with 5-alkylidenedihydrotetrazoles.[83]

The regiochemistry of the cycloaddition reactions has also been rationalized in terms of frontier molecular orbital (FMO) theory.[4, 5, 11, 84] As predicted, addition of unsymmetrically substituted olefins or alkynes usually yields the 5-substituted pyrazolines or pyrazoles as the major product. However, in the case of *C,N*-bis(silyl)nitrile imine **62n**, the 4-substituted pyrazole **97** becomes the major isomer;[54] this finding is also in agreement with theory, since the silyl groups raise the FMO energies. Nitrile imine **46n** reacts with methyl isocyanate only with the C=N and not with the C=O double bond, as expected for a HOMO(dipole)-controlled cycloaddition and in contrast to the results observed with transient nitrile imines.[5, 6] (The isolated product **99** results from the insertion of a second molecule of isocyanate into the P–N bond of the primary product **98**)[49] (Scheme 31). To summarize, both transient and stable



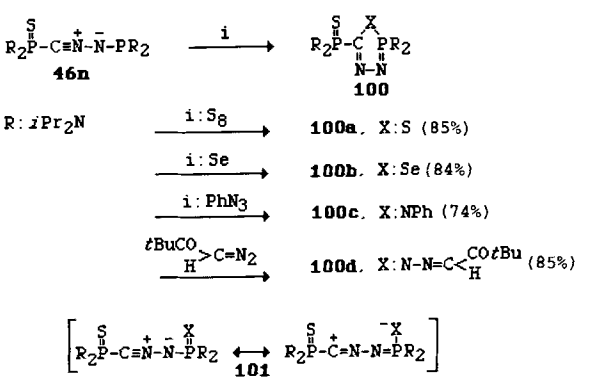
Scheme 31. Examples of the regioselectivity of [2 + 3] cycloaddition reactions of nitrile imines **62n** and **46n**.

nitrile imines have similar reactivities with 1,3-dipoles, although, not surprisingly, the stable nitrile imines are somewhat less reactive.

6.2. Reactions Involving the CNN Skeleton and a Heteroatom Substituent

As described in Section 5, the structure of nitrile imines is not strongly perturbed by heteroatom substituents. However, one of the important questions was whether the heteroatom bonded to the CNN moiety could extend the scope of nitrile imine reactions.

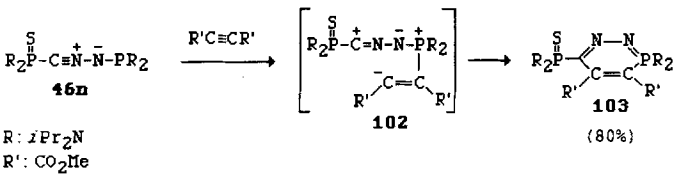
Indeed, reactions involving both the CNN unit and a λ^3-phosphorus atom bound to the nitrogen terminus have been reported.[52, 64a] Nitrile imine **46n** reacts with sulfur, selenium, phenyl azide, and pivaloyldiazomethane at room temperature to afford 1,3,4,2λ^5-thiadiazaphosphole **100a**, 1,3,4,2λ^5-selenadiazaphosphole **100b**, and 1,2,4,3λ^5-triazaphospholes **100c** and **100d**, respectively, in good yields. Adducts **100** formally result from a [4 + 1] cycloaddition. But actually a two-step mechanism is most likely involved: electrophilic attack of sulfur, selenium, phenyl azide, or diazo compound on the phosphorus lone pair, which is activated by the electron-rich nitrile imine moiety, leads to intermediates **101**, which undergo 1,5-electrocyclization[47] (Scheme 32). These reactions can be compared with the formation of 1,3,4-thiadiazoles and 1,3,4-triazoles from unstable *N*-thiocarbonyl-[85] and *N*-iminonitrile imines,[86] respectively.



Scheme 32. Formal [1 + 4] cycloaddition reactions of nitrile imine **46n**.

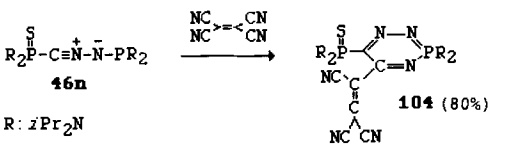
The four reagents used in the above reactions are known to react with the phosphorus lone pair and not with the nitrile imine moiety. In contrast, a dipolarophile such as dimethyl acetylenedicarboxylate could react both with the lone pair[87] and with the 1,3-dipole. In fact, the reaction of **46n** with this electron-poor alkyne affords the 1,2,3λ^5-diazaphosphinine **103** (Scheme 33).[52, 64a] Although heterocycle **103** formally results from a [4 + 2] cycloaddition process, it is likely that the first mechanistic step is the electrophilic attack of the alkyne on the phosphorus lone pair of **46n**, followed by the 1,6 ring closure of **102**. This is the first example of 1,6-electrocyclization involving nitrile imines.

A similar reaction has been observed between nitrile imine **46n** and tetracyanoethylene giving rise to **104**.[52, 64a] Although



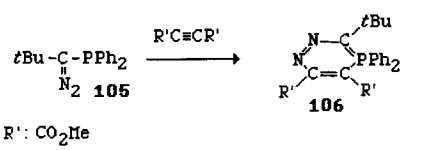
Scheme 33. Formal [2 + 4] cycloaddition reaction of nitrile imine **46n** with dimethyl acetylenedicarboxylate.

addition and cycloaddition reactions of tetracyanoethylene usually proceed with high selectivity at the C–C double bond,[88] in this case the reaction involves the nitrile group[89] (Scheme 34).



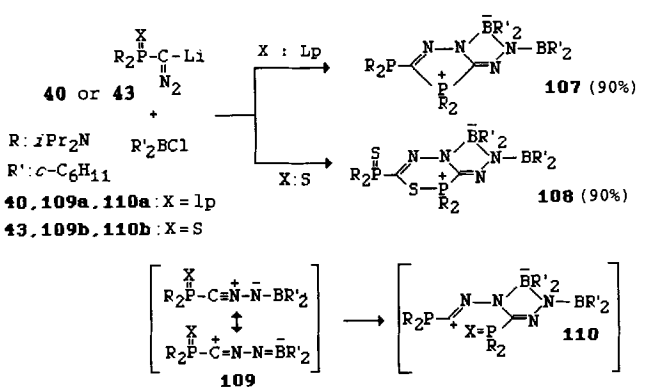
Scheme 34. Formal [2 + 4] cycloaddition reaction of nitrile imine **46n** with tetracyanoethylene.

Recently Regitz et al. reported a formal [2 + 4] cycloaddition reaction involving phosphinodiazomethane **105** (Scheme 35).[90] All these reactions are of synthetic interest, since the resulting heterocycles **100**, **103**, **104**, and **106** are hardly available by classical routes.



Scheme 35. Formal [2 + 4] cycloaddition reaction of phosphanyldiazomethane **105**.

An atypical dimerization of nitrile imines involving the *N*-heteroatom substituent is noteworthy.[91] The reactions of the lithium salts of phosphinodiazomethane and thiophosphinoyldiazomethane, **40** and **43**, respectively, with chlorodicyclohexylborane lead to bicyclic compounds **107** and **108**, respectively (Scheme 36). It is quite likely that the first step of these



Scheme 36. Atypical dimerization of nitrile imines **109**.

reactions is the formation of nitrile imines **109a** and **109b**, which possess a formal boron–nitrogen double bond. Thus, the CNN unit of one molecule can react as a 1,3-dipole with the boron–nitrogen double bond of a second molecule giving intermediates **110a** and **110b** having a carbocation center, which react with the phosphorus or sulfur atoms to give the observed products.

Lastly, as already mentioned Section 4.3, the heteroatom substituents can be employed in the preparation of other stable nitrile imines.

7. Rearrangements of Nitrile Imines

In this review only the rearrangements of the nitrile imine skeleton, and not those involving the substituents bonded to the carbon or nitrogen termini, will be discussed.

Theoretical studies on the relative stabilities of the various possible ground state isomers of CH_2N_2 have been published.[92] Interestingly, 1*H*-diazirine is found to be of only slightly higher energy than the parent formonitrile imine **2n**: +14.2 kcal mol^{-1} at the HF/6-31G level,[92c] +8.4 kcal mol^{-1} at the HF/3-21G* level (with electron correlation),[92b] and +1.1 kcal mol^{-1} at the G2(MP2) level[92d]. Diazomethane is significantly more stable, and carbodiimide is the most stable of these isomers (cyanamide is the global minimum) (Fig. 4).

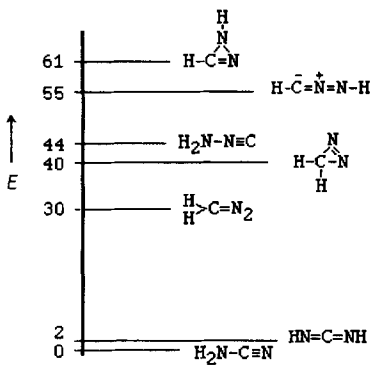
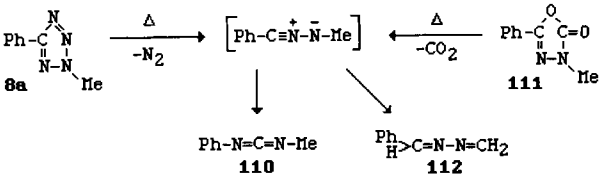


Fig. 4. Calculated relative energies [kcal mol^{-1}] of H_2CN_2 isomers (G2(MP2) level [92d]).

Therefore, considering the thermodynamics, it is not surprising that nitrile imines rearrange to diazo compounds and carbodiimides. The nitrile imine → carbodiimide rearrangement was postulated to proceed through a 1*H*-diazirine intermediate, which by ring-opening would lead to an imidoylnitrene;[42] the Wolff-type rearrangement of imidoylnitrenes to carbodiimides is well known.[42, 93] Ab initio calculations indicate high energy barriers for the ring closure of nitrile imine to 1*H*-diazirine and for the 1,3-hydrogen shift leading to diazomethane (Fig. 4).[92b, d] Nevertheless, there is some experimental evidence for such rearrangements.

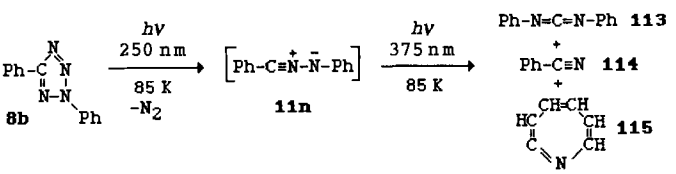
7.1. Rearrangements of Nitrile Imines to Carbodiimides and N–N Bond Cleavage

The thermal rearrangement of nitrile imines to carbodiimides (both systems are isoelectronic to those in the nitrile oxide → isocyanate rearrangement)[93] has been postulated to explain the formation of methylphenylcarbodiimide (**110**) on flash vacuum thermolysis of 2-methyl-5-phenyltetrazole (**8a**) or 3-methyl-5-phenyl-1,3,4-oxadiazol-2(3*H*)-one (**111**) (Scheme 37).[42] The yield of this reaction is rather low (1–8%) but can be increased when the reaction is conducted photochemically.[69] In the thermal reaction, azine **112**, which results from a 1,4-hydrogen shift, was also obtained in 10% yield.[42]



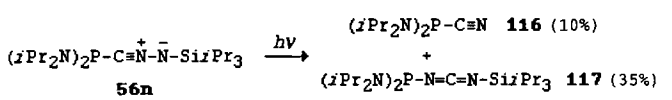
Scheme 37. Thermal rearrangement of transient *N*-methyl-*C*-phenylnitrile imine.

In a very elegant paper[37] Holm et al. demonstrated the photochemical rearrangement of a nitrile imine to a carbodiimide. Diphenylnitrile imine (**11n**) was generated in PVC matrix at 85 K by photolysis of 2,5-diphenyltetrazole (**8b**) at 250 nm. **11n** was characterized by IR and UV spectroscopy (ν = 2228 cm^{-1}; λ_{max} = 378 nm). Continued irradiation (λ = 370 nm) of nitrile imine **11n** led to diphenylcarbodiimide (**113**), along with benzonitrile (**114**) and 1-aza-1,2,4,6-cycloheptatetraene (**115**) (Scheme 38). The structures **11n** and **113**–**115** were confirmed by ^{15}N-labeling experiments. Compound **115** originates from rearrangement of the initially formed phenyl nitrene.[73] Thus, the rearrangement of the nitrile imine to carbodiimide competes with nitrogen–nitrogen bond cleavage.



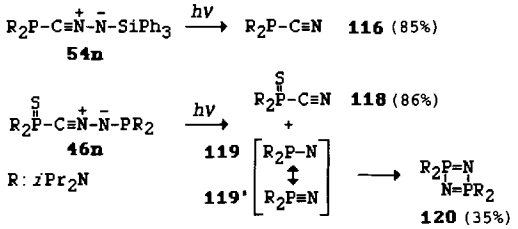
Scheme 38. Photochemical rearrangement of diphenylnitrile imine **11n**.

For nitrile imines that are stable at room temperature, competing reactions of this type have only been observed on irradiation of *C*-[bis(diisopropylamino)phosphino]-*N*-triisopropylsilylnitrile imine (**56n**), which led to phosphinonitrile **116** and carbodiimide **117** (Scheme 39).[54]



Scheme 39. Photochemical rearrangement of nitrile imine **56n**.

All the other photolyses reported with stable nitrile imines unequivocally led to carbodiimides, except in the cases of *C*-phosphino-*N*-triphenylsilylnitrile imine **54n**[54] and *N*-phosphino-*C*-thiophosphinoylnitrile imine **46n**[49] which underwent nitrogen–nitrogen bond cleavage. The photolysis of nitrile imine **54n** gave phosphinonitrile **116** in 85% yield along with several



Scheme 40. Photochemical rearrangement of nitrile imines **54n** and **46n**.

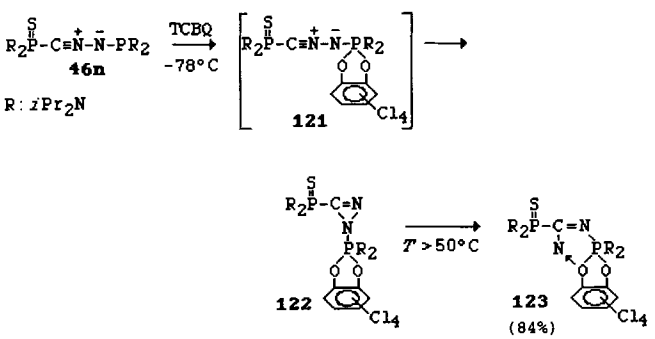
silylated products which were not isolated (Scheme 40). Irradiation of **46n** at 300 nm led to thiophosphinoylnitrile **118** and to phosphinonitrene **119** which dimerizes into the cyclodiphosphazene **120**. It has already been shown that **119**, generated by photolysis of bis(diisopropylamino)phosphanyl-azide, behaves as "phosphonitrile" **119'**,[94] and dimerizes to give the four-membered ring compound **120**[95] (Scheme 40).

The photochemical rearrangement of nitrile imines to carbodiimides seems to be rather general. As indicated in Scheme 41, the reaction is possible for compounds with a wide variety of substituents at the carbon and nitrogen termini.[54, 58, 63, 69]

X	Y	$\tilde{\nu}$ [cm^{-1}]
$(i\mathrm{Pr}_2\mathrm{N})_2\mathrm{P(S)}$	$\mathrm{Si}i\mathrm{Pr}_3$	2200
$(i\mathrm{Pr}_2\mathrm{N})_2\mathrm{P(S)}$	$\mathrm{B(N}i\mathrm{Pr}_2)_2$	2200
$(i\mathrm{Pr}_2\mathrm{N})_2\mathrm{P}$	$\mathrm{B(N}i\mathrm{Pr}_2)_2$	2210
$i\mathrm{Pr}_3\mathrm{Si}$	$\mathrm{Si}i\mathrm{Pr}_3$	2200
$i\mathrm{Pr}_3\mathrm{Si}$	$\mathrm{B(N}i\mathrm{Pr}_2)_2$	2200
$i\mathrm{Pr}_3\mathrm{Si}$	GeRR'R"	2165
RR'R"Ge	GeRR'R"	2106
$(i\mathrm{Pr}_2\mathrm{N})_2\mathrm{B}$	$\mathrm{B(N}i\mathrm{Pr}_2)_2$	2252

Scheme 41. Photochemical rearrangement of nitrile imines into carbodiimides. Wavenumbers of IR absorption bands of the carbodiimides are given in the right column.

As mentioned above, the nitrile imine → carbodiimide rearrangement was postulated to proceed through an 1*H*-diazirine intermediate which leads to an imidoylnitrene by ring opening.[42] Interestingly, one piece of evidence for this mechanism has been reported.[96] Addition of tetrachloro-*o*-benzoquinone to nitrile imine **46n** led to compound **123**, which was isolated after workup (Scheme 42). This compound can be regarded as an imidoylnitrene stabilized by donor–acceptor interaction with an oxygen atom (the stabilization of nitrenes by

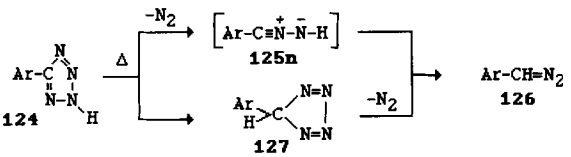


Scheme 42. Evidence for the rearrangement nitrile imine → isodiazirine → imidoylnitrene.

coordination at nitrogen is known).[97] Moreover, when the reaction was monitored by NMR spectroscopy at −50 °C, an intermediate tentatively assigned as isodiazirine **122** was detected. Many questions remain concerning the factors influencing the photochemical reactions of nitrile imines.

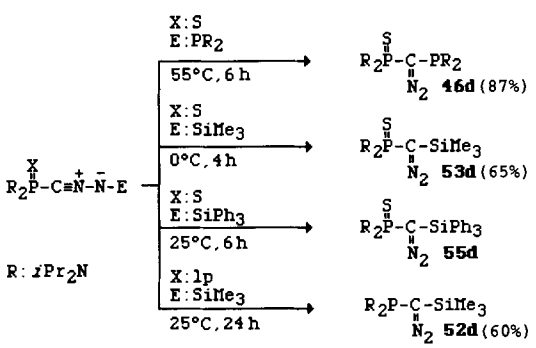
7.2. Rearrangement of Nitrile Imines to Diazo Compounds

The possible existence of a diazomethane–nitrile imine equilibrium was described in Section 2 [Eq. (1)]. Nitrile imine → diazoalkane rearrangements have been postulated to explain the products obtained in the thermolysis of potential nitrile imine precursors.[98, 99] However, the nitrile imines were never observed, and apart from one case[98] the resulting diazo compounds were also not stable under the experimental conditions. Moreover, even the thermolysis of 5-aryltetrazole **124**[98] leading to the isolable diazo compound **126** may proceed by an alternative mechanism that bypasses nitrile imine **125n** and involves instead the tautomeric 5*H*-tetrazole **127** (Scheme 43). Recent ab initio calculations support the latter mechanism.[100]



Scheme 43. Formation of diazo derivatives from 5-aryltetrazoles.

The first definitive proof for the nitrile imine → diazoalkane rearrangement was reported in 1988.[50] Indeed, nitrile imine **46n**, which was fully characterized (including single-crystal X-ray diffraction), rearranged on heating in chloroform (55 °C, 6 h) to the stable phosphino(thiophosphinoyl)diazomethane **46d** (Scheme 44). However, this rearrangement does not appear

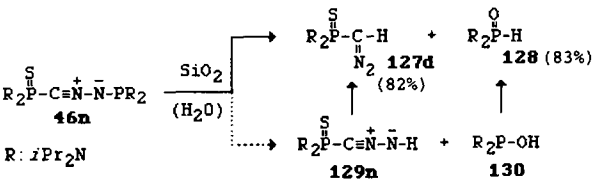


Scheme 44. Rearrangement of stable nitrile imines into diazo compounds.

to be general. So far, only three other examples have been published, and all of them involve *C*-phosphorus-*N*-silyl-substituted nitrile imines.[54]

For the sake of comprehensiveness, the formation of bis(diisopropylamino)thiophosphinoyldiazomethane (**127d**) and phosphane oxide **128** from hydrolysis of nitrile imine **46n** should

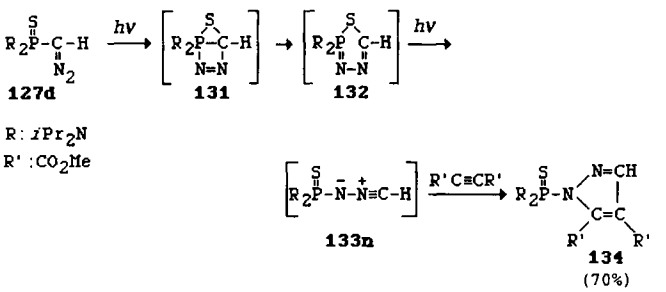
be mentioned. This reaction takes place on silica gel and has been rationalized in terms of a nitrile imine → diazoalkane rearrangement.[50] The first step could be the hydrolysis of the phosphorus–nitrogen bond leading to the *N*-unsubstituted nitrile imine **129n** and the hydroxyphosphane **130**, followed by isomerization to **127d** and **128**, respectively (Scheme 45).



Scheme 45. Hydrolysis of nitrile imine **46n**.

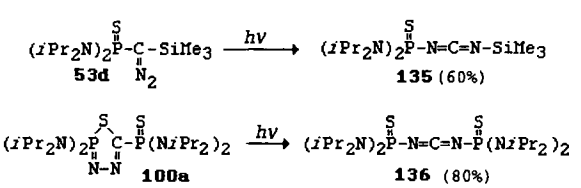
The factors governing the rearrangement of nitrile imines to diazo compounds are not understood. At the most, it seems that the larger the substitutent on the nitrogen atom, the slower the rearrangement.

The reverse rearrangement of diazo compounds to nitrile imines has been postulated to explain the formation of *N*-(thiophosphinoyl)pyrazole **134** from the photolysis of thiophosphinoyldiazomethane **127d** in the presence of dimethyl acetylenedicarboxylate.[101] Pyrazole **134** is the expected product of the [2 + 3] cycloaddition of nitrile imine **133n** and the alkyne, and it could well be that the diazo → nitrile imine rearrangement proceeds via **131** and **132** (Scheme 46). In other words, this rearrangement would be assisted by the presence of the phosphorus–sulfur double bond.



Scheme 46. Example of a diazo compound → nitrile imine rearrangement.

This mechanistic hypothesis is corroborated by the formation of carbodiimides **135** and **136** on photolysis of (trimethylsilyl)(thiophosphinoyl)diazomethane **53d** and 1,3,4,2λ⁵-thiadiazaphosphole **100a**, respectively.[101] In fact, these reactions could be examples of the rearrangement of a diazoalkane to a nitrile imine to a carbodiimide (Scheme 47).



Scheme 47. Rearrangements of diazo compound **53d** and thiadiazaphosphole **100a** to carbodiimides.

Numerous questions remain concerning mechanisms of the rearrangements of the various isomers of nitrile imine. One of the most fundamental ones is whether they are intra- or intermolecular. Future work in our laboratories will address such questions.

8. Conclusion and Outlook

Nitrile imines were only accessible as reactive intermediates until a few years ago, and since then many stable compounds of this type have been prepared. Some of them are solids, others distillable liquids. Most of the stable nitrile imines have been prepared by nonclassical routes, and these compounds are now available in multigram quantities. Their stabilization is determined largely by steric interactions. For this reason, the isolable nitrile imines tend to be less reactive. They are also less ambiphilic than their transient counterparts; that is, they are usually nucleophilic, with the exception of the positively charged *N*-phosphonionitrile imine **78n**, which is strongly electrophilic.

The question of concertedness in 1,3-dipolar cycloaddition reactions was previously much debated. The addition of the stable nitrile imine **46n** to dimethyl maleate has been shown to be nonconcerted. Examples of nonconcerted cycloaddition of other 1,3-dipoles have been reported previously.

A striking feature of stable nitrile imines is the possibility of reactions at the periphery of the CNN skeleton, which allow the synthesis of other nitrile imines. Reactions involving the nitrile imine moiety and a heteroatom substituent are also noteworthy.

X-ray crystal structures have now been obtained for several stable nitrile imines. While all of these compounds possess nonplanar, allenic structures, electron-withdrawing substituents promote a partial linearization in the direction of the propargylic structure. This is the case of the *C,N*-bis(boryl) compound **85n** and the *N*-phosphonio derivative **78n**. These unusual structures have generated a renewed interest in high-level ab initio calculations of nitrile imines. While calculations at the Hartree–Fock level indicate that the allenic and the propargylic forms can coexist as discrete minima, incorporation of electron correlation with Møller–Plesset perturbation theory leads to the prediction that only the allenic form should be stable. However, substituents on the CNN framework can strongly modify the geometry. The agreement between experimentally determined structures and those calculated for model compounds is excellent. These results will prompt further high-level calculations of structures and energies for nitrile imines.

The variability of structure between the allenic and propargylic extremes makes a rigorous interpretation of the infrared spectra difficult. Both theoretical and experimental work is needed here, in particular regarding the hitherto elusive *C*-arylnitrile imines.

Another area of interplay theory and experiment concerns the rearrangement of nitrile imines to diazo compounds and to carbodiimides. Theory predicts a very high activation energy both for the 1,3-hydrogen shift (by either concerted or homolytic pathways) and for the ring closure to the 1 *H*-diazirine intermediate. However, there are several examples of such rearrangements taking place under mild conditions. Further studies of their mechanisms are highly desirable.

The story of nitrile imines clearly illustrates that heteroatoms are wonderful tools for stabilizing highly reactive species. The variety of easily available heteroatom substituents with disparate electronic effects allows a ready understanding of the factors that influence the stability of the compounds. This simplifies the choice of the right organic substituents required for the synthesis of purely organic, stable species.

It is now clear that nitrile imines are no longer laboratory curiosities; they are easily available and storable, and their use as building blocks for organic synthesis or for polymeric materials is anticipated.

We would like to thank the Centre National de la Recherche Scientifique (CNRS) for a Visitor's Fellowship (to C. W.) which made this collaboration possible. Thanks are due also to our coworkers A. Baceiredo, R. Réau, G. Sicard, M. Granier, F. Castan, M. P. Arthur, K. Horchler von Locquenghien, M. Soleilhavoup, and G. Veneziani in Toulouse, and G. G. Qiao, R. Leung-Toung, and M. W. Wong in Brisbane, without whom this work would never have come to fruition. The financial support of the experimental work in Toulouse by the CNRS and Pierre Fabre Médicaments is greatfully acknowledged.

Received: January 14, 1993 [A 932 IE]
German version: *Angew. Chem.* **1994**, *106*, 549

[1] a) R. Huisgen, M. Seidel, J. Sauer, J. W. McFarland, G. Wallbillich, *J. Org. Chem.* **1959**, *24*, 892; b) R. Huisgen, M. Seidel, G. Wallbillich, H. Knupfer, *Tetrahedron* **1962**, *17*, 3.
[2] R. Huisgen, *Angew. Chem.* **1963**, *27*, 604; *Angew. Chem. Int. Ed. Engl.* **1963**, *2*, 565.
[3] R. Huisgen, *Angew. Chem.* **1963**, *27*, 741; *Angew. Chem. Int. Ed. Engl.* **1963**, *2*, 633.
[4] R. Huisgen, *J. Org. Chem.* **1976**, *41*, 403.
[5] R. Huisgen in *1,3-Dipolar Cycloaddition Chemistry* (Ed.: A. Padwa), Wiley, New York, **1984**, Chapter 1, p. 1 ff.
[6] P. Caramella, P. Grünanger in *1,3-Dipolar Cycloaddition Chemistry* (Ed.: A. Padwa), Wiley, New York, **1984**, Chapter 3, p. 291 ff.
[7] R. N. Butler, F. L. Scott, *Chem. Ind. (London)* **1970**, 1216; Yu. P. Kitaev, B. I. Buzykin, *Russ. Chem. Rev. (Engl. Transl.)* **1972**, *41*, 495; A. S. Shawali, C. Parkanyi, *J. Heterocycl. Chem.* **1980**, *17*, 833.
[8] R. A. Firestone, *J. Org. Chem.* **1968**, *33*, 2285; *ibid.* **1972**, *37*, 2181; *Tetrahedron* **1977**, *33*, 3009.
[9] P. Caramella, K. N. Houk, *J. Am. Chem. Soc.* **1976**, *98*, 6397; P. Caramella, R. W. Gandour, J. A. Hall, C. G. Deville, K. N. Houk, *ibid.* **1977**, *99*, 385.
[10] Cf. also P. C. Hiberty, C. Leforestier, *J. Am. Chem. Soc.* **1978**, *100*, 2012; P. C. Hiberty, C. Ohanessian, *ibid.* **1982**, *104*, 66; C. Thomson, C. Glidewell, *J. Comput. Chem.* **1983**, *4*, 1.
[11] K. N. Houk, K. Yamaguchi in *1,3-Dipolar Cycloaddition Chemistry* (Ed.: A. Padwa), Wiley, New York, **1984**, Chapter 13, p. 407 ff.
[12] M. W. Wong, C. Wentrup, *J. Am. Chem. Soc.* **1993**, *115*, 7743.
[13] E. Müller, W. Kreutzmann, *Justus Liebigs Ann. Chem.* **1934**, *512*, 264.
[14] E. Müller, P. Kästner, R. Beutler, W. Rundel, H. Suhr, B. Zeeh, *Justus Liebigs Ann. Chem.* **1968**, *713*, 87.
[15] For a definitive structure determination of isocyanamide H_2N-NC see E. Schäfer, M. Winnewisser, *Ber. Bunsenges. Phys. Chem.* **1982**, *86*, 780.
[16] J.-P. Anselme, *J. Chem. Educ.* **1977**, *54*, 296.
[17] a) An IR band at 2169 cm^{-1} obtained on photolysis of diazomethane at 4 K was tentatively ascribed to HCNNH: J. F. Ogilvie, *Photochem. Photobiol.* **1966**, *9*, 65; cf. J. F. Ogilvie, *J. Mol. Spectrosc.* **1969**, *3*, 513. However, this band was possibly due to carbodiimide HN=C=NH, which absorbs at 2097 and 2169 cm^{-1} in Ar matrix [17b]. Diazomethane itself absorbs at 2099 cm^{-1} at 4 K and thus would mask the band at 2097 cm^{-1}; b) S. T. King, J. H. Strope, *J. Chem. Phys.* **1971**, *54*, 1289. For the gas-phase IR spectrum of HN=C=NH (2105 and ca. 2177 cm^{-1}) see also M. Birk, M. Winnewisser, *Chem. Phys. Lett.* **1986**, *123*, 386; c) For earlier suggestions of the formation of formonitrile imine HCNNH in photolyses of diazomethane, see D. E. Milligan, G. C. Pimentel, *J. Chem. Phys.* **1958**, *29*, 1405; I. M. Mills, H. W. Thompson, *Trans. Faraday Soc.* **1954**, *50*, 1270. However, the presence of any tautomer was discounted by G. B. Moore, G. C. Pimentel, *J. Chem. Phys.* **1964**, *40*, 329, 342.
[18] W. Beck, K. Feldl, *Angew. Chem.* **1966**, *78*, 746; *Angew. Chem. Int. Ed. Engl.* **1966**, *5*, 722; W. Beck, P. Swoboda, K. Feldl, R. S. Tobias, *Chem. Ber.* **1971**, *104*, 533. For the history of fulminic acid and its structure, see M. Winnewisser, B. P. Winnewisser, *Chem. Listy* **1976**, *70*, 785.
[19] R. Fusco, R. Justoni, *Gazz. Chim. Ital.* **1937**, *67*, 3; R. Fusco, *Pyrazoles* in *The Chemistry of Heterocyclic Compounds, Vol. 22* (Ed.: A. Weissberger), Wiley, New York **1967**, pp. 1–176.
[20] R. Fusco, R. Romani, *Gazz. Chim. Ital.* **1946**, *76*, 439; **1948**, *78*, 342.
[21] a) E. Bamberger, J. Grob, *Ber. Dtsch. Chem. Ges.* **1901**, *34*, 523; b) "The sodium salt of the isonitro compound decomposes to nitrile and the molecular residue $C_6H_5-C-N=N-C_6H_5$, which immediately polymerizes to the tetrazoline derivative".
[22] J. S. Clovis, W. Fliege, R. Huisgen, *Chem. Ber.* **1983**, *116*, 3062.
[23] R. Huisgen, J. Sauer, M. Seidel, *Chem. Ber.* **1961**, *94*, 2503.
[24] R. Huisgen, J. Sauer, M. Seidel, *Justus Liebigs Ann. Chem.* **1962**, *654*, 146.
[25] P. Scheiner, J. F. Dinda, *Tetrahedron* **1970**, *26*, 2619.
[26] M. Märky, H. Meier, A. Wunderli, H. Heimgartner, H. Schmid, H.-J. Hansen, *Helv. Chim. Acta* **1978**, *61*, 1477.
[27] M. Ruccia, N. Vivona, *Chim. Ind. (Milan)* **1966**, *48*, 147.
[28] H. Meier, W. Heinzelmann, H. Heimgartner, *Chimia* **1980**, *34*, 506. See also H. Meier, H. Heimgartner, *Helv. Chim. Acta* **1977**, *60*, 3035.
[29] C. Grundmann, K. Flory, *Justus Liebigs Ann. Chem.* **1969**, *721*, 91.
[30] W. A. F. Gladstone, *J. Chem. Soc. Chem. Commun.* **1969**, 179; W. A. F. Gladstone, J. B. Aylward, R. O. C. Norman, *J. Chem. Soc. C* **1969**, 2587.
[31] a) Y. Huseya, A. Chinune, M. Ohta, *Bull. Chem. Soc. Jpn.* **1971**, *44*, 1667; *ibid.* **1972**, *45*, 3203; b) C. S. Angadiyavar, M. V. George, *J. Org. Chem.* **1971**, *36*, 1589; c) M. Märky, H.-J. Hansen, H. Schmid, *Helv. Chim. Acta* **1971**, *54*, 1275.
[32] a) J. Sauer, K. K. Mayer, *Tetrahedron Lett.* **1968**, 32; b) see also G. Westphal, D. Schlangstedt, *Z. Chem.* **1979**, *19*, 217.
[33] H. Reimlinger, J. J. M. Vanderwalle, G. S. D. King, W. R. F. Lingier, R. Merenyi, *Chem. Ber.* **1970**, *103*, 1918.
[34] J. H. Boyer, P. S. Ellis, *J. Chem. Soc. Perkin Trans 1* **1979**, 483; J. H. Boyer, P. J. A. Frints, *J. Heterocycl. Chem.* **1970**, *7*, 71.
[35] J. W. Lown, B. E. Landberg, *Can. J. Chem.* **1975**, *53*, 3782.
[36] H. Meier, W. Heinzelmann, H. Heimgartner, *Chimia* **1980**, *34*, 504.
[37] N. H. Toubro, A. Holm, *J. Am. Chem. Soc.* **1980**, *102*, 2093.
[38] a) A. Padwa, P. H. J. Carlsen, *J. Am. Chem. Soc.* **1976**, *98*, 2006; **1979**, *99*, 1514; b) J. Fischer, W. Steglich, *Angew. Chem.* **1979**, *91*, 168; *Angew. Chem. Int. Ed. Engl.* **1979**, *18*, 167; c) A. Padwa in *1,3-Dipolar Cycloaddition Chemistry* (Ed.: A. Padwa), Wiley, New York, **1984**, Chapter 12, pp. 277–406; d) A. Padwa, *Angew. Chem.* **1976**, *88*, 131; *Angew. Chem. Int. Ed. Engl.*, **1976**, *15*, 123.
[39] C. Wentrup, A. Damerius, W. Reichen, *J. Org. Chem.* **1978**, *43*, 2037.
[40] C. Wentrup, J. Benedikt, *J. Org. Chem.* **1980**, *45*, 1407.
[41] W. Reichen, *Helv. Chim. Acta* **1976**, *59*, 1636.
[42] S. Fischer, C. Wentrup, *J. Chem. Soc. Chem. Commun.* **1980**, 502.
[43] C. Wentrup, S. Fischer, A. Maquestiau, R. Flammang, *Angew. Chem.* **1985**, *97*, 74; *Angew. Chem. Int. Ed. Engl.* **1985**, *24*, 56.
[44] H. Bock, R. Dammel, S. Fischer, C. Wentrup, *Tetrahedron Lett.* **1987**, *28*, 617.
[45] A. Baceiredo, A. Igau, G. Bertrand, M. J. Menu, Y. Dartiguenave, J. J. Bonnet, *J. Am. Chem. Soc.* **1986**, *108*, 7868.
[46] G. Sicard, A. Baceiredo, G. Bertrand, *J. Am. Chem. Soc.* **1988**, *110*, 2663.
[47] For a review see, for example, E.C. Taylor, I. J. Turchi, *Chem. Rev.* **1979**, *79*, 181.
[48] S. Patai, *The Chemistry of Diazonium and Diazo Groups*, Wiley, New York, **1978**; M. Regitz, *Diazoalkanes*, Thieme, Stuttgart, **1977**; M. Regitz, G. Maas, *Diazo Compounds, Properties and Synthesis*, Academic Press, Orlando, FL, USA, **1986**.
[49] M. Granier, A. Baceiredo, Y. Dartiguenave, M. J. Menu, G. Bertrand, *J. Am. Chem. Soc.* **1990**, *112*, 6277.
[50] M. Granier, A. Baceiredo, G. Bertrand, *Angew. Chem.* **1988**, *100*, 1397; *Angew. Chem. Int. Ed. Engl.* **1988**, *27*, 1350.
[51] A. Baceiredo, M. Granier, F. Castan, J. M. Sotiropoulos, G. Sicard, G. Bertrand, *Phosphorus Sulfur Silicon Relat. Elem.* **1990**, *49*, 131.
[52] F. Castan, M. Granier, T. A. Straw, A. Baceiredo, K. B. Dillon, G. Bertrand, *Chem. Ber.* **1991**, *124*, 1739.
[53] G. Bertrand, *Heteroat. Chem.* **1991**, *2*, 29.
[54] F. Castan, A. Baceiredo, D. Bigg, G. Bertrand, *J. Org. Chem.* **1991**, *56*, 1801.
[55] M. J. Menu, M. Dartiguenave, Y. Dartiguenave, J. J. Bonnet, G. Bertrand, A. Baceiredo, *J. Organomet. Chem.* **1989**, *372*, 201.
[56] R. Réau, G. Veneziani, G. Bertrand, *J. Am. Chem. Soc.* **1992**, *114*, 6059.
[57] F. Castan, A. Baceiredo, G. Bertrand, *Angew. Chem.* **1989**, *101*, 1253; *Angew. Chem. Int. Ed. Engl.* **1989**, *28*, 1250.
[58] M. P. Arthur, H. Goodwin, A. Baceiredo, K. B. Dillon, G. Bertrand, *Organometallics* **1991**, *10*, 3205.
[59] M. P. Arthur, A. Baceiredo, G. Bertrand, *J. Am. Chem. Soc.* **1991**, *113*, 5856.
[60] J. Lorberth, S. H. Shin, H. Donath, S. Wocadlo, W. Massa, *J. Organomet. Chem.* **1991**, *407*, 167; A. Fadini, E. Glozbach, P. Krommes, J. Lorberth, *ibid.* **1978**, *149*, 297.
[61] M. F. Lappert, J. Lorberth, J. S. Poland, *J. Chem. Soc. A* **1970**, 2954.
[62] R. Réau, G. Veneziani, F. Dahan, *Angew. Chem.* **1992**, *104*, 481; *Angew. Chem. Int. Ed. Engl.* **1992**, *31*, 439.

[63] C. Leue, P. Jutzi, R. Réau, G. Bertrand, unpublished results.
[64] a) M. Granier, A. Baceiredo, M. Nieger, G. Bertrand, *Angew. Chem.* **1990**, *102*, 1185; *Angew. Chem. Int. Ed. Engl.* **1990**, *29*, 1123; b) M. Granier, A. Baceiredo, G. Bertrand, V. Huch, M. Veith, *Inorg. Chem.* **1991**, *30*, 1161.
[65] F. Castan, A. Baceiredo, F. Dahan, N. Auner, G. Bertrand, *J. Chem. Soc. Chem. Commun.* **1992**, 1274.
[66] M. P. Arthur, A. Baceiredo, J. Fischer, A. De Cian, G. Bertrand, *Synthesis* **1992**, 43.
[67] N. Dubau, A. Baceiredo, F. Dahan, G. Bertrand, unpublished results.
[68] R. H. Hout, B. A. Levi, W. J. Hehre, *J. Comput. Chem.* **1982**, *3*, 234.
[69] G. G. Qiao, C. Wentrup, unpublished results.
[70] R. A. Evans, P. Lorencak, K. T. Ha, C. Wentrup, *J. Am. Chem. Soc.* **1991**, *113*, 7261, and references therein.
[71] M. Shiro, M. Yamakawa, T. Kubota, H. Koyama, *J. Chem. Soc. Chem. Commun.* **1968**, 1409; K. H. Bodenseh, K. Morgenstern, *Z. Naturforsch. A* **1970**, *25*, 150; M. Winnewisser, *Chem. Phys. Lett.* **1971**, *11*, 579.
[72] J. H. Teles, G. Maier, B. A. Hess, L. J. Schaad, M. Winnewisser, B. P. Winnewisser, *Chem. Ber.* **1989**, *122*, 753.
[73] O. L. Chapman, J.-P. LeRoux, *J. Am. Chem. Soc.* **1978**, *100*, 282.
[74] E. P. Janulis, S. R. Wilson, A. J. Arduengo, *Tetrahedron Lett.* **1984**, *25*, 405.
[75] A. J. Arduengo, private communication.
[76] C. Wentrup, S. Fischer, H.-M. Berstermann, M. Kuzaj, H. Lüerssen, K. Burger, *Angew. Chem.* **1986**, *98*, 99; *Angew. Chem. Int. Ed. Engl.* **1986**, *25*, 85.
[77] H.-J. Hansen, H. Heimgartner in *1,3-Dipolar Cycloaddition Chemistry* (Ed.: A. Padwa), Wiley, New York, **1984**, Chapter 2, pp. 177–290.
[78] K. Horchler von Locquenghien, R. Réau, G. Bertrand, *J. Chem. Soc. Chem. Commun.* **1991**, 1192.
[79] F. de Sarlo, A. Brandi, A. Guarna, N. Niccolai, *J. Magn. Reson.* **1982**, *50*, 64.
[80] R. Sustmann, *Pure Appl. Chem.* **1974**, *40*, 569.
[81] A. Eckell, R. Huisgen, R. Sustmann, G. Wallbillich, D. Grashey, E. Spindler, *Chem. Ber.* **1967**, *100*, 2192.
[82] R. Huisgen, G. Mloston, E. Langhals, *J. Am. Chem. Soc.* **1986**, *108*, 6401; *J. Org. Chem.* **1986**, *51*, 4085; R. Huisgen, E. Langhals, H. Nöth, *Tetrahedron Lett.* **1986**, *27*, 5475; G. Mloston, E. Langhals, R. Huisgen, *ibid.* **1989**, *30*, 5373.
[83] H. Quast, D. Regnat, E. M. Peters, K. Peters, H. G. von Schnering, *Angew. Chem.* **1990**, *102*, 724; *Angew. Chem. Int. Ed. Engl.* **1990**, *29*, 695.
[84] K. N. Houk, J. Sims, C. R. Watts, L. J. Luskus, *J. Am. Chem. Soc.* **1973**, *95*, 7301; K. N. Houk, J. Sims, R. E. Duke, R. W. Strozier, J. K. George, *ibid.* **1973**, *95*, 7287.
[85] R. Huisgen, H. J. Sturm, M. Seidel, *Chem. Ber.* **1961**, *94*, 1555.
[86] R. Huisgen, J. Sauer, M. Seidel, *Chem. Ber.* **1960**, *93*, 2885; H. Reimlinger, J. J. M. Vandewalle, G. S. D. King, W. R. F. Lingier, R. Merenyi, *ibid.* **1970**, *103*, 1918; H. Reimlinger, J. J. M. Vandewalle, W. R. F. Lingier, *ibid.* **1970**, *103*, 1960; M. S. Gibson, *Tetrahedron* **1963**, *19*, 1587.
[87] R. Luckenbach, *Dynamic Stereochemistry of Pentacoordinated Phosphorus and Related Elements*, Thieme, Stuttgart, **1973**.
[88] For a review of cycloaddition reactions of tetracyanoethylene see, for example, A. J. Fatiadi, *Synthesis* **1987**, 749.
[89] Very few examples of [3 + 2] and [4 + 2] cycloaddition reactions with the nitrile group of tetracyanoethylene have been reported: J. E. Franz, R. K. Howe, H. K. Pearl, *J. Org. Chem.* **1976**, *41*, 620; M. Brown, R. E. Benson, *ibid.* **1966**, *31*, 3849; K. Burger, H. Schickaneder, M. Prinzel, *Liebigs Ann. Chem.* **1976**, 30; K. Burger, H. Goth, *Angew. Chem.* **1980**, *92*, 836; *Angew. Chem. Int. Ed. Engl.* **1980**, *19*, 810; K. Burger, H. Goth, W. Schöntag, J. Firl, *Tetrahedron* **1982**, *38*, 287.
[90] T. Facklam, O. Wagner, H. Heydt, M. Regitz, *Angew. Chem.* **1990**, *102*, 316; *Angew. Chem. Int. Ed. Engl.* **1990**, *29*, 314.
[91] N. Dubau, A. Baceiredo, F. Dahan, G. Bertrand, unpublished results.
[92] a) C. Thomson, C. Glidewell, *J. Comput. Chem.* **1983**, *4*, 1; b) C. Guimon, S. Khayar, F. Gracian, M. Begtrup, G. Pfister-Guillouzo, *Chem. Phys.* **1989**, *138*, 159; c) J. B. Moffat, *J. Mol. Struct.* **1979**, *52*, 275; d) R. Leung-Toung, M. W. Wong, C. Wentrup, unpublished results.
[93] For a review, see C. Wentrup, *Adv. Heterocycl. Chem.* **1981**, *28*, 231.
[94] G. Sicard, A. Baceiredo, G. Bertrand, J. P. Majoral, *Angew. Chem.* **1984**, *96*, 450; *Angew. Chem. Int. Ed. Engl.* **1984**, *23*, 459.
[95] A. Baceiredo, G. Bertrand, J. P. Majoral, G. Sicard, J. Jaud, J. Galy, *J. Am. Chem. Soc.* **1984**, *106*, 6088; A. Baceiredo, G. Bertrand, J. P. Majoral, F. El Anba, G. Manuel, *ibid.* **1985**, *107*, 3945.
[96] M. Granier, A. Baceiredo, H. Grützmacher, H. Pritzkow, G. Bertrand, *Angew. Chem.* **1990**, *102*, 671; *Angew. Chem. Int. Ed. Engl.* **1990**, *29*, 659.
[97] P. A. S. Smith in *Azides and Nitrenes* (Ed.: E. F. V. Scriven), Academic Press, London **1984**.
[98] C. Wentrup, *Helv. Chim. Acta* **1978**, *61*, 1755.
[99] A. Padwa, T. Caruso, D. Plache, *J. Chem. Soc. Chem. Commun.* **1980**, 1229; A. Padwa, T. Caruso, S. Nahm, *J. Org. Chem.* **1980**, *45*, 4065; A. Padwa, T. Caruso, S. Nahm, A. Rodriguez, *J. Am. Chem. Soc.* **1982**, *104*, 2865.
[100] M. W. Wong, R. Leung-Toung, C. Wentrup, *J. Am. Chem. Soc.* **1993**, *115*, 2465.
[101] M. Soleilhavoup, A. Baceiredo, F. Dahan, G. Bertrand, *Inorg. Chem.* **1992**, *31*, 1500.

Just what does a referee system achieve?

Regular readers of "Angewandte" are well aware that Dr. Hans-Dieter Daniel has researched this question using *Angewandte Chemie* as example. The preliminary results were presented in a communication on this topic (Issue 2/93). Now the complete analysis by Daniel is available in book form: "The Guardians of Science: Fairness and Reliability in Peer Review" by H.-D. Daniel, foreword by H. Nöth (VCH, Weinheim, 1993, ISBN 3-527-29041-9, DM 78.—).

Novel Carbon Compounds with "Naked" C_n Units

Heinrich Lang*

A new class of compounds interesting in view of their new material properties[1] and as model systems for surface carbides in heterogeneous catalysis[2, 3] has become significant: compounds in which linear carbon chains C_n ($n = 1-5$) bridge different organometallic building blocks. Whereas compounds with "naked" C_n units ($n = 1, 2, 4$) and identical terminal metal complex fragments have already been well studied,[3] complexes with C_n bridges ($n = 1-5$) which link different transition metal complex building blocks have only recently become accessible.[1e, 3-18]

With regard to the synthesis of complexes with C_n bridges a formal classification of these compounds into those with an even number of C_{2n} ($n = 1, 2, \ldots$) bridges and those with an odd number of C_{2n+1} ($n = 0, 1, 2, \ldots$) bridges is possible.

Transition Metal Complexes with C_{2n+1} Units ($n = 0, 1, 2$)

C_1 Bridges: Organometallic compounds with a single carbon atom between two different metal atoms are of interest as model systems for surface carbides.[1e, 2-5] The two-coordinate carbon atom may be part of a 1,3-dimetallaallene system as in **1**[3, 4] or part of a C-metalated carbyne complex (**2**).[5]

Whereas the synthesis, the reaction behavior, and the structural features of 1,3-dimetallaallenes of the higher homologues of carbon have been well-studied,[19-22] only few examples of isolated and structurally characterized carbon compounds such as **1** are known.[3, 4] One of these compounds is the 1,3-dimetallaallene **1a** synthesized by W. Beck et al., which contains the shortest metal–carbon bond (Fe–C: 161 pm) known so far.[4] Compound **1a** was obtained by the reaction of the dichlorocarbene complex $[(tpp)Fe{=}CCl_2]$ (tpp = tetraphenylporphyrinate) with $[Re(CO)_5]^-$. The extension of

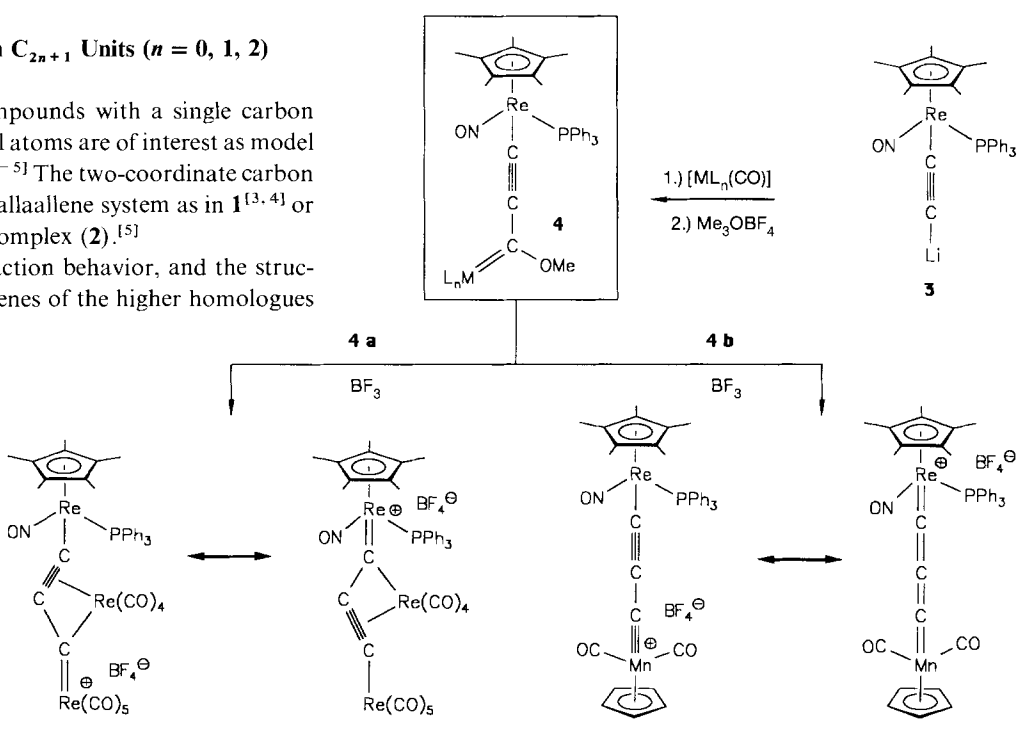
$[(tpp)Fe{=}C{=}ML_n]$ $[L_nM{\equiv}C{-}M'L_n]$

1 **2**

1a: $ML_n = Re_2(CO)_9$ [4]
1b: $ML_n = Mn_2(CO)_9$ [3]
1c: $ML_n = Cr(CO)_5$ [3]
1d: $ML_n = Fe(CO)_4$ [3]
2a: $ML_n = HB(pz)_3(CO)_2Mo$; $M'L_n = FeCp(CO)_2$ [5a]
2b: $ML_n = HB(pz)_3(CO)_2Mo$; $M'L_n = PtBr(PPh_3)_2$ [5b]
2c: $ML_n = (Me_3CO)_3W$; $M'L_n = RuCp(CO)_2$ [5c]

this synthetic method to the carbonyl metalates $[Mn(CO)_5]^-$, $[Cr(CO)_5]^{2-}$, and $[Fe(CO)_4]^{2-}$ leads to the compounds **1b–d**.[3]

The complex **2a** can be prepared by nucleophilic substitution of $[\{HB(pz)_3\}(CO)_2Mo{\equiv}CCl]$ (pz = 3,5-dimethylpyrazolyl) with $K[FeCp(CO)_2]$;[5a] **2b** is formed by the reaction of the analogous bromocarbyne with "$Pt(PPh_3)_2$".[3, 5b] A particularly elegant synthetic method makes use of the alkyne-analogous reactivity of $[(Me_3CO)_3W{\equiv}CEt]$ which in the metathesis with the alkyne complex $[Cp(CO)_2Ru{-}C{\equiv}CMe]$ affords the C-metalated carbyne complex **2c**.[5c]



5a **5b** **6a** **6b**

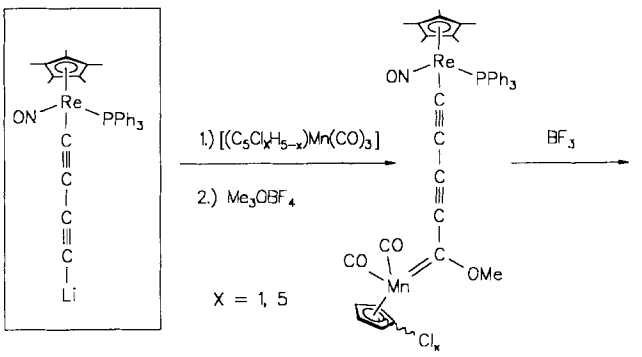
Scheme 1. **4a**: $ML_n = Re(CO)_4Re(CO)_5$; **4b**: $ML_n = CpMn(CO)_2$; **4c**: $ML_n = W(CO)_5$; **4d**: $ML_n = Fe(CO)_4$.

[*] Priv.-Doz. Dr. H. Lang
Anorganisch-chemisches Institut der Universität
Im Neuenheimer Feld 270, D-69120 Heidelberg (FRG)
Telefax: Int. code + (6221)56-4197

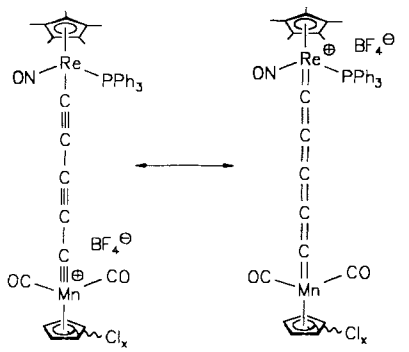
C_3 and C_5 Bridges: By using the classic Fischer–carbene and -carbyne synthesis,[6] J. A. Gladysz et al. were able to prepare complex **5** in a two-step reaction sequence; this compound exhibits a novel nonlinear form of a C_3 bridge (Scheme 1).[7] The synthesis of this compound is achieved by treating the acetylide complex **3** first with $[Re_2(CO)_{10}]/Me_3OBF_4$ and subsequently with BF_3. If the mononuclear carbonyl complexes $[CpMn(CO)_3]$, $[Fe(CO)_5]$, or $[W(CO)_6]$ are used instead of $[Re_2(CO)_{10}]$, initially compounds **4b–d** are formed by an analogous reaction pathway; subsequent reaction of **4b** with BF_3 leads to the cationic complex **6**,[7a] which, in contrast to **5**, has a linear, terminally bound C_3 chain.

The structures of compounds **5** and **6** have been confirmed by X-ray structure analyses.[7] Thus, the structure of compound **6** can best be described by the "cumulene formula" **6b**.[7] The Re–C and C–C distances in **5** correspond best to the limiting structure **5b**,[7b] which is consistent with the stronger donor properties of the Ph_3P- and Cp*-substituted rhenium atom.

The successful strategy for the preparation of complexes **5** and **6** could be extended to the synthesis of compound **9** containing a C_5 chain.[8] A decision as to which of the two given limiting formulae is more important for **9** may only be reached by a structure analysis.[8]



7 8

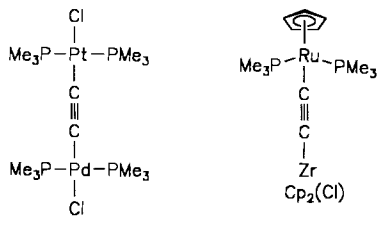


9

Transition Metal Complexes with C_{2n} Units ($n = 1, 2$)

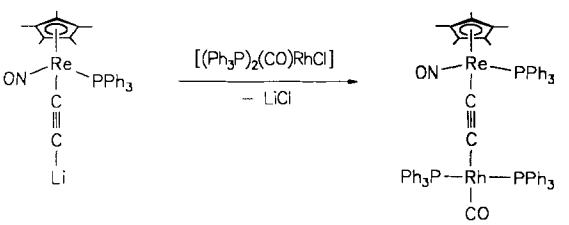
C_2 Bridges: Complexes with a C_2 bridge are a rapidly developing class of compounds.[3] The C_2 building blocks can be readily obtained from acetylene derivatives. Thus, compounds are usually formed in which two identical organometallic substituents are bound to the C_2 unit, such as in $[(CO)_5Re-C\equiv C-Re(CO)_5]$.[9]

In general, the synthesis of compounds with two different metal complex fragments at the C_2 building block requires first the preparation of the organometallic-substituted alkyne. Compound **10** is formed in this way by the reaction of $[(Me_3P)_2(Cl)Pt-C\equiv CH]$ with $[(Me_3P)_2PdCl_2]$ in the presence of Cu^ICl and $HNEt_2$;[10] compound **11** forms from $[Cp(Me_3P)_2Ru-C\equiv CH]$ and $[Cp_2Zr(Cl)(NMe_2)]$ with the elimination of $HNMe_2$.[11]



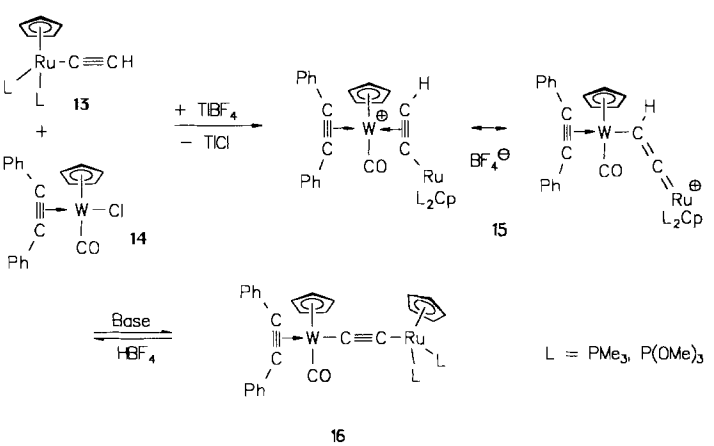
10 11

The reaction of the rhenium complex **3** with $[(Ph_3P)_2(CO)RhCl]$ to give **12** is an example of the reaction of terminal lithiated alkynyl building blocks.[12]



3 12

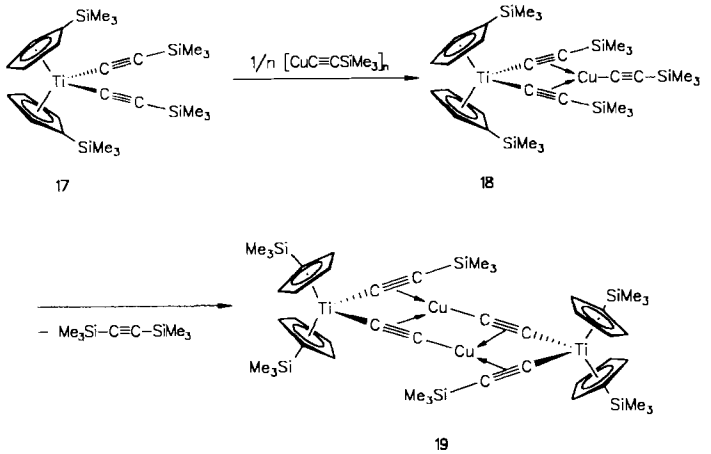
An interesting reaction sequence, which finally leads to complex **16** containing a linear C_2 bridge, was recently developed by J. P. Selegue et al.[13]



13 14 15 16

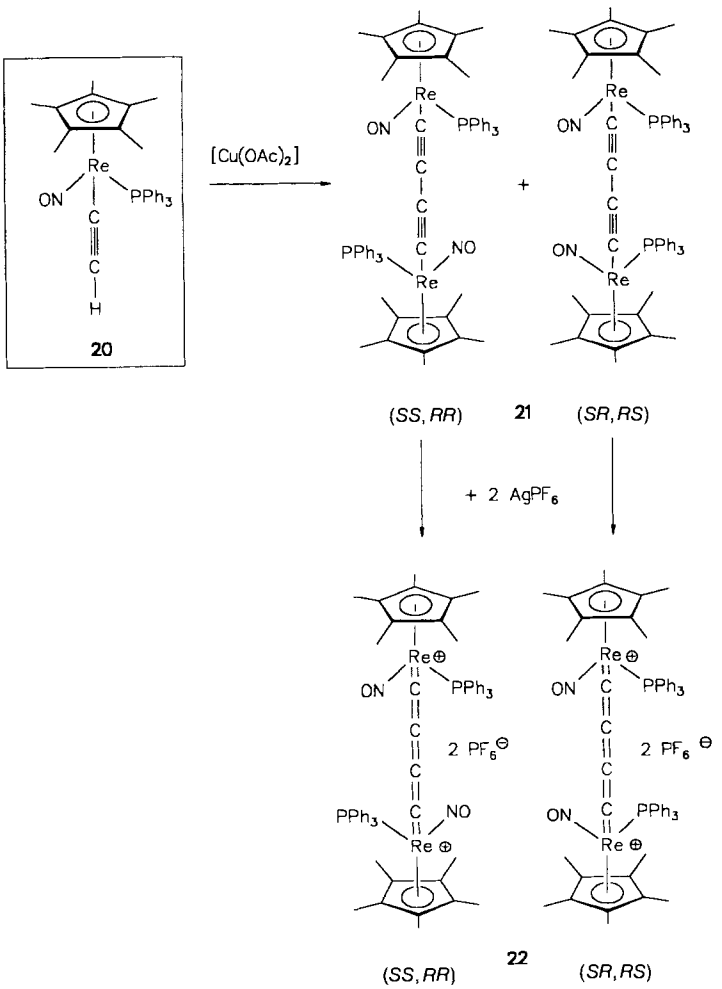
The reaction of the titanium complex **17** with $[CuC\equiv CSiMe_3]_n$ illustrates that compounds with different metal complex fragments attached to the C_2 building block can also be prepared from (silylalkynyl) complexes.[14]

C_4 Bridges: The elegant synthesis of compound **21** shows that metal-bound alkynyl groups can be coupled in a way very sim-



17 18 19

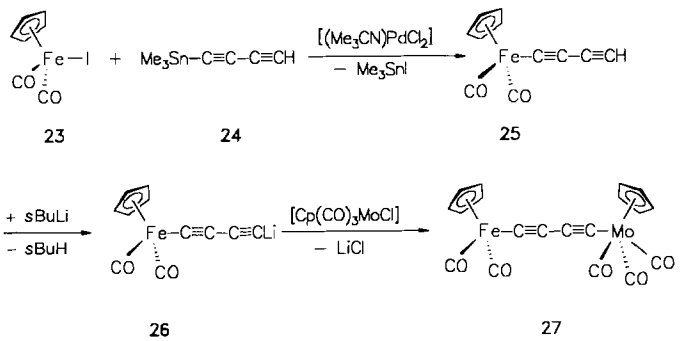
ilar to that of free alkynes. Since **20** is chiral, two diastereomers are formed, which can be separated by crystallization.[1e, 15] The bond lengths in **21** are appropriate for the given formulation of the complex with two alkyne functions. The dications **22** are obtained by oxidation of **21**; the Re–C and C–C distances in **22** can be assigned to a cumulene system.[15]



20 (SS,RR) 21 (SR,RS) (SS,RR) 22 (SR,RS)

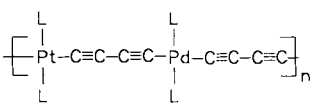
Compounds of the type **21** are also known with a range of other organometallic terminal groups.[3] Emphasis here should also be placed on complexes with different terminal transition metal fragments at the 1,3-butadiyne-1,4-diyl bridging ligands.[13, 16, 17]

For the preparation of compounds similar to **27**, usually building blocks are employed which already contain a C_4 chain. In this way the coordination of different organometallic terminal groups can be achieved.[16]



23 24 25 26 27

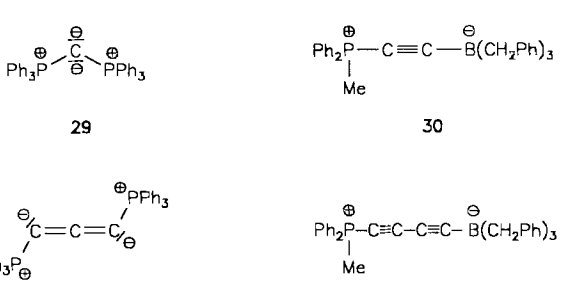
The preparation of polymers in which the C_4 building blocks are linked in a continuous chain as *trans* ligands by ML_2 building blocks is of great interest with regard to new materials.[1, 18] The square-planar coordination exhibited by the d^8 metals (M^{II} ions) makes them suitable for such linkages. An elegant synthesis for such compounds was described previously by N. Hagihara et al., who showed that $[L_2Pt(C{\equiv}C{-}C{\equiv}CH)_2]$ reacts with $[L_2PdCl_2]$ (L = PBu_3) to give the polymer **28**.[18] In this way an ordered series of different metal bridges can be built into the polymer.



28

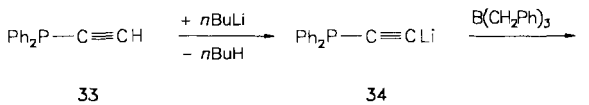
C_n Chains ($n = 1-4$) with Terminal Main Group Element Units

Polyalkyne derivatives X-C_n-Y whose terminal groups X and Y are main group element units can be prepared by numerous, in some cases well-developed, procedures.[1c] The compounds **29**–**32** are particularly interesting examples in phosphorus chemistry.[23–25] The chemistry of these compounds has been intensively studied by the groups of H. J. Bestmann and H. Schmidbaur.

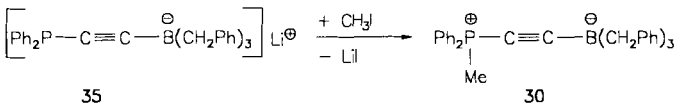


29 30 31 32

The compounds with C_1 or C_3 building blocks can be considered as bis-ylides. The compounds with C_2 or C_4 building blocks are zwitterions with charge centers more widely separated from one another. The preparation of such compounds is exemplified by the synthesis of **30**.[24] The structures of **30** and **32** determined by X-ray analysis support the formulation of the given valence formulae.[24, 25]

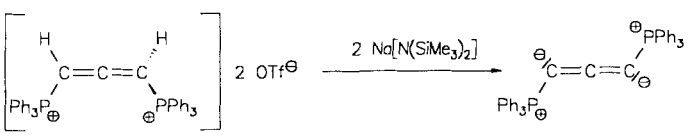


33 34



35 30

Whereas the preparation of **30** and **32** is relatively simple, the synthesis of **31** is more difficult. Compound **31** is obtained by the reaction of the allene-1,3-diylbisphosphonium salt **36** with two equivalents of sodium [bis(trimethylsilyl)amide].[25]



36 31

Outlook

The isolation of the compounds described reveals that the highly reactive carbon units C_n ($n = 1-5$) can be stabilized by suitable terminal building groups. The synthesis of these new compounds particularly for those containing organometallic substituents is often surprisingly simple.

The synthesized alkyne complexes offer a fascinating perspective for the preparation of novel organic compounds. In a wider sense it is also conceivable that alkyne-containing metal complexes with conjugated carbon bridges between different terminal groups could be used as signal transformers in nonlinear optical materials (NLO) and perhaps even as molecular wires. Finally, applications in the field of material science may also be possible in which the inherent mechanical stability of the C_n chains plays an essential role.

German version: *Angew. Chem.* **1994**, *106*, 569

[1] See for example: a) M. H. Chisholm, *Angew. Chem.* **1991**, *103*, 690–691; *Angew. Chem. Int. Ed. Engl.* **1991**, *30*, 673; b) H. S. Nalua, *Appl. Organomet. Chem.* **1991**, *5*, 349–377; c) F. Diederich, Y. Rubin, *Angew. Chem.* **1992**, *104*, 1123–1146; *Angew. Chem. Int. Ed. Engl.* **1992**, *31*, 1101, and references therein; d) G. Frapper, M. Kertesz, *Inorg. Chem.* **1993**, *32*, 732–740; e) Y. Zhou, J. W. Seyler, W. Weng, A. M. Arif, J. A. Gladysz, *J. Am. Chem. Soc.* **1993**, *115*, 8509–8510.

[2] See for example: a) R. B. Anderson, *The Fischer-Tropsch Synthesis*, Academic Press, London **1984**; b) H. Pines, *The Chemistry of Catalytic Hydrocarbon Conversions*, Academic Press, London, **1981**; c) C. Masters, *Adv. Organomet. Chem.* **1979**, *17*, 61–103.

[3] W. Beck, B. Niemer, M. Wieser, *Angew. Chem.* **1993**, *105*, 969–996; *Angew. Chem. Int. Ed. Engl.* **1993**, *32*, 923, and references therein.

[4] W. Beck, W. Knauer, C. Robl, *Angew. Chem.* **1990**, *102*, 331–333; *Angew. Chem. Int. Ed. Engl.* **1990**, *29*, 293.

[5] a) M. Etienne, P. S. White, J. L. Templeton, *J. Am. Chem. Soc.* **1991**, *113*, 2324–2325; b) W. Beck, J. Breitmair, W. Knauer, T. Weidmann, *Transition Metal Carbyne Complexes* (Ed.: F. R. Kreissl), Kluwer, Dordrecht, **1993**, p. 189–199; c) S. L. Latesky, J. P. Selegue, *J. Am. Chem. Soc.* **1987**, *109*, 4731–4733.

[6] a) K. H. Dötz, H. Fischer, P. Hofmann, F. R. Kreissl, U. Schubert, K. Weiss, *Transition Metal Carbene Complexes*, VCH, Weinheim, **1983**; b) H. Fischer, P. Hofmann, F. R. Kreissl, R. R. Schrock, U. Schubert, K. Weiss, *Carbyne Complexes*, VCH, Weinheim, **1988**.

[7] a) W. Weng, J. A. Ramsden, A. M. Arif, J. A. Gladysz, *J. Am. Chem. Soc.* **1993**, *115*, 3824–3825; b) W. Weng, A. M. Arif, J. A. Gladysz, *Angew. Chem.* **1993**, *105*, 937–939; *Angew. Chem. Int. Ed. Engl.* **1993**, *32*, 891.

[8] J. A. Gladysz, University of Utah, Salt Lake City, personal communication.

[9] a) J. Heidrich, M. Steinmann, M. Appel, W. Beck, J. R. Phillips, W. C. Trogler, *Organometallics* **1990**, *9*, 1296–1300; b) W. Beck, B. Niemer, J. Breitmair, J. Heidrich, *J. Organomet. Chem.* **1989**, *371*, 79–83.

[10] a) H. Ogawa, T. Joh, S. Takahashi, K. Sonogashira, *J. Chem. Soc., Chem. Commun.* **1985**, 1220–1221; b) H. Ogawa, K. Onitsuka, T. Joh, S. Takahashi, Y. Yamamoto, H. Yamazaki, *Organometallics* **1988**, *7*, 2257–2260; c) K. Onitsuka, T. Joh, S. Takahashi, *Bull. Chem. Soc. Jpn.* **1992**, *65*, 1179–1181; d) *Angew. Chem.* **1992**, *104*, 893–894, *Angew. Chem. Int. Ed. Engl.* **1992**, *31*, 851–852.

[11] a) R. M. Bullock, F. R. Lemke, D. J. Szalda, *J. Am. Chem. Soc.* **1990**, *112*, 3244–3245; b) F. R. Lemke, D. J. Szalda, R. M. Bullock, *ibid.* **1991**, *113*, 8466–8477.

[12] J. A. Ramsden, W. Weng, A. M. Arif, J. A. Gladysz, *J. Am. Chem. Soc.* **1992**, *114*, 5890–5891.

[13] K. G. Frank, J. P. Selegue, *J. Am. Chem. Soc.* **1990**, *112*, 6414–6416.

[14] H. Lang, M. Herres, L. Zsolnai, M. D. Janssen, G. van Koten, unpublished.

[15] J. W. Seyler, W. Weng, J. Zhou, J. A. Gladysz, *Organometallics* **1993**, *12*, 3802–3804.

[16] See for example: a) A. Wong, P. C. W. Kang, C. D. Tagge, D. R. Leon, *Organometallics* **1990**, *9*, 1992–1994, and references therein; b) S. J. Davies, B. F. G. Johnson, J. Lewis, M. S. Khan, *J. Organomet. Chem.* **1991**, *401*, C43–C47, and references therein.

[17] N. Le Narvar, C. Lapinte, *J. Chem. Soc. Chem. Commun.* **1993**, 357–359.

[18] a) K. Sonogashira, S. Kataoka, S. Takahashi, N. Hagihara, *J. Organomet. Chem.* **1978**, *160*, 319–327; b) N. Hagaihara, K. Sonogashira, S. Takahashi, *Adv. Polym. Sci.* **1980**, *41*, 149; c) S. Takahashi, H. Monmoto, E. Murato, S. Kataoka, K. Sonogashira, N. Hagihara, *J. Polym. Sci. Polym. Chem. Ed.* **1982**, *20*, 565; d) T. Kaharu, H. Matsubara, S. Takahashi, *J. Mater. Chem.* **1991**, *1*, 145–146; e) J. Lewis, M. S. Khan, A. K. Kakkar, B. F. G. Johnson, T. B. Marder, H. B. Fyde, F. Wittmann, R. H. Friend, A. E. Dray, *J. Organomet. Chem.* **1992**, *425*, 165–176; f) M. S. Khan, S. J. Davies, A. K. Kakkar, D. Schwartz, B. Ling, B. F. G. Johnson, J. Lewis, *ibid.* **1992**, *424*, 87–97; g) M. S. Khan, D. J. Schwartz, N. A. Paska, A. K. Kakkar, B. Lin, P. R. Raithby, J. Lewis, *Z. Anorg. Allg. Chem.* **1992**, *616*, 121–124; h) S. J. Davies, B. F. G. Johnson, M. S. Khan, J. Lewis, *J. Chem. Soc. Chem. Commun.* **1991**, 187–188.

[19] C. Zybill, D. L. Wilkinson, G. Müller, *Angew. Chem.* **1988**, *100*, 574–575; *Angew. Chem. Int. Ed. Engl.* **1988**, *27*, 583.

[20] a) W. Gäde, E. Weiss, *J. Organomet. Chem.* **1981**, *213*, 451–460; b) D. Melzer, E. Weiss, *ibid.* **1984**, *263*, 67–73.

[21] a) J. D. Korp, I. Bernal, R. Hörlein, R. Serrano, W. A. Herrmann, *Chem. Ber.* **1985**, *118*, 340–347; b) W. A. Herrmann, H. J. Kneuper, E. Herdtweck, *Angew. Chem.* **1985**, *97*, 1060–1061; *Angew. Chem. Int. Ed. Engl.* **1985**, *24*, 1062; c) *Chem. Ber.* **1989**, *122*, 445–451; d) *ibid.* **1989**, *122*, 433–436.

[22] a) F. Ettel, G. Huttner, L. Zsolnai, *Angew. Chem.* **1989**, *101*, 1525–2527; *Angew. Chem. Int. Ed. Engl.* **1989**, *28*, 1496; b) F. Ettel, G. Huttner, W. Imhof, *J. Organomet. Chem.* **1990**, *397*, 299–307; c) F. Ettel, G. Huttner, L. Zsolnai, C. Emmerich, *J. Organomet. Chem.* **1991**, *414*, 71–87.

[23] H. Schmidbaur, *Nachr. Chem. Tech. Lab.* **1979**, *27*, 620–622, and references therein.

[24] H. J. Bestmann, H. Behl, M. Bremer, *Angew. Chem.* **1989**, *101*, 1303–1304; *Angew. Chem. Int. Ed. Engl.* **1989**, *28*, 1219.

[25] H. J. Bestmann, D. Hadawi, H. Behl, M. Bremer, F. Hampel, *Angew. Chem.* **1993**, *105*, 1198–1200; *Angew. Chem. Int. Ed. Engl.* **1993**, *32*, 1205.

 © VCH Verlagsgesellschaft mbH, D-69451 Weinheim, 1994 0570-0833/94/0505-0550 $ 10.00+.25/0

Enzyme Mimics

Anthony J. Kirby*

One of the great intellectual challenges presented to Science by Nature is a proper understanding of how enzymes work. At one level we can "explain" enzyme catalysis—what an enzyme does is bind, and thus stabilize selectively, the transition state for a particular reaction.[1] But our current level of understanding fails the more severe, practical test—that of designing and making artificial enzyme systems with catalytic efficiencies which rival those of natural enzymes.

Enzyme mimics have long been high-profile targets for bioorganic chemists. The picture to date has been the familiar one of steady progress, with occasional flashes of inspiration, and a heightening awareness of just how complex the problem is. But two recent reports[2, 3]—approaching the problem from completely different directions—claim catalytic efficiencies in artificial systems which are extraordinary in terms of conventional wisdom. First we should set the scene.

The "conventional wisdom" is based on the one hand on mechanistic work on enzymes, and on the other hand on (mostly separate) studies of binding and catalysis in simpler, artificial systems. Enzymes are of course more than just highly evolved catalysts: they also recognize and respond to molecules other than their specific substrate and product, as part of the control mechanisms of the cell. But the evolution of enzyme mimics is at a stage where the efficient combination of binding and catalysis is the main objective. A starting point may be a system which shows efficient binding; or the mechanism of the reaction concerned, since it is the rate-determining transition state which is the most important target for the binding process. Eventually the two approaches must converge if a genuine enzyme mimic is to emerge. This sort of work holds out the promise of artificial catalysts, which may be more robust than proteins, for unnatural reactions of interest. On the other hand, the most natural basis for an enzyme mimic is inevitably a real enzyme. All these approaches are currently producing interesting results.

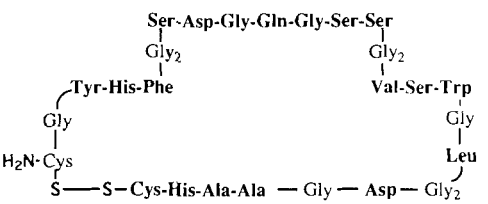
Enzyme-Based Mimics

It is possible to modify a natural enzyme, chemically or more commonly by the methods of protein engineering, in such a way that its specificity is altered, even to the point that the modified system will catalyze a new reaction. Such systems are modified enzymes rather than enzyme mimics, which to qualify in this context should have been constructed artificially.

When it became possible to identify the functional groups in enzyme active sites it was natural to look at small peptides containing active-site sequences of amino acids as possible catalysts. The results of this sort of work were uniformly negative. We know now that a working enzyme active site has its functional groups disposed in a specific, dynamic three-dimensional array, with significant interactions with the rest of the protein; this cannot successfully be modeled in two dimensions.

[*] Dr. A. J. Kirby
University Chemical Laboratory
GB-Cambridge CB2 1EW (UK)
Telefax: Int. code +(223) 336362

A true enzyme-based mimic might try to reproduce the three-dimensional arrangement of the functional groups of the active site in a synthetic framework. The reasoning is simple; turning the idea into real molecules less so. However, what appears to be a major success for this approach is the report of Atassi and Manshouri[2] on the preparation of two so-called "pepzymes", modeled from the active site structures of trypsin and chymotrypsin by "surface-simulation". This involved the design and synthesis of a series of relatively small (29 residue) peptides containing the key catalytic and binding amino acid sequences of the enzymes. These were connected by glycine spacers so as to model the three-dimensional arrangement known from the X-ray structures of the enzyme and its complexes with substrate analogues. An early version which showed some trypsin-like binding activity was modified systematically to the point where the peptide (native active site residues indicated in bold) shows extraordinary catalytic activity, specifically in the cyclic (disulfide) form **A**.



A

Not only does this molecule hydrolyze the simple trypsin "substrate" *N*-tosyl-L-arginine methyl ester with k_{cat} and K_m comparable to those of the native enzyme, but it also hydrolyzes test proteins to give similar peptide profiles. A peptide closely related to **A** based on the chymotrypsin active site had similar activity and the expected, different specificity.

It must be said that this level of activity is surprising, especially against amide bonds, and intensive efforts to repeat the results are under way. If confirmed this work will be seen as an important advance: the design stage may be complex, but with modern synthetic methods peptides of this sort of size are quite reasonable synthetic targets. A practical limitation, as always with enzyme-based mimics, is that—at this stage of development at least—complete success simply means doing a reaction as well as an available natural catalyst.

Mechanism-Based Mimics

At the other extreme, it is possible to achieve enormous rate accelerations in quite simple systems by by-passing the binding process and making reactions intramolecular, that is, by bringing the functional groups concerned together on the same molecule.[4] Typically, making the reaction of interest part of a thermodynamically favorable cyclization can produce systems in which the extraordinarily stable groups of structural biology (amides, glycosides, and phosphate esters have half-lives of many years under physiological conditions near pH 7) can be

 © VCH Verlagsgesellschaft mbH, D-69451 Weinheim, 1994 0570-0833/94/0505-0551 $ 10.00+.25/0

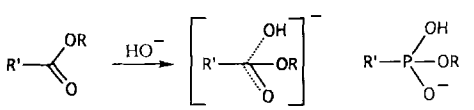
cleaved in a fraction of a second. Detailed chemical mechanisms of catalysis can then be worked out for specific reactions, studied under the same conditions and proceeding at similar rates as the same reactions between the same two (or more) functional groups in enzyme active sites. Two measures of catalytic efficiency are relevant: the effective molarity (EM), that is the effective concentration of the catalytic group, that would be needed to make an intermolecular reaction go at the rate of the intramolecular one,[4] and, of course, the absolute rate of the reaction. Because reactions in enzyme active sites are very fast: fast enough for many enzymes to have reached evolutionary perfection, defined by Albery and Knowles[5] as catalytic efficiency so high that the rate-determining step of the reaction concerned is diffusion away of the products.

EM values as high as $10^{13}-10^{14}$ M—meaning half-lives of the order of a second—can be attained in systems where on ordinary aliphatic amide is forced into close proximity with a COOH group,[5, 6] or a phosphate diester unit with a neighboring OH,[7] and it is possible to define detailed mechanisms for such model reactions. These serve as an essential basis for the discussion of the mechanisms of the same reactions in enzyme active sites, or for the design of enzyme mimics. It is not possible– so far at least—to attain rate-enhancements of anything like this magnitude when the reacting groups are brought together by noncovalent binding.

Binding-Step Based Mimics

A minimum requirement for a true enzyme mimic is a binding interaction between two molecules prior to the catalytic reaction, indicated by Michaelis–Menten kinetics. Intramolecular systems can support very rapid reactions because we can use synthesis to bring groups together into close and unavoidable proximity. But an enzyme must select and bind its substrate noncovalently in a dynamic equilibrium. The chemistry of the molecular recognition processes involved is one of the most active areas of current research, and a popular topic for meetings,[8, 9] highlights,[10] and reviews.[11] As with chemical catalysis, much of our understanding of noncovalent interactions comes from studies of simple systems designed to answer specific questions about the basic processes. More directly relevant to the development of enzyme mimics are systems designed to achieve catalysis by binding, that is without specific catalytic groups built in. These fall into two important classes: synthetic hosts designed to bring two reactants into close and productive proximity, and most catalytic antibodies.

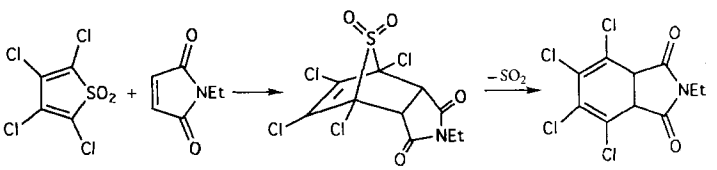
The majority of catalytic antibodies[12, 13] so far known have been designed to catalyze the hydrolysis of carboxylic acid derivatives, and have been raised against phosphonate haptens **2**, which model the structure of the tetrahedral transition states involved (**1**). Catalysis of ester hydrolysis is rather reliably obtained with suitable haptens (and substrates), with the nucleophile coming from the solvent. More ambitious systems with catalytic groups built-in can, in principle, be obtained by careful



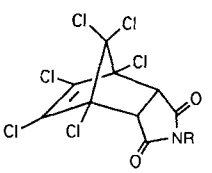
1 **2**

hapten design (coupled with a large slice of luck); or from an existing catalytic antibody by protein engineering. This is an area of definite promise, and much current activity.

Careful hapten design also allowed the preparation of an antibody that catalyzed the Diels–Alder reaction of tetrachlorothiophene dioxide **3** and *N*-ethylmaleimide.[14] Again, catalysis results simply from productive binding (an EM of >110 M is estimated): turnover depends on the instability of the initial adduct **4**, which loses SO_2 very rapidly to give the product **5**. This avoids product inhibition, which is a common problem with such potential catalytic systems: the hapten **6** ($R=(CH_2)_5CO_2H$) is a reasonable transition state analogue, but geometrically very different from the final product.

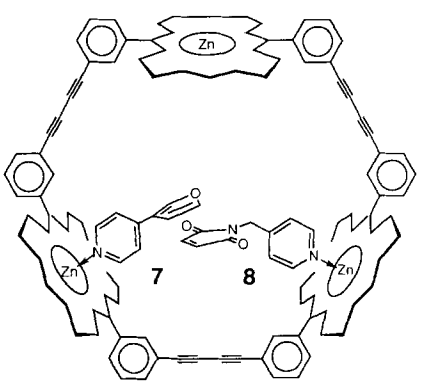


3 **4** **5**



6

The Diels–Alder reaction can also be catalyzed by simple artificial systems. A recent example is the reversible reaction between **7** and **8**, which is accelerated by (stoichiometric amounts of) a cyclic zinc-porphyrin trimer host which binds pyridine derivatives inside the cavity.[16] The product is the *exo*



7 **8**

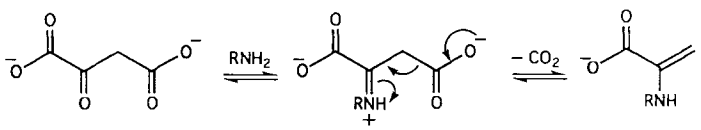
adduct, produced up to 1000 times faster than the corresponding *endo* isomer (which is obtained as the kinetic product in the absence of the macrocycle). This corresponds to an EM of about 20 M. The system is not catalytic because of product inhibition (as was an early example using the cavity of a cyclodextrin as host[17]).

Enzyme Mimics Showing Binding and Catalysis

Many of the most successful enzyme mimics have involved functionalized cyclodextrins, and the work of Breslow et al., in

particular, is familiar to anyone who has followed the field.[18] These hosts bind aromatic rings within a hydrophobic cavity. In another seminal contribution Lehn et al.[19, 20] used polyammonium macrocycles to catalyze phosphate transfer reactions of ATP, demonstrating that multiple hydrogen bonds can also be an effective source of binding between flexible systems in aqueous solution.

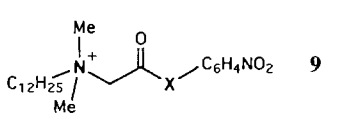
A different approach has been reported by Benner et al.,[20] who based the design of a synthetic decarboxylase on the known properties of proteins and the mechanism of amine-catalyzed decarboxylation of β-ketoacids. Their enzyme mimics are 14-residue peptides (called oxaldie 1 and 2) based on leucine and lysine, in a sequence known to favor α-helix formation, and thus expected to adopt protein-like conformations, with a hydrophobic core and a hydrophilic exterior. They catalyze the decarboxylation of oxalylacetate by the expected mechanism (see Scheme 1), with the cationic lysine side chains presumably involved in binding the two carboxylates of both substrate and transition state (acetoacetate, with a single carboxylate group, is not a substrate). Michaelis–Menten kinetics are observed and



Scheme 1. Decarboxylation of oxalylacetate catalyzed by an enzyme mimic. R = lysine side chain.

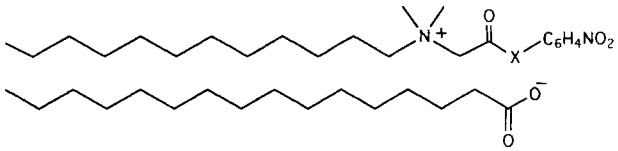
imine formation is 10^3–10^4 times faster than with simple amine catalysts. Also the activity does indeed seem to depend on the degree of α-helix formation.

The simplest, and one of the most remarkable, new enzyme mimics has emerged from a piece of "lateral thinking" by Menger and Fei.[3] No synthesis is involved. These authors simply mixed long-chain carboxylic acids, amines, alcohols, and alkylimidazoles, of the sort known to form aggregates, and eventually micelles, in aqueous solution: then screened large numbers of such mixtures for catalytic activity. The test reaction was the hydrolysis of the reactive ester **9** (X = O), which is easily followed above pH 7 by the release of the *p*-nitrophenolate chromophore. Some of the mixtures used effected the hydrolysis of **9** (X = O) at rates too fast to measure manually. Remarkably this was also true in the presence of a single component when this was the hexadecanoate anion, and this system also effects the hydrolysis of the *p*-nitroanilide (**9**, X = NH). This is an activated amide, but one that is not hydrolyzed detectably in the presence of 0.2 M acetate at pH 7 (25 °C). But under similar conditions, in the presence of just 2×10^{-5} M hexadecanoate its half-life is only three minutes.



9

Only nucleophilic catalysis can account for such an efficient process.[4] No EM can be calculated as no data are available for a suitable comparison, but hexadecanoate is at least 10^8 times more effective than acetate. Interestingly the reaction is stoichiometric: though a mixed anhydride is almost certainly an intermediate, its hydrolysis must be rate-determining in the overall hydrolysis of the anilide. The authors suggest that the reaction takes place in submicellar aggregates or "clumps", in which hydrophobic association of the long alkyl chains brings anilide carbonyl and hexadecanoate carboxylate groups into close and remarkably productive proximity (see Scheme 2). (Simply adding three methylene groups to the substrate [**9**, X = $(CH_2)_3NH$] eliminates the observed reaction.)



Scheme 2. Hydrophobic association between **9** and hexadecanoate.

Two points are of special interest here: the high reactivity, which is much greater than previously observed for such apparently loosely-associated systems: and the principle of screening large numbers of simple systems, rather than actually synthesizing complex, carefully designed ones. The newer approach supplements existing ways of thinking, and practical applications may result.

German version: *Angew. Chem.* **1994**, *106*, 573

[1] A. R. Fersht, *Enzyme Structure and Mechanism*, second edition, W. H. Freeman, New York, **1985**.
[2] M. Z. Atassi, T. Manshouri, *Proc. Natl. Acad. Sci. USA*, **1993**, *90*, 8282–8286.
[3] F. Menger, Z. X. Fei, *Angew. Chem.* **1994**, *106*, 329; *Angew. Chem. Int. Ed. Engl.* **1994**, *33*, 346.
[4] A. J. Kirby, *Effective molarities for intramolecular reactions* (*Adv. Phys. Org. Chem.* **1980**, *17*, 183–278).
[5] W. J. Albery, J. R. Knowles, *Biochemistry* **1976**, *15*, 5631.
[6] F. M. Menger, M. Ladika, *J. Am. Chem. Soc.* **1988**, *110*, 6794.
[7] K. N. Dalby, A. J. Kirby, F. Hollfelder, *J. Chem. Soc. Perkin Trans. 2* **1993**, 1269.
[8] *Host-Guest Interactions: from Chemistry to Biology* (Eds.: D. J. Chadwick, K. Widdows) (*Ciba Found. Symp.* **1991**, *158*).
[9] *The Chemistry of Biological Molecular Recognition* (Eds.: A. J. Kirby, D. H. Williams) (*Philos. Trans. R. Soc. London A* **1993**, *345*, 1–164).
[10] H.-J. Schneider, *Angew. Chem.* **1993**, *105*, 890; *Angew. Chem. Int. Ed. Engl.* **1993**, *32*, 848.
[11] R. J. Pieters, J. Rebek, *Recl. Trav. Chim. Pays-Bas* **1993**, *112*, 330; I. Chao, F. Diederich, *ibid.* **1993**, *112*, 335.
[12] P. G. Schultz, *Angew. Chem.* **1989**, *101*, 1336; *Angew. Chem. Int. Ed. Engl.* **1989**, *28*, 1283.
[13] U. K. Pandit, *Recl. Trav. Chim. Pays-Bas* **1993**, *112*, 431.
[14] D. Hilvert, K. W. Hill, K. D. Narel, M.-T. M. Auditor, *J. Am. Chem. Soc.* **1989**, *111*, 9261; see also [15].
[15] A. C. Braisted, P. G. Schultz, *J. Am. Chem. Soc.* **1992**, *112*, 7431.
[16] C. J. Walter, H. L. Anderson, J. K. M. Sanders, *J. Chem. Soc. Chem. Commun.* **1993**, 458, and references therein.
[17] D. Rideout, R. Breslow, *J. Am. Chem. Soc.* **1980**, *102*, 7816.
[18] For recent references and a review see: R. Breslow, P. J. Duggan, J. P. Light, *J. Am. Chem. Soc.* **1992**, *114*, 3982; R. Breslow in [8], p. 115.
[19] M. W. Hosseini, J.-M. Lehn, K. C. Jones, K. E. Plute, K. B. Mertes, M. P. Mertes, *J. Am. Chem. Soc.* **1989**, *111*, 6330–6335; M. P. Mertes, K. B. Mertes, *Acc. Chem. Res.* **1990**, *23*, 413–418.
[20] K. Johnsson, R. K. Allemann, H. Widmer, S. Benner, *Nature (London)* **1993**, *365*, 530–532.

 © VCH Verlagsgesellschaft mbH, D-69451 Weinheim, 1994 0570-0833/94/0505-0553 $ 10.00+.25/0

Molecular Solids as Ligands in Organometallic Chemistry: $[Cp^*_6Ti_6Na_7F_{19}\cdot 2.5thf]$ ($Cp^* = C_5Me_5$) and $[Cp^*_4Ti_4Mg_2F_{12}\cdot 7thf]$, Links Between Ionic Solids and Organometallic Compounds**

Feng-Quan Liu, Annja Kuhn, Regine Herbst-Irmer, Dietmar Stalke, and Herbert W. Roesky*

We previously reported the isolation of inclusion complexes from the reaction of $[Cp^*TiF_3]$ (**1**) ($Cp^* = C_5Me_5$) with NaF in acetonitrile. These complexes can be considered as analogues of crown ethers;[1] encapsulation of the Na^+ ion by two $[(Cp^*TiF_3)_2F]^-$ fragments corresponds to that in $[Na([12]crown\text{-}4)_2]^+$. Here, the nucleophilic host has a fluoride surface which surrounds the sodium ion. The reaction of $[Cp^*TiF_3]$ with sodium metal in THF in a 1:1 molar ratio results in the formation of NaF and the expected reduction of Ti^{IV} to Ti^{III}. Surprisingly, no NaF precipitates out during this synthesis. If the solution is left to stand for an extended period of time, green crystals of composition $[Cp^*_6Ti_6Na_7F_{19}\cdot 2.5thf]$ (**2**) are formed.

The structure of **2** has been determined by a single-crystal X-ray analysis,[2] and its central inorganic structural unit is depicted in Figure 1. The structure has a noncrystallographic two-fold axis which runs through Na1 and F19. The six Cp^*TiF_2 groups almost completely enclose seven NaF molecules such that a "molecular NaF structure" is formed within the aggregate. Here, however, a different coordination is found than that in crystalline NaF. Only F19 is octahedrally coordinated; all other fluorine atoms exhibit lower coordination. Thus, F9 and F15 have the coordination number five, F3 and F6 the coordination number four, and the remaining fluorides exhibit a coordination number of three. Although Na1, Na6, and Na7 are six-coordinate, their coordination polyhedra are distorted in such a way as to prohibit their description as octahedra. While Na2 and Na3 are seven-coordinate, the peripherally "naked" atoms Na4 and Na5 are each coordinated to four fluorine atoms and one oxygen atom (from a THF molecule). The average Na–F bond length (234.9 pm) is similar to that in solid NaF (231 pm),[3] but significantly shorter than that in $[tBu_2SiFNaNtBu]_2$ (243.4 pm and 332.5 pm),[4] $[2,4,6\text{-}(CF_3)_3C_6H_2ONa\cdot 2thf]_2$ (266.4 and 272.0 pm),[5] or $[2,4,6\text{-}(CF_3)_3C_6H_2SNa\cdot 2thf]_x$ (243.4 to 257.1 pm).[5] The Ti–F distances in **2** (204.6 pm) are similar to those in $[(Cp_2TiF_2)_3Ti]$ (209.4 pm; $Cp = C_5H_5$).[6] In the crystal of **2**, a THF molecule is trapped between two $[Cp^*_6Ti_6Na_7F_{19}\cdot 2thf]$ units in such a way that the molecule is disordered with its oxygen atom directed towards one of the sodium atoms (Fig. 2). The Na–O bond to this molecule is about 30 pm longer than those to the rigidly coordinated THF molecules.

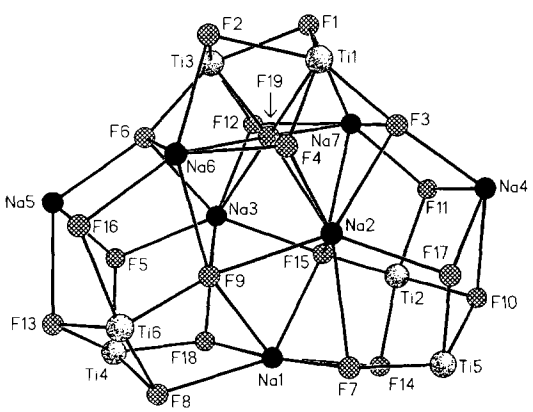


Fig. 1. Structure of the central inorganic unit of **2** in the crystal. Selected bond lengths [pm]: Ti–F 204.6* (194.7–215.2), $Ti\text{–}Cp^*_{(center)}$ 203.2*, Na–F 234.9* (215.3–275.1), Na4–O1 229.1(4), Na5–O2 231.9(4), Na7–O9 263(2). The values marked with a * are average values.

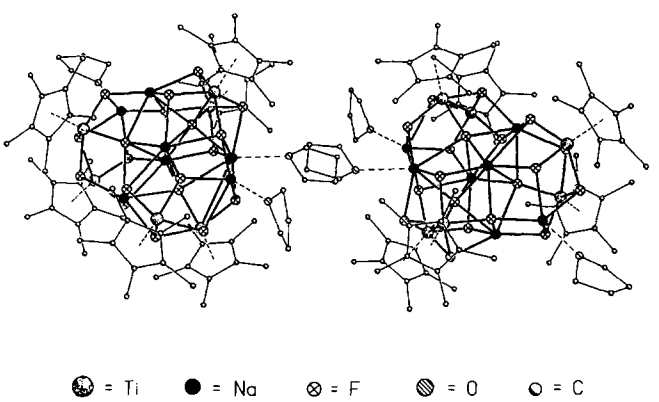


Fig. 2. Arrangement of two molecules of **2** about a trapped THF molecule.

We then investigated whether the coordination pattern found in **2** would also be exhibited by Group 2 elements. $[Cp^*TiF_3]$ (**1**) reacted with magnesium metal in THF to form **3** [Eq. a]. In this

$$4\,[Cp^*TiF_3] + 2\,Mg \xrightarrow{thf} [Cp^*_4Ti_4Mg_2F_{12}\cdot 7thf] \qquad (a)$$

1 → **3**

reaction, two magnesium atoms are incorporated between four $[Cp^*TiF_3]$ units. The single-crystal X-ray structure analysis of **3**[2] (Fig. 3) revealed a six-coordinate magnesium atom similar to that in solid MgF_2.[3] Two of the six coordination sites in **3**, however, are occupied by THF molecules. Whereas the THF molecules containing O1 and O2 are each bound to one magnesium atom as terminal ligands, the O3-containing THF molecule bridges the two Mg atoms. To our knowledge, such μ_2-

[*] Prof. Dr. H. W. Roesky, Dr. F.-Q. Liu, A. Kuhn, Dr. R. Herbst-Irmer, Priv.-Doz. Dr. D. Stalke
Institut für Anorganische Chemie der Universität Göttingen
Tammannstrasse 4, D-37077 Göttingen (FRG)
Telefax: Int. code + (551)39-2582

[**] This work was supported by the Deutsche Forschungsgemeinschaft, the Volkswagen Stiftung, the Fonds der Chemischen Industrie, and the Hoechst AG.

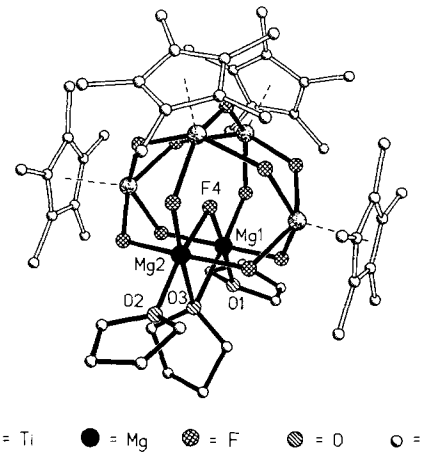


Fig. 3. Structure of **3** in the crystal. Selected bond lengths [pm]: Ti–F 202.5* (200.4–203.6). Ti–$Cp^*_{(centerr)}$ 204.6*. Mg–O(1,2) 206.0*, Mg1–O3 226.8(3), Mg2–O3 235.8(4), Mg1–F4 202.6(3), Mg2–F4 201.8(3), Mg–F 190.5* (190.0–190.9). The values marked with a * are average values.

bridging THF molecules in alkaline earth metal compounds are unknown to date. Although the Mg–F distances to the Mg bridging fluorine atom F4 (202.2 pm) correspond to the distances in the rutile lattice of MgF_2 (205 pm),[7] the remaining Mg–F bond lengths in **3** (mean 190.5 pm) are significantly shorter. The central $Ti_4Mg_2F_{12}$ inorganic core is outwardly shielded by both the Cp* groups and the coordinated THF molecules. Four Ti, two Mg, and twelve F atoms build a cage-like framework whose cavity has a μ_2-bridging fluorine atom (Mg1–F4–Mg2) projecting into it.

With these examples, we have shown for the first time that molecular solids can function as ligands in organometallic chemistry. Continuing investigations are aimed at determining how the size of the aggregates can be influenced by, for example, changes in the ligands, the solvent, or through template effects as well as whether corresponding oxide systems can be prepared.

Experimental Procedure

2: A solution of **1** (0.72 g, 3 mmol) in THF (40 mL) was added dropwise to a suspension of Na (0.07 g, 3 mmol) and mercury (10 g) in THF (20 mL) at 0 °C. The reaction must be carried out under careful exclusion of water and oxygen. The mixture was stirred for 12 h, filtered, and the solvent was then removed in vacuum. Crystalline **2** (0.52 g, 65% yield) was obtained by recrystallizing the green residue from THF/hexane (20 mL/40 mL). M.p. 204 °C (decomp). The decomposition temperature refers to the solvent-free compound, which is obtained by evacuation of **2** (10^{-2} mbar, 25 °C, 12 h). Correct elemental analyses. IR (Nujol): $\tilde{\nu}$[cm^{-1}] = 1497(m), 1260(m), 1061(s), 1027(s), 815(s), 545(s), 507(s), 494(s), 471(s).

3: A solution of **1** (0.72 g, 3 mmol) in THF (40 mL) was added dropwise to Mg (0.35 g, 14 mmol) in THF (20 mL) under an inert atmosphere. The magnesium was first activated with $HgCl_2$ (5 mg). The mixture was stirred for 12 h at room temperature, filtered, and the solvent was then removed in vacuum. The residue was recrystallized from THF/hexane (40 mL/20 mL) which yielded 0.5 g of **3** (75%). M.p. 240 °C. Correct elemental analyses from the solvent-free compound (10^{-2} mbar, 25 °C, 12 h). IR (Nujol): $\tilde{\nu}$[cm^{-1}] = 1498(m), 1260(m), 1031(s), 801(s), 519(s); MS(El) *m/z*: 873 (M–Cp*, 1.2%), 135 (Cp*, 100%).

Received: October 2, 1993 [Z 6386IE]
German Version: *Angew. Chem.* **1994**, *106*, 577

[1] H. W. Roesky, M. Sotoodeh, M. Noltemeyer, *Angew. Chem.* **1992**, *104*, 869; *Angew. Chem. Int. Ed. Engl.* **1992**, *31*, 864.

[2] Crystal data for **2**: $C_{68}H_{100}F_{19}Na_7O_2Ti_6 + 1/2$ thf, $M_r = 1800.91$, triclinic, space group $P\bar{1}$, $a = 1195.0(2)$, $b = 1407.7(2)$, $c = 2670.9(5)$ pm, $\alpha = 80.99(1)$, $\beta = 77.67(1)$, $\gamma = 72.46(1)°$, $V = 4.165(1)$ nm^3, $Z = 2$, $\rho_{calcd} = 1.436$ $g\,cm^{-3}$, F(000) = 1860, $\lambda = 71.073$ pm, $\mu(Mo_{K\alpha}) = 0.668$ mm^{-1}. The data were collected on a Stoe-Siemens-Huber four-circle diffractometer. The intensities were determined at −120 °C from a rapidly cooled crystal in a drop of oil [8] having dimensions of $0.4 \times 0.3 \times 0.2$ mm by the $2\theta/\omega$ method over the range $8° \leq 2\theta \leq 45°$. A semiempirical absorption correction method was applied to the 10922 independent reflections from the 18706 collected. 10920 of the independent reflections and 5683 restraints were used in the refinement of 1143 parameters. Largest minimum and maximum in the final difference-Fourier synthesis: 460 and −480 $e\,nm^{-3}$, respectively. $R1(F > 4\sigma(F)) = 0.046$ and $wR2 = 0.128$ (for all data). **3**: $C_{52}H_{84}F_{12}Mg_2O_3Ti_4 + 4$ thf, $M_r = 1513.83$, monoclinic, space group $P2_1/m$, $a = 1470.9(1)$, $b = 1679.8(2)$, $c = 1539.5(2)$ pm, $\beta = 105.53(1)°$, $V = 3.6649(7)$ nm^3, $Z = 2$, $\rho_{calcd} = 1.372$ $g\,cm^{-3}$, F(000) = 1600, $\lambda = 71.073$ pm, $\mu(Mo_{K\alpha}) = 0.517$ mm^{-1}. The data were collected on a Stoe-Siemens-AED four-circle diffractometer. The intensities were determined at −120 °C from a drop of oil [8] having dimensions of $0.2 \times 0.2 \times 0.1$ mm by the $2\theta/\omega$ method over the range $8° \leq 2\theta \leq 50°$. From the 6666 independent reflections out of the 8199 collected, 6663 were used together with 1416 restraints in the refinement of 696 parameters. Largest minimum and maximum in the final difference-Fourier synthesis: 600 and −380 $e\,nm^{-3}$, respectively. $R1(F > 4\sigma(F)) = 0.048$ and $wR2 = 0.140$ (for all data). The values for $R1$ and $wR2$ were defined as $R1 = \Sigma||F_o| - |F_c||/[\Sigma|F_o|]$; $wR2 = \{[\Sigma w(F_o^2 - F_c^2)^2/[\Sigma w(F_o^2)^2]\}^{1/2}$. The structures were solved by direct methods (SHELXS-90) [9] and refined by least-squares methods (SHELXS-93) [10]. The hydrogen positions were refined by a riding model in which CH_3 groups can rotate about their local threefold axes. Further details of the crystal structure investigations may be obtained from the Director of the Cambridge Crystallographic Data Centre, 12 Union Road, GB-Cambridge CB2 1EZ on quoting the complete literature citation.

[3] A. F. Wells, *Structural Inorganic Chemistry*, 5th ed., Oxford University Press, Oxford, **1984**.
[4] U. Pieper, D. Stalke, S. Vollbrecht, U. Klingebiel, *Chem. Ber.* **1990**, *123*, 1039.
[5] S. Brooker, F. T. Edelmann, T. Kottke, H. W. Roesky, G. M. Sheldrick, D. Stalke, K. H. Whitmire, *J. Chem. Soc. Chem. Commun.* **1991**, 144.
[6] F.-Q. Liu, H. Gornitzka, D. Stalke, H. W. Roesky, *Angew. Chem.* **1993**, *105*, 447; *Angew. Chem. Int. Ed. Engl.* **1993**, *32*, 441.
[7] R. D. Shannon, C. T. Prewitt, *Acta Crystallogr. Sect. B* **1969**, *25*, 925.
[8] T. Kottke, D. Stalke, *J. Appl. Crystallogr.* **1993**, *26*, 615.
[9] G. M. Sheldrick, *Acta Crystallogr. Sect. A* **1990**, *46*, 467.
[10] G. M. Sheldrick, *SHELXL-93*, Göttingen, **1993**.

Kinetic Resolution of the Acrolein Dimer by Asymmetric Horner–Wadsworth–Emmons Reactions**

Tobias Rein,* Nina Kann, Reinhard Kreuder, Benoit Gangloff, and Oliver Reiser*

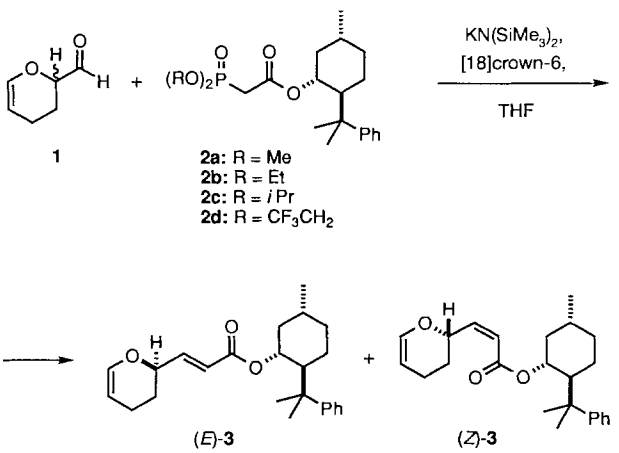
Dedicated to Professor Björn Åkermark on the occasion of his 60th birthday

The Diels–Alder dimer of acrolein **1**[1] is available in bulk quantities and has great potential as a synthetic building block[2] because of its aldehyde and enolether functionality.

[*] Dr. T. Rein, Dipl.-Chem. N. Kann
Organic Chemistry, Royal Institute of Technology
S-100 44 Stockholm (Sweden)
Telefax: Int. code + (8)791 23 33
Dr. O. Reiser, R. Kreuder[+1]
Institut für Organische Chemie der Universität
Tammanstrasse 2, D-37077 Göttingen (FRG)
Telefax: Int. code + (551)39 94 75
B. Gangloff[+1]
Université de Marseille, Marseille (France)
[+] Erasmus exchange students at the Royal Institute of Technology, Stockholm.

[**] We thank the Swedish Natural Sciences Research Council, the Deutsche Forschungsgemeinschaft (Re 948/1-2), Carl Tryggers Foundation for Scientific Research, the Foundation Bengt Lundqvists Minne, Helge Axson Johnsons Foundation, and the Royal Institute of Technology for financial support. Dr. D. Yu, Degussa AG, Germany, is acknowledged for a generous sample of aldehyde **1**. Travel grants from the Erasmus program for student exchange (B. G.) and the Bundesamt für Ausbildungsförderung Flensburg (R. K.) are gratefully acknowledged. We also thank Professors B. Åkermark, Royal Institute of Technology, Stockholm, A. de Meijere, Göttingen, and P. Helquist, University of Notre Dame IN, USA, for their continued interest and support, and Ms. Gurli Hammarberg for assistance with spectroscopic analyses.

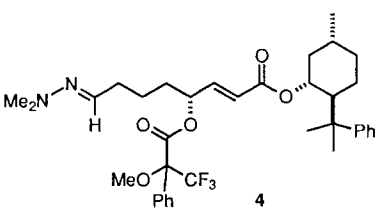
However, **1** has not yet found wide application since it is not available in optically pure form. As part of our ongoing studies regarding asymmetric alkene synthesis[3] and the utilization of vinyl-substituted dihydropyrans as homoaldol equivalents,[4] we have studied kinetic resolutions of racemic **1** by reactions with chiral phosphonate reagents. In all previously reported cases of kinetic resolution by asymmetric alkene synthesis,[5] the substrates used have been ketones. In this paper, we report that kinetic resolutions of the aldehyde **1** can give high diastereoselectivities, and furthermore that either (*E*)-**3** or (*Z*)-**3** can be obtained as the main product.

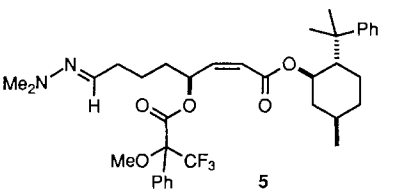


Initial studies were performed by using the chiral phosphonate **2a**[6] which has previously been used[7] in asymmetric alkene synthesis with ketone substrates, and has also given good results in our studies of reactions with *meso* dialdehydes.[3] The reaction of **1** with **2a** gave high diastereoselectivities for both (*E*)-**3** and (*Z*)-**3** (Table 1, entry 1), however, the (*E*)/(*Z*) ratio was only modest (39:61).[8, 9] To study the influence of variations in the phosphonate structure on the selectivity,[10] the new phosphonate **2b**[11] and the previously known reagent **2c**[6] were synthesized in the same manner as **2a**. Use of **2b** favored formation of the (*E*) isomer (entry 2), and performing the reaction at lower temperature (entry 3) gave a good yield of (*E*)-**3**[11] with high diastereomeric purity (88% *de*) after chromatography. Reactions with phosphonate **2c** (entries 4 and 5) gave even higher (*E*)/(*Z*) selectivity, but the diastereoselectivities were lower.[12]

It is known that the formation of (*Z*) alkenes in Horner–Wadsworth–Emmons reactions is favored by using trifluoroethoxy substituents on phosphorus.[13] In order to enable selective preparation of the (*Z*) product, we thus synthesized the new phosphonate reagent **2d**[11] by the same method as used for the other reagents **2**. To our delight, **2d** gave high diastereoselectivity for the (*Z*) product, together with useful double bond selectivity (entries 6 and 7). After chromatography, high yields of (*Z*)-**3**[11] with excellent diastereomeric purity (96–98% *de*) were obtained.

Our assignments of the absolute configurations of the condensation products are based on the NMR analysis[14] of the Mosher ester derivatives **4** and **5** obtained from (*E*)-**3** and (*Z*)-**3**, respectively, by straightforward transformations. This analysis shows that the (*E*) and (*Z*) products are formed from different enantiomers of the starting material **1**. Further support for this conclusion comes from the reaction in entry 8, in which only one equivalent of **1** was used, also indicating that the (*E*) and (*Z*) isomers are formed from different enantiomers of the starting aldehyde. The alternative explanation of a fast racemization of the aldehyde in the course of the reaction is unlikely since similar (*E*)/(*Z*) selectivites and yields would be expected in entries 6 and 8 if racemization was faster than the condensation process.





Concerning the mechanistic reasons behind the observed selectivities, there are several points that need to be investigated further before any well-founded rationalizations can be made.[10] It is not clear which reaction step is the rate-determining one for a given combination of reactants, the initial addition of the phosphonate anion to the aldehyde or the subsequent elimination step. Also, the analysis is complicated by the fact that each alkene isomer might in theory have been formed from either of two different diastereomeric β-alkoxy anion precursors.

We are presently studying the possibility of using other types of aldehydes as substrates in these reactions, as well as synthetic applications. We believe that kinetic resolutions of this type should have considerable synthetic potential.

Table 1. Reactions of phosphonates **2** with racemic aldehyde **1**. [a]

Entry	Phosphonate	*T* [°C]	(*E*)/(*Z*) ratio, crude [b]	Diast. ratio, crude (*E*) [b]	Diast. ratio, isol. (*E*) [b]	Yield, (*E*) [%] [c]	Diast. ratio, crude (*Z*) [b]	Diast. ratio, isol. (*Z*) [b]	Yield, (*Z*) [%] [c]
1	**2a**	−78	39:61	95:5	96:4	20	91:9	91:9	55
2	**2b**	−78	73:27	92:8	92:8	70	82:18	81:19	24
3	**2b**	−100	68:32	93:7	**94:6**	**68**	90:10	90:10	29
4	**2c**	−78	95:5	84:16	87:13	89	72:28	69:31	3
5	**2c**	−100	91:9	79:21	80:20	81	86:14	88:12	8
6	**2d**	−78	20:80	96:4	96:4	20	98:2	98:2	77
7	**2d**	−100	15:85	96:4	97:3	14	99:1	**99:1**	**81**
8 [d]	**2d**	−78	44:56	95:5	95:5	43	92:8	92:8	52

[a] General conditions: 2.1–3 equiv of **1**, 1.1 equiv of phosphonate, 1.0 equiv of potassium hexamethyl disilazide (KHMDS), 5 equiv of [18]crown-6, 0.01–0.02 M in THF. [b] Determined by ^{1}H NMR spectroscopy at 400 MHz (integrals of olefin protons). For entries 2 and 7, the diastereomeric ratios were confirmed by HPLC analysis (Chiralcel OD column). [c] Isolated yields, after chromatography (>95% pure by NMR and TLC). [d] Only 1.0 equivalent of **1** was used.

 © VCH Verlagsgesellschaft mbH, D-69451 Weinheim, 1994 0570-0833/94/0505-0557 $ 10.00+.25/0

Experimental Procedure

To a solution of the phosphonate reagent **2** (1.1 equiv, 0.01–0.02 M) and [18]crown-6 (5 equiv) in THF at −78 C under argon was added 1.0 equiv of $KN(SiMe_3)_2$ (0.5 M in toluene). After 30 min, the resulting solution/slurry was added by cannula to a precooled (−78 or −100 C) solution of **1** (2.1–3.0 equiv) in THF. The reaction mixture was stirred for 2–4 h at −78 or −100 C and then quenched with 1 M acetic acid in MeOH followed by pH 7 phosphate buffer. Extractive workup (ethyl acetate), drying ($MgSO_4$), and concentration gave the crude condensation product which was purified by flash chromatography on silica gel by using 2% EtOAc in hexanes. Selected ^{1}H NMR data (400 MHz, $CDCl_3$): (*E*)-**3**: δ = 6.57 (dd, J = 15.8, 4.4 Hz, 1 H, C*H*=CHC(O), major diastereomer), 6.37 (dd, J_1 = 5 Hz, J_2 not measurable (overlapping signals), 1 H, C*H*=CHC(O), minor diastereomer), 6.35 (dt, J = 6.2, 1.9 Hz, 1 H), 5.50 (dd, J = 15.7, 1.8 Hz, 1 H), 4.84 (td, J = 10.7, 4.4 Hz, 1 H), 4.70 4.66 (m, 1 H), 4.40–4.34 (m, 1 H); (*Z*)-**3**: δ = 6.33 (dd, J = 6.2, 1.7 Hz, 1 H), 6.11 (dd, J = 11.7, 7.3 Hz, 1 H), 5.22 (tm, J = 8.1 Hz, 1 H), 5.16 (dd, J = 11, 2 Hz, 1 H, CH=C*H*C(O), minor diastereomer), 5.09 (dd, J = 11.8, 2.0 Hz, 1 H, CH=C*H*C(O), major diastereomer), 4.78 (td, J = 10.7, 4.4 Hz, 1 H), 4.73 4.68 (m, 1 H).

Received: September 17, 1993 [Z 6363 IE]
German version: *Angew. Chem.* **1994**, *106*, 597

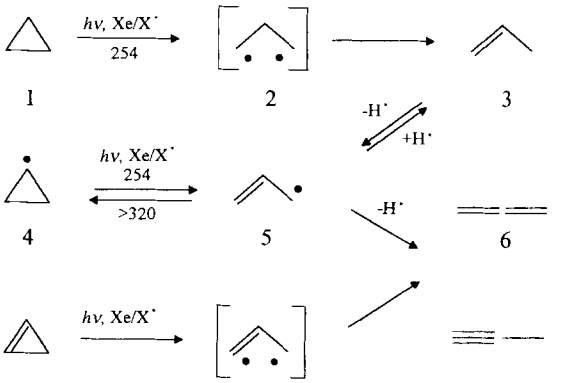
[1] R. W. Fourie, G. H. Riesser in *Acrolein* (Ed.: C. W. Smith), Wiley, New York, **1962**, pp 181–210.
[2] A. C. Oehlschlager, S. M. Singh, *Can. J. Chem.* **1988**, *66*, 209–213, and references therein.
[3] N. Kann, T. Rein, *J. Org. Chem.* **1993**, *58*, 3802–3804.
[4] S. Hillers, A. Niklaus, O. Reiser, *J. Org. Chem.* **1993**, *58*, 3169–3171.
[5] a) S. Musierowicz, A. Wróblewski, H. Krawczyk, *Tetrahedron Lett.* **1975**, 437–440; b) S. Hanessian, S. Beaudoin, *ibid.* **1992**, *33*, 7655–7658; c) C. R. Johnson, N. A. Meanwell, *J. Am. Chem. Soc.* **1981**, *103*, 7667–7669; d) C. R. Johnson, R. C. Elliott, N. A. Meanwell, *Tetrahedron Lett.* **1982**, *23*, 5005 5008.
[6] S. Hatakeyama, K. Satoh, K. Sakurai, S. Takano, *Tetrahedron Lett.* **1987**, *28*, 2713–2716.
[7] a) H.-J. Gais, G. Schmiedl, W. A. Ball, J. Bund, G. Hellmann, I. Erdelmeier, *Tetrahedron Lett.* **1988**, *29*, 1773–1774; b) H. Rehwinkel, J. Skupsch, H. Vorbrüggen, *ibid.* **1988**, *29*, 1775–1776.
[8] Since the aldehyde **1** is quite sensitive towards decomposition, a slight excess (2.1 3 equivalents) was used. We have not determined the *ee* of remaining unreacted aldehyde in any case.
[9] Only the major diastereomers of (*E*)-**3** and (*Z*)-**3** [i.e. (*R*,*E*)-**3** and (*S*,*Z*)-**3**, respectively] have been illustrated. The (*E*)/(*Z*) ratio for the crude product refers to the total amounts of (*E*) and (*Z*) products. Strictly speaking, all four isomeric products are diastereomers; for clarity, however, we have only given diastereomeric ratios between products with the same alkene geometry [that is the comparison of (*R*,*E*)-**3** with (*S*,*E*)-**3** and of (*S*,*Z*)-**3** with (*R*,*Z*)-**3**].
[10] For recent reviews covering the Horner–Wadsworth–Emmons reaction, including mechanistic aspects, see: a) B. E. Maryanoff, A. B. Reitz, *Chem. Rev.* **1989**, *89*, 863–927; b) S. E. Kelly in *Comprehensive Organic Synthesis*; *Vol. 1* (Eds.: B. M. Trost, I. Fleming), Pergamon Press, Oxford, **1991**, pp 761–773.
[11] Spectroscopic and analytical data (^{1}H and ^{13}C NMR, IR, MS, elemental analysis) in accordance with the structure were obtained for this compound.
[12] An initial attempt to increase the (*E*) selectivity further by using phosphonate **2b** in combination with *n*-butyllithium as base, instead of potassium hexamethyl disilazide (KHMDS)/[18]crown-6, gave a much lower diastereomeric ratio for the (*E*) product.
[13] W. C. Still, C. Gennari, *Tetrahedron Lett.* **1983**, *24*, 4405–4408.
[14] a) J. A. Dale, H. S. Mosher, *J. Am. Chem. Soc.* **1973**, *95*, 512–519; b) I. Ohtani, T. Kusumi, Y. Kashman, H. Kakisawa, *ibid.* **1991**, *113*, 4092–4096 and references therein.

Ring Opening of Cyclopropane at 10 K**

Günther Maier* and Stefan Senger

We recently reported the irradiation of methylenecyclopropane in a halogen-doped xenon matrix, which surprisingly leads to trimethylenemethane.[1, 2] To explore the potential of this unusual C–C bond cleavage, we have subjected cyclopropane **1** to the same conditions. This molecule does not absorb light in the UV region and has a considerable energy barrier to thermally induced ring opening.[3] Nonetheless, even at 10 K a C–C bond was easily broken with this new fragmentation method.

Cyclopropane (**1**) is inert at 10 K with respect to irradiation with 254 nm light in a xenon matrix. This changes drastically when bromine is mixed into the xenon matrix (ratio bromine:cyclopropane:xenon ≈ 1:1.5:1000), and subsequently bromine atoms are generated by irradiating with light (254 nm) from a mercury-vapor lamp. After only 30 min, bands corresponding to propene (**3**) and allyl radical (**5**)[4] are visible in the IR spectrum. After 24 h irradiation, the cyclopropane is completely consumed. Alongside the bands for **3** and **5**, those from allene (**6**), propyne (**9**), and small amounts of acetylene and methane can be seen in the IR spectrum.[5] Interestingly, irradiation of **1** in a xenon matrix doped with Cl$^\bullet$, Br$^\bullet$ or I$^\bullet$ at wavelengths greater than 270 nm (mercury-vapor lamp with cutoff filter) produces propene (**3**) exclusively. The other products are only formed if the irradiation is changed to a shorter wavelength (254 nm). Control experiments (dependence of the appearance and disappearance of the relevant signals on wavelength and irradiation time) show that the first observable product is always propene (**3**). The allyl radical (**5**) is formed from this product by loss of a hydrogen atom. Radical **5** splits off a second H atom in forming allene (**6**), which then isomerizes to propyne (**9**, Scheme 1). A C–C bond cleavage can also occur in **5**, which leads eventually to acetylene and methane (probably via a methyl radical).



Scheme 1.

If the allyl radical (**5**) is generated by pyrolysis of a mixture of allyl iodide and xenon gas at 850 °C and immediately cooled to 10 K, then the product mixture subsequently formed in the I$^\bullet$-doped xenon matrix by irradiation is dependent on the wavelength of light used. Irradiation at 254 nm gives, as in the presence of Br$^\bullet$ atoms, allene (**6**), propyne (**9**), acetylene, methane, and, contrary to expectations, traces of propene (**3**) by trapping of an H atom.

The initial step in the transformation of cyclopropane (**1**) should be a C–C bond cleavage. The dissociation energy of the C–H bond is roughly 30 kcal mol^{-1} higher than for the C–C bond, so formation of the cyclopropyl radical (**4**) is unlikely. In spite of this, we examined the behavior of **4** in a halogen-doped matrix. The cyclopropyl radical **4**[6] was produced by irradiation into the long wavelength band of the allyl radical **5** at

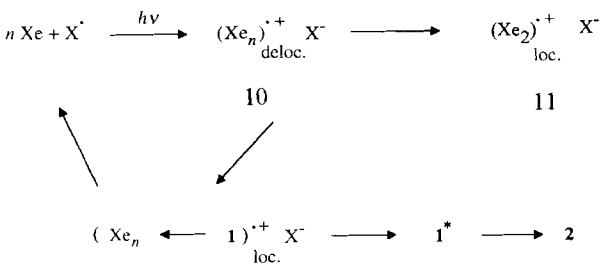
[*] Prof. G. Maier, S. Senger
Institut für Organische Chemie der Universität
Heinrich-Buff-Ring 58, D-35392 Giessen (FRG)
Telefax: Int. code + (641)702-5712

[**] Small Rings, Part 81. This work was supported by the Fonds der Chemischen Industrie. Part 80: G. Maier, R. Wolf, H.-O. Kalinowski, *Chem. Ber.*, in press.

(λ_{max} = 408.5 nm[4a]). This isomerization also occurs relatively quickly (1 h) when **5** is irradiated at >320 nm (mercury-vapor lamp with cutoff filter) in an I$^{\bullet}$-doped xenon matrix. A rapid reverse reaction of **4** to **5** is observed if the wavelength is subsequently changed to 254 nm. However, it cannot be concluded that propene (**3**) formation from irradiating cyclopropane (**1**) occurs by the pathway **1** → **4** → **5** → **3**, because the quantity of propene produced by the irradiation of cyclopropane is much greater than that produced in the irradiation of allyl radical **5**, carried out in a control experiment.

In addition to cyclopropane, cyclopropene (**7**) was also irradiated under the same conditions (Scheme 1). In the gas phase, **7** shows an UV absorption maximum at 190 nm[7] and also a noticeable end absorption above 200 nm. As a consequence, **7** is not stable with respect to 254 nm light in an argon matrix and affords allene (**6**) and propyne (**9**).[8] This photoisomerization proceeds much more easily in a xenon matrix. However, **7** is stable if the irradiating wavelength is 313 nm. In a Br$^{\bullet}$-doped xenon matrix, **7** is efficiently isomerized to **6** and **9** at both wavelengths, but faster at the shorter wavelength. Use of light of 254 nm leads to almost complete conversion after 2.5 hours.

What is the mechanism for the ring-opening of cyclopropane (**1**) and cyclopropene (**7**)? Our working hypothesis is the following: initially, exciplexes of type **10** are formed by excitation of the available halogen atoms (Scheme 2). This species is a hole/



Scheme 2.

anion pair in which the hole is delocalized in the valence band of the xenon and the anion is fixed. When no other partner is available, **10** relaxes to the more stable exciplex **11** in which the hole is also localized (by self-capture) in the form Xe_2^{+} (as partner to the ion X^-). The formation of **11** is confirmed by observation of the appropriate emissions.[1, 9a, b] The opportunity to perform chemistry with the delocalized hole **10** is new. If a suitable substrate molecule, like **1**, is available as a donor molecule, the delocalized hole in the xenon valence band can perform a capture reaction with it. The localized charge-transfer complex $(Xe_n \leftarrow \mathbf{1})^{\bullet +}$ is well away from the fixed X^- ion. Nonetheless, neutralization between the complex $(Xe_n \leftarrow \mathbf{1})^{\bullet +}$ and X^- can take place, because electron transfer can occur over large distances.[10] The energy stored in the charge separation of the cation radical and anion is thereby released. The energy contained in **12**, which is released instantaneously on neutralization, is sufficient to bring the substrate molecule to such a high vibrational state that bond cleavage results. For **1**, the barrier to be overcome is 65.0 kcal mol^{-1}.[3] This reaction probably proceeds via the diradical **2**,[11] or, starting from cyclopropene **7**, diradical **8** (vinylcarbene)[11] (activation energies E_A (**7** → **9**) = 34.7, E_A (**7** → **6**) = 43.4 kcal mol^{-1}[12]). In this manner the seemingly paradoxical result arises in which, in a thermal reaction at 10 K, **1** and **7** overcome a considerable energy barrier to break a C–C bond. The higher the excitation energy, the further apart the hole **10** and the halogen ion are separated from each other and the greater the stored energy. The following findings support this hypothesis: the formation of the exciplex **10** is indicated by a characteristic absorption maximum (Xe/I$^{\bullet}$: λ_{max} = 280 nm; Xe/Br$^{\bullet}$: λ_{max} = 310 nm; Xe/Cl$^{\bullet}$: λ_{max} = 354 nm). In principle, irradiation with light of this wavelength should be the most efficient for opening cyclopropane (**1**). Strangely, this is not the case. Photoexcitation of **1** with 313 nm light (mercury-vapor lamp, monochromator) in a Br$^{\bullet}$-doped xenon matrix gave absolutely no reaction, even though the wavelength employed corresponds to the absorption optimum. Only after changing to light of higher energy (254 nm) is the opening of **1** to **2** induced.

Received: October 2, 1993 [Z 6387 IE]
German version: *Angew. Chem.* **1994**, *106*, 605

[1] G. Maier, H. P. Reisenauer, K. Lanz, R. Troß, D. Jürgen, B. A. Hess, Jr., L. J. Schaad, *Angew. Chem.* **1993**, *105*, 119–121; *Angew. Chem. Int. Ed. Engl.* **1993**, *32*, 74–76.

[2] Doping of the xenon matrix with halogen atoms was carried out either by irradiation of the halogen molecules in the xenon matrix (bromine and chlorine) or by pyrolytic generation of BX$^{\bullet}$ and immediate cooling to 10 K (bromine and iodine). Since then we have discovered that the halogen-doping necessary for converting methylenecyclopropane into trimethylenemethane can also be achieved by irradiation of hydrogen bromide in the xenon matrix. The simultaneously generated H atom forms a Xe_2H^+ type ion with xenon (H. Kunttu, J. Seetula, M. Räsänen, V. A. Apkarian, *J. Chem. Phys.* **1992**, *96*, 5630–5635). These ions as well as the simultaneously formed hydrogen dibromide ion HBr_2^- (M. Räsänen, J. Seetula, H. Kunttu, *ibid* **1993**, *98*, 3914–3918) can be identified by using IR spectroscopy: G. Maier, D. Jürgen, unpublished results.

[3] T. S. Chambers, G. B. Kistiakowsky, *J. Am. Chem. Soc.* **1934**, *56*, 399–405.

[4] a) G. Maier, H. P. Reisenauer, B. Rohde, K. Dehnicke, *Chem. Ber.* **1983**, *116*, 732–740; b) A. K. Mal'tsev, V. A. Korolev, O. M. Nefedov, *Izv. Akad. Nauk SSSR Ser. Khim.* **1982**, 2415; *Bull. Acad. Sci. USSR Div. Chem. Sci. Engl. Transl.* **1982**, *31*, 2131.

[5] Only one band at 644 cm^{-1} could not be assigned to a plausible product.

[6] K. Holtzhauer, C. Cometta-Morini, J. F. M. Oth, *J. Phys. Org. Chem.* **1990**, *3*, 219–229.

[7] M. B. Robin, H. Basch, N. A. Kuebler, K. B. Wiberg, G. B. Ellison, *J. Chem. Phys.* **1969**, *51*, 45–52.

[8] O. L. Chapman, *Pure Appl. Chem.* **1974**, *40*, 511–523.

[9] a) M. E. Fajardo, V. A. Apkarian, *J. Chem. Phys.* **1986**, *85*, 5660–5681; b) *ibid.* **1988**, *89*, 4102–4123; c) *ibid.* **1988**, *89*, 4124–4136; d) I. Last, T. F. George, *ibid.* **1987**, *86*, 3787–3794; e) I. Last, T. F. George, M. E. Fajardo, V. A. Apkarian, *ibid.* **1987**, *87*, 5917–5927.

[10] a) J. R. Miller, J. A. Peeples, M. J. Schmitt, G. L. Closs, *J. Am. Chem. Soc.* **1982**, *104*, 6488–6493; b) L. T. Calcaterra, G. L. Closs, J. R. Miller, *ibid.* **1983**, *105*, 670–671.

[11] The structures **2** and **8**, shown for the primary ring-opened products, are merely formal. As these species could not be directly observed it is impossible to say anything about their exact nature (spin multiplicity, intermediate or transition state, number of stationary points on the reaction coordinate).

[12] R. Walsh, *J. Chem. Soc. Faraday Trans. 1* **1976**, *72*, 2137–2138; I. M. Bailey, R. Walsh, *ibid.* **1978**, *74*, 1146–1158.

Buckminsterfullerene Adducts from *Ortho*-Quinodimethanes**

Andreas Gügel, Alexander Kraus,
Jochen Spickermann, Pavel Belik, and Klaus Müllen*

Covalent-bonded fullerene adducts can be synthesized by the reaction of the fullerene C_{60} (**1**) with arynes,[1] carbenes,[2] or

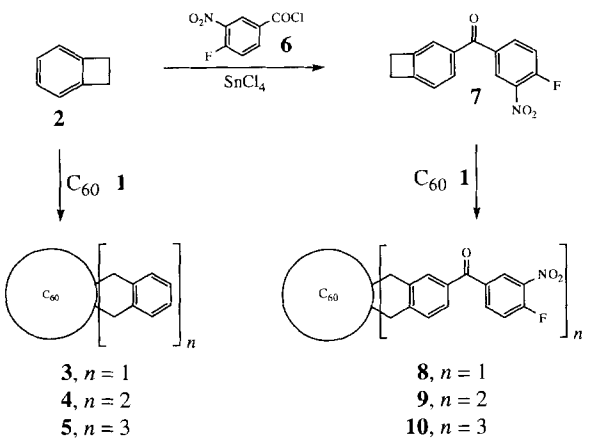
[*] Prof. Dr. K. Müllen, Dipl.-Chem. A. Gügel, Dipl-Chem. A. Kraus
Dipl.-Chem. J. Spickermann, Dipl.-Chem. P. Belik
Max-Planck-Institut für Polymerforschung
Ackermannweg 10, D-55128 Mainz (FRG)
Telefax: Int. code + (6131)379350

[**] This work was supported by the Bundesministerium für Forschung und Technologie (grant no. 13N6076).

organometallic reagents.[3] The Diels–Alder reaction of **1** with *o*-quinodimethane described by us, leads to thermally stable and soluble cycloadducts **3**,[6] **4**,[6] and **5** in high yields. It has now become apparent that modified fullerenes can be obtained from functionalized *o*-quinodimethanes. The former provide access to a broad spectrum of stable fullerene adducts by subsequent nucleophilic aromatic substitution. Thus it becomes possible to link C_{60} (**1**) in a simple way through bridging groups with chromophoric, electrophoric, or ionophoric units.

Functionalized derivatives of *o*-quinodimethane[4] can be obtained (under reaction conditions which are tolerated by **1**) by thermolysis of the corresponding derivatives of 3-isochromanone,[5] 1,2-dihydrocyclobutabenzene **2**, or 1,3-dihydrobenzo[*c*]thiophene-2,2-dioxide.[5] The thermolysis is thus an alternative to iodide-induced bromine elimination from 1,2-bis(bromomethyl)benzene derivatives.[6]

If C_{60} (**1**) is treated with 1.5 equivalents of unsubstituted **2** (accessible by flash vacuum pyrolysis of 2-methylbenzyl chloride[7]) in boiling 1,2,4-trichlorobenzene for 8 h, the monoadduct **3** (70%), the bisadduct **4** (27%; each based on converted C_{60}), and traces of the trisadduct **5** are formed. About 10% of unconverted C_{60} was recovered. The separation of the Buckminsterfullerene adducts **3**–**5** was achieved by chromatography on polystyrene gel by using toluene or chloroform as eluents.[5] The regioisomers of **4** and **5**, however, cannot be separated in this way.



Compound **2** can be transformed into **7** by a Friedel–Crafts reaction with the readily accessible carboxylic acid chloride **6**[8] (tin tetrachloride as catalyst *and* solvent). The reaction of **7** with **1** affords in quantitative yield (based on converted C_{60}) a mixture of the mono- (**8**) and bisadduct (**9**) as well as traces of the trisadduct **10**. The [4 + 2]cycloaddition involves exclusively the 6-6 bonds without the occurrence of subsequent ring openings (Fig. 1). The products were separated by chromatography on polystyrene gel with chloroform as the mobile phase. The very good solubility of the adducts in chloroform (ca. 20 mg mL^{-1}) as well as the good peak separation allowed the separation of up to 30 g crude material on a 20 × 600 mm 100 Å polystyrene gel column per day. All adducts **8**–**10** are thermally very stable, as supported by the thermogravimetric analysis of **9**; decomposition takes place first above 400 °C. Compound **8** can be detected in an almost unfragmented form by field desorption mass spectrometry.

The high activation of the fluorine-substituted phenyl ring by the nitro and keto group allows nucleophilic aromatic substitution of adducts **8**–**10** in almost quantitative yields.[9] The highly nucleophilic aliphatic amines such as 7,16-diaza[18]crown-6 (**11**)

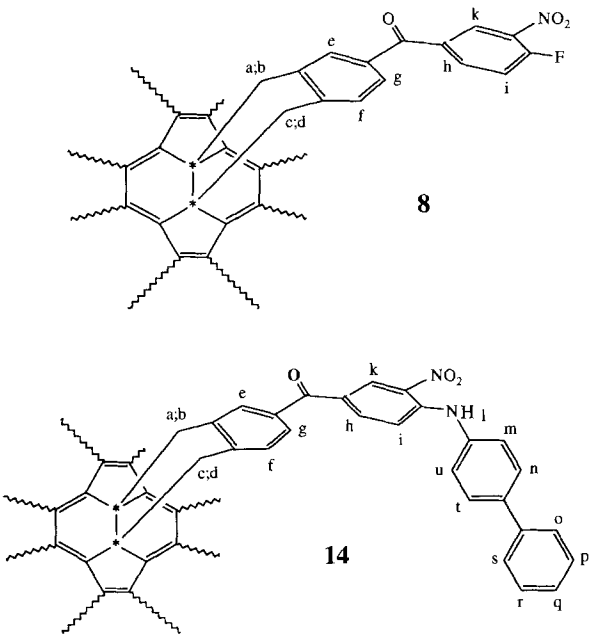
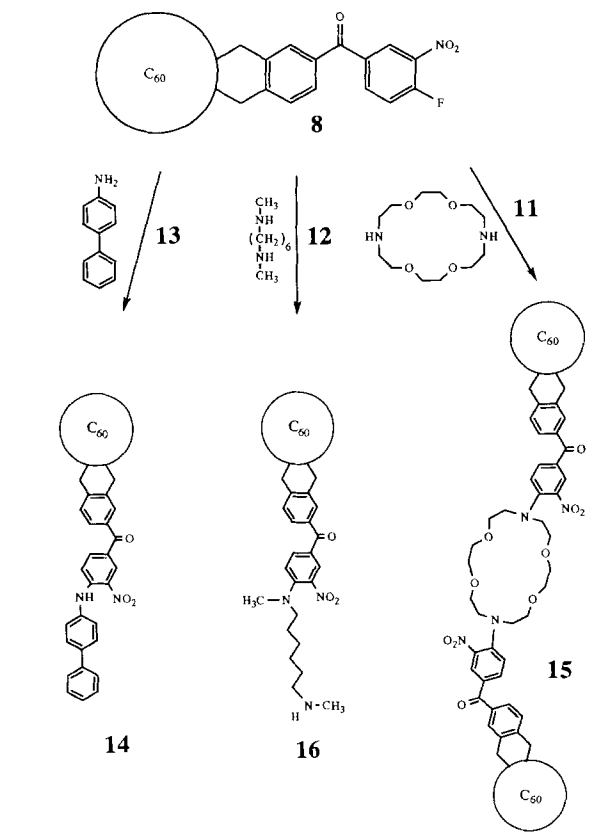


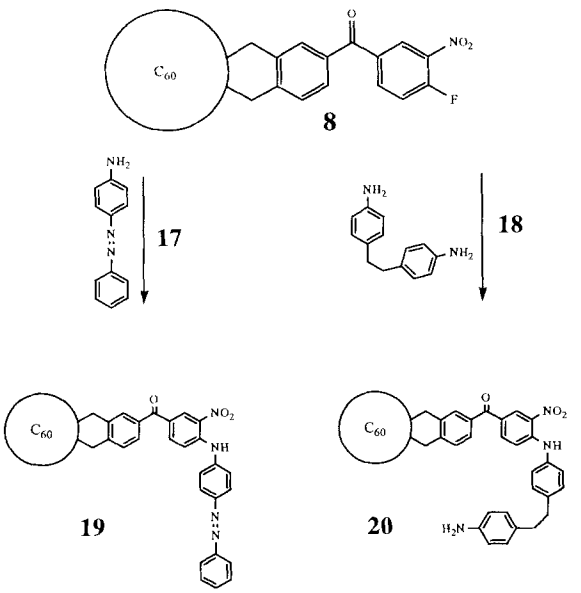
Fig. 1. Sections of **8** and **14** with the protons a–k and a–u, respectively.

or 1,6-bis(methylamino)hexane (**12**) react at room temperature within only a few minutes with **8**, whereas the less nucleophilic aromatic amines such as 4-aminobiphenyl (**13**) require significantly longer reaction times. The resulting mono- or bisfullerene adducts **14** and **16** and **15**, respectively are stable like the starting material **8**. They can also be separated readily from the starting materials by chromatography on polystyrene gel. The reaction of **8** with **11** occurs kinetically in a very unusual way. In contrast



 © VCH Verlagsgesellschaft mbH, D-69451 Weinheim, 1994 0570-0833/94/0505-0560 $ 10.00+.25/0

to the reaction of **12** with **8**, the bis-substitution product **15** forms almost exclusively even when the diamine **11** is present in a 100-fold excess and **8** is added very slowly. On the other hand, the monosubstitution product of **11** is always formed in only trace amounts. Besides the compounds described, a large number of other aromatic amines such as 4-aminoazobenzene (**17**) and 4,4'-diaminobibenzyl (**18**) were treated with **8**, leading to the formation of the adducts **19** and **20**, respectively.



The functionalization method chosen by us is limited by the electronic properties of C_{60} (**1**). Thus, the reaction of **8** with 1,3-benzenedithiol does not give the expected substitution product but leads to oligophenylenedisulfides by oxidative coupling (C_{60} and its derivatives are weak oxidizing agents). Likewise the reaction of 4-*tert*-butylphenol with potassium carbonate and **8** at 70 °C does not afford the expected adduct but a fragmentation of the C_{60} framework takes place. By the nucleophilic aromatic substitution of **8** and **9** it is now possible to bind primary and secondary amines covalently to Buckminsterfullerenes. From an electronic standpoint it is important to link the electron acceptor C_{60} with electron donors, since this provides substrates for the study of electron- and energy-transfer processes. In **15** two C_{60} units are bound by an ionophore. Furthermore, as a result of their functionalization, the mono- and bisadducts **8** and **9** are suitable for the incorporation of C_{60} as an active unit in side and main chain polymers.

Experimental Procedure

Reaction of 1 with 7: C_{60} (**1**) and **7** (1.5 equiv) were heated under reflux in 1,2,4-trichlorobenzene (1 mL per 6 mg **1**) for 8 h. The solution turned dark brown. The batch was concentrated to dryness at 100 °C/10^{-2} Torr, the brown solid taken up in chloroform, and the brown solution filtered through an 0.25 μm Teflon membrane filter. After chromatography on polystyrene gel the fractions were precipitated with methanol and the brown solid was dried for 4 h at 100 °C/10^{-2} Torr. The adducts **8**–**10** were usually prepared in 1–2 g quantities. The yield of **8** was 65% and of **9** 31% (each based on converted C_{60}). About 10% C_{60} (based on the C_{60} used) could be recovered. Compound **10** was formed in traces.

UV/VIS: The UV/VIS spectra of all the compounds described are similar to that of C_{60}. All monoadducts show an absorption band at 435 nm; for the higher adducts this band is missing. Compound **15** shows an additional weak absorption band at 701 nm.

MS(FD) (molecular ion peaks, *m/z*): **8**: 720 (**1**$^+$, 30%), 991.1 (**8**, M^+, 100%), 1262 (**9**$^+$, 10%). **9**: 720 (**1**$^+$, 30%), 991 (**8**$^+$, 7%) 1262.2 (**9**, M^+, 100%). **10**: 1262 (**9**$^+$, 10%) 1536 (**10**. M^+, 100%). **14**: 570.2 (**14**. M^{2+}, 15%), 720 (**1**$^+$, 5%), 1139.6 (**14**. M^+, 100%).

^1H NMR (δ values, 500 MHz, $C_2D_2Cl_4$, 28 °C; for **8** and **14** see Fig. 1): **8**: arom. H: 7.45 (t, 1H, 9 and 10 Hz, i), 7.8 (d, 1H, 8 Hz, f), 7.89 (d, 1H, 8 Hz, g), 8.04 (s, 1H, e), 8.18 (m, 1H, h), 8.53 (dd, 1H, 2 and 7 Hz, k); benzyl. H: 4.48 (b, 2H), 4.81 (b, 2H). **14**: N-H: 9.85 (s, 1H); arom. H: 7.3–7.43 (m, 6H, i, o, p, q, r, s), 7.57 (d, 2H, 7 Hz, m, u), 7.65 (d, 2H, 8 Hz, n, t), 7.78 (d, 1H, 8 Hz, f), 7.89 (dd, 1H, 2 and 8 Hz, g), 7.98 (dd, 1H, 2 and 8 Hz h), 8.02 (s, 1H, e), 8.75 (d, 1H, 2 Hz, k); benzyl. H: 4.48 (b, 2H), 4.82 (b, 2H). **15**: arom. H: 7.26 (d, 1H, 9 Hz), 7.76 (d, 1H, 8 Hz), 7.87 (d, 1H, 8 Hz), 7.96 (dd, 1H, 2 and 9 Hz), 8.0 (s, 1H), 8.20 (d, 1H, 2 Hz); benzyl. H: 4.46 (b, 2H), 4.80 (b, 2H); aliph. H: 3.54 (b, 8H, O-CH_2), 3.66 (b, 4H, N-CH_2). **16**: N-H: 4.07 (m, 1H); arom. H: 7.05 (d, 2H, 9 Hz), 7.81 (d, 1H, 7.5 Hz), 8.05 (dd, 1H, 2 and 9 Hz), 8.09 (b, 2H), 8.36 (d, 1H, 2 Hz); benzyl. H: 4.55 (b, 2H), 4.89 (b, 2H); aliph. H: 0.93 (b, 8H, CH_2), 2.34 (d, 3H, N-CH_3, 9 Hz), 2.94 (b, 3H, N-CH_3), 3.65 (s, 3H, N-CH_3), 4.23 (t, 2H, N-CH_2, 5 Hz).

^{13}C NMR (δ values, 125 MHz, $C_2D_2Cl_4$, 28 °C): *means: several superimposed signals. **8**: CO: 195.90; quart. non-aliph. C: 136.75, 137.5, 137.52, 138.69, 141.06, 142.20, 143.20* (b), 144.69* (b), 145.11* (b), 145.17, 145.19, 145.64, 146.16* (b), 147.42, 147.72, 147.75, 148.52* (b), 149.32, 149.53, 149.55, 150.75, 150.77; quart. arom. C: 119.4, 119.65, 126.65; arom. CH: 122.08, 122.25, 128.49, 131.23, 131.40, 131.60, 132.23, 132.29, 132.83 (b), 133.06, 140.10, 140.18; quart. aliph. C_{60}: 68.51, 68.56; aliph. C: 47.97, 48.19. **14**: CO: 196.37; quart. non-aliph. C: 139.61, 139.99, 141.06, 141.80, 142.77, 142.86, 143.24* (b), 144.66* (b), 145.11, 145.21, 145.25, 145.61, 146.16* (b), 146.27, 147.72, 147.77, 148.51, 149.01, 149.29* (b), 149.54* (b), 150.73, 150.76; quart. arom. C: 129.75, 134.96; arom. CH: 119.3, 128.42, 128.49, 130.11, 130.88, 131.4, 131.7, 132.12, 132.23, 132.65, 133.62, 139.87; quart. aliph. C_{60}: 68.63, 68.68; aliph. C: 48.04, 48.01.

Chromatography [10]: Elution pump: Master pump M 305 with a 25 SC pump head; injection pump: M 306 with a 25SC pump head; detector: UV DAD detector L-3000 with preparative flow-through type cell (light path: 0.1 mm) and DAD manager software; fraction collector: 201 C; column: 20 × 600 mm filled with polystyrene gel (5μm, 100 Å); amount injected: 2–6 mL of a saturated solution of the adducts in the mobile phase; mobile phase: 7 mL min^{-1} $CHCl_3$. Retention volumes (injection: 1 mL of a saturated solution) for all compounds described: **1**: 129.3 mL; **3**: 101.1 mL; **4**: 105.7 mL; **5**: 101.1 mL; **8**: 100.5 mL; **9**: 89.4 mL; **10**: 84.1 mL; **14**: 92.9 mL; monosubstitution product of **11**: 91.4 mL; **15**: 85.9.

Received: August 25, 1993 [Z6268IE]
German version: *Angew. Chem.* **1994**, *106*, 601

[1] S. H. Hoke, J. Molstad, D. Dilettato, M. J. Jay, D. Carlson, B. Kahr, R. G. Cooks, *J. Org. Chem.* **1992**, *57*, 5069–5071; J. Spickermann, Diplomarbeit, **1993**, Universität Mainz.

[2] A. Vasella, P. Uhlmann, C. A. A. Waldraff, F. Diederich, C. Thilgen, *Angew. Chem.* **1992**, *104*, 1383–1385; *Angew. Chem. Int. Ed. Engl.* **1992**, *31*, 1388–1390; T. Suzuki, Q. Li, K. C. Khemani, F. Wudl, *J. Am. Chem. Soc.* **1992**, *114*, 7300–7301; F. Wudl, *Acc. Chem. Res.* **1992**, *25*, 157–161; S. Shi, K. C. Khemani, Q. "Chan" Li, F. Wudl, *J. Am. Chem. Soc.* **1992**, *114*, 10656–10657.

[3] A. L. Balch, V. J. Catalano, J. W. Lee, M. M. Olmsted, *J. Am. Chem. Soc.* **1992**, *114*, 5455–5457; J. M. Hawkins, *Acc. Chem. Res.* **1992**, *25*, 150–156; A. Hirsch, A. Soi, H. R. Karfunkel, *Angew. Chem.* **1992**, *104*, 808–810; *Angew. Chem. Int. Ed. Engl.* **1992**, *31*, 766–768.

[4] a) Reviews on *ortho*-quinodimethanes: J. L. Charlton, M. M. Alauddin, *Tetrahedron* **1987**, *43*, 2873-2889; P. G. Sammes, *ibid.* **1976**, 32, 405-422; K. P. C. Vollhardt, *Angew. Chem.* **1984**, *96*, 525-541; *Angew. Chem. Int. Ed. Engl.* **1984**, *23*, 539-556; J. J. McCullough, *Acc. Chem. Res.* **1980**, *13*, 270-276; b) *ortho*-quinodimethanes from 1,2-dihydrocyclobutabenzene derivatives: T. A. Upshaw, J. K. Stille, J. P. Droske, *Macromolecules* **1991**, *24*, 2143-2150; R. P. Thummel, *Acc. Chem. Res.* **1980**, *13*, 70-76; I. L. Klundt, *Chem. Rev.* **1970**, *70*, 471-486; c) *ortho*-quinodimethanes from 1,3-dihydrobenzo[*c*]thiophene-2,2-dioxide derivatives: W. Oppolzer, D. A. Roberts, T. G. C. Bird, *Helv. Chim. Acta* **1979**, *62*, 2017-2021; W. Oppolzer, D. A. Roberts, *ibid.* **1980**, *63*, 1703-1705; K. C. Nicolaou, W. E. Barnette, P. Ma, *J. Org. Chem.* **1980**, *45*, 1463-1470; d) *ortho*-quinodimethanes from 3-isochromanone derivatives: R. J. Spangler, B. G. Beckmann, J. H. Kim, *J. Org. Chem.* **1977**, *42*, 2989-2996.

[5] By the reaction of C_{60} with 3-isochromanone and its core-substituted derivatives as well as with 1,3-dihydrobenzo[*c*]thiophene-2,2-dioxide and its derivatives numerous other Buckminsterfullerene adducts have been prepared by us in good yields and separated: A. Gügel, K. Müllen, *Chromatographia*, **1993**, *37*, 387–391.

[6] P. Belik, A. Gügel, J. Spickermann, K. Müllen, *Angew. Chem.* **1993**, *105*, 95-97; *Angew. Chem. Int. Ed. Engl.* **1993**, *105*, 78-80; similar reactions: Y. Rubin, S. I. Khan, D. I. Freedberg, C. J. Yeretzian, *J. Am. Chem. Soc.* **1993**, *115*, 344-345; S. I. Khan, A. M. Oliver, M. N. Paddon-Row, Y. Rubin, *ibid.* **1993**, *115*, 4919-4920.

[7] K. A. Walker, L. J. Markoski, J. S. Moore, *Synthesis* **1992**, 1265-1268.

[8] Compound **6** can be obtained by the reaction of commercially available carboxylic acid (Aldrich) with thionyl chloride under reflux.

[9] J. March *Advanced Organic Chemistry*, Wiley, **1985**, 576-607.

[10] Separation of fullerenes: A. Gügel, M. Becker, D. Hammel, L. Mindach, J. Räder, T. Simon, M. Wagner, K. Müllen, *Angew. Chem.* **1992**, *104*, 666-667; *Angew. Chem. Int. Ed. Engl.* **1992**, *31*, 644-645; A. Gügel, K. Müllen, *J. Chromatogr.* **1993**, *628*, 23-29.

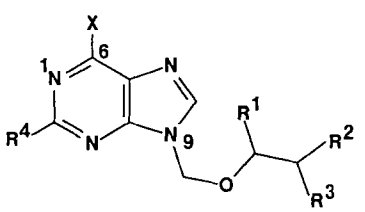
Regioselective Synthesis and Antiviral Activity of Purine Nucleoside Analogues with Acyclic Substituents at N7**

Gerhard Jähne,* Herbert Kroha, Armin Müller, Matthias Helsberg, Irvin Winkler, Gerhard Gross, and Thomas Scholl

Classic antiviral purine nucleosides such as 9-[(2-hydroxyethoxy)methyl]guanine (Aciclovir, ACV, **1a**),[1] 9-[(1,3-dihydroxy-2-propoxy)methyl]guanine (Ganciclovir, GCV, **1b**),[2] and 9-[(2,3-dihydroxy-1-propoxy)methyl]guanine (**1c**)[3] have an acyclic side chain linked to the N9 position of the natural heterocycle guanine instead of the D-ribofuranose residue of guanosine; in **1a** this substituent is a C1′-O-C4′-C5′ chain,[***] in **1b** a branched C1′-O-C4′-(C5′,C3′) chain.[***] The guanine derivatives **1a,b** are important in the treatment of viral diseases caused by herpes viruses including the herpes simplex virus 1 (HSV-1), herpes simplex virus 2 (HSV-2), varicella zoster virus (VZV), and the human cytomegalovirus.[4]

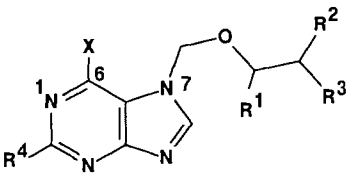
Since the discovery of the selective antiherpes action of **1a**[5] a multitude of purine and pyrimidine nucleoside analogues have been described.[6] In the synthesis of these purine nucleosides with acyclic substituents the N9 regioselectivity of the coupling of the heterocycle with the acyclic residue was considered essential, as natural purine nucleosides are substituted at N9. It was simply assumed that the analogous N7 regioisomers would not display antiviral activity. Indeed, this assumption was found to hold for the few hitherto isolated and characterized N7-substituted purines.[7] We report here on a regioselective route to purine nucleoside analogues having acyclic substituents at N7 and on the antiviral activity of one compound in this new class of drugs.

Guanine derivatives having carboacyclic substituents, in which the oxygen atom of the C1′-O-C4′-C5′ chain at N7 is replaced by a methylene group, can be prepared with moderate regioselectivity.[8] However, the synthetic route cannot be applied to the synthesis of purine nucleosides with acyclic substituents at N7. In contrast, the regioselective preparation of the N7 isomer of guanosine is known: a solution of persilylated N^2-acetylguanine and tetra-*O*-acetyl-β-D-ribofuranose in acetonitrile at room temperature is treated with a fivefold excess of tin tetrachloride.[9]



1

	X	R^1	R^2	R^3	R^4
1a [1]	OH	H	H	OH	NH_2
1b [2]	OH	CH_2OH	H	OH	NH_2
1c [3]	OH	H	OH	CH_2OH	NH_2
1d	OH	CH_2OiPr	H	O*i*Pr	$NHC(O)CH_3$
1e [16]	H	CH_2OiPr	H	O*i*Pr	NH_2
1f [7b]	NH_2	CH_2OH	H	OH	H
1g [14]	H	H	H	OH	NH_2
1h [7b]	H	CH_2OH	H	OH	NH_2



2

	X	R^1	R^2	R^3	R^4
2a	OH	CH_2OiPr	H	O*i*Pr	$NHC(O)CH_3$
2b	Cl	CH_2OiPr	H	O*i*Pr	$NHC(O)CH_3$
2c	Cl	CH_2OiPr	H	OCH_2Ph	$NHC(O)CH_3$
2d	Cl	CH_2OCH_2Ph	H	OCH_2Ph	$NHC(O)CH_3$
2e	Cl	CH_2OEt	H	OEt	$NHC(O)CH_3$
2f	Cl	H	OCH_2Ph	CH_2OiPr	$NHC(O)CH_3$
2g	Cl	H	O*i*Pr	H	$NHC(O)CH_3$
2h	H	CH_2OiPr	H	O*i*Pr	$NHC(O)CH_3$
2i	H	CH_2OiPr	H	O*i*Pr	NH_2
2k	H	CH_2OH	H	OH	NH_2
2l	H	CH_2OH	H	OH	$NHC(O)CH_3$
2m [7b]	OH	CH_2OH	H	OH	NH_2

We first examined the analogous reaction of persilylated N^2-acetylguanine with 1,3-diisopropoxy-2-methylthiomethoxypropane or 2-acetoxymethoxy-1,3-diisopropoxypropane (**3**)[10] under the same reaction conditions. A 1:1 mixture of the N9 isomer **1d** and the N7 isomer **2a** was obtained in good overall yield (80%). By modification of the starting materials, reagents, and conditions a regioselectivity of 9:1 could be obtained for the N7/N9 substitution. Persilylated N^2-acetylguanine was replaced with persilylated 2-acetamido-6-chloropurine (**4**), instead of a fivefold excess of tin tetrachloride 1–1.2 equivalents of trimethylsilyl trifluoromethanesulfonate (TMSOTf) was employed as the Lewis acid, 1,2-dichloroethane (DCE) served as the solvent rather than acetonitrile, and the reaction temperature was reduced to −30 °C. Under these conditions the N7 regioisomer **2b** was isolated as the kinetic reaction product in 65% yield (Scheme 1).[11] Following this procedure, compounds with related activated side chain components could be prepared regioselectively. Derivatives with other 1,3-dialkoxy-2-propoxymethyl side chains (**2c–2e**), the isomeric 2,3-dialkoxy-1-propoxymethyl side chain (**2f**), and a simple 2-alkoxyethoxymethyl side chain (**2g**) were synthesized.[11] A further advantage in the application of **4** instead of of N^2-acetylguanine is that the chloro substituent of **4** is conducive to a large number of modifications of the purine system. For example, **2b** can be converted into **2h** by hydrogenolysis and then into **2i** by subsequent aminolysis (Scheme 1). Diol **2k**, an isoster of the N9-substituted adenine derivative **1f**, which has only weak antiviral activity,[7b] is obtained by ether cleavage of **2h** with boron trichloride followed by removal of the *N*-acetyl protective group.

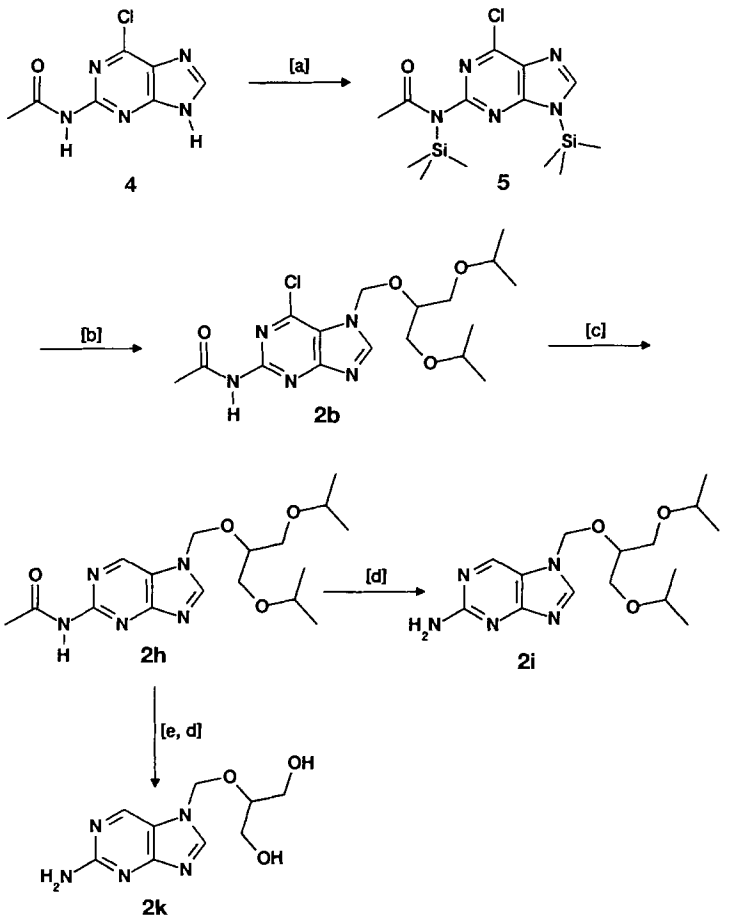
The N7- and N9-substituted products **2i** and **1e** (HOE 602), respectively, can be distinguished by their ^1H and ^{13}C NMR spectra.[12a] The spectroscopic data are in accord with those of other purine derivatives.[12b]

The antiviral activity of these compounds was measured in vitro with Vero cells infected with HSV-1 and HSV-2. We found that the N7-substituted purine derivative **2k** has a minimal inhibitory concentration (MIC) of 3.99 μM for HSV-1 and 6.9 μM for HSV-2. (The MIC is the concentration at which half of the

[*] Dr. G. Jähne, H. Kroha, A. Müller, Dr. M. Helsberg, Dr. I. Winkler
Hoechst AG, SGE Antiinfektiva-Forschung, G838
D-65926 Frankfurt am Main (FRG)
Telefax: Int. code + (69)305-331399
Dr. G. Gross, Dr. T. Scholl
Hoechst AG, Radiochemisches Labor

[**] We thank Dr. H.-W. Fehlhaber, Dr. H. Kogler, and M. Weber, Hoechst AG, Allgemeine Pharma Forschung, Analytisches Labor, for measuring the ^1H and ^{13}C NMR and mass spectra of the new compounds.

[***] The numbers refer to positions in the ribofuranose residue.



Scheme 1. Regioselective synthesis of 2-amino-7-[(1,3-dihydroxy-2-propoxy)-methyl]purine (**2k**). [a] $NH(SiMe_3)_2$, xylene, $(NH_4)_2SO_4$ cat., N_2, reflux, quantitative; [b] 2-acetoxymethoxy-1,3-diisopropoxypropane (**3**), TMSOTf, −30 °C, DCE, 65%; **2b**: m.p. 70–71 °C; [c] Pd/C (10%), H_2, MeOH, NEt_3, 91%; **2h**: m.p. 94 °C; [d] H_2NCH_3/H_2O, MeOH, reflux, 80%; **2i**: m.p. 154 °C; [e] BCl_3 in CH_2Cl_2, −40 °C, 78%; **2k**: m.p. 180 °C.

infected cells no longer show the cytopathogenetic effects caused by the virus.) The analogous inhibition values for **1a** are 2.42 and 1.7 μM, those for **1b** are 0.7 and 7.56 μM, respectively. N9-substituted purines like **1g** and **1e** are known to function in vivo as prodrugs of the corresponding guanine derivatives **1a** and **1b**, respectively. Xanthine oxidase converts **1g** into **1a**,[13] whereas in the bioconversions acting on **1e** this first anabolic step is followed by the cleavage of two isopropyl ether groups by enzymes of the P_{450} system.[14] Thus the excellent antiherpes action of **2k** might possibly be explained by its in vivo oxidation to **2m**, the N7 regioisomer of **1b**, or by the in vivo rearrangement of **2m** to give **1b** or of **2k** to provide **1h** followed by oxidation with xanthine oxidase yielding **1b**. The first hypothesis does not explain the antiviral action, as the antiherpes activity of **2m** has an MIC of ≥1.57 mM for HSV-1 and HSV-2. Preliminary studies of the metabolism of compound **2k** in vitro and in vivo do not indicate that the other possible processes occur.[15]

Thus we have developed a new regioselective synthesis of 2-aminopurine nucleoside analogues. One of these, **2k**, which displays promising antiviral activity (possibly after intracellular phosphorylation to the triphosphate ester), was shown not to be converted into a N9-substituted isomer. We are now examining the suitability of **2k** and its derivatives as new orally active antiviral drugs.

Received: August 19, 1993 [Z6300IE]
German version: *Angew. Chem.* **1994**, *106*, 603

[1] H. J. Schaeffer, L. Beauchamp, P. de Miranda, G. B. Elion, D. J. Bauer, P. Collins, *Nature* **1978**, *272*, 583–585.
[2] a) K. K. Ogilvie, U. O. Cheriyan, B. K. Radatus, K. O. Smith, K. S. Galloway, W. L. Kennell, *Can. J. Chem.* **1982**, *60*, 3005–3010; b) W. T. Ashton, J. D. Karkas, A. K. Field, R. L. Tolman, *Biochem. Biophys. Res. Commun.* **1982**, *108*, 1716–1721; c) J. C. Martin, C. A. Dvorak, D. F. Smee, T. R. Matthews, J. P. H. Verheyden, *J. Med. Chem.* **1983**, *26*, 759–761.
[3] W. T. Ashton, L. F. Canning, G. F. Reynolds, R. L. Tolman, J. D. Karkas, R. Liou, M.-E. M. Davies, C. M. DeWitt, H. C. Perry, A. K. Field, *J. Med. Chem.* **1985**, *28*, 926–933.
[4] M. S. Hirsch, J. C. Kaplan in *Virology, Vol. 1* (Eds.: B. N. Fields, D. M. Knipe, R. M. Chanock, M. S. Hirsch, J. L. Melnick, T. P. Monath, B. Roizman), Raven, New York, **1990**, pp. 441–468.
[5] G. B. Elion, P. A. Furman, J. A. Fyfe, P. de Miranda, L. Beauchamp, H. J. Schaeffer, *Proc. Natl. Acad. Sci. USA* **1977**, *74*, 5716–5720.
[6] C. K. Chu, S. J. Cutler, *J. Heterocycl. Chem.* **1986**, *23*, 289–319.
[7] a) K. K. Ogilvie, H. R. Hanna, *Can. J. Chem.* **1984**, *62*, 2702–2706; b) K. K. Ogilvie, N. Nguyen-Ba, M. F. Gillen, B. K. Radatus, U. O. Cheriyan, H. R. Hanna, K. O. Smith, K. S. Galloway, *ibid.* **1984**, *62*, 241–252; c) J. T. Kusmierek, B. Czochralska, N. G. Johansson, D. Shugar, *Acta Chem. Scand. Ser. B* **1987**, *41*, 701–707.
[8] a) J. Kjellberg, N. G. Johansson, *J. Heterocycl. Chem.* **1986**, *23*, 625–627; b) J. L. Sessler, D. J. Magda, V. Lynch, G. M. Schiff, G. I. Bernstein, *Nucleosides Nucleotides* **1989**, *8*, 431–448; c) G. R. Geen, T. J. Grinter, P. M. Kincey, R. L. Jarvest, *Tetrahedron* **1990**, *46*, 6903–6914.
[9] P. Garner, S. Ramakanth, *J. Org. Chem.* **1988**, *53*, 1294–1298.
[10] W. Hertzsch, G. Jähne (Hoechst AG), EP-A 448006, **1990**.
[11] G. Jähne, M. Rösner, I. Winkler, M. Helsberg, T. Scholl (Hoechst AG), EP-A 452680, **1990**.
[12] a) ^{1}H NMR (270 MHz, [D$_6$]DMSO, 25 °C, TMS): **2i**: δ = 8.65 (s, 1H; H-6), 8.38 (s, 1H; H-8), 6.22 (s, 2H; NH_2), 5.67 (s, 2H; H-1'), 3.65 (m, 1H; H-2'), 3.32 (m, 4H; H-3'), 3.42 (m, 2H; H-4'), 1.00 (q, 12H; H-5'); **1e**: δ = 8.59 (s, 1H; H-6), 8.16 (s, 1H; H-8), 6.52 (s, 2H; NH_2), 5.53 (s, 2H; H-1'), 3.80 (m, 1H; H-2'), 3.30 (m, 4H; H-3'), 3.43 (m, 2H; H-4'), 0.98 (d, 12H; H-5'); ^{13}C NMR (67.93 MHz, [D$_6$]DMSO, 25 °C, TMS): **2i**: δ = 162.74 (C-4), 161.00 (C-2), 147.54 (C-6), 142.30 (C-8), 118.47 (C-5), 76.99 (C-2'), 74.52 (C-1'), 71.05 (C-4'), 67.45 (C-3'), 21.71 (C-5'); **1e**: δ = 160.63 (C-2), 153.06 (C-4), 148.92 (C-6), 142.71 (C-8), 126.78 (C-5), 77.58 (C-2'), 71.41 (C-1'), 70.96 (C-4'), 67.36 (C-3'), 21.68 (C-5'); b) J. Kjellberg, N. G. Johansson, *Tetrahedron* **1986**, *42*, 6541–6544.
[13] T. A. Krenitsky, W. W. Hall, P. de Miranda, L. M. Beauchamp, H. J. Schaeffer, P. D. Whiteman, *Proc. Natl. Acad. Sci. USA* **1984**, *81*, 3209–3213.
[14] G. Gross, M. Helsberg, G. Jähne, M. Rösner, T. Scholl, I. Winkler, unpublished.
[15] G. Gross, M. Helsberg, G. Jähne, T. Scholl, I. Winkler, unpublished.
[16] a) E. Winkelmann, I. Winkler, H. Rolly, M. Rösner, G. Jähne, *Arzneim. Forsch.* **1988**, *38*, 1545–1548; b) I. Winkler, E. Winkelmann, T. Scholl, M. Rösner, G. Jähne, M. Helsberg, *Antiviral Res.* **1990**, *14*, 61–74.

The Influence of Charge Distribution on Bond Lengths in the P_4O_6 Framework in Compounds of the Type P_4O_6X**

Max Mühlhäuser, Bernd Engels, Christel M. Marian, Sigrid D. Peyerimhoff,* Pablo J. Bruna, and Martin Jansen

The occupation of orbitals in a molecule is a determining factor for the geometry of the nuclear framework. For this reason, electronic excitations often lead to significant changes in the molecular structure. Continuous changes in the charge distribution through various substituents can also cause noticeable

[*] Prof. Dr. S. D. Peyerimhoff, Dipl.-Chem. M. Mühlhäuser
Priv.-Doz. Dr. B. Engels, Priv.-Doz. Dr. C. M. Marian, Dr. P. J. Bruna
Institut für Physikalische und Theoretische Chemie der Universität
Wegelerstrasse 12, D-53115 Bonn (FRG)
Telefax: Int. code + (228)73-2551
Prof. Dr. M. Jansen
Institut für Anorganische Chemie der Universität Bonn (FRG)

[**] This work was supported by the Deutsche Forschungsgemeinschaft within the framework of the Sonderforschungsbereich 334.

alterations in the nuclear framework. These alterations need not necessarily be effected in the immediate vicinity of the disturbance. A marked example for this is the cage structure of phosphorus oxides and phosphorus oxide sulfides with the general formula $P_4O_6X_n$ (X = O, S; n = 0–4). The structures of these compounds can be derived from the adamantane-like P_4O_6 central framework, which has taken up oxygen or sulfur atoms at terminal positions on phosphorus.

The highly symmetrical P_4O_6 structure (T_d symmetry) is characteristically distorted in the monosubstituted compounds P_4O_6X, as can be seen in Figure 1. Both the first and second coordination spheres of the attacked phosphorus atom are changed upon transition from $P^{III} \rightarrow P^V$. The bonds between P^V and the nearest oxygen neighbours (P–O bonds) are now shorter, whereas the bonds between the bordering oxygen centers and the remaining phosphorus atoms (O–P bonds) are longer than in P_4O_6 (Table 1). Rather surprisingly, the alterations effected by the sulfur and oxygen substituents are of almost equal size. The small differences in the bond lengths found in phosphorus oxides and phosphorus oxide sulfides are in agreement with the situation found in numerous phosphoryl and thiophosphoryl compounds[4] and in P_4O and P_4S.[5]

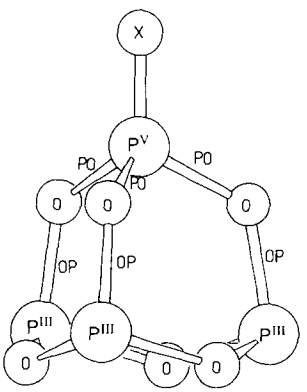


Fig. 1. Structure of P_4O_6X.

We have now carried out quantum chemical calculations which should help elucidate by which mechanisms the shortening of the P–O bond and lengthening of the O–P bond are effected, and whether the changes are directly connected, as had been assumed.[6] The deviations of the calculated structural data from the experimentally determined data are small, as can be seen in Table 1. This means that our Hartree–Fock calculations in a DZP (double zeta plus polarization) basis [7] are of sufficient accuracy to correctly describe the geometrical distortions in a qualitative manner.

Table 1. Comparison of the equilibrium geometries of P_4O_6, P_4O_7, and P_4O_6S as determined experimentally by X-ray structure investigations [1–3] and calculated theoretically (bond lengths in pm, bond angles in degrees).

Equilibrium geometry	P_4O_6 Exp. [a]	P_4O_6 Theor. [b]	P_4O_7 Exp. [c]	P_4O_7 Theor. [b]	P_4O_6S Exp. [d]	P_4O_6S Theor. [b]
$r(P^V\text{-X})$	-	-	145.0	143	189.0	188
$r(P^V\text{-O})$	165.5 [e]	165	159.4	160	159.6	161
$r(O\text{-}P^{III})$	165.5	165	168.4	166	167.8	166
$r(P^{III}\text{-O})$	165.5	165	164.6	165	163.7	165
$\sphericalangle$ O-P^V-O	99.5 [e]	98	103.5	101	103.1	100
$\sphericalangle$ P^V-O-P^{III}	127.0 [e]	129	123.9	127	124.2	128
$\sphericalangle$ O-P^{III}-O	99.5	98	98.9	98	98.9	98

[a] ref. [1]. [b] Hartree–Fock calculation in DZP AO basis. [c] ref. [2]. [d] ref. [3]. [e] In these cases P^V denotes the apical P atom.

In order to clarify whether the size of the distortion of the central P_4O_6 framework is directly related with the electron-attracting capability of the substituent X, geometry optimizations for P_4O_6X were performed by using a series of substituents, X, whose electronegativities stretched over a wide range. These included strongly electron-attracting substituents such as F^+ and H^+, and the electron-repelling N^-. As can be seen in Figure 2, there is a relationship between the charge density on the P^V center and the change in the P–O bond length. The shifts of the 1s orbital energies of P^V in P_4O_6X, as compared to its 1s orbital energy in the undisturbed P_4O_6 molecule, were used as a measure for the extent of the changes in the charge distribution. Population analyses that we carried out (Mulliken and Roby–Davidson) did not deliver reliable results due to the high polarity of the compounds involved. The 1s orbital energy of phosphorus can be expressed as in Equation (1);[10] where $\varepsilon_{1s}(P^{13+})$

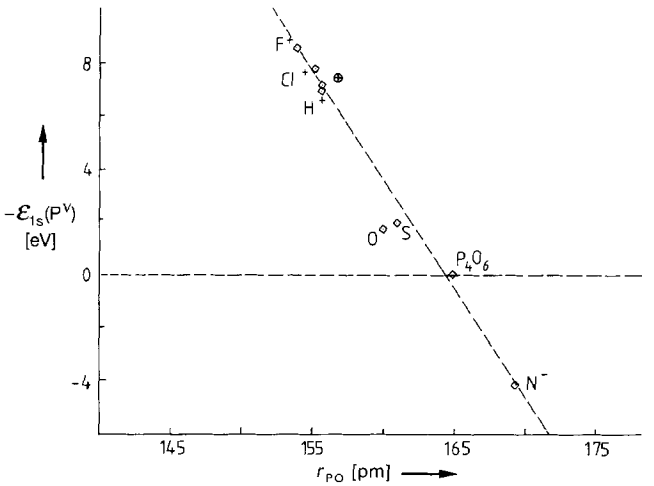


Fig. 2. Relationship between the 1s orbital energy $-\varepsilon_{1s}$ of the P^V center and the shortening of the P–O bond. The 1s orbital energies of the P^V center in P_4O_6X are plotted relative to its 1s orbital energy in the undisturbed P_4O_6 molecule. The sign has been chosen so that positive energy differences correspond to a more positive P^V center relative to P_4O_6. The individual compounds are denoted by the terminal substituent, the cation $P_4O_6^+$ by the symbol ⊕.

$$-\varepsilon_{1s}(P) = -\{\varepsilon_{1s}(P^{13+}) + V_{val} + V_{ext}\} \quad (1)$$

is the energy of the 1s electron of atomic phosphorus after removal of all outer electrons. V_{val} is the potential energy of the 1s electron in the mean field of the valence electrons on phosphorus, and V_{ext} the potential energy in the field of the electrons and nuclei of the other atoms. The last two terms are directly dependent on the electronic environment of the phosphorus; the 1s orbital energy is proportionally lower according to the increase in the positive partial charge on the phosphorus. The change in the 1s orbital energy of a particular center can, therefore, be regarded as a theoretical analogue to the chemical shift in ESCA (electron spectroscopy for chemical analysis) spectroscopy.[11, 12, 13] As can be seen in Figure 2, the P–O bond lengths vary considerably (> 15 pm), and this variation bears a direct correlation with the change in the electron density on the P^V center caused by the substituents. Particularly noteworthy is the observation that the reduction in P–O bond lengths, as found for the electron-attracting substituents, turns into an elongation for the electron-repelling N^-.

P_4O_6S and P_4O_7 deviate slightly from the correlation lines. As a result of the high electronegativity of oxygen, one would at first expect a significantly stronger electron-attracting effect and therefore a larger shift of the 1s orbital energy. According to Equation (1), however, the high electron density on the terminal P=O bond works to counteract this. In the case of P_4O_6S, the greater polarizability of sulfur allows the electrons to be distributed over a greater spatial volume, thus causing the effective charge densities to be approximately equal in both compounds. For this reason, sulfur has to be assigned the same effective electronegativity as oxygen in phosphorus-containing compounds. The relationship between the electron density in the

 © VCH Verlagsgesellschaft mbH, D-69451 Weinheim, 1994 0570-0833/94/0505-0564 $ 10.00+.25/0

terminal bond and the shift in the 1s orbital energy becomes particularly apparent when the atoms involved in a P–O bond are displaced (artificially) from their equilibrium positions. If the P–X distance is held constant and the P–O bond length is varied, the following picture (Fig. 3) ensues: The electron density on the phosphorus center is small for large P–O bond lengths ($r_{PO} > 165$ pm), and one obtains, as expected, a greater shift in the 1s orbital energy of P_4O_7 than in P_4O_6S; shorter PO bond lengths (< 165 pm), corresponding to higher electron densities on phosphorus, reverses this trend, as the electrons can be more easily shifted towards sulfur.

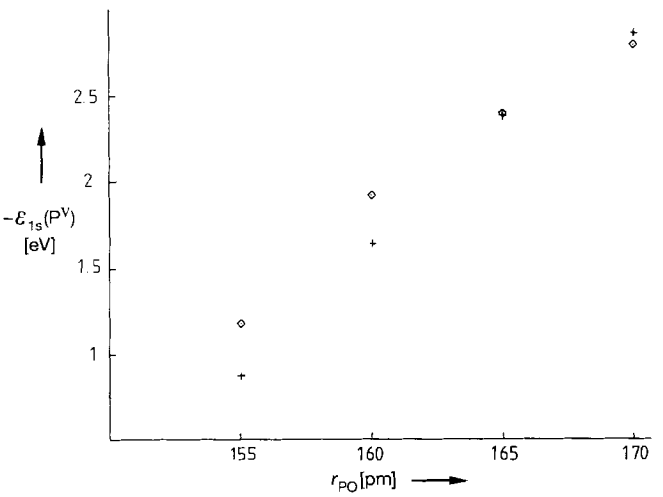


Fig. 3. Change of the 1s orbital energy of the P^V center in P_4O_6S (◇) and P_4O_7 (+) caused by an artificial distortion of the P–O bond. The sum of the P–O and the O···P bond lengths were held constant.

A correlation between the shortening of the P–O bond lengths and the elongation of the O···P bonds can be clearly seen in Figure 4. Whereas both bond lengths vary considerably in the series investigated, their sums remain virtually constant. This relationship, which is often employed in solid-state chemistry,[6] can be confirmed quite impressively here. The propagation of the disturbance arising on the P^V center into the P_4O_6 framework manifests itself in that the withdrawal of charge from P^V results in a more positive partial charge (with respect to P_4O_6) on the other phosphorus centers (Fig. 5). This shift in charge is

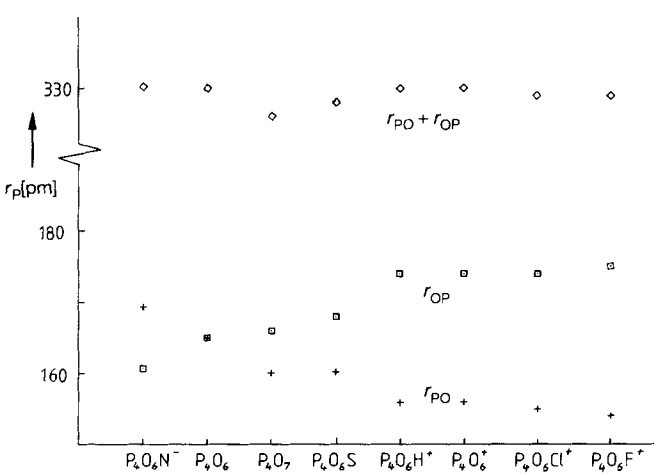


Fig. 4. Relationship between the shortening of the P–O bond and the elongation of the O···P bond. The individual bond lengths PO (+), OP (⊡) and their sums (◇) are plotted according to the substituents X.

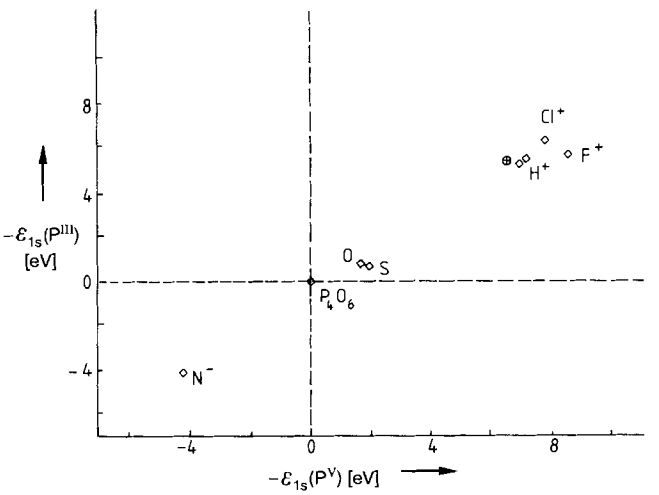


Fig. 5. Relationship between the charge density on P^V and the other phosphorus centers. The dimensions are defined in Figure 2.

more readily propagated for $X = Cl^+$ than for $X = F^+$, which indicates that both inductive and mesomeric effects play a role. The oxygen atoms which connect the P^V center with the remaining phosphorus centers take the role of a mediator such that no net charge displacement can be observed on them.

The comprehension of the individual form of a chemical bond in a defined environment, in such a way as to enable the construction of cause–effect relationships, has only been partially successful as yet. Our quantum chemical analyses on the phosphorus oxides and phosphorus oxide sulfides, which are particularly suited for this treatment, have shown that: 1) The change in bond lengths can be described in terms of the amount of charge transferred on substitution, which is documented by the 1s orbital energies, and 2) a strongly electron-repelling substituent, $X = N^-$, causes an elongation of the P–O bonds of the substituted P atom.

The synthesis and structural characterization of $P_4O_6N^-$ is therefore a great challenge for the preparative chemist, while at the same time being an acid test for the models proposed in this article.

Received: September 15, 1993 [Z 6358 IE]
German version: *Angew. Chem.* **1994**, *106*, 578

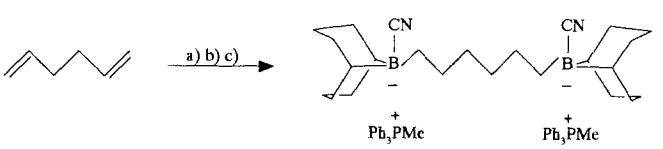
[1] M. Jansen, M. Voss, H.-J. Deiseroth, *Angew. Chem.* **1981**, *93*, 1023; *Angew. Chem. Int. Ed. Engl.* **1981**, *20*, 965; M. Jansen, M. Möbs, *Inorg. Chem.* **1984**, *23*, 4486.
[2] M. Jansen, M. Voss, *Angew. Chem.* **1981**, *93*, 120; *Angew. Chem. Int. Ed. Engl.* **1981**, *20*, 100; M. Jansen, M. Möbs, *Z. Anorg. Allg. Chem.* **1984**, *514*, 39.
[3] F. Frick, M. Jansen, P. J. Bruna, S. D. Peyerimhoff, *Chem. Ber.* **1991**, *124*, 1711.
[4] E. Fluck, D. Weber, *Z. Anorg. Allg. Chem.* **1975**, *412*, 47.
[5] P. J. Bruna, S. D. Peyerimhoff, *Chem. Phys.* **1991**, *149*, 325.
[6] M. O'Keefe, A. Navrotsky, *Structure and Bonding in Crystals*, Academic Press, New York, **1981**.
[7] The geometries were fully optimized at the Hartree–Fock level under retention of C_{3v} symmetry using the TURBOMOLE program package [8]. Contracted Gaussian orbital DZP basis sets were used [9]: H: (4s1p/2s1p) with $\alpha_p = 0.8$; (8s4p1d/4s2p1d) for the second-row elements, $\alpha_d = \{0.8(N), 1.2(O), 1.4(F)\}$; (11s7p1d/6s4p1d) for the third-row elements, with $\alpha_d = \{0.45(P), 0.55(S), 0.65(Cl)\}$.
[8] M. Häser, R. Ahlrichs, *J. Comput. Chem.* **1989**, *10*, 104.
[9] S. Huzinaga, *Approximate Atomic Wavefunctions I, II*, Dept. of Chemistry Report, University of Alberta, Alberta, Canada, **1965**.
[10] R. McWeeny, *Coulsons Chemische Bindung*, Hirzel, Stuttgart, **1984**, p. 187.
[11] K. Siegbahn, *ESCA: Atomic, Molecular and Solid-State Structure Studied by Means of Electron Spectroscopy*, Almqvist and Wicksells, Uppsala, **1967**.
[12] R. J. Buenker, S. D. Peyerimhoff, *Chem. Phys. Lett.* **1969**, *3*, 37; *J. Chem. Phys.* **1966**, *45*, 3682.
[13] Z. B. Maksić, *Molecular Spectroscopy, Electronic Structure and Intramolecular Interactions*, Springer, Berlin, **1991**, p. 290.

The First Water-Dependent Liquid Clathrate: X-Ray Evidence in the Solid for a C–H···π(Heteroarene)···H–C Interaction**

Roger Hunter*, Renate H. Haueisen, and Anne Irving

In spite of the explosion in supramolecular chemistry in recent years, few examples of boron host compounds[1] have emerged in the literature, presumably because of the air sensitivity of many of the boron-containing functionalities. In this regard, boronic acid derivatives[2] have found favor because of their relative air stability. To our knowledge the only host compound with borate units known to date has been reported by Nassimbeni et al.[3] They showed that certain tetraalkylammonium tetraalkylborates form liquid clathrates with a variety of hydrocarbons. However, the borate derivatives were difficult to purify and no satisfactory X-ray analysis could be obtained. Here we report on the synthesis of the first air- and water-stable cyanoborate[4] clathrand **1** which forms both a liquid and solid clathrate with furan depending on water content. An X-ray analysis[5] of the solid clathrate of **1** with furan has revealed an interesting C–H···π(heteroarene)···H–C interaction.

Bis-hydroboration of 1,5-hexadiene with 9-borabicyclo-[3.3.1]nonane (9-BBN) followed by cyanidation with sodium cyanide in *N,N*-dimethylformamide (DMF) and cation exchange with methyltriphenylphosphonium bromide furnished the air-stable clathrand bis(methyltriphenylphosphonium) *B,B'*-dicyano-*B,B'*-hexamethylenebis(9-boratabicyclo[3.3.1]nonane) **1** in 76% overall yield (Scheme 1). The ^1H and ^{13}C NMR spectra were in agreement with the proposed formula and compound **1** analyzed as **1** · H_2O.[6] The complete removal of water was followed by thermal gravimetric analysis (TGA) and required heating **1** in vacuo (0.5 mm Hg) at 70 °C for 16 h.



1

Scheme 1. a) 9-BBN (2 equiv), THF, 0 °C to 25 °C; b) NaCN (2 equiv), DMF; c) $PMePh_3Br$ (2 equiv), MeOH.

A study of the clathrate behavior of **1** with furan revealed it to be highly dependent on the water content in the sample of **1** · nH_2O. Samples of **1** with different n values were obtained by varying the drying temperature and n was determined by TGA. A completely anhydrous sample did not dissolve in furan, whereas warming of a sample with $n = 1$ with furan resulted in rapid formation of a slightly yellow-colored liquid clathrate beneath a colorless furan layer. The ^1H NMR spectrum indicated that the liquid clathrate contained about eight furan units per borate host, and IR and ^1H NMR spectroscopic investigations of the two layers indicated that the water resided in the liquid clathrate layer. The cut-off point for formation of a liquid clathrate was around $n = 0.8$, while much higher values of n than 1 promoted the formation of three layers, one being water.

[*] Prof. Dr. R. Hunter, Dipl.-Chem. R. H. Haueisen, Dr. A. Irving
Chemistry Department, University of Cape Town
Rondebosch 7700 (Republic of South Africa)
Telefax: Int. code +(21) 6503788

[**] This work was supported by Dynamic Power Systems Anglo American and the Foundation for Research and Development Pretoria. We thank L. Barbour for the data collection and Prof. L. R. Nassimbeni for helpful discussions.

This result is striking since, although a number of groups[7] have discovered liquid clathrate sustaining salts which are considerably more air- and water-stable than those of Atwood's original alkylaluminates[8], **1** constitutes the first example of a salt forming a water-dependent liquid clathrate. A further important aspect is that over a period of time (at least two days) beautiful transparent crystals of a solid clathrate appeared from the liquid clathrate layer; the crystallization time decreases with diminishing n. By ^1H NMR spectroscopy and TGA, the host–guest ratio in the solid clathrate was established as 1:2. Furthermore, water, although necessary for the formation of the liquid clathrate, was absent in the solid clathrate structure according to TGA, IR, and ^1H NMR. The result of an X-ray structure analysis of the solid clathrate is shown in Figure 1.

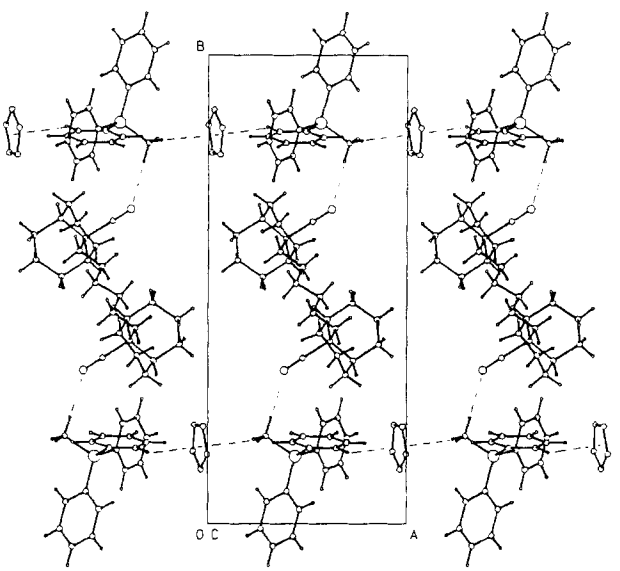


Fig. 1. Packing of **1** · $2C_4H_4O$ in the crystal. The view down Z0 showing the C–H···π···H–C and C–H···N hydrogen bonding scheme of the centrosymmetric ions solvated with furan.

Several features of the X-ray structure deserve mentioning. In contrast to aromatic compounds, very few structure analyses have been carried out on compounds involving furan as either a π ligand or as a guest in a solvate.[9] The cyanoborate clathrate is an example of a coordinatoclathrate[10] in a coordination-assisted host–lattice. The latter is provided by hydrogen bonding between a nitrogen atom[11] of a cyano group and a hydrogen atom of a phosphonium methyl group. The furan unit interacts with two hydrogen atoms from opposite faces of the plane of the heteroarene ring (see Fig. 1).[12] The hydrogen atoms involved in this C–H···π(heteroarene)···H–C interaction originate from the methyl group and the *ortho* position of a phenyl group of different phosphonium ions. Thus, the phosphonium ion plays a pivotal structural role in this clathrate and lends itself to future design characteristics.

C–H···π(arene) interactions have been of much interest recently[13] and are encountered when there is a deficiency of hydrogen bond acceptors.[14] Such interactions have been frequently reported for calixarene cavitates[15] involving π-electron-rich phenolic rings. We believe this to be the first example of a C–H···π(arene)···H–C interaction[16] and this may be due primarily to the π-excessive nature of the heteroaromatic guest. This interaction, however, is spatially analogous, although not electronically so, to a C–H···π(arene)···Cl–C interaction recently reported.[17]

In summary, this work extends the important contributions on the clathrate chemistry of organic onium compounds made by Vögtle et al.[18] Furthermore, clathrate activity is not just restricted to furan. Compound **1** also forms water-dependent liquid clathrates with benzene and thiophene, and normal solid clathrates with a range of aromatic compounds. The average guest:host (G:H) ratios of some examples were as follows benzene (0.8), *o*-, *m*-, and *p*-xylene (all ≈ 0.3), mesitylene (0.2), anisole (0.5), and *N*,*N*-dimethylaniline (1.0). Changing the cation of **1** to benzyltriphenylphosphonium extended the solid clathrate activity towards the recognition of more polar guests with higher G:H ratios compared to **1**. For instance, ether was included from the extraction procedure in a 0.4–0.8 G:H ratio and only released at 80–100 °C according to TGA. Some examples of other guests included were anisole (G:H ratio 2), benzothiazole (2.5), DMF (1.2). Hence, these phosphonium cyanoborates constitute a new family of clathrands whose activity (solid/liquid and selectivity) may be controlled by appropriate functional group changes. In our case the borate anion plays an important structural role and phosphonium is preferred over the ammonium cation. Further results on these interesting cyanoborates as novel clathrands will be communicated in due course.

Experimental Procedure

1: To a solution of 9-BBN (0.5 M in THF, 60 mL, 30 mmol) cooled to 0 °C was added 1,5-hexadiene (1.8 mL, 15 mmol) with a syringe. The mixture was stirred overnight at room temperature before the THF was removed by distillation at atmospheric pressure followed by pumping in vacuo. To the resulting liquid was added dry, deoxygenated DMF (1.5 mL) and dry NaCN (1.8 g, 36.7 mmol), and the mixture stirred until the reaction had cooled to room temperature. Na^+ ion exchange was carried out by adding methyltriphenylphosphonium bromide (10.72 g, 30.0 mmol) dissolved in MeOH (25 mL) to the borate mixture and stirring until a homogeneous mixture had formed. MeOH was removed under vacuum and ether and water were added resulting in the formation of three layers. Addition of solid NaCl (0.1 g) assisted in salting out the borate. The lower aqueous layer was separated and extracted twice with ether (2×30 mL). The combined ether extracts together with the oily middle layer from the first extraction were then washed three times with water (3×30 mL). This usually resulted in the formation of crystals from the middle layer. The combined ether extracts together with the oily middle layer and the crystals were kept at room temperature for all the precipitate to form. If solid did not form, all the aqueous and organic extracts were combined and left at 0 °C to precipitate out. The solid was filtered, washed with ether and water twice and vacuum dried to afford **1** · H_2O (10.56 g, 76%; m.p. 110–113 °C) as clear crystals. The included H_2O was removed under vacuum (0.5 mm Hg) at 70 °C for 16 h to afford anhydrous **1**. Correct C,H,N elemental analyses. ^{1}H NMR (200 MHz, $CDCl_3$, 25 °C): $\delta = 0.14$ (m, 4H), 0.35 (br.s, 4H), 0.95–2.12 (m, 32H), 2.89 (d, ^2J(P,H) = 13.3 Hz, 6H), 7.48–7.87 (m, 30H); ^{13}C NMR (50 MHz, $CDCl_3$, 25 °C): $\delta = 9.9$ (^1J(C,P) = 58 Hz), 24.6, 25.6, 26.5, 28.7, 30.7, 34.6, 35.9, 118.6 (^1J(C,P) = 88 Hz), 130.5 (^2J(C,P) = 12.9 Hz), 132.9 (^3J(C,P) = 10.8 Hz), 135.2, 150.0 (CN); IR (THF): $\tilde{\nu}$[cm^{-1}] = 2906, 2826, 2146 (CN), 1437, 1114.

Received: June 15, 1993
Revised version: September 4, 1993 [Z 6141 IE]
German version: *Angew. Chem.* **1994**, *106*, 588

[1] a) A. S. Fletcher, W. E. Paget, K. Smith, *Heterocycles* **1982**, *18*, 107; b) R. Köster, W. Schüssler, R. Boese, D. Bläser, *Chem. Ber.* **1991**, *124*, 2259.

[2] a) H. E. Katz, *J. Org. Chem.* **1989**, *54*, 2179; b) K. Tsukagoshi, S. Shinkai, *J. Org. Chem.* **1991**, *56*, 4089; c) M. T. Reetz, C. M. Niemeyer, M. Hermes, R. Goddard, *Angew. Chem.* **1992**, *104*, 1053; *Angew. Chem. Int. Ed. Engl.* **1992**, *31*, 1017.

[3] D. R. Bond, G. E. Jackson, H. C. João, M. N. Hofmeyer, T. A. Modro, L. R. Nassimbeni, *J. Chem. Soc. Chem. Commun.* **1989**, 1910.

[4] A. Pelter, K. Smith, M. G. Hutchings, K. Rowe, *J. Chem. Soc. Perkin Trans. 1* **1975**, 129.

[5] Crystallographic data for the clathrate of **1** with furan: $C_{62}H_{76}B_2N_2P_2 \cdot 2C_4H_4O$: monoclinic, $P2_1/n$, $a = 10.181(1)$, $b = 23.310(4)$, $c = 13.182(4)$ Å, $\beta = 91.07(2)°$, $Z = 2$, $\rho_{calcd} = 1.14$ Mg m^{-3}, $\mu(Mo_{K\alpha}) = 0.08$ mm^{-1}, $F(000) = 1148$, $\lambda(Mo_{K\alpha}) = 0.71069$ Å, $T = 25$ °C. Measurements were made with an Enraf–Nonius CAD4 diffractometer. 5903 reflections, 4540 unique, 3397 with $I > 2\sigma(I)$ considered as observed. Solution by direct methods and refinement with SHELX-76. $R = 0.053$, $R_w = 0.065$, $w = 1/[\sigma^2(F_o) + 0.0052(F_o^2)]$. All non-hydrogen atoms, except those for the furan molecule, anisotropic. Constained isotropic refinement of hydrogen atoms. Furan ring disordered, refined as regular pentagon, hydrogen atoms not placed. Two positions of furan ring (0.54:0.46) related by a rotation of 35° by the plane of the ring round the normal through the centroid. Further details of the crystal structure investigation are available on request from the Director of the Cambridge Crystallographic Data Centre, 12 Union Road, GB-Cambridge CB2 1EZ, UK, on quoting the names of the authors, and the full journal citation.

[6] This was corroborated by an X-ray structure which will be reported elsewhere.

[7] a) S. Christie, R. H. Dubois, R. D. Rogers, P. S. White, M. J. Zaworotko, *J. Inclusion Phenom. Mol. Recognit. Chem.* **1991**, *11*, 103; b) A. Alvanipour, H. Zhang, J. L. Atwood, *J. Organomet. Chem.* **1988**, *358*, 295; c) S. A. Sangokoya, G. H. Robinson, *J. Inclusion Phenom. Mol. Recognit. Chem.* **1990**, *9*, 85.

[8] J. L. Atwood in *Inclusion Compounds, Vol. 4* (Eds.: J. L. Atwood, J. E. D. Davies, D. D. MacNicol), Academic Press, New York, **1984**, p. 375.

[9] a) B. Chaudret, F. A. Jalon, *J. Chem. Soc. Chem. Commun.* **1988**, 711; b) S. E. Biali, B. Kahr, Y. Okamoto, R. Aburatani, K. Mislow, *J. Am. Chem. Soc.* **1988**, *110*, 1917.

[10] E. Weber, H. P. Josel, *J. Inclusion Phenom.* **1983**, *1*, 79.

[11] D. S. Reddy, B. S. Goud, K. Panneerselvam, G. R. Desiraju, *J. Chem. Soc. Chem. Commun.* **1993**, 663.

[12] The position of the *ortho* phenyl proton H(O) and of the methyl proton H(M) from two different phosphonium ions with respect to the furan ring suggests that C–H···π interactions are possible here, since the hydrogen atoms are vertically above and below the plane of the ring and, at a distance from it less than the sum of the van der Waals distances for a π bond and a hydrogen atom (1.77 + 1.17) Å. Geometric parameters for H(M) and H(O) are respectively: perpendicular distance from the plane of the furan ring 2.67, 2.79 Å; H···ring-centroid 2.79, 2.80 Å; angle between the C–H bond and the perpendicular from the hydrogen atom to the ring plane 148, 144°; C–H···ring-centroid 132, 140°; range of distances from the furan ring atoms 2.73 to 3.32, 2.96 to 3.10 Å. The H···ring-centroid···H angle is 165°. The C–H···π interaction of chloroform with benzene has been known for a long time [13b]. Accordingly, the generality of the $(Cl_3C)H\cdots\pi$(arene) interaction was probed with the 1992 version of the Cambridge Structural Database [19] (102 103 entries). 153 error-free, non-disordered structures, $R < 0.100$, were used. Intermolecular contacts were evaluated from normalized hydrogen positions with GSTAT90. The angle between the C–H bond and the perpendicular from the H atom to the plane of the aromatic ring was constrained to lie between 100 and 180°. The distances of the hydrogen atom to each of the six ring carbon atoms were restricted to the range 2.0 to 4.0 Å to ensure that the H atom was vertically over the inside of the periphery of the ring. Three hits (refcodes: DAJLOP, FECTAI, DUYXEA) were obtained and these were scrutinized manually. The results in Table 1 show that the parameters for the C–H···π(heteroarene)···H–C interaction fit very neatly into the pattern for $(Cl_3)C$–H···π(arene) interactions.

Table 1. Some geometric parameters for C–H···π interactions.

	H···π [a] [Å]	Angle [b] [°]	Range of H···C(π) [Å]
DAJLOP	2.35	170	2.57–4.03
FECTAI	2.42	173	2.59–3.08
Ref. [17]	2.60	158	2.76–3.16
DUYXEA	2.65	143	2.68–3.61
H(M)	2.67	148	2.73–3.32
H(O)	2.79	144	2.96–3.10

[a] Perpendicular distance of the hydrogen atom to the ring. [b] Angle between the C–H bond and the perpendicular from the hydrogen atom to the ring plane.

Further support for the C–H···π(heteroarene)···H–C interaction is given from work reported on the geometry of interactions of X–H (X = O, N) with π-electron systems [20]. A second hydrogen atom of the phosphonium methyl group forms a hydrogen bond to the cyano nitrogen atom; C(H)···N 3.425(3), H···N 2.46 Å, C–H···N 177°.

[13] a) K. Kobayashi, Y. Asakawa, Y. Kikuchi, H. Toi, Y. Aoyama, *J. Am. Chem. Soc.* **1993**, *115*, 2648; b) M. Nishio, M. Hirota, *Tetrahedron* **1989**, *45*, 7201.

[14] L. R. Hanton, C. A. Hunter, D. H. Purvis, *J. Chem. Soc. Chem. Commun.* **1992**, 1134.

[15] a) M. A. McKervey, E. M. Seward, G. Ferguson, B. L. Ruhl, *J. Org. Chem.* **1986**, *51*, 3581; b) P. Soncini, S. Bonsignore, E. Dalcanale, F. Ugozzoli, *ibid.* **1992**, *57*, 4608; c) G. D. Andreetti, O. Ori, F. Ugozzoli, C. Alfieri, A. Pochini, R. Ungaro, *J. Inclusion Phenom.* **1988**, *6*, 523; d) R. Ungaro, A. Pochini, G. D. Andreetti, P. Domiano, *J. Chem. Soc. Perkin Trans. 2* **1985**, 197.

[16] For the first example of two π-arene···H interactions, in an inclusion complex involving CH_2Cl_2 as the guest, see: J. L. Atwood, S. G. Bott, C. Jones, C. L. Raston, *J. Chem. Soc. Chem. Commun.* **1992**, 1349.

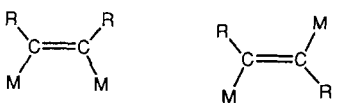
 © VCH Verlagsgesellschaft mbH, D-69451 Weinheim, 1994 0570-0833/94/0505-0567 $ 10.00+.25/0

[17] A. Irving, H. M. N. H. Irving, *J. Crystallogr. Spectrosc. Res.* **1993**, *23*, 725.
[18] F. Vögtle, H. G. Löhr, J. Franke, D. Worsch, *Angew. Chem.* **1985**, *97*, 721; *Angew. Chem. Int. Ed. Engl.* **1985**, *24*, 727.
[19] F. H. Allen, S. Bellards, M. D. Brice, B. A. Cartwright, A. Doubleday, H. Higgs, T. Hummelink, B. G. Hummelink-Peters, O. Kennard, W. D. Motherwell, J. R. Rodgers, D. G. Watson, *Acta Crystallogr. Sect. B* **1979**, *35*, 2331.
[20] M. A. Viswamitra, R. Radhakrishnan, J. Bandekar, G. R. Desiraju, *J. Am. Chem. Soc.* **1993**, *115*, 4868.

Reactions at Both Ends of a Dimetalated Olefin: CS_2 Insertion into and Atom Transfer Reactions of $[Re(CO)_4\{trans\text{-}\mu\text{-}HC{=}C(CO_2Me)\}Re(CO)_4(NCMe)]$**

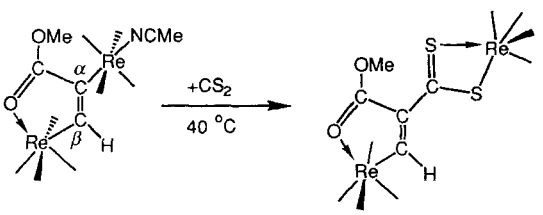
Richard D. Adams,* Linfeng Chen, and Wengan Wu

Polynuclear metal complexes with bridging alkyne ligands are of great interest in organic synthesis.[1-3] Dimetalated olefins **A** and **B** are a special class of di-σ-coordinated alkyne complexes whose organic chemistry has not yet been widely studied.[4, 5]



A B

We have now found an interesting combination of reagents that permits the functionalization of a dimetalated olefin at both ends of the ligand. Complex **1**[5a] reacts readily with carbon disulfide to yield the new complex **2** (78% yield) by insertion of the CS_2 molecule exclusively into the Re–C_α bond of **1**.



1 2

Compound **2** has been structurally characterized by X-ray diffraction methods (Fig. 1).[6] The structures of **2** and the related complex $[Re(CO)_4\{(E)\text{-}HC{=}C(CO_2Me)C{=}N(C_6H_4\text{-}p\text{-}Me)S\}Re(CO)_4]$ formed by the reaction of *p*-tolylisothiocyanate with **1** are very similar.[5b] The two $Re(CO)_4$ groups in **2** are linked by an (*E*)-methylcarboxylate-substituted dithiocarboxylatovinyl unit. The dithiocarboxylate group is chelated to the Re1 center (Re1–S1 2.496(2) and Re1–S2 2.495(2) Å). The C–C distances indicate that the C2–C3 bond is a double bond (1.35(1) Å) and that the C1–C2 bond is a single bond (1.47(1) Å). The methylcarboxylate group is coordinated by its ketonic oxygen atom to Re2 as in **1** (Re2–O1 2.201(5) Å).

Most interestingly, compound **2** subsequently reacts with the atom transfer reagents, pyridine-*N*-oxide and ethylenesulfide, to

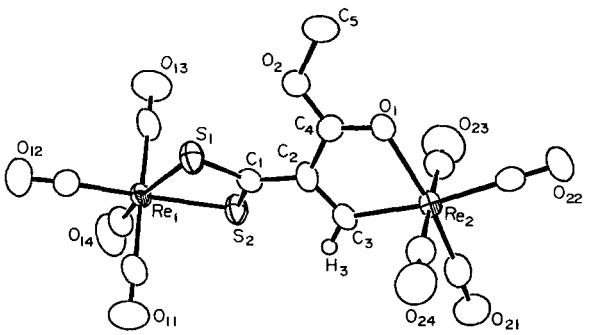
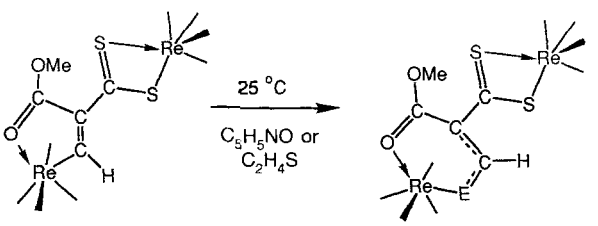


Fig. 1. Molecular structure of **2** (ORTEP, 50% probability thermal ellipsoids). Selected interatomic distances [Å]: Re1–S1 2.496(2), Re1–S2 2.495(2), Re2–C3 2.125(9), Re2–O1 2.201(5), C1–C2 1.47(1), C2–C3 1.35(1), C1–S1 1.686(8), C1–S2 1.696(9), C2–C4 1.45(1).

insert a heteroatom into the Re–C_β bond. Treatment of **2** with pyridine-*N*-oxide at 25 °C afforded the new complex **3a** in 97% yield, the reaction with ethylenesulfide at 25 °C gave compound **3b** in 50% yield. Both compounds were characterized by IR and ^{1}H NMR spectroscopy and elemental analyses. Compound **3b**



2 **3a,b:** E = O, S

was further characterized by a single-crystal X-ray diffraction analysis (Fig. 2).[6] The structures of **2** and **3b** have many common structural features; the most noticeable difference is that in **3b** a sulfur atom S3 has been inserted into the Re2–C3 bond

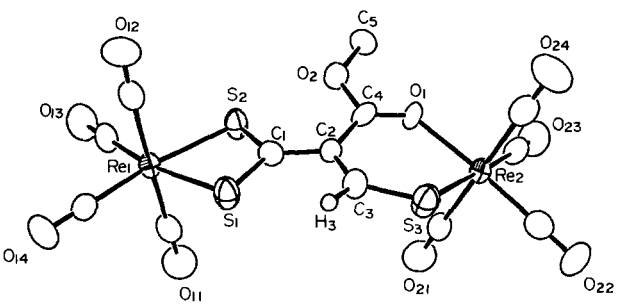


Fig. 2. Molecular structure of **3b** (ORTEP, 50% probability thermal ellipsoids). Selected interatomic distances [Å]: Re1–S1 2.495(2), Re1–S2 2.481(2), Re2–S3 2.452(2), Re2–O1 2.163(5), C1–C2 1.46(1), C2–C3 1.38(1), C1–S1 1.713(7), C1–S2 1.702(7), C3–S3 1.676(8), C2–C4 1.47(1).

(Re2–S3 2.452(2) Å). The C2–C3 distance in **3b** is short (1.38(1) Å), likewise the C3–S3 distance is also short (1.676(8) Å), and is even shorter than the C–S distances in the dithiocarboxylate group (1.713(7) and 1.702(7) Å). Thus, this C–S bond may also contain some multiple bond character.

An increasing number of studies have focused on the oxygenation of organic ligands in metal complexes by atom transfer.[7] We are unaware of any previous studies that demonstrate

[*] Prof. R. D. Adams, L. Chen, W. Wu
Department of Chemistry and Biochemistry
University of South Carolina, Columbia, SC 29208 (USA)
Telefax: Int. code + (803)777-6781

[**] This research was supported by the Office of Basic Energy Sciences of the US Department of Energy.

both oxygen and sulfur atom insertions occurring at the same transition metal–carbon bond.

Experimental Procedure

2: **1** (100.0 mg, 0.139 mmol) and CS_2 (100.0 μL, 1.660 mmol) were dissolved in CH_2Cl_2 (200 mL) and heated to reflux for 4 h. The product was separated by TLC on silica gel to give 82.8 mg **2** (orange, 78%). IR (hexane): $\tilde{\nu}$(C=O) [cm^{-1}] = 2098(w), 2008(s), 1995(m), 1959(s), 1582(w); ^1H NMR ($CDCl_3$): δ = 11.65 (s, 1H, C*H*), 4.09 (s, 3H, O*Me*); MS: *m/z* = 758 (M^+, ^{187}Re) and ions corresponding to the loss of eight carbonyl ligands; correct elemental analysis.

3a: **2** (20.0 mg, 0.026 mmol) in CH_2Cl_2 (30 mL) was allowed to react with C_5H_5NO (3.0 mg, 0.032 mmol) at 25 °C for 20 min. The product was separated by TLC on silica gel to give 19.8 mg **3a** (yellow, 97% yield). IR (hexane): $\tilde{\nu}$(C=O) [cm^{-1}] = 2120(vw), 2101(w), 2018(s), 2002(s), 1991(s), 1958(s), 1605(m). ^1H NMR ($CDCl_3$): δ = 9.64 (s, 1H, C*H*), 3.92 (s, 3H, O*Me*); MS: *m/z* = 774 (M^+, ^{187}Re) and ions corresponding to the loss of six carbonyl ligands; correct elemental analysis.

3b: **2** (20.0 mg, 0.026 mmol) in hexane (20 mL) was allowed to react with C_2H_4S (20.0 μL, 0.336 mmol) at 25 °C for 3 h. The product was separated by TLC on silica gel to give 10.2 mg **3b** (orange, 50% yield). IR (hexane): $\tilde{\nu}$(C=O) [cm^{-1}] = 2114(vw), 2101(w), 2019(s), 2004(s), 1993(m), 1963(s), 1958(m), 1585(w). ^1H NMR (C_6D_6) **3b**: δ = 10.17 (s, 1H, C*H*), 2.82 (s, 3H, O*Me*); correct elemental analysis.

Received: August 21, 1993 [Z 6309 1E]
German version: *Angew. Chem.* **1994**, *106*, 591

[1] N. E. Schore, *Chem Rev.* **1988**, *88*, 1081.
[2] G. Palyi, G. Vardi, L. Markó in *Stereochemistry of Organometallic and Inorganic Compounds Vol. 1* (Ed.: I. Bernal), Elsevier, Amsterdam, **1986**, p. 358.
[3] E. Sappa, A. Tiripicchio, P. Braunstein, *Chem Rev.* **1983**, *83*, 203.
[4] F. R. Lemke, D. J. Szalda, R. M. Bullock, *J. Am. Chem. Soc.* **1991**, *113*, 8466.
[5] a) R. D. Adams, L. Chen, W. Wu, *Organometallics* **1993**, *12*, 1623; b) *ibid.* **1993**, *12*, 2404.
[6] **2**: Orange crystals: $Re_2S_2O_{10}C_{13}H_4$, M_r = 756.70, monoclinic, 20 °C, space group $C2/c$, a = 1865.1(3), b = 1151.3(3), c = 1795.2(2) pm, β = 97.54(1)°, Z = 8, ρ_{calcd} = 2.63 $g cm^{-3}$, $Mo_{K\alpha}$ radiation, $2\theta_{max}$ = 46°, 2320 reflections ($I > 3\sigma I$), number of variables 248, empirical absorption correction (Ψ scans), R = 0.028, R_w = 0.032.–**3b**: Orange crystals: $Re_2S_3O_{10}C_{13}H_4$, M_r = 788.76, triclinic, 20 °C, space group $P\bar{1}$, a = 1236.3(2), b = 1388.0(3), c = 597.3(1) pm, α = 93.09(2), β = 101.06(1), γ = 77.81(1)°, Z = 2, ρ_{calcd} = 2.66 $g cm^{-3}$, $Mo_{K\alpha}$ radiation, $2\theta_{max}$ = 45°, 2126 reflections, number of variables 269, empirical absorption correction (Ψ scans), R = 0.020, R_w = 0.022. Programs: TEXSAN structure solving program library (V 5.0) of the Molecular Structure Corp., The Woodlands, TX. Further details of the crystal structure investigations are available on request from the Director of the Cambridge Crystallographic Data Centre, 12 Union Road, GB-Cambridge, CB2 1EZ, (UK), on quoting the full journal citation.
[7] a) J. Muzart, A. Riahi, *Organometallics* **1992**, *11*, 3478; b) T. V. Lubben, P. T. Wolczanski, *J. Am. Chem. Soc.* **1987**, *109*, 424; c) P. L. Alsters, J. Boersma, G. van Koten, *Organometallics* **1993**, *12*, 1629; d) C. Sinha, D. Bandyopadhyay, A. Chakravorty, *Inorg. Chem.* **1988**, *27*, 1173; e) A. K. Mahapatra, D. Bandyopadhyay, P. Bandyopadhyay, A. Chakravorty, *Inorg. Chem.* **1986**, *25*, 2214; f) C. Sinha, D. Bandyopadhyay, A. Chakravorty, *J. Chem. Soc. Chem. Commmun.* **1988**, 468; g) A. K. Mahapatra, D. Bandyopadhyay, P. Bandyopadhyay, A. Chakravorty, *ibid.* **1984**, 999; h) P. T. Matsunaga, G. L. Hillhouse, *J. Am. Chem. Soc.* **1993**, *115*, 2075.

$[SbN(SbCl)_3(NSbCl_2)(NSiMe_3)_2 \cdot SbCl_3]$, an Unusual Nitridoantimony Complex with a Heterocubane Structure

Markus Rhiel, Frank Weller, Jürgen Pebler, and Kurt Dehnicke*

Nitrido complexes of main group elements in their highest oxidation states, in particular of the heavy elements, are rare,[1] in contrast to the many such examples of complexes of transition metals.[2] One of the reasons is considered to be the instability of the element's bond to nitrogen—these complexes are energetically favored only by a lowering of the basicity of the nitrogen atoms by electron-withdrawing groups or through mesomeric effects.[1] One example is the imidoantimony(v) complex **1**, which has an Sb_4N_4-heterocubane structure.[3] This

$[(CH_3NSbCl_3)_4]$ **1**

tendency also seems to be present in the nitrides of main group elements in lower oxidation states, as the comparison of explosive Se_4N_4 with the distinctly more stable chloronitride Se_2NCl_3 shows.[4]

This concept was confirmed in the first nitrido–antimony(III) complex, which we have now synthesized, whose nitride moiety is apparently stabilized by the other units of the heterocubane structure. Compound **2** is formed almost quantitatively from antimony trichloride and tris(trimethylsilyl)amine in dichloromethane as sparingly soluble, white, moisture-sensitive precipitate [Eq. (a)]. In spite of the complexity of this reaction, the

$$6\,SbCl_3 + 4\,N(SiMe_3)_3 \longrightarrow [SbN(SbCl)_3(NSbCl_2)(NSiMe_3)_2 \cdot SbCl_3] + 10\,ClSiMe_3 \quad (a)$$

2

same product arises irrespective of the relative amounts of the starting materials. Single crystals of **2** were obtained from dilute solution by mixing the reactants at −60 °C and subsequent very slow warming to 20 °C.

According to the results of the crystal structure analysis,[5] **2** has the heterocubane structure reproduced in Figure 1. Each

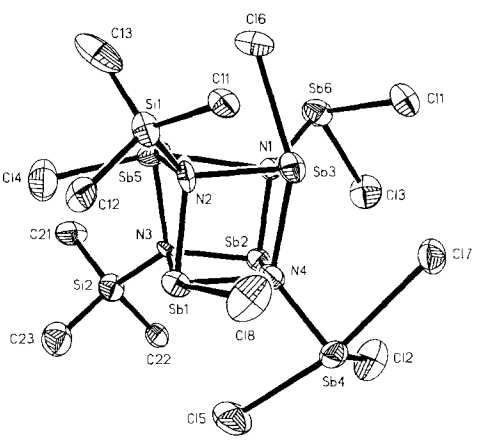


Fig. 1. Molecular structure of **2** in the crystal. Ellipsoids of thermal vibration represent 50% probability at 19 °C. Selected distances [pm] and angles [°]: Sb1-Cl8 261.4(5), Sb1-N4 209(1), Sb(2)···Cl7 315.6(5), Sb2-N1 209(1), Sb3-Cl6 271.3(5), Sb2-N3 209(1), Sb4-Cl2 240.0(6), Sb2-N4 213(1), Sb4-Cl5 254.5(6), Sb3-N1 211(1), Sb4-Cl7 279.0(5), Sb3-N2 216(1), Sb5-Cl4 247.4(6), Sb3-N4 234(1), Sb6-Cl1 240.7(5), Sb4-N4 208(1), Sb6-Sl3 239.1(6), Sb5-N1 258(1), Sb6···Cl7 315.5(6), Sb5-N2 214(1), Sb1-N2 217(1), Sb5-N3 213(1), Sb1-N3 235(1), Sb6-N1 200(1); Sb1-N4-Sb2 104.8(6), Sb2-N4-Sb3 97.7(5), Sb1-N4-Sb3 97.1(5), Sb2-N4-Sb4 119.1(6), Sb1-N4-Sb4 113.0(7), Sb3-N4-Sb4 121.7(6).

individual molecule is chiral; the symmetry constraints, however, require that a racemate is present in the unit cell. Of the four nitrogen atoms of the heterocubane framework, only the N4 atom has nitride character (N^{3-}); the other three N atoms have imide character. To each of N2 and N3 is bound a trimethylsilyl group ($NSiMe_3^{2-}$), whereas N1 bears a dichloro-

[*] Prof. Dr. K. Dehnicke, Dipl.-Chem. M. Rhiel, Dr. F. Weller, Prof. Dr. J. Pebler
Fachbereich Chemie der Universität
D-35032 Marburg (FRG)
Telefax: Int. code + (6421)28-8917

 © VCH Verlagsgesellschaft mbH, D-69451 Weinheim, 1994 0570-0833/94/0505-0569 $ 10.00+.25/0

antimony substituent ($NSbCl_3^{2-}$). In the nitride unit, N4 achieves the coordination number 4 by addition of an $SbCl_3$ molecule, but displays a strikingly short Sb–N bond of 208 pm for this bond type. Typical Sb–N distances in donor–acceptor complexes of $SbCl_3$ are 253 pm in [$SbCl_3$·aniline[6]] and 224.5 and 231.7 pm in [$SbCl_3$(2,2′–bpy)] (**3**, bpy = bipyridine[7]). The T-shaped arrangement of the chlorine atoms of the $SbCl_3$ molecule bound to N4 is surprising. Such a geometry was also observed in the chelate complex **3**,[7] but monofunctional donor molecules bound to $SbCl_3$ give rise, in general, to pyramidal structures.[6, 8] With the exception of the Sb–N bonds of the heterocubane framework (Sb1–N3, Sb3–N4 and Sb5–N1), in which the bond lengths are 235, 234, and 258 pm, respectively, the Sb–N bond lengths of between 200 and 217 pm hardly differ from one another. They correspond well with the

[$SbCl_3$(2,2′-bpy)] **3** [{$SbCl_2(NSMe_2NSiMe_3)$}$_2$] **4**

distances observed for the folded Sb_2N_2 four-membered ring in **4** (206.4 and 223.2 pm).[9] Similar Sb–N distances are also displayed by the heterocubane **1** (215–219 pm),[3] in which the antimony atoms are in a distorted octahedral environment.

In **2** all six antimony atoms are in a distorted pseudo-trigonal-bipyramidal environment; the antimony atoms Sb2 and Sb6 achieve this coordination through strong intermolecular interactions with the chlorine atom Cl7, to which Sb···Cl contacts of 315.6 and 315.5 pm are formed along the lattice vector [101]. These contacts are far shorter than the sum of the van der Waals radii of 400 pm.[10] The polymeric association coupled with this phenomenon also explains the low solubility of **2** in organic solvents. However, **2** dissolves extremely well in dichloromethane on addition of only the equimolar amount of tetraphenylphosphonium chloride, and the salt PPh_4^+[**2**·Cl^-] is formed. In the process the cubane framework in the chloro complex [**2**·Cl^-] is retained.[11] Presumably the chloride ion adds to the Sb2 atom; thus, all antimony atoms of the heterocubane become equivalent. As a consequence of the intermolecular bridging function of the Cl7 atom in **2**, the Sb4–Cl7 distance is stretched to 279.0 pm, the longest direct Sb–Cl bond in **2**.

The ^{121}Sb Mössbauer spectrum of **2**[12] reflects the pseudo-trigonal-bipyramidal surroundings of all six nonequivalent antimony atoms (Fig. 2). The Lorentz fit (solid curve) provides an average value for the isomeric shift of $\delta_{IS} = -13.4(4)$ mm s^{-1} and for the quadrupole splitting of $\Delta E^Q = 18.4(4)$ mm s^{-1}, which has a positive sign for all Sb atoms. The size of the isomeric shift fits well with those measured for **4** (13.5(1) mm s^{-1}[9]) and for **5**

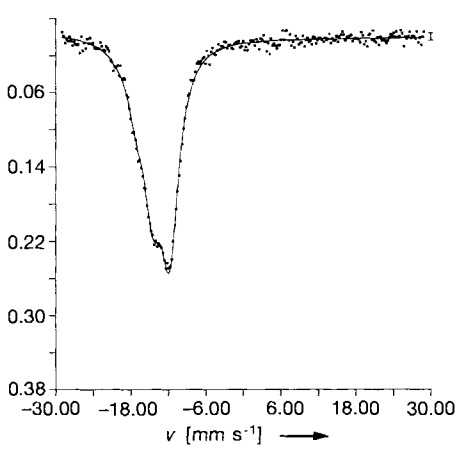


Fig. 2. ^{121}Sb Mössbauer spectrum of **2** at 4.2 K. The x axis represents the relative speed of the source relative to the absorber, and the y axis the absorption.

[Ph–C(NSiMe$_3$)$_2$SbCl$_2$] **5**

(−13.2(1) mm s^{-1}[13]). In both complexes the antimony atoms are surrounded by a pseudo-trigonal-pyramid of Cl and N atoms, as in **2**. The large quadrupole splitting in the Mössbauer spectrum of **2** upon coordination of the Sb atoms by N and Cl atoms is, because of the only slight difference in electronegativity, in essence attributable to the steric requirements of the lone pairs on the antimony atoms, according to all experience.[9, 13–15] Similarly large values for the quadrupole splitting are found in the Mössbauer spectra of amidinatoantimony(III) complexes in which the coordination environment at the antimony atoms resembles that of **2**[16] (for example, $\Delta E^Q = 15.5$ mm s^{-1} in **5**[13]).

Experimental Procedure

2·CH_2Cl_2: A solution of $N(SiMe_3)_3$ (3.53 g, 15.1 mmol) in CH_2Cl_2 (20 mL) was added dropwise to a stirred solution of $SbCl_3$ (5.18 g, 22.7 mmol) in CH_2Cl_2 (30 mL). The initially clear solution was slowly allowed to warm to 20 °C without stirring and was then filtered under a dry nitrogen atmosphere, washed with CH_2Cl_2, and dried under vacuum. Yield 4.43 g (90%). Correct elemental analysis for C, H, N, Cl, Si.

Received: October 6, 1993
Revised version: October 26, 1993 [Z6396IE]
German version: *Angew. Chem.* **1994**, *106*, 599

[1] W. Schnick, *Angew. Chem.* **1993**, *105*, 846–858; *Angew. Chem. Int. Ed. Engl.* **1993**, *32*, 806–818.
[2] K. Dehnicke, J. Strähle, *Angew. Chem.* **1992**, *104*, 978–1000; *Angew. Chem. Int. Ed. Engl.* **1992**, *31*, 955–978, and references therein.
[3] W. Neubert, H. Pritzkow, H. P. Latscha, *Angew. Chem.* **1988**, *100*, 298–299; *Angew. Chem. Int. Ed. Engl.* **1988**, *27*, 287–288.
[4] R. Wollert, A. Höllwarth, G. Frenking, D. Fenske, H. Goesmann, K. Dehnicke, *Angew. Chem.* **1992**, *104*, 1216–1218; *Angew. Chem. Int. Ed. Engl.* **1992**, *31*, 1251–1253.
[5] Crystallographic data of **2**·CH_2Cl_2 (19 °C): space group $P2_1/n$, $a = 983.5(2)$, $b = 2726.2(5)$, $c = 1187.7(2)$ pm, $\beta = 98.32(3)°$, $Z = 4$, Enraf-Nonius CAD4 four-circle diffractometer, $Mo_{K\alpha}$ radiation, graphite monochromator, ω scan, $\theta = 3.1$–$24.7°$, 5149 independent reflections of which 3140 were observed ($F_0 > 5\sigma(F_0)$), 282 refined parameters, positions of the H atoms isotropic, empirical absorption correction, $\mu(Mo_{K\alpha}) = 60.0$ cm^{-1}, $R = 0.063$, $R_w = 0.045$, residual electron density 2.2 e Å^{-3}. Further details of the crystal structure investigation may be obtained from the Fachinformationszentrum Karlsruhe, Gesellschaft für wissenschaftlich-technische Information mbH, D-76344 Eggenstein-Leopoldshafen (FRG) on quoting the depository number CSD-57955, and the journal citation.
[6] R. Hulme, J. C. Scruton, *J. Chem. Soc. (A)* **1968**, 2448–2452.
[7] A. Lipka, H. Wunderlich, *Z. Naturforsch. B* **1980**, *35*, 1548–1551.
[8] B. Rubin, F. J. Heldrich, W. K. Dean, D. J. Williams, A. Viehbeck, *Inorg. Chem.* **1981**, *20*, 4434–4437; E. Hough, D. G. Nicholson, *J. Chem. Soc. Dalton Trans.* **1981**, 2083–2087.
[9] H. W. Roesky, K. Hübner, M. Noltemeyer, M. Schäfer, *Angew. Chem.* **1991**, *103*, 856–857; *Angew. Chem. Int. Ed. Engl.* **1991**, *30*, 860–862.
[10] A. F. Wells, *Structural Inorganic Chemistry*, Clarendon, Oxford, **1984**.
[11] M. Rhiel, Diplomarbeit, Universität Marburg, **1993**.
[12] Source ($Ba^{121}SnO_3$) temperature and absorber temperature 4.2 K, NaI(Tl) scintillation detector, measured data relative to $BaSnO_3$. Both the 37.2 keV Mössbauer transition and that of the escape peak of the NaI crystal at about 8 keV were used for the measurement; 512 channel analyser.
[13] M. Schäfer, Diplomarbeit, Universität Marburg, **1989**.
[14] M. Alamgir, P. W. C. Barnard, J. D. Donaldson, *J. Chem. Soc. Dalton Trans.* **1980**, 1542–1544.
[15] M. Schäfer, J. Pebler, B. Borgsen, F. Weller, K. Dehnicke, *Z. Naturforsch. B* **1990**, *45*, 1243–1250; M. Schäfer, G. Frenzen, B. Neumüller, K. Dehnicke, *Angew. Chem.* **1992**, *104*, 354–355; *Angew. Chem. Int. Ed. Engl.* **1992**, *31*, 334–335.
[16] C. Ergezinger, F. Weller, K. Dehnicke, *Z. Naturforsch. B* **1988**, *43*, 1119–1124; U. Patt-Siebel, U. Müller, C. Ergezinger, B. Borgsen, K. Dehnicke, D. Fenske, G. Baum, *Z. Anorg. Allg. Chem.* **1990**, *582*, 30–36.

 © VCH Verlagsgesellschaft mbH, D-69451 Weinheim, 1994 0570-0833/94/0505-0570 $ 10.00+.25/0

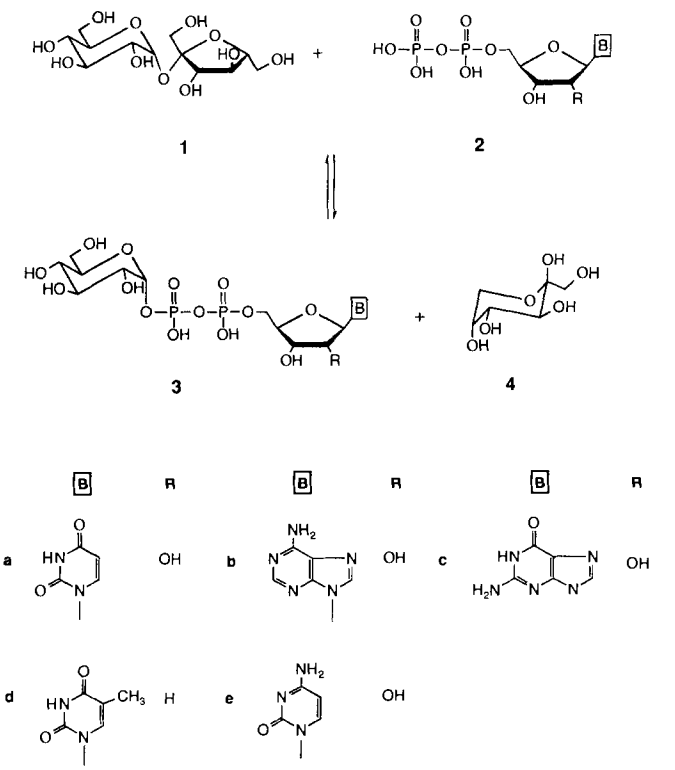
Continuous Enzymatic Synthesis of 2′-Deoxythymidine-5′-(α-D-glucopyranosyl)diphosphate**

Astrid Zervosen, Lothar Elling, and Maria-Regina Kula*

2′-Deoxythymidine-5′-(α-D-glucopyranosyl)diphosphate (dTDP-Glucose) **3d** belongs to the primary nucleotide sugars whose existence and importance in the biosynthesis of glycosylated compounds was recognized in 1950 by Leloir et al.[1] In current basic research the role of complex glycoconjugates in intercellular and immunological recognition events in biological systems is being closely studied.[2] In the course of this development enzymatic synthesis of oligosaccharide structures with glycosyl transferases[3] and glycosidases[4] have assumed ever greater importance in comparison with labor-intensive chemical syntheses with their extensive use of protective groups.[5] The use of a glycosyl transferase depends on the availability of a suitable nucleosidediphosphate sugar. In recent years several activated sugars have been synthesized in preparative amounts by means of pyrophosphorylases.[6]

We have, for the first time, used sucrose synthase (EC 2.4.1.13), which catalyzes both the synthesis and the cleavage of a disaccharide, for the preparation of dTDP-glucose. Starting from dTDP-glucose a series of activated deoxy sugars (e.g. dTDP-dihydrostreptose, dTDP-L-rhamnose) are obtainable, which are components of particular antibiotics[7] or of lipopolysaccharides of enterobacteria.[2] The purified sucrose synthase, isolated from rice grains, cleaves sucrose in the presence of uridine-5′-(UDP) (**2a**), 2′-deoxythymidine-5′(dTDP) (**2d**), adenosine-5′-(ADP) (**2b**), cytidine-5′-(CDP) (**2e**), and guanosine-5′-(GDP) diphosphate (**2c**) (Scheme 1) and is, thereby, a candidate for the synthesis of primary nucleotide sugars.[8] The enzyme can be used in glycosyl transferase catalyzed reactions for the in situ regeneration of dTDP-glucose. In contrast, dTDP-glucose pyrophosphorylase,[9] which catalyzes the reaction of dTDP with glucose-1-phosphate, cannot be used for coupled reactions because of the as yet unsolved problem of the enzymatic regeneration of dTTP from dTDP.

The first continuous enzymatic synthesis of a nucleosidediphosphate sugar in preparative amounts was realized with an enzyme membrane reactor (EMR). The sucrose synthase was purified from rice with the elimination of contaminating phosphatases and invertases.[10] Under the conditions for synthesis (200 mM 2-[4-(2-hydroxyethyl)piperazin-1-yl]ethanesulfonic acid (Hepes)–NaOH buffer, pH 7.0, 30 °C), the measured half-life for the activity of the enzyme was 119 h. Under these conditions dTDP-glucose is stable whereas 1% of the substrate dTDP is hydrolysed to 2′-deoxythymidine-5′-monophosphate (dTMP) during the synthesis in the EMR. The conversion of 5 mM dTDP (**2d**) and 350 mM sucrose (**1**) gave a maximum yield of 89.6% dTDP-glucose **3d** in the EMR (Fig. 1). This corresponds to a space–time yield of 98.1 $g L^{-1} d^{-1}$ (about 1 $g d^{-1}$ dTDP-glucose in the reactor used). In comparison with syntheses carried out in parallel in a batch reactor, the enzyme consumption can



Scheme 1. Synthesis of nucleoside diphosphate sugars with sucrose synthase from rice.

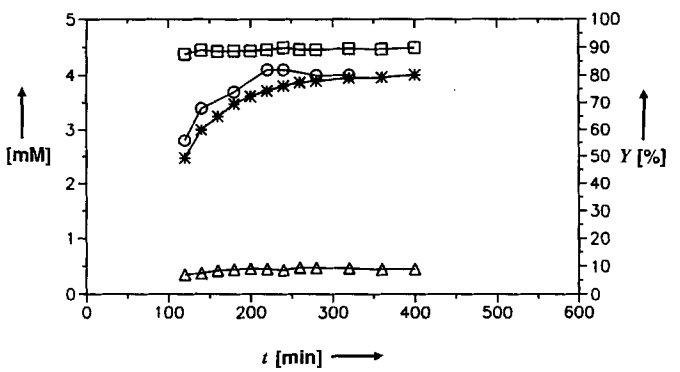


Fig. 1. Concentration/time curves for the continuous synthesis of dTDP-glucose **3d** (*) in an enzyme membrane reactor; starting concentrations: 5 mM dTDP **2d** (△), 350 mM sucrose **1**, 200 mM Hepes–NaOH; pH 7.0; 30 °C; 990 mU sucrose synthase; residence time: 0.67 h. D-fructose (○); **Y**: Yield (□).

be lowered from 3.9 $U g^{-1}$ dTDP-glucose to 1 $U g^{-1}$. Aliquots of the dTDP-glucose **3d** synthesized in the EMR were worked up by two different purification methods. dTDP-Glucose was isolated by ion exchange chromatography. In the subsequent lyophilization, the amount of decomposition of the dTDP-glucose was decreased by maintaining a pH of 7.0. As an alternative to the desalting of the lyophilizate by gel filtration precipitation with ethanol/acetone was carried out, which has the advantage of an easy scale-up. Both purification procedures can still be improved. On account of the high yield of almost 90% dTDP-glucose, the product can be used without prior purification for further enzymatic conversions. The enzymatically prepared dTDP-glucose (purification method 2) was characterized by means of ^1H and $^{13}C\{^1H\}$ NMR spectroscopy (Table 1).

[*] Prof. Dr. M.-R. Kula, Dipl. Chem. A. Zervosen, Dr. L. Elling
Institut für Enzymtechnologie der Universität Düsseldorf im Forschungszentrum Jülich
Postfach 2050, D-52404 Jülich (FRG)
Telefax: Int. code + (2461)61-2490

[**] We thank Dr. W. Klaffke (Universiät Hamburg) for recording the NMR spectra and for his help in their interpretation, and Dr. U. Kragl (Institut für Biotechnologie, Forschungszentrum, Jülich) for making an enzyme membrane reactor available.

Table 1. NMR data of dTDP-glucose **3d** in D_2O. ^1H NMR: 400 MHz; $^{13}C\{^1H\}$ NMR: 100 MHz; [11].

^1H NMR (400 MHz, D_2O): $\delta = 7.80$ (s, 1H; H-6'), 6.40 (dd, $^3J(1,2a) \approx {}^3J(1,2b) \approx 7.0$ Hz, 1H; H-1), 5.65 (dd, $^3J(1'',2'') \approx 3.6$ Hz, $^3J(1'',P) = 7.1$ Hz, 1H; H-1''), 4.80 (HDO), 4.66 (m, 1H; H-4), 4.25 (m, 2H; H-5a, 5b), 4.02–3.86 (m, $^2J(6_a'',6_b'') = 12.7$ Hz, 2H; H-5'', H-$6_a''$), 3.86–3.79 (m, $^3J(3'',4'') = 9.2$ Hz, $^3J(4'',5'') = 8.7$ Hz, $^3J(5'',6_b'') \approx 4.6$ Hz, $^2J(6_a'',6_b'') = 12.7$ Hz, 2H; H-4'', H-$6_b''$), 3.58 (ddd, $^3J(1'',2'') = 3.6$ Hz, $^3J(2'',3'') = 9.7$ Hz, $^4J(2'',P) = 3.4$ Hz, 1H; H-2''), 3.51 (dd, $^3J(2'',3'') = 9.7$ Hz, $^3J(3'',4'') = 9.2$ Hz, 1H; H-3''), 2.43 (m, 2H; H-2a, b), 1.98 (s, 3H; 5'-CH_3)

$^{13}C\{^1H\}$ NMR (100 MHz, D_2O): $\delta = 156.1$ (C-5'), 137.6 (C-6'), 95.8 (d, $^3J(C\text{-}1'', P) = 6.5$ Hz, C-1''), 85.5 (C-1), 73.1 (C-5''), 71.8 (d, $^4J(C\text{-}2'',P) = 8.5$ Hz, C-2''), 71.4 (C-3), 71.2 (C-4), 69.5 (C-3''), 65.7 (d, $^3J(C\text{-}5,P) = 6.5$ Hz, C-5), 60.6 (C-6'') 38.8 (C-2), 11.9 (5'-CH3)

Experimental Procedure

The reaction was carried out in Hepes-NaOH buffer (200 mM, pH 7.0) at 30 °C. At the start 990 mU of purified sucrose synthase [10] and 10 mg bovine serum albumin were injected through a sterile filter (0.2 μm, Sartorius, Göttingen) into the sterile EMR filled with buffer solution (volume 10 mL; Bioengineering, Wald, Switzerland). Subsequently the substrate solution (100 mL) with dTDP (**2d**, Na^+ salt, 230 mg, Sigma) and sucrose (**1**, 11.98 g, 350 mM) was pumped continuously through the reactor in which the enzyme was retained by means of an ultrafiltration membrane (YM 10, Amicon, Witten), with a flow rate of 15 mL h^{-1}. The synthesis was monitored for 400 min (ten residence times) by means of regular sampling. The nucleoside phosphates and nucleotide sugar were separated and quantitatively analyzed by ion-pair HPLC [10]. Aliquots of the dTDP-glucose were worked up with different procedures. Method 1 (84.4 mg crude product): First dTDP, the sugar, and the buffer were separated by ion exchange chromatography on Sepharose Q in the Cl^- form (1.8 × 30 cm, gradient: 55–200 mM LiCl at pH 5.0). The separation of dTMP was achieved with Dowex 1 × 2 in the Cl^- form (100–200 mesh, 2.6 × 7.0 cm, gradient: 55–350 mM LiCl with 3 mM HCl). After lyophilization the product was desalted by gel filtration chromatography (G-10, 1.6 × 30 cm). (Yield of purified product: 39.1 mg, 46.4%).

Method 2 (57.8 mg, crude product): After ion exchange chromatography on Sepharose Q, dTMP was removed with Dowex 1 × 2 in the Cl^- form (100–200 mesh, 2.6 × 7.0, 0–500 mM LiCl). After lyophilization the lyophilizate was dissolved in ethanol. The dTDP-glucose was precipitated by the addition of 2.5 times the amount of acetone, filtered off, and dried. (Yield of purified product: 24.5 mg, 42.4%) $[\alpha]_d^{22.5} = 48.1$ (c = 4.6 mM in H_2O). The product contained 6.5% dTMP according to HPLC analysis [10].

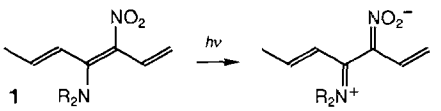
Received: October 2, 1993 [Z 6388 1E]
German version: *Angew. Chem.* **1994**, *106*, 592

[1] C. E. Cardini, R. Caputto, A. C. Paladini, L. F. Leloir, *Nature* **1950**, *165*, 191–192.
[2] H. Paulsen, *Angew. Chem.* **1982**, *94*, 184–201; *Angew. Chem. Int. Ed. Engl.* **1982**, *21*, 155–173; K. Marumo, L. Lindqvist, N. Verma, A. Weintraub, P. R. Reeves, A. A. Lindberg, *Eur. J. Biochem.* **1992**, *240*, 539–545.
[3] Y. Ichikawa, G. C. Look, C.-H. Wong, *Anal. Biochem.* **1992**, *202*, 215–238.
[4] K. G. I. Nilsson, *Trends Biotechnol.* **1988**, *6*, 256–264.
[5] H. Waldmann, *Nachr. Chem. Tech. Lab.* **1992**, *40*, 828.
[6] J. E. Heidlas, K. W. Williams, G. M. Whitesides, *Acc. Chem. Res.* **1992**, *25*, 307–314.
[7] H. Grisebach, *Adv. Carbohydr. Chem. Biochem.* **1978**, *35*, 81–126.
[8] L. Elling, M. Grothus, M.-R. Kula, *Glycobiology* **1993**, *3*, 349–355; L. Elling, M.-R. Kula, *Enzyme Microb. Technol.* **1993**, in press.
[9] S. Kornfeld, L. Glaser, *J. Biol. Chem.* **1961**, *236*, 1791–1794.
[10] L. Elling, M.-R. Kula, *J. Biotech.* **1993**, *29*, 277–286.
[11] The NMR data correspond with those of dTDP-glucose synthesized chemically (Dr. W. Klaffke, personal communication).

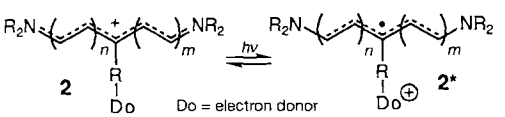
Phenothiazinyl-Substituted Cyanines: Model Compounds for Molecular Switches**

Agnes Ehmann, Rudolf Gompper,* Horst Hartmann, Thomas J. J. Müller, Kurt Polborn, and Reiner Schütz

Conjugated π-electron systems such as polyacetylene, polypyrrole, polythiophene, polyaniline, and polyphenylenevinylene,[1] which are electrically conducting in either their doped or undoped state, have paved the way to molecule-based electronic devices.[2] Molecular switches are one of the essential components of molecular electronics, and proposals for such systems have been made.[3–6] (The term switch is defined in ref. [5].) One of these model systems is polyacetylene **1** with donor and acceptor substituents. The conjugation in the "molecular wire" can be



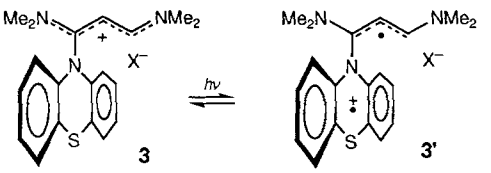
interrupted by the interaction of light with the β-nitroenamine chromophore.[2b, 3] This model has been criticized[3] in part because of anticipated difficulties in its synthesis (cf. solid-state polymerization of a push–pull diacetylene[7]). But it is also doubtful, for example, whether the donor–acceptor portion of the molecule can be excited selectively and whether the radical cation or cationic center generated at the terminus of the polyene would be sufficiently localized for the migration of a soliton through the system (resonance delocalization of the soliton is more likely). Thus we propose system **2**; the electric conductivity of this molecule is controlled by photoinduced electron transfer (PET) from a donor group not involved in π-conjugation to the "molecular wire" of the polymethinecyanine framework (**2** → **2***).



Reaction of (2-substituted) vinamidinium salts with, for example, *p*-phenylenediamine, provides polyvinamidines, which have high electrical conductivities[8] (undoped 10^{-5} to 0.15 S cm^{-1}, doped 0.03 to 50 S cm^{-1}). For this reason we used the vinamidinium salts **3** as model systems for **2**. Instead of the porphyrin group frequently employed in π-σ-π electron systems,[9–12] we chose the phenothiazinyl group. Phenothiazines are known to give rise to stable radical cations and dications[13–17] as well as charge transfer complexes.[18, 19] Phenothiazinyl-substituted ligands in metal complexes have served as probes in UV/VIS studies of electron transfer processes.[20, 21]

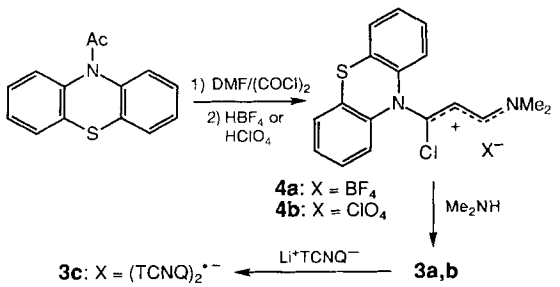
[*] Prof. R. Gompper, Dipl.-Chem. A. Ehmann, Dr. T. J. J. Müller, Dr. K. Polborn
Institut für Organische Chemie der Universität
Karlstrasse 23, D-80333 München (FRG)
Telefax: Int. code + (89) 5902-420
Prof. H. Hartmann, Dr. R. Schütz
Martin-Luther-Universität
Geusaer Strasse, D-06217 Halle-Wittenberg (FRG)

[**] This research was supported by the Deutsche Forschungsgemeinschaft and the Fonds der Chemischen Industrie. T. J. J. M. thanks the State of Bavaria for a Stipendium zur Förderung des künstlerischen und wissenschaftlichen Nachwuchses. We thank Dr. A. Lerf, Hahn-Meitner-Institut, Garching (FRG), for conducting the conductivity measurements.



In contrast to most of the systems used in studies of charge separation in PET processes, the phenothiazinyl group in **3** is coupled directly to the vinamidinium system. Selective oxidation of the phenothiazinyl group should be possible owing to the stability of the phenothiazinyl radical cation, especially if the phenothiazine and vinamidinium systems are not coplanar. We report here on the synthesis of **3** and on our findings that the π-electron systems are mutually orthogonal and that photoinduced electron transfer most likely gives **3'**.

Reaction of 10-acetylphenothiazine with *N*,*N*-dimethylformamide chloride at room temperature in chloroform and subsequent workup with aqueous tetrafluoroboric acid or perchloric acid furnished the 3-chloro-3-phenothiazinylpropeniminium salts **4** in good to excellent yields (cf. chloroformylation of *N*,*N*-disubstituted acetamides[22] and the analogous reaction of *N*-acetylphenoxazine[23]). The 1-phenothiazinylvinamidinium salts **3a**, **b** were obtained by treatment of **4** with ethanolic dimethylamine at room temperature. When hot ethanolic solutions of **3a** and lithium tetracyanoquinodimethane (Li^+TCNQ^-) were combined and cooled, salt **3c** formed as blue-black crystals.



In the X-ray structure analysis of **4b**[24] (Fig. 1) the W form typical for vinamidinium salts[25] is evident, and the phenothiazinyl unit is almost coplanar with the allyl cation moiety. Since the C1–N1 bond is considerably longer than the C3–N2 bond (134.8 vs 129.4 pm), the phenothiazinyl group rotates about the C1–N1 bond more readily than the dimethylamino group about the C3–N2 bond. Consequently only one set of signals is seen for the phenothiazine C atoms in the room-temperature ^{13}C NMR spectrum, whereas the dimethylamino C atoms give rise to two signals. The phenothiazinyl group is thus conjugated with the trimethine system, but the dimethylamino group is more so.

The crystal structure of **3b**[26] (Figs. 2–4) shows that the phenothiazine and cyanine unit are almost orthogonal. The cyanine system (plane 1: N2, C13, C14, C15, N3) is planar and the CC and CN bond lengths (136.9, 137.5 and 131.0, 132.4 pm, respectively) are characteristic of a trimethinecyanine (139, 132 pm).

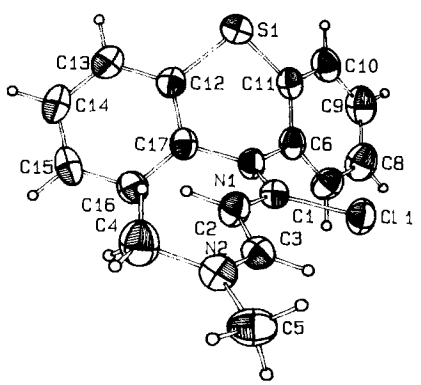


Fig. 1. X-ray structure of the cation of **4b** (ORTEP); selected bond lengths [pm] and angles [°]: C1-N1 134.8(5), C3-N2 129.4(5), C1-C2 135.9(5), C2-C3 138.9(5), C1-Cl1 172.3(4); N1-C1-C2 124.9(4), C1-C2-C3 123.7(4), C2-C3-N2 126.1(4).

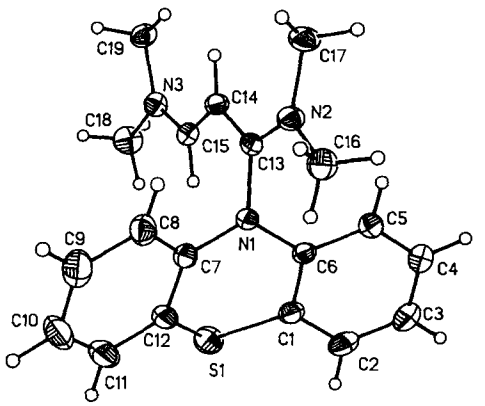


Fig. 2. X-ray structure of the cation of **3b** (ORTEP); selected bond lengths [pm] and angles [°]: N1-C13 142.4(5), N2-C13 132.4(6), N3-C15 131.0(6), C13-C14 136.9(6), C14-C15 137.5(7); N2-C13-C14 124.6(4), C13-C14-C15 120.2(4), C14-C15-N3 126.4(4).

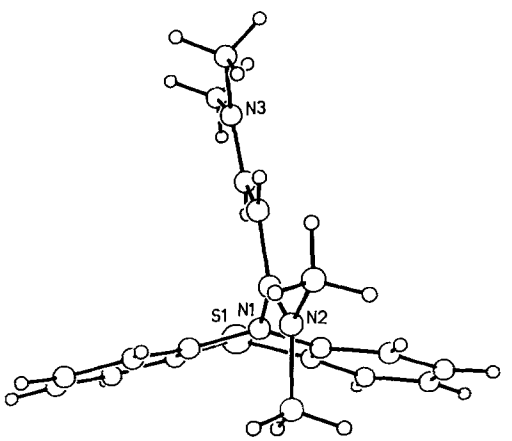


Fig. 3. ORTEP representation of the cation of **3b**; view along the N2–C13 bond.

The angle between plane 2 (S1, N1, C1, C2, C3, C4, C5, C6; maximum deviation 6.24 pm) and plane 3 (S1, N1, C7, C8, C9, C10, C11, C12; maximum deviation 3.20 pm) is 151.7°, close to that in monoclinic phenothiazine[28] (153.3°). The S and N atoms of the butterfly-shaped phenothiazinyl unit (cf. ref.[29]) do not quite lie in the plane of the central six-membered ring, which is found in a tub conformation.

Planes 1 and 2 form an angle of 82.6°. The distance between N1 and C13 (142.4 pm) is significantly larger than the corresponding distance in **4b** (134.8 pm) and lies in the range of $C(sp^2)$–$N(sp^2)$ single bonds.[30] Thus, the phenothiazine unit in **3b**, in contrast to **4b**, is not in conjugation with the cyanine system. It should therefore be possible to oxidize **3** to the radical dication without the unpaired electron being delocalized in the cyanine system.

 © VCH Verlagsgesellschaft mbH, D-69451 Weinheim, 1994 0570-0833/94/0505-0573 $ 10.00+.25/0

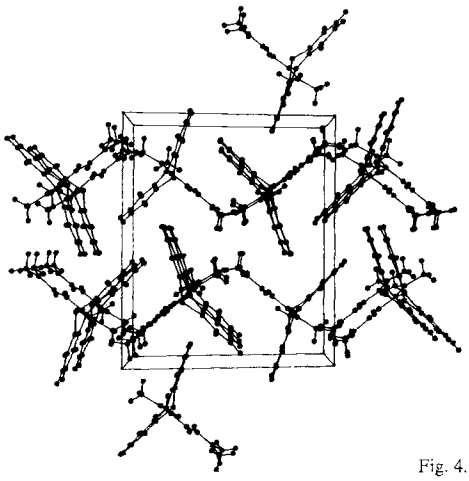
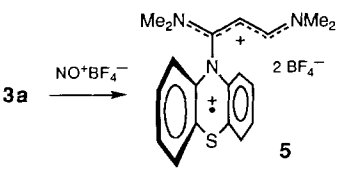


Fig. 4. X-ray structure of **3b**.

The head-to-tail arrangement of the cations is evident in Figure 4; the direction of this arrangement alternates in adjacent chains.

Oxidation of **3a** at −30 °C in dichloromethane with nitrosyl tetrafluoroborate provided the black-violet salt **5** of the radical cation, which is stable under exclusion of air and moisture.

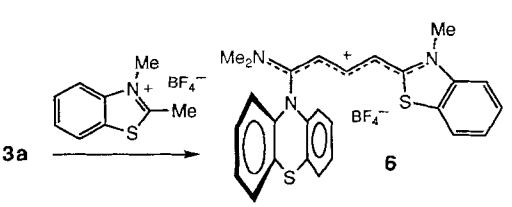


The radical structure is supported by the ESR spectrum of a solution of **5** in acetonitrile, which shows a broad triplet (a_N = 5.13 G; g = 2.0724). Although a high-resolution ESR spectrum could not be obtained even in degassed acetonitrile, the distribution of the bands indicates that **5** is a typical phenothiazine radical cation.[17]

In the UV/VIS spectrum of **5** bands characteristic of the phenothiazine radical cation[17, 31] occur at 276, 522, and 815 nm. The band with the greatest extinction coefficient is that of the cyanine system at 330 nm. Bands that would indicate the interaction of the radical cation with the cyanine system are not evident. Apparently the phenothiazine radical cation unit and the cyanine moiety in **5** are orthogonal as in **3a**.

Structural derivatives of salts **3a, b** can also be prepared. When, for example, **3a** was heated with dimethylbenzothiazolium tetrafluoroborate in ethanol in the presence of triethylamine, the cyanine salt **6** was obtained as fine red needles with a metallic green shimmer (λ_{max} (lgε) [DMSO] = 512 nm (4.592), 558 (S, 3.799)). Other spectroscopic data indicate that the structure of **6** is similar to that of **3**.

The electron spectrum of **3c** has bands at 376, 392, 417, 432, and 663, 679, 726, 742, 760 nm, which are typical for TCNQ and



TCNQ$^{\cdot-}$. The cyanine band of **3a** occurs at 331 nm, which rules out the interaction of the cyanine system in **3a** with TCNQ or TCNQ$^{\cdot-}$. Since the phenothiazinyl radical cation absorbs at 522 nm, the phenothiazinyl group and TCNQ apparently do not interact either.

The single-crystal conductivity of **3c** is 10^{-7} Scm^{-1}, which is relatively low compared to the conductivities of salts with TCNQ anions.[32]

The cyclic voltammograms of **3a** and **6** display reversible one-electron waves at 0.84 and 0.79 V, respectively. A quasireversible transition at 1.32 V is observed for **3a**; an irreversible transition at 1.11 V is evident for **6**. In the reduction range **3a** gives rise to a quasireversible transition at −1.32 v, **6** an irreversible transition at −0.96 V.

As the potentials for the oxidation of **3a** (0.84 V) and **6** (0.79 V) to the respective radical ions are in the same range, the phenothiazine unit in both **6** and **3** must be orthogonal to the cyanine moiety. The oxidation potentials of **3a** and **6** are anodically shifted relative to those of phenothiazine[14] (0.27 V) and *N*-methylphenothiazine;[14] in other words, oxidation to the radical cations is hampered by the cationic cyanine substituent.

The reduction potentials of **3a** (−1.32 V) and 3-chloro-3-dimethylamino-*N*,*N*-dimethylpropenium perchlorate[33] (−1.37 V) are very similar. This finding along with the NMR and electron spectra indicate that the phenothiazinyl group exerts the same electronic effect on the cyanine system as a chlorine atom; put simply, the negative induction effect of the phenothiazine N atom dominates in **3a**.

Salt **4a** (E_2 = 1.19 V) is considerably more difficult to oxidize than **3a** (E_2 = 0.84 V). The phenothiazine N atom in **4a** is involved with the conjugated π-electron system of the trimethine unit, and the radical cation is thus less stable than that of **3a** (**4a** could not be oxidized with nitrosyl tetrafluoroborate).

Time-resolved spectroscopy: The phenothiazine radical cation also forms upon irradiation of a solution of phenothiazine in chloroform.[31] The radical cation is evident by its intense orange-red color, and like the radical cations of its derivatives, can be recognized by time-resolved spectroscopy. The kinetics of its decomposition can be obtained from the decay rates.[20d]

A solution of **3a** in acetonitrile was examined at room temperature under argon by time-resolved spectroscopy. A weak transient absorption with a maximum at about 500 nm was observed, which is assigned to a T–T process because of the lifetime and sensitivity to oxygen. The decay follows strict first-order kinetics and is assigned to an intersystem crossing (ISC) process $T_1 \rightarrow S_0$, which has a surprisingly small rate constant $k_1 = 36\ s^{-1}$. The corresponding lifetime for the T_1 state, which probably corresponds to structure **3′**, is 28 ± 2 ms. The S_1 lifetime of **3a** could not be determined because of the lack of fluorescence.

The transient absorption of **3a** in 1,2-dibromoethane occurs at the same wavelength, is stronger than in acetonitrile, and can be detected even in dilute solution and in the presence of oxygen. The decay follows strict second-order kinetics. Owing to technical problems only the product of the corresponding rate constant k_2 and the extinction E_m of the sample could be determined ($k_2 E_m = (5.1 \pm 1.5) \times 10^3$). Apparently this decay is related to an $S_1 \rightarrow T_n$ process initiated by the heavy atoms in the solvent, which leads to the efficient population of the corresponding T_1 state. This state is deactivated by means of a triplet–triplet annihilation process.

PPP-π-SCF calculations were carried out based on force field calculations, in which a twisted structure analogous to the X-ray structure was used for the starting geometry. In these calculations the two lowest lying S_1 and T_1 states are characterized as

 © VCH Verlagsgesellschaft mbH, D-69451 Weinheim, 1994 0570-0833/94/0505-0574 $ 10.00+.25/0 Angew. Chem. Int. Ed. Engl. 1994, 33, No. 5

charge transfer states, in which one electron from the HOMO, which is localized primarily in the phenothiazine unit, is transferred to the LUMO, which is localized predominantly in the trimethine unit. Thus, the electronic properties of both units change during the relatively long lifetime of the T_1 state. If it were possible to produce polyvinamidines[8] from **3**, then this change in the electronic properties should be apparent, for example, as a change in the electric conductivity.

Thus the 1-phenothiazinylvinamidinium salt **3a** can be considered to be a model of a molecular switch; flash excitation induces the transfer of an electron from the phenothiazine moiety to the cyanine unit, whereby the properties of both units change reversibly.

Experimental Procedure

4b: *N,N*-dimethylformamide (9.3 mL, 25 mmol) in anhydrous chloroform (10 mL) was mixed with oxalyl chloride (2.2 mL, 25 mmol) in chloroform (10 mL) at 0 °C. To this solution was added dropwise a solution of 10-acetylphenothiazine (2.11 g, 10 mmol) in anhydrous chloroform (10 mL). After 12 h the solvent was removed under vacuum at room temperature, and the residue was treated with ice water and 70% aqueous perchloric acid (2 mL). Yield: 2.18 g (52%); yellow crystals, m.p. 205 °C (acetonitrile/ether). ^{1}H NMR (CD_3CN): δ = 3.06 (s, 3H, NCH_3), 3.48 (s, 3H, NCH_3), 5.73 (d, J = 11.2 Hz, 1HJ, CCHC), 7.49–7.71 (m 8H, benzo-H), 8.19 (d, J = 11.2 Hz, 1H, NCHC).

3b: A suspension of **4b** (0.83 g, 2 mmol) in ethanol (5 mL) was treated with 33% ethanolic dimethylamine (5 mL). After 12 h the precipitate was removed by vacuum filtration. Yield: 0.50 g (70%); yellow crystals, m.p. 187–188 °C (methanol). ^{1}H NMR ($CDCl_3$): δ = 3.29 (s, 9H, NCH_3), 3.40 (s, 3H, NCH_3), 5.68 (d, J = 12 Hz, 1H, CCHC), 6.45–7.18 (m, 8H, benzo-H), 7.73 (d, J = 12 Hz, 1H, NCHC).

5: A suspension of **3a** (0.41 g, 1 mmol) in anhydrous dichloromethane (20 mL) was cooled to −30 °C and stirred while nitrosyl tetrafluoroborate (0.12 g, 1.1 mmol) was added in portions. The reaction mixture was allowed to warm to room temperature over 30 min. The precipitate was removed by vacuum filtration after 6 h. Yield 0.09 g (18%); black-violet needles (acetonitrile/ether), m.p. 185–186 °C (decomp). UV/VIS (MeCN): λ_{max} (lg ε) = 211 (4.473), 256 (4.427), 276 (4.438), 330 (4.619), 522 (3.978), 815 (2.903) nm.

Correct elemental analyses were obtained for all compounds.

Received: September 8, 1993 [Z 6349 IE]
German version: *Angew. Chem.* **1994**, *106*, 581

[1] A. O. Patil, A. J. Heeger, F. Wudl, *Chem. Rev.* **1988**, *88*, 183; H. Naarmann, *Adv. Mater.* **1990**, *2*, 345; S. Roth, M. Filzmoser, *ibid.* **1990**, *2*, 356; L. M. Tolbert, *Acc. Chem. Res.* **1992**, *25*, 561.

[2] a) J. S. Miller, *Adv. Mater.* **1990**, *2*, 98, 378, 495, 601; b) F. Garnier, *Angew. Chem.* **1989**, *101*, 529; *Angew. Chem. Int. Ed. Engl.* **1989**, *28*, 513.

[3] F. L. Carter in *Molecular Electronic Devices* (Ed.: F. L. Carter), Dekker, New York, **1982**, p. 51.

[4] a) *Molecular Electronic Devices II* (Ed.: F. L. Carter), Dekker, New York, **1987**; b) D. K. Campbell, *Solitons and Polarons in Quasi-One-Dimensional Conducting Polymers and Related Materials* in [4a], p. 111; c) F. L. Carter, A. Schultz, D. Duckworth, *Soliton Switching and Its Implication for Molecular Electronics* in [4a], p. 149; d) M. P. Groves, *Dynamic Circuit Diagrams for Some Soliton Switching Devices* in [4a], p. 183.

[5] K. Schaumburg, J.-M. Lehn, V. Goulle, S. Roth, H. Byrne, S. Hagen, J. Poplawsky, K. Brunfeldt, K. Beechgard, T. Bjørnholm, P. Frederiksen, M. Jørgensen, K. Lerstrup, P. Sommer-Larsen, O. Goscinsky, J.-L. Calais, L. Erikson, *Switching Molecules for Molecular Electronics: Esprit BR Action MOLSWITCH* in *Nanostructures Based on Molecular Materials* (Eds.: W. Göpel, C. Ziegler), VCH, Weinheim, **1992**, p. 153; definition of a switch (p. 154): "A molecular switch is defined as a molecule which under external influence may switch to a metastable state. The lifetime relevant to qualify as metastable is to be defined by the application. The molecular switch is required to have distinct properties in the two states, permitting a 'read' operation to determine the state of the switch."

[6] a) A. Aviram, *J. Am. Chem. Soc.* **1988**, *110*, 5687; b) N. S. Hush, A. T. Wong, G. S. Bacskay, J. R. Reimers, *ibid.* **1990**, *112*, 4192; c) A. Farazdel, M. Dupuis, E. Clementi, A. Aviram, *ibid.* **1990**, *112*, 4206; d) J. M. Tour, R. Wu, J. S. Schumm, *ibid.* **1990**, *112*, 5662; e) J. Guay, A. Diaz, R. Wu, J. M. Tour, *ibid.* **1993**, *115*, 1869; f) J. Nakayama, T. Fujimoro, *J. Chem. Soc. Chem. Commun.* **1991**, *1614*.

[7] R. Galli, M. Neuenschwander, P. Engel, *Helv. Chim. Acta* **1989**, *72*, 1324.

[8] T. J. Müller, Dissertation, Universität München, **1992**.

[9] A. R. McIntosh, A. Siemiarczuk, J. R. Bolton, M. J. Stillman, T.-F. Ho, A. C. Weedon, *J. Am. Chem. Soc.* **1983**, *105*, 7215.

[10] A. D. Joran, B. A. Leland, G. G. Geller, J. J. Hopfield, P. B. Dervan, *J. Am. Chem. Soc.* **1984**, *106*, 6090.

[11] A. Osuka, K. Maruyama, I. Yamazaki, N. Tamai, *J. Chem. Soc. Chem. Commun.* **1988**, 1243; T. A. Moore, T. Gust, P. Mathis, J.-C. Mialocq, C. Chachaty, R. V. Bensasson, E. J. Land, D. Doizi, P. A. Liddell, W. R. Lehman, G. A. Nemeth, A. L. Moore, *Nature* **1984**, *307*, 630.

[12] Molecular shift register: J. J. Hopfield, J. N. Onuchic, D. N. Beratan, *Science* **1988**, *241*, 817.

[13] C. O. Okafor, *Heterocycles* **1990**, *31*, 793.

[14] J.-C. Moutet, G. Reverdy, *Nouv. J. Chim.* **1983**, 105.

[15] I. Forrest, F. Forrest, *Biochim. Biophys. Acta* **1958**, *29*, 105.

[16] Y. Iida, *Bull. Chem. Soc. Jpn.* **1971**, *44*, 663.

[17] L. Michaelis, S. Granick, M. P. Schubert, *J. Am. Chem. Soc.* **1941**, *63*, 351; B. C. Gilbert, P. Hanson, R. O. C. Norman, *Chem. Commun.* **1966**, 161; H. J. Shine, W. W. Wendlandt, *U.S. Dep. Commer.* **1966**, AD 639685 (*Chem. Abstr.* **1967**, *66*, 115211z); M. Kamiya, T. Mitsui, Y. Akahori, *Bull. Chem. Soc. Jpn.* **1973**, *46*, 1577; M. H. Litt, J. Radovic, *J. Phys. Chem.* **1974**, *78*, 1750; K. Yasukouchi, I. Taniguchi, H. Yamaguchi, J. Ayukawa, K. Ohtsuka, Y. Tsuruta, *J. Org. Chem.* **1981**, *46*, 1679; D. M. Chapman, A. C. Buchanan III, G. P. Smith, G. Mamantov, *J. Am. Chem. Soc.* **1986**, *108*, 654.

[18] R. C. Wheland, J. L. Gillson, *J. Am. Chem. Soc.* **1976**, *98*, 3916.

[19] P. Berges, J. Kudnig, G. Klar, E. Sanchez Martinez, R. Diaz Callaja, *Synth. Met.* **1992**, *46*, 207.

[20] a) R. Duesing, G. Tapolsky, T. J. Meyer, *J. Am. Chem. Soc.* **1990**, *112*, 5378; b) W. E. Jones, Jr., P. Chen, T. J. Meyer, *ibid.* **1992**, *114*, 387; c) A. M. Brun, A. Harriman, V. Heitz, J.-P. Sauvage, *ibid.* **1991**, *113*, 8657; d) H. D. Burrows, T. J. Kemp, M. J. Welbourn, *J. Chem. Soc. Perkin Trans. 2* **1973**, 969.

[21] J.-P. Collin, S. Guillerez, J.-P. Sauvage, *J. Chem. Soc. Chem. Commun.* **1989**, 776.

[22] J. Liebscher, H. Hartmann, *Synthesis* **1979**, 241.

[23] A. Kirschner, Dissertation, Technische Universität München, **1969**.

[24] X-ray structure analysis of **4b**: Enraf–Nonius CAD-4 diffractometer, $\mu(Mo_{K\alpha})$ = 4.983 cm^{-1}, single crystal of dimensions 0.17 × 0.3 × 0.5 mm, T = 294 K. Crystal data: M_r = 415.30, ρ_{calcd} = 1.539 g cm^{-3}, monoclinic, space group $P2_1/c$ (No. 14), a = 8.241(2), b = 15.379(3), c = 14.606 Å, β = 104.456(2)°, V = 1.7925 nm^3, Z = 4. Collection of ω-data: 2θ = 4–46°, maximum measuring time 60 s, scan width 0.6° + 0.36 tanθ. 2708 measured, 2597 independent reflections, of which 2290 were considered observed [$I > 2\sigma(I)$]. Refined parameters: 235. Structure solution: SHELXS-86, refinement MOLEN. R = 0.0643, R_w = 0.0980; max./min. residual electron density + 0.535/−0.792 10^{-6} e pm^{-3}. Further details of the crystal structure investigation may be obtained from the Fachinformationszentrum Karlsruhe, D-76344 Eggenstein-Leopoldshafen (FRG) on quoting the depository number CSD-57944, the names of the authors, and the journal citation.

[25] D. Lloyd, H. McNab, *Angew. Chem.* **1976**, *88*, 496; *Angew. Chem. Int. Ed. Engl.* **1976**, *15*, 459.

[26] X-ray structure analysis of **3b**: Enraf–Nonius CAD-4 diffractometer, $\mu(Mo_{K\alpha})$ = 2.917 cm^{-1}, single crystal of dimensions 0.13 × 0.4 × 0.53 mm, T = 294 K. Crystal data: M_r = 455.96, ρ_{calcd} = 1.351 g cm^{-3}, monoclinic, space group $P2_1/n$ (No. 14), a = 1021.4, b = 1624.2, c = 1375.4 pm, β = 100.75°, V = 2.2417 nm^3, Z = 4. Collection of ω-data: 2θ = 4–42°, maximum measuring time 180 s, scan width 0.80° + 0.35 tanθ. 2693 measured ($\pm h, +k, +l$), 2258 independent reflections, of which 1987 were considered observed [$I > 2\sigma(I)$]. Refined parameters: 271. Structure solution: SHELX-86, refinement SHELXTL-PLUS. R = 0.0576, R_w = 0.0576; residual electron densities + 0.34 and −0.39 10^{-6} e pm^{-3} [24].

[27] B. W. Matthews, R. E. Stenkamp, P. M. Colman, *Acta Crystallogr. Sect. B* **1973**, *29*, 449.

[28] J. D. Bell, J. F. Blount, O. V. Briscoe, H. C. Freeman, *Chem. Commun.* **1968**, 1656.

[29] E. Ragg, G. Fronza, R. Mondelli, G. Scapini, *J. Chem. Soc. Perkin Trans. 2* **1983**, 1289.

[30] H.-L. Ammon, *Acta Crystallogr. Sect. B* **1974**, *30*, 1731.

[31] G. P. Brown, J. W. Cole, Jr., T. I. Crowell, *J. Org. Chem.* **1955**, *20*, 1772.

[32] J. H. Perlstein, *Angew. Chem.* **1977**, *100*, 534; *Angew. Chem. Int. Ed. Engl.* **1977**, *16*, 519; L. R. Melby, R. J. Harder, W. R. Hertler, W. Mahler, R. E. Benson, W. E. Mochel, *J. Am. Chem. Soc.* **1982**, *84*, 3374.

[33] E. Bacher, R. Gompper, R. Mertz, H.-U. Wagner, *Z. Naturforsch. B.* **1989**, *44*, 839.

 © VCH Verlagsgesellschaft mbH, D-69451 Weinheim, 1994 0570-0833/94/0505-0575 $ 10.00+.25/0

Reactions of C_3O_2 with Stabilized Triphenylphosphoranes $Ph_3P{=}CHX$ (X = CN, COMe, COPh)**

Luciano Pandolfo,* Giacomo Facchin,* Roberta Bertani, Paolo Ganis, and Giovanni Valle

Dedicated to Professor Gastone Paiaro on the occasion of his 65th birthday

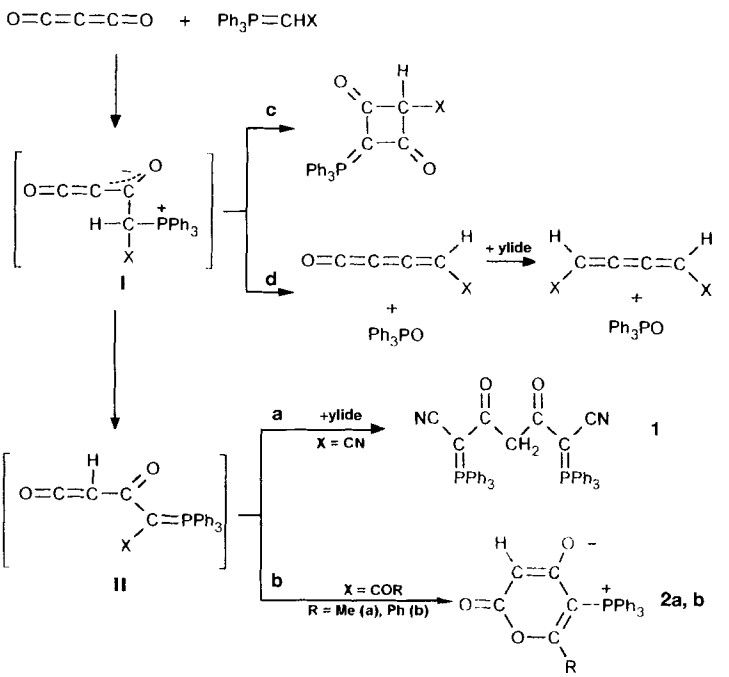
Carbon suboxide, C_3O_2, ist an extremely reactive "clean" compound, suitable for various organic and organometallic syntheses.[1] By reaction with nucleophiles a great variety of either open chain malonic acid derivatives, or heterocycles can be obtained depending on the reagents and reaction conditions used.[1]

Phosphorus ylides are quite versatile nucleophiles, whose electronic and steric properties can be modulated by changing the substituents on the ylidic carbon atom.[2]

A few reactions between C_3O_2 and ylides have been published;[3] however, the results of these are not completely in agreement with each other. Excluding the earlier report,[3a] in which the formation of a cyclobutanedione derivative was postulated, the reaction of C_3O_2 with ylides has been applied to prepare pentatetraenic systems (C_5 compounds with four double bonds) through the Wittig reaction. However, well-defined cumulenic products were obtained only in the case of ylides without hydrogen substituents on the ylidic carbon atom.[3b, c]

Here we report the reactions between C_3O_2 and the stabilized ylides $Ph_3P{=}CHX$ (X = CN, COMe, COPh). The reactions, performed in toluene at room temperature or at 80 °C or in 1,2-dichloroethane, give, depending on the ylide used, linear (**1**) or cyclic (**2**) compounds in nearly quantitative yields. Several routes are possible for this reaction and these are summarized in Scheme 1. Very likely the first step consists of a nucleophilic attack of the ylidic carbon atom on one carbonyl group of C_3O_2,[1] forming the intermediate **I**. This is followed by different reactions or rearrangements. There is no evidence of the Wittig reaction as a main process and high yields of stable linear malonic acid derivatives or zwitterionic pyrone-like compounds are obtained.

Cyanomethylenetriphenylphosphorane ($Ph_3P{=}CHCN$) reacts with C_3O_2 to give exclusively the malonic acid derivative **1** (route a of Scheme 1). The reaction proceeds at room temperature in 1:2 ratio (C_3O_2/ylide) and is complete within a few minutes. The molecular structure of **1**[4] is depicted in Figure 1. The molecule shows virtual C_2 symmetry, with the twofold axis passing through the C4 atom. The bond lengths P1–C1 and P2–C6, both of about 1.75 Å, are indicative of some double



Scheme 1. Possible pathways for the reaction between C_3O_2 and ylides.

bond character. The bond lengths C1–C3 (1.434(8) Å) and C5–C6 (1.421(8) Å) indicate partial double bond character as expected in the presence of adjacent CO groups.[5] The C–O bond

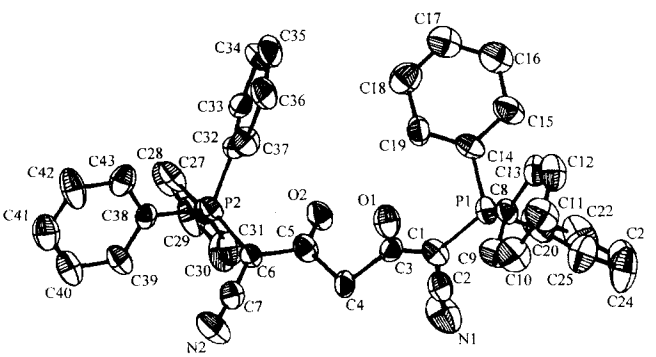


Fig. 1. Molecular structure of **1** (thermal ellipsoids at 30% probability level) with atom numbering. Selected distances [Å] and angles [°] with standard deviations in parentheses: P1-C1 1.754(8), P1-C8 1.787(6), P1-C14 1.783(7), P1-C20 1.775(7), P2-C6 1.746(8), P2-C26 1.795(5), P2-C32 1.787(6), P2-C38 1.793(7), C1-C2 1.403(8), C1-C3 1.434(8), C2-N1 1.152(7), C3-O1 1.226(7), C3-C4 1.528(9), C5-C4 1.543(8), C5-O2 1.231(7), C5-C6 1.421(8), C6-C7 1.416(9), C7-N2 1.156(8); P1-C1-C3 118.4(7), P1-C1-C2 118.4(9), C2-C1-C3 122.9(7), P2-C6-C5 115.0(9), P2-C6-C7 121.1(8), C7-C6-C5 123.4(7), C6-C5-O2 119.4(7), C6-C5-C4 120.5(7), O2-C5-C4 120.0(7), C1-C3-O1 123.4(8), C1-C3-C4 116.9(7), O1-C3-C4 119.6(8), C3-C4-C5 107.9(8).

lengths are almost normal for keto groups; these are oriented in such a way as to bisect the bond angles C8-P1-C14 and C26-P2-C32, probably in order to favor a positive interaction between $P^{\delta+}$ and $O^{\delta-}$. The resulting "eclipsed" conformation of the cyano groups with respect to the bonds P1–C20 and P2–C38 gives rise to nonbonding distances C2···C20 and C7···C38 of about 3.05 Å. The crystal structure contains 1.5 molecules of toluene per molecule of **1**.

The ^{31}P NMR spectrum of **1** shows a singlet at $\delta = 20.37$, which is high-field shifted with respect to the ylide signal at $\delta = 23.18$, and is in the range expected for a phosphonium

[*] Dr. L. Pandolfo, Prof. P. Ganis
Dipartimento di Chimica Inorganica, Metallorganica e Analitica
Università di Padova
Via Marzolo, 1, I-35131 Padova (Italy)
Telefax: Int. code + (49)831249
Dr. G. Facchin, Dr. R. Bertani
Centro di Chimia e Tecnologia dei Composti Metallorganici degli Elementi di Transizione del CNR
Istituto di Chimica Industriale, Università di Padova
Via Marzolo, 9, I-35131 Padova (Italy)
Telefax: Int. code + (49) 831680
Dr. G. Valle
Centro di Studio sui Biopolimeri, (CNR) Padova (Italy).

[**] This work was supported by the Ministero dell'Università e della Ricerca Scientifica e Technologica (MURST) and by the Consiglio Nazionale delle Ricerche (CNR). P. G. is on sabbatical leave from Università di Napoli (Italy).

system. This is in agreement with the relatively long P–C bonds, as found in the X-ray determination. In the ^{1}H NMR spectrum of **1**, recorded in CD_2Cl_2 or in $CDCl_3$, signals originating from a possible keto–enol equilibrium are not detected.

By reacting C_3O_2 with $Ph_3P{=}CHCOR$ (R = Me, Ph) in toluene, the cyclic derivatives **2a** and **2b** are obtained in high yields. The reactions proceed in a stoichiometric ratio 1:1, resulting in the formation of the heterocyclic systems after a nucleophilic intramolecular attack of the ylidic carbonyl group (COR) on the ketene moiety in **II** (route b, Scheme 1). Closely related behavior was previously reported in the reaction of C_3O_2 with 1,3-dicarbonilyl compounds.[6]

The molecular structure[4] of **2a** is shown in Figure 2. The six-membered ring is almost planar and the same plane also contains the atoms P1 and C7. The bond lengths C2–O1

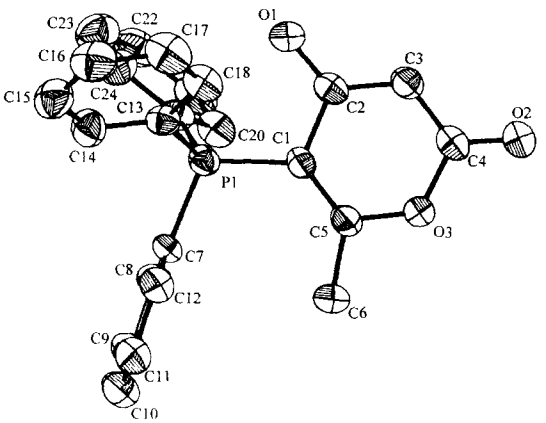


Fig. 2. Molecular structure of **2a** (thermal ellipsoids at 30% probability level) with atom numbering. Selected distances [Å] and angles [°] with standard deviations in parentheses: P1-C1 1.787(3), P1-C7 1.800(4), P1-C13 1.796(4), P1-C19 1.804(4), C1-C2 1.492(5), C2-C3 1.354(4), C2-O1 1.251(4), C3-C4 1.404(5), C4-O2 1.218(4), C4-O3 1.380(4), C5-O3 1.387(4), C5-C6 1.494(6), C5-C1 1.349(4); P1-C1-C5 128.4(4), P1-C1-C2 111.1(2), C1-C5-C6 131.7(4), C1-C5-O3 118.9(4), C6-C5-O3 109.5(3), C5-O3-C4 124.0(3), C3-C4-O3 116.2(4), C3-C4-O2 123.9(5), O3-C4-O2 119.8(3), C2-C3-C4 124.0(4), C1-C2-O1 118.2(4), C1-C2-C3 116.4(3), O1-C2-C3 125.3(4).

[1.251(4) Å] and C4–O2 [1.218(4) Å] support the zwitterionic character of the molecule, confirmed also by the P1–C1 distance of 1.787(3) Å which falls in the range of bond lengths reported for phosphonium ions.[7] Noteworthy is the eclipsed conformation of the bonds P1–C7 and C1–C5, as found for **1**, and the relatively short intramolecular nonbonding distance between C7 and C6 (ca. 3.13 Å). The conformation, such as obtained through a rotation of 180° about the P1–C1 bond and with analogous distortions of the angles C1-C2-O1 and P1-C1-C2, would be certainly preferred on the basis of mere intramolecular van der Waals interactions, but it would probably oppose the stabilizing ionic interaction between $P1^+$ and $O1^-$, which in **2a** are 2.78 Å apart. The crystal structure contains two solvent molecules of CH_2Cl_2 per molecule of **2a**.

^{31}P NMR spectra of **2a** and **2b** show a singlet at $\delta = 16.16$ and 17.31, respectively, characteristic for phosphonium systems.[2]

We have tried to force the Wittig reaction (route d) by heating compounds **1** and **2** under reflux in 1,2-dichloroethane for three days. The solution of **1** remains unchanged, whereas solutions of **2a, b** become red, slowly releasing CO_2 (evidenced by IR spectra) which possibly originates from the decomposition of the α-pyronic ring. TLC of the resulting solutions show the presence of several compounds, which were not further characterized.

The present work shows that the reactions of C_3O_2 with ylides bearing a hydrogen atom on the ylidic carbon atom follow alternative routes with respect to those previously reported for different ylides without H substituents.[3] A fundamental role seems to be played by the easily displaceable hydrogen atom. It migrates to the carbanionic carbon atom in the intermediate **I** forming the ylide **II**. This process is similar to that reported for the reaction of ylides with electron-poor olefins.[8] For X = CN intermediate **II** reacts with a second molecule of cyanomethylenetriphenylphosphorane to yield **1** (route a, Scheme 1). For X = COR an intramolecular nucleophilic attack of the carbonyl oxygen atom of the ylide moiety on the carbonyl carbon atom of the ketene occurs, (route b) leading to the pyrone derivatives **2**. In all cases, we have not found any evidence for a Wittig reaction (route d), or for the formation of cyclobutanedione derivatives (route c).

Experimental Procedure

1: The ylide $Ph_3P{=}CHCN$ (0.550 g, 1.82 mmol) was dissolved in 50 mL of a toluene/CH_2Cl_2 solution (5/1) and a solution of C_3O_2 in toluene (3.2×10^{-2} M, 28.5 mL, 0.91 mmol) was added at room temperature under stirring. The solution became light yellow and the IR spectra revealed the disappearance of C_3O_2. The solution was concentrated under vacuum at room temperature to 40 mL, the white solid obtained was filtered off, washed with toluene, and dried under vacuum. Yield 0.450 g (73%). Compound **1** was also obtained when the reaction was performed in 1,2-dichloroethane, yield 85%. M.p. 243–244 °C (decomp). Correct C,H,N analysis. IR(nujol) [cm^{-1}]: 2175 (CN), 1565 (CO); ^{1}H NMR (200 MHz, CD_2Cl_2, 25 °C): $\delta = 4.01$ (s, CH_2), 7.72–7.46 (m, C_6H_5), ^{13}C NMR (CD_2Cl_2, 25 °C): $\delta = 49.63$ (d, ^1J(CP) = 126.70 Hz, CP), 51.30 (t, ^3J(CP) = 7.04 Hz, CH_2), 191.04 (dt, ^2J(CP) = 5.84, ^2J(CH) = 5.39 Hz, CO), CN (signal too weak to be observed). ^{31}P NMR ($CDCl_3$, 25 °C) $\delta = +20.37$(s). FAB MS in glycerol: *m/z* (%): 671 (13.7) [$M - H^+$], 670 (0.1) [M^+].

2: The ylide ($Ph_3P{=}CHCOMe$ (**a**) or $Ph_3P{=}CHCOPh$ (**b**)) was dissolved in anhydrous toluene, an equimolecular amount of C_3O_2 [9] dissolved in toluene was added at room temperature and the solution was stirred for 3 h. The solvent was partially removed under vacuum, and pale yellow crystals were obtained which were filtered, washed with toluene at 0 °C, and dried under vacuum. Yield: **2a**: 91%, **2b**: 96%. **2a** and **2b** were obtained, with similar yields, also when the reactions were performed in 1,2-dichloroethane at room temperature or in toluene at 80 °C.

2a: M.p. 213–215 °C (decomp). Correct C, H analysis. IR(nujol) [cm^{-1}]: 1693 (CO). ^{1}H NMR (200 MHz, CD_2Cl_2, 25 °C): $\delta = 1.52$ (d, ^4J(HP) = 1.42 Hz, CH_3), 5.00 (d, ^4J(HP) = 3.59 Hz, CH), 7.69–7.16 (m, C_6H_5). ^{13}C NMR (CD_2Cl_2, 25 °C): $\delta = 20.05$ (q, ^1J(CH) = 130.25 Hz, CH_3), 84.32 (dd, ^1J(CH) = 165.15 Hz, ^3J(CP) = 3.59 Hz, CH), 100.76 (d, ^1J(CP) = 116.70 Hz, =CP), 165.18 (d, ^2J(CH) = 3.80 Hz, CO^-), 172.63 (dq, ^2J(CP) = 28.68 Hz, ^2J(CH) = 5.38 Hz, Me-C-O-), 177.13 (d, ^2J(CH) = 3.59 Hz, C=O). ^{31}P NMR ($CDCl_3$, 25 °C): $\delta = +16.16$(s). FAB MS in glycerol *m/z* (%): 387 (0.3) [$M - H^+$], 386 (0.4) [M^+].

2b: M.p. 216–218 °C (decomp). Correct C, H analysis. IR(nujol) [cm^{-1}]: 1706 (CO). ^{1}H NMR (200 MHz, CD_2Cl_2, 25 °C): $\delta = 5.13$ (d, ^4J(HP) = 3.59 Hz, CH), 7.57–6.89 (m, C_6H_5). ^{13}C NMR (CD_2Cl_2, 25 °C): $\delta = 85.78$ (dd, ^1J(CH) = 165.16, ^3J(CP) = 4.20 Hz, CH), 100.35 (dd, ^1J(CP) = 113.58, ^3J(CH) = 4.25 Hz, =CP), 165.08 (d, ^2J(CH) = 3.52 Hz, CO^-), 173.39 (dt, ^2J(C,P) = 17.97, ^3J(CH) = 8.43 Hz, Ph-C-O-), 177.35 (d, ^2J(CH) = 3.20 Hz, C=O). ^{31}P NMR ($CDCl_3$, 25 °C): $\delta = +17.31$(s). FAB MS in glycerol *m/z* (%): 449 (0.1) [$M - H^+$], 448 (0.05) [M^+].

Received: September 7, 1993 [Z 6345 IE]
German version: *Angew. Chem.* **1994**, *106*, 586

[1] a) T. Kappe, E. Ziegler, *Angew. Chem.* **1974**, *86*, 529; *Angew. Chem. Int. Ed. Engl.* **1974**, *13*, 491; b) G. Paiaro, L. Pandolfo, *Comments Inorg. Chem.* **1991**, *12*, 213.

[2] A. W. Johnson, *Ylides and Imines of Phosphorus*, Wiley, New York, **1993**, and references therein.

[3] a) H. F. Van Woerden, N. Cerfontain, C. F. Van Valkenburg, *Recl. Trav. Chim. Pays-Bas* **1969**, *88*, 158; b) F. W. Nader, A. Brecht, *Angew. Chem.* **1986**, *98*, 105; *Angew. Chem. Int. Ed. Engl.* **1986**, *25*, 93; c) L. Bonsignore, G. Loy, D. Secci, S. Cabiddu, *Gazz. Chim. Ital.* **1987**, *117*, 625.

[4] X-ray structure analyses: Philips-PW 1100 computer-controlled four-circle diffractometer; graphite monochromator $Mo_{K\alpha}$, (0.71073 Å), 298 K; θ 2θ scan methods; solution and refinement by standard Patterson methods and subsequent Fourier recycling. **1**: $C_{43}H_{32}O_2N_2P_2 \cdot 1.5\,C_7H_8$; $M = 808.89$, triclinic, $P\bar{1}$; $a = 10.202(3)$, $b = 10.533(3)$, $c = 23.884(7)$ Å, $\alpha = 77.80(5)$, $\beta = 86.50(5)$, $\gamma = 62.60(6)°$; $V = 2225.20(9)$ Å^3, $Z = 2$, $\varrho_{calcd} = 1.210$ g cm^{-3}, $\mu = 1.03$ cm^{-1}. 2θ range 3–45°. Suitable crystals (0.25 × 0.35 × 0.20 mm) were obtained by recrys-

tallization from a CH_2Cl_2/toluene solution and sealed in a Lindeman capillary tube. $F(000) = 850$. 5401 unique reflections and 2527 assumed as observed with $I \geq 3\sigma(I)$. Least-square refinements with anisotropic thermal parameters for all non-hydrogen atoms (except the atoms of the solvent) gave $R(F_0) = 0.062$ and $R_w(F_0) = 0.075$. **2**: $C_{24}H_{19}O_3P \cdot 2CH_2Cl_2$; $M = 556.24$, triclinic, $P\bar{1}$; $a = 14.838(4)$, $b = 11.109(4)$, $c = 8.215(2)$ Å, $\alpha = 104.30(8)$, $\beta = 91.20(7)$, $\gamma = 96.30(7)^\circ$; $V = 1302.6(9)$ Å^3, $Z = 2$, $\varrho_{calcd} = 1.418$ g cm^{-3}, $\mu = 3.94$ cm^{-1}. 2θ range 3–45°. Suitable crystals (0.30 × 0.30 × 0.20 mm) were obtained by recrystallization from a CH_2Cl_2/heptane solution and sealed in a Lindeman capillary tube. F(000) = 572. 4102 unique reflections and 3917 assumed as observed with $I \geq 3\sigma(I)$. Least-square refinements with anisotropic thermal parameters for all non-hydrogen atoms gave $R(F_0) = 0.059$ and $R_w(F_0) = 0.070$. Further details of the crystal structure investigation are available on request from the Director of the Cambridge Crystallograpic Data Centre, 12 Union Road, GB-Cambridge CB21EZ (UK), on quoting the full journal citation.

[5] a) *Interatomic Distances and Configuration in Molecules and Ions*, Chemical Society Special Publ., London, **1958**; b) *International Tables for X-Ray Crystallography*, Riedel, Boston, MA, **1983**.

[6] a) F. Hradetzky, E. Ziegler, *Monatsh. Chem.* **1966**, *97*, 398; b) A. Omori, N. Sonoda, S. Tsutsumi, *J. Org. Chem.* **1969**, *34*, 2480; c) L. Pandolfo, G. Paiaro, *J. Mol. Catal.* **1984**, *27*, 343.

[7] a) H. Schmidbaur, G. A. Bowmaker, U. Deschler, C. Doezerbach, R. Herr, B. Milewski-Marla, A. Schier, G. Zybill, *Phosphorus Sulfur* **1983**, *18*, 167; b) J. J. Daly, *Perspective in Structural Chemistry, Vol. 3*, Wiley, New York, **1969**; c) D. J. H. Smith in *Comprehensive Organic Chemistry, Vol. 2*, (Eds.: D. Barton, W. D. Ollis), Pergamon, Oxford, **1979**, p. 1313.

[8] H. J. Bestmann, G. Schmid, L. Kisielowski, *Isr. J. Chem.* **1982**, *22*, 45.

[9] By performing the reactions in 1:2 ratio (C_3O_2:ylide) only **2a** and **2b** were obtained and unreacted ylides were recovered.

Reactivity of a Phosphanylcarbene (λ^5-Phosphaacetylene) with Lewis Acids: X-Ray Crystal Structures of the First Carbene–Gallane Complex and *C*-Gallyl-Substituted Phosphorus Ylide**

Alan H. Cowley,* François P. Gabbaï, Carl J. Carrano, Ladd M. Mokry, Marcus R. Bond, and Guy Bertrand*

So far, only two types of stable carbene are known.[1, 2] Although both of them are heteroatom-substituted, their structures, as shown by molecular orbital calculations[3, 4] and reactivity studies, are significantly different. Arduengo et al.[5] have recently reported the synthesis of an alane-imidazol-2-ylidene complex, which is in fact the only structurally characterized carbene–Lewis acid adduct. In contrast, phosphanylcarbene–borane complexes are unstable and undergo a variety of rearrangements.[6] Herein, we report that phosphanylcarbenes exhibit a remarkably diverse reactivity depending on the nature of the Lewis acid employed, and of particular interest, we describe the synthesis of a stable phosphanylcarbene–Lewis acid complex.

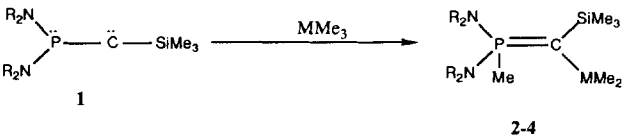
[*] Prof. A. H. Cowley, F. P. Gabbaï
Department of Chemistry and Biochemistry
The University of Texas at Austin
Austin, TX 78712 (USA)
Telefax: Int. code + (512)471-6822

Dr G. Bertrand
Laboratoire de Chimie de Coordination du CNRS
205, route de Narbonne, F-31077 Toulouse Cédex (France)
Telefax: Int. code + (61)553003

Prof. C. J. Carrano, L. M. Mokry, Dr. M. R. Bond
Department of Chemistry
Southwest Texas State University, San Marcos, TX 78666 (USA)
Telefax: Int. code + (512)245-2374

[**] This work was supported by the National Science Foundation, the Robert A. Welch Foundation and the Centre National de la Recherche Scientifique. We thank Mr. Harold S. Isom for conducting the variable temperature NMR experiments.

[Bis(dicyclohexylamino)phosphanyl](trimethylsilyl)carbene (**1**) reacts cleanly with $AlMe_3$, $GaMe_3$, and $InMe_3$ in Et_2O at −78 °C to afford the corresponding 1:1 adducts **2**, **3**, and **4**, respectively (Scheme 1). The similarity of the NMR data[7] for



Scheme 1. R = *cyclo*-C_6H_{11}; M = Al (**2**), Ga (**3**), In (**4**).

2, **3**, and **4** suggests that they possess comparable structures. For compound **3**, the presence of a doublet at $\delta = 1.61$ ($J_{PH} = 11.7$ Hz) in the ^{1}H NMR spectrum and a doublet at $\delta = 22.37$ ($J_{PC} = 84.4$ Hz) in the ^{13}C NMR spectrum indicated the presence of a methyl group directly bonded to phosphorus. The X-ray structure analysis[8] of the gallium compound **3** confirmed that formal Me–$GaMe_2$ addition across the phosphorus–carbon bond had taken place (Fig. 1). A number of

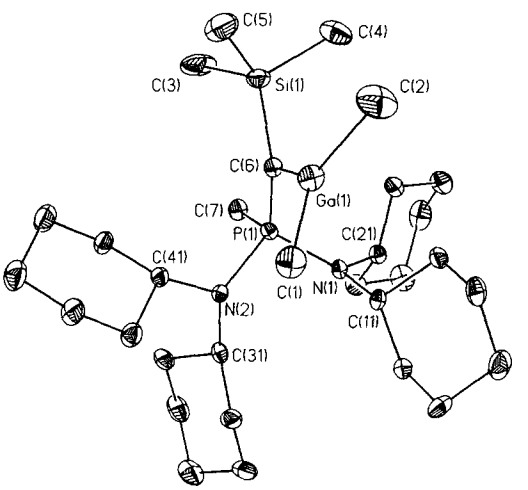
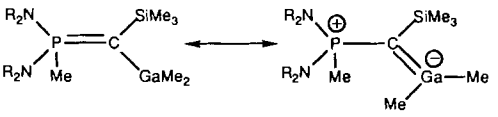


Fig. 1. View (ORTEP) of **3** showing the atom labeling scheme. Important bond lengths [Å] and angles [°]: P-C6 1.658(7), P-C7 1.808(6), P-N1 1.693(5), P-N2 1.690(5), C6-Si1 1.829(7), C6-Ga1 1.935(6), Ga1-C1 1.994(8), Ga1-C2 1.988(10); C6-P1-C7 113.4(3), C6-P1-N1 118.1(3), C6-P1-N2 112.6(3), C7-P1-N1 103.8(3), C7-P1-N2 105.3(3), N1-P1-N2 102.2(3), Ga1-C6-P1 120.0(4), Ga1-C6-Si1 110.3(3), Si1-C6-P1 129.1(4), C1-Ga1-C2 112.1(4), C1-Ga1-C6 125.4(3), C2-Ga1-C6 122.5(3).

structural aspects merit comment. The Ga1–C6 distance (1.935(6) Å) is appreciably shorter than those of the Ga1–C1 and the Ga1–C2 bonds (av. 1.991(10) Å), C6 and Ga1 both adopt a trigonal planar geometry (sums of angles = 359.4(4)° and 360.0(4)°, respectively) and the dihedral angle between the C1-Ga1-C2 and P1-C6-Si1 planes is small (36.7°). Taken collectively, this suggests a modicum of π-type interaction between C6 and Ga1 (canonical form **3B**; Scheme 2). However, the P1–C6 distance (1.658(7) Å) is shorter than that observed in the analogous boron system (1.696(2) Å), where such a π-type interaction has been demonstrated[9] thus favoring canonical form **3A**. In variable-temperature ^{1}H NMR experiments, we have found that the methyl groups of the $GaMe_2$ moiety become nonequivalent only below −85 °C.



3 A 3 B

Scheme 2. Possible canonical formulae of **3**.

The reactions of **1** with the analogous chlorinated Lewis acids $AlCl_3$, $GaCl_3$, and $InCl_3$ in Et_2O solution at 25 °C likewise afford 1:1 adducts, namely **5**, **6**, and **7**, respectively (Scheme 3).



5-7

Scheme 3. M = Al (**5**), Ga (**6**), In (**7**).

However, the ^{31}P chemical shifts[7] of the products are distinctly different from those of the carbene–MMe_3 adducts. The X-ray structure analysis of **6**[8] indicated that **6** is the first carbene–gallane adduct (Fig. 2). Examination of the molecular structure

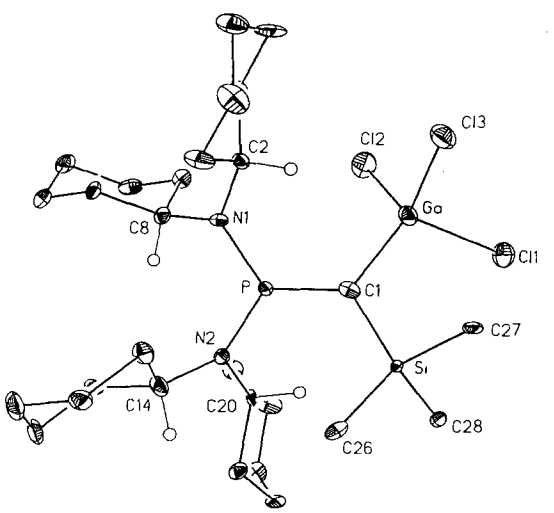
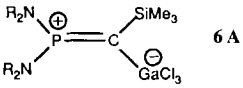


Fig. 2. View (ORTEP) of **6**·CH_2Cl_2 showing the atom labeling scheme. Important bond lengths [Å] and angles [°]: P-C1 1.601(9), P-N1 1.622(7), P-N2 1.619(8), C1-Si 1.886(8), C1-Ga 1.978(10), Ga-Cl1 2.210(3), Ga-Cl2 2.179(3), Ga-Cl3 2.198(3); N1-P-N2 113.4(4), N1-P-C1 125.1(5), N2-P-C1 121.4(4), P-C1-Si 121.8(6), P-C1-Ga 122.6(5), Si-C1-Ga 115.7(5), C1-Ga-Cl1 111.4(3), C1-Ga-Cl2 113.9(3), C1-Ga-Cl3 112.8(3), Cl1-Ga-Cl2 105.49(11), Cl1-Ga-Cl3 104.35(12), Cl2-Ga-Cl3 108.19(12).

of **6** reveals the following salient points: 1) the phosphorus and carbon atoms both adopt a trigonal planar geometry (sums of the angles = 359.8(8) and 360.0(8)°, respectively), 2) the phosphorus–carbon bond length of 1.610(15) Å, together with a rather small torsional angle of 34.1°, are indicative of a bond order of two, 3) the geometry at gallium is tetrahedral, thus implying that **6** is best described by a zwitterionic methylenephosphonium canonical form **6A** (Scheme 4).[10] Evidently, a similar structure persists in solution; the deshielded ^{31}P chemical shift of $\delta = 130$ is consistent with the presence of a double bond and positive charge development at phosphorus. Moreover, since the ^{31}P chemical shift and $^3J_{PH}$ coupling con-



6 A

Scheme 4. Predominant canonical formula of **6**.

stants for **5** and **7** are virtually identical to those of **6**, similar structures can be proposed for these adducts.[7] Compounds **5**–**7** are evidently the first examples of neutral zwitterionic methylenephosphonium compounds. However, an uneven charge distribution has been implied previously in the cation $[(iPr_2N)_2P{=}C(SiMe_3)_2]^+$.[10]

Overall, the present results demonstrate that the reactions of phosphanylcarbenes with Lewis acids are highly versatile and that the outcomes are based on subtle interplays of thermodynamic and steric effects.

Experimental Procedure

3: An excess of neat trimethylgallium (0.50 mL, 5.0 mmol) was added to a solution of **1** (1.0 mmol) in Et_2O (15 mL) at −78 °C. The reaction mixture was allowed to warm to 25 °C. The solvent and volatiles were then evaporated yielding a microcrystalline residue which was washed with pentane (5 mL) to afford 0.38 g (65% yield) of pale yellow microcrystalline **3** (m.p. 146–148 °C). X-ray quality crystals were grown by cooling a saturated toluene solution of **3** to −20 °C for two weeks. Compounds **2** and **4** were prepared by a similar procedure.

6: A solution of gallium trichloride (0.176 g, 1.0 mmol) in toluene (3 mL) was added to a solution of **1** (1.0 mmol) in Et_2O (15 mL) at 25 °C. The reaction mixture was stirred for 20 minutes during which time a precipitate was formed. The solution was removed with a cannula and the precipitate was washed with Et_2O (5 mL) affording 0.52 g (79% yield) of pale yellow solid **6** (m.p. 110 °C, decomp). X-ray quality crystals of **6**·CH_2Cl_2 were grown from a dichloromethane solution by slow evaporation of the solvent. Compounds **5** and **7** were prepared by a similar procedure.

Received: September 25, 1993 [Z 6378 IE]
German version: *Angew. Chem.* **1994**, *106*, 584

[1] A. J. Arduengo III, R. L. Harlow, M. Kline, *J. Am. Chem. Soc.* **1991**, *113*, 361; A. J. Arduengo III, H. V. R. Dias, R. L. Harlow, M. Kline, *ibid.* **1992**, *114*, 4430.

[2] A. Igau, H. Grützmacher, A. Baceiredo, G. Bertrand, *J. Am. Chem. Soc.* **1988**, *110*, 6463; A. Igau, A. Baceiredo, G. Trinquier, G. Bertrand, *Angew. Chem.* **1989**, *101*, 617; *Angew. Chem. Int. Ed. Engl.* **1989**, *28*, 621; G. Gillette, A. Baceiredo, G. Bertrand, *ibid.* **1990**, *102*, 1486 and **1990**, *29*, 1429; M. Soleilhavoup, A. Baceiredo, O. Treutler, R. Ahlrichs, M. Nieger, G. Bertrand, *J. Am. Chem. Soc.* **1992**, *114*, 10959.

[3] D. A. Dixon, A. J. Arduengo III, *J. Phys. Chem.* **1991**, *95*, 4180.

[4] M. T. Nguyen, M. A. McGinn, A. F. Hegarty, *Inorg. Chem.* **1986**, *25*, 2185; K. D. Dobbs, D. A. Dixon, A. J. Arduengo III, G. Bertrand *J. Am. Chem. Soc.* **1991**, *113*, 8782; M. R. Hoffmann, K. Kuhler, *J. Chem. Phys.***1991**, *94*, 8029; O. Treutler, R. Ahlrichs, M. Soleilhavoup, *J. Am. Chem. Soc.* **1993**, *115*, 8788.

[5] A. J. Arduengo III, H. V. R. Dias, J. C. Calabrese, F. Davidson, *J. Am. Chem. Soc.* **1992**, *114*, 9724.

[6] G. Alcaraz, R. Reed, A. Baceiredo, G. Bertrand, *J. Chem. Soc. Chem. Commun.* **1993**, 1354.

[7] ^{31}P NMR (121.5 MHz, Et_2O, 295 K, 85% H_3PO_4 ext.): **2**: $\delta = 56$. **3**: $\delta = 57$. **4**: $\delta = 59$. **5**: $\delta = 129$. **6**: $\delta = 130$. **7**: $\delta = 131$.^1H NMR (300.15 MHz, 295 K, TMS ext.): **3** (C_6D_6): $\delta = 0.40$ (s, 6H, $Ga(CH_3)_2$), 0.47 (s, 9H, $Si(CH_3)_3$), 0.80 to 2.00 (m, 40H, $NCCH_2$), 1.61 (d, 3H, $^2J(PH) = 11.7$ Hz, PCH_3), 3.64 (m, 4H, $^3J(PH) = 12.0$ Hz, NCH). **6** (CD_2Cl_2): $\delta = 0.40$ (s, 9H, $Si(CH_3)_3$), 1.00 to 2.50 (m, 40H, $NCCH_2$), 3.77 (m, 4H, $^3J(PH) = 10.8$ Hz, NCH). ^{13}C NMR (75.47 MHz, 295 K, TMS ext.): **3**: (C_6D_6): $\delta = 3.33$ (br, $Ga(CH_3)_2$), 6.65 (d, $^3J(PC) = 8.2$ Hz, $Si(CH_3)_3$), 22.37 (d, $^1J(PC) = 84.4$ Hz, PCH_3), 26.50 ($C\gamma$), 27.83 and 28.05 ($C\delta$), 36.39 and 36.80 ($C\beta$), 57.13 (d, $^2J(PC) = 5.4$ Hz, $C\alpha$), GaCP not detected. **6** (CD_2Cl_2): $\delta = 3.20$ (d, $^3J(PC) = 7.5$ Hz, $Si(CH_3)_3$), 25.53 and 25.80 ($C\delta$), 27.08 ($C\gamma$), 34.63 and 34.92 ($C\beta$), 57.16 (d, $^2J(PC) = 5.3$ Hz, $C\alpha$), 84.16 (d, $^1J(CP) = 83.4$ Hz, GaCP). MS (CI, CH_4): **3**: *m/z* 591 ($M^+ + 1$), 494 ($M^+ - N(C_6H_{11}) + 1$), 477 ($M^+ - GaMe_3 + 1$). **6**: m/z 651 ($M^+ + 1$).

[8] Crystal structure data for **3**: $C_{31}H_{62}GaN_2PSi$, monoclinic, space group $P2_1/n$, $Z = 4$, $a = 14.358(2)$, $b = 15.673(5)$, $c = 15.006(2)$ Å, $\beta = 92.36(2)°$, $V = 3374(6)$ Å^3, $\rho_{calcd} = 1.165$ g cm^{-3}, $Mo_{K\alpha}$, $\lambda = 0.71073$ Å, $\mu = 0.919$ mm^{-1}. 4376 unique data were collected (θ-2θ scan technique, $3.5 < 2\theta < 45°$) of which 2626 had $I > 2\sigma(I)$ and were used for structure solution and refinement, $R = 0.0559$. Crystal structure data for **6**·CH_2Cl_2, monoclinic, space group

$P2_1/c$, $Z = 4$, $a = 10.1310(12)$, $b = 19.028(2)$, $c = 19.442(3)$ Å, $\beta = 104.083(10)°$, $V = 3635.2(8)$ Å^3, $\rho_{calcd} = 1.35$ g cm^{-3}, $Mo_{K\alpha}$, $\lambda = 0.71073$ Å, $\mu = 1.222$ mm^{-1}. 5543 unique data were collected (ω scan technique, $4.0 < 2\theta < 47.5°$) of which 2416 had $I > 2\sigma(I)$ and were used for structure solution and refinement, $R = 0.0684$. Further details of the crystal structure investigations may be obtained from the Fachinformationszentrum Karlsruhe, D-76344 Eggenstein-Leopoldschafen (FRG), on quoting the depository number CSD-57775, the names of the authors and, the journal citation.

[9] K. Horchler von Locquenghien, A. Baceiredo, R. Boese, G. Bertrand, *J. Am. Chem. Soc.* **1991**, *113*, 5062.

[10] A. Igau, A. Baceiredo, H. Grützmacher, H. Pritzkow, G. Bertrand, *J. Am. Chem. Soc.* **1989**, *111*, 6853; H. Grützmacher, H. Pritzkow, *Angew. Chem.* **1991**, *103*, 721; *Angew. Chem. Int. Ed. Engl.* **1991**, *30*, 709; M. Ehrig, H. Horn, C. Kölmel, R. Ahlrichs, *J. Am. Chem. Soc.* **1991**, *113*, 3701.

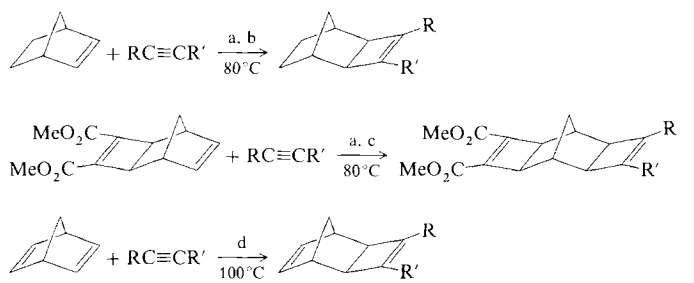
[2 + 2]Cycloaddition of Norbornenes with Alkynes Catalyzed by Ruthenium Complexes**

Take-aki Mitsudo,* Hiroshi Naruse, Teruyuki Kondo, Yoshihiko Ozaki, and Yoshihisa Watanabe*

The [2 + 2]cycloaddition of olefins and/or alkynes is a versatile method for preparation of cyclobutane derivatives, and the cycloaddition has been achieved by thermal reactions via biradical intermediates,[1] photoreactions,[2] and transition-metal-catalyzed reactions.[3] Among them, ruthenium-complex-catalyzed cycloaddition of norborn*enes* (bicyclo-[2.2.1]heptene derivatives) with ethynedicarboxylates is a unique reaction.[3] The catalyst was $[RuH_2(CO)(PPh_3)_3]$ or [Ru(cod)(cot)] (cod = 1,5-cyclooctadiene, cot = 1,3,5-cyclooctatriene)]/PR_3), and the reaction was applied to the preparation of pseudo-ladder compounds.[4, 5] However, the reaction had a severe limitation: only ethynedicarboxylates could be used. We now report that [Cp*RuCl(cod)][6] (**1**, Cp* = pentamethylcyclopentadienyl) is an excellent catalyst for the [2 + 2]cycloaddition of norbornenes with various alkynes. Further, the analogous reaction of terminal alkynes with norborn*adiene* (nbd, bicyclo[2.2.1]hepta-2,5-diene) gives 1,3-disubstituted benzene as well as the [2 + 2] adducts.

Both aliphatic and aromatic internal alkynes readily reacted with norbornene in the presence of a catalytic amount of **1** at 80 °C to give the corresponding [2 + 2]cycloadducts, *exo*-3,4-disubstituted tricyclo[4.2.1.0.^{2,5}]non-3-enes in high yields (Scheme 1, **A**/**B**). The *exo* structure of the adducts was confirmed by ^{1}H NMR spectroscopy; no coupling of the 2,5-protons with those at the bridgehead was observed.[7] Unsymmetrical internal alkynes as well as symmetric ones reacted successfully. Furthermore, a double cross-adduct was also prepared by a stepwise reaction (run 7).

Complex, **1** also catalyzed the reaction of internal alkynes with norborn*adiene* (Scheme 1, **C**) to give the corresponding [2 + 2]cycloadducts, and the complex was completely converted into [Cp*RuCl(nbd)] in the reaction. Since the formed [Cp*RuCl(nbd)] is more stable than **1**, the rate of [2 + 2]cycloaddition of diphenylethyne with norbornadiene (run 11) was slower than that in the reaction with norbornene (run 1). However, alkynes with electron-withdrawing groups such as methyl 2-butynoate (run 9), and ethyl 3-phenylprop-2-ynolate (run 10) readily reacted to give the corresponding adducts in high yields.



No.	R	R′	t [h]	Yield	
1	Ph	Ph	15	88 (91)	**A**
2	Ph	Me	15	87	**A**
3	C_5H_{11}	C_5H_{11}	20	40	**A**
4	Et	$CH(OEt)_2$	15	62	**A**
5	Ph	CO_2Et	15	60	**A**
6	Me	CO_2Me	15	79	**A**
7	Ph	Ph	20	74	**B**
8	CO_2Me	CO_2Me	24	37	**C**
9	Me	CO_2Me	24	87	**C**
10	Ph	CO_2Et	24	74	**C**
11	Ph	Ph	120	23	**C**

Scheme 1. [Cp*RuCl(cod)]-catalyzed [2 + 2]cycloaddition of norbornenes and norbornadiene with alkynes. The reactions were performed in an argon atmosphere. a) 4.0 mmol norbornene, 2.0 mmol ethyne, 0.1 mmol [Cp*RuCl(cod)] (**1**); b) 1.5 mL NEE_3 as solvent; c) 1 mL benzene as solvent; d) 10.0 mmol norbornadiene, 2.0 mmol alkyne, 0.1 mmol **1**, no solvent. The yields are based on the alkyne concentration. The yield in parentheses was determined by gas chromatography.

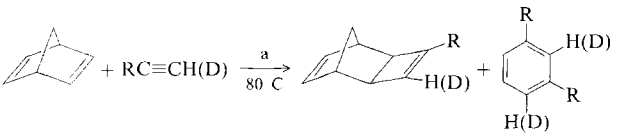
Effects of solvents and additives on the [2 + 2]cycloaddition reaction of diphenylethyne with norbornene (run 1) catalyzed by **1** were examined. The reaction proceeded smoothly at 80 °C for 15 h in *n*-hexane (85% yield determined by gas chromatography), benzene (83%), triethylamine (91%), and THF (85%), but when pyridine (2%) or DMSO (0%) was employed as a solvent, the reaction was suppressed. Although phosphane ligands had been quite effectively employed in the reaction of dimethyl ethynedicarboxylate with norbornenes catalyzed by [Ru(cod)(cot)]/P*n*Bu$_3$ or $[RuH_2(CO)(PPh_3)]$ etc.,[3] in the present reaction addition of PPh_3 to the benzene solution resulted in the decease of the yield to 51% for PPh_3/Ru = 1.0 mol/mol and to 26% for PPh_3/Ru = 2.0 mol/mol. Cyclopentadienyl–phosphane complexes such as $[CpRuCl(PPh_3)_2]$ were inactive. Treating catalyst **1** with $AgOSO_2CF_3$ in triethylamine to generate a cationic $[Cp^*Ru]^+$ species[8] also decreased the catalytic activity (26% yield). These results strongly suggest that an active species of this reaction is a *neutral* "[Cp*RuCl]" moiety.

Both aromatic and aliphatic substituted terminal alkynes also reacted readily with norborn*adiene* in the presence of a catalytic amount of **1** at 80 °C to give the corresponding [2 + 2]cycloadducts accompanied by the formation of unexpected 1,3-disubstituted benzene derivatives (Scheme 2). Neither the 1,4- nor 1,2-disubstituted isomer was detected at all.

If the alkyne used in this reaction is [D_1]phenylethyne, in the [2 + 2]cycloadduct the expected position was labeled by deuterium, and in the 1,3-disubstituted benzene, *m*-terphenyl, the 2- and 4-positions were selectively labeled. Furthermore, dicyclopentadiene formed by Diels–Alder reaction of cyclopentadiene was detected in the reaction mixture. These results demonstrate that the source of the carbon atoms C5 and C6 in *m*-terphenyl is norbornadiene (olefinic carbons) and that C1 to C4 originate from two alkyne molecules.

[*] Prof. Dr. T. Mitsudo, Prof. Dr. Y. Watanabe, H. Naruse, Dr. T. Kondo, Y. Ozaki
Division of Energy and Hydrocarbon Chemistry
Graduate School of Engineering, Kyoto University
Sakyo-ku, Kyoto, 606-01 (Japan)
Telefax Int. code +(75)753-4976

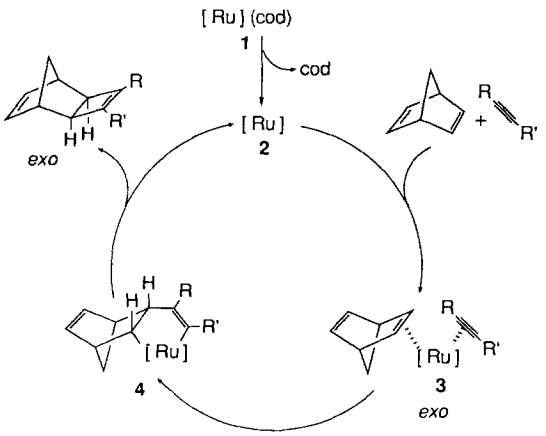
[**] This work was partially supported by the Ministry of Education, Science, and Culture, Japan (Grant-in-Aid for Scientific Research No. 04650732, 05403024).



No.	R	t [h]	Yield (add.)	Yield (arene)
12	Ph	16	44	26
13	n-C_8H_{17}	40	23	20
14	n-$C_{10}H_{21}$	40	23	12

Scheme 2. [Cp*RuCl(cod)]-catalyzed reaction of norbornadiene with terminal alkynes. The yields were determined by gas chromatography. a) 10 mmol norbornadiene, 2 mmol alkyne, 0.10 mmol **1**. add. = [2 + 2]cycloaddition product, arene = 1,3-disubstituted benzene product.

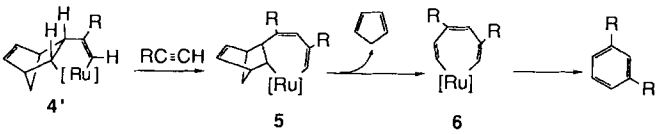
Although mechanism of the [2 + 2]cycloaddition has not yet been clarified, one of plausible possibilities is illustrated in Scheme 3. At first an unsaturated complex, [Cp*RuCl] (**2**), is formed by dissociation of cod from **1**; then norbornene and the alkyne coordinate at the unsaturated sites to form **3**. The coordination of norbornenes was invariably *exo* because π-electron density of the *exo* face of norbornenes is higher than that of the *endo* face.[9] A ruthenacyclopentene complex **4** is formed by oxidative cyclization. By successive reductive elimination, the *exo*[2 + 2]cycloadduct is formed, and unsaturated **2** is regenerated. The related reaction intermediates to the ruthenacyclopentene intermediate **4** in dimerization of norbornadiene with Ir[10] or Ni[11] catalyst have been isolated.



Scheme 3. Possible mechanism for the [2 + 2]cycloaddition. [Ru] = Cp*RuCl.

With an excess amount of norbornadiene, after the alkyne was completely consumed, [Cp*RuCl(nbd)], in which norbornadiene replaced 1,5-cyclooctadiene, was formed and recovered; therefore no deactivation of the catalyst was observed. However, with an excess of norbor*nene*, neither [Cp*RuCl(norbornene)$_2$] nor [Cp*RuCl(cod)] was detected after the reaction at all. The catalytic activity of [Cp*RuCl(cod)] was so high that ruthenacyclopentene complex **4** could not be detected. Furthermore, when the stoichiometric reaction of [Cp*RuCl(nbd)] with diphenylethyne was monitored by ^{1}H NMR at 100 °C, only the signals for the substrates, [Cp*RuCl(nbd)], and the product were observed. The complexes **3** and **4** could not be detected, which suggests that the rate-determining step of this reaction is the simultaneous coordination of the norbornadiene and the alkyne to **3**.

The formation of 1,3-disbustituted benzene is rationalized by the route shown in Scheme 4 via the ruthenacyclopentene com-



Scheme 4. Possible mechanism for the formation of 1,3-disubstituted benzenes. [Ru] = Cp*RuCl.

plex **4'**. The second alkyne molecule inserts into **4'** to form **5**, then cyclopentadiene is eliminated from **5** by a retro-Diels–Alder reaction,[12] followed by reductive elimination to produce 1,3-disustituted benzene. These reactions are, to our knowledge, the first examples of carbon–carbon bond-forming reactions efficiently catalyzed by a neutral Cp*–ruthenium complex.

Received: September 16, 1993 [Z 6359IE]
German version: *Angew. Chem.* **1994**, *106*, 595

[1] J. E. Baldwin in *Comprehensive Organic Synthesis, Vol. 5* (Eds.: B. M. Trost, I. Fleming, L. A. Paquette), Pergamon, Oxford, **1991**, p. 63.
[2] M. T. Crimmins in *Comprehensive Organic Synthesis, Vol. 5* (Eds.: B. M. Trost, I. Fleming, L. A. Paquette), Pergamon, Oxford, **1991**, p. 123.
[3] T. Mitsudo, K. Kokuryo, T. Shinsugi, Y. Nakagawa, Y. Watanabe, Y. Takegami, *J. Org. Chem.* **1979**, *44*, 4492, and references therein; T. Mitsudo, Y. Hori, Y. Watanabe, *J. Organomet. Chem.* **1987**, *334*, 157.
[4] R. N. Warrener, I. G. Pitt, D. N. Butler, *J. Chem. Soc. Chem. Commun.* **1983**, 1340.
[5] H. Oevering, M. N. Paddon-Row, M. Heppener, A. M. Oliver, E. Cotsaris, J. W. Verhoeven, N. S. Hush, *J. Am. Chem. Soc.* **1987**, *109*, 3258.
[6] N. Oshima, H. Suzuki, Y. Moro-oka, *Chem. Lett.* **1984**, 1161.
[7] C. D. Smith, *J. Am. Chem. Soc.* **1966**, *88*, 4273; J. Meinwald, J. C. Meinwald, T. N. Baker, *ibid.* **1964**, *86*, 4074.
[8] K. Masuda, H. Ohkita, S. Kurmatani, K. Itoh, *Organometallics* **1993**, *12*, 2221, and references therein; R. Carreno, B. Chaudret, D. Labroure, S. Sao-Etienne, *ibid.* **1993**, *12*, 13; B. M. Trost, A. Indolese, *J. Am. Chem. Soc.* **1993**, *115*, 4361.
[9] S. Inagaki, H. Fujimoto, K. Fukui, *J. Am. Chem. Soc.* **1976**, *98*, 4054.
[10] A. R. Fraser, P. H. Bird, S. A. Bezman, J. R. Sharpley, R. White, J. A. Osborn, *J. Am. Chem. Soc.* **1973**, *95*, 597.
[11] M. J. Doyle, J. McMeeking, P. Binger, *J. Chem. Soc. Chem. Commun.* **1976**, 376.
[12] The possibility of a retro-Diels–Alder reaction after the reductive elimination of **5** should be mentioned. No cyclohexadiene derivative derived from the reductive elimination of complex **5** was detected at all. Details will be discussed in a full paper.

Activation of Glutathione Reductase by Light: A Novel Approach to Design Redox Photo-Enzymes**

Itamar Willner* and Eran Zahavy

Dedicated to Professor Mordecai Rabinovitz on the occasion of his 60th birthday

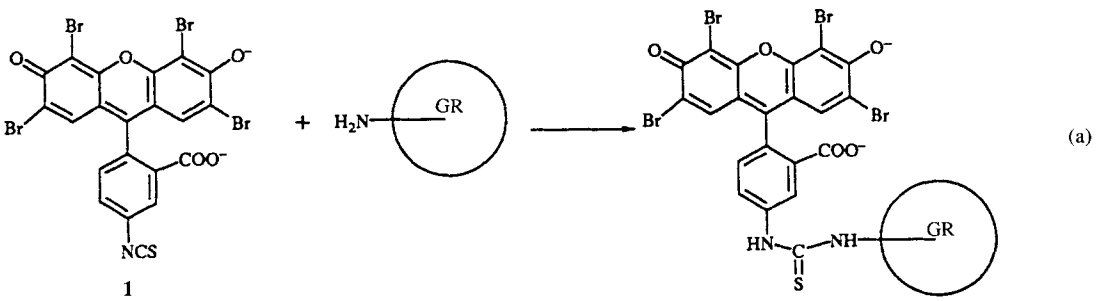
Photoactivation of proteins has been the subject of extensive research efforts.[1] Reversible "ON–OFF" activation of enzymes[2] and other proteins[3] has recently been achieved by covalent linkage of photoisomerizable (photochromic) units to

[*] Prof. I. Willner, E. Zahavy
Institute of Chemistry and Farkas Center for Light-Induced Processes
The Hebrew University of Jerusalem
Jerusalem 91904 (Israel)
Telefax: Int. code + (2)585345

[**] This research was supported by a grant from the Bundesministerium für Forschung und Technologie (BMFT), Germany, and by the National Council for Research and Development, the Ministry of Science and Technology, Israel.

the proteins. The participation of redox enzymes in light-induced electron transfer processes was accomplished by chemical modification of the protein in electron relay units.[4] In these studies protein-anchored electron acceptors acted as quenchers for the excited state of a diffusional photosensitizer and as electron mediators for transporting the electron to the enzyme active site. Here we report on the conversion of the enzyme glutathione reductase (GR) to a photoactive biocatalyst by covalent attachment of eosin to the protein. This modified enzyme is activated (switched "ON") by light. The light-induced redox process is followed by an electron transfer within the protein, and this leads to a biotransformation of the biocatalyzed reduction of oxidized glutathione (GSSG). Till now proteins with light-sensitive components have been modified to study electron transfer pathways in proteins.[5, 6] Our results highlight the possibility of coupling light-induced electron transfer with chemical transformations.

GR (from bakers yeast, EC 1.6.4.2, Sigma) was allowed to react with eosin isothiocyanate (**1**) to form the xanthene-dye-modified protein [Eq. (a)]. The loading of the enzyme corresponds to two units of eosin per protein. The eosin-modified enzyme Eo^{2-}-GR retains 50% of the activity of the native GR protein.[7] Illumination ($\lambda > 475$ nm) of our photosystem that includes Eo^{2-}-GR in a phosphate buffer solution (pH = 7.5) as well as Na_2EDTA (EDTA = ethylenediaminetetraacetic acid) as sacrificial electron donor and oxidized glutathione (GSSG), results in the formation of reduced glutathione GSH. The rate of GSH[8] formation as a function of illumination time is shown in Figure 1a. No GSH formation is observed in the dark or when Na_2EDTA is excluded from the system. These results indicate that GSH is formed by a photoinduced electron transfer. Indeed, stepwise illumination of the photosystem (Fig. 1b) reveals that GSH is formed upon exposure of the system to light and that the process is switched-off in the dark. Based on the amount of GSH formed after 200 minutes of illumination, we estimate 75 cycles of the enzyme active site (the molecular weight of GR used for this calculation was MW = 118000 g mole^{-1}[7]). Thus, Eo^{2-}-GR acts as a photocatalyst in this light-induced transformation.



Illumination of a photosystem ($\lambda > 475$ nm) that includes the native enzyme GR and eosin as a diffusional photosensitizer in the presence of Na_2EDTA and GSSG results in only trace amounts of GSH (Fig. 1c). The rate of GSH formation with the xanthene-dye-modified protein is about fivefold enhanced as compared to the diffusional biocatalyst–dye assembly. This improved yield with the covalently modified Eo^{2-}-GR is attributed to facilitated electron transfer communication within the protein. It should be noted, however, that the photosystem with Eo^{2-}-GR is about 1000-fold less active towards reduction of GSSG than the activity of the native enzyme that utilizes NADPH as electron donor.

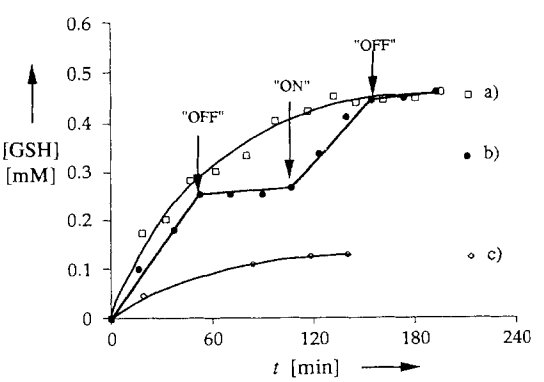


Fig. 1. Rates of GSH formation as a function of illumination time ($\lambda > 475$ nm): a) Photosystem consists of Eo^{2-}-GR (1 mg mL^{-1}), Na_2EDTA (1×10^{-2} M), and GSSG (1×10^{-2} M). b) The photosystem includes similar components as in (a). Arrows indicate the times when the light is switched "ON" or "OFF". c) Photosystem consists of GR, Eo^{2-} (1.7×10^{-5} M), Na_2EDTA (1×10^{-2} M), and GSSG (1×10^{-2} M). Phosphate buffer solutions (pH = 7.5) are used in all photosystems. All experiments were performed under an inert argon atmosphere.

A detailed flash photolysis study has allowed us to elucidate the electron transfer mechanism. The triplet lifetime of Eo^{2-}-GR is 36 μS. The primary process involves the intra-protein electron transfer quenching of the excited Eo^{2-}-GR state to generate the xanthene dye ion pair $Eo^{\bullet-}$ and $Eo^{3\bullet-}$ [Eq. (b)].[9] In the absence of the sacrificial electron donor Na_2EDTA, and GSSG, back electron transfer of the photogenerated products occurs [Eq. (c); $k_b = 2 \times 10^3\ s^{-1}$].[10] In the presence of added Na_2EDTA, oxidation of the sacrificial electron donor, [Eq. (d)] competes with the back reaction, and $Eo^{3\bullet-}$ is accumulated,

$$(^{T}Eo^{2-} + Eo^{2-}) - GR_{ox} \rightarrow (Eo^{\bullet-} + Eo^{3\bullet-}) - GR_{ox} \quad \text{(b)}$$

$$(Eo^{\bullet-} + Eo^{3\bullet-}) - GR_{ox} \xrightarrow{k_b} (Eo^{2-} + Eo^{2-}) - GR_{ox} \quad \text{(c)}$$

$$(Eo^{\bullet-} + Eo^{3\bullet-}) - GR_{ox} + Na_2EDTA \xrightarrow{k_{ox}} (Eo^{2-} + Eo^{3\bullet-}) - GR_{ox} + Na_2EDTA_{ox} \quad \text{(d)}$$

$$\downarrow$$

decomposition products

$$(Eo^{2-} + Eo^{3\bullet-}) - GR_{ox} \xrightarrow{k_{et}} (Eo^{2-} + Eo^{2-}) - GR_{red} \quad \text{(e)}$$

$$(Eo^{2-} + Eo^{2-}) - GR_{red} + GSSG + 2H^{+} \longrightarrow (Eo^{2-} + Eo^{2-}) - GR_{ox} + GSH \quad \text{(f)}$$

$k_{ox} = 3.8 \times 10^4\ s^{-1}$. In the presence of GSSG and Na_2EDTA, the photogenerated reduced product $Eo^{3\bullet-}$ decays. This process corresponds to electron transfer from the ion pair to the enzyme redox site, [Eq. (e); $k_{et} = 1.7 \times 10^2\ s^{-1}$] where reduction of

 © VCH Verlagsgesellschaft mbH, D-69451 Weinheim, 1994 0570-0833/94/0505-0582 $ 10.00+.25/0

GSSG occurs [Eq. (f)]. The electron transfer rate constant from $Eo^{3\bullet-}$ to the protein active site is small in comparison to previously reported values.[11]

It should be noted that the active site of GR is composed of an isoalloxazine unit, which is a part of the flavine adenine dinucleotide (FAD) cofactor, and a disulfide bond between Cys58 and Cys63.[12] We assume that electron transfer from $Eo^{3\bullet-}$ to the disulfide bond is mediated by the isoalloxazine unit.

This postulated kinetic scheme for electron transfer [Eq. (b)–(f)] was further supported by modification of α-chymotrypsin with eosin isothiocyanate. The α-chymotrypsin acts as hydrolytic protein and lacks an active redox center. Accordingly, the electron transfer reactions in this xanthene-dye-modified protein follow Equations (b)–(d). Nonetheless, since this enzyme lacks the active site, $Eo^{3\bullet-}$ (λ_{max} = 400 nm) is accumulated upon flash photolysis of the system in the presence of Na_2EDTA without noticeable decay.

We thus conclude that modification of GR with the photoactive eosin units converts the biocatalyst into a photostimulated protein. The covalently associated dye functions by two complementary pathways: It initiates the photoinduced electron transfer and acts as a relay unit within the protein backbone that facilitates electrical communication with the enzyme redox center. Nonetheless, the biocatalytic performance of Eo^{2-}-GR is substantially lower than that of the native enzyme and its NADPH cofactor. Linkage of chromophores to the protein exhibiting longer tethers may improve the electrical communication within the protein and also the activity of the photoenzyme. We suggest that such chromophore-modified proteins could provide a basic principle for designing novel photosynthetic devices.[13] By coupling two redox enzymes (an oxidative and a reductive protein) and their modification with appropriate light-active compounds, cyclic photosynthetic systems can be envisaged.

Received: September 6, 1993 [Z 6339 IE]
German version: *Angew. Chem.* **1994**, *106*, 594

[1] I. Willner, B. Willner in *Bioorganic Photochemistry. Biological Application of Photochemical Switches, Vol. 2* (Ed.: H. Morrison), Wiley, New York, **1993**, pp. 1–110.
[2] a) I. Willner, S. Rubin, A. Riklin, *J. Am. Chem. Soc.* **1991**, *113*, 3321–3325; b) N. A. Porter, J. O. Bruhnke, *Photochem. Photobiol.* **1991**, *51*, 37–43.
[3] a) I. Willner, S. Rubin, *J. Am. Chem. Soc.* **1992**, *114*, 3150–3151; b) I. Willner, S. Rubin, Y. Cohen, *ibid.* **1993**, *115*, 4937–4938.
[4] I. Willner, N. Lapidot, *J. Am. Chem. Soc.* **1991**, *113*, 3625.
[5] a) S. L. Mayo, W. R. Ellis, R. J. Crutchley, H. B. Gray, *Science* **1986**, *233*, 948; b) B. Durham, L. P. Pal, J. E. Long, F. Millett, *Biochemistry* **1989**, *28*, 8659; c) R. A. Scott, D. W. Conrad, M. K. Eidsness, A. C. F. Gorren, S. A. Wallin in *Metal Ions in Biological Systems. Electron Transfer Reactions in Metalloproteins* (Eds.: H. Sigel, A. Sigel), Dekker, New York, **1991**, pp. 199–222.
[6] a) D. N. Beratan, J. N. Betts, J. N. Onuchic, *Science* **1991**, *252*, 1285; b) L. P. Pan, M. Fram, B. Durham, D. Davies, F. Millett, *Biochemistry* **1990**, *29*, 3231; c) H. J. Therien, J. Chang, A. L. Raphael, B. E. Bowler, H. B. Gray, *Struct. Bonding* **1991**, *75*, 109; d) D. N. Beratan, J. N. Onuchic, J. N. Betts, B. E. Bowler, H. B. Gray, *J. Am. Chem. Soc.* **1990**, *112*, 7915.
[7] a) R. F. Colman in *Method in Enzymology, Vol. 17B* (Eds.: S. P. Colomick, N. O. Kaplan), Academic Press, New York, **1971**; b) R. F. Colman in [7a], p. 500; c) C. H. Williams, Jr., L. O. Arscott in [7a], p. 503.
[8] GSH concentration was determined by the Ellman method. Cf. G. L. Ellman, *Arch. Biochem. Biophys.* **1959**, *82*, 70.
[9] Intermolecular electron transfer of xanthene dyes in constrained media have been reported previously: a) L. Lindqvist, *Ark. Kemi*, **1960**, *16*, 79–137; b) V. Kasche, L. Lindqvist, *Photochem. Photobiol.* **1965**, *4*, 923–933; c) L. Flamigni, *J. Phys. Chem.* **1992**, *96*, 3331–3337; d) P. Bilsk, R. Dabestani, C. F. Chignell, *ibid.* **1991**, *95*, 5784–5791; e) J. C. Mialocq, P. Hébert, X. Armand, R. Bonneau, J. P. Morand, *J. Photochem. Photobiol. A: Chem.* **1991**, *56*, 323–338; f) V. E. Korobov, A. K. Chibisov, *J. Photochem.* **1978**, *9*, 411–424.
[10] The transient of recombination fits a monoexponential decay. The rate is independent of the enzyme concentration within the range 10^{-5}–10^{-6} M, implying that recombination proceeds within the protein backbone and does not involve a bimolecular pathway.
[11] The slow electron transfer rate constant might be attributed to the bulkiness of the charge carrier $Eo^{3\bullet-}$. Intra-protein steric constraints that could be involved in attaining appropriate orientations for electron transfer between the charge mediator and enzyme redox center may lead to such low electron transfer rates. See: D. W. Conrad, H. Zhang, D. E. Stewart, R. A. Scott, *J. Am. Chem. Soc.* **1992**, *114*, 9909.
[12] a) P. A. Karplus, G. E. Schultz, *J. Mol. Biol.* **1987**, *195*, 701; b) *ibid.* **1989**, *210*, 163; c) G. E. Schulz, R. H. Schirmer, W. Sachsenheimer, E. F. Pai, *Nature* **1978**, *273*, 120.
[13] I. Willner, B. Willner, *Top. Curr. Chem.* **1991**, *159*, 153–218.

 © *VCH Verlagsgesellschaft mbH, D-69451 Weinheim, 1994* *0570-0833/94/0505-0583 $ 10.00+.25/0*

From Inorganic Materials to Carbohydrates

Inorganic Materials. Edited by *D. W. Bruce* and *D. O'Hare*. Wiley, Chichester, 1992. XIV, 543 pp., hardcover £ 55.00.– ISBN 0-471-92889-5

This book is another attempt to meet the need, which has become much more pressing in the last few years, for a modern presentation of inorganic chemistry and its close interaction with materials science. However, the title is to some extent misleading, as the nine chapters are concerned not so much with individual compounds as with areas of inorganic chemistry where there is activity in research and applications developments. Thus the book is in direct competition, both in its general subject area and detailed contents, with "Compounds", edited by A. K. Cheetham and P. Day, the recently published second volume in the series "Solid State Chemistry" (see *Angew. Chem.* **1993**, *105*, 472; *Angew. Chem. Int. Ed. Engl.* **1992**, *31*, 1396). In their choice of authors the editors have concentrated mainly on younger scientists, giving them the opportunity to present their specialist areas from their individual viewpoints. The result is a collection of articles that are concise, free from unnecessary verbiage, and sometimes unconventional but nevertheless highly competent. Often the individual chapters begin with a brief review of the historical development of the area under discussion, including definitions of the main terms used and an explanation of the necessary limitations on the choice of subject matter. This is followed by a more detailed treatment of a class of compounds, usually molecular.

Thus P. Cassoux and L. Valade, in their chapter entitled "Molecular Inorganic Superconductors" (58 pp.), place the main emphasis on $M(dmit_2)$ complexes (dmit = 4,5-dimercapto-1,3-dithiole-2-thionato), while O. Kahn, Y. Pei, and Y. Journaux in "Molecular Inorganic Magnetic Materials" (56 pp.) are concerned mainly with the ferri- and ferromagnetic properties of one-dimensional and discrete transition metal complexes. In "Metal-Containing Materials for Nonlinear Optics" (50 pp.), S. R. Marder first lays the foundation with an excellent introduction to the theory then deals mainly with second- and third-order nonlinear optical effects in organometallic compounds. D. O'Hare's survey of "Inorganic Intercalation Compounds" (71 pp.) is virtually all-embracing, though with a clear emphasis on intercalation phenomena in two-dimensional host lattices. In the chapter on "Biogenic Inorganic Materials" (58 pp.) S. Mann deals mainly with purely inorganic materials such as gypsum, magnetite, and calcite; in particular he discusses the different types and functions of these materials and their biological control mechanisms. In the chapter entitled "Clay Chemistry" (57 pp.) R. W. McCabe first describes the structures of these materials then discusses organic reactions that take place at their surfaces. The contribution by G. E. Kellogg and J. Gaudiello on "Polymeric Coordination Complexes" (52 pp.) is subtitled "Bridging Molecular Metals and Conductive Polymers", and takes up the theme of the metallophthalocyanines already mentioned in an earlier chapter, going into greater detail with regard to their synthesis and physical characterization. In the chapter on "Metal-Containing Liquid Crystals" (86 pp.) by D. W. Bruce the main focus is on mesomorphic coordination complexes with divalent ligands, while in "Precursors for Electronic Materials" (45 pp.) P. O'Brian is concerned mainly with small single-source molecules for the production of II/VI and III/V semiconductors.

In view of the limited length of the individual chapters it is understandable that an exhaustive treatment of all the interesting and important details has not been possible. On the other hand, there are some apparently inexplicable editorial failings which greatly detract from the effective use of the book. One such concerns the scanty index of only slightly more than six pages, which is also very superficial and unevenly compiled. Some important terms and substances are missing, and in other cases not all the relevant passages are listed. It would have been preferable to have two separate indexes for keywords and substances. Another deficiency is undoubtedly the abbreviations used for journals, which often do not follow international conventions and even differ within a single chapter. Abbreviations in the names of authors and journals are invariably given without periods (full stops), which may be the recommended practice nowadays, but takes a little getting used to and also sacrifices clarity. Yet another problem is the inconsistent treatment of abbreviations in the names of substances, so that whereas some of these are never explained, others are explained each time they appear. Here it would have been useful to include a separate list of such abbreviations, either with each chapter or for the book as a whole. Again, whereas one normally expects the figures to clarify points in the text, in this book they do not always succeed in doing so, as the figure captions are often too brief and superficial. Moreover, the device of distinguishing the different types of atoms in a compound by different filling colors has not been applied consistently, and sometimes degenerates into a chemical puzzle because the color codes are not explained. Also each figure or table needs to be mentioned in the text. The typeface is unnecessarily large. A more compact presentation would have significantly reduced the number of pages and also the price.

Notwithstanding these criticisms regarding the editorial and production aspects of the book, it must be said that the authors have devoted much effort to providing a thorough treatment not only of the physical properties of the materials but also of the chemical and preparatve aspects.

To summarize, the individual chapters give brief but mainly excellent introductions to important areas of research in inorganic chemistry, providing newcomers and non-specialists with an initial over-

This section contains book reviews and a list of new books received by the editor. Book reviews are written by invitation from the editor. Suggestions for books to be reviewed and for book reviewers are welcome. Publishers should send brochures or (better) books to the Book Editor, Dr. Gerhard Karger, Redaktion Angewandte Chemie, Postfach 101161, D-69451 Weinheim, Federal Republic of Germany. The editor reserves the right of selecting which books will be reviewed. Uninvited books not chosen for review will not be returned.

 © VCH Verlagsgesellschaft mbH, D-69451 Weinheim, 1994 0570-0833/94/0505-0585 $ 10.00+.25/0

view and some insights. To that extent the book fulfills the aims set out by the editors in the preface. Those wishing to study the subject in greater depth will need to extend their reading to advanced monographs and more detailed texts, helped by the numerous literature references given (nearly 1500). Although not suitable as a student textbook, the work certainly offers students with sufficient previous knowledge an excellent resource for stimulating an interest in inorganic chemistry with regard both to materials and applications.

Hans Reuter
Institut für Anorganische Chemie
der Universität Osnabrück (FRG)

Thermal Analysis—Techniques and Applications. Edited by *E. L. Charsley* and *S. B. Warrington*. Royal Society of Chemistry, Cambridge, 1992. VIII, 296 pp., hardcover £ 45.00.—ISBN 0-85186-375-2

This multiauthor work is based on a course held in 1992 by the Thermal Analysis Consulting Service. It aims to provide an overview of the most important methods used in thermal analysis (TA) and to acquaint the reader with some recent advances and applications.

A brief (and superficial) introduction to TA methods is followed by chapters on differential thermal analysis and dynamic difference calorimetry (too brief and too qualitative), thermogravimetry, supplementary methods (not exhaustive, but up-to-date), evolved gas analysis, thermomechanical analysis and dynamic mechanical analysis (not enough relevant literature references), controlled rate TA (an important and valuable introduction to this new technique), applications of TA to polymers (informative, but lacking enough references to more advanced and detailed literature), TA in pharmacy (superficial and does not give an up-to-date review), applications of TA in metallurgy and materials science (very specialized), applications to minerals and fossil fuels, applications of TA to catalysts (does not remotely live up to what the title of the chapter promises), and quality control by TA (a first introduction to this important area, though it does not treat it in much depth).

Unfortunately the chapters concerned with fundamentals are not by themselves adequate in either their breadth of coverage or depth of treatment to enable the reader to apply TA methods. On the other hand, the chapters on applications are very uneven in quality. In some cases the authors are content to merely list examples of applications, and in others only a few examples are discussed in detail (as in the case of magnetic resonance TA, a technique which has probably scarcely been used by anyone other than the inventor and author of the article). There has evidently been insufficient discussion between the authors of the individual chapters, resulting in much unnecessary repetition and a lack of consistency in nomenclature. The quality of printing is good, despite the fact that the manuscripts have been reproduced in ordinary typescript characters (surprising in view of modern text-processing technology), with some of the chapters in justified style and others with an irregular right-hand margin. Some of the equations have been very carelessly typed.

Thus we have here a review volume which is of rather uneven quality (though inexpensive). It can serve as an introduction to this field, though not in much depth.

Heiko K. Cammenga
Institut für Physikalische und
Theoretische Chemie
der Technischen Universität
Braunschweig (FRG)

Determination of Thermodynamic Properties. 2nd Edition. (Series: Physical Methods of Chemistry, Vol. 6) Edited by *B. W. Rossiter* and *R. C. Baetzold*. Wiley, Chichester, 1992. XI, 743 pp., hardcover £ 157.00.—ISBN 0-471-57087-7

At a time when the primary literature is expanding at a near-explosive rate, whereas library budgets are suffering deep cuts, handbooks have become even more important than they were, say, 20 years ago. Such classics as the *Physical Methods of Chemistry* series aim to provide scientists involved in research and applications with a comprehensive, accurate, and concise introduction to the theory, methodology, and applications of measurement techniques, thus enabling them to select the most suitable ones for particular problems, and to consult the specialist literature before applying them.

Volume 6 of this 12-volume handbook is concerned with the determination of thermodynamic properties (although, regrettably, it does not cover the subject anywhere near exhaustively). In the chapter on "Mass and Density Determinations" R. S. Davies and W. F. Koch give a thoroughly adequate description of the most important methods of determining mass, together with their fundamental basis, including secondary effects on the weighing operation. However, in some places they might have brought out more clearly the advantages and disadvantages of the different weighing principles. The use of weighing methods in applications such as density measurement, and the measurement of partial molar volumes, moisture contents, and specific surface areas, are treated in appropriate detail. However, for many other applications, such as the determination of surface tension and contact angle, not even literature references are given. In the chapter "Pressure and Vacuum Measurements" C. R. Tilford treats the physical aspects of the measurement methods thoroughly, but includes almost nothing on applications, nor on the suitability of the methods for particular measurement tasks, aspects that the chemist wishing to determine properties would expect to find included. For example, there is not a word about vapor pressure measurements! P. J. Dunlop, K. R. Harris, and D. J. Young, in their chapter "Methods for Studying Diffusion in Gases, Liquids, and Solids", give a lucid introduction to the theory of diffusion (including ternary systems) and describe in great detail the experimental methods for gases, liquids, and solids. D. K. Wyatt and L. T. Grady contribute a chapter on "Determination of Solubility" (regrettably with some printing errors that should have been corrected) in which they review the classical methods. Here the authors could have shortened some of the material included in the previous edition and instead given more detail on, for example, gas-chromatographic and optical methods, the currently important topic of determining solubilities in liquified and supercritical gases, and continuous methods. Appropriate space is devoted to the determination of the rate of dissolution of solids in liquids. In the chapter on "Viscosity and its Measurement" J. Greener gives a good and detailed (perhaps even too detailed) theoretical treatment of the viscous behavior of fluids, and devotes special attention to the various sources of error in viscosity measurements. Unfortunately, though, measurements on gases are generally not discussed in enough detail. In the chapter on "Temperature Measurement with Application to Phase Equilibria Studies" J. B. Ott and J. R. Goates give a good introduction to this subject of great practical importance, with a wealth of important literature references, and their account of the application of temperature measurements to investigating phase equilibria is lucidly presented. However, it is unfortunate that in deriving thermodynamic relationships for mixed

 © VCH Verlagsgesellschaft mbH, D-69451 Weinheim, 1994 0570-0833/94/0505-0586 $ 10.00+.25/0

systems they have mainly limited their treatment to the ideal cases that so seldom occur in practice. J. L. Oscarson and R. M. Izatt, in their contribution on "Calorimetry", give most emphasis to descriptions of types of calorimeters, with less attention to the principles and applications of calorimetry, with the result that the chapter is more a list of publications than an aid to the user. The chapter "Differential Thermal Methods", by J. Boerio-Goates and J. E. Callenan, is of very uneven quality, with numerous printing errors (including some in equations), an inadequately researched literature coverage, and not enough references to up-to-date monographs and reviews dealing with new techniques and their applications.

These eight contributions together make up a volume in which much of the material is of excellent quality but some is in need of improvement. The editors ought to have paid attention to achieving better coordination between the contributions (and less repetition), ensuring that the same symbols were used for the same quantities throughout, eliminating obsolete units, and above all ensuring appropriate coverage of published work from outside the USA (especially when highly relevant). However, although the volume leaves much to be desired, it and the series to which it belongs should be in every library.

Heiko K. Cammenga
Institut für Physikalische
und Theoretische Chemie
der Technischen Universität
Braunschweig (FRG)

Solid Supports and Catalysts in Organic Synthesis. (Organic Chemistry Series.) Edited by *K. Smith*. Ellis Horwood/Prentice Hall, New York, 1992. XIV, 338 pp., hardcover $ 85.00. ISBN 0-13-639998-3

As K. Smith explains in the preface to this book on solid phase reagents and catalysts, it has been written especially with the needs of organic chemists in mind. It can be said at the outset that this aim has been very well fulfilled. The twelve chapters by eminent authors provide the reader with information on almost every aspect of solid phase reagents in organic and bioorganic synthesis. The individual contributions together make up a well rounded work, a praiseworthy achievement by the editor.

The first part (61 pp.) describes the most commonly used solid phases. The discussion is divided into inorganic phases (P. Diddams) and organic phases (J. M. Maud), affording an insight into the structures and properties of silica gels, aluminas, graphites, clays, and zeolites, as well as a variety of polymers, mostly polystyrene-based. The tables detailing and comparing the different phases are an especially pleasing feature; the wealth of useful information provided includes structural type, pore size, specific surface area, acidity, manufacturers (!), and names of commercial products (!).

The second part (130 pp.) describes "conventional" organic reactions using solid state reagents. These are discussed according to the types of support materials, namely amorphous inorganic supports (M. Butters), clays and graphites (J. A. Ballantine), zeolites (M. Butters), and polymers (J. M. Maud), rather than under reaction types. This arrangement gives a good overview of the areas of application of each type of solid phase, but for the user wishing to carry out a particular transformation it is undeniably rather inconvenient. This would not be a serious shortcoming if there were a good index enabling one to find particular reaction types. Here, however, one of the book's few weaknesses becomes apparent, as the subject index is much too sparse and does not even enable one to find relevant sections. For example, if one is seeking information about the oxidation of alcohols, under this heading the index refers one only to Section 3.10.1 (oxidation of alcohols on SiO_2), failing to mention Sections 5.12.1 (oxidation of alcohols on zeolites) or 9.6 (oxidation of alcohols using biocatalysts). Under "Alcohols" one finds no entry at all on this topic. Regrettably, any number of such examples could be given, and this diminishes the value of the book.

The third part (80 pp.) is devoted to biological applications, consisting of detailed treatments of solid phase peptide syntheses (J. S. Davies), oligonucleotide syntheses (H. A. White), and immobilized biocatalysts (J. M. Woodley). Nonspecialists too will benefit from reading these clear and readily understandable chapters.

Last but not least, the fourth part (52 pp.) describes special applications. It begins with a chapter by M. E. Fakley and F. King on hydrogenations, which is unfortunately rather too brief. In the report on microreactors by P. Laszlo which follows, one would again have liked some more detailed information on the types and applications of such systems. The book ends with an excellent chapter on the use of microwave radiation to activate reactions on solid phases (G. Bram, A. Loupy, and D. Villemin), including many examples illustrating the considerable potential of this method, which has so far been little exploited.

Despite some weaknesses (notably the subject index), a few printing errors, and minor inelegancies (floating substituents in some of the structure diagrams), the organic chemist will find in this book a wealth of useful examples of reactions on solid phases. The numerous literature references will be an additional aid to readers seeking to become involved in the world of supported reagents and catalysts.

Oliver Reiser
Institut für Organische Chemie
der Universität Göttingen (FRG)

Solid State Chemistry. An Introduction. By *L. Smart* and *E. Moore*. Chapman and Hall, London, 1992. XII, 292 pp., paperback £ 15.95. ISBN 0-412-40040-5

L. Smart and E. Moore have set themselves the task of writing an *introductory* textbook on solid state chemistry specially for students following a basic chemistry course. It can be said at the outset that they have succeeded very well. Each of the eight chapters introduces its subject matter at a basic level, assuming very little previous knowledge.

Chapter 1 is concerned with simple crystal structures, which are described in terms of the occupancy of the holes in a close-packed arrangement of spheres. The two-color illustrations (in green and gray) are clear and self-explanatory. The only structure diagram that I would criticize is that for quartz, in which the helical connection of the tetrahedra is not obvious. Chapter 2 treats bonding in solids on the basis of the band structure model, then Chapter 3 discusses lattice defects and nonstoichiometric compounds. The authors constantly seek to relate the subject to modern technological applications; in this chapter, for example, they describe oxygen ion conductors and the sodium–sulfur accumulator. Chapter 4 deals with low-dimensional solids such as polyacetylene and the tetracyanoplatinates, and discusses their anisotropic physical properties. Chapter 5 introduces the structural chemistry of zeolites, including also modern techniques for the elucidation of zeolite structures such as solid-state ^{29}Si NMR spectroscopy. Applications of zeolites are discussed, with the main emphasis on their catalytic properties. Chapter 6 is concerned with the optical properties of solids, and again these

 © *VCH Verlagsgesellschaft mbH, D-69451 Weinheim, 1994* *0570-0833/94/0505-0587 $ 10.00+.25/0*

are related to modern technological applications, with lucid explanations of the mechanisms of light-emitting diodes (LEDs) and diode lasers. Chapter 7 deals with the magnetic properties of solids. A short introduction to the different types of magnetic materials is followed by a discussion of some applications, for example, data storage using ferromagnetic materials such as CrO_2 or ferrimagnetic materials as the basis for magnetic bubble data stores. The book ends with Chapter 8 on superconductivity. The treatment of this highly topical subject consists of a historical survey of the discovery and development of superconducting materials, followed by a lucid but rather superficial account of the Bardeen–Cooper–Schrieffer (BCS) theory, and a detailed discussion of the structures of oxide superconductors. Each chapter ends with a list of references for further reading, with comments, and a set of carefully chosen questions that can be used to test one's knowledge, together with answers.

In a book of fewer than 300 pages it is inevitable that there are some gaps. For example, the ligand field theory is not discussed, nor are preparative aspects of solid state chemistry such as chemical transport reactions. However, the authors have not aimed to write a comprehensive work on solid state chemistry; instead they have accomplished the rare trick of producing a textbook that is a pleasure to read and is capable of arousing in students an interest in the supposedly "dry" but highly topical subject of solid state chemistry.

Johannes Beck
Institut für Anorganische und
Analytische Chemie
der Universität Gießen (FRG)

Carbohydrates—Synthetic Methods and Applications in Medicinal Chemistry. Edited by *H. Ogura, A. Hasegawa* and *T. Suami*. VCH Verlagsgesellschaft, Weinheim/VCH Publishers, New York/Kodansha, Tokyo, 1992. XIII, 406 pp., hardcover DM 208.00.—ISBN 3-527-29012-5/1-56081-701-1/4-06-205807-3

This book is a summary of twenty essays presented at "Fuji 90", a post-symposium of the 15th International Carbohydrate Symposium. It is intended mainly for scientists in synthetic and medicinal chemistry. Without claiming completeness, the authors discuss some highly topical aspects of the latest state of knowledge on the synthetic applications and biological functions of carbohydrates. While research on carbohydrates was in the past directed mainly towards their utilization in agriculture, manufacturing, and construction, present day research focusses on the use of carbohydrates as cheap enantiomerically pure raw materials for stereocontrolled syntheses of complex biologically active molecules. Recent developments in carbohydrate structural analysis and synthetic methodology benefit biochemists and medicinal chemists in their studies on cell–cell interactions at the molecular level in the search for new therapeutic agents.

The book is organized in four general topics: Synthetic Methods for Chemical Modification of Carbohydrates; Synthetic Methods for Enzymatic Modification of Carbohydrates; Synthetic and Biological Studies of Sialic Acid; Functional and Biological Studies on Glyco-Conjugates.

The first topic includes nine articles related to the conversion of mono- and disaccharides into suitably functionalized enantiopure building blocks for the synthesis of various non-sugar target molecules or different types of carbohydrate analogs. Since there is an enormous amount of literature on natural products synthesized via this approach, the authors focus on selected examples including marine natural products, macrolides, antibiotics, and alkaloids. Special attention is paid to transformations of carbohydrates involving their anomeric center, such as glycosylation reactions, C-glycosyl bond formation, and radical spirocyclization. The examples given demonstrate the efficient application of modern preparative organic methodology, thus reflecting the state of the art in the subject.

As a logical continuation of the first topic, articles contained in the second topic deal with combined synthetic and enzymatic methods for construction of oligosaccharides by glycosylation of monosaccharides or degradation of polysaccharides. Following the biochemical pathways of carbohydrate metabolism, the practical use of enzymes such as glycohydrolases and glycosyltransferases is discussed. Heterooligosaccharides such as glycoproteins and glycolipids are chosen as synthetic targets due to their significant role in processes of intercellular recognition, cell differentiation, and growth.

A third main theme of the book is the chemistry and biology of the cell surface located sialic acids as the most important terminal units of glycolipids and glycoproteins. Sialic acids are involved in a series of important regulatory processes such as membrane permeability, intercellular interactions, suppression of immune reactions, and protection of glycoproteins such as enzymes against too rapid proteolysis. On the other hand, pathological disorders of sialic acid metabolism are connected with many diseases caused by viruses, bacteria, and toxins. Therefore, the extensively described up-to-date synthetic and biological studies on various analogs and derivatives of sialic acids offer possibilities for a better understanding of their structural and functional role in cell biology and for the development of novel medicinal therapeutic strategies.

In the last three chapters the biological significance of cell surface carbohydrates in cell adhesion and binding is reviewed. Interaction of cell surface carbohydrates with biologically active proteins, such as immunoglobulins, triggers lymphocyte differentiation resulting in an immune response. Different oligosaccharide ligands are synthesized and their bindings with homologous monoclonal antibodies are studied in order to determine the bonding and nonbonding interactions between the antigen and the combining region of the immunoglobulin. The final chapter of this book is devoted to chemical and enzymatic methods for depolymerization and modification of heparin for the preparation of structurally well-defined low molecular weight heparins with new or improved chemical and biological properties.

Leaving aside some printing errors and inaccurate numbering of a few molecules in the text and the illustrations, the book has an excellent layout. A pleasing feature is the standard format of each article consisting of an introduction, main text, conclusion, and extensive bibliography. Usually the references include articles pertaining to the author's own research as well as the most relevant papers by others, thus directing the reader to suitable background reading on topics that may be unfamiliar.

The choice and variety of the topics and the quality of the presentations make this book a valuable source of information and new ideas for synthetic and medicinal chemists involved in the expanding field of research on carbohydrates and glycobiology.

Vassil I. Ognyanov, Alan P. Kozikowski
Neurochemistry Research
Mayo Clinic, Jacksonville (USA)

 © VCH Verlagsgesellschaft mbH, D-69451 Weinheim, 1994 0570-0833/94/0505-0588 $ 10.00+.25/0

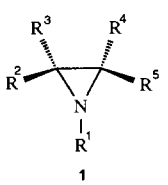
Chiral Aziridines—Their Synthesis and Use in Stereoselective Transformations

David Tanner*

The preparation of enantiomerically pure compounds is one of the major areas of organic chemistry. Much emphasis is placed on the elaboration of naturally occurring starting materials and on the development of techniques for enantioselective transformations of achiral substrates. In this field, chiral aziridines form an attractive class of compounds, since they are available in enantiomerically pure (or highly enriched) form by a variety of procedures and can be used for asymmetric synthesis in a number of different ways. The chemistry of aziridines is dominated by ring-opening reactions, the driving force for which is relief of ring strain. By suitable choice of substituents on the carbon and nitrogen atoms, excellent stereo- and regiocontrol can be attained in ring-opening reactions with a wide variety of nucleophiles, including organometallic reagents; this makes chiral aziridines useful as *substrates* for the synthesis of important biologically active species including alkaloids, amino acids, and β-lactam antibiotics. Substrate-controlled diastereoselective synthesis is also possible by use of aziridines as removable chiral *auxiliaries*, while metalation at a ring carbon atom allows aziridines to be used as chiral *reagents* for asymmetric synthesis. Chiral bisaziridines can act as *ligands* for transition metals, and applications in the challenging field of enantioselective catalysis can be envisioned. *Today, the exclusion of three-membered carbo- and heterocycles from the arsenal of the organic chemist is inconceivable.*[1]

1. Introduction

Aziridines **1** are saturated three-membered heterocycles containing one nitrogen atom. This class of compounds dates back to 1888, when Gabriel (unwittingly) synthesized the parent member.[2] Like other three-membered rings such as cyclopropanes and epoxides, aziridines are highly strained.[3] Ring strain renders aziridines susceptible to the ring-opening reactions that dominate their chemistry and, as shown below, makes them useful synthetic intermediates that fully deserve a prominent place in the arsenal of the organic chemist.



1

In view of the long history of aziridine chemistry, it is not surprising that the literature on the subject is very extensive. For the interested reader requiring a general introduction, several excellent discussions are available.[4] The present review of chiral aziridines is thus intended to be representative rather than comprehensive, and the selection of material inevitably reflects the author's own interests and/or prejudices. The discussion will deal mainly (but not exclusively) with nonracemic aziridines, and an attempt will be made to illustrate their great potential and versatility as chiral *substrates, auxiliaries, reagents,* and *ligands* in the field of stereoselective synthesis.

[*] Dr. D. Tanner
Department of Organic Chemistry
University of Uppsala
Box 531, S-751 21 Uppsala (Sweden)

2. Synthesis of Chiral Nonracemic Aziridines

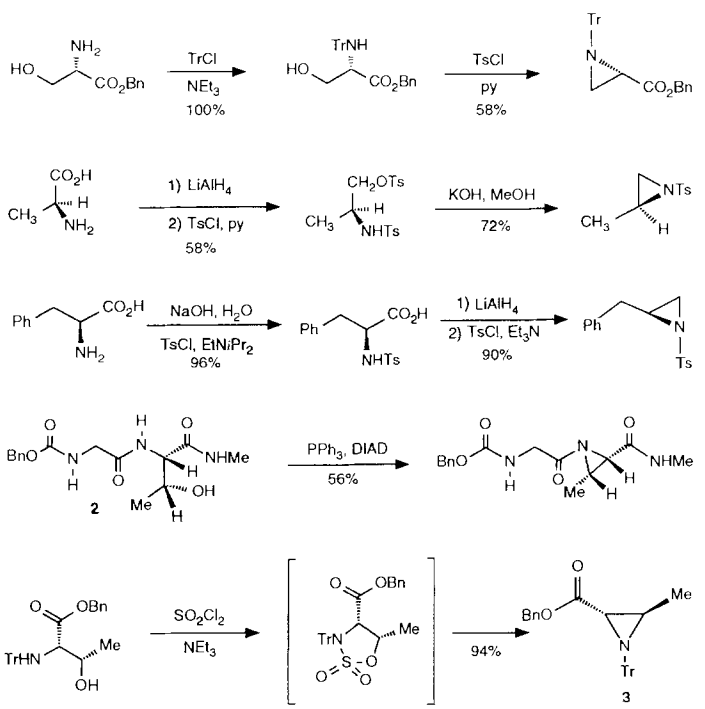
A variety of routes[5] to chiral nonracemic aziridines is available, most of which rely either on the availability of enantiomerically pure starting materials from natural sources (amino acids, carbohydrates, hydroxy acids) or on asymmetric transformations of C–C or C–N double bonds. These two general approaches are discussed below, together with some recent methods for efficient enantiomer separation and enzymatic transformations.

2.1. Synthesis from Amino Acids

Since the ring closure of 1,2-amino alcohols or suitable derivatives thereof[6] provides a convenient and usually efficient synthesis of aziridines, it is not surprising that amino acids are widely used as chiral starting materials. Some representative examples are shown in Scheme 1.

The first three sequences[7–9] can be conducted easily on a multigram scale with good overall yields. The conditions used by Wipf and Miller[10] to cyclize the threonine moiety of the peptide **2** provided some insight on the factors governing the steric course of such Mitsunobu-type[11] reactions (see also Scheme 4). The "one-pot" method developed by the Dutch group[12] for the synthesis of **3** is noteworthy for its simplicity and efficiency.

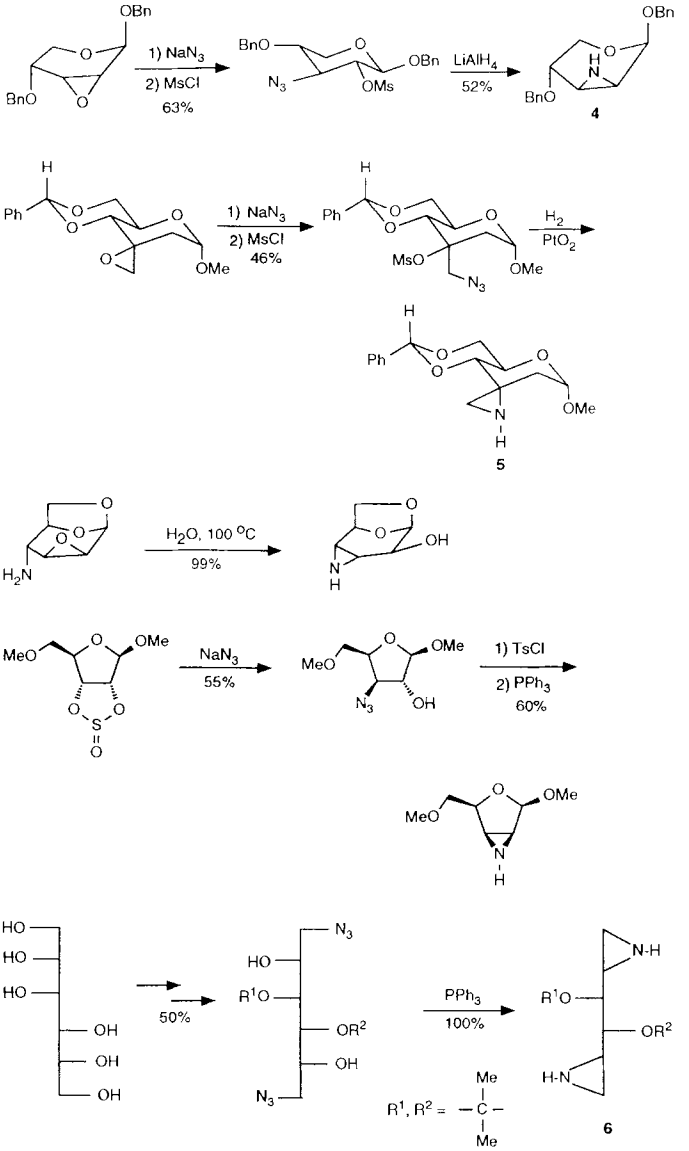
 © VCH Verlagsgesellschaft mbH, D-69451 Weinheim, 1994 0570-0833/94/0606-0599 $ 10.00+.25/0



Scheme 1. Synthesis of enantiomerically pure aziridines from amino acids. Bn = CH_2Ph, Ts = SO_2Tol, DIAD = diisopropyl azidocarboxylate, Tr = CPh_3, py = pyridine.

2.2. Synthesis from Carbohydrates

By taking advantage of steric, stereoelectronic, and conformational effects, the regio- and stereoselective manipulation of the various hydroxyl groups in carbohydrates is possible.[13] Sugar derivatives are thus attractive chiral starting materials for a wide variety of synthetic purposes, including the preparation of aziridines; Scheme 2 shows just a few[14–18] of the many possibilities. As is the case for the amino acids, the major drawback to the use of carbohydrates as starting materials is that usually only one of a given pair of enantiomeric starting compounds is easily or cheaply available. The unusual regiochemistry of the subsequent ring opening[14] of aziridine **4** will be discussed in Section 4.2. Spiroaziridines such as **5**[15] are very useful intermediates in the synthesis of important branched-chain amino sugars (Section 5.2), and the chiral bisaziridines **6**[18] provide an elegant route to α-amino acids and aldehydes



Scheme 2. Synthesis of enantiomerically pure aziridines from carbohydrates. Ms = SO_2Me.

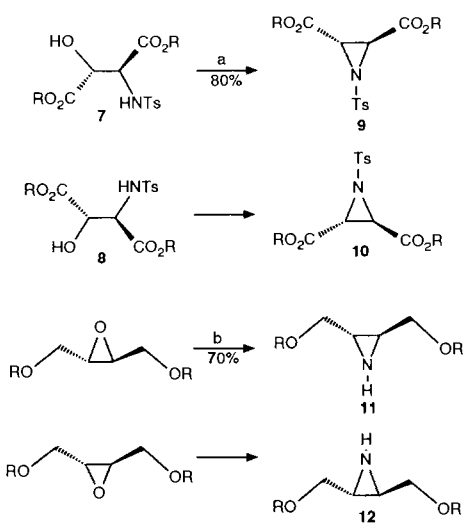
(Section 5.3). Further references to the ring closure of azido alcohols to aziridines by use of organophosphorus reagents can be found in references [19–21].



David Tanner was born in 1955 in Inverness, Scotland, and studied chemistry at the University of Edinburgh (B. Sc. 1977). He then moved to Göteborg, Sweden, where he obtained his doctorate in 1981 under the supervision of O. Wennerström. After a one-year postdoctoral stay with K. C. Nicolaou at the University of Pennsylvania, he returned to Göteborg in 1983 to pursue independent research; he received the title of "Docent" from Chalmers University of Technology in 1986. In 1988 he was appointed to a lectureship at the University of Uppsala, where he also currently holds a personal research position in organic synthesis awarded by the Swedish Natural Science Research Council.

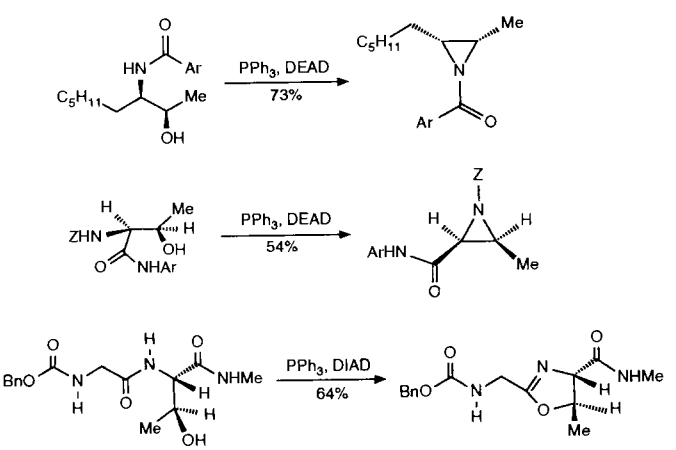
2.3. Synthesis from Hydroxy Acids

The hydroxy acid most familiar to organic chemists is no doubt tartaric acid, derivatives of which are not only of great historical importance[22] but also allow access to an impressive variety of enantiomerically pure "building blocks" for synthesis.[23] Tartaric acid is also used to provide the chiral environment for the Sharpless asymmetric epoxidation reaction discussed in the next section. Both enantiomers of tartaric acid are readily available and can be converted to the enantiomerically pure pairs of aziridines **9** and **10**,[24] and **11** and **12**[25] shown in Scheme 3. Some applications of these C_2-symmetric compounds in asymmetric synthesis will be demonstrated in Sections 4.4 and 6.



Scheme 3. Synthesis of C_2-symmetric aziridines from tartaric acid. a) PPh_3, diethyl azodicarboxylate (DEAD); b) 1. NaN_3, 2. MsCl, 3. $LiAlH_4$. R = Et, CH_2Ph. Compound **7** and the precursor of **11** were obtained from (+)-tartaric acid, compound **8** and the precursor of **12** from (−)-tartaric acid.

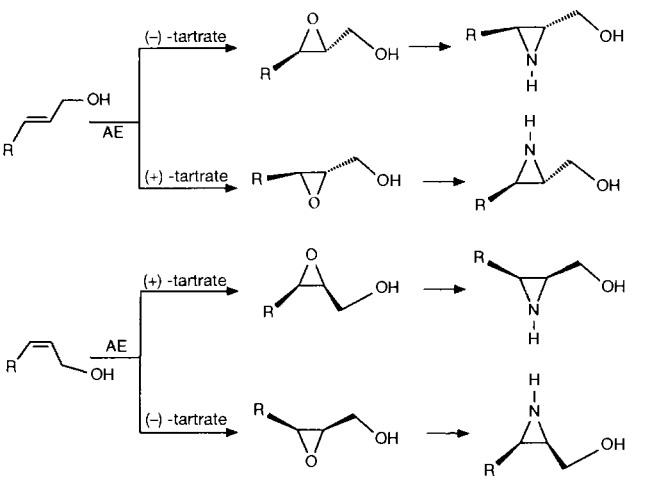
The Mitsunobu-type reactions used for the ring closure[26] of the hydroxy sulfonamides **7** and **8** are stereospecific and occur with inversion at the carbon center bearing the OH group. The results of the related reactions shown in Scheme 4 can be compared[27, 28] and contrasted[10] with that shown for cyclization of **2** in Scheme 1.



Scheme 4. Some stereospecific intramolecular Mitsunobo reactions. Ar = aryl, Z = benzyloxycarbonyl.

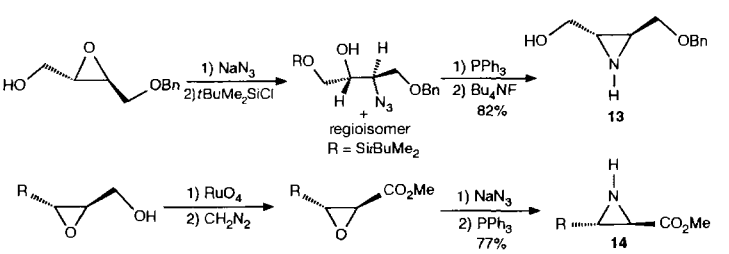
2.4. Synthesis from Alkenes via Chiral Epoxides and 1,2-Diols

As emphasized in Schemes 2 and 3, ring opening of epoxides by nitrogen nucleophiles followed by ring closure of the resultant 1,2-amino alcohol derivatives is an attractive route to aziridines. Although epoxides had long been regarded as versatile intermediates and had been used extensively in synthesis,[29] their potential was increased enormously in the 1980s by the discovery of the asymmetric epoxidation (AE) reaction of allylic alcohols by Sharpless et al.[30]. This epoxidation is mediated by a titanium(IV) alkoxide and *tert*-butyl hydroperoxide in the presence of a tartrate ester. As outlined in Scheme 5, this catalytic asymmetric synthesis provides a general route to all possible stereoisomers of a given hydroxymethylaziridine ("2,3-aziridino alcohol").



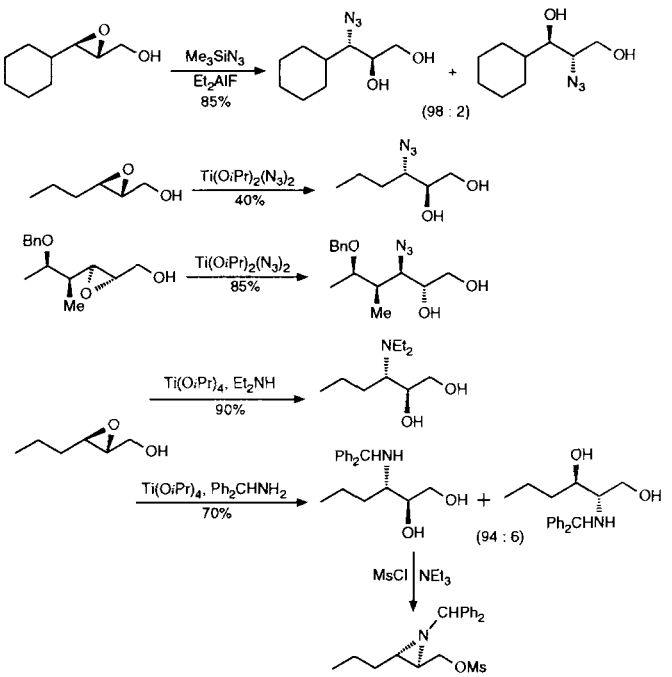
Scheme 5. A general route to chiral 2,3-aziridino alcohols by the Sharpless asymmetric epoxidation (AE).

One of the many advantages associated with the Sharpless AE reaction is that both enantiomers of the product are available equally easily from a common starting material. As pointed out above, azide ion is often an excellent nucleophile for the ring opening of epoxides, and azido alcohols can then be converted to aziridines; the overall epoxide → aziridine transformation is thus stereospecific (inversion at both carbon atoms of the original epoxide). Some examples[31, 32] are shown in Scheme 6. Aziridino alcohols and esters such as **13** and **14** are very useful chiral intermediates (see Sections 4.3 and 4.4).



Scheme 6. Synthesis of chiral, nonracemic aziridino alcohols and esters via epoxides available by the Sharpless AE reaction.

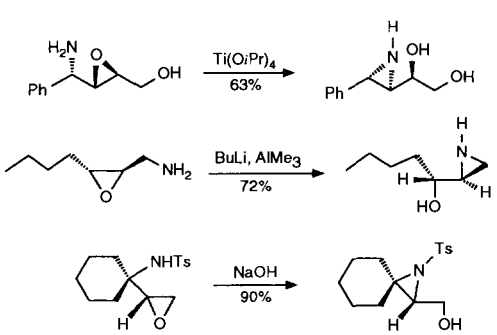
It is usually of little consequence that the ring-opening reactions shown in Scheme 6 are not regioselective, since both regioisomers of a given azido alcohol eventually yield the same aziridine. However, in the case of epoxy alcohols, the sequence does entail temporary protection of the primary hydroxyl group. Regioselectivity in the ring opening by azide[33–35] and secondary[36] or primary[37] amines is possible if the reaction is mediated by aluminum or titanium complexes. The products from the primary amines have been converted[38] to aziridines (Scheme 7). Good to excellent regioselectivity in the C-3 ring



Scheme 7. Regioselective ring opening of epoxy alcohols.

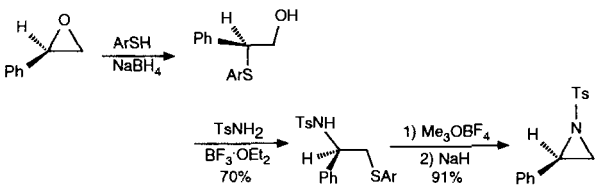
opening of 2,3-epoxy acids and amides by amines[39] and the C-2 ring opening of 2,3-epoxy esters by azide[40] has also been demonstrated.

A useful tactic in epoxy alcohol chemistry is use of the Payne rearrangement.[41] As shown in Scheme 8, amino epoxides can perform in an analogous fashion in the presence of complexes of titanium[42] or aluminum.[43] *N*-Tosylamino epoxides undergo the same type of rearrangement simply upon treatment with base (Scheme 8).[44]



Scheme 8. Chiral aziridines by Payne-type rearrangement of amino epoxides.

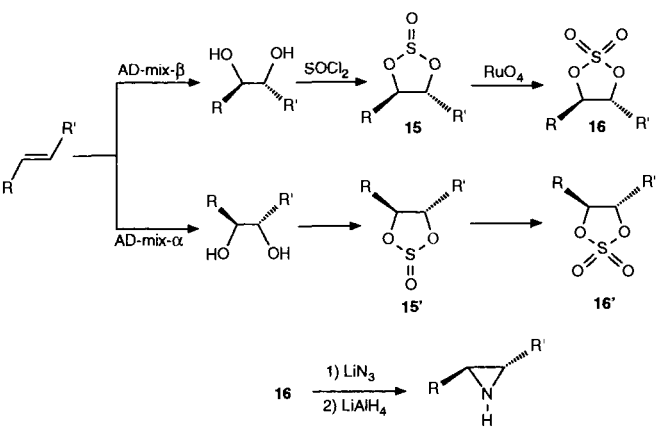
The epoxide → aziridine transformations outlined in Schemes 6–8 involve overall inversion of configuration. However, an interesting method for conversion of a terminal epoxide to the corresponding *N*-tosyl aziridine with overall retention[45] was introduced recently (Scheme 9). This use of sulfur chemistry



Scheme 9. Conversion of a terminal epoxide to an *N*-tosyl aziridine with retention of configuration.

nicely complements the methods that proceed with overall inversion and thus allows the synthesis of both enantiomers of a given terminal aziridine from a single chiral epoxide.

While the Sharpless AE reaction is a beautiful example of catalytic asymmetric synthesis, its major limitation is that the substrate must contain a "handle" in the form of an allylic hydroxyl goup. Chiral terminal epoxides such as those shown in Scheme 9 are thus not available directly by the AE method, and indeed the direct asymmetric epoxidation of "nonfunctionalized" olefins remains a major challenge.[46] However, Sharpless et al. have provided a very attractive indirect solution to this problem which relies on cyclic sulfates of chiral 1,2-diols. These compounds are now easily available in enantiomerically pure (or highly enriched) form by the osmium-catalyzed asymmetric dihydroxylation (AD) reaction[47] shown in Scheme 10; the chiral ligands



Scheme 10. Sharpless asymmetric dihydroxylation (AD) as a route to chiral, nonracemic aziridines. The mixtures of reagents used here are denoted AD-mix-α and AD-mix-β.

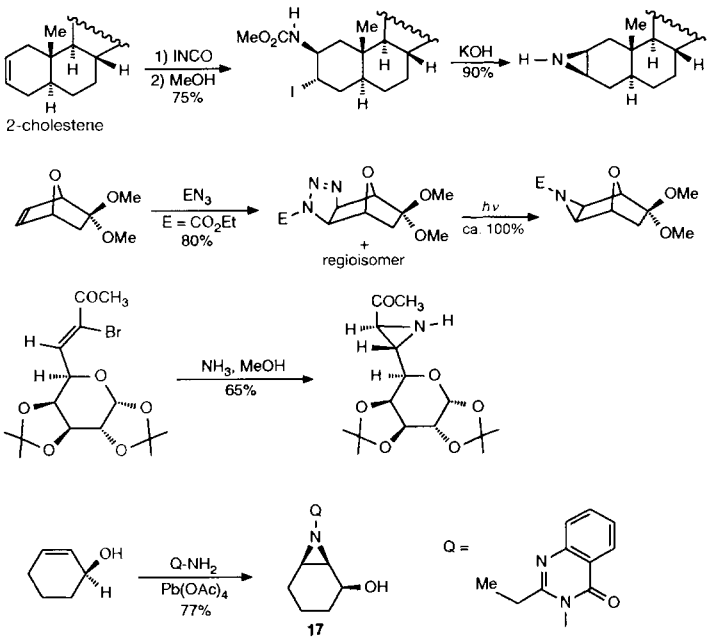
in the AD-mix reagents are based on hydroquinidine and hydroquinine. The cyclic sulfates **16** in many ways surpass the corresponding epoxides in terms of reactivity ("like epoxides only more reactive"[48]), and aziridines are readily available[49] from these intermediates. The cyclic sulfites **15** can also be used for aziridine formation.[50]

Although the two types of ligands employed in the AD-mix formulations[47] are not enantiomers, they actually behave as if they were, and the process provides equally easy access to both enantiomers of a given 1,2-diol from the same olefin. In connection with the AD reaction, it may be mentioned here that osmium also mediates the stereospecific oxyamination of olefins and thus provides another stereospecific synthesis of aziridines.[51] However, no enantioselective version of this reaction has yet been reported.

2.5. Other Asymmetric Transformations of C–C Double Bonds

Some of the well-established methods[5] for the synthesis of aziridines from olefins are: 1) addition of IN_3 or INCO followed by reductive or hydrolytic ring closure; 2) 1,3-dipolar cycloaddition of azides followed by decomposition of the intermediate triazoles; 3) addition of a primary amine to a suitably 2-substituted acrylic acid derivative or Michael addition of a nitrogen nucleophile followed by expulsion of a leaving group at nitrogen; and 4) direct addition of nitrene species. These general methods for aziridine formation can be used to exemplify the "hierarchy" of asymmetric synthesis, which ranges from substrate control, through reagent control, to enantioselective catalysis.

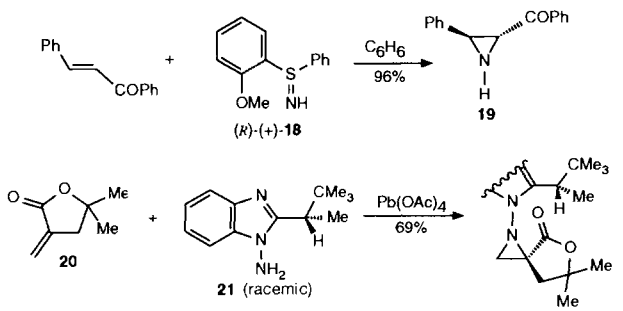
Some examples[52–55] of substrate control are presented in Scheme 11. Although the starting material for the synthesis of



Scheme 11. Asymmetric synthesis of aziridines by substrate control.

17[55] was racemic, optically pure 2-cyclohexen-1-ol is available.[56] Good to excellent diastereoselectivity in the addition of nitrenes to chiral enoates has been described by the Dreiding group.[57]

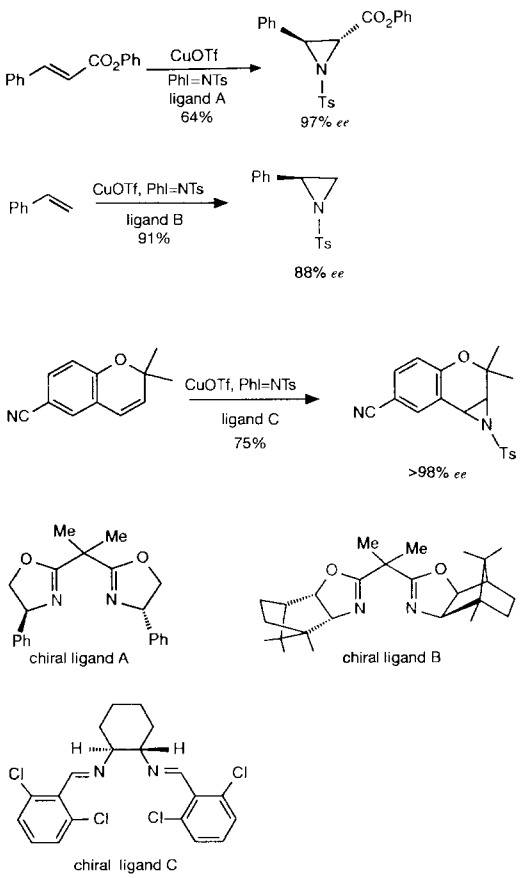
Two examples of reagent control are given in Scheme 12. The chiral sulfimide reagent **18**[58] yields aziridine **19** with only modest enantioselectivity (30% *ee*), whereas asymmetric induction is



Scheme 12. Asymmetric synthesis of aziridines by reagent control.

complete in the nitrene reaction[59, 60] of alkene **20**. Reagent **21** has not yet been prepared in enantiomerically pure form, but some asymmetric induction has been claimed[61] for an interesting variant of this reaction, in which an optically active oxidant (lead tetra-(*S*)-2-methylbutanoate) was used.

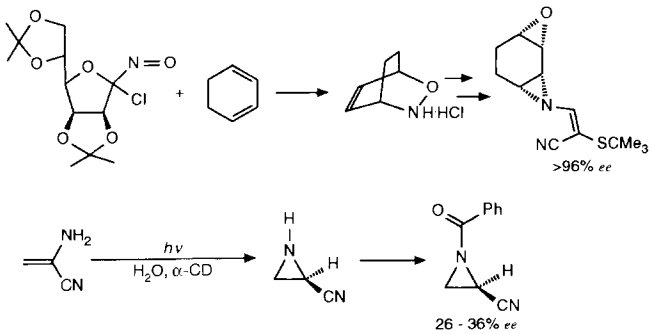
In the previously mentioned "hierarchy" of asymmetric synthesis, enantioselective catalysis is at the very top. Two examples (the Sharpless AE and AD reactions, Section 2.4) have already been discussed, and three very exciting developments in catalytic asymmetric aziridination[62–64] are shown in Scheme 13. For



Scheme 13. Asymmetric synthesis of aziridines by enantioselective catalysis.

related work on the direct (nonenantioselective) aziridination of alkenes, including catalysis by metalated porphyrins, see references [65–70].

This section concludes with the two interesting aziridination reactions depicted in Scheme 14. The highly diastereo- and enantioselective functionalization[71] of all four carbon atoms in

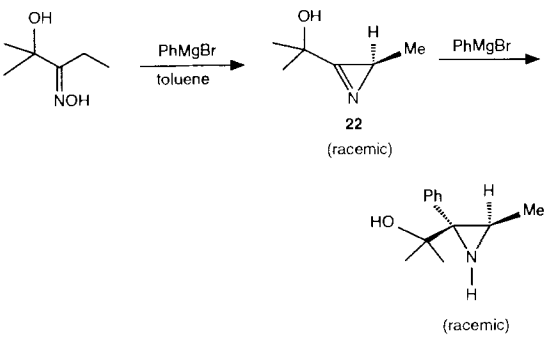


Scheme 14. Chiral aziridines by asymmetric cycloaddition with a chiral auxiliary (top) and by enantioselective photocyclization (bottom).

the diene unit of cyclohexadiene relied on the use of a chiral auxiliary derived from a carbohydrate.[72] The enantioselective photocyclization reaction in the presence of α-cyclodextrin (α-CD)[73] was performed in connection with studies of compounds of potential interest to prebiotic chemistry.

2.6. Asymmetric Transformations of C–N Double Bonds

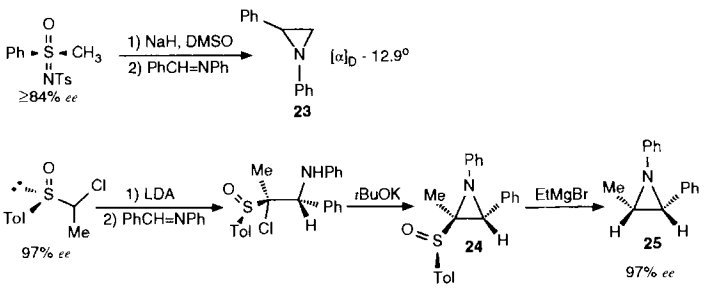
Aziridines are available by reaction of α-hydroxy oximes with Grignard reagents via azirine intermediates (Scheme 15). The



Scheme 15. Diastereofacial selectivity in the conversion of an azirine to an aziridine.

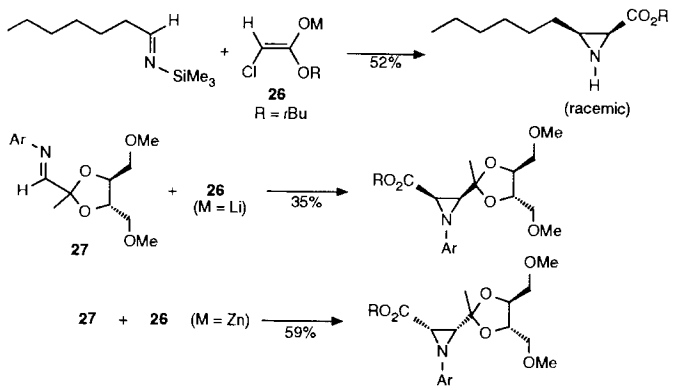
results of an interesting study[74] on the diastereofacial selectivity of this reaction were interpreted in terms of complexation of the Grignard reagent to the alcohol function of **22** followed by intramolecular delivery of the nucleophile to the less hindered face of the C–N double bond.

Two examples of reagent control are presented in Scheme 16. In the first, an *N*-tosylsulfoximine[75] was used as a chiral nucleophilic alkylidene transfer reagent; unfortunately, the enantiomeric purity of aziridine **23** was not determined. The second example[76] shows a very efficient asymmetric synthesis based on the chemistry of chiral sulfoxides in which a stereospecific desulfinylation reaction of **24** gives aziridine **25**. The proposed intermediate is a chiral metalated aziridine, an interesting type of nucleophilic species which is discussed in more detail in Section 7.



Scheme 16. Reagent control in the asymmetric transformation of a C–N double bond. DMSO = dimethyl sulfoxide. LDA = lithium diisopropylamide.

Scheme 17 shows two analogues of the Darzens reaction.[77] For the first,[78] which is highly diastereoselective, the authors suggested a cyclic transition state to explain the observed *cis* selectivity. They also pointed out that this type of reaction should be amenable to the preparation of nonracemic aziridines. The second example,[79] in which a chiral auxiliary is used, shows that this is indeed the case. It is remarkable that complete "stereodivergence" is possible here simply by switching the metal counterion of the enolate from lithium to zinc!

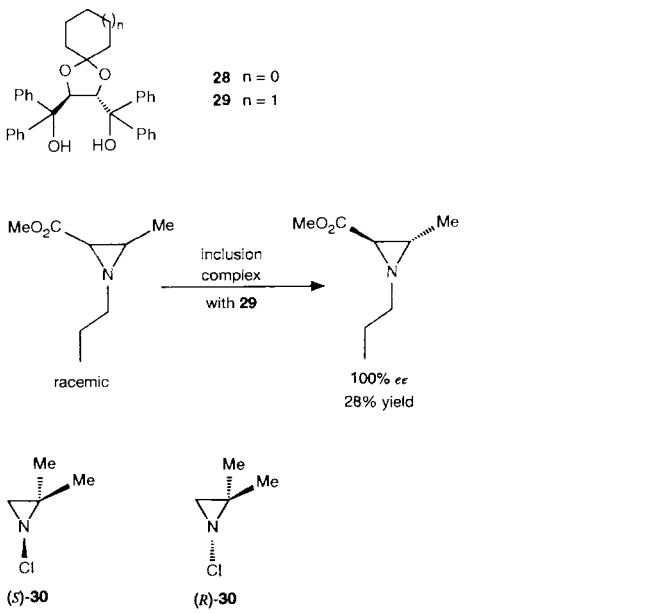


Scheme 17. Synthesis of chiral aziridines by Darzens-type reactions. M in **26**: Li.

2.7. Chiral Aziridines by Resolution of Racemates

Early attempts[80] at direct optical resolution of chiral aziridines were not promising. But recently Mori and Toda[81] reported an efficient method based on the formation of inclusion complexes between certain aziridines and the optically active host compounds **28** and **29**, which are derived from tartaric acid. Enantiomeric purities up to 100% were obtained (Scheme 18).

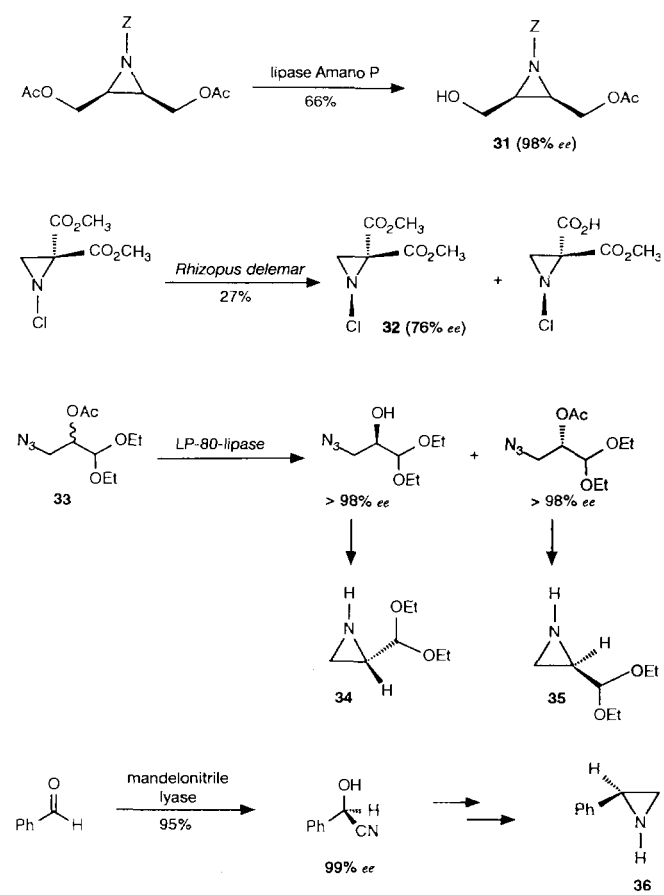
An important structural feature of aziridines is the high barrier[82] to pyramidal inversion at the ring nitrogen atom when it is bonded to alkyl or aryl groups or, especially, to heteroatomic moieties such as Cl, OR, or NH_2. This has allowed the separation[83] of the enantiomers (invertomers) of, for example, 1-chloro-2,2-dimethylaziridine (**30**, Scheme 18) by complexation gas chromatography. This elegant study also allowed accurate determination of the inversion barrier, which earlier had been estimated[84] from ^{1}H NMR spectroscopic data.



Scheme 18. Two methods for the resolution of racemic aziridines.

2.8. Enzymatic Routes to Chiral Aziridines

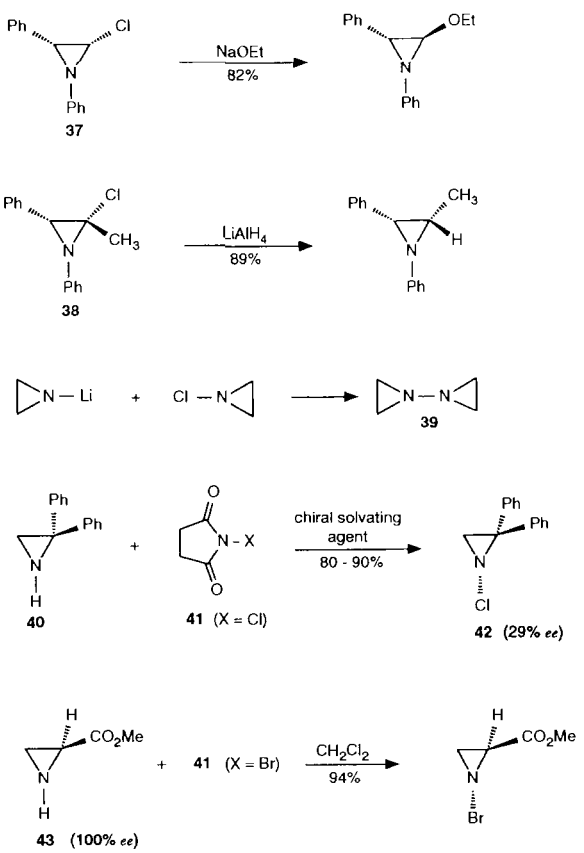
In recent years the use of enzymes in synthetic organic chemistry has increased steadily.[85] A popular technique is the enantioselective hydrolysis of *meso* diesters, exemplified[86] by the reaction yielding aziridine **31** in Scheme 19. Enzymes were also employed[87] in the preparation (by selective hydrolysis) of aziridine **32**, which is chiral solely because of slow nitrogen inversion. Wong et al.[88] prepared the enantiomerically pure aziridines **34** and **35** by enantioselective hydrolysis of **33**, and Effenberger et al.[89, 90] have reported the synthesis of enantiomerically pure aziridine **36** by a sequence involving enzyme-catalyzed cyanohydrin formation.



Scheme 19. The use of enzymes in the synthesis of enantiomerically pure aziridines.

3. Stereoselective Transformations at Ring Atoms and in Side Chains without Ring Opening

As will be discussed in Section 4, ring opening occurs in many of the reactions of aziridines. However, for "nonactivated" aziridines (see Section 4) it is possible to perform stereoselective transformations either at ring atoms (carbon or nitrogen) or in side chains without disrupting the ring. Some examples are shown in Schemes 20 and 21.

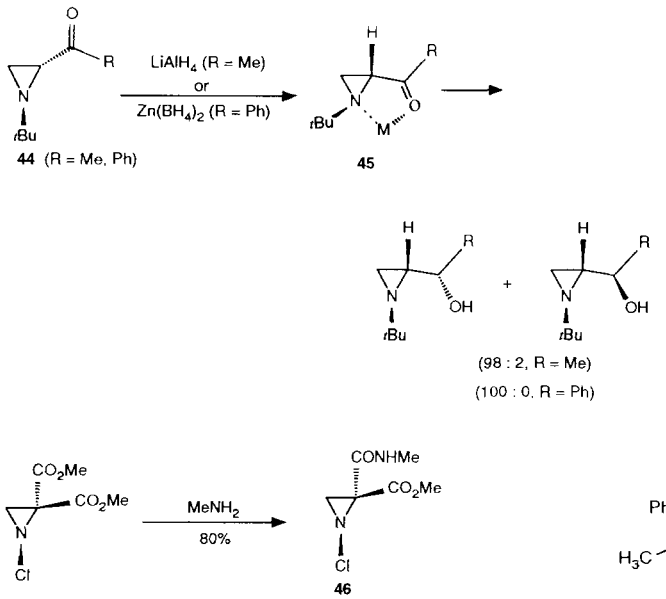


Scheme 20. Stereoselective transformations at ring atoms of aziridines.

The first examples of facile nucleophilic displacements at the carbon atoms in three-membered rings were provided by Deyrup and Greenwald,[91] who showed that the products of displacement reactions on **37** and **38** were formed with clean inversion. As far as the present author is aware, no nonracemic derivatives of the interesting 1,1'-diaziridine **39**[92] have been reported. Attempted asymmetric chlorination at the nitrogen atom in **40** in the presence of a chiral solvating agent gave **42** with only modest

enantioselectivity.[93] However, *N*-bromination[94] of optically pure **43** was completely stereoselective (Scheme 20).

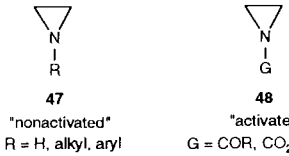
The reactions depicted in Scheme 21 show that aziridines with suitable substituents on the nitrogen atom may react with powerful nucleophiles such as metal hydrides[95, 96] without ring opening. Pierre et al.[97] and Laurent et al.[98] both explained the results of reduction of **44** by $LiAlH_4$ or $Zn(BH_4)_2$ by the intermediacy of chelate **45**. Modest diastereoselectivity was also observed in the reaction of aziridino aldehydes with Grignard reagents.[99] The aminolysis that yields **46** is completely diastereoselective.[100]



Scheme 21. Stereoselective transformations in side chains of aziridines.

4. Ring-Opening Reactions

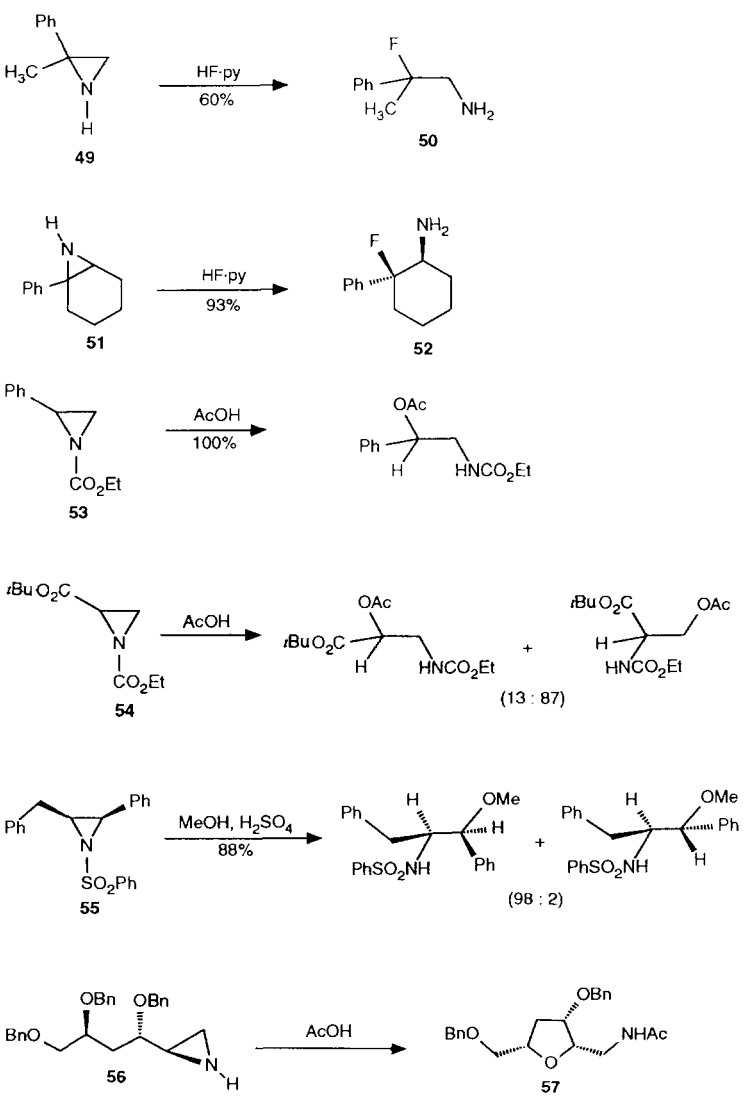
As a consequence of the ring strain present in aziridines and related three-membered rings, ring-opening reactions are a dominant feature of their chemistry. In this respect, aziridines can be divided into two main groups,[101] according to the nature of the substituent on nitrogen. The first group, "nonactivated" aziridines, **47**, contain a basic nitrogen atom, and ring-opening reactions usually occur only after protonation, quaternization, or formation of a Lewis acid adduct. The second group, "activated" aziridines, **48**, contain a substituent which can conjugatively stabilize the negative charge that develops on the nitrogen atom in the transition state for ring opening by a nucleophile. (It may also be noted here that the nitrogen lone pair in aziridines has increased s character as compared to other aliphatic secondary amines, which results in lower basicity and reduced π-donor ability.[102])



If aziridines, whether activated or not, are to be of use in synthesis, it is of prime importance to be able to control the stereochemistry and the regiochemistry of the ring-opening process. The issues of stereo- and regioselectivity will be emphasized in the following discussion, which will deal mainly with activated aziridines.

4.1. Acid-Catalyzed Ring Opening

The detailed mechanism of acid-catalyzed ring-opening reactions of aziridines has been the subject of much debate.[103] Some examples for both nonactivated and activated aziridines are shown in Scheme 22. Wade[104] interpreted the formation of **50** and **52** from **49** and **51**, respectively, in terms of an S_N1 mechanism (see, however, ref. [105]). Acetolysis of **53** and **54** was proposed[106] to occur by an A-2 pathway, in which the acetoxy group preferentially attacks the carbon atom best able to ac-



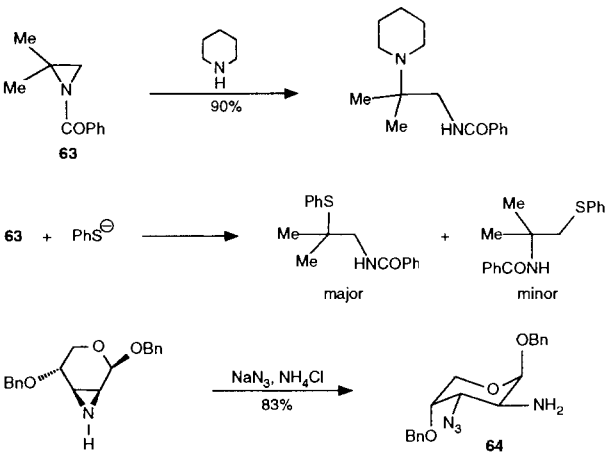
Scheme 22. Acid-catalyzed ring opening of aziridines.

commodate some carbenium ion character. Borderline behavior was observed[107] for the alcoholysis of *cis*-aziridine **55**, which was cleaved completely regioselectively with nearly complete inversion (98:2 ratio of diastereoisomers). Finally, the completely stereo- and regioselective conversion of **56** to **57** provides an interesting and unusual example of neighboring group participation of benzyl ethers.[108]

4.2. Nucleophilic Ring Opening of Activated Aziridines

The reaction mechanism for the nucleophilic ring opening[109] of activated aziridines is more clear-cut than that for nonactivated species, and some generalizations can be made. For monocyclic aziridines, nucleophilic attack is expected to occur by an S_N2-like mechanism with inversion. Monosubstituted aziridines are expected to be attacked predominantly or exclusively at the methylene carbon atom. In analogy with epoxides, fused bicyclic aziridines may be expected to obey the Fürst–Plattner rule[110] for *trans*-diaxial ring opening. Scheme 23 shows some examples of "normal" nucleophilic ring-opening reactions. The *cis*/*trans* isomers **58** and **59** underwent a clean S_N2 reaction[111] with complete Walden inversion; the monosubstituted aziridines **60** and **61** were attacked exclusively[112–114] at the less hindered site; and the sugar aziridine **62** gave predominantly the product of diaxial ring opening.[115]

Some "abnormal" nucleophilic ring openings are presented in Scheme 24. Stamm et al.[116,117] have explained the unusual ring opening of **63** both as a single electron transfer process and also as a borderline S_N2 reaction, depending on the nucleophile used. The anti-Fürst–Plattner ring opening that yields **64**[14] is more difficult to explain.[118,119]



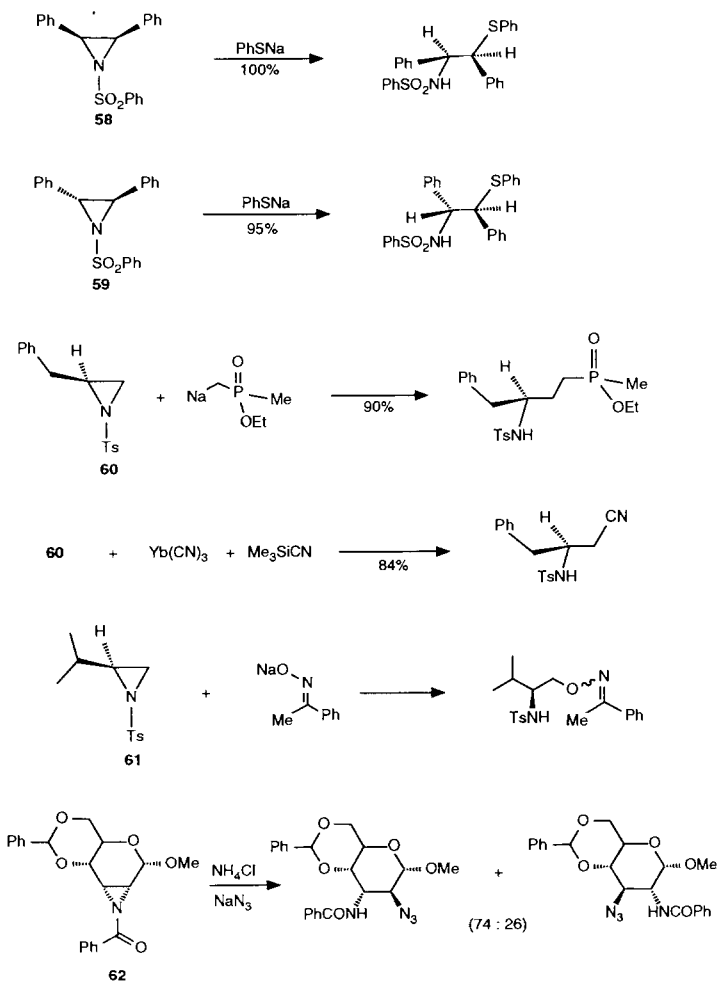
Scheme 24. Some "abnormal" nucleophilic ring-opening reactions.

Since organometallic reagents offer a host of possibilities for selective carbon–carbon bond formation, often under mild reaction conditions, the ring opening of chiral three-membered heterocycles by organometallic compounds should be an attractive tactic in stereoselective synthesis. While such reactions of epoxides were quite well explored at a relatively early stage,[120] the corresponding aziridine chemistry developed more slowly. The difficulties associated with the use of aziridines stem mainly from the inherently low reactivity of the unactivated heterocycles and the ambident nature of activated species such as aziridinecarbamates and *N*-acylaziridines. Some of the problems and solutions are depicted in Scheme 25.

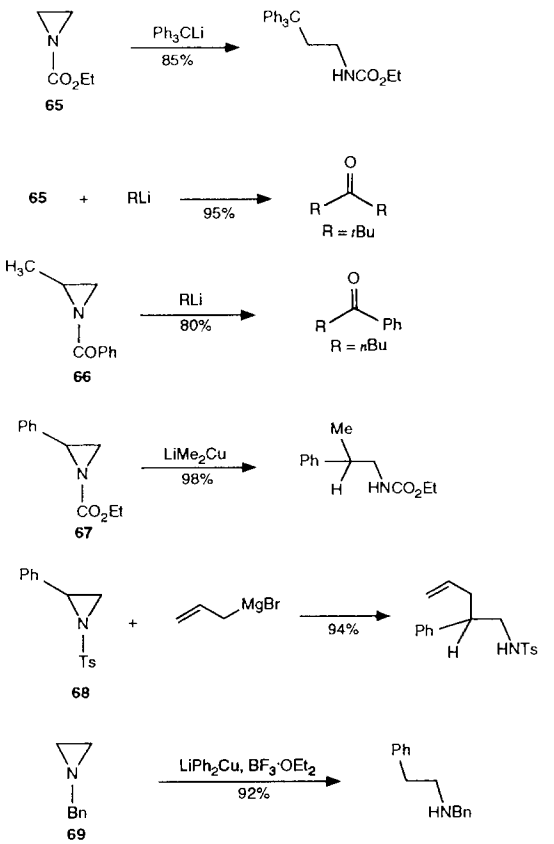
The work of Hassner and Kascheres[121] on aziridinecarbamate **65** clearly demonstrates the ambident electrophilic nature of the substrate. In addition to the convenient synthesis of ketones shown, *N*-acylaziridines such as **66**[122] provide a route to aldehydes.[123] The study conducted by Kozikowski et al.[124] on the ring opening of **67** and **68** underscores the chemoselectivity of cuprate reagents and also the greater activating power of the sulfonyl group relative to the acyl and alkoxycarbonyl groups. The compatability of cuprates with certain Lewis acids allows smooth ring opening of the unactivated aziridine **69** under very mild conditions.[125] Reactions of more elaborate aziridines with organometallic reagents are discussed in Sections 4.3–4.5 and 5.4.

4.3. Ring Opening of Aziridino Alcohols

Thanks to the experimental simplicity and excellent enantioselectivity of the Sharpless asymmetric epoxidation, 2,3-epoxy alcohols have rapidly gained importance in stereoselective synthesis.



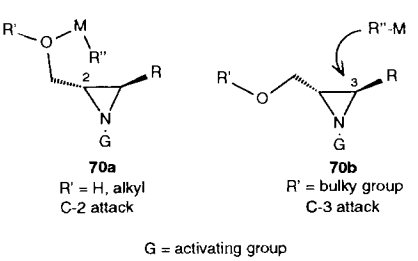
Scheme 23. Nucleophilic ring opening of activated aziridines.



Scheme 25. Reaction of aziridines with some organometallic reagents.

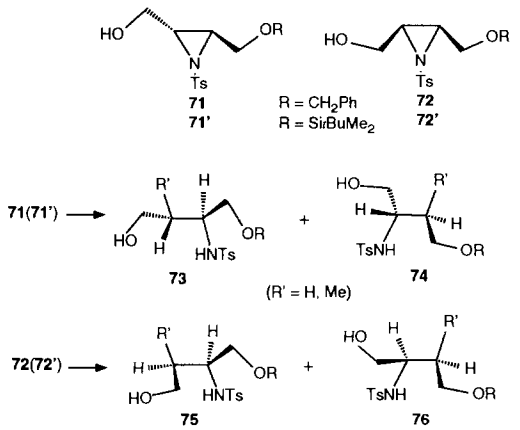
hols have rapidly gained importance in stereoselective synthesis. Much of their chemistry is based on regioselective ring-opening reactions,[126] and in this section it will be demonstrated that their aziridine counterparts, readily available in enantiomerically pure form (see Scheme 6), are also attractive as chiral building blocks.

The basic concept is illustrated by structure **70**, in which G is a strongly activating group which can control *stereochemistry*



by promoting clean S_N2-type attack under as mild conditions as possible; *regiochemistry* is controlled by the substituent on the oxygen atom, which can be used to direct the incoming nucleophile to C-2 (by complexation to the attacking species) or to C-3 (by exerting steric effects).

The substrates chosen[31, 127] were the two *trans*/*cis*-pairs **71**/**72** and **71'**/**72'**; the reagents were either complex hydrides, organocuprates, or organoaluminum compounds (Scheme 26). The results of the ring opening of **71** and **72** by the complex hydrides Red-Al (sodium bis(2-methoxyethoxy)aluminum hydride), $LiAlH_4$, and DIBAL (diisobutylaluminum hydride) are shown in Table 1. Excellent C-2 regioselectivity was observed in the reactions with Red-Al (entries 1 and 2); none of the products of ring opening at C-3 could be detected by high-field ^1H NMR spectroscopy. Since the corresponding epoxy alcohols[128–130] behave in the same way, it seems reasonable to suggest that the free hydroxyl group first coordinates to the reagent, which thus allows intramolecular delivery of the hydride to the proximal carbon atom via a five-membered cyclic transition state.



Scheme 26. Possible regioisomers from the ring opening of *trans* and *cis* aziridino alcohols.

Table 1. Ring opening of **71** and **72** by hydride reagents (R' = H).

Entry	Substrate	Reagent/Conditions	73:74	75:76	Yield [%]
1	**71**	Red-Al, THF, −78 °C	>99:1		86
2	**72**	Red-Al, THF, −78 °C		>99:1	81
3	**71**	$LiAlH_4$, THF, −20 °C	>99:1		80
4	**72**	$LiAlH_4$, THF, −20 °C		>99:1	70
5	**71**	DIBAL, THF, −78 °C → RT [a]	>99:1		30 [b]
6	**72**	DIBAL, THF, −78 °C → RT [a]		58:42	19 [b]
7	**71**	DIBAL, C_6H_6, 0 °C → RT [a]	50:50		20 [b]
8	**72**	DIBAL, C_6H_6, 0 °C → RT [a]		70:30	53 [b]

[a] RT = room temperature. [b] Incomplete reaction.

The same high levels of regioselectivity were obtained in the reactions with $LiAlH_4$ (entries 3 and 4). This also parallels the behavior of the corresponding epoxy alcohols[128] and can be explained in the same way as the Red-Al results. Interestingly, the regioselectivity is much better for the reactions of aziridines, which can be conducted at lower temperatures thanks to the strongly activating *N*-tosyl group. Epoxy alcohols usually undergo selective C-3 attack by DIBAL,[129] but aziridines **71** and **72** do not mimic this behavior, for reasons which are not yet clear (entries 5–8). However, in the case of epoxides, regioselectivity is probably determined to some extent by complexation of Lewis acidic reagents such as DIBAL to the epoxide oxygen atom. Such complexation is less likely for the *N*-tosyl groups of **71** and **72**.

Reactions with alkyl nucleophiles are synthetically more interesting, since the products of ring opening retain two contiguous stereocenters. The reagents chosen were the Gilman cuprate $LiMe_2Cu$,[131] the Lipshutz "higher order" cyanocuprate Li_2Me_2CuCN,[132] and trimethylaluminum. The results for the *trans*-aziridines **71** and **71'** are collected in Table 2. Both types of

Table 2. Ring opening of **71** and **71′** by methylation reagents (R′ = Me).

Entry	Substrate	Reagent/Conditions	**73**:**74**	Yield [%]
1	**71**	$LiMe_2Cu$, Et_2O, −20 °C	>99:1	80
2	**71′**	$LiMe_2Cu$, Et_2O, −20 °C	>99:1	98
3	**71**	Li_2Me_2CuCN, THF, −20 °C	92:8	81
4	**71′**	Li_2Me_2CuCN, THF, −20 °C	>99:1	92
5	**71**	$AlMe_3$, toluene, 75 °C	<1:99	71
6	**71′**	$AlMe_3$, toluene, 75 °C	15:85	82

cuprate reagents gave very satisfactory C-2 regioselectivity (entries 1–4) irrespective of the substituent on C-4. Once again, it seems plausible to suggest that initial complexation of the reagent to the C-1 hydroxyl group is followed by intramolecular attack at C-2. The corresponding epoxy alcohols behave similarly. It is noteworthy, however, that in the reaction with $LiMe_2Cu$ aziridine **71** shows much higher regioselectivity than its epoxide counterpart.[133, 134] On the other hand, trimethylaluminum gave good to excellent C-3 selectivity (entries 5 and 6). Thus, for the ring opening of aziridine **71** complete regiocontrol can be exercised (cf. entries 1 and 5). Presumably the first equivalent of the reagent forms an aluminum alcoholate by removal of the OH proton. This alcoholate is expected to transfer a methyl group more slowly than a trialkylaluminum species.[135, 136] A second equivalent of the reagent then forms a Lewis acid–base complex with the benzyloxy group on C-4, which is followed by intramolecular delivery of a methyl group to the proximal (C-3) carbon. Entry 6 is in line with this reasoning, since the *tert*-butyldimethylsiloxy group in **71′** should be a poorer Lewis base than the benzyloxy group.[137] As for the reaction with $LiMe_2Cu$, the ring opening of **71** by $AlMe_3$ proceeds with much better regioselectivity than that of the corresponding epoxy alcohol.[134]

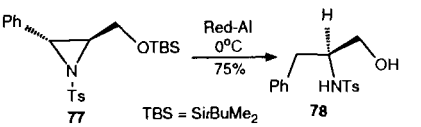
The results of the ring-opening reactions of the *cis*-aziridines **72** and **72′** are shown in Table 3. Inspection of entries 1–4 shows

Table 3. Ring opening of **72** and **72′** by methylation reagents (R′ = Me).

Entry	Substrate	Reagent/Conditions	**75**:**76**	Yield [%]
1	**72**	$LiMe_2Cu$, Et_2O, −20 °C	– [a]	–
2	**72′**	$LiMe_2Cu$, Et_2O, −20 °C	78:22	87
3	**72**	Li_2Me_2CuCN, THF, −20 °C	79:21	73
4	**72′**	Li_2Me_2CuCN, THF, −20 °C	88:12	68
5	**72**	$AlMe_3$, toluene, 75 °C	<1:99	92
6	**72′**	$AlMe_3$, toluene, 75 °C	33:66	60

[a] No reaction.

the general trend of poorer regioselectivity (and lower reactivity, entry 1) for the reactions of **72** and **72′** as compared to the *trans* isomers **71** and **71′**. Presumably if complexation of the organometallic reagent to the free hydroxyl group is important for the regiochemistry of the ring scission, the poorer performance of the *cis* isomers is mainly due to steric effects. However, ring opening of **72** with trimethylaluminum gave the same excellent C-3 selectivity as observed for the *trans* isomer **71**; the importance of having a good Lewis base at the C-4 position is again underlined by comparison of entries 5 and 6. Applications of this ring-opening methodology to the enantioselectivity synthesis of some natural products are described in Section 5.4.



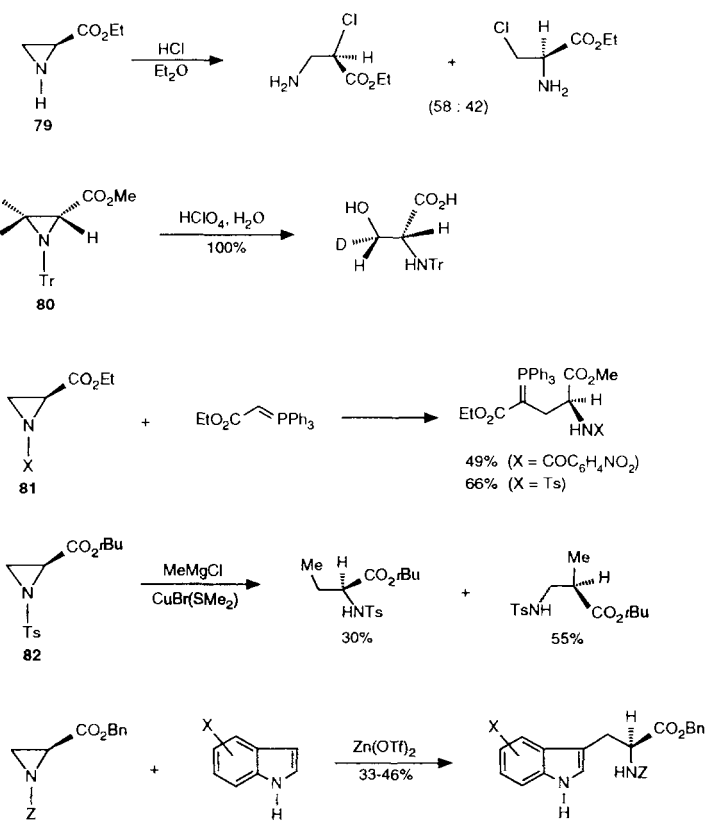
Scheme 27. Regioselective ring opening of **77** accompanied by cleavage of a silyl ether. TBS = *tert*-butyldimethylsilyl.

The transformation[138] shown in Scheme 27 illustrates complete selectivity for ring opening at the benzylic position of **77** and also the sometimes surprising lability[139] of silyl ethers towards complex hydrides.

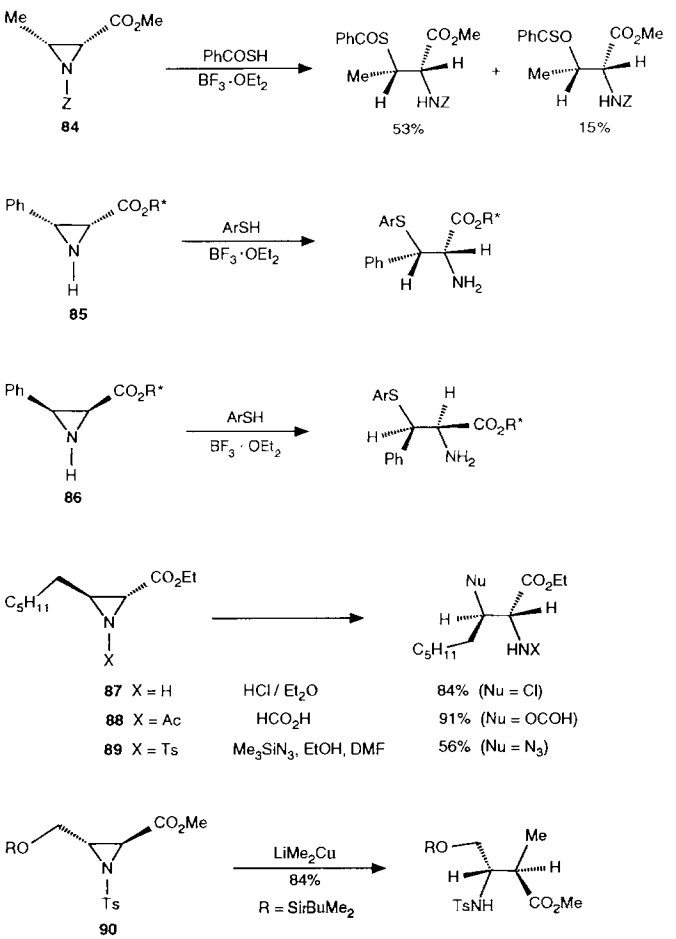
4.4. Ring Opening of Aziridine-2-carboxylates

Aziridino esters (aziridine-2-carboxylates) are potentially very useful synthetic intermediates, since enantioselective routes to unusual amino acids (by regioselective ring-opening reactions) can be envisaged. Leading references can be found in the recent paper by Zwanenburg et al.,[140] who have developed a convenient route to enantiomerically pure aziridino esters (see Scheme 6). Some representative examples of the ring opening of both activated and nonactivated substrates are shown in Schemes 28 and 29.

As discussed in Sections 4 and 4.1, the mechanism and regioselectivity of the acid-catalyzed ring opening of nonactivated aziridines may vary, depending on the exact conditions used. This is



Scheme 28. Regioselective ring opening of aziridine-2-carboxylates. DMF = dimethylformamide.

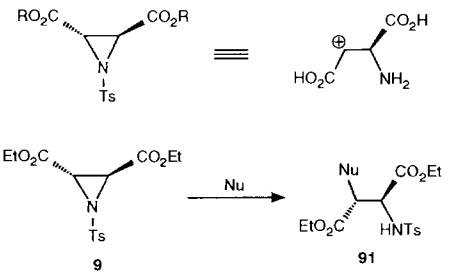


Scheme 29. Regioselective ring opening of 3-substituted aziridine-2-carboxylates. In **85** and **86** R* = (−)-menthyl.

nicely demonstrated by the reactions of aziridines **79**[141] and **80** (Scheme 28).[142] The latter reaction provides convenient access to stereospecifically labeled amino acids. Baldwin et al. have described the ring opening of the activated species **81** with Wittig reagents[143] (see also Section 5.3) and the copper-catalyzed reaction of **82** with Grignard reagents.[144] Unfortunately, the nonactivated *N*-benzyl analogue of **82** was not a good substrate for organometallic reagents, even in the presence of Lewis acids.[125] In studies directed toward the synthesis of biologically active natural products, Sato and Kozikowski[145] showed that the reaction of **83** with a variety of substituted indoles was highly dependent on the nature of the Lewis acid used to promote the reaction.

The ring opening of disubstituted aziridino ester **84**[146] (Scheme 29) was completely regioselective but illustrates the complications associated with ambident nucleophiles. Interestingly, a peptide analogue of **84** gave a single regioisomer with sole formation of the *S*-acyl derivative, without the need for Lewis acid catalysis.[146] In the nonactivated series, Marquet et al.[147] observed complete stereo- and regioselectivity in the ring opening of **85** and **86** by a thiol; the corresponding *trans* isomers behaved similarly. (For the ring opening of nonactivated aziridinecarboxylic acids with thiols under mild conditions, see ref. [148]). Zwanenburg et al.[140] have published an extensive study of 3-alkylaziridine-2-carboxylic esters such as **87**–**89**. Scheme 29 shows some examples of the excellent stereo- and regioselectivity obtained in the ring-opening reactions of both nonactivated and activated substrates. Complete C-2 regioselectivity was observed[149] for the ring opening of **90** by a cuprate reagent, a result that may be compared to those listed in Tables 2 and 3.

In Section 2.3 the synthesis of the C_2-symmetric aziridine **9** (Scheme 30) from tartaric acid was described. The C_2 symmetry



Scheme 30. The C_2-symmetric aziridine **9** is a synthetic equivalent for the β cation of L-aspartic acid; *ent*-**9**, the synthetic equivalent of the β cation of D-aspartic acid, can be used analogously.

removes the question of regioselectivity as far as ring opening is concerned, and the three electron-withdrawing groups in **9** make this substrate highly susceptible to attack by nucleophiles.[24] Some results are shown in Table 4. In each case, ring opening occurred with inversion under very mild conditions, which reflects the combined activating effects of the three substituents. As sketched in Scheme 30, the diester **9** and its enantiomer can be considered as synthetic equivalents for the β-cation of L- and D-aspartic acid, respectively. This approach to stereospecifically substituted aspartic acid derivatives complements the work of Baldwin et al.[150] and Hanessian et al.,[151] who independently developed synthetic equivalents of the corresponding anionic synthons.

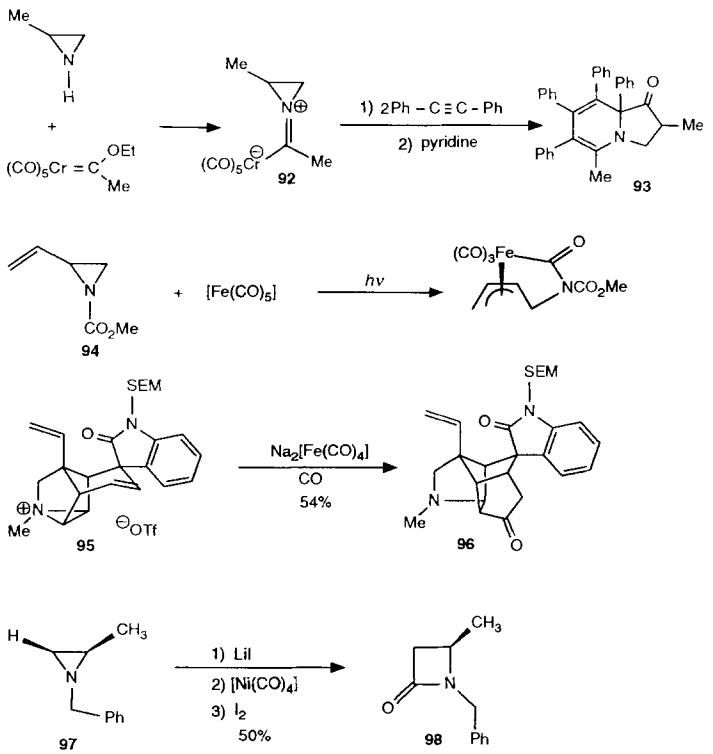
Table 4. Ring opening of aziridine **9**.

Entry	Reagent	Product	Nu	Yield [%]
1	$LiMe_2Cu$	**91a**	Me	68
2	$LiBu_2Cu$	**91b**	Bu	54
3	Li_2Bu_2CuCN	– [a]		
4	NaN_3	**91c**	N_3	81
5	MgI_2	**91d**	I	72
6	$MgBr_2$	**91e**	Br	76

[a] Decomposition.

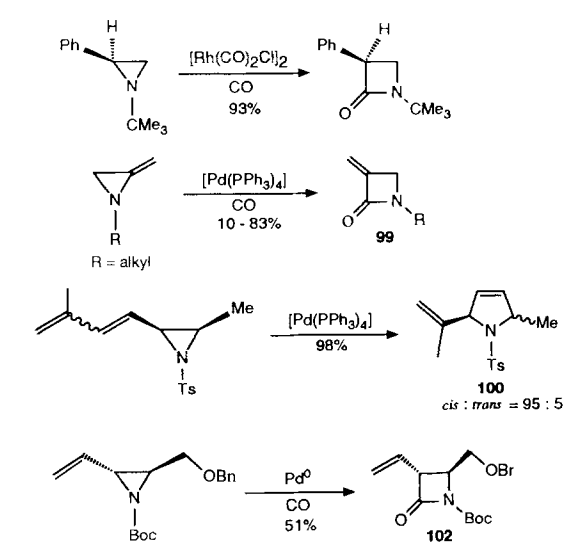
4.5. Ring Opening Promoted by Transition Metal Complexes

The development of organo transition metal chemistry[152] has brought new dimensions to organic synthesis and greatly expanded the repertoire of techniques available for chemo-, regio-, and stereoselective transformations. Some reactions of aziridines mediated by transition metal complexes are depicted in Schemes 31 and 32; particularly attractive are the *catalytic* procedures shown in Scheme 32.



Scheme 31. Reactions of aziridines with transition metal complexes. SEM = trimethylsilylethoxymethyl.

The ring expansion of aziridine **92** to give bicyclic compound **93** can be regarded as an "organometallic analogue" of the Stevens rearrangement of ammonium ylides.[153] The process involves the insertion of two molecules of diphenylacetylene and a single molecule of carbon monoxide. The reaction of **94** with $[Fe(CO)_5]$ was one of the first applications of vinylaziridines.[154] The pathway proposed[155] for the remarkable transformation of aziridinium ion **95** into **96** provides a good demonstration of the mechanistic diversity exhibited by organometallic complexes. The type of nickel-mediated ring expansion used to transform aziridine **97** into β-lactam **98** was shown to be both regio- and stereoselective.[156]



Scheme 32. Regio- and stereoselective transformations of aziridines catalyzed by transition metals.

In the catalytic procedures shown in Scheme 32, the rhodium-mediated ring expansion developed by Alper et al.[157] was shown to be both stereo- and enantiospecific, and occurred with retention of configuration. This reaction could also be used for kinetic resolution of aziridines, when menthol was added as chiral ligand. In a similar type of reaction, palladium was used[158] to catalyze the formation of α-methylene-β-lactams **99**. Palladium was also employed by Oshima et al.[159] in an excellent synthesis of vinylpyrrolines such as **100** from dienylaziridines. Vinylaziridines[160] are also substrates of interest, and the palladium-catalyzed reaction[161] of **101** was regio- and stereoselective, yielding an azetidinone (**102**) of considerable synthetic potential. A related reaction conducted with diastereo- and enantiomerically pure material is discussed in Section 5.4.

5. Chiral Aziridines and Aziridinium Ions in Total Synthesis

It should be clear from the foregoing sections that chiral aziridines are attractive building blocks for organic synthesis. In the following discussion, representative applications of chiral aziridines and aziridinium ions in the total synthesis of some natural products and their analogues will be presented. In most of these syntheses nonracemic materials were employed. This section is subdivided according to the types of target molecules.

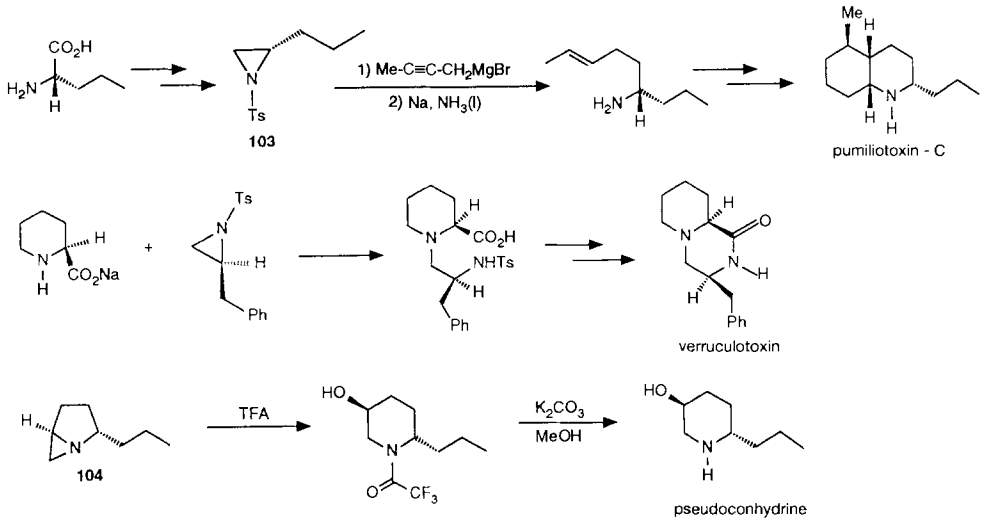
5.1. Alkaloids

Oppolzer and Flaskamp[162] used the chiral aziridine **103** (Scheme 33) in an enantioselective total synthesis of pumiliotoxin-C. This elegant piece of work allowed unambiguous assignment of the absolute configuration of the natural product and was also one of the first applications of an organometallic reagent for the ring opening of an activated aziridine. Scheme 33 also shows a convenient enantiospecific synhesis of verruculotoxin[163] as well as a route to racemic pseudoconhydrine,[164] which made use of the thermodynamic control of the ring opening of bicyclic aziridine **104**.

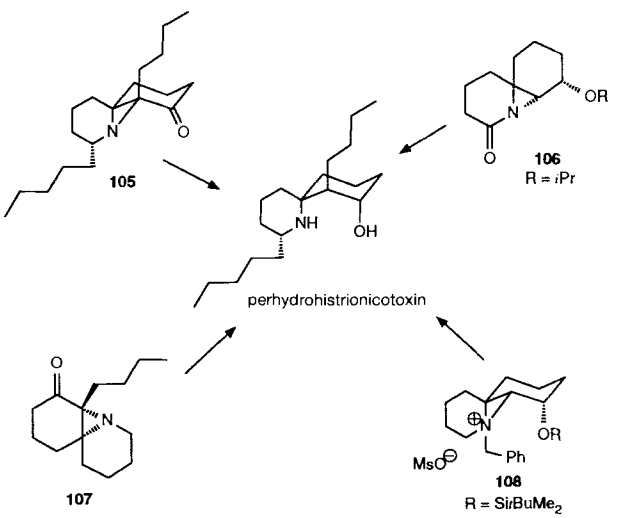
Tricyclic aziridines **105**,[165] **106**,[166] and **107**[167] and aziridinium ion **108**[168] have all featured in routes to the synthetically challenging histrionicotoxin family of spirocyclic alkaloids (Scheme 34).

The synthesis of (+)-croomine[169] shown in Scheme 35 involved the one-pot conversion of **109** into the target molecule by intramolecular capture of the aziridinium species **110**.

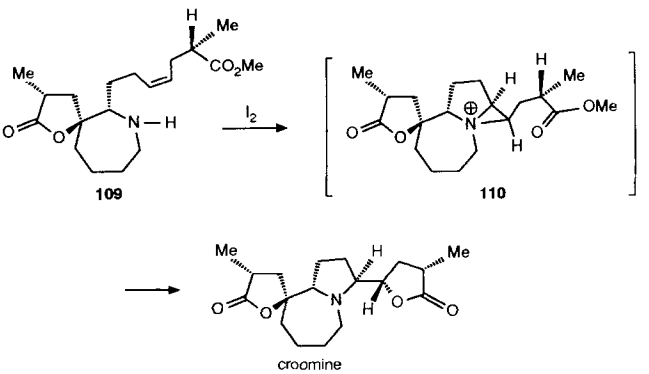
Hudlicky et al.[170] have developed an ingenious and efficient enantiodivergent route to the pyrrolizidine alkaloid trihydroxyheliotridane (Scheme 36). Starting from chlorobenzene, which was subjected to enantioselective microbial oxidation, the synthesis diverged to give protected derivatives of both L- and D-erythrose. Elaboration of both enantiomers of bicyclic vinylaziridine **111** was followed by thermal rearrangement to provide the desired bicyclic ring systems.



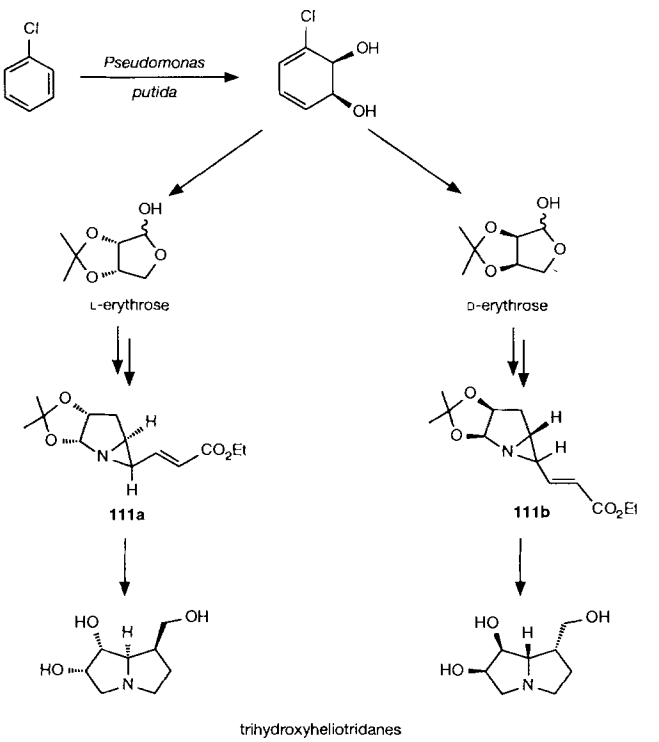
Scheme 33. Stereoselective synthesis of some alkaloids from chiral aziridines. TFA = trifluoroacetic acid.



Scheme 34. Aziridine-based routes to the alkaloid perhydrohistrionicotoxin.



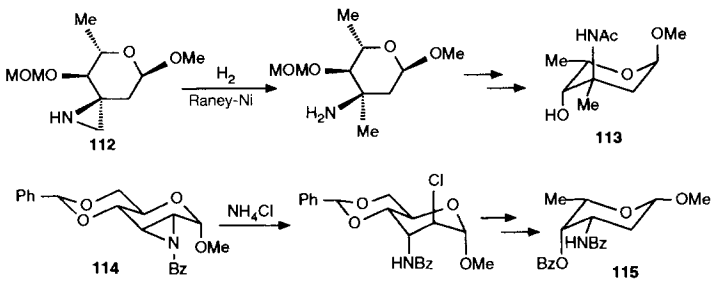
Scheme 35. An aziridinium ion as a key intermediate in the enantioselective total synthesis of the alkaloid croomine.



Scheme 36. Synthesis of trihydroxyheliotridanes via enantiomeric vinylaziridines.

5.2. Amino Sugars

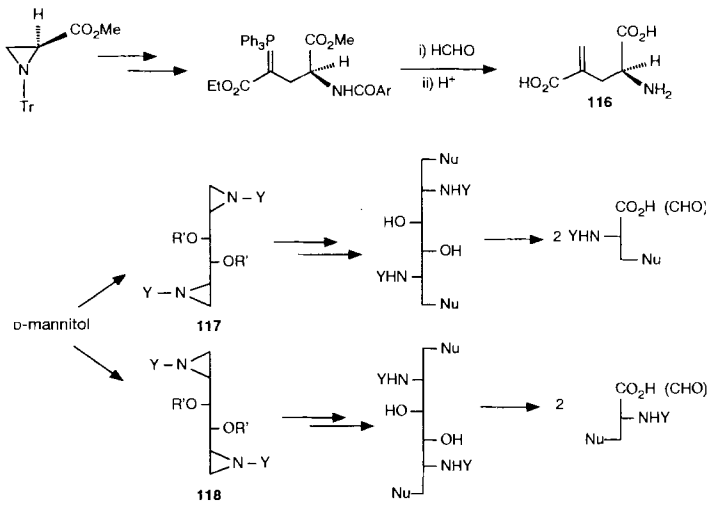
Sugar aziridines (cf. Scheme 2) often provide convenient access to the amino sugars found in many naturally occurring antibiotics. Two examples, in which the ring opening of both spiro and fused bicyclic aziridines are utilized, are shown in Scheme 37. The synthesis[171] of the branched-chain amino sugar **113** included hydrogenolysis of aziridine **112** over Raney nickel; the route[172] to the daunosamine deriative **115** proceeded via the Fürst–Plattner regioisomer (cf. Section 4.2) from the ring opening of fused aziridine **114**.



Scheme 37. Chiral aziridines in the synthesis of enantiomerically pure amino sugars. MOM = methoxymethyl, Bz = benzoyl.

5.3. Amino Acids and Derivatives

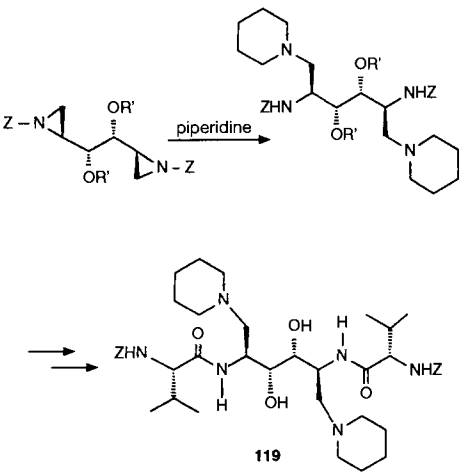
Baldwin et al.[143] have used the ring opening of aziridine-2-carboxylates by Wittig reagents (Section 4.4) as a key step in the synthesis of naturally occurring unsaturated amino acids (synthesis of **116**, Scheme 38). In Section 2.2, a general synthesis of chiral



Scheme 38. Chiral aziridines in the synthesis of amino acids and their derivatives. Nu = alkyl, halide, N_3^-, PhS^-.

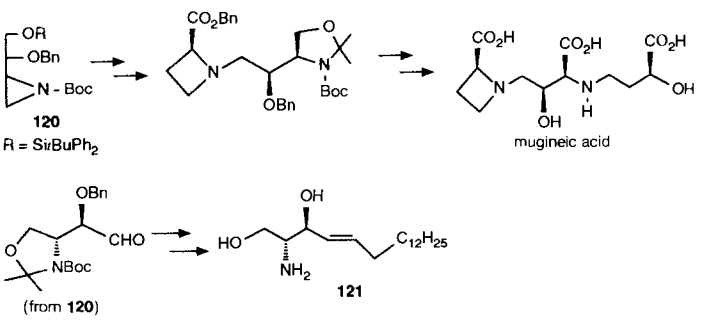
bisaziridines from mannitol was presented (cf. **117** and **118**, Scheme 38). These form the basis of the elegant and convenient route[173] to α-amino acids and aldehydes shown in Scheme 38. The best activating groups (Y) were tosyl and benzyloxycarbonyl, and a very thorough study of twofold ring-opening reactions with a wide range of nucleophiles was performed. Oxidative cleavage of the central 1,2-diol moiety finally provided two molecules of chiral product per molecule of substrate. The same mannitol derivatives could be used for the synthesis[174] of C_2-symmetric inhibitors of HIV-1 protease (**119**, Scheme 39, cf. [175]).

The Paris group[176] has also reported an enantioselective approach toward mugineic acid. The chiral aziridine **120** (Scheme 40) was synthesized from 2-*O*-benzyl-L-threitol and could be converted in a few steps (including regioselective ring opening by phenylthiolate) to an advanced key intermediate. Aziridine **120** is also a possible precuror to optically active *erythro*-sphingosine (**121**).[177]



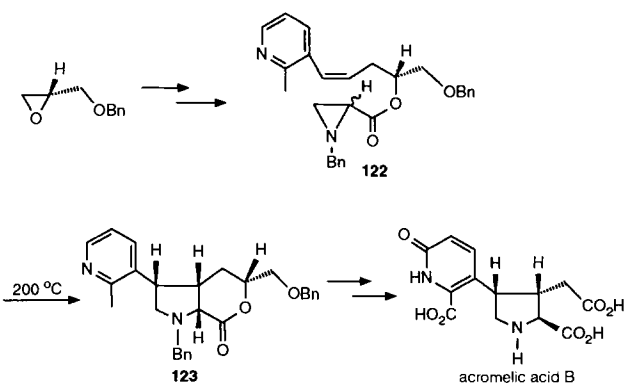
Scheme 39. Synthesis of an inhibitor of HIV-1 protease (**119**) via a chiral bisaziridine. Z = benzyloxycarbonyl.

The 1,3-dipolar cycloaddition reactions of azomethine ylides produced by thermolysis of aziridines have been studied very thoroughly by Huisgen et al.[178] An interesting intramolecular version of this reaction was used by Takano et al.[179] as a key step in the enantioselective total synthesis of acromelic acid B



Scheme 40. Enantioselective routes to mugineic acid and *erythro*-sphingosine (**121**) via chiral aziridine **120**.

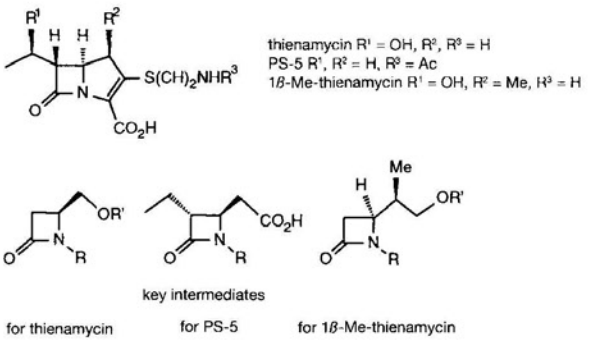
from (*S*)-*O*-benzylglycidol (Scheme 41). Thermolysis of a 50:50 mixture of aziridine epimers **122** gave a single stereoisomer of pyrrolidine **123**, which was then elaborated to the target molecule by a sequence involving epimerization at C-2.



Scheme 41. Aziridine **122** as a key intermediate in the enantioselective total synthesis of acromelic acid B.

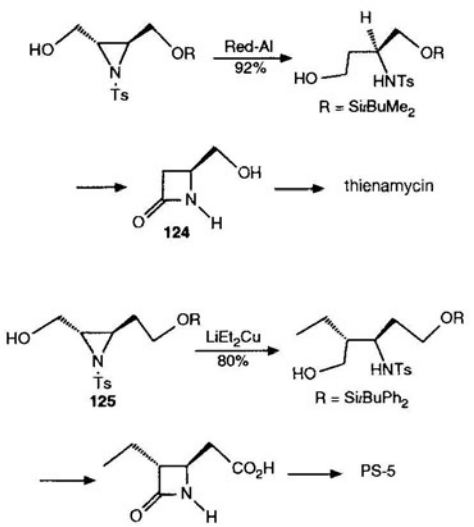
5.4. β-Lactam Antibiotics

In Sections 2.4 and 4.3 the synthesis and ring-opening reactions of enantiomerically pure 2,3-aziridino alcohols were described. It will now be demonstrated how this methodology can be applied to the enantioselective synthesis of some members of the important class of carbapenem antibiotics. The target molecules and the types of key intermediates for their total synthesis are shown in Scheme 42.



Scheme 42. Key intermediates for the enantioselective synthesis of some carbapenem antibiotics.

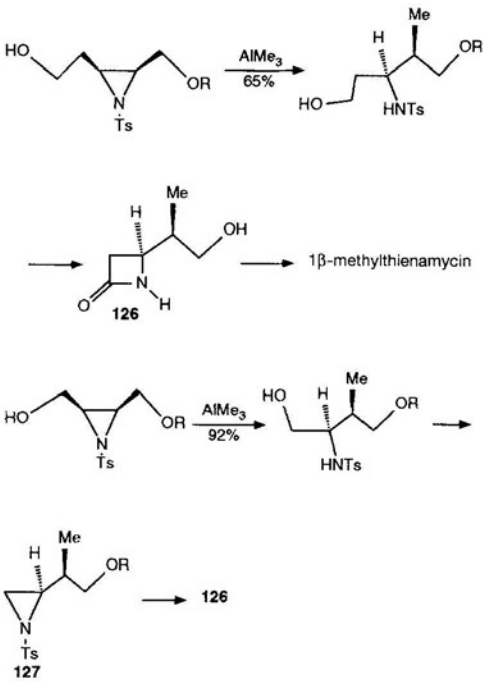
The synthesis of these three key intermediates relies on the regio- and stereoselective ring opening of suitable aziridino alcohols by Red-Al, $LiEt_2Cu$, and $AlMe_3$, respectively. *trans*-Aziridines were used in the routes to thienamycin, via **124**,[31] and PS-5, from **125**[180] (Scheme 43). The C-2 regioselectivity was



Scheme 43. Enantiomerically pure *trans* aziridino alcohols provide a route to the carbapenem antibiotics thienamycin and PS-5.

excellent in both cases, presumably owing to the directing effects of the free hydroxyl group (cf. Section 4.3).

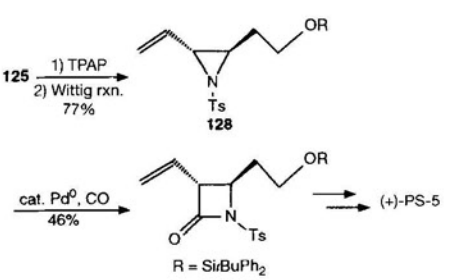
cis-Aziridines were used in two approaches[181] to 1β-methylthienamycin (via key intermediate **126**); the second route involved chiral aziridines at two different stages (Scheme 44). The regioselectivity of the ring opening, now dictated by the benzyl moiety (Section 4.3), is complete in both cases. The route via **127** is particularly efficient in terms of overall yield.[181]



Scheme 44. Use of *cis* aziridino alcohols in the synthesis of 1β-methylthienamycin. R = $PhCH_2$.

All four of the required aziridino alcohols can be obtained in >90% *ee* from the corresponding epoxides. The tosyl group not only activates the ring toward nucleophilic attack but also is important for efficient closure of the azetidinone ring under mild conditions.[182] Non-natural analogues of these antibiotics are equally easily available by this route simply by suitable permutations of the *cis* or *trans* geometry of the allylic alcohol used in the Sharpless AE reaction, the (+) or (−) enantiomer of the tartrate ester serving as a ligand in the AE reaction, and the nature of the nucleophile used in the ring opening of the activated aziridine.

A complementary method[183] for the synthesis of PS-5 is shown in Scheme 45. Key steps in this stereoselective route are

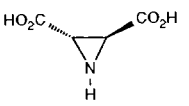


Scheme 45. A stereoselective palladium-catalyzed transformation of a vinylaziridine to an enantiomerically pure β-lactam. TPAP = tetra-*n*-propylammonium perruthenate, R = Si^tBuPh_2.

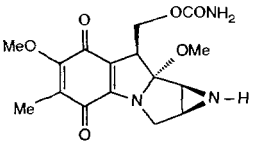
the palladium-catalyzed ring opening of vinylaziridine **128**, followed by insertion of CO and ring closure to the β-lactam (cf. Section 4.5).

5.5. Some Natural Products Containing Aziridine Units

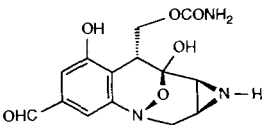
The C_2-symmetric aziridine **129** can be synthesized[184] in a few steps from (+)-tartaric acid (cf. Scheme 3). Not surprisingly, the other much more intricate structures have prompted much synthetic activity; the most effort[185] has been devoted to the



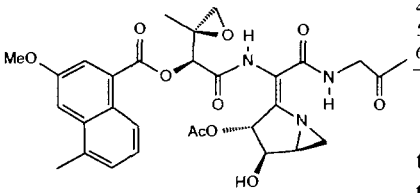
129



130 mitomycin A



131 FR-900482

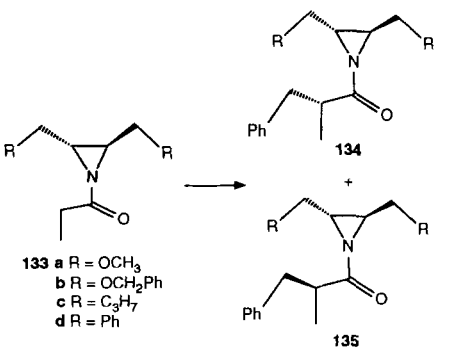


132 azinomycin A

mitomycins. (The first total synthesis of racemic mitomycin A was accomplished by Kishi et al.[186] as early as 1977.) Racemic FR-900482 was synthesized very recently by Fukuyama et al.,[187] and an enantiospecific approach from L-methionine (via an aziridine closely related to compound **31** in Scheme 19) has also been reported.[188] Coleman and Carpenter[189] have disclosed a stereoselective route from D-glucosamine to the aziridine substructure of the azinomycins.

6. Aziridines as Chiral Auxiliaries for Asymmetric Synthesis

As shown in Section 2.3, tartaric acid provides convenient access to C_2-symmetric chiral aziridines. Scheme 46 shows how these materials can be used as chiral auxiliaries[25] for diastereoselective alkylation. The enolates of amides **133a–d** were formed at low temperature and allowed to react with various electrophiles. Results from the alkylations with benzyl bromide (Table 5) illustrate some of the interesting features of the reaction. The lithium enolates of aziridines **133a** and **133b**, which have ether side chains, reacted with complete diastereoselectivity to give the alkylated products with the absolute configuration shown for **134** (Table 5, entries 1 and 2). For **133b** the effect of varying the counterion of the enolate was studied; lithium was found to be far superior to sodium or potassium (entries 2–4). The importance of the nature of the cation and insensitivity of the steric bulk of the alkoxy group suggests that a chelate is formed between the metal ion and an oxygen atom in the enolate and one in the side chain. This hypothesis was tested by studying



133 a R = OCH_3
b R = OCH_2Ph
c R = C_3H_7
d R = Ph

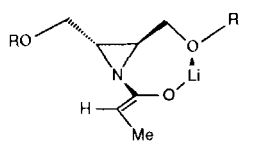
134 + **135**

Scheme 46. Use of C_2-symmetric aziridines as chiral auxiliaries for diastereoselective alkylation with alkali metal bis(trimethylsilyl)amides and benzylbromide.

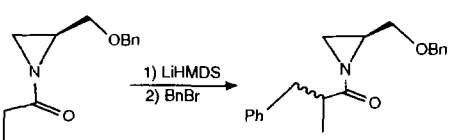
Table 5. Diastereoselective alkylation of **133** with $MN(SiMe_3)_2$ and $PhCH_2Br$.

Entry	Substrate	$M^{\oplus}$	**134**:**135**
1	**133a**	Li	>99:1
2	**133b**	Li	>99:1
3	**133b**	Na	75:25
4	**133b**	K	67:33
5	**133c**	Li	80:20
6	**133d**	Li	75:25

the reaction of aziridines **133c** and **133d** (available in enantiomerically pure form by the Sharpless asymmetric dihydroxylation procedure),[190] which have two relatively bulky side chains with no donor atoms for chelate formation (entries 5 and 6). A simple model[25] to explain the results is provided by structure **136**. Under the reaction conditions used, the (*Z*) enolate is formed,[191] and the enolate species is presumed[192] to have a pyramidalized nitrogen atom. Chelation of the metal ion (expected to be most favorable for lithium) then directs the incoming electrophile to the opposite face of the enolate, which results in the absolute configuration observed in the products. Since the substrate has C_2 symmetry, it makes no difference on which face of the aziridine ring the chelate is formed. The importance of the symmetry element[193] is emphasized by the results of the reaction shown in Scheme 47.

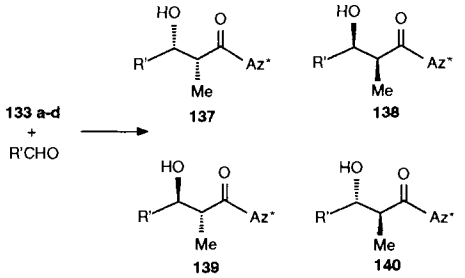


136



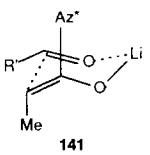
Scheme 47. Poor diastereoselectivity (75:25) in the alkylation of a non-C_2-symmetric substrate. LiHMDS = lithium hexamethyl disilazide.

Much effort has been expended on the development of asymmetric versions of the aldol reaction.[191] Since many of the most successful approaches are based on the use of chiral auxiliaries, it was of interest to test the performance of the C_2-symmetric aziridines. Four diastereomeric products are possible for the aldol reactions (Scheme 48).



Scheme 48. Four possible diastereomers may result from an aldol reaction in which a chiral aziridine auxiliary (Az*) is used.

One important stereochemical factor is the enolate geometry. (*Z*) Enolates of the type used here tend to give *syn*-aldol products under conditions of kinetic control. The Zimmerman–Traxler model of the transition state (**141**) has gained widespread use for explaining the stereochemical outcome.[191] A selection of results[25, 190] is shown in Table 6.



141

Table 6. Diastereoselective aldol reactions of **133** and R'CHO.

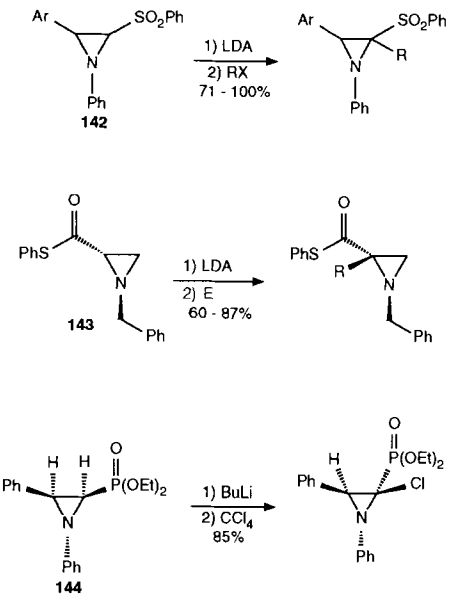
Entry	Substrate	R'	**137**:**138**:**139**:**140**
1	**133a**	Ph	87:13:<1:<1
2	**133b**	Ph	99:1:<1:<1
3	**133c**	Ph	>99:<1:<1:<1
4	**133d**	Ph	91:9:<1:<1
5	**133b**	Et	40:40:10:10
6	**133c**	Et	87:13:<1:<1
7	**133d**	Et	85:15:<1:<1

Bis(benzyloxymethyl)aziridine **133b** gave excellent results only with relatively bulky aldehydes (cf. entries 2 and 5), while the bis(methoxymethyl) species **133a** was even less selective (entry 1). This behavior does not parallel that observed for the alkylation reactions (cf. Table 5). Another significant difference is the much improved performance of auxiliaries having side chains not containing oxygen atoms (entries 3, 4, 6, 7). For the Zimmerman–Traxler mechanism to be operative, the metal ion must be able to coordinate simultaneously to both the enolate and the aldehyde oxygen atoms. This is not possible if the metal ion is already coordinated to the side chain of the auxiliary. In the special case of the reaction between **133b** and benzaldehyde (entry 2) the diastereoselectivity appears to be entirely due to steric effects on the approach of the aldehyde to the enolate. For the reactions involving auxiliaries without oxygen atoms in their side chains, the Zimmerman–Traxler transition structure (**141**) is assumed.

The C_2-symmetric aziridines discussed here thus fulfill the usual requirements for a good chiral auxiliary: both enantiomeric forms are readily available; they give good to excellent *de* in subsequent reactions; and they can be removed easily[194] in a nondestructive manner.

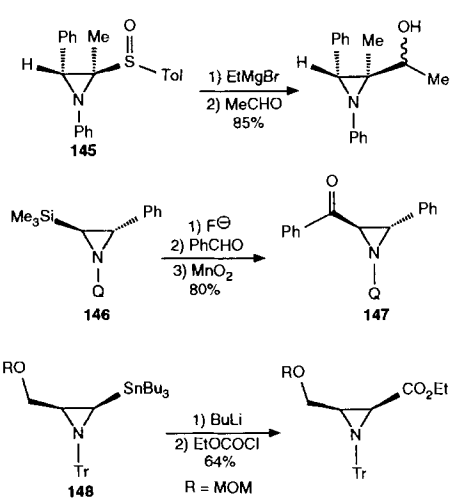
7. Aziridines as Chiral Reagents

The reaction of chiral metalated aziridines with electrophiles has obvious potential for stereoselective synthesis. However, as summarized by Seebach and Häner,[195] the generation and handling of "carbanionic" three-membered heterocycles can be problematic. Some successful solutions to this problem are discussed below (Schemes 49 and 50).



Scheme 49. Stereoselective reactions with metalated aziridines as chiral intermediates. Top: R = CH_3, $C_6H_5CH_2$, CH_2=$CHCH_2$; middle: E = MeI, $C_6H_5CH_2Br$, C_6H_5CHO, β-nitrostyrene.

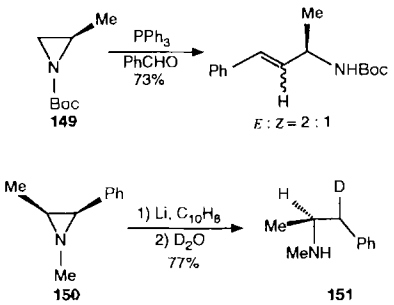
The 2-phenylsulfonylaziridine **142** could be metalated and then alkylated with reactive alkyl halides in excellent yield (Scheme 49).[196] Racemic compounds were used and, unfortunately, no stereochemical information was provided. Seebach et al. have published the results of a careful study of the lithiation and subsequent reactions of both racemic[195] and enantiomerically pure[197] (*S*)-phenyl aziridinecarbothiates **143**; electrophilic substitution was shown to occur with retention of configuration. Lithiated (racemic) aziridinylphosphonate **144** could not be alkylated or trapped by aldehydes but did react with carbon tetrachloride; in this case, inversion of configuration was suggested.[198]



Scheme 50. Further examples of the use of configurationally stable "carbanionic" aziridine species. Q is given in Scheme 11.

The sulfinylaziridine **145** (which can be obtained in enantiomerically pure form, see Section 2.6) was transformed to the corresponding Grignard reagent, which could be trapped by acetaldehyde but not with alkyl halides (Scheme 50).[76] An aziridinyl carbanion was implicated in the efficient sequence[199] leading from **146** to **147**. Vedejs and Moss[200] have described the preparation of configurationally stable (racemic) aziridinyllithium reagents by tin–lithium exchange[201] on aziridines such as **148**; the lithiated species could be trapped efficiently by a range of electrophiles, and an interesting anionic Stevens rearrangement was also observed.

Two interesting examples of chiral reagents formed from ring-opening reactions of aziridines are shown in Scheme 51. A chiral

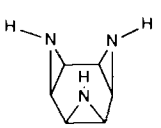


Scheme 51. Formation and reaction of chiral reagents from the ring opening of aziridines.

Wittig reagent was prepared from the enantiomerically pure aziridine **149** and used for the synthesis of optically active allylic amines.[202] Yus et al. obtained a single diastereomer of **151** from the naphthalene–lithium catalyzed ring opening[203] of (racemic) aziridine **150** followed by quenching with D_2O.

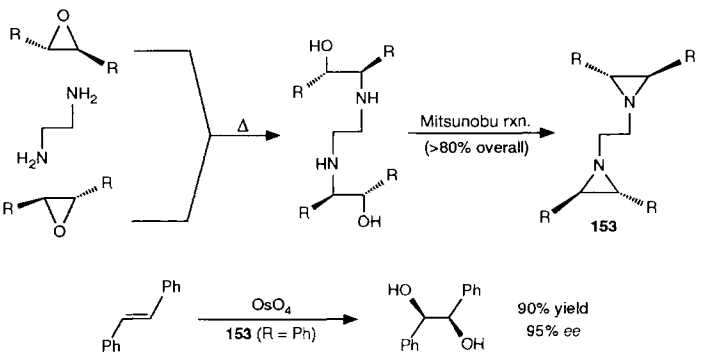
8. Aziridines as Chiral Ligands. Toward Enantioselective Catalysis

Many of the most exciting recent developments in stereoselective organic synthesis are based on transition metal catalyzed processes, and the rational design of chiral ligands for enantioselective catalysis presents a formidable challenge.[204] Aziridines can be employed not only in the preparation of such chiral species[205, 206] but should also be useful ligands in their own right. Trisaziridine **152** is an (achiral) ligand and just one of a series of fascinating compounds prepared and studied by Prinzbach et al.[207]



152

A general approach[208] to C_2-symmetric bisaziridine ligands is shown in Scheme 52. Two equivalents of a *trans*-epoxide are ring-opened by one equivalent of a diamine, and the resultant species is subjected to a double Mitsunobu ring closure. In a stoichiometric reaction ligand **153** mediates the enantioselective *syn*-dihydroxylation of *trans*-stilbene in excellent chemical yield and with 95% *ee*. Current work focuses on the development of catalytic procedures for this and other reactions, for example enantioselective cyclopropanation and aziridination.



Scheme 52. Synthesis of C_2-symmetric bisaziridine ligands and their use in enantioselective synthesis.

9. Summary and Outlook

Chiral aziridines are readily available in enantiomerically pure form by a variety of procedures, and the reactivity of these three-membered heterocycles can be modified by suitable choice of the substituent on the nitrogen atom. Regio- and stereoselective ring-opening reactions with many types of nucleophiles provide access to a great number of useful synthetic intermediates. In addition to being attractive substrates or "building blocks" for the organic chemist, aziridines can also function as chiral auxiliaries, chiral reagents, and chiral ligands for asymmetric synthesis.

The utility of chiral aziridines in organic synthesis will be further enhanced by the development of improved general procedures for the catalytic enantioselective aziridination of olefins. But it seems appropriate even now to close this review by paraphrasing the title of an article by Sharpless et al.[48]: *Chiral aziridines—like epoxides only even more versatile.*

It is a pleasure to acknowledge the experimental and intellectual contributions of the following co-workers: Dr. Peter Somfai (Lund Institute of Technology), Dr. Hua Ming He, Dr. Carin Birgersson, Adrian Harden, and Hardip K. Dhaliwal. Prof. K. B. Sharpless and Prof. E. N. Jacobsen very kindly provided copies of manuscripts prior to publication. I also thank Prof. Tomas Trnka for an extensive list of references to sugar aziridines, Ms. Anita Meurling for the literature search, and Mr. Olle Eriksson for the drawings. Generous financial support was provided by the University of Uppsala and the Swedish Natural Science Research Council.

Received: May 12, 1993 [A 933 IE]
German version: *Angew. Chem.* **1994**, *106*, 625

[1] H. Heimgartner, *Angew. Chem.* **1991**, *103*, 271; *Angew. Chem. Int. Ed. Engl.* **1991**, *30*, 238.
[2] S. Gabriel, *Ber. Dtsch. Chem. Ges.* **1888**, *21*, 1049.
[3] a) T. L. Gilchrist, *Heterocyclic Chemistry*, 2nd ed., Longman, Harlow, **1992**, p. 38; b) "Strain-Assisted Syntheses" (Tetrahedron Symposia-in-Print No. 38; Guest Ed.: L. Ghosez), *Tetrahedron*, **1989**, *45*, 2875ff. (entire issue).
[4] a) H. W. Heine, *Angew. Chem.* **1962**, *74*, 772; *Angew. Chem. Int. Ed. Engl.* **1962**, *1*, 528; b) O. C. Dermer, G. E. Ham, *Ethylenimine and Other Aziridines*, Academic, New York, **1969**; c) J. A. Deyrup in *Small Ring Heterocycles, Vol. 1* (Ed.: A. Hassner), Wiley, New York, **1983**, p. 1; d) A. Padwa, A. D. Woolhouse in *Comprehensive Heterocyclic Chemistry, Vol. 7* (Eds.: A. R. Katritzky, C. W. Rees), Pergamon, Oxford, **1984**, p. 47; e) W. B. Jennings, D. R. Boyd in *Cyclic Organonitrogen Stereodynamics* (Eds.: J. Lambert, Y. Takeuchi), VCH, New York, **1992**, p. 119; f) J. Backes in *Houben-Weyl: Methoden der Organischen Chemie, Vol. E 16 c* (Ed.: D. Klamann), Thieme, Stuttgart, **1992**, p. 370.

[5] J. E. G. Kemp in *Comprehensive Organic Synthesis, Vol. 7* (Eds.: B. M. Trost, I. Fleming), Pergamon, Oxford, **1991**, p. 469.
[6] J. W. Kelly, N. L. Eskew, S. A. Evans, Jr., *J. Org. Chem.* **1986**, *51*, 95.
[7] K. Nakajima, F. Takai, T. Tanaka, K. Okawa, *Bull. Chem. Soc. Jpn.* **1978**, *51*, 1577.
[8] G. W. Daub, D. A. Heerding, L. E. Overman, *Tetrahedron* **1988**, *44*, 3919.
[9] M. B. Berry, D. Craig, *Synlett* **1992**, 41.
[10] P. Wipf, C. P. Miller, *Tetrahedron Lett.* **1992**, *33*, 6267.
[11] O. Mitsunobu, *Synthesis* **1981**, 1.
[12] E. Kuyl-Yeheskiely, M. Lodder, G. A. van der Marel, J. H. van Boom, *Tetrahedron Lett.* **1992**, *33*, 3013.
[13] S. Hanessian, *Total Synthesis of Natural Products: The ‚Chiron' Approach*, Pergamon, Oxford, **1983**.
[14] H. Paulsen, H. Patt, *Liebigs Ann. Chem.* **1981**, 1633.
[15] J. S. Brimacombe, K. M. M. Rahman, *Carbohydr. Res.* **1983**, *113*, C6.
[16] I. Černy, M. Budešínsky, T. Trnka, M. Černy, *Carbohydr. Res.* **1984**, *130*, 103.
[17] L. Dubois, R. H. Dodd, *Tetrahedron* **1993**, *49*, 901.
[18] A. Duréault, C. Greck, J. C. Depezay, *Tetrahedron Lett.* **1986**, *27*, 4157.
[19] Y. Ittah, Y. Sasson, I. Shahak, S. Tsaroom, J. Blum, *J. Org. Chem.* **1978**, *43*, 4271.
[20] E. P. Müller, *Helv. Chim. Acta* **1982**, *65*, 1617.
[21] P. Pöchlauer, E. P. Müller, P. Peringer, *Helv. Chim. Acta* **1984**, *67*, 1238.
[22] M. J. T. Robinson, *Tetrahedron* **1974**, *30*, 1499.
[23] D. Seebach, E. Hungerbühler, *Modern Synth. Methods* **1980**, *2*, 91.
[24] D. Tanner, C. Birgersson, H. K. Dhaliwal, *Tetrahedron Lett.* **1990**, *31*, 1903.
[25] D. Tanner, C. Birgersson, *Tetrahedron Lett.* **1991**, *32*, 2533.
[26] J. R. Henry, L. R. Marcin, M. C. McIntosh, P. M. Scola, G. D. Harris, Jr., S. M. Weinreb, *Tetrahedron Lett.* **1989**, *30*, 5709.
[27] D. H. Boschelli, *Synth. Commun.* **1988**, *18*, 1391.
[28] A. K. Bose, D. P. Sahu, M. S. Manhas, *J. Org. Chem.* **1981**, *46*, 1229.
[29] J. G. Smith, *Synthesis*, **1984**, 629, and references therein.
[30] R. A. Johnson, K. B. Sharpless in *Comprehensive Organic Synthesis, Vol. 7* (Eds.: B. M. Trost, I. Fleming), Pergamon, Oxford, **1991**, p. 389.
[31] D. Tanner, P. Somfai, *Tetrahedron Lett.* **1987**, *28*, 1211.
[32] J. Legters, L. Thijs, B. Zwanenburg, *Tetrahedron Lett.* **1989**, *30*, 4881.
[33] K. Maruoka, H. Sano, H. Yamamoto, *Chem. Lett.* **1985**, 599.
[34] M. Caron, P. R. Carlier, K. B. Sharpless, *J. Org. Chem.* **1988**, *53*, 5185.
[35] T. Inghardt, T. Frejd, G. Svensson, *Tetrahedron* **1991**, *47*, 6469.
[36] M. Caron, K. B. Sharpless, *J. Org. Chem.* **1985**, *50*, 1557.
[37] M. Canas, M. Poch, X. Verdaguer, A. Moyano, M. A. Pericàs, A. Riera, *Tetrahedron Lett.* **1991**, *32*, 6931.
[38] M. Poch, X. Verdaguer, A. Moyano, M. A. Pericàs, A. Riera, *Tetrahedron Lett.* **1991**, *32*, 6935.
[39] J. M. Chong, K. B. Sharpless, *J. Org. Chem.* **1985**, *50*, 1560.
[40] S. Saito, N. Takahashi, T. Ishikawa, T. Moriwake, *Tetrahedron Lett.* **1991**, *32*, 667.
[41] G. B. Payne, *J. Org. Chem.* **1962**, *27*, 3819.
[42] H. Urabe, Y. Aoyama, F. Sato, *Tetrahedron* **1992**, *48*, 5639.
[43] R. Najime, S. Pilard, M. Vaultier, *Tetrahedron Lett.* **1992**, *33*, 5351.
[44] J. Moulines, P. Charpentier, J.-P. Bats, A. Nuhrich, A.-M. Lamidey, *Tetrahedron Lett.* **1992**, *33*, 487.
[45] A Toshimitsu, H. Abe, C. Hirosawa, S. Tanimoto, *J. Chem. Soc. Chem. Commun.* **1992**, 284.
[46] E. N. Jacobsen, W. Zhang, A. R. Muci, J. R. Ecker, L. Deng, *J. Am. Chem. Soc.* **1991**, *113*, 7063.
[47] a) K. B. Sharpless, W. Amberg, Y. L. Bennani, G. A. Crispino, J. Hartung, K.-S. Jeong, H.-L. Kwong, K. Morikawa, Z.-M. Wang, D. Xu, X.-L. Zhang, *J. Org. Chem.* **1992**, *57*, 2768; b) B. B. Lohray, *Tetrahedron Asymmetry* **1992**, *3*, 1317; c) R. A. Johnson, K. B. Sharpless in *Catalytic Asymmetric Synthesis* (Ed.: I. Ojima), VCH, New York, **1993**, p. 447.
[48] Y. Gao, K. B. Sharpless, *J. Am. Chem. Soc.* **1988**, *110*, 7538.
[49] B. B. Lohray, Y. Gao, K. B. Sharpless, *Tetrahedron Lett.* **1989**, *30*, 2623.
[50] B. B. Lohray, J. R. Ahuja, *J. Chem. Soc. Chem. Commun.* **1991**, 95.
[51] J. E. Bäckvall, K. Oshima, R. E. Palermo, K. B. Sharpless, *J. Org. Chem.* **1979**, *44*, 1953.
[52] A. Hassner, C. Heathcock, *J. Org. Chem.* **1964**, *29*, 3640.
[53] a) J.-L. Reymond, P. Vogel, *Tetrahedron Lett.* **1988**, *29*, 3695; b) P. Vogel, D. Fattori, F. Gasparini, C. Le Drian, *Synlett* **1990**, 173.
[54] J. M. J. Tronchet, M. A. M. Massoud, *Heterocycles* **1989**, *29*, 419.
[55] R. S. Atkinson, B. J. Kelly, *J. Chem. Soc. Perkin Trans. 1* **1989**, 1515.
[56] T. Sato, Y. Goto, M. Watanabe, T. Fujisawa, *Chem. Lett.* **1983**, 1533.
[57] Z. Chilmonczyk, M. Egli, C. Beringer, A. S. Dreiding, *Helv. Chim. Acta* **1989**, *72*, 1095.
[58] N. Furukawa, T. Yoshimura, M. Ohtsu, T. Akasaka, S. Oae, *Tetrahedron* **1980**, *36*, 73.
[59] R. S. Atkinson, J. Fawcett, D. R. Russell, G. Tughan, *J. Chem. Soc. Chem. Commun.* **1986**, 832.
[60] For evidence against a nitrene intermediate, see: R. S. Atksinson, B. J. Kelly, *J. Chem. Soc. Chem. Commun.* **1987**, 1362.
[61] G. V. Zhalnina, M. A. Kuznetsov, V. V. Semenovskii, G. V. Shustov, *Vestn. Leningr. Univ. Ser. 4 Fiz. Khim.* **1990**, 72 (*Chem. Abstr.* **1991**, *114*, 163892d).
[62] D. A. Evans, M. M. Faul, M. T. Bilodeau, B. A. Anderson, D. M. Barnes, *J. Am. Chem. Soc.* **1993**, *115*, 5328.
[63] R. E. Lowenthal, S. Masamune, *Tetrahedron Lett.* **1991**, *32*, 7373.
[64] Z. Li, K. R. Conser, E. N. Jacobsen, *J. Am. Chem. Soc.* **1993**, *115*, 5326.
[65] J. C. Bottaro, *J. Chem. Soc. Chem. Commun.* **1980**, 560.
[66] J. T. Groves, T. Takahashi, *J. Am. Chem. Soc.* **1983**, *105*, 2073.
[67] J.-P. Mahy, G. Bedi, P. Battioni, D. Mansuy, *J. Chem. Soc. Perkin Trans. 2*, **1988**, 1517.
[68] V. F. Rudchenko, S. M. Ignatov, R. G. Kostyanovsky, *J. Chem. Soc. Chem. Commun.* **1990**, 261.
[69] D. A. Evans, M. M. Faul, M. T. Bilodeau, *J. Org. Chem.* **1991**, *56*, 6744.
[70] E. Vedejs, H. Sano, *Tetrahedron Lett.* **1992**, *33*, 3261.
[71] J.-L. Vaerman, H. G. Viehe, *Tetrahedron* **1989**, *45*, 3183.
[72] Review: H. Kunz, K. Rück, *Angew. Chem.* **1993**, *105*, 355; *Angew. Chem. Int. Ed. Engl.* **1993**, *32*, 336.
[73] S. Drenkard, J. Ferris, A. Eschenmoser, *Helv. Chim. Acta* **1990**, *73*, 1373.
[74] A. Laurent, A. Marsura, J.-L. Pierre, *J. Heterocycl. Chem.* **1980**, *17*, 1009.
[75] C. R. Johnson, R. A. Kirchhoff, R. J. Reischer, G. F. Katekar, *J. Am. Chem. Soc.* **1973**, *95*, 4287.
[76] T. Satoh, T. Sato, T. Oohara, K. Yamakawa, *J. Org. Chem.* **1989**, *54*, 3973.
[77] G. Berti, *Top. Stereochem.* **1973**, *7*, 210.
[78] G. Cainelli, M. Panunzio, D. Giacomini, *Tetrahedron Lett.* **1991**, *32*, 121.
[79] T. Fujisawa, R. Hayakawa, M. Shimizu, *Tetrahedron Lett.* **1992**, *33*, 7903.
[80] S. Fujita, K. Imamura, H. Nozaki, *Bull. Chem. Soc. Jpn.* **1971**, *44*, 1975.
[81] K. Mori, F. Toda, *Tetrahedron: Asymmetry* **1990**, *1*, 281.
[82] For a discussion see ref. [4e].
[83] V. Schurig, U. Leyrer, *Tetrahedron: Asymmetry* **1990**, *1*, 865.
[84] J. M. Lehn, J. Wagner, *J. Chem. Soc. Chem. Commun.* **1968**, 148.
[85] a) J. B. Jones, *Tetrahedron* **1986**, *42*, 3351; b) M. Ohno, M. Otsuka, *Org. React.* **1989**, *37*, 1; c) A. M. Klibanov, *Acc. Chem. Res.* **1990**, *23*, 114.
[86] K. Fuji, T. Kawabata, Y. Kiryu, Y. Sugiura, T. Taga, Y. Miwa, *Tetrahedron Lett.* **1990**, *31*, 6663.
[87] M. Bucciarelli, A. Forni, I. Moretti, F. Prati, *Tetrahedron Asymmetry* **1990**, *1*, 5.
[88] R. L. Pederson, K. K.-C. Liu, J. F. Rutan, L. Chen, C.-H. Wong, *J. Org. Chem.* **1990**, *55*, 4897.
[89] F. Effenberger, T. Ziegler, S. Förster, *Angew. Chem.* **1987**, *99*, 491; *Angew. Chem. Int. Ed. Engl.* **1987**, *26*, 458.
[90] F. Effenberger, U. Stelzer, *Angew. Chem.* **1991**, *103*, 866; *Angew. Chem. Int. Ed. Engl.* **1991**, *30*, 873.
[91] J. A. Deyrup, R. B. Greenwald, *J. Am. Chem. Soc.* **1965**, *87*, 4538.
[92] A. F. Graefe, R. E. Meyer, *J. Am. Chem. Soc.* **1958**, *80*, 3939.
[93] M. Bucciarelli, A. Forni, I. Moretti, G. Torre, *J. Org. Chem.* **1983**, *48*, 2640.
[94] G. V. Shustov, G. K. Kadorkina, R. G. Kostyanovsky, A. Rauk, *J. Am. Chem. Soc.* **1988**, *110*, 1719.
[95] R. von Capeller, R. Griot, M. Häring, T. Wagner-Juaregg, *Helv. Chim. Acta* **1957**, *40*, 1652.
[96] A. G. Davies, R. Sutcliffe, *J. Chem. Soc. Perkin Trans. 2* **1982**, 1483.
[97] H. Handel, J. L. Pierre, *Tetrahedron* **1975**, *31*, 997.
[98] R. Bartnik, A. Laurent, S. Lesniak, *J. Chem. Res., Synop.* **1982**, 287.
[99] L. Wartski, *Bull. Soc. Chim. Fr.* **1973**, 2466.
[100] L. Antolini, M. Bucciarelli, A. Forni, I. Moretti, F. Prati, *J. Chem. Soc. Chem. Commun.* **1991**, 538.
[101] a) G. E. Ham, *J. Org. Chem.* **1964**, *29*, 3052; b) O. Mitsunobu in *Comprehensive Organic Synthesis, Vol. 7* (Eds.: B. M. Trost, I. Fleming), Pergamon, Oxford, **1991**, p. 65.
[102] See ref. [3a], p. 41.
[103] See ref. [4b], Chapter 3.
[104] T. N. Wade, *J. Org. Chem.* **1980**, *45*, 5328.
[105] Y. Girault, S. Geribaldi, M. Rouillard, M. Azzaro, *Tetrahedron* **1987**, *43*, 2485.
[106] H. Takeuchi, K. Koyama, *J. Chem. Soc. Perkin Trans. 2* **1981**, 121.
[107] H. Stamm, D. Speth, *Arch. Pharm. (Weinheim)* **1989**, *322*, 277.
[108] H. Dehmlow, J. Mulzer, C. Seilz, A. R. Strecker, A. Kohlmann, *Tetrahedron Lett.* **1992**, *33*, 3607.
[109] M. J. S. Dewar, G. P. Ford, *J. Am. Chem. Soc.* **1979**, *101*, 783.
[110] N. R. Williams, *Adv. Carbohydr. Chem. Biochem.* **1970**, *25*, 109.
[111] T. Mall, H. Stamm, *Chem. Ber.* **1988**, *121*, 1353.
[112] M. E. Duggan, D. S. Karanewsky, *Tetrahedron Lett.* **1983**, *24*, 2935.
[113] S. Matsubara, T. Kodama, K. Utimoto, *Tetrahedron Lett.* **1990**, *31*, 6379.
[114] S. Itsuno, K. Tanaka, K. Ito, *Chem. Lett.* **1986**, 1133.
[115] R. D. Guthrie, G. J. Williams, *J. Chem. Soc. Perkin Trans. 1* **1976**, 801.
[116] H. Stamm, P. Assithianakis, B. Buchholz, R. Weiss, *Tetrahedron Lett.* **1982**, *23*, 5021.
[117] P.-Y. Lin, K. Bellos, H. Stamm, A. Onistschenko, *Tetrahedron* **1992**, *48*, 2359.
[118] U. Spohr, W. Meyer zu Reckendorf, *Liebigs Ann. Chem.* **1982**, 1375.
[119] H. Hashimoto, K. Araki, K. Miyazawa, J. Yoshimura, *Carbohydr. Res.* **1982**, *99*, 59.
[120] See, for example: R. W. Herr, C. R. Johnson, *J. Am. Chem. Soc.* **1970**, *92*, 4979.
[121] A. Hassner, A. Kascheres, *Tetrahedron Lett.* **1970**, 4623.
[122] S. Wattanasin, F. G. Kathawala, *Tetrahedron Lett.* **1984**, *25*, 811.

[123] H. C. Brown, A. Tsukamoto, *J. Am. Chem. Soc.* **1961**, *83*, 4549.
[124] A. P. Kozikowski, H. Ishida, K. Isobe, *J. Org. Chem.* **1979**, *44*, 2788.
[125] M. J. Eis, B. Ganem, *Tetrahedron Lett.* **1985**, *26*, 1153.
[126] a) C. H. Behrens, K. B. Sharpless, *Aldrichim. Acta* **1983**, *16*, 67; b) C. H. Behrens, S. Y. Ko, K. B. Sharpless, F. J. Walker, *J. Org. Chem.* **1985**, *50*, 5687; c) C. H. Behrens, K. B. Sharpless, *ibid.* **1985**, *50*, 5696.
[127] D. Tanner, H. M. He, P. Somfai, *Tetrahedron* **1992**, *48*, 6069.
[128] P. Ma, V. S. Martin, S. Masamune, K. B. Sharpless, S. M. Viti, *J. Org. Chem.* **1982**, *47*, 1378.
[129] J. M. Finan, Y. Kishi, *Tetrahedron Lett.* **1982**, *23*, 2719.
[130] S. M. Viti, *Tetrahedron Lett.* **1982**, *23*, 4541.
[131] See for example: G. H. Posner, *Org. React.* **1972**, *19*, 1.
[132] B. H. Lipshutz, R. S. Wilhelm, J. A. Kozlowski, *Tetrahedron* **1984**, *40*, 5005.
[133] D. Tanner, P. Somfai, *Tetrahedron* **1987**, *43*, 4395.
[134] W. R. Roush, M. A. Adam, S. M. Peseckis, *Tetrahedron Lett.* **1983**, *24*, 1377.
[135] T. Inghardt, T. Frejd, *J. Org. Chem.* **1989**, *54*, 5539.
[136] T. Suzuki, H. Saimoto, H. Tomioka, K. Oshima, H. Nozaki, *Tetrahedron Lett.* **1982**, *23*, 3597.
[137] S. Shambayati, J. Blake, S. Wierschke, W. Jorgensen, S. Schreiber, *J. Am. Chem. Soc.* **1990**, *112*, 697.
[138] D. Tanner, H. M. He, unpublished.
[139] E. J. Corey, G. B. Jones, *J. Org. Chem.* **1992**, *57*, 1028.
[140] J. Legters, J. G. H. Willems, L. Thijs, B. Zwanenburg, *Recl. Trav. Chim. Pays-Bas* **1992**, *111*, 59.
[141] E. Kyburz, H. Els, S. Majnoni, G. Englert, C. von Planta, A. Fürst, P. A. Plattner, *Helv. Chim. Acta* **1966**, *49*, 359.
[142] B. S. Axelsson, K. J. O'Toole, P. A. Spencer, D. W. Young, *J. Chem. Soc. Chem. Commun.* **1991**, 1085.
[143] J. E. Baldwin, R. M. Adlington, N. G. Robinson, *J. Chem. Soc. Chem. Commun.* **1987**, 153.
[144] J. E. Baldwin, R. M. Adlington, I. A. O'Neil, C. Schofield, A. C. Spivey, J. B. Sweeney, *J. Chem. Soc. Chem. Commun.* **1989**, 1852.
[145] K. Sato, A. P. Kozikowski, *Tetrahedron Lett.* **1989**, *30*, 4073.
[146] T. Wakamiya, K. Shimbo, T. Shiba, K. Nakajima, M. Neya, K. Okawa, *Bull. Chem. Soc. Jpn.* **1982**, *55*, 3878.
[147] O. Ploux, M. Caruso, G. Chassaing, A. Marquet, *J. Org. Chem.* **1988**, *53*, 3154.
[148] Y. Hata, M. Watanabe, *Tetrahedron* **1987**, *43*, 3881.
[149] D. Tanner, P. Somfai, unpublished.
[150] J. E. Baldwin, M. G. Moloney, M. North, *Tetrahedron* **1989**, *45*, 6309.
[151] S. Hanessian, K. Sumi, B. Vanasse, *Synlett* **1992**, 33.
[152] a) J. P. Collman, L. S. Hegedus, J. R. Norton, R. G. Finke, *Principles and Applications of Organotransition Metal Chemistry*, University Science Books, Mill Valley, CA, **1987**; b) P. J. Harrington, *Transition Metals in Total Synthesis*, Wiley, New York, **1990**; c) F. J. McQuillin, D. G. Parker, G. R. Stephenson, *Transition Metal Organometallics for Organic Synthesis*, Cambridge University Press, Cambridge, **1991**.
[153] B. Denise, A. Parlier, H. Rudler, J. Vaissermann, J. C. Daran, *J. Chem. Soc. Chem. Commun.* **1988**, 1303.
[154] R. Aumann, K. Fröhlich, H. Ring, *Angew. Chem.* **1974**, *86*, 309; *Angew. Chem. Int. Ed. Engl.* **1974**, *13*, 275.
[155] L. E. Overman, M. J. Sharp, *J. Org. Chem.* **1992**, *57*, 1035.
[156] W. Chamchaang, A. R. Pinhas, *J. Org. Chem.* **1990**, *55*, 2943.
[157] S. Calet, F. Urso, H. Alper, *J. Am. Chem. Soc.* **1989**, *111*, 931.
[158] H. Alper, N. Hamel, *Tetrahedron Lett.* **1987**, *28*, 3237.
[159] K. Fugami, K. Miura, Y. Morizawa, K. Oshima, K. Utimoto, H. Nozaki, *Tetrahedron* **1989**, *45*, 3089.
[160] a) A. Hassner, J. Keogh, *Tetrahedron Lett.* **1975**, 1575; b) R. Chaabouni, A. Laurent, *Synthesis* **1975**, 464; c) R. E. Dolle, C.-S. Li, A. N. Shaw, *Tetrahedron Lett.* **1989**, *30*, 4723; d) Y.-L. Li, K. Luthman, U. Hacksell, *ibid.* **1992**, *33*, 4487.
[161] G. W. Spears, K. Nakanishi, Y. Ohfune, *Synlett* **1991**, 91.
[162] W. Oppolzer, E. Flaskamp, *Helv. Chim. Acta* **1977**, *60*, 204.
[163] J. Martens, M. Scheunemann, *Tetrahedron Lett.* **1991**, *32*, 1417.
[164] K. E. Harding, S. R. Burks, *J. Org. Chem.* **1984**, *49*, 40.
[165] E. J. Corey, R. D. Balanson, *Heterocycles* **1976**, *5*, 445.
[166] M. Aratani, L. V. Dunkerton, T. Fukuyama, Y. Kishi, H. Kakoi, S. Sugiura, S. Inoue, *J. Org. Chem.* **1975**, *40*, 2009.
[167] C.-K. Sha, S.-L. Ouyang, D.-Y. Hsieh, R.-C. Chang, S.-C. Chang, *J. Org. Chem.* **1986**, *51*, 1490.
[168] D. Tanner, P. Somfai, *Tetrahedron* **1986**, *42*, 5657.
[169] D. R. Williams, D. L. Brown, J. W. Benbow, *J. Am. Chem. Soc.* **1989**, *111*, 1923.
[170] T. Hudlicky, H. Luna, J. D. Price, F. Rulin, *J. Org. Chem.* **1990**, *55*, 4683.
[171] J. S. Brimacombe, R. Hanna, L. C. N. Tucker, *J. Chem. Soc. Perkin Trans. 1* **1983**, 2277.
[172] M. K. Gurjar, V. J. Patil, J. S. Yadav, A. V. Rama Rao, *Carbohydr. Res.* **1984**, *129*, 267.
[173] A. Duréault, I. Tranchepain, J.-C. Depezay, *J. Org. Chem.* **1989**, *54*, 5324.
[174] P. K. Jadhav, F. J. Woerner, *Bioorg. Med. Chem. Lett.* **1992**, *2*, 353.
[175] T. K. Chakraborty, K. K. Gangakhedkar, *Tetrahedron Lett.* **1991**, *32*, 1897.
[176] F. Carreaux, A. Duréault, J. C. Depezay, *Synlett* **1992**, 527.
[177] G. Cardillo, M. Orena, S. Sandri, C. Tomasini, *Tetrahedron* **1986**, *42*, 917.
[178] R. Huisgen, K. Matsumoto, C. H. Ross, *Heterocycles* **1981**, *15*, 1131, and references therein.
[179] S. Takano, S. Tomita, Y. Iwabuchi, K. Ogasawara, *Heterocycles* **1989**, *29*, 1473.
[180] D. Tanner, P. Somfai, *Tetrahedron* **1988**, *44*, 619.
[181] D. Tanner, H. M. He, *Tetrahedron* **1992**, *48*, 6079.
[182] D. Tanner, P. Somfai, *Tetrahedron* **1988**, *44*, 613.
[183] D. Tanner, P. Somfai, *Bioorg. Med. Chem. Lett.*, **1993**, *3*, 2415.
[184] J. Legters, L. Thijs, B. Zwanenburg, *Tetrahedron* **1991**, *47*, 5287.
[185] Review: W. A. Remers, B. S. Iyengar in *Recent Progress in the Chemical Synthesis of Antibiotics* (Eds.: G. Lukacs, M. Ohno), Springer, Berlin, **1990**, p. 415.
[186] T. Fukuyama, F. Nakatsubo, A. J. Cocuzza, Y. Kishi, *Tetrahedron Lett.* **1977**, 4295.
[187] T. Fukuyama, L. Xu, S. Goto, *J. Am. Chem. Soc.* **1992**, *114*, 383.
[188] R. J. Jones, H. Rapoport, *J. Org. Chem.* **1990**, *55*, 1144.
[189] R. S. Coleman, A. J. Carpenter, *J. Org. Chem.* **1992**, *57*, 5813.
[190] D. Tanner, C. Birgersson, unpublished.
[191] D. A. Evans, J. V. Nelson, T. R. Taber, *Top. Stereochem.* **1982**, *13*, 1.
[192] a) V. G. Matassa, P. R. Jenkins, A. Kumin, L. Damm, J. Schreiber, D. Felix, E. Zass, A. Eschenmoser, *Isr. J. Chem.* **1989**, *29*, 321; b) W. Oppolzer, G. Poli, C. Starkemann, G. Bernardinelli, *Tetrahedron Lett.* **1988**, *29*, 3559; c) T. Laube, J. D. Dunitz, D. Seebach, *Helv. Chim. Acta* **1985**, *68*, 1373; d) D. Seebach, *Angew. Chem.* **1988**, *100*, 1685; *Angew. Chem. Int. Ed. Engl.* **1988**, *27*, 1624.
[193] J. K. Whitesell, *Chem. Rev.* **1989**, *89*, 1581.
[194] a) See ref. [123]; b) D. A. Evans, T. C. Britton, J. A. Ellman, *Tetrahedron Lett.* **1987**, *28*, 6141.
[195] D. Seebach, R. Häner, *Chem. Lett.* **1987**, 49.
[196] V. Reutrakul, V. Prapansiri, C. Panyachotipun, *Tetrahedron Lett.* **1984**, *25*, 1949.
[197] R. Häner, B. Olano, D. Seebach, *Helv. Chim. Acta* **1987**, *70*, 1676.
[198] P. Coutrot, A. Elgadi, C. Grison, *Heterocycles* **1989**, *28*, 1179.
[199] R. S. Atkinson, B. J. Kelly, *Tetrahedron Lett.* **1989**, *30*, 2703.
[200] E. Vedejs, W. O. Moss, *J. Am. Chem. Soc.* **1993**, *115*, 1607.
[201] For similar work on lithiated epoxides: P. Lohse, H. Loner, P. Acklin, F. Sternfeld, A. Pfaltz, *Tetrahedron Lett.* **1991**, *32*, 615.
[202] J. F. Dellaria, Jr., K. J. Sallin, *Tetrahedron Lett.* **1990**, *31*, 2661.
[203] J. Almena, F. Foubelo, M. Yus, *Tetrahedron Lett.* **1993**, *34*, 1649.
[204] See, for example: E. J. Corey, R. K. Bakshi, S. Shibata, *J. Am. Chem. Soc.* **1987**, *109*, 5551.
[205] K. Saito, S. Saijo, K. Kotera, T. Date, *Chem. Pharm. Bull.* **1985**, *33*, 1342.
[206] S. Jugé, J. P. Genêt, *Tetrahedron Lett.* **1989**, *30*, 2783.
[207] R. Schwesinger, K. Piontek, W. Littke, H. Prinzbach, *Angew. Chem.* **1985**, *97*, 344; *Angew. Chem. Int. Ed. Engl.* **1985**, *24*, 318.
[208] D. Tanner, P. Somfai, A. Harden, unpublished.

Theoretical Definition of a Functional Group and the Molecular Orbital Paradigm

Richard Frederick William Bader,* Paul Lode Albert Popelier, and Todd Alan Keith

It is the purpose of this review to demonstrate that the empirical classification of the observations of chemistry in terms of the properties assigned to functional groups is a consequence of and is predicted by physics. This is accomplished by showing that the atoms and functional groups of chemistry can be identified with bounded space-filling objects whose properties are defined by quantum mechanics. The quantum mechanical definition of a group is combined with a new pictorial representation of its form to obtain a unified picture which should make it eminently recognizable to chemists. This picture, when combined with the demonstrated ability of these groups to recover the measured properties of atoms in molecules, is offered as one which meets the expectations a chemist associates with the concept of a functional group. The manner in which this physical definition of a group differs fundamentally from models of functional groups based upon molecular orbital theory is discussed.

1. Introduction

1.1. Does Chemistry Have a Basis in Physics?

It is reasonable to ask why it has taken considerable time to arrive at a possible quantum mechanical definition of a functional group, and why there has evolved instead a prevailing opinion that this fundamental operational concept of chemistry, while unquestionably useful, would find no firm basis in physics. First, it has taken a reformulation of physics, as afforded by the work of Feynman[1] and Schwinger,[2] to provide us with the necessary quantum mechanical framework for asking the question "are there atoms in molecules?" Second, as so eloquently expressed and illustrated by Kuhn[3] with examples from all branches of science, is the phenomenon of the resistance accorded a new theory because of the conceptual bias exerted by existing paradigms. The paradigm of molecular orbital theory effectively filters out the hope of establishing a quantum mechanical basis for functional groups.

This review summarizes the evidence in favor of the identification of quantum subsystems with the functional groups of chemistry. Quantum subsystems are defined as regions of real space. A new pictorial representation of a quantum subsystem is presented to complement the demonstration of their equality with a chemist's mental and physical model of a group. This summary is prefaced with a discussion of why molecular orbital theory, whose components are rooted in the mathematical Hilbert space, appears to be at variance with this identification. It is shown that this conflict is a result of insisting that all chemical concepts be cast in the orbital mold, thereby requiring that the orbital model be applied beyond its intended scope.

[*] Prof. R. F. W. Bader, Dr. P. L. A. Popelier, T. A. Keith
Department of Chemistry, McMaster University
Hamilton, Ontario, L8S 4M1 (Canada)
Telefax: Int. code + (905)522-2509

1.2. Classification as a Definition of Science

A scientific discipline begins with the empirical classification of observations. It becomes exact in a predictive sense, when these observations are classified in such a way as to reflect the physics governing its behavior. In this limiting situation, prediction and classification are synonymous and the classification is based upon what physics predicts can be observed. This situation is exemplified in quantum mechanics by the classification of a given state in terms of the eigenvalues of the maximal commuting set of observables which constitute the measurable properties specific to that state.[4] In this sense, science is classification.

1.3. Classification in Chemistry

The observations of chemistry are classified empirically in terms of the properties exhibited by functional groups. In chemistry we recognize the presence of a group in a given system and predict its effect upon the static and dynamic properties of the system in terms of the characteristic set of properties assigned to that group. The functional group is the central concept in the working hypothesis of chemistry, the molecular structure hypothesis. According to this hypothesis, which rests upon the accumulated observations of experimental chemistry, the properties of matter are a consequence of the atoms it contains and of the network of bonds that link them. It is the purpose of this

 © VCH Verlagsgesellschaft mbH, D-69451 Weinheim, 1994 0570-0833/94/0606-0620 $ 10.00+.25/0 Angew. Chem. Int. Ed. Engl. 1994, 33, 620-631

article to demonstrate that the classification based upon the properties of functional groups is a consequence of and is predicted by physics, and that the classification is therefore, fundamental.[5]

2. The Molecular Orbital Paradigm

The molecular orbital point of view and its associated paradigm that is used to argue against the possibility of establishing a physical basis for functional groups, is illustrated by a quotation from a paper by Libit and Hoffmann.[6] It follows a paragraph in which they stress that it is the logic of substituent effects that has made possible the great strides in synthetic and mechanistic organic and inorganic chemistry: "Nothing like this logic comes out of molecular orbital calculations. Every molecule is treated as a whole and no set of transferable properties associated with a functional group emerges." This statement appears as true or false depending upon the role one assigns to the molecular orbitals (MOs) used in the calculation. If the orbitals are used not only to calculate the state function, but are in addition used in the search for properties to be assigned to an individual atom or group which forms a part of the real space of the molecule, the statement is true, since the orbitals, like the state function they are used to approximate, are necessarily delocalized over the whole system. If, however, the role of the molecular orbitals is confined to the determination of the state function and the electronic structure of the system, the statement is false. A state function contains the necessary information for the exhaustive partitioning of the real space of a molecule into separate regions whose properties reflect the very transferability associated with functional groups.[5, 7] It is the demonstration of this fact that will relieve chemists of the dilemma of having to contend with the coexistence in their minds of two apparently mutually exclusive models: one experimentally based, which provides the framework for the ordering of their observations and another, mathematically based, which when improperly applied, suggests that this framework has no basis in theory.

2.1. Molecular Orbital Theory as a Model of Electronic Structure

Mulliken[8] and Hund[9] developed molecular orbital theory to obtain a classification and understanding of band spectra. Molecular orbitals provide the basis for a model of the electronic structure of molecules. The molecular orbital model provides an excellent example of a classification scheme which parallels the predictions of theory. This model, when applied to the oxygen diatomic molecule for example, enables one to predict without the necessity of calculation that this sixteen-electron system will possess a ground state of $^3\Sigma_g^-$ symmetry followed by $^1\Delta_g$ and $^1\Sigma_g^+$ excited states. This classification is precisely what quantum mechanics predicts can be observed experimentally, the spin and orbital angular momentum operators, along with the symmetry operations, forming a maximal commuting set with the Hamiltonian operator.[10]

The use of orbital theory for the calculation of approximate state functions was initiated by Hartree[11] who introduced the concept of the self-consistent field (SCF) in the numerical determination of atomic orbitals. The incorporation of exchange was accomplished by Fock[12] and by Slater,[13] the latter through the specific variation of the spin orbitals in a determinantal wave function. The possibility of applying the Hartree–Fock method to the calculation of molecular orbitals was accomplished by Roothaan[14] and Hall,[15] by showing how the orbitals could be expanded in a set of basis functions. Their work and its extension by others, has made it practicable to calculate state functions for molecules to any desired degree of accuracy within the extended framework of orbital theory.

Molecular orbitals are used for purposes other than as a basis for the classification and calculation of electronic states. The orbitals themselves can be classified as bonding or antibonding, a classification which correlates with observed changes in bond lengths and dissociation energies of new states generated by changes in occupation of a particular orbital.[16] Because of their delocalized nature, there was an original reluctance on the part of chemists to embrace the molecular orbital model and use it in place of the valence bond approach which provided a quantum mechanical basis for the Lewis model of the electron pair and its directed properties.[17, 18] This reluctance was overcome in part by the introduction of equivalent orbitals by Lennard-Jones[19] and their subsequent evolution into localized orbitals. Lennard-Jones emphasized that any unitary transformation amongst a set of orbitals leaves all properties, including the total charge density, unchanged and that such transformations must be interpreted with caution.[20]

Wigner and Witmer introduced the use of group theory into chemistry in 1928 by deriving a set of rules for determining what types of states for diatomic molecules result from given states



Dr. Richard F. W. Bader was born in Kitchener, Ontario in 1931. He received his B.Sc. and M.Sc. from McMaster University and his Ph.D. in 1957 from the Massachusetts Institute of Technology (MIT) working with Professor C. G. Swain. He did post doctoral work at MIT from 1957 to 1958 and at Cambridge University from 1958 to 1959 in the Laboratory of Professor H. C. Longuet-Higgins. He began his scientific career as a physical organic chemist. He was at the University of Ottawa from 1960 to 1963 and then moved to McMaster University, where he remains today. His research interests are centered on the continued development of the theory of atoms in molecules and its application to chemistry.

of the separate atoms.[21] The first symmetry rule for molecular reactions appeared in 1962.[22] It predicts the reaction coordinate in terms of the symmetry of the transition density obtained by mixing in the first excited electronic state in a second-order perturbation expansion of the energy, expressed in terms of the nuclear displacements. This model likens the instability of a system for motion along a reaction coordinate to a pseudo Jahn–Teller effect. It is the nature of the first excited state of proper symmetry which determines the course of a chemical reaction.[22] Molecular orbital theory in combination with group theory is indispensable in predicting the ordering and symmetries of electronic states, as first demonstrated by Mulliken,[23] and the transition density itself can be usefully approximated in terms of the product of relevant orbitals which in many cases corresponds to the HOMO–LUMO product. In this manner the symmetry rule justifies the assumptions of frontier molecular orbital theory.[24] The same phase information of molecular orbitals provides the basis for the success of the concept of the conservation of orbital or state symmetry in the prediction of the course of a chemical reaction.[25] In these and other related approaches to reactivity and discussions of bonding, the orbitals are properly used in their capacity to provide information regarding the electronic structure of a system.

2.2. Looking for Atoms in Molecular Orbitals

A significant breach of the model occurs when physical significance is ascribed to particular choices of nuclear-centered basis functions used in the expansion of the molecular orbitals. An orbital describes the motion of a single electron in the field of all the nuclei and in the self-consistently determined average field of the remaining electrons. It is obtained by solving a set of coupled integral–differential equations whose solutions for an atom are called atomic orbitals and for a molecule, molecular orbitals.[26] The solutions to these equations are independent of the method used to obtain them, whether it be numerical or expressed in terms of an expansion.

The acronym LCAO-MO (linear combination of atomic orbitals for molecular orbitals) grew naturally out of early attempts to gain some understanding of the form of an MO in terms of its correlated one-electron states at infinite separation,[26] an idea first introduced by Lennard-Jones in 1929.[27] The pioneer workers, however, very much appreciated that this manner of representing a molecular orbital was meant to provide no more than a crude model of its form and that it did not imply the presence of an atomic component in a molecular orbital. Mulliken described how atomic orbitals (AOs) to be used as basis functions in the expansion of a molecular orbital, should be suitably modified for the molecule and not identified with the atomic case. He then continued with the statement,[28] "However, it should be kept in mind that the concept of an SCF MO is an independent one, and thus the use of a linear combination of AO's or STO's (Slater type orbitals) as building blocks to construct an MO is merely a convenience." In this same paper Mulliken presents an explanation as to why no physical significance should be ascribed to an atomic population based on an LCAO expansion. This acronym, for the sake of clarity of thought, should be changed to LCBF (linear combination of basis functions). In a later paper[29] Mulliken et al. completely disowned the concept of a population analysis upon the demonstration that it bore no relation to the form of the total charge distribution, as evidenced by the statement "It should be possible to avoid such inconsistent and unsatisfactory results by computing atomic charges directly from the molecular charge distribution." It is more than a question of semantics to understand that basis functions are not atomic orbitals. There are no atomic orbitals in a molecule, nor is there any overlap of atomic components.

It is perhaps asking too much of some that they give up the notion that a molecular orbital is a linear combination of atomic orbitals and indeed it is not necessary that they do so. It is only necessary that they not insist that the only chemical concepts capable of definition are those which survive the filtering through the successive levels of approximation within the molecular orbital model, as outlined above. The delocalized nature of molecular orbitals and of the basis functions employed in their expansion, which are associated with truncated portions of the mathematical Hilbert space, should not be used to exclude the possibility of identifying atoms or functional groups with bounded regions of real space. There is no question concerning the possibility of obtaining a quantum mechanical definition of uniquely defined regions of real space.[5, 30] The answer to the question of whether or not these regions correspond to the atoms of chemistry should not to be prejudiced by any existing orbital-based paradigm, but rather be determined solely by comparison of their predicted properties with the observed properties of matter.

3. Observational Constraints on the Definition of a Functional Group

Before proceeding with the quantum mechanical development, it is imperative to state what are the essential requirements imposed upon the definition of an atom in a molecule by the observations of chemistry. The first stems from the necessity that two identical pieces of matter exhibit identical properties. Since the form of matter is determined by the distribution of charge throughout real space, two objects are identical only if they possess identical charge distributions. This parallelism of properties with form exists not only at the macroscopic level, but as originally postulated by Dalton, is assumed to exist at the atomic level as well. It demands that an atom be a function of its form in real space, requiring that it be defined in terms of the charge distribution. It follows that if an atom exhibits the same form in the real space of two systems, or at two different sites within a crystal, it contributes identical amounts to the total value of every property in each case. This requirement demands in turn that the atomic contributions sum to yield the total value for the system, that is, the atomic contributions to a property must be additive. Only atoms meeting these two requirements can account for the observation of so-called additivity schemes wherein the atomic properties appear to be transferable as well as additive. Finally, the boundary defining an atom or functional group must be such as to maximally preserve its form and thereby maximize the transfer of chemical information from one system to another.

These are the there requirements that must be satisfied if one is to predict that atoms and functional groupings of atoms contribute characteristic and measurable sets of properties to every system in which they occur. It is because of the direct relationship between the spatial form of a group and its properties that we are able to identify it in different systems. Since the purpose of quantum mechanics is to predict the measurable properties of a system, it is reasonable to suppose that these observational constraints will be met by the quantum definition of an atom.

4. From Dirac's Theory to the Theory of Atoms in Molecules

Our goal here is not to review the mathematical foundation of the theory of a quantum subsystem. This has been done previously in a number of references.[5, 31] Here we wish to concentrate on its underlying ideas. We preface this discussion with a brief synopsis of this discussion for readers who wish to proceed directly to Section 4.3. Central to the new approach to physics developed by Feynman[1] and Schwinger[2] is the principle of least action, the idea that there exists a quantity called the action whose minimization yields the equation describing the motion of a system. The action itself is a quantity which is determined by the evolution in time of a system in real space and it thus defines a space–time volume. Schwinger showed how one can obtain all the laws of physics by extremizing this space–time volume in a general way. If one desires a definition of an atom based on physics, the atom must generate its own space–time volume and its boundaries must therefore, be defined in real space. This is the reasoning underlying the basic tenet of the theory of atoms in molecules, which is that atoms be defined as pieces of real space.[5]

4.1. From Dirac's to Schwinger's Theory

The historical development of the ideas that led to Schwinger's formulation of physics began with Dirac. Dirac demonstrated the equivalence of Schrödinger's wave mechanics and Heisenberg's matrix mechanics, both of which are firmly rooted in classical Hamiltonian dynamics.[32] Dirac's work went beyond this demonstration of equivalence, and in particular he introduced the theory of unitary transformations to parallel the canonical transformations of classical theory. Unitary or canonical transformations enable one to obtain equivalent descriptions of a system by passing from one representation to another.

In 1933, in what was to be a paper of singular importance,[33] Dirac posed and answered the question of what would correspond in the quantum theory to the Lagrangian method of classical mechanics and its associated action integral, a formulation of mechanics he considered to be more fundamental than that based on Hamiltonian theory. The answer to this question is provided by the so-called multiplicative law. This law provides the possibility of expressing a probability amplitude connecting two states as a product of contributions connecting intermediate states. As a consequence of this theorem, the associated action can be expressed as a sum of corresponding contributions. It is upon these ideas that both Feynman[1] and Schwinger[2] based their new formulations of quantum mechanics.[34a] These approaches are equivalent in that Schwinger's "fundamental dynamical principle" is a differential statement of Feynman's "path integral", but Schwinger's approach is specifically formulated to enable one to ask new questions of physics. It is this aspect of Schwinger's work that is not fully appreciated. One cannot find atoms in pre-Schwinger quantum mechanics. If one tries, one is simply led to his formulation.

4.2. From Schwinger's Theory to the Theory of Atoms in Molecules

Central to the Lagrangian approach is the principle of least action described above. Within quantum mechanics, the extremization of the action can be accomplished by varying the state function in the action integral. In extending the principle to a subsystem of a total system, one must necessarily retain these variations on the surface of the subsystem. But, retaining the variations on the boundary of the system is the very step which Schwinger purposefully makes in his generalization of the action principle. He does this to introduce Dirac's transformation theory, a step he accomplishes by identifying the variations with the generators of unitary transformations. Such generators describe all possible transformations, and hence all physical changes a system can possibly undergo. With their introduction, Schwinger generalizes the action principle to obtain quantum mechanics from a single dynamical principle.[34b] In particular, the extended action principle defines the observables of quantum mechanics, their equations of motion and their expectation values, in addition to the commutation relations. These are precisely the properties which must be established and defined for a subsystem if one wishes to obtain a quantum prescription for an atom in a molecule.

The possibility of defining the action for a subsystem is a consequence of its fundamental additive nature. The variation of the action for a subsystem leads one down the same road traversed by Schwinger, but one does not arrive at the same destination and recover his principle unless the subsystem satisfies a particular boundary condition. This condition is imposed as a constraint on the variation of the action and it requires that the subsystem be bounded by a surface through which there is a zero flux in the gradient vector field of the electron density $\varrho(\boldsymbol{r})$ [Eq. (a)], where $\boldsymbol{n}$ is the unit vector normal to the surface.

$$\nabla\varrho(\boldsymbol{r}) \cdot \boldsymbol{n}(\boldsymbol{r}) = 0 \text{ at every point on the surface} \qquad \text{(a)}$$

Because the boundary condition is stated in terms of the electron density, a quantum subsystem is defined in real space, as it must be if its properties are to be defined as quantum mechanical expectation values. Indeed there is no such thing as an isolated system, and all systems are subsystems with varying degrees of interaction through their shared zero-flux surfaces.

4.3. Defining a Group by Applying the Quantum Boundary Condition

The application of the boundary condition defining a quantum subsystem, the zero-flux requirement in Equation (a), leads to a disjoint partitioning of the space of a molecule into a set of atomic basins.[5, 35] This is a consequence of the principal topological property exhibited by the electron density; that is, it exhibits local maxima at the positions of the nuclei. A nucleus thus serves as an attractor in the $\nabla\varrho$ field, and the region of space traversed by the trajectories of $\nabla\varrho$ that terminate at a nuclear maximum defines the basin of the atom. The basin is necessarily bounded by a zero-flux surface.[5, 35]

A representation of a group as a space-filling object with zero-flux surfaces separating it from the remainder of the molecule, is shown in Figures 1a and 1b. The group is the central

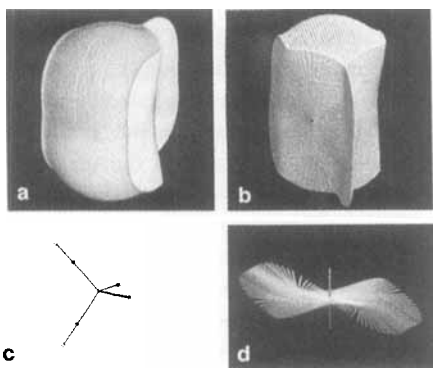


Fig. 1. A view of the transferable methylene group of the hydrocarbons with a) the van der Waals surface of the two hydrogen atoms, and b) the two C|C surfaces displayed in the foreground. The bond critical point is denoted by a dot for one C|C surface. c) The portion of the molecular graph that defines the methylene group up to the two bond critical points (denoted by dots) in the C|C interatomic surfaces. d) A display of the individual trajectories of $\nabla\varrho$ which terminate at a bond critical point and define a C|C interatomic surface. Also illustrated is the unique pair of trajectories which originate at the critical point and define the bond path. The shape of this surface is characteristic of surfaces between saturated carbon atoms, including that found in the diamond lattice.

methylene in pentane. It is obtained by separating the basins of the two neighboring carbon atoms in the hydrocarbon chain at their common interatomic surfaces. The group is represented symbolically by $|C(H_2)|$, the vertical bars denoting the C|C interatomic surfaces, and graphically (see Fig. 1a, b) by showing the two interatomic surfaces and their intersection with a surface on which the electron density attains a prescribed value, in this case 0.001 au. This envelope of electron density determines the van der Waals shape of the group[36] and is used to replace those portions of the atomic surfaces which occur infinitely far from the nuclei.

Illustrated in Figure 1d is the manner in which a C|C interatomic surface is defined by the set of trajectories of $\nabla\varrho$ which terminate at a bond or (3,−1) critical point of the electron density (a point where $\nabla\varrho = 0$), as well as the unique pair of trajectories which originate at this point and terminate at each of the neighboring nuclei. They define the bond path, the line of maximum charge density linking the carbon nucleus to its bonded C neighbors. The network of bond paths determines the molecular graph which in turn defines the molecular structure.[5, 35] That portion of the molecular graph which defines the methylene group up to its interatomic surfaces is shown in Figure 1c. In agreement with the chemical definition, a functional group is a linked set of atoms, bounded by a zero-flux surface.

Aside from the interatomic surfaces being curved rather than flat, this representation of the methylene group is similar in all respects to the space-filling models of atoms that chemists link together to represent a group or molecule. The boundaries between the atoms in the van der Waals envelope defined by the electron density are in general, less pronounced than when they are approximated by using van der Waals atomic spheres.[36] A group identical to that in Figure 1, bound only to other methylenes, is found in all *n*-hydrocarbons following and including pentane. In terms to its spatial representation and its other properties, it fulfills the chemist's expectations of the transferable methylene group of the hydrocarbons; it possesses a zero net charge, as it must if it is to be the repeating building block of the *n*-hydrocarbons. It makes a constant contribution to the molar volume as anticipated by the experiments of Kopp in 1855. Its energy equals the energy increment between successive pairs of hydrocarbons in agreement with the heats of formation of the hydrocarbons measured by Rossini et al.[37] Its polarizability and magnetic susceptibility reproduce the measured values of these field-induced properties for the methylene group.[38, 39]

This group serves as an example of the groups that are defined by theory and demonstrates their ability to reproduce the quantitative as well as the qualitative properties of the groups of chemistry. The classification and identification of a group in terms of its properties is the central idea in the application of quantum mechanics to the study of functional groups. Thus, the quantum mechanical concepts underlying the definition of the measurable properties of a system deserve careful consideration.

5. Definition of Group Properties

5.1. Observables and Expectation Values

Associated with every measurable property of a system is a linear Hermitian operator, an observable. An oft repeated statement concerns the impossibility of defining an atom or its properties, an atomic population for example, because they are not "quantum observables".[40] Part of the problem with such statements arises from their misuse of the language of quantum mechanics, and one again turns to Dirac for a clear statement of the principles involved. Dirac defines an *observable* to be a real dynamical variable, that is, a linear Hermitian operator, whose eigenstates form a complete set.[32] The *measurable* value of a property is one of the eigenvalues of the corresponding observable, an expectation value being the average value obtained by repeated measurement.[32]

Properly stated, the electron density is the measurable *expectation value* of the density operator, a quantum mechanical *observable*.[41] Thus an atom is defined in terms of the expectation value of a quantum observable. To state, as some do, that "an atom or its population is not a quantum observable" is to say

that neither is a linear Hermitian operator, which while true, is not a meaningful statement. The quantum boundary condition defining an atom [Eq. (a)] can be stated in terms of the density operator and thus an atom can be defined directly in terms of the action of a quantum observable.[30] Similarly, an electron population is defined as the expectation value of the number operator, the integral form of the density operator, and again a quantum observable.[41] It will yield an atomic population if one can obtain a quantum definition of its expectation value for atoms in molecules.

5.2. Atomic Expectation Values

As discussed above, Schwinger's formulation of quantum mechanics[2] does indeed enable one to define expectation values for a subsystem which satisfies the boundary conditions [Eq. (a)]. The required statement obtained from the generalized variation of the action integral is given in Equation (b).[5, 30, 31] In this equation the symbol $\mathscr{L}[\Psi,\Omega,t]$ denotes the Lagrange integral for a system Ω bounded by a zero-flux surface, the quantity whose integral over time yields the action. The Hamiltonian operator is denoted by $\hat{H}$, and $\hat{G}$ denotes any quantum observable. The important point to note about Equation (b) is that the commutator $[\hat{H},\hat{G}]$, when multiplied by i/h, gives the time rate-of-change of $\hat{G}$, the Heisenberg equation of motion. Thus, Equation (b) is a variational derivation of the equation of motion for the average value of an observable.

$$\delta\mathscr{L}[\Psi,\Omega,t] = (\varepsilon/2)\{i/h)\langle\Psi|[\hat{H},\hat{G}]|\Psi\rangle_\Omega + \text{complex conjugate}\} \quad \text{(b)}$$

The equation applies to any region of space bounded by a surface of zero-flux in the gradient vector field of ϱ [Eq. (a)]. It applies equally to the total system and to every atom within the system. Thus an atomic expectation value is defined on an equal footing with the expectation value of the same property for the total system. An important consequence of the averaging implied in Equation (b) is that the expectation value of any observable $\hat{M}$ for the total system is given by the sum of the corresponding atomic values $M(\Omega$ [Eq. (c)].

$$\langle\hat{M}\rangle = \sum_{\Omega} M(\Omega) \quad \text{(c)}$$

6. Atomic Theorems

6.1. Atomic Populations

Setting the observable $\hat{G}$ in Equation (b) equal to the number operator yields not only a definition of an atomic population, as the integral of the electron density over the atomic basin, but also an equation for its time rate-of-change, the integrated equation of continuity.[5, 41] It is a general result that a single variation principle [Eq. (b)] defines an observable's expectation value and yields a theorem governing its behavior, for both the total system and for its constituent atoms.[5, 42]

6.2. Atomic Force Theorem

The time rate-of-change of the momentum is force, and setting the generator $\hat{G}$ equal to $\hat{p}$, the momentum operator for an electron, yields the atomic force theorem. This is the Ehrenfest force,[43] the average force exerted on the electron density. In a stationary state this theorem establishes that the force acting on an atomic basin is determined by the flux in the force through its atomic surface, and is equal and opposite to that exerted by its bonded neighbors. Thus an atom and its properties respond only to changes in the total Ehrenfest force acting on each element of its surface, and hence only to changes in its surface. By preserving the interatomic surface characteristic of a given interaction, the properties of the group are preserved whether or not the bonded neighbor is considered to be present.

Using this property it is not necessary to "cap" a group when only a fragment of a larger system is to be studied, as exemplified by the isolation of the single peptide group from a polypeptide shown in Figure 2b. The alanyl group is obtained by separating the basins of neighboring N and C atoms at their common interatomic surfaces in the two amide bonds which link the group to a polypeptide chain. The alanyl group, like the other peptide groups investigated so far, possesses a zero net charge,[44, 45] and a peptide unit can serve as a building block of a polypeptide chain. The C|N interatomic surface of the amide bond undergoes only minor change, primarily in its outer reaches far from the bond critical point, as the substituent R is changed and different peptide units can be linked together to form a polypeptide with only minor modifications in their form and properties.[44, 45]

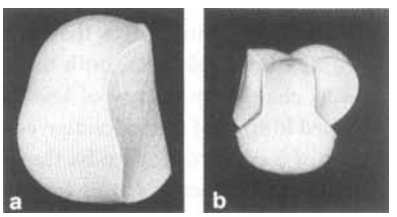


Fig. 2. a) A representation of the transferable methyl group of saturated hydrocarbons with its single interatomic surface. This group and its properties is found in all *n*-hydrocarbons following and including propane. b) A representation of the alanyl group, |NHCHRC(=O)|. R = CH_3. The -C(=O)| surface is on the right, the -HN| surface on the left, and the CHR group is in the foreground with the methyl group pointing down. Figure 2b is drawn to half scale relative to Figure 2a.

The sensitivity of an interatomic surface to changes in neighboring atomic basins acts as probe for spatially isolating changes within a system. Thus a rotation about the C–N bond of formamide causes only minor changes to the C|O and C|H surfaces, but results in a substantial shift in the C|N surface towards the N nucleus. As anticipated on the basis of these findings, the properties of the carbonyl oxygen and hydrogen atoms, their charges, energies, and associated bond lengths, are largely unaffected by the rotation, the major changes occurring within the basins of the C and N atoms and primarily in the region of their interatomic surface.[46]

6.3. Atomic Virial Theorem

Setting the generator equal to the operator $\hat{r} \cdot \hat{p}$, where $\hat{r}$ is an electronic position coordinate, yields the atomic statement of the virial theorem. Since this generator has the dimensions of action, its time derivative is energy. Thus this theorem defines the atomic averages of the electronic kinetic and potential energies. The potential energy, which is determined by the interactions between all the particles in a system, is defined to be the virial of the Ehrenfest force, a local property. Thus the total energy, like all properties, is given by a sum of atomic contributions.

An atomic energy exhibits the necessary property of being as transferable as is the electron density itself. As discussed above, when the physical form of any object, including an atom, is the same in two situations, observation requires that all of its properties, including its energy, must remain unchanged.[47] This requirement is fulfilled by the energies of the transferable methyl and methylene groups depicted in Figures 1 and 2a.[48–51] While there is no known functional relation between the electron density and the total energy, the properties of the quantum atom speak for its existence and ultimate discovery. The total energies of the methyl and methylene groups are in the tens of thousands of $kJ\,mol^{-1}$, yet they are transferable amongst the *n*-hydrocarbon molecules, both theoretically and experimentally, with changes in energy of less than four $kJ\,mol^{-1}$. This is observed in spite of the individual contributions to the potential energy of a group changing by thousands of $kJ\,mol^{-1}$ between succeeding members of the homologous series. The glycyl group, with an energy of approximately 524000 $kJ\,mol^{-1}$, can be transferred from formylglycylamine to triglycyl with a change of only $24\,kJ\,mol^{-1}$.[45]

By reason of their definition in terms of the zero-flux surface[5] and by demonstration,[7, 36, 44, 45, 48–51] the atoms and groups of theory are the most transferable pieces of a system definable in an exhaustive partitioning of real space. If perturbations are relatively small, groups respond so as to minimize the total change resulting from their interaction. Thus, the methyl group of ethane necessarily withdraws a small amount of electronic charge from the methylene group when transferred to propane, but not only is charge conserved, so is the energy. The energy lost by the methylene group equals the energy gained by each methyl group, and a similar conservation of charge and energy occurs for methylene groups bonded to a single methyl group in succeeding members of the homologous series. Thus additivity of energy is preserved in spite of the methyl group in ethane necessarily being unique.[48–51]

6.4. Atomic Current Theorem

The time rate-of-change of position is velocity and setting the generator in Equation (b) equal to $\hat{r}$ yields the theorem governing the average velocity of the electrons in the basin of an atom. In the presence of a constant uniform applied magnetic field, this velocity corresponds to the average of the electronic current induced over the basin of the atom. Equation (b) shows this atomic average of the electronic velocity to be equal to the flux in the position-weighted current through the surface of the atom.[42] The contribution of this flux to the mean atomic magnetic susceptibility $\bar{\chi}(\Omega)$, becomes vanishingly small when the current flow, like the charge density, is localized within the atomic basins, as illustrated for the ionic system LiH in Figure 3a. It becomes appreciable and comparable in magnitude to the basin contribution to $\bar{\chi}(\Omega)$ in systems with shared atomic interactions, as found in methane (Fig. 3b). The flux in the current flow across the interatomic surfaces for a linked ring of atoms dominates $\bar{\chi}$ in molecules such as benzene.[52, 53] Equation (b) also demonstrates that in a steady magnetic field there is local conservation of the current over each atomic basin.

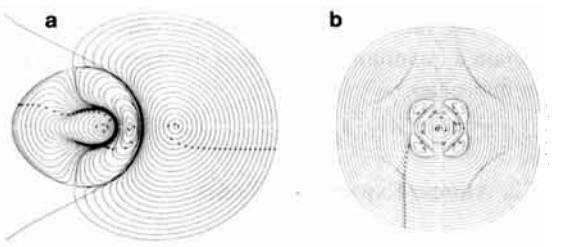


Fig. 3. a) The current density induced by an externally applied magnetic field for a symmetry plane containing the nuclei in LiH; the Li nucleus is on the left. The direction of flow within a current loop, for a field applied perpendicular to and into the plane, is indicated by an arrow. The positively charged Li atom has both diamagnetic and paramagnetic currents induced in its basin, the paramagnetic loops being isolated from the diamagnetic flow in the basin of the negatively charged H atom by the interatomic surface. This localized atomic behavior of the current flows and the presence of a paramagnetic component in the basin of the electropositive atom is typical of molecules with closed-shell (ionic) or intermediate (polar) interactions [5] and reflects the corresponding localization of the electron density. b) The current flow in an alternating plane of symmetry containing the carbon nucleus in the methane molecule, showing the intersection of the C|H interatomic surfaces. In this molecule with shared (covalent) atomic interactions [5] there is a substantial flow of current across the interatomic surfaces.

The electronic current density and its derived properties induced by a magnetic field for an atom in a molecule exhibit the same degree of transferability as does the charge density itself. Thus the methyl and methylene groups of Figures 1a, b and 2a contribute constant amounts to the magnetic susceptibilities of the members of the homologous series of hydrocarbons, confirming Pascal's values[39] for the group susceptibilities.[53] The same constancy in group contributions is found for the mean polarizability when the molecules are in the presence of an applied electric field.[50] Thus even in the presence of external fields, the atoms of theory behave as required by observation; their field-induced properties reflecting the form of the atom in the field-free case.

6.5. Atoms in Crystals

The idea of individual atoms being the source of the scattering of X-rays in a crystal dates back to Laue and Bragg.[54] A carbon atom in the face-centered cubic structure of diamond is shown in Figure 4.[55] It is completely bounded by its four interatomic surfaces, each of which is curved in the form of a chaise-longue. This atom, of T_d symmetry, linked to a mirror-image neighbor at one of its interatomic surfaces, defines a Wigner–Seitz cell of D_{3d} symmetry for the crystal. This cell is the smallest connected set of atomic basins which preserves the translational

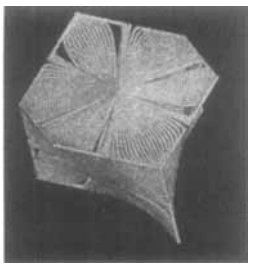


Fig. 4. A representation of a carbon atom of T_d symmetry in the diamond lattice. It is linked by bond paths to four other atoms, each bond path originating at the critical point defining the associated interatomic surface.

invariance of the lattice. The *single* atom depicted in Figure 4 determines all of the bulk properties of the lattice in terms of its quantum mechanical expectation values, including the scattering of X-rays and the appearance of the "forbidden" 222 reflection.

Any and all expectation values and their associated theorems are defined by Equation (b) for an atom, a linked grouping of atoms, or for the complete molecule or crystal. The above examples illustrate how the theory of atoms in molecules enables one to apply the theorems and principles governing the behavior of quantum mechanical observables to the functional groups of chemistry, and do so in precisely the same manner as is done for the total system. In what follows a survey of the form and properties of some atoms and common functional groups is presented to demonstrate how they recover and expand upon our understanding of this basic chemical concept.

7. Form and Properties of Functional Groups

The periodic variations in the form of the A and H atoms in the second-row hydrides AH_n are displayed in Figure 5 and selected properties are given in Table 1. The properties of the atoms in LiH, BeH_2, and BH_3 reflect the hydridic nature of these compounds. There is an abrupt change in the form of the H atom at methane, reflecting a change to a nonpolar interaction that is characterized by a nearly equal sharing of the valence charge density. The decreasing size of the H atom in NH_3, H_2O, and HF reflects the increasing polarity of the atomic interactions and the resultant acidity in these latter members. The atomic first moment $\boldsymbol{M}(\Omega)$ measures the dipolar polarization of an atomic density relative to its nucleus. The directions of $\boldsymbol{M}$(H) reflect the interatomic charge transfers, the H atoms being polarized towards the positively charged A atoms preceeding carbon and away from those bearing a negative charge following it. The atomic susceptibilities also parallel the characteristics of the atomic charge distributions. The currents localized in the basins of the A atoms in the hydridic molecules correspond to opposing paramagnetic and diamagnetic flows, as illustrated for LiH in the Figure 3a. The resulting cancellation leads to a small negative value of $\bar{\chi}$(A) for Li and positive or paramagnetic contributions for Be and B.

The boron and hydrogen atoms in B_2H_6, and the apical H-B| group in $B_6H_6^{2-}$ are displayed in Figure 6. The stability of these electron-deficient compounds is a consequence of the delocalization of electronic charge over the surfaces of the three- and four-membered rings of atoms.[56] A boron atom in B_2H_6 is a member of a single four-membered ring. The apical boron atom in B_5H_9 shares in four four-membered rings, possesses 0.90 more electrons on average, and is more stable by

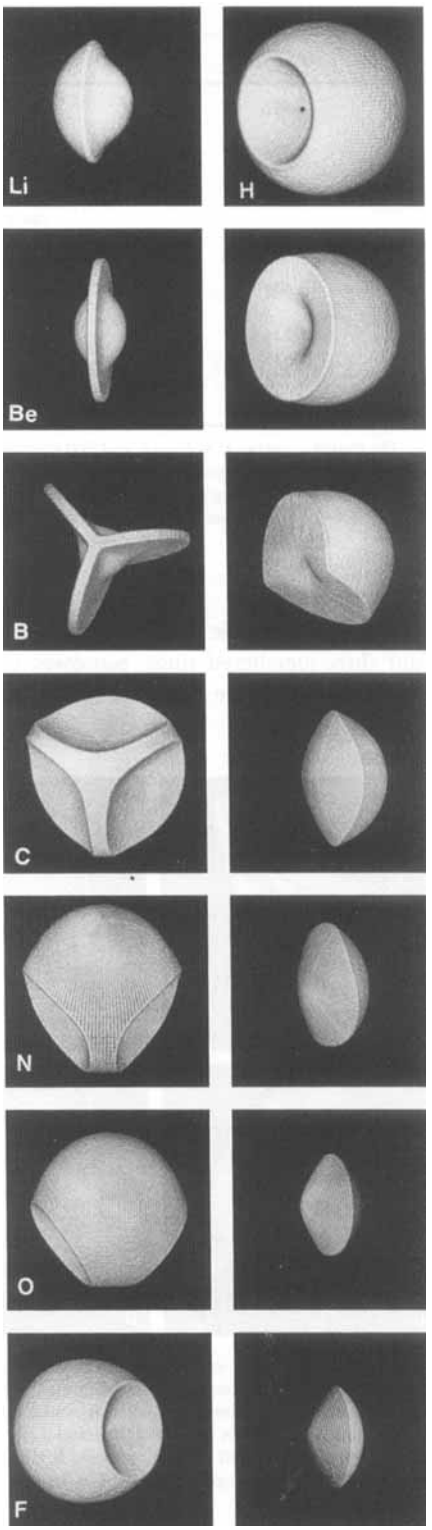


Fig. 5. Representations of the atoms in the second-row hydrides AH_n. In the hydridic members, LiH, BeH_2, and BH_3, the A atom consists primarily of a core of decreasing radius, dressed with some residual valence density. The form and properties of the atoms undergo a marked change at methane, a nonpolar molecule: no core is visible on the C atom, and the H atoms, considerably reduced in size and population, now lie on the convex side of the interatomic surface. The increasing polarity of the remaining members is reflected in the decreasing size of the H atom and the increasing convexity of its interatomic surface.

Table 1. Atomic properties of hydrides AH_n computed at 6-311++G(2d,2p)//6-311++G(2d,2p) level [a].

AH_n	q(A)	E(A)	v(A) [b]	M(A) [c]	$\bar{\chi}$(A)	q(H)	E(H)	v(H)	M(H) [d]	$\bar{\chi}$(H)
LiH	0.912	−7.3662	30.79 (99.30)	+0.005	−0.81	−0.912	−0.6198	195.82 (91.97)	−0.407	−11.8
BeH_2	1.725	−14.2353	19.54 (100.00)	0.000	1.66	−0.862	−0.7682	139.16 (95.96)	−0.566	−6.39
BH_3	2.112	−23.7822	23.17 (99.92)	0.000	1.94	−0.704	−0.8724	88.14 (97.44)	−0.395	−3.79
CH_4	0.175	−37.6601	76.85 (99.70)	0.000	−15.8	−0.044	−0.6381	51.45 (97.62)	+0.126	−3.62
NH_3	−1.048	−54.7472	137.64 (99.33)	−0.172	−21.9	0.349	−0.4905	32.17 (97.52)	+0.186	−2.04
OH_2	−1.254	−75.3719	149.83 (99.39)	+0.351	−20.8	0.627	−0.3428	18.97 (97.37)	+0.153	−1.11
FH	−0.779	−99.8149	130.44 (99.51)	+0.456	−16.7	0.779	−0.2416	11.49 (97.20)	+0.102	−0.80

[a] The charge q, energy E, volume v, and first moment M are in atomic units (au), the magnetic susceptibility $\bar{\chi}$ is in 10^{-29} J (Tesla)$^{-2}$. [b] Volume is determined by the 0.001 au density envelope. The number in parentheses is the fraction of the atomic population contained within this envelope. [c] A negative sign denotes a polarization of the electron density of A along the principal symmetry axis in a direction away from the protons, a positive sign the reverse. [d] A negative sign denotes a polarization of the electron density of H towards A along the A–H bond direction, a positive sign the reverse.

1070 kJ mol^{-1}, while a boron atom in $B_6H_6^{2-}$ participates in four three-membered rings, possesses 1.66 more electrons on average, and is more stable by 1730 kJ mol^{-1}.

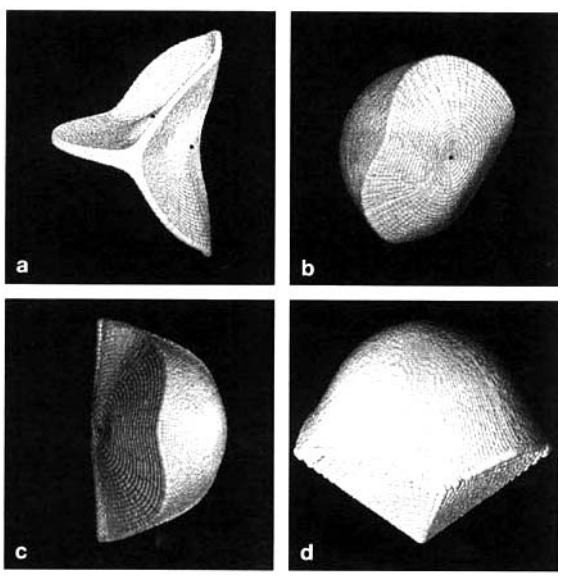


Fig. 6. a) The boron atom in diborane. The two terminal hydrogen atoms lie in the plane of the diagram and one such B|H interatomic surface is shown on the left. An interatomic surface for a bridging hydrogen, which will project out of the plane of the diagram, is also shown. b) and c) A terminal and a bridging hydrogen atom, respectively, in diborane. d) A H–B| group of $B_6H_6^{2-}$ showing two of its four B|B interatomic surfaces. A cage critical point is located at the apex where the four surfaces intersect.

The carbon and hydrogen atoms of ethane, benzene, ethene, and ethyne are displayed in Figure 7 and properties are given in Table 2. The value of ϱ at the C|C bond critical point, the quantity ϱ_b, increases throughout this series and yields bond orders of 1.0, 1.6, 2.0, and 3.0, respectively. The decreasing extent of charge transfer from C to H evidenced in the atomic charges q(H), reflects the increase in the electronegativity of the carbon atom with change in hybridization from sp^3 to sp. The sp^2 carbon atom in benzene is more stable than that in ethene.

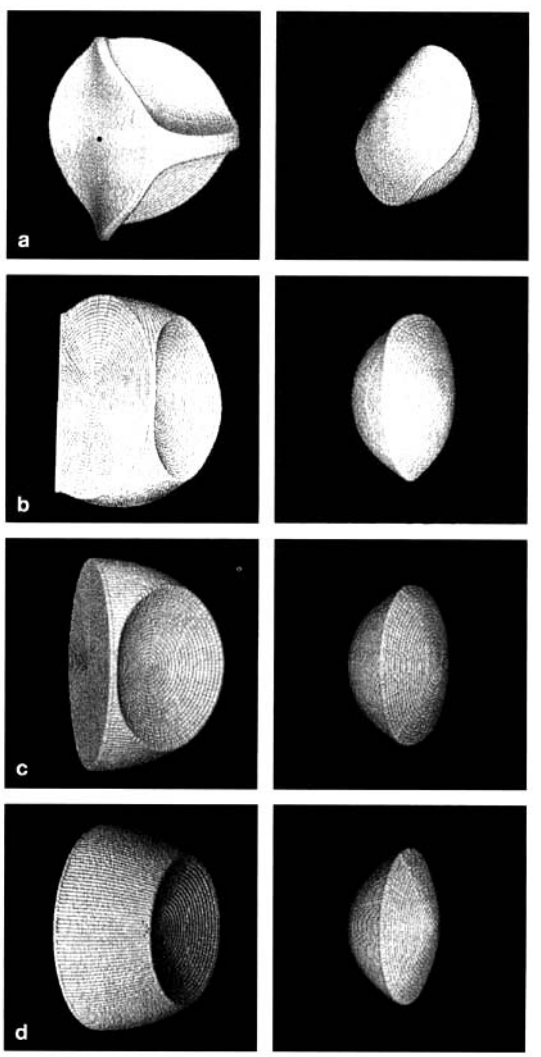


Fig. 7. The C and H atoms in ethane (a), benzene (b), ethene (c), and ethyne (d), respectively. The C|C surface in ethane is similar in shape to that found in methyl or methylene groups and diamond (Figs. 2a, 1a, b, 4). The C|C surfaces in the remaining molecules are planar as a consequence of symmetry. Note that the H atom is largest in ethane and smallest in ethyne.

Table 2. Atomic properties of C and H atoms in hydrocarbons computed at 6-311++G(2d,2p)//6-311++G(2d,2p) level [a].

Molecule	q(C)	E(C)	v(C) [b]	M(C) [c]	$\bar{\chi}$(C)	q(H)	E(H)	v(H)	M(H) [d]	$\bar{\chi}$(H)
C_2H_6	0.184	−37.6720	64.74 (99.85)	−0.029	−13.5	−0.061	−0.6522	51.45 (97.76)	+0.127	−3.39
C_6H_6	0.020	−37.8246	83.08 (99.68)	+0.051	−13.6	−0.020	−0.6371	49.76 (97.76)	+0.119	−2.94
C_2H_4	0.035	−37.7651	96.28 (99.06)	+0.006	−11.2	−0.017	−0.6328	49.89 (97.64)	+0.120	−2.96
C_2H_2	−0.136	−37.8642	126.04 (99.12)	+0.126	−15.8	0.136	−0.5593	41.92 (95.87)	+0.111	−2.61
CH_3^+	0.179	−37.7439	93.41 (99.52)	0.000	–	0.274	−0.5000	35.42 (97.73)	+0.106	
$CH_3^{\cdot}$	−0.035	−37.7399	116.81 (99.22)	−0.001		0.012	−0.6113	49.22 (97.53)	+0.131	
CH_3^-	−0.422	−37.5359	182.24 (97.95)	−1.513	–	−0.193	−0.6609	68.45 (96.37)	+0.258	

[a], [b] See footnotes to Table 1. [c] A negative sign denotes a polarization of the electron density of C along the principal symmetry axis in a direction away from the protons, a positive sign the reverse. [d] A negative sign denotes a polarization of the electron density of H towards C along the C–H bond direction, a positive sign the reverse.

Bridgehead carbon atoms in [1.1.1]bicyclopentane and [1.1.1]propellane are shown in Figure 8a and c. In addition to the C|H surface, the carbon atom in the bicyclic compound has

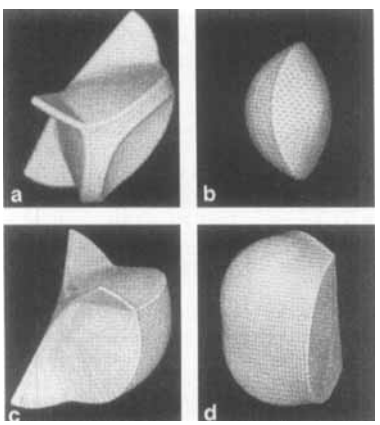


Fig. 8. a) A bridging C atom and b) its H atom in [1.1.1]bicyclopentane, c) a bridging C atom in [1.1.1]propellane, and d) a methylene group in cyclopropane. For details see text. The carbon atom in (a) is capped by electron density bound to a proton in the basin of a hydrogen atom (b). The carbon atom in (c) exhibits a bulge of nonbonded density, which the Laplacian of the charge density shows to be a nonbonded charge concentration, a site of electrophilic attack [5].

three C|C interatomic surfaces with the methylene carbon atoms. Their common point is a cage critical point where the electronic charge density attains a local minimum value of 0.098 au.[57] The carbon atom in the propellane molecule, in addition to three similar C|C surfaces with methylene carbon atoms, shares a fourth surface with the second brighehead carbon atom. This surface, the flat inner triangle bounded by three ring critical points, while of rather limited spatial extent, represents a significant accumulation of electronic charge. The value of ϱ at the ring critical points is only 0.004 au less than its value of 0.203 au at the central bond critical point, of bond order 0.7 (0.6 with a GVB wave function[57]), where ϱ attains its maximum value in the interatomic surface. The result is a *triangular* accumulation of electronic charge linking the bridgehead carbon atoms, in place of the usual *line* of maximum of charge density. Note the significant accumulation of electronic charge in the nonbonded region of the propellane carbon atom[57] whose presence accounts for its susceptibility to electrophilic attack.[58]

In Figure 8d a methylene group from cyclopropane is shown. It differs from the standard transferable methylene groups displayed in Figure 1 by having planar C|C interatomic surfaces. Subjecting the standard group to the geometrical constraints of a three-membered ring results in a strain-induced transfer of charge from H to C within the CH_2 group. This leads to an increase of 38.7 kJ mol^{-1} in its total energy relative to the standard group and to a total strain energy three times this, or 116.1 kJ mol^{-1},[48, 50] in agreement with the experimental value of 115.1 kJ mol^{-1}.[59] This is another example of an experimentally measured property being recovered in terms of a group defined as a quantum subsystem. Figure 9 gives representations of the carbon atom in the methyl cation, the methyl radical, and the methyl anion. Atomic properties are given in Table 2. The atomic forms provide a vivid display of the growth of the nonbonded charge on the carbon atom.

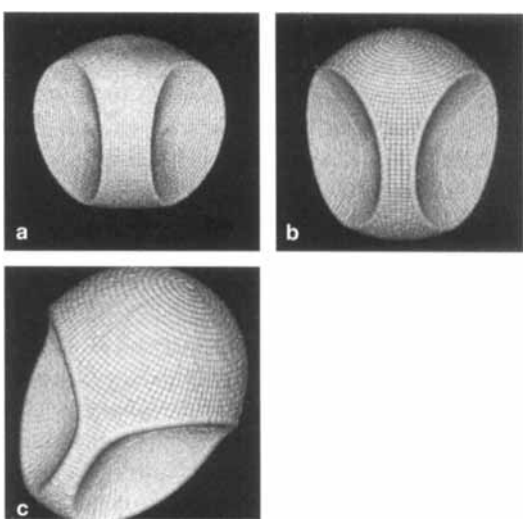


Fig. 9. The carbon atoms in the methyl cation (a), radical (b), and anion (c), respectively. A comparison of (a) with (c) adds to the understanding of the differing properties of cationic nd anionic carbon atoms.

8. Summary and Outlook

This article has presented the quantum mechanical definition of a subsystem and its properties made possible by Schwinger's reformulation of physics. It has shown that the properties of these subsystems meet the constraints imposed on the definition of atoms in molecules by the observations of chemistry. Their properties and physical forms are compatible with a chemist's expectations regarding the behavior of a functional group. In particular, the subsystem expectation values for the historically important additive and transferable properties of volume, energy, polarizability, and magnetic susceptibility, agree with the experimental values obtained for the homologous series of *n*-hydrocarbons. Agreement with experiment is the ultimate test of any theory.

It has been demonstrated that the classification and prediction of chemical behavior afforded by the concept of a functional group is contained within the quantum mechanical framework of observables and their equations of motion. This extension of the predictions of quantum mechanics to include the atoms that make up a total system increases the input of physics into chemistry and complements the information obtained from theories and models of electronic structure. The literature now contains many examples of how the properties of atoms in molecules can be used to increase our understanding of chemistry.

Perhaps because of its use of a new and unfamiliar principle of physics, there is a tendency to ignore the quantum basis of the theory as exemplified in reference [40], or to overlook this basis and instead refer to it as an "electron density analysis".[60] The theory is a generalization of quantum mechanics to a subsystem, enabling one to apply physics to the total molecule or to its constituent atoms on an equal footing. The electron density enters through the statement of the boundary condition,[61] a condition necessarily expressed in terms of the density if the theory is to apply to real physical systems. The boundary condition is identical to that used by Wigner and Seitz[62] in the definition of an atomic cell in their historic quantum investigation of the properties of metallic sodium within the one-electron model. The boundary condition is of profound physical importance. It not only defines atoms in molecules, but further study of the gradient vector field of the electron density leads to a complete theory of structure and structural stability.[5] The resulting unified theory of molecular structure is obtained because the definition of an atom given in Equation (a) is a consequence of the fundamental form exhibited by matter at the atomic level.

In outlook, one can anticipate an increase in the effectiveness of the functional group concept, through the replacement of the present qualitative and largely empirically derived knowledge of group properties by the predictions of quantum mechanics. Since theory predicts what can be observed, one should eventually be able to do everything with the functional groups of theory that one does with them in the laboratory, including their use[44, 45] as synthons.[63] It is perhaps our ability to design the synthesis of a desired molecule in terms of the successive linking of chemical transformations, each step depending upon the particular characteristics of a given functional group, that represents the crowning achievement of the functional group concept. The synthesis of a given molecule from a bank of theoretically defined groups will require further advances in subsystem quantum mechanics in the form of a variation or perturbation theory to predict the changes undergone by a group when it is placed in a new environment,[64] as required in the synthesis. It is to be hoped that the recognition of the theory of atoms in molecules as an extension of quantum mechanics to the atomic domain[65] will spur workers entering the field to further explore and develop subsystem quantum mechanics, enabling physics to be put to its fullest use in chemistry, in the design and synthesis of new molecules.

The authors wish to acknowledge helpful discussions with Dr. Richard G. A. Bone. One of us (R. F. W. B.) would like to thank Mr. G. Reading for restimulating his interest in Kuhn's thesis regarding the influence of existing paradigms on new developments in science.

Received: December 17, 1992 [A 934 IE]
German version: *Angew. Chem.* **1994**, *106*, 647

[1] R. P. Feynman, *Rev. Mod. Phys.* **1948**, *20*, 367–387.
[2] J. Schwinger, *Phys. Rev.* **1951**, *82*, 914–927.
[3] T. S. Kuhn, *The Structure of Scientific Revolutions*, *2nd ed.*, University of Chicago Press, Chicago, **1970**.
[4] The dynamical state of a system is completely determined by specifying the eigenvalues of the complete set of commuting observables. This is the maximum information which can be gained about a quantized system. A. Messiah, *Quantum Mechanics, Vol. 1*, Wiley, New York, **1958**, p. 204 and 301; P. Roman, *Advanced Quantum Theory*, Addison-Wesley, Reading, MS, USA, **1965**, p. 13.
[5] R. F. W. Bader, *Atoms in Molecules – A Quantum Theory*, Oxford University Press, Oxford, **1990**.
[6] L. Libit, R. Hoffmann, *J. Am. Chem. Soc.* **1974**, *96*, 1370–1383.
[7] R. F. W. Bader, P. M. Beddall, *J. Chem. Phys.* **1972**, *56*, 3320–3329.
[8] R. S. Mulliken, *Phys. Rev.* **1928**, *32*, 186; *Rev. Mod. Phys.* **1930**, *2*, 60–115; *ibid.* **1931**, *3*, 89–155.
[9] F. Hund, *Z. Phys.* **1928**, *51*, 759; *Handbuch der Physik*, *24*, *2nd edition*, Springer, Berlin, **1933**, p. 561.
[10] In his reminiscences, Mulliken notes that as a youth he spent much time examining the local flora on Plum island, near to his home and goes on to state that "I had even become an amateur taxonomist", defined as one who is a "scientific classifier". R. S. Mulliken in *Selected Papers of Robert S. Mulliken, Part I* (Eds.: D. A. Ramsay, J. Hinze), The University of Chicago Press, Chicago, **1975**, p. 4.
[11] D. R. Hartree, *Proc. Cambridge Philos. Soc.* **1928**, *24*, 111–132.
[12] V. Fock, *Z. Phys.* **1930**, *61*, 126–148.
[13] J. C. Slater, *Phys. Rev.* **1930**, *35*, 210–211.
[14] C. C. J. Roothaan, *Rev. Mod. Phys.* **1951**, *23*, 69–89.
[15] G. G. Hall, *Proc. R. Soc. London A* **1951**, *205*, 541–552.
[16] R. S. Mulliken, *Rev. Mod. Phys.* **1932**, *4*, 1–86; *Phys. Rev.* **1939**, *56*, 778–787.
[17] L. Pauling, *J. Am. Chem. Soc.* **1931**, *53*, 1367–1400.
[18] J. C. Slater, *Phys. Rev.* **1931**, *37*, 481–489.
[19] J. E. Lennard-Jones, *Proc. R. Soc. London A* **1949**, *198*, 14–26.
[20] J. E. Lennard-Jones, *J. Chem. Phys.* **1952**, *20*, 1024–1029. Lennard-Jones pointed out that the degree to which electrons are localized in pairs is determined by the pair density. The physical localization determined in this manner demands a corresponding localization of the Fermi correlation hole, a condition which within the orbital model, requires that the orbitals be localized to separate regions of space [5]; R. F. W. Bader, M. E. Stephens, *J. Am. Chem. Soc.* **1975**, *97*, 7391–7399. This condition is, in general, not satisfied by localized valence moleular orbitals because they exhibit significant absolute overlap and such orbitals do not represent spatially localized pairs of electrons [5].
[21] E. Wigner, E. E. Witmer, *Z. Phys.* **1928**, *51*, 859.
[22] R. F. W. Bader, *Can. J. Chem.* **1962**, *40*, 1164–1175.
[23] R. S. Mulliken, *Phys. Rev.* **1932**, *40*, 55–62; *ibid.* **1932**, *41*, 49–71, and 751–758; *ibid.* **1933**, *43*, 279–302; *J. Chem. Phys.* **1933**, *1*, 492–503.
[24] K. Fukui, *Acc. Chem. Res.* **1971**, *4*, 57–64.
[25] R. B. Woodward, R. Hoffmann, *J. Am. Chem. Soc.* **1965**, *87*, 395–397; R. Hoffmann, R. B. Woodward, *Acc. Chem. Res.* **1968**, *1*, 17–22; H. C. Longuet-Higgins, E. W. Abrahamson, *J. Am. Chem. Soc.* **1965**, *87*, 2045–2048.
[26] R. S. Mulliken, Nobel-lecture, reprinted in *Science* **1967**, *157*, 13–24; *Angew. Chem.* **1967**, *79*, 541–554.
[27] J. E. Lennard-Jones, *Trans. Faraday Soc.* **1929**, *25*, 668–686.
[28] R. S. Mulliken, *J. Chem. Phys.* **1962**, *36*, 3428–3439.
[29] P. Politzer, R. S. Mulliken, *J. Chem. Phys.* **1971**, *55*, 5135–5136.

[30] S. Srebrenik, R. F. W. Bader, *J. Chem. Phys.* **1975**, *63*, 3945–3961; S. Srebrenik, R. F. W. Bader, T. T. Nguyen-Dang, *ibid.* **1978**, *68*, 3667–3679; R. F. W. Bader, S. Srebrenik, T. T. Nguyen-Dang, *ibid.* **1978**, *68*, 3680–3691; R. F. W. Bader, T. T. Nguyen-Dang, *Adv. Quantum Chem.* **1981**, *14*, 63–124; P. F. Zou, R. F. W. Bader, *Int. J. Quantum Chem.* **1992**, *43*, 677–699.

[31] R. F. W. Bader, *Chem. Rev.* **1991**, *91*, 893–928.

[32] P. A. M. Dirac, *The Principles of Quantum Mechanics*, Oxford University Press, Oxford, **1958**.

[33] P. A. M. Dirac, *Phys. Z. Sowjetunion* **1933**, *3*, 64.

[34] a) To quote from Feynman [1]: "We shall see that it is the possibility of expressing S (the action) as a sum, and hence Φ (the probability amplitude for a single path) as a product of contributions from successive sections of the path, which leads to the possibility of defining a quantity having the properties of a wave function." b) To quote from Schwinger [2]: "Quantum mechanics involves two distinct sets of hypotheses – the general mathematical scheme of linear operators and state vectors with its associated probability interpretation and the commutation relations and equations of motion for specific dynamical systems. It is the latter aspect that we wish to develop, by substituting a single quantum dynamical principle for the conventional array of assumptions based on classical Hamiltonian dynamics and the correspondence principle." The fundamental dynamical principle is stated as a variational equation for the transformation function connecting eigenvectors associated with different spacelike surfaces, which describe the temporal development of the system.

[35] R. F. W. Bader, T. T. Nguyen-Dang, Y. Tal, *Rep. Prog. Phys.* **1981**, *44*, 893–948.

[36] R. F. W. Bader, M. T. Carroll, J. R. Cheeseman, C. Chang, *J. Am. Chem. Soc.* **1987**, *109*, 7968–7979; R. F. W. Bader, W. H. Henneker, P. E. Cade, *J. Chem. Phys.* **1967**, *46*, 3341–3363.

[37] F. D. Rossini, *J. Res. Natl. Bur. Stand. (US)* **1931**, *6*, 37; *ibid.* **1931**, *7*, 329; *ibid.* **1934**, *13*, 21–35; E. J. Prosen, W. H. Johnson, F. D. Rossini, *ibid.* **1946**, *37*, 51–56.

[38] R. J. W. LeFevre, *Adv. Phys. Org. Chem.* **1965**, *3*, 1.

[39] P. Pascal, *Ann. Chim. Phys.* **1910**, *19*, 5; P. Pascal, F. Gallais, S. F. Labarre, *C. R. Hebd. Seances Acad. Sci.* **1961**, *252*, 2644.

[40] For example: "Although the total electron density ϱ is a quantum mechanical observable atomic charges are not, since it is arbitrary how the electron density is apportioned to atoms" (C. L. Perrin, *J. Am. Chem. Soc.* **1991**, *113*, 2865, and references therein.

[41] R. F. W. Bader, P. F. Zou, *Chem. Phys. Lett.* **1992**, *191*, 54–58.

[42] R. F. W. Bader, P. L. A. Popelier, *Int. J. Quantum Chem.* **1993**, *45*, 189–207.

[43] P. Ehrenfest, *Z. Phys.* **1927**, *45*, 455.

[44] C. Chang, R. F. W. Bader, *J. Phys. Chem.* **1992**, *96*, 2654–2662.

[45] R. F. W. Bader, P. L. A. Popelier, C. Chang, *J. Mol. Struct. (THEOCHEM)* **1992**, *255*, 145–171.

[46] K. B. Wiberg, K. E. Laidig, *J. Am. Chem. Soc.* **1987**, *109*, 5935–5943.

[47] One cannot observe perfect transferability, since if $\varrho(r)$ and its derivatives are identical over arbitrarily small regions of space in two systems, the two systems must be identical. (J. Riess, W. Münch, *Theor. Chim. Acta* **1981**, *58*, 295–300; R. F. W. Bader, P. Becker, *Chem. Phys. Lett.* **1988**, *148*, 452–458). No restriction is imposed on how closely this limit can be approached however, and from an operational point of view, two atoms may appear identical to within experimental accuracy.

[48] K. B. Wiberg, R. F. W. Bader, C. D. H. Lau, *J. Am. Chem. Soc.* **1987**, *109*, 1001–1012.

[49] R. F. W. Bader, A. Larouche, C. Gatti, M. T. Carroll, P. J. MacDougall, K. B. Wiberg, *J. Chem. Phys.* **1987**, *87*, 1142–1152.

[50] R. F. W. Bader, T. A. Keith, K. M. Gough, K. E. Laidig, *Mol. Phys.* **1992**, *75*, 1167–1189.

[51] R. F. W. Bader, *Can. J. Chem.* **1986**, *64*, 1036–1045.

[52] T. A. Keith, R. F. W. Bader, *Chem. Phys. Lett.* **1992**, *194*, 1–8.

[53] T. A. Keith, R. F. W. Bader, *J. Chem. Phys.* **1993**, *99*, 3669–3682; R. F. W. Bader, T. A. Keith, *ibid.*, **1993**, *99*, 3683–3693.

[54] W. H. Bragg, *Philos. Trans. R. Soc. London A* **1915**, *215*, 153; *Proc. Phys. Soc. London* **1921**, *33*, 304–311.

[55] P. F. Zou, R. F. W. Bader, *Acta Crystallogr. B*, submitted.

[56] R. F. W. Bader, D. A. Legare, *Can. J. Chem.* **1992**, *70*, 657–676.

[57] K. B. Wiberg, R. F. W. Bader, C. D. H. Lau, *J. Am. Chem. Soc.* **1987**, *109*, 985–1001; C. Gatti, P. J. MacDougall, R. F. W. Bader, *J. Chem. Phys.* **1988**, *88*, 3792–3804.

[58] K. B. Wiberg, F. H. Walker, *J. Am. Chem. Soc.* **1982**, *104*, 5239–5240.

[59] K. B. Wiberg, *Angew. Chem.* **1986**, *98*, 312–322; *Angew. Chem. Int. Ed. Engl.* **1986**, *25*, 312–322.

[60] W. Kutzelnigg, *Angew. Chem.* **1992**, *104*, 1423; *Angew. Chem. Int. Ed. Engl.* **1993**, *32*, 128. In this review of the book listed in reference [5] the theory is referred to as "der Bader-Analyse der Elektronendichte". No mention is made of the theory being based upon a generalization of Schwinger's action principle to a subsystem, nor is any mention made of the development of the quantum mechanical description of atoms in molecules. The essence of the theory, as stated in the title of the book, is not discussed.

[61] Every variational result is obtained subject to boundary conditions. The derivation of Schrödinger's equation from the restricted variation of the action integral for the total system, requires the vanishing of $\boldsymbol{V}_i\psi \cdot \boldsymbol{n}\delta\psi$ on the infinite boundary of the system, as obtained by requiring that $\boldsymbol{V}_i\psi \cdot \boldsymbol{n} = 0$ for all particles. These terms are retained in Schwinger's generalization of the action principle, see Equations 2.17 and 2.19 of reference [2]. Their retention and combination with the terms derived from the boundary condition Equation (a), that $\boldsymbol{V}\varrho \cdot \boldsymbol{n}$ vanish on the surface of the atom, leads to the extension of the generalized action principle to an atom in a molecule. It is this marriage of surface terms which yields the fundamental relation between the variation in the energy or action, and the infinitesimal flux in the current density through the surface of the subsystem.

[62] E. Wigner, F. Seitz, *Phys. Rev.* **1933**, *43*, 804–810.

[63] E. J. Corey, *Pure Appl. Chem.* **1967**, *14*, 19–37.

[64] P. F. Zou, *Int. J. Quantum Chem.* **1992**, *44*, 997–1013; P. F. Zou, Thesis, McMaster University, Hamilton, Ontario, Kanada, **1993**.

[65] An essential part of physics is the possibility it provides of proving a proposed theory or conjecture wrong. Either the generalization of the quantum action principle, subject to the boundary condition given in Equation (a) to yield Equation (b), the atomic generalization of Schwinger's variation principle, is correct, or it can be disproven.

Opportunities for New Chemical Libraries: Unnatural Biopolymers and Diversomers

Rob M. J. Liskamp*

The solid-phase methodology for the synthesis of biopolymers is nowadays indispensable in chemistry, pharmacology, immunology, physiology, biology, and biophysics. Using this fantastic tool,[1] it is not only possible to prepare (large) peptides in a (semi)automatic manner in which amino acids and other reagents are added, and excess of reagents and waste are removed (without the tedious purification of intermediates), but this methodology has also been successfully applied to the synthesis of nucleic acids and recently carbohydrates.[2, 3] Once developed the next logical step was the adaptation of the efficient solid-phase methodology to the *simultaneous* synthesis of *several* peptides. This led to the development of several multiple peptide synthesis strategies with a large range of applications.[4] A significant step further are the peptide libraries, for example, aimed at the systematic synthesis of many –if not all– possible peptides of a certain length. When each amino acid residue is one of the 20 proteinogenic L-amino acids, there are 400 possible dipeptides, 8000 possible tripeptides etc. in a library: with each amino acid increment the number of peptides increases 20-fold. However, there will be intrinsic difficulties in preparing and handling such large libraries,[4] in addition to difficulties in identification, selection, and enrichment of promising compounds from a library. In order to facilitate identification and enrichment, encoded libraries might be very interesting. In one particular promising type of these libraries a chemically synthesized entity, for example a peptide, is linked to a particular oligonucleotide sequence. It is proposed that the use of the encoding genetic tag should serve to identify and to enrich the promising compounds from the library.[5, 6] Peptide libraries are undeniably useful in the discovery of chemical lead compounds. However, the chemical lead discoveries from these libraries still require extensive modifications before suitable drug candidates are produced. This is due to the disadvantages of peptides, such as their water solubility and in many cases their facile degradation by proteases, which limit their use in biological systems. Therefore the results described by Cho et al. and Hobbs DeWitt et al. are the next significant steps on the way to new libraries,[7, 8] which first may—to a certain extent—circumvent these disadvantages, second provide lead compounds, possibly requiring less extensive modifications, and third may provide new frameworks for generating macromolecules with novel properties.

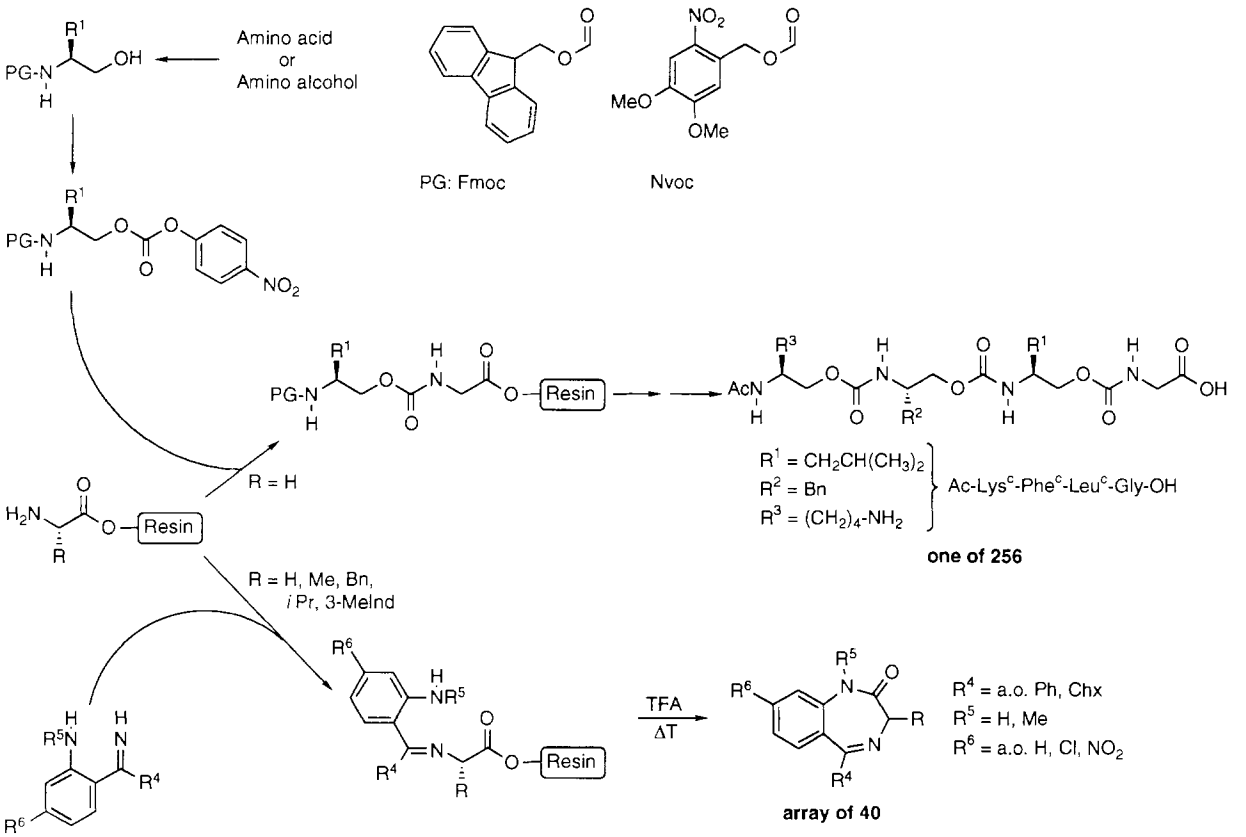
Cho et al. described the principles of the solid-phase synthesis of an oligocarbamate as well as the generation of an oligocarbamate library.[7] This oligocarbamate was referred to as "an unnatural biopolymer",[9] "unnatural" because it is obviously not found in nature and "biopolymer" to hint at the origin of the monomers which were derived from proteinogenic amino acids. The term "biopolymer mimetic" is perhaps a better alternative, as "unnatural biopolymer" is a contradiction in itself. The monomeric, *N*-protected aminoalkylcarbonates were conveniently prepared from the corresponding *N*-protected amino acids or from amino alcohols derived from amino acids (Scheme 1). By using the base-labile Fmoc-protecting group, an oligocarbamate was synthesized by standard solid-phase methods; the coupling yields were greater than 99% per step. Even more interesting was the use of the photolabile nitroveratryloxycarbonyl (Nvoc) amino-protecting group (Scheme 1). This enabled the authors to prepare a library containing 256 oligocarbamates, by employing a binary masking strategy as was described by Fodor et al. in their light-directed parallel synthesis of libraries of oligopeptides and oligonucleotides.[10] The library contains all of the compounds that can be formed by deleting one or more carbamate units from the parent sequence Ac-Tyr^c-Phe^c-Ala^c-Ser^c-Lys^c-Ile^c-Phe^c-Leu^c (the superscript "c" indicates the presence of a carbamate linkage). The library was attached to a glass surface of approximately 1.3 cm by 1.3 cm and screened for its ability to bind a monoclonal antibody against Ac-Tyr^c-Lys^c-Phe^c-Leu^c. It was found that the oligocarbamates Ac-Lys^c-Phe^c-Leu^c-Gly-OH (Gly is the linker in the keyhole limpet hemocyanin conjugate of this oligocarbamate), Ac-Phe^c-Lys^c-Phe^c-Leu^c-Gly-OH, Ac-Tyr^c-Lys^c-Phe^c-Leu^c-Gly-OH, Ac-Ala^c-Lys^c-Phe^c-Leu^c-Gly-OH, and Ac-Ile^c-Phe^c-Leu^c-Gly-OH were among the ten highest affinity ligands based on fluorescence intensities. Competitive enzyme-linked immunosorbent assay experiments in solution using the free oligocarbamates resulted in IC_{50} values between 60 and 180 nM. It was therefore suggested that the dominant epitope of the antibody was Phe^c-Leu^c. Although, Ac-Tyr^c-Phe^c-Leu^c-Gly-OH containing this epitope did bind in solution with an IC_{50} value of about 160 nM, the fluorescence signal associated with this oligocarbamate on the solid support, that is the glass surface in the library,

[*] Dr. R. M. J. Liskamp
Utrecht Institute for Pharmaceutical Sciences
Department of Pharmaceutics, Section Organic and
Medicinal Chemistry, Utrecht University
P.O. Box 80082, NL-3508 TB Utrecht (The Netherlands)
Telefax: Int. code + (30)516674

ranked in the bottom 30%. This suggests that the conformation of the oligocarbamate on the solid support may be different from that in solution. This problem certainly has to be addressed in the future before a general application of the use of libraries can be recommended for affinity studies.[11]

compounds (comparable to an in-house sample collection of a pharmaceutical company), which can be offered to the often automated, fast high throughput biological screening assays.

In contrast to the well-known procedure in which polyethylene rods or pins were used as a solid support for mul-



Scheme 1. Solid-phase synthesis of oligocarbamates and benzodiazepines starting with a resin-bound amino acid. The Fmoc-protected 4-nitrophenyl carbonate monomers derived from amino acids or amino alcohols were used in a normal solid-phase synthesis of an oligocarbamate, whereas the corresponding Nvoc-protected monomers were used in the generation of a library of 256 oligocarbamates of which one representative (Ac-Lysᶜ-Pheᶜ-Leuᶜ-Gly-OH) is shown. An array of 40 diazepines was synthesized by reacting the resin-bound amino acid with eight different 2-aminobenzophenone imines followed by cyclization. Ind = indolyl. Chx = cyclohexyl.

Although the oligocarbamate differs significantly from the corresponding polypeptide, for example, it is more extended (that is there are four atoms located between the side chains instead of two atoms as in a peptide), some inherent disadvantages of peptides seem to be less pronounced in oligocarbamates: a) the oligocarbamates are significantly more hydrophobic, as was determined from a comparison of the water/octanol partitioning coefficients; b) the oligocarbamates are resistant to degradation by trypsin and pepsin.

Contrary to the Berkeley and Affymax report, the diversomer paper by Hobbs De Witt et al. placed no emphasis on the preparation of an oligomer library but focussed entirely on the generation of a library of diverse, albeit related, organic compounds called "diversomers".[8] An important reason for the creation of these libraries is to discover lead compounds, which will be structurally more related to the ultimate drug, since lead compounds discovered from peptide or nucleotide libraries still require extensive modifications (vide supra). Another equally important reason is to rapidly obtain a large library of organic

tiple peptide synthesis in the "PEPSCAN" method,[4, 12] hollow pins, ending in a glass frit were used, each containing approximately 100 mg resin to which a Fmoc amino acid was attached by a linker. The removal of the Fmoc-group from eight amino acid resins and treatment of each resin with five different isocyanates followed by cyclization led to 39 of the 40 desired hydantoins in 4–81% yield. Similarly, by starting from Boc-protected amino acid Merrifield resins (five), 40 different benzodiazepines were synthesized by reacting with eight different 2-aminobenzophenone imines followed by cyclization (Scheme 1). The 40 products were obtained in 9–63% yield and their purity was typically >90% (determined by ^{1}H NMR spectroscopy). These compounds were then used in an assay for inhibition of fluoronitrazepam. A report by Bunin and Ellman had earlier described the solid-phase synthesis of ten benzodiazepine derivatives using an alternative approach.[13]

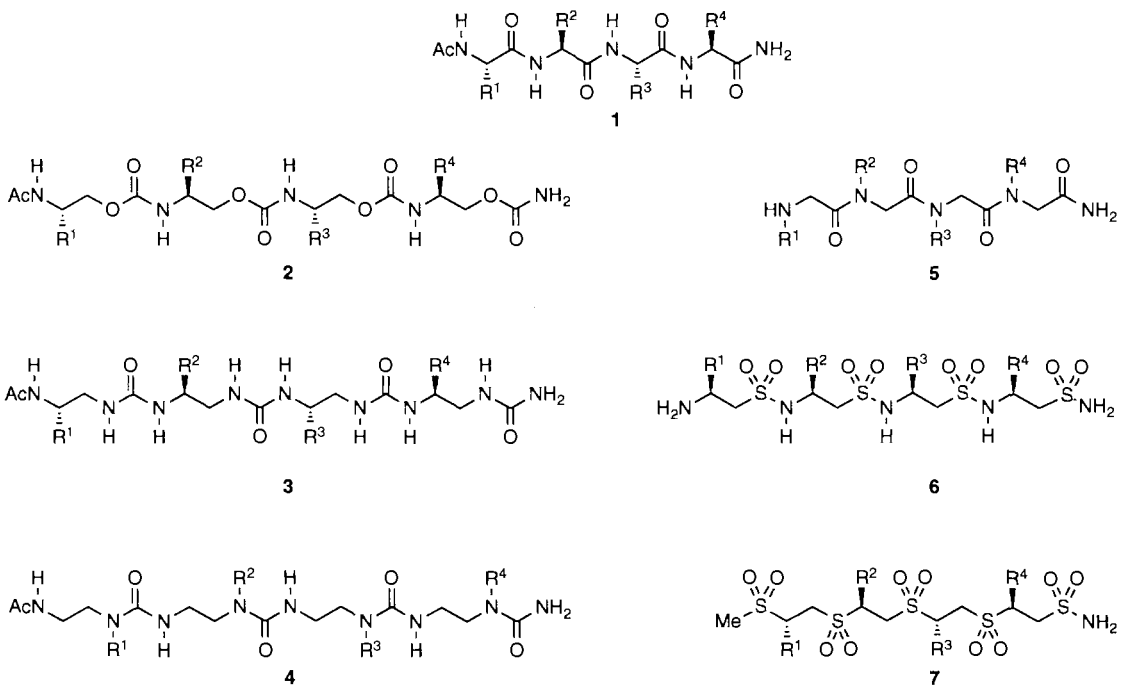
An important message from the reports is that the authors are able by carrying out synthesis on a solid support—to prepare an array of unnatural compounds, which can be used for screen-

ing purposes to discover new lead compounds. These lead compounds may then be closer to ultimate drugs, because they are obtained from an array of compounds further removed from natural systems such as peptides and nucleotides.

Using the solid-phase strategy also libraries of other biopolymer mimetics may become accessible, for example, oligoureas, oligosulfones, peptidosulfonamides,[14] peptidophosphoramidates, and peptoids (Scheme 2).[15] These compounds will undoubtedly provide new biologically active compounds and also opportunities for the construction of biopolymers with novel properties.

tance of creating library compounds with defined conformations that are similar if not identical in different environments.

The scientist has an innate desire to be able to *rationally* design a compound with a predicted (biological) activity. Computer-assisted molecular modeling techniques, X-ray crystallographic analysis, and NMR methods have intensified this desire and the belief that this should ultimately be possible for all drugs. Nevertheless, many of the current drugs or at least the lead compounds which initiated their development have been obtained by screening approaches, that is, by an "*irrational*" approach. Although it is expected that the rational design of



Scheme 2. A peptide (**1**), the corresponding oligocarbamate (**2**), oligoureas (**3** and **4**), peptoid (**5**), peptidosulfonamide (**6**), and oligosulfone (**7**).

The diversomer library shows that an array of organic compounds can be synthesized, and, although the number is much smaller than that which can be achieved by most of the current methods for generating peptide libraries, a significant number of structural analogues can be obtained in a faster way than is the case when each of the compounds is synthesized separately. Furthermore, it should be possible to adapt the method to many more organic reactions, so that it is likely that a number of diversomer libraries will be appear in the near future.

Another challenge is the development of "conformationally restricted" libraries in which the conformation of an oligomer is more accurately defined, for example, by introducing rigid monomers at different locations in an oligomer. This is noteworthy, since there is ample evidence in the literature that in many cases merely the presence of functional groups delivered, for example, by an amino acid sequence is not sufficient for an optimal biological activity, but that a proper orientation of functional groups is essential too.[16] In addition, the conformation on the solid support of the library may be different from that in solution (vide supra), which may diminish the reliability of a library for the selection process. This underlines the importance of drugs will become increasingly important, screening approaches will gain more momentum too, since they will contribute to a faster and more direct access to information. Therefore the rational design of irrational screening procedures holds promises for the future, and as a result there will be plenty of opportunities for the creation and applications of new libraries.[17]

German version: *Angew. Chem.* **1994**, *106*, 661

[1] R. B. Merrifield, *J. Am. Chem. Soc.* **1963**, *85*, 2149; *Angew. Chem.* **1985**, *97*, 801; *Angew. Chem. Int. Ed. Engl.* **1985**, *24*, 799.

[2] For a recent review: S. L. Beaucage, R. P. Iyer, *Tetrahedron* **1993**, *48*, 2223.

[3] R. Verduyn, P. A. M. van der Klein, M. Douwes, G. A. van der Marel, J. H. van Boom, *Recl. Trav. Chim. Pays-Bas* **1993**, *112*, 464; S. J. Danishefsky, K. F. McClure, J. T. Randolph, R. B. Ruggeri, *Science* **1993**, *260*, 1307; S. P. Douglas, D. M. Whitfield, J. J. Krepinsky, *J. Am. Chem. Soc.* **1991**, *113*, 5095; G. H. Veeneman, R. M. J. Liskamp, G. A. van der Marel, J. H. van Boom, *Tetrahedron Lett.* **1987**, *28*, 6695.

[4] For a recent review on multiple peptide synthesis: G. Jung, A. G. Beck-Sickinger, *Angew. Chem.* **1992**, *104*, 375; *Angew. Chem. Int. Ed. Engl.* **1992**, *31*, 367.

[5] S. Brenner, R. A. Lerner, *Proc. Natl. Acad. Sci USA* **1992**, *89*, 5381; I. Amato, *Science* **1992**, *257*, 330; J. Nielsen, S. Brenner, K. D. Janda, *J. Am. Chem. Soc.* **1993**, *115*, 9812

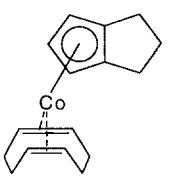
[6] In principle, it should also be possible to assign coding elements to compounds other than peptides, for example, carbohydrates, for the identification of a

compound. This would expand the possibilities for the creation of new libraries.
[7] C. Y. Cho, E. J. Moran, S. R. Cherry, J. C. Stephans, S. P. A. Fodor, C. L. Adams, A. Sundaram, J. W. Jacobs, P. G. Schultz, *Science* **1993**, *261*, 1303.
[8] S. Hobbs DeWitt, J. S. Kiely, C. J. Stankovic, M. C. Schroeder, D. M. Reynolds Cody, M. R. Pavia, *Proc. Natl. Acad Sci. USA* **1993**, *90*, 6909.
[9] The antisense oligonucleotides are an earlier category of "unnatural biopolymers": A. Peyman, *Chem. Rev.* **1990**, *90*, 543.
[10] S. P. A. Fodor, J. L. Leighton Read, M. C. Pirrung, L. Stryer, A. T. Lu, D. Solas, *Science* **1991**, *251*, 767; a highlight was devoted to this topic: G. von Kiederowksi, *Angew. Chem.* **1991**, *103*, 839; *Angew. Chem. Int. Ed. Engl.* **1991**, *30*, 822.
[11] This is one the critical questions raised in the highlight by von Kiederowski [10].
[12] H. M. Geysen, R. H. Meloen, S. J. Barteling, *Proc. Natl. Acad. Sci. USA* **1984**, *81*, 3998.
[13] B. A. Bunin, J. A. Ellman, *J. Am. Chem. Soc.* **1992**, *114*, 10997.
[14] R. M. J. Liskamp, W. J. Moree, unpublished results.
[15] Peptoids were recently highlighted by H. Kessler, *Angew. Chem.* **1993**, *105*, 572; *Angew. Chem. Int. Ed. Engl.* **1993**, *32*, 543.
[16] See for example the recent review on peptidomimetics: A. Giannis, T. Kolter, *Angew. Chem.* **1993**, *105*, 1303; *Angew. Chem. Int. Ed. Engl.* **1993**, *32*, 1244.
[17] A highlight was devoted to the "rationality of random screening": A. Plückthun, L. Ge, *Angew. Chem.* **1991**, *103*, 301; *Angew. Chem. Int. Ed. Engl.* **1991**, *30*, 296.

Construction of Carbon Frameworks with the Help of Ruthenium Complexes: 1,5-Cyclooctadiene as a Reagent in Transition Metal Catalyzed Reactions

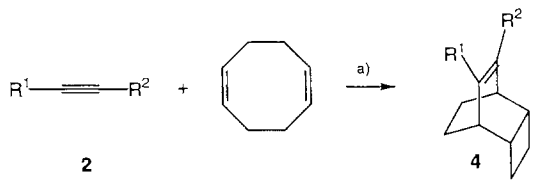
Holger Butenschön*

A communication by B. M. Trost et al.[1] which appeared last year is one of several important papers that have been published recently from the rapidly developing area of ruthenium–organic chemistry. 1,5-Cyclooctadiene (COD) is frequently used in transition metal complexes as a bidentate, neutral ligand, which can be removed again often under mild conditions with the formation of free coordination sites. The perfect example of this is bis(1,5-cyclooctadiene)nickel(0) as a precursor of "naked nickel", with which G. Wilke et al. carried out a large number of important reactions and thus emphasized the special value of organometallic chemistry for the synthesis of organic compounds at a very early stage.[2] It is noteworthy that there have been very few reports on the reactions of COD at the metal center despite its frequent use as a ligand. One such example is the formation of the bicyclo[3.3.0]octadienylcobalt complex **1** from the reaction of cobalt reagents with COD, as reported by Lehmkuhl et al. as well as Otsuka et al.[3–5]



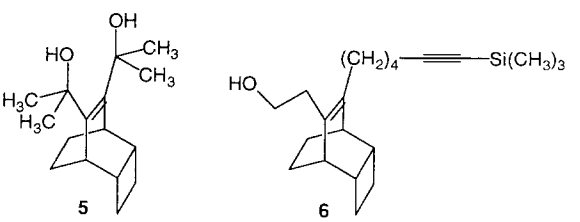
1

The relatively narrow spectrum of the organic chemistry of COD has been considerably extended by B. M. Trost et al.[1] who discovered that COD can formally function as a bis-homodiene in metal-catalyzed [4 + 2]cycloadditions. A 0.1 M solution of the alkyne **2** reacts with 1.1 equivalents of COD in the presence of 5 mol% chloro(η^4-cyclooctadiene)(η^5-cyclopentadienyl)ruthenium(II) [CpRu(COD)Cl] (**3**)[6] in boiling methanol to give derivatives **4** of tricyclo[4.2.2.$0^{2,5}$]dec-7-ene (Scheme 1). Yields of between 78 and 100% are achieved in seven out of eight examples, in the other case the yield is only 22% (however, as the authors note, this is in fact "65% yield brsm", where brsm stands for "based on recovered starting material"). Electron-deficient alkynes react particularly slowly and no reaction takes place with dimethyl butynedioate. Steric hindrance slows down the reaction; **5** is obtained only in 51% (98% brsm) after 80 h at reflux. This can, however, be used for the differentiation of triple bonds in alkynes with several triple bonds, as shown by the selective formation of **6** in 63% (72% brsm, Scheme 2).



2 **4**

Scheme 1. a) 5% [CpRu(COD)Cl] (**3**), MeOH; R^1 = Me, Et, $CH_2OSi(iPr)_3$, *p*-$CH_2C_6H_4OCH_3$, H; R^2 = CH_2OH, $CH_2OSi(iPr)_3$, CH_2CH_2OH, *p*-$CH_2C_6H_4OCH_3$, CO_2Me, $CH_2CH_2CH_2CO_2Me$; 78–100% (see text).

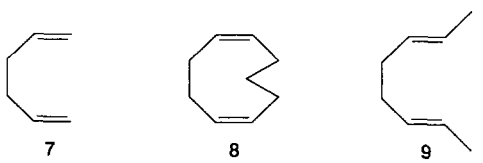


5 **6**

The catalytic cycle proposed by the authors starts from a cationic cyclopentadienylruthenium complex, bearing one COD ligand and one solvent molecule. The latter is displaced by the alkyne, which subsequently reacts with a double bond of the COD ligand to give a metallacyclopentene. An intramolecular carbometalation of the remaining double bond of the eight-membered ring with successive reductive elimination leads to the elimination of the products **4**; renewed complexation of a COD molecule regenerates the catalytically active species. The authors point out that the reaction is also catalyzed by other coordinatively highly unsaturated ruthenium complexes and fi-

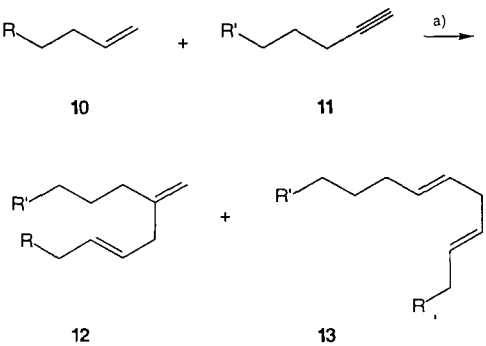
[*] Prof. Dr. H. Butenschön
Institut für Organische Chemie der Universität
Schneiderberg 1B, D-30167 Hannover (FRG)
Telefax: Int. code + (511)762-3011

nally make the important remark that the ease of the reactions observed by them suggests that a range of other ruthenium-catalyzed reactions of COD may well be possible. They assume that the coordination properties of COD cannot only be derived from the entropic effect of the spatial arrangement of the two double bonds in COD. Possibly electronic effects similar to those in norbornadiene exist in an attenuated form in COD. This is in agreement with the fact that the dienes **7**–**9** do not undergo the reaction found with COD.[7]



7 **8** **9**

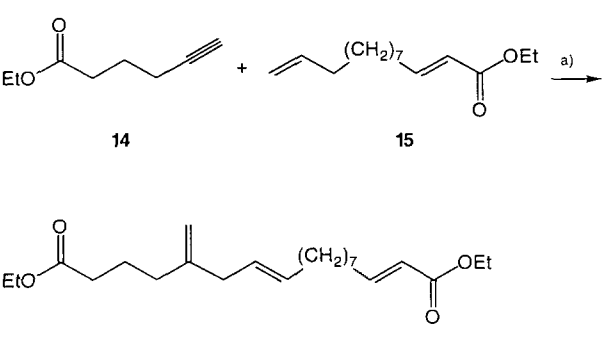
The ruthenium catalyst **3** was recently used by B. M. Trost et al. also for coupling reactions of alkenes **10** with alkynes **11**.[8] These reactions lead to the branched coupling products **12** as well as the linear isomers **13** (Scheme 2). The yields lie between



10 **11** **12** **13**

Scheme 2. a) 5% **3**, dimethylformamide (DMF)/H_2O 3:1, 100 °C, 2 h; R = Bu, CH_2CH_2OH, COMe, $(CH_2)_3CO_2Me$; R′ = Pr, $CH_2OTBDMS$, CO_2Et; 60–90%.

60 and 90%, and in most cases the branched isomer **12** is formed preferentially (**12**:**13** up to 6:1). Substituents at the propargyl position of **11** reduce the regioselectivity, and the presence of propargylic oxygen substituents even leads to an inversion of the selectivity in favor of the linear coupling products. The chemoselectivity of the reaction is impressively underlined by the reaction of **14** with the $\alpha\beta$-unsaturated ester **15** to give exclusively **16** in 70% yield (Scheme 3).

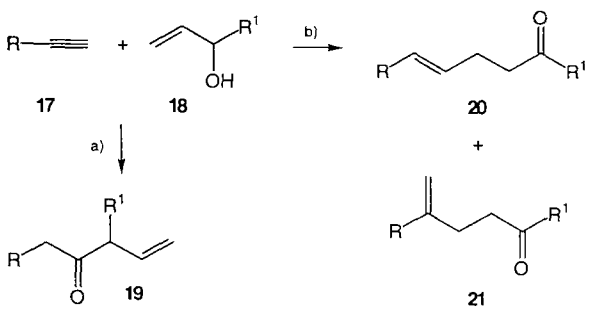


14 **15** **16**

Scheme 3. a) 5% **3**, DMF/H_2O 3:1, 100 °C, 2 h, 70%.

Also in these reactions the authors assume that a cationic cyclopentadienylruthenium complex is the catalytically active species, the only difference here being that in addition to the chloro ligand also the COD ligand is decomplexed and all three free coordination sites are filled by readily displaceable solvent molecules. After the complexation of the alkene component, the latter is transformed into an allyl ligand and the hydrogen atom released is bound to the metal as a hydrido ligand. After coordination, the alkyne is either intramolecularly hydrometalated or carbometalated starting from the allyl ligand. From both intermediates the reaction product, still coordinated to ruthenium, can be easily formed, which is then released with the regeneration of the above-mentioned catalytically active species.

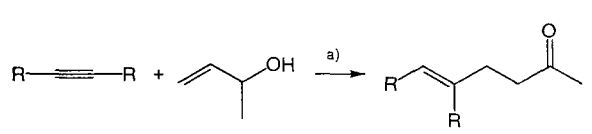
Several years ago B. M. Trost et al.[9] reported on the coupling of terminal alkynes **17** with allyl alcohols **18** in the presence of NH_4PF_6. This reaction is catalyzed by $[(PPh_3)_2CpRuCl]$ and leads to the formation of $\beta\gamma$-unsaturated ketones **19** (Scheme 4). A mechanistic study reveals that vinylidene complexes are formed as intermediates from the terminal alkynes.[10] Also allyl alcohols can be isomerized with $[(PPh_3)_2CpRuCl]$ directly to give saturated ketones.[11] Interestingly, compound **3**, which is different from $[(PPh_3)_2CpRuCl]$ only in that instead of the two phosphane ligands a COD ligand is present, catalyzes the coupling of alkynes **17** and allyl alcohols **18** in 51–85% yields to give $\gamma\delta$-unsaturated ketones **20** and **21** (Scheme 4).[12]



17 **18** **19** **20** **21**

Scheme 4. a) 6% $[(PPh_3)_2CpRuCl]$, 10% NH_4PF_6, 100 °C, 10 h, 44–74%; b) 10% **3**, 10–20%, NH_4PF_6, 100 °C, 1–2 h; R = $C_{10}H_{21}$, C_6H_{13}, $CH(OH)C_5H_{11}$, $C(C_2H_5)(OH)C_5H_{11}$; R^1 = Me, *i*Pr, cyclohexyl, $C_{11}H_{23}$; 51–85%.

From the fact that in the reaction catalyzed by **3** also internal alkynes **22** can react to give ketones **23** (Scheme 5), the authors conclude that in this case no vinylidene complex acts as an intermediate. Apparently, its formation is favored by the presence of phosphane ligands, and in their absence other reaction paths are followed. The regioselectivity of the reaction as well as its yield can be increased if a mixture of water and DMF is used as solvent. The reaction functions also with alkynes whose triple bond is conjugated to an ester group. The chemoselectivity of the reaction was demonstrated by the coupling of a steroid side



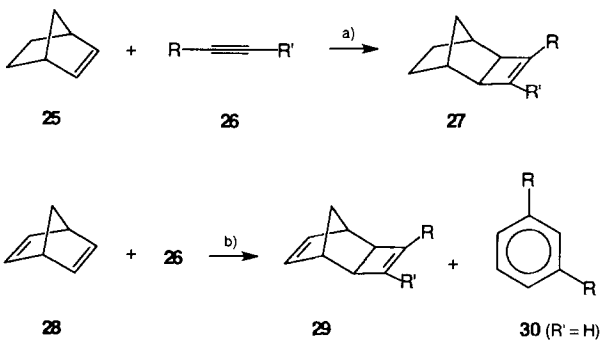
22 **18** ($R^1 = CH_3$) **23**

Scheme 5. a) 10% **3**, 10–20% NH_4PF_6, 100 °C, 1–2 h, R = Bu (45%), Ph (50%).

 © VCH Verlagsgesellschaft mbH, D-69451 Weinheim, 1994 0570-0833/94/0606-0637 $ 10.00+.25/0

chain with an allyl alcohol; one $\alpha\beta$-unsaturated carbonyl functionality present in the steroid part remained unaltered.

The significance of ruthenium-catalyzed reactions is also emphasized by a very recent publication by T. Mitsudo et al.,[13] who achieved [2 + 2]cycloadditions of norbornene **25** and norbornadiene **28** with a range of alkynes **26**. These reactions are catalyzed by chloro(η^4-cyclooctadiene)(η^5-pentamethylcyclopentadienyl)ruthenium(II) [Cp*Ru(COD)Cl] (**24**)[14] and give **27** and **29**, respectively in good yields (Scheme 6). Ru-catalyzed



Scheme 6. a) 5% [Cp*Ru(COD)Cl] **24**, 80 °C, 15–20 h, NEt_3, R, R′ = Me, Et, Ph, C_5H_{11}, $CH(OEt)_2$, CO_2Me, CO_2Et, 40–88%; b) 5% **24**, 100 °C, 24–120 h, R, R′ = H, Me, Ph, CO_2Me, CO_2Et, C_8H_{17}, $C_{10}H_{21}$, 23–87% **29**, 12–26% **30** (R′ = H).

[2 + 2]cycloadditions of norbornene with butynedioates have been known for a long time.[15, 16] However, what is new is that the reaction, which was successful with other ruthenium catalysts only with butynedioates, now functions with a whole series of different alkynes, and that not only norbornene **25**, but also norbornadiene **28** can be used. In this way in the course of the reaction [Cp*RuCl(nbd)] (nbd = norbornadiene) is formed, which is more stable than **3**. Thus, slightly higher reaction temperatures are required for reactions with norbornadiene. In addition to the adducts **29** to norbornadiene, *meta*-disubstituted arenes **30** are also formed. The use of phenylethyne which is deuterated at the terminal alkyne position reveals that the additional C_2 building block present in **30** stems from norbornadiene. In agreement with a retro-Diels–Alder reaction, di(cyclopentadiene) was detected in the reaction mixtures.

As a possible mechanism for the reaction the authors propose that **24** releases the COD ligand with the formation of the catalytically active species and the two free coordination sites are then filled by norbornadiene and the alkyne. From this a metallacyclopentene is formed, which either reacts by reductive elimination to give the [2 + 2]cycloadduct or by insertion of a further alkyne molecule forms a metallacycloheptadiene. The latter then releases cyclopentadiene in a retro-Diels–Alder reaction and is thus transformed into the metallacycloheptatriene, the direct precursor of **30**.

Interestingly, the only difference between the catalysts used by B. M. Trost et al. (**3**) and T. Mitsudo et al. (**24**) is that an unsubstituted cyclopentadienyl ligand is present in **3** and a pentamethylcyclopentadienyl ligand in **24**. The electronic and steric differences of the two ligands are well known; in light of the papers presented here the question arises as to how the spectrum of ruthenium-catalyzed reactions may be extended by the use of a new ligand recently described by P. Gassman et al.;[17] the title of the work read as follows: "1,2,3,4-Tetramethyl-5-(trifluoromethyl)cyclopentadienide: A Unique Ligand with the Steric Properties of Pentamethylcyclopentadienide and the Electronic Properties of Cyclopentadienide".

That the Cp*Ru fragment can also be used to break down carbon frameworks was shown at the beginning of 1993 by B. Chaudret et al.[18], who, using an example from steroid chemistry, achieved the elimination of methane from a methyl-substituted cyclohexadiene with consequent aromatization.

German version: *Angew. Chem.* **1994**, *106*, 664

[1] B. M. Trost, K. Imi, A. F. Indolese, *J. Am. Chem. Soc.* **1993**, *115*, 8831–8832.
[2] Summary: G. Wilke, *Angew. Chem.* **1988**, *100*, 189–211; *Angew. Chem. Int. Ed. Engl.* **1988**, *27*, 185–206.
[3] S. Otsuka, T. Taketomi, *J. Chem. Soc. Dalton Trans.* **1972**, 1879–1882.
[4] H. Lehmkuhl, H. W. Leuchte, E. Janssen, *J. Organomet. Chem.* **1971**, *30*, 407–409.
[5] H. W. Leuchte, Dissertation, Universität Bochum, **1971**.
[6] M. O. Albers, D. J. Robinson, A. Shaver, E. Singleton, *Organometallics* **1986**, *5*, 2199–2205
[7] B. M. Trost, personal communication.
[8] B. M. Trost, A. Indolese, *J. Am. Chem. Soc.* **1993**, *115*, 4361–4362.
[9] B. M. Trost, G. Dyker, R. J. Kulawiec, *J. Am. Chem. Soc.* **1990**, *112*, 7809–7811.
[10] B. M. Trost, R. J. Kulawiec, *J. Am. Chem. Soc.* **1992**, *114*, 5579–5584.
[11] B. M. Trost, R. J. Kulawiec, *J. Am. Chem. Soc.* **1993**, *115*, 2027–2036.
[12] B. M. Trost, J. A. Martinez, R. J. Kulawiec, A. F. Indolese, *J. Am. Chem. Soc.*, in press.
[13] T. Mitsudo, H. Naruse, T. Kondo, Y. Ozaki, Y. Watanabe, *Angew. Chem.* **1994**, *106*, 595–597; *Angew. Chem. Int. Ed. Engl.* **1994**, *33*, 580–581.
[14] N. Oshima, H. Suzuki, Y. Moro-oka, *Chem. Lett.* **1984**, 1161–1164.
[15] T. Mitsudo, K. Kokuryo, T. Shinsugi, Y. Nakagawa, Y. Watanabe, Y. Takegami, *J. Org. Chem.* **1979**, *44*, 4492–4496.
[16] T. Mitsudo, Y. Hori, Y. Watanabe, *J. Organomet. Chem.* **1987**, *334*, 157–167.
[17] P. G. Gassman, J. W. Mickelson, J. R. Sowa, Jr., *J. Am. Chem. Soc.* **1992**, *114*, 6942–6944.
[18] M. A. Halcrow, F. Urbanos, B. Chaudret, *Organometallics* **1993**, *12*, 955–957.

 © VCH Verlagsgesellschaft mbH, D-69451 Weinheim, 1994 0570-0833/94/0606-0638 $ 10.00+.25/0

A Novel Open-Framework Cobalt Phosphate Containing a Tetrahedrally Coordinated Cobalt(II) Center: $CoPO_4 \cdot 0.5\ C_2H_{10}N_2$ **

Jiesheng Chen, Richard H. Jones, Srinivasan Natarajan, Michael B. Hursthouse, and John Meurig Thomas*

The ever-growing family of microporous aluminophosphates, first synthesized in 1982,[1] continues to stimulate synthesis of other novel compounds with open-framework structures comparable to the naturally occurring zeolites. Among the so-called ALPO family ($AlPO_4$-*n*, where *n* signifies a distinct framework structure) some members have structures exactly analogous to those of zeolites (for example, $AlPO_4$-17 has the erionite structure[2] and $AlPO_4$-20 is isostructural with sodalite[1]), whereas others (such as VPI-5[3] and JDF-20[4]) have no naturally occurring counterparts. Notable examples of newly synthesized open-framework structures containing elements other than Si and Al are the gallophosphate cloverite, which has 20-membered rings as openings,[5] and $Zn_7[P_{12}N_{24}]Cl_2$ (which consists of sodalite units constructed with P–N linkages),[6] germanium dioxides,[7] and several beryllium and zinc phosphates.[8–11] The formation of open-framework structures with transition metal phosphates was first demonstrated for iron.[12] Recent work by Haushalter and co-workers has opened up a rich chemistry with molybdenum compounds.[13–15] It has also proved possible to introduce relatively low concentrations of transition metals into various members of the $AlPO_4$-*n* family,[16, 17] and there are structures in which the transition metal is found in a quite high concentration.[18] To our knowledge, however, there are no reported examples of an open framework constructed from transition metal phosphate in which the transition metal is exclusively in a tetrahedral environment and is present in a metal/P ratio of unity. Here we report the first framework structure based on cobalt, phosphorus, and oxygen only, which is, additionally, the first cobalt phosphate of any type that has the metal exclusively in a tetrahedral environment. The compound is designated DAF-2 (Davy Faraday number 2; DAF-1 is a magnesium aluminum phosphate[19] with a framework composition of $Mg_{0.22}Al_{0.78}PO_4$).

The deep blue DAF-2 crystallizes in the monoclinic space group *I*2/*b* (nonstandard setting) with $a = 14.719(6)$, $b = 14.734(5)$, $c = 17.891(6)$ Å, $\gamma = 90.02(2)°$. The structure is based on a network of strictly alternating CoO_4 and PO_4 tetrahedra in which all the vertices are shared (Fig. 1). It thus differs markedly from other transition metal phosphates or arsenates with an open-framework structure[12–15, 20] where there is octahedral coordination of the metal. DAF-2 is similar to microporous phosphates with other divalent nontransition metals, such as beryllium, and zinc.[8–11] The formula of the anionic structure is $[CoO_2PO_2]^-$, and its stoichiometry is similar to that found in the zinc and beryllophosphates. This composition results in the same anionic charge as found for Lowenstein-limited zeolites with an Al:Si ratio of 1:1, $[AlO_2SiO_2]^-$.[11] The charge neutrality for DAF-2 is achieved by incorporation of the template in its protonated form: there are 0.5 $[H_2en]^{2+}$ ions per framework formula unit (en = ethylenediamine).

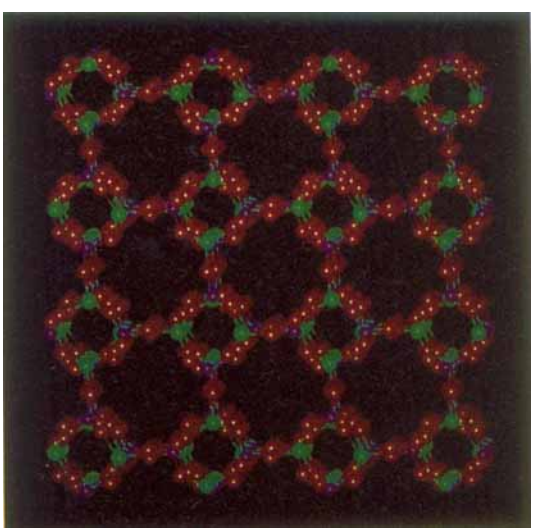


Fig. 1. The framework structure of DAF-2 viewed along the [001] axis. Red: oxygen; green: cobalt; violet: phosphorus. For clarity, the template molecules occluded in the framework channels are omitted. The channel window contains eight T atoms (T = Co and P) which are strictly alternated.

The framework structure consists of three systems of channels with windows containing eight T-atoms (T = Co and P) parallel to each of the crystallographic axes. The channels which are in the [001] direction have fairly regular windows with O–O distances which lie between 3.9 and 4.7 Å. The structure is pseudotetragonal; the channels in the [100] and [010] directions have similar characteristics (Fig. 2). The windows of these latter channels which do not intersect with each other, are irregular in shape with O–O contacts which vary between 1.9 and 4.8 Å. These channels do, however, intersect with those parallel to [001] giving rise to a three-dimensional open network, at the junctions of which the diprotonated ethylenediamine cations are preferentially accommodated. The organic cations are hydrogen-bonded to the oxygen atoms of the framework. The structure can be related to a previously predicted 4.8.8 net[21] in the (001) plane. These net layers are linked through the four-mem-

[*] Prof. Sir John Meurig Thomas, Dr. J. Chen, Dr. S. Natarajan
Davy Faraday Research Laboratory
The Royal Institution of Great Britain
21 Albemarle Street, London W1X 4BS (UK)
Telefax: Int. code +(71)629-3569
Dr. R. H. Jones
Department of Chemistry, Keele University
Staffordshire ST5 5BG (UK)
Prof. M. B. Hursthouse
Department of Chemistry, University of Wales,
College of Cardiff
PO Box 68, Cardiff CF1 3XA (UK)

[**] This work was supported by Science and Engineering Research Council (SERC), the Royal Society, and Unilever plc. We thank Dr. R. G. Bell for technical help.

 © VCH Verlagsgesellschaft mbH, D-69451 Weinheim, 1994 0570-0833/94/0606-0639 $ 10.00+.25/0

bered rings arranged in an "untwisted" manner with respect to the layer below. Structures based upon the idealised 4.8.8 net have also been found for both naturally occurring and synthetic compounds[11, 22–24]

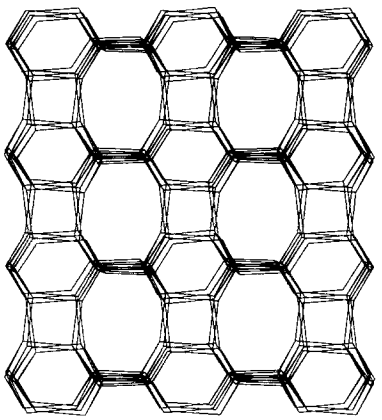


Fig. 2. The framework structure of DAF-2 depicting only (Co P) atoms viewed along either the [100] or the [010] direction.

In previously synthesized cobalt phosphates, the Co^{II} centers were coordinated to five or six oxygen atoms.[25, 26] And although it is possible to introduce Co^{II} into three-dimensional open-framework structures where the Co atom resides in a tetrahedral environment,[16–18] in none of these compounds does the Co/P ratio approach unity. Thus DAF-2 is the first cobalt(II) phosphate in which Co is found exclusively in a tetrahedral site and there is a Co/P ratio of unity. The Co–O distances vary from 1.906 to 1.992 Å, and the average (1.95 Å) is in good agreement with those for Co tetrahedrally coordinated to four oxygen atoms, for example, 1.947 Å in Co_3O_4.[27] The P–O distances are within the range 1.480–1.576 Å, and the average (1.53 Å) is quite similar to that seen in cobalt phosphates (for example, 1.538 Å in $Co_3(PO_4)_2$) and comparable to that in berlinite (1.516 Å), which is the aluminum phosphate analogue of quartz.[28]

Differential thermal analysis and thermal gravimetric analysis shows that the template ethylenediamine occluded in DAF-2 structure decomposes endothermically at 400–500 °C, which gives rise to a marked weight loss. At 600–700 °C, the compound undergoes recrystallization, as indicated by an intense exothermic effect without significant weight loss. After the template decomposes, DAF-2 becomes X-ray amorphous; thus, as expected, the thermal stability of DAF-2 is inferior to that of most members of the $AlPO_4$-*n* family and the newly synthesized magnesium aluminum phosphate[19] DAF-1. When held for prolonged periods at the recrystallization temperature, DAF-2 converts via an amorphous phase into a crystalline phase of composition $Co_2P_2O_7$ and known structure.[29]

Whilst it has not yet proved possible to remove the template of this solid thermally to obtain a microporous material, we are currently investigating chemical routes to achieve this goal, which would open up many intriguing possibilities in materials chemistry. Preliminary magnetic measurements with a SQUID magnetometer under an applied field of 100 G, down to 1 K, reveal that the solid exhibits classic Curie–Weiss paramagnetism down to about 5 K. At 2 K, the solid orders antiferromagnetically.

Experimental procedure

DAF-2 was synthesized hydrothermally from a cobalt phosphate gel containing ethylenediamine as a structure-directing template. Thus, cobalt carbonate hydrate, phosphoric acid (85%), ethylenediamine (en), and water in the ratio $CoO:0.9P_2O_5:1.0en:1.0H_2CO_3:25H_2O$ were mixed and stirred until homogeneous. The mixture was sealed in a PTFE-lined stainless steel autoclave and heated at 190 °C for 3 days. Pure deep blue crystals suitable for X-ray analysis were recovered by filtering off the solid products. The blue colour is indicative of the presence of tetrahedrally coordinated cobalt(II) centers. Chemical analysis yields an empirical formula of $CoHPO_4 \cdot 0.5en$ for the compound. Single crystal diffraction data were collected with an Enraf-Nonius FAST diffractometer with Mo(Kα) radiation ($\lambda = 0.71069$ Å). A total of 15310 reflections were collected of which 8992 satisfied the criterion for measurement. These were merged to give 4960 unique data of which 1730 were considered to be observed with $I > 3\sigma(I)$. The structure was refined by full-matrix least squares to $R = 0.073$ and $R_w = 0.057$ with a total of 170 parameters. During the final stages of refinement a total of 8 reflections with $F_o \ll F_c$ were omitted. A nonstandard setting of *I*2/*b* was chosen because of the pseudotetragonal nature of the structure. Whilst the structure can be refined in space group $I4_1/a$, the *R* values at all corresponding stages of the refinement were much higher, and the model required a disordered arrangement of the template molecule. Further details of the crystal structure investigation may be obtained from the Director of the Cambridge Crystallographic Data Centre, 12 Union Road, GB-Cambridge CB2 1EZ on quoting the full literature citation.

Received: September 1, 1993 [Z 6328 IE]
German version: *Angew. Chem.* **1994**, *106*, 667

[1] S. T. Wilson, B. M. Lok, C. A. Messina, T. R. Cannan, E. M. Flanigen, *J. Am. Chem. Soc.* **1982**, *104*, 1146.
[2] J. J. Pluth, J. V. Smith, J. M. Bennett, *Acta Crystallogr. Sect. C* **1986**, *42*, 283.
[3] M. E. Davis, C. Saldarriaga, C. Montes, J. Garces, C. Growder, *Nature* **1988**, *331*, 698.
[4] R. H. Jones, J. M. Thomas, J. Chen, R. Xu, Q. Huo, S. Li, Z. Ma, A. M. Chippendale, *J. Solid State Chem.* **1993**, *102*, 204.
[5] M. Esterman, L. B. McCusker, C. Baerlocher, A. Merrouche, H. Kessler, *Nature* **1991**, *352*, 320.
[6] W. Schnick, J. Lücke, *Angew. Chem.* **1992**, *104*, 208; *Angew. Chem. Int. Ed. Engl.* **1992**, *31*, 213.
[7] R. H. Jones, J. Chen, J. M. Thomas, A. George, M. B. Hursthouse, R. Xu, S. Li, Y. Lu, G. Yang, *Chem. Mater.* **1992**, *4*, 808.
[8] T. E. Gier, G. D. Stucky, *Nature* **1991**, *349*, 508.
[9] T. M. Nenoff, W. T. A. Harrison, T. E. Gier, G. D. Stucky, *J. Am. Chem. Soc.* **1991**, *113*, 378.
[10] W. T. A. Harrison, T. E. Gier, G. D. Stucky, *J. Mater. Chem.* **1991**, *1*, 153.
[11] W. T. A. Harrison, T. E. Martin, T. E. Gier, G. D. Stucky, *J. Mater. Chem.* **1992**, *1*, 175.
[12] D. R. Corbin, J. F. Whitney, W. C. Fulz, G. D. Stucky, M. M. Eddy, A. K. Cheetham, *Inorg. Chem.* **1986**, *25*, 2279.
[13] R. C. Haushalter, K. G. Strohmaier, F. W. Lai, *Science* **1989**, *246*, 1289.
[14] H. E. King, Jr., R. C. Haushalter, L. A. Mundi, K. G. Strohmaier, *J. Solid State Chem.* **1991**, *92*, 154.
[15] L. A. Meyer, R. C. Haushalter, *Inorg. Chem.* **1993**, *32*, 1579.
[16] S. T. Wilson, E. M. Flanigen, US-A 4567029, **1986**.
[17] J. Chen, G. Sankar, J. M.Thomas, R. Xu, G. N. Greaves, D. Waller, *Chem. Mater.* **1992**, *4*, 1373.
[18] J. M. Bennet, B. K. Marcus in *Innovation in Zeolite Materials Science* (Eds.: P. J. Grobet, W. J. Mortier, G. Schulz-Ekloff), Elsevier, Amsterdam, **1988**, p. 269.
[19] P. A. Wright, R. H. Jones, S. Natarajan, R. G. Bell, J. Chen, M. B. Hursthouse, J. M. Thomas, *J. Chem. Soc. Chem. Commun.* **1993**, 633.
[20] M. J. Buerger, W. A. Dollase, I. Garayochea-Wittke, *Z. Kritsallogr.* **1967**, *125*, 92.
[21] J. V. Smith, *Am. Mineral.* **1978**, *63*, 960.
[22] J. M. Bennett, W. J. Dytrych, J. J. Pluth, J. W. Richardson, Jr., J. V. Smith, *Zeolites* **1986**, *6*, 349.
[23] J. V. Smith, *Chem. Rev.* **1988**, *88*, 149.
[24] A. J. Alberti, G. Vezzalini, *Acta Crystallogr. Sect. B* **1979**, *35*, 2866.
[25] P. Lightfood, A. K. Cheetham, *Acta Crystallogr. Sect. C* **1988**, *44*, 1331.
[26] B. B. Anderson, E. Kostiner, M. C. Miller, J. R. Rea, *J. Solid State Chem.* **1975**, *14*, 372.
[27] J. P. Picard, G. Baud, J. P. Besse, R. Chevalier, *J. Less-Common Metals* **1980**, *75*, 99.
[28] D. Schwarzenbach, *Z. Kristallogr.* **1966**, *123*, 161.
[29] J. B. Forsyth, C. Wilkinson, S. Paster, B. M. Wanklyn, *J. Phys. C.* **1989**, *1*, 169.

 © VCH Verlagsgesellschaft mbH, D-69451 Weinheim, 1994 0570-0833/94/0606-0640 $ 10.00+.25/0

Ionization and Delocalization in Potassium Zeolite L: A Combined Neutron Diffraction and Electron Spin Resonance Study**

Paul A. Anderson,* A. Robert Armstrong, and Peter P. Edwards*

On account of their regular intracrystalline channels and cavities, and consequent large internal surface area, zeolites – powerful catalysts in their own right – have found increasing use as supports for dispersed metal catalysts.[1] Since alkali metals are paramagnetic in states of aggregation ranging from the free atom to bulk metal itself, electron spin resonance (ESR) spectroscopy is particularly suited to the study of dispersions of these metals in zeolites.[2–5] Although single-line ESR spectra for such materials have been widely attributed to the presence of metal clusters or particles within the zeolite pores,[2–4] some recent work has questioned this interpretation.[5,6] Here we present the results of the first combined structural and spectroscopic study of an alkali metal dispersed in a zeolite support. The interaction of potassium vapor with zeolite L leads to spontaneous ionization of the guest metal atoms and delocalization of the resulting electrons among the potassium cations that line the one-dimensional channels of the zeolite host.

The pale blue solid K_1/K_9-L was prepared through the controlled reaction of dehydrated potassium LTL (K_9-L) with a calibrated amount of potassium vapor equivalent to one potassium atom per unit cell. Rietveld refinement of neutron diffraction data from unloaded K_9-L and from K_1/K_9-L converged to yield the final parameters given in Tables 1 and 2, respectively; calculated diffractograms and the corresponding difference profiles of both materials are shown in Figure 1. In both dehydrated K_9-L and K_1/K_9-L potassium was located in only three sites, K(2), K(3), and K(4), which correspond to cation positions B, C, and D, respectively[7] (Fig. 2). The conversion of K_9-L to K_1/K_9-L through the inclusion of potassium metal resulted in a small decrease in both lattice parameters a and c, but the most significant structural change was an increase in the partial occupancy of the K(4) site in the large channels from 0.72(7) to 0.92(6), which accounts neatly for the extra potassium atom incorporated from the vapor phase.

Table 1. Structural parameters for K_9-L (space group $P6/mmm$, $a = 18.483(1)$, $c = 7.4938(4)$ Å).

Atom	Position	x/a	y/b	z/c	B_{iso} [Å^2]	Occupancy
Si(1)/Al(1)	12 q	0.0921(6)	0.3546(6)	0.5000	2.0(2)	0.75/0.25
Si(2)/Al(2)	24 r	0.1666(5)	0.4990(4)	0.2110(7)	0.9(1)	0.75/0.25
O(1)	6 k	0.0000	0.2749(5)	0.5000	1.2(1)	
O(2)	6 m	0.1657(3)	0.3313(6)	0.5000	2.3(2)	
O(3)	12 o	0.2653(2)	0.5307(4)	0.2576(9)	1.7(1)	
O(4)	24 r	0.1004(4)	0.4143(4)	0.3225(6)	2.4(1)	
O(5)	12 o	0.4261(2)	0.8521(5)	0.2720(9)	2.4(1)	
O(6)	12 p	0.1457(4)	0.4779(4)	0.0000	1.7(1)	
K(2)	2 d	0.3333	0.6667	0.5000	2.0(5)	
K(3)	3 g	0.0000	0.5000	0.5000	3.5(6)	
K(4)	6 j	0.0000	0.3156(14)	0.0000	2.5(7)	0.72(7)

[a] $R_P = 0.043$, $R_{WP} = 0.029$, $R_E = 0.028$, $R_I = 0.070$.

Table 2. Structural parameters for K_1/K_9-L (space group $P6/mmm$, $a = 18.4503(5)$, $c = 7.4852(2)$ Å).

Atom	Position	x/a	y/b	z/c	B_{iso} [Å^2]	Occupancy
Si(1)/Al(1)	12 q	0.0911(4)	0.3553(4)	0.5000	1.5(1)	0.75/0.25
Si(2)/Al(2)	24 r	0.1673(3)	0.4999(3)	0.2113(5)	0.5(1)	0.75/0.25
O(1)	6 k	0.0000	0.2739(4)	0.5000	0.9(1)	
O(2)	6 m	0.1651(2)	0.3303(4)	0.5000	1.8(1)	
O(3)	12 o	0.2652(1)	0.5303(3)	0.2569(7)	1.8(1)	
O(4)	24 r	0.1011(2)	0.4148(3)	0.3191(4)	1.9(1)	
O(5)	12 o	0.4267(2)	0.8534(4)	0.2728(7)	2.2(1)	
O(6)	12 p	0.1457(3)	0.4777(3)	0.0000	1.5(1)	
K(2)	2 d	0.3333	0.6667	0.5000	0.9(3)	
K(3)	3 g	0.0000	0.5000	0.5000	3.3(4)	
K(4)	6 j	0.0000	0.3138(11)	0.0000	5.6(8)	0.92(6)

[a] $R_P = 0.055$, $R_{WP} = 0.046$, $R_E = 0.030$, $R_I = 0.061$.

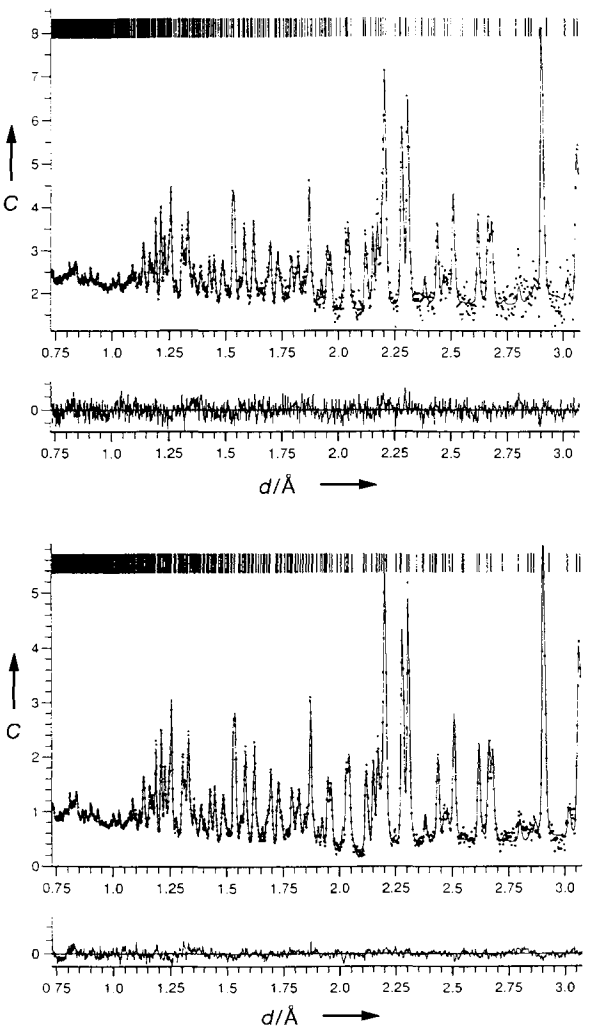


Fig. 1. Observed and calculated neutron diffraction patterns for dehydrated K_9-L (top) and K_1/K_9-L (bottom), and the corresponding difference profiles. C = normalized neutron counts.

[*] Prof. Dr. P. P. Edwards
School of Chemistry, University of Birmingham
Edgbaston, GB-Birmingham B15 2TT (UK)
Telefax: Int. code +(21)414-4403
Dr. P. A. Anderson[+]
University Chemical Laboratory
Lensfield Road, GB-Cambridge CB2 1EW (UK)
Dr. A. R. Armstrong
Rutherford Appleton Laboratory, Chilton, Didcot (UK)
[+] Present address: School of Chemistry, University of Birmingham (UK)

[**] This work was supported by the British Science and Engineering Research Council, which also provided the neutron beam facilities. P. A. A. thanks the Royal Society for the award of a University Research Fellowship.

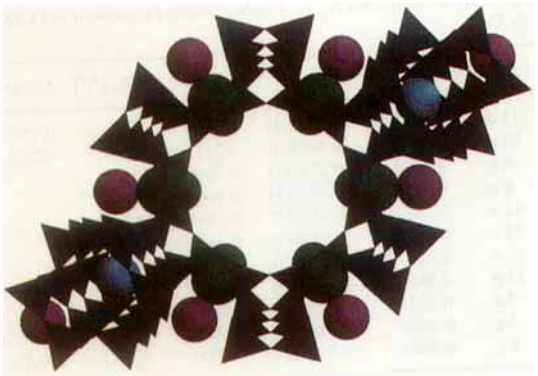


Fig. 2. The structure of zeolite L viewed along the c axis, showing the three potassium sites K(2), K(3), and K(4) in pale blue, purple, and green, respectively.

Observation of the included potassium in K_1/K_9-L in a conventional ionic site on the zeolite framework is convincing proof that ionization of the incoming potassium atoms has occurred. Presumably in return for a framework coordination site, the guest atoms give up their valence electrons, which then interact with the framework cations. This process has been proposed in other sodium and potassium zeolites, where it leads to the creation of paramagnetic centers of the form $(M^+)_n e^-$ consisting of an electron delocalized over a well-defined number of cations.[2, 8, 9] In the case of K_1/K_9-L, however, ESR measurements were unable to detect centers of this kind. Moreover, although the ESR spectrum of K_1/K_9-L (Fig. 3) was consistent ($g = 1.9995 \pm 0.0003$, $\Delta H_{pp} = 2.65 \pm 0.05$ mT) with those of metallic clusters or small particles of potassium located within zeolite pores,[2, 4] the diffraction data provided no evidence for clustering or particle formation.

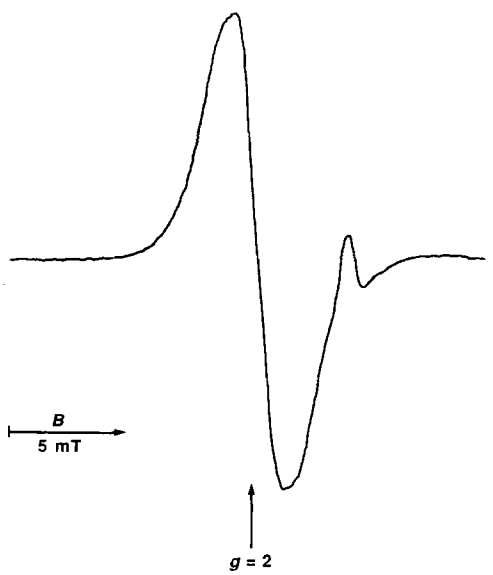


Fig. 3. The ESR spectrum of K_1/K_9-L at 77 K.

Using linewidth and hyperfine splitting parameters measured from the K_4^{3+} center ($n = 4$),[2] we have simulated (see Fig. 4) ESR spectra for a zeolite in which an electron interacts with different numbers of potassium ions. We conclude that the observed spectrum results from electron spins delocalized over a sufficiently large number of cations such that individual hyperfine splittings cannot be resolved. In such cases Anderson et al.[5] showed how the number of ions involved may be estimated from the observed ESR linewidth; a figure of $n \approx 30$–40 is estimated for K_1/K_9-L. In this case the ESR spectrum also exhibits a secondary feature at high field ($g = 1.9739 \pm 0.0005$), which is probably indicative of anisotropy in the sample (Fig. 3). Although this phenomenon has not to our knowledge been observed before in alkali metal zeolites, it is consistent with the one-dimensional channel structure of zeolite L (Fig. 2). As diffraction data clearly locates the included potassium ions in the large channels of zeolite L, for reasons of charge balance it is likely that released valence electrons interact primarily with the potassium cations at K(4) positions there. In order to interact

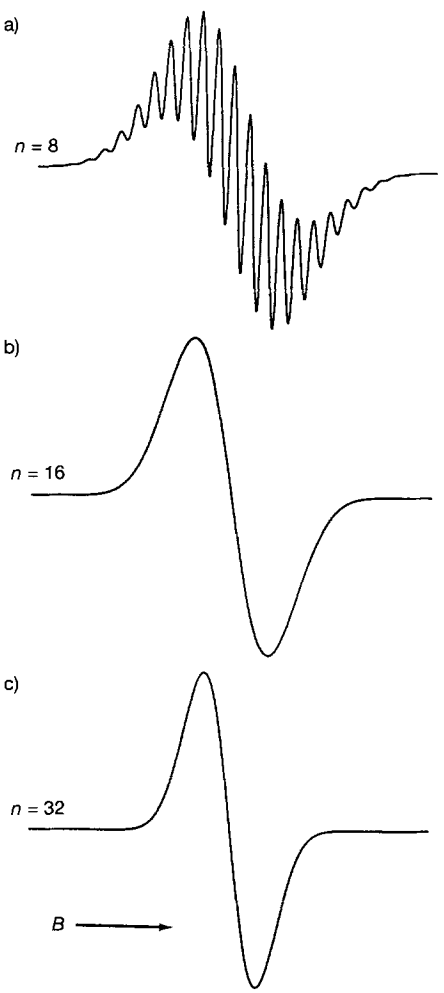


Fig. 4. Simulated ESR spectra ($\Delta H_{pp} = 0.8$ mT, $a = 1.71 \times 4/n$ mT) for $(K^+)_n e^-$. a) $n = 8$, b) $n = 16$, and c) $n = 32$.

with 30–40 such cations, each electron if confined to a single channel would have to be effectively delocalized over a distance of 6–8 unit cells or 4.5–6.0 nm. Through careful fine-tuning of the concentration of electrons in the one-dimensional channels of zeolite L it may be possible to engineer charge transport along the channels and produce a unique compound comprising a

 © VCH Verlagsgesellschaft mbH, D-69451 Weinheim, 1994 0570-0833/94/0606-0642 $ 10.00+.25/0

precise array of ultrafine, atomic-scale conducting wires embedded in the aluminosilicate zeolite framework.

Experimental Procedure

The compound K_1/K_9-L was prepared through the controlled reaction (in sealed quartz reaction tubes) of dehydrated potassium zeolite LTL (K_9-L) (supplied by Laporte) with an amount of potassium vapor equivalent to one potassium atom per zeolite unit cell; the general procedure has been described in detail elsewhere [5]. The ESR spectrum of the resultant pale blue powder was recorded on a Varian E-109 spectrometer operating at X-band frequencies (9.3 GHz) witb 100 kHz field modulation. The microwave frequency was measured with a Hewlett-Packard 5342A frequency counter to an accuracy of ± 1 kHz, and g-values were determined through comparison of the resonant field with that of the 1,1-diphenyl-2-picrylhydrazyl (DPPH) radical ($g = 2.0036$).

Neutron diffraction measurements were performed at room temperature on the POLARIS diffractometer at the ISIS pulsed source of the Rutherford Appleton Laboratory. Since the alkali metal loaded zeolites exhibit great air sensitivity, and dehydrated zeolites readily absorb water, the materials were studied in their original quartz reaction vessels. In order to eliminate the background signals of amorphous silicon dioxide, data were also collected from an empty sample tube. These data were then smoothed, appropriately scaled, and subtracted from the zeolite diffraction patterns to produce an essentially flat background. Rietveld refinement of the structure used the least squares program TF14LS based on the Cambridge Crystallographic Subroutine Library [10]. Scattering lengths for K, Si, Al, and O were taken to be 0.367, 0.41534, 0.3449, and 0.5803×10^{-12} cm, respectively [11]. The structure was refined in the space group *P6/mmm* as reported in previous studies by Barrer and Villiger [7], and Newsam [12]. The positions of the framework atoms were refined before introduction of the potassium cations. Although Newsam [12b] reported different site preferences for silicon and aluminium, in view of the similarity in scattering lengths, we fixed the Si:Al ratio at the theoretical value of 3.0 for both sites throughout the analyses. Difference Fourier methods were used to search for additional potassium sites in K_1/K_9-L.

Received: November 2, 1993 [Z6471 IE]
German version: *Angew. Chem.* **1994**, *106*, 669

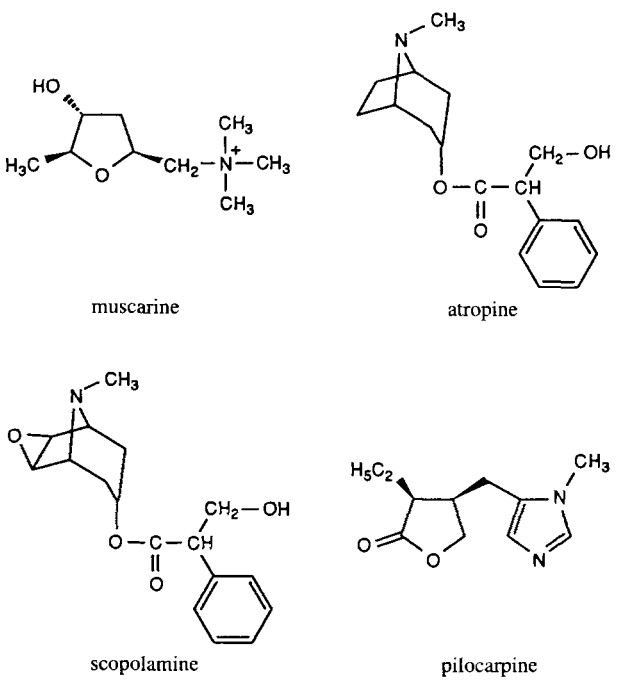
[1] A. Dyer, *An Introduction to Zeolite Molecular Sieves*, Wiley, New York, **1988**, p. 117.
[2] P. P. Edwards, M. R. Harrison, J. Klinowski, S. Ramdas, J. M. Thomas, D. C. Johnson, C. J. Page, *J. Chem. Soc. Chem. Commun.* **1984**, 982–984; M. R. Harrison, P. P. Edwards, J. Klinowski, J. M. Thomas, D. C. Johnson, C. J. Page, *J. Solid State Chem.* **1984**, *54*, 330–341.
[3] L. R. M. Martens, P. J. Grobet, W. J. M. Vermeiren, P. A. Jacobs, *Stud. Surf. Sci. Catal.* **1986**, *28*, 935–941; P. J. Grobet, L. R. M. Martens, W. J. M. Vermeiren, D. R. C. Huybrechts, P. A. Jacobs, *Z. Phys. D. At. Mol. Clusters* **1989**, *12*, 37–40; R. E. H. Breuer, E. De Boer, G. Geismar, *Zeolites* **1989**, *9*, 336–340; F. Blatter, K. W. Blazey, A. M. Portis, *Phys. Rev. B. Condens. Matter* **1991**, *44*, 2800–2802.
[4] K. W. Blazey, K. A. Müller, F. Blatter, E. Schumacher, *Europhys. Lett.* **1987**, *4*, 857–861; Y. Katayama, K. Maruyama, H. Endo, *J. Non-Cryst. Solids* **1990**, *117*, 485–488; B. Xu, L. Kevan, *J. Chem. Soc. Faraday Trans.* **1991**, *87*, 2843–2847; *J. Phys. Chem.* **1992**, *96*, 2642–2645.
[5] P. A. Anderson, P. P. Edwards, *J. Am. Chem. Soc.* **1992**, *114*, 10608–10618.
[6] G. Schäfer, W. W. Warren, P. A. Anderson, P. P. Edwards, *J. Non-Cryst. Solids* **1993**, *156–158*, 803–806.
[7] R. M. Barrer, H. Villiger, *Z. Kristallogr.* **1969**, *128*, 352–370.
[8] J. A. Rabo, C. L. Angell, P. H. Kasai, V. Schomaker, *Discuss. Faraday Soc.* **1966**, *41*, 328–349; P. A. Anderson, P. P. Edwards, *J. Chem. Soc. Chem. Commun.* **1991**, 915–917; P. A. Anderson, D. Barr, P. P. Edwards, *Angew. Chem.* **1991**, *103*, 1511–1512; *Angew. Chem. Int. Ed. Engl.* **1991**, *30*, 1501–1502.
[9] P. A. Anderson, R. J. Singer, P. P. Edwards, *J. Chem. Soc. Chem. Commun.* **1991**, 914–915.
[10] J. C. Matthewman, P. Thompson, P. J. Brown, *J. Appl. Crystallogr.* **1982**, *15*, 167–173; P. J. Brown, J. C. Matthewman, Rutherford Appleton Laboratory Report, RAL-87-010, **1987**.
[11] V. F. Sears, *Neutron News* **1992**, *3* (3), 26.
[12] a) J. M. Newsam, *Mater. Res. Bull.* **1986**, *21*, 661–672; b) J. M. Newsam, *J. Phys. Chem.* **1989**, *93*, 7689–7694.

Mapping the Electrostatic Potential of Muscarinic and Nicotinic Agonists with Artificial Neural Networks**

Johann Gasteiger* and Xinzhi Li

Signals in biological neural networks are transmitted between neurons by chemicals, called neurotransmitters, that are released at the terminus of the axon of one neuron, cross the synaptic gap, and then bind to receptors in the postsynaptic membrane of a dendrite of another neuron where they cause an electrical signal. Acetylcholine is such a neurotransmitter occurring in a variety of neuron types of the sympathetic and parasympathetic nervous system. It binds to at least two different receptors, the muscarinic and the nicotinic receptor.

The ring system makes muscarine structurally fairly rigid; thus it can only bind to the receptor that has been given its name. Scheme 1 shows muscarine and three other molecules that are agonists of muscarine and likewise bind only to the muscarinic receptor.

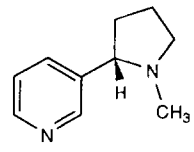


Scheme 1. Muscarine and three of its agonists, atropine, scopolamine, and pilocarpine.

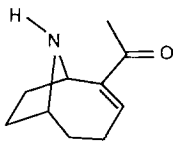
Similarly, nicotine has such a rigid structure that it binds only to the nicotinic receptor as do the other three molecules of Scheme 2.

[*] Prof. Dr. J. Gasteiger,[+] Dr. X. Li
Organisch-chemisches Institut der Technischen Universität München
Lichtenbergstrasse 4, D-85747 Garching (FRG)
[+] New address:
Computer-Chemie-Centrum
Universität Erlangen-Nürnberg
Nägelsbachstrasse 25, D-91052 Erlangen (FRG)
Telefax: Int. code +(9131)856566

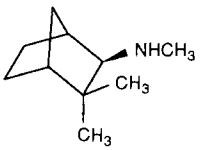
[**] Support of this work by the Bundesministerium für Forschung und Technologie, FRG is gratefully acknowledged. We appreciate helpful discussions with Prof. J. Zupan, National Institute of Chemistry, Ljubljana, Slovenia, and the contribution of Dr. J. Sadowski in the calculation of molecular surfaces and electrostatic potentials.



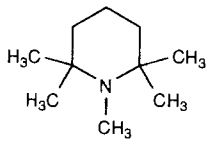
nicotine



(+)-anatoxin-a



mecamylamine



pempidine

Scheme 2. Four molecules that only bind to the nicotinic receptor: nicotine, anatoxin-a, mecamylamine, and pempidine.

In this study we report how similarities in the compounds that bind either to the muscarinic or nicotinic receptor can be found. Furthermore, dissimilarities between these two classes of compounds can be recognized.

The investigation of molecular electrostatic potentials (MEPs) is a commonly used method for unraveling the secrets of biological activity. Particularly, the MEP on a molecular surface is calculated and visualized by projection onto a computer screen. However, such projections are linear transformations and thus can only provide insight into one part of the three-dimensional molecular surface. To obtain a full picture of the entire MEP a series of observation points and associated projections is needed. We will show here that maps of the MEP obtained by Kohonen neural networks indicate characteristics common to musearinic agonists or to nicotinic agonists. The neural network paradigm that was developed by Kohonen models an important feature of the human brain, namely, the development of maps of the sensory environment in the cortex of the brain.[1, 2] The Kohonen network employs a competitive learning method that maps a point of a space (body, measurement space) into a single neuron of a two-dimensional network while conserving the topology of the information, that is, the neighborhood relationship of the points in the space.

The self-organizing formation of topological feature maps of Kohonen neural networks can be utilized as a method for the nonlinear transformation of a high-dimensional space into a one- or two-dimensional network.[3, 4] In our application, points of the three-dimensional van der Waals surface of a molecule are mapped into a two-dimensional space. In order to have a two-dimensional space in which each neuron has the same number of neighbors the projection was made onto a space without boundaries: the surface of a torus. For easier visualization the torus will be cut along two perpendicular lines and the surface spread out to form a plane which gives a rectangular array of neurons (Fig. 1).[3, 4]

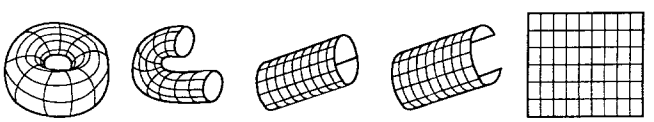


Fig. 1. The surface of a torus is cut along two perpendicular lines and spread into a plane. The little boxes of the rectangle symbolize the neurons of the network.

Learning in a Kohonen network is an unsupervised process. In our case, only the three Cartesian coordinates of the points on the van der Waals surface of a molecule are used, but not the property existing at such a point (e.g., the MEP). With three input variables, each neuron j also has three weights $\boldsymbol{w}_j = (w_{j1}, w_{j2}, w_{j3})$. Each point $\boldsymbol{x}_s = (x_{s1}, x_{s2}, x_{s3})$ on the surface will be mapped into that central neuron c_s that has weights, $\boldsymbol{w}_{c_s} = (w_{c_s1}, w_{c_s2}, w_{c_s3})$, closest to $\boldsymbol{x}_s$ with respect to the Euclidean distance [Eq. (1)]. The neuron c_s is usually referred to as the winning

$$\| \boldsymbol{x}_s - \boldsymbol{w}_{c_s} \| = \min_j \| \boldsymbol{x}_s - \boldsymbol{w}_j \| \qquad (1)$$

neuron of the input $\mathbf{x}_s$. The weights of all neurons are adjusted in the learning process iteratively for each randomly selected point $\mathbf{x}_s$ on the molecular surface.

The basic methodology for obtaining Kohonen maps of the MEP of the molecules shown in Schemes 1 and 2 is as follows:

1. Three-dimensional atomic coordinates are calulated by the automatic 3D-structure generator CORINA.[5, 6]

2. Partial atomic charges are calculated by the empirical PEOE procedure.[7, 8]

3. The electrostatic potential at points of the van der Waals surface is calculated as classical coulomb potential. (Clearly, more sophisticated quantum mechanical methods and other molecular surfaces, such as the solvent accessible surface,[9] can be used as well.)

4. 20000 points are randomly selected from the van der Waals surface with a grid of 100 points per Å^2 and used for training a Kohonen map with 100×100 neurons.

In the self-organization of the Kohonen map, points that are elose to each other on the van der Waals surface are mapped into the same or nearby neurons.

Two methods are used for visualizing the mapping of a molecular surface. In the first approaeh, a neuron of the two-dimensional Kohonen network (it is, in fact, the surface of a torus) is colored aceording to the value of the eleetrostatic potential observed at the points on the van der Waals surface that have been mapped into this neuron. A strongly negative potential is indicated in red; in order, yellow, green, blue, and purple indicate increasingly morc positive values of the MEP. This leads to maps of the MEP of the entire molecular surface.

In the second approach, the van der Waals surface is dissected into areas originating from the individual atoms of a molecule. Those parts of the surface belonging to a specific atom or group of atoms are distinguished by color. A neuron of a Kohonen map is colored according to the particular atom surface assignment (ASA) of the origin of the point mapped into this neuron. In this way, the nonlinear mapping of certain parts of the molecular surface can be identified.

Figure 2a shows a Kohonen map of the MEP on the van der Waals surface of muscarine. With this map, the entire MEP can be viewed in a *single* picture, quite in contrast to the usual representations of MEP that need a series of different viewpoints to obtain an overall impression of the MEP.

The map of Figure 2a was obtained by cutting the surface of a torus at two perpendicular lines (see Fig. 1). Such cuts can be made at arbitrary lines and thus the map of Figure 2a can be shifted into any direction. In fact, Figure 2a was obtained by centering the map on the large positive part of the MEP of muscarine—effectively putting the positively charged nitrogen into the center of the map. Figure 2b shows the same map, now centered on the negative part of the MEP. In order to show this self-containment of the Kohonen maps we have found it quite useful to put several identical maps together like tiles. This is

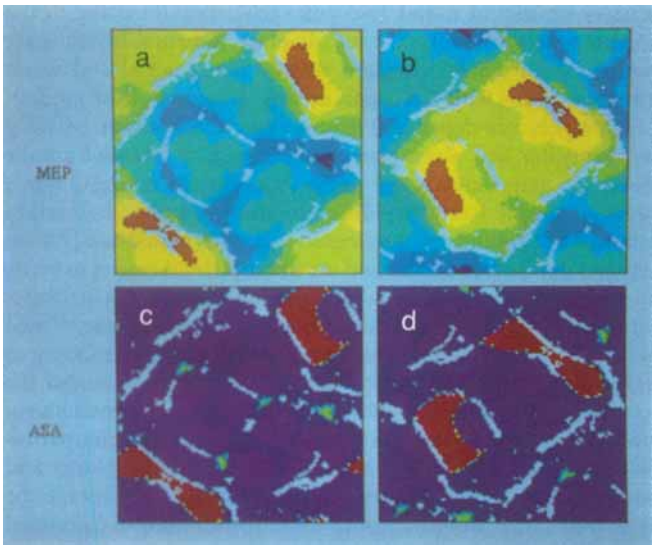


Fig. 2. Maps of the van der Waals surface of muscarine. For details see text.

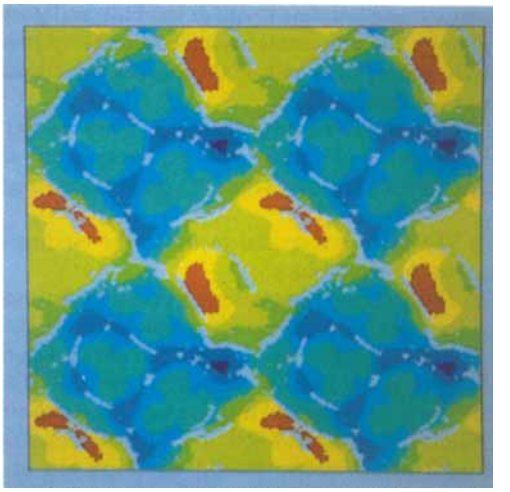


Fig. 3. Four identical maps of the MEP of muscarine put together like tiles.

shown in Figure 3 where Figure 2a has been replicated four times. Both Figure 2a and 2b can clearly be distinguished as parts of Figure 3.

While the neurons in the Kohonen map of Figure 2a and Figure 2b have been identified by the MEP observed at the points on the van der Waals surface, these Kohonen maps can be associated with any other molecular surface property. Figure 2c and Figure 2d show the very same maps of Figures 2a and 2b, now indicating the atomic surface assignment (ASA).

These ASA maps give a clearer picture of how the nonlinear transformation leads to the self-organization of the neurons. The representative surface was colored in such a way that those parts mapped by hydrogen are shown in purple and those by carbon in dark blue. The contribution of nitrogen to the van der Waals surface is indicated in green and that of the two oxygen atoms in red. Clearly, the van der Waals surface is dominated by hydrogen atoms. The carbon atoms, and particularly the nitrogen atom, are buried deeper in the molecule and are much less visible, but can still be located. The two oxygen atoms, on the other hand, can be clearly identified.

The Kohonen maps of the electrostatic potential on the van der Waals surfaces of the eight structures shown in Schemes 1 and 2 are given in Figure 4. To allow for a correct comparison, the neutral molecules were protonated at the most basic site, since this also occurs when they are bound to their receptors.[10, 11] The large positive MEP associated with the positively charged quaternary nitrogen atom clearly has a profound influence on the binding of these substrates to their respective receptors. Therefore, the maps of the MEP of these eight molecules have been arranged so that this positive MEP is in the center of the image in order to see variations at this binding site most directly.

A detailed discussion of these Kohonen maps goes beyond the scope of this paper. However, it can be seen that the maps of the four muscarinic compounds shown in the top row have some distinct common features. A regular rhomboid pattern of white lines indicating empty neurons is centered in the map. These empty neurons result from topological distortions occurring during the mapping of the molecular surface onto the topologically different surface of a torus.[12] The rhomboid pattern of empty neurons in the maps of the muscarinic compounds encloses the blue area of the positive MEP.

The maps of the four nicotinic compounds in the bottom row of Figure 4 have rather irregular patterns of empty neurons. The topological distortions indicated by these empty neurons occur directly adjacent to those parts of the molecular surface having the largest positive MEP; that is, the pattern of the white lines

VCH-YEK (KM/KE) W650/54 Aon 0/79 (Jnn Lonn) (20/04/79) 0155

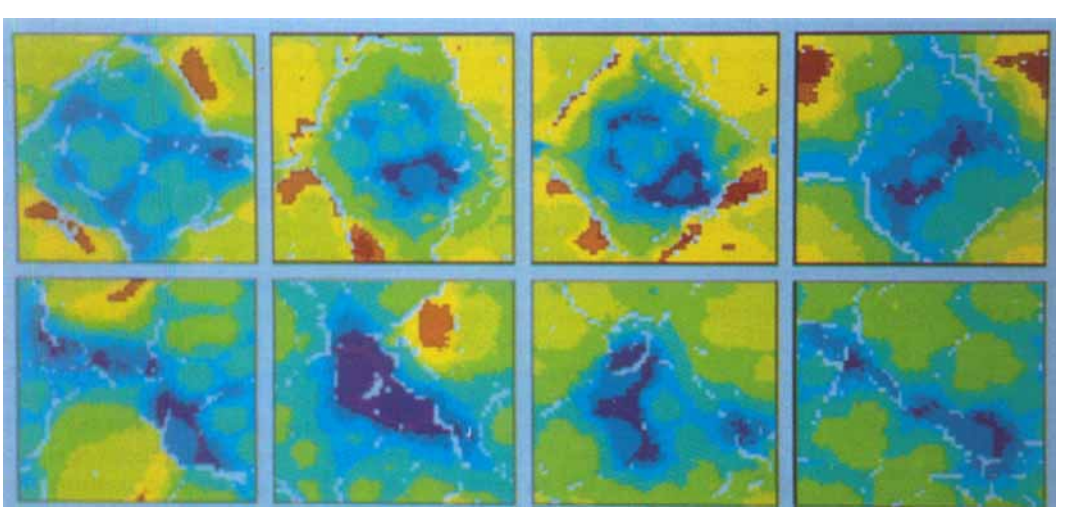


Fig. 4. Kohonen maps of (top row) muscarine and the protonated forms of atropine, scopolamine, pilocarpine and of (bottom row) the protonated form of nicotine, anatoxin-a, mecamylamine, and pempidine.

 © VCH Verlagsgesellschaft mbH, D-69451 Weinheim, 1994 0570-0833/94/0606-0645 $ 10.00+.25/0

of empty neurons cuts through the blue and purple areas. Furthermore, the blue areas are more elongated than for the muscarinic compounds and in some cases extend across the entire area of the map.

The similarities in the Kohonen maps of the MEPs of the agonists either of muscarine or of nicotine, and the clear differences between the two series of compounds suggest the following:

1. The MEP is a crucial factor in the binding of these molecules to their receptors.

2. The Kohonen maps retain essential features of the MEP and thus can help in screening biologically active compounds.

The self-organization in Kohonen networks enables the projection of properties of molecular surfaces. The mapping of MEP can give important insights into the similarity of molecules essential for biological activity. The present study shows that artificial neural networks can be employed to shed light on essential mechanisms of information processing in biological neural networks.

Received: November 16, 1993 [Z 6504 IE]
German version: *Angew. Chem.* **1994**, *106*, 671

[1] T. Kohonen, *Biol. Cybernetics* **1982**, *43*, 59–69.
[2] T. Kohonen, *Proc. IEEE* **1990**, *78*, 1464–1480.
[3] J. Gasteiger, J. Zupan, *Angew. Chem.* **1993**, *105*, 510–536; *Angew. Chem. Int. Ed. Engl.* **1993**, *32*, 503–527.
[4] J. Zupan, J. Gasteiger, *Neural Networks for Chemists: An Introduction*, VCH, Weinheim, **1993**.
[5] J. Gasteiger, C. Rudolph, J. Sadowski, *Tetrahedron Comput. Methodol.* **1990**, *3*, 537–547.
[6] J. Sadowski, C. Rudolph, J. Gasteiger, *Anal. Chim. Acta* **1992**, *265*, 233–241.
[7] J. Gasteiger, M. Marsili, *Tetrahedron*, **1980**, *36*, 3219–3228.
[8] J. Gasteiger, H. Saller, *Angew. Chem.* **1985**, *97*, 699–701; *Angew. Chem. Int. Ed. Engl.* **1985**, *24*, 687–689.
[9] M. J. Connolly, *Science* **1983**, *221*, 709–713.
[10] A. Maelicke *Angew. Chem.* **1984**, *96*, 193–219; *Angew. Chem. Int. Ed. Engl.* **1984**, *23*, 195–221.
[11] C. E. Spivak, J. A. Waters, R. S. Aronstam, *Mol. Pharmacol.* **1989**, *36*, 177–184.
[12] X. Li, J. Gasteiger, J. Zupan, *Biol. Cybernetics* **1993**, *70*, 189–198.

The Equilibrium Distribution of Semivolatile Organochloro Compounds between Atmosphere and Surface Water in the Atlantic Ocean**

Jörn Schreitmüller and Karlheinz Ballschmiter*

The distribution of chemicals in the environment is described with several unit-world models,[1] of which the fugacity approach of Mackay is the most universal. This model attributes the distribution of a substance to the tendency to achieve the same chemical potential and thus attain a thermodynamic equilibrium in all relevant environmental compartments.

For the abundance of anthropogenic or biogenic trace substances in the marine atmosphere, three situations that are interconvertible must be discussed: 1. a temporally and spatially fluctuating content as a result of varying uptake through the aerial transport path (Schlieren model; an example is the short-term, massive uptake of α and also γ-hexachlorocyclohexane in the northern hemisphere); 2. a steady-state nonequilibrium state caused by an almost constant uptake along aerial and water transport paths with the ocean as sink or source (flow model); 3. a temperature-dependent equilibrium distribution between surface water and atmosphere with only a differential uptake along the aerial and water paths (equilibrium model). For a constant supply from very different sources and a slow establishment of equilibrium, a potential thermodynamic equilibrium between the oceanic system and the atmosphere is easiest to verify by measurements in regions far from the sources. An air/water equilibrium for the distribution of hexachlorocyclohexane,[3] used as insecticide, has already been discussed in the Arctic Ocean as well as in the eastern North Pacific.[4] We have measured the content of α- and γ-hexachlorocyclohexane (HCH), pentachloromethoxybenzene (pentachloroanisol, PCA) and tetrachloro-1,4-dimethoxybenzene (TMB) in air and water of the North and South Atlantic (Fig. 1); in the process we did not average the measured values in order not to lose the information contained in the individual results.

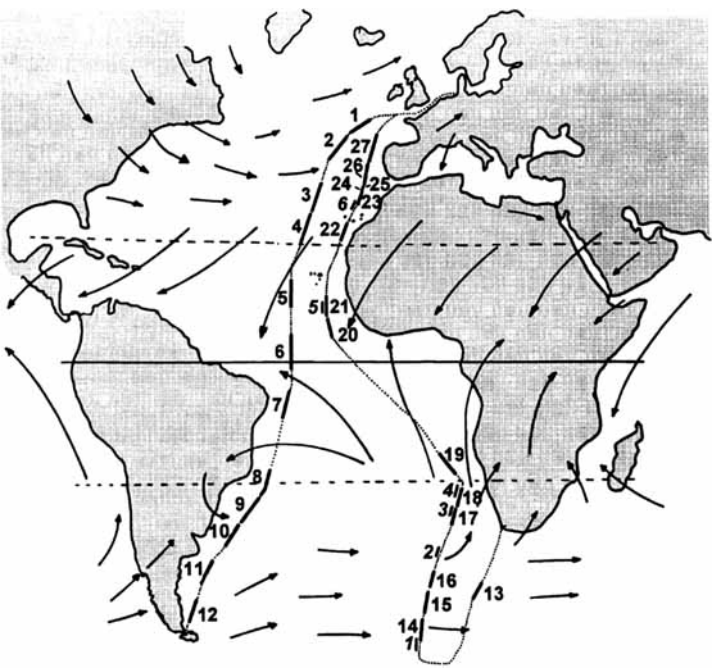


Fig. 1. Sampled zones for air samples (1–27) and water samples (1–6) in the Atlantic Ocean on the north/south cruises of the research vessel "Polarstern". The air samples 1–12 were taken in autumn 1990 on the voyage ANT IX/1 from Bremerhaven to Punta Arenas (Chile), the air samples 13–27 and the water samples 1–6 on the voyage ANT IX/4 from Cape Town to Bremerhaven. The prevailing wind directions are indicated by arrows.

The semivolatile organochloro compounds were determined in the lower troposphere and in surface water (6–8 m depth) of the Atlantic Ocean between 50 °N and 50 °S. The sampling region includes both the northern hemisphere in which the majority of the anthropogenic compounds are taken up,[1] and the southern hemisphere which functions as a global dilution zone. The two chloromethoxybenzenes are considered products of the biotransformation of pentachlorophenol[5] and via this intermediate also as metabolites of hexachlorobenzene[6] and the HCH isomers.[7] The close correlation of the concentrations of α- and γ-HCH with those of PCA and TMB in marine air confirms this interrelationship (Fig. 2).

[*] Prof. Dr. K. Ballschmiter, Dipl.-Chem. J. Schreitmüller
Abteilung Analytische Chemie und Umweltchemie der Universität
D-89069 Ulm (FRG)
Telefax: Int. code + (731)502-2763

[**] This work was supported by the Deutsche Forschungsgemeinschaft and the Fonds der Chemischen Industrie. We thank the Alfred-Wegener-Institut für Polar- und Meeresforschung, Bremerhaven, for their valued support.

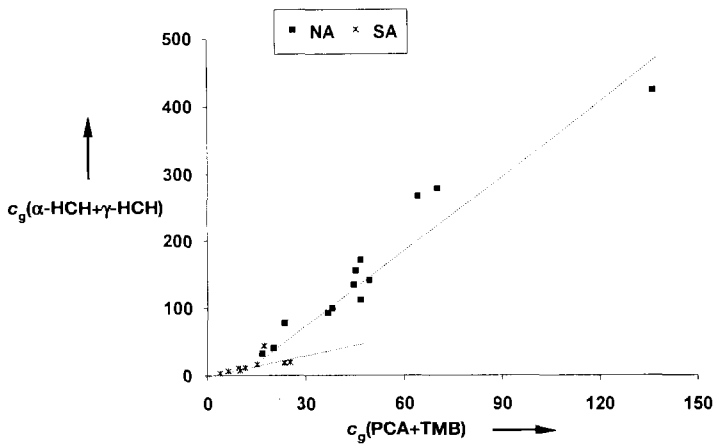


Fig. 2. Correlation of the sum of the concentrations c_g [pg m^{-3}] of α- and γ-HCH with those of pentachloromethoxybenzene and tetrachloro-1,4-dimethoxybenzene in the troposphere of the Atlantic Ocean. NA: North Atlantic, SA: South Atlantic.

The assignment of a vast meridional gradient of organochloro compounds in the lower atmosphere to a temperature-regulated, thermodynamically determined equilibrium of the air/water exchange will be described here for the first time. In addition the burden of the South Atlantic with the compounds mentioned above is documented for the first time.

The relation (1), where ΔG is the Gibbs partition energy, R the gas constant, and T the absolute temperature, is generally valid for the temperature dependence of an equilibrium constant K.

$$\ln K = -\Delta G\,(RT)^{-1} \tag{1}$$

Accordingly Equation (2), where ΔH_{gw} is the gas/water partition enthalpy and ΔS_{gw} the gas/water partition entropy, is valid

$$\ln K_{gw} = -\Delta H_{gw}\,(RT)^{-1} + \Delta S_{gw} R^{-1} \tag{2}$$

for the equilibrium distribution between atmosphere and surface water, described by the gas/water partition coefficients $K_{gw} = a_g a_w^{-1} = f_g c_g (f_w c_w)^{-1}$, ($a_g$, a_w are activities in the gaseous and aqueous phases, respectively; f_g, f_w: activity coefficients; c_g, c_w: concentrations).

The assumption f_g, $f_w = 1$ allows Equation (2) to be transformed into Equations (3.1) and (3.2), in which $A = -\Delta H_{gw} R^{-1}$ and $B = \Delta S_{gw} R^{-1}$. For a value of the gas/water partition coefficient K_{gw} of less than 10^{-2}, the change in the concentration in water resulting from evaporation or absorption as a consequence of the temperature dependence of K_{gw} is not measurable. Assumption of a virtually constant concentration in the surface water leads to the form (3.3) for Equation (3.2) ($C = \Delta S_{gw} R^{-1} + \ln c_w \approx$ constant). The slope of the linear regression function thus corresponds to $-\Delta H_{gw} R^{-1}$ and the intercept to $\Delta S_{gw} R^{-1} + \ln c_w$.

$$\ln c_g = -\Delta H_{gw}\,(RT)^{-1} + \Delta S_{gw} R^{-1} + \ln c_w \tag{3.1}$$

$$\ln c_g = A\,T^{-1} + B + \ln c_w \tag{3.2}$$

$$\ln c_g = A T^{-1} + C \tag{3.3}$$

Different contents in water at a distribution equilibrium and the same partition enthalpy are recognizable by the presence of parallel lines [Eq. (3.1)]. A plot of $\ln c_g$ vs. the reciprocal average temperature of the surface water in Kelvin yields the relationships depicted in Figures 3a–d for the studied compounds in

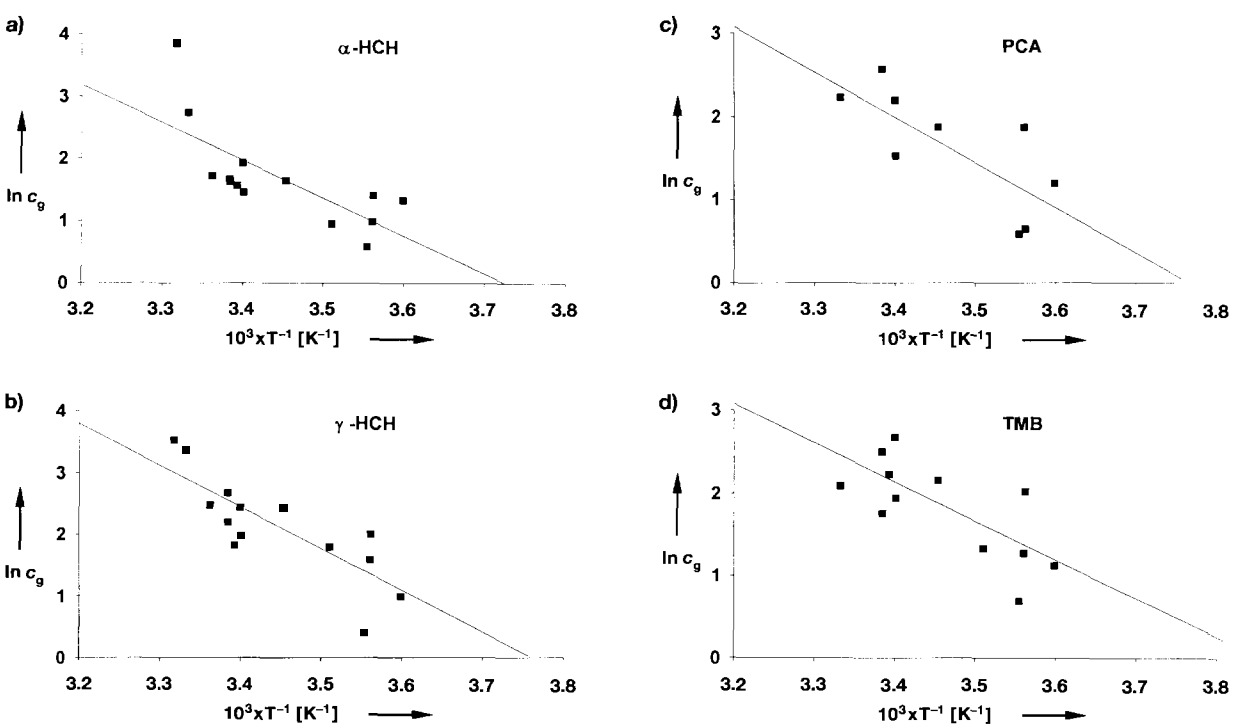


Fig. 3. Relationship between the concentrations c_g [pg m^{-3}] of α-HCH (a), γ-HCH, (b) pentachloromethoxybenzene (c), and tetrachloro-1,4-dimethoxybenzene (d) in the lower layer of the troposphere of the South Atlantic (air samples 6–12 and 13–19 from Fig. 1) and the reciprocal average water temperature at which each air sample was taken. Linear regression functions: a) $\ln c_g = -6170 \times T^{-1} + 22.94$, $r = -0.73$; b) $\ln c_g = -7130 \times T^{-1} + 26.68$, $r = -0.82$; c) $\ln c_g = -5380 \times T^{-1} + 20.31$, $r = -0.75$; d) $\ln c_g = -4730 \times T^{-1} + 18.20$, $r = -0.72$.

 © VCH Verlagsgesellschaft mbH, D-69451 Weinheim, 1994 0570-0833/94/0606-0647 $ 10.00+.25/0

the South Atlantic. All air samples collected on both cruises of the "Polarstern" south of the high-rising, intertropical convergence zone (ITCZ) formed by the convergence of the north eastern and south eastern Trades[11] were plotted. For the South Atlantic it was shown that a largely uniform distribution of the four compounds in water is valid.

Deviations from linearity according to Equation (3.3) result from a not yet completely established equilibrium. This situation can arise, for instance, when rapid air movements bring air masses from colder or warmer regions, and the equilibrium with the water has not yet compensated the depleted or enriched contents in the atmosphere. On the other hand, interactions in the aqueous phase lead to a decrease in activities ($a_w = f_w c_w$ in which $f_w < 1$), and also noticeable fluctuations in the concentrations in surface water itself, cause apparent deviations from the equilibrium state, because then the conditions for Equation (3.3) no longer hold. Despite these fundamental parameters of influence, the observed relationship over a large region of the South Atlantic is surprisingly close to the linear behavior of Equation (3.3).

From the slopes of the lines, ΔH_{gw} was determined and compared with measured values (Table 1).[8] The data calculated from our measurements in the environment for the HCH isomers correspond to a good approximation with the values determined experimentally in the laboratory for the partition enthalpies.

Table 1. Comparison of the partition enthalpies from environmental measurements in the South Atlantic with experimentally determined partition enthalpies [8]. The calculated values for the chloromethoxybenzenes have no laboratory counterpart yet.

	K_{gw} (20 °C, sea water [8])	ΔH_{gw} [a] (South Atlantic) [kJ mol^{-1}]	ΔH_{gw} [b] (Laboratory [8]) [kJ mol^{-1}]
α-HCH	3.2×10^{-3}	51 ± 11	55 ± 4
γ-HCH	2.4×10^{-3}	59 ± 11	52.5 ± 5.5
TMB		38 ± 11	
PCA		45 ± 11	

[a] The deviation is the consequence of a statistical error of ±20% in the results of the analyses. [b] The values were calculated from the Henry constants given in ref. [8] (sea water between 0.5 and 23 °C).

Furthermore, the content in the atmosphere was compared with the equilibrium concentrations defined by the physical and chemical properties of the substances under investigation. From the measured content in six water samples and the experimentally determined values for K_{gw} of HCH at each water temperature,[8] the corresponding equilibrium concentration in the air was calculated. The results are depicted in Figure 4. Only the air samples taken on the same section of the cruise as the water samples are considered ("Polarstern" ANT IX/4 from Cape Town to Bremerhaven, air samples 13–27, water samples 1–6). In the northern hemisphere the equilibrium values in air calculated from the water samples for α-HCH are lower than the measured values; that is, the surface water is distinctly depleted with respect to α-HCH.[9] Besides the decomposition by OH radicals (lifetime τ_{OH} = 25 days[10]), a net loss of this compound from the atmosphere by gas diffusion into the surface water takes place. In contrast, in the southern hemisphere to a large extent an equilibrium between α-HCH concentrations in air and surface water exists. The surface water functions as source and balances the loss in the atmosphere caused by decomposition by OH radicals. For γ-HCH the air/water system in the North Atlantic—with the exception of areas characterized by a large continental uptake of γ-HCH—approaches the equilibrium state, whereas in the South Atlantic the air/water equilibrium, as for α-HCH, has been established. For both HCH isomers the establishment of the air/water equilibrium must be faster than the loss by decomposition by OH radicals.

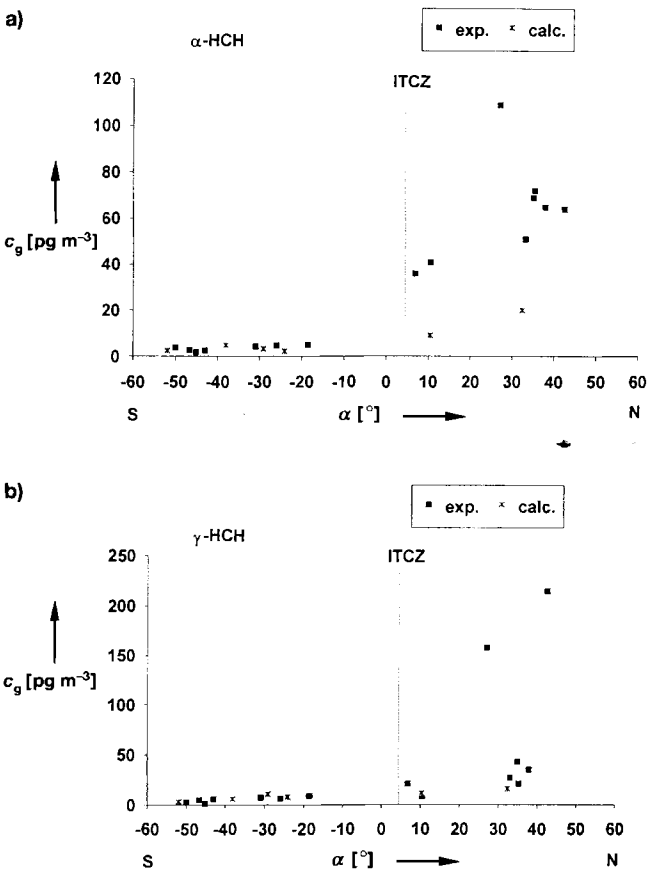


Fig. 4. Comparison of measured concentrations c_g of α-HCH (a) and γ-HCH (b) in the lower layer of the troposphere in the Atlantic (air samples 13–27) with calculated concentrations obtained from the water samples 1–6 from experimentally determined, temperature-dependent gas/water partition coefficients K_{gw} (from ref. [8]). exp.: measured concentrations; calc. calculated concentrations, α: degree of latitude.

The proof of a temperature-regulated equilibrium in the sense of classical thermodynamics of anthropogenic environmental chemicals between the atmosphere and surface water for the global dimension of the South Atlantic has far-reaching practical consequences for the interpretation of measured content of anthropogenic as well as biogenic trace substances in the marine atmosphere of the southern hemisphere and beyond. Current uptake of contaminated air from the continents and also of undercontaminated or noncontaminated air from the backstream from the stratosphere in the region of the subtropic high-pressure zones would be recognizable as deviations from the equilibrium concentrations till relaxation of the disturbed air/water equilibri-

um occurs.[11] Furthermore, the long-term role of the oceans as sink and as source for the uptake into the atmosphere becomes clear. The results show that with correct and significant data—a prerequisite demanded of the analytical processes of modern analytical chemistry—general chemical relationships for global environmental chemistry become clear. They are then able to be modeled on facts, and thus some aspects become predictable.

Experimental Procedure

Details of sampling on board the "Polarstern" on cruises from Bremerhaven to Punta Arenas (Chile) in 1990 (air samples 1–12) and from Cape Town to Bremerhaven in 1991 (air samples 13–27, water samples 1–6) may be found in ref. [12, 13]. The sampling zones are shown in Figure 1.

Further details on the determination of the atmospheric trace substances by adsorption from high-volume samples (500–1000 m^3) on prepurified silica gel and sample workup under strict control for potential contamination, preseparation by adsorption liquid chromatography, and separation and detection by high-resolution capillary gas chromatography with electron-capture detection (HRGC–ECD) are described in ref. [13]. The hexachlorocyclohexanes in surface water were analyzed according to a method described in ref. [14] (adsorption on prepurified polystyrene–divinylbenzene copolymer (XAD-2), sample workup and determination with HRGC–ECD) [12].

Received: September 30, 1993 [Z 6382 IE]
German version: *Angew. Chem.* **1994**, *106*, 688

[1] This review provides access to a wide spectrum of the relevant literature in this context.

[2] D. Mackay, *Multimedia Environmental Models: the Fugacity Approach*, Lewis Publishers, Chelsea, MI, USA, **1991**; D. Mackay, S. Paterson, *Environ. Sci. Technol.* **1991**, *25*, 427–436.

[3] *Lindan-Informationen über einen Wirkstoff* (Ed.: Centre International d'Etudes du Lindan (C.I.E.L.)), Schillinger, Freiburg, **1983**.

[4] D. A. Hinckley, T. F. Bidleman, C. P. Rice, *J. Geophys. Res.* **1991**, *96*, 7201–7213; W. E. Cotham, T. F. Bidleman, *Chemosphere* **1991**, *22*, 165–188; D. A. Kurtz, E. L. Atlas in *Long Range Transport of Pesticides* (Ed.: D. A. Kurtz), Lewis Publishers, Chelsea, MI, USA, **1990**, pp. 143–160.

[5] K. Rango Rao, *Pentachlorophenol: Chemistry, Pharmacology and Environmental Toxicology*, Plenum, New York, **1978**, pp. 402; *Stoffbericht Pentachlorphenol*, (Ed.: Gesellschaft Deutscher Chemiker, Beratergremium für umweltrelevante Altstoffe (BUA)), VCH, Weinheim, **1986**, pp. 55–64.

[6] *Stoffbericht Hexachlorbenzol* (Ed.: Gesellschaft Deutscher Chemiker, Beratergremium für umweltrelevante Altstoffe (BUA)), S. Hirzel, Stuttgart, **1993**, in press.

[7] R. Engst, R. M. Macholz, M. Kujawa, *Res. Rev.* **1977**, *68*, 59–90.

[8] J. R. Kucklick, D. A. Hinckley, T. F. Bidleman, *Mar. Chem.* **1991**, *34*, 197–209.

[9] These results modify and refine the basically identical statements by H. Iwata, S. Tanabe, N. Sakai, R. Tatsukawa, *Environ. Sci. Technol.* **1993**, *27*, 1080–1098.

[10] Calculated for an average concentration of 1.5×10^6 OH radicals per cm^3 and a reaction rate constant for α- and γ-HCH of 0.6×10^{-12} $cm^3 s^{-1}$ (C. Zetsch, *Z. Umweltchem. Ökotoxikol.* **1991**, *3*, 59–64).

[11] The mass flow in the atmosphere and in the global oceanic system has scarcely been considered previously in the discussion of the spread of organic trace substances [1]. The exchange of air masses between troposphere and stratosphere is often underestimated (E. R. Reiter, *Rev. Geophys. Space Phys.* **1975**, *13*, 459–474). We could test by measurement of the content in the air in a sufficiently wide region along the coast of Chile whether a similar temperature-regulated air/water equilibrium to that of the South Atlantic is present in the eastern South Pacific. The content in surface water then can be calculated from the values in the air alone. The concept of a global environmental chemistry, which we dubbed the "Ulmer 4-W approach" (Was, Wieviel, Wo, Warum: what, how much, where, why) that attempts to relate the chemistry of studied compounds and the global mass-flow phenomena on the basis of an efficient analytical chemistry is confirmed in the results described here in an exemplary manner.

[12] J. Schreitmüller, Dissertation, Universität Ulm, **1994**.

[13] R. Wittlinger, K. Ballschmiter, *Chemosphere* **1987**, *16*, 2497–2513; J. Schreitmüller, K. Ballschmiter, *Fresenius J. Anal. Chem.* **1994**, *348*, 226–239.

[14] W. Krämer, Dissertation, Universität Ulm, **1987**.

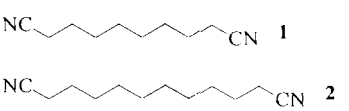
Zigzag Channels in the Structure of Sebaconitrile/Urea **

Mark D. Hollingsworth,* Bernard D. Santarsiero, and Kenneth D. M. Harris

Dedicted to the memory of Professor Margaret C. Etter

Since their discovery by Bengen and Schlenk,[1] hundreds of urea inclusion compounds have been studied by various techniques. In these crystals, long-chain alkanes and their substituted analogues are enclosed within continuous, linear hexagonal channels formed by a hydrogen-bonded array of urea molecules. Because the internal diameter of the channel (about 5.3–5.7 Å) is somewhat larger than the van der Waals envelope of an alkyl chain, the guest molecules are held loosely, and typically undergo substantial translational and reorientational motions.[2] Thus far, with the exception of urea inclusion compounds with trioxane,[3] 5-undecanone[4] and certain short-chain α,ω-dihaloalkanes,[5] the incommensurate[6] repeat distances of host and guest along the channel is a common feature of virtually all urea inclusion compounds, and the guest molecules pack within van der Waals contact of each other. In some cases particularly at low temperatures, the host is distorted slightly, but the repeat length along the channel axis is uniformly close to the standard value of 11.0 Å.[7] If a guest species cannot be accommodated by the conventional hexagonal channel, it is ordinarily not included within urea,[8] and either separate phases or specific cocrystals[9] are formed.

Our cross-polarization magic angle spinning (CP-MAS) NMR studies of urea inclusion compounds have focused on interactions between functional groups that are isolated as pairs within the urea channels.[10] For the incommensurate urea inclusion compounds, ^{13}C MAS NMR ordinarily yields extremely narrow bands with characteristic chemical shifts for given pairs of functional groups. However, we were intrigued by the unusual behavior of the sebaconitrile/urea (**1**/urea) inclusion compound. For guest molecules in **1**/urea, chemical shifts of the nitrile and α carbons are different from those in the doubly homologous 1,10-dicyanodecane/urea (**2**/urea). Magnetic field dependence (Fig. 1) and ^{15}N-labeling experiments demonstrate that the $^{13}C-^{14}N$ residual dipolar splittings[11] of the nitrile carbon are much larger in **1**/urea, and suggest substantial loss of motional freedom for this shorter guest molecule.[12] Although the crystal habit of **1**/urea (flat hexagonally shaped plate instead of



[*] Prof. M. D. Hollingsworth[+]
Department of Chemistry
Indiana University
Bloomington, IN 47405 (USA) (present address)
and
Department of Chemistry, University of Alberta (Canada)
Dr. B. D. Santarsiero
Molecular Structure Corporation
and
Department of Chemistry, University of Alberta (Canada)
Dr. K. D. M. Harris
Department of Chemistry, University College London (UK)

[+] Fellow of the Alfred P. Sloan Foundation

[**] We thank the donors of the Petroleum Research Fund, administered by the American Chemical Society (#24396-AC4), the Natural Sciences and Engineering and Research Council of Canada and the Alfred P. Sloan Foundation for financial support and Drs. John C. Huffman and Natsuko Cyr for their help with this work.

 © VCH Verlagsgesellschaft mbH, D-69451 Weinheim, 1994 0570-0833/94/0606-0649 $ 10.00+.25/0

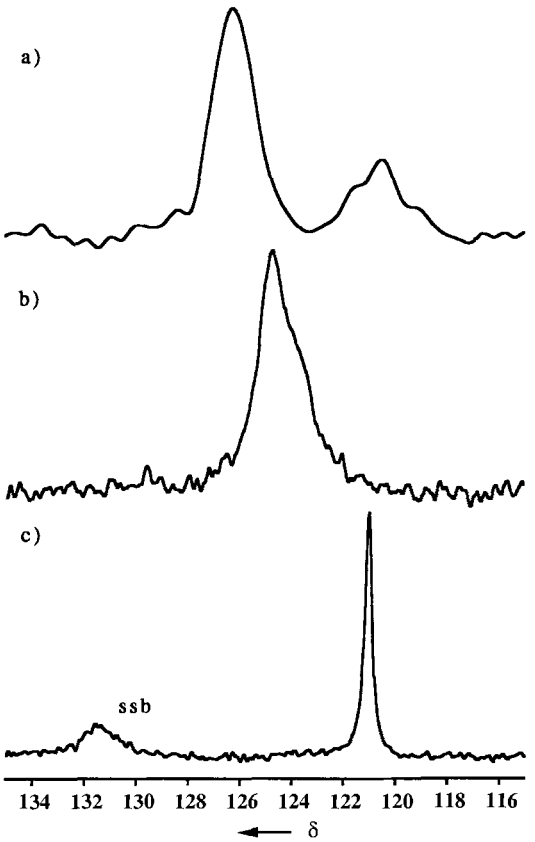


Fig. 1. Nitrile carbon region of ^{13}C CP-MAS NMR spectra of **1** urea at 50.3 MHz (a) and at 125.7 MHz (b), and of **2**/urea at 125.7 MHz (c). In **2**/urea (c), which is typical of incommensurate nitrile/urea systems, large amplitude motions of the nitrile group average the residual dipolar interaction between ^{13}C and ^{14}N to less than 30 Hz. In contrast, the spectra of **1**/urea show much larger residual dipolar interactions. ssb = spinning side band.

the typical hexagonal needle) might have been rationalized in terms of poisoning of the {0001} faces of a normal urea inclusion compound by **1**, the birefringence exhibited for light entering normal to the plate face could not be understood in terms of a simple uniaxial (hexagonal) crystal.[15]

Our X-ray diffraction investigations reveal that **1** forms commensurate inclusion compounds with urea, and although this structure exhibits a number of features common to conventional urea inclusion compounds, the differences are striking: the structure[16] is monoclinic, not hexagonal, and though the stoichiometry (**1**: urea = 1:6) suggests a commensurate structure, the unit cell axes have no simple relationship to the normal 11.0 Å repeat along the channel axis. A view down the channel axis (Fig. 2) shows only modest distortions from the conventional hexagonal host structure near the middle of the sebaconitrile molecule. However, at the junction between adjacent antiparallel nitriles within a channel, the linear channel structure is interrupted by a *kink* in which two linear, parallel segments are offset by significant amounts. Although one might expect that the kink in the channel is caused by the steric bulk of the nitriles (which should be tethered strongly by dipole–dipole interactions),[14] these two groups are well beyond van der Waals contact from each other. (For adjacent nitriles, the interatomic distances are 3.841(7) Å (C–C), 3.911(7) Å (C–N), and 4.290(6) Å (N–N). Instead, and in contrast with urea inclusion compounds studied previously, there is hydrogen bonding between the host and guest, and each nitrile is tethered to two different urea molecules in the next segment of the channel (Fig. 3). This hydrogen bonding disrupts the network of urea molecules and gives rise to a longer repeat distance of 13.26 Å (usual: 11.0 Å) in each channel segment. As a result, the guest molecules are significantly bowed along the *b* axis by several small angle torsions near the chain termini.

Thus, the nitrile–urea hydrogen bonding is the dominant source of the restricted motion that gives rise to the large residual dipolar splitting in the MAS NMR spectrum. The consequential disruption of host–host hydrogen bonding is presumably the source of the unusual flat plate habit of these crystals, in which material is added preferentially to the sides of the channels instead of along their long axes. However, the exact reasons for the morphology change are unknown.

Apart from an uncharacterized premelting transition within 5° of the melting point,[16] differential scanning calorimetry (DSC) shows no discernible phase transitions above 220 K. Lattice parameters also show smooth temperature dependences from 97–312 K. To date, we have not been able to generate the normal hexagonal form of **1**/urea, even by seeding with hexagonal urea inclusion compounds, by grinding, or by growing crystals from solutions containing small amounts of guests that ordinarily form hexagonal urea inclusion compounds. However, we have been able to form hexagonal needles of **1**/[D_4]urea (from MeOD solution), quite reliably by seeding with tiny amounts of hexagonal inclusion compounds of 1-cyanooctadecane/urea or its [D_4]-urea analogue. (The long chain guests impart low solubility to the seed crystals.) Unless they are collected immediately after they are formed, these hexagonal needles of **1**/[D_4]urea undergo a solvent-mediated phase transition to the monoclinic plate form.

DSC on the three available crystal forms provides some clues about the nature of the isotope effect in this system. Although the

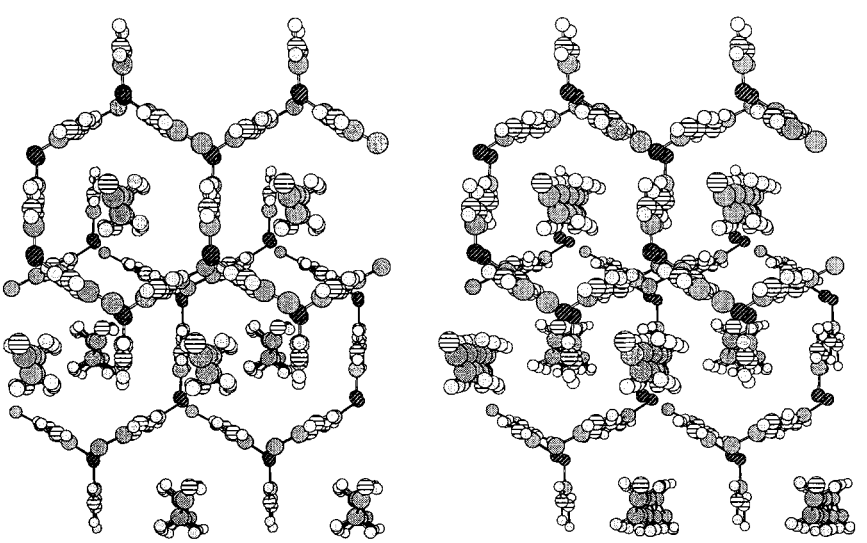


Fig. 2. Stereoview down the channel axis of two unit cells of **1**/urea. The (doubled) *b* axis is horizontal, and the view is 29° from the *c* axis of the crystal. The rear channel segment is offset by 2.3 Å along *b*, and by 0.9 Å along the vertical direction of this diagram. Nitriles in the front segment of the channel are bowed by 0.55 Å along *b* so that their nitrile groups can hydrogen bond with urea molecules of the rear channel segment. Guests in the rear segment are bowed along $-b$. The offset channels bring nitriles in *adjacent* channels to within 5 Å of each other. (Oxygen: dark diagonally hatched circles, nitrogen: horizontally hatched circles, carbon: mottled gray, hydrogen: light gray.)

protiated plates melt at a higher temperature than the deuterated plates (onsets at 371.2 and 364.2 K, respectively; 5 K min^{-1}), the measured enthalpy of melting (or decomposition) is *lower* for the protiated form (11.8 vs. 17.7 cal g^{-1}), indicating a process controlled by entropy. At the same time, cell constants for the deuterated and protiated forms are identical between 97 and 312 K,[19] which suggests that zero-point energies, not equilibrium structures, constitute the main differences between these isotopomorphs. The melting transition occurs at a lower temperature for the **1**/[D_4]urea needles (onset at 351.5 K) but the heat of fusion (14.1 cal g^{-1}) and melting temperature cannot be interpreted in the absence of similar data for the protiated needles.

Even though the solvent-mediated phase transition severely limits the size of hexagonal needles of **1**/[D_4]urea that one can grow, these crystals are stable in the absence of water vapor, and can be studied by X-ray diffractometry at room temperature. Although the metric propeties of the guest structure have not yet been determined, diffractometry shows that the host retains its normal channel structure, but that the channel diameter is approximately 0.05 Å wider, and the periodic repeat distance is about 0.04 Å shorter than the hexagonal channels formed in the presence of 'typical' guests.[20] The wider channels can probably better accommodate the molecules of **1**, which are expected to exhibit rhombohedral interchannel ordering that occurs for $NC(CH_2)_{10}CN$ and several other guests of the formula $X(CH_2)_nX$.[21] If they could be prepared, the hexagonal crystals of **1**/urea would show whether these cell constant differences were due to the strain induced by the guest, or to the replacement of hydrogen by deuterium. Our diffractometric studies of deuterated and protiated forms of several other hexagonal inclusion compounds suggest the former.[22] Further studies of this unusual system, including deuterium fractionation and spectroscopic and structural measurements, will appear in forthcoming publications.

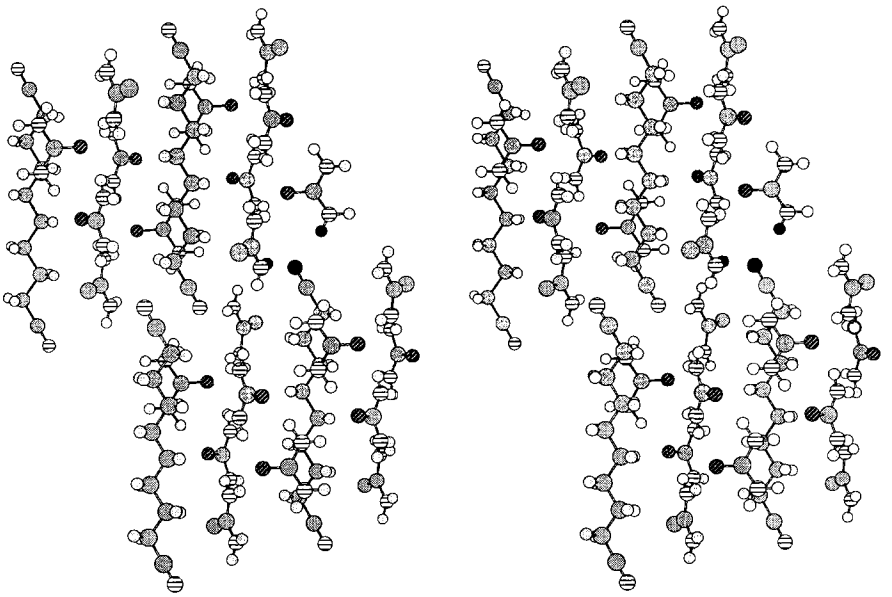


Fig. 3. Stereoview down the *b* axis of **1**/urea. The vertical axis (which lies very close to the bisector of *a* and *c*) gives the repeat of the two segments. One set of atoms involved in host-guest hydrogen bonding is shaded black. Distances between the nitrile and urea protons are N···H(syn) 2.36(4) Å, N···H(anti) 2.45(4)) angles are C–N···H(syn) 117.2(10)°, C–N···H(anti) 119.4(10)°, N–H(anti)···N 159(9), and N–H(syn)···N 157(7)°.

Experimental Procedure

[1,8-$^{13}C_2$]Sebaconitrile (98.4% enrichment) was prepared by heating $Na^{13}CN$ (0.126 g, 2.52 mmol) and 1,8-dibromooctane (0.329 g, 1.21 mmol) in DMF (6.8 mL) for 5 h at 115 °C. After addition of H_2O (25 mL), the product was extracted with pentane/diethyl ether (1:2), dried, and then distilled (92–96 °C/0.05 mm Hg) to give 0.60 g (93.1%) of a clear oil. [$^{15}N_2$]Sebaconitrile (99.0% enrichment) was prepared by a similar procedure. Inclusion compounds were formed by dissolving **1** (0.10 g) in a solution of urea (1.8 M) in MeOH (2.3 mL) at 26 °C and then slowly cooling to 5 °C over a period of 8–10 hours. Although hexagonal **1**/[D_4]urea could be formed from MeOD by the same method, these crystals were formed most reliably by adding **1** (0.7 mL) to a hot solution (70 °C) of [D_4]urea (0.45 g) in MeOD (1.33 g) and then cooling with seeding to 40 °C over 20–25 min. The ratio of MeOD to guest in these crystals was in some cases as large as 1:5. The sebaconitrile used in these experiments was made highly pure by dissolving monoclinic **1**/urea crystals in H_2O, extracting with diethyl ether, drying, and condensing.

Received: May 24, 1993
Revised: December 17, 1993 [Z 6103IE]
German version: *Angew. Chem.* **1994**, *106*, 698

[1] W. Schlenk, Jr., *Justus Liebigs Ann. Chem.* **1949**, *565*, 204.
[2] S. P. Smart, F. Guillaume, K. D. M. Harris, C. Sourisseau, A. J. Dianoux, *Physica B* **1992**, *180–181*, 687.
[3] a) R. Claude, R. Clement, A. Dworkin, *J. Chem. Thermodyn.* **1977**, *9*, 1199; b) R. Clement, C. Mazieres, L. Guibe, *J. Solid State Chem.* **1972**, *5*, 436.
[4] M. D. Hollingsworth, C. R. Goss, *Mol. Cryst. Liq. Cryst.* **1992**, *219*, 43.
[5] J. Otto, *Acta Crystallogr. Sect. B* **1972**, *28*, 543. Our complete crystal structures of $Br(CH_2)_6Br$/urea, $Br(CH_2)_6Cl$/urea, $Cl(CH_2)_6Cl$/urea, $NC(CH_2)_6CN$/urea and $Cl(CH_2)_6CN$/urea will be reported shortly.
[6] By incommensurate we mean that the repeat distances of host and guest along the channel axis (c_h and c_g) do not satisfy the relationship $n\,|c_h| \approx m|c_g|$ for reasonably small integers *m* and *n*.
[7] a) A. E. Smith, *Acta Crystallogr.* **1952**, *5*, 224; b) F. Laves, N. Nicolaides, K. C. Peng, *Z. Kristallogr.* **1965**, *121*, 258; c) H.-U. Lenné, *ibid.* **1963**, *118*, 439, 454; d) R. Forst, H. Boysen, F. Frey, H. Jagodzinski, *J. Phys. Chem. Solids* **1986**, *47*, 1089; e) K. D. M. Harris, M. D. Hollingsworth, *Proc. R. Soc. (London) Ser. A* **1990**, *431*, 245; f) K. D. M. Harris, J. M. Thomas, *J. Chem. Soc. Faraday Trans.* **1990**, *86*, 2985.
[8] See K. Takemoto, N. Sonoda in *Inclusion Compounds, Vol. 2* (Eds.: J. L. Atwood, J. E. Davies, D. D. MacNicol), Academic Press; Orlando, FL, USA **1984**, p. 47 ff.
[9] M. D. Hollingsworth, B. D. Santarsiero, H. Oumar-Mahamat, C. J. Nichols, *Chem. Mater.* **1991**, *3*, 23; X. Zhao, Y.-L. Chang, F. W. Fowler, J. W. Lauher, *J. Am. Chem. Soc.* **1990**, *112*, 6627, and references therein.
[10] M. D. Hollingsworth, N. Cyr, *Mol. Cryst. Liq. Cryst.* **1990**, *187*, 135.
[11] See a) J. G. Hexem, M. H. Frey, S. J. Opella, *J. Am. Chem. Soc.* **1981**, *103*, 224; b) A. Naito, S. Ganapathy, C. A. McDowell, *J. Chem. Phys.* **1981**, *74*, 5393; c) J. G. Hexem, M. H. Frey, S. J. Opella, *ibid.* **1982**, *77*, 3847; d) A. C. Olivieri, L. Frydman, L. E. Diaz, *J. Magn. Reson.* **1987**, *75*, 50.
[12] An earlier study [13] of stearonitrile/urea concluded that at 50.3 MHz, the 92 Hz splitting in the nitrile ^{13}C resonance was due to residual dipolar coupling between ^{13}C and ^{14}N that had been attenuated by the motional averaging of the nitrile group in the channel. Our field dependence and ^{15}N labeling studies show that for this unsymmetric nitrile, this 92 Hz splitting is actually due to two different arrangements of guests (head to head or head to tail), and that for incommensurate urea inclusion compounds containing nitriles, large amplitude motions of the nitrile collapse the residual dipolar interactions to within the linewidth of each individual resonance. See also ref. [14].
[13] M. Okazaki, A. Naito, C. A. McDowell, *Chem. Phys. Lett.* **1983**, *100*, 15.
[14] M. D. Hollingsworth, A. R. Palmer, *J. Am. Chem. Soc.* **1993**, *115*, 5881.
[15] N. H. Hartshorne, A. Stuart, *Crystals and the Polarising Microscope*, 4th ed., Edward Arnold Publishers London, **1970**, pp. 112–116.
[16] $C_{10}H_{16}N_2 \cdot 6CH_4N_2O$ (melts with irreversible complex decomposition at 98 °C) monoclinic, *C*2/*c*, a = 14.872(3), *b* = 7.807(3), *c* = 25.626(3) Å, β = 103.213(12)°, *V* = 2896 Å^3 (for reflections from 9.0° < θ < 19.8°), ρ_{calcd} = 1.204 g cm^{-3}, *Z* = 8 for $C_8H_{20}N_7O_3$, λ ($Mo_{K\alpha}$) = 0.7107 Å, μ = 0.55 cm^{-1}, 3578 reflections ($2\theta_{max} \leq 50°$ for *h*, *k*, ±*l*, −20 °C, Enraf–Nonius CAD4) were averaged over 2/*m* symmetry to give 2741 averaged observations, of which 1238 reflections with $I > 3\sigma(I)$ were used in the final cycles of refinement. The structure was solved by direct methods (MITHRIL 83) [17] using an empirical absorption correction.[18] Non-hydrogen atoms were refined with anisotropic

Gaussian displacement parameters. Methylene hydrogen atoms were constrained with a riding model (at 0.95 Å), whereas urea hydrogen atoms were refined with isotropic terms and no restraints in the final cycle; goodness of fit = 1.77, $R_F = 0.046$, $R_{WF} = 0.060$. The highest peak in the final difference Fourier map has a density of 0.08(2) e Å^{-3}. Further details of the crystal structure investigation are available on request from the Director of the Cambridge Crystallographic Data Centre, 12 Union Road, GB-Cambridge CB2 1EZ (UK), on quoting the full journal citation.

[17] C. J. Gilmore, MITHRIL 83, A Multiple Solution Direct Methods Program, University of Glasgow, **1983**.

[18] N. Walker, D. Stuart, *Acta Crystallogr. Sect. A* **1983**, *39*, 158.

[19] At 22 °C, **1**/[D_4]urea gives $a = 14.844(3)$, $b = 7.879(1)$, $c = 25.623(5)$ Å, $\beta = 103.14(1)°$, whereas **1**/urea gives $a = 14.839(3)$, $b = 7.883(1)$, $c = 25.616(6)$ Å, $\beta = 103.10(1)°$.

[20] **1**/[D_4]urea (hexagonal form) cell constants at 23 °C: $a = b = 8.270(2)$ Å, $c = 10.977(4)$ Å. Compare octyl acetate/urea at 20 °C: $a = b = 8.221(2)$ Å, $c = 11.015(3)$ Å, and other given in references [3–5].

[21] K. D. M. Harris, S. P. Smart, M. D. Hollingsworth, *J. Chem. Soc. Faraday Trans.* **1991**, *87*, 3423.

[22] a) S. J. Peters, M. D. Hollingsworth, J. C. Huffman, unpublished; b) see A. B. Jaffe, D. S. Malament, E. P. Slisz, J. M. McBride, *J. Am. Chem. Soc.* **1972**, *94*, 8515 for a counter example.

A Novel Route to Diastereomerically Pure (*E*)-Alkene Dipeptide Isosteres from β-Aziridinyl-α,β-enoates by Treatment with Organocopper Reagents**

Toshiro Ibuka,* Kazuo Nakai, Hiromu Habashita, Yuka Hotta, Nobutaka Fujii,* Norio Mimura, Yoshihisa Miwa, Tooru Taga,* Yoshinori Yamamoto*

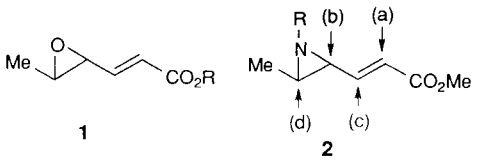
Dedicated to Professor Reinhard W. Hoffmann on the occasion of his 60th birthday

The growing importance of peptide mimetics[1] in synthetic and medicinal chemistry has created a need for efficient routes to the (*E*)-alkene dipeptide isosteres.[2] We have been interested in the synthetically useful ring-opening reactions of N-activated aziridines in connection with studies on peptide isosteres with stereochemically well-defined structures. Although the ring-opening reactions of γ,δ-epoxy-α,β-enoates **1** with a variety of organometallic reagents have found widespread application in the stereocontrolled synthesis of many acyclic systems,[3] prior to the initiation of our studies no information was available regarding the regio- and stereochemistry of organocopper-mediated reaction of β-aziridinyl-α,β-enoates such as **2**. Very recently, a report on the palladium-catalyzed selective hydrogenolysis of β-aziridinyl-α,β-enoates with formic acid appeared.[4]

[*] Prof. Dr. Ibuka, Prof. Dr. N. Fujii, K. Nakai, H. Habashita, Y. Hotta
Faculty of Pharmaceutical Sciences, Kyoto University
Sakyo-Ku, Kyoto 606 (Japan)
Telefax: Int. code + (75)753-4570
Prof. Dr. T. Taga, N. Mimura, Dr. Y. Miwa
Graduate School of Pharmaceutical Sciences, Kyoto University
Kyoto 606 (Japan)
Prof. Dr. Y. Yamamoto
Department of Chemistry, Tohoku University
Sendai 980 (Japan)

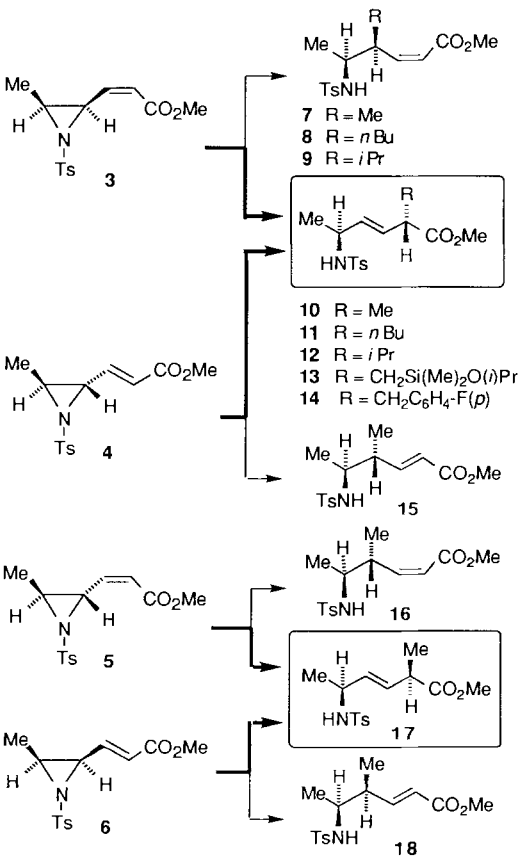
[**] This work was supported in part by Grants-in-Aid for Scientific Research from the Japanese Ministry of Education, Science and Culture and by the CIBA-GEIGY Foundation.

In principle, there are four reactive positions for nucleophilic attack (denoted by a, b, c, and d in enoate **2**). Thus, it is not an easy matter to predict where attack occurs primarily in the reaction of **2** with organocopper reagents. The S_N2' reaction of δ-*tert*-butoxycarbonylamino-γ-mesyloxy-α,β-enoates with organocopper reagents offers a valuable route to (*E*)-alkene dipeptide isosteres, though, in some cases, its application is hindered by rather low stability of the γ-mesyloxy-α,β-enoates.[5]



From an experimental point of view, the β-(*N*-tosylaziridinyl)-α,β-enoates **2**, R = Tos, have the advantage that they are more stable and are readily purified by recrystallization. The present study had two goals: 1) to find reaction conditions whereby (*E*)-alkene dipeptide isosteres can be synthesized from readily available β-aziridinyl-α,β-enoates in high chemical yields, and 2) to examine the stereochemical relationship between substrate and product stereochemistry.

We report here on a new synthesis of (*E*)-alkene dipeptide isosteres suitable for large-scale preparation by an anti-S_N2' reaction of diastereomerically pure β-aziridinyl-α,β-enoates with organocopper reagents (Scheme 1). The requisite four diastereomerically pure stereoisomeric starting materials **3**–**6** were readily prepared in acceptable yields from either L-threonine or



Scheme 1. Ts = *p*-toluenesolfonyl.

D-allothreonine according to the usual method.[6] To test the feasibility of an organocopper-mediated allylic substitution for the synthesis of (*E*)-alkene dipeptide isosteres, we examined the reaction of **3** with a variety of organocopper reagents (see Table 1). Selection of the organometallic reagent is very important and holds the key to success. Enoate **3** reacted smoothly with both Me_3ZnLi in the presence of 30 mol% of CuCN and MeCu(CN)Li to give the required N-protected isostere **10** in high yields along with small amounts of **7** (entries 1 and 4 in Table 1).[7] A comparable result was obtained by reaction of **3** with Me_2Zn in the presence of 20 mol% of CuCN (entry 3 in Table 1). This strategy allows flexibility in introducing substituents such as *n*Bu, *i*Pr, $iPrOSi(Me)_2CH_2$, and *p*-F-C_6H_4-CH_2 at the position α to the ester group merely by changing the reagent (entries 5–8 in Table 1). In a similar manner, exposure of isomeric enoates **4**–**6** to either Me_2Zn in the presence of 20 mol% of CuCN or MeCu(CN)Li gave the expected (*E*)-alkene dipeptide isosteres as the major products in very high yields and with high optical purity (diastereoselectivity >99:1; entries 9–14 in Table 1).

Table 1. Reaction of β-(*N*-tosylaziridinyl)-α,β-enoates **3**–**6** with organometallic reagents[a].

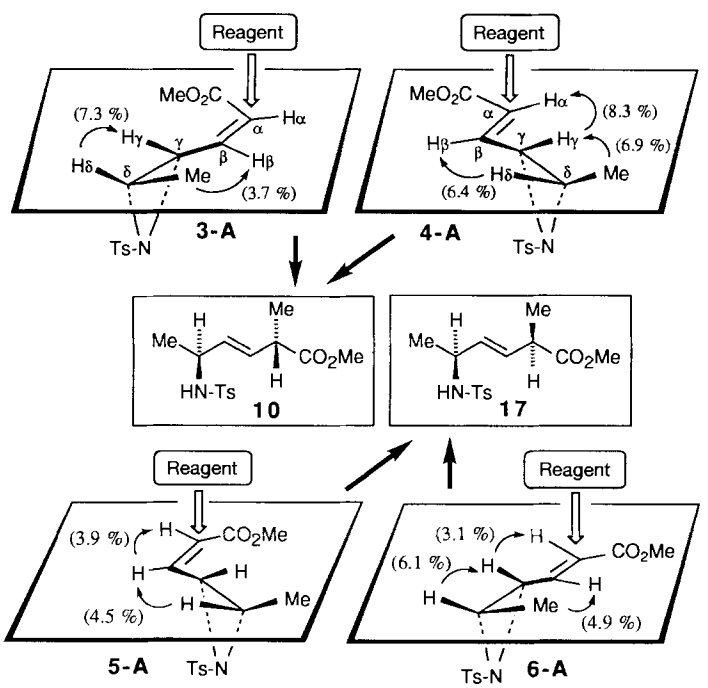
Entry	Cmpd.	Reagent [b]	Products (yield [%]) [c] S_N2 product	*anti*-S_N2' product
1	**3**	Me_3ZnLi; 30 mol % CuCN	**7** (4)	**10** (90)
2	**3**	Me_3ZnLi; 3 mol % CuCN	**7** (3)	**10** (81)
3	**3**	Me_2Zn; 20 mol % CuCN	**7** (4)	**10** (94)
4	**3**	MeCu(CN)Li	**7** (6)	**10** (93)
5	**3**	nBu_3ZnLi; 30 mol % CuCN	**8** (1)	**11** (97)
6	**3**	*i*PrCu(CN)MgCl·2LiCl	**9** (2)	**12** (98)
7	**3**	$iPrOSi(Me)_2CH_2Cu(CN)MgCl\cdot 2LiCl$	– [d]	**13** (75)
8	**3**	*p*-F-$C_6H_4CH_2Cu(CN)MgCl\cdot 2LiCl$	– [d]	**14** (98)
9	**4**	Me_2Zn; 20 mol % CuCN	**15** (3)	**10** (92)
10	**4**	MeCu(CN)Li	**15** (3)	**10** (92)
11	**5**	Me_2Zn; 20 mol % CuCN	**16** (5)	**17** (95)
12	**5**	MeCu(CN)Li	**16** (4)	**17** (82)
13	**6**	Me_2Zn; 20 mol % CuCN	**18** (2)	**17** (88)
14	**6**	MeCu(CN)Li	**18** (3)	**17** (92)

[a] Reaction conditions: −78 °C, 30 min (exception, entry 7: 0 °C, 30 min), 3–4 mol equiv of reagents in THF/Et_2O (ca. 5/1, entries 1–5 and 9–14) or THF (entries 6–8). [b] Me_3ZnLi and Me_2Zn were prepared as LiBr complexes from $ZnCl_2$ and MeLi in Et_2O. MeCu(CN)Li was prepared as the LiBr complex from CuCN and MeLi in Et_2O. [c] All the new compounds were fully characterized by spectroscopy and their composition determined by high-resolution mass spectrometry and/or elemental analysis. Diastereoisomeric purities (>99%) of all isolated compounds were determined by HPLC. [d] Could not be isolated.

The desired (*E*) configuration of the double bond in isosteres **10**–**14** and **17** was easily established from the coupling constant (ca. 15.5 Hz) of the two olefinic protons in the ^1H NMR spectra. The absolute configuration of the alkylated carbon center at the α position in isosteres **10**–**14** and **17** was conveniently determined by a circular dichroism (CD) measurement.[8] The structure and stereochemistry of the S_N2 side products **7**, **15**, **16**, and **18** were confirmed by comparison of their spectral data (^1H NMR, IR) and HPLC retention times with those of authentic samples prepared by an unambiguous, independent synthetic route.[16]

As mentioned previously, enoates **3** and **4**, and **5** and **6** gave dipeptide isosteres **10**–**14** and **17**, respectively, as the major products upon treatment with organozinc reagents in the presence of CuCN or lower order organocyanocuprates. The question remains of why both the (*E*)- and (*Z*)-α,β-enoates are transformed into the (*E*)-alkene isosteres. Is there any logical reason why enoates **3** and **4** yield **10**–**14** and the isomeric enoates **5** and **6** give **17**? In the preferred conformation of many olefins containing a propene moiety a hydrogen atom at the sp^3 carbon in the propene unit eclipses the double bond.[9] In this conformation allylic 1,3 strain is minimized.[10] Hoffmann has recently reviewed the use of allylic 1,3 strain as a controlling factor in highly stereoselective reactions of alkenes and heteroalkenes.[11] The preferred conformations of the four stereoisomeric compounds **3**–**6** have been determined by variable-temperature ^1H NMR spectroscopy[12] in $[D_8]THF$ (all reactions were carried out in solvent mixtures containing THF). In addition, an X-ray analysis of the (*Z*)-enoate **3** and (*E*)-enoate **4** has been carried out.[13]

The ^1H-^1H COSY and selective decoupling experiments for **3**–**6** suggest that the preferred conformations are **3-A**, **4-A**, **5-A**, and **6-A** (Scheme 2). These are in agreement with the preferred conformations in related systems such as vinylcyclopropane[14] and vinyloxiranes.[15] The X-ray structure analyses of **3** and **4** indicate that the conformation in the crystal is quite similar to that in solution (Fig. 1). Thus organocopper reagents attack the α position on the most abundant conformer **3-A**–**6-A** *anti* to the C_γ–N bond that breaks to give the anti-S_N2' products **10**–**14** and **17**, respectively, as the major products.



Scheme 2. Preferred conformations **3-A**, **4-A**, **5-A**, and **6-A** of compounds **3**–**6** in solution ($[D_8]THF$, 600 MHz, 300 K). The NOE values are given in parentheses.

In summary, the reaction of N-sulfonylated β-aziridinyl-α,β-enoates with organometallic reagents (Scheme 1 and Table 1) provides a simple and efficient route to diastereomerically pure (*E*)-alkene dipeptide isosteres that may have biological significance. The absolute configuration at the alkylated α position and the (*E*) configuration of the S_N2' products completely reflect the most abundant conformation of substrates **3**–**6**.

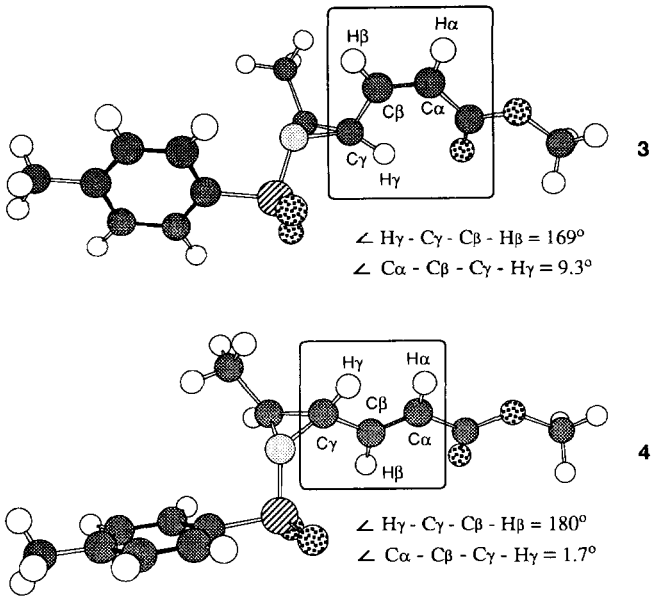


Fig. 1. Crystal structures of **3** and **4** with the values of the angles relevant to the conformation of the propene unit.

Experimental Procedure

Representative procedure for the synthesis of (*E*)-alkene dipeptide isosteres, compound **14** (Table 1, entry 8): To a stirred solution of CuCN (358 mg, 4 mmol) and LiCl (339 mg, 8 mmol) in 5 mL of dry THF at −78 °C was added by syringe 5.33 mL (4 mmol) of 0.75 M *p*-fluorobenzylmagnesium chloride in THF. The mixture was allowed to warm to 0 °C and was stirred at this temperature for 10 min. A solution of enoate **3** (295 mg, 1 mmol) in dry THF (2 mL) was added dropwise to the above reagent at −78 °C with stirring, and the stirring was continued for 30 min followed by quenching at −78 °C with 4 mL of a mixture of saturated NH_4Cl solution and 28% NH_4OH solution (1/1). The mixture was extracted with Et_2O/CH_2Cl_2 (4/1), and the extract was washed with brine and dried over $MgSO_4$. The solvent was removed under reduced pressure, and the residue was purified by flash chromatography on silica gel (*n*-hexane/EtOAc 3/1) to give 397 mg (98% yield) of **14** as a colorless oil. This compound was fully characterized by spectroscopic means (IR ($CHCl_3$), ^1H and ^{13}C NMR ($CDCl_3$), CD (isooctane), and MS). Diastereomeric purity (>99%) was determined by HPLC (chiral column: Chiralcel OD).

Received: October 25, 1993
Revised: December 13, 1993 [Z6444 IE]
German version: *Angew. Chem.* **1994**, *106*, 693

[1] For a review on the stereoselective synthesis of dipeptide mimetics see A. Spatola in *Chemistry and Biochemistry of Amino Acids, Peptides and Proteins, Vol. 7*, (Ed.: B. Weinstein); Marcel Dekker, New York **1983**, p. 267; see also M. T. Reetz, *Angew. Chem.* **1991**, *103*, 1559; *Angew. Chem. Int. Ed. Engl.* **1991**, *30*, 1531; for nomenclature see IUPAC-IUB Joint Commission on Biochemical Nomenclature, *Eur. J. Biochem.* **1984**, *138*, 9.

[2] For a review on the synthesis of (*E*)-alkene dipeptide isosteres see T. Ibuka, *J. Synth. Org. Chem. Jpn.*, **1992**, *50*, 953; for recent reports see R. Beresis, J. S. Panek, *Bioorg. Med. Chem. Lett.* **1993**, *3*, 1609; A. C. Bohnstedt, J. V. N. Vara Prasad, D. H. Rich, *Tetrahedron Lett.* **1993**, *34*, 5217; N. Fujii, K. Nakai, H. Habashita, H. Yoshizawa, T. Ibuka, F. Garrido, A. Mann, Y. Chounan, Y. Yamamoto, *ibid.* **1993**, *34*, 4227.

[3] a) Samarium(II): G. A. Molander, B. E. LaBell, G. Hahn, *J. Org. Chem.* **1986**, *51*, 5259; b) copper(I): T. Ibuka, M. Tanaka, H. Nemoto, Y. Yamamoto, *Tetrahedron* **1989**, *45*, 435; c) palladium(0): I. Shimizu, T. Maruyama, T. Makuta, A. Yamamoto, *Tetrahedron Lett.* **1993**, *34*, 2135, and references therein; d) Al(Me)$_3$: M. Miyashita, K. Yoshihara, K. Kawamine, M. Hoshino, H. Irie, *ibid.* **1993**, *34*, 6285, and references cited therein.

[4] I. Shimizu, A. Satake, A. Yamamoto, *7th IUPAC Symposium on Organometallic Chemistry directed towards Organic Synthesis*, **1993**, Kobe, Japan, Abstracts p. 349; for reports on the ring-opening reaction of alkenylaziridines see: [Fe(CO)$_5$]: R. Aumann, K. Fröhlich, H. Ring, *Angew. Chem.* **1974**, *86*, 309; *Angew. Chem. Int. Ed. Engl.* **1974**, *13*, 275; BH_3: R. Chaabouni, A. Laurent, B. Marquet, *Tetrahedron Lett.* **1976**, 757.

[5] T. Ibuka, H. Habashita, S. Funakashi, N. Fujii, Y. Oguchi, T. Uyehara, Y. Yamamoto, *Angew. Chem.* **1990**, *102*, 816; *Angew. Chem. Int. Ed. Engl.* **1990**, *29*, 801; T. Ibuka, H. Habashita, A. Otaka, N. Fujii, Y. Oguchi, T. Uyehara, Y. Yamamoto, *J. Org. Chem.* **1991**, *56*, 4370.

[6] Synthesis of the starting compounds: **3** and **6**: L-Threonine methyl ester hydrochloride (1 equiv), prepared by reaction of L-threonine (1 equiv) with $SOCl_2$ (2 equiv) in MeOH under reflux for 2.5 h, was tosylated with *p*-toluenesulfonyl chloride (1 equiv) and Et_3N (3 equiv) in dimethylformamide at 25 °C for 18 h to give *N*-*p*-toluenesulfonyl-L-threonine methyl ester (78% yield, m.p. 99 °C (*n*-hexane/Et_2O 1/1), $[\alpha]_D^{20} = -3.27$ ($c = 0.917$ in $CHCl_3$)). Diethyl azodicarboxylate (1.5 equiv) was added dropwise to a stirred mixture of the above ester (1 equiv) and PPh_3 (1.5 equiv) in THF at 0 °C, and the mixture was stirred for 18 h at room temperature. The mixture was concentrated under reduced pressure, and the residual oil was purified by flash chromatography on silica gel (*n*-hexane/EtOAc 3/1) to yield (3*S*)-methyl-*N*-*p*-toluenesulfonylaziridine-(2*S*)-carboxylic acid methyl ester (92% yield, m.p. 61 °C (*n*-hexane/Et_2O 1/4), $[\alpha]_D^{20} = -38.9$ ($c = 0.81$ in $CHCl_3$), >99% *de* (HPLC, Chiralcel OD)). Diisobutylaluminum hydride in toluene (1.1 equiv) was added dropwise to a stirred solution of the above aziridine (1 equiv) in CH_2Cl_2 at −78 °C, and the mixture was stirred for 2 h. The reaction was quenched with a saturated NH_4Cl solution at −78 °C with vigorous stirring. After the addition of (methoxycarbonylmethylene)triphenylphosphorane (1 equiv) at −78 °C, the reaction mixture was stirred for 18 h and allowed to warm to room temperature. The inorganic salts were removed by filtration through Celite. The usual workup of the filtrate gave a yellow, oily residue, which was purified by flash chromatography on silica gel (*n*-hexane/EtOAc 3/1) to yield, in order of elution, **6** (6% yield) and **3** (91% yield). The (*E*)-enoate 6 can be obtained as the major product (**6**:**3** = 83:17; 92% combined yield) by the use of a sodium salt of trimethylphosphonoacetate instead of (methoxycarbonylmethylene)triphenylphosphorane. In a similar manner, the β-aziridinyl-α,β-enoates **4** and **5** were synthesized via *N*-*p*-toluenesulfonyl-D-*allo*-threonine methyl ester (m.p. 100 °C (*n*-hexane/Et_2O 1/10), $[\alpha]_D^{20} = -20.7$ ($c = 0.987$ in $CHCl_3$)) and (3*S*)-methyl-*N*-*p*-toluenesulfonylaziridine-(2*R*)-carboxylic acid methyl ester (colorless oil, $[\alpha]_D^{20} = 15.6$ ($c = 1.2$ in $CHCl_3$), >99% *de* (HPLC, Chiralcel OD)) from D-*allo*-threonine in comparable yields. – **3**: m.p. 75–77 °C (*n*-hexane/Et_2O/CH_2Cl_2 4/4/1), $[\alpha]_D^{27} = 10.1$ ($c = 0.915$ in $CHCl_3$), >99% *de* (HPLC, Chiralcel OD); **4**: m.p. 84 °C (Et_2O), $[\alpha]_D^{20} = 28.4$ ($c = 1.07$ in $CHCl_3$), >99% *de* (HPLC, Chiralcel OD); **5**: m.p. 51 °C (*n*-hexane/Et_2O 1/2), $[\alpha]_D^{20} = -181$ ($c = 1.13$ in $CHCl_3$), >99% *de* (HPLC, Chiralcel OD); **6**: m.p. 92–93 °C (*n*-hexane/Et_2O 2/1), $[\alpha]_D^{32} = -89$ ($c = 0.725$ in $CHCl_3$), >99% *de* (HPLC, Chiralcel OD).

[7] For reviews on the use of organozinc reagents in the presence of CuCN see B. H. Lipshutz, S. Sengupta in *Organic Reactions, Vol. 41* (Ed.: L. A. Paquette), Wiley, New York, **1992**, p. 135; P. Knochel, R. D. Singer, *Chem. Rev.* **1993**, *93*, 2117, and references therein; for recent publications see E. Nakamura, K. Sekiya, M. Arai, S. Aoki, *J. Am. Chem. Soc.* **1989**, *111*, 3091; L. Zhu, R. M. Wehmeyer, R. D. Rieke, *J. Org. Chem.* **1991**, *56*, 1445; Y. Yamamoto, M. Tanaka, T. Ibuka, *ibid.* **1992**, *57*, 1024.

[8] T. Ibuka, H. Habashita, S. Funakoshi, N. Fujii, K. Baba, M. Kozawa, Y. Oguchi, T. Uyehara, Y. Yamamoto, *Tetrahedron Asymmetry* **1990**, *1*, 389; T. Ibuka, T. Taga, H. Habashita, K. Nakai, H. Tamamura, N. Fujii, Y. Chounan, H. Nemoto, Y. Yamamoto, *J. Org. Chem.* **1993**, *58*, 1207, and references therein.

[9] E. L. Eliel, N. L. Allinger, *Top. Stereochem.* **1970**, *5*, 187; E. Testa, in *Principles of Organic Stereochemistry* (Ed.: P. G. Gassman),, Marcel Dekker, New York, **1979**, p. 95.

[10] N. C. Gonnella, K. Nakanishi, V. S. Martin, K. B. Sharpless, *J. Am. Chem. Soc.* **1982**, *104*, 3775; Z. Smith, N. Carballo, E. B. Wilson, K.-M. Marstokk, H. Møllendal, *J. Am. Chem. Soc.* **1985**, *107*, 1951.

[11] R. W. Hoffmann, *Chem. Rev.* **1989**, *89*, 1841; *Angew. Chem.* **1992**, *104*, 1147; *Angew. Chem. Int. Ed. Engl.* **1992**, *31*, 1124; see also J. L. Broeker, R. W. Hoffmann, K. N. Houk, *J. Am. Chem. Soc.* **1991**, *113*, 5006.

[12] a) B. W. Gung, M. A. Wolf, K. Ohm, A. J. Peat, *Tetrahedron Lett.* **1993**, *34*, 1417. b) B. W. Gung, M. A. Wolf, Z. Zhu, *J. Org. Chem.* **1993**, *58*, 3350.

[13] The X-ray structure analysis showed that enoate **4** has two conformers in its unit cell. Interestingly, the dihedral angle (H_β-C_β-C_γ-H_γ) of both conformers is 180°. The two conformers of **4** differ slightly in the orientation of the *N*-*p*-toluenesulfonyl moiety. Consequently, only one conformer is shown in Figure 1. Further details of the crystal structure investigations are available on request from the Director of the Cambridge Crystallographic Data Centre, University Chemical Laboratory, 12 Union Road, GB-Camhridge CB2 1EZ (UK), on quoting the full journal citation.

[14] For rotational isomerism in vinylcyclopropane see G. R. De Mare, J. S. Martin, *J. Am. Chem. Soc.* **1966**, *88*, 5033; A. de Meijere, W. Lüttke, *Tetrahedron* **1969**, *25*, 2047.

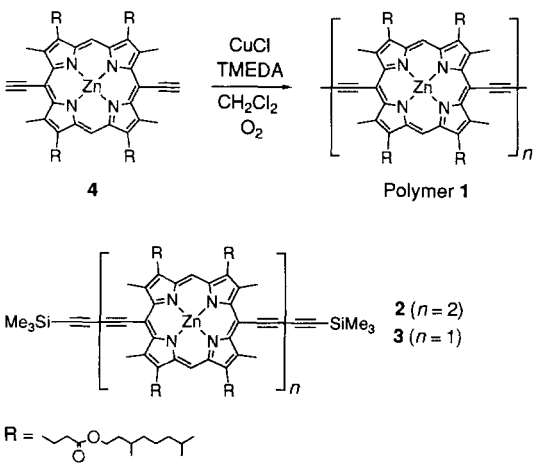
[15] J. A. Marshall, J. D. Trometer, B. E. Blough, T. D. Crute, *J. Org. Chem.* **1988**, *53*, 4274.

[16] T. Ibuka, K. Nakai, H. Habashita, Y. Hotta, N. Fujii, N. Mimura, Y. Miwa, T. Taga, Y. Yamamoto, unpublished.

Synthesis and Third-Order Nonlinear Optical Properties of a Conjugated Porphyrin Polymer**

Harry L. Anderson,* Simon J. Martin, and Donal D. C. Bradley*

Materials with large third-order optical nonlinearity are potentially useful for the fabrication of fast optical switches, but very few materials have sufficiently high susceptibility, $\chi^{(3)}$. There is particular demand for materials with high $\chi^{(3)}$ ($> 10^{-8}$ esu) in the near IR region (ca. 1 μm wavelength) for telecommunication switches. The molecular design features for a high $\chi^{(3)}$ material are poorly understood, although long conjugation lengths and low HOMO–LUMO gaps both appear to be important.[1] Porphyrins are appealing units from which to build high $\chi^{(3)}$ materials because of their large polarizable π systems. Here we report the synthesis of a conjugated porphyrin polymer (**1**), which exhibits an unusually high susceptibility $\chi^{(3)}$, as revealed by its electroabsorption (Stark effect) spectrum, which is much more intense than those of model compounds such as the dimer **2** and the monomer **3**.



Compound **1** is the first soluble conjugated porphyrin polymer. Edge-fused conjugated porphyrin oligomers, and an insoluble polymer, have previously been synthesized.[2] Coordination polymers have also been investigated[3] in which the metalloporphyrins are linked face-to-face; these exhibit much less intermacrocycle electronic coupling than polymer **1**, in which the π systems are edge-to-edge. Compound **1** was synthesized by Glaser–Hay coupling of the *meso*-diethynyl zinc porphyrin **4**.[4] Hay's coupling conditions were originally developed for polymer synthesis[5] and have previously been used to prepare high molecular weight conjugated polymers from simple heterocycles.[6] The polymer **1** is extremely soluble in chlorinated solvents in the presence of a ligand such as pyridine which can coordinate to the zinc sites. Solutions of the polymer are viscous, which broadens the NMR signals; at 100 °C the ^{1}H NMR line widths (in $C_2D_2Cl_4/C_5D_5N$) are around 65 Hz, but the expected features are evident, including a signal at $\delta = 10.1$ characteristic for the *meso* protons. The ^{13}C NMR spectrum shows sharp signals for the mobile sidechain carbon atoms (ca. 3 Hz line width), and broader signals for the pyrrole ring, the ring methyl and the propanoate methylene groups (ca. 30 Hz); the acetylene and *meso* carbon atoms on the backbone of the polymer are even broader (ca. 50 Hz) and are difficult to identify. The similarity between the chemical shifts for the polymer and those of model compounds, **2** and **3**, supports the proposed structure. The NMR line widths and the high intrinsic viscosity ($[\eta] = 180 \pm 10$ mL g^{-1})[7] are consistent with a polymeric structure. The presence of the butadiyne link is demonstrated by a band at 2120 cm^{-1} in the IR spectrum. Neither in the IR nor in the NMR spectrum are any signals from acetylene end-groups detected, which indicates a degree of polymerization greater than 10.[8]

Simple porphyrins, such as zinc octaethylporphyrin (ZnOEP), show two $\pi-\pi^*$ absorption bands: a Soret, or B, band at about 400 nm and a weaker Q band at about 600 nm.[9] The absorption spectrum of the polymer **1** in solution is compared with those of the dimer **2** and the monomer **4** in Figure 1. As the conjugation

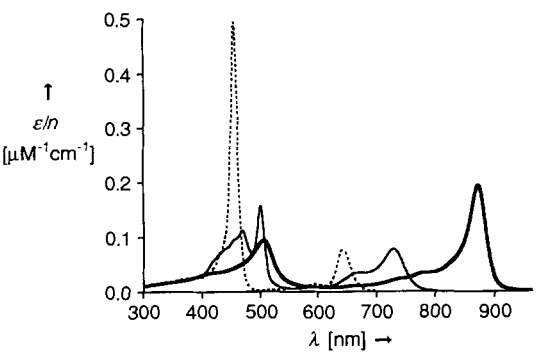


Fig. 1. Absorption spectra of **1** (bold), **2**, and **4** (dashed) in 1% pyridine/dichloromethane (extinction coefficient per porphyrin unit).

length is increased there is a dramatic red shift and intensification of the Q band; in the polymer this is the most intense peak and occurs in the infra red region. Even the Q band of the bisacetylenic monomer **4** is red shifted and intensified when compared with that of ZnOEP. This can be seen from the dipole strengths[10] per porphyrin unit and band energies in Table 1.

Table 1. Transition dipole strengths and energies for porphyrin B and Q bands [a].

Porphyrin	μ_B^2 [D^2]	μ_Q^2 [D^2]	E_B [eV]	E_Q [eV]
ZnOEP	83	10	3.0	2.3, 2.1
4	106	14	2.9	2.1, 2.0
3	142	32	2.7	2.2, 1.9
2	123	58	2.6, 2.5	1.7
1	102	100	2.5	1.4

[a] All spectra were recorded in 1% pyridine/dichloromethane at 25 °C.

[*] Dr. H. L. Anderson[+]
University Chemical Laboratory
Lensfield Road, GB-Cambridge CB2 1EW (UK)
Dr D. D. C. Bradley,[*] S. J. Martin
Cavendish Laboratory
Madingley Road, GB-Cambridge CB3 0HE (UK)
[+] Present address:
Laboratorium für Organische Chemie, ETH-Zentrum Universitätstrasse 16, CH-8092 Zürich (Switzerland)
Telefax: Int. code + (1)261-3524
[*] Present address: Department of Physics, University of Sheffield
Hicks Building
Hounsfield Road, GB-Sheffield S3 7RH (UK)
Telefax: Int. code + (742)728079

[**] This work was supported by Magdalene College Cambridge, Toshiba Corporation and European Office of Aerospace Research and Development (EOARD) (90-0213). Dr J. K. M. Sanders provided generous laboratory support.

The Soret dipole strengths, μ_B^2, are fairly constant, although they increase with the conjugation length per porphyrin, in the order ZnOEP < **4** ≈ **1** < **2** < **3**. In contrast, the Q dipole strengths μ_Q^2 increase with the total conjugation length of the molecule in the order ZnOEP < **4** < **3** < **2** < **1**. The energy of the Q band, and to a lesser extent the B band, decreases as the total conjugation length increases. The low Q band intensity of simple porphyrins is a consequence of accidental degeneracy between the two highest occupied π orbitals $3a_{2u}$ and $1a_{1u}$.[9] In **1** the Q and B bands have similar dipole strength, so this degeneracy must have been removed, which is not surprising because the $3a_{2u}$ orbital has large coefficients at the *meso* carbon atoms whereas the $1a_{1u}$ orbitals has nodes at these positions. However, the total dipole strength of **1** per porphyrin ($\mu_B^2 + \mu_Q^2$) is more than twice that of ZnOEP, indicating that the electronic structure of **1** is too different from that of a simple porphyrin for it to be treated as a slight perturbation of the "four-orbital" model.

The electronic structure of **1** was also investigated by using electroabsorption spectroscopy. This is a useful technique for probing the details of electronic transitions and determining the spectral dependence of the quadratic electrooptic susceptibility $\chi^{(3)}(-\omega;0,0,\omega)$[11-13] which can be related to the nonlinear refractive index n_2, the response of importance in optical switching. In probing electronic spectra the technique allows identification of charge transfer bands,[14,15] discrimination between exciton and band-to-band transitions, and, through its symmetry breaking effect, allows the observation of dipole-forbidden transitions to states of the same parity as the ground state. Electroabsorption spectra show the change in absorbance of a sample in response to a sinusoidal electric field of frequency f (in this work 5 kHz, 10–100 kVcm^{-1}). Centrosymmetric materials give no linear response at the incident frequency f, but only a quadratic response at the second harmonic $2f$.

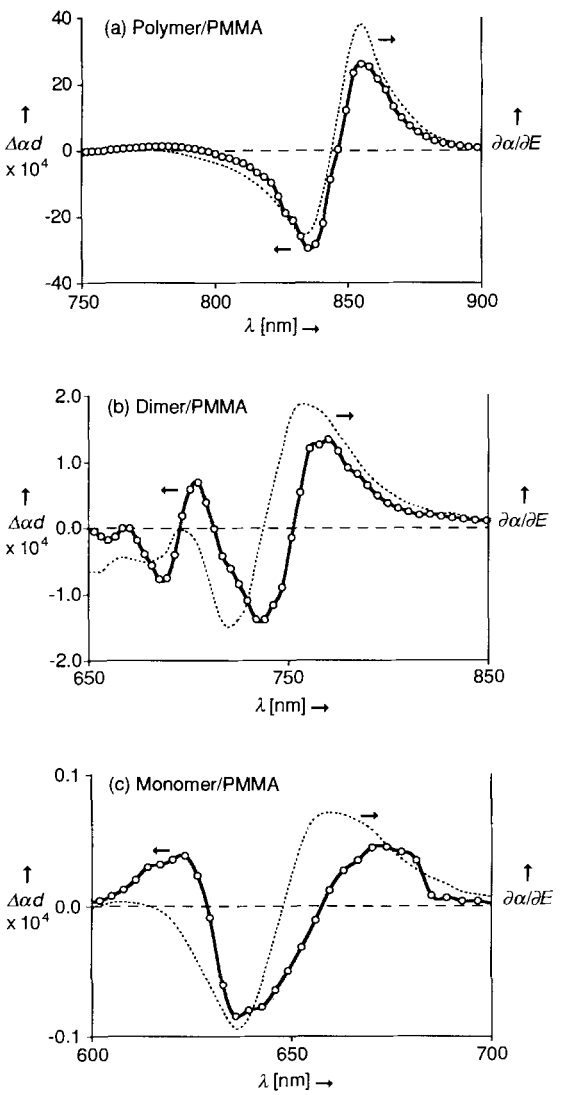


Fig. 2. Electroabsorption spectra ($\Delta\alpha d$, bold) and the first derivative absorption spectra ($\delta\alpha/\delta E$) of (a) **1**, (b) **2** and (c) **3** as thin films of 10% porphyrin/PMMA (all scaled to 35 kVcm^{-1} field strength; **1** and **2** are at 77 K, **3** is at 300 K).

The electroabsorption spectra of the polymer **1**, the dimer **2**, and the monomer **3** are compared with the first derivatives of their absorption spectra, $\delta\alpha/\delta E$, in Figure 2 ($\Delta\alpha$ is the field-induced change in absorption, d is the film thickness). These spectra were recorded on solutions of the porphyrins in polymethylmethacrylate (10% porphyrin/PMMA, spun cast from solution in 10% $C_5H_5N/CHCl_3$). All films gave $2f$ responses proportional to the square of the electric field strength, but the shapes of the spectra were field-independent. The polymer **1** gave a strong response closely resembling $\delta\alpha/\delta E$, which shows that the absorption is due to neutral localized excitons, whereas the monomer **3** gave a much weaker response resembling the second derivative of its absorption spectrum, $\delta^2\alpha/\delta E^2$, implying that its transitions have more charge transfer character.[14] The magnitude of the electrooptic response decreases with decreasing conjugation length in the order **1** > **2** > **3**.

High-quality thin films of the pure polymer are readily cast from solution. The electroabsorption spectra of these films are similar to those of **1** in PMMA, but they are more readily transformed into quadratic electrooptic susceptibilities.[16] The real and imaginary components of $\chi^{(3)}(-\omega;0,0,\omega)$ calculated[11] from these spectra are plotted in Figure 3. The peak resonant

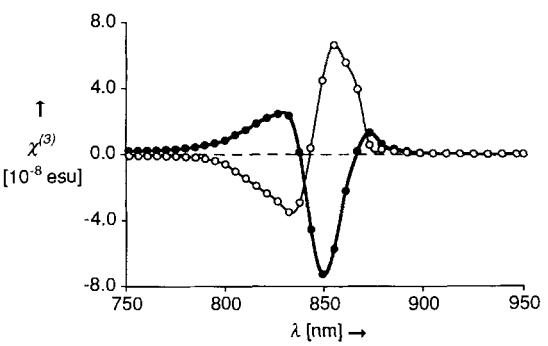


Fig. 3. Real (bold) and imaginary $\chi^{(3)}(-\omega;0,0,\omega)$ spectra of pure **1** calculated from the electroabsorption spectra (35 kVcm^{-1}, 77 K, 800 Å thick, spun coated on spectrosil from a 1% solution in 10% $C_5H_5N/CHCl_3$).

$\chi^{(3)}(-\omega;0,0,\omega)$ of **1**, (7.3×10^{-8} esu) compares favorably with those of other conjugated polymers such as polyacetylene (2.5×10^{-8} esu),[12] polydiacetylene (2×10^{-8} esu),[13] and polythienylenevinylene (7×10^{-9} esu).[11,17] The high near-IR $\chi^{(3)}$ of this new type of conjugated polymer opens the way for the development of a new class of material for nonlinear optics applications.

Experimental Procedure

1: A solution of **4** (400 mg, 0.3 mmol) in dichloromethane (400 mL) was vigorously stirred with CuCl (2.4 g, 24 mmol) and *N,N,N',N'*-tetramethylethylenediamine (TMEDA) (3.4 mL, 22 mmol) under dry air. The green solution became brown and viscous, and no unreacted **4** could be detected by TLC after 5 min. After 30 min the mixture was washed with water (3 × 500 mL) and passed through a silica flash column, eluting with 1% pyridine/dichloromethane to remove baseline contaminants. The eluate was centrifuged (2.2 kG, 2 × 20 min) to remove colloidal copper salts, then treated with methanol (20 mL) to precipitate the polymer. The product was isolated by centrifugation (2.2 kG, 20 min), washed with methanol and diethyl ether, and dried in vacuo to yield 230 mg (58%) of a leathery lustrous green solid. m.p. > 300 °C; ^{1}H NMR (400 MHz, $C_2D_2Cl_4/C_5D_5N$, 100 °C): δ = 0.8–1.5 (76 H), 3.3 (8 H), 4.1–4.5 (28 H), 10.1 (2 H); ^{13}C NMR (100 MHz, $C_2D_2Cl_4/C_5D_5N$, 100 °C): δ = 16.6, 19.3, 21.9, 22.2, 24.2, 27.5, 30.0, 35.6, 37.0, 37.2, 39.0, 63.1, 81.2 (v br), 92.8, (v br) 99.5 (v br), 138.0, 141.3, 145.5, 151.1, 172.6; IR (1% C_5H_5N/CCl_4): $\tilde{\nu}$[cm^{-1}] = 2120 (C≡C), 1730 (C=O); UV/VIS (1% C_5H_5N/CH_2Cl_2): λ_{max} [nm] (log ε) = 505 (4.97), 873 (5.29); correct C, H, N analysis for $C_{80}H_{114}N_4O_8Zn$. Electroabsorption spectra were recorded and transformed into $\chi^{(3)}$ spectra as described previously [11].

Received: September 30, 1993 [Z 6381 IE]
German version: *Angew. Chem.* **1994**, *106*, 711

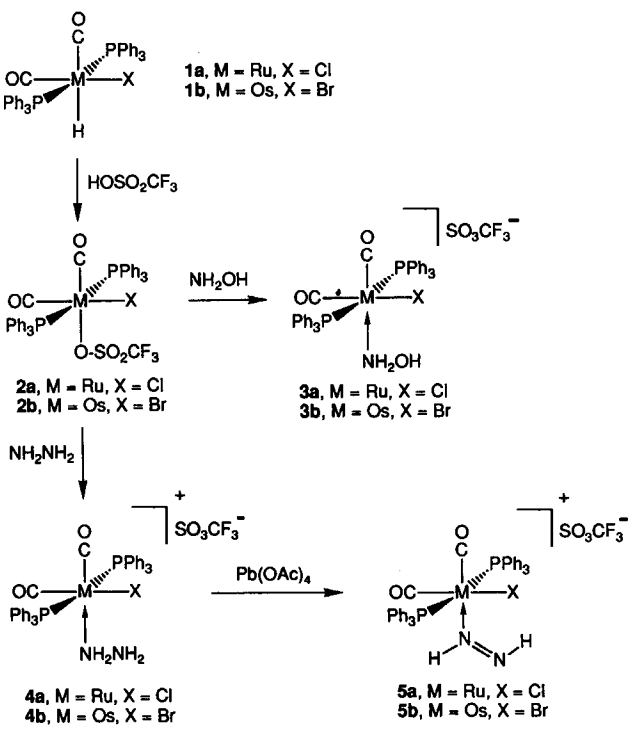
[1] H. S. Nalwa, *Adv. Mater.* **1993**, *5*, 341–357.
[2] Crossley and Burn have reported the preparation of an insoluble porphyrin polymer, and some soluble conjugated oligomers: M. J. Crossley, P. L. Burn, *J. Chem. Soc. Chem. Commun.* **1987**, 39–40; *ibid* **1991**, 1569–1571.
[3] For reviews of coordination-linked porphyrin and phthalocyanine oligomers see E. Kellogg, J. G. Gaudiello in *Inorganic Materials* (Eds.: D. W. Bruce, D. O'Hare), Wiley, Chichester, **1992**, pp 353–396; M. Hanack, S. Deger, A. Lange, *Coord. Chem. Rev.* **1988**, *83*, 115–136.
[4] The synthesis of **2**, **3**, and **4** are to be published elsewhere: H. L. Anderson, *Inorg. Chem.* **1994**, *33*, 982–993.
[5] A. S. Hay, *J. Org. Chem.* **1960**, *25*, 1275–1276.
[6] M. R. Callstrom, T. X. Neenan, G. M. Whitesides, *Macromolecules* **1988**, *21*, 3528–3530; D. R. Rutherford, J. K. Stille, C. M. Elliot, V. R. Reichert, *ibid* **1992**, *25*, 2294–2306.
[7] The intrinsic viscosity was measured at 25.0 °C in 20% pyridine/1,2,4-trichlorobenzene (concentration 1–6 mg mL^{-1}) by extrapolating both the viscosity number and the logarithmic viscosity number to infinite dilution.
[8] Preliminary small angle neutron scattering measurements on solutions of **1** in $CHCl_3/C_5H_5N$ indicate the degree of polymerization is in the range 7–15. We thank Dr A. R. Rennie, Cavendish Laboratory, GB-Cambridge, for these measurements.
[9] M. Gouterman in *The Porphyrins Vol. 3* (Ed.: D. Dolphin), Academic Press, New York, **1978**, pp. 1–166.
[10] Transition dipole strengths were calculated by integrating extinction coefficient divided by wavenumber, $\varepsilon(\tilde{\nu})/\tilde{\nu}$ versus $\tilde{\nu}$, using the equation $\mu^2 = (9.188 \times 10^{-3}/n_0)\int\{\varepsilon(\tilde{\nu})/\tilde{\nu}\}d\tilde{\nu}$, where n_0 is the solvent's refractive index (1.42 for CH_2Cl_2) and μ^2 is the dipole strength in D^2 (D = Debye).
[11] O. M. Gelsen, D. D. C. Bradley, H. Murata, N. Takada, T. Tsutsui, S. Saito, *J. Appl. Phys.* **1992**, *71*, 1064–1066.
[12] S. D. Phillips, R. Worland, G. Yu, T. Hagler, R. Freedman, Y. Cao, V. Yoon, J. Chiang, W. C. Walker, A. J. Heeger, *Phys. Rev. B Condens. Matter* **1989**, *40*, 9751–9759.
[13] T. Hasegawa, K. Ishikawa, T. Koda, K. Takeda, H. Kobayashi, K. Kubodera, *Synth. Met.* **1991**, *43*, 3151–3156.
[14] L. Sebastian, G. Weiser, H. Bässler, *Chem. Phys.* **1981**, *61*, 125–135.
[15] D. J. Lockhart, S. G. Boxer, *Proc. Natl. Acad. Sci. USA* **1988**, *85*, 107–111.
[16] We have not yet calculated $\chi^{(3)}(-\omega;0,0,\omega)$ for the porphyrin/PMMA films because the algorithm we use to compute linear optical constants, by iterative Kramers–Kronig analysis of the transmission data, does not converge well when the absorption per unit thickness is small.
[17] The $\chi^{(3)}$ values reported for most porphyrins are less than 10^{-10} esu; a few give $\chi^{(3)}(-\omega;\omega,\omega,-\omega)$ of up to 10^{-7} esu (A. Grund, A. Kaltbeitzet, A. Mathy, R. Schwarz, Ç. Bubeck, P. Vermehren, M. Hanack, *J. Phys. Chem.* **1992**, **96**, 7450–7454), but for a given material these three-photon resonant $\chi^{(3)}(-\omega;\omega,\omega,-\omega)$ values are expected to be much larger than one-photon resonant $\chi^{(3)}(-\omega;0,0,\omega)$ values (A. Willetts, J. E. Rice, D. M. Burland, D. P. Shelton, *J. Chem. Phys.* **1992**, *97*, 7590–7599).

Hydroxylamine, Hydrazine, and Diazene as Unidentate Ligands in Osmium and Ruthenium Complexes**

Tan-Yun Cheng, Adrian Ponce, Arnold L. Rheingold, and Gregory L. Hillhouse*

Diazene NH=NH is one of the most reactive of the nitrogen hydrides, undergoing disproportionation at −150 °C in the condensed phase to N_2 and N_2H_4.[1] Nevertheless, it is a molecule of fundamental importance, useful as a reagent in stereoselective *cis* hydrogenation of unsaturated organic compounds, and of possible relevance to inorganic and bioinorganic N_2-reduction processes.[2] The stability of diazene is greatly enhanced in solution, especially in liquid ammonia,[3] and by coordination to transition metals (usually in a bimetallic fashion through both nitrogen lone pairs).[4] Herein we report the syntheses of new diazene complexes of Ru and Os, including the first structural characterizations of complexes containing η^1-coordinated H_2NNH_2 and HN=NH ligands.

The hydrido complexes **1a** and **1b** react with trifluoromethanesulfonic acid (triflic acid) to give H_2 and the corresponding trifluoromethanesulfonato complexes **2a** ($\tilde{\nu}$(CO) = 2071, 2006; $\tilde{\nu}(OSO_2CF_3)$ = 1329 cm^{-1}) and **2b** ($\tilde{\nu}$(CO) = 2054, 1985; $\tilde{\nu}(OSO_2CF_3)$ = 1335 cm^{-1}). Hydroxylamine and hydrazine displace the triflate ligands in these complexes to afford the salts **3**



[*] Prof. G. L. Hillhouse, T.-Y. Cheng, A. Ponce
Searle Chemistry Laboratory, Department of Chemistry
The University of Chicago
5735 S. Ellis Avenue, Chicago, IL 60637 (USA)
Telefax: Int. code + (312)702-0805
Prof. A. L. Rheingold
Department of Chemistry, University of Delaware
Newark, DE 19716 (USA)

[**] This work was supported by the US National Institutes of Health (GM-41650 to G. L. H.) and an undergraduate research fellowship from the Amoco Foundation (to A. P.).

and **4**, in which hydroxylamine and hydrazine, respectively, coordinate in a unidentate fashion to the metal center through one of the nitrgen atoms. The spectroscopic data of the complexes are summarized in Table 1. The hydrazine complexes **4** can be oxidized with $Pb(OAc)_4$ at low temperature to give the stable diazene complexes **5**. The complexes **5** exhibit lowfield ($\delta = 17-15$) ABX_2 patterns in their ^1H NMR spectra characteristic of the diazene protons of unidentate *trans*-HN=NH ligands coupled to two equivalent ^{31}P atoms.[5] This synthetic protocol is analogous to that used to prepare the related diazene complex $[W(HN{=}NH)(CO)_2(NO)(PPh_3)_2][SO_3CF_3]$ which we recently reported.[5] We have not yet been successful in isolating stable complex cations containing nitrosyl hydride ligands (M←NH=O) from the analogous oxidation of **3a** or **3b**, although a similar neutral Os complex with this ligand, $[Os(Cl)_2(CO)(NH{=}O)(PPh_3)_2]$ (**6**), is known.[6]

Table 1. IR, ^{31}P and ^1H NMR spectroscopic data.

	3a	**3b**	**4a**	**4b**	**5a**	**5b**
$\tilde{\nu}$(CO) [a]	2069, 2012	2055, 1992	2070, 2010	2058, 1985	2070, 2019	2061, 2001
$\delta(^{31}P\{^1H\})$ [b]	24.86 (s)	−2.24 (s)	27.09 (s)	−2.65 (s)	25.56 (s)	−1.65 (s)
^1H NMR: [c]						
δ(M–NH_2Y)	5.50 (t)	5.46 (t)	4.33 (br. m)	4.35 (br. m)	–	–
(Y = OH,NH_2)	$^3J_{PH} = 4.3$	$^3J_{PH} = 4.4$				
δ(M–NH_2Y)	8.22 (br.)	8.66 (br.)	3.35 (t)	3.56 (t)	–	–
(Y = O*H*:N*H*$_2$)			$^3J_{HH} = 4.9$	$^3J_{HH} = 4.5$		
δ(MN*H* = NH)	–	–	–	–	16.64 (d)	16.60 (d)
					$^3J_{HH} = 29.3$	$^3J_{HH} = 29.4$
δ(MNH = N*H*)	–	–	–	–	15.43 (dt)	15.53 (dt)
					$^3J_{HH} = 29.3$,	$^3J_{HH} = 29.4$,
					$^4J_{PH} = 1.9$	$^4J_{PH} = 2.2$

[a] Fluorolube mull, in cm^{-1}. [b] 202 MHz, CD_2Cl_2 solution, 20 °C. [c] 500 MHz, CD_2Cl_2 solution, 20 °C, coupling constants in Hz.

The molecular structures of **4b** and **5b** have been determined by X-ray diffraction analyses and are interesting because they allow for comparison of hydrazine (**4b**) and diazene (**5b**) ligands in identical coordination environments.[7] Both complex cations are pseudooctahedral with *cis* carbonyl and *trans* phosphane ligands. The Os–N (2.181(3) Å) and N–N (1.451(7) Å) bonds in **4b** are in the normal range for single bonds (Fig. 1); the Os-N-N angle (119.3(3)°) is somewhat opened from the tetrahedral value.[8]

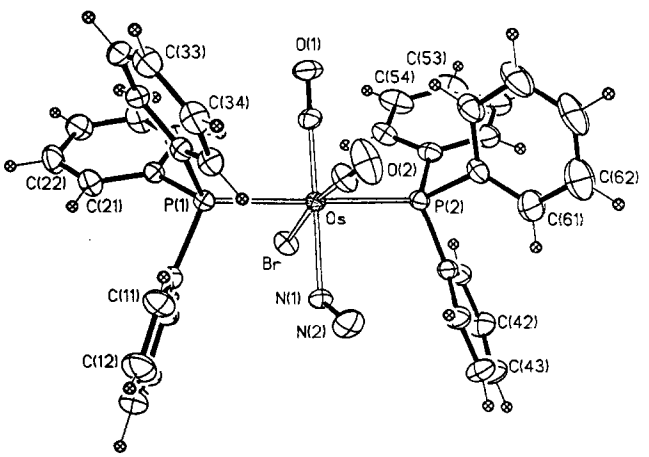


Fig. 1. A perspective view of the complex cation of **4b**.

The most significant structural feature of **5b** (Fig. 2) is the unambiguously characterized unidentate *trans*-HN=NH ligand coordinated to the Os atom. The positions of the H atoms of the diazene were located and refined.[9] The N–N (1.166(17) Å) bond length in **5b** is short, but it is within experimental error of that expected for a N=N bond. The Os–N (2.118(12) Å) bond length is shorter than that in **4b**, consistent with the smaller covalent radius for the sp^2-hybridized N atom in diazene compared to the sp^3-hybridized N atom in hydrazine. The Os-N-N angle (135.9(10)°) in **5b** is significantly more obtuse than the idealized 120° trigonal value. A comparison of the metrical parameters of the diazene ligand of **5b** with those of the isoelectronic HN=O ligand in **6** (in which the nitrosyl hydride ligand is also unidentate) reveals striking similarities: in **6**, N–O 1.193(7), Os–N 1.915(6) Å, and ∢ Os-N-O 136.9(6)°.[6]

It is noteworthy that while monosubstituted diazenes usually coordinate to metals as *cis*-NH=NR ligands,[10] complexes of the parent diazene show only *trans*-HN=NH ligation. With several complexes containing diazene ligands coordinated in a unidentate fashion now in hand, we are currently exploring the reaction chemistry of these molecules.

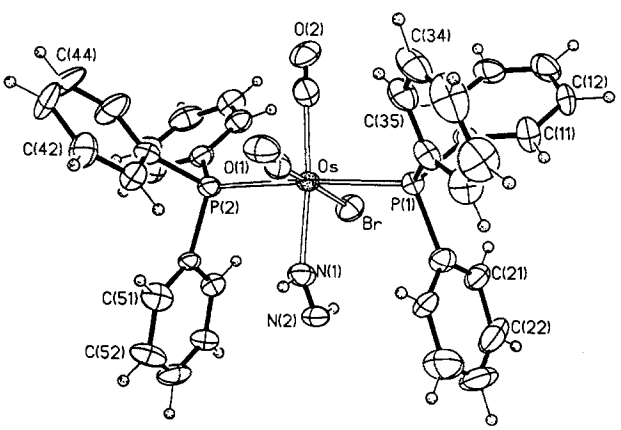


Fig. 2. A perspective view of the complex cation of **5b**.

Experimental Procedure

All reactions were carried out under argon using dry, air-free solvents.

2b: To a stirred solution of **1b** (1.00 g, 1.17 mmol) [11] in CH_2Cl_2 (35 mL) was added $HOSO_2CF_3$ (0.11 mL). When gas evolution ceased, the solvent volume was reduced and Et_2O was added to precipitate 0.88 g (75% yield) of **2b** as white crystals. **2a** was prepared analogously in 70% yield from **1a**.

3b: To a stirred solution of **2b** (0.15 g, 0.15 mmol) in CH_2Cl_2 (10 mL) was added NH_2OH (0.025 g, 0.75 mmol) [12]. The solution was stirred for 15 min, additional NH_2OH (0.025 g) was then added, and stirring was continued for 10 min. The reaction mixture was filtered through Celite, the volume of the filtrate was reduced, and Et_2O was added to precipitate 0.077 g (50% yield) of **3b** as a white powder. **3a** was prepared analogously in 90% yield from **2a**.

4b: To a solution of **2b** (0.50 g, 0.50 mmol) in CH_2Cl_2 (30 mL) was added 98% NH_2NH_2 (1.24 mL, 0.75 mmol). The solution was stirred for 15 min, additional NH_2NH_2 (0.5 mL) was then added, and stirring was continued for 15 min. The solution was filtered, the solvent volume was reduced, and Et_2O was added to precipitate 0.41 g (80% yield) of **4b** as a white powder. **4a** was prepared analogously in 90% yield from **2a**.

5b: A sample of **4b** (0.10 g, 0.10 mmol) was placed in a two-necked 25 mL flask fitted with a solids–addition sidearm containing $Pb(OAc)_4$ (0.05 g, 0.12 mmol). The system was evacuated, $CHCl_3$ (5 mL) was vacuum transferred at −40 °C into the flask, and the $Pb(OAc)_4$ was added portionwise to the cold, stirred solution. After 10 min, the solvent was removed under vacuum, and the residue was extracted with CH_2Cl_2 (10 mL). The solution was filtered, the solvent volume was reduced, and petroleum ether was added to precipitate 0.064 g (64% yield) of **5b** as a pale yellow

powder. **5a** was prepared analogously in 40% yield from **4a**, except that the reaction temperature was maintained at −78 °C.

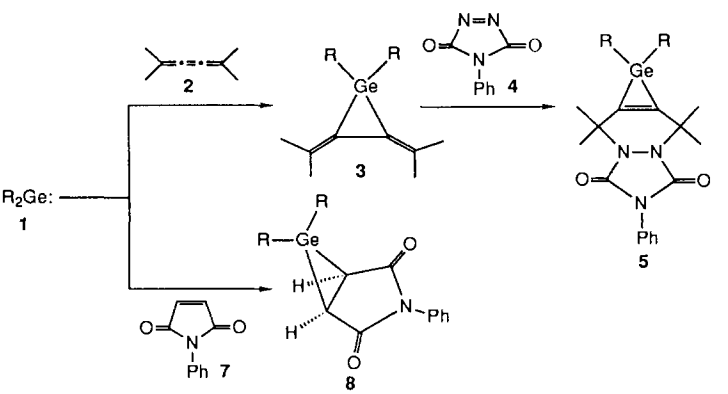
Received: October 5, 1993 [Z 6394 IE]
German version: *Angew. Chem.* **1994**, *106*, 703

[1] N. Wiberg, H. Bachhuber, G. Fischer, *Angew. Chem.* **1972**, *84*, 889; *Angew. Chem. Int. Ed. Engl.* **1972**, *11*, 829.
[2] R. A. Back, *Rev. Chem. Intermed.* **1984**, *5*, 293; S. Hünig, H. R. Müller, W. Thier, *Angew. Chem.* **1965**, *77*, 368; *Angew. Chem. Int. Ed. Engl.* **1965**, *4*, 271; C. E. Miller, *J. Chem. Educ.* **1965**, *42*, 254; J. M. Manriquez, R. D. Sanner, R. E. Marsh, J. E. Bercaw, *J. Am. Chem. Soc.* **1976**, *98*, 3042; D. Coucouvanis, *Acc. Chem. Res.* **1991**, *24*, 1; R. N. F. Thorneley, R. R. Eady, D. J. Lowe, *Nature (London)* **1978**, *272*, 5578; R. A. Henderson, G. J. Leigh, C. J. Pickett, *Adv. Inorg. Chem. Radiochem.* **1983**, *27*, 198.
[3] C. Willis, R. A. Back, *Can. J. Chem.* **1973**, *51*, 3605; R. A. Back, C. Willis, *ibid.* **1974**, *52*, 2513.
[4] D. Sellmann, A. Brandl, R. Endell, *Angew. Chem.* **1973**, *85*, 1122; *Angew. Chem. Int. Ed. Engl.* **1973**, *12*, 1019; D. Sellmann, K. Jödden, *ibid.* **1977**, *89*, 480 and **1977**, *16*, 464; D. Sellmann, E. Böhlen, M. Waeber, G. Huttner, L. Zsolnai, *ibid.* **1985**, *97*, 984 and **1985**, *24*, 981; D. Sellmann, W. Soglowek, F. Knoch, M. Moll, *ibid.* **1989**, *101*, 1244 and **1989**, *28*, 1271; G. Huttner, W. Gartzke, K. Allinger, *ibid.* **1974**, *86*, 860 and **1974**, *13*, 822; D. Sellmann, *J. Organomet. Chem.* **1972**, *44*, C46; G. Huttner, W. Gartzke, K. Allinger, *ibid.* **1975**, *91*, 47; D. Sellmann, A. Brandl, R. Endell, *ibid.* **1973**, *49*, C22; J. P. Collman, J. E. Hutchison, M. A. Lopez, R. Guilard, R. A. Reed, *J. Am. Chem. Soc.* **1991**, *113*, 2794.
[5] M. R. Smith III, T.-Y. Cheng, G. L. Hillhouse, *J. Am. Chem. Soc.* **1993**, *115*, 8638.
[6] K. R. Grundy, C. A. Reed, W. R. Roper, *J. Chem. Soc. Chem. Commun.* **1970**, 1501; R. D. Wilson, J. A. Ibers, *Inorg. Chem.* **1979**, *18*, 336.
[7] Further details of the crystal structure investigations are available on request from the Director of the Cambridge Crystallographic Data Centre, 12 Union Road, GB-Cambridge CB2 1EZ (UK), on quoting the full journal citation.
[8] Crystal data for **4b**: $C_{39}H_{34}BrF_3N_2O_5OsP_2S$, triclinic, $P\bar{1}$, $a = 11.434(3)$, $b = 13.718(4)$, $c = 13.859(3)$ Å, $\alpha = 98.17(2)$, $\beta = 100.31(2)$, $\gamma = 104.13(2)°$, $V = 2034.2(9)$ Å^3, $Z = 2$, $\rho_{calcd} = 1.685$ g cm^{-3}, $\mu(Mo_{K\alpha}) = 43.04$ cm^{-1}, $T = 296$ K. Of 12316 data collected (Siemens P3, $2\theta_{max} = 60°$), 11865 were independent and 8878 were observed ($5\sigma F_o$). All non-hydrogen atoms were anisotropically refined and phenyl hydrogen atoms were treated as idealized contributions; those of the hydrazine molecule were ignored. The phenyl rings were constrained to rigid planar hexagons. SHELXTL software was used for all calculations. At convergence: $R(F) = 0.0371$, $R(wF) = 0.0430$.
[9] Crystal data for **5b**: $C_{39}H_{32}BrF_3N_2O_5OsP_2S$, monoclinic, $P21/c$, $a = 11.219(2)$, $b = 14.165(3)$, $c = 25.410(6)$ Å, $\beta = 93.370(2)°$, $V = 4031.2(15)$ Å^3, $Z = 4$, $\rho_{calcd} = 1.697$ g cm^{-3}, $\mu(Mo_{K\alpha}) = 43.44$ cm^{-1}, $T = 296$ K. Of 5774 data collected (Siemens P4, $2\theta_{max} = 45°$), 5272 were independent, and 3701 were observed ($4\sigma F_o$). All non-hydrogen atoms were anisotropically refined, and hydrogen atoms were idealized except for the diazene hydrogen atoms which were located and refined. SHELXTL software was used for all calculations. $R(F) = 0.0537$, $R(wF) = 0.0624$.
[10] M. R. Smith III, T.-Y. Cheng, G. L. Hillhouse, *Inorg. Chem.* **1992**, *31*, 1535, and references therein.
[11] K. R. Laing, W. R. Roper, *J. Chem. Soc. (A)* **1969**, 1889; B. R. James, L. D. Markham, B. C. Hui, G. L. Rempel, *J. Chem. Soc. Dalton Trans.* **1973**, 2247.
[12] C. H. Hurd, *Inorg. Syn.* **1939**, *1*, 87.

Stable Germirane Derivatives**

Wataru Ando,* Harunobu Ohgaki, and Yoshio Kabe

1,2-Additions of carbene analogues of the heavier group 14 elements with alkenes and alkynes have been used for the synthesis of the corresponding three-membered metallacycles.[1] Germirane (germacyclopropane) has been proposed to exist as an intermediate in reactions of germanediyls ("germylenes") with alkenes, dienes, and enones, but they have never been isolated.[2] Neumann et al.[2e] proposed a germirane or germylene–olefin complex as a intermediate in the reaction of dimethylgermylene with styrene, which resulted in the formation of a germacyclopentane. Several other approaches for the preparation of germiranes have been unsuccessful, for example, reductive elimination of bromine from di(bromomethyl)germanes by Seyferth et al.,[2d] CH insertion of germylcarbenes by M. Jones, Jr. et al.,[2c] and extrusion of N_2 from a germapyrazoline from Nefedov, Krebs, et al.[2f] and Satge et al.[2g,h] In every case only olefins and polygermanes were detected. These experimental results were supported by recent ab initio calculations which indicated that germiranes are the most likely of the group 14 metallacycles to undergo cycloelimination.[3] Herein we describe the reactions of the stable germylene **1**[4] with 2,5-dimethyl-2,3,4-hexatriene ("tetramethylbutatriene" **2**) and *N*-phenylmaleimide (**5**) which yield the first isolable germirane derivatives, bis(alkylidene)germirane **3** and bicyclic germirane **8** (Scheme 1), which were characterized by X-ray crystallography.



Scheme 1. R = $(Me_3Si)_2CH$.

Our first approach was the construction of a germirane with two alkylidene substituents. Tetramethylbutatriene **2** was thought to be a suitable electron-rich triene for the introduction of *exo*-alkylidene moieties to germirane. Similar reactions have been successful in the preparation of bis(alkylidene)silirane.[1h] Thus when a yellow solution of **1** in benzene was treated with tetramethylbutatriene **2**, immediate decolorization was observed and **3** was isolated from the reaction mixture in 33% yield. The

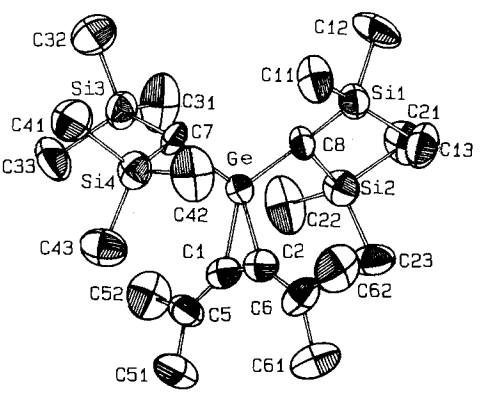


Fig. 1. Crystal structure of **3** (ORTEP). Selected bond lengths [Å] and angles [°]: Ge-C(1) 1.95(1), Ge-C(2) 1.96(1), Ge-C(7) 1.95(9), Ge-C(8) 1.99(1), C(1)-C(2) 1.46(2), C(1)-C(5) 1.34(2), C(2)-C(6) 1.33; C(1)-Ge-C(2) 44.0(5), Ge-C(1)-C(2) 68.3(7), Ge-C(2)-C(1) 67.7(7), Ge-C(1)-C(5) 148(1), Ge-C(2)-C(6) 146(1), C(1)-C(2)-C(6) 140(1), C(2)-C(1)-C(5) 138(1).

[*] Prof. Dr. W. Ando, H. Ohgaki, Dr. Y. Kabe
Department of Chemistry, University of Tsukuba
Tsukuba, Ibaraki 305 (Japan)
Telefax: Int. code + (298)53-6503

[**] This work was supported by a Grant-in-Aid for Scientific Research for Ministry of Education, Science and Culture of Japan. The authors are greatful to Asai Germanium Institute, Shin-Etsu Co. Ltd., and Tosoh Akzo Corp. for generous gifts of trichlorogermane, chlorosilanes, and alkyllithium.

^{1}H NMR spectra of compound **3** exhibit one signal for the $SiMe_3$ groups and two signals for the alkylidene CH_3 groups, which indicates that the molecule has C_{2v} symmetry.[5] Conclusive evidence for **3** was obtained by X-ray analysis (Fig. 1).[6] Compound **3** underwent [4 + 2] cycloaddition with 4-phenyl-1,2,4-triazoline-3,5-dione (TAD, **4**) to afford the tricyclic germirene **5**[5] in 48% yield; this compound was also characterized by X-ray structure analysis (Fig. 2).[6] On hydrolysis of **3** the

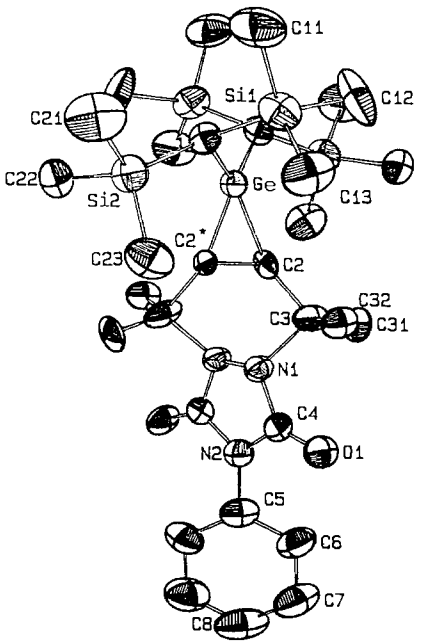
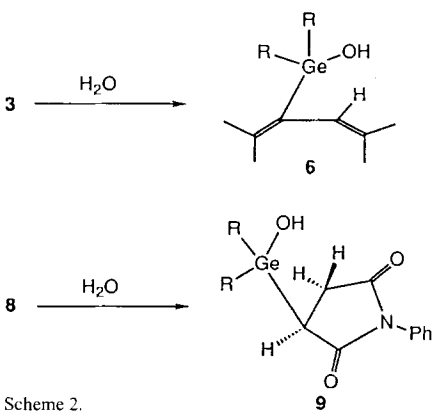


Fig. 2. Crystal stucture of **5** (ORTEP). The molecule has C_2 symmetry; the twofold axis passes through Ge, N(2), C(5), and C(8). Selected bond lengths [Å] and angles [°]: Ge-C(1) 1.93(1), Ge-C(2) 1.88(1), C(2)-C(2)* 1.39(1), C(2)-C(3) 1.55(1); C(2)-Ge-C(2)* 43.2(2), Ge-C(2)-C(2)* 68.4(2), Ge-C(2)-C(3) 161.4(7).

Ge–C bond was cleaved to give the corresponding germanol **6** quantitatively (Scheme 2).[5]



Scheme 2.

Dialkylgermylenes such as **1** are known to undergo [4+1] cycloadditions with acyclic electron-deficient enones.[2a] Since this reaction is not possible for cyclic enediones such as *N*-phenylmaleimide (**7**), one might expect a [2 + 1] cycloaddition of germylene to a C–C double bond. Indeed after treatment of *N*-phenylmaleimide (**7**) with **1** in benzene, the bicyclic germirane **8** was isolated (Scheme 1) as moderately air- and moisture-sensitive colorless crystals in 78% yield and purified by repeated recrystallization from hexane. The most characteristic signals in the ^{1}H and ^{13}C NMR spectra of **8** are sets of resonances for the germirane protons and carbon atoms at $\delta = 2.70$ and 29.4, respectively.[5] The two signals each for the CH and Me_3Si groups of the $(Me_3Si)_2CH$ substituents are consistent with the C_s molecular symmetry of **8**.[5] Hydrolysis of **8** yielded germanol **9** quantitatively (Scheme 2), which exhibits four resonances for the Me_3Si groups and three doublet of doublets for the CH and CH_2 protons in the five-membered ring.[5]

The X-ray structure analysis of **8** (Fig. 3)[6] was hampered by the small data set, which was caused by decomposition of the crystal in the X-ray beam and the existence of two independent molecules. Nevertheless, it is evident that the average Ge–C and

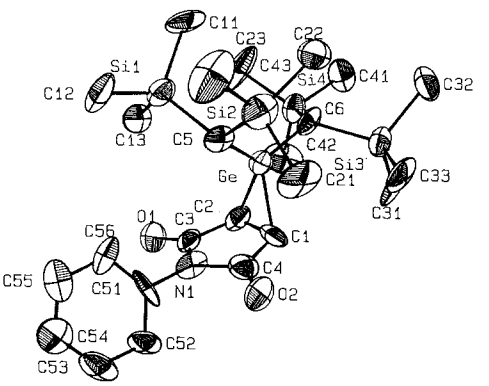


Fig. 3. Crystal structure of **8** (ORTEP). Since two independent molecules are present in the asymmetric unit, the following bond lengths [Å] and angles [°] are given in pairs: Ge-C(1) 1.92(2)/1.97(2), Ge-C(2) 1.98(2)/2.07(2), Ge-C(5) 1.90(2)/1.99(2), Ge-C(6) 1.90(2)/1.93(2), C(1)-C(2) 1.51(3)/1.62(3), C(1)-C(4) 1.42(3)/1.46(3), C(2)-C(3) 1.46(3)/1.55(3); C(1)-Ge-C(2) 45.0(8)/47.7(8), Ge-C(1)-C(2) 68(1)/71(1), C(5)-Ge-C(6) 126.5(8)/123.5(7), Ge-C(2)-C(1) 61.4(9)/67(1), Ge-C(1)-C(4) 115(1)/118(1), Ge-C2-C3 111(2)/113(1), C(1)-C(2)-C(3) 102(1)/104(2), C(2)-C(1)-C(4) 104(1)/107(2).

C–C bond lengths of 1.99 Å and 1.56 Å, respectively, fall within the range of normal Ge–C (1.96–2.01 Å) and C–C (1.44–1.54 Å) separations. Furthermore, among the germirane and germirene derivatives **3**, **5**, and **8** the C-Ge-C bond angles as well as C–C bond lengths decrease in the order **8** (averaged values for two molecules 46.3°, 1.56 Å), **3** (44.0°, 1.46 Å), and **5** (43.2°, 1.387 Å). The smallest values (40.5°, 1.33 Å) were observed for a germirene isolated by Krebs et al. and Nefedov et al.[1m,n] Of particular interest is that the ring Ge–C bond lengths of **3** (1.95 Å) and **5** (1.88 Å) are, as predicted, shorter than those of **8** (averaged values for two molecules 1.99 Å). This observation implies that these unsaturated ring systems are somewhat stabilized by delocalization.

Now that the first germiranes **3** and **8** have been isolated and characterized, the higher homologues, stanniranes (stannacyclopropanes), should be of great interest.

Received: September 21, 1993 [Z 6370 IE]
German version: *Angew. Chem.* **1994**, *106*, 723

[1] a) Review: W. Ando, Y. Kabe, *Small-Ring Organo-Silicon, Germanium and Tin Compounds* (*Adv. Strain Org. Chem.* **1993**, *3* in press); b) siliranes: G. L. Delker, Yu. Wang, G. D. Stucky, R. L. Lambert, Jr., C. K. Hass, D. Seyferth, *J. Am. Chem. Soc.* **1976**, *98*, 1779; c) D. Seyferth, D. C. Annarelli, S. C. Vick, P. Duncan, *J. Organomet. Chem.* **1980**, *201*, 179; d) W. Ando, M. Fujita, H. Yoshida, A. Sekiguchi, *J. Am. Chem. Soc.* **1988**, *110*, 3310; e) P. Boujouk, E. Black, R.

Kumarathasan, *Organometallics* **1991**, *10*, 2095; f) D. H. Pae, M. Xiao, M. Y. Chiang, P. P. Gasper, *J. Am. Chem. Soc.* **1991**, *113*, 1281; g) alkylidenesiliranes: H. Saso, W. Ando, K. Ueno, *Tetrahedron* **1989**, *45*, 1929; h) bis(alkylidene)siliranes: T. Yamamoto, Y. Kabe, W. Ando, *Organometallics* **1993**, *12*, 1996; i) silirenes: R. T. Conlin, P. P. Gasper, *J. Am. Chem. Soc.* **1976**, *98*, 3715; j) H. Sakurai, Y. Kamiyama, Y. Nakadaira, *ibid.* **1977**, *99*, 3879; k) K. Hirotsu, T. Higuchi, M. Ishikawa, H. Sugisawa, M. Kumada, *J. Chem. Soc. Chem. Commun.* **1982**, 726; l) D. Seyferth, D. C. Annarelli, S. C. Vick, *J. Organomet. Chem.* **1984**, *272*, 123; m) germirenes: A. Krebs, J. Berndt, *Tetrahedron Lett.* **1983**, *24*, 4083; n) M. P. Egorov, S. P. Kolensnikov, Y. T. Struchkov, M. Y. Antipin, S. V. Sereda, O. M. Nefedov, *J. Organomet. Chem.* **1985**, *290*, C27; o) stannirenes: L. R. Sita, R. D. Bickerstaff, *J. Am. Chem. Soc.* **1988**, *110*, 5208.

[2] Reviews: a) W. P. Neumann, *Chem. Rev.* **1991**, *91*, 311; b) J. Barrau, J. Escudie, J. Satge, *ibid.* **1990**, *90*, 283. Germirane intermediates were proposed in the following reports: c) E. B. Norsoph, B. Coleman, M. Jones, Jr., *J. Am. Chem. Soc.* **1978**, *100*, 994; d) D. Seyferth, M. Massol, J. Barrau, S. Monteverdi, *J. Organomet. Chem.* **1980**, *185*, 307; e) J. Köcher, W. P. Neumann, *Organometallics* **1985**, *4*, 400; f) M. P. Egorov, S. P. Kolesnikov, O. M. Nefedov, A. Krebs, *J. Organomet. Chem.* **1989**, *375*, C5; g) M. Lazraq, J. Escudie, C. Couret, J. Satge, M. Soufianoui, *ibid.* **1990**, *397*, 1; h) M. Lazraq, C. Couret, J. P. Declercq, A. Dubourg, J. Escudie, M. Rivieve-Baudet, *Organometallics* **1990**, *9*, 845; i) K. L. Bobbitt, V. M. Maloney, P. P. Gaspar, *ibid.* **1991**, *10*, 2772.

[3] D. A. Horner, R. S. Grev, H. F. Schaefer III, *J. Am. Chem. Soc.* **1992**, *114*, 2093.

[4] D. E. Goldbeg, P. B. Hitchcock, M. F. Lappert, K. M. Thomas, A. J. Thorne, T. Fjeldberg, A. Haaland, B. E. R. Schilling, *J. Chem. Soc. Dalton Trans.* **1986**, 2387.

[5] **3**: Colorless crystals, m.p. 118.5 °C; ^{1}H NMR (500 MHz, C_6D_6): $\delta = 0.10$ (s, 2H), 0.32 (s, 36H), 2.04 (s, 6H), 2.16 (s, 6H); ^{13}C NMR (125 MHz, C_6D_6): $\delta = 3.1$ (q), 7.7 (d), 24.9 (q), 28.9 (q), 129.0 (s), 135.7 (s); MS: *m/z*: 500 (M^+), 485 ($M^+ - Me$). – **5**: Colorless crystals, m.p. 189.3–189.5 °C; ^{1}H NMR (400 MHz, C_6D_6): $\delta = -0.01$ (s, 2H), 0.24 (s, 36H), 1.97 (s, 12H), 7.04 (t, 1H), 7.18 (t, 2H), 7.80 (d, 2H); ^{13}C NMR (100 MHz, C_6D_6): $\delta = 3.4$ (q), 14.1 (d), 25.3 (q), 63.9 (s), 125.9 (d), 127.5 (d), 128.8 (d), 132.7 (s), 135.3 (s), 157.5 (s); MS: *m/z*: 675 (M^+), 660 ($M^+ - Me$). – **6**: Colorless oil; ^{1}H NMR (500 MHz, C_6D_6): $\delta = 0.30$ (s, 2H), 0.35 (s, 18H), 0.41 (s, 18H), 0.60 (s, 1H), 1.55 (d, 3H), 1.64 (d, 3H), 1.79 (d, 3H), 1.98 (d, 3H), 6.00 (d, 1H); ^{13}C NMR (125 MHz, C_6D_6): $\delta = 3.8$ (q), 4.3 (q), 11.6 (d), 20.7 (q), 23.7 (q), 25.7 (q), 26.4 (q), 126.9 (d), 134.0 (s), 138.1 (s), 141.7 (s); MS: *m/z*: 518 (M^+), 503 ($M^+ - Me$); HRMS: calcd. for $C_{22}H_{52}OSi_4{}^{74}Ge$ 518.2307, found 518.2308. In the COLOC spectra of **6** olefinic CH and the neighboring quaternary carbons ($\delta = 126.9$ and $\delta = 134.0$, respectively) show cross peaks to two CH_3 protons ($\delta = 1.55$, 1.79), while the other olefinic quaternary carbons ($\delta = 138.1$, 141.7) correlated with two other CH_3 protons ($\delta = 1.64$, 1.98). – **8**: Colorless crystals; decomp. 108.7 °C; ^{1}H NMR (400 MHz, C_6D_6): $\delta = -0.03$ (s, 1H), 0.07 (s, 1H), 0.15 (s, 18H), 0.24 (s, 18H), 2.70 (d, 2H), 7.05 (t, 1H), 7.27 (t, 2H), 7.8 (d, 2H); ^{13}C NMR (100 MHz, C_6D_6): $\delta = 3.1$ (q), 3.5 (q), 3.7 (d), 7.1 (d), 29.4 (d), 126.3 (d), 127.3 (d), 128.3 (s), 128.8 (d), 173.9 (s); MS: *m/z*: 565 (M^+), 550 ($M^+ - Me$). – **9**: Colorless powder; ^{1}H NMR (400 MHz, C_6D_6): $\delta = 0.02$ (s, 1H), 0.14 (s, 9H), 0.22 (s, 9H), 0.26 (s, 9H), 0.36 (s, 9H), 0.45 (s, 1H), 2.32 (s, 1H), 2.72 (dd, 1H, $J_{AB} = 10.1$ Hz, $J_{BC} = 17.7$ Hz), 2.81 (dd, 1H, $J_{AB} = 10.1$ Hz, $J_{AC} = 4.90$ Hz), 2.93 (dd, 1H, $J_{AC} = 4.90$ Hz, $J_{BC} = 17.7$ Hz), 7.05 (t, 1H), 7.22 (t, 2H), 7.53 (d, 2H); ^{13}C NMR (100 MHz, C_6D_6): $\delta = 3.3$ (q), 3.5 (q), 3.6 (q), 3.8 (q), 9.5 (d), 11.6 (d), 32.3 (t), 34.9 (d), 126.5 (d), 128.2 (d), 128.9 (d), 133.0 (s), 175.0 (s), 178.6 (s); MS: *m/z*: 583 (M^+), 568 ($M^+ - Me$); HRMS: calcd. for $C_{24}H_{47}O_3NSi_4{}^{74}Ge$ 583.1844, found 583.1844. In the C-H COSY spectra of **9** the signal for the CH_2 carbon ($\delta = 32.3$) shows cross peaks to H^B ($\delta = 2.72$) and H^C ($\delta = 2.93$). The *J* values of H^A (2.81 Hz), H^B, and H^C establish the proton connectivities and the *trans* relationship between H^A and H^C. The four Me_3Si signals in the ^{1}H and ^{13}C NMR spectra of **9** are assigned to the two diastereotopic $(Me_3Si)_2CH$ groups, since the carbon attached to germyl substituent is chiral and each Me_3Si group is also diastereotopic due to the unsymmetrically substituted germanium.

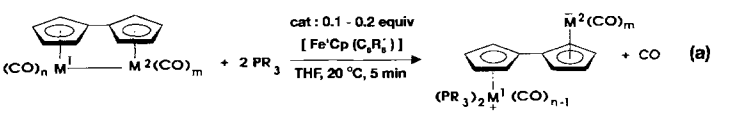
[6] Crystal data: **3**: $C_{22}H_{50}GeSi_4$, $M_r = 499.6$, triclinic with $a = 9.217(6)$, $b = 11.384(8)$, $c = 15.861(9)$ Å, $\alpha = 76.60(4)$, $\beta = 87.33(4)$, $\gamma = 72.78(5)°$, $V = 1545.9$ Å^3, space group *P*-1, $Z = 2$, $\mu(Mo_{K\alpha}) = 11.4$ cm^{-1}, $\varrho_{calcd} = 1.15$ g cm^{-3}. **5**: $C_{30}H_{55}GeSi_4N_3O_2$, $M_r = 674.73$, orthorhombic with $a = 15.157(1)$, $b = 15.546(1)$, $c = 16.059(1)$ Å, $V = 3784.1$ Å^3, space group *Pbcn*, $Z = 4$, $\mu(Mo_{K\alpha}) = 9.5$ cm^{-1}, $\varrho_{calcd} = 1.189$ cm^{-3}. **8**: $C_{29}H_{45}NO_2Si_4Ge$, $M_r = 624.62$, triclinic with $a = 9.454(1)$, $b = 15.905(3)$, $c = 21.086(4)$ Å, $\alpha = 87.50(2)$, $\beta = 79.04(1)$, $\gamma = 88.90(1)°$, $V = 3109.8$ Å^3, space group *P*-1, $Z = 4$, $\mu(Mo_{K\alpha}) = 11.5$ cm^{-1}, $\varrho_{calcd} = 1.33$ g cm^{-3}. The 2175 (**3**), 1411 (**5**), and 2637 (**8**) independent reflections [$2\theta \leq 50°$; $|F_o 2| > 3\sigma|F_o 2|$] were measured on an Enraf–Nonius CAD4 diffractometer using $Mo_{K\alpha}$ irradiation and ω-2θ scan. An empirical absorption correction based on a series of Ψ-scans were applied to the data (0.82/1.00 for **3**; 0.92/1.00 for **5**; 0.863/0.999 for **8**). The structures were solved by direct methods, and all non-hydrogen atoms were refined anisotropically to $R = 0.065$ ($R_w = 0.076$), $R = 0.066$ ($R_w = 0.077$) and $R = 0.066$ ($R_w = 0.081$) for **3**, **5**, and **8**, respectively. Further details of the crystal structure investigation may be obtained from the Fachinformationszentrum Karlsruhe, D-76344 Eggenstein-Leopoldshafen (FRG), on quoting the depository number CSD-57793, the names of the authors, and the journal citation.

Electron-Reservoir Complexes [Fe^{I}Cp(arene)] as Selective Initiators for a Novel Electron Transfer Chain Catalyzed Reaction: General Synthesis of Fulvalene-Bridged Homo- and Heterodinuclear Zwitterions**

David S. Brown, Marie-Hélène Delville-Desbois, Roland Boese, K. Peter C. Vollhardt,* and Didier Astruc*

Dedicated to Professor Henri Bouas-Laurent on the occasion of his 60th birthday

Many non-redox reactions proceed by the electron-transfer chain (ETC) mechanism.[1, 2] We now report ETC catalysis of a redox reaction, the intramolecular disproportionation of dinuclear fulvalene carbonyl complexes in the presence of PR_3 (R = Me, OMe).[3] The result is the cleavage of the metal–metal bond, replacement of one CO by two PR_3 ligands at a single metal center, and intramolecular electron transfer [Eq. (a); R′ = H, Me in the Fe catalyst]. The starting materials and products are listed in Table 1.



(a)

Table 1. Summary of the starting materials and products for reaction (a).

Starting material	Product	M^1	M^2	*n*	*m*	R
1	**2**	Mo	Mo	3	3	Me
3	**4**	W	W	3	3	Me
5	**6**	Fe	W	2	3	OMe
5	**8**	Fe	W	2	3	Me
9	**10**	Ru	Mo	2	3	Me
11	**13**	Ru	W	2	3	Me

Electron-reservoir complexes [Fe^{I}Cp(C_6R_6)],[4] the most electron-rich, stable neutral compounds known (based on ionization potential values[5b]), are ideal mediators allowing reduction at very negative potentials ($E^0 = -1.3$ to -1.9 V vs. SCE).[5] They can be used in precise amounts, and their redox potentials

[*] Prof. K. P. C. Vollhardt, Dr. D. S. Brown
Department of Chemistry, University of California
and
Chemical Sciences Division, Lawrence Berkeley Laboratory
Berkeley CA 94720 (USA)
Telefax: Int. code + (510)643-5208

Prof. D. Astruc, Dr. M.-H. Delville-Desbois
Laboratoire de Chimie Organique et Organométallique
URA CNRS n° 35, Université Bordeaux I
351 Cours de la Libération, F-33405 Talence Cédex (France)
Telefax: Int. code + 56846646

Priv.-Doz. R. Boese
Institut für Anorganische Chemie der Universität-Gesamthochschule Essen
Universitätsstrasse 3–5, D-45117 Essen (FRG)
Telefax: Int. code + (201)183-2535

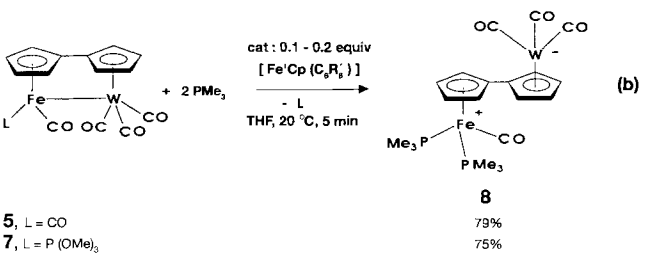
[**] This work was supported by the University of California at Berkeley and the Université Bordeaux I, the Centre National de la Recherche Scientifique (CNRS), the Région Aquitaine, the National Science Foundation (NSF), NATO (CRG 900479), and the Director of the Office of Energy Research, Office of Basic Energy Sciences, Materials Science Division of the US Department of Energy (DE-AC-03 76SF00098).

$E^0_{Fe^I/Fe^{II}}$ can be adjusted by the choice of the ring substituents, which provides selectivity, as will be shown here.[5]

With these Fe^I initiators, the ETC-catalyzed synthesis of fulvalene-bridged homo- and heterobimetallic zwitterions proceeds very smoothly (20 °C, a few minutes) in good yields. The ready synthesis of organometallic zwitterions bridged by a ligand and with a delocalized π-electron system has potential, for instance, for the preparation of materials with nonlinear optical properties.[6] Some of the zwitterions could be synthesized thermally, but the reactions needed heating for days, gave low yields, and required decomplexation of one metal center.[7]

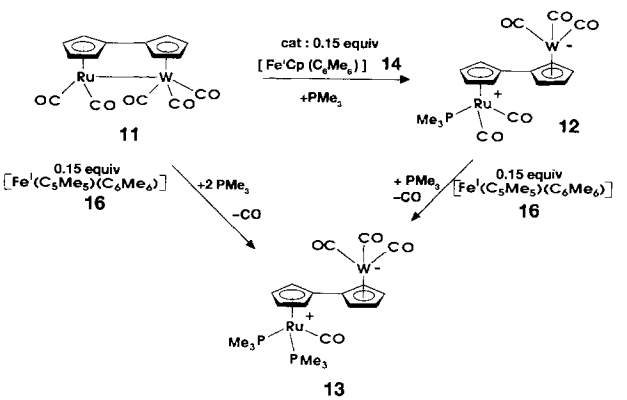
The respective prototypical homodinuclear Mo and W fulvalene carbonyl complexes **1** and **3**[8] react with excess PMe_3 in THF in the presence of 0.1–0.2 equiv $[Fe^ICp(C_6Me_6)]$ (**14**) ($E^0 = -1.55$ V vs. SCE, in dimethylformamide (DMF)) to give the zwitterions **2** (60%) and **4** (70%), respectively, in a few minutes at 20 °C. Monophosphane zwitterions are not detected.

For the heterobimetallic FeW complex **5**,[8] we know that reduction differentiates the two metal centers (recognition), since two distinct one-electron waves were found (W reduction at −1.05 V vs. SCE, Fe reduction at −1.6 V vs. SCE, in THF).[9] Thus, single-electron reduction of **5** provides the radical anion $Fe^{\bullet}W^-$, and the ligand-exchange reactions with PR_3 (R = Me, OMe) proceed at the radical iron center in the chain propagation step. ETC catalysis can be initiated by either **14** or $[Fe^ICp(C_6H_6)]$ (**15**) ($E^0 = -1.30$ V vs. SCE, in DMF), owing to an exergonic electron transfer in the initiation step ($\Delta G^0 < -24$ kJ mol^{-1} with **15**). Not unexpectedly, cobaltocene proved an inefficient initiator, since its E^0 value (−0.9 V vs. SCE) is too low.[10] Complex **7** undergoes (like **5**) ETC reaction initiated with **14** to give zwitterions **6** and **8** [Eq. (b); R′ = H, Me in the Fe catalyst]. Only the bis-PMe_3 complex **8** forms upon reaction with PMe_3, which indicates that PMe_3 displaces $P(OMe)_3$ during the ETC reaction.



Of particular interest is the RuW complex **11**, since differentiation between the two metal centers is not observed by cyclic voltammetry; instead an irreversible two-electron reduction to the dianion $[Fv\{W(CO)_3^-\}\{Ru(CO)_2^-\}]$ occurs.[9] The ETC reaction, however, does differentiate between the two metal centers, since two PMe_3 ligands are bound regiospecifically at the Ru center [Eq. (a)]. ETC-catalyzed syntheses provide either the monophosphane zwitterion **12** (the only one in the series) or the diphosphane zwitterion **13**, depending on the reductive power of the electron-reservoir complex. Using **14** as the initiator specifically leads to **12**, whereas the use of $[Fe^I(C_5Me_5)(C_6Me_6)]$ (**16**) ($E^0 = -1.85$ V vs. SCE in DMF) provides only **13**. Accordingly, it is also possible to synthesize **13** from **12** when **16** is used as the ETC initiator (Scheme 1).

Note that the first reaction (**11** → **12**) represents an ETC catalysis of net phosphane addition, a simple but new reaction, whereas the second (**12** → **13**) is only a classical substitution of CO by PMe_3. Despite the simplicity of ETC-catalyzed substitution reactions, there are very few reports of such a reaction for



Scheme 1. ETC reactions starting with **11**.

mononuclear complexes.[2b, 11] This is because of side reactions of the radical anion involved in the chain propagation step. The efficiency in the reactions described here is explained by the effectiveness of the fulvalene ligand as an electron sink, similar to clusters.[2a, 12] The remarkable selectivity indicates that the electron transfer between **12** and **14** is too endergonic to occur.[13] Since Cp permethylation (**14** → **16**) shifts the E^0 value of the initiator negatively by 300 mV, reduction of **11** by **16** is exergonic, thus very efficient.

The molecular structure of the zwitterions was proven by elemental analysis, high-resolution ^1H, ^{13}C, and ^{31}P NMR spectroscopy, and mass spectrometry.[14] In the case of **8**, the X-ray crystal structure[15] shows the *anti* conformation of the two metal complex fragments (Fig. 1), which is most probably common to all the zwitterions reported here. Cyclic voltammetry was used to monitor the ETC-catalyzed process by following the disappearance of the starting complexes and appearance of the zwitterions. (Details will be provided in a full paper.)

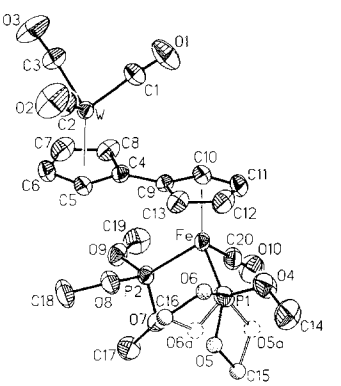


Fig. 1. Crystal structure of **8** (ORTEP).

In conclusion, we have carried out a series of ETC-catalyzed reactions providing fulvalene-bridged homo- and heteronuclear zwitterions. The selectivity, generality, and efficiency of this reaction, as well as the role of three Fe^I electron-reservoir ETC initiators, was demonstrated.

Experimental Procedure

Under inert gas a Schlenk tube was charged with the fulvalene dimetal carbonyl complex (0.1 mmol) and THF (10 mL); PR_3 (100 μL, 1 mmol) was added by syringe, followed by a solution of Fe^I complex (0.01 mmol) in dimethoxyethane. After 5 min analysis by thin-layer chromatography (silica gel, 1/1 THF/hexane) indicated that no starting material remained. The solvent was removed in vacuo. The residue was dissolved in MeCN and filtered through a plug of Celite (1 × 4 cm). The solvent was removed in vacuo and the residue recrystallized from acetone/ether at −78 °C or −30 °C.

Received: October 6, 1993 [Z 6400 IE]
German version: *Angew. Chem.* **1994**, *106*, 715

[1] a) The first ETC-catalyzed reaction: H. Taube, R. L. Rich, *J. Am. Chem. Soc.* **1954**, *76*, 2608; b) comparative review of ETC catalysis in molecular chemistry: M. Chanon, *Acc. Chem. Res.* **1980**, *13*, 23; c) L. Eberson, *Electron Transfer*

Reactions in Organic Chemistry, Springer, Berlin, **1987**; d) J.-M. Savéant, *Acc. Chem. Res.* **1980**, *13*, 323; e) J. K. Kochi, *J. Organomet. Chem.* **1986**, *300*, 139.
[2] a) D. Astruc, *Angew. Chem.* **1988**, *100*, 666; *Angew. Chem. Int. Ed. Engl.* **1988**, *27*, 643; *Comments Inorg. Chem.* **1987**, *6*, 61; *Acc. Chem. Res.* **1991**, *24*, 36; b) W. Kaim, *J. Organomet. Chem. Libr.* **1980**, *22*, 173; c) J. Heinze, *Angew. Chem.* **1984**, *96*, 823; *Angew. Chem. Int. Ed. Engl.* **1984**, *23*, 831.
[3] For the photochemically initiated disproportionation of metal carbonyls, see: a) D. R. Tyler, *Prog. Inorg. Chem.* **1988**, *36*, 125; b) D. R. Tyler, F. Mao, *Coord. Chem. Rev.* **1985**, *97*, 199.
[4] Besides ETC initiation, the two major functions of electron-reservoir complexes are: 1) stoichiometric electron transfer for the activation of molecules and in material science, and 2) redox catalysis: D. Astruc, *Acc. Chem. Res.* **1986**, *19*, 377; *New J. Chem.* **1992**, *16*, 305.
[5] a) J.-R. Hamon, D. Astruc, P. Michaud, *J. Am. Chem. Soc.* **1981**, *103*, 758; b) J. Green, M. R. Kelly, M. P. Payne, E. A. Seddon, D. Astruc, P. Michaud, *Organometallics* **1983**, *2*, 211; c) for the preparation of the Fe^{I} complexes, see ref. [5a] and D. Astruc, J.-R. Hamon, M. Lacoste, M.-H. Desbois, A. M. Madonik, E. Román in *Organometallic Synthesis, Vol. 4* (Ed.: R. B. King), Elsevier, Amsterdam, **1988**, pp. 172–187.
[6] a) R. W. Boyd, *Nonlinear Optics*, Academic Press, New York, **1992**; b) S. R. Marder, D. N. Beratan, L. T. Cheng, *Science* **1991**, *252*, 103; c) W. M. Laidlaw, R. G. Denning, *Nature* **1993**, *363*, 58.
[7] a) For instance, the non-ETC-catalyzed synthesis of **10** required heating $[Ru_2(Fv)(CO)_4]$ (Fv = fulvalene) with PMe_3 for 2d to give $[Ru(Fv)(CO)(PMe_3)_2]$, which was then metalated with $[Mo(CO)_3(MeCN)_3]$: M. A. Huffman, D. A. Newman, M. Tilset, W. B. Tolman, K. P. C. Vollhardt, *Organometallics* **1986**, *5*, 1926; b) M. Tilset, K. P. C. Vollhardt, *ibid.* **1985**, *4*, 2230.
[8] K. P. C. Vollhardt, T. W. Weidman, *Organometallics* **1984**, *3*, 82.
[9] a) M.-H. Delville-Desbois, D. Brown, K. P. C. Vollhardt, D. Astruc, *J. Chem. Soc. Chem. Commun.* **1991**, 1355; b) D. Brown, M.-H. Delville-Desbois, K. P. C. Vollhardt, D. Astruc, *New J. Chem.* **1992**, *16*, 899.
[10] a) W. E. Geiger, *J. Am. Chem. Soc.* **1974**, *96*, 2632; for the electrochemistry of di- and polynuclear organometallic complexes see: b) W. E. Geiger, *Prog. Inorg. Chem.* **1985**, *33*, 275; c) W. E. Geiger, N. G. Connelly, *Adv. Organomet. Chem.* **1985**, *24*, 87; d) P. Lemoine, *Coord. Chem. Rev.* **1982**, *58*, 55; *ibid.* **1988**, *64*, 169.
[11] a) P. Lahuerta, M. Latorre, H. Sanau, H. Kisch, *J. Organomet. Chem.* **1985**, *280*, C27; b) B. Olbrich-Deussner, R. Gross, W. Kaim, *ibid.* **1989**, *366*, 155.
[12] For a comprehensive example of study of ETC exchange of CO by phosphanes in clusters see: K. Hinkelmann, J. Heinze, H. T. Schacht, T. S. Field, H. Vahrenkamp, *J. Am. Chem. Soc.* **1989**, *111*, 5078.
[13] a) R. A. Marcus, *J. Chem. Phys.* **1956**, *24*, 966; b) R. A. Marcus, N. Sutin, *Biochem. Biophys. Acta* **1985**, *811*, 265.
[14] **2:** See ref. [7b]. – **4:** M. Tilset, Dissertation, University of California at Berkeley, **1986**. **6:** M.p. 128–129 °C; ^1H NMR (400 MHz, CD_3CN): $\delta = 5.63$ (t, $J = 2.4$ Hz, 2H), 5.14 (t, $J = 2.4$ Hz, 2H), 5.12 (m, 2H), 4.96 (t, $J = 1.9$ Hz, 2H), 3.68 (m, 18H); $^{13}C\{^1H\}$ NMR (100 MHz, CD_3CN): $\delta = 225.86$, 215.06, 106.61, 90.75, 86.55, 86.32, 83.92, 79.48, 54.45 (t, $J(P,C) = 3.7$ Hz); $^{31}P\{^1H\}$-NMR (121.5 MHz, CD_3CN): $\delta = 167.97$; IR (CH_3CN): $\tilde{\nu} = 1985$, 1895, 1783 cm^{-1} (CO); MS: *m/z* (%): 700 (10) ($M^+ - CO$), 672 (26.2) ($M^+ - 2CO$), 616 (36.8) ($M^+ - 4CO$), 520 (18.1) ($M^+ - P(OMe)_3 - 3CO$), 492 (34.4) ($M^+ - P(OMe)_3 - 4CO$); satisfactory C,H analysis. – **8:** M.p. >250 °C (decomp without melting); ^1H NMR (400 MHz, CD_3CN): $\delta = 5.57$ (t, $J = 2.3$ Hz, 2H), 5.12 (t, $J = 2.3$ Hz, 2H), 4.87 (t, $J = 2.0$ Hz, 2H), 4.81 (t, $J = 2.3$ Hz, 2H), 1.48 (m, 18H); $^{13}C\{^1H\}$ NMR (100 MHz, CD_3CN): $\delta = 226.20$, 217.32, 105.08, 92.93, 86.26, 85.87, 84.93, 78.27, 21.28 (t, $J(P,C) = 16.2$ Hz); $^{31}P\{^1H\}$ NMR (121.5 MHz, CD_3CN): $\delta = 25.33$; IR (CH_3CN): $\tilde{\nu} = 1958$, 1895, 1785 cm^{-1} (CO); FAB-MS (nitrobenzylalcohol): *m/z*: 632 (M^+); satisfactory C,H analysis. – **10, 13:** see ref. [7a]. – **12:** M.p. >300 °C (decomp.); ^1H NMR (400 MHz, CD_3CN): $\delta = 5.69$ (t, $J = 2.1$ Hz, 2H), 5.62 (t, $J = 2.4$ Hz, 2H), 5.57 (t, $J = 2.1$ Hz, 2H), 5.14 (t, $J = 2.4$ Hz, 2H), 1.68 (d, $J = 11.5$ Hz, 9H); $^{13}C\{^1H\}$ NMR (100 MHz, CD_3CN): $\delta = 245.82$, 225.54, 110.44, 89.13, 86.84, 86.24, 85.63, 81.61, 20.76 (d, $J(P,C) = 36.7$ Hz); $^{31}P\{^1H\}$ NMR (121.5 MHz, CD_3CN): $\delta = 6.62$. IR (CH_3CN): $\tilde{\nu} = 2003$, 1899, 1796, 1789 cm^{-1} (CO); high-resolution MS (FAB): MH^+ calcd for $C_{18}H_{18}O_5P^{99}Ru^{182}W$ 625.9433; found 625.9431.
[15] X-ray structure determination of **8**: A crystal with the approximate dimensions of $0.39 \times 0.31 \times 0.23$ mm^3 was measured on a Nicolet R3m/V diffractometer with $Mo_{K\alpha}$ radiation at room temperature. Cell dimensions, refined from the diffractometer angles of 50 centered reflections, are $a = 9.766(1)$, $b = 10.973(1)$, $c = 12.536(2)$ Å, $\alpha = 77.60(1)$, $\beta = 73.43(1)$, $\gamma = 81.13(1)°$, $V = 1242.5(3)$ $Å^3$ with $Z = 2$, $\varrho_{calcd} = 1.720$ gcm^{-3}, $\mu = 5.33$ mm^{-1} in space group $P\bar{1}$; $R = 0.0393$ and $R_w = 0.0426$ for 8250 reflections with $F \geq 4\sigma(F)$. Further details of the crystal structure investigation are available on request from the Fachinformationszentrum Karlsruhe, D-76344 Eggenstein-Leopoldshafen, on quoting the following number CSD-57238, the names of the authors, and the journal citation.

3-Phosphonio-1,2-diphosphaindenides and the Electrophilic Substitution of *C*-Phenyl-Substituted Ylides**

Georg Jochem, Alfred Schmidpeter,* Martina Thomann, and Heinrich Nöth

A *C*-phenyl-substituted phosphonium ylide $R_3P{=}CR{-}C_6H_5$ can also be regarded as an ylide-substituted benzene. Although textbooks do not include ylides in the list of substituents affecting electrophilic aromatic substitution, indubitably they should belong to the class of rate-increasing, *o,p*-directing substituents. Indeed, CNDO calculations on compounds of this type indicate a strong perturbation of the benzene π-electron system by an ylide substituent, which is in agreement with their photoelectron spectra. In addition, upfield shifts of the ^{13}C NMR signals relative to the benzene resonance confirm the calculated charge transfer from the ylide carbon atom to the carbon atoms in the *ortho* and *para* positions.[1] To our surprise we could not find any examples of electrophilic substitution reactions at the *C*-phenyl ring of an ylide. During the preparation of *C*-chlorophosphino- and *C*-bromophosphino-ylides[2] we recently encountered an unexpected side reaction, which comprises this type of substitution. Further examples were found during model reactions to determine the reaction pathway.

The reaction of benzyltriphenylphosphonium bromide (**1**) with phosphorus trichloride or tribromide and triethylamine leads to the *C*-dihalophosphino-*C*-phenyl ylides **2**.[2] In addition, in both cases the formation of a further product, which presents a conspicuous ABC spin system in its $^{31}P\{^1H\}$ NMR spectrum, is observed and was identified as 1,2-dihalo-3-triphenylphosphoranediyl-1,2-diphosphaindane **3** (Table 1).[3] Its yield increases

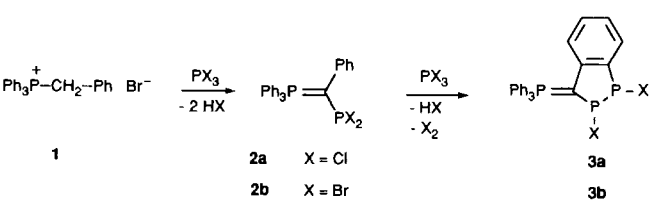


Table 1. ^{31}P NMR data for the 1,2-diphosphaindanes **3** and **5**, and the 1,2-diphosphaindenes **6** in CH_2Cl_2. Coupling constants *J* in Hz.

Cmpd.	δ(P-2)	δ(P-1)	δ(P-3)	^1J(PP)	^2J(PP)	^3J(PP)	^3J(PH)
3a	132.4	78.7	18.6	249.7	96.7		
3c [a]	134.3	78.9	18.3	248.6	97.6		
3d [a]	130.8	75.8	18.5	256.3	96.1		
3b	154.2	61.0	17.7	236.5	91.4	3.8	4.5
3e [a]	156.8	61.8	17.2	235.8	91.5	3.0	
3f [a]	155.8	57.6	17.4	242.7	9.0	3.0	
5	178.6	6.9	17.3	262.5	86.2		
6a	317.1	229.4	14.9	480.2	87.5	6.1	6.9
6b [a]	314.7	229.1	14.0	476.1	87.0	6.1	
6c [a]	309.2	218.8	14.4	477.6	87.0	4.5	

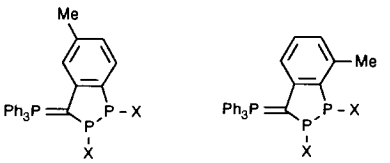
[a] The assignment as the 5-methyl and 7-methyl isomers is preliminary.

[*] Prof. Dr. A. Schmidpeter, Dipl.-Chem. G. Jochem, Dr. M. Thomann, Prof. Dr. H. Nöth
Institut für Anorganische Chemie der Universität
Meiserstrasse 1, D-80333 München (FRG)
Telefax: Int. code + (89) 5902-578

[**] This work was supported by the Deutsche Forschungsgemeinschaft and the Fonds der Chemischen Industrie. We wish to thank Dr. Karaghiosoff for obtaining the 2D NMR spectra, which were essential for the structural elucidation of **10b**.

with reaction time, and for X = Br product **3** can account for up to 50% of the reacted trihalide.

The corresponding reactions of (3-methylbenzyl)triphenylphosphonium bromide (≙ **1**, with 3-$MeC_6H_4CH_2$ instead of $PhCH_2$) with PCl_3 and PBr_3 yield the isomer mixtures **3c**, **d** and **3e**, **f**, respectively, as side products (Table 1). This type of side product is not observed in analogous reactions of other phosphonium bromides of type **1**, in which the benzyl group bears a $-M$ group (NO_2) or in which both *ortho* positions have chlorine substituents.

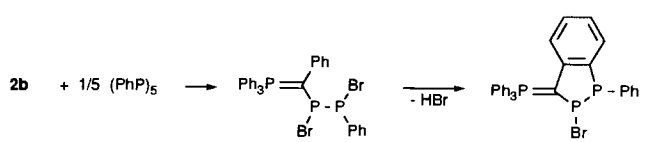


3c X = Cl **3d**

3e X = Br **3f**

Compounds **3** are most likely formed from **2** by *ortho* substitution of the phenyl ring and reduction. A second molecule of **1** acts as reductant and is transformed into the *C*-halo-substituted ylide.[4] Alternatively, added triphenylphosphane can act as reductant, whereby it is transformed into the dihalide. The first alternative was found to be more suitable for workup. To demonstrate that the formation of **3** from **1** proceeds via **2**, we showed that isolated **2b** can be transformed into **3b** in the same manner. For instance, **3b** is formed when a suspension of **2b** in benzene is simply heated to reflux for several days.

The order in which substitution and reduction occur cannot be determined unequivocally; the fact that only *ortho* substitution and no *para* substitution is observed supports an initial P–P linkage. This is expected for an intramolecular reaction but not for an intermolecular process (see below). The proposed intramolecular substitution[5] is further supported by the formation of 2-bromo-1-phenyl-3-triphenylphosphoranediyl-1,2-diphosphaindane (**5**) in the reaction of **2b** with phenyldibromophosphane, triphenylphosphane, and triethylamine, or with pentaphenylcyclopentaphosphane and triethylamine. In the second synthesis **4** is the only reasonable intermediate formed in a precedented manner from **2b** by the insertion of a phosphinidene unit into the P–Br bond.[6]



4 **5**

The values of the $^1J_{PP}$ coupling constants for **3** and **5** (Table 1) confirm the expected *trans* arrangement of the substituents on the phosphorus atoms. The unusually small shielding of P-2, especially compared to P-1, should also indicate structural differences. According to the crystal structure of **3b**,[7] the diphosphaindane backbone, including the exocyclic phosphorus atom, is essentially planar and has bromine atoms located *trans* to each other (Fig. 1). The two P–Br bonds are very different; the bond directly adjacent to the ylide carbon atom is longer (2.42 Å) than

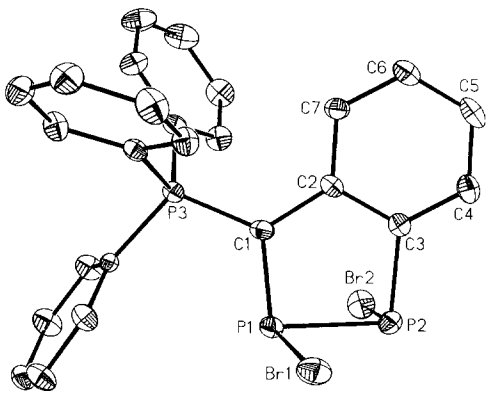
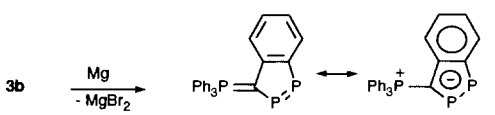


Fig. 1. Crystal structure of **3** (thermal ellipsoids with 50% probability). Selected bond lengths [Å] and angles [°]: P1-Br1 2.424(2), P2-Br2 2.303(2), P1-P2 2.201(3), P2-C3 1.819(6), P1-C1 1.733(6), P3-C1 1.726(6), C1-C2 1.470(7), C2-C3 1.410(9); C1-P1-P2 93.9(2), C1-P1-Br1 103.6(2), Br1-P1-P2 85.8(1), P1-P2-C3 93.0(2), P1-P2-Br2 92.5(1), C3-P2-Br2 97.9(2), P3-C1-P1 118.8(3), P3-C1-C2 123.6(4), P1-C1-C2 117.5(4).

all P–Br bonds previously reported.[8, 9] This can be attributed to its nearly parallel orientation to the p_z orbital of the ylide carbon atom, which enables some charge transfer from there into the antibonding orbital of the P–Br bond.[10]

Compound **3b** can be reduced with magnesium in THF to yield **6a**. This is the first example for formation of a diphosphene by the reduction of a dihalodiphosphane.[11] **6a** is obtained as orange-yellow crystals from THF and as yellow-green crystals upon recrystallization from benzene. **6a** and its 5-methyl (**6b**) and 7-methyl (**6c**) derivatives[12] (Table 1) are also formed as side products in the reaction of **2a** or the corresponding *meta*-tolyl compound (≙ **2a**, with 3-MeC_6H_4 instead of Ph) with Na_2S or Na_2Se.[13]



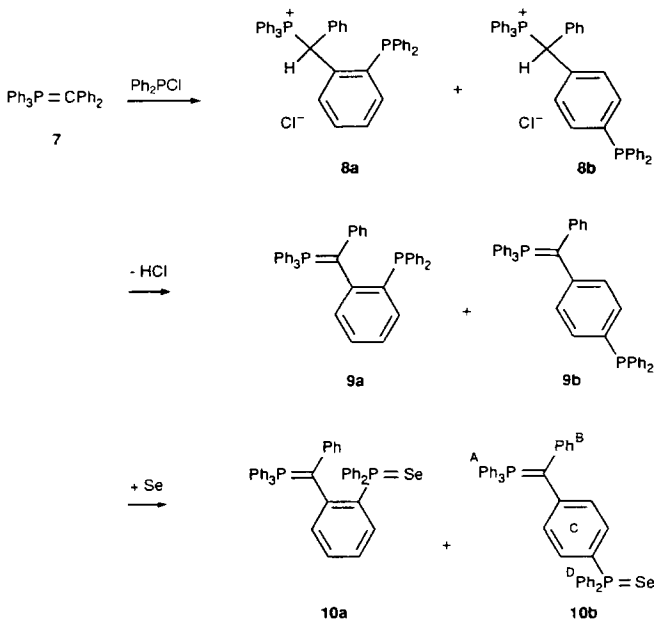
6a

According to the resonance formula on the right, **6a** can be viewed as a 3-phosphonio-1,2-diphosphaindenide with a ring structure isoelectronic to 2,3-diphosphaindole.[14] In fact, the ^{31}P NMR spectra of both compounds are in good agreement with respect to the different downfield shifts and the strong coupling of the signals stemming from the phosphorus atoms in the ring. The $^2J_{PP}$ coupling constant corresponds to that in a diphosphonio-isophosphindolide.[15] In addition, the downfield shift of the ^{13}C NMR signal of C-3, compared to that in **3b**, also indicates the formation of a cyclic conjugated system.

We assumed the electrophilic substitution on the phenyl ring of the ylide to be the crucial step in the formation of the five-membered rings in **3** and **5**. The question arose whether such a substitution by a phosphorus(III) halide could also be realized independent of ring formation. Indeed, PCl_3 adds smoothly at room temperature to triphenylphosphonio-diphenylmethanide (**7**) with PCl_2 substitution in the *para* position of one *C*-phenyl ring and a proton shift to the ylide carbon atom.[16] Even the significantly less electrophilic diphenylchlorophosphane is added in the same fashion with substitution in the *ortho* and *para* positions. The two isomeric phosphonium chlorides **8** are formed in a mole ratio of

 © VCH Verlagsgesellschaft mbH, D-69451 Weinheim, 1994 0570-0833/94/0606-0664 $ 10.00+.25/0

9:10. Ylides **9**, the neutral substitution products, can be obtained by treatment of **8** with sodium bis(trimethylsilyl)amide. After selenation to give **10** one of the isomers can be crystallized in pure form and is identified as the *para* compound **10b**. This enables the assignment of the ^{31}P NMR signals also in the mixtures of **8**, **9**, and **10**.



Experimental Procedure

3b: A suspension of 30.60 g (71.0 mmol) of **1** in 150 mL of dichloromethane and 80 mL of benzene was stirred for one day at about 20 °C with 14.40 g (142.0 mmol) of Et_3N and 19.22 g (71.0 mmol) of PBr_3. The reaction mixture slowly turned red and was filtered. Cooling the filtrate to 0 °C led to the separation of **3b**·$2C_6H_6$ as red platelets. The mother liquor was concentrated and cooled again to give a second fraction. Yield 8.75 g (34%), m.p. 205–206 °C, correct C,H, Br analysis. ^1H NMR (CD_2Cl_2): δ = 6.45 (m, 1H), 6.94 (m, 2H), 7.31 (s, 12H; C_6H_6), 7.60 (m, 6H; *m*-H), 7.70–7.80 (m, 9H; *o*,*p*-H), 7.96 (m, 1H); $^{13}C\{^1H\}$ NMR (CD_2Cl_2): δ = 69.4 (ddd, $^1J(PC)$ = 98.6 Hz, $^1J(PC)$ = 70.1 Hz, $^2J(PC)$ = 50.0 Hz; C-3), 121.4 (dd, $J(PC)$ = 8.5 Hz, $J(PC)$ = 1.9 Hz), 122.8(t, $J(PC)$ = 4.2 Hz), 123.8 (dd, $^1J(CP)$ = 89.6 Hz, $^3J(PC)$ = 6.1 Hz; *i*-C), 128.4 (s, C_6H_6), 129.6 (d, $^3J(PC)$ = 12.3 Hz, *m*-C), 131.0 (d, $J(PC)$ = 1.9 Hz), 133.7 (d, $^4J(PC)$ = 2.9 Hz; *p*-C), 134.0 (d, $J(PC)$ = 3.8 Hz), 134.2 (dd, $^2J(PC)$ = 10.4 Hz; $^4J(PC)$ = 1.4 Hz; *o*-C), 142.1 (dd, $^1J(PC)$ = 52.2 Hz, $^2J(PC)$ = 17.8 Hz; C-7a), 153.4 (ddd, $^2J(PC)$ = 13.8 Hz, $^2J(PC)$ = 7.6 Hz, $^2J(PC)$ = 2.8 Hz; C-3a).

6a: A solution of 3.70 g (6.5 mmol) of **3b** in 40 mL of THF was stirred for 15 h at 20 °C with 0.16 g (6.5 mmol) of magnesium shavings. After solvent removal under vacuum, the residue was extracted three times with 30 mL of hot benzene. Light green prisms of **6a**·$1/2C_6H_6$ separated from the extract. Yield 2.21 g (75%), m.p. 198–200 °C, correct C,H analysis. ^1H NMR ([D_8]THF): δ = 6.73 (t, $^3J(HH)$ = 7.6 Hz, 1H) 6.86 (t, $^3J(HH)$ = 7.5 Hz, 1H), 7.15 (d, $^3J(HH)$ = 7.7 Hz, 1H; 4-H), 7.24 (s, 3H, C_6H_6), 7.52 (m, 6H; *m*-H), 7.63–7.68 (m, 9H; *o*, *p*-H), 8.12 (t, $^3J(PH)$ = $^3J(HH)$ = 7.7 Hz, 1H; 7-H); $^{13}C\{^1H\}$ NMR ([D_8]THF): δ = 103.1 (dd, $^1J(PC)$ = 84.4 Hz, $^1J(PC)$ = 82.0 Hz; C-3), 117.6 (d, $^3J(PC)$ = 14.7 Hz; C-4), 121.8 (s), 122.8 (s), 125.9 (d, $^1J(PC)$ = 88.7 Hz; *i*-C), 130.0 (d, $^3J(PC)$ = 12.3 Hz; *m*-C), 130.8 (d, $^2J(PC)$ = 26.5 Hz; C-7), 133.9 (d, $^4J(PC)$ = 2.8 Hz; *p*-C), 135.1 (d, $^2J(PC)$ = 10.0 Hz, *o*-C), 151.1 (dd, $^2J(PC)$ = 13.7 Hz, $^2J(PC)$ = 8.1 Hz; C-3a), 164.2 (dd, $^1J(PC)$ = 61.1 Hz, $^2J(PC)$ = 23.2 Hz; C-7a).

10b: A solution of 3.44 g (15.6 mmol) of Ph_2PCl in 20 mL of CH_2Cl_2 was added over 1 h to a stirred solution of 6.68 g (15.6 mmol) of **7** in 100 mL of CH_2Cl_2. After 15 h at room temperature the solvent was removed under vacuum. The residue was stirred with 2.43 g (13.3 mmol) of $NaN(SiMe_3)_2$ for 15 h at room temperature. Removal of all volatiles under vacuum yielded a red oil, which solidified upon tituration with 50 mL of pentane. 2.58 g of the resulting orange-red powder was dissolved in benzene and stirred at room temperature with 0.45 g (5.7 mmol) of gray selenium. After 15 min the suspension was heated to 50 °C and filtered while hot. $^{31}P\{^1H\}$ NMR: **10a**: δ = 10.2, 34.4 ($^1J(SeP)$ = 731.4 Hz); **10b**: δ = 10.3, 33.7 ($^1J(SeP)$ = 719.2 Hz). A total of 0.82 g of **10b**·C_6H_6 crystallized as orange-red needles from the filtrate, m.p. 201–203 °C, correct C,H analysis. ^1H NMR (CD_2Cl_2): δ = 6.40 (m, 2H; *o*-H^C), 6.92–6.97 (m, 3H; *p*-H^B + *m*-H^C), 7.03 (t, $^3J(HH)$ = 7.3 Hz, 2H; *m*-H^B), 7.07 (dt, $^3J(HH)$ = 8.3 Hz, $^4J(HH)$ = $^4J(PH)$ = 1.7 Hz, 2H; *o*-H^B), 7.28 (s, 6H; C_6H_6), 7.39–7.47 (m, 12H; *m*-H^A + *m*,*p*-H^D), 7.54 (tq, $^3J(HH)$ = 5.6 Hz, $^4J(HH)$ = $^5J(PH)$ = 2.0 Hz, 3H; *p*-H^A), 7.60 (m, 6H; *o*-H^A), 7.68 (m, 4H; *o*-H^D). $^{13}C\{^1H\}$ NMR (CD_2Cl_2): δ = 49.3 (d, $^1J(PC)$ = 124.6 Hz; C(ylide)), 110.4 (d, $^1J(PC)$ = 89.6 Hz; *p*-C^C), 120.0 (dd, $^3J(PC)$ = 10.4 Hz, $^3J(PC)$ = 13.3 Hz; *o*-C^C), 125.0 (d, $^5J(PC)$ = 2.4 Hz; *p*-C^B), 127.2 (d, $^1J(PC)$ = 86.7 Hz; *i*-C^A), 128.3 (d, $^3J(PC)$ = 12.3 Hz; *m*-C^D), 128.5 (s, C_6H_6), 128.5 (s, *m*-C^B), 128.9 (d, $^3J(PC)$ = 11.8 Hz; *m*-C^A), 131.0 (d, $^4J(PC)$ = 2.9 Hz, *p*-C^D), 132.0 (d, $^2J(PC)$ = 14.2 Hz; *m*-C^C), 132.1 (s, *p*-C^A), 132.6 (d, $^2J(PC)$ = 10.4 Hz, *o*-C^D), 134.1 d, $^2J(PC)$ = 9.5 Hz; *o*-C^A), 134.1 (d, $^1J(PC)$ = 76.3 Hz; *i*-C^D), 136.3 (d, $^3J(PC)$ = 3.8 Hz; *o*-C^B), 141.3 (d, $J(PC)$ = 15.2 Hz; *i*-C^B), 151.6 (dd, $^2J(PC)$ = 13.7 Hz, $^4J(PC)$ = 2.4 Hz; *i*-C^C); $^{31}P\{^1H\}$ NMR (CD_2Cl_2): δ = 10.5 (s, 50%), 33.3 (s 47%, d 3%, $^1J(SeP)$ = 718.5 Hz). (C_6H_6): δ = 10.1, 34.3 ($^1J(SeP)$ = 735.4 Hz); $^{77}Se\{^1H\}$ NMR (CD_2Cl_2): δ = −258.9 (d, $^1J(SeP)$ = 712.2 Hz).

Received: October 7, 1993 [Z 6398 IE]
German version: *Angew. Chem.* **1994**, *106*, 708

[1] K.-H. A. Ostoja Starzewski, H. Bock, H. tom Dieck, *Angew. Chem.* **1975**, *87*, 197–198; *Angew. Chem. Int. Ed. Engl.* **1975**, *14*, 173–174; K.-H. A. Ostoja Starzewski, H. Bock, *J. Am. Chem. Soc.* **1976**, *98*, 8486–8494; K.-H. A. Ostoja Starzewski, H. tom Dieck, *Phosphorus Relat. Group V Elem.* **1976**, *6*, 177–189.
[2] A. Schmidpeter, G. Jochem, *Tetrahedron Lett.* **1992**, *33*, 471–474.
[3] The formation of **3** from **1** is reminiscent of the Herz reaction, in which 1,2,3-benzodithiazolium chloride is formed from aniline and disulfur dichloride: W. K. Warburton, *Chem. Rev.* **1957**, *57*, 1011–1020.
[4] H. J. Bestmann, R. Zimmermann *Methoden Org. Chem. (Houben-Weyl) 4th ed. 1952–*, Vol. E1, **1982**, pp. 616–782.
[5] Recently an $AlCl_3$-induced reversible intramolecular addition to the *ortho* position of an ylide phenyl residue was reported; a subsequent base-catalyzed proton shift converts the reaction into a substitution: U. Heim, H. Pritzkow, U. Fleischer, H. Grützmacher, *Angew. Chem.* **1993**, *105*, 1400–1402; *Angew. Chem. Int. Ed. Engl.* **1993**, *32*, 1359–1361.
[6] A. Hinke, W. Kuchen, *Chem. Ber.* **1983**, *116*, 3003–3010.
[7] Crystal structure analysis of **3b**·$2C_6H_6$: red plates, $C_{37}H_{31}Br_2P_3$, M = 728.4, crystal size 0.35 × 0.17 × 0.55 mm^3, triclinic, space group $P\bar{1}$: a = 9.997(4), b = 10.245(5), c = 18.306(8) Å, α = 101.91(4), β = 95.47(3), γ = 111.72(3)°, V = 1673.6(13) Å^3, Z = 2, ρ_{calcd} = 1.445 g cm^{-3}, $F(000)$ = 736, μ = 25.63 cm^{-1}. 5659 reflections (5273 independent) were measured on a Siemens R3m/V diffractometer ($Mo_{K\alpha}$ radiation, graphite monochromator) using ω scans in the range of $2.0° \le 2\theta \le 48.0°$, with h, $\pm k$, $\pm l$; 3620 reflections with $F > 3.0\sigma(F)$. The structure was solved by direct methods (SHELXTL PLUS) and refined using anisotropicic thermal parameters for the non-hydrogen atoms (H atoms were placed at calculated positions and included in the refinement using a riding model). Final R = 0.048 and R_w = 0.046. Further details of the crystal structure investigation may be obtained from the Fachinformationszentrum Karlsruhe, D-76344 Eggenstein-Leopoldshafen (FRG) on quoting the depository number CSD-57824, the names of the authors, and the journal citation.
[8] In PBr_3 the P–Br distance was found by electron diffraction to be 2.220 Å: K. Kuchitsu, T. Shibata, A. Yokozeki, *Inorg. Chem.* **1971**, *10*, 2584–2587.
[9] Under the influence of *two* immediately adjacent ylide groups, P^{III} halogen bonds become ionic[2,15].
[10] Cf. the increase in bond lengths in cyclic α-haloethers in the context of the anomeric effect: A. J. Kirby, *The Anomeric Effect and Related Stereoelectronic Effects at Oxygen*, Springer, Berlin, **1983**, pp. 37, 52.
[11] M. Yoshifuji in *Multiple Bonds and Low Coordination in Phosphorus Chemistry* (Eds.: M. Regitz, O. J. Scherer), Thieme, Stuttgart, **1990**, pp. 321–337.
[12] While 1,3-diphospholes can be considered a well-examined class of compounds by now, compounds **6** are the first examples of free 1,2-diphospholes. Previously this ring system was synthesized only in the coordination sphere of Fe and was known in the form of 1,2-diphosphaferrocenes: L. Weber, R. Kirchhoff, R. Boese, H.-G. Stammler, *J. Chem. Soc. Chem. Commun.* **1991**, 1293–1295; E. Niecke, D. Schmidt, *ibid.* **1991**, 1659–1660.
[13] G. Jochem, H. Nöth, A. Schmidpeter, *Angew. Chem.* **1993**, *105*, 1117–1119; *Angew. Chem. Int. Ed. Engl.* **1993**, *32*, 1089–1091.
[14] M. R. Mazières, K. Rauzy, J. Bellan, M. Sanchez, G. Pfister-Guillouzo, A. Senio, *Phosphorus Sulfur Silicon Relat. Elem.* **1993**, *76*, 45–48.
[15] A. Schmidpeter, M. Thiele, *Angew. Chem.* **1991**, *103*, 333–335; *Angew. Chem. Int. Ed. Engl.* **1991**, *30*, 308–310.
[16] Recently the linking of two molecules of **7** in the *para* position was observed formally by loss of hydride: D. Hesse, H. W. Roesky, M. Noltemeyer, *Chem. Ber.* **1992**, *125*, 833–834.

 © VCH Verlagsgesellschaft mbH, D-69451 Weinheim, 1994 0570-0833/94/0606-0665 $ 10.00+.25/0

Chemistry within a Unimolecular Micelle Precursor: Boron Superclusters by Site- and Depth-Specific Transformations of Dendrimers**

George R. Newkome,* Charles N. Moorefield, John M. Keith, Gregory R. Baker, and Gregory H. Escamilla

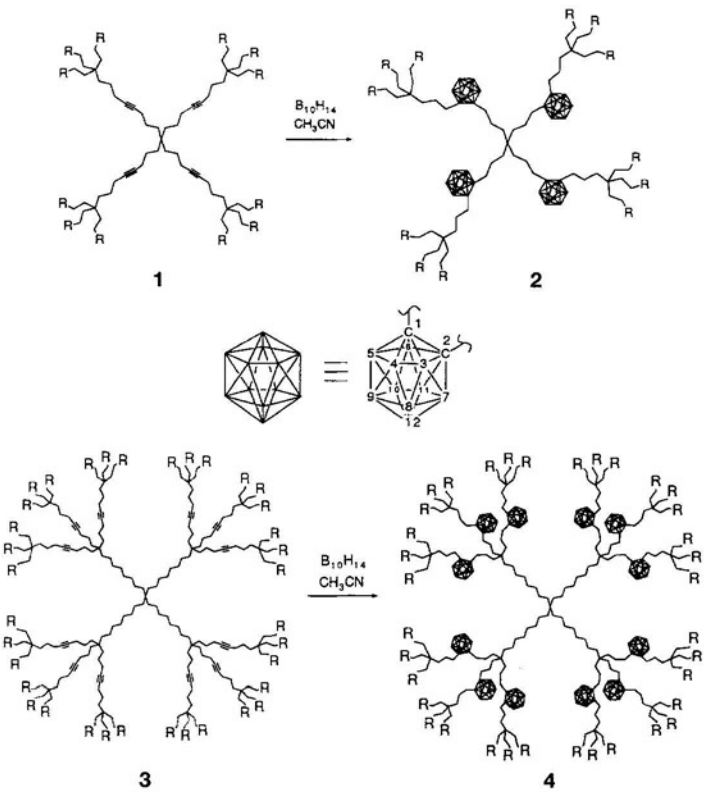
To date, researchers concerned with dendritic (cascade) polymer chemistry have primarily focused on the preparation of new materials based upon the sequential connection of monomeric building blocks to affect properties in the interior or on the surface of the new macromolecule, such as flexibility, solubility, porosity, and lipophilicity. Monomer addition, and thus cascade construction, have been achieved by convergent and divergent approaches, as well as combinations of the two.[1] Also, the ability of molecules to penetrate the interior of the cascade framework, through nonbonding interactions, has demonstrated the unimolecular micelle concept.[2] Elegant exploitation of this concept was recently reported;[3] the solubility of polyaromatic hydrocarbons in water was effected by a polyether cascade. Investigations into the potential to specifically incorporate and manipulate functionality in the interior of the cascade molecule have been largely neglected except for the interesting case of "superbases" acting on poly(benzyl ether) dendrimers for internal electrophilic introduction.[4] However, these transformations were not tier- or group-specific. We herein report our preliminary results on the ability to transform sites of reactivity between branching centers chemically[5] after cascade construction, without branch degradation. Ramifications include the precise placement of covalently bonded organic, inorganic, and metal-containing moieties, or any compatible combination at different generations, within a cascade superstructure; the aim is ultimately to provide a method for concentrating aqueous or nonaqueous insoluble functionality within a desired medium.

The creation in our laboratories of the hydrocarbon-based, unimolecular micelles, termed micellanes,[2] provided the impetus to employ internal functionality for *endo*- and *regio*-specific[6] chemical modifications in the interior of the cascade infrastructure. During micellane construction, facile, palladium-catalyzed, heterogeneous reduction of interior alkyne moieties to produce saturated hydrocarbon branches attest to reactivity in the interior of the cascade molecule, which suggested that branches are flexible and the cascade molecule permeable. Initial experiments focused on the first and second generation polyalkyne, the micellanoic acid precursors **1** and **3** (Scheme 1), and capitalized on the propensity of alkyne moieties to react with decaborane, $B_{10}H_{14}$, to afford 1,2-dicarba-*closo*-dodecaboranes (*o*-carboranes). The potential to render boron clusters soluble in an aqueous environment is of interest because of their use in cancer treatment by Boron Neutron Capture Therapy[7] (BNCT) and in catalysis.[8]

[*] Prof. G. R. Newkome, J. M. Keith, Dr. G. R. Baker, G. H. Escamilla
Center for Molecular Design and Recognition
Department of Chemistry, University of South Florida
Tampa, FL 33620 (USA)
Telefax: Int. code + (813)-974-4962
Dr. C. N. Moorefield
Tampa Bay Research Corporation

[**] Chemistry of Micelles, Part 37. This work was supported by the National Science Foundation (DMR-92-17331; 92-08925; 89-06792) and the Petroleum Research Fund administered by the American Chemical Society. Part 36: G. R. Newkome, F. Cardullo, E. C. Constable, C. N. Moorefield, A. M. W. Cargill Thompson, *J. Chem. Soc. Chem. Commun.* **1993**, 925.

Treatment of the tetra- and dodecaalkynes **1** and **3** with excess $B_{10}H_{14}$, activated by acetonitrile, in toluene under reflux for 24 h gave the corresponding tetra- and dodeca-*o*-carboranes **2** and **4** (89% and 77%, respectively),[9] as viscous oils. Excess decaborane was decomposed by the addition of 10% HCl and MeOH followed by heating under reflux for 24 h.



Scheme 1. Preparation of *o*-carborane superclusters **2** and **4** by treatment of polyalkyne cascade precursors **1** and **3** with $B_{10}H_{14}$. Also depicted is the *o*-carborane numbering scheme. R = $CH_2OCH_2C_6H_5$.

Evidence for the transformations (Table 1) was provided by the disappearance of ^{13}C NMR signals at $\delta = 19.3$ ($C{\equiv}CCH_2$) and 80.9 ($C{\equiv}C$), as well as the appearance of new peaks at $\delta = 23.5$ ($B_{10}H_{10}C_2CH_2CH_2$ and CH_2CH_2O) and 29.5 ($B_{10}H_{10}C_2CH_2$). The expected resonances (^{13}C NMR) at $\delta = 71.2$ (CH_2O) and 72.8 ($OCH_2C_6H_5$) were also observed. Broadening of the ^{13}C NMR signals for the first- and second-generation, boron superclusters was observed, although it was more pronounced in the dodeca-*o*-carborane (**4**) spectrum. The absence of ^{13}C NMR peaks assigned to the *o*-carborane carbons ($B_{10}H_{10}C_2$) was attributed to the rapid quadrupolar relaxation of the connected ^{11}B nuclei, as well as the multiplicity of the signal.[10]

Broadened signals in the ^1H NMR spectrum of both **2** and **4** were recorded at the expected chemical shifts [$\delta = 3.40$ (CH_2O) and 4.46 ($OCH_2C_6H_5$)], including a hydrocarbon envelope centered at $\delta = 1.51$ (**2**, 136 H; **4**, 472 H), while the IR spectra exhibited prominent peaks at 2575 cm^{-1} (ν_{B-H}). The symmetry of both the ^{13}C and ^1H NMR spectra of **1** and **3** was maintained in the spectra of **2** and **4**, which further supports complete transformation of the cascade interior; however, the broadened resonances suggested decreased chain flexibility.

The ^1H decoupled ^{11}B NMR spectra[11] of the poly(*o*-carboranes) **2** and **4** displayed similar patterns; peaks occur at $\delta =$

Table 1. Spectroscopic data for boron superclusters **2** and **4**–**6** [a].

2: ^{13}C NMR: δ = 23.5 ($B_{10}H_{10}C_2CH_2CH_2$ CH_2CH_2O), 29.6 ($B_{10}H_{10}C_2CH_2$), 32.4 ($CH_2CH_2CH_2O$), 36.5 (C_4, $B_{10}H_{10}C_2CH_2CH_2CH_2$), 71.2 ($CH_2O$), 72.8 ($OCH_2C_6H_5$), 127.3, 127.4, 128.3, 138.6 (C_6H_5); ^{1}H NMR: δ = 0.85–2.10 [m, $(CH_2)_3B_{10}H_{10}C_2(CH_2)_3C\{CH_2CH_2\}_3$, 136 H], 3.40 (br. s, CH_2O, 24 H), 4.46 (br. s, $OCH_2C_6H_5$, 24 H), 7.30 (br. s, C_6H_5, 60 H); ^{11}B NMR (^{1}H-decoupled): δ = −19.6 (s, $B_{3,6}$), 0.5 (m, $B_{4,5,7,11}$), 23.6 (s, $B_{8,10}$), 35.6 (br. s, $B_{9,12}$); ^{11}B NMR: (^{1}H-coupled) δ = −19.6 (d, $B_{3,6}$, J = 145.2 Hz), 0.5 (m, $B_{4,5,7,11}$), 23.6 (d, $B_{8,10}$, J = 119.5 Hz), 35.6 (br. s, $B_{9,12}$); IR $\tilde{\nu}$ = 3080, 3030, 2920, 2860, 2575, 1100, 745, 700 cm^{-1}.

4: ^{13}C NMR: δ = 22.5 [$C(CH_2CH_2)_4^{int}$], 23.5 [$C(CH_2CH_2)_4^{ext}$, CH_2CH_2O], 29.0 [$C(CH_2CH_2CH_2CH_2)_4^{int}$], 29.5 ($B_{10}H_{10}C_2CH_2$), 31.5 [$C(CH_2CH_2CH_2)_4^{int}$], 32.6 ($CH_2CH_2CH_2O$), 36.6 [m, C_4, $C_4(CH_2)_4$], 71.3 (CH_2O), 72.8($OCH_2C_6H_5$), 127.3, 127.4, 128.3, 138.6 (C_6H_5); ^{1}H NMR: δ = 0.70–2.15 [br. s, $(CH_2)_8^{int}$, $(CH_2)_3B_{10}H_{10}C_2(CH_2)_3C\{CH_2CH_2\}_3^{ext}$, 372 H], 3.41 (br. s, CH_2O, 72 H), 4.47 (br. s, $OCH_2C_6H_5$, 70 H), 7.30 (br. s, C_6H_5, 180 H); ^{11}B NMR (^{1}H-decoupled): δ = −19.6 (s, $B_{3,6}$), 0.5 (m, $B_{4,5,7,11}$), 23.6 (s, $B_{8,10}$), 35.6 (br. s, $B_{9,12}$); IR: $\tilde{\nu}$ = 3080, 3030, 2920, 2860, 2575, 1100, 745, 700 cm^{-1}.

5: ^{13}C NMR (D_3COD): δ = 27.4 (CH_2CH_2OH), 30.6 ($B_{10}H_{10}C_2CH_2CH_2$), 33.6 ($CH_2CH_2CH_2O$, $B_{10}H_{10}C_2CH_2CH_2$), 37.9 (C_4), 64.0 (CH_2OH); ^{1}H NMR (D_3COD): δ = 1.05–1.80(m, $(CH_2)_3B_{10}H_{10}C_2(CH_2)_3C\{CH_2CH_2\}$, 136H), 3.44 (br. t, CH_2OH, 24H); ^{11}B NMR (D_3COD): δ = −14.5 (br. s, $B_{3,6}$), −6.2 (br. s, $B_{4,5,7,11}$), 22.4 (s, $B_{8,10}$), 35.8 (br. s, $B_{9,12}$); IR: $\tilde{\nu}$ = 3700–3000, 2570 cm^{-1}.

6: ^{13}C NMR: δ = 27.5 ($CH_2CH_2CH_2O$), 29.0 [$C(CH_2CH_2CH_2)_4^{int}$], 30.7 ($B_{10}H_{10}C_2CH_2CH_2$), 33.6 [$CH_2CH_2CH_2O$, $C(CH_2)_4$], 37.6 (C_4), 63.8(CH_2OH); ^{1}H NMR: δ = 0.90–1.90 [br. envelope, $(CH_2)_8^{int}$, $(CH_2)_3B_{10}H_{10}C_2(CH_2)_3C\{CH_2CH_2\}_3^{ext}$, 472H], 3.41 (br. t, CH_2OH, 72H); ^{11}B NMR (^{1}H-decoupled) δ = −14.6 (br. s, $B_{3,6}$), −6.2 (br. s, $B_{4,5,7,11}$), 22.6 (s, $B_{8,10}$), 35.8 (br. s, $B_{9,12}$); IR: $\tilde{\nu}$ = 3700–3000, 2920, 2860, 2575 cm^{-1}.

[a] Acceptable spectral and analytical data was obtained for the new materials. All NMR data were recorded on a Bruker 360 MHz AMX spectrometer. Solvent: $CDCl_3$ (^{13}C NMR, δ = 77.0); internal standards: Me_4Si (^{1}H NMR, δ = 0) or $BF_3 \cdot Et_2O$ (^{11}B NMR, δ = 0).

−19.6, 0.5, 23.6, and 35.6 ($B_{3,6}$, $B_{4,5,7,11}$, $B_{8,10}$, and $B_{9,12}$, respectively). The observed absorptions attributed to the boron nuclei at carborane positions 4, 5, 7, and 11 (Fig. 1) are not significantly different, as might be expected, considering that two atoms are oriented toward the core and the other two toward the exterior. It is assumed that these positions are in similar environments because they are surrounded by similar bishomoneopentyl moieties. The ^{1}H-coupled ^{11}B NMR spectrum of **2** displays doublets at δ = −19.6 ($B_{3,6}$, J = 145.2 Hz) and 23.6 ($B_{8,10}$, J = 119.5 Hz).

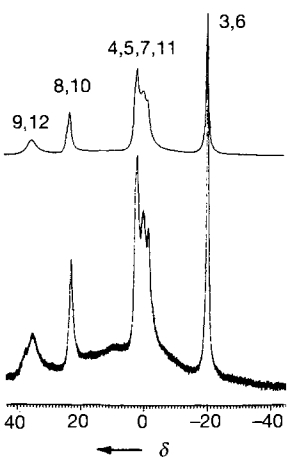
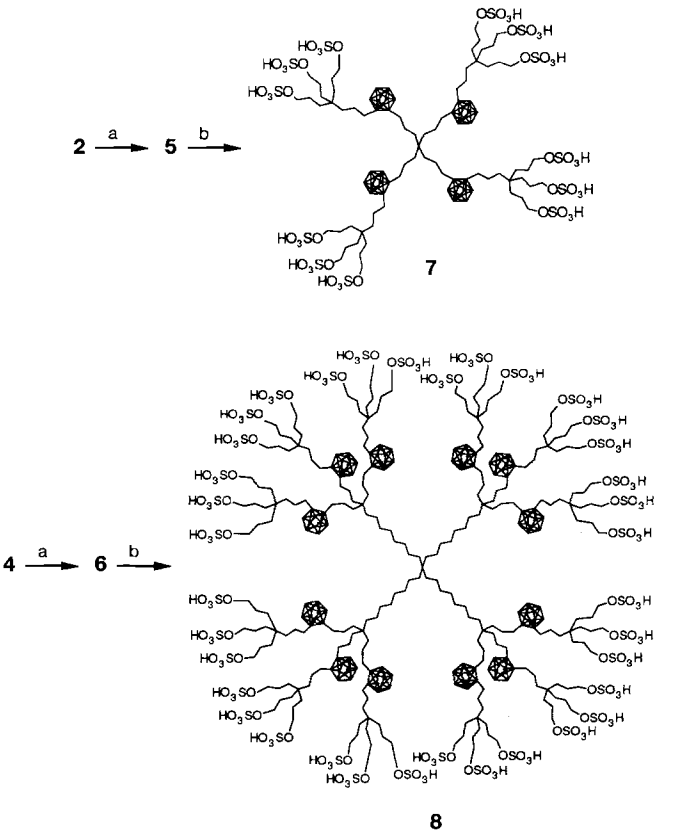


Figure 1. ^{1}H-decoupled ^{11}B NMR spectra of **2** (top) and **4** (bottom). The numbers indicate the assigned boron atoms.

The stability of carborane moieties under diverse reaction conditions is well documented.[12] Thus reaction of **2** with $PdO_2 \cdot xH_2O$, cyclohexene, and EtOH[13] smoothly afforded the dodecaalcohol **5** (yield 91%, Scheme 2). Salient features on comparison of the ^{13}C NMR spectra of **2** and **5** included the disappearance of peaks in the arene region as well as at δ = 71.2 and 72.8 and the appearance of signals at 63.8 (CH_2OH), 33.6 ($CH_2CH_2CH_2O$), and 27.4 (CH_2CH_2O). The ^{1}H NMR spectrum exhibited a poorly resolved triplet at δ = 3.43 (CH_2OH) and no downfield signals, which further supports complete deprotection. Resonances in the ^{11}B NMR spectrum were observed at δ = 37.8 ($B_{9,12}$) and 22.4 ($B_{8,10}$) that were nearly identical to those recorded for the precursor **2**; however, resonances assigned to $B_{4,5,7,11}$ (δ = −6.2) and $B_{3,6}$ (δ = −14.5) appeared as severely broadened envelopes. Treatment of **4** under the same reductive conditions yielded the polyol **6** (87%) that was characterized by virtually identical ^{13}C, ^{1}H, and ^{11}B NMR spectra to that observed for first tier polyol **5**.



Scheme 2. Syntheses of water-soluble boron superclusters **7** and **8** by transformation of the termini of the polyols **5** and **6** into sulfate moieties. a: $PdO2 \cdot xH_2O$, cyclohexene, EtOH, 4 days under reflux; b: $ClSO_3H$, 0 °C, 1 hour.

Water solubility (at high and low pH) was imparted to the carborane polyols **5** and **6** by reaction with $ClSO_3H$[14] (0 °C, 1 h) to afford the corresponding polysulfates **7** and **8** (Scheme 2). Evidence for the transformation of the alcohols to the desired boron superclusters included ^{13}C NMR spectra showing peaks at δ = 68.5 (CH_2OSO_3H) and 29.5 ($B_{10}H_{10}C_2CH_2$), and ^{1}H NMR spectra with broad signals at 3.72 (CH_2OSO_3H) and 1.35 [$(CH_2)_3B_{10}H_{10}C_2(CH_2)_3C\{CH_2CH_2\}_3$]. Raising the pH of a D_2O solution of the dodecasulfatetetra-*o*-carborane **7** with solid Na_2CO_3 produced a downfield shift of the ^{1}H NMR signal assigned to the terminal sulfatomethylene moieties to δ = 3.98.

Computer-generated space-filling models[15] of the superclusters, with termini soluble either in aqueous or nonaqueous media, reveal ample cascade "*void volume*" for the placement of multiple, icosahedral, *o*-carborane units within the cascade framework. Models of individual icosahedrons were created by using X-ray diffraction data;[16] they possess a diameter of 5.6 Å. In a fully extended conformation, the distances between branching centers of interest, before and after treatment with $B_{10}H_{14}$, were determined to be 11.1 and 9.6 Å, respectively.

In summary, we have demonstrated the ability to modify the cascade interior at precise depths on the macromolecular framework. Well-conceived cascade construction should allow the covalent incorporation of a variety of metals and nonmetals at predetermined sites provided that dense packing limits have not been reached. The attachment of different, as well as similar, guests onto successive generations should also be possible. Construction of cascades bearing interior, covalently bonded metallic or organic species is currently in progress.

Received: October 11, 1993 [Z 6405 IE]
German version: *Angew. Chem.* **1994**, *106*, 701

[1] For a recent review, see: H.-B. Mekelburger, W. Jaworek, F. Vögtle, *Angew. Chem.* **1992**, *104*, 1606; *Angew. Chem. Int. Ed. Engl.* **1992**, *31*, 1571.
[2] G. R. Newkome, C. N. Moorefield, G. R. Baker, A. L. Johnson, R. K. Behera, *Angew. Chem.* **1991**, *103*, 1205; *Angew. Chem. Int. Ed. Engl.* **1991**, *30*, 1176; G. R. Newkome, C. N. Moorefield, G. R. Baker, M. J. Saunders, S. H. Grossman, *ibid.* **1991**, *103*, 1207 and **1991**, *30*, 1178; G. R. Newkome, C. N. Moorefield, US-A 5154853, October 13, **1992**.
[3] C. J. Hawker, K. Wooley, J. M. J. Fréchet, *J. Chem. Soc. Perkin Trans. 1* **1993**, 1287.
[4] L. Lochmann, K. L. Wooley, P. T. Ivanova, J. M. J. Fréchet, *J. Am. Chem. Soc.* **1993**, *115*, 7043.
[5] G. R. Newkome, C. N. Moorefield, *Polym. Prep. Am. Chem. Soc. Div. Polym. Chem.* **1993**, *34*, 75.
[6] Terms *endo* and *regio* here describe reactions that occur on the internal cascade superstructure and at specific sites, respectively.
[7] M. F. Hawthorne, *Angew. Chem.* **1993**, *105*, 997; *Angew. Chem. Int. Ed. Engl.* **1993**, *32*, 950; H. Nemoto, J. G. Wilson, H. Nakamura, Y. Yamamoto, *J. Org. Chem.* **1992**, *57*, 435; M. Miura, D. Gabel, G. Oenbrink, R. G. Farichild, *Tetrahedron Lett.* **1990**, *31*, 2247; H. Ketz, W. Tjarks, D. Gabel, *ibid.* **1990**, *31*, 4003.
[8] J. Plešek *Chem. Rev.* **1992**, *92*, 269.
[9] Nomenclature for cascade macromolecules: G. R. Newkome, G. R. Baker, J. K. Young, J. G. Traynham, *J. Polym. Sci. Part A: Polym. Chem.* **1993**, *31*, 641. Accordingly, **4** is termed as [36-cascade:methane[4]:(nonylidine):(5,6-(1,2-dicarbo-*closo*-dodecaborane)-nonylidine):(2-oxapentyl)benzene].
[10] H. Nötz, B. Wrackmeyer in *Nuclear Magnetic Resonance Spectroscopy of Boron Compounds* (Eds.: P. Diehl, E. Fluck, R. Kosfeld), Springer, New York, **1978**, pp. 103–104.
[11] G. A. Olah, K. Wade, R. E. Williams in *Electron Deficient Boron And Carbon Clusters*, Wiley-Interscience, New York, **1991**, pp. 105–110.
[12] R. N. Grimes in *Carboranes* (Eds.: P. M. Maitlis, F. G. A. Stone, R. West), Acedemic Press, New York, **1970**, Chapter 6.
[13] G. M. Anantharamaiah, K. M. Sivanandaiah, *J. Chem. Soc. Perkins Trans. 1* **1977**, 490.
[14] S. R. Sandler, W. Karo *Organic Functional Group Preparations, Vol 12-III* (Ed.: H. H. Wasserman), Academic Press, New York, **1989**, p. 141.
[15] Theoretical measurements and space-filling models were obtained at a Silicon Graphics 4D50GT graphics workstation with Quanta molecular modeling software, available from Molecular Simulations.
[16] D. Voet, W. B. Lipscomb, *Inorg. Chem.* **1964**, *3*, 1679.

1(9)-Homocubene and 9-Homocubylidene: Theoretical Investigation of Structures, Energies, and Rearrangement Reactions**

Max C. Holthausen and Wolfram Koch*

The synthesis of 1(9)-homocubene (**1**) was described both by Eaton and Hoffmann and by Chen and Jones.[1] **1** is an unusual olefin: the double bond is located at a bridgehead atom contrary to Bredt's rule and is also extremely twisted. The 2p atomic orbitals of this π bond are rotated by almost 90° to each other, such that no bonding overlap is possible. Thus, the question arises of the extent **1** may still be described as an olefin in the singlet state, or if it more closely resembles a singlet diradical. Closely associated with the electronic structure of the "double bond" in **1** are its equilibrium geometry and, in particular, the length of the C1–C9 bond. Unfortunately no experimental information is available. The unusual bonding situation in **1** is also evident from its reversible rearrangement[2] into the isomeric carbene 9-homocubylidene (**2**).[1] This type of rearrangement of an olefin into a carbene is extremely rare. Eaton and White have carried out in-depth experiments on the mechanism for the analogous rearrangement of 9-phenyl-1(9)-homocubene using isotopically

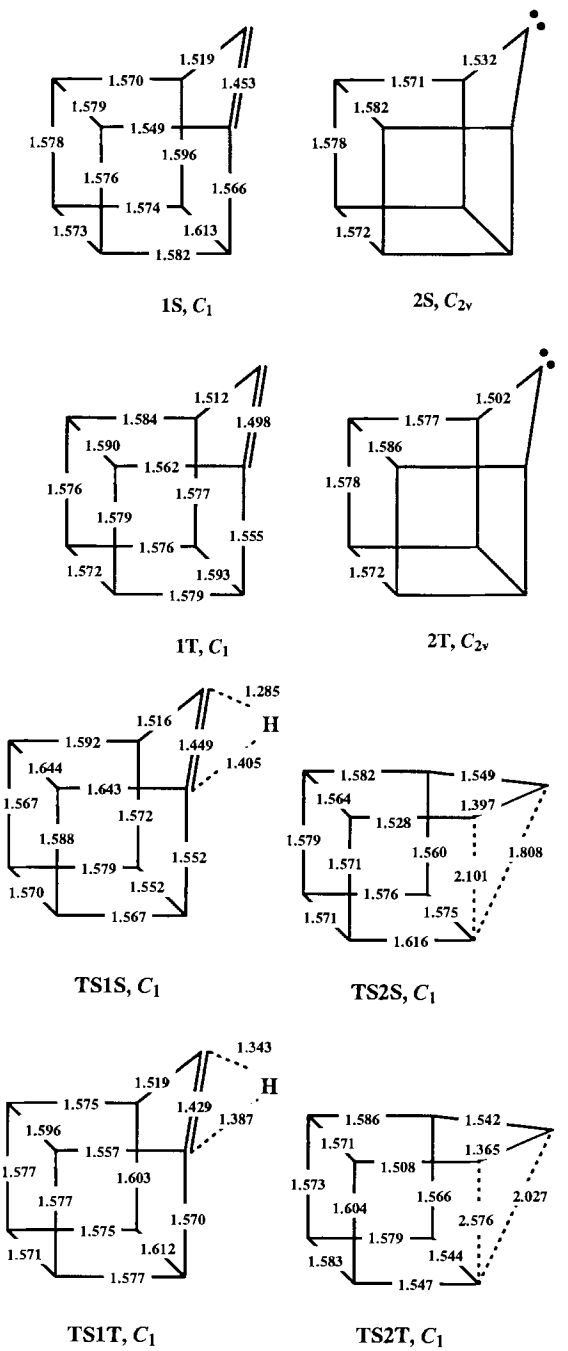


Fig. 1. Optimized bond lengths [Å] for compounds **1** and **2**, and for the transition states **TS1** and **TS2**.

[*] Prof. Dr. W. Koch, Dipl.-Chem. M. C. Holthausen
Institut für Organische Chemie der Technischen Universität
Strasse des 17. Juni 135, D-10623 Berlin (FRG)
Telefax: Int. code + (30)314-21102

[**] This work was supported by the Fonds der Chemischen Industrie and by the Gesellschaft der Freunde der Technischen Universität Berlin. We thank R. Hertwig for assistance with the preparation of the figures.

labeled compounds.[3] They found that the reaction proceeds by a C–C bond shift in the homocubane skeleton rather than by phenyl migration. We report here on quantum chemical ab initio calculations of the equilibrium geometries of the singlet and triplet ground states of 1(9)-homocubene (**1S** and **1T**, respectively) and of 9-homocubylidene (**2S** and **2T**, respectively), and those of the intermediates for the H migration and the C–C shift which revisibly interconvert **1** and **2**.[4]

The calculated equilibrium geometry of the singlet ^1A ground state of **1S** shown in Figure 1 confirms that the C1–C9 bond (1.453 Å) differs markedly from a conventional double bond (1.34 Å). This is a consequence of the strong twisting of both of the R_2C units at the bond.

As is apparent in the Newman projection in Figure 2, both carbon atoms of the C=C bond are distinctly pyramidalized. The orbitals forming the double bond are not coplanar, as is necessary for optimal overlap; but form an angle of 49.7°. Figure 3 depicts the (formally) highest occupied (HOMO) and the lowest unoccupied (LUMO) molecular orbitals, which show the reduced overlap. A CASSCF calculation shows that **1** cannot be regarded as having a conventional closed-shell singlet state, and that **1** exhibits distinct diradical character. The Hartree–Fock (HF) configuration, which corresponds to that of a conventional double bond, is weighted only 71%, whilst the configuration in which two electrons have been excited from the HOMO into the LUMO accounts for 28% of the wave function. The HOMO is occupied by merely 1.43 electrons instead of by 2, and the LUMO, which is unoccupied in the HF description, shows an increased occupancy of 0.57.

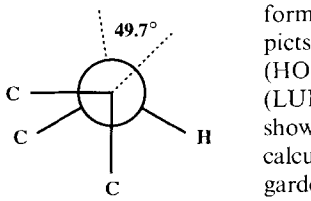


Fig. 2. Newman projection along the C1–C9 bond in structure **1S**.

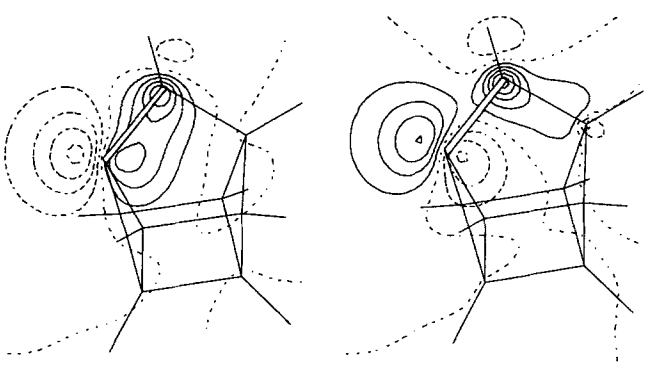


Fig. 3. Contour plots of the HOMO (left) and LUMO (right) of **1**.

The diradical character of **1S** is also revealed by the very small difference in energy to the corresponding triplet state **1T**, which is calculated to be only 1.5 kcal mol^{-1} less stable than **1S** (Table 1). The HOMO and LUMO in **1T** are each singly occupied, and the C1–C9 bond has no double bond character. The geometries of **1T** and **1S** differ only marginally. The C1–C9 bond in **1T** (ca. 1.50 Å) is somewhat longer than that in **1S**. These results lead to the conclusion that 1(9)-homocubene (**1**) is indeed formally an olefin; however, it has no double bond and is therefore better described as a singlet diradical. The Mulliken partial charges at the C1 and C9 centers are + 0.02 (+ 0.03) and −0.04 (− 0.06) for **1S** (**2T**), respectively.

Table 1. Calculated relative energies [kcal mol^{-1}] of **1** and **2**.

State	Singlet CASSCF/ 3-21G	CASSCF/ DZP	State	Triplet ROHF/ 3-21G	ROHF/ DZP
1S	0.0 [a]	0.0 [b]	**1T**	1.3	1.5
2S	2.2	−3.1	**2T**	−4.1	−2.0
TS1S	97.3	88.5	**TS1T**	98.2	93.5
TS2S	25.8	23.5	**TS2T**	34.5	34.8

[a] E_{tot} = − 343.31570 Hartree. [b] E_{tot} = − 345.18936 Hartree.

The C_{2v}-symmetrical 9-homocubylidene (**2S**), which is isomeric to **1**, is structurally much less different from carbenes than **1S** is from olefins (Fig. 1). The bond angle at the carbene center in **2S** is somewhat reduced compared to an open-chain carbene because of ring strain (96.6 compared to 103.2° in methylene).[5] The carbene character of **2S** is also evident in the CASSCF wave function of the $^1A_1$ state. In analogy to methylene, the formal b_1 LUMO in **2S** is partly occupied at the expense of the a_1 HOMO (calculated occupancy: 1.93 (HOMO), 0.07 (LUMO) for **2S**; 1.92 (HOMO) and 0.08 (LUMO) for CH_2). **2S** is calculated (DZP basis set) to be roughly 1.1 kcal mol^{-1} more stable than the corresponding **2T** state; in other words, the singlet state is the stable species here in contrast to methylene. (With the smaller 3-21G basis set the relative stabilities are also close together; however, **2T** is calculated to be more stable than **2S**, which in turn is less stable than **1T**.) The calculational level used is insufficient for quantitative evaluations about the singlet/triplet energy difference (at the same level the $^3B_1$ state in methylene is 13.9 kcal mol^{-1} more stable than the $^1A_1$ state, whereas the experimental energy difference is 9 kcal mol^{-1} [6]). However, the finding that the singlet and triplet states of **2** are energetically close to each other is certainly correct. For ethylidene, for example, the triplet state is only 3 ± 2 kcal mol^{-1} more stable than the singlet state.[7] Furthermore, the effect of ring strain on the carbene angle destabilizes the triplet state more than the singlet state, because triplet carbenes usually have bond angles of 130°;[5] in **2T** this angle is only 101.7°. Our calculations also show **2S** to be slightly more stable than **1S**, which is in accord with the observed reversible rearrangement **1** → **2**.

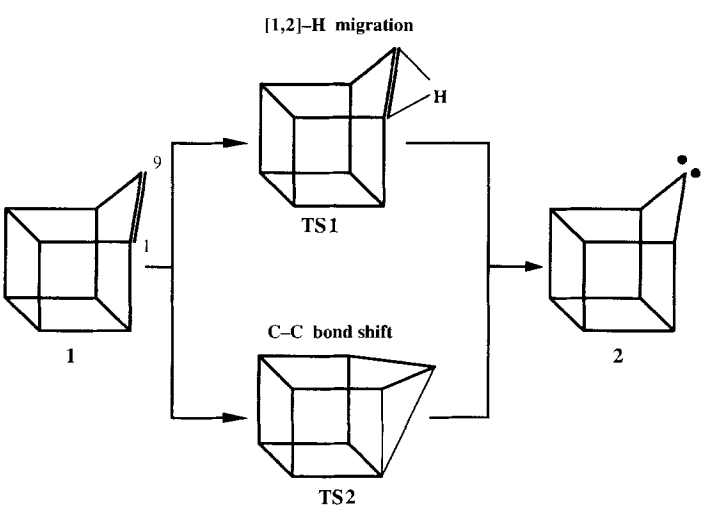


Fig. 4. Possible rearrangement mechanism **1** ⇌ **2**.

 © VCH Verlagsgesellschaft mbH, D-69451 Weinheim, 1994 0570-0833/94/0606-0669 $ 10.00+.25/0

By which mechanism does this rearrangement occur? Two possibilities are conceivable: either a [1,2]-H migration or a C–C bond shift (Fig. 4). For both alternative pathways the saddle points were located and characterized by analysis of the force constant matrix as unambiguous transition structures (one negative eigenvalue). The saddle point associated with the [1,2]-H migration, **TS1S**, is very high in energy (88.5 kcal mol^{-1} higher than **1S**); in comparison that associated with the C–C bond shift, **TS2S**, is clearly more favorable (23.5 kcal mol^{-1} higher in energy than **2S**). As is clear from Table 1, **TS1T** is also much higher in energy than **TS2T**. The quantitative energy differences may be somewhat different at a higher level of theory, but the qualitative result that the C–C bond shift is clearly favored over H migration should remain unchanged. This result confirms the experimental findings of Eaton and White[3] for the 9-phenyl-substituted derivative of **1** and **2**.

Because of the extremely strained structure, the double bond character of **1** is significantly reduced, and **1S** is only a formal olefin. As a result of the destabilization of **1S**, the isomeric **2S** becomes similar in energy, which is reflected in the reversible rearrangement **1** $\rightleftharpoons$ **2** observed experimentally. This rearrangement occurs by a C–C bond shift with a relatively low activation barrier.

Received: October 13, 1993 [Z 6413 IE]
German version: *Angew. Chem.* **1994**, *106*, 682

[1] P. E. Eaton, K.-L. Hoffmann, *J. Am. Chem. Soc.* **1987**, *109*, 5285; M. Jones, Jr., N. Chen, *J. Phys. Org. Chem.* **1988**, *1*, 305; *Tetrahedron Lett.* **1989**, *30*, 6969. For a general review on cubane chemistry see: P. E. Eaton, *Angew. Chem.* **1992**, *104*, 1447; *Angew. Chem. Int. Ed. Engl.* **1992**, *31*, 1421.
[2] P. E. Eaton, R. B. Appell, *J. Am. Chem. Soc.* **1990**, *112*, 4055.
[3] P. E. Eaton, A. J. White, *J. Org. Chem.* **1990**, *55*, 1321.
[4] The geometry optimizations were carried out by employing analytical gradients and the 3-21G basis set[8]. The diradical character of the singlet wave function was determined by a multiconfigurational SCF calculation of the CASSCF type[9]. The two molecular orbitals relevant for the diradical were selected as active. The occupation of these two orbitals by two electrons leads to a maximum of three configurations in the CASSCF calculation. The ROHF approximation was used in the calculation of the triplet states. Energy calculations were then carried out with the same approximations on the optimized geometries by using the DZP basis set (polarization functions only at the carbon atoms)[10]. Additional, more accurate calculations were not possible because of the size and low symmetry of the molecules, but qualitative trends should be reproduced correctly. Software packages GAMESS[11], GAUSSIAN-92[12], and MOLCAS-2[13] were used.
[5] For a general discussion of carbenes and their theoretical description see: J. F. Liebman, J. Simons in *Molecular Structure and Energetics* (Eds.: J. F. Liebman, A. Greenberg), VCH, Deerfield Beach, **1986**.
[6] D. G. Leopold, K. K. Murray, W. C. Lineberger, *J. Chem. Phys.* **1984**, *81*, 1048; D. G. Leopold, K. K. Murray, A. E. S. Miller, *ibid.* **1985**, *83*, 4849.
[7] S. Khodabandeh, E. A. Carter, *J. Phys. Chem.* **1993**, *97*, 4360.
[8] J. S. Binkley, J. A. Pople, W. J. Hehre, *J. Am. Chem. Soc.* **1980**, *102*, 939.
[9] See for example B. O. Roos, *Lect. Notes Quantum Chem., Lect. Notes Chem.*, **1992**, *58*.
[10] A. Schäfer, H. Horn, R. Ahlrichs, *J. Chem. Phys.* **1992**, *97*, 2571.
[11] M. W. Schmidt, K. K. Baldridge, J. A. Boatz, J. H. Jensen, S. Koseki, M. S. Gordon, K. A. Nguyen, T. L. Windus, S. T. Elbert, *QCPE Bull.* **1990**, *10*, 52.
[12] M. J. Frisch, G. W. Tucks, M. Head-Gordon, P. M. W. Gill, M. W. Wong, J. B. Foresman, B. G. Johnson, H. B. Schlegel, M. A. Robb, E. S. Replogle, R. Gomperts, J. L. Andres, K. Raghavachari, J. S. Binkley, C. Gonzalez, R. L. Martin, D. J. Fox, D. J. DeFrees, J. Baker, J. J. P. Stewart, J. A. Pople, Gaussian 92, Rev. A; Gaussian Inc. Pittsburgh, PA, 1992.
[13] K. Andersson, M. R. A. Blomberg, M. P. Fülscher, V. Kellö, R. Lindh, P.-A. Malmqvist, J. Noga, J. Olsen, B. O. Roos, A. J. Sadlej, P. E. M. Siegbahn, M. Urban, P.-O. Widmark, MOLCAS, Version 2, University of Lund, Sweden, 1991.

Fairly Strong Ferromagnetic Interactions between Imino Nitroxide Ligands through a Diamagnetic Cu^{I} Ion in $[Cu^{I}(im\text{-}mepy)_2](PF_6)$**

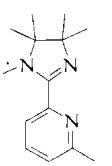
Hiroki Oshio,* Takashi Watanabe, Akihiro Ohto, Tasuku Ito,* and Umpei Nagashima

Molecular units which exhibit inter- or intramolecular ferromagnetic interactions are indispensable for the construction of molecular-based ferromagnets. In order to attain magnetic ordering at high temperature, strong ferromagnetic interactions are necessary. These propagate if the magnetic orbitals are orthogonal.[1] The orthogonal arrangement of the paramagnetic building blocks has been used to attain the parallel spin alignment in paramagnetic compounds, for instance, in Cu^{II}–$V{=}O^{IV}$[2] and Cr^{III}–Ni^{II}[3] systems. Recently this approach has also been applied to diamagnetic metal complexes with organic radicals. In Ti^{IV}–[4] and Ga^{III}–semiquinone complexes,[5] the semiquinone ligands show ferromagnetic interactions, and magnetic susceptibility measurements gave exchange coupling constants J of $-56\ cm^{-1}$ ($H = JS_1S_2$) and $7.8\ cm^{-1}$ ($H = -2J\Sigma S_iS_j$), respectively.

Nitronyl nitroxide and imino nitroxide radicals were first prepared by Ullman et al.,[6] and their paramagnetic metal complexes have been extensively studied, and some of these have been reported to show spontaneous magnetization.[7] Cu^{I} ions are known to favor a tetrahedral coordination geometry;[8] when two bidentate radical ligands complete the tetrahedral coordination sphere, two planes of the two ligands form a dihedral angle of 90° (or two magnetic orbitals on the radical ligands are orthogonal), hence, the interaction between the two ligands should be ferromagnetic. Here we report on a fairly strong ferromagnetic interaction of this type between two imino nitroxide ligands in the Cu^{I} complex **1**.

$[Cu^{I}(im\text{-}mepy)_2](PF_6)$ **1**

im-mepy =



Complex **1** was synthesized by adding the bidentate radical ligand im-mepy[10] (0.32 g) to a solution of $[Cu^{I}(CH_3CN)_4](PF_6)$[9] (0.25 g) in ethanol (25 mL) under a nitrogen atmosphere. The reaction mixture was allowed to stand overnight during which time dark red crystals precipitated which were then filtered. The results of the X-ray structural analysis of **1**[11] are shown in Figure 1. The copper atom sits on a twofold axis and is coordinated by two im-mepy ligands, which are thus related by the twofold symmetry. The tetrahedral coordination sphere of the copper atom is completed by four nitrogen atoms from the imino and pyridyl groups. The dihedral angle between the two planes Cu-N2-C7-N3-O1 and Cu-N2*-C7*-N3*-O1* is 88.7°.

The UV/VIS spectrum of **1** in acetonitrile shows absorption bands at 464 nm ($\varepsilon = 6300\ M^{-1}cm^{-1}$) and 766 nm ($\varepsilon = 5000\ M^{-1}cm^{-1}$) which are assigned to the charge transfer bands

[*] Prof. H. Oshio, Prof. T. Ito, T. Watanabe, A. Ohto
Department of Chemistry, Faculty of Science
Tohoku University
Aoba-ku, Sendai 980 (Japan)
Telefax: Int. code + (22)262-1077
Prof. U. Nagashima
Department of Information Sciences, Faculty of Science
Ochanomizu University, Tokyo 112 (Japan)
Telefax: Int. code + (3)3942-2815

[**] This work was in part supported by a Grant-in-Aid for Scientific Research on Priority Area "Molecular Magnetism" (Area No. 228/No. 05226203) and No. 05453039 from the Ministry of Education, Science and Culture, Japan.

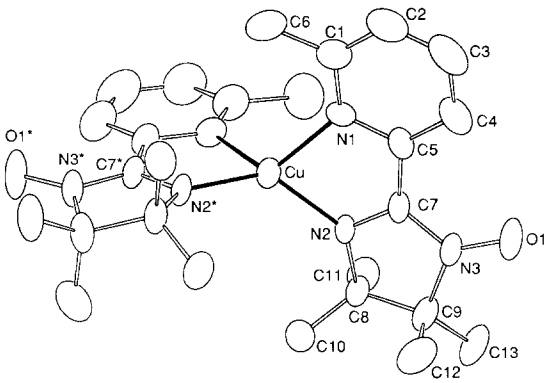


Fig. 1. The crystal structure of the cation of **1** (ORTEP; 30% thermal ellipsoids). Important bond lengths [Å] and angles [°]: Cu-N1 2.081(6), Cu-N2 1.953(5), O1-N3 1.273(7), N2-C7 1.271(7); N1-Cu-N2 81.1(2), N1-Cu-N1* 116.8(2), N1-Cu-N2 126.0(2), N2-Cu-N2* 131.2(2), Cu-N1-C1 128.4(6), Cu-N1-C5 111.9(4), C1-N1-C5 119.7(7), Cu-N2-C7 114.2(4), Cu-N2-C8 135.3(4), O1-N3-C7 126.1(7), N2-C7-N3 112.5(6).

from the copper (dπ) to ligand π* orbitals primarily localized on pyridyl imine[12] and imino nitroxide moieties,[13] respectively. The temperature dependence of the magnetic susceptibility was measured down to 2.0 K; a plot of $\chi_m T$ vs. T is shown in Figure 2 (χ_m = molar magnetic susceptibility). The $\chi_m T$ values

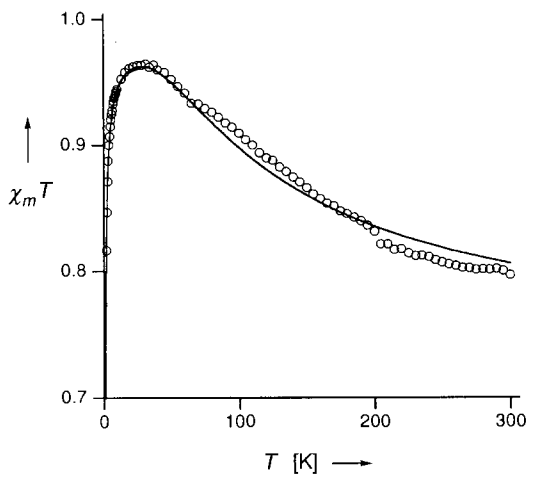


Fig. 2. Temperature dependence of $\chi_m T$ [emu mol^{-1} K] for **1**. The solid line corresponds to the least-squares fit obtained by using the Bleaney-Bowers equation and the parameters described in the text.

show a gradual increase as the temperature decreases, reaching a plateau (0.96 emu mol^{-1} K) at 40 K; the spin-only value for $S = 1$ is 1.0 emu mol^{-1} K. The copper(I) cation (d^{10} configuration) is diamagnetic and a solution of **1** in ethanol is ESR inactive at 293 K. Thus, it is concluded that the magnetic behavior of **1** indicates an intramolecular ferromagnetic interaction between the imino nitroxide ligands. An abrupt decrease of the $\chi_m T$ values below 20 K might be due to an intermolecular antiferromagnetic interaction. The magnetic susceptibility data were analyzed by using a Bleaney-Bowers equation ($H = -2JS_1S_2$) of the form (1),[14] where the contribution of the

$$\chi_m = \frac{Ng^2\beta^2}{k(T-\theta)}\left[\frac{2}{3+\exp(-2J/kT)}\right] \quad (1)$$

intermolecular antiferromagnetic interaction was included in the term θ. The best-fit parameters were $2J = +102(2)$ cm^{-1}, $g = 1.977(3)$, and $\theta = -0.36(2)$ K.

Magnetic interactions occurring between paramagnetic metal ions through a diamagnetic metal ion have been considered to be negligibly small or weakly antiferromagnetic. Trinuclear systems such as dimethylglyoximato-bridged Cu^{II}-Ni^{II}(LS)-Cu^{II}[15] (LS = low spin) and Fe^{III}-Fe^{II}(LS)-Fe^{III} complexes[16] show weak antiferromagnetic interactions ($J = -2.6$ and -4.4 cm^{-1}, respectively) between terminal metal ions, while a moderately strong antiferromagnetic interaction ($J = -36$ cm^{-1}) in an analogous Cu^{II}-Pd^{II}-Cu^{II} complex is exceptional.[15] In diamagnetic semiquinone–metal complexes,[4, 5] however, the occurrence of ferromagnetic interactions between the semiquinone ligands was due to their orthogonal arrangement. The Cu^{I}–imino nitroxide complex reported here shows a fairly strong ferromagnetic interaction ($2J = +102(2)$ cm^{-1}; $H = -2JS_1S_2$) compared with that of Ti^{IV}- and Ga^{III}-semiquinone complexes, which can be interpreted by the orthogonal arrangement of the radical ligands. Furthermore, a strong charge transfer interaction between the copper dπ to radical π* orbitals may play an important role in stabilizing the high-spin state. Thus, the copper(I) cation appears particularly suitable for linking organic radicals and in this way for building molecular-based ferromagnets.

Received: October 11, 1993 [Z 6406 IE]
German version: *Angew. Chem.* **1994**, *106*, 691

[1] *Magnetic Molecular Materials* (Eds.: D. Gatteschi, O. Kahn, J. S. Miller, F. Palacio), Kluwer, Dordrecht, **1991**; C. Kollmar, O. Kahn, *Acc. Chem. Res.* **1993**, *26*, 259; O. Kahn, *Molecular Magnetism*, VCH, Weinheim, **1993**.
[2] O. Kahn, J. Galy, Y. Journaux, J. Jaud, I. Morgenstern-Badarau, *J. Am. Chem. Soc.* **1982**, *104*, 2165.
[3] Y. Pei, Y. Journaux, O. Kahn, *Inorg. Chem.* **1989**, *28*, 100; H. Tamaki, Z. J. Zhong, N. Matsumoto, S. Kida, M. Koikawa, N. Achiwa, Y. Hashimoto, H. Okawa, *J. Am. Chem. Soc.* **1992**, *114*, 6974.
[4] A. Caneschi, A. Dei, D. Gatteschi, *J. Chem. Soc. Chem. Commun.* **1992**, 630.
[5] D. M. Adams, A. L. Rheingold, A. Dei, D. N. Hendrickson, *Angew. Chem.* **1993**, *105*, 434; *Angew. Chem. Int. Ed. Engl.* **1993**, *32*, 391.
[6] J. H. Osiecki, F. E. Ullman, *J. Am. Chem. Soc.* **1968**, *90*, 1078; F. E. Ullman, J. H. Osiecki, D. G. B. Boocock, R. Darcy, *ibid.* **1972**, *94*, 7049; E. F. Ullman, L. Call, J. H. Osiecki, *J. Org. Chem.* **1970**, *35*, 3623.
[7] A. Caneschi, D. Gatteschi, J. P. Renard, P. Rey, R. Sessoli, *Inorg. Chem.* **1989**, *28*, 1976; A. Caneschi, D. Gatteschi, J. P. Renard, P. Rey, R. Sessoli, *ibid.* **1989**, *28*, 3314; A. Caneschi, D. Gatteschi, R. Sessoli, P. Rey, *Acc. Chem. Res.* **1989**, *22*, 392.
[8] F. A. Cotton, G. Wilkinson, *Advanced Inorganic Chemistry 5th edition*; Wiley, New York, **1988**.
[9] G. J. Kubas, B. Monzyk, A. L. Crumbliss, *Inorg. Synth.* **1979**, *19*, 90.
[10] A. Caneschi, D. Gatteschi, P. Rey, *Prog. Inorg. Chem.* **1991**, *39*, 331.
[11] Crystal data: ($C_{26}H_{36}CuF_6N_6O_2P$), orthorombic space group *Pba*2, $a = 11.251(2)$, $b = 14.745(3)$, $c = 9.747(2)$ Å, $V = 1617.0(5)$ Å^3, $\varrho_{calcd} = 1.382$ g cm^{-3}, and $Z = 2$. Data were collected on a Rigaku AFC5R diffractometer at 223 K with $Cu_{K\alpha}$ ($\lambda = 1.54178$ Å) radiation. The structure was solved by Patterson methods and refined to $R = 0.044$, $R_w = 0.053$, for 991 unique reflections with $F_o > 6\sigma(F_o)$ and 191 parameters. Further details of the crystal structure investigation may be obtained from the Fachinformationszentrum Karlsruhe, D-76344 Eggenstein-Leopoldshafen (FRG), on quoting the depository number CSD-57958.
[12] S. Kitagawa, M. Munakata, *Inorg. Chem.* **1981**, *20*, 2261.
[13] M. Moscherosch, J. S. Field, W. Kaim, S. Kohlmann, M. Krejcik, *J. Chem. Soc. Dalton Trans.* **1993**, 211; C. Vogler, H. D. Hausen, W. Kaim, S. Kohlmann, H. E. A. Kramer, J. Rieker, *Angew. Chem.* **1989**, *101*, 1734; *Angew. Chem. Int. Ed. Engl.* **1989**, *28*, 1659.
[14] B. Bleaney, K. D. Bowers, *Proc. R. Soc. London A* **1952**, *214*, 451.
[15] P. Chaudhuri, M. Winter, B. P. C. Della Védova, E. Bill, A. Trautwein, S. Gehring, P. Fleischhauer, B. Nuber, J. Weiss, *Inorg. Chem.* **1991**, *30*, 2148.
[16] P. Chaudhuri, M. Winter, P. Fleischhauer, W. Haase, U. Flörke, H.-J. Haupt, *J. Chem. Soc. Chem. Commun.* **1990**, 1728.

 © VCH Verlagsgesellschaft mbH, D-69451 Weinheim, 1994 0570-0833/94/0606-0671 $ 10.00+.25/0

Synthesis and Crystal Structure of a Monocarbene Complex of Copper

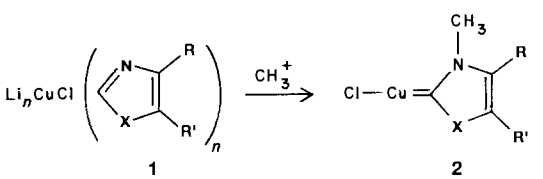
Helgard G. Raubenheimer,* Stephanie Cronje, Petrus H. van Rooyen, Pierre J. Olivier, and James G. Toerien

Dedicated to Professor E. O. Fischer on the occasion of his 75th birthday

In certain copper(I)-catalyzed reactions, such as the cyclopropanation of alkenes and alkynes with diazoalkanes and diazoketones,[1] and the formation of formamides from isocyanides and alcohols,[2] the existence of copper–carbene intermediates have been proposed. Recently Arduengo et al.[3] reported the preparation of the first isolable homoleptic copper–carbene and silver–carbene complexes. However, no X-ray crystal structure was reported for the copper complex. We now report a simple new route to an unusual thiazolylidene complex of copper(I), which has been extended to include imidazolylidene Cu^{I} complexes, as well as the first X-ray crystal structure of a copper–carbene complex.

The treatment of [Au(Cl)tht] (tht = tetrahydrothiophene) with two equivalents of a lithiated thiazole leads to the formation of aurates, which can be protonated or alkylated to produce stable mono- or biscarbene complexes of gold(I) in high yields.[4] Similarly, it is possible to form cuprates[5] by treating a suspension of CuCl in THF with lithiated thiazoles or imidazoles.[6]

Alkylation of the cuprate **1** (Scheme 1) with CF_3SO_3H afforded a clear solution from which the crystalline air-sensitive copper–carbene **2a** was obtained.[7, 8] By contrast, protonation



1 2

Scheme 1. **a**, X = S, R, R' = CH_3; **b**, X = S, R' = CH_3, R' = H; **c**, X = S, R, R' = $-(CH)_4-$; **d**, X = NCH_3, R, R' = H; **e**, X = NCH_3, R, R' = $-(CH)_4-$.

of the 4,5-dimethylthiazolyl, 4-methylthiazolyl, or benzothiazolyl cuprate with CF_3SO_3H did not yield the expected copper–carbene complexes. Instead complexes of the type $[\{Cu(\mu\text{-Cl})(thiazole)_2\}_2]$ were obtained; protonation had clearly occurred on the metal-bonded C^2 atom.

The exact composition of the 4,5-dimethylthiazolyl cuprate **1** is not known,[5] but it represents an aggregate containing chloride ions that are also present in the products obtained after alkylation or acidification.

The X-ray structure of **2a**[9] (Fig. 1) indicates that the copper atom is essentially two-coordinate, bonded to the carbene carbon of the thiazolylidene ligand (Cu–C1 1.888(6) Å)[10] and a chloride (Cu–Cl 2.122(2) Å)[11] in an approximately linear fashion (C1-Cu-Cl 166.9(2)°).[12] However, association of the copper atom and the chloride of adjacent molecule (Cu···Cl 2.905 Å)[13] results in the apparent dimeric nature of the compound in the solid state. The two molecules constituting the "dimer" lie in a plane; the largest deviation from the best-fit plane as defined by the non-hydrogen atoms is 0.087 Å for the two Cl atoms. None of the other atoms deviate more than 0.03 Å from the plane.

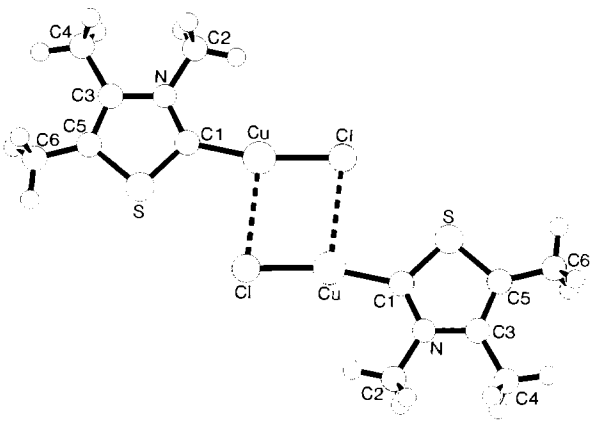


Fig. 1. Crystal structure of **2a** (SCHAKAL representation). Selected distances [Å] and angles [°]: Cu–Cl 2.122(2), Cu-Cl 1.888(6), C1-N 1.350(6), C1-S 1.665(6), Cl-Cu-C1 166.9(2), Cu-C1-N 128.0(5).

Experimental Procedure

2a: A suspension of CuCl (0.37 g, 3.7 mmol) in THF (40 mL) was added to 4,5-dimethylthiazol-2-yllithium, prepared from 4,5-dimethylthiazole (0.80 mL, 7.6 mmol) and 1.6 M *n*BuLi in hexane (4.6 mL, 7.4 mmol) in THF (40 mL), at −80 °C. The mixture was stirred for 2 h before adding $CF_3SO_3CH_3$ (0.40 mL, 3.6 mmol) at −80 °C. Stirring was continued at this temperature for 1 h, then for 1.5 h at −50 °C, and finally at −20 °C for 1 h, before the mixture was warmed to room temperature. After filtration through anhydrous $MgSO_4$ (18 g) and concentration in vacuo to about 75 mL, light brown crystals (0.46 g, 55%) formed at −20 °C. Crystals suitable for X-ray structure determination were obtained from the mother liquor of the first crystallization.

Received: October 8, 1993 [Z 6404 IE]
German version: *Angew. Chem.* **1994**, *106*, 687

[*] Prof. Dr. H. G. Raubenheimer, Dr. S. Cronje, Mr. P. J. Olivier, Dr. J. G. Toerien
Department of Chemistry and Biochemistry, Rand Afrikaans University
P.O. Box 524, Aucklandpark 2006 (South Africa)
Telefax: Int. code (011)489 2363
Prof. Dr. P. H. van Rooyen
Department of Chemistry, University of Pretoria (South Africa)

[1] D. S. Wulfman, B. Poling in *Reactive Intermediates, Vol. 1* (Ed.: R. A. Abramovitch), Plenum Press, New York, **1980**, p. 321; P. J. Pérez, M. Brookhart, J. L. Templeton, *Organometallics* **1993**, *12*, 261; M. P. Doyle, *Chem. Rev.* **1986**, *86*, 919.
[2] J. A. McCleverty, M. M. M. da Mota, *J. Chem. Soc. Dalton Trans.* **1973**, 2571.
[3] A. J. Arduengo, H. V. Rasika Dias, J. C. Calabrese, F. Davidson, *Organometallics* **1993**, *12*, 3405.
[4] H. G. Raubenheimer, F. Scott, M. Roos, R. Otte, *J. Chem. Soc. Chem. Commun.* **1990**, 1722; H. G. Raubenheimer, F. Scott, G. J. Kruger, J. G. Toerien, R. Otte, W. van Zyl, I. Taljaard, P. Oliver, L. Linford, *J. Chem. Soc. Dalton Trans.*, in press.
[5] B. H. Lipshutz, S. Sengupta, *Org. React. N.Y.* **1992**, *41*, 135.
[6] F. Bonati, A. Burini, B. R. Pietroni, B. Bovio, *J. Organomet. Chem.* **1989**, *375*, 147; *ibid.* **1991**, *408*, 271.
[7] **2a**: M.p. 143 °C (decomp.); ^{1}H NMR (200 MHz, CD_2Cl_2, 25 °C): δ = 4.08 (s, 3H; NCH_3), 2.32 (s, 6H; CCH_3); $^{13}C\{^1H\}$ NMR (50 MHz, CD_2Cl_2, 15 °C): δ = 198.3 (s, CuC), 140.9 (s, NC), 131.7 (s, SC), 44.7 (s, NCH_3), 12.5, 12.2 (s, CCH_3); MS (70 eV): *m/z* (%): 226(91) [M^+], 191(56) [M^+ − Cl], 127(37) [M^+ − Cl − Cu].
[8] The compounds **2b**–**2e** were prepared in a similar fashion to **2a** starting with the corresponding thiazolyl or imidazolyl cuprates and have all been fully characterized.
[9] Crystallographic data for **2a**: $C_6H_9ClCuNS$, M_r = 226.21, triclinic, $P\bar{1}$, a = 7.562(1), b = 7.954(2), c = 8.604(2) Å, α = 63.25(2), β = 71.75(1), γ = 69.83(2)°, based on 25 reflections with 12 < θ < 15°, V = 426.0(2) Å^3, Z = 2, ρ_{calcd} = 1.76 g · cm^{-3}, $F(000)$ = 227.97, μ = 2.93 mm^{-1}. Intensity data were collected on an Enraf Nonius CAD4 diffractometer, T = 297 K, with $Mo_{K\alpha}$ radiation (λ = 0.7107 Å), graphite monochromator, 3 < θ < 30°, 2488 unique reflections measured of which 1378 were considered as observed with $|I| > 3\sigma|I|$. All the non-hydrogen atoms were refined anisotropically, and the hydrogen atoms were included in the refinement in calculated positions, riding on their associated heavy atoms but with the isotropic thermal parameters free

to refine independently. A total of 101 parameters were refined and convergence was reached at $R_w = 0.042$ ($R = 0.058$) by using $\sigma(F_o)^{-2}$ weights. Further details of the crystal structure investigation are available on request from the Director of the Cambridge Crystallographic Data Centre, 12 Union Road, GB-Cambridge, CB2 1EZ (UK), on quoting the full journal citation.

[10] This bond is shorter than known Cu-C bonds. a) G. Nardin, L. Randaccio, E. Zangrando. *J. Organomet. Chem.* **1974**, *74*, C23: Cu–C = 1.962(15) Å in $[\{Cu[(CH_3)_2P(CH_2)_2]\}_2]$; b) A. Toth, G. Floriani, A. Chiesi-Villa, C. Guastini, *J. Chem. Soc. Dalton Trans.* **1988**, 1599: Cu–C = 1.918(2) Å in $[Cu_2(\mu\text{-}Cl)_2\{(p\text{-}CH_3C_6H_4)NC\}_4]$; c) H. Schmidbaur, C. E. Zybill, G. Müller, C. Krüger, *Angew. Chem.* **1983**, *95*, 753; *Angew. Chem. Int. Ed. Engl.* **1983**, *22*, 729: Cu–C 1.906(2) Å in $[Cu(Cl)C(PPh_3)_2]$.

[11] Known Cu–Cl bond lengths are similar. a) G. Müller, C. Krüger, C. Zybill, H. Schmidbaur, *Acta Crystallogr. Sect. C* **1986**, *40*, 1141: Cu–Cl = 2.113(1) Å in $[Cu(Cl)C(PPh_3)_2]$; b) J. S. Thompson, J. F. Whitney, *ibid.* **1984**, *40*, 756: Cu–Cl = 2.155(1) Å in $[Cu(HBpz_3)(C_6H_{10})CuCl]$, $HBpz_3$ = hydrotris(1-pyrazolyl)borate.

[12] The bond angle is larger than the N-Cu-Cl angle (159.24(4)°) in $[Cu(HBpz_3)(C_6H_{10})CuCl]$ (see [11b]) and smaller than the C-Cu-Cl angle (178.2(1)°) in $[Cu(Cl)C(PPh_3)_2]$ (see [11a]).

[13] The distances of 2.905 Å is too great to consider the copper to be three-coordinate. a) P. C. Healy, J. D. Kildea, A. H. White, *Aust. J. Chem.* **1989**, *42*, 137: Cu–Cl = 2.177(3), 2.475(3), 2.168(3), and 2.510(3) Å in [(oha)$CuCl_2$Cu(oha)], oha = 1,2,3,4,5,6,7,8-octahydroacridine; b) see also [11a], Cu···Cl 2.618(1) Å in $[Cu(HBpz_3)(C_6H_{10})CuCl]$.

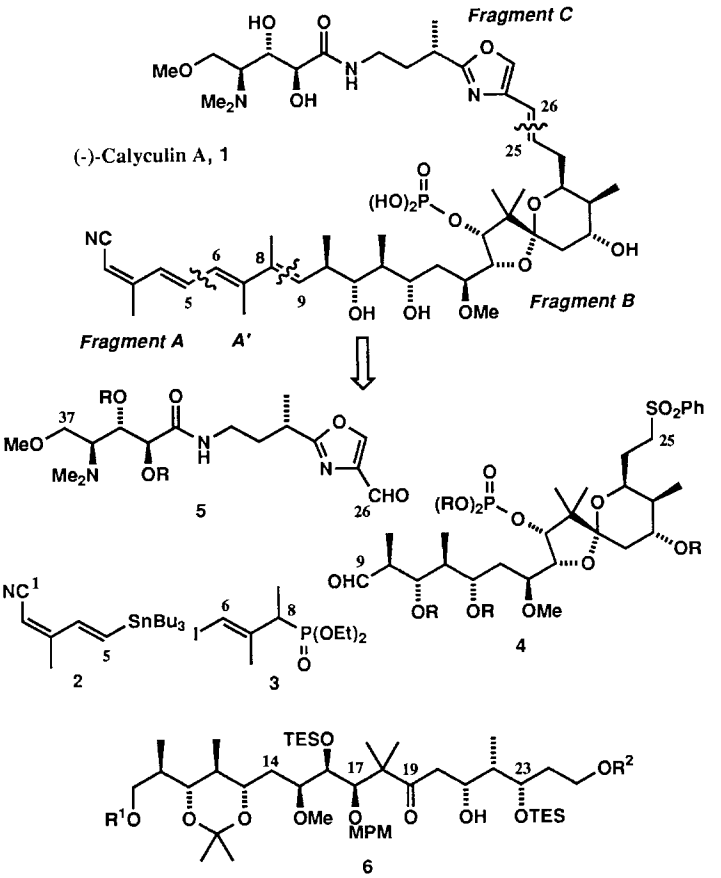
The Synthesis of Naturally Occurring (−)-Calyculin A**

Norihiko Tânimoto, Samuel W. Gerritz, Akiyoshi Sawabe, Takeshi Noda, Sandra A. Filla, and Satoru Masamune*

Calyculin A (**1**), isolated in 1986 from the marine sponge *Discodermia calyx*,[1] has aroused considerable interest among synthetic chemists mainly for two reasons: 1) this marine product exhibits striking biological activity exemplified by the inactivation of the serine/threonine protein phosphatases 1 and 2A,[2] and 2) it possesses a functionally and stereochemically unique structure as demonstrated by X-ray crystallography (which clarified the relative stereochemistry).[1] In late 1991 two studies[3] established the absolute stereochemistry as shown in **1**, which was enantiomeric to that depicted in the original 1986 report. While all synthetic efforts recorded thus far[4] had selected *ent*-**1** as the target molecule, we promptly modified our synthetic plan towards **1** and now describe the synthesis of *naturally occurring* calyculin A (**1**).

As noted previously,[5] retrosynthetic dissection as shown by the wavy lines superimposed on **1** provides fragments A (**2**, C1–C5), A′ (**3**, C6–C8), B (**4**, C9-C25), and C (**5**, C26-C37). As shown in Equation (a), the order of fragment coupling was carefully selected so that the sensitive tetraene portion (C1–C8) was introduced at a late stage in the synthesis. Since fragments A, A′, and C were already available,[5] the synthesis of fragment B and the assembly of calyculin A are outlined below. Several aldol reactions used for the fragment B construction address a previously unsolved problem in this methodology: the stereoselective coupling of chiral fragments through the aldol reaction.[6]

$$B \xrightarrow{C} BC \xrightarrow{A'} A'BC \xrightarrow{A} AA'BC \qquad (a)$$

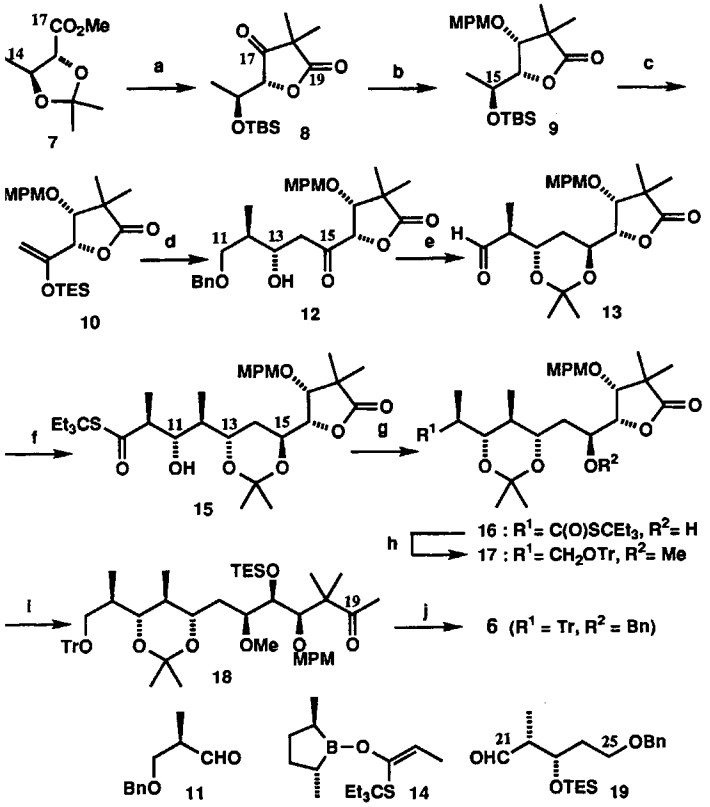


All stereocenters embedded in fragment B (**4**) are contained in the acyclic intermediate **6** (TES = triethylsilyl, MPM = *p*-methoxyphenylmethyl), which was selected after numerous model studies and prepared according to Scheme 1. The initial task was the construction of the central portion C14–C19 of **6** through a sequence of standard conversions: a) the Claisen condensation of **7** with the lithium enolate derived from methyl isobutyrate followed by lactonization and alcohol protection to provide **8** (TBS = *tert*-butyl(dimethyl)silyl), b) stereoselective (>10:1) reduction of the C17-ketone and MPM-protection of the resulting alcohol to afford **9**,[7] and c) liberation of the C15 alcohol, Swern oxidation, and enol silylation to provide **10**. The Ti^{IV}-mediated, chelation-controlled, Mukaiyama-type aldol reaction of aldehyde **11** with **10** proceeded smoothly to provide **12** with 10:1 diastereoselection (step d). Apparently the chirality present in **10** has a limited effect on the diastereoselectivity of the reaction,[8] an important observation for the stereoselective coupling of two *chiral* components. The C11, C13, and C15 oxygen functionalities in **12** were modified to those shown in **13** (step e). This modification set the stage for the subsequent aldol reaction, which involved the construction of the 10,11-*anti*, 11,12-*anti*, 12,13-*anti* aldol **15**, the 'worst' mismatched pair possible for a product of the aldol reaction.[9] Fortunately, the extraordinarily high diastereoselectivity of the *E*(O) enolate **14** (derived from propanethiolate with (*R*,*R*)-2,5-dimethylboro-

[*] Prof. S. Masamune, Dr. N. Tanimoto, Dr. S. W. Gerritz, Dr. A. Sawabe, Dr. T. Noda, S. A. Filla
Department of Chemistry
Massachusetts Institute of Technology
Cambridge, MA 02139 (USA)
Telefax: Int. code + (617)253-1340

[**] This work was supported by the National Institutes of Health, USA (CA 48175). We gratefully acknowledge valuable contributions made by Drs. H. A. Vaccaro, T. Jaetsch, D. E. Levy, E. Parmee, and L.-Y. Chen in the early stage of the synthesis. A sample of (−)-calyculin of natural origin was made available to us by Professor N. Fusetani as a generous gift.

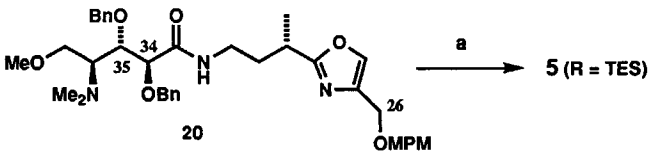
lanyl triflate)[10] overrode that (1:4) of **13** to provide **15** with 12:1 diastereoselection (step f). All other chiral reagents tested failed to provide the desired diastereomer as the major product.[11] The above successful stereochemical control to form an *anti, anti, anti* product represents one of the rare recorded examples of this case. With all the carbons in place, **15** was further modified: conversion of the 13,15-*anti* acetonide into the more stable 11,13-*syn* acetonide (**16**) (step g), followed by reduction of the thiol ester[12] to the corresponding C9 primary alcohol, and finally the protection of the C9 and C15 alcohol groups with trityl (Tr) and methyl groups, respectively, to provide **17** (step h).[7]



Scheme 1. Synthesis of intermediate **6**; reagent, conditions, and yield. a) 1. Methyl isobutyrate, lithium diisopropylamide (LDA), THF/hexane, then **7**, −78 °C–25 °C; 2. Dowex-50 × 8 (H^+), MeOH; 3. *t*BuMe$_2$SiOTf, 2,6-lutidine, CH_2Cl_2, 25 °C (84%, three steps). b) 1. KEt$_3$BH, THF, −78 °C, then AcOH (85%); 2. MPMBr, *n*Bu$_4$NI, KH, THF (82%); c) 1. *n*Bu$_4$NF, THF, 25 °C; 2. Swern oxidation; 3. Et$_3$SiOTf, 2,6-lutidine, CH_2Cl_2 (83%, three steps). d) **11**, $TiCl_4$, CH_2Cl_2, then **10**, −78 °C (84%, 13*S*:13*R* = 10:1); e) 1. Me$_4$NHB(OAc)$_3$, CH_3CN-AcOH (1:1), 2. Me$_2$C(OMe)$_2$, TsOH (83%, two steps); 3. W-2 Raney Ni, EtOH; 4. Swern oxidation (89%, two steps). f) (*E*)-enolate **14**, hexane/CH_2Cl_2, −78 °C (82%, 11,12-*anti*:11,12-*syn* = 12:1); g) camphorsulfonic acid (CSA), acetone, 25 °C (100%). h) 1. Hg(CF$_3$CO$_2$)$_2$, NaH$_2$PO$_4$, THF (98%; 2. ClCO$_2$Et, Et$_3$N, THF, then NaBH$_4$, H_2O (85%); 3. Ph$_3$CCl, Et$_3$N, 4-dimethylaminopyridine (DMAP), 4. KH, [18]-crown-6, MeI, THF (86%, two steps). i) 1. LiOH, *t*BuOH-H_2O, 2. CH_2N_2, Et$_2$O; 3. reagents as for c, 3; 4. Me$_3$SiCH$_2$Li, THF, then MeOH (95%, four steps). j) (cHex)$_2$BCl, Et$_3$N, CH_2Cl_2, then **19** (93%). Tf = trifluoromethanesulfonate, Ts = tosyl.

The utility of the above acetonide migration strategy deserves a special note, as it enables us to differentiate between the secondary hydroxyl groups at C11 and C15, thereby freeing the C15 hydroxyl group for subsequent methylation as required in **1**. Transformation of **17** into the methyl ketone **18** was effected with a set of standard reactions (step i), and then the coupling of the two chiral fragments **18** and **19** (C21–C25)[13] constituted the final aldol reaction needed for the assembly of **6**. The $BF_3 \cdot OEt_2$-promoted aldol reaction[14] of the TMS enol ether of **18** (TMS = trimethylsilyl) proceeded slowly (5–7 days) and in low yield (about 50%) prompting an investigation of the aldol reaction mediated by a variety of achiral boron reagents. This survey of boron reagents revealed that the size of the alkyl ligands on boron had a pronounced effect on the diastereoselectivity of the aldol reaction; the increase in the size of the ligands attached to B enhanced the ratio of **6** to its 21-epimer (**6a**). Thus, the use of the bulky reagent dicyclohexyl boron chloride brought about the exclusive formation of **6**, the C21 stereochemistry of which was confirmed by its conversion into the corresponding spiroketal **21** (see below).

Precursor **20** to fragment C prepared from D-galactose by analogy to our previously reported synthesis of *ent*-**20**,[5] was futher modified to **5** (R = TES) (Scheme 2) in order to secure a fragment BC suitable for final coupling with fragments A and A′. It is noteworthy that selective deprotection of the C34 and



Scheme 2. Synthesis of fragment C, reagents, conditions, and yield. a) 1. 10% Pd/C, 4.4% HCO_2H/MeOH (63%); 2. Et$_3$SiOTf, 2,6-lutidine, CH_2Cl_2 (81%); 3. dichlorodicyanoquinone (DDQ), CH_2Cl_2/H_2O/*i*PrOH (62%), 4. Swern oxidation (89%).

C35 benzyloxy groups in the presence of the C26 OMPM group was not a trivial task and proceeded under the unusual conditions specified in Scheme 2, step i.[15]

Table 1. Stereoscopic data of selected synthetic intermediates (**5**, **21**, and **26**).

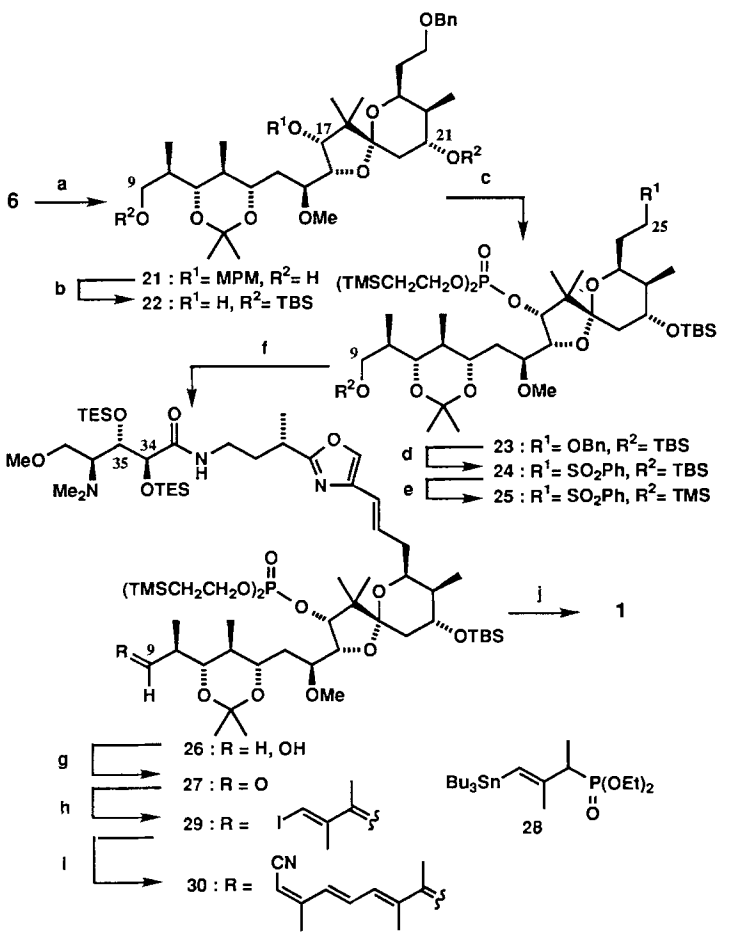
5 (R = TES): $[\alpha]_D^{22} = -2.6$ ($c = 0.94$, $CHCl_3$); ^{1}H NMR (300 MHz, C_6D_6): $\delta = 0.68$ (q, $J = 7.8$ Hz, 6H), 1.01 (t, $J = 7.8$ Hz, 9H), 1.07 (q, $J = 7.8$ Hz, 9H), 1.12 (d, $J = 6.9$ Hz, 3H), 1.68 (m, 1H), 1.96 (m, 1H), 2.45 (s, 6H), 2.86 (m, 1H), 3.09 (s, 3H), 3.18–3.36 (m, 2H), 3.43 (ddd, $J = 3.3$, 6.9, 9.6 Hz, 1H), 3.58 (dd, $J = 3.3$, 12 Hz, 1H), 3.60 (dd, $J = 6.9$, 12 Hz, 1H), 4.37 (dd, $J = 1.2$ Hz, 1H), 6.58 (br t, 1H), 9.67 (s, 1H). MS (EI): *m/z* calcd for $C_{28}H_{55}N_3O_6Si_2$ 585.3629, found 585.3635.

21: $[\alpha]_D^{22} = -66.8$ ($c = 1.30$, CH_2Cl_2); ^{1}H NMR (300 MHz, C_6D_6): $\delta = 0.59$ (d, $J = 6.8$ Hz, 3H), 0.66 (s, 3H), 0.72 (d, $J = 7.3$ Hz, 3H), 1.11 (s, 3H), 1.15 (d, $J = 7.4$ Hz, 3H), 1.16 (s, 3H), 1.17 (s, 3H), 1.32 (m, 3H), 1.52 (t, $J = 3.3$ Hz, 2H), 1.54–1.70 (m, 3H), 1.78 (m, 1H), 2.50 (m, 1H), 3.08 (d, $J = 5.2$ Hz, 1H), 3.34 (s, 3H), 3.37 (m, 1H), 3.4–3.6 (m, 3H), 3.80 (dt, $J = 8.1$, 2.1 Hz, 1H), 3.89 (m, 3H), 4.10 (m, 3H), 4.20 (d, $J = 9.7$ Hz, 1H), 4.30 (d, $J = 10.0$ Hz, 1H), 4.39 (d, $J = 12.2$ Hz, 1H), 4.73 (d, $J = 10.6$ Hz, 1H), 6.95 (d, $J = 8.4$ Hz, 2H), 7.1–7.3 (m, 3H), 7.34 (d, $J = 7.3$ Hz, 2H), 7.40 (d, $J = 8.5$ Hz, 2H); ^{13}C-NMR (75 MHz, C_6D_6): $\delta = 11.0$, 12.1, 15.7, 17.6, 19.0, 23.1, 29.9, 30.6, 33.6, 35.2, 36.6, 37.2, 38.6, 50.8, 54.8, 60.5, 63.5, 64.0, 68.1, 70.6, 71.4, 72.7, 75.3, 77.8, 79.8, 86.5, 86.8, 98.3, 108.7, 114.0, 127.3, 127.6, 128.5, 128.6, 130.5, 140.0, 160.0, MS (EI): *m/z* calcd for $C_{41}H_{62}O_{10}$ 714.4343 found 714.4351.

26: ^{1}H NMR (500 MHz, C_6D_6): $\delta = -0.019$ (s, 9H), 0.071 (s, 9H), 0.100 (s, 3H), 0.164 (s, 3H), 0.679 (d, $J = 6.4$ Hz, 3H), 0.704 (q, $J = 7.8$ Hz, 6H), 0.773 (q, $J = 7.8$ Hz, 6H), 0.795 (s, 3H), 0.832 (d, $J = 6.8$ Hz, 3H), 1.033 (t, $J = 7.8$ Hz, 9H), 1.061 (s, 9H), 1.087 (t, $J = 7.8$ Hz, 9H), 1.178(d, $J = 7.3$ Hz, 3H), 1.244 (d, $J = 7.3$ Hz, 3H), 1.369 (s, 3H), 1.433 (s, 3H), 1.484 (s, 3H), 1.662–1.710 (m, 2H), 1.750–1.841 (m, 2H), 1.894 (m, 1H), 2.067 (m, 1H), 2.175 (ddd, $J = 2.0$, 10.5, 13.5 Hz, 1H), 2.286 (ddd, $J = 7.5$, 7.5, 15.5 Hz, 1H), 2.463 (s, 6H), 2.607 (m, 1H), 2.968 (tq, $J = 7.5$, 6.5 Hz, 1H), 3.111 (s, 3H), 3.315 (m, 1H), 3.383 (m, 1H), 3.408–3.461 (m, 3H), 3.587–3.650 (m, 3H), 3.763 (s, 3H), 3.791 (br d, $J = 3.0$ Hz, 1H), 3.906–3.995 (m, 3H), 4.271–4.321 (m, 2H), 4.370 (m, 1H), 4.397 (d, $J = 9.8$ Hz, 1H), 4.463 (dt, $^3J_{P-H} = 10.3$, $J_{H-H} = 7.3$ Hz, 2H), 4.620 (s, 1H), 4.801 (dd, $J = 4.4$, 9.3 Hz, 1H), 4.866 (ddd, $J = 2.0$, 7.3, 7.3 Hz, 1H), 6.577 (d, $J = 16.0$ Hz, 1H), 6.596 (br, t, $J = 6.0$ Hz, 1H), 6.771 (ddd, $J = 5.4$, 8.3, 15.6 Hz, 1H), 7.591 (s, 1H). MS (*FAB*) *m/z* calcd for $C_{70}H_{141}N_3O_{16}Si_5P$ (MH^+) 1450.8896, found 1450.8904.

 © VCH Verlagsgesellschaft mbH, D-69451 Weinheim, 1994 0570-0833/94/0606-0674 $ 10.00+.25/0

Intermediate **6** to fragment B also had to undergo several critical manipulations. Thus, removal of the TES groups at C16 and C23 from **6** followed by treatment with 1:1 formic acid/ether[16] provided the single spiroisomer **21** (Scheme 3, step a; 70% yield),[17] the stereochemistry of which was ascertained by extensive nuclear Overhauser enhancement (NOE) experiments.[7] After silylation of the C9 and C21 hydroxyl groups and oxidative removal of the C17 MPM group (step b), the liberated C17 alcohol was converted to its bis(2-trimethylsilylethyl)phosphate triester (**23**, step c) as described earlier.[18] The transformation of the C25 benzyl group of **23** into the C25 sulfone group (**24**) proceeded in the usual manner (step d). The selection of a protecting group for the C9 hydroxyl function proved to be problematic, because the group must be stable to the Julia-Lythgoe coupling[19] conditions, yet more labile than the C34 and C35 OTES groups. After extensive experimentation, a TMS group was found to satisfy these requirements, and compound **25** (step e) was ready for the B–C coupling.



Scheme 3. Synthesis of fragment B and subsequent reactions leading to calyculin A **1**; reagents, conditions, and yield. a) 1. nBu$_4$NF, THF, 0 °C (95%); 2. HCO_2H-Et_2O (1:1), 25 °C (70%). b) 1. tBuMe$_2$SiOTf, 2,6-lutidine, CH_2Cl_2; 2. DDQ, CH_2Cl_2/H_2O (10:1) (75%, two steps); c) $Me_3SiCH_2CH_2OPCl_2$, pyridine, 0 °C, then $Me_3SiCH_2CH_2OH$, 25 °C, then 30% H_2O_2 (70%, two steps) d) 1. 10% Pd/C, H_2, MeOH (92%); 2. MsCl, Et_3N, CH_2Cl_2, 0 °C; 3. PhSNa, DMF, 4. *meta*-chlorperbenzoic acid (mCPBA), CH_2Cl_2 (92%, three steps). e) 1. HF-pyridine, THF-pyridine, 2. Me_3SiCl, Et_3N, CH_2Cl_2 (93%, two steps). f) 1. PhLi, THF, −78 °C, then **5** (56%). 2. PhCOCl, Et_3N, DMAP, CH_2Cl_2; 3. Na-Hg, MeOH-EtOAc, −20 °C (68%, two steps). g) Swern oxidation (82%). h) **28**, PhLi, THF, −78 °C, then **27**, 0 °C, then I_2 (53%). i) **2**, $[Pd(Ph_3P)_2Cl_2]$, DMF (67%); j) CH_3CN/47%HF/H_2O 85:5:10 (57%).

The anion derived from **25** with phenyllithium reacted with aldehyde **5** to provide the corresponding adduct (step f) without losing the C9 TMS group, and the adduct, after benzoylation, was subjected to reductive elimination with sodium amalgam to provide the *E*-olefin **26** as the predominant product ($J_{25,26}$ = 16.0 Hz). The C9 OH group was liberated in this last step of the Julia coupling. Since the nucleophilic attack of the anion of **25** on **5** proceeded much faster than deprotonation of the amide group present in **5**, temporary protection of the amide was unnecessary. With the BC fragment fully protected except for the C9 alcohol, the construction of the tetraene moiety on **26** was carried out as shown earlier.[5] Thus, the Horner–Emmons reaction of **27**, derived from **26** (Swern oxidation, step g), with the anion generated from **28** with phenyllithium provided the unstable vinyltin intermediate, which was converted in situ into the corresponding iodide **29**. The product was almost exclusively the *E,E* isomer. The final coupling utilized the Stille coupling[20] of **29** and **2** with the aid of $[PdCl_2(Ph_3P)_2]$, and complete removal of all the protecting groups of **30** with CH_3CN/HF completed the synthesis of (−)-**1**, which was found to be identical in every respect to naturally occurring calyculin A.

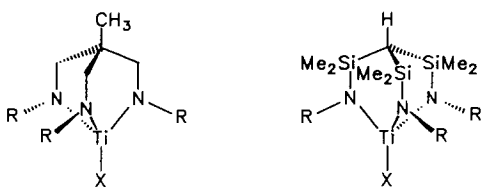
Received: October 11, 1993 [Z 6409 IE]
German version: *Angew. Chem.* **1994**, *106*, 674

[1] Y. Kato, N. Fusetani, S. Matsunaga, K. Hshimoto, S. Fujita, T. Furuya, *J. Am. Chem. Soc.* **1986**, *108*, 2780–2781.
[2] H. Ishibara, B. L. Martin, D. L. Brautigan, H. Karaki, H. Ozaki, Y. Kato, N. Fusetani, S. Watabe, K. Hashimoto, D. Uemura, D. J. Hartshorne, *Biochem. Biophys. Res. Commun.* **1989**, *159*, 871–877. For a recent study, see: M. Suganuma, H. Fujiki, S. Okabe, S. Nishiwaki, D. Brautigan, T. S. Ingebritsen, M. R. Rosner, *Toxicon* **1992**, *30*, 873–878.
[3] a) S. Matsunaga, N. Fusetani, *Tetrahedron Lett.* **1991**, *32*, 5605–5606; b) Y. Hamada, Y. Tanada, F. Yokokawa, T. Shioiri, *ibid.* **1991**, *32*, 5983–5986.
[4] The total synthesis of nonnatural (+)-calyculin A (*ent*-**1**) was reported in 1992: a) D. A. Evans, J. R. Gage, J. L. Leighton, *J. Am. Chem. Soc.* **1992**, *114*, 9434–9453. Leading references to other synthetic approaches to *ent*-**1**: b) J. Matsubara, K. Nakao, Y. Hamada, T. Shioiri, *Tetrahedron Lett.* **1992**, *33*, 4187–4190; c) A. B. Smith, III, J. J.-W. Duan, K. G. Hull, B. A. Salvatore, *ibid.* **1991**, *32*, 4855–4858; d) R. W. Armstrong, J. A. DeMattei, *ibid.* **1991**, *32*, 5749–5752; e) A. M. P. Koskinen, J. Chen, *ibid.* **1991**, *32*, 6977–6980; f) A. G. M. Barrett, J. J. Edmunds, K. Horita, C. J. Parkinson, *J. Chem. Soc. Chem. Commun.* **1992**, 1236–1238.
[5] H. A. Vaccaro, D. E. Levy, A. Sawabe, T. Jaetsch, S. Masamune, *Tetrahedron Lett.* **1992**, *33*, 1937–1940. The synthesis of **20** has been improved significantly compared with that of *ent*-**20** described in this reference.
[6] A. J. Duplantier, M. H. Nantz, J. C. Roberts, R. P. Short, P. Somfai, S. Masamune, *Tetrahedron Lett.* **1989**, *30*, 7357–7360.
[7] Evidence to confirm the indicated stereochemical assignment of **9**, **17**, and **21** was presented to the editors and reviewers.
[8] The Ti^{IV}-mediated aldol reaction between **11** and achiral silyl enol ethers proceeded with similar diastereoselectivity: M. T. Reetz, K. Kesseler, *J. Chem. Soc. Chem. Commun.* **1984**, 1079.
[9] For a review, see: W. R. Roush, *J. Org. Chem.* **1991**, *56*, 4151–4157.
[10] S. Masamune, T. Sato, B.-M. Kim, T. A. Wollmann, *J. Am. Chem. Soc.* **1986**, *108*, 8279–8281.
[11] For instance, utilization of the *E*-crotyl Roush reagent derived from (*S,S*)-diisopropyl tartrate (W. R. Roush, K. Ando, D. B. Powers, A. D. Palkowitz, R. L. Halterman, *J. Am. Chem. Soc.* **1990**, *112*, 6339–6348) gave a 2:1 mixture of diastereomers favoring the undesired 11,12-*syn* adduct.
[12] S. Masamune, M. Hirama, S. Mori, S. A. Ali, D. S. Garvey, *J. Am. Chem. Soc.* **1981**, *103*, 1568–1571.
[13] S. Masamune, W. Choy, F. A. J. Kerdesky, B. Imperiali, *J. Am. Chem. Soc.* **1981**, *103*, 1566–1568.
[14] C. H. Heathcock, L. A. Flippin, *J. Am. Chem. Soc.* **1983**, *103*, 1667–1668.
[15] B. ElAmin, G. M. Anantharamaiah, G. P. Royer, G. E. Means, *J. Org. Chem.* **1979**, *44*, 3442–3444.
[16] M. Bessodes, D. Komiotis, K. Antonakis, *Tetrahedron Lett.* **1986**, *27*, 579–581.
[17] This formation of a single spiroketal **21** is in accord with Smith's [4c], but somewhat different from Evans's results [4a].
[18] A. Sawabe, S. A. Filla, S. Masamune, *Tetrahedron Lett.* **1992**, *33*, 7685–7686. Cf. [4a] for different phosphate protecting groups.
[19] M. Julia, *Pure Appl. Chem.* **1985**, *57*, 763–768.
[20] J. K. Stille, B. L. Groh, *J. Am. Chem. Soc.* **1987**, *109*, 813–817.

Titanium Complexes with Tripodal Amido Ligands: Building Blocks for Stable Bimetallic Coordination Compounds Containing Highly Polar Metal–Metal Bonds**

Stefan Friedrich, Harald Memmler, Lutz H. Gade,* Wan-Sheung Li, Mary McPartlin

Focusing the chemical reactivity at an early transition metal center upon a single "activated" site while effectively shielding the remaining coordination sphere is an underlying motivation of the recent interest in the development of polydentate amido ligands.[1] A notable example is the reactivity of a series of complexes containing the silylated tren ligand (tren = tris(2-aminoethyl)-amine) of the type $[N\{CH_2CH_2NSiRMe_2\}_3MX_n]$ (R = Me, *t*Bu; M = Ti, V, Cr, Mn, Fe, Ta; X = Cl, PR; n = 0, 1, 2) reported by Schrock et al.[2] The anticipated stabilization of a high-valent early transition metal shielded, and thus kinetically stabilized, by a polyfunctional ligand appeared to us to provide the key to a general strategy for the synthesis of thermally stable dinuclear complexes containing highly polar unsupported metal–metal bonds. Despite the activities in the chemistry of early–late heterobimetallics there are still but a few stable species of this kind,[3] and their different sets of ligands have hampered a systematic comparative study of their structure and reactivity.[4] This led us to develop new tripodal amides[5] (type **A**) which leave a greater coordination arc at the reactive center than the tren derivatives (Fig. 1)[6], thus potentially facilitating M–M′ bond formation. These complexes indeed satisfied the expectations.



A **B**

Fig. 1. Titanium-containing building blocks of type **A** and **B** for the synthesis of stable heterobimetallic complexes with unsupported metal–metal bonds.

We have now extended this approach to the synthesis of a new class of titanium amido halides (type **B**) and report the synthesis of one member, **2**.[7]

The amido titanium bromide **2** is readily obtained by reaction of the trilithiated amino-functionalized trisilylmethane with $[TiBr_4(thf)_2]$ [Eq. (a)].

$$[HC(SiMe_2N(Li)C_6H_4CH_3)_3] \xrightarrow{[TiBr_4(thf)_2]} [HC(SiMe_2NC_6H_4CH_3)_3TiBr] \quad (a)$$
2

The spectroscopic data of the moisture-sensitive, red, crystalline compound (Table 1) are in accordance with the structure depicted in Figure 1. Reaction of the complex **1**[6a] or **2** with carbonyl metallate derivatives according to Scheme 1 leads to the coupled heterobimetallic, dinuclear complexes **3**–**5** and **6**–**8**, respectively. The Ti–Fe complexes, **3** and **6** are the first compounds with an unsupported Ti–Fe bond that are stable in solution at ambient temperatures and chemically fairly robust towards attack by weak nucleophiles unless activated thermally or photochemically.[8]

Table 1. Selected spectroscopic data. NMR spectra recorded at 200.13 MHz (^{1}H), 50.32 MHz (^{13}C), 77.78 MHz (^{29}Si), and 81.03 MHz (^{31}P) in C_6D_6. Correct elemental analyses were obtained for all compounds.

2: ^{1}H NMR: $\delta = -0.28$ (s, HC(Si...)$_3$), 0.37 (s, Si(CH$_3$)$_2$), 2.07 (s, 4-CH_3C$_6$H$_4$), 6.98 (d, $^3J_{HH} = 8.2$ Hz, H2$_{tol}$), 7.10 (d, H3$_{tol}$); ^{13}C NMR: $\delta = 3.8$ (Si(CH$_3$)$_2$), 9.9 (HC(Si...)$_3$), 20.8 (4-CH$_3$C$_6$H$_4$), 123.1, 130.3, 133.4, 148.1 (C2, C4, C3, C1 tolyl); ^{29}Si NMR: $\delta = 6.5$

3: ^{1}H NMR: $\delta = 0.41$ (s, Si(CH$_3$)$_3$), 0.70 (s, CH$_3$-C), 3.10 (s, CH$_2$N), 4.59 (s, C$_5$H$_5$); ^{13}C NMR: $\delta = 2.2$ (Si(CH$_3$)$_3$), 26.7 (CH$_3$-C), 49.5 (CH$_3$-C), 60.5 (CH$_2$N), 84.4 (C$_5$H$_5$), 216.6 (CO); ^{29}Si NMR: $\delta = 2.5$; IR(toluene): ν(CO) = 1968(s), 1916(s)

4: ^{1}H NMR: $\delta = 0.40$ (s, Si(CH$_3$)$_3$), 0.72 (s, CH$_3$-C), 3.14 (s, CH$_2$N), 4.99 (s, C$_5$H$_5$); ^{13}C NMR: $\delta = 2.3$ (Si(CH$_3$)$_3$), 26.5 (CH$_3$-C), 50.3 (CH$_3$-C), 60.6 (CH$_2$N), 87.2 (C$_5$H$_5$), 205.6 (CO); ^{29}Si NMR: $\delta = 1.9$; IR(n-hexane): ν(CO) = 1988(s), 1932(s)

5: ^{1}H NMR: $\delta = 0.46$ (s, Si(CH$_3$)$_3$), 0.85 (s, CH$_3$-C), 3.39 (s, CH$_2$N), 6.96–7.09, 7.51–7.61 (m, phenyl); ^{13}C NMR: $\delta = 1.3$ (Si(CH$_3$)$_3$), 26.4 (CH$_3$-C), 50.2 (CH$_3$-C), 61.5 (CH$_2$N), 128.7, 130.1, 133.3 (d, $^2J_{PC} = 12.5$ Hz), 135.5 (d, $^1J_{PC} = 39.7$ Hz) (C3, C4, C2, C1 phenyl), 206.6 (CO, $^2J_{PC}$ not resolved); ^{29}Si NMR: $\delta = 2.6$; ^{31}P NMR: $\delta = 56.0$; IR(n-hexane): ν(CO) = 1930(vs)

6: ^{1}H NMR: $\delta = -0.78$ (s, HC(Si...)$_3$), 0.33 (s, Si(CH$_3$)$_2$), 2.21 (s, 4-CH_3C$_6$H$_4$), 3.55 (s, C$_5$H$_5$) 7.24 (d, $^3J_{HH} = 8.2$ Hz, H2$_{tol}$), 7.56 (d, H3$_{tol}$); ^{13}C NMR: $\delta = 4.0$ (Si(CH$_3$)$_2$), 6.7 (HC(Si...)$_3$), 21.0 (4-CH$_3$C$_6$H$_4$), 85.3 (C$_5$H$_5$), 126.4, 130.3, 132.2, 150.8 (C2, C4, C3, C1 tolyl), 213.2 (CO); ^{29}Si NMR: $\delta = 2.0$; IR(benzene): ν(CO) = 1975(s), 1928(s)

7: ^{1}H NMR: $\delta = -0.68$ (s, HC(Si...)$_3$), 0.36 (s, Si(CH$_3$)$_2$), 2.20 (s, 4-CH_3C$_6$H$_4$), 4.07 (s, C$_5$H$_5$), 7.23 (d, $^3J_{HH} = 8.2$ Hz, H2$_{tol}$), 7.52 (d, H3$_{tol}$); ^{13}C NMR: $\delta = 4.0$ (Si(CH$_3$)$_2$), 7.1 (HC(Si...)$_3$), 20.9 (4-CH$_3$C$_6$H$_4$), 87.6 (C$_5$H$_5$), 126.1, 130.0, 132.2, 149.5 (C2, C4, C3, C1 tolyl), 202.8 (CO); ^{29}Si NMR: $\delta = 2.6$; IR(KBr): ν(CO) = 1990(s), 1932(s)

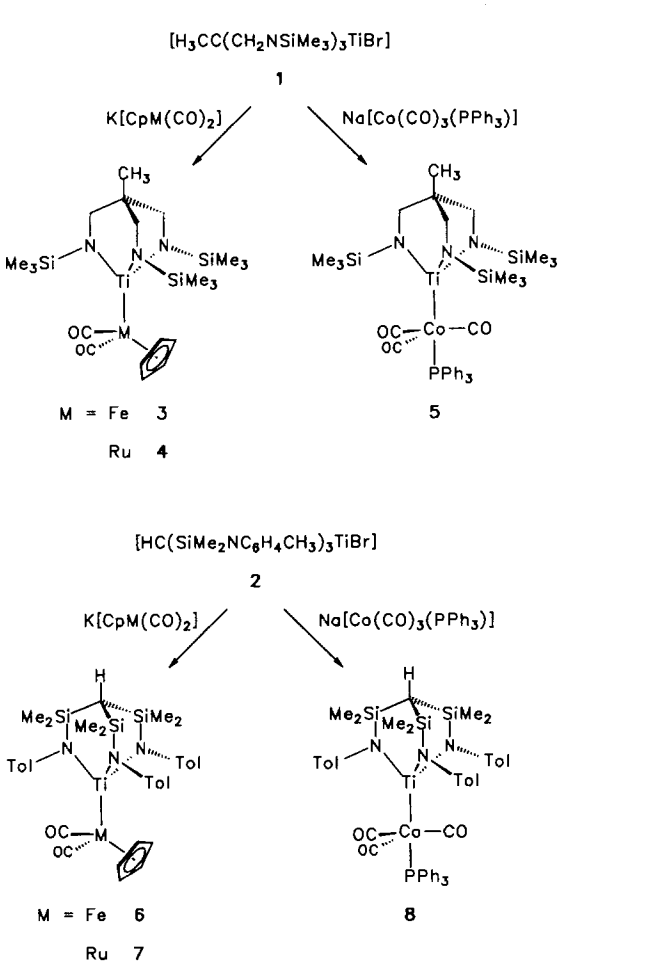
8: ^{1}H NMR: $\delta = -0.53$ (s, HC(Si...)$_3$), 0.43 (s, Si(CH$_3$)$_2$), 2.28 (s, 4-CH_3C$_6$H$_4$), 6.69–6.99 (m, phenyl), 7.19 (d, $^3J_{HH} = 8.0$ Hz, H2$_{tol}$), 7.61 (d, H3$_{tol}$); ^{13}C NMR: $\delta = 4.2$ (Si(CH$_3$)$_2$), 8.6 (HC(Si...)$_3$), 21.1 (4-CH$_3$C$_6$H$_4$), 125.7, 129.4, 132.0, 150.5 (C2, C4, C3, C1 tolyl), 129.3, 129.8, 133.4 (d, $^2J_{PC} = 12.5$ Hz), 134.4 (d, $^1J_{PC} = 40.0$ Hz) (C4, C3, C2, C1, phenyl), 205.1 (d, $^2J_{PC} = 16.4$ Hz, CO); ^{29}Si NMR: $\delta = 3.8$; ^{31}P NMR: $\delta = 56.7$; IR(benzene): ν(CO) = 2003(w), 1938(vs)

The existence of Ti–M bonds in **3**–**8** was initially established by IR spectroscopy. The ν_{CO} bands of the dimers are shifted to higher wavenumbers relative to those of the alkali metal salts of the anions,[8, 9] as would be expected for metal–metal bonded structures (Table 1). The absence of ν_{CO} absorptions attributable to bridging carbonyl or isocarbonyl ligands supports the structural arrangements shown in Scheme 1. Free rotation about the Ti–M bonds is inferred from the effective threefold symmetry of the titanium–amide moiety observed in the NMR spectra. Cooling solutions of **3**, **4**, **6** and **7** in [D$_8$]toluene 190 K leads to a broadening of the resonances assigned to the amido ligand; however, it proved impossible to reach the low temperature limit.

Single crystal X-ray structure analyses of **3** and **4**[10] have established that while the compounds differ significantly with regard to their packing in the crystal and thus space group symmetry, their molecular structures are very similar (Fig. 2). The central structural unit is the free Ti–M bond (M = Fe, Ru), which is effectively shielded by the tripodal amido ligand at the Ti center as well as the set of ligands coordinated to the late

[*] Dr. L. H. Gade, S. Friedrich, H. Memmler
Institut für Anorganische Chemie der Universität
Am Hubland, D-97074 Würzburg (FRG)
Telefax: Int. code + (931)888 4605
W.-S. Li, Prof. M. McPartlin
School of Chemistry, University of North London
Holloway Road, GB-London N7 8DB (UK)

[**] This work was supported by the Fonds der Chemischen Industrie (L. H. G.), the Deutsche Forschungsgemeinschaft (L. H. G., S. F.) and the Scientific and Engineering Research Council (SERC) (M. McP.). We thank Prof. H. Werner for his support. We are also grateful to Wacker Chemie AG and Degussa AG for gifts of basic chemicals.



Scheme 1. Condensation of **1** (type **A**) and **2** (type **B**) with late transition metal carbonylates.

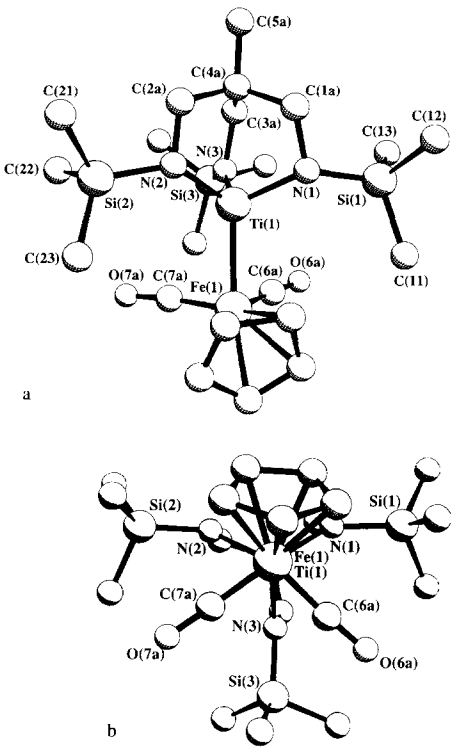


Fig. 2. a) Molecular structure of **3**; b) view along the Fe–Ti axis of **3**. Selected mean bond lengths [Å] and interbond angles [°] for the two independent molecules in the asymmetric unit: Ti-Fe 2.433(5), Fe-C6 1.73(2), Fe-C7 1.68(2), Ti-N1 1.90(2), Ti-N2 1.88(2), Ti-N3 1.89(2); Ti-Fe-C6 81.3(8), Ti-Fe-C7 83.8(8), C6-Fe-C7 96(1), Fe-Ti-N1 114.1(5), Fe-Ti-N2 116.1(5), Fe-Ti-N3 117.3(6). Corresponding bond parameters of **4**, which has a very similar molecular structure (but only one molecule in the asymmetric unit): Ti-Ru 2.527(1), Ru-C6 1.840(9), Ru-C7 1.835(9), Ti-N1 1.907(5), Ti-N2 1.905(6), Ti-N3 1.907(6); Ti-Ru-C6 79.6(3), Ti-Ru-C7 81.9(3), C6-Ru-C7 93.1(4), Ru-Ti-N1 118.1(2), Ru-Ti-N2 115.3(2), Ru-Ti-N3 113.1(2).

transition metal. The average Ti–Fe distance of 2.433 Å in the structure of **3** and the Ti–Ru distance of 2.527(1) Å in that of **4** are significantly shorter than the corresponding bond lengths observed in $[Cp(CO)_2MTi(NMe_2)_3]$ [d_{av}(Ti–Fe) = 2.568,[4b] d(Ti–Ru) = 2.663(1) Å][11a] and $[Cp(CO)_2RuTi(NMe_2)(2,6\text{-}Me_2C_6H_3O)_2]$ [d(Ti–Ru) = 2.573(1) Å].[11b] In fact, the Ti–Fe bond length in **3** is the shortest hitherto observed for an unsupported transition metal–metal single bond in a molecule,[12] a consequence both of the high bond polarity and the low steric hindrance of the two halves of the molecule.[13]

The essentially linear carbonyl ligands lean markedly towards the Ti atoms [mean Ti-Fe-CO 82.6° (**3**); mean Ti-Ru-CO 80.8° (**4**)], but the Ti $\cdots$ CO distance of about 2.8 Å in each compound precludes any "semi-bridging" interaction[14] and indicates that the disposition of these ligands is largely determined by the steric requirements of the bulky cyclopentadienyl group. Repulsion between this ligand and the large N-bonded Me_3Si groups at the other side of the Ti–Fe or Ti–Ru bond results in two silyl groups being forced apart (as can be seen in Fig. 2b), thus breaking the otherwise threefold symmetry of the Ti complex fragment. The polydentate triamido ligand is clearly sufficiently flexible to accommodate these distortions without a significant destabilization of the bimetallic molecule.

In order to establish the basic structural arrangement in the bimetallic complexes derived from **2**, an X-ray structure analysis of **7** was carried out (Fig. 3).[15] A striking feature is the lampshade arrangement of the tripodal amide in which the tolyl groups are oriented almost orthogonally to the radial planes spanned by the Ti, N, and Si atoms.[16] That this orientation of the amido tolyl groups is retained in solution may be inferred from the shift of the signals of the Cp protons in the ^{1}H NMR spectrum of **7** to higher field (δ = 4.07 in comparison to 4.99 in **4**). The Ti–Ru bond therefore appears less shielded than in **4**, and it may be due to this situation that the metal–metal bond [d(Ti–Ru) = 2.503(4) Å] is even shorter than that observed in **4**. All other structural features related to the metal–metal bond

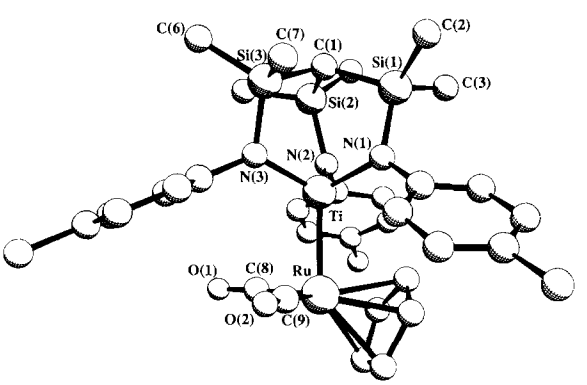


Fig. 3. Molecular structure of **7** in the crystal. Selected bond lengths [Å] and interbond angles [°]: Ti-Ru 2.503(4), Ru-C8 1.81(2), Ru-C9 1.80(2), Ti-N1 1.93(1), Ti-N2 1.90(1), Ti-N3 1.90(1); Ti-Ru-C8 87.8(7), Ti-Ru-C9 88.4(8), C8-Ru-C9 91.2(8), Ru-Ti-N1 113.9(4), Ru-Ti-N2 112.7(5), Ru-Ti-N3 117.7(5).

resemble those of **3** and **4**. In view of the similarity of the NMR data of **6** and **7** as well as the band-to-band analogy of the IR spectra, an almost identical structure may be assumed for the Fe analogue **6**.

The general applicability of the concept of Ti–M bond stabilization by use of Ti complex fragments containing polydentate amido ligands was demonstrated by the synthesis of the Ti–Co species **5** and **8**. Stable dinuclear compounds with this structural element have been elusive until recently[17] due to their extreme thermal lability. Both **5** and **8** can be readily handled in solution and were found to be sufficiently stable at ambient temperature to enable a systematic investigation into their reactivity.[18] In general, type **A** and **B** Ti amides therefore appear to "do the trick" in stabilizing Ti–M (M = late transition metal) heterobimetallics.

Experimental Procedure

2: A 2.5 M solution of *n*-butyllithium in hexanes (5.72 mL) was added to a mixture of $HC(SiMe_2NHC_6H_4CH_3)_3$ (2.41 g, 4.72 mmol) [5b] in pentane (30 mL) and diethyl ether (2 mL), which was cooled at −50 °C. The reaction mixture was subsequently warmed and stirred at room temperature for 2 h. The resulting lithium amide suspension was then cooled to −50 °C, solid $[TiBr_4(thf)_2]$ (2.69 g = 5.25 mmol) was added, and the reaction mixture warmed to room temperature over 20 h. Evaporation of the solvent, extraction of the residue with toluene (20 mL), and filtration yielded a deep red filtrate, which was concentrated to 10 mL and stored at −40 °C to yield **2** as red crystals. Yield: 1.65 g (55%).

3–**8**: Solid alkali carbonyl metalate (1 mmol) was added to a solution of **1** or **2** (1 mmol; for **1** 458 mg, for **2** 631 mg) in toluene (30 mL) cooled at −70 °C, and the reaction mixture warmed to room temperature over a period of 20 h. Evaporation of the solvent, extraction of the residue with pentane (20 mL), and subsequent filtration yielded yellow-orange solutions of the heterobimetallic complexes. Evaporation of the solvent yielded the reaction products as microcrystalline solids, which were washed with cold pentane; isolated yields: **3** 59%, **4** 68%, **5** 48%, **6** 61%, **7** 73%, **8** 39%. Single crystals suitable for X-ray crystallography were obtained by slow cooling of solutions of the compounds in toluene.

Received: October 13, 1993 [Z 6414 IE]
German version: *Angew. Chem.* **1994**, *106*, 705

[1] W. M. P. B. Menge, J. G. Verkade, *Inorg. Chem.* **1991**, *30*, 4628; A. A. Naiini, W. M. P. B. Menge, J. G. Verkade, *ibid.* **1991**, *30*, 5009; J. G. Verkade, *Acc. Chem. Res.* **1993**, *26*, 483.

[2] C. C. Cummins, R. R. Schrock, W. M. Davis, *Organometallics* **1992**, *11*, 1452; C. C. Cummins, J. Lee, R. R. Schrock, W. M. Davis, *Angew. Chem.* **1992**, *104*, 1510; *Angew. Chem. Int. Ed. Engl.* **1992**, *31*, 1501; C. C. Cummins, R. R. Schrock, W. M. Davis, *ibid.* **1993**, *105*, 758 and **1993**, *32*, 756.

[3] D. W. Stephan, *Coord. Chem. Rev.* **1989**, *95*, 41.

[4] a) C. P. Casey, *J. Organomet. Chem.* **1990**, *400*, 205 and references therein; b) W. J. Sartain, J. P. Selegue, *Organometallics* **1987**, *6*, 1812.

[5] a) L. H. Gade, N. Mahr, *J. Chem. Soc. Dalton Trans.* **1993**, 489; b) L. H. Gade, C. Becker, J. W. Lauher, *Inorg. Chem.* **1993**, *32*, 2308.

[6] a) S. Friedrich, L. H. Gade, A. J. Edwards, M. McPartlin, *Chem. Ber.* **1993**, *126*, 1797; b) *J. Chem. Soc. Dalton Trans.* **1993**, 2861.

[7] Bürger et al. have reported the unsuccessful attempt to coordinate the in situ lithiated $HC(SiMe_2NHMe)_3$ to titanium(IV) centers: a) H. Bürger, R. Mellies, K. Wiegel, *J. Organomet. Chem.* **1977**, *142*, 55. We have found that the use of various aryl-substituted amines of this type leads to stable titanium complexes: b) H. Memmler, L. H. Gade, J. W. Lauher, *Inorg. Chem.*, submitted.

[8] The only known example of a titanium compound of that type, Selegue's $[Cp(CO)_2FeTi(NMe_2)_3]$, was reported to decompose rapidly in solution at ambient temperature [4b]. Casey et al. reported the synthesis of $[Cp_2Zr(R)\{Fe(CO)_2Cp\}]$ (R = CH_3, O*t*Bu) and $[Cp_2Zr\{Fe(CO)_2Cp\}_2]$. The latter is only stable in solution at temperatures below −20 °C: C. P. Casey, R. F. Jordan, A. L. Rheingold, *J. Am. Chem. Soc.* **1983**, *105*, 665; *Organometallics* **1984**, *3*, 504.

[9] M. Brookhart, W. B. Studabaker, R. Husk, *Organometallics* **1987**, *6*, 1141.

[10] Crystals of **3** suitable for X-ray studies were difficult to obtain and diffracted only poorly. This resulted in relatively high standard deviations on all parameters, but the main features of the structure are well established. Crystal data of **3**: $C_{21}H_{41}N_3O_2Si_3TiFe$, monoclinic, space group $P2_1/n$, $a = 15.496(3)$, $b = 12.983(3)$, $c = 29.219(3)$ Å, $\beta = 104.518(2)°$, $M = 555.57$, $V = 5690.71$ Å^3, $Z = 8$, $\varrho_{calcd} = 1.297$ g cm^{-3}, $F(000) = 2352$, $R = 0.0699/R_w = 0.0709$ for 2101 reflections with $I/\sigma(I) > 3.0$ corrected for absorption [$\mu(Mo_{K\alpha}) = 9.1$ cm^{-1}]. Crystal data of **4**: $C_{21}H_{41}N_3O_2Si_3TiRu$, monoclinic, space group $P2_1/c$, $a = 12.977(3)$, $b = 12.084(3)$, $c = 18.217(3)$ Å, $\beta = 91.33(2)°$, $M = 600.73$, $V = 2855.91$ Å^3, $Z = 4$, $\varrho_{calcd} = 1.397$ g cm^{-3}, $F(000) = 1248$, $R = 0.0484/R_w = 0.0518$ for 2903 reflections with $I/\sigma(I) > 3.0$ corrected for absorption [$\mu(Mo_{K\alpha}) = 9.0$ cm^{-1}].

[11] a) W. S. Sartain, J. P. Selegue, *J. Am. Chem. Soc.* **1985**, *107*, 5818; b) *Organometallics* **1989**, *8*, 2153.

[12] Cambridge Structural Database, Cambridge University, **1993**.

[13] Whether d_π–d_π backbonding plays a role in these heterobimetallics as invoked for the ligand-bridged Zr–Rh complex $[Cp^*Zr(\mu\text{-}OCH_2Ph_2P)_2RhMe_2]$ [*d*(Zr–Rh) = 2.444(1) Å] (G. S. Ferguson, P. T. Wolczanski, L. Párkányi, M. C. Zonnevylle, *Organometallics* **1988**, *7*, 1967) remains to be investigated in MO calculations of appropriate model systems.

[14] See, for example, F. A. Cotton, *Prog. Inorg. Chem.* **1976**, *21*, 1; F. A. Cotton, J. M. Troup, *J. Am. Chem. Soc.* **1974**, *96*, 1233; W. I. Bailey, D. M. Collins, F. A. Cotton, *J. Organomet. Chem.* **1977**, *135*, C53.

[15] Crystal data of **7**: $C_{35}H_{45}N_3O_2Si_3TiRu$, monoclinic, space group $I2/c$, $a = 24.473(3)$, $b = 15.417(3)$, $c = 20.783(4)$ Å, $\beta = 104.20(2)°$, $M = 772.92$, $V = 7601.84$ Å^3, $Z = 8$, $\varrho_{calcd} = 1.351$ g cm^{-3}, $F(000) = 3200$, $R = 0.0663/R_w = 0.0667$ for 1904 reflections with $I/\sigma(I) > 3.0$ corrected for absorption [$\mu(Mo_{K\alpha}) = 6.9$ cm^{-1}]. Further details of the crystal structures are available on request from the Director of the Cambridge Data Centre, 12 Union Road, Cambridge CB2 1EZ, UK on quoting the full journal citation.

[16] A preliminary X-ray structure analysis of the sterically less crowded precursor **2** has revealed a similar arrangement of the tolyl groups [7b], which is therefore not to be interpreted as solely a consequence of the steric interaction with the Ru complex fragment.

[17] D. Selent, R. Beckhaus, J. Pickardt, *Organometallics* **1993**, *12*, 2857. The only other structurally characterized example of a compound containing an unsupported Ti–Co bond was reported by G. Schmid, B. Stutte, R. Boese, *Chem. Ber.* **1978**, *111*, 1239.

[18] If solutions of **5** or **8** in benzene are stirred at room temperature over a period of *several days*, slow decomposition sets in and generates $[\{Co(CO)_3(PPh_3)\}_2]$ which precipitates from the solution.

Direct Metal–Metal Bonds Between High and Low Valent Complex Fragments: The Reaction of Metal Bases with the Metal Acids $[Re(NR)_3]^+$ and $[Mo(NR)_2]^{2+}$ **

Jörg Sundermeyer,* Diane Runge, and John S. Field

Dedicated to Professor Wolfgang Sundermeyer on the occasion of his 65th birthday

The synthesis of heterobimetallic complexes in which a metal center deficient in d-electrons (f block element, metal of the group 4 or 5) with a complex fragment rich in d-electrons (typically a metal of group 8) fixed in close proximity is enjoying steadily growing interest. The combination of antipodes of the periodic system (early–late heterobimetallics)[1] holds the promise of cooperative behavior on the part of the metal centers in the activation of smaller molecules,[2] an increased catalytic activity in the homogeneous phase, or at least an insight into the interaction of immobilized catalysts with oxide support materials.[3] Comparable synergistic effects could also be achieved by the combination of the same metal, or of two metals close to one another

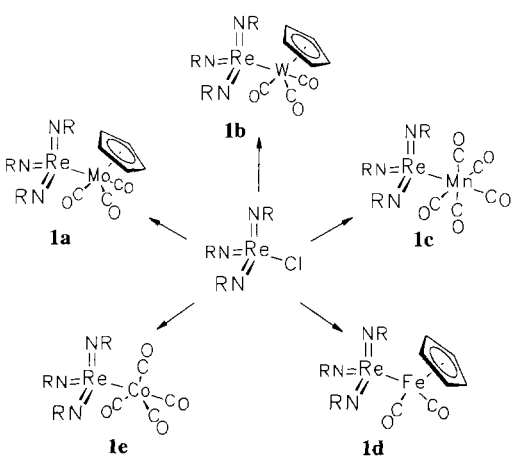
[*] Dr. J. Sundermeyer, Dipl.-Chem. D. Runge
Institut für Anorganische Chemie der Universität
Am Hubland
D-97074 Würzburg (FRG)
Telefax: Int. code + (931)888-4605
Prof. J. S. Field
Department of Chemistry and Chemical Technology
University of Natal
P. O. Box 375, Pietermaritzburg 3200 (South Africa)

[**] Höhervalente Derivate der d-Metall-Säuren, Part 9. This work was supported by the Deutsche Forschungsgemeinschaft, the Fonds der Chemischen Industrie, the South African Foundation for Research Development, and the University of Natal. We would like to thank Prof. Helmut Werner for his support and Dr. Lutz Gade for his expert debates. Part 8: J. Sundermeyer, K. Weber, K. Peters, H. G. von Schnering, *Organometallics*, submitted.

in the periodic system. A prerequisite for this, however, is that one metal center may be considered as electron-deficient because of its formally high oxidation state ($\geq +5$), the other as low valent and electron-rich (oxidation state +1, 0). Unequivocal evidence of a direct interaction between the metal atoms would be a M–M′ bond wholly unsupported by bridging ligands. The only compound which, to our knowledge, fulfills these criteria, is the complex [Cp*W(O)$_2$–W(CO)$_3$Cp*] (Cp* = η^5-C$_5$Me$_5$), which was synthesized by autoxidation of [{Cp*W(CO)$_2$}$_2$] by H. Alt et al.[4] This was reason enough for us to search for synthesis strategies for the isoelectronically related compounds of the type [L$_x$(O)$_y$M]–[M′(CO)$_m$L′$_n$] and [L$_x$(RN)$_y$M]–[M′(CO)$_m$L′$_n$].

Nucleophilic substitution reactions compete with electron-transfer processes in the reaction of electron-deficient oxo complexes with potentially reducing nucleophiles as a matter of course. The selectivity in favor of the substitution increases when the oxo function, O^{2-}, is replaced by the isoelectronic, yet more strongly π-basic imido function, $(RN)^{2-}$. A very fruitful branch of organometallic chemistry has developed in the last few years, in which reactions of high valent imido complexes with carbanions[5–7] and phosphorus ylides [8], as well as the activation of C–H bonds,[9] stand in the foreground. The imido function continued to prove itself as a useful protecting group in the masking of oxo functions, for example in the synthesis of organometallic functionalized oxometalates, such as NBu$_4$[Cp*MO$_3$] (M = Mo, W)[7] through selective hydrolysis of the imido precursors. For this reason, we directed our attention primarily at metalated imido complexes.

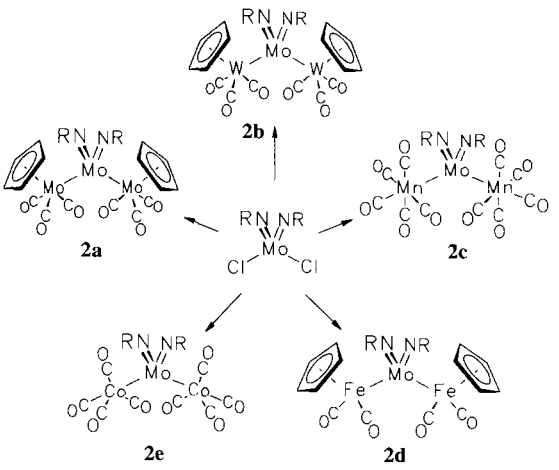
Recent works by R. R. Schrock,[10] G. Wilkinson,[11] and M. L. H. Green[12] report that, in the reduction of high valent imido complexes with Na/Hg or [Co$_2$(CO)$_8$], Re–Hg, Re–Co and Mo–Hg bonds can be formed. A first early–late heterobimetallic complex containing bridging imido ligands has just been described by R. G. Bergman et al.[13] In the following we report on a series of bimetallic compounds which have been prepared in good yields in targeted syntheses by reactions of [Re(N*t*Bu)$_3$Cl][5b] and [Mo(N*t*Bu)$_2$Cl$_2$][5c] with carbonyl metalates of groups 6–8 (Schemes 1 and 2). Compounds **1a–e** and



Scheme 1. Reaction of [(*t*BuN)$_3$ReCl] with the carbonyl metalates.

2a–e were obtained in adequate purity for analytical purposes after workup by sublimation, crystallization, or column chromatography. A selection of spectroscopic and analytical data is shown in Table 1.

The absence of a tendency for the complexes to form clusters of higher nuclearity by loss of carbonyl groups under normal conditions, as is observed in the reaction of [Re(N*t*Bu)$_3$Cl] with [Co$_2$(CO)$_8$],[11] is rather surprising. Only rotamers can be identified spectroscopically; no isomers with bridging carbonyl, isocarbonyl,[14] or imido ligands can be identified even at low temperatures. This explains why no spontaneous redox reaction takes place through intramolecular ligand exchange under normal conditions.[15]



Scheme 2. Reaction of [(*t*BuN)$_2$MoCl$_2$] with the carbonyl metalates.

Compounds **1a–e** and **2a–e** are formed by metalation of the formally heptavalent and hexavalent cationic Lewis acids, $[Re(NR)_3]^+$ and $[Mo(NR)_2]^{2+}$ respectively, with carbonyl complex fragments isolobal with CH_3^-. The compounds **1a–e** can be described as a combination of a 16 VE (valence electron) and an 18 VE building block. The donor and acceptor centers are connected to one another by a polar metal–metal bond, which is not supported by ligand bridges. The recently reported homobinuclear d^1–d^1 dimer [(ArN)$_3$Tc–Tc(NAr)$_3$] (Ar = 2,6-*i*Pr$_2$C$_6$H$_3$)[16] is comparable in its overall electron balance. In contrast, **2a–e** are electronically unsaturated. Even if both imido ligands are considered as using their donor capability to the full extent, that is, one σ and two π bonds each, only 16 VE can be assigned to the central molybdenum atom in each case. The difference $\Delta\delta$ in the ^{13}C resonance signals of the quaternary and primary carbon atoms in *tert*-butylimido complexes is a useful spectroscopic probe for the estimation of the electron density on the metallic center.[17] The $\Delta\delta$ values for **1a–e** and **2a–e** correlate with the M′H acidities of the corresponding metal carbonyl hydrides.[18] As the metal basicity and σ-donor ability (nucleophilicity) of metal carbonyl fragments are influenced to varying extents by steric factors, a tendency,[19] but not a linear correlation of $\Delta\delta$(M=N*t*Bu)/pK_s(M′H), can be recognized (Table 1).

Additional evidence for the structures given in Schemes 1 and 2 is provided by the results of crystal structure analyses on single crystals of **1a** (Fig. 1) and **2a** (Fig. 2).[20] The molecular framework of **1a** has C_s symmetry in the crystalline state. A mirror plane runs through the atoms Re, Mo, C2, O2, C8, N1, and C9. The Re–Mo distance of 2.844(1) Å is considerably shorter than comparable Re–Mo single bonds. The metal–metal bond of 3.12 Å in [(OC)$_5$Re–Mo(CO)$_3$Cp][21] for example, in which none of the ligands plays a bridging role, or the asymmetrical CO-bridged bond of 2.959(1) Å in [CpRe(μ-CO)$_2$MoCp$_2$][22] are significantly longer. Considered separately, neither of the metal

Table 1. Experimental data from **1** and **2**.

Compound (R = *t*Bu)	ν(CO) [a]	ν(M = NC) [b]	$\delta(C_\alpha)$	$\delta(C_\beta)$	$\Delta\delta$ [c]	pK_s [d]	M^+ [e] ($M^+ - CO$)	Color, Yield, M.p.
$[(RN)_3Re-Mo(CO)_3Cp]$	1993 vs, 1924 s,	1228 s	68.65	30.90	37.75	13.9	645.0	yellow, 72%,
1a	1912 vs	1211 s						121 °C [f]
$[(RN)_3Re-W(CO)_3Cp]$	1992 vs, 1916 s,	1226 s	68.61	30.78	37.83	16.1	(705.1)	yellow, 64%,
1b	1909 vs	1211 s						134 °C
$[(RN)_3Re-Mn(CO)_5]$	2079 m, 1997 vs,	1227 s	69.03	31.00	38.03	15.1	594.8	yellow, 34%,
1c	1990 s	1209 s						56 °C
$[(RN)_3Re-Fe(CO)_2Cp]$	1994 vs, 1949 vs	1229 s	67.63	31.34	36.29	19.4	577.2	orange-yellow, 83%,
1d		1211 s						105 °C
$[(RN)_3Re-Co(CO)_4]$	2072 s, 2011 s,	1225 s	69.03	30.71	38.32	8.3	570.9	orange, 91%,
1e	1994 vs	1205 s						63 °C
$[(RN)_2Mo\{Mo(CO)_3Cp\}_2]$	2023 m, 1982 vs,	1240 s	71.99	30.96	41.03	13.9	731.7	orange, 43%,
2a	1946 s, 1912 m,	1202 s						172 °C [f]
	1888 m							
$[(RN)_2Mo\{W(CO)_3Cp\}_2]$	2022 s, 1962 s,	1242 s	71.62	30.66	40.96	16.1	(876.0)	orange, 31%,
2b	1939 vs, 1913 s,	1204 s						199 °C [f]
	1903 m							
$[(RN)_2Mo\{Mn(CO)_5\}_2]$	2079 m, 2054 s,	1231 s	72.16	31.43	40.73	15.1	-	dark red, 63%,
2c	2019 m, 1989 vs,	1200 s						64 °C [f]
	1971 vs, 1926 m							
$[(RN)_2Mo\{Fe(CO)_2Cp\}_2]$	1978 s, 1969 vs,	1247 s	68.78	31.83	36.95	19.4	593.8	orange, 71%,
2d	1926 vs	1204 s						144 °C [f]
$[(RN)_2Mo\{Co(CO)_4\}_2]$	2078 m, 2059 vs	1239 s	72.84	30.97	41.87	8.3	581.7	red, 66%,
2e	2039 s, 2017 s, 1999 vs	1202 s						68 °C [f]

[a] In cm^{-1}; **1a–e**, **2c–e** in *n*-hexane. **2a, b** in methylcyclohexane. [b] In cm^{-1}; nujol mull. [c] $^{13}C\{^1H\}$ NMR (100.6 MHz): **1a–e**, **2d** in $CDCl_3$; **2a–c, e** in C_6D_6: $C_\alpha = CMe_3$, $C_\beta = CMe_3$, $\Delta\delta = \delta(C_\alpha)-\delta(C_\beta)$. [d] p$K_s$ of M'H [18]. [e] EI-MS (70 eV); most intensive signal shown, correct isotope distribution. [f] decomposition.

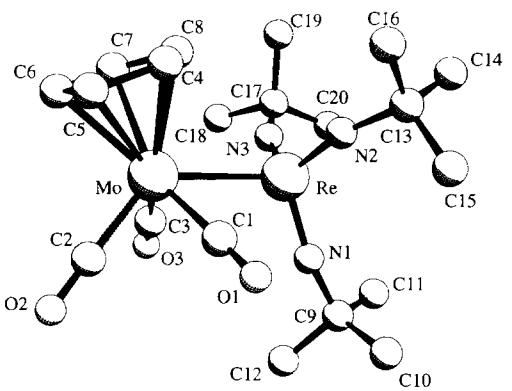


Fig. 1. Crystal structure of **1a** (SCHAKAL image [20d]): View perpendicular to the mirror plane; selected distances [Å] and angles [°]: Re-Mo 2.844(1), Re-N1 1.720(13), Re-N2 1.737(14), Re-N3 1.760(15), Mo-C1 2.01(2), Mo-C2 1.97(2), Mo-C3 1.96(2); Mo-Re-N1 108.8(4), Mo-Re-N2 103.4(4), Mo-Re-N3 104.0(4), N1-Re-N2 111.9(7), N1-Re-N3 112.1(7), N2-Re-N3 115.7(7), Re-N1-C9 165.6(12), Re-N2-C13 164.0(11), Re-N3-C17 164.2(13), C1-Mo-C3 105.2(7), Re-Mo-C2 128.9(4).

complex fragments is found to deviate characteristically from known structures of the respective homonuclear complexes.[5b, 23] Compound **2a** has crystallographically imposed C_2 symmetry. The Mo1 center has distorted tetrahedral coordination; the two-fold screw axis bisects the extended angles Mo2-Mo1-Mo2′ and N-Mo1-N′ (124.7(1)° and 114.6(6)°, respectively). The carbonyl groups C1–O1 and C2–O2 formally fulfill the criteria[24] for semibridging CO ligands. This can be regarded as a possible mechanism by which the molecule compensates the different charge densities on the Mo1 and Mo2 centers. The interactions are so weak, however, that they can equally plausibly be explained by the forced spatial proximity of four CO groups to the sterically shielded Mo1 center. The Mo1–Mo2 distance of 2.875(1) Å is considerably shorter than other known Mo–Mo single bond values in the absence of ligand bridges. Examples are $[Cp(CO)_3Mo-Mo(CO)_3Cp]$[23] (3.235(1) Å) and $[CpMo(CO)_3Mo-Mo(CAr_2)(NNCAr_2)Cp]$[24] (3.052(1) Å).

We assume that the very short M–M distances are due to coulombic forces; more precisely, due to the electrostatic attraction in the dipolar structural unit $M^{\delta+}-Mo^{\delta-}$. The smaller radii of Re^{7+}/Re^{6+} and Mo^{6+}/Mo^{4+} as compared to the zero valent and monovalent metal centers also contribute to the shortening of the M–M bond. Just how large the difference between formal oxidation state and the distribution of real charge density actually is in these simply built, symmetrical molecules remains a domain reserved for the analysis of photoelectron spectra and quantum mechanical calculations.

The electronically unsaturated character and the low coordination number of the central diimido unit in compounds **2a–e** promises further interesting chemistry when these are used as starting materials. We have these reactions currently under investigation with particular attention to the linking of imido and

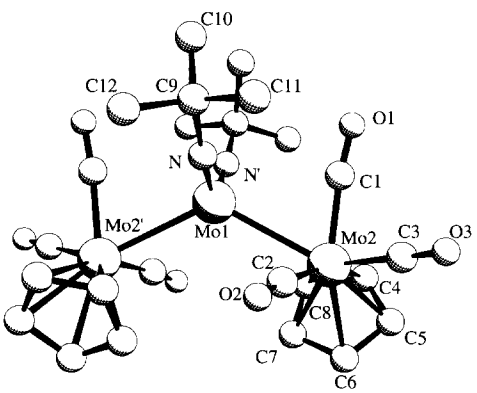


Fig. 2. Crystal structure of **2a** (SCHAKAL image [20d]): View perpendicular to the crystallographically imposed C_2 axis; selected distances [Å] and angles [°]: Mo1-Mo2 2.875(1), Mo1-N 1.721(8), Mo2-C1 1.983(12), Mo2-C2 1.939(11), Mo2-C3 1.999(13); Mo2-Mo1-N 101.9(3), Mo2-Mo1-Mo2′ 124.7(1), N-Mo1-N′ 114.6(6), Mo1-N-C9 166.5(8); Mo1-Mo2-C3 127.6(3), C1-Mo2-C2 102.2(5).

 © VCH Verlagsgesellschaft mbH, D-69451 Weinheim, 1994 0570-0833/94/0606-0680 $ 10.00+.25/0 Angew. Chem. Int. Ed. Engl. 1994, 33, No. 6

carbonyl ligands through the mediation of the metal centers to give isocyanates. It is also hoped that selective hydrolysis or metathesis reactions will provide a general preparative route to mixed metal carbonyl–oxo complexes containing M–M′ bonds. Furthermore, the especially volatile compounds **1a–e**, **2c**, and **2e** are promising starting materials for the deposition of thin layers $[M_mM'_nN_x]$ from the gas phase using the metal-organic chemical vapor deposition technique.

Received: October 15, 1993 [Z 6424 IE]
German version: *Angew. Chem.* **1994**, *106*, 679

[1] D. W. Stephan, *Coord. Chem. Rev.* **1989**, *95*, 41–107.
[2] R. M. Bullock, C. P. Casey, *Acc. Chem. Res.* **1987**, *20*, 167–173.
[3] a) B. Imelik, C. Naccache, G. Coudurier, H. Praliaud, P. Gallezot, G. A. Martin, J. C. Verdrine, *Metal-Support and Metal-Additive Effects in Catalysis*, Elsevier, New York, **1982**; b) V. W. Day, W. G. Klemperer, *Science* **1985**, *228*, 533–541.
[4] a) H. G. Alt, H. I. Hayen, R. D. Rogers, *J. Chem. Soc. Chem. Commun.* **1987**, 1795–1796; b) H. G. Alt, H. I. Engelhardt, H. I. Hayen, R. D. Rogers, *J. Organomet. Chem.* **1989**, *366*, 287–295; c) $[Cp^*Re_2(O)_2(CO)_3]$, an intermediate in the photo-oxidation of $[Cp^*Re(CO)_3]$, very probably has a structure containing a symmetrically bridging oxo ligand and a semibridging CO ligand. This ligand arrangement leads to a Re^{II}/Re^{IV} species and not to the more polar Re^{I}/Re^{V}: W. A. Herrmann, *ibid.* **1986**, *300*, 111–137.
[5] Selected examples: a) M. B. Hursthouse, M. Motevalli, A. C. Sullivan, G. Wilkinson, *J. Chem. Soc. Chem. Commun.* **1986**, 1398–1399; b) A. A. Danopoulos, C. J. Longley, G. Wilkinson, B. Hussain, M. B. Hursthouse, *Polyhedron* **1989**, *8*, 2657–2670; c) G. Schoettel, J. Kress, J. A. Osborn, *J. Chem. Soc. Chem. Commun.* **1989**, 1062–1063; d) N. Meijboom, C. J. Schaverien, A. G. Orpen, *Organometallics* **1990**, *9*, 774–782; e) R. R. Schrock, R. T. DePue, J. Feldman, K. B. Yap, D. C. Yang, W. M. Davis, L. Park, M. DiMare, M. Schofield, J. Anhau, E. Walborsky, E. Evitt, C. Krüger, P. Betz, *ibid.* **1990**, *9*, 2262–2275; f) R. R. Schrock, J. S. Murdzek, G. C. Bazan, J. Robbins, M. DiMare, M. O'Regan, *J. Am. Chem. Soc.* **1990**, *112*, 3875–3886; g) W. A. Herrmann, G. Weichselbaumer, R. A. Paciello, R. A. Fischer, E. Herdtweck, J. Okuda, D. W. Marz, *Organometallics* **1990**, *9*, 489–496.
[6] a) J. Sundermeyer, *Chem. Ber.* **1991**, *124*, 1977–1979; b) U. Radius, J. Sundermeyer, *ibid.* **1992**, *125*, 2183–2186.
[7] a) J. Sundermeyer, U. Radius, C. Burschka, *Chem. Ber.* **1992**, *125*, 2379–2384; b) M. S. Rau, C. M. Kretz, G. L. Geoffroy, A. L. Rheingold, *Organometallics* **1993**, *12*, 3447–3460.
[8] a) J. Sundermeyer, K. Weber, O. Nürnberg, *J. Chem. Soc. Chem. Commun.* **1992**, 1631–1633; b) J. Sundermeyer, K. Weber, H. Pritzkow, *Angew. Chem.* **1993**, *105*, 751–753; *Angew. Chem. Int. Ed. Engl.* **1993**, *32*, 731–733; c) L. K. Johnson, M. Frey, T. A. Ulibarri, S. C. Virgil, R. H. Grubbs, J. W. Ziller, *J. Am. Chem. Soc.* **1993**, *115*, 8167–8177.
[9] a) C. C. Cummins, S. M. Baxter, P. T. Wolczanski, *J. Am. Chem. Soc.* **1988**, *110*, 8731–8733; b) C. C. Cummins, C. P. Schaller, G. D. Van Duyne, P. T. Wolczanski, A. W. E. Chan, R. Hoffmann, *ibid.* **1991**, *113*, 2985–2994; c) P. J. Walsh, F. J. Hollander, R. J. Bergman, *ibid.* **1988**, *110*, 8729–8731; d) P. J. Walsh, A. M. Baranger, R. J. Bergman, *ibid.* **1992**, *114*, 1708–1719; e) D. S. Glueck, J. Wu, F. J. Hollander, R. G. Bergman, *ibid.* **1991**, *113*, 2041–2054; f) J. de With, A. D. Horton, *Angew. Chem.* **1993**, *105*, 958–960; *Angew. Chem. Int. Ed. Engl.* **1993**, *32*, 903–905.
[10] D. S. Williams, J. T. Anhaus, M. H. Schofield, R. R. Schrock, W. M. Davis, *J. Am. Chem. Soc.* **1991**, *113*, 5480–5481.
[11] V. Saboonchian, A. Gutierrez, G. Wilkinson, B. Hussain-Bates, M. B. Hursthouse, *Polyhedron* **1991**, *10*, 1423–1425.
[12] M. L. H. Green, P. Konidaris, P. Mountford, S. J. Simpson, *J. Chem. Soc. Chem. Commun.* **1992**, 256–259.
[13] A. M. Baranger, F. J. Hollander, R. G. Bergman, *J. Am. Chem. Soc.* **1993**, *115*, 7890–7891.
[14] Isocarbonyl bridges [M′]–C≡O–[M] are often found for very hard Lewis acids [M], or for [M] fragments with high steric requirements. They are a result of the ambident character of the metal nucleophiles. For a representative example, see D. M. Hamilton, Jr., W. S. Willis, G. D. Stucky, *J. Am. Chem. Soc.* **1981**, *103*, 4255–4256.
[15] Interestingly, bridging imido and carbonyl ligands were recently identified in homobinuclear Mo and W complexes with more strongly balanced charge densities on both metal centers: M. D. Curtis, M. S. Hay, W. M. Butler, J. Kampf, A. L. Rheingold, B. S. Haggerty, *Organometallics* **1992**, *11*, 2884–2892.
[16] a) A. K. Burrell, J. C. Bryan, *Angew. Chem.* **1993**, *105*, 85–86; *Angew. Chem. Int. Ed. Engl.* **1993**, *32*, 94–95; b) In contrast, the combination of two 17 VE $[(tBu_3N)_3Re]$ radicals led to the formation of a d^1–d^1 dimer with bridging imido ligands (two edge-sharing tetrahedra). See also [5b].
[17] W. A. Nugent, R. J. McKinney, R. V. Kasovski, F. A. Van-Catledge, *Inorg. Chim. Acta* **1982**, *65*, L91–L93.
[18] E. J. Moore, J. M. Sullivan, J. R. Norton, *J. Am. Chem. Soc.* **1986**, *108*, 2257–2263.
[19] As expected, the weakest metal base $[Co(CO)_4]^-$ led to the largest $\Delta\delta$ value, and the strongest metal base $[CpFe(CO)_2]^-$ to the smallest. When the pK_s values show only small differences from one another, the σ-donor capability is found to be largely dependent on the steric requirements of the metal carbonyl fragments.
[20] a) Crystal structure analysis of **1a**: $C_{20}H_{32}MoN_3O_3Re$, $M = 644.64\ g\,mol^{-1}$, orthorhombic, space group: *Pbca*, $a = 8.866(2)$, $b = 17.262(3)$, $c = 33.519(6)$ Å, $V = 5130(2)$ Å^3, $Z = 8$, $\rho_{calcd} = 1.669\ g\,cm^{-3}$, crystal size = 0.75 × 0.15 × 0.19 mm, $\mu(Mo_{K\alpha}) = 54.94\ cm^{-1}$. Intensity measurement: Enraf-Nonius CAD4 diffractometer, $Mo_{K\alpha}$ radiation, 22 °C, $2\theta_{max} = 46°$, 2864 reflections measured, of which 1953 observed ($I > \sigma_I$), semi-empirical absorption correction (ψ scan). Structure refinement: H atoms were not found. C atoms of the *t*Bu group were input as part of a rigid group. All atoms other than hydrogen were refined anisotropicically. $R = 0.0409$, $R_w = 0.0423$, $w = 1/[\sigma^2(F) + 0.0007F^2]$ max. shift/e.s.d. = 0.518, 235 parameters, remaining electron density = 0.86 e Å^{-3}. b) Crystal structure analysis of **2a**: $C_{24}H_{28}Mo_3N_2O_6$, $M = 742.33\ g\,mol^{-1}$, monoclinic, space group: *C2/c*, $a = 17.725(3)$, $b = 16.107(3)$, $c = 9.588(3)$ Å, $\beta = 91.95(3)°$, $V = 2735(1)$ Å^3, $Z = 4$, $\rho_{calcd} = 1.803\ g\,cm^{-3}$, crystal size = 0.42 × 0.31 × 0.25 mm, $\mu(Mo_{K\alpha}) = 13.72\ cm^{-1}$. Intensity measurement: Enraf-Nonius CAD4 diffractometer, $Mo_{K\alpha}$ radiation, 22 °C, $2\theta_{max} = 46°$, 2488 reflections measured, of which 1425 observed ($I > 3\sigma_I$), semi-empirical absorption correction (ψ-scan). Structure refinement: H atom positions were calculated. Methyl C and H atoms were input as part of a rigid group. All atoms other than hydrogen were refined anisotropicically, H atoms were refined isotropically. $R = 0.0492$, $R_w = 0.0481$, $w = 1/[\sigma^2(F) + 0.0010F^2]$ max. shift/e.s.d. = 0.128, 187 parameters, remaining electron density = 1.0 e Å^{-3}. The programs SHELX-86 and SHELX-76 were used to solve and refine both structures [20c]. Further details of the crystal structure investigations may be obtained from the Fachinformationszentrum Karlsruhe, D-76344 Eggenstein-Leopoldshafen (FRG) on quoting the depository number CSD-57867 and the journal citation. c) G. M. Sheldrick, *SHELX-86*, Universität Göttingen, **1986**; *SHELX-76*, University of Cambridge, **1976**; d) E. Keller, *SCHAKAL*, Universität Freiburg, **1990**.
[21] Y. T. Struchkov, K. N. Anisimov, O. P. Osipova, N. E. Kolobova, A. N. Nesmeyanov, *Dokl. Akad. Nauk SSSR Ser. Khim.* **1967**, *172*, 107; G. Wilkinson, F. G. A. Stone, E. W. Abel, *Comprehensive Organometallic Chemistry, Vol. 6*, Pergamon, Oxford, **1982**, p. 802f.
[22] R. I. Mink, J. J. Welter, P. R. Young, G. D. Stucky, *J. Am. Chem. Soc.* **1979**, *101*, 6928–6933.
[23] R. D. Adams, D. M. Collins, F. A. Cotton, *Inorg. Chem.* **1980**, *19*, 1086–1090.
[24] a) R. J. Klingler, W. M. Burtler, M. D. Curtis, *J. Am. Chem. Soc.* **1978**, *100*, 5034–5039; b) M. D. Curtis, K. R. Han, W. M. Burtler, *Inorg. Chem.* **1980**, *19*, 2096–2101.
[25] M. D. Curtis, L. Messerle, *Organometallics* **1987**, *6*, 1713–1717.

Tetrakis(hypersilyl)dithallium(*Tl–Tl*): A Divalent Thallium Compound**

Sonja Henkel, Karl Wilhelm Klinkhammer,* and Wolfgang Schwarz

Molecular compounds with divalent boron have been known for a long time in the form of diboranes(4), whereas Uhl et al. achieved the first preparation and unequivocal characterization of element-homologous dialuminum, digallium, and diindium compounds only a few years ago.[1] Hitherto, only for the heaviest element of the third main group, thallium, were no analogous compounds known.[2] We report here on the synthesis and structural characterization of one such dithallium compound.

Organothallium(I) compounds with σ-bound substituents and corresponding derivatives with Tl–Si bonds have so far not been synthesized,[3] in contrast, the related trivalent thallium com-

[*] Dr. K. W. Klinkhammer, Dr. W. Schwarz
Institut für Anorganische Chemie der Universität
Pfaffenwaldring 55, D-70550 Stuttgart (FRG)
Telefax: Int. code + (711)685-4241
S. Henkel
Institut für Organische Chemie der Universität Stuttgart (FRG)

[**] For the term "hypersilyl" see ref. [5].

pounds have been prepared, for example, from bis(triorganylsilyl)mercury derivatives and trimethylthallium.[4]

A feasible route to kinetically stabilized, silyl-substituted thallium(I) compounds would be the reaction of thallium(I) halides with metal derivatives of a sterically demanding silane. Corresponding experiments with alkali metal derivatives of tris(trimethylsilyl)silane ("hypersilane"),[5] however, did not lead to a compound with a Tl–Si bond but, analogous to the corresponding reactions with lead(II) halides, to the silane **1** and elemental thallium [Eq. (a)].[6]

$$2\,TlX + 2\,MSi(SiMe_3)_3 \longrightarrow 2\,Tl + 2\,MX + \underset{\mathbf{1}}{(Me_3Si)_3Si\text{–}Si(SiMe_3)_3} \quad (a)$$

X = Cl, I; M = Li, Na, K, Rb, Cs

However, if, instead of a thallium(I) halide, the thallium(I) bis(trimethylsilyl)amide (**2**), soluble in hydrocarbon solvents and readily accessible from thallium(I) chloride and $LiN(SiMe_3)_2$ in toluene, is used, initially no metal precipitates out but a clear blood red solution is formed.

The expected thallium(I) derivative has, however, so far not been isolated nor spectroscopically detected. Also in this case already after a few minutes elemental thallium is precipitated, but without a loss of color of the solution [Eq.(b)].[3] A fractionating crystallization from *n*-pentane affords in addition to the colorless, sparingly soluble rubidium bis(trimethylsilyl)amide, dark red, platelike crystals of tetrakis(hypersilyl)dithallium(*Tl–Tl*) (**3**).

$$4\,(Me_3Si)_3SiRb + 4\,TlN(SiMe_3)_2 \longrightarrow \underset{\mathbf{2}}{} \quad (b)$$

$$4\,RbN(SiMe_3)_2 + \underset{\mathbf{3}}{[(Me_3Si)_3Si]_2Tl\ Tl[Si(SiMe_3)_3]_2} + 2\,Tl$$

The thallium(II) compound **3** dissolves well in aliphatic and aromatic hydrocarbons but only sparingly in polar solvents such as diethyl ether or acetonitrile. On standing a renewed temperature-dependent deposition of thallium is observed from these solutions. This takes place already after a few minutes at $+20\,^{\circ}C$ or after a few hours at $-60\,^{\circ}C$, and proceeds with a continual clarification of the solution. In addition, the simultaneously formed silane **1** can be detected by NMR spectroscopy.

As a result of its readiness to decompose in solution, compound **3** has so far not been satisfactorily characterized by spectroscopy. Furthermore, in the NMR spectra there are indications of dynamic processes, which we are currently investigating in more detail. Surprisingly, no radicals with longer lifetimes seem to participate in the decomposition of the compound, since the solution in *n*-pentane is ESR inactive, even after irradiation with shortwave UV light.

Raman spectra of compound **3** could only be obtained from concentrated *n*-pentane solutions and even then only under constant rotation of the sample tube, since the crystalline compound decomposes very rapidly in laser light with the deposition of thallium and the formation of a colorless material. In addition to a few low-intentsity bands, a very intense absorption band is found at 78 cm^{-1}, which we assign to the Tl–Tl vibrational stretch. Correspondingly, the IR spectrum also shows a medium-strong, broad absorption band in this range, at about 82 cm^{-1}. Since the dithallium compound **3** can be handled in the crystalline state without any visible decomposition (also in air!) for quite some time, it was investigated by X-ray crystallography (Fig. 1).[7] The central structural element of the compound is a dumbbell constructed from two trigonal-planar coordinated thallium atoms. The angle between the two planes which are each defined by a thallium atom and the bound silicon atoms

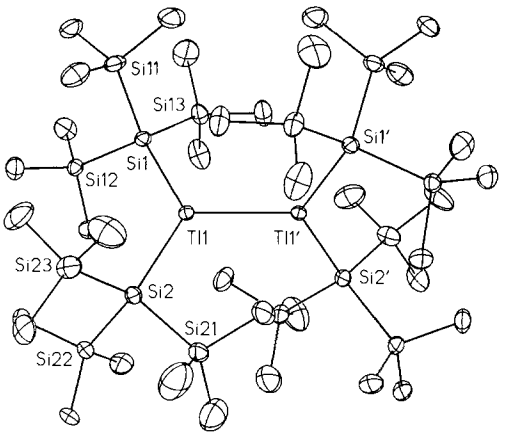


Fig. 1. Molecular structure of **3** in the crystal (thermal ellipsoids at 30% probability level). Selected bond lengths [pm] and angles [°]: Tl1-Tl1' 291.42(5), Tl1-Si1 266.4(2), Tl1-Si2 268.5(2), Si1-Si11 236.1(3), Si1-Si12 234.2(2), Si1-Si13 235.5(3), Si2-Si21 237.4(4), Si2-Si22 236.0(4), Si2-Si23 235.5(4), Si1-Tl1-S2 125.07(8), Si1-Tl1-Tl1' 116.85(4), Si2-Tl1-Tl1' 118.06(7), Si11-Si1-Tl1 117.12(8), Si12-Si1-Tl1 111.71(7), Si13-Si1-Tl1 107.95(8), Si21-Si2-Tl1 107.6(1), Si22-Si2-Tl1 119.2(2), Si23-Si2-Tl1 112.1(1), Si1-Tl1-Tl1'-Si1' +78.1(1).

is 78.1° (Fig. 2). The molecule has crystallographically imposed C_2 symmetry and its Tl_2Si_8 framework even shows approximate D_2 symmetry. In the tetraaryldigallium and -diindium compounds recently synthesized by Power et al. and Cowley et al. the substituents are also staggered.[8] According to ab initio

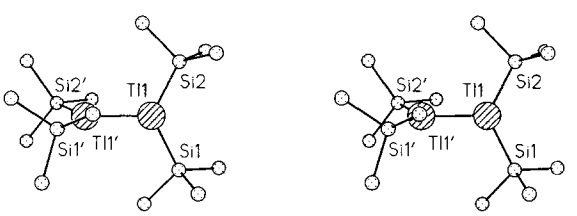


Fig. 2. Stereoscopic representation of the molecular framework of **3**. Only the thallium and silicon atoms are represented (as spheres of arbitrary sizes).

calculations by Treboux and Barthelat this staggered arrangement is also the energetically most favorable for the parent compounds M_2H_4.[9a] Only the tetraalkyldialuminum, -digallium, and -diindium compounds prepared by Uhl et al. exhibit an almost planar C_4M_2 framework, probably as result of hyperconjugative interactions of the empty p orbitals of the central metal atoms with the substituents.[1] The Tl–Tl bond length in **3** is 291.4 pm at $-100\,^{\circ}C$.[10] This value is about 20 pm less than twice the value of the covalent radius of the element (310 pm[11]).[12] The Tl–Tl distance in the comparable Tl_2 dumbbell of the molybdate $Sn_{0.8}Tl_{0.6}Mo_7O_{11}$ studied by Simon and Dronskowski is about an additional 7 pm less;[13] the latter value is in excellent agreement with the bond length (284 pm) for Tl_2H_4 optimized with SCF calculations at the Hartree–Fock and MP2 level.[9d] The distances of the thallium atoms to the central silicon atoms of the hypersilyl group (Σr_{cov} = 272 pm[11]) also appear slightly shortened (267 pm). The Si–Si bond lengths (236 pm) lie in the expected range. As a consequence of the greater electronegativity of thallium, the Si-Si-Si angles are somewhat larger (105 to 108°) than the Si-Si-Si angles of corresponding alkali metal derivatives.[14] The comparatively small angle (125°) between the sterically very demanding hypersilyl groups leads to the tilting of the

substituents away from the Si–Tl bond, which results in an increase of one Tl-Si-Si angle to almost 120°. Only in bis(hypersilyl)lead(II) do even smaller Si-Pb-Si angles of about 115° lead to even greater distortions in the geometry of the ligand.[15]

Experimental Procedure

3: A solution of $TlN(SiMe_3)_2$ [16] (0.438 g, 1.201 mmol) in *n*-pentane (10 mL) at −30 °C was quickly added dropwise to a solution of $RbSi(SiMe_3)_3$ [14c] (0.400 g, 1.201 mmol) in toluene (10 mL) and stirred. The solution immediately turned blood red. In the course of 14 h at −60 °C most of the $RbN(SiMe_3)_2$ precipitated in the form of colorless crystals. After repipetting the solution and removal of the solvent under vacuum at room temperature, the residue was taken up in *n*-pentane (10 mL) and the solution formed was filtered off from the insoluble gray solid. After a further 14 h, in addition to thallium, dark red, square platelets of **3** precipitated; 0.197 g, 0.300 mmol, yield 47%, based on the $RbSi(SiMe_3)_3$ used, m. p. 130 °C; correct elemental analysis; ^1H NMR (60 MHz, [D$_6$]benzene, 22 °C, TMS): $\delta = 0.46$ (br); ^{13}C NMR (50.324 MHz, [D$_8$]toluene, 27 °C, TMS): $\delta = 5.9$ (d(br), $^3J(CTl) = 48.2$ Hz); ^{29}Si NMR (39.761 MHz, [D$_8$]toluene, 27 °C, octamethylcyclotetrasilonane (OMCT)): $\delta = 2.42$ (d(br), $^2J(SiTl) = 22.4$ Hz, Si_3Si; $Si_3\mathit{Si}$ not observed); IR (Nujol, FT, 20–500 cm^{-1}): $\tilde{\nu}$[cm^{-1}] = 465(w), 443(sh), 434(vs), 386(m), 286(s), 260(w), 232(sh), 220(s), 146(mw, br), 80(m); Raman (*n*-pentane, FT): $\tilde{\nu}$[cm^{-1}] = 380(w, br), 280(mw), 144(sh), 133(m), 78(vs).

Received: October 16, 1993 [Z 6427 IE]
German version: *Angew. Chem.* **1994**, *106*, 721

[1] W. Uhl, *Z. Naturforsch. B* **1988**, *43*, 1113; W. Uhl, M. Layh, T. Hildenbrand, *J. Organomet. Chem.* **1989**, *364*, 289; W. Uhl, M. Layh, W. Hiller, *ibid.* **1989**, *368*, 139; review: W. Uhl, *Angew. Chem.* **1993**, *105*, 1449; *Angew. Chem. Int. Ed. Engl.* **1993**, *32*, 1386.

[2] G. E. Coates and K. Wade cited in *Organometallic Compounds* Vol. 1 (Eds.: G. E. Coates, R. L. H. Green, K. Wade), 3rd edition, Methuen, London, **1967**, p. 372, a personal communication by C. A. Wilkie and J. P. Oliver, according to which the latter are supposed to have prepared a thallium(II) salt of the composition $K_2Tl_2Me_6$ with a Tl–Tl bond by reduction of trimethylthallium with potassium in 1,2-dimethoxyethane. However, to our knowledge this work has never been published.

[3] During the reaction of thallium(I) halides with organolithium or -magnesium compounds disproportionation reactions also take place (see for example: H. Gilman, R. G. Jones, *J. Am. Chem. Soc.* **1946**, *68*, 517; G. Bähr, P. Burba, *Methoden Org. Chem. (Houben-Weyl) 4th ed. 1952-*, Bd. 13/4, **1970**, p. 369). However, to date in these cases no thallium(II) derivatives have been detected; instead the corresponding, apparently thermodynamically favored organothallium(III) compounds are formed. For the hypersilyl substituent, bowever, the formation of a thallium(III) derivative may well be kinetically hindered because of a steric overloading of the thallium atom with these sterically extremely demanding groups. The reaction of bis(hypersilyl)lead [15], also synthesized by us, with hypersilyl alkali metal derivatives to give tris(hypersilyl)plumbates $MPb[Si(SiMe_3)_3]_3$ (M = K, Cs) shows that an arrangement of three hypersilyl groups [5] around an atom of the size of thallium is in principle possible.

[4] E. A. V. Ebsworth, A. G. Lee, G. M. Sheldrick, *J. Chem. Soc. A.* **1969**, 1052.

[5] We adopt here the nomenclature, proposed by N. Wiberg at the Xth International Symposium on Organosilicon Chemistry in Poznan (Poland) in August 1993, according to which for the differentiation of the substituents $(Me_3C)_3Si$ and $(Me_3Si)_3Si$ corresponding compounds should be termed supersilyl and hypersilyl derivatives, respectively.

[6] S. P. Mallela, I. Bernal, R. A. Geanangel, *Inorg. Chem.* **1992**, *31*, 1626.

[7] Crystal data of **3**: dark red, square platelets, monoclinic, space group *C*2/*c* (no. 15), $a = 28.254(3)$, $b = 12.935(2)$, $c = 23.346(2)$ Å, $\beta = 126.048(7)°$, $V = 6898.5(14)$ Å^3, $Z = 4$, $\mu = 4.97$ mm^{-3}, $\rho_{calcd} = 1.347$ g cm^{-3}. Four-circle diffractometer P2$_1$ (Syntex), Wyckoff scan, $T = -100$ °C; 7078 independent reflections, ($Mo_{K\alpha}$; $2\theta_{max} = 55°$); absorption correction with ψ scan (platelets correction; glancing angle 4°; min./max. transmission: 0.27/0.78), 328 parameters, 88 restraints. The structure was solved by direct methods (SHELXTL Plus) and refined with full-matrix least-squares based on F_o^2 values (SHELXL 93). Tl, Si, and C atoms were refined anisotropically, hydrogen atoms isotropically at idealized positions. A tris(trimethylsilyl)silyl group shows a static position disorder; the occupation factor of the preferred orientation was determined to 0.837(4). *R*1 [$F_o > 4\sigma(F_o)$] = 0.041, *wR*2 [$F_o^2 > -3\sigma(F_o^2)$] = 0.105, GOF = 1.16. Further details of the crystal structure investigation may be obtained from the Fachinformationszentrum Karlsruhe, D-76344 Eggenstein-Leopoldshafen (FRG) on quoting the depository number CSD-57881, the names of the authors, and the journal citation.

[8] X. He, R. A. Bartlett, M. M. Olmstead, K. Ruhlandt-Senge, B. E. Sturgeon, P. P. Power, *Angew. Chem.* **1993**, *105*, 761; *Angew. Chem. Int. Ed. Engl.* **1993**, *32*, 717; R. D. Schluter, A. H. Cowley, D. A. Atwood, R. A. Jones, M. R. Bond, C. J. Carrano, *J. Am. Chem. Soc.* **1993**, *115*, 2070.

[9] a) G. Treboux, J.-C. Barthelat, *J. Am. Chem. Soc.* **1993**, *115*, 4870; b) P. Schwerdtfeger, *Inorg. Chem.* **1991**, *30*, 1660; c) C. Janiak, R. Hoffmann in *Unkonventionelle Wechselwirkungen in der Chemie metallischer Elemente* (Ed.: B. Krebs), VCH, Weinheim, **1992**, p. 45; d) K. W. Klinkhammer, P. Pyykkö; unpublished results. Recently Treboux and Barthelat did calculations on the same system employing different pseudo potentials and basis sets, but the optimized Tl–Tl bond length (277.6 pm) seems to be too short [9a].

[10] The Tl–Tl (293.5) and Tl–Si (270 pm) bond lengths determined for the same crystal by an additional measurement at + 22 °C are slightly longer than those determined at −100 °C; otherwise no significant changes in the molecular structure are observed.

[11] J. Emsley, *The Elements*, 2nd edition, Clarendon, Oxford, **1991**, p. 2.

[12] In the last few years similar short Tl···Tl distances (400 pm ≥ *d*(Tl···Tl) ≥ 316 pm) have been determined in several Tl(I) compounds, which have led to an intensive, partly controversial discussion on the bonding in such systems [9].

[13] R. Dronskowski, A. Simon, *Angew. Chem.* **1989**, *101*, 775; *Angew. Chem. Int. Ed. Engl.* **1989**, *28*, 758.

[14] a) G. Becker, H. M. Hartmann, A. Münch, H. Riffel, *Z. Anorg. Allg. Chem.* **1985**, *530*, 29; b) A. Heine, R. Herbst-Irmer, G. M. Sheldrick, D. Stalke, *Inorg. Chem.* **1993**, *32*, 2694; c) K. W. Klinkhammer, W. Schwarz, *Z. Anorg. Allg. Chem.* **1993**, *619*, 1777.

[15] K. W. Klinkhammer, W. Schwarz, unpublished results.

[16] K. W. Klinkhammer, S. Henkel, *J. Organomet. Chem.*, submitted.

Asymmetric Synthesis of Highly Substituted Pyrrolidines by 1,3-Dipolar Cycloadditions of Azomethine Ylides with *N*-Acryloylproline Benzyl Ester**

Herbert Waldmann,* Edwin Bläser, Martin Jansen, and Hans-Peter Letschert

Dedicated to Professor János Rétey on the occasion of his 60th birthday

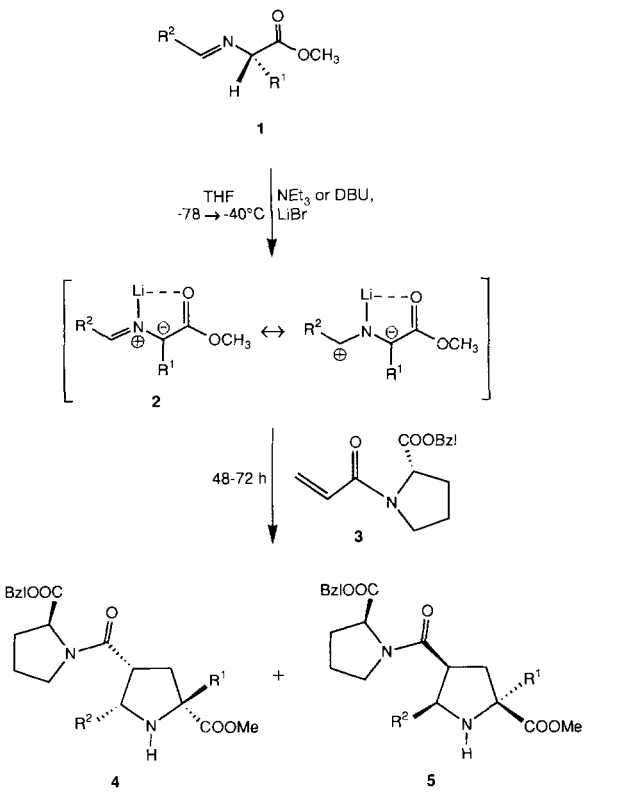
1,3-Dipolar cycloadditions are among the most efficient methods of organic synthesis. For example, the reaction of azomethine ylides with alkenes makes possible the simultaneous construction of up to four stereocenters and thus provides a direct and efficient entry to highly substituted pyrrolidines.[1] These heterocycles occur as structural elements in several biologically significant alkaloids[1] and are also of considerable interest in the field of medicinal chemistry, for example as highly effective glycosidase inhibitors[2] and as antagonists of excitatory amino acids.[3] Cycloadditions of azomethine ylides are thus increasingly important as key steps in the synthesis of complex natural products and pharmaceuticals.[4] Thus, the development of efficient chiral auxiliaries, with which the stereochemical path of these reactions can be controlled, has recently been intensively investigated. Despite these efforts, the results obtained have been mixed.[5] We have now found that highly stereoselective 1,3-dipolar cycloadditions of azomethine ylides can be successfully carried out with proline benzyl ester as chiral auxiliary.[6]

Schiffs bases **1** of amino acid esters can be prepared simply by condensation of the appropriate aldehyde and an amino acid ester in dichloromethane in the presence of $MgSO_4$ as water absorbent.[7] These imines are then converted by deprotonation

[*] Prof. Dr. H. Waldmann, Dipl.-Chem. E. Bläser
Institut für Organische Chemie der Universität
Richard-Willstätter-Allee 2, D-76128 Karlsruhe (FRG)
Telefax: Int. code +(721)608-4825
Prof. Dr. M. Jansen, Dipl.-Chem. H. Letschert
Institut für Anorganische Chemie der Universität Bonn (FRG)

[**] This work was funded by the Deutsche Forschungsgemeinschaft and by the Fonds der Chemischen Industrie. We thank Degussa AG for the donation of chemicals.

with triethylamine or 1,8-diazabicyclo[5.4.0]undec-7-ene (DBU) to the azomethine ylides, which give metalated 1,3-dipoles of fixed configuration in the presence of anhydrous LiBr (Scheme 1).[8]

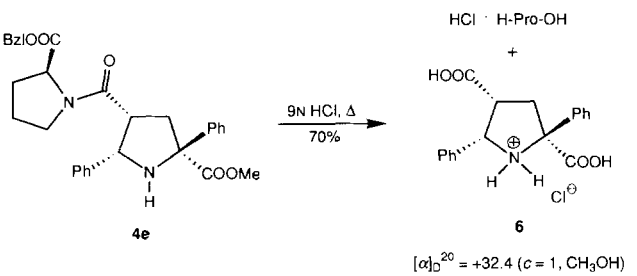


Scheme 1. Asymmetric 1,3-dipolar cycloadditions between *N*-acryloyl-(*S*)-proline benzyl ester and metalated azomethine ylides. Bzl = benzyl.

The complexes **2** react with *N*-acryloyl-(*S*)-proline benzyl ester **3** in THF to give the pyrrolidines **4** and **5** in satisfactory yields and very high stereoselectivity even at temperatures between $-78\,^{\circ}C$ to $-40\,^{\circ}C$ (Table 1). In each case only four of the eight possible diastereoisomers could be detected; one stereoisomer of each was always formed in large excess. When lithium diisopropylamide was used as base and for the formation of the metal complex,[9] or when acetonitrile was used as solvent, mixtures of products were formed in which the stereoselectivity was lower.

Imines of aliphatic and aromatic amino esters can be used as precursors to the 1,3-dipoles (Table 1). In each case the desired cycloadduct is formed with almost complete *endo*/*exo* selectivity (regularly >99:1). Only in the case of **4f** is the *exo* adduct detected. In the case of the asymmetric cycloadditions of proline benzyl ester **3**, the prefered *endo* isomers **4** are formed with excellent diastereomeric excesses. The stereoselectivity of the reaction increases as the steric demands of the amino acid side chains of the 1,3-dipole increase (Table 1). Thus **4a** and **4b**, which are derived from the benzaldimines of glycine and alanine methyl esters, are formed with diastereomeric ratios of 93:7 and 91:9 respectively. (Table 1, Nos. 1 and 2). On the other hand, the Schiffs bases obtained from the methyl esters of valine, isoleucine, and phenylglycine deliver products with isomeric ratios of >95:5 to >99:1 (Nos. 3–7). In the cases of pyrrolidines **4c**, **4d**, and **4e**, the corresponding *endo* isomer **5** was completely undetectable. The ratios of stereoisomers were determined by high performance liquid chromatography (HPLC) of the crude reaction mixtures. The major isomers could be easily separated by simple flash chromatography as colorless solids. Their absolute configurations were unambiguously assigned by crystal structure analysis of the pyrrolidine **4e**.[10]

The removal of the chiral auxiliary from the cycloaddition products was carried out in high yield simply by acid hydrolysis of the proline amide bond with the concomitant hydrolysis of the ester group of the pyrrolidine. This approach is exemplified by compound **4e** in Scheme 2. The liberated proline can easily be recovered, for example, by chromatography.



$[\alpha]_D^{20} = +32.4$ ($c = 1$, CH_3OH)

Scheme 2. Removal of the chiral auxiliary from the cycloadducts.

Enantiomerically pure pyrrolidine-2,4-dicarboxylic acids such as **6** are of interest not only as precursors in the field of alkaloid synthesis,[1, 2] but also in their own right as potential pharmaceuticals, since they act as antagonists of the excitatory glutamic acid and can be used in the study of the glutamic acid receptor.[3]

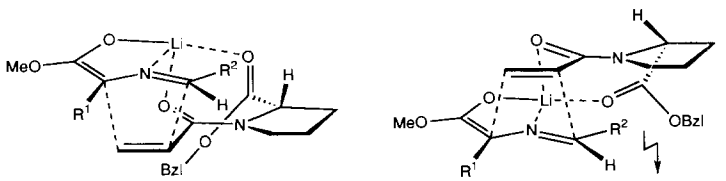
In order to explain the almost total *endo*/*exo* selectivity and the very high face selectivity attained through the 1,3-dipolar cycloaddition of the α,β-unsaturated proline benzyl ester amide **3** with the metalated azomethine ylides **2**, we assume that the reaction proceeds preferentially via the highly ordered *endo*

Table 1. Results of the 1,3-dipolar cycloadditions between azomethine ylides (**2**) and *N*-acryloyl-(*S*)-proline benzyl ester (**3**) yielding the pyrrolidines **4** and **5**.

No.	Cmpd.	R^1	R^2	*T* [°C]	Reaction time [h]	$[\alpha]_D^{25}$ ($c = 2$, CH_2Cl_2)	M.p. [°C]	Yield [%] [a]	*endo*/*exo*-ratio	**4**:**5** [b]
1	**4a**	H	Ph	−78 → 25	72	−99.3	87	43	>99:1	93:7
2	**4b**	CH_3	Ph	−40 → 25	72	−251.0	Öl	48	>99:1	91:9
3	**4c**	*i*Pr [c]	Ph	−40 → 25	72	−128.0	95	30	>99:1	>99:1
4	**4d**	*i*Bu [c]	Ph	−40	72	−153.5	119	30	>99:1	>99:1
5	**4e**	Ph	Ph	−78 → 25	48	−74.8	115	67	>99:1	>99:1
6	**4f**	Ph	4-NO_2Ph	−40	48	−77.5	160	60	93:7	97:3
7	**4g**	Ph	4-MeOPh	−40	48	−79.8	53	65	>99:1	95:5

[a] The yields are based on pure diastereoisomer **4** after chromatographic purification. All pyrrolidines **4** were identified from 400 MHz NMR spectra ($CDCl_3$), and all gave the correct elemental analyses. [b] Determined from the crude reaction mixture by HPLC. [c] DBU was used as base.

transition states **A** and **B** (Fig. 1). In both these transition states the lithium cation is coordinated to the azomethine ylide and to the dipolarophile, in such a way that a compact and efficient ordering of the reaction partners results. If the dipole had an *exo*



A **B**

Fig. 1. Possible transition states consistent with the stereoselection found in the 1,3-dipolar cycloadditions between *N*-acryloyl-(*S*)-proline benzyl ester and metalated azomethine ylides.

orientation, such double coordination would not be possible. To allow the lithium cation to coordinate through the amide and ester carbonyl groups of the dipolarophile, the acrylamide must assume the proposed *cis–anti* conformation.[6] In the corresponding *cis-syn* configuration the dipoles of the carbonyl groups would, for electrostatic reasons, lie in an antiparallel, and therefore more favorable, conformation. However, this effect is overridden by the additional coordination of the lithium cation by the ester group. Of the two *endo* transition states, **A** is the energetically more favorable, because in **B** the group R^2 of the dipole lies close to the COOBzl group of the proline benzyl ester, while in **A** only an interaction with the sterically undemanding α-hydrogen of the proline has to be considered.

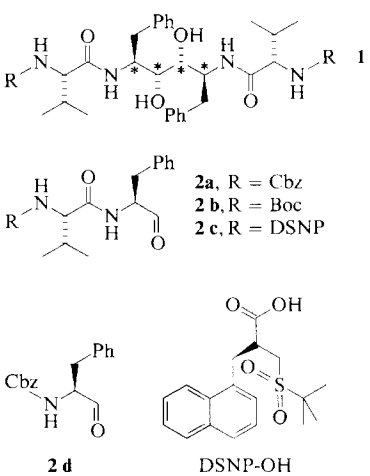
Received: October 21, 1993 [Z 6437 IE]
German version: *Angew. Chem.* **1994**, *106*, 717

[1] Review article: W. J. Lown in *1,3-Dipolar Cycloaddition Chemistry, Vol. 1.* (Ed.: A. Padwa), Wiley, New York, **1984**. See also detailed references in [5c].
[2] Reviews: G. W. Fleet, *Top. Med. Chem.* **1988**, *65*, 149; b) R. T. Schwarz, R. Datema, *Trends Biochem. Sci.* **1984**, 32. For more recent work see: V. Wehner, V. Jäger, *Angew. Chem.* **1990**, *102*, 1180; *Angew. Chem. Int. Ed. Engl.* **1990**, *29*, 1169, and references therein.
[3] See, for example, R. J. Bridges, F. E. Lovering, J. M. Humphrey, M. S. Stanley, T. N. Blakely, M. F. Cristofaro, A. R. Chamberlin, *Biorg. Med. Chem. Lett.* **1993**, *3*, 115, and references therein.
[4] See, for example, a) G. A. Kraus, J. A. Nagy, *Tetrahedron* **1985**, *41*, 3537; b) P. DeShong, D. A. Kell, *Tetrahedron Lett.* **1986**, *27*, 3979; c) C.-L. Wang, W. C. Ripka, P. N. Confalone, *ibid* **1984**, *25*, 4613; d) P. N. Confalone, R. A. Earl, *ibid.* **1986**, *27*, 2695; e) P. Garner, W. B. Ho, H. Shin, *J. Am. Chem. Soc.* **1992**, *114*, 2767, and references therein; f) S. Takano, K. Samizu, K. Ogasawara, *Chem. Lett.* **1990**, 1239.
[5] Chiral auxiliaries in 1,3-dipoles: P. Deprez, J. Royer, H.-P. Husson, *Tetrahedron: Asymmetry* **1991**, *2*, 1189; A. S. Anslow, L. M. Harwood, H. Philips, D. Watkin, L. F. Wong, *ibid.* **1991**, *2*, 1343; R. M. Williams, W. Zhai, D. J. Aldous, S. C. Aldous, *J. Org. Chem.* **1992**, *57*, 6527. Chiral auxiliaries in dipolarophiles: P. Garner, W. B. Ho, *ibid.* **1990**, *55*, 3973; S. Kanemasa, T. Hayashi, J. Tanaka, H. Yamamoto, T. Sakurai, *ibid.* **1991**, *56*, 4473; D. A. Barr, M. J. Dorrity, R. Grigg, J. F. Malone, V. Sridharan, *ibid.* **1991**, *32*, 5417; A. H. Fray, A. I. Meyers, *ibid.* **1992**, *33*, 3575.
[6] Use of proline benzyl ester as chiral auxiliary in carbo-Diels–Alder reactions: H. Waldmann, *J. Org. Chem.* **1988**, *53*, 6133; *Liebigs Ann. Chem.* **1990**, 671; in 1,3-dipolar cycloadditions of nitrile oxides: H. Waldmann, *ibid.* **1990**, 1013; in radical additions to carbonyl groups: H. Waldmann, *Synlett* **1990**, 627; *Liebigs Ann. Chem.* **1991**, 1317. Reviews of the use of amino esters as chiral auxiliaries: H. Waldmann, M. Braun, *Gazz. Chim. Ital.* **1991**, *121*, 277; H. Waldmann, *Kontakte* **1993** (1), 58; *ibid.* **1993** (2), 34.
[7] a) H. Takashi, H. Omatsu, *Chem. Pharm. Bull.* **1978**, *26*, 466; b) G. Grundke, W. Keese, M. Rippler, *Synthesis* **1987**, *12*, 1115.
[8] K. Amornraksa, D. Barr, G. Donegan, R. Grigg, P. Ratananukul, V. Sridharan, *Tetrahedron* **1989**, *45*, 4649, and references therein.
[9] D. A. Barr, R. Grigg, H. Q. Nimal Gunaratne, J. Kemp, P. McMeekin, V. Sridharan, *Tetrahedron* **1988**, *44*, 557 and references therein.
[10] Crystal data: $C_{31}H_{32}N_2O_5$, orthorhombic crystals, space group $P2_1/m$ (no. 11), with $a = 8.473(5)$, $b = 17.736(3)$, $c = 8.927(2)$ Å, $Z = 2$, $\beta = 95.32(1)°$. 2807 reflections were measured (quadropole diffractometer Enraf Nonius (No. CAD4, $Mo_{K\alpha}$ radiation, graphite monochromator), of which 2717 were independent with $I > 2\sigma(I)$. The structure determination was carried out with direct methods (SHELX-76 and SHELXL-93), $R = 0.0547$, $R_w = 0.0838$, $w = 1/\sigma^2 F) + 0.0001 F^2$. All C, N, and O atoms were anisotropically refined. The hydrogen atoms are found in the calculated sites with the appropriate isotropic temperature factors for CH, CH_2, CH_3, and phenyl H. Further details of the crystal structure investigation may be obtained from the Fachinformationszentrum Karlsruhe, D-76344 Eggenstein-Leopoldshafen (FRG) on quoting the depository number CSD-58112 and the journal citation.

Vanadium(II)- and Niobium(III)-Induced, Diastereoselective Pinacol Coupling of Peptide Aldehydes to C_2-Symmetrical HIV-Protease Inhibitors**

Bernhard Kammermeier,* Gerhard Beck, Detlev Jacobi, and Heiner Jendralla*

In 1993 fifteen European and American pharmaceutical companies decided to collaborate on medicinal AIDS control.[1] Possible synthetic approaches to finding a method for chemotherapeutic intervention in the complex reproduction cycle of the Human Immunodeficiency Virus (HIV) are both diverse and beset with problems. They range from blocking of the viral gp120 surface structure to the inhibition of the virus-specific enzyme reverse transcriptase (RT) or to inhibition of the HIV protease, an aspartyl protease whose structure was elucidated in 1989, and which is essential for the maturation of infectious virus particles.[2] In particular, inhibition of the C_2-symmetrical HIV protease by compounds with structures of type **1** (see Scheme 1)[3] has crystallized as a promising therapeutic target. This is primarily for two reasons. First, proteases of the host organism are unable to carry out the proteolytic tasks of an inhibited HIV protease, and second, the aspartyl protease class, which also includes renin and pepsin, for example, is a class of mechanistically well-characterized proteolytic enzymes.



2a, R = Cbz
2b, R = Boc
2c, R = DSNP

2d DSNP-OH

Scheme 1. HIV protease inhibitors **1** and "half" precursor molecules **2**. Cbz: benzyloxycarbonyl, Boc: *tert*-butyloxycarbonyl.

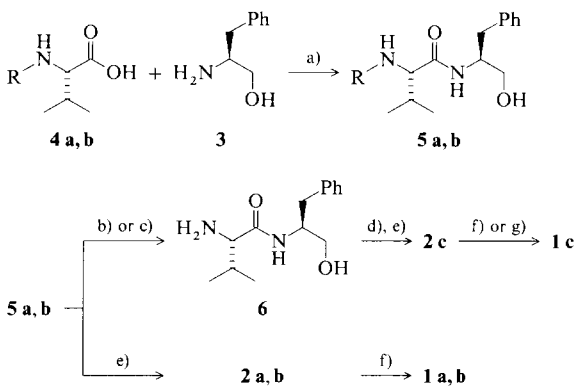
C_2-symmetrical inhibitors were first synthesized and their biological activity studied by Kempf and Erickson et al. in 1990.[4] A crucial problem in the synthesis of these aminodiols is stereoselective access to the most effective diastereomer type **1**.[5] Because of the molecular symmetry of the com-

[*] Dr. B. Kammermeier, Priv.-Doz. Dr. H. Jendralla, Dr. G. Beck
Pharma-Forschung, Hoechst AG
Postfach 800320, D-65926 Frankfurt am Main (FRG)
Telefax: Int. code + (69)331369
Dr. D. Jacobi
Landes-Entwicklungs-Gesellschaft, D-70182 Stuttgart (FRG)

pounds, a synthesis based on the two "molecular halves" **2** (Scheme 1) characteristically requires very few synthetic steps. The customary reductive dimerizations do not in this case lead to the target: both titanium(III)-catalyzed McMurry couplings[6] and samarium(II)-induced dimerizations[3] yield only diastereomeric mixtures that are difficult to separate.

We report here on vanadium- and niobium-induced couplings of homochiral peptide aldehydes, which proceed in high yield and diastereoselectively to afford inhibitors of type **1**, from the readily available compounds of type **2**. The dimerization takes place with simultaneous control of all four stereo centers shown in **1**. According to Pedersen and Konradi,[7] pinacol coupling of **2d** to **1d** with $[V_2Cl_3(thf)_6]_2[Zn_2Cl_6]$ proceeds in 76% yield. Using a catalyst generated in situ, we were now able to couple homochiral peptide aldehydes as large as the formal tripeptide aldehyde **2c** and dimerize these to the vicinal aminodiol **1c**. These reactions are also practicable on a kilogram scale.[8]

The synthetic route (Scheme 2) starts with the phosphonic anhydride-induced peptide coupling of (*S*)-phenylalaninol (**3**) and N-terminal protected (*S*)-valine (**4**), leading to the protected dipeptide analogs **5** in at least 94% yield. Under Swern-oxida-



Scheme 2. Diastereoselective synthesis of C_2-symmetrical HIV protease inhibitors (R see Scheme 1): a) *n*-propyl phosphonic anhydride, NEt_3, EtOAc, room temperature (RT), 94%; b) HCl(gas), MeOH, RT, 92%; c) MeOH/HCl (pH 6), H_2, Pd/C, RT, 94%; d) dicyclohexylcarbodiimide, hydroxybenzotriazole, DSNP-OH, RT, 75%; e) $(COCl)_2$, dimethylsulfoxide (DMSO), NEt_3, CH_2Cl_2, −60 °C, 72–89%; f) VCl_3, Zn, 1,3-dimethyl-2-imidazolidinone, THF, reflux, 62–72%; g) $[NbCl_3(dme)]$, THF, reflux, 40%.

tion conditions, these can be directly transformed to the aldehydes **2a** and **2b** (72–89% yield). However, depending on the protecting group used, **5** can also be deprotected at the amino-terminus by hydrogenolysis or protonation (>92% yield). The free amine **6** is now coupled either to a further amino acid unit or to another carboxylic acid, such as DSNP-OH (see Scheme 1),[9a] through its active ester.[9] This affords the corresponding alcohol, which is formally a tripeptide alcohol (75%yield). The product is then subjected to a Swern oxidation that has been optimized for use on a kilogram scale to give rise to the diastereomerically pure peptide aldehyde **2c** in the (*S,S,S*)-form (72% yield). In the key reaction of the synthetic sequence, the peptide aldehydes **2** are reductively dimerized by using a vanadium complex (55–76% yield). The procedure used here is significantly different in several aspects from the known methods for amino aldehydes. Since the catalyst is generated in situ, it is possible to avoid both the isolation of oxygen-sensitive complexes like $[VCl_3(thf)_3]_{10}$ and the change to chlorinated solvents.

For the dimerization, VCl_3 is heated at reflux for five hours in THF, followed by addition of 0.5 equivalents zinc powder, 1,3-dimethyl-2-imidazolidinone as a complexing agent, and aldehyde **2c**, for example. The reaction is heated for a further hour at reflux, and then subjected to an aqueous workup. This one-pot method yields the diol **1c** with the desired configuration and with good diastereoselectivity[11] in 65% yield, and is practicable on a kilogram scale.[5] From the increasing size of the aldehydes **2d**[7] to **2c** which can be reductively dimerized, it is clear that the amino protecting groups in **2b** and **2c** can also be replaced by further amino acid units or by "chain-lengthening" carboxylic acids. The reaction mechanism itself does not restrict the nature of the aldehydes to be dimerized at all. Clearly, the amide units function in the transition state as good chelating groups for the dinucleate vanadium(II) complex.[7]

Remarkably, **2c** could also be transformed to **1c** on a gram scale by the niobium(III) complex ($[NbCl_3(dme)]$, dme = dimethoxyethane) introduced by Pederson et al.[12] for the reductive coupling of imines with aldehydes. The dimerization catalyst is in this case freshly prepared before the coupling reaction. $NbCl_5$ is added to a solution of Bu_3SnH in DME at −78° C, and the brick-red precipitate is filtered off under inert gas. Compound **2c** is then heated at reflux in THF with an equimolar amount of the freshly prepared niobium catalyst. This represents – despite the low yield of barely 40% of **1c**—the first coupling of homochiral peptide aldehydes with this niobium catalyst, which in addition proceeds with higher diastereoselectivity.[13, 14]

These results demonstrate that the application spectrum for both these dimerization reagents is broad, both with respect to the scale of the reaction and to the size of the substrate and its functional groups. Both types of catalysts are simple to synthesize, and the vanadium complex, at least, can also be generated in situ. Finally, the higher selectivity of these reducing agents for activated aldehyde functional groups has the advantage that dimerizations can also be carried out in the presence of other functional groups such as amides and sulfones within the molecule concerned.

Experimental Procedure

1c: VCl_3 (678 g, 4.3 mol) were heated at reflux in anhydrous THF (24 L) under nitrogen for 5 h. Zinc powder (160 g, 2.4 mol), 1,3-dimethyl-2-imidazolidinone (1.6 L), and **2c** (1.2 kg, 2.1 mol) in THF (6 L) were then added to the mixture. The reaction was heated for 1 h at reflux, cooled to room temperature, and diluted with 10% aqueous citric acid (19 L) and ethyl acetate (18 L). After separating the phases, the organic phase was washed several times with water, dried over Na_2SO_4, filtered, and the solvent removed under vacuum. The solid residue was recrystallized first from ethanol and then from ethyl acetate, and yielded 720 g **1c** as colorless crystals; m.p. 189 °C [14].

Received: October 25, 1993 [Z6445IE]
German version: *Angew. Chem.* **1994**, *106*, 719

[1] "Firms unit for Aids Cure", *Chem. Br.* **1993**, *29*, 465.
[2] a) A. G. Tomasselli, W. J. Howe, A. Wlodawer, R. L. Heinrikson, *Chim. Oggi* **1991**, May 6–27; b) D. W. Norbeck, D. J. Kempf, *Annu. Rep. Med. Chem.* **1991**, *26*, 141; c) D. Häbich, *Chem. Unserer Zeit* **1991**, *25*, 295.
[3] a) K. H. Budt, A. Peyman (Hoechst AG), EP-A 0435059, **1990**; *Chem. Abstr.* **1991**, *115*, P163862u; b) D. Enders, U. Jegelka, B. Dücker, *Angew. Chem.* **1993**, *105*, 423; *Angew. Chem. Int. Ed. Engl.* **1993**, *32*, 423; c) K.-H. Budt, J. Knolle, C. Meichsner, D. Ruppert, B. Stowasser, I. Winkler, A. Paessens, J. Hansen (Hoechst AG), EP-A 0428849, **1990**; *Chem. Abstr.* **1992**, *116*, P214912m; c) K.-H. Budt, J. Hansen, J. Knolle, C. Meichsner, A. Paessens, D. Ruppert, *Abstr. Pap. IXth Int. Conf. on AIDS-IVth World Congress*, Berlin, June 7–11, **1993**, PO-A25-0613.
[4] J. Erickson, D. J. Neidhart, J. VanDrie, D. J. Kempf, X. C. Wang, D. W. Norbeck, J. J. Plattner, J. W. Rittenhouse, M. Turon, N. Wideburg, W. E. Kohlbrenner, R. Simmer, R. Helfrich, D. A. Paul, M. Knigge, *Science* **1990**, *249*, 527.

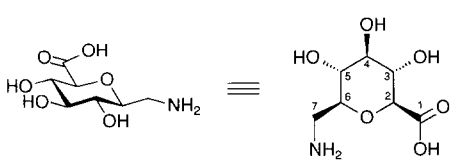
 © VCH Verlagsgesellschaft mbH, D-69451 Weinheim, 1994 0570-0833/94/0606-0686 $ 10.00+.25/0

[5] For the ordering of the activity (*S,R,R,S*) > (*S,S,S,S*) see [3] and A. Peyman, K.-H. Budt, J. Spanig, D. Ruppert, *Angew. Chem.* **1993**, *105*, 1852; *Angew. Chem. Int. Ed. Engl.* **1993**, *32*, 1720.
[6] D. J. Kempf, D. W. Norbeck, L. M. Codacovi, X. C. Wang, W. E. Kohlbrenner, N. E. Wideburg, D. A. Paul, M. Knigge, S. Vasavanonda, A. Craig-Kennard, A. Saldivar, W. Rosenbrock, J. J. Clement, J. J. Plattner, J. Erickson, *J. Med. Chem.* **1990**, *33*, 2687.
[7] A. W. Konradi, S. F. Pedersen, *J. Org. Chem.* **1992**, *57*, 28.
[8] D. Jacobi, H. Jendralla, B. Kammermeier (Hoechst AG), EP-A 0503561, **1992**.
[9] a) G. Beck, H. Jendralla, B. Kammermeier, *Tetrahedron*, submitted for publication; b) for coupling of activated amino acids with amino alcohols and subsequent Swern oxidation see: M. T. Reetz, *Angew. Chem.* **1992**, *104*, 1638; *Angew. Chem. Int. Ed. Engl.* **1993**, *32*, 1626.
[10] L. E. Manzer, *Inorg. Synth.* **1982**, *21*, 135.
[11] Relative to the four stereocenters of the newly formed hexane skeleton, the following diastereomeric ratios were measured for crude product mixtures from the synthesis of **1a**, **1b**, and **1c**: **1a**: *SRRS*:*SSSS* = 5.5:1; **1b**: *SRRS*:*SSSS* = 6.5:1; **1c**: *SRRS*:*SSSS* = 8.7:1.
[12] E. J. Roskamp, S. F. Pedersen, *J. Am. Chem. Soc.* **1987**, *109*, 6551.
[13] D. Jacobi, H. Jendralla, B. Kammermeier, Hoechst AG, EP-A 0541946, **1992**.
[14] Spectroscopic data for all novel compounds agree with the proposed structures. These, and detailed experimental procedures, may be found in refs. [8] and [13].

A Sugar Amino Acid as a Novel Peptidomimetic**

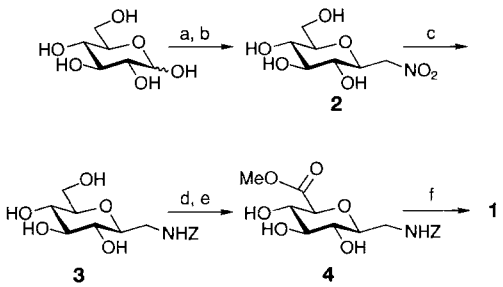
Erich Graf von Roedern and Horst Kessler*

Amino acids and peptide units with nonnatural structures are being employed with increasing frequency as components of peptide-based drugs, since they can be used to modify pharmacokinetics and metabolic stability.[1] We report here on the simple synthesis of the sugar amino acid H-Gum-OH **1**,[2] a new type of dipeptide isostere. We demonstrate the effect of H-Gum-OH **1** on the structural and biological properties of peptides with cyclic somatostatin analogues and a linear enkephalin analogue. H-Gum-OH **1**, which can be prepared from glucose in four steps, is characterized structurally by the rigid, pyranoid framework of the sugar residue. The conformations of peptides containing **1** are thus restricted. The free hydroxyl groups increase the hydrophilicity of the peptides; with nonpolar protective groups the opposite effect can be induced.



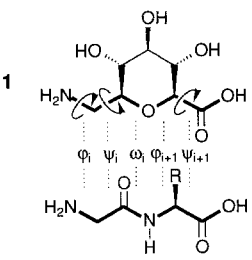
1

Although pyranoid rings are found frequently in natural products of therapeutic importance,[3] we know of only one case in which this structure occurs in a peptide chain.[4] Glucose has already been used as the framework of a nonpeptidic peptidomimetic[5] but not to modify a peptide backbone. H-Gum-OH **1** was synthesized (Scheme 1) in only 12% overall yield; however, since glucose and the reagents employed are inexpensive, the synthesis can be conducted on a large scale.



Scheme 1. a) CH_3NO_2, NaOMe; b) H^+/H_2O, ΔT; c) H_2, Pd/C, Z-Cl (Z = benzyloxycarbonyl); d) O_2, Pt/C; e) MeOH, DCC/DMAP (dicyclohexylcarbodiimide/*N*,*N*-dimethylaminopyridine); f) NaOH, H_2, Pd/C.

Analysis of the $^3J_{H,H}$ coupling constants[6] of **1** indicates that the pyranoid ring is in the all-equatorial chair conformation typical for sugars ($^4C_1$ analogues). The backbone bonds and the dihedral angles of the dipeptide isostere **1** are compared to those of a natural dipeptide in Scheme 2. The cyclic structure of H-Gum-OH **1** fixes the ω_i angle at 180°, which corresponds to a *trans* amide bond. The φ_{i+1} angle in **1** is also fixed at 180°; this is often found in natural β-sheet structures. However, **1** is not a β-sheet mimetic, since it has no amide groups for hydrogen bonding. **1** has "free rotation" about the φ_i angle and both ψ angles. Accordingly, peptidomimetic **1** can be used to replace two adjacent amino acids having conformational restriction at the ω_i and φ_{i+1} angles. A comparison of the "side chains" of **1** with those of a natural dipeptide shows that **1** is structurally related to H-Gly-Ser-OH and H-Gly-Thr-OH (Scheme 2). To determine



Scheme 2. Comparison of the torsion angles of H-Gum-OH **1** with those of a dipeptide (H-Gly-AA-OH (AA = amino acid)). The freely rotating bonds of **1** are marked with arrows.

the effect that H-Gum-OH **1** exerts on the conformation of a peptide, we incorporated **1** into a cyclic hexapeptide[7] by replacing two neighboring amino acids (Table 1).

Table 1. The synthesized cyclopeptides, the reference peptide **8**, and their activities as somatostatin analogues.

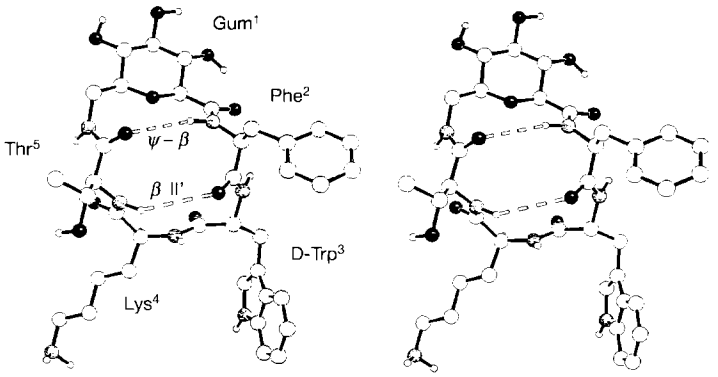
Compound [a]	IC_{50}[μM] [b]
cyclo(-Gum^1-Phe^2-D-Pro^3-Ala^4-Phe^5-) **5**	[c]
cyclo(-Gum^1-Tyr^2-D-Trp^3-Lys^4-Val^5-) **6**	0.47
cyclo(-Gum^1-Phe^2-D-Trp^3-Lys^4-Thr^5-) **7**	0.15
cyclo(-Pro-Phe-D-Trp-Lys-Thr-Phe-) **8** [d]	0.002

[a] The amino acids in compounds **5**, **6**, and **7** at a given position are abbreviated in the text as Xxx^N. [b] Inhibition constant IC_{50} for the release of growth hormone measured with a cell line obtained from mouse pituitary. [c] Model peptide; activity was not tested; D-Pro in the $(i+1)$ position strongly induces a βII′ loop. [d] Reference peptide for the activity determination [9].

[*] Prof. Dr. H. Kessler, Dipl.-Ing. E. Graf von Roedern
Institut für Organische Chemie und Biochemie
der Technischen Universität München
Lichtenbergstrasse 4, D-85747 Garching (FRG)
Telefax: Int. code + (89)3209-3210

[**] We thank Dr. B. Kutscher and Dr. M. Bernd, Asta Medica AG, Frankfurt am Main (FRG), for providing the biological somatostatin tests, and Prof. Dr. P. W. Schiller, Clinical Research Institute of Montreal, for measuring the biological activity of the enkephalin analogue.

Interproton distances were determined by 250 MHz ROESY (rotating frame Overhauser effect spectroscopy) and 500 MHz NOESY (nuclear Overhauser effect spectroscopy); these served as restrains in the force field in molecular dynamics (MD) simulations (programs DISCOVER and GROMOS[10]) in dimethyl sulfoxide (DMSO).[11] The structure of cyclo(-Gum^1-Phe^2-D-Trp^3-Lys^4-Thr^5-) **7** is shown in Figure 1 as an example of the synthesized cyclic peptides.



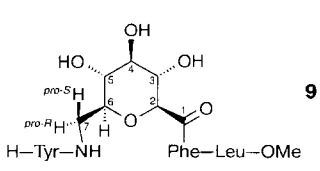
7

Fig. 1. Stereoplot of the average structure of **7** (80 ps MD simulation); for clarity only the polar hydrogen atoms are shown.

In the cyclic peptides the six-membered ring of Gum^1 is found in the chair conformation described above and occupies the $(i+1)$ and $(i+2)$ positions of a pseudo-β turn. Since Gum^1 is only a weak hydrogen bond acceptor (ring oxygen atom), owing to its lack of an amide group, and does not have any hydrogen bond donor groups, stabilizing hydrogen bonds can form only between Xxx^2 and Xxx^4 (Table 1). As expected, D-Xxx^3, which induces the βII′ turn, is in the $(i+1)$ position. The peptide ring is distinctly bent because of the steric repulsion of the ring oxygen atom of **1** and the carbonyl oxygen atom of the neighboring Xxx^5 (Fig. 1). In contrast, the two β turns in a "normal" cyclic hexapeptide with six natural amino acids are almost coplanar.[12]

Most of the the known active somatostatin analogues contain the partial sequence -Phe-D-Trp-Lys-Thr- or -Tyr-D-Trp-Lys-Val- forming a βII′ turn.[9] Peptides **6** and **7** (Table 1) are derivatives of cyclic somatostatin analogues, in which the cyclizing amino acids -Pro-Phe- or a cystine disulfide bridge are replaced by Gum. **6** and **7** are biologically active in the submicromolar range for the inhibition of the release of growth hormone (Table 1). In fact, compound **7** is only 75 times less active than the highly potent somatostatic analogue **8**. This is particularly remarkable, since **7** does not have the lipophilic residues on both sides of the active tetrapeptide sequence that are important for the increase in somatostatin activity.[9]

The effect of Gum on linear peptides was examined with the Leu-enkephalin analogue **9**, in which the Gly-Gly unit of natural Leu-enkephalin is replaced by **1**. The homonuclear $^3J_{H,H}$ coupling constants between the methylene protons on C7 and 6-H in **9** are 1.0 and 8.5 Hz. This indicates that the free rotation about the C6–C7 bond in **9** is restricted such that one of the two methylene protons is antiperiplanar to 6-H. The assignment of the two diastereotopic protons on C7 is difficult, owing to the overlap with the chemical shifts of the ring protons of Gum. However, the interproton distances obtained from a 500 MHz NOESY spectrum assign *pro-S*7-H to be antiperiplanar to 6-H, as shown in the structural formula. Thus Gum most likely forms a loop-type structure in linear peptides as well. Compound **9** does not show biological activity analogous to that of enkephalin up to a concentration of 10^{-5} M.



9

The easily accessible sugar amino acid **1** is the first example, in which a basic sugar unit is employed as a peptidomimetic within a peptide chain. It most likely functions as a dipeptide isostere and induces a β turn in linear peptides, even though it has only partial conformational restriction. Gum is the first of a series of sugar-based peptide building blocks that can be used to adjust the structures and properties of peptides. Thus not only can the secondary structure be influenced (e.g. turn mimetics), peptide side chains can also be mimicked by the selective functionalization of the OH groups of sugar amino acids.

Experimental Procedure

A solution of D-β-Glucopyranosylnitromethane (**2**)[13] (5 g) in methanol (80 mL) and water (20 mL) was hydrogenated with 10% Pd-C (3 g, Degussa, ca. 50% H_2O) under an atmosphere of hydrogen for 24 h (H_2 consumption ca. 3.5 L)[14]. The catalyst was filtered off and washed. The filtrate was treated with $NaHCO_3$ (10.5 g) and benzyl chloroformate (17 mL) and stirred vigorously. After 1 h H_2O (50 mL) was added to the reaction mixture, and the methanol was removed under vacuum. The aqueous solution was washed with diethyl ether and concentrated to dryness under vacuum. The residue was taken up in anhydrous acetone (80 mL), and the inorganic salts were removed by filtration and washed with acetone. The filtrate was concentrated under vacuum and dried giving 7.21 g (98.5%) of **3** as a colorless, hard foam.

Compound **3** (5 g) was dissolved in H_2O (100 mL) and stirred with 10% Pt-C (2.5 g, Degussa, ca. 50% H_2O) at 90 °C under a steady stream of O_2[15]. The gas was pumped through the closed apparatus and purified by passing it through 4 N NaOH. The pH of the reaction mixture was maintained between 7 and 8 by addition of 10% $NaHCO_3$ every hour. Catalyst was added after 8 and 18 h (2 g each time). After the reaction was complete (monitored by TLC), ion-exchange resin (10 g, Aldrich, Amberlyst 15, strongly acidic, H^+ form) was added and the reaction mixture stirred for 10 min. The ion-exchange resin was filtered off and washed with H_2O. The filtrate was concentrated under vacuum and lyophilized. The powdery residue was dissolved in anhydrous methanol (100 mL), DCC (2.9 g) and DMAP (0.2 g) were added, and the reaction mixture was stirred for 1 h. Insoluble residue was removed by filtration, and the filtrate was concentrated almost to dryness under vacuum. The resulting syrup was chromatographed on silica gel (100 g silica gel, eluent $CHCl_3$/methanol 9/1) and then recrystallized from H_2O to provide 1.9 g (34%) of **4**[16] as colorless needles. The methyl ester was prepared, since it is more readily purified and isolated. After saponification of the ester in methanol with 1 N NaOH (1.1 equiv) and cleavage of the Z protective group by hydrogenation, H-Gum-OH **1** was obtained quantitatively in crystalline form ($[\alpha]_D^{20} = -41.2$)[17].

Received: October 16, 1993 [Z 6428 IE]
German version: *Angew. Chem.* **1994**, *106*, 684

[1] A. Giannis, T. Kolter, *Angew. Chem.* **1993**, *105*, 1303–1326; *Angew. Chem. Int. Ed. Engl.* **1993**, *32*, 1244–1267.

[2] The abbreviation "H-Gum-OH" for **1** is derived from glucosyluronic acid methylamine. The systematic name following IUPAC recommendations is 7-amino-L-*glycero*-L-*gulo*-2,6-anhydro-7-deoxyheptoic acid.

[3] The immunosuppressive FK506 is a notable example: H. Tanaka, A. Kuroda, H. Marusawa, H. Hatanaka, T. Kino, T. Goto, M. Hashimoto, *J. Am. Chem. Soc.* **1987**, *109*, 5031–5033.

[4] Galantinic acid, the component of the natural peptide galantine I, is this one known case: N. Sakai, Y. Ohfune, *J. Am. Chem. Soc.* **1992**, *114*, 998–1010.

[5] R. Hirschmann, K. C. Nicolaou, S. Pietranico, E. M. Leahy, J. Salvino, B. Arison, M. A. Cichy, P. G. Spoors, W. C. Shakespeare, P. A. Sprengeler, P. Hamley, A. B. Smith III, T. Reisine, K. Raynor, L. Maechler, C. Donaldson, W. Vale, R. M. Freidinger, M. R. Cascieri, C. D. Strader, *J. Am. Chem. Soc.* **1993**, *115*, 12550–12568. R. Hirschmann, K. C. Nicolaou, S. Pietranico, J. Salvino, E. M. Leahy, P. A. Sprengeler, G. Furst, A. B. Smith, C. D. Strader, M. A. Cascieri, M. R. Candelore, C. Donaldson, W. Vale, L. Maechler, *J. Am. Chem. Soc.* **1992**, *114*, 9217–9218.

[6] The coupling constants of **1** correspond to those listed for the protected compound **4** in ref. [16].

[7] a) H. Kessler, *Angew. Chem.* **1982**, *94*, 509–520; *Angew. Chem. Int. Ed. Engl.* **1982**, *21*, 512–523; b) for the conformation of cyclic hexapeptides: M. Kurz, Dissertation, Technische Universität München, **1991**; c) for the cyclization of

peptides: S. Zimmer, E. Hoffmann, G. Jung, H. Kessler, *Liebigs Ann. Chem.* **1993**, 497–501.
[8] The peptides were synthesized in solution (*DMF/THF* mixtures). EDCI/HOBT (1-ethyl-3-[3-(dimethylamino)propyl]carbodiimide/*N*-hydroxybenzotriazole) was used as a coupling agent, and the cyclization step was activated with TBTU (2-([1*H*]-benzotriazol-1-yl)-1,1,3,3-tetramethyluronium tetrafluoroborate).
[9] a) Our source for **8** is Calbiochem-Novabiochem, Bad Soden/Taunus (FRG); b) an overview on somatostatin analogues is provided by D. F. Veber in *Peptides, Chemistry and Biology, Proceedings of the Twelfth American Peptide Symposium* (Eds.: J. A. Smith, J. E. Rivier), Escom, Leiden, **1992**, pp. 3–14.
[10] a) The program DISCOVER is a product of Biosym Technologies, San Diego, CA, USA; b) W. F. van Gunsteren, H. J. C. Berendsen, *Groningen Molecular Simulation (GROMOS) Library Manual Biomos*, Groningen, **1987**.
[11] D. F. Mierke, H. Kessler, *J. Am. Chem. Soc.* **1991**, *113*, 9466–9470.
[12] M. Kurz, D. F. Mierke, H. Kessler, *Angew. Chem.* **1992**, *104*, 213–214; *Angew. Chem. Int. Ed. Engl.* **1992**, *31*, 210–212.
[13] L. Petrus, S. Bystricky, T. Sticzay, V. Bilik, *Chem. Zvesti* **1982**, *36* (1), 103–110.
[14] L. Petrus, V. Mihalov, *Collect. Czech. Chem. Commun.* **1983**, *48*, 1867–1871; L. Petrus et al. use Fe^{2+} to reduce the nitro group; however, catalytic hydrogenation is preferable.
[15] K. Heyns, H. Paulsen, *Adv. Carbohydr. Chem.* **1962**, *17*, 169–221.
[16] Physical data for the protected compound **4**, the starting compound for the peptide synthesis: $[\alpha]_D^{20} = 21.7$ ($c = 1$ in H_2O); m.p. 164 °C; FAB-MS: *m/z* 356 ($M - H^+$); ^{1}H NMR (250 MHz, [D$_6$]DMSO + 10% D$_2$O, 300 K): δ = 7.29–7.40 (m, 5H, Ph), 4.99 (s, 2H, Ph-CH_2), 3.63 (s, 3H, OMe), 3.63 (d, 1H, 2-H), 3.47 (dd, 1H, 7a-H), 3.29 (dd, 1H, 3-H), 3.20 (ddd, 1H, 6-H), 3.18 (dd, 1H, 4-H), 2.96 (dd, 1H, 5-H), 2.95 (dd, 1H, 7b-H); $J(2,3) = 9.7$, $J(3,4) = 9.1$, $J(4,5) = 8.7$, $J(5,6) = 9.7$, $J(6,7a) = 2.3$, $J(6,7b) = 8.2$, $J(7a,7b) = 14.1$ Hz; ^{13}C NMR (62.5 MHz, DMSO, 300 K): δ = 169.9 (C-1), 156.5(C = O), 128.5–127.8 (Ph), 79.3 (C-2), 79.2 (C-6), 77.2 (C-3), 71.9 (C-4), 71.7 (C-5), 65.5 (Ph-CH_2), 52.0 (OMe), 42.5 (C-7).
[17] E. F. Fuchs, J. Lehmann, *Chem. Ber.* **1975**, *108*, 2254–2260; Fuchs and Lehmann prepared the enantiomer of **1** by a completely different route in eleven steps starting from glucose; however, they did not use the product as a peptide building block.

Discrete M_6N Octahedra in the Subnitrides $Na_{16}Ba_6N$ and $Ag_{16}Ca_6N$: A Reconsideration of the Ag_8Ca_3 Structure Type**

G. Jeffrey Snyder and Arndt Simon*

The suboxides[1] of the heavy alkali metals are remarkable for the occurrence of ion clusters interacting through metallic bonding, leading to some unique physical properties. We have recently expanded this chemistry to barium subnitrides with the discovery of the infinite chain subnitride $NaBa_3N$.[2] Here we report the structure of $Na_{16}Ba_6N$ which contains discrete Ba_6N octahedral clusters. The existence of the isotypic $Ag_{16}Ca_6N$, previously known as Ag_8Ca_3,[3] indicates that subnitride chemistry may be more common than expected.

$Na_{16}Ba_6N$ was discovered in a capillary size sample, prepared as described for the single-crystal investigation of Na_2Ba.[4] Nitrogen originated from traces present in argon freed from water (molecular sieve) and oxygen (oxisorb catalyst[5]). A single crystal of $Na_{16}Ba_6N$[6] was found near the tip of the sample, together with sodium and polycrystalline NaBa[7] and Na_2Ba.

$Na_{16}Ba_6N$ has the metal atom arrangement as described for Ag_8Ca_3. The Ba–Ba distance (3.99 Å) is rather short compared to the distances of 4.54 and 4.52 Å found in the binary intermetallic compounds NaBa and Na_2Ba, respectively, but comparable to the average distance of 3.93 Å in $NaBa_3N$. This and the significant electron density of 3.3 e Å^{-3} at the center of the barium octahedron clearly indicate the presence of a light atom at this position. Refining the data with a nitrogen atom at this position significantly reduces $wR2$ from 0.159 ($R1 = 0.061$) to 0.119 ($R1 = 0.051$). After concluding that the Ba_6 octahedron in $Na_{16}Ba_6N$ must be occupied, we predicted that the center of the Ca_6 octahedron in "Ag_8Ca_3" should also be centered by a nitrogen atom, using the same bond length argument as above, only for Ca–Ca distances.

The structure of Ag_8Ca_3 had been solved by using film methods.[3] Analysis of the starting materials had revealed 0.01% nitrogen; however, after alloying, nitrogen was found "at the 0.1% level".[3] $Ag_{16}Ca_6N$ requires only 0.7% nitrogen.

Following the synthetic procedure for "Ag_8Ca_3"[3] in the absence of nitrogen produced Ag_7Ca_2 and no $Ag_{16}Ca_6N$. However, if the reaction is carried out under an N_2/Ar atmosphere,[8] $Ag_{16}Ca_6N$ is produced as a majority phase. $Ag_{16}Ca_6N$ forms golden metallic air-stable crystals, which are relatively brittle. Grinding the sample and removing malleable intermetallic byproduct (most likely Ag_7Ca_2) resulted in essentially phase pure $Ag_{16}Ca_6N$. The cell and atomic parameters given for "Ag_8Ca_3" are within one standard deviation of our data for $Ag_{16}Ca_6N$.[9] Refining the structure without nitrogen results in a residual electron density peak of 10 e Å^{-3} at the 2*a* position with $wR2 = 0.052$ ($R1 = 0.027$), while placing a nitrogen at this position reduces $wR2$ to 0.026 ($R1 = 0.017$).

The structure of $Na_{16}Ba_6N$ [and $Ag_{16}Ca_6N$] contains discrete regular octahedra of barium [calcium] atoms surrounding a central nitrogen atom. Figure 1 illustrates how these octahedra are separated by the matrix of sodium [silver] atoms. The Na1 [Ag1] atoms cap the faces of two opposing Ba_6N [Ca_6N] octahedra in a trigonal antiprismatic arrangement. The Na2 and [Ag2] atoms not only cap the faces of the Ba_6N [Ca_6N] octahedra, but are also arranged in a square. The metal coordination spheres for "Ag_8Ca_3" were well-described by Pearson.[10]

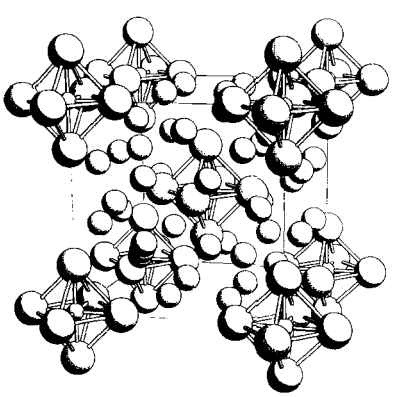


Fig. 1. Structure of $Na_{16}Ba_6N$ showing the Ba_6N octahedra drawn with bonds. The smaller nonconnected spheres represent sodium atoms.

The interatomic distances in $Na_{16}Ba_6N$ and $Ag_{16}Ca_6N$ indicate that there is ionic bonding within the subnitride units and metallic bonding outside. For $Na_{16}Ba_6N$ the Ba–Na and Na–Na average distances (4.48 Å and 3.62 Å, respectively) are similar to those found in the intermetallic phases NaBa (4.27, 3.72 Å) and Na_2Ba (4.32, 3.70 Å), and close to the sum of metal-

[*] Prof. Dr. A. Simon, G. J. Snyder
Max-Planck-Insitut für Festkörperforschung
Heisenbergstrasse 1, D-70569 Stuttgart (FRG)
Telefax: Int. code + (0711)689-1642

[**] We thank Dr. H. Borrmann and Dr. K. Peters for single-crystal data collection, Dr. P. Rauch and T. Gulden for starting materials and helpful discussion and the Hertz Foundation for financial support.

lic radii[10] (4.15, 3.82 Å). As mentioned above, the Ba–Ba distance is closer to those of the subnitrides than those of the binary intermetallic phases of Ba. The Ba–N distance (2.82 Å) is somewhat longer than the corresponding distance in $NaBa_3N$ (2.73 Å) or in Ba_2N (2.76 Å).[11]

For $Ag_{16}Ca_6N$, the average Ca–Ag and Ag–Ag distances (3.38, 2.89 Å) compare well with those of the intermetallic phases AgCa[12] (3.20, 2.88 Å), Ag_7Ca_2 (3.27, 2.92 Å), and the sum of metallic radii (3.42, 2.89 Å). The Ca–Ca distance in $Ag_{16}Ca_6N$ is considerably shorter (3.55 Å) than in the element (3.95 Å) or in the intermetallic phases AgCa (3.99 Å) and Ag_7Ca_2 (3.80 Å), but rather similar to that found in the phases Ca_3XN,[13, 14] which range from 3.4 to 3.5 Å. The Ca–N distance of 2.51 Å found in $Ag_{16}Ca_6N$ is longer than those of the more oxidized compounds Ca_3XN, ranging from 2.41 to 2.48 Å.

The molar volume of $Na_{16}Ba_6N$ can be well-described by using pure sodium metal and partially oxidized barium as a model. Subtracting the contribution due to metallic sodium leaves

$$V_m(Na_{16}Ba_6N) - 16\,V_m(Na) = V_m(Ba_6N) = 211\ cm^3 \cdot mol^{-1},$$

while summing the molar volumes [15] for the individual ions and atoms gives

$$\tfrac{2}{3}V_m(Ba^{2+}) + V_m(N^{3-}) + \tfrac{9}{2}V_m(Ba) = 209.5\ cm^3 \cdot mol^{-1}.$$

Heteropolarity of the bond between Ag and Ca, in contrast to the Na/Ba system,[4] leads to a volume contraction of about 11% for the intermetallic compounds, thus making further volume calculations for $Ag_{16}Ca_6N$ difficult.

Both $Na_{16}Ba_6N$ and $Ag_{16}Ca_6N$ must be metals. The expected metallic behavior is confirmed by four-probe electrical resistivity measurements[16] on $Ag_{16}Ca_6N$ (Fig. 2). The resistivity at room temperature is comparable with that of silver, 1.51×10^{-6} cm.

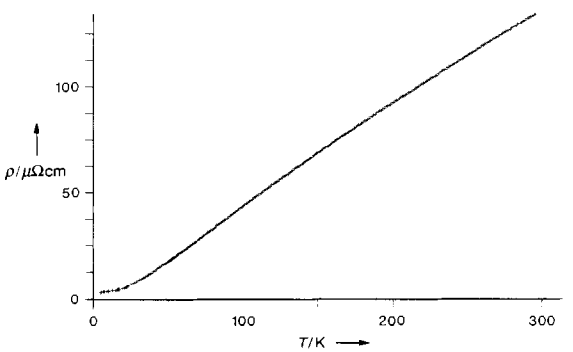


Fig. 2. Resistivity vs. temperature for a sample of $Ag_{16}Ca_6N$ (four-probe measurement) $0.5 \times 0.5 \times 0.5\ mm^3$ in size.

Numerous other phases have been considered to have the Ag_8Ca_3 structure type, $Ni_6Si_2(RE)_3$ (RE = Ce, Pr, Nd, Sm, Eu, Gd, Tb, Dy, Ho, Er, Tm, Yb, Lu),[17] $Ni_6Ga_2(RE)_3$ (RE = Y, Pr, Nd, Sm, Gd, Tb, Dy, Ho, Er, Tm),[18] and $Ni_6Al_2(RE)_3$ (RE = Y, Gd, Tb, Dy, Er, Tm).[19] The question then arises whether the $(RE)_6$ octahedra are empty. So far only the series of compounds $(RE)_6Fe_{16}O_x$ ($x \leq 1$; RE = Gd, Tb, Dy, Ho, Er)[20] have been reported to have the Ag_8Ca_3 structure, but containing an oxygen or some other metalloid atom in the center of the rare-earth atom octahedron. Neutron powder diffraction data[21] on $Ho_6Fe_{16}O$ were consistent with full oxygen occupancy.

The discovery of $Na_{16}Ba_6N$ expands the realm of barium subnitride chemistry. Layers of edge-condensed Ba_6N octahedra are found in Ba_2N,[11] while these octahedra share faces to form chains in $NaBa_3N$ and Na_5Ba_3N, and now discrete Ba_6N octahedra have been found in $Na_{16}Ba_6N$. The existence of oligomeric clusters formed by a limited number of Ba_6N units may be anticipated, as found frequently with transition metals.[22]

The discrete Ba_6N subnitride unit in $Na_{16}Ba_6N$ also supplies the missing piece in suboxide cluster chemistry. The Rb suboxides, Rb_9O_2 and Rb_6O, contain two such face-sharing M_6O units. The Cs suboxides, $Cs_{11}O_3$, Cs_7O, and Cs_4O continue this condensation, combining three face-sharing M_6O units to form $Cs_{11}O_3$ clusters. The segregation of the sodium atom around an individual subnitride cluster in $Na_{16}Ba_6N$ is analogous to that of the rubidium atoms which surround a $Cs_{11}O_3$ cluster in $Rb_xCs_{11}O_3$ ($x = 1, 2, 7$).

Hypermetalated species such as Li_6C have been studied in the gas phase.[23] $Na_{16}Ba_6N$ and $Ag_{16}Ca_6N$ serve as examples where such hypermetalated species are stabilized in the solid state by insertion into a purely metallic matrix.

There is also the promise of other nitrides in the Ag-Ca-N system,[24] possibly with a similarly large variety of structures as seen in the Na-Ba-N system. The accessibility of air-stable single crystals of $Ag_{16}Ca_6N$ will allow detailed investigations on a system that may be termed a "void metal". At a microscopic level the compound is a metal with a periodic sublattice of N^{3-} ions 8.5 Å apart, which are repulsive to conduction electrons. As a consequence quantum size effects can be expected, as they have been demonstrated for related systems like $Cs_{11}O_3$.[25]

Received: December 2, 1993 [Z 6531 IE]
German version: *Angew. Chem.* **1994**, *106*, 713

[1] A. Simon, *Struct. Bonding* **1979**, *36*, 81.
[2] P. E. Rauch, A. Simon, *Angew. Chem.* **1992**, *104*, 1505; *Angew. Chem. Int. Ed. Engl.* **1992**, *31*, 1519.
[3] L. D. Calvert, C. Rand, *Acta Crystallogr.* **1964**, *17*, 1175.
[4] G. J. Snyder, A. Simon, *Z. Naturforsch.*, in press.
[5] H. L. Krauss, H. Stach, *Z. Anorg. Allg. Chem.* **1969**, *366*, 34.
[6] a) Crystal data for $Na_{16}Ba_6N$: $Im\bar{3}m$; $a = 12.5266(5)$; $Z = 2$; $\varrho_c = 2.037\ g\,cm^{-3}$; Na1 in 8*c*, Na2 in 24*h* ($y = 0.3480(9)$), Ba in 12*e* ($x = 0.2255(3)$), N in 2*a*; $R1 = 0.051$, $wR2 = 0.119$ [$I > 4\sigma(I)$]; $R1 = 0.067$, $wR2 = 0.143$ (all data); 134 observed reflections, averaged from 631 measured ($R_{int} = 0.106$); extinction coefficient 0.0006(3); CAD4 diffractometer, $Mo_{K\alpha}$ radiation, 2θ-range of 4.6 to 43.4°; SHELX93. b) Further details of the crystal structure investigation may be obtained from the Fachinformationszentrum Karlsruhe, D-76344 Eggenstein-Leopoldshafen (FRG) on quoting the depository number CSD-57937.
[7] G. J. Snyder, A. Simon, *J. Chem. Soc. Dalton Trans.* in press.
[8] Distilled calcium metal (0.0897 g) and silver shot (0.7125 g) were melted together in a Ta crucible at 780 °C under one atmosphere of purified argon. Cooling to 700 °C, the argon pressure was reduced to 1 mbar and 0.00522 g nitrogen gas added to the system raising the pressure to 15 mbar. After four days at 700 °C, the final pressure was 11 mbar.
[9] Crystal data for $Ag_{16}Ca_6N$: $Im\bar{3}m$; $a = 9.7845(2)$; $Z = 2$; $\varrho_{calcd.} = 7.021\ g\,cm^{-3}$; Ag1 in 8*c*, Ag2 in 24*h* ($y = 0.3467(1)$), Ca in 12*e* ($x = 0.2565(2)$), N in 2*a*; $R1 = 0.017$, $wR2 = 0.026$ [$I > 4\sigma(I)$]; $R1 = 0.021$, $wR1 = 0.026$ (all data); 162 unique reflections, averaged from 792 measured ($R_{int} = 0.034$); extinction coefficient 0.0043(2); CAD4 diffractometer, $Mo_{K\alpha}$ radiation, 2θ-range of 6 to 60°; SHELX-93 [6b].
[10] W. B. Pearson, *The Crystal Chemistry and Physics of Metals and Alloys*, Wiley Interscience, London, **1972**.
[11] H.-T. Künzel, Thesis, Universität Stuttgart, **1980**.
[12] F. Merlo, *J. Less-Common Met.* **1982**, *86*, 241.
[13] X = P, As, Sb, Bi, Ge, Sn, Pb: M. Y. Chern, D. A. Vennos, F. J. DiSalvo, *J. Solid State Chem.* **1992**, *96*, 415.
[14] X = Au: J. Jäger, D. Stahl, P. C. Schmidt, R. Kniep, *Angew. Chem.* **1993**, *105*, 738; *Angew. Chem. Int. Ed. Engl.* **1993**, *32*, 709.
[15] W. Biltz, *Raumchemie der festen Stoffe*, Leopold Voss, Leipzig, **1934**.
[16] Constant D. C. current of 10 mA, using silver epoxy contacts.

 © VCH Verlagsgesellschaft mbH, D-69451 Weinheim, 1994 0570-0833/94/0606-0690 $ 10.00+.25/0

[17] E. I. Hladyschewskyj, P. I. Krypiakewytsch, O. I. Bodak, *Z. Anorg. allg. Chem.* **1966**, *344*, 95.
[18] J. P. Jarmoljuk, J. N. Gryn', E. I. Gladyshevskij, *Dopov. Akad. Nauk Ukr. RSR, Ser. A: Fiz. Mat. Tekh. Nauki* **1978**, *40*, 759.
[19] R. M. Rykhal', O. S. Zarechnjuk, V. M. Mandzyn, *Dopov. Akad. Nauk Ukr. RSR Ser. A: Fiz.-Mat. Tekh. Nauki* **1980**, *42*, 77; O. S. Zarechnjuk, R. M. Rykhal', V. A. Romaka, O. K. Koval'skaja, A. I. Sharabura, *ibid.* **1982**, *44*, 81; R. M. Rykhal', O. S. Zarechnjuk, O. M. Marich, *ibid.* **1978**, *40*, 853; R. M. Rykhal', O. S. Zarechnjuk, *ibid.* **1977**, *39*, 375; R. M. Rykhal', O. S. Zarechnjuk, V. S. Protasov, V. A. Romaka, *Dopov. Akad. Nauk Ukr. RSR, Ser. B: Geol. Khim. Biol. Nauki* **1982**, 43.
[20] M. P. Dariel, M. R. Pickus, *J. Less-Common Met.* **1976**, *50*, 125.
[21] M. Melamud, M. P. Dariel, H. Shaked, *J. Appl. Phys.* **1979**, *50*, 1978.
[22] A. Simon, *Angew. Chem.* **1988**, *100*, 163; *Angew. Chem. Int. Ed. Engl.* **1988**, *27*, 159.
[23] P. von R. Schleyer in *New Horizons of Quantum Chemistry* (Eds.: P.-O. Löwdin, B. Pullman), Reidel, Dordrecht, **1983**, p. 95.
[24] See reference [15], footnote 4.
[25] M. G. Burt, V. Heine, *J. Phys. C* **1978**, *11*, 961.

A Clathrate Hydrate of Nitric Oxide**

Andreas Hallbrucker*

Nitric oxide (NO) recently was found to be of crucial importance in biochemical processes.[1] The interaction of NO with the solvent water is one of its basic physical properties important in this context. However, measurements are scarce, for example, the stretching vibration of NO dissolved in water at ambient temperature, which might serve as an indicator for its perturbation by the solvent, has not been reported so far, probably because of experimental difficulties. The solvent–solute interaction of nonpolar or slightly polar gases in aqueous solution is often considered to resemble the arrangement of molecules in crystalline water clathrates.[2, 3] In the absence of experimental data, the interaction of NO with liquid water may be approximately described by this system. I show here that the clathrate hydrate of NO is prepared by adsorption of NO in highly porous, amorphous solid water at 77 K and subsequent heating of the sample to 197 K. It is characterized by X-ray diffraction and Raman spectra of the NO vibration. Unlike CO,[4] a molecule with very similar physical properties, NO is shown to form a clathrate hydrate of structure II.

Gas hydrates of small guests such as O_2, N_2, and CO are usually prepared by grinding ice at about 243 K under pressures >150 bar for several days.[5] Evidently, this method is only suitable for stable and inert guest gases. Only recently a new method for preparing these clathrate hydrates at low temperatures and pressures from microporous, amorphous solid water (ASW) was established.[6] ASW is formed by slow deposition of water vapor on a substrate held at 77 K in a vacuum system and exposed to moderate pressures of gas (<1 bar). On heating to about 120 K considerable amounts of this gas are irreversibly trapped in the ice matrix and transformed to a clathrate hydrate on further heating in vacuo.[6]

Samples of ASW with enclosed NO were initially prepared, by the method already described for O_2, N_2, CO, and Ar clathrate hydrates,[6] on an X-ray sample holder and on small brass plates for Raman probes. Briefly, water vapor was admitted to a vacuum system and condensed on the substrate cooled to 77 K at low base pressure (ca. 10^{-6} mbar) for about 6 h. This gave an amorphous ice layer of about 1 mm thickness. Subsequently, NO gas was condensed onto the ASW layer for 3 h at equally low base pressure. Practical grade NO was taken from a tank (Messer Griesheim, purity >99.85%), and purified by fractionating condensation.[7] The purity (i.e. the absence of N_2O and NO_2) was checked by IR spectroscopy. The samples were then heated to 140 K at which temperature considerable amounts of NO are irreversibly trapped in the pores and micropores of ASW. After recooling to liquid nitrogen temperature, sample holders were removed from the vacuum apparatus and transferred to the precooled X-ray camera, or into the cryostat for Raman measurements. All Raman spectra were recorded at 130 K, after recooling, because irradiation at elevated temperatures leads to reaction of NO.

The X-ray diffractogram of the sample after transfer to the X-ray camera and heating to 130 K is depicted in Figure 1, curve 1. Only two broad peaks at $2\theta = 24$ and 43° are observable, characteristic for ASW. In Figure 2, curve 1, the Raman spectrum of the NO stretching vibration region is represented, exhibiting two sharp peaks at 1868.8 and 1858.8 cm^{-1} and one broad and weak absorption band at about 1840 cm^{-1}. On heating to 173 K ASW largely crystallizes to cubic ice (Ic), evident by the sharp reflections in the X-ray diffractogram in Figure 1, curve 2. In Figure 2, curve 2, the Raman spectrum of the sample after heating to 173 K and recooling to 130 K is shown: it also exhibits three absorption bands at nearly the same positions (1868.1, 1858.6, and 1836.6 cm^{-1}) as those in curve 1 but with significant changes of their intensities. Whereas the total area under the three bands is almost unchanged, the intensity of the band at highest frequency is decreased, mainly at the expense of the band near 1858 cm^{-1}. The intensity of the band at lowest frequency is only slightly increased. Raman and X-ray samples were then heated to 197 K and recooled to 130 K. Four clearly

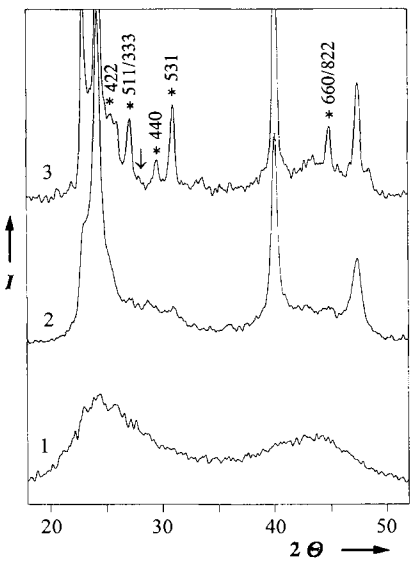


Fig. 1. X-ray diffractograms of amorphous solid water with enclosed NO recorded at 130 K: 1) on first heating starting from about 80 K, 2) after partial crystallization to cubic ice by heating to 173 K, and 3) after formation of NO clathrate hydrate at 197 K. Reflections due to NO clathrate hydrate are marked with * in curve 3 and indexed for a structure II clathrate hydrate. Curves are represented on the same scale with constant ordinate offset. The diffractograms were recorded with Kristalloflex 4 (Siemens) by using $Cu_{K\alpha}$ radiation.

[*] Dr. A. Hallbrucker
Institut für Allgemeine, Anorganische und Theoretische Chemie
der Universität
Innrain 52a, A-6020 Innsbruck (Austria)
Telefax: Int. code + (512) 507-3223

[**] This work was supported by the Forschungsförderungsfonds of Austria (project no. 9175-PHY).

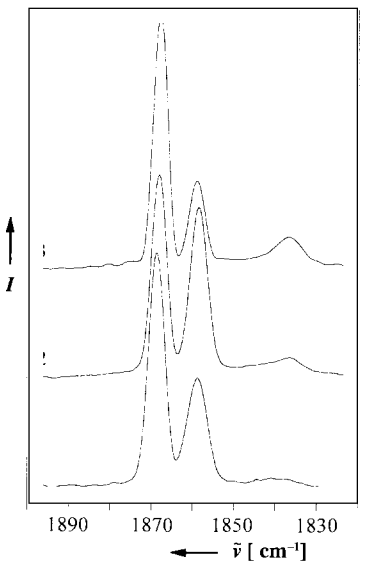


Fig. 2. Raman spectra of the NO stretching vibration region of NO absorbed in the micropores of amorphous solid water recorded at 130 K: 1) on first heating starting from about 80 K, 2) after crystallization to cubic ice by heating to 173 K, and 3) after formation of NO clathrate hydrate of strucutre II at 197 K. Curves were drawn on the same scale. All spectra were measured at 130 K on a Coderg PHO instrument with double monochromator and photon counting, slit with 4 cm^{-1}, 488 nm argon laser excitation with a power of 500 mW.

observable additional reflections in the diffractogram of this sample in Figure 1, curve 3, at $2\theta = 27.14$, 29.60, 31.01, and 44.89° indicate the formation of NO clathrate hydrate.[8] Clathrate hydrates formed this way from ASW necessarily contain a large amount of cubic and/or hexagonal ice, because it stabilizes the clathrate hydrate.[6] The four additional reflections mentioned above, which are clearly separated from the ice reflections, must be due to NO clathrate hydrate because they grow and disappear at the same rate, and formation of other clathrate hydrates by contaminants such as N_2, O_2, N_2O, NO_2, and CO, has been carefully excluded by Raman spectroscopy. A fifth reflection due to NO clathrate hydrate, at $2\theta = 25.50°$, is partly superimposed by the ice reflections at $2\theta = 24.38°$ (off scale) and 25.98°, but is also formed at a similar rate as the other four reflections due to NO clathrate hydrate. Its peak position is retained in diffractograms bandnarrowed by deconvolution. The total area under five NO clathrate hydrate reflections accounts for about 10% of the total area under the diffraction curve, this can also be used as the lower limit of the amount of clathrate hydrate formed.[6]

The assignment of NO clathrate hydrate to a clathrate hydrate of structure type II is based on the following, and its reflections (see Fig. 1) are indexed accordingly: 1) Whereas three of the well-separated clathrate hydrate reflections have counterparts at similar positions in the diffractogram of a clathrate hydrate of structure I, the reflection at $2\theta = 29.60°$ (index 440 for structure II) has none. This reflection clearly shows up in all of the common structure II clathrate hydrates with about half of the intensity of the reflections at 27.14 and 31.01° (index 511/333 and 531, respectively) at only slightly varying position.[6, 8, 9] 2) The most intense peak in clathrate hydrates of type I (index 321) is absent! Since the size of the cubic unit cell for clathrate hydrates of type I is always close to 11.9 Å, largely independent of the size and type of the guest molecule, this reflection (321) is always found at about 28.1°. At this position, which is marked by an arrow in Figure 1, curve 3, no intense peak is recognizable. For CO, a molecule resembling NO in size and polarity, but forming a clathrate hydrate of structure I, it occurs at 28.115° with maximum intensity.[4] The absence of this reflection is a strong argument in favor of a clathrate hydrate of type II, because this reflection is calculated and consistently observed as the most intense one in clathrate hydrates of type I.[4, 8, 10] 3) The reflection at $2\theta = 25.50°$, which is partly superimposed by the ice reflections, can easily be assigned to a clathrate hydrate peak of type II, with index 422.[9] In CO clathrate hydrate of type I the closest peak is at $2\theta = 25.98°$[4] which is outside the range expected for differences in lattice parameters.

In Figure 2, curve 3, the Raman spectrum of the sample containing NO clathrate hydrate is shown. It also exhibits three bands with maxima shifted only slightly (with respect to curve 2) to lower frequencies (1867.8, 1858.8, and 1836.6 cm^{-1}). The total area under the three absorption bands has decreased by about 13%, apparently due to loss of NO during clathrate hydrate formation. However, only the intensity of the band at the intermediate position has decreased, whereas the intensities of the bands at high and low frequency have in fact increased. The band at 1836.6 cm^{-1} is assigned to NO encaged in the lattice of the clathrate hydrate, because its absolute area increases from curve 1 to curve 3, parallel to the increase in clathrate hydrate formation observed by diffraction. This is not the case for the other two intense bands at about 1869 cm^{-1} and about 1859 cm^{-1}, which are observable already in the fully amorphous ASW sample (curve 1). These two bands are assigned to NO in two distinct trapping sites. In curve 1 a very weak and broad band at about 1840 cm^{-1} further indicates the presence of a third trapping site in the amorphous ice matrix which has a similar frequency to that of NO in the clathrate hydrate.

The stretching vibration of gaseous NO at 300 K is centered at 1877 cm^{-1}[11] and at 1875 cm^{-1} for NO in an Ar matrix at 4.2 K.[12] The frequency of the stretching vibration of the condensed states $(NO)_2$ is lowered to 1866 cm^{-1},[13] similar in frequency to one of the bands observed in the ice matrix. It is very unlikely, however, that considerable amounts of NO dimer exist at 130 K.[7] Moreover, a Raman spectrum recorded at 173 K gave the same pattern as curve 2 in Figure 2. The frequency of the stretching vibration of NO, enclosed in the cages of the clathrate hydrate, is further lowered to 1836.6 cm^{-1}. This indicates considerable interactions with the hydrate matrix. The shift of the NO stretching vibration by about 40 cm^{-1} to lower frequency, compared to the gas phase value, is much higher than the shift of about 10 cm^{-1} observed for O_2 clathrate hydrate.[14] Force constant calculations from observed frequencies give 1.45×10^3 N m^{-1} for $^{14}N^{16}O$ clathrate hydrate and 1.55×10^3 N m^{-1} for $^{14}N^{16}O$ in the gas phase or in an Ar matrix.

While originally the size of the guest molecule was anticipated to determine the structure of the hydrate formed, with small molecules forming type I,[15] clathrate hydrates of N_2 and O_2 were identified as being type II.[5, 6] Somewhat surprisingly CO clathrate hydrate proved to be type I.[4, 6] A small dipole moment, and a slightly higher quadrupole moment and molecular polarizability than O_2 and N_2 were considered to be responsible for this fact by Davidson et al.[4] This must now be considered inconclusive, since NO, with very similar properties to CO, forms a clathrate hydrate of structure type II.

Received: September 17, 1993 [Z 6362 IE]
German version: *Angew. Chem.* **1994**, *106*, 677

[1] J. S. Stamler, D. J. Singel, J. Loscalzo, *Science* **1992**, *258*, 1898–1902; see also the highlight by H.-J. Galla, *Angew. Chem.* **1993**, *105*, 399; *Angew. Chem. Int. Ed. Engl.* **1993**, *32*, 378.

[2] L. Pauling, *Science* **1961**, *134*, 15–21.
[3] W. J. Moore, *Physikalische Chemie*, 2nd edition, de Gruyter, Berlin, **1976**, p. 275.
[4] D. W. Davidson, M. A. Desando, S. R. Gough, Y. P. Handa, C. I. Ratcliffe, J. A. Ripmeester, J. S. Tse, *Nature* **1987**, *328*, 418–419.
[5] D. W. Davidson, Y. P. Handa, C. I. Ratcliffe, J. A. Ripmeester, J. S. Tse, J. R. Dahn, F. Lee, L. D. Calvert, *Mol. Cryst. Liq. Cryst.* **1986**, *141*, 141–149.
[6] A. Hallbrucker, E. Mayer, *J. Chem. Soc. Faraday Trans.* **1990**, *86*, 3785–3792.
[7] C. E. Dinerman, G. E. Ewing, *J. Chem. Phys.* **1970**, *53*, 626–631.
[8] M. von Stackelberg, H. R. Müller, *Z. Elektrochem.* **1954**, *58*, 25–45.
[9] J. E. Bertie, S. M. Jacobs, *J. Chem. Phys.* **1978**, *69*, 4105–4113.
[10] J. E. Bertie, F. E. Bates, D. K. Hendricksen, *Can. J. Chem.* **1975**, *53*, 71–75.
[11] G. Herzberg, *Molecular Spectra and Molecular Structure, I. Spectra of Diatomic Molecules*, 2nd edition, van Nostrand, Toronto, Canada, **1967**, p. 62.
[12] W. G. Fateley, H. A. Bent, B. Crawford, Jr., *J. Chem. Phys.* **1959**, *31*, 204–217.
[13] E. M. Nour, L. H. Chen, M. M. Strube, J. Laane, *J. Phys. Chem.* **1984**, *88*, 756–759.
[14] A. Hallbrucker, *J. Chem. Soc. Faraday Trans.* **1994**, *90*, in press.
[15] D. W. Davidson in *Water – A Comprehensive Treatise, Vol. 2* (Ed.: F. Franks), Plenum, New York, **1972**, Ch. 3.

Rearrangement and Selective Transmetalation of Bis(pyridyl)methyllithium**

Heinz Gornitzka and Dietmar Stalke*

Recently we investigated the crystal structure of bis([12]crown-4)lithium bis[*N*,*N*′-bis(trimethylsilyl)phenylsulfinamidinato]lithiate.[1] The two inequivalent lithium atoms in $[Li([12]crown\text{-}4)_2]^+[Li(\{N(SiMe_3)\}_2SPh)_2]^-$ and the lithium atom in the transformation product $[PhS\{(Me_3Si)N\}_2$-Li([12]crown-4)] gave rise to three separate signals resolved for the first time in a ^7Li quadrupole nutation MAS NMR spectrum (MAS = magic angle spinning).

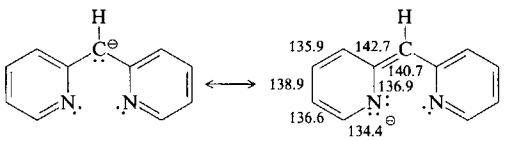
To elucidate the nature of the transformation in more detail, we synthesized bis(2,2′-pyridyl)methylbis(tetrahydrofuran)-lithium (**1**) and the corresponding lithium-lithiate compound **2**.

$[Li\{(2\text{-}NC_5H_4)_2CH\}(thf)_2]$ **1**

$[Li([12]crown\text{-}4)_2][Li\{(2\text{-}NC_5H_4)_2CH\}_2]$ **2**

In contrast to, for example, triphenylmethyl alkali metal derivatives,[2] in which the lithium atom is coordinated by the central carbon atom[3] or the heavier alkali metal atoms are coordinated by a phenyl ring,[4] the bis(2,2′-pyridyl)methyl substituent provides two additional nitrogen atoms in the heteroarene rings for coordination.

If bis(2,2′-pyridyl)methane[5–7] is treated with *n*BuLi, the central carbon atom of the CH_2 group of the starting material is deprotonated. However, as the crystal structure[8] of **1** shows, the deprotonated ligands contain in a formal sense a carbanionic noncoordinated center.[9] The average bond lengths (see **B**) in the bis(pyridyl)methyl ligands of the compounds **1**, **2**, and **4** show that the carbanionic mesomeric structure **A** with the double bonds at the positions 2 and 4 in the pyridine ring provides an inadequate description of the ligands; the mesomeric structure **B** describes the bonding better.



A **B**

As expected, the lithium atom is exclusively coordinated to the two nitrogen atoms of the pyridine rings and to two THF molecules (Fig. 1a). The lithium atom is within the plane of the chelating ligand, and one of the THF molecules lies above and one below that plane.[10] The Li–N bonds (196.6 and 197.3 pm) are of normal length.[11]

Compound **2** forms a solvent-separated ion-pair in the solid state (Fig. 1b).[8] Only two related structures of this lithium-lithiate type compound are known.[1, 12] The Li1 atom is coordinated to two $HC(2\text{-}NC_5H_4)_2$ ligands, giving the overall singly charged anion. The Li2 atom is complexed by two crown ether molecules, giving a singly charged cation. The Li–N bonds in **2** are slightly longer than those in **1**, reflecting the higher steric requirement of the two bis(pyridyl)methyl ligands coordinated

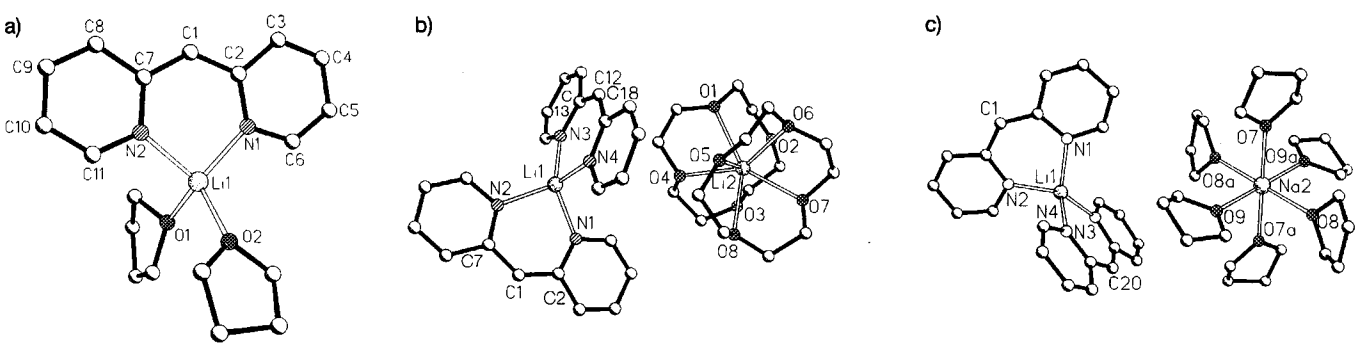


Fig. 1. a) The crystal structure of **1**; selected bond lengths [pm] and angles [°]: Li1-N1 196.6(4), Li1-N2 197.3(4), Li1-O1 199.4(4), Li1-O2 196.5(3); N1-Li1-N2 96.4(2), O1-Li1-O2 98.9(2), C2-C1-C7 130.9(2). b) The crystal structure of **2**; selected bond lengths [pm] and angles [°]: Li1-N1 201.5(5), Li1-N2 202.6(5), Li1-N3 200.1(5), Li1-N4 200.3(5), Li2-O 236.5(5) (average) (range 221.9–252.3); N1-Li1-N2 92.6(2), N3-Li1-N4 93.6 (2), C2-C1-C7 130.3(2), C13-C12-C18 130.8(2). c) The crystal structure of **4**; selected bond lengths [pm] and angles [°]: Li1-N1 201.0(5), Li1-N2 200.0(5), Li1-N3 200.4(5), Li1-N4 198.5(5), Na-O 237.8(2) (average); N1-Li1-N2 93.6(2), N3-Li1-N4 94.0(2).

[*] Priv.-Doz. Dr. D. Stalke, Dipl.-Chem. H. Gornitzka
Institut für Anorganische Chemie der Universität
Tammannstrasse 4, D-37077 Göttingen (FRG)
Telefax: Int. code + (551)39-2582

[**] This work was supported by the Deutsche Forschungsgemeinschaft and the Fonds der Chemischen Industrie. We are grateful to Mr. W. Zolke for recording the ^6Li CP/MAS NMR spectra.

to just one lithium atom. The Li1 ··· C1 vector intersects the Li1 ··· C12 vector at an angle of 159.8°, and the planes of the anions are not exactly perpendicular (82.3°). We synthesized ^6Li-enriched **2** to investigate the dynamic behavior of the compound in solution and in the solid state by ^6Li NMR experiments. Unfortunately, **2** is not soluble enough in hydrocarbons

 © VCH Verlagsgesellschaft mbH, D-69451 Weinheim, 1994 0570-0833/94/0606-0693 $ 10.00+.25/0

to record the ^{6}Li NMR spectrum in solution. In [D$_8$]THF solution the different environments of the two lithium atoms level out giving rise to a single resonance signal at $\delta = 3.25$. As expected, the solid-state structure is not retained in donor solvents. Two resonance signals are observed in the ^{6}Li CP/MAS NMR spectrum (CP = cross polarization) at $\delta = -2.5$ and 3.3 (Fig. 2a). The spectrum a was recorded from a freshly crystallized sample ($t_0 = 0$). Even in this spectrum a broad signal at $\delta = 1.4$ indicates a third ^{6}Li magnetic environment. After the first measurement the rotor with the sample was stored for 3 h at room temperature in a dry argon atmosphere. The spectrum recorded subsequently (Fig. 2b) shows the growth of the signal at $\delta = 1.4$; storage for 12 h under the same conditions leads to further growth of the third signal (Fig. 2c). The spectra d and e in Figure 2 depict the ^{6}Li CP/MAS NMR spectra after additional warming to +50 °C for 2 h and 12 h, respectively. The spectrum e represents the end of the phase transition at +50 °C. Longer warming gives rise to the same signal pattern.

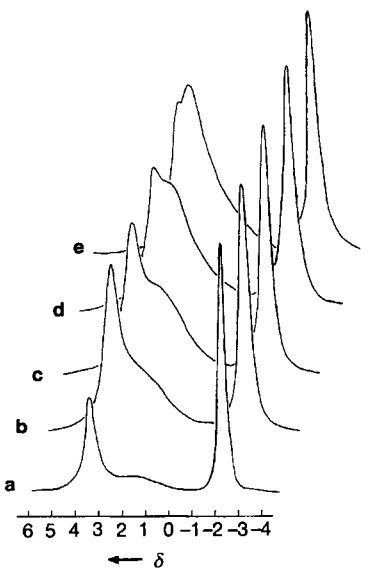
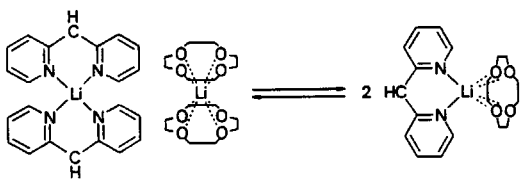


Fig. 2. The ^{6}Li CP/MAS NMR spectrum ($^6LiCO_3$ as external standard) depicting the partial transformation of **2** to **3**. a) Two signals at $t_0 = 0$ and $\delta = -2.5$, 3.3; b) $t_1 = t_0 + 3$ h; c) $t_2 = t_0 + 16$ h; d) $t_3 = t_2 + 2$ h at +50 °C; e) $t_4 = t_3 + 12$ h at +50 °C.

To explain the alterations in the spectra we suggest a rearrangement equilibrium of **2** to **3**, where in the product **3** one bis(pyridyl)methyl ligand and one crown ether molecule are coordinated to the lithium atom.



2 **3**

Compound **2** gives rise to two resonance signals, whereas **3** leads to a single resonance signal in the ^{6}Li CP/MAS NMR spectrum. After the experiment the orange powder of compound **2** consists of two phases. Compound **3** forms a purple semiplastic phase on the inner wall of the NMR rotor, while unrearranged **2** remains in the center of the rotor. Apparently, the considerable mechanical strain (12000 revs. s^{-1}) promotes the rearrangement of **2** to **3**.

Treatment of **1** with one equivalent of NaO*t*Bu in THF surprisingly leads to the first sodium lithiate complex **4** rather than to the total metal exchange product.

$$\underset{\mathbf{1}}{2[Li\{(2\text{-}NC_5H_4)_2CH\}(thf)_2]} \xrightarrow[-\ LiO\mathit{t}Bu\ -\ NaO\mathit{t}Bu]{\text{in THF}\ +\ 2\ NaO\mathit{t}Bu} \underset{\mathbf{4}}{[Na(thf)_6][Li\{(2\text{-}NC_5H_4)_2CH\}_2]}$$

Crystals of **4** were obtained at −35 °C from THF. The low melting single crystals (m.p. < −30 °C) were selected and transferred to the diffractometer at −80 °C.[13] To our knowledge **4** is the first example of a sodium lithiate although a few mixed lithium/sodium complexes are known.[14] The anion in **4** is very similar to the one in **2** (Fig. 1c). Formally the Li([12]crown-4)$_2$ cation in **2** is replaced by the very unusual [Na(thf)$_6$] cation.[15] The Li1 ··· C1 vector intersects the Li1 ··· C20 vector at an angle of 162.6° and, in contrast to **2**, the mean planes of the anions are almost perpendicular (91.7°).

Apparently, two CH(2-NC$_5$H$_4$)$_2$ anions accommodate a single Li cation so well that this structural motif is present in **2** and **4**. This might be the reason why complete metal exchange does not occur. Hence this reaction and the structure of **4** provide some insight to the function of superbases.[16] In the mixture of RLi/NaO*t*Bu the R$^-$ ion does not necessarily have to be a classical carbanion like Me$^-$ or Bu$^-$. The very attractive Li–O interaction is often regarded as the driving force in this type of reaction. Compound **4** appears to be the first example in which only one Li–O bond but six Na–O bonds are formed. With the right shape and basisity of the carbanion, selective transmetalation can be achieved. We are currently investigating the steric and electronic requirements necessary to vary the anion R$^-$ of the organolithium component RLi in other selective transmetalations by KO*t*Bu, RbO*t*Bu, and CsO*t*Bu.

Experimental Procedure

1: H$_2$C(2-NC$_5$H$_4$)$_2$ (0.681 g, 4 mmol) in THF (25 mL) was treated with the equimolar amount of *n*BuLi (1.74 mL of a 2.3 M solution) at −80 °C. Evaporating off the solvent gave an orange precipitate, which was washed twice with pentane (10 mL). Crystallization from THF yielded X-ray quality crystals. Yield 0.858 g; 67%, m.p. 40 °C. Decomposition at $T \geq 70$ °C, ^{1}H NMR ([D$_8$]THF, room temperature,TMS ext.): $\delta = 1.77$, 3.58 (THF), 4.63 (s, H1), 5.80 (ddd, $^3J_{5,4} = 6.61$, $^3J_{5,6} = 5.31$, $^4J_{5,3} = 1.11$ Hz; H5), 6.28 (ddd, $^3J_{3,4} = 8.65$, $^4J_{3,5} = 1.11$, $^4J_{3,1} = 1.11$ Hz; H3), 6.74 (ddd, $^3J_{4,3} = 8.65$, $^3J_{4,5} = 6.61$, $^4J_{4,6} = 1.91$ Hz; H4), 7.59 (dd, $^3J_{6,5} = 5.31$, $^4J_{6,4} = 1.91$ Hz; H6); ^{13}C NMR (THF/C$_6$D$_6$, room temperature, TMS. ext.): $\delta = 88.4$ (s, C1), 110.7 (s, C5), 122.8 (s, C3), 135.6 (s, C4), 141.2 (s, C6), 155.1 (s, C2); ^{7}Li NMR ([D$_8$]THF, room temperature, LiCl ext.): $\delta = 3.25$.

2 H$_2$C(2-NC$_5$H$_4$)$_2$ (1.702 g, 10 mmol) in hexane (30 mL) was treated with *n*Bu^{6}Li (5.4 mL, 1.85 M solution) at −80 °C. After stirring for 2 h [12]crown-4 (2.000 g, 11.349 mmol) was added. The reaction mixture was warmed to room temperature and the precipitate was redissolved in a small amount of THF. Storage at −35 °C yielded X-ray quality single crystals, yield 2.995 g; 85%, m.p. 193 °C. Decomposition at $T \geq 215$ °C. **2** is insoluble in hydrocarbons and NMR investigations in THF show similar chemical shifts as **1**.

4 NaO*t*Bu (0.769 g, 8 mmol) and Li(2-NC$_5$H$_4$)$_2$CH (1.409 g, 8 mmol) were stirred in THF (30 mL) at room temperature. The reaction mixture was directly transferred to a deep freezer. After three days at −35 °C colorless crystals were obtained; melting point about −30 °C; all NMR data were obtained from the vacuum-dried THF-free powder (decomp $T > 270$ °C). ^{1}H NMR ([D$_8$]THF, room temperature, TMS ext.): $\delta = 4.61$ (s, H1), 5.70 (ddd, $^3J_{5,4} = 6.55$, $^3J_{5,6} = 5.30$, $^4J_{5,3} = 1.1$ Hz; H5), 6.23 (d, $^3J_{3,4} = 8.60$ Hz, H3), 6.69 (ddd, $^3J_{4,3} = 8.60$, $^3J_{4,5} = 6.55$, $^4J_{4,6} = 1.99$ Hz; H4), 7.59 (dd, $^3J_{6,5} = 5.30$, $^4J_{6,4} = 1.99$ Hz, H6); ^{13}C NMR ([D$_8$]THF, room temperature, TMS ext.): $\delta = 87.8$ (s, C1), 105.9 (s, C5),120.1 (s, C3), 132.8 (s, C4), 148.1 (s, C6), 160.2 (s, C2); ^{7}Li NMR ([D$_8$]THF, room temperature, LiCl ext.): $\delta = 2.34$ (s); ^{23}Na NMR ([D$_8$]THF, room temperature, NaCl ext.): δ −0.49 (s, br.).

Received: October 25, 1993 [Z 6442 IE]
German version: *Angew. Chem.* **1994**, *106*, 695

[1] F. Pauer, J. Rocha, D. Stalke, *J. Chem. Soc. Chem. Commun.* **1991**, 1477.
[2] Review: E. Weiss, *Angew. Chem.* **1993**, *105*, 1565; *Angew. Chem. Int. Ed. Engl.* **1993**, *32*, 1501.
[3] J. J. Brooks, G. D. Stucky, *J. Am. Chem. Soc.* **1972**, *94*, 7333.
[4] D. Hoffmann, W. Bauer, P. von R. Schleyer, U. Pieper, D. Stalke, *Organometallics* **1993**, *12*, 1193.
[5] C. Osuch, R. Levine, *J. Am. Chem. Soc.* **1956**, *78*, 1723.
[6] A. J. Canty, N. J. Minchin, *Aust. J. Chem.* **1986**, *39*, 1063.
[7] F. R. Keene, E. R. T. Tiekink, *Acta Crystallogr. Sect. C* **1990**, *46*, 1562.
[8] Crystal data for **1** (−120 °C): $C_{19}H_{25}LiN_2O_2$, $M = 320.35$, orthorhombic, space group $P2_12_12_1$, $a = 970.4(1)$, $b = 1305.3(1)$, $c = 1354.3(3)$ pm, $V = 1.716(1)$ nm^3, $Z = 4$, $\varrho_{calcd} = 1.240$ Mg m^{-3}, $\mu = 0.08$ mm^{-1}, 3712 measured reflections, 3264 independent, 3260 employed in the refinement, $2\theta_{max} = 55°$, $R1 = \Sigma||F_o| - |F_c||/\Sigma F_o = 0.040$ ($F > 4\sigma F$) and $wR2 = [\Sigma w(F_o^2 - F_c^2)^2/(\Sigma wF_o^4)]^{1/2} = 0.152$ (all data) of $w^{-1} = \delta^2(F_o^2) + (g1 \cdot P)^2 + g^2 \cdot P$ with $P = (F_o^2 + 2F_c^2)/3$ and $g1 = 0.035$, $g^2 = 0.380$, max. residual density: 1.3×10^2 e nm^{-3}; **2** (−120 °C): $C_{38}H_{50}Li_2N_4O_8$, $M = 704.3$, monoclinic, space group $P2_1/c$, $a = 1194.1(6)$, $b = 2404.9(12)$, $c = 1320.8(7)$ pm, $\beta = 101.74(3)°$, $V = 3.714(3)$ nm^3, $Z = 4$, $\varrho_{calcd} = 1.260$ Mg m^{-3}, $\mu = 0.09$ mm^{-1}, 7744 measured reflections, 6512 independent, 6508 employed in the refinement, $2\theta_{max} = 50°$, $R1 = 0.050$ and $wR2 = 0.159$ (all data, $g1 = 0.050$, $g2 = 1.07$; same definitions as above), max. residual density: 2.0×10^2 e nm^{-3}; **4** (−120 °C): $C_{50}H_{74}LiN_4O_7Na$, $M = 873.06$, triclinic, space group $P\bar{1}$, $a = 1132.4(5)$, $b = 1407.3(7)$, $c = 1788.5(9)$ pm, $\alpha = 93.49(2)$, $\beta = 106.73(2)$, $\gamma = 112.76(2)°$, $V = 2.469(3)$ nm^3, $Z = 2$, $\varrho_{calcd} = 1.175$ Mg m^{-3}, $\mu = 0.09$ mm^{-1}, 8151 measured reflections, 6405 independent, 6404 employed in the refinement, $2\theta_{max} = 45°$, $R1 = 0.055$ and $wR2 = 0.155$ (all data, $g1 = 0.078$, $g2 = 1.93$; same definitions as above), max. residual electron density: 3.7×10^2 e nm^{-3}. Data of all discussed structures were collected on a Stoe-Siemens diffractometer. Intensities of a rapidly cooled crystal in an oil drop [13] were collected by using graphite-monochromated $Mo_{K\alpha}$ radiation ($\lambda = 71.073$ pm). The structures were solved by direct methods (SHELXS-90) [17]. All non-hydrogen atoms were refined anisotropically on (F^2) [18]. The absolute structure of **1** could not be established by refinement of an inversion twin parameter [19] [$x = -0.32(13)$, where $x = 0$ for the correct absolute structure and -1 for the inverted structure]. Further details of the crystal investigations are available on request from the Director of the Cambridge Crystallographic Data Centre, 12 Union Road, GB-Cambridge CB2 1EZ, by quoting the full journal citation.
[9] U. Pieper, D. Stalke, *Organometallics* **1993**, *12*, 1201.
[10] A. Steiner, D. Stalke, *J. Chem. Soc. Chem. Commun.* **1993**, 444.
[11] K. Gregory, P. von R. Schleyer, R. Snaith, *Adv. Inorg. Chem.* **1991**, *37*, 47.
[12] C. Eaborn, P. B. Hitchcock, J. D. Smith, A. C. Sullivan, *J. Chem. Soc. Chem. Commun.* **1983**, 827.
[13] T. Kottke, D. Stalke, *J. Appl. Crystallogr.* **1993**, *26*, 615.
[14] a) K. Jonas, D. J. Brauer, C. Krüger, P. J. Roberts, Y. H. Tsay, *J. Am. Chem. Soc.* **1976**, *98*, 74; b) E. Weiss, G. Sauermann, G. Thirase, *Chem. Ber.* **1983**, *116*, 74; c) W. Clegg, R. E. Mulvey, R. Snaith, G. E. Toogood, K. Wade, *J. Chem. Soc. Chem. Commun.* **1986**, 1740; d) N. G. Furmanova, V. I. Andrianiv, G. F. Dobrzhanskii, *Kristallografiya* **1986**, *31*, 175; e) C. L. Raston, C. R. Whitaker, A. H. White, *Aust. J. Chem.* **1988**, *41*, 823; f) U. Schümann, E. Weiss, *Angew. Chem.* **1988**, *100*, 573; *Angew. Chem. Int. Ed. Engl.* **1988**, *27*, 584; g) D. Barr, W. Clegg, R. E. Mulvey, R. Snaith, *J. Chem. Soc. Chem. Commun.* **1989**, 57; h) S. Freitag, W. Kolodziejski, F. Pauer, D. Stalke, *J. Chem. Soc. Dalton Trans.* **1993**, 3479.
[15] A. Steiner, D. Stalke, *Inorg. Chem.* **1993**, *32*, 1977.
[16] S. Harder, A. Streitwieser, *Angew. Chem.* **1993**, *105*, 1108; *Angew. Chem. Int. Ed. Engl.* **1993**, *32*, 1066.
[17] G. M. Sheldrick, *Acta Crystallogr. Sect. A* **1990**, *46*, 467.
[18] G. M. Sheldrick, SHELXL-93, Program for crystal structure refinement, **1993** University of Göttingen.
[19] H. D. Flack, *Acta Crystallogr. Sect. A* **1983**, *39*, 876.

How do they fit so much in?



Keep up with the latest developments in all areas of chemistry.
Order your own personal subscription.

Just fax

USA	Fax: (3 05)	428-82 01
UK	Fax: (02 23)	31 32 21
Japan	Fax: (03)	38 16 37 58
Rest of world	Fax: (0 11 49)	62 01-606-184

VCH

Simulation of Liquids

Theoretical Treatment of Liquids and Liquid Mixtures. (Series: Studies in Physical and Theoretical Chemistry, Vol. 80.) By *C. Hoheisel*. Elsevier, Amsterdam, 1992. XVI, 362 pp., hardcover HFl 320.00, $ 200.00.— ISBN 0-444-89835-2

This monograph is intended for scientists and students who already have a good knowledge of statistical mechanics. It is especially concerned with theoretical concepts for describing liquid mixtures. The introduction to statistical mechanics has therefore been kept very brief, and is confined to the fundamental relationships between the thermodynamic potentials and the quantities describing the canonical ensemble. The author then continues with some general observations regarding computer simulations. The next two chapters deal with Monte Carlo (MC) and molecular dynamics (MD) simulation methods, including fundamental relationships involving the properties of Markov chains and principles of simulations. Discussions of intermolecular interaction potentials are interspersed with descriptions of the MD method and of simulation techniques. At this point it is already becoming apparent that the main content of the book is devoted to descriptions of results obtained by simulation methods.

After looking through these first four chapters, which are evidently intended as an introduction, one has the impression that the style of presentation is sadly inferior to that in other monographs on the subject. Descriptions that are more didactically sound and understandable by the reader can be found in books such as K. Lucas's *Angewandte Statistische Thermodynamik* or D. Chandler's *Introduction to Modern Statistical Mechanics*. The reader seeking a systematic introduction to simulations of liquid systems would be better advised to consult *Computer Simulation of Liquids*, by Allen and Tildesley.

Chapter 5 deals with all the equilibrium properties, structures, and thermodynamics of liquid systems, Here the contradictions between the aims expressed in the preface and the actual content of the book become clearly evident. The descriptions of integral equation theories are very brief, and correspond to the state of knowledge about ten years ago. The detailed discussion of hard-sphere models includes comparisons with simulations using Percus–Yevick and hypernetted chain (HNC) calculations. Lennard–Jones systems are then treated in the same way. The emphasis here is on the discussion of additive and nonadditive mixtures. The author makes no reference to more recent developments such as the application of integral equations to inhomogeneous systems, rapid methods for the solution of the Ornstein–Zernike equation, or the LHNC and RHNC methods. Consequently, Figure A 33 and others give an outdated impression of the capabilities of theoretical treatments. The advice (e.g., on p. 115) in the phrase "The reader is referred to the existing relevant literature" hardly makes up for these deficiencies. Much more seriously, though, the author says nothing at all about polar systems, and devotes only five pages to molecular liquids. Here results from more recent theoretical developments are neglected, and the citations are limited to a few of the author's own papers.

The choice and style of treatment of the literature references invite criticism. Lists of publications are scattered throughout the chapters, but there are hardly any corresponding references in the text, so that the reader is left to decide which citations relate to which parts of the text. After reading Part A the verdict must be that the contents do not live up to the promise of the book's title.

At first sight the idea of treating equilibrium properties together with the dynamics of liquid systems appears promising, especially as the theoretical concepts overlap. However, to treat these two topics together in detail is a very ambitious task. Part B of the book, with 200 pages, is the main part both in length and subject matter. The main emphasis is again on simulations and their evaluation. However, close examination reveals some gaps and inadequacies in the descriptions of the theory and in the arrangement of material. Unfortunately, the theory is only treated in the amount of detail needed to interpret the simulations. There are frequent references to more detailed treatments in later chapters (e.g., on pp. 165, 182, 183, 185, 187, 188, 192, 244), giving the impression of a lack of systematization.

An introduction including continuity equations and examples of applications of the Navier–Stokes equation is followed by a chapter on time-correlation functions, which glosses over many of the points too briefly. The treatment of self-diffusion includes numerous simulations for Lennard–Jones systems, from which autocorrelation functions are derived and diffusion coefficients are determined. These values are then compared with results from the Enskog theory and the kinetic mean field theory, but not with experimental values (except in Table B 3). In (9.3.1.1.10) the last equations given appear to contain printing errors. The next chapter is devoted to transport coefficients. Starting from the Green–Kubo equations, simulations of Lennard–Jones mixtures are used to derive diffusion coefficients, viscosities, and thermal conductivities. Here the author makes systematic comparisons with the Enskog and kinetic theories, the Rice–Allnatt approximation, and the Gaussian memory function model, and discusses the results. The book concludes with discussions of nonequilibrium simulations and calculations of transport coefficients. Here, for the first time, comparisons with experimental data are introduced, enabling one to evaluate the simulation methods.

If the numerous references in this book to more advanced monographs and original publications are to be taken seriously, one must conclude that it would be better to simply read these sources instead.

Jochen Winkelmann
Institut für Physikalische Chemie
der Universität Halle-Wittenberg (FRG)

This section contains book reviews and a list of new books received by the editor. Book reviews are written by invitation from the editor. Suggestions for books to be reviewed and for book reviewers are welcome. Publishers should send brochures or (better) books to the Book Editor, Dr. Gerhard Karger, Redaktion Angewandte Chemie, Postfach 101161, D-69451 Weinheim, Federal Republic of Germany. The editor reserves the right of selecting which books will be reviewed. Uninvited books not chosen for review will not be returned.

Stereocontrolled Synthesis of Oligo(nucleoside phosphorothioate)s

Wojciech J. Stec,* Andrzej Wilk

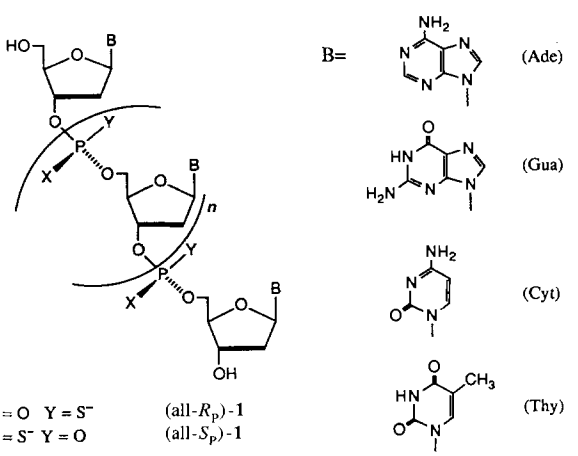
Encouraging results obtained for modulation of gene expression by antisense oligonucleotides and their analogues have kindled hopes for a new generation of therapeutics against viral infections, cancer, and many other diseases. Among such analogues, oligo(nucleoside phosphorothioate)s (Oligo-S) have generally shown the highest efficacy in inhibiting the biosynthesis of "unwanted" proteins. The first clinical trials of antisense agents are now in progress using Oligo-S against genital warts and acute myeloid leukemia, and tests of Oligo-S against AIDS should follow soon. Nevertheless, their mechanism of action, internalization, cellular trafficking, subcellular localization, and interaction with cellular proteins is still poorly understood. It is assumed a priori that application involves rapid and efficient molecular recognition of target RNA by Oligo-S; however, the effects of the chirality of Oligo-S have so far been unappreciated, because Oligo-S has not yet been synthesized with stereocontrol. Indeed, the diastereomeric composition of Oligo-S has never been determined, primarily because of the lack of appropriate analytical methods. Since each of the diastereomers is a stereochemically unique chemical entity, questions arise as to which diastereomer is responsible for an observed biological response, including positive (curative) or possibly negative (toxic) side effects.

In this review we intend provide a perhaps somewhat speculative assessment of the problems associated with the stereocontrolled synthesis of Oligo-S and to discuss the state-of-the-art in this field including strategies that may lead to Oligo-S of predetermined chirality. This article is not intended to discourage researchers from further studies of diasteromeric mixtures of Oligo-S as potential pharmaceuticals. Throughout the history of medicinal chemistry numerous useful medicines were discovered, developed, and employed without the detailed knowledge of their structure. Indeed, the composition of the vaccines discovered by Pasteur is a subject of vigorous study still today.

1. Introduction

Since the discovery that Oligo-S **1** can effectively protect cells from the lethal action of the HIV-1 virus,[1] a number of reports have appeared concerning improvements in their synthesis,[2] their purification and analysis,[3] cellular uptake, pharmacokinetics and toxicity,[4] mechanism of action,[5] and potential therapeutic applications.[6] In the first enzymatic[7] and chemical[8] syntheses of Oligo-S it was recognized that stereodefined 3′-*O*-deoxyribosyl and 5′-*O*-deoxyribosyl moieties surround the phosphorus atom of each phosphorothioate unit, and because of the stereogenicity of phosphorus, new centers of chirality are created in each molecule of **1**.

However, relatively little attention has been paid to the structural and biochemical consequences of this diastereomerism. The aim of the present review is to focus the attention of researchers, who are applying Oligo-S to antisense technology[9] and/or ribozyme technology,[10] on the problem of the polydiastereomerism of **1**, and to critically evaluate the potential strategies for stereocontrolled synthesis of Oligo-S leading to pure products with defined chirality at each phosphorus atom.



Scheme 1. Oligo(nucleoside phosphorothioate)s **1** and bases B.

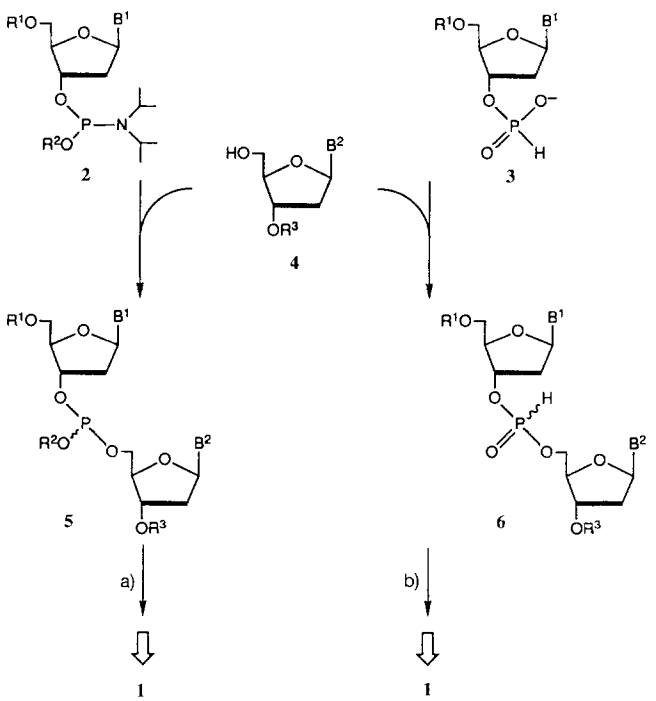
[*] Prof. Dr. W. J. Stec, Dr. A. Wilk
Polish Academy of Sciences
Centre of Molecular and Macromolecular Studies
Department of Bioorganic Chemistry
Sienkiewicza 112, PL-90-363 Lodz (Poland)
Telefax: Int. code +(42)815483

 © *VCH Verlagsgesellschaft mbH, D-69451 Weinheim, 1994* *0570-0833/94/0707-0709 $ 10.00+.25/0*

2. Nonstereocontrolled Synthesis of Oligo(nucleoside phosphorothioate)s

Antisense Oligo-S **1** are relatively short oligonucleotides (ca. 15- to 30-mers) with a defined sequence of nucleobases complementary to RNA (or ssDNA) in which each internucleotide phosphate is replaced by a phosphorothioate moiety. The sequence of nucleobases between the 5′-OH and 3′-OH end groups in these molecules is responsible for recognition of a complementary target RNA and specific alignment governed by Watson–Crick hydrogen bond formation.[11]

Oligo-S have been prepared until now by primarily two methodologies: a) stepwise phosphoroamidite coupling[12] followed by sulfurization[8, 13] of the intermediate *O*-alkylphosphite **5**, and b) tandem sulfurization of oligo(nucleoside *H*-phosphonate)s[2b, 14] bound to the solid support (Scheme 2). Sulfurization of either *O*,*O*,*O*-trialkylphosphites or *O*,*O*-dialkyl-*H*-phosphonates is itself stereoretentive.[15] Assuming that both methodologies are neither stereospecific nor stereoselective and that each *O*-alkyl phosphite internucleotide bond (as in **5**) or each *H*-phosphonate bond (as in **6**) is formed in a nonstereoselective manner, the resulting Oligo-S consists of a mixture of 2^n diastereomers, where n is the number of phosphorothioate internucleotide bonds. The content of any single diastereomer in this mixture should therefore be 2^{-n}. However, even from the pioneering works of Burgers and Eckstein[16] and Marlier and Benkovic[17] on the synthesis the stereoisomers **12**, $U_{PS}A$ and $A_{PS}A$, respectively, it was known that the quantities of diastereomers (R_P) and (S_P) were not equimolar. By applying phosphorodichloridite coupling (by means of **9**) followed by sulfurization of phosphite **10**, both groups independently obtained diastereomers of diribonucleoside 3′,5′-phosphorothioates **12** (Scheme 3) and assigned the configuration at the phosphorus atom. Moreover, recent studies have shown that condensation of 5′-*O*-DMT-nucleoside 3′-*O*-(*O*-2-cyanoethyl-*N*′,*N*′-diisopropylphosphoramidite)s with 5′-OH nucleoside bound to a solid support through the 3′-O atom gives after deprotection the diastereomeric mixtures of (R_P)- and (S_P)-dinucleoside 3′,5′-phosphorothioates in the ratios listed in the Table 1. (This condensation must be performed according to the generally accepted protocol for the synthesis of oligonucleotides, with the exception that the oxidation step with iodine is replaced by sulfurization.[8, 12g]) It was demonstrated earlier[8c] that the diastereomeric composition of the starting 5′-*O*-DMT-*N*-benzoylcytidine 3′-*O*-(*O*-methyl-*N*′,*N*′-diisopropylphosphoroamidites) does not influence the ratio of the resulting diastereomers of dicytidine 3′,5′-phosphorothioate.



Scheme 2. Synthesis of **1** with the phosphoroamidite (a) and *H*-phosphonate methods (b). a) 1. Sulfurization, 2. capping of the unreacted 5′-OH group, 3. removal of the 5′-trityl group, 4. condensation with **2**/tetrazole, 5. steps 1–4 are repeated n times. b) 1. Removal of the 5′-trityl group, 2. condensation with **3**/pivaloyl (adamantoyl) chloride, 3. capping of the unreacted 5′-OH group, 4. steps 1–3 are repeated n times, 5. final sulfurization. For both methods the product is then cleaved from the solid support, deprotected, and purified. R^1 = 4,4′-dimethoxytrityl (DMT); R^2 = CH_2CH_2CN, Me; R^3 = long chain amine controlled pore glass (LCA-CPG); B^1,B^2 = AdeBz, Gua*i*Bu, CytBz, Thy.

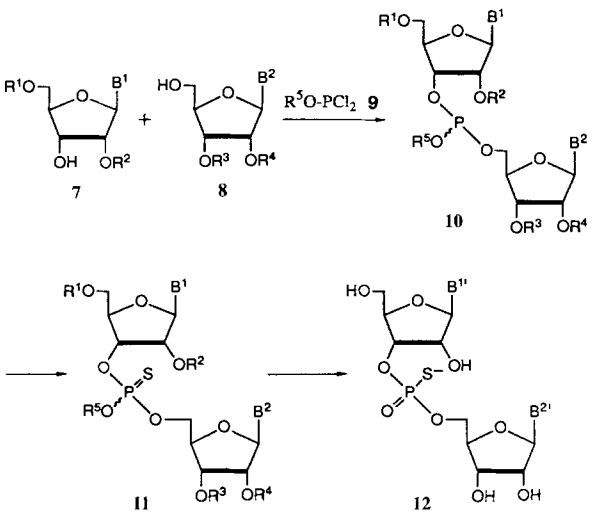
The composition of the mixture of diastereomers obtained with (R_P) diastereoselectivity x and (S_P) diastereoselectivity y ($y = 1 - x$) preserved at each of n couplings can be calculated from the polynomial Equation (a). The following example is

$$(x + y)^n = x^n + \binom{n}{1} x^{n-1} y + \cdots + \binom{n}{n-1} x y^{n-1} + y^n \qquad \text{(a)}$$

calculated for the pentamer (e.g. d[$(C_{PS})_4$C]) obtained with diastereoselectivity $x = 0.6$: $(x + y)^4 = x^4 + 4x^3y + 6x^2y^2 +$



Wojciech J. Stec was born in Warsaw, Poland, in 1940. He obtained his M. S. (1963) and Ph.D. (1968) from the Technical University of Lodz. After postdoctoral work at Vanderbilt University, Nashville, TN, USA (1970), he returned to Lodz and became Associate Professor in 1974. In 1979 he became Full Professor and Head of the Department of Bioorganic Chemistry. His research activity is focused on the synthesis and stereochemistry of organophosphates, the stereochemical analysis of cyclic phosphates, isotope labeling, the mechanism of action of alkylating anticancer drugs, and the stereoselective activity of enzymes. Recently he became involved in protein bioengineering and "antisense" technology. From 1983 to 1984 he was a Senior Visiting Scientist at the U.S. Food and Drug Administration; in 1992–1993 he was appointed Scholar-in-Residence at the U.S. National Institutes of Health. He was elected member of the Societas Scientiarum ac Litterarum Varsoviensis in 1981.



Scheme 3. The phosphite method used by Eckstein (a) and Benkovic (b) for the synthesis of diribonucleoside 3',5'-phosphorothioates [16, 17]. a) R^1 = *p*-chlorophenoxyacetyl; R^2 = methoxytetrahydropyranyl; R^3,R^4 = *O*-methoxymethylidene; R^5 = phenyl; B^1 = $B^{1'}$ = Ura; B^2 = N^6-benzoyl-Ade; $B^{2'}$ = Ade. b) R^1 = methoxytrityl; R^2 = *O*-nitrobenzyl; R^3,R^4 = benzoyl; R^5 = methyl; B^1 = N^6-benzoyl-Ade; B^2 = N^6,N^6-dibenzyl-Ade; $B^{1'}$ = $B^{2'}$ = Ade.

Table 1. Proportions of the (R_P) isomer in dinucleoside 3',5'-phosphorothioates ($N_{PS}N'$) in percent [a].

N'/N	dA	dG	dC	dT
dA	51.7	42.6	53.4	53.8
dG	55.3	51.0	55.2	56.0
dC	57.0	48.6	59.7	62.7
dT	58.6	50.8	60.0	59.6

[a] Dinucleoside 5',3'-phosphorothioates ($N_{PS}N'$ where N is at the 5'-end) were prepared according to the standard coupling method (DNA synthesizer, Applied Biosystems model 380 B), followed by sulfurization with a 0.08 M solution of bis-(diisopropoxyphosphinothioyl) disulfide in acetonitrile/pyridine (2/1) for 45 s (ca. 400 μL). The 5'-dimethoxytrityl group was removed in the final step in the synthesis. Crude mixtures were analyzed by HPLC (Supelcosil RP-18 column (5 μ, 2.3 mm × 250 mm), acetonitrile gradient in 0.1 M TEAB from 0%, 0.5% CH_3CN min^{-1}, flow rate 1 mL min^{-1}). The percent of the (R_P) isomer was obtained from peak integration. The coupling efficiency was not lower than >98%.

$4xy^3 + y^4 = 0.1296 + (4 \times 0.0864) + (6 \times 0.0576) + (4 \times 0.0384) + 0.0256$. Thus the mixture of sixteen diastereomers (2^4) contains 12.96% (all-R_P), 2.56% (all-S_P), four possible "(all-R_P) but one" diastereomers, each formed in 8.64% yield, six fragments with equal numbers of (R_P) and (S_P) internucleotide bonds, each with a yield of 5.76%, and four possible "(all-S_P) but one" diastereomers, each formed in 3.84% yield. It is worth mentioning that in the above example the ratio of (all-R_P) to (all-S_P) diastereomers is 5:1.

Indeed, it has been demonstrated roughly that the ratios of diastereomers of $d(C_{PS}C_{PS}C)$ are in agreement with calculated values: (R_P,R_P):(S_P,R_P):(R_P,S_P):(S_P,S_P) = (0.6 × 0.6):(0.6 × 0.4):(0.4 × 0.6):(0.4: × 0.4) (Fig. 1).[18] This assignment also indicates that the diastereoselectivity of subsequent steps of the coupling process is, in the case of cytidine components, nearly the same. That means that in oligo(cytidine phosphorothioate)s the ratio of phosphorothioates with (R_P) configuration at a particular position in the chain to those with (S_P) configuration will be close to 60:40. Further experimental data indicate that for oligo(deoxyadenosine phosphorothioate)s the relative ratio

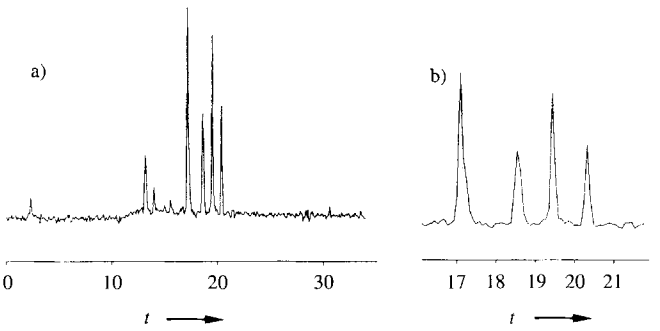


Fig. 1. Chromatogram from a RP-HPLC separation of the four diastereomers of $d(C_{PS}C_{PS}C)$ from the sample prepared by the phosphoroamidite method. For experimental details see Table 1. a) Entire chromatogram of crude material; b) expanded section showing the baseline separated peaks for the diastereomers. Retention time *t* in min.

(R_P):(S_P) is 52:48 in the case of dimer formation (see Table 1) but increases roughly 1% per coupling. Thus, the second coupling occurs with 53% (R_P) selectivity, the third with 54%, etc. If this trend can be extrapolated, the 49th coupling should be 100% (R_P) diastereoselective. Perhaps the most convincing demonstration of the effect of the variable diastereoselectivity of the coupling process on the final composition of diastereomers is given in Figure 2. Here it is evident that even during the

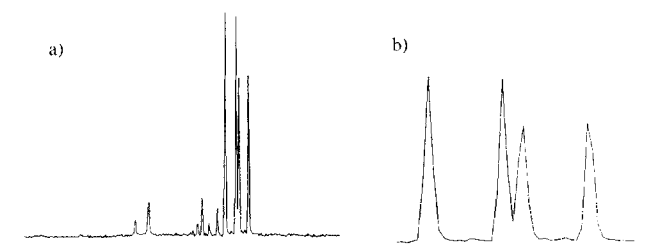


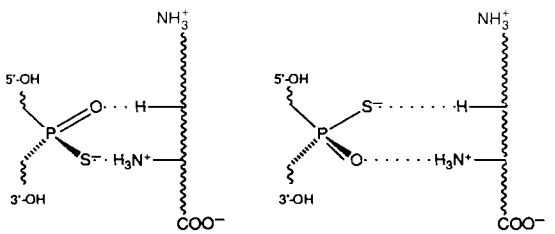
Fig. 2. RP-HPLC trace of crude trimer $d(A_{PS}A_{PS}A)$ prepared and analyzed as indicated in Figure 1. Complete baseline separation of (R_P,S_P) and (S_P,R_P) diastereomers (peaks in the middle of b) was not possible. Retention time *t* in min.

synthesis of the trimer $d(A_{PS}A_{PS}A)$ the ratio of the diastereomers obtained (R_P,R_P):(R_P,S_P):(S_P,R_P):(S_P,S_P) is 29.1:26.1:22.7:22.1.[18]

3. Biological Implications of the Chirality of Oligo-S

What are the consequences of a nonstatistical distribution of individual diastereomers in such constructs as **1**? One must accept the fact that if antisense oligonucleotides **1** are considered as potential therapeutics, their contact with proteins is unavoidable after introduction to the body. Recent results indicate that Oligo-S like $d[(C_{PS})_nC]$ with $n \geq 14$ can inhibit human DNA polymerase and RNase activities.[5a] Therefore, the most problematic consequence of varying the distribution of particular diastereomers of **1** may be the batch-to-batch irreproducibility of biological effects resulting from the different activity of individual diastereomers towards the variety of proteins in the inter-

and intracellular media. From the work initiated by studies of Eckstein,[19] Benkovic et al.,[20] and Frey[21] it is known that functional proteins such as polymerases and nucleases interact with phosphorothioate analogues of biophosphates in a diastereoselective manner.[22] However, the diastereoselectivity is not predictable, since for each enzyme it results from different spatial arrangements of functional groups in proteins (including orientations of peptide bonds), which can interact with phosphate oxygen atoms by means of hydrogen bonds and salt bridges.[23] Recently it has been hypothesized that the diastereoselectivity of enzyme-catalyzed processes in the degradation of oligonucleotides bearing phosphorothioate functions results from directional two-point interactions between the phosphorothioate unit and the protein (Scheme 4).[22f] This hypothesis is well



Scheme 4. Representation of the hypothetical directional two-point interaction between the phosphorothioate group and a protein, which is responsible for the diastereoselective action of some nucleases. Left: arrangement leading to a "productive" interaction of a phosphorothioate function with a protein (as seen with the natural oligonucleotide); right: arrangement leading to an "unproductive" arrangement.

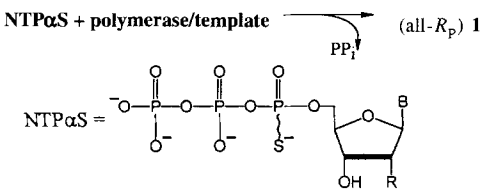
supported by the results of studies on the interactions between oligonucleotides bearing the $^{5'-OH}\cdots GAATTC\cdots{}^{3'-OH}$ sequence and the restriction enzyme *Eco*RI. Replacement of the $\cdots A_pT\cdots$ internucleotide group with $\cdots A_{PS}T\cdots$ having an (S_P) configuration improves the binding between oligonucleotide and this particular enzyme.[22g] Moreover, the proposal that cellular uptake of oligonucleotide involves a specific receptor or transporting protein[4b, 24] implies that the passage through the cell membranes (either inward or outward) may be diastereoselective because of the chirality of both receptors and transporting proteins. This diastereoselectivity could be cell- or species-dependent and could affect both pharmacokinetics and biodistribution.

Finally, the principle of antisense activity of **1** implies the affinity of **1** towards target RNA (or DNA).[9] It is tempting to postulate, even on the basis of early, simplistic model studies,[25] that this affinity is also dependent on the configuration of the phosphorus atom (vide infra). On the other hand, it is reasonable to consider, in light of the unpredictable influence of the chirality of **1** on their interactions with proteins and/or RNA, that the most reliable approach to obtaining active antisense agents is to provide the living system with the pool of diastereomers of **1**. Then the competitive, natural selection of effective diastereomers in each step of the overall process would lead to biological activity. This assumes that the other "incorrect" components of this diastereomeric mixture neither prevent activity nor are harmful to the biological system. It should be emphasized that all biological results reported thus far, including those on the inhibitory effects of Oligo-S on protein biosynthesis, were obtained with diastereomeric mixtures of **1**.[4–6] Although the legal regulations[26] for a new potential drug insist on the precise stereochemical description of the molecule when and if possible, scholarly attitude alone requires chemists to work out the ideal solution—to design a methodology for the synthesis of **1** in a stereocontrolled manner which leads to a single desired diastereomer of **1**.

4. Stereocontrolled Chemical Synthesis of Oligo(nucleotide phosphorothioate)s

One approach to the stereocontrolled synthesis of organic molecules is to use enzymes. For the synthesis of **1** polymerases, transferases, and nucleases can be considered,[27] since these classes of enzymes can assist in the synthesis and degradation of phosphorothioate moieties.

The first synthesis of **1** performed enzymatically (with polymerase) proved to be (R_P) stereoselective (Scheme 5). The use of



Scheme 5. Enzymatic synthesis of (all-R_P)-poly(nucleoside phosphorothioate)s. Template = DNA; R = H, B = Ade, Gua, Cyt, Thy or R = OH, B = Ade, Gua, Cyt, Ura.

endonucleases for diastereoselective degradation of **1** having undesired (R_P) or (S_P) configurations has been studied but is limited in practice to short homopolymers like penta(cytidine phosphorothiate)s, $d[(C_{PS})_4C]$.[18, 28] A diastereomeric mixture of $d[(C_{PS})_4C]$ was exposed to endonuclease P1, which selectively cleaves all phosphorothioate diesters with (S_P) configuration.[22k] Besides intact (all-R_P)-$d[(C_{PS})_4C]$, the accompanying diastereomerically pure 5'-phosphorothioylated units were converted by alkaline phosphatase to the corresponding 5'-OH dimer, trimer, and tetramer having only (R_P)-configurated internucleotide phosphorothioate groups (Fig. 3). Diastereoselective degradation of Oligo-S with the "wrong" configuration at phosphorus is limited to phosphorothioates prepared diastereoselectively, in other words, Oligo-S with mainly (R_P) or (S_P) configuration. If this were not the case, diastereoselective enzymatic digestion would be impractical for most purposes, because in the statistically simplest case the desired product is only a small fraction (2^{-n}) of the starting mixture. Moreover, since an endonuclease with diastereoselectivity opposite to that of nuclease P1 has not been found, recovery of oligonucleotide **1** of (all-S_P) configuration, even from a mixture of diastereomers of predominantly (S_P) configuration, is not yet possible. Therefore, the only rational approach to the synthesis of Oligo-S having a predetermined sequence of nucleobases and predetermined chirality at each phosphorus atom is a stereocontrolled, and highly stereoselective chemical method.

What are the potential strategies for the synthesis of Oligo-S with defined stereochemistry at the phosphorus centers? Method-

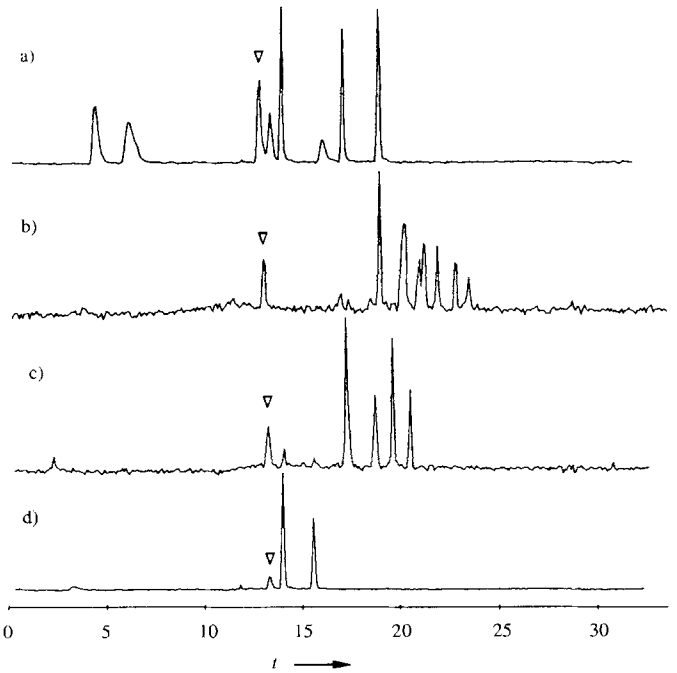


Fig. 3. RP-HPLC traces of a) the parent tetramer d($C_{PS}C_{PS}C_{PS}C$) after digestion with nuclease P1/alkaline phosphatase; b) crude tetramer d($C_{PS}C_{PS}C_{PS}C$) (mixture of eight diastereomers); c) crude trimer d($C_{PS}C_{PS}C$) (four diastereomers); d) crude dimer d($C_{PS}C$) (two diastereomers). Dimer, trimer, and tetramer were prepared by the phosphoroamidite/sulfurization method and analyzed as described in Table 1 with the exception that the gradient was 0.66% min^{-1}. Retention time t in min. Peaks marked with a triangle correspond to benzamide.

ologies developed during 100 years of phosphorus chemistry[29] that may be employed for the stereocontrolled synthesis of diastereomerically pure **1** are based on a) stereoselective or stereospecific nucleophilic substitution at tricoordinate phosphorus, b) stereoselective synthesis or stereoselective sulfurization of intermediates containing internucleotide *H*-phosphonates, c) stereoselective or stereospecific nucleophilic substitution at tetracoordinate phosphorus.

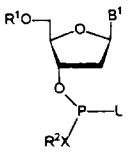
In choosing a potential strategy, one must consider that the diastereomeric purity (*dp*) of **1** is described by Equation (b).

$$dp = p_1 \cdot p_2 \cdot p_3 \ldots p_n \qquad \text{(b)}$$

If $p_1 = p_2 = \ldots = p_n$, then $dp = p^n$, where n is the number of internucleotide phosphorothioate units and $p_1, p_2, \ldots p_n$ designate diastereoselectivities of particular coupling steps. It is obvious that the diastereoselectivity of any single coupling must be greater than 0.95 for the effective application of this strategy.

4.1. Nucleophilic Substitution at Tricoordinate Phosphorus Centers

Stereoselective/stereospecific syntheses of **1** utilizing substrates **13** (Scheme 6), which contain a tricoordinate phosphorus center (P^{III}), have the following limitations: substrate **13** must be separable into its P enantiomers, the R^1 group must be an acid-labile protecting group, X must be an oxygen or sulfur atom, and R^2

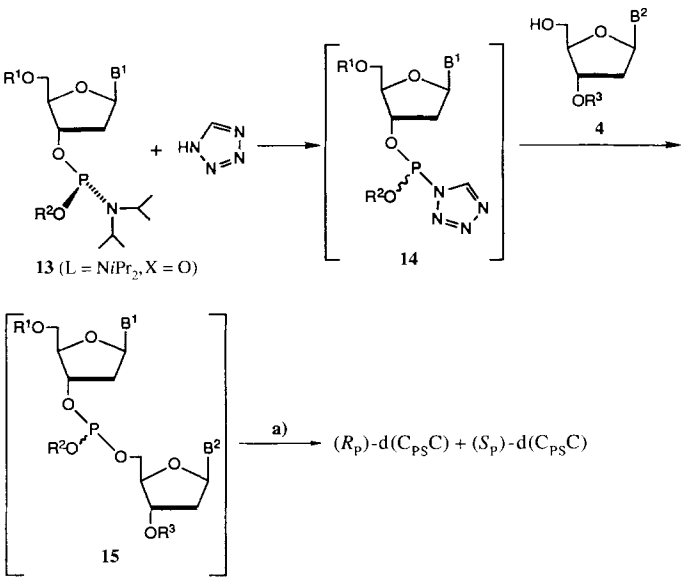


Scheme 6. R^1 = DMT, pixyl, etc.; R^2 = alkyl, aryl; X = S, O or R^2X = Me; B^1 = protected Ade, Gua, Cyt, Thy; L = leaving group.

13

should be removable by cleavage of the X–R^2 bond. If R^2X = L, prochiral **13** offers the possibility for diastereoselective exchange (replacement) of (*pro-R*) or (*pro-S*) groups.

In early attempts at the diastereoselective synthesis of **1**[8c] substrates **13** (R^1 = DMT, R^2X = MeO, L = iPr_2N, B^1 = CytBz) were obtained in diastereomerically pure form, but their activation by tetrazole appeared to cause P-epimerization. Besides protonation, activation of **13** by tetrazole also involves the substitution of the $NiPr_2$ group by tetrazole. Intermediate phosphorotetrazolidites **14** undergo fast P-epimerization in the presence of an excess of tetrazole, most probably by rapid exchange of substituents (Scheme 7).



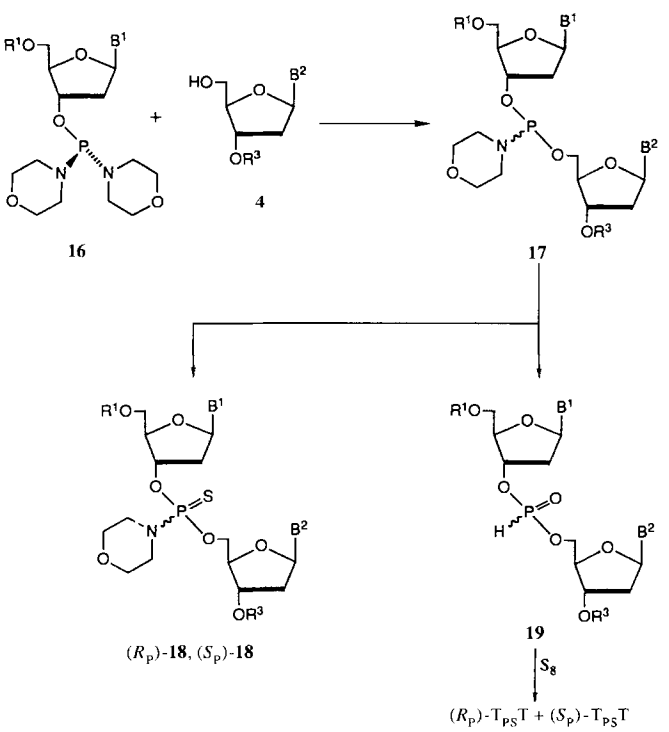
Scheme 7. Diastereomerically pure **13** undergoes P-epimerization in the presence of tetrazole, which impedes the stereocontrolled synthesis of **1** by phosphoroamidite methodology. a) 1. S_8, 2. deprotection. R^1 = DMT; R^2 = Me; R^3 = LCA-CPG; B^1 = B^2 = CytBz.

Detailed mechanistic studies confirmed this early hypothesis.[30] Accordingly, the resulting intermediate dinucleoside 3′,5′-*O*-methylphosphite **15** consists of a mixture of diastereomers. Stereoretentive sulfurization of **15** followed by deprotection of amino and hydroxyl functions, and cleavage from the solid support gave dicytidine 3′,5′-phosphorothioates with the ratio of diastereomers (R_P):(S_P) = 60:40. In similar studies on the diastereoselective synthesis of dinucleoside 3′,5′-methanephosphonates, Lebedev et al.[31] used diastereomeric substrates **13** (R^2X = Me, L = iPr_2N). The nucleoside component in this reaction was 5′-*O*-trifluoroacetyl-3′-*O*-acetylthymidine, and 4-dimethylaminopyridine (DMAP) was used as the catalyst. After mild oxidation and deprotection, the resulting dinucleoside

3′,5′-methanephosphonate appeared to consist of a 1:1 mixture of diastereomers.

These discouraging attempts obviously do not preclude success with other P^{III} compounds. Perhaps substrates **13** bearing bulky and/or chiral R^2 groups (but offering selective R^2–X bond cleavage) can be constructed. Compounds with a different leaving group L may require a different type of activation than that used for substrates with L = NR_2. Alternatively, NR_2 groups that do not undergo ready exchange should be employed. A potentially good leaving group is 4-nitrophenoxyl,[32] but only under the condition that the resulting 4-nitrophenoxide ion is removed from the reaction medium immediately after release; otherwise, it may cause epimerization of **13**.

Selectivity may also be attained by the diastereoselective reactions of prochiral P^{III} substrates (**13**, R^2X = L) with the 5′-OH function of the nucleoside component. Diastereoselectivity within the coupling process is possible since both reagents (3′-*O*-phosphitylated nucleoside and 5′-OH nucleoside) bear chiral auxiliaries (2′-deoxyribosyl moieties), and one of the two competing routes (leading to the (S_P) and (R_P) diastereomers) can be considered to be kinetically favored. In the course of the development of the phosphorodiamidite approach to oligonucleotide synthesis[33] 5′-*O*-DMT-thymidine 3′-*O*-phosphorodimorpholidite **16** was synthesized and coupled with 3′-*O*-acetylthymidine **4** in the presence of tetrazole as the catalyst (Scheme 8). Unfortunately, neither phosphorothioate **18** nor *H*-phosphonate **19** were enriched in one diastereomer to a meaningful extent.[34] These results strengthen the hypothesis that any phosphoroamidite substrate like **13**, which is activated by an acid nucleophilic catalyst, is prone to P-epimerization.

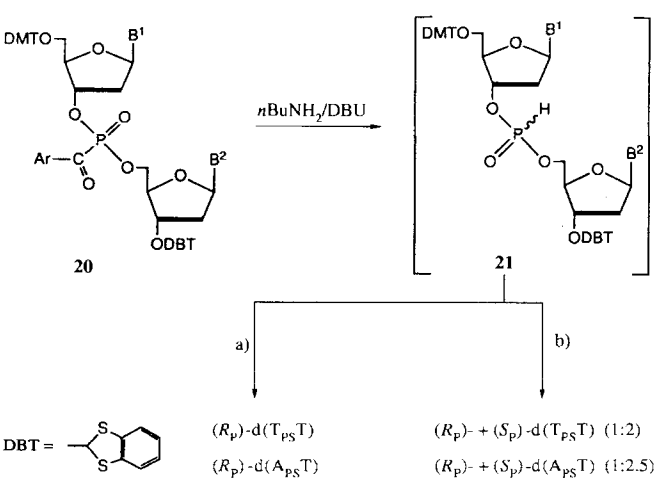


Scheme 8. The synthesis of Oligo-S with the phosphoroamidite method could not be conducted diastereoselectively. R^1 = DMT; R^3 = Ac; B^1,B^2 = Thy. (R_P)-/(S_P)-**18** and (R_P)-/(S_P)-$T_{PS}T$ are both formed in approximately 1:1 ratios.

4.2. Stereoselective Formation and Sulfurization of Oligo(nucleoside *H*-phosphonate)s

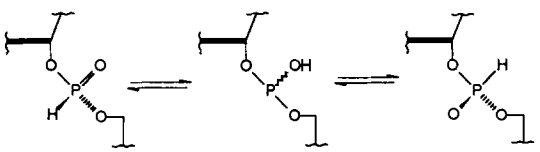
The *H*-phosphonate approach to oligonucleotide synthesis involves 5′-*O*-DMT-nucleoside 3′-*O*-(H-phosphonate)s as P-prochiral substrates **3**. Their activation with sterically demanding pivaloyl[35a] or adamantoyl[35c] chloride may, in principle, be stereoselective and lead to chiral oligo(nucleoside *H*-phosphonate)s bound to the solid support. These, after tandem sulfurization, cleavage from the support, and nucleobase deprotection, give Oligo-S.[36] However, the ratio of diastereomers of di(deoxyribonucleoside) 3′,5′-*H*-phosphonates **6** is known to be close to 1:1,[37] which dictates that a similar ratio of the corresponding diastereomeric dinucleoside 3′,5′-phosphorothioates results from subsequent sulfurization.[36b] Very recently Stawinski et al. reported that diribonucleoside 3′,5′-*H*-phosphonate $C_{PH}U$ prepared by his method[35] consists of a mixture of diastereomers in the ratio 6:1.[38] Independently, it has been demonstrated that diastereomers of dinucleoside 3′,5′-*H*-phosphonates **6** can be separated by silica gel chromatography[37, 38] and sulfurized with retention of configuration. This P-configurational stability of unsymmetrical *O*,*O*-dialkyl *H*-phosphonates was, however, not surprising in light of classical studies on the preparation of diastereomerically pure *O*-menthylphenylphosphonates[39] and enantiomeric *O*-isopropylmethylphosphonates.[40] Moreover, sulfurization of P-chiral *O*,*O*-dialkyl *H*-phosphonates is known to be a stereoretentive process.[15] Therefore, stereocontrolled synthesis of oligo(nucleoside *H*-phosphonate)s as convenient precursors of Oligo-S (or other P-chiral analogues of oligonucleotides) seems to be a still-unexplored avenue that deserves more attention, especially in view of results reported by Hata et al.[41] and recently by Battistini et al.[42]

Hata et al. found that degradation of dinucleoside 3′,5′-α-ketophosphonates **20** by treatment with *n*-butylamine and 1,8-diazabicyclo[5,4,0]undec-7-ene (DBU) is stereoselective (Scheme 9). In these studies intermediate *H*-phosphonates **21** were not isolated but treated with trimethylsilyl chloride and sulfurized with



Scheme 9. The DBU-catalyzed aminolysis of phosphonates **20** was remarkably diastereoselective, as shown by the diastereomeric ratio of the sulfurized product. a) 1. S_8, 2. deprotection of OH groups; b) 1. deprotection of OH groups, 2. $Me_3SiCl/Et_3N + S_8$. B^1 = Ade, Thy; B^2 = Thy; Ar = phenyl, *p*-chlorophenyl.

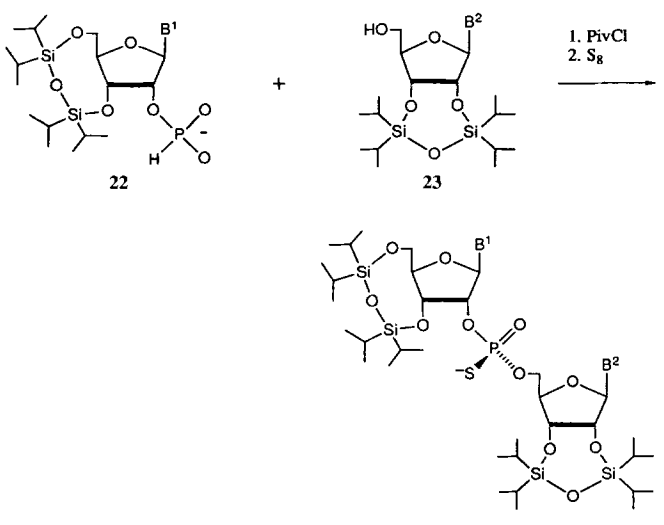
elemental sulfur. Depending on the kind of protective groups and the sequence of deprotection/sulfurization steps, either pure (R_P)-dinucleoside 3',5'-phosphorothioate or a significantly enriched mixture of diastereomers [(S_P):(R_P) = 2.5:1] was obtained. As pointed out by the authors[41b] in the case of d(T_{PS}T), when a benzoyl or *tert*-butyldimethylsilyl group was used as the 3'-terminal protecting group instead of 1,3-benzodithiol-2-yl (DBT), the formation of the phosphorothioates was not stereoselective. Because the starting α-ketophosphonates **20** were used as a mixture of diastereomers for the DBU-catalyzed aminolysis, the conclusion drawn was that DBU influences the configurational equilibration of the resulting *H*-phosphonates **21** (Scheme 10). Hata et al. postulated[41b] that DBU, generally



Scheme 10. The effect of DBU in shifting the configurational equilibrium of **21**.

considered to be a nonnucleophilic base,[43] interacts with *H*-phosphonates to form pentacoordinated intermediates which epimerize at the phosphorus center by pseudorotation to give the thermodynamically more stable isomers. The thermodynamic preference is dictated by steric demands of bulky ligands (augmented by sterically demanding protecting groups at the 5'-*O* and 3'-*O* positions).[44]

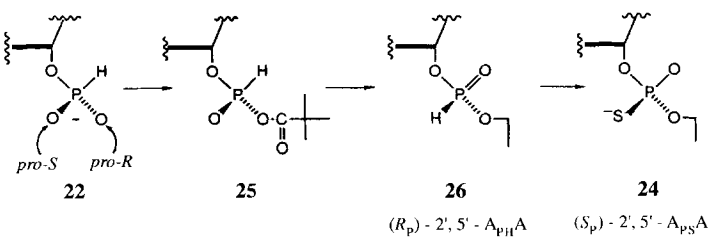
A different explanation must be given for the stereoselectivity in the synthesis of 2',5'-(A_{PS}A) reported by Battistini et al.[42] Condensation of N^6-benzoyl-3',5'-*O*,*O*-tetraisopropyldisiloxane adenosine 2'-*O*-(*H*-phosphonate) (**22**) with **23** in the presence of pivaloyl chloride provides exclusively (S_P)-configurated diadenosine 2',5'-phosphorothioate **24** after sulfurization (Scheme 11). Interestingly, introduction of a *tert*-butyldimethylsilyl protective group at 2'-O, which has more conformational



Scheme 11. Stereoselective synthesis of 2',5'-A_{PS}A. B^1 = B^2 = AdeBz; Piv = pivaloyl.

freedom than the cyclic 3',5'-*O*,*O*- or 2',3'-*O*,*O*-1,1,3,3-tetraisopropyl-1,3-disiloxanediyl protective groups, causes a reduction in diastereoselectivity [(S_P):(R_P) = 70:30].

These intriguing observations can be interpreted in terms of diastereoselective activation of the *H*-phosphonate function of protected **22** owing to the presence of sterically demanding protective groups at the nucleoside components. Presumably, for steric reasons, acylation of anionic **22** occurs exclusively at the (*pro-R*) oxygen atom, and anhydride **25** reacts stereospecifically with **23** leading to (R_P)-2',5'-A_{PH}A **26**; subsequent stereoretentive sulfurization gives (S_P)-**24** (Scheme 12). This explanation



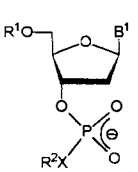
Scheme 12. (*pro-R*)-*O*-Acylation of **22** responsible for the diastereoselective synthesis of 2',5'-A_{PS}A.

implies that nucleophilic substitution at the phosphorus center in **25** occurs with an inversion of configuration; however, no examples of stereochemical transformations of compounds of type **25** have been reported thus far.

In light of the results of Hata et al. in the stereoselective synthesis of oligo(nucleoside phosphorothioate)s by DBU-catalyzed stereoselective epimerization of the internucleotide *H*-phosphonate functions, one should consider introducing specially designed sterically and/or stereoelectronically demanding protective groups into the participating nucleosides (nucleotides). In our own research a variety of potential catalysts for shifting the (R_P):(S_P) equilibrium of **21** have been studied, including optically active and sterically demanding acids and bases, but so far the process is not controllable.[34]

4.3. Diastereoselective Activation of Prochiral Substrates with Tetracoordinate Phosphorus Centers

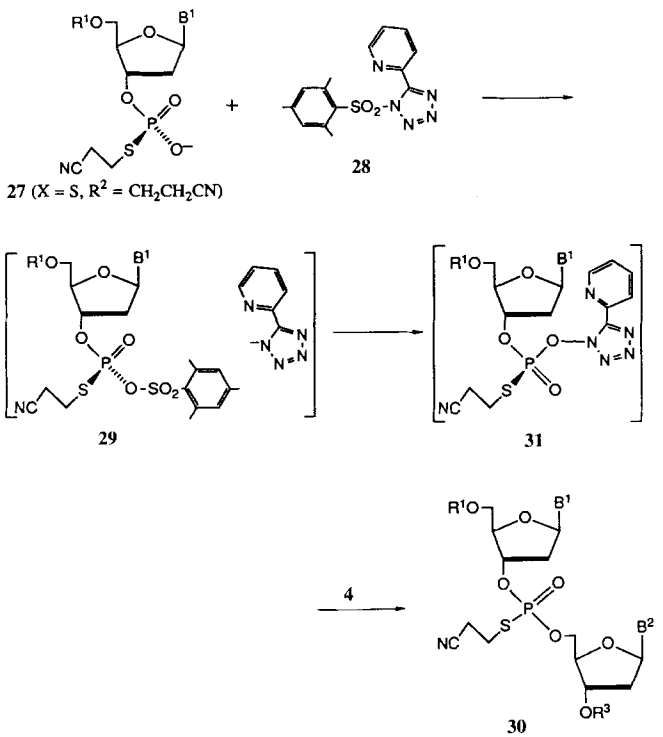
The P-prochiral substrates **27** (Scheme 13) are employed in the phosphotriester approach to oligonucleotide synthesis.[45] When R^2X was an alkoxy or aryloxy group, activation of phosphate function led to the formation of P-chiral dinucleoside 3',5'-*O*-aryl(alkyl)phosphates. Since the synthesis requires the subsequent removal of the *O*-aryl function, the diastereomeric ratio of the intermediate triester was not of interest. However, the prochirality of **27** suggests that the activation process could



Scheme 13. R^1 = DMT, pixyl, etc.; R^2 = alkyl, aryl; X = O; B^1 = protected Ade, Gua, Cyt, Thy.

27

be diastereoselective. Indeed, in one well-documented case, Ohtsuka et al.[46] proved that the condensation of N^6,5′-*O*-bis-(dimethoxytrityl)adenosine 3′-*O*-[(*O*-2-chlorophenyl)phosphate] with N^6,3′-*O*-bis(dimethoxytrityl)adenosine in the presence of 1-(2,4,6-triisopropylbenzenesulfonyl)-5-(pyridin-2-yl)tetrazole as the activating agent gives, after deprotection, dideoxyadenosine 3′,5′-*O*-(2-chlorophenyl)phosphate with (S_P) configuration. This particular finding prompted Cosstick and Williams[47] to study the diastereoselective activation of **27** (B^1 = CytBz; Scheme 14). They demonstrated that reaction of

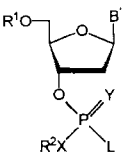


Scheme 14. Diastereoselective activation of P-prochiral phosphorothioate **27** by 1-(2,4,6-trimethylphenylsulfonyl)-5-(pyridin-2-yl)tetrazole.

27 with 3′-*O*-acetylthymidine (**4**, R^3 = Ac, B^1 = Thy) in the presence of **28** leads to the formation of the corresponding dinucleoside **30**, which after decyanoethylation at sulfur consists of the diastereomeric mixture of d(C_{PS}T) with a distinctive preponderance of the (S_P) diastereomer. In the best case the ratio of diastereomers (S_P):(R_P) was 79:21. Such enrichment, although not satisfactory in terms of a stereocontrolled synthesis of **1**, is worth deeper consideration and perhaps more extensive study. If the mechanism of activation of **27** involves stereoselective formation of the mixed phosphorothioic sulfonic anhydride **29**, and this undergoes double nucleophilic substitutions (first by **28** with transient formation of phosphorotetrazolidate **31** and subsequent reaction with **4** to give phosphorothioate triesters **30**), attempts at introducing sterically demanding protective groups on nucleobases and hydroxyl functions not participating in the coupling process increase the probability of diastereoselective formation of dinucleoside 3′,5′-phosphorothioates. This promising scenario must be taken with caution, because earlier studies of Knorre, Zarytova, et al. indicated that the phosphorylating intermediates in the triester approach to oligonucleotide synthesis are pyrophosphates;[48] their intermediacy and the possibility of equilibration at the phosphorus stereocenter may cancel the effects of diastereoselective activation of **27**.[49]

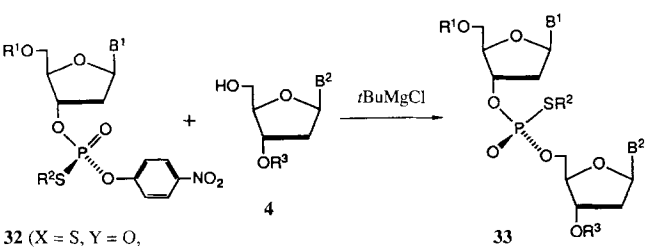
4.4. Stereoselective Nucleophilic Substitution at Tetracoordinate Phosphorus Centers

The most promising and straightforward approach to stereocontrolled synthesis of Oligo-S involves substrates **32** bearing leaving group L (R^2 = aryl, X = O, Y = S or R^2 = alkyl, X = S, Y = O; Scheme 15), which in the process of nucleophilic



Scheme 15. R^1 = DMT, pixyl, etc.; R^2 = alkyl, aryl; X,Y = S,O (X ≠ Y); B^1 = protected Ade, Gua, Cyt, Thy; L = leaving group.

substitution at the phosphorus atom can be replaced by the 5′-OH function of the nucleoside or oligonucleotide in stereodefined manner. Such substrates **32** (R^2X = MeS, Y = O, L = 4-$NO_2C_6H_4O$) were first described by Lesnikowski et al.[50] The separated diastereomers of **32** reacted with 3′-*O*-acetyl nucleosides in the presence of *t*BuMgCl to give dinucleoside 3′,5′-(*S*-methyl)phosphorothioates **33** (Scheme 16). Cleavage of the CH_3–S bond (phosphorothioate deprotection) was achieved in a later step with PhSH/NEt_3. The coupling occurs with inversion of configuration at phosphorus with a stereospecificity of >95% and furnishes **33** in about 70% yield.

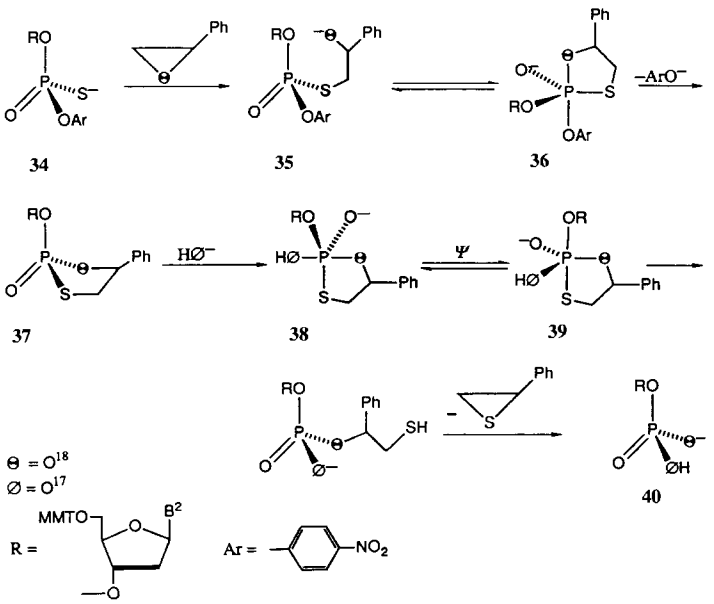


Scheme 16. Stereoselective nucleophilic substitution at the phosphorus center in **32**. This reaction is used for the synthesis of short Oligo-S. R^1 = monomethoxytrityl (MMT); R^2 = Me; R^3 = Ac; B^1 = B^2 = Thy.

Although this methodology cannot be used in solid-phase synthesis, Lesnikowski et al. were able to demonstrate that preparation of stereochemically pure trimers d($T_{PS}T_{PS}T$) and tetramers d($T_{PS}T_{PS}T_{PS}T$) is feasible if protective groups such as 4-chlorobenzyl are introduced at sulfur. Very recently, this strategy was applied to the synthesis of (R_P,R_P)- and (S_P,S_P)-$U_{PS}U_{PS}U$.[50c] In spite of efforts to find other catalysts, *t*BuMgCl, which was introduced for oligonucleotide chemistry by Hayakawa et al.[51] is the catalyst of choice; other catalysts such as *t*BuOK, DMAP, and DBU gave unsatisfactory yields or led to P-epimerization.[52]

4.5. Oxathiaphospholane Method for the Synthesis of Oligo-S

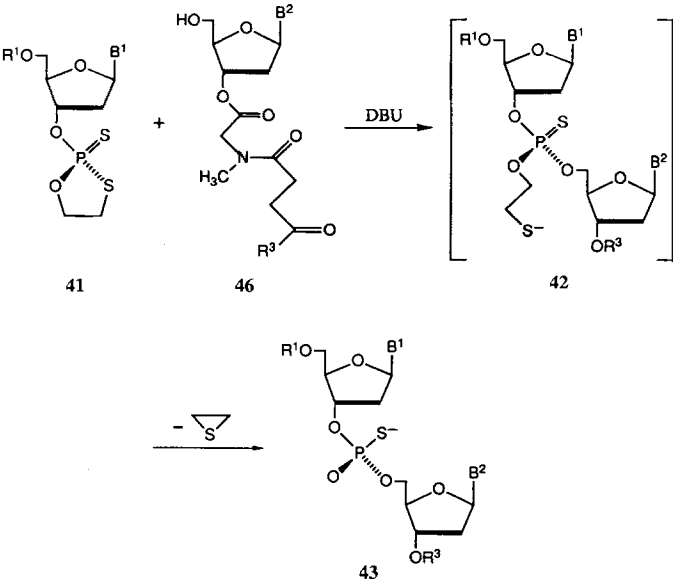
A novel strategy leading to stereodefined Oligo-S based on nucleophilic substitution at tetracoordinate phosphorus centers was elaborated following studies on the conversion of *O,O*-dialkylphosphorothioates into the corresponding [^{18}O]-phosphates.[53] Okruszek et al. observed that *O*-alkyl-*O*-arylphosphorothioates **34** undergo reaction with [^{18}O]styrene oxide/[^{17}O]water with replacement of sulfur by [^{18}O] and of the aryloxy group by [^{17}O]OH, respectively. Both replacements occur with full stereospecificity (Scheme 17).



Scheme 17. Proposed mechanism for the stereocontrolled synthesis of nucleoside 3'-[^{16}O,^{17}O,^{18}O]phosphates **40**.

Detailed mechanistic studies showed that the initial attack of the sulfur atom of **34** on the carbon atom of styrene oxide results in intermediate **35**. Subsequent attack of the β-alkoxyl anion on the phosphorus center and elimination of ArO^- from **36** gives intermediate **37**. In the hydrolysis of oxathiaphospholane **37** by [^{17}O]H_2O the five-membered ring opens exclusively by cleavage of the P–S bond. Intermediate **38** is formed by attack of the water molecule on **37** from the side opposite to the endocyclic P–O bond. Pseudorotation then places the leaving group in an apical position in **39**. Cleavage of the P–S bonds is followed by fast elimination of the alkylene episulfide.

Following the stereocontrolled synthesis of monoalkyl-[^{16}O,^{17}O,^{18}O]phosphates **40**, the construction of oxathiaphospholanes such as **41** and their reaction with alcohols were of interest.[28] 5'-*O*-DMT-nucleoside 3'-*O*-(2-thio-1,3,2-oxathiaphospholane)s **41** were prepared and treated with 3'-*O*-acetylthymidine. In this case, the attack of the hydroxyl group on the phosphorus atom requires a basic catalyst. Although the reaction occurs in the presence of triethylamine (room temperature, 24 h, 5% yield) and diisopropylamine (room temperature, 4 h, 38% yield), DBU was the catalyst of choice. With DBU as catalyst a single coupling required 5 min and, after removal of protective groups, dinucleoside 3',5'-phosphorothioate **43** was obtained with >95% yield (Scheme 18). Separation of the diastereomers of **41** (B^1 = AdeBz, Gua*i*Bu, CytBz, Thy) was followed by studies of the stereoselectivity of the oxathiaphospholane ring opening, which was found to be higher than 98%.[28]



Scheme 18. Base-catalyzed alcoholysis of 1,3,2-oxathiaphospholanes **41**. R^1 = DMT; R^3 = Ac; B^1 = B^2 = Thy.

Model studies of (R_P,R_C)-2-[*N*-(α-naphthyl)ethylamino-2-thio]-1,3,2-oxathiaphospholane **44**[54] have shown that the ring opening with MeOH/DBU occurs by attack of the base-activated hydroxyl function of MeOH on phosphorus from the side opposite to the endocyclic P–O bond (Scheme 19). Collapse of



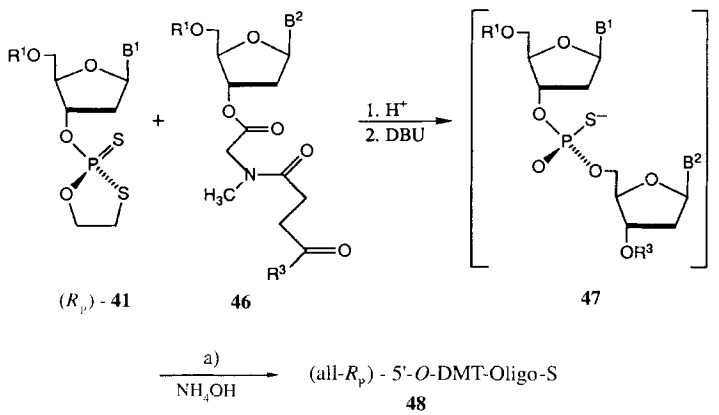
(R_P,R_C)-**44** (S_P,R_C)-**45**

Scheme 19. DBU-catalyzed methanolysis of **44**. α-$C_{10}H_7$ = α-naphthyl.

the pentacoordinate intermediate requires, according to Westheimer's rules,[55] pseudorotation placing the endocyclic P–S bond to be cleaved in the apical position. Cleavage of the P–S bond is followed by fast elimination of ethylene episulfide. The assignment of absolute configuration of substrates and products, namely (R_P,R_C)-**44** and (S_P,R_C)-**45** (resulting from *S*-methylation of the product of DBU-catalyzed methanolysis of **44**), and the analysis of the stereochemical course of the conversion of **44** into **45** also allowed tentative assignment of the absolute configuration at phosphorus in **41**. The quickly eluting diastereomers of **41**, which react with 5'-OH nucleosides to give (S_P)-d(N_{PS}N'), have (S_P) configuration at phosphorus, whereas the slowly eluting diastereomers of **41** have (R_P) configuration.[54]

Detailed knowledge of the stereochemistry of substrates and products of the oxathiaphospholane method leading stereo-

selectively to dinucleoside 3',5'-phosphorothioates was still not sufficient for the stereocontrolled synthesis of Oligo-S. Since the succinyl linker typically used with solid supports is cleaved in the presence of DBU,[56] a succinylsarcosinyl type of linker was employed,[56c] which survives in 0.1 M DBU in acetonitrile during the solid-phase synthesis of oligonucleotides.[56d] All four support-bound nucleosides **46** were prepared and used for the DBU-catalyzed reaction with separated diastereomers of **41** (Scheme 20). Penta(deoxycytidine-, octa(thymidine-, and dodeca(deoxyadenosine phosphorothioate)s have been obtained in diastereomerically pure form.[28, 57] Following stereocontrolled synthesis of (all-R_P)- and (all-S_P)-d[$(A_{PS})_{11}$A] it was shown that the alignment of (all-S_P)-d[$(A_{PS})_{11}$A] to complementary dodecathymidylic acid is more effective (T_m = 34.4 °C) than that of (all-R_P)-d[$(A_{PS})_{11}$A] (T_m = 30.0 °C).[59] This experimental result is in agreement with the analysis of model duplexes of B conformation, which indicated that duplexes formed by Oligo-S with (R_P) configuration and the sulfur atoms directed "inward" relative to the axis of the double helix are sterically less favorable than those formed by (all-S_P)-Oligo-S in which all sulfur atoms are directed "outward". The higher steric demands of phosphorothioates in comparison to phosphates were also evident from earlier results concerning the synthesis, molecular mechanics calculations, and biological properties of adenosine-3',5'-cyclic phosphorodithioate.[60] Recent molecular mechanics and dynamics calculations on a simulated complete helical turn of DNA duplexes formed by unmodified oligonucleotide as well as homochiral (all-R_P)- or (all-S_P)-Oligo-S[61] confirmed the results of intuitive analysis and experimental facts. Independently, NMR spectroscopic[62] and T_m[63] studies of oligonucleotides containing phosphorodithioate functions also indicated a destabilizing effect of sulfur atoms on double-stranded constructs.



(R_p) - **41** **46** **47** **48**

Scheme 20. Stereocontrolled oxathiaphospholane method for the synthesis of **1**. a) 1. H$^+$; 2. **41** + DBU; 3. capping; 4. steps 1–3 are repeated n times. R^1 = DMT; R^3 = LCA-CPG, B^1 = B^2 = AdeBz, Gua*i*Bu, CytBz, Thy.

Unfortunately, the synthesis and isolation of satisfactorily pure Oligo-S longer than 12-mers by using oxathiaphospholane methodology is still difficult. Single-step coupling efficiency sometimes substantially lower than 96% may be responsible for the presence of "failed" sequences ($n-1$, $n-2$, $n-3$...), especially if the "capping" step is not 100% effective. Recently, acetic anhydride/*N*-methylimidazole, which was originally reported[28] for the capping of unreacted 5'-OH groups by acylation, has been replaced by acetic anhydride/4-dimethylaminopyridine. Moreover, because the water content in solvents and reagents is most likely a critical parameter (traces of water in the presence of DBU can initiate ring-opening polymerization of 1,3,2-oxathiaphospholanes), special precautions and strictly anhydrous reagents have been used. Also, the time of the coupling step has been shortened from 600 to 200 seconds. Although the conditions and parameters for the oxathiaphospholane method are still not completely optimized, Grajkowski et al. have accomplished, starting from diastereomerically pure substrates **41** (B^1 = CytBz), the synthesis of (all-R_P) and (all-S_P) diastereomers of d[$(C_{PS})_{27}$C] with 86% and 82% chain integrity, respectively, as proved by polyacrylamide gel electrophoresis (PAGE).[58] Analysis of the crude product by ^{31}P NMR spectroscopy did not show any evidence of phosphate contaminants, which are unavoidable when Oligo-S is prepared by other methods.[3c] Grajkowski et al. also prepared, starting from diastereomeric mixtures of **41**, a "mixed-sequence" 26-mer Oligo-S containing six dC, six dG, ten dT, and four dA, which by PAGE was comparable to the 26-mer prepared by the phosphoramidite/sulfurization method. Current efforts are being directed at further improving the yield of single steps and elucidating the structures of the products resulting from unexpected, obscure side reactions.

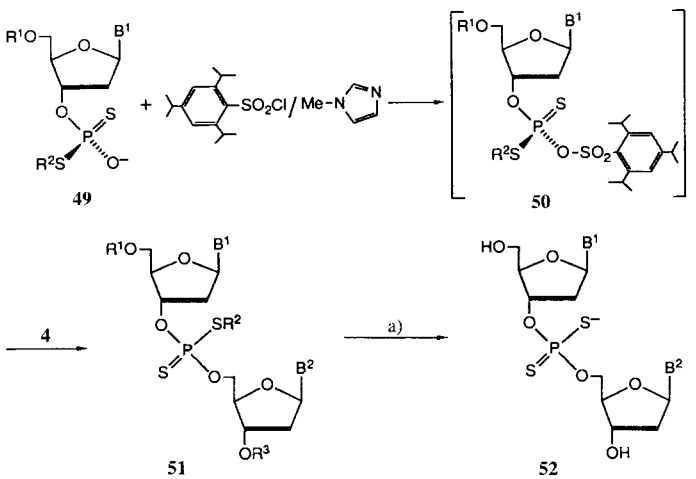
What kind of side reactions may be envisioned? An obvious one starts with the formation of an internucleotide phosphorothioate triester function containing the charged $CH_2CH_2S^-$ group, as in **42**. This moiety, although expected to be eliminated, may instead attack the nearest 5'-*O*-phosphorus-bound 5'-carbon atom, such that the phosphorothioate–carbon skeleton is extended by one CH_2CH_2S unit. This side reaction may proceed through a thermodynamically unfavorable seven-membered ring-transition state, and the enzymatic hydrolysis of the final Oligo-S should give modified nucleosides(tides), which does not appear to be the case. However, this possibility requires further investigation, since these contaminants are characterized by the same base composition and net negative charge as the expected product. Also under investigation is the possibility of "decapping" the 5'-*O*-acetyl group with DBU, which could be responsible for unwanted formation of ($n-1$), ($n-2$), ($n-3$) Oligo-S.[64]

Other studies in progress focus on the preparation of substrates like **41** without amide hydrogens, since activation by DBU and creation of the possible branching sites for growing polymer would be avoided. Efforts are also being made to construct the C-substituted oxathiaphospholanes **41**, which would still react with 5'-OH group, but the ring opening should not be followed by subsequent elimination of episulfide. S-Acylation of an intermediate like **42** would preserve the triester moiety until the end of desired chain extention, but one would also expect an increase in the undesired attack on the 5'-carbon atom as discussed above.[64]

Although beyond of the scope of this review, it is worth mentioning that modification of the oxathiaphospholane method by use of 5'-*O*-DMT-nucleoside 3'-*O*-(2-thiono-1,3,2-dithiaphospholane)s has allowed the preparation of oligo(nucleoside phosphorodithioate)s **52**.[65]

4.6. Other Possible Strategies for the Stereocontrolled Synthesis of Oligo(nucleoside phosphorothiate)s

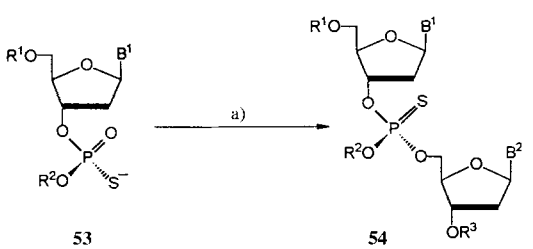
Since we wish to direct the attention of phosphorus and biopolymer chemists to the problem of the stereocontrolled synthesis of Oligo-S and related DNA or RNA congeners, other, yet unexplored routes to P-chiral oligonucleotide analogues should be mentioned. A mixture of diastereomers of 5′-*O*-DMT-nucleoside 3′-*O*-[*S*-(2,4-dichlorobenzyl)phosphorodithioate] **49** was treated with 2,4,6-triisopropylbenzenesulfonyl chloride (TIPS-Cl) and *N*-methylimidazole to give 97% activation of the oxygen atom of the phosphorodithioate moiety as opposed to activation of the sulfur atom (Scheme 21). Although reaction of **50**



Scheme 21. Activation of phosphorodithioate **49** by TIPS-Cl/*N*-methylimidazole occurs in 97% at oxygen.

with 5′-OH nucleoside **4** gives a diastereomeric mixture of dinucleotide **51**, these undergo S-deprotection and provide P-achiral dinucleoside 3′,5′-phosphorodithioates **52**.[66]

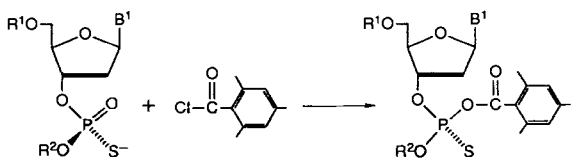
This chemoselective activation, unexpected in the light of earlier works on the activation of ambident phosphorothioate anions,[49, 67] kindled some hopes that substrates **53** with OR^2 groups such as OMe, OEt, or OBn, after separation into diastereomeric species, could undergo selective activation of phosphorothioate anions at the oxygen center; subsequent reaction at phosphorus with an OH-nucleoside may then lead to diastereomerically pure (or highly enriched) dinucleoside 3′,5′-*O*-alkylphosphorothioates **54** (Scheme 22). Removal of the phosphorothioate protecting groups by attack on the carbon



Scheme 22. Phosphorothioates **53** are potential substrates for the stereocontrolled synthesis of **1**. a) 1. TIPS-Cl/*N*-methylimidazole; 2. **4**. R^1 = DMT; R^2 = Me, Et, Bz, allyl; R^3 = Ac; B^1 = B^2 = Thy.

atom should lead to Oligo-S. However, if a pyrophosphorothioate intermediate[48] follows the formation of thiophosphoric sulfonic anhydrides, this approach to the stereocontrolled synthesis of Oligo-S may fail.

Another possibility involves acylation of appropriately protected nucleoside 3′-*O*-(*O*-alkyl)phosphorothioate **53** with sterically demanding, substituted benzoyl chlorides and subsequent reaction of the resulting mixed anhydride **55** with a 5′-OH function of a nucleoside or or oligonucleotide (Scheme 23). Al-



Scheme 23. Anhydrides **55** are potential substrates for the stereocontrolled synthesis of **1**.

though mixed phosphoric carboxylic anhydrides are known to exhibit both acylating and phosphorylating properties,[68] there are few well-documented examples of their exclusive phosphorylating activity. Jackson et al.[68c] have pointed out the important change in regioselectivity depending on the nature of the nucleophile: aminolysis occurs by an attack at the carbonyl carbon, whereas alcoholysis takes place by an attack at phosphorus. Moreover, Lambie[68e] demonstrated that *O*-pentachlorobenzoyl *O*,*O*-diethylphosphate reacts as a phosphorylating reagent even with aniline. This distinctive phosphorylating ability prompted Wozniak to synthesize P-diastereomerically pure forms of nucleoside 3′-*O*-(methanethiophosphonic) carboxylic anhydrides as the potential substrates for the stereocontrolled synthesis of oligo(nucleoside methanethiophosphonate)s. So far, reactions of aforementioned mixed anhydrides with 5′-OH nucleosides 3′-*O*-bound to the solid support lead to the desired product in miserable yields that are unacceptable for repetitive multistep synthesis. The search for an appropriate catalyst for this reaction is in progress and, if successful, efforts will be undertaken to synthesize analogous substrates applicable to the synthesis of **1**.[69]

5. Analysis of the Diastereomeric Purity of Oligo-S

In the introduction to this review we mentioned how difficult it is to determine the diastereomeric purity of Oligo-S. Figure 4 presents our best results obtained to date for the RP-HPLC separation of eight diastereomers of $d[C_{PS})_4C]$ (Fig. 4a, b) and an HPL chromatogram of $d[(C_{PS})_4C]$ (Fig. 4c, d); both products were prepared by the nonstereoselective phosphoroamidite method. Figure 4b clearly indicates the limit of RP-HPLC for the separation of small Oligo-S.[18] Our earlier results also indicated that in the case of Oligo-S with (R_P) configuration at each internucleotide phosphorothioate, digestion with endonuclease P1 can be used to prove its structure. It can also be useful as a "purification" process because under appropriate conditions every phosphorothioate of (S_P) configuration is cleaved.[22k]

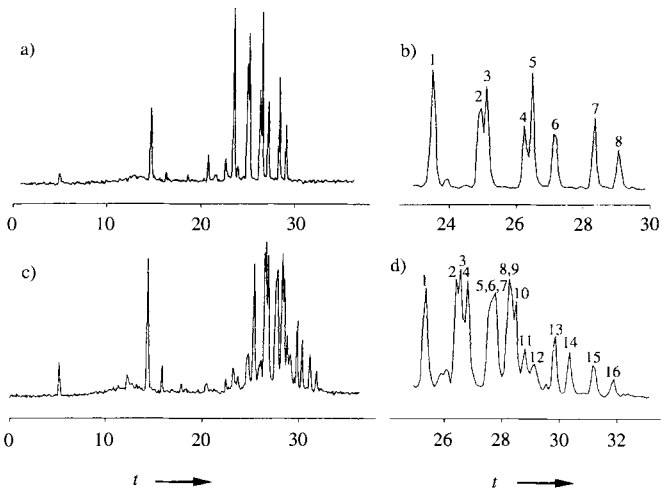


Fig. 4. RP-HPLC traces of tetramer d($C_{PS}C_{PS}C_{PS}C$): a) entire chromatogram; b) expanded section showing the presence of all eight diastereomers; c) and d) show the partial separation of 16 diastereomers of pentamer d($C_{PS}C_{PS}C_{PS}C_{PS}C$). For HPLC conditions see Table 1. Retention time t in min.

Moreover, exposure of d[$(C_{PS})_nC$] ($n = 1-4$, prepared as diastereomeric mixtures) to nuclease P1 followed by alkaline phosphatase gave the product, which was separated by RP-HPLC to give pure (R_P)-d($C_{PS}C$), (R_P,R_P)-d($C_{PS}C_{PS}C$), (R_P,R_P,R_P)-d($C_{PS}C_{PS}C_{PS}C$), and (R_P,R_P,R_P,R_P)-d[$(C_{PS})_4C$]. Similar treatment of the aforementioned diastereomeric mixtures of Oligo-S by means of snake venom phosphodiesterase (SVPDE), which is known to be (R_P) selective,[22i, j] was limited to digestion of 3'-terminal (R_P) internucleotide phosphorothioate because the enzyme has no endonucleolytic activity.[70]

Very distinctive differences in electrophoretic mobilities between (all-R_P)- and (all-S_P)-d[$(C_{PS})_9C$] have been found under nondenaturing conditions (Fig. 5). This observation could possibly indicate different self-organization (e.g. by base stacking) or interactions with a gel, which occur in P-homochiral Oligo-S, and may be considered as an indirect example of the effect of the chirality of Oligo-S on mobility. Important parameters such as cell membrane permeability may be influenced as well.

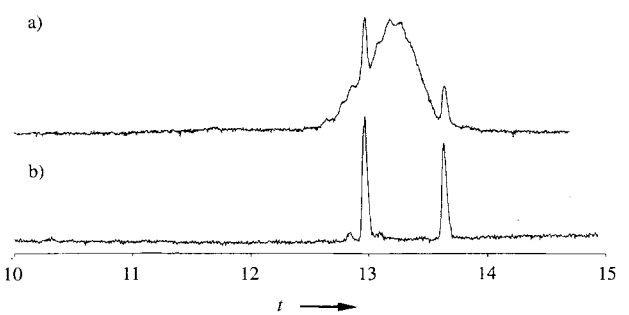


Fig. 5. High-performance capillary electrophoresis analyses were performed on an Applied Biosystems 270A-HT capillary electrophoresis instrument with MICRO-GEL_{100} (Applied Biosystems Inc., Foster City, CA) gel-filled capillaries (50 μm ID, effective length 27 cm; running buffer: 75 mM TRIS phosphate, pH 7.6, 10% methanol). Detection was at 260 nm, voltage 15 kV. Two individual diastereomers (all-R_P)- and (all-S_P)-d[$(C_{PS})_9C$] were mixed (b) and compared with the mixture of both diastereomers added to the sample of d[$(C_{PS})_9C$] prepared by phosphoroamidite/sulfurization method (512 diastereomers) (a).

6. Conclusions

Besides the biological consequences of the defined chirality of Oligo-S, there is another unanswered question: how far are we from solving the problem of the stereocontrolled synthesis of **1**? For oligopeptides it took nearly a century to solve the synthetic problem, and new enzymatic methods are being developed for enantiospecific synthesis.[71] As pointed out earlier, in every multistep synthesis the diastereomeric purity dp of the n-mer is roughly p^{n-1}, such that for a 28-mer prepared with $p = 0.98$ the $dp = 0.98^{27} = 0.56$. Therefore, is diastereoselective synthesis of chiral Oligo-S possible? Eckstein et al.[7] demonstrated that the polymerase-based synthesis of **1** with α-dNTPS leads to (all-R_P)-poly(nucleoside phosphorothioate)s. This type of enzymatic preparation of Oligo-S would be limited to the preparation of (all-R_P)-Oligo-S. In this review it has also been indicated that chemically synthesized (all-R_P)-Oligo-S can be stereochemically purified by digestion of contaminating (S_P)-phosphorothioates with nuclease P1. The next few years may bring the discovery of an effective (R_P)-diastereoselective endonuclease, or an appropriate enzyme may be developed by biotechnology. Such an endonuclease would not only be very useful for analytical purposes but would also be valuable for purification of (all-S_P)-Oligo-S contaminated with diastereomers possessing (R_P)-phosphorothioates. However, even if such endonucleases become available, their application in stereochemical degradation would not allow practical production of (all-S_P)-Oligo-S, since the content of the fraction with the desired homochirality in the diastereomeric mixture is approximately 2^{-n}. Efforts should also be directed toward the search for conditions under which a stereoselective endonuclease can work in a reversible manner. One can envision that matrix-directed synthesis of Oligo-S by means of phosphorothioate transferases will become feasible if studies are focused on, for example, the reversibility of the action of nucleases or phosphotransferases.

Alternatively, chemists must master the art of constructing substrates that allow the synthesis of Oligo-S with a diastereoselectivity >99% and a predetermined chirality at each internucleotide phosphorothioate function. However, progress seems to be rather slow on this front. Ten years after the first stereocontrolled synthesis of both diastereomers of dithymidine 3',5'-phosphorothioate[72] the demonstrated ability of stereocontrolled synthesis of **1** has extended only to dodecamers.[28] Undoubtedly, economic interests may provide enough incentive for the solution of this very challenging problem. If Oligo-S or synthetic ribozyme constructs containing nuclease-resistant components **1** responsible for recognition of appropriate target sequence within mRNA or pre-mRNA, are further evaluated as useful oligonucleotide therapeutics, then the stereocontrolled synthesis of **1** will be facilitated. Should that not be the case, there is still intellectual curiosity, which has always been an important factor in purely fundamental studies. Mission-oriented projects may not always succeed if they are not enforced by intellectual challenge.

This review was completed during the one-year appointment of one of the authors (W.J.S.) as Fogarty Scholar-in-Residence at the National Institutes of Health (NIH), Bethesda, MD (USA). We thank several colleagues and collaborators who contributed to the development of the first stereocontrolled methods for the syn-

thesis of Oligo-S; their names are given in the relevant references. Research projects were supported by the State Committee for Scientific Research (grant no. 0034/PZ/92/03). We would also like to express our gratitude to Dr. Gerald Zon of Lynx Therapeutics, Inc., Foster City, CA (USA) and to Dr. Jack Schmidt, Fogarty International Center, NIH, for critically reading several "mutations" of this review, and to Ms. Malgorzata Stec for typing this manuscript. We thank an anonymous referee for suggestions concerning another side reaction that may accompany the oxathiaphospholane ring-opening process.

Received: February 12, 1993 [A 935 IE]
German version: *Angew. Chem.* **1994**, *106*, 747

[1] a) M. Matsukura, K. Shinozuka, G. Zon, H. Mitsuya, M. Reitz, J. S. Cohen, S. Broder, *Proc. Natl. Acad. Sci. USA* **1987**, *84*, 7706; b) M. Matsukura, G. Zon, K. Shinozuka, M. Robert-Guroff, T. Shimada, C. A. Stein, H. Mitsuya, F. Wong-Staal, J. S. Cohen, S. Broder, *ibid.* **1989**, *86*, 4244; c) S. Agrawal, J. Goodchild, M. P. Civeira, A. H. Thornton, P. S. Sarin, P. C. Zamecnik, *ibid.* **1988**, *85*, 7079; d) S. Agrawal, T. Ikeuchi, D. Sun, P. S. Sarin, A. Konopka, J. Maizel, P. C. Zamecnik, *ibid.* **1989**, *86*, 7790.

[2] a) G. Zon, W. J. Stec in *Oligonucleotides and Their Analogues: A Practical Approach* (Ed.: F. Eckstein), IRL, Oxford, **1991**, p. 87; b) G. Zon, T. G. Geiser, *Anti-Cancer Drug Des.* **1991**, *6*, 539; c) T. Geiser, *Aids: Anti-HIV Agents, Therapies and Vaccines* (*Ann. N.Y. Acad. Sci. N. Y.* **1990**, *616*, 173).

[3] a) J. W. Efcavitch in *Gel Electrophoresis of Nucleic Acids* (Eds.: D. Rickwood, B. D. Hannes), IRL, Oxford, **1990**, p. 125; b) V. Metelev, S. Agrawal, *Anal. Biochem.* **1992**, *200*, 342; c) B. J. Bergot, W. Egan, *J. Chromatogr.* **1992**, *599*, 35; d) G. Zon in *High-Performance Liquid Chromatography in Biotechnology* (Ed.: W. S. Hancock), Wiley, New York, **1990**, p. 310; e) J. Tang, A. M. Roskey, S. Agrawal, *Anal. Biochem.* **1993**, *212*, 134.

[4] a) C. A. Stein, K. Mori, S. L. Loke, K. Subasinghe, J. S. Cohen, L. M. Neckers, *Gene* **1988**, *72*, 333; b) S. L. Loke, C. A. Stein, X. H. Zhang, K. Mori, M. Nakanishi, C. Subasinghe, J. S. Cohen, L. M. Neckers, *Proc. Natl. Acad. Sci. USA* **1989**, *86*, 3474; c) P. L. Iversen, *Anti-Cancer Drug Des.* **1991**, *6*, 531; d) P. L. Iversen, S. Zhu, A. Meyer, G. Zon, *Antisense Res. Dev.* **1992**, *2*, 211; e) P. L. Iversen, D. Crouse, G. Zon, G. Perry, *ibid.* **1992**, *2*, 223; f) G. Marti, W. Egan, P. Noguchi, G. Zon, M. Matsukura, S. Broder, *ibid.* **1992**, *2*, 27; g) S. Agrawal, J. Temsamani, J. Y. Tang, *Proc. Natl. Acad. Sci. USA* **1991**, *88*, 7595; h) D. J. Chin, G. A. Green, G. Zon, F. C. Szoka, R. M. Straubinger, *New Biol.* **1990**, *2*, 1091; i) W.-I. Gao, C. Storm, W. Egan, Y.-C. Cheng, *Mol. Pharmacol.* **1993**, *43*, 45; j) P. T. C. Ho, T. A. Bacon, E. Wickstrom, A. C. Sartorelli, *J. Cell Biol.* **1989**, *109*, 329; k) J. M. Campbell, T. A. Bacon, E. Wickstrom, *J. Biochem. Biophys. Methods* **1990**, *20*, 259; l) Q. Zhao, S. Matson, C. J. Herrera, E. Fisher, H. Yu, A. M. Krieg, *Antisense Res. Dev.* **1993**, *3*, 53; m) C. A. Stein, A. M. Cleary, L. Yakubov, S. Lederman, *ibid.* **1993**, *3*, 19.

[5] a) C. Cazenave, C. A. Stein, N. Loreau, N. T. Thuong, L. M. Neckers, C. Subasinghe, C. Helene, J. S. Cohen, J. J. Toulme, *Nucleic Acids Res.* **1989**, *17*, 4255; b) P. J. Furdon, A. Dominski, R. Kole, *ibid.* **1989**, *17*, 9193; c) W.-Y. Gao, F. Han, C. Storm, W. Egan, Y.-C. Cheng, *Mol. Pharmacol.* **1991**, *41*, 223; d) M. Chiang, H. Chan, M. A. Zounes, S. M. Freier, W. F. Lima, C. F. Bennett, *J. Biol. Chem.* **1991**, *266*, 18162; e) T. M. Woolf, D. A. Melton, C. B. G. Jennings, *Proc. Natl. Acad Sci. USA* **1992**, *89*, 7305; f) C. A. Stein, J. L. Tonkinson, L. Yakubov, *Pharmacol. Ther.* **1991**, *52*, 365; g) M. K. Ghosh, K. Ghosh, J. S. Cohen, *Antisense Res. Dev.* **1992**, *2*, 111.

[6] a) M. Z. Ratajczak, J. A. Kant, S. M. Luger, N. Hijiya, J. Zhang, G. Zon, A. M. Gewirtz, *Proc. Natl. Acad. Sci. USA* **1992**, *89*, 11823; b) M. Simons, E. R. Edelman, J. DeKeyser, R. Langer, R. D. Rosenberg, *Nature* **1992**, *352*, 67; c) K. D. Kumble, P. L. Iversen, J. K. Vishwanatha, *J. Cell Sci.* **1992**, *101*, 35; d) M. Simons, R. D. Rosenberg, *Circ. Res.* **1992**, *70*, 835; e) G. Citro, D. Perrotti, C. Cucco, I. D'Agnano, A. Sacchi, G. Zupi, B. Calabretta, *Proc. Natl. Acad. Sci. USA* **1992**, *89*, 7031; f) K. H. Schlingensiepen, W. Brysch in *Gene Regulation: Biology of Antisense RNA and DNA* (Eds.: R. P. Erickson, J. G. Izant), Raven, New York, **1992**, p. 317; g) Y. Shi, J. M. Glynn, L. J. Guilbert, T. G. Cotter, R. P. Bismonette, D. R. Green, *Science* **1992**, *257*, 212; h) P. H. Watson, R. T. Pon, R. P. Shiu, *Cancer Res.* **1991**, *51*, 3996; i) L. Whitesell, D. Geselowitz, C. Chavany, B. Fahmy, S. Walbridge, J. R. Alger, L. M. Neckers, *Proc. Natl. Acad. Sci. USA* **1993**, *90*, 4665; j) J. Lisziewicz, D. Sun, M. Klotman, S. Agrawal, P. Zamecnik, R. Gallo, *ibid.* **1992**, *89*, 11209; k) S. Agrawal, J. Y. Tang, *Antisense Res. Dev.* **1992**, *2*, 261; l) I. Katajima, T. Shinohara, T. Minor, L. Bibbs, J. Bilakovics, M. Nerenberg, *J. Biol. Chem.* **1992**, *267*, 25881; m) M. Hikida, K.-i. Haruma, H. Ohmori, *Immunol. Lett.* **1992**, *34*, 297; n) M. Ebbecke, C. Unterberg, A. Buchwald, S. Stohr, V. Wiegand, *Basic Res. Cardiol.* **1992**, *87*, 585; o) B. J. Chiasson, M. L. Hooper, P. R. Murphy, H. A. Robertson, *Eur. J. Pharmacol.* **1992**, *227*, 451; p) B. C. Paria, S. K. Dey, G. K. Andrews, *Proc. Natl. Acad. Sci. USA* **1992**, *89*, 10051; q) T. Lallier, M. Bronner-Freser, *Science* **1993**, *259*, 692; r) A. Colige, B. P. Sokolov, P. Nugent, R. Baserga, D. J. Prockop, *Biochemistry* **1993**, *32*, 8; s) L. M. Cowsert, M. C. Fox, G. Zon, C. K. Mirabelli, *Antimicrob. Agents Chemother.* **1993**, *37*, 171; t) H. Yokozaki, A. Budillon, G. Tomtora, S. Meissner, S. L. Beaucage, K. Miki, Y. S. Cho-Chung, *Cancer Res.* **1993**, *53*, 868; u) J. M. E. Leitler, S. Agrawal, P. Palese, P. C. Zamecnik, *Proc. Natl. Acad. Sci. USA* **1990**, *87*, 3430; v) J. W. Jaroszewski, O. Kaplan, J.-L. Syi, M. Sehested, P. L. Faustino, J. S. Cohen, *Cancer Commun.* **1990**, *2*, 287; w) E. Rapaport, K. Misiura, S. Agrawal, P. Zamecnik, *Proc. Natl. Acad. Sci. USA* **1992**, *89*, 8577; x) J. C. Reed, C. A. Stein, C. Subasinghe, S. Haldar, C. M. Croce, S. Yum, J. S. Cohen, *Cancer Res.* **1990**, *50*, 6565; y) J. Lisziewicz, D. Sun, V. Metelev, P. Zamecnik, R. C. Gallo, S. Agrawal, *Proc. Natl. Acad. Sci. USA* **1993**, *90*, 3860; z) E. Bayever, M. R. Boshop, G. Zon, J. Spinolo, A. Kessinger, *Proc. Am. Cancer Res.* **1993**, *34*, 593; A. Gewirtz, *ibid.* **1993**, *34*, 595.

[7] a) F. Eckstein, H. Gindl, *Eur. J. Biochem.* **1970**, *13*, 558; b) F. Eckstein, W. Armstrong, H. Sternbach, *Proc. Natl. Acad. Sci. USA* **1976**, *73*, 2987; c) T. A. Kunkel, F. Eckstein, A. S. Mildvan, R. M. Koplitz, L. Loeb, *ibid.* **1981**, *78*, 6734; d) L. J. P. Latimer, K. Hampel, J. S. Lee, *Nucleic Acids Res.* **1989**, *17*, 1549.

[8] a) W. J. Stec, G. Zon, W. Egan, B. Stec, *J. Am. Chem. Soc.* **1984**, *106*, 6077; b) W. J. Stec, G. Zon, *Tetrahedron Lett.* **1984**, *25*, 5275; c) *ibid.* **1984**, *25*, 5279; d) W. J. Stec, G. Zon, B. Uznanski, *J. Chromatogr.* **1985**, *326*, 263.

[9] a) G. Zon, *Pharm. Res.* **1988**, *5*, 539; b) C. A. Stein, J. S. Cohen, *Cancer Res.* **1988**, *48*, 2659. c) J. S. Cohen in *Oligonucleotides: Antisense Inhibitors of Gene Expression* (Ed.: J. S. Cohen), Macmillan, London, **1989**, p. 12; d) E. Uhlmann, A. Peyman, *Chem. Rev.* **1990**, *90*, 544; e) U. Englisch, D. H. Gauss, *Angew. Chem.* **1991**, *103*, 629; *Angew. Chem. Int. Ed. Engl.* **1991**, *30*, 613; f) M. Ghosh, J. S. Cohen, *Prog. Nucleic. Acid. Res. Mol. Biol.* **1992**, *42*, 79; g) S. Agrawal, *Trends Biotechnol.* **1992**, *10*, 152.

[10] a) T. R. Cech, *Curr. Opin. Struct. Biol.* **1992**, *2*, 605; b) S. M. Edgington, *Biotechnology* **1992**, *10*, 256; c) N. Sarver, *Antisense Res. Dev.* **1991**, *1*, 373; d) J. Goodchild, *Nucleic Acids Res.* **1992**, *20*, 4607; e) K. Taira, S. Nishikawa in *Gene Regulation: Biology of Antisense RNA and DNA* (Eds.: R. P. Erickson, J. G. Izant), Raven, New York, **1992**, p. 35.

[11] a) W. Saenger, *Principles of Nucleic Acid Structure*, Springer, New York, **1984**; b) N. T. Thuong, C. Hélène, *Angew. Chem.* **1993**, *105*, 697; *Angew. Chem. Int. Ed. Engl.* **1993**, *32*, 666.

[12] a) S. L. Beaucage, M. H. Caruthers, *Tetrahedron Lett.* **1981**, *22*, 1859; b) M. H. Caruthers, *Science* **1985**, *230*, 281; c) S. L. Beaucage, R. P. Iyer, *Tetrahedron* **1992**, *48*, 2233.

[13] a) M. Vaman Rao, C. B. Reese, Z. Zhengyun, *Tetrahedron Lett.* **1992**, *33*, 4839; b) R. P. Iyer, W. Egan, J. B. Ryan, S. L. Beaucage, *J. Am. Chem. Soc.* **1990**, *112*, 1253; c) R. P. Iyer, L. R. Phillips, E. Egan, J. B. Regan, S. L. Beaucage, *J. Org. Chem.* **1990**, *32*, 4693; d) H. Vu, B. L. Hirschbein, *Tetrahedron Lett.* **1991**, *32*, 3005; e) H. C. P. F. Roelen, P. C. J. Kamer, H. van den Elst, G. A. van der Marel, J. H. van Boom, *Recl. Trav. Chim. Pays-Bas* **1991**, *110*, 325; f) P. C. J. Kamer, H. C. P. F. Roelen, H. van den Elst, G. A. van der Marel, J. H. van Boom, *Tetrahedron Lett.* **1989**, *30*, 6757; g) W. J. Stec, B. Uznanski, A. Wilk, B. L. Hirschbein, K. L. Fearon, B. J. Bergot, *Tetrahedron Lett.* **1993**, *34*, 5317.

[14] a) B. C. Froehler, *Tetrahedron Lett.* **1986**, *27*, 5575; b) B. C. Froehler, M. D. Matteucci, *ibid.* **1986**, *27*, 469.

[15] a) L. Horner, *Pure Appl. Chem.* **1964**, 225; b) W. C. McEwen in *Topics in Phosphorus Chemistry, Vol. 2* (Eds.: M. Grayson, E. J. Griffith), Interscience, New York, **1965**, p. 25; c) W. Bentrude, L. H. Hargis, P. E. Rusek, *J. Chem. Soc. D* **1969**, 296; d) M. Mikolajczyk, J. Luczak, *Tetrahedron* **1972**, *28*, 5411; e) W. J. Stec, A. Okruszek, J. Michalski, *Angew. Chem.* **1971**, *83*, 491; *Angew. Chem. Int. Ed. Engl.* **1971**, *10*, 494; f) W. J. Stec, A. Okruszek, M. Mikolajczyk, *Z. Naturforsch. B* **1971**, *26*, 855; g) L. J. Szafraniec, L. L. Szafraniec, H. S. Aaron, *J. Org. Chem.* **1982**, *47*, 1936.

[16] P. M. J. Burgers, F. Eckstein, *Tetrahedron Lett.* **1978**, 3835.

[17] J. F. Marlier, S. J. Benkovic, *Tetrahedron Lett.* **1980**, *21*, 1121.

[18] A. Wilk, W. J. Stec, unpublished.

[19] F. Eckstein, *Annu. Rev. Biochem.* **1985**, *54*, 376.

[20] F. R. Bryant, S. J. Benkovic, *Biochemistry* **1979**, *18*, 2825.

[21] P. A. Frey in *New Comprehensive Biochemistry* (Eds.: A. Neuberger, L. L. L. van Deenen), Elsevier, Amsterdam, **1982**, p. 204.

[22] a) P. M. J. Burgers, F. Eckstein, *Biochemistry* **1979**, *18*, 450; b) B. A. Connolly, B. V. L. Potter, F. Eckstein, A. Pingoud, L. Grotjahn, *ibid.* **1984**, *23*, 3443; c) G. Slim, M. J. Gait, *Nucleic Acids Res.* **1991**, *19*, 1183; d) P. M. J. Burgers, F. Eckstein, D. H. Hunneman, *J. Biol. Chem.* **1979**, *254*, 7476; e) B. V. L. Potter, B. A. Connolly, F. Eckstein, *Biochemistry* **1983**, *22*, 1369; f) M. Koziolkiewicz, W. J. Stec, *ibid.* **1992**, *31*, 9460; g) D. R. Lesser, A. Grajkowski, M. R. Kurpiewski, M. Koziolkiewicz, W. J. Stec, L. Jen-Jacobson, *J. Biol. Chem.* **1992**, *267*, 24510; h) A. Gupta, C. DeBrosse, S. J. Benkovic, *ibid.* **1982**, *257*, 7689; i) P. M. J. Burgers, F. Eckstein, D. H. Hunneman, *ibid.* **1979**, *254*, 7476; j) B. V. L. Potter, B. A. Connolly, F. Eckstein, *Biochemistry* **1983**, *22*, 1369; k) A. D. Griffiths, B. V. L. Potter, I. C. Eperon, *Nucleic Acids Res.* **1987**, *15*, 4145; l) A. P. Gupta, P. A. Benkovic, S. J. Benkovic, *ibid.* **1984**, *12*, 5897.

[23] Z. Otwinowski, R. W. Schervitz, R. G. Zhang, C. L. Lawson, A. Joachimiak, R. Q. Marmorstein, B. F. Luisi, P. B. Sigler, *Nature* **1988**, *335*, 321.

[24] L. A. Yakubov, E. A. Deeva, V. F. Zarytova, E. M. Ivanova, A. S. Ryte, L. V. Yurchenko, V. V. Vlassov, *Proc. Natl. Acad. Sci. USA* **1989**, *86*, 6454.

[25] G. Zon, M. F. Summers, K. A. Gallo, K.-L. Shao, M. Koziolkiewicz, B. Uznanski, W. J. Stec in *Biophosphates and Their Analogues – Synthesis, Structure, Metabolism and Activity* (Eds.: K. S. Bruzik, W. J. Stec), Elsevier, Amsterdam, **1987**, p. 165.

[26] a) FDA's Policy Statement for Development of New Stereoisomeric Drugs, Food and Drug Administration: Rockville, MD, May **1992**; b) I. Amato, *Science* **1992**, *256*, 964; c) J. Hodgson, *Biotechnology* **1992**, *10*, 1093; d) A. G. Petsko, *Science* **1992**, *256*, 1403; e) S. C. Stinson, *Chem. Eng. News* **1992**, *71*, 46; f) W. A. Nugent, T. V. RajanBabu, M. J. Burk, *Science* **1993**, *259*, 479; g) U. Hacksell, S. Ahlenius, *Trends Biotechnol.* **1993**, *11*, 73.

[27] J. A. Gerlt, J. A. Coderre, S. Mehdi, *Adv. Enzymol.* **1983**, *55*, 279.

[28] a) W. J. Stec, *Nucleic Acids Symp. Ser.* **1991**, *23*, 171; b) W. J. Stec, A. Grajkowski, M. Koziolkiewicz, B. Uznanski, *Nucleic Acids Res.* **1991**, *19*, 5883.

[29] D. Valentine in *Asymmetric Synthesis 1983–1984* **1985**, *4*, 263.

[30] a) S. Berner, K. Muhlegger, H. Seliger, *Nucleic Acids Res.* **1989**, *17*, 853; b) B. H. Dahl, J. Nielsen, O. Dahl, *ibid.* **1987**, *15*, 1729; c) Y. Watanabe, *J. Chem. Soc. Perkin Trans 1* **1992**, 1879.

[31] A. V. Lebedev, J. P. Rife, H. W. Seligsohn, G. R. Wensinger, E. Wickstrom, *Tetrahedron Lett.* **1990**, *31*, 855.

[32] a) T. Tanaka, S. Tamatsukuri, M. Ikehara, *Tetrahedron Lett.* **1986**, *27*, 199; b) J. Helinski, W. Dabkowski, J. Michalski, *ibid.* **1991**, *32*, 4981.

[33] B. Uznanski, A. Wilk, W. J. Stec, *Tetrahedron Lett.* **1987**, *28*, 3401.

[34] B. Uznanski, A. Wilk, W. J. Stec, unpublished.

[35] a) P. J. Garegg, T. Regberg, J. Stawinski, E. Stomberg, *Chem. Scr.* **1985**, *25*, 280; b) P. J. Garegg, I. Lindh, T. Regberg, J. Stawinski, R. Stromberg, *Tetrahedron Lett.* **1986**, *27*, 4051; c) A. Andrus, J. W. Efcavitch, L. McBride, B. Gusti, *ibid.* **1988**, *29*, 861.

[36] a) B. C. Froehler, P. G. Ng, M. D. Matteucci, *Nucleic Acids Res.* **1986**, *14*, 160; b) C. A. Stein, C. Subasinghe, K. Shinozuka, J. S. Cohen, *ibid.* **1988**, *16*, 3209.

[37] a) F. Seela, U. Kretschmer, *Nucleosides Nucleotides* **1991**, 10, 711; b) *J. Chem. Soc. Chem. Commun.* **1990**, 1154; c) *J. Org. Chem.* **1991**, *56*, 3861.

[38] a) J. Stawinski, R. Stromberg, R. Zain, *Tetrahedron Lett.* **1992**, *33*, 3185; b) H. Almer, J. Stawinski, R. Stromberg, M. Thelin, *J. Org. Chem.* **1992**, *57*, 6163.

[39] a) W. B. Farnham, R. K. Murray, K. Mislow, *J. Am. Chem. Soc.* **1970**, *92*, 5809; b) J. Donohue, N. Mandel, W. B. Farnham, M. H. Murray, K. Mislow, H. P. Benschop, *ibid.* **1971**, *93*, 3792.

[40] a) L. P. Reiff, H. S. Aaron, *J. Am. Chem. Soc.* **1970**, *92*, 5275; b) L. J. Szafraniec, L. P. Reiff, H. S. Aaron, *ibid.* **1970**, *92*, 6391.

[41] a) M. Fujii, K. Ozaki, A. Kume, M. Sekine, T. Hata, *Tetrahedron Lett.* **1986**, *26*, 935; b) M. Fujii, K. Ozaki, M. Sekine, T. Hata, *Tetrahedron* **1987**, *43*, 3395.

[42] a) C. Battistini, M. G. Brasca, S. Fustinoni, *Nucleosides Nucleotides* **1991**, *10*, 723; b) C. Battistini, M. G. Brasca, S. Fustinoni, E. Lazzari, *Tetrahedron* **1992**, *48*, 3209.

[43] H. Oediger, F. Moller, K. Eiter, *Synthesis* **1972**, 591.

[44] The influence of DBU on configurational stability of *P*-chiral organophosphates requires further study. Unpublished results from our laboratory (Z. J. Lesnikowski, L. Wozniak) indicate that diastereomers of dinucleoside 3',5'-methanephosphonates are not epimerized in the presence of DBU under conditions that lead to complete P-epimerization of diastereomerically pure nucleoside 3'-*O*-(*O*-4-nitrophenylmethanephosphonate)s or nucleoside 3'-*O*-(Se-methyl-methanephosphonate)s. Therefore, these last results can be explained in terms of DBU-catalyzed hydrolysis caused by traces of water; released *p*-nitrophenoxide ion or methylselenenyl ion, respectively, may cause epimerization of parent compounds in the presence of DBU by a ping-pong type mechanism.

[45] a) C. B. Reese, *Tetrahedron* **1978**, *34*, 3143; b) M. Ikehara, E. Ohtsuka, A. F. Markham, *Adv. Carbohydr. Chem. Biochem.* **1978**, *36*, 135; c) R. Wu, C. Bahl, S. A. Narang, *Prog. Nucleic Acid Res. Mol. Biol.* **1978**, *21*, 101; d) K. Itakura, A. D. Riggs, *Science* **1980**, *209*, 1401; e) S. A. Narang, *Tetrahedron* **1983**, *39*, 3; f) B. S. Sproat, M. J. Gait in *Oligonucleotide Synthesis; A Practical Approach* (Ed.: M. J. Gait), IRL, Oxford, **1984**; g) J. E. Marugg, C. Van Den Bergh, J. Tromp, G. G. Van Der Marel, J. Van Zoest, J. H. Van Boom, *Nucleic Acids Res.* **1984**, *12*, 9095.

[46] E. Ohtsuka, M. Shiraishi, M. Ikehara, *Tetrahedron Lett.* **1985**, *41*, 5271.

[47] R. Cosstick, D. M. Williams, *Nucleic Acids Res.* **1987**, *15*, 9921.

[48] a) D. G. Knorre, A. V. Lebedev, A. V. Zarytova, *Nucleic Acids Res.* **1976**, *3*, 1401; b) D. G. Knorre, V. F. Zarytowa in *Phosphorus Chemistry Directed Towards Biology* (Ed.: W. J. Stec), Pergamon, Oxford, **1979**, p. 13; c) E. H. Ivanova, L. M. Khalimskaya, V. P. Romanienko, V. F. Zarytova, *Tetrahedron Lett.* **1982**, *23*, 5447; d) V. F. Zarytova, D. G. Knorre, *Nucleic Acids Res.* **1984**, *12*, 2091.

[49] W. Niewiarowski, Z. J. Lesnikowski, A. Wilk, P. Guga, A. Okruszek, B. Uznanski, W. J. Stec, *Acta Biochim Pol* **1987**, *34*, 217.

[50] a) Z. J. Lesnikowski, A. Sibinska, *Tetrahedron* **1986**, *42*, 5025; b) Z. J. Lesnikowski, M. Jaworska, *Tetrahedron Lett.* **1989**, *30*, 3821, c) Z. J. Lesnikowski, *Nucleosides Nucleotides* **1992**, *11*, 1621.

[51] a) Y. Hayakawa, M. Uchiyama, R. A. Noyori, *Tetrahedron Lett.* **1984**, *25*, 4003; b) M. Uchiyama, Y. Aso, R. Noyori, Y. Hayakawa, *J. Org. Chem.* **1993**, *58*, 373.

[52] M. Jaworska-Maslanka, *Ph. D. Thesis*, University of Lodz, **1992**.

[53] a) P. Guga, W. J. Stec, *Tetrahedron Lett.* **1983**, *24*, 3899; b) A. Okruszek, P. Guga, W. J. Stec, *J. Chem. Soc. Chem. Commun.* **1985**, 1225; c) A. Okruszek, P. Guga, W. J. Stec in *Biophosphates and Their Analogues – Synthesis, Structure, Metabolism and Activity* (Eds.: K. S. Bruzik, W. J. Stec), Elsevier, Amsterdam, **1987**, p. 247; d) A. Okruszek, P. Guga, W. J. Stec, *J. Chem. Soc. Chem. Commun.* **1987**, 5957; e) *Heteroat. Chem.* **1991**, *2*, 561.

[54] B. Uznanski, A. Grajkowski, B. Krzyzanowska, A. Kazmierkowska, W. J. Stec, M. W. Wieczorek, J. Blaszczyk, *J. Am. Chem. Soc.* **1992**, *114*, 10197.

[55] F. H. Westheimer in *Rearrangements in Ground & Exited States* (Ed.: P. de Mayo), Academic Press, New York, **1980**, p. 229.

[56] a) K.-P. Stengele, W. Pfleiderer, *Nucleic Acids Symp. Ser.* **1989**, *21*, 101; b) *Tetrahedron Lett.* **1990**, *31*, 2549; c) T. Brown, C. E. Pritchard, G. Turner, S. A. Salisbury, *J. Chem. Soc. Chem. Commun.* **1989**, 891; d) C. Lehman, Y.-Z. Xu, C. Christoloulos, Z. K. Tan, M. J. Gait, *Nucleic Acids Res.* **1989**, *17*, 2379.

[57] A. Suska, A. Grajkowski, A. Wilk, B. Uznanski, J. Blaszczyk, M. Wieczorek, W. J. Stec, *Pure Appl. Chem.* **1993**, *65*, 707.

[58] A. Grajkowski, A. Wilk, M. Koziolkiewicz, W. J. Stec, unpublished.

[59] The T_m value for heteroduplex (all-R_P)-d[$(A_{PS})_{11}$A]/T_{12} given in ref. [57] was determined incorrectly. All measurements were repeated with diastereomeric dodeca(adenosine phosphorothioate)s of size-homogeneity >99% as checked by capillary electrophoresis. The diastereomeric purity the of (all-R_P) diastereomer was proven by its treatment with nuclease P1. Material recovered by RP-HPLC was converted into sodium salt by precipitation. Measurements were performed in HEPES buffer (pH 5.4, 100 mM HEPES, 20 mM $MgCl_2$, 200 mM NaCl) with direct temperature monitoring inside the UV cell. The results are as follows: dA_{12}/dT_{12} 37.4 °C, d[$(A_{PS})_{11}$A] (mixture of all diastereomers, ca. 58% (R_P) configuration)/dT_{12} 31.6 °C; (all-R_P)-d[$(A_{PS})_{11}$A]/dT_{12} 30.0 °C; (all-S_P)-d[$(A_{PS})_{11}$A]/dT_{12} 34.4 °C.

[60] L. H. Parker-Botelho, L. C. Webster, J. D. Rothemel, J. Baraniak, W. J. Stec, *J. Biol. Chem.* **1988**, *263*, 5301.

[61] J. W. Jaroszewski, J.-J. Syi, J. Maizel, J. S. Cohen, *Ant-Cancer Drug Des.* **1992**, *7*, 253.

[62] M. E. Piotto, J. N. Granger, Y. Cho, N. Farshtschi, D. G. Gorenstein, *Tetrahedron* **1991**, *47*, 2449.

[63] a) M. H. Caruthers, G. Beaton, L. Cummins, *Nucleosides Nucleotides* **1991**, *10*, 47; b) K. Bjergarde, B. H. Dahl, O. Dahl, *ibid.* **1991**, *10*, 461; c) K. Bjergarde, O. Dahl, *Nucleic Acids Res.* **1991**, *19*, 5843.

[64] B. Karwowski, A. Kobylanska, A. Sierzchala, A. Okruszek, W. J. Stec, unpublished.

[65] A. Okruszek, A. Sierzchala, M. Sochacki, W. J. Stec, *Tetrahedron Lett.* **1992**, *33*, 7585.

[66] E. K. Yan, Y.-X. Ma, M. A. Caruthers, *Tetrahedron Lett.* **1990**, *31*, 1953.

[67] W. Dabkowski, A. Lopusinski, J. Michalski, C. Radziejewski, *Phosphorus Sulfur Relat. Elem.* **1980**, *8*, 375.

[68] a) G. H. Smith, C. N. Cauhlan, F. Ramirez, S. Glaser, P. Stern, *J. Am. Chem. Soc.* **1974**, *96*, 2698, and references therein.; b) R. Ramage in *Organophosphorus Reagents in Organic Synthesis* (Ed.: J. I. G. Cadogan), Academic Press, **1979**, p. 511; c) A. G. Jackson, G. W. Kenner, G. A. Moore, R. Ramage, *Tetrahedron Lett.* **1976**, 3627; d) P. C. Crofts, *Org. Phosphorus Comp. 1972–1976* **1973**, *6*, 51; e) A. J. Lambie, *Tetrahedron Lett.* **1966**, 3709; f) N. E. Jacobsen, P. A. Bartlett, *J. Am. Chem. Soc.* **1983**, *105*, 1613, g) *ibid.* **1983**, *105*, 1619.

[69] L. Wozniak, W. J. Stec, unpublished.

[70] G. M. Richards, G. du Vair, M. Laskowski, Sr., *Biochemistry* **1965**, *4*, 501.

[71] W. Kullmann, *Enzymatic Peptide Synthesis*, CRC, Boca Raton, FL, **1987**.

[72] B. Uznanski, W. Niewiarowski, W. J. Stec, *Tetrahedron Lett.* **1982**, *23*, 4289.

Ladder Sequencing of Peptides and Proteins—A Combination of Edman Degradation and Mass Spectrometry

Jörg W. Metzger*

The most important method for the determination of the primary structure of proteins is the stepwise chemical degradation developed by Edman in 1950 (Edman degradation).[1] Reaction of the N-terminal amino group of the peptide or protein with phenylisothiocyanate gives the phenylthiocarbamoyl peptide **1**, which in acidic solution is cleaved to form a 2-anilinothiazolin-5-one **2**, and the peptide chain shortened by one amino acid **3** (Fig. 1). Thiazolinone **2** hydrolyzes to give the phenylthiocarbamoyl amino acid (PTC amino acid) **4**, which is converted by

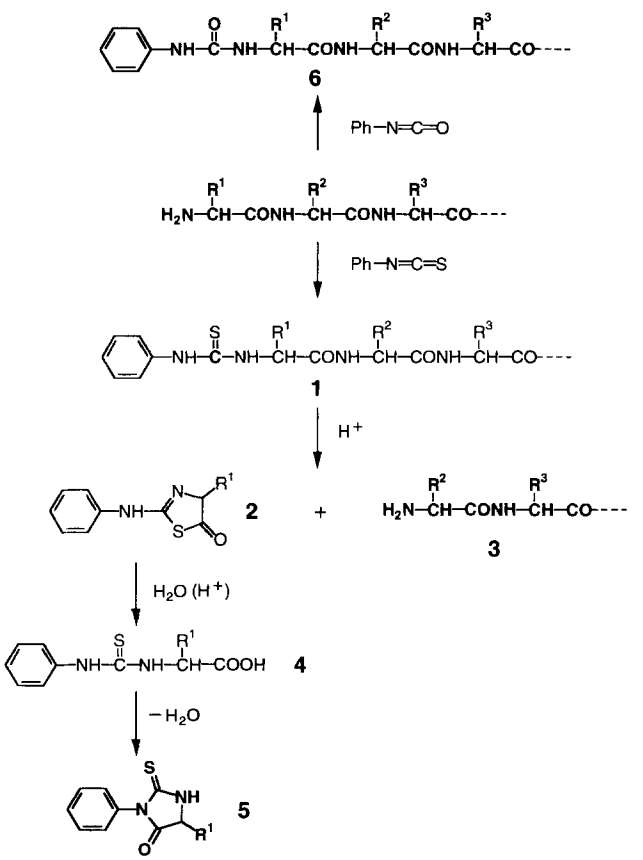


Fig. 1. Generation of the peptide ladder by Edman degradation in the presence of phenylisocyanate as the terminating reagent.

ring formation into the 3-phenyl-2-thiohydantoin (PTH amino acid) **5**. The PTH amino acid **5** is extracted and identified chromatographically. A major disadvantage of the fully automated Edman degradation by on-line HPLC is the relatively low sample throughput; even with the short analysis times possible by optimized chemical and analytical cycles, only about 60 residues per day can be determined.[2] Many unusual amino acids cannot be identified, and modified amino acids (e.g. phosphorylated amino acids) only with especially elaborated analytical procedures.[3]

Because of the excellent suitability of novel ionization techniques like matrix-assisted laser desorption (MALDI)[4] and electrospray ionization (ESI)[5] for peptide and protein analysis, mass spectrometric sequencing methods are gaining increasing importance. Tandem mass spectrometry[6] is used for obtaining sequence information for peptides and proteins.[7] This technique requires two mass analyzers (MS-MS). The molecular ion formed by ionization is selected in the first mass analyzer and reaches a collision cell, where it is fragmented by collision with argon atoms (collision-induced dissociation; CID). The fragment ions are separated according to their m/z ratio in the second mass analyzer and are registered in a "product" or "daughter ion" mass spectrum. Depending on the peptide sequence, this spectrum contains a series of N-terminal, C-terminal, or internal fragment ions formed by cleavage of bonds along the peptide backbone. In favorable cases it is possible to determine the entire sequence from the observed mass differences between corresponding mass peaks in the daughter ion spectrum. Depending on the collision energy, high- and low-energy CID spectra can be distinguished.

The potential of protein sequencing by tandem mass spectrometry is restricted because 1) many peptides undergo only a limited extent of fragmentation, 2) the interpretation of tandem mass spectra is often not trivial and unambiguous, and 3) the applicability is usually restricted to peptides with molecular masses of not more than 3000–4000 u.[7] However, fragmentation of multiply charged ions, as they are commonly found in ESI-MS, may provide sequence information for larger peptides and even proteins.[8] Usually, however, larger peptides are cleaved into smaller peptides by chemical or enzymatic degradation prior to tandem mass spectrometric investigation.

Mass spectrometric sequencing methods are also suitable for the sequencing of N-terminally blocked peptides and for the determination of posttranslational modification sites (acylation, phosphorylation, glycosylation, farnesylation, etc.). The amino acids Ile and Leu, which have the same nominal mass (isobaric

[*] Dr. J. W. Metzger
Institut für Organische Chemie der Universität
Auf der Morgenstelle 18, D-72076 Tübingen (FRG)
Telefax: Int. code + (7071) 29-6925

 © VCH Verlagsgesellschaft mbH, D-69451 Weinheim, 1994 0570-0833/94/0707-0723 $ 10.00+.25/0

amino acids) can be distinguished by their different side-chain fragmentation patterns in the high-energy CID experiment (e.g. by using a four-sector instrument).[7] Lysine can be differentiated from isobaric glutamine after acetylation of the ε-amino group.[7]

The novel method of sequencing peptides by means of metastable ions in a time-of-flight mass spectrometer is quite promising.[9] This technique is characterized by high sensitivity, allowing sequencing in the femtomole range.

In other approaches Edman degradation and mass spectrometry are combined. Here, the basic idea is to replace the slow HPLC analysis of the PTH amino acids by a quicker mass spectrometric analysis. In order to determine the sequence of a peptide, either the mass of the cleaved PTH amino acid[10] or of the remaining peptide[11] can be determined after each degradation step. A modified Edman reagent containing a quaternary ammonium group was recently introduced to enhance the sensitivity of the detection step with ESI-MS.[10]

Chait et al. recently introduced the interesting method of ladder sequencing[12] which consists of two steps: 1. the chemical degradation of the protein into peptide fragments, each of which differ by one amino acid (generation of the "peptide ladder"). 2. readout of the sequence from the MALDI mass spectrum, which results from the mass differences between adjacent mass peaks. To generate the ladder stepwise Edman degradation with phenylisothiocyanate is performed in the presence of phenylisocyanate as the terminating reagent (ratio of phenylisothiocyanate to phenylisocyanate is ca. 95:5). The phenylcarbamoyl peptide (PC peptide) **6** is stable in acidic solution, whereas the phenylthiocarbamoyl peptide **1** is degraded (see Fig. 1). Thus, in each cycle a small amount of peptide is blocked N-terminally by PhNCO and protected from further Edman degradation. A defined number of degradation cycles (**1**–**5**) is performed without isolating and analyzing the reaction products formed with PhNCS. Only at the end is a MALDI mass spectrum of the whole mixture recorded. The spectrum contains the mass peaks of the individual phenylcarbamoyl peptides **6**. The mass difference of adjacent mass peaks corresponds to one particular amino acid residue, the order of their occurrence defines the sequence of the original peptide chain (Fig. 2).

The readout of the sequence in a single step is similar to the method of DNA sequencing by chain fragmentation developed by Maxam and Gilbert[13] and accelerates sequencing substantially. As the remaining peptide and not the cleaved amino acid is detected, the acid-catalyzed conversion step (1 M HCl or 25% trifluoroacetic acid, ca. 60 °C), which generates the stable PTH amino acid, is unnecessary (cf. Fig. 2). Thus, acid-labile phosphorylated amino acids like phosphoserine remain intact and can be identified directly by the respective mass difference in the spectrum. A further advantage is that the reaction yield does not have to be as high as in conventional Edman degradation. However, all peptides should be present quantitatively as carbamoyl peptides; this can be achieved by repeating the treatment of the reaction mixture with phenylisocyanate before analysis.

The potential of mixture analysis by MALDI mass spectrometry and the principle feasability of ladder sequencing was demonstrated by the investigation of a synthetic peptide mixture consisting of more than 30 peptides.[12] Although mass spectrometric discrimination effects are common for surface ionization techniques, each component gave a clear mass peak and total

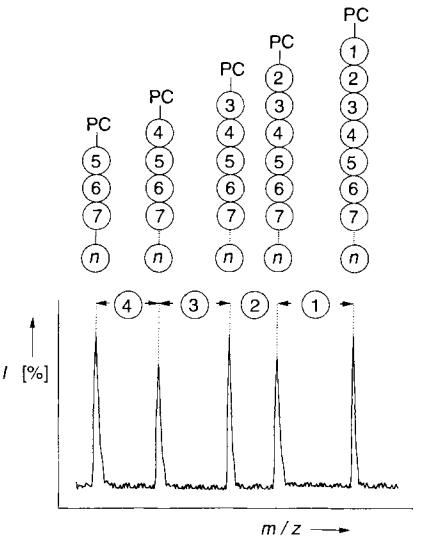


Fig. 2. Readout of a partial sequence of a peptide containing n amino acids by means of the MALDI mass spectrum (PC = phenylcarbamoyl). The mass difference between adjacent mass peaks corresponds to a particular amino acid (modified or unusual residues can also be determined; residues with the same nominal mass cannot be distinguished; N-terminally blocked peptides cannot be sequenced). The direction of readout of the sequence is from higher to lower mass, owing to the degradation from the N- to the C-terminus.

suppression of single components was not observed. Ladder sequencing with MALDI-MS is also suitable for larger peptides; however, the inaccuracy of the determination of individual residues increases with increasing molecular mass (up to 0.9 u for peptides with relative molecular masses >3500).[12] Due to the limited resolution of the mass analyzer, the residues Asp and Asn, Gln and Glu present in a ladder peptide of this high mass cannot be unambiguously differentiated. In contrast to tandem mass spectrometry, ladder sequencing does not allow the sequencing of N-terminally blocked peptides, because these are not amenable to the ladder-generating chemistry. The maximal sequencable length of a peptide by this technique is comparable to that achieved by conventional Edman degradation (the authors consider ca. 60 residues to be the limit).[12] On the other hand, a much higher sample throughput can be achieved.

Ladder sequencing could become an alternative to the slower Edman degradation in the HPLC-equipped protein sequencer, if it is possible to perform and fully automate the chemistry at a picomole scale. Recently, it was shown that the peptide ladder can be generated in a commercial protein sequencer.[14] Interestingly, the ladder could also be generated in the absence of a terminating agent by using very short contact times of the Edman reagent with the protein during the degradation steps.[14] On account of the high sensitivity in the mass spectrometric readout step (low femtomole range), no more than 10–100 picomoles of peptide is needed for the ladder-generating chemistry. ESI mass spectrometry, which also proved to be a highly potent technique for mixture analysis,[15] could also be used for the mass determination of ladder peptides. However, the occurence of multiply charged ions, which are commonly observed with this technique, might complicate the readout of the sequence. In addition, ESI is usually employed with quadrupole instruments, which usually have a slightly better mass resolution than the time-of-flight analyzers used with MALDI, but which

also have a limited mass range ($< m/z$ 4000, usually ca. 2000–3000). For the sequencing of larger peptides a time-of-flight analyzer, which in principle has no upper mass limit, is advantageous. Because of the rapid development of time-of-flight analyzers, development of novel matrices, and improvement of sample preparation,[16] considerable improvements in the mass accuracy and resolution can be expected in the near future.

The development of a fully automated protein sequencer with mass spectrometric detection based on the chemistry of ladder sequencing is feasible. However, it can be expected that the cost of such an analytical instrument will be clearly higher than that of conventional sequencers equipped with HPLC, because of the relatively expensive mass analyzers. Despite the high price, such instruments would be very interesting for peptide and protein chemists, especially because of the expected high sample throughput and the possibility of sequencing modified peptides and peptides with unusual amino acids.

German version: *Angew. Chem.* **1994**, *106*, 763

[1] a) P. Edman, G. Begg, *Eur. J. Biochem.* **1967**, **1**, 80–91; b) P. Edman, *Acta Chem. Scand.* **1950**, *4*, 283–293.

[2] N. F. Totty, M. D. Waterfield, J. J. Hsuan, *Protein Sci.* **1992**, *1*, 1215–1224.

[3] a) H. E. Meyer, E. Hoffmann-Posorske, H. Korte, L. M. G. Heilmeyer, *FEBS Lett.* **1986**, *204*, 61–66; b) H. E. Meyer, E. Hoffmann-Posorske, A. Donella-Deana, H. Korte, *Methods Enzymol.* **1991**, *201*, 206–224.

[4] a) M. Karas, D. Bachmann, U. Bahr, F. Hillenkamp, *Int. J. Mass Spectrom. Ion Processes* **1987**, *78*, 53–68; b) M. Karas, F. Hillenkamp, *Anal. Chem.* **1988**, *60*, 2299–2301; c) M. Karas, U. Bahr, A. Ingendoh, F. Hillenkamp, *Angew. Chem.* **1989**, *101*, 805–806; *Angew. Chem. Int. Ed. Engl.* **1989**, *28*, 760–761.

[5] a) M. Yamashita, J. B. Fenn, *J. Phys. Chem.* **1984**, *88*, 4451–4459; b) **1984**, *88*, 4671–4675; c) A. P. Bruins, T. R. Covey, J. D. Henion, *Anal. Chem.* **1987**, *59*, 2642–2646.

[6] *Mass Spectrometry/Mass Spectrometry: Techniques and Applications in Tandem Mass Spectrometry* (Eds.: K. L. Busch, G. L. Glish, S. A. McLuckey), VCH, New York, **1988**.

[7] K. Biemann, *Methods Enzymol.* **1990**, *193*, 455–479.

[8] a) C. J. Barinaga, C. G. Edmonds, H. R. Udseth, R. D. Smith, *Rapid Commun. Mass Spectrom.* **1989**, *3*, 160–164; b) R. D. Smith, C. J. Barinaga, H. R. Udseth, *J. Phys. Chem.* **1989**, *93*, 5019–5022; c) R. D. Smith, C. J. Barinaga, *Rapid Commun. Mass Spectrom.* **1990**, *4*, 54–57; d) J. A. Loo, C. G. Edmonds, R. D. Smith, *Anal. Chem.* **1991**, *63*, 2488–2499; e) K. J. Light-Wahl, J. A. Loo, C. G. Edmonds, R. D. Smith, H. E. Witkowska, C. H. L. Shakleton, C.-S. C. Wu, *Biol. Mass Spectrom.* **1993**, *22*, 112–120.

[9] a) B. Spengler, D. Kirsch, R. Kaufmann, *J. Phys. Chem.* **1992**, *96*, 9678–9684; b) B. Spengler, D. Kirsch, R. Kaufmann, E. Jaeger, *Rapid Commun. Mass Spectrom.* **1992**, *6*, 105–108; c) R. Kaufmann, B. Spengler, F. Lützenkirchen, *ibid.* **1993**, *7*, 902–910.

[10] R. Aebersold, E. H. Bures, M. Namchuk, M. H. Goghari, B. Shushan, T. C. Covey, *Protein Sci.* **1992**, *1*, 494–503.

[11] I. Katakuse, T. Matsuo, H. Matsuda, Y. Shimonishi, Y.-M. Hong, Y. Izumi, *Biomed. Mass Spectrom.* **1982**, *9*, 64–68.

[12] a) B. T. Chait, R. Wang, R. C. Beavis, S. B. H. Kent, *Science* **1993**, *262*, 89–92; b) *Proceedings of the 40th ASMS Conference on Mass Spectrometry and Allied Topics* **1992**, Washington, DC, May 31–June 5, pp. 1939–1940.

[13] A. M. Maxam, W. Gilbert, *Proc. Natl. Acad. Sci. USA* **1977**, *74*, 560–564.

[14] R. Wang, S. Walker, R. C. Beavis, S. B. H. Kent, B. T. Chait, *Proceedings of the 41th ASMS Conference on Mass Spectrometry and Allied Topics*, **1993**, San Francisco, California, May 31–June 4, p. 658.

[15] a) J. W. Metzger, K.-H. Wiesmüller, V. Gnau, J. Brünjes, G. Jung, *Angew. Chem.* **1993**, *105*, 901–903; *Angew. Chem. Int. Ed. Engl.* **1993**, *32*, 894–896; b) J. W. Metzger, C. Kempter, K.-H. Wiesmüller, G. Jung, *Anal. Biochem.*, in press.

[16] T. W. Hutchens, T.-T. Yip, *Rapid Comm. Mass Spectrom.* **1993**, *7*, 576–580.

A Structural Model for the Water-Oxidizing Manganese Cluster in Photosystem II

Karl Wieghardt*

Higher plants and cyanobacteria can generate chemical energy from light. In the water-oxidizing photosynthesis[1] this conversion proceeds by light-induced, transmembrane charge separation of protons and electrons at the reaction centers photosystem I and photosystem II (PS I, PS II) (Fig. 1), during which the water is oxidized in the active site of PS II at a (probably[2]) tetranuclear manganese cluster [Eq. (a)].

$$2\,H_2O \rightarrow O_2 + 4\,H^+ + 4\,e^- \qquad (a)$$

Pioneering work by Joliot and Kok has shown[3] that the O_2 cleavage occurs periodically after four light flashs.[3] In the catalytic cycle of Kok (Fig. 2) five oxidation states are therefore defined in the manganese-containing center in PS II, S_0–S_4; the four oxidation equivalents accumulate stepwise (one electron after the other is relinquished to PS I) and stored until in the

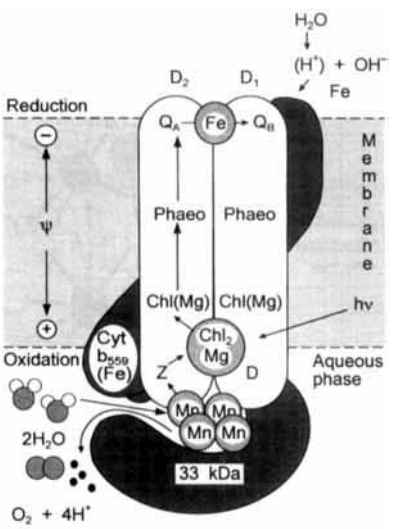


Fig. 1. Schematic arrangement of the proteins of PS II in the membrane: Chl = chlorophyll, Phaeo = phaeophytin, Q = quinone, Z = a tyrosine radical. Adapted from J. J. R. Frausto da Silva, R. J. P. Williams, *The Biological Chemistry of the Elements*, Clarendon, Oxford, **1991**.

[*] Prof. Dr. K. Wieghardt
Lehrstuhl für Anorganische Chemie I der Universität
Universitätsstrasse 150, D-44780 Bochum (FRG)
Telefax: Int. code + (234)7094-109

 © VCH Verlagsgesellschaft mbH, D-69451 Weinheim, 1994 0570-0833/94/0707-0725 $ 10.00+.25/0

transition $S_4 \rightarrow S_0$ molecular oxygen is released, and the cycle begins again. This cycle, which is responsible for all life on our planet (formation of an O_2-containing atmosphere) is still not understood on a molecular level, mainly because the structure of the manganese cluster is unknown. Also the role of the essential cofactors, the chloride and calcium ions, is not precisely known. The two ions can be replaced by bromide and strontium ions, respectively, without loss of function,[4] but fluoride ions inhibit O_2 evolution. PS I from *Synechococcus sp.* has been crystallized and its structure determined with 6 Å resolution by an X-ray structure analysis.[5] Such definitive experiments for PS II are still not available, although recently a three-dimensional structure of PS II at 2 nm resolution (!) was reported. These data were collected from electron-microscopic images of ordered two-dimensional arrangements of PS II in spinach chloroplast membranes,[5b] but still do not permit any statement on the structure of the manganese cluster.

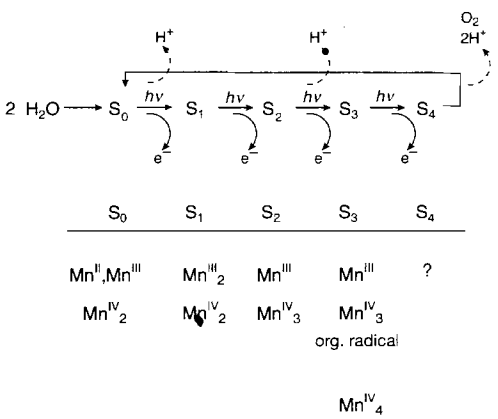


Fig. 2. Representation Kok's catalytic cycle. The scheme given at the bottom shows the most likely (according to present information) distribution of the oxidation steps in the tetranuclear manganese cluster in the S_0 to S_4 states of PS II [6].

At last the Berkeley group of K. Sauer and M. P. Klein has now published their structural model for the tetranuclear manganese cluster (Fig. 3),[6] which has been discussed for two years in the circle of PS II fans and which graced the cover of a book published as early as 1992.[7] It is the result of many years of

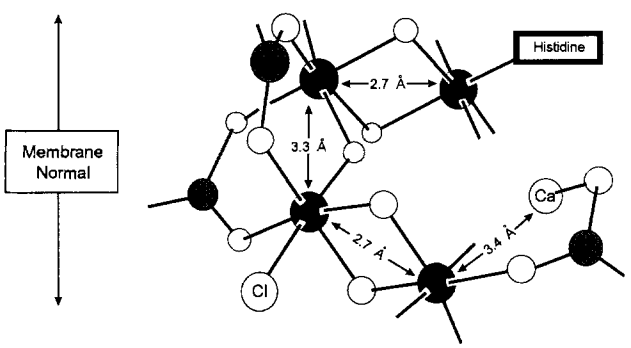


Fig. 3. Schematic representation of the Berkeley model [6] of a potential spatial arrangement of four manganese ions in PS II. According to this, the cofactors Ca^{2+} and Cl^- are also in the vicinity of the Mn cluster or coordinatively bound to a Mn ion. The N-coordination of a histidine residue has been proven by spectroscopy [15]; the nature and number of the bridging carboxylato groups is unknown. Black spheres = Mn centers, white spheres = O centers, cross-hatched spheres = C centers.

spectroscopic studies such as electron spin resonance (ESR) and, in particular, analyses of the Fourier transformed fine structure of the manganese X-ray absorption edge (EXAFS) of membrane-oriented preparations of PS II in S_0, S_1, S_2, and S_3 states and of synthesized model complexes with low molecular weight, which have contributed much to the calibration of these methods. The combination of these two manganese-specific spectroscopic methods enables conclusions to be drawn on 1) the oxidation state of the manganese ions in S_0, S_1, S_2, and—in a limited sense—S_3 states (S_4, as intermediate, cannot be isolated and therefore has not yet been characterized), 2) the electronic structure of the manganese cluster, and 3) (again with limitations) the spatial arrangement of the four manganese ions relative to one another.

That the four oxidation equivalents are stored stepwise, each after a light flash, is an intuitively obvious concept that is apparently difficult to prove. Witt et al. made this deduction indirectly, from changes in the UV absorption spectra and the electrochromic absorptions during the catalytic cycle.[8] In contrast, Klein et al.[9] concluded from changes in Mn near-edge X-ray absorption spectroscopy (XANES) that, for *cryogenic* temperatures, though the light-induced transitions $S_0 \rightarrow S_1$ and $S_1 \rightarrow S_2$ do result in the oxidation of the manganese cluster, during the transition $S_2 \rightarrow S_3$ an organic radical (perhaps a histidine radical?) is formed without further oxidation of the manganese cluster and gives rise to an ESR signal, at least in Ca^{2+}-free preparations.[10] Repetition of the XANES measurements in which the S_x states ($x = 0-3$) were generated at *physiological* temperatures led to the conclusion that the $S_2 \rightarrow S_3$ transition is also associated with a further oxidation of the manganese cluster.[11]

This apparent contradiction is closely related to the problem of the generation of pure S_x states. In the dark adapted PS II samples are in the S_1 state, which, as Dexheimer and Klein[12] could prove by ESR spectroscopy, had a paramagnetic ground state probably with $S = 1$; in contrast, Brudvig et al.[13] postulated a diamagnetic ground state ($S = 0$) from measurements of the dipolar spin–lattice relaxation rate of the stable tyrosine radical in Mn-containing and Mn-free PS II in the S_1 state (resting state). Klein et al. must then have studied an active S_1 state that differs from Brudvigs only by the duration of the dark adaptation of PS II (?).

The ESR-active S_2 state is generated from the dark-adapted PS II by light flashs at 273 K or by continuous illumination during rapid freezing.[14] The famous ESR multiline spectrum discovered by Dismukes and Siderer[16] containing at least 19 manganese hyperfine lines at $g \approx 2.0$ has been the best studied. Attempts to simulate[17] this signal, as well as a theoretical analysis of the possible spin states have shown quite unambiguously that all four manganese ions of the cluster must be electronically coupled to each other and that they are present exclusively in the oxidation states + III and + IV.

A particularly interesting development in the synthesis of pure PS II in a defined S_x state is described by Bocarsly and Brudvig.[18] They succeeded in preparing the S_3 state in large yields in concentrated PS II preparations by the addition of redox-active herbicides that bind to the Q_B site (Fig. 1) and interrupt the catalytic electron transfer turnover.[18] The control of the catalytic turnover of PS II is very promising, because now the more

exact spectroscopic characterization of this and perhaps the S_0 and S_4 states will be possible.

The burgeoning development starting in about 1983 of the coordination chemistry of Mn^{III} and Mn^{IV} led to the synthesis and X-ray structural analysis of stable tetranuclear oxo-bridged complexes with adamantane, cubane, and butterfly frameworks (structures **A**, **B**, and **E** in Fig. 4),[19] which then became models for the first formulations of the catalytic cycles on the molecular level for the water oxidation in PS II.[20] Two of these suggestions, namely those of Brudvig and Crabtree[20a]on one hand and of Vincent and Christou[20b] on the other, immediately found their way into textbooks, not least because of their aesthetic qualities; however, it rapidly became clear that the EXAFS data of PS II could not be well correlated with those of the model complexes. These models are too symmetric.

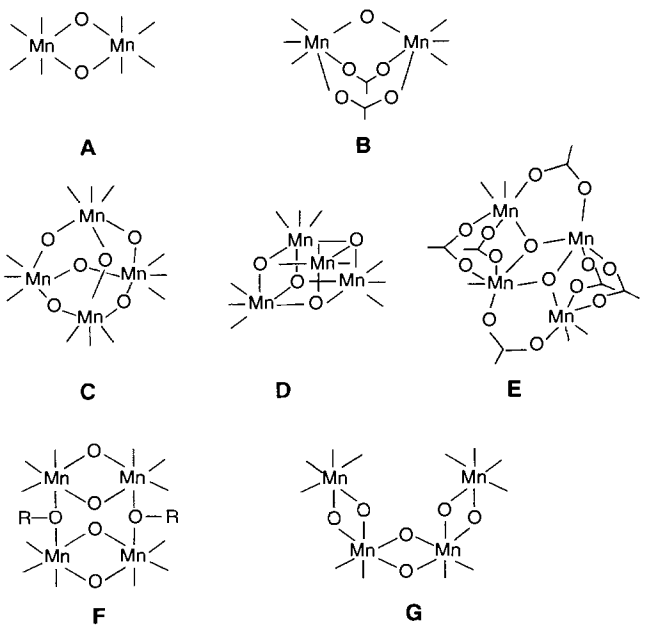


Fig. 4. Important structural types of Mn^{III} and Mn^{IV} complexes with oxo and alkoxo bridges characterized by X-ray analysis: **A**: edge-sharing, octahedral with Mn···Mn ≈ 2.7 Å; **B**: μ-oxo-di-μ-carboxylatodimanganese complexes with Mn···Mn 3.0–3.5 Å; **C**: adamantane-like $Mn_4^{IV}(\mu_2\text{-}O)_6$ skeleton; **D**: cubane skeleton $Mn_4^{IV}(\mu_3\text{-}O)_4$; **E**: butterfly framework $Mn_4(\mu_3\text{-}O)_2$; **F**: di-μ-alkoxo-bridged pair of di-μ-oxodimanganese units [21]; **G**: open-chain arrangement of four Mn^{IV} ions with six oxo bridges [22].

All EXAFS studies on PS II are in accord that the four manganese ions are situated in a ligand sphere consisting predominantly of oxygen donor atoms (oxo and carboxylato groups) and are bound to few, if any, nitrogen atoms. Furthermore, they show that on transitions $S_1 \rightarrow S_2$ and $S_2 \rightarrow S_3$, the structure of the manganese cluster changes only slightly; so no fundamental structural reorganization of the cluster takes place during the accumulation of the oxidation equivalents.

Interestingly an unambiguous Mn···Mn distance of 2.7 Å and a less certain and still controversial one of 3.3 Å, which can also be attributed to a Mn···Ca distance, were detected. The shorter Mn···Mn vector is typical for di-μ-oxodimanganese complexes (Fig. 4, structure **A**) with short $Mn-O_{oxo}$ distances of 1.8 Å, whereas in dinuclear μ-oxo-bis(μ-carboxylato)dimanganese complexes (Fig. 4, structure **B**) Mn–Mn distances between 3.0 and 3.5 Å were measured, depending on the oxidation state of the manganese ions. A combination of these two structural types leads logically to the Berkeley model in Figure 3.

Several other finer points should be mentioned: From the observed dichroism of these Mn···Mn vectors in ordered, oriented membranes with PS II in the EXAFS experiment, information on their spatial arrangement relative to each other in the S_1 state could be obtained. From the sensitivity of the EXAFS spectra (which are specific for manganese) to a substitution of the cofactor Ca^{2+} by Sr^{2+} the conclusion could be drawn that a Ca^{2+} ion must be coordinated in the vicinity of the manganese cluster. A similar situation occurs for Cl^- ions, because their substitution by Br^- likewise causes effects—though very small ones—in the Mn EXAFS spectrum.

The Berkeley group[6] itself warned of an overinterpretation of the attractive model in Figure 3. "Although we have provided evidence for the tetranuclear Mn model and the presence of Ca, halide, and histidine, we do not know their positions relative to each other at this time." This means that the actual structure could look significantly different. The recently characterized complexes $[(Mn_2O_2)_2(tphpn)_2]^{2+}$ (tphpn = *N*,*N*,*N*′,*N*′-tetra(2-methylpyridyl)-2-hydroxypropanediamine; Fig. 4, type **F**)[21] and $[Mn_4^{IV}O_6(bpy)_6]^{4+}$ (bpy = bipyridine; Fig. 4, type **G**)[22] are interesting, novel structural types, because they satisfy several EXAFS characteristics of PS II, and the former, as mixed valent $(Mn^{III}\text{–}Mn^{IV})_2$ complex models the electronic structure of PS II in the active S_1 state amazingly precisely—it has an electronic $S = 1$ ground state and shows an astoundingly similar ESR spectrum to that reported by Klein et al.[12] for PS II in the S_1 state.

Naturally, several questions remain open, which biochemists or biophysicists must answer together with inorganic chemists. For instance, the mechanism on a molecular level of the important step $S_4 \rightarrow S_0$ remains an enigma: when and how is the first O–O bond of the oxo groups or coordinated H_2O molecules formed? The coordination chemists are also challenged: why have we till today not been able to come up with a good tetranuclear water-oxidizing model complex in homogeneous phase? An attempt from theoretical chemistry to give answers to the last two questions has been published recently.[23] Here it is shown that the tri- or tetracoordination of a peroxo ligand to manganese ions facilitates its two-electron oxidation to molecular oxygen. Perhaps not surprising. The solution of the structure of an active site of a metalloprotein from spectral data in many respects resembles the building of a three-dimensional puzzle in which even a few spurious pieces (information) are included (that is, are wrong). I wonder whether in the near (or distant) future the crystallization of PS II and an X-ray structure analysis with sufficient resolution to recognize the manganese cluster will be achieved. It would be great!

German version: *Angew. Chem.* **1994**, *106*, 765

[1] G. Renger, *Angew. Chem.* **1987**, *99*, 660; *Angew. Chem. Int. Ed. Engl.* **1987**, *26*, 643; b) G. Renger, T. Wydrzynski, *Biol. Met.* **1991**, *4*, 73; c) R. J. Debus, *Biochim. Biophys. Acta* **1992**, *1102*, 269.

[2] Although the number of manganese ions in PS II is generally accepted to be four, this is not completely uncontroversial, because every PS II preparation contains *inactive* particles whose manganese content cannot be determined independently. See S. Pauly, H. T. Witt, *Biochim. Biophys. Acta* **1992**, *1099*, 211, who suggest six Mn sites in active PS II.

[3] P. Joliot, B. Kok, *Oxygen Evolution in Photosynthesis* in *Bioenerg. Photosynth.* **1975**, 387.

[4] a) D. F. Ghanotakis, G. T. Babcock, C. F. Yocum, *FEBS* Lett. **1984**, *167*, 127; b) the role of F^-, Cl^-, and Br^- ions in PS II was summarized by W. J. Coleman (*Photosynth. Res.* **1990**, *23*, 1).
[5] a) N. Krauss, W. Hinrichs, I. Witt, P. Fromme, W. Pritzkow, Z. Danter, C. Betzel, K. S. Wilson, H. T. Witt, W. Saenger, *Nature* **1993**, *361*, 326; b) A. Holzenburg, M. C. Bewley, F. H. Wilson, W. V. Nicholson, R. C: Ford, *Nature* **1993**, *363*, 470.
[6] V. K. Yachandra, V. J. DeRose, M. J. Latimer, I. Mukerji, K. Sauer, M. P. Klein, *Science* **1993**, *260*, 675.
[7] *Manganese Redox Enzymes* (Ed.: V. L. Pecoraro), VCH, New York, **1992**.
[8] H. Kretschmann, H. T. Witt, *Biochim. Biophys. Acta* **1993**, *1144*, 331.
[9] R. D. Guiles, J.-L. Zimmermann, A. E. McDermott, V. K. Yachandra, J. L. Cole, S. L. Dexheimer, R. D. Britt, K. Wieghardt, U. Bossek, K. Sauer, M. P. Klein, *Biochemistry* **1990**, *29*, 471.
[10] A. Boussac, J.-L. Zimmermann, A. W. Rutherford, J. Lavergne, *Nature* **1990**, *347*, 303.
[11] T. One, T. Noguchi, Y. Inoue, M. Kusunoki, T. Matsushita, H. Oyanagi, *Science* **1992**, *258*, 1335.
[12] S. L. Dexheimer, M. P. Klein, *J. Am. Chem. Soc.* **1992**, *114*, 2821.
[13] D. Koulougliotis, D. J. Hirsh, G. W. Brudvig, *J. Am. Chem. Soc.* **1992**, *114*, 8322.
[14] a) G. C. Dismukes, Y. Siderer, *FEBS Lett.* **1980**, *121*, 78; b) Ö. Hansson, L. E. Andreasson, *Biochim. Biophys. Acta* **1982**, *679*, 261.
[15] V. J. DeRose, V. K. Yachandra, A. E. McDermott, R. D. Britt, K. Sauer, M. P. Klein, *Biochemistry* **1991**, *30*, 1335.
[16] G. C. Dismukes, Y. Siderer, *Proc. Natl. Acad. Sci. USA* **1981**, *78*, 274.
[17] J. Bonvoisin, G. Blondin, J. J. Girerd, J.-L. Zimmermann, *Biophys. J.* **1992**, *61*, 1076.
[18] J. R. Bocarsly, G. W. Brudvig, *J. Am. Chem. Soc.* **1992**, *114*, 9762.
[19] a) V. L. Pecoraro, *Photochem. Photobiol.* **1988**, *48*, 249; b) G. Christou, *Acc. Chem. Res.* **1989**, *22*, 328; c) K. Wieghardt, *Angew. Chem.* **1989**, *101*, 1179; *Angew. Chem. Int. Ed. Engl.* **1989**, *28*, 1153; d) G. W. Brudvig, R. H. Crabtree, *Progr. Inorg. Chem.* **1989**, *37*, 99; e) G. C. Dismukes, *Bioinorganic Catalysis* (Ed.: J. Reedijk), Dekker, New York, **1993**.
[20] a) G. W. Brudvig, R. H. Crabtree, *Proc. Natl. Acad. Sci. USA* **1986**, *83*, 4586; b) J. B. Vincent, G. Christou, *Inorg. Chim. Acta* **1987**, *136*, L 41.
[21] M. L. Kirk, M. K. Chan, W. H. Armstrong, E. I. Solomon, *J. Am. Chem. Soc.* **1992**, *114*, 10432.
[22] C. Philouze, G. Blondin, S. Menage, N. Auger, J.-J. Girerd, D. Vigner, M. Lance, M. Nierlich, *Angew. Chem.* **1992**, *104*, 1643; *Angew. Chem. Int. Ed. Engl.* **1992**, *31*, 1629.
[23] D. M. Proserpio, R. Hoffmann, G. C. Dismukes, *J. Am. Chem. Soc.* **1992**, *114*, 4374.

Resolution of Racemates by Distillation with Inclusion Compounds

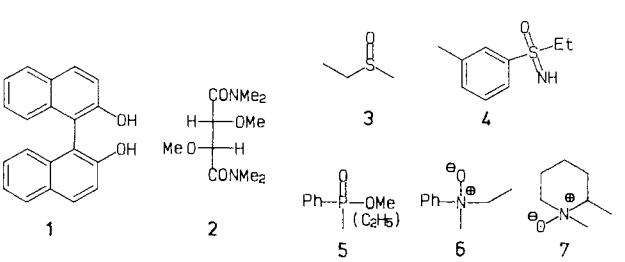
Gerd Kaupp*

Chiral drugs and additives are generally not permitted to be used in racemic form (most important exception: DL-methionine) so that unintended side effects and unnecessary environmental hazards are avoided. Larger amounts of enantiomerically pure compounds are economically produced by fermentation or (complete) enzymatic conversion of racemates into the desired enantiomer. Thus, since 420000 t of L-glutamic acid and large quantities of L-aspartic acid and L-phenylalanine (for the sweetener aspartame) and D-phenylglycine are produced annually, excessive amounts of waste should and can be prevented.[1]

Absolute asymmetric synthesis, a rapidly developing field, is a simple approach to the synthesis of enantiomerically pure compounds and has low environmental impact; however, enantiomorphic crystals (with a chiral space group) are required, which are not necessarily formed by all compounds with prochiral centers.[2] Enantioselective syntheses with chiral auxiliaries and "without biology" have been fine-tuned most impressively and have a longer tradition,[3] but are still usually very costly and time-consuming. Several approaches to chemical synthesis may be outlined: the synthesis is conducted in chiral media (recently inclusion compounds have been shown to be efficient[4]) or with chiral catalysts. Alternatively, an optically active starting material is employed in a diastereoselective synthesis, and the portion of the molecule with the initial chiral center is cleaved off afterwards. This can be done with loss of chirality in the auxiliary (e.g. with the Seebach method[3]) or without loss (e.g. with the Schöllkopf method[5]); however, recovery of the auxiliary from small-scale reactions does not appear to be very worthwhile.[3] Upscaling for industrial applications is still problematic.[6] Apparently resolution of racemates following straightforward synthesis remains the most frequently applied method.

Supramolecular chemistry introduced new possibilities; inclusion compounds were systematically examined, and versatile clathrating agents were designed and employed.[7] These findings have been used since the early 1980s to selectively and reversibly include chiral guest molecules in host lattices of chiral molecules.[4] In contrast to the formation of diastereomeric salts, compounds with almost any functional group can be treated. The enantiomerically pure host and the racemic guest (or the racemic host and the enantiomerically pure guest) are dissolved, the inclusion compound composed of the better fitting set of enantiomers is allowed to precipitate, and the crystalline material is removed by filtration. The two enantiomers of the guest are obtained from the filtrate and from a solution of the crystals after the host is removed by chromatography on SiO_2, respectively.

The enantiomers (atropisomers) of 2,2′-dihydroxy-1,1′-binaphthyl (**1**) do not interconvert at normal temperatures. If a chiral compound like (*R*,*R*)-**2** (or *N*-benzylcinchonidinium chloride)[8] is dissolved with *rac*-**1**, only one of the diastereomeric inclusion compounds crystallizes on account of chiral recognition. (−)-**1**

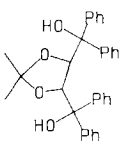


1 2 3 4 5 6 7

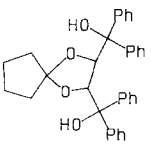
[*] Prof. Dr. G. Kaupp
FB9 - Organische Chemie I der Universität
Postfach 2503, D-26111 Oldenburg (FRG)
Telefax: Int. code + (441) 798-3409

(and (+)-**1**) is obtained with >99% *ee* (from benzene) and separated from **2** by chromatography on SiO_2. The enantiomerically pure host (−)-**1** (and (+)-**1**) can now be used for a variety of difficult chiral resolutions (>99% *ee*) by inclusion crystallization, for example the resolution of racemic sulfoxides like **3**, sulfoximines like **4**, phosphinates/phosphanoxides like **5**, and aminoxides like **6** and **7**. Hundreds of resolutions of very diverse racemic compounds have been reported with a broad range of hosts.[4]

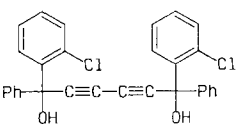
Recently an improvement in this separation technique was reported, which seemed to indicate that enantioselective inclusion in the lattices of chiral hosts could be employed on a large scale.[9] When crystalline hosts such as (*R*,*R*)-(−)-**8** (m.p. 196 °C),[10] (*R*,*R*)-(−)-**9** (m.p. 165 °C),[10] and (*S*,*S*)-(−)-**10** (m.p. 128 °C) are suspended in hexane or water, chiral guest molecules form the same inclusion compounds as in solution. This is by no



8



9

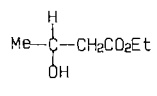


10

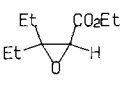
means self-evident, since inclusion compounds usually have different crystal lattices than the pure host crystals. Thus crystal/liquid reactions occur, and phase rebuildings analogous to those observed in gas/solid reactions[11] must take place. Yet this suspension technique is more selective and more effective than the initially developed solution technique. Numerous racemic alcohols like **11**, β-hydroxy esters like **12**, epoxy esters like **13**, and epoxy ketones like **14** were stirred a few hours with appropriate hosts (suspensions of **8**, **9**, and **10**) and formed 1:1 complexes that could be filtered off in yields of >85% and with *ee* values of >97% (the complex of **12** and **9** formed in hexane only; 80% *ee* in one step). Recrystallization of the inclusion compounds is not generally necessary; (−)-**11**, (+)-**12**, (+)-**13**, and (+)-**14** are released by heating under vacuum. Hosts **8**, **9**, and **10** can



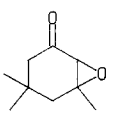
11



12



13



14

then be used again in further resolutions. The procedure is simple, cheap, and environmentally safe. Of course, as with other resolutions, the undesired enantiomer must be disposed of, or better yet, converted into a racemic mixture and resolved again.

Another advantage of the new technique is the possibility of using a stoichiometric amount of the host relative to the racemate (in other words, in excess). The resolution can then be achieved by fractional (Kugelrohr) distillation. For example, 2 mmol of *rac*-**11** and 2 mmol of crystalline **8** in 1 mL of hexane were stirred for 1 h at room temperature and the mixture subsequently distilled. At approximately 70 °C uncomplexed (+)-**11** was collected with 59% *ee*; the distillation of the residue provided (−)-**11** in 69% yield and with 97% *ee* at roughly 150 °C. In a similar fashion fractional vacuum distillation of *rac*-**14** and **10** gave (−)-**14** (68% *ee*) and 63% (+)-**14** with 95% *ee*. If the process with the enantiomeric host is repeated, both enantiomers of the guest can be isolated in pure form. Since the hosts are not consumed and do not racemize, they can be employed in subsequent separations.

As upscaling this method for industrial applications is of particular interest, initial tests cannot be far off. In the distillation the heat transfer to the solid should not present any difficulties up to the kg scale, and technical solutions should be possible for larger scale separations.

It can be expected that the Toda procedure for obtaining enantiomerically pure compounds will find broad application very soon. This development could make preparative HPLC with chiral columns obsolete and be applied to distillable amino acid derivatives. After all, analytical resolution of amino acids was quite successful by host/guest complexation chromatography with reversed-phase packings loaded with Cram's chiral 1,1′-binaphthyl crown ethers (similar to **1**).[12]

German version: *Angew. Chem.* **1994**, *106*, 768

[1] Fonds der Chemischen Industrie, *Aminosäuren – Bausteine des Lebens* (Folienserie 11 des Fonds der Chemischen Industrie), Frankfurt, **1993**; R. M. Williams, *Synthesis of Optically Active α-Amino Acids*, Pergamon Press, Oxford, **1989**, Chapter 7, p. 257; I. Shiio, S. Nakamori in *Fermentation Process Development of Industrial Organisms* (Ed.: J. O. Neway), Marcel Dekker, New York, **1989**, p. 133; R. Biegelis in *Biotechnology, Vol. 7b* (Eds.: H. J. Rehm, G. Reed), VCH, Weinheim, **1989**, p. 229.

[2] Highlight: G. Kaupp, M. Haak, *Angew. Chem.* **1993**, *105*, 727; *Angew. Chem. Int. Ed. Engl.* **1993**, *32*, 694; L. Caswell, M. A. Garcia-Garibay, J. A. Scheffer, J. Trotter, *J. Chem. Educ.* **1993**, *70*, 785.

[3] Recent example: S. Blank, D. Seebach, *Angew. Chem.* **1993**, *105*, 1780; *Angew. Chem. Int. Ed. Engl.* **1993**, *32*, 1765, and references therein.

[4] D. Worsch, F. Vögtle, *Top. Curr. Chem.* **1987**, *140*, 22; F. Toda, *ibid.* **1987**, *140*, 43; F. Toda in *Inclusion Compounds, Vol. 4* (Eds. J. L. Atwood, J. E. D. Davies, D. D. MacNicol), Oxford University Press, Oxford, **1991**, p. 126; F. Toda, *Adv. Supramol. Chem.* **1992**, *2*, 141.

[5] K. Busch, U. M. Groth, W. Kühnle, U. Schöllkopf, *Tetrahedron* **1992**, *48*, 5607, and references therein.

[6] Of course this is not true for the diastereoselective reactions of chiral natural products, for example, steroids.

[7] See for example E. Weber, *Top. Curr. Chem.* **1987**, *140*, 2.

[8] K. Tanaka, T. Okada, F. Toda, *Angew. Chem.* **1993**, *105*, 1266; *Angew. Chem. Int. Ed. Engl.* **1993**, *32*, 1147, and references therein. Synthesis of **2** and **3** from tartaric acid: D. Seebach, H.-D. Kalinowski, B. Bastani, G. Crass, H. Daum, H. Dörr, N. P. Duprez, V. Ehsig, W. Langer, C. Nüssler, H.-A. Dei, M. Schmidt, *Helv. Chim. Acta* **1977**, *60*, 301.

[9] F. Toda, Y. Tohi, *J. Chem. Soc. Chem. Commun.* **1993**, 1238; synthesis of **8** and **9**: A. K. Beck, B. Bastani, D. A. Plattner, W. Letter, D. Seebach, H. Braunschweiger, P. Gysi, L. La Vecchia, *Chimia* **1991**, *45*, 238, and references therein.; synthesis of **10**: F. Toda, K. Tanaka, K. Omata, T. Nakamura, T. Oshima, *J. Am. Chem. Soc.* **1983**, *105*, 5151. – Spontaneous inclusion of guests from suspensions of achiral components is only rarely reported: F. Toda, K. Tanaka, G. U. Daumas, M. C. Sachez, *Chem. Lett.* **1983**, 1521; H. R. Allcock in *Inclusion Compounds, Vol. 1* (Eds.: J. L. Atwood, J. E. D. Davies, D. D. MacNichol), Oxford University Press, Oxford, **1984**, p. 351.

[10] The molecule in ref.[9] (there **1a,b,c**) is shown with the (*S*,*S*) configuration but labeled "(*R*,*R*)". Upon subsequent inquiry the correspondence author replied that "(*R*,*R*)-(−)" is correct. The optical rotations in the table apply to this configuration.

[11] G. Kaupp, J. Schmeyers, *Angew. Chem.* **1993**, *105*, 1656; *Angew. Chem. Int. Ed. Engl.* **1993**, *32*, 1587, and references therein.

[12] T. Shinbo, T. Yamaguchi, K. Nishimura, M. Sugiura, *J. Chromatogr.* **1987**, *405*, 145, and references therein.

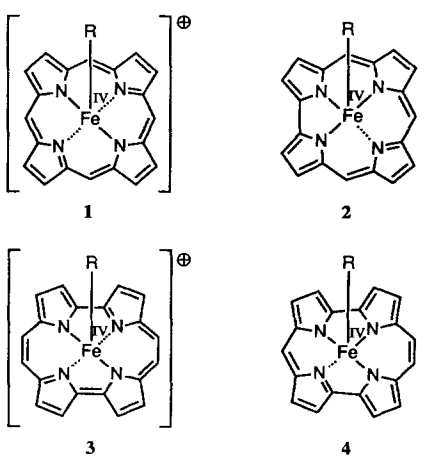
 © VCH Verlagsgesellschaft mbH, D-69451 Weinheim, 1994 0570-0833/94/0707-0729 $ 10.00+.25/0

Metallocorroles with Formally Tetravalent Iron

Emanuel Vogel,* Stefan Will, Andreas Schulze Tilling, Ludger Neumann, Johann Lex, Eckhard Bill, Alfred X. Trautwein, and Karl Wieghardt

Dedicated to Professor Ernst Otto Fischer on the occasion of his 75th birthday

The coordination chemistry of metals in unusual oxidation states is a fascinating aspect of research in the field of metalloporphyrins. Of particular significance in this respect are oxoiron porphyrins containing tetravalent iron, since complexes of this sort occur as reactive intermediates in numerous biological and biomimetic oxidation processes.[1] Iron(IV) porphyrins, in which the metal is not present as part of a [Fe=O] unit, are likewise known, but are rare species. To the best of our knowledge cationic σ-phenyliron(IV) porphyrins (type **1** in Scheme 1)[2] and dimethoxyiron(IV) porphyrins,[3] both of which are only stable at low temperatures, as well as some μ-nitrido- and μ-carbidoiron(IV) complexes[4] are the only representatives of this class of compounds so far characterized. A route to iron(IV) porphycenes (type **3**), constituting analogues of **1**, has very recently been opened up.[5]



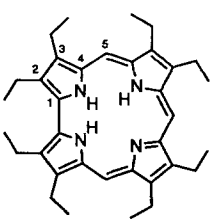
1 **2**

3 **4**

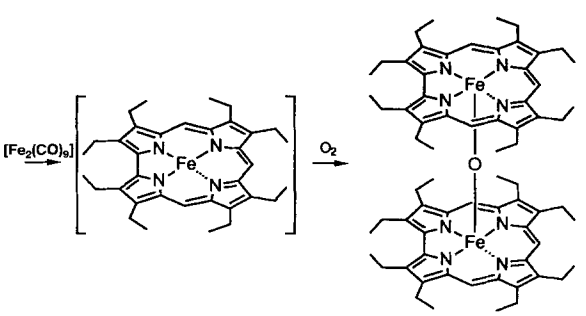
Scheme 1. Models of the iron(IV) complexes of porphyrin (**1**), corrole (**2**), porphycene (**3**), and isocorrole (**4**) with axial ligands (R = aryl, alkyl, and other substituents).

The existence of cationic iron(IV) complexes of types **1** and **3** suggested the possibility that the potentially trianionic porphyrinoids corrole[6]—the aromatic parent substance of corrin, the ring system of vitamin B_{12}—and isocorrole[7] may enable the preparation of the corresponding neutral complexes, that is, types **2** and **4**, respectively. This supposition appeared to be substantiated all the more so, as it was recently shown that stable iron(IV) complexes with ligands based on pentane-2,4-dione-bis(*S*-alkylisothiosemicarbazides)—which are also trianionic—could be synthesized.[8, 9] We have now found that octaethylcorrole **5** can be readily converted into the triad of stable complexes **7**–**9**, all of which contain formally tetravalent iron.[10] Furthermore, the existence of the iron corrole **10** (bearing an axial pyridine ligand) with a formal oxidation state of the metal of + III was corroborated.

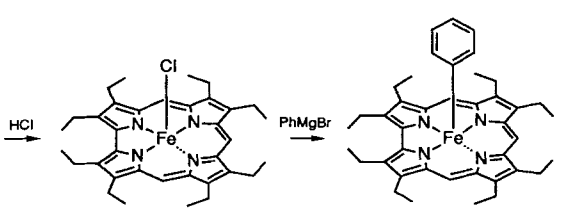
Iron(III) corroles, which might serve as starting materials for the synthesis of iron(IV) corroles, have already been described in the literature several times.[11] However, it is only recently that they have been thoroughly characterized spectroscopically, in work by T. Boschi et al.[11c, d] According to these investigations octamethylcorrole undergoes smooth metalation with iron trichloride or iron pentacarbonyl to give the neutral iron(III) corrole, which, on the basis of ^{1}H NMR spectroscopic findings, has a pronounced tendency to bind ligands in the axial position. Indications of a possible oxidation of iron(III) to iron(IV) corroles cannot be found in any of the published work. Two reasons led us to use the octaethyl compound **5**[12] rather than the



5



6 **7**



8 **9**

[*] Prof. Dr. E. Vogel, Dipl.-Chem. S. Will, Dipl.-Chem. A. Schulze Tilling, Dr. L. Neumann, Dr. J. Lex
Institut für Organische Chemie der Universität
Greinstrasse 4, D-50939 Köln (FRG)
Telefax: Int. code + (221) 470-5102
Prof. Dr. A. X. Trautwein, Dr. E. Bill
Institut für Physik der Universität Lübeck (FRG)
Prof. Dr. K. Wieghardt
Lehrstuhl für Anorganische Chemie I der Universität Bochum (FRG)

 © VCH Verlagsgesellschaft mbH, D-69451 Weinheim, 1994 0570-0833/94/0707-0731 $ 10.00+.25/0

octamethyl compound as corrole ligand: first, the substantially better solubility of **5** and its metal complexes; second, a planned parallel study in the isocorrole series, for which the octaethyl compound corresponding to **5** was at our disposal.[7b]

The choice of **5** proved to be fortunate. As it turned out, treatment of **5** with nonacarbonyldiiron in toluene at 100–110 °C (2 h) under an argon atmosphere, followed by a workup with admission of air (causing a change in the color of the solution from brown to red), yielded as the only defined product the oxygen-bridged binuclear iron(IV) complex **7**, μ-oxo-bis[(octaethylcorrolato)iron(IV)]. This must have arisen from the spontaneous air oxidation of the iron(III) octaethylcorrole **6**, the assumed primary product. The new iron(IV) complex **7** can be easily isolated and is stable. After crystallization from hexane, it is obtained as black rhombohedra (m.p. >300 °C, yield 58%, see Experimental Procedure).

In the reaction of octamethylcorrole with iron transfer agents, the poor solubility of the intermediate Fe^{III} corrole complex slows down the air oxidation, and thus the Fe^{III}/Fe^{IV} conversion, which under suitable conditions is also observed in this system, was not detected.

A crystal structure analysis[13] of complex **7** (Fig. 1 and Table 1) confirms its molecular structure. The iron atoms in **7**

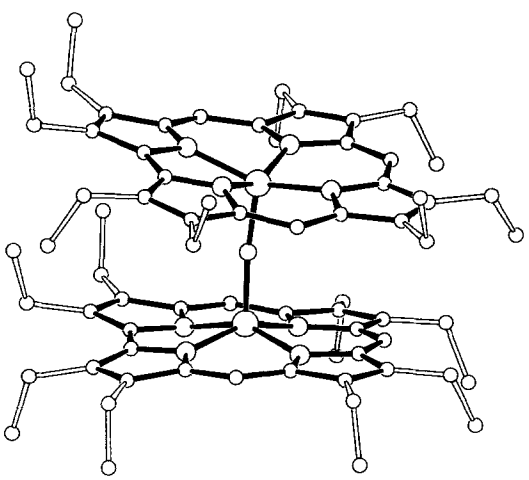


Fig. 1. Structure of the μ-oxodiiron(IV) corrole complex **7** in the crystal. Perspective view (without hydrogen atoms).

are coordinated in an approximately square-pyramidal fashion. The corrole ligands have—mainly because of steric interactions between the ethyl groups in the top and bottom halves of the molecule—ring frameworks that are twisted to varying degrees. However, in comparison to the free corrole, in which the spatial requirement of the imino hydrogen atoms causes a considerable deviation of the framework from planarity,[14] the corrole ligands in **7** have experienced a certain degree of flattening. The iron atoms are situated 0.403 Å (average value) above the planes formed by the N-donor atoms. The Fe–N bond lengths, which are within the range of those of known iron(IV) compounds,[8, 9] are significantly shorter than those in iron(III) porphyrins (1.96–2.09 Å).[15] The Fe–O bonds in **7** are also noticeably short [1.706 vs. 1.757 Å in the μ-oxodiiron(III) complex[16] derived from octaethylporphyrin]. The Fe-O-Fe angle is 170.0°, even though one would expect from theoretical arguments that a complex such as **7**, which has a (d^4–d^4) electronic configuration [as compared to μ-oxodiiron(III) porphyrins which have a (d^5–d^5) configuration], would exhibit a linear Fe-O-Fe unit.[17]

The magnetic susceptibility (measured in the range of 81–293 K)[18] and the ^{1}H NMR spectrum of **7** (Tables 2 and 3), which displays well-defined signals with small linewidth, indicate that the compound is effectively diamagnetic. The protons of the perimeter give rise to sharp singlets at $\delta = 6.66$ (H-5,15) and 6.62 (H-10), while those from the ethyl substituents appear as multiplets in the range $\delta = 2.82$–2.56 and as triplets at $\delta =$ 1.25, 1.17, 1.15, and 1.14. The shift of the resonances of the perimeter protons to higher field by no less than 2.7 ppm as compared to those of free octaethylcorrole, tantamount to substantial loss of the diamagnetic ring current of the ligand, demands interpretation by theory.[19] The ^{13}C NMR spectrum of **7** shows the expected 18 signals—again in the range in which diamagnetic compounds resonate. That the resonances of the *meso*-carbon atoms C-5,15 and C-10 have undergone a pronounced low-field shift of 17 and 21 ppm, respectively, compared with those in the uncomplexed **5** seems noteworthy. The singlet ground state ($S = 0$) observed for **7** at room temperature is caused by a very strong intramolecular antiferromagnetic coupling of the two iron(IV) ions with $S = 1$ ground states. It is interesting that in the analoguous μ-oxodiiron(III) porphyrins this coupling is considerably weaker,[20] since in these cases the ground state ($S = 0$), due to antiferromagnetic coupling of the two high-spin iron(III) ions ($S = 5/2$), is only observed at low temperatures ($T < 50$ K).

Table 1. Selected bond lengths and distances Δ (in Å) in the iron corrole complexes **7**–**10**. L = axial ligand at the iron center.

	7		**8**	**9**	**10**
	ligand 1 [a]	ligand 2			
Fe-N [b]	1.904(2)	1.904(2)	1.906(2)	1.871(3)	1.893(2)
Fe-L	1.705(2)	1.706(2)	2.256(1)	1.984(3)	2.188(2)
$\Delta(N_4)$ [c]	0.406(1)	0.400(1)	0.422(1)	0.272(1)	0.273(1)
Δ(core) [d]	0.436(1)	0.418(1)	0.533(1)	0.318(1)	0.425(1)
Δ_{max} [e]	0.164(2)	0.193(2)	0.139(3)	0.077(3)	0.219(2)

[a] Ligand 1 indicates the upper corrole unit of **7** in Fig. 1. [b] Average values. [c] Distance of the iron atom from the mean plane of the four pyrrole nitrogen atoms. [d] Distance of the iron atom from the mean plane of the ring framework (core). [e] Maximum distance of the carbon and nitrogen atoms from the average plane of the ring framework.

Table 2. Selected ^{1}H NMR data (room temperature, 300 MHz) of ligand **5** and iron corroles **7**–**10**.

	5 ($CDCl_3$)	**7** (C_6D_6)	**8** ($CDCl_3$)	**9** ($CDCl_3$)	**10** ([D_5]pyridine)
H-5,15	9.38	6.66	177	54.5	-15.9
H-10	9.21	6.62	189	49.3	-62.2
CH_2	3.9–4.1	2.6–2.8	-5.7–29.9	-8.4–98.1	1.9–67.7
CH_3	1.7–2.0	1.1–1.3	-0.3–2.5	3.0–7.3	3.2–3.8

In analogy to μ-oxodiiron(III) porphyrins and porphycenes,[21] **7** experiences cleavage by acids to yield mononuclear complexes.[22] When, for example, **7** is allowed to react in dichloromethane with 1 M hydrochloric acid at room temperature, chloro(octaethylcorrolato)iron(IV) (**8**) is formed, which crystallizes from hexane/dichloromethane as black needles (m.p. >300 °C, yield 84%). Treatment of solutions of the chloro complex **8** with aqueous sodium hydroxide leads to the rapid reformation of **7**.

Chloro(octaethylcorrolato)iron(IV) (**8**) invited attempts to exchange the axial halogen ligand for aryl and alkyl groups by reaction with Grignard reagents, and thus provide access to the

organometallic σ-aryl- and σ-alkyl(octaethylcorrolato)iron(IV) complexes, respectively. Indeed, **8** could be smoothly transformed into the σ-phenyl complex **9** when it was treated with four equivalents of phenylmagnesium bromide (in ether) in dichloromethane. Crystallization of the product from hexane/dichloromethane afforded **9** as gray rhombohedra with metallic luster (decomp. >185 °C, yield 75%).

The isolation of complex **9** as a stable compound is surprising, considering the fact that cationic σ-phenyliron(IV) complexes in the porphyrin series (type **1**) rearrange rapidly even at room temperature to *N*-phenylated iron(II) complexes.[2] Whether a similar phenyl migration is possible in **9** at higher temperatures or by electrochemical means is currently under investigation. Insertion of oxygen into the iron–carbon bond, a reaction typical for σ-phenyliron(III) porphyrins,[23] has not been observed for **9**, since complex **9** is relatively air-stable in solution.

X-ray crystal structure analyses allowed an insight into the molecular structure of complexes **8** and **9** (Figs. 2 and 3, respectively, and Table 1).[13] In the chloroiron(IV) complex **8** the coordinative environment of the iron center corresponds to that found in the μ-oxo compound **7**, but the nitrogen atoms are better orientated towards the metal, allowing the ligand to adopt a more symmetric conformation. Otherwise **8** is characterized by a relatively long iron–chlorine bond [2.256 vs. 2.231 Å in high-spin chloro(octaethylporphyrinato)iron(III)[24]]. The phenyliron complex **9** is distinguished from **7** and **8** in so far as the distance between the metal and the N_4 plane is reduced to 0.272 Å (compared with 0.403 Å and 0.422 Å in **7** and **8**, respectively). Consequences of this are not only the shortening of the Fe–N distances, but also the almost complete flattening of the ring framework. Additionally, it is worth noting that **9**, in contrast to **8**, exists in the crystal as a π–π dimer with laterally shifted ring frameworks (intermolecular distance between the ring frameworks: 3.5–3.6 Å; Fe···Fe distance 5.437 Å).[15c]

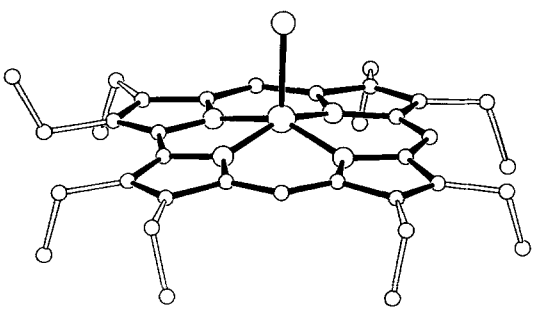


Fig. 2. Structure of the chloroiron(IV) corrole complex **8** in the crystal. Perspective view (without hydrogen atoms).

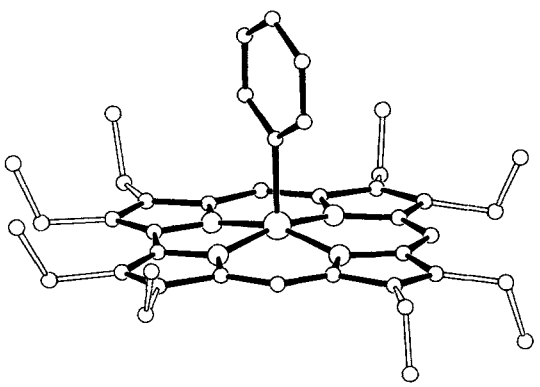


Fig. 3. Structure of the σ-phenyliron(IV) corrole complex **9** in the crystal. Perspective view (without hydrogen atoms).

The ^{1}H NMR spectra of complexes **8** and **9** are—in striking contrast to that of **7**—characteristic for paramagnetic compounds with broad unstructured signals over a wide range of absorptions (Tables 2 and 3).[25] In the case of **9** three further signals are observed at $\delta = -4.0$, -77.0, and -153.6, which can be attributed to the protons at the *meta*, *para*, and *ortho* positions, respectively, of the axially bound phenyl ligand.[26] The paramagnetism in **8** and **9** was confirmed by measurement of their magnetic susceptibility, from which it is evident that both complexes, similar to other iron(IV) compounds, exist in a spin triplet ground state ($S = 1$) ($\mu_{eff} = 2.97$ and $2.89\ \mu_B$, respectively, at 293 K).[8c] The Mössbauer spectra of **7**–**9**, measured at 4.2 and 77 K,[18] are in agreement with the formulation of these compounds as iron(IV) complexes. Small isomer shifts in the range $\delta_{Fe} = -0.11$ to -0.19 mm s^{-1} and relatively large quadrupole splittings $\Delta E_q = 2.35$–3.72 mm s^{-1} were observed (Table 3). Similar Mössbauer parameters have been reported for compounds I and II of heme peroxidases and related porphyrin model complexes.[27]

Table 3. Selected physical data for **7**–**10**. ^{1}H NMR: 300 MHz; ^{13}C NMR: 75.5 MHz; IR: CsI. The isomer shifts δ_{Fe} are relative to α-iron at 298 K. OEC = trianion of octaethylcorrole, py = pyridine

7: M.p. > 300 °C (hexane); ^{1}H NMR (C_6D_6): δ = 6.66 (s, 2H; H-5,15), 6.62 (s, 1H; H-10), 2.82 (m, 4H; H-2a,18a), 2.69 (m, 4H; H-3a,17a), 2.60 (m, 4H; H-8a,12a), 2.56 (m, 4H; H-7a,13a), 1.25 (t, 6H; H-3b, 17b), 1.17 (t, 6H; H-2b,18b), 1.15 (t, 6H; H-7b,13b), 1.14 (t, 6H; H-8b,12b); ^{13}C NMR (C_6D_6): δ = 146.29, 145.58, 145.34, 140.95, 135.76, 135.41, 134.21, 130.23, 110.13 (C-10), 109.78 (C-5,15), 19.77, 18.71, 18.54, 18.37, 17.71, 17.48, 17.04, 16.87; MS (EI, 70 eV): *m/z* (%): 575 (100) [M^+ − OFe(OEC)]; IR: $\tilde{\nu}$ = 2963, 2929, 2869, 1469, 1450, 1272, 1232, 1059, 1013, 957, 833, 805 cm^{-1}; UV/VIS (*n*-hexane): λ_{max} (ε) = 310 (53000), 369 (105800), 537 nm (16500); magnetic moment (293 K): $\mu_{eff} = 0.69\ \mu_B$; Mössbauer parameters (77 K): $\delta_{Fe} = 0.02$ mm s^{-1}, $\Delta E_q = 2.35$ mm s^{-1}.

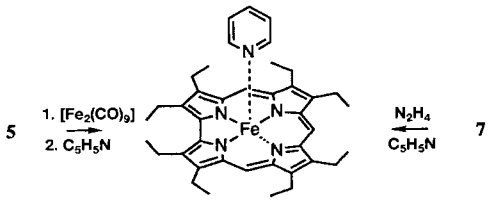
8: M.p. > 300 °C (hexane/dichloromethane); ^{1}H NMR ($CDCl_3$): δ = 189 (br. s, 1H; H-10), 177 (br. s, 2H; H-5,15), 29.9, 27.8, 21.3, 17.7, 15.8, 3.7 (br. s, each 2H; CH_2), 2.5, 1.3 (br. s, each 6H; CH_3), 0.9 (br. s, 2H; CH_2), 0.6, −0.3 (br. s, each 6H; CH_3), −5.7 (br. s, 2H; CH_2); MS (EI, 70 eV): *m/z* (%) 612/610 (5/9) [M^+], 575 (100) [M^+ − Cl]; IR: $\tilde{\nu}$ = 2964, 2930, 2869, 1466, 1374, 1155, 1055, 1011, 952, 876, 785, 759, 316 cm^{-1} (Fe-Cl); UV/VIS (CH_2Cl_2): λ_{max} (ε) = 302 (25200) sh, 338 (39200) sh, 371 (57400), 465 (10900) sh, 516 (8000) sh, 602 nm (3000); magnetic moment (293 K): $\mu_{eff} = 2.97\ \mu_B$; Mössbauer parameters (77 K): $\delta_{Fe} = 0.19$ mm s^{-1}, $\Delta E_q = 2.99$ mm s^{-1}.

9: Decomp. >185 °C (hexane/dichloromethane); ^{1}H NMR ($CDCl_3$): δ = 98.1, 65.6, 56.5 (br. s, each 2H; CH_2), 54.5 (br. s, 2H; H-5,15), 49.3 (br. s, 1H; H-10), 34.1, 28.2, 13.6 (br. s, each 2H; CH_2), 7.3 (br. s, 6H; CH_3), 6.4 (br. s, 2H; CH_2), 4.1, 3.7, 3.0 (br. s, each 6H; CH_3), −4.0 (br. s, 2H; phenyl, *m*-H), −8.4 (br. s, 2H; CH_2) −77.0 (br. s, 1H; phenyl, *p*-H), −153.6 (br. s, 2H; phenyl, *o*-H); MS (EI, 70 eV): *m/z* (%) 652 (8) [M^+], 575 (21) [M^+ − Ph], 154 (100) [biphenyl]; IR: $\tilde{\nu}$ = 3044, 2964, 2930, 2869, 1551, 1461, 1056, 1024, 1005, 986, 957, 833, 722 cm^{-1}; UV/VIS (CH_2Cl_2): λ_{max} (ε) = 251 (24100) sh, 340 (34300) sh, 380 (66100), 507 (14900), 668 nm (2300); magnetic moment (293 K): $\mu_{eff} = 2.89\ \mu_B$; Mössbauer parameters (77 K): $\delta_{Fe} = -0.11$ mm s^{-1}, $\Delta E_q = 3.72$ mm s^{-1}.

10: Decomp. >160 °C (methanol/pyridine); ^{1}H NMR ([D_5]pyridine): δ = 67.7, 37.9, 28.5 (br. s, each 4H; CH_2), 5.3, 3.8 (br. s, each 6H; CH_3), 3.2 (br. s, 12H; CH_3), 1.9 (br. s, 4H; CH_2), −15.9 (br. s, 2H; H-5,15), −62.2 (br. s, 1H; H-10); ^{1}H NMR (CS_2, $C_6H_{6int.}$): δ = 114 (br. s, 2H; py, α-H), 77.1 (br. s, 2H; py, β-H), 70.2, 38.7, 28.3 (br. s, each 4H; CH_2), 5.6, 4.0 (br. s, each 6H; CH_3), 3.4 (br. s, 12H; CH_3), 2.0 (br. s, 4H; CH_2), −3.3 (br. s, 1H; py, γ-H), −14.6 (br. s, 2H; H-5,15), −59.1 (br. s, 1H; H-10); MS (FAB): *m/z* (%): 575 (100) [M^+ − py]; IR: $\tilde{\nu}$ = 2962, 2930, 2868, 1596, 1482, 1445, 1155, 1056, 1024, 1009, 959, 807, 754, 694 cm^{-1}; UV/VIS (pyridine): λ_{max} (ε) = 397 (67200), 482 (8850), 547 (15200), 640 (3200), 670 (2900) sh, 720 nm (2000); magnetic moment (293 K): $\mu_{eff} = 3.80\ \mu_B$; Mössbauer parameters (77 K): $\delta_{Fe} = -0.09$ mm s^{-1}, $\Delta E_q = 3.88$ mm s^{-1}.

 © VCH Verlagsgesellschaft mbH, D-69451 Weinheim, 1994 0570-0833/94/0707-0733 $ 10.00+.25/0

The possibility of stabilizing iron(III) corrole complexes by an axial pyridine ligand was demonstrated some time ago by Y. Murakami et al. with the example of 7,8,12,13-tetraethyl-2,3,17,18-tetramethylcorrole, but no details were given about the characterization of the complex.[11b] In parallel to this we have established that the product obtained from the metalation of **5** with nonacarbonyldiiron and subsequent removal of the solvent under vacuum yields the monopyridine complex **10** when treated with pyridine prior to the admission of air.



Alternatively, **10** can be obtained by reduction of **7** with hydrazine in the presence of pyridine. Complex **10** is stable in the solid state; however, in solution devoid of pyridine slow oxidation occurs to yield **7**. Treatment of a solution of **10** in dichloromethane with dilute hydrochloric acid leads to the immediate formation of the chloro complex **8**.

An X-ray crystal structure analysis[13] could also be carried out on complex **10** (Fig. 4 and Table 1). The distance between the iron atom and the N_4 plane (0.273 Å) is small and is similar to that in the phenyl compound **9**. Although all the nitrogen atoms

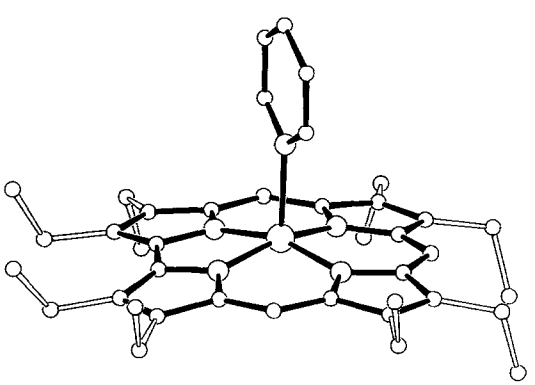


Fig. 4. Structure of the pyridine iron(III) corrole complex **10** in the crystal. Perspective view (without hydrogen atoms).

are in good alignment with the metal, the ring framework in **10** deviates from planarity more pronouncedly (the maximum distance of the C and N atoms from the mean plane of the ring is 0.219 Å) than is the case in the mononuclear complexes **8** and **9**. The Fe–N bond lengths in **10** are virtually the same as those found in the iron(IV) complexes **7**–**9**. This is unexpected, since one would have predicted an elongation towards the distances found in iron(III) porphyrins. The Fe–N distance between the iron atom and the pyridine ligand (2.188 Å) is similar to that in the cationic (3-chloropyridine)iron(III) complex of octaethylporphyrin (2.126 Å).[28] Finally, it should be noted that $\pi-\pi$ dimer formation in crystals of **10** is encountered by analogy to the situation in **9** (intermolecular separation of the ring frameworks: 3.6–3.7 Å; Fe···Fe distance: 6.221 Å).[15c]

The ^{1}H NMR spectrum of **10** (in [D_5]pyridine) corresponds in its kind to that expected for pentacoordinated paramagnetic high-spin iron(III) porphyrins:[25] the *meso* protons absorb at high field, the protons of the ethyl groups, on the other hand, at low field (Tables 2 and 3). On measuring the spectrum in carbon disulfide, three additional signals appear at $\delta = 11.4$, 7.7.1, and -3.3, which correspond to the protons in the α, β, and γ positions, respectively, of the axially coordinated pyridine ligand.[26] The positions of the resonances of the ligand protons change only slightly on altering the solvent from [D_5]pyridine to carbon disulfide; a tendency for **10** to form a six-coordinate dipyridine complex is thus not evident. Susceptibility measurements[18] indicate that **10** has a $S = 3/2$ ground state due to the observed temperature-independent magnetic moment of 3.80 μ_B (81–293 K). To our surprise, the Mössbauer spectrum of **10** exhibits parameters ($\delta_{Fe} = -0.09$ mm s^{-1} and $\Delta E_q = 3.88$ mm s^{-1} at 77 K) which are difficult to reconcile with the assumption of an iron(III) complex with a $S = 3/2$ ground state.[29] The observed isomer shifts and quadrupole splittings correspond rather as has also been established for the Fe–N bond lengths—to those in complexes **7**–**9**. We must therefore entertain the possibility that the formal Fe^{III} complex **10** should actually be considered as an Fe^{IV} corrole anion radical complex, whose magnetic properties ($S = 3/2$) come about as a result of ferromagnetic spin coupling of an iron(IV) metal center ($S = 1$) with a corrole anion radical ($S = 1/2$). Theoretical studies should shed further light on the electron distribution in **10**.

The synthesis of the iron(IV) corrole complexes **7**–**9** makes it conceivable that corroles might allow also the stabilization of unusual oxidation states of metals other than iron.[30] This possibility is directed, in particular, to the already well-known corrole complexes of copper and nickel, which, on the basis of chemical, UV/VIS, and ESR spectroscopic studies, have long been assumed to contain the metal in a divalent state.[6, 12] The conjecture that these complexes are actually Ni^{III} and Cu^{III} compounds is presently under investigation.

We are confident that research efforts in the field of metallocorroles, which have long stood in the shadow of metalloporphyrins, will now receive renewed impetus as a result of the access to iron(IV) complexes.

Experimental Procedure

7: Octaethylcorrole (**5**) (523 mg, 1 mmol) and nonacarbonyldiiron (1.8 g, 5 mmol) were heated together in toluene (25 mL) for two hours at 100–110 °C under an atmosphere of argon. Subsequently, the solution was concentrated under vacuum to 5 mL and air was introduced over 20 min, causing a change in color from brown to red. After filtration, the solution was stirred intensively for a further two hours under a current of air to complete the oxidation. The solvent was removed and the residue was subjected twice to chromatographic filtration (aluminum oxide, Woelm activity I, 10 × 2 cm, eluent diethyl ether). The μ-oxo complex **7** was eluted as an intensely red fraction, from which black rhombohedra were obtained after crystallization from hexane; m.p. >300 °C; yield 336 mg (58%).

8: A solution of the μ-oxo complex **7** (233 mg, 0.2 mmol) in dichloromethane (20 mL) was thoroughly stirred with hydrochloric acid (1 M, 20 mL) for 5 min. The organic phase was dried over sodium sulfate, and the residue obtained after removal of the solvent was chromatographically filtered (silica gel, 4 × 2 cm, eluent dichloromethane). The chloro complex **8** was eluted as the only fraction, which, after crystallization from hexane/dichloromethane (9:1), was obtained as small black needles; m.p. >300 °C; yield 204 mg (84%).

9: The chloro complex **8** (122 mg, 0.2 mmol) in dichloromethane (10 mL) was treated with four equivalents of phenylmagnesium bromide (solution in diethyl ether, ca. 0.5 M) over 5 min. After addition of water, the organic phase was separated, dried over sodium sulfate, and the solvent removed under vacuum. A chromatographic filtration (aluminum oxide, Woelm activity I, 10 × 2 cm, eluent diethyl ether) of the residue gave a red-orange eluate. This contained the phenyl complex **9**, which, after crystallization from hexane/dichloromethane (9:1), was recovered as gray rhombohedra with metallic luster; decomp. >185 °C; yield 98 mg (75%).

10: A solution of the μ-oxo complex **7** (233 mg, 0.2 mmol) in pyridine (5 mL) was treated with hydrazine hydrate (0.2 mL) and thereafter stirred for 5 min. After the addition of methanol (50 mL), the pyridine complex **10** was allowed to crystallize out at -30 °C. Subsequent crystallization from methanol/pyridine (5:1) gave **10** as gray rhombohedra with metallic luster; decomp. >160 °C; yield 210 mg (80%). All compounds gave correct elemental analyses (C, H, N, Cl).

Received: July 29, 1993 [Z 6244 IE]
Publication delayed at authors' request
German version: *Angew. Chem.* **1994**, *106*, 771

[1] P. R. Ortiz de Montellano, *Cytochrome P-450; Structure, Mechanism and Biochemistry*, Plenum, New York, **1986**; R. H. Holm, *Chem. Rev.* **1987**, *87*, 1401; B. Meunier, *ibid.* **1992**, *92*, 1411; D. Ostovic, T. Bruice, *Acc. Chem. Res.* **1992**, *25*, 314.

[2] D. Lançon, P. Cocolios, R. Guilard, K. M. Kadish, *Organometallics* **1984**, *3*, 1164; *J. Am. Chem. Soc.* **1984**, *106*, 4472; A. L. Balch, M. W. Renner, *ibid.* **1986**, *108*, 2603; a stable (at room temperature; in solution) σ-phenyliron(IV) porphyrin has in the meantime been reported: K. M. Kadish, E. Van Caemelbecke, F. D'Souza, C. J. Medforth, K. M. Smith, A. Tabard, R. Guilard, *Organometallics* **1993**, *12*, 2411.

[3] J. T. Groves, R. Quinn, T. J. McMurry, M. Nakamura, G. Lang, B. Boso, *J. Am. Chem. Soc.* **1985**, *107*, 354; J. T. Groves, J. A. Gilbert, *Inorg. Chem.* **1986**, *25*, 123.

[4] D. Mansuy, J.-P. Lecomte, J.-C. Chottard, J.-F. Bartoli, *Inorg. Chem.* **1981**, *20*, 3119; K. M. Kadish, R. K. Rhodes, L. A. Bottomley, H. M. Goff, *ibid.* **1981**, *20*, 3195; V. L. Goedken, M. R. Deakin, L. A. Bottomley, *J. Chem. Soc. Chem. Commun.* **1982**, 607; D. R. English, D. N. Hendrickson, K. S. Suslick, *Inorg. Chem.* **1983**, *22*, 367; *ibid.* **1985**, *24*, 121.

[5] R. Guilard, University of Burgundy, Dijon, personal communication.

[6] A. W. Johnson, I. T. Kay, *J. Chem. Soc.* **1965**, 1620; A. W. Johnson in *Porphyrins and Metalloporphyrins* (Ed.: K. M. Smith), Elsevier, Amsterdam, **1975**, p. 729; R. Grigg in *The Porphyrins, Vol. II* (Ed.: D. Dolphin), Academic Press, New York, **1978**, p. 327; N. S. Genokhova, T. A. Melent'eva, V. M. Berezovskii, *Usp. Khim.* **1980**, *49*, 2132 [*Russ. Chem. Rev. (Engl. Transl.)* **1980**, *49*, 1056]; T. A. Melent'eva, *ibid.* **1983**, *52*, 1136 [and **1983**, *52*, 641]; K. M. Kadish, W. Koh, P. Tagliatesta, D. Sazou, R. Paolesse, S. Licoccia, T. Boschi, *Inorg. Chem.* **1992**, *31*, 2305; R. Paolesse, S. Licoccia, M. Fanciullo, E. Morgante, T. Boschi, *Inorg. Chim. Acta* **1993**, *203*, 107.

[7] a) S. Will, A. Rahbar, H. Schmickler, J. Lex, E. Vogel, *Angew. Chem.* **1990**, *102*, 1434; *Angew. Chem. Int. Ed. Engl.* **1990**, *29*, 1390; b) E. Vogel, *Pure Appl. Chem.* **1993**, *65*, 143.

[8] a) V. M. Leovac, R. Herak, B. Prelesnik, S. R. Niketic, *J. Chem. Soc. Dalton Trans.* **1991**, 2295; b) N. V. Gerbeleu, Y. A. Simonov, V. B. Arion, V. M. Leovac, K. I. Turta, K. M. Indrichan, D. I. Gradinaru, V. E. Zavodnik, T. I. Malinovskii, *Inorg. Chem.* **1992**, *31*, 3264; c) U. Knof, T. Weyhermüller, T. Wolter, K. Wieghardt, E. Bill, C. Butzlaff, A. X. Trautwein, *Angew. Chem.* **1993**, *105*, 1701; *Angew. Chem. Int. Ed. Engl.* **1993**, *32*, 1635.

[9] Further examples of non-porphyrinoid iron(IV) complexes with N_4 ligands: W. Hiller, J. Strähle, A. Datz, M. Hanack, W. E. Hatfield, L. W. ter Haar, P. Gütlich, *J. Am. Chem. Soc.* **1984**, *106*, 329; T. J. Collins, K. L. Kostka, E. Münck, E. S. Uffelman, *ibid.* **1990**, *112*, 5637; T. J. Collins, B. G. Fox, Z. G. Hu, K. L. Kostka, E. Münck, C. E. F. Rickard, L. J. Wright, *ibid.* **1992**, *114*, 8724; K. L. Kostka, B. G. Fox, M. P. Hendrich, T. J. Collins, C. E. F. Rickard, L. J. Wright, E. Münck, *ibid.* **1993**, *115*, 6746. For other Fe^{IV} compounds see: F. M. Nelson in *Comprehensive Coordination Chemistry, Vol. 4* (Eds.: G. Wilkinson, R. D. Gillard, J. A. McCleverty), Pergamon, Oxford, **1987**, p. 217; D. Sellmann, M. Geck, F. Knoch, G. Ritter, J. Dengler, *J. Am. Chem. Soc.* **1991**, *113*, 3819.

[10] It should be noted here, that in the case of complexes containing ligands having extended π systems (so-called noninnocent ligands) the metal cannot be assigned a definite oxidation state—the reason for this is the mixing of metal and ligand orbitals. For discussion of this subtle problem see: F. C. Anson, T. J. Collins, T. G. Richmond, B. D. Santarsiero, J. E. Toth, B. G. R. T. Treco, *J. Am. Chem. Soc.* **1987**, *109*, 2974; reference [8c].

[11] a) M. Conlon, A. W. Johnson, W. R. Overend, D. Rajapaksa, C. M. Elson, *J. Chem. Soc. Perkin Trans. 1* **1973**, 2281; b) Y. Murakami, Y. Aoyama, M. Hayashida, *J. Chem. Soc. Chem. Commun.* **1980**, 501; c) T. Boschi, S. Licoccia, R. Paolesse, P. Tagliatesta, M. A. Tehran, G. Pelizzi, F. Vitali, *J. Chem. Soc. Dalton Trans.* **1990**, 463; d) S. Licoccia, M. Paci, R. Paolesse, T. Boschi, *ibid.* **1991**, 461.

[12] Y. Murakami, Y. Matsuda, K. Sakata, S. Yamada, Y. Tanaka, Y. Aoyama, *Bull. Chem. Soc. Jpn.* **1981**, *54*, 163. The synthesis of octaethylcorrole **5** by oxidative intramolecular coupling of 1,19-dideoxyoctaethylbiladiene-*ac*-dihydrobromide proceeds as follows: the tetrapyrrole starting material in methanol is treated with chloranil at room temperature in the presence of potassium hydrogen carbonate (5 min). After addition of hydrazine (to deprotonate the corrole hydrobromide and to reduce the excess chloranil) the corrole **5** separates, and is crystallized from methanol/chloroform (9:1) to give pure material; m.p. 226–227 °C (yield is increased from 19 to 60% compared with the previous method).

[13] **7**: $C_{70}H_{86}Fe_2N_8O$, crystals from hexane; monoclinic, space group $P2_1/n$, a = 15.589(4), b = 15.950(4), c = 25.933(7) Å, β = 90.84(2)°, Z = 4; ρ_{calcd} = 1.202 g cm^{-3}, μ_{Mo} = 4.98 cm^{-1}; 10412 observed reflections; θ_{max} = 27°; $R1$ = 0.0421, $wR2$ = 0.1178. **8**: $C_{35}H_{43}ClFeN_4 \cdot C_6H_6$, crystals from benzene; triclinic, space group $P\bar{1}$, a = 10.191(2), b = 13.973(3), c = 14.684(3) Å, α = 82.62(2), β = 71.19(2), γ = 69.65(2)°, Z = 2; ρ_{calcd} = 1.234 g cm^{-3}, μ_{Mo} = 5.12 cm^{-1}; 5844 observed reflections; θ_{max} = 27°; $R1$ = 0.0646, $wR2$ = 0.1614. **9**: $C_{41}H_{48}FeN_4$, crystals from hexane/ether; triclinic, space group $P\bar{1}$, a = 11.989(2), b = 12.443(2), c = 14.970(2) Å, α = 60.39(2), β = 68.50(2), γ = 67.88(2)°, Z = 2; ρ_{calcd} = 1.237 g cm^{-3}; μ_{Mo} = 4.64 cm^{-1}; 4908 observed reflections; θ_{max} = 25°; $R1$ = 0.0644, $wR2$ = 0.1882. **10**: $C_{40}H_{48}FeN_4$, crystals from pentane/pyridine; monoclinic, space group $P2_1/n$, a = 12.761(3), b = 14.644(4), c = 18.662(5) Å, β = 95.58(2)°, Z = 4; ρ_{calcd} = 1.253 g cm^{-3}, μ_{Mo} = 4.70 cm^{-1}; 6186 observed reflections; θ_{max} = 27°; $R1$ = 0.0361, $wR2$ = 0.1121. The measurement of the reflection intensities was carried out on an Enraf-Nonius CAD4 diffractometer (room temperature, $Mo_{K\alpha}$ radiation λ = 0.71069 Å). The structures were solved with direct methods and refined with F^2 for all independently observed reflections with ($F_o^2 > 2\sigma F_o^2$) (heavy atoms with anisotropic, H atoms with isotropic temperature factors); $wR2 = [\Sigma w(F_o^2 - F_c^2)^2/\Sigma(F_o^2)^2]^{1/2}$. Programs used: for solving the structures MolEN (Enraf-Nonius) and for the refinement SHELXL-93 (G. M. Sheldrick, Universität Göttingen). Further details of the crystal structure investigations may be obtained from the Fachinformationszentrum Karlsruhe, D-76344 Eggenstein-Leopoldshafen (FRG) on quoting the depository number CSD-57965.

[14] For the only X-ray structure analysis of an uncomplexed corrole so far, that of 8,12-diethyl-2,3,7,13,17,18-hexamethylcorrole, see: H. R. Harrison, O. J. R. Hodder, D. C. Hodgkin, *J. Chem. Soc. B* **1971**, 640.

[15] a) W. R. Scheidt, C. A. Reed, *Chem. Rev.* **1981**, *81*, 543; b) W. R. Scheidt, M. Gouterman in *Iron Porphyrins, Part I* (Eds.: A. B. P. Lever, H. B. Gray), Addison-Wesley, Reading/Massachusetts, **1983**, p. 89; c) W. R. Scheidt, Y. J. Lee, *Struct. Bonding (Berlin)* **1987**, *64*, 1.

[16] W. R. Scheidt, B. Cheng, M. K. Safo, F. Cukiernik, J.-C. Marchon, P. G. Debrunner, *J. Am. Chem. Soc.* **1992**, *114*, 4420 (ref. [8g]).

[17] K. Tatsumi, R. Hoffman, *J. Am. Chem. Soc.* **1981**, *103*, 3328. In an μ-oxodiiron complex containing a pentane-2,4-dione-bis(*S*-alkylisothiosemicarbazonate) ligand, described in reference [8b], the Fe-O-Fe angle is only 153.7°.

[18] The susceptibility measurements were carried out on powdered samples in the temperature range of 81 to 293 K on a Faraday balance; the diamagnetic correction was calculated by using Pascal constants. The Mössbauer experiments were carried out on powdered samples at 4.2 K and 77 K in zero field.

[19] The perimeter protons in metalloporphyrin dimers are shifted to highfield due to the magnetic anisotropicy of the ligands. This shift amounts to about 0.5 ppm in the case of the *meso* protons in the μ-oxodiscandium complex of octaethylporphyrin (see ref. [22]). By the clamping together of two porphyrin units, the distance between the ring frameworks is reduced to 3.4 Å. In this way shifts of up to 1.5 ppm are observed (see M. O. Senge, K. R. Gerzevske, M. G. H. Vicente, T. P. Forsyth, K. M. Smith, *Angew. Chem.* **1993**, *105*, 745; *Angew. Chem. Int. Ed. Engl.* **1993**, *32*, 750). Since the average separation of the ring frameworks in **7** is 4.3 Å, it seems unlikely that the shifts encountered in this work are solely due to a conventional anisotropy effect.

[20] D. M. Kurtz, Jr., *Chem. Rev.* **1990**, *90*, 585.

[21] M. Lausmann, J. Zimmer, J. Lex, H. Lueken, K. Wieghardt, E. Vogel, *Angew. Chem.* **1994**, *106*, 776; *Angew. Chem. Int. Ed. Engl.* **1994**, *33*, 736.

[22] J. W. Buchler, H. H. Schneehage, *Z. Naturforsch. B* **1973**, *28*, 433.

[23] R. D. Arasasingham, A. L. Balch, R. L. Hart, L. Latos-Grazynski, *J. Am. Chem. Soc.* **1990**, *112*, 7566.

[24] J. Ernst, J. Subramanian, J.-H. Fuhrhop, *Z. Naturforsch. A* **1977**, *32*, 1129.

[25] G. N. La Mar, F. A. Walker (Jensen) in *The Porphyrins, Vol. IV* (Ed.: D. Dolphin), Academic Press, New York, **1979**, p. 61; H. M. Goff in *Iron Porphyrins, Part I* (Eds.: A. B. P. Lever, H. B. Gray), Addison-Wesley, Reading/Massachusetts, **1983**, p. 237.

[26] The ^{1}H NMR spectrum of **9** was assigned by comparison with those of the [D_5]phenyl derivative, the *m*-tolyl compound, and the complex **9** deuterated in the *meso* positions; in the case of **10**, the ^{1}H NMR spectra of the [D_5]pyridine complex and the 3-methylpyridine derivative served as references.

[27] E. Bill, X.-Q. Ding, E. L. Bominaar, A. X. Trautwein, H. Winkler, D. Mandon, R. Weiss, A. Gold, K. Jayaraj, W. E. Hatfield, M. L. Kirk, *Eur. J. Biochem.* **1990**, *188*, 665.

[28] W. R. Scheidt, D. K. Geiger, Y. J. Lee, C. A. Reed, G. Lang, *Inorg. Chem.* **1987**, *26*, 1039.

[29] P. G. Debrunner in *Iron Porphyrins, Part III* (Eds.: A. B. P. Lever, H. B. Gray), VCH, New York, **1989**, p. 137.

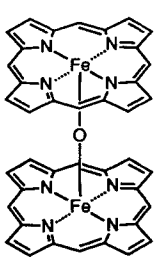
[30] The only previous example of this is the oxochromium(V) complex of 7,8,12,13-tetraethyl-2,3,17,18-tetramethylcorrole: Y. Matsuda, S. Yamada, Y. Murakami, *Inorg. Chim. Acta* **1980**, *44*, L309.

 © VCH Verlagsgesellschaft mbH, D-69451 Weinheim, 1994 0570-0833/94/0707-0735 $ 10.00+.25/0

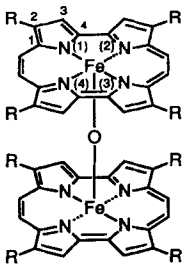
μ-Oxodiiron(III) Complexes of Porphycenes

Michael Lausmann, Ingeborg Zimmer, Johann Lex, Heiko Lueken, Karl Wieghardt, and Emanuel Vogel*

Porphyrin complexes with divalent iron, the highly reactive hemes, are the prosthetic groups of hemoglobin and myoglobin and, as such, are capable of reversibly binding dioxygen.[1] This function of the hemoprotein metal center was successfully simulated in the groups of Collman[2a] and Baldwin[2b] with the design and synthesis of the "picket fence" and "capped" porphyrins.[2c] In the case of simple iron(II) porphyrinates, the reversible binding of dioxygen is suppressed by the alternative irreversible oxidation step. The thermodynamically stable μ-oxodiiron(III) porphyrin complexes of type **1**,[3] the so-called μ-oxo dimers, are thus formed. Because of the role they play in dioxygen binding, their varied chemistry, and not least because of their interesting electronic structure and the magnetic interactions between the two Fe^{III} centers,[4] the μ-oxo dimers rank among the important iron porphyrin complexes.



1



2: R = *n*-C_3H_7
3: R = *t*-C_4H_9

In view of the similarity between metalloporphycenes and the corresponding metalloporphyrins,[5] it is very likely that iron(II) porphycenates, tailored after the heme models in their molecular architecture, are also capable of reversibly binding dioxygen. While porphycenates of this type still await synthesis, we report here on the preparation and properties of the first μ-oxodiiron(III) porphycene complexes; the sterically complementary complexes **2** and **3** of 2,7,12,17-tetra-*n*-propylporphycene (**4**)[5a] (H_2TPrPc) and 2,7,12,17-tetra-*tert*-butylporphycene (**5**) (H_2TBuPc), respectively.

The μ-oxodiiron(III) porphycenates **2** and **3** can readily be made following a well-established procedure for the synthesis of μ-oxodiiron(III) porphyrinates.[3] Porphycenes **4** and **5** were heated under reflux with tris(acetylacetonato)iron(III) in phenol to give the corresponding (phenolato)iron(III) porphycenates, which, after removal of the solvent, were treated with an aqueous sodium hydroxide solution. Chromatography and recrystallization furnished **2** and **3** in yields of 81 and 67%, respectively, (see Experimental Procedure) as stable compounds [**2**: violet-black, parallelepiped-shaped crystals (from benzene/pentane); m.p. 266–268 °C; **3**: violet, parallelepiped-shaped crystals (from hexane/dichloromethane); m.p. > 300 °C (decomp.)].

[*] Prof. Dr. E. Vogel, Dr. M. Lausmann, Dr. I. Zimmer, Dr. J. Lex
Institut für Organische Chemie der Universität
Greinstrasse 4, D-50939 Köln (FRG)
Telefax: Int. code + (221)470-5102
Prof. Dr. H. Lueken
Institut für Anorganische Chemie der Technischen Hochschule Aachen (FRG)
Prof. Dr. K. Wieghardt
Lehrstuhl für Anorganische Chemie I der Universität Bochum (FRG)

Due to the presence of the paramagnetic iron(III) ions, the ^{1}H NMR spectra (300 MHz, $CDCl_3$, room temperature) of the μ-oxodiiron(III) complexes **2** and **3** show unstructured, broadened resonance signals with unusual chemical shifts.[6] Signal assignments must therefore be based on an analysis of linewidths and comparison with the spectra of reference compounds.[7] The signals in the spectrum of **2** (Table 1) at $\delta = 14.4$ and 6.9 are thus assigned to the perimeter protons H-3,6,13,16 and H-9,10,19,20, respectively, while those at $\delta = 6.6$ and 5.4 (splitting caused by diastereotopism), 2.5, and 1.4 correspond to the α-CH_2, β-CH_2, and methyl protons, respectively. Since the spectra of **2** and **3** are, as far as they are comparable, very similar, the spectral assignment for **3** follows by analogy from that described above for **2**. An indication of how closely complexes **2** and **3** are related to μ-oxodiiron(III) porphyrinates in NMR-spectroscopic terms is provided by the observation that the two types of μ-oxo complexes have comparable isotropic shifts.[6] The electronic spectra of **2** and **3** exhibit porphyrinoid features, with a Soret band (at 367 and 370 nm, respectively) and a broad band at longer wavelength (632 and 628 nm, respectively). The Mössbauer spectra of **2** and **3** at room temperature show a near-symmetrical quadrupole split doublet with isomer shifts (δ_{Fe}) of 0.24 and 0.25 mm s^{-1}, respectively, and electric quadrupole splittings (ΔE_q) of 0.58 and 0.52 mm s^{-1}, respectively. These δ_{Fe} and ΔE_q values lie in the range characteristic of μ-oxo porphyrin complexes ($0.23 \leq \delta_{Fe} \leq 0.39$ mm s^{-1} and $0.54 \leq \Delta E_q \leq 0.74$ mm s^{-1} at $T = 298$ K[8]), and thus attest to the similarities between the porphycene complexes and their porphyrin counterparts already evident from the other spectral findings.

Cyclovoltammetric investigations, on the other hand, revealed remarkable differences in the redox behavior of μ-oxodiiron(III) porphycenates and μ-oxodiiron(III) porphyrinates. Compounds **2** and **3** both undergo four reversible one-electron oxidations and four reversible one-electron reductions. Four reversible one-electron oxidations are also observed for the porphyrin complexes, yet only one reversible one-electron reduction can be detected.[9]

The X-ray structure analysis of μ-oxodiiron(III) porphycenate complex **2** (Fig. 1) confirms its molecular structure.[10] Each of the iron atoms in **2** is coordinated in a square-pyramidal geome-

Table 1. Selected physical data of new compounds **2**, **3**, **5**, **7**–**9**. ^{1}H NMR: 300 MHz, room temperature; ^{13}C NMR: 75.5 MHz; MS: EI, 70 eV; IR: CsI; UV/VIS: CH_2Cl_2. Isomer shifts are quoted relative to α-iron at 298 K.

2: M.p. 266–268 °C (benzene/pentane); ^{1}H NMR ($CDCl_3$): $\delta = 14.4$ (br. s, 8H; H-3,6,13,16), 6.9 (br. s, 8H; H-9,10,19,20), 6.6 (br. s, 8H; α-CH_2), 5.4 (br. s, 8H; α-CH_2), 2.5 (br. s, 16H; β-CH_2), 1.4 (br. s, 24H; CH_3); MS: *m/z* (%): 1080 (24) [M^+], 532 (100) [M^+ – Fe(TPrPc)O]; IR: $\tilde{\nu} = 2957$, 2929, 2868, 1466, 1241, 1044, 968, 913, 844 [$\tilde{\nu}_{as}$(Fe-O-Fe)], 812 cm^{-1}; UV/VIS: $\lambda_{max}(\varepsilon) = 342$ (86100) sh, 367 (99600), 427 (23600) sh, 632 nm (55500); Mössbauer parameters (298 K): $\delta_{Fe} = 0.24$ mm s^{-1}, $\Delta E_q = 0.58$ mm s^{-1}

3: Decomp. > 300 °C (hexane/dichloromethane); ^{1}H NMR ($CDCl_3$): $\delta = 14.4$ (br. s, 8H; H-3,6,13,16), 7.3 (br. s, 8H; H-9,10,19,20), 2.5 (br. s., 72H; CH_3); MS: *m/z* (%): 1192 (48) [M^+], 588 (100) [M^+ – Fe(TBuPc)O]; IR: $\tilde{\nu} = 2963$, 2909, 2871, 1464, 1189, 1039, 1010, 976, 902, 823, 805 cm^{-1}; UV/VIS: $\lambda_{max}(\varepsilon) = 370$ (123000), 430 (21000) sh, 580 (31600) sh, 628 nm (89000); Mössbauer parameters (298 K): $\delta_{Fe} = 0.25$ mm s^{-1}, $\Delta E_q = 0.52$ mm s^{-1}

5: M.p. > 300 °C (acetonitrile/dichloromethane); ^{1}H NMR ($CDCl_3$): $\delta = 10.2$ (s, 4H; H-9,10,19,20), 9.4 (s, 4H; H-3,6,13,16), 3.6 (br. s, 2H; NH), 2.3 (s, 36H; CH_3); ^{13}C NMR ($CDCl_3$): $\delta = 153.5$, 142.5, 132.8, 121.9, 112.6, 34.3, 33.8; MS: *m/z* (%): 534 (100) [M^+]; IR: $\tilde{\nu} = 2960$, 2867, 1462, 1363, 1228, 1181, 1034, 999, 887, 823, 808 cm^{-1}; UV/VIS: $\lambda_{max}(\varepsilon) = 370$ (147000), 384 (96300) sh, 562 (33700), 601 (35300), 632 nm (48500)

7: M.p. 160–162 °C (methanol); ^{1}H NMR ($CDCl_3$): $\delta = 7.55$, 7.50, 7.40, 7.17, 5.87

8: Decomp. > 195 °C (pentane); ^{1}H NMR ($CDCl_3$): $\delta = 7.85$, 6.50, 6.10, 1.25

9: M.p. 299–301 °C (ethanol/dichloromethane); ^{1}H NMR ($CDCl_3$): $\delta = 12.40$, 10.03, 6.34, 1.46

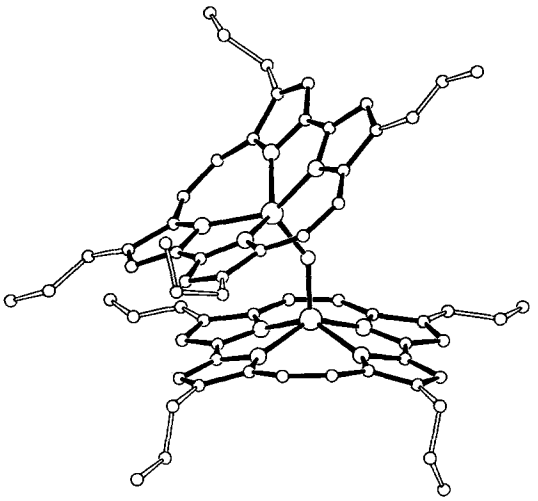


Fig. 1. Structure of the μ-oxodiiron(III) complex **2** in the crystal. Perspective view (hydrogen atoms omitted). Selected bond lengths and distances [Å] (mean values), and bond angles [°]: Fe–O 1.770, Fe–N 2.052, Fe···N_4 plane 0.670; Fe-O-Fe 145.3.

try. The porphycene ligand has a dome-shaped framework, and thus differs significantly from the free ligand 2,7,12,17-tetra-*n*-propylporphycene (**4**), in which—just like in its nickel(II) complex[5a]—the framework is planar. As can be deduced from Figure 1, the changes in the geometry of the macrocycle resulting from complexation can largely be explained in terms of the tendency shown by the nitrogen electron pairs and bonds to align themselves in such a way as to maximize bonding with the metal center. As a result, the ratios of the lengths of the sides in the N_4 core are reversed [N(1)···N(2)/N(1)···N(4): 2.629/2.851 Å; **4**: 2.831/2.651 Å], a phenomenon also observed in other metallo-2,7,12,17-tetra-*n*-propylporphycenes (nickel complex: 2.554/2.801 Å).[5a, 11] The distances of the iron atoms from the N_4 mean planes and from the mean planes of the ring frameworks of 0.67 and 0.84 Å, respectively (mean values), are noticeably larger than the corresponding values for the μ-oxodiiron(III) porphyrin complexes (0.50–0.54 Å and 0.42–0.67 Å).[12] The iron–nitrogen distances are, in contrast, slightly shorter than those observed in their porphyrin counterparts (2.052 and 2.078 Å, respectively, mean values).

According to an X-ray structure analysis,[10] the μ-oxodiiron(III) complex **3** (Fig. 2 top) of the tetra-*tert*-butylporphycene **5** has a crystallographic twofold axis of symmetry which bisects the angle of the Fe-O-Fe bridging unit. In the structural unit comprising the ligand and the incorporated iron atom, distances and bond lengths involving iron are very similar to those of **2**; however, the deviation from planarity of the ring framework is less pronounced (maximum deviation of the C and N atoms from the mean plane: ±0.26 Å vs. ±0.40 Å for **2**).

The most conspicuous result to emerge from the X-ray structure analyses of **2** and **3** is that the Fe-O-Fe angles in the two compounds differ substantially. Whereas the Fe-O-Fe unit in **2** is, as anticipated from theoretical considerations,[13] bent (at an angle of 145.3°), it is almost linear in **3** (178.5°). Steric interactions between the bulky *tert*-butyl groups, which are staggered (the porphycene ligands are twisted with respect to each other by ca. 39° in **3** and ca. 31° in **2**), evidently disfavor an approach of the two porphycene ligands, and thus prevent bending in the Fe-O-Fe unit of **3** (Fig. 2 bottom).[14] The Fe–O bond lengths in **2** and **3** are 1.770 and 1.748 Å, respectively. It is interesting to compare these values with the Fe-O-Fe bond angle of 171.8° and

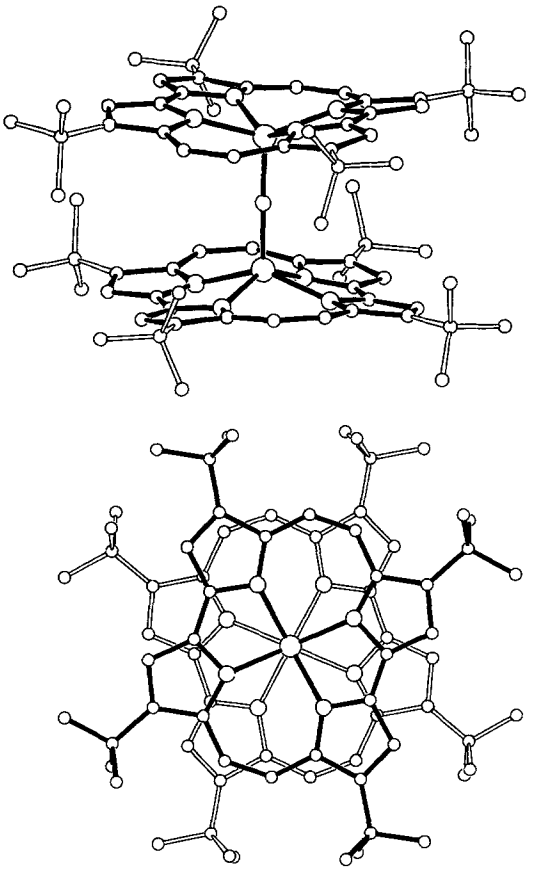


Fig. 2. Structure of the μ-oxodiiron(III) complex **3** in the crystal. Top: Perspective view (hydrogen atoms omitted); bottom: top view (hydrogen atoms omitted). Selected bond lengths and distances [Å] (mean values), and bond angles [°]: Fe–O 1.748, Fe–N 2.056, Fe···N_4 plane 0.600; Fe-O-Fe 178.5.

the Fe–O bond lengths of 1.754 and 1.760 Å found in the μ-oxodiiron(III) complex of octaethylporphyrin.[12d]

In order to determine the strength of the spin-spin interaction between the paramagnetic d^5 iron(III) centers in the dinuclear μ-oxo complexes **2** and **3**, the magnetic susceptibility[15] χ_M of both complexes was measured over the temperature range from 3.0 to 294 K (Fig. 3).[16] On application of the isotropic Heisenberg–Dirac–van Vleck model, the temperature-dependence in

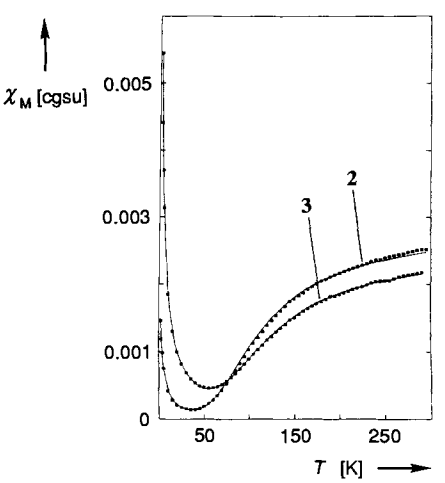


Fig. 3. Temperature dependence of the molar susceptibilities of the μ-oxodiiron(III) porphycenates **2** and **3**.

 © VCH Verlagsgesellschaft mbH, D-69451 Weinheim, 1994 0570-0833/94/0707-0737 $ 10.00+.25/0

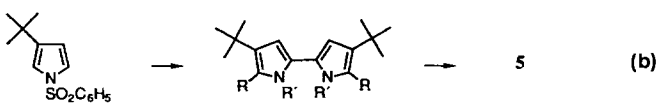
both series of measurements can readily be fitted to the spin-Hamiltonian operator $\mathscr{H} = -2J\boldsymbol{S}_1\cdot\boldsymbol{S}_2$ with $S_1 = S_2 = 5/2$, where $\boldsymbol{S}_1$ and $\boldsymbol{S}_2$ are the total spins of the interacting ions 1 and 2, respectively, and J is the spin-exchange coupling constant. Using the Landé factor $g = 2.0$ and assuming that samples of **2** and **3** are contaminated with a small percentage α of a paramagnetic mononuclear iron(III) porphycenate with $S = 5/2$, the following numerical values for J were obtained: for **2**: $-114\ cm^{-1}$ ($\alpha = 0.1\%$) and for **3**: $-129\ cm^{-1}$ ($\alpha = 0.2\%$). These values suggest an intramolecular antiferromagnetic coupling between the iron(III) ions (d^5 high-spin electron configuration[17]) in **2** and **3**. The spin-exchange coupling constant J for **2** and **3** fall within the range reported for numerous Fe^{III}-O-Fe^{III}-bridged complexes.[3c] According to theoretical considerations[13, 18] and experimental data,[19] the dominant factor influencing the magnitude of J is the mean Fe–O bond length; the shorter the Fe–O distance the stronger the coupling. As indicated by the Fe–O distances observed for **2** and **3** (see discussion of the X-ray structure analyses), the coupling in **3** is slightly stronger than that in **2**.

These investigations emphasize, once again, the far-reaching parallels existing between the porphycenes and porphyrins, including their metal complexes. μ-Oxodiiron(III) porphycenates resemble the corresponding μ-oxodiiron(III) porphyrinates not only in most of the physical properties discussed here, close agreement is also observed in their chemical behavior. The fact that μ-oxodiiron(III) porphycenates are solvolyzed in weakly acidic media by compounds HX to yield mononuclear iron(III) porphycenates bearing an axial ligand X^--analogous to the class of compounds referred to as hemins—lends support to this statement. Further investigations into this type of complex, many examples of which have been prepared starting from **2** with the model compound **4** (H_2TPrPc) as ligand [Eq. (a)],[20] will be reported in another context.

$$(TPrPcFe)_2O \xrightarrow{HX} TPrPcFeX \quad (X = Cl, Br, N_3, O_2CCH_3, O_2CCF_3, OC_6H_5) \qquad (a)$$

Experimental Procedure

5: The ligand 2,7,12,17-tetra-*tert*-butylporphycene (**5**) was prepared according to Equation (b):



6[21]

7: R' = $SO_2C_6H_5$; R = H
8: R' = R = H
9: R' = H; R = CHO

6 → **7**: *n*-Butyllithium, 2,2,6,6-tetramethylpiperidine, THF, −78 °C, 1 h, then $CuCl_2$, −78 °C, 2 h; workup by hydrolysis with aqueous glycine solution (46%); **7** → **8**: KOH, methanol, reflux, 8 h (89%); **8** → **9**: $POCl_3$, dimethylformamide, 3 h, 60 °C; CH_3COONa, H_2O, 30 min, 90 °C (85%); **9** → **5**: $TiCl_4$, Zn, CuCl, THF, reflux, 1 h; hydrolysis with aqueous NH_3 solution (20%).

2: A mixture of 2,7,12,17-tetra-*n*-propylporphycene (**4**)[5a] (120 mg, 0.25 mmol), tris(acetylacetonato)iron(III) (265 mg, 0.75 mmol), and phenol (2.5 g) was maintained at 210 °C for 3 h. The phenol was removed by sublimation at 50 °C under high vacuum. The residue was dissolved in dichloromethane (60 mL), and the resulting solution was stirred with 10% aqueous sodium hydroxide solution (60 mL) for 30 min. After extraction with dichloromethane, the crude product was chromatographed on aluminum oxide (Woelm, neutral, act. IV, column: 3.5 × 30 cm). Unreacted porphycene **4** was eluted with hexane/dichloromethane (4:1). The μ-oxo complex **2** was then eluted with dichloromethane. Finally, crystallization from benzene/pentane gave **2** as violet-black, elongated parallelepiped-shaped crystals (109 mg, 81%); m.p. 266–268 °C.

3: The μ-oxo complex **3** of the tetra-*tert*-butylporphycene **5** was prepared from **5** by an analogous procedure to that described for the propyl compound **2**. Crystallization from hexane/dichloromethane (2:1) gave **3** as violet, parallelepiped-shaped crystals (100 mg, 67%); m.p. > 300 °C (decomp.).

All compounds gave correct elemental analyses (C, H, N).

Received: November 29, 1993 [Z 6525 IE]
German version: *Angew. Chem.* **1994**, *106*, 776

[1] C. Ho, *Hemoglobin and Oxygen Binding*, Elsevier/North Holland, Amsterdam **1982**; R. E. Dickerson, I. Geis, *Hemoglobin: Structure, Function, Evolution and Pathology*, Benjamin/Cummings, Menlo Park, **1983**; M. F. Perutz, *Q. Rev. Biophys.* **1989**, *22*, 139; *Annu. Rev. Physiol.* **1990**, *52*, 1.

[2] a) J. P. Collman, R. R. Gagne, T. R. Halbert, J.-C. Marchon, C. A. Reed, *J. Am. Chem. Soc.* **1973**, *95*, 7868; J. P. Collman, K. S. Suslick, *Pure Appl. Chem.* **1978**, *50*, 951; J. P. Collman, J. I. Brauman, T. J. Collins, B. L. Iverson, G. Lang, R. B. Pettman, J. L. Sessler, M. A. Walters, *J. Am. Chem. Soc.* **1983**, *105*, 3038; J. P. Collman, J. I. Brauman, B. L. Iverson, J. L. Sessler, R. M. Morris, Q. H. Gibson, *ibid.* **1983**, *105*, 3052; b) J. Almog, J. E. Baldwin, R. L. Dyer, M. Peters, *ibid.* **1975**, *97*, 226; J. E. Baldwin, P. Perlmutter, *Top. Curr. Chem.* **1984**, *121*, 181; J. E. Baldwin, J. H. Cameron, M. J. Crossley, I. J. Dagley, S. R. Hall, T. Klose, *J. Chem. Soc. Dalton Trans.* **1984**, 1739; c) see also the reviews: T. G. Traylor, *Acc. Chem. Res.* **1981**, *14*, 102; B. Morgan, D. Dolphin, *Struct. Bonding* **1987**, *64*, 115.

[3] a) J. W. Buchler in *Porphyrins and Metalloporphyrins* (Ed.: K. M. Smith), Elsevier, Amsterdam, **1975**, p. 157; b) J. W. Buchler in *The Porphyrins, Vol. I* (Ed.: D. Dolphin), Academic Press, New York, **1978**, p. 389; c) D. M. Kurtz, Jr., *Chem. Rev.* **1990**, *90*, 585.

[4] For the significance of oxo-bridged bi- and polyiron centers in biology and chemistry, see: J. Lippard, *Angew. Chem.* **1988**, *100*, 353; *Angew. Chem. Int. Ed. Engl.* **1988**, *27*, 344.

[5] For comparison between the physical properties of metalloporphycenes and metalloporphyrins, see a) E. Vogel, M. Balci, K. Pramod, P. Koch, J. Lex, O. Ermer, *Angew. Chem.* **1987**, *99*, 909; *Angew. Chem. Int. Ed. Engl.* **1987**, *26*, 928; b) E. Vogel, M. Köcher, J. Lex, O. Ermer, *Isr. J. Chem.* **1989**, *29*, 257; c) M. W. Renner, A. Forman, W. Wu, C. K. Chang, J. Fajer, *J. Am. Chem. Soc.* **1989**, *111*, 8618; d) M. Toporowicz, H. Ofir, H. Levanon, E. Vogel, M. Köcher, K. Pramod, R. W. Fessenden, *Photochem. Photobiol.* **1989**, *50*, 37; e) L. R. Furenlid, M. W. Renner, K. M. Smith, J. Fajer, *J. Am. Chem. Soc.* **1990**, *112*, 1634; f) J. Schlüpmann, M. Huber, M. Toporowicz, M. Plato, M. Köcher, E. Vogel, H. Levanon, K. Möbius, *ibid.* **1990**, *112*, 6463; g) E. Vogel, *Pure Appl. Chem.* **1990**, *62*, 557; h) J. P. Gisselbrecht, M. Gross, M. Köcher, M. Lausmann, E. Vogel, *J. Am. Chem. Soc.* **1990**, *112*, 8618; i) W. A. Oertling, W. Wu, J. J. López-Garriga, Y. Kim, C. K. Chang, *ibid.* **1991**, *113*, 127; j) J. Waluk, M. Müller, P. Swiderek, M. Köcher, E. Vogel, G. Hohlneicher, J. Michl, *ibid.* **1991**, *113*, 5511; k) A. Berman, A. Michaeli, J. Feitelson, M. K. Bowman, J. R. Norris, H. Levanon, E. Vogel, P. Koch, *J. Phys. Chem.* **1992**, *96*, 3041; l) Z.-Y. Li, J.-S. Huang, C.-M. Che, C. K. Chang, *Inorg. Chem.* **1992**, *31*, 2670; m) K. M. Kadish, E. Van Caemelbecke, P. Boulas, F. D'Souza, E. Vogel, M. Kisters, C. J. Medforth, K. M. Smith, *ibid.* **1993**, *32*, 4177.

[6] G. N. La Mar, F. A. Walker (Jensen) in *The Porphyrins, Vol. IV* (Ed.: D. Dolphin), Academic Press, New York, **1979**, p. 61; H. M. Goff in *Iron Porphyrins, Part I* (Eds.: A. B. P. Lever, H. B. Gray), Addison-Wesley, Reading/Massachusetts, **1983**, p. 237.

[7] The reference compounds used were μ-oxobis[(9,10,19,20-tetra-*n*-propylporphycenato)iron(III)] (M. Köcher, dissertation, Universität Köln, **1988**) and μ-oxobis[(2,3,6,7,12,13,16,17-octaethylporphycenato)iron(III)] (P. Koch, dissertation, Universität Köln, **1990**).

[8] J. R. Sams, T. B. Tsin in *The Porphyrins, Vol. IV* (Ed.: D. Dolphin), Academic Press, New York, **1979**, p. 425; P. G. Debrunner in *Iron Porphyrins, Part III* (Eds.: A. B. P. Lever, H. B. Gray), VCH, New York, **1989**, p. 137. We thank Dr. A. Hirsch (Universität Tübingen) and Dr. E. Bill (Medizinische Universität Lübeck) for the recording and interpretation of the Mössbauer spectra of **2** and **3**.

[9] Unpublished experiments from the groups of M. Gross (Universite Louis Pasteur de Strasbourg) and K. M. Kadish (University of Houston); see also R. Cosmo, C. Kautz, K. Meerholtz, J. Heinze, K. Müllen, *Angew. Chem.* **1989**, *101*, 638; *Angew. Chem. Int. Ed. Engl.* **1989**, *28*, 604.

[10] **2**: $C_{64}H_{72}Fe_2N_8O$, crystals from benzene/pentane; triclinic, space group $P\bar{1}$, $a = 13.543(3)$, $b = 15.067(4)$, $c = 16.115(4)$ Å, $\alpha = 108.39(2)$, $\beta = 111.56(2)$, $\gamma = 90.19(2)$°, $Z = 2$; $\rho_{calcd} = 1.248\ g\,cm^{-3}$; $\mu_{Mo} = 5.53\ cm^{-1}$; 5015 observed reflections; $\theta_{max} = 27$°; $R1 = 0.074$, $wR2 = 0.114$. **3**: $C_{72}H_{88}Fe_2N_8O$, crystals from dichloromethane/hexane; monoclinic, space group $C2/c$, $a = 18.570(4)$, $b = 13.544(3)$, $c = 27.345(6)$ Å, $\beta = 103.64(2)$°, $Z = 4$; $\rho_{calcd} = 1.186\ g\,cm^{-3}$; $\mu_{Mo} = 4.79\ cm^{-1}$; 3517 observed reflections; $\theta_{max} = 25$°; $R1 = 0.081$, $wR2 = 0.193$. Measurements of reflection intensities were carried out on an Enraf-Nonius CAD4 diffractometer (room temperature, $Mo_{K\alpha}$ radiation $\lambda = 0.71069$ Å). The structures were solved by direct methods and refined with F^2 for all independent observed reflections ($F_o^2 > 2\sigma F_o^2$) (heavy atoms with anisotropic, H atoms with isotropic temperature factors); $wR2 = [\Sigma w(F_o^2 - F_c^2)^2/\Sigma w(F_o^2)^2]^{1/2}$. Programs used: for structure solution MolEN (Enraf-Nonius) and for refinement SHELXL-93 (G. M. Sheldrick, Universität Göttingen). Further details of the crystal structure investigations may be ob-

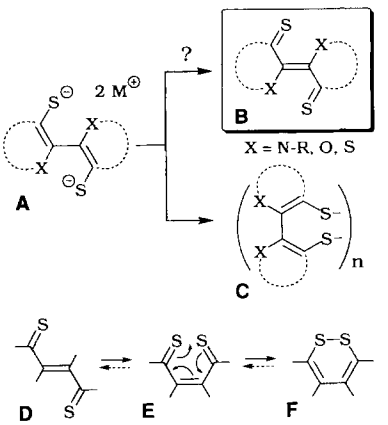
tained from the Fachinformationszentrum Karlsruhe, D-76344 Eggenstein-Leopoldshafen (FRG), on quoting the depository number CSD-57964.
[11] E. Vogel, P. Koch, X.-L. Hou, J. Lex, M. Lausmann, M. Kisters, M. A. Aukauloo, P. Richard, R. Guilard, *Angew. Chem.* **1993**, *105*, 1670; *Angew. Chem. Int. Ed. Engl.* **1993**, *32*, 1600.
[12] a) W. R. Scheidt, M. Gouterman in *Iron Porphyrins, Part I* (Eds.: A. B. P. Lever, H. B. Gray), Addison-Wesley, Reading/Massachusetts, **1983**, p. 89; b) A. Gold, K. Jayaraj, P. Doppelt, J. Fischer, R. Weiss, *Inorg. Chim. Acta* **1988**, *150*, 177; c) M. A. Ivanca, A. G. Lappin, W. R. Scheidt, *Inorg. Chem.* **1991**, *30*, 711; d) W. R. Scheidt, B. Cheng, M. K. Safo, F. Cukiernik, J.-C. Marchon, P. G. Debrunner, *J. Am. Chem. Soc.* **1992**, *114*, 4420 (ref. [8g]).
[13] K. Tatsumi, R. Hoffmann, *J. Am. Chem. Soc.* **1981**, *103*, 3328. According to the calculations of these authors concerning the dependence of the potential energy of μ-oxodiiron(III) porphyrinates on the Fe-O-Fe angle, a very flat energy minimum (hardly more than 1 kcal mol^{-1}) is expected for angles marginally below 150°. For a discussion of Fe-O-Fe angles in oxo-bridged dinuclear iron complexes in proteins, see J. Sanders-Loehr, W. D. Wheeler, A. K. Shiemke, B. A. Averill, T. M. Loehr, *ibid.* **1989**, *111*, 8084.
[14] A crystal structure analysis was also possible for μ-oxobis[(2,3,6,7,12,13,16,17-octaethylporphycenato)iron(III)]. A bent arrangement of the Fe-O-Fe unit (Fe-O-Fe angle: 180°) is, here too, prevented by intramolecular steric interactions between the alkyl groups; E. Vogel, M. Kisters, J. Lex, unpublished results.
[15] S. Mitra in *Iron Porphyrins, Part II* (Eds.: A. B. P. Lever, H. B. Gray), Addison-Wesley, Reading/Massachusetts, **1983**, p. 1.
[16] We thank Dipl.-Phys. C. Butzlaff (Medizinische Universität Lübeck) for the low-temperature magnetic susceptibility measurements on the μ-oxodiiron(III) complex **3**.
[17] W. R. Scheidt, C. A. Reed, *Chem. Rev.* **1981**, *81*, 543. In agreement with this is the observation that, of all mononuclear (porphycenato)iron complexes examined to date, the mononuclear complex phenolato(2,7,12,17-tetra-*n*-propylporphycenato)iron(III) with the relatively strong π-donating phenolato ligand in the axial position has the highest temperature-dependent magnetic moment [μ_{eff} = 5.2 μ_B (293 K) and 4.9 μ_B (81 K)]. Chloro(2,7,12,17-tetra-*n*-propylporphycenato)iron(III), in contrast, has a μ_{eff} of 3.5 μ_B (250 K); K. Wieghardt, E. Vogel, M. Lausmann, unpublished results.
[18] J. R. Hart, A. K. Rappé, S. M. Gorun, T. H. Upton, *Inorg. Chem.* **1992**, *31*, 5254.
[19] S. M. Gorun, S. J. Lippard, *Inorg. Chem.* **1991**, *30*, 1625.
[20] M. Lausmann, dissertation, Universität Köln, **1993**. The direct synthesis of chloro(tetra-*n*-propylporphycenato)iron(III) (TPrPcFeCl) by the acetate method (reported by A. Oertling et al. [5i]), with iron(III) chloride as the metal carrier and refluxing acetic acid as solvent, offers no advantage over the synthesis via **2**.
[21] H. J. Anderson, C. E. Loader, R. X. Xu, N. Lê, N. J. Gogan, R. McDonald, L. G. Edwards, *Can. J. Chem.* **1985**, *63*, 896.

Concerning the Questionable Existence of Thioxoindigoid Compounds**

Werner Schroth,* Ekkehard Hintzsche, Michael Felicetti, Roland Spitzner, Joachim Sieler, and Rhett Kempe

Dedicated to Professor Hans Gross on the occasion of his 65th birthday

Indigoid compounds with thioxo instead of oxo groups as in **B** (Scheme 1) are probably[1] still unknown, although they should provide interesting information on structure–color relationships.[1, 2] Their synthesis is difficult, since the 1,4-dithioxo-2-butene structural element **D** incorporated in **B** is closely related, through its valence-isomeric *cis* form **E**, to the (colored) 1,2-dithiine type **F**, which is not known to undergo electrocyclic ring opening to **E** in either the solid state or solution.[3] In fact, oxidation of alkali metal dithiolates **A**, even though they are thio analogues of leucoindigo, does not lead to thioxoindigoid compounds **B** but rather, depending on the heteroatom X, to valence isomers or oligomeric cyclic dialkenyldisulfides **C**.



Scheme 1.

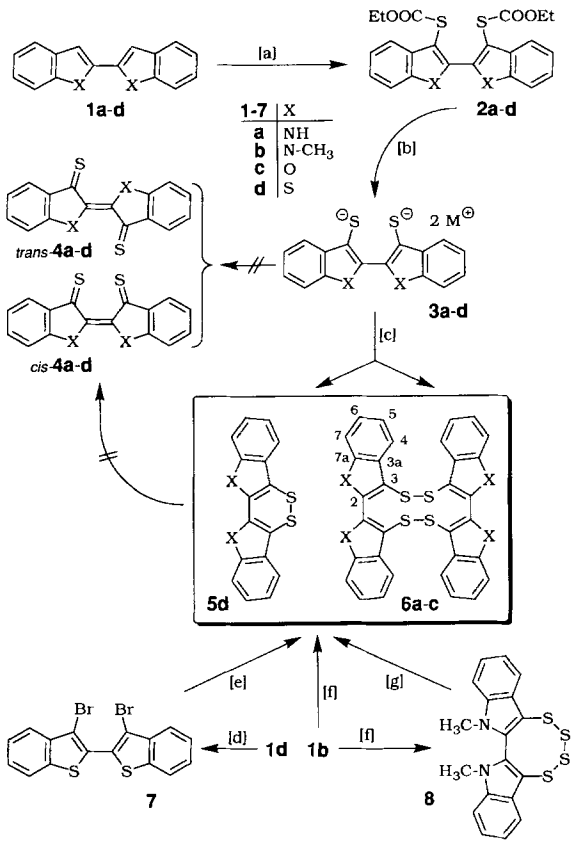
The dipotassium 3,3′-dithiolates **3a–d** corresponding to **A** were obtained by the conversion of 2,2′-biheteroaryls **1a–d**[4] into the 3,3′-di(ethoxycarbonylthio) derivatives **2a–d** by treatment with ethoxycarbonylsulfenyl chloride (Scheme 2). Saponification of **2a–d** with ethanolic potassium hydroxide[5] and in situ oxidation with aerial oxygen or $K_3[Fe(CN)_6]$ did not lead to the thioxoindigoid compounds **4a–d**, rather the following results were obtained:

a) For X = S, the di(benzo[*b*]thieno)-annelated 1,2-dithiine **5d**, a valence isomer of *cis*-**4d**, was formed exclusively as deep red needles [λ_{max}(MeCN) = 465 nm, lg ε = 4.413], which can be easily reduced back to dithiolate **3d** with $NaBH_4$. In addition **5d** was obtained by bromination of **1d** to give the 3,3′-dibromo derivative **7** followed by halogen–lithium exchange with *n*BuLi to provide 3,3′-dilithio-2,2′-di(benzo[*b*]thienyl) and, finally, by reaction with elemental sulfur.[6] The product proved to be identical with that obtained by heating 3-mercaptobenzo[*b*]thiophene and morpholine in toluene,[1b] which was referred to by the authors as "dithioxothioindigo" *trans*-**4d**. The results of an X-ray structure analysis (nonplanar ring, C-S-S-C dihedral angle 53.1°; S–S bond length 2.062 Å), the preparation, and the reactions are described in reference [7]. Unlike the nonannelated 1,2-dithiines,[3a, b] **5d** shows no tendency to extrude sulfur.

b) For X = NCH_3, O the relatively insoluble cyclic bisdisulfides **6b, c** predominate.[8, 9] According to the X-ray structure analysis of **6b** (Fig. 1),[10] two heteroarene rings (twisted relative to one other by ca. 180°) face each another, while the planes of the other two are tilted outwards; the planes of the 2,2′-biheteroaryl units are significantly twisted, in **6b** by 113.7°, in **6c** by 160.9° (C-S-S-C dihedral angles 89.5 and 75.4°, respectively). The ^1H and ^{13}C NMR spectra (Table 1) are characteristic of a dynamic structural system. In the electron impact mass spectrum (EI-MS) of **6b,c** the base peaks corresponding to the masses of **4b,c**/**5b,c** (*m*/*z* 322 and 296, respectively, are derived from twofold S–S cleavage.[11] The reaction of **1b** with S_2Cl_2 at −20 to −60 °C gave a mixture of products, from which **6b** and the cyclic tetrasulfide **8** were isolated in low yield; the structure of **8** was confirmed by X-ray structure analysis (twist of the indolyl planes 67.6°, S-S-S-S dihedral angle 78.6°). Reduction of **8** with $NaBH_4$ and subsequent aerial oxidation regenerated **6b**.

[*] Prof. Dr. W. Schroth, Dr. E. Hintzsche, Dipl.-Chem. M. Felicetti, Dr. habil. R. Spitzner
Institut für Organische Chemie der Universität Halle-Wittenberg
D-06099 Halle (FRG)
Telefax: Int. code + (345) 649-065
Prof. Dr. J. Sieler, Dr. R. Kempe
Institut für Anorganische Chemie der Universität Leipzig

[**] This work was supported by the Fonds der Chemischen Industrie.



Scheme 2. [a] **2a**: 2 equiv ClSCOOEt, CH_2Cl_2/HCOOH (2:1), 90 min −10 °C, 4 h 20 °C; 100%, m.p. 215 °C (decomp); **2b**: same as **2a**, 83%, m.p. 139 °C; **2c**: 2 equiv ClSCOOEt, $CH_2Cl_2/BF_3 \cdot Et_2O$, 1 h 20 °C, 6 h reflux; 60%, m.p. 139–140 °C; **2d**: 2 equiv ClSCOOEt, 2 equiv $TiCl_4$, $CHCl_3$, 3 h 20 °C, 1 h reflux; 87%, m.p. 98–100 °C. [b]/[c] 3 equiv KOH/EtOH, argon, 1 h reflux, 20 °C, bubbled with air; 100% **5d**, **6a**, 86% **6b**, 70% **6c**. [d] 2 equiv Br_2, $CHCl_3$, 0 °C, 3 h 20 °C; 78% **7**, m.p. 177–178 °C. [e] 1. 2 equiv *n*BuLi/Et_2O, 2.5 h −70 °C; 2. S_8, 3 h −10 °C; 3. 10% NaOH/H_2O; 4. $K_3[Fe(CN)_6]$; 61% **5d**. [f] 1 equiv S_2Cl_2, CH_2Cl_2, 6 h −60 °C; 10% **6b**; −20 °C: 16% **8**. [g] $NaBH_4$ (excess), EtOH; bubbled with air.

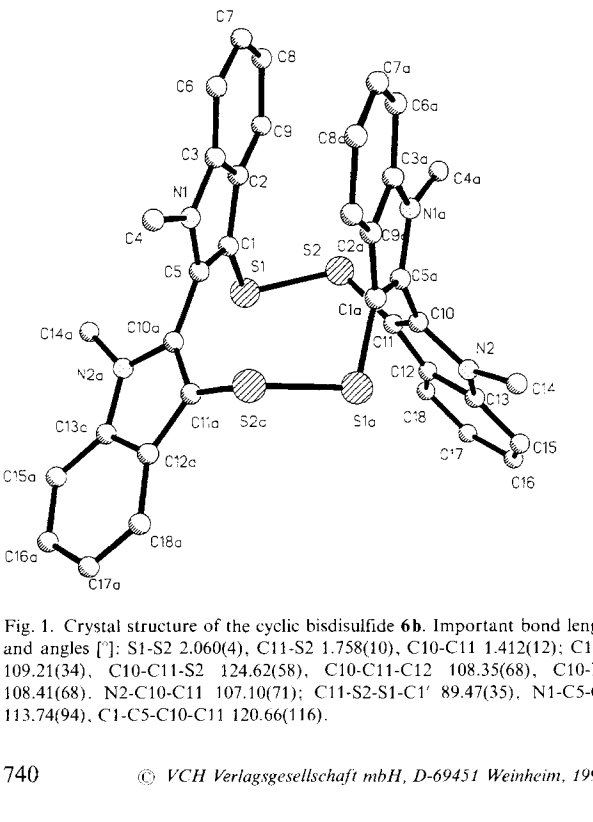


Fig. 1. Crystal structure of the cyclic bisdisulfide **6b**. Important bond lengths [Å] and angles [°]: S1-S2 2.060(4), C11-S2 1.758(10), C10-C11 1.412(12); C11-S2-S1 109.21(34), C10-C11-S2 124.62(58), C10-C11-C12 108.35(68), C10-N2-C13 108.41(68), N2-C10-C11 107.10(71); C11-S2-S1-C1′ 89.47(35), N1-C5-C10-N2 113.74(94), C1-C5-C10-C11 120.66(116).

Table 1. Physical and spectroscopic data for selected compounds [a].

5d: Deep red needles; m.p. 215 °C (ref. [1b]: 213–215 °C). UV (MeCN): λ_{max} (lgε) = 227 (4.582), 244 (4.347, sh), 274 (4.045), 331 (4.240), 465 nm (4.413); ^{1}H NMR ($CDCl_3$): δ = 7.30–7.50 (m, 4H, arene H), 7.75–7.86 (m, 4H, arene H) (multiplets in a 1:1 ratio, ABCD spectrum); ^{13}C NMR ($CDCl_3$): δ = 120.9 (C-3), 122.8 (C-7), 123.4 (C-4), 125.5, 125.8 (C-5/C-6 exchangeable signals), 134.1 (C-2), 137.0 (C-3a), 138.5 (C-7a); MS (70 eV): *m/z* (%): 328 (100) [M^+], 296 (50) [M^+ − S], 164 (14) [$M/2^+$].

6a: Yellow powder, insoluble; m.p. >360 °C (decomp). MS (70 eV): *m/z* (%): 588 (5) [M^+], 556 (9) [M^+ − S], 294 (100) [$M/2^+$], 261 (29) [$M/2^+$ − SH].

6b: Yellow plates; m.p. 319–320 °C (decomp). UV ($CHCl_3$): λ_{max} (lgε) = 235.5 (4.54), 300 nm (4.27); ^{1}H NMR ([D_{18}]HMPT, 500 MHz): δ = 3.45 (s, 12H, $4CH_3$), 7.09–7.30 (m, 12H, arene H), 7.74–7.81 (m, 4H, arene H); ^{13}C NMR ([D_{18}]HMPT, 500 MHz): δ [b] = 133.9, 132.0, 132.1 (C-2), 112.0, 106.9, 110.4 (C-3), 123.6, 123.4, 123.2/121.5, 120.6, 120.5/119.4, 118.9, 118.4 (C-4, C-5, C-6), 111.4, 111.2, 109.5 (C-7), 139.3, 137.9, 138.5 (C-7a), 128.5, 126.5, 127.9 (C-3a), 31.8, 31.5, 31.2 (CH_3); MS (70 eV) [c]: *m/z* (%): 644 (6) [M^+], 612 (23) [M^+ − S], 580 (19) [M^+ − 2S], 548 (45) [M^+ − 3S], 322 (100) [$M/2^+$].

6c: Brick-red needles; m.p. 244 °C (decomp). UV (CH_2Cl_2): λ_{max} (lgε) = 243 (4.14), 334 (4.13), 473 nm (3.26); ^{1}H NMR ([D_{18}]HMPT, 500 MHz): δ = 6.73–6.74 (m, 4H, C-4-H), 7.29–7.30 (m, 4H, C-6-H), 7.57–7.60 (m, 4H, C-5-H), 7.88–7.90 (m, 4H, C-7-H); ^{13}C NMR ([D_{18}]HMPT, 500 MHz): δ [b] = 148.8, 145.6 (C-2), 115.6, 109.7 (C-3), 120.2, 120.9 (C-4), 125.0, 125.3/128.3, 127.6 (C-5, C-6), 112.7, 111.2 (C-7), 154.1, 155.1 (C-7a), 128.6, 125.2 (C-3a); MS (70 eV) [c]: *m/z* (%): 592 (8) [M^+], 296 (100) [$M/2^+$], 264 (9) [$M/2^+$ − S].

8: Pale yellow prisms; m.p. 303–304.5 °C (decomp). UV ($CHCl_3$): λ_{max} (lgε) = 235 (4.31), 295 nm (4.18); MS (70 eV): *m/z* (%): 386 (17) [M^+], 322 (99) [M^+ − 2S], 290 (100) [M^+ − 3S], 274 (61) [M^+ − 3S − CH_4].

11a: Brick-red needles; m.p. 66 °C. UV (MeCN): λ_{max} (lgε) = 260 (3.54, sh), 307 (3.98), 425 nm (3.22); ^{1}H NMR ($CDCl_3$): δ = 6.83, 6.85, (d, 2H, arene H; J = 4.0 Hz), 7.21, 7.23 (d, 2H, arene H; J = 4.0 Hz); ^{13}C NMR ($CDCl_3$): δ = 123.8, 125.1, 126.7, 134.3 (4C, arene C); MS (70 eV): *m/z* (%): 228 (100) [M^+], 196 (20) [M^+ − S], 164 (4) [M^+ − 2S], 151 (16) [M^+ − C_6H_5].

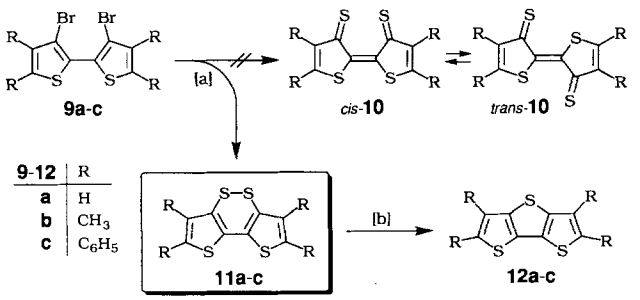
11b: Red blocks; m.p. 202–203 °C. UV (MeCN): λ_{max} (lgε) = 238 (4.22, sh), 296 (4.21), 335 (4.18), 441 nm (3.52); ^{1}H NMR ($CDCl_3$): δ = 1.79 (s, 6H, $2CH_3$), 1.74 (s, 6H, $2CH_3$); ^{13}C NMR ($CDCl_3$): δ = 12.8, 13.5 ($2CH_3$), 125.3, 130.5, 131.4, 131.8 (arene C); MS (70 eV): *m/z* (%): 284 (100) [M^+], 269 (16) [M^+ − CH_3], 252 (40) [M^+ − S], 251 (61) [M^+ − SH].

11c: Orange-red needles; m.p. 304–306 °C. UV ($CHCl_3$): λ_{max} (lgε) = 290 (4.29), 401 nm (4.08); ^{1}H NMR ($CDCl_3$): δ = 7.08–7.37 (m, 20H, arene H); ^{13}C NMR ($CDCl_3$): δ = 127.4, 127.6, 127.9, 128.3, 128.4, 128.9, 130.1, 130.7 (8C, phenyl), 133.2, 134.5, 136.8, 138.7 (4C, thiophene rings); MS (70 eV): *m/z* (%): 532 (100) [M^+], 500 (50) [M^+ − S], 466 (13) [M^+ − 2SH].

[a] Correct elemental analyses were obtained for all compounds. [b] Three sets of signals for **6b** (relative intensities A ≈ B > C) and two sets of signals for **6c** (relative intensities: A > B), reversible increase of C (**6b**) or B (**6c**) at increased temperature (80 °C); assignments based on the attached proton test (APT) in the ^{13}C NMR spectrum. [c] Cf. ref. [11b].

c) When X = NH, oxidation led to an amorphous and extremely insoluble mixture of products which melted above 360 °C over a wide range and was separated into its components only with difficulty. The same result was obtained from the stepwise reaction of **1a** with iodine and thiourea followed by alkaline hydrolysis and oxidation analogous to the procedure in reference [12]. The mass spectrum up to *m/z* 600 contains a peak consistent with **6a** (*m/z* 588) together with a base peak corresponding to **4a**/**5a** (*m/z* 294). Reduction of the product with $NaBH_4$ regenerated the starting material **3a**. The presence of oligomeric cyclic disulfides including **6a** can be inferred (associated by intermolecular NH hydrogen bonds according to the IR spectrum: strong NH bands at 2700 ± 50 and 3340 cm^{-1}).

Similarly in the 2,2′-dithienyl series no thioxoindigoid compounds of type *cis*- or *trans*-**10** were obtained (Scheme 3): the reaction of 3,3′-dibromo-2,2′-dithienyls **9a–c**[13] with *n*BuLi and elemental sulfur and subsequent oxidation of the 3,3′-dithiolate salts thus formed led to the valence isomeric dithieno-2,2′-dithiines **11a–c**. The cyclic disulfide structure appeared both in solution (no indication in the ^{13}C NMR spectrum of a C=S group as in **10**) and the solid state. The X-ray structure analysis showed a C-S-S-C dihedral angle of 50.85° for **11a** and 52.55°



Scheme 3. [a] 1. 2 equiv nBuLi/Et_2O, 2.5 h, −70 °C; 2. S_8, 3 h −10 °C; 3. 10% NaOH/H_2O; 4. $K_3[Fe(CN)_6]$; 19% **11a**, 64% **11b**, 61% **11c**. [b] Cu powder (mixed), 45 min 200 °C, extraction with hot $CHCl_3$; 47% **12a** (m.p. 64–66 °C, ref. [19]: 66.5–67 °C); 50% **12b** (m.p. 206–207 °C); 69% **12c** (m.p. 298 °C).

for **11b** (see Fig. 2).[10] Although colored like the 3,6-disubstituted 1,2-dithiines,[3a,e] compounds **11** do not spontaneously extrude sulfur under mild conditions (in daylight in solution at room temperature). Only with copper bronze at high temperatures (melt) could the sulfur be removed with the formation of dithieno[3,2-*b*;2′,3′-*d*]thiophenes **12a–c**.[14]

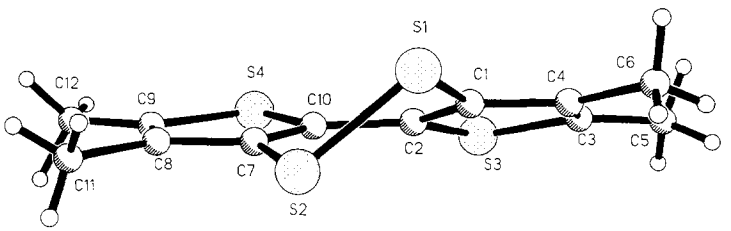


Fig. 2. Crystal structure of the thieno-annelated 1,2-dithiine **11b**. Important bond lengths [Å] and angles [°]: S1-S2 2.059(1), S2-C7 1.763(2), S1-C1 1.761(2), C7-C10 1.365(3), C1-C2 1.376(3), C2-C10 1.450(3); S1-C1-C2 120.99(13), C1-C2-C10 125.06(16), C1-C2-S3 109.98(14), C2-S3-C3 92.65, C4-C3-S3 111.54(14); C1-S1-S2-C7 52.55(10), C1-C2-C10-C7 21.45(26).

Attempts to convert the cyclic disulfides **5**, **6**, and **11** to **4** and **10**, respectively, by heating them above their melting points or in high boiling solvents (e.g. decalin) have so far not succeeded. From our results it can be concluded that thioindigoid compounds **B** (≡ **4a–d**, **10**) cannot be prepared by the "classical" route (oxidation of thioanalogues of leuco compounds) and that their ability to exist at all, either in the solid state or in solution at room temperature, is questionable.[15] It remains to be seen whether compounds of type **B** can be generated and spectroscopically characterized in low-temperature matrices.

The predominance of the cyclic disulfides **5**, **6**, and **11** as opposed the open-ring thioxo valence isomers finds parallels in some other S-heterocycles such as 1,2-dithietes,[16] 1,2-dithiolium-3-olates,[17] 1,2-dithiolo[3,4-*d*]-1,2-dithioles,[18] 1,2-dithiapentalenes,[19] and 1,7,8-trithiapentalenes.[20]

Received: October 25, 1993 [Z 6447 IE]
German Version: *Angew. Chem.* **1994**, *106*, 808

[1] a) Compare the failed attempts to prepare dithioxoindigo by thionating indigo with the transfer of sulfur: H. Sieghold, Dissertation, Universität Göttingen, **1973**; b) H. Hartmann, S. Scheithauer, *J. Prakt. Chem.* **1969**, *311*, 827–843 (corrected in favor of the valence isomeric 1,2-dithiine structure **5d**; see the following text and ref. [7]); c) G. Glas, R. Gompper, M. Junius, R. Mertz, H.-U. Wagner, H. Nöth, R. Staudigl, *ibid.* **1990**, *332*, 949–967 (strictly speaking this deals with N-isoindigoid species, cf. ref. [15]); d) cf. further statements which justify considerable doubts: L. Raffa, *Gazz. Chim. Ital.* **1942**, *72*, 549–557 [*Chem. Abstr.* **1944**, *38*, 5499 b (thioxoindigo and dithioxoisoindigo as a green powder); A. A. El-Kateb, I. T. Hennawy, R. Shabana, F. H. Osman, *Phosphorus Sulfur Relat. Elem.* **1984**, *20*, 329–332 (dithioxoisoindigo as a gray crystalline product); A. A. El-Kateb, R. Shabana, F. H. Osman, *Z. Naturforsch. B* **1984**, *39*, 1614–1616 (as a gray powder).

[2] Concerning the thioxo function as a chromophoric structural element: a) J. Voss, *Methoden Org. Chem. (Houben-Weyl) 4th ed. 1952* · Vol. E11, part 1, **1985**, p. 195 ff.; b) A. Maciejewski, R. P. Steer, *Chem. Rev.* **1993**, *93*, 67–98; c) J. Fabian, H. Viola, R. Mayer, *Tetrahedron* **1967**, *23*, 4323–4329.

[3] a) Synthesis and characterization: W. Schroth, F. Billig, H. Langguth, *Z. Chem.* **1965**, *5*, 353–354, W. Schroth, F. Billig, G. Reinhold, *Angew. Chem.* **1967**, *79*, 685–686; *Angew. Chem. Int. Ed. Engl.* **1967**, *6*, 698–699; b) see also: H. Behringer, E. Meinetsberger, *Liebigs Ann. Chem.* **1981**, 1729–1750; *ibid.* **1981**, 1928–1959; *ibid.* **1982**, 315–341; J. R. Moran, R. Huisgen, I. Kalwinsch, *Tetrahedron Lett.* **1985**, *26*, 1849–1852; K. Hartke, E. Pfleging, *Liebigs Ann. Chem.* **1988**, 933–941; c) as a compound in plants: F. Bohlmann, K.-M. Kleine, *Chem. Ber.* **1965**, *98*, 3081–3086; J. T. Mortensen, J. S. Sørensen, N. A. Sørensen, *Acta Chem. Scand.* **1964**, *18*, 2392–2394; G. H. N. Towers, Z. Abramowski, A. J. Finlayson, A. Zucconi, *Planta Med.* **1985**, *51*, 225–229; d) on the preference of **F** versus **E**/**D** in solution: R. Radeglia, H. Poleschner, W. Schroth, *Z. Naturforsch. B* **1988**, *43*, 605–610; e) on color theory (λ_{max} = 450–550 nm) and molecular structure: R. Borsdorf, H.-J. Hofmann, H.-J. Köhler, M. Scholz, J. Fabian, *Tetrahedron* **1970**, *26*, 3227–3231; J. Fabian, P. Birner, *Collect. Czech. Chem. Commun.* **1988**, *53*, 2096–2115; R. Cimiraglia, J. Fabian, B. A. Hess, Jr., *J. Mol. Struct.* **1991**, *230*, 287–293; f) cf. reviews: U. Eisner, T. Krishnamurthy, *Int. J. Sulfur Chem. Part B* **1972**, *7*, 101–107; F. Freeman, D. S. H. L. Kim, E. Rodriguez, *Sulfur Rep.* **1989**, *9*, 207–256.

[4] a) Approach to **1a**: W. Madelung, *Justus Liebigs Ann. Chem.* **1924**, *405*, 58–95; b) to **1b**: J. Bergman, N. Eklund, *Tetrahedron* **1980**, *36*, 1439–1443; c) to **1c**: F. Toda; M. Nakagawa, *Bull. Chem. Soc. Jpn.* **1958**, *32*, 514–516; d) to **1d**: L. J. Pandya, D. S. Rao, B. D. Tilak, *J. Sci. Ind. Res. Sect. B.* **1959**, *18*, 516–521 (*Chem. Abstr.* **1960**, *54*, 17391 d) or analogous to the method in ref. [13b].

[5] Example with arenes: W. Schroth, M. Hassfeld, W. Schiedewitz, C. Pfotenhauer, *Z. Chem.* **1977**, *17*, 411–413; analogous thiolation of enolizable ketones: Y. Sanemitsu, S. Kawamura, Y. Tanabe, *J. Org. Chem.* **1992**, *57*, 1053–1056.

[6] Comparable synthesis of dibenzo[*c*,*e*]-1,2-dithiine from 2,2′-dibromodiphenyl: S. Cossu, G. Delogu, D. Fabbri, P. Maglioli, *Org. Prep. Proced. Int.* **1991**, *23*, 455–457.

[7] W. Schroth, E. Hintzsche, H. Viola, R. Winkler, H. Klose, R. Boese, R. Kempe, J. Sieler, *Chem. Ber.* **1994**, *127*, 401–408.

[8] Compare also the reactions of 2,2′-dilithio-1,1′-binaphthyl with S_8 to give dinaphtho[2,1-*c*;1′,2′-*e*]-1,2-dithiine and with selenium to give the "dimeric" cyclic bis-diselenide: S. Murata, T. Suzuki, A. Yanagisawa, S. Suga, *J. Heterocycl. Chem.* **1991**, *28*, 433–438.

[9] **6c** is red both in solution and in the solid state (see Table 1); this color is usually characteristic of the 1,2-dithiine system [3a, e]; however, such a system (like **5c**) can be disregarded, cf. ref. [11b].

[10] Crystal structure data: **6b** (Fig. 1): $C_{36}H_{28}N_4S_4$; triclinic, *C*2/*c* (No. 15), a = 22.523(6), b = 9.378(3), c = 18.956(6) Å, V = 3087.6 Å^3, R = 0.0406, R_w = 0.036, Z = 4. **11b** (Fig. 2): $C_{12}H_{12}S_4$; triclinic, $P\bar{1}$ (No. 2), a = 7.637, b = 7.921(1), c = 12.08(1) Å, V = 648.3 Å^3, R = 0.0318, R_w = 0.0367, Z = 2. Diffractometer: STADI4 (Fa. STOE), radiation: $Mo_{K\alpha}$ (λ = 0.71069 Å), program: SHELXS, SHELXS76. Further details of the crystal structure investigation may be obtained from the Fachinformationszentrum Karlsruhe, D-76344 Eggenstein-Leopoldshafen (FRG), on quoting the depository number CSD-57853, the names of the authors, and the journal citation.

[11] These base peaks appear in the mass spectra of **2b**, **c** without any recognizable intermediate degradation steps, which is evidence for the thermodynamic preference of the **4**/**5** structural system in the dilute gas phase. b) Mass-analyzed ion kinetic energy (MIKE) spectra, low-voltage mass spectra (20 eV) and mass chromatography (plot of the intensity of selected ions in the EI mass spectra versus time) demonstrate the absence of any noteworthy amounts of **4b**, **c** or **5b**, **c** in the mixture.

[12] R. G. Woodbridge, III, G. Dougherty, *J. Am. Chem. Soc.* **1950**, *72*, 4320–4322.

[13] a) Approach to **9a**: E. Khor, S. C. Ng, H. C. Li, S. Chai, *Heterocycles* **1991**, *32*, 1805–1812; b) to **9b**: S. Gronowitz, A. Wiersema, *Acta Chem. Scand.* **1970**, *24*, 2593–2611; c) to **9c**: E. Hintzsche, Dissertation, Universität Halle-Wittenberg, **1993**.

[14] Independent syntheses: F. Stoyanovich, F. Fedorov, *J. Org. Chem. USSR Engl. Transl.* **1965**, *1*, 1296; F. de Jong, M. J. Janssen, *J. Org. Chem.* **1971**, *36*, 1645–1648.

[15] Compounds of the N-isoindigoid series are known (thioamide resonance): W. Schroth, M. Felicetti, E. Hintzsche, R. Spitzner, J. Sieler, M. Pink, unpublished; cf. also ref. [1c].

[16] Cf. W. Kusters, P. de Mayo, *J. Am. Chem. Soc.* **1974**, *96*, 3502–3511; F. Diehl, H. Meyer, A. Schweig, B. A. Hess, Jr., J. Fabian, *J. Am. Chem. Soc.* **1989**, *111*, 7651–7653.

[17] R. Mayer, J. Fabian, H. Viola, J. Jakisch, *Phosphorus Sulfur Relat. Elem.* **1987**, *31*, 109–122.

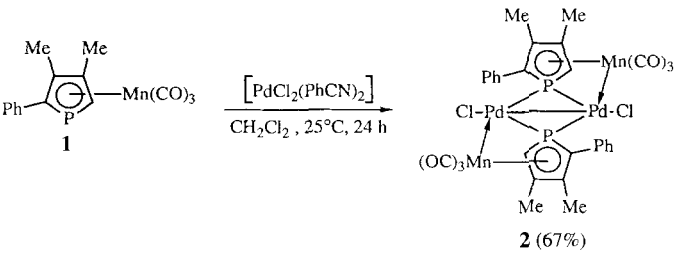
[18] H.-D. Stachel, M. Schorp, T. Zoukas, *Liebigs Ann. Chem.* **1992**, 1039–1044.

[19] K. Hafner, B. Stowasser, V. Sturm, *Tetrahedron Lett.* **1985**, *26*, 189–192.

[20] See also the general problems of "no bond resonance" in comparable disulfide systems: G. Calzaferri, R. Gleiter, *J. Chem. Soc. Perkin Trans. 2* **1975**, 559–566; R. Gleiter, R. Gygax, *Top. Curr. Chem.* **1976**, *63*, 51–88.

The Reactivity of Phosphacymantrenes towards Palladium(II) and Palladium(0) Compounds: Synthesis, Structure, and Chemistry of Pd_2Mn_2 and Pd_3Mn_4 Arrays**

Lionel Brunet, François Mercier, Louis Ricard, and François Mathey*



The presence of nonbonding e_{2g} electrons on the iron atom of ferrocene implies the possibility of dative bonds between iron and electron-deficient transition metal centers. Indeed, such compounds have been found for gold(I)[1], mercury(II)[2], palladium(II),[3-5] and platinum(II).[4] In order to prevent both the dissociation of such complexes and redox processes yielding ferricinium salts, cyclopentadienyl ligands with chelating substituents are generally used to hold the electron-accepting metal center close to the iron center. In 1986 Roberts, Silver, and Wells[6] demonstrated that 1,1'-diphosphaferrocenes also form such complexes with copper(I) and silver(I), but these complexes were not structurally characterized. Their results reflect the similarity of the electronic structures of ferrocene and diphosphaferrocene[7] and the greater resistance of diphosphaferrocene toward oxidation.[8]

Theoretically, the manganese center in phosphacymantrenes should also be able to participate in their coordination chemistry, since their HOMOs have predominantly 3d(Mn) character.[9] A priori, either a two-electron donation by manganese or an insertion into the P–Mn bond might be observed. These two possibilities have indeed found to occur with palladium as the electron-accepting metal center.

With palladium(II), the most satisfactory results were obtained with 3,4-dimethyl-2-phenylphosphacymantrene (**1**).[10] The reaction of **1** with $[PdCl_2(PhCN)_2]$ in dichloromethane at room temperature was monitored by ^{31}P NMR spectroscopy. Initially, the resonance of **1** at $\delta = -35$ disappears, and two new signals appear at $\delta = 12.9$ and 24.6. These most likely arise from two classical isomeric or diastereomeric $[Pd(\mathbf{1})_2Cl_2]$ complexes. After some time these complexes disappear, and a new complex **2** is formed with a signal at $\delta(^{31}P) = 116.5$.

The X-ray crystal structure analysis of **2** indicates the presence of a Mn-Pd-Pd-Mn chain and a completely planar $Mn_2Pd_2Cl_2P_2$ core (Fig. 1). At 2.8373(3) Å the Pd–Pd separation is shorter than the Pd–Pd bonds in some Pd_3 clusters with phosphido bridges.[12] Similarly, the Pd–Mn separation (2.7812(6) Å) falls in the range of genuine Pd–Mn bonds.[13] The Pd–P bond lengths are in the normal range,[12] although significantly different (2.286(1) and 2.2268(9) Å). The most fascinating observation concerns the P–Mn separation, which at 2.3712(9) Å clearly indicates that there is still a bond between phosphorus and manganese. For 2,5-diphenylphosphacymantrene (**4**) we have recorded a P–Mn distance of 2.392(1) Å,[14] and a value of 2.376(3) Å was reported for $[W(\mathbf{4})(CO)_5]$.[15] Since manganese is still η^5-bonded to the phospholyl ring, and since both IR and X-ray analysis exclude bridging carbonyl ligands, the Pd–Mn bond necessarily corresponds to the donation of two electrons by manganese to palladium. The carbonyl ligands are a sensitive probe for this transfer of electrons away from manganese. The CO stretching frequencies (Table 1) increase from 2017.2 and 1937.7 in **1** to 2018.2 and 1964.8 cm^{-1} in **2**. The $\delta(^{13}CO)$ signal shifts from 224 in **1** to 220 in **2**. The Mn–CO separations are 1.791–1.794(4) in **4** and 1.804–1.825(4) Å in **2**; the corresponding CO bond lengths are 1.149–1.155(5) in **4** and 1.132–1.149(5) Å in **2**. All these data suggest that the carbonyl ligands are significantly less polarized in **2** than in **1**, which indicates a lower electronic density on manganese. From another standpoint, in **2** phosphorus shares its two nonbonding electrons with the two palladium atoms.

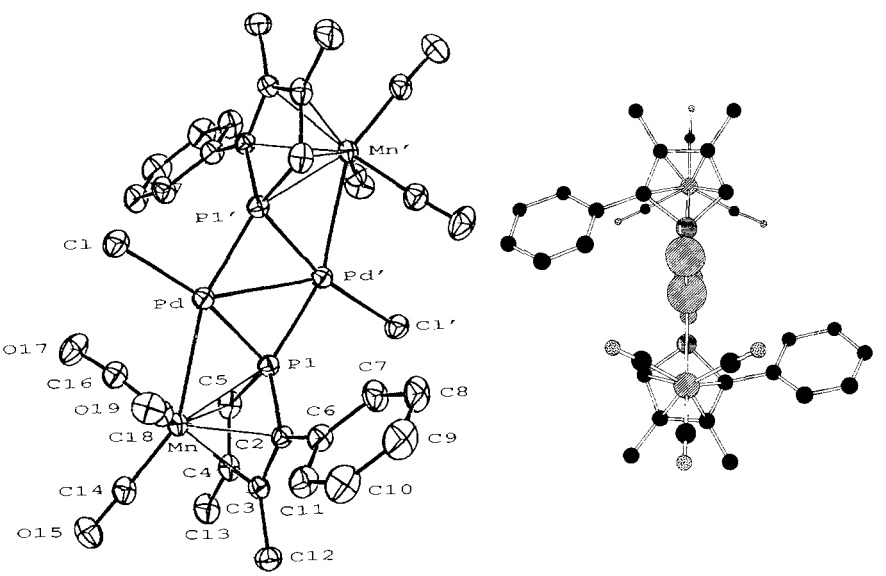


Fig. 1. Left: Crystal structure of **2** [11] (ellipsoids at the 50% probability level, hydrogen atoms omitted for clarity). Important bond lengths [Å] and angles [°]: Pd-Pd' 2.8373(3), Pd-Mn 2.7812(6), Pd-Cl 2.338(1), Pd-P1 2.286(1), Pd-P1' 2.2268(9), Mn-P1 2.3712(9), Mn-C2 2.227(3), Mn-C3 2.208(3), Mn-C4 2.180(4), Mn-C5 2.186(4), P1-C2 1.773(3), P1-C5 1.756(3), C2-C3 1.411(5), C3-C4 1.450(5), C4-C5 1.409(6); Pd'-Pd-Mn 104.87(1), Pd'-Pd-Cl 142.77(2), Pd'-Pd-P1 50.12(2), Pd'-Pd-P1' 51.97(2), Mn-Pd-P1 54.76(2), Mn-Pd-P1' 156.83(3), Cl-Pd-P1 167.09(3), Cl-Pd-P1' 90.81(3), P1-Pd-P1' 102.09(3), Pd-P1-Pd' 77.91(3), C2-P1-C5 92.1(2). Right: A Chem-Draw view of one molecule of **2** showing its perfect symmetry and the planarity of the $Mn_2Pd_2Cl_2P_2$ core.

This kind of bonding has some precedent for two-coordinate phosphorus centers.[16] Finally, the ^1H and ^{13}C NMR spectra of crude **2** (Table 1) indicate the presence of a second isomer in which the two phenyl groups are probably on the same side of the $Mn_2Pd_2Cl_2P_2$ plane.

[*] Prof. Dr. F. Mathey, L. Brunet, Dr. F. Mercier, Dr. L. Ricard
Laboratoire "Hétéroéléments et Coordination" URA 1499 CNRS
DCPH, Ecole Polytechnique
F-91128 Palaiseau Cedex (France)
Telefax: Int. code + (1)69333010

[**] This research was supported by Air Liquide (grant to L. B.).

Table 1. Selected spectroscopic data for **1**–**12** [a].

1: δ^{31}P ($CDCl_3$) = – 35.3; ^{1}H NMR ($CDCl_3$): δ = 2.13 (s, CH_3), 2.18 (s, CH_3), 4.52 (d, ^2J(H,P) = 35.1 Hz, CHP); ^{13}C NMR ($CDCl_3$): δ = 13.40 (s, Me), 16.07 (s, Me), 95.28 (d, ^1J(C,P) = 62.6 Hz, CHP), 110.11 (d, ^2J(C,P) = 7.1 Hz, *C*Me), 111.79 (d, ^2J(C,P) = 4.5 Hz, *C*Me), 119.97 (d, ^1J(C,P) = 59.2 Hz, PhCP), 135.01 (d, ^2J(C,P) = 17.3 Hz, Ph, *i*-C), 224.08 (s, CO); IR (CH_2Cl_2): $\tilde{\nu}$(CO) = 2017.2 (vs), 1937.7 (vs br) cm^{-1}

2: δ^{31}P(CH_2Cl_2) = 116.5; ^{1}H NMR ($CDCl_3$) (M = major, m = minor isomer): δ = 2.32 (s, Me, m), 2.37 (s, Me, M), 4.36 (pseudo-t, $\sum|^2J$(H,P) + ^4J(H,P)| = 32.4 Hz, CHP, m), 4.60 (pseudo-t, $\sum|^2J$(H,P) + ^4J(H,P)| = 32.0 Hz, CHP, M); ^{13}C NMR ($CDCl_3$): δ = 13.42 (s, Me), 16.41 (s, Me), 86.62 (pseudo-t, $\sum|^1J$(C,P) + ^3J(C,P)| = 16.4 Hz, CHP), 103.24 (s, *C*Me, M), 104.02 (s, *C*Me, m), 104.27 (pseudo-t, *C*Me, m), 104.85 (pseudo-t, $\sum|^2J$(C,P) + ^4J(C,P)| = 14.2 Hz, *C*Me, M), 112.44 (pseudo-t, $\sum|^1J$(C,P) + ^3J(C,P)| = 18.5 Hz, PhCP, M), 113.00 (pseudo-t, PhCP, m), 220.09 (s, CO); IR (CH_2Cl_2): $\tilde{\nu}$(CO) = 2018.2 (vs), 1964.8 (vs br) cm^{-1}

3: δ^{31}P (CH_2Cl_2) = 135.3 (M), 136.2 (m); ^{13}C NMR ($CDCl_3$): δ = 12.82 (s, Me), 15.8 (s, Me), 83.22 (pseudo-t, CH-P, m), 83.72 (pseudo-t, $\sum|^1J$(C,P) + ^3J(C,P)| = 18.4 Hz, CHP, M), 101.80 (s, *C*Me, M), 102.77 (pseudo-t, $\sum|^2J$(C,P) + ^4J(C,P)| = 13.5 Hz, *C*Me, m), 103.18 (s, *C*Me, m), 103.69 (pseudo-t, $\sum|^2J$(C,P) + ^4J(C,P)| = 12.6 Hz, *C*Me, M), 108.12 (pseudo-t, PhCP, m), 108.35 (pseudo-t, $\sum|^1J$(C,P) + ^3J(C,P)| = 18.6 Hz, PhCP, M); IR (CH_2Cl_2): $\tilde{\nu}$(CO) = 2016.5 (vs), 1957.8 (s br) cm^{-1}

4: δ^{31}P ($CDCl_3$) = – 29.7; ^{1}H NMR ($CDCl_3$): δ = 5.95 (s, CH); ^{13}C NMR ($CDCl_3$): δ = 90.85 (d, ^2J(C,P) = 5.2 Hz, CH), 120.00 (d, ^1J(C,P) = 62.0 Hz, PCPh), 134.88 (d, ^2J(C,P) = 16.3 Hz, Ph, *i*-C), 223.16 (s, CO); IR (CH_2Cl_2): $\tilde{\nu}$(CO) = 2022.5 (vs), 1946.7 (vs br) cm^{-1}

5: δ^{31}P ($CDCl_3$) = + 12.2 (br); ^{1}H NMR ($CDCl_3$): δ = 5.61 (s br, 1 H, CH), 5.96 (s br, 1 H, CH) (the two sides of the ring are nonequivalent because of the torsion of the molecule about Pd1); ^{13}C NMR ($CDCl_3$): δ = 87.23 (s), 107.54 (m, PCPh), 134.36 (s, Ph, *i*-C), 223.97 (s, CO); IR (CH_2Cl_2): $\tilde{\nu}$(CO) = 2011.5 (vs), 1996.2 (s), 1949.3 (vs br) cm^{-1}

6: δ^{31}P ($CDCl_3$) = + 20.4; ^{1}H NMR (C_4D_8O): δ = 6.01 (d, ^3J(H,P) = 19.4 Hz, CH); ^{13}C NMR (C_4D_8O): δ = 74.19 (d, ^1J(C,P) = 51.3 Hz, PCPh), 78.61 (d, ^2J(C,P) = 12.9 Hz, CH), 224.23 (CO); IR (CH_2Cl_2): $\tilde{\nu}$(CO) 2010.9 (vs), 1953.0 (s br) cm^{-1}

7: δ^{31}P (CH_2Cl_2) = 16.6; ^{13}C NMR (C_4D_8O): δ = 76.04 (d, ^1J(C,P) = 53.2 Hz, PCPh), 80.05 (d, ^2J(C,P) = 13.3 Hz, CH)

8: δ^{31}P(CH_2Cl_2) = 13.5; ^{1}H NMR (C_4D_8O): δ = 2.17 (d, ^2J(H,P) = 10.7 Hz, CH_3), 5.90 (d, ^3J(H,P) = 20.5 Hz, CH); ^{13}C NMR (C_4D_8O): δ = 74.95 (d, ^1J(C,P) = 51.9 Hz, PCPh), 78.96 (d, ^2J(C,P) = 13.7 Hz, CH); IR (CH_2Cl_2): $\tilde{\nu}$(CO) = 2011.4 (s), 1951.5 (vs br) cm^{-1}

9: δ^{31}P (CH_2Cl_2) = 28.0; ^{1}H NMR ($CDCl_3$): δ = 3.97 (m, CH_2), 5.28 (d, ^3J(H,P) = 20.6 Hz, CH); ^{13}C NMR (CD_2Cl_2): δ = 37.52 (s, CH_2), 74.59 (d, ^1J(C,P) = 50.5 Hz, PCPh), 79.14 (d, ^2J(C,P) = 12.1 Hz, CH); IR (CH_2Cl_2): $\tilde{\nu}$(CO) = 2011.7 (vs), 1953.5 (s br) cm^{-1}

10: δ^{31}P ($CDCl_3$): ABX: δ_A = 34.7, δ_B = 36.2, δ_X = 62.81, J_{AB} = 46, J_{BX} = 9 Hz

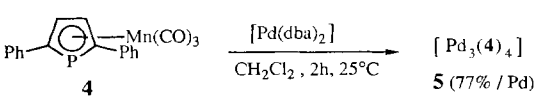
11: δ^{31}P (CD_2Cl_2): ABX: δ_A = 26.7, δ_B = 27.7, δ_X = 63.27, J_{AB} = 43.8, J_{AX} = 12.3 Hz; ^{1}H NMR ($CDCl_3$): δ = 5.27 (d, ^3J(H,P) = 21.8 Hz, CH); ^{13}C NMR ($CDCl_3$): δ = 64.67 (d, ^1J(C,P) = 118.9 Hz, PCPh), 76.18 (d, ^2J(C,P) = 33.1 Hz, CH), 229.04 (CO); IR (CH_2Cl_2): $\tilde{\nu}$(CO) = 1976.0 (vs), 1894.7 (vs), 1871.6 (s) cm^{-1}

12: δ^{31}P (CH_2Cl_2): ABX: δ_A = 33.9, δ_B = 34.8, δ_X = 62.2, J_{AB} = 43.7, J_{AX} = 8.5 Hz

[a] 200.13 MHz ^{1}H, 50.32 MHz ^{13}C, 81.01 MHz ^{31}P NMR spectra.

A similar reaction with PdI_2 gave complex **3**, which according to spectroscopic data (Table 1) has a $[Pd_2(\mathbf{1})_2I_2]$ formulation similar to that of **2**. As expected, **3** is formed as a mixture of two isomers.

With palladium(0) the most satisfactory results were obtained with 2,5-diphenylphosphacymantrene (**4**).[17] The reaction with $[Pd(dba)_2]$ (dba = dibenzylideneacetone) essentially gives one product, **5**, with a 3:4 stoichiometry. A clue to the best formula-



4 **5** (77% / Pd)

tion of **5** comes from the comparison of its structure (Fig. 2) with those of free **4**[14] and $[W(\mathbf{4})(CO)_5]$.[15] Whereas the overall structure of **4** does not change drastically (in particular, the P–C

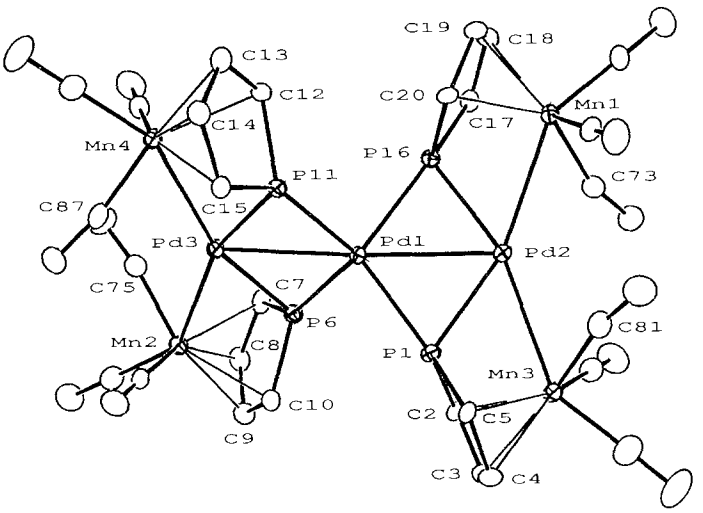
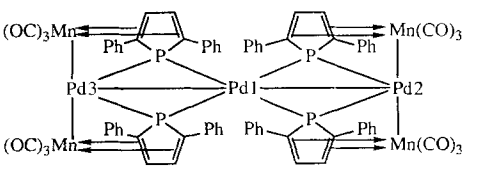


Fig. 2. Crystal structure of **5** [18] (ellipsoids at the 50% probability level, hydrogen atoms and phenyl groups omitted for clarity). Important distances [Å] and angles [°]: Pd1-Pd2 2.8004(5), Pd1-Pd3 2.7877(5), Pd1-P1 2.355(1), Pd1-P6 2.352(1), Pd1-P11 2.384(1), Pd1-P16 2.362(1), Pd2-Mn1 2.7939(8), Pd2-Mn3 2.8142(9), Pd2-P1 2.359(1), Pd2-P16 2.343(1), Pd3-Mn2 2.7332(9), Pd3-Mn4 2.8297(8), Pd3-P6 2.374(1), Pd3-P11 2.322(1), Mn1···P16 2.474(1), Mn2···P6 2.470(2), Mn3···P1 2.473(1), Mn4···P11 2.489(1), P1-C2 1.791(5), P1-C5 1.799(5), P6-C7 1.803(5), P6-C10 1.795(5), P11-C12 1.795(5), P11-C15 1.800(5), P16-C17 1.807(5), P16-C20 1.800(5); Pd2-Pd1-Pd3 176.67(2), P1-Pd1-P16 106.78(5), P6-Pd1-P11 106.85(4), P1-Pd2-P16 107.27(5), P6-Pd3-P11 108.21(5); interplane angle P6-Pd1-P16/P6-Pd1-P11: 60.15 ± 0.05.

and C–C separations within the ring remain almost the same), the P–Mn separations are significantly larger in **5** than in either **4** or $[W(\mathbf{4})(CO)_5]$; **5**: 2.470(2)–2.489(1) Å; **4**: 2.392(1) Å; $[W(\mathbf{4})(CO)_5]$: 2.376(3) Å. Simultaneously, the folding of the phospholyl ring about the C_α–C_γ axis and away from manganese is more pronounced in **5**: 2.54 ± 2.88, 5.68 ± 1.86, 5.75 ± 1.59, and 5.96 ± 1.52°; **4**: 0.87 ± 0.32°. These observations suggest that the phospholyl ring acts as two distinct subunits: an η^4-diene and a μ-phosphido ligand with no P–Mn bonding. Such situations have already been described.[19, 20] On the other hand, a significant interaction exists between the external palladium atoms Pd2, Pd3 and the vicinal manganese atoms: the Pd–Mn separations (2.733(1)–2.829(1) Å) are in the range of genuine Pd–Mn bonds.[13] Similarly, the Pd–Pd separations of 2.8004(5) and 2.7877(5) Å are less than those reported for some phosphido-bridged Pd–Pd bonds in trinuclear clusters.[12] Besides, the distorted tetrahedral coordination of Pd1 and the diamagnetism of **5** exclude a 16-electron configuration for Pd1. Taking all these observations into account, we propose the formulation for **5** depicted in Scheme 1.

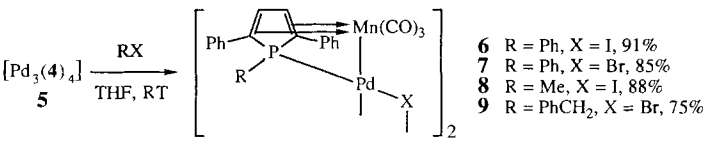


Scheme 1. Proposed formulation for **5**.

Basically, this formulation indicates that an insertion of Pd^0 into the P–Mn bond of **4** has taken place with disruption of the delocalization in the phospholyl ring. That the electronic situation within the phospholyl rings of **5** is dramatically different from that in **2** is clear from the ^{31}P NMR data: δ^{31}P = 12.2 (**5**),

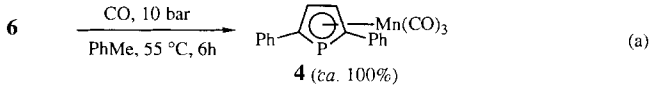
116.5 (**2**). The reduction in the electron transfer from manganese to palladium in **5** is also suggested by the IR and ^{13}C NMR data: IR: $\tilde{\nu}$(CO; CH_2Cl_2, *E* band): 1949.3 (**5**), 1964.8 cm^{-1} (**2**); ^{13}C NMR: δ(CO; $CDCl_3$): 224 (**5**), 220 (**2**). The manganese atoms appear to be more electron-rich in **5** than in **2**, as suggested by the higher polarization of the carbonyl ligands and in agreement with the presence of dative Mn → Pd bonds in **2** and apolar Mn–Pd bonds in **5**. Thus the phosphacymantrene ligand in **5** acts as a (3 + 1)-electron donor and in **2** as a (2 + 2)-electron donor.

The disruption of the P–Mn bond and of the electronic delocalization of the phospholyl rings upon formation of **5** also has a dramatic effect on the chemistry of ligand **4**. Whereas phosphorus is electrophilic in **4**,[21] it is nucleophilic in **5**, and easy arylation and alkylation at phosphorus can be performed (Scheme 2).



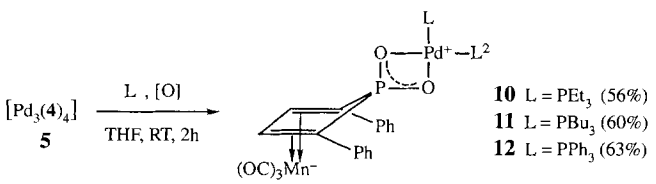
Scheme 2. Electrophilic substitution at the phosphorus center of **5**. RT = room temperature.

The formulation of the products is based on the X-ray crystal structure analysis of **6** (Fig. 3). These arylation/alkylations probably proceed by the oxidative addition of R–X to the 16-electron Pd2 and Pd3 centers followed by the collapse of the Pd1-Pd2-Pd3 unit and the migration of R from Pd to P. A curious finding was that the treatment of **6** with an excess of a two-electron ligand (CO or PBu_3) regenerates **4**, through cleavage of the P–Ph bond and rearomatization of the ring [Eq. (a)]. This observation cast some light on the mechanism of the synthesis of phosphacymantrenes by reaction of $[Mn_2(CO)_{10}]$ with phospholes.[21]



(a)

Another interesting aspect of the chemistry of **5** concerns its reaction with phosphanes (Scheme 3). All the products (**10**–**12**) display very similar ABX ^{31}P NMR spectra. The formulation of these species is based on an X-ray crystal structure analysis of **11** (Fig. 4). The Pd–Mn separation of 5.209 Å implies the absence of any bond between these atoms and hence a zwitterionic formulation. The shift of the CO stretching frequencies to lower energies further suggests the presence of partial negative charge on the manganese atom. The folding of the phosphole ring about the C_α–$C_{\alpha'}$ axis is now 27.85 ± 0.64°, which is in the normal range for such systems.[23]



Scheme 3. Reactions of **5** with phosphanes.

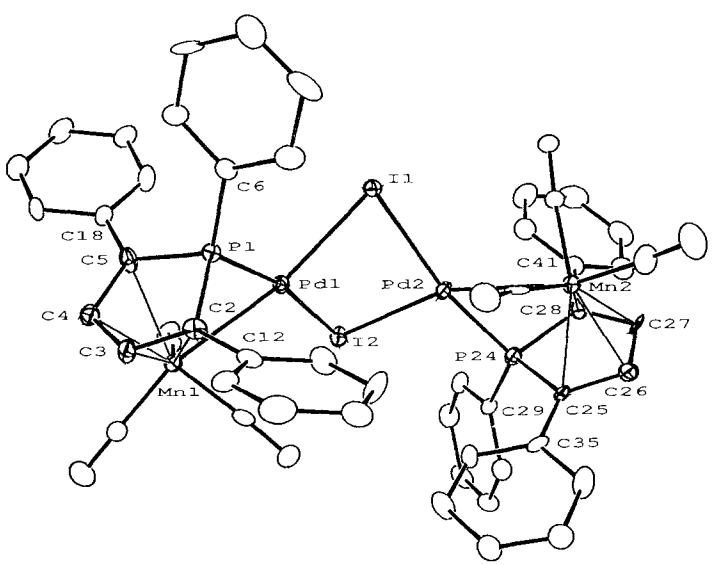


Fig. 3. Crystal structure of **6** [22a] (ellipsoids at the 50% probability level). Important distances [Å] and angles [°]: Pd1 ··· Pd2 3.494(2), Pd1-I1 2.676(1), Pd1-I2 2.715(1), Pd1-P1 2.176(3), Pd1-Mn1 2.708(2), Pd2-I1 2.721(1), Pd2-I2 2.664(1), Pd2-P24 2.172(3), Pd2-Mn2 2.719(2), P1-C2 1.79(1), P1-C5 1.76(1), P1-C6 1.80(1), P1 ··· Mn1 2.497(3), P24-C25 1.81(1), P24-C28 1.78(1), P24-C29 1.81(1), P24 ··· Mn2 2.494(3); I1-Pd1-I2 89.48(3), I1-Pd1-P1 102.27(8), I1-Pd1-Mn1 162.54(5), I2-Pd1-P1 167.91(8), I2-Pd1-Mn1 107.97(5), P1-Pd1-Mn1 60.33(8), Pd1-I1-Pd2 80.67(3), Pd1-I2-Pd2 81.01(3), I1-Pd2-I2 89.59(3), Pd1-P1-C2 108.1(5), Pd1-P1-C5 107.9(4), Pd1-P1-C6 119.4(3), Pd1-P1-Mn1 70.45(9), C2-P1-C5 90.9(6), C2-P1-C6 114.6(5), C5-P1-C6 112.2(7); interplane angle Pd1-I1-I2/Pd2-I1-I2 48.08 ± 0.04, Pd1-I1-I2/Pd1-Mn1-P1 3.55 ± 0.18.

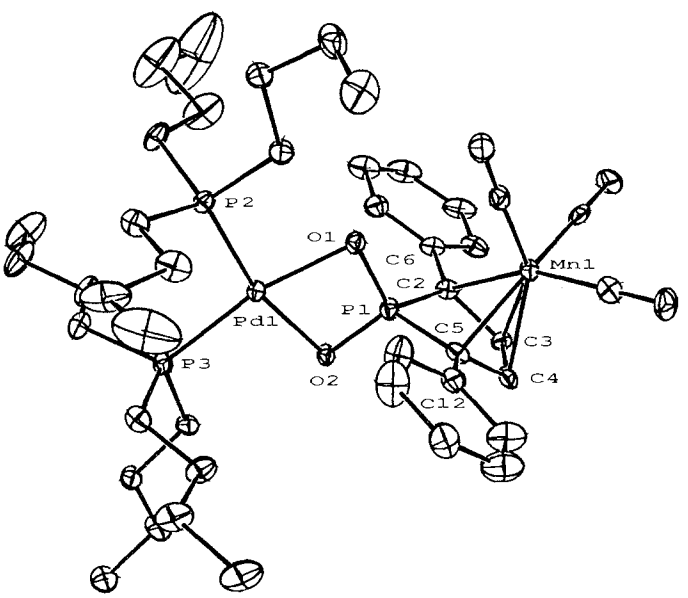


Fig. 4. Crystal structure of **11** [22b] (ellipsoids at the 40% probability level). Important bond lengths [Å] and angles [°] in one of the two molecules of the asymmetric unit: Pd1-O1 2.087(5), Pd1-O2 2.099(5), Pd1-P2 2.242(2), Pd1-P3 2.232(2), P1-O1 1.561(5), P1-O2 1.560(6), P1-C2 1.770(9), P1-C5 1.772(7), C2-C3 1.46(1), C3-C4 1.44(1), C4-C5 1.46(1), C2-Mn1 2.202(8), C3-Mn1 2.099(8), C4-Mn1 2.080(8), C5-Mn1 2.168(8), Mn1-CO 1.790(8), 1.82(1), 1.788(8); O1-Pd1-O2 71.2(2), O1-Pd1-P2 93.6(2), O1-Pd1-P3 168.2(2), O2-Pd1-P2 164.7(2), O2-Pd1-P3 97.4(2), P2-Pd1-P3 97.80(8), O1-P1-O2 102.6(3), C2-P1-C5 91.5(3), P1-C2-C3 108.1(6), C2-C3-C4 111.2(7), C3-C4-C5 112.9(6), C4-C5-P1 107.0(5).

 © VCH Verlagsgesellschaft mbH, D-69451 Weinheim, 1994 0570-0833/94/0707-0744 $ 10.00+.25/0

The first palladium η^2-phosphinate has been described very recently.[24] The analogous complexes **10**–**12** are probably formed via an intermediate $[Pd(\mathbf{4})(L)_2]$ complex in which the palladium atom is inserted into the P–Mn bond of **4**. Then, coordination of oxygen as an η^2 species,[25] could take place followed by intramolecular oxidation of phosphorus. It must be noted here that the direct reaction of $[Pd(PPh_3)_4]$ with **4** also gives **12**.

We have described two new coordination modes of phosphacymantrenes: complexation at manganese and insertion into the P–Mn bond. High-valent Pd^{2+} prefers the first mode, whilst low-valent Pd^0 favors the second. In the second case, umpolung of the phosphorus center from electrophilic to nucleophilic is observed, and alkylation, arylation, and oxidation at phosphorus is then possible. This series of results probably can be transposed to other η^5-phospholyl complexes, thus extending significantly the coordination chemistry of this class of compounds.

Experimental Procedure

2: To phosphacymantrene **1** (1 g, 3.1×10^{-3} mol) in CH_2Cl_2 (30 mL) was added $[PdCl_2(PhCN)_2]$ (1 g, 2.6×10^{-3} mol) in CH_2Cl_2 (30 mL) dropwise. After stirring at room temperature under dry nitrogen for 24 h, the solvent was evaporated and the residue washed several times with diethyl ether. Yield of **2**: 0.8 g (67%).

3: To PdI_2 (0.2 g, 5.5×10^{-4} mol) in acetone (10 mL) was added **1** (0.27 g, 8.3×10^{-4} mol). After stirring at room temperature for 5 h under nitrogen, the solution was filtrated and evaporated. The residue was washed with hexane to remove excess **1**. Complex **3** is less stable than complex **2**.

5: To the palladium(0) complex $[Pd(dba)_2]$ (1 g, 1.8×10^{-3} mol) in CH_2Cl_2 (30 mL) was added phosphacymantrene **4** (1.1 g, 3×10^{-3} mol) in CH_2Cl_2 (20 mL). After stirring at room temperature under dry nitrogen for 2 h, the solvent was evaporated and the residue treated with diethyl ether (20 mL). The pale red precipitate of **5** was recovered (0.84 g, 77%/Pd); m.p. 192 °C (decomp).

6: To **5** (1 g, 5.5×10^{-4} mol) in freshly distilled and degassed THF (30 mL) was added iodobenzene (0.35 g, 1.7×10^{-3} mol). The mixture was stirred at room temperature under dry nitrogen for 2 h. The solution was concentrated to one-third of its volume. Then, 20 mL of distilled and degassed hexane was added and the precipitate filtered. Yield of **6**: 1.1 g (91.7%), m.p. 200 °C (decomp).

7: Same procedure as for **6**, reaction time 24 h. From 1 g of **5** and 0.31 g of PhBr was obtained 0.9 g of **7** (85%); m.p. ≈190 °C (decomp).

8: Same procedure as for **6**, reaction time 48 h. From 0.2 g of **5** and 0.1 g of MeI was obtained 0.18 g of **8** (88%); m.p. ≈200 °C (decomp).

9: Same procedure as for **6**, reaction time 24 h. From 0.1 g of **5** and 0.05 g of $PhCH_2Br$ was obtained 0.09 g of **9** (75%); m.p. ≈180 °C (decomp).

10: To **5** (0.1 g, 5.5×10^{-5} mol) in freshly distilled and degassed THF (10 mL) was added triethylphosphane (5×10^{-2} g, 4×10^{-4} mol). The mixture was stirred at room temperature in a Schlenk tube under nitrogen for 2 h. After evaporation, The residue was treated with diethyl ether (10 mL). The precipitate was recovered.

11: Same procedure as for **10**. From 0.2 g of **5** and 0.13 g of PBu_3 was obtained 0.185 g of **11** (60%); m.p. ≈215 °C (decomp).

12: Same procedure as for **10**. From 0.5 g of **5** and 0.87 g of PPh_3 was obtained 0.53 g of **12** (63%); m.p. ≈196 °C (decomp).

Received: October 16, 1993
Revised: November 29, 1993 [Z 6430/6431 IE]
German version: *Angew. Chem.* **1994**, *106*, 812

[1] V. G. Andrianov, Yu. T. Struchkov, E. R. Rossinskaja, *J. Chem. Soc. Chem. Commun.* **1973**, 338.
[2] R. M. G. Roberts, J. Silver, *J. Organomet. Chem.* **1981**, *209*, 385; M. Watanabe, H. Ichikawa, I. Motoyama, H. Sano, *Bull. Chem. Soc. Jpn.* **1983**, *56*, 3291.
[3] D. Seyferth, B. W. Hames, T. G. Rucker, M. Cowie, R. S. Dickson, *Organometallics* **1983**, *2*, 472.
[4] S. Akabori, T. Kumagai, T. Shirahige, S. Sato, K. Kawazoe, C. Tamura, M. Sato, *Organometallics* **1987**, *6*, 526.
[5] M. Sato, K. Suzuki, S. Akabori, *Chem. Lett.* **1987**, 2239.
[6] R. M. G. Roberts, J. Silver, A. S. Wells, *Inorg. Chim. Acta* **1986**, *119*, 165.
[7] N. M. Kostić, R. F. Fenske, *Organometallics* **1983**, *2*, 1008; C. Guimon, D. Gonbeau, G. Pfister-Guillouzo, G. de Lauzon, F. Mathey, *Chem. Phys. Lett.* **1984**, *104*, 560; M.-D. Su, S.-Y. Chu, *J. Phys. Chem.* **1989**, *93*, 6043.
[8] P. Lemoine, M. Gross, P. Braunstein, F. Mathey, B. Deschamps, J. H. Nelson, *Organometallics* **1984**, *3*, 1303.
[9] C. Guimon, G. Pfister-Guillouzo, F. Mathey, *Nouv. J. Chim.* **1979**, *3*, 725.
[10] F. Mercier, S. Holand, F. Mathey, *J. Organomet. Chem.* **1986**, *316*, 271.
[11] Crystals of $\mathbf{2} \cdot 2CH_2Cl_2$, $C_{32}H_{28}Cl_2Mn_2O_6P_2Pd_2 \cdot 2CH_2Cl_2$, were grown from a dichloromethane solution of the compound. Data were collected at -150 ± 0.5 °C. The compound crystallizes in space group $P2_1/c$, $a = 10.927(1)$, $b = 14.404(1)$, $c = 13.152(1)$ Å, $\beta = 109.96(1)°$; $V = 1945.61(58)$ Å^3; $Z = 2$; $\rho_{calc} = 1.936$ g cm^{-3}; $\mu = 20.5$ cm^{-1}; $F(000) = 1116$. A total of 5668 unique reflections were recorded in the range $2° \le 2\theta \le 60.0°$, of which 4121 were used for solution and refinement. The structure was solved by Patterson methods (localization of the Pd, P, and Cl atoms). The hydrogen atoms were included as riding atoms in the final stages of least-squares refinement. A non-Poisson weighting scheme was applied with a p factor of 0.08; $R = 0.033$, $Rw = 0.054$, GOF = 1.12 [26].
[12] G. W. Bushnell, K. R. Dixon, P. M. Moroney, A. D. Rattray, Ch'eng Wan, *J. Chem. Soc. Chem. Commun.* **1977**, *709*.
[13] P. Braunstein, J.-M. Jud, J. Fischer, *J. Chem. Soc. Chem. Commun.* **1983**, 5.
[14] We have recorded the X-ray crystal structure of **4** for comparison. The structure of 2-benzoyl-3,4-dimethylphosphacymantrene was already described: F. Mathey, A. Mitschler, R. Weiss, *J. Am. Chem. Soc.* **1978**, *100*, 5748.
[15] A. G. Ginzburg, A. S. Batsanov, Yu. T. Struchkov, *Metallorg. Khim.* **1991**, *4*, 854.
[16] O. J. Scherer, R. Konrad, E. Guggolz, M. L. Ziegler, *Angew. Chem.* **1982**, *94*, 309; *Angew. Chem. Int. Ed. Engl.* **1982**, *21*, 297; B. Schmid, L. M. Venanzi, T. Gerfin, V. Grumlich, F. Mathey, *Inorg. Chem.* **1992**, *31*, 5117.
[17] A. Brèque, F. Mathey, C. Santini, *J. Organomet. Chem.* **1979**, *165*, 129.
[18] Crystals of $\mathbf{5} \cdot C_2H_4Cl_2 \cdot Et_2O$, $C_{76}H_{48}Mn_4O_{12}P_4Pd_3 \cdot C_2H_4Cl_2 \cdot C_4H_{10}O$, were grown from a dichloroethane/ether solution of the compound. Data were collected at -150 ± 0.5 °C. The compound crystallizes in space group $Pca2_1$, $a = 20.347(2)$, $b = 16.145(2)$, $c = 22.716(2)$ Å; $V = 7462.23(2.31)$ Å^3; $Z = 4$; $\rho_{calc} = 1.770$ g cm^{-3}; $\mu = 15.5$ cm^{-1}; $F(000) = 3960$. A total of 11117 unique reflections were recorded in the range $2° \le 2\theta \le 60.0°$, of which 8548 were used for solution and refinement. The structure was solved by direct methods (localization of the Pd and Mn atoms). Hydrogen atoms were included as fixed contributions with set positions and temperature factors in the final stages of least-squares refinement. A non-Poisson weighting scheme was applied with a p factor of 0.04; $R = 0.029$, $Rw = 0.035$, GOF = 1.03 [26].
[19] J. M. Rosalky, B. Metz, F. Mathey, R. Weiss, *Inorg. Chem.* **1977**, *16*, 3307.
[20] S. Holand, F. Mathey, J. Fischer, A. Mitschler, *Organometallics* **1983**, *2*, 1234.
[21] F. Mathey, A. Mitschler, R. Weiss, *J. Am. Chem. Soc.* **1978**, *100*, 5748.
[22] a) Crystals of $\mathbf{6} \cdot CH_2Cl_2$, $C_{50}H_{34}I_2Mn_2O_6P_2Pd_2 \cdot CH_2Cl_2$, were grown from a dichloromethane/methanol solution of the compound. Data were collected at -150 ± 0.5 °C. The compound crystallizes in space group $P2_12_12_1$, $a = 14.138(1)$, $b = 17.238(2)$, $c = 21.617(2)$ Å; $V = 5268.24(1.47)$ Å^3; $Z = 4$; $\rho_{calc} = 1.833$ g cm^{-3}; $\mu = 24.8$ cm^{-1}; $F(000) = 2808$. A total of 8351 unique reflections were recorded in the range $2° \le 2\theta \le 60.0°$, of which 5325 were used for solution and refinement. The structure was solved by Patterson methods (localization of the Pd and I atoms). The hydrogen atoms were included as fixed contributions with set positions and temperature factors in the final stages of least-squares refinement. A non-Poisson weighting scheme was applied with a p factor of 0.08; $R = 0.041$, $Rw = 0.057$, GOF = 1.06 [26]. b) Crystals of $\mathbf{11} \cdot THF$, $C_{43}H_{66}MnO_5P_3Pd \cdot C_4H_8O$, were grown from a warm THF solution of the compound. Data were collected at -150 °C ± 0.5 °C. The compound crystallizes in space group $P2_1/c$, $a = 25.645(2)$, $b = 16.163(1)$, $c = 25.083(2)$ Å; $\beta = 100.95(1)°$; $V = 10207.59(2.58)$ Å^3; $Z = 8$; $\rho_{calc} = 1.288$ g cm^{-3}; $\mu = 7.2$ cm^{-1}; $F(000) = 4160$. A total of 12461 unique reflections were recorded in the range $2° \le 2\theta \le 44.0°$, of which 8428 were used for solution and refinement. The structure was solved by Patterson method (hydrogen atoms were ignored). A non-Poisson weighting scheme was applied with a p factor of 0.08; $R = 0.061$, $Rw = 0.090$, GOF = 1.82.
[23] K. Yasufuku, A. Hamada, K. Aoki, H. Yamazaki, *J. Am. Chem. Soc.* **1981**, *102*, 4363.
[24] P. Leoni, F. Marchetti, M. Pasquali, *J. Organomet. Chem.* **1993**, *451*, C25.
[25] η^2-O_2 Palladium complexes are well known, see: T. Yoshida, K. Tatsumi, M. Matsumoto, K. Nakatsu, A. Nakamura, T. Fueno, S. Otsuka, *Nouv. J. Chim.* **1979**, *3*, 761.
[26] Enraf–Nonius CAD4 diffractometer, structures solved and refined with the program MOLEN; $Mo_{K\alpha}$ radiation ($\lambda = 0.71073$ Å), graphite monochromator; only reflections with $F^2 \le 3.0\,\sigma(F^2)$ were considered observed. All non-hydrogen atoms were refined with anisotropic temperature factors. Further details of the crystal structure investigations may be obtained from the Fachinformationszentrum Karlsruhe, D-76344 Eggenstein-Leopoldshafen (FRG), on quoting the depository number CSD-57959.

New Sulfur- and Selenium-Bridged Copper Clusters; Ab Initio Calculations on $[Cu_{2n}Se_n(PH_3)_m]$ Clusters **

Stefanie Dehnen, Ansgar Schäfer, Dieter Fenske,* and Reinhart Ahlrichs

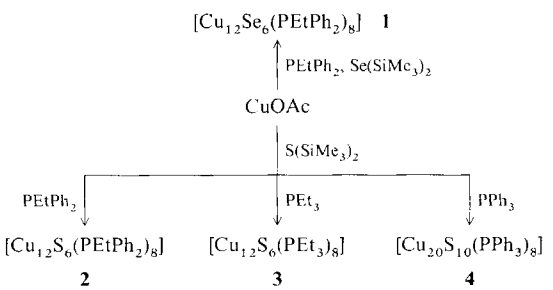
Copper(I) chloride reacts with tertiary phosphanes and $Se(SiMe_3)_2$ with the elimination of $SiMe_3Cl$ to give selenium-bridged copper cluster complexes.[1] Hitherto only metal-rich copper clusters have been observed and characterized as reaction products for these reactions. Examples of these include:[1]

$[Cu_{30}Se_{15}(PiPr_3)_{12}]$ $[Cu_{70}Se_{35}(PEt_3)_{22}]$ $[Cu_{146}Se_{73}(PPh_3)_{30}]$

In contrast, it has not been possible to isolate intermediates of these reactions, as has been achieved in the synthesis of tellurium-bridged copper clusters.[2]

In 1991 I. G. Dance et al. reported the existence of smaller copper chalcogenide cluster ions, such as $[Cu_{11}E_6]^-$, $[Cu_{12}E_7]^-$, and $[Cu_{19}E_{10}]^-$, which were produced after laser ablation of the elements or of the binary chalcogenides, and subsequently could be detected by mass spectrometry.[3] This encouraged us to search for synthetic methods for ligand-protected copper clusters of this type.

In order to synthesize these intermediates as well as the sulfur-bridged species still missing in the series of chalcogenide-bridged copper clusters, copper(I) acetate was treated with PR_2R' (R, R' = Ph, Et) and $E(SiMe_3)_2$ (E = S, Se) in diethyl ether or THF. In this way compounds **1**–**4** were isolated and characterized by X-ray crystal structure analyses (see Figs. 3 and 4).[4, 5]



Compounds **2**, **3**, and **4** are the first sulfur-bridged copper clusters which could be prepared in this way and characterized. Compounds **1** and **4** precipitate in the form of red crystals from dark brown solutions; **2** forms red and **3** forms violet crystals, which were each isolated from colorless reaction solutions. The IR spectra of the compounds are not very informative, since they only contain characteristic vibrations for the phosphane ligands.

After the synthesis of **1**, ab initio calculations for $[Cu_{12}Se_6]$ were carried out parallel to and independent of the crystal structure analysis of **1**. The structural features and energetics of such molecules had been investigated previously as part of a systematic study of small $[Cu_2Se]_n$ clusters with and without phosphane ligands.[6] The calculations were carried out with the TURBOMOLE[7] program at the MP2 approximation,[8] which had proved successful for the above study, whereas the SCF method had proved to be insufficient.

Several important structure principles shall be outlined by using clusters **5**–**8** (Fig. 1) as examples; each of these form local minima on the energy hypersurface. More accurate calculations were also carried out for **5** at the coupled cluster level (CCSD(T)), from which errors in the Cu–Cu (±5 pm) and Cu–Se (±3 pm) bond lengths of the MP2 structures can be estimated.

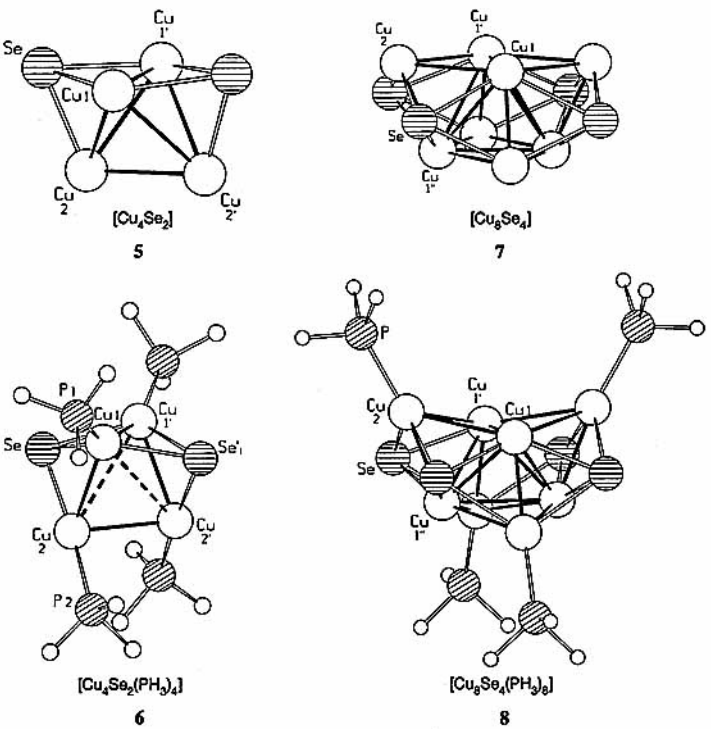


Fig. 1. Structures of **5**–**8** resulting from MP2 calculations. Selected bond lengths [pm] (error ±5 pm) and angles [°]: **5**: Cu1–Cu1′ 221.6, Cu1–Cu2 260.2, Cu2–Cu2′ 261.2, Cu1–Se 237, Cu2–Se 222.8. - **6**: Cu1–Cu1′ 244.4, Cu1–Cu2 251, Cu1–Cu2′ 323.9, Cu2–Cu2′ 260.4, Cu1–Se′ 237.7, Cu1–Se 244.3, Cu2–Se 222.7, Cu1–P1 218.3, Cu2–P2 216; Se-Cu2-P2 172. - **7**: Cu1–Cu1′ 262.6, Cu1–Cu1″ 275.4, Cu1–Cu2 260.1, Cu1″–Cu2 223.8, Cu1–Se 245.2, Cu2–Se 233.1. - **8**: Cu1–Cu1′ 280.4, Cu1–Cu1″ 260.5, Cu1–Cu2 271.2, Cu1″–Cu2 234.7, Cu1–Se 232.2, Cu2–Se 246.5, Cu2–P 219.

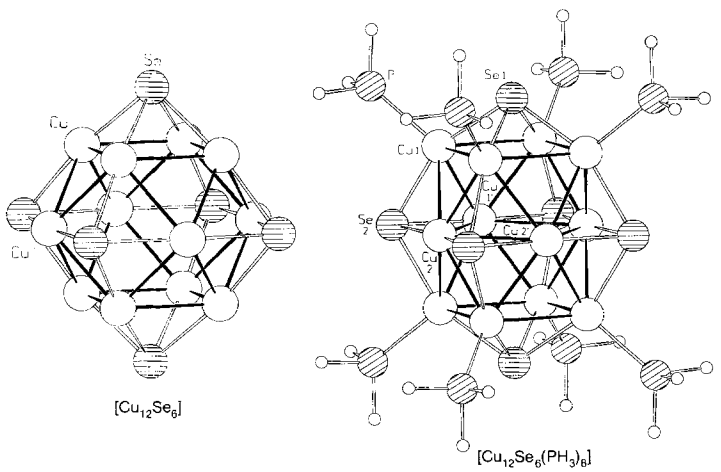
For at least three, but mostly four Cu–Se contacts per selenium atom, the structure with the maximum number of short Cu–Cu contacts (< 260 pm) is always preferred. Generally, this leads to structures with relatively high symmetry. Accordingly, a distorted Cu_4 tetrahedron exists in **5** in which two Cu_3 faces are capped by μ_3-selenido ligands. In contrast, in **7** a highly distorted cube of copper atoms is observed, whose two selenium-free faces are deformed to rhombuses that are rotated by 90° relative to each other. The Cu–Cu interaction exhibits marginal covalent contributions and is best considered as a dispersion interaction of the d^{10} systems.[9]

The PH_3 ligands in **6** and **8** coordinate to exposed sites on the cluster framework and favor—as far as possible—a linear Se-Cu-P arrangement (the Se-Cu2-P2 angle in **6** is 172°); this tendency is typical for the coinage metals in the oxidation state +I.[10] For increased loading with Se ligands, trigonal-planar coordination at the Cu centers is preferred (in **8** P projects 21.5°

[*] Prof. Dr. D. Fenske, Dipl.-Chem. S. Dehnen, Dipl.-Chem. A. Schäfer, Prof. Dr. R. Ahlrichs
Institut für Anorganische Chemie der Universität
Engesserstrasse, Gebäude-Nr. 30.45, D-76131 Karlsruhe (FRG)
Telefax: Int. code + (721)661-921

[**] This work was supported by the Deutsche Forschungsgemeinschaft (SFB 195).

above the Se–Cu2–Se plane). The rules found for smaller molecules, regarding the choice of the most stable arrangement of copper and selenium atoms, support the structure of **9** (Fig. 2). Other considered structures always gave higher energy. Compound **9** has O_h symmetry and can be described as a Cu_{12} cubooctahedron with Se-capped square faces or as a Se_6 octahedron whose edges are linked by Cu atoms.



9 **10**

Fig. 2. Structures of **9** and **10**, resulting from MP2 calculations. Selected bond lengths [pm] (error ±5 pm): **9**: Cu–Cu′ 252, Cu–Se 233.3; **10**: Cu1–Cu1′ 275.2, Cu1–Cu2 256.5, Cu2–Cu2′ 283.4, Cu1–Se1 234.5, Cu1–Se2 242.1, Cu2–Se2 227.6, Cu1–P 232.6.

For the calculation of the structure of the ligand-clad cluster framework of **9**, PH_3 was used as a model ligand and the highest possible symmetry, D_{4h}, was assumed for the resulting molecule **10**. This considerably reduced the effort required for the calculation. The structure of **10** (Fig. 2) determined in this way is in agreement with (within the limits of the methods) the molecular structure of **1** (cf. Fig. 3)[4] determined by crystal structure analysis. The calculated Cu–Se distances in **10** lie in the range of measured values of **1** or slightly above (< 2 pm). The calculated Cu–P bond is at least 3 pm longer than that found in **1**, which can be attributed to the fact that substituted phosphanes are stronger donors than PH_3. Slightly larger deviations occur for several Cu–Cu distances; the greatest difference (11 pm) between the calculated and measured values is found for Cu1–Cu2 (see Fig. 3). Here, however, very soft modes are observed—in the small clusters they typically lie at 100 cm^{-1}; as a result packing effects might play a role in the crystal.

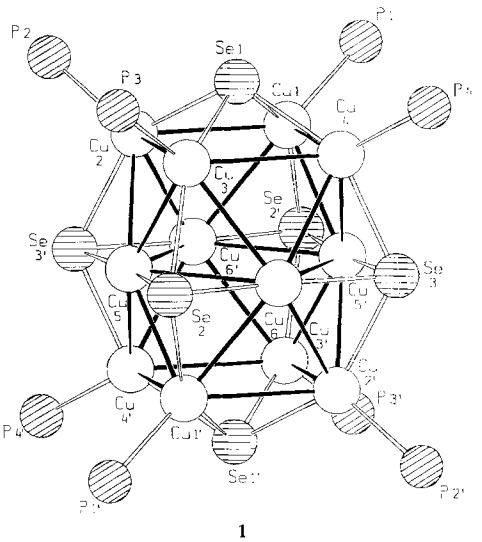
The PH_3 ligands lead to a distortion of the Cu_{12} framework in **9**, in such a way that two face-shared Cu_8 antiprisms are formed in **10**. The copper atoms bearing phosphane ligands (Cu1–Cu4 in **1**) in **10** and **1** are positioned further away from the center of the cluster than in **9** and adopt trigonal-planar coordination. In contrast, the four remaining copper atoms (Cu5, Cu6 and inverted positions in **1**) are shifted further towards the center of the cluster, retaining almost linear Se-Cu-Se arrangements (the angle is about 167° in **10**); as a result the coordination of additional ligands to these atoms is prevented.

The stabilization energy E_n of the naked clusters **5**, **7**, and **9** is calculated to be −160, −302, and −427 kJ mol^{-1}, respectively.[*] The bond energy of the naked clusters increases with growing cluster size; thus, these clusters are not thermodynamically stable systems.

$$E_n = \frac{1}{n} E[Cu_{2n}Se_n] - E[Cu_2Se]$$

From the calculated total energies (MP2) of **6**, **8**, and **10**, the following bond energies of the Cu–P bonds result: 103, 98, and 50 kJ mol^{-1}. The Cu–P bond becomes weaker as the size of the cluster increases, since the copper atoms are then loaded with selenium neighbors, and thus, the ideal (linear) Se-Cu-P arrangements are no longer formed. This also explains why the PR_3 ligands preferably bind to the exposed copper atoms. The low bond energy of the Cu–P bond (50 kJ mol^{-1}) in **10** clarifies why **1** must be prepared with cooling.

The structural buildup of **1**, **2**, and **3** is the same. The molecular structures of these compounds in the crystal is exemplified in Figure 3, which shows the structure of **1**. Compounds **1**, **2**, and



1

Fig. 3. Structure of $[Cu_{12}Se_6(PEtPh_2)_8]$ **1** in the crystal (without ethyl and phenyl groups, Cu–Cu distances up to 318 pm are drawn). Selected bond lengths [pm] and angles [°] (error ±0.9 pm and ±0.3°, respectively): Cu(1,2,3,4)–Cu 257.2–292.8, Cu5–Cu(6,6′) 296.2 and 286.9, Se1–Cu 232.9–233.9, Se2–Cu 220–245, Se3–Cu 216.5–239.3, P–Cu 226.2–229.1; Se1-Cu-Se 143.4–147.4, Cu1-Se2′-Cu3′ 123.2, Cu2-Se3′-Cu4′ 127.9, Se1-Cu-P 115.7–120.9, Cu1-Cu5′-Cu3′ 113.2.

3 have an inversion center. The copper part of the framework consists of two face-shared, slightly distorted square antiprisms. This rare structural fragment exists, however, in a highly deformed form, for example, in $[Rh_{12}C_2(CO)_{24}]^{2-}$, $[Rh_{12}C_2(CO)_{23}]^{3-}$, and $[Rh_{12}C_2(CO)_{23}]^{4-}$.[5] The distances of the copper atoms from the inversion center range from 205.4–300 pm in **1**, 206.4–295.9 pm in **2**, and 203.8–310 pm in **3**. The atoms of the middle Cu_4 faces (Cu5, Cu5′, Cu6, Cu6′) are each closer to the center than those of the basal faces (Cu1–Cu4). Thus, the copper part of the framework cannot be described as a distorted cubooctahedron; cubooctrahedral cluster compounds or structural fragments always have almost identical distances between the apecies of the polyhedron and the center. One example of this is the framework of copper atoms in $[Cu_{12}(PPh)_6(PPh_3)_6]$.[2]

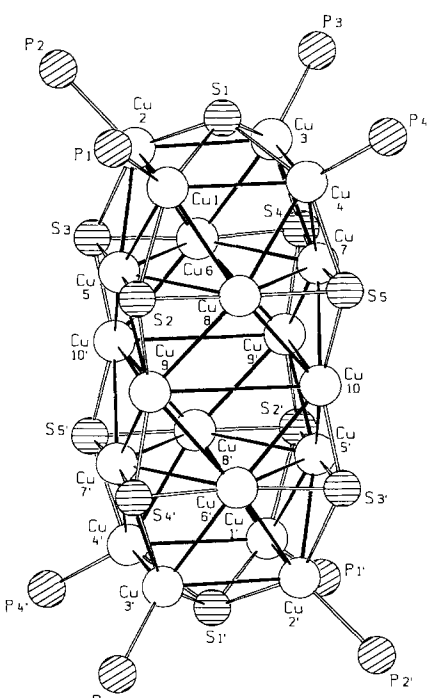
[*] The calculated total energies (MP2) of the naked clusters **5**, **7**, and **9** using the basis set given in [6] are −220.962573, −442.141384, and −663.497772 au, respectively; 1 au (atomic unit) = 2625.5 kJ mol^{-1}. For the ligand-clad clusters **6**, **8**, and **10** values of −253.693704, −474.865664, and −728.799384 au are obtained.

 © VCH Verlagsgesellschaft mbH, D-69451 Weinheim, 1994 0570-0833/94/0707-0747 $ 10.00+.25/0

The eight phosphane ligands in **1**, **2**, and **3** coordinate to the eight copper atoms of the two basal faces. The sulfur and selenium atoms always act as μ_4-bridging ligands. Together they form a slightly distorted octahedron. The copper atoms of the outer faces (Cu1–Cu4) are each bound to two chalcogen atoms and one phosphorus atom (E-Cu-E = 142–147°, E-Cu-P = 112–122°, and 95–105°). The copper atoms of the middle face are each coordinated by two chalcogen atoms, leading to an almost linear E-Cu-E arrangement (172–176°). In the equatorial face of the chalcogen octahedron an eight-membered Cu_4E_4 metallacycle (Cu5, Cu6, E2, E3 and inverted positions) is found. Cu_4R_4 metallacycles without additional coordination are known for R = CH_2SiMe_3 or R = *O-tert*-butyl.[11] The ability of chalcogen atoms to adopt higher coordination enables the formation of the three-dimensional structures for the cluster complexes presented here.

In addition to differences in bond lengths, compounds **1**, **2**, and **3** show different degrees of tetragonal distortion. In this way the molecules (without taking the organic groups into consideration) do not achieve D_{4h} symmetry, but only D_{2h} symmetry. The Cu–Cu distances in all of the compounds are too large (255–354 pm) to be considered as bonding interactions. The Cu–Cu and the Cu–E distances found in **1**–**3** are of the same order of magnitude as those in binary chalcogenides. This was also established for other copper–selenide clusters.[1]

The molecular structure of the cluster complex **4** (Fig. 4) can now be derived in a simple way from the structures of **1**, **2**, and **3**: in **4**, two Cu_{12} fragments were formally linked through one of the Cu_4 faces previously described as basal faces. The sulfur atoms which are arranged above these faces in **1**, **2**, and **3** and the eight phosphane molecules bound to the corresponding copper atoms are no longer present after this formal cluster condensation. Instead the new, almost square Cu_4 face is extended; thus, the framework of copper atoms in **4** forms an arrangement of four square antiprisms linked through three Cu_4 faces. An inversion center is also present in **4**.



4

Fig. 4. Structure of $[Cu_{20}S_{10}(PPh_3)_8]$ **4** in the crystal (without phenyl groups, Cu–Cu distances up to 354 pm are drawn). Selected bond lengths [pm] and angles [°] (error ±0.9 pm and ±0.4°, respectively): Cu(1,2,3,4)–Cu 264.1–290, Cu(9,10)–Cu 267.7–354.4, S1–Cu 224.5–226.1, S2–Cu 214.2–235.8, S3–Cu 215.7–235.1, S4–Cu 215.7–234.8, S5–Cu 214.9–235.2, P–Cu 227.3–229.6; S1-Cu-S 140.2–152, Cu1-S2-Cu9 140.1, Cu2-S3-Cu10' 138.9, Cu3-S4-Cu9' 140.6, Cu4-S5-Cu10 140, S1-Cu-P 117.2–120.2, Cu1-Cu5-Cu9 103.5, Cu1-Cu8-Cu9 105, Cu2-Cu5-Cu10' 104.8, Cu2-Cu6-Cu10' 103.2, Cu3-Cu6-Cu9' 105.4, Cu3-Cu7-Cu9' 102.3, Cu4-Cu7-Cu10 105.1, Cu4-Cu8-Cu10 102.9.

There are numerous examples of the condensation of cluster fragments to larger units. Face-shared octahedra exist, for example, in the species $[Cs_{11}O_3]$ and $[Rb_9O_3]$,[12,13] described by A. Simon; examples for the formation of strands of octahedra by face-sharing include the Chevrel phases $[Mo_{12}Se_{14}]^{2-}$, $[Mo_{18}Se_{20}]^{4-}$, $[Mo_{24}Se_{26}]^{6-}$, and $[Mo_{30}Se_{32}]^{8-}$.[12,14,15] Cluster complexes which exhibit this building principle are also known for cobalt and nickel: $[Co_9Se_{11}(PPh_3)_6]$, $[Ni_{15}Se_{15}(PPh_3)_6]$, and $[Ni_{12}Se_{12}(PEt_3)_6]$.[16] Ecliptic stacking of trigonal prisms through triangular faces has been described for $[Pt_{15}(CO)_{30}]^{3-}$.[5]

The linkage of more than three tetragonal antiprisms is, however, new in cluster chemistry. Besides icosahedral (e.g. $[Ni_{10}As_2(CO)_{18}(CH_3)_2]^{2-}$) and anticubooctahedral structures (e.g. $[PtRh_{12}(CO)_{24}]^{4-}$) as well as polyhedra consisting of three face-shared octahedra (e.g. $[Ir_{12}(CO)_{26}]^{2-}$) also many, far less symmetrical arrangements (e.g. $[Co_3Ni_9C(CO)_{20}]^{3-}$ and $[Os_{11}CuC(CO)_{27}(CH_3CN)]^{-}$)[5] of twelve metal atoms in cluster compounds have been observed. For the few known metal clusters with 20 metal atoms so far no uniform structural principle has been formulated.

If it is assumed that in **1**–**4** the chalcogenido ligands exist as Se^{2-} or S^{2-}, the copper fragments of the compounds carry the formal charges Cu_{12}^{12+} and Cu_{20}^{20+}. Consequently, the copper atom in the cluster complexes can be assigned the formal oxidation state +1 (d^{10} configuration). This supports the assumption that metal–metal bonding can be ruled out in these systems, and that at most weak interactions exist between the copper atoms. There are, however, several cases in which d^{10}–d^{10} interactions contribute to metal bonding.[11,17]

Compounds **1**–**4** are possibly intermediates in the synthesis of larger cluster compounds. This is indicated first by the dark brown color of the reaction mixtures from which the red crystals of **1** and **4** were isolated, and second the compounds are more readily decomposed than known large cluster complexes. There is still a lack of concrete evidence for the formation of larger cluster complexes in the colorless reaction mixtures from which **2** and **3** were isolated.

Experimental Procedure

1: $PEtPh_2$ (1.61 mL, 6 mmol) was added to a suspension of CuAc (0.37 g, 3 mmol) in diethyl ether (25 mL), which resulted in the dissolution of the CuAc. The reaction mixture was cooled to −65 °C and treated with (0.37 mL, 1.5 mmol) $Se(SiMe_3)_2$. The solution was allowed to warm to room temperature over 4 d, during which time it had turned dark brown and red needles of **1** had crystallized out (yield 5%).

2: $PEtPh_2$ (1.61 mL, 6 mmol) was added to a suspension of CuAc (0.37 g, 3 mmol) in diethyl ether (25 mL), which resulted in the dissolution of the CuAc. $S(SiMe_3)_2$ (0.31 mL, 1.5 mmol) was added to the solution at −78 °C, and the reaction mixture was subsequently allowed to warm to −20 °C over 4 d. Cherry red rhombuses of **2** crystallized from the colorless solution (yield 100%).

3: PEt_3 (1.18 mL, 8 mmol) was added to a suspension of CuAc (0.25 g, 2 mmol) in diethyl ether (40 mL), which resulted in the dissolution of the CuAc. $S(SiMe_3)_2$ (0.21 mL, 1 mmol) was added to the solution at −78 °C, and the reaction mixture was subsequently allowed to warm to −20 °C over 4 d. In this way violet square crystals of **3** were obtained in 82% yield.

4: PPh_3 (1.31 g, 5 mmol) was added to a suspension of CuAc (0.12 g, 1 mmol) in THF (20 mL), which resulted in the dissolution of the CuAc. Subsequently, $S(SiMe_3)_2$ (0.10 mL, 0.5 mmol) was added, which caused the reaction mixture to turn dark brown. The mixture was cooled to −40 °C, and after 7 d a powdery precipitate was filtered off. Red octahedra of **4** crystallized out after a further 6 d at −20 °C.

Received: October 25, 1993 [Z6448IE]
German version: *Angew. Chem.* **1994**, *106*, 786

[1] D. Fenske, H. Krautscheid, S. Balter, *Angew. Chem.* **1990**, *102*, 799–801; *Angew. Chem. Int. Ed. Engl.* **1990**, *29*, 796–798 D. Fenske, H. Krautscheid, *ibid.* **1990**, *102*, 1513–1515 and **1990**, *29*, 1452–1454; H. Krautscheid, D. Fenske, G. Baum, M. Semmelmann, *ibid.* **1993**, *105*, 1364–1367 and **1993**, *32*, 1303–1305.

[2] D. Fenske, J.-C. Steck, *Angew. Chem.* **1993**, *105*, 254–257; *Angew. Chem. Int. Ed. Engl.* **1993**, *32* 238–242.

[3] J. H. El Nakat, I. G. Dance, K. J. Fisher, G. D. Willet, *Inorg. Chem.* **1991**, *30*, 2958.

[4] X-ray structure analyses: STOE IPDS; $Mo_{K\alpha}$, 213 K; data collection and refinement: **1**: $a = 1380.3(10)$, $b = 1452.6(12)$, $c = 1733.9(12)$ pm, $\alpha = 107.5(4)$, $\beta = 101.11(4)$, $\gamma = 112.18(4)^\circ$, $V = 2880(4) \times 10^6$ pm^3, $P\bar{1}$ (no. 2), $Z = 1$, $\mu(Mo_{K\alpha}) = 41.23$ cm^{-1}, $2\theta_{max} = 52^\circ$; 20613 reflections, 10232 of which are independent, 2245 with $I > 6\sigma(I)$, 622 parameters (Se, Cu, P, C anisotropicically refined). $R = 0.082$. As a result of the very low scattering power of the crystals so far no better data set has been obtained. An isotropic refinement of the C atoms leads to $R = 0.093$. - **2**: $a = 1377.0(11)$, $b = 1441.0(10)$, $c = 1731.0(12)$ pm, $\alpha = 106.96(6)$, $\beta = 101.52(4)$, $\gamma = 112.11(4)^\circ$, $V = 2852(4) \times 10^6$ pm^3, $P\bar{1}$ (no. 2), $Z = 1$, $\mu(Mo_{K\alpha}) = 24.05$ cm^{-1}, $2\theta_{max} = 56^\circ$; 22531 reflections, of which 12363 are independent, 5096 with $I > 6\sigma(I)$, 622 parameters (S, Cu, P, C anisotropicically refined), $R = 0.063$. - **3**: $a = 1203.4(12)$, $b = 1254.5(10)$, $c = 1492.8(10)$ pm, $\alpha = 66.03(4)$, $\beta = 68.14(7)$, $\gamma = 78.4(6)^\circ$, $V = 1908(3) \times 10^6$ pm^3, $P\bar{1}$ (no. 2), $Z = 1$, $\mu(Mo_{K\alpha}) = 35.57$ cm^{-1}, $2\theta_{max} = 61^\circ$; 32712 reflections, of which 8370 are independent, 5387 with $I > 6\sigma(I)$, 242 parameters (S, Cu, P anisotropicically refined; the ethyl groups are partly double disordered, their atomic positions were refined isotropically), $R = 0.072$. - **4**·8THF: $a = 2526(2)$, $b = 2798.1(8)$, $c = 2899(2)$ pm, $V = 20489(22) \times 10^6$ pm^3, $Pbca$ (no. 61), $Z = 4$, $\mu(Mo_{K\alpha}) = 21.79$ cm^{-1}, $2\theta_{max} = 42^\circ$; 74443 reflections, of which 10857 are independent, 3249 with $I > 6\sigma(I)$, 396 parameters (S, Cu, P anisotropicically refined; phenyl rings refined as rigid groups). $R = 0.094$. Four solvent molecules were located per asymmetric unit. Further details of the crystal structure investigations may be obtained from the Fachinformationszentrum Karlsruhe, D-76344 Eggenstein-Leopoldshafen (FRG) on quoting the depository number CSD-57883.

[5] D. F. Shriver, H. D. Kaesz, R. D. Adams, *The Chemistry of Metal Cluster Complexes*, VCH, New York, **1990**.

[6] A. Schäfer, C. Huber, J. Gauss, R. Ahlrichs, *Theor. Chim. Acta* **1993**, *87*, 29; A. Schäfer, R. Ahlrichs, unpublished.

[7] R. Ahlrichs, M. Bär, M. Häser, H. Horn, C. Kölmel, *Chem. Phys. Lett.* **1989**, *162*, 165; F. Haase, R. Ahlrichs, *J. Comput. Chem.* **1993**, *14*, 907.

[8] MP2 denotes the treatment of electron correlation in the second order of perturbation theory starting from a Hartree–Fock wave function: C. Møller, M. S. Plesset, *Phys. Rev.* **1934**, *46*, 618. Relativistically corrected pseudopotentials with 18 core electrons for Cu and 28 core electrons for Se were used for the calculations; M. M. Hurley, L. F. Pacios, P. A. Christiansen, R. B. Ross, W. C. Ermler, *J. Chem. Phys.* **1986**, *84*, 6840. The basis sets Cu: (3s2p6d)/[2s2p2d] and Se: (3s3p1d)/[2s2p1d] were optimized for the atoms at the SCF level, polarization functions for Cu_2Se at the MP2 level [7]. A pseudopotential with 10 core electrons was used for P; W. R. Wadt, P. J. Hay, *J. Chem. Phys.* **1985**, *82*, 284. The associated basis set was further optimized (changes 5%) and supplemented with a set of d functions ($\eta_d = 0.45$). A 3s basis set was optimized for H and contracted to one function.

[9] C. Kölmel, R. Ahlrichs, *J. Phys. Chem.* **1990**, *94*, 5536.

[10] A. Grohmann, J. Riede, H. Schmidbaur, *Nature* **1990**, *345*, 140.

[11] F. A. Cotton, G. Wilkinson, *Advanced Inorganic Chemistry*, 5. edition, Wiley, New York, **1988**.

[12] A. Simon, *Angew. Chem.* **1981**, *93*, 23–44; *Angew. Chem. Int. Ed. Engl.* **1981**, *20*, 1–22; *ibid.* **1988**, *100*, 163–188 and **1988**, *27*, 159–183.

[13] A. Simon, *J. Solid State Chem.* **1985**, *57*, 2.

[14] O. Bars, J. Guilleric, D. Grandjean, *J. Solid State Chem.* **1973**, *6*, 6; R. Chevrel, P. Gougeon, M. Potel, M. Sergent, *ibid.* **1985**, *57*, 25; R. Chevrel, M. Sergent, B. Seeber, O. Fischer, A. Grüttner, K. Yvon, *Mater. Res. Bull.* **1979**, *14*, 567; A. Grüttner, K. Yvon, R. Chevral, M. Potel, M. Sergent, B. Seeber, *Acta Crystallogr. Sect. B* **1979**, *35*, 285; M. Potel, R. Chevrel, M. Decroux, O. Fischer, *C. R. Hebd. Séances Acad. Sci. Ser. C* **1979**, *288*, 429.

[15] W. Honle, H. G. von Schnering, A. Lipka, K. Yvon, *J. Less-Common Met.* **1980**, *71*, 135.

[16] D. Fenske, J. Ohmer, J. Hachgenei, K. Merzweiler, *Angew. Chem.* **1988**, *100*, 1300–1320; *Angew. Chem. Int. Ed. Engl.* **1988**, *27*, 1277–1296.

[17] F. A. Cotton, X. Feng, M. Matusz, R. Poli, *J. Am. Chem. Soc.* **1988**, *110*, 7077; R. Mason, D. M. P. Mingos, *J. Organomet. Chem.* **1973**, *50*, 53; P. K. Mehrotra, R. Hoffmann, *Inorg. Chem.* **1978**, *17*, 2187; K. M. Merz, R. Hoffmann, *ibid.* **1988**, *27*, 2120.

Borophosphates—A Neglected Class of Compounds: Crystal Structures of $M^{II}[BPO_5]$ (M^{II} = Ca, Sr) and $Ba_3[BP_3O_{12}]$**

Rüdiger Kniep,* Güller Gözel, Brigitte Eisenmann, Caroline Röhr, Matthias Asbrand, and Meral Kizilyalli

Given all the current activity in the field of microporous solids, it is remarkable that intermediate phases of the $M^I_2O/M^{II}O$-B_2O_3-P_2O_5(-H_2O) systems (M^I = alkali metal, M^{II} = alkaline earth metal) have been "forgotten". Bauer[1, 2] (1965/1966) reported the synthesis and X-ray diffraction patterns of the isostructural (hexagonal) phases $M^{II}[BPO_5]$ (M^{II} = Ca, Sr, Ba). Ramamoorthy and Rockett[3] (1974) confirmed the existence of $Ca[BPO_5]$ from phase equilibria studies on the system CaO-B_2O_3-P_2O_5 at 900 °C. Liebertz and Stähr[4] (1982) reported on the compound $Mg_3[BPO_7]$ (dimorphous; isostructural with α-/β-$Zn_3[BPO_7]$). Rulmond and Tarte[5] (1988) studied the borophosphates $M^{II}[BPO_5]$ synthesized by Bauer[1, 2] and assumed that they crystallized in the stillwellite type[6] ($Ce[BSiO_5]$). The neutral borophosphate BPO_4[7–9] is of particular interest because of its isostructural relationship to the polymorphic modifications of SiO_2.[10]

$Ca[BPO_5]$ and $Sr[BPO_5]$ were obtained as single-phase microcrystalline powders, as outlined in Equations (a) and (b) respectively, in platinum crucibles at 900 °C, following the procedures described by Bauer.[1]

$$CaHPO_4 \cdot 2H_2O + H_3BO_3 \longrightarrow Ca[BPO_5] + 4H_2O \quad (a)$$

$$SrCO_3 + H_3BO_3 + (NH_4)_2HPO_4 \longrightarrow Sr[BPO_5] + 3H_2O + 2NH_3 + CO_2 \quad (b)$$

Well-ground mixtures were used in the mole equivalents given in Equations (a) and (b). $Ca[BPO_5]$ was synthesized by heating the reaction mixture at a rate of 2 K min^{-1} to 900 °C and then cooling to room temperature at the same rate. For the synthesis of $Sr[BPO_5]$ the reaction mixture was heated at 2 K min^{-1} to 600 °C, cooled to room temperature, and ground up again; the reaction was completed by heating at 900 °C for 24 h. According to DTA experiments the borophosphates melt incongruently at 1025 °C ($Ca[BPO_5]$) and 1092 °C ($Sr[BPO_5]$).

Single-phase samples of the compound $Ba[BPO_5]$ could not be synthesized under the same conditions. Experiments employing an excess of $(NH_4)_2HPO_4$ as a flux medium or a solvent provided single crystals of the new compound $Ba_3[BP_3O_{12}]$: mixtures of $BaCO_3$, H_3BO_3, and $(NH_4)_2HPO_4$ in the mole ratio 2:1:3 were heated to 1300 °C over 4 h in a platinum crucible and were kept at this temperature for 8 h. After a further 24 h at 1000 °C the mixtures were cooled to room temperature over 4 h. A glassy matrix was formed in which were embedded elongated orthorhombic prisms of $Ba_3[BP_3O_{12}]$; $Ba_2[P_2O_7]$ was detected as an additional crystalline side product by X-ray powder diffraction studies. The crystal structures of the isostructural phases $Ca[BPO_5]$ and $Sr[BPO_5]$ were refined with X-ray powder data[10] (see also Fig. 1); the crystal structure of $Ba_3[BP_3O_{12}]$ was determined by single-crystal methods.[11]

[*] Prof. Dr. R. Kniep, Dr. G. Gözel,[+] Priv.-Doz. Dr. B. Eisenmann, Dr. C. Röhr, Dipl.-Ing. M. Asbrand, Prof. Dr. M. Kizilyalli[+]
Eduard-Zintl-Institut der Technischen Hochschule
Hochschulstrasse 10, D-64289 Darmstadt (FRG)
Telefax: Int. code + (6151)16-4073

[**] This work was supported by the Pinguin-Stiftung (Düsseldorf). G. G. thanks TÜBITAK for a grant for a research stay at the TH Darmstadt.

[+] Permanent address: Middle East Technical University
Department of Chemistry, TR-06531 Ankara (Turkey)

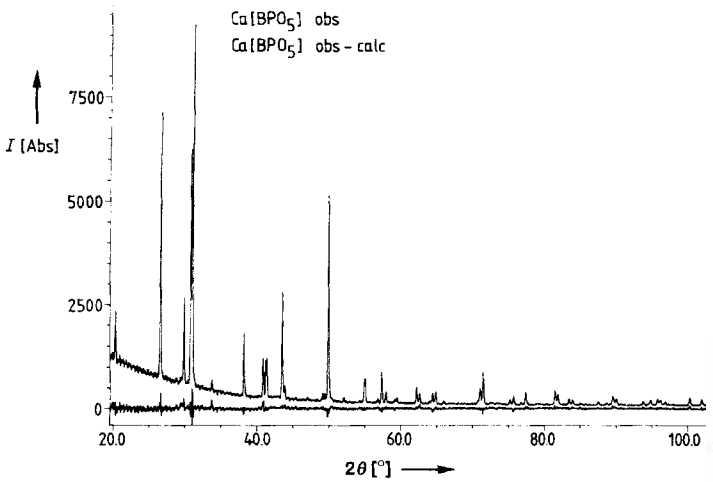


Fig. 1. Top: X-ray powder diffraction pattern of $Ca[BPO_5]$ ($Cu_{K\alpha}$ radiation). Bottom: difference diagram (measured − calculated).

The crystalline phases $Ca[BPO_5]$ ($Sr[BPO_5]$) and $Ba_3[BP_3O_{12}]$ contain $^1_\infty$anionic units of BO_4 and PO_4 tetrahedra joined by common vertices (Figs. 2 and 3). The $M^{II}[BPO_5]$ compounds, which crystallize in the stillwellite type,[6] contain central "dreier" single chains of BO_4 tetrahedra running parallel to [001], which are linked to terminal PO_4 tetrahedra to form loop-branched chains.[13] The polymeric assembly of tetrahedral anions in crystalline $Ba_3[BP_3O_{12}]$ consists of central "vierer" single chains (BO_4 and PO_4 in alternation) which run parallel to [001]; the two free vertices of each BO_4 tetrahedron are connected with terminal PO_4 tetrahedra, resulting in "zweifach" open branched "vierer" single chains.[13] Tetrahedral connections of this kind were hitherto unknown. $Ba_3[BP_3O_{12}]$ contains wide channels in which the barium ions are located.

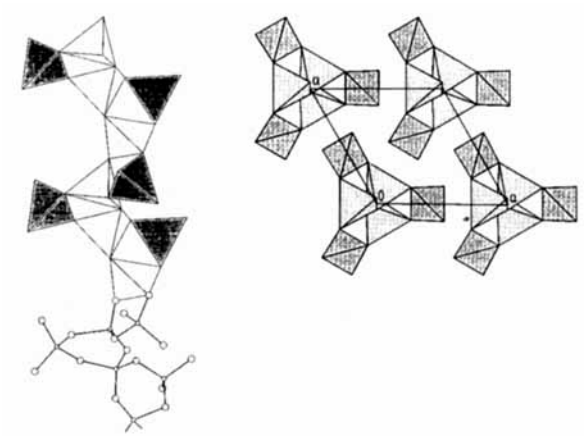


Fig. 2. Section of the crystal structure of $Ca[BPO_5]$ ($Sr[BPO_5]$). Left: loop-branched chains of tetrahedra $^1_\infty[BPO_5^{2-}]$ running parallel to [001]: light tetrahedra: BO_4; dark tetrahedra: PO_4. Right: packing of the chains of tetrahedra $^1_\infty[BPO_5^{2-}]$; view along [001].

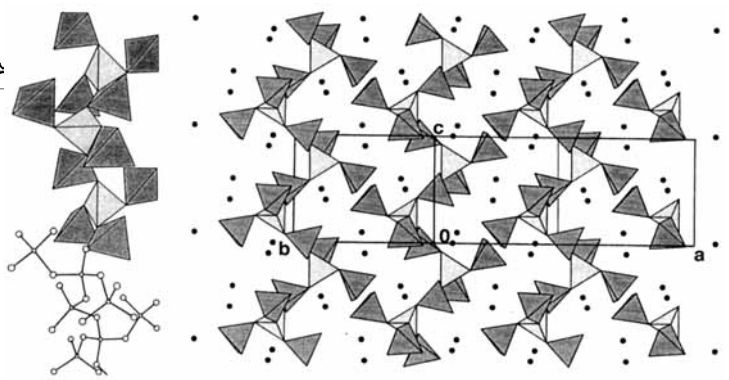


Fig. 3. Section of the crystal structure of $Ba_3[BP_3O_{12}]$. Left: "zweifach" open branched chains of tetrahedra $^1_\infty[BP_3O_{12}^{6-}]$; light tetrahedra: BO_4; dark tetrahedra: PO_4. Right: arrangement of chains of tetrahedra in the crystal structure; Ba^{2+} ions (black circles) within wide channels.

The bond lengths and angles in the polymeric tetrahedral anions of these borophosphates are quite similar to those in known polyphosphates and borates with a tetrahedrally coordinated central atom (see Table 1).

Given the results presented here and considering the known linking modes of tetrahedral groups, the formation of borophosphates with layered or framework structures or structures containing cavities may also be envisaged. The variety of possible structural linking patterns is certainly increased, since boron displays the trigonal-planar arrangement as well as the tetrahedral coordination by oxygen. In this context the "microporous" zincoborate $Zn_4O(BO_3)_2$[17] should be mentioned; here ZnO_4 tetrahedra and trigonal-planar BO_3 groups from a three-dimensional network with large cavities running through it. The technological importance of the incorporation of boron into microporous structures composed of tetrahedra (e.g. alu-

Table 1. Bond lengths [pm] and angles [°] of the three borophosphates presented here together with those of some related compounds. The abbreviations br and term stand for bridging and terminal.

	B-O_{br}	P-O_{br}	P-O_{term}	O-B-O	B-O-B	O-P-O	P-O-P	B-O-P
$Ba_3[BP_3O_{12}]$	144(2)	158(2)	151(2)	107(2)–		103(1)–		130(2)
	145(2)	162(2)	156(2)	111(2)		114(1)		
$[B_5O_6(OH)_4]^-$	144.2(1)–			107.9(1)	121.5(1)–			
[14]	147.9(1)			110.2(1)	124.5(1)			
$AgM[PO_3]_2$		160.1(3)	147.9(3)–			101.9(1)–	129.6(2)	
[15]		161.7(3)	149.3(3)			120.8(2)	134.5(2)	
$Ca[BPO_5]$	146(6)	149(3)	149(3)	102(2)–	122(1)	106(1)		126(1)
	158(6)			116(2)		113(1)		
$Sr[BPO_5]$	149(9)	150(4)	143(4)	104(3)–	122(1)	104(1)–		129(2)
	151(9)			112(3)		121(1)		
$Na_2[ZnPO_4(OH)]$		154.7(4)	152.8(4)			108.1(2)–		
$\cdot 7H_2O$ [16] [a]		154.8(4)	153.1(4)			111.4(2)		

[a] The crystal structure contains central "zweier" single chains of $ZnO_2(OH)_2$ tetrahedra, which are loop-branched through terminal PO_4 groups.

mosilcates) has already been shown, for example, with "boron/MFI-zeolite".[18]

Received: October 20, 1993 [Z 6436 IE]
German version: *Angew. Chem.* **1994**, *106*, 791

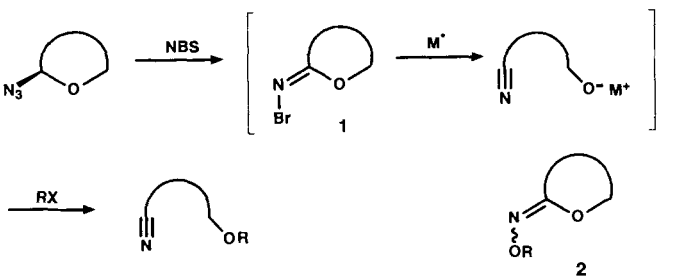
[1] H. Bauer, *Z. Anorg. Allg. Chem.* **1965**, *337*, 183–190.
[2] H. Bauer, *Z. Anorg. Allg. Chem.* **1966**, *345*, 225–312.
[3] P. Ramamoorthy, T. J. Rockett, *J. Am. Ceram. Soc.* **1974**, *57*, 501–502.
[4] J. Liebertz, S. Stähr, *Z. Kristallogr.* **1982**, *160*, 135–137.
[5] A. Rulmont, P. Tarte, *J. Solid State Chem.* **1988**, *75*, 244–250.
[6] A. A. Voronkov, Yu. A. Pyatenko, *Kristallografiya* **1967**, *12*, 258–265; *Sov. Phys. Crystallogr.* **1967**, *12*, 214–220.
[7] G. E. R. Schulze, *Z. Phys. Chem.* **1934**, *B24*, 215–240.
[8] J. D. Mackenzie, W. L. Roth, R. H. Wentorf, *Acta Crystallogr.* **1959**, *12*, 79.
[9] F. Dachille, L. S. Dent Glasser, *Acta Crystallogr.* **1959**, *12*, 820–821.
[10] a) $Ca[BPO_5]$ ($Sr[BPO_5]$): Space group $P3_121$; a = 667.99(2) (684.88(1)), c = 661.21(3) (681.59(2)) pm; Z = 3; ϱ_{calcd} = 2.53 (3.19) $g\,cm^{-3}$; Stoe diffractometer 6.11.1, position-sensitive detector, $Cu_{K\alpha}$ radiation; 2θ range/step width 10 to 103°/0.02° (18° to 105°/0.02°); number of measurements used for refinement: 4138 (4006); structural refinement using the Rietveld method [12] (isotypic relation to stillwellite [6]; number of refined profile parameters: 16 (15); number of refined structural parameters: 16 (16); R_{wp} = 0.079 (0.11), $R(I, hkl)$ = 0.073 (0.077). (b) Further details of the crystal structure investigation may be obtained from the Fachinformationszentrum Karlsruhe, D-76344 Eggenstein-Leopoldshafen (FRG) on quoting the depository number CSD-57927, the names of the authors, and the journal citation.
[11] $Ba_3[BP_3O_{12}]$: Space group $Ibca$; a = 2221.1(8), b = 1429.6(6), c = 710.(4) pm; Z = 8; ϱ_{calcd} = 4.17 $g\,cm^{-3}$; 1328 independent observed reflections ($I \geq 2\sigma(I)$); Philips PW 1100 diffractometer, 2θ range from 5° to 60°; $Mo_{K\alpha}$ radiation; R = 0.075; residual electron density $+3.2/-4.9\ e^-\ 10^{-6}$ pm^{-3} [10b].
[12] H. M. Rietveld, *J. Appl. Crystallogr.* **1969**, *2*, 65–71.
[13] Nomenclature according to F. Liebau, *Structural Chemistry of Silicates*, Springer, Berlin, **1985**.
[14] M. Wiebcke, C. C. Freyhardt, J. Felsche, G. Engelhardt, *Z. Naturforsch. B*, in press.
[15] M. T. Averbuch-Pouchot, *J. Solid State Chem.* **1993**, *102*, 93–99.
[16] W. T. A. Harrison, T. M. Nenoff, T. E. Gier, G. D. Stucky, *Inorg. Chem.* **1993**, *32*, 2437–2441.
[17] W. T. A. Harrison, T. E. Gier, G. D. Stucky, *Angew. Chem.* **1993**, *105*, 788–790; *Angew. Chem. Int. Ed. Engl.* **1993**, *32*, 724–726.
[18] D. S. Santilli, S. I. Zones in *Synthesis of Microporous Materials: Vol. 1: Molecular Sieves* (Eds.: M. L. Occelli, H. E. Robson), Van Nostrand Reinhold, New York, **1992**, p. 373.
[19] Note added in proof: A recent, more extensive literature search revealed the structure determinations of the minerals lüneburgite ($Mg_3(H_2O)_6[B_2(OH)_6(PO_4)_2]$) and seamanite ($Mn_3(OH)_2[B(OH)_4][PO_4]$). Lüneburgite contains dimeric tetrahedral units $[BPO_7]^{6-}$ (P. K. S. Gupta, G. H. Swikart, R. Dimitrijević, M. B. Hossain, *Amer. Mineral.* **1991**, *76*, 1400–1407)), whereas the crystal structure of seamanite contains isolated BO_4 and PO_4 tetrahedra (P. B. Moore, S. Ghose, *Amer. Mineral.* **1971**, *56*, 1527–1538.).

Conversion of Glycosyl Azides via *N*-Bromoglycosylimines to Aldononitriles

Alois Fürstner* and Jean-Pierre Praly*

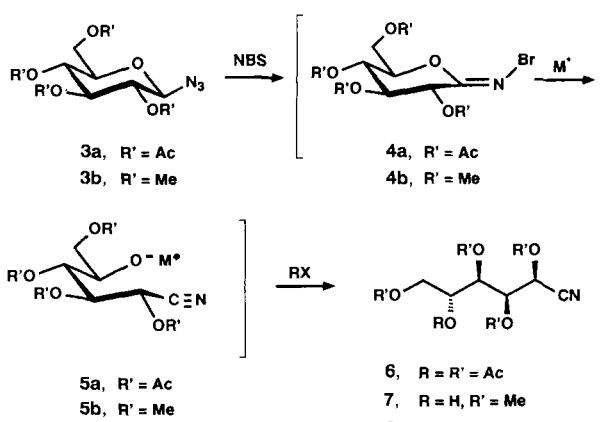
N-bromosuccinimide (NBS) reacts with β-glycosyl azides to afford *N*-bromoglycosylimines **1** in good yield,[1] the chemistry of which is completely unexplored. Their similarity with (*Z*)-hydroxyiminoglyconolactones **2**, which have been used, for example, for the synthesis of spiro sugars, carbohydrate derived oxazoles, glycosylidene carbenes, and ring-expanded structures,[2] makes it worthwhile to explore the reactivity of **1** in more detail. Any synthetic application, however, must take their hydrolytic lability and low thermal stability into account. We report here on a metal-triggered reaction which converts these sensitive compounds to substituted aldononitriles.

The extraordinary reactivity of metal-graphite reagents makes them suitable for inducing many transformations under neutral conditions in aprotic media at low reaction temperatures; therefore, they can be applied nicely to hydrolytically labile substrates.[3] Furthermore, they are compatible with a variety of functional groups and can thus also be applied to complex natural products.[4] Deoxyhalo sugars, for example, on treatment with either C_8K or Zn/Ag-graphite are prone to reductive eliminations, resulting in the smooth ring opening of the carbohydrate precursors.[5] *N*-bromoglycosylimines may also undergo such dealkoxyhalogenations, if clean *N*-metalation can be achieved (Scheme 1).



Scheme 1. Successive reaction of glycosyl azides with NBS and metal-graphite (M*) (schematic representation). The structural analogy between *N*-bromoglycosylimines **1** and (*Z*)-hydroxyiminoglyconolactones **2** is evident.

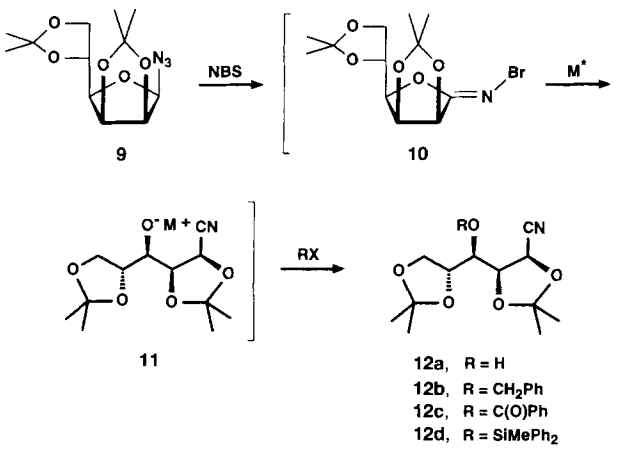
The reaction of 2,3,4,6-tetra-*O*-acetyl-β-D-glucopyranosyl azide **3a**[6] with NBS and azobisisobutyronitrile (AIBN) in CCl_4 according to the literature procedure[11] and the subsequent treatment of the crude bromoimine derivative **4a** with an excess of Zn/Ag-graphite in THF, however, did not lead to a clean transformation. Since the NMR study of the crude product indicated the presence of several aldononitrile derivatives, the mixture was acetylated (Ac_2O/pyridine), affording penta-*O*-acetylgluconolactone **6**[7] in 71% isolated yield (Scheme 2). Since partial migration of the acetyl groups in the intermediate ring-opened zinc alcoholate **5a** (M = ZnBr) apparently accounted for the observed mixture, we chose azides stable to basic conditions, such as **3b** and **9** (Scheme 3),[8] as substrates. In fact, after



Scheme 2. Reactions according to Scheme 1 in the glucose series; M* = Zn/Ag-graphite or $2C_8K$ (see Table 1).

[*] Univ.-Doz. Dr. A. Fürstner
Max-Planck-Institut für Kohlenforschung
Kaiser-Wilhelm-Platz 1, D-45470 Mülheim/Ruhr (FRG)
Telefax: Int. code + (208)306-2980
Dr. J.-P. Praly
Université Claude Bernard Lyon 1
Laboratoire de Chimie Organique Associé au CNRS, ESCIL
43, Boulevard du 11 Novembre 1918, F-69622 Villeurbanne (France)

 © VCH Verlagsgesellschaft mbH, D-69451 Weinheim, 1994 0570-0833/94/0707-0751 $ 10.00+.25/0



Scheme 3. One-pot conversion of mannofuranosyl azide **9** to protected mannononitriles **12**. M* = Zn/Ag-graphite or $2C_8K$ (see Table 1).

conversion to the corresponding bromoimines, both nicely gave the respective nitriles in good yield upon reaction with either Zn/Ag-graphite or C_8K (Table 1). The use of C_8K provided the additional advantage that the intermediate potassium alcoholates **5b** and **11** (M = K) may be trapped in situ with electrophiles, thus affording differently protected aldononitriles in one high-yielding step (Table 1). The synthetic potential of these highly functionalized sugar derivatives previously prepared by multistep approaches has been outlined recently.[10]

Table 1. Preparation of aldononitriles from glycosyl azides.

Substrate	M*-Graphite	RX	Product (Yield)
3a	Zn/Ag	Ac_2O [a]	**6** (71%)
3b	C_8K	CS_2/MeI	**7** (10%), **8** (62%)
9	Zn/Ag	– [b]	**12a** (87%)
9	C_8K	– [b]	**12a** (90%)
9	C_8K	$C_6H_5CH_2Br$	**12b** (76%)
9	C_8K	C_6H_5COCl	**12c** (80%)
9	C_8K	$Ph_2MeSiCl$	**12d** (86%)

[a] Acetylation using Ac_2O (5 equiv) in pyridine. [b] Moisture of solvents used for workup as proton source.

Attempts to cyclize xanthate **8**, obtained by quenching the potassium alcoholate **5b** (M = K) with CS_2 followed by alkylation with methyl iodide, under radical conditions failed.[11]

In summary, we describe the first transformations of sensitive *N*-bromoglycosylimines. Upon treatment with metal-graphite reagents these carbohydrate derivatives can be reductively ring-opened to aldononitriles, with an additional option for in situ derivatization if C_8K is used as the reducing agent. The reaction sequence constitutes not only a high-yielding approach to enantiomerically pure open-chain building blocks from sugars, but also proves for the first time that dealkoxyhalogenations can occur along (hetero) double-bond systems.

Experimental Procedure

12c: To a solution of 2,3:5,6-di-*O*-isopropylidene-β-D-mannofuranosyl azide **9** (300 mg, 1.05 mmol) [8] in CCl_4 (40 mL) was added NBS (393 mg, 2.21 mmol) and AIBN (10 mg). The mixture was stirred at room temperature until TLC showed complete conversion of the substrate and the appearance of a faint brown color in the reaction medium indicated the end of the conversion (2–3 h). The insoluble residues were filtered off, rinsed with CCl_4 (10 mL), the solvent removed in vacuo at < 20 °C (bath temperature), and the residue coevaporated twice with THF (3 mL each) to ensure complete removal of the CCl_4 from the syrup. The crude **10** thus obtained was dissolved in THF (3 mL) and added to a suspension of C_8K (426 mg, 3.15 mmol) [5, 9] in THF (20 mL) under argon. TLC showed rapid conversion (< 5 min) to a more polar compound. After addition of benzoyl chloride (300 mg, 2.13 mmol) in THF (1 mL), the reaction mixture was stirred for 1 h at room temperature, filtered, the solvent evaporated, and the residue purified by flash chromatography affording **12c** as colorless crystals (304 mg, 80%).

Table 2. Physical and analytical data of **3b**, **6**–**8**, and **12a**–**d**.

3b: Syrup; $[\alpha]_D^{20} = -22$ ($c = 2$ in $CHCl_3$); IR: $\tilde{\nu} = 2110\ cm^{-1}$ (N_3); ^1H NMR (200 MHz, C_6D_6): $\delta = 2.91$ (t, $J(2,3) = 8.5$, 1H, H-2), 3.06 (t, $J(3,4) = 8.8$, 1H, H-3), 3.06 (m, $J(5,6) = 1.5$, $J(5,6') = 3.8$, 1H, H-5), 3.14 (s, 3H, OMe), 3.22 (t, $J(4,5) = 9.5$, 1H, H-4), 3.38, 3.40 (s, each 3H, OMe), 3.41 (m, 2H, H-6,6'), 3.50 (s, 3H, OMe), 4.12 (d, $J(1,2) = 8.4$, 1H, H-1); ^{13}C NMR (50 MHz, C_6D_6): $\delta = 59.17$, 60.25, 60.37, 60.75, 71.27, 77.49, 79.29, 83.90, 87.30, 90.13.

6: M.p. 83–85 °C (ref. [7]: 82–84 °C); $[\alpha]_D^{20} = +46.9$ ($c = 0.6$ in CH_2Cl_2) (ref. [7]: +47.3); ^1H NMR (300 MHz, $CDCl_3$): $\delta = 5.56$ (dd, $J(3,4) = 2.6$, $J(4,5) = 8.3$, 1H, H-4), 5.48 (d, $J(2,3) = 6.3$, 1H, H-2), 5.37 (dd, 1H, H-3), 5.11 (ddd, $J(5,6) = 2.9$, $J(5,6') = 5$, 1H, H-5), 4.08, 4.22 (dAB, $J(6,6') = 12.5$, 2H, H-6,6'), 2.14, 2.12, 2.11, 2.03, 2.02 (s, each 3H, MeCOO); ^{13}C NMR (75 MHz, $CDCl_3$): $\delta = 170.41$ (s), 169.60 (s), 169.46 (s), 169.41 (s), 168.24 (s), 114.11 (s), 68.22 (d), 67.19 (d), 67.10 (d), 61.61 (t), 58.90 (d), 20.62 (q), 20.31 (q), 20.05 (q).

7: Syrup; $[\alpha]_D^{20} = +62$ ($c = 0.2$ in CH_2Cl_2); ^1H NMR (300 MHz, $CDCl_3$): $\delta = 4.37$ (d, $J(2,3) = 6.8$, 1H, H-2), 3.88 (dt, $J = 4, 8$, 1H, H-5), 3.79 (dd, $J = 2.6, 7$, 1H), 3.45–3.62 (m, 4H), 3.57, 3.54, 3.47, 3.38 (s, each 3H, OMe); ^{13}C NMR (75 MHz, $CDCl_3$): $\delta = 116.87$ (s), 80.98 (d), 79.85 (d), 73.22 (t), 72.19 (d), 69.50 (d), 61.29 (q), 60.51 (q), 59.19 (q), 58.84 (q).

8: Syrup; $[\alpha]_D^{20} = +10.4$ ($c = 4.9$ in CH_2Cl_2); ^1H NMR (300 MHz, $CDCl_3$): $\delta =$ 5.80 (dt $J = 3, 6.6$, 1H, H-5), 4.31 (d, $J(2,3) = 7$, 1H, H-2), 3.96 (dd, $J = 2.6, 7$, 1H, H-3), 3.80, 3.63 (dAB, $J(5,6) = 2.6$, $J(5,6') = 3.8$, $J(6,6') = 11.6$, 2H, H-6,6'), 3.48 (2s, m, 7H, H-4, 2-OMe), 3.40, 3.30 (s, each 3H, OMe), 2.51 (s, 3H, C(S)SMe); ^{13}C NMR (75 MHz, $CDCl_3$): $\delta = 215.22$ (s), 116.37 (s), 80.77 (d), 80.61 (d), 78.25 (d), 71.73 (d), 69.68 (t), 61.08 (q), 61.02 (q), 59.17 (q), 58.74 (q), 19.28 (q).

12a: M.p. 97–98 °C; $[\alpha]_D^{20} = +62.4$ ($c = 1.2$ in CH_2Cl_2); ^1H NMR (300 MHz, $CDCl_3$): $\delta = 4.81$ (d, $J(2,3) = 5$, 1H, H-2), 4.15 (ddd, $J(3,4) = J(4,5) = 8.2$, $J(4,-OH) = 1.5$, 1H, H-4), 4.07 (dd, 1H, H-3), 3.78–3.95 (m, 3H, H-5, H-6,6'), 3.21 (bs, 1H, OH), 1.53, 1.39, 1.34, 1.27 (s, each 3H, Me); ^{13}C NMR (75 MHz, $CDCl_3$): $\delta = 117.12$ (s), 111.53 (s), 110.43 (s), 79.50 (d), 75.69 (d), 72.55 (d), 68.02 (t), 66.37 (d), 26.97 (q), 25.92 (2q), 25.16 (q).

12b: M.p. 74–76 °C; $[\alpha]_D^{20} = +71.5$ ($c = 1.2$ in CH_2Cl_2); ^1H NMR (300 MHz, $CDCl_3$): $\delta = 7.35–7.39$ (m, 5H, -Ph), 5.00, 4.70 (AB, $J(AB) = 11.4$, 2H, CH_2Ph), 4.89 (d, $J(2,3) = 4.9$, 1H, H-2), 4.24 (dd, $J(3,4) = 8.5$, 1H, H-3), 4.18 (dd, $J(4,5) = 6.5$, 1H, H-4), 3.98 (ddd, $J(5,6) = J(5,6') = 8.7$, 1H, H-5), 3.82 (dd, $J(6,6') = 8.7$, 1H, H-6), 3.74 (dd, 1H, H-6'), 1.68, 1.46, 1.45, 1.34 (s, each 3H, Me); ^{13}C NMR (75 MHz, $CDCl_3$): $\delta = 138.05$ (s), 128.61 (d), 128.42 (d), 128.29 (d), 128.17 (d), 117.55 (s), 111.65 (s), 110.72 (s), 81.08 (d), 79.97 (d), 75.42 (d), 74.75 (d), 68.50 (t), 67.04 (d), 27.26 (q), 26.22 (q), 25.90 (q), 25.44 (q).

12c: M.p. 131–132 °C; $[\alpha]_D^{20} = +20.8$ ($c = 0.3$ in CH_2Cl_2); ^1H NMR (300 MHz, $CDCl_3$): $\delta = 7.45–8.09$ (m, 5H, Ph), 5.57 (dd, $J(3,4) = J(4,5) = 8.3$, 1H, H-4), 4.96 (d, $J(2,3) = 5.2$, 1H, H-2), 4.48 (dd, 1H, H-3), 4.11–4.28 (m, 2H, H-6,6'), 4.02 (dd, $J(5,6) = J(5,6') = 8.6$, 1H, H-5), 1.59, 1.50, 1.40, 1.38 (s, each 3H, Me); ^{13}C NMR (75 MHz, $CDCl_3$): $\delta = 165.49$ (s), 133.61 (d), 130.18 (d), 129.75 (s), 128.70 (d), 116.92 (s), 112.18 (s), 110.95 (s), 77.79 (d), 75.04 (d), 72.67 (d), 67.89 (t), 66.48 (d), 27.10 (q), 26.26 (2q), 25.74 (q).

12d: Syrup $[\alpha]_D^{20} = +42.2$ ($c = 0.7$ in CH_2Cl_2); ^1H NMR (300 MHz, $CDCl_3$): $\delta = 7.41–7.69$ (m, 10H, Ph); 4.87 (d, $J(2,3) = 3.3$, 1H, H-2), 4.08–4.21 (m, 4H), 3,72 (dd, 1H), 1.58, 1.45, 1.38, 1.25 (s, each 3H, Me); ^{13}C NMR (75 MHz, $CDCl_3$): $\delta = 138.02$ (s), 137.98 (s), 134.60 (d), 134.50 (d), 134.14 (d), 130.16 (d), 129.91 (d), 128.05 (d), 127.64 (d), 117.32 (s), 111.11 (s), 110.66 (s), 80.32 (d), 76.59 (d), 75.04 (d), 68.86 (t), 66.64 (d), 27.07 (q), 25.76 (2q), 25.56 (q), -2.24 (1q).

Received: October 28, 1993 [Z 6460 IE]
German version: *Angew. Chem.* **1994**, *106*, 779

[1] a) J.-P. Praly, C. Di Stefano, L. Somsak, G. Descotes, *J. Chem. Soc. Chem. Commun.* **1992**, 200–201; b) J.-P. Praly, D. Senni, R. Faure, unpublished results.

[2] a) D. Beer, A. Vasella, *Helv. Chim. Acta* **1985**, *68*, 2254–2274; b) E. Bozo, A. Vasella, *ibid.* **1992**, *75*, 2613–2633; c) A. Vasella, *Pure Appl. Chem.* **1991**, *63*, 507–518; d) M. Yokoyama, K. Sujino, M. Irie, N. Yamazaki, T. Hiyama, N. Yamada, H. Togo, *J. Chem. Soc. Perkin Trans. 1* **1991**, 2801–2809; e) M. Yokoyama, M. Irie, K. Sujino, T. Kagemoto, H. Togo, M. Funabashi, *ibid.* **1992**, 2127–2134.

[3] A. Fürstner, *Angew. Chem.* **1993**, *105*, 171–197; *Angew. Chem. Int. Ed. Engl.* **1993**, *32*, 164–189.

[4] a) A. Fürstner, J. Baumgartner, *Tetrahedron*, **1993**, *49*, 8541–8560; b) R. E. Ireland, T. K. Highsmith, L. D. Gegnas, J. L. Gleason, *J. Org. Chem.* **1992**, *57*, 5071–5073.
[5] a) A. Fürstner, H. Weidmann, *J. Org. Chem.* **1989**, *54*, 2307–2311; b) A. Fürstner, D. N. Jumbam, J. Teslic, H. Weidmann, *ibid.* **1991**, *56*, 2213–2217; c) A. Fürstner, *Tetrahedron Lett.* **1990**, *31*, 3735–3738.
[6] H. Paulsen, Z. Györgydeak, M. Friedmann, *Chem. Ber.* **1974**, *107*, 1568–1578.
[7] R. Kuhn, J. C. Jochims, *Chem. Ber.* **1960**, *93*, 1047–1052.
[8] Compound **9**: W. Schörkhuber, E. Zbiral, *Liebigs Ann. Chem.* **1980**, 1455–1469. Compound **3b** was prepared by Zemplen deacetylation of **3a**, followed by methylation (NaH/MeI in dimethylformamide); for physical data see Table 2.
[9] Similar trapping experiments were successfully used in glycal syntheses, see: a) A. Fürstner, H. Weidmann, *J. Carbohydr. Chem.* **1988**, 7, 773–783; b) A. Fürstner, *Liebigs Ann. Chem.* **1993**, 1211–1217.
[10] P. Ermert, A. Vasella, *Helv. Chim. Acta* **1991**, *74*, 2043–2053.
[11] Successful cyclizations by the addition of carbon-centered radicals onto nitriles: a) D. L. J. Clive, P. L. Beaulieu, L. Set, *J. Org. Chem.*, **1984**, *49*, 1313–1314; b) J. K. Dickson, R. Tsang, J. M. Llera, B. Fraser-Reid, *ibid.* **1989**, *54*, 5350–5356; c) H. Pak, J. K. Dickson, B. Fraser-Reid, *J. Am. Chem. Soc.* **1989**, *54*, 5357–5364; d) R. A. Alonso, C. S. Burgey, B. V. Rao, G. D. Vite, R. Vollerthun, M. A. Zottola, B. Fraser-Reid, *ibid.* **1993**, *115*, 6666–6672; similar failures e) N. S. Simpkins, S. Stokes, A. J. Whittle, *J. Chem. Soc. Perkin Trans. 1* **1992**, 2471–2477; f) J. Marco-Contelles, C. Pozuelo, M. L. Jimeno, L. Martinez, A. Martinez-Grau, *J. Org. Chem.* **1992**, *57*, 2625–2631; g) B. W. A. Yeung, J. L. M. Contelles, B. Fraser-Reid, *J. Chem. Soc. Chem. Commun.* **1989**, 1160–1161.

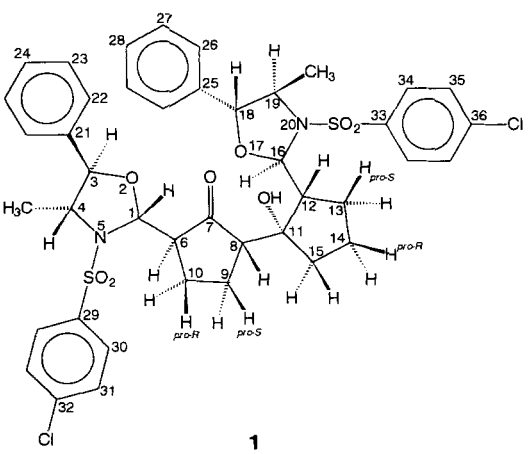
Determination of the Relative Configuration by Distance Geometry Calculations with Proton–Proton Distances from NOESY Spectra**

Michael Reggelin,* Matthias Köck, Kilian Conde-Frieboes, and Dale Mierke

Investigations of the structures of reactive organometallic compounds such as lithiated or titanated 2-alkenylsulfoximides[1] are quite difficult. Studies of these species under the conditions required for their reaction, in other words at low temperatures and in solution, are particularly problematic. Here NMR spectroscopy is the method of choice, since in principle the reaction dynamics (e.g. conformational flexibility, configurational behavior) of the metalated intermediates can be examined, which may aid in the interpretation of the stereochemical outcome of the reaction.[1] Often when no other method is available, only the relationship between the configuration of the metalated intermediates and the stereochemistry of the products of a stereoselective organometallic reaction can provide information on the stereochemistry of these intermediates. Thus, the development of a method independent of postulated models of transition states (e.g. Zimmerman–Traxler model) would be very valuable.

The obvious question is how NMR data (H–H distances, coupling constants) can be used to determine the relative configurations of molecules that may be flexible. To answer this question we conducted "NOE-restrained" molecular dynamics calculations with heavily weighted experimental distances.[2] The problem of the parametrization of the force field prevents the general application of this approach. Since suitable parameters are not available for many interesting systems such as polar organometallic compounds, alternative procedures had to be developed. The best approach appeared to be the application of as many actual measurable quantities, in other words H–H distances, as possible.

In principle conformations can be determined from distance data by distance geometry (DG) calculations,[3, 4] a procedure used for the NMR spectroscopic structure determination of biopolymers.[3] The absolute configuration of a stereogenic center is determined by the sign of the "chiral volume" (V_C)[5] taken up by the atoms bound to this chiral center. Typically a constant value is maintained for the chiral volume in the calculations to ensure the stereochemical integrity of the stereogenic center under consideration. If this chiral restraint is removed, the sense of chirality can be inverted and a new conformational space is opened up, within which a conformation can be found that optimally fits the distances obtained from the NOESY data. This method was applied for the assignment of diastereotopic protons in proteins,[6] and we have demonstrated its suitability for the determination of the configuration of a model compound.[7] Since the stereogenic centers of interest were in a section of the molecule that could be determined quite well from NOEs (bridgehead positions), we wondered if this method was generally applicable. To find out more about the potential of DG calculations for the determination of relative configurations we chose the much more flexible bisoxazolidine **1**.[8]



1

In addition to the known stereogenic centers in the norpseudoephedrin section of the molecule, **1** has six additional centers with unknown configurations. Two-dimensional NMR spectroscopy was used for the assignment of all of the protons in **1**.[9] The analysis began with the differentiation of the two quasisymmetric halves of the molecule. The OH-bearing carbon atom (C-11) was easy to identify, because it does not give rise to a cross peak in the proton-detected H–C correlation spectrum (HMQC[10]). This atom has a heteronuclear long-range correlation ($^3J_{C,H}$) with the proton at C-16 (HMBC[11]), which was used to identify the halves of the molecule. The ^{1}H signals within each half were assigned based on DQF-COSY and TOCSY experiments.[12] The arene protons were assigned with a selective HMBC experiment (excitation with a 270° Gaussian pulse[13]). Seven 400 MHz NOESY spectra were recorded for the determi-

[*] Dr. M. Reggelin, Dr. M. Köck, Dr. K. Conde-Frieboes
Institut für Organische Chemie der Universität
Marie-Curie-Strasse 11, D-60439 Frankfurt am Main (FRG)
Telefax: Int. code + (69) 5800-9128
Dr. D. F. Mierke[+]
Organisch-chemisches Institut der Technischen Universität München
Lichtenbergstrasse 4, D-85747 Garching (FRG)
[+] Present address:
Department of Chemistry, Clark University
Worcester, MA 01610 (USA)

[**] This work was supported by the Deutsche Forschungsgemeinschaft and the Fonds der Chemischen Industrie (Habilitation fellowship for M. R. and postdoctoral fellowship for M. K.). We thank Prof. Dr. C. Griesinger and Prof. Dr. H. Kessler for their generous support.

nation of the H–H distances (mixing times: $\tau_{mix} = 100, 200, 300, 400, 500, 800, 1200$ ms). The cross peak between the geminal protons on C-10 was used as a calibration peak ($r = 178$ pm), and the distances corresponding to the volume integrals of the other cross peaks were calculated. Only results that were independent of the mixing time (generally up to $\tau_{mix} = 500$ ms, initial rate approximation) were used for the determination of the distances.

The DG calculations were conducted with a modified version[7, 15] of the DISGEO program.[3, 14] Ninety-nine structures were calculated by "random metrization", optimized[15, 16] with "distance bounds driven dynamics" (DDD)[17, 18] in four-dimensional space, and finally reduced to three-dimensional space with the "embed" algorithm. These structures were again refined with DDD.[19] The planarity of amide functions and aromatic rings, as well as the configurations of carbon atoms of known chirality, were secured with a penalty function.[20] The chiral volumes of the six centers of unknown absolute configuration were removed from the list of chiral restraints.

The 99 structures generated could be divided into three structure families according to their "pseudoenergies"[20] from the DDD calculations. The family with the lowest pseudoenergies (between 47 and 52) consists of 70 structures, the next has 11 structures (pseudoenergies between 67 and 95), and the last family comprises 18 structures with very high pseudoenergies (between 121 and 261). All the structures in the first two families except one (in the second family) have the same absolute configurations at the six unknown stereogenic centers as in the crystal structure.[21] Even in the third, energetically unfavorable family two structures (of 18) have the correct configurations. In the superpositioned structures from the first family shown in Figure 1a the conformations of the two inner five-membered rings of oxazolidine **1** are close to those in the structure determined by X-ray analysis. The intramolecular hydrogen bond between the acidic hydrogen atom and the carbonyl oxygen atoms is also accurately reproduced (Fig. 1c, d).

The distinct structural fluctuations in the arene region, which affect the precision of the description of the oxazolidine rings, are a consequence of the *o*- and *m*-protons. For this reason no individual distances from these protons are available. The average chiral volumes for the first family and for all calculated structures as well as the minimum and maximum volumes are listed in Table 1.

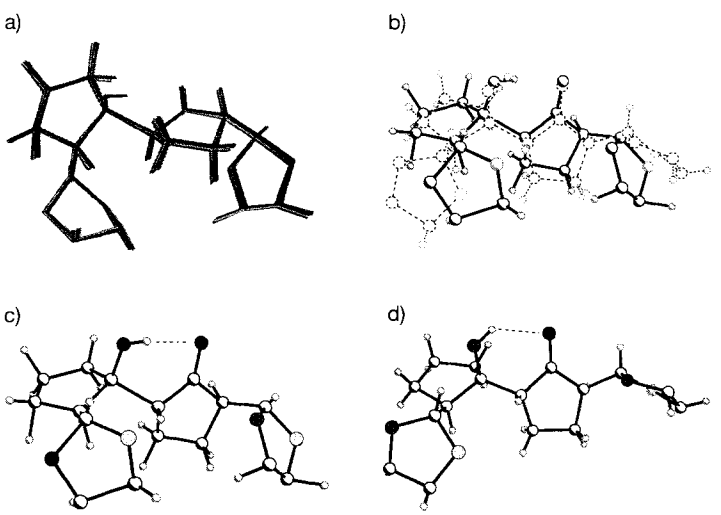


Fig. 1. a) Superposition of 43 randomly chosen structures from the first structure family obtained from DG calculations. b) Superposition of the crystal structure of **1** (dotted lined) and the DG structure (without the arene units). c) The intramolecular hydrogen bond is reproduced in the DG structure. d) The corresponding section of the crystal structure with the hydrogen bond drawn in. (Nitrogen: light gray circles, oxygen: dark gray circles).

Table 1. Calculated chiral volumes V_C of the six unknown stereogenic centers in **1**.

Atom no.	[b]		[c]		[d]	
	V_C	σ	V_C	σ	V_C^{min}	V_C^{max}
1	5.499	0.083	4.895	0.257	−6.417	7.162
6	7.752	0.020	6.924	0.244	−9.146	8.291
8	8.651	0.009	7.848	0.240	−9.156	7.108
11	5.074	0.010	4.291	0.351	−8.150	7.156
12	−4.944	0.009	−4.647	0.136	−3.313	5.843
16	5.129	0.008	4.926	0.108	−1.296	6.684

[a] Here positive values correspond to an (*R*)-configurated chiral center. σ = standard deviation. [b] Average chiral volume from the 70 structures of the first family. [c] Average chiral volume from all 99 structures. [d] Minimum and maximum volumes for all 99 structures.

Even after averaging over *all* structures, including those with large deviations from the required distances, the correct absolute configurations are obtained for the previously unknown chiral centers. This may be traced back to the fact that in general even in the "high-energy family" only one stereogenic center is determined incorrectly.

Received: September 6, 1993
Revised version: December 17, 1993 [Z6344IE]
German version: *Angew. Chem.* **1994**, *106*, 822

[1] M. Reggelin, H. Weinberger, *Angew. Chem.* **1994**, *106*, 489–491; *Angew. Chem. Int. Ed. Engl.* **1994**, *33*, 444–446.
[2] M. Reggelin, H. Hoffmann, M. Köck, D. F. Mierke, *J. Am. Chem. Soc.* **1992**, *114*, 3272–3277.
[3] G. M. Crippen, T. F. Havel, *Distance Geometry and Molecular Conformation*, Research Studies Press, Somerset, UK, **1988**.
[4] I. D. Kuntz, J. F. Thomason, C. M. Oshiro, *Methods Enzymol.* **1989**, *177B*, 159–204.
[5] A, B, C, and D are the ligands on the stereogenic center X in order of decreasing priority. The chiral volume (V_C) spanned by these four points is one-sixth of the oriented volume of the vectors extending from one point to the other three: $V_C = 1/6\ \vec{AD} \cdot [\vec{BD} \otimes \vec{CD}]$. If the vectors $\vec{AD}$, $\vec{BD}$, $\vec{CD}$ form a right-handed coordinate system, the volume is positive ((*S*) configuration), if they form a left-handed system, the volume is negative ((*R*) configuration).
[6] P. L. Weber, R. Morrison, D. Hare, *J. Mol. Biol.* **1988**, *204*, 483–487.
[7] D. F. Mierke, M. Reggelin, *J. Org. Chem.* **1992**, *57*, 6365–6367.
[8] K. Conde-Frieboes, Dissertation, Universität Kiel, **1992**.
[9] ^{1}H NMR (400 MHz, $CDCl_3$, 300 K, TMS): $\delta = 1.57$ (19-CH_3), 1.58 (4-CH_3), 1.59/1.89 (2H-14), 1.66/2.56 (H-9^{pro-S}/H-9^{pro-R}), 1.76/1.76 (2H-15), 1.82/1.96 (H-13^{pro-R}/H-13^{pro-S}), 2.13/2.38 (H-10^{pro-S}/H-10^{pro-R}), 2.30 (H-12), 3.10 (H-6), 3.25 (H-8), 3.44 (H-19), 3.76 (H-4), 4.02 (11-OH), 4.63 (H-18), 4.85 (H-3), 5.58 (H-1), 5.85 (H-16), 6.64 (H-26), 6.84 (H-22), 7.14 (H-23), 7.17 (H-27), 7.20 (H-24), 7.22 (H-28), 7.24 (H-31), 7.43 (H-35), 7.56 (H-30), 7.74 (H-34). – ^{13}C NMR (100 MHz, $CDCl_3$, 300 K, TMS): $\delta = 20.51$ (19-CH_3), 20.56 (C-14), 20.71 (C-10), 21.53 (4-CH_3), 23.88 (C-9), 24.98 (C-13), 36.68 (C-15), 51.26 (C-12), 55.62 (C-8), 56.30 (C-6), 62.48 (C-4), 63.14 (C-19), 81.72 (C-11), 85.02 (C-3), 85.17 (C-18), 90.06 (C-1), 91.40 (C-16), 124.79 (C-22), 125.31 (C-26), 127.59 (C-24), 128.16 (C-28), 128.49 (C-27), 128.60 (C-23), 128.89 (C-30), 129.26 (C-31), 129.43 (C-35), 129.76 (C-34), 133.85 (C-32), 134.80 (C-36), 137.75 (C-25), 137.96 (C-21), 139.90 (C-29/C-33).
[10] HMQC = Heteronuclear Multiple Quantum Coherence: A. Bax, S. Subramanian, *J. Magn. Reson.* **1986**, *67*, 565–569.
[11] HMBC = Heteronuclear Multiple-Bond Correlation: A. Bax, D. Marion, *J. Magn. Reson.* **1988**, *78*, 186–191; A. Bax, M. F. Summers, *J. Am. Chem. Soc.* **1986**, *108*, 2093–2094.
[12] DQF = Double Quantum Filter, TOCSY = Total correlation spectroscopy; A. Bax, D. G. Davis, *J. Magn. Reson.* **1985**, *65*, 355–360.
[13] L. Emsley, G. Bodenhausen, *J. Magn. Reson.* **1989**, *82*, 211–221; H. Kessler, P. Schmieder, M. Köck, M. Kurz, *ibid.* **1990**, *88*, 615–618.
[14] T. F. Havel, DISGEO, Quantum Chemistry Program Exchange (QCPE) No. 507, Indiana University, **1986**.
[15] T. F. Havel, *Prog. Biophys. Mol. Biol.* **1991**, *56*, 43–78.
[16] T. F. Havel, *Biopolymers* **1990**, *29*, 1565–1585.

[17] R. Kaptein, R. Boelens, R. M. Scheek, W. F. van Gunsteren, *Biochemistry* **1988**, *27*, 5389–5395.
[18] R. M. Scheek, W. F. van Gunsteren, R. Kaptein, *Methods Enzymol.* **1989**, *177*, 204–218.
[19] Both DDD refinements were conducted with 2500 steps and a step width of 20 fs using the SHAKE algorithm (J. P. Ryckaert, G. Ciccotti, H. J. C. Berendsen, *J. Comput. Phys.* **1977**, *23*, 327–341) at a temperature of 300 K with a strong coupling to a temperature bath (every 10 steps) (H. J. C. Berendsen, J. P. M. Postma, W. F. van Gunsteren, A. DiNola, J. R. Haak, *J. Chem. Phys.* **1984**, *81*, 3684–3690. The temperature was then reduced to 1 K, and the structures were DDD-refined with another 1000 steps and a weak coupling to the temperature bath (every 50 steps).
[20] The pseudoenergy E_{pseudo} is a dimensionless number obtained from the following calculation: $E_{pseudo} = 0.5k_{dis}(r - r^{exp})^2 + 0.5k_{chir}(V_C - V_C^{exp})^2$. k_{dis} is the force constant for weighting the difference between the calculated distance r and the experimentally determined distance r^{exp}. k_{chir} is the force constant for weighting the difference between the calculated chiral volume V_C and the chiral volume of the initial structure V_C^{exp}. All values are derived from the DG structure refinement.
[21] Further details of the crystal structure investigation may be obtained from the Fachinformationszentrum Karlsruhe, D-76344 Eggenstein-Leopoldshafen (FRG) on quoting the depository number CSD-57938, the names of the authors, and the journal citation; J. Hirschler, B. Berger, M. Bolte, *Acta Crystallogr. Sect. C*, submitted.

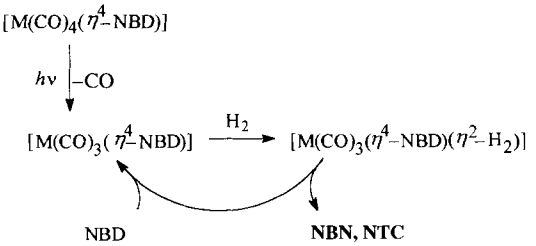
In Situ NMR Investigations of Photocatalyzed Hydrogenations with Parahydrogen in the Presence of Metal Carbonyl Compounds of Group 6**

Angelika Thomas, Mathias Haake, Friedrich-Wilhelm Grevels, and Joachim Bargon*

Hydrogenations with parahydrogen (p-H_2) lead to nuclear spin polarization effects in ^{1}H NMR spectra.[1, 2] The extreme sensitivity of this method enables organometallic-catalyzed hydrogenations to be investigated. The amplification of the signal by up to 10^5 fold, the PASADENA effect (*P*arahydrogen *A*nd *S*ynthesis *A*llows *D*ramatically *E*nhanced *N*uclear *A*lignment), results from the breakdown of the H_2 symmetry during the hydrogenation;[1] the in situ NMR method based on this is called parahydrogen induced polarization (PHIP)[2–5] and is suitable for the detection of short-lived reaction intermediates.

A detailed analysis of the nuclear spin polarization pattern of the reaction products (or intermediates) identifies directly the positions of the transferred H_2 protons and thus indirectly allows conclusions about the nature of the intermediary binding of the H_2 molecule to the organometallic complex.[3b] Labeling experiments with D_2 are therefore unnecessary.

The systems studied previously were concerned with thermally induced hydrogenations in the presence of metal complexes of Groups 8–10, which activate the H_2 molecule by an oxidative addition.[2–7] In this communication, the hydrogenation of norbornadiene (NBD) is used as example to show that also in the photolytic activation of metal carbonyls of Group 6, the nuclear spin polarization of p-H_2 is transferred to the reaction products. The metal carbonyl compounds were used in the form of $[M(CO)_4(\eta^4\text{-NBD})]$ complexes (M = Cr, Mo). From an earlier study it is known that NBD is hydrogenated in the presence of the Mo complex mainly to give norbornene (NBN), whereas in the presence of the Cr complex the hydrogenation leads to nortricyclene (NTC) and NBN in the ratio of 3:1 (see Fig. 1).[8] The activation here results from photolytic cleavage of a CO ligand from the $[M(CO)_4(\eta^4\text{-NBD})]$ complex.[9] An H_2 molecule can be coordinated to the resulting free coordination site of the $[M(CO)_3(\eta^4\text{-NBD})]$ fragment, leading to the formation of the nonclassical hydrogen complex $[M(CO)_3(\eta^4\text{-NBD})(\eta^2\text{-}H_2)]$.[10] The other steps of the catalytic cycle, in which the $M(CO)_3$ group is the repeating unit, are shown in Scheme 1.



Scheme 1. Activation and catalytic cycle for the hydrogenation of NBD in the presence of carbonyl complexes of group 6.

The polarization signals of the 1,2-hydrogenation product NBN and also those of the homo-1,4-hydrogenation product NTC were detected (Fig. 1). The PHIP signals of NBN are identical with those which occur during thermally activated hydrogenations with the cationic rhodium catalyst $[Rh(NBD)(PPh_3)_2]PF_6$,[3b] although the H_2 molecule is activated in different ways. The analysis of the polarization pattern as an eight-spin system with a computer program (PHIP 9, J. Kandels, dissertation, Universität Bonn, FRG, 1992) developed for the PHIP NMR method confirms the formation of *cis-endo* hydrogenated NBN (Fig. 2). The necessary NMR parameters were taken from the literature (Scheme 2).[12]

A prerequisite for the computer-assisted evaluation of the experimental PHIP spectra is the assumption of a spontaneous hydrogenation.[3c] Spontaneous hydrogenation means that the breakdown of the symmetry of the H_2 molecule occurs on product formation. Thus, the H_2 molecule then cannot be bound hydridically to the catalyst for a longer period of time, which for $[RhCl(PPh_3)_3]$ is several milliseconds, since this would have resulted in the loss of the phase correlation because of the different chemical shifts of the two protons by different precession frequencies. Also in the case of a classical dihydrido complex, only an extremely short residence time of p-H_2 at the catalyst can prevent a loss of the phase correlation, otherwise both hydrogen atoms stemming from H_2 must be in chemically equivalent positions. Since the latter should apply for a η^2-H_2 complex, in this case the phase correlation of the nuclear spin is retained. A product molecule with an AA'BB' nuclear spin system or one with a partial spin system, as formed by the *endo*/*exo* protons of NBN, is a particularly sensitive probe for exploring the chemical environment in which the H_2 atoms occur in the course of the hydrogenation.[3c] A loss of the phase correlation of the H_2 atoms prior to their transfer to the substrate (NBD) would lead to considerable changes of the polarization pattern (Fig. 2c). The best agreement between experiment and simulation occurs under the assumption of spontaneous hydrogenation (see Fig. 2), that is, the bond of the H_2 molecule in the intermediate catalyst

[*] Prof. Dr. J. Bargon, Dipl.-Chem. A. Thomas, M. Haake
Institut für Physikalische Chemie der Universität
Wegelerstrasse 12, D-53115 Bonn (FRG)
Telefax: Int. code + (228)732-551
Prof. Dr. F.-W. Grevels
Max-Planck-Institut für Strahlenchemie, Mülheim an der Ruhr (FRG)

[**] This work was supported by the Fonds der Chemischen Industrie and the Bundesministerium für Bildung und Wissenschaft (Graduiertenkolleg "Spektroskopie isolierter und kondensierter Moleküle").

complex remains unbroken; thus, an oxidative addition of H_2 to the catalyst does not take place.[3c]

The quantitative analysis of polarization spectra permits statements about the nature and the reaction path of isomeric reaction products. Thus, the hydrogenation with $[Mo(CO)_4(\eta^4\text{-NBD})]$ only leads to polarization signals of the NBN formed by *cis-endo* hydrogenation (see Fig. 1a). In contrast, for the hydrogenation

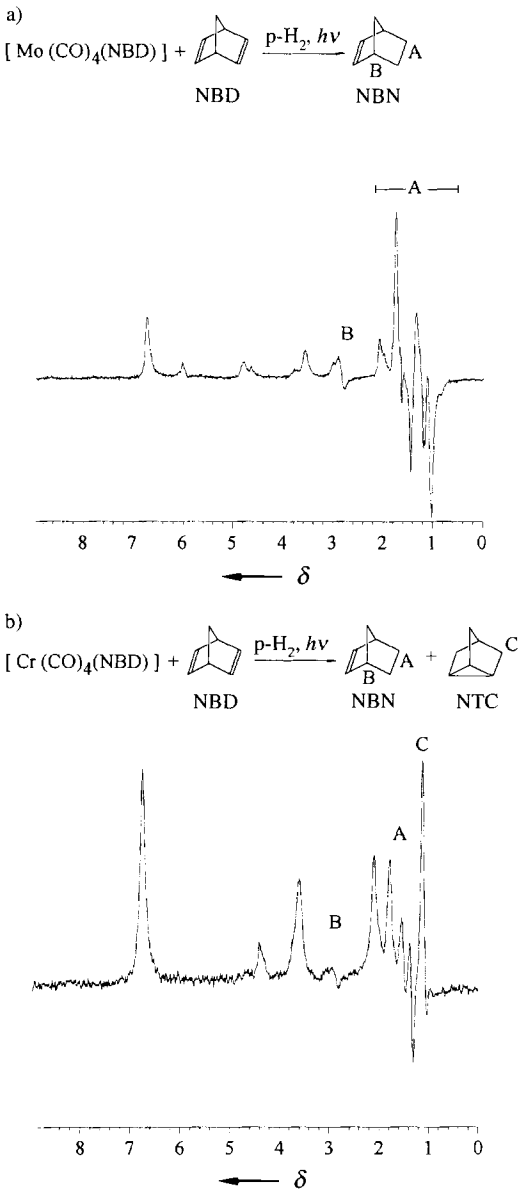


Fig. 1. Experimental PHIP spectra of the photocatalytic hydrogenation of norbornadiene in the presence of a) $[Mo(CO)_4(\eta^4\text{-NBD})]$ (165 accumulations, pulse delay 10 s, $\pi/4$ pulse) and b) $[Cr(CO)_4(\eta^4\text{-NBD})]$ (50 accumulations, pulse delay 10 s $\pi/4$ pulse). The spectra show in addition to the thermal signals of the reactants the polarization signals of protons of the nortricyclene (C: CH_2) and of the norbornene (A: *endo/exo* protons, B: bridgehead protons).

with $[Cr(CO)_4(\eta^4\text{-NBD})]$, in addition to a low polarization of the 1,2-hydrogenation product NBN mainly a polarization of the methylene protons of the homo-1,4-hydrogenation product NTC is detected. The formation of NBN can be detected above all as a result of the polarization of the bridgehead protons (group B in Fig. 1b), which show a coupling with the *endo/exo* proton system.

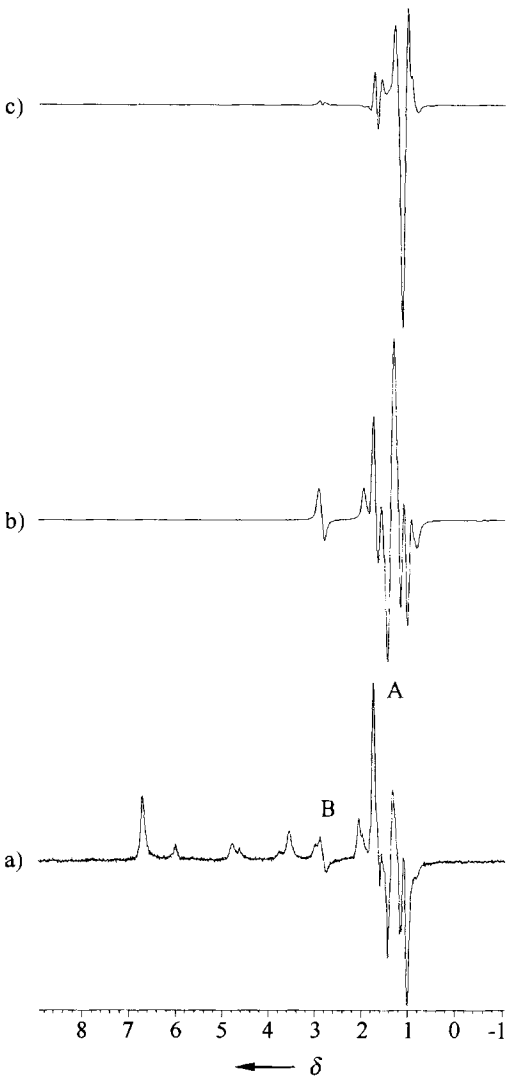
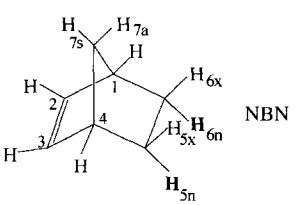


Fig. 2. Photocatalytic hydrogenation of norbornadiene in the presence of $[Mo(CO)_4(\eta^4\text{-NBD})]$. Experimental PHIP spectrum with polarization in the *endo/exo* protons (A) and the bridgehead protons (B) of NBN (a). Simulated PHIP spectra of the norbornene formed by *cis-endo* hydrogenation (b) under the assumption of spontaneous hydrogenation with additional W_2 relaxation of the geminal protons 5x, 5n and 6x, 6n as well as W_0 relaxation of the protons 1, 6x and 4, 5x (numbering see Scheme 2) ($W_0 = 0.16$, $W_2 = 0.15$), c) under the assumption of no spontaneous hydrogenation with a S/T_0 mixture of 1/1 [3c] during the hydrogenation and with the analogous assumption for the relaxation as for (b).

For both catalyst systems polarization signals occur only after an irradiation period of about 20 s. The hydrogenation with $[Mo(CO)_4(\eta^4\text{-NBD})]$ under continuous irradiation can be followed over 2.5 h by means of the polarization signals of the product (NBN). If the photoactivation is interrupted, the polar-



Scheme 2. Hydrogenation product norbornene: n = *endo*, x = *exo*, s = *syn*, a = *anti*.

ization signals for the two catalytic systems decrease over a period of 60 s; however, they can be reactivated by renewed irradiation.

The in situ PHIP NMR method allows a dynamic determination of the hydrogenation activity of catalysts. Recombination of the photoactivated catalyst with its original CO ligand or complex binding of olefinic substrates, that is, the formation of $[M(CO)_3(\eta^4\text{-NBD})(\eta^2\text{-L})]$ (L = NBN or NBD) lowers the catalytic activity.[11] Additional PHIP measurements at various CO pressures and NBD concentrations are required for the differentiation of these deactivation steps.

Experimental Procedure

The experiments were performed in a 80 MHz FT-^{1}H NMR spectrometer. For this, a pressure sample head with continuous flow system was used, which ensured the exclusion of O_2. This was important, since the catalysts employed are considerably air sensitive after photoactivation. The closed system enables continuous irradiation during the hydrogenation process as well as quantitative statements. The experimental set up and the p-H_2 enrichment have been described previously [5,8]. The reactions were carried out at room temperature and under atmospheric pressure with a solution of norbornadiene (2.0×10^{-3} M) and catalyst (8.0×10^{-4} M) in [D_{12}]cyclohexane. In control experiments with p-H_2 and pressure up to 10 bar without UV irradiation, it was shown that the catalyst systems proved to be inert. The samples were irradiated through a Pyrex window in the pressure probe head with unfiltered light from a 500 W-Hg lamp (Osram XBO 162).

Received: October 25, 1993 [Z 6443 IE]
German version: *Angew. Chem.* **1994**, *106*, 820

[1] C. R. Bowers, D. P. Weitekamp, *Phys. Rev. Lett.* **1986**, *57*, 2645–2648; C. R. Bowers, D. N. Jones, H. D. Kurur, J. A. Labinger, M. G. Pravica, D. P. Weitekamp, *Adv. Magn. Reson.* **1990**, *14*, 279–291.

[2] T. C. Eisenschmid, R. U. Kirss, P. P. Deutsch, S. I. Hommeltoft, R. Eisenberg, J. Bargon, R. G. Lawler, A. L. Balch, *J. Am. Chem. Soc.* **1987**, *109*, 8089–8091.

[3] a) J. Bargon, J. Kandels, K. Woelk, *Angew. Chem.* **1990**, *102*, 70–71; *Angew. Chem. Int. Ed. Engl.* **1990**, *29*, 58–59; b) J. Bargon, J. Kandels, P. Kating, A. Thomas, K. Woelk, *Tetrahedron Lett.* **1990**, *31*, 5721–5724; c) J. Kandels, P. Kating, J. Bargon, *J. Chem. Phys.* **1993**, *98*, 6150–6153; d) P. Kating, A. Wandelt, R. Selke, J. Bargon, *J. Phys. Chem.* **1993**, *97*, 13313–13317.

[4] R. Eisenberg, *Acc. Chem. Res.* **1991**, *24*, 110–116.

[5] J. Bargon, J. Kandels, K. Woelk, *Z. Phys. Chem.* **1993**, *180*, 65–93.

[6] C. R. Bowers, D. P. Weitekamp, *J. Am. Chem. Soc.* **1987**, *109*, 5541–5542.

[7] R. U. Kirss, R. Eisenberg, *J. Organomet. Chem.* **1989**, *359*, C22–C26; S. B. Duckett, R. Eisenberg, *J. Am. Chem. Soc.* **1993**, *115*, 5292–5293, and references therein.

[8] K. Woelk, J. Bargon, *Rev. Sci. Instrum.* **1992**, *63*, 3307–3310.

[9] G. Platbrood, L. Wilputte-Steinert, *Bull. Soc. Chim. Belg.* **1973**, *82*, 733–735; *J. Organomet. Chem.* **1974**, *70*, 393–405; D. J. Darensbourg, H. H. Nelson III, M. A. Murphy, *J. Am. Chem. Soc.* **1977**, *99*, 896–903; M. J. Mirbach, D. Steinmetz, A. Saus, *J. Organomet. Chem.* **1979**, *168*, C13–C19; D. Chmielewski, F.-W. Grevels, J. Jacke, K. Schaffner, *Angew. Chem.* **1991**, *103*, 1361–1363; *Angew. Chem. Int. Ed. Engl.* **1991**, *30*, 1343–1345; F.-W. Grevels in *Photoprocesses in Transition Metal Complexes, Biosystems and Other Molecules. Experiment and Theory (NATO ASI Ser. Ser. C* **1992**, 376), 856–861.

[10] S. A. Jackson, P. M. Hodges, M. Poliakoff, J. J. Turner, F.-W. Grevels, *J. Am. Chem. Soc.* **1990**, *112*, 1221–1233.

[11] P. M. Hodges, S. A. Jackson, J. Jacke, M. Poliakoff, J. J. Turner, F.-W. Grevels, *J. Am. Chem. Soc.* **1990**, *112*, 3307–3310.

[12] R. J. Abraham, J. Fisher, *Magn. Reson. Chem.* **1985**, *23*, 856-861. Chemical shifts and coupling data for NBN (^{1}H NMR) used in the simulation: δ = 0.952 (H-5n, 6x), 1.074 (H-7a), 1.314 (H-7s), 1.6042 (H-5x, 6n), 2.842 (H-1, 4) coupling constants: $J(1,4) = 1.19$, $J(1,7s) = 1.83$, $J(1,7a) = 1.51$, $J(1,5x) = -0.15$, $J(1,6x) = 3.66$, $J(1,6n) = 0.55$, $J(1,5n) = -0.08$, $J(7s,7a) = -8.03$, $J(7s,6x) = 0.00$, $J(7s,6n) = 2.37$, $J(7a,6n) = 2.37$, $J(7a,6x) = 0.00$, $J(5x,6x) = 9.38$, $J(5x,6n) = 3.91$, $J(5x,5n) = -11.29$, $J(5n,6n) = 9.02$ Hz.

The Oxovanadium–Organophosphonate System: Complex Cluster Structures $[(VO)_6(t\text{BuPO}_3)_8\text{Cl}]$, $[(VO)_4\{\text{PhP(O)}_2\text{OP(O)}_2\text{Ph}\}_4\text{Cl}]^-$, and $[V_{18}O_{25}(H_2O)_2(\text{PhPO}_3)_{20}\text{Cl}_4]^{4-}$ with Encapsulated Chloride Anions Prepared from Simple Precursors**

José Salta, Qin Chen, Yuan-Da Chang, and Jon Zubieta*

Current interest in the oxovanadium–organophosphonate system $V/O/RPO_3^{2-}$ is based on the practical applications of such materials as sorbents[1,2] and their diverse structural types. Recent developments in the chemistry of the $V/O/RPO_3^{2-}$ system have revealed the dinuclear complexes **1** and **2**, fully oxidized clusters **3** and **4**, mixed-valence clusters **5**–**7**, and layered compounds **8** and **9**.

$[(VO)_2Cl_2(RPO_3H)_2Y_2]^{n-}$[3] **1**

$[(VO_2)_2(RPO_3)_2]^{2-}$[3] **2**

$[V_5O_7(OCH_3)_2(PhPO_3)_5]^{1-}$[4] **3**

$[V_7O_{12}(PhPO_3)_6Cl]^{2-}$[5] **4**

$[H_{12}(VO_2)_{12}(PhPO_3)_8]^{4-}$[6] **5**

$[H_6(VO_2)_{16}(CH_3PO_3)_8]^{8-}$[7] **6**

$[(NH_4)_2Cl_2V_{14}O_{22}(OH)_4(H_2O)_2(PhPO_3)_8]^{6-}$[8] **7**

$VO(PhPO_3)] \cdot H_2O$[1] **8**

$[(VO)_2\{CH_2(PO_3)_2\}_2] \cdot 4H_2O$[9] **9**

These studies indicate that the composition and structure of the products isolated are critically dependent on solvent, temperature, and the presence or absence of templates. While the large mixed-valence clusters were obtained from hydrothermal reactions,[10,11] the penta- and heptanuclear complexes were prepared in organic solvents by conventional methods;[4,5] the dinuclear species was isolated under strictly controlled conditions in the presence of a bulky organic cation.[3] In solvothermal reactions with organic solvents intermediate temperatures and pressures are accessible, which should allow the isolation of metastable phases not accessible by conventional or hydrothermal techniques.[11] Furthermore, while controlled linkage of simple molecular units to form oligomers or solid phases remains elusive, the condensation of vanadium coordination polyhedra with organophosphonate tetrahedra to form aggregates can be directed to some extent by anionic templates. Directed condensations of this type were noted for the "naked" or predominantly inorganic clusters with a $[V_xO_yE]^{n-}$ core (E = encapsulated anionic unit) described by Müller et al.[12] and for oxovanadium phosphate phases.[13] We report here on the syntheses and structures of a series of clusters (**10**–**13**) of the $V/O/RPO_3^{2-}$ system,

$[(VO)_6(t\text{BuPO}_3)_8\text{Cl}]$ **10**

$[Ph_4P][(VO)_4\{\text{PhP(O}_2\text{)OP(O)}_2\text{Ph}\}_4\text{Cl}]$ **11**

$[Ph_4P][V_5O_7(OCH_3)_2(PhPO_3)_5]$ **12**

$[Ph_4P]_4[V_{18}O_{25}(H_2O)_2(\text{PhPO}_3)_{20}\text{Cl}_4] \cdot 6CH_3CN \cdot 2CH_3OH$ **13**

[*] Prof. J. Zubieta, J. Salta, Q. Chen, Y.-D. Chang
Department of Chemistry, Syracuse University
Syracuse, NY 13244-4100 (USA)
Telefax: Int. code + (315)443-4070

[**] This work was supported by the National Science Foundation (Grant CHE 9119910).

 © VCH Verlagsgesellschaft mbH, D-69451 Weinheim, 1994 0570-0833/94/0707-0757 $ 10.00+.25/0

in which the outer framework, which is constructed from the corner-sharing of vanadium-centered square pyramids and/or octahedra and organophosphonate tetrahedra, encloses chloride ions.

The solvothermal reaction of tBuPO$_3$H$_2$ with [Ph$_4$P][VO$_2$Cl$_2$][14] in acetonitrile yields lustrous dark green crystals of the mixed-valence cluster [(V^{V}O)$_5$(V^{IV}O)(tBuPO$_3$)$_8$Cl] (**10**).[15] X-ray crystallographic analysis of **10**[16] revealed that its structure (Fig. 1) consists of a spherical V/P/O shell of corner-sharing vanadium-centered square pyramids and organophosphonate tetrahedra encapsulating a chloride anion, which seems to serve as a template for cluster formation.[17] Although the structure of

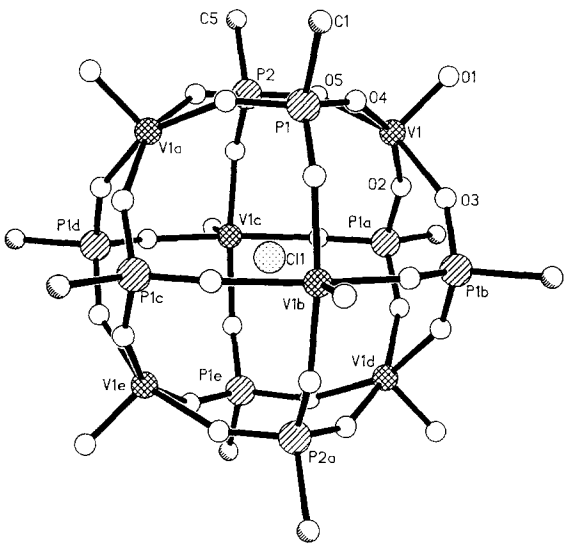


Fig. 1. A view of the structure of **10**. Selected bond lengths [Å] and angles [°]: V1-O1 1.563(7), V1-O2 1.850(3), V1-O3 1.863(8), V1-O4 1.860(5), V1-O5 1.848(9), P-O (average) 1.494(10); O(apical)-V1-O(plane) (average) 101.2(6). The central chloride ion lies on a crystallographic threefold inversion axis; P2 lies on a crystallographic threefold axis. Consequently, all atomic positions are related by to the unique set labeled V1 through C5 and shown in the upper right quadrant of the spherical shell.

10 is somewhat reminiscent of those of [V$_7$O$_{12}$(PhPO$_3$)$_6$Cl]$^{2-}$[5] and [V$_{15}$O$_{36}$Cl]$^{6-}$,[18] its topological details are distinct. The structure of [V$_{15}$O$_{36}$Cl]$^{6-}$ is constructed exclusively from {VO$_5$} square pyramids in a highly symmetrical arrangement of approximate D_{3h} symmetry; the faces of the sphere consist of two {V$_3$O$_3$}, three {V$_4$O$_4$}, and eighteen {V$_2$O$_2$} rings. The structure of [V$_7$O$_{12}$(PhPO$_3$)$_6$]$^-$ is much less symmetrical, exhibiting C_2 symmetry and faces constructed from {V$_2$PO$_3$}, {V$_2$P$_2$O$_4$}, {V$_3$PO$_4$}, and {V$_3$P$_2$O$_5$} rings. The structure of **10** exhibits idealized D_{4h} symmetry, and the shell is constructed exclusively from twelve {V$_2$P$_2$O$_4$} faces. In contrast to the structure of [V$_7$O$_{12}$(PhPO$_3$)$_6$]$^-$, **10** does not possess {V-O-V} bridges, and the vanadium centers are isolated from each other. The structural relationship of **10** to the dinuclear complexes of the type [(VO)$_2$Cl$_4$(tBuPO$_3$H)$_2$]$^{2-}$[3] is also apparent. Formally, the shell of **10** is constructed from the condensation of three such units with concomitant loss of HCl and incorporation of two additional tBuPO$_3^{2-}$ groups. The structure of **10** is also related to that of the layered phase VO(PhPO$_3$) · H$_2$O, since cleavage of three V – O(phosphonate) bonds in **10** and flattening of the cage produces a motif seen in the layered phase. These compounds display an unusually broad range of compositions: [V$_7$O$_{12}$(PhPO$_3$)$_6$Cl]$^{2-}$ exhibits a V:P ratio of 7:6, in **10** this ratio is 3:4, and ratios of 9:10, 1:1, 3:2, 7:4, and 2:1 have now been reported for V/O/RPO$_3^{2-}$ clusters.

Relatively minor changes in the starting materials in the solvothermal synthesis often lead to dramatically different products. Thus, the reaction of PhPO$_3$H$_2$ with [Ph$_4$P][VO$_2$Cl$_2$] under identical conditions to those employed for the synthesis of **10** results in the isolation of green crystals of the V^{IV} species **11**. The structure of **11**[19] consists of discrete Ph$_4$P$^+$ cations and [(VO)$_4${PhP(O)$_2$OP(O)$_2$Ph}$_4$Cl]$^-$ anions (Fig. 2). In this instance, the shell is constructed from vanadium-centered square pyramids and the fused tetrahedra of the pyrophosphonate ligands [PhP(O)$_2$OP(O$_2$)Ph]$^{2-}$, which are formed in a metal-mediated, thermally induced condensation process.[20] As in the structure of **10**, the structure of **11** exhibits isolated vanadium-centered square pyramids with no {V-O-V} interactions. Each vanadium center is bonded to the oxygen donors of three neighboring pyrophosphonate ligands; two ligands are each bonded through one O atom and the third through two O atoms to form a {V-O-P-O-P-O-} ring. The V/P/O shell of **11** acts as a cage for a Cl$^-$ ion. The V···Cl distances in **11** are 3.07 Å compared to 3.39 Å for **10**.

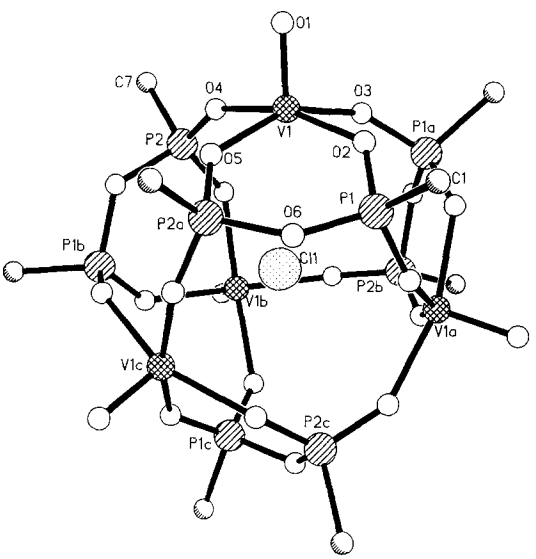


Fig. 2. A view of the anion of **11**. Selected bond lengths [Å] and angles [°]: V1-O1 1.571(10), V1-O2 1.981(8), V1-O3 2.003(9), V1-O4 1.977(9), V1-O5 1.986(8), P1-O6 1.607(9), P2-O6 1.603(9), P-O(other) (average) 1.499(12); O(apical)-V1-O(plane) (average) 100.7(8). The central chloride ion lies on a crystallographic fourfold inversion axis. The V/O/P shell of **11** is thus generated by symmetry from the unique quadrant.

The reaction of [Ph$_4$P][VO$_2$Cl$_2$] with PhPO$_3$H$_2$ in methanol yields [Ph$_4$P][V$_5$O$_7$(OCH$_3$)$_2$(PhPO$_3$)$_5$] (**12**),[21] which contains the same anion as described previously for [nBu$_4$N][V$_5$O$_7$-(OCH$_3$)$_2$(PhPO$_3$)$_5$].[4] However, when **12** is heated in acetonitrile at reflux, deep red crystals of the octadecanuclear species **13** are isolated. The structure of **13**[22] consists of discrete Ph$_4$P$^+$ cations and {V$_{18}$O$_{25}$(H$_2$O)$_2$(PhPO$_3$)$_{20}$}^{0} groups which encapsulate four chloride anions (Fig. 3 top). The structure of the anion of **13** may be described as a cyclic arrangement of four {V$_4$O$_6$(PhPO$_3$)$_5$}$^{2-}$ clusters linked through four P-O-V interactions and fused through eight V – O(phosphonate) bonds to a central {V$_2$O(H$_2$O)$_2$}$^{8+}$ moiety. The four chloride ions occupy the resulting four cavities.

The structural relationship of the anion of **13** to [V$_5$O$_7$(PhPO$_3$)$_5$]$^-$, shown in the lower part of Figure 3, is apparent. Removal of the pendant {VO(OCH$_3$)} group of **12** frees three phosphonate oxygen atoms to condense to additional vanadium atoms. One phosphonate oxygen atom displaces a

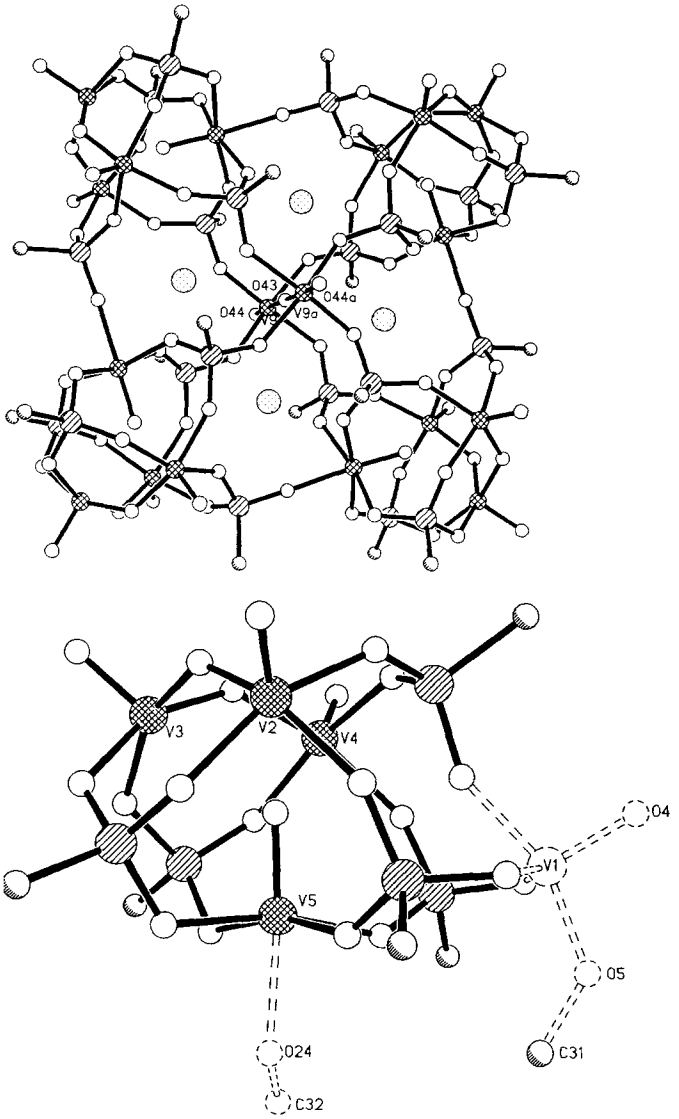


Fig. 3. Top: A view of the anion of **13**. Selected bond length ranges [Å]: Square-pyramidal V sites, V1-V6: V-O(terminal): 1.56–1.58; V-O(bridging): 1.71–1.81; V-O(phosphonate): 1.90–2.00; octahedral sites in the $\{V_4O_6(PhPO_3)_5\}^{2-}$ units, V7 and V8: V-O(terminal): 1.62; V-O(phosphonate, *trans* to oxo): 2.09; V-O(phosphonate, other): 1.99–2.03; central octahedral site, V9: V-O(oxo): 1.60; V-O(phosphonate): 1.96–2.02; V-O44 (aqua): 2.012. Bottom: A view of the anion of **13**, showing the $\{VO(OCH_3)_3\}^{2+}$ unit and the methoxy group which are displaced in the aggregation process to form the "supercluster."

methoxy group from the site *trans* to the interior-directed V=O unit of a $\{VO(OCH_3)(PhPO_3)_4\}$ center of a second $\{V_4O_6(OCH_3)(PhPO_3)_5\}$ unit; the remaining two P—O groups are utilized in bonding to the central $\{V_2O(H_2O)_2\}^{8+}$ moiety. Two of these $[\{V_4O_6(PhPO_3)_5\}_2]^{4-}$ units are then organized about the central $\{V_2O(H_2O)_2\}^{8+}$ fragment to form the cluster shell. It is noteworthy that the unusual $\{V=O\}$ units, which are directed toward the interior of the subunit cavities and which were first described for $[V_5O_7(OCH_3)_2(PhPO_3)_5]^-$, are retained in the structure of the supercluster. The anion in **13** may be considered a "cluster of clusters" and demonstrates that small oligomers may be linked by appropriate ligand types to form clusters of nanometer dimensions by more or less rational synthetic routes.

While the clusters of this study appear to organize about chloride anions, the roles of different anions as templates for the formation of various $V/O/RPO_3^{2-}$ materials remain largely unexplored. The topological and electronic diversity of the $V/O/RPO_3^{2-}$ system may rival or even exceed that of the "naked" V/O cluster system.[12, 23] The introduction of organophosphonate tetrahedra as a new type of polyhedra for cluster construction expands the structural possibilities, as does the ability of RPO_3^{2-} groups to bridge cluster subunits to form superclusters and undergo condensation reactions to form polyphosphonate species. These interesting features of the $V/O/RPO_3^{2-}$ system are even more forcefully demonstrated in the $V/O/RAsO_3^{2-}$ system and will be discussed in the immediately following report.[24]

Experimental Procedure

10: A suspension of $[Ph_4P][VO_2Cl_2]$ (0.65 g, 1.25 mmol) and $tBuPO_3H_2$ (0.341 g, 2.47 mmol) in acetonitrile (6 mL), was transferred to a thick-walled glass tube. After evacuation, the tube was sealed and placed in an oven for 36 h at 100 °C. After cooling to room temperature, dark green crystals of **10** were collected by filtration. Yield: 0.0808 (25% based on V). Correct C,H,P analysis. IR (KBr): $\tilde{\nu}$[cm^{-1}]: 2969(m), 2870(w), 1480(m), 1461(w), 1395(w), 1365(w), 1206(m), 1159(s), 1037(s), 1005(s), 935(m), 832(m), 666(m), 600(m), 467(s). Manganometric titration confirmed the presence of one V^{IV} atom per cluster.

11: A suspension of $[Ph_4P][VO_2Cl_2]$ (0.605 g, 1.23 mmol) and $PhPO_3H_2$ (0.395 g, 2.80 mmol) in acetonitrile (6 mL) was transferred to a thick-walled glass tube. After evacuation and sealing, the tube was heated for 36 h at 100 °C. After cooling to room temperature, green needles of **11** were collected. Yield: 34% (0.191 g). Correct C,H,P analysis. IR (KBr): $\tilde{\nu}$[cm^{-1}]: 3078(m), 1594(m), 1486(m), 1439(s), 1248(s), 1183(s), 1148(s), 1105(s), 1070(m), 1028(m), 998(s), 954(s), 764(m), 746(m), 721(m), 695(s), 618(w), 594(s), 561(w), 521(s), 460(m). Manganometric titration confirmed that all vanadium atoms are V^{IV}.

12: $[Ph_4P][VO_2Cl_2]$ (0.712 g, 1.45 mmol) and $PhPO_3H_2$ (0.205 g, 1.45 mmol) were refluxed in methanol for 6 h. After filtration and evaporation to dryness, the red powder was dissolved in CH_3CN (5 mL) and this solution carefully layered with diethyl ether. After standing at room temperature for two weeks, red crystals of **12** were isolated in 45% yield. X-ray quality crystals were grown by slow diffusion of methanol into a CH_2Cl_2 solution of **12** to give red blocks of $[Ph_4P][V_5O_7(OCH_3)_2(PhPO_3)_5] \cdot MeOH \cdot 0.5CH_2Cl_2$ (**12a**). Correct C,H,P analysis. IR (KBr): $\tilde{\nu}$[cm^{-1}]: 3058(w), 1484(w), 1438(m), 1262(w), 1138(vs), 1108(s), 1037(sh), 1007(vs), 990(vs), 753(m), 723(m), 691(m), 587(sh), 572(m), 527(m).

13: Method 1: Compound **12** (0.512 g, 0.32 mmol) was dissolved in acetonitrile (5 mL) and placed in a thick-walled glass tube. After evacuation and sealing, the tube was heated for 36 h at 100 °C. After cooling to room temperature, red needles of **13** were collected in 53% yield. (0.296 g).

Method 2: Under a nitrogen atmosphere, a solution of $[Ph_4P][VO_2Cl_2]$ (1.90 g, 3.9 mmol) in methanol (20 mL) was added to a solution of $PhPO_3H_2$ (1.20 g, 7.7 mmol) in methanol (25 mL). Upon addition of Et_3N (0.80 g, 7.7 mmol) with stirring, the red-orange color of the solution darkened to an intense red. After 48 h of stirring at room temperature, a dark red solid was collected, washed with diethyl ether, and dried. Recrystallization from CH_3CN/CH_3OH at 0 °C gave red translucent needles of **13** in 58% yield (0.794 g). Correct C,H,P analysis. IR (KBr): $\tilde{\nu}$[cm^{-1}]: 3058(w), 1484(m), 1438(s), 1314(w), 1178(vs), 1132(vs), 1040(vs), 1020(vs), 990(vs), 833(m), 753(m), 722(m), 689(m), 553(m), 526(s), 492(m).

Received: October 15, 1993 [Z 6423 IE]
German version: *Angew. Chem.* **1994**, *106*, 781

[1] G. H. Huan, A. J. Jacobson, J. W. Johnson, E. W. Corcoran, Jr., *Chem. Mater.* **1990**, *2*, 2.
[2] J. W. Johnson, A. J. Jacobson, W. M. Butler, S. E. Rosenthal, J. F. Brody, J. T. Lewandowski, *J. Am. Chem. Soc.* **1989**, *111*, 381.
[3] Q. Chen, J. Salta, J. Zubieta, *Inorg. Chem.* **1993**, in press.
[4] Q. Chen, J. Zubieta, *Angew. Chem.* **1993**, *105*, 304; *Angew. Chem. Int. Ed. Engl.* **1993**, *32*, 261.
[5] Y. Chang, J. Salta, J. Zubieta, *Angew. Chem.* **1994**, *106*, 347; *Angew. Chem. Int. Ed. Engl.* **1994**, *33*, 325.
[6] G. H. Huan, A. J. Jacobson, V. W. Day, *Angew. Chem.* **1991**, *103*, 426; *Angew. Chem. Int. Ed. Engl.* **1991**, *30*, 422.
[7] G. Huan, V. W. Day, A. J. Jacobson, D. P. Goshorn, *J. Am. Chem. Soc.* **1991**, *113*, 3188.
[8] A. Müller, K. Hovemeier, R. Rohlfing, *Angew. Chem.* **1992**, *104*, 1214; *Angew. Chem. Int. Ed. Engl.* **1992**, *31*, 1192.
[9] G. Huan, J. W. Johnson, A. J. Jacobson, J. S. Merola, *J. Solid State Chem.* **1990**, *89*, 220.
[10] M. Figlarz, *Chim. Scr.* **1988**, *28*, 3.
[11] R. A. Laudise, *Chem. Eng. News* **1987**, *65*(39), 30.
[12] A. Müller, R. Rohlfing, E. Krichemeyer, H. Bögge, *Angew. Chem.* **1993**, *105*, 916; *Angew. Chem. Int. Ed. Engl.* **1993**, *32*, 909, and references therein.
[13] V. Soghomonian, Q. Chen, R. C. Haushalter, J. Zubieta, *Angew. Chem.* **1993**, *105*, 601; *Angew. Chem. Int. Ed. Engl.* **1993**, *32*, 611.

[14] D. Fenske, A.-F. Shihada, H. Schwab, K. Dehniche, *Z. Anorg. Allg. Chem.*, **1986**, *471*, 140.
[15] The oxidation state assignment is consistent with the formulation of **10**, which is confirmed by X-ray structure analysis, elemental analyses, manganometric titration of V^{IV}, and the room-temperature susceptibility of 1.73 BM per formula unit.
[16] a) X-ray structure analysis of **10**: rhombohedral space group $R\bar{3}$ with $a = 14.604(2)$, $c = 25.154(5)$ Å, $V = 4646(2)$ Å^3, $Z = 3$, $\varrho_{calc} = 1.636$ g cm^{-3}, $\mu(Mo_{K\alpha}) = 17.97$ cm^{-1}; $R = 0.0687$ for 1065 reflections with $2\theta < 45^\circ$ and $I_o \geq 3\sigma(I_o)$; Rigaku AFC5S diffractometer, graphite-monochromated $Mo_{K\alpha}$ radiation. The structure was solved using direct methods with the SHELXTL program package. No anomalies were encountered in the refinement. b) Further details of the crystal structure investigation may be obtained from the Fachinformationszentrum Karlsruhe, D-76344 Eggenstein-Leopoldshafen (FRG) on quoting the depository number CSD-57868, the names of the authors, and the journal citation.
[17] H. Reuter, *Angew. Chem.* **1992**, *104*, 1210; *Angew. Chem. Int. Ed. Engl.* **1992**, *31*, 1185.
[18] A. Müller, M. Penk, R. Rohlfing, E. Krickemeyer, J. Döring, *Angew. Chem.* **1990**, *102*, 927; *Angew. Chem. Int. Ed. Engl.* **1990**, *29*, 926.
[19] X-ray structure analysis of **11**: tetragonal space group $P\bar{4}$ with $a = 12.127(2)$, $c = 13.094(3)$ Å, $V = 1926(1)$ Å^3, $Z = 1$, $\varrho_{calc} = 1.576$ g cm^{-3}, $\mu(Mo_{K\alpha}) = 7.69$ cm^{-1}; $R = 0.0687$ for 1660 reflections with $2\theta < 45^\circ$ and $I_o \geq 3\sigma(I_o)$. All other conditions and information as in reference [16].
[20] The organophosphonate forms only in the presence of vanadium. Although no organic condensation products were isolated in the absence of vanadium, condensation products were observed under solvothermal conditions in the presence of catalytic amounts of V^V.
[21] X-ray structure analysis of **12a**: monoclinic space group $P2_1/n$ with $a = 21.360(4)$, $b = 13.134(3)$, $c = 26.583(5)$ Å, $\beta = 112.20(3)^\circ$, $V = 6905(3)$ Å^3, $Z = 4$, $\varrho_{calc} = 1.564$ g cm^{-3}, $\mu(Mo_{K\alpha}) = 9.07$ cm^{-1}; $R = 0.0764$ for 4395 reflections with $2\theta < 45^\circ$ and $I_o \geq 3\sigma(I_o)$. All other conditions and information as in reference [16].
[22] X-ray structure analysis of **13**: orthorhombic space group *Pbca* with $a = 38.750(6)$, $b = 17.048(2)$, $c = 39.526(6)$ Å, $V = 26111(1)$ Å^3, $Z = 4$, $\varrho_{calc} = 1.519$ g cm^{-3}, $\mu = 8.80$ cm^{-1}; $R = 0.072$ for 5187 reflections with $2\theta < 45^\circ$ and $I_o \geq 3\sigma(I_o)$. The positions of V9 and O44 in the central $\{V_2O(H_2O)_2\}$ unit are disordered along the crystallographic y axis. This is a consequence of the unequal V–O distances in the $\{V{=}O43\cdots V\}$ unit which, because of the center of symmetry coincident with the location of O43, results in two locations for V9 and O44, each with 0.5 occupancy. The V9–O44 distance and valence sum calculations for V9 and O44 identify O44 as an aqua ligand. This assignment is consistent with the diamagnetism of **13** and the charge requirements of the cluster which identify all V atoms as V^V.
[23] M. T. Pope, A. Müller, *Angew. Chem.* **1991**, *103*, 56; *Angew. Chem. Int. Ed. Engl.* **1991**, *30*, 34.
[24] M. I. Khan, J. Zubieta, *Angew. Chem.* **1994**, *106*, 784; *Angew. Chem. Int. Ed. Engl.* **1994**, *33*, 760.

The Oxovanadium–Organoarsonate System: $[2CH_3OH \subset V_{12}O_{14}(OH)_4(PhAsO_3)_{10}]^{4-}$ and $[2H_2O \subset V_{12}O_{12}(OH)_2(H_2O)_2(PhAsO_3)_{10}(PhAsO_3H)_4]^{2-}$, Clusters with Nanometer Dimensions and Cavities for Neutral Molecules**

M. Ishaque Khan and Jon Zubieta*

The complex cage and cluster structures adopted by polyoxovanadates have been extensively studied,[1–3] but recent developments have shown that these compounds exhibit structures beyond such classical structural types as the Keggin core[4] and the closely related $[V_{18}O_{42}]^{12-}$ cage;[5] a variety of novel structural types[6–10] have been found including frameworks with readily accessible cavities.[11–15] Clusters such as $[CH_3CN \subset V_{12}O_{32}]^{4-}$,[11] $[Me_4N^+ \subset H_6V_{16}O_{24}(MePO_3)_8]^{7-}$,[14] $[2NH_4^+, 2Cl^- \subset V_{14}O_{22}(OH)_4(H_2O)_2(PhPO_3)_8]^{6-}$,[15] and $[4Cl \subset V_{18}O_{25}(H_2O)_2(PhPO_3)_{20}]^{4-}$[10] are examples of new classes of polyoxoanions serving as hosts for neutral and charged species with vastly different cavity requirements. Although the fusing of vanadium-centered square pyramids and octahedra in "naked core" polyoxovanadium clusters $[V_xO_y]^{n-}$ provides a series of possible complex host shells, the introduction of bridging ligating moieties such as the tetrahedral organophosphonate group may dramatically expand the structural possibilities.[9–10] Frameworks constructed from square-pyramidal, octahedral, tetrahedral units are well documented in the solid-state phases of the V/O/P system,[16] and recent investigations demonstrate that a variety of cluster cores organize about anionic templates in the V/O/organophosphonate system.[14, 15] In contrast, the chemistry of the oxovanadium–organoarsonate system V/O/$RAsO_3^{2-}$ remains largely unexplored and is represented only by the mixed-valence cluster $[V_6O_{10}(PhAsO_3)_4(PhAsO_3H)_2]^{2-}$ and the decanuclear V^V species $[V_{10}O_{24}(NH_2C_6H_4AsO_3)_3]^{4-}$.[17] Whereas the hexanuclear cluster forms exclusively in organic solvents under conventional conditions, other compounds in the V/O/$RAsO_3^{2-}$ system may be accessible by solvothermal synthesis.[18] The potential of this approach is demonstrated in the organization of clusters **1**–**3** of nanometer dimensions which serve as "hosts"[15] for neutral template molecules.

$[H_7O_3]_2[n\mathrm{Bu}_4\mathrm{N}]_2[2CH_3OH \subset V_{12}O_{14}(OH)_4(PhAsO_3)_{10}] \cdot H_2O$ **1**

$[PhCH_2NEt_3]_2[PhCH_2NMe_3]_4[2CH_3CN \subset V_{14}O_{22}(OH)_4(PhPO_3)_8] \cdot 2CH_3CN \cdot 2CH_3OH \cdot 2H_2O$ **2**

$[Et_4N]_2[2H_2O \subset V_{12}O_{12}(OH)_2(H_2O)_2(PhAsO_3)_{10}(PhAsO_3H)_4] \cdot 6H_2O$ **3**

The solvothermal reaction of $[n\mathrm{Bu}_4\mathrm{N}]_3[H_3V_{10}O_{28}]$ with phenylarsonic acid in methanol/water yields translucent light green crystals of **1**. The IR spectrum of **1** exhibits a strong bands at 1093 cm^{-1} and 998 cm^{-1}, associated with the $\{PhAsO_3\}^{2-}$ group and the $\nu(V^{IV}{=}O)$ stretching vibration, respectively.

The anion of **1**[19] (Fig. 1 top) lies on a crystallographic inversion center and possesses approximate D_{2h} symmetry. The structure is constructed from edge- and corner-sharing vanadium-centered square pyramids, organoarsonate tetrahedra, and arsonate square pyramids, and may be described as two $\{V_4^{IV}O_5(PhAsO_3)\}$ units bridged by two dinuclear $[V_2^{IV}O_2(OH)_2(PhAsO_3)_4]^{6-}$ moieties. The cavity formed encloses two methanol molecules. While the structure of **1** is clearly related to that of $[V_{14}O_{22}(OH)_4(H_2O)_2(PhPO_3)_8]^{6-}$,[15] there are a number of significant differences. In the organophosphonate cluster the vanadium centers in the bridging dinuclear $[V_2O_2(OH)_2(H_2O)(PhPO_3)_4]^{6-}$ units have octahedral coordination because of a bridging aqua ligand; since **1** lacks this bridging water molecule, the vanadium centers of the corresponding dinuclear units have square-pyramidal coordination. Consequently, the interior of the cluster shell may be less polar in **1** than in the organophosphonate analogue, a situation which favors enclosure of neutral organic molecules; in contrast inorganic cation/anion pairs are encapsulated in the hydrophilic cavity of $[V_{14}O_{22}(OH)_4(H_2O)_2(PhPO_3)_8]^{6-}$. It is also noteworthy that the $\{V_5O_9\}^{3+}$ fragments in $[V_{14}O_{22}(OH)_4(H_2O)_2(PhPO_3)_8]^{6-}$ and common to the structures of $[V_5O_9(\text{thiophene-2-carboxylate})]^{2-}$[13] and $[H_4V_{18}O_{42}Cl]^{2-}$[2] are replaced in **1** by $\{V_4O_5(PhAsO_3)\}^{4+}$ fragments. Thus, in a topological sense, the $\{VO\}^{3+}$ unit is equivalent to $\{RAs\}^{4+}$. In fact, valence bond arguments indicate that the lengths of As^V–O and V^V–O single bonds should be nearly identical,[20] which confirms the geometric equivalence of these groups. Since the P^V–O bond is 0.15 Å

[*] Prof. J. Zubieta, Dr. M. I. Khan
Department of Chemistry, Syracuse University
Syracuse, New York 13244-4100 (USA)
Telefax: Int. code + (315) 443-4070

[**] This work was supported by the National Science Foundation (Grant CHE 9119910).

shorter than the As^V–O, organophosphonate analogues of **1** containing the hypothetical $\{V_4O_5(PhPO_3)\}^{4+}$ unit will be inaccessible.

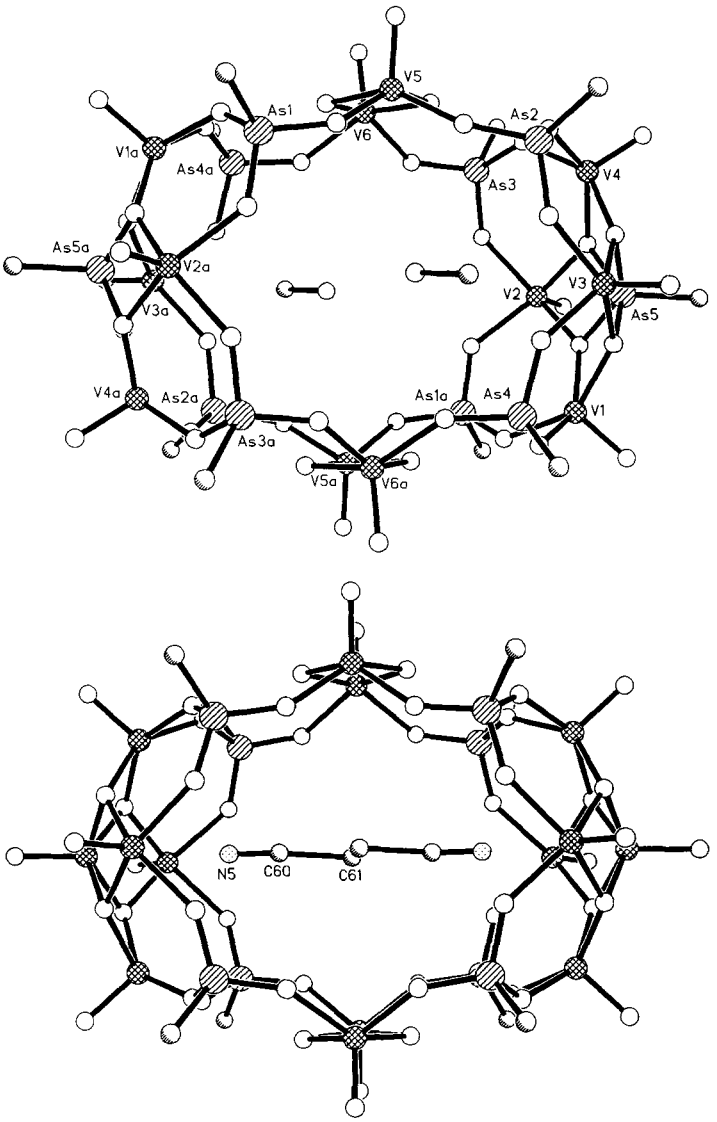


Fig. 1. Top: A view of the structure of anion in **1**. Selected bond lengths [Å]: V-O(terminal), 1.55–1.65(2); V-O(arsonate, μ^2), 1.92–1.99(2); V-O(arsonate, μ^3) 1.95–2.03(2); As1-O, 1.80–1.82(2); As(other)-O, 1.65–1.68(2); V5-O(H), 1.96(2) and 1.98(2); V6-O(H), 1.96(2) and 1.97(2). Bottom: A view of the anion in **2**. Selected bond lengths [Å]: V-O(terminal), 1.56–1.60(1); V-O(bridging), 1.88–1.99(1); V-O(phosphonate), 1.95–1.99(1); P-O, 1.51–1.53(1); V-O(H), 1.96–1.97(1).

The isolation of **1** did, however, suggest that the analogous $[V_{14}O_{22}(OH)_4(PhPO_3)_8]^{6-}$ shell should be formed about neutral organic templates in the absence of inorganic cations and in nonaqueous reaction media. Indeed, **2** was prepared from the solvothermal reaction of $[nBu_4N]_3[H_3V_{10}O_{28}]$, phenylphosphonic acid, $PhCH_2NMe_3Cl$ and $PhCH_2NEt_3Cl$ in CH_3CN/MeOH at 120 °C. The IR spectrum of **2** exhibits four characteristic bands for the PO_3 group of the $(PhPO_3)^{2-}$ ligands in the 1000–1200 cm^{-1} region and a feature at 996 cm^{-1} associated with the $\nu(V^{IV}{=}O)$ stretch.

The structure of the anion shell of **2** (Fig. 1 bottom) is identical to that of $[2NH_4^+, 2Cl^- \subset V_{14}O_{22}(OH)_4(H_2O)_2(PhPO_3)_8]^{6-}$ [15] except that the bridging aqua ligands in the dinuclear moieties are lacking. In **2** the shell has organized about two CH_3CN molecules, which are aligned within the cavity so as to nestle the nitrogen in the polar cavity of the $\{V_5O_9\}$ basket and direct the methyl group toward the relatively open and nonpolar central region of the framework. The acetonitrile molecules interact only weakly with the vanadium centers of the $\{V_5O_9\}$ unit (average V···N distance 3.21 Å), which is reminiscent of the $[CH_3CN \subset V_{12}O_{32}]^{4-}$ inclusion complex.[11]

The synthesis of **2** establishes that the $[V_{14}O_{22}(OH)_4(PhPO_3)_8]^{6-}$ shell may organize about different templates. While the template effect is well known for cluster shells of this type, the mechanism is not well understood. Both charge-compensation and space-filling effects play a role,[22] and the relative importance of these influences may reflect the synthetic conditions. It is noteworthy that the same shell may enclose species as diverse as neutral organic molecules and inorganic cations and anions.

Small variations in the conditions of solvothermal synthesis often result in novel products, as was found in the preparation of **3**. The reaction of $[nBu_4N]_3[H_3V_{10}O_{28}]$, $PhAsO_3H_2$, and CH_3OH/H_2O under identical conditions to those employed for the synthesis of **1** yields shiny green crystals of **3**. Incorporation of the $PhAsO_3^{2-}$ ligand into the framework is confirmed by the presence of a strong band at 1093 cm^{-1} in the IR spectrum, and the very strong absorption at 987 cm^{-1} is consistent with the $\nu(V^{IV}{=}O)$ stretch.

The structure of the anion of **3**[23] (Fig. 2) is constructed from vanadium-centered square pyramids and octahedra, and organoarsonate tetrahedra and square pyramids. The dominant structural motifs are two $\{V_5^{IV}O_6(PhAsO_3)_3\}^{2+}$ units bridged by two $\{V^{IV}(OH)(H_2O)(PhAsO_3)_2(PhAsO_3H)_2\}^{3-}$ groups. The shell encloses two water molecules, which are confined to the rather restricted free volume of the interior and strongly hydrogen-bonded to the hydroxo groups of the central bridging units.

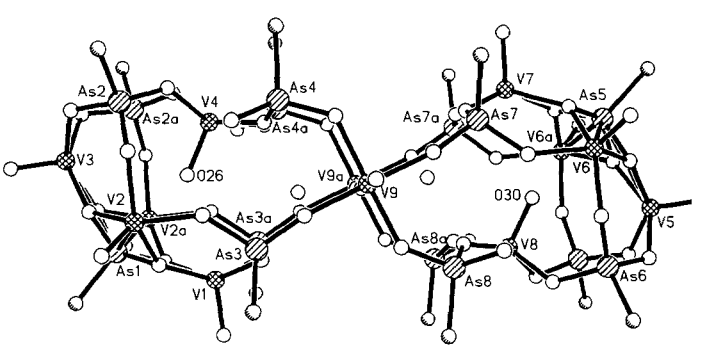


Fig. 2. The structure of the anion in **3**. Selected bond lengths [Å]: V-O(terminal), 1.55–1.67(3); V-O(arsonate, μ^2), 1.92–2.01(3); V-O(arsonate, μ^3), 1.92–2.10(3); As-O(μ^3), 1.73–1.81(3); As-O(H), 1.72–1.75(3); As-O(other), 1.60–1.70(3); V9-O(H), 1.74(3); V9-O(aqua), 2.24(5).

These hydroxo groups, as well as the oxo groups of one vanadium center in each $\{V_5O_6(PhAsO_3)_3\}^{2+}$ unit, are directed toward the interior of the cavity and thus reduce the volume accessible to guest molecules. The core of the $\{V_5O_6(PhAsO_3)_3\}^{2+}$ unit consists of four vanadium-centered square pyramids which

 © VCH Verlagsgesellschaft mbH, D-69451 Weinheim, 1994 0570-0833/94/0707-0761 $ 10.00+.25/0

share edges with a central $\{PhAsO_4\}$ square pyramid. This is yet another structural motif first observed in **1**. Two $\{PhAsO_3\}^{2-}$ tetrahedra each bridge three vanadium centers of this core and provide linkage to the fifth vanadium center. Reminiscent of the structures of $[V_5O_7(PhPO_3)_5]^-$[7] and $[V_{18}O_{25}(H_2O)_2(PhPO_3)_{20}Cl_4]^{4-}$,[10] the oxo group of this vanadium center is directed into the interior of the shallow bowl formed by the $\{V_4O_5(PhAsO_3)\}$ fragment and interacts weakly with the four vanadium atoms in this fragment. An oxo group with such an orientation was first described only recently, but it appears to be a common structural motif in the chemistry of the V/O/organophosphonate and V/O/organoarsonate systems. The central $\{V(OH)(H_2O)\}$ fragments are each linked to these $\{V_5O_6(PhAsO_3)_3\}^{2+}$ units by two $(PhAsO_3)^{2-}$ and two $(PhAsO_3H)^-$ groups. The protonated oxygen atoms are identified by the relatively long As–O distances and the pendant position.

The structural variety of the "naked" polyoxovanadium clusters $\{V_xO_y\}^{n-}$ is well documented. However, the compositional diversity of the $V/O/RPO_3^{2-}$ and $V/O/RAsO_3^{2-}$ systems may well exceed that of the naked clusters. The connectivity possibilities for the construction of cluster frameworks are expanded by the incorporation of $\{REO_3\}$ tetrahedra (E = P or As) and $\{RAsO_4\}$ square pyramids. Furthermore, thermally induced condensations of the $\{REO_3\}$ groups can provide polyphosphonate and polyarsonate units[24] which also enhance the structural possibilities. Solvothermal reactions may provide access to metastable species not available through conventional or hydrothermal techniques.

Certain target molecules are suggested by the analogy of the $V/O/RPO_3^{2-}$ and $V/O/RAsO_3^{2-}$ systems. These include organoarsonte analogues of $[V_2O_2Cl_2(PRO_3H)_2(H_2O)_2]$ and $[V_2O_2Cl_4(RPO_3H)_2]^{2-}$,[9] $[(VO)_6(RPO_3)_8Cl]$,[10] and $[V_7O_{12}(PhPO_3)_8Cl]^{-2}$.[25] Similarly, since $[V_5O_7(OCH_3)_2(PhPO_3)_5]^-$ and $[V_{18}O_{25}(H_2O)_2(PhPO_3)_{20}Cl_4]^{4-}$ are chemically and structurally related,[10] we expect that by analogy to the $\{V_5O_6(PhAsO_3)_3\}^{2+}$ unit of **3** a species of the type $[V_6O_7(RAsO_3)_7]^{n-}$ should exist. Likewise, aggregation of multiple units of $[V_6O_7(RAsO_3)_7]^{n-}$ would provide "clusters of clusters" in a fashion akin to that observed for the $V/O/RPO_3^{2-}$ system. Such rational design of superclusters and even solid phases from simple inorganic building blocks remains the elusive but ultimate objective of these investigations.[9]

Experimental Section

Compounds **1**, **2**, and **3** were characterized by C,H,N analyses, manganometric titration of the V^{IV} content, thermogravimetric determination of water content, IR spectroscopy, single-crystal X-ray crystallography, and the determination of bond valence sums.

1: A mixture consisting of $[nBu_4N]_3[H_3V_{10}O_{28}]$ (0.30 g, 0.18 mmol), $PhAsO_3H_2$ (0.40 g, 1.98 mmol) and CH_3OH/H_2O (2 mL, 99:1) was placed in a thick-walled pyrex tube (27 cm long, 8 mm inner diameter). The contents of the tube were frozen in liquid nitrogen, and the tube was sealed under vacuum. After the mixture was allowed to warm to room temperature, the tube was heated at 100 °C for 17 h. The resultant dark brown-black solution was then heated for 3 d at 120 °C. Upon cooling to room temperature, light green needles of **1** were filtered from the green mother liquor. The crystals of **1** were separated manually from an amorphous gray material and stored in the mother liquor. Yield: 20% based on vanadium. The crystals are slightly soluble in CH_3CN. Exposure to air or to other solvents such as alcohols, acetone, or water causes the crystals to become opaque. IR (KBr): ν[cm^{-1}]: 1482(m), 1438(s), 1093(s), 998(vs), 895(sh), 840(vs), 740(m), 690(s), 639(vs), 503(s).

2: A mixture of $[nBu_4N]_3[H_3V_{10}O_{28}]$ (0.33 g, 0.19 mmol), $PhPO_3H_2$ (0.158 g), $PhCH_2NMe_3Cl$ (0.370 g), $PhCH_2NEt_3Cl$ (0.454 g, 2.00 mmol), CH_3CN (4 mL), and CH_3OH (1 mL) was placed in a Teflon-lined Parr acid digestion vessel and heated at 120 °C for 87 h. After cooling to room temperature, dark green blocklike crystals of **2** were collected in 60% yield. IR (KBr): ν[cm^{-1}]: 1121(s, broad), 1097(vs), 1068(m), 1032(m), 1015(s), 996(vs), 751(m), 720(m), 698(s), 645(m), 619(m), 609(s), 559(s), 523(s).

3: A mixture of $[nBu_4N]_3[H_3V_{10}O_{28}]$ (0.30 g), $PhAsO_3H_2$ (0.20 g), Et_4NCl (0.30 g) and CH_3OH/H_2O (4 mL, 99:1) was treated according to the procedure described for **1**. Light green needles of **3** were manually separated from an amorphous black powder and stored in the light green mother liquor. Yield: 30% based on vanadium. Exposure to air or other organic solvents results in opacity of the solid. IR (KBr): ν[cm^{-1}]: 1483(m), 1438(s), 1093(s), 1012(s), 987(vs), 895(sh), 840(vs), 812(sh), 740(s), 690(s), 637(vs), 507(s).

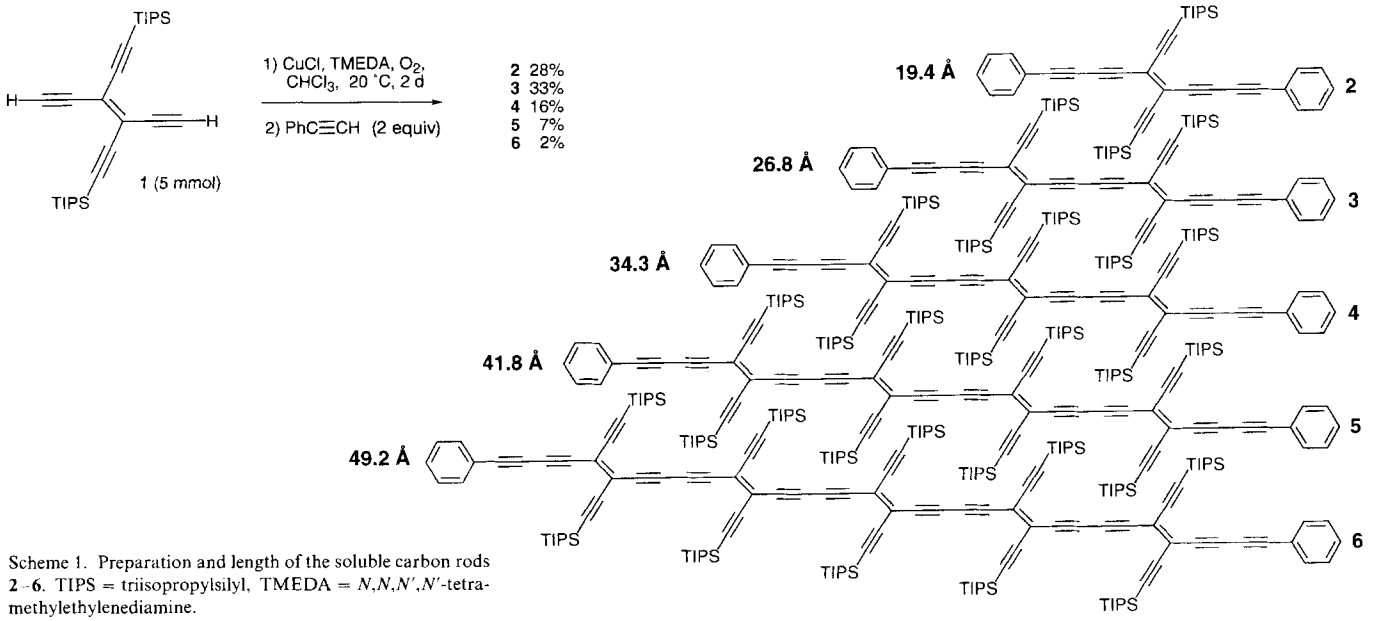
Received: October 25, 1993 [Z 6449 IE]
German version: *Angew. Chem.* **1994**, *106*, 784

[1] M. T. Pope, A. Müller, *Angew. Chem.* **1990**, *103*, 56; *Angew. Chem. Int. Ed. Engl.* **1990**, *30*, 34.
[2] A. Müller, M. Penk, R. Rohlfing, E. Krichemeyer, J. Döring, *Angew. Chem.* **1990**, *102*, 927; *Angew. Chem. Int. Ed. Engl.* **1990**, *29*, 926.
[3] W. G. Klemperer, T. A. Marquart, O. M. Yaghi, *Angew. Chem.* **1992**, *104*, 51; *Angew. Chem. Int. Ed. Engl.* **1992**, *32*, 49.
[4] P. Kato, A. Kobayashi, Y. Sasaki, *J. Am. Chem. Soc.* **1980**, *102*, 6571.
[5] G. K. Johnson, E. O. Schlemper, *J. Am. Chem. Soc.* **1978**, *100*, 3645.
[6] G. Huan, V. W. Day, A. J. Jacobson, D. P. Goshorn, *J. Am. Chem. Soc.* **1991**, *113*, 3188.
[7] Q. Chen, J. Zubieta, *Angew. Chem.* **1993**, *105*, 304; *Angew. Chem. Int. Ed. Engl.* **1993**, *32*, 261.
[8] A. Müller, P. Rohlfing, E. Krickemeyer, H. Bögge, *Angew. Chem.* **1993**, *105*, 916; *Angew. Chem. Int. Ed. Engl.* **1993**, *32*, 909.
[9] Q. Chen, J. Salta, J. Zubieta, *Inorg. Chem.* **1993**, in press.
[10] J. Salta, Y.-D. Chang, Q. Chen, J. Zubieta, unpublished.
[11] V. W. Day, W. G. Klemperer, O. M. Yaghi, *J. Am. Chem. Soc.* **1989**, *111*, 5959.
[12] Q. Chen, J. Zubieta, *Inorg. Chem.* **1989**, *28*, 4433.
[13] D. D. Heinrich, K. Folting, W. E. Streib, J. C. Huffman, G. Christou, *J. Chem. Soc. Chem. Commun.* **1989**, 1411.
[14] G. H. Huan, A. J. Jacobson, V. W. Day, *Angew. Chem.* **1991**, *103*, 426; *Angew. Chem. Int. Ed. Engl.* **1991**, *30*, 422.
[15] A. Müller, K. Hovemeier, R. Rohlfing, *Angew. Chem.* **1992**, *104*, 1214; *Angew. Chem. Int. Ed. Engl.* **1992**, *31*, 1192.
[16] V. Soghomonian, Q. Chen, R. C. Haushalter, J. Zubieta, *Angew. Chem.* **1993**, *105*, 601; *Angew. Chem. Int. Ed. Engl.* **1993**, *32*, 610, and references therein.
[17] M. I. Khan, Y.-D. Chang, Q. Chen, H. Höpe, S. Parkin, D. P. Goshorn, J. Zubieta, *Angew. Chem.* **1992**, *104*, 1236; *Angew. Chem. Int. Ed. Engl.* **1992**, *31*, 1197.
[18] M. Figlarz, *Chem. Scr.* **1988**, *28*, 3.
[19] a) Crystal data for **1**: triclinic space group $P\bar{1}$ with $a = 14.138(3)$, $b = 16.567(3)$, $c = 17.990(4)$ Å, $\alpha = 65.82(2)$, $\beta = 71.28(2)$, $\gamma = 65.58(2)°$, $V = 3441.3(12)$ Å^3, $Z = 1$, $\rho_{calc} = 1.710$ gcm^{-3}, $\mu(Mo_{K\alpha}) = 35.39$ cm^{-1}; $R = 0.067$ for 3786 reflections with $2\theta < 45°$ and $I > 3\sigma(I)$; Rigaku AFC5S diffractometer, graphite-monochromated $Mo_{K\alpha}$ radiation. The structure was solved using direct methods with the SHELXTL program package. The identity of the $(H_7O_3)^+$ ions is confirmed by the charge requirements of the compound and by the structural parameters associated with the O···O···O framework, which are nearly identical to those previously reported for $[H_7O_3]_2[NEt_4]_2[Ru_3Cl_{12}]$: A. Bino, F. A. Cotton, *J. Am. Chem. Soc.* **1980**, *102*, 608. The $(H_7O_3)^+$ ions serve as "goalkeepers" for the anionic cluster and are centrally situated above and below the open faces of the cavity of the cluster. b) Further details of the crystal structure investigations may be obtained from the Fachinformationszentrum Karlsruhe, D-76344 Eggenstein-Leopoldshafen (FRG) on quoting the depository number CSD-57869, the names of the authors, and the journal citation.
[20] I. D. Brown, *Structure and Bonding in Crystals, Vol. 4* (Eds.: M. O'Keefe, A. Navrotskyk), Academic Press, New York, **1981**, p. 1.
[21] Crystal data for **2**: triclinic space group $P\bar{1}$ with $a = 15.068(3)$, $b = 15.861(3)$, $c = 18.336(4)$ Å, $\alpha = 70.56(2)$, $\beta = 70.23(2)$, $\gamma = 84.12(2)°$, $V = 3889(2)$ Å^3, $Z = 1$, $\rho_{calc} = 1.551$ gcm^{-3}, $\mu(Mo_{K\alpha}) = 11.65$ cm^{-1}; $R = 0.071$ for 4462 reflections with $2\theta < 45°$ and $I > 3\sigma(I)$. All other conditions and informations as in reference [19].
[22] A. Stein, S. W. Keller, T. E. Mallouk, *Science* **1993**, *259*, 1558.
[23] Crystal data for **3**: orthorhombic space group *Pnma* with $a = 44.411(8)$, $b = 14.798(2)$, $c = 24.366(4)$ Å, $V = 16013(15)$ Å^3, $Z = 4$, $\rho_{calc} = 1.693$ gcm^{-3}, $\mu(Mo_{K\alpha}) = 36.2$ cm^{-1}; $R = 0.079$ for 2895 reflections with $I > 3\sigma(I)$. All other conditions and informations as in reference [19]. The Et_4N^+ cation is so highly disordered that the carbon sites must be fixed at idealized positions.
[24] J. Salta, Y.-D. Chang, Q. Chen, J. Zubieta, unpublished.
[25] J. Salta, Y.-D. Chang, J. Zubieta, *Angew. Chem.* **1994**, *106*, 347; *Angew. Chem. Int. Ed. Engl.* **1994**, *33*, 325.

Stable Soluble Conjugated Carbon Rods with a Persilylethynylated Polytriacetylene Backbone**

John Anthony, Corinne Boudon, François Diederich,* Jean-Paul Gisselbrecht, Volker Gramlich, Maurice Gross, Markus Hobi, and Paul Seiler

Rigid acetylenic frameworks are being used with increasing frequency for the fabrication of molecular nanostructures.[1] Here we report the preparation of the conjugated, nanometer-sized molecular rods[2] **2**–**6** through end-capping polymerization of *trans*-bis(triisopropylsilyl)-protected tetraethynylethene **1** (Scheme 1).[3, 4]

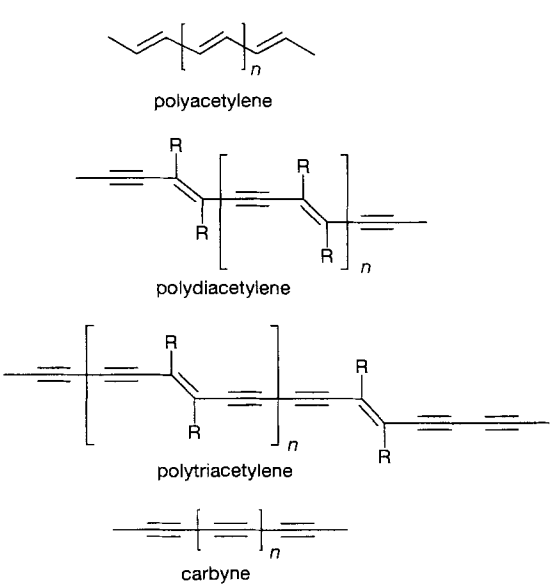


Scheme 1. Preparation and length of the soluble carbon rods **2**–**6**. TIPS = triisopropylsilyl, TMEDA = *N*,*N*,*N*′,*N*′-tetramethylethylenediamine.

Oligomers **2**–**6** are polytriacetylenes and are thus intermediate between polyacetylene[5] and polydiacetylene,[6] and carbyne (Scheme 2).[7] Derivatives of **2**–**6** could exhibit interesting nonlinear optical properties[8] and function as molecular wires.[9]

trans-Bis(triisopropylsilyl)-protected tetraethynylethenes are readily prepared in multigram quantities by the general synthetic route shown in Scheme 3. Both the diester **14** and the free diethynyl derivative **1** were characterized by X-ray crystallography (Figs. 1 and 2).[10] In the crystal, the carboxyl groups of **14** are twisted out of the plane of the tetraethynylethene backbone because of steric hindrance between the ester residue and the neighboring TIPS group. The angle between the least-squares planes passing through C(2), C(1), O(1), O(2), and the tetraethynylethene fragment is 42(1)°. The stability of crystalline **1** is quite remarkable, since bisdeprotected *trans*-enediynes typically polymerize rapidly upon concentration of solutions.[11] An analysis of the crystal packing shows that the stability of **1** is related to the "insulating effect" of the TIPS groups, which we had previously found to stabilize crystals of a persilylethynylated tetradehydro[12]annulene.[12] The molecules of **1** align in a herringbone fashion with the reactive free ethynyl groups pointing directly towards the silyl groups of neighboring molecules.

End-capping reactions are used in polymer chemistry to control polymer length.[13] When phenylacetylene was added to the oxidative polymerization of **1** (Scheme 1), a mixture of oligomers was obtained, from which compounds **2**–**6** were isolated by chromatography (SiO_2, hexanes). If a large excess of phenylacetylene (6 equiv) was added at the beginning of the reaction, **2** was the only compound isolated. If phenylacetylene (2 equiv) was added after 6 to 8 h, oligomers **2**–**4** were isolated in fair yields. For the preparation of the larger derivatives **5** and **6** the oxidative coupling had to be allowed to run for at least 24 h before the end-capping reagent was added.

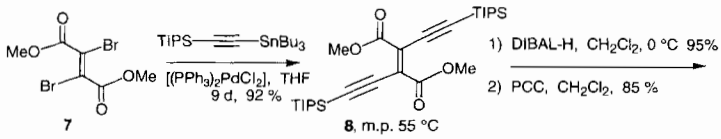


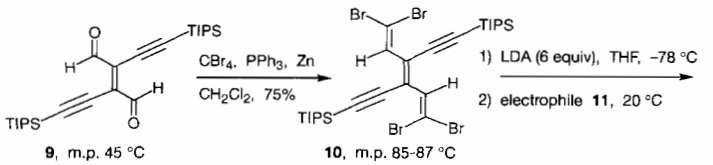
Scheme 2. Progression of polymeric backbones from polyacetylene to carbyne.

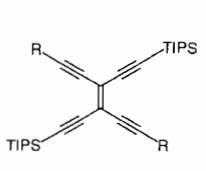
[*] Prof. F. Diederich, J. Anthony, M. Hobi, P. Seiler
Laboratorium für Organische Chemie
ETH-Zentrum
Universitätstrasse 16, CH-8092 Zürich (Switzerland)
Telefax: Int. code + (1) 261-3524
Dr. V. Gramlich
Institut für Kristallographie und Petrographie
ETH-Zentrum
Sonneggstrasse 5, CH-8092 Zürich (Switzerland)
Prof. M. Gross, C. Boudon, J.-P. Gisselbrecht
Laboratoire d'Electrochimie et de Chimie Physique du Corps Solide
U.R.A. au C.N.R.S. n° 405
Faculté de Chimie, Université Louis Pasteur
1 et 4, rue Blaise Pascal B.P. 296
F-67008 Strasbourg Cedex (France)

[**] This work was supported by the Swiss National Science Foundation.

 © VCH Verlagsgesellschaft mbH, D-69451 Weinheim, 1994 0570-0833/94/0707-0763 $ 10.00+.25/0







	R	Yield [%]	M.p. [°C]
1	H	95	76
12	I	23	88-90
13	$CH(OH)CH_3$	81	104-106
14	$CO_2CH_2CH(CH_3)_2$	65	81
15		79	174-175

Scheme 3. Synthesis of *trans*-bis(triisopropylsilyl)-protected tetraethynylethene derivatives. **10** was metalated and then treated with the following electrophiles H^+, I_2, acetaldehyde, isobutyl chloroformate, fluorenone. DIBAL-H = diisobutylaluminum hydride, PCC = pyridinium chlorochromate, LDA = lithium diisopropylamide.

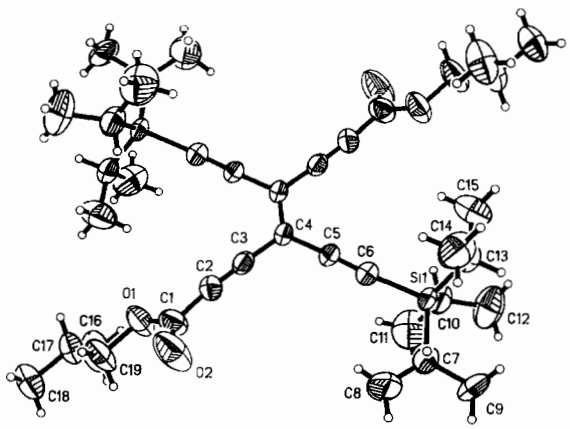


Fig. 1. Crystal structure of **14**. Selected bond lengths [Å] and angles [°]: C(2)-C(3) 1.173(8), C(3)-C(4) 1.436(7), C(4)-C(5) 1.426(6), C(5)-C(6) 1.204(6), C(4)-C(4A) 1.353(11); C(1)-C(2)-C(3) 175.9(6), C(2)-C(3)-C(4) 176.7(5), C(3)-C(4)-C(4A) 121.4(4), C(3)-C(4)-C(5) 116.5(5), C(4A)-C(4)-C(5) 122.0(5), C(4)-C(5)-C(6) 178.2(6), C(5)-C(6)-Si(1) 174.8(4).

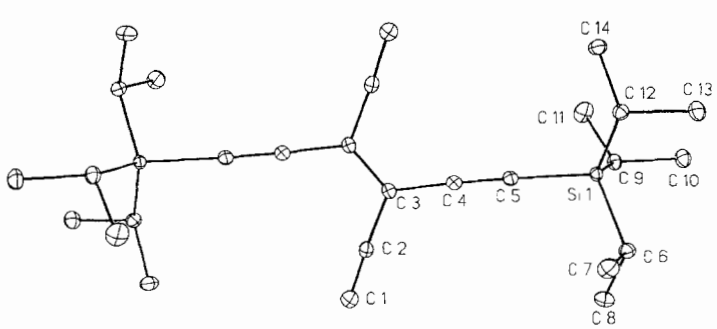


Fig. 2. Crystal structure of **1**. Selected bond lengths [Å] and angles [°]: C(1)-C(2) 1.194(4), C(2)-C(3) 1.431(4), C(3)-C(3A) 1.368(5), C(3)-C(4) 1.437(3), C(4)-C(5) 1.207(3), C(5)-Si(1) 1.850(2); C(1)-C(2)-C(3) 177.3(3), C(2)-C(3)-C(3A) 121.9(3), C(2)-C(3)-C(4) 116.8(2), C(3A)-C(3)-C(4) 121.3(3), C(3)-C(4)-C(5) 177.1(3), C(4)-C(5)-Si(1) 175.4(2).

Oligomers **2**–**6** are amazingly stable, high-melting materials (Table 1) that remain unchanged for months at room temperature when exposed to air and light. The TIPS groups both stabilize the extended conjugated chromophores and render them soluble in common solvents. The shorter derivatives **2**–**4** dissolve in hexane, while all five molecular rods are soluble in chloroform,

Table 1. Selected physical data of compounds **2**–**6**[a-c].

2: Golden yellow crystals, m.p. 142–143 °C. FT-IR (KBr): $\nu = 2220$ (C≡C) cm^{-1}; ^1H NMR (200 MHz): $\delta = 1.16$ (s, 42H), 7.37 (m, 6H), 7.50 (m, 4H); ^{13}C NMR (125.76 MHz): $\delta = 11.24$, 18.62, 74.16, 76.99, 84.56, 86.91, 101.8, 104.2, 119.8, 121.5, 128.5, 129.9, 132.5; UV/VIS ($CHCl_3$): λ_{max} [nm] = 256 ($\varepsilon = 36700$), 275 (28100), 290 (25300), 306 (20000), 325 (15600), 394 (34000), 422 (35500), 479 (1600)); MALDI-TOF-MS: m/z 637 (M^-).

3: Orange-yellow crystals, m.p. 180 °C (decomp.). FT-IR (KBr): $\nu = 2200$ (C≡C) cm^{-1}; ^1H NMR (200 MHz): $\delta = 1.16$ (s, 42H), 1.17 (s, 42H), 7.36 (m, 6H), 7.50 (m, 4H); ^{13}C NMR (125.76 MHz): $\delta = 11.17$, 11.22, 18.57, 18.60, 74.17, 78.86, 83.83, 84.29, 85.04, 87.24, 101.4, 101.7, 104.4, 105.0, 119.5, 120.6, 121.5, 128.5, 129.6, 132.5; UV/VIS ($CHCl_3$): λ_{max} [nm] = 270 ($\varepsilon = 21000$), 290 (21000), 309 (19000), 329 (18000), 384 sh (15000), 440 (28000), 478 (31000); MALDI-TOF-MS: m/z 1073 (M^-).

4: Red crystals, m.p. 245 °C (decomp.). FT-IR (KBr): $\nu = 2179$, 2177, 2133 (C≡C) cm^{-1}; ^1H NMR (200 MHz): $\delta = 1.11$ (s, 42H), 1.14 (s, 42H), 1.16 (s, 42H), 7.37 (m, 6H), 7.50 (m, 4H); ^{13}C NMR (125.76 MHz): $\delta = 11.16$, 11.21, 18.56, 18.60, 74.15, 78.85, 83.90, 84.15, 84.25, 84.75, 85.10, 87.29, 101.3, 101.4, 101.7, 104.5, 105.1, 105.2, 119.4, 120.1, 120.7, 121.5, 128.5, 129.6, 132.5; UV/VIS ($CHCl_3$): λ_{max} [nm] = 274 ($\varepsilon = 40500$), 290 (41000), 311 (40100), 330 (39900), 368 (28600), 480 (63800), 506 sh (51500); MALDI-TOF-MS: m/z 1507 (M^-), 1463 (M^- − isopropyl), 1419 (M^- − 2isopropyl).

5: Red crystals, m.p. 250 °C (decomp.). FT-IR (KBr): $\nu = 2200$, 2177, 2133 (C≡C) cm^{-1}; ^1H NMR (200 MHz): $\delta = 1.117$ (s, 42H), 1.119 (s, 42H), 1.123 (s, 42H), 1.14 (s, 42H), 7.37 (m, 6H), 7.50 (m, 4H); ^{13}C NMR (125.76 MHz): $\delta = 11.19$, 11.25, 18.54, 18.57, 74.17, 78.89, 83.90, 84.20, 84.21, 84.25, 84.67, 84.79, 85.10, 87.29, 101.31, 101.35, 101.5, 101.7, 104.5, 105.1, 105.3, 105.35, 119.3, 120.0, 120.1, 120.7, 121.5, 128.5, 129.6, 132.5; UV/VIS ($CHCl_3$): λ_{max} [nm] = 272 ($\varepsilon = 40900$), 291 (40300), 317(39400), 327 (38000), 366 (28300), 392 (28900), 416 sh (30600), 484 (53600) 511 sh (44600); MALDI-TOF-MS: m/z 1937 (M^-).

6: Dark red crystals, m.p. 250 °C (decomp.). FT-IR (KBr): $\nu = 2199$, 2168, 2152, 2130 (C≡C) cm^{-1}; ^1H NMR (200 MHz): $\delta = 1.116$ (br. s, 84H), 1.118 (s, 42H), 1.123 (s, 42H), 1.142 (s, 42H), 7.37 (m, 6H), 7.50 (m, 4H); ^{13}C NMR (125.76 MHz): $\delta = 11.23$, 11.30, 11.46, 18.58, 18.61, 74.21, 78.93, 83.899, 84.191, 84.229, 84.289, 84.646, 84.665, 84.737, 84.801, 85.108, 87.296, 101.299 (2 ×), 101.337, 101.443, 101.712, 104.506, 105.128, 105.329, 105.344, 105.394, 119.33, 119.98, 120.11, 120.20, 120.69, 121.56, 128.5, 129.6, 132.5; UV/VIS ($CHCl_3$): λ_{max} [nm] = 290 ($\varepsilon = 25300$), 320 (25800), 329 (25700), 367 sh (18200), 390 sh (17800), 419 sh (19700), 490 (37500), 514 sh (38700); MALDI-TOF-MS: m/z 2376 (M^-).

[a] All NMR spectra were recorded in $CDCl_3$. [b] Matrix for MALDI-TOF mass spectrometry: 9-nitroanthracene; we thank L. Isaacs for recording these spectra. [c] All new compounds were fully characterized by ^1H and ^{13}C NMR, FT-IR, and UV/VIS spectroscopy, EI-MS or MALDI-TOF MS, and correct elemental analysis.

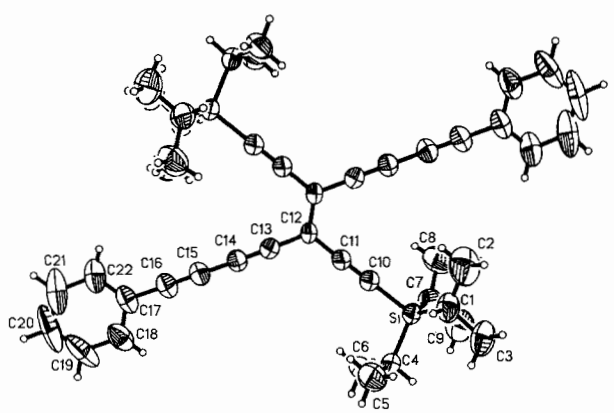


Fig. 3. Crystal structure of **2**. Selected bond lengths [Å] and angles [°]: Si-C(10) 1.853(6), C(10)-C(11) 1.190(6), C(11)-C(12) 1.426(6), C(12)-C(12A) 1.368(7), C(12)-C(13) 1.429(6), C(13)-C(14) 1.188(6), C(14)-C(15) 1.376(6), C(15)-C(16) 1.190(6), C(16)-C(17) 1.431(6); Si-C(10)-C(11) 178.6(3), C(10)-C(11)-C(12) 177.9(4), C(11)-C(12)-C(13) 118.2(3), C(11)-C(12)-C(12A) 121.4(4), C(12A)-C(12)-C(13) 120.4(4), C(12)-C(13)-C(14) 179.2(4), C(14)-C(15)-C(16) 178.1(4), C(15)-C(16)-C(17) 176.5(4).

 © VCH Verlagsgesellschaft mbH, D-69451 Weinheim, 1994 0570-0833/94/0707-0764 $ 10.00+.25/0

which allowed their full analytical characterization (Table 1). Mass spectra of **2**–**6** with the molecular ions as parent ions were obtained by matrix-assisted laser desorption ionization time-of-flight mass spectrometry (MALDI-TOF-MS) with detection in the negative ion mode. Upon recrystallization from hexane, the shorter rods **2** and **3** formed crystals suitable for X-ray analysis (Figs. 3 and 4). The conjugated carbon frames of both molecules, including the phenyl rings, are nearly perfectly planar with a maximum deviation from the least-squares plane passing through the entire carbon chromophore of 0.22 Å in **2** and only 0.03 Å in **3**.[3] Distances between the *para*-phenyl C atoms at the termini of the rods are 19.37 Å (in **2**) and 26.84 Å (in **3**), which is in agreement with the calculated values in Scheme 1.[14]

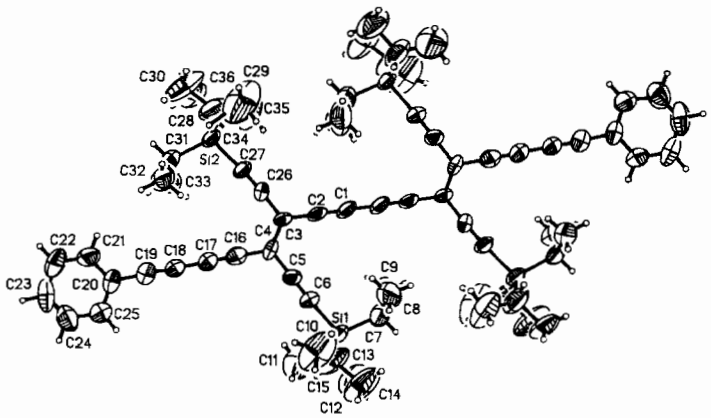


Fig. 4. Crystal structure of **3**. Selected bond lengths [Å] and angles [°]: C(1)-C(1A) 1.368(3), C(2)-C(3) 1.432(2), C(3)-C(4) 1.352(2), C(4)-C(5) 1.452(2), C(5)-C(6) 1.175(2), C(6)-Si(1) 1.852(2), C(4)-C(16) 1.424(2), C(16)-C(17) 1.192(2), C(17)-C(18) 1.371(2), C(18)-C(19) 1.197(2), C(19)-C(20) 1.429(2), C(3)-C(26) 1.441(2), C(26)-C(27) 1.187(2), C(27)-Si(2) 1.844(2); C(1)-C(2)-C(3) 176.4(2), C(2)-C(3)-C(4) 119.5(2), C(3)-C(4)-C(5) 121.8(1), C(4)-C(5)-C(6) 179.6(1), C(5)-C(6)-Si(1) 175.9(8), C(3)-C(4)-C(16) 121.9(2), C(4)-C(16)-C(17) 179.6 (2), C(16)-C(17)-C(18) 178.1(2), C(17)-C(18)-C(19) 178.0(2), C(18)-C(19)-C(20) 178.4(2), C(2)-C(3)-C(26) 118.1(1), C(3)-C(26)-C(27) 176.0(1), C(26)-C(27)-Si(2) 175.8(1), C(4)-C(3)-C(26) 122.4(1).

In the electronic absorption spectra of **2**–**6** (Fig. 5) the wavelength of the end absorption increases with the length of the oligomeric chain. It is well known that the band gap E_g of a polymer can be determined from plots of the longest wavelength UV/VIS absorption for a series of related oligomers versus the length of the oligomers.[15] When the end absorptions of **2**–**6** were plotted against the inverse of the oligomeric length, a straight line was obtained ($r^2 = 0.996$) with an intercept at 540 nm (2.3 eV), which corresponds to the longest wavelength absorption cutoff for an infinite polymer in solution, in other words, its solution band gap. This band gap is comparable to that of many polydiacetylenes ($E_g \approx 2.1$ eV).

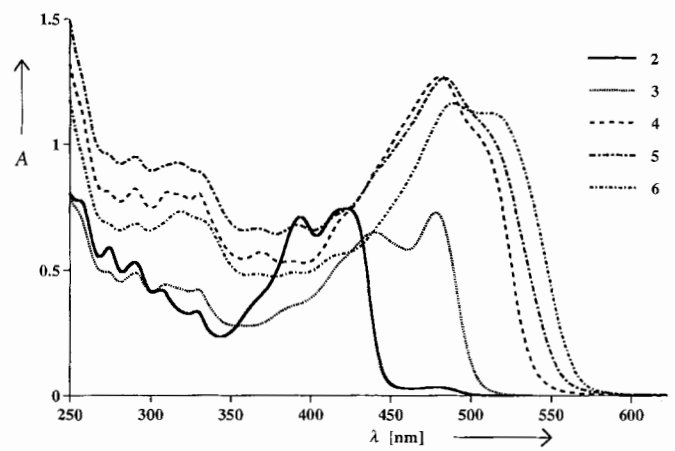


Fig. 5. Electronic absorption spectra of **2**–**6** in $CHCl_3$, $c = 2.3 \times 10^{-5}$ M, $T = 293$ K.

Of particular interest were the redox properties of the conjugated rods, which were examined by polarography and cyclic voltammetry in THF with $Bu_4N^+PF_6^-$ (0.1 M) as the supporting electrolyte.[16] While none of the oligomers **2**–**5** could be oxidized below +1.0 V (vs ferrocene), which helps explain their stability in air, they were all readily reduced with the number of reversible one-electron reduction steps corresponding to the number of tetraethynylethene moieties in each rod.[17] For longer oligomers the first reduction occurred at increasingly less negative potentials (Fig. 6). A plot of reduction potential vs 1/(oligomer length) gave nearly identical first and second reduction potentials of −1.01 V and −1.05 V, respectively, for an infinite polymer.[18]

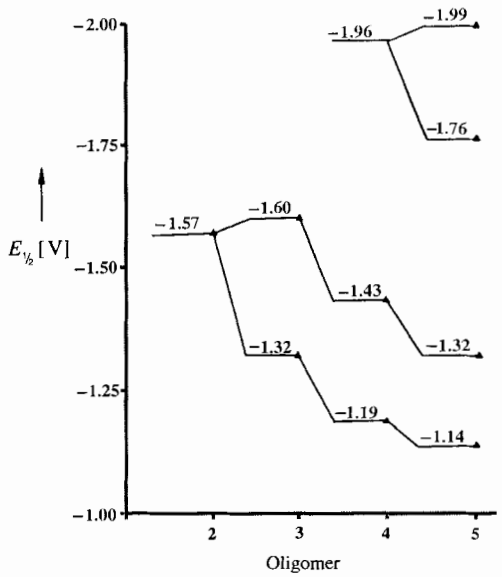
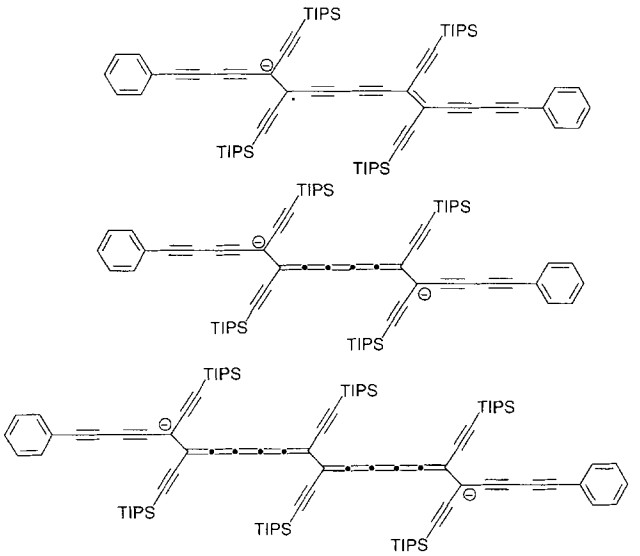


Fig. 6. Reduction potentials $E_{1/2}$ (V, vs ferrocene) for **2**–**5** in THF with $Bu_4N^+PF_6^-$ (0.1 M) as the electrolyte.

A closer inspection of the reduction potentials shows an interesting trend (Fig. 6). The monomeric compound **2** undergoes one reversible one-electron reduction at −1.57 V. The first reduction potential of dimeric **3** is significantly less negative (−1.32 V) and the second reduction step occurs at a potential (−1.60 V) similar to that for the reduction of **2**. The trimeric compound **4** undergoes a facile first (−1.19 V) and second (−1.43 V) reduction, but the third reduction occurs at significantly higher energy (−1.96 V). Tetramer **5** undergoes its fourth one-electron reduction (−1.99 V) at nearly the same potential as the third one-electron reduction in **4** (−1.96 V). This "pairwise" reduction behavior is best explained by especially stable dianions and tetraanions. In the first one-electron reduction, a radical anion forms which is delocalized over the entire backbone (Scheme 4). We propose that in the dianion the anionic centers are separated by a [5]cumulene unit. In such a structure the anionic centers are held far apart, minimizing repulsive electrostatic interactions. Furthermore, the negative charges are delocalized over what are essentially dialkynylmethyl moieties, which have been shown previously to form quite stable anions.[19] In the trimer **the negative**



Scheme 4. Proposed structures of the radical anion of **3** (top) and the dianions of **3** (middle) and **4** (bottom).

charges of a dianion are localized on the dialkynylmethyl moieties on opposite ends of the molecule (Scheme 4). A third electron would have to add to the central dicumulenic unit, which explains the difficulty in forming the trianion.

Because of their remarkable stability, oligomers such as **2**–**6** could become useful in the field of molecular electronics. Other substituents may also be attached to the end of the rods by changing the end-capping reagent. The properties of these nanometer-scale materials could be easily altered by exchanging the silyl groups for other substituents. This study of new oligomeric rods has allowed us to predict interesting properties of the corresponding polymers, on which we will report in due course.

Received: November 6, 1993 [Z 6482 IE]
German version: *Angew. Chem.* **1994**, *106*, 794

[1] Z. Wu, S. Lee, J. S. Moore, *J. Am. Chem. Soc.* **1992**, *114*, 8730–8732.
[2] a) J.-M. Lehn, *Angew. Chem.* **1988**, *100*, 91–116; *Angew. Chem. Int. Ed. Engl.* **1988**, *27*, 89–112; b) P. Kaszynski, A. C. Friedli, J. Michl, *J. Am. Chem. Soc.* **1992**, *114*, 601–620, and references cited therein; c) J. Müller, K. Base, T. F. Magnera, J. Michl, *ibid.* **1992**, *114*, 9721–9722; d) X. Yang, W. Jiang, C. B. Knobler, M. F. Hawthorne, *ibid.* **1992**, *114*, 9719–9721; e) J. Guay, A. Diaz, R. Wu, J. M. Tour, *ibid.* **1993**, *115*, 1869–1874.
[3] A. M. Boldi, J. Anthony, C. B. Knobler, F. Diederich, *Angew. Chem.* **1992**, *104*, 1270–1273; *Angew. Chem. Int. Ed. Engl.* **1992**, *31*, 1240–1242.
[4] The potential of substituted tetraethynylethenes as monomers for new polymers has been independently recognized: H. Hopf, M. Kreutzer, P. G. Jones, *Chem. Ber.* **1991**, *124*, 1471–1475.
[5] A. J. Heeger, A. G. McDiarmid in *The Physics and Chemistry of Low Dimensional Solids* (Ed.: L. Alcacer), Reidel, Dordrecht, **1980**, pp. 353–391.
[6] a) G. Wegner, *Angew. Chem.* **1981**, *93*, 352–371; *Angew. Chem. Int. Ed. Engl* **1981**, *20*, 361–381; b) G. Adler, *Mol. Cryst. Liq. Cryst (Part A)* **1983**, *96*, 1–412.
[7] A. M. Sladkov, *Sov. Sci. Rev. Sect. B* **1981**, *3*, 75–110.
[8] H. S. Nalwa, *Adv. Mater.* **1993**, *5*, 341–358.
[9] a) F. L. Carter, *Molecular Electronic Devices II*, M. Dekker, New York, **1987**; b) *Nanostructures Based on Molecular Materials* (Eds.: W. Göpel, C. Ziegler), VCH, Weinheim, **1992**.
[10] X-ray crystal data for **14** ($C_{38}H_{60}O_4Si_2$, $M_r = 637.0$): Monoclinic space group $P2_1/c$ (No. 14), $\rho_{calc} = 1.046\ g\,cm^{-3}$, $Z = 2$, $a = 13.896(12)$, $b = 10.810(10)$, $c = 14.999(11)$ Å, $\beta = 116.16(6)^\circ$, $V = 2022(3)$ Å^3, $Mo_{K\alpha}$ radiation, $2\theta \leq 40^\circ$, 1900 unique reflections, $T = 293$ K. The structure was solved by direct methods (SHELXTL PLUS) and refined by full-matrix least-squares analysis using experimental weights (heavy atoms anisotropic, H atoms fixed, whereby H positions are based on stereochemical considerations). Final $R(F) = 0.047$, $wR(F) = 0.060$ for 199 variables and 1307 observed reflections with $F > 4\sigma(F)$. – **1** ($C_{28}H_{44}Si_2$, $M_r = 436.8$): Monoclinic space group $P2_1/c$ (No. 14) $\rho_{calc} = 1.03\ g\,cm^{-3}$, $Z = 2$, $a = 13.443(4)$, $b = 11.762(5)$, $c = 8.904(1)$ Å, $\beta = 92.85(0)^\circ$, $V = 1406.13$ Å^3, $Mo_{K\alpha}$ radiation, $2\theta \leq 50^\circ$, 2447 unique reflections, $T = 100$ K. The structure was solved by direct methods (SHELXTL PLUS) and refined by full-matrix least-squares analysis using an isotropic extinction coefficient and an exponentially modified weight factor with $r = 5$ Å^2 (heavy atoms anisotropic, H atoms isotropic, whereby H positions are based on stereochemical considerations). Final $R(F) = 0.038$, $wR(F) = 0.039$ for 159 variables and 1578 observed reflections with $I > 3\sigma(I)$. – **2** ($C_{44}H_{52}Si_2$, $M_r = 637.0$): Monoclinic space group $P2_1/c$ (No. 14), $\rho_{calc} = 1.046\ g\,cm^{-3}$, $Z = 2$, $a = 8.40(2)$, $b = 15.570(6)$, $c = 15.57(4)$ Å, $\beta = 96.7(2)^\circ$, $V = 2023(7)$ Å^3, $Mo_{K\alpha}$ radiation, $2\theta \leq 45^\circ$, 2635 unique reflections, $T = 293$ K. The structure was solved by direct methods (SHELXTL PLUS) and refined by full-matrix least-squares analysis using experimental weights (heavy atoms anisotropic, H atoms fixed, whereby H positions are based on stereochemical considerations). Final $R(F) = 0.052$, $wR(F) = 0.050$ for 208 variables and 2008 observed reflections with $F > 4\sigma(F)$. – **3** ($C_{72}H_{94}Si_4$, $M_r = 1071.8$): Triclinic space group $P\bar{1}$, $\rho_{calc} = 1.029\ g\,cm^{-3}$, $Z = 1$, $a = 12.021(6)$, $b = 12.249(7)$, $c = 13.597(5)$ Å, $\alpha = 105.07(4)$, $\beta = 109.46(3)$, $\gamma = 101.53(4)^\circ$, $V = 1730.2(15)$ Å^3, $Mo_{K\alpha}$ radiation, $2\theta \leq 45^\circ$, 4537 unique reflections, $T = 293$ K. The structure was solved by direct methods (SHELXTL PLUS) and refined by full-matrix least-squares analysis using unit weights (heavy atoms anisotropic, H atoms fixed, whereby H positions are based on stereochemical considerations). Final $R(F) = 0.052$, $wR(F) = 0.053$ for 343 variables and 1280 observed reflections with $F > 4\sigma(F)$. We thank I. Steiner, A. Kramer, and S. Zürcher for help with the X-ray crystal structure analyses. Further details of the crystal structure investigations are available on request from the Director of the Cambridge Crystallographic Data Centre, 12 Union Road, GB-Cambridge CB2 1EZ (UK), on quoting the full journal citation.
[11] J. A. Walker, S. P. Bitler, F. Wudl, *J. Org. Chem.* **1984**, *49*, 4733–4734.
[12] a) J. Anthony, C. B. Knobler, F. Diederich, *Angew. Chem.* **1993**, *105*, 437–440; *Angew. Chem. Int. Ed. Engl.* **1993**, *32*, 406–409; b) J. Anthony, F. Diederich, unpublished.
[13] See: T. X. Neenan, M. R. Callstrom, L. M. Scarmoutzos, K. R. Stewart, G. M. Whitesides, V. R. Howes, *Macromolecules* **1988**, *21*, 3525–3528.
[14] CVFF force field, Biosym Technologies, San Diego.
[15] J. L. Brédas, R. Silbey, D. S. Boudreaux, R. R. Chance, *J. Am. Chem. Soc.* **1983**, *105*, 6555–6559.
[16] In the electrochemical investigations of **2**–**5** polarography and cyclic voltammetry gave concurring results. In THF with 0.1 M $Bu_4N^+PF_6^-$ as the supporting electrolyte the accessible potential range on mercury was +0.15 to −3.4 V vs ferrocene. In a standard three-electrode cell, the working electrode was a dropping mercury electrode, the counter electrode a mercury pool, and the pseudo-reference electrode a silver wire dipped in a solution of supporting electrolyte. Under these conditions, ferrocene, used as an internal standard, is oxidized at 0.87 V vs Ag. Similar results were also obtained in THF with a platinum working electrode (available potential range +1.0 to −2.2 V vs ferrocene). A detailed account on the electrochemical properties of **2**–**5**, including spectroelectrochemical studies, will be given elsewhere.
[17] a) J. Heinze, J. Mortensen, K. Müllen, R. Schenk, *J. Chem. Soc., Chem. Commun.* **1987**, 701–703; b) R. Schenk, H. Gregorius, K. Meerholz, J. Heinze, K. Müllen, *J. Am. Chem. Soc.* **1991**, *113*, 2634–2647.
[18] P. Bäuerle, *Adv. Mater.* **1992**, *4*, 102–107.
[19] H. Hauptmann, *Tetrahedron Lett.* **1974**, *40*, 3593–3596.

1,1-Dimethyl-1*H*-silirene**

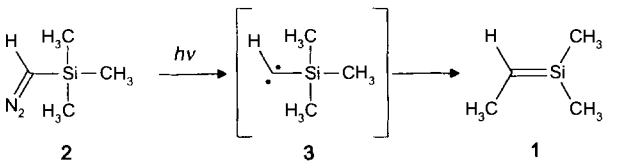
Martin Trommer, Wolfram Sander,* and Claudia Marquard

Silyldiazo compounds are frequently used as precursors for the synthesis of silaethenes (silenes). For instance, 1,1,2-trimethylsilene (**1**), the first silene characterized spectroscopically, was obtained by irradiation of trimethylsilyldiazomethane (**2**) in an argon matrix.[1] Carbene **3**, formulated as an intermediate in this reaction, is produced only in a very low stationary concentration and could be detected by ESR but not by IR spec-

[*] Prof. Dr. W. Sander,[+] Dipl.-Chem. M. Trommer, C. Marquard
Institut für Organische Chemie der Technischen Universität
Hagenring 30, D-38106 Braunschweig (FRG)
[+] New address: Organische Chemie II, Ruhr-Universität Bochum
Universitätsstrasse 150, D-44780 Bochum (FRG)
Telefax: Int. code + (234)7094-353

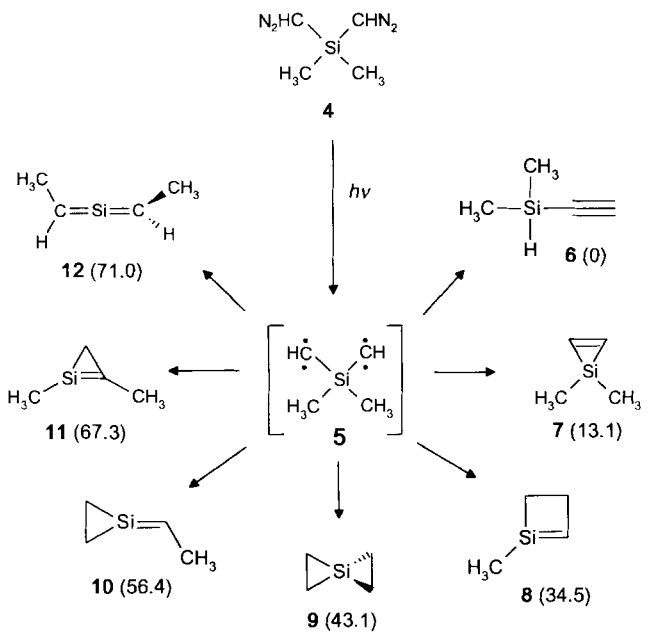
[**] This work was supported by the Deutsche Forschungsgemeinschaft and the Fonds der Chemischen Industrie.

troscopy.[1b] In an analogous way, a series of other silenes was produced in solution and these were characterized indirectly by trapping experiments.[2, 3]



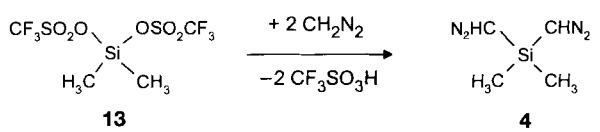
2 3 1

We report here on the photochemistry of 2-sila-1,3-bis(diazo)propane (**4**). The elimination of nitrogen from **4** should lead to biscarbene **5** or its rearrangement products **6**–**12** (Scheme 1).



Scheme 1. Possible rearrangement products of biscarbene **5**; only closed-shell molecules were considered. The HF energies (kcal mol^{-1}) calculated by ab initio methods (RHF/6-31G(d,p)) relative to **6** are given in parentheses.

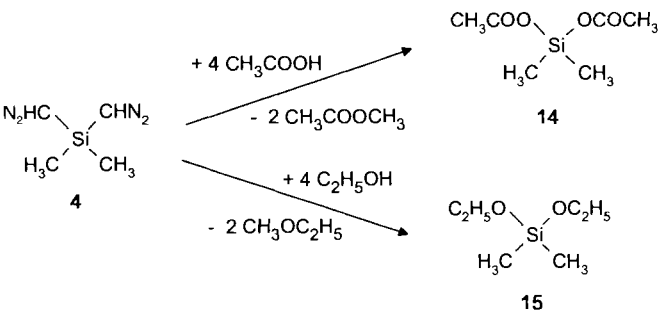
The bisdiazo compound **4** was synthesized by treating dimethylsilanediylbis(trifluoromethanesulfonate) (**13**) with diazomethane[4] in diethyl ether at $-60\,^{\circ}C$ and was purified by preparative gas chromatography (yellow oil). Compound **4** is stable at room



13 4

temperature for short periods and can be stored for several months at $-78\,^{\circ}C$ without decomposition. As expected, two singlets are observed in the ^1H NMR spectrum of **4** at $\delta = 0.29$ and 2.72 (ratio 1:3), and two signals are found in the ^{13}C NMR spectrum at $\delta = -2.14$ and 19.8. The mass spectrum shows a peak for the molecular ion at $m/z = 140$ as well as the expected fragmentation pattern. The most intense absorptions in the IR spectrum (2082 and 2073 cm^{-1}) were assigned to the N=N stretching vibration of the diazo groups. Solutions of **4** lose color rapidly on irradiation or by addition of acids, with the evolution of gas.

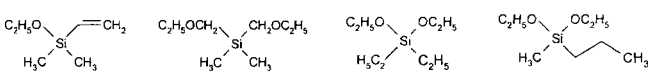
The major products of the reaction of **4** with acetic acid are dimethylsilanediyldiacetate (**14**) and methyl acetate. Compound **4** reacts with ethanol slowly at room temperature to give diethoxydimethylsilane (**15**). Thus, **4** behaves like other silyldiazo compounds towards protic compounds.[5]



4 14 15

If the diazo compound **4** is irradiated ($\lambda \geq 305$ nm) in ethanol or EPA glasses[6] at 77 K, four products are observed after warming to room temperature (yields >95% determined by gas chromatography), none of which contain nitrogen (GC-MS). At the same time a large amount of gas (probably N_2) is evolved. These products were characterized as ethenylethoxydimethylsilane (**16**), bis(ethoxymethyl)dimethylsilane (**17**), diethoxydiethylsilane (**18**), and diethoxymethylpropylsilane (**19**) (Table 1). In order to elucidate the mechanism for the formation of these products, the photolyses were also carried out in C_2H_5OD and C_2D_5OD.

Vinylsilane **16** is formed in ethanol or EPA glasses (irradiation at 77 K) in 46% yield and is the trapping product of 1,1-dimethyl-1*H*-silirene (**7**). Photolysis of **4** at 273 K leads to a considerable reduction in the yield of **16** (Table 1). After irradiation in



16 17 18 19

Table 1. Yields of the trapping products determined by gas chromatography for irradiation ($\lambda \geq 305$ nm) of **4** in ethanol at various temperatures.

Compound	Product [a]	Yield [%] 77 K	170 K	273 K
7	**16**	46	45	30
5	**17**	14	5	3
9, 10, 12	**18**	23	25	28
8	**19**	13	15	19

[a] The yields were determined by gas chromatography. The total yield of **16**–**19** was 96% at 77 K, and decreases to 90% at 170 K, and further to 80% at 273 K. The by-products that occur at higher temperatures have so far not been identified unequivocally.

C_2H_5OD, a deuterium atom is found in the vinyl group. The addition of alcohols under cleavage of a Si–C bond and the formation of vinylsilanes is characteristic for 1*H*-silirenes.[7, 8] Dimethylsilane **17** is the formal reaction product of biscarbene **5** with ethanol (the release of N_2 from **4** can, however, also occur stepwise); with C_2H_5OD as trapping reagent, as expected, one deuterium atom is found in each of the methylene groups adja-

 © VCH Verlagsgesellschaft mbH, D-69451 Weinheim, 1994 0570-0833/94/0707-0767 $ 10.00+.25/0

cent to the Si atom. The yield of **17** is highly temperature-dependent and decreases from 14% at 77 K to 3% at 273 K (Table 1).

The formation of **18** is indicative of a precursor which contains two C_2 units. This precursor could be 1-silaspiropentane (**9**), 2-sila-2-ethylidenecyclopropane (**10**), or 3-sila-2,3-pentadiene (**12**) (Table 1). With C_2H_5OD and C_2D_5OD, the expected deuterated isotopomers of **18** are formed, each with one deuterium atom in the ethyl groups adjacent to the Si atom (C_2H_5OD) and with additional perdeuterated ethoxy groups (C_2D_5OD), respectively.

The propyl group in **19** can only stem from a precusor which already contains a C_3 unit. The best candidate for this is 1-methylsilacyclobutene (**8**), which can be formed from biscarbene **5** by a [1,2] methyl shift followed by an insertion of the remaining carbene center in a terminal C–H bond of the ethylidene group.

Evidently, carbene **5** can follow several reaction pathways. In order to elucidate which is the primary photolysis product of the bisdiazo compound **4**, we have studied the photochemistry in an argon matrix at 10 K and have followed the course of the reaction by IR and UV/VIS spectroscopy. Irradiation of **4** for several hours with $\lambda \geq 305$ nm results in the disappearance of all of the IR bands assigned to the diazo compound, and a single photoproduct is formed, which is assigned the structure of silirene **7** by comparison of the experimental and ab initio-calculated (RHF/6-31G(d,p))[9] IR spectra (Fig. 1, Table 2). Other structures, such as silirene **11**, silaallene **12**, silacyclopropane **10**, or silaspiropentane **9** could be ruled out after comparison of the experimental IR spectrum with the spectra calculated for these compounds.

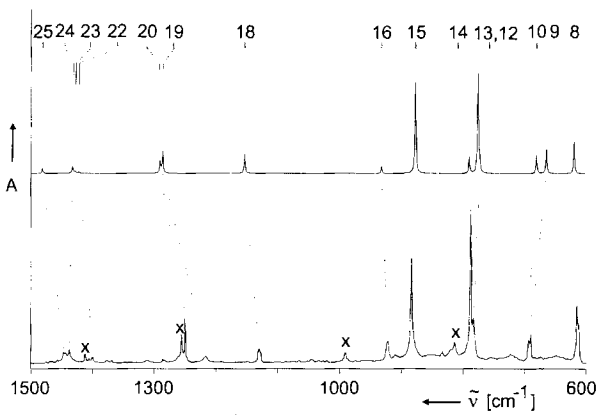


Fig. 1. IR spectrum of 1,1-dimethyl-1*H*-silirene (**7**), matrix-isolated in argon at 10 K (bottom) and ab-initio-calculated at the RHF/6-31(d,p) level (top). Tentative assignment based on the band position and band intensity. The calculated spectrum was scaled by a factor of 0.9 to allow the direct comparison with the experimental spectrum, and a Lorentz band shape was simulated with a half-value width of 2 cm^{-1}. The bands labeled with X were assigned to the solvent.

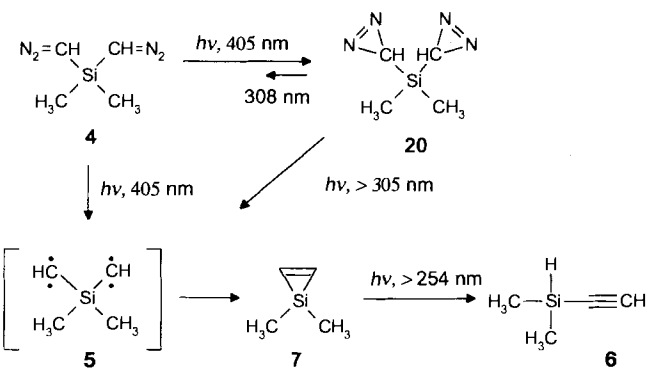
Irradiation of compound **4** with blue light (λ = 405 nm) initially leads only to the formation of a small amount of **7**; however, instead, an additional photoproduct, **20**, is obtained, which on short wavelength irradiation (λ > 305 nm) also results in **7**. The IR and UV spectrum of **20** reveal that this compound is a diazirine. Whether **20** is the bisdiazirine shown or a monodiazirine cannot be determined unambiguously from the IR and UV/VIS spectra. The formation of **20** is partially reversible, and on irradiation at 308 nm (XeCl excimer laser) in addition to **7** also small quantities of **4** are reformed. This is in agreement with the photochemistry of other silyl-substituted diazomethanes, for which a photostationary equilibrium between diazomethanes and diazirines is frequently observed.[1, 10] On irradiation

Table 2. IR spectroscopic data of 1,1-dimethyl-1*H*-silirene (**7**). Experimental data in argon at 10 K, calculated data with a RHF/6-31G(d,p) basis set.

No. [a]	Argon, 10 K ν[cm^{-1}]	I [b]	ab initio 6-31G(d,p) ν[cm^{-1}] [c]	I [b]	Assignment [d]
33	3023.1	9	3033.3	9	asym. =C-H str.
29	2992.5	10	2914.7	25	sym. C-H str.
26	2959.1	9	2853.2	5	asym. C-H str.
25	1447.1	10	1482.3	5	C=C str.
24	1444.2	10	1433.0	7	CH_3 def.
23	1438.1	12	1429.4	2	CH_3 def.
22	1400.2	7	1423.2	1	CH_3 def.
21	–	–	1421.4	0	CH_3 def.
20	1250.2	32	1290.8	12	
19	1216.1	7	1287.0	22	
	1132.0	12			asym. H-C= bend.
18	1129.8	12	1153.6	19	
	1127.7	10			
17	–	–	985.7	0	asym. H-C= out-of-plane
	991.6	10			
16	922.1	17	932.8	7	sym. H-C= bend.
15	884.1	71	878.2	92	
14	–	–	790.7	16	
13	788.4	100	777.4	100	
12	784.9	31	774.1	11	
11	–	–	732.7	0	
10	694.1	17	681.7	19	sym. Si-C str.
9	691.1	21	666.2	24	asym. Si-C str.
8	616.1	39	620.7	32	sym. C-H out-of-plane
	613.7	28			

[a] Number of calculated vibration (ab initio). The assignment of the experimental to the calculated vibrations is based on the comparison of band positions and relative intensities and is—particularly in the range of the C–H stretching vibrations—only tentative. [b] Relative intensities based on the most intense band (100%). [c] Calculated frequencies are scaled by 0.9. [d] Assignment of vibrations from the calculated spectrum (cf. Fig. 1).

with short-wavelength UV light ($\lambda \geq$ 254 nm), silirene **7** finally rearranges into dimethyl(ethynyl)silane (**6**), which was characterized by comparison with an authentic matrix-isolated sample. The formation of **6** provides further evidence that for the photolysis in an argon matrix—in contrast to the photolysis in an ethanol glass—no migration of the methyl groups to the carbene center occurs. Silane **6** is also the main product of the flash vacuum pyrolysis (500 °C, 10^{-4} mbar) of **4**.



The synthesis of **7** described here is a new, high-yield route to 1*H*-silirenes. Compound **7** is the first silirene without substituents at the double bond, which could be proven unambiguously. We are currently investigating whether this synthesis can also be applied to other silirenes—in particular, to the as yet unknown parent compound.

 © VCH Verlagsgesellschaft mbH, D-69451 Weinheim, 1994 0570-0833/94/0707-0768 $ 10.00+.25/0

Experimental Procedure

All operations were carried out under the exclusion of moisture and under inert gas in glass apparatus with silylated surfaces (through treatment of the glass surfaces with hexamethyldisilazane). The photolyses were performed with a 500 W-Hg high-pressure lamp (Oriel) in combination with cut-off and interference filters. For a description of the matrix apparatus see ref. [11]. The ethynylsilane **6** and the ethanol adducts **16**, **18**, and **19** were characterized by comparison with authentic samples, and **17** by mass spectrometry of the three isotopomers obtained with C_2H_5OH, C_2H_5OD, and C_2D_5OD.

4: A solution of **13** (4.0 g, 1 equiv) [12, 13] in dry pentane (50 mL) was added slowly dropwise to a solution of diazomethane (1.0 g, 2.15 equiv) in Et_2O (80 mL) and ethyldicyclohexylamine (5.0 g, 2.1 equiv) at $-50\,^{\circ}C$ and stirred vigorously for 1 h. The ammonium salt precipitated during the reaction was separated from the yellow solution by rapid filtration with a frit. The solution was subsequently concentrated under vacuum to about 6 mL at $-45\,^{\circ}C$. The yellow concentrate was separated from a nonvolatile residue by one recondensation under vacuum (0.5 mbar) and subsequently separated by gas chromatography (Shimadzu GC-8a, column: 3m SE 30, 80 °C, det./inj.: 140 °C). **4** was obtained as a yellow liquid, which was stable for several weeks in $CDCl_3$ at $-10\,^{\circ}C$. The yield determined by gas chromatography was 14%. ^1H NMR (400 MHz, $CDCl_3$): $\delta = 0.29$ (s, 6H, CH_3), 2.72 (s, 2H, CH); ^{13}C NMR (100 MHz, $CDCl_3$); $\delta = -2.14$, 19.8; IR (Ar, 10 K): $\tilde{\nu}$ (%) = 2082.5 (100, N=N), 2073.3 (99, N=N), 1267.5 (36), 1263.6 (34), 1262.3 (28), 840.8 (23), 837.4 (9), 832.1 (35), 828.8 (15), 822.5 (6), 810.9 (7), 794.1 (14), 727.0 (4), 518.2 (4), 514.1 (13), 480.9 (3); UV/VIS (EPA glass, 77 K): $\lambda_{max} = 398$ nm; EI-MS: *m/z* (%): 140 (4) $[M^+]$, 125 (8) $[M^+ - CH_3]$, 112 (2) $[M^+ - N_2]$, 99 (5) $[M^+ - CHN_2]$, 84 (24) $[M^+ - 2N_2]$, 58 (60) $[SiC_2H_6^+]$, 43 (100) $[SiCH_3^+]$.

A mixture of **20** and **7** was obtained by irradiation ($\lambda \geq 360$ nm) of **4** in argon at 10 K; irradiation at $\lambda \geq 305$ nm afforded **7** quantitatively. Irradiation at 254 nm led finally to the formation of **6**.

20: IR (Ar, 10 K): 3013.3 (14), 3003.3 (16), 1642.6 (22), 1638.9 (22), 1636 (22), 1297.7 (19), 1261.6 (38), 968.3 (57), 962.3 (54), 960.4 (78), 957.4 (51), 954.1 (35), 949.2 (38), 945.2 (30), 845.2 (65), 842.3 (54), 828.3 (73), 825 (51), 797.8 (57), 795.3 (100), 718.3 (19), 705.3 (16); UV/VIS (Ar, 10 K): $\lambda_{max} = 320$ nm.

6: IR (Ar, 10 K): 3318.4 (11), 3316.1 (10), 3312.6 (9), 2159.5 (11), 2142.5 (32), 2052.9 (17), 2050.7 (10), 2048.9 (11), 1336.3 (7), 1257.9 (7), 1253.9 (31), 899.4 (55), 889.4 (69), 886.1 (100), 843.2 (50), 775.1 (35), 773.1 (38), 745.2 (12), 739.6 (26), 684 (14), 678.5 (21), 675.8 (43), 584.2 (14).

Received: October 29, 1993 [Z 6469 IE]
German version: *Angew. Chem.* **1994**, *106*, 816

[1] a) O. L. Chapman, C. C. Chang, J. Kolc, M. E. Jung, J. A. Lowe, T. J. Barton, M. L. Tumey, *J. Am. Chem. Soc.* **1976**, *98*, 7844–7846; b) M. R. Chedekel, M. Skoglund, R. L. Kreeger, H. Shechter, *ibid.* **1976**, *98*, 7846–8748.
[2] A. Sekiguchi, W. Ando, *Chem. Lett.* **1986**, 2025–2026.
[3] A. Sekiguchi, W. Ando, *Organometallics* **1987**, *6*, 1857–1860.
[4] For example, for the electrophilic diazoalkane substitution with silyl triflates see: a) M. Martin, *Synth. Commun.* **1983**, *13*, 809–811; b) T. Allspach, H. Gümpel, M. Regitz, *J. Organomet. Chem.* **1985**, *290*, 33–39.
[5] a) L. Berseck, K.-D. Kaufmann, W. Jugelt, *Z. Chem.* **1970**, *10*, 150–151; b) K.-D. Kaufmann, K. Rühlmann, *ibid.* **1968**, *8*, 262–263.
[6] Organic glass (generally at 77 K) consisting of ethanol, isopentane, and diethyl ether in the ratio 2:5:5.
[7] R. T. Conlin, P. P. Gaspar, *J. Am. Chem. Soc.* **1976**, *98*, 3715–3716.
[8] D. Seyferth, D. C. Annarelli, S. C. Vick, *J. Organomet. Chem.* **1984**, *272*, 123–139.
[9] All ab initio calculations were carried out with Gaussian 92, revision C, on a RISC workstation (Silicon Graphics). M. J. Frisch, G. W. Trucks, M. Head-Gordon, P. M. W. Gill, M. W. Wong, J. B. Foresman, B. G. Johnson, H. B. Schlegel, M. A. Robb, E. S. Replogle, R. Gomperts, J. L. Andres, K. Raghavachari, J. S. Binkley, C. Gonzalez, R. L. Martin, D. J. Fox, D. J. Defrees, J. Baker, J. J. P. Stewart, J. A. Pople, *Gaussian 92*, Gaussian Inc., Pittsburgh, **1992**.
[10] a) W. Sander, W. Trommer, *Chem. Ber.* **1992**, *125*, 2813–2815; b) M. Trommer, W. Sander, A. Patyk, *J. Am. Chem. Soc.* **1993**, *115*, 11775–11783.
[11] W. Sander, *J. Org. Chem.* **1989**, *54*, 333–339.
[12] A. R. Bassindale, T. Stout, *J. Organomet. Chem.* **1984**, *271*, C1–C3.
[13] M. Schmeißer, P. Sartori, B. Lippsmeier, *Chem. Ber.* **1970**, *103*, 868–879.

Aurophilicity at Sulfur Centers: Synthesis and Structure of the Tetragold(I) Species $[(Ph_3PAu)_4S](CF_3SO_3)_2 \cdot 2CH_2Cl_2$**

Fernando Canales, M. Concepción Gimeno, Peter G. Jones, and Antonio Laguna*

The structural chemistry of gold(I) complexes shows many examples of inter- and intramolecular contacts of about 3 Å between the formally closed-shell (d^{10}) metal centers. This phenomenon is based on relativistic effects that cause a contraction of the 6s orbital of the heavy elements; these effects reach a maximum for gold.[1–3]

In the last few years Schmidbaur et al. have shown that (phosphane)gold(I) cations can coordinate to main group elements, often giving structures with high coordination numbers in which the main group elements do not always show classical bonding configurations. Thus, in addition to complexes with more conventional stoichiometry,[4a] interesting hypercoordinated species such as $[(LAu)_5C]^+$, $[(LAu)_6C]^{2+}$, $[(LAu)_5N]^{2+}$, $[(LAu)_5P]^{2+}$,[4a] and $[(LAu)_6P]^{3+}$[4b] have been described.

In the sixth main group, compounds of the type $[(LAu)_3X]^+$ (X = O, S, Se) have been reported,[5–8] but further coordination around the central atom has not yet been achieved. Here we report the synthesis and structural characterization of the tetranuclear cationic species tetrakis(triphenylphosphanegold)sulfonium, which can be isolated as its bis-triflate salt **1**. The most common quadruply bridging forms for the sulfido ligand are the tetrahedron[9] or square pyramid.[10, 11] In the former the sulfido ligand serves as an eight-electron donor, while in the latter it is believed to serve as a six-electron donor, and therefore a lone pair of electrons has to be located in the apical position.

$[(Ph_3PAu)_4S](CF_3SO_3)_2$ **1**

The reaction of $[(Ph_3PAu)_2S]$[8] with two equivalents of $[AuPPh_3(CF_3SO_3)]$ in dichloromethane affords a solution from which the colorless air- and moisture-stable complex **1** can be isolated in 73% yield. Solutions of **1** in acetone show conductivities typical of 1:2 electrolytes.[12] The $^{31}P\{^1H\}$ NMR spectrum shows one unique resonance at $\delta = 32.5$ for the four phosphorus atoms, shielded in comparison to the starting material.

Crystals of **1** suitable for X-ray structure analysis[13] were obtained from dichloromethane/hexane. The structure of the cation of **1** is shown in Figure 1; it possesses a tetragonal pyramidal framework, with the sulfur atom occupying the apical position. The SAu_4 core of **1** thus has to be regarded as electron-deficient, since only three bonding molecular orbitals under approximate local C_{4v} symmetry are occupied. The Au-S-Au angles in **1** (73.5(2) to 75.6(2)°) are smaller than those in $[(Ph_3PAu)_3S]^+$ (82.9(3)–95.0(3)°).[6, 7] This leads to short metal–metal distances between adjacent Au atoms (2.883(2)–2.938(2) Å) and longer ones (ca. 3.4 Å) between opposite Au atoms in the base of the pyramid. The Au atoms are arranged in a butterfly form

[*] Prof. Dr. A. Laguna, F. Canales, Dr. M. C. Gimeno
Departamento de Química Inorgánica
Instituto de Ciencia de Materiales de Aragón
Universidad de Zaragoza-C. S. I. C.
E-50009 Zaragoza (Spain)
Telefax: Int code + (76)567920
Prof. Dr. P. G. Jones
Institut für Anorganische und Analytische Chemie
der Technischen Universität
Postfach 3329, D-38023 Braunschweig (FRG)

[**] This work was supported by the Dirección General de Investigación Científica y Técnica (PB91-0122) and the Fonds der Chemischen Industrie.

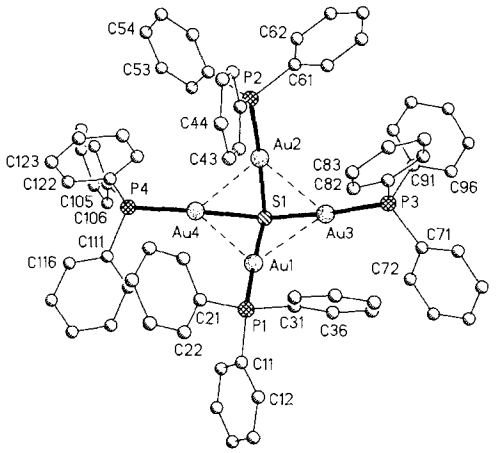


Fig. 1. The structure of the cation of **1** in the crystal. The radii are arbitrary, and the H atoms are omitted for clarity. Selected bond lengths [Å] and angles [°]: Au1-P1 2.270(6), Au2-P2 2.266(6), Au3-P3 2.273(5), Au4-P4 2.272(6), Au1-S1 2.362(5), Au2-S1 2.388(5), Au3-S1 2.429(5), Au4-S1 2.417(5), Au1-Au4 2.911(2), Au2-Au3 2.883(2), Au1-Au3 2.938(2), Au2-Au4 2.907(2); P1-Au1-S1 175.8(2), P2-Au2-S1 176.2(2), P3-Au3-S1 171.2(2), P4-Au4-S1 175.1(2), Au2-S1-Au4 74.5(2), Au2-S1-Au3 73.5(2), Au1-S1-Au4 75.0(2), Au1-S1-Au3 75.6(2).

with a hinge angle of 30°. The deviations of the Au atoms from the best Au_4 plane are ± 0.3 Å, where the S atom lies 1.3 Å out of the same plane. There are two distinctive pairs of Au-Au-Au angles in the framework: about 75° at Au3 and Au4 and about 100° at Au1 and Au2. It is probable that the Au···Au interactions at the base of the S-capped pyramid contribute strongly to the stability of **1**, as was suggested for the similar As-centered complex $[(Ph_3PAu)_4As]^+$.[14]

The Au–P bond lengths in **1** fall into the expected range for two-coordinate gold(I) and are very similar to those in $[(Ph_3PAu)_3S]^+$, although the Au–S distances, which vary from 2.362(5) to 2.429(5) Å, are, as expected, longer than in the latter complex.

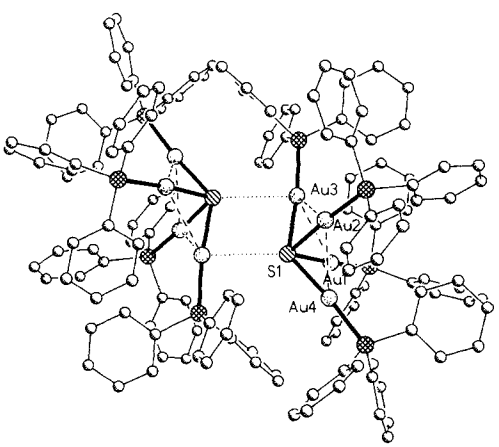


Fig. 2. The weak association of two cations of **1** in the crystal. The $CF_3SO_3^-$ ions and the CH_2Cl_2 molecules have been omitted.

In the crystal the cations of **1** are paired across symmetry centers (Fig. 2); the intermolecular S···Au3′ and Au3···Au3′ contacts are 3.202 and 4.256 Å, respectively. A similar arrangement was observed in $[(Ph_3PAu)_4As]^+$.[14]

Received: October 19, 1993 [Z 6433 IE]
German version: *Angew. Chem.* **1994**, *106*, 811

[1] H. Schmidbaur, *Gold Bull. Gold Pat. Dig.* **1990**, *23*, 11-21.
[2] H. Schmidbaur, *Interdisc. Sci. Rev.* **1992**, *17*, 213–220.
[3] P. Pyykkö, *Chem. Rev.* **1988**, *88*, 563–594.
[4] a) Review: H. Schmidbaur, *Pure Appl. Chem.* **1993**, *65*, 691–698, and references therein. b) E. Zeller, H. Schmidbaur, *J. Chem. Soc. Chem. Comm.* **1993**, 69–70.
[5] A. N. Nesmeyanov, E. G. Perevalova, Yu. T. Struchkov, M. Yu. Antipin, K. I. Grandberg, V. P. Dyadchenko, *J. Organomet. Chem.* **1980**, *201*, 343–349.
[6] P. G. Jones, G. M. Sheldrick, E. Hädicke, *Acta Crystallogr. Sect. B* **1980**, *36*, 2777–2779.
[7] H. Schmidbaur, A. Kolb, E. Zeller, A. Schier, H. Beruda, *Z. Anorg. Allg. Chem.* **1993**, *619*, 1575–1579.
[8] C. Lensch, P. G. Jones, G. M. Sheldrick, *Z. Naturforsch. B* **1982**, *37*, 944–949.
[9] R. D. Adams, D. F. Foust, *Organometallics* **1983**, *2*, 323–327.
[10] R. D. Adams, I. T. Horváth, B. E. Segmüller, L. W. Yang, *Organometallics* **1983**, *2*, 1301–1308.
[11] R. D. Adams, *Polyhedron* **1985**, *4*, 2003–2005.
[12] Compound **1** was satisfactorily characterized by elemental analysis (C,H,S), IR spectroscopy, and its $^{31}P\{^1H\}$ NMR spectrum in $CDCl_3$.
[13] Crystal data: $\mathbf{1}\cdot 2CH_2Cl_2$, $C_{76}H_{64}Au_4Cl_4F_6O_6P_4S_3$, $P2_1/n$, $a = 16.439(5)$, $b = 23.161(7)$, $c = 20.311(6)$ Å, $\beta = 91.34(3)°$, $V = 7731(4)$ Å^3, $Z = 4$, $\mu = 7.9$ mm^{-1}, $T = -100$ °C. A colorless tablet $0.6 \times 0.2 \times 0.1$ mm was mounted in inert oil (type RS3000, donated by Riedel de Haën). Using $Mo_{K\alpha}$ radiation on a Siemens R3 diffractometer, 11768 intensities were measured to $2\theta_{max}$ 47°, of which after absorption corrections 11327 were unique ($R_{int} = 0.040$) and 11265 used for all calculations (program SHELXL-93). The structure was solved by direct methods and refined anisotropically on F^2. H atoms were included with a riding model. The final $wR(F^2)$ was 0.185, with conventional $R(F)$ 0.052 for 918 parameters and 830 restraints. Further details of the crystal structure investigation may be obtained from the Fachinformationszentrum Karlsruhe, D-76344 Eggenstein-Leopoldshafen (FRG), on quoting the depository number CSD-400453.
[14] E. Zeller, H. Beruda, A. Kolb, P. Bissinger, J. Riede, H. Schmidbaur, *Nature* **1991**, *352*, 141–143.

A Building Principle of Amorphous Chalcogenides of Transition Metals: The "Extrusion" of the Electron-Rich Cluster $[Re_4S_2(SO_2)_4(CN)_{10}]^{8-}$ from a-Re_2S_7**

Achim Müller,* Erich Krickemeyer, Hartmut Bögge, Henryk Ratajczak, and Anja Armatage

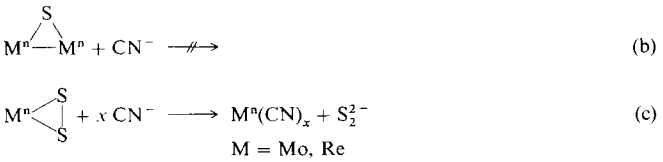
Amorphous sulfides of Groups 5–7 are of fundamental interest due to,among other things, their significance as catalysts,[1] their material properties,[1] their occurrence as minerals, for example jordisite (MoS_2), as well as their application in classical separation processes. Since their structures have been up to now controversially debated, we looked at the question whether one could obtain chemically, for instance, through cyanolysis—at least in some special cases—supplemental structural information. Furthermore, we were interested in the question whether a uniform structural principle exists. In this context, a decisive factor is the well-known stability of the M(μ_2-S)M and (μ_3-S)M_3 cluster fragments as well as clusters composed thereof (M = Mo, W, Re) against nucleophilic attack by CN^- [2] corresponding to the schematic reaction equations (a)–(c) (Scheme 1).

[*] Prof. Dr. A. Müller, E. Krickemeyer, Dr. H. Bögge, A. Armatage
Fakultät für Chemie der Universität, Lehrstuhl für Anorganische Chemie 1
Postfach 100131, D-33501 Bielefeld (FRG)
Telefax: Int. code + (521)1066003
Prof. Dr. H. Ratajczak
Department of Chemistry, University of Wrocław
14 Joliot Curie Str., PL-50-383 Wrocław (Poland)

[**] a-Re_2S_7 symbolizes amorphous metal sulfide. We thank Mr. D. Sölter for the MO calculations and Degussa AG for a gift of rhenium compounds.

$$M^n\text{–}S + CN^- \longrightarrow M^{n-2} + NCS^- \quad \text{(a)}$$

(Two-electron metal-reduction/ligand-oxidation process with atom transfer.)



(b)

(c)

M = Mo, Re

Scheme 1. Reactions of cluster fragments with cyanide ions. *n* is the oxidation number.

We have obtained the diamagnetic compounds **1a**, **1b** (brown), and **2** (green) through the reaction of either **3**[3] or amorphous Re_2S_7[4] with aqueous CN^- solution at 85 °C (Fig. 1) and characterized them by electronic and IR spectroscopy as well as single-crystal X-ray structure analysis.[5] In the reaction of **3** to **1a**, the central $\{Re_4^{IV}S_4\}^{8+}$ cluster (cf. structure of the cluster anion of **1a** in Fig. 1) remains intact as expected—that is, according to our working hypothesis and the reaction type (b) and (c)—whereas in the reaction with a-Re_2S_7 **2** is formed in addition to **1b** which has the same anion as **1a**.[6] This compound contains a noteworthy, novel, electron-rich, mixed-valent, tetranuclear cluster anion (see the reaction scheme in Fig. 1).

The structure of the rhombic anion in **2** (Fig. 2) with approximate C_{2h} symmetry can be (formally) obtained by condensing two trinuclear $\{Re_3(\mu_3\text{-}S)(\mu_2\text{-}S)_3(CN)_9\}$ clusters that are isostructural with $[Mo_3S_4(CN)_9]^{5-}$.[2c] The anion of **2** is obviously formed from the "intermediate product" $[Re_4(\mu_3\text{-}S)_2(\mu_2\text{-}S)_4(CN)_{10}]^{8-}$ through the oxidation of the four $(\mu_2\text{-}S)^{2-}$ ligands, which show a higher electron density than the $(\mu_3\text{-}S)^{2-}$ ligands.

$K_4[Re_4^{IV}S_4(CN)_{12}] \cdot 4\,H_2O$ **1a**

$K_4[Re_4^{IV}S_4(CN)_{12}] \cdot 6\,H_2O$ **1b**

$K_8[Re_2^{III}Re_2^{IV}S_2(SO_2)_4(CN)_{10}] \cdot 5\,H_2O$ **2**

$(NH_4)_4[Re_4^{IV}S_4(S_3)_6] \cdot 2\,H_2O$ **3**

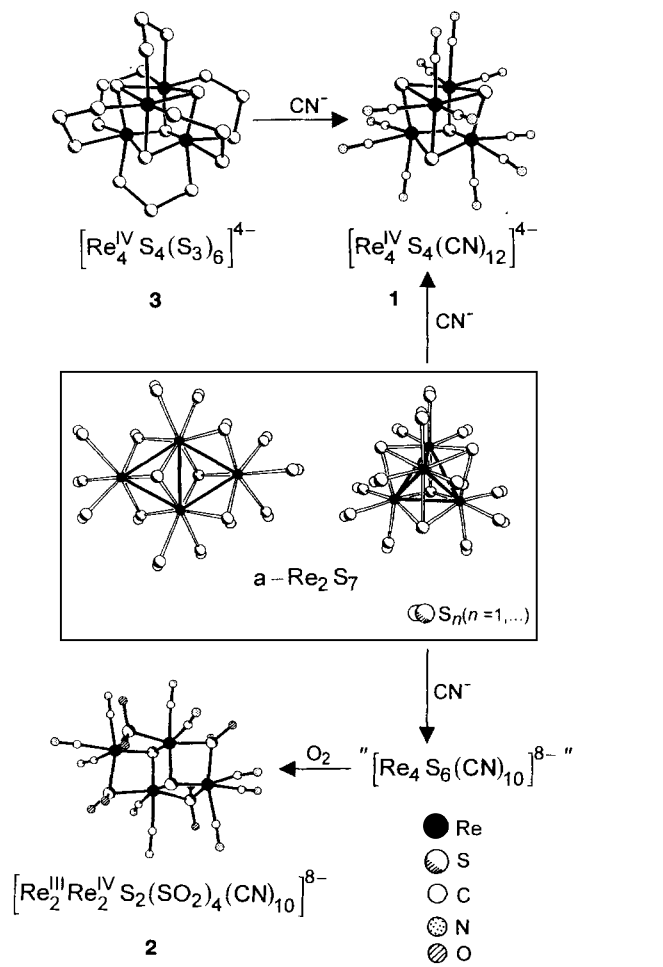


Fig. 1. An illustrative reaction scheme for the cyanolysis of **3** and a-Re_2S_7 (**1**, **2**, and **3** shown without Re–Re bonds, cations, and water molecules) and the structure of $[Re_4S_4(CN)_{12}]^{4-}$ in the crystals of **1a**; range of bond lengths [pm] (values for **1b** in parentheses): Re–Re 274.5(1)–275.6(1) (273.9(1)–275.3(1)), Re–S 234.3(2)–235.1(2) (233.9(4)–234.9(3)), Re–C 210.8(10)–211.5(10) (209.0(16)–212.4(17)), C–N 113.7(15)–115.4(13) (112.7(12)–117.4(13)); range of bond angles [°]: S-Re-S 105.2(1)–106.0(1), C-Re-S 84.2(3)–86.1(3) and 159.7(3)–162.2(3), C-Re-C 79.7(4)–81.1(4), Re-S-Re 71.5(1)–71.9(1), Re-C-N 176.4(9)–178.4(9).[5] For the structure of the anion in **2** see Fig. 2.

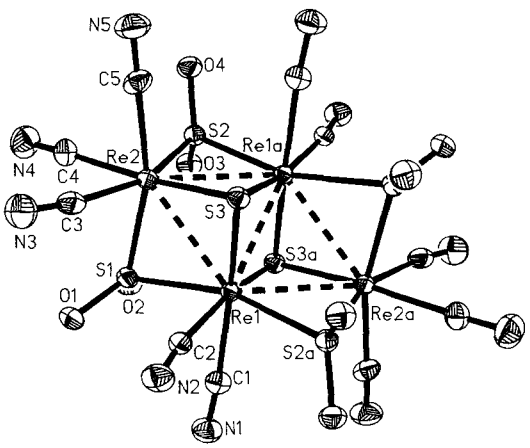


Fig. 2. Structure of the anion $[Re_4S_2(SO_2)_4(CN)_{10}]^{8-}$ in the crystals of **2**. Selected distances [pm] and angles [°]: Re1-Re1a 274.0(1), Re1-Re2 283.7(1), Re1-S1 238.7(2), Re1-S3 236.6(2), Re2-S1 231.7(2), Re2-S3 236.8(2), Re1-C1 209.1(8), S1-O1 149.3(5), C1-N1 116.9(11); S1-Re1-S3 103.4(1), S1-Re1-S2a 162.9(1), S3-Re1-S2a 86.4(1), S1-Re2-S3 105.5(1), S1-Re1-C1 79.8(2), S1-Re1-C2 89.3(2), S3-Re1-C1 165.2(2), C1-Re1-C2 81.7(3), O1-S1-O2 108.2(3), Re1-S1-O2 117.9(2), Re1-S1-Re2 74.2(1), Re1-C1-N1 175.3(6).

Metal clusters with planar M_4 rhombuses are rare (see, for example, the notable compound $CsNb_4Hal_{11}$[7] which shows bridged Nb_4Hal_{16} rhombuses). The electronic structure of clusters of this type is especially interesting, because on one hand—particularly for the previously unknown electron-rich systems—the planarity of the four-membered ring of metal atoms allows for very strong metal–metal interaction, and on the other hand, in the case of strong transannular interactions, nonequivalent metal centers must be present. The mixed valent cluster of **2** is electron-rich and is indeed the first of this type (electron configuration $\{Re_4\}^{14}$), since the formation of the five Re–Re bonds—like that in the case of the Nb_4 cluster mentioned above—requires only ten electrons in the appropriate d levels. The short transannular Re–Re distance is indicative of considerable double-bond character. EH-SCCC MO calculations on the $\{Re_4S_2(SO_2)_4\}^{2+}$ fragment found in **2** confirm this, but also reveal an increase in the (negative) charge of the two central Re atoms (formally Re^{III} according to Fig. 3) relative to the others, along with a pronounced delocalization of the HOMOs over the Re centers. The distance to the LUMO, the "transannular π^* orbital" is only about 1.3 eV. The assignment of the band with the longest wave-

 © VCH Verlagsgesellschaft mbH, D-69451 Weinheim, 1994 0570-0833/94/0707-0771 $ 10.00+.25/0

length in the VIS spectrum follows accordingly. This band is missing, as expected, in the spectra for **1a** and **1b**, in which the metal clusters do not contain π orbitals. This explains why **2** has a different color. The above-mentioned charge distribution corresponds to a formulation as SO_2^{2-}, which follows from all data, for example, from the position of the ν(SO) frequency and the results of earlier investigations.[2e] The high electron density, related to the electron richness of the ring system, on the sulfur centers of the "intermediate product $[Re_4(\mu_3\text{-}S)_2(\mu_2\text{-}S)_4(CN)_{10}]^{8-}$" explains the easy oxidizability of the μ_2-S centers.[8]

The Re_4S_6 fragment in **2** interestingly corresponds to a section of the ReS_2 or $ReSe_2$ lattice,[9] in which comparable rhombohedral Re_4 cluster units are present and linked through (additional) Re–Re bonds, which are, however, longer than the bonds in the Re_4 units (cf. Fig. 3).[9] ReS_2 and $ReSe_2$ crystallize like, for example, MoS_2 (in which the metal centers, however, have trigonal-prismatic coordination geometry), in an XMX layered lattice with a van der Waals gap between the X layers. The greater number of valence electrons ($5d^3$) in the rhenium chalcogenides results in strong metal–metal bonding, which is further strengthened because the 5d–5d overlap is larger than the 4d–4d overlap.

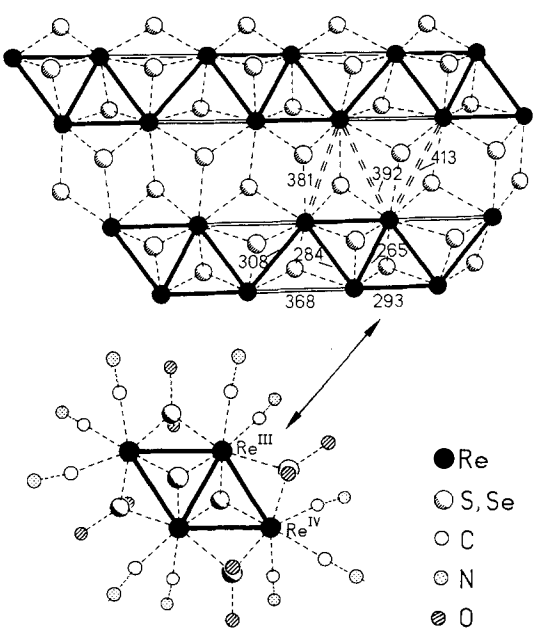


Fig. 3. A descriptive illustration of the relationship between **2** (bottom) and the structure of ReS_2 ($ReSe_2$) (top) [9], which in close approximation possesses a zigzag type of linking between the Re_4 rhombuses (bond lengths in pm). The assignment Re^{IV}/Re^{III} reflects the predominant character of the metal center.

Re_nS_m clusters—like those in **1b** ($\{Re^{IV}\}_4$) and **2** ($\{Re_2^{III}Re_2^{IV}\}$)—can be "extruded" through cyanolysis out of amorphous Re–S phases like Re_2S_7 while apparently retaining their topology, so long as the clusters are not connected through additional Re–Re bonds like in crystalline ReS_2, which does not react in an analogous manner with CN^-. The cluster anion of **1** is formed from a-Re_2S_7 only when the reduction according to Equation (a) (which leads to the formation of **2**) does not occur simultaneously. Obviously, 12-electron Re_4 clusters exist in Re_2S_7,[10] which are linked irregularly through S_x^{2-} ligands. This has a certain amount of similarity to the linking principle found for the structure of $CsNb_4Hal_{11}$.[7] An analogous cluster $[Mo_3^{IV}S_4(CN)_9]^{5-}$, which (besides $[Mo_4^{III}S_4(CN)_{12}]^{8-}$) is generated from the Mo_3^{IV} cluster through a reduction of type (a)) can be extruded by cyanolysis[2b,e] from the phases a-MoS_3 and a-MoS_2 in which Mo_3 clusters[11] are not linked by MoS_xMo bonds with metal–metal interactions.

Our investigations indicate that cyanolysis supplements other physical methods for the characterization of amorphous metal sulfide phases of early transition elements and relevant catalysts, as well as metalloenzymes with metal sulfide bonds in the active center. a-Re_2S_7—but also other analogous amorphous sulfides of electron-poor transition metals—can obviously be considered (formally) a "quasi-solid" solution of clusters linked irregularly through S_x^{2-} ligands. The reason for this is the well-known pronounced tendency to form clusters with metal centers in intermediate oxidation states.[12] Such clusters also form in solution under comparable conditions. Trinuclear clusters are formed preferentially for Mo/W (d^2), tetranuclear for Tc/Re (d^3).[12] This corresponds to the "precise electron count", an approximate rule that is valid for clusters of the transition elements of Groups 5–7.[12]

The structure principle introduced here also explains why the sulfides discussed above and the corresponding selenides, do not crystallize upon annealing. The S_n^{2-} units transform upon decomposition into S^{2-} and S_{n-1}^0 to form—it is even possible to observe—elemental sulfur. The fact that amorphous phases like MoS_3, WS_3, Tc_2S_7 and Re_2S_7 and the corresponding selenides have compositions which formally correspond to the highest possible valence of the metal has often led to misconceptions in the past.[13] The presence of reduced metal centers in such amorphous metal sulfides became obvious for the first time through the generation of discrete polythiometalates (from mononuclear species), which is, notably, achieved under similar conditions as the formation of the amorphous sulfides.[14] In both cases an intramolecular redox process involving S^{2-} oxidation and M^{n+} reduction takes place, a process which is often associated with the generation of metal–metal bonds.[14] The presence of metal–metal bonds in the sulfides is concluded from the unequivocal evidence obtained from pair distribution functions, as determined from the Debye reflections of the amorphous materials (see, for example, [4b]).

In general, discrete metal clusters can exist in virtually pure form, for example, in the gas phase or in a noble gas matrix, in classical chemical form (that is, ligand stabilized) in solution or in the corresponding crystalline arrangement, but also as described here, in a quasi-solid solution. Condensed clusters in solid state structures are not included in this context.

Experimental Procedure

1b, **2**: A solution of KCN (16.0 g, 245.7 mmol) in H_2O (80 mL) was mixed with Re_2S_7 [4] (2.0 g, 3.35 mmol) and kept for 24 h at 85 °C on a hot plate (without stirring) in a 100 mL Erlenmeyer flask (wide neck, covered with a watch glass). (Re_2S_7 was not dried over P_4O_{10}, but instead, after washing, dried under a stream of inert gas). Subsequently, the mixture was concentrated by evaporation to a volume of 75 mL in a open vessel at the same temperature. After cooling to 20 °C brown crystals of **1b** precipitated, which were filtered off after 1–1.5 weeks and dried in air on filter paper. Yield **1b**: 0.40 g (16.5 % based on the amount of Re_2S_7 used). Dark green crystals of **2** (apart from some KCN) slowly precipitate out of the mother liquor kept on a hot plate without stirring at 85 °C (evaporation from a 100 mL Erlenmeyer flask covered with a watch glass). These were filtered from the hot solution and recrystallized in water. Yield **2**: 0.35 g (12.1 % based on the amount of Re_2S_7 used).

Main IR absorption bands (solid state/KBr pellet/[cm^{-1}]) for **2**: ca. 2130(sh), 2120(s), 2100(m)(ν(CN)), 1147(m), 1110(m), 1015(s), 1000(s)(ν(SO)). Bands in electronic absorption spectra (solid state/reflectance/[nm]) for **1**: 550, ca. 465(sh), 420, 375, ca. 320, and for **2**: ca. 700(sh), 615, 465, ca. 350(br).

Received: September 4, 1993
Revised: December 15, 1993 [Z 6338 IE]
German version: *Angew. Chem.* **1994**, *106*, 800

[1] Re–S phases like Re_2S_7 and ReS_2 have interesting catalytic properties (V. I. Nefedov, N. P. Sergushin, N. M. Zhavoronkov, *J. Anal. Chem. USSR (Engl. Transl.)* **1974**, *29*, 196); Re_2S_7 has also semiconducting properties (F. Hulliger, *Struct. Bonding* **1968**, *4*, 83.

[2] a) M. G. B. Drew, P. C. H. Mitchell, C. F. Pygall, *Angew. Chem.* **1976**, *88*, 855; *Angew. Chem. Int. Ed. Engl.* **1976**, *15*, 784; *J. Chem. Soc. Dalton Trans.* **1977**, 1071; cf. also A. Müller, P. Christophliemk, *Angew. Chem.* **1969**, *81*, 752; *Angew. Chem. Int. Ed. Engl.* **1969**, *8*, 753; b) A. Müller, W. Eltzner, H. Bögge, R. Jostes, *ibid.* **1982**, *94*, 783 and **1982**, *21*, 795; *Angew. Chem. Suppl.* **1982**, 1643; c) A. Müller, R. Jostes, W. Eltzner, C.-S. Nie, E. Diemann, H. Bögge, M. Zimmermann, M. Dartmann, U. Reinsch-Vogell, S. Che, S. J. Cyvin, B. N. Cyvin, *Inorg. Chem.* **1985**, *24*, 2872; d) A. Müller, E. Krickemeyer, R. Jostes, H. Bögge, E. Diemann, U. Bergmann, *Z. Naturforsch. B* **1985**, *40*, 1715; A. Müller, E. Krickemeyer, H. Bögge, D. Rehder, *Chimia* **1992**, *46*, 386; e) A. Müller, W. Eltzner, R. Jostes, H. Bögge, E. Diemann, J. Schimanski, H. Lueken, *Angew. Chem.* **1984**, *96*, 355; *Angew. Chem. Int. Ed. Engl.* **1984**, *23*, 389. In [2a–2c] relations to possible prebiotic processes are made.

[3] A. Müller, E. Krickemeyer, H. Bögge, *Angew. Chem.* **1986**, *98*, 258; *Angew. Chem. Int. Ed. Engl.* **1986**, *25*, 272; detailed synthesis in *Z. Anorg. Allg. Chem.* **1987**, *554*, 61.

[4] a) H. Müller in *Handbuch der Präparativen Anorganischen Chemie, Vol. 3* (Ed.: G. Brauer), Enke, Stuttgart, **1981**, p. 1619; b) E. Diemann, *Z. Anorg. Allg. Chem.* **1977**, *431*, 273.

[5] **1a**: $I4_1/a$, $a = 1460.7(2)$, $c = 1369.3(4)$ pm, $V = 2921.5(14) \times 10^6$ pm^3, $Z = 4$, $\mu = 176.4$ cm^{-1}; measurement temperature: 294 K; $R = 0.036$ for 1264 independent reflections ($F_0 > 4\sigma(F_0)$); **1b**: $P\bar{1}$, $a = 1242.1(2)$, $b = 1245.1(2)$ $c = 1303.0(2)$ pm, $\alpha = 106.28(1)$, $\beta = 109.98(1)$, $\gamma = 109.25(1)^\circ$, $V = 1602.9(4) \times 10^6$ pm^3, $Z = 2$, $\mu = 160.9$ cm^{-1}; measurement temperature: 294 K; $R = 0.043$ for 5733 independent reflections ($F_0 > 4\sigma(F_0)$); **2**: $C2/c$, $a = 1829.0(3)$, $b = 1026.8(2)$, $c = 1962.0(4)$ pm, $\beta = 102.77(1)^\circ$, $V = 3593.8(11) \times 10^6$ pm^3, $Z = 4$, $\mu = 149.5$ cm^{-1}; measurement temperature: 294 K; $R = 0.031$ for 3368 independent reflections ($F_0 > 4\sigma(F_0)$); Siemens R3m/V diffractometer, $Mo_{K\alpha}$ radiation, graphite monochromator. The powder diffraction patterns calculated from the single crystal data agree with the measured patterns. Further details of the crystal structure investigations of **1a**, **1b**, and **2** may be obtained from the Fachinformationszentrum Karlsruhe, D-76344 Eggenstein-Leopoldshafen (FRG) on quoting the depository number CSD-58049 and the journal citation.

[6] With respect to the structure of $(PPh_4)_4[Re_4S_4(CN)_{12}] \cdot 3H_2O$ cf. also M. Laing, P. M. Kiernan, W. P. Griffith, *J. Chem. Soc. Chem. Commun.* **1977**, 221.

[7] A. Broll, A. Simon, H. G. von Schnering, H. Schäfer, *Z. Anorg. Allg. Chem.* **1969**, *367*, 1.

[8] See also A. Müller, E. Krickemeyer, V. Wittneben, H. Bögge, M. Lemke, *Angew. Chem.* **1991**, *103*, 1501; *Angew. Chem. Int. Ed. Engl.* **1991**, *30*, 1512.

[9] J. C. Wildervanck, F. Jellinek, *J. Less-Common Met.* **1971**, *24*, 73; N. W. Alcock, A. Kjekshus, *Acta Chem. Scand.* **1965**, *19*, 79; V. J. Fedorov, *Chalcogenides of Refractory Transition Metals. Quasi One-dimensional Compounds (russ.)*, "Nauka", Novosibirsk, **1988**.

[10] The metal centers in Re_2S_7 should be present in (approximately) a formal oxidation state of about + IV according to ESCA data (E_B value in eV; Re $4f_{7/2}$): Re_2S_7: 41.8 (Au $4f_{7/2}$, 84.0); for comparison: $Re^{IV}S_2$: 42.0(Au $4f_{7/2}$, 84.0), $(PPh_4)[Re^{VII}S_4]$: 43.6 (C ls_{int}, 285.0), $(PPh_4)[Re^{V}S(S_4)_2]$: 43.0 (C ls_{int}, 285.0), **3**: 42.3 (C ls_{cent}, 285.0).

[11] A. Müller, V. Fedin, K. Hegetschweiler, W. Amrein, *J. Chem. Soc. Chem. Commun.* **1992**, 1795; A. Müller, E. Diemann, E. Krickemeyer, H.-J. Walberg, H. Bögge, A. Armatage, *Eur. J. Solid State Inorg. Chem.* **1993**, *30*, 565; see also S. P. Cramer, K. S. Liang, A. J. Jacobson, C. H. Chang, R. R. Chianelli, *Inorg. Chem* **1984**, *23*, 1215.

[12] A. Müller, R. Jostes, F. A. Cotton, *Angew. Chem.* **1980**, *92*, 921; *Angew. Chem. Int. Ed. Engl.* **1980**, *19*, 875. This is in accordance with the finding that trinuclear Mo^{IV} clusters are formed from $[MoO_4]^{2-}$ by heating $[MoO_4]^{2-}$ solutions in the presence of S_x^{2-} (even nearly quantitatively!: A. Müller, E. Krickemeyer, *Inorg. Synth.* **1990**, *27*, 47) and tetranuclear Re^{IV} clusters from $[ReO_4]^-$ [3].

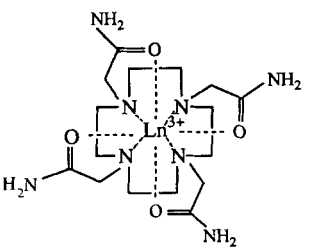
[13] See, for example, A. F. Holleman, E. Wiberg, *Lehrbuch der Anorganischen Chemie*, 91st–100th ed., de Gruyter, Berlin **1985**, p. 1099.

[14] Observed for the first time during the formation of $[W_3S_9]^{2-}$ and $[Mo_2O_2S_2(S_2)_2]^{2-}$ from tetrahedral d^0 thioanions (cf. references in A. Müller, *Polyhedron* **1986**, *5*, 323.)

Lanthanide(III) Tetraamide Macrocyclic Complexes as Synthetic Ribonucleases: Structure and Catalytic Properties of $[La(tcmc)(CF_3SO_3)(EtOH)](CF_3SO_3)_2$**

Shahid Amin, Janet R. Morrow,* Charles H. Lake, and Melvyn Rowen Churchill

Trivalent lanthanide ions (Ln^{3+}) efficiently promote RNA cleavage by phosphate ester transesterification.[1] Our interest lies in the design of ligands that strongly bind lanthanide ions without inhibiting their catalytic properties.[2] Such catalysts tethered to nucleic acid recognition agents may find application as RNA sequence-specific cleaving agents for antisense oligonucleotide strategies.[3] Our efforts have focused on the synthesis of robust cationic Ln^{3+} complexes that may be effective catalysts in vivo.[2a] Recently we have synthesized Ln^{3+} complexes of macrocyclic ligands that are structurally similar to dota (1,4,7,10-tetraazacyclododecane-1,4,7,10-tetraacetate), but, instead of acetate groups, contain neutral amide or hydroxyethyl groups.[2b,c] Here we report on Ln^{3+} tetraamide macrocyclic complexes that are remarkably inert to dissociation in water (**1**, Ln = La, Eu, Dy). Only $[La(tcmc)]^{3+}$ efficiently promotes RNA cleavage. Its X-ray crystal structure features a ten-coordinate La^{3+} cation.



1

The tcmc ligand and $[Ln(tcmc)](CF_3SO_3)_3$ complexes were prepared in good yield and characterized as detailed in the Experimental Procedure. Potentiometric titrations of 1.0 mM solutions of the La^{3+} and Eu^{3+} complexes indicate there are no ionizable protons in the pH region between 4.0 and 9.0. For $[Ln(tcmc)](CF_3SO_3)_3$ (Ln = La, Eu), plots of molar conductivity versus the square root of concentration give slopes of 3200 and 1600 cm^2 L$^{1/2}$ mol$^{-3/2}$ ohm^{-1} with intercepts of 350 and 308 cm^2 mol^{-1} ohm^{-1}, respectively, consistent with 3:1 electrolytes.[4] $[La(tcmc)]^{3+}$ has ^{1}H and ^{13}C NMR properties that support strong coordination of the amide groups and demonstrate the rigidity of the tcmc macrocycle. At $-10\,^\circ$C, the ethylenic units of the cyclen ring are rigid on the NMR time scale and are present in the highly symmetric [3333] square conformation. There is a dynamic process, similar to that for $[La(dota)]^-$,[5] that involves a change in conformation of the ethylenic units in concert with movement of the pendant groups. The ^{13}C NMR

[*] Prof. J. R. Morrow, S. Amin, C. H. Lake, Prof. M. R. Churchill
Chemistry Department, Acheson Hall
State University of New York at Buffalo,
3435 Main Street, Buffalo, NY 14214 (USA)
Telefax: Int. code + (716)829-2960

[**] This research was supported by the National Institutes of Health (GM-46539). Upgrade of the diffractometer was made possible by Grant 89-13733 from the Chemical Instrumentation Program of the National Science Foundation.

tcmc = 1,4,7,10-tetrakis(carbamoylmethyl)-1,4,7,10-tetraazacyclododecane. Cyclen is the trivial name for the unsubstituted macrocyclic ligand.

resonances for the ethylenic carbons ($\delta = 50.1$ and 54.3 at $-20\,^{\circ}C$) broaden ($0\,^{\circ}C$) and coalesce. An activation energy of $56.1 \pm 0.5\ kJ\,mol^{-1}$ is calculated at coalescence ($22\,^{\circ}C$). $[La(dota)]^-$ and $[La(thed)]^{3+}$ (thed = 1,4,7,10-tetrakis(2-hydroxyethyl)-1,4,7,10-tetraazacyclododecane) have activation energies of 60.7 and 52.0 $kJ\,mol^{-1}$ for similar dynamic processes;[2b, 5] the order $[La(dota)]^- > [La(tcmc)]^{3+} > [La(thed)]^{3+}$ may reflect stronger coordination of acetate and amide groups than hydroxyethyl groups, which is in accord with formation constants for similar macrocycles.[6-8] In [D$_6$]DMSO an activation barrier of $82.6 \pm 0.3\ kJ\,mol^{-1}$ for rotation about the C–N bond was calculated from the slow-exchange line-broadening approximation ($115\,^{\circ}C$). The large activation energy for this rotation in $[La(tcmc)]^{3+}$ compared to that of the free tcec ligand (tcec = 1,4,7,10-tetrakis(2-carbamoylethyl)-1,4,7,10-tetraazacyclododecane, $70.5 \pm 0.5\ kJ\,mol^{-1}$)[2c] is attributed to polarization of the C=O bond and an increase in C–N double-bond character due to coordination.

Lanthanide complexes must be robust if they are to be useful as catalysts. The kinetic inertness of a complex to dissociation may correlate better than thermodynamic stability with the ability of a complex to remain intact in vivo.[9] Although poly(aminocarboxylate) ligands containing one or two amide groups and three acetate groups bind strongly to Ln^{3+},[8, 10] our initial studies with ligands containing four amide groups (tcec) failed to produce complexes that remained intact in water.[2c] In contrast, tcmc complexes do not dissociate in water at $37\,^{\circ}C$, pH 6.0, as determined by studies with excess Cu^{2+} as a trapping agent. First-order rate constants are 1.2×10^{-6} and $4.4 \times 10^{-7}\ s^{-1}$ ($t_{1/2}$ = 6.7 and 18 days) for $[La(tcmc)]^{3+}$ and $[Dy(tcmc)]^{3+}$, respectively. For $[La(tcmc)]^{3+}$ the rate of dissociation is independent of Cu^{2+} concentration, consistent with a process that is not assisted by Cu^{2+}. $[Eu(tcmc)]^{3+}$ did not dissociate over a period of 6 weeks (<1%). A rate constant of $1.6 \times 10^{-7}\ s^{-1}$ ($t_{1/2}$ = 50 days) at pH 2.0 and $60\,^{\circ}C$ indicates that $[Eu(tcmc)]^{3+}$ is as inert as the agent $[Gd(dota)]^-$ used in magnetic resonance imaging experiments.[6]

$[La(tcmc)]^{3+}$ promotes rapid cleavage of RNA oligomers. The pseudo-first-order rate constant ($0.57\ h^{-1}$) for cleavage of oligomers of adenylic acid (A_{12}–A_{18}) by 0.200 mM $[La(tcmc)]^{3+}$ at $37\,^{\circ}C$ and pH 7.6 is similar to that for the highly efficient Eu^{3+} Schiff-base catalyst.[2a, 11] $[La(tcmc)]^{3+}$ (1.00 mM) also promotes rapid transesterification of the RNA model substrate, the phosphate diester **2**, at pH 7.4 and $37\,^{\circ}C$ ($k = 5.8 \times 10^{-2}\ h^{-1}$). That

$[P(O)_2(4\text{-}NO_2C_6H_4O)(OCH_2CH(CH_3)OH)]^-$ **2**

0.02 mM ethylenediaminetetraacetate (EDTA) has no effect on RNA cleavage rates, nor 0.5 mM EDTA on the rate of transesterification of **2** indicates that catalysis is not due to trace free La^{3+}.[12] Under similar conditions, $[Eu(tcmc)]^{3+}$ or $[Dy(tcmc)]^{3+}$ neither promote RNA cleavage in the presence of 0.02 mM EDTA over 8 h nor the transesterification of **2** over 1 h. These differences in catalytic activity are unusual. Past studies have shown that there is little difference in the extent of RNA cleavage with various Ln^{3+} salts; generally the later Ln^{3+} ions are better promoters because of their greater Lewis acidity.[1a, b] One explanation for the different catalytic activity lies in the fact that octadentate ligands such as tcmc nearly encapsulate Ln^{3+} ions. The larger La^{3+} ion may attain a higher coordination number and thus has more coordination sites remaining for binding substrate and for catalysis. Structural data support this argument. Gd^{3+} and Eu^{3+} complexes of similar macrocycles are all nine-coordinate with an octadentate macrocycle and a water molecule. These include Eu^{3+} and Gd^{3+} complexes of dota, dota-like macrocycles containing an amide pendant group, and thp (thp = 1,4,7,10-tetrakis(2-hydroxypropyl)-1,4,7,10-tetraazacyclododecane).[2d, 8, 13, 14] Recent X-ray diffraction studies indicate that the Eu^{3+} complex ion of $[Eu(tcmc)(H_2O)](CF_3SO_3)_3 \cdot 2CH_3OH$ is nine-coordinate.[15]

The single-crystal X-ray structure of $[La(tcmc)(EtOH)(CF_3SO_3)](CF_3SO_3)_2$ features a ten-coordinate La^{3+} ion. The crystallographic asymmetric unit consists of one $[La(tcmc)(EtOH)(SO_3CF_3)]^{2+}$ ion and two triflate counterions.[16] The ten-coordinate La^{3+} ion is bound to four nitrogen atoms and four oxygen atoms from the tcmc ligand, an oxygen atom of the coordinated ethanol molecule and an oxygen atom of a coordinated trifluoromethylsulfonate ion (Fig. 1). The coordinated

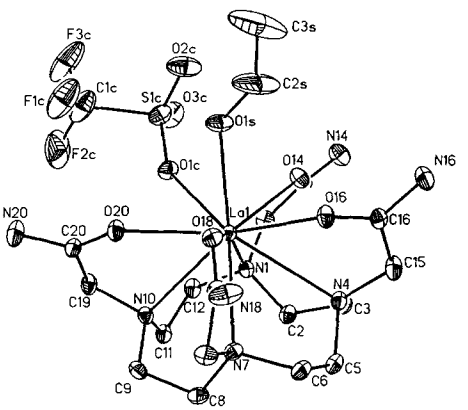


Fig. 1. Structure of the $[La(tcmc)(EtOH)(SO_3CF_3)]^{2+}$ ion. Selected distances [Å] and angles [°]: La1-O14 2.492(3), La1-O16 2.496(3), La1-O18 2.582(2), La1-O1c 2.600(3), La1-O1s 2.524(4), La1-O20 2.551(3), La1-N4 2.950(4), La1-N1 2.858(3), La1-N7 2.757(4), La1-N10 2.853(4); N1-La1-N7 97.2(1), N4-La1-N10 98.5(1), N7-La1-N10 65.8, O14-La1-O16 73.6(1), O20-La1-O1s 78.3(1), N1-La1-O14 61.5(1).

atoms are arranged about the La^{3+} ion in an unusual 1,5,4 geometry. The six oxygen atoms form a pentagonal pyramid with that from ethanol providing the cap (rms deviation of the other oxygens from the pentagonal plane is 0.133 Å). The pentagonal pyramid is stacked base upon apex on top of a square pyramid with the four nitrogen atoms forming the base and the La^{3+} ion occupying the vertex (rms deviation of the nitrogen atoms from a plane is 0.017 Å). The regularity of the pentagonal plane can be shown by examining the angles formed with the centroid of the pentagonal plane: O14-centroid-O16 = 74.2, O16-centroid-O18 = 68.8, O18-centroid-O20 = 70.2, O20-centroid-O1c = 74.0, and O1c-centroid-O14 = 74.0°. (For a regular pentagon the angles are all 72°.) The centroid of the pentagonal plane is 1.151 Å from the lanthanum(III) ion. The square arrangement of nitrogen atoms is oriented relative to the pentagonal arrangement of oxygen atoms such that N7 is eclipsed with O18. The centroid of the four nitrogen atoms lies 1.875 Å from the lanthanum(III) ion, and the dihedral angle formed by the intersection of the plane of nitrogen atoms and the plane of oxygen atoms is only 3.5°.

Studies of phosphate ester and nucleic acid binding to $[Ln(tcmc)]^{3+}$ are underway to elucidate differences in catalytic properties and to further our efforts in catalyst design.

Experimental Procedure

Cyclen (0.500 g, 2.91 mmol), bromoacetamide (1.810 g, 13.12 mmol), and triethylamine (2 mL, 14.38 mmol) were heated at reflux in anhydrous ethanol for 4 h. The

 © VCH Verlagsgesellschaft mbH, D-69451 Weinheim, 1994 0570-0833/94/0707-0774 $ 10.00+.25/0

tcmc ligand precipitated out during the course of the reaction and was recrystallized from boiling ethanol/water; yield 61%. Synthesis of a similar ligand has been reported [19]. $Ln(SO_3CF_3)_3$ (0.63 mmol) in 75 mL of anhydrous ethanol was treated with tcmc (0.250 g, 0.63 mmol) in 225 mL of ethanol. The mixture was heated at reflux under nitrogen for 3.5 h following the dissolution of tcmc. The solution was concentrated in vacuo, and hexane was added until cloudiness was observed. For Eu^{3+} and La^{3+} complexes, crystals formed within about 12 h. The Dy^{3+} complex was isolated as a powder. Yields were greater than 55%. Satisfactory microanalytical data were obtained for all compounds. ^1H NMR (CD_3CN): [La(tcmc)]-$(CF_3SO_3)_3$ (−10 °C): δ = 2.42 (NCH_2 (equatorial), d, J(C,H) = 14.8 Hz), 2.56 (NCH_2 (equatorial), d, J(C,H) = 13.6 Hz), 2.85 (NCH_2 (axial), pseudo t), 3.35 (NCH_2 and $CH_2C(O)NH_2$, m), 3.84 ($CH_2C(O)NH_2$, d, J(C,H) = 16.4 Hz), 7.27 (NH_2, s), 7.81 (NH_2, s); (75 °C): 2.69 (NCH_2, br.), 3.03 (NCH_2, br.), 3.65 ($CH_2C(O)NH_2$, s), 7.08 (NH_2, s), 7.68 (NH_2, s). ^{13}C NMR (CD_3CN): [La(tcmc)]-$(CF_3SO_3)_3$ (−20 °C): δ = 50.1, 54.3 (NCH_2, ring), 58.9 (NCH_2, amide), 178.8 ($C(O)NH_2$); [Eu(tcmc)]$(CF_3SO_3)_3$ (19 °C): δ = 76.3, 91.5, 110 (NCH_2 ring and amide), 198.3 ($C(O)NH_2$). Kinetic measurements of RNA cleavage were made as described previously [2a, 20].

Received: September 20, 1993
Revised: December 15, 1993 [Z 6368 IE]
German version: *Angew. Chem.* **1994**, *106*, 824

[1] a) R. Breslow, D.-L. Huang, *Proc. Natl. Acad. Sci. USA* **1991**, *88*, 4080; b) M. Komiyama, K. Matsumura, Y. Matsumoto, *J. Chem. Soc. Chem. Commun.* **1992**, 640; c) B. F. Rordorf, D. R. Kearns, *Biopolymers* **1976**, *15*, 1491.

[2] a) J. R. Morrow, L. A. Buttrey, V. M. Shelton, K. A. Berback, *J. Am. Chem. Soc.* **1992**, *114*, 1903; b) J. R. Morrow, K. O. A. Chin, *Inorg. Chem.* **1993**, *32*, 3357; c) J. R. Morrow, S. Amin, C. H. Lake, M. R. Churchill, *ibid.* **1993**, *32*, 4566; d) K. O. A. Chin, J. R. Morrow, C. H. Lake, M. R. Churchill, *Inorg. Chem.* **1994**, *33*, 656.

[3] a) C. A. Stein, J. S. Cohen, *Cancer Res.* **1988**, *48*, 2659; b) E. Uhlmann, A. Peyman, *Chem. Rev.* **1990**, *90*, 544; c) J. Goodchild, *Bioconjugate Chem.* **1990**, *1*, 165; d) U. English, *Angew. Chem.* **1991**, *103*, 629; *Angew. Chem. Int. Ed. Engl.* **1991**, *30*, 613.

[4] a) J. A. Davies, F. R. Hartley, S. G. Murray, *Inorg. Chim. Acta* **1980**, *43*, 69; b) V. N. Krishnamurthy, S. Soundararajan, *J. Inorg. Nucl. Chem.* **1967**, *29*, 517.

[5] J. F. Desreux, *Inorg. Chem.* **1980**, *19*, 1319.

[6] X. Wang, T. Jin, V. Comblin, A. Lopez-Mut, E. Merciny, J. F. Desreux, *Inorg. Chem.* **1992**, *31*, 1095.

[7] C. A. Chang, *Eur. J. Solid State Inorg. Chem.* **1991**, *28*, 237.

[8] S. Aime, P. L. Anelli, M. Botta, F. Fedeli, M. Grandi, P. Paoli, F. Uggeri, *Inorg. Chem.* **1992**, *31*, 2422.

[9] M. F. Tweedle, J. J. Hagan, K. Kumar, S. Mantha, C. A. Chang, *Magn. Reson. Imaging* **1991**, *9*, 409.

[10] M. S. Konings, W. C. Dow, D. B. Love, K. N. Raymond, S. C. Quay, S. M. Rocklage, *Inorg. Chem.* **1990**, *29*, 1488.

[11] In buffered solutions (10 mM (4-(2-hydroxyethyl)piperazino)ethanesulfonic acid (Hepes)) at 37 °C, first-order rate constants for cleavage of A_{12} to A_{18} oligomers at pH 7.6 and for transesterification of **2** at pH 7.4 in the absence of catalyst are 2.3×10^{-3} h^{-1} and 5.4×10^{-4} h^{-1}, respectively. Because the pseudo-first-order rate constant for the catalyzed reaction is dependent on the concentration of lanthanum complex, calculation of rate enhancements awaits the determination of true first-order rate constants for catalysis, which may be obtained through saturation kinetic studies or by the determination of binding constants.

[12] $[Ln(edta)]^-$ complexes are inactive in RNA cleavage (ref. [2a]).

[13] M.-R. Spirlet, J. Rebizant, J. F. Desreux, M.-F. Loncin, *Inorg. Chem.* **1984**, *23*, 359.

[14] C. A. Chang, L. C. Francesconi, M. F. Malley, K. Kumar, J. Z. Gougoutas, M. F. Tweedle, D. W. Lee, L. J. Wilson, *Inorg. Chem.* **1993**, *32*, 3501.

[15] S. Amin, J. R. Morrow, C. H. Lake, M. R. Churchill, unpublished results.

[16] Colorless crystals ($0.4 \times 0.27 \times 0.2$ mm) were mounted on an upgraded Siemens $P2_1/P3$ diffractometer. Data were collected through the use of the coupled $2\theta/\omega$ scan technique. A total of 5469 reflections were collected ($Mo_{K\alpha}$, λ = 0.71073, 2θ = 5–45°) and were merged into a unique set of 5061 reflections (R_{int} = 0.0126). All data were corrected for Lorentz and polarization effects. An empirical absorption correction was also applied to the data set. The crystal belongs to the triclinic system, space group $P\bar{1}$, a = 10.019(1), b = 12.754(2), c = 16.116(3) Å, α = 96.614(14), β = 92.035(13), γ = 108.960(12)°, V = 1928.8(6) Å^3 and Z = 2. All crystallographic calculations were carried out with the Siemens SHELXTL PLUS program package [17]. The analytical scattering factors for neutral atoms were corrected for both the $\Delta f'$ and $i\Delta f''$ components of anomalous dispersion [18]. The structure was solved by means of a Patterson map. Refinement of parameters was achieved through the minimization of the function $\sum w(|F_o|-|F_c|)^2$. The extreme features on the final difference-Fourier map were a peak of height 0.53 eÅ^{-3} and a negative feature of −0.84 eÅ^{-3}. Refinement converged with R = 0.0260 and R_w = 0.0283 for 542 parameters refined against those 4169 reflections with $|F_o| > 6\sigma|F_o|$ and R = 0.0358 for all 5061 data. Further details are available on request from the Director of the Cambridge Crystallographic Data Centre, 12 Union Road, GB-Cambridge CB2 1EZ (UK).

[17] SHELXTL PLUS, Siemens Analytical Instruments, Madison, WI, USA, **1990**.

[18] *International Tables for X-ray Crystallography Vol. 4*, Kynoch, Birmingham, UK, **1974**; Vol. 4, pp 99–101, 149–150.

[19] R. Kataky, D. Parker, A. Teasdale, J. P. Hutchinson, H. J. Buschmann, *J. Chem. Soc. Perkin Trans. 2* **1992**, 1347.

[20] M. K. Stern, J. K. Bashkin, E. D. Sall, *J. Am. Chem. Soc.* **1990**, *112*, 5357.

Jacobson and Heintschel Peroxides**

Sei-Hum Jang, Prakash Gopalan, James E. Jackson,* and Bart Kahr*

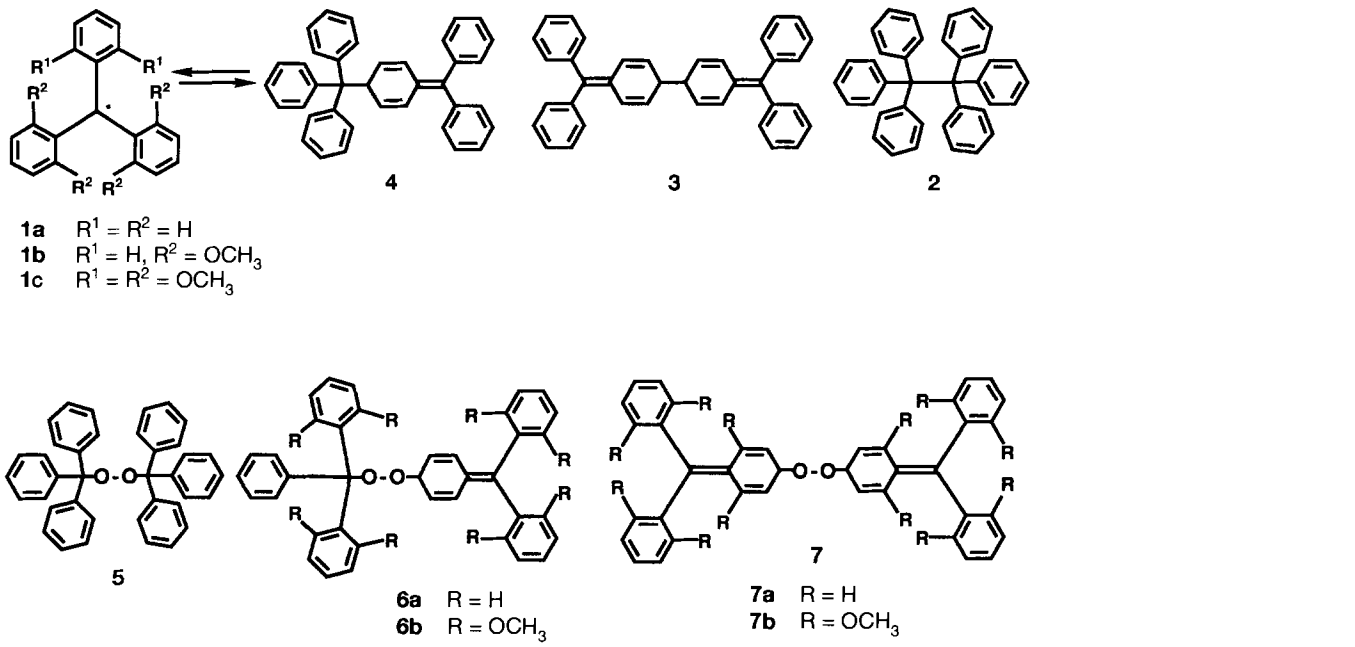
In 1908, Schmidlin[1] titrated solutions of Gomberg's[2] triphenylmethyl radical (**1a**) with oxygen and demonstrated that the revolutionary, hypovalent carbon species was in equilibrium with an unreactive one. Molecular weight determinations in anaerobic solutions[3] indicated a dimer for which several structures had been proposed: Markownikoff (1902) insisted upon hexaphenylethane (**2**),[4] Heintschel (1903) proposed a "tail-to-tail" or *para*–*para* coupling (**3**),[5] and Jacobson (1905) favored a "head-to-tail" or methyl–*para* coupling (**4**).[6] After a decade, Gomberg settled on **2**, which became entrenched as the consensus choice.[7] However, NMR studies in 1968 confirmed Jacobson's proposal (**4**), much to the surprise of the many scientists who had assumed that **2** was the correct structure.[8] In his 1974 review, McBride uncovered neglected chemical evidence that should have supported Jacobson, and argued that democracy is not always the best way to make scientific judgements.[9]

Another dimer—bis(triphenylmethyl)peroxide (**5**)[10]—was the product in Schmidlin's titration. In fact, the ready formation of this peroxide on exposure of solutions of triphenylmethyl to air forced Gomberg to conclude that he had prepared a novel, reactive species in 1900.[2] It since has been assumed that only methyl–methyl coupled peroxides, like **5**, are produced from triarylmethyls and oxygen. Herein, we describe the preparation and characterization of Jacobson and Heintschel peroxides in which triarylmethyl radicals add oxygen between methyl–*para* (**6**) and *para*–*para* positions (**7**), respectively. Presumably, analogous peroxides long have been present in many triarylmethyl radical oxidations.

We recently proposed a scheme for assembling molecular magnetic materials based on complexation of the stable free radical, tris(2,6-dimethoxyphenyl)methyl (**1c**), with metal cations.[11] As part of this work we determined the crystal structure of **1c**.[12] It displays an anomalous conformation far from the symmetrical D_3 ground state expected from ESR spectroscopy[13, 14] (Fig. 1) and molecular orbital calculations (see next paragraph). Two aryl rings are twisted out of the plane of

[*] Prof. Dr. J. E. Jackson, Dr. S.-H. Jang
Department of Chemistry and Center for Fundamental Materials Research
Michigan State University
East Lansing, MI 48824-1322 (USA)
Telefax: Int. code + (517)353-1793
Prof. Dr. B. Kahr, Dr. P. Gopalan
Department of Chemistry, Purdue University
West Lafayette, IN 47907-1393 (USA)
Telefax: Int. code + (317)494-0239

[**] This work was supported by the National Science Foundation.



Scheme 1. Triarylmethyl dimers and peroxides.

coordination of the central carbon atom by 61°, while the third ring is twisted by only 12°. This conformation is similar to the transition state structure for the two-ring flip enantiomerization mechanism in Ar_3Z propellers.[15]

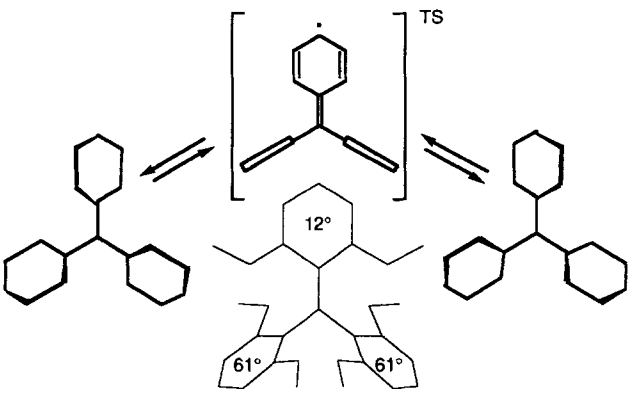


Fig. 1. Schematic illustration of the two-ring flip enantiomerization showing the near equivalence of the transition state (TS) with the conformation of **1c** in the crystal (bottom).

We surmised that a tetra-*ortho*-substituted radical such as **1b** might have a ground state geometry that resembled the crystallographic conformation of **1c**. ENDOR studies of **1b** by Ishizu et al.[16] qualitatively support these expectations, yielding twist angles of 65° for the substituted rings and 30° for the unsubstituted rings. Calculations of the molecular structure of **1b** with the AM1 Hamiltonian[17] were consistent with the ENDOR geometry. The structure was found to have C_2 symmetry with twists of 10° for the unsubstituted ring and 61° for the substituted rings. By contrast, the calculated ring twists for the hexamethoxy radical (**1c**) were 46°.[18]

In **1b**, the twist angles of two rings are increased, relative to those of the unsubstituted triphenylmethyl, by the out-of-plane deforming *ortho* substituents; the unique ring can now turn to an orientation nearly in the plane of coordination of the methyl carbon. In this way, **1b** maximizes its spin density at the *para* position of one ring while sterically hindering the methyl center.[19] The reactivity of such a radical should be concentrated at this *para* position.

Solutions of **1b** were allowed to stand in air for three days after which yellow-brown crystals were collected. Single-crystal X-ray analysis revealed a Jacobson peroxide **6b** (Fig. 2) in which oxygens link the central methyl position of one and the *para* position of the other triarylmethyl subunit.[20] In contrast to **5**, which was centrosymmetric in the crystal with a peroxide dihedral angle of 180°, C17-O10-O9-C20 was measured as 127.6(4)° in **6b**. The latter is much closer to the standard value of approximately 110° for the skew conformation in dialkyl peroxides.[21] Other geometric parameters such as the O–O bond length and C-O-O valence angles compare favorably with **5** (see legend to Fig. 2).

Martin et al. noted that solutions of **1c** react slowly with oxygen in the air to give an orange-brown precipitate.[13] Our attempts to recrystallize this material gave single crystals too small for X-ray analysis. As with **6b**, acid treatment of the oxidation product of **1c** gives the corresponding triarylmethyl

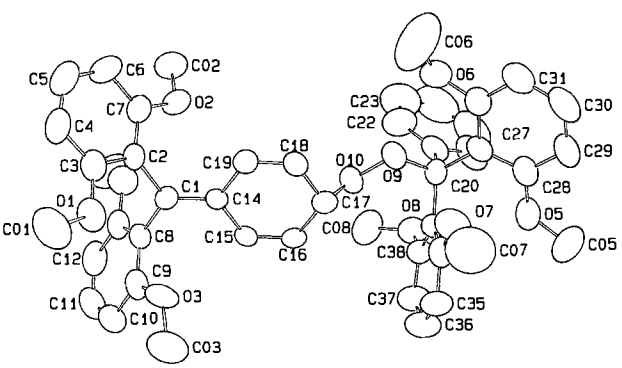


Fig. 2. ORTEP representation (50% probability ellipsoids) of the crystal structure of **6b**. Selected bond lengths [Å] and angles [°] are followed by the corresponding parameters for bis(triphenylmethyl)peroxide in square brackets. O9–O10 1.473(5) [1.480], C17–O10 1.466(6) and C20–O9 1.471(6) [1.461] C17–O10–O9 106.7(4)° C20–O9–O10 108.1(4)° [107.5].

 © VCH Verlagsgesellschaft mbH, D-69451 Weinheim, 1994 0570-0833/94/0707-0776 $ 10.00+.25/0

cation. Elemental analysis and FAB mass spectrometry established the composition as $C_{50}H_{54}O_{14}$, consistent with a peroxide. The structure of **7b** was determined by ^{1}H NMR spectroscopy. *Para* attachment is indicated by the presence of the methine and olefinic protons giving the pattern characteristic of an AA'BB'C spin system. This spectrum, in contrast to that of **6b**, results from a symmetric or Heintschel peroxide; the radical **1c** undoubtedly forms a compound in which the dioxygen bridge joins *para* positions.

Like the Jacobson dimer of triarylmethyl radicals, Jacobson and Heintschel peroxides, the common oxidation products in a variety of triarylmethyl radical studies, have escaped the attention of chemists for generations. These structures raise a concern: Why are not all bis(triarylmethyl)peroxides methyl–*para*-coupled in a Jacobson configuration? It previously has been shown that large radicals such as the *tert*-butoxy radical prefer to attach to *para* positions of triarylmethyls.[22] Such behavior has not been observed for oxygen. But since the first formed peroxy radical (a large radical by most standards) must attach to the second triarylmethyl radical we always might expect attack at the less hindered *para* site. Experiments are in progress to determine the first position bound in the formation of **6b**.

Experimental Procedure

Bis(2,6-dimethoxyphenyl)phenylmethanol (**1b**-OH): A solution of 1,3-dimethoxyphenyllithium was prepared by addition of 2.5 M *n*BuLi (34.8 mL, 86.9 mmol) in *n*-hexane to a solution of 1,3-dimethoxybenzene (10 g, 72.4 mmol) in anhydrous diethyl ether at −78 °C. The mixture was stirred at room temperature under argon for 48 h. Methylbenzoate (3.13 g, 23.0 mmol) in benzene (20 mL) was added, and the reaction solution was heated at reflux for 3 days under argon. The reaction mixture was poured into 200 mL of water, and the organic layer was dried and concentrated to yield the methanol as an oil. The oil was crystallized in CH_2Cl_2 and hexane. Mp 104 °C, 46% yield. ^{1}H NMR ($CDCl_3$, 299.95 MHz): δ = 3.38 (s, 12H), 6.43 (s, 1H), 6.54 (d, J = 8 Hz, 4H), 7.11 (t, J = 8 Hz, 2H), 7.13 (m, 1H), 7.21 (m, 2H), 7.46 (m, 2H); ^{13}C{^{1}H}NMR ($CDCl_3$, 75.46 MHz): δ = 56.5, 79.5, 106.74, 125.37, 126.31, 126.50, 126.63, 127.28, 149.5, 158.5.

1b$^+ \cdot$ **BF**$_4^-$: A solution of **1b**-OH (500 mg, 1.31 mmol) in 150 mL diethyl ether was treated with 0.1 mL of 48% HBF_4. The resulting crystalline blue precipitate was filtered and dried to give the BF_4^- salt of bis(2,6-dimethoxyphenyl)phenylmethyl cation quantitatively. Mp 142–143 °C. ^{1}H NMR ($CDCl_3$, 299.95 MHz): δ = 3.54 (s, 12H), 6.63 (d, J = 8 Hz, 4H), 7.44 (m, 4H); 7.61 (m, 1H), 7.79 (t, J = 8 Hz, 2H); ^{13}C{^{1}H} NMR ($CDCl_3$, 75.46 MHz): δ = 56.83, 105.36, 125.00, 129.09, 134.59, 137.02, 145.90, 163.79, 191.58.

1b: Compound **1b**$^+ \cdot$ **BF**$_4^-$ (200 g) was reduced by a 5 M $CrCl_2$ solution (20 mL, prepared with $CrCl_3 \cdot 6H_2O$ and Zn/Hg in 10% HCl solution), extracted with CH_2Cl_2, washed with water, and dried with $MgSO_4$. The solution was chromatographed over silica gel to give the radical (35%, based on SQUID measurement (SQUID = Superconducting Quantum Interference Device), μ_{eff} = 0.61 μ_B); m.p. 155–157 °C.

6b: Solutions of **1b** were allowed to stand in air for 3 days. Red-orange crystals of the peroxide precipitated during this time. Mp 121 °C; ^{1}H NMR ($CDCl_3$, 299.95 MHz): δ = 3.40 (s, 12H), 3.58(d, J = 2 Hz, 12H), 4.82 (m, 1H), 5.54 (m, 2H), 6.12 (m, 2H), 6.44 (m, 8H), 6.55 (m, 2H), 7.03 (t, J = 6 Hz, 4H), 7.05 (m, 1H0, 7.11 (t, J = 6 Hz, 2H), 7.68(d, J = 6 Hz, 2H); ^{13}C{^{1}H} NMR ($CDCl_3$, 75.46 MHz): δ = 55.94, 56.33, 103.94, 104.13, 106.47, 117.50, 124.71, 125.63, 125.85, 126.15, 127.07, 127.88, 127.99, 130.05, 147.20, 154.50, 158.43, 158.50; IR (KBr): $\tilde{\nu}$ = 2992, 2936, 2832, 1586, 1472, 1430, 1288, 1252, 1110, 1030, 928, 780, 726 cm^{-1}.

7b: Tris(2,6-dimethoxyphenyl)methyl (**1c**) was prepared as described previously [11]. A pale orange solid (**7c**) precipitated from ether solutions that stood in air for 3 days. The solid was washed with diethyl ether and recrystallized from THF. Mp > 300 °C; correct C,H elemental analyses. ^{1}H NMR ($CDCl_3$, 299.95 MHz): δ = 3.13 (s, 12H), 3.52 (d, J = 2 Hz, 24H), 5.02 (d, J = 8 Hz, 4H), 5.34 (t, J = 8 Hz, 2H), 6.39 (d, J = 8 Hz, 8H), 6.99 (d, J = 8 Hz, 4H); satisfactory C,H analysis; IR (KBr): $\tilde{\nu}$ = 2928, 2828, 1654, 1611, 1584, 1470, 1431, 1382, 1298, 1249, 1219, 1108, 912, 742 cm^{-1}.

Received: October 11, 1993 [Z 6408 IE]
German version: *Angew. Chem.* **1994**, *106*, 826

[1] a) J. Schmidlin, *Ber. Dtsch. Chem. Ges.* **1908**, *41*, 2471. b) This equilibrium was first proposed by B. Flürscheim, *J. Prakt. Chem.* **1905**, *71*, 497; *Ber. Dtsch. Chem. Ges.* **1908**, *41*, 2746.
[2] M. Gomberg, *Ber. Dtsch. Chem. Ges.* **1900**, *33*, 3150; *J. Am. Chem. Soc.* **1900**, *22*, 757.
[3] M. Gomberg, *Ber. Dtsch. Chem. Ges.* **1901**, *34*, 2726; M. Gomberg, L. H. Cone, *ibid.* **1904**, *37*, 2033.
[4] V. W. Markownikoff, *Zh. Russ. Fiz.-Khim. O-va.* **1902**, *34*, 140.
[5] E. Heintschel, *Ber. Dtsch. Chem. Ges.* **1903**, *36*, 320, 579.
[6] P. Jacobson, *Ber. Dtsch. Chem. Ges.* **1905**, *38*, 196.
[7] M. Gomberg, *J. Am. Chem. Soc.* **1914**, *36*, 1144.
[8] H. Lankamp, W. T. Nauta, C. MacLean, *Tetrahedron Lett.* **1968**, 249; H. Lankamp, Dissertation, Freie Universität Amsterdam, **1970**; see also: H. Volz, W. Lotsch, H.-W. Schell, *Tetrahedron* **1970**, *26*, 5343.
[9] J. M. McBride, *Tetrahedron* **1974**, *30*, 2009.
[10] For crystal structures of bis(triphenylmethyl)peroxide (**5**) see C. Glidewell, D. C. Liles, D. J. Walton, G. M. Sheldrick, *Acta Crystallogr. Sect. B* **1979**, *35*, 500; A. I. Yanovskii, T. V. Timofeeva, N. G. Furmanova, Yu. T. Struchkov, L. Yu. Ukhin, V. V. Bessonov, *Sov. Phys. Crystallogr. Engl. Transl.* **1981**, *26*, 112.
[11] S.-H. Jang, R. A. Bertsch, J. E. Jackson, B. Kahr, *Mol. Cryst. Liq. Cryst.* **1992**, *211*, 289.
[12] B. Kahr, J. E. Jackson, D. L. Ward, S.-H. Jang, *Acta Crystallogr. Sect. B* **1992**, *48*, 324; For a comparison of triarylmethyl geomtries in the solid state see B. Kahr, D. Van Engen, P. Gopalan, *Chem. Mater.* **1993**, *5*, 729.
[13] J. C. Martin, R. G. Smith, *J. Am. Chem. Soc.* **1964**, *86*, 2252.
[14] M. J. Sabacky, C. S. Johnson, Jr., R. G. Smith, H. S. Gutowsky, J. C. Martin, *J. Am. Chem. Soc.* **1967**, *89*, 2054.
[15] K. M. Mislow, *Acc. Chem. Res.* **1976**, *9*, 26.
[16] K. Ishizu, K. Mukai, A. Shibayama, K. Kondo, *Bull. Chem. Soc. Jpn.* **1977**, *50*, 2269.
[17] M. J. S. Dewar, E. G. Zoebisch, E. F. Healy, J. J. P. Stewart, *J. Am. Chem. Soc.* **1985**, *107*, 3902.
[18] This value is in excellent agreement with the twist angle originally predicted by ESR data [14].
[19] It would have an electronic structure that would mimic the transition state in the two-ring flip enantiomerization (see Fig. 1).
[20] Crystals of **6b** suitable for single crystal X-ray analysis were obtained as described in the Experimental Procedure. $C_{46}H_{46}O_{10}$, M = 758.87 g · mol^{-1}, monoclinic, a = 9.398(1) Å, b = 27.900(2), c = 15.259(2) Å, β = 96.87(1), V = 3972(1) Å^3, space group $P2_1/n$, Z = 4, $\mu(Cu_{K\alpha})$ = 6.88 cm^{-1}, ϱ_{calcd} = 1.269 g cm^{-3}, 3031 unique, observed ($I > 3.0\sigma(I)$) reflections with $2\theta < 116°$, R = 0.062, R_w = 0.080. The intensities were measured on an Enraf-Nonius CAD4 diffractometer with ω-2θ scans. The structure was solved by direct methods (SHELX-86: G. M. Sheldrick, Institut for Anorganische Chemie der Universitat Gottingen, F.R.G. 1986) and non-H atoms were refined anisotropically using the programs in MolEN (C. K. Fair, MolEN Structure Determination system, Delft Instruments, Delft, The Netherlands (1990). Further details of the crystal structure investigation are available on request from the Director of the Cambridge Crystallographic Data Centre, 12 Union Road, GB-Cambridge CB21EZ (UK) on quoting the full journal citation.
[21] S. Matsugo, I. Saito in *Organic Peroxides* (Ed.: W. Ando), Wiley, Chichester, **1992**.
[22] J. A. Kampmeier, R. R. Geer, A. J. Meskin, R. M. D'Silva, *J. Am. Chem. Soc.* **1966**, *88*, 1257; J. P. Lorand, P. D. Bartlett, *ibid* **1966**, *88*, 3294; J.-J. L. Fu, W. G. Bentrude, *ibid.* **1972**, *94*, 7710.

The First Isolable Dithiirane by Oxidation of a Dithietane

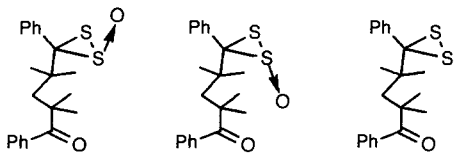
Akihiko Ishii, Toru Akazawa, Teruo Maruta, Juzo Nakayama,* Masamatsu Hoshino, and Motoo Shiro

The smallest cyclic disulfides, the dithiiranes, are of interest as isomers of thiocarbonyl *S*-sulfides (thiosulfines) and dithioesters.[1, 2] In dithiiranes the dihedral angle of 0° leads to significant repulsive lone pair–lone pair interactions in addition to large angle strains,[3] and therefore, although several dithiiranes have been recognized as elusive intermediates, no isolable ex-

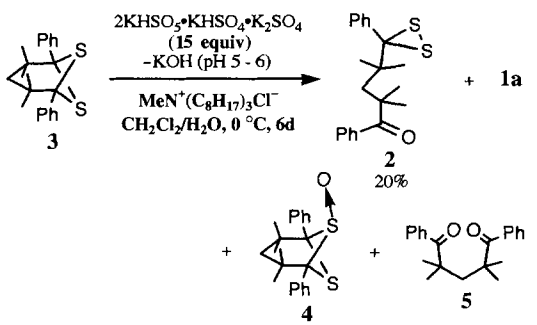
[*] Prof. Dr. J. Nakayama, Dr. A. Ishii, T. Akazawa, T. Maruta, Prof. Dr. M. Hoshino
Department of Chemistry
Faculty of Science, Saitama University
Urawa, Saitama 338 (Japan)
Telefax: Int. code + (48)858-3698
Dr. M. Shiro
Rigaku Corporation (Japan)

 © VCH Verlagsgesellschaft mbH, D-69451 Weinheim, 1994 0570-0833/94/0707-0777 $ 10.00+.25/0

amples (including their oxidized derivatives)—with the exception of **1**[4]—were reported in spite of much effort.[1] In contrast, the oxygen analogues, the dioxiranes are known and used as oxidizing reagents, though they are not very stable molecules for similar reasons.[5] We report here on the synthesis of the first isolable, *unoxidized* dithiirane **2** by oxidation of the bicyclic 1,3-dithietane **3**[6] with potassium peroxomonosulfate (OXONE, Aldrich, $2KHSO_5 \cdot KHSO_4 \cdot K_2SO_4$)[7, 8] and its chemical properties, for example the thermal isomerization to the corresponding thiocarbonyl *S*-sulfide.



Treatment of the bicyclic 1,3-dithietane **3** with OXONE (pH 5–6) and a catalytic amount of $[MeN(C_8H_{17})_3]Cl$ led to **2** in 20% yield (Scheme 1).[9] The dithiirane **2** is an orange crys-



Scheme 1. Synthesis of the dithiirane **2**.

talline compound that is stable at room temperature in air but decomposes to give the thioketone **6**[10] (see Scheme 2) and elemental sulfur when heated at 68–75 °C in a capillary tube. The structure of **2** was determined by spectroscopy and X-ray single-crystal structure analysis (Fig. 1).[11] In the UV/VIS spectrum, the longest absorption maximum was observed at 452 nm. This absorption corresponds to the first electronic transition ($n_\pi \rightarrow$ (S-S, S-C)σ^*, 422 nm) of the parent dithiirane calculated by Snyder and Carlsen with the CNDO/S-CI method.[3a] The X-ray structure analysis shows that no unusual bond lengths and angles are observed in the dithiirane ring of **2**. The S–S bond length (2.073 Å) corresponds to the mean value (2.070 Å)[12] of S–S bond lengths found in disulfides in which the dihedral angles between two C–S bonds are constrained to 0–20° and the two C–S bond lengths (1.821 and 1.814 Å) are very similar to that of the parent thiirane (1.815 Å).[13]

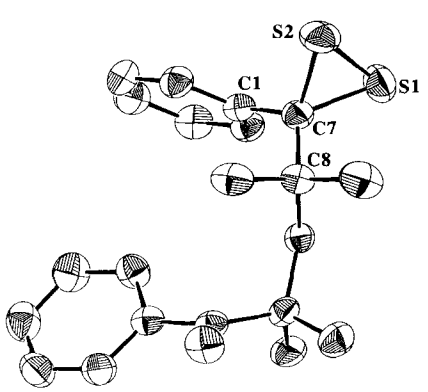
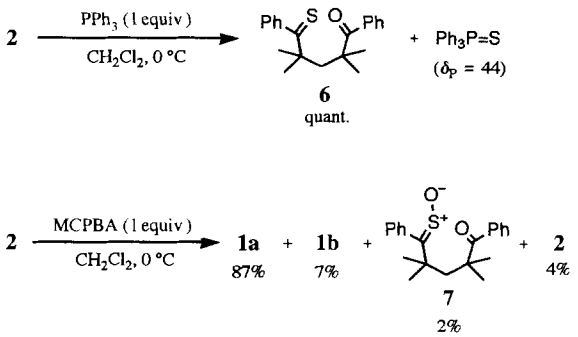


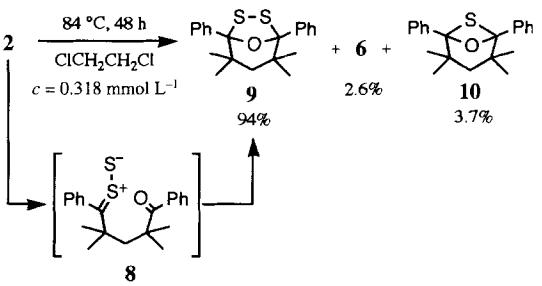
Fig. 1. ORTEP view of dithiirane **2**. Selected bond lenghts [Å] and angles [°]: S1-S2 2.073(2), S1-C7 1.821(2), S2-C7 1.814(3), C1-C7 1.515(3), C7-C8 1.566(3); S2-S1-C7 55.07(8), S1-S2-C7 55.37(8), S1-C7-S2 69.55(9), S1-C7-C1 113.1(2), S1-C7-C8 117.0(2), S2-C7-C1 113.2(2), S2-C7-C8 118.0(2), C1-C7-C8 117.2(2).

Dithiirane **2** is rather inert to acids such as *para*-toluenesulfonic acid, but very sensitive to nucleophiles such as amines and phosphanes. Thus, **2** decomposed quickly by treatment with triethylamine or triphenylphosphane to give the thioketone **6** quantitatively. Oxidation of **2** with an equimolar amount of *m*-CPBA (*meta*-chloroperoxybenzoic acid) gave the corresponding sulfoxides **1a** and **1b** in addition to small amounts of the sulfine **7**[4] and the starting material (Scheme 2).



Scheme 2. Reactions of the dithiirane **2**.

We next examined the thermal isomerization of **2** to the corresponding thiocarbonyl *S*-sulfide or dithioester. Thus, a dilute solution of **2** in 1,2-dichloroethane (0.318 mmol L^{-1}) was heated at 84 °C for 48 h. The ^1H NMR spectroscopic analysis of the residue after removal of the solvent revealed that the bicyclic 1,3,4-oxadithiolane **9**[10] was formed in high yield along with **6** and the 1,3-oxathietane **10**. The most straightforward explanation for the formation of **9** involves the isomerization of **2** to the thiocarbonyl *S*-sulfide **8** followed by an intramolecular 1,3-dipolar cycloaddition between the thiocarbonyl *S*-sulfide and carbonyl moieties. Interestingly, the yield of **9** markedly de-



creased to 27% with increased yields of **6** (51%) and **10** (22%), when the thermolysis of **2** was carried out in refluxing benzene (0.290 mmol L^{-1}). This influence of the solvent polarity can be attributed to the polar character of the thiocarbonyl *S*-sulfide functional group. An attempt to trap **8** by intermolecular cycloaddition with dimethyl acetylenedicarboxylate was unsuccessful.

 © VCH Verlagsgesellschaft mbH, D-69451 Weinheim, 1994 0570-0833/94/0707-0778 $ 10.00+.25/0

Thiocarbonyl *S*-sulfides have been considered thermodynamically less stable than the corresponding dithiiranes.[3b] The driving force of the thermal isomerization of **2** to **9** is probably attributed to the rapid intramolecular ring closure, leading to thermodynamically far more stable **9**, even when the equilibrium concentration of **8** is very low. Incidentally, no isomerization of **2** to the corresponding dithioester was detected.

Experimental Procedure

2: A solution of **3** (681 mg, 2 mmol) in CH_2Cl_2 (500 mL), an aqueous solution (180 mL) of OXONE (18.4 g, 30 mmol) whose pH was adjusted to 5–6 by adding 1 M KOH, and a catalytic amount of $[MeN(C_8H_{17})_3]Cl$ were stirred vigorously at 0 °C for 6 d. During the reaction, 1 M KOH (2–3 mL) was added once or twice a day to maintain the pH of the aqueous layer between 5–6. The orange organic layer was separated, washed with cold water, dried over anhydrous $MgSO_4$, and evaporated under reduced pressure at 0 °C. The residue was dissolved in CH_2Cl_2 (2–3 mL) and the solution diluted with hexane. The resulting mixture was allowed to stand in a refrigerator and the first white crystalline crop, which consisted of by-products, was removed by filtration and the filtrate was cooled again in the refrigerator for 2 d. The orange crystals separated were collected by filtration and purified by medium-pressure liquid chromatography (silica gel, CH_2Cl_2) to give 146 mg of **2**. By-products of this oxidation consisted of the dithiirane oxide **1a**, the sulfoxide **4**, and the dicarbonyl compound **5**, whose yields were not determined.

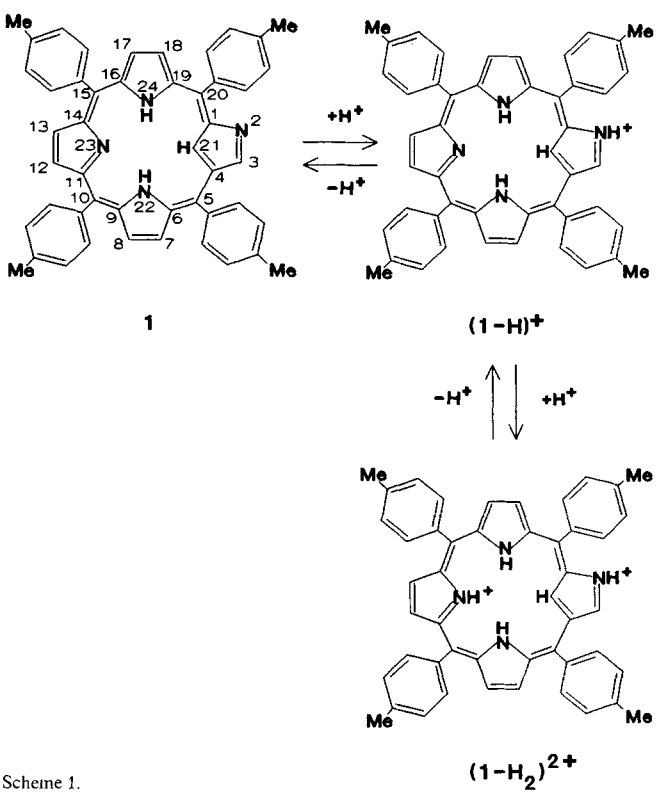
Received: November 8, 1993 [Z 6484 IE]
German version: *Angew. Chem.* **1994**, *106*, 829

[1] A. Senning, H. C. Hansen, M. F. Abdel-Megeed, W. Mazurkiewicz, B. Jensen, *Tetrahedron* **1986**, *42*, 739; A. Senning, *Sulfur Lett.* **1986**, *4*, 213; *ibid.* **1990**, *11*, 83; G. W. Kutney, K. Turnbull, *Chem. Rev.* **1982**, *82*, 333.
[2] R. Huisgen, J. Rapp, *J. Am. Chem. Soc.* **1987**, *109*, 902.
[3] a) J. P. Snyder, L. Carlsen, *J. Am. Chem. Soc.* **1977**, *99*, 2931; b) S. P. So, *J. Mol. Struct. (THEOCHEM)* **1986**, *148*, 153; c) R. M. Wilson, D. N. Buchanan, J. E. Davis, *Tetrahedron Lett.* **1971**, 3919, and references therein.
[4] A. Ishii, T. Akazawa, M.-X. Ding, T. Honjo, J. Nakayama, M. Hoshino, M. Shiro, *J. Am. Chem. Soc.* **1993**, *115*, 4914.
[5] R. W. Murray, *Chem. Rev.* **1989**, *89*, 1187; W. Adam, R. Curci, J. O. Edwards, *Acc. Chem. Res.* **1989**, *22*, 205; J. O. Edwards, R. H. Pater, R. Curci, F. DiFuria, *Photochem. Photobiol.* **1979**, *30*, 63.
[6] A. Ishii, J. Nakayama, M.-X. Ding, N. Kotaka, M. Hoshino, *J. Org. Chem.* **1990**, *55*, 2421.
[7] For oxidation of sulfides with OXONE see R. J. Kennedy, A. Stock, *J. Org. Chem.* **1960**, *25*, 1901; B. M. Trost, D. P. Curran, *Tetrahedron Lett.* **1981**, *22*, 1287.
[8] Attempted preparation of **2** by deoxygenation of **1** with phenylsilane was unsuccessful.
[9] The mechanism for the formation of **2** is not clear. A mechanism similar to that presented for the formation of **1a, b** may be operative [4].
[10] A. Ishii, M.-X. Ding, J. Nakayama, M. Hoshino, *J. Chem. Soc. Chem. Commun.* **1992**, 7.
[11] Selected spectral data of **2**: ^{1}H NMR ($CDCl_3$, 400 MHz): δ = 1.11 (s, 6H), 1.33 (s, 6H) 2.25 (s, 2H), 7.21 (t, J = 7.9 Hz, 2H), 7.27 (t, J = 7.9 Hz, 1H), 7.32–7.36 (m, 4H), 7.43 (t, J = 7.9 Hz, 1H), 7.59 (d, J = 7.9 Hz, 2H); ^{13}C NMR ($CDCl_3$, 100.6 MHz): δ = 26.3 (CH_3), 29.2 (CH_3), 42.6 (C), 48.5 (C), 50.1 (CH_2), 80.6 (S-C-S), 126.5 (CH), 127.9 (CH), 128.0 (CH), 128.3 (CH), 130.9 (CH), 132.1 (CH), 138.7 (C), 141.2 (C), 208.5 (C=O). IR (KBr): $\tilde{\nu}$ = 1669 cm^{-1} (C=O). UV/VIS (CH_2Cl_2): $\lambda_{max}(\varepsilon)$ = 452 nm (104). Crystal data for **2**: triclinic, $P\bar{1}$; a = 9.927(5), b = 10.593(10), c = 9.810(6) Å, α = 108.22(5)°, β = 108.29(4)°, γ = 90.64(7)°, V = 923(1) Å^3, Z = 2, ρ_{calcd} = 1.282 g cm^{-3}, $\mu(Cu_{K\alpha})$ = 25.83 cm^{-1}. The structure was solved by using direct methods (SIR88) and refined by a full-matrix least-squares procedure, using 2284 data, to a conventional R value of 0.047 (R_w = 0.071). Further details of the crystal structure investigation are available on request from the Director of the Cambridge Crystallographic Data Centre, 12 Union Road, GB-Cambridge CB21EZ (UK), on quoting the full journal citation.
[12] F. H. Allen, O. Kennard, D. G. Watson, L. Brammer, A. Guy Orpen, R. Taylor, *J. Chem. Soc. Perkin Trans. 2* **1987**, S1.
[13] K. Okiya, C. Hirose, D. G. Lister, J. Sheridan, *Chem. Phys. Lett.* **1974**, *24*, 111.

Tetra-*p*-tolylporphyrin with an Inverted Pyrrole Ring: A Novel Isomer of Porphyrin**

Piotr J. Chmielewski, Lechosław Latos-Grażyński,* Krystyna Rachlewicz, and Tadeusz Głowiak

In our search of core-modified tetraarylporphyrin and metallotetraarylporphyrin analogs we have discovered a novel isomer of 5,10,15,20-tetra-*p*-tolyl-porphyrin ($TTPH_2$), namely 2-aza-21-carba-5,10,15,20-tetra-*p*-tolylporphyrin ($CTTPH_2$) (**1**, Scheme 1).[***] The interest in this new macrocycle centers on its remarkable ability – as a tetradentate ligand to form carbon–metal bond. Spectral properties of **1** highlight to its potential applications as the photosensitizer in photodynamic therapy.



Scheme 1.

Since its discovery by Rothemund,[1] 5,10,15,20-tetraphenylporphyrin and its substituted analogs have become the most ubiquitous models of the coordination centers of hemoproteins in biomimetic chemistry and in investigations on metalloporphyrin catalyzed oxidation. Conventional syntheses of tetra-

[*] Prof. Dr. L. Latos-Grażyński, Dr. P. J. Chmielewski, Dr. K. Rachlewicz, Prof. Dr. T. Głowiak
Institute of Chemistry, University of Wrocław
14 F. Joliot-Curie Street, Wrocław 50383 (Poland)
Telefax: Int. code +(71)222-348

[**] This work was supported by the State Committee for Scientific Research KBN (Grant 207329101).

[***] Note added in proof: After acceptance of this paper, the synthesis and the X-ray structure analysis of 2-aza-21-carbatetraphenylporphyrin were reported by H. Furuta, T. Asano, and T. Ogawa (*J. Am. Chem. Soc.* **1994**, *116*, 767). Our conclusions concerning the dissociation scheme (the protonation of the peripheral nitrogen in the first step) and the condensation mechanism of $CTTPH_2$ contradict suggestions of Furuta et al. – Editorial comment: Both papers will be comprehensively discussed in a Highlight on "New Porphyrin Isomers" (J. L. Sessler, *Angew. Chem.* **1994**, *106*, in press; *Angew. Chem. Int. Ed. Engl.* **1994**, *33*, in press).

 © VCH Verlagsgesellschaft mbH, D-69451 Weinheim, 1994 0570-0833/94/0707-0779 $ 10.00+.25/0

meso-substituted prophyrins involve one- or two-step condensation of pyrrole and suitable aldehydes,[2–5] a stepwise route[6] to control substitutions of β-positions,[6] or a modification[7] of the coordination core.

The isomer **1** of $TTPH_2$ can be formally constructed by an interchange of a β-methine moiety and pyrrolic nitrogen within the pyrrole ring while preservation of the general pattern of the porphyrin skeleton. Mechanistically, the synthesis of the isomeric porphyrin requires one β-condensation instead of the typical all α-condensation at the pyrrole nuclei.

The reaction of *p*-tolylaldehyde with excess pyrrole in dichloromethane, catalyzed by BF_3 Et_2O, yields the usual tetra-*p*-tolylporphyrin and its novel isomer **1** (Table 1). An electronic spectrum of **1** (Fig. 1) is porphyrin-like with the characteristic band at 730 nm. Its ^{1}H NMR spectrum exhibits three AB patterns of regular pyrrole protons (Fig. 2A). The inverted pyrrole ring contributes one proton signal. Two protons located on inner pyrrole nitrogens gave a broad singlet at 25 °C, but presented two well-separated singlets at −50 °C. The definitive confirmation of the structure is provided by the enormous upfield shift of the unique 21-CH proton ($\delta = -5.083$, $CDCl_3$, −50 °C) of the inverted pyrrole ring, spin-spin-coupled to 3-H, and showing strong nuclear Overhauser effects (NOE) to 22-NH and 24-NH. The NH protons ($\delta = -2.588$, -2.672) can be easily exchanged by deuterium of D_2O to leave only the 21-CH resonance in the upfield region. Heating of **1** in $CDCl_3$/CH_3COOD mixture (95:5 volume ratio, 0.5 h, 60 °C) finally introduced deuterium in the 21-position. The molecule **1** preserves the aromaticity, because all outer pyrrole and *p*-tolyl resonances are strongly downfield shifted due to the ring current effect, which is also demonstrated by the remarkable shift difference ($\Delta\delta \approx 14$) between outer and inner pyrrolic resonances. The full assignments have been obtained by 2D ^{1}H NMR COSY and NOESY experiments.

Table 1. Selected physical data of **1**, $(1\text{-H})^+$, $(1\text{-H}_2)^{2+}$, and **2**.

1: ^{1}H NMR (300 MHz, $CDCl_3$, −50 °C): δ = 8.990 (7-H), 8.614 (8-H) (J(AB) = 5.0 Hz), 8.925 (18-H), 8.582 (17-H), (J(AB) = 5.0 Hz), 8.578, 8.556 (12, 13-H) (J(AB) = 4.8 Hz), 8.694 (s, 3-H), -2.558(24-NH), -2.672 (22-NH), -5.083 (21-CH); UV/VIS (CH_2Cl_2): λ_{max} [nm] ($\varepsilon \cdot 10^{-3}$) = 383(sh), 440 (Soret) (96.8), 506 (4.7), 543 (7.5), 585 (10.9), 672 (2.8), 730 (9.7); MS (EI): m/z (%) = 670 (100), HR-MS: m/z = 670.309557 (found for M^+) 670.30965 (calcd for $C_{48}H_{38}N_4$); correct elemental analysis for $CTTPH_2 \cdot MeOH$

$(1\text{-H})^+$: ^{1}H NMR (300 MHz, $CDCl_3$, −50 °C, 2 equiv, CF_3COOH): δ = 8.995, 8.497 (J(AB) = 4.8 Hz), spin-spin-coupled to NH at -1.155, 8.852, 8.468 (J(AB) = 5.2 Hz) spin-spin-coupled to NH at -1.237, 8.376 (unresolved, 12,13-H), 8.391 (s, 3H), 16.670 (s, 2-NH), -3.854 (21-CH). 3-H, 2-NH, and 21-CH are spin-spin coupled.

$(1\text{-H}_2)^{2+}$: ^{1}H NMR (300 MHz, $CDCl_3$, −50 °C, 30 equiv CF_3COOH): δ = 8.580 (d, J(AB) = 4.0 Hz, pyrrole), 8.470 (d, J(AB) = 4.3 Hz, pyrrole). The unresolved multiplet in the δ = 8.3–7.4 range is attributable to pyrrole and tolyl resonances, 11.669 (2-NH), 2.034, 1.877, 1.612 (22,23,24-NH), -1.611 (21-CH)

2: ^{1}H NMR (300 MHz, $CDCl_3$, 20 °C): δ = 8.029, 7.750 (J(AB) = 5.0 Hz, 7,8-H), 7.996, 7.798 (J(AB) = 5.0 Hz, 17,18-H), 7.877, 7.874 (J(AB) = 5 Hz, 12,13-H), 10.034 (2-NH), 8.485 (3-H) (J(AX) = 3.4 Hz); UV/VIS ($CHCl_3$): λ_{max} [nm] ($\varepsilon \cdot 10^{-3}$) = 359 (48.5), 426 (Soret) (88), 460 (sh), 515 (10.7), 557 (10.3), 595 (11.4), 660 (sh), 718 (6.9), 789 (7.1); MS (EI): m/z(%) = 726 (M^+, 100)

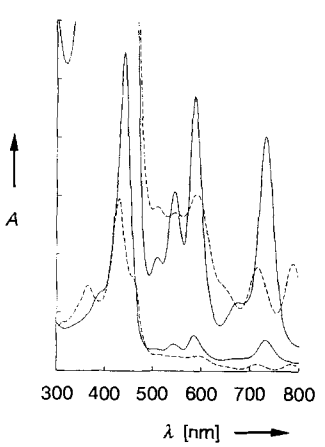


Fig. 1. The electronic spectra of **1** (solid line) and **2** (dashed line) in dichloromethane.

Two discrete stages of the protonation of **1** in chloroform have been demonstrated (−50 °C). The addition of the first proton to the outer nitrogen has been confirmed by the downfield shift of the 2-NH resonance (δ = 16.670) of $(1\text{-H})^+$ (Scheme 1 and Fig. 2B). The second titration step $(1\text{-H}_2)^{2+}$ completely protonates the inner nitrogens (δ = 2.034, 1.877, 1.611).

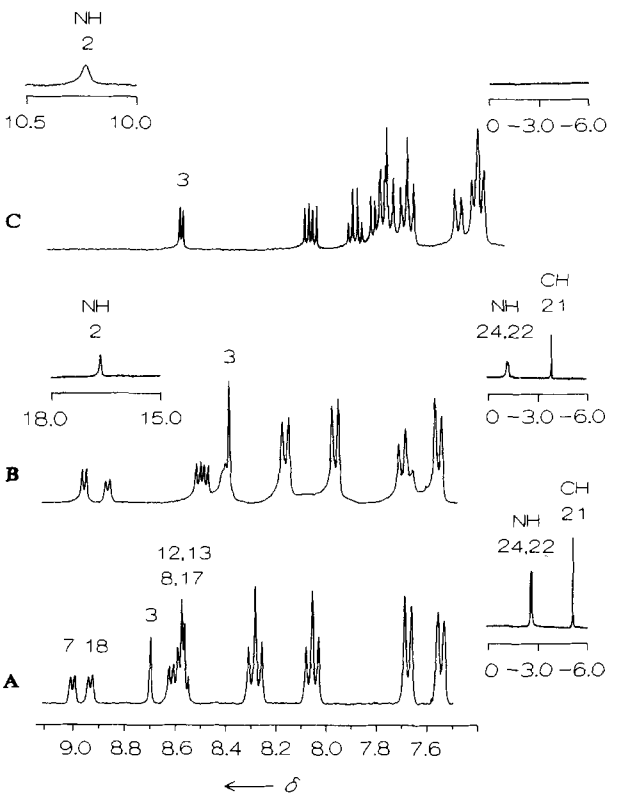


Fig. 2. The ^{1}H NMR spectra (300 MHz) (selected downfield and upfield regions presented) of **1** in $CDCl_3$ at −50 °C (A) $(1\text{-H})^+$ in $CDCl_3$ containing 2 equiv CF_3COOH(B), and **2** in CD_2CL_2 at 20 °C (C). Resonance assignments follow the systematic numbering of porphyrin positions.

The insertion of nickel (II) ions into **1** under mild conditions results in the formation of $[Ni^{II}(CTTP)]$ (**2**). The electronic spectrum of **2** contains features expected for metalloporphyrins (see Fig. 1). The ^{1}H NMR spectrum of the diamagnetic species **2** (Fig. 2C), resembles that of $(1\text{-H}_2)^{2+}$. The 2-NH proton (δ = 10.208, CD_2Cl_2, 20 °C) is spin-spin-coupled to 3-H (δ = 8.553) and exchangeable for deuterium of D_2O. The most notable feature of the nickel (II) complex **2** is coordination through the unprotonated β-carbon in the equatorial plane deduced from the disappearance of the 21-H resonance in the ^{1}H NMR spectrum of **2**. This observation implies unusual labilization of the inner C–H bond.

The structure of **2** was determined by X-ray crystallography (Fig. 3).[8] The average distances of Ni···N and Ni···C of 1.955(3) and 1.963(3) Å are comparable to the Ni···N distances in the nearly planar $[Ni^{II}(OEP)]$ derivative (1.958(2) Å, OEP = octaethylporphyrin dianion),[9] and are in the range of Ni^{II}–C bond lengths (1.87–1.97 Å).[10]

 © VCH Verlagsgesellschaft mbH, D-69451 Weinheim, 1994 0570-0833/94/0707-0780 $ 10.00+.25/0

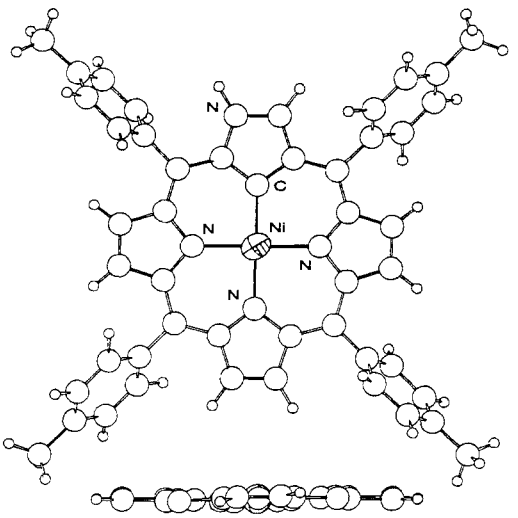
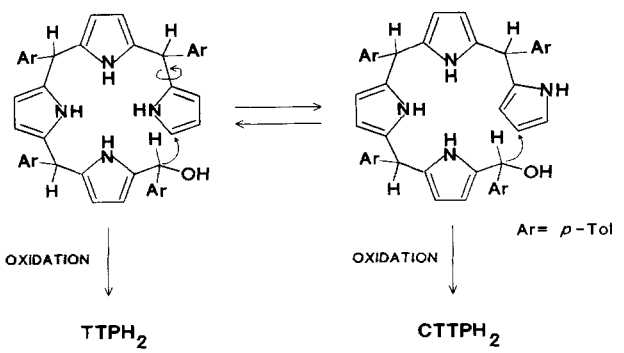


Fig. 3. Crystal structure of **2** (top). A projection emphasizing the planar nature of **2** (bottom). Phenyl groups are omitted from the side view for clarity. Only one of eight possible forms is shown.

To summarize, the typical pyrrole–arylaldehyde condensation provides a convenient access to the new family of core-modified porphyrins exemplified here by a tetra-*p*-tolylporphyrin containing one inverted pyrrole ring. This „carbaporphyrin" is structurally different from the other isomer, porphycene.[11]

For the mechanism of carbaporphyrin formation we suggest that two helical conformations of tetrapyrromethane differing only by a single 180 °C rotation of the terminal pyrrole ring around the *α-meso* carbon bond contribute in the porphyrinogen ring closure.[5, 12–14]. They provide two optimal orientations for the macrocyclic ring closure at the pyrrole α- or β-positions, both susceptible to electrophilic attack[5, 12–14] to afford regular or inverted porphyrinogen, and on oxidation of it, $TTPH_2$ or inverted $CTTPH_2$, respectively.



Experimental procedure

The condensation of *p*-tolylaldehyde (40 mmol) and pyrrole (70 mmol) in dichloromethane (1L) catalyzed by $BF_3 \cdot Et_2O$ (8 mmol), conducted over 1 h under nitrogen at room temperature, followed by oxidation with *p*-chloranil (8 g) carried out under reflux for 1 h, produced a mixture of $TTPH_2$ and **1** (4:1 molar ratio). The solution was evaporated to dryness, and the solid material subjected to chromatography on basic Al_2O_3 to remove tar products. The crude porphyrin products were eluted with dichloromethane. Small amount of basic Al_2O_3 was added to the solution, followed by removal of solvent by rotary evaporation. The solid material was deposited on the top of a column packed with basic Al_2O_3 and eluted with tetrachloromethane. The first eluted band contained $TTPH_2$. The second brown band of **1** was eluted with tetrachloromethane/dichloromethane (4/1 v/v). The fraction containing **1** was evaporated to dryness, and the product recrystallized from benzene/methanol to give **1** in 4% yield (0.27 g). Only a trace amount (less than 1% of the overall macrocycle crop) of **1** can be detected by ^1H NMR in the tail of the $TTPH_2$ chromatographic band if a 1:1 pyrrole/*p*-tolyladehyde molar ratio is used, as typical in the $TTPH_2$ synthesis described by Lindsey et al.[5].

Insertion of nickel(II): A mixture of **1** (0.12 mM) in $CHCl_3$ was heated at reflux with an ethanolic solution of $NiCl_2 \cdot 6H_2O$ (1.2 mM) for 0.5 h. After evaporation of the solution, the residue was subjected to chromatography on silica with dichloromethane as an eluent. The first green band was collected, and the solvent removed. The product Ni^{II} (CTTP) (**2**, 40% yield) was recrystallized from pyridine.

Received: November 23, 1993 [Z 6506 IE]
German version: *Angew. Chem.* **1994**, *106*, 805

[1] P. Rothemund, *J. Am. Chem. Soc.* **1936**, *58*, 625; *ibid.* **1939**, *61*, 2912.
[2] A. D. Adler, F. R. Longo, W. Shergalis, *J. Am. Chem. Soc.* **1964**, *86*, 3145; A. D. Adler, F. R. Longo, J. D. Finarelli, J. Goldmacher, J. Assour, L. Korsakoff, *J. Org. Chem.* **1967**, *32*, 476; A. D. Adler, L. Sklar, F. R. Longo, J. D. Finarelli, M. G. Finarelli, *J. Heterocycl. Chem.* **1968**, *5*, 669.
[3] D. Dolphin, *J. Heterocycl. Chem.* **1970**, *7*, 275.
[4] A. M. d'A. Rocha Gonsalves, M. M. Pereira, *J. Heterocycl. Chem.* **1985**, *22*, 931; A. M. d'A. Rocha Gonsalves, J. M. T. B. Varejão, M. M. Pereira, *ibid.* **1991**, *28*, 635.
[5] J. S. Lindsey, H. C. Hsu, I. C. Schreiman, *Tetrahedron Lett.* **1986**, *27*, 4969; J. S. Lindsey, I. C. Schreiman, H. C. Hsu, P. C. Kearney, A. M. Marguerettaz, *J. Org. Chem.* **1987**, *52*, 827; J. S. Lindsey, R. W. Wagner, *ibid.* **1989**, *54*, 828.
[6] D. M. Wallace, K. M. Smith, *Tetrahedron Lett.* **1990**, *31*, 7265.
[7] L. Latos-Grażyński, J. Lisowski, M. M. Olmstead, A. L. Balch, *J. Am. Chem. Soc.* **1987**, *109*, 4428.
[8] Dark-brown bricks of **2** were grown directly in the NMR tube by the slow evaporation of CD_2CCl_2 after the identity of **2** was confirmed with ^1H NMR spectroscopy. The crystals belong the to the monoclinic space group $P2_1/c$ (no. 14) with $a = 14.151(4)$, $b = 8.600(3)$, $c = 15.727(4)$ Å, $\beta = 95.19(3)$°, $Z = 2$ at 20 °C. Refinement of 3228 reflections with $I > 4\sigma(I)$ and 241 parameters gave $R = 0.058$. There is a center of symmetry at the center of the macrocycle; hence the 21-C and 2-N atoms are disordered and not distinguishable in the X-ray structure. Further details of the crystal structure investigation are available on request from the Director of the Cambridge Crystallographic Data Centre, 12 Union Road, GB-Cambridge CB2 1EZ (UK) on quoting the full journal citation.
[9] D. R. Cullen, E. F. Meyer, Jr., *J. Am. Chem. Soc.* **1974**, *96*, 2095.
[10] P. W. Jolly in *Comprehensive Organometallic Chemistry Vol. 6* (Eds.: G. Wilkinson, F. G. A. Stone, E. W. Abel), Pergamon, Oxford, **1982**, p. 37.
[11] E. Vogel, M. Köcher, H. Schmickler, J. Lex, *Angew. Chem.* **1986**, *98*, 262; *Angew. Chem. Int. Ed. Engl.* **1986**, *25*, 257.
[12] a) B. Franck, *Angew. Chem.* **1982**, *92*, 327; *Angew. Chem. Int. Ed. Engl.* **1982**, *21*, 343; b) K.-H. Schumacher, B. Franck, *ibid.* **1989**, *101*, 1292 and **1989**, *28*, 1243.
[13] A. R. Battersby, M. G. Baker, H. A. Broadbent, J. R. Fookes, F. J. Leeper, *J. Chem. Soc. Perkin Trans. 1* **1987**, 2027.
[14] A. R. Battersby, F. J. Leeper, *Chem. Rev.* **1990**, *90*, 1261.

Synthesis of the Anthraquinone Framework of Dynemicin A**

K. C. Nicolaou,* Jonathan L. Gross, Michael A. Kerr, Robert H. Lemus, Kiyoshi Ikeda, Kouichi Ohe

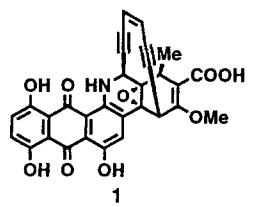
Dynemicin A (**1**), a naturally occurring enediyne anticancer antibiotic, is characterized by a unique molecular architecture and an interesting biological profile.[1] Dynemicin's antibiotic and antitumor activities stem from its ability to generate, upon in vivo activation, benzenoid diradicals that damage DNA.[1–3] Numerous efforts directed towards the total synthesis of **1** and

[*] Professor Dr. K. C. Nicolaou, J. L. Gross, M. A. Kerr, R. H. Lemus, K. Ikeda, K. Ohe
Department of Chemistry, The Scripps Research Institute
10666 N. Torrey Pines Road, La Jolla, CA 92037 (USA)
and
Department of Chemistry, University of California, San Diego
9500 Gilman Drive, La Jolla, CA 92093 (USA)

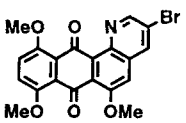
[**] We thank The Scripps Research Institute and the National Institutes of Health, USA for financial support. JLG thanks Pfizer, Inc., USA for a Predoctoral Fellowship (1992-93).

 © VCH Verlagsgesellschaft mbH, D-69451 Weinheim, 1994 0570-0833/94/0707-0781 $ 10.00+.25/0

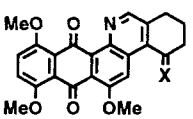
towards various model systems and biological mimics have been reported.[2, 4] Particularly impressive are Schreiber's recent advances in the field, which include the construction of the angular anthraquinone **2**[5] and of methylated forms of the natural product.[6] In this communication we report our synthesis of dynemicin A polycyclic frameworks, compounds **3** and **4**, by chemistry that should serve as a prelude to a projected total synthesis of the naturally occurring compound.



1

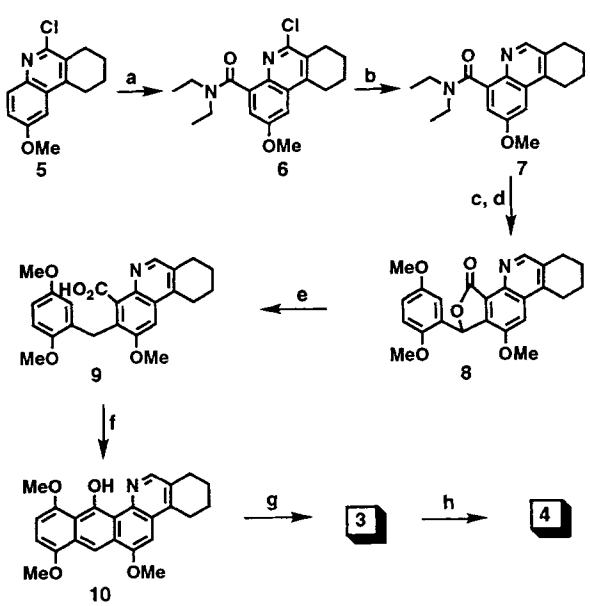


2



3: X = H_2; **4**: X = O

The synthesis of the target compounds **3** and **4** began with the tricyclic intermediate **5**[7] (Scheme 1). Thus regioselective metalation of compound **5** with *sec*-BuLi in the presence of *N*,*N*,*N*′,*N*′-tetramethyl-1,2-ethanediamine (TMEDA) followed by quenching with diethylcarbamoyl chloride gave diethyl amide **6** in 84% yield. The chloro substituent was then reductively removed from **6** by hydrogenolysis of the carbon–chlorine bond with Pd/C and hydrogen to yield quinoline derivative **7** in 92% yield. A second metalation[8] of quinoline **7** at the available position adjacent to the amide side chain, and facilitated by it, followed by addition of 2,5-dimethoxybenzaldehyde and subsequent exposure to *p*-toluenesulfonic acid (TsOH) at 110 °C furnished the γ-lactone **8** in 65% overall yield. In preparation for the construction of the final ring of the desired anthraquinone skeleton, the γ-lactone was reductively opened by treatment of compound **8** with Zn dust in 10% aqueous NaOH solution at reflux, which resulted in the smooth formation of carboxylic acid **9** by cleavage of the benzylic C–O bond (98% yield). Finally, ring closure of the carboxylic acid group in **9** onto the dimethoxy aromatic ring under the influence of trifluoroacetic anhydride, followed by treatment with base, furnished the pentacyclic system **10** in 93% yield. The oxidation of **10** with Jones reagent at 0 °C led to the anthraquinone system **3** (58% yield). Compound **3** could be oxidized further to the keto derivative **4** by prolonged treatment with CrO_3 in acetic acid (50% yield).



Scheme 1. Synthesis of the pentacyclic anthraquinone compounds **3** and **4**. Reagents and conditions: a) 1.2 equiv TMEDA, 1.15 equiv *s*BuLi, THF, −78 °C, 1 h, then 1.15 equiv diethylcarbamoyl chloride, 25 °C, 16 h, 84%; b) H_2, 10% Pd on charcoal, 1.0 equiv KOH, EtOH, 25 °C, 24 h, 92%; c) 1.2 equiv TMEDA, 1.15 equiv *s*BuLi, −78 °C, 1 h, then 1.15 equiv 2,5-dimethoxybenzaldehyde, 25 °C, 16 h; d) 0.1 equiv TsOH, toluene, 110 °C, 6 h, 65%; e) 5.0 equiv Zn dust, excess of NaOH, H_2O, 100 °C, 8 h, 98%; f) 3.0 equiv trifluoroacetic anhydride, CH_2Cl_2, 0 °C, 2 h, 93%; g) excess of Jones reagent, acetone, 0 °C, 2 h, 58%; h) excess of CrO_3, acetic acid, 25 °C, 24 h, 50%.

The reported chemistry represents a facile entry into anthraquinone systems and culminates in the rapid assembly of pentacyclic frameworks relevant to the total synthesis of the enediyne anthraquinone antibiotic dynemicin A (**1**). Thus, combining this strategy with that already reported for the enediyne segment of **1** should open a viable route to advanced dynemicin A systems and to the natural product itself. Furthermore, the synthesized molecules **3** and **4** are quite interesting in their own right as potential intercalating agents to double stranded DNA and as useful biological tools.[9, 10]

Received: November 11, 1993
Revised: December 6, 1993 [Z 6492 IE]
German version: *Angew. Chem.* **1994**, 106, 790

[1] M. Konishi, K. Matsumoto, T. Tsuno, H. Kanei, T. Miyaki, T. Oki, H. Kawaguchi, G. D. VanDuyne, J. Clardy, *J. Antibiot.* **1989**, *42*, 1449; M. Konishi, H. Ohkuma, T. Tsuno, T. Oki, G. D. VanDuyne, J. Clardy, *J. Am. Chem. Soc.* **1990**, *112*, 3715; Y. Sugura, T. Shiraki, M. Konishi, T. Oki, *Proc. Natl. Acad. Sci. USA* **1990**, *87*, 3831; T. Shiraki, Y. Sugiura, *Biochemistry* **1990**, *29*, 9795.

[2] Reviews: a) K. C. Nicolaou, W.-M. Dai, *Angew. Chem.* **1991**, *103*, 1453; *Angew. Chem. Int. Ed. Engl.* **1991**, *30*, 1387; b) K. C. Nicolaou, A. L. Smith, *Acc. Chem. Res.* **1993**, *25*, 497; c) K. C. Nicolaou, A. L. Smith, E. W. Yue, *Proc. Natl. Acad. Sci. USA* **1993**, *90*, 5881.

[3] R. G. Bergman, *Acc. Chem. Res.* **1973**, *6*, 25.

[4] J. A. Porco, Jr., F. J. Schoenen, T. J. Stout, J. Clardy, S. L. Schreiber, *J. Am. Chem. Soc.* **1990**, *112*, 7410; K. C. Nicolaou, C.-K. Hwang, A. L. Smith, S. V. Wendeborn, *ibid.* **1990**, *112*, 7416; P. A. Wender, C. K. Zercher, *ibid.* **1991**, *113*, 2311; P. Magnus, S. M. Fortt, *J. Chem. Soc. Chem. Commun.* **1991**, 544; J. L. Wood, J. A. Porco, J. Taunton, A. Y. Lee, J. Clardy, S. L. Schreiber, *J. Am. Chem. Soc.* **1992**, *114*, 5898.

[5] H. Chikashita, J. A. Porco, T. J. Stout, J. Clardy, S. L. Schreiber, *J. Org. Chem.* **1991**, *56*, 1692.

[6] J. Taunton, J. L. Wood, S. L. Schreiber, *J. Am. Chem. Soc.* **1993**, *115*, 10378.

[7] K. C. Nicolaou, P. Maligres, T. Suzuki, S. V. Wendeborn, W.-M. Dai, R. K. Chadha, *J. Am. Chem. Soc.* **1992**, *114*, 8890.

[8] V. Snieckus, *Chem. Rev.* **1990**, *90*, 879; P. Blake, R. A. Brown, *J. Org. Chem.* **1982**, *47*, 34.

[9] All new compounds exhibited satisfactory spectral and analytical and/or exact mass data. Yields refer to chromatographically and spectroscopically homogeneous materials.

[10] Selected physical and spectroscopic data for compounds **8**–**10**, **3** and **4**. **8**: R_f = 0.53 (silica, ethyl acetate); IR ($CDCl_3$): $\tilde{\nu}_{max}$[cm^{-1}] = 1763 (C=O); ^{1}H NMR (400 MHz, $CDCl_3$): δ = 8.77 (s, 1H), 7.33 (s, 1H), 6.77–6.88 (m, 3H), 6.37 (d, *J* = 2.6 Hz, 1H), 3.83 (s, 3H), 3.82 (s, 3H), 3.61 (s, 3H), 3.05–3.14 (m, 2H), 2.94 (br t, *J* = 5.9 Hz, 2H), 1.88–2.02 (m, 4H); ^{13}C NMR ($CDCl_3$): δ = 168.8, 153.4, 152.4, 152.0, 151.9, 144.2, 144.14, 137.7, 131.3, 130.0, 124.3, 123.2, 115.1, 114.1, 112.7, 106.6, 75.2, 56.7, 55.9, 55.7, 27.2, 25.6, 22.3, 22.0; MS: *m*/*z* (*M*$^+$) calcd 428.1474, found 428.1461. **9**: R_f = 0.54 (silica, 10% methanol in ethyl acetate: 1% acetic acid); IR ($CDCl_3$): $\tilde{\nu}_{max}$[cm^{-1}] = 1699 (C=O); ^{1}H NMR (400 MHz, [D$_6$]DMSO): δ = 8.46 (s, 1H), 7.28 (s, 1H), 6.85 (d, *J* = 8.8 Hz, 1H), 6.66 (d, *J* = 8.8, 3.1 Hz, 1H), 6.10 (br s, 1H), 3.98 (s, 2H), 3.83 (s, 3H), 3.79 (s, 3H), 3.49 (m, 3H), 3.07 (br t, *J* = 6.2 Hz, 2H), 2.85 (br t, *J* = 5.1 Hz, 2H), 1.80–1.91 (m, 4H); ^{13}C NMR ([D$_6$]DMSO): δ = 169.5, 155.7, 152.4, 150.9, 149.4, 139.7, 138.3, 129.8, 128.9, 126.9, 115.2, 110.7, 109.8, 101.0, 55.9, 55.0, 27.2, 26.5, 24.5, 21.9, 21.8, 20.9; MS: *m*/*z* (*M*$^+$)

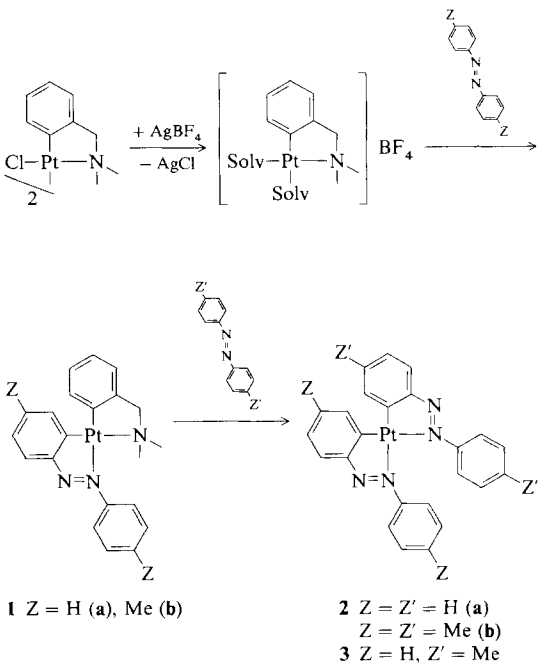
calcd 408.1811, found 408.1825. **10**: $R_f = 0.65$ (silica, diethyl ether); IR ($CDCl_3$): $\tilde{\nu}_{max}$[cm^{-1}] = 1621; ^{1}H NMR (400 MHz, $CDCl_3$): δ = 8.56 (s, 1H), 8.27 (s, 1H), 6.80 (d, J = 8.4 Hz, 1H), 6.76 (d, J = 8.4 Hz, 1H), 6.72 (s, 1H), 4.09 (s, 3H), 4.08 (s, 3H), 4.04 (s, 3H), 3.02 (br t, J = 6.2 Hz, 2H), 2.92 (br t, J = 6.2 Hz, 2H), 1.94–2.01 (m, 2H), 1.85–1.91 (m, 2H); ^{13}C NMR ($CDCl_3$): δ = 159.2, 155.1, 152.4, 149.5, 143.5, 141.2, 140.9, 130.0, 128.0, 126.1, 125.3, 115.8, 111.5, 103.9, 103.8, 103.7, 94.5, 56.7, 55.8, 55.5, 27.1, 25.8, 22.6, 22.1; MS: m/z (M^+) calcd 390.1705, found 390.1715. **3**: $R_f = 0.50$ (silica, 10% methanol in ethyl acetate); IR ($CDCl_3$): $\tilde{\nu}_{max}$[cm^{-1}] = 1682 (quinone); ^{1}H NMR (400 MHz, $CDCl_3$): δ = 8.76 (s, 1H), 7.37 (s, 1H), 7.14 (s, 2H), 4.05 (s, 3H), 3.94 (s, 6H), 3.00 (br t, J = 6.2 Hz, 2H), 2.88 (br t, J = 6.2 Hz, 2H), 1.94–2.02 (m, 2H), 1.85–1.92 (m, 2H); ^{13}C NMR ($CDCl_3$): δ = 185.3, 183.4, 154.4, 153.0, 151.6, 151.4, 139.4, 137.7, 132.0, 131.7, 126.8, 125.5, 124.9, 118.1, 118.0, 110.2, 106.4, 56.8, 56.7, 56.3, 27.1, 25.0, 22.2, 21.9; HR MS (FAB) m/z (M^+) calcd 404.1498, found 404.1515. **4**: $R_f = 0.50$ (silica, 10% methanol in ethyl acetate); IR ($CDCl_3$): $\tilde{\nu}_{max}$[cm^{-1}] = 1680 (C=O); ^{1}H NMR (400 MHz; $CDCl_3$): δ = 9.14 (s, 1H), 9.06 (s, 1H), 7.18 (s, 2H), 4.11 (s, 3H), 3.97 (s, 3H), 3.96 (s, 3H), 3.15 (br t, J = 6.0 Hz, 2H), 2.84 (br t, J = 6.0 Hz, 2H), 2.24–2.33 (m, 2H); ^{13}C NMR ($CDCl_3$): δ = 200.5, 184.9, 183.0, 156.7, 153.1, 151.7, 139.9, 139.5, 134.9, 132.1, 129.7, 128.4, 126.9, 125.3, 118.3, 118.2, 110.2, 56.9, 56.8, 56.5, 40.9, 28.0, 22.6; HR MS (FAB) m/z (M^+) calcd 418.1291, found 418.1308.

An Easy Route to Homo- and Heteroleptic Biscycloplatinated Complexes without Recourse to Organolithium Compounds**

Alexander D. Ryabov* and Rudi van Eldik

Cycloplatination reactions are characterized by a diversity of mechanisms for C–H bond cleavage[1] on one hand, and low yields of platinacycles formed[2] on the other. Moreover, certain types of complexes, such as *cis*-[Pt(C ~ N)$_2$], have not yet been prepared by metalation of C–H bonds. These homoleptic species were obtained by lithiation of organic ligands followed by interaction with the appropriate platinum(II) derivatives.[3] The synthesis of heteroleptic species of the type *cis*-[Pt(C ~ N)(C* ~ N)] is even more laborious.[4] Such homo- and heteroleptic complexes exhibit remarkable stereochemistry,[5] photochemistry, and chemical reactivity,[3] but the synthetic difficulties limit their wide use.

We report here on facile cycloplatinations through C–H bond cleavage leading to both homo- and heteroleptic complexes, as well as on novel exchange of cycloplatinated ligands, similar to that observed in palladium(II) complexes.[6] The platination of C–H bonds is expected to be easier when promoted by abstraction of the chloro ligands by $AgNO_3$.[7] We have found that it is even more advantageous to use $AgBF_4$ instead of $AgNO_3$. The role of the silver salts is obvious: they create coordinative unsaturation at platinum(II) and thus increase the electrophilicity of the metal center. Naturally, higher efficiency is anticipated with a poorly coordinating anion, BF_4^-, as Ag^+ counterion. The principal results are shown in Scheme 1. A solution of the chloro-bridged diplatinum complex $[Pt(C_6H_4CH_2NMe_2)Cl]_2$[8] in CH_2Cl_2 or C_6H_6 was treated with $AgBF_4$ dissolved in acetone. Addition of azobenzene, after filtering off AgCl, triggered a reaction which occurred readily at 25–50 °C. The main products are *cis* complexes **1a** and **2a**. When using 4,4′-azotoluene, the corresponding complexes **1b** and **2b** were isolated. The $^3J_{Pt,H}$ coupling constants clearly show that *cis* species are formed under these conditions.[9a] Such complexes usually have *cis* geometry,[3] but *trans* compounds are also known.[9] Complexes **1** and, in particular, **2** display properties typical of biscycloplatinated compounds.[3] Their UV/VIS spectra contain many bands, and in addition, **2a** shows fluorescence in CH_2Cl_2 at room temperature with a maximum at 359 nm when excited with light with wavelength λ = 254 nm.



Scheme 1. A new route to homo- and heteroleptic monomeric biscycloplatinum complexes.

The data in Figure 1 suggest that complex **1a** is formed first and is then converted into **2a**, a novel example for the exchange of cyclometalated ligands in platinum(II) complexes. It illustrates an easy way to the heteroleptic biscycloplatinated compounds, since the primary product **1a**, if treated with a ligand other than azobenzene, could afford the heteroleptic complex after dissoci-

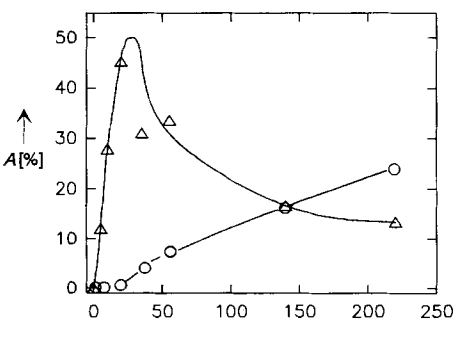


Fig. 1. The course of the formation of **1a** (Δ) and **2a** (O) from [Pt(C$_6$H$_4$CH$_2$NMe$_2$)(Solv)$_2$]BF$_4$ and azobenzene in C_6H_6/acetone (1:1 v/v) at 50 °C monitored by UV/VIS spectroscopy; [Pt(II)] = [azobenzene] = 1.09×10^{-2} M.

[*] Prof. A. D. Ryabov,[+] Prof. R. van Eldik
Institut für Anorganische Chemie der Universität Witten/Herdecke
Stockumer Strasse 10, D-58453 Witten (FRG)

[+] Permanent address:
Division of Chemistry, G. V. Plekhanov Russian Economic Academy
Stremyanny per. 28, 113054, Moscow (Russia)

[**] We are grateful to Prof. Paul S. Pregosin for his persistent advice to test the use of silver salts in these systems and to R. Wimmer for experiments with proton scavengers. A stipend (1991–1993) from the Alexander von Humboldt Foundation for ADR is gratefully acknowledged.

ation of *N*,*N*-dimethylbenzylamine. We attempted to carry out this transformation by treating **1a** with 4,4′-azotoluene under exactly the same conditions: in CH_2Cl_2/acetone or C_6H_6/acetone mixtures at 50 °C. Surprisingly, there was no exchange. Assuming that there was a catalytic process, we tried unsuccessfully to induce the reaction by addition of $AgBF_4$, $[Pt(C_6H_4CH_2NMe_2)Cl]_2$, or both to the reaction mixture. What was then responsible for the exchange? The analogy with the palladium(II) reactions helped to solve the problem.[6] The first cycloplatination to form **1** from the solvento complex (Scheme 1) must generate a strong acid, HBF_4, which in turn is able to cleave the more basic dimethylaminomethylbenzenido ligand of **1**, as does acetic acid as cosolvent in related palladium(II) complexes.[10] Since the acid anion is noncoordinating, the product $[Pt(C_6H_4N{=}NPh)(Solv)_2]BF_4$ is able to cyclometalate the next azobenzene molecule to form **2**.

If this rationalization is correct, the following two processes must occur: Firstly, strong acids with noncoordinating anions should induce the conversion of **1** into **2** and, secondly, heteroleptic compounds could be generated under the same conditions as in Scheme 1 from the cycloplatinated azobenzene dimer $[Pt(C_6H_4N{=}NPh)Cl]_2$.[11] We were, in fact, able to carry out both these reactions. The exchange, achieved by addition of stoichiometric amounts of F_3CSO_3H to the mixture of **1a** and 4,4′-azotoluene, and direct cycloplatination of the same ligand by the solvento complex derived from $[Pt(C_6H_4N{=}NPh)Cl]_2$ gave the identical heteroleptic complex **3**.

One of the referees of this paper raised the question whether it is possible to preclude the formation of **2** by addition of a "proton sponge" to the reaction mixture. Therefore, 1,8-bis(dimethylamino)naphthalene or 2,6-di-*tert*-butylpyridine was added to the solvento species to bind the acid liberated in subsequent reaction with azobenzene. However, these nitrogen ligands themselves react instantaneously with $[Pt(C_6H_4CH_2NMe_2)(Solv)_2]BF_4$ affording dark brownish complexes. No attempt was made to characterize these species.

The formation of homoleptic complexes **2** from the *N*,*N*-dimethylaminomethylbenzenide complex (Scheme 1) is a unique example of "suicidal" cyclometalation, since the activation of C–H bonds by electrophilic substitution generates a strong acid which then "kills" the more basic ligand of the primary product **1**. Azobenzenes are less basic than tertiary amines, and this makes complexes **2** and **3** more resistant to small concentrations of strong acids. The exchange reaction resembles processes that are well-known in palladium(II) chemistry.[6] The principal difference is that the exchange reactions of the platinum complexes involve monomeric biscycloplatinum complexes of the type [Pt(C ~ N)(C* ~ N)]. In the palladium(II) case, however, exclusively monometalated dimeric complexes of the type [Pd(C ~ N)X]$_2$, in which only organic ligand is bound to the metal center, participate. Related monometalated platinum(II) dimers are insufficiently labile to undergo the proton-induced exchange and react with azobenzenes in a different way.[12] The Pt–C bond of one platinacycle is needed to increase the lability of the other cycloplatinated leaving ligand toward proton attack. We have recently shown that the kinetic labilization brought about by orthoplatination (that is, labilization by the Pt–C bond *trans* to the leaving ligand) increases the reactivity by four orders of magnitude, with the result that the anation rate of platinum(II) complexes reaches that of analogous [Pd(dien)] complexes.[13] In the present case, the Pt–C bond of azobenzene labilizes the *trans*, Pt–N bond of the leaving dimethylaminomethylbenzenido ligand. The corresponding Pt–C bond becomes less stabilized by chelation and is easily cleaved by the acid.

Experimental Procedure

The typical procedure was as follows: the solution of $[Pt(C_6H_4CH_2NMe_2)Cl]_2$ (0.080 mmol) in CH_2Cl_2 (1.5 mL) was mixed with $AgBF_4$ (0.164 mmol) dissolved in acetone (1 mL); AgCl was removed, and azobenzene (0.170 mmol) was added. The mixture was kept for 18 min at 30 °C, then cooled in ice, and the products were separated by preparative TLC (SiO_2, C_6H_6). If the goal is the isolation of **1**, as in this example, TLC operations must be carried out fast. Azobenzene is eluted first, then **2a** (brown band) followed by **1a** (orange). The products were washed off with $CHCl_3$ and recrystallized from $EtOH/H_2O$ after removal of the solvent. A brownish red material that was difficult to elute from SiO_2 was always present. Its ^1H NMR spectrum showed a mixture of compounds which was not investigated further. Yields: **1a** 53%, **2a** 7%. Satisfactory C,H,Pt analyses were obtained;

1a: ^1H NMR ($CDCl_3$): $\delta = 2.41$ (s, $^3J(Pt,H) = 16.1$ Hz, NCH_3), 3.85 (s, $^3J(Pt,H) = 20.4$ Hz, NCH_2), 7.06 (t, H4 ("dimethylbenzylamine", dmba)), 7.12 (d, H3 (dmba)), 7.20 (t, H5 (dmba)), 7.21 (td, H4 ("azobenzene", azb)), 7.34 (td, H5 (azb)), 7.45 (t, H4′(azb)), 7.51 (d, H2′,6′(azb)), 7.56 (t, H3′,5′ (azb)), 8.00 (d, $^3J(Pt,H) = 53.0$ Hz, H6(azb)), 8.02 (d, $^3J(Pt, H) = 53.5$ Hz, H6 (dmba)), 8.02 (dd, H3 (azb)); IR (KBr): $\tilde{\nu} = 699$, 769 (monosubstituted azb ring), 721 (1,2-disubstituted azb ring), 742 cm^{-1} (1,2-disubstituted dmba ring)[12]; UV/VIS (CH_2Cl_2): λ_{max} (ε[$M^{-1}cm^{-1}$]) = 474 (5300), 394 (4250), 334 (8500) nm. – **2a**: ^1H NMR: $\delta = 7.01$ (t, H3′,5′), 7.11 (t, H4′), 7.31 (t, H4), 7.49 (d, H2′,6′), 7.50 (t, H5), 8.13 (d, H3), 8.21 (d, $^3J(Pt,H) = 47.3$ Hz, H6); IR: $\tilde{\nu} = 691$, 762 (monosubstituted ring), 718 cm^{-1} (1,2-disubstituted ring); UV/VIS λ_{max} (ε) = 600sh, 513 (6900), 377 (16000), 337 (15100), 317 (14700), 284 (19400), 251 (19700) nm. – **1b**: ^1H NMR: $\delta = 2.41$ (s, CCH_3), 2.43 (s, NCH_3), 2.45 (s, CCH_3), 3.85 (s, $^3J(Pt,H) = 20.05$ Hz, NCH_2), 6.99 (d, H4 ("azotoluene", azt)), 7.06 (t, H4 (dmba)), 7.12 (d, H3 (dmba)), 7.22 (t, H5 (dmba)), 7.32 (d, H3′,5′ (azt)), 7.40 (d, H2′,6′(azt)), 7.78 (s, $^3J(Pt,H) = 54.4$ Hz, H6 (azt)), 7.87 (d, H3 (azt)), 8.01 (d, $^3J(Pt,H) = 45.39$ Hz, H6(dmba)); IR: $\tilde{\nu} = 741$ (1,2-disubstituted dmba ring), 804, 820, 844 cm^{-1}(azt); UV/VIS: λ_{max} (ε) = 454 (5100), 342 (9700), 281 (12000) nm. – **2b**: ^1H NMR: $\delta = 2.26$ (s, CCH_3), 2.52 (s, CCH_3), 6.78(d, H3′,5′), 7.10 (d, H4), 7.32 (d, H2′,6′), 7.97 (d, H3), 7.97 (s, $^3J(Pt,H) = 48.6$ Hz, H6); IR: $\tilde{\nu} = 805$, 820 cm^{-1}; UV/VIS: λ_{max} (ε) = 597 (2350), 510 (7800), 393 (21000), 359 (18600), 325 (22900), 289 (23200), 259 (22200) nm. – **3**: ^1H NMR: $\delta = 2.24$ (s, CCH_3), 2.52 (s, CCH_3), 6.76 (d, H3′,5′ (azt)), 7.00 (t, H3′,5′ (azb)), 7.10 (d, H4 (azt)), 7.11 (t, H4′ (azb)), 7.31 (t, H5 (azb)), 7.34 (d, H2′,6′ (azt)), 7.46 (d, H2′,6′ (azb)), 7.51 (td, H4 (azb)), 7.98 (s; $^3J(Pt,H) = 49.1$ Hz, H6 (azt)), 7.98 (d, H3 (azt)), 8.14 (dd, H3 (azb)), 8.20 (d, $^3J(Pt,H) = 46.6$ Hz, H6 (azb)); IR: $\tilde{\nu} = 692$, 766 (monosubstituted azb ring), 718 (1,2-disubstituted azb ring), 823 cm^{-1} (azt); UV/VIS: λ_{max} (ε) = 590sh, 512 (3600), 387 (8700), 359 (8500), 322 (9000), 286 (10500), 257 (10100) nm.

The data shown in Figure 1 were obtained from samples (0.10 mL) withdrawn intermittantly from the reaction mixture and purified on Merck silica gel 5 × 10 cm aluminium sheets for TLC (eluted with benzene). The brown and orange bands of **2a** and **1a**, respectively, were cut out, the products washed off with $CHCl_3$, and their concentrations determined by UV/VIS spectroscopy.

Received: May 8, 1993
Revised version: December 1, 1993 [Z 6070 IE]
German version: *Angew. Chem.* **1994**, *106*, 798

[1] A. D. Ryabov, *Chem. Rev.* **1990**, *90*, 403–424.
[2] J. Dehand, M. Pfeffer, *Coord. Chem. Rev.* **1976**, *18*, 327–352; M. I. Bruce, *Angew. Chem.* **1977**, *89*, 75–84; *Angew. Chem. Int. Ed. Engl.* **1977**, *16*, 73–86; I. Omae, *Chem. Rev.* **1979**, *79*, 287–331.
[3] Review: M. Maestri, V. Balzani, C. Deuschel-Cornioley, A. von Zelewsky, *Adv. Photochem.* **1992**, *17*, 1–68.
[4] C. Deuschel-Cornioley, R. Lüönd, A. von Zelewsky, *Helv. Chim. Acta* **1989**, *72*, 377–382.
[5] C. Deuschel-Cornioley, H. Stoeckli-Evans, A. von Zelewsky, *J. Chem. Soc. Chem. Commun.* **1990**, 121–122.
[6] Review: A. D. Ryabov in *Perspectives in Coordination Chemistry* (Eds.: A. F. Williams, C. Floriani, A. E. Merbach), Verlag Helvetica Chimica Acta, Basel VCH, Weinheim, **1992**, pp. 271–292.
[7] P. S. Pregosin, F. Wombacher, A. Albinati, F. Lianza, *J. Organomet. Chem.* **1991**, *418*, 249–267.
[8] A. C. Cope, E. C. Friedrich, *J. Am. Chem. Soc.* **1968**, *90*, 909–913.
[9] a) G. Longoni, P. Fantucci, P. Chini, F. Canziani, *J. Organomet. Chem.* **1972**, *39*, 413–425; b) H.-P. Abicht, K. Issleib, *J. Organomet. Chem.* **1985**, *289*, 201–213.
[10] A. D. Ryabov, A. K. Yatsimirsky, H.-P. Abicht, *Polyhedron* **1987**, *6*, 1619–1620.
[11] A. C. Cope, R. W. Siekman, *J. Am. Chem. Soc.* **1965**, *87*, 3272–3273.
[12] A. D. Ryabov, L. G. Kuz'mina, N. V. Dvortsova, D. Stufkens, R. van Eldik, *Inorg. Chem.* **1993**, *32*, 3166–3174.
[13] M. Schmülling, A. D. Ryabov, R. van Eldik, *J. Chem. Soc. Chem. Commun.* **1992**, 1609–1611.

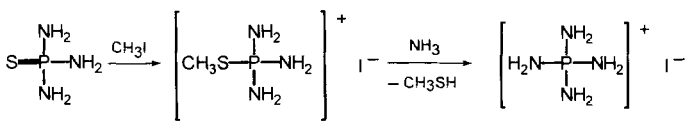
Synthesis and Crystal Structure of the First Tetraaminophosphonium Salt $P(NH_2)_4I$**

Wolfgang Schnick,* Stefan Horstmann, and Alfred Schmidpeter

Dedicated to Professor Otto J. Scherer on the occasion of his 60th birthday

The characteristic building blocks in phosphorus(v) nitrides are PN_4 tetrahedra. Linkage of these structural elements through common corners allows access to a large number of condensation degrees. This is reminiscent of the varied structural chemistry of the silicates and phosphates.[1] One of the extremes in the series of differently condensed phosphorus nitrides is the ionic compound Li_7PN_4, which comprises "isolated" PN_4^{7-} ions.[2] Due to its extremely high formal charge, no indications for the existence of this anion in solution have yet been found; therefore, Li_7PN_4 is accessible only by solid-state reaction of the corresponding binary nitrides. Thus, the certainly high synthetic potential of isolated PN_4 groups in solution for the formation of well-defined P–N solid compounds has remained unexplored.

The salt Li_7PN_4 is derived from the hypothetical acid H_7PN_4, which is suspected to be an unstable monophosphazene intermediate during ammonolysis of PCl_5.[3] However, due to its high basicity and tendency to undergo condensation reactions it has not yet proven possible to isolate imidophosphoric acid triamide, H_7PN_4. With $P(NH_2)_4I$ (**C**) we report the first successful synthesis and structural proof of a tetraaminophosphonium salt, which can be regarded as a hydroiodide of H_7PN_4. The synthesis followed the modification of a procedure[4] that starts from phosphorothionic triamide (**A**).[5] Methylation of the sulphur atom in **A** with methyl iodide and careful subsequent ammonolysis of **B** readily yields the desired product **C**. As the last



A **B** **C**

reaction step is a heterogeneous solid–liquid reaction, **C** is obtained as a sparingly-soluble, fine-crystalline powder. The crystal growth of tetraaminophosphonium iodide was severely hampered by the fact that **C** is insoluble in most solvents and that, due to its reactivity, it easily undergoes hydrolysis and condensation reactions. In the past methanol had been suggested as a solvent for **C**. However, according to our investigations prolonged exposure of **C** to methanol leads to the formation of tetramethylammonium iodide [Eq. (a)]. Sufficiently large single crystals of **C** were obtained by crystallization from dry acetonitrile employing a temperature gradient between 70 °C and room temperature. Obviously, tetraaminophosphonium iodide is sufficiently soluble at the higher temperature.

$$4P(NH_2)_4I + 4CH_3OH \longrightarrow (CH_3)_4NI + 4OP(NH_2)_3 + 3NH_4I \qquad (a)$$

[*] Prof. Dr. W. Schnick, Dipl.-Chem. S. Horstmann
Laboratorium für Anorganische Chemie der Universität
D-95440 Bayreuth (FRG)
Telefax: Int. code + (921)55-2531

Prof. Dr. A. Schmidpeter
Institut für Anorganische Chemie der Universität München (FRG)

[**] This work was supported by the Deutsche Forschungsgemeinschaft and the Fonds der Chemischen Industrie. We thank Dr. W. Milius, Universität Bayreuth, for help with and discussion of the X-ray structure analysis.

Unprecedented in chemistry, the acid–base pair $H_8PN_4^+$/PN_4^{7-} enables structural comparison over a range of eight successive dissociation steps: According to the results of the X-ray structure analysis,[6] $P(NH_2)_4^+$ and I^- ions form a CsCl-analogous arrangement in the solid. The P–N bond length (160.7(2) pm) (Fig. 1) represents the shortest P–NH_2 bond distance reported to date. The valence sum for the phosphorus center (5.56), calculated from the four P–N bonds according to O'Keeffe et al.,[7] is indicative of significant polar bonding or multiple bonds between the phosphorus and nitrogen atoms. The electrostatic repulsion between the nitrogen atoms in PN_4^{7-} (P–N: 171 pm[2]) is obviously compensated by the interaction between the nitrogen atoms and the terminal protons of the tetraaminophosphonium ion. This results in a marked shortening of the P–N bonds by approximately 10 pm. In accord with these short P–N bond lengths the H-N-H and H-N-P bond angles (114(3)° and 120(2)°, respectively) in the tetraaminophosphonium ion indicate a significant P–N double-bond character. Even though there are no N–H···N hydrogen bonds present between the cations, the NH_2 groups are fixed with regard to rotation around the P–N bonds. Accordingly, it was possible to locate the positions of the hydrogen atoms unambiguously[8] during X-ray structure analysis by difference-Fourier synthesis.

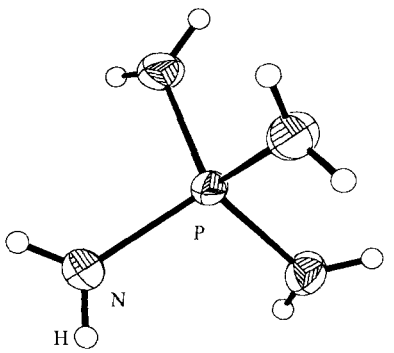


Fig. 1. Structure of the tetraaminophosphonium cation in $P(NH_2)_4I$. Distances [pm] and angles [°]: P–N 160.7(2), N–H 74.9(26), N-P-N 124.2(2) and 102.7(1), H-N-H 114(3), P-N-H 120(2).

Experimental Procedure

$SP(NH_2)_3$ (4.53 g, 0.04 mol) was treated with CH_3I (8.17 g, 0.06 mol) in dry acetonitrile (25 mL) for 6 days at room temperature. The resulting solid **B** (yield: 76%) was separated and washed with diethyl ether. ^{31}P NMR (36.9 MHz, $CDCl_3$, 25 °C): $\delta = 48.1$ (*s*). **B** (4.82 g, 0.02 mol) was suspended in 100 mL of dichloromethane and treated at room temperature (duration: 3 h) with a vigorous stream of NH_3 (KOH drying column). The resulting solid **C** was separated off and washed with diethyl ether (yield: 96%). For purification and crystal growth, 1.0 g of **C** in 25 mL acetonitrile was transferred to a Schlenk tube, and a temperature gradient (bottom: 70 °C, top: 25 °C) was applied to the supernatant. Coarse-crystalline, colorless **C** deposited at the cooler end. According to X-ray powder diffraction studies and ^{31}P NMR MAS measurements the product was obtained as a single phase. IR(KBr): $\tilde{\nu}$ [cm^{-1}] = 3378 (NH), 3280 (NH), 3097 (NH), 1078 (PN), 946 (PN). $T = 180$ °C (10^{-3} mbar, decomposition). All reactions were carried out in dry solvents under an inert argon atmosphere.

Received: November 9, 1993 [Z 6475 IE]
German version: *Angew. Chem.* **1994**, *106*, 818

[1] W. Schnick, *Angew. Chem.* **1993**, *105*, 846; *Angew. Chem. Int. Ed. Engl.* **1993**, *32* 806.
[2] W. Schnick, J. Lücke, *J. Solid State Chem.* **1990**, *87*, 101.
[3] M. Becke-Goehring, K. Niedenzu, *Chem. Ber.* **1957**, *90*, 2072.

[4] A. Schmidpeter, C. Weingand, *Angew. Chem.* **1968**, *80*, 234; *Angew. Chem. Int. Ed. Engl.* **1968**, *7*, 210.
[5] W. Schnick, *Z. Naturforsch. B* **1989**, *44*, 942.
[6] X-ray structure analysis of C: H_8PN_4I, $M = 221.9\,g\,mol^{-1}$, space group *P4/nbm*, $Z = 2$, $a = 842.6(2)$, $c = 486.7(2)$ pm, $V = 345.5 \times 10^6$ pm^3, $\rho_{calcd} = 2.133\,g\,cm^{-3}$, $F(000) = 208$, $\lambda = 71.073$ pm, $T = 173$ K, $\mu(Mo_{K\alpha}) = 4.76\,mm^{-1}$, Siemens P4 diffractometer, crystal dimensions (mm): $0.24 \times 0.20 \times 0.20$, 2θ-θ scan, $4.0^\circ \leq 2\theta \leq 60.0^\circ$, 1260 observed reflections, 282 symmetry-independent reflections ($R_{int} = 0.007$), structure solution with direct methods, H-atoms by difference-Fourier synthesis, structure refinement with full matrix by the least-squares method (16 parameters), all atoms anisotropic, H-atoms isotropic, $R = 0.022$, $wR = 0.013$. Further details of the crystal structure investigation may be obtained from the Fachinformationszentrum Karlsruhe, D-76344 Eggenstein-Leopoldshafen (FRG), on quoting the depository number CSD-400461 and the journal citation.
[7] N. E. Brese, M. O'Keeffe, *Acta Crystallogr. Sect. B* **1991**, *47*, 192.
[8] The X-ray structure analysis gave a N–H bond length of 74.9(26) pm.

$C_{60}H_4$: Kinetics and Thermodynamics of Multiple Addition to C_{60}**

Craig C. Henderson, Celeste McMichael Rohlfing, Roger A. Assink, and Paul A. Cahill*

The regiochemistry of addition of X_2 to fullerenes has now been thoroughly investigated through both theory and experiment.[1–3] In C_{60} and C_{70}, and presumably in the higher fullerenes, both the kinetic and thermodynamic products are derived from "localized" addition, that is, 1,2 addition across 6-6 bonds or 1,4 addition across six-membered rings. In C_{70}, addition to the 6-6 bonds closest to the poles of the molecule leads to the most stable products by both calculation and experiment. However, products resulting from 1,4 addition to the six-membered ring spanning the equatorial region of C_{70} are predicted to lie only slightly higher in energy. Questions of the regiochemistry of both the kinetic and thermodynamic products of multiple additions to C_{60} and C_{70} have not yet been resolved and are highly relevant to the chemical modification of fullerenes for applications ranging from pharmaceuticals to materials science. We report here the synthesis, isolation, characterization, and equilibration of several isomers of $C_{60}H_4$ which, in combination with ab initio Hartree–Fock computations, have yielded insight into the regiochemistry of multiple additions to C_{60}. Remarkably, the major kinetic product of hydroboration *and* the thermodynamically most stable isomer of $C_{60}H_4$ is 1,2,3,4-$C_{60}H_4$ (**1**) (Fig. 1), in which the four hydrogens atoms have added to adjacent 6-6 bonds.[4, 5]

Hydroboration of C_{60} and C_{70} has led to the isolation of one isomer of $C_{60}H_2$[1] and two isomers of $C_{70}H_2$,[2] all of which have been shown to be products resulting from 1,2 addition to 6-6 bonds. These products are the thermodynamically most favored isomers at all levels of calculation. For $C_{60}H_4$, Matsuzawa et al.[6] have reported semiempirical calculations that suggest that only 3.5 kcal mol^{-1} separate the heats of formation of the highest and lowest energy isomers in which addition is limited to 6-6 bonds (Fig. 1a). Four of these eight isomers are predicted to lie within 0.6 kcal mol^{-1} of the lowest energy isomer **4** ("orthogonal" addition of the H_2 pairs, see Fig. 1a). However, these values are suspect because recent results indicate that semiempirical calculations are unreliable for closely spaced fullerene isomer energies.[7, 8] We therefore undertook an ab initio study of the previously identified isomers in concert with our experimental work.

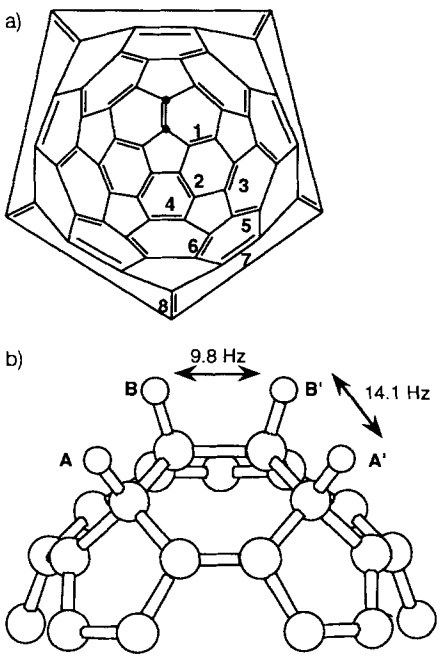


Fig. 1. a) Illustration of the eight isomers of $C_{60}H_4$ which arise from 1,2 additions to 6-6 bonds of C_{60}. The numbers correspond to those in the text for isomerically related formulae [6]. b) Part of the structure of 1,2,3,4-$C_{60}H_4$ (**1**); ^3J(H,H) values given as shown.

The theoretical methodology employed here is similiar to that described previously in our study of isomers of $C_{60}H_2$ and $C_{70}H_2$.[7] These eight isomers of $C_{60}H_4$ were investigated by using ab initio methods within the GAUSSIAN 92 series of programs.[9]

Complete geometry optimizations were performed at the Hartree–Fock (HF) level using the 3-21G and 6-31G* basis sets, the latter containing one set of spherical harmonic d functions on each carbon. The relative HF/6-31G* energies obtained are very likely to be reliable estimates of the relative free energies of the $C_{60}H_4$ isomers because this approach previously yielded relative isomer energies for $C_{70}H_2$ with chemical accuracy.[8] In marked disagreement with the MNDO-PM3 results, both levels of ab initio theory predict the lowest energy isomer to be 1,2,3,4-$C_{60}H_4$ (**1**) (Table 1). This structure is favored over the next

Table 1. Relative energies (kcal mol^{-1}) for $C_{60}H_4$ isomers **1**–**8**, based on fully optimized geometries at each level of theory.

Isomer	H on C	MNDO-PM3[6]	HF/3-21G	HF/6-31G*
1	1,2,3,4	3.3	0.0	0.0
2	1,2,7,21	3.5	6.1	6.6
3	1,2,16,17	2.4	8.1	8.5
4	1,2,18,36	0.0	3.2	4.0
5	1,2,34,35	0.2	4.1	4.9
6	1,2,33,50	0.4	3.5	4.2
7	1,2,51,52	0.6	3.9	4.8
8	1,2,55,60	0.5	3.9	4.8

[*] Dr. P. A. Cahill, Dr. C. C. Henderson, Dr. C. M. Rohlfing, Dr. R. A. Assink
MS 0368, Chemistry of Organic Materials
Sandia National Laboratories
Albuquerque, NM 87185-0368 (USA)
Telefax: Int. code + (505)844-9624

[**] This work was supported at Sandia National Laboratories under the Laboratory Directed Research and Development Program by the US Department of Energy under contract DE-AC04-94AL85000.

lowest lying isomer, **4**, and the highest lying isomer, **3**, by 4.0 and 8.5 kcal mol^{-1}, respectively, at the HF/6-31G* level.[10]

The reaction of BH_3·THF (1 equiv) with $C_{60}H_2$ in toluene afforded a complex mixture of the six products (NMR data listed in Table 2), with 1,2,3,4-$C_{60}H_4$ (**1**), accounting for approximately 50% of the total $C_{60}H_4$ product. The chromatogram of the reaction mixture after chromatographic removal of most of the starting material revealed, however, only the three products shown in Figure 2. Isomer **1** (= C) is the last compound to elute on a Buckyclutcher I stationary phase[11] with a toluene/hexane (1/1) isocratic mobile phase, and is well-separated from the other $C_{60}H_4$ products. The total yield of $C_{60}H_4$ products based on uncorrected peak areas is less than 2% from C_{60}, but is 10% when $C_{60}H_2$ is used as a starting material. A mixture of $C_{60}H_4$ isomers A and B isomerizes on a Pt-contaminated Buckyclutcher I column to **1** (= C). This suggests that **1** is the thermodynamically most stable isomer, a result consistent with ab initio calculations.

Table 2. ^{1}H NMR data (400 MHz, [D$_8$]toluene, 25 °C, TMS, unless otherwise noted), structural assignments, and percent composition of the mixture for the $C_{60}H_4$ products observed by hydroboration of $C_{60}H_2$ in toluene.

Product	Spectroscopic data	Isomer	Percentage [%]	Isolable [a]
A	δ = 5.55 (AB quartet, $\Delta\delta$ = 0.18, ^3J(H,H) = 15.8 Hz)	unknown	20	yes
B	δ = 5.36 (2H, s) δ = 5.05 (AB quartet, $\Delta\delta$ = 0.24, ^3J(H,H) = 15.5 Hz)	**4**	20	yes
C	δ = 5.03 (AA'BB', $\Delta\delta$ = 0.75, ^3J(AB) = 14.1 ± 0.5, ^3J(BB') = 9.8 ± 0.5, ^4J(AB') = − 0.2 ± 0.5, ^5J(AA') = 1.7 ± 0.2 Hz)	**1**	50	yes
D	δ = 5.85 (AB quartet, 200 MHz, $\Delta\delta$ = 0.15, ^3J(H,H) = 15.5 Hz)	unknown	7	no
E	δ = 5.59 (AB quartet, 200 MHz, $\Delta\delta$ = 0.15, ^3J(H,H) = 16.3 Hz)	unknown	2	no
F	δ = 6.33 (s, 200 MHz)	**8**	1	no

[a] Nonisolable products either isomerize or decompose upon separation.

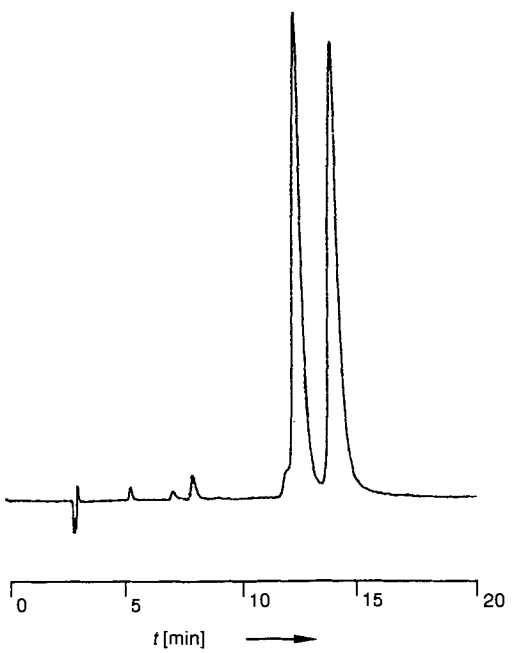


Fig. 2. Chromatogram of the product mixture resulting from the reaction of BH_3 with $C_{60}H_2$, detected at 340 nm, pre-purified to remove most starting materials (Buckyclutcher I, 10 mm × 25 cm column with hexane/toluene (1/1), flow rate 4.5 mL min^{-1}). Compound (elution time [min]): solvent spike (3.05), C_{60} (5.24), C_{70} (7.07), $C_{60}H_2$ (7.96), shoulder of product E followed by a mixture of products A and B (12.44), C (= **1**) (13.97). Products A and B were separated by using 18:82 CH_2Cl_2:hexane as the eluent *after* removal of **1**.

The 400 MHz ^{1}H NMR spectrum of **1** in [D$_8$]toluene shows an AA'BB' spin system centered at δ = 5.03 (Fig. 3a). Simulation of this spectrum led to the spectrum shown in Figure 3b, and the high quality of agreement between the two spectra provides strong evidence of the product's structure. The parameters used to simulate the spectrum are $\Delta\delta$ = 300 Hz, $^3J_{AB}$ = 14.1 ± 0.5, $^3J_{BB'}$ = 9.8 ± 0.5, $^4J_{AB'}$ = − 0.2 ± 0.5, and $^5J_{AA'}$ = 1.7 ± 0.2 Hz. Variations in these values beyond the stated error limits led to significant differences between the observed and simulated spectra.

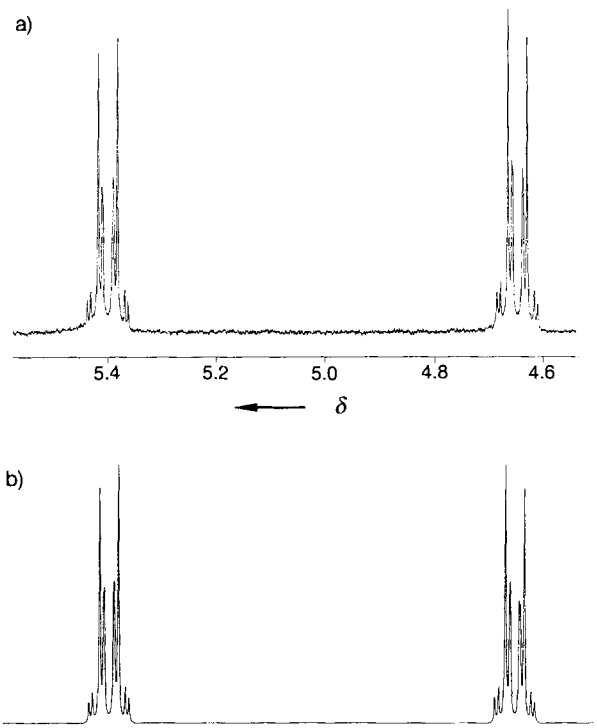


Fig. 3. a) ^{1}H NMR spectrum of **1** (400 MHz, [D$_8$]toluene, 25 °C, TMS). b) Simulated spectrum. A line broadening of 0.1 Hz was used. Coupling constants see Table 2. The related coupling constant for $C_{60}H_2$ is ^3J(A,B) = 15.7 Hz (6-6 bond).

The AB coupling between the hydrogen atoms across the 6-6 bond is 14.1 Hz, similar to the value of 15.7 Hz observed in $C_{60}H_2$. The BB' coupling between the hydrogen atoms across the 6-5 bond is 9.8 Hz. The reason for this smaller coupling constant is unclear, but the value is not unreasonable for *cis*, vicinal H_2 substitution. The AB' coupling constant at −0.2 Hz is near zero, again consistent with the assigned geometry between the two C–H bonds.[12] Finally, the terminal AA' hydrogen atoms are coupled through the double bond in the six-membered ring giving rise to a small, positive coupling constant of 1.7 ± 0.2 Hz. The observed spectrum is confidently assigned to the 1,2,3,4 isomer **1**. The only other possible structure that could lead to such a spectrum is the 1,6,7,8 isomer which would result

 © VCH Verlagsgesellschaft mbH, D-69451 Weinheim, 1994 0570-0833/94/0707-0787 $ 10.00+.25/0

from 1,2 H_2 additions to adjoining 6-5 bonds. The formation of this isomer is, however, unlikely because isolated X_2 addition to 6-5 bonds of C_{60} has never been observed and is calculated to be at least 20 kcal mol^{-1} less stable than addition to 6-6 bonds at all levels of theory.

The coupling constants observed in the ^{1}H NMR spectra of the isomers A–E are all consistent with 1,2 addition to 6-6 bonds. The assignment of product F with a resonance signal at $\delta = 6.33$ to **8** is tentative, but is consistent with the exceptionally low-field resonance signal of $C_{60}H_2$ at $\delta = 5.93$. All other resonance signals observed for $C_{60}H_4$ products are upfield from that observed for $C_{60}H_2$. The structure of B can be unambiguously assigned to **4**, but the structures of the products A, D, and E are consistent with any of the remaining five isomers. We plan to assign structures to these isomers through crystallographic analysis.

Experimental Procedure

To a solution of $C_{60}H_2$ [1] (10 mg, 14 μmol) in toluene (15 mL) was added BH_3 (14 μL, 1.0 M solution in THF) at 0 °C under argon. The mixture was stirred at 0 °C for 45 min, warmed to room temperature for 45 min, and quenched by addition of water (1.0 mL). The organic layer was separated, dried over $MgSO_4$, and the $C_{60}H_4$ fraction isolated by preparative chromatography on a Buckyclutcher I column (10 mm × 25.0 cm) with a toluene/hexane (1/1) mobile phase. The total yield of $C_{60}H_4$ products is 10%, less than the 20–30% yields of $C_{60}H_2$ that are obtained from C_{60} under similar conditions ($C_{60}H_4$ isomers were first obtained as side products in <1% yields in this reaction). Positive-ion FAB MS (for the mixture): observed, 724.0309, calculated 724.0313 (no evidence for $C_{60}H_6$). From this mixture three $C_{60}H_4$ isomers were separated (Table 2). The UV/VIS spectrum of C (= **1**) in toluene/hexane (1/1) tails from 290 nm with a shoulder at 342 nm and a distinct absorption at 442 nm, both of which may be diagnostic for this substitution pattern. Positive-ion FAB MS: observed, 724.0309; calculated, 724.0313. Similar for A, distinct maximum at 325 nm and weak absorption maxima at 410 and 430 nm. For B, distinct maxima are absent, shoulders at 330, 380, 425, and a broad feature at 475 nm are observed. Isolation of the materials is limited to concentrated solutions (1 mg mL^{-1}) which are handled routinely in light and air. Such solutions may be stored indefinitely at −20 °C, but removal of the solvent leads to solids which do not completely redissolve. Products A and B that were previously separated from C (**1**) were eluted on a Buckyclutcher I column that contained an unusually high amount of residual platinum from the preparation of the Buckyclutcher ligand. Repeated elutions resulted in conversion of A and B to C.

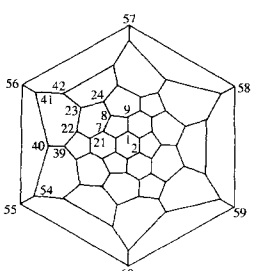
Received: October 28, 1993
Revised: December 27, 1993 [Z 6462 IE]
German version: *Angew. Chem.* **1994**, *106*, 803

[1] For $C_{60}XY$, see a) C. C. Henderson, P. A. Cahill, *Science* **1993**, *259*, 1885; b) A. Hirsch, A. Soi, H. R. Karfunkel, *Angew. Chem.* **1992**, *104*, 808; *Angew. Chem. Int. Ed. Engl.* **1992**, *31*, 766; c) A. Hirsch, T. Grosser, A. Skiebe, A. Soi, *Chem. Ber.* **1993**, *126*, 1061; d) N. Matsuzawa, D. A. Dixon, T. Fukunaga, *J. Phys. Chem.* **1992**, *96*, 7594; e) C. C. Henderson, P. A. Cahill, *Chem. Phys. Lett.* **1992**, *198*, 570; f) S. Ballenweg, R. Gleiter, W. Krätschmer, *Tet. Lett.* **1993**, *34*, 3737.

[2] For $C_{70}XY$, see ref. [7]; H. R. Karfunkel, A. Hirsch, *Angew. Chem.* **1992**, *104*, 1529; *Angew. Chem. Int. Ed. Engl.* **1992**, *31*, 1468; ref. [1c]; C. C. Henderson, C. M. Rohlfing, P. A. Cahill, presented to the American Chemical Society, August 1993.

[3] For a recent reviews of fullerene chemistry see R. Taylor, D. R. M. Walton, *Nature* **1993**, *363*, 685; A. Hirsch, *Angew. Chem.* **1993**, *105*, 1189; *Angew. Chem. Int. Ed. Engl.* **1993**, *32*, 1138.

[4] The numbering used is that in Fig. 2b of R. Taylor, *J. Chem. Soc. Perkin Trans. 2* **1993**, 813. See diagram below.



[5] The isolation of this product was first presented to the Materials Research Society at the spring meeting in San Francisco, CA, USA, April 1993. The formation of several $C_{60}H_4$ and $C_{70}H_4$ isomers by diimide reduction has also been reported: R. Taylor, presented to the American Chemical Society, August 1993; A. G. Avent, A. D. Darwish, D. K. Heimbach, H. W. Kroto, M. F. Meidine, J. P. Parsons, C. Remars, R. Roers, O. Ohashi, R. Taylor, D. R. M. Walton, *J. Chem. Soc. Perkin Trans. 2*, **1994**, 15. In their Table 1, isomer 1,2,57,58 should read 1,2,55,60. We thank R. Taylor for a preprint of this work.

[6] N. Matsuzawa, T. Fukunaga, D. A. Dixon, *J. Phys. Chem.* **1992**, *96*, 10747.

[7] C. C. Henderson, C. M. Rohlfing, and P. A. Cahill, *Chem. Phys. Lett.* **1993**, *213*, 383.

[8] Equilibration of 7,8- and 1,9-$C_{70}H_2$ led to excellent agreement between the observed free energy difference (1.4 ± 0.2 kcal mol^{-1}) and calculated ab initio HF/6-31G* total energy difference (1.3 kcal mol^{-1}): C. C. Henderson, C. M. Rohlfing, K. T. Gillen, P. A. Cahill, *Science*, in press. The 1,9 isomer is both the kinetic product of hydroboration/hydrolysis and the thermodynamically most stable isomer.

[9] GAUSSIAN 92: M. J. Frisch, G. W. Trucks, M. Head-Gordon, P. M. W. Gill, M. W. Wong, J. B. Foresman, B. G. Johnson, H. B. Schlegel, M. A. Robb, E. S. Replogle, R. Gomberts, J. L. Andres, K. Raghavachari, J. S. Binkley, C. Gonzalez, R. L. Martin, D. J. Fox, D. J. DeFrees, J. Baker, J. J. P. Stewart, and J. A. Pople, Gaussian, Inc., Pittsburgh, PA, 1992.

[10] Note that other $C_{60}H_4$ isomers, in particular, those with a 1,4-addition pattern, may have relative energies within the span of isomer energies presented in Table 1.

[11] C. J. Welch, W. H. Pirkle, *J. Chromatogr.* **1992**, *609*, 89.

[12] L. M. Jackman, S. Sternhell, *Applications of Nuclear Magnetic Resonance Spectroscopy in Organic Chemistry*, 2nd ed., Pergamon, Oxford, **1969**, p. 336.

Liquid Sulfur Dioxide as a Lewis-Acidic Solvent for the Alkylation and Alkoxyalkylation of Allylsilanes**

Herbert Mayr,* Gorden Gorath, and Bernhard Bauer

The use of metal halides as Lewis acids for Friedel–Crafts and related reactions is increasingly criticized because of the nonrecyclable salts produced in the usual aqueous workup. In particular, in reactions which require stoichiometric quantities of Lewis acid, this presents an ecological and financial problem. Sulfur dioxide (SO_2) has a high ionizing power because it can act as an electron pair acceptor. Although this property has been known for a long time,[1] it has rarely been used to replace metal halides in electrophilic alkylations or acylations.[2]

Using liquid SO_2 as solvent makes an aqueous workup superfluous and should enable the recondensed SO_2 to be recycled. For these reasons we decided to study its use as a solvent for the alkylation and alkoxyalkylation of allylsilanes. In this case, reactions with acetals are of particular interest because they generally require stoichiometric quantities of $TiCl_4$[1,3] but examples with catalytic amounts of acids have been reported.[4]

If acetals **1a–1e** are treated with 1.2 equivalents of allyltrimethylsilane (**2a**) in liquid SO_2 at −60 °C the homoallyl ethers **3a–3e** are obtained in good yield (Table 1). The reaction of **1e** with **2a** shows that the reaction can also be carried out at room temperature. Due to the low vapor pressure of SO_2 at 20 °C (about 3 bar at 20 °C),[5a] thick-walled glass vessels with a screw-top were employed,[5b] which were cooled for filling and emptying and covered with a protective metal casing during the reaction. Based on the high yields for these reactions and on earlier investigations on the electrophilicity of acetals,[6] it is expected that all ordinary acetals will react under these conditions.

Table 1 shows that alkylations with the corresponding chlorides **1f–i** were also successful. The failure of 1-chloro-1-phenylethane and *tert*-butyl chloride to react under these conditions suggests that only alkyl chlorides with high S_N1 reactivities ($k_1 > 10^{-6}$ s^{-1} in EtOH, 25 °C) are reactive under these conditions.[7]

[*] Prof. Dr. H. Mayr, Dipl.-Chem. G. Gorath, B. Bauer
Institut für Organische Chemie der Technische Hochschule
Petersenstrasse 22, D-64287 Darmstadt (FRG)
Telefax: Int. code + (6151)16-5591

[**] This work was supported by the Fonds der Chemischen Industrie. We would also like to thank Dr. W. Siegel and Dr. M. Eggersdorfer, BASF AG, for stimulating this investigation.

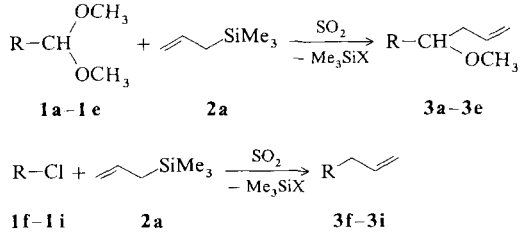


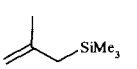
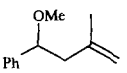
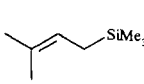
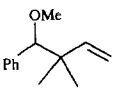
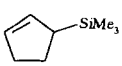
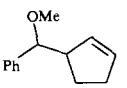
Table 1. Reactions of acetals **1a–e** and alkyl chlorides **1f–i** with allyltrimethylsilane in liquid SO_2.

R	Reactant/Product	T[°C]	t[h][a]	Yield [%]
C_6H_5	**1a/3a**	−60	18	96
p-MeC_6H_4	**1b/3b**	−60	72	98
p-$MeOC_6H_4$	**1c/3c**	−60	22	83
n-C_5H_{11}	**1d/3d**	−60	72	93
n-C_6H_{13}	**1e/3e**	20	46	86[b]
$(C_6H_5)_3C$	**1f/3f**	20	330	80
$(p$-$MeC_6H_4)_2CH$	**1g/3g**	−60	48	85
$(C_6H_5)Me_2C$	**1h/3h**	−60	20	76
$(p$-$MeOC_6H_4)CH_2$	**1i/3i**	20	185	93

[a] Reaction times have not been optimized. [b] With a trace of I_2 present.

As shown in Table 2, other allylsilanes also react with benzaldehyde dimethyl acetal in SO_2. However, it is unclear why prenyltrimethylsilane **2c** reacts significantly more slowly than would be expected from its high nucleophilicity observed in other reactions.[8] Formation of allylsilane/SO_2 copolymers[9] was occassionally observed for which a radical chain process or an ionic mechanism could be envisaged. In the reaction of **1e** with **2a** the formation of copolymers could be suppressed by the addition of a tiny crystal of I_2, indicating the operation of a radical mechanism for copolymerization.

Table 2. Reactions of benzaldehyde dimethyl acetal (**1a**) with allylsilanes in liquid SO_2.

Reactant		Product		T[°C]	t[h] [a]	Yield [%]
	**2b**		**4b**	−60	24	85
	**2c**		**4c**	20	452	56
	**2d**		**4d**	−60	23	41

[a] Reaction times have not been optimized.

Preliminary experiments of the alkylation and alkoxyalkylation of silylenol ethers and/or electron-rich arenes were also successful. It can therefore be assumed that the solvent SO_2 could replace metal halides as Lewis acids in numerous reactions. Addition of catalytic quantities of 2,6-di-*tert*-butyl-4-methylpyridine inhibits product formation, suggesting that the ionization is catalyzed by traces of acid (possibly H_2SO_3).

Experimental Procedure

Dry SO_2 (10 mL) was condensed in a Schlenk tube at −40 °C under a nitrogen atmosphere. Benzaldehyde dimethyl acetal (1.31 g, 8.61 mmol) and allyltrimethylsilane (1.18 g, 10.3 mmol) were then dissolved with stirring and the reaction mixture allowed to stand at −60 °C. After 18 h the SO_2 was allowed to evaporate at room temperature and the residue was distilled; yield: 1.34 g (96%) *rac*-4-methoxy-4-phenyl-1-butene (**3a**).

Received: October 26, 1993 [Z6451IE]
German version: *Angew. Chem.* **1994**, *106*, 793

[1] N. N. Lichtin in *Carbonium Ions, General Aspects and Methods of Investigation, Vol. 1* (Eds.: G. A. Olah, P. von R. Schleyer), Wiley, New York, **1968**, pp. 135–151; D. F. Burow ("Liquid Sulfur Dioxide") in *Chemistry of Nonaqueous Solvents, Vol. 3* (Ed.: J. J. Lagowski), Academic Press, New York, **1970**.
[2] N. Tokura, *Synthesis* **1971**, 639–645.
[3] a) H. Sakurai, *Pure Appl. Chem.* **1985**, *57*, 1759–1770; b) T. Mukaiyama, M. Murakami, *Synthesis* **1987**, 1043–1054; c) E. W. Colvin, *Silicon in Organic Synthesis*, Butterworths, London, **1981**; d) W. P. Weber, *Silicon Reagents for Organic Synthesis*, Springer, Berlin, **1983**; e) I. Fleming in *Comprehensive Organic Chemistry, Vol. 3* (Eds.: D. H. R. Barton, W. D. Ollis), Pergamon, Oxford, **1979**, pp. 541; f) H. Sakurai, *Pure Appl. Chem.* **1982**, *54*, 1–22; g) D. Schinzer, *Synthesis* **1988**, 263–273; i) I. Fleming, J. Dunogues, R. Smithers, *Org. React. N.Y.* **1989**, *37*, 57; j) R. Eaborn, W. Bott in *Organometallic Compounds of the Group IV Elements, Vol. 1*, (Ed.: A. G. Mac-Diarmid), Marcel Dekker, New York, **1968**, Part 1; k) I. Fleming in *Comprehensive Organic Synthesis, Vol. 2* (Eds.: B. M. Trost, I. Fleming, C. H. Heathcock), Pergamon, Oxford, **1991**, pp. 563–593.
[4] a) T. Tsunoda, M. Suzuki, R. Noyori, *Tetrahedron Lett.* **1980**, *21*, 71–74; b) H. Sakurai, K. Sasaki, A. Hosomi, *ibid.* **1981**, *22*, 745–748; c) T. Mukaiyama, H. Nagaoka, M. Murakami, M. Ohshima, *Chem. Lett.* **1985**, 977–980.
[5] a) Gmelin-Institut for Inorganic Chemistry of the Max-Planck-Gesellschaft zur Förderung der Wissenschaften, *Gmelin-Handbuch der Anorganischen Chemie, Schwefeloxide, Vol. 3*, 8th ed., Springer, Berlin, **1980**, p. 95; b) M. Begtrup, *J. Chem. Educ.* **1987**, *64*, 974.
[6] a) U. von der Brüggen, R. Lammers, H. Mayr, *J. Org. Chem.* **1988**, *53*, 2920–2925; b) H. Mayr, J.-P. Dau-Schmidt, *Chem. Ber.* **1994**, *127*, 213–217.
[7] a) J.-P. Dau-Schmidt, H. Mayr, *Chem. Ber.* **1994**, *127*, 205–212; b) H. Mayr, *Angew. Chem.* **1981**, *93*, 202–204; *Angew. Chem. Int. Ed. Engl.* **1981**, *20*, 184–186; c) H. Mayr, W. Striepe, *J. Org. Chem.* **1983**, *48*, 1159–1165.
[8] a) H. Mayr, R. Pock, *Tetrahedron* **1986**, *42*, 4211–4214; b) G. Hagen, H. Mayr, *J. Am. Chem. Soc.* **1991**, *113*, 4954–4961.
[9] H. F. Mark, N. G. Gaylord, N. M. Bikales, *Encyclopedia of Polymer Science and Technology, Vol. 9*, Intersience Publ., New York, **1968**.

 © VCH Verlagsgesellschaft mbH, D-69451 Weinheim, 1994 0570-0833/94/0707-0789 $ 10.00+.25/0

From Aluminum Compounds to Drug Design and Action

Coordination Chemistry of Aluminum. Edited by *G. H. Robinson*. VCH Verlagsgesellschaft, Weinheim/VCH Publishers, New York, 1993. XIII, 234 pp., hardcover DM 189.00, $ 115.00.—ISBN 3-527-28149-5/1-56081-059-9

This book is mainly concerned with the properties and structures of organoaluminum compounds, and constitutes an important survey of this highly topical field of research, which has grown at a remarkable rate in the last few years.

In the first chapter A. Haaland classifies the different types of interactions between atoms of Main Groups 5 and 6 and aluminum, and thereby succeeds in bringing order to the confusing variety of examples which show a remarkably wide range of bond lengths. The division into covalent and dative bonding types or mixtures of the two seems rather arbitrary at first sight, but leads to a very simple and graphic picture which, except in very few cases, affords a description of even quite small effects.

In the second chapter G. H. Robinson describes the fascinating variety of structural types that are now recognized in aluminum–nitrogen chemistry. It has been found that reacting trialkylaluminum compounds with simple amines or chelating amines yields species ranging from monomeric aluminum amides to clusters with up to eight Al–N units. In the next chapter, deviating somewhat from the mainly organo-element orientated content of the book, C. Orvig reports on the coordination chemistry of aluminum in aqueous solutions, a research topic that has been badly neglected in the current euphoria about the chemistry of Main Group 3 elements. As the author impressively shows, very interesting results continue to emerge in this area; as expected, kinetic and thermodynamic data provide the main focus of interest. In addition this relates to the highly topical theme of the transport mechanisms of aluminum ions in the human body, which are being intensively studied in connection with Alzheimer's disease.

A. R. Barron gives a very good review of compounds containing aluminum in unusual oxidation states, which were obtained in pure forms stable at room temperature only within the last few years. More remarkably, the author also reports in detail here on unstable species that can only be prepared and studied in a solid matrix, such as those formed by aluminum with CO or C_2H_4. For completeness it would have been useful to also include here a short description of species prepared and studied under extreme conditions in the gas phase. After treating compounds containing Al–Al bonds and clusters of aluminum atoms, which have only recently been isolated and characterized by crystal structure analysis, Barron moves on to paramagnetic species. Here it is found in many cases that the unpaired electrons are centered on the ligands and the aluminum atom is actually in the normal trivalent form. Here this referee takes the opportunity to suggest a minor correction. It is stated in the article, on the basis of results found for $R_2Al-AlR_2$ [where $R = CH(SiMe_3)_2$], that a criterion for the presence of an isolated Al–Al bond is a downfield shift of the α-carbon resonance in the ^{13}C NMR spectrum. This is certainly not the case, since all aluminum compounds with a three-coordinated aluminum atom and a bis(trimethylsilyl)-methyl group show a similar downfield shift.

In the remaining two chapters J. P. Oliver et al. and J. L. Atwood contribute detailed and very lucid reports on alkoxides and thiolates and on cationic and anionic organoaluminum compounds respectively. The latter chapter includes a very detailed treatment of the formation of clathrates from anionic binuclear aluminum compounds. However, cationic species are treated somewhat too briefly; although these have been known for a long time, not all have been studied by crystal structure analysis. In particular I feel that there should have been a mention of the reaction of $AlCl_3$ with pyridine, which was reported in detail (including the crystal structure of the product) as long ago as 1982.

To summarize, this easily readable book gives an excellent survey of the subject. At the cost of some loss of tidiness and clarity, it could perhaps have been enlarged to include compounds of aluminum with, for example, phosphorus, arsenic, transition metals, or alkyl groups. As someone already familiar with the subject, I found the book very enjoyable to read, leaving aside the inevitable errors. However, the book is suitable not only for specialists in the chemistry of Main Group 3 elements but also as a work of reference for more general use, as it comprehensively covers the literature in this rapidly advancing field up to 1991, with detailed and clear presentation of results, often including tables and figures.

Werner Uhl
Fachbereich Chemie
der Universität Oldenburg (FRG)

Biosensors. Theory and Applications. By *D. G. Buerk*. Technomic, Basel, 1993. 232 pp., hardcover SwFr 187.00.—ISBN 0-87762-975-7

The title of this book leads one to expect a survey bringing together the main principles and applications of biosensors. Such a book is especially welcome in view of the wealth of literature on biosensors that has already appeared, and the progressive introduction of yet more novel physical principles into the development of biosensors. A look at the list of contents reinforces this expectation. After an introduction there are chapters on electrochemical methods and transducers, the incorporation of these into enzyme electrodes, biosensors based on optical and other principles, immunosensors, and sensors that use whole cells. The book ends with a chapter on likely future developments. Thus it appears at first glance that

This section contains book reviews and a list of new books received by the editor. Book reviews are written by invitation from the editor. Suggestions for books to be reviewed and for book reviewers are welcome. Publishers should send brochures or (better) books to the Book Editor, Dr. Gerhard Karger, Redaktion Angewandte Chemie, Postfach 101161, D-69451 Weinheim, Federal Republic of Germany. The editor reserves the right of selecting which books will be reviewed. Uninvited books not chosen for review will not be returned.

the author has succeeded in providing an account of all the most important biosensor principles and their present and potential applications.

However, on looking through the book in more detail one discovers that many of the expectations are not fulfilled. Both the structure of the book and its detailed contents invite criticism. It consists of ten chapters, each of which is divided into sections varying in number from seven to thirteen. These are further divided into as many as nineteen subsections. Some of these consist of fewer than ten lines of text, while in other cases the first such subsection is not followed by a second one. This impression of a not always appropriate arrangement of the material is further reinforced on noting that, for example, there are three sections on glucose sensors (Sections 4.3, 4.4, and 4.5) which all employ the same principle but are applied to different problems. These are followed by sections on sensors for urea (Sect. 4.6) and for alcohols (Sect. 4.7), on multienzyme sensors (Sect. 4.9), and on carbon electrodes for enzymes (Sect. 4.10), despite the fact that the exclusion of these sensors from earlier sections was not mentioned, and without referring to the existence of glucose and alcohol sensors based on carbon electrodes. Similar inconsistencies can be found in other chapters. A clearer way of arranging the subject matter, and its inclusion in full in the list of contents, would have helped the reader considerably.

Furthermore, of the eight chapters that describe the current state of progress in biosensor developments, four are concerned exclusively with electrochemical principles and enzyme electrodes. Since immunosensors and sensors using whole cells also employ electrochemical methods, this means that these topics occupy more than half the book. Consequently the author fails to do justice to other techniques, in particular to the optical methods that are now so important in immunosensors. Thus the main emphasis in the book is on measurements using electrochemical principles. The historical survey in the introduction begins with the development of the acid–base theory, and mentions various fundamental developments in electrochemistry, whereas other detection methods are ignored. The chapters that follow contain explanations of some of the theoretical fundamentals; sometimes these are so brief that non-electrochemists will have difficulty in understanding them in detail, and in any case they are not essential for understanding biosensors. The applications described nearly all belong to the medical field; this emphasis is carried to such lengths that, for example, in relation to oxyhemoglobin and oximetry, the author describes methods that may well be important for blood investigations, but have not so far proved useful in biosensor technology. On the other hand, some important aspects of biosensors are not covered. Topics that are only treated very briefly or omitted altogether include the use of mediators as artificial electron acceptors, successful experiments on direct electron transfer from enzymes to electrodes, fabrication techniques not based on thin film technology, and optical methods such as interferometry.

Each chapter ends with a list of references, including some that are very recent, although regrettably the overwhelming emphasis is on work in the USA. Few citations of work by Japanese or European groups are included, even for groups that have developed sensors for medical applications. Moreover, there are no references to any commercial enzyme analyzers or sensors other than those made by Yellow Springs Instruments.

To summarize, the high expectations raised by the book's title fail to materialize. An indication in the title that the subject matter is restricted to medical applications and electrochemical methods would have given a better idea of the author's research interests, and would have served these topics more effectively, as they could then have been given the more detailed treatment promised by the title.

Ursula Bilitewski
Bereich Enzymtechnologie/
Naturstoffchemie
Gesellschaft für Biotechnologische
Forschung mbH
Braunschweig (FRG)

The Organic Chemistry of Drug Design and Drug Action. By *R. B. Silverman.* Academic Press, New York, 1992. XIV, 422 pp., hardcover $ 55.00.—ISBN 0-12-643 730-0

It was the author's expressed intent in writing this book to create a text through which "a student or a scientist interested in entering the field of medicinal chemistry" would learn to look at the drug development process as basically a problem in mechanistic organic chemistry. In this endeavor, Dr. Silverman has been successful and then some. A range of topics is covered and explored in a reasonable level of detail in a text of 422 pages. Specifically, there are chapters on the general principles of receptors and drug–receptor complexes, enzymes and enzyme inhibition, and DNA and drug–DNA interactions. The references are comprehensive enough for the book to serve to jumpstart a literature search in the areas that are included, although the cited literature cuts off in 1989. Interesting historical background information is included in many chapters, which enhances the reader's appreciation of why the drug discovery process evolved the way it did in certain areas. The author has also included chapters which give a reasonable overview of how a typical prototype compound is discovered, and of concepts such as bioisosterism and QSAR as they relate to structure optimization. However, there is sufficient mathematics in the discussion of physicochemical parameters to slake the typical medicinal chemist's thirst for such. The chapter on drug metabolism may perhaps overemphasize the importance of this area relative to absorption, tissue distribution, and excretion phenomena as they relate to a medicinal chemist's concerns about a compound's pharmacokinetic and pharmacodynamic behavior. However, in keeping with the book's purpose, metabolism is better understood and more easily explained in terms of the principles of organic chemistry than these other (equally important) aspects of pharmaceutical research and development. The discussion of prodrugs is an especially handy reference for browsing.

"The Organic Chemistry of Drug Design and Drug Action" is very well written, nicely indexed, and generally free of typographical errors. Naturally, since it was conceived as a text for an introductory course in medicinal chemistry, there are numerous subjects which are either treated very lightly or not at all. For the experienced medicinal chemist, this book will never replace texts such as Goodman and Gilman's "The Pharmacological Basis of Therapeutics" as a resource. Nevertheless, I believe that this book is so readable that it will prove to be a welcome addition to the library of any medicinal chemist, regardless of experience.

James B. Doherty
Merck & Co., Inc.
Rahway NJ (USA)

 © VCH Verlagsgesellschaft mbH, D-69451 Weinheim, 1994 0570-0833/94/0707-0792 $ 10.00+.25/0

Cyclodextrins as Building Blocks for Supramolecular Structures and Functional Units

Gerhard Wenz*

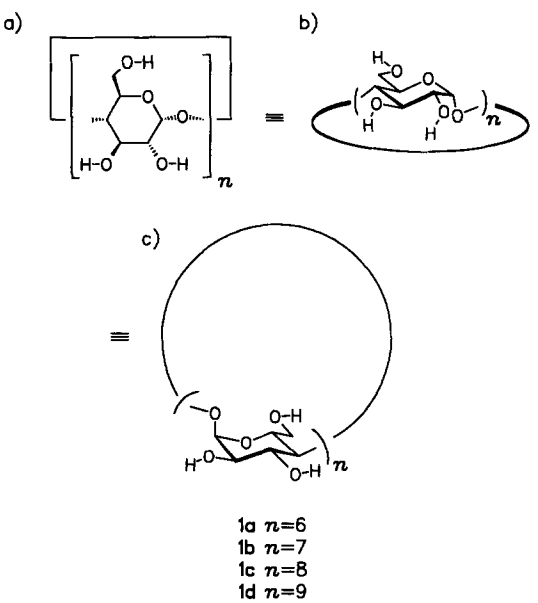
Cyclodextrins are frequently used as building blocks, because they can be linked both covalently and noncovalently with specificity. Thus one, two, three, seven, fourteen, eighteen, or twenty substituents have been linked to one β-cyclodextrin molecule in a regioselective manner. Furthermore, cyclodextrins may serve as organic host molecules. Their internal cavity is able to accommodate one or two guest molecules. Conversely, suitable guest molecules can be used to thread one, two, or many (one hundred or more) cyclodextrin rings. The resulting supramolecular structures are often formed in solution, which allows characterization by high-resolution spectroscopic methods. Chemical conversion of these structures provides molecular architectures such as catenanes, rotaxanes, polyrotaxanes, and tubes, which are not readily prepared by other methods. The particular properties of cyclodextrins can also be employed, for example, for the chromatographic separation of complex mixtures of substances, even racemates, by molecular recognition. Cyclodextrins and their derivatives have been found to be remarkably active catalysts as well. Finally, since cyclodextrins can favorably influence the release of drugs, many new applications will certainly be developed in the near future.

1. Introduction

Cyclic oligomers of amylose are referred to as cyclooligoamyloses, cyclomaltooligosaccharides, or cyclodextrins (α-, β-, γ-, and δ-cyclodextrin **1a**, **1b**, **1c**, and **1d**, respectively; Scheme 1). Since their discovery by Villiers[1] in 1891, interest in these cyclic carbohydrates has increased steadily. Why?

Cyclodextrins are of interest for synthetic chemists because they are chemically stable and can be modified in a regioselective manner. Cyclodextrins are of great importance for supramolecular chemistry, since they form a homologous series of water-soluble and chiral host molecules which can be used as models for studying weak interactions. In addition, their low price provides motivation for the discovery of new applications. Thus cyclodextrins are used for the solubilization and encapsulation of drugs, perfumes, and flavorings. Their toxicity is low, and they are biodegradable. Finally, they are of interest because they are obtained from a renewable resource, starch.[2]

The last review on cyclodextrins in *Angewandte Chemie* was written by Wolfram Saenger in 1979 and entitled "Cyclodextrin Inclusion Compounds in Research and Industry".[3] Since then many (about 7000[4]) publications have appeared in this field, some of them very exciting, and it appears worthwhile to survey this field once more.[5]



1a $n=6$
1b $n=7$
1c $n=8$
1d $n=9$

Scheme 1. Structure of the cyclodextrins. Projections a) 90°, b) 45°, and c) 0° to the C_n axis.

2. Synthesis, Structure, and Physical Properties of the Cyclodextrins

The enzymatic degradation of starch affords a mixture of cyclic and linear maltooligosaccharides. The enzymes used are cyclodextrin glucosyl transferases (CGTases) of bacterial origin, for example from *Bacillus macerans* and *alcaliphilic bacilli*.[6] They

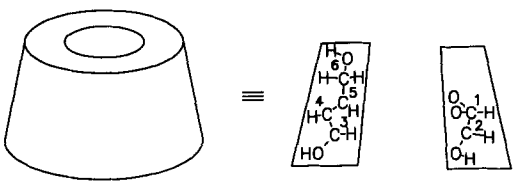
[*] Prof. Dr. G. Wenz
Polymer-Institut der Universität
Hertzstrasse 16, D-76187 Karlsruhe (FRG)
Telefax: Int. code + (721)608-4421

are in general unspecific with respect to ring size.[7] The isolation of a particular cyclodextrin is carried out by the addition of selective precipitating agents.[6] Since the various cyclodextrins are interconverted by CGTases, the final product is the one that is continuously removed from the reaction mixture by selective precipitation. Thus cyclodextrins can be obtained in remarkable yields and high homologous purity (ca. 99%) (Table 1).[7, 8] Owing to the biological origin of cyclodextrins, only dextrorotatory enantiomers are formed. The levorotatory enantiomers could only be obtained by synthetic procedures, but at present an economical total synthesis does not appear feasible. D-**1a** and D-**1c** have been obtained from D-maltose in multistep procedures with overall yields of $\leq 0.3\%$.[9]

Table 1. Synthesis of cyclodextrins by enzymatic degradation of starch.

Cyclodextrin	Precipitating agent	Yield [%]	Ref.
1a	1-decanol	40	[8b]
1b	toluene	50–60	[8a]
1c	cyclohexadec-8-en-1-one	40–50	[7]

Crystalline cyclodextrins bind 6–13 wt% water, depending on ring size. The structures of **1a**·$6H_2O$,[10] **1a**·$7.57H_2O$,[11] **1b**·$12H_2O$,[12] **1c**·$13.3H_2O$,[13] and **1d**·$13.75H_2O$[14] have been determined by X-ray and neutron diffraction. These structures show that a cyclodextrin molecule resembles a hollow truncated cone (torus) and has approximate C_n symmetry (Scheme 2).



Scheme 2. Schematic representation of the shape of a cyclodextrin molecule. Two halves of two opposite glucose units are shown in cross section.

The primary hydroxyl groups are located on the narrower side of the torus and the secondary hydroxyl groups on the broader side. Because of the conical shape of the cyclodextrins and deviations from ideal C_n symmetry, their dimensions can be obtained only to within roughly ± 0.3 Å. The internal diameter increases with the number of glucose units (**1a**: 4.9 Å, **1b**: 6.2 Å, **1c**: 7.9 Å), while the height remains constant at 7.9 Å.[3, 15] All the glucopyranoside building blocks are relatively rigid and exist in a $^4C_1$ chair conformation. The secondary hydroxyl groups OH(2) and OH(3) are in equatorial positions; OH(2) groups point in towards the cavity and OH(3) groups point outwards. Since the torus bears twice as many hydroxyl groups on one side as on the other, the dipole moment is relatively large (calculated: 10–15 D,[16] found: ca. 5 D[17]) and directed along the C_n axis.

Cyclodextrins are poorly to moderately soluble in water,[18] methanol, and ethanol, and readily soluble in strongly polar aprotic solvents like dimethyl sulfoxide (DMSO), dimethylformamide (DMF), *N*,*N*-dimethylacetamide, and pyridine[19] and mixtures of these.[20] The shape of cyclodextrin molecules can be approximated by means of molecular dynamics simulations.[21] Although the torus is stabilized by intramolecular hydrogen bonds, it is still flexible enough to permit considerable deviations from regular toroidal shape.[21] However, the time-averaged structure has C_n symmetry, such that, for example, all the glucose building blocks are equivalent by ^1H and ^{13}C NMR spectroscopy.[22] Complete rotation of a glucose unit about the C(1)-O-C(4′) bonds is not possible for steric reasons. Thus protons H(3) and H(5) are always situated within the torus, whereas protons H(1), H(2), and H(4) always point outwards.

3. Synthesis of Cyclodextrin Derivatives

Cyclodextrins are derivatized in order to vary their solubility behavior, to modify their complexation properties, and to introduce groups with certain specific (e.g. catalytic) functions.

3.1. Survey of Possible Reactions

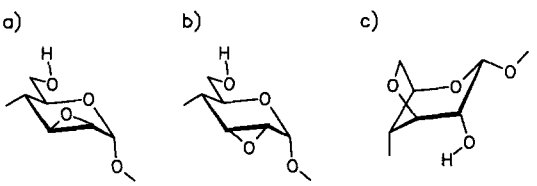
Since cyclodextrins are polyfunctional, they can undergo a wide variety of reactions;[23] these may involve cleavage of either O–H, C–O, C–H, or C–C bonds.

The reaction type most frequently studied is electrophilic attack at the OH groups. Reactions of **1** with alkyl halides,[24] epoxides,[25] acyl derivatives,[24a, 26] isocyanates,[26b] and inorganic acid derivatives such as sulfonic acid chlorides,[27] phosphoric acid chlorides,[28] phosphonic acid chlorides,[29] silyl chlorides,[30] and nitric acid[31] lead to cyclodextrin ethers and esters.



Gerhard Wenz was born in 1953 in Mainz, Germany, and studied chemistry from 1972 to 1979 at the Universities of Mainz and Freiburg. He received his Ph.D. in 1984 for research with G. Wegner in Freiburg on the polymerization of diacetylenes. He then spent a year as a reseach assistant at the Hermann-Staudinger-Institut, Freiburg, and studied discotic polymeric liquid crystals. During a subsequent one-year postdoctoral stay with D. J. Cram at the University of California, Los Angeles, he worked on the synthesis of a chymotrypsin model. In 1986 he moved to the Max-Planck-Institut für Polymerforschung in Mainz. In 1993 he completed his habilitation in organic chemistry at the University of Mainz and accepted a position as Professor of Macromolecular Chemistry at the University of Karlsruhe. His research focuses on the supramolecular chemistry of polymers and carbohydrates.

The nucleophilic cleavage of a C–OH bond requires activation of the oxygen atom by an electron-withdrawing group. Thus the reactions of cyclodextrin-6-*O*-sulfonates with nucleophiles such as azide ions,[32] halide ions,[33] thiols,[34] thiourea,[34b] and amines[35] generally afford the corresponding 6-deoxy derivatives.[36] 6-Azido-6-deoxycyclodextrins can be reduced to the preparatively important 6-amino-6-deoxycyclodextrins.[35, 37] The attack of imidazole on a β-cyclodextrin-2-*O*-sulfonate affords the 2-(1-imidazolyl)-deoxy-β-cyclodextrin.[38] This substitution occurs with retention, presumably due to the neighboring group effect of OH(3). In contrast, the attack of aqueous bases on cyclodextrin-2-*O*-sulfonates leads to an *intra*molecular nucleophilic substitution by OH(3) to give 2,3-anhydrocyclodextrins with *manno* configuration (Scheme 3a).[27b, 39] In analogy,



Scheme 3. a) 2,3-*manno*-, b) 2,3-*allo*-, c) 3,6-anhydrocyclodextrins.

the intramolecular substitution of sulfonate groups in position 3 by OH(2) leads to 2,3-anhydrocyclodextrins with *allo* configuration (Scheme 3b).[39c, 40] The intramolecular nucleophilic attack of OH(3) on 6-*O*-sulfonates[41] and 6-deoxyiodides[42] leads to the relatively stable 3,6-anhydrocyclodextrins (Scheme 3c). Nucleophilic attack on 2,3-*manno*-anhydrocyclodextrins opens the epoxide ring with formation of an allose unit substituted in the 3-position.[43]

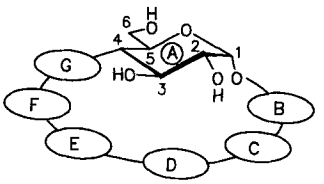
Electrophilic attack at a C-O-C bond leads to decomposition of the cyclodextrin molecule. Cyclodextrins are, however, remarkably stable towards aqueous acids; for example, the half-life of **1b** in 1.15 M HCl at 80 °C is 1.6 h.[44] On the other hand, electrophilic attack by Lewis acids under aprotic conditions in the presence of a reducing agent (e.g. $BF_3 \cdot Et_2O$/triethylsilane or trimethylsilyl triflate/triethylsilane) affords smooth cleavage of the C(1)-O-C(4) bonds without affecting the glucose units and their substituents. This method is therefore used for the analytical determination of the distribution of substituents in cyclodextrin derivatives.[45] Alternatively, the C(1)–O(5) bonds can be cleaved selectively by 9-borabicyclo[3.3.1]nonyl trifluoromethanesulfonate/ethyldiborane.[46]

The H atoms are exchanged on Raney nickel for deuterium atoms (preferably in the 2-position).[47] Treatment with N_2O_4 or Pt/O_2 causes oxidation of CH_2(6) to a carboxylic acid group.[48]

All C(2)–C(3) bonds of **1b** are cleaved upon oxidation with periodate, which leads to the formation of a derivative of [35]crown-7.[49]

3.2. The Problem of Positional Isomerism

Many of the cyclodextrin derivatives described in the literature[23a] are complex mixtures of compounds, since a large number of positional isomers within the cyclodextrin framework are possible. The number of possible positions for a substituent is given by the number of possible positions at a glucose unit (three: 2, 3, and 6) multiplied by the number of different glucose units A, B, C... in the cyclodextrin (Scheme 4). The number of combinations increases rapidly with each further substituent. The number of possible positional isomers, N_i, is shown as a function of the number of substituents, N_s, in Figure 1. In the case of **1b**, N_i reaches a maximum (50388) for the substitution



Scheme 4. Labeling of the positions in the cyclodextrin molecule.

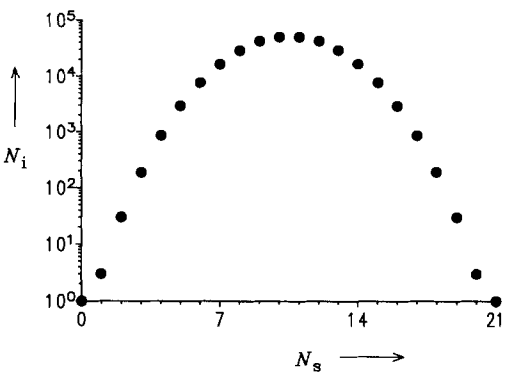


Fig. 1. Number of positional isomers, N_i, as a function of the number of identical substituents, N_s, in **1b**.

of half of the hydroxyl groups.[24a] Thus the probability of synthesizing and isolating a uniform product decreases with the increasing number of isomers. A further difficulty is that homologous derivatives with a lower or higher degree of substitution are also formed in addition to the product, and separation is required. Thus the synthesis of uniform cyclodextrin derivatives is a daunting task. Only since the advent of powerful analytical methods[45c] such as gas chromatography (after degradation),[45] high-pressure liquid chromatography,[50] mass spectrometry,[51] and high-resolution ^{13}C NMR spectroscopy has it become possible to obtain unequivocal proof of the uniformity of a reaction product. By using these methods several reaction products that had long been considered to be uniform were shown to be mixtures.[51, 52, 53]

3.3. General Strategies for Regioselective Substitution

The synthesis of uniform cyclodextrin derivatives requires regioselective reagents, optimization of the reaction conditions, and good separability of the products. Bulky reagents react preferentially at the primary hydroxyl groups OH(6), since these are the most accessible. The secondary hydroxyl groups OH(2) have the highest acidity ($pK_a = 12.2$).[22c, 54] Under anhydrous conditions they can be selectively deprotonated and allowed to react with electrophilic reagents.[55] The secondary hydroxyl groups OH(3) are the least reactive and can be reacted selectively only after OH(2) and OH(6) have been blocked.[56]

The product distribution can be greatly influenced by the reaction conditions. Monosubstitution of a cyclodextrin is achieved by using less than one equivalent of the reagent, and its slow addition can also be advantageous.[57] The presence of a large excess of the reagent must be avoided when the uniform mono- or disubstitution of *all* glucose units in a cyclodextrin is required, since otherwise the reaction may go too far. The optimum reaction time is determined by carefully monitoring the reaction progress, for example by thin-layer chromatography[58] or high-pressure liquid chromatography. These reaction times are often not reproducible; this may be due to the undefined water content of the reaction mixture.[58]

The complete substitution of all hydroxyl groups requires drastic reaction conditions such as a large excess of the reagent, increased reaction temperature, and complete exclusion of water.[59]

Since mixtures of cyclodextrin derivatives are generally formed, chromatographic separation is typically required. Homologous derivatives can be separated only if the polarity of the substituent differs significantly from that of cyclodextrin. Thus the separation of derivatives with hydrophobic substituents (e.g. butyl,[58] benzoyl,[52] and tosyl[60]) is easier than that of derivatives with less hydrophobic substituents (e.g. hydroxypropyl[25b] and methyl[50a, 53]).

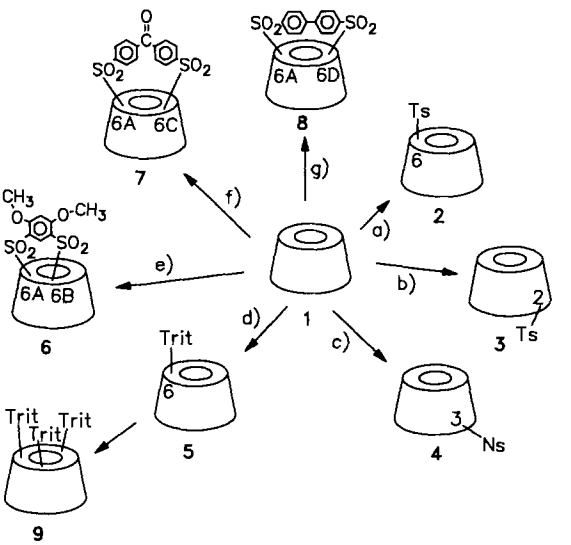
In the following sections we shall discuss methods for regioselective derivatization, classified according to the degree of substitution; we shall also distinguish between activating and blocking substituents.

3.4. Mono-, Di-, and Trisubstituted Cyclodextrins

A cyclodextrin bearing one, two, or three substituents gives extremely complex NMR spectra because of its low symmetry; these can be assigned only by means of multidimensional methods such as ^{1}H-^{1}H or ^{1}H-^{13}C COSY.[39b, 61]

The most important cyclodextrins with *one* activating substituent (Scheme 5) are the cyclodextrin tosylates. The reaction of **1a**, **b** with tosyl chloride in pyridine affords the 6-*O*-tosylates **2a** and **2b** in 10–30% yield.[37, 60] (The ring sizes 6, 7, and 8 are denoted throughout the text by a, b, and c, respectively.) In contrast, esterification with 3-nitrophenyltosylate in DMF/water at pH 10 leads to the 2-*O*-tosylates **3a** and **3b**.[27a, 39b, 62] When **1a**, **b** is treated with tosyl chloride in aqueous NaOH,[27a] **3a** and **2b**[35] are obtained.[27a] Topochemical reaction control might be the case here. In other words, the reagent might be included in the cyclodextrin, and esterification would then occur preferentially within the inclusion compound. Therefore the orientation of the reagent in the cyclodextrin ring determines the position to be attacked. The reaction of dibutyltin oxide with **1** gives cyclic 2,3-*O*-stannates, which can be converted selectively (30% yield) with tosyl chloride into the 2-*O*-tosylates **3**.[63] The selective deprotonation of OH(2) in **1b** with NaH and subsequent reaction with tosyl chloride also leads to **3b**.[55] The 3-position of **1** can be activated by 2-naphthalenesulfonyl chloride in acetonitrile/water at pH 12 to furnish 3-*O*-(2-naphthalenesulfonates) **4a**,[40a] **4b**,[40b] and **4c**.[39c]

The etherification of **1a**, **b** with the sterically demanding trityl chloride leads to the singly blocked 6-*O*-tritylcyclodextrins



Scheme 5. Specific introduction of one, two, or three substituents to cyclodextrins. a) TsCl/Py [37,60], b) 3-nitrophenyltosylate/DMF/H_2O (pH 10) [27a,62], c) NsCl/MeCN/H_2O (pH 12) [39c,40,69b], d) TritCl/Py [37,64b,70], e) [67], f) and g) [66b], Ts = 4-toluenesulfonyl, Ns = 2-naphthalenesulfonyl, Trit = triphenylmethyl, Py = pyridine.

5a[37] and **5b**, respectively.[64] Similarly, **1b** undergoes regioselective reaction with *tert*-butyldimethylsilyl chloride at low temperatures to give 6-*O*-*tert*-butyldimethylsilyl-β-cyclodextrin.[65]

Disubstituted cyclodextrins are obtained most easily by bridging the cyclodextrin molecule with difunctional reagents. Thus Tabushi et al. allowed **1b** to react with arenedisulfonic acid chlorides; depending on the distance between the sulfonyl chloride groups, they obtained A,B-, A,C-, and A,D-disubstituted cyclodextrin sulfonates **6**, **7**, and **8**, respectively, with yields of up to 40%.[66] Such derivatives are referred to as capped cyclodextrins. The introduction of methoxy groups on the aryl residue can increase the stability of the disulfonates and thus facilitate their purification.[67] The reaction of cyclodextrins with monofunctional acid chlorides leads to mixtures of mono-, di-, and higher substituted cyclodextrins, which can be separated by preparative reversed-phase chromatography. Depending on the reaction conditions, the substituents can be directed to positions O(6),[68] O(2),[27b, 40] and O(3).[40b]

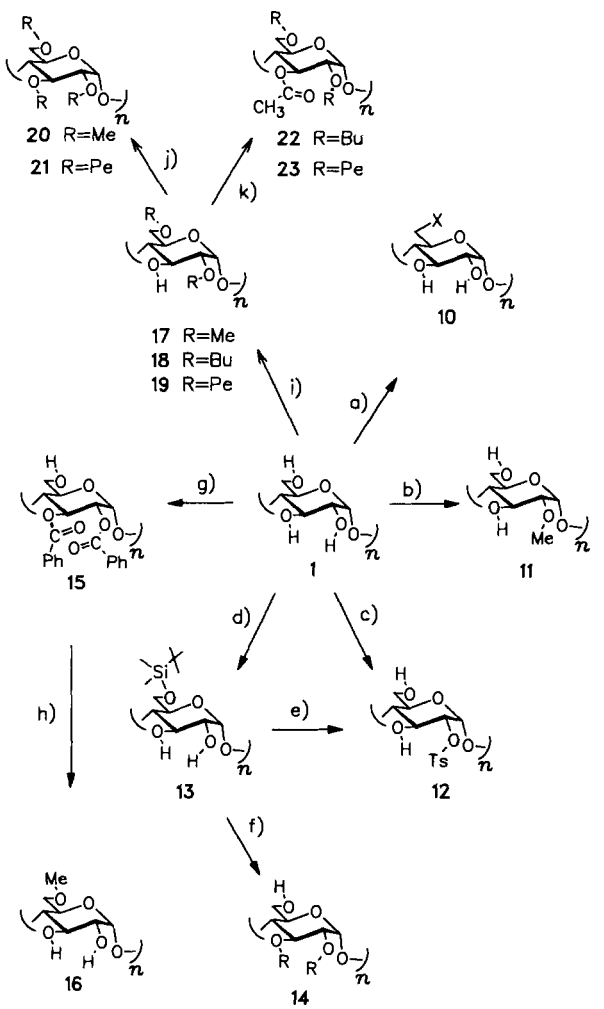
The synthesis and isolation of *trisubstituted* cyclodextrins is very difficult because of the large number of positional isomers and homologues possible. Tosylation of **1b** leads to 6^A,6^C,6^E-tri-*O*-tosyl-β-cyclodextrin in only 2.6% yield.[69] In contrast, tritylation of **1a** gives the 6^A,6^C,6^E-trityl derivative **9** in a respectable yield of 23%.[70] A remarkable alternative method should also be mentioned here: Cottaz and Driguez obtained 6^A,6^C,6^E-tri-*O*-methyl-α-cyclodextrin in 43% yield from enzymatic cyclotrimerization of 6-*O*-methylmaltose.[71]

3.5. Cyclodextrins with Uniform Mono-, Di-, and Trisubstituted Glucose Units

Since C_n symmetry is preserved if all the glucose units in cyclodextrin are substituted in the same way, these derivatives generally crystallize more easily and show simpler NMR spectra than the unsymmetrical derivatives.

Complete tosylation of all primary hydroxyl groups is difficult; because of the increasing bulk of the cyclodextrin upon substitution, the first secondary hydroxyl groups may be attacked before the last primary hydroxyl groups have completed reaction.[41] Reactions that proceed via an intermediate with bulky substituents but lead to a final product with only small substituents are more favorable. Thus **1a** and **1b** were converted by triphenylphosphane/bromine (or iodine) into the per(6-deoxy-6-halo)-cyclodextrins **10a** and **10b** in 80 and 88% yield, respectively (Scheme 6).[42]

Selective deprotonation of all the hydroxyl groups OH(2) of **1b** with NaH and etherification with methyl iodide affords heptakis(2-*O*-methyl)-*β*-cyclodextrin **11b**.[55] Heptakis(2-*O*-tosyl)-*β*-cyclodextrin **12b** was obtained in an analogous manner.[55] All the hydroxyl groups in position 6 can be blocked by treatment with *tert*-butyldimethylsilyl chloride (formation of **13**).[30, 33, 65]



Scheme 6. Homogeneous, regioselective derivatization of all the glucose units of a cyclodextrin. a) PPh_3/X_2/DMF with X = Br, I [42], b) NaH/DMSO, MeI [55], c) NaH/DMSO, TsCl [55], d) TBDMSCl/Py [30,33,65], e) TsCl/DMAP/Py [73], f) NaH/RI/DMF (R = Me, Pe), Bu_4NF [33,74], PheCOCl/Py, *i*PrOK/*i*PrOH [24a], h) $CH_2N_2/CHCl_3$, KOH/EtOH [24a], i) $BaO/Ba(OH)_2 \cdot 8H_2O/R_2SO_4$/DMSO/DMF for R = Me [24a,75] Et [51b,76], Bz [56], otherwise NaOH/RBr/DMSO (R = Pr, Bu, Pe, Dodec) [58], j) RBr or RI/NaH/DMF [24b,77] or THF [59] (R = Me, Pe). k) Ac_2O/DMAP/Et_3N/CH_2Cl_2 [78a,c,e] or R'COCl/Py (R' = Ph, *t*Bu) [52,78b]. TBDMSCl = *tert*-butyldimethylsilyl chloride, Ts = 4-toluenesulfonyl, Bz = benzyl, Pr = propyl, Bu = butyl, Pe = pentyl, Dodec = dodecyl, Ph = phenyl, Py = pyridine, DMAP = 4-(dimethylamino)pyridine.

The remaining hydroxyl groups can be either selectively benzylated[72] or tosylated[73] at OH(2), or completely alkylated.[33, 74] The 2-*O*-tosylates **12** and the 2,3-di-*O*-alkylethers **14** are obtained after removal of the TBDMS groups.

Lehn et al. synthesized a cyclodextrin (**15**) blocked at all OH(2) and OH(3) positions by saponification of the more reactive ester groups at position 6 from per(2,3,6-tri-*O*-benzoyl)cyclodextrin.[24a] Methylation of the OH(6) hydroxyl groups with diazomethane and subsequent cleavage of the benzoyl groups furnishes the per(6-*O*-methyl)cyclodextrins **16**.[24a]

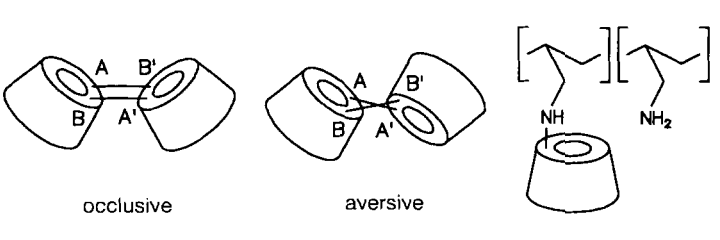
Alkylation of all OH(2) and OH(6) groups is carried out by treating **1** with alkyl halides or alkyl sulfates and a hydroxide. Thus with dimethyl sulfate, $Ba(OH)_2 \cdot 8H_2O$, and BaO in DMF/DMSO the per(2,6-di-*O*-methyl)cyclodextrins **17** are formed;[24, 75] with diethyl sulfate the analogous ethyl derivatives are obtained.[51, 76] The introduction of longer alkyl chains in positions 2 and 6 is possible by treating **1** with primary alkyl bromides and NaOH in DMSO (**18**, **19**).[58] Whereas both methylation and ethylation yield mixtures of isomers and homologous substitution products which are difficult to separate,[50, 53] the longer chain per(2,6-di-*O*-alkyl) derivatives (in particular per(2,6-di-*O*-butyl)cyclodextrins **18**) can be obtained readily in pure form. In contrast to **1** the latter are soluble in most organic solvents, even in hexane, but are completely insoluble in water.[58]

Per(2,6-di-*O*-alkyl)cyclodextrins can be completely alkylated in a subsequent step with strict exclusion of water to give per-(2,3,6-tri-*O*-alkyl)cyclodextrins (e.g. permethyl and perpentyl derivatives **20** and **21**).[24b, 59, 77] Benzyl groups serve as protecting groups for OH(2) and OH(6) in the synthesis of per(3-*O*-methyl)cyclodextrins.[56] Acylation of per(2,6-di-*O*-alkyl)cyclodextrins leads to per(3-*O*-acyl-2,6-di-*O*-alkyl)cyclodextrins such as **22** and **23**.[52, 78]

3.6. Cyclodextrin-Containing Oligomers and Polymers

Reactions of monofunctional cyclodextrin derivatives (e.g. **2a**, **b**) with difunctional nucleophiles (*α*,*ω*-diamines, *α*,*ω*-disulfides, *α*,*ω*-dicarboxylic acids) lead to singly bridged cyclodextrin dimers.[79] Breslow et al. obtained the doubly bridged cyclodextrin dimer **24** from $6^A,6^B$-diiodo-*β*-cyclodextrin and a difunctional nucleophile. Dimer **24** exists in two stable conformations: in the occlusive conformation the two rings are inclined towards each other, in the aversive conformation they tilt away from each other.[80]

For the synthesis of linear cyclodextrin polymers, polyallylamine was treated with **2b** to give **25**;[81] the radical polymerization of vinyl-substituted cyclodextrins also provided linear cyclodextrin polymers.[82]



24 **25**

3.7. Statistically Substituted Monomeric and Polymeric Cyclodextrins for Technical Applications

There are many reasons for synthesizing uniform cyclodextrin derivatives. The procedures can be reproduced more consistently, and the products often crystallize better and are easier to identify than mixtures. However, statistical mixtures of substituted cyclodextrins also have advantages: they can be prepared much more simply, and the reactions can often be carried out in water rather than in expensive inert solvents such as DMSO. Complicated chromatographic separations are also unnecessary. In addition, statistically substituted cyclodextrins are often much more soluble than pure compounds because of their poorer tendency to crystallize.[50a] Thus until now only statistically substituted derivatives have been used industrially (see Section 8).[5c]

Hydroxypropylcyclodextrins are the statistically substituted derivatives of greatest technical interest so far. They are obtained in large quantities by adding propylene oxide to **1** in aqueous sodium hydroxide[25a, 83] and are readily soluble in water. Depending on the reaction conditions, up to two hydroxyl groups per glucose unit are etherified. Pitha et al. studied the product distribution as a function of the reaction conditions in detail.[51, 84] The substitution pattern at the glucose unit is determined most easily by degradative analysis.[45a, 45c] The hydroxypropyl substituents can be directed to certain positions by regulating the pH.[25b]

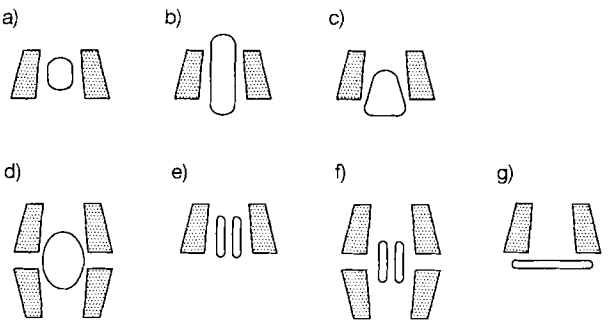
Methylation of cyclodextrins with dimethyl sulfate in aqueous solution also leads to a statistical mixture of *O*-methylcyclodextrins with a degree of substitution of 1–2 per glucose unit.[85] Enzymatic linkage of maltose oligomers to **1** leads to mixtures of branched cyclodextrins which, like the hydroxypropyl derivatives, are readily soluble in water.[51c, 86] Depending on the reaction conditions, the reaction of difunctional reagents such as epichlorohydrin,[87] diisocyanates,[88] and dicarboxylic acid dichlorides[89] with **1** affords either soluble[87b, 90] or insoluble[91] branched products.

4. Supramolecular Structures Derived from Cyclodextrins

A supramolecular structure results from defined noncovalent interactions between several individual molecules.[92] Host–guest complexes[93] are important examples of this type of structure. The host molecule offers the guest molecule a suitable environment, generally a cavity. The driving force for complexation can arise from Coulombic, dipole–dipole, van der Waals, solvatophobic, or hydrogen bonding interactions between host and guest.[94] The outer sphere of the host should be compatible with the required solvent in order to avoid aggregation or insolubility problems. In the following sections we shall distinguish between cyclodextrin derivatives, which according to their solvent compatibility are "exohydrophilic", "exolipophilic", or "amphiphilic" hosts, and describe some examples of supramolecular structures.

4.1. Cyclodextrins as Exohydrophilic Hosts

Since the exterior of cyclodextrin molecules is hydrophilic, they can form adducts with guest molecules in aqueous solution.[3, 95] These adducts can consist of one or more cyclodextrin or guest molecules. If the guest is situated within the cavity (Scheme 7a–f), these adducts are termed *inclusion compounds* according



Scheme 7. Topology of cyclodextrin adducts with a) complete, b) axial, c) partial, and d) sandwich-type inclusion; e) 1:2 and f) 2:2 inclusion compounds; g) lidlike association compound.

to the nomenclature proposed by Cramer et al.[96] On the other hand, if the guest molecule lies outside the cavity, the compounds are referred to as *association compounds* (Scheme 7g). The packing of the cyclodextrin adducts is determined predominantly by the dimensions of the guest relative to those of the cavity. The guest can be either completely or partially surrounded by the host molecule. A long, thin guest can form an axial inclusion compound, whereas a short thick guest forms a sandwichlike structure.[97] In general the stability of cyclodextrin inclusion compounds increases with the extent to which the cavity is filled by the hydrophobic part of the guest.

In order to cover the plethora of results in the literature in as brief a manner as possible, we shall first describe methods for the preparation and characterization of the cyclodextrin adducts and then consider rules for packing behavior.

4.1.1. Preparation of Cyclodextrin Adducts

Cyclodextrin adducts are usually prepared in water; the partners must only be minimally soluble. Other solvents such as DMSO are less suitable than water, since the stability of the adducts in these is much lower.[98] Even the addition of small amounts of short-chain alcohols to the aqueous solution lowers the adduct stability considerably.[99, 100] The more hydrophilic substituents on the guest or cyclodextrin molecule, the more readily soluble the adducts are in water. Thus the adducts of paraffins and **1a** are almost insoluble in water,[19, 101] while those of the short-chain alcohols,[102] acids,[103] and α,ω-diols[104] are readily soluble. Cyclodextrins with hydrophilic substituents such as sulfopropyl-α-cyclodextrin[105] or hydroxypropylcyclodextrin[25b] can solubilize even completely hydrophobic molecules such as paraffins or toluene. In heterogeneous systems the rate of adduct formation is determined by the rate of dissolution. In homogeneous solution most adducts form very quickly, generally within micro- or milliseconds.[106]

4.1.2. Methods for Determining the Topology of the Adducts

Precise information on the topology of cyclodextrin adducts can be obtained from X-ray structural analysis of single crystals (Table 2).[107] Not only the position of the guest molecule with respect to the cavity but also its mobility can be determined. Neutron diffraction also provides information on the positions and motion of the protons.

Table 2. Topology of cyclodextrin adducts from X-ray structure analysis.

Host	Guest	H:G	Type	Ref.
1a	4-iodaniline	1:1	complete	[107a]
1a	4-nitrophenol	1:1	complete	[107b]
1a	3-nitrophenol	1:1	partial	[107c]
1a	$[Rh(cod)(NH_3)_2]PF_6$ [a]	1:1	partial	[107i]
1a	ferrocene	2:1	sandwich	[107p, q]
1b	1,4-butanediol	1:1	axial	[107r]
1b	1,4-diazabicyclo[2.2.2]octane	1:1	complete	[107g]
1b	hexamethylenetetramine	1:1	complete	[107h]
1b	2-(3-phenoxyphenyl)propionic acid	1:1	axial	[107m, n]
17b	4-nitrophenol	1:1	association	[107j]
1c	[12]crown-4	1:1	complete	[107l]
1c	[12]crown-4 · NaCl	3:3:1	sandwich	[107o]
1c	1-propanol	undefined	loose	[107d]

[a] cod = 1,5-cyclooctadiene.

The topology of cyclodextrin adducts can also be determined in solution. The interactions between host and guest may lead to characteristic shifts in the ^1H and ^{13}C NMR spectra that might give information on the packing.[108] Nuclear Overhauser effects provide more precise information,[109] since their magnitudes are a measure of the distance between the protons of host and guest. As the positions of almost all the protons in the cyclodextrin molecule are well defined, the location of the guest in the cyclodextrin can be determined.

The circular dichroism induced by the chiral cyclodextrin on an achiral guest affords information on the topology of the adducts, if the orientation of the transition dipole moment of the guest is known.[108b, 110] Positive circular dichroism indicates that the transition dipole moment in the cavity lies along the C_n axis (axial).[110a, 111] Negative circular dichroism indicates that the transition dipole moment is either within the cavity and perpendicular to the C_n axis or external and parallel to the axis.[112]

The proximity of *two* chromophores included in *one* cyclodextrin molecule can favor the formation of excimers[113] or exciplexes,[114] which can be detected by fluorescence spectroscopy.[115]

4.1.3. Methods for Determining the Thermodynamic Stability of the Adducts

The formation of the adducts is described by the law of mass action. The equilibrium constant K_s, also known as the stability constant, is a measure of the thermodynamic stability of the cyclodextrin adducts. Any physical property of the host or guest that changes on formation of the adduct can in principle be used for the determination of K_s.[116]

The choice of the method to be used depends on the expected value of K_s. The larger the K_s value, the more sensitive the method must be, since the concentrations of the free species decrease with increasing K_s. The physical properties that may be used are listed in order of increasing sensitivity: solubility,[117] vapor pressure,[105b] chemical shifts of ^1H and ^{13}C NMR signals,[109e, 118], circular dichroism,[119] optical absorption,[120] acidity,[121] conductivity,[121, 122] fluorescence.[123] Common to all these methods is their limited scope of application. A much more general method, which is also more precise, is the determination of the heat of formation with the help of a microcalorimeter.[104, 124] The evaluation of the concentration dependence of the heat evolution affords not only the binding constant but also the enthalpy and entropy changes associated with the formation of the adduct.[104, 116b]

The displacement of an included probe molecule by a guest molecule can also be used for the determination of K_s.[117b, 125] Probes used in the case of α-cyclodextrin include methyl orange (detection by means of optical absorption)[117b] and 3-nitrophenyl acetate (rate of solvolysis),[126] and for β-cyclodextrin phenolphthalein,[102, 125a] methyl orange[127] (optical absorption), naphthalene derivatives (fluorescence),[128] and 3-nitrophenyl acetate (rate of solvolysis).[129]

4.1.4. Methods for Studying the Kinetics of Adduct Formation

Information on the kinetics of adduct formation can be obtained by the temperature-jump[106a, 130] and stopped-flow[131] methods; the adduct yield is detected as the change in optical absorption or conductivity. In addition, dynamic NMR spectroscopy affords at least qualitative information. Depending on whether separate[132] or averaged[109c, 118e, 133] signals are observed, the adduct formation is either slow or fast on the NMR timescale.

4.1.5. The Inclusion of Monomeric Guest Molecules

Unbranched alkyl chains fit best into α-cyclodextrin **1a**. The stability constant K_s increases rapidly with increasing chain length k and reaches values of up to $K_s = 10^4\ M^{-1}$ (Fig. 2). This indicates that hydrophobic interactions are the main driving force. Neutral hydrophilic groups at the ends of longer alkyl chains have little influence on the stability, presumably because they are situated outside the cavity in the inclusion compound. Charged

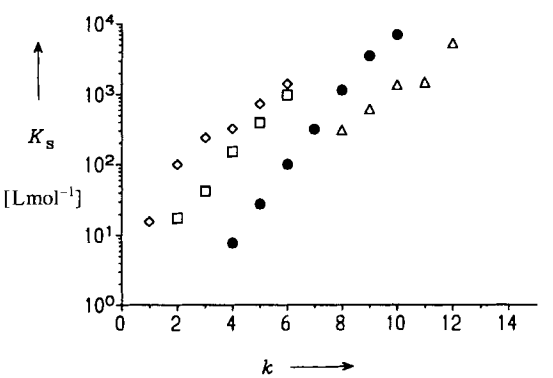


Fig. 2. Stability constants K_s of the inclusion compounds of $HOOC-(CH_2)_k-COOH$ (◇), $HOOC-(CH_2)_k-COO^-$ [134a] (□), $HO-(CH_2)_k-OH$ [104] (●), and $^-OOC-(CH_2)_k-COO^-$ [132b] (△) in **1a** as a function of the spacer length k.

terminal groups lower the stability.[104, 121, 131, 132b, 134] If substituents are present at both ends of the chain, they can have a considerable influence on the inclusion kinetics. For example, inclusion of 1,10-decanediol and decamethylenediamine[135] is so fast that signal averaging is observed in the NMR spectra. In contrast, this process is so slow for 1,1′-decamethylenedipyridinium[132a] and 1,10-decanedicarboxylic acid[132b] that averaging is not observed. Instead, the methylene groups give rise to two sets of signals, because of the removal of mirror symmetry upon inclusion in the asymmetric host.[132a] In the case of decamethylenebis(trimethylammonium) the end groups are so large that inclusion in **1a** takes several minutes.[135] Thus the ionic end groups can provide significant steric hindrance to the inclusion and dissociation processes. When the ion passes through the ring, its hydrate shell must be shed. This also shows quite clearly that axial inclusion compounds are actually formed (Scheme 7b). This finding has been confirmed by NOE measurements[132b] and X-ray structure analysis.[107r]

Although benzene is already too large for **1a**, benzene derivatives (e.g. *p*-dibromobenzene, $K_s = 913\ M^{-1}$) can undergo inclusion.[117b, 136] The cyclodextrin apparently sticks preferentially over one of the substituents and is deformed to give an ellipse.[137] 4,4′-Bis(aminomethyl)biphenyl is already too large for **1a** ($K_s = 8\ M^{-1}$),[138] probably because the two benzene rings are not coplanar. On the other hand, azobenzene derivatives form stable axial inclusion compounds with **1a**[139] (e.g. methyl orange, $K_s = 10^{-5}\ M^{-1}$),[120b] most likely because they are planar and dumbbell-shaped.

Bulky benzene derivatives do fit into β-cyclodextrin **1b** (e.g. 4-*tert*-butylphenol, $K_s = 36300\ M^{-1}$),[140] as do naphthalene derivatives.[141] However, the cavity in **1b** is filled by molecules with a cylindrical shape better than by flat arenes. Thus derivatives of perfluoroalkyl chains,[122a] adamantane,[127] and ferrocene,[142] as well as transition metal complexes of cyclic dienes,[143, 144] form stable inclusion compounds with **1b**. Although the relatively thin, linear alkyl derivatives are included by **1b** just as well as by **1a**, virtually no spectroscopic changes occur because of the loose packing, and inclusion can be detected only indirectly, for example, by the displacement of a probe molecule.[102, 125a]

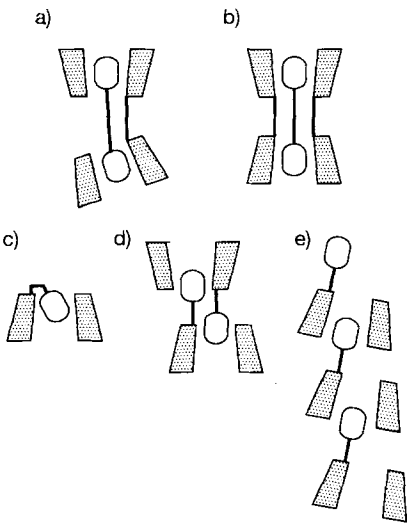
γ-Cyclodextrin **1c** is large enough to take up polyannelated ring systems such as pyrene,[145] benzpyrene,[119c] and even steroids.[146] [12]Crown-4 and its alkali metal complexes form sandwichlike inclusion complexes.[107l, o, 147] Even coronene[148] and buckminsterfullerene C_{60}[149] form stable inclusion compounds with two molecules of **1c** (Scheme 7d). **1c** is also able to take up two guest molecules (e.g. anthracene derivatives[115, 150]) simultaneously (Scheme 7e,f).

Amylose, the polymeric analogue of the cyclodextrins, often also forms similar inclusion complexes.[151] In contrast to the cyclodextrins the internal diameter of the amylose helix is not defined. The conformation of the amylose molecule can adapt itself to the size and shape of the guest molecule.[152] The selectivity of amylose is thus much lower than that of the cyclodextrins.

4.1.6. Covalently Linked Cyclodextrins and Guest Molecules

The formation of covalent bonds between building blocks provides additional possibilities for constructing supramolecular structures. Not only can two cyclodextrins or two guest molecules be linked together, equally feasible is linking a cyclodextrin and a guest molecule.

Harada et al. and Breslow et al. described the binding potential of singly[79a, 153] and doubly[80] bridged cyclodextrin dimers (Schemes 8a and 8b). Such molecules are referred to as ditopic hosts,[92b] since they are able to include two hydrophobic guests or a guest with two hydrophobic binding sites (a ditopic guest). In the latter case the stability constants can be particularly high ($K_s \geq 10^{10}\ M^{-1}$). As such systems also have a high recognition potential for guest molecules, they are also referred to as artificial receptor molecules.[80]

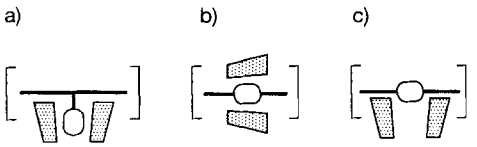


Scheme 8. Topology of inclusion compounds from a) covalently linked hosts and guests and b) ditopic host plus ditopic guest; c) monomeric, d) dimeric, and e) polymeric complexes of a host–guest conjugate.

A unique situation arises when a cyclodextrin molecule and a guest molecule are covalently linked. Such cyclodextrin–guest conjugates can organize themselves either intramolecularly to give monomeric inclusion compounds or intermolecularly to give dimeric or polymeric inclusion compounds[34a, 35, 154] (Scheme 8c–e). A covalently bonded guest molecule can be displaced from the cyclodextrin cavity by a free guest molecule. Since this displacement process can be detected spectroscopically by either optical absorption,[155] fluorescence,[156] or circular dichroism,[157] such cyclodextrin–guest conjugates can be used as sensor molecules, for example, for steroids.[155b, 156]

4.1.7. The Inclusion of Polymeric Guest Molecules

A polymer can by complexed by many host molecules if it has a corresponding number of binding sites, in other words, if it functions as a polytopic guest molecule. The binding sites can lie along the main chain as well as in the side chains. Since such polymers can form both inclusion and addition compounds with cyclodextrins, several arrangements are possible (Scheme 9). The axial inclusion of the main chain of a polymer (Scheme 9b) leads to a special topology: the rings are "threaded" onto a chain. This means that a threaded ring is not undergoing dynamic exchange with the free rings, unless it occupies



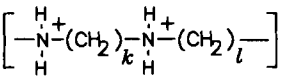
Scheme 9. Topology of cyclodextrin inclusion compounds with polymeric guest molecules. a) Inclusion of the side chain, b) axial inclusion of the main chain, c) addition to the main chain.

the position at the end of the chain. The threaded rings can only migrate along the chain or rotate about it; they are thus confined to one-dimensional space with respect to the polymer chain.

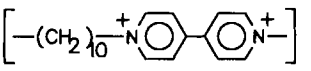
The formation of inclusion compounds with polymers has been carried out by free radical polymerization,[158] polycondensation,[159] and polyaddition[160] in the presence of cyclodextrins or hydrophilic cyclodextrin derivatives. Since the resulting polymeric adducts could not be clearly characterized owing to their poor solubility and structural heterogeneity, their topology is still unclear.

In the interactions between poly(styrenesulfonic acid)[161] or poly(*N*-alkyl-4-vinylpyridinium bromide)s[130] and cyclodextrins the side chains probably undergo inclusion (Scheme 9a). According to Harada et al., polyethylene glycol and **1a**,[162] polypropylene glycol and **1b**,[163] and poly(methyl vinyl ether) and **1c** form scarcely water-soluble adducts above a chain length of ten monomer units. The formation of these adducts is highly specific; for example, polyethylene glycol interacts only with **1a** but not with **1b** or **1c**. These adducts contain two ethylene oxide units or three ethylene units per cyclodextrin molecule. The length of these two or three repeat units (7.5 Å) and the height of the cyclodextrin torus are almost identical. Hence, it seems reasonable to suppose that the polymer chains pass through stacks of cyclodextrins. This hypothesis was supported by the X-ray powder diffractogram of the adduct of polyethylene glycol and **1a**, which is comparable to those found for axial inclusion compounds with long guest molecules like polyiodide[3, 165] in **1**. Final proof of the axial topology (Scheme 9b) of these inclusion compounds was provided by the fact that termination of the polymer chains with bulky 3,5-dinitrobenzoyl groups inhibits their formation completely.

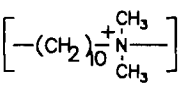
We have used polymers with alternating hydrophobic and hydrophilic segments to construct water-soluble polymeric inclusion compounds. The hydrophobic segments (oligomethylene units) are intended to function as binding sites for **1a**. The hydrophilic segments (secondary or quaternary ammonium groups) should ensure solubility in water. The protonated poly(imino-oligomethylene)s **26**[166] and the polymeric compounds with quaternary ammonium groups, **27**[167] and **28**,[168] are sufficiently soluble in water that the interaction with **1a** occurs in a homogeneous phase. The ^{1}H NMR spectrum shows new signals due to the included oligomethylene units and the occupied rings. The induced signal shifts are independent of the concentration and resemble those of monomeric model compounds (e.g. decamethylenediamine[135] and 1,1′-decamethylenedipyridinium[132a] in **1a**). The observed signal doubling in the aliphatic range of the ^{1}H NMR spectrum is characteristic of the axial inclusion of the chain.[132a] In comparison with the formation of monomeric inclusion compounds the reaction of



26A $k = l = 6$
26B $k = l = 11$
26C $k = 10$, $l = 3$



27



28

1a with polymers **26**, **27**, and **28** is astonishingly slow; we have measured reaction times between one hour and six months. The rate of reaction decreases rapidly with the increasing bulk of the cationic groups, thus confirming the axial chain inclusion.

The polymers **26C** and **28** included in **1a** are released so slowly that excess free cyclodextrin molecules can be separated readily by dialysis or gel permeation chromatography (GPC). Like the slow threading, the slow release of **1a** is attributed to the slow migration rate of the rings along the polymer chain. This migration is probably hampered by the bulky hydrate shells around the cationic groups.

As with monomeric guest molecules, the final extent of inclusion increases dramatically with the increasing length of the hydrophobic segments. While no inclusion is observed when the chain is only six methylene units long (polymer **26A**), all water-soluble polymers with more than nine methylene groups undergo inclusion.[166–168] For example, polymer **26B** (45 mM solution in water) undergoes complexation to the extent of 68% when an equimolar amount of **1a** is added.[166] Almost complete coverage of the chain can be achieved when an excess of **1a** is used. The driving force for the threading of **1a** onto the polymer chain is a gain in enthalpy; for the polymeric inclusion compound **1a**·**26B** the enthalpy of formation is $-20\ kJ\ mol^{-1}$.[169] This value lies in the range of the enthalpies of formation of analogous monomeric systems.[104]

Our observation that the inclusion of a polymer in **1a** requires the alkyl group to be at least ten methylene groups long appears to contradict the results of Harada et al., who detected inclusion of even ethylene segments in **1a**.[162] Probably the two systems are topologically quite different. In our systems the ammonium ions form steric barriers that separate the threaded rings from each other. In contrast the neutral systems studied by Harada permit a close packing of the rings, which are linked by hydrogen bonds, along the chain.[170]

The threading of the larger host **1b** onto polymers **26C** and **28** cannot be detected by either NMR spectroscopy or microcalorimetry. In order to prove the inclusion of polymer **28** in **1b** we made use of the fact that threaded rings cannot pass one another. Polymer **28** was allowed to interact with **1b** and **1a** successively in aqueous solution; the free rings were removed afterwards by dialysis. In the product the chain is occupied up to 60% by **1b** and 7.5% by **1a**. Thus the rings **1b** are threaded rapidly onto the polymer chain, and the "slower" rings **1a** prevent them from slipping off.[168, 169]

4.2. Cyclodextrins as Exolipophilic Hosts

The binding capability of lipophilic cyclodextrins was first studied by Menger and Dulany.[77] They found that a polar guest molecule such as 4-nitrophenol is complexed by heptakis(3-*O*-butyl-2,6-di-*O*-methyl)-β-cyclodextrin in organic solvents. In contrast to the hydrophilic systems here the stability constant K_s *increases* with decreasing solvent polarity; in nonpolar solvents such as heptane the stability constant for the inclusion of 4-nitrophenol is quite high ($K_s = 2600\ M^{-1}$).[77] The main driving force for the complexation is thought to be provided by dipole–dipole interactions and hydrogen bonds.[77] Thus the cyclodextrin ether behaves as an exolipophilic host.

Polar substituents directed towards the interior of the cavity increase the complexation ability of lipophilic cyclodextrins. The following values for the complexation of 4-nitrophenol in cyclohexane have been measured:[171] per(2,3,6-tri-*O*-pentyl)-β-cyclodextrin **21b** $K_s = 3560\ M^{-1}$, per(2,6-di-*O*-pentyl)-β-cyclodextrin **19b** $K_s = 6000\ M^{-1}$, and per(2,6-di-*O*-pentyl-3-*O*-acetyl)-β-cyclodextrin **23b** $K_s \geq 10000\ M^{-1}$.

The complexation of cations by the lipophilic cyclodextrins per(2,3,6-tri-*O*-acetyl)- and per(2,3,6-tri-*O*-phenylcarbamoyl)-β-cyclodextrin in organic solvents was first proven by Komiyama et al.[26b] However, the quantification of the complexation ability with the picrate extraction method[172] showed that per(di-*O*-alkyl)-, per(tri-*O*-alkyl)-, and per(tri-*O*-acyl)cyclodextrins interact only weakly with cations. In contrast, per(3-*O*-acyl-2,6-di-*O*-alkyl)-β-cyclodextrins give quite stable complexes with alkali metal ions; they are in fact even superior to the standard crown ethers,[173] though they are not as specific (Fig. 3).[174] Even very large cations such as the tetramethylammonium ion or 4,4'-bipyridinium dications[78e] are complexed by **22b**. The good complexing ability of **22b** and **23b** can be traced back to the ester carbonyl groups, which according to the *trans* rule[175] should be directed preferably towards the C_7 axis (Scheme 10). Carbonyl oxygen atoms are known to interact strongly with cations.[176]

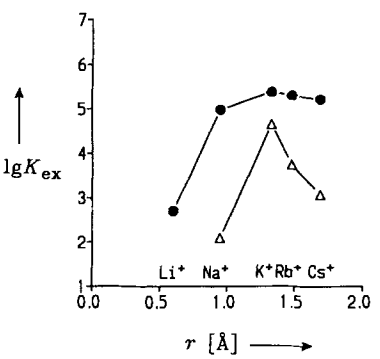
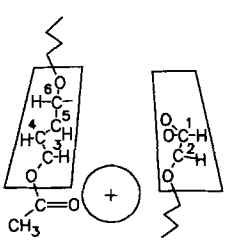


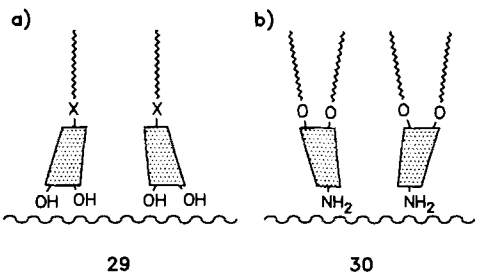
Fig 3. Complexation ability (picrate extraction coefficient K_{ex}) as a function of the cation radius r for **23b** in toluene [174] (•) and for dibenzo[18]crown-6 in benzene [173] (Δ).



Scheme 10. Possible location of an alkali metal ion in a per(3-*O*-acetyl-2,6-di-*O*-alkyl)-cyclodextrin.

4.3. Cyclodextrins as Building Blocks for Mono- and Multilayer Systems

Apart from host–guest complexes, other supramolecular structures such as monolayers and multilayers have been derived from cyclodextrin building blocks. Kawabata et al. showed for the first time that the amphiphilic cyclodextrins **29** and **30** undergo self-organization at the air–water interface to give stable monolayers analogous to crystals.[177] The area A occupied by a molecule at the water surface increases with increasing ring size (**29a**: $A = 173$, **29b**: $A = 210$, **29c**: $A = 281\ Å^2$) but varies little with changes in the length of the alkyl chain. Consequently, the cyclodextrin rings swim flat on the water surface, and the secondary hydroxyl groups are oriented towards the water (Scheme 11). In contrast, the amphiphilic cyclodextrin **30** forms



Scheme 11. Arrangement of amphiphilic cyclodextrins at the water/air interface. X = S, NH [177, 32c].

monolayers in which the side with the primary functional groups is directed towards the water.[32c]

Guest molecules such as azo dyes can be incorporated into the monolayers formed by cyclodextrins. As the area occupied by each host molecule does not increase on complexation, the guest molecule is situated inside the host cavity.[177b, 178] Such monolayers together with their included guests can be transferred repeatedly by means of the Langmuir–Blodgett technique to planar hydrophobic substrates such as glass slides precoated with cadmium icosanate.[177a] It is thus possible to produce multilayers composed of a defined number of monolayers on such a substrate. The guest molecules incorporated into the multilayer still have enough space to undergo photochemical isomerization. For instance, included azobenzene molecules can be switched photochemically between the *trans* and *cis* configurations.[179] Such systems could in principle serve as information storage media.[180]

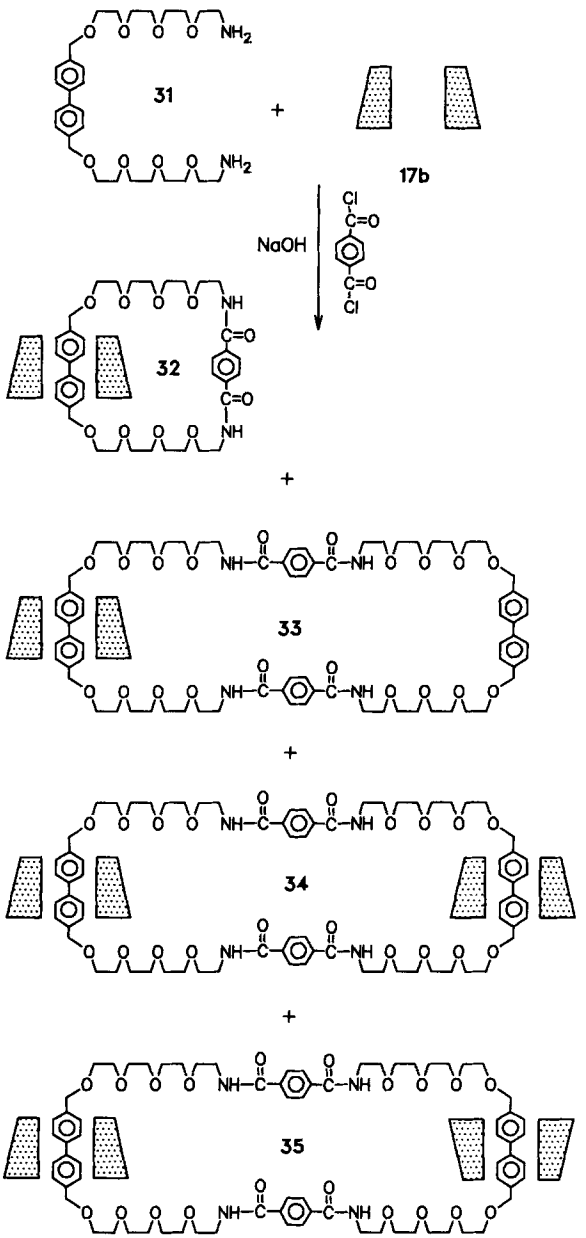
Monolayers composed of cyclodextrins are also produced by adsorption.[181] For example, cyclodextrins containing thiol groups have been adsorbed on a gold surface.[182] The formation of inclusion compounds at these monolayers can be detected by surface analysis (e.g. with plasmon spectroscopy).[182] Applications of such systems as sensors are conceivable.

5. The Construction of Molecular Architectures by Supramolecular Positioning

The great interest that supramolecular chemistry has found in the last few years arises from the idea of building up complex molecular structures from simple building blocks. The classical stepwise construction of structures by the formation of covalent bonds is replaced by the planned positioning of large units by means of secondary valence forces and their subsequent covalent linkage.[183] Whereas a large number of reactions are required in classical organic synthesis to generate, link, convert, protect, and cleave functional groups, supramolecular synthesis requires predictable forms of self-organization to bring building blocks into position in a defined manner prior to the necessary formation of covalent bonds. The tremendous power of the supramolecular approach has been demonstrated by the efficient syntheses of catenanes,[122a, 184] rotaxanes,[185] polyrotaxanes,[185] and knots[187] by Sauvage, Stoddart, and others.[92e] In the following sections we shall discuss the conditions necessary for the construction of catenanes, rotaxanes, and tubes from cyclodextrin inclusion compounds.

5.1. Synthesis of Catenanes

As early as 1957 Lüttringhaus, Cramer, Prinzbach, and Henglein attempted to synthesize a [2]catenane by ring closure of a long guest molecule included in **1a**.[188] This attempt was unsuccessful, perhaps because the guest molecule (28 bonds in length) was not long enough to circle the wall of the cyclodextrin molecule. Thirty-five years later Stoddart et al. synthesized two [2]catenanes, **32** and **33**, and two [3]catenanes, **34** and **35**, from the inclusion compound of the bitolyl derivative **31** in heptakis(2,6-di-*O*-methyl)-β-cyclodextrin **17b** (Scheme 12).[189] The cyclization of the guest was carried out by acylation of the two terminal amino groups with terephthaloyl dichloride, a reaction which also proceeds in good yields in aqueous solution. The catenanes formed can be readily separated from the reaction mixture because of their amphiphilic nature. Thus the requirements for supramolecular positioning, for the ring-closing reaction, and for the separation of the target compound were fulfilled; however, the yield of catenane **32** was only a disappointing 3% in spite of the stability of **17b**·**31** ($K_s \geq 10000\ M^{-1}$). It is possible that in **17b**·**31** the reactivity of the amino groups is diminished even though the guest **31** is 35 bonds in length. Amazingly, the catenanes **33**, **34**, and **35** with 84-membered rings could also be detected in yields of about 1%, even though their formation requires the formation of four bonds rather than two.

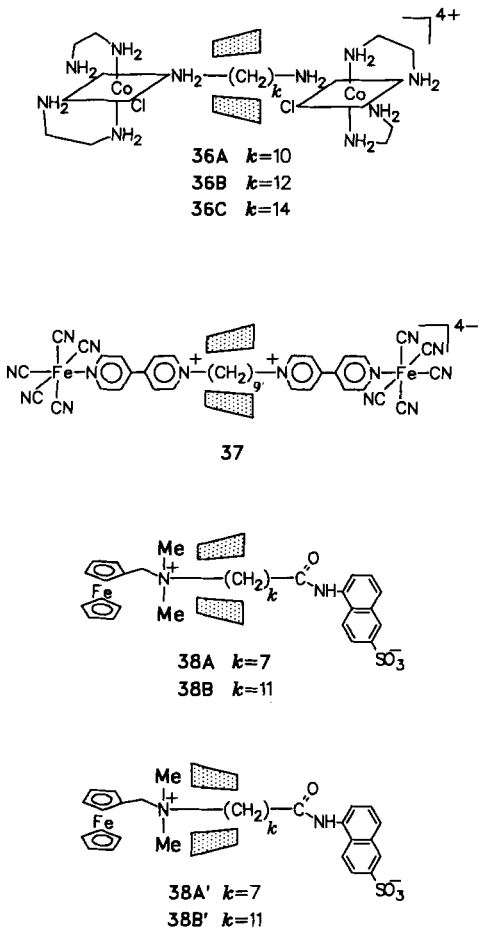


Scheme 12. Synthesis of [2]- and [3]catenanes from **17b** [189].

5.2. Synthesis of [2]Rotaxanes

In 1981 Ogino and Ohata reported that α,ω-alkanediyldiamines, included in **1a** or **1b**, react with bulky cobalt(III) complexes at both ends to give [2]rotaxanes **36** (Scheme 13).[190] The yield increased with decreasing ring size and depended on the length k of the alkyl chain, reaching a maximum of 19% at $k = 12$ (Table 3).[190b] If the chain is too short ($k = 8$), the amino groups are probably too strongly shielded by the host; if it is too long, the alkyl chains may associate. The solvent used was DMSO. Since the stability constants in this solvent are very low,[191] it is necessary to use very high concentrations of both host and guest. In a similar manner Wylie and Macartney obtained [2]rotaxane **37** by treating the inclusion compound of 1,1′-nonamethylenebis(4,4′-bipyridinium) and **1a** with a bulky iron(II)cyano complex in aqueous solution.[192] Since the iron complex formed is kinetically unstable ($k_d = 1.5 \times 10^{-3}\ s^{-1}$), there is a very slow exchange between the rotaxane **37** and the uncomplexed dumbbell-shaped compound and **1a**.[192]

Stable rotaxanes are formed only when the blocking groups are covalently linked to an included guest molecule. Isnin and Kaifer obtained a mixture of the two isomeric [2]rotaxanes **38A** and **38A′** as well as **38B** and **38B′** in 15% yield by forming an



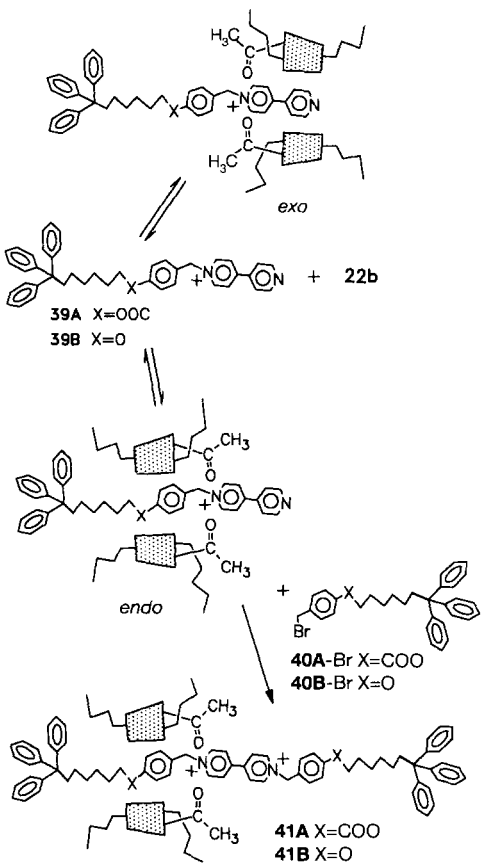
Scheme 13. Hydrophilic [2]rotaxanes from cyclodextrins [190–193].

Table 3. Synthesis of [2]rotaxanes according to Ogino and Ohata [190b].

Host	k in H_2N-$(CH_2)_k$-NH_2	[2]Rotaxane	Yield [%]
1a	8	–	0
1a	10	**36A**	5.7
1a	12	**36B**	19
1a	14	**36C**	12
1b	12	**36D**	6.7

amide bond. Surprisingly isomer **38A** is stable, in other words it is a rotaxane, whereas the other isomer **38A'** dissociates slowly into the dumbbell and **1a**.[194] It seems that the steric hindrance towards unthreading depends on the orientation of the cyclodextrin.

The main difficulty in these rotaxane syntheses is that the conditions for the bond-forming reaction must be favorable for the host–guest interaction as well. Although water is the best solvent for the formation of inclusion compounds, it is not very well suited as a reaction medium for the attachment of the blocking groups, as the reagents are generally only poorly soluble and can be consumed by hydrolysis. It thus appeared of interest to attempt constructing [2]rotaxanes in inert organic solvents with exolipophilic cyclodextrins. Per(3-*O*-acyl-2,6-di-*O*-alkyl)cyclodextrins such as **22b** are indeed able to complex guests such as the 4,4'-bipyridinium ions **39**, which are blocked on one side (Scheme 14). Two orientations of the host **22b** (the



Scheme 14. Synthesis of lipophilic [2]rotaxanes from *endo* complexes of bipyridinium ions blocked at one end [78e, 108e].

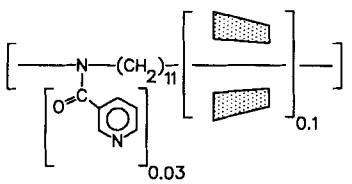
exo and the *endo* form) with respect to the guest can be distinguished in the ^{1}H NMR spectrum.[108e] Attachment of the blocking group **40A** (as the bromide) to the complexed guest **22b**·**39A** furnished the lipophilic [2]rotaxane **41A** in 19% yield.[78e] The yield of the analogous [2]rotaxane **41B** starting from the building blocks **39B** and **40B** was even better (^{1}H NMR: 50%, isolated 36%).[108e] The ^{1}H NMR spectra of both rotaxanes **41** show the distinct doubling of signals for the protons on the dumbbell axis. Together with NOE studies this signal doubling indicates that the cyclodextrin molecule is not situated in the middle of the dumbbell but towards one side of it. The two halves of the dumbbell were differentiated by deuteration of the benzylic methylene group of the blocking group **40B**. It could then be shown that in the rotaxane the host is located only on the side of the original guest molecule **39B**. Thus only the *endo* complex reacts with the blocking group **40**-Br. In the case of the *exo* complex the terminal pyridine group is probably shielded from attack of **40**-Br by the host.[108e] This selective reaction of a host–guest compound with one orientation could be used for the construction of uniform [2]rotaxanes with an unsymmetrical dumbbell component.

5.3. Synthesis of Polyrotaxanes

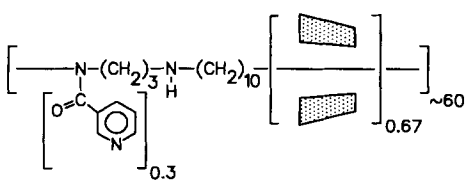
Polyrotaxanes can be prepared by reactions between axial polymeric inclusion compounds with blocking groups or by

polymer-analogous reactions of polymers with monomeric inclusion compounds. In the former case the rotaxane axes lie along the polymer main chain (main-chain polyrotaxanes), while in the latter they branch off from it as side chains (side-chain polyrotaxanes).

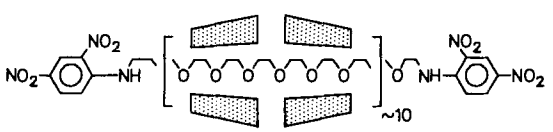
Starting from the inclusion compounds of the polyamines **26B** and **26C** with **1a**, we obtained the water-soluble main-chain polyrotaxanes **42** in good yields by partial polymer-analogous reaction of the amino groups with nicotinoyl chloride (Scheme 15).[166] The products were readily purified by dialysis. In the case of **42B** about forty rings were held permanently on the chain. Nicotinoyl groups are too small, however, to block the larger rings **1b**, and larger substituents such as 2,4-dinitro-5-aminophenyl groups had to be used instead.[169]



42A

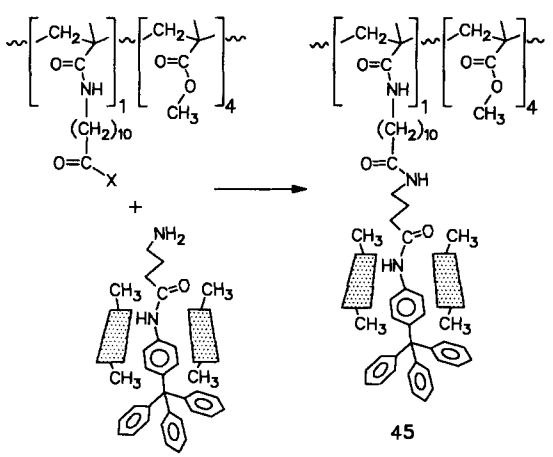


42B



43

Scheme 15. Main-chain polyrotaxanes from **1a** [166, 195].



17b·44 **45**

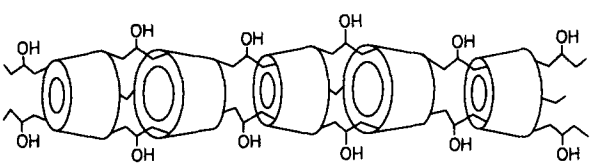
Scheme 16. A side-chain polyrotaxane from **17b** [196]. X = O-COOEt.

Harada et al. synthesized the polyrotaxane **43** with about twenty rings on the chain by reacting the terminal amino groups of a polyethylene oxide included in **1a** with Sanger's reagent.[195] This rotaxane is soluble in water at pH > 12 and in DMSO; it was purified by GPC.

The synthesis of a side-chain polyrotaxane (Scheme 16) was achieved by Ritter et al. by the reaction between the guest in **44·17b** and the side groups of a reactive comb polymer; the polymeric product **45** was purified by multiple precipitation.[196]

5.4. Synthesis of Tubular Polymers

We have so far discussed only syntheses in which a chemical reaction was carried out at an included guest molecule. We shall now turn our attention to the covalent linkage of threaded rings to give tubular polymers. The polymeric "thread" has the function of arranging stacks of rings. Harada et al. treated a solution of polyrotaxane **43** in 10% NaOH with epichlorohydrin.[197] By using gel permeation chromatography they were able to show that cross-linking occurs only along the polymer chain with formation of hydroxypropylene bridges. The blocking groups were then cleaved with 25% NaOH and the threads removed by GPC. The final product was the tube **46** consisting of about fifteen multiply bridged cyclodextrin units.[197]

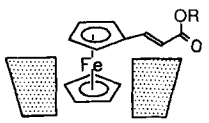


46

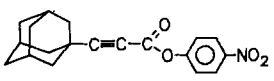
6. Host–Guest Catalysis

The defined spatial relationship between the building blocks of a supramolecular structure makes it possible to carry out reactions under topochemical[198] control. The influence of the host on reactions at the guest (host–guest catalysis) has been the subject of many investigations.[199] We shall now discuss the most important catalytic functions of cyclodextrins.

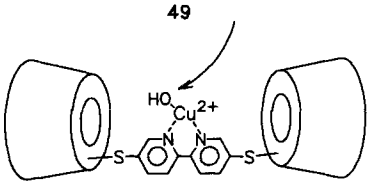
The term *covalent catalysis* is used when the catalysis involves a temporary covalent bond between host and guest. Most studies have focused on the catalytic activity of cyclodextrins in ester hydrolysis. Cyclodextrins accelerate the alkaline (pH > 11) saponification of esters of carboxylic acids,[200] phosphoric acids,[201] and sulfuric acid.[202] A deprotonated secondary hydroxyl group, probably OH(2), serves as the nucleophile, since it has the highest acidity. This hydroxyl group forms a cyclodextrin ester, which then hydrolyzes to the cyclodextrin and the free acid.[140, 203] The catalytic activity of the cyclodextrin increases with the stability of the inclusion compound[204] and with decreasing distance between OH(2) and the ester group of the guest in the inclusion compound.[140] Optimization of the structure of the guest leads to esters that are cleaved very rapidly by **1b**. For instance, the cleavage of ferrocene ester **47** (Scheme 17)



47 + 1b



49



48

Scheme 17. Catalysts based on cyclodextrins[205,211]. R = p-NO_2-C_6H_4.

can be accelerated by **1b** by a factor of 10^5.[205] The cyclodextrin is consumed in this process, since the cleavage of the cyclodextrin ester formed is very slow.

Cyclodextrins (pK_a = 12.2) are catalysts for ester cleavage at pH values above 11. Since it would be more useful to have such catalysis at lower pH values, functional groups that are deprotonated more easily were attached to the cyclodextrins. When the imidazole moiety (pK_a = 7.04)[206] was used, the catalytic activity of the cyclodextrin increased considerably and the optimum pH shifted to 8.[38, 203, 207] The activity depends on the position of the imidazole moiety on the cyclodextrin: an imidazole group on the side with the secondary OH groups causes a greater increase in the reaction rate than one on the side of the primary OH groups.[38, 207c] The highest activity, an increase in the rate of hydrolysis of 4-nitrophenyl acetate by a factor of 1100, was observed by Toda et al. for a heptakis(2,6-di-*O*-methyl)-β-cyclodextrin with a 4-imidazoylethyl group at O(3).[207c] Since one equivalent of this compound effected the saponification of one hundred equivalents of the ester, it is evident that the covalent intermediate is also rapidly cleaved.

Transition metal ions such as Zn^{2+} and Cu^{2+} can be coordinated to amine-functionalized cyclodextrins in order to mimic metalloenzymes. Such complexes have been used to catalyze the cleavage of esters,[208] cyclic phosphates,[209] and the hydration of carbon dioxide.[210] Very recently, the ditopic catalyst **48** was introduced, which increases the rate of hydrolysis of suitable esters like **49** at pH 7 by a factor of up to 220000.[211] Unfortunately, all such advances have so far been limited to the saponification of a few activated esters (e.g. *p*-nitrophenolates). Therefore application of these catalysts is still not feasible.[212]

Cyclodextrins can catalyze other reactions besides the saponification of esters. For example, pyridoxamine-substituted cyclodextrins catalyze the reduction of α-ketocarboxylic acids,[67] while alkenes can be converted to epoxides with porphyrin-substituted cyclodextrins.[213]

Cyclodextrins can also increase the rate of reactions without the formation of a covalent bond to the included guest; here the cyclodextrin serves as a "reaction vessel". Thus electrophilic substitution of arenes (e.g. chlorination,[214] carboxylation,[215] and azo coupling[216]) can be catalyzed by cyclodextrins. The σ complex is apparently stabilized in the inclusion compound by the donor action of the cyclodextrin. Such stabilization can even allow spectroscopic characterization of the σ complex.[217] Inclusion generally leads to a decrease in the amount of *ortho* and *meta* products because of shielding of these positions by the host.[214, 218] The regio-[219] and enantioselectivity[220] of a number of other reactions has also been influenced by the inclusion of starting materials in cyclodextrins.

When two guest molecules are included in the same cavity (cf. Scheme 7e), they are compressed, which facilitates pericyclic reactions. Inter-[221] and intramolecular[222] [4 + 2] Diels–Alder reactions and [2 + 2] photodimerizations[113b, 150b, 223] are accelerated by **1b** and **1c**, and the yields are increased. Both regio- and enantioselectivity are influenced as well.[222, 221]

7. Physical Functions of Supramolecular Structures Derived from Cyclodextrins

In addition to the chemical functions of supramolecular structures we must also mention the physical functions such as recognition[92b] and translocation (retention or transport) of guest molecules.[224] The combination of these functions is of great practical interest, since it can be employed for the separation of compounds.

7.1. Molecular Recognition

A host that forms complexes of different stabilities with two similar guests is said to display molecular recognition. Cyclodextrins detect not only the length and thickness of a guest but also distinguish between enantiomeric guest molecules owing to their chirality. Diastereomeric host–guest complexes are known both for hydrophilic[28, 141, 225] and lipophilic cyclodextrins.[226] The interactions that determine chiral recognition have been studied by computer simulations.[21, 226, 227]

7.2. Selective Retention of Guest Molecules by Immobilized Cyclodextrins

A guest molecule can be retained in a molecular current only if the host is bound to a solid substrate. The stronger the interaction between the guest and the immobilized host, the slower the guest proceeds in the current. Armstrong et al. were the first to immobilize hydrophilic cyclodextrins on silica gel and to use them for the separation of a variety of guest molecules (in particular racemates) by liquid chromatography.[228] König, Wenz, et al. showed that coatings of lipophilic cyclodextrins (e.g. **21a**,[229] **21b**,[230] **21c**,[231] **23a**,[232] and **23b**[233]) inside long capillaries form excellent stationary phases for the gas-chromatographic separation of enantiomers. The more polar permethylated cyclodextrins **20** also show very good separation performance in a lipophilic medium.[234] Immobilized permethyl-β-cyclodextrin can also be used for supercritical fluid chromatography, a method that also permits the high-resolution separation of nonvolatile substances.[234d, e] Chromatographic separation on cyclodextrin-containing stationary phases has become a widely applied analytical method for substances of general importance such as flavorings,[236] pheromones,[237] anaesthetics,[238] drugs,[239] and agrochemicals,[240] as well as for pollutants.[241]

7.3. Transport of Guest Molecules by Means of Mobile Cyclodextrins

The transport of a guest molecule in or through a liquid phase relies primarily on an increase in its solubility by the formation of a host–guest complex. This transport can be used for phase-transfer catalysis of chemical reactions[26a, 242] and for the separation of different guest molecules.[243] Hydrophilic cyclodextrins were used to transport hydrophobic guest molecules across an aqueous phase,[242a, c, 243] lipophilic cyclodextrins to transport ionic guest molecules across a lipophilic phase,[26a] and an amphiphilic derivative to transport cations across a liposome membrane.[244] Charged cyclodextrins can effect the transport of included neutral guest molecules in an electrical field.[245]

8. Applications

Cyclodextrins and their derivatives are already in use throughout the world for the formulation of drugs[83a, 246] and cosmetics[247] and for technical purposes.[248] With the exception of the latter area these applications must generally be approved by national licensing authorities. Detailed studies on the toxicity, mutagenicity, teratogenicity, and carcenogenicity of cyclodextrins, in particular hydroxypropyl-β-cyclodextrin, have thus been carried out.[249] So far cyclodextrins have been found to be non-hazardous with the exception that high concentrations of **1a**, **1b**, and **1c** cause damage to human erythrocytes.[250] However, even this can be avoided with hydroxypropyl derivatives.[7] At present cyclodextrins have general approval for use as food additives in Japan and Hungary and approval for specific applications in France and Denmark. Cyclodextrins often have advantages over starch, which might have similar inclusion properties, since they do not provide a culture medium for microorganisms.

In most of the applications, cyclodextrin inclusion compounds are formed for the modification of physical or chemical properties of the guest molecules. Analytical applications have already been mentioned. Cyclodextrins can be used for both increasing and decreasing the availability of an active substance and for protecting it from degradation.

8.1. Increasing the Availability of Drugs

The solubility of hydrophobic drugs in water can be increased by inclusion in cyclodextrins. The increase in solubility facilitates simpler formulation and an improved uptake of the drug.[251] Tensides are also used for this purpose, but cyclodextrins are more compatible with sensitive biological systems such as erythrocyte cell membranes.[249] Hydroxypropylcyclodextrins are used for solubilizing drugs that are administered parenterally.[252] Recently there has been great interest in the solubilization of insulin[253] and steroid hormones[254] as well as antiviral drugs[255] for nasal application.

Even small amounts of lipophilic cyclodextrin derivatives such as **22b** accelerate the solidification of cyanoacrylate adhesives. The acceleration of this polymerization probably results from the solubilization of ionic initiators.[256]

8.2. Reducing or Retarding the Availability of Active Substances

The formation of poorly soluble cyclodextrin derivatives, in particular starting from **1b**, can be used for removing undesired substances (e.g. cholesterol from liquid egg,[247] aromatic compounds from wastewater,[257] and nicotine and condensate from cigarette smoke[258]) and for encapsulating active substances. Encapsulation can be used to slow down the rate of release and thus increase the duration of effectiveness.[259] The vapor pressure of guest molecules can also be lowered by inclusion in cyclodextrins. This is employed for the carefully dosed long-lasting release of pleasant aromatic compounds such as chamomile, rose, lemon, and peppermint oil.[260] For this purpose cyclodextrins can also be immobilized on consumer goods such as textiles.[261] At the other extreme, unpleasant odors such as those of metabolic by-products and mercaptans in hair care products can be masked by cyclodextrins.[262]

Even the viscosity of polymeric thickening agents can be adjusted by cyclodextrins. The addition of **1** leads to readily processable solutions of low viscosity of otherwise associating polymers. The inclusion of polymer side chains probably decreases polymer–polymer interactions; however, as soon as the host is saturated by a monomeric guest, the polymer side chains are released and highly viscous solutions result.[248]

8.3. Stabilization of Active Substances

Cyclodextrins protect the included guest molecule from degradation by autoxidation, photolysis, and hydrolysis, particularly in the crystalline state. For example it is possible to stabilize sensitive flavorings such as those in onions, dill, garlic and horseradish,[262] and also vitamins[263] over a long period of time by forming cyclodextrin inclusion compounds.

9. Future Prospects

Developments shall continue at a great pace in the next few years, particularly if cyclodextrins are licensed for further applications in food and drug production.

For the synthesis of cyclodextrins the development of simpler, more easily reproducible procedures will be important. All available chromatographic and spectroscopic methods will be required for characterizing new products. Standard measurement and evaluation protocols should be developed for the determination of the stoichiometry and stability of cyclodextrin inclusion compounds to ensure the comparability of the data. Of the methods available at present, ^{1}H NMR spectroscopy and microcalorimetry are of particular importance, as they are almost universally applicable.

The boundaries drawn here, which indeed still exist, between preparative, physical, theoretical, macromolecular, biomimetic, analytic, and physiological chemistry will be fascinating to cross. For example, catalytically active catenanes and rotaxanes appear feasible. Rotaxanes and cyclodextrin catalysts could also be built into larger supramolecular structures such as monolayers and vesicles in order to carry out specific operations. Poly-

mers of defined length could be synthesized in tube-shaped polymers. The programmed release of several active substances could be achieved by the slow unthreading from polymer chains. Because of the common solvent, water, it even appears rewarding to forge a link to biochemistry. The imagination knows no limits!

I thank my co-workers and the research group of Prof. W. A. König, Universität Hamburg, for discussions and for reading this manuscript. I am also indebted to Wacker Chemie GmbH, München, and Henkel KGaA, Düsseldorf, as well as to the Bundesministerium für Forschung und Technologie (Projekt BEO 22/0319055A) and the Max-Planck-Institut für Polymerforschung for the generous support of my work in this field.

Received: December 21, 1992 [A 936 IE]
German version: *Angew. Chem.* **1994**, *106*, 851
Translated by: Dr. T. N. Mitchell, Dortmund (FRG)

[1] A. Villiers, *C. R. Hebd. Seances Acad. Sci.* **1891**, *112*, 536.
[2] *Nachwachsende Rohstoffe – Perspektiven für die Chemie* (Eds.: M. Eggersdorfer, S. Warwel, G. Wulff), VCH, Weinheim, **1993**.
[3] W. Saenger, *Angew. Chem.* **1980**, *92*, 343; *Angew. Chem. Int. Ed. Engl.* **1980**, *19*, 344.
[4] Chemical Abstracts Service registered 7131 publications on cyclodextrins between 1979 and August 30, 1993.
[5] Other reviews: a) M. L. Bender, M. Komiyama, *Cyclodextrin Chemistry*, Springer, Berlin, **1978**; b) J. Szejtli, *Cyclodextrins and their Inclusion Complexes*, Akademia Kiado, Budapest, **1982**; c) "Cyclodextrin Technology": J. Szejtli in *Topics in Inclusion Science* (Ed.: J. E. D. Davies), Kluwer, Dordrecht, **1988**; d) R. J. Clarke, J. H. Coates, S. F. Lincoln, *Adv. Carbohydr. Chem. Biochem.* **1988**, *46*, 205.
[6] Ref. [5c], p. 26.
[7] Recently CGTases have been isolated that preferably produce one particular ring size: a) *New Trends in Cyclodextrins and Derivatives* (Ed.: D. Duchêne), Editions de Santé, Paris, **1991**; G. Schmid in [7a], p. 25.
[8] a) H. Vakaliu, M. Miskolci-Torok, J. Szejtli, M. Jarai, G. Seres (Chinoin), HU-B 16098, **1977** [*Chem. Abstr.* **1979**, *91*, 91923]; b) E. Flaschel, J. P. Landert, A. Renken in *Proc. 1st Int. Symp. on Cyclodextrins* (Ed.: J. Szejtli), Reidel, Dordrecht, **1982**, p. 41.
[9] a) Y. Takahashi, T. Ogawa, *Carbohydr. Res.* **1987**, *164*, 277; b) *ibid.* **1987**, *169*, 127.
[10] P. C. Manor, W. Saenger, *J. Am. Chem. Soc.* **1974**, *96*, 3630.
[11] K. K. Chacko, W. Saenger, *J. Am. Chem. Soc.* **1981**, *103*, 1708.
[12] a) K. Lindner, W. Saenger, *Angew. Chem.* **1978**, *90*, 738; *Angew. Chem. Int. Ed. Engl.* **1978**, *17*, 694; b) *Carbohydr. Res.* **1982**, *99*, 103; c) C. Betzel, W. Saenger, B. E. Hingerty, G. M. Brown, *J. Am. Chem. Soc.* **1984**, *106*, 7545; d) V. Zabel, W. Saenger, S. A. Mason, *ibid.* **1986**, *108*, 3664.
[13] K. Harata, *Chem. Lett.* **1984**, 641.
[14] T. Fujiwara, N. Tanaka, S. Kobayashi, *Chem. Lett.* **1990**, 739.
[15] W. Saenger in *Inclusion Compounds* (Eds.: J. L. Atwood, J. E. D. Davies, D. D. MacNicol), Academic Press, London, **1984**, p. 231.
[16] a) M. Kitagawa, H. Hoshi, M. Sakurai, Y. Inoue, R. Chujo, *Carbohydr. Res.* **1987**, *163*, c1; b) M. Sakurai, M. Kitagawa, Y. Inoue, R. Chujo, *ibid.* **1990**, *198*, 181.
[17] G. Wenz, C. Apel, unpublished.
[18] M. J. Jozwiakowski, K. A. Connors, *Carbohydr. Res.* **1985**, *143*, 51.
[19] D. French, M. L. Levine, J. H. Pazur, E. Norberg, *J. Am. Chem. Soc.* **1949**, *71*, 353.
[20] A. K. Chatjigakis, C. Donze, A. W. Coleman, P. Cardot, *Anal. Chem.* **1992**, *64*, 1632.
[21] a) J. E. H. Koehler, W. Saenger, W. F. van Gunsteren, *J. Mol. Biol.* **1988**, *203*, 241; b) K. B. Lipkowitz, *J. Org. Chem.* **1991**, *56*, 6357; c) W. Linert, P. Margl, I. Lukovits, *Comput. Chem.* **1992**, *16*, 61.
[22] a) D. J. Wood, F. E. Hruska, W. Saenger, *J. Am. Chem. Soc.* **1977**, *99*, 1735; b) M. Vincendon, *Bull. Soc. Chim. Fr.* **1981**, 129; c) R. I. Gelb, L. M. Schwartz, D. A. Laufer, *Bioorg. Chem.* **1982**, *11*, 274.
[23] Reviews: a) A. P. Croft, R. A. Bartsch, *Tetrahedron* **1983**, *39*, 1417; b) M. Yalpani, *ibid.* **1985**, *41*, 2957.
[24] a) J. Boger, R. J. Corcoran, J.-M. Lehn, *Helv. Chim. Acta* **1978**, *61*, 2190; b) J. Szejtli, A. Liptak, I. Jodal, P. Fügedi, P. Nanasi, A. Neszmelyi, *Starch/Stärke* **1980**, *32*, 165.
[25] a) B. W. Müller, U. Brauns, *Pharm. Res.* **1985**, 309; b) C. T. Rao, B. Lindberg, J. Lindberg, J. Pitha, *J. Org. Chem.* **1991**, *56*, 1327.
[26] a) N. Kunieda, H. Taguchi, S. Shiode, M. Kinoshita, *Makromol. Chem. Rapid Commun.* **1982**, *3*, 395; b) M. Komiyama, H. Yamamoto, H. Hirai, *Chem. Lett.* **1984**, 1081; c) H. Ryoshi, N. Kunieda, M. Kinoshita, *Makromol. Chem. Rapid Commun.* **1985**, 263.
[27] a) K. Takahashi, K. Hattori, F. Toda, *Tetrahedron Lett.* **1984**, *25*, 3331; b) K. Fujita, T. Ishizu, K. Oshiro, K. Obe, *Bull. Chem. Soc. Jpn.* **1989**, *62*, 2960.
[28] K. Kano, K. Yoshiyasu, S. Hashimoto, *J. Chem. Soc. Chem. Commun.* **1989**, *17*, 1278.
[29] T. Eiki, T. Horiguchi, Y. Karawazaki, W. Tagaki, *Mem. Fac. Eng. Osaka City Univ.* **1984**, *24*, 573.
[30] a) K. Takeo, H. Mitoh, K. Uemura, *Carbohydr. Res.* **1989**, *187*, 203; b) P. Fügedi, *ibid.* **1989**, *192*, 366.
[31] S. Bulusu, T. Axenrod, B. Liang, Y. He, L. Yuan, *Magn. Reson. Chem.* **1991**, *29*, 1018.
[32] a) Y. Kuroda, O, Kobayashi, Y. Suzuki, H. Ogoshi, *Tetrahedron Lett.* **1989**, *30*, 7225; b) Z. Szurmai, A. Liptak, J. Szejtli, *Starch/Stärke* **1990**, *42*, 447; c) H. Parrot-Lopez, C. C. Ling, P. Zhang, A. Baszkin, G. Albrecht, C. D. Rango, A. W. Coleman, *J. Am. Chem. Soc.* **1992**, *114*, 5479.
[33] K. Takeo, K. Uemura, H. Mitoh, *J. Carbohydr. Chem.* **1988**, *7*, 293.
[34] a) S. Kamitori, K. Hirotsu, T. Higuchi, K. Fujita, H. Yamamura, T. Imoto, I. Tabushi, *J. Chem. Soc. Perkin Trans. 2* **1987**, 7; b) J. Defaye, A. Gadelle, A. Guiller, R. Darcy, T. O'Sullivan, *Carbohydr. Res.* **1989**, *192*, 251.
[35] R. C. Petter, J. S. Salek, C. T. Sikorski, G. Kumaravel, F.-T. Lin, *J. Am. Chem. Soc.* **1990**, *112*, 3860.
[36] The 3,6-anhydro product can be formed as a by-product: G. Wenz, G. Nelles, unpublished.
[37] L. D. Melton, K. N. Slessor, *Carbohydr. Res.* **1971**, *18*, 29.
[38] K. R. Rao, T. N. Srinivasan, N. Bhanumathi, P. B. Sattur, *J. Chem. Soc. Chem. Commun.* **1990**, 10.
[39] a) R. Breslow, A. W. Czarnik, *J. Am. Chem. Soc.* **1983**, *105*, 1390; b) H. Ikeda, Y. Nagano, Y.-Q. Du, T. Ikeda, F. Toda, *Tetrahedron Lett.* **1990**, *31*, 5045; c) T. Tahara, K. Fujita, T. Koga, *Bull. Chem. Soc. Jpn.* **1990**, *63*, 1409; d) A. R. Khan, L. Barton, V. T. D'Souza, *J. Chem. Soc. Chem. Commun.* **1992**, 1112; e) A. W. Coleman, P. Zhang, C.-C. Ling, J. Mahuteau, H. Parrot-Lopez, M. Miocque, *Supramol. Chem.* **1992**, *1*, 11.
[40] a) K. Fujita, S. Nagamura, T. Tahara, T. Koga, *J. Am. Chem. Soc.* **1985**, *107*, 3233; b) K. Fujita, T. Tahara, T. Imoto, T. Koga, *ibid.* **1986**, *108*, 2030.
[41] P. R. Ashton, P. Ellwood, I. Staton, J. F. Stoddart, *Angew. Chem.* **1991**, *103*, 96; *Angew. Chem. Int. Ed. Engl.* **1991**, *30*, 80.
[42] A. Gadelle, J. Defaye, *Angew. Chem.* **1991**, *103*, 94; *Angew. Chem. Int. Ed. Engl.* **1991**, *30*, 78.
[43] a) R. Breslow, S. Chung, *Tetrahedron Lett.* **1989**, *30*, 4353; b) H. Ikeda, Y. Nagano, Y.-Q. Du, T. Ikeda, F. Toda, *ibid.* **1993**, in press.
[44] Ref. [5c], p. 19.
[45] a) P. Mischnick, *Carbohydr. Res.* **1989**, *192*, 233; b) P. Mischnick, R. Krebber, *ibid.* **1989**, *187*, 197; c) P. Mischnick in [7a], p. 249.
[46] A. Hernandez, M. Alonso-Lopez, M. Martin-Lomas, C. Pascual, S. Penades, *Tetrahedron* **1987**, *43*, 5457.
[47] F. Djedaini, J. Desalos, B. Perly, *J. Labelled Compd. Radiopharm.* **1990**, *28*, 785.
[48] B. Casu, G. Scovenna, A. J. Cifonelli, A. S. Perlin, *Carbohydr. Res.* **1978**, *63*, 13.
[49] J. Szejtli, L. Kandra, *J. Inclusion Phenom.* **1987**, *5*, 639.
[50] a) Y. Kubota, T. Tanimoto, S. Horiyama, K. Koizumi, *Carbohydr. Res.* **1989**, *192*, 159; b) T. Tanimoto, Y. Kubota, N. Nakanishi, K. Koizumi, *Chem. Pharm. Bull.* **1990**, *38*, 318.
[51] a) J. Pitha, L. Szabo, H. M. Fales, *Carbohydr. Res.* **1987**, *168*, 191; b) T. Irie, K. Fukunaga, J. Pitha, K. Uekama, H. M. Fales, E. A. Sokolowski, *ibid.* **1989**, *192*, 167; c) Y. Kubota, T. Tanimoto, S. Horiyama, K. Koizumi, *ibid.* **1989**, *192*, 159; d) K. Koizumi, T. Tanimoto, Y. Okada, N. Nakanishi, N. Kato, Y. Tagaki, H. Hashimoto, *ibid.* **1991**, *215*, 127.
[52] C. M. Spencer, J. F. Stoddart, R. Zarzycki, *J. Chem. Soc. Perkin Trans. 2* **1987**, 1323.
[53] K. Koizumi, Y. Kubota, T. Utamura, S. Horiyama, *J. Chromatogr.* **1986**, *368*, 329.
[54] R. I. Gelb, L. M. Schwartz, J. J. Bradshaw, D. A. Laufer, *Bioorg. Chem.* **1980**, *9*, 299.
[55] D. Rong, V. T. D'Souza, *Tetrahedron Lett.* **1990**, *31*, 4275.
[56] J. Canceill, L. Jullien, L. Lacombe, J. M. Lehn, *Helv. Chim. Acta* **1992**, *75*, 791.
[57] B. Pöpping, A. Deratani, *Makromol. Chem. Rapid Commun.* **1992**, *13*, 237.
[58] G. Wenz, *Carbohydr. Res.* **1991**, *214*, 257.
[59] G. Wenz, P. Mischnick, P. Krebber, M. Richters, W. A. König, *J. High Resolut. Chromatogr.* **1990**, *13*, 724.
[60] S. F. Lincoln, J. H. Coates, C. J. Easton, S. J. van Eyk, B. M. May, P. Singh, M. A. Stile, M. L. Williams (Australian Commercial Research and Development Ltd.), WO-B 9002141, **1990** [*Chem. Abstr.* **1991**, *114*, 88647].
[61] B. Perly, F. Djedaini, P. Berthault in [7a], p. 179.
[62] A. Ueno, R. Breslow, *Tetrahedron Lett.* **1982**, *23*, 3451.
[63] T. Murakami, K. Harata, S. Morimoto, *Tetrahedron Lett.* **1987**, *28*, 321.
[64] a) M. Tanaka, Y. Kawaguchi, T. Niinae, T. Shono, *J. Chromatogr.* **1984**, *314*, 193; b) S. Cottaz, H. Driguez, *Synthesis* **1989**, *10*, 755.
[65] P. Fügedi, P. Nanasi, *Carbohydr. Res.* **1988**, *175*, 173.

[66] a) I. Tabushi, K. Shimokawa, K. Fujita, *Tetrahedron Lett.* **1977**, *18*, 1527; b) I. Tabushi, K. Yamamura, T. Nabeshima, *J. Am. Chem. Soc.* **1984**, *106*, 5267.

[67] R. Breslow, J. W. Canary, M. Varney, S. T. Waddell, D. Yang, *J. Am. Chem. Soc.* **1990**, *112*, 5212.

[68] K. Fujita, A. Matsunaga, T. Imoto, *Tetrahedron Lett.* **1984**, *25*, 5533.

[69] a) K. Fujita, T. Tahara, T. Koga, *Chem. Lett.* **1989**, 821; b) K. Fujita, T. Tahara, H. Yamamura, T. Imoto, T. Koga, T. Fujioka, K. Mihashi, *J. Org. Chem.* **1990**, *55*, 877.

[70] J. Boger, D. G. Brenner, J. R. Knowles, *J. Am. Chem. Soc.* **1979**, *101*, 7630.

[71] S. Cottaz, H. Driguez, *J. Chem. Soc. Chem. Commun.* **1989**, *16*, 1088.

[72] a) *Minutes of the 6th International Symposium on Cyclodextrins* (Ed.: A. R. Hedges), Editions de Santé, Paris, **1992**; b) D. Icheln, T. Runge, B. Gehrcke, W. A. König in [72a], p. 616.

[73] A. W. Coleman, P. Zhang, H. Parrot-Lopez, C. C. Ling, M. Miocque, L. Mascrier, *Tetrahedron Lett.* **1991**, *32*, 3997.

[74] W. A. König, D. Icheln, T. Runge, I. Pforr, A. Krebs, *J. High Resolut. Chromatogr.* **1990**, *13*, 702.

[75] B. Casu, M. Reggiani, G. R. Sanderson, *Carbohydr. Res.* **1979**, *76*, 59.

[76] K. Uekama, N. Hirashima, Y. Horiuchi, F. Hirayama, T. Ijitsu, M. Ueno, *J. Pharm. Sci.* **1987**, *76*, 660.

[77] F. M. Menger, M. A. Dulany, *Tetrahedron Lett.* **1985**, *26*, 267.

[78] a) W. A. König, G. Wenz, S. Lutz, E. von der Bey (Macherey-Nagel), DE-B 3810737, **1988** [*Chem. Abstr.* **1989**, *113*, 24434x]; b) D. R. Alston, P. R. Ashton, T. H. Lilley, J. F. Stoddart, R. Zarzycki, A. M. Z. Slawin, D. J. Williams, *Carbohydr. Res.* **1989**, *192*, 259; c) E. von der Bey, M. Gottlieb, G. Wenz in *Minutes of the 5th International Symposium on Cyclodextrins* (Ed.: D. Duchêne), Editions de Santé, Paris, **1990**, p. 82; d) H. G. Schmarr, B. Maas, A. Mosandl, S. Bihler, H. P. Neukom, K. Grob, *J. High Resolut. Chromatogr.* **1991**, *14*, 317; e) G. Wenz, E. von der Bey, L. Schmidt, *Angew. Chem.* **1992**, *104*, 758; *Angew. Chem. Int. Ed. Engl.* **1992**, *31*, 783.

[79] a) A. Harada, M. Furue, S.-I. Nozakura, *Polym. J. Tokyo* **1980**, *12*, 29; b) K. Fujita, S. Ejima, T. Imoto, *J. Chem. Soc. Chem. Commun.* **1984**, 1277; c) J. H. Coates, C. J. Easton, S. J. van Eyk, S. F. Lincoln, B. L. May, C. B. Whalland, M. L. Williams, *J. Chem. Soc. Perkin Trans. 1* **1990**, 2619; d) R. C. Petter, C. T. Sikorski, D. H. Waldeck, *J. Am. Chem. Soc.* **1991**, *113*, 2325.

[80] R. Breslow, S. Chung, *J. Am. Chem. Soc.* **1990**, *112*, 9659.

[81] T. Seo, T. Kajihara, T. Iijima, *Makromol. Chem.* **1987**, *188*, 2071.

[82] a) A. Harada, M. Furue, S.-I. Nozakura, *Macromolecules* **1976**, *9*, 701; b) Y. Kawakami, H. Kamiya, Y. Yamashita, *J. Polym. Sci. Polym. Symp.* **1986**, *74*, 291.

[83] a) U. Brauns, B. W. W. Müller (Janssen Pharmaceutica), EP-B 0149197 B1, **1984** [*Chem. Abstr.* **1985**, *103*, 166168f]; b) L. Szente, C. E. Strattan in [7a], p. 55.

[84] a) B. Lindberg, J. Pitha (Janssen Pharmaceutica), WO-B 9012035, **1990** [*Chem. Abstr.* **1991**, *114*, 143910e]; b) J. Pitha, C. Rao, B. Lindberg, P. Seffers, *Carbohydr. Res.* **1990**, *200*, 429.

[85] a) K. Hattori, K. Takahashi (Japan Maize Products), JP-B 62/59601 A2, **1987** [*Chem. Abstr.* **1987**, *107*, 60951y]; b) K. Yamamoto, A. Matsuda, Y. Tsuchiyama, M. Sato, Y. Yagi, T. Ishikura (Sannaku Co., Ltd.), JP-B 63041505, **1988** [*Chem. Abstr.* **1988**, *108*, 206598].

[86] a) Y. Yamamoto, Y. Inoue, R. Chujo, S. Kobayashi, *Carbohydr. Res.* **1987**, *166*, 156; b) H. Hashimoto in [7a], p. 97.

[87] a) J. Szejtli, E. Fenyvesi, B. Zsadon, *Starch/Stärke* **1978**, *30*, 127; b) T. Cserhati, G. Oros, E. Fenyvesi, J. Szejtli, *J. Inclusion Phenom.* **1984**, *1*, 395.

[88] H. Hirai, M. Komiyama, H. Yamamoto, *J. Inclusion Phenom.* **1984**, *2*, 655.

[89] H. Zemel, M. B. Koch (UOP Inc.), US-A 4958015, **1990** [*Chem. Abstr.* **1991**, *114*, 45364k].

[90] B. F. L. Sebille, A. L. E. Deratani, N. Thuaud, G. R. Lelievre (Centre National de la Recherche Scientifique), FR-B 2671087, **1992** [*Chem. Abstr.* **1993**, *118*, 171408y].

[91] B. Zsadon, M. Szilasi, F. Tudos, E. Fenyvesi, J. Szejtli, *Starch/Stärke* **1979**, *31*, 11.

[92] a) J.-M. Lehn, *Science* **1985**, *227*, 849; b) *Angew. Chem.* **1988**, *100*, 91; *Angew. Chem. Int. Ed. Engl.* **1988**, *27*, 89; c) *ibid.* **1990**, *102*, 1347 and **1990**, *29*, 1304; d) J. Rebek, Jr., *ibid.* **1990**, *102*, 245 and **1990**, *29*, 261; e) F. Vögtle, *Supramolekulare Chemie*, 2nd ed., Teubner, Stuttgart, **1992**; *Supramolecular Chemistry*, Wiley, New York, **1991**.

[93] a) D. J. Cram, J. M. Cram, *Science* **1974**, *183*, 803; b) *Acc. Chem. Res.* **1978**, *11*, 8.

[94] H.-J. Schneider, *Angew. Chem.* **1991**, *103*, 1419; *Angew. Chem. Int. Ed. Engl.* **1991**, *30*, 1417.

[95] K. Freudenberg, M. Meyer-Delius, *Ber. Dtsch. Chem. Ges. B* **1938**, *71*, 1596.

[96] a) F. Cramer, *Chem. Ber.* **1951**, *84*, 851; b) F. Cramer, F. M. Henglein, *ibid.* **1957**, *90*, 2561.

[97] The classification used here takes into account only the relation of the guest to the host and can thus be applied for both the crystalline and the solution state. Inclusion compounds can also be classified according to the arrangement of the rings in the crystal: see ref. [15].

[98] B. Siegel, R. Breslow, *J. Am. Chem. Soc.* **1975**, *97*, 6869.

[99] K. A. Connors, M. J. Mulski, A. Paulson, *J. Org. Chem.* **1992**, *57*, 1794.

[100] Only in exceptional cases did the addition of small amounts of alcohols lead to an increase in stability due to specific interactions: a) G. Nelson, G. Patonay, I. M. Warner, *J. Inclusion Phenom.* **1988**, *6*, 277; b) G. Nelson, I. M. Warner, *J. Phys. Chem.* **1990**, *94*, 576.

[101] A. Wishnia, S. J. Lappi, *J. Mol. Biol.* **1974**, *82*, 77.

[102] A. Buvari, J. Szejtli, L. Barcza, *J. Inclusion Phenom.* **1983**, *1*, 151.

[103] H. Schlenk, D. M. Sand, *J. Am. Chem. Soc.* **1961**, *83*, 2312.

[104] M. Bastos, L. E. Briggner, I. Shehatta, I. Wadsoe, *J. Chem. Thermodyn.* **1990**, *22*, 1181.

[105] a) J. N. J. J. Lammers, J. L. Koole, J. Hurkmans, *Starch/Stärke* **1971**, *23*, 167; b) J. N. J. J. Lammers, J. L. Koole, A. J. G. van Diemen, *Recl. Trav. Chim. Pays-Bas* **1972**, *91*, 483.

[106] a) F. Cramer, W. Saenger, H.-C. Spatz, *J. Am. Chem. Soc.* **1967**, *89*, 14; b) N. Yoshida, A. Seiyama, M. Fujimoto, *J. Phys. Chem.* **1990**, *94*, 4246.

[107] a) K. Harata, H. Uedaira, *Nature* **1975**, *253*, 190; b) K. Harata, *Bull. Chem. Soc. Jpn.* **1977**, *50*, 1416; c) K. Harata, H. Uedaira, J. Tanaka, *ibid.* **1978**, *51*, 1627; d) K. Lindner, W. Saenger, *Biochem. Biophys. Res. Commun.* **1980**, *92*, 933; e) K. Harata, K. Uekama, M. Otagiri, F. Hirayama, H. Ogino, *Bull. Chem. Soc. Jpn.* **1981**, *54*, 1954; f) K. Harata, K. Uekama, M. Otagiri, F. Hirayama, *ibid.* **1982**, *55*, 3904; g) K. Harata, *ibid.* **1982**, *55*, 2315; h) *ibid.* **1984**, *57*, 2596; i) D. R. Alston, A. M. Z. Slawin, J. F. Stoddart, D. J. Williams, *Angew. Chem.* **1985**, *97*, 771; *Angew. Chem. Int. Ed. Engl.* **1985**, *24*, 786; j) K. Harata, *Bull. Chem. Soc. Jpn.* **1988**, *61*, 1939; k) D. R. Alston, A. M. Z. Slawin, J. F. Stoddart, D. J. Williams, *J. Chem. Soc. Chem. Commun.* **1985**, 1602; l) K. Hirotsu, S. Kamitori, T. Higuchi, *ibid.* **1986**, 690; m) J. A. Hamilton, L. Chen, *J. Am. Chem. Soc.* **1988**, *110*, 5833; n) *ibid.* **1988**, *110*, 4379; o) S. Kamitori, K. Hirotsu, T. Higuchi, *Bull. Chem. Soc. Jpn.* **1988**, *61*, 3825; p) Y. Odagaki, K. Hirotsu, T. Higuchi, A. Harada, S. Takahashi, *J. Chem. Soc. Perkin Trans. 1* **1990**, *4*, 1230; q) B. Klingert, G. Rihs, *J. Inclusion Phenom. Mol. Recognit. Chem.* **1991**, *10*, 255; r) T. Steiner, G. Koellner, W. Saenger, *Carbohydr. Res.* **1992**, *228*, 321.

[108] a) M. Sakurai, H. Hoshi, Y. Inoue, R. Chujo, *Chem. Phys. Lett.* **1989**, *163*, 217; b) N. Kobayashi, T. Osa, *Carbohydr. Res.* **1989**, *192*, 147; c) M. Sakurai, M. Kitagawa, H. Hoshi, Y. Inoue, R. Chujo, *Bull. Chem. Soc. Jpn.* **1989**, *62*, 2067; d) D. Wouessidjewe, A. Crassous, D. Duchene, A. Coleman, N. Rysanek, G. Tsoucaris, B. Perly, F. Djedaini, *Carbohydr. Res.* **1989**, *192*, 313; e) G. Wenz, F. Wolf, *New J. Chem.* **1993**, *17*, 729.

[109] a) Y. Yamamoto, M. Onda, M, Kitagawa, Y. Inoue, R. Chujo, *Carbohydr. Res.* **1987**, *167*, C11; b) Y. Inoue, Y. Kanda, Y. Yamamoto, R. Chujo, S. Kobayahsi, *ibid.* **1989**, *194*, C8; c) C. Jaime, J. Redondo, F. Sanchez-Ferrando, A. Virgili, *J. Org. Chem.* **1990**, *55*, 4772; d) H. Parrot-Lopez, F. Djedaini, B. Perly, A. W. Coleman, H. Galons, M. Micoque, *Tetrahedron Lett.* **1990**, *31*, 1999; e) F. Djedaini, B. Perly in [7a], p. 215.

[110] a) K. Harata, H. Uedaira, *Bull. Chem. Soc. Jpn.* **1975**, *48*, 375; b) M. Ata, Y. Kubuzono, Y. Suzuki, M. Aoyagi, Y. Gondo, *ibid.* **1989**, *62*, 3706; c) M. Kamiya, S. Mitsuhashi, M. Makino, H. Yoshioka, *J. Phys. Chem.* **1992**, *96*, 95.

[111] M. Kajtar, C. Horvath-Toro, E. Kuthi, J. Szejtli, *Acta Chim. Acad. Sci. Hung.* **1982**, *110*, 327.

[112] M. Kodaka, *J. Phys. Chem.* **1991**, *95*, 2110.

[113] a) A. Ueno, K. Takahashi, T. Osa, *J. Chem. Soc. Chem. Commun.* **1980**, 921; b) T. Tamaki, T. Kokubu, *J. Inclusion Phenom.* **1984**, *2*, 815.

[114] a) S. Hamai, *Bull. Chem. Soc. Jpn.* **1982**, *55*, 2721; b) G. S. Cox, N. J. Turro, N. C. Yang, M.-J. Chen, *J. Am. Chem. Soc.* **1984**, *106*, 422; c) S. Hamai, *Bull. Chem. Soc. Jpn.* **1991**, *64*, 431.

[115] T. Tamaki, *Chem. Lett.* **1984**, 53.

[116] a) K. A. Connors, *Binding Constants: The Measurement of Molecular Complex Stability*, Wiley, New York, **1987**; b) T. Wiseman, S. Williston, J. F. Brandts, L.-N. Lin, *Anal. Biochem.* **1989**, *179*, 131.

[117] a) T. Higuchi, K. A. Connors, *Adv. Anal. Chem. Instrum.* **1965**, *4*, 117; b) K. A. Connors, D. A. Pendergast, *J. Am. Chem. Soc.* **1984**, *106*, 7607; c) Y. Wu, K. Ishibashi, T. Deguchi, I. Sanemasa, *Bull. Chem. Soc. Jpn.* **1990**, *63*, 3450.

[118] a) G. Longhi, G. Zerbi, G. Peterlini, L. Ricard, S. Abbate, *Carbohydr. Res.* **1987**, *161*, 1; b) B. Casu, A. Grenni, A. Naggi, G. Torri, M. Virtuani, B. Focher, *ibid.* **1990**, *200*, 101; c) F. Garcia-Tellado, S. Goswami, S. K. Chang, S. J. Geib, A. D. Hamilton, *J. Am. Chem. Soc.* **1990**, *112*, 7393; d) F. Djedaini, B. Perly, *Magn. Reson. Chem.* **1990**, *28*, 372; e) J. Lehmann, E. Kleinpeter, J. Krechl, *J. Inclusion Phenom. Mol. Recognit. Chem.* **1991**, *10*, 233.

[119] a) K. Harata, K. Tsuda, K. Uekama, M. Otagiri, F. Hiryama, *J. Inclusion Phenom.* **1988**, *6*, 135; b) H. Yamaguchi, M. Higashi, J. Nakayama, M. Hoshino, *J. Inclusion Phenom. Mol. Recognit. Chem.* **1990**, *9*, 253; c) G. Patonay, M. I. Warner, *ibid.* **1991**, *11*, 313; d) K. Harata, *ibid.* **1992**, *13*, 77.

[120] a) H. A. Benesi, J. H. Hildebrand, *J. Am. Chem. Soc.* **1949**, *71*, 2703; b) W. Broser, W. Lautsch, *Z. Naturforsch. B* **1953**, *8*, 711; c) L. Barcza, A. Buvari-Barcza, *Carbohydr. Res.* **1989**, *192*, 103; d) N. Yoshida, T. Shirai, M. Fujimoto, *ibid.* **1989**, *192*, 291.

[121] a) R. I. Gelb, L. M. Schwartz, R. F. Johnson, D. A. Laufer, *J. Am. Chem. Soc.* **1979**, *101*, 1869; b) I. Satake, T. Ikenoue, T. Takeshita, K. Hayakawa, T. Maeda, *Bull. Chem. Soc. Jpn.* **1985**, *58*, 2746.

[122] a) R. Palepu, V. C. Reinsborough, *Can. J. Chem.* **1989**, *67*, 1550; b) E. Saint Aman, D. Serve, *J. Colloid Interface Sci.* **1990**, *138*, 365; c) C. D. Lavandier, M. P. Pelletier, V. C. Reinsborough, *Aust. J. Chem.* **1991**, *44*, 457.

[123] a) N. J. Turro, T. Okubo, C.-J. Chung, *J. Am. Chem. Soc.* **1982**, *104*, 3954; b) G. Nelson, G. Patonay, I. M. Warner, *Appl. Spectrosc.* **1987**, *41*, 1235; c) F. V. Bright, G. C. Catena, J. Huang, *J. Am. Chem. Soc.* **1990**, *112*, 1343; d) J. M. Schütte, T. Ndou, A. M. d. la Pena, K. L. Greene, C. Williamson, I. M. Warner, *J. Phys. Chem.* **1991**, *95*, 4897; e) H.-J. Schneider, T. Blatter, S. Simova, *J. Am. Chem. Soc.* **1991**, *113*, 1996.

[124] a) G. Barone, G. Castronuovo, V. Di Ruocco, V. Elia, C. Giancola, *Carbohydr. Res.* **1989**, *192*, 331; b) E. Siimer, M. Kobu, M. Kurvits, *Thermochim. Acta* **1990**, *170*, 89; c) A. F. Danil de Namor, R. Traboulssi, D. F. V. Lewis, *J. Am. Chem. Soc.* **1990**, *112*, 8442; d) S. Takagi, M. Fujisawa, T. Kimura, *Thermochim. Acta* **1991**, *183*, 289.

[125] a) K. Sasaki, S. D. Christian, E. E. Tucker, *Fluid Phase Equilib.* **1989**, *49*, 281; b) J. S. Alper, R. I. Gelb, D. A. Laufer, L. M. Schwartz, *Anal. Chim. Acta* **1989**, *220*, 171.

[126] R. L. VanEtten, J. F. Sebastian, G. A. Clowes, M. L. Bender, *J. Am. Chem. Soc.* **1967**, *89*, 3242.

[127] R. I. Gelb, L. M. Schwartz, *J. Inclusion Phenom. Mol. Recognit. Chem.* **1989**, *7*, 537.

[128] a) I. Tabushi, K. Shimokawa, N. Shimizu, H. Shirakata, K. Fujita, *J. Am. Chem. Soc.* **1976**, *98*, 7855; b) J. W. Park, H. J. Song, *J. Phys. Chem.* **1989**, *93*, 6454; c) M. D. Johnson, V. C. Reinsborough, *Aust. J. Chem.* **1992**, *45*, 1961.

[129] O. S. Tee, J. J. Hoeven, *J. Am. Chem. Soc.* **1989**, *111*, 8318.

[130] T. Okubo, M. Kuroda, *Macromolecules* **1989**, *22*, 3936.

[131] a) M. Fujimoto, N. Yoshida, A. Seiyama, *Chem. Lett.* **1984**, 703; b) T. Okubo, Y. Maeda, H. Kitano, *J. Phys. Chem.* **1989**, *93*, 3721.

[132] a) H. Saito, H. Yonemura, H. Nakamura, T. Matsuo, *Chem. Lett.* **1990**, 535; b) M. Watanabe, H. Nakamura, T. Matsuo, *Bull. Chem. Soc. Jpn.* **1992**, *65*, 164.

[133] a) R. I. Gelb, L. M. Schwartz, D. A. Laufer, *J. Am. Chem. Soc.* **1978**, *100*, 5875; b) N. Yoshida, A. Seiyama, M. Fujimoto, *J. Phys. Chem.* **1990**, *94*, 4254.

[134] a) A. Aversa, W. Etter, R. I. Gelb, L. M. Schwartz, *J. Inclusion Phenom. Mol. Recognit. Chem.* **1990**, *9*, 277; b) S. Takagi, M. Fujisawa, T. Kimura, *Chem. Express* **1991**, *6*, 93.

[135] At pH 9, G. Wenz, B. Keller, unpublished.

[136] K. A. Connors in *The Bioorganic Chemistry of Enzymatic Catalysis: An Homage to Myron L. Bender* (Eds.: V. T. D'Souza, J. Feder), CRC Press, Boca Raton, FL, USA; **1992**, p. 13.

[137] W. Saenger, K. Beyer, P. C. Manor, *Acta Crystallogr. B* **1976**, *32*, 120.

[138] A. Meister, Dissertation, Mainz, **1991**.

[139] K. Harata, *Bull. Chem. Soc. Jpn.* **1976**, *49*, 1493.

[140] Y. Matsui, T. Nishioka, T. Fujita, *Top. Curr. Chem.* **1985**, *128*, 61.

[141] a) N. Kobayashi, S. Minato, T. Osa, *Makromol. Chem.* **1983**, *184*, 2123; b) Y. Yamashoji, M. Tanaka, T. Shono, *Chem. Lett.* **1990**, 945.

[142] S. McCormack, N. R. Russell, J. F. Cassidy, *Electrochim. Acta* **1992**, *37*, 1939.

[143] A. Harada, S. Takahashi, *J. Chem. Soc. Chem. Commun.* **1986**, *16*, 1229.

[144] For a survey on included metal complexes see: J. F. Stoddart, R. Zarzycki, *Recl. Trav. Chim. Pays-Bas* **1988**, *107*, 515.

[145] A. Munoz de la Pena, T. Ndou, J. B. Zung, I. M. Warner, *J. Phys. Chem.* **1991**, *95*, 3330.

[146] a) M. Kempfle, R. Müller, R. Palluk, *Fresenius Z. Anal. Chem.* **1984**, *317*, 700; b) A. Ueno, I. Suzuki, T. Osa, *Anal. Chem.* **1990**, *62*, 2461.

[147] S. Kamitori, K. Hirotsu, T. Higuchi, *J. Am. Chem. Soc.* **1987**, *109*, 2409.

[148] S. Hamai, *J. Inclusion Phenom. Mol. Recognit. Chem.* **1991**, *11*, 55.

[149] T. Andersson, K. Nilsson, M. Sundahl, G. Westman, O. Wennerstroem, *J. Chem. Soc. Chem. Commun.* **1992**, *8*, 604.

[150] a) N. Kobayashi, A. Ueno, T. Osa, *J. Chem. Soc. Chem. Commun.* **1981**, 340; b) T. Tamaki, T. Kokuku, K. Ichimura, *Tetrahedron* **1987**, *43*, 1485.

[151] J. Szejtli, E. Banky-Elöd, *Starch/Stärke* **1978**, *30*, 85.

[152] a) G. Wulff, S. Kubik, *Makromol. Chem.* **1992**, *193*, 1071; b) *Carbohydr. Res.* **1992**, *237*, 1.

[153] R. Breslow, N. Greenspoon, T. Guo, R. Zarzycki, *J. Am. Chem. Soc.* **1989**, *111*, 8296.

[154] K. Hirotsu, T. Higuchi, K. Fujita, T. Ueda, A. Shinoda, T. Imoto, I. Tabushi, *J. Org. Chem.* **1982**, *47*, 1143.

[155] a) A. Ueno, F. Moriwaki, T. Matsue, T. Osa, *Makromol. Chem. Rapid. Commun.* **1985**, *6*, 231; b) A. Ueno, T. Kuwabara, A. Nakamura, F. Toda, *Nature* **1992**, *356*, 136.

[156] a) A. Ueno, S. Minato, I. Suzuki, M. Fukushima, M. Ohkubo, T. Osa, F. Hamada, K. Murai, *Chem. Lett.* **1990**, 605; b) A. Ueno, I. Suzuki, T. Osa, *Anal. Chem.* **1990**, *62*, 2461.

[157] Q. Chen, I. Suzuki, T. Osa, A. Ueno, *Makromol. Chem. Rapid. Commun.* **1991**, *12*, 113.

[158] M. Maciejewski, A. Gwidzowski, P. Peczak, A. Pietrzak, *J. Macromol. Sci. Chem. A* **1979**, *13*, 87.

[159] N. Ogata, K. Sanui, J. Wada, *J. Polym. Sci. Polym. Lett. Ed.* **1976**, *14*, 459.

[160] H. Chakihara, N. Kunieda, M. Kinoshita, *Mem. Fac. Eng. Osaka City Univ.* **1987**, *28*, 121.

[161] T. Seo, T. Kajihara, T. Iijima, *Makromol. Chem.* **1990**, *191*, 1665.

[162] A. Harada, M. Kamachi, *Macromolecules* **1990**, *23*, 2821.

[163] A. Harada, M. Kamachi, *J. Chem. Soc. Chem. Commun.* **1990**, *19*, 1322.

[164] A. Harada, J. Li, M. Kamachi, *Chem. Lett.* **1993**, 237.

[165] M. Noltemeyer, W. Saenger, *Nature* **1976**, *259*, 629.

[166] G. Wenz, B. Keller, *Angew. Chem.* **1992**, *104*, 201; *Angew. Chem. Int. Ed. Engl.* **1992**, *31*, 197.

[167] B. Keller, G. Wenz in [72a], p. 192.

[168] G. Wenz, B. Keller, *Polym. Prepr. Am. Chem. Soc. Div. Polym. Chem.* **1993**, *34*, 62.

[169] G. Wenz, B. Keller, unpublished.

[170] If the formation of these hydrogen bonds is hindered by substituents at the host, polyethylene glycol is not complexed: A. Harada, private communication, **1992**.

[171] a) *Proceedings of the 4th International Symposium on Cyclodextrins* (Eds.: O. Huber, J. Szejtli), Kluwer, Dordrecht, **1988**; G. Wenz, E. von der Bey in [171a] p. 133.

[172] H. K. Frensdorff, *J. Am. Chem. Soc.* **1971**, *93*, 4684.

[173] Y. Takeda, *Top. Curr. Chem.* **1984**, *121*, 1.

[174] a) *Minutes of the 5th International Symposium on Cyclodextrins* (Ed.: D. Duchêne), Editions de Santé, Paris, **1990**; b) A. Hochgesand, G. Wenz in [174a], p. 322.

[175] R. Huisgen, H. Ott, *Tetrahedron* **1959**, *6*, 253.

[176] a) R. J. M. Nolte, D. J. Cram, *J. Am. Chem. Soc.* **1984**, *106*, 1416; b) L. Echegoyen, G. W. Gokel, M. S. Kim, E. M. Eyring, S. Petrucci, *J. Phys. Chem.* **1987**, *91*, 3854.

[177] a) Y. Kawabata, M. Matsumoto, M. Tanaka, H. Takahashi, Y. Irinatsu, S. Tamura, W. Tagaki, H. Nakahara, K. Fukuda, *Chem. Lett.* **1986**, 1933; b) Y. Kawabata, M. Takanaka, Y. Ishizuka, M. Matsumoto, T. Nakamura, A. Yabe, H. Nakanishi, H. Takahashi, S. Tamura, W. Tagaki, H. Nakahara, K. Fukuda, *ibid.* **1987**, 1307; c) Y. Kawabata, M. Matsumoto, M. Tanaka, T. Nakamura, E. Manda, *Thin Solid Films* **1988**, *159*, 353; d) Y. Kawabata, *7th Symposium on Future Electron Devices* **1988**, 109.

[178] S. Taneva, K. Argia, Y. Okahata, *Langmuir* **1989**, *5*, 111.

[179] A. Yabe, Y. Kawabata, H. Niino, M. Matsumoto, A. Ouchi, H. Takahashi, S. Tamura, W. Tagaki, H. Nakahara, K. Fukuda, *Thin Solid Films* **1988**, *160*, 33.

[180] Y. Kawabata, M. Matsumoto, M. Tanaka, Y. Ishizuka, H. Nakanishi (Agency of Industrial Sciences and Technology), DE-B 3710569 A1, **1987** [*Chem. Abstr.* **1988**, *109*, 131146].

[181] C. D. Bain, E. B. Troughton, Y.-T. Tao, J. Evall, G. M. Whitesides, R. G. Nuzzo, *J. Am. Chem. Soc.* **1989**, *111*, 321.

[182] C. Chung, (Dissertation, Iowa State University, Ames, IA, USA), *Report* **1991** (*Emergy Res. Abstr.* **1991**, *16*, No. 14982) [*Chem. Abstr.* **1992**, *115*, 287853g].

[183] D. Philp, J. F. Stoddart, *Synlett* **1991**, *7*, 445.

[184] a) C. O. Dietrich-Buchecker, J. P. Sauvage, J. M. Kern, *J. Am. Chem. Soc.* **1984**, *106*, 3043; b) P. R. Ashton, T. T. Goodnow, A. E. Kaifer, M. V. Reddington, A. M. Z. Slawin, N. Spencer, J. F. Stoddart, C. Vicent, D. J. Williams, *Angew. Chem.* **1989**, *101*, 1404; *Angew. Chem. Int. Ed. Engl.* **1989**, *28*, 1396; c) P. R. Ashton, C. L. Brown, E. J. T. Chrystal, K. P. Parry, M. Pietraszkiewicz, N. Spencer, J. F. Stoddart, *ibid.* **1991**, *103*, 1058 and **1991**, *30*, 1042; d) P. R. Ashton, C. L. Brown, E. J. T. Chrystal, T. T. Goodnow, A. E. Kaifer, K. P. Parry, A. M. Z. Slawin, N. Spencer, J. F. Stoddart, D. J. Williams, *ibid.* **1991**, *103*, 1055 and **1991**, *30*, 1039; e) C. O. Dietrich-Buchecker, J.-P. Sauvage, *Chem. Rev.* **1987**, *87*, 795.

[185] a) P. L. Anelli, P. R. Ashton, R. Ballardini, V. Balzani, M. Delgado, M. T. Gandolfi, T. T. Goodnow, A. E. Kaifer, D. Philp, M. Pietraszkiewicz, L. Prodi, M. V. Reddington, A. M. Z. Slawin, N. Spencer, J. F. Stoddart, C. Vicent, D. J. Williams, *J. Am. Chem. Soc.* **1992**, *114*, 193; b) P. R. Ashton, D. Philp, N. Spencer, J. F. Stoddart, *J. Chem. Soc. Chem. Commun.* **1992**, 1124; c) P. R. Ashton, M. R. Johnston, J. F. Stoddart, M. S. Tolley, J. W. Wheeler, *ibid.* **1992**, 1128; d) J. C. Chambron, V. Heitz, J. P. Sauvage, *ibid.* **1992**, 1131.

[186] a) H. W. Gibson, Y. X. Shen, *Macromolecules* **1992**, *25*, 2058; b) H. W. Gibson, H. Marand, *Adv. Mater.* **1993**, *5*, 11.

[187] a) C. O. Dietrich-Buchecker, J.-P. Sauvage, *Angew. Chem.* **1989**, *101*, 192; *Angew. Chem. Int. Ed. Engl.* **1989**, *28*, 189; b) C. O. Dietrich-Buchecker, J.-P. Sauvage, J. P. Kintzinger, P. Maltese, C. Pascard, J. Guilhem, *New J. Chem.* **1992**, *16*, 931.

[188] a) A. Lüttringhaus, F. Cramer, H. Prinzbach, *Angew. Chem.* **1957**, *69*, 137; b) A. Lüttringhaus, F. Cramer, H. Prinzbach, F. M. Henglein, *Justus Liebigs Ann. Chem.* **1958**, *613*, 185.

[189] D. Armspach, P. R. Ashton, C. P. Moore, N. Spencer, J. F. Stoddart, T. J. Wear, D. J. Williams, *Angew. Chem.* **1993**, *105*, 944; *Angew. Chem. Int. Ed. Engl.* **1993**, *32*, 854.

[190] a) H. Ogino, *J. Am. Chem. Soc.* **1981**, *103*, 1303; b) H. Ogino, K. Ohata, *Inorg. Chem.* **1984**, *23*, 3312.

[191] For **1**·decamethylenediamine $K_s = 3\ \text{M}^{-1}$: A. Meister, Dissertation, Mainz (FRG), **1991**.

[192] R. S. Wylie, D. H. Macartney, *J. Am. Chem. Soc.* **1992**, *114*, 3136.

[193] R. Isnin, A. E. Kaifer, *J. Am. Chem. Soc.* **1991**, *113*, 8188.

[194] J. F. Stoddart, *Angew. Chem.* **1992**, *104*, 860; *Angew. Chem. Int. Ed. Engl.* **1992**, *31*, 846.

[195] A. Harada, J. L. M. Kamachi, *Nature* **1992**, *356*, 325.

[196] M. Born, H. Ritter, *Makromol. Chem. Rapid Commun.* **1991**, *12*, 471.
[197] A. Harada, J. Li, M. Kamachi, *Nature* **1993**, *364*, 516.
[198] The term comes from solid-state chemistry and describes the effect of the packing of the reactant on the reaction rate: a) G. H. J. Schmidt in *Solid-State Photochemistry* (Ed.: D. Ginsburg), Verlag Chemie, Weinheim, **1976**, p. 2; b) G. Wegner, *Z. Naturforsch. B* **1969**, *24*, 824.
[199] For further information see the following reviews: a) D. W. Griffiths, M. L. Bender, *Adv. Catal.* **1973**, *23*, 209; b) I. Tabushi, *Tetrahedron* **1984**, *40*, 269; c) R. Breslow in *Inclusion Compounds, Vol. 3* (Eds.: J. L. Atwood, J. E. D. Davies, D. D. MacNicol), Academic Press, London, **1984**, p. 473; d) O. S. Tee, *Carbohydr. Res.* **1989**, *192*, 181.
[200] a) F. Cramer, G. Mackensen, *Angew. Chem.* **1966**, *78*, 641; *Angew. Chem. Int. Ed. Engl.* **1966**, *5*, 601; b) R. L. VanEtten, G. A. Clowes, J. F. Sebastian, M. L. Bender, *J. Am. Chem. Soc.* **1967**, *89*, 3253; c) O. Tee, C. Mazza, X. Du, *J. Org. Chem.* **1990**, *55*, 3603.
[201] a) N. Hennrich, F. Cramer, *J. Am. Chem. Soc.* **1967**, *87*, 1121; b) M. Komiyama, *Carbohydr. Res.* **1989**, *192*, 97; c) A. C. Hengge, W. W. Cleland, *J. Org. Chem.* **1991**, *56*, 1972.
[202] J. M. Dabis, D. R. Cameron, J. M. Kubanek, L. Mizubayu, G. R. J. Thatcher, *Tetrahedron Lett.* **1991**, *32*, 2205.
[203] a) V. T. D'Souza, M. L. Bender, *Acc. Chem. Res.* **1987**, *20*, 146; b) R. L. VanEtten, G. A. Clowes, J. F. Sebastian, M. L. Bender, *J. Am. Chem. Soc.* **1967**, *89*, 3253.
[204] Cases are also known in which the catalysis is **not** due to the inclusion of the guest: see ref. [129].
[205] a) R. Breslow, M. F. Czarniecki, *J. Am. Chem. Soc.* **1978**, *100*, 7771; b) G. L. Trainor, R. Breslow, *ibid.* **1981**, *103*, 154; c) R. Breslow, G. Trainor, A. Ueno, *ibid.* **1983**, *105*, 2739.
[206] M. L. Bender, B. W. Turnquest, *J. Am. Chem. Soc.* **1957**, *79*, 1656.
[207] a) T. Ikeda, R. Kojin, C.-J. Yoon, H. Ikeda, M. Iijima, K. Hattori, F. Toda, *J. Inclusion Phenom.* **1984**, *2*, 669; b) T. Ikeda, R. Kojin, C.-J. Yoon, H. Ikeda, M. Iijima, F. Toda, *ibid.* **1987**, *5*, 93; c) H. Ikeda, R. Kojin, C.-J. Yoon, T. Ikeda, F. Toda, *J. Inclusion Phenom. Mol Recognit. Chem.* **1989**, *7*, 117.
[208] a) M. I. Rosenthal, A. W. Czarnik, *J. Inclusion Phenom. Mol. Recognit. Chem.* **1991**, *10*, 119; b) H. J. Schneider, F. Xiao, *J. Chem. Soc. Perkin Trans. 2* **1992**, *3*, 387; c) A. W. Czarnik, E. U. Akkaya, *J. Phys. Org. Chem.* **1992**, *5*, 540.
[209] Y. Matsumoto, M. Komiyama, *J. Mol. Catal.* **1990**, *61*, 129.
[210] I. Tabushi, Y. Kuroda, *J. Am. Chem. Soc.* **1984**, *106*, 4580.
[211] R. Breslow, B. Zhang, *J. Am. Chem. Soc.* **1992**, *114*, 5882.
[212] F. M. Menger, M. Ladika, *J. Am. Chem. Soc.* **1987**, *109*, 3145.
[213] a) Y. Kuroda, T. Hiroshige, H. Ogoshi, *J. Chem. Soc. Chem. Commun.* **1990**, *22*, 1594; b) S. Mosseri, J. C. Mialocq, B. Perly, P. Hambright, *J. Phys. Chem.* **1991**, *95*, 2196.
[214] R. Breslow, P. Campbell, *J. Am. Chem. Soc.* **1969**, *91*, 3085.
[215] M. Komiyama, H. Hirai, *J. Am. Chem. Soc.* **1984**, *106*, 174.
[216] H. Ye, D. Rong, V. T. D'Souza, *Tetrahedron Lett.* **1991**, *32*, 5231.
[217] H. Ye, W. Tong, V. T. D'Souza, *Tetrahedron Lett.* **1992**, *33*, 6271.
[218] a) M. Komiyama, H. Hirai, *J. Am. Chem. Soc.* **1983**, *105*, 2018; b) M. Komiyama, *J. Chem. Soc. Perkin Trans. 1*, **1989**, 2031.
[219] a) M. S. Syamala, V. Ramamurthy, *Tetrahedron* **1988**, *44*, 7232; b) M. S. Syamala, B. N. Rao, V. Ramamurthy, *ibid.* **1988**, *44*, 7234; c) J.-T. Lee, H. Alper, *J. Org. Chem.* **1990**, *55*, 1854.
[220] a) N. Kunieda, S. Yamane, H. Taguchi, M. Kinoshita, *Makromol. Chem. Rapid. Commun.* **1983**, *4*, 57; b) R. Fornasier, F. Reniero, P. Scrimin, U. Tonellato, *J. Chem. Soc. Perkin Trans. 2* **1987**, 1121; c) M. Barra, R. H. de Rossi, E. B. de Vargas, *J. Org. Chem.* **1987**, *52*, 5004; d) Y. Zhang, W. Xu, *Synth. Commun.* **1989**, *19*, 1291; e) M. Barra, R. H. de Rossi, *J. Org. Chem.* **1989**, *54*, 5020; f) K. Hattori, K. Takahashi, M. Uematsu, N. Sakai, *Chem. Lett.* **1990**, 1463; g) S. Colonna, A. Manfredi, R. Annunziata, N. Gaggero, L. Casella, *J. Org. Chem.* **1990**, *55*, 5862; h) H. Sakuraba, Y. Tananaka, F. Toda, *J. Inclusion Phenom. Mol. Recognit. Chem.* **1991**, *11*, 195.
[221] a) D. C. Rideout, R. Breslow, *J. Am. Chem. Soc.* **1980**, *102*, 7816; b) H.-J. Schneider, N. K. Sangwan, *J. Chem. Soc. Chem. Commun.* **1986**, 1787; c) *Angew. Chem.* **1987**, *99*, 924; *Angew. Chem. Int. Ed. Engl.* **1987**, *26*, 896; d) D. L. Wernick, A. Yazbek, J. Levy, *J. Chem. Soc. Chem. Commun.* **1990**, *14*, 956.
[222] D. D. Sternbach, D. M. Rossana, *J. Am. Chem. Soc.* **1982**, *104*, 5853.
[223] J. N. Moorthy, K. Venkatesan, R. G. Weiss, *J. Org. Chem.* **1992**, *57*, 3292.
[224] B. Dietrich, T. M. Fyles, M. W. Hosseini, J.-M. Lehn, K. C. Kaye, *J. Chem. Soc. Chem. Commun.* **1988**, 691.
[225] a) K. Harata, K. Uekama, M. Otagiri, F. Hirayama, *Bull. Chem. Soc. Jpn.* **1987**, *60*, 497; b) K. Harata, *J. Chem. Soc. Perkin Trans. 2* **1990**, *5*, 799; c) H. Dodziuk, J. Sitkowski, L. Stefaniak, J. Jurczak, D. Sybilska, *J. Chem. Soc. Chem. Commun.* **1992**, *3*, 207.
[226] J. E. H. Köhler, M. Hohla, M. Richters, W. A. König, *Angew. Chem.* **1992**, *104*, 362; *Angew. Chem. Int. Ed. Engl.* **1992**, *31*, 319.
[227] a) A. Venema, H. Henderiks, R. Van Geest, *J. High Resolut. Chromatogr.* **1991**, *14*, 676; b) K. B. Lipkowitz, S. Raghothama, J.-A. Yang, *J. Am. Chem. Soc.* **1992**, *114*, 1554; c) N. K. de Vries, B. Coussens, R. J. Meier, G. Heemels, *J. High Resolut. Chromatogr.* **1992**, *15*, 499.
[228] a) D. W. Armstrong, *J. Liq. Chromatogr.* **1984**, *7*, 353; b) W. L. Hinze, T. E. Riehl, D. W. Armstrong, W. DeMond, A. Alak, *Anal. Chem.* **1985**, *57*, 237; c) D. W. Armstrong, T. J. Ward, R. D. Armstrong, E. Beesley, *Science* **1986**, *232*, 1132; d) D. M. Han, Y. I. Han, D. W. Armstrong, *J. Chromatogr.* **1988**, *441*, 376; e) D. W. Armstrong, X. Yang, S. M. Han, R. A. Menges, *Anal. Chem.* **1987**, *59*, 2594.
[229] a) W. A. König, S. Lutz, P. Mischnick-Lübbecke, B. Brassat, G. Wenz, *J. Chromatogr.* **1988**, *447*, 193; b) W. A. König, S. Lutz, G. Wenz, *Angew. Chem.* **1988**, *100*, 989; *Angew. Chem. Int. Ed. Engl.* **1988**, *27*, 979.
[230] a) J. Ehlers, W. A. König, S. Lutz, G. Wenz, H. tom Dieck, *Angew. Chem.* **1988**, *100*, 1614; *Angew. Chem. Int. Ed. Engl.* **1988**, *27*, 1556; b) W. A. König, S. Lutz, M. Hagen, R. Krebber, G. Wenz, K. Baldenius, H. tom Dieck, *J. High Resolut. Chromatogr.* **1989**, *12*, 35.
[231] D. Kappes, H. Gerlach, P. Zbinden, M. Dobler, W. A. König, R. Krebber, G. Wenz, *Angew. Chem.* **1989**, *101*, 1744; *Angew. Chem. Int. Ed. Engl.* **1989**, *28*, 1657.
[232] a) W. A. König, S. Lutz, C. Colberg, N. Schmidt, G. Wenz, E. von der Bey, A. Mosandl, C. Günther, A. Kustermann, *J. High Resolut. Chromatogr.* **1988**, *11*, 621; b) W. A. König, S. Lutz, P. Mischnick-Lübbecke, B. Brassat, E. von der Bey, G. Wenz, *Starch/Stärke* **1988**, *40*, 472.
[233] a) W. A. König, S. Lutz, G. Wenz, E. v. d. Bey, *HRC & CC, J. High Resolut. Chromatogr. Commun.* **1988**, *11*, 506; b) A. Mosandl, U. Hener, U. Hagenauer-Hener, A. Kustermann, *J. High Resolut. Chromatogr.* **1989**, *12*, 532.
[234] a) V. Schurig, H.-P. Nowotny, D. Schmalzing, *Angew. Chem.* **1989**, *101*, 785; *Angew. Chem. Int. Ed. Engl.* **1989**, *28*, 736; b) H.-P. Nowotny, D. Schmalzing, D. Wistuba, V. Schurig, *J. High Resolut. Chromatogr.* **1989**, *12*, 383; c) V. Schurig, M. Jung, D. Schmalzing, M. Schleimer, J. Duvekot, J. C. Buyten, J. A. Peene, P. Mussche, *ibid.* **1990**, *13*, 470; d) V. Schurig, Z. Juvancz, G. J. Nicholson, D. Schmalzing, *ibid.* **1991**, *14*, 58; e) V. Schurig, D. Schmalzing, M. Schleimer, *Angew. Chem.* **1991**, *103*, 994; *Angew. Chem. Int. Ed. Engl.* **1991**, *30*, 987.
[235] a) M. L. Hilton, D. W. Armstrong in [7a], p. 515; b) V. Schurig, H.-P. Nowotny, *Angew. Chem.* **1990**, *102*, 969; *Angew. Chem. Int. Ed. Engl.*, **1990**, *29*, 939; c) W. A. König, *Gas Chromatographic Enantiomer Separation with Modified Cyclodextrins*, Hüthig, Heidelberg, **1992**; d) S. Li, W. C. Purdy, *Chem. Rev.* **1992**, 1457.
[236] a) A. Mosandl, *J. Chromatogr.* **1992**, *624*, 267; b) W. A. König, B. Gehrcke, D. Icheln, P. Evers, J. Dönnecke, W. Wang, *J. High Resolut. Chromatogr.* **1992**, *15*, 367; c) W. A. König, A. Krüger, D. Icheln, T. Runge, *ibid.* **1992**, *15*, 184.
[237] a) W. Boland, W. A. König, R. Krebber, D. G. Müller, *Helv. Chim. Acta* **1989**, *72*, 1288; b) S. Schulz, W. Francke, W. A. König, V. Schurig, K. Mori, R. Kittmann, D. Schneider, *J. Chem. Ecol.* **1990**, *16*, 3511.
[238] J. Meinwald, W. R. Thompson, D. L. Pearson, W. A. König, T. Runge, W. Francke, *Science* **1991**, *251*, 560.
[239] a) A. Berthod, H. L. Jin, T. E. Beesley, J. D. Duncan, D. W. Armstrong, *J. Pharm. Biomed. Anal.* **1990**, *8*, 123; b) W. A. König, S. Lutz, P. Evers, J. Knabe, *J. Chromatogr.* **1990**, *503*, 256.
[240] W. A. König, D. Icheln, T. Runge, B. Pfaffenberger, P. Ludwig, H. Hühnerfuss, *J. High Resolut. Chromatogr.* **1991**, *14*, 530.
[241] a) J. Faller, H. Hühnerfuss, W. A. König, P. Ludwig, *Mar. Pollut. Bull.* **1991**, *22*, 82; b) R. Kallenborn, H. Hühnerfuss, W. A. König, *Angew. Chem.* **1991**, *30*, 328, *Angew. Chem. Int. Ed. Engl.* **1991**, *103*, 320.
[242] a) A. Z. Trifonov, T. T. Nikiforov, *J. Mol. Catal.* **1984**, *24*, 15; b) L. Fenichel, P. Bako, L. Toke, L. Szente, J. Szejtli in [171a], p. 113; c) S. Shimizu, Y. Sasaki, C. Hirai, *Bull. Chem. Soc. Jpn.* **1990**, *63*, 176.
[243] D. W. Armstrong, H. L. Jin, *Anal. Chem.* **1987**, *59*, 2237.
[244] M. J. Pregel, L. Jullien, J.-M. Lehn, *Angew. Chem.* **1992**, *104*, 169; *Angew. Chem. Int. Ed. Engl.* **1992**, *31*, 1637.
[245] Y. Kawaguchi, M. Tanaka, M. Nakae, K. Funazo, T. Shono, *Anal. Chem.* **1983**, *55*, 1852.
[246] a) P. Chiesi, V. Servadio (G. Bianchetti), EP-B 0153998, **1984** [*Chem. Abstr.* **1985**, *102*, 226056j]; b) W. A. J. J. Hermens, F. W. H. M. Merkur, EP-B 0349091 B1, **1990**, [*Chem. Abstr.* **1990**, *113*, 65253f].
[247] J. Cully, H.-R. Vollbrecht (SKW Trostberg AG), DE-A 4013367 A1, **1990**, [*Chem. Abstr.* **1992**, *116*, 40116n].
[248] E. K. Eisenhart, R. F. Merritt, E. A. Johnson (Rohm and Haas Co.), EP-A 0460896 A2, **1991** [*Chem. Abstr.* **1992**, *116*, 85880y].
[249] M. E. Brewster in [7a], p. 313.
[250] Y. Ohtani, T. Irie, K. Uekama, K. Fukunaga, J. Pitha, *Eur. J. Biochem.* **1989**, *186*, 17.
[251] Ref. [5c], p. 186.
[252] An inclusion compound is marketed by Schwarz Pharma, Monheim (FRG) under the name Prostaglandin E1.
[253] H. Arima, K. Wakamatsu, H. Aritomi, T. Irie, K. Uekama in [174a], p. 487.
[254] B. Pfannemüller, W. Burchard, *Makromol. Chem.* **1969**, *121*, 1.
[255] W. Al-Nakib, P. G. Higgins, G. I. Barrow, D. A. J. Tyrell, K. Andries, G. V. den Bussche, N. Taylor, P. A. J. Janssen, *Antimicrob. Agents Chemother.* **1989**, *33*, 522.
[256] G. Wenz, K. Engelskirchen, H. Fischer, H. C. Nicolaisen, S. Harris (Henkel KGaA, Düsseldorf, Max-Planck-Gesellschaft, Göttingen), DE-A 4009621 A1, **1990**, [*Chem. Abstr.* **1992**, *116*, 42807n].

[257] a) J. C. Fetzer (Chevron Research and Technology Company), US-A 5190663, **1992**; [*Chem. Abstr.* **1993**, *118*, 240099n]; b) J. Kiji, H. Konishi, T. Okano, T. Terashima, K. Motomura, *Angew. Makromol. Chem.* **1992**, *199*, 207.
[258] K. Murakawa, H. Muraoka, H. Kiyama, *Jpn. Kokai Tokkyo Koho* 85156761 [*Chem. Abstr.* **1985**, *104*, 111337].
[259] a) J. Szejtli, *J. Inclusion Phenom.* **1983**, *1*, 135; b) H. G. Hassan, H. Renck, B. Lindberg, H. Lindquist, B. Aackerman, *Acta Anaestesiol. Scand.* **1985**, *29*, 380.
[260] T. Osato, S. Takeuchi, S. Esumi, C. Higashikaze (Institute of Physical and Chemical Research; Kaken Chemical Co.), JP-B 55038338, **1980** [*Chem. Abstr.* **1980**, *93*, 95580w].
[261] a) D. Knittel, H.-J. Buschmann, E. Schollmeyer, *Textilveredlung* **1991**, *26*, 92; b) D. Knittel, H.-J. Buschmann, E. Schollmeyer, *B + W Forum Bekleidung and Textil* **1992**, *12*, 34.
[262] Ref.[5c], p. 307.
[263] a) J. Szejtli, E. Bolla-Pusztai, P. Szabo, T. Ferenczy, *Pharmazie* **1980**, *35*, 779; b) M. T. Lengyel, J. Szejtli, *J. Inclusion Phenom.* **1985**, *3*, 1.

ANGEWANDTE
CHEMIE
International Edition in English



Twice a month in 1994

To start your personal subscription please contact:

VCH, Reader Service
P.O. Box 10 11 61, D-69451 Weinheim
Federal Republic of Germany
Telephone: +49 (6201) 60 64 27
Fax: +49 (6201) 60 61 17

VCH
8 Wellington Court
Cambridge CB1 1HZ, UK
Fax: (0223) 31 33 21
(for customers in the UK)

VCH
220 East 23rd Street
New York, NY 10010-4606, USA
Fax: (212) 481 0897
(for customers in the USA and Canada)

VCH
Hardstrasse 10, Postfach
CH-4020 Basel, Switzerland
Fax: (061) 2 71 06 18
(for customers in Switzerland)

VCH

Determination of Reaction Paths for Pentacoordinate Metal Complexes with the Structure Correlation Method

Thomas Auf der Heyde*

Dedicated to Professor Hans-Beat Bürgi

Crystal structures potentially deliver far more information than is present in the average structural communication—if sufficient structural data on closely related molecules or molecular fragments are available, it may be possible to infer details of geometric changes occurring along certain reaction pathways for the species of interest. This geometric information is extrapolated from an analysis of the similarities between the structures of the fragment in the various crystalline environments, by a method that is now known as structure correlation analysis. Since it was first proposed twenty years ago, the method has been applied to a large variety of chemical systems, but none have received as much attention as the class of five-coordinate compounds. Comparative analyses of the structures of pentacoordinate complexes have yielded information about the intimate mechanisms of substitution and addition/elimination reactions at tetrahedral and square-planar complexes, and about intramolecular isomerizations of five-coordinate compounds. Since its inception, the structure correlation method has gradually adapted techniques from other branches of science, in particular group-theoretical and multivariate statistical techniques, which have been shown to be enormously powerful tools for probing geometrically complex systems. This review traces the development of the method of structure correlation and the evolution of these co-opted techniques, with a specific emphasis on studies of five-coordinate metal complexes.

1. Introduction

One of the most irksome and paradoxical shortcomings of the molecular approach to chemistry that is currently prevalent in the discipline[1] is the lack of a suitable technique for directly observing changes occurring at the molecular level during the course of a chemical reaction. In this context, the geometric characteristics of a particular reaction are usually inferred from dynamic NMR or kinetic studies, or from volume of activation measurements, for example. In some cases they may be obtained from the results of ab initio calculations, but even the unprecedented development of computational technology in the last few years has not yet enabled a quantum chemical solution for most of the real systems that the discipline has turned its attention to.[2]

Although direct *observation* of a chemical molecule along a given reaction coordinate does not seem feasible, its *visualization* at least does. The structure correlation hypothesis[3, 4] assumes that the geometric changes that a given molecular fragment would undergo along a specific reaction coordinate are mirrored by the gradual distortion or static deformation manifested by that fragment collectively over a large variety of crystalline environments. The various crystal or molecular structures are considered to constitute a series of "frozen-in" points, or snapshots, taken along the reaction pathway, which, when viewed in the correct order, yield a cinematic film of the reaction.

The rationale behind the hypothesis is enticingly simple. Crystalline structures represent stable atomic arrangements—their representative points on the Born–Oppenheimer potential energy surface will consequently tend to aggregate around local potential minima, either a "well", a "dip", or a point in a "valley". Crystal structures of closely related molecular fragments will be represented by points variously displaced from the potential minima, *along pathways of minimum energy*. Arranged in the correct sequence, then, these fragments can be assumed to map such pathways, their static deformation mirroring that expected along the coordinate. This idea has found expression in the structure correlation hypothesis: If a correlation can be found between two or more independent parameters describing the structure of a given structural fragment in a variety of environments, then the correlation function maps a minimum energy path in the corresponding parameter space.[4c]

Essentially, the method of structure correlation involves choosing a suitable data set comprising crystal or molecular structures[5] that are closely related to the fragment of interest, and then searching for correlations (similarities) between them. In the twenty years since the first paper explicitly outlining the idea of structure correlation was published,[3] the method has been applied to a wide variety of chemical systems, including organic,

[*] Dr. T. Auf der Heyde
Department of Chemistry, University of Cape Town
Rondebosch, Cape Town 7700 (South Africa)
Telefax: Int. code + (21)650-3788

 © VCH Verlagsgesellschaft mbH, D-69451 Weinheim, 1994 0570-0833/94/0808-0823 $ 10.00+.25/0

inorganic, organometallic, and cluster compounds. During this time it has undergone considerable development involving the application of sophisticated multivariate statistical techniques, and group-theoretical methods. Some of the earlier studies have already been reviewed,[4a, b] and a book covering later work, with a comprehensive summary of the methods that have been developed during this time, appeared in late 1993.[6]

Undoubtedly, the class of compounds that has been most frequently and intensively studied by the technique of structure correlation is that of pentacoordinate complexes, which contains both main group elements and transition metals; indeed, the first paper in this area examined five-coordinate cadmium complexes.[3] Because these compounds have been so widely studied, the various papers offer interesting historical comparisons: 1) collectively they trace the various stages in the development of the structure correlation method (SCM), and 2) they illustrate how successively more complex methods of correlation analysis have yielded significantly greater insight into the stereochemistry of pentacoordination. This paper reviews structure correlation studies of pentacoordinate metal[7] complexes with these two aspects in mind. Papers dealing with nonmetal complexes will not be discussed here since they have received attention elsewhere[8] and in any event, do not add significant information, nor do they shed more light on the development of the SCM. We begin with a brief overview of the techniques that have proved useful in structure correlation studies.[9]

2. The Method of Structure Correlation

2.1. Representing Molecular Structures

Chemists represent molecules in many ways;[10] for the purposes of the SCM, their "depiction" in terms of a set of numbers is the most convenient for the subsequent statistical correlation analysis. This requirement necessitates an important conceptual leap in that the molecules comprising a given data set are no longer regarded as three-dimensional objects embedded in Cartesian space; they are, instead, represented by points in a multidimensional space spanned by a set of parameters (or variables) that are capable of defining the molecular geometry. In general, $3N-6$ such parameters are necessary for the complete description of an N-atom fragment.[11] Both internal coordinates (for example, bond angles and distances) and external coordinates such as fractional (crystallographic) coordinates can serve this function, but in almost all cases published thus far, the former have been used to represent the molecular geometry.[12] Bond angles and distances and other internal coordinates like them have the advantage of being easy to use and to visualize, and of appealing readily to the chemist's intuition, but they do suffer from several disadvantages that may introduce bias in comparative studies. Firstly, in general, no unique set of $3N-6$ parameters can be chosen to describe the molecular structure, so the selection will be biased by an arbitrary choice of parameters. But this choice is not always easy to make, since the larger the molecule, the greater the number of alternative parameters,[13] and the more complicated and opaque the geometric relations between them become; this complicates the identification of redundant or dependent coordinates. Secondly, in crystal structure analyses the internal coordinates are not the original refined parameters, and their errors are not directly estimated; an error in one coordinate may be coupled with errors in others, and there is no guarantee that such an effect will be obvious. Finally, the parameters are usually not all of the same type or have the same units (scale), and this can severely distort an analysis of covariance.

Where observed molecular geometries need to be referred to an idealized or a reference molecule, deformation coordinates or symmetry coordinates (SCs)—originally developed for use in vibrational spectroscopy—are very useful.[14] SCs are, for example, linear combinations of internal coordinates that transform according to the irreducible representations of the point group **G** of the chosen reference molecule; their derivation is described in most textbooks on applied group theory.[15] They are closely related to normal coordinates, and thus to the vibrational modes of the molecule.

As an example, consider an analysis of triatomic molecules that attempts to describe their deformations in relation to a reference molecule XYX with $\mathbf{G} = C_{2v}$; any such molecule is fully described by two bond-length increments (r_1 and r_2) and the increment in the bond angle ($\Delta\theta$), relative to the respective bond lengths and the bond angle in the reference structure. These (internal) coordinates transform as $2A_1 + B_2$ under C_{2v} symmetry, and the corresponding SCs are given in Scheme 1. Any given molecule would be represented by a particular point in the (three-dimensional) space spanned by S_1, S_2, and S_3. A dis-



Born in South Africa in 1958, Thomas Auf der Heyde studied chemistry at the University of Cape Town (UCT). As an undergraduate he worked for two years as a research assistant in coordination chemistry with D. A. Thornton. After obtaining his Honours degree (1981) he took up a lectureship at the University of the Western Cape (UWC), completing his Masters and Ph.D. degrees with L. R. Nassimbeni (1988). During this time he spent some months in Berne, Switzerland, with H.-B. Bürgi as pre-doctoral fellow. He returned to Berne after completing his studies, and subsequently worked with F. A. Allen in Cambridge at the Crystallographic Data Centre and with K. Mislow in Princeton. At the end of 1992 he resigned as associate professor at UWC and has since been visiting at UCT. His main research interests revolve around issues of molecular structure, incorporating areas such as the stereochemistry of coordination compounds, extraction of information about the dynamic behavior of molecules from their solid-state structure, and the quantification of chirality.

$S_1(A_1) = \Delta\theta$

$S_2(A_1) = (1/\sqrt{2})(r_1 + r_2)$

$S_3(B_2) = (1/\sqrt{2})(r_1 - r_2)$

Scheme 1.

placement along the positive S_1 coordinate would correspond to an opening of the X-Y-X angle relative to its value in the reference structure, a displacement along the S_2 axis corresponds to a symmetric stretch—both r_1 and r_2 increase or decrease simultaneously—while a displacement along S_3 represents an antisymmetric stretch.

In general, the geometry of an observed triatomic molecule would not correspond to that of the reference molecule, and its representative point in the space spanned by the symmetry coordinates would not coincide with the origin, which represents the undistorted reference. However, the coordinates of the representative point, given by its displacements (d_i) along the SCs ($\boldsymbol{S}_i$), can be used to define both the *type* of distortion and its *extent*: 1) A displacement along an S_i transforming as Γ_j under **G** would indicate that the corresponding molecule has retained the Γ_j symmetry of the reference molecule;[16] 2) the total molecular distortion can be described in terms of a displacement vector $\boldsymbol{D} = d_i\boldsymbol{S}_i$, which measures the overall displacement of the point representing the molecule from the origin, that is, the deformation of the given molecule away from the reference geometry.

Although SCs have proved extremely useful in structure correlation studies, their use does have limitations. The main restriction is that a symmetrical reference geometry needs to be chosen. This condition is not always possible to achieve, especially for large molecules, and often the choice is not straightforward, as for example when dealing with highly flexible molecules.[17]

2.2. Data Analysis: Statistical Methods[18]

Once a coordinate system has been chosen and a suitable data set comprising the fragment of interest and closely related ones in a variety of crystalline environments has been compiled,[19, 20] There may be a need to standardize or scale the data.[21, 22] The subsequent data analysis can be conveniently broken down into two stages. In the first, the behavior of individual geometric parameters, or pairs of them, is analyzed in order to identify systematic effects on the distribution of observed values, that is, to detect the existence of environmental effects. For this analysis univariate and bivariate statistics are generally sufficient. In the second stage the distributions of the molecular geometries as a whole are evaluated, that is, the types of conformation present in the data set are identified. This stage requires multivariate statistical techniques, since at this point one is dealing with complete representations of the molecules in $(3N - 6)$-dimensional parameter space.

2.2.1. *Univariate and Bivariate Statistics*

In addition to positional coordinates or bond lengths and angles and derived parameters, X-ray or electron diffraction studies yield estimated standard deviations (e.s.d.'s) that give an indication of the experimental error associated with a particular observation. A comparison of these individual e.s.d.'s with the sample variance can indicate the presence either of experimental error or environmental factors such as crystal lattice effects, or of geometric constraints on the fragment under investigation that may emanate from some residual part of the molecule.[23] Thus, if a particular squared e.s.d. is much larger than the sample variance for a given parameter, this could indicate a gross experimental error in that measurement only. On the other hand, a large sample variance relative to the e.s.d.'s indicates structural variance that may warrant further investigation. A second criterion for absence of environmental effects hinges on the calculation of the weighted sum of squares of deviations, which should approximately follow a χ^2 distribution if environmental effects are negligible.[24] (Effectively, this test evaluates whether the observations agree with one another as closely as might be expected from their e.s.d.'s.)

Histograms and two-dimensional scatter plots may be very useful in identifying clusters of data points or outliers, which may arise from experimental error, unusual structural features, or unique molecular environments. Possible linear correlations between pairs of observed parameters can be investigated through an analysis of covariance: a strong correlation would suggest that a reduction in dimensionality of the problem is possible, since some linear combination of the two parameters could adequately represent them. But since in most cases $3N - 6$ parameters are required for a molecular representation, multivariate statistical analysis should usually be performed.

2.2.2. *Principal Component Analysis*[25]

Reduction in dimensionality of the problem is generally possible only after a principal component analysis (PCA) has been performed.[9, 18, 22a, 26] Instead of breaking the data set down into two-dimensional subsets—as in covariance analysis or scatterplots—PCA searches for correlations among all $3N - 6$ parameters simultaneously, extracting linear combinations of highly correlated variables that describe, in turn, the greatest sample variance, the next greatest (orthogonal to the first), and so on. The consecutive linear combinations are called the principal components (PCs), and they appear as linear combinations of the original variables (a, b, c,...) [Eq. (1)].

$$\mathrm{PC}_n = \lambda_1 a + \lambda_2 b + \lambda_3 c + \ldots \quad (1)$$

$$n = 1, 2, \ldots, 3N - 6$$

The variables a, b, c,... that appear in any particular PC are called its components, while the coefficients λ_1, λ_2, λ_3, ... are called the loadings of the PC, and they indicate the relative importance of the corresponding variable in the PC. In addition, the technique yields the percentage of total sample variance accounted for by each PC, so it is possible to reduce the dimensionality of the problem to less than $3N - 6$ by choosing only the first k PCs ($k < 3N - 6$) that together account for, say, 90% of the variance, and ignoring the others.

Mathematically, PCA is accomplished through an eigenanalysis of the covariance or correlation matrix.[27] This process corresponds to a rotation of the original $3N - 6$ orthogonal parameter axes into $3N - 6$ new axes, the PCs, which lie along directions of maximal variance.

2.2.3. *Cluster Analysis*

The aim of cluster analysis (CA) is to cluster together similar points (observations) and/or clusters in the multidimensional parameter space, thereby yielding clusters of data points that have something in common.[9, 18, 22a, 28] Clustering algorithms differ in the criteria used for establishing similarity and in the rationale according to which clusters are fused together. They may be divided into two types: hierarchical and nonhierarchical. In hierarchical clustering each observation is initially considered either as a cluster on its own, and the most similar clusters are successively merged together in subsequent steps until all of the data points are in one large cluster; or, conversely, each point is initially considered part of the same large cluster, which is then progressively subdivided into smaller ones until, finally, each observation is again in a cluster of its own. Nonhierarchical techniques partition a data set either into some pre-set number of disjoint clusters, or into clusters situated at some user-specified locations in the multidimensional parameter space; in both cases the partitioning is done in a single step, rather than a number of hierarchical stages.

All these methods initially require the calculation of a similarity matrix whose elements are numbers indicating the similarity between each pair of observations (molecular structures) in the data set. The similarity between any two structures k and l is generally measured by a distance d_{kl} between their representative points [Eq. (2)], where x_{kj} is the value of the j-th parameter

$$d_{kl} = \left[\sum_{j=1}^{3N-6} |x_{kj} - x_{lj}|^n \right]^{1/n} \quad (2)$$

for observation (structure) k. For $n = 2$ Equation (2) yields the Euclidian distance in $3N - 6$ dimensions, while for $n = 1$ the resulting measure is called the "city-block" metric. It is important that the parameters used in a clustering analysis are suitably scaled, if not standardized, for the distance measure to be a good reflection of the relation between representative points in the multidimensional data space.[29]

CA is less objective than PCA, since the user needs to make a number of decisions, each of which could affect the outcome of a CA. Thus, once the similarity criterion has been defined, there are a large number of different linkage criteria—at what stage to link together clusters?—from which to choose. Because of the large number of user-defined variables in CA, it is good practice to apply different clustering techniques to the same body of data wherever possible.

2.3. Symmetry Considerations

For a given N-atom fragment there are, in general, $N!$ permutations of the atom labels on the molecular skeleton. This means that for each such molecule, $N!$ possible representative points exist in the parameter space.[30] Which to choose? Murray-Rust examined this problem in detail, and suggested two ways in which to deal with it.[23e] In the first a unique system of nomenclature is developed to ensure that every individual molecule is labeled in exactly the same way. In practice this may not always be possible; moreover this approach has implications for the statistical evaluation in that the distribution of the observed parameters, artificially skewed by the nomenclature, will not reflect the true distribution.

A second approach that has been widely applied in structure correlation studies makes explicit use of the symmetry of the reference molecule in generating all symmetry-equivalent permutations of the atomic labels on the molecular skeleton. This permutation has the effect of generating all symmetry-related siblings for each representative point, and it is tantamount to a symmetry expansion of the data set, in which each representative point is transformed according to the operations of the reference point group **G**.[31] While the method of symmetry expansion multiplies the number of data points by the order of **G**, it does not add any new data, but merely brings into prominence the symmetry that is implicitly assumed through the use of the group **G** as a reference group. Moreover, the explicit symmetry of the data expansion must reappear in the results of PCA and CA, thereby yielding an indicator as to the correctness of the results.

3. Proposed Reaction Paths for Five-Coordinate Metal Complexes

Complexes with the ML_5 composition (M = metal atom, L = any ligating atom) have been postulated and demonstrated to be intermediates or transition states for many ligand exchange reactions of tetracoordinate metal complexes.[32] Historically these reactions have been divided into three main groups: nucleophilic substitution, electrophilic substitution, and oxidative addition followed by reductive elimination. It has become fairly clear, though, that a relationship exists between many types of reactions previously classified quite separately.[33] Often this relationship results from geometrically similar reaction paths involving the formation of a five-coordinate species, which could be either a true intermediate in an associative nucleophilic substitution, an early transition state in an oxidative addition, or a solvento species in a dissociative substitution, for example. In this sense then, many if not most reactions of four-coordinate complexes can be deemed at some stage to involve the formation of a five-coordinate species (Scheme 2).

$$XML_3 + Y \rightarrow [XML_3Y] \rightarrow X + ML_3Y$$

Scheme 2. X and L represent any coordinated ligands, and Y is either X, L, or a solvent molecule.

Figure 1 depicts the reaction paths that have most commonly been invoked in mechanistic explanations of these ligand exchange processes at tetracoordinate metals. From a purely geometric perspective, step A maps the addition of a fifth donor to a square-planar complex—or the reverse (elimination) reaction—such as might occur for the d^8 metals. The incipient stages of this path are characterized by pentacoordinate complexes whose metal atom lies close to the base of a square pyramid (SQP); such conformers will be dubbed flattened square pyramids (fSQP). As the atom of the fifth ligand becomes more firmly bonded to the metal, the latter is drawn away from the

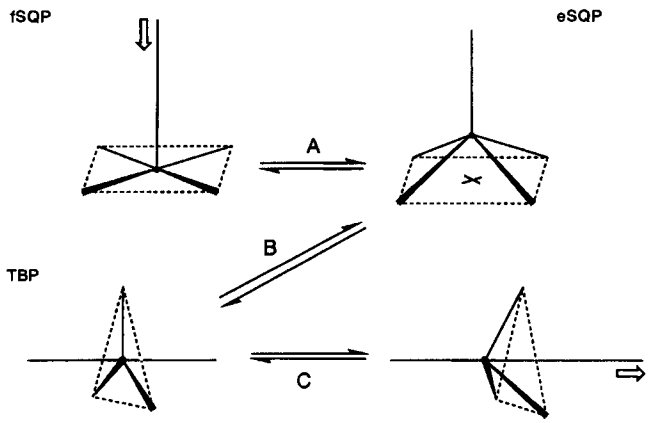


Fig. 1. Deformation and reaction pathways of five-coordinate complexes. fSQP = flattened square pyramid, eSQP = elevated square pyramid, TBP = trigonal bipyramid.[34a] Path A maps a reversible addition/elimination reaction at a square-planar metal complex, path B represents half of the Berry coordinate (Fig. 2), while path C depicts a reversible nucleophilic substitution at a tetrahedral center.

basal plane of the fSQP to form what is termed an elevated SQP (eSQP).[34a] Step B maps half of the Berry intramolecular rearrangement[35] whereby a trigonal bipyramid (TBP) deforms into a SQP by concerted bends in the axial angle and one of the equatorial angles of the TBP.[34b] The Berry mechanism[36] was originally proposed in an attempt to explain the NMR equivalence of axial and equatorial fluorine atoms in PF_5 at ambient temperature, and it offers a pathway[37, 38] for the continuous deformation of one TBP into another, through a SQP intermediate (Fig. 2). Finally, step C maps the addition of a fifth ligand

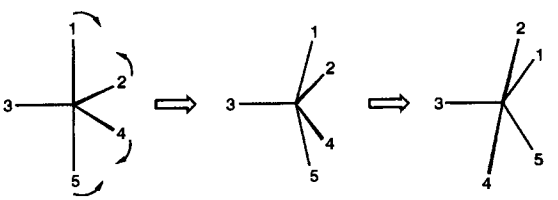


Fig. 2. The Berry intramolecular exchange mechanism. The atom labeling shown is used throughout this paper.

to a tetrahedral complex, yielding a TBP, or the reverse elimination; this path is equivalent to the S_N2 reaction coordinate of organic chemistry, and it might be expected for those metals whose tetracoordinate complexes adopt tetrahedral configurations. The two structures of highest symmetry, usually chosen as reference geometries for ML_5 complexes, are the TBP (D_{3h} symmetry) and the SQP (C_{4v}); while the angular geometry of the TBP is fixed by its symmetry, the same is not true for the SQP, which can adopt any value for the angles between *trans* ligands in the eSQP, so long as these angles are equal to each other.

4. Reaction Paths Derived from Crystal Structures

4.1. Laying the Foundations

Soon after Bürgi published the first paper outlining and explicitly employing what has since come to be known as the structure correlation method,[3] Muetterties and Guggenberger similarly applied the new idea to a study of five-coordination, but focused on a different deformation path.[39] In his paper, Bürgi viewed a series of five-coordinate metal complexes as essentially adopting TBP configuration, and then extracted an S_N2 reaction pathway (path C in Fig. 1) from correlations between them. Muetterties and Guggenberger, on the other hand, examined deformations away from TBP configuration, establishing a Berry pathway in the process (path B). Between them, the methods developed in these two papers laid the foundations for many of the subsequent structure correlation studies of pentacoordinate metal (and nonmetal) complexes, and because of their seminal importance, we shall dwell on them at some length below.

4.1.1. Bürgi's Cadmium Study—the S_N2 Pathway

The original paper examined eleven approximately trigonal bipyramidal cadmium complexes with equatorial thioglycolate ligands, and iodine, sulphur, or oxygen as axial ligands. The coordination polyhedra were simply described by internal coordinates, and correlations were mainly analyzed by means of scatterplots. The most telling correlations were those between the out-of-plane displacement (Δz) of the central Cd atom, and the distance increments[40] of the two axial bonds (Δx, Δy). This correlation is depicted in Figure 3. The results were interpreted

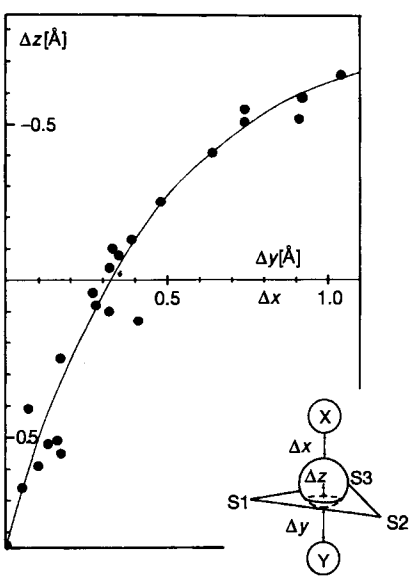


Fig. 3. The correlation between axial distance increments (Δx or Δy) and out-of-plane displacement (Δz) of the Cd atom. The distortion maps an S_N2 coordinate equivalent to step C in Figure 1.

in terms of an S_N2 distortion coordinate equivalent to step C (Fig. 1): beginning with a TBP distorted toward C_{3v} symmetry—that is, a TBP that could be viewed as a tetrahedron with a fifth ligand at one of the tetrahedral faces—one axial bond (Δx) becomes longer, as the other (Δy) shortens, while the metal is concomitantly drawn into the equatorial plane of the TBP. In the intermediate or transition state the two axial bonds are lengthened from their respective "standard" lengths by about 0.32 Å each, and the metal atom is situated exactly in the equatorial plane. An analysis of the variation in the internal angles

that accompanies the bond length changes, reveals the typical "umbrella-type" motion whereby a tetrahedron inverts during a classic organic S_N2 reaction.

An analytic expression [Eq. (3)], which parallels that proposed by Pauling [Eq. (4)],[41] was used to describe a geometric distortion coordinate along which changes in interatomic distance Δd are related to bond numbers n. On the basis of the

$$\Delta x, \Delta y = g(\pm \Delta z) = -1.5 \lg[(\pm \Delta z + 0.84)/1.68] \quad (3)$$

$$\Delta d = C \lg n \qquad 0 < n < 1 \quad (4)$$

analytic expression Bürgi was able to show that bond number n is linearly dependent on Δz, and that the sum of the axial bond numbers (n_x, n_y) equals unity at each stage of the reaction, which implies that the bond between the incoming ligand and cadmium is strengthened at the expense of that between the departing group and the metal. The bond variations observed by Bürgi have since been approximated by Burdett in an angular-overlap molecular orbital study, in which he modeled distortions with C_{3v} symmetry for ML_5 fragments with D_{3h} symmetry (corresponding to step C in Fig. 1), as well as coupled distortions along paths A and B.[42] Despite discrepancies between his calculated curves and those of Bürgi and others, Burdett[42] reports a fairly good qualitative reproduction of the observed bond shortenings and elongations.

Apart from the proposal of mapping reaction paths from crystal structures, Bürgi's initial paper also for the first time introduced the idea of using symmetry coordinates to describe molecular deformations in the solid state. He suggested that an alternative way of looking at the nucleophilic addition was to view it as the reverse of the decay of the TBP, mapped by the SCs collated in Scheme 3, where $\Delta\alpha_{nX}$, $\Delta\alpha_{nY}$ represents the deviation

$$S_2(A_1') = (\Delta y + \Delta x)/\sqrt{2}$$
$$S_3(A_2'') = (\Delta y - \Delta x)/\sqrt{2}$$
$$S_4(A_2'') = (\Delta\alpha_{1X} - \Delta\alpha_{1Y} + \Delta\alpha_{2X} - \Delta\alpha_{2Y} + \Delta\alpha_{3X} - \Delta\alpha_{3Y})/\sqrt{6}$$

Scheme 3.

of the observed angle between the n-th equatorial ligand and the axial ligands, either X or Y, from their values in the reference structure (the TBP). Figure 4 depicts the correlations between these coordinates for the eleven structures of the study. The smooth curves were obtained by regression from Equation (2) and the corresponding expressions for the SCs, and they were interpreted as follows: The decay of the TBP is initiated by antisymmetric stretching of the axial bonds (S_3, Fig. 4 top) coupled to out-of-plane bending of the CdS_3 moiety (S_4). Initially—for values of S_3 smaller than about 0.2 Å—the complex hardly deforms along the symmetric stretch coordinate (S_2, Fig. 4 bottom), but as the decay proceeds this stretch becomes more pronounced.

Another novel idea in the paper was explored in the attempt to estimate the relative magnitude of quadratic and cubic potential (force) constants for the displacement reaction, by modeling the reaction coordinate—the smooth curves in Figure 4—by equations describing a principal axis of the potential energy

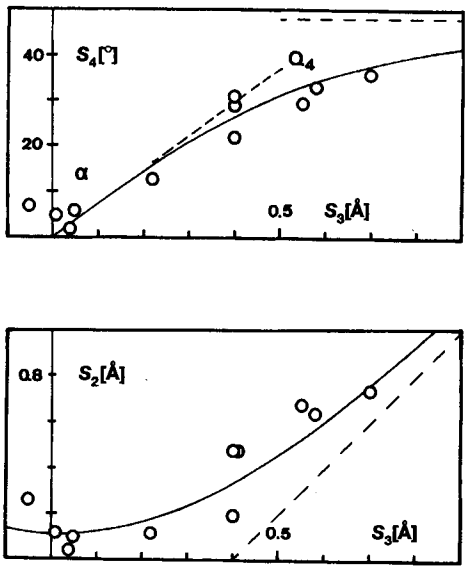


Fig. 4. Top: correlations between the SCs S_3 (XCdY, antisymmetric stretch) and S_4 (CdS_3, out-of-plane bend); bottom: correlations between S_3 (XCdY, antisymmetric stretch) and S_2 (XCdY, symmetric stretch). The solid curves were obtained by regression.

ellipsoid, and making certain simplifying assumptions. Although this approach has since been criticized,[43] it suggested the beguiling notion of extracting data on the topography of the potential energy surface of the ML_5 fragment from the experimental (crystallographic!) information at a time when such data would have been very difficult to come by computationally. Recently this idea has again been given some attention,[44, 45] though there has as yet been no further attempt to obtain empirical information on the potential energy surface for pentacoordinate metal complexes.

4.1.2. Muetterties and Guggenberger—the Berry Rearrangement

Although Bürgi's study revealed convincing correlations, it ignored certain deformations of the coordination polyhedron, by assuming that the complexes all approached at least C_{3v} symmetry. A careful analysis of the data reveals, however, that some of the complexes are quite significantly distorted away from this symmetry; the angle between axial ligands can be as low as 161°. Muetterties and Guggenberger[39] explicitly set out to deal with this problem of approximate configurations.[46] From a structural examination of a large number of coordination complexes they identified a "surprising consistency of shape", in that for compounds of the type ML_n, the n ligating atoms generally describe a polytope in which all faces are equilateral triangles or nearly so. They further found that while the fully triangulated form is always the favored one, there are alternate polyhedra (polytopal isomers[47]) for all commonly observed classes of complexes containing n ligating atoms that may be generated from the favored forms by minor bending–stretching modes. The favored form of ML_5 complexes is the TBP; the SQP is formed when two of the adjacent triangular faces of the TBP become coplanar in a square face during the (Berry) polyhedral rearrangement. As shape parameters Muetterties and Guggenberger proposed the dihedral angles between

the normals to adjacent polytopal faces, coupled with associated angles subtended at the central metal. With reference to Figure 2, the angle (δ_{24}) between the normals to the faces 124 and 524, which share the common edge 24, changes from 53.1° to zero as the TBP deforms to the SQP along the Berry coordinate. This change is accompanied by a concomitant change in the angles θ_{15} (from 180° to about 155°) and θ_{24} (from 120° to also about 155°). By correlating these three angles, Muetterties and Guggenberger were able to arrange seven pentacoordinate complexes containing six different central atoms[48] into a series convincingly mimicking the Berry path. The corresponding diagram (Fig. 5) beautifully illustrates how the individual molecular

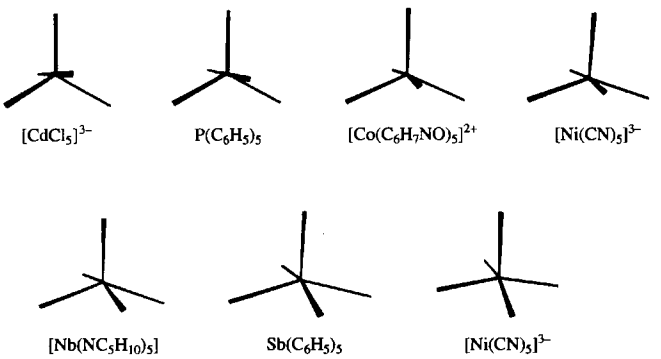


Fig. 5. Muetterties and Guggenberger's arrangement of five-coordinate complexes, which mimic the Berry mechanism, that is, the progression from D_{3h} to C_{4v} symmetry.

structures yield a cinematic film of the reaction, when they are strung together in the right order.[49]

4.1.3. Extension of the Dihedral Angle Technique

For a number of years after the two papers discussed in Sections 4.1.1. and 4.1.2. were published, little or no further attention was given to pentacoordinate metal complexes. Nonmetal compounds, however, were fairly intensively investigated by Holmes, Deiters, and co-workers (see ref. [8]), who developed an extension of Muetterties and Guggenberger's dihedral angle method, which allows a quantification of the extent to which a given molecule has traversed the TBP → SQP divide.[50] Instead of (subjectively) focusing on just two or three of the internal coordinates, Holmes and Deiters included all nine dihedral angles (between normals) in their shape parameter.[51] In their method the sum of the differences between the angles δ_{ij}(C) for each edge ij in the observed structures C and the corresponding angles in the reference polyhedra [δ_{ij}(SQP) and δ_{ij}(TBP), respectively] is determined. For the concerted axial and equatorial bends accompanying the Berry rearrangement, a plot of $217.9° - \sum_{ij}|\delta_{ij}(C) - \delta_{ij}(SQP)|$ versus $\sum_{ij}|\delta_{ij}(C) - \delta_{ij}(TBP)|$, where $217.9° = \sum_{ij}|\delta_{ij}(TBP) - \delta_{ij}(SQP)|$, should then theoretically yield a straight line with unit slope and length $(217.9°)/\sqrt{2}$. The percentage displacement of a given representative point along this coordinate—that is, the percentage displacement of the particular structure along the TBP → SQP pathway—is then easily expressed as a proportion of the length of this line.

4.2. Applications of the Early Methods

4.2.1. Nickel Complexes

The structures of 78 five-coordinate nickel complexes have been examined along similar lines to those discussed in Section 4.1.[52] The molecular geometries were described by internal coordinates (bond distances being expressed as increments relative to the respective standard bond lengths[40]), and no special account was taken of symmetry considerations of the kind mentioned in Section 2.3. The data comprised all five-coordinate nickel entries deposited in the Cambridge Structural Database at that time,[19, 20] but excluded allylic complexes.[53] Scatterplots revealed that 34 of the compounds mapped an association reaction for tetrahedral nickel complexes (path C in Fig. 1), while the remaining 44 structures lay along a reaction coordinate depicting an addition reaction at square-planar centers (path A). This finding is, of course, reconcilable with the fact that four-coordinate nickel complexes can adopt either tetrahedral or square-planar configuration, and ligand substitutions at such centers must therefore necessarily proceed at least partly by different pathways.

The reaction coordinate for square-planar complexes can be suitably described by a correlation between the angular parameters defined on the right of Figure 6; the corresponding scatter-

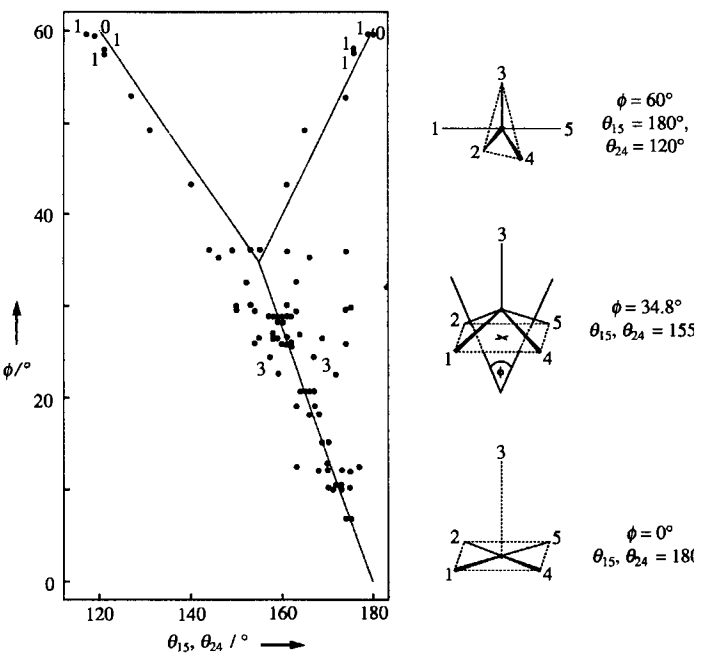


Fig. 6. Deformation of nickel complexes mapped by the bond angles θ_{15}, θ_{24} and the parameter ϕ (defined on the right of the diagram). Points on the lower right of the plot represent fSQPs, those in the center eSQPs, and those at the top right and left TBP conformers. The solid line maps the theoretical coordinate for the deformation described on the right of the scatterplot. The numbers give the oxidation state of the metal.

plot is shown on the left. The solid line represents the theoretical deformation pathway for the scheme shown on the right of the figure. In the scatterplot, points on the lower right represent compounds mapping the incipient stages of step A, that is, flattened SQPs, those at the center represent elevated SQPs, while points in the upper right and left represent TBP complexes; the

split part of the coordinate corresponds to the Berry pathway. The data are fairly evenly spread along the theoretical trajectory, which suggests that there may only be a very small energy difference between the fSQP and the eSQP, and that the activition barrier for the transformation of the one into the other is very small. However, it is not clear how to interpret the scatter about the theoretical coordinate: the phenomenon may arise from structural variations that are not adequately modeled by the method, which includes only three geometric parameters and may therefore be biased by the choice of variables.

The S_N2 pathway was mapped in reverse—that is, an axial ligand in a TBP was removed along the C_3 axis—by correlating the normalized shift parameter $s = (d_{eq} - 3z)/d_{eq}$ with the sum of the angles at the metal atom along $[\sum\theta_{1e}]$ and around $[\sum\theta_{ee}]$ the threefold axis, according to Equation (5) and Equation (6), respectively.[54] The parameter d_{eq} is the average equatorial bond length, z the displacement of the nickel atom out of the equatorial plane. Figure 7 depicts the corresponding scatterplot

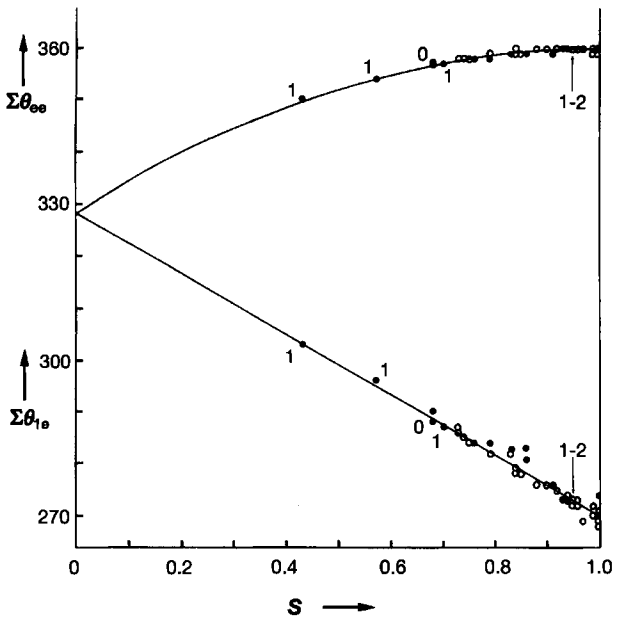


Fig. 7. Adherence of nickel compounds to the coordinate mapping the transition from C_{3v} to T_d symmetry (solid line), that is, the reverse of path C. The numbers indicate the oxidation states of the metal. $\sum\theta_{1e}$ is the sum of the angles [°] at the metal atom along the threefold axis [Eq. (5)], $\sum\theta_{ee}$ the sum of the equatorial angles [Eq. (6)], and s a normalized shift parameter (see text). The numbers indicate the oxidation state of the metal.

for the 34 complexes that mapped this pathway; the solid line represents the theoretical coordinate. Complexes containing Ni^I atoms are indicated by the numbers in the diagram, and lie furthest along the dissociation pathway. This may indicate that in those cases where homolytic bond cleavage results in Ni^I species, it will be an axial bond in a TBP that will cleave.

$$\Sigma\theta_{1e} = \theta_{12} + \theta_{13} + \theta_{14} \quad (5)$$

$$\Sigma\theta_{ee} = \theta_{23} + \theta_{34} + \theta_{24} \quad (6)$$

Finally, the Berry mechanism was found to be a viable pathway for intramolecular exchange in these complexes: a plot of

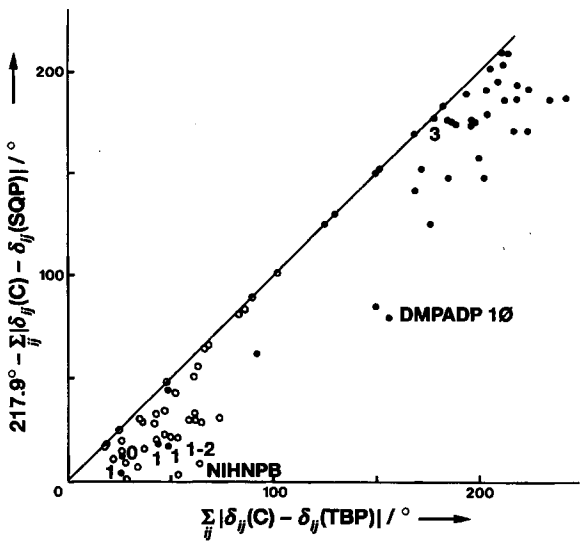


Fig. 8. Adherence of nickel complexes to the Berry coordinate (solid line). Filled circles correspond to structures mapping the association reaction at square-planar nickel, empty circles to those that do not. The numbers indicate oxidation state of the metal. NIHNPB and DMPADP are outliers.

$217.9° - \sum_{ij}|\delta_{ij}(C) - \delta_{ij}(SQP)|$ versus $\sum_{ij}|\delta_{ij}(C) - \delta_{ij}(TBP)|$ revealed a reasonable adherence of the structures to the Berry coordinate depicted by the solid line in Figure 8, in which the origin corresponds to a TBP and the upper end of the straight line at (217.9°; 217.9°) to a SQP. The fairly even clustering of the data around both ends of the coordinate suggests a small energy difference between the TBP and SQP, since a large difference would presumably result in preferred clustering of observed geometries about the lower energy conformer, and a relative paucity of points around the higher energy one. The two outliers could easily be accounted for by unique, highly restrictive structural features that would be expected to distort them away from a minimum energy pathway.

A number of different explanations could account for the scatter in Figure 8. In the paper it was suggested that the complexes that do not map the association reaction for square-planar centers (empty circles) possibly exhibit slightly less scatter than those that do (filled circles). This would make sense, since from a geometric perspective one could argue that structures distorted toward C_{3v} symmetry—that is, those lying along path C (see Fig. 1) and closer to the origin in Figure 8—would more readily undergo Berry exchange than would fSQPs, which lie along path A and at the upper right of Figure 8. Indeed, the fact that the fSQPs lie at the bottom right of Figure 6, displaced from the Berry coordinate, substantiates this suggestion. A certain amount of the scatter is also likely to arise randomly from the different crystalline environments. But another factor that complicates all studies of five-coordinate complexes is that the geometry of the SQP is not uniquely fixed by its symmetry, as is the case for the TBP. In the SQP one degree of freedom remains: the *trans*-basal angles (θ_{15} and θ_{24}, Fig. 6) can adopt any value under C_{4v} symmetry, provided that they are equal. This implies that an arbitrary choice has to be made about the constitution of the "reference SQP" and the values of its angles. Clearly, this affects the calculation of Holmes and Deiters's shape parameters; specifically, the length of the Berry coordinate in plots like

that of Figure 8 and the coordinates of the representative points in these diagrams would be affected.[55]

4.2.2. Zinc, Molybdenum, and Iron Complexes

Scatterplots and the application of the dihedral angle method to a sample of 33 pentacoordinate zinc compounds (represented by their internal coordinates) has enabled a mapping of steps B and C in Figure 1.[56] Results are similar to those for the cadmium complexes and the 78 nickel complexes described earlier, with the exception that in the S_N2 pathway the TBP intermediate was shown to be distorted (with an axial angle of about 163°), as a consequence of the directional preferences of the substitution pathway. There are two extreme approach trajectories of the incoming nucleophile N with respect to the ZnL_4 tetrahedron: for an ideal 'face' approach (F) one N-Zn-L angle would be 180° and three 70.5°, while an ideal 'edge' attack (E) gives rise to two pairs of angles of 125.3° and 54.7°. Figure 9 reveals that the nucleophile approaches the tetrahedron at an oblique angle, midway between F and E, which may well cause the observed distortion of the intermediate. An absence of correlations for the more square pyramidal configurations of the data set suggests that in the case of Zn^{II} complexes any dissociation must occur from the axial positions of a TBP (path C), as opposed to the apical position of an SQP (path A): hence, for the substitution reaction, Berry deformation of a complex towards an SQP leads into a cul-de-sac.

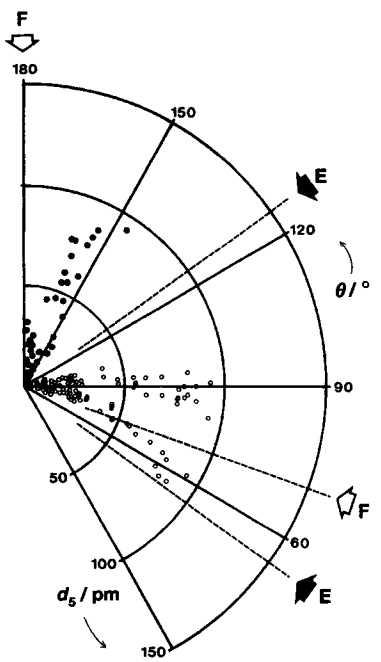


Fig. 9. Scatterplot showing the dependence of the angle of nucleophilic attack on the distance increment [40] of the Zn-to-nucleophile bond. Filled circles plot θ_{15}, open circles θ_{25}, θ_{35}, and θ_{45} (see Fig. 2 for nomenclature). F = face attack, E = edge attack.

A sample of 44 five-coordinate molybdenum complexes has been very similarly treated, and coordinates for an S_N2 reaction and a Berry exchange were obtained.[57] A Berry coordinate has also been mapped from an analysis of nine structures of the type $[Fe(CO)_3P_2]$, where P_2 represents either a bidentate or two monodentate phosphane ligands.[58] In this case, the data were symmetry-expanded according to C_s symmetry. The distribution of the resulting 18 data points was fairly even along the TBP → SQP pathway, again suggesting a low energy barrier for this deformation; indeed, two of the compounds are fluxional even at temperatures as low as −80 °C. This result was not reproduced in a study of twelve $[Fe(CO)_4L]$ complexes (L = monodentate ligand), which found that most of them clustered around the TBP configuration, though some displacement along the Berry coordinate was observed.[59] The aim of the latter study was to establish correlations between the geometric deformations of these complexes and certain Mössbauer parameters, in an attempt to relate their electronic nature to their structure. The results of the study led the authors to predict that axial ligands whose π-acceptor qualities are similar to those of CO would facilitate the Berry mechanism, whereas strong σ-donor ligands would present barriers to the intramolecular exchange. Kinetic and dynamic NMR data to verify this speculation are yet to be forthcoming.

4.2.3. Copper Complexes

Complexes of copper(II) exhibit a wide variety of regular and nonregular stereochemistries, partially as a result of the lack of spherical symmetry of this d^9 ion. In particular, it is often impossible to distinguish between penta- and hexacoordination. This feature has led to attempts[60] to classify these complexes as (4 + 2) when there are four short and two long bonds, or as (4 + 1 + 1*) when there are four short bonds, one long bond, and one (1*) of intermediate length. These configurations could alternatively also be considered as a perturbed ML_4 geometry (4 + 2 or 4 + 1 + 1*), perturbed ML_5 (4 + 1 + 1*), or distorted ML_6 (4 + 2 or 4 + 1 + 1*). Such a structural spectrum invariably invites attempts to map deformation pathways. But it might also frustrate those attempts, since the broad range of configurations could be indicative of a flat potential energy surface, in which case correlations may not be easily identifiable. In the following we concentrate only on those complexes that are readily identifiable as pentacoordinate.

The geometry of the $[Cu(bpy)_2Cl]^+$ ion (bpy = 2,2′ bipyridyl) has been shown to be closer to TBP, though distorted towards SQP, in a series of five complexes with various anions.[60–63] Correlations between some of the internal parameters of the CuN_4Cl chromophore led Hathaway et al. to suggest that these structures map out a TBP → SQP transformation. In terms of the Berry mechanism there are three possible deformations of a trigonal bipyramidal CuN_4Cl polyhedron, of which two are equivalent (Fig. 10). The data for the five $[Cu(bpy)_2Cl]^+$ complexes seemed to map pathway E (or the symmetry-equivalent path F), but not path D. Since the distortion along path E does

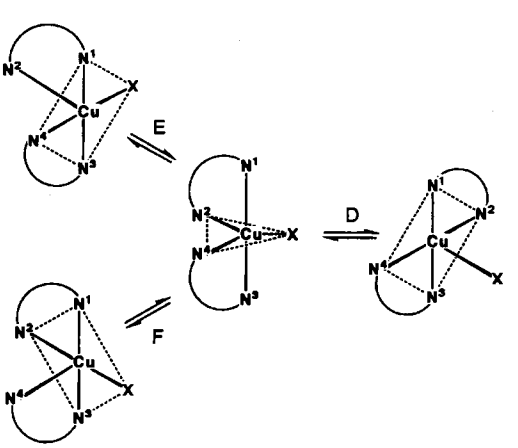


Fig. 10. Possible deformation modes of trigonal bipyramidal complex $[Cu(bpy)_2X]^+$. Path D maintains C_{2v} symmetry, while the symmetry-equivalent paths E and F do not.

not maintain C_2 or C_{2v} symmetry, Hathaway rationalized the deformation as a linear combination of the normal modes of vibration of a trigonal bipyramidal $[CuN_4Cl]^+$ ion, rather than as a Berry mechanism. Path D, however, retains C_2 symmetry, and can hence "be considered as a Berry twist-type mechanistic pathway"; the latter path is mapped by three out of four $[Cu(bpy)_2(OH_2)]^{2+}$ complexes.[61]

Extended Hückel molecular orbital calculations were then used to estimate the relative total energies for a $[Cu(NH_3)_4Cl]^+$ ion as a function of one of the N-Cu-N angles, defined as α_3 (equivalent to the angle N2-Cu-N4 in Fig. 10).[62, 63] The resulting energy profile is shown in Figure 11. Plotted onto the profile

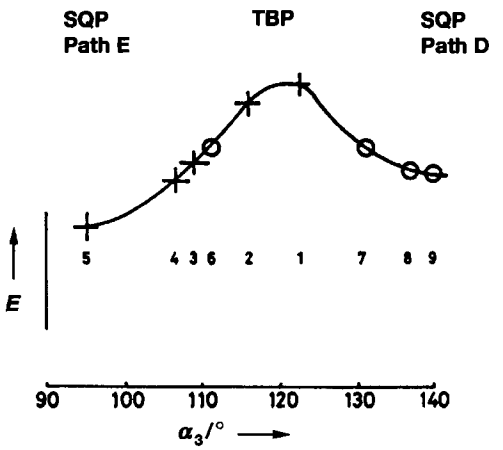


Fig. 11. The extended Hückel energy profile for the model complex $[Cu(NH_3)_4Cl]^+$, as a function of the N2-Cu-N4 angle (α_3) in Figure 10. The crosses represent the observed values of α_3 for complexes $[Cu(bpy)_2X]^+$ in which X = Cl, the circles those in which X = OH_2.

are the values of α_3 for the chloro complexes (crosses) and the aqua complexes (circles). The diagram should not be misconstrued as the correlation between the observed values of α_3 and the energy of the complex, but it does serve to illustrate one possible approach to empirical potential energy surfaces: if a large enough sample pertains, it might be possible to model the data distribution density along the reaction coordinate and thereby perhaps obtain information about the topography of the energy well (or minimum energy path). However, in this case the calculations tellingly revealed the TBP to be of slightly higher energy than the SQP, even though most of the structures approximate more closely to the TBP than the SQP; perhaps this illustrates the point that the potential energy surfaces for the various observed structures and the model complex are significantly different, even though the complexes have similar compositions.[43] In a subsequent paper the results of variable temperature NMR experiments on the $[Cu(bpy)_2X]^+$ ions (X = Cl or I) are reported, and it is shown that they exhibit no fluxionality;[64] in view of this, it is not clear how to interpret the structural correlations obtained for these molecules in the earlier reports. In another study, Hathaway et al. have proposed that three related complexes the CuN_5-containing chromophore may be viewed as stationary points along a Berry pathway, but no further reports have emerged for this system.[65] All of the studies discussed so far in this section suffer from the drawback that they included only very limited numbers of structures, and the conclusions—as far as there are any—must therefore be treated with a certain amount of caution.

In a separate report,[66] brief mention is made of a principal component analysis (PCA) of 26 $[Cu(L)_2X]$ complexes (L = bpy or 1,10-phenanthroline (phen)), which revealed that the structural variance for these compounds essentially lies in a plane in the 15-dimensional data space[67] that was analyzed. The plane is described by two axes that correspond to the eigenvectors for the two deformations depicted in Figure 10, that is, the symmetric (Berry) pathway (path D), and the asymmetric (non-Berry) deformation (path E). Hathaway's conclusion that the structures of this type of complex can be discussed in terms of these two deformation paths has therefore been borne out by the PCA. A more recent study[68] suggests, however, that the true deformation pathway for complexes of this kind is intermediate between the symmetry-equivalent paths E and F. In the latter case, 36 bpy and phen complexes were analyzed on the basis of their internal coordinates, specifically the equatorial angles around the metal atom. The conclusion about the nature of the deformation path may be doubtful though, because of certain problems in the geometric treatment.[69] In a slight contradiction of the above suggestion, the study also concluded that $[Cu(L)_2X]$ complexes do not readily distort toward SQP through the symmetric deformation, whereas they do through path E. This observation was rationalized by the argument that the $Cu(L)_2$ chromophores cannot be planar—as they would be along path D—because of steric hindrance between the hydrogen atoms near the pyridinic nitrogen atoms.

The studies on five-coordinate copper complexes that have been mentioned here barely scratch the surface of the data that are available: less than forty, highly select complexes have been examined. It seems that the complexity of the problem—emphasized by the confused results and conclusions from the different studies—calls for the application of far more sophisticated methods of analysis than have thus far been brought to bear on these structures.

4.3. The Application of Multivariate Techniques: d^8 Metal Complexes

Perhaps the most comprehensive analysis of an ML_5 system to date can be found in a study involving the multivariate analysis of a data set comprising 196 pentacoordinate d^8 complexes containing the metals nickel, palladium, platinum, rhodium, and iridium.[70, 71] Bond distances were expressed as increments,[40] and angles were all scaled to the approximate dimension of the average bond distance in the data set.[21] The coordination geometries were expressed by means of a complete set of symmetry coordinates for both TBP and SQP configurations. Each ML_5 fragment was thus represented by a point in two different 12-dimensional parameter spaces: *T-space*, where each structure is related to a TBP, and *S-space*, where each is related to a SQP. A novel feature of this analysis is that no "ideal" value of the *trans*-basal angle (θ_{15} and θ_{24}, Fig. 2) in the reference SQP had to be assumed, since the evaluation of the SCs does not require a value for this angle: even though it is the increments r or deviations Δ of the observed values from the reference values that appear in the SC expressions (see Section 2.1), the

reference values cancel for all but the totally symmetric representations.[72, 73] The atom labeling problem (Section 2.3) was explicitly discussed: the 120 (= 5!) possible permutations of the labels give rise to ten and fifteen groups, respectively, of twelve and eight so-called permutationally equivalent isomers—structures that are represented by identical lengths, but different senses, of the total distortion vector (Section 2.1), that is, they are equally deformed from the reference TBP or SQP, but their atom labels are permuted according to the symmetry of the reference point groups.

For both spaces the data were symmetry-expanded (D_{3h} and C_{4v} symmetry), leading to 2352 and 1568 data points in T- and S-space, respectively. Univariate and bivariate statistics (analysis of variance and covariance) suggested the importance of deformations along paths B and C (Fig. 1) for the data in T-space, while in S-space deformations along paths A and B predominated.

The resultant twelve-dimensional data distributions were then analyzed by both hierarchical and nonhierarchical cluster analysis (CA), and the Euclidian distance was chosen as a measure of similarity. The method of nonhierarchical CA classified the data set into a user-specified number of clusters, while hierarchical CA employed a method called "Ward's method".[74] The search for the "ideal" number of clusters was fairly random in the initial stages, but a solution was soon found by use of the symmetry criterion, namely that the symmetry of the data distribution made explicit by the symmetry expansion must reappear in the results of CA. An additional criterion, implementable because two different clustering algorithms were employed, was that the classification of data points had to be identical, or very nearly so, for both methods.[75] Four clusters were identified in both spaces (see Fig. 12): in T-space a central cluster (cluster T3) representing an ideal TBP is surrounded by three identical clusters (T1, T2, T4) whose median configurations (archetypes) are distorted SQPs. Interestingly, the three SQPs represented by these clusters correspond to the alternate SQPs that could be obtained from the central TBP (cluster T3) by means of the Berry mechanism. In S-space, the data cluster about an fSQP and an eSQP archetype (S2 and S4), as well as two permutationally equivalent TBP archetypes (S1, S3)—the latter again correspond to the two TBPs that could ideally be formed from the eSQP. Note how the symmetry of the data distribution reflects the symmetry of the reference point groups.

The study interestingly revealed a strong homogeneity of the clusters. Histograms displaying the distance of each observation from the cluster center in most cases revealed no more than two or three outliers, and for all of these it was possible to rationalize why they appeared on the fringes of the clusters: in some cases the points corresponded to structures that were intermediate between SQP and TBP, or between fSQP and eSQP, while in others peculiar structural features of the compounds deformed them away from the minimum energy path.

An interesting comparison can be made between the scatterplots for the addition reaction at a nickel center in a square-planar environment in the earlier study[52] (Fig. 6) and the corresponding diagram for the study discussed here (Fig. 12, right). In the former, where only three geometric parameters are employed in the analysis, a distinction between the eSQP and the fSQP is hardly possible, whereas the clustering algorithm has been able to subdivide the group of square-pyramidally disposed structures into the two classes automatically. This speaks volumes for the power of this form of analysis, since the distinction between these two forms would appear to be a totally arbitrary one on the basis of a graphical analysis only: the representative points for the eSQP and the fSQP are likely to be separated by only a very small potential barrier on the Born-Oppenheimer potential energy surface for the ML_5 fragment, and the spread of observed molecular structures around these points can be expected to be large and diffuse, with no clear boundaries between the two distributions. Purely graphical techniques would consequently be unlikely to suffice as a means of differentiation. This point becomes clear when one compares the average sizes[76] of S2 and S4 (0.697 and 0.932 Å) with the distance between them (0.833 Å)—possibly the clouds of data points diffuse into each other. Despite this, the statistical technique evidently succeeded in fixing the positions of the archetypal configurations somewhere in the center of the cloud of data points surrounding them.

Principal component analysis did not enable a dramatic reduction in dimensionality, but it did reveal chemically meaning-

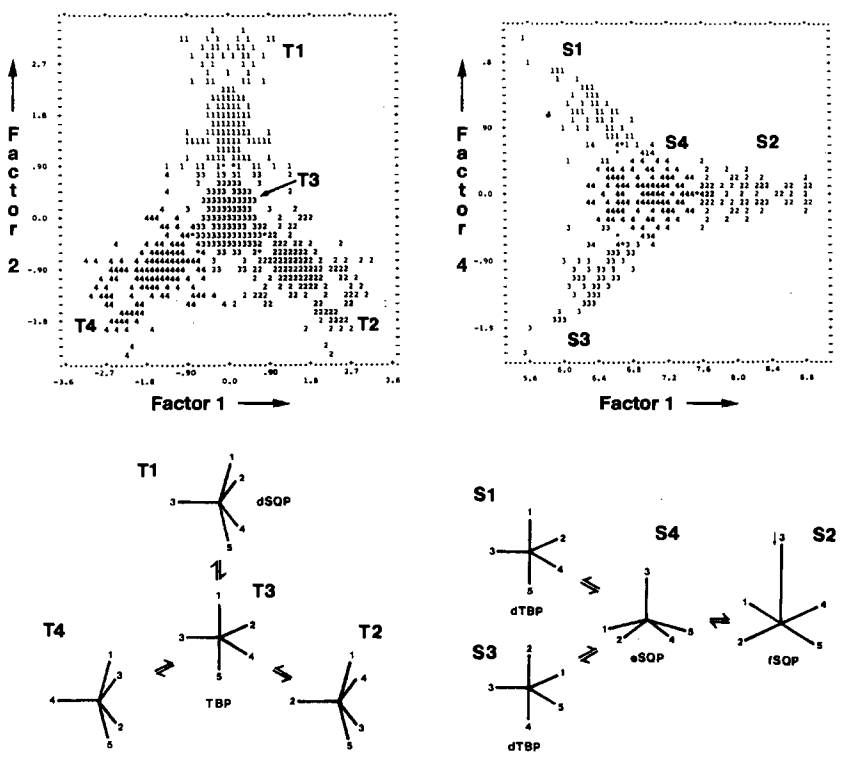


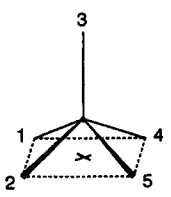
Fig. 12. Results of cluster analysis of d^8 metal complexes. The scatterplot on the left shows the clusters formed in T-space, that on the right those formed in S-space. Below each scatterplot is a qualitative interpretation of the cluster archetypes, and the deformation coordinates relating them.

ful results. For the TBP the two most important distortions are the S_N2 and the Berry deformations (steps C and B in Fig. 1), accounting for 15 and 24% of the variance, respectively. The eSQP was shown to distort along both the addition/elimination pathway (step A, 14%) and the Berry coordinate (12%). In an interesting contrast, the fSQP maps only the incipient stages of the addition/elimination reaction (14% of variance), and was not seen to distort along the Berry path. In this analysis, symmetry considerations also played an important role, in that only SCs of identical symmetry appeared together in the same PC. As an example, consider the first two PCs for the eSQP [Eq. (7a, b)]

$$PC1 = 0.888S_1 - 0.879S_2 + 0.879S_3 \quad (7a)$$

$$PC2 = 0.837S_4 + 0.837S_5 \quad (7b)$$

where the SCs (S_i) are defined as in Figure 13. The component SCs of PC1, mapping the addition/elimination deformation, are all of A_1 symmetry, while those of PC2, describing the Berry coordinate, all have B_1 symmetry, that is, no mixing of symmetries is observed.



$S_1(A_1) = r_3$

$S_2(A_1) = \frac{1}{2}(r_1 + r_2 + r_4 + r_5)$

$S_3(A_1) = (1/\sqrt{2})(\Delta\theta_{15} + \Delta\theta_{24})$

$S_4(B_1) = \frac{1}{2}(r_1 - r_2 - r_4 + r_5)$

$S_5(B_1) = (1/\sqrt{2})(\Delta\theta_{15} - \Delta\theta_{24})$

Fig. 13. Examples of some of the SCs used to represent the structures of observed pentacoordinate complexes. SCs shown are those derived for the SQP reference geometry; the atom numbering scheme is indicated. Their symmetries are given in the brackets.

Chemically, the results suggested interesting new possibilities: 1) the fact that the TBP cluster distorts along the S_N2 coordinate suggests that five-coordinate Rh and Ir compounds, which are significantly represented in this cluster, may undergo dissociation by an S_N2 mechanism via a (short-lived) tetrahedral intermediate, even though this may not be evident from the chemistry of their (square-planar) tetracoordinate complexes; 2) since the fSQP is not seen to map the Berry coordinate, other mechanisms may be operable in fluxional pentacoordinate Pt and Pd complexes (which are principally represented in this cluster), or at least, the complexes may have to undergo a considerable distortion of their coordination sphere to an eSQP before this mechanism can operate. This observation may be the reason for the lack of unambiguous experimental results that indicate Berry fluxionality in complexes of these metals.[70c]

5. Comparison of Structural Results with Theoretical Models

Ab initio calculations on compounds of the type dealt with in this paper are—arguably—only just becoming computationally feasible, and no real comparisons are yet possible between that type of theoretical approach, and the results of the structural analyses. However, studies involving simpler theoretical models are available. Kepert et al. have developed a simple repulsion model in which the ligand donor atoms, regarded as point charges, are assumed to be distributed on the surface of a hard sphere at the center of which the metal is sited.[77] The main purpose of this model is to classify, rationalize, and predict the stereochemistries of $[ML_n^x]$ complexes, where L represents either unidentate ($x = 1$), bidentate ($x = 2$), or less commonly, tridentate ligands ($x = 3$). For the composition $[ML_5^1]$, for instance, the data, which include both transition and nontransition metals, appear to fall into two categories: those that map the TBP → SQP transition, and those that do not; the latter to a large extent map the departure of an apical ligand from a SQP instead.[77, 78] This finding was later[52] corroborated in the analysis of 78 five-coordinate nickel complexes discussed in Section 4.2.1, where just under half the complexes were found to lie along paths B and C of Figure 1, while the rest map paths A and B.

In their study of $[ML_5^1]$ complexes, Favas and Kepert[78] defined an axis in the TBP, such that the angles between this axis and each of the ligand atoms A, B, and C, are all equal; angles ϕ_D and ϕ_E are then measured between this axis and the bonds to D and E. Figure 14 depicts the potential energy surface (PES)

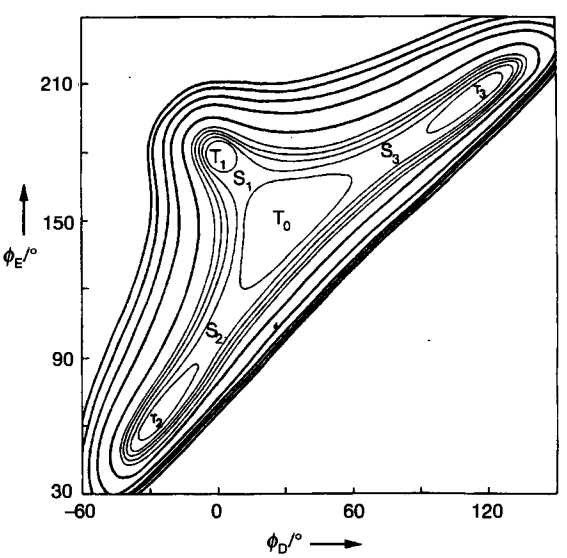


Fig. 14. Potential energy surface for $[ML_5^1]$ complexes. T_0, T_1, T_2, and T_3 represent TBP conformers that may be interconverted through SQP intermediates, represented by S_1, S_2, and S_3. The angular parameters ϕ_D and ϕ_E are described in the text.

for $[ML_5^1]$ molecules with C_s symmetry, projected onto the ϕ_D/ϕ_E plane. The positions of the TBPs and SQPs are shown by T and S, respectively, and the PES is symmetrical about the line $\phi_E = 180° - \phi_D$. The topography of this PES is mirrored in a scatterplot (Fig. 15, left) of the structural data for 33 zinc complexes (Section 4.2.2), in which the data have been projected onto a plane that is almost equivalent to the ϕ_D/ϕ_E plane, but is defined in terms of bond angles in the structures.[56]

For complexes of the type $[MA_2B_3]$, where A and B are unidentate, the PES has similar general features to those shown in Figure 14, but the relative energies of stereochemically distinct TBPs and SQPs, that is, of the potential minima (T_0, T_1,

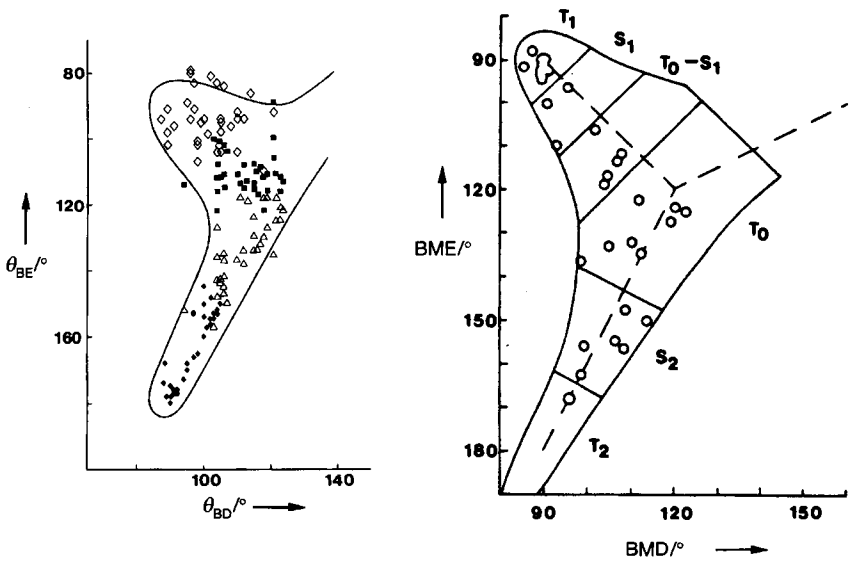


Fig. 15. Left: scatterplot of bond angles θ_{23} (equivalent to θ_{BE}) and θ_{34} (θ_{BD}) (see atom numbering in Fig. 2) for 33 zinc complexes [56]. The different symbols represent different permutations of the atom labels on the same molecular skeleton. Right: the same angular data for 51 mixed $[MA_2B_3]$ complexes (A, B = monodentate ligands) [78]. Note the similarity between the outlines of the distributions in these diagrams, and those of the potential energy surface in Figure 14.

T_2, T_3) and the saddle points (S_1, S_2, S_3), depend on the relative lengths of the M–A and M–B bonds. It is therefore not possible to obtain a unique representation of the PES for this model. Nonetheless, a plot of the angular data for 51 mixed complexes of this kind[78] reproduces the broad outlines of the PES for these $[ML_5]$ complexes (Fig. 15, right).[79] An analysis, along similar lines, of 16 $[ML^3L_2^1]$ compounds with a variety of transition and nontransition metals has provided an empirical mapping of a stereochemical interconversion of two distorted TBPs via a SQP intermediate, that maintains C_s symmetry.[80] The process is not equivalent to the Berry mechanism and has no readily recognizable counterpart among postulated $[ML_5]$ reaction mechanisms. Nevertheless, the data partially lie along troughs in the PES for this system, as established by using Kepert's model. Lastly, the amount of square-pyramidal distortion of eleven $[Cu(planar\text{-}L^3)L_2^1]$ complexes has been analyzed and quantified with the dihedral angle method of Muetterties and Guggenberger (Section 4.1.2), and the data distribution compared to the PES for this system according to Kepert's model.[81] A comparison of results showed that the ordering of the complexes along the TBP → SQP coordinate from the approach of Muetterties and Guggenberger was similar to the ordering that emerged from Kepert's model.

It has long been suggested that the geometry of ML_5 conformers will be dependent on the metal's d electron configuration;[82, 83] specifically the degree of 'flatness' of the SQP, and the ratios of the apical/basal and axial/equatorial bond lengths[84] in the SQP and TBP, respectively, are influenced by this factor. On the basis of an extended Hückel molecular orbital analysis of a $[PtL_5]^{3-}$ model, and considering only σ-bond strength,[85] Rossi and Hoffmann[83] predicted that the apical bond in a square-pyramidal d^8 complex would be longer than the basal bonds, while in the corresponding TBP the axial bonds would be shorter than those in equatorial positions. An empirical analysis by Holmes[86, 87] confirmed these predictions, but in that instance only fairly small samples were analyzed.[88] In the case of the multivariate analysis discussed in Section 4.3, the average axial bond in the TBP was found to be 0.030 Å longer than its usual reference value, while the equatorial bonds were 0.025 Å shorter, in contradiction to both the earlier empirical analysis and the theoretical predictions. In the case of the SQP, however, the results for the larger data set corresponded with those of Holmes, and with those of the theoretical prediction: for the eSQP the apical bond will be 0.030 Å longer, the basal bonds 0.008 Å shorter than the references, while the fSQP will have apical bonds that are on average 0.692 Å longer and basal bonds 0.165 Å shorter than their standard lengths.

According to Rossi and Hoffmann's calculations the "ideal" *trans*-basal bond angle (θ_{tb}) for a SQP environment of a d^8 metal center is 164°, but their model did not include the effect of spin. In his analysis, Holmes subdivided the compounds for which the spin state was known into low-spin and high-spin complexes (fourteen and nine compounds, respectively) and showed that low-spin complexes have a preference for the fSQP configuration (average $\theta_{tb} = 173°$), and high-spin complexes for the eSQP (average $\theta_{tb} = 161°$). The multivariate analysis revealed $\theta_{tb} = 171°$ for the fSQP (cluster S2 in Fig. 12; 39 structures), and $\theta_{tb} = 163°$ for the eSQP (S4; 88 structures), but it was not possible to correlate these values with spin state, since for most of the structures in the data set spin was not measured or reported. In addition, Holmes predicted that high-spin d^8 complexes would preferentially adopt SQP configuration over TBP, and his data seem to agree with this assertion. In the more recent study (Section 4.3) approximately twice as many compounds were classified as SQP than as TBP, and when regarding the individual metals, it is obvious that this tendency for the second- and third-row elements, which are more likely to be low-spin, is more pronounced than for nickel. Once again, without more knowledge of the spin states of the complexes, little can be definitely said about the conformational preferences of different spin states.

6. Discriminating Between Reaction Mechanisms: Metal Cluster Rearrangements

In previous sections we have focused on complexes in which the central metal atom is surrounded by five ligand donor atoms; here we shall be looking at one example of a metal cluster, where, although the metal atoms are not five-coordinate, the cluster framework nevertheless adopts regular polyhedral shapes known from pentacoordinate metal complexes. Metal clusters containing trigonal bipyramidal M_2Ru_3 fragments (M = Cu, Ag, Au) have been shown to exhibit dynamic behavior in solution, involving an intramolecular site exchange of the M atoms in the TBP.[89] In the absence of any geometric information about the interconversion pathways, Rodger and

Johnson have put forward three hypotheses concerning possible mechanisms for such polyhedral rearrangements.[90] They postulate that there are only two possible mechanisms[91] for site exchange in pentaatomic clusters: the first involves the stepwise cleavage and subsequent formation of a polyhedral edge, with an edge-bridged tetrahedral intermediate, while the second involves a concerted process and a SQP intermediate, akin to the Berry process. These alternative mechanisms are depicted in Figure 16.

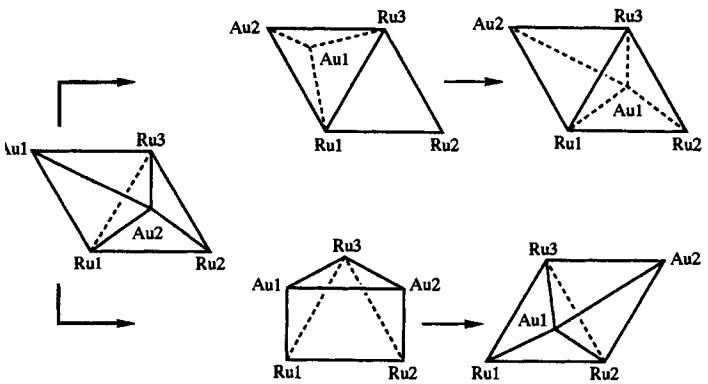


Fig. 16. Possible mechanisms for site exchange in Au_2Ru_3 clusters. Top: stepwise mechanism with edge-bridged intermediate; bottom: Berry process. The molecular fragments were defined by the lengths of the nine edges indicated for the TBP on the left, plus the distance Au1–Ru2.

An examination[92] of the structures of 19 Au_2Ru_3 fragments contained in clusters with a variety of carbonyl, phosphane, and μ_3-ligands (e.g. S, COMe) has revealed that site exchange most likely occurs by the Berry process. It proved possible to rule out tetrahedral edge-bridged intermediates and the alternative turnstile mechanism[37, 38] on the basis of the structural evidence. The data, composed of interatomic distances and selected bond and dihedral angles, were symmetry-expanded according to the C_s symmetry group common to the idealized TBP and SQP clusters, and the analysis included multivariate techniques and scatterplots. A dihedral angle plot, in which the dihedral angle between the planes Au1-Ru1-Au2 and Ru2-Ru1-Au2 (Fig. 16) —equivalent to the dihedral angle δ_{24} of Section 4.1.2. and Figure 2—is plotted against the corresponding bond angles θ_{15} and θ_{24}, reveals the typical 'V-shaped' Berry coordinate (Fig. 17). Corroborating evidence comes from the PCA, which yielded one PC accounting for 92% of the variance in the ten metal–metal distances chosen to represent the fragments (Fig. 16); the major components of this PC are the symmetry equivalent distances Au1–Ru2 and Au2–Ru1. The proposed mechanism is fully consistent with the results of NMR studies on the dynamic behavior of these fragments in solution.[89]

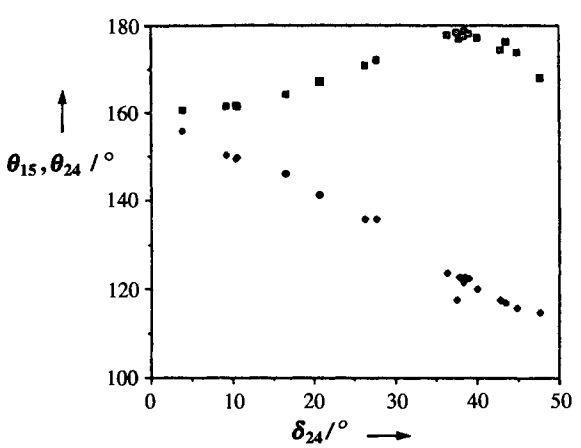


Fig. 17. Dihedral angle plot for Au_2Ru_3 clusters. The angles δ_{24} and θ_{15}, θ_{24} are described in the text.

7. Summary and Outlook

In retrospect, by and large the various structure correlation studies on pentacoordinate complexes have served to substantiate earlier hypotheses (made on the strength of (indirect) evidence from solution studies) about the likely geometric route that reaction pathways of ML_5 or (ML_4 + L) systems might take. Whereas those studies employing simpler two- or three-dimensional methods of analysis may not have significantly deepened our understanding of the mechanisms even though they have lent support to the structure correlation hypothesis, the multidimensional analysis revealed geometric details which suggest that these reaction mechanisms require more careful study with techniques that extend to shorter time-scales. Questions remain, for example, about the viability of the Berry pathway for isomerization reactions of platinum and palladium complexes, or about the possible existence of short-lived tetrahedral rhodium and iridium intermediates in substitution reactions of (square-planar) compounds of these metals. There may also be a need to reinvestigate the possible correspondence (or lack of it) between theoretical predictions[83] about ratios between axial/equatorial and apical/basal bond lengths and the empirical results.[70]

Even the application of the structure correlation method to ML_5 complexes has not yet been exhausted, since pentacoordinate copper complexes still seem to offer a fruitful field of research, for example. Another area of great interest would be an analysis of site preferences for various classes of ligands,[93] particularly in complexes of the d^8 metals; this could yield information about the *trans* effect in square-planar complexes, since five-coordinate intermediates are often invoked in mechanistic explanations of this phenomenon. Future work might focus more on obtaining energetic information along with geometric detail by combining kinetic and structural data to construct individual reaction-path and energy profiles.[45] It might also take advantage of the recent dramatic increases in availibility of computers with high performance to compare structural results with ab initio calculations on some of the systems discussed here. Connected to this is the use of results from structure correlation studies in the optimization of molecular modeling software: the averaged geometries obtained from structure correlation studies represent, at least, local potential minima, and can therefore be used in the process of minimization.[94]

Finally, without being able to offer an answer but in the hope that it may spur more work in the area, I wish to close with what appears to me a fundamental paradox. No single molecular Hamiltonian exists for the series of [ML_n] complexes, and hence there can be no potential energy surface for this "system". Why

is it, then, that these complexes exhibit such consistent correlations, when at most what they have in common is a metal atom surrounded by n coordinated ligand atoms?

I wish to thank the Chemistry Department, University of Cape Town, for hosting me so generously, thereby affording me the opportunity to do what most academic chemists can only dream of—completing unfinished manuscripts.

Received: June 7, 1993 [A 21E]
German version: *Angew. Chem.* **1994**, *106*, ■

[1] This approach allows us to represent a molecule in terms of classical concepts of shape and structure, that is, as an ensemble of nuclei that vibrate with small amplitudes around well-defined positions in space. From this notion arises the possibility of depicting a molecule by a model in which the time-averaged nuclear positions are made to coincide with well-defined points in space. Notwithstanding its success, it should not be forgotten that this molecular theory has its origin in the Born–Oppenheimer approximation to the molecular Hamiltonian, according to which electronic and nuclear motions may be separated—and the latter largely ignored—or that there may also be other molecular theories that give rise to nonclassical interpretations and models; see S. J. Weininger, *J. Chem. Educ.* **1984**, *61*, 939–944; R. G. Wooley, *ibid.* **1985**, *62*, 1083–1084; R. G. Wooley, *New Sci.* **1988**, *22*, 53–57; A. Amann, W. Gans, *Angew. Chem.* **1989**, *101*, 277–285; *Angew. Chem. Int. Ed. Engl.* **1989**, *28*, 268–276; A. Amann, *S. Afr. J. Chem.* **1992**, *45*, 29–38; J. C. A. Boeyens, *Struct. Bonding (Berlin)* **1985**, *63*, 65–101.

[2] a) D. G. Truhlar, R. Steckler, M. S. Gordon, *Chem. Rev.* **1987**, *87*, 217–236; b) W. F. van Gunsteren, H. J. C. Berendsen, *Angew. Chem.* **1990**, *102*, 1020–1052; *Angew. Chem. Int. Ed. Engl.* **1990**, *29*, 992–1023.

[3] H.-B. Bürgi, *Inorg. Chem.* **1973**, *12*, 2321–2326.

[4] a) H.-B. Bürgi, *Angew. Chem.* **1975**, *87*, 461–474; *Angew. Chem. Int. Ed. Engl.* **1975**, *14*, 460–473; b) H.-B. Bürgi, J. D. Dunitz, *Acc. Chem. Res.* **1983**, *16*, 153–161; c) *J. Am. Chem. Soc.* **1975**, *97*, 921–922.

[5] For the remainder of this paper, such structures will collectively be referred to as "molecular structures".

[6] *Structure Correlation* (Eds.: H.-B. Bürgi, J. D. Dunitz), VCH, Weinheim, **1993**.

[7] Transition metals, including zinc and cadmium.

[8] Antimony compounds: R. R. Holmes, R. O. Day, V. Chandrasekhar, J. M. Holmes, *Inorg. Chem.* **1987**, *26*, 163–168; germanium compounds: A. O. Mozzchukhin, A. A. Macharashvili, V. E. Shklover, Yu. T. Struchkov, A. G. Shipov, V. N. Sergeev, S. A. Artamkin, S. V. Pestunovich, Yu. I. Baukov, *J. Organomet. Chem.* **1991**, *408*, 305–322; silicon compounds: M. J. Barrow, E. A. V. Ebsworth, M. M. Harding, *J. Chem. Soc. Dalton Trans.* **1980**, 1838–1844; F. Liebau, *Inorg. Chim. Acta* **1984**, *89*, 1–7; R. R. Holmes, R. O. Day, V. Chandrasekhar, J. J. Harland, J. M. Holmes, *Inorg. Chem.* **1985**, *24*, 2016–2020; G. Klebe, *J. Organomet. Chem.* **1987**, *332*, 35–46; A. A. Macharashvili, V. E. Shklover, Yu. T. Struchkov, G. I. Oleneva, E. P. Kramarova, A. G. Shipov, Yu. I. Baukov, *J. Chem. Soc. Chem. Commun.* **1988**, 683–685; G. Klebe, *Struct. Chem.* **1990**, *1*, 597–616; R. R. Holmes, *Chem. Rev.* **1990**, *90*, 17–31; V. F. Sidorkin, V. V. Vladimirov, M. G. Voronkov, V. A. Pestunovich, *J. Mol. Struct. (THEOCHEM)* **1991**, *228*, 1–9; K. Tamao, T. Hayashi, Y. Ito, M. Shiro, *Organometallics* **1992**, *11*, 2099–2114; phosphorus compounds: R. R. Holmes, *Acc. Chem. Res.* **1979**, *12*, 257–276; tin compounds: D. Britton, J. D. Dunitz, *J. Am. Chem. Soc.* **1981**, *103*, 2971–2979; U. Kolb, M. Dräger, B. Jousseaume, *Organometallics* **1991**, *10*, 2737–2742; S. A. Jackson, O. Eisenstein, J. D. Martin, A. A. Albeniz, R. H. Crabtree, *ibid.* **1991**, *10*, 3062–3069; see also ref. [6], Chapter 8, for a further review of silicon and germanium complexes.

[9] For more comprehensive reviews: a) ref. [6], Chapters 1, 2, and 4; b) T. Auf der Heyde, *S. Afr. J. Chem.*, in press.

[10] For example, structural diagrams, chemical formulas, bond distances, and angles. For a descriptive review, see R. Hoffmann, P. Laszlo, *Angew. Chem.* **1991**, *103*, 1–17; *Angew. Chem. Int. Ed. Engl.* **1991**, *30*, 1–16.

[11] Under specific constraints, such as those imposed by symmetry considerations or those resulting from limitations on certain geometrical parameters, it may be possible to reduce the number of degrees of freedom from $3N-6$. For example, the imposition of T_d symmetry on a five-atom fragment reduces the number of parameters needed from nine to only one (the bond length); see J. D. Dunitz, *X-Ray Analysis and the Structure of Organic Molecules*, Cornell University Press, Ithaca, **1979**, Chapter 9.

[12] For one example of a structure correlation analysis involving positional coordinates see P. Murray-Rust, J. Raftery, *J. Mol. Graphics* **1985**, *3*, 50–59.

[13] For example, the number of internal distances of $N(N-1)/2$ is much larger than the number of degrees of freedom $(3N-6)$.

[14] a) P. Murray-Rust, H.-B. Bürgi, J. D. Dunitz, *Acta Crystallogr. Sect. B* **1978**, *34*, 1787–1793; b) P. Murray-Rust, H.-B. Bürgi, J. D. Dunitz, *ibid.*, 1793–1803; c) *Acta Crystallogr. Sect. A* **1979**, *35*, 703–713.

[15] a) F. A. Cotton, *Chemical Applications of Group Theory*, 3rd ed., Wiley, New York, **1990**; b) S. F. A. Kettle, *Symmetry and Structure*, Wiley, Chichester, **1985**; c) E. B. Wilson, J. C. Decius, P. C. Cross, *Molecular Vibrations—The Theory of Infrared and Raman Vibrational Spectra*, McGraw–Hill, London, **1955**; d) D. Wald, *Gruppentheorie für Chemiker*, 1st ed., VCH, Weinheim, **1985**.

[16] With reference to the case cited in the text, for example, any molecules whose representative points fall exactly onto the S_1 or S_2 coordinates would exhibit full C_{2v} symmetry, since these coordinates transform as A_1. Expressed differently, any such molecules would differ from the reference structure only in their bond angle (S_1), or in the length of the two $X-Y$ bonds (each being shortened or lengthened by the same amount; S_2); both of these deformations maintain C_{2v} symmetry.

[17] In such cases it may be necessary to refer to the group theory of "nonrigid" molecules, see H. C. Longuet-Higgins, *Mol. Phys.* **1963**, *6*, 445–460; H. Frei, A. Bauder, H. H. Günthard, *Top. Curr. Chem.* **1977**, *81*, 1–97; R. L. Flurry, *J. Chem. Educ.* **1984**, *61*, 663–665.

[18] Statistical methods suitable for structure correlation studies have been reviewed in T. P. E. Auf der Heyde, *J. Chem. Educ.* **1990**, *67*, 461–469 and in ref. [9a, b].

[19] Crucial tools for this stage are the Cambridge Structural Database [20], which contains crystallographic data for a large number of organic and organometallic compounds, or the Inorganic Crystal Structure Database [G. Bergerhoff, R. Hundt, R. Sievers, I. D. Brown, *J. Chem. Inf. Comput. Sci.* **1983**, *23*, 66–69], housing data on inorganic structures. The databases allow the user to define a search fragment, and then retrieve all crystallographic structures that contain that fragment. The choice of a search fragment needs to be a judicious compromise between a definition that is too narrow in its scope, thereby precluding the retrieval of entries whose distortions might be of extreme interest and importance, and one that is so broadly stated as to include fragments which add nothing to the analysis—apart, that is, from time and effort spent on it.

[20] a) F. H. Allen, O. Kennard, R. Taylor, *Acc. Chem. Res.* **1983**, *16*, 146–153; b) *Cambridge Structural Database (CSD) User Manual, Version 4.2*, Crystallographic Data Center, Cambridge, **1990**.

[21] Angular and distance measurements, for example, are not directly comparable. Angles may be *scaled* to about the same range as distances, by expressing them as radial displacements α on a circle whose radius r is equal to the average bond distance in the data set: $\alpha = 2\pi r\,(\theta/360°)$. Alternatively, the data may be *standardized* to unit variance and zero mean, by using the z-transformation; see ref. [22] for other suitable scaling and standardization techniques. For an example of the z-transformation applied to crystallographic data in a structure correlation study, see R. Taylor, *J. Mol. Graphics* **1986**, *4*, 123–131.

[22] a) D. L. Massart, B. G. M. Vandeginste, S. N. Deming, Y. Michotte, L. Kaufman, *Chemometrics*, Elsevier, Amsterdam, **1988**; b) R. L. Anderson, *Practical Statistics for Analytical Chemists*, Reinhold, New York, **1987**; c) R. M. Bethea, B. S. Duran, T. L. Boullion, *Statistical Methods for Engineers and Scientists*, Dekker, New York, **1975**; d) R. Caulcutt, R. Boddy, *Statistics for Analytical Chemists*, Chapman and Hall, London, **1983**.

[23] a) P. Murray-Rust, W. D. S. Motherwell, *Acta Crystallogr. Sect. B* **1978**, *34*, 2518–2526; b) P. Murray-Rust, R. Blaha, *ibid.* **1978**, *34*, 2527–2533; c) P. Murray-Rust, W D. S. Motherwell, *ibid.* **1978**, *34*, 2534–2546; d) *J. Am. Chem. Soc.* **1979**, *101*, 4374–4376; e) P. Murray-Rust, *Acta Crystallogr. Sect. B* **1982**, *38*, 2765–2771; f) P. Murray-Rust, J. Raftery, *J. Mol. Graphics* **1985**, *3*, 60–68.

[24] R. Taylor, O. Kennard, *Acta Crystallogr. Sect. B* **1983**, *39*, 517–525.

[25] Principal component analysis is often referred to as factor analysis, a generically related, but distinct, method: C. Chatfield, A. J. Collins, *Introduction to Multivariate Analysis*, Chapman and Hall, London, **1980**.

[26] E. R. Malinowski, D. G. Howery, *Factor Analysis in Chemistry*, Wiley, New York, **1980**.

[27] The matrix (**E**) composed of the normalized eigenvectors is multiplied by the diagonal matrix ($\mathbf{\Lambda}^{1/2}$) of the square roots of the eigenvalues: $\mathbf{P} = \mathbf{E}\cdot\mathbf{\Lambda}^{1/2}$. The PCs are then obtained from the columns of the resulting $(3N-6)\times(3N-6)$ matrix (**P**), while the eigenvalue associated with each PC represents the proportion of the total sample variance accounted for by that PC.

[28] D. L. Massart, L. Kaufman, *The Interpretation of Analytical Chemical Data by the Use of Cluster Analysis*, Wiley, New York, **1983**; J. Zupan, *Clustering of Large Data Sets*, Research Studies Press (Wiley), Chichester, **1982**.

[29] For instance, a pair of otherwise identical structures may differ by 0.5 Å in a particular bond distance, while another pair differs only by 10° in a given bond angle. Without suitable scaling or standardization, the representative points for the first pair will be closer to each other than those of the second pair, even though the molecules of the first pair differ more than those of the second in a chemical sense.

[30] In crystallographic terms this is equivalent to the problem of ensuring that wherever possible all the atoms listed for a given molecule are found within the same asymmetric unit and not distributed over symmetry-equivalent positions throughout the crystal lattice, which would give rise to a disjoint molecule.

[31] In the case of the triatomic molecules discussed in Section 2.1, for example, this means that four points would be generated for any given structure, one for each of the four operations of the point group (C_{2v}). However, in this instance, the permutations for the operations E and $\sigma(xy)$ will generate the same coordinates for the representative point because the molecules are planar; the same goes for

the permutations brought about by the operations C_2 and $\sigma'(yz)$. The points will all be equidistant from the origin, that is, equally distorted with respect to the reference molecule, since they represent symmetry-equivalent permutations of the labeling of the atoms on the same molecular skeleton.

[32] See, for example, a) F. Basolo, R. G. Pearson, *Mechanisms of Inorganic Reactions*, 2nd ed., Wiley, New York, **1967**; b) G. K. Anderson, R. J. Cross, *Chem. Soc. Rev.* **1980**, *9*, 185–215; c) *Mechanisms of Inorganic and Organometallic Reactions*, Vol. 2 (Ed.: M. V. Twigg), Plenum, New York, **1984**; d) R. J. Cross, *Adv. Inorg. Chem.* **1989**, *34*, 219–292.

[33] G. K. Anderson, R. J. Cross, *Acc. Chem. Res.* **1984**, *17*, 67–74; R. J. Cross, *Chem. Soc. Rev.* **1985**, *14*, 197–223; R. J. Cross in ref. [32c], Chapter 5.

[34] a) Clearly, when the ligands are not all identical in the tetravalent complex the symmetry of the SQP will be lower (than C_{4v}). The term SQP then implies that all apical equatorial angles are only approximately equal. b) The SQP → TBP rearrangement implies that pairs of opposite apical-equatorial angles remain approximately equal during the process.

[35] R. S. Berry, *J. Chem. Phys.* **1960**, *32*, 933–938.

[36] The Berry deformation has been inappropriately called a "pseudorotation"; the latter term was borrowed from work on the fluxional puckering motion of cyclopentane (see J. E. Kilpatrick, K. S. Pitzer, R. Spitzer, *J. Am. Chem. Soc.* **1947**, *69*, 2483–2488), where it denotes an *equipotential* process in which the motion of the atoms is *perpendicular* to the direction of pseudorotation. As early as 1970 Muetterties pointed out that "the terminology is imprecise and should be dropped" (see footnote [44] in E. L. Muetterties, *Acc. Chem. Res.* **1970**, *3*, 266–273).

[37] Another mechanism proposed for such an intramolecular exchange process is the turnstile rearrangement [38]. However, two independent ab initio examinations, one on the model compound PH_5 (J. A. Altmann, K. Yates, I. G. Csizmadia, *J. Am. Chem. Soc.* **1976**, *98*, 1450–1454), and the other on PF_5 (P. Russegger, J. Brickmann, *Chem. Phys. Lett.* **1975**, *30*, 276–278), have shown that this mechanism requires a considerably higher activation energy and is not a strictly different pathway, but can be regarded as a distortion away from the minimum energy path of the Berry coordinate. Both studies conclude that a turnstile mechanism will only be realized for structurally restricted systems, and that the true saddle point corresponds to the square-pyramidal intermediate with C_{4v} symmetry. For the remainder of this paper we shall focus on the Berry process, referring to the turnstile mechanism only where explicit mention is made of it in the study under review.

[38] I. Ugi, D. Marquarding, H. Klusacek, P. Gillespie, F. Ramirez, *Acc. Chem. Res.* **1971**, *4*, 288–296.

[39] E. L. Muetterties, L. J. Guggenberger, *J. Am. Chem. Soc.* **1974**, *96*, 1748–1756.

[40] The increment in the observed bond distance between two atoms A and B is established relative to the length of a "standard" covalent A–B bond length. Standard bond lengths can be obtained from any number of tables, such as those compiled by L. Pauling, *The Nature of The Chemical Bond*, 3rd ed., Cornell University Press, Ithaca, **1960**. A comprehensive set of bond distances has recently been collected in A. G. Orpen, L. Brammer, F. H. Allen, O. Kennard, D. G. Watson, R. Taylor, *J. Chem. Soc. Dalton Trans.* **1989**, S1–S83; F. H. Allen, O. Kennard, D. G. Watson, L. Brammer, A. G. Orpen, R. Taylor, *J. Chem. Soc. Perkin Trans. 2* **1987**, S1–S19.

[41] L. Pauling, *J. Am. Chem. Soc.* **1947**, *69*, 542–553.

[42] J. K. Burdett, *Inorg. Chem.* **1979**, *18*, 1024–1030.

[43] Insofar as the reaction coordinates are obtained from a correlation analysis of all the structures comprising the data set, the underlying assumption behind this kind of approach (see also ref. [44]) is that the potential energy surface for each observed structure has exactly the same topography. This is clearly an untenable assumption, given the widely divergent compounds involved; the shortcomings of this approach have since been discussed in H.-B. Bürgi, J. D. Dunitz, *Acta Crystallogr. Sect. B* **1988**, *44*, 445–448.

[44] F. Pavelcik, E. Luptakova, *Collect. Czech. Chem. Commun.* **1990**, *55*, 1427–1434.

[45] H.-B. Bürgi, K. C. Dubler-Steudle, *J. Am. Chem. Soc.* **1988**, *110*, 4953–4957.

[46] They complained of the "irksome phrase...'the molecule is a *distorted* trigonal bipyramid'...encumbered with imprecise English and often encountered in structural papers" [author's emphasis], while admitting to using such language themselves.

[47] The term "polytopal isomer" was first coined by Muetterties in 1969 (E. L. Muetterties, *J. Am. Chem. Soc.* **1969**, *91*, 1636–1643), and it refers to a class of stereoisomers "of idealized polygons or polyhedra whose vertices are defined by the ligand atom positions in coordination compounds".

[48] Cadmium, phosphorus, cobalt, nickel, niobium, and antimony.

[49] This diagram has even found its way into an inorganic chemistry textbook; see J. E. Huheey, *Inorganic Chemistry*, 2nd ed., Harper and Row, New York, **1979**, p. 196.

[50] R. R. Holmes, J. A. Deiters, *J. Am. Chem. Soc.* **1977**, *99*, 3318–3326.

[51] A critique that might be raised here is that the nine dihedral angles described by the shape of the TBP polyhedron are not all independent.

[52] T. P. E. Auf der Heyde, L. R. Nassimbeni, *Inorg. Chem.* **1984**, *23*, 4525–4532.

[53] Allylic compounds were excluded from all the papers reviewed here, because it is difficult to identify a definite atom or point of ligation in such structures.

[54] A. Gleizes, A. Kerkeni, M. Dartiguenave, Y. Dartiguenave, H. F. Klein, *Inorg. Chem.* **1981**, *20*, 2372–2391.

[55] In this case the value of the *trans*-basal angle was chosen as 105°, which is the value obtained when placing the metal atom at the center of mass of an L_5 square pyramid.

[56] T. P. E. Auf der Heyde, L. R. Nassimbeni, *Acta Crystallogr. Sect. B* **1984**, *40*, 582–590.

[57] D. Liao, H. Fu, Y. Tang, *Wuli Huaxue Xuebao* **1987**, *3*, 449–452; *Chem. Abstr.* **1988**, *108*, 119883.

[58] C. P. Casey, G. T. Whiteker, C. F. Campana, D. R. Powell, *Inorg. Chem.* **1990**, *29*, 3376–3381.

[59] G. H. M. Dias, M. K. Morigaki, *Polyhedron* **1992**, *11*, 1629–1636.

[60] B. J. Hathaway, *Coord. Chem. Rev.* **1982**, *41*, 423–487.

[61] a) W. D. Harrison, D. M. Kennedy, M. Power, R. Sheahan, B. J. Hathaway, *J. Chem. Soc. Dalton Trans.* **1981**, 1556–1564; b) S. Tyagi, B. J. Hathaway, *ibid.* **1981**, 2029–2033.

[62] B. J. Hathaway, *Struct. Bonding (Berlin)* **1984**, *57*, 55–118.

[63] W. D. Harrison, D. M. Kennedy, B. J. Hathaway, *Inorg. Nucl. Chem. Lett.* **1981**, *17*, 87–90.

[64] S. Tyagi, B. J. Hathaway, S. Kremer, H. Stratemeier, D. Reinen, *J. Chem. Soc. Dalton Trans.* **1984**, 2087–2091.

[65] N. J. Ray, L. Hulett, R. Sheahan, B. J. Hathaway, *J. Chem. Soc. Dalton Trans.* **1981**, 1463–1469.

[66] E. Müller, C. Piguet, G. Bernardinelli, A. F. Williams, *Inorg. Chem.* **1988**, *27*, 849–855.

[67] This representation included 15 parameters (five distances and ten angles), of which only twelve are independent.

[68] O. Carugo, C. B. Castellani, *J. Chem. Soc. Dalton Trans.* **1990**, 2895–2902.

[69] The main problem in this study lies with the conceptualization of the parameter space, which is defined in terms of "three coplanar axes at 120°", and yet is treated as an orthogonal "three-dimensional" space. The three axes are defined by the differences between the observed angles and the values they would adopt in a presumed SQP, each axis corresponding to a different permutation of the ligand labels in the complex. It is not clear that the three coplanar axes represent truly independent coordinates, and, moreover, in the hypothetical case of an observed complex having exactly the same geometry as the reference SQP, the denominator in the shape parameter becomes zero, rendering the parameter space ill-defined.

[70] a) T. P. E. Auf der Heyde, H.-B. Bürgi, *Inorg. Chem.* **1989**, *28*, 3960–3969; b) *ibid.* **1989**, *28*, 3970–3981; c) *ibid.* **1989**, *28*, 3982–3989.

[71] The data were retrieved from the July 1984 version of the CSD [20] and comprised 113 nickel, 15 palladium, 9 platinum, 28 rhodium, and 31 iridium structures.

[72] With regard to the SCs of Section 2.1, for instance, the length of the reference bond (in the calculation of the distance increment [40]) would cancel in S_3, which transforms as B_2, but not in S_2, which is totally symmetric (A_1).

[73] The fact that no "ideal" SQP needs to be defined also means, however, that there is no single representative point for this conformer in the corresponding 12-dimensional parameter space. Instead, all allowed SQPs with C_{4v} symmetry will lie along a continuous line, which reflects the one degree of freedom that this symmetry allows the SQP (see Section 3).

[74] L. Nørskov-Lauritsen, H.-B. Bürgi, *J. Comput. Chem.* **1985**, *6*, 216–228.

[75] A given structure whose representative point is clustered together with the points for all the other SQPs in the data set should, in general, be classified in this way, irrespective of the kind of algorithm employed.

[76] The size is defined as the average distance [Å] of cluster members from the center of the cluster.

[77] D. L. Kepert, *Inorganic Stereochemistry*, Heidelberg, Springer, Berlin, **1982**, and references therein.

[78] M. C. Favas, D. L. Kepert, *Prog. Inorg. Chem.* **1980**, *27*, 325–463.

[79] The angles BME and BMD are defined within the same plane in the structures as the angles ϕ_D and ϕ_E; the two pairs of angular parameters are therefore geometrically related.

[80] D. L. Kepert, E. S. Kucharski, A. H. White, *J. Chem. Soc. Dalton Trans.* **1980**, 1932–1938.

[81] J. L. Mesa, M. I. Arriortua, L. Lezama, J. L. Pizarro, T. Rojo, D. Beltran, *Polyhedron* **1988**, *7*, 1383–1388.

[82] a) R. J. Gillespie, *J. Chem. Soc.* **1963**, 4679–4685; b) J. K. Burdett, *Adv. Inorg. Chem. Radiochem.* **1978**, *21*, 113–134.

[83] A. R. Rossi, R. Hoffmann, *Inorg. Chem.* **1975**, *14*, 365–374.

[84] In line with our use of these terms in earlier papers [70], we refer to the apical bond in a SQP, and the axial bonds in a TBP.

[85] Rossi and Hoffmann also include π-donor and -acceptor effects in their analysis, but insofar as most of the complexes in the studies considered here would have minimal π-bonding ligands (see ref. [53]), these effects will not be discussed at this point.

[86] In these papers [87], Holmes presents a comprehensive overview of his structural work specifically with compounds containing pentacoordinate phosphorus and other main-group elements, as well as a compilation of studies on five-coordinate transition metal complexes. He compares the observed structures to those predicted by Rossi and Hoffmann [83] for a variety of different

d-orbital configurations, and interprets the observed conformations in terms of repulsions between nonbonding electrons in d-orbitals and electrons in bonding orbitals.
[87] a) R. R. Holmes, *Prog. Inorg. Chem.* **1984**, *32*, 119–235; b) R. R. Holmes, *J. Am. Chem. Soc.* **1984**, *106*, 3745–3750.
[88] Twenty-eight nickel, four platinum, five iridium, and seven rhodium complexes.
[89] See, for example, C. P. Blaxill, S. S. D. Brown, J. C. Frankland, I. D. Salter, V. Sik, *J. Chem. Soc. Dalton Trans.* **1989**, 2039–2047, and references therein; S. S. D. Brown, I. D. Salter, V. Sik, I. J. Colquhoun, W. McFarlane, P. A. Bates, M. B. Hursthouse, M. Murray, *ibid.* **1988**, 2177–2185; L. J. Farrugia, M. J. Freeman, M. Green, A. G. Orpen, F. G. A. Stone, I. D. Salter, *J. Organomet. Chem.* **1983**, *249*, 273–288.
[90] A. Rodger, B. F. G. Johnson, *Polyhedron* **1988**, *7*, 1107–1120.
[91] See also D. Britton, J. D. Dunitz, *J. Am. Chem. Soc.* **1975**, *97*, 3836.
[92] A. G. Orpen, I. D. Salter, *Organometallics* **1991**, *10*, 111–117.
[93] How do the π and σ properties of ligands affect their positions in the TBP and SQP, and how do they correlate with the stereochemistry of the complexes? Such an analysis would require algorithms capable of handling categorical variables (for the different sites or the different kinds of ligands) as opposed to continuous variables. For example, the influence of σ-donor capability on the dynamic stereochemistry of $[Ni(CH_3)_2A_3]$, where A is a weaker σ donor than CH_3, has been examined in K. Tatsumi, A. Nakamura, S. Komiya, A. Yamamoto, T. Yamamoto, *J. Am. Chem. Soc.* **1984**, *106*, 8181–8188.
[94] A. Vedani, D. W. Huhta, *J. Am. Chem. Soc.* **1990**, *112*, 4759–4767.

A stop-gap solution?



If the latest library copy of Angewandte spends more time off the shelf than on, stop the gap with a personal subscription.

Just call or fax

VCH

USA: Tel. 1-(800) 422-8824; Fax (305) 428-8201
UK: Tel. (0223) 321111, Fax (0223) 313221

X-Ray Structure Analysis of Methane Monooxygenase: An Important Step toward Understanding the Oxidation of Methane in Biological Systems

Bernt Krebs* and Norbert Sträter

Metalloenzymes catalyze a variety of elementary chemical transformations in biological systems. Frequently the task of these highly active and efficient catalysts is to activate small and often also quite unreactive substrates like CO, CO_2, H_2, CH_4, NO, N_2, O_2, and H_2O. Besides the fundamental increase in knowledge about the construction of the active site, the determination of the structure of these proteins often also provides the key to the mode of action of the enzyme. In addition, the metal centers in biological systems can be imitated by synthetic biomimetic coordination compounds and thus serve as models for new, more active or more specific technical catalysts. Whereas the inference of exact structural information from spectroscopic data—with the exception of the data from multidimensional NMR spectroscopy—is very difficult, the complete three-dimensional structure of a biomolecule can be determined with crystal structure analysis. With the X-ray structure elucidation of the hydroxylase component of the methane monooxygenase (MMO) from *Methylococcus capsulatus* (Bath), the comprehensive characterization of an interesting active site that contains two iron atoms has now been achieved.[1] The structural basis for the mechanism of the difficult transformation of the nonpolar molecules CH_4 and O_2 under physiological conditions could be clarified.

The element iron is ubiquitous in virtually all living systems and performs very different functions, which, apart from its abundant availability in the biosphere, can be attributed to its redox behavior (most often Fe^{II}/Fe^{III}) and its varied coordination chemistry. The binuclear iron proteins have formed a particular research priority in recent years, arousing interest because of their broad distribution and the diverse modes of action. They participate in the reversible binding of oxygen (hemerythrin), in DNA synthesis (ribonucleotide reductase), in phosphate ester hydrolysis (purple acid phosphatases), in electron transport (rubrerythrin), and in hydroxylation of alkanes (methane monooxygenase). The crystal structures of hemerythrin[2] and ribonucleotide reductase[3] have already been elucidated (Fig. 1), and also the crystallization of rubrerythrin[4] and the purple acid phosphatase from kidney beans[5] has been achieved as a first step toward the X-ray structure analysis of these proteins that is underway.

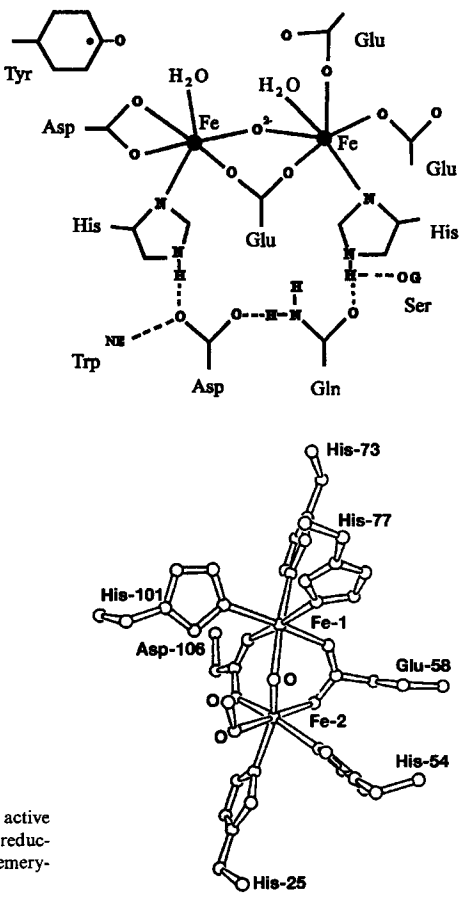


Fig. 1. Structure of the active site of ribonucleotide reductase [3] (top) and oxyhemerythrin [2] (bottom).

Methanotrophic bacteria can exploit methane as the only source of energy and carbon. They play an important role in the carbon cycle of the biosphere, because they limit the release of this greenhouse gas into the atmosphere. Apart from methane, monooxygenases can, however, also oxidize longer hydrocarbons. The methanotrophic bacteria have become technically important for the biological regeneration of ground polluted with oil[6] and for the oxidative removal of trichloroethylene from potable water.[7]

In the conversion of methane to methanol MMO catalyzes the first and indeed the most difficult step of the oxidation of hydrocarbons to carbon dioxide under physiological conditions [Eq. (a)]. The catalytic function of the metal center may be seen

[*] Prof. Dr. B. Krebs, N. Sträter
Anorganisch-chemisches Institut der Universität
Wilhelm-Klemm-Strasse 8, D-48149 Münster (FRG)
Telefax: Int. code + (251)83-8366

 © VCH Verlagsgesellschaft mbH, D-69451 Weinheim, 1994 0570-0833/94/0808-0841 $ 10.00+.25/0

$$CH_4 + NADH + H^+ + O_2 \longrightarrow CH_3OH + NAD^+ + H_2O \quad (a)$$

as the activation of the oxygen molecule for the reaction with the likewise rather inert C–H bond of methane. The MMO from *M. capsulatus* consists of three proteins: the hydroxylase (protein A, $M_r \approx 251$ kDa) that incorporates the iron-containing active center, the reductase (protein C, 38.6 kDa) that transfers the electrons from NADH to the hydroxylase, and a regulatory protein (B) with a molecular weight of 15.5 kDa. The hydroxylase in turn consists of three peptide chains with $\alpha_2\beta_2\gamma_2$ stoichiometry.

The structure of the hydroxylase complex was determined at a crystallographic resolution of 2.2 Å, which allows details to be discussed on an atomic level. Two αβγ protomers are linked through a noncrystallographic twofold rotation axis and form a relatively compact heart-shaped molecule of dimensions 60 × 100 × 200 Å. At the interface between the αβγ protomers is a large canyon; this, however, does not provide direct access to the active site. The secondary structures of the three subunits are strongly dominated by α-helices. The structure of the α and β subunits closely resembles the ribonucleotide reductase in terms of the arrangement of the secondary structure elements. The active site containing two iron centers is completely integrated into the α subunit (Fig. 2), with the result that four iron atoms are present per $\alpha_2\beta_2\gamma_2$ dimer. This result contradicts studies by atomic absorption spectroscopy, which yield an iron content of 2.3 mol per dimer.[8]

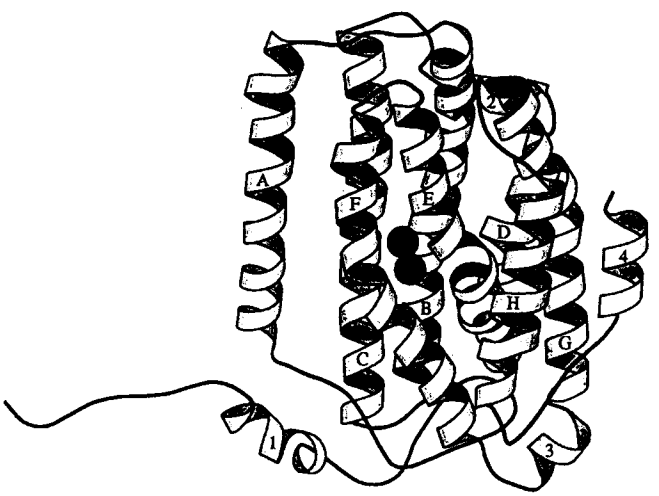


Fig. 2. Secondary structure of the α-subunit of the hydroxylase component of methane monooxygenase [1].

A model for the active site, proposed after determining and comparing the amino acid sequences of MMO from *M. capsulatus* with that of ribonucleotide reductase, was confirmed by structure elucidation.[9] The Fe^{III}–Fe^{III} distance was refined to 3.4 Å and is thus in good agreement with the interpretation of EXAFS data, which yield a distance of 3.42 Å.[8] In comparison, the metal–metal distances in the ribonucleotide reductase and in hemerythrin are 3.3 and 3.32 Å, respectively. Both iron atoms are in an approximately octahedral environment and are bridged by two exogenic ligands, which the authors interpret as a hydroxide and a bidentate acetate ion (Fig. 3). Since ammonium acetate was also present in the crystallization buffer, this ligand may not be coordinated to the enzyme in the cell. Possibly the methoxide ion binds as an oxidized substrate at this position before it is protonated and leaves the active site. A terminal aqua ligand is bound to the Fe(1) atom. The binding site for the oxygen molecule may also be localized here. This picture of the diiron site of hydroxylase is in agreement with EXAFS, ENDOR, UV/VIS, EPR, and Mössbauer studies that have been performed on the enzyme in solution.

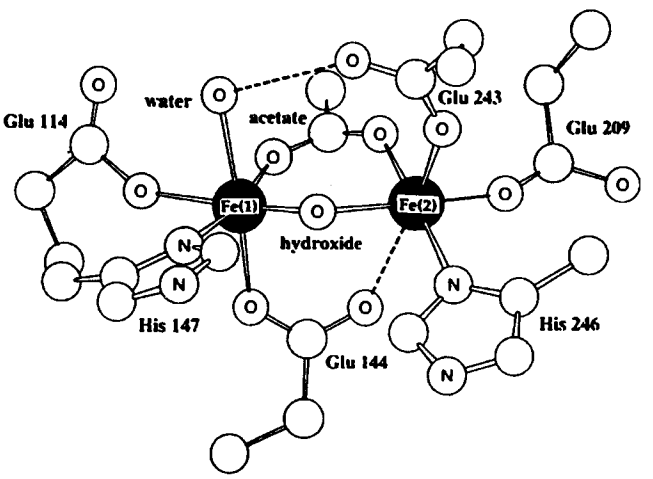


Fig. 3. Structure of the active site of methane monooxygenase [1].

Interestingly, the tyrosine radical important for the reaction mechanism of the structurally similar ribonucleotide reductase is replaced in MMO by a cysteine unit. A redox-active role for this SH group has been proposed, and the authors announce that further evidence will be published soon. Besides this cysteine unit, a threonine group is the only other protonated side chain in the vicinity of the active site. This group might thus have the function of providing the proton in the reaction. A cavity close to the active site is formed by predominantly hydrophobic side chains. Possibly the alkanes are preoriented here for conversion with the activated oxygen molecule at the Fe(2) atom. Because no direct access from the surface of the protein to the active center is present, the binding of the substrate must be made possible by a change in conformation of the enzyme, which is probably induced by interaction with the regulatory protein B. The presence of this protein also causes large changes in the spectroscopic properties of the hydroxylase, the rate of conversion, and the regioselectivity of substrate oxidation. This influence of protein B on the active site is probably transmitted through the helices E and F exposed to the large cavity at the αβγ dimer interface (Fig. 2); thus the binding of the B component in this cavity can be postulated.

This structure elucidation is a decisive step on the way to understanding the molecular mechanism of the oxidation of methane to methanol in biological systems. The structure provides the basis for a deeper interpretation of the available spectroscopic measurements and gives important impetus to further investigations. Also interesting is the structural relationship between MMO and ribonucleotide reductase, which gives us a new instructive example of how nature employs available structural

 © VCH Verlagsgesellschaft mbH, D-69451 Weinheim, 1994 0570-0833/94/0808-0842 $ 10.00+.25/0

features—here both the tertiary structure and the active site—in the catalysis of completely different reactions. The future will certainly bring further structural analyses: for example, if samples crystallized in another buffer or containing the active site in a reduced state were to be analyzed, more detailed hypotheses of the reaction mechanism could be proposed. Possibly a larger complex of proteins A, B, and C could be crystallized, above all to study the immense influence of the regulatory protein on the structure of the active site.

German version: *Angew. Chem.* **1994**, *106*, 889

[1] A. C. Rosenzweig, C. A. Frederick, S. J. Lippard, P. Nordlund, *Nature* **1993**, *366*, 537–543.
[2] M. A. Holmes, I. L. Trong, S. Turley, L. C. Sieker, R. E. Stenkamp, *J. Mol. Biol.* **1991**, *218*, 583–593.
[3] P. Nordlund, H. Eklund, *J. Mol. Biol.* **1993**, *232*, 123–164.
[4] L. C. Sieker, S. Turley, B. C. Prickril, J. LeGall, *Proteins: Struct. Funct. Genet.* **1988**, *3*, 184–186.
[5] N. Sträter, R. Fröhlich, A. Schiemann, B. Krebs, M. Körner, H. Suerbaum, H. Witzel, *J. Mol. Biol.* **1992**, *224*, 511–513.
[6] P. H. Pritchard, C. F. Costa, *Environ. Sci. Technol.* **1991**, *25*, 372–379.
[7] J. Green, H. Dalton, *J. Biol. Chem.* **1989**, *264*, 17698–17703.
[8] J. G. DeWitt, J. G. Bentsen, A. C. Rosenzweig, B. Hedman, J. Green, S. Pilkington, G. C. Papaefthymiou, H. Dalton, K. O. Hodgson, S. J. Lippard, *J. Am. Chem. Soc.* **1991**, *113*, 9219–9235.
[9] P. Nordlund, H. Dalton, H. Eklund, *FEBS Lett.* **1992**, *307*, 257–262.

Fullercages without Carbon—Fulleranes, Fullerenes, Space-filler-enes?

Reinhard Nesper*

Is the fullerene structural principle, revealed in recent years with the new modifications of carbon, of far more wide-ranging significance than has previously been assumed? Can the special geometry of fullercages form the basis for energetically favorable, or at the very least kinetically stable structures, with elements quite different from carbon? Such questions relate not only to derivatives of carbon fullerenes with metallic or organometallic species but also to what has previously been known as incorporation, or the replacement of carbon in fullerenes with heteroatoms. A new study by Corbett and Sevov entitled "Carbon-Free Fullerenes" has now provided further food for thought in a quite different direction.[1]

The two authors describe the ternary indides $Na_{172}In_{197}Ni_2$ and $Na_{96}In_{97}Z_2$ (Z = Ni, Pd, Pt), in which $Na_{12}In_{48}$, In_{70}, and In_{74} cages, each with fullerene-type structures, form characteristic structural elements. The fullercages are present, however, not as isolated clusters, but as two-dimensional layers in a quasi-closest-packed arrangement, connected through In–In bonds. The spaces between the layers are filled by the Na and Z atoms.

The fullercages in these indides are not empty. They contain additional interesting polyhedra, whose corners are located beneath the surface of the larger external polyhedra, in accord with the duality principle. These enclosed polyhedra can be designated endohedral units, thereby leading to the formulations $Na_{32}@[Na_{12}In_{48}]$, $Na_{37}@In_{70}$, and $Na_{39}@In_{74}$. The inner polyhedra are still fairly large and are each filled with one additional smaller polyhedron. In this way one of the most important structural principles of the intermetallic phases is also adhered to: a quasi-closest-packed arrangement in every sense. For the larger cages the overall structure of the multilayered polyhedra can, with respect to the central atom Z, be represented as $In_{10}@Na_{32}@[Na_{12}In_{48}]$, $Ni@In_{10}@Na_{37}@In_{70}$, and $Z@In_{10}@Na_{39}@In_{74}$ (Fig. 1c). The discrepancies with the overall formulas are due to additional interstitial atoms.

Substitution of spheres for the large cages in $Na_{96}In_{97}Z_2$ gives rise to an arrangement that corresponds very well to the nickel arsenite structure. The expression "hierarchical structures" was recently used by von Schnering et al. to describe arrangements in which large units containing many atoms, in this case fullerspheres, take the place of smaller, topologically similar species, here, simple atoms.[2] This comparison points to the fact that compounds that differ both in terms of stoichiometry and chemistry can apparently exist in similar arrangements, if these arrangements prove to be particularly favorable in a number of respects. Thus, a kind of fractal behavior or scale-symmetry is indicated in structural chemistry.[3]

We now come to the question as to whether fullercages are among the more favored arrangements. I believe so. Upon close scrutiny of the literature, it becomes clear that such polyhedra have indeed been frequently detected in chemical compounds since the 1950s; the first unambiguous example was β-rhombohedral boron.[4] However, intermetallic compounds may also contain fullercages (Table 1) formed between the more electronegative components in each compound, in which homopolar bonds are preferred.

In β-rhombohedral boron a B_{60} fullercage is present as the doubly endohedrally filled unit $B_{12}@B_{12}@B_{60}$ with connections in three dimensions (Fig. 1a).[4] As all the atoms are of the same type, all the bonds are covalent, even the shorter, stronger bonds between the B_{12} polyhedra. It is therefore difficult to consider the B_{60} polyhedra as distinct units in a chemical bond-

[*] Prof. Dr. R. Nesper
Laboratorium für Anorganische Chemie
Eidgenössische Technische Hochschule, ETH Zentrum
CH-8092 Zürich (Switzerland)
Telefax: Int. code + (1)262-0718

 © VCH Verlagsgesellschaft mbH, D-69451 Weinheim, 1994 0570-0833/94/0808-0843 $ 10.00+.25/0

Table 1. Intermetallic compounds with endohedrally filled fullercages N_{60}, N_{70}, N_{74}, and N_{76}. The maximum average number of electrons per atom of the electronegative component is calculated assuming a complete transfer of charge from the electropositive component (d electrons are not taken into account for Cu, Zn, and Cd).

Compound	Fullercage	Symmetry	VEC_{max} [a]	Ref.
Li_3CuAl_5	$(Cu,Al)_{60}$	$T_d - \bar{4}3m$	3.0	[10]
$(Al,Zn)_{49}Mg_{32}$ [b]	$(Zn,Al)_{60}$	$T_d - \bar{4}3m$	3.0	[11]
$Li_{13}Cu_6Ga_{21}$	$(Ga)_{60}$	$T_d - \bar{4}3m$	3.0	[12]
$Li_{38}Zn_{34}Ga_{67}$	$(Zn,Ga)_{60}$	$D_{3h} - \bar{6}m2$	3.0	[13]
$Na_{35}Cd_{24}Ga_{56}$	$(Cd,Ga)_{60}$	$D_{3d} - \bar{3}m$	3.1	[14]
$Na_{13}K_4Ga_{49.6}$	$(Ga)_{60}$	$D_{3d} - \bar{3}m$	3.3	[15]
$Na_{172}In_{197}Ni_2$	$(In)_{70}$	$C_{2v} - 2m$	3.9	[1]
$Na_{96}In_{97}Z_2$	$(Na,In)_{60}$	$D_{3d} - \bar{3}m$	4.0	[1]
	$(In)_{74}$	$D_{3h} - \bar{6}m2$		
$LiMgAl_2$	$(Al)_{76}$	$C_{3v} - 3m$	4.5	[3, 7]

[a] VEC = valence electron number = average number of electrons per atom. [b] see Fig. 1b.

ing sense. Quantum mechanical investigations have not yet been carried out for the fullerpolyhedra in this boron modification—an additional challenge for courageous theoreticians.

What is certain is that the average number of valence electrons—three per boron atom—does not suffice for the formation of a fullerene or hence a system with VEC = 4. At first glance, the inwardly and outwardly orientated terminal bonds present a confusing picture (see Fig. 1a). Upon closer examination, however, multicenter and two-electron/two-center bonds can be assigned, in accordance with the Wade rules for electron-deficient polyhedra. All the five-membered rings, and hence all the bonds in the five-membered rings, comprise constituent parts of icosahedra, and thus Wade polyhedra. All other bonds, in other words those joining the five-membered rings, bridge the icosahedra and are thereby among the stronger two-electron/two-center bonds. It may be coincidental that the shorter and longer bonds in C_{60} and B_{60} are topologically equivalent.

On the basis of these considerations and by analogy with boranes the B_{60} polyhedron may be considered an electron-deficient fullerane with free terminal valences rather than a fullerene. Fulleranes constructed with single bonds and terminally linked on all sides have the same theoretical electron requirement as isolated fullerenes—VEC = 4. Thus, the boron structure has too few electrons for either structural form. However, boron may compensate for this through the formation of electron-deficient polyhedra, in this case icosahedra, which as a consequence must be integrated into the fullerane surface. Should β-rhombohedral boron therefore be perceived as a polymeric, electron-deficient variation of C_{60}? As is the case for the boron fullercage, N_{60} polyhedra are present in many of the compounds shown in Table 1. These polyhedra should correspond to the stronger covalent interactions, as in each case they are composed of the more electronegative components Al and Ga and display relatively short edge-dimensions.

Although all the phases listed in Table 1 display intermetallic character, the partial transfer of charge from the more strongly electropositive alkali and alkaline earth elements should be taken into account. But the charge transfer should be less pronounced than that in Zintl phases. Thus, it is not clear how many electrons are available for a given fullercage, in other words, how many electronic states are occupied. For the novel indides[1] and $LiMgAl_2$[5] only simplified theoretical investigations have been conducted to date with the extended-Hückel method. The maximum average number of electrons possible for the electronegative components, VEC_{max}, is attained when all the valence electrons are assigned to these atoms (see Table 1). Thus for N_{60} fulleranes (N = Al, Ga) $VEC_{max} = 3.0-3.3$; for the In_{70}, In_{74}, and $(Na,In)_{60}$ fulleranes in $Na_{96}In_{97}Z_2$ and $Na_{172}In_{197}Ni_2$ $VEC_{max} \approx 4$; and finally for Al_{76} in $LiMgAl_2$, the largest metal fullerane known to date, $VEC_{max} = 4.5$.

The indium atoms in these phases can thus formally obtain up to about four valence electrons, thereby permitting fullerane- or fullerene-type structures. No inward homopolar interactions are present, because no indium atoms are contained within the middle inner polyhedron; however, there are many terminal In–In bonds to the neighboring cages. Multiple bonding should be absent here, as a consequence of the low tendency towards such interactions among the heavy main-group elements, and thus, in analogy to the boron polyhedron, a fullerane formulation is proposed.

The largest cages to date are the doubly endohedrally filled Al_{76} fulleranes in $LiMgAl_2$, $Al_3M_7@M_{40}@Al_{76}$, where M = Li, Mg (Fig. 1d).[3, 7] Its size is compared to that of C_{60} in Figure 1f. The Al_{76} cages form a quasi-cubic-closest-packed arrangement, again in line with the hierarchical structure relationship. Since all the Al_{76} cages are linked through Al–Al bonds, there should be no double bonding contribution, and the large cage can be termed a fullerane. The results of simplified band structure calculations indicate that the fullerane Al atoms have an electron requirement of VEC $\approx$ 4 to achieve optimal bonding.[5] The electronic prerequisites for this are derived from the stoichiometry (see Table 1). In this way, only a single formal transfer of charge, $(Li,Mg)^+$ Al^-, is required per formula unit.

With this relatively simple classification of such phases by means of a more or less estimated valence electron count, it is clear that only a limited understanding of the chemical bonding can be achieved; however, this may still be useful for the synthesis of new compounds of similar type. In support of this preliminary qualitative hypothesis, we should emphasize that the structures of many aluminides, gallides, and indides can be rationalized by simple, formal charge-transfers and the Wade rules. Thus, the phases discussed here are not exceptional.[6–8]

The formation of metal fulleranes appears to begin with an icosahedral cluster which forms the innermost shell of a three-layer cluster that is typically completed by a fullerane sphere. For phases that obey this construction principle the term "icosogene" has been coined.[9] The shell-like construction, in which electropositive and electronegative atoms are segregated into different layers, is strongly reminiscent of tenside emulsions and micellar systems. For the two metal fulleranes the formation of the inner surfaces seems to be of considerable significance. Viewed superficially, the phases NaIn and $Na_{96}In_{97}Z_2$ scarcely differ from one another in stoichiometry and valence electron count; however, the latter phase contains Z atoms as nucleation centers.

This leads to the obvious question: when does growth from nucleation centers of icosahedral or pentagonal symmetry result in classical crystals and when in quasi-crystals? Interestingly, quasi-crystalline $LiMgAl_2$ has also recently been reported[16] (see also ref.[3]). One wonders whether fullerenes can also serve as nuclei for the growth of quasi-crystals.

 © VCH Verlagsgesellschaft mbH, D-69451 Weinheim, 1994 0570-0833/94/0808-0844 $ 10.00+.25/0 Angew. Chem. Int. Ed. Engl. 1994, 33, No. 8

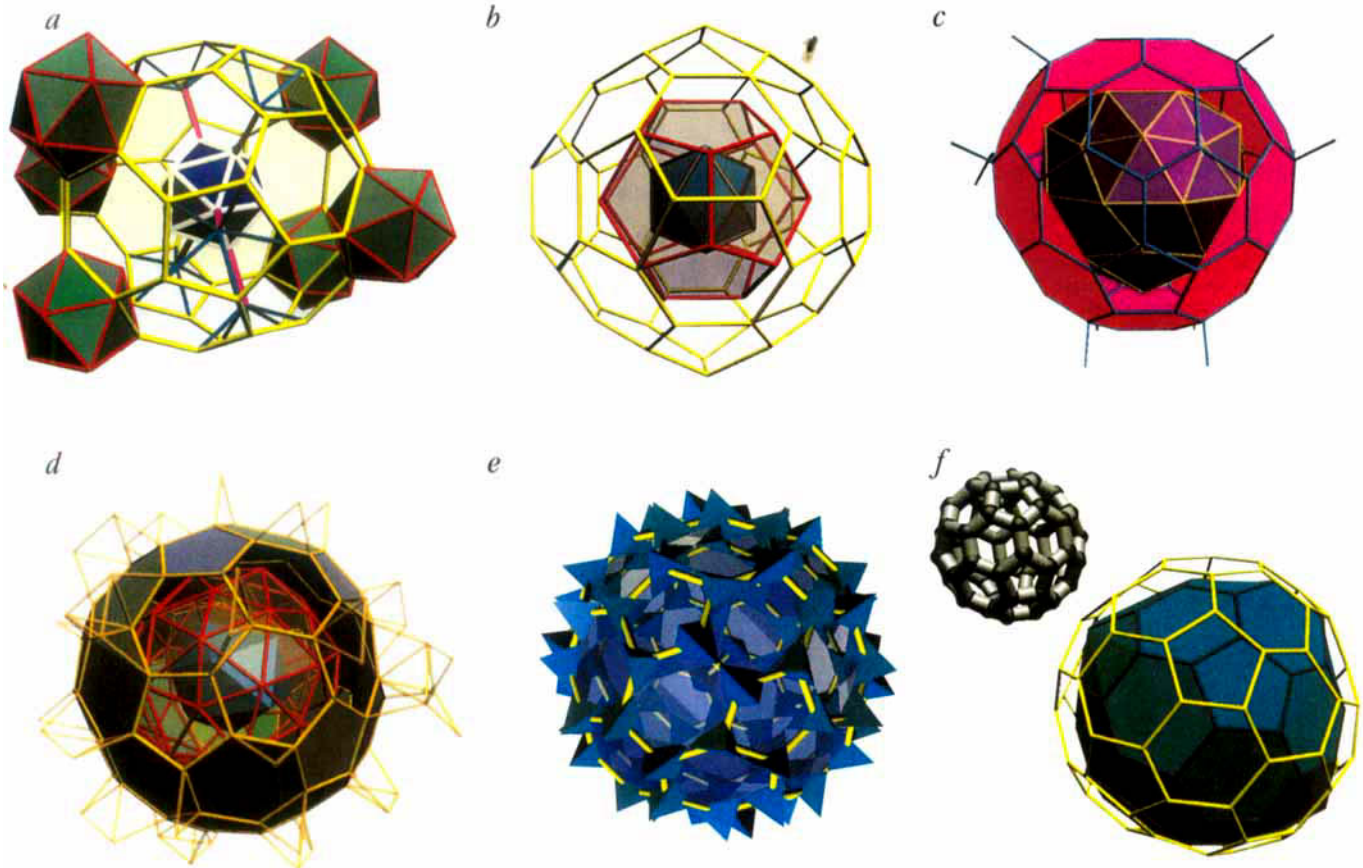


Fig. 1. Structures of endohedrally filled fullercages: a) β-rhombohedral boron. In the fullercage B_{60} all the five-membered rings form part of B_{12} icosahedra (red and blue rods; yellow rods for the corresponding fullerene five-membered rings), of which only half are represented completely. The central icosahedron (white rods) is linked through terminal bonds (thick magenta rods; only half are depicted for clarity) to all the icosahedra in the B_{60} surface. b) $(Al,Zn)_{49}Mg_{32}$ with $(Al,Zn)_{60}$ fullerane cage. The pentagon dodecahedron shown in red corresponds to the layer of atoms between the fullercage and the inner icosahedron. The fullercage shows distinct deformations which displace the atoms from the mean plane of the surface of the sphere. c) Multiply endohedrally filled $Na_{96}In_{97}Z_2$: $Z@In_{10}@Na_{39}@In_{74}$. Only the middle inner polyhedron Na_{39} is visible as depicted. The outwardly bridging In–In bonds are indicated. d) $LiMgAl_2$ with a doubly endohedrally filled Al_{76} fullerane: $Al_3M_7@M_{40}@Al_{76}$ (M = Li, Mg). The outwardly bridging Al–Al bonds (transparent golden rods) are shown on the fullerene surface (yellow rods). e) $Al_{84}O_{210}$ polyhedra in $Sr_{36}Bi_{22}Al_{48}O_{141}$ with AlO_4 tetrahedra (violet). This polyhedron is also filled by two further polyhedron shells, but these are not shown here. Since the polyhedron surfaces of the fullercage are depicted as transparent, the tilting of the AlO_4 tetrahedra can be discerned clearly. f) Comparison between C_{60} (left) and, Al_{60} (in $(Al,Zn)_{49}Mg_{32}$, solid, blue-green) in Al_{76} (right, yellow rods). The average sphere radii are 3.4, 6.8, and 7.4 Å.

Fullercages have already been identified in the structures of insulators, again in an arrangement in which distinct interactions lead to onion-skin-like constructions on the molecular scale. The compound $Sr_{36}Bi_{22}Al_{48}O_{141}$ is a complex oxide composed of a doubly endohedrally filled $Al_{48}O_{210}$ polyhedron with 12 five-membered rings and 32 six-membered rings[17] (Fig. 1e). Here, each O atom is situated not quite midway between two Al atoms ($Al_{84}O_{116}$). The three-way coordination of the Al atoms on the surface of the fullercage is increased to tetrahedral ($Al_{84}O_{210}$) through a further, terminal oxygen atom, whereby the linked AlO_4 tetrahedra give rise to a complex fullercage. It is therefore reasonable to anticipate more such structures in the chemistry of heteropolyanions.

Multiply endohedrally filled units are likewise known for the larger C_n fullerenes, for example, the "onion-skin fullerenes" constructed entirely from carbon atoms.[19] It is, however, also possible to include here other molecular species that form van der Waals complexes with C_n fullerenes, in other words, host–guest compounds. Access to clathrates of this type is not very likely with the Krätschmer process,[18] as few potential guest molecules have sufficiently high thermal stability. Rather, fullerenes must first be synthesized at significantly lower temperatures before such inclusion compounds would appear completely conceivable.

Finally, there remains the question as to whether other heavy elements are able to form fullerenes or fulleranes. Since silicon and germanium tolerate a greater range of bond angles, they would be expected to form cages that would be geometrically stabilized by endohedral filling. Whether a multiply bonded structure would have any energetic chance over a singly bonded fullerane is another open question. For the tricoordinate elements phosphorus, arsenic, antimony, and bismuth, endohedrally stabilized fulleranes seem entirely imaginable.

But why should we stop here? A great number of multicomponent compounds can be discussed in this manner and may even have been prepared in a few laboratories. Binary compounds are suitable only with certain preconditions because of the unavoidable frustration in the five-memberd rings. Perhaps other large polyhedra with rings having an even number of members and whose geometry and solid-state structure are also

 © VCH Verlagsgesellschaft mbH, D-69451 Weinheim, 1994 0570-0833/94/0808-0845 $ 10.00+.25/0

known are more favorable—they do not always have to form fullercages!

German version: *Angew. Chem.* **1994**, *106*, 891

[1] S. C. Sevov, J. D. Corbett, *Science* **1993**, *262*, 880.
[2] W. Carillo-Cabrera, N. Caroca-Canales, K. Peters, H. G. von Schnering, *Z. Anorg. Allg. Chem.* **1993**, *619*, 1556.
[3] R. Nesper, *Angew. Chem.* **1991**, *103*, 805; *Angew. Chem. Int. Ed. Engl.* **1991**, *30*, 789.
[4] B. Kolakowski, *Acta Phys. Pol.* **1962**, *22*, 439; J. L. Hoard, D. B. Sullenger, C. H. L. Kennard, R. E. Hughes, *J. Solid State Chem.* **1970**, *1*, 268; D. Geist, R. Kloss, H. Follner, *Acta Crystallogr. Sect. B* **1970**, *26*, 1800; J. Donohue, *Structures of the Elements*, Krieger, Malaba, FL, USA, **1974**, S. 61.
[5] R. Nesper, unpublished results.
[6] C. Belin, M. Tillard-Charbonnel, *Prog. Solid State Chem.* **1993**, *22*, 59.
[7] R. Nesper, *Jahrb. Akad. Wiss. Göttingen*, Vandenhoek & Ruprecht, Göttingen, **1989**, S. 15; R. Nesper, Habilitationschrift, Universität Stuttgart, **1988**; R. Nesper, *Prog. Solid State Chem.* **1990**, *20*, 1.
[8] U. Frank-Cordier, G. Cordier, H. Schäfer, *Z. Naturforsch. B* **1982**, *37*, 119, 127; W. Blase, G. Cordier, *ibid.* **1989**, *44*, 1011–1014.
[9] R. B. King, *Inorg. Chem.* **1989**, *28*, 2796.
[10] H. K. Hardy, J. M. Silcock, *J. Inst. Met.* **1956**, *24*, 423.
[11] G. Bergman, J. L. T. Waugh, L. Pauling, *Acta Crystallogr.* **1957**, *10*, 254.
[12] M. Tillard-Charbonnel, C. Belin, *J. Solid State Chem.* **1991**, *90*, 270.
[13] M. Tillard-Charbonnel, N. Chouaibi, C. Belin, J. Lappaset, *Eur. J. Solid State Inorg. Chem.* **1992**, *29*, 347.
[14] M. Tillard-Charbonnel, N. Chouaibi, C. Belin, *Mater. Res. Bull.* **1992**, *27*, 1277.
[15] C. Belin, M. Charbonnel, *J. Solid. State Chem.* **1993**, *64*, 57.
[16] A. Niikura, A. P. Tsai, A. Inoue, T. Masumoto, A. Yamamoto, *Jpn. J. Appl. Phys. Part 2* **1993**, *32*, 1160.
[17] H. G. von Schnering, T. Popp, unpublished; T. Popp, Dissertation, Universität Stuttgart, **1990**.
[18] W. Krätschmer, L. D. Lamb, K. Fostiropoulos, D. R. Huffman, *Nature* **1990**, *347*, 354.
[19] D. Ugarte, *Nature* **1992**, *359*, 707.

How do they fit so much in?



Keep up with the latest developments in all areas of chemistry.
Order your own personal subscription.

Just fax

USA	Fax: (305)	428-8201
UK	Fax: (0223)	313221
Japan	Fax: (03)	38163758
Rest of world	Fax: (0 1149)	6201-606-184

VCH

 © *VCH Verlagsgesellschaft mbH, D-69451 Weinheim, 1994* *0570-0833/94/0808-0846 $ 10.00+.25/0*

Organoplatinum Dendrimers Formed by Oxidative Addition**

Sudhir Achar and Richard J. Puddephatt*

Dendrimers are branched molecules the synthesis and characterization of which are of great current interest.[1-7] Most known dendrimers are organic compounds, but those containing inorganic functional groups are also of interest. Recently dendrimers containing ruthenium(II) coordination centers,[6] organosilicon centers,[4] and (η-arene)η-cyclopentadienyliron centers[4] have been reported but there appear to be no examples of dendrimers containing alkyltransition metal groups.[1,7] Hitherto, dendrimers were synthesized by one of two stepwise approaches, namely the divergent method[1] (construction from the center outwards) and the convergent method[2,3] (construction from the outside to the center). To be successful, both methods require that very high yields are obtained for the individual steps and this is difficult to achieve in many organometallic reactions. We report here a new method of synthesis which has yielded the first polynuclear, dendritic organotransition metal complexes. This synthetic method is based on two known reactions. First, the displacement of the SMe_2 ligands from $[Pt_2Me_4(\mu\text{-}SMe_2)_2]$ (**1**) by diimines is easy and essentially quantitative and yields $[PtMe_2(diimine)]$.[8] Second, oxidative addition of benzyl bromide and related molecules to $[PtMe_2(diimine)]$ occurs quantitatively to give $[PtBrMe_2(benzyl)(diimine)]$.[9,10] In particular, $[PtMe_2(bu_2bpy)]$ (**2**), (bu_2bpy = 4,4′-di-*tert*-butyl-2,2′-bipyridine) is very reactive towards oxidative addition and the products are more soluble than those obtained by using $[PtMe_2(bpy)]$, (bpy = 2,2′-bipyridine).[10] The oxidative additions are readily monitored by a change in color from orange-red for the platinum(II) complexes such as **2** to pale yellow for the platinum(IV) products,[11] and by a decrease in the coupling constant $^2J(Pt,H)$ for the methylplatinum groups in the ^1H NMR spectrum from 84–86 Hz in **2** to 69–70 Hz in the platinum(IV) products.[8-10]

The reaction sequence leading to the organoplatinum dendrimer is shown in Scheme 1 (the black circles represent the *tert*-butyl groups). Oxidative addition of the C–Br bonds of 4,4′-bis(bromomethyl)-2,2′-bipyridine (**3**)[12] to the platinum(II) centers of **2**[11] gave the binuclear platinum(IV) complex **4**, which was isolated as a pale yellow solid. Complex **4**, which contains two stable platinum(IV) centers and a free diimine functionality, is formed selectively by *trans* oxidative addition.[13] The subsequent reaction of **4** with **1** occurred with displacement of $PtMe_2(SMe_2)_2$ to give the trinuclear complex **5**.[13] Complex **5** is orange-red and contains a new, reactive platinum(II) center with similar reactivity to that in **2**. This represents the end of the first growth cycle in which the platinum nuclearity is first doubled, then increased by one with regeneration of the platinum(II) center required to participate in the next cycle (in Scheme 1, the new diimine derived from **3** is color-coded red to aid identification in later steps).

In the second growth cycle, trinuclear **5** reacted in a 2:1 molar ratio with **3** (color-coded blue in the Scheme 1), with doubling of the nuclearity to give the pale yellow hexanuclear platinum(IV) complex **6**,[14] which again contains a free diimine group. Reaction of **6** with **1** adds a new platinum(II) center and leads to the orange-red heptanuclear **7**.[14]

In the third growth cycle, heptanuclear **7** reacted cleanly in a 2:1 molar ratio with **3** (color-coded green in Scheme 1) to give the pale yellow Pt_{14} cluster **8**.[15] After this stage the reactions occurred less cleanly. Thus, reaction of **8** with **1** did not occur quantitatively, and reaction of this impure product with more **2** failed to give the desired Pt_{30} complex. This limit to growth can be understood in terms of steric hindrance. Thus the synthetic method shown in Scheme 1 is convergent[2,3] with the result that the reaction center becomes more sterically hindered with each growth cycle until a limit is reached at which further reaction is suppressed. In our sequence, modification of the reagents to reduce steric hindrance is required to achieve growth beyond the Pt_{14} dendrimer.

An uncontrolled dendrimeric growth is observed on reaction of **1** with **3**. The first step is substitution of the SMe_2 ligands of **1** by the diimine to give the red $[PtMe_2(\mathbf{3})]$ which then reacts by intermolecular oxidative addition of the C–Br bonds to give an insoluble yellow polymer.

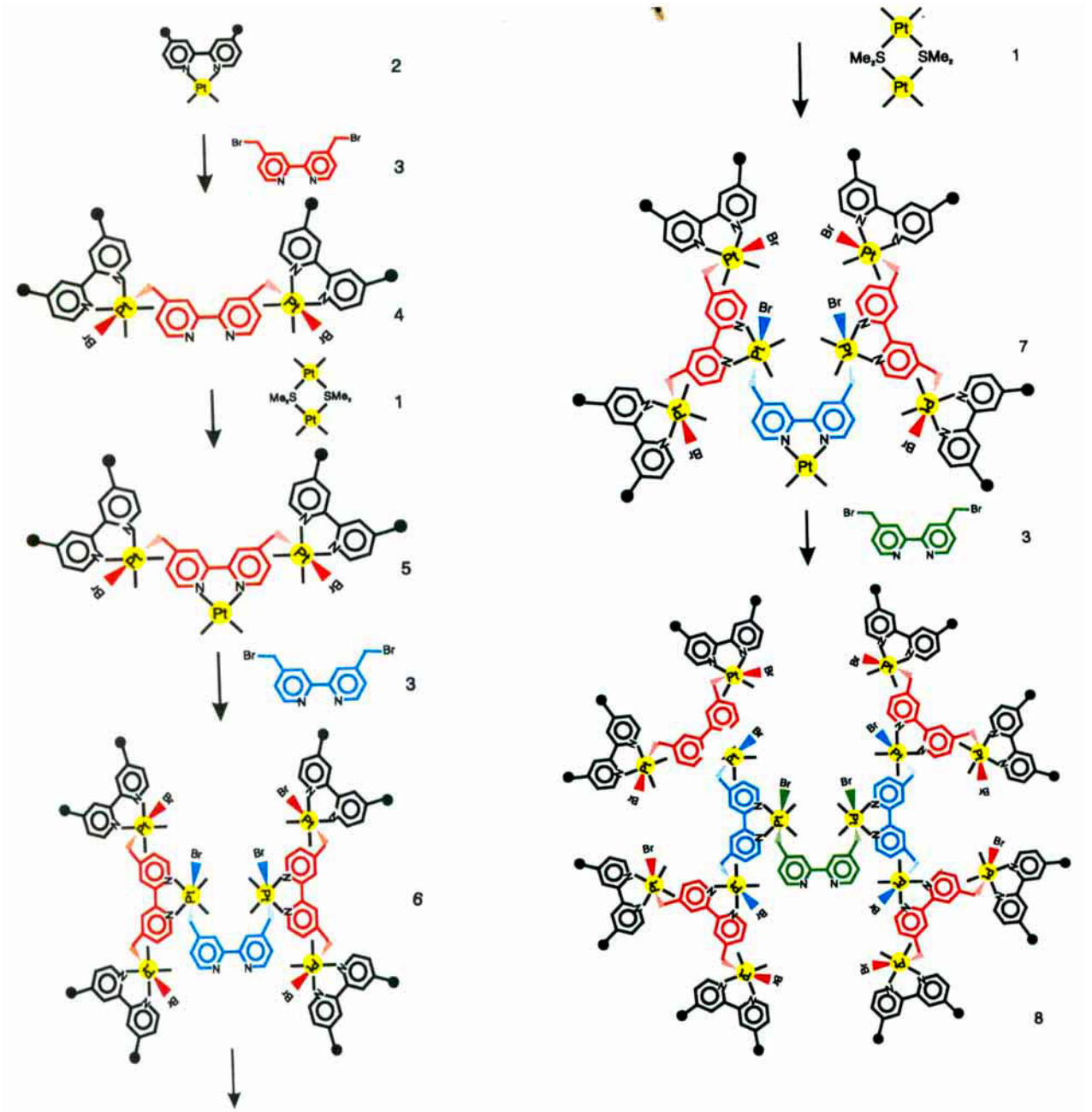
The new dendrimers are characterized by several methods. The formation and reaction of the platinum(II) centers can be monitored by UV/VIS spectroscopy by the growth and decay, respectively, of the metal to ligand charge transfer band [5d(Pt^{II}) to π^*(diimine)] at 430–470 nm in acetone solution. Analytical and NMR spectroscopic data are particularly useful. The NMR spectra become more complex as the molecular size increases. For complexes **4** and **5**, complete assignments including $^{195}Pt,^1H$ coupling constants can be made; for complexes **6** and **7**, almost all proton resonances can be assigned but peak broadening makes assignment of $^{195}Pt,^1H$ couplings difficult; for complex **8**, peaks are further broadened but peak integration is still useful and the interpretation of the spectra is fully consistent with the proposed structure. The increase in molecular weight on going from **7** to **8** can be monitored by gel permeation chromatography (GPC). The apparent molecular weight by GPC referenced to polystyrene standards was 1700 for **7** and 2900 for **8**, fully consistent with a doubling of molecular size.[16] The solubilities of the complexes follow the sequence **8** $\gg$ **7**, **6** $\gg$ **5**, **4** $\ll$ **1**, as expected since the greater solubility associated with the branched dendrimeric structures is only expected at the second growth cycle.[1-7]

In summary, it is clear that the methodology described above has succeeded in the synthesis of the first alkyltransition metal dendrimers. The highest nuclearity obtained is Pt_{14} but modification of the method should lead to controlled synthesis of even higher nuclearity dendrimers. The stuctures of these molecules not only have considerable aesthetic appeal but add a new dimension to the range of potentially useful dendrimers.[1-7]

[*] Prof. Dr. R. J. Puddephatt, S. Achar
Department of Chemistry, The University of Western Ontario,
London, Ontario, N6A 5B7 (Canada)
Telefax: Int. code + (519)661-3022

[**] This work was supported by Natural Sciences and Engineering Research Council (Canada) and 3M (Canada).

Received: November 8, 1993 [Z 6485IE]
German version: *Angew. Chem.* **1994**, *106*, 895



[1] D. A. Tomalia, A. M. Naylor, W. A. Goddard III, *Angew. Chem.* **1990**, *102*, 119; *Angew. Chem. Int. Ed. Engl.* **1990**, *29*, 138-175.
[2] C. J. Hawker, J. M. J. Fréchet, *J. Am. Chem. Soc.* **1992**, *4*, 8405-8413.
[3] T. M. Miller, E. W. Knock, T. X. Neenan, *Macromolecules*, **1992**, *25*, 3143-3148.
[4] A. W. van der Made, P. W. N. M. van Leeuwen, J. C. de Wide, R. A. C. Brander, *Adv. Mater.* **1993**, *5*, 466-468; F. Mouline, B. Gloaguen, D. Astruc, *Angew. Chem.* **1992**, *104*, 452; *Angew. Chem. Int. Ed. Engl.* **1992**, *31*, 458.
[5] H.-B. Mekelburger, W. Jaworek, F. Vögtle, *Angew. Chem.* **1992**, *104*, 1609; *Angew. Chem. Int. Ed. Engl.* **1992**, *31*, 1571-1576.
[6] S. Serroni, G. Denti, S. Campagna, A. Juris, M. Ciano, V. Balzani, *Angew. Chem.* **1992**, *104*, 1540; *Angew. Chem. Int. Ed. Engl.* **1992**, *31*, 1493-1495; G. R. Newkome, F. Cardullo, E. C. Constable, C. N. Moorefield, A. M. W. C. Thompson, *J. Chem. Soc. Chem. Comm.* **1993**, 925.
[7] Z. Xu, J. S. Moore, *Angew. Chem.* **1993**, *105*, 261; *Angew. Chem. Int. Ed. Engl.* **1993**, *32*, 246-248.
[8] J. D. Scott, R. J. Puddephatt, *Organometallics* **1983**, *2*, 1643.
[9] S. Achar, J. D. Scott, R. J. Puddephatt, *Organometallics* **1992**, *11*, 2325.
[10] K.-T. Aye, A. J. Canty, M. Crespo, R. J. Puddephatt, J. D. Scott, A. A. Watson, *Organometallics* **1989**, *8*, 1518.
[11] a) V. F. Sutcliffe, G. B. Young, *Polyhedron* **1984**, *3*, 87; b) N. Chaudhury, R. J. Puddephatt, *J. Organomet. Chem.* **1975**, *84*, 105.
[12] S. Gould, G. F. Strouse, T. J. Meyer, B. P. Sullivan, *Inorg. Chem.* **1991**, *30*, 2942-2949.
[13] Complex **4**: ^{1}H NMR (300 MHz, $CDCl_3$): δ = 1.13 (s, 36H, *t*Bu), 1.48 (s, 12H, ^2J(Pt,H) = 69 Hz, Pt-CH_3), 2.73 (s, 4H, ^2J(Pt,H) = 98 Hz, Pt-CH_2), 6.45 (dd, 2H, ^2J(H-5,H-6) = 5 Hz, H-5, H-5′ of first generation diimine), 6.64 (s, 2H, H-3, H-3′ of first generation diimine), 7.28 (dd, 4H, ^2J(H-5,H-6) = 6 Hz, ^4J(H-5,H-3) = 1.5 Hz, H-5, H-5′ of bu_2bpy), 7.63 (s, 4H, H-3, H-3′ of bu_2bpy), 7.76 (d, 2H, ^2J(H-6,H-5) = 5 Hz, H-6, H-6′ of first generation diimine), 8.48 (d, 4H, ^{2}J(H-6,H-5) = 6 Hz, ^3J(Pt,H) = 18 Hz, H-6, H-6′ of bu_2bpy); FAB-MS; *m/z* (%) = 1329 (10) [M^+]; 1269 (100) [M^+ − Br], 1154 (50) [M^+ − (2 Br + Me)]. Complex **5**: ^{1}H NMR (300 MHz, $CDCl_3$): δ = 0.77 (s, 6H, ^2J(Pt,H) = 86 Hz, Pt^{II}-CH_3), 1.36 (s, 36H, *t*Bu), 1.50 (s, 12H, ^2J(Pt,H) = 69 Hz, Pt^{IV}-CH_3), 2.80 (s, 4H, ^2J(Pt,H) = 100 Hz, Pt^{IV}-CH_2); UV/VIS (CH_3CN): λ_{max} = 470 nm.
[14] Complex **6**: ^{1}H NMR (300 MHz, $CDCl_3$): δ: 1.2–1.37 (72H, *t*Bu), 1.12, 1.4–1.6 (36H, Pt^{IV}-CH_3), 2.1–3.0 (12H, Pt^{IV}-CH_2), 8.40, 8.68 (d, 4H each, H-6, H-6′ of bu_2bpy); 8.05 (s, 8H, H-3, H-3′ of bu_2bpy); 7.28, 7.58 (d, 4H each,

 © VCH Verlagsgesellschaft mbH, D-69451 Weinheim, 1994 0570-0833/94/0808-0848 $ 10.00+.25/0

H-5, H-5′ of bu_2bpy)], [5.71 (d, 4H, H-5, H-5′ of first generation diimine), 6.83 (s, 4H, H-3, H-3′ of first generation diimine), 8.11 (d, 4H, H-6, H-6′ of first generation diimine)]; [6.65 (d, 2H, H-6, H-6′ of second generation diimine); 6.48 (s, 2H, H-3, H-3′ of second generation diimine), note that the signals of H-5 and H-5′ of second generation diimine are obscured. Complex **7**: ^{1}H NMR (200 MHz, [D_6]acetone): $\delta = 0.65$ (s, Pt^{II}-CH_3), 1.1–1.7 (108 H, *t*Bu and Pt^{IV}-CH_3), 2.5–3.4 (12 H, Pt^{IV}-CH_2); UV/VIS (CH_3CN): $\lambda_{max} = 430$ nm.

[15] Complex **8**: ^{1}H NMR (200 MHz, $CDCl_3$): δ: 1.0–1.8 (228 H, 144 in *t*Bu and 84 in Pt^{IV}-CH_3), 2.5–3.1 (28 H, Pt^{IV}-CH_2), 6.0–8.8 (m, 90 H, aromatic CH). Note the absence of a CH_2Br resonance, which would be present if only partial oxidative addition occurred, and the absence of a MLCT band in the UV/VIS which would be present if some Pt^{II} centers remained unreacted.

[16] GPC analysis was performed in THF employing polystyrene standards. The absolute molecular weights cannot be expected to be correct since the standards are linear and organic, while **7** and **8** are more spherical with heavy metal content. Nevertheless, GPC is shown to be useful for characterization of organometallic dendrimers.

[17] Editorial note: Y.-H. Liao and J. R. Moss recently reported on organoruthenium dendrimers with Ru–C bonds (*J. Chem. Soc. Chem. Commun.* **1993**, 1774). In these dendrimers the organoruthenium units are, however, exclusively functional groups on the dendrimer surface.

$[Mo_{57}Fe_6(NO)_6O_{174}(OH)_3(H_2O)_{24}]^{15-}$: A Highly Symmetrical Giant Cluster with an Unusual Cavity and the Possibility of Positioning Paramagnetic Centers on Extremely Large Cluster Surfaces**

Achim Müller,* Winfried Plass, Erich Krickemeyer, Stephan Dillinger, Hartmut Bögge, Anja Armatage, Anna Proust, Christian Beugholt, and Ulf Bergmann

Dedicated to Professor Otto Scherer on the occasion of his 60th birthday

How is it possible to synthesize larger and larger molecular constructions, for example clusters, in a range we shall call mesoscopic? It certainly would be of considerable importance if one could obtain relatively large intermediates by a self-assembly process;[1] these quasi-preorganized building blocks could then be combined to giant molecules, a step that, of course, requires a detailed knowledge of the system. Significant in this context is that extraordinary and novel properties—for example magnetic and electronic—can be expected for mesoscopic compounds. This is especially true, if the relevant compounds do not represent a section of a solid-state structure.

The following novel route can be pursued for this: Substitution of more positive by less positive metal centers M′—for example, molybdenum(VI) by vanadium(IV) centers in oxometalates of the α-Keggin type anion $[Mo_{12}XO_{40}]^{3-}$ (X = P, As)—results in highly negatively charged (that is, nucleophilic) intermediates. These can either be stabilized by cationic species or, as here, connected to give larger moieties. In the case of $[Mo_{12}AsO_{40}]^{3-}$ the intermediate $[Mo_8^{VI}V_4^{IV}As^{V}O_{40}]^{11-}$, formed according to above formalism, can be stabilized in aqueous solution, for example by As^{3+}, affording the $[As_2^{III}Mo_8^{VI}V_4^{IV}As^{V}O_{40}]^{5-}$ cluster.[2] In the absence of arsenic further condensation occurs;[2] hence, it stabilizes the α-Keggin ion. As intended, a large polymolybdate is formed as an intermediate that, as a reactive, highly negatively charged ligand can be connected in various ways by metal cations M′ or cationic groups (e.g., $VO^{2+}/Fe^{3+}/MoO_2^{2+}$) to yield large molecular constructions. In this way one arrives at giant (metal) clusters with open d-shells and/or novel band structures and probably also at compounds with unusual material properties.

Heating an aqueous, hydrochloric acid solution of sodium molybdate dihydrate and iron(III) nitrate nonahydrate with hydroxylammonium chloride under reflux results in the formation of **1**. This highly symmetrical ($\bar{6}m2$; D_{3h}) torus-like giant cluster anion with a size in the nanometer range comprises 276 atoms (excluding H atoms) and has a molecular weight of 9250.9 Da (Fig. 1). Six Fe^{3+} centers and three (formally) cationic $[Mo\text{-}(\mu\text{-}H_2O)_2(\mu\text{-}OH)Mo]^{9+}$ moieties connect three Mo_{17} ligands, $[Mo_{15}^{VI}(MoNO)_2^{3+}O_{58}(H_2O)_2]^{20-}$. This now allows for exchange and positioning of cationic centers M′ with open d-shells while at the same time retaining the Mo_{17} moieties as spacers.

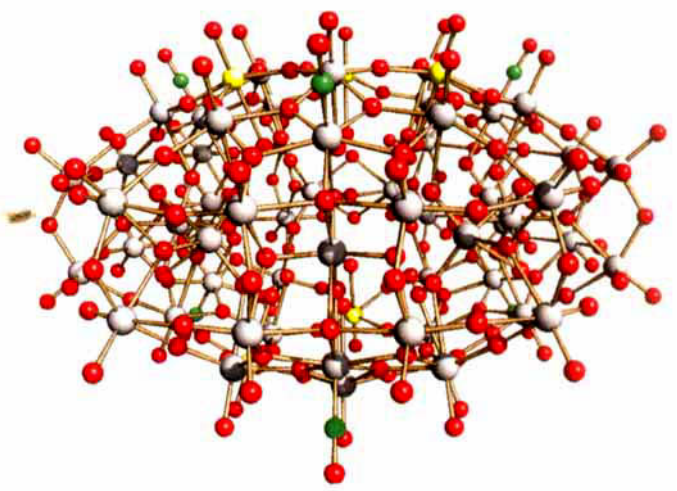


Fig. 1. Ball-and-stick model of the cluster anion of **1** viewed (approximately) along one of the $2(C_2)$ axes (outer diameter: ca. 2.5 nm; color code: Mo light gray, Fe yellow, O red, and N green).

$Na_3(NH_4)_{12}[Mo_{57}Fe_6(NO)_6O_{174}(OH)_3(H_2O)_{24}] \cdot 76H_2O$ **1**

Characterization—especially determining the kind of protonation and the oxidation states of the metal centers—has, due to the size of **1**, required the application of numerous methods: elemental analysis (including determination of NH_4^+ by Kjeldahl nitrogen analysis), single-crystal X-ray structure analysis,[3] calculation of the bond valence sum for the metal and oxygen atoms, redox titration (manganometric), thermogravimetry, magnetochemical measurements as well as UV/VIS/NIR, IR, Raman, ^{57}Fe Mössbauer, and ESR spectroscopy.[4] Limiting oneself to the results of the X-ray structure analysis can lead to extreme possibilities for mistakes as work by Zhang et al.[5] clearly shows. For compounds **2** and **3** the authors published completely wrong results: for **2** a cluster charge of 6– instead of 21– and incorrect cations were reported, while for the highly negatively charged cluster in **3**, the structure was

$(NH_4)_{21}[Mo_{57}V_6(NO)_6O_{180}(OH)_3(H_2O)_{18}] \cdot 65H_2O$ **2**

$(NH_4)_{12}[Mo_{36}(NO)_4O_{108}(H_2O)_{16}] \cdot 33H_2O$ **3**

[*] Prof. Dr. A. Müller,* Dr. W. Plass, E. Krickemeyer, Dipl.-Chem. S. Dillinger, Dr. H. Bögge, A. Armatage, Dr. A. Proust, C. Beugholt, U. Bergmann
Fakultät für Chemie der Universität
Lehrstuhl für Anorganische Chemie I
Postfach 100131, D-33501 Bielefeld (FRG)
Telefax: Int. code + (521)106-6003

[**] We thank Prof. Dr. A. X. Trautwein and Dr. M. Lengen, Lübeck, for measurement of the Mössbauer spectra and Prof. Dr. K. Wieghardt and Mr. H. Espey, Bochum, for carrying out the magnetic measurements.

 © VCH Verlagsgesellschaft mbH, D-69451 Weinheim, 1994 0570-0833/94/0808-0849 $ 10.00+.25/0

incorrectly described and was formulated as a neutral unit.[5] This is a particularly serious error since different formulations correlate with completely different expectations for the important magnetic and electronic properties.

Compound **1** exhibits a multitude of different coordination polyhedra (Fig. 2). In the Mo_{17} moieties a central heptamolybdate fragment is discernible, which contains two $(MoNO)^{3+}$ groups as pentagonal bipyramids. An additional interesting

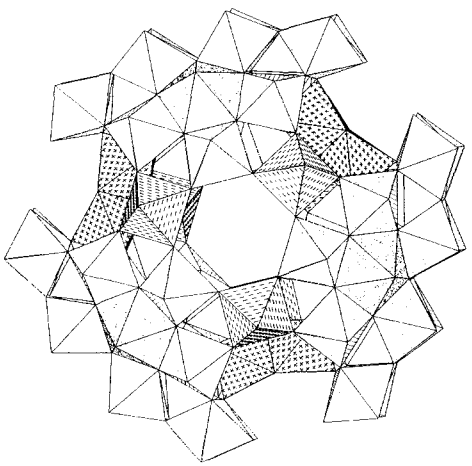


Fig. 2. Polyhedral representation of the cluster anion of **1** showing the three Mo_{17} units. The $Fe^{III}O_4(OH_2)_2$ octahedra are shown with broken lines, the $[Mo(\mu\text{-}H_2O)_2(\mu\text{-}OH)Mo]$ moieties with crosses, the pentagonal $Mo(NO)_6$ bipyramids are randomly dotted and the MoO_6 octahedra have a regular pattern of dots (selected distances: Mo–N 171.4(11); N–O 126.2(16); Fe–$(OH_2)_{term}$ 204.1(9); 217.7(9); Fe–O_{6r} 194.0(7), 195.0(7) pm); the distances for M=O- and Mo-O-Mo moieties are within the expected range.

structural element are two alternating Fe-O-Mo-O twelve-membered rings perpendicular to the $\bar{6}(S_3)$ axis. Inside the cluster anion is a relatively large cavity, which is formed by a central O_{33} polyhedron (cf. Fig. 3). Two planar H_2O six-membered

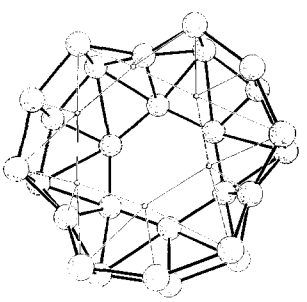


Fig. 3. Characterization of the cavity in the cluster anion of **1** (diameter normal to the $\bar{6}(S_3)$ axis ca. 0.9 and parallel ca. 0.5 nm, without taking the hydrogen atoms into account), formed by the central O_{33} polyhedron (consisting of twelve terminal H_2O molecules, three μ_2-OH groups of the $[Mo(\mu\text{-}H_2O)_2(\mu\text{-}OH)Mo]$ moieties and eighteen μ_2-O atoms).

rings each lying beneath the Fe-O-Mo-O twelve-membered rings are integrated in the O_{33} polyhedron. Since, here similar structural elements are observed as for a modification of ice, the H_2O six-membered rings possibly have a template effect for the formation of the shell structures (remarkable in this regard is the observation that the cluster anion in **1** is apparently *not* formed in D_2O as the reaction medium). Furthermore, the formation of hydrogen bonds of the H_2O molecules which border the cavity points to an interesting relation with clathrates (Fig. 3).[7] Clathrates are namely crystalline framework inclusion compounds whose host structures are constructed in such a way that isolated or bound cavities form, which can contain partly or completely small, in general, uncharged guest species. Since in the main only weak van der Waals interactions exist between the host matrix and the guests, it often happens that the guest species are disordered.[7] Evidently, in connection with the possible presence of H_2O molecules,[3] **1** can be classed as a molecular model for clathrates.

Magnetic measurements for compound **1** at room temperature gave a value of $\mu_{eff} = 15.1\ \mu_B$, as expected for the presence of six high-spin iron(III) centers (expected spin-only value for six uncorrelated $S = 5/2$ centers: $\mu_{eff} = 14.5\ \mu_B$).[8] The temperature-dependence of μ_{eff} between room temperature and 80 K is indicative of a weak, but significant exchange interaction of antiferromagnetic type with small coupling constants. The interpretation of the ESR spectrum recorded at room temperature is consistent with this small exchange interaction. The presence of iron(III) centers can also be confirmed by Mössbauer data (at 100 K: isomer shift $\delta = 0.50 \pm 0.02\ mm\,s^{-1}$ vs. α-Fe and quadrupole splitting $\Delta E_Q = 1.14 \pm 0.01\ mm\,s^{-1}$) as well as by bond valence sum calculations.

Vibrational spectra (IR and Raman spectra) of **1** show the characteristic bands for the Mo_{17} moieties,[4] as well as the characteristic band for the ν(NO) stretching vibration, which proves the presence of a linear $(MoNO)^{3+}$ moiety.[9] On the basis of this data **1** can be described as follows:

$$Na_3(NH_4)_{12}[\{Fe^{III}(H_2O)_2\}_6\{Mo(\mu\text{-}H_2O)_2(\mu\text{-}OH)Mo\}_3\text{-}\{Mo^{VI}_{15}(MoNO)^{3+}_2O_{58}(H_2O)_2\}_3]\cdot 76H_2O \quad \mathbf{1}$$

From bond valence sum calculations the cationic group can be approximately formulated as a $[Mo^{V}(\mu\text{-}H_2O)_2(\mu\text{-}OH)Mo^{V}]$ moiety. This implies that the 4d electrons are only predominantly located on the relevant Mo centers. The results of additional spectroscopic investigations, the interpretation of which with regard to the electronic properties is extremely difficult due to the size of the cluster, will be correlated with the interesting material properties in the future.

It is especially efficient, if the range of nanostructures that is of interest to molecular materials becomes, as here, accessible by a self-assembly process.[10] Polyoxometalates are premier objects of investigation, since between the limiting cases of "molecular" systems (type MO_4^{n-}) and oxidic solids, there are mesoscopic forms with a fascinating structural variety and unusual material properties.[11] It must be emphasized that the last two classes of compounds are formed by the same chemical process, that is acidification of a solution containing MO_4^{n-} anions.[11]

Another interesting aspect of the underlying concept is the possibility of positioning several, especially paramagnetic, metal centers M′ at well-defined locations, employing the Mo_{17} moieties as ligands or spacers. This allows one to influence the topology or structure of the M'_n polyhedron due to the different coordination behavior of M′. In turn insights into interesting exchange interactions—for instance, in polyoxometalates and specifically across the Mo_{17} moiety—can be obtained. This particular aspect is also of relevance to comparable arrangements of paramagnetic metal centers on molybdenum oxide surfaces (cf. the model function of **1** for the Fe^{III}/polymolybdate catalyst used industrially in the Formox process for the oxidation of methanol to formaldehyde[12, 13]).

Finally, it is worth pointing out the possibility of developing an interesting host–guest chemistry in connection with the relatively large cavity in **1**[3]—however, also its model character for clathrates. It will be the goal of a future synthesis plan to produce even larger clusters. Since, however, with increasing cluster size their solubility (and thus possible growth) decreases, at-

tempts will be made to produce even more highly negatively charged species, whose solubility is increased as a result of large hydration.

Experimental Procedure

A mixture of $Na_2MoO_4 \cdot 2H_2O$ (12.00 g, 49.6 mmol), $Fe(NO_3)_3 \cdot 9H_2O$ (9.50 g, 23.5 mmol), $NH_2OH \cdot HCl$ (16.00 g, 230.2 mmol), H_2O (250 mL), and 3.5% HCl (12.5 mL) was stirred rapidly and heated to reflux (The initially formed precipitate, redissolved: the solution changed color from brown to dark green, brown to green-brown; intermittently strong effervescence) until brown vapors appeared at the upper end of the reflux condenser (duration: ca. 20 min). The beige-brown precipitate was filtered hot and the filtrate, after cooling to 20 °C, was allowed to stand for 2 d in an open 400-mL beaker and was then filtered again. Brown, hexagonal crystals (stroke color: green-brown) of **1** precipitated within 3–4 d from the solution, which was stored in a closed vessel at 5 °C. Yield: 0.6 g (ca. 6.0% based on the amount of Mo used).

Received: September 17, 1993
Revised: December 23, 1993 [Z 6365 IE]
German version: *Angew. Chem.* **1994**, *106*, 897

[1] J. S. Lindsey, *New J. Chem.* **1991**, *15*, 153.

[2] A. Müller, E. Krickemeyer, S. Dillinger, unpublished results. In that case compound **2** is formed.

[3] Crystal structure analysis: $P6_3/mmc$, $a = 2380.6(5)$, $c = 2763.4(7)$ pm, $V = 13563(5) \times 10^6$ pm^3, $Z = 2$, $\rho_{calcd} = 2.67$ g cm^{-3}; temperature: 193 K; structure solution with direct methods, $R = 0.063$ for 3377 independent reflections ($F_0 > 4\sigma(F_0)$). Details of the crystal structure and particularly of the complex cation lattice (particularly spectacular and grave errors in [5], which cannot be discussed in this work) of **1** are to be published in detail elsewhere. An important piece of information is, for example, that there is a significantly low occupation of the Na positions. No significant residual electron density could be located inside the cavity. The question of whether possibly "water" is present in the cavity, cannot be answered conclusively either with the help of the X-ray crystal structure analysis (possible disorder) or hy taking into consideration the thermogravimetric data (mass contribution per H_2O molecule is only ca. 0.2%). Further details of the crystal structure investigation may be obtained from the Fachinformationszentrum Karlsruhe, D-76344 Eggenstein-Leopoldshafen (FRG), on quoting the depository number CSD-57983.

[4] Additional characterization of **1** not mentioned in the text: correct elemental analysis for $H_{251}N_{18}Fe_6Mo_{57}Na_3O_{283}$ (H,N,Fe); IR (KBr pellet, some characteristic bands): $\tilde{\nu} = 1600$ (m, $\delta(H_2O)$ and $\nu(NO)$), 945 (m), 910 (sh), 880 (vs, all $\nu(Mo{=}O)$); characteristic bands in the Raman spectrum ($\lambda = 1064$ nm): 960 (vs), 930 (m), 880 cm^{-1} (m, all $\nu(Mo{=}O)$). The presence of (formally) six Mo^V and six $(MoNO)^{3+}$ centers can be deduced from the redox titration with permanganate. An increasing delocalization of the 4d electrons, which are obviously influenced in large species of the type **1** by the cation lattice, seems to reduce the degree of protonation of the μ-OH group in the $[Mo(\mu\text{-}H_2O)_2(\mu\text{-}OH)Mo]$ moieties. The balance of charges might then take place by an increase of the number of cations—in the present case by further occupation of the Na positions [3].

[5] S. Zhang, G. Huang, M. Shao, Y. Tang, *J. Chem. Soc. Chem. Comm.* **1993**, 37; *ibid.* **1986**, 835. The compound "$[H_3O^+]_6[Mo_{57}V_6O_{183}(NO)_6(H_2O)_{18}]^{6-} \cdot 89H_2O$" given there is obviously false with respect to its composition, structure, and the oxidation states of the metal centers. Also, the synthesis of this compound was not reproducable following the procedure provided by the authors: personal communication by P. Gouzerh, University Pierre et Marie Curie, Paris. The correct formulation for a compound obtained by us: $(NH_4)_{21}[\{V^{IV}O(H_2O)\}_6\{Mo^V(\mu\text{-}H_2O)_2\text{-}(\mu\text{-}OH)Mo^V\}_3\{Mo^{VI}_{15}(MoNO)^{3+}_2O_{58}\text{-}(H_2O)_2\}_3] \cdot 65H_2O$ (**2**)) [6]. The compound formulated as a neutral (!) complex by Zhang et al. $(NH_4)_{12}[(Mo^{VI}O_2)_2\{H_{12}Mo^{VI}_{15}(MoNO)^{3+}_2O_{58}(H_2O)_2\}_2] \cdot 33H_2O$ (**3**), which contains the same Mo_{17} ligand was described—unlike **2**—even with a false macrostructure. Compounds **2** and **3** were recently obtained by us in relatively high yields following a different route [6].

[6] A. Müller, E. Krickemeyer, S. Dillinger, H. Bögge, A. Proust, W. Plass, R. Rohlfing, *Naturwissenschaften*, **1993**, *80*, 560 (a provisional formulation for compounds **2** and **3**, without physical data and justification, has already been given here); for more recent details see A. Müller, E. Krickemeyer, S. Dillinger, A. Bögge, W. Plass, A. Proust, L. Dloczik, C. Menke, J. Meyer, R. Rohlfing, *Z. Anorg. Allg. Chem.* **1994**, *620*, 599.

[7] A. F. Wells, *Structural Inorganic Chemistry*, 5th ed., Clarendon, Oxford, **1984**; F. Vögtle, Supramolekulare Chemie, Teubner, Stuttgart, 1989; A. Müller, H. Reuter, S. Dillinger, unpublished results.

[8] Within in the range of measurement the Mo centers do not make a significant positive contribution to the χ value, that is, the 4d-electrons are spin-paired as observed for the two- and fourfold reduced Keggin ions (A. Müller, E. Krickemeyer, M. Penk, V. Wittneben, J. Döring, *Angew. Chem.* **1990**, *102*, 85; *Angew. Chem. Int. Ed. Engl.* **1990**, *29*, 88).

[9] $(MoNO)^{3+}$ [electron configuration $(MoNO)^4$] has a considerable tendency of formation in mono- and polynuclear chalkogometalate systems: P. Gouzerh, Y. Jeannin, A. Proust, F. Robert, *Angew. Chem.* **1989**, *101*, 1377; *Angew. Chem. Int. Ed. Engl.* **1989**, *28*, 1363; A. Müller, W. Eltzner, S. Sarkar, H. Bögge, P. J. Aymonino, N. Mohan, U. Seyer, P. Subramanian, *Z. Anorg. Allg. Chem.* **1983**, *503*, 22; A. Müller, W. Eltzner, H. Bögge, E. Krickemeyer, *Angew. Chem.* **1983**, *95*, 905; *Angew. Chem. Int. Ed. Engl.* **1983**, *22*, 884; A. Müller, W. Eltzner, W. Clegg, G. M. Sheldrick, *ibid.* **1982**, *94*, 555 and **1982**, *21*, 535. Some of the compounds described herein have been used as models or standards in the aforementioned titration.

[10] An essential aspect is that clear quality and property changes or jumps (incidentally a fundamental problem in science) and, furthermore, also an increase in information in the sense of the definition given by C. F. von Weizsäcker emanate starting from a simple molecular region. This applies even more, if the resulting systems do not represent a section of a typical solid-state structure with approximated translational symmetry, which also—according to von Weizsäckers approach—reduces the number of decision points. It is referred here to the concept of information as defined by von Weizsäcker since it will become important for the classification of molecular materials in the future (C. F. von Weizsäcker: a.) "Information is the measure of amount of *form*. . . .matter has form. . ." b.) "The more decisions can be made about an object, the more form in a general, not necessarily spacial sense of the word can he recognized about it. This amount of form is, as just stated, a property of the object. . ." (From C. F. von Weizsäcker, *Aufbau der Physik*, 1st ed., dtv, Stuttgart, **1988**, p. 167 with the authentic definition in German.)). In this context the following statement by R. Feynman is of interest: "I can hardly doubt that when we have some control of the arrangement of things on a small scale we will get an enormously greater range of possible properties that substances can have." (cited from: R. W. Siegel, *Physics Today* **1993**, *46* (October), 64). These statements are of special relevance to polyoxometalates with their structural and functional variety and with respect to the resulting numerous possible applications [11].

[11] M. T. Pope, A. Müller, *Angew. Chem.* **1991**, *103*, 56; *Angew. Chem. Int. Ed. Engl.* **1991**, *30*, 34.

[12] H. Adkins, W. P. Peterson, *J. Am. Chem. Soc.* **1931**, *53*, 1512; *Ullmans Encyclopedia of Industrial Chemistry, Vol A11*, 5th edition, VCH, Weinheim, **1988**, p. 628.

[13] In addition, it should be mentioned that studies regarding the interaction of the Co^{II} centers in hydrodesulfurization (HDS) catalysts (nanometer-size molyhdenum disulfide crystallites with Co^{II} centers on the edges) have been carried out in order to understand the electronic/magnetic state of the catalyst system in correlation to its activity. In this system the Co^{II}—Co^{II} distances of the catalyst, which regularly shows a high degree of saturation for edge sites, are of the same magnitude as the Fe^{III}—Fe^{III} distances in **1** (H. Topsøe, R. Candia, N.-Y. Topsøe, B. B. Clausen, *Bull. Soc. Chim. Belg.* **1984**, *93*, 783). Remarkably, the size of the crystallites of the HDS catalyst is comparable to that of the cluster anion in **1** [14].

[14] E. Diemann, T. Weber, A. Müller, *J. Catal.*, in press.

Synthesis and Properties of 2,4,6-Trimethylphenylborane (Mesitylborane), a Stable Alternative to Thexylborane**

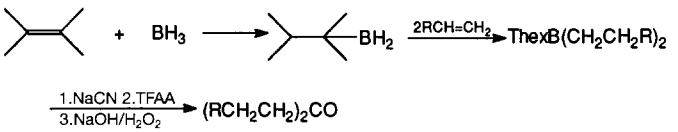
Keith Smith,* Andrew Pelter,* and Zhao Jin

Thexylborane[1, 2] (1,2,2-trimethylpropylborane)[***] has been extensively used in synthesis. This is due to a combination of its ability to add two alkenes of little or moderate steric hindrance and the low migratory aptitude of the thexyl group in such important reactions as the cyanoborate process[3] and carbonylation[4] of organoboranes [Eq. (a), TFAA = trifluoroacetic anhydride]. However, thexylborane suffers from some major disadvantages. It must be made at low temperatures and used immediately or else the boron group wanders, by retrohy-

[*] Prof. K. Smith, Prof. A. Pelter, Z. Jin
University College of Swansea
Singleton Park, Swansea SA2 8PP (UK)
Telefax: Int. code + (792)295747.

[**] Hindered Organoboranes in Organic Chemistry, Part 26. Part 25: A. Pelter, K. Smith, S. Elgendy, *Tetrahedron*, **1993**, *49*, 7119.

[***] For convenience monoorganoboranes are referred to as though they were monomers although in fact all are dimers.

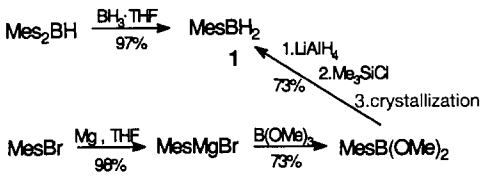


(a)

droboration–hydroboration, to the primary carbon atoms. Two different alkenes can be added sequentially only if the first is somewhat hindered; on the other hand two slightly hindered alkenes cannot be added without substantial displacement of tetramethylethene. These disadvantages limit the variety of products that can be made using thexylborane.

Monoarylboranes cannot undergo retrohydroboration and could possibly be stabilized by 2,6-disubstitution.[5] They thus present attractive possibilities and we have previously reported on 2,4,6-triisopropylphenylborane (tripylborane).[6] We now record that 2,4,6-trimethylphenylborane, mesitylborane (**1**), is a readily available, crystalline, stable borane that can replace thexylborane for most purposes. In addition **1** has special properties not shared by thexylborane and also shows significant advantages compared with tripylborane.

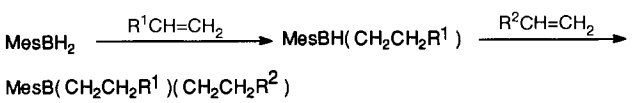
Mesitylborane (**1**) (m.p. 46 °C) is made by either of the two routes shown in Scheme 1. Commercially available dimesitylborane[7] undergoes ready redistribution with borane–THF to give **1**. Alternatively mesityl dimethoxyborane, a useful relay compound, may be converted to **1** by conventional methods.[6]



Scheme 1. Synthesis of mesitylborane **1**.

Crystalline **1** showed no sign of decomposition, isomerization, or redistribution after 24 h at room temperature, and after 10 days retained 93% of its original hydride activity. In THF after seven days at room temperature there was a 16% loss of hydride activity, but no redistribution or isomerization. From a two week old solution of **1** in THF, pure crystalline **1** is readily recovered in 75% yield. This is in great contrast to methylborane[8] or thexylborane,[1, 2] both of which must be made in solution and used at once.

The first notable point about the chemistry of **1** is that it hydroborates 1-alkenes in a sequential fashion (Eq. (b), Table 1, exp. 6; also exp. 1, 2, 7 were carried out in a sequential fashion).



(b)

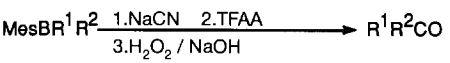
The second is that the regioselectivity of each step of the hydroboration is around 99%. Furthermore, there is no displacement of the aromatic group even on addition of two secondary alkyl groups (exp. 3–5, 8) though it was noted that α-pinene was displaced by cyclohexene during the final hydroboration step following initial hydroboration of α-pinene by mesitylborane (exp. 9).

Table 1. Hydroboration of alkenes with $MesBH_2$ (**1**).

Exp.	Alkene A	Alkene B	Yield [%] [a] MesOH	R^AOH	R^BOH
1	1-octene	1-octene	88	91	
2	1-hexene	1-hexene	94	91	
3	cyclohexene	cyclohexene	92	90	
4	2-methyl-1-pentene	2-methyl-1-pentene	94	87	
5	1-methylcyclopentene	1-methylcyclopentene	91	73	
6	1-octene	1-hexene	92	93	91
7	1-octene	cyclohexene	93	89	91
8	α-pinene	1-hexene	93	88	93
9	α-pinene	cyclohexene	91	[b]	43

[a] Yield after oxidation of the triorganoboranes determined by gas chromatography. [b] 81% α-pinene.

To show that the organoboranes $MesBR^1R^2$ can be put to synthetic use, examples were transformed to ketones by the cyanoborate process [Eq. (c)].[3] The results (Table 2) show that ketones are produced in yields at least as good as those obtained by using thexylborane[3] and in higher purity due to the greater regiospecificity shown by mesitylborane in hydroboration reactions. There was no evidence of scrambling of alkyl groups, nor



(c)

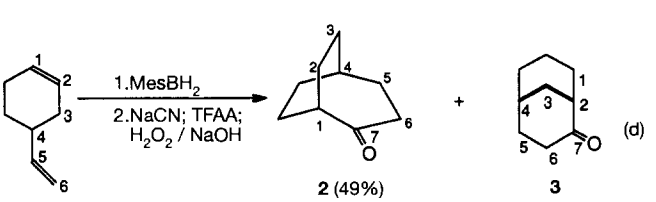
Table 2. Conversions of $MesBR^AR^B$ to ketones according to Equation (c).

Exp.	Alkene A	Alkene B	Yield [%] [a] R^ACOR^B	MesOH
10	1-hexene	1-hexene	81	84
11	cyclohexene	cyclohexene	87	93
12	cyclohexene	1-octene	77	91
13	1-octene	1-hexene	86	92

[a] Yields determined by gas chromatography and based on $MesBH_2$.

were there any ketone products derived by migration of the mesityl group. The synthesis of unsymmetrical linear ketones (previously only available by circuitous routes[9, 10]) greatly enlarges the scope of reactions such as the cyanoborate process.

Cyclic hydroboration followed by replacement of the boron atom by a carbonyl group is an important process.[3] This is readily accomplished by hydroboration with mesitylborane followed by the cyanoborate process as illustrated by the reaction of vinylcyclohexene to give the bicyclic ketone **2** with only a trace of the alternative product **3** [Eq. (d)]. The corresponding

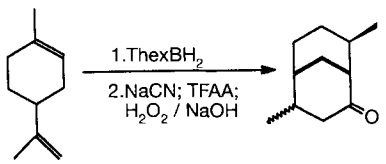


(d)

reaction using thexylborane gave about the same yield of ketonic product but this consisted of approximately equal amounts of **2** and **3**.

 © VCH Verlagsgesellschaft mbH, D-69451 Weinheim, 1994 0570-0833/94/0808-0852 $ 10.00+.25/0

The cyanoborate process on limonene [Eq. (e)], successful with thexylborane,[3] essentially failed for mesitylborane. This might be due to the greater facility of thexylborane, as compared to mesitylborane, for the hydroboration of more hindered alkenes. It defines at least one area in which thexylborane will retain an advantage over mesitylborane.



(e)

We next examined the displacement of the mesityl group from dialkylmesitylboranes, and found two unusual and highly selective processes that further enhance the usage of mesitylborane. The first method consisted of the addition of bromine in methanol to the dialkylmesitylboranes [Eq. (f)]. This caused cleavage of the mesityl group with production of bromomesitylene and dialkylmethoxyboranes, oxidation of which gave the corresponding alcohols in overall yields of 82–87%.

$$MesBR^1R^2 \xrightarrow[MeOH]{Br_2/} MesBr + MeOBR^1R^2 \xrightarrow{[O]} R^1OH + R^2OH \quad (f)$$

More importantly, the intermediate dialkylmethoxyboranes can be reacted directly with a Grignard reagent to give fully mixed organoboranes, in which all the alkyl groups can be primary. These in turn can be readily converted to the corresponding tertiary alcohols[11] [Eq. (g)]. When R^1 = *n*-octyl, R^2 = *n*-hexyl, R^3 = *n*-butyl, the overall yield of isolated carbinol, based on $MesBH_2$ is 69%, which implies a highly efficient process given the seven steps involved.

$$MesBR^1R^2 \xrightarrow{Br_2/MeOH} MeOBR^1R^2 \xrightarrow{R^3MgBr} BR^1R^2R^3 \xrightarrow[H_2O_2 / NaOH]{NaCN; TFAA;} HOCR^1R^2R^3 \quad (g)$$

A different method of releasing the mesityl group is through direct reaction with an alkyl or aryllithium (e.g. Eq. (h)). Butylhexyloctylborane produced from the initial reaction was converted to the corresponding carbinol by the cyanoborate process in 78% yield showing that there had been little, if any, scrambling of the alkyl groups. The mesityl group, presumably displaced as mesityllithium, was recovered as mesitylene in 88% yield.

$$MesB(Oct)(Hex) \xrightarrow{BuLi} BuB(Oct)(Hex) \xrightarrow[H_2O_2 / NaOH]{NaCN; TFAA;} HOC(Bu)(Hex)(Oct) \quad (h)$$

Our studies show that mesitylborane is readily available and its hydroborating properties, as well as the properties of the derived organoboranes, should render it a useful addition to the armoury of organic reagents.

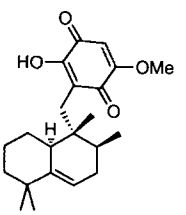
Received: November 13, 1993 [Z 6500 IE]
German version: *Angew. Chem.* **1994**, *106*, 913

[1] A. Pelter, K. Smith, H. C. Brown, *Borane Reagents*, Academic Press, London, **1988**.
[2] E. Negishi, H. C. Brown, *Synthesis* **1980**, 153.
[3] A. Pelter, K. Smith, M. G. Hutchings, K. Rowe, *J. Chem. Soc. Perkin Trans. 1* **1975**, 129.
[4] H. C. Brown, E. Negishi, *Synthesis* **1972**, 196.
[5] A. Pelter, B. Singaram, L. Warren, J. W. Wilson, *Tetrahedron* **1993**, *49*, 2965.
[6] A. Pelter, K. Smith, D. Buss, Zhao Jin, *Heteroat. Chem.* **1992**, *3*, 275.
[7] A. Pelter, S. Singaram, H. C. Brown, *Tetrahedron Lett.* **1983**, *24*, 1433.
[8] M. Srebnik, T. E. Cole, H. C. Brown, *J. Org. Chem.* **1990**, *55*, 5051.
[9] S. U. Kulkarni, H. D. Lee, H. C. Brown, *J. Org. Chem.* **1980**, *45*, 4542.
[10] G. Zweifel, N. R. Pearson, *J. Am. Chem. Soc.* **1980**, *102*, 5919.
[11] A. Pelter, M. G. Hutchings, K. Rowe, K. Smith, *J. Chem. Soc. Perkin Trans. 1* **1975**, 138.

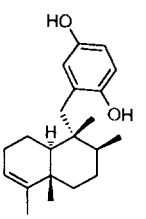
A Concise Total Synthesis of (±)-Mamanuthaquinone by Using an *exo*-Diels–Alder Reaction**

Taeyoung Yoon, Samuel J. Danishefsky,* and Susan de Gala

An interesting class of sesquiterpenoid quinones and hydroquinones has been isolated from various marine sponges.[1] Certain members of this family exhibit profiles of cytotoxity,[2] antimicrobial activity,[2b, 3] and inhibition of reverse transcriptase action.[4] Among the novel compounds in this subgroup is mamanuthaquinone **1**[5] isolated from *Fasciospongia sp.*, a sponge isolated from Mamanutha Island in the Fiji chain. Mamanuthaquinone exhibits moderate cytotoxity toward human colon tumor cell lines (HCT-116). Also, the structurally related avarol **2** and its quinone analogue have been proposed as promising anti-AIDS drugs,[4a] though their clinical usefulness is far from demonstrated.[6]



1 mamanuthaquinone



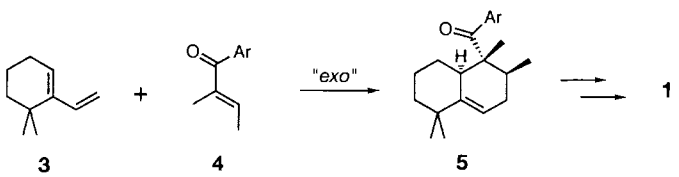
2 avarol

In considering a total synthesis of mamanuthaquinone **1** an obvious, if speculative possibility presented itself (Scheme 1). In

[*] Prof. S. J. Danishefsky,[+] T. Yoon
Department of Chemistry, Yale University
New Haven, CT 06511 (USA)
Telefax: Int. code + (212)772-8691
S. de Gala
Yale Chemical Instrumentation Center
New Haven, CT 06511 (USA)
[+] New addresses: Memorial Sloan-Kettering Cancer Center
1275 York Avenue, New York, NY 10021 (USA)
Telefax: Int. code + (212)772-8691
and
Department of Chemistry, Havemeyer Hall
Columbia University, New York, NY 10027 (USA)
Telefax: Int. code + (212)854-7142

[**] This research was supported by Public Health Service (PHS) Grant CA28824. NMR spectra were obtained through the auspices of the Northeast regional National Science Foundation (NSF)/NMR Facility at Yale University, which was supported by NSF Chemistry Division Grant CHE 7916210.

principle, the generalized system **5** can be assembled from diene **3** and dienophile **4**. With a properly chosen aroyl function, **1** might well be quickly derivable from the adduct **5**. However, in such a Diels–Alder reaction an *exo* transition state is required to reach the stereochemistry required for **1**.



Scheme 1. *Exo*-Diels–Alder approach for **1**.

The well-known preference for *endo* topology in the Diels–Alder reaction[7] is most pervasive with relatively unhindered cyclic dienophiles (e.g., maleic anhydride, *p*-benzoquinone, etc.) and homoannular dienes.[8] Nevertheless, *endo* orientation is still preferred in most intermolecular processes and if it is not dominant, the cycloadditions tend toward stereorandomness. However, the attractive forces of secondary orbital interaction to which the selectivity is generally attributed[9] are rather weak and can be easily overridden by seemingly minor structural changes.[10] Indeed, almost exclusive *exo* additivity has been exhibited by the reaction of cyclopentadiene and acyclic dienophiles having an alkyl substituent on the carbon bearing the activating group (e.g., methacrolein).[11] While the origin of this "abnormal" tendency is not clear, the anomaly had been mostly confined to reactions utilizing cyclopentadiene as the diene partner. Conceivably, it could be the consequence of the steric repulsion between the methylene group of cyclopentadiene and the α-substituent of dienophiles in the transition state leading to *endo* adduct.[12] For instance, the same catalytic system that produces only *exo* adduct from the cycloaddition of methacrolein with cyclopentadiene[11e] gave rise to nearly complete *endo* preference with acyclic dienes such as 1-methoxybutadiene.[13]

We were also mindful, on the other hand, that with the parent 1-vinylcyclohexene, Diels–Alder reaction had been reported to yield cleanly the *endo* product.[14] However, in the case at hand (**3** + **4**), we hoped to extend the "cyclopentadiene effect" by taking particular advantage of the quaternary carbon of the diene in conjunction with a sterically demanding aroyl group on the dienophile. In such a cycloaddition, the *endo* mode might be highly disfavored due to repulsion of the aryl group with the dimethylcyclohexenyl array (Fig. 1). Thus, the use of a maximally substituted aroyl function in the Diels–Alder reaction seemed to be in keeping with the stereochemical rationale, while holding promise for simplifying the late stages of reaching **1**. In this communication we describe the first total synthesis of mamanuthaquinone in a remarkably concise way drawing upon this reasoning (Scheme 2).

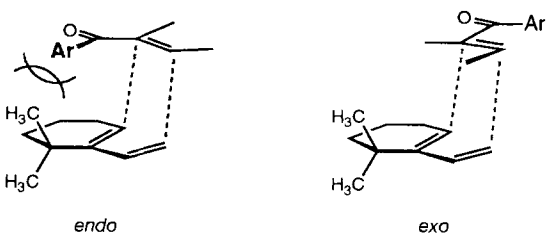
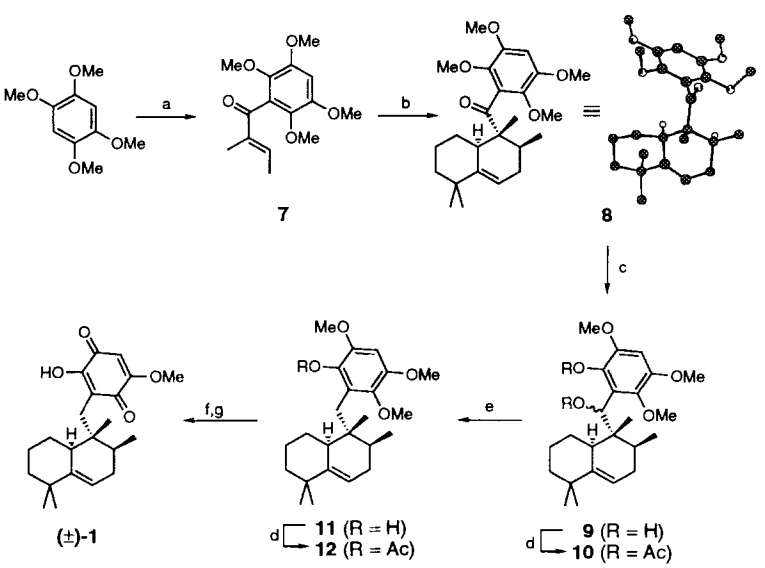


Fig. 1. *Exo* addition of **3** to **4** is favored over *endo* addition.

The requisite dienophile **7** was obtained in one step (77% yield) from the reaction of the aryl lithio derivative of 1,2,4,5-tetramethoxybenzene[15] and **6**, which was in turn prepared from the reaction of tigloyl chloride with *N*,*O*-dimethylhydroxylamine following the protocols of Weinreb.[16] Cycloaddition of **7** with **3**[17] under mediation by ethylaluminum dichloride/THF in dichloromethane afforded an 85% yield of a single cycloadduct. The presence of THF resulted in a doubling of the yield; without it, decomposition of the diene competed quite significantly, which was so extensive with other Lewis acids such as boron triflouride etherate or titanium tetrachloride that the desired cycloaddition did not proceed at all. The regiochemistry of the cycloaddition was well compliant with the precedents and no other regio- or stereoisomers were detected. Compound **8** was characterized by X-ray crystallography.[18]



Scheme 2. Synthesis of (±)-mamanuthaquinone **1**. a) *n*BuLi, LiCl, THF, 0 °C → room temperature, 1 h; then (*E*)-$CH_3CH{=}CCH_3CON(CH_3)OCH_3$ **6**, −78 °C → room temperature, 12 h; b) **3** (2 equiv), $EtAlCl_2$ (1.5 equiv.), THF (1 equiv), CH_2Cl_2, room temperature, 6 h; c) $LiAlH_4$, THF, reflux, 2.5 d; d) Ac_2O, Et_3N, cat. 4-dimethylaminopyridine, CH_2Cl_2, room temperature, 4 h; e) Li (10 equiv), NH_3, −78 °C, 10 min; NaOBz; NH_4Cl; f) $(NH_4)_2Ce(NO_3)_6$ (2.5 equiv), aq. MeCN; g) K_2CO_3, MeOH, room temperature, 1 h.

With the three stereogenic centers installed in the required configuration, a straightforward end game sequence was implemented. Treatment of **8** with lithium aluminum hydride resulted, not only in reduction of the ketone, but also in demethylation of one of the *ortho* methoxy groups. Acetylation of diastereomers **9** gave **10**, whose de-acetoxylation as shown afforded **11**, which was then acetylated to give **12** (55% based on **8**). Oxidative demethylation of **12** with ceric ammonium nitrate followed by de-acylation (K_2CO_3 in MeOH) afforded (±)-mamanuthaquinone (85% based on **12**; m.p. 114–116 °C, the enantiomerically pure natural product:[5] m.p. 108.5–109.5 °C).[19]

In summary, the total synthesis of **1** has been accomplished in eight steps in 32% yield from 1,2,4,5-tetramethoxybenzene. We hope to sort out the factors which were responsible for the apparent *exo* selectivity of this Diels–Alder reaction. For instance, assigning the relative importance of the geminal dimethyl center of **3** and the two vinyl methyl groups of **7**

would be helpful in planning extensions of these findings. Studies addressed to such issues as well as to proposals relating to the mode of action of mamanuthaquinone are in progress.

Experimental Procedure

8: To an ice-cold solution containing **7** (208 mg, 0.74 mmol) and THF (0.06 mL, 1 equiv) in CH_2Cl_2 (5 mL) was added 1.8 M $EtAlCl_2$ in toluene (0.60 mL, 1.5 equiv), followed by slow dropwise addition of **3** (0.20 g, 2 equiv) in CH_2Cl_2 (2 mL). After the addition was complete, the mixture was allowed to warm to room temperature and stirred for 6 h. The reaction was quenched by cautious addition of saturated NH_4Cl at 0 °C. The aqueous layer that separated was extracted with CH_2Cl_2 and the combined organic phases were dried (Na_2SO_4), concentrated in vacuo, and chromatographed on silica (10/1 to 4/1 hexane/EtOAc) to give 263 mg of **8** as a white solid (84%): m.p. 122–124 °C (CH_2Cl_2/hexane); IR ($CDCl_3$): $\tilde{\nu}_{max}$ = 2939, 1680, 1484, 1465, 1424, 1257, 1225, 1197 cm^{-1}; ^1H NMR (300 MHz, $CDCl_3$): $\delta \approx 6.55$ (s, 1 H, phenyl), 5.43 (d, J = 4.3 Hz, 1 H, vinyl), 3.87 (s, 6 H), 3.73 (s, 3 H), 3.70 (s, 3 H), 2.60 (d, J = 12.3 Hz, 1 H), 2.25 (m, 1 H), 2.0–1.7 (m, 3 H), 1.2–1.0 (m, 3 H), 1.07 (s, 3 H), 1.02 (s, 3 H), 0.92 (d, J = 6.9 Hz), 0.89 (s, 3 H); ^{13}C NMR (75 MHz, $CDCl_3$): δ = 213.2, 149.2, 148.8, 145.7, 138.9, 138.5, 132.8, 115.6, 99.6, 62.0, 61.5, 56.6, 54.9, 42.5, 41.2, 36.5, 33.9, 31.2, 30.3, 29.8, 28.0, 22.7, 17.1, 12.0; MS (20 eV EI): *m/z* (rel. int.): 416 (1) [M^+], 280 (1), 225 (100) [aroyl$^+$], 210 (6), 191 (4); high-resolution FAB MS for $C_{25}H_{36}O_5$, calcd 416.2564, found 416.2540; correct elemental analysis.

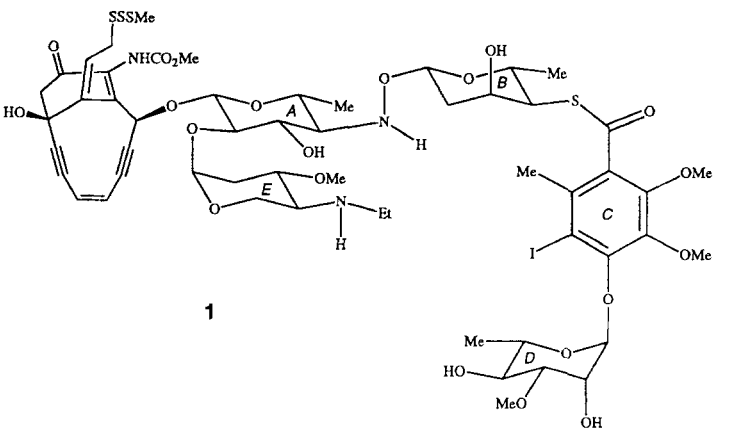
Received: November 26, 1993 [Z6516IE]
German version: *Angew. Chem.* **1994**, *106*, 923

[1] For a series of reviews on marine natural products including those from sponges, see: D. J. Faulkner, *Nat. Prod. Reports* **1992**, *9*, 323 and its forerunners.
[2] a) M. Kondracki, M. Guyot, *Tetrahedron* **1989**, *45*, 1995; b) M. Kondracki, M. Guyot, *Tetrahedron Lett.* **1987**, 5815; c) J. Rodriguez, E. Quinoa, R. Riguera, B. M. Peters, L. M. Abrell, P. Crews, *Tetrahedron* **1992**, *48*, 6667.
[3] B. W. Sullivan, D. J. Faulkner, G. K. Matsumoto, H. Cun-heng, J. Clardy, *J. Org. Chem.* **1986**, *51*, 4568.
[4] a) P. S. Sarin, D. Sun, A. Thornton, W. E. G. Müller, *JNCI, J. Natl. Cancer Inst.* **1987**, *78*, 633; b) S. Loya, A. Hizi, *FEBS Lett.* **1990**, *269*, 131.
[5] J. C. Swersey, L. R. Barrows, C. M. Ireland, *Tetrahedron Lett.* **1991**, 6687.
[6] See footnote 3 of ref. [2c].
[7] K. Alder, G. Stein, *Angew. Chem.* **1937**, *50*, 510.
[8] "*Intermolecular Diels–Alder Reactions*": W. Oppolzer in in *Comprehensive Organic Synthesis, Vol. 5* (Ed.: B. M. Trost); Pergamon, London, **1991**, Chapt. 4.1.
[9] R. B. Woodward, T. J. Katz, *Tetrahedron* **1959**, *5*, 70.
[10] J. G. Martin, R. K. Hill, *Chem. Rev.* **1961**, *61*, 537.
[11] a) Y. Kobuke, T. Fueno, J. Furukawa, *J. Am. Chem. Soc.* **1970**, *92*, 6548; for more recent examples employing Lewis acid catalysts, see b) F. Ribiere, O. Riant, H. B. Kagan, *Tetrahedron Asymmetry* **1990**, *1*, 199; c) K. Furuta, S. Shimizu, Y. Miwa, H. Yamamoto, *J. Org. Chem.* **1989**, *54*, 1483; d) H. Takemura, N. Komeshima, I. Takahashi, S. Hashimoto, N. Ikota, K. Tomioka, K. Koga, *Tetrahedron Lett.* **1987**, 5687; e) M. Reetz, S. Kyung, C. Bolm, T. Zierke, *Chem. Ind. London* **1986**, 834.
[12] The concept of a specific *endo*-orienting preference of methyl groups by a σ interaction has been suggested [11a]. However, the explanation given in the text, which is based on steric interactions, seems more likely in the light of the fact that a similar *exo* preference is exhibited by α-haloacrylic acids (see [10]). Also, quite recently, Lewis acid controlled variation of *endo*/*exo* selectivity in a hetero-Diels–Alder reaction has been reported: L. F. Tietze, C. Schneider, *Synlett* **1992**, 755.
[13] K. Mikami, M. Terada, Y. Motoyama, T. Nakai, *Tetrahedron Asymmetry* **1991**, 643.
[14] E. J. Corey, M. C. Desai, *Tetrahedron Lett.* **1985**, 5747.
[15] F. Benington, R. D. Morin, L. C. Clark, Jr., *J. Org. Chem.* **1955**, *20*, 102.
[16] S. Nahm, S. M. Weinreb, *Tetrahedron Lett.* **1981**, 3815.
[17] S. P. Tanis, Y. M. Abdallah, *Synth. Commun.* **1986**, 251.
[18] X-ray crystal structure analysis of compound **8**: $C_{25}H_{36}O_5$, triclinic, space group $P\bar{1}$ (no. 2), a = 9.9014(6), b = 10.322(1), c = 12.188(1) Å, α = 85.161(7), β = 69.095(6), γ = 87.714(7)°, V = 1159.4(4) Å^3, Z = 2, ρ_{calcd} = 1.193 g cm^{-3}, $\mu(Mo_{K\alpha})$ = 0.8 cm^{-1}. Of the 4548 reflections collected, 4294 were unique and 2526 reflections with $I > 3\sigma(I)$ were used in the refinement of the structure; R = 0.045, Rw = 0.055. The residual electron density was less than 0.15 e Å^{-3}, Enraf-Nonius CAD4 diffractometer, $Mo_{K\alpha}$ irradiation, $2\theta_{max}$ = 50°, sturcture determination by direct methods (MITHRIL), all hydrogen atoms were included in calculated positions, except those belonging to methyl groups in which case one hydrogen atom of the methyl group was located in the difference map and included to set the orientation of the other two hydrogen atoms. Further details of the crystal structure investigation are available on request from The Director of the Cambridge Crystallographic Centre, 12 Union Road, Cambridge CB2 1EZ (UK) on quoting the full jounal citation.
[19] While we were unable to obtain a sample of the natural product, our assignment is secure given the crystallographically verified structure of **8** and the complete correspondence of the high-field ^1H and ^{13}C NMR spectra of synthetic **1** with those reported.

On the DNA Recognition Role of the Carbohydrate Sector in Calicheamicin: A Comparison of DNA Cleaving Capacity of Enantiomeric Calicheamicinones**

Jayshree Aiyar, Stephen A. Hitchcock, Derek Denhart, Kevin K. C. Liu, Samuel J. Danishefsky,* and Donald M. Crothers

The antitumor activity of the naturally occurring drug calicheamicin γ_1^I (**1**) is believed to operate through its efficient cleavage of duplex DNA in a double-stranded, highly sequence-selective fashion.[1, 2] The drug is comprised of an aryl tetrasaccharide carbohydrate region tethered to an enediyne-containing aglycone moiety. The latter, which is termed calicheamicinone, was synthesized first in our laboratory as its racemate[3] (**2**/**3**) and subsequently in the enantiomerically pure form corresponding to the natural product, by Nicolaou et al.[4]



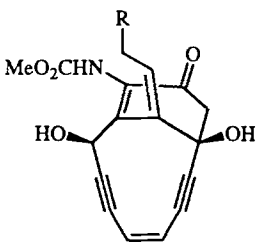
1

Calicheamicin γ_1^I reacts with supercoiled phage DNA to produce a ratio of double- to single-stranded cuts of 1:2.[5] The

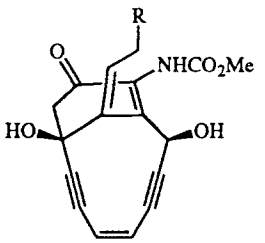
[*] Prof. S. J. Danishefsky,[+] Dr. J. Aiyar, Dr. S. A. Hitchcock, Dr. D. Denhart, Dr. K. K. C. Liu, Prof. D. M. Crothers
Department of Chemistry, Yale University
New Haven, CT 06511 (USA)
Telefax: Int. code + (203)432-5098
[+] New addresses: Memorial Sloan-Kettering Cancer Center
1275 York Avenue, New York, NY 10021 (USA)
Telefax: Int.code + (212)772-8691
and
Department of Chemistry, Havemeyer Hall
Columbia University, New York, NY 10027 (USA)
Telefax: Int. code + (212)854-7142

[**] This research was supported hy the National Institutes of Health (Grants No. CA 28824 and GM-21966). A NATO/SERC (Science and Engineering Research Council (UK)) Fellowship to S. A. H., a National Research Council (Canada) Predoctoral Fellowship to D. D.

propensity for this enediyne drug to exact double-stranded cuts is more pronounced than that of many other DNA cleaving agents.[6] In contrast, racemic calicheamicinone (**2**/**3**), which lacks the carbohydrate sector, exhibits sharply reduced capacity to effect such double-stranded cleavage[5] and furthermore exhibits none of the sequence selectivity displayed by the intact drug itself. Nonetheless, quantifiable genuine double-stranded cutting events are detected with the aglycone racemate (the ratio of double-stranded to single-stranded cuts is about 1:30).[5] In addition, reaction of DNA with racemic calicheamicinone, under conditions where the enediyne sector suffers reductive cyclization, leads to only 10% hydrogen incorporation into the aglycone by direct transfer from DNA.[5] This is in contrast to the situation in **1**, where 80–90% hydrogen incorporation by transfer from deoxyribose residues is observed in the course of reductive aromatization.[7]

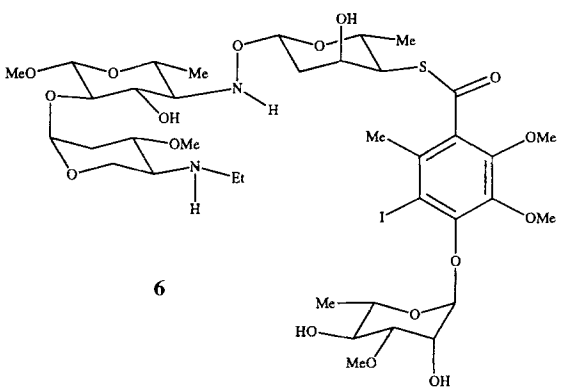


2 R = SSSMe
4 R = AcS



3 R = SSSMe
5 R = AcS

Preincubation of linear duplex DNA with the carbohydrate domain of calicheamicin in the form of its methyl glycoside **6**,[8] followed by incubation with racemic calicheamicinone led to modulation[9a] of the virtually uniform cleavage pattern observed in the absence of the carbohydrate.[9] A similar capacity is exhibited by the racemic *S*-acetate (**4**/**5**), a precursor of calicheamicinone. However, in contrast to calicheamicinone, which relies on a trisulfide trigger, the racemic *S*-acetate **4**/**5** has the advantage of being readily activated for diyl formation at pH 8 without recourse to exogenous reducing agents.[5]



6

The experiments described herein assess the contributions of each of the aglycone *S*-acetate enantiomers (**4** and **5**) to the double-stranded cutting and sequence selectivity observed in our previous studies with the racemate.[5] Compounds **4** and **5** have been prepared in enantiomerically pure form by total synthesis and converted to the two antipodes of calicheamicinone (**2** and **3**).[10, 11]

The kinetics of supercoiled phage DNA cleavage were monitored in experiments in which *S*-acetate enantiomers of natural (**5**) and unnatural absolute configuration (**4**) were incubated with DNA. Figure 1 shows that the two enantiomers displayed different degrees of double-stranded cleavage. Surprisingly, the unnatural enantiomer, **4**, with a double- to single-stranded cutting ratio of about 1:20 is four to five times more efficient in this sense than is the natural enantiomer (ratio of about 1:90 at the same concentration). On the other hand, the overall cleavage rate, the sum of single- and double- stranded cutting rates, does not differ detectably for the two enantiomers.

The absolute amount of double-stranded cutting measured in these experiments using the *S*-acetates **4** and **5**, though still formidable relative to conventional reagents, is small compared with calicheamicin itself. Therefore we do not presently propose a detailed model to explain the significant and reproducible difference in the double-stranded cleaving capacities of the two enantiomers. A possible direction for interpretation of the trend could be the presence of hydrophobic pockets in the minor groove which favor the free unnatural *S*-acetate **4** over its natural counterpart **5** in certain conformations, which allow for double-stranded cleavage.[12] We note that the possibility of enantioselective bias in the interaction of ligands with oligonucleotide hosts has been addressed in the elegant investigations of Barton et al.[13] and more recently by Boger et al.[14] However, this is the first such finding in the enediyne drug area.

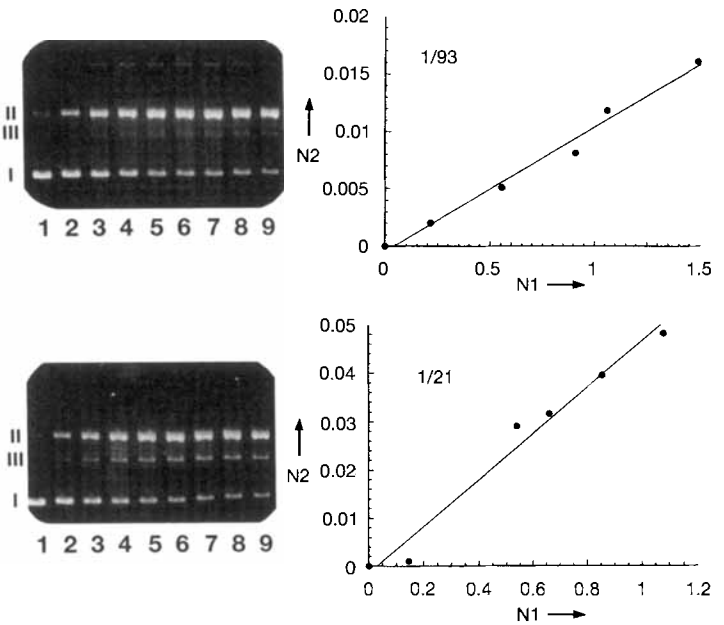


Fig. 1. Agarose gels illustrating the different degrees of double-stranded cleavage displayed by the enantiomeric aglycones **4** (bottom) and **5** (top). Supercoiled ΦX174(RFI) DNA (40 μM in nucleotides) was incubated with 0.2 mM **4** or **5** in 50 mM tris(hydroxymethyl)aminomethane (Tris), pH 8.0 at room temperature. At various times, 3 μL aliquots of each reaction mixture were added to 3 μL loading dye (0.02% bromophenol blue in 80% glycerol) and resolved on a 1% agarose gel in 1X TAE buffer (40 mM Tris acetate/2 mM EDTA) run at 6–8 Vcm^{-1}. The gels were stained in a 1.3 $\mu g mL^{-1}$ ethidium bromide solution and photographed with Polaroid 665 film. Negatives were scanned by using a model 1650 scanning densitometer (Hoefer). The average number of single-stranded (N1) and double-stranded (N2) cuts per molecule were calculated as discussed earlier [5], assuming a Poisson distribution for the formation of Form II (nicked circular) and Form III (linear) cleaved products from Form I (supercoiled) DNA. The data from the first 5–7 min of the reactions can be fitted to a linear equation (top and bottom right, respectively), giving the ratio of the average number of double- to single-stranded cuts per molecule. For both gels, lane 1: untreated DNA, lanes 2–9: extent of the reaction at 1, 2, 3, 5, 7, 10, 15, and 20 min, respectively.

 © VCH Verlagsgesellschaft mbH, D-69451 Weinheim, 1994 0570-0833/94/0808-0856 $ 10.00+.25/0

When the DNA was preincubated with the methyl glycoside of the aryl tetrasaccharide domain of calicheamicin γ_1^I **6** (5 μM), prior to addition of the aglycone, it was found that the double- to single-stranded cutting ratios decreased in both **4** and **5** (to ca. 1:50 and 1:200 respectively, Fig. 2). Possibly the carbohydrate preferentially binds the phage DNA at sites which would otherwise be targeted for double-stranded cutting by the aglycone.[12] However, the unnatural *S*-acetate enantiomer **4**, retained its greater efficacy as a double-stranded cleaving agent relative to the natural antipode **5** even under these conditions.

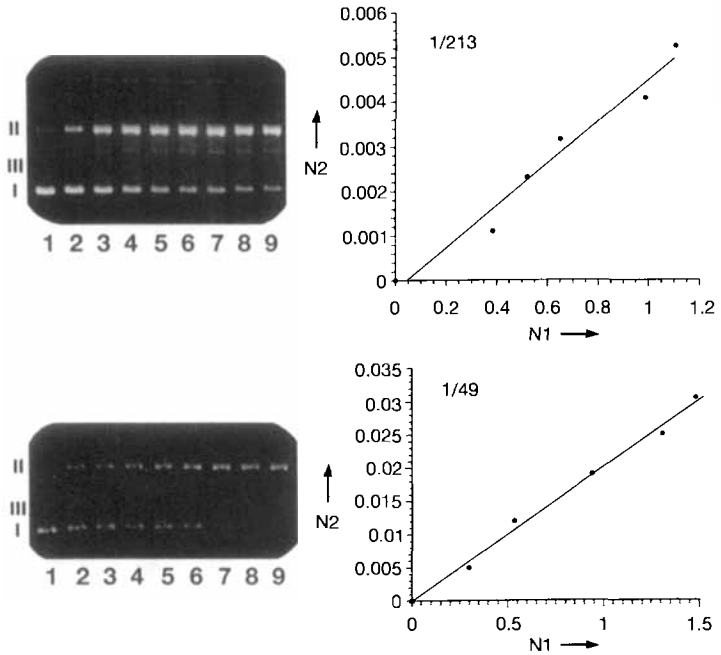


Fig. 2. Chiral preference of the aglycones **4** (bottom) and **5** (top) in the presence of the saccharide **6** in the double-stranded cleavage of DNA (agarose gel chromatographs, left). Reactions were carried out as described in Figure 1, except that the DNA was preincubated with 5 μM **6** for 15 min prior to addition of **4** or **5**. Data were analyzed as described in Figure 1, and are represented quantitatively in the top and bottom right panels. For both gels, lane 1: untreated DNA + **6**, lanes 2–9: extent of the reaction at 1, 4, 7, 10, 15, 20, 25, and 30 min, respectively. The ratio of double to single-stranded cuts is equal to the slope of the line, and is accurate to about ±15%.

Thus, the carbohydrate domain, when bound to DNA, does not appear to modulate the relative binding characteristics of the two *S*-acetate aglycone enantiomers. In addition, preincubation of the linear duplex DNA used in earlier studies[5, 9a] with methyl glycoside **6** prior to addition of either **4** or **5** gave rise to the same enhanced cutting sites flanking the carbohydrate-protected regions as were found with the racemate (Fig. 3). As before, the most prominent of the enhanced sites is at the underlined G in the CGGA sequence (marked by the lower bracket on the right side of Fig. 3). This sequence serves as one of the calicheamicin recognition domains included in the design of the DNA fragment.[5] Quantitative analysis of the gel chromatographic data (not shown) gives enhancement patterns for the two enantiomers (lanes 9–12, 14–18) which are indistinguishable from the results we reported earlier[9a] for the racemic mixture (lanes 1–4). Note that the enhanced sites (marked by arrows) are adjacent to, but frequently do not correspond exactly to calicheamicin γ_1^I cleavage sites, which can best be seen in lane 13.

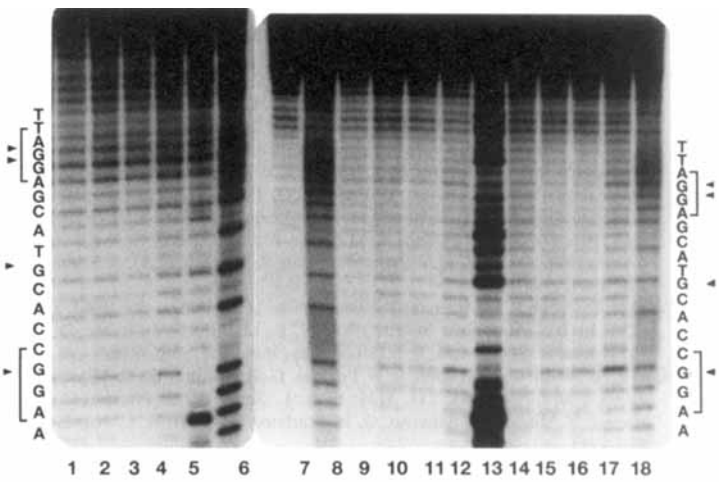


Fig. 3. Sequence selectivity of the aglycones in the presence of aryl tetrasaccharide **6** bound to DNA. The DNA sequence [5,9a] was designed to include several calicheamicin cleavage sites. Oligosaccharide and [3′-^{32}P] bottom-strand labeled DNA duplex ("bottom" with respect to orientation of calicheamicin γ_1^I at the recognition sites) were preincubated in 10 mM Tris·HCl (pH 8.0), 1 mM EDTA, 2% THF for 15 min at 25 °C. Aglycones **4**, **5**, or a racemic mixture of **4** and **5** (3.2 mM) were added to the reactions, and incubation continued for 2 h. The DNA in each reaction was ethanol-precipitated, resolved by electrophoresis on a 10% denaturing polyacrylamide gel, and autoradiographed. Lanes 1–4, reaction with racemic mixture of **4** and **5**: lane 1, DNA + aglycone; lane 2, DNA preincubated with 20 μM oligosaccharide + aglycone; lane 3, same as lane 2, but with 0.1 mM oligosaccharide; lane 4, same as lane 2, but with 0.5 mM oligosaccharide; lane 5, DNA + 5 μM **1** + (dithiothreitol) DTT, reacted at room temperature for 5 min; lane 6, A + G marker ladder. Lanes 9–12 and 14–18, reactions with individual enantiomers **5** and **4**, respectively: lane 7, untreated DNA; lane 8, A + G marker ladder; lane 9, DNA + **5**; lane 10, DNA preincubated with 20 μM oligosaccharide + **5**; lane 11, same as lane 10, but with 0.1 mM oligosaccharide; lane 12, same as lane 10, but with 0.5 mM oligosaccharide; lane 13, DNA + 5 μM **1** + DTT, reacted at room temperature for 15 min; lane 14, DNA + **4**; lane 15, DNA preincubated with 20 μM oligosaccharide + **4**; lane 16, same as lane 15, but with 0.1 mM oligosaccharide; lane 17, same as lane 15, but with 0.5 mM oligosaccharide; lane 18, A + G marker ladder. Brackets indicate strong calicheamicin γ_1^I recognition sites within the DNA sequence used in these experiments. Arrows point to strong aglycone-mediated cleavage sites adjacent to protected regions, in the presence of the oligosaccharide.

In summary, it is clear that the carbohydrate sector provides the bulk of the DNA recognition of the drug. Yet, in the absence of a covalent link between the recognition and effector (enediyne) domains, the carbohydrate is unable to override or measurably modify the inherent differences of the antipodal *S*-acetate:DNA interactions. It would therefore be of great interest to determine whether the carbohydrate domain when covalently joined to each of the enantiomeric aglycone antipodes, could modulate the characteristics of the drugs through their enediyne sectors.

Clearly the covalent attachment of the *ent* effector to the natural recognition domains can only be accomplished through the medium of organic synthesis. Another fascinating synthetic goal is that of creating hybrid agents where the effector domains of established clinically useful drugs are joined to the powerful carbohydrate recognition domain of calicheamicin.[15] On the basis of ongoing experiments, we have reason to believe that such goals are not unrealistic.

Received: January 8, 1994 [Z 6534 IE]
German version: *Angew. Chem.* **1994**, *106*, 925

[1] a) For a critical review of the field of endiyne antibiotics see: K. C. Nicolaou, W.-M. Dai, *Angew. Chem.* **1991**, *103*, 1453; *Angew. Chem. Int. Ed. Engl.* **1991**, *30*, 1387; b) For the total synthesis of calicheamicin see: K. C. Nicolaou, C. W. Hummel, M. Nakada, K. Shibayama, E. N. Pitsinos, H. Saimoto, Y. Mizuno, K.-U. Baldenius, A. L. Smith, *J. Am. Chem. Soc.* **1993**, *115*, 7625, and references therein.

[2] a) M. D. Lee, T. S. Dunne, C. C. Chang, M. M. Siegel, G. O. Morton, G. A. Ellestad, W. J. McGahren, D. B. Borders, *J. Am. Chem. Soc.* **1992**, *114*, 985; b) M. D. Lee, G. A. Ellestad, D. B. Borders, *Acc. Chem. Res.* **1991**, *24*, 235; c) M. D. Lee, T. S. Dunne, M. M. Siegel, C. C. Chang, G. O. Morton, D. B. Borders, *J. Am. Chem. Soc.* **1987**, *109*, 3464; d) M. D. Lee, T. S. Dunne, C. C. Chang, G. A. Ellestad, M. M. Siegel, G. O. Morton, W. J. McGahren, D. B. Borders, *ibid.* **1987**, *109*, 3466; e) J. Golik, J. Clardy, G. Dubay, G. Groenewold, G. H. Kawaguchi, M. Konishi, M. B. Krishnan, H. Ohkuma, K.-I. Saitoh, T. W. Doyle, *ibid.* **1987**, *109*, 3461; f) J. Golik, G. Dubay, G. Groenewold, H. Kawaguchi, M. Konishi, B. Krishnan, H. Ohkuma, K.-I. Saitoh, T. W. Doyle, *ibid.* **1987**, *109*, 3462; f) N. Zein, A. M. Sinha, W. J. McGahren, G. A. Ellestad, *Science* **1988**, *240*, 1198; g) N. Zein, M. Poncin, R. Nilakantan, G. A. Ellestad, *ibid.* **1989**, *244*, 697.

[3] a) M. P. Cabal, R. S. Coleman, S. J. Danishefsky, *J. Am. Chem. Soc.* **1990**, *112*, 3253; b) J. N. Haseltine, M. P. Cabal, N. B. Mantlo, N. Iwasawa, D. S. Yamashita, R. S. Coleman, S. J. Danishefsky, *ibid.* **1991**, *113*, 3850.

[4] a) A. L. Smith, C.-K. Hwang, E. N. Pitsinos, G. R. Scarlato, K. C. Nicolaou, *J. Am. Chem. Soc.* **1992**, *114*, 3134; b) A. L. Smith, E. N. Pitsinos, C.-K. Hwang, Y. Mizuno, H. Saimoto, G. R. Scarlato, T. Suzuki, K. C. Nicolaou, *ibid.* **1993**, *115*, 7612.

[5] J. Drak, N. Iwasawa, S. J. Danishefsky, D. M. Crothers, *Proc. Natl. Acad. Sci. USA* **1991**, *88*, 7464.

[6] a) L. F. Povirk, W. Wubker, W. Johnlein, F. Hutchinson, *Nucleic Acids Res.* **1977**, 4, 3573; b) P. C. Dedon, I. H. Goldberg, *J. Biol. Chem.* **1990**, *265*, 14713.

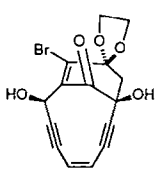
[7] a) N. Zein, W. J. McGahren, G. O. Morton, J. Ashcroft, G. A. Ellestad, *J. Am. Chem. Soc.* **1989**, *111*, 6888; b) C. A. Townsend, J. J. De voss, W.-D. Ding, G. O. Morton, G. A. Ellestad, N. Zein, A. B. Tabor, S. L. Schreiber, *ibid.* **1990**, *112*, 9669.

[8] For syntheses of the carbohydrate sector see: a) R. D. Groneberg, T. Miyazaki, N. A. Stylianides, T. J. Schulze, W. Stahl, E. P. Schreiner, T. Suzuki, Y. Iwabuchi, A. L. Smith, K. C. Nicolaou, *J. Am. Chem. Soc.* **1993**, *115* 7593; b) K. C. Nicolaou, R. D. Groneberg, T. Miyazaki, N. A. Stylianides, T. J. Schulze, W. Stahl, *ibid.* **1990**, *112*, 8193; c) R. L. Halcomb, S. H. Boyer, S. J. Danishefsky, *Angew. Chem. Int. Ed. Eng.* **1992**, *31*, 338.

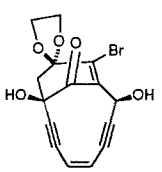
[9] For DNA binding studies see: a) J. Aiyer, S. J. Danishefsky, D. M. Crothers, *J. Am. Chem. Soc.* **1992**, *114*, 7552; b) K. C. Nicolaou, S.-C. Tsay, T. Suzuki, G. F. Joyce, *ibid.* **1992**, *114*, 7555.

[10] For the synthesis of enantiomerically pure intermediates toward calicheamicinone see: V. P. Rocco, S. J. Danishefsky, *Tetrahedron Lett.* **1991**, *32*, 6671.

[11] The enantiomerically pure ketones **7** and **8** were obtained as previously described [10] by resolution of a racemic precursor. The ketones **7** and **8** were then employed to access the *ent* and natural *S*-acetate congeners **4** and **5**, respectively, by the method disclosed for the corresponding racemate [3]. The original surmise [10] concerning the absolute configurations of **7** and **8** has now been reversed.



7



8

[12] For a detailed proposed binding model for calicheamicin with DNA see: R. C. Hawley, L. L. Kiessling, S. L. Schreiber, *Proc. Natl. Acad. Sci. USA* **1989**, *86*, 1105.

[13] a) M. D. Purugganan, C. V. Kumar, N. J. Turro, J. K. Barton, *Science* **1988**, *241*, 1645; b) H. Y. Mei, J. K. Barton, *Proc. Natl. Acad. Sci. USA* **1988**, *85*, 1339; c) J. K. Barton, J. M. Goldberg, C. V. Kumar, N. J. Turro, *J. Am. Chem. Soc.* **1986**, *108*, 2081; d) J. K. Barton, E. Lolis, *ibid.* **1985**, *107*, 708; e) J. K. Barton, J. J. Dannenberg, A. L. Rapheal, *ibid.* **1982**, *104*, 4967.

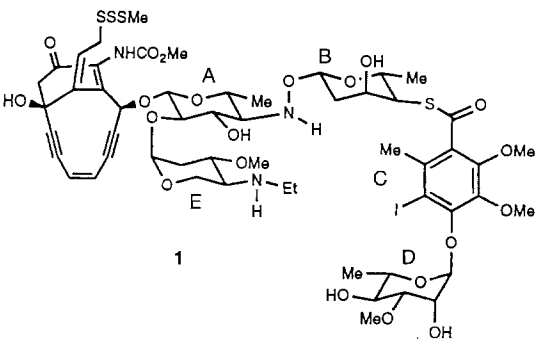
[14] D. L. Boger, K. Machiya, D. L. Hertzog, P. A. Kitos, D. Holmes, *J. Am. Chem. Soc.* **1993**, *115*, 9025. See also D. L. Boger, D. S. Johnson, W. Yun, C. M. Tarby, *Bioorg. Med. Chem. Lett.* **1994**, in press; D. L. Boger, D. S. Johnson, W. Yun, *J. Am. Chem. Soc.* **1994**, *116*, in press.

[15] For hybrids of synthetic DNA cleaving agents with the calicheamicin oligosaccharide region see: K. C. Nicolaou, E. P. Schreiner, Y. Iwabuchi, T. Suzuki, *Angew. Chem.* **1992**, *104*, 317; *Angew. Chem. Int. Ed. Engl.* **1992**, *31*, 340.

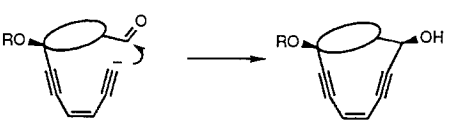
A Convergent Total Synthesis of Calicheamicin γ_1^I**

Stephen A. Hitchcock, Serge H. Boyer, Margaret Y. Chu-Moyer, Steven H. Olson, and Samuel J. Danishefsky*

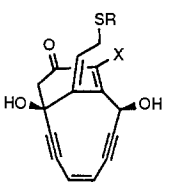
We have been concerned with the total synthesis of the enediyne antibiotic calicheamicin γ_1^I (**1**).[1, 2] In 1988 we described the first construction of a functionalized core structure corresponding to the aglycone sector of the drug. This synthesis showed the feasibility of assembling such structures by a cyclization of the type **a** → **b**, and the stereochemical ramifications of such a process at the emerging secondary alcohol.[3] Subsequently, related cyclizations have found application in a variety of other programs in the enediyne area.[4] Exploiting these findings, we accomplished the synthesis of descarbamoylcalicheamicinone (**2**)[5] and, finally, calicheamicinone (**3**)[6] both in racemic form. It was shown that these systems, lacking the carbohydrate domains,



1



a **b**



2 X = H, R = SSMe
3 X = $NHCO_2Me$, R = SSMe
4 X = H, R = Ac
5 X = $NHCO_2Me$, R = Ac

[*] Prof. S. J. Danishefsky,[+] Dr. S. A. Hitchcock, S. H. Boyer, M. Y. Chu-Moyer, S. H. Olson
Department of Chemistry, Yale University
New Haven, CT 06511 (USA)
Telefax: Int. code + (203)432-5098

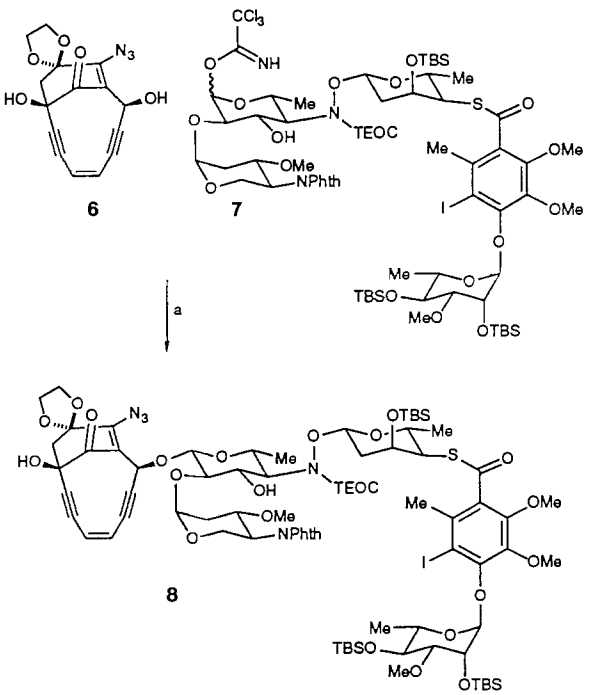
[+] New addresses: Memorial Sloan-Kettering Cancer Center
1275 York Avenue, New York, NY 10021 (USA)
Telefax: Int. code + (212)772-8691
and
Department of Chemistry, Havemeyer Hall
Columbia University, New York, NY 10027 (USA)
Telefax: Int. code + (212)854-7142

[**] This research was supported by National Institutes of Health (Grant No. CA 28824). A NATO/SERC (Science and Engineering Research Council (UK)) Fellowship to S. A. H., a Kent Fellowship to S. H. B. and M. Y. C.-M., and an NSF Predoctoral Fellowship to M. Y. C.-M. are gratefully acknowledged.

still retain significant double-stranded DNA-cleaving capacity, albeit in significantly reduced potency relative to the drug and with no appreciable sequence selectivity.[7, 8] During the course of these studies,[7] it was also demonstrated that S-acetates **4** and **5** were more readily actuated for Bergman cyclization[11] and diyl formation than were the corresponding trisulfide aglycones **2** and **3**, respectively.

From these studies we undertook a program to access enantiomerically pure versions of these aglycone derivatives. This effort culminated in the synthesis of (−)-calicheamicinone (having the absolute configuration corresponding to the natural product), as well as its (+)-enantiomer.[9, 10] As a consequence of this initiative,[9] aglycone analogues bearing the unnatural absolute configuration also became available for the first time with some surprising implications. The double-stranded DNA-cleaving capacity of these unnatural aglycone congeners was demonstrated to be significantly more effective than that of their counterparts in the natural series; thus providing the incentive to attach the enantiomeric effectors to the carbohydrate region of the natural drug.

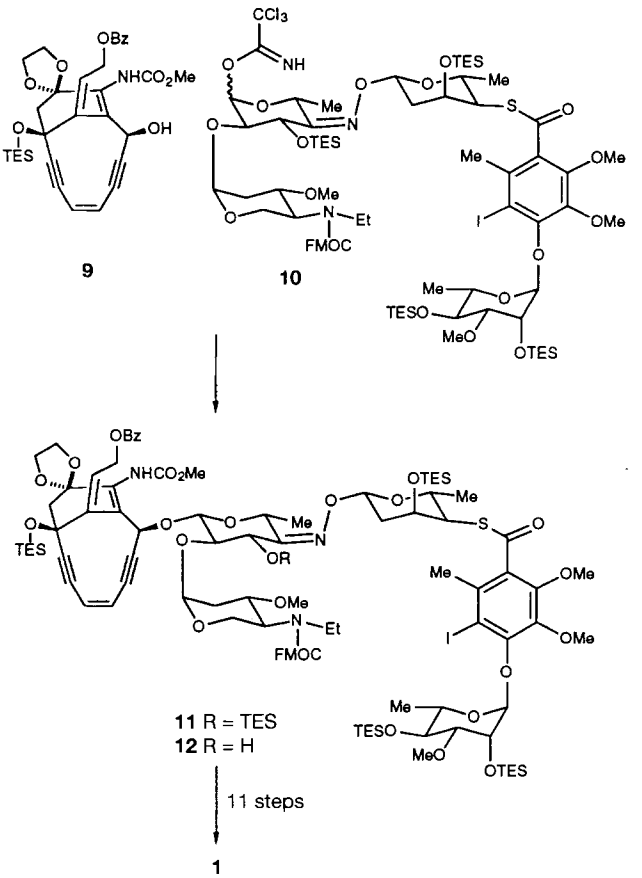
As for the carbohydrate sector, we showed (by analogy with esperamicin) that coexistence of the reducing hydroxyl and the NH function of the hydroxylamine connector would be extremely unlikely.[11] We demonstrated that the free "reducing" hydroxyl could be sustained and activated if the hydroxylamine NH group were protected, for instance, as a 2-trimethylsilylethoxycarbonyl (TEOC) function. Using these principles, we effected coupling of calicheamicinone precursor **6** with a fully functionalized pentacyclic aryl tetrasaccharide domain (see trichloroacetimidate **7**, Scheme 1).[12, 13] While this was, at the



Scheme 1. a) $BF_3 \cdot OEt_2$, Et_2O, CH_2Cl_2, −78 °C (25%). Phth = phthaloyl; TBS = *tert*-butyldimethylsilyl.

time, the most advanced coupling of its kind, it transpired that the chemistry of the steps required to get from **8** → **1** was too extensive and complex to allow for survival of the aglycone sector and the various glycosidic bonds.

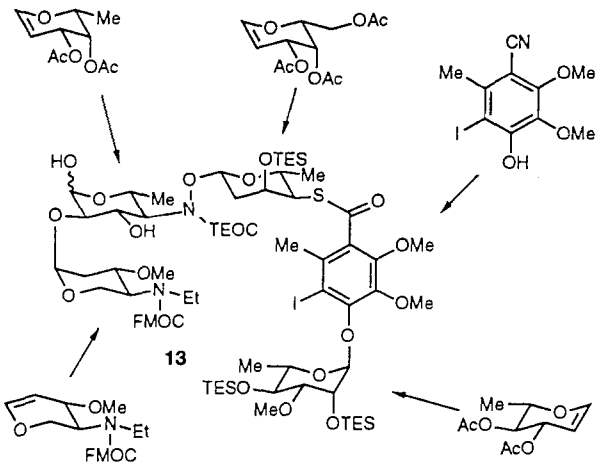
In the interim, Nicolaou et al. succeeded in coupling aglycone precursor **9** with the oxime-linked donor **10** (Scheme 2). In an experimental tour de force, adduct **11** was converted to calicheamicin (**1**) in an 11-step sequence. In that way the first total synthesis of calicheamicin was accomplished.[2]



Scheme 2. a) $BF_3 \cdot OEt_2$, CH_2Cl_2, −40 °C (40% of **11** plus 36% of **12**). TES = triethylsilyl.

Our own efforts were deployed toward determining the latest point in the synthesis in which coupling could be accomplished. For ultimate convergence, it would be necessary to fashion a glycosyl donor containing the fully functionalized pentacyclic domain at the required oxidation level. The blocking group strategy had to take into account the need to protect the hydroxylamine nitrogen, as discussed above. It was also necessary to protect the amino function of the E-ring with something other than a phthalimide since it was found that deprotection of such a nitrogen (by hydrazinolysis) would not be compatible with the labile functionality present in the aglycone. Experience gathered in our synthetic program had revealed that liberation of the axial alcohols in the B- and D-rings, from the corresponding *tert*-butyldimethylsilyl derivatives, would also not be possible in the latter stages of the synthesis for the same reason. With these considerations in mind, and with helpful precedents from the Nicolaou synthesis available,[2] donor **13** was synthesized and employed. The construction of **13** (Scheme 3) followed very closely from the glycal assembly method used in the related construction of the previously mentioned donor **7**.[12]

To achieve maximum convergency we employed a very mild trichloroacetimidate glycosylation promoter which, we hoped,

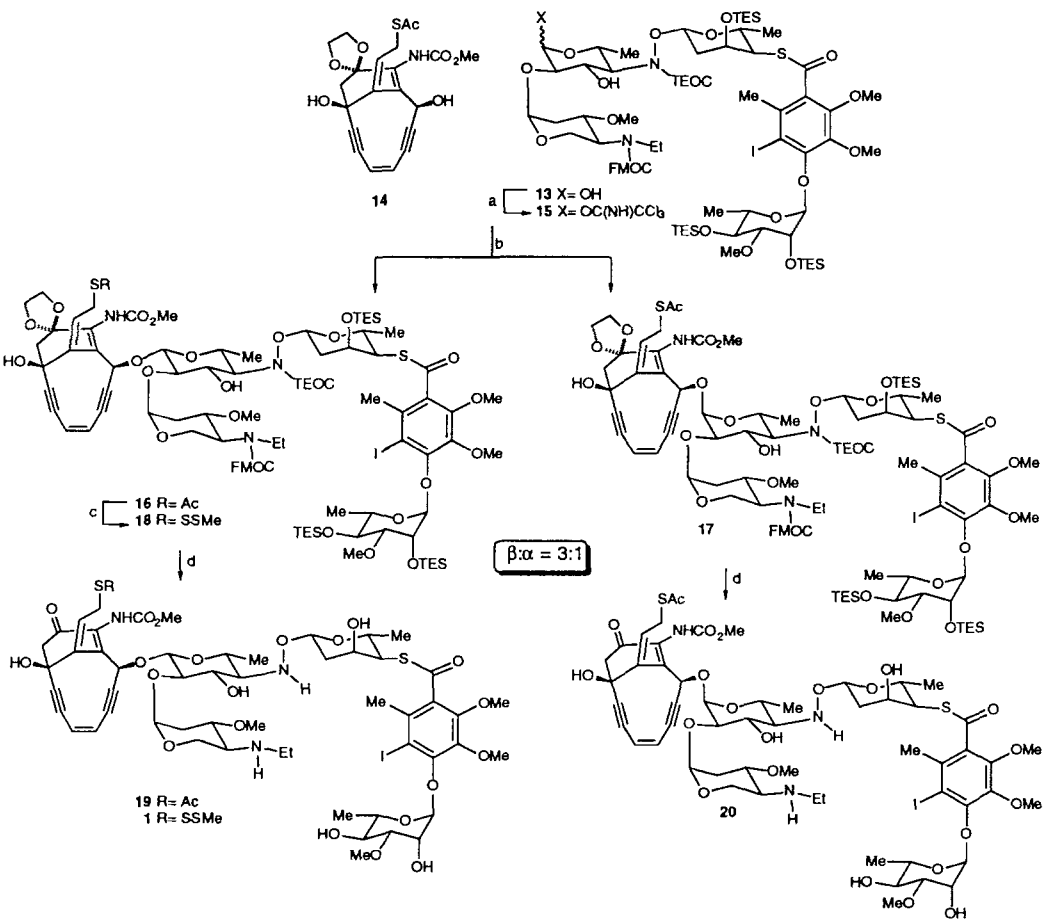


Scheme 3. Synthesis of the carbohydrate domain from four glycals and an aryl iodide.

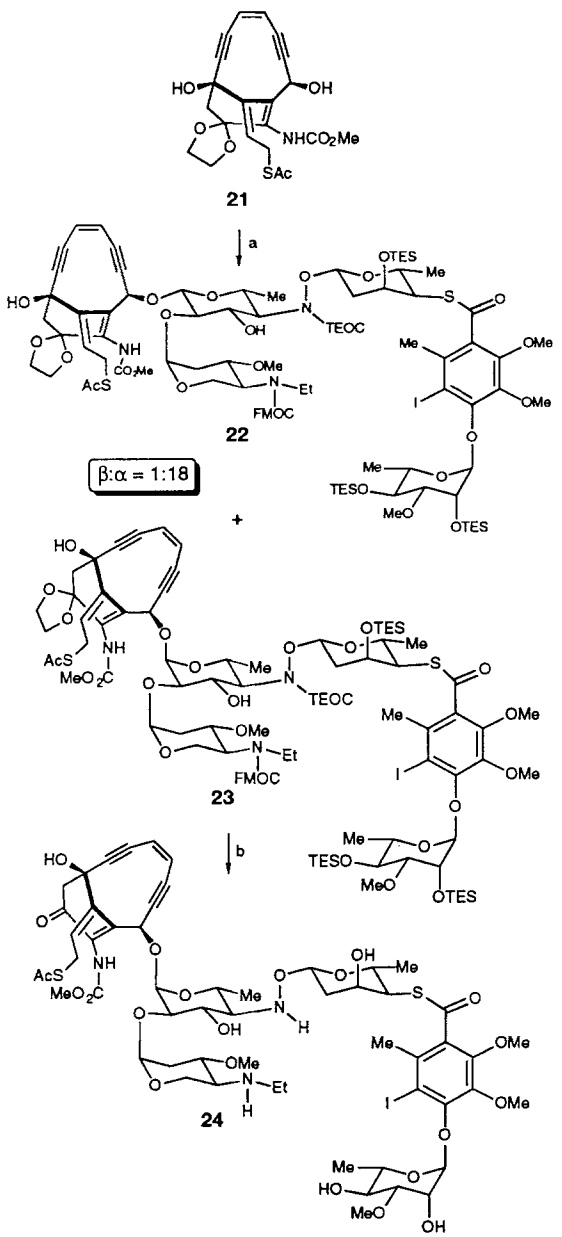
would be compatible with the highly sensitive functionality which would be contained in the acceptor (vide infra). A gratifying success was realized in the coupling of **15** with the optically pure (−)-S-acetate intermediate **14** prepared en route to **3**, as discussed above (Scheme 4). Under mediation by silver(I) triflate, in the presence of molecular sieves, a 58% yield of a separable 3:1 mixture of **16** and the corresponding α-anomer **17** was obtained.[14] Compound **16** was transformed to the corresponding trisulfide **18** as shown. Deketalization of **18**, which was accompanied by partial desilylation, was followed by tetra-*n*-butylammonium fluoride (TBAF)-induced removal of all remaining silyl groups as well as the TEOC *and* 9-fluorenylmethoxycarbonyl (FMOC) urethane protecting groups in a single step. This concise two-step deprotection sequence afforded calicheamicin γ_1^I (**1**) identical with an authentic sample[15] of the natural product by physical and spectroscopic data (TLC, $[\alpha]_D^{25}$, ^{1}H NMR, MS, and IR).

A similar two-step deprotection of **16** itself, led to **19** which is the S-acetate congener of **1**. As an additional source of corroboration for this structure, the high-field ^{1}H NMR spectrum of our synthetically prepared compound compared identically with a spectrum kindly provided by Professor K. C. Nicolaou.[16] By the same token, treatment of α-glycoside **17** afforded **20** which differs from the drug congener **19** only at the anomeric center at the A-ring of the carbohydrate sector.

A most remarkable finding was encountered in the glycosylation of the *ent*-version of **15** (i.e., **21**)[9] with the same glycosyl donor **15** (Scheme 5). The hope had been to construct a system which would be comprised of the carbohydrate domain of calicheamicin in its natural configuration, glycosidically linked to an *ent*-aglycone sector either as a trisulfide (corresponding to the *ent*-aglycone version of **1**) or as an S-acetate corresponding to the *ent*-aglycone version of **19**. Coupling of **15** with **21** gave a 38% yield of a separable mixture of two anomers (in a ratio of 1:18). Amazingly, the minor product corresponded to the β-glycoside **22** while the major product was the α-glycoside



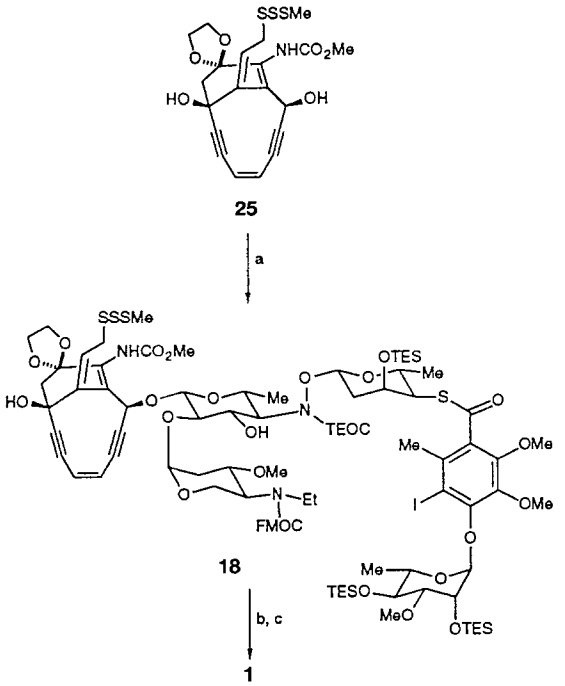
Scheme 4. Coupling of **15** with the (−)-S-acetate **14**. a) Cs_2CO_3, Cl_3CCN, CH_2Cl_2, 25 °C, 4 h (91%); b) AgOTf (Tf = trifluoromethanesulfonyl), 4 Å molecular sieves, CH_2Cl_2, 25 °C, 12 h (58%); c) diisobutylaluminum hydride (DIBAL), CH_2Cl_2, −78 °C, 0.5 h, then *N*-(methyldithio)phthalimide, CH_2Cl_2, 25 °C, 0.5 h (54%); d) camphorsulfonic acid (CSA), THF, H_2O, 25 °C, 96 h, then TBAF, THF, 0 °C, 15 min, R = Ac (40% overall), R = SSMe (37% overall).



Scheme 5. Coupling of **15** with the (+)-S-acetate **21**. a) **15**, AgOTf, 4 Å molecular sieves, CH_2Cl_2, 25 °C, 12 h (38%); b) CSA, THF, H_2O, 25 °C, 96 h, then TBAF, 0 °C, 15 min (40% overall).

23.[17] This compound was deprotected in the usual two-step sequence giving rise to **24** which is seen to be the α-glycoside version of **20** bearing the *ent*-effector domain. The evaluation of the *ent*-aglycone α-glycoside and α- and β-glycoside versions of the S-acetate drugs is now under way.

Finally, we were emboldened to attempt glycosylation at an even more advanced stage, that is, that of trisulfide **25** (Scheme 6). In the event, a 34% yield of **18** was obtained.[18] The feasibility of this coupling with the allylic trisulfide in place is eloquent testimony to the mildness of the conditions which have been devised. We note that the route communicated herein embodies ultimate convergence for the synthesis of **1**. The aglycone portion is unveiled in a single deketalization step. The entire carbohydrate domain of calicheamicin is delivered in a form where it is retrieved in a single *step* (TBAF). The success of these experiments suggests that it will be possible to attach a



Scheme 6. Glycosidation of the trisulfide aglycone **25**. a) **15**, AgOTf, 4 Å molecular sieves, CH_2Cl_2, 25 °C, 12 h (34%); b) CSA, THF, H_2O; 25 °C, 96 h; c) TBAF, THF, 15 min (32%).

variety of other carbohydrate permutants to **25** in an effort to assess the relationship of carbohydrate structure to drug performance.

Received: December 22, 1993 [Z 6576 1E]
German version: *Angew. Chem.* **1994**, *106*, 928

[1] For a critical review of the field of enediyne antibiotics, see: a) K. C. Nicolaou, *Angew. Chem.* **1993**, *105*, 1462; *Angew. Chem. Int. Ed. Engl.* **1993**, *32*, 1377; b) K. C. Nicolaou, W.-M. Dai, *ibid.* **1991**, *103*, 1453 and **1991**, *30*, 1387.

[2] For the only total synthesis of calicheamicin, see: a) K. C. Nicolaou, C. W. Hummel, E. N. Pitsinos, M. Nakada, A. L. Smith, K. Shibayama, H. Saimoto, *J. Am. Chem. Soc.* **1992**, *114*, 10082; b) R. D. Groneberg, T. Miyazaki, N. A. Stylianides, T. J. Schulze, W. Stahl, E. P. Schreiner, T. Suzuki, Y. Iwabuchi, A. L. Smith, K. C. Nicolaou, *ibid.* **1993**, *115*, 7593; c) A. L. Smith, E. N. Pitsinos, C.-K. Hwang, Y. Mizuno, H. Saimoto, G. R. Scarlato, T. Suzuki, K. C. Nicolaou, *ibid.* **1993**, *115*, 7612; d) K. C. Nicolaou, C. W. Hummel, M. Nakada, K. Shibayama, E. N. Pitsinos, H. Saimoto, Y. Mizuno, K.-U. Baldenius, A. L. Smith, *ibid.* **1993**, *115*, 7625.

[3] a) S. J. Danishefsky, N. B. Mantlo, D. S. Yamashita, G. Schulte, *J. Am. Chem. Soc.* **1988**, *110*, 6890; b) For a related cyclization of a less advanced model, see: A. S. Kende, C. A. Smith, *Tetrahedron Lett.* **1988**, *29*, 4217.

[4] Calicheamicin: a) C. Crévisy, J.-M. Beau, *Tetrahedron Lett.* **1991**, *32*, 3171; b) M. F. Semmelhack, J. J. Gallager, T. Minami, T. Date, *J. Am. Chem. Soc.* **1993**, *115*, 11618. Dynemicin: c) K. C. Nicolaou, C.-K. Hwang, A. L. Smith, S. V. Wendeborn, *J. Am. Chem. Soc.* **1990**, *112*, 7416; d) T. Nishikawa, M. Isobe, T. Goto, *Synlett* **1991**, 393; e) P. A. Wender, C. K. Zercher, *J. Am. Chem. Soc.* **1991**, *113*, 2311; f) P. A. Wender, C. K. Zercher, S. Beckham, E.-M. Haubold, *J. Org. Chem.* **1993**, *58*, 5867. Neocarzinostatin chromophore: g) A. G. Myers, P. M. Harrington, E. Y. Kuo, *J. Am. Chem. Soc.* **1991**, *113*, 694.

[5] a) J. N. Haseltine, S. J. Danishefsky, G. Schulte, *J. Am. Chem. Soc.* **1989**, *111*, 7638; b) J. N. Haseltine, S. J. Danishefsky, *J. Org. Chem.* **1990**, *55*, 2576. For the first synthesis of a trisulfide, see: c) P. Magnus, R. T. Lewis, F. Bennett, *J. Chem. Soc. Chem. Commun.* **1989**, 916.

[6] a) M. P. Cabal, R. S. Coleman, S. J. Danishefsky, *J. Am. Chem. Soc.* **1990**, *112*, 3253; b) J. N. Haseltine, M. P. Cabal, N. B. Mantlo, N. Iwasawa, D. S. Yamashita, R. S. Coleman, S. J. Danishefsky, G. K. Schulte, *ibid.* **1991**, *113*, 3850.

[7] J. Drak, N. Iwasawa, S. J. Danishefsky, D. M. Crothers, *Proc. Natl. Acad. Sci. USA* **1991**, *88*, 7464.

[8] a) J. Aiyar, S. J. Danishefsky, D. M. Crothers, *J. Am. Chem. Soc.* **1992**, *114*, 7552; b) K. C. Nicolaou, S.-C. Tsay, T. Suzuki, G. F. Joyce, *ibid.* **1992**, *114*, 7555.

[9] J. Aiyar, S. A. Hitchcock, D. J. Denhart, K. K.-C. Liu, S. J. Danishefsky, D. M. Crothers, *Angew. Chem.* **1994**, *106*, 925; *Angew. Chem. Int. Ed. Engl.* **1994**, *33*, 855.
[10] For the first total synthesis of (−)-calicheamicinone, see: A. L. Smith, C.-K. Hwang, E. N. Pitsinos, G. R. Scarlato, K. C. Nicolaou, *J. Am. Chem. Soc.* **1992**, *114*, 3134.
[11] a) R. L. Halcomb, M. D. Wittman, S. H. Olson, S. J. Danishefsky, J. Golik, H. Wong, D. Vyas, *J. Am. Chem. Soc.* **1991**, *115*, 5080. For the first synthesis of the carbohydrate domain of calicheamicin as its methyl glycoside, see: b) K. C. Nicolaou, R. D. Groneberg, T. Miyazaki, N. A. Stylianides, T. J. Schulze, W. Stahl, *J. Am. Chem. Soc.* **1990**, *112*, 8193.
[12] R. L. Halcomb, S. H. Boyer, S. J. Danishefsky, *Angew. Chem.* **1992**, *104*, 314; *Angew. Chem. Int. Ed. Engl.* **1992**, *31*, 338.
[13] Carbohydrate domain **9** (vide infra) was coupled through a spacer to a dynemicin model: K. C. Nicolaou, E. P. Schreiner, Y. Iwabuchi, T. Suzuki, *Angew. Chem.* **1992**, *104*, 317; *Angew. Chem. Int. Ed. Engl.* **1992**, *31*, 340.
[14] S. P. Douglas, D. M. Whitfield, J. J. Krepinsky, *J. Carb. Chem.* **1993**, *12*, 131.
[15] We thank Drs. G. A. Ellestad and D. B. Borders of Lederle Laboratories for supplying an authentic sample of calicheamicin γ_1^I.
[16] We thank Professor K. C. Nicolaou for apprising us of the existence of this compound and of its potent biological activity prior to publication. See also K. C. Nicolaou, T. Li, M. Nakada, C. W. Hummel, A. Hiatt, W. Wrasidlo, *Angew. Chem.* **1994**, *106*, 195; *Angew. Chem. Int. Ed. Engl.* **1994**, *33*, 183.
[17] For a previous example of double stereodifferentiation in glycosylation, see: N. M. Spijker, C. A. A. van Boeckel, *Angew. Chem.* **1991**, *103*, 179; *Angew. Chem. Int. Ed. Engl.* **1991**, *30*, 180.
[18] None of the corresponding α-anomer has been detected as of this writing.

Donor-Stabilized Aluminum(II) Bromide**

Mario Mocker, Christian Robl, and Hansgeorg Schnöckel*

Dedicated to Professor Helmut Werner on the occasion of his 60th birthday

Boron and gallium dihalides have been known for a long time; however, hitherto no evidence could be found for AlX_2 compounds (X = halogen) in the condensed phase.[1] AlX_2 structures are of particular interest: whereas boron dihalides, such as BCl_2, exist as dimers with a boron–boron bond (B_2Cl_4), solid $GaCl_2$ must be formulated, for example, as $Ga^I[Ga^{III}Cl_4]$. The latter compound, however, can be converted into a molecular species with a Ga–Ga bond (e.g. $Cl_2GaGaCl_2 \cdot 2$dioxane) by addition of suitable bases.[4, 5] Thus, boron and gallium are similiar to each other with regard to their ability to form element–element bonds. Hence corresponding base-stabilized species $Al_2X_4 \cdot 2$donor with an Al–Al bond are to be expected also in the case of aluminum. This expectation was intensified by the characterization of an Al–Al bond in Al_2R_4 (R = $CH(SiMe_3)_2$) by Uhl et al.[7] We report here on the preparation and structure of the first base-stabilized Al^{II} halide.

The title compound was prepared by depositing the high-temperature molecule AlBr[8] together with anisole on a surface cooled with liquid nitrogen.[10] By warming this mixture above the melting point of anisole a red solution of AlBr is obtained, which on further warming to room temperature decomposes within a few days. This process is, however, so slow at −30 °C that $AlBr_2$ can form continuously from AlBr and the $AlBr_3$ (max. 10%) which is present as a consequence of the method of preparation. $AlBr_2$ crystallizes in the form of yellow needles of the composition $Al_2Br_4 \cdot 2$anisole **1** on slow condensation of pentane into the mixture [Eq. (a)]. In this way the major product AlBr is deposited as a red oil on the walls of the flask.[13]

$$AlBr + AlBr_3 \xrightarrow[-30\,^\circ C]{\text{anisole}} \underset{\mathbf{1}}{Al_2Br_4 \cdot 2\,\text{anisole}} \qquad \text{(a)}$$

In the solid state **1** can be stored at room temperature and can be prepared in a glove box for additional investigations (e.g. X-ray diffraction, Raman spectroscopy). On warming solid **1** above 100 °C, however, significant decomposition takes place. In toluene or C_6D_6, **1** disproportionates at room temperature within a few hours. The ^{27}Al NMR spectrum of a freshly prepared sample of **1** shows a broad signal at $\delta \approx 130$ as well as an additional signal at $\delta = 95$, which is assigned to the adduct $AlBr_3 \cdot$anisole and which indicates the beginning of the disproportionation.[14] In the Raman spectrum the totally symmetric $AlBr_2$ stretching vibration is found at 188 cm^{-1} and the Al–Al vibration at 510 cm^{-1}.[15] In the mass spectrometer **1** cannot be vaporized without decomposition, the heaviest fragment to appear is $[M^+ - OCH_2]$.[18]

The molecular structure of **1** resulting from the X-ray structure analysis is illustrated in Figure 1.[19] The Al–Br distance

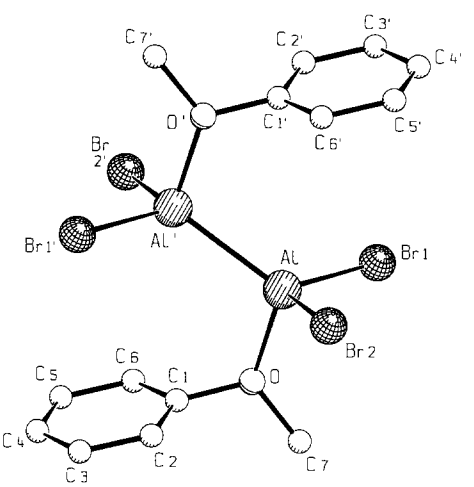


Fig. 1. Molecular structure of **1** in the crystal (hydrogen atoms are not shown). Selected bond lengths [pm] and angles [°] (standard deviations in parentheses): Al–Al' 252.7(6), Al–Br1 229.9(4), Al–Br2 231.2(4), Al–O 193.0(8); Br1-Al-Br2 108.4(1), Br1-Al-O 100.6(3), Br2-Al-O 100.8(3), Br1-Al-Al' 119.2(2), Br2-Al-Al' 117.8(2), O-Al-Al' 106.9(3).

(230 pm) is, as expected, longer than the Al–Br distance found in $AlBr_3$.[20] The $Br_2AlAlBr_2$ framework has approximate C_{2h} symmetry; the $AlBr_2$ planes are each bent by 35° away from the line through the bond between the two aluminum centers. The coordination of anisole results in a distorted tetrahedral environment for each Al atom. The Al–O bond (193 pm) is short in comparison to the Al–O bond of $AlMe_3 \cdot Me_2O$ (201 pm[23]). There is no corresponding structural data available for an adduct $AlBr_3 \cdot R_2O$ which would be more suitable for comparison.[24] A comparison of the dissociation enthalpies ($AlBr_3 \cdot Et_2O$: 36.5/39.1 kcal mol^{-1}, $AlMe_3 \cdot Et_2O$: 20.2 kcal mol^{-1}[26]), however, indicates a strengthening of the Al–O bond in the adduct $AlBr_3 \cdot$ether.

[*] Prof. Dr. H. Schnöckel
Institut für Anorganische Chemie der Universität
Engesserstrasse 1, Geb.-Nr. 30.45, D-76131 Karlsruhe (FRG)
Telefax: Int. code + (721)608-4854
Dipl.-Chem. M. Mocker, Prof. Dr. C. Robl
Institut für Anorganische und Analytische Chemie der Universität Jena (FRG)

[**] This work was supported by the Deutsche Forschungsgemeinschaft and the Fonds der Chemischen Industrie.

The most remarkable structural feature of **1** is the short Al–Al bond (252.7 pm). This bond is comparable in length to the Al–Al bond in the radical anion $[R_2AlAlR_2]^{\bullet-}$ (R = $CH(SiMe_3)_2$) (253 pm) which is strengthened by π bonding contributions.[27] The single occupation of a bonding π orbital for R_2AlAlR_2 ($d_{(Al-Al)}$ = 266 pm[7]) thus leads to the same increase in bond strength as the replacement of the substituents R by bromine atoms and at the same time to donor stabilization by anisole. Apparently, in both cases repulsive Al–Al interactions, which arise from positive partial charges, are weakened in the same way. In contrast, the Al–Al bond in the radical anion $[Trip_2AlAlTrip_2]^{\bullet-}$ (Trip = 2,4,6-*i*$Pr_3C_6H_2$) of 247 pm is significantly shorter than that of **1**; the Al–Al bond length in the neutral $Trip_2AlAlTrip_2$ of 264.7 pm differs only slightly from that in R_2AlAlR_2 (R = $CH(SiMe_3)_2$).[28] Comparable relationships are also observed in the analogous gallium compounds. For instance, the Ga–Ga distance in the radical anion $[Trip_2GaGaTrip_2]^{\bullet-}$ (234.3 pm)[29] is considerably shorter than that in $Ga_2Br_4 \cdot 2$dioxane (239 pm[30]).

The preparation and characterization of **1** shows that with this synthesis strategy both additional R_2AlAlR_2 species and additional aluminum(II) halides and chalcogenides should be accessible.

Received: November 10, 1993 [Z 6489 IE]
German version: *Angew. Chem.* **1994**, *106*, 946

[1] Molecular $AlCl_2$ has been detected in low concentrations in addition to AlCl and $AlCl_3$ in high-temperature equilibria [2]; in noble gas matrices it is formed from aluminum atoms and Cl_2 [3]. It is questionable whether, as described in [3], $AlCl_2$ and $AlBr_2$ can be prepared at temperatures from 120 °C to 570 °C. According to our observations a rapid disproportionation into aluminum and AlX_3 (X = Cl, Br) occurs under these conditions.

[2] a) B. J. Chai, H. C. Ko, M. A. Greenbaum, M. Farber, *J. Phys. Chem.* **1967**, *71*, 3331; b) M. Farber, S. P. Harris, *High Temp. Sci.* **1971**, *3*, 231.

[3] G. A. Olah, O. Farooq, S. M. F. Farnia, M. R. Bruce, F. L. Clouet, P. R. Morton, G. K. Surya Prakash, R. C. Stevens, R. Bau, K. Lammertsma, S. Suzer, L. Andrews, *J. Am. Chem. Soc.* **1988**, *110*, 3231.

[4] J. C. Beamish, R. W. Small, I. J. Worrall, *Inorg. Chem.* **1979**, *18*, 220.

[5] The addition of halide ions also leads to species with Ga–Ga bonds, for example, $Ga_2Cl_6^{2-}$ [6].

[6] W. Hönle, G. Miller, A. Simon, *J. Solid State Chem.* **1988**, *75*, 147.

[7] W. Uhl, *Z. Naturforsch. B* **1988**, *43*, 1113.

[8] AlBr was prepared analogously to AlCl [9] from Al and HBr.

[9] M. Tacke, H. Schnöckel, *Inorg. Chem.* **1989**, *28*, 2895.

[10] The deposition of gaseous $AlBr_2$ is not suitable for the preparation of solid $AlBr_2$ in preparative quantities, since the concentration of this species in comparison to the concentration of AlBr under our preparation conditions is very low (in earlier experiments for the preparation of AlBr in matrices no indications of $AlBr_2$ were found [11]). If the equilibrium distribution is roughly estimated for $AlCl_2$ (only for this species are thermodynamic data known [12]), it is shown that in the presence of AlCl and liquid aluminum at about 1200 K, the concentration of $AlCl_2$ is only about 0.1 % of the concentration of AlCl.

[11] H. Schnöckel, *Z. Naturforsch. B* **1976**, *31*, 1291.

[12] M. W. Chase, Jr., C. A. Davies, J. R. Downey, Jr., D. J. Frurip, R. A. McDonal, A. N. Syverud, *JANAF Thermochemical Tables*, 3rd edition, ACS, AIP, NBS, Midland, MI, **1985**.

[13] We also expect a structure stabilized by the formation of Al–Al bonds or by coordination of anisole for AlBr. We are currently trying to further purify and to fully characterize this compound.

[14] NMR spectra (Jeol-GSX-270, C_6D_6, 25 °C): $\delta(^{27}Al)$ = 130 ($\omega_{1/2}$ = 3000 Hz), 95 (based on $[Al(H_2O)_6]^{3+}$ as external standard); $\delta(^1H)$ = 3.52 (3 H), 6.81, 6.92 (5 H) (based on TMS).

[15] This assignment is based on a comparison of the observed bands of stronger intensity [16] in the low-frequency region between 510 and 85 cm^{-1} with the Raman frequencies of Si_2Br_6: ν(SiSi) 562, $\nu_s(SiBr_3)$ 229, $\delta_s(SiBr_3)$ 80, $\nu_{as}(SiBr_3)$ 479, $\delta_{as}(SiBr_3)$ 134, ρ($SiBr_3$) 89 cm^{-1} [17]. After an additional comparison with a section from the Raman spectrum of anisole (108, 266, and 444 cm^{-1}) the following assignment seems plausible for several of the remaining bands: 85 cm^{-1}: ρ($AlBr_2$) or $\delta_s(AlBr_2)$; 137 cm^{-1}: $\delta_{as}(AlBr_2)$; 492 cm^{-1}: $\nu_{as}(AlBr_2)$.

[16] Raman spectrum: Bruker FT Ramanscope IFS66/FRA 106, Nd: YAG laser, 1064 nm. $\tilde{\nu}$[cm^{-1}] (rel. int.) = 3066(6.5), 3042(1.5), 2955(3), 2832(0.5), 1599(1.5), 1585(1.5), 1449(0.5), 1428(0.5), 1205(0.5), 1168(1), 1156(1), 1138(2), 1069(0.5), 1021(1), 1005(5), 945(1.5), 792(1), 760(2), 691(0.5), 612(1), 510(2), 492(0.5), 392(0.5), 300(1), 236(0.5), 220(2), 188(10), 137(6), 109(5), 85(7).

[17] F. Höfler, W. Sawodny, E. Hengge, *Spectrochim. Acta Part A* **1970**, *26*, 819.

[18] Mass spectrum: Finnigan MAT MS 71 (EI, 70 eV), *m/z* (%) 560 (29) $[M^+ - 0CH_2]$, 292 (22) $[M^+ - OCH_2 - AlBr_3]$, 280 (17) $[AlBr_2OC_6H_5^+]$, 94 (100) $[C_6H_5OH^+]$.

[19] X-ray structure analysis: $C_{14}H_{16}O_2Al_2Br_4$, molecular weight 589.9 $g\,mol^{-1}$, monoclinic, space group $P2_1/n$, a = 790.9(3), b = 1550.2(7), c = 873.0(4) pm, β = 95.98(4)°, V = 1064.6(8) × 10^6 pm^3, Z = 2, ρ_{calcd} = 1.840 $g\,cm^{-3}$, $F(000)$ = 564, μ = 2.34 cm^{-1} ($Mo_{K\alpha}$), 295 K, ($\omega/2\theta$) scan, θ_{max} = 25°, measurement rate 3.45–14.65 ° min^{-1}, scan width 1.5°, Siemens R3m/V diffractometer, graphite monochromator, of 2106 measured reflections, 1876 are symmetry independent, R_{int} = 0.0859; 1320 reflections with $|F| > 3\sigma_{|F|}$ were classified as observed. Calculations with SHELXTL PLUS, 102 parameters, H atoms geometrically positioned, non-hydrogen atoms refined anisotropically, empirical absorption correction; R = 0.0763, R_w = 0.0542, R_g = 0.0468, $w = \sigma|F|^{-2}$. Limits of the final difference Fourier synthesis + 0.83/−0.87 e × 10^{-6} pm^3. Further details of the crystal structure investigation may be obtained from the Fachinformationszentrum Karlsruhe, D-76344 Eggenstein-Leopoldshafen (FRG) on quoting the depository number CSD-58057.

[20] The structure of $AlBr_3$ in the gas phase has so far not been investigated. However, the Al–Br distance should correspond to that of the terminal Al–Br bond in Al_2Br_6 (222 pm [21]), since the terminal Al–Cl distance in Al_2Cl_6 corresponds to that in $AlCl_3$ [22].

[21] P. A. Akishin, N. G. Rambidi, E. Z. Zasovin, *Sov. Phys. Crystallogr. Engl. Transl.* **1959**, *4*, 167.

[22] I. Hargittai, M. Hargittai, *J. Chem. Phys.* **1974**, *60*, 2563.

[23] A. Haaland, S. Samdal, O. Stokkeland, J. Weidlein, *J. Organomet. Chem.* **1977**, *134*, 165.

[24] In the only X-ray crystallographic investigation of $AlBr_3 \cdot Et_2O$ [25] of which we are aware, no Al–O distance was given.

[25] K. N. Semenenko, E. B. Lobkovskii, V. N. Fokin, *Russ. J. Inorg. Chem. Engl. Transl.* **1973**, *18*(*10*), 1443.

[26] A. Haaland in *Coordination Chemistry of Aluminum* (Ed.: G. H. Robinson), VCH, New York, **1993**, p. 9.

[27] C. Pluta, K.-R. Pörschke, C. Krüger, K. Hildenbrand, *Angew. Chem.* **1993**, *105*, 451; *Angew. Chem. Int. Ed. Engl.* **1993**, *32*, 388.

[28] R. J. Wehmschulte, K. Ruhlandt-Senge, M. M. Olmstead, H. Hope, B. E. Sturgeon, P. P. Power, *Inorg. Chem.* **1993**, *32*, 2983.

[29] X. He, R. A. Bartlett, M. M. Olmstead, K. Ruhandt-Senge, B. E. Stargeon, P. P. Power, *Angew. Chem.* **1993**, *105*, 761; *Angew. Chem. Int. Ed. Engl.* **1993**, *32*, 717.

[30] R. W. H. Small, I. J. Worrall, *Acta Crystallogr. B* **1982**, *38*, 250.

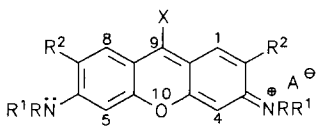
3,6-Diazaxanthylium Salts: Dyes with a New Chromophore**

Lutz Eggers, Walter Grahn,* Wolfgang Lüttke, Burkhard Knieriem, Peter G. Jones, and Axel Chrapkowski

Amongst xanthene dyes[1] rhodamines (**1**) are of scientific interest[2] and have found diverse commercial applications[3] (e.g., since 1967 as laser dyes[2b, 4]); this is particularly so for rhodamine B (**1a**) and rhodamine 6G (**1b**).[2, 3] We were interested in potential changes in the properties of **1** if the nitrogen atoms were not bonded peripherally to the xanthylium framework as in **1**, but instead formed part of the tricyclic framework as in the 3,6-diazaxanthylium salts (**2**). Heterocycles with the parent framework of **2** were previously unknown.

[*] Priv.-Doz. Dr. W. Grahn, Dipl.-Chem L. Eggers
Institut für Organische Chemie der Technischen Universität
Hagenring 30, D-38106 Braunschweig (FRG)
Telefax: Int. code + (531)391-5388
Prof. Dr. W. Lüttke, Dr. B. Knieriem
Institut für Organische Chemie der Universität Göttingen (FRG)
Prof. Dr. P. G. Jones, A. Chrapkowski
Institut für Anorganische und Analytische Chemie
der Technischen Universität Braunschweig (FRG)

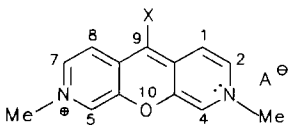
[**] Part of the Ph.D. thesis of L. Eggers, Technische Universität Braunschweig, **1993**. We thank Priv.-Doz. Dr. H. G. Löhmannsröben and Dipl.-Chem. J. Küster, Institut für Physikalische und Theoretische Chemie der Technischen Universität Braunschweig, for recording the fluorescence spectra.



1

1a X = 2-COOH-C_6H_4
R = R^1 = Et, R^2 = H, A = Cl

1b X = 2-COOEt-C_6H_4
R = H, R^1 = Et, R^2 = Me, A = Cl



2

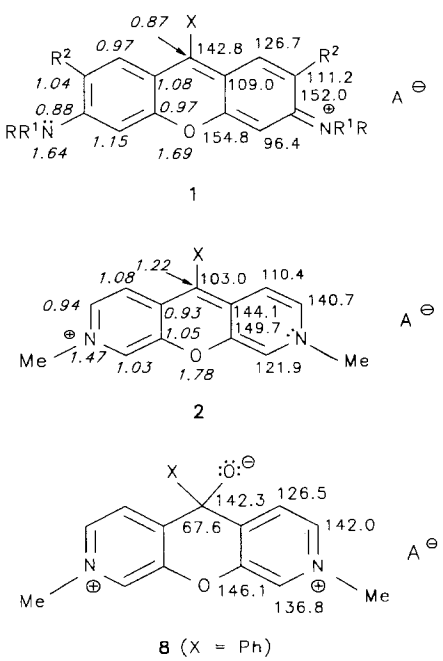
2a X = Ph, A = BF_4
2b X = 4-CF_3-C_6H_4, A = BF_4

In order to be able to make a prediction about the absorption of light, we calculated the positions of the electronic absorption bands of **1** and **2** using the PPP method[5] (Table 1 , Scheme 1).

Table 1. Longest wavelength absorption maxima λ_A, fluorescence maxima λ_F, and fluorescence quantum yields ϕ_F of **1**, **2**, and **8a**; A^- = counterion.

No.	X (R,R^1,R^2)	A^-	λ_A [nm] (ε_{max})	λ_F [nm] (ϕ_F)	Solvent	
1'	H (R = R^1 = R^2 = H)	–	495 (36300)	–	–	[a]
1a	2-COOH-C_6H_4 (R = R^1 = Et, R^2 = H)	Cl	554 (106000)	576 (0.54)	EtOH/H^+	[2b]
1b	2-COOEt-C_6H_4 (R = H, R^1 = Et, R^2 = Me)	Cl	530 (111000)	553 (0.95)	EtOH	[2b]
2'	H		649 (6800)	–	–	[a]
2a	Ph	BF_4	630 (24100)	654 (0.17)	CH_2Cl_2	[b]
2b	4-CF_3-C_6H_4	BF_4	614 (19400)	645 (0.12)	Me_2CO	[b]
8a	Ph	BF_4	268 (20700)		CH_2Cl_2	

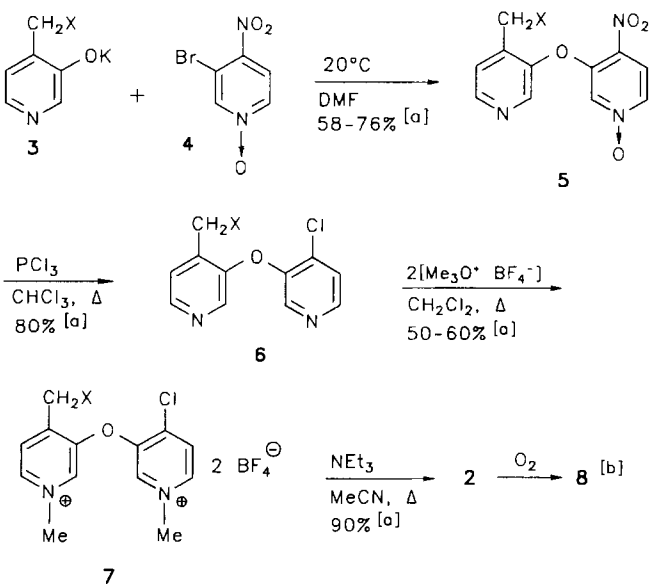
[a] Calculated by the PPP method [5]. [b] Quantum corrected.



Scheme 1. Compounds **1**, **2**, and **8a**: Chemical shifts δ of the methine C atoms and π-charge densities q_π (numbers in italics) at the centers of the tricyclic frameworks in the ground state, calculated by the PPP method [5] (except for **8a**). [**1**: q_π : **1'** (X = H); δ(^{13}C NMR): **1a**(X = 2-COOH-C_6H_4) [6]. **2**: q_π : **2'** (X = H); δ(^{13}C NMR): **2a**(X = Ph)].

We found that **2**, despite its smaller π-electron system, should absorb at considerably longer wavelengths than **1** (**2**: λ_{max}(PPP) = 649 nm, **1**: λ_{max}(PPP) = 495 nm; **2**: 16 π electrons, 14 π orbitals, **1**: 18 π electrons, 16 π orbitals). This unexpected prediction prompted us to synthesize two compounds of type **2**, and to investigate them by X-ray crystallography, spectroscopically, and with regard to their reactivity.

Starting materials for the synthesis of **2** were the 3,4-disubstituted pyridines **3** and **4** (Scheme 2). In addition to the pyridine nitrogen atom, potassium-4-benzyl-3-pyridinolate (**3**)[7] contains two further nucleophilic centers, namely the pyridinolate oxygen atom and (in the latent form) the methylene group. 3-Bromo-4-nitropyridine-1-oxide (**4**) undergoes regioselective nucleophilic attack by **3** at the 3-position with formation of 3,3'-oxybispyridine (**5**) at room temperature in dimethylformamide (DMF). Subsequent heating of **5** with phosphorus trichloride yields the ether **6** by deoxygenation[8] and replacement of the nitro group by chlorine. The dicationic salt **7**, the methylene protons of which are more acidic than those of **6**, is produced by forming two quaternary nitrogen atoms using Meerwein's reagent. If **7** is treated with triethylamine in a polar solvent such as acetonitrile, the reaction solution turns blue. The initially formed benzyl anion nucleophilically attacks the C atom bearing the chlorine substituent. After elimination of HCl, the salts **2** can be isolated as violet crystals with a metallic luster. Attempts to obtain the parent compound **2** (X = H) from the dication **7** with X = H have as yet been unsuccessful.[9]



Scheme 2. Synthesis of the 3,6-diazaxanthylium salt **2**. [a] Yield for X = phenyl; [b] the structure of **8** is shown in Scheme 1.

The cations of **2a** and **2b** contain a previously unreported heterocyclic central framework. The structures of **2a,b** may be deduced from spectroscopic and X-ray data: In the FAB^+ mass spectra (matrix: 3-nitrobenzyl alcohol) of **2a** and **2b**, the base peaks occur at the expected m/z values of 289 and 357, respectively. The ^{1}H and ^{13}C NMR spectra of **2a** and **2b** differ significantly from those of their respective precursors **7** and are only consistent with a symmetrical structure.

The structures of both dyes **2** were confirmed by X-ray structural analyses at −130 (**2a**) and −100 °C (**2b**).[10] Suitable crystals were obtained by using tetraphenylborate as counterion.

The chemically equivalent bonds of **2a** and **2b** are the same length as those of **1b**[11a] to within about 1 pm. Unlike the exactly planar tricyclic parent framework of the xanthene dye **1b**,[11a] both cations are clearly tilted about the central axis O10 · · · C9; the left and right halves are planar to within 1 pm and form an interplanar angle of 5°. The phenyl substituents are positioned similarly as for xanthenes (**1**), approximately perpendicular to the best plane through the tricycle (interplanar angles 83° and 75°, respectively; cf. Fig. 1). The following aryl torsion angles were observed for xanthenes (**1**): **1b**: 82°,[11a] **1** (X = 2-(fluorosulfonyl)-4-sulfophenyl): 86°.[11b]

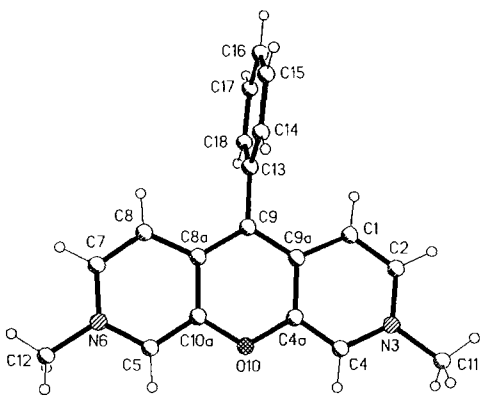


Fig. 1. Structure of the cation of **2a** in the crystal. Selected distances [pm]: N3–C2 134.8(3), C2–C1 136.1(3), C1–C9a 141.4(3), C9a–C9 140.2(3), N3–C4 136.6(3), C4–C4a 134.6(3), C4a–C9a 142.0.

The signals of the equivalent protons 1-H and 8-H which appear in the ^{1}H NMR spectra of **2a,b** at remarkably high field (δ = 5.50 and 5.58, respectively) imply that they lie in the shielding region of the anisotropy effect originating from the phenyl substituents X. This is only possible if the phenyl ring in solution is also positioned orthogonally to the chromophore for **2a,b**. The ^{13}C chemical shifts correlate with the π-charge densities q_π obtained by PPP calculations and show alternating π densities which are inverted for corresponding centers of **1** and **2** (see Scheme 1).

The UV/VIS spectra of **2** are of particular interest compared to those of the rhodamines **1** (**1a**: λ_{max} = 554 nm). The intense band of **2a** with the longest wavelength (Fig. 2) appears at 630 nm (ε = 24100); its position corresponds very well to the theoretical prediction (Table 1). The absorption of **2** at considerably longer wavelength than **1** is explained by the fact that the ether bridge, as a donor, influences the chromophores differently at different positions in the framework according to the Dewar rules.[12] Thus, a donor at C-4a (or C-10a) should cause hypsochromism for **1**, and bathochromism for **2**, in comparison to their respective basic chromophores.

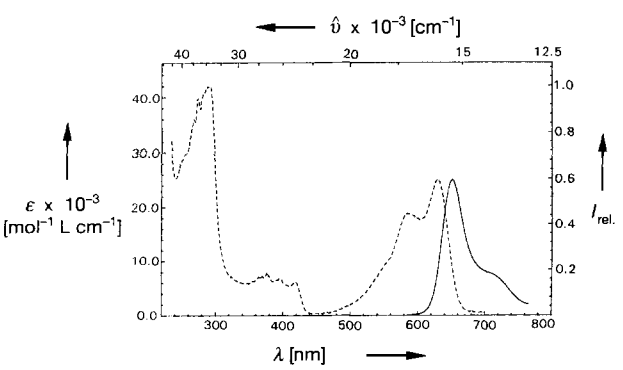


Fig. 2. Absorption (· · ·) and fluorescence (—) spectrum of **2a** where A = BF_4^- in dichloromethane; $c = 1.40 \times 10^{-6}$ mol L^{-1}; λ_{EX} = 390 nm.

The extinction coefficients of the absorption maxima of **2** with the longest wavelengths are considerably lower than those of **1** (Table 1). Differences in the transition moments of **1** and **2** are responsible for this. According to the PPP calculations of the π-charge densities q_π for the S_0 and S_1 state, a strong shift of charge takes place from both of the amino nitrogen atoms in the tricyclic framework following excitation of **1**. This is not possible for compounds **2**, since their nitrogen atoms are incorporated into the aromatic system. On excitation of **2**, a markedly smaller shift of charge, polarized perpendicular to the long axis of the molecule, results within the xanthylium ion.

Since many xanthene dyes such as **1a,b** show intense fluorescence with a mainly small Stokes shift (Table 1), the fluorescence of **2a,b** was determined. For each of the dyes **2** we also observed a fluorescence band, which was only slightly shifted compared to the absorption band with the longest wavelength; the quantum yields ϕ_F are considerably smaller than for rhodamines (**1**) (Table 1).

The dyes **2** have high melting points and are stable for a few months in the crystalline form and in solution, but only with the exclusion of oxygen. As crystals, they decompose and decolorize in air (without exposure to light) within days or weeks, but in solution within a few minutes or hours. The constitution of the non-analytically pure oxidation product **8a** of **2a**, which can be isolated as a colorless substance, indicates why these dyes are sensitive to oxygen. The ^{1}H and ^{13}C NMR spectra of **8a** are consistent with a symmetrical structure. The NMR signal of the central atom C-9 experiences a distinct high-field shift from 103.0 in **2a** to 67.6 in **8a**; the oxygen therefore attacks at C-9, which has a high π-electron density according to the PPP calculations (see Scheme 1). In contrast to **2**, oxidation of rhodamines (**1**) occurs preferentially when exposed to light; a structurally asymmetrical oxidation product results by attack at C-3 or C-6.[13]

Experimental Procedure

2a: The following operations were all carried out using N_2 as the inert gas (strict O_2 exclusion). Triethylamine (0.25 mL, 1.7 mmol) was added to a solution of **7a** (360 mg, 0.72 mmol) in dry acetonitrile (25 mL) and heated under reflux with stirring for 2 h. The solution was then concentrated and chromatographed on about 50 g neutral Al_2O_3 (activity 90) with dichloromethane/acetone ≈ 3:2. After the solvents were distilled off, the residue was dissolved in dichloromethane (50 mL) and extracted once with water (20 mL); yield: 243 mg (90%). Analytically pure **2a** was obtained by recrystallization from chloroform [14].

2a: M.p. 219–222 °C (BPh_4^- as anion); ^{1}H NMR (CD_2Cl_2): δ = 3.33 (s, 6H; CH_3), 5.50 (d, ^3J(H,H) = 6.8 Hz, 2H; 1/8-H), 6.28 (d, ^4J(H,H) = 1.7 Hz, 2H; 4/5-H), 6.59 (dd, ^3J(H,H) = 6.8, ^4J(H,H) = 1.7, 2H; 2/7-H), 6.99–7.01 (m, 2H; 14/18-H), 7.25–7.27 (m, 1H; 16-H), 7.35–7.39 (m, 2H, 15/17-H); ^{13}C NMR (CD_2Cl_2): δ = 44.33 (C-11/12), 103.00 (C-9), 110.36 (C-1/8), 121.92 (C-4/5), 128.40 (C-16), 129.93 (C-14/18), 130.33 (C-15/17), 132.99 (C-13), 140.65 (C-2/7), 144.13 (C-8a/9a), 149.74 (C-4a/10a).

2b: M.p. 186–188 °C (BF_4^- as anion); ^{1}H NMR (CD_2Cl_2): δ = 3.44 (s, 6H; CH_3), 5.58 (d, ^3J(H,H) = 6.9 Hz, 2H; 1/8-H), 6.42 (d, ^4J(H,H) = 1.6 Hz, 2H; 4/5-H), 6.76 (dd, ^3J(H,H) = 6.9, ^4J(H,H) = 1.6 Hz, 2H; 2/7-H), 7.25 (m, 2H; 14/18-H), 7.70 (m, 2H; 15/17-H); ^{13}C NMR (CD_2Cl_2): δ = 44.43 (C-11/12), 100.96 (C-9), 109.99 (C-1/8), 122.39 (C-4/5), 124.41 (^1J(C,F) = 272 Hz, C-19), 127.27 (^3J(C,F) = 3.7 Hz, C-15/17), 130.04 (^2J(C,F) = 35.2 Hz, C-16), 130.72 (C-14/18), 137.34 (C-13), 140.90 (C-2/7), 143.87 (C-8a/9a), 149.52 (C-4a/10a).

5a: M.p. 126 °C; ^{1}H NMR ($CDCl_3$): δ = 4.02 (s, 2H; CH_2), 7.10–7.24 (m, 5H; Ph), 7.29 (d, ^3J(H,H) = 4.9 Hz, 1H; 5-H), 7.36 (d, ^4J(H,H) = 1.8 Hz, 1H; 2'-H), 7.81

 © VCH Verlagsgesellschaft mbH, D-69451 Weinheim, 1994 0570-0833/94/0808-0865 $ 10.00+.25/0

(dd, ^3J(H,H) = 7.2, ^4J(H,H) = 1.8 Hz, 1H; 6'-H), 7.90 (d ^3J(H,H) = 7.2 Hz, 1H; 5'-H), 8.32 (s, 1H; 2-H), 8.50 (d, ^3J(H,H) = 4.9 Hz, 1H; 6-H); ^{13}C NMR ($CDCl_3$): δ = 36.06 (C-7), 122.06 (C-5'), 126.20 (C-5), 127.04 (C-11), 128.77 (C-10/12), 128.93 (C-9/13), 130.54 (C-2'), 133.86 (C-4'), 134.16 (C-6'), 136.89 (C-8), 142.25 (C-2), 142.42 (C-4), 148.27 (C-6), 148.57 (C-3), 149.63 (C-3').

6a: M.p. 42–43 °C; b.p.: 200–220 °C/0.2 mbar (Kugelrohr); ^{1}H NMR ($CDCl_3$): δ = 4.06 (s, 2H; CH_2), 7.14 (d, ^3J(H,H) = 4.9 Hz, 1H; 5-H), 7.19–7.21 (m, 3H; 9/11/13-H), 7.22–7.30 (m, 2H; 10/12-H), 7.41 (d, ^3J(H,H) = 5.1 Hz, 1H; 5'-H), 8.07 (s, 1H; 2-H), 8.08 (s, 1H; 2'-H), 8.30 (d, ^3J(H,H) = 5.1 Hz, 1H; 6'-H), 8.33 (d, ^3J(H,H) = 4.9 Hz, 1H; 6-H); ^{13}C NMR ($CDCl_3$): δ = 35.41 (C-7), 125.437 (C-5'), 125.444 (C-5), 126.74 (C-11), 128.68 (C-10/12), 129.07 (C-9/13), 134.49 (C-4'), 137.73 (C-4), 139.46 (C-2), 140.57 (C-8), 141.44 (C-2'), 145.82 (C-6'), 145.87 (C-6), 149.32 (C-3), 150.88 (C-3').

7a: M.p. 210–213 °C; ^{1}H NMR (CD_3NO_2): δ = 4.33 (s, 3H; CH_3), 4.42 (s, 3H; CH_3), 4.45 (s, 2H; CH_2), 7.27–7.37 (m, 5H; Ph), 8.12 (d, ^3J(H,H) = 6.2 Hz, 1H; 5-H), 8.25 (d, ^3J(H,H) = 6.5 Hz, 1H; 5'-H), 8.32 (d, ^4J(H,H) = 1.4 Hz, 1H; 2'-H), 8.55 (s, 1H; 2-H), 8.59 ("dt", ^3J(H,H) = 6.5, ^4J(H,H) = 1.1, ^4J(H,H) = 0.6 Hz, 1H; 6'-H), 8.70 (dd, ^3J(H,H) = 6.2, ^4J(H,H) = 0.7 Hz, 1H; 6-H); ^{13}C NMR (CD_3NO_2): δ = 37.48 (C-7), 49.78 (CH_3), 50.10 (CH_3), 129.05 (C-11), 130.55 (C-10/12), 130.96 (C-9/13), 131.49 (C-5'), 131.57 (C-5), 137.10 (C-8), 137.79 (C-2'), 137.80 (C-2), 144.28 (C-6'), 144.74 (C-6), 146.13 (C-4'), 152.32 (C-3'), 152.86 (C-3), 154.67 (C-4).

Received: October 22, 1993 [Z 6440IE]
German version: *Angew. Chem.* **1994**, *106*, 903

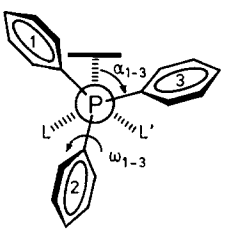
[1] H. Zollinger, *Color Chemistry*, 2nd edition, VCH, Weinheim, **1991**.
[2] a) O. Valdes-Aquilera, D. C. Neckers, *Acc. Chem. Res.* **1989**, *22*, 171–177; b) J. Arden, G. Deltau, V. Huth, U. Kringel, D. Peros, K. H. Drexhage, *J. Lumin.* **1991**, *48–49*, 352–358; c) R. Sens, Strahlungslose Desaktivierung in Xanthen-, Oxazin- und Carbazinfarbstoffen, Dissertation, Universität-Gesamthochschule Siegen, **1984**.
[3] R. E. Farris, *Kirk-Othmer Encycl. Chem. Technol.* **1984**, *24*, 664–668.
[4] a) M. Maeda, *Laser Dyes*, Academic Press, Tokyo, **1984**, 22, Table 12; b) K. H. Drexhage in *Dye Lasers* (F. P. Schäfer), 3rd edition, Springer, Berlin, **1990**, 175–180.
[5] PPP program PCSCF3D by U. Wild, Zürich, Version 4/1993 B. Knieriem, Universität Göttingen. In the calculation the parameters of R. Zahradnik and R. Gleiter (personal communication) were used. The configuration interaction takes into account the 50 singly excited states with lowest energy.
[6] Fachinformationszentrum Karlsruhe, Reference No. STCC-70159-025, **1986**.
[7] According to T. L. Shing, W.-L. Chia, M.-J. Shiao, T.-Y. Chau (*Synthesis*, **1991**, 849–850) 4-benzyl-3-benzyloxypyridine is synthesized from 3-benzyloxypyridine and benzylbromide with *p*-chloranil (instead of sulfur) as the oxidizing agent. This forms **3** after hydrogenation with H_2/Pd (10% on activated carbon) according to D. L. Comins, E. D. Stroud (*J. Heterocycl. Chem.* **1985**, *22*, 1419–1420) and then treatment with KOH according to E. Butler, B. P. H. Poschel, J. G. Marriot (*J. Med. Chem.* **1981**, *24*, 346–350).
[8] E. Ochiai, *J. Org. Chem.* **1953**, *18*, 534–551.
[9] Synthesis of the compound without an oxygen bridge: I. H. Leubner, *J. Org. Chem.* **1973**, *38*, 1098–1102.
[10] Crystal data for **2a** at −130 °C: triclinic, $P\bar{1}$, a = 1140.4(3), b = 1227.5(3), c = 1278.0(4) pm, α = 94.77(2), β = 101.98(2), γ = 111.58(2)°, Z = 2, $Mo_{K\alpha}$ radiation, $2\theta_{max}$ = 50°. Refinement on F^2: H atoms with a riding model, $wR(F^2)$ = 0.131 for all 5648 reflections, $R(F)$ = 0.049. Diffractometer: Stoe STADI-4. Refinement programm: SHELXL-93 (G. M. Sheldrick, *J. Appl. Cryst.* **1994**, submitted). Crystal data for **2b**·CH_2Cl_2 at −100 °C: triclinic, $P\bar{1}$, a = 1125.8(5), b = 1283.6(4), c = 1439.4(4) pm, α = 85.18(3), β = 70.67(3), γ = 77.91(3)°, Z = 2, $Mo_{K\alpha}$ radiation, $2\theta_{max}$ = 50°. Refinement on F^2: H atoms with a riding model, $wR(F^2)$ = 0.240 for all 6756 reflections, $R(F)$ = 0.070. The CF_3 group is disordered over two alternative positions. Diffractometer: Siemens R3. Program: as above. Further details of the crystal structure investigations may be obtained from the Fachinformationszentrum Karlsruhe, D-76344 Eggenstein-Leopoldshafen, on quoting the depository numbers CSD-400511 and 400512.
[11] a) H. Möller, G. Deltau, K. H. Drexhage, Universität-Gesamthochschule Siegen, personal communication, June 1993; b) I. N. Polyakova, Z. A. Starikova, B. V. Parusnikov, I. A. Krasavin, *Zh. Strukt. Khim.* **1985**, *26*, 125–131; *J. Struct. Chem. Engl. Trans.* **1986**, *26*, 600–605.
[12] M. J. S. Dewar, *J. Chem. Soc.* **1950**, 2329; *ibid.* **1952**, 3532, 3544.
[13] N. Kuznetsova, O. Kaliya, E. Luk'yanets in *Chemistry of Functional Dyes* (Eds.: Z. Yoshida, T. Kitao), Mita, Tokyo, **1989**, pp. 183–185.
[14] The spectroscopic data [IR, UV/VIS, ^{1}H NMR (400 MHz; TMS), ^{13}C NMR (100 MHz) spectroscopy and mass spectrometry] and the correct elemental analyses indicate the structures of the new compounds **5**–**7** and **2**. The NMR signals were assigned by using 2D spectra (CH-COSY, COLOC) and HOMO decoupling.

Propeller Isomerism of the Triphenylphosphane Ligand in Half-Sandwich Ru^{II} Complexes**

Henri Brunner,* Ralf Oeschey, and Bernd Nuber

Dedicated to Professor Helmut Werner on the occasion of his 60th birthday

The phenyl rings of triphenylphosphane adopt a propeller-like arrangement in both the free and the complex-bound state.[1, 2] In organometallic complexes, the configuration of the three phenyl rings in the crystal is primarily determined by intramolecular interactions and not by packing forces.[3–6] Here, the phenyl rings in half-sandwich complexes deviate from a staggered conformation with respect to the other ligands in a characteristic way (Scheme 1); one phenyl ring is arranged face-exposed (Ph 1) and the other is arranged edge-exposed (Ph 3) to the π-bound arene ligand.[3–6] The *gauche* angles α_{1-3} therefore lie in the ranges 24–58°, 145–179°, and 262–302°.[3, 4, 6] The sign of the torsion angles ω_{1-3} of the phenyl rings about the C_{ipso}–P axes determines the configuration of the two possible enantiomeric propeller arrangements *M* (Scheme 1) or *P*.[3, 4]



Scheme 1. Left-handed helical *M* configuration of PPh_3 on the complex fragment [(arene)MLL'].

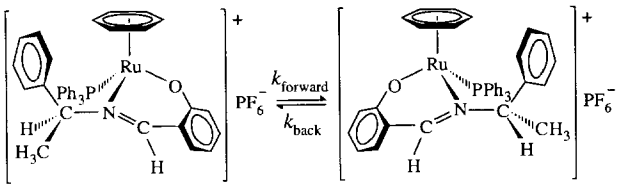
The energy barriers for the rotation of the PPh_3 ligand about the M–L axis (determined by variable-temperature $^{13}C\{^1H\}$ NMR spectroscopy) for the complexes $[CpFe(CO)(COMe)PPh_3]$[5] and $[(\eta^6\text{-}C_6Me_6)Cr(CO)_2PPh_3]$[7] are 43.1 and 28.2 kJ mol^{-1}, respectively. Complex fragments with a stereogenic metal atom of given configuration form diastereomers with triphenylphosphane which only differ in terms of the sense of the propeller of the PPh_3 ligand. Although the calculated energy difference between the two diastereomers is small, in all of the previously reported cases only one of the two possible diastereomers occurs in the solid state, probably the more stable one.[4–6] We report here on half-sandwich Ru^{II} complexes containing the triphenylphosphane ligand. In the synthesis of these complexes initially the diastereomer with the more unstable propeller arrangement forms (kinetic product), which is subsequently converted into the diastereomer with the more stable propeller arrangement (thermodynamic product) at higher temperatures. Both isomers were characterized by X-ray crystal structure analyses.

In the cation, compound **1** contains the anion of *S*-(+)-1-phenylethylsalicylaldimine (pesa) as a chirally modified N,O chelate ligand. In accordance with the synthesis of the corresponding *p*-cymol complexes,[8] **1** is obtained from the neutral complex $[(\eta^6\text{-}C_6H_6)Ru(pesa)Cl]$ by halogen abstraction with $AgPF_6$ and subsequent addition of PPh_3 at −35 °C. Compound **1** forms two diastereomers (R_{Ru},S_C) and (S_{Ru},S_C), which differ from each other in terms of the configuration at the ruthenium

[*] Prof. Dr. H. Brunner, Dipl.-Chem. R. Oeschey
Institut für Anorganische Chemie der Universität
D-93040 Regensburg (FRG)
Telefax: Int. code + (941)943-4439
Dr. B. Nuber
Anorganisch-chemisches Institut der Universität Heidelberg (FRG)

[**] Optically Active Transition Metal Complexes, Part 105. This work was supported by the Deutsche Forschungsgemeinschaft and the Fonds der Chemischen Industrie. We thank the BASF AG for donating chemicals. Part 104: H. Brunner, S. Forster, B. Nuber, *Organometallics* **1993**, *12*, 3819.

atom (Scheme 2). At room temperature the equilibrium ratio determined by the integration of the ^{1}H NMR signals of the η^6-arene protons is 93:7 in [D$_6$]acetone and 95:5 in $CDCl_3$.



(R_{Ru}, S_C)-**1** (S_{Ru}, S_C)-**1**

Scheme 2.

Compound **1** crystallizes in a diastereomerically pure form from $CHCl_3$/petroleum ether as deep red, air-stable tetrahedra (**1a**), if, after synthesis at $-35\,^\circ C$, the solution is kept at $5\,^\circ C$. If, on the other hand, the initially bright red solution of **1a** in $CHCl_3$ is warmed to higher temperatures, epimerization takes place, which can be followed by ^{1}H NMR spectroscopy and occurs first order,[9] the solution changing color to red-brown, only observable in thick layers. If the solution is cooled to $5\,^\circ C$, after a period of more than ten half-lives, red-brown tablets of **1b** crystallize.[9] Both modifications, **1a** and **1b**, show the same ^{1}H, ^{31}P{^{1}H}, and ^{13}C{^{1}H} NMR spectra in solution up to $-90\,^\circ C$.[10] Also no differences in the chemical shifts of the phosphorus signals were observed in the ^{31}P CP/MAS solid-state NMR spectra (CP/MAS = cross polarization/magic angle spinning),[11] and the IR spectra of **1a** and **1b** were identical both in a KBr matrix and in $CHCl_3$ solution. Within the error limits the same is true for the angle of rotation as well as the circular dichroism and UV spectra.[12]

The X-ray structure analyses of the tetrahedral and tablet modifications, **1a** and **1b**, respectively, revealed both to have the (R_{Ru},S_C) configuration (Fig. 1). They differ only in terms of the chirality of the propeller of the PPh_3 ligand; the rest of the complex cation is almost the same in both cases.[13]

Noteworthy in the structures is that in **1a** the P1–Ru1 bond is 0.037(4) Å longer and the N1–Ru1 bond 0.04(1) Å shorter than in **1b**. Furthermore, the P1-Ru1-N1 angle in **1b** is 2.6(4)° smaller than in **1a**. The shape of the thermal ellipsoids for the η^6-arene carbon atoms in **1b** indicates a disorder in terms of a rotation about the sixfold Ru1–arene axis. In **1a** the arene ring is not planar, since the distances Ru1–C36 and Ru1–C37 are up to 0.06(2) Å longer than the other Ru1–C(arene) distances because of the *trans* effect of PPh_3.[14]

(R_{Ru},S_C)-**1a** and (R_{Ru},S_C)-**1b** differ with respect to the propeller configuration of the PPh_3 ligand. In comparison to **1a**, the PPh_3 fragment in **1b** is rotated anticlockwise about the M–L axis by 53°. This is accompanied by a rotation of the phenyl "rotor blades" about their C_{ipso}–P axes, which causes the inversion of the propeller from the *M* arrangement in **1a** to *P* in **1b**. The edge arrangement of the phenyl ring C16–C21 relative to the arene ligand in **1a** changes into the face arrangement in **1b**; the opposite is true for the phenyl ring C10–C15. For the edge-exposed phenyl rings the dihedral angle C21-P1-Ru1-arene(centr) in **1a** (− 82°) is slightly smaller than the dihedral angle C15-P1-Ru1-arene(centr) of 89° in **1b**.[15] Thus, the distance of the *ortho* proton at C20 in **1a** (2.34 Å) to the protons of the arene ligand is slightly smaller than for the corresponding proton at C14 in **1b** (2.40 Å). The difference between the minimum H···H distances of the methyl protons at C3 and the next- nearest protons on the phenyl rings of the PPh_3 ligand is significantly greater, namely 2.43 Å for H3···H8 in **1a** and 3.20 Å for H3···H5 in **1b**.[15] These intramolecular interactions provide an explanation why the initially formed **1a** is thermodynamically unstable in comparison to **1b**.

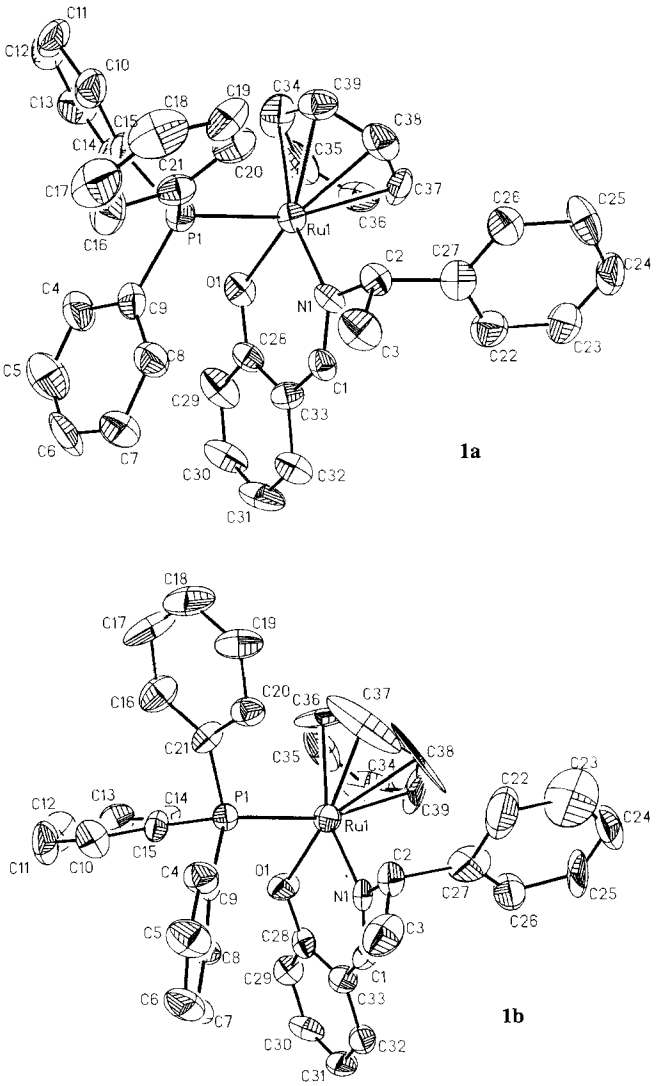


Fig. 1. Crystal structures of **1a** and **1b** (thermal ellipsoids at 50% probability level). The PF_6 anions and the hydrogen atoms were omitted for clarity. Selected distances [Å] and angles [°] in **1a**: Ru1-P1 2.392(4), Ru1-O1 2.063(8), Ru1-N1 2.063(8), Ru1-N1 2.09(1), Ru1-C34 2.22(2), Ru1-C35 2.21(2), Ru1-C36 2.28(2), Ru1-C37 2.27(2), Ru1-C38 2.24(1), Ru1-C39 2.21(1), N1-C1 1.28(2); P1-Ru1-N1 88.8(5), P1-Ru1-O1 82.3(4), O1-Ru1-N1 89.4(4); **1b**: Ru1-P1 2.355(4), Ru1-O1 2.057(9), Ru1-N1 2.13(1), Ru1-C34 2.18(3), Ru1-C35 2.20(3). Ru1-C36 2.18(4), Ru1-C37 2.21(2), Ru1-C38 2.28(3), Ru1-C39 2.17(4); P1-Ru1-N1 90.6(3), P1-Ru1-O1 82.3(2), O1-Ru1-N1 86.8(4).

The conformations found in the molecular structures of **1a** and **1b** in regard to the stereogenic center C2 are also preferred in solution. This is revealed by the ^{1}H NMR signals of the methyl protons at C3 and of the methine proton at C2, which, in comparison to those of the likewise (R_{Ru},S_C)-configurated starting material [(η^6-C_6H_6)Ru(pesa)Cl], are shifted by more than $\Delta\delta = 0.8$ to higher field. The molecular structures in the crystal clearly show that the methyl and methine protons are situated within the anisotropy cone of the phenyl ring C16–C21 of **1a** and of the phenyl ring C4–C9 of **1b**. The weak attraction between the π-bound six-membered ring and the phenyl group C22–C27 of the 1-phenylethyl group, known as the "β-phenyl effect", seems to determine the conformation.[16]

 © VCH Verlagsgesellschaft mbH, D-69451 Weinheim, 1994 0570-0833/94/0808-0867 $ 10.00+.25/0

Red tetrahedra of **1a** crystallize at 5 °C from a $CHCl_3$ solution of **1a**, which has been kept at −25 °C for several days. In this case, neither the helicity of the PPh_3 nor the Ru configuration has changed. If crystallization is effected after adjustment of the diastereomeric equilibrium $(R_{Ru},S_C) \rightleftharpoons (S_{Ru},S_C)$, red-brown tablets of **1b** are obtained containing the thermodynamically more stable propeller configuration of the triphenylphosphane ligand. The course of the exchange experiments with tri(*p*-tolyl)phosphane can be followed by ^{1}H NMR spectroscopy. The results suggest that the epimerization of **1a** and **1b**, and therefore also the change of the propeller configuration, occurs by a rate-determining dissociation of the PPh_3 ligand.[9, 17]

Inversion of the propeller configuration in the complexes $[CpFe(CO)(COMe)PPh_3]$[5] and $[(\eta^6\text{-}C_6Me_6)Cr(CO)_2PPh_3]$[7] occurs rapidly and intramolecularly; this inversion is hindered, but not prevented, by the Cp and arene ligands and, depending on their size, also by the other ligands. In **1a**, in contrast, the $CHCH_3$ group of the 1-phenylethyl group blocks the intramolecular propeller inversion, which is only made possible by the triphenylphosphane dissociation.

Experimental Procedure

$[(\eta^6\text{-}C_6H_6)Ru(pesa)Cl]$: Synthesis in accordance with the preparation of the analogous cymol complex [8] (synthesis at room temperature, workup by repeated precipitation from CH_2Cl_2/acetone/hexane). The compound was obtained crystalline and diastereomerically pure in 45% yield with (R_{Ru},S_C) configuration [18] in the crystalline state; in contrast, in $CDCl_3$ solution a diastereomeric ratio of 86:14 is found. ^{1}H NMR (250 MHz, $CDCl_3$, 25 °C, TMS) (values for the (S_{Ru},S_C) diastereomer in parentheses): δ = 7.99 (s, 1H, N=CH), 7.67–6.39 (m, 9H, arene-H), 5.97 (5.68), (q, ^3J(H,H) = 6.9 Hz, 1H, CH), 5.31 (5.54) (s, 6H, C_6H_6), 1.77 (2.00), (d, ^3J(H,H) = 6.9 Hz, 3H, CH_3); correct elemental analysis.

$[(\eta^6\text{-}C_6H_6)Ru(pesa)PPh_3]PF_6$ **1**: $AgPF_6$ (429 mg, 1.7 mmol) was added to a suspension of $[(\eta^6\text{-}C_6H_6)Ru(pesa)Cl]$ (744 mg, 1.7 mmol) in acetone (120 mL) at −35 °C and stirred (N_2 atmosphere). Subsequently, after 45 min PPh_3 (525 mg, 2.0 mmol) was added which caused the mixture to turn yellow immediately. After the mixture had been stirred for 30 min at −35 °C, it was filtered through Celite, concentrated to a few mL, and precipitated by the addition of petroleum ether. Several precipitations from CH_2Cl_2/petroleum ether gave **1** as an orange-yellow, microcrystalline powder in almost quantitative yield. The crystallization of each 100 mg **1** from 1.9 mL $CHCl_3$/0.4 mL petroleum ether at 5 °C after 3 d yielded red, air-stable tetrahedra of **1a** (73%). Tablets of **1b** were formed after warming a solution of **1** at 40 °C for 50 min or 5 h stirring at 12 °C and subsequent crystallization at 5 °C (80% yield of red-brown, air-stable tablets within 3 d). ^{1}H NMR (250 MHz, $CDCl_3$, 25 °C, TMS) (values for (S_{Ru},S_C)-**1** in parentheses): δ = 7.78 (d, ^4J(H,P) = 0.7 Hz, 1H, N=CH, 7.65–6.44 (m, 24H, arene-H), 5.33 (5.83) (d, ^3J(H,P) = 0.7 Hz, 6H, C_6H_6), 5.21 (q, ^3J(H,H) = 7.0 Hz, 1H, CH), 1.04 (1.93) (d, ^3J(H,H) = 7.0 Hz, 3H, CH_3); $^{31}P\{^1H\}$ NMR (161.8 MHz, [D$_6$]acetone, 25 °C, 85% H_3PO_4 ext.): δ = 35.8 (28.8) (s, 1P), −142.6 (sept, ^1J(P,F) = 707 Hz, 1P, PF_6); $^{13}C\{^1H\}$ NMR (100.6 MHz, $CDCl_3$, 25 °C): δ = 165.7 (s, C1), 164.8 (s, C28), 142.6 (s, C33), 135.9, 134.8 (s, C30, C31), 133.9 (d, ^2J(C,P) = 10 Hz, C4/8/10/14/16/20), 131.5 (d, ^4J(C,P) = 2.4 Hz, C6/12/18), 130.2 (d, ^1J(C,P) = 47.5 Hz, C9/15/21), 129.8 (s, C23/25), 129.1 (d, ^2J(C,P) = 10 Hz, C5/7/11/13/17/19), 128.5 (s, C24), 125.7 (s, C22/26), 122.6 (s, C32), 121.7 (s, C27), 115.8 (s, C29), 90.3 (90.8) (d, ^2J(C,P) = 3 Hz, C34/35/36/37/38/39), 77.6 (d, ^3J(C,P) = 1.8 Hz, C2), 25.0 (s, C3); correct elemental analysis.

Received: July 22, 1993
Revised version: January 11, 1994 [Z6227IE]
German version: *Angew. Chem.* **1994**, *106*, 941

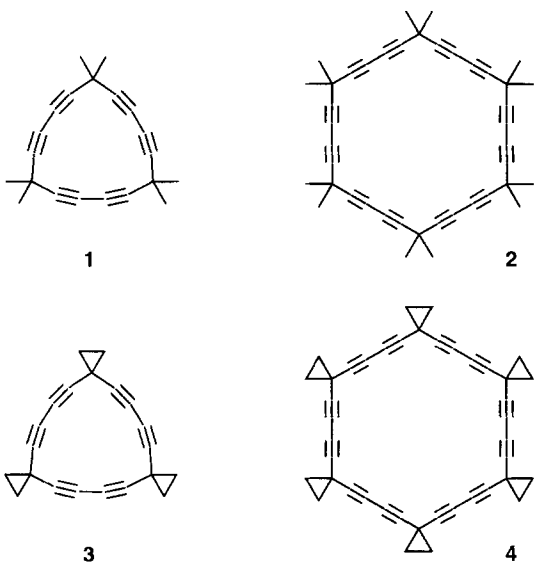
[1] K. Mislow, D. Gust, *J. Am. Chem. Soc.* **1973**, *95*, 1535; K. Mislow, D. Gust, P. Finocchiaro, R. J. Boettcher, *Top. Curr. Chem.* **1974**, *47*, 1; K. Mislow, *Acc. Chem. Res.* **1976**, 9, 26; F. Strohbusch, *Tetrahedron*, **1972**, *28*, 1915.
[2] J. J. Daly, *J. Chem. Soc.* **1964**, 3799; M. R. Churchill, T. A. O' Brien, *J. Chem. Soc. Sect. A* **1970**, 161.
[3] H. Brunner, B. Hammer, C. Krüger, K. Angermund, I. Bernal, *Organometallics* **1985**, 4, 1063.
[4] J. Polowin, S. C. Mackie, M. C. Baird, *Organometallics* **1992**, *11*, 3724.
[5] S. G. Davies, A. E. Derome, J. P. McNally, *J. Am. Chem. Soc.* **1991**, *113*, 2854.
[6] S. E. Garner, A. G. Orpen, *J. Chem. Soc. Dalton Trans.* **1993**, 533.
[7] G. Hunter, T. J. R. Weakley, W. Weissensteiner, *J. Chem. Soc. Dalton Trans.* **1987**, 1545; J. A. Chudek, G. Hunter, R. L. MacKay, P. Kremminger, K. Schlögel, W. Weissensteiner, *ibid.* **1990**, 2001.
[8] S. K. Mandal, A. K. Chakravarty, *J. Organomet. Chem.* **1991**, *417*, C59; *J. Chem. Soc. Dalton Trans.* **1992**, 1627.
[9] The kinetics of the epimerization is followed based on the decrease of the η^6-C_6H_6 signal of **1a** in $CDCl_3$ at 12 ± 2 °C. The analysis of the data affords $k_{rate} = (2.28 \pm 0.02) \times 10^{-2}$ min^{-1}, which corresponds to a half-life $\tau_{1/2}$ = (30.4 ± 0.4) min. By using the equilibrium constant $K = [(S_{Ru},S_C)\text{-}\mathbf{1}]/[(R_{Ru},S_C)\text{-}\mathbf{1}] = 0.046 \pm 0.003$, the rate constants of the forward and back reaction can be calculated: $k_{forward} = (1.00 \pm 0.08) \times 10^{-3}$, $k_{back} = (2.18 \pm 0.03) \times 10^{-2}$ min^{-1}. The kinetic parameters determined with **1b** ($k_{rate} = 2.31 \pm 0.03) \times 10^{-2}$ min^{-1}, $\tau_{1/2}$ = (30.1 ± 0.3 min) correspond with those determined for **1a** within the limits of error.
[10] On cooling, a reversible signal broadening of the ^{13}C resonances of the triphenylphosphane ligand, particularly the C_{ortho} signals, occurs.
[11] ^{31}P CP/MAS NMR (121.5 MHz, ν_{rot} = 3340 Hz for **1a**, 3266 Hz for **1b**): **1a**: δ = 33.5 (s, 1P), −143.7 (sept, ^1J(P,F) = 712 Hz, 1P, PF_6); **1b**: 33.4 (s, 1P), −143.8 (sept, ^1J(P,F) = 712 Hz, 1P, PF_6). We thank Prof. Dr. A. Sebald, Bayreuth, for recording the spectra.
[12] UV/VIS (−10 °C, $CHCl_3$): **1a**/**1b**: λ_{max} (ε = 418 (3000); by raising the temperature to 25 °C after 30 min: 410 (2600); angle of rotation: **1a**/**1b**: $[\alpha]_D^{-18}$ = −1076°, $[\alpha]_{578}^{-18}$ = −1276°, $[\alpha]_{546}^{-18}$ = −2072°; CD (−20 °C, CH_2Cl_2): **1a**/**1b**: λ_{max}; λ_0 ($\Delta\varepsilon$ [° L mol^{-1} cm^{-1}]) 443 (−14.6), 393 (12.2), 352 (−5.8), 305 (5.1); 414, 369, 327.
[13] Crystal structure analyses: Syntex-Nicolet R3 four-circle diffractometer, $Mo_{K\alpha}$ radiation (λ = 0.71073 Å), empirical absorption correction, SHELXTL-PLUS program on a Microvax II workstation, structure solution by Patterson Fourier and least squares methods, positions of the H atoms were calculated with the option HFIX. **1a**: $C_{39}H_{35}F_6NOP_2Ru$, M_r = 810.72, crystals: red tetrahedra, 0.2 × 0.2 × 0.2 mm^3, monoclinic, space group $P2_1$, a = 10.436(5), b = 19.39(1), c = 10.518(5) Å, β = 119.62(4)°, V = 1850.7 Å^3, Z = 2, ρ_{calcd} = 1.45 g cm^{-3}, $\mu(Mo_{K\alpha})$ = 0.56 mm^{-1}; transmission factors: 0.92–1.00, ω scan, 3.0° < 2σ_i < 52.5°. 2198 independent reflections with $I > 2.5\theta$, refinement with 451 variables: R = 0.051, R_w = 0.043, GOF = 1.63, residual electron density 0.43/−0.38 eÅ^{-3}, determination of the absolute configuration by comparison of the R values for the two possibilities. The refinement of the variables η according to Sheldrick did not result in any reliable conclusion. PF_6 slightly disordered. **1b**: $C_{39}H_{35}F_6NOP_2Ru$, M_r = 810.72, crystals: red-brown tablets, 0.02 × 0.1 × 0.6 mm^3, monoclinic, space group $P2_1$, a = 10.01(1), b = 18.073(9), c = 10.472(7) Å, β = 96.78(7)°, V = 1881.2 Å^3, Z = 2, ρ_{calcd} = 1.43 g cm^{-3}, $\mu(Mo_{K\alpha})$ = 0.55 mm^{-1}; transmission factors: 0.92–1.00, ω scan, 3.0° < 2σ_i < 42.0°. 2743 independent reflections with $I > 2.5\theta$ (h,k,l: min: 0/0/−11, max: 11/19/11), refinement with 451 variables: R = 0.060, R_w = 0.049, GOF = 1.48, residual electron density 0.50/−0.62 eÅ^{-3}, determination of the absolute configuration by measurement of a section of Friedel pairs (20.0° < 2θ < 45.0°, $h/k/l$: min: 0/−20/−12, max: 11/−1/12) and refinement up to η = 1.2 ± 0.2, since, because of the small size of the crystal, the reflection intensities of the crystallographically independent unit were relatively weak. The arene ligand is disordered in terms of a rotation about the sixfold Ru1-centr axis. Further details of the crystal structure investigations may be obtained from the Fachinformationszentrum Karlsruhe, D-76344 Eggenstein-Leopoldshafen (FRG) on quoting the depository number CSD-57948.
[14] M. A. Bennett, G. B. Robertson, A. K. Smith, *J. Organomet. Chem.* **1972**, *43*, C41.
[15] The torsion angles and nonbonding H ··· H distances were calculated from the atomic parameters [13] with the software package PCMODEL, Serena Software, Bloomington, IN. We thank Dr. W. Leitner for providing us with necessary computer time (centr corresponds to the center of the arene ligand).
[16] H. Brunner, *Angew. Chem.* **1983**, *95*, 921; *Angew. Chem. Int. Ed. Engl.* **1983**, *22*, 897.
[17] The exchange experiment was carried out with **1a** at 11 ± 2 °C in $CDCl_3$ by addition of a fivefold molar excess of tri(*p*-tolyl)phosphane. The decrease in the concentration of (R_{Ru},S_C)-**1** occurs first order and gives a rate constant $k = (2.26 \pm 0.01) \times 10^{-3}$ min^{-1}, which correlates well with the rate-determining $k_{forward}$ of the epimerization [9].
[18] H. Brunner, R. Oeschey, B. Nuber, unpublished results.

Hexaspiro[2.4.2.4.2.4.2.4.2.4.2.4]dotetraconta-4,6,11,13,18,20,25,27,32,34,39,41-dodecayne —An Exploding [6]Rotane**

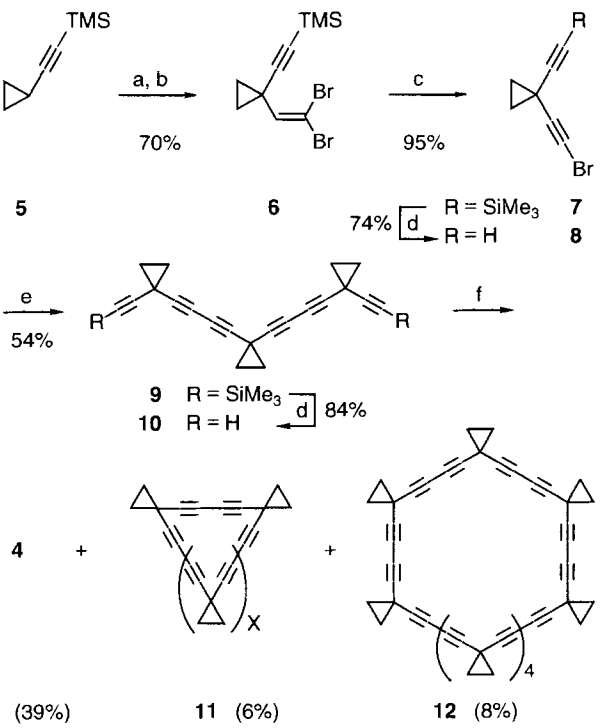
Armin de Meijere,* Sergei Kozhushkov, Carsten Puls, Thomas Haumann, Roland Boese, Mark J. Cooney, and Lawrence T. Scott*

Dedicated to Professor Mordecai Rabinovitz on the occasion of his 60th birthday

Substantial electronic interactions have been evidenced in per-*gem*-dimethyl-substituted macrocyclic oligoalkynes ("pericyclynes")[1-3] and oligoalkadiynes[4] such as **1** and **2**. Since the highest occupied molecular orbitals (HOMOs) of a cyclopropane ring[5] are much closer in energy to the π MOs of an acetylene unit than the σ MOs of a *gem*-dimethyl group are, we thought that considerably stronger homoconjugative effects ought to be shown by perspirocyclopropanated pericyclynes[6] and perspirocyclopropanated macrocyclic oligoalkadiynes such as **3** and **4**. This expectation is based on the observation that the splitting between the π MOs parallel to the plane of the ring in 1,1-diethynylcyclopropane is much larger (1.4 eV) than in 3,3-dimethylpenta-1,4-diyne (0.6 eV).[7]



3,3:8,8:13,13-Trisethanopentadecahexayne (**10**) should be a more appropriate building block than 1,1-diethynylcyclopropane[8] for compounds of type **3** and **4**. Hexayne **10** was assembled in six steps from (trimethylsilylethynyl)cyclopropane (**5**).[9] The sequence began with the deprotonation of **5** with butyllithium in diethyl ether and subsequent formyl group transfer with dimethylformamide. The resulting aldehyde was converted into the dibromoethenyl derivative **6** by treatment with a mixture of carbon tetrabromide, triphenylphosphane, and zinc[10] (70% overall yield) and this in turn dehydrobrominated to give the 1,1-diethynylcyclopropane derivative **7** (95%). This compound was desilylated to provide **8**, which was first treated with two equivalents each of butyllithium, then cuprous chloride, and finally diethynylcyclopropane derivative **7**. This Cadiot–Chodkiewicz coupling[11] led to the silylated acyclic dehydrotrimer **9** of 1,1-diethynylcyclopropane in 54% yield, and desilylation gave **10** (84%) (Scheme 1). When a solution of **10** in pyridine was added over a period of three days to a slurry of cuprous chloride and cupric acetate in pyridine,[12] and the mixture was stirred at ambient temperature for an additional four days, three cyclic dehydro oligomers of 1,1-diethynylcyclopropane were isolated in 6, 39, and 8% yield, respectively, by column chromatography and/or recrystallization. All three were characterized by their diagnostically simple ^1H and ^{13}C NMR spectra (Table 1). Attempts to determine their molecular masses by mass spectrometry with common ionization methods (electron ionization, chemical ionization, direct chemical ionization, field desorption) failed, as the compounds apparently decompose irreproducibly in the inlet system of the mass spectrometer.[13] The relative molecular masses of the two major compounds were, however, determined by vapor pressure osmometry in dichloromethane solution to be 529 and 783 g mol^{-1}, which indicated that they correspond to the cyclic dehydrohexamer **4** (calcd for $C_{42}H_{24}$: 528 g mol^{-1}) and the cyclic dehydrononamer **12** (calcd for $C_{63}H_{36}$: 793 g mol^{-1}) of 1,1-diethynylcyclopropane. While attempts to grow high-quali-



Scheme 1. a: 1) *n*BuLi, Et_2O, 20 °C, 14 h; 2) DMF, 0 °C. b: Zn, Ph_3P, CBr_4, CH_2Cl_2, 20 °C, 30 h. c: *t*BuOK, THF, −78 °C, 5 h. d: 3 equiv KF·$2H_2O$, DMF, 20 °C, 3 h. e: 1) 2 equiv *n*BuLi, Et_2O, 0 °C, 0.5 h; 2) 2 equiv CuCl, THF, 0 °C, 2 h; 3) 2 equiv. **7**, pyridine, 20 °C, 4 h. f: 11.6 equiv CuCl, 16 equiv. $Cu(OAc)_2$, pyridine, 20 °C, 7 d (inverse addition of **10** over 3 d).

[*] Prof. Dr. A. de Meijere, Dr. S. Kozhushkov, Dr. C. Puls
Institut für Organische Chemie der Universität
Tammannstrasse 2, D-37077 Göttingen (FRG)
Telefax: Int. code + (551)39-9475
Prof. Dr. L. T. Scott, M. J. Cooney
Department of Chemistry, Merkert Chemistry Center
Boston College
Chestnut Hill, MA 02167-3860 (USA)
Dipl.-Chem. T. Haumann, Priv.-Doz. Dr. R. Boese
Institut für Anorganische Chemie
der Universität-Gesamthochschule Essen

[**] This work was supported by the Deutsche Forschungsgemeinschaft (Projekt Me 405/15-1,2), the Fonds der Chemischen Industrie, the U. S. National Science Foundation, and NATO. C. P. thanks the Deutsche Forschungsgemeinschaft for a postdoctoral fellowship, S. K. is indebted to the Alexander-von-Humboldt Foundation for a research fellowship.

Table 1. Physical and spectroscopic data of the new compounds **4** and **6**–**12**. NMR spectra: $CDCl_3$, 250 MHz (^1H), 62.9 MHz (^{13}C, additional DEPT).

6: White crystals, m.p. 46–47 °C. ^1H NMR: $\delta = 0.11$ (s, 9 H, $SiMe_3$), 0.98–1.30 (AA'BB', 4 H, CH_2), 6.40 (s, 1 H, CH); ^{13}C NMR: $\delta = 0.12$ (CH_3), 18.80 (CH_2), 137.14 (CH), 15.10, 81.36, 94.80, 107.23 (C).
7: White crystals, m.p. 36–38 °C. ^1H NMR: $\delta = 0.13$ (s, 9 H, $SiMe_3$), 1.24 (s, 4 H, CH_2); ^{13}C NMR: $\delta = 0.01$ (CH_3), 20.51 (CH_2), 4.55, 35.99, 80.60, 81.08, 105.99 (C).
8: Colorless liquid, b.p. 35–40 °C. ^1H NMR: $\delta = 1.27$ (s, 4 H, CH_2), 2.00 (s, 1 H, CH); ^{13}C NMR: $\delta = 19.59$ (CH_2), 84.02 (CH), 3.29, 36.31, 65.13, 80.04 (C).
9: White powder, m.p. 112–114 °C. ^1H NMR: $\delta = 0.12$ (s, 18 H, $SiMe_3$), 1.27 (s, 4 H, CH_2), 1.29 (s, 4 H, CH_2); ^{13}C NMR: $\delta = 0.05$ (CH_3), 21.33 (CH_2), 3.86, 4.03, 61.47, 62.54, 77.22, 77.42, 79.15, 105.30 (C).
10: White powder, m.p. 101–102 °C. ^1H NMR: $\delta = 1.28$ (s, 8 H, CH_2), 1.30 (s, 4 H, CH_2), 1.98 (s, 2 H, CH); ^{13}C NMR: $\delta = 20.67$, 21.32 (CH_2), 83.71 (CH), 3.00, 3.82, 61.76, 62.36, 65.42, 77.27, 78.69 (C).
11: White crystals, decomp > 90 °C. ^1H NMR: $\delta = 1.25$ (s); ^{13}C NMR: $\delta = 20.38$ (CH_2), 3.93, 62.90, 78.08 (C).
4: White crystals, decomp > 130 °C. ^1H NMR: $\delta = 1.27$ (s); ^{13}C NMR: $\delta = 21.02$ (CH_2), 3.91, 62.52, 77.77 (C).
12: White powder, decomp > 100 °C. ^1H NMR: $\delta = 1.29$ (s); ^{13}C NMR: $\delta = 21.30$ (CH_2), 3.87, 62.41, 77.73 (C).

ty crystals of the unidentified product **11** and nonamer **12** failed, "expanded [6]rotane" **4** crystallized well from chloroform and benzene. The structure of the crystals containing two molecules of chloroform per molecule of **4** was analyzed by X-ray diffraction at 200 K and refined to $R = 0.047$ (Fig. 1).[14]

The thirty-membered ring of compound **4** has a chair conformation (Fig. 1 bottom), but with an average torsional angle of $\varphi = 41.4(4)°$ it is less puckered than cyclohexane ($\varphi = 55.1°$)[15] and [6]rotane ($\varphi = 54.6°$).[16] Therefore, a maximum overlap between the Walsh orbitals of the spirocyclopropane units and the π orbitals of the adjacent ethynyl groups is not realized. In fact, the bond angle in the "expanded" six-membered ring of **4**

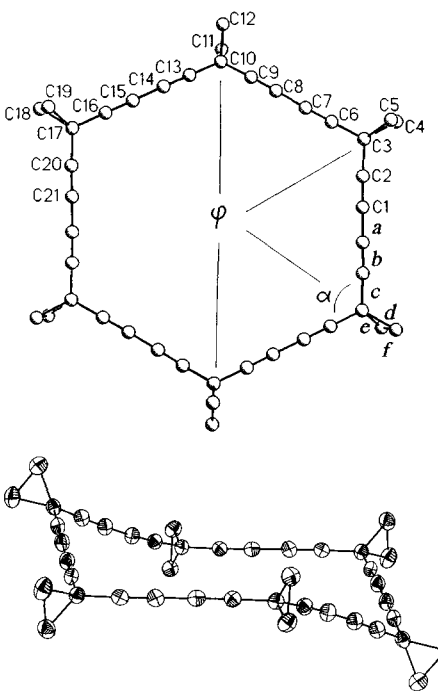


Fig. 1. Crystal structure of hexaspiro[2.4.2.4.2.4.2.4.2.4.2.4]dotetraconta-4,6,11,13,18,20,25,27,32,34,39,41-dodecayne $C_{42}H_{24}$ (**4**)[14]. The numbering in the upper part of the figure does not follow that recommended by IUPAC. Bond lengths [Å] and angles [°] (averaged over D_{3d} symmetry): $a = 1.379(4)$, $b = 1.190(3)$, $c = 1.443(2)$, $d = 1.529(4)$ (axial position), $e = 1.523(3)$ (equatorial position), $f = 1.467(3)$; $\alpha = 115.5(4)$, $\varphi = 41.1(4)$. In the bottom section **4** is shown with thermal probability ellipsoids (50% probability level) and without hydrogen atoms.

($\alpha = 115.5°$), which is also the exocyclic angle of the spirocyclopropanes, is virtually the same as that between the two exocyclic carbon–carbon bonds in 1,1-diethynylcyclopropane (115.5°).[17] This causes the macrocycle **4** to be less puckered than the six-membered rings in cyclohexane ($\alpha = 111.4°$)[15] and in [6]rotane ($\alpha = 111.5°$).[16] The ethynyl groups on the cyclopropane rings in **4** apparently exert an electron-withdrawing effect, as the lengths of the proximal and the distal bonds in the three-membered rings are found to be significantly different [1.526(4) versus 1.467(3) Å]. This lengthening of the proximal and the shortening of the distal bond is also observed in 1,1-diethynylcyclopropane [1.526(1) versus 1.483(1) Å],[17] and it is consistent with the known effects of electron-withdrawing substituents on a cyclopropane[18] as put forward by MO theory.[19] This type of bond differentiation is not observed in [5]- and [6]rotane,[16] and it is opposite to that in [3]rotane, in which the proximal bonds are shortened and the distal bonds are lengthened.[20] The electron donor action of the spirocyclopropane groups in **4**, on the other hand, does not affect the C≡C bond lengths.

Surprisingly, the UV spectra for the basic chromophore 1,4-dicyclopropylbutadiyne, the acyclic dehydrotrimer **10**, and macrocycles **4** and **12** look quite similar in the long-wavelength region, with bathochromic shifts of about 2 nm for the absorption maxima of **4** and **12** (Fig. 2). The intense main absorptions

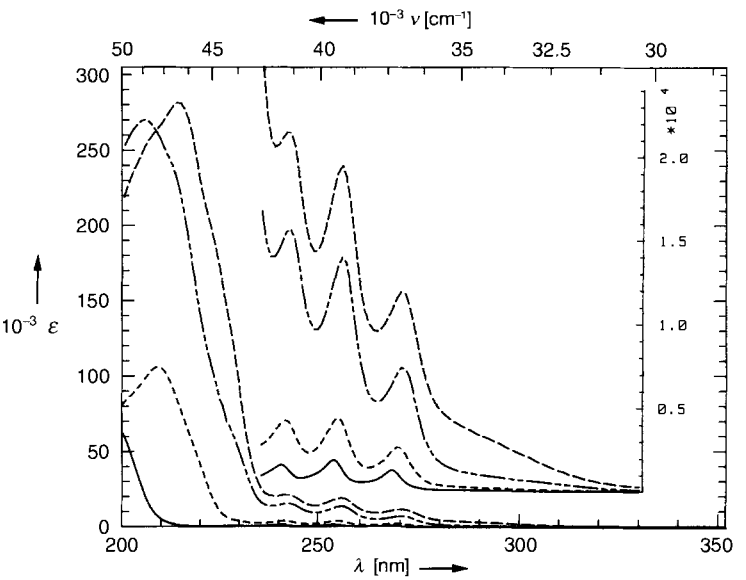


Fig. 2. UV spectra of 1,4-dicyclopropylbutadiyne (—) in methanol, 3,3:8,8:13,13-trisethanopentadecahexayne **10** (----), hexaspirodotetracontadodecayne **4** (— —), and nonaspirotrihexacontaoctadecayne **12** (– –) in *tert*-butyl methyl ether.

at 200–220 nm ($\varepsilon = 250000$–450000), however, are strikingly different. A distinct bathochromic shift is observed on going from 1,4-dicyclopropylbutadiyne to **10** and, more interestingly, this absorption splits into two bands for both macrocycles **4** and **12** but with different magnitudes. This is most likely linked to the expected increased homoconjugative interaction between ethynyl units in **4** and **12**, as corresponding effects are not observed in the UV spectra of the analogous permethylated macrocycles **1** and **2**.

Another striking feature of the "expanded [6]rotane" **4** is its shock sensitivity: When a sample was struck hard with a spatula, a pestle, or a falling metal ball, it flared and turned into black soot. This unusual behavior must be attributed to the presence

of the six three-membered rings, as analogous behavior has not been observed for the permethylated derivative **2**.[4]

Received: November 13, 1993 [Z 6498 IE]
German version: *Angew. Chem.* **1994**, *106*, 934

[1] a) L. T. Scott, G. J. DeCicco, J. L. Hyun, G. Reinhardt, *J. Am. Chem. Soc.* **1983**, *105*, 7760; b) L. T. Scott, G. J. DeCicco, J. L. Hyun, G. Reinhardt, *ibid.* **1985**, *107*, 6546.
[2] K. N. Houk, L. T. Scott, N. G. Rondan, D. C. Spellmeyer, G. Reinhardt, J. L. Hyun, G. J. DeCicco, R. Weiss, M. H. M. Chen, L. S. Bass, J. Clardy, F. S. Jorgensen, T. A. Eaton, V. Sarkozi, C. M. Petit, L. Ng, K. D. Jordan, *J. Am. Chem. Soc.* **1985**, *107*, 6556.
[3] L. T. Scott, M. J. Cooney, D. W. Rogers, K. Dejroongruang, *J. Am. Chem. Soc.* **1988**, *110*, 7244. See also: L. J. Schaad, B. A. Hess Jr., L. T. Scott, *J. Phys. Org. Chem.* **1993**, *6*, 316.
[4] L. T. Scott, M. J. Cooney, D. Johnels, *J. Am. Chem. Soc.* **1990**, *112*, 4054.
[5] A. de Meijere, *Angew. Chem.* **1979**, *91*, 867; *Angew. Chem. Int. Ed. Engl.* **1979**, *18*, 809.
[6] C. Otte, R. Gleiter, L. T. Scott, A. de Meijere, unpublished results.
[7] a) M. Eckert-Maksič, R. Gleiter, N. S. Zefirov, S. I. Kozhushkov, T. S. Kuznetsova, *Chem. Ber.* **1991**, *124*, 371; b) R. Gleiter, J. Spanget-Larsen, *Adv. Strain Org. Chem.* **1992**, *2*, 143.
[8] N. S. Zefirov, S. I. Kozhushkov, T. S. Kuznetsova, R. Gleiter, M. Eckert-Maksič, *Zh. Org. Khim.* **1986**, *22*, 110; *J. Org. Chem. USSR* **1986**, *22*, 95.
[9] H.-C. Militzer, S. Schömenauer, C. Otte, C. Puls, J. Hain, S. Bräse, A. de Meijere, *Synthesis* **1993**, 998.
[10] E. J. Corey, P. L. Fuchs, *Tetrahedron Lett.* **1972**, 3769.
[11] See P. Cadiot, W. Chodkiewicz In *Chemistry of Acetylenes* (Ed.: H. G. Viehe), M. Dekker, New York, **1969**, p. 630 ff.
[12] These conditions for oxidative coupling of terminal acetylenes were adopted from: D. O'Krongly, S. R. Denmeade, M. Y. Chiang, R. Breslow, *J. Am. Chem. Soc.* **1985**, *107*, 5544.
[13] The molecular mass of compound **4**, but not of **12**, was determined by matrix-assisted laser desorption time-of-flight mass spectrometry (MALD-TOF-MS) (9-nitroanthracene matrix). We are grateful to Armen Boldi and Prof. Dr. François Diederich, ETH, Zürich.
[14] Structure determination of **4**: Diffractometer Nicolet R 3m/V, $\lambda(Mo_{K\alpha})$, graphite monochromator, Wyckoff scan, $3^\circ \leq 2\theta \leq 50^\circ$, direct methods (SHELXTL-PLUS). Crystal dimensions $0.65 \times 0.52 \times 0.45$ mm^3, space group $P2_1/n$, $Z = 2$, $T = 200$ K; cell dimensions: $a = 6.053(2)$, $b = 21.121(8)$, $c = 15.161(4)$ Å, $\alpha = \gamma = 90^\circ$, $\beta = 92.34(2)^\circ$, $\rho_{calcd} = 1.36$ g cm^{-3}. 3397 Independent reflections, of which 2566 were considered observed ($F_0 \geq 4\sigma(F)$), 229 parameters for the structure refinement, all non-hydrogen atoms anisotropic, $R = 0.047$, $R_w = 0.047$. Further details of the crystal structure investigation may be obtained from the Fachinformationszentrum Karlsruhe, D-76344 Eggenstein-Leopoldshafen, on quoting the depository number CSD-400451, the names of the authors, and the journal citation.
[15] R. Kahn, R. Fourme, D. Andrè, M. Renaud, *Acta Crystallogr. Sect. B* **1973**, *29*, 131.
[16] T. Prangé, C. Pascard, A. de Meijere, U. Behrens, J.-P. Barnier, J.-M. Conia, *Nouv. J. Chim.* **1980**, *4*, 321.
[17] R. Boese, T. Haumann, S. Kozhushkov, A. de Meijere, unpublished results.
[18] R. Pearson, Jr., A. Choplin, V. W. Laurie, *J. Chem. Phys.* **1975**, *62*, 4859; R. Pearson, Jr., A. Choplin, V. W. Laurie, J. Schwartz, *ibid.* **1975**, *62*, 2949, and references therein.
[19] R. Hoffmann, *Tetrahedron Lett.* **1970**, 2907; H. Günther, *ibid.* **1970**, 5173.
[20] R. Boese, T. Miebach, A. de Meijere, *J. Am. Chem. Soc.* **1991**, *113*, 1743. See also: R. Boese, *Adv. Strain Org. Chem.*, **1992**, *2*, 191.

Enzymatic Grooming of Organic Thin Films**

James K. Whitesell,* Hye Kyung Chang, and Christopher S. Whitesell

We recently described the preparation of new materials consisting of helical peptides arranged nearly vertically and unidirectionally from the surface of gold and of indium–tin oxide (ITO) glass.[1] These layers were produced by polymerization of the N-carbonic anhydride of amino acids, and although they are composed of essentially completely helical structures, the polypeptide chains appeared not to be monodisperse. We report here that these synthetic, oriented peptide layers can be manipulated enzymatically to clip selectively the longer peptide chains, providing a more uniform layer without concurrently destroying bulk material or adversely influencing the high levels of helicity of the layers. These results are significant from two perspectives. First, we have demonstrated that enzymes can be used to manipulate the macroscopic features of bulk materials, in this case resulting in the smoothing of an uneven polymer surface. Second, we have shown that bulk materials comprised of natural substrates for enzymes are resistant to natural enzymatic degradation when formed in a tightly organized array.

Through the use of suitable starting "seeds" of different size, we have been able to define an area on the surface that is appropriate for the helical secondary structure of polyphenylalanine, polyethylglycine, and polyleucine on gold (as a thin layer on chromium-coated silicon) and of polyalanine on both ITO glass and gold (Fig. 1).[1, 2] Possible applications of these polypeptide

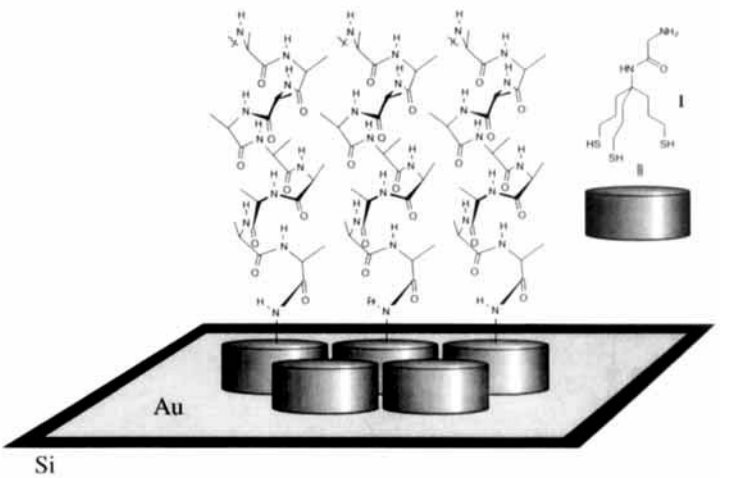


Fig. 1. Schematic representation of a layer of helical polyalanine formed by polymerization of the N-carbonic anhydride starting with a monolayer of aminotrithiol **1** as a "seed" bound to a gold layer on silicon with an intervening layer of chromium. For clarity, **1** is shown as a cylinder on the surface.

layers include waveguide optical switches based on nonlinear optical properties inherent in materials with unidirectional alignment of polarizability vectors.[3–6] Our method for constructing relatively thick layers of highly ordered and directionally aligned materials complements other techniques that depend upon a discrete, layer-by-layer assembly, and has the distinct advantage that the layers are constructed in a single operation; it has the disadvantage that there is no inherent means to produce material composed of chains of all the same length. Thus, although the layers formed in this way are composed almost exclusively of helical peptide units oriented nearly perpendicular to the surface, the lengths of the individual chains (and, therefore, the height above the surface) are uneven. Indeed, attempts to measure thickness of these polypeptide layers using ellipsometry[7] were unsuccessful as the data was highly variable across the surface and not interpretable. Nonetheless, we were able to make an estimate of average thickness of the layers by comparing their IR absorbance with that of a layer consisting of 24 alanines prepared by the sequential addition of trialanine units using Merrifield-like technology. Each amino acid residue in a helical

[*] Prof. J. K. Whitesell, Dr. H. K. Chang, C. S. Whitesell
Department of Chemistry, The University of Texas at Austin
Austin, TX 78712 (USA)
Telefax: Int. code + (512)471-7791

[**] We are grateful to the National Science Foundation (Small Grant for Exploratory Research DMR-9014026) and the Robert A. Welch Foundation (Grant F-626) for financial support of this research.

polypeptide contributes approximately 1.5 Å to the length of the helix, and thus with our system and measurement technique (80°, grazing angle reflection IR spectroscopy with vertically polarized light), each 0.1 absorbance unit (for the amide I band) corresponds to approximately 300 Å of thickness. We have thus far been able to grow layers thicker than 3000 Å that are optically clear.

For practical use as waveguide materials, it is desirable that the surface be as uniform as possible to minimize light loss. Thus, we began to examine methods which allow the longer chains to be selectively shortened. Because the bulk of the layer is apparently composed of tightly packed, helical polypeptide polymers, we reasoned that only the longer chains protruding above the surface of the bulk layer would be exposed to possible hydrolytic cleavage. However, attempted hydrolysis with aqueous sodium hydroxide led to rapid attack of the silicon–chromium interface and physical destruction of the gold overlayer.

Thus, we turned to the use of enzymes in order to achieve hydrolysis under conditions that would be more selective for cleavage of only the peptide amide bonds exposed to the solution. Indeed, treatment of a layer of polyalanine on gold with alanine aminopeptidase[8] led to rapid removal of a small fraction of the peptide layer. A plot of absorbance versus time (Fig. 2) reveals that the initial rapid rate of loss of material dropped dramatically and stopped after approximately 12% of the material was removed. (Fresh enzyme was added at 10 h intervals to insure that the decrease in removal rate did not result from inactivation of the enzyme by either denaturation or product inhibition.[9])

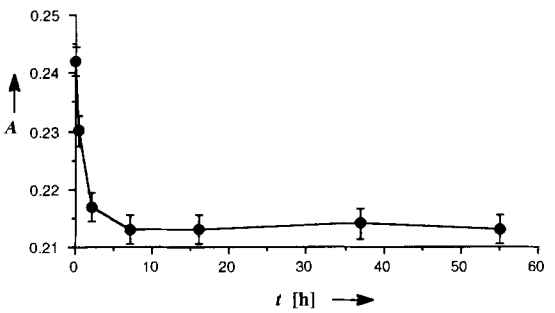


Fig. 2. Plot of absorbance A (amide I band) versus time t for a 300 Å thick layer of polyalanine on gold upon treatment with alanine aminopeptidase in water at pH 6.8 and 37 °C.

By modification of the procedure used to prepare polyalanine layers, we have also been able to construct thin films of peptides derived from other amino acids, including phenylalanine and leucine.[11] Treatment of the layer of polyleucine with leucine aminopeptidase[10] also resulted in a rapid decrease in IR absorbance with no further change observed after 1 h; approximately 11% of the total thickness was removed by the enzyme.

These results are consistent with the selective removal of residues only from the longer chains, a process that must stop when the amino terminus of the peptide can no longer reach the active site of the enzyme. We have represented this concept schematically in Figure 3. Indeed, after enzymatic treatment, the layers were amenable to ellipsometry. We conclude that the longer chains form a disordered mass on the surface and that this overlayer of helical peptides contributes dramatically to the degree of rotation of the laser beam used in the ellipsometric measurement. After enzymatic grooming, thickness values of about 300 Å per 0.1 absorbance units were obtained for the polyalanine films, in reasonable agreement with the estimate made above based upon the discretely prepared, 24-mer of polyalanine.[11] Furthermore, measurement of the contact angle with water[12] before treatment gave values that ranged from 23–61°, consistent with a highly variable surface. After enzymatic grooming, the contact angle was 55–56° uniformly over the surface.

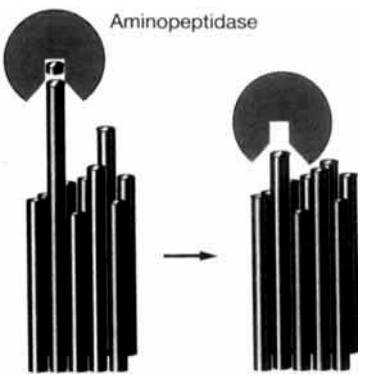


Fig. 3. Schematic representation of the selective action of alanine and leucine aminopeptidases on those polypeptide chains that extend significantly above the bulk layer.

Leucine aminopeptidase is the only aminopeptidase for which a crystal structure has been obtained.[13] The distance of the active site of this enzyme from the surface is approximately ten amino acid residues (in an extended, β-conformation). In the α-helical conformation, ten residues contribute 15 Å to the length of the peptide. However, we hesitate to suggest that variation in lengths of our surface-bound peptide layers have been reduced to this amount, because the mode of action of leucine aminopeptidase is not yet known in detail.[14] It is interesting that the same percentage of the surface-bound peptide is removed from both the polyalanine and polyleucine layers.

Experimental Procedure

Polyalanine and polyleucine layers on gold were prepared as previously described [1]. A solution of tris(hydroxymethyl)methylamine (3 mM) and $CoCl_2$, $MnCl_2$, and $MgCl_2$ (each 5 mM) was prepared and adjusted to pH 6.8 with dilute HCl. Alanine aminopeptidase (5 mg) was added and the solution was warmed at 37 °C for 20 min. The plate coated with the polyalanine layer was immersed in this solution, and periodically removed, rinsed with water and then ethanol, and analyzed by grazing angle IR spectrospcopy. Additional enzyme was added at 10 h intervals. The commericial solution of leucine aminopeptidase was used as obtained from Sigma at 37 °C. Fresh solution was used after each measurement.

Received: October 13, 1993 [Z 6416 IE]
German version: *Angew. Chem.* **1994**, *106*, 921

[1] J. K. Whitesell, H. K. Chang, *Science* **1993**, *261*, 73.
[2] The mean spacing of Si–OH groups on a glass surface is approximately 10 Å, the same as that required by helical polyalanine. However, these groups are not uniformly spaced and, as a result, the layers on ITO glass are not as well ordered as those on gold.
[3] D. F. Eaton, *Science* **1991**, *253*, 281.
[4] *Non-Linear Optical Properties of Organic Molecules and Crystals, Vol. 1, 2* (Eds.: D. S. Chemla, J. Zyss), Academic Press, New York, **1987**.
[5] *Non-Linear Optical Properties of Organic and Polymeric Materials* (Ed.: D. J. Williams) (*ACS Symp. Ser.* **1983**, *233*).
[6] D. J. Williams, *Angew. Chem.* **1984**, *96*, 637; *Angew. Chem. Int. Ed. Engl.* **1984**, *23*, 690.
[7] K. Rielding, *Ellipsometry for Industrial Applications*, Springer, Wien, **1988**. R. Collins, Y.-T. Kim, *Anal. Chem.* **1990**, *62*, 887A.
[8] W. L. Starnes, F. J. Behal, *Biochemistry* **1974**, *13*, 3221. The enzyme used was extracted from bovine intestinal mucosa (Sigma).
[9] The amount of enzyme used was orders of magnitude more than necessary to remove all of the peptide layer.

[10] M. M. Bradford, *Anal. Biochem.* **1974**, *13*, 3221. The enzyme used was extracted from porcine kidney (type III-CP, Sigma).
[11] This comparison is not ideal because the layers that we have built by sequential addition do not exhibit as high a level of helicity as those prepared by polymerization. We rationalize this difference as resulting from low levels of partial racemization during the multistep operations, where a single amino acid of the opposite hand inhibits formation of the helical secondary structure for several residues to both sides of the defect.
[12] A. W. Adamson, *Physical Chemistry of Surfaces*, 5th ed. Wiley Interscience, New York, **1990**, pp. 332-368. R. H. Dettre, R. E. Johnson, Jr., *J. Phys. Chem.* **1965**, *69*, 1507.
[13] S. K. Burley, P. R. David, A. Taylor, W. N. Lipscomb, *Proc. Natl. Acad. Sci. USA* **1990**, *87*, 6878. This crystal structure was obtained on peptidase obtained from bovine lense—that used in our experiments was obtained from porcine kidney. It has been suggested that these enzymes are very similar, if not identical. See: F. Jurnak, A. Rich, L. van Loon-Klaassen, H. Bloemendal, A. Taylor, F. H. Carpenter *J. Mol. Biol.* **1977**, *112*, 149 and ref. [14].
[14] W. N. Lipscomb, H. Kim, *Biochemistry* **1993**, *32*, 8465; W. N. Lipscomb, personal communication.

An Extremely Long-Lived Triplet Carbene; Reactivity, Optical Absorption Spectrum, and Kinetics of Highly Congested Diarylcarbenes**

Hideo Tomioka,* Hidetsumu Okada, Tetsuya Watanabe, and Katsuyuki Hirai

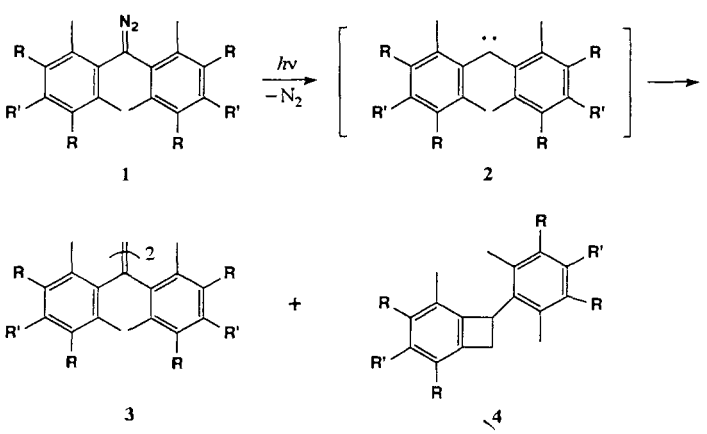
In contrast to the long history of persistent radicals,[1] which started with the work of Moses Gomberg in 1890, that of persistent carbenes is much shorter. Only a few years ago "bottleable" carbenes were first isolated.[2, 3] These carbenes are stabilized not only by bulky protecting groups but also by heteroatom substituents directly connected to the carbenic carbon atom. Owing to these substituents, these carbenes have singlet ground states. But their electronic configurations are still a topic of debate.[4] The next challenge is the stabilization of a carbene hopefully having a triplet ground state by all-carbon substituents. The most persistent triplet carbene known so far is dimesitylcarbene (**2a**), which was first generated by Zimmerman and Paskovich[5] in 1964. The congestion at the carbene center in **2a** is reflected in its unique behavior, for example its proclivity to dimerize and reluctance to attack secondary carbon–hydrogen bonds. Carbene **2a** was not stable enough to be isolated, and systematic kinetic studies were also not conducted for further characterization. If four additional methyl groups are introduced at the *meta* positions, the carbenic center would be more crowded, because of the "buttressing effect" on the four *ortho* methyl groups.[6] In view of the scarcity of the data in this field despite recent growing interest in triplet carbenes as potential organic ferromagnets,[7] we became interested in designing and generating persistent triplet carbenes. Thus, we have generated a series of polymethylated diphenylcarbenes **2a–c** and investigated their reactivities by flash photolysis techniques. We have found that they are exceptionally long-lived for diarylcarbenes with lifetimes on the order of seconds.

The new precursor diazomethanes **1b, c** were prepared by essentially the same procedure[5, 8] employed for dimesityldiazomethane. The polymethylated diphenylcarbenes were then generated either by thermolysis or by photolysis of the diazomethanes, and the products were analyzed by conventional methods (Table 1). The reactions observed with didurylcarbene

Table 1. Conditions and product distribution for the decomposition of diazo compounds **1** [a].

Diazo cmpd	Conditions	Yield [%] [b] 3	4
1a	C_6H_6/140 °C	14	63
1b	C_6H_6/140 °C	0	96
1c	C_6H_6/140 °C	0	90
1a	$h\nu/C_6H_6$/10 °C	61	0
1b	$h\nu/C_6H_6$/10 °C	29	41
1c	$h\nu/C_6H_6$/10 °C	5	79

[a] Irradiations were carried out on a 20 mM solution of **1** in degassed benzene with a 300 W Hg lamp and a Pyrex filter. Thermolyses were performed in degassed benzene and in a sealed Pyrex tube. [b] Determined by gas chromatography and NMR spectroscopy.



(**2b**) and decamethyldiphenylcarbene (**2c**) were analogous to those observed with dimesitylcarbene (**2a**). These carbenes did not react with the diazomethane precursors to give ketazines. Instead they reacted either by dimerization to form tetraarylethylene **3** or by attack at an *ortho* methyl group to give 1,2-dihydrocyclobutabenzene ("benzocyclobutene") **4**. A key difference is found, however, in the formation of **4**. In the case of **2a**, **4a** was produced only by thermolysis at 140 °C, and **2a** underwent mainly dimerization when photolyzed at room temperature. On the other hand, in the case of **2b**, benzocyclobutene **4b** was produced not only by thermolysis but also by photolysis along with the dimer. Compound **2c** produced **4c** as major product at the expense of **3a** even in the photolytic run.

Irradiation ($\lambda > 300$ nm) of **1a** in a 2-methyltetrahydrofuran (MTHF) glass at 4 K gave a paramagnetic species readily characterized from its EPR spectrum as triplet didurylcarbene **2a**. The EPR signals from **2** were stable for at least several hours at this temperature and survived even at 110 K. These observations established the triplet as the ground state of this carbene.[9]

Optical spectroscopy in the frozen medium gave analogous but more intriguing results. Figure 1b shows the absorption spectrum obtained after irradiation of **1b** in a MTHF glass at 77 K. The spectrum displays two distinct features: two sharp, intense UV bands with maxima at 321 and 335 nm, and in the

[*] Prof. Dr. H. Tomioka, H. Okada, T. Watanabe, K. Hirai
Chemistry Department for Materials, Faculty of Engineering
Mie University
Tsu, Mie 514 (Japan)
Telefax: Int. code + (592)31-9471

[**] This work was supported by the Japanese Ministry of Education, Science, and Culture.

visible portion of the spectrum two weak, broad, overlapping bands with apparent maxima at 466 and 495 nm. The glassy solution did not exhibit any changes in its absorption spectrum for several hours when kept at 77 K. However, when it was allowed to warm to room temperature and then cooled to 77 K, the characteristic absorption bands disappeared (vide infra). The absorption spectra of several aryl carbenes in frozen media have been reported.[10] Typically, they display an intense UV band and a weak visible transition. These features are present in the spectrum obtained in the photolysis of **1b**. Moreover, the product analysis of the reaction solution showed the presence of dimer **3b** as well as benzocyclobutene **4b**. Thus, the absorption spectrum can be attributed to didurylcarbene (**2b**) generated by the photodissociation of **1b**.

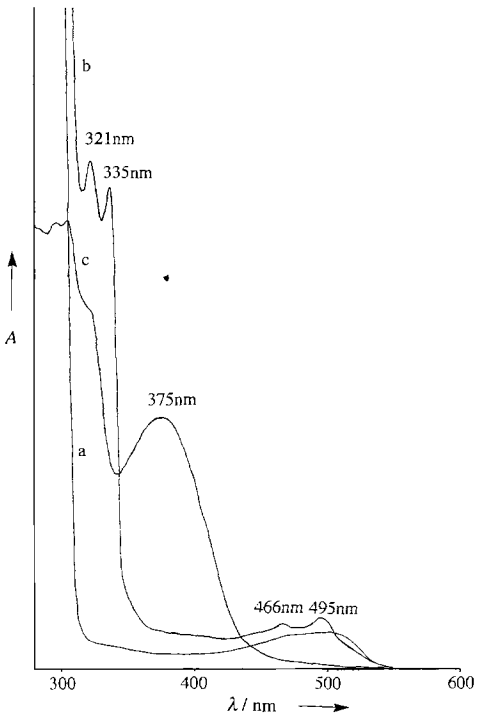
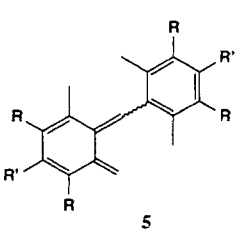


Fig. 1. a) UV/VIS spectrum of **1a** in MTHF at 77 K. b) Same sample after 6 min irradiation ($\lambda > 300$ nm). c) Same sample after the matrix was warmed to 110 K.

The spectral changes of the matrix were carefully monitored as a function of temperature as the matrix thawed. At higher temperatures a new broad absorption at 375 nm appeared and increased as carbene absorption bands decreased (Fig. 1c). The species responsible for this new absorption showed appreciable thermal stability; even at room temperature it persisted a few seconds before decaying. These observations suggest that the absorption at 375 nm must be due to an intermediate formed from the initially generated triplet carbene that leads to the final products.

A plausible candidate for the intermediate, which also explains the formation of benzocyclobutene, is *o*-xylylene **5b**, formed by intramolecular 1,4 H shift from an *ortho*-methyl group to the carbenic center of **2b**. Coincidently, the formation of *o*-xylylene from *o*-tolylmethylene and its subsequent cyclization was demonstrated by matrix isolation spectroscopy in inert gas matrices at low temperature both upon photolysis and upon thawing the matrix.[11] Moreover, several *o*-xylylenes have been reported to exhibit a broad absorption band centered at around 350 to 460 nm depending on the substituents.[12]



5

Flash photolysis of **1b** (1.0×10^{-4} M) in a degassed benzene solution at room temperature with a xenon flash lamp (pulse width of 10 μs) produced a transient species absorbing at 310–350 nm; the apparent maximum at around 335 nm was coincident with the xenon pulse (Fig. 2). The decay kinetics of the

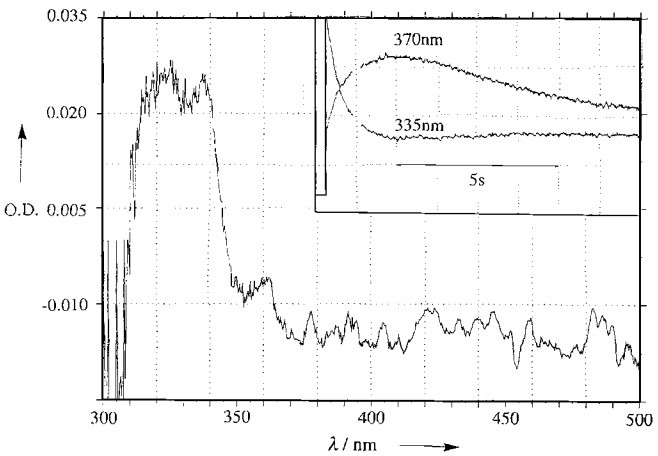


Fig. 2. Absorption spectra of the intermediates formed by irradiation of **1b** in degassed benzene, recorded 50 μs after the photolysis pulse. The inset in the upper right shows the time course of the absorptions at 335 and 370 nm (oscillogram traces). O.D. = optical density.

transients indicates that the absorption at 335 nm decays within 1 s and a new species with an absorption maximum at around 370 nm arises, which is too long-lived to be monitored by our system. Product analysis of the spent solution showed the presence of **3b** and **4b**. Thus, on the basis of the low-temperature spectrum coupled with chemical analysis, we assign the initially formed transient with a maximum at 335 nm to carbene **2b** and the second to *o*-quinodimethane **5b**. This interpretation is supported by the trapping experiments using oxygen. In the flash photolysis of an oxygen-saturated benzene solution of **1b** a broad absorption band with a maximum at 390 nm appeared at the expense of the absorption due to the carbene. The reaction mixture was found to contain octamethylbenzophenone as the main product. It is well documented that diarylcarbenes with triplet ground states are readily trapped by oxygen to generate the corresponding diarylketone oxides.[13] Thus, our observation can be interpreted as indicating that the triplet carbene **2b** is trapped by oxygen to form the carbonyl oxide, which confirms that the transient absorption quenched by oxygen is due to **2b**. The rate constant for the quenching of **2b** by oxygen was determined to be $7.1 \times 10^7\ M^{-1} s^{-1}$. The inset in Figure 2 shows the decay of **2b** and the formation of **5b** over time and indicates that the decay of **2b** is kinetically correlated with the growth of **5b**. The decay rate constant was determined to be $2.1 \pm 0.1\ s^{-1}$, while the growth rate constant was $1.8 \pm 0.2\ s^{-1}$. Since the product analysis shows that carbene **2b** decays not only by intramolecular H abstraction but also by dimerization, the difference in the rate constants can be ascribed to the dimerization rate constant (k_d) under the assumption that the rate constant for the formation of **5b** is identical with that for H abstraction (k_i). Since the difference in the rate constants, $0.3\ s^{-1}$, is equal to $k_d[\mathbf{2b}]$, k_d is determined to be $6.4 \pm 0.7 \pm 10^4\ M^{-1} s^{-1}$ by

 © VCH Verlagsgesellschaft mbH, D-69451 Weinheim, 1994 0570-0833/94/0808-0874 $ 10.00+.25/0

using [**2b**] obtained from the extinction coefficient of **2b** and absorbance after the pulse. A half-life ($t_{1/2}$) of roughly 310 ms was determined for **2b** from the decay curve, while the lifetime based on k_i was estimated to be 555 ± 62 ms. Similar measurements for the carbenes **2a** and **2c** gave values of k_d, k_i, and $t_{1/2}$ (τ) for **2a** of $7.3 \pm 1.5 \times 10^5\ M^{-1} s^{-1}$, $3.1 \pm 0.4\ s^{-1}$, and 210 (323 ± 42) ms, respectively, while **2c** decayed unimolecularly with $k_i = 6.9 \pm 0.5\ s^{-1}$ ($\tau = 145 \pm 10$ ms).

These results indicate that when four methyl groups are introduced at the *meta* positions of the *ortho*-methylated diphenylcarbene, the carbenic center is more effectively blocked by the four *ortho* methyl groups presumably owing to the buttressing effect exerted by the *meta* substituents. Didurylcarbene is found to be some five orders of magnitude longer lived than the parent diphenylcarbene (2 μs in cyclohexane).[14] However, when two more methyl groups are introduced at the *para* positions, the carbenic center is forced to react with the *ortho* methyl groups, which are brought much closer to the carbene, and the carbene is shorter lived.

Support is lent to this explanation by semiempirical calculations. Optimized geometries calculated for a series of polymethylated phenylcarbenes with the programm PM3-ROHF/CI (4×4)[15] indicate that the distances between carbenic carbon and *o*-methyl carbon atom for mesityl-, duryl-, and pentamethylphenylcarbenes are 2.8461, 2.7942, and 2.7778 pm, respectively.

The present study reveals that polymethylated diphenylcarbenes are exceptionally long-lived for diarylcarbenes, although they are not persistent enough to be isolable. The buttressing effects effectively strengthen the *ortho* effect that protects the reactive center. This strategy may prove successful in the preparation of a "bottleable" triplet carbene.

Received: October 27, 1993 [Z 6455 IE]
German version: *Angew. Chem.* **1994**, *106*, 944

[1] Reviews: A. R. Forrester, J. M. Hay, R. H. Thomson, *Organic Chemistry of Stable Radicals*, Academic Press, London, **1968**; D. Griller, K. U. Ingold, *Acc. Chem. Res.* **1976**, *9*, 13; M. Ballester, *ibid.* **1985**, *18*, 380.

[2] A. Igau, H. Grützmacher, A. Baceiredo, G. Bertrand, *J. Am. Chem. Soc.* **1988**, *110*, 6463; A. Igau, A. Baceiredo, G. Trinquier, G. Bertrand, *Angew. Chem.* **1989**, *101*, 617; *Angew. Chem. Int. Engl.* **1989**, *28*, 621; G. R. Gilette, A. Baceiredo, G. Bertrand, *ibid.* **1990**, *102*, 1486 and **1990**, *29*, 1429; D. A. Dixon, K. D. Dobbs, A. J. Arduengo, III, G. Bertrand, *J. Am. Chem. Soc.* **1991**, *113*, 8782.

[3] A. J. Arduengo, III, R. L. Harlow, M. Kline, *J. Am. Chem. Soc.* **1991**, *113*, 361; A. J. Arduengo, III, M. Kline, J. C. Calabrese, F. Davidson, *ibid.* **1991**, *113*, 9704; A. J. Arduengo, III, H. V. Rasika Dias, R. L. Harlow, M. Kline, *ibid.* **1992**, *114*, 5530.

[4] M. Regitz, *Angew. Chem.* **1991**, *103*, 691; *Angew. Chem. Int. Ed. Engl.* **1991**, *30*, 674; R. Dagani, *Chem. Eng. News* **1991**, *69*, No. 4, p. 19.

[5] H. E. Zimmerman, D. H. Paskovich, *J. Am. Chem. Soc.* **1964**, *86*, 2149.

[6] a) See for instance, L. N. Ferguson, *The Modern Structural Theory of Organic Chemistry*, Prentice-Hall, Englewood-Cliffs, NJ, USA, **1963**, Chapters 3 and 5; b) for the buttressing effect in carbene chemistry see: H. Tomioka, K. Kimoto, H. Murata, Y. Izawa, *J. Chem. Soc. Perkin Trans. 1* **1991**, 471, and references therein.

[7] For a review see: H. Iwamura, *Pure Appl. Chem.* **1986**, *58*, 187; *Adv. Phys. Org. Chem.* **1990**, *26*, 179.

[8] Diazomethanes **2b**, **c** were prepared by the treatment of diarylketimine with N_2O_4 followed by the reduction of the corresponding *N*-nitrosoketimine with $LiAlH_4$. They could be purified by gel permeation chromatography. **2b**: Orange crystals, m.p. 168.0–169.0 °C: ^1H NMR (CCl_4) $\delta = 1.98$ (s, 12H), 2.10 (s, 12H), 6.78 (br, s, 2H); IR (KBr): $\nu = 2038\ cm^{-1}$; **2c**: orange crystals, m.p. 141.2–144.0 °C: ^1H NMR (CCl_4): $\delta = 2.10$ (s, 12H), 2.22 (s, 12H), 2.26 (s, 6H); IR (KBr): $\nu = 2040\ cm^{-1}$.

[9] H. Tomioka, T. Takui, K. Itoh, unpublished.

[10] See for example A. Trozzolo, *Acc. Chem. Res.* **1968**, *1*, 329.

[11] R. J. McMahon, O. L. Chapman, *J. Am. Chem. Soc.* **1987**, *109*, 683; O. L. Chapman, J. W. Johnson, R. J. McMahon, P. R. West, *ibid.* **1988**, *110*, 501.

[12] a) K. K. de Fonseka, J. J. McCullough, A. J. Yarwood, *J. Am. Chem. Soc.* **1979**, *101*, 3277; b) G. Quinkert, *Angew. Chem.* **1975**, *87*, 790; *Angew. Chem. Int. Ed. Engl.* **1975**, *14*, 851; c) V. Wintgens, J. C. Netto-Ferreira, H. L. Casal, J. C. Scaiano, *J. Am. Chem. Soc.* **1990**, *112*, 2363, and references therein; d) J. C. Netto-Ferreira, V. Wintgens, J. C. Scaiano, *Tetrahedron Lett.* **1989**, *30*, 6851; e) H. G. Korth, K. U. Ingold, R. Sustman, H. de Groot, H. Sies, *Angew. Chem.* **1992**, *104*, 915; *Angew. Chem. Int. Ed. Engl.* **1992**, *31*, 891.

[13] For a review see: W. Sander, *Angew. Chem.* **1990**, *102*, 362; *Angew. Chem. Int. Ed. Engl.* **1990**, *29*, 344.

[14] L. M. Hadel, V. M. Maloney, M. S. Platz, W. G. McGimpsey, J. C. Scaiano, *J. Phys. Chem.* **1986**, *90*, 2488.

[15] J. J. P. Stewart, *J. Compt. Chem.* **1989**, *10*, 209, 221; MOPAC version 6.01 (JCPE # PO44), was used.

Ether-Solvated Sodium Ions in Salts Containing π-Hydrocarbon Anions: Crystallization, Structures, and Semiempirical Solvation Energies**

Hans Bock,* Christian Näther, Zdenek Havlas, Andreas John, and Claudia Arad

Dedicated to Professor Heinz Nöth on the occasion of his 65th birthday

In numerous reactions in solution, the solvation of cations[1] can exert influence on the multidimensional network of interrelated equilibria of electron transfer, ion pair formation, or aggregation[1e] and, therefore, control processes from a geochemical[1f] to a biochemical[1g] nature. The selection of the $Na^{\oplus}$ ion is advantageous for the investigation of the complex interdependencies, because, due to its small ionic radius and high solvation enthalpy[2] together with the relatively low reduction potential of sodium metal,[2] this cation forms countless salts[3a] and compounds[1e, 3b] of impressive structural diversity. Using $Na^{\oplus}$ as example, we report on a method to specifically prepare optimally ether-solvated metal cations by one-electron reduction of unsaturated hydrocarbons with alkali metals in ether solution and to crystallize the solvent-separated π-hydrocarbanion salts (Scheme 1).

Under aprotic reduction conditions the π-hydrocarbons (Scheme 1) selectively form their radical anions, which, due to the extensive delocalization of the negative charge in their rather large π-systems, no longer possess negatively charged centers[1e, g] suited to form contact ion pairs **A**, and therefore crystallize as solvent-separated ion pairs **B**[4]. One of the many possible variations is demonstrated by fluorene (Scheme 1), the sodium reduction of which leads to H_2 formation.[4]

$[Met^{\oplus}\{RO(CH_2CH_2O)_{x-1}\}_y C_n H_m^{\bullet\ominus}]$ **A**

$[Met^{\oplus}\{RO(CH_2CH_2O)_{x-1}\}_y][C_n H_m^{\bullet\ominus}]$ **B**

[*] Prof. Dr. H. Bock, Dipl.-Chem. C. Näther, Dipl.-Chem. A. John, Dipl.-Chem. C. Arad
Chemisches Institut der Universität
Marie-Curie-Strasse 11, D-60439 Frankfurt am Main (FRG)
Telefax: Int. code + (069)5800-9188
Dr. Z. Havlas
Institute of Organic Chemistry and Biochemistry of the Czech Academy of Sciences, Prague (Czech Republic).

[**] Structures of Charge-Perturbed and Sterically Overcrowded Molecules as well as Interactions in Crystals, Part 31. The investigations have been supported by the A. Messer Foundation, the Bundesland Hessen, the Deutsche Forschungsgemeinschaft, and the Fonds der Chemischen Industrie. – Part 30: H. Bock, I. Göbel, C. Näther, Z. Havlas, A. Gavezzotti, G. Filippini, *Angew. Chem.* **1993**, *105*, 1823; *Angew. Chem. Int. Ed. Engl.* **1993**, *32*, 1755.

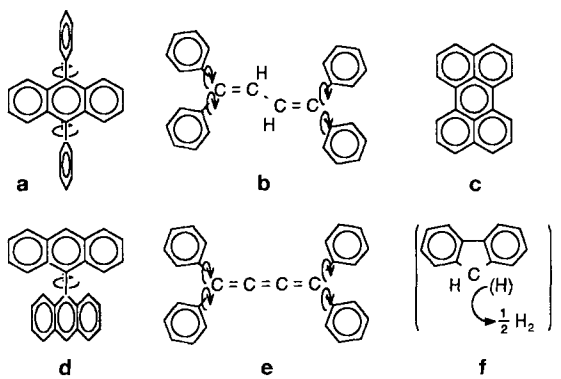
Redox half-reaction I:

$$[Met]_{\infty} + y\ solvent \rightleftharpoons [Met^{\oplus}(solvent)_y] + e^{\ominus}$$

Redox half-reaction II:

$$C_nH_m + e^{\ominus} \rightleftharpoons [C_nH_m^{\bullet\ominus}]$$

$[C_nH_m^{\bullet\ominus}]$:



Scheme 1. Preparation of solvent-separated radical anion salts $[Met^{\oplus}(solvent)_y][C_nH_m^{\bullet\ominus}]$ with optimally solvated metal cations $Met^{\oplus}$ by one-electron transfer from alkali metals $[Met]_x$ to unsaturated hydrocarbons C_nH_m containing extended π-systems, partly sterically shielded because of twisting effects, for example, in ether as solvent. (For $Met^{\oplus} = Na^{\oplus}$, see Fig. 1 and text). **a**: 9,10-diphenylanthracene$^{\bullet\ominus}$, **b**: 1,1,4,4-tetraphenyl-1,3-butadiene$^{\bullet\ominus}$, **c**: perylene$^{\bullet\ominus}$, **d**: bianthryl$^{\bullet\ominus}$, **e**: 1,1,4,4-tetraphenylbutatriene$^{\bullet\ominus}$, (**f**: fluorenyl$^{\bullet\ominus}$).

In the solvates **1**–**5** with various ethers (Fig. 1), the coordination number n of the $Na^{\oplus}$ center increases from the frequently observed[3] 6 in **1**, **2**, and **3** to 7 in the cryptand-221-solvate **4** and to 8 in the bis(triglyme) solvate **5**. Despite largely comparable dihedral angles ω(OC-CO) = 59 ± 2° in polyethers,[5] the average contact distances $Na^{\oplus} \cdots O$ increase with the coordination number from 239 ± 4 pm for $n = 6$ to 248 ± 9 pm for $n = 7$ and to 262 ± 13 pm for $n = 8$. An almost octahedral arrangement is observed only in the solvent complex $[Na^{\oplus}(thf)_6]$ (**1**, Fig. 1), which exhibits angles $ONa^{\oplus}O$ of 90 ± 3°. All the other coordination polyhedra $Na^{\oplus}O_n$ are distorted: The angles $ONa^{\oplus}O$ vary in $[Na^{\oplus}(dme)_3]$ (**2**) between 69 and 104°, in $[Na^{\oplus}(diglyme)_2]$ (**3**) between 80° and 138°, in $[Na^{\oplus}$(cryptand-221)] (**4**) between 68° and 124°, and in the eight-coordinate $[Na^{\oplus}(triglyme)_2]$ (**5**) between 61 and 93° (Fig. 1).

The different solvent shells around the $Na^{\oplus}$ ions (Fig. 1) can be discussed with regard to MNDO enthalpies of formation (Table 1), which have been approximated from the structural coordinates[6] (Scheme 2).

Table 1. Characteristic MNDO differences in heats of formation, $\Delta\Delta H_f^{MNDO}$, [6c] and average bond energies BE^{MNDO} [$Na^{\oplus} \cdots O(N)$] (each in kJ mol^{-1}) for the solvated complexes $[Na^{\oplus}\{RO(CH_2CH_2O)_{x-1}R\}_y]$ (cf. Scheme 2).

Cation	$n_{Coord.}$	Ether	(Solvent shell)	$\Delta\Delta H_f^{MNDO}$ (Solvent repulsion)	(Free ether)	BE^{MNDO} [$Na^{\oplus} \cdots O$]
1	6	6 THF	−830	+243	−587	−98
2	6	3 DME	−771	+100	−671	−112
3	6	2 Diglyme	−743	+66	−677	−113
4	7	1 Cryptand-221			−804	(−115)
5	8	2 Triglyme	−859	+151	−708	−89

The MNDO heats of formation[6] (Scheme 2 and Table 1) for the solvent complexes $[Na^{\oplus}\{RO(CH_2CH_2O)_{x-1}R\}_y]$ provide, in particular, the following information:

1) The best complexing agent for $Na^{\oplus}$ is the cryptand-221 (Table 1; $\Delta\Delta H_f^{MNDO}$ (free ethers) = − 804 kJ mol^{-1}), as expected.

2) If the coordination number of the cation is kept constant, the repulsive interactions within the solvent shell are clearly

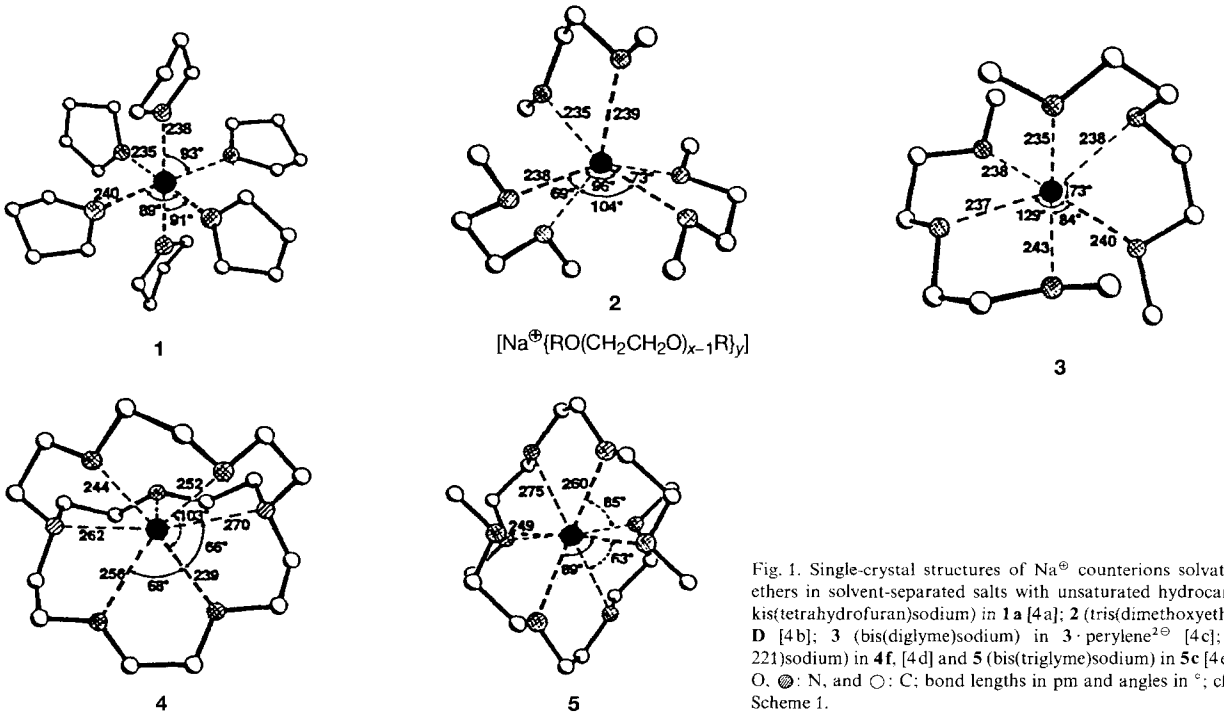
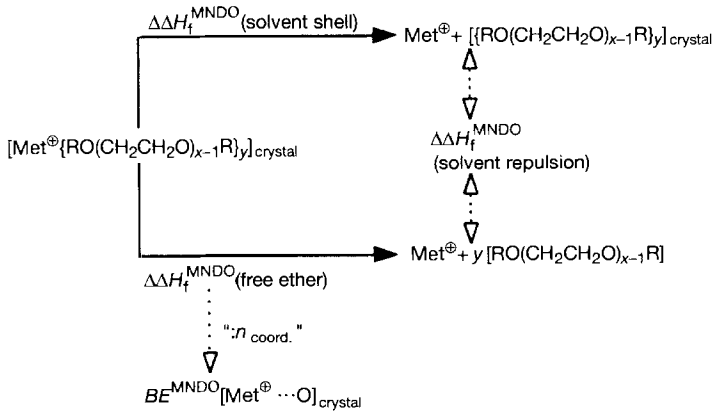


Fig. 1. Single-crystal structures of $Na^{\oplus}$ counterions solvated by different ethers in solvent-separated salts with unsaturated hydrocarbons: **1** (hexakis(tetrahydrofuran)sodium) *in* **1a** [4a]; **2** (tris(dimethoxyethane)sodium) *in* **D** [4b]; **3** (bis(diglyme)sodium) in **3**·perylene$^{2\ominus}$ [4c]; **4** ((cryptand-221)sodium) in **4f**, [4d] and **5** (bis(triglyme)sodium) in **5c** [4e]. ●: $Na^{\oplus}$, ◍: O, ◎: N, and ○: C; bond lengths in pm and angles in °; cf. text. **a**–**f**: See Scheme 1.



Scheme 2. Approximate calculation of MNDO heats of formation from the crystal structure data (Fig. 1): Removal of the cation $Met^{\oplus}$ from the solvated complex $[Met^{\oplus}\{RO(CH_2CH_2O)_{x-1}R\}_y]$ yields the heats of formation difference $\Delta\Delta H_f^{MNDO}$ (solvent shell) if the solvent shell does not change, and analogously if the shell breaks up into individual ether molecules, $\Delta\Delta H_f^{MNDO}$ (free ethers); the difference between them can be defined as $\Delta\Delta H_f^{MNDO}$ (solvent repulsion). An average bond energy BE^{MNDO} $[Met^{\oplus} \cdots O]$ in the solvated complexes can be estimated from the value $\Delta\Delta H_f^{MNDO}$ (free ether) on dividing it by the coordination number $n_{coord.}$.

noticeable: Thus $Na^{\oplus}$ is encapsulated by three molecules of dimethoxyethane energetically more favorably than by six molecules of tetrahydrofuran (Fig. 1, **1** and **2**, as well as Table 1, $\Delta\Delta H_f^{MNDO}$ (solvent repulsion) = +100 and +243 kJ mol^{-1}). This further substantiates the laboratory experience that DME is better suited than THF to crystallize thermally stable $Na^{\oplus}$ salts of organometallic anions.

3) For comparable solvation, the size of the cation plays an important role. For instance, for the solvent complex $[Li^{\oplus}(dme)_3]$[7] the MNDO bond energy ($Li^{\oplus} \cdots O$) is estimated to be only −42 kJ mol^{-1} (cf. Table 1, $[Na^{\oplus}(dme)_3]$ with BE^{MNDO} ($Na^{\oplus} \cdots O$) = −112 kJ mol^{-1}), and the repulsion between the surrounding dimethoxyethane molecules, which is enhanced by the decrease of the cation radius from 97 to 68 pm,[2] increases by about 90 kJ mol^{-1}.[8]

The last remark also reveals that the method for preparation and crystal growth of salts with optimally solvated cations (Scheme 1) exemplified here for $Na^{\oplus}$ can be applied to other metals that can reduce unsaturated hydrocarbons. The same holds for other solvents such as ethylenediamine derivatives $R_2N(CH_2CH_2NR)_xR$.[9]

For the fascinating phenomenon of cation solvation, (macroscopic) thermodynamic data dominate the literature to date. For a 'microscopic' structural picture, serendipitous discoveries such as the simultaneous 1:1 crystallization of tetraphenylbutadiene disodium from dimethoxyethane both as a solvent-sharing contact ion aggregate **C** as well as a solvent-separated ion triple **D**[1k] can add novel and essential facets: The equilibria

$[\{Na^{\oplus}(dme)_2\}_2C_{28}H_{22}^{2\ominus}]$ **C**

$[\{Na^{\oplus}(dme)_3\}_2][C_{28}H_{22}^{2\ominus}]$ **D**

between the multiple solvation of metal cations and the competing formation of contact ion triples with a shared solvent shell is further affected by an energetically favorable lattice packing.[10]

Experimental Procedure

For the preparation of solvent-separated ion pairs freshly cut sodium (0.5 to 1 mmol, about 12 mg) degreased with *n*-hexane was placed in a Schlenk trap under argon, and a sodium metal mirror was generated at 10^{-4} mbar by heating with a hot air blower. Thereafter, an equimolar amount of the hydrocarbon was weighed into the trap under Ar, and the appropriate solvent, carefully dried ($c_{H^{\oplus}} < 1$ ppm) and repeatedly degassed at 10^{-4} mbar was added dropwise. The quantity is selected so that the hydrocarbon concentration essential for the crystal growth amounts to approximately 1 to 2×10^{-2} mol L^{-1}. Under the above conditions crystals of $[Na^{\oplus}(thf)_6]$[9,10-diphenylanthracene$^{\cdot\ominus}$] and of $[Na^{\oplus}(dme)_3][9,9'$-bianthryl$^{\cdot\ominus}]$ with dimensions between 0.3 and 0.5 mm and a reflection profile suited for structure determination grow within 2 to 20 days. Advisable for reactions with perylene is a sixfold metal surplus and for those requiring lithium metal for reaction activation an initial ultrasonic treatment (50 W) of 2 to 5 minutes. For the crystal growth of the sodium salts, the solutions have to be covered by a 5 to 10 mL layer of carefully purified *n*-hexane.

Received: September 11, 1993
Revised version: January 11, 1994 [Z 6353 IE]
German version: *Angew. Chem.* **1994**, *106*, 931

[1] From the extensive literature are selected: a) *Ions and Ion Pairs in Organic Reactions*, Vol. 1, 2 (Ed.: M. Swarc), Wiley-Interscience, New York, **1972**, **1974**; b) Y. Marcus, *Ion Solvation*, Wiley, Chichester, **1985**; c) J. M. Lehn, *Angew. Chem.* **1988**, *100*, 91; *Angew. Chem. Int. Ed. Engl.* **1988**, *27*, 89; d) *Cation Binding by Macrocycles* (Eds.: Y. Inoue, G. W. Gokel), M. Dekker, New York, **1990**; e) H. Bock, K. Ruppert, C. Näther, Z. Havlas, H.-F. Herrmann, C. Arad, I. Göbel, A. John, J. Meuret, S. Nick, A. Rauschenbach, W. Seitz, T. Vaupel, B. Solouki, *Angew. Chem.* **1992**, *104*, 564; *Angew. Chem. Int. Ed. Engl.* **1992**, *31*, 560; f) N. Wiberg, *Holleman/Wiberg: Lehrbuch der Anorganischen Chemie*, 91–100. ed., de Gruyter, Berlin, **1985**; g) W. Kaim, B. Schwederski, *Bioanorganische Chemie*, Teubner, Stuttgart **1991**; h) H. Kurreck, B. Kirste, W. Lubitz, *Electron Nuclear Double Resonance Spectroscopy of Radicals in Solution*, VCH, New York, **1988**; i) H. Bock, H.-F. Herrmann, *J. Am. Chem. Soc.* **1989**, *111*, 7622; k) H. Bock, C. Näther, K. Ruppert, Z. Havlas, *J. Am. Chem. Soc.* **1992**, *114*, 6907, and the references in each paper.

[2] According to transference measurements, $Li^{\oplus}$ and $Na^{\oplus}$ move in aqueous solution as the ions $[Li^{\oplus}(H_2O)_{25}]$ and $[Na^{\oplus}(H_2O)_{17}]$ surrounded by presumably up to three solvent shells; their ionic radii increase from 68 and 97 pm for the "naked" ions to 340 and 276 pm [1 f]. The different enthalpies of hydration of −500 kJ mol^{-1} for $Li^{\oplus}$ and of −390 kJ mol^{-1} for $Na^{\oplus}$ contribute to the reason why the metal reduction potentials in water [$E(Li/Li^{\oplus}_{aq}) = -3.05$ V and $E(Na/Na^{\oplus}_{aq}) = -2.71$ V [1 f]] have a reversed sequence to the atomic ionization potentials $IE_I^V(Li) = 5.39$ eV and $IE_I^V(Na) = 5.14$ eV.

[3] Reviews: a) A. F. Wells, *Structural Inorganic Chemistry*, 5th ed., Oxford University Press, Oxford, **1987**; b) C. Schade, P. von R. Schleyer, *Adv. Organomet. Chem.* **1987**, *27*, 169; W. N. Setzer, P. von R. Schleyer, *ibid.*, **1985**, *24*, 353.

[4] The ether-solvated $Na^{\oplus}$ counterions crystallize (cf. Experimental) as follows: a) **1** with the 9,10-diphenylanthracene radical anion **a**, black blocks from THF (H. Bock, A. John, C. Näther, Z. Havlas, E. Mihokova, *Helv. Chim. Acta* **1994**, *77*, 41); b) **2** with the 1,1,4,4-tetraphenyl-1,3-butadiene dianion (cf. **D**), dark violet blocks from dimethoxyethane [1 k]. Solvent-separated ions $[Na^{\oplus}(dme)_3]$ (**2**) also crystallize with the tetraphenyl butatriene radical anion **e** (H. Bock, C. Arad, C. Näther, unpublished; cf. [1 e]) or with the bianthryl radical anion **d** (H. Bock, A. John, C. Näther, L. Walz, unpublished); c) **3** with perylene dianion, violet prisms from diglycol dimethyl ether (diglyme); $C_{20}H_{12}Na_2 \cdot 4C_6H_{14}O_3$, $a = 1611.2(1)$, $b = 2017.1(1)$, $c = 1412.0(1)$ pm, $V = 4589.0 \times 10^6$ pm^3 (160 K), $\rho_{calcd} = 1.209$, space group $Pna2_1$, $Z = 4$, 5675 measured reflections between $3^\circ < 2\theta < 50^\circ$, of which 4239 are independent and $4097 > 0.5\sigma(I)$, NP = 532, $R = 0.0634$, $R_w = 0.0540$, residual electron density 0.41/−0.27 e Å^{-3}, (H. Bock, C. Näther, unpublished; in addition, the salt of **3** can be crystallized with the perylene radical anion); d) **4** with the fluorenyl anion, yellow blocks from dimethoxyethane solution on addition of cryptand-221; $C_{13}H_9Na \cdot C_{16}H_{32}O_5N_2$, $a = 1334.9(1)$, $b = 1206.2(2)$, $c = 1738.6(1)$ pm, $\beta = 96.58(1)^\circ$, $V = 2780.1 \times 10^6$ pm^3 (100 K), $\rho_{calcd} = 1.186$, space group: $P2_1/n$, 7742 measured reflections between $3^\circ < 2\theta < 53^\circ$, of which 5777 are independent and $3152 > 2\sigma(I)$, NP = 321, $R = 0.0598$, $R_w = 0.0634$, residual electron density 0.59/−0.28 e Å^{-3} (H. Bock, C. Näther, unpublished). For other structure determinations of [$Na^{\oplus}$ cryptand-221)] cf., for example, D. J. Darensbourg, C. J. Bischoff, J. H. Reibenspies, *Inorg. Chem.* **1991**, *30*, 1144; D. J. Darensbourg, M. Pala, *J. Am. Chem. Soc.* **1985**, *107*, 5687; D. J. Darensbourg, R. Rokicki, R. Kudaroski, *Organometallics* **1982**, *1*, 1161; F. Mathieu, B. Metz, D. Moras, R. Weiss, *J. Am. Chem. Soc.* **1978**, *100*, 4412. e) **5** with the perylene radical anion **c**, green blocks from triglyme, $2C_{20}H_{12} \cdot Na \cdot 2C_8H_{18}O_4$, $a = 1200.1(1)$, $b = 1687.0(1)$, $c = 2320.2(1)$ pm, $V = 4697.3 \times 10^6$ pm^3 (150 K), $\rho_{calcd} = 1.250$, space group $Pccn$, $Z = 4$, 8389 measured reflections between $3^\circ < 2\theta < 50^\circ$, of which 4626 are independent and $3142 > 1\sigma(I)$, NP = 314, $R = 0.0533$, $R_w = 0.0447$, residual electron density 0.29/−0.29 e Å^{-3} (H. Bock, C. Näther, unpublished). All structures were determined with a Siemens-AED II four-cycle diffractometer ($Mo_{K\alpha}$ radiation) and were solved by direct methods (SHELXTL-PLUS). Further details of the crystal structure investigations may be obtained from the Fachinformationszentrum Karlsruhe, D-76344 Eggenstein-Leopoldshafen (FRG), on quoting the depository number CSD-58122 and the literature citation.

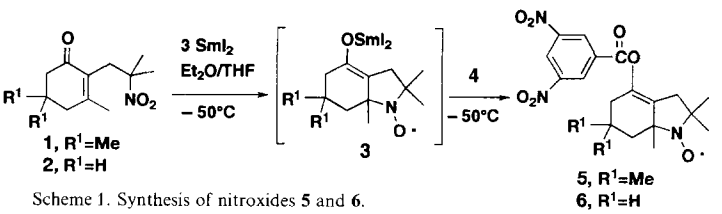
[5] H. Bock, K. Ruppert, *Inorg. Chem.* **1992**, *31*, 5094.
[6] According to literature the neglected entropy contributions are presumably small: a) For the crystallization of hydrocarbons or ketones at 300 K values for ΔTS are estimated at between 2 and 4 kJ mol^{-1} (M. S. Searle, D. H. Williams, *J. Am. Chem. Soc.* **1992**, *114*, 10690. b) On complexation of cations by cryptands, enthalpy contributions [7] also dominate (J. M. Lehn, *Acc. Chem. Res.* **1978**, *11*, 49). c) For the Na parametrization within the MNDO procedure: Z. Havlas, S. Nick, H. Bock, *J. Int. Quantum Chem.* **1992**, *44*, 449. The CH bond lengths have been corrected to 109 pm.
[7] Cf., for example, H. Schumann, W. Genthe, E. Hahn, M. B. Hossain, D. van der Helm, *J. Organomet. Chem.* **1986**, *299*, 67, or the complex [perylene$^{\bullet\ominus}$][Li$^{\oplus}$(dme)$_3$] (H. Bock, C. Näther, unpublished).
[8] H. Bock, *Jahrb. Dtsch. Akad. Naturforsch.* Leopoldina, Halle/Saale, **1992**; LEOPOLDINA **1993**, *38*, 221.
[9] Na$^{\oplus}$ solvation with ethylenediamine derivatives $R_2N(CH_2CH_2NR)_xR$: E. Weiss, *Angew. Chem.* **1993**, *105*, 1565; *Angew. Chem. Int. Ed. Engl.* **1993**, *32*, 1501, and references therein; H. Bock, C. Arad, C. Näther, Z. Havlas, unpublished.
[10] Cf., for example, *Organic Solid State Chemistry* (Ed.: G. R. Desiraju), Elsevier, Amsterdam, **1987**; G. R. Desiraju, *Crystal Engineering* (*Mat. Sci. Monogr.* **1989**, *54*).

Preparation of Chiral Nitroxide Radicals and Spontaneous Optical Resolution by Recrystallization**

Rui Tamura,* Shinsuke Susuki, Nagao Azuma, Akira Matsumoto, Fumio Toda, Akio Kamimura, and Kenzi Hori

Nitroxides protected by bulky substituents continue to play an important role not only as stable free radicals for spin-labeling experiments[1] and trapping reactions[2] but also as spin sources for the elaboration of organic magnetic materials[3] and more recently as organic oxidants.[4] The vast majority of nitroxides have been synthesized by oxidation of secondary amines or hydroxylamines.[5] We describe here the preparation, properties, and crystal structure of nitroxide radicals that are obtained as conglomerates (racemic mixtures); the synthesis is based upon the mechanistic studies of a newly found $S_{RN}1$ reaction.[6] Furthermore, we discuss the formation of the radical conglomerates in terms of the unique molecular and crystal structure. To the best of our knowledge no report has appeared to date on the preparation of stable free radical as conglomerates and their spontaneous optical resolution, although two types of optically active nitroxide radicals were obtained from an optically active compound[7] and from diastereomeric derivatives after optical resolution.[8]

When nitroenones **1** ($E^{red}_{1/2} = -1.68$ V)[6] and **2** were treated with 3.0 equiv of SmI_2 ($E^{ox}_{1/2} = -1.55$ V)[9] in THF/Et_2O (3/1, v/v) at $-50\,^{\circ}C$, the fairly stable radical anion **3**[10] was produced (Scheme 1). Subsequent addition of powdered 3,5-dinitrobenzoyl chloride (**4**) all at once at $-50\,^{\circ}C$[11] and warming to $25\,^{\circ}C$ resulted in the O-acylation of the enolate moiety of **3**. Analytically pure cyclic nitroxides **5** and **6** were obtained in 75 and 70% yield, respectively (Table 1), after purification by flash column chromatography on silica gel (hexane/EtOAc, 19/1) and recrystallization from Et_2O. An X-ray analysis of a single



Scheme 1. Synthesis of nitroxides **5** and **6**.

Table 1. Melting points and spectroscopic data of **5** and **6**.

Cmpd.	M.p. [°C]	$[\alpha]_D^{25}$	$\tilde{\nu}$ [cm^{-1}] (KBr)	ESR [a] g	a_N [G]
5	150.0 [b] 147.5–148.5 [d]	+20 or −20 [b, c] 0 [d]	1729, 1630, 1544, 1455, 1362, 1346, 1273, 1158, 917	2.0059	14.6
6	146.0–146.5 [b] 143.5–144.5 [d]	+30 or −30 [b, e] 0 [d]	1738, 1630, 1544 1458, 1363, 1345, 1270, 1158, 916	2.0057	14.2

[a] In THF at 25 °C. [b] Enantiomers resolved by recrystallization. [c] In THF, $c = 0.03$. [d] Conglomerate. [e] In THF, $c = 0.01$.

crystal of **5** established the nitroxide structure unequivocally (Fig. 1),[12] which is in accord with the consumption of 3.0 equiv of SmI_2. Both the X-ray structure[13] and the ab initio molecular orbital calculations[14] of **1** show short intramolecular contacts (3.20–3.26 Å) between one of the nitro oxygen atoms and ethylenic carbon atoms of the enone moiety. This conformation and the reducing power of SmI_2 toward **1** and **2**[15] should be responsible for the efficient formation of the cyclic nitroxides, although the detailed mechanism is not yet fully understood.

Spontaneous optical resolution occurred during recrystallization of **5** and **6**[12]. The properties of **5** and **6** are summarized in Table 1. The single crystal of **5** that was examined consisted of a single enantiomer, as was evident from its point and space group ($P3_1$ or $P3_2$, $Z = 3$) and was indeed optically active. The melting points of the pure enantiomers of **5** and **6** were higher than those of the respective mixtures. Moreover, the pattern of the X-ray powder diffraction spectra of mixtures of the enantiomeric crystals of **5** and **6** obtained by recrystallization was identical with those of the respective unrecrystallized materials.

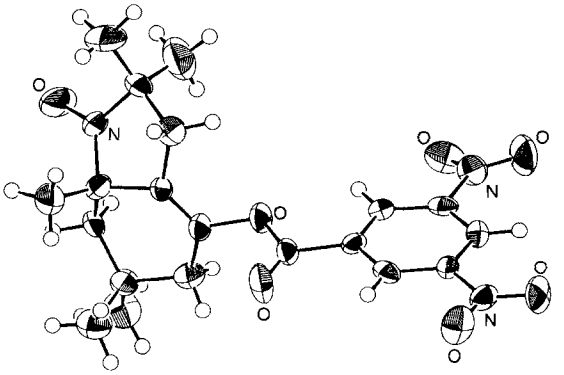


Fig. 1. Molecular structure of **5** in the crystal (ORTEP).

[*] Dr. R. Tamura, Dr. N. Azuma, Prof. A. Matsumoto
Department of Chemistry, Faculty of General Education, Ehime University
Matsuyama 790 (Japan)
Telefax: Int. code + (899)23-1071
S. Susuki, Prof. F. Toda
Department of Applied Chemistry, Faculty of Engineering, Ehime University
Dr. A. Kamimura, Dr. K. Hori
Department of Chemistry, Faculty of Liberal Arts, Yamaguchi University

[**] This work was supported by the Japanese Ministry of Education, Science and Culture (Grand-in-Aids for Scientific Research on Priority Area "Molecular Magnetism", No. 228/05234220), the Yamada Science Foundation (R. T.), and the Computer Center at the Institute for Molecular Science, Okazaki National Research Institute (Japan) (use of the HITAC M-600 and S-820/80 computers). We also thank Prof. K. Mukai, Ehime University, and Prof. T. Takui, Osaka City University, for helpful discussions.

Consequently, we conclude that nitroxides **5** and **6** form conglomerates consisting of a mixture of two enantiomeric crystals.

In the chiral molecule **5** (Fig. 1) the mean plane of the fused rings forms an angle of 76° with the 3,5-dinitrobenzoyl group so as to avoid steric repulsion; the dihedral angle between the mean plane of the nitroxide portion (C-NO-C) and the 3,5-dinitrobenzoyl group is 51°. More interesting is the crystal structure of **5** with two threefold screw axes along the *c* axis in the trigonal unit cell (Fig. 2). The molecules are arranged around one axis be-

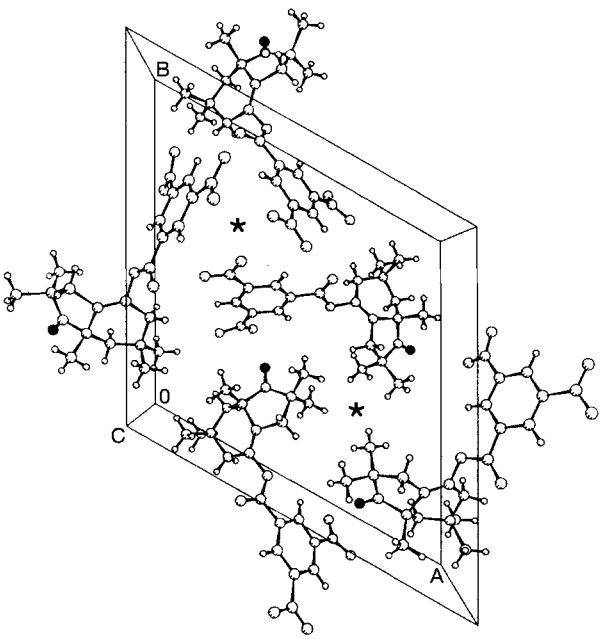


Fig. 2. Crystal structure of **5**. ⋆: Points corresponding to the threefold screw axes; •: O atoms of the NO groups.

cause of the electrostatic intermolecular interaction between the nitroxide oxygen atom and the nitrogen atom of one of two nitro groups on the benzene ring (2.87 Å), whereby a head-to-tail arrangement results. The other axis is surrounded by the other nitro group owing to another electrostatic intermolecular interaction between the nitro groups (3.02 Å), giving a tail-to-tail arrangement. Thus, the unique molecular asymmetry and arrangement seems to be responsible for the helical crystal structure and hence leads to the formation of conglomerates of the stable free radical.

Solutions of **5** and **6** in THF display an intense 1:1:1 triplet in their ESR spectra at 25 °C (Table 1), and the powdered materials exhibit exchange-narrowed spectra (**5**: $\Delta H \approx 12$ G, $g = 2.007$; **6**: $\Delta H \approx 16$ G, $g = 2.007$) at 25 °C. The radical purity of **5** and **6** was determined to be approximately 100% by magnetic susceptibility measurements by means of a Faraday balance (55 K $\leq T \leq$ 250 K); in other words, the temperature dependence of the static magnetic susceptibility of **5** and **6** follow the Curie–Weiss law; the Curie constants are approximately 0.38 ± 0.01 K emu mol^{-1} (theoretical value, 0.377).

The methods described here have provided conglomerates of stable radicals with a unique crystal structure that leads to spontaneous optical resolution. The scope, limitations, and the reaction mechanism of this synthetic method along with the precise magnetic properties of the newly prepared nitroxides are under investigation.

Received: October 19, 1993
Revised: December 1, 1993 [Z 6432 IE]
German version: *Angew. Chem.* **1994**, *106*, 914

[1] G. I. Likhtenstein, *Pure Appl. Chem.* **1990**, *62*, 281; D. Marsh, *ibid.* **1990**, *62*, 265; C. Degrand, B. Limoges, R. L. Blankespoon, *J. Org. Chem.* **1993**, *58*, 2573.
[2] H. G. Aurich in *Nitrones, Nitronates and Nitroxides* (Eds.: S. Patai, Z. Rappoport), Wiley, New York, **1989**, pp. 313, 371.
[3] H. Iwamura, *Adv. Phys. Org. Chem.* **1990**, *26*, 179; A. Rassat, *Pure Appl. Chem.* **1990**, *62*, 223; R. Chiarelli, M. A. Novak, A. Rassat, J. L. Tholence, *Nature* **1993**, *363*, 147; M. Tamura, Y. Nakazawa, D. Shiomi, K. Nozawa, Y. Hosokoshi, M. Ishikawa, M. Takahashi, M. Kinoshita, *Chem. Phys. Lett.* **1991**, *186*, 401.
[4] M. Yamaguchi, T. Miyazawa, T. Takata, T. Endo, *Pure Appl. Chem.* **1990**, *62*, 217.
[5] E. G. Rozantsev, V. D. Sholle, *Synthesis* **1971**, 190, 401; H. G. Aurich, W. Weiss, *Top. Curr. Chem.* **1975**, *59*, 65; see also ref. [2].
[6] R. Tamura, K. Yamawaki, N. Azuma, *J. Org. Chem.* **1991**, *56*, 5743; R. Tamura, M. Kohno, S. Utsunomiya, K. Yamawaki, N. Azuma, A. Matsumoto, Y. Ishii, *ibid.* **1993**, *58*, 3953.
[7] Y. Brunel, H. Lemaire, A. Rassat, *Bull. Soc. Chim. Fr.* **1964**, 1895.
[8] J. S. Roberts, C. Thomson, *J. Chem. Soc. Perkin Trans. 2* **1972**, 2129.
[9] J. L. Namy, P. Girard, H. B. Kagan, *Nouv. J. Chem.* **1981**, *5*, 479.
[10] The ESR spectrum of **3** ($g = 2.0059$, $a_N = 14.4$ G) in the reaction mixture was detected even at 25 °C in the presence of atmospheric oxygen, and no noticeable decrease of the spectral intensity was noted after 1 h at 25 °C.
[11] The use of powdered **4** and THF/Et_2O was essential to avoid the undesired one-electron transfer from **3** to **4**.
[12] A mixture (conglomerate) of two enantiomeric single crystals of **5** or **6** was obtained by very slow evaporation of the saturated ether solution of **5** or **6** at 25 °C. Crystal data for **5**: $C_{20}H_{24}N_3O_7$, trigonal, $P3_1$ or $P3_2$, $a = 17.274$ (6), $c = 6.166$ (2) Å, $V = 1593$ Å^3, $Z = 3$, $\rho_{calcd} = 1.308$ g cm^{-3}, $\mu(Mo_{K\alpha}) = 0.94$ cm^{-1}, 910 observed reflections ($I > 3.00\,\sigma(I)$, $T = 298$ K) were used for the solution and refinement of the structure. $R = 0.045$, $R_w = 0.041$; $R = (\Sigma\|F_o| - |F_c\|/\Sigma|F_o|)$, $R_w = [\Sigma w(|F_o| - |F_c\|)^2/\Sigma wF_o^2]^{1/2}$. Further details of the crystal structure investigation are available on request from the Director of the Cambridge Crystallographic Data Centre, 12 Union Road, GB-Cambridge CB2 1EZ(UK), on quoting the full journal citation.
[13] N. Azuma, T. Ozama, K. Yamawaki, R. Tamura, *Bull. Chem. Soc. Jpn.* **1992**, *65*, 2860.
[14] The MO calculations were performed with a 3-21G basis set (J. S. Binkley, J. A. Pople, W. J. Hehre, *J. Am. Chem. Soc.* **1980**, *102*, 939) and the Gaussian 90 program.
[15] S. Kende, J. S. Mendoza, *Tetrahedron Lett.* **1991**, *14*, 1699.

Cyclotrimerization of Ethyne on the Complex Fragment [(η^1-*t*Bu$_2$PCH$_2$P*t*Bu$_2$)Ni^0] with Formation of an η^6-Benzene–Nickel(0) Complex**

Thomas Nickel, Richard Goddard, Carl Krüger, and Klaus-Richard Pörschke*

For a number of years we have directed our efforts to modifying the properties of nickel(0) centers with mono- and bidentate ligands, for example, with the phosphanes PR_3 (R = Me, Et, Ph, *i*Pr),[1] $Me_2PCH_2PMe_2$,[2] and *t*Bu$_2$PC$_2$H$_4$P*t*Bu$_2$.[3] Ethene and ethyne are especially interesting coligands. For the ligand combination *t*Bu$_2$PCH$_2$P*t*Bu$_2$ (dtbpm)[4] and stilbene or diphenylacetylene, activated by electron-withdrawing substituents, Hofmann et al. first obtained nickel(0) complexes with dtbpm as a chelating ligand.[5] We report here on novel nickel(0) complexes in which only *one* phosphorus atom of the bidentate dtbpm ligand is coordinated to the nickel(0) center.

[*] Priv.-Doz. Dr. K.-R. Pörschke, Dipl.-Chem. T. Nickel, Dr. R. Goddard, Prof. Dr. C. Krüger
Max-Planck-Institut für Kohlenforschung
D-45466 Mülheim an der Ruhr (FRG)
Telefax: Int. code + (208) 306-2984

[**] Part of the planned dissertation of T. Nickel. This work was supported by the Fonds der Chemischen Industrie and by the Volkswagen-Stiftung.

 © VCH Verlagsgesellschaft mbH, D-69451 Weinheim, 1994 0570-0833/94/0808-0879 $ 10.00+.25/0

When a solution of equimolar amounts of $[Ni(C_2H_4)_3]$[6] and $tBu_2PCH_2PtBu_2$ in ether is cooled from $-10\,^{\circ}C$ to temperatures between -30 and $-78\,^{\circ}C$, large yellow cubes of **1** form in 65% yield [Eq.(a)]. When heated rapidly, **1** decomposes at $70\,^{\circ}C$; the compound can be stored for longer periods only below $0\,^{\circ}C$. Complex **1** is stabilized in solution by addition of ethene.

$$[Ni(C_2H_4)_3] + tBu_2PCH_2PtBu_2 \longrightarrow [(\eta^1\text{-}tBu_2PCH_2PtBu_2)Ni(C_2H_4)_2] + C_2H_4 \quad (a)$$

In the 300 MHz ^1H NMR spectrum ([D$_8$]THF) of **1** at $-80\,^{\circ}C$ two signals are observed at $\delta = 2.60$ and 2.51, which are assigned to the "inner" and "outer" protons, respectively, of two equivalent ethene ligands in a trigonal-planar L-Ni$(C_2H_4)_2$ complex.[7] The phosphane ligand gives rise to two equally intense methyl signals; the broad signal ($\delta = 1.35$) is attributed to a coordinated $PtBu_2$ group, the sharp one ($\delta = 1.18$) to a noncoordinated $PtBu_2$ group. Corresponding signals are found in the ^{13}C NMR spectrum (75.5 MHz, $-80\,^{\circ}C$). In the ^{31}P NMR spectrum ($-80\,^{\circ}C$) the coordinated and the noncoordinated phosphorus atoms of the dtbpm ligand give rise to an AX system [$\delta = 63.5, 23.8$; $^2J(PP) = 17$ Hz]. In the ^1H and ^{13}C NMR spectra at $-30\,^{\circ}C$ the ethene signals are coalesced, and both $PtBu_2$ signals are sharp. Apparently, for solutions of **1** the rotation of the ethene ligands about the bond axis to the nickel atom is restricted at low temperatures, and in addition the mobility of the *tert*-butyl groups of the coordinated phosphorus atom is reduced; when the temperature is increased the ethene ligands and the *tert*-butyl groups undergo facile rotation. A (fast) exchange of the phosphorus atoms is not observed at $-30\,^{\circ}C$.

The results of the crystal structure analysis of **1**[8a] are summarized in Figure 1. The Ni atom is coordinated in a trigonal-planar fashion by two ethene molecules and one P atom of the diphosphane ligand [Ni–P1 2.238(1) Å]. The second P atom of the phosphane ligand is far enough from the Ni center [Ni···P2 4.696(1) Å] that both intramolecular and intermolecular Ni···P2 interactions in the crystal lattice can be discounted. The fact that the dtbpm ligand in **1** does not act as a chelating ligand with formation of a NiPCP ring, even though the Ni center is unsaturated (16e), is explained by the high conformational strain connected with this coordination mode.[9]

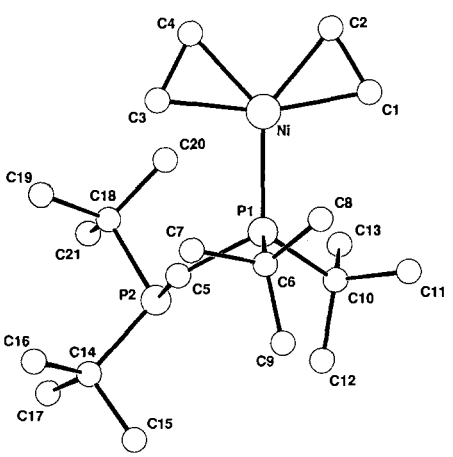


Fig. 1. Crystal structure of **1**. Selected bond lengths [Å], angles [°], and torsion angles [°] (Ca,b: midpoint between atoms Ca and Cb): Ni-P1 2.238(1), Ni-C1 2.013(2), Ni-C2 2.000(2), Ni-C3 2.016(2), Ni-C4 1.999(2), P1-C5 1.872(2), P2-C5 1.877(2), Ni-C1,2 1.883(4), Ni-C3,4 1.886(4), C1,2···C3,4 3.319(6), Ni···P2 4.696(1), Ni-P1-C5 116.5(1), P1-C5-P2 125.9(1), C5-P2-C14 98.2(1), C5-P2-C18 104.7(1), P1-Ni-C1,2 120.3(1), P1-Ni-C3,4 116.0(1), C1,2-Ni-C3,4 123.5(1), Ni-P1-C5-P2 89.7(2), C3,4-Ni-P1-C5 29.5(2).

When a yellow solution of **1** in pentane with an excess of ethyne is warmed from -78 to $-55\,^{\circ}C$, it becomes dark and a few flakes of red-colored polyacetylene precipitate. At $-78\,^{\circ}C$ and in the course of several days, orange rosette-shaped crystals of the benzene–nickel(0) complex **2** form in 50% yield.[10a] According to these results, the ethene ligands of **1**[10b] are displaced, and ethyne is cyclotrimerized on the 12e $[(\eta^1\text{-}tBu_2PCH_2PtBu_2)Ni]$ complex fragment to give a benzene ligand [Eq.(b)].[10c,d]

$$1 + 3\,HC{\equiv}CH \longrightarrow [(\eta^1\text{-}tBu_2PCH_2PtBu_2)Ni(\eta^6\text{-}C_6H_6)] + 2\,C_2H_4 \quad (b)$$

Crystalline **2** melts at $83\,^{\circ}C$ with decomposition. In the EI mass spectrum ($80\,^{\circ}C$) the molecular ion (440) undergoes cleavage of benzene to give the complex fragment $[(dtbpm)Ni]^+$ (362); benzene cation gives rise to the base peak. Complex **2** decomposes in solution (THF) above $-30\,^{\circ}C$, presumably by release of the benzene ligand.[11] In the 400 MHz ^1H and 75.5 MHz ^{13}C NMR spectra at $-80\,^{\circ}C$ very sharp singlets at $\delta(H) = 5.95$ and $\delta(C) = 92.0$ are observed for the benzene ligand; the chemical shifts and the coupling constant $J(CH) = 168$ Hz are comparable to those of $[(C_6H_6)Cr(CO)_3]$ [$\delta(H) = 5.67$; $\delta(C) = 95.5$; $J(CH) = 175$ Hz].[12] Thus for **2** in solution the benzene ligand is η^6-coordinated to the nickel atom. Since the ^1H and ^{13}C NMR signals of the *tert*-butyl groups occur in pairs, only *one* phosphorus atom of the bidentate dtbpm ligand in **2** is bound to the nickel(0) center [^{31}P NMR ($-80\,^{\circ}C$): $\delta = 53.4, 19.1$; $^2J(PP) = 37$ Hz]. Within the temperature range at which the complex is stable the phosphorus ligand was not observed to change hapticity (accompanied by plausible η^4-coordination of the benzene ligand), nor could an exchange of the benzene ligand with free benzene be proved by NMR spectroscopy.

The crystal structure of **2**[8b] is shown in Figure 2. The benzene ligand is planar [maximum deviation (C2): 0.005 Å] and symmetrically coordinated to the Ni atom [average Ni–C bond length: 2.138(6) Å]; the center D of the C_6 ring is 1.606(5) Å away from the Ni atom.[13] The C–C bonds within the six-membered ring [1.41(1) Å] are all the same length within the margin of error. In addition the P1 atom of the dtbpm ligand is coordi-

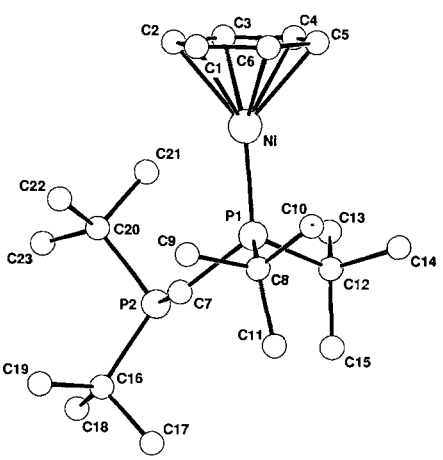


Fig. 2. Crystal structure of **2**. Selected bond lengths [Å], angles [°], and torsion angles [°] (D: center of the six-membered ring (C1–C6): Ni-P1 2.111(1), Ni-C1 2.140(4), Ni-C2 2.128(5), Ni-C3 2.136(5), Ni-C4 2.143(5), Ni-C5 2.142(5), Ni-C6 2.136(5), Ni-D 1.606(5), Ni···P2 4.507(1), P1-C7 1.867(4), P2-C7 1.867(4); D-Ni-P1 174.2(2), Ni-P1-C7 122.2(1), P1-C7-P2 123.6(2), Ni-P1-C7-P2 74.6(7).

nated to the Ni center. The Ni–P1 bond of 2.111(1) Å is relatively short, and the D-Ni-P1 angle is 174.2(2)°. The coordination geometry of the nickel atom can be considered pseudo-linear. The torsion angle Ni-P1-C7-P2 [74.6(7)°] is smaller than the related angle in **1** [89.7(2)°]; this can be explained by the reduced spatial requirement of the (η^6-C_6H_6)Ni unit in comparison to that of the $(C_2H_4)_2$Ni unit. The P-C-P angles in **1** [125.9(1)°] and **2** [123.6(2)°] are similar and markedly larger than the P-C-P angles in transition metal complexes with a tBu$_2$PCH$_2$PtBu$_2$ chelating ligand [95.5(2)–99.2(2)°].[5, 14] Force field calculations[15] on the uncomplexed tBu$_2$PCH$_2$PtBu$_2$ molecule indicate a P-C-P angle of 122.3° [P–C 1.89 Å, P···P 3.30 Å]. The calculated molecule has a twofold rotational axis that bisects the P-C-P angle. In the related diphosphane (c-C_6H_{11})$_2$PCH$_2$P(c-C_6H_{11})$_2$ this angle is determined to be 120.5(1)°[16] (calcd: 120.6°).[15]

Nickel(0) complexes with benzene or other arene ligands have been relatively uncommon. Jonas prepared the first complexes of the type [{R$_2$P(CH$_2$)$_n$PR$_2$}Ni(arene)] by reducing [{R$_2$P(CH$_2$)$_n$PR$_2$}NiCl] (R = c-C_6H_{11}; n = 2, 3) with lithium in the presence of benzene (or other arenes).[17] The bidentate phosphane ligand is presumably bound to the nickel(0) center in a chelating fashion and the arene ligand like an alkene (η^2 or η^4) (NMR data are not available). This coordination mode was proven for the analogous naphthalene[18] and anthracene complexes[19] by NMR spectra and crystal structures. In contrast, the benzene ligand in **2** serves as a six-electron ligand for the nickel atom, which attains an 18e configuration including the electron pair of the coordinating phosphorus atom. Complex **2** completes the series of complexes of the type [L$_n$M(η^6-C_6H_6)], n = 2–4, with the parent structure, n = 1. The reaction providing **2** [Eq.(b)] at temperatures below −50 °C (!) may serve as a model[10c] for a reaction step in Reppe's nickel(0)-catalyzed cyclotrimerization of ethyne to benzene.[20]

Experimental Procedure

1: A solution of [Ni(C_2H_4)$_3$][6] in ether (30 mL), prepared from [Ni(*trans*,*trans*,*trans*-1,5,9-cyclododecatriene)] (1.165 g, 5.0 mmol) and ethene, was combined with a solution of dtbpm (1.522 g, 5.0 mmol) in ether (20 mL) at −10 °C. The solution was filtered through a cooled D4 frit to remove insoluble impurities; large yellow cubes formed at −30 °C. The crystallization was completed at −78 °C; the mother liquor was removed from the crystals with a capillary, and the crystals were washed twice with cold pentane and dried at −30 °C under vacuum (oil pump). Yield 1.36 g (65%). – Correct elemental analyses; m.p. 70 °C (decomp); ^{1}H NMR (300 MHz, −80 °C): δ = 2.60, 2.51 (4H each, H_2C=CH_2'); 2.05 (2H, PCH_2P'), 1.35 (d, 18 H, PtBu$_2$ complexed), 1.18 (d, 18H, PtBu$_2$ free); (− 30 °C): 2.58 (8H, C_2H_4), 2.07 (2H, PCH_2P'), 1.37 (d, 18H, PtBu$_2$ complexed), 1.17 (d, 18H, PtBu$_2$ free); ^{13}C NMR (75.5 MHz, −80 °C): δ = 54.3, 50.5 (2C each, H_2C=CH_2); 38.1 (2C, sharp, PCMe_3), 34.0 (2C, br. P'CMe_3), 30.2 (12C, br, CH_3 and CH_3'), 18.0 (1C, ^1J(PC) = 50; 2 Hz, PCH_2P'); (− 30 °C): δ = 52.7 (4C, C_2H_4); 38.1, 34.0 (2C each, sharp, PCMe_3 and P'C'Me_3), 30.7, 30.5 (6C each, CH_3 and CH_3'), 18.2 (1C, PCH_2P'); ^{31}P NMR (121.5 MHz, −80 °C): δ = 63.5, 23.8 (^2J(PP) = 17 Hz).

2: A yellow solution of **1** (419 mg, 1.0 mmol) in pentane (25 mL), which was prepared at 0 °C, was exposed to ethyne (100 mL, 4 mmol) at −78 °C. The reaction mixture was stirred and warmed to −55 °C. Any **1** that had precipitated then redissolved. The solution became dark, and a red precipitate of polyacetylene formed. At −78 °C orange, rosette-shaped crystals form over the course of several days, which were washed twice with ether at −78 °C and dried under vacuum (oil pump) at −30 °C. Yield 220 mg (50%). – Correct elemental analyses, m.p. 83 °C; EI-MS (80 °C): m/z = 440 ([M]$^+$, 2), 362 ([(dtbpm)Ni]$^+$, 4), 78 ([C_6H_6]$^+$, 100); IR (KBr): 3060 (ν(=C-H)), 1748, 1585 cm^{-1} (ν(C=C); C_6H_6); ^{1}H NMR (400 MHz, −80 °C): δ = 5.95 (s, 6H, C_6H_6), 1.58 (2H, PCH_2P), 1.24, 1.18 (each 18H, C(CH_3)$_3$ and C(CH_3')$_3$); ^{13}C NMR (75.5 MHz, −80 °C): δ = 92.0 (6C, ^1J(CH) = 168 Hz, C_6H_6), 35.9 (2C, PCMe_3), 33.1 (2C, P'C'Me_3), 34.0, 32.2, 30.7 (2C each, C(CH_3)$_3$), 30.8 (6C, C(CH_3')$_3$), 15.6 (1C, PCH_2P); ^{31}P NMR (121.5 MHz, −80 °C): δ = 53.4, 19.1 (^2J(PP) = 37 Hz).

Received: November 9, 1993 [Z 6487 IE]
German version: *Angew. Chem.* **1994**, *106*, 908

[1] a) K.-R. Pörschke, Y.-H. Tsay, C. Krüger, *Angew. Chem.* **1985**, *97*, 334; *Angew. Chem. Int. Ed. Engl.* **1985**, *24*, 323; b) K.-R. Pörschke, *J. Am. Chem. Soc.* **1989**, *111*, 5691.
[2] a) K.-R. Pörschke, Y.-H. Tsay, C. Krüger, *Inorg. Chem.* **1986**, *25*, 2097; b) K.-R. Pörschke, R. Mynott, *Z. Naturforsch. B* **1987**, *42*, 421.
[3] K.-R. Pörschke, C. Pluta, B. Proft, F. Lutz, C. Krüger, *Z. Naturforsch. B* **1993**, *48*, 608.
[4] H. H. Karsch, *Z. Naturforsch. B* **1983**, *38*, 1027.
[5] a) P. Hofmann, L. A. Perez-Moya, M. E. Krause, O. Kumberger, G. Müller, *Z. Naturforsch. B* **1990**, *45*, 897; b) P. Hofmann, L. A. Perez-Moya, O. Steigelmann, J. Riede, *Organometallics* **1992**, *11*, 1167.
[6] K. Fischer, K. Jonas, G. Wilke, *Angew. Chem.* **1973**, *85*, 620; *Angew. Chem. Int. Ed. Engl.* **1973**, *12*, 565.
[7] For comparison (Me$_3$P)Ni(C_2H_4)$_2$: K.-R. Pörschke, G. Wilke, R. Mynott, *Chem. Ber.* **1985**, *118*, 298.
[8] a) Crystal structure analysis of **1**: $C_{21}H_{46}NiP_2$, M_r = 419.3 g mol^{-1}, crystal dimensions 0.28 × 0.42 × 0.53 mm, a = 13.471(1), b = 8.342(1), c = 21.504(2) Å, β = 103.48(1)°, V = 2350.0 Å^3, ρ_{calcd} = 1.18 g cm^{-3}, μ = 9.65 cm^{-1}, F(000) = 920 e, Z = 4, crystal system monoclinic, space group $P2_1/n$ (No. 14), Enraf–Nonius CAD-4 diffractometer, λ = 0.71069 Å, method of measurement ω – 2θ, 5882 measured reflections ($\pm h, +k, +l$), $[(\sin\theta)/\lambda]_{max}$ = 0.65 Å^{-1}, 5360 independent and 4747 observed reflections ($I > 2\sigma I$), 217 refined parameters; heavy atom method, H atom positions calculated and included in the least-squares refinement, R = 0.030, R_w = 0.040 [$w = 1/\sigma^2(F_0)$], maximum residual electron density 0.38 e Å^{-3}. b) Crystal structure analysis of **2**: $C_{23}H_{44}NiP_2$, M_r = 441.3 g mol^{-1}, crystal dimensions 0.39 × 0.46 × 0.28 mm, a = 11.113(2), b = 15.355(2), c = 14.154(3) Å, β = 93.84(2)°, V = 2409.9 Å^3, ρ_{calcd} = 1.22 g cm^{-3}, μ = 24.35 cm^{-1}, F(000) = 960 e, Z = 4, crystal system monoclinic, space group, $P2_1/n$ (No. 14), Enraf–Nonius CAD-4 diffractometer, λ = 1.54178 Å, method of measurement ω – 2θ, 5508 measured reflections ($\pm h, +k, +l$), $[(\sin\theta)/\lambda]_{max}$ = 0.63 Å^{-1}, 4953 independent and 4680 observed reflections ($I > 2\sigma I$), 259 refined parameters; heavy atom method, positions of H1–H6 were found and refined isotropically, the positions of the other H atoms were calculated and not included in the least-squares refinement, R = 0.066, R_w = 0.125 [$w = 1/\sigma^2(F_0)$], maximum residual electron density 1.04 e Å^{-3}. Further details of the crystal structure investigation may be obtained from the Fachinformationszentrum Karlsruhe, D-76344 Eggenstein-Leopoldshafen (FRG) on quoting the depository number CSD-57884, the names of the authors, and the journal citation.
[9] The monoethene complex [(dtbpm)Ni(C_2H_4)] with dtbpm as a chelating ligand can be prepared from **1** by a laborious procedure. This complex converts back to **1** immediately upon treatment with ethene. This implies that bidentate coordination of dtbpm on the nickel(0) center with ethene as a coligand is possible but high in energy. In contrast, activated alkenes acting as strong acceptors stabilize the chelating coordination of dtbpm on nickel(0)[5], since they take up the excess charge pushed onto the nickel(0) center by the two phosphorus atoms.
[10] a) Uncomplexed benzene in the reaction mixture was evident in the ^{1}H and ^{13}C NMR spectra. b) The mixed ethene/ethyne complex [(η^1-tBu$_2$PCH$_2$PtBu$_2$)-Ni(CH$_2$=CH$_2$)(HC≡CH)] was isolated in crude form as an intermediate in the displacement reaction at −78 °C and characterized by ^{1}H and ^{31}P NMR spectroscopy. c) It was shown qualitatively (^{1}H, ^{31}P NMR) that the benzene complex **2** catalyzes the cyclotrimerization of ethyne at −50 °C to give benzene. d) For comparison [(tBu$_2$MeP)Ni(C_2H_4)$_2$] was prepared as a model compound for **1** and treated with ethyne under the same conditions. The formation of benzene was also observed, but a benzene complex analogous to **2** was not found. Benzene is also formed as a side product in the synthesis of the bis(ethyne) complexes [(R$_3$P)Ni(HC≡CH)$_2$] (R = Me, Et, etc.)[1b].
[11] Upon warming to −30 °C the red solutions of **2** turn yellow. According to the ^{31}P NMR spectrum a number of compounds are formed, which have not yet been identified.
[12] The ^{1}H and ^{13}C NMR signals of [(C_6H_6)Cr(CO)$_3$] are shifted upfield from those of uncomplexed benzene [δ(H) = 7.35; δ(C) = 129.0; J(CH) = 159 Hz]; this is explained by the increased charge density on the C atoms as a result of backbonding. This is apparently accompanied by an increase in the s character of the C–H bonds, which leads to a stronger coupling J(CH). R. Aydin, H. Günther, J. Runsink, H. Schmickler, H. Seel, *Org. Magn. Reson.* **1980**, *13*, 210.
[13] The corresponding distances in the Ni^{II} complexes [(C_6F_5)$_2$Ni(η^6-toluene)] [13a] and [(C_6F_5)$_2$Ni(η^6-mesitylene)][13b] are considerably longer (1.693 and 1.691 Å, respectively); moreover, the η^6-bound six-membered rings are not planar. a) L. J. Radonovich, K. J. Klabunde, C. B. Behrens, D. P. McCollor, B. B. Anderson, *Inorg. Chem.* **1980**, *19*, 1221; b) L. J. Radonovich, F. J. Koch, T. A. Albright, *ibid.* **1980**, *19*, 3373.
[14] a) P. Hofmann, C. Meier, U. Englert, M. U. Schmidt, *Chem. Ber.* **1992**, *125*, 353; b) P. Hofmann, H. Heiss, G. Müller, *Z. Naturforsch. B* **1987**, *42*, 395; c) P. Hofmann, H. Heiss, P. Neiteler, G. Müller, J. Lachmann, *Angew. Chem.* **1990**, *102*, 935; *Angew. Chem. Int. Ed. Engl.* **1990**, *29*, 880.
[15] SYBYL 6.0, Tripos Associates, Inc., St. Louis, MO, USA. C,H: Tripos force field; P: F. Lutz, Dissertation, Universität Wuppertal, **1993**. Minimization algorithm: BFGS. Convergence criterion: rms gradient

 © VCH Verlagsgesellschaft mbH, D-69451 Weinheim, 1994 0570-0833/94/0808-0881 $ 10.00+.25/0

< 0.01 kcal mol^{-1} Å^{-1}. Nonbonded cutoff: 8 Å, steric demands of the phosphorus lone pair were taken into account.

[16] Crystal data (EDD investigation): $C_{25}H_{46}P_2$, $M_r = 408.6$ g mol^{-1}, crystal dimensions $0.06 \times 0.35 \times 0.33$ mm, $a = 9.718(2)$, $b = 10.423(2)$, $c = 12.775(1)$ Å, $\alpha = 98.21(1)$, $\beta = 96.84(1)$, $\gamma = 105.23(1)^\circ$, $V = 1218.8$ Å^3, $\rho_{calcd} = 1.11$ g cm^{-3}, $\mu = 1.81$ cm^{-1}, $F(000) = 452$ e, $Z = 2$, crystal system triclinic, space group $P\bar{1}$ (No. 2), Enraf–Nonius CAD-4 diffractometer, $\lambda = 0.71069$ Å, method of measurement $\omega - 2\theta$, 68524 measured reflections ($\pm h, \pm k, \pm l$), $[(\sin\theta)/\lambda]_{max} = 1.0$ Å^{-1}, 18953 independent ($R_{av} = 0.05$) and 8822 observed reflections ($I > 2\sigma I$), 428 refined parameters; direct methods, H atom positions found and included in the least-squares refinement, $R = 0.060$, $R_w = 0.051$ [$w = 1/\sigma^2(F_o)$], maximum residual electron density 1.09 e Å^{-3}.

[17] K. Jonas, *J. Organomet. Chem.* **1974**, *78*, 273.

[18] a) R. Benn, R. Mynott, I. Topalovic, F. Scott, *Organometallics* **1989**, *8*, 2299; b) F. Scott, C. Krüger, P. Betz, *J. Organomet. Chem.* **1990**, *387*, 113.

[19] a) D. J. Brauer, C. Krüger *Inorg. Chem.* **1977**, *16*, 884; b) A. Stanger, *Organometallics* **1991**, *10*, 2979; c) A. Stanger, R. Boese, *J. Organomet. Chem.* **1992**, *430*, 235; d) R. Boese, A. Stanger, P. Stellberg, A. Shazar, *Angew. Chem.* **1993**, *105*, 1500; *Angew. Chem. Int. Ed. Engl.* **1993**, *32*, 1475.

[20] See P. W. Jolly in *Comprehensive Organometallic Chemistry, Vol. 8* (Eds.: G. Wilkinson, F. G. A. Stone, E. W. Abel), Pergamon, Oxford, **1982**, p. 649ff., and references therein.

The Absolute Configuration of (+)-α-1,2,3,4,5,6-Hexachlorocyclohexane, and Its Permeation through the Seal Blood–Brain Barrier**

Kattrin Möller, Cornelia Bretzke, Heinrich Hühnerfuss,* Roland Kallenborn, Jochen N. Kinkel, Jürgen Kopf, and Gerhard Rimkus

Because of its ubiquitous nature and its relative persistence, α-1,2,3,4,5,6-hexachlorocyclohexane (α-HCH) plays an important role in most studies of the "fate" of organic pollutants in marine and terrestrial ecosystems. In Western Europe its direct application mixed with the insecticide γ-hexachlorocyclohexane (γ-HCH, lindane) is no longer permitted, but in other parts of Europe, especially in eastern Europe, it may still be entering the environment by way of such formulations. In the marine environment γ-HCH is also transformed to α-HCH by marine microorganisms. The amounts involved are very low, but they may be significant over longer periods of time.[1]

In the last two years, α-HCH has received additional attention in process studies, because it is the only one of the eight possible HCH isomers which is chiral, and can therefore be studied by chiral gas chromatography. The cyclodextrin separation phases which have recently been developed[2] have made it possible to distinguish between enzymatic and nonenzymatic degradation processes.[3] This method has been used to study the pathways of microbial degradation of α-HCH in North Sea water, and its enzymatic degradation in marine and terrestrial organisms from various trophic levels.[3–5] In the liver of the common eider duck, for example, preferential degradation of (−)-α-HCH was demonstrated.[6]

During analysis of brain tissue from the harbor seal (*Phoca vitulina*) we encountered a surprising phenomenon. In brain samples from eight Icelandic seals we detected almost exclusively (+)-α-HCH (the values for the enantiomer ratio (+)-α-HCH/(−)-α-HCH were 55.6, 66.2, and six values of 100:0; Fig. 1). In contrast, blubber tissue from the same animals yielded enantiomer ratios of only 1.2 to 1.4. This finding is especially interesting because of the widespread hypothesis that the blood–brain barrier is also partially effective towards certain fat-soluble organic pollutants. The "blood–brain barrier" is normally understood as mechanisms which greatly inhibit the transport of *non*-lipid-soluble substances such as proteins from blood vessels into the surrounding interstitial nervous system tissue (glia) and the capillary endothelium. These mechanisms thus ensure a constant environment for the neurons.[7] The respiratory gases carbon dioxide and oxygen, however, can cross the capillary walls with ease. The exact mechanisms involved, especially for the selective inhibition of entry for certain lipid-soluble pollutants into the brain tissue, still require more detailed study. Whether the barrier effect is enhanced by enzymes in the endothelial cells (enzyme barrier) also still appears controversial.

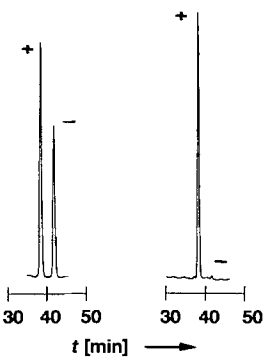


Fig. 1. Comparison of chromatograms for *n*-hexane extracts of blubber (left) and brain tissue (right) from the harbor seal (*Phoca vitulina*). For experimental conditions see Experimental Procedure.

Concentrations of polychlorinated biphenyls (PCBs) in brain tissue have been found to be a factor of ten lower than those found in other organs of the same animals.[8] This well-known effect is also often ascribed to the influence of the blood–brain barrier. Other authors, however, have shown that α-HCH is accumulated very efficiently in the brain tissue of mice and rats[9] and of fur seals.[10] The brain samples from rats[9a] and two of the fur seal samples[10] also revealed the first indications of preferential accumulation of (+)-α-HCH. The systematic investigation of eight Icelandic seals carried out in the present study shows that this phenomenon can obviously be generalized, at least for the less pollutant-exposed Icelandic animals. In addition, our studies show that as for the PCBs, γ-HCH is present at much lower concentrations in the brain samples than in other organs of the same animals. Such extreme concentration differences between γ-HCH and α-HCH, when comparing values from brain and other organs, have also been reported by Mössner et al. for fur seals.[10] However, these results are difficult to reconcile with our previous experience with enzymatic and nonenzymatic degradation processes for HCH isomers. We therefore interpret the enantioselective enrichment of (+)-α-HCH in seal brain tissue less as the result of enzymatic degrada-

[*] Priv.-Doz. Dr H. Hühnerfuss, Dipl.-Chem. K. Möller, Dr. R. Kallenborn
Institut für Organische Chemie der Universität
Martin-Luther-King-Platz 6, D-20146 Hamburg (FRG)
Telefax: Int. code + (40)4123-2893

C. Bretzke, Priv.-Doz. Dr J. Kopf
Institut für Anorganische und Angewandte Chemie
der Universität Hamburg (FRG)

Dr. J. N. Kinkel
Abt. FO REAG CHROM, E. Merck (FRG)

Dr. G. Rimkus
Lebensmittel- und Veterinäruntersuchungsamt
des Landes Schleswig-Holstein (FRG)

[**] Chromatographic Separation of Enantiomers of Chiral Organic Pollutants, Part 7. This work was supported by the Ministry of Research and Technology. Part 6: [4].

tion processes, and rather as a "preferential permeability of the blood–brain barrier" for (+)-α-HCH. However, we can not of course exclude the possibility that enzyme processes acting in the same direction also enhance this effect.

Preliminary studies with brain tissue from the common eider duck and sheep also indicated preferential enrichment of (+)-α-HCH, and support the findings obtained in this study.[11] A similar protective mechanism is also presumed for humans, though a systematic study at this trophic level has yet to be carried out.

A more detailed discussion of this phenomenon has been impossible until now, because the absolute configurations of the α-HCH enantiomers were unknown. A first step in this direction required development of a method for separating sufficient quantities of the α-HCH enantiomers for crystallization. X-ray crystal structure analysis should then permit assignment of absolute configuration to the (+)-α-HCH enantiomer.

Attempts to separate the α-HCH enantiomer with an optically active base, (+)-brucine, using the method described by Cristol[12] proved to be very time-consuming. After several weeks and repeated workup of the reaction mixture, (−)-α-HCH was obtained in 96% purity. The (+)-α-HCH enantiomer was lost in this procedure. By modifying the reaction and using the (−)-enantiomer of an optically active base it may have been possible to synthesize the (+)-α-HCH enantiomer in an analogous manner.

The two α-HCH enantiomers were accessible by high performance liquid chromatography (HPLC) in a much more elegant manner, in a matter of hours. The enantiomer separation was carried out using a preparative column with the chiral stationary phase ChiraDex (Merck). An HPLC chromatogram of α-HCH obtained with an analytical version of this column is shown in Figure 2.

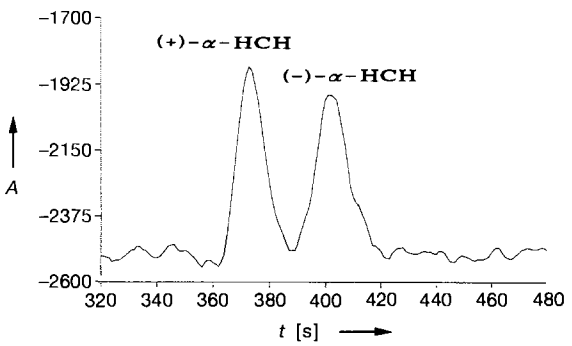


Fig. 2. HPLC chromatogram (Absorption A versus time t) for enantiomer separation of *rac*-α-HCH . For experimental conditions see Experimental Procedure.

Five cycles with a preparative Chiradex 250–50 column yielded about 20 mg of α-HCH of ≥99% purity. Recrystallization from ether at 277 K afforded single crystals of this enantiomer which were suitable for X-ray analysis. Figure 3 shows the SCHAKAL representation of the α-HCH structure thus obtained.[13] Following the extended priority rules of Cahn, Ingold, and Prelog,[14] the absolute structure of (+)-α-HCH was therefore assigned the configuration (+)-α-1*S*,2*R*,3*R*,4*S*,5*S*,6*S*-hexachlorocyclohexane.

In summary, we conclude that (+)-α-1*S*,2*R*,3*R*,4*S*,5*S*,6*S*-hexachlorocyclohexane is enantioselectively accumulated in the brain tissue of seals. From the data so far available, we assume that the blood–brain barrier of the seal is enantioselectively permeable for this α-HCH enantiomer. Further studies will be required to determine whether other pollutants can also cross the blood–brain barrier enantioselectively, whether similar structural elements are required, and to what extent this finding can be extended to all organisms of higher trophic levels, including humans.

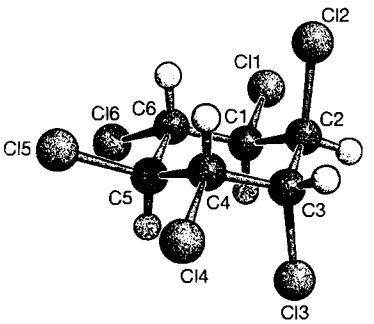


Fig. 3. The molecular structure of (+)-α-1*S*,2*R*,3*R*,4*S*,5*S*,6*S*-hexachlorocyclohexane. Bond lengths [pm] and selected bond angles [°]: Cl1-C1 178.3, Cl2-C2 179.3, Cl3-C3 178.5, Cl4-C4 179.3, Cl5-C5 178.5, Cl6-C6 178.8, C1-C2 152.3, C2-C3 151.6, C3-C4 152.8, C4-C5 152.1, C5-C6 153.1, C6-C1 151.7, all C–H bond lengths are 98.0 pm; Cl1-C1-C2 110.0, Cl2-C2-C3 108.0, Cl3-C3-C4 112.0, Cl4-C4-C5 109.9, Cl5-C5-C6 109.8, Cl6-C6-C1 109.9.

Experimental Procedure

Preparation of brain samples (homogenization, extraction, chromatographic purification, fractionation by HPLC) was carried out by the procedures described for the common eider duck [6]. The (+)-α-HCH fraction was measured by gas chromatography under the following conditions: fused silica capillary column: 25 m, i.d. 0.25 mm, stationary phase 50% octakis(3-*O*-butyryl-2,6-di-*O*-pentyl)-γ-cyclodextrin and 50% OV-1701, carrier gas helium 60 kPa, Vega gas chromatograph Carlo Erba, 2 μL on-column injection, ^{63}Ni-ECD with nitrogen as make-up gas.

The HPLC separation of the (+)-α-HCH enantiomers was carried out on an LiChrocart 250-4 ChiraDex (5 μm) analytical column from Merck, Darmstadt, under the following conditions: eluent MeOH/H_2O 75/25 (v/v): flow rate 0.8 mL min^{-1}; pressure 1.27×10^7 Pa, 3 μg *rac*-α-HCH sample; sample loop 200 μL; detector spectrophotometer. For the preparative 250-50 column with the same stationary phase, the following conditions were used; pump L-6200 (Merck–Hitachi), equipped with a preparative pump head; eluent MeOH/H_2O 75/25 isocratic; flow rate 15 mL min^{-1}; 16.5–20 mg *rac*-α-HCH sample; after five applications of sample, about 20 mg of (+)-α-HCH was isolated, purity ≥99%. Recrystallization from ether at 277 K afforded single crystals of this enantiomer which were suitable for X-ray analysis. The optical rotation in hexane solution was determined with a Perkin–Elmer polarimeter 243 (c = 2.5 mg L^{-1}): $[\alpha]_D^{20}$ = 117.4.

CAS Registry numbers: α-HCH , 319-84-6; (+/-)-α-HCH, 60291-32-9; (+)-α-HCH, 119911-69-2; (−)-α-HCH, 119911-70-5.

Received: October 28, 1993
Revised: November 26, 1993 [Z6458IE]
German version: *Angew. Chem.* **1994**, *106*, 911

[1] H. Hühnerfuss, J. Faller, W. A. König, P. Ludwig, *Environ. Sci. Technol.* **1992**, *26*, 2127–2133.
[2] a) W. A. König, R. Krebber, P. Mischnik, *J. High Resolut. Chromatogr.* **1989**, *12*, 732–738; b) W. A. König, *Nachr. Chem. Tech. Lab.* **1989**, *37*, 471–476; c) V. Schurig, H.-P. Nowotny, *Angew. Chem.* **1990**, *102*, 969–986; *Angew. Chem. Int. Ed. Engl.* **1990**, *29*, 939–957, and references therein.
[3] H. Hühnerfuss, J. Faller, R. Kallenborn, W. A. König, P. Ludwig, B. Pfaffenberger, M. Oehme, G. Rimkus, *Chirality* **1993**, *5*, 393–399, and references therein.
[4] B. Pfaffenberger, H. Hühnerfuss, R. Kallenborn, A. Köhler-Günther, W. A. König, G. Krüner, *Chemosphere* **1992**, *25*, 719–725.
[5] H. Hühnerfuss, R. Kallenborn, *J. Chromatogr.* **1992**, *580*, 191–214, and references therein.
[6] R. Kallenborn, H. Hühnerfuss, W. A. König, *Angew. Chem.* **1991**, *103*, 328–329; *Angew. Chem. Int. Ed. Engl.* **1991**, *30*, 320–321.
[7] a) H. Greiling, A. M. Gressner, *Lehrbuch der Klinischen Chemie und Pathobiochemie*, 2nd ed., Schattauer, Stuttgart, **1989**, p. 860; b) A. Faller, *Der Körper des Menschen*, 9th edition, Thieme, Stuttgart, **1980**, p. 335.
[8] a) K. Ronald, R. J. Frank, J. L. Dougan, R. Frank, H. E. Braun, *Sci. Total Environ.* **1984**, *38*, 133–152; b) R. Kallenborn, *Untersuchungen von ausgewählten chlorierten Schadstoffen im ökologischen Umfeld der Eiderenten (Somateria mollissima (L.)) aus norddeutschen Küstengebieten*, Dissertation, Universität Hamburg, **1993**.
[9] a) J. Portig, K. Stein, H. W. Vohland, *Xenobiotica* **1989**, *19*, 123–130; b) W. Koransky, S. Ullberg, *Biochem. Pharmacol.* **1964**, *13*, 1537–1538; c) E. Nakajima, H. Shindo, N. Kurihara, *Radioisotopes* **1970**, *19*, 60–66.

 © VCH Verlagsgesellschaft mbH, D-69451 Weinheim, 1994 0570-0833/94/0808-0883 $ 10.00+.25/0

[10] S. Mössner, T. R. Spraker, P. R. Becker, K. Ballschmiter, *Chemosphere* **1992**, *24*, 1171–1180.
[11] K. Möller, H. Hühnerfuss, G. Rimkus, *J. High Resolut. Chromatogr.* **1993**, *16*, 672–673.
[12] J. S. Cristol, *J. Am. Chem. Soc.* **1949**, *71*, 1894.
[13] Crystal structure analysis of (+)-α-HCH: space group $P2_12_12_1$, $a = 738.0(1)$, $b = 805.3(1)$, $c = 1802.5(2)$ pm, $V = 1071.25 \times 10^6$ pm^3, $Z = 4$, measured crystal $0.4 \times 0.4 \times 0.3$ mm^3, 293 K, $Cu_{K\alpha}$ radiation, Enraf-Nonius-CAD4 diffractometer, 2248 symmetry independent reflections, structure solved with SHELXS-90, structure refined with SHELXL-93, $R = 0.0571$ for all reflections and $R = 0.0546$ for 2173 significant reflections [$|F| > 4\,\sigma(F)$]. Flack-parameter: $x = -0.02(4)$. Further details of the crystal structure investigation may be obtained from the Fachinformationszentrum Karlsruhe, D-76344 Eggenstein-Leopoldshafen (FRG) on quoting the depository number CSD-400418.
[14] a) R. S. Cahn, C. K. Ingold, V. Prelog, *Experientia* **1956**, *12*, 81–124; b) *Angew. Chem.* **1966**, *78*, 413–447; *Angew. Chem. Int. Ed. Engl.* **1966**, *5*, 385–415; c) V. Prelog, G. Helmchen, *ibid.* **1982**, *94*, 614–631 and **1982**, *21*, 567–583.

Cellulose in Schweizer's Reagent: A Stable, Polymeric Metal Complex with High Chain Stiffness**

Walther Burchard,* Norbert Habermann, Peter Klüfers,* Bernd Seger, and Ulf Wilhelm

Cellulose is the biogenic raw material that nature provides us with the largest quantities of. The search for solvents for cellulose has always been closely associated with the development of new applications and has also served in the chemical and physical characterization of cellulose. One of the longest known solvents for cellulose is Schweizer's reagent, an aqueous ammoniacal solution of copper(II) hydroxide ("cuoxam"). This reagent was discovered in the middle of the 1800s[1] and has been employed since the turn of the century in the cuprammonium process. The alkaline variant is used today, in particular for the preparation of membranes from (modified) cellulose for hemodialysis and hemofiltration.[2] In polymer analysis both cuoxam and "cuen" (copper(II) hydroxide in aqueous ethylenediamine (en)) are used for the determination of the degree of polymerization of cellulose.

The numerous conjectures regarding the fundamental molecular aspects of the cuprammonium process and the applications in polymer analysis are, for the most part, not backed up by experiment. Recently we showed that carbohydrates in aqueous alkaline solution are multiply deprotonated in the presence of copper(II) ions and form chelate complexes.[3] We report here on our first investigation of the solution equilibria in the systems polyol/Cu^{II}/NH_3 and polyol/Cu^{II}/en, on preliminary light-scattering experiments on cellose in cuoxam, and on a structural model of the cellulose–copper complex, which can be used to link the values from coordination chemistry with parameters from polymer chemistry.

The formation constants of polyolato–copper complexes were determined for the polyols anhydroerythritol (*meso*-oxolane-3,4-diol; AnEryt) and methyl-4-*O*-methyl-β-D-glucopyranoside (Me-β-D-Glc*p*4Me) by spectral photometry.[4] (The latter polyol was included because of its close structural resemblance to cellulose.) The structural formulas show both polyols along with a monomeric unit from cellulose from the middle of the chain (anhydroglucose, Glc_C).

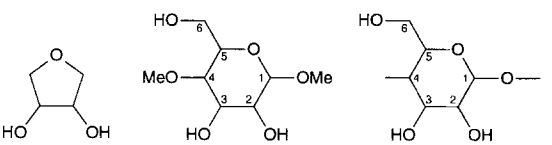


Table 1 lists the constants for the system Cu^{II}/NH_3/AnEryt (1/500/3), $c_0(Cu) = 1$ mM, that are used in the calculation of the distribution curves. The distribution of species[5] as a function of the pH value is shown on the left side of Figure 1. The known amminecopper complexes are the dominant species up to pH ≈ 11; the polyol is doubly deprotonated at higher pH values, and the resulting *meso*-oxolanediolate(2−) ion displaces ammonia with formation of the ternary complex $[(NH_3)_2Cu(AnErytH_{-2})]$. The formation of the $AnErytH_{-2}$ ligand in aqueous solution is in accord with the observed formation of crystalline oxolanediolato(2−)cuprates from aqueous media.[3]

Table 1. Indices of the formula $Cu_i(NH_3)_j(AnErytH_{-2})_kH_l$, mixed stability constants ("Brønsted constants") as $\log\beta$ and λ_{max} [nm], in parentheses: ε_{max} [M^{-1}cm^{-1}][a]. The following relationship holds (without charges):

$$\beta = \frac{c([Cu_i(NH_3)_j(AnErytH_{-2})_kH_l])}{c^i(Cu)\,c^j(NH_3)\,c_k(AnErythH_{-2})\,c^l(H)}$$

The constants used for the calculation of the distribution of noncolored species: 0101 9.53[b], 0011 13.6 (estimated), 0012 27.0 (first step determined by the Michaelis method[c]), 000−1 14.0; $I_0 = 0.75$ M (ammonium sulfate).

ijkl	$\log\beta$	$\lambda_{max}(\varepsilon)$
1100	4.0	752 (19)
1200	7.4	702 (30)
1300	10.2	642 (42)
1400	12.0	583 (55)
1500	11.1	653 (130)
1210	18.2	611 (44)
1020	22.0	632 (37)
102 − 2	−5.8	687 (38)

[a] The values for the five amminecopper ions were determined in the binary ammonia–copper system; in the evaluation of the ternary system fixed values were used and variables were also refined. Maximum deviations between the two calculations: 0.1 for $\log\beta$, 2 nm for λ_{max}, and 2 M^{-1} for ε. [b] I. Nagypál, F. Debreczeni, *Inorg. Chem. Acta* **1984**, *81*, 69–74. [c] L. Michaelis *Ber. Dtsch. Chem. Ges.* **1913**, *46*, 3683–3693.

The unexpected thermodynamic stability of polyolatocopper complexes is emphasized on the right side of Figure 1. In an excess of components AnEryt and en, $AnErytH_{-2}$ displaces ethylenediamine from the stable $[Cu(en)_2]^{2+}$ complex above pH ≈ 11 with formation of the ternary complex; above pH ≈ 13 en-free bis(polyolato)cuprates are formed despite the excess of en. In the investigation of the system Cu^{II}/NH_3/Me-β-D-

[*] Prof. Dr. W. Burchard, Dipl.-Chem. B. Seger
Institut für Makromolekulare Chemie der Universität
Sonnenstrasse 5, D-79104 Freiburg (FRG)
Telefax: Int. code + (761)276453
Prof. Dr. P. Klüfers, Dr. N. Habermann, Dr. U. Wilhelm
Institut für Anorganische Chemie der Universität
Engesserstrasse, Gebäude 30.45, D-76128 Karlsruhe (FRG)
Telefax: Int. code + (721)608-4290

[**] Polyol–Metal Complexes, Part 7. This work was supported by the Bundesministerium für Forschung und Technologie (Förderkennzeichen 0319368A) and Akzo AG, Wuppertal (FRG). We thank Prof. Dr. A. Zuberbühler, Basel (Switzerland), for supporting our work and for an expanded version of the program SPECFIT. – Part 6: M. Klaassen, P. Klüfers, *Acta Crystalogr. Sect. C*, **1994**, 50, 175–178.

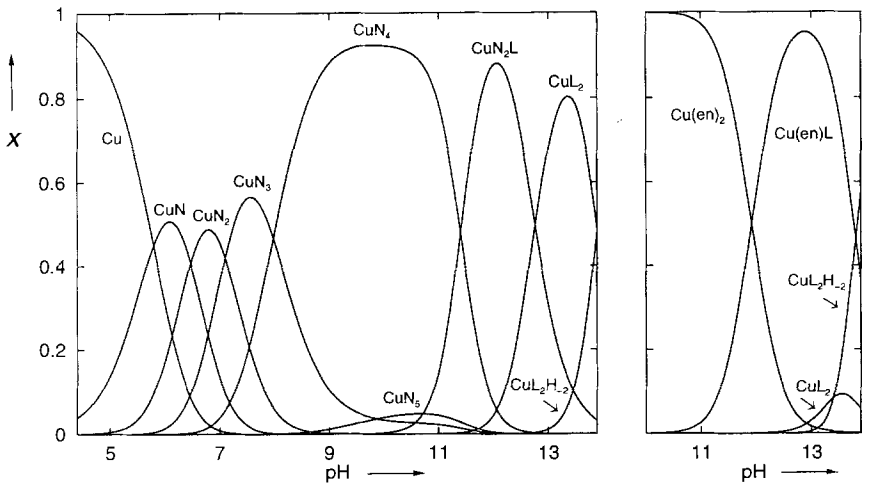


Fig. 1. Left: Plot of the molar ratio x of a species relative to the total amount of copper as a function of the pH for the system Cu^{II}/NH_3/AnEryt (1/500/3); $c_0(Cu) = 1$ mM and ionic strength $I_0 = 0.75$ M; in the notation used for the individual species N stands for NH_3 and L for anhydroerythritol. Right: Species distribution for the system Cu^{II}/en/AnEryt (1/3/3); $c_0(Cu) = 1$ mM and $I \approx 0$; values of logβ (indices based on the formula $Cu_i(en)_j(AnEryrH_{-2})_kH_l$): 0101 9.93, 0102 16.78 [16]; 1200 18.95, 1110 21.9, 1020 21.6, 102−2 −5.2.

Glc$p$4Me (1/100/1), $c_0(Cu) = 1$ mM, an equimolar copper:polyol ratio was chosen so as to model the cellulose-saturated cuoxam solutions. No new species of particular stability were found, and the constants of the complexes formed with doubly deprotonated glucoside are comparable to those with AnEryt.[6]

What form does cellulose take in Schweizer's reagent? Investigations with simple polyols suggest that the monomer should be formulated as $(NH_3)_2Cu(Glc_c2,3H_{-2})$ with deprotonated O-2 and O-3. Owing to the high stability of polyolatocopper complexes, it is expected that in not-too-dilute solutions of sufficiently high pH most anhydroglucose units are complexed. Rough numerical approximations for solutions with concentrations typically used in polymer characterization can be obtained by transferring the formation constants from dilute solution. For the conditions given in Figure 2—these concentrations are also used in the dilution series in the light-scattering experiments described below—almost complete complexation occurs even in concentrated ammonia solutions, and complexation increases as the diol concentration decreases. Thus cellulose forms a stable polymeric metal complex in cuoxam.

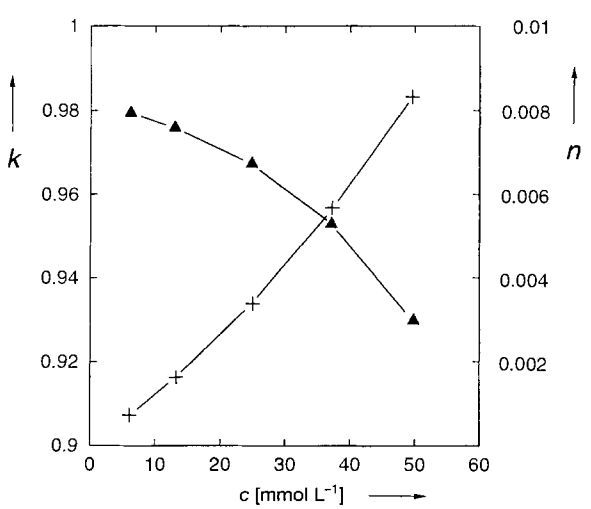
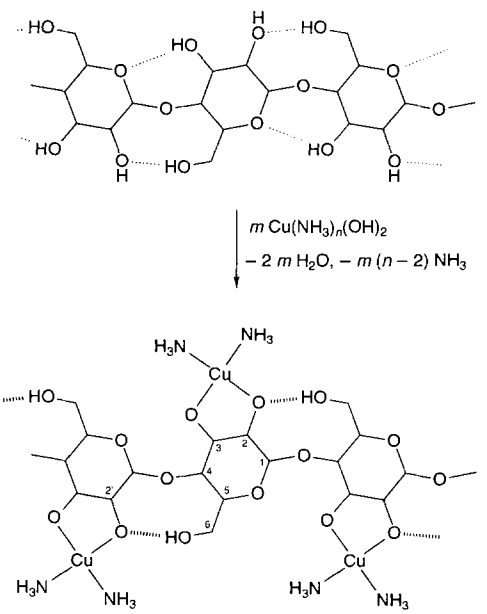


Fig. 2. Plot of the degree of complexation k (k = proportion of the metal-bound diol units [triangles] and degree of cross-linking n ($n = 0.5 \times$ proportion of diol units in bis(diolato) complexes [crosses]) versus AnEryt concentration c; calculated from the values of logβ from Table 1 and for the concentrations used in the light scattering measurements (0.1025 M $Cu(OH)_2$, 14.7 M NH_3, 0.0063–0.0496 M diol).

A preliminary model for the structure of the polymeric complex can be sketched in which the monomeric units are disposed following a construction principle that we observed recently for a related cyclodextrin complex. There, the alkoxide functions serve as acceptors in intramolecular hydrogen bonds of the type $O-H\cdots O^-$.[7] In the bottom part of Scheme 1 a cellulose chain is shown in which the monomer units are linked by O-6–$H\cdots$O-2′ bonds in addition to the glycosidic bond. The special



Scheme 1.

characteristic of cellulose is obvious: in the cyclodextrin complex a compromise is drawn between the complexation of as many copper ions as possible and the stabilization of the alkoxide functions by the formation of hydrogen bonds. In contrast, in the cellulose complex *all* the diol functions are engaged in complexation and *also* in formation of hydrogen bonds of the type $O-H\cdots O^-$. Remarkably the conformation of the cellulose chain generally assumed[8] (Scheme 1, top) does not change upon complexation. According to our model the number of hydrogen bonds in the complex is less than in cellulose, but these remaining hydrogen bonds are stronger owing to the deprotonation of the acceptor.

 © VCH Verlagsgesellschaft mbH, D-69451 Weinheim, 1994 0570-0833/94/0808-0885 $ 10.00+.25/0

One should bear in mind that the notion that the polymer is fixed in *one* conformation by strong hydrogen bonds holds only for those sections of the macromolecule in which adjacent anhydroglucose units bind copper ions. However, as the degree of complexation k is less than 1, copper-free monomeric units occur which can be considered to be flaws. In these positions more than one conformation with $O-H\cdots O^-$ bonds is possible, and the complexed cellulose chain has a "joint" at this point. The degree of complexation under the chosen experimental conditions is thus an important parameter for characterizing the polymer and should correlate with chain stiffness.

A second parameter that connects coordination and polymer chemistry is the degree of cross-linking, also defined in Figure 2. Analysis of the solution equilibria show that even with an excess of copper and ammonia a small amount of the polyol exists as bis(polyolato) complexes, which corresponds to the cross-linking of cellulose strands or sections of strands through copper.

Our proposed model can be tested by light-scattering (LS) experiments. Up until now LS experiments were not possible because of the deep-blue color of the copper complexes. We were able to conduct the first analyses of this type with a strong Ar ion laser (absorption correction, $\lambda_0 = 457.9$ nm). With modern LS techniques the mean geometrical molecular radius R_g can be ascertained as well as a molecular radius determined by hydrodynamics R_h.[9] These two radii and the angle dependence of the scattering intensity are used to determine chain stiffness. The measurements were conducted with cellulose of different molecular weights; a polydispersity of $M_w/M_n = 2$ was assumed.

The term "chain stiffness" can be understood by examination of Figure 3. A chain with unrestricted mobility forms a relatively tight knot. If the mobility of individual members of the chain (here the anhydroglucose units) is hampered, the knot expands to a wormlike chain. In a mathematical description in 1934

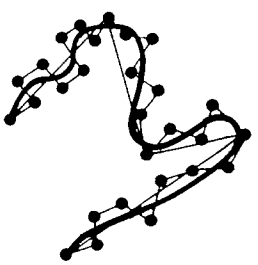


Fig. 3. Schematic representation of chain stiffness (flexible chains: short lines connecting the dots; chain in the Kuhn model: long, thin lines; wormlike chain: long, thick lines.

Kuhn[10] introduced the concept of a statistically preferred length, which is referred to today as the Kuhn segment length l_k (long lines in Fig. 3). This extended length, which joins a number of monomeric units into an almost rigid segment, requires free and independent mobility of the new segments. Identical results were obtained from the analysis of the scattering data[11] by three methods employing: 1) the radius of gyration R_g defined by Benoit and Doty,[12a] 2) the characteristic ratio C_∞ according to Flory,[12b] and 3) the angle dependence of the scattering intensity with application of the Koyame theory.[12c] The analysis (for details see ref.[12d]) yielded a Kuhn segment length of $l_k = 26(\pm 6)$ nm; in other words, approximately 50 monomeric units form a relatively rigid segment. These results become more meaningful upon comparison to the known values for polystyrene: $l_k = 2$ nm and roughly 10 units per segment.[13] Thus cellulose in cuoxam shows an unexpectedly high chain stiffness, in accord with the proposed model.

A further question was whether cross-linkage through the formation of bis(polyolato) complexes can be proved by LS experiments. Figure 4 shows a plot of the radius of gyration R_g and the hydrodynamic radius R_h versus chain length. Polymers with constant segment densities give straight lines over the entire range in such plots. In Figure 4 the plot clearly deviates from linearity for samples with greater molecular weights. This implies an increase in the segment density with high degree of polymerization and is an indication of intramolecular cross-linking. This type of exclusively intramolecular cross-linking is possible only in highly dilute solution.[14] Intermolecular cross-linking between chains should occur at higher concentrations, especially when the so-called overlap concentration c^*[15] is exceeded. Indeed, this effect is observed: cluster formation and finally gelling take place.

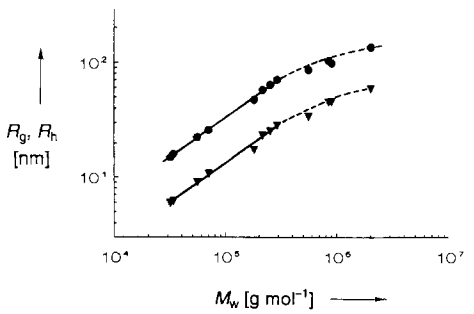


Fig. 4. Plot of the molecular radii R_g (circles) and R_h (triangles) versus molecular weight M. The anomalies at high molecular weights result from the contraction of the molecular knot as a consequence of intramolecular cross-linking.

These results show that a structural model of cellulose derived from single-crystal data from cyclodextrin complexes links values from coordination chemistry with parameters from polymer chemistry. It should be noted that the model itself and the values shown in Figure 2 are preliminary. For a more precise description of the complex equilibria further investigations that include the concentration range of the polymer analysis are necessary. The compensation of various errors is likely to be crucial in the uniform values we obtained (50 anhydroglucose units in the rigid sections versus an extent of complexation of 98% at high dilution).

Received: November 11, 1993 [Z 6491 IE]
German version: *Angew. Chem.* **1994**, *106*, 936

[1] E. Schweizer, *J. Prakt. Chem.* **1857**, *72*, 109–111.
[2] G. von Sengbusch, H. D. Lemke, J. Viencken in *Uremia Therapy* (Ed.: H. J. Gurland), Springer, Berlin, **1987**, pp. 111–124.
[3] M. Klaassen, P. Klüfers, *Z. Anorg. Allg. Chem.* **1993**, *619*, 661–668.
[4] Titration of an appropriate solution under inert gas and recording of the VIS spectra (Varian Cary 3 with extended sample cell, 10-cm flow cuvette) within the given pH limits (monitored with Orion 960 with EA 940 pH meter, Orion "Ross" electrode 8102 SC), $T = 25\,^{\circ}C$; the conditions at the start of the measurements are referred to in the text by the subscript 0 for concentration c and ion strength I. Analysis with the program SPECFIT (H. Gampp, M. Maeder, C. J. Meyer, A. Zuberbühler, *Talanta* **1985**, *32*, 257–264, 1133–1139; *ibid.* **1986**, *33*, 943–951.
[5] The curves were fitted with SPE (A. Martell, R. Motekaitis, *Determination and Use of Stability Constants*, VCH, Weinheim, **1988**, pp. 197–208; figures with GNUPLOT.
[6] $\log\beta_{1210} = 17.5$, $\log\beta_{101\ -2} = -10.8$, indices *ijkl* from the molecular formula $Cu_i(NH_3)_j$(Me-β-D-Glcp4MeH$_{-2}$)$_k$H$_l$, $I_0 = 0.15$ M (ammonium sulfate), $c_0(Cu) = 2$ mM; dihydroxo-glucosidatocuprate (species 101–2) is not formed completely in the pH range examined (up to 13.76).
[7] R. Fuchs, N. Habermann, P. Klüfers, *Angew. Chem.* **1993**, *105*, 895–897; *Angew. Chem. Int. Ed. Engl.* **1993**, *32*, 852–854.
[8] See for example: A. Sarko in *Cellulose* (Eds.: R. A. Young, R. M. Powell), Wiley, New York, **1986**, pp. 29–49; the formulation of the hydrogen bonds is a topic of debate (cf. G. A. Jeffrey, W. Saenger, *Hydrogen Bonding in Biological Structures*, Springer, Berlin, **1991**, pp. 216–218.

 © VCH Verlagsgesellschaft mbH, D-69451 Weinheim, 1994 0570-0833/94/0808-0886 $ 10.00+.25/0

[9] See for example: M. B. Huglin, *Light Scattering from Polymer Solutions*, Academic Press, London, **1972**, pp. 89–164; B. J. Berne, R. Pecora, *Dynamic Light Scattering*, Wiley, New York, **1976**, pp. 53–91.
[10] W. Kuhn, *Kolloid-Z.* **1934**, *68*, 2–15.
[11] The measurements were conducted in the concentration range 1–10 g L^{-1} cellulose with scattering angles from 30 to 150° in 10° increments and extrapolated to $c = 0$ by analysis of the Zimm plot. The limiting concentration is independent of interactions between the macromolecules and served as the basis for the structure analysis of the individual molecules.
[12] a) H. Benoit, P. Doty, *J. Phys. Chem.* **1953**, *57*, 958–963; b) P. J. Flory, *Statistical Mechanics of Chain Molecules*, Interscience, New York, **1969**, pp. 16–18; c) R. Koyama, *J. Phys. Soc. Jpn.* **1973**, *34*, 1029–1036; d) P. Denkinger, W. Burchard, *J. Polym. Sci. Part B: Polym. Phys.* **1991**, *29*, 589–600.
[13] J. Bandrup, E. H. Immergut, *Polymer Handbook*, Wiley, New York, **1975**, pp. IV-40–IV-41.
[14] The degree of cross-linking n is the sum of an intramolecular and an intermolecular term. It should be noted that the extrapolation to $c = 0$ in the polymer analysis does not imply an analogous extrapolation in the $n(c)$ diagram. The limiting case there corresponds to infinitesimally few diol units near the amminecopper units and thus to $n \rightarrow 0$ for $c \rightarrow 0$. In contrast, extrapolation in polymer analysis allows a description of the behavior of isolated cellulose molecules in solution; however, in this case a finite number of diol units are available for complex equilibria. Under these conditions n corresponds to the extent of *intra*molecular cross-linking.
[15] P. G. de Gennes, *Scaling Concepts in Polymer Physics*, Cornell University Press, Ithaca, **1979**, pp. 76–80.
[16] R. M. Smith, A. E. Martell, *Critical Stability Constants, Vol. 2*, Plenum, New York, **1975**, p. 37; *Critical Stability Constants, Vol. 6*, **1989**, pp. 181, 439.

A Mixed-Valent, Unsymmetrical $Fe^{II}Fe^{III}$ Complex with a Terminal Phenolato Ligand as a Model for the Active Site of Purple Acid Phosphatases**

Elisabeth Bernard, William Moneta, Jean Laugier, Sylvie Chardon-Noblat, Alain Deronzier, Jean-Pierre Tuchagues, and Jean-Marc Latour*

Purple acid phosphatases (PAP) are non-heme proteins with an active site containing two iron atoms; these enzymes catalyze the hydrolysis of activated phosphoric acid esters.[1] Two forms of the diiron unit have been characterized: the oxidized inactive $Fe^{III}Fe^{III}$ center and the reduced active $Fe^{II}Fe^{III}$ unit. The diiron(II) form of the protein is unstable, and release of Fe^{II} ions is observed upon reduction of the oxidized protein with dithionite.[1] X-ray structure analysis has not yet been possible for any PAP enzyme; however, EXAFS[2] and NMR[3] studies indicate that the Fe_2 center has an oxygen-rich coordination environment similar to that in ribonucleotide reductase.[4] A bridging hydroxo ligand has been proven in the reduced form of the protein, but some controversy still exists on the nature of the bridging ligands at the oxidized center.[1, 5] A distinctive feature of these proteins is the tyrosine residue bound to one of the iron atoms, which contributes to their color through a Tyr-to-Fe^{III} charge transfer transition at 550 nm in the oxidized protein. Upon one-electron reduction the charge transfer band moves to 510 nm while retaining its intensity, which indicates that the Tyr residue is bound to the nonelectroactive Fe^{III} ion.

Two approaches have been used for modeling the PAP active site. The dinuclear iron(III) complex with a phenolato ligand has been used to mimic the coordination of the tyrosine residue. But a symmetrical complex was obtained in which each Fe^{III} atom is ligated by a phenolato ligand.[6] In another approach phosphate bridges have been incorporated into μ-oxodiiron(III) cores[7] and into mixed-valent $Fe^{II}Fe^{III}$ complexes of μ-phenolato ligands containing four pyridine rings.[8] In all instances symmetrical complexes were obtained.

In this communication we describe the structural and magnetic characterization of the unsymmetrical mixed-valent $Fe^{II}Fe^{III}$ complex **1**. This complex is the first to reproduce the coordination of a terminal tyrosine residue to a diiron center as found in the PAP enzymes. This compound was derived from a new unsymmetrical heptadentate ligand (H_2L) constructed by introducing two different complexing "arms" (bis(2-pyridylmethyl)aminomethyl and (2-pyridylmethyl)(2-hydroxyphenyl)-aminomethyl) at the *ortho* positions of *p*-cresol.[9] In addition, the results of an electrochemical study of **1** help explain the instability of the reduced diiron(II) form of the PAP enzymes.

Reaction of one equivalent of H_2L with two equivalents of $Fe(NO_3)_3 \cdot 9H_2O$ and one equivalent of disodium 1,3-benzenedipropionate (Na_2mpdp) affords a violet solution, which yields a violet precipitate of **1** upon addition of sodium tetraphenylborate. Elemental analysis of **1** shows that it is the

$[Fe^{II}Fe^{III}L(mpdp)]BPh_4$ **1**

mixed-valent complex with the above formulation, which is confirmed by solid-state magnetic studies. Recrystallization of this powder from acetonitrile/ethanol affords violet crystals suitable for X-ray structure analysis.[10] The structure of **1** is represented in Figure 1. The complex consists of discrete diiron complex

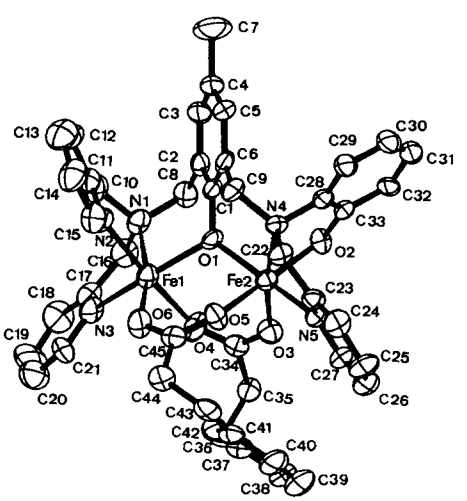


Fig. 1. Structure of the cation $[Fe_2L(mpdp)]^+$ of **1** in the crystal. Important bond lengths [Å] and angles [°]: Fe1 ··· Fe2 3.417(1), Fe1-O1 2.073(3), Fe1-O4 2.037(3), Fe1-O6 2.178(4), Fe1-N1 2.238(5), Fe1-N2 2.170(4), Fe1-N3 2.118(4), Fe2-O1 1.949(3), Fe2-O2 1.936(3), Fe2-O3 2.053(3), Fe2-O5 1.965(4), Fe2-N4 2.244(4), Fe2-N5 2.147(5), Fe1-O1-Fe2 116.4.

[*] Dr. J.-M. Latour, E. Bernard, Dr. W. Moneta
Département de Recherche Fondamentale sur la Matière Condensée
Laboratoire de Chimie de Coordination, C.E.N.G.
F-85 X 38041 Grenoble Cedex (France)
Telefax: Int. code + 76 88 50 90
J. Laugier
Département de Recherche Fondamentale sur la Matière Condensée
Laboratoire Structures, C.E.N.G., Grenoble
Dr. S. Chardon-Noblat, Dr. A. Deronzier
Laboratorie d'Electrochimie Organique et de Photochimie Rédox
Université Joseph Fourier, Grenoble
Prof. J.-P. Tuchagues
Laboratoire de Chimie de Coordination du CNRS, Toulouse

[**] This research was supported by the Centre National de la Recherche Scientifique (URA 1194 and GDR Métalloprotéines).

cations and tetraphenylborate counterions. The two iron atoms have substantially different coordination environments. Fe1 is surrounded by a distorted N_3O_3 octahedron consisting of three nitrogen atoms from one "arm" of L and two oxygen atoms from two carboxylate groups of mpdp, and the oxygen atom from the cresolato ligand. Fe2, on the other hand, is in an N_2O_4 environment made up of two nitrogen atoms from the other "arm" of L, two oxygen atoms from two carboxylate groups of mpdp, one from the cresolato ligand, and one from the terminal phenolate group (terminal with respect to coordination to the iron center and the ligand system). The two iron atoms are bridged by the two carboxylate groups and the oxygen atom of the cresolate. The Fe–Fe distance amounts to 3.417 Å, which compares favorably with those determined in symmetrical bis-μ-carboxylato-μ-phenolato complexes [3.39(3) Å][11] and in reduced uteroferrin [3.52 Å] from EXAFS measurements.[2] It is worth noting that the Fe-O-Fe unit is strongly asymmetric; the Fe2–O1 distance is 0.124 Å shorter than Fe1–O1 separation. The same trend is observed for the other metal–ligand distances and leads to the conclusion that the valences of the iron ions are localized; the Fe2 center is in the +III oxidation state, Fe1 in the +II oxidation state.

The localization of valences in **1** is supported by the Mössbauer spectra (range 300–80 K), which at 80 K exhibit two doublets split by quadrupole interactions with isomer shifts of 0.490 and 1.124 mm s^{-1} (relative to metallic iron at room temperature), splittings of 0.594 and 2.376 mm s^{-1}, and relative areas of 50.6 and 49.4%, respectively. The first doublet is attributed unambiguously to the trivalent Fe2 center, while the second one corresponds to the divalent Fe1 center. Similar Mössbauer parameters have been obtained for various PAP enzymes. Magnetization studies have been performed over the temperature range 2–300 K. The product of the molar susceptibility and the temperature is equal to 6.8 μ_B at 300 K and decreases slightly with temperature to 5.4 μ_B at 100 K. It then decreases more abruptly to reach roughly 0.4 μ_B at 2 K. This behavior is consistent with the occurrence of a moderate antiferromagnetic interaction between the Fe^{II} and Fe^{III} centers. The data were fitted to the equation deduced from application of the Heisenberg spin Hamiltonian $\mathcal{H} = -2JS_1S_2$ to a pair of spins $S_1 = 5/2$ and $S_2 = 2$. The best fit was obtained with the values $g = 2.0$ and $J = -3.8$ cm^{-1}.[12] This exchange interaction compares more favorably with that calculated for the phosphate derivative ($J = -3.0$ cm^{-1}) than that determined for the uncomplexed form ($J = -9.9$ cm^{-1}) of the PAP from porcine uterus.[13]

The electrochemical properties of **1** were investigated in 0.1 M tetrabutylammonium perchlorate in acetonitrile. In this medium the electronic absorption spectrum of **1** comprises three bands in the range 300–800 nm: at 374 nm ($\varepsilon \approx 2200$), 405 nm ($\varepsilon \approx 2000$), and 535 nm ($\varepsilon \approx 1700$) (Fig. 2, curve a). Comparison of this spectrum with those of complexes of μ-phenolato ligands leads to the tentative assignment of the bands at 405 and 535 nm to charge-transfer transitions from the terminal and the bridging phenolates to the Fe ion, and the absorption at 374 nm to a charge transfer from the Fe^{II} ion to the pyridine groups.[11]

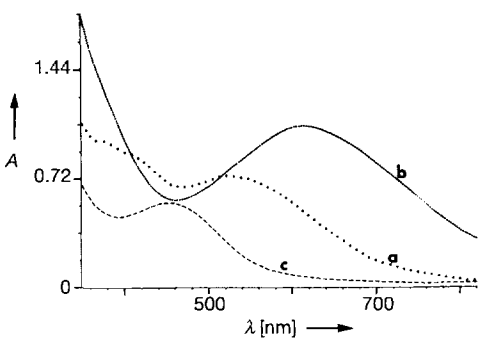


Fig. 2. Electronic absorption spectra in a 0.1 M solution of tetrabutylammonium perchlorate (TBAP) in acetonitrile at ambient temperature: a) solution of **1** (0.97 mM); b) solution from a) after one-electron oxidation; c) solution from a) after one-electron reduction.

A reversible oxidation wave is observed in the cyclic voltammogram of **1** (Fig. 3, curve a) at $E_{1/2} = 0.12$ V. Coulometric analysis shows that this process is a one-electron transfer, and it is therefore assigned to the $Fe^{II}Fe^{III}/Fe^{III}Fe^{III}$ transition (e.g. the oxidation of the Fe^{II} ion). The solution of the oxidized complex shows an enhanced charge-transfer band at 618 nm ($\varepsilon \approx 2600$; Fig. 2, curve b). The reduction of **1** at $E_{1/2} = -0.88$ V is reversible, but following this reduction a second wave appears at a slightly less negative potential $E_{1/2} = -0.72$ V (Fig. 3, curve b). Exhaustive electrochemical reduction of **1** at −1.2 V requires one electron per molecule, and the resulting solution shows the presence of the two $Fe^{II}Fe^{II}$ species in roughly a 1:1 ratio (Fig. 3, curve c). The electronic spectrum of the reduced

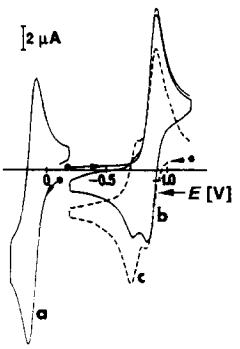


Fig. 3. Cyclic voltammetry with a glassy carbon electrode (diameter 3 mm) of a 0.84 mM solution of **1** versus Ag/10 mM Ag^+ reference in acetonitrile/0.1 M TBAP; $v = 100$ mV s^{-1}. Curve a: Scan between −0.10 V and +0.30 V; curve b: two successive scans between −0.20 V and −1.20 V; curve c: obtained after controlled potential reduction at −1.20 V of the initial solution.

solution presents an absorption at 452 nm ($\varepsilon \approx 1100$). Reoxidation at −0.45 V or at −0.8 V (the potential at which only the most readily oxidized species is oxidized) regenerates essentially the starting solution. This behavior is consistent with the existence of two $Fe^{II}Fe^{II}$ compounds **2** in equilibrium; **2b** results from a chemical transformation of **2a** [Eq. (a)].

$$\underset{\mathbf{1}}{Fe^{II}Fe^{III}} + e^- \rightleftharpoons [\underset{\mathbf{2a}}{Fe^{II}Fe^{II}} \rightleftharpoons \underset{\mathbf{2b}}{(Fe^{II}Fe^{II})}] \qquad \text{(a)}$$

Several hypotheses can be made about the nature of the chemical transformation **2a** → **2b**. Comparison of the structures of the mixed-valence and diiron(II) complexes with the μ-phenolato ligand containing four pyridine units indicates that the structures do not change greatly upon reduction.[14] This indicates that a drastic structural change is also unlikely to occur in the reduction of **1**. On the other hand, the electrochemical study shows that the high electron density resulting from both the coordination of the second phenolato ligand and the transfer of an electron strongly destabilizes the diiron(II) center.[15] The dissociation of an anionic ligand (carboxylate or phenolate) would therefore release some electron density from the diiron site. The small stabilization of the second reduced species (160 mV) is more consistent with dissociation of a carboxylato than that of the terminal phenolato ligand. This ligand would bind again when the diiron(II) center is reoxidized, making the

 © VCH Verlagsgesellschaft mbH, D-69451 Weinheim, 1994 0570-0833/94/0808-0888 $ 10.00+.25/0

overall process chemically reversible. Further work is in progress to fully characterize the second reduced species **2b**.

In summary, complex **1** is the first structurally characterized model complex of a PAP enzyme that reproduces the unsymmetrical coordination of a terminal phenolato ligand to a diiron center. Solid-state magnetic studies have shown that the electronic structure of complex **1** is similar to that of the active site of the enzyme. Electrochemical studies have demonstrated that **1**, like the PAP enzymes, has stable $Fe^{III}Fe^{III}$ and $Fe^{II}Fe^{III}$ forms, and that the terminal phenolato ligand destabilizes the diiron(II) state, both in terms of electrochemical potentials and of chemical reactivity. The latter finding rationalizes the observation that reduction of porcine PAP is accompanied by release of iron ions.[1]

Experimental Procedure

To a solution of 1 g (1.88 mmol) of H_2L in 75 mL of CH_3OH were added successively a solution of 1.52 g (3.76 mmol) of $Fe(NO_3)_3 \cdot 9H_2O$ in 50 mL of CH_3OH and a solution of 550 mg (2.48 mmol) of Na_2mpdp [16] in 50 mL of CH_3OH. Addition of a solution of 2.6 g (7.6 mmol) of sodium tetraphenylborate in 30 mL of CH_3OH induced the precipitation of **1** (1.25 g) as a black powder. Recrystallization from acetonitrile/ethanol gave black crystals suitable for X-ray analysis.

Received: November 2, 1993 [Z 6472 IE]
German version: *Angew. Chem.* **1994**, *106*, 914

[1] a) J. Sanders-Loehr in Iron Carriers and Iron Proteins (Ed.: T. M. Loehr), VCH, New York, **1989**, p. 373; b) L. Que, A. E. True, *Prog. Inorg. Chem.* **1990**, *38*, 97; c) J. B. Vincent, G. L. Olivier-Lilley, B. A. Averill, *Chem. Rev.* **1990**, *90*, 1447.
[2] A. E. True, R. C. Scarrow, R. C. Holz, L. Que, *J. Am. Chem. Soc.* **1993**, *115*, 4246.
[3] Z. Wang, L.-J. Ming, L. Que, J. B. Vincent, M. W. Crowder, B. A. Averill, *Biochemistry* **1992**, *31*, 5263.
[4] P. Nordlund, H. Eklund, B.-M. Sjöberg, *Nature* **1990**, *345*, 593.
[5] M. Dietrich, D. Münstermann, H. Suerbaum, H. Witzel, *Eur. J. Biochem.* **1991**, *199*, 105.
[6] S. Yan, L. Que, L. F. Taylor, O. P. Anderson, *J. Am. Chem. Soc.* **1988**, *110*, 5222.
[7] a) P. N. Turowski, W. H. Armstrong, M. E. Roth, S. J. Lippard, *J. Am. Chem. Soc.* **1990**, *112*, 681; b) S. Drüecke, K. Wieghardt, K. Nuber, J. Weiss, H.-P. Fleischhauer, S. Gehring, W. Haase, *J. Am. Chem. Soc.* **1989**, *111*, 8622; c) R. E. Norman, S. Yan, L. Que, G. Backes, J. Ling, J. Sanders-Loehr, J. H. Zhang, C. J. O'Connor, *J. Am. Chem. Soc.* **1990**, *112*, 1554.
[8] a) K. Schepers, B. Bremer, B. Krebs, G. Henkel, E. Althaus, B. Mosel, W. Müller-Warmuth, *Angew. Chem.* **1990**, *102*, 582; *Angew. Chem. Int. Ed. Engl.* **1990**, *29*, 531; b) L.-J. Ming, H. G. Jang, L. Que, *Inorg. Chem.* **1992**, *31*, 359.
[9] The ligand H_2L was obtained from 2,6-bis(hydroxymethyl)-4-methylphenol by the following sequence of reactions: 1) oxidation of one hydroxymethyl group by manganese dioxide; 2) chlorination of the remaining hydroxymethyl group with hydrogen chloride; 3) amination with bis(2-pyridylmethyl)amine; 4) reduction of the formyl group with sodium borohydride; 5) chlorination of the remaining hydroxymethyl group with thionyl chloride; 6) amination with (2-hydroxyphenyl)(2-pyridylmethyl)amine. Mass spectrum (FAB^+, dichloromethane/nitrobenzyl alcohol): 532 ($M - H^+$).
[10] Crystal structure data of **1**: monoclinic, space group $P21/a$, $a = 22.038(9)$, $b = 16.195(8)$, $c = 16.536(7)$ Å, $\beta = 97.26°$, $Z = 4$, $V = 5854.5$ Å^3, measuring temperatue 294 K, $Mo_{K\alpha}$ radiation, ($\lambda = 0.7107$ Å), 14375 symmetry independent reflections, 6583 with $F > 4^*\sigma(F)$, $R = 0.052$, $R_w = 0.042$, structure solution by direct methods, H atoms at calculated positions. Further details of the crystal structure investigation are available on request from the Director of the Cambridge Crystallographic Data Centre, 12 Union Road, GB-Cambridge CB21EZ (UK), on quoting the full journal citation.
[11] a) A. S. Borovik, V. Papaefthymiou, L. F. Taylor, O. P. Anderson, L. Que, *J. Am. Chem. Soc.* **1989**, *111*, 6183; b) M. S. Mashuta, R. J. Webb, K. J. Oberhausen, J. F. Richardson, R. M. Buchanan, D. N. Hendrickson, *ibid.* **1989**, *111*, 2745.
[12] In cases where the exchange integral J is as small as here, the zero-field splitting parameter of the Fe^{II} ion is likely to be of the same order of magnitude and should be taken into account. Accordingly, the Heisenberg spin Hamiltonian furnishes only a crude estimate of J. A more sophisticated treatment of the field and temperature dependences of the magnetization of **1** is currently underway and will be reported in due course.
[13] E. P. Day, S. S. David, J. Peterson, W. R. Dunham, J. J. Bonvoisin, R. H. Sands, L. Que, *J. Biol. Chem.* **1988**, *263*, 15561.
[14] A. S. Borovik, M. P. Hendrich, T. R. Holman, E. Münck, V. Papaefthymiou, L. Que, *J. Am. Chem. Soc.* **1990**, *112*, 6031.
[15] Compared to the complexes of the μ-phenolato ligand systems containing four pyridine rings, the diiron(III) state of **1** is stabilized by 0.28 V, while the diiron(II) form is destabilized by 0.58 V. As a consequence, the mixed-valence state **1** has a larger stability domain $\Delta E = 1.0$ V (**1**) versus ca. 700 mV (other complexes).
[16] R. H. Beer, W. B. Tolman, S. G. Bott, S. J. Lippard, *Inorg. Chem.* **1989**, *28*, 4557.

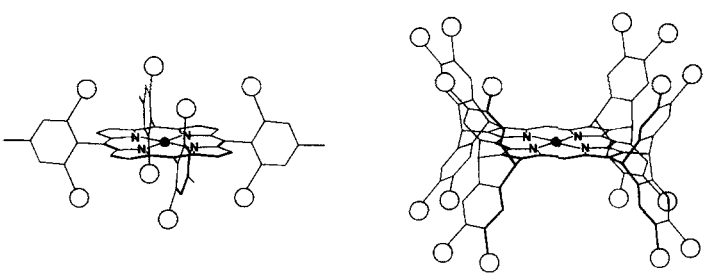
Porphyrins with Biconcave Frameworks**

Yvan Ramondenc, Reinhold Schwenninger, Thao Phan, Karl Gruber, Christoph Kratky, and Bernhard Kräutler*

Dedicated to Professor Hans Gruber on the occasion of his 65th birthday

Recently new porphyrin-like compounds such as Franck's "vinylogous" porphyrins,[1] the "extended" porphyrins, for example, those of Woodward et al., Sessler et al., and Gossauer et al.,[2] and Vogel's "porphycenes"[3] have drawn attention to the considerable number of possible forms which can arise just from their two-dimensional structures. However, the structuring of the third dimension through covalently bonded, peripheral substituents was of crucial importance in Collman's "picket fence" porphyrin.[4] In the *meso*-aryl porphyrin used there, the aryl substituents were the basis for the buildup of the framework in the third dimension. This construction principle was used in (nearly) all[5] three-dimensionally structured porphyrins prepared later[6] (Scheme 1 left).

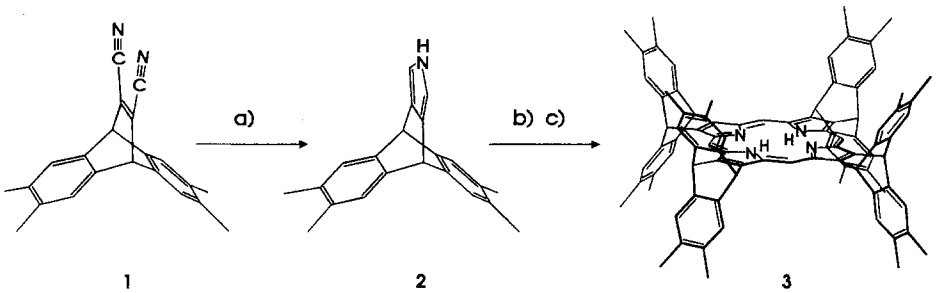
We report here on a second, widely applicable strategy for the synthesis of three-dimensionally structured porphyrins, using porphyrins with "biconcave" frameworks as examples (Scheme 1 right). Cycloadditions provided access to new bulky pyrroles with an oligocyclic structure. The synthesis of the β,β'-disubsti-



Scheme 1. Basic framework of *meso*-aryl porphyrins (left) and of "biconcave" porphyrins (right).

[*] Prof. Dr. B. Kräutler, Dr. Y. Ramondenc, Mag. R. Schwenninger, Dipl.-Ing. T. Phan
Institut für Organische Chemie der Universität
Innrain 52a, A-6020 Innsbruck (Austria)
Telefax: Int. code + (512)507-3303
Mag. K. Gruber, Doz. Dr. C. Kratky[+]
Institut für Physikalische Chemie der Universität
Heinrichstrasse 28, A-8010 Graz (Austria)
Telefax: Int code + (316)32248
[+] Address for correspondence concerning the X-ray crystallographic analysis.

[**] We would like to thank Dr. W. Amrein and R. Häfliger (ETH, Zürich) and E. Williams (Fisons Instruments) for measuring mass spectra. This work was supported by the Jubiläumsfonds der Österreichischen Nationalbank (Proj. Nr. 4194).



Scheme 2. Preparation of pyrrole **2** and its tetramerization to porphyrin **3**. a) DIBAH, −20 °C; b) 30% formaldehyde solution, acetic acid, room temperature, 7 d; c) DDQ, room temperature, 2 h.

tuted pyrroles necessary for this was achieved with oligocyclic-substituted maleic acid dinitriles whose reduction provided a new route to pyrroles.[7, 8] The dinitrile **1** (from acetylenedicarbonitrile and 2,3,6,7-tetramethylanthracene analogous to ref. [9]) could be reduced with diisobutylaluminum hydride (DIBAH) to give pyrrole **2** (Scheme 2) in about 33% yield. Pyrrole **2** has a framework similar to that of triptycene. According to an X-ray crystal structure analysis (Fig. 1), the angle between the planes of the two central phenyl rings in **2** is 115.5°; the distances C2–C7 and C2′–C7′ are 6.52 and 8.68 Å, respectively.[10]

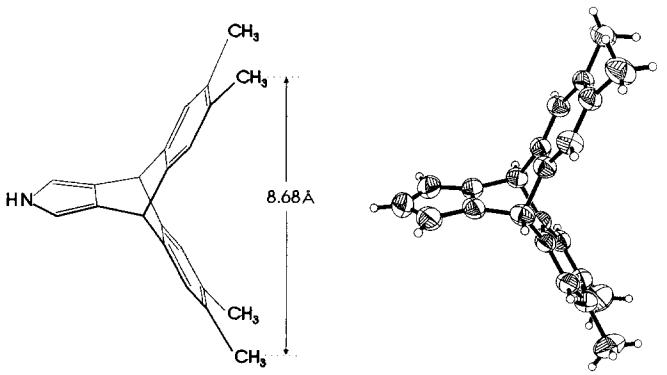


Fig. 1. Left: Structural formula of pyrrole **2**; right: Crystal structure of **2** (projection of one of the three crystallographically independent molecules; thermal ellipsoids at 50% probability level).

Tetramerization of pyrrole **2** by condensation with formaldehyde and subsequent oxidation gave, analogous to a well-known method,[11] reddish, fluorescent, biconcave tetrakis-(9,10-dihydro-9,10-anthraceno)porphyrin **3** in 72% yield. The structure of **3** was deduced from UV/VIS, FAB-MS, and ^{1}H NMR spectra (Table 1).

Compound **3**, like other porphyrins, is an excellent ligand for transition metal ions; for example, in the successful preparation[12] of the Co^{II}-porphyrinate **4**. In the NMR spectrum of the paramagnetic Co^{II} complex **4**, the signals of the hydrogen atoms of the porphyrin ligands show characteristic anisotropic shifts.[13] The light-sensitive, diamagnetic 8-iodooctylporphyrinatocobalt(III) **5** could be prepared from **4** by reduction and subsequent reaction with 1,8-diodooc-

Table 1. Selected spectroscopic data for **1**–**5**.

1: Colorless crystals, m.p. 237 °C; ^{1}H NMR: δ = 2.20 (s, 12H), 5.27 (s, 2H), 7.18 (s, 4H); ^{13}C NMR: δ = 19.38 (q), 53.37 (d), 113.92 (CN), 125.51 (d), 134.44 (s), 137.34 (s), 138.97 (s); IR(KBr): $\tilde{\nu}$ = 2222 cm^{-1}; MS: *m/z* (%): 310 (100) [M^+], 234 (45) [$M^+ - 76$].

2: Colorless crystals, m.p. 277 °C (decomp); ^{1}H NMR: δ = 2.17 (s, 12H), 5.19 (s, 2H), 6.50 (d, 2H, J = 2.9 Hz), 7.12 (s, 4H); ^{13}C NMR: δ = 19.37 (q), 46.32 (d), 109.16 (d), 124.63 (d), 131.26 (s), 132.19 (s), 144.99 (s); IR(KBr): $\tilde{\nu}$ = 3421, 3377 cm^{-1}. UV/VIS (CH_2Cl_2): λ_{max} (log ε) = 263.0 (3.39), 272.0 (3.52), 281.0 (3.58), 289.0 nm (3.71); MS: *m/z* (%): 299 (63.0) [M^+], 284 (100.0) [$M^+ - 15$].

3: Red-brown powder, m.p. >280 °C (decomp); ^{1}H NMR: δ = −4.93 (s, 2H, NH), 2.18 (s, 48H), 6.94 (s, 8H), 7.63 (s, 16H), 10.46 (s, 4H, *meso*-H); IR(KBr): $\tilde{\nu}$ = 3318, 1468, 1454 cm^{-1}. UV/VIS (CH_2Cl_2): λ_{max} (log ε) = 398.0 (5.39), 500.5 (4.32), 532.5 (3.87), 569.5 (3.88), 623.5 nm (2.95); FAB-MS: *m/z* (%): 1240.7 (88), 1239.7 (100) [M^+].

4: Bright red crystals (CH_2Cl_2/hexane); ^{1}H NMR: δ = 2.64 (s, 48H), 10.38 (s, 16H), 14.31 (s, 8H), 30.95 (s, br, 4H); UV/VIS (CH_2Cl_2): λ_{max} (log ε) = 402.5 (5.42), 514.0 (4.16), 546.0 nm (4.17); FAB-MS: *m/z* (%): 1298.6 (26), 1297.6 (62), 1296.6 (100) [M^+], 1295.6 (86).

5: Red crystals; ^{1}H NMR (cf. fig. 2): δ = −5.83 (quint, 2H), −4.40 (t, 2H), −2.16 (quint, 2H), −1.23 (quint, 2H), −0.62 (quint, 2H), 0.10 (quint, 2H), 1.03 (quint, 2H), 2.13 (s, 24H), 2.23 (s, 24H), 2.69 (t, 2H), 6.85 (s, 8H), 7.54 (s, 8H), 7.65 (s, 8H), 10.38 (s, 4H).

[a] ^{1}H NMR (300 MHz) and ^{13}C NMR (75 MHz): Bruker AM 300, $CDCl_3$, 30 °C. FT-IR: Mattson 3000. UV/VIS: Hitachi U-3000. Positive-ion-FAB-MS: ZAB-2 SEQ (NOBA matrix). EI-MS (70 eV) VARIAN MAT 44/S.

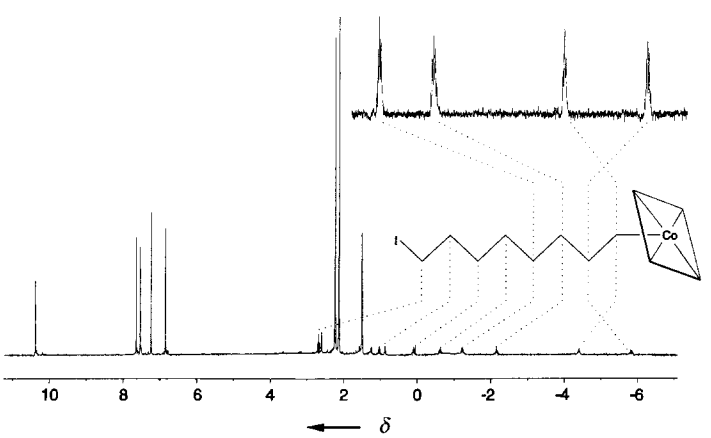
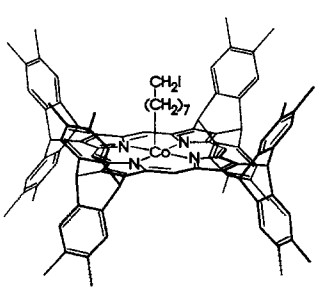


Fig. 2. ^{1}H NMR spectrum of 8-iodooctylporphyrinatocobalt(III) **5** (300 MHz, $CDCl_3$, $\delta(CHCl_3)$ = 7.24; signal assignment in the high-field region from H,H-COSY spectra).

tane. In the NMR spectrum of **5**, the signals of the alkyl groups bonded to cobalt show a characteristic high-field shift (to $\delta \approx -5.8$, Fig. 2).

In metalloporphyrins like **4** and **5**, which are derived from biconcave porphyrins, the peripheral ring of substituted phenyl rings shields the central metal ion from both sides. The biconcave framework prevents dimerization and can be used for a spatially controlled uptake of organic guest molecules. According to preliminary investigations,[14a] in the solid, large guest molecules (such as fullerenes) are incorporated into the structured cavities.[14b]



5

The new approach for the preparation of β,β'-disubstituted pyrroles presented here opens up a rational, and multifacetted direct route to porphyrins with a three-dimensionally structured periphery. This has led to the preparation of the first biconcave metalloporphyrins, whose frameworks promise interesting catalyst properties.

Experimental Procedure

1: Acetylenedicarbonitrile (234 mg, 3.08 mmol) in benzene (5 mL) was added dropwise over 4 h (under N_2) to a heated (80 °C) suspension of 2,3,6,7-tetramethylanthracene (452 mg, 1.93 mmol) [15] in benzene (5 mL). The reaction mixture was heated under reflux for an additional 10 h. After cooling and concentration of the mixture, column chromatography (silica gel, CH_2Cl_2/petroleum ether 1/1) and crystallization from CH_2Cl_2 yielded 562 mg (1.81 mmol, 94%) **1**.

2: DIBAH (12 mmol, 1 M in hexane) was treated with **1** (0.60 g, 1.93 mmol) in dry CH_2Cl_2 (20 mL) under N_2 at −20 °C and stirred. The mixture was stirred at −20 °C for 3.5 h, treated with aqueous citric acid (0.5 M, 16 mL) and diluted with aqueous citric acid (0.5 M, 12 mL) and CH_2Cl_2 (12 mL) at room temperature. The organic phase was concentrated and purified by column chromatography (silica gel, CH_2Cl_2/petroleum ether 1/1). The colorless pyrrole **2** (190.5 mg, 0.64 mmol) crystallized from CH_2Cl_2/hexane (1:5) in 33% yield.

3: A solution of **2** (81 mg, 0.27 mmol) in CH_2Cl_2 (0.6 mL) was treated under N_2 with CH_3OH (0.84 mL), acetic acid (78 μL), and 30% formaldehyde solution (111 μL). The mixture was protected from light, stirred for 7 d at room temperature under N_2, and then concentrated. The residue was dissolved in benzene (2 mL) under N_2 and treated with dichlorodicyanobenzoquinone (DDQ) (42.3 mg, 0.18 mmol) in benzene (4 mL). After 2.5 h at room temperature, the solution was diluted with CH_2Cl_2 (2 mL) and shaken with phosphate buffer (pH 7) (0.1 M 3 mL). The organic phase was separated by column chromatography (CH_2Cl_2). Microcrystalline **3**, 60 mg (72%), was obtained from the red porphyrin fraction after concentration and precipitation from CH_2Cl_2/hexane.

4: **3** (90 mg, 74 μmol) was dissolved in dry THF (20 mL) under N_2 and treated with anhydrous Co^{II} bromide (283 mg, 1.3 mmol) and triethylamine (200 μL, 1.4 mmol) in THF (15 mL). The mixture was stirred at room temperature for 6 h, concentrated under vacuum, and the residue was extracted with CH_2Cl_2 (200 mL). The extract was worked up in water, concentrated, and filtered through an aluminum oxide column. The red fraction (**4**) was concentrated under vacuum and dried. The Co^{II} porphyrinate **4**, 83 mg (88.9%), was obtained as a red-brown powder.

5: This was obtained with a yield of 48% by the reduction of **4** and alkylation with 1,8-diiodooctane (analogous with ref. [16]).

Received: November 10, 1993 [Z 6490 IE]
German version: *Angew. Chem.* **1994**, *106*, 939

[1] a) B. Franck, M. Gosmann, *Angew. Chem.* **1986**, *98*, 1107; *Angew. Chem. Int. Ed. Engl.* **1986**, *25*, 1100; b) B. Frank, G. Knübel, *ibid.* **1988**, *100*, 1203 and **1988**, *27*, 1170.

[2] a) V. J. Bauer, D. R. Clive, D. Dolphin, J. B. Paine, F. L. Harris, M. M. King, J. Loder, S.-W. C. Wang, R. B. Woodward, *J. Am. Chem. Soc.* **1983**, *105*, 6429; b) H. Furuta, M. J. Cyr, J. Sessler, *ibid.* **1991**, *113*, 6677; c) H. Rexhausen, A. Gossauer, *J. Chem. Soc. Chem. Commun.* **1983**, 275.

[3] E. Vogel, *Pure Appl. Chem.* **1993**, *65*, 143.

[4] J. P. Collman, *Acc. Chem. Res.* **1977**, *10*, 265.

[5] Exceptions: Porphyrin dimers and oligomers: a) J. P. Collman, P. Denisevich, Y. Konai, M. Marrocco, C. Koval, F. C. Anson, *J. Am. Chem. Soc.* **1980**, *102*, 6027; b) J.-M. Lehn, *Angew. Chem.* **1988**, *100*, 91; *Angew. Chem. Int. Ed. Engl.* **1988**, *27*, 89; c) G. M. Dubowchik, A. D. Hamilton, *J. Chem. Soc. Chem. Commun.* **1987**, 293; d) C. A. Hunter, M. N. Meah, J. K. M. Sanders, *ibid.* **1988**, 692.

[6] a) Dimers: J. P. Collman, C. M. Elliot, T. R. Halbert, B. S. Tovrog, *Proc. Natl. Acad. Sci. USA* **1980**, *74*, 18; b) "chiral wall" porphyrins: S. O'Malley, T. Kodadek, *J. Am. Chem. Soc.* **1989**, *111*, 9116; c) "vaulted" porphyrins: J. T. Groves, P. Viski, *J. Org. Chem.* **1990**, *55*, 3628; d) "bis-pocket" porphyrins: K. S. Suslick, M. M. Fox, *J. Am. Chem. Soc.* **1983**, *105*, 3507; e) "basket-handle" porphyrins: M. Momenteau, *Pure Appl. Chem.* **1986**, *58*, 1493.

[7] A. Gossauer, *Chemie der Pyrrole*, Springer, Berlin, **1974**.

[8] First experiments on the formation of type **2** pyrroles by cycloaddition: F. Roth-Kutter, B. Kräutler, unpublished results; F. Roth-Kutter, Diplomarbeit, ETH, Zürich, **1987**.

[9] C. D. Weis, *J. Org. Chem.* **1962**, *28*, 74.

[10] Crystal structure analysis of **2**. Crystallization from *n*-hexane/$CHCl_3$; space group $P\bar{1}$; $a = 6.972(1)$, $b = 20.611(4)$, $c = 20.864(4)$ Å, $\alpha = 117.73(3)$, $\beta = 90.96(3)$, $\gamma = 90.56°$, $V = 2652.9(8)$ Å, $Z = 6$ for $C_{22}H_{21}N$, $M_r = 299.4$ (three molecules in the asymmetric unit), $\rho_{calcd} = 1.124\ g\,cm^{-3}$, $\mu(Cu_{K\alpha}) = 4.90\ cm^{-1}$; structure determination with 9206 measured and 6942 symmetry independent reflections ($Cu_{K\alpha}$ radiation, $\lambda = 1.5418$ Å, $T = 298$ K); $R = 0.049$ for 5329 reflections ($F_o > 4\sigma(F_o)$) and 713 parameters. Further details of the crystal structure investigation may be obtained from The Director of the Cambridge Crystallographic Data Centre, 12 Union Road, GB-Cambridge CB2 1EZ, UK on quoting the complete journal citation.

[11] a) D. O. Cheng, E. Le Goff, *Tetrahedron Lett.* **1977**, 1469; b) A. Treibs, N. Häberle, *Justus Liebigs Ann. Chem.* **1968**, *718*, 183.

[12] Similar conditions for the incorporation of cobalt: "*Die Porphyrinogen↔Pyrrocorphin-Tautomerisation*": R. Waditschatka, dissertation, ETH, Zürich, **1985**.

[13] G. La Mar, F. A. Walker in *The Porphyrins, Vol. 4*, (Ed.: D. Dolphin), Academic Press, New York, **1979**, p.61.

[14] a) R. Schwenniger, J. Maynollo, B. Kräutler, K. Gruber, C. Kratky, unpublished results. b) The investigation of solvent-containing single crystals of porphyrin are described by M. P. Byrn, C. J. Curtis, I. Goldberg, Y. Hsiou, S. I. Khan, P. A. Swain, S. K. Tenfick, C. E. Strouse, *J. Am. Chem. Soc.* **1991**, *113*, 6549.

[15] D. Bender, K. Müllen, *Chem. Ber.* **1988**, *121*, 1187.

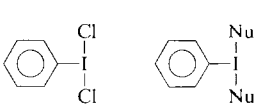
[16] H. Ogoshi, E. Watanabe, N. Koketesu, Z. Yoshida, *Bull. Chem. Soc. Jpn.* **1976**, *49*, 2529.

Electrostatic Activation of Hypervalent Organo-Iodine Compounds: Bis(onio)-Substituted Aryliodine(III) Salts

Robert Weiss* and Jörg Seubert

The massive use of electrostatic effects is an option for the control of structure and reactivity which has to date been used remarkably little. Using organic π systems we have already been able to demonstrate that the complete conversion of a set of neutral ligands to a set of a cationic ligands (e.g. by poly(onio) substitution) confers a dramatically increased electrophilicity and electron affinity on the π template.[1] This effect is predominantly caused by the electrostatic effect (field effect)[2] of the positively charged ligands and should thus not show a saturation effect nor be limited to organic π systems. The latter conclusion has already been confirmed for poly(onio)-substituted derivatives of phosphorous in several oxidation states.[3] In view of the current significance of hypervalent organo-iodine(III) compounds[4] as multifaceted redox reagents in organic synthesis, the question was now posed as to whether their reactivity and synthetic potential could not also be increased by electrostatic activation. We report here on the first synthesis of bis(onio)-substituted aryliodine(III) salts and demonstrate their potential in organic synthesis with a few examples.

The starting point of modern organo-iodine(III) chemistry is still Willgerodt's (dichloro-iodo)benzene **1**.[5] A large number of publications have reported on the transformation of this system into reagents of type **2** using O, C, or N nucleophiles within the framework of $S_N(I)$ reactions.[4] Onio-substituted aryliodine(III) salts were, however, not accessible by this route. However, the first examples of this new class of compounds can be prepared under mild conditions and in high yields according to the various syntheses shown in Scheme 1.[6]



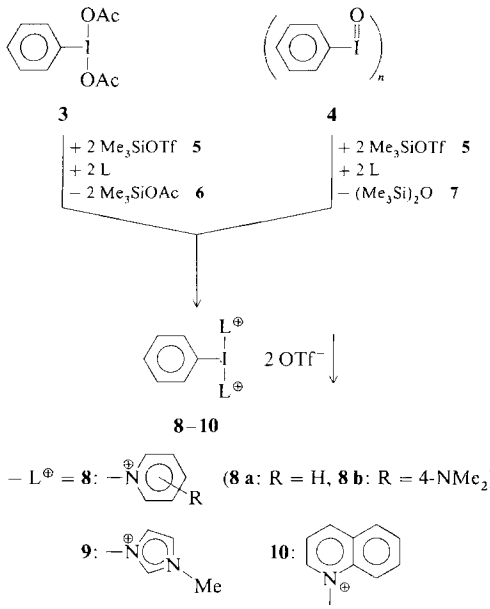
1 **2**

$Nu^{\ominus}$ = O, C, N nucleophile

Treatment of diacetoxyiodobenzene (**3**) or iodosobenzene (**4**) with trimethylsilyl trifluoromethanesulfonate (**5**)/N-heteroarene

[*] Prof. Dr. R. Weiss, Dipl.-Chem. J. Seubert
Institut für Organische Chemie der Universität Erlangen-Nürnberg
Henkestrasse 42, D-91054 Erlangen (FRG)
Telefax: Int. code + (9131) 859 132

 © VCH Verlagsgesellschaft mbH, D-69451 Weinheim, 1994 0570-0833/94/0808-0891 $ 10.00+.25/0



Scheme 1. OTf = O_3SCF_3.

(L) in a mol ratio of 1:2 leads, within a few minutes at room temperature, to the precipitation of the title compounds **8–10** as triflate salts which are sparingly soluble in CH_2Cl_2. They are completely stable in the absence of moisture and can be stored. According to this procedure their synthesis is coupled in a thermodynamically favorable way with the simultaneous (practically quantitative) formation of the products **6** and **7** containing low-energy Si–O bonds. This is crucial for the success of the synthesis, since **3** does not react with ligands such as L without the addition of **5**; incidentally, **1** does not react even with the addition of **5**. The formation of **6** and **7** can easily be controlled by ^{1}H NMR spectroscopy.[7]

Table 1. Yields and spectroscopic data for the compounds **8–10** [a]. Correct C,H,N analyses were obtained.

8a: Yield: 98%; ^{1}H NMR: δ = 7.65 (dd, ^3J = 6.6, 6.0 Hz, 2H; H-3/H-5 Ph), 7.80 (m, 5H; H-4 Ph, H-3/H-5 pyridine), 8.36 (t, ^3J = 7.7 Hz; 2H; H-4 pyridine), 8.69 (d, ^3J = 7.7 Hz, 2H; H-2/H-6 Ph), 9.00 (d, ^3J = 4.9 Hz, 4H, H-2/H-6 pyridine); ^{13}C NMR: δ = 121.86 (q, ^1J(C,F) = 320 Hz; CF_3), 124.67 (C-1 Ph), 129.87 (C-3/C-5 pyridine), 134.37 (C-3/C-5 Ph), 135.95 (C-4 Ph), 136.73 (C-2/C-6 Ph), 146.14 (C-4 pyridine), 148.58 (C-2/C-6 pyridine)

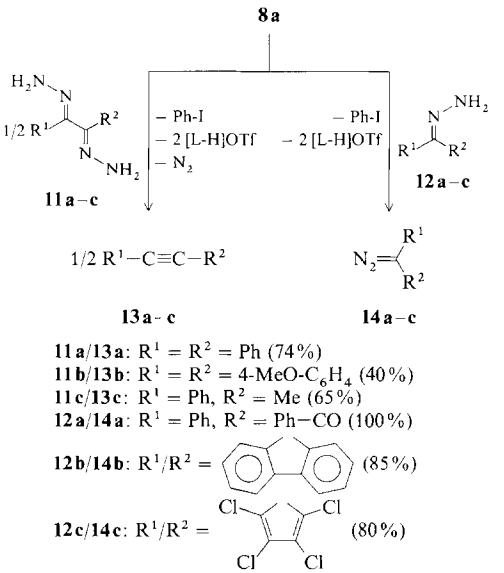
8b: Yield: 80%; ^{1}H NMR: δ = 3.08 (s, 12H, NMe_2), 7.47 (AA'BB', ^3J = 7.7 Hz, 8H; DMAP), 7.59 (dd, ^3J = 8.2, 7.7 Hz, 2H; H-3/H-5 Ph), 7.72 (t, ^3J = 7.7 Hz, 1H; H-4 Ph), 8.48 (d, ^3J = 8.2 Hz, 2H; H-2/H-6 Ph); ^{13}C NMR: δ = 40.28 (NMe_2), 109.66 (C-3/C-5 DMAP), 122.00 (q, ^1J(C,F) = 320 Hz; CF_3), 123.60 (C-1 Ph), 133.77 (C-3/C-5 Ph), 134.88 (C-4 Ph), 135.15 (C-2/C-6 Ph), 145.94 (C-2/C-6 DMAP), 157.14 (C-4 DMAP)

9: Yield: 93%; ^{1}H NMR: δ = 3.76 (s, 6H; Me), 7.27 (d, ^3J = 89.6 Hz, 4H; H-4/H-5 imidazole), 7.61 (dd, ^3J = 8.2, 7.7 Hz, 2H; H-3/H-5 Ph), 7.76 (t, ^3J = 7.7 Hz, 1H; H-4 Ph), 8.42 (s, 2H; H-2 imidazole), 8.52 (d, ^3J = 7.7 Hz, 2H; H-2/H-6 Ph); ^{13}C NMR: δ = 36.38 (Me), 122.00 (q, ^1J(C,F) = 320 Hz; CF_3), 124.80 (C-1 Ph), 126.30 (C-4/C-5 imidazole), 133.74 (C-3/C-5 Ph), 134.97 (C-4 Ph), 135.66 (C-2/C-6 Ph), 140.11 (C-2 imidazole)

10: Yield: 81%; ^{1}H NMR: δ = 7.45 (dd, ^3J = 8.2, 7.7 Hz, 2H; H-3 quinoline), 7.58 (dd, ^3J = 7.7, 7.1 Hz, 2H; H-3/H-5 Ph), 7.89 (m, 3H; H-4 Ph, H-6 quinoline), 8.17 (d, ^3J = 7.7 Hz, 2H; H-5 quinoline), 8.24 (dd, ^3J = 8.8, 7.1 Hz, 2H; H-7 quinoline), 8.72 (d, ^3J = 7.7 Hz, 2H; H-2/H-6 Ph), 8.80 (d, ^3J = 8.8 Hz, 2H; H-8 quinoline), 8.96 (d, ^3J = 8.2 Hz, 2H; H-4 quinoline), 10.00 (d, ^3J = 5.5 Hz, 2H; H-2 quinoline); ^{13}C NMR: δ = 121.86 (q, ^1J(C,F) = 320 Hz; CF_3), 124.61 (C-3 quinoline), 125.10 (C-1 Ph), 125.89 (C-6 quinoline), 131.13 (C-5 quinoline), 131.49 (C-4a quinoline), 134.12 (C-3/C-5 Ph), 135.66 (C-4 Ph), 135.99 (C-7/C-8 quinoline), 136.69 (C-2/C-6 Ph), 141.71 (C-4 quinoline), 147.93 (C-8a quinoline), 153.94 (C-2 quinoline)

[a] ^{1}H NMR (400 MHz, CD_3CN, 25 °C, TMS), ^{13}C NMR (100 MHz, CD_3CN, 25 °C, TMS).

Because of the irreversibility of the electron acceptance in the new bis(onio)iodine(III) compounds, no cyclic voltametric redox potentials could be determined for **8–10**. A clear indication of the efficiency of the electrostatic increase of the electron affinity by poly(onio) substitution is given by a comparison of polarographic measurements on **3** and **8a**. According to these, the $E_{1/2}$ value for the acceptance of the first electron in the transition from **3** to **8a** is shifted by about 1.3 V) towards more positive potential (from −1.0 to +0.34 V)![8] This severely increased oxidation power of **8a** relative to **3**, combined with the basic nature of the free ligand, pyridine, enables the valuable use of this reagent in synthesis. Thus, 1,2-bishydrazones **11** could be cleanly oxidized to alkynes **13** by using **8a** (Scheme 2).[9] Under analogous conditions, and using **3** as oxidant, this reaction leads to totally unsatisfactory results with respect to yield, reaction time, and the formation of by-products.[10] This is, therefore, further proof of the electrostatic activation in compounds **8–10**. In several cases the dehydrogenation of monohydrazones **12** afforded the diazo compounds **14** (Scheme 2).[11]



Scheme 2.

Both reactions occur spontaneously at room temperature in mainly good to very good yields[12] and are notable for the ease of workup of the reaction mixture and the avoidance of toxic heavy metal reagents (e.g. HgO), which are used, in general, in the conventional dehydrogenations of this type.

We have obtained many new bis(onio)-substituted aryliodine(III) salts by structural variation of the parent iodoarene and the N-heteroarene. The synthetic potential of these new reagents is currently under investigation.[13]

Experimental Procedure

All reactions were carried out under nitrogen in dried solvents (exception: workup of **13** and **14**). No melting points were determined on account of the extreme hygroscopic nature of compounds **8–10**. Compounds **13** and **14** were characterized by comparison of their physical data with those in the literature.

8–10: **3** or **4** (2.5 mmol) in CH_2Cl_2 (20 mL) was treated with **5** (5 mmol). The N-heteroarene (5 mmol) in CH_2Cl_2 (10 mL) was added dropwise to this solution. The colorless (**8b** beige) precipitate was filtered, washed with CH_2Cl_2, and dried at 0.01 Torr.

13: **8a** (3 mmol) was suspended in CH_2Cl_2 (40 mL) and was treated with a solution of **11a–c** (1.5 mmol) in CH_2Cl_2 (10 mL) with strong evolution of N_2. After 1 h the solution was treated with petroleum ether and the residue filtered off. After distilling off the solvent, the product was purified by sublimation at 0.01 Torr (**13a, b**) or by Kugelrohr distillation (**13c**) (**13c** was obtained as a 1:2 mixture with iodobenzene).

14: **8a** (2 mmol) was suspended in CH_2Cl_2 (30 mL) and treated dropwise with a solution of **12a–c** (2 mmol) in CH_2Cl_2 (10 mL). After 1 h the solvent was removed at 20 Torr and the residue taken up in Et_2O. After filtration and renewed removal of the solvent at 20 Torr, the product was recrystallized from petroleum ether (**14b**) or MeOH (**14c**). Crude **14a** was transferred on to a silica gel column and washed with a large quantity of petroleum ether. Subsequently the product was eluted with CH_2Cl_2 and dried after removal of the solvent at 20 Torr.

Received: September 21, 1993
Revised: December 9, 1993 [Z 6369 IE]
German version: *Angew. Chem.* **1994**, *106*, 900

[1] a) R. Weiss, N. J. Salomon, G. E. Miess, R. Roth, *Angew. Chem.* **1986**, *98*, 925–926; *Angew. Chem. Int. Ed. Engl.* **1986**, *25*, 917–919; b) R. Weiss, R. Roth, *Synthesis* **1987**, 870–872; c) R. Weiss, R. Roth, R. H. Lowack, M. Bremer, *Angew. Chem.* **1990**, *102*, 1164–1166; *Angew. Chem. Int. Ed. Engl.* **1990**, *29*, 1132–1134; d) R. Weiss, R. Roth, *J. Chem. Soc. Chem. Commun.* **1987**, 317–318.

[2] R. W. Taft, R. D. Topsom, *Prog. Phys. Org. Chem.* **1987**, *16*, 6.

[3] a) R. Weiss, S. Engel, *Synthesis* **1991**, 1077–1079; b) *Angew. Chem.* **1992**, *104*, 239–240; *Angew. Chem. Int. Ed. Engl.* **1992**, *31*, 216–217.

[4] Reviews: a) C. Willgerodt, *Die Organischen Verbindungen mit Mehrwertigem Iod*, Enke, Stuttgart, **1914**; b) R. M. Moriarty, O. Prakash, *Acc. Chem. Res.* **1986**, *19*, 244–250; c) A. Varvoglis, *Synthesis* **1984**, 709–726; d) G. F. Koser in *The Chemistry of Functional Groups, Supplement D* (Eds.: S. Patai, Z. Rappoport), Wiley, Chichester, **1983**, pp. 1265–1351; e) A. Varvoglis, *Chem. Soc. Rev.* **1982**, *10*, 377–407; f) R. M. Moriarty, R. K. Vaid, *Synthesis* **1990**, 431–447; g) D. F. Banks, *Chem. Rev.* **1966**, *66*, 243–266; h) R. M. Moriarty, R. K. Vaid, G. F. Koser, *Synlett* **1990**, 365–383; i) P. J. Stang, *Angew. Chem.* **1992**, *104*, 281–292; *Angew. Chem. Int. Ed. Engl.* **1992**, *31*, 274–285; j) A. Varvoglis, *The Organic Chemistry of Polycoordinated Iodine*, 1st edition, VCH, Weinheim, **1992**.

[5] C. Willgerodt, *J. Prakt. Chem.* **1886**, *33*, 154.

[6] J. Seubert, Diplomarbeit, Universität Erlangen-Nürnberg, **1992**.

[7] ^1H NMR (δ value): **5**: 0.53, **6**: 0.27, **7**: 0.01 ($SiMe_3$).

[8] The redox potentials of the other compounds are of the same order of magnitude. Due to the irreversibility of the acceptance of an electron, no precise value can be expected. A quantitative comparison of the values is thus not possible.

[9] V. Jäger, H. G. Viehe, *Methoden Org. Chem. (Houben-Weyl) 4th edition 1952–*, Bd V/2a, **1977**, p. 188–193, and references therein.

[10] Thus, for example, a complex mixture of substances was obtained from the reaction of **3** with **11a** after several hours. In addition to small amounts of product **13a**, large quantities of the starting material **3**, and an as yet unidentified diazo compound were isolated.

[11] a) M. Regitz, G. Maas, *Diazo Compounds*, 1st edition, Academic Press, Orlando, **1986**, pp. 233–256, and references therein; b) M. Böhshar, J. Fink, H. Heydt, O. Wagner, M. Regitz, *Methoden Org. Chem. (Houben-Weyl) 4th edition 1952–*, Bd. E14b, **1990**, p. 996–1010, and references therein. The dehydrogenation of a monohydrazone with **3** has so far only been reported for one example: P. A. S. Smith, E. M. Bruckmann, *J. Org. Chem.* **1974**, *39*, 1047.

[12] The yields were not optimized.

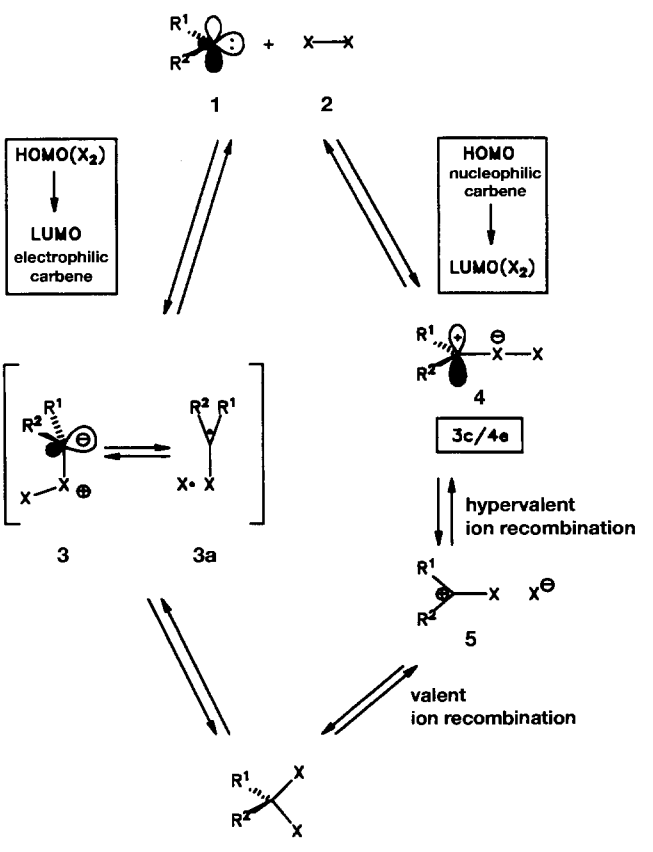
[13] In preliminary experiments electron-deficient hydroquinones, for example *o*- and *p*-tetrachlorohydroquinone and even 2,3-dichloro-5,6-dicyano-1,4-hydroquinone could be oxidized to the corresponding quinones. In reactions with activated arenes (e.g. anisole) under mild conditions (room temperature) the corresponding diaryliodonium systems were obtained.

Concerning the Mechanism of α-Elimination: Hypervalent Ion Pairing in an Iodocarbenium Iodide**

Robert Weiss,* Michael Rechinger, and Frank Hampel

Although the α-addition of a halogen to a carbene and the corresponding α-elimination are important basic reactions in organic chemistry, little experimentally confirmed information is available concerning the thermal pathway of these reactions.[1] From a mechanistic point of view a general reaction coordinate, which is characterized by two electronically complementary limiting cases, can be formulated for these processes. R. Hoffmann et al. have considered (qualitative theory) one of these limiting cases by using the example of chlorine addition to difluorocarbene (Scheme 1, left branch).[2] According to these studies the polar α-addition of the halogen molecule X_2 **2** is initiated by a valent (i.e. 2c/2e) LAB (Lewis Acid Base) interaction between the π^* orbital of the halogen (HOMO) and the $2p_z$ orbital of the (S)-carbene **1** (LUMO), from which primarily the halonium ylide **3** should result.[2] Its conversion to the methane derivative **6** can now proceed by the familiar route of sigmatropic 1,2-shifts in ylides. As in the Stevens rearrangement the latter process could also involve radical pairs (in our case **3a**)—a mechanistic option not discussed by Hoffmann.[3]

In this case the reaction between **1** and **2** would be initiated by a hypervalent LAB-interaction between the sp_2 lone pair of the carbene and the σ^* LUMO of the halogen (Scheme 1, right branch). This interaction should initially lead to the hypervalent 3c/4e situation **4** within the framework of an S_N2 reaction at the halogen X. Depending on the substituents R^1/R^2 as well as the



Scheme 1.

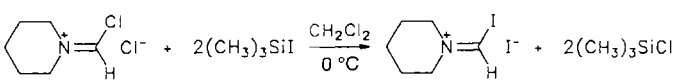
halogen X, the latter structure should either have the character of an intermediate or a transition state on the way to the inner ion pair **5** and/or the methane derivative **6**. If one uses the relative stabilities of the structurally related trihalides X_3^- as a guide,[4] the formal combination of a nucleophilic carbene with molecular iodine should give the best chance of obtaining systems of the type **4** and thus of being able to study them experimentally. In earlier work we have repeatedly pointed out the possibility that certain anomalies in the chemical behavior of

[*] Prof. Dr. R. Weiss, Dipl.-Chem. M. Rechinger, Dipl.-Chem. F. Hampel
Institut für Organische Chemie der Universität Erlangen-Nürnberg
Henkestrasse 42, D-91054 Erlangen (FRG)
Telefax: Int. code + (9131) 859132

[**] Iodocarbenium Ions, Part 4. This work was supported by the Fonds der Chemischen Industrie. Part 3: [5c].

donor-substituted iodocarbenium iodides of the general type **5** might be explained by the assumption of n-σ* contacts between the oppositely polarized iodine centers.[5] However, the experimental material did not allow any statements about the nature and structural consequences of these hypervalent contacts. We have now for the first time succeeded in obtaining a crystalline simple donor-substituted iodocarbenium iodide and in answering, with the aid of a crystal structure analysis, some of the questions raised above.

N-(Iodomethylene)piperidinium iodide (*N,N*-pentamethylene(iodomethylene)iminium iodide) (**8**) served as a model system. This compound could be obtained readily from the corresponding dichlorine system 7 by a halogen exchange reaction with Me_3SiI in CH_2Cl_2 and subsequent precipitation with Et_2O.[6]



7 **8**

On cooling the reaction mixture to −18 °C, **8** precipitates as yellow needles, suitable for X-ray structure analysis.[7] The structure of **8** is shown in Figure 1.

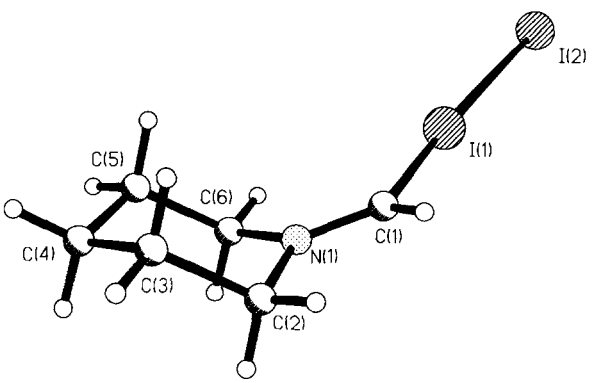


Fig. 1. Crystal Structure of **8**. Important distances [Å] and angles [°]: C1–I1 2.132, I1–I2 3.330, C1–N1 1.461; C1–I1–I2 176.8, N1–C1–I1 125.7

The asymmetric unit consists of four molecules whose C–I and I–I distances differ somewhat (C–I: 2.063–2.132 Å; I–I: 3.330–3.440 Å). The C-I-I bond angles vary between 171.3 and 177.5°. The C–I distances in **8** are clearly longer than the typical vinylic C–I bond lengths of approximately 2.03 Å.[8] With an average length of 3.37 Å, the I–I bond lengths in **8** almost correspond to the arithmetic mean of the I–I distance in molecular iodine (2.66 Å)[9] and the I–I distance of 4.3 Å[9] of the inner ion pair expected on the basis of the sum of the van der Waals radii. Accordingly, with its almost linear C-I-I sequence, the structure has the characteristics of a new type of hypervalent 3c/4e bonding system. The latter corresponds to a "frozen transition state" of I_2-elimination from a donor-stabilized diiodomethane and marks for the first time a characteristic point on the reaction coordinate of the polar α-elimination. An ab initio calculation on the structural analogue *N,N*-dimethyl(iodomethylene)iminium iodide confirms, in principle, our experimental findings.[10] The difference between the I–I distances calculated for the gas phase (3.01 Å) in $Me_2\overset{+}{N}{=}CHI\ I^-$ and the crystallographically determined I–I bond lengths in the analogous system **8** can be explained by the occurrence of additional secondary donor–acceptor interactions in the crystal, between an available lone pair at the terminal iodine and the empty p_z orbital at the carbenium center of the unit lying underneath it (C–I distance: ≈3.5 Å). These intermolecular interactions should cause a weakening of the n–σ* contacts discussed above. This again results in a shorter experimental C–I bond length than that calculated ($C-I_{calculated}$: 2.25 Å). The system calculated for the gas phase is thus already more advanced on the reaction coordinate of the α-elimination. A further consequence of this association is the low solubility of **8** in common organic solvents, which we have already observed with other iodocarbenium iodides.[5]

G. Maier et al. reported in 1986 on the photochemical generation and matrix isolation of the parent compound of the iodocarbenium iodides, $CH_2I^+\ I^-$.[11] The authors concluded from spectroscopic studies that this species has the character of a contact ion pair of type **5**, and not that of a hypervalent system of type **4**. These results contrast markedly to our findings on the donor-substituted iodocarbenium iodide **8**, for which one would a priori expect ion pair character rather than for $CH_2I^+I^-$ due to its internal mesomeric stabilization. Effects of the medium could be responsible for this divergence, alternatively the possibility exists that the species produced by Maier et al. rather has the character of a halonium ylide of type **3**. Theoretical calculations by these authors in a later publication also indicate this possibility.[12]

Experimental Procedure

All manipulations were carried out under nitrogen in dried N_2-saturated solvents. A solution of Me_3SiI (0.9 mL, 1.22 g, 6.1 mmol) in CH_2Cl_2 (5 mL) was added dropwise to a solution of 7 [13] (0.512 g, 3.05 mmol) in CH_2Cl_2 (20 mL) at 0 °C. After stirring at 20 °C for 12 h, **8** was precipitated as a yellow solid from the solution with diethyl ether. Subsequently the product was dried for 8 h under high vacuum. Yield: 0.984 g (92%). Single crystals of **8** were obtained after storing the filtrate at −20 °C for two months. Correct C,H,N elemental analyses. ^{1}H NMR (400 MHz; SO_2, −60 °C, [D_6]acetone): δ = 10.56 (s, 1H; CHI), 4.45 (br, s, 4H; CH_2), 2.18 (br, s, 6H; CH_2); ^{13}C NMR (100 MHz; SO_2, −60 °C, [D_6]acetone: δ = 143.4 (CHI), 66.3 (CH_2), 61.8 (CH_2), 26.8 (CH_2), 26.2 (CH_2), 22.6 (CH_2); IR (KBr): ν[cm^{-1}] = 2947m, 2863m, 1695s, 1608m, 1443m, 1370m, 1347m, 1295m, 1021m, 1000s, 954m, 909m, 859m, 843m, 805m, 767m, 634m, 605m, 559br, 434s, 335m.

Received: November 6, 1993 [Z 6480 IE]
German version: *Angew. Chem.* **1994**, *106*, 901

[1] W. Kirmse, *Angew. Chem.* **1965**, *77*, 1; *Angew. Chem. Int. Ed. Engl.* **1965**, *4*, 1.
[2] S. R. Cain, R. Hoffmann, E. R. Grant, *J. Phys. Chem.* **1981**, *85*, 4046.
[3] a) U. Schöllkopf, U. Ludwig, *Chem. Ber.* **1968**, *101*, 2224; b) W. D. Ollis, M. Rey, I. O. Sutherland, *J. Chem. Soc. Perkin Trans. 1* **1983**, 1009, 1049.
[4] E. E. Genser, R. E. Connick, *J. Chem. Phys.* **1971**, *58*, 990.
[5] a) R. Weiss, H. Wolf, U. Schubert, T. Clark, *J. Am. Chem. Soc.* **1981**, *103*, 6142; b) A. E. Reed, F. Weinhold, R. Weiss, J. Macheleid, *J. Phys. Chem.* **1985**, *89*, 2688; c) R. Weiss, G.-E. Miess, A. Haller, W. Reinhardt, *Angew. Chem.* **1986**, *98*, 102; *Angew. Chem. Int. Ed. Engl.* **1986**, *25*, 103.
[6] The prototype of this compound class (Me_2NCHI_2) was already prepared by Arnold from HI and the corresponding dichlorine compound: Z. Arnold, A. Holly, *Collect. Czech. Chem. Commun.* **1962**, *27*, 2886.
[7] Crystal structure analysis of **1** ($C_6H_{11}I_2N$): M = 351.0, triclinic, space group $P\bar{1}$, a = 8.274(5), b = 10.670(5), c = 24.790(10) Å, α = 85.34(5), β = 84.50(5), γ = 76.37(5)°, V = 2129(4) Å^3, Z = 8, $\varrho_{calcd.}$ = 2.189 Mgm^{-3}, 12052 collected reflections (3.0° < 2θ < 54.0°), 9276 independent and 7433 observed reflections ($F > 4\sigma(F)$), 325 refined parameters. R = 0.063 (wR = 0.074); all data were collected on a Nicolet-R3m/V diffractometer at 200 K with $Mo_{K\alpha}$ radiation (λ = 0.71073 Å). The structure was solved with direct methods (SHELXTL PLUS (VMS)). All non-hydrogen atoms were refined anisotropically, hydrogen atoms isotropically in fixed, idealized positions (riding model). Further details of the crystal structure investigation may be ob-

tained from the Fachinformationszentrum Karlsruhe, D-76344 Eggenstein-Leopoldshafen (FRG) on quoting the depository number CSD-57882.
[8] A. S. Rajput, S. Chandra, *Bull. Chem. Soc. Jpn.* **1966**, *39*, 1854.
[9] a) N. N. Greenwood, A. Earnshaw, *Chemistry of the Elements*, Pergamon, **1984**, p. 934; b) C. A. McAuliffe, B. Beagley, G. A. Gott, A. G. Mackie, P. P. MacRory, P. G. Pritchard, *Angew. Chem.* **1987**, *99*, 237; *Angew. Chem. Int. Ed. Engl.* **1987**, *26*, 26.
[10] We thank Dipl.-Chem. J. Kapp for the ab initio calculations. The calculations were carried out with the program package Gaussian 92, using the 6-31G* standard basis set for H; semi-relativistic pseudopotentials and [5s5p1d]/(3s3p1d) (DZ + P) basis sets were used for I, C, and N. The geometry was fully optimized at MP2 level.
[11] G. Maier, H. P. Reisenauer, *Angew. Chem.* **1986**, *98*, 829; *Angew. Chem. Int. Ed. Engl.* **1986**, *25*, 814.
[12] G. Maier, H. P. Reisenauer, J. Hu, B. A. Hess, Jr., L. J. Schaad, *Tetrahedron Lett.* **1989**, *30*, 4105.
[13] H. H. Bosshard, R. Mory, M. Schmid, H. Zollinger, *Helv. Chim. Acta* **1959**, *42*, 1653; H. H. Bosshard, H. Zollinger, *ibid.* **1959**, *42*, 1659.

Reductive Disproportionation of NO Mediated by Copper Complexes: Modeling N_2O Generation by Copper Proteins and Heterogeneous Catalysts**

Christy E. Ruggiero, Susan M. Carrier, and William B. Tolman*

Copper ion-mediated reduction of nitric oxide (NO) to nitrous oxide (N_2O) or dinitrogen (N_2) is important in biological denitrification, whereby anaerobic organisms utilize nitrogen oxides as electron acceptors for metabolism,[1] and in heterogeneous catalytic processes useful for pollution control.[2] Although mechanistic investigations have implicated copper/NO interactions in the generation of N_2O and/or N_2 by metalloenzymes (e.g., nitrite reductase)[3] and heterogeneous catalysts (e.g., copper-exchanged zeolites),[4] there is a general lack of knowledge of the chemistry of $Cu-N_xO_y$ species with which to evaluate the plausibility of postulated reaction pathways.[5] As part of our efforts to provide such a chemical foundation, we have isolated and determined the geometric and electronic structures of mononuclear copper nitrosyl complexes ([$Tp^{RR'}$CuNO], where R = *t*Bu, R′ = H, or R = R′ = Ph, and $Tp^{RR'}$ refers to the tris(1-pyrazolyl)hydroborate anion; R and R′ denote the substituents at the 3- and 5-positions of the pyrazole rings, respectively),[6] that provide the chemical precedent for NO binding to single copper ions in proteins and in zeolites.[7] These novel compounds were reversibly formed upon treatment of [$Tp^{RR'}Cu^{I}$] precursors with NO (g). In the presence of excess NO and in the absence of dioxygen or added ligands such as CH_3CN or CO, [Tp'^{BuH}CuNO] exists unchanged in solution for longer than a day. Here we report that when Cu^{I} complexes of the less sterically hindered supporting ligands Tp^{Ph2} or Tp^{Me2} are allowed to stand under an excess of NO (1 atm), the initially formed NO adducts cleanly convert to Cu^{II} nitrite complexes and N_2O in a well-defined disproportionation reaction that models possible copper-mediated N_2O formation routes in biological and heterogeneous catalytic systems.

Exposure of colorless solutions of [$Tp^{Me2}Cu]_2$ (**1**)[8] or [$Tp^{Ph2}Cu(CH_3CN)$] (**2**)[9] in CH_2Cl_2 to excess NO (1 atm) resulted in the rapid (within 5 min) formation of equilibrium quantities of [$Tp^{R2}Cu(NO)$] (**3**, R = Me, or **4**, R = Ph), which were identified by diagnostic metal-to-ligand charge transfer (MLCT) features at 494 nm or 478 nm in their respective UV/VIS spectra.[7] Upon standing, the NO-saturated solutions of **3** or **4** turned green or yellow, respectively, and generated one equivalent of N_2O [90–95% yield, based on copper; determined by GC; Eq. (a)]. The colored products were identified as nitrito

$$\underset{\text{or}}{\tfrac{1}{2}[(Tp^{Me2}Cu)_2]\ \mathbf{1}} \quad \underset{[Tp^{Ph2}Cu(CH_3CN)]\ \mathbf{2}}{} \quad + 3\,NO \longrightarrow [Tp^{R2}Cu(NO_2)] + N_2O \qquad \begin{matrix}\mathbf{5}\ (R = Me)\\ \mathbf{6}\ (R = Ph)\end{matrix} \qquad (a)$$

complexes (**5**, R = Me; **6**, R = Ph) by comparison of their spectroscopic properties to independently synthesized samples, and were shown by UV/VIS and EPR spectroscopies to be produced in quantitative yields. When $^{15}N^{18}O$ was used as substrate in the reaction with **1**, fully labeled products predominated,[10] a result that argues against involvement of other N- or O-containing species in the reaction (for example, possible contaminants N_2, N_2O, or O_2) and confirms that both N_2O and NO_2^- arise from NO. Although NO-disproportionation reactions are known for other transition metals,[11] to our knowledge well-defined examples of such a transformation mediated by copper complexes have not been reported.[12]

An X-ray crystal structure determination of **5** revealed symmetric, bidentate binding of nitrite to a square-pyramidal Cu^{II} ion (Fig. 1).[13] The coordination geometry of **5** contrasts with

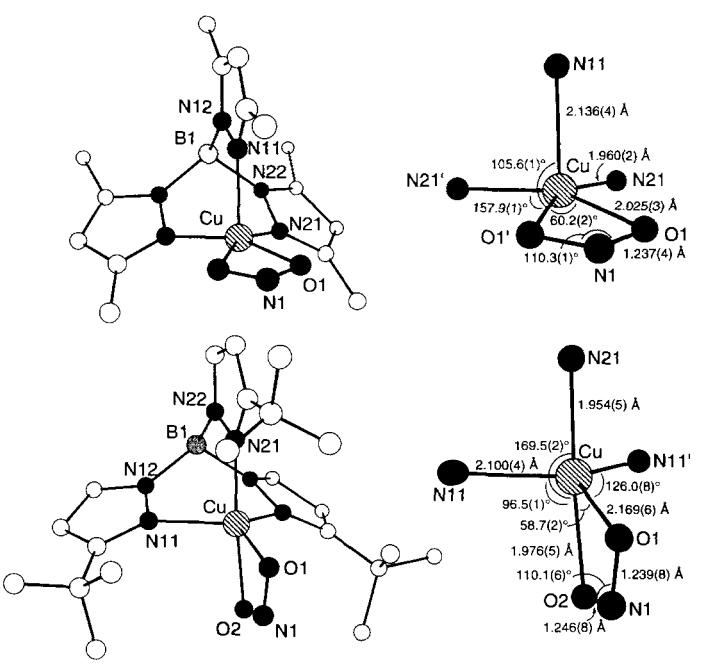


Fig. 1. X-ray crystal structures of **5** (top) and [$Tp'^{BuH}Cu(NO_2)$] (bottom, from ref. [5b]), with full views on the left and views of the copper coordination spheres on the right (selected bond distances [Å] and angles [°] given; hydrogen atoms omitted for clarity).

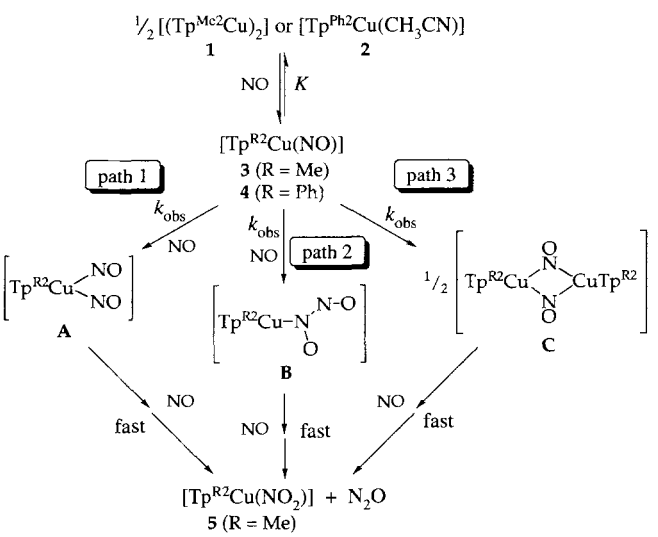
[*] Prof. W. B. Tolman, C. E. Ruggiero, S. M. Carrier
Department of Chemistry, University of Minnesota
207 Pleasant Street S. E., Minneapolis, MN 55455 (USA)
Telefax: Int. code + (612)626-7541.

[**] This work was supported by the National Institutes of Health (GM47365), the Searle Scholars Program/Chicago Community Trust, the National Science Foundation (National Young Investigator Award), and the University of Minnesota. We thank Professor Doyle Britton for his work on the X-ray structure of 5.

 © VCH Verlagsgesellschaft mbH, D-69451 Weinheim, 1994 0570-0833/94/0808-0895 $ 10.00+.25/0

that of the previously characterized analog $[Tp^{tBuH}Cu(NO_2)]$,[5b] reproduced for comparison in Figure 1, which exhibits differing $Cu^{II}-O_{nitrite}$ bond lengths and a distorted trigonal-bipyramidal structure. These structural differences, which presumably result from divergent steric influences of the Tp substituents, are reflected in disparate EPR spectroscopic properties for the two complexes; the signal of **5** is axial ($g_\perp = 2.09$, $g_\parallel = 2.32$, $A_\parallel = 128$ G, $A_{N\perp} = 14$ G) while that of $[Tp^{tBuH}Cu(NO_2)]$ is distinctively rhombic.[5b] Either complex can be envisioned as a speculative model for the substrate adduct to the monocopper site of nitrite reductases,[5b, 14] and we suggest on the basis of the observed differences between the synthetic analogues that similar variability in nitrite orientation and/or Cu^{II} coordination geometry is possible in the enzymes.

Mechanisms for the copper-mediated disproportionation reaction may be envisioned that involve binding of a second NO molecule to the copper ion of the initial nitrosyl complex to afford a *cis*-dinitrosyl compound (**A**, path 1, Scheme 1), direct attack on the coordinated nitrosyl to form a monocopper N_2O_2 adduct (**B**, path 2), or dimerization of the copper nitrosyl compound to generate a μ_2-$(NO)_2Cu_2$ unit (**C**, path 3). An intermediate like **C** was previously suggested to be involved in the reaction of a Cu^I_2 compound with NO that afforded N_2O and a $Cu^{II}-O-Cu^{II}$ complex.[5a] Subsequent N–N bond formation from **A** or **C** could generate mono- or dinuclear $Cu-N_2O_2$ species like **B**. Analogous complexes with $N_2O_2^{n-}$ ligands ($n = 0$, 1, or 2) have been generated from NO[15] and have been proposed as intermediates in NO disproportionation reactions catalyzed by other transition metals[11, 16] and by zeolites,[4] as well as in the formation of N_2O by both iron and copper nitrite reductases.[17] Rapid electron transfer from Cu^I to generate Cu^{II} and a $N_2O_2^-$ adduct, elimination of N_2O, and reaction with a third NO molecule to give NO_2^- may be envisioned to occur subsequently in all cases (paths 1–3) in some (undefined) order.



Scheme 1. Possible mechanisms for the disproportionation reaction (R = R′ = Ph or Me; $Tp^{RR'}$ refers to the tris(1-pyrazolyl)hydroborate anion, and R and R′ denote the substituents on the 3- and 5-positions of the pyrazole rings, respectively). Oxidation states of the metal and nitrogen oxide ligands are not shown due to potential ambiguities inherent in such assignments for these redox active species (see ref. [7]).

Monitoring UV/VIS spectroscopic changes as a function of time allowed calculation of a pseudo-first-order rate constant for the reaction of **4** (R = Ph) with excess NO ($k_{obs} = 1.3(2) \times 10^{-4}$ sec^{-1} at 24 °C; $t_{1/2} = 1.5$ h), which remained constant within experimental error when the copper concentration was varied (10-fold range) and when either loss of **4** ($\lambda_{max} = 478$ nm) or gain of **6** ($\lambda_{max} = 798$ nm) was followed (Fig. 2). Thus, the order of the reaction with respect to the copper nitrosyl precursor is one, clearly ruling out dimerization of copper species as a rate limiting step and, assuming that the subsequent steps are relatively fast, supporting the initial mononuclear paths 1 or 2 (Scheme 1). Kinetic analysis of the faster ($t_{1/2} \approx 8$ min) reaction of **3** (R = Me) was complicated by the similarity between the rate at which the **1**/**3** equilibrium (K) was reached (k_1 step) and the rate of formation of **5** and N_2O (k_2 step). Nonetheless, reasonable preliminary fits of the data to yield pseudo-first-order rate constants $k_{obs(1)} \approx k_{obs(2)} \approx 3 \times 10^{-3}$ sec^{-1} at 24 °C were obtained using a kinetic scheme involving preequilibrium formation of **3** followed by irreversible reaction with additional NO molecules, consistent with paths 1 or 2 (Scheme 1).[18] Further work directed toward isolation of possible reaction intermediates and acquisition of more detailed kinetic information is underway.

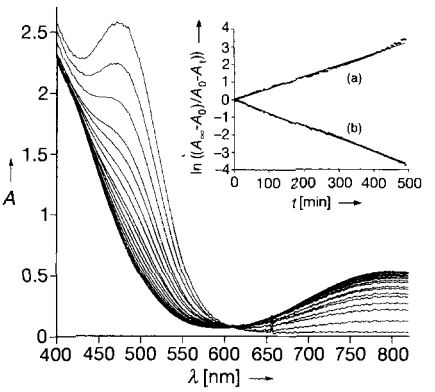


Fig. 2. Electronic absorption spectra showing the loss of **4** (478 nm) and the formation of **6** (798 nm) as a function of time. Spectra are shown at 30 min intervals. Inset: First-order plots for loss of **4** (a) and gain of **6** (b).

Experimental Procedure

5: Solutions of $CuCl_2 \cdot 2H_2O$ (490 mg, 2.90 mmol) in MeOH (1 mL) and $NaNO_2$ (399 mg, 5.79 mmol) in MeOH (5 mL) were simultaneously added to a solution of KTp^{Mc2} [8] (650 mg, 1.93 mmol) in CH_2Cl_2 (15 mL). The solution immediately turned green, and a precipitate formed. After stirring for 10 min, the solution was filtered, the filtrate was concentrated to 5 mL, and 1 mL MeOH was added. The solution was further concentrated until green microcrystals formed. The crystals were collected by filtration (408 mg, 52% yield). X-ray quality crystals were obtained in 50% yield by recrystallization from CH_2Cl_2/Et_2O. IR (KBr): $\tilde{\nu}$[cm^{-1}] = 2931, 2518 (B-H), 1541, 1450, 1419, 1386, 1351, 1291, 1197, 1067, 1048, 982, 877, 846, 805, 768, 689, 669, 644; UV/VIS (CH_2Cl_2): λ_{max} [nm] (ε) = 260 (800), 306 (1000), 370 (420), 800 (110); EPR (9.47 GHz, CH_2Cl_2/toluene, 77 K): $g_\perp = 2.06$, $g_\parallel = 2.33$, $A_\parallel = 145$ G, $A_{N\perp} = 14$ G, $A_{N\parallel} = 12$ G; correct C,H,N analysis.

6: This complex was prepared analogously to **5**, except anhydrous $CuCl_2$ was used, and the product was initially precipitated from cold (−20 °C) CH_2Cl_2 prior to CH_2Cl_2/Et_2O recrystallization (53% yield). **6**: IR (KBr): $\tilde{\nu}$[cm^{-1}] = 3062, 2623 (B-H), 1546, 1474, 1426, 1364, 1283, 1283, 1234, 1173, 1070, 1011, 917, 878, 808, 762, 570; UV/VIS (CH_2Cl_2): λ_{max} [nm] (ε) = 258 (19000), 300 (sh, 1500), 400 (400), 798 (100); EPR (9.47 GHz, CH_2Cl_2/toluene, 77K): $g_\perp = 2.09$, $g_\parallel = 2.32$, $A_\parallel = 128$ G, $A_{N\perp} = 14$ G; correct C,H,N analysis.

Received: November 29, 1993 [Z 6517 IE]
German version: *Angew. Chem.* **1994**, *106*, 917

[1] P. M. H. Kroneck, J. Beuerle, W. Schumacher in *Degradation of Environmental Pollutants by Microorganisms and their Metalloenzymes, Vol. 28* (Eds.: H. Sigel, A. Sigel), Dekker, New York, **1992**, p. 455–505; P. M. H. Kroneck, W. G. Zumft in *Denitrification in Soil and Sediment* (Ed.: N. P. Revsbech, J. Sorensen), Plenum, New York, **1990**, p. 1–20.

[2] *Nitrogen Oxides and Their Effects on Health* (Ed.: S. D. Lee), Ann Arbor Science, Ann Arbor, **1980**; M. Iwamoto, *Stud. Surf. Sci. Catal.* **1990**, *54*, 121–143.

[3] R. W. Ye, I. Toro-Suarez, J. M. Tiedje, B. A. Averill, *J. Biol. Chem.* **1991**, *266*, 12848–12851; M. A. Jackson, J. M. Tiedje, B. A. Averill, *FEBS Lett.* **1991**, *291*, 41–44; E. Libby, B. A. Averill, *Biochem. Biophys. Res. Commun.* **1992**, *187*, 1529–1535.

[4] E. Giamello, D. Murphy, G. Magnacca, C. Morterra, Y. Shioya, T. Nomura, M. Anpo, *J. Catal.* **1992**, *136*, 510–520; Y. Li, W. K. Hall, *ibid.* **1991**, *129*, 202–215; M. Iwamoto, H. Yahiro, N. Mizuno, W.-X. Zhang, Y. Mine, H. Furukawa, S. Kagawa, *J. Phys. Chem.* **1992**, *96*, 9360–9366; C. C. Chao, J. H. Lunsford, *ibid.* **1972**, *76*, 1546–1548.

[5] a) P. P. Paul, K. D. Karlin, *J. Am. Chem. Soc.* **1991**, *113*, 6331–6332; b) W. B. Tolman, *Inorg. Chem.* **1991**, *30*, 4878–4880, and references therein.

[6] S. Trofimenko, *Chem. Rev.* **1993**, *93*, 943–980.

[7] S. M. Carrier, C. E. Ruggiero, W. B. Tolman, G. B. Jameson, *J. Am. Chem. Soc.* **1992**, *114*, 4407–4408; W. B. Tolman, S. M. Carrier, C. E. Ruggiero, W. E. Antholine, J. W. Whittaker in *Bioinorganic Chemistry of Copper* (Ed.: K. D. Karlin, Z. Tyeklár), Chapman & Hall, New York, **1993**, p. 406–418; C. E. Ruggiero, S. M. Carrier, W. E. Antholine, J. W. Whittaker, C. J. Cramer, W. B. Tolman, *J. Am. Chem. Soc.* **1993**, *115*, 11285–11298.

[8] C. Mealli, C. S. Arcus, J. L. Wilkinson, T. J. Marks, J. A. Ibers, *J. Am. Chem. Soc.* **1976**, *98*, 711–718.

[9] S. M. Carrier, C. E. Ruggiero, R. P. Houser, W. B. Tolman, *Inorg. Chem.* **1993**, *32*, 4889–4899.

[10] Mass spectrometric analysis of N_2O produced from 99.9% ^{15}N and 96.2% ^{18}O nitric oxide indicated ~85% $^{15}N_2{}^{18}O$, ~10% $^{15}N_2{}^{16}O$, and ~5% $^{14,15}N_2{}^{18}O$. Attempts to obtain a parent ion of $[Tp^{Me2}Cu(NO_2)]$ using mass spectrometry (EI, CI, and FAB) were unsuccessful. However, the product was determined to contain predominantly $^{15}N^{18}O_2$ on the basis of two new intense bands in the IR spectrum at 1143 and 831 cm^{-1} that were not present in the spectra of independently synthesized $[Tp^{Me2}Cu(^{15}N^{16}O_2)]$ and $[Tp^{Me2}Cu(^{14}N^{16}O_2)]$.

[11] Lead references: F. Bottomley in *Reactions of Coordinated Ligands, Vol. 2*, (Ed.: P. S. Braterman), Plenum, New York, **1989**, pp. 115–222. G. B. Richter-Addo, P. Legzdins, *Metal Nitrosyls*, Oxford University, New York, **1992**.

[12] Some copper complexes of polypyridyl ligands have been shown to reduce NO to N_2O. See ref. [5a] and N. Komeda, H. Nagao, G. Adachi, M. Suzuki, A. Uehara, K. Tanaka, *Chem. Lett.* **1993**, 1521–1524. Generation of N_2O from NO has also been observed with other systems that contain copper and other metals: C. H. Cheng, K. S. Sun, *Inorg. Chem.* **1990**, *29*, 2547–2548. T. L. Nunes, R. E. Powell, *ibid.* **1970**, *9*, 1912–1916; M. Kubota, K. J. Evans, C. A. Koerntgen, J. C. J. Marsters, *J. Am. Chem. Soc.* **1978**, *100*, 342–343; M. Kubota, K. J. Evans, C. A. Koerntgen, J. C. Marsters, Jr., *J. Mol. Catal.* **1980**, *7*, 481–486.

[13] Crystal data for **5** ($C_{15}H_{22}N_7O_2BCu$): green prism, size 0.600 × 0.500 × 0.450 mm, $M_r = 406.74$, space group *Pnma* (No. 62), $a = 18.192(6)$ Å, $b = 13.504(6)$ Å, $c = 7.970(3)$ Å, $V = 1958(3)$ Å^3, $Z = 4$, $\rho_{calcd} = 1.380$ g cm^{-1}. For a total of 2050 unique, observed reflections with $I > 2.00\,\sigma(I)$ and 134 variable parameters, the discrepancy indices are $R = 0.048$ and $R_w = 0.053$. Further details of the crystal structure investigation are available on request from the Director of the Cambridge Crystallographic Data Centre, 12 Union Road, GB-Cambridge, CB21EZ (UK), on quoting the full journal citation.

[14] J. W. Godden, S. Turley, D. C. Teller, E. T. Adman, M. Y. Liu, W. J. Payne, J. LeGall, *Science* **1991**, *253*, 438–442; E. T. Adman, S. Turley in *Bioinorganic Chemistry of Copper* (Ed.: K. D. Karlin, Z. Tyeklár), Chapman & Hall, New York, **1993**, p. 397–405.

[15] P. Gans, *J. Chem. Soc. A* **1967**, 943–946; B. F. Hoskins, F. D. Whillans, D. H. Dale, D. C. Hodgkin, *J. Chem. Soc. Chem. Commun.* **1969**, 69–70; S. Bhaduri, B. F. G. Johnson, A. Pickard, P. R. Raithby, G. M. Sheldrick, C. I. Zuccaro, *ibid.* **1977**, 354–355; R. Bau, I. H. Sabherwahl, A. B. Burg, *J. Am. Chem. Soc.* **1971**, *93*, 4926–4928.

[16] M. Gargano, P. Giannoccaro, M. Rossi, A. Sacco, G. Vasapoilo, *Gazz. Chim. Ital.* **1975**, *105*, 1279–1290; E. L. Loechler, A. M. Schneider, D. B. Schwartz, T. C. Hollocher, *J. Am. Chem. Soc.* **1987**, *109*, 3076–3087.

[17] B. A. Averill, J. M. Tiedje, *FEBS Lett.* **1982**, *138*, 8–12; E. Weeg-Aerssens, J. Tiedje, B. A. Averill, *J. Am. Chem. Soc.* **1988**, *110*, 6851–6856; J. Goretski, T. C. Hollocher, *J. Biol. Chem.* **1990**, *265*, 889–895.

[18] J. H. Espenson, *Chemical Kinetics and Reaction Mechanisms*, McGraw Hill, New York, **1981**, p. 71.

Evidence of Room-Temperature Superconductivity in the Bi-Sr-Cu-O System**

Richard S. Burrows, Darl H. McDaniel*

In 1988, H. G. von Schnering et al.[1] reported the observation of superconductivity with an onset temperature of 140 K and zero resistivity at 80 K in a sample of $Bi_2Sr_2(Ca_{trace})CuO_x$ (Bi2202, $x = 6 + \delta$). No repetitions of this observation have been reported until now. Using a sol-gel preparative route,[2] we have observed the 140 K superconducting phase a number of times, with evidence of both higher T_c and lower T_c phases being present as well. We describe here the preparation and characterization of these samples and present a possible explanation for the evolution of the superconducting phases. Figure 1 shows the magnetic susceptibility vs. temperature with significant abrupt decreases below 150 K and 50 K, Figure 2 shows a magnetization curve at 130 K displaying hysteretic behavior characteristic

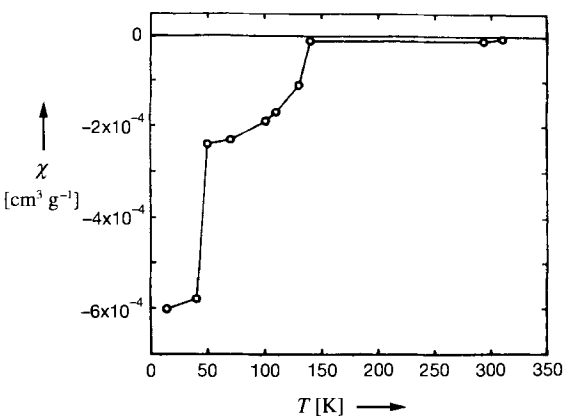


Fig. 1. Magnetic susceptibility vs. temperature of a nominal $Bi_2Sr_2CuO_6$ prepared by a sol–gel route indicating a negative susceptibility at 300 K.

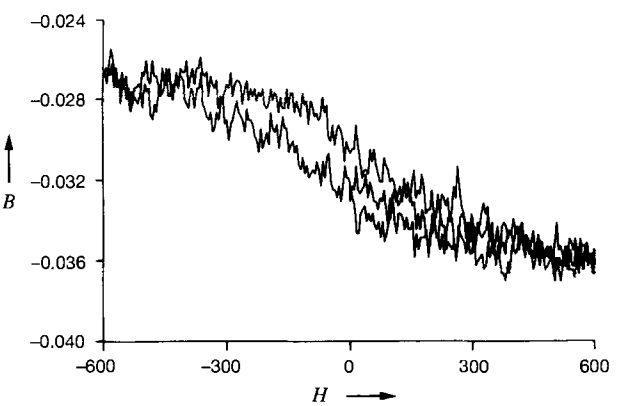


Fig. 2. A magnetization curve obtained at 130 K displaying hysteretic behavior characteristic of flux pinning of Type II superconductors. B in emu g^{-1} (emu = Am^2), H in oersted (1 Oe = 79.6 A m^{-1}).

[*] Prof. D. H. McDaniel, R. S. Burrows
Department of Chemistry, Mail Location 172
University of Cincinnati, Cincinnati, OH 45221 (USA)
Telefax: Int. code + (513)556-9239

[**] We would like to acknowledge the contributions of Mr. Mahjoub Abdelgadir for help in data collection, Prof. Punit Boolchand for his comments and use of laboratory facilities, and Prof. Warren Huff for access to the powder X-ray diffractometer in the Geology Department. We also would like to acknowledge the Office of the Vice President and University Dean for Graduate Studies and Research at the University of Cincinnati for support of this work.

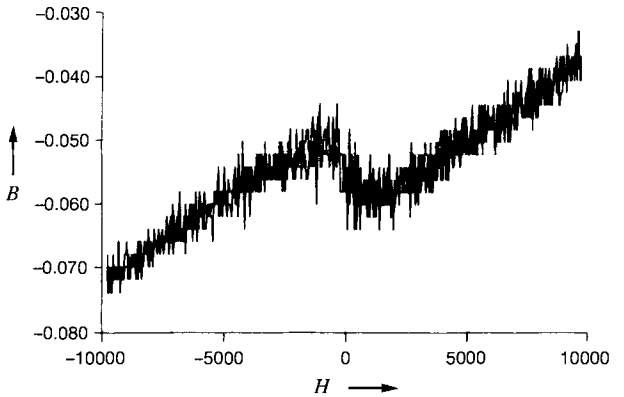


Fig. 3. A magnetization curve at room temperature showing the persistence of diamagnetism with induced paramagnetic behavior at higher field strength (B and H, see Fig. 2).

of flux pinning of Type II superconductors, and Figure 3 shows a room temperature curve displaying the persistence of diamagnetism with induced paramagnetic behavior at higher field strength. The observed phenomena in this sample persisted for over one month, during which time the sample was kept in a Kel-F holder. The sample was removed at that time to check the background of the holder, which was found to be very slightly paramagnetic. On returning the sample to the holder, the previously observed diamagnetic signal had disappeared.

Figure 4 depicts a hysteresis loop obtained by vibrating sample magnetometry for another nominal Bi2201 sample at room temperature, the thermal limit of our instrument (EG & G ORTEC). Using a thermogravimetic analyzer (Perkin

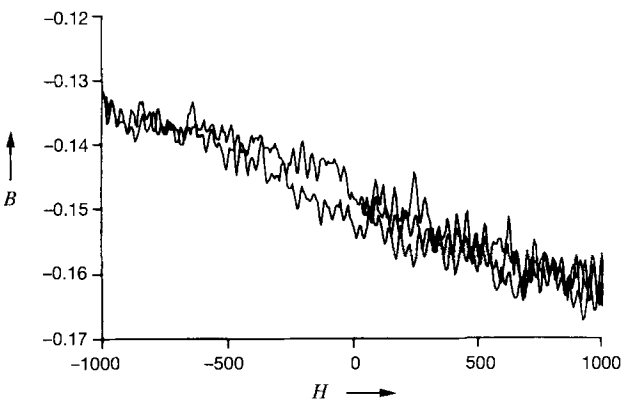


Fig. 4. A magnetization curve obtained at 300 K displaying hysteretic behavior for a second sample of nominal $Bi_2Sr_2CuO_6$ composition (B and H, see Fig. 2).

Elmer), we determined what we believe to be the superconducting critical temperature of this second sample. By placing a magnet just below the sample, we observed an apparent weight loss which was reversible after removing the magnet from the sample proximity and which was not due to interactions of the platinum cup or stirrup with the magnetic field. Upon warming the sample, we observed a weight increase until 350 K whereupon, the sample began to lose weight. We interpret the weight gain as a loss of superconducting volume fraction as a function of temperature until the T_c was achieved at 350 K. We have now prepared a total of eight Bi2201 samples (some with Pb or Li doping) showing evidence of room temperature superconductivity, and an additional 14 samples showing superconductivity between 25 and 110 K. (The literature T_c values for Bi2201 range from 4 to 18 K.[3–7]) All of our high-temperature superconducting samples exhibit temporal instability with the superconducting signal disappearing within hours to days.

The following procedure has shown a success rate of about 10% in yielding superconducting samples with T_c above 50 K. Chemicals used in this work were commercial reagent grade materials (Aldrich, Fisher Scientific, and Baker) and were used as received. Oxides and carbonates were individually dissolved in near stoichiometric amounts of 8 M nitric acid (slight excess in the case of bismuth) and each metal solution subsequently diluted to 0.1 M. Half-molar ethylenediaminetetraacetic acid (EDTA) solution was prepared by adding enough 6 M aqueous ammonia to bring about dissolution. Each solution of metal ions was individually chelated with stoichiometric amounts of EDTA solution. The chelated-metal salt solutions were then mixed and the pH adjusted to near 7.0, after which, the solution was evaporated at 40–60 °C until a blue gel formed. The gel was then charred between 250 and 300 °C in a 250 mL crucible in an electrically heated sand bath. The crucible mouth was covered by a watch glass to prevent excessive air flow over the hot char material. (**Caution:** Excess acid in the dissolution stage should be avoided as ammonium nitrate which is formed upon neutralization leads to flashing of the sample near 160 °C.) After charring, the cooled ash was ground using an agate mortar and pestle to reduce the sample volume and increase sample homogeneity. The ashed sample was then transferred to a combustion boat and annealed at temperatures between 795 and 840 °C under air. Although char colors varied from black to yellow/green, the yellow/green samples were discarded due to the presence of phase-separated Bi_2O_3. Dark brown colored chars gave the most favorable results. Annealed samples which were black with a slight brown tint gave the best magnetic characteristics. Annealing and cooling conditions used in this work are summarized in Table 1. We had no success in preparing superconducting pellet samples from previously calcined material. Pellets were made from pressed precursor ash, but exhibited microcracks and porosity. On two occasions, metal-like conductivities were measured, but neither sample indicated temperature dependence between 77 and 300 K. On one of these trials, the temperature sensor failed on attempting a 400 K measurement.

Table 1. Annealing conditions for the nominal Bi-Sr-Cu-O samples.

Nominal stoichiometry	T [°C]	Duration [h]	T [°C]	Duration [h]	Cool cycle [a]
Bi2201	800	10.00	320	12	p/q
$Bi_2Sr_{1.9}Li_{0.1}CuO_6$	805	4.75	–	–	f/c A
Bi2201	813	0.50	–	–	quench
Bi2201	796	1.33	–	–	quench
Bi2201	750	6.20	–	–	B
$Bi_2Sr_{1.8}Pb_{0.2}CuO_6$	840	22.00	–	–	f/c
$Bi_2Sr_{1.8}Pb_{0.2}CuO_6$	825	2.50	844	22	f/c
$Bi_2Sr_{1.8}Pb_{0.2}CuO_6$	840	17.83	–	–	quench

[a] P/q: A partial quench from 300 °C. f/c: Samples cooled over a period of nearly 30 min. A: Cooled under an oxygen atmosphere. B: Slow cooled to 560 °C under O_2 and to room temperature under nitrogen over a seven hour period.

Powder X-ray patterns (Siemens) made from 10-hour scans of the superconducting samples were assigned to five different phases. The majority phase was the Bi2201 material; the signals of the minority phases (three of which were strontium cuprates) were nearly equivalent in intensity. Our findings are consistent with the conclusions of Schlichemaier et al.[8] who reported that

Bi2201 cannot be prepared phase pure. Lattice parameters for the alkaline-earth metal cuprate systems in this work closely match those previously reported for alkaline-earth metal cuprates.[9–12] Table 2 summarizes the phases fit to the X-ray diffraction patterns. The unknown phase is believed to be a "doubling" of the Bi2201 unit cell along the c axis. This c axis length is approximately the same length reported by Michel et al.[3]

Table 2. Lattice parameters for the phases fit to nominal $Bi_2Sr_2CuO_6$ samples.

Phase	a [Å]	b [Å]	c [Å]	Ref.
Bi2201	5.392	5.394	24.45	[3–7]
$SrCuO_2$ [a]	3.56	16.32	3.92	[13, 15]
$SrCuO_2$ [b]	3.90	3.90	3.35	[15, 17]
Sr_2CuO_3	12.7	3.5	3.9	[14, 16–18]
[c]	–	–	47.6	[3]

[a] Orthogonal phase. [b] Tetragonal phase. [c] This unknown phase was fit with only lattice parameters of (00l).

Although the crystal structures of alkaline-earth metal cuprates[9, 10] have been known for some time, reports of new synthetic routes, solid solutions, and defect studies have recently appeared.[11–14] Azuma et al.[15] indicate that the tetragonal $Sr_{1-x}Ca_xCuO_2$ phase is responsible for superconducting behavior observed up to 110 K, which has been improved to 180 K by Li et al. in $Ca_{1-x}Sr_xCuO_2$.[16] Undoped $SrCuO_2$ has also been reported by Hiroi et al.[17] to superconduct at 100 K. Since we have observed reflections of tetragonal $SrCuO_2$ in all but one of our high-temperature superconducting samples by X-ray diffraction, the tetragonal $SrCuO_2$ is a good candidate for the high-temperature superconducting component produced in our samples. The $SrCuO_2$ may grow selectively on the surface of a Bi2201 template. Strain would be introduced by the mismatch in the lattices between the two phases at their interface. The $SrCuO_2$ superconducting properties would therefore be subject to the stresses of the aging Bi2201 template as well as any degradation caused by the ambient atmosphere, resulting in temporal instability. While von Schnering found superconductivity at 140 K in Bi2201 containing a trace of calcium, we found no evidence of calcium incorporation in our samples to form $Bi_2Sr_2CaCu_2O_8$ by X-ray diffraction and believe that the presence of calcium in von Schnering's 140 K sample may be coincidental to its superconductivity. Hagberg et al.[18] described the observation of a "hyper-diamagnetic" signal at 240 K in nominal $Bi_{1.9}Pb_{0.4}Sr_{1.9}Ca_{2.0}Cu_{3.2}O_x$. Some very low intensity reflections in powder X-ray diffraction patterns reported by Hagberg et al.[18] appear to be assignable to phase-separated strontium cuprate which might be responsible for their observed signal. Laguës et al.[19] have recently found evidence of superconductivity at 250 K in an artificially layered BiSrCaCuO system. Their high-temperature superconductor also appears to be a small volume fraction of their sample.

Received: December 9, 1993 [Z 6550 IE]
German version: *Angew. Chem.* **1994**, *106*, 906

[1] H. G. von Schnering, L. Walz, M. Schwarz, W. Becker, M. Hartweg, T. Popp, B. Hettich, P. Müller, G. Kämpf, *Angew. Chem.* **1988**, *100*, 604; *Angew. Chem. Int. Ed. Engl.* **1988**, *27*, 574.
[2] J. Fransaer, J. R. Roos, L. Delaey, O. van der Biest, O. Arkens, J. P. Celis, *J. Appl. Phys.* **1989**, *65*, 3277.
[3] C. Michel, M. Hervieu, M. Borel, A. Grandin, F. Deslandes, J. Provost, B. Raveau, *Z. Phys. B.* **1987**, *68*, 421.
[4] R. M. Fleming, S. A. Sunshine, L. F. Schneemeyer, R. B. van Dover, R. J. Cava, P. M. Marsh, J. V. Waszczak, S. H. Glarum, S. M. Zahurak, F. J. DiSalvo, *Physica C* **1991**, *173*, 37.
[5] L. F. Schneemeyer, S. A. Sunshine, R. M. Fleming, S. H. Glarum, R. B. van Dover, P. Marsh, J. V. Waszczak, *Appl. Phys. Lett.* **1990**, *57*, 2362.
[6] B. C. Chakoumakos, P. S. Ebey, B. C. Sales, E. Sonder, *J. Mater. Res.* **1989**, *4*, 767.
[7] Y. Ikeda, H. Ito, S. Shimomura, Y. Oue, K. Inaba, Z. Hiroi, M. Takano, *Physica C* **1989**, *159*, 93.
[8] M. Schlichenmaier, W. Wischert, S. Kemmler-Sack, *Ann. Phys. (Leipzig)* **1992**, *1*, 321.
[9] C. L. Teske, Hk. Müller-Buschbaum, *Z. Anorg. Allg. Chem.* **1970**, *379*, 234.
[10] C. L. Teske, Hk. Müller-Buschbaum, *Z. Anorg. Allg. Chem.* **1969**, *371*, 325.
[11] C. Niu, C. M. Lieber, *J. Am. Chem. Soc.* **1992**, *114*, 3570.
[12] C. Krüger, W. Reichert, A. Almes, U. König, H. Oppermann, H. Scheler, *J. Solid State Chem.* **1992**, *96*, 67.
[13] S. Takeno, S. Nakamura, Y. Terashima, T. Miura, *Physica C* **1993**, *206*, 75.
[14] M. Xu, E. T. Voiles, L. S. Chumbley, A. I. Goldman, D. K. Finnemore, *J. Mater. Res.* **1992**, *7*, 1283.
[15] M. Azuma, Z. Hiroi, M. Takano, Y. Bando, Y. Takeda, *Nature* **1992**, *356*, 775.
[16] X. Li, T. Kawai, S. Kawai, *Jpn. J. Appl. Phys.* **1992**, *31*, L934, and references therein.
[17] Z. Hiroi, M. Takano, M. Azuma, Y. Takeda, Y. Bando, *Physica C* **1991**, *185–189*, 523.
[18] J. Hagberg, E. Lähderanta, G. Zsolt, S. Leppävuori, I. Kirschner, R. Laiho, A. Uusimäki, T. Porjesz, I. Dódony, Gy. Kovács, J. Levoska, T. Kármán, *J. Less Common Met.* **1990**, *164/165*, 730.
[19] M. Laguës, X. M. Xie, H. Tebbji, X. Z. Xu, V. Mairet, C. Hatterer, C. F. Beuran, C. Deville-Cavellin, *Science* **1993**, *262*, 1850.

 © VCH Verlagsgesellschaft mbH, D-69451 Weinheim, 1994 0570-0833/94/0808-0899 $ 10.00+.25/0

History of Chemistry

Histoire de la chimie. By *B. Bensaude-Vincent* and *I. Stengers*. La Découverte, Paris, 1992. 360 pp., paperback FF 180.00.—ISBN 2-7071-2192-4

The Fontana History of Chemistry. By *W. H. Brock*. Fontana Press, London, 1992. 744 pp., paperback £ 8.99.—ISBN 0-00-686173-3

We chemists are fascinated by our history. An historical approach to teaching gives depth and perspective to the subject. It provides role models and helps to start vocations. It brings in the human element, indeed a humanistic touch. In research, the historical dimension reframes one's own efforts. It can give ideas. A paper by Naumann in the 1904 *Berichte* helped us to devise the new reagent "clayfen." Furthermore, there may be lessons in the constantly reshuffling history of the subject that we never learned from, or were never taught by our mentors. And, now that we live in a global village, past histories, centered on Europe in the ninetheenth century, are too restrictive.

Before reading the two books reviewed, I drew up a check-list consisting of these ten items: coverage of ancient Chinese alchemy and chemistry; of Arabic alchemy; chlorine bleaching (Scheele, 1773; Berthollet, 1785); Humphrey Davy's diamond combustion; Ampère and representative shapes for molecules (1814); Faraday's isolation of benzene; Ostwald's role in the birth of physical chemistry; Ehrlich's devising of drugs for tropical diseases; the phase rule; Bayer's invention of the polyurethanes. Then I graded each book, from 0 (no mention) to 10 (adequate coverage) on each item. By this method, coverage by the French book scores 20%, that by the British book 47%. To be fair, however, *History* gave itself, justifiably, twice the space of *Histoire*.

Chemists are being eased out from their own history. In spite of the living tradition of chemists as historians of their own discipline—contemporary examples include Joseph Needham, Joseph S. Fruton, and the ACS books edited by Jeffrey I. Seeman—historians of chemistry claim the field as their own. The strategy can be blunt, or it can be more subtle. *Histoire* states emphatically that chemists in our century are no longer engaged in history of chemistry. Counter-examples include J. R. Partington, as well as the above short list! *Histoire* denies an identity to chemistry. It claims conversely that chemistry reduces to its history alone. And this history is defined, prior to being set in concrete by the pure historians. *Histoire* tells the same traditional and rather boring history that originates with Partington and overemphasizes such topics as nomenclature, the Leblanc and Solvay processes, and the Berthelot contributions to organic synthesis; to the detriment of stereochemistry, coordination chemistry (*Histoire* does not even mention Werner's name), catalysis, rare gas chemistry, or the Dow chlorine chain. An additional ploy of historians to wrest the field from the chemists is to end the narrative in the 1930s, so as to avoid tempting living chemists to jut in and to set the record straight.

Histoire is marred by careless mistakes: *Roger* B. Woodward and Ro*n*ald Hoffma*n*: Kekul*e*; *V*an't Hoff. The tone of ironic condescension, such as the constant reference to "professorial chemistry", grates.

Histoire is organized in 32 tripartite chapters. Such segmentation makes for easy reading; each episode is narrated and analyzed in a couple of pages. Some are done in an exemplary manner: the reception in France of Dalton's atomic theory, for example. These discursive segments were composed, it appears, almost exclusively from secondary sources; virtually all quotations from primary material are borrowed from other historians rather than from the properly acknowledged original.

History is a very different book, delightful to read, with little one can take issue with. The author not only avoids denigrating chemists, he understands chemistry. The format he has chosen explains his success: each chapter is centered on a seminal textbook. Thus, Brock goes in succession through Multhauf's and Partington's histories, Boyle's *Sceptical Chymist*, Lavoisier's *Traité Élémentaire*, Dalton's *A New System of Chemical Philosophy*, Liebig's *Anleitung zur Analyse organischer Körper*, Laurent's *Méthode de chimie*, James Sheridan Muspratt's *Chemistry: Theoretical, Practical and Analytical as applied and relating to the Arts and Manufactures*, Mendeleev's *Principles of Chemistry*, John Servos's *Physical Chemistry from Ostwald to Pauling: The Making of a Science in America*, Cannizzaro's *Sketch of a Course of Chemical Philosophy*, Pauling's *Nature of the Chemical Bond*, Ingold's *Structure and Mechanism in Organic Chemistry*, and Nyholm's *Renaissance of Inorganic Chemistry*. This organization gives autonomy to the chapters; each reads like a small essay (plus the final bibliographical essay, hard to fault in coverage).

The writing is consistently pleasurable, with the occasional chuckle (arsole, p. 603). Some features are genuine finds, such as the parallel between Australian and Japanese chemistries, or the percipient note on the dominance of the teaching market by American books since the 1960s. Conversely, *History* is a bit fastidious on academic moves, and exaggerates the importance of University College, London, in 20th century chemistry. I felt that Brock struggled with the problem of fitting into his intricate patchwork at least a passing mention of every crucial name. I did not find howlers, only irritants. Carothers's suicide had reasons more complex than feelings of inadequacy as a scientist: he had been aggrieved by his sister's death, and his new director of research at DuPont was giving him a hard time. Mukaiyama's name is misspelt. An obsolete graphical symbol for benzene is still used (p. 622). And C_{60} can be argued to be a natural molecule (soot, rocks, interstellar matter) rather than an "invented" one.

To sum up on these two books: condescension backlashes, admiration does not err.

Pierre Laszlo
Laboratoire de chimie
École polytechnique, Palaiseau (France)

This section contains book reviews and a list of new books received by the editor. Book reviews are written by invitation from the editor. Suggestions for books to be reviewed and for book reviewers are welcome. Publishers should send brochures or (better) books to the Book Editor, Dr. Gerhard Karger, Redaktion Angewandte Chemie, Postfach 101161, D-69451 Weinheim, Federal Republic of Germany. The editor reserves the right of selecting which books will be reviewed. Uninvited books not chosen for review will not be returned.

New Books

Dynamics of Excited Molecules. Edited by **K. Kuchitsu.** Elsevier, Amsterdam, **1994.** 620 pp., hardcover, Dfl. 495.00.—ISBN 0-444-81796-4

Theories and Mechanism of Phase Transitions, Heterophase Polymerizations, Homopolymerization, Addition Polymerization. (Advances in Polymer Science, Vol. 112). Edited by **A. Abe, H. Benoit, H.-J. Cantow et al.** Springer, Heidelberg, **1994.** 307 pp., hardcover, DM 198.00.—ISBN 3-540-57236-8

Polymer Synthesis. (Advances in Polymer Science, Vol. 111). Edited by **A. Abe, H. Benoit, H.-J. Cantow et al.** Springer, Heidelberg, **1994.** 227 pp., hardcover, DM 188.00.—ISBN 3-540-57198-1

Luftreinhaltung, 3rd Ed. By **G. Baumbach.** Springer, Heidelberg, **1994.** 461 pp., paperback, DM 78.00.—ISBN 3-540-56823-9

Ab Initio Variational Calculations of Molecular Vibrational-Rotational Spectra. (Lecture Notes in Chemistry, Vol. 61). By **D. J. Searles, E. I. v. Nagy-Felsobuki.** Springer, Heidelberg, **1993.** 186 pp., paperback, DM 58.00.—ISBN 3-540-57465-4

Stereoselective Synthesis. Edited by **E. Ottow, K. Schöllkopf, B.-G. Schulz.** Springer, Heidelberg, **1993.** 136 pp., hardcover, DM 128.00.—ISBN 3-540-57202-3

TA-Siedlungsabfall. Kommentar unter Berücksichtigung der aktuellen Gesetzeslage. Edited by **Bundesverband der Deutschen Entsorgungswirtschaft e. V.** Merz Verlag, Bonn, **1994.** Paperback, DM 32.50.—ISBN 3-926108-26-6

Metalloporphyrins Catalyzed Oxidations. (Catalysis by Metal Complexes, 17). Edited by **F. Montanari, L. Casella.** Kluwer, Dordrecht, **1994.** 368 pp., hardcover, Dfl. 240.00. —ISBN 0-7923-2657-1

Cyclodextrins in Pharmacy. (Topics in Inclusion Science, 5). By **K.-H. Frömming, J. Szejtli.** Kluwer, Dordrecht, **1993.** 228 pp., hardcover, Dfl. 160.00.—ISBN 0-7923-2139-1

Conceptual Trends in Quantum Chemistry. Edited by **E. S. Kryachko, J. L. Calais.** Kluwer, Dordrecht, **1994.** 264 pp., hardcover, Dfl. 165.00.—ISBN 0-7923-2621-0

Oxygenates by Homologatin or CO Hydrogenation with Metal Complexes. (Catalysis by Metal Complexes, 16). Edited by **G. Braca.** Kluwer, Dordrecht, **1994.** 240 pp., hardcover, Dfl. 160.00.—ISBN 0-7923-2628-8

Spectra for the Identification of Monomers in Food Packaging. By **J. Bush, J. Gilbert, X. Goenaga.** Kluwer, Dordrecht, **1993.** 448 pp., hardcover, Dfl. 320.00.—ISBN 0-7923-2400-5

Fluorescent Chemosensors for Ion and Molecule Recognition. (ACS Symposium Series No. 538). Edited by **A. W. Czarnik.** American Chemical Society, Washington (USA), **1993.** 243 pp., hardcover, $ 69.95.—ISBN 0-8412-2728-4

Thermally Generated Flavors. (ACS Symposium Series No. 543). Edited by **T. H. Parliment, M. J. Morello, R. J. McGorrin.** American Chemical Society, Washington (USA), **1993.** 488 pp., hardcover, $ 109.95.—ISBN 0-8412-2742-X

Silk Polymers. (ACS Symposium Series No. 544). Edited by **D. Kaplan et al.** American Chemical Society, Washington (USA), **1993.** 253 pp., hardcover, $ 94.95.—ISBN 0-8412-2743-8

The Anomeric Effect and Associated Stereoelectronic Effects. (ACS Symposium Series No. 539). Edited by **G. R. J. Thatcher.** American Chemical Society, Washington (USA), **1993.** 290 pp., hardcover, $ 74.95.—ISBN 0-8412-2729-2

Physical Properties of Polymers, 2nd Ed. By **J. E. Mark et al.** American Chemical Society, Washington (USA), **1993.** 409 pp., hardcover, $ 59.95.—ISBN 0-8412-2505-2

Polymers for Microelectronics. (ACS Symposium Series No. 537). Edited by **L. F. Thompson, C. G. Willson, S. Tagawa.** American Chemical Society, Washington (USA), **1993.** 554 pp., hardcover, $ 119.95.—ISBN 0-8412-2721-7

Thin-Layer Chromatography, 3rd Ed. (Chromatographic Science Series, 66). By **B. Fried, J. Sherma.** Marcel Dekker, New York, **1994.** 464 pp., hardcover, $ 165.00.—ISBN 0-8247-9171-1

NMR Techniques in Catalysis. (Chemical Industries Series, 55). Edited by **A. T. Bell, A. Pines.** Marcel Dekker, New York, **1994.** 448 pp., hardcover, $ 165.00.—ISBN 0-8247-9173-8

Stoffe E-O. Hagers Handbuch der Pharmazeutischen Praxis, Vol. 8, 5th Ed. Edited by **F. v. Bruchhausen et al.** Springer, Heidelberg, **1993.** 1293 pp., hardcover, DM 610.00.—ISBN 3-540-52640-4

Solid-State NMR I: Methods. (NMR - Basic Principles and Progress, Vol. 30). Edited by **B. Blümich.** Springer, Heidelberg, **1994.** 281 pp., hardcover, DM 248.00.—ISBN 3-540-57189-2

Solid-State NMR II: Inorganic Matter. (NMR - Basic Principles and Progress, Vol. 31). Edited by **B. Blümich.** Springer, Heidelberg, **1994.** 215 pp., hardcover, DM 248.00.—ISBN 3-540-57190-6

Protein Purification, 3rd Ed. By **R. K. Scopes.** Springer, Heidelberg, **1994.** 380 pp., hardcover, DM 88.00.—ISBN 3-540-94072-3

Crystallography. By **W. Borchardt-Ott.** Springer, Heidelberg, **1993.** 303 pp., paperback, DM 44.00.—ISBN 3-540-56679-1

Quality Assessment of Textiles. By **K. Mahall.** Springer, Heidelberg, **1993.** 227 pp., hardcover, DM 148.00.—ISBN 3-540-57390-9

The Barbier Reaction and Related One-Step Processes. (Reactivity and Structure: Concepts in Organic Chemistry, Vol. 31). By **C. Blomberg.** Springer, Heidelberg, **1993.** 183 pp., hardcover, DM 186.00.—ISBN 3-540-57169-8

New Gmelin Volumes:

B Boron Compounds. Suppl. Vol. 4, Part 2. By **G. Heller.** Springer, Heidelberg, **1993.** 297 pp., hardcover, DM 1780.00.—ISBN 3-540-93673-4

N Nitrogen. Suppl. Vol. B, Part 2. Edited by **P. Merlet, D. Koschel, A. Wietelmann.** Springer, Heidelberg, **1993.** 188 pp., hardcover, DM 1140.00.—ISBN 3-540-93672-6

OS Organoosmium Compounds. Suppl. Vol. B, Part 6. Edited by **K. Behrends, J. Füssel, C. Weber.** Springer, Heidelberg, **1993.** 248 pp., hardcover, DM 1485.00.—ISBN 3-540-93671-8

Physical Properties of High Temperature Superconductors. (High Temperature Superconductivity, Vol. 4). Edited by **D. M. Ginsberg.** World Scientific, Singapore, **1994.** 650 pp., hardcover, £ 70.00.—ISBN 981-02-1637-8

Rohstoffe und Umwelt. (Geologie und Ökologie im Kontext, Vol. 2). Edited by **E. Speetzen.** Ernst & Sohn, Berlin, **1994.** 222 pp., hardcover, DM 118.00.—ISBN 3-433-01521-X

Gentechnik als eine Herausforderung in Deutschland. (Nova Acta Leopoldina, NF, Vol. 70, No. 286). Edited by **E.-L. Winnacker.** Barth Verlag, Leipzig, **1993.** 74 pp., DM 9.80.—ISBN 3-335-00393-4

Advances in Transport Processes IX. Edited by **A. S. Mujumdar, R. A. Mashelkar.** Elsevier, Amsterdam, **1993.** 586 pp., hardcover, Dfl. 595.00.—ISBN 0-444-89737-2

Relaxation in Polymers. Edited by **T. Kobayashi.** World Scientific, Singapore, **1993.** 340 pp., £ 64.00.—ISBN 981-02-1373-5

Advances in Thermochemical Biomass Conversion. Edited by **A. V. Bridgwater.** Chapman & Hall, London, **1993.** 1760 pp., hardcover, £ 195.00.—ISBN 0-7514-0171-4

Gas Cleaning at High Temperatures. Edited by **R. Clift, J. P. K. Seville.** Chapman & Hall, London, **1993.** 696 pp., hardcover, £ 99.00.—ISBN 0-7514-0178-1

Chemical Chaos. (International Series of Monographs on Chemistry No. 24). By **S. K. Scott.** Oxford University Press, Oxford, **1993.** 470 pp., paperback, £ 22.50.—ISBN 0-19-855658-6

Introduction to Modern Colloid Science. By **R. J. Hunter.** Oxford University Press, Oxford, **1993.** 346 pp., hardcover, £ 35.00.—ISBN 0-19-855387-0

Protein Structure: In Focus. By **N. J. Darby, T. E. Creighton.** Oxford University Press, Oxford, **1993.** 120 pp., paperback, £ 8.95.—ISBN 0-19-963310-X

Maintenance-Free Batteries - A Handbook of Battery Technology. By **D. Berndt.** Research Studies Press, Chichester, Great Britain, **1993.** 384 pp., £ 65.00.—ISBN 0-86380-143-9

Organic Chemistry, 2nd Ed. By **K. P. C. Vollhardt, N. E. Schore.** Freeman, Oxford, **1993.** 1312 pp., hardcover, £ 24.95.—ISBN 0-7167-2010-8

Quantum Mechanics in Chemistry. By **G. C. Schatz, M. A. Ratner.** Prentice Hall, Englewood Cliffs, USA, **1993.** 325 pp., hardcover, $ 88.30.—ISBN 0-13-747585-3

Fish and Fish Products. By **B. Holland, J. Brown, D. H. Buss.** Royal Society of Chemistry, Cambridge, **1993.** 135 pp., paperback, £ 24.50.—ISBN 0-85186-421-X

 © VCH Verlagsgesellschaft mbH, D-69451 Weinheim, 1994 0570-0833/94/0808-0902 $ 10.00+.25/0

Turning Points in Catalysis**

John Meurig Thomas*

This personal journey through the enlarging landscape of heterogeneous catalysis, pure and applied, starts with the discovery in 1823 of a dramatic example of the synthesis of water that was to serve as the basis of the first commercial exploitation of catalysis, Dobereiner's lighter (tinder box). The quickening pace of successive industrial innovations and of academic insight during the intervening 170 years are summarized and the turning points, both major and minor, identified. Although new concepts and new ideas emerged in relative profusion, few exhibited the longevity predicted for them at birth by their proponents. Some concepts, like broken milestones on a vanished road, have ceased to retain their significance. Some have survived, even flourished. But in catalysis, as in most other branches of natural science, new tools and new techniques, rather than new concepts, tend to hold sway. And just as experimental advances in enzymology and immunology have led to the design of remarkable new biocatalysts so also, but not yet at the same level of delicate control, have the tools and techniques of solid-state chemistry (including novel preparative and computational procedures), generated many powerful rationally designed inorganic catalysts.

1. Introduction

It is not an excess of multinational European fervor but a sense of innocent pride mingled with a respect for historical exactitude that prompts me to begin by recalling that Europe has been the crucible and fulcrum for change in the science and technology of catalysis for more than two centuries. Nowadays, however, catalysis has been so extensively woven into the fabric of life in all the industrialized nations that the practice and pursuit of the subject transcends both national and continental boundaries.

Although *concepts* and *ideas* occupy a central place in the grand sweep of our understanding of the nature of the world around us, it is a mistake to imagine that they play a greater role than *tools* and *techniques* in achieving scientific progress. Few scientific revolutions are concept-driven. They invariably grow and are ultimately accomplished through the agency of experiment. In the tortuous paths from genesis to maturity in most disciplines and topics, more profound influences are exerted by the arrival of new instruments, new techniques, and the discoveries that they engender, than by the formulation of new ideas.

Galileo's telescope played as crucial a role in the consolidation of the heliocentric view of the universe as did Copernicus's theory, which was, in any case, based on prior observations. Likewise, the optical micoscope of Leeuwenhoek, no less than the electron microscope of Ruska, and all the dazzling succession of microscopes now at our disposal, have revolutionized our appreciation of the architecture and texture of the invisible. And when Röntgen discovered X-rays and W. H. Bragg invoked a mathematical tool (invented by a famous Frenchman) to represent the intensities of diffraction spots in terms of Fourier series, machinery was set in motion that now gives us the means to derive electron distributions in solids and molecules and in individual chemical bonds—the very essence of our present-day interpretations of catalysis.

Mathematical tools such as the transform and series associated with Fourier's name, like the more tangible tools of the chemist such as chromatography and spectroscopy, can set us off in new directions. And even the identification of simple physical phenomena can, in certain contexts, constitute major turning points.[1]

So much for general observations. When we focus on catalysis we have to cope with a vast corpus of information. Besides the simple and complicated facts pertaining to its occurrence and practice—as well as the impressive armory of tools and techniques with which to pursue manifestations of the phenomenon—we have, in addition, another factor which is so pervasive and so much taken for granted that we tend to discount it as a determinant in the growth of the subject. This is the desire to exploit catalysis for practical purposes. The urge to gain mastery over, or to harness the forces of, nature and to exploit one's discoveries for practical or commercial ends is

[*] Prof. Sir John Meurig Thomas
Davy Faraday Research Laboratory
The Royal Institution of Great Britain
21 Albemarle Street, London W1X 4BS (UK)
Telefax: Int. code + (71)629-3569
and
The Master's Lodge
Peterhouse
Cambridge CB2 1QY (UK)

[**] This review is based on the opening lecture at the first European Congress on Catalysis (EUROPACAT-1), Montpellier, 12–17 September 1993.

 © VCH Verlagsgesellschaft mbH, D-69451 Weinheim, 1994 0570-0833/94/0909-0913 $ 10.00+.25/0

irrepressible.[2] This urge is itself the engine of change, which brings forth new turning points.

1.1 The Early Days of Heterogeneous Catalysis and the First Commercial Exploitation: Döbereiner's Lighter

Even before Berzelius in 1835 coined the word catalysis in its modern connotation, applied catalysis was already a reality (Table 1). The writings of the Arabic alchemist, Jabir ibn Haiyan (Geber) in the eighth century reveal that mineral acid was then used as a catalyst for the production of ether by the dehydration of alcohol. Davy's discovery (at the Royal Institution, in 1817) consisted essentially in the observation that a pre-heated length of fine platinum wire could be made to glow in a mixture of air with coal gas, carbon monoxide, alcohol vapor, or similar substances, and that the glowing continued until all the inflammable material was consumed.[5]

Table 1. Historical overview of applied catalysis up to about 1900.

Jabir Ibn Haiyan (Geber)	8th Century	ether from alcohol (sulfuric acid catalyzed)
Kirchhoff	1814	acid-catalyzed hydrolysis of starch
Davy	1817–26	hot platinum, air, and coal gas
Döbereiner	1820s	tinder box (Feuerzeug)
Grove	1840	electrocatalysis, fuel cell
Phillips	1840s	$SO_2 \rightarrow SO_3$; sulfuric acid synthesis (Pt on montmorillonite as catalyst)
Mége-Mouries	1869	catalytic hydrogenation of oils
Normann	1901	octadecenoic acid to stearic acid

Over a period of seven days in late July–early August 1823 Döbereiner produced a dramatic example of the catalyzed synthesis of water. He directed a fine jet of hydrogen at a powdered platinum catalyst from a distance of four or so centimeters. The finely divided catalyst instantly became white hot and, with a strong jet, the hydrogen caught fire. This was the scientific principle that led Döbereiner in due course to produce his famous lighter—the forerunner of the matchstick—the so-called "feuerzeug" or tinder box.[6, 7] Scientific aspects of Döbereiner's discovery were pursued by Michael Faraday;[6] but another Englishman, one Alexander Garden, "a scientific chemist in Oxford Street, London"[7] was more concerned about its practical applications and, specifically, in "the idea of employing it for the instantaneous production of fire and light". By 1828, hundreds of thousands of Döbereiner's lighters had been mass produced by Gottfried Piegler in Schleiz (on the edge of the Thüringer Wald between Hof and Gera): some 20000 were in use in England alone that year.[7] One of them, which was received as a gift from Döbereiner by Faraday,[8] and which is now a treasured antique in the Director's flat at the Royal Institution, is shown in Figure 1. Döbereiner's lighter is reminiscent of the Kipp's apparatus for the generation of hydrogen sulfide: hydrogen is produced by the action of sulfuric acid on granules of zinc. The pressure of hydrogen that builds up stops the acid from continuing to fall on the zinc until a stopcock, releasing the hydrogen which impinges upon the platinum catalyst, is opened.

His lighter brought Döbereiner great fame.[7] It might also have brought him considerable fortune, but he characteristically refused to take out a patent, published all his designs, and spurned a large offer from an Englishman named Robinson for monopoly rights with the words "I love science more than money".[9] (Humphry Davy a little earlier had refused to patent his invention of the miners' safety lamp for similar reasons.[10] The desire to make money is not the only stimulus for technological enterprise!) Robinson prospered from the manufacture of Döbereiner tinder boxes (lighters), as did many others throughout Western Europe. This was the first example of the commercial exploitation of heterogeneous catalysis. And in spite of the invention of the safety match in 1848, by one of his former pupils, Böttger, the Döbereiner lighter retained its popularity for a long time and was still in use at the beginning of the First World War.[11]



John Meurig Thomas was born in South Wales in 1932 and took his initial degree in the University College of Swansea. For twenty years, after completing his Ph.D. in London, he taught in the University of Wales, first at Bangor, later as Professor and Head of Chemistry in Aberystwyth where his work in solid-state and surface chemistry led to his election as Fellow of the Royal Society in 1977. Called to the University of Cambridge to succeed Jack Linnett in 1978 he headed the Department of Physical Chemistry and was Professorial Fellow of King's College for nine years before taking over the Directorship of the Royal Institution of Great Britain in London where, as Fullerian Professor he continues his researches. He has received numerous awards, both nationally and internationally, including the premier one awarded every three years (Faraday medal) of the Royal Society of Chemistry, and the Messel Gold Medal of the Society of Chemical Industry. He has been elected honorary foreign member of six national academies and is the recipient of many honorary degrees. He has lectured extensively overseas, and gave the Baker Lectures at Cornell University on Solid State Chemistry in 1983. Author of several books (including one on 'Michael Faraday and the Royal Institution: the Genius of Man and Place') and over 700 articles, he was knighted for his services to chemistry and the popularization of science in 1991. For the last three years he has served as Deputy Pro-Chancellor of the University of Wales, and in 1993 was elected Master of the oldest College in Cambridge, Peterhouse. The book entitled "Principles and Practice of Heterogeneous Catalysis", which he wrote together with W. John Thomas, Bath, is due to be published at the end of 1994 by VCH.



Fig. 1. Michael Faraday received this "tinder box" (fire lighter) from Döbereiner, its inventor, in the late 1820s. In Döbereiner's lighter, the first example of the commercial exploitation of heterogeneous catalysis, a jet of hydrogen, which is generated by the action of acid on zinc, is allowed to impinge upon divided platinum. The catalyst becomes white hot and so the hydrogen catches fire.

In the late 1830s my countryman Grove pioneered the use of platinum as an electrocatalyst. He also demonstrated that platinum could equally readily catalyze the thermal decomposition of water vapor into hydrogen and oxygen as it could the combustion of hydrogen to water. Grove described his famous "gas battery" or fuel cell, of which he was the inventor, in a charming letter to Michael Faraday written in October 1842.[12]

W. R. Grove to M. Faraday
London Institution
Saturday Oct 22 1842
My dear Sir

I have just completed a curious voltaic pile which I think you would like to see, it is composed of alternate tubes of oxygen and hydrogen through each of which passes platina foil so as to drop into separate vessels of water acidulated with sulphuric acid the liquid just touching the extremities of the foil as in the rough figure below [see ref. [8]].

The platina is platinized so as to expose by capillary attraction a greater surface of liquid to the gas. With 60 of these alternations I get an unpleasant shock and decompose not only iodide of potassium but water so plainly that a continuous stream of thin bubbles ascends from each electrode. Thus water is decomposed by its composition—no oxidable metal is employed. I have reversed the tubes and tried all the counter expts but the phenomena are too marked I think to render any mistakes possible. Mr Gassiot was with me today and saw the Expts. Can you spare me an hour next week on Tuesday if it suits you or any day except Wednesday at any hour from 11 to 3— at the Laboratory of the London Institution. I cannot but regard the experiment as an important one both as to the chemical and other theories of the pile and as to the catalytic effects of the combination of the gases by platina.
I remain my dear Sir
yours very sincerely
W. R. Grove

In the early 1830s, Peregrine Phillips, an enterprising Englishman, patented a catalyst consisting of finely divided platinum supported on montmorillonite clay for the conversion of sulfur dioxide to the trioxide, thereby paving the way for the manufacture of sulfuric acid.

We must not forget, in France of all places, that it was a Frenchman, rejoicing in the name Hippolyte Mége-Mouries, who, in 1869, was the recipient of Napoleon III's prize for the best substitute for butter: he succeeded in catalytically hydrogenating natural oils thereby inventing margarine. Processes of this kind were to benefit greatly from the catalytic investigations of the German worker Normann more than thirty years later. It was Normann who, inter alia, succeeded in converting octadecanoic acid to stearic acid. Such processes were also much facilitated by the techniques of catalytic hydrogenation using metallic nickel pursued by Sabatier in France in the 1900s.

1.2. Heterogeneous Catalysis from the End of the Last Century to the End of the Second World War

Of the various landmarks summarized in Table 2, one notes that many of these processes are of vital importance even today. Working from the bottom up, the significance of the achievements of Lewis and Gilleland in the USA was that they introduced a fundamentally new kind of chemical engineering process, namely *fluidized catalytic cracking*. This certainly marked a turning point, not only because of its commercial efficiency and repercussions, but because it drew particular attention to the need in such operations for the catalyst particles used in the fluidized bed to possess an irreducible minimum attrition resistance. *Catalytic cracking* itself, using a fixed-bed reactor, had been introduced in 1936 by Houdry, a motor-racing enthusiast obsessively motivated by the desire to produce better -higher octane-rating- -fuel.

Table 2. Historical overview of applied catalysis 1900–1945.

Haber	1909	ammonia synthesis
Ostwald	1910...	nitric acid from ammonia
BASF	1920...	methanol synthesis
Fischer and Tropsch	1922	syngas chemistry
Union Carbide	1937	ethylene oxide (Ag)
Houdry	1930–40	fixed-bed catalytic cracking of oils → fuels
Ipatieff and Pines	1940	solid acid catalysts
Lewis and Gilleland	1941	fluidized catalytic cracking

The "*solid acid catalysts*" produced in the early 1940s in the USA by the Russian emigre Ipatieff and his coworker Pines, consisted of diatomeceous earth (kieselguhr) laced with concentrated phosphoric acid. This catalyst proved remarkably effective in a variety of isomerizations, oligomerizations, and alkylations, which, in turn, greatly improved the quality of aviation fuel.

Fischer–Tropsch chemistry is still of primary concern in the chemical and petrochemical industry. It represents a milestone in applied catalysis in that it opened the way for the conversion of essentially all sources of carbon —coal, oil, biomass, and natural gas— via synthesis gas ("syngas", i.e. $CO + H_2$ mixtures) to alkanes, alkenes, and alkanols, depending upon the choice of

catalyst. With the need to minimize the sulfur and nitrogen content of fuels, Fischer–Tropsch catalysis is nowadays an attractive means of producing environmentally clean fuels, quite apart from its pivotal role in the generation of chemical commodities.

The success of *the Haber process*, initiated in 1909, for the *synthesis of ammonia*,[12] and subsequent improvements to it, is in large measure responsible for the feeding of mankind. In 1990 over 100 million tonnes of ammonia were synthesized worldwide. This figure grows annually by some two per cent. The vast majority of the ammonia ends up as fertilizer, and the onset of the use of this *fertilizer* is now and will forever be inscribed in the biological record- -see the striking dendochronological picture of growth rings in the trunk of a tree from a Norwegian forest (Fig. 2).

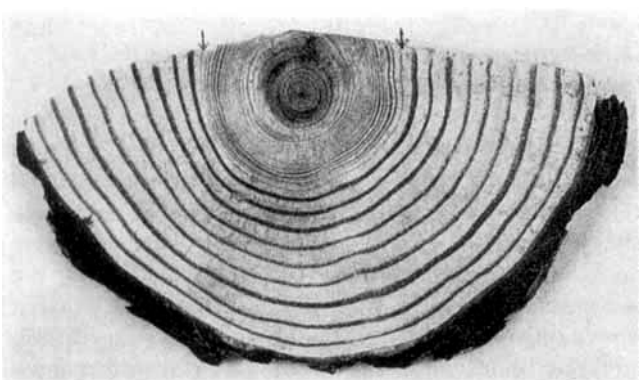


Fig. 2. An eloquent illustration of the impact of ammonia on the biological record. This section is of a tree from a Norwegian forest after about 35 years growth. Nitrogenous fertilizer was administered annually from the air after about 25 years initial growth. The enormously increased rate of growth under fertilization is apparent from the much wider spacing of the annual growth ring from the start of fertilization (indicated by arrows).

It has frequently been argued that the success of applied catalysis owes very little to pure, laboratory-based research and much more to industrial innovation. Paraphrasing a well-known aphorism among engineers—that science owes more to the steam engine than the steam engine does to science—the tacit implication among proponents of this view is that "science owes more to industrial catalysts than industrial catalysts owe to science". Indeed, in the context of the ammonia synthesis the case has recently been made[13] that the best catalysts were arrived at "by purely empirical methods and countless screening experiments". Whilst there is some truth in this statement for the development of ammonia (as well as other) industrial catalysts, one must not conclude that the design and practice of industrially viable modern catalysts is bereft of scientific principle. To be sure, it is undeniable that the majority of the catalysts appearing in Tables 1 and 2 were the product of largely empirical investigation. It is, however, equally indisputable[4] that a high proportion of the industrial catalysts of the last fifty years (see Tables 3 and 4) and especially of the catalysts introduced from 1980 onwards (see Table 9) emerged from pre-meditated scientific analysis and application.[14–18] Later in this article (see Section 5) several examples of designed heterogeneous catalysts are given.

To revert to Table 2, the mechanism of the copper-based methanol synthesis (ICI process) is now reasonably well understood, as are the broad features of catalytic cracking of hydrocarbons and their synthesis by Fischer–Tropsch reaction—even to the extent that the Shell Company could recently (and rapidly) set up a manufacturing facility for sulfur-free hydrocarbon fuels from syngas using a "formulated" Fischer–Tropsch catalyst based on cobalt. Major progress, much of it based on pre-meditated formulation and dextrous chemical synthesis, has also been achieved in the development of new solid acid catalysts.[16]

2. Highlights in Industrial Catalysis 1945–1985

Many of the key industrial catalytic processes introduced in this period have themselves served as turning points, judging by the considerable intellectual and technological stimulus that they have provided. Taking the enumerations of Tables 3 and 4, we first note the major impact of the independent work of Barrer and colleagues[19] in England and of Breck,[20] Rabo,[21] Milton, and others in the USA in preparing highly pure and highly crystalline analogues of naturally occurring, as well as uniquely new, *zeolitic molecular-sieve catalysts*. Mordenite is a typical example in the first category, zeolites X, Y, and L in the second. Zeolites constituted an impressive new kind of cracking, alkylation, and isomerization catalyst, much more active, and appreciably more specific than the acidic silica-alumina gel catalysts that they supplanted. In the hands of Plank and Rosinsky, zeolite-Y preparations were fine-tuned to be powerful fluidized cracking catalysts. A second generation of zeolitic catalysts, nowadays termed pentasils and typefied by ZSM-5, were brought forth by Weisz, Kerr, Haag,[22–24] and co-workers in the early 1970s. Their hallmark was shape-selectivity, a key quality to which we return later in Section 5.

Table 3. Historical overview of applied catalysis after 1945, part 1.

Rabo, Barrer, Breck, Milton	zeolites for isomerization and as replacement
Plank and Rosinsky	for silica-alumina in catalytic cracking.
Weisz, Haag...	alkylation, etc.
Haensel	Pt on acidic supports for catalytic reforming
Chevron, Exxon (Sinfelt)	refinements in reforming; hydrodesulfurization (hydro-treating)
Phillips	triolefin process (supported $Mo(CO)_6$ and $W(CO)_n$)
Ziegler and Natta Kaminsky and Sinn	stereoregular polymerization

Table 4. Historical overview of applied catalysis after 1945, part 2.

Katchalski (Nelson and Griffin)	immobilized enzymes (sensors)
Beecham and Bayer Tanabe Seiyaku	pharmaceutical and foodstuff production
Johnson Matthey, Engelhardt, etc.	auto-exhaust catalysts
Knowles, Noyori, Sharpless...	enantioselective synthesis
Grätzel...	photocatalysis
	alkane activation
	new acid catalysts
	catalytic distillation and reverse configuration reactors

Haensel's introduction of *reforming catalysts*, in which, inter alia, linear alkanes were converted to branched ones (with improved octane ratings), brought into the arena of catalysis the notion of *bifunctionality*. Not only did the comminuted platinum, supported on high-area oxides such as alumina, provide the platform for such processes as hydrogenation and dehydrogenation, but the acidic support, the other functionality, facilitated both the formation and rearrangement of cationic organic moieties present as intermediates at the catalyst surface.

Ziegler (in Mülheim) and Natta (in Milan) were responsible for a major advance in 1953 with their discovery of *stereoregular polymerization*. This marked the introduction of the control of tacticity of synthetic polymers. It was Natta who first realized that the precise nature of the catalyst crucially governed the type of polymer that was produced. An appropriate choice of catalyst could, for example, increase the polymer density and tensile strength. The length of the polymer chain determines such properties as the transparency, stiffness, brittleness, and strength of the material. The catalyst used by Ziegler consisted of $TiCl_4$ and alkylaluminum compounds. The modern version of the Ziegler–Natta catalyst is a $MgCl_2$-supported $TiCl_3$ complex, and a great deal is now known about the individual steps in the overall catalytic process.

In the 1980s Kaminsky, Ewen, Brintzinger, and Sinn produced an impressive new family of homogeneous organometallic *metallocene catalysts* for the stereoregular polymerization of propene. Catalysts such as [ethylenebis-(4,5,6,7-tetrahydro-1-indenyl)]zirconium dichloride in the presence of an aluminum compound such as methyl alumoxane ($(CH_3AlO)_n$) were shown by Kaminsky et al. to be highly efficient for stereoregular polymerization.[25, 26] They regarded this as a key advance from the heterogeneous Ziegler–Natta catalysts in that, being homogeneous, the new catalysts are relatively straightforward to study because every one of the active sites has the same molecular structure, and, more important operationally, there is a well-defined chiral center in each catalytic molecular entity so that stereopreference inevitably ensues during chain growth as implied in the schematic representation of Figure 3. It is energeticallly favored for the monomer to be bound to the zirconacene catalyst in one of the two possible modes.

Of more ancient lineage but of no lesser importance at present than stereoregular polymerization is catalysis by *immobilized enzymes*. A pioneeering paper by the American workers Nelson and Griffin in 1916 showed that when invertase is grafted on to a high-area microporous charcoal, no loss of enzymatic activity is observed. In the mid 1940s invertase immobilized on high-area solids was used as an industrial biocatalyst for the decolorization of golden syrup (by the inversion of sucrose). Katchalski and coworkers[27] in Israel and many other investigators, including the groups of Lilly and Dunnill in London and of some industrial companies in Japan, Europe, and North America brought immobilized enzymes into a high degree of performance. Noteworthy achievements were the use of immobilized penicillin amidase to convert benzylpenicillin to 6-aminopenicillanic acid (thereby leading to the production of semi-synthetic penicillins), and of immobilized glucose isomerase for the isomerization of glucose to fructose. These two examples led the way to the ever-increasing use of immobilized biocatalysts in the food and pharmaceutical industries, uses that are now burgeoning.[28]

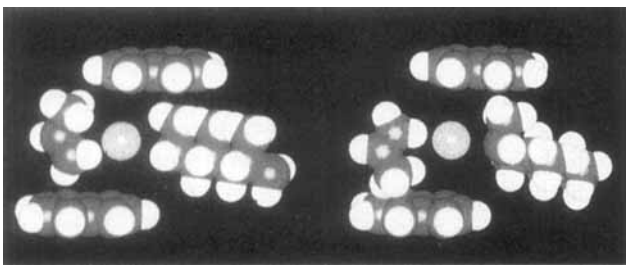


Fig. 3. On the left is shown the energetically favored, on the right the unfavored manner for a propylene molecule to be attached to the central atom of the zirconium catalyst. This energetic preference is the root cause of the stereoregular polymerization of propylene with a Brintzinger–Kaminsky catalyst. The growing polymer is on the right of the central atom (see text). (Picture by R. S. Bell and J. M. Thomas based on F. Kübor *New Sci.* **1993**, *139* (1986), 28).

Auto-exhaust catalysts have been fashioned on the basis of steadily increased knowledge of the individual mechanistic steps associated with the combined objective of eliminating nitric oxide, carbon monoxide, and incompletely combusted hydrocarbons from the exhaust. As well as utilizing rhodium, palladium, and platinum, which are well known for their ability to cope catalytically with the above gases, advantage has been taken of the propensity exhibited by some metal oxides, of which CeO_2 is a notable example, to *release* oxygen from its structure in a sacrificial manner when gas-phase oxygen is depleted, as is often the case, in the exhaust environment.

Catalytic, enantioselective synthesis of organic compounds of increasingly impressive specificity was introduced in the interval in question by adroit choice of transition metal or noble metal complexes typefied by the rhodium complexes of Knowles in the US, the BiNAP reagent developed by Noyori,[29] and the elegant work of Sharpless, Collman, and others on regio- and enantioselective epoxidations.[30] Efforts to perfect *selective oxidation* of methane on an industrial scale were not successful. It is easier to find catalysts for the more effective complete combustion of this hydrocarbon than for its selective transformation to C_2 building blocks and higher homologues. Likewise laboratory (model) systems for the activation of the C–H bond in alkanes depend heavily on pointers provided by biological catalysts.

Catalytic distillation, a relatively new chemical engineering strategem, utilized early on by the Enichem Company in Italy, combines distillation and catalysis into one operation. The aim here, as in the use of *catalytic membranes* pioneered by Gryaznov in Moscow, is to increase the efficiency of the overall operation. Other strategies entailing new chemical engineering practices were incorporated into the so-called *catalytic heat generator* (CHG) developed in Novosibirsk.[31, 32] This specially designed heat generator greatly reduces emission of carbon dioxide in the burning of fuel. The CHG combines in one reactor various energy-consuming processes (such as heating or evaporation of water and other liquids, drying, and thermal treatment of solid powders) with catalytic oxidation (combustion) of the fuel in a fluidized bed. Catalytic heat generators, like the rapidly expanding field of solid acid catalysts,[33] are likely to play an ever-increasing role in the *clean technology* of the future.

3. Everything Is Interesting: Not Everything Is Important

On contemplating the vast canvas of catalysis and the enormous and growing wealth of facts pertaining to the phenomenon, it is prudent to remind ourselves that, in catalysis, almost everything we investigate is interesting. But not everything is important. It is also salutory to recall that we have had conspicuously more success in discovering new catalysts than in explaining old ones.

These thoughts came forcibly to mind when, in preparing this lecture, I consulted the monograph published by Georg-Maria Schwab in 1931 (Fig. 4). This book was an important milestone.

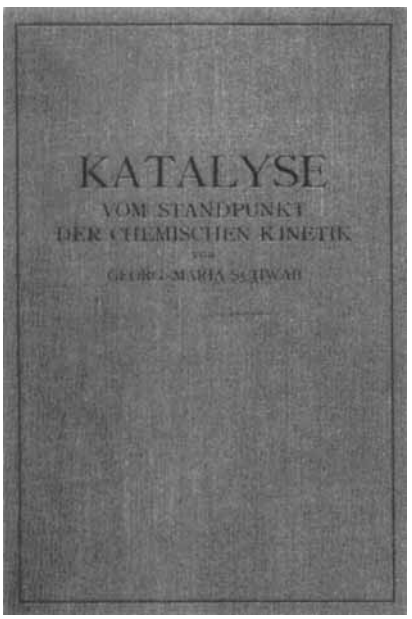


Fig. 4. Title page of the English of Georg-Maria Schwab's monograph on "Catalysis From The Standpoint of Chemical Kinetics" (published by Macmillan, London) translated by H. S. Taylor and R. Spence.

It was composed by the thirty-year-old Schwab with all the scholarship and authority associated with teutonic thoroughness. The fact that H. S. Taylor, a major figure in catalysis at that time and head of a thriving school in Princeton, saw fit immediately to translate it into English with R. Spence[34] testifies to the esteem with which Schwab's work was held by his scientific peers. Schwab's book makes fascinating reading even now, and I take comfort from one of his early caveats:

"*In this section particularly, a certain subjectivity of standpoint can be excused as essentially unavoidable*"

In catalysis, as in many other subjects, it was ever thus! Overwhelmingly, Schwab's book views the world of catalysis, as his title made explicit, from the perspective of chemical kinetics. He attempts to encompass all aspects of the subject, including processes in the homogeneous gas phase as well as in the homogeneous liquid phase. But he says very little about biological catalysis, evidently because of its then bewildering nature. He highlights the contributions of Langmuir especially and of Hinshelwood in the domain of kinetics. He also focuses on the "active sites" concept proposed by H. S. Taylor in the early 1920s. He underlined the importance of many other topics that are still relevant to discussions of the subject: heats of adsorption (and the value of calorimetry and thermodynamics in retrieving such heats), intermediate "compounds" of various kinds as envisaged by Van't Hoff, Arrhenius, and Sabatier, and the "activation" of a catalysts or the conversion of a precursor solid into an active catalyst by heating.[35]

It is interesting to reflect that biological catalysis, which seemed to Schwab to be of such complexity that it was omitted from his monograph, has been so greatly clarified in the intervening years that it is now perhaps better understood, and certainly more amenable to subtle modification and prior design than any other form of heterogeneous catalysis (see Section 5.1). Schwab also wrote:

"*The somewhat pessimistic conclusion which we have already reached from the present conditions of our knowledge, that there is not a single mechanism of catalysis, naturally does not exclude the possibility that a quite general correlation of the pertinent phenomena covering a whole series of items, can be given*".

It still remains true –and not unexpectedly so in view of the wide spectrum of different reactions amenable to catalysis– that there is no single, all-embracing theory of catalysis, in the sense that we have other comprehensive theories (of evolution or relativity, for example). Schwab's reminder about general correlations is therefore relevant.[36]

3.1. Important Tools and Techniques

In the intervening years since the appearance of Schwab's seminal work, enormous power has been added to the armory of those who investigate the science and technology of catalysis (Table 5). On the spectroscopic front, as well as in the field of imaging and in numerous aspects of diffraction, *ultrasensitivity of detection* or *identification* and *ultrarapidity of operation* have been the hallmarks, and there has been a concomitant florescence in *computation and simulation*. Particular examples, be they spectroscopic, diffractive, or concerned with imaging, are of greatest value when they can be applied to catalysts operating under realistic conditions. In situ studies, including the use of chemical reactions themselves as probes of catalytic performance, have been rather slow in reaching maturity. If we concern ourselves excessively with model systems operating under rarefied conditions –both in the literal and metaphorical

Table 5. Modern equipment for the study of catalysts.

Tools	Sensitivity and speed
Instruments for	
spectroscopy	ultra-high structural and spatial resolution
diffraction	extraordinary sensitivity of detection
imaging	
computation	fast retrieval from data bases
simulation	

sense—we run the risk of abandoning studies of catalysis per se in favor of pursuing phenomena such as adsorption, surface structure, and the dynamics and physics of two-dimensional arrays. So tempting and seductive are the appearance of meretricious new methods and so tantalizing is the glamor of new techniques that we can be readily diverted from our original intentions. So intoxicated do we become by the lure of the new that we tend to jettison our long-term policy and replace it by a perpetual programme of improvisation.

In contemplating the choice of tools currently at our disposal, it is chastening to recall that, whereas spectroscopic and all other experiments can fail as well as succeed, in the practices of computation and simulation the criteria—even the awareness—of failure are less sharply defined.[37]

It is a little difficult to identify the precise turning points in the recent explosive growth of computational techniques. Several factors have converged to change the overall climate: the integrated circuit, the fast Fourier transform, the parallel processor, each have had their part to play. All this has meant that ab initio and other quantum mechanical calculations have become more manageable if not routine. Monte Carlo and molecular dynamics (MD) calculations are now regularly performed by non-experts. A major turning point in this area was the introduction by Car *and* Parrinello[38] in 1985 of the *ab initio molecular dynamics* method, based on the local density approximation.[39] Car and Parrinello procedures now permit us to "test" the existence of vast new ranges of solids not hitherto prepared (or imagined). Nesper et al.,[40] for example, have recently explored the stability of hypothetical, microporous modifications of carbon derived from zeolitic frameworks.

Table 6 lists some of the more important tools and techniques that have been the agents of progress in catalysis. But this list is not complete; electron microscopy in all its numerous modes[41–43] and scanning tunneling and atomic force microscopy, Raman spectroscopy as well as other powerful tools[44] are omitted. Working upwards in Table 6, one recognizes that photoelectron and high-resolution electron-energy-loss spectroscopy (*with or without angular variation*[45]), as well as conventional or tensor low-energy electron diffraction (LEED and TLEED, respectively) are not suited for in situ studies of catalysts because of limitations imposed by the mean free path of the electron. Nevertheless these tools are admirable for the investigation of model systems, and they yield invaluable pointers pertaining to the performance of real catalysts. Brief statements summarising the contributions of each of the items listed in Table 6 are as follows:

Table 6. Impetus of some new techniques and tools.

Brunauer–Emmett–Teller (BET) theory
calorimetry
H/D and o/p-H_2 exchange
radio and stable isotopic labeling (^{14}C, ^{13}C, ^{18}O)
multinuclear NMR spectroscopy with high-resolution (MAS-NMR, DOR, ^2H, and 2D)
IR, FT-IR, DRIFTS, spectator species
synchrotron (rotating-anode) sources, combined X-ray absorption and diffraction, NEXAFS
neutron scattering
transient kinetics and in-situ methods
molecular dynamics, Monte Carlo methods
(XPS-UPS, HREELS, TLEED, etc, suitable only for model systems)

[a] Abbreviations see text.

- *X-ray induced photoelectron spectroscopy* (XPS) made it possible to study submonolayer amounts on solids of exceptionally low area (ca 1 cm^2),[46–48] and in so doing revealed the nature of the bonding of the bound state and set limits on its sticking coefficient. The same, essentially, can be said of high-resolution electron-energy loss spectroscopy (HREELS).[44, 49]
- *UV-induced photoelectron spectroscopy* (UPS) and its angular dependence[45] in association with XPS, definitively established that those metals active as Fischer–Tropsch catalysts facilitated dissociative chemisorption of carbon monoxide. Metals that were not active favored adsorption of CO in the molecular state.[48]
- *Monte Carlo* and *MD*, together with other computational techniques such as docking and energy-minimization calculations, are now so well advanced that they can yield diffusivities of reactant and product species (in zeolitic catalysts, for example[50]) with a precision rivalling that of direct measurement. Computer simulation in catalysis is a burgeoning field.[51, 52]
- *Transient kinetics* studies, using isotopically labeled reactants in interrupted flow, as carried out by Tamaru[53] in Japan, offers access to both turnover number and the concentration of active intermediates at a particular catalyst surface.
- *Neutron scattering* has broadly two major advantages to offer in the in situ study of catalysts. First, since neutrons freely penetrate stainless steel yet are readily scattered by hydrogen and deuterium, in situ high-pressure studies of, for example, hydrodesulfurization (HDS) (MoS_2) catalysts, may be made by inelastic neutron scattering.[54] Second, by focusing on elastic neutron scattering (diffraction that is), the detailed atomic structure of a working catalyst, along with the subtle changes it undergoes during activation, may be refined by the Rietveld method from the profile of the powder diffraction pattern recorded under operating conditions.[55, 56]
- *Synchrotron radiation* with its unparalleled angular resolution, monochromaticity, polarization, and wavelength tunability has had a profound impact on our knowledge of catalysis;[57, 58] and again is usable under working conditions. Not only does it make it possible to record ultra-high-resolution diffractograms of working catalysis prior to, during, and after activation[16, 59]—and thereby yield (by Rietveld analysis) unique insights into the delicate structural changes accompanying the conversion of an inert, precursor solid into an active catalyst—it also affords direct information on the valence state, the environment, and coordination numbers in the first and second coordination spheres of a metal center. Furthermore, it is now possible to chart both the short-range order and properties of a key element in a particular catalyst while at the same time obtain information about long-range (crystallographic and related) order by doing combined X-ray diffraction analysis and X-ray absorption spectroscopy (the so-called XRD/EXAFS approach).[60–65] Near-edge X-ray absorption spectroscopy (NEXAFS), employing fluorescence emission from light elements (such as C, N, and O) in

small molecular species undergoing adsorption at metal surfaces, has yielded[66, 67] quantitative data about bond lengths in the chemisorbed state.

- The analytical value of infrared (IR) spectroscopy, rendered much more sensitive by Fourier transform (FT) operation, is incontestable. It has uncovered modes of bonding hitherto unknown. It has shown (by the reflection-absorption procedure) that even an atomically flat single crystal metal surface is energetically nonuniform. It has proved invaluable in the identification of acidic and other sites at catalyst surfaces. But it must not be thought that a well-defined surface species identified by IR is directly implicated in the act of catalytic turnover. One must be wary of *spectator species*: the ethylidene species formed at metal surfaces during catalytic hydrogenation of ethene for example thought to be is no more than a spectator, as was demonstrated by J. T. Yates by using a combination of surface spectroscopy, isotopic labeling, and transient kinetics.
- *Multinuclear NMR spectroscopy* is an indispensable tool to monitor the progress of solid-catalyzed gas-phase or liquid-phase reactions.[68, 69] The advent of FT methods (by Ernst, who demonstrated that natural-abundance ^{13}C NMR measurements largely dispensed with the need for the use of ^{14}C radio-labeled compounds) as well as magic-angle spinning NMR,[70] and other sophisticated variants like double-rotation NMR developed jointly by Lippmaa in Tallinn and Pines in Berkeley, makes it possible to devise elegant in situ experiments in heterogeneous catalysis.
- *Deuterium exchange* and labeling experiments were devised by H. S. Taylor and members of his school of acolytes at Princeton shortly after Urey discovered the isotope. These experiments did much to confirm the reality of dissociative absorption of polyatomic species and the atomic-scale scrambling within intermediates at catalyst surfaces. The ortho/para hydrogen exchange, especially in the hands of Farkas and Eley, shed light on the magnetic properties and degree of chemical unsaturation of various surfaces.
- *Calorimetry*, as noted by Schwab in his book, directly reveals the energetic uniformity or, more usually, heterogeneity of a catalyst surface. Nowadays, extremely minute areas of catalyst can be quantitatively investigated, as shown by King et al[71] using their novel micro-calorimeter for Ni surfaces.

The *Brunauer–Emmett–Teller (BET) theory* introduced in the late 1930s of multilayer adsorption gave rise to a reasonably reliable method of measuring the true area of a catalyst (or any solid) from the uptake of gas as a function of pressure. Modest as it may, at first sight, seem, this marked a turning point in the progress of catalysis for it provided a quantitative means of comparing one catalyst, in terms of its genuine surface activity, with another.

Other techniques, not listed in Table 6, are also of great value in investigating model or real-life catalysts. These include a family of temperature-programmed procedures (desorption, reduction, sulfidation, etc) the majority of which are applicable to operating, practical catalysts. There are also a variety of techniques better suited—or even solely suited, owing to their intrinsic character—to probe the properties of model catalysts. These encompass Auger electron spectroscopy (AES), ion scattering spectroscopy (ISS), and secondary ion mass spectrometry (SIMS) and most variants of electron microscopy. These days, X-ray diffraction, thanks to the availability of powerful (rotating-anode) laboratory X-ray sources, may be routinely deployed to identify and characterize mono- or multiphasic solid catalysts under operating conditions[72, 73] and to do so with essentially immediate computer access to powder-diffractogram data bases. Specialist techniques, based on Mössbauer spectroscopy or Rutherford back-scattering, are also available.[74]

I wish to draw attention to the special status occupied by zeolitic and some other solid catalysts. These are best described as *uniform heterogeneous catalysts*[14, 75] and are monophasic crystalline solids in which the active sites are distributed in a spatially uniform manner throughout their bulk. Shape-selective catalysts, discussed further in Section 5, also fall into this category. Because such catalysts have the overwhelming fraction of the surface area *inside* the bulk (being microporous and crystalline), the surface and the bulk of such solids are effectively synonymous. It follows that the techniques of solid-state chemistry and solid-state physics are also applicable for the study of the surfaces of these uniform heterogeneous catalysts. All the panoply of spectroscopic, diffraction-based, and computational techniques deployed for the solid state are therefore appropriate for uniform heterogeneous catalysts. It follows, for example, that when the surface is inside the bulk, as in a zeolitic catalyst, a projected high-resolution image of the solid, as shown in Figure 5, faithfully reflects the projected surface characteristics of this catalyst.

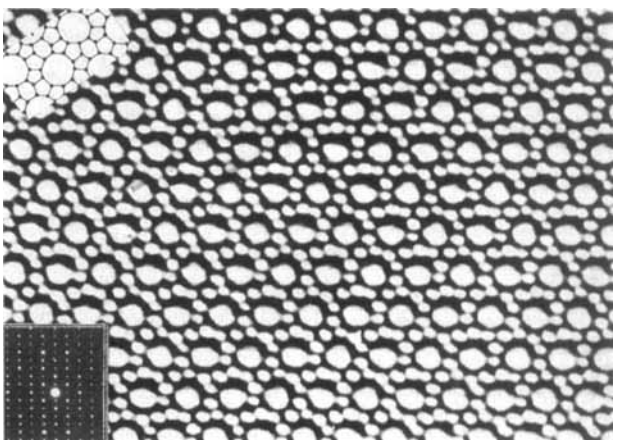


Fig. 5. High-resolution electron micrograph of a zeolitic acid catalyst (see also section 5) showing projected structure of pores lined with active sites. Large pores are 5.5 Å in diameter (from J. M. Thomas, P. L. Gai-Boyes, *Nature* **1993**, *364*, 478).

Zeolitic and other molecular-sieve crystalline solids occupy a unique place in the science and technology of catalysis in that they can function equally as faithful models for, and as actual examples of, practical catalysts.[76]

3.2. Important Concepts and Phenomena

Several concepts of ancient vintage in the surface chemistry of solids are still central to contemporary catalysis (see Table 7 for

Table 7. Concepts and phenomena of surface chemistry and catalysts as well as their proponents.

monolayers	Langmuir
kinetics of reactions involving monolayers	Langmuir Hinshelwood Rideal, Eley
active Site, poisoning heterogeneity	Taylor (Henry, Faraday)
potential energy diagrams	Lennard, Jones
surface reorganization and reconstruction	Germer
definition of catalysis	Berzelius, Ostwald
equilibrium unaffected by presence of catalyst	Lemoine
a catalyst for the forward reaction is also one for the reverse	Grove

several examples). The notion of chemisorbed *monolayers*, first introduced by Langmuir nearly eighty years ago, is an integral part of the language and interpretations of catalysis, and it is through this notion that reaction mechanisms for kinetically zero, first, or fractional order are formulated.

Langmuir–Hinshelwood mechanisms of surface-catalyzed reactions predicate the co-adsorption of two (or more) reactants. The *Rideal–Eley mechanism*, on the other hand, requires only one of the reactants to be chemisorbed: the other reactant simply suffers a rather sticky collision with the bound species (or with the interstices in the incomplete adsorbed layer) thereby leading to reaction. Experiment indicates that the majority of catalytic reactions comply more with the Langmuir–Hinshelwood than with the Rideal–Eley mechanism. It is also a great convenience in chemical engineering practice to express overall rate equations in the format associated with Langmuir–Hinshelwood mechanisms.[77] Such rate equations facilitate the scale-up of laboratory and pilot-plant studies into their mature, industrial-scale operation.[78, 79]

There were (comparatively sterile) periods in the history of catalysis when too much emphasis was placed on kinetic and not enough on structural studies. These periods have now passed.[80, 81] It is, however, surprising that, notwithstanding the preoccupation with kinetic studies that dominated catalysis research for so long, it was not until quite recently that chemical oscillations and instabilities, of the kind now recognized to be so pervasive and responsible for nonlinear behavior in chemical phenomena generally,[82] were discovered (see Section 4).

The term *active site* in heterogeneous catalysis by solid is inextricably associated with the work of H. S. Taylor in the 1920s. Such sites were initially regarded as those of high heats of adsorption. Nowadays, recognizing that a bound state needs to be neither too strongly nor too weakly bound to a catalyst surface, active sites have almost the opposite connotation from that originally propounded by Taylor. Of key significance and lasting validity was Taylor's view, subsequently confirmed by experiment, that at a particular catalyst there could be different types of active sites for different catalyzed reactions. This neatly explained why different poisons or inhibitors[83] exert different effects on different reactions. In biological catalysis, the active site is so central a concept that its structure and accessibility are the principal objectives in its study.

Surface heterogeneity in inorganic, especially metallic catalysts, originally implied the topographical irregularities of terraces, kinks, corners on or point defects and emergent dislocation at a crystal face, or different kinds of crystallographic faces.[84] Whilst such a description is still valid and logically leads to the notion of coordinative unsaturation, it is now recognized that even an atomically flat solid surface has intrinsic energetic heterogeneity because of the scope for a multiplicity of different kinds of bonding.

Potential energy diagrams entered the literature of catalysis soon after they were introduced in 1932 by Lennard-Jones to explain the peculiarities of adsorption isobars and, in particular, the observed differences in amounts adsorbed at a fixed external pressure (of, typically, hydrogen in contact with a polycrystalline metal) as the temperature rose from that of liquid air upwards.

Prior to the explosion of information that ultimately occurred following the seminal work of Germer in the USA on low-energy electron diffraction (LEED) from surfaces, and prior to the appreciation of all the surface structural subtleties that LEED subsequently revealed—supermeshes, commensurate and incommensurate two-dimensional repeats, surface Debye–Waller factors, and the like—it had long been realized that:

1) The position of equilibrium for a given reaction was unaffected by the presence or not of an appropriate catalyst. Lemoine, a French chemist, had established this fact in 1877 by elegant work on the system $2HI \rightleftharpoons H_2 + I_2$.
2) A catalyst for a forward reaction is also one for the back reaction. The principle of microscopic reversibility demands this. But before that principle was explicitly enunciated, Grove in the 1840s, had demonstrated it for $2H_2O \rightleftharpoons 2H_2 + O_2$.

Table 7 is selective rather than comprehensive. It omits the not unimportant mechanism of oxidation first identified by Mars and van Krevelen[85] who observed that certain oxides readily release their structural oxygen to an incoming reactant and subsequently make good the loss by assimilating oxygen from the gas phase. For reasons that are not clear, metal oxides that possess the perovskite, fluorite, or pyrochlore structures are prone to exhibit this property. Such *sacrificial mechanisms* often loom large in the catalytic oxidation of some hydrocarbons[86] and carbon monoxide.[87] Another omission from Table 7 is the useful subdivision, introduced by Boudart,[88] by which supported catalysts are termed either *structure-sensitive* or *structure-insensitive*.[89] A catalytic reaction is said to be structure-sensitive if its rate changes markedly as the particle size of the (supported) catalyst is changed, or as the crystallographic face of a (single-crystal) catalyst is altered. Conversely, the rate of a structure-insensitive reaction is not significantly modified by such changes. The hydrogenolysis of ethane ($C_2H_6 + H_2 \rightarrow 2CH_4$) and the synthesis of ammonia are good examples of structure-sensitive reactions:[90] the hydrogenation of ethene or benzene and the oxidation of carbon monoxide, on the other hand, are examples of structure-insensitive reactions.[91]

3.3. Broken Milestones on a Vanished Road

Blessed with the wisdom of hindsight it is easy to see which of the teeming variety of concepts, hypotheses, and principles for

mulated in earlier eras have stood the test of time. Some have survived, some have been resuscitated and injected with renewed vitality, others have died and now appear like broken milestones on a vanished road. Notions such as the "dislocation hypothesis" and "disruptive action of catalysts", propounded by Boeseken, no less than the "spatial factors" proposed by Biltz, along with suggestions pertaining to the mechanical or magnetic effects of catalysis and many other notions[92] are heard no more.

Of those that have survived it is instructive to elaborate their usefulness.

4. Some Illustrative Examples and Summarizing Statements

The idea that some solid catalysts possess *bifunctional* or *multifunctional* character is an important one. The recognition that supported metal catalysts (e.g., Pd or Pt on Al_2O_3 or zeolites) behave in a clearly identified dual fashion has greatly assisted designers of catalytic reactors. In the hydro-processing of petrochemicals, for example, the metal serves to dissociate H_2 as well as to facilitate the equilibration of alkanes, alkenes, and alkynes, whereas the acid support serves to catalyze the build-up of vital carbocationic intermediates. We note that the support functions not only to stabilize the highly dispersed catalyst (thereby retaining high surface area), to prevent poisoning by facilitating removal of deposited coke for example, and to activate the metal by electron transfer between it and metal, but it also can be directly involved in crucial elementary steps in overall reactions such as that shown in Figure 6.[93] Implicit in this picture is the "*spillover*" of hydrogen atoms that are generated by dissociation of H_2 at the metal particle. The dissociated atoms are mobile on the support, to a degree that depends on the nature of the latter—the H atoms are more mobile on WO_3 than on SiO_2 for instance—and play an important role in many heterogeneously catalyzed hydrogenations.

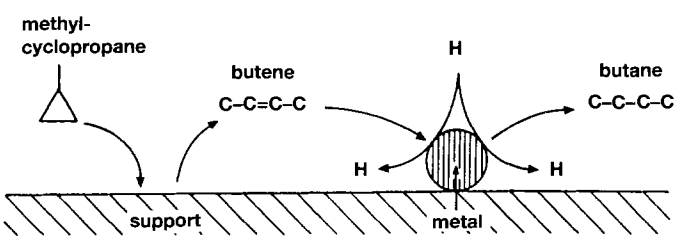


Fig. 6. A bifunctional catalyst such as platinum on silica facilitates the isomerization of methylcyclopropane to but-2-ene as well as the hydrogenation of the latter to butane. Dissociated hydrogen, facilitated at the metal, "spillover" on to the support (after Boudart [93]).

Consideration of bifunctional catalysts raise other relevant issues. *Metal-support interaction*, for example, influences both the electronic state of the metal along with its precise morphology. When finely divided chromium is dispersed over either SiO_2 or Al_2O_3 high area supports, there is little doubt (from the observed magnetic properties) that the chromium exists predominantly in the Cr^{II} state. Whereas the SiO_2 support provides a strong ligand field, thereby favoring the low-spin configuration for the octahedrally bonded $3d^4$-Cr^{II} ion, the Al_2O_3 support provides a weak ligand field, thereby favoring the high-spin state of the Cr^{II}. Metal-support interaction can be very strong, as was first recognized by Schwab and Solymosi.[94a] It has been further studied by Tauster et al.,[94b] who found that the catalytic activity for alkane hydrogenolysis, for example, can be suppressed if the supported catalyst is subjected to high-temperature pretreatment in H_2. The probable cause of the diminution in catalytic activity is the migration of species from the oxide support on to the exposed surface of the otherwise active metal. This is an example of strong-metal-support interaction (SMSI) about which a great deal is heard these days. Supported rhodium, for example, is a component of the automotive exhaust catalyst[95] (the three-way one) responsible for the reduction of NO by CO. It is also a viable catalyst for the conversion of syngas to oxyproducts such as ethanol and acetaldehyde.[96] This catalyst exhibits strong-metal-support interaction following high-temperature treatment in H_2, and minute particles of it tend to disintegrate further in atmospheres of CO. The morphology of supported metals can take up a multiplicity of types, from discrete, well-defined polyhedral, to discrete fluxional (though still polyhedral) to monolayer form. All this has emerged from a combined use of high-resolution electron microscopy,[97-99] EXAFS,[90] and X-ray diffraction.[99]

The realization that surfaces could be pre-treated so as to endow them with properties that they lacked in their pristine state constitutes another turning point in catalysis, and it is especially well-reflected in the development of *solid enantioselective catalysts*. The scope for tailoring metal catalysts by pre-adsorbing upon their surfaces bulky organic molecules which create prochiral cavities for the incoming reactant is considerable.[100] Wells et al.[101] have re-examined the Orito reaction[102] in which platinum, modified by the presence of presorbed cinchonidine becomes active for the stereoselective hydrogenation of an α-ketoester (e.g. methyl pyruvate) to an optically active product, for example, (*R*)-(+)-methyllactate (Fig. 7). My colleagues and I have explored, by computer graphics, the way in which this stereoselective process might proceed. The plausible assumption here is that cinchonidine forms an ordered, well spaced out array of interstices in the adsorbed layer. The interstices permit ingress of the methyl pyruvate in a preferred fashion so as to pre-ordain the formation of a given enantiomer.[15] There is little doubt, however,

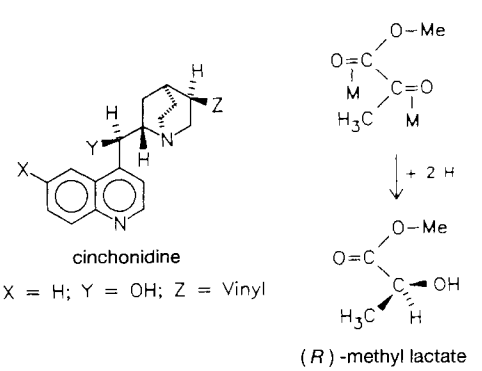
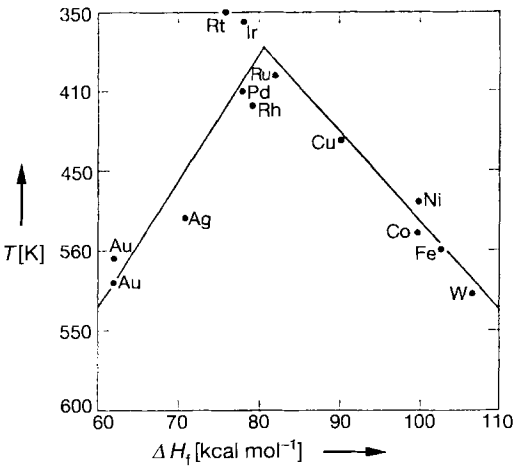


Fig. 7. Cinchonidine preadsorbed on a platinum catalyst favors the steroselective hydrogenation of a co-adsorbed α-ketoester to the optically active (*R*)-methyl lactate. See also ref. [15] and there particularly Figure 4.

that enantioselective catalysts of this kind will soon be superseded by more reliable, active, and selective ones, such as chiral metal complexes and a wide variety of stereoselective biocatalysts (see Section 5).

Another concept, stemming originally from the Russian worker Balandin, and later taken up by the Dutch school (notably Schuit and Sachtler) in the early 1960s is that of the use *volcano plots* (Figs. 8, 9). In reality, this concept encapsulates



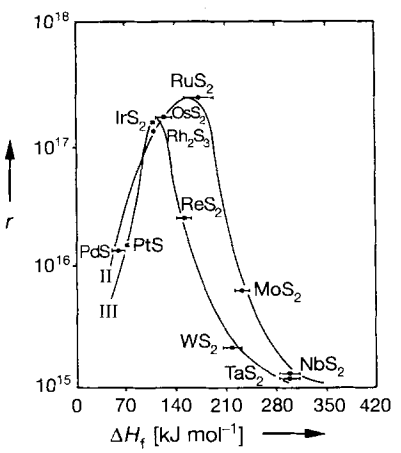


Fig. 8 (top) and 9 (bottom). Volcano plots, first proposed by the Russian worker Balandin, emphasize that catalytic activity is optimal when the enthalpy of formation ΔH_f of the surface intermediate compound is neither too great nor too small (see text). The dependence of the formation enthalpy of the formate on the temperature at which a certain rate of reaction is achieved is plotted in Figure 8. Details of Figure 9 are given in ref. [103].

the view that an intermediate surface compound, a metal formate, for example, when formic acid is catalytically decomposed at metal surfaces, is formed on the catalyst. This view, in a sense, is an updated version of Sabatier's original idea. The stability of this two-dimensional compound should be neither too high nor too low to secure maximal activity. Volcano plots have wide applicability. That reproduced in Figure 9 is taken from the work of Chianelli et al.[103] whose work on metal sulfides has done much to elucidate the mechanisms of hydrodesulfurization. This topic is one in which the Topsøe group[104, 105] in Denmark has made valuable contributions.

Whilst the idea of the *electronic factor* in catalysis, espoused by Hauffe, Wolkenstein, Weisz, and Stone in the 1950s, proved valuable for the interpretation of catalysis at oxide semiconductors,[106, 107] and whilst it served[108] as a useful basis for rationalizing trends for catalytic performance among families of alloy and bimetallic phases, it is now recognized that the term as such lacks precision and provides little predictive power in handling the massive corpus of inorganic catalytic phenomena.[109] Specific interactions between solid surfaces and molecules that impinge upon it are now handled quantum mechanically at various levels of sophistication from semi-empirical to rigorous ab initio treatments.[110–113]

Band theory tended to dominate discussions on catalysis by solids in the period 1950 to 1965. Far less is heard of it nowadays, chiefly because the local density of states at individual atoms or small clusters is now demonstrably more appropriate. There is, however, one area of catalysis, of growing practical importance, where band-structure considerations hold sway, and this is in *photocatalysis*. Gerischer, Parmon, Cunningham, and others have carried out a great deal of research in this field.

A knowledge of the magnitude of the electronic band gap and precise positions of the top of the valence band and the bottom of the conduction band edges—the analogue for an extended system of the HOMO–LUMO gap in a molecule—together with estimates of band bending that inevitably occurs owing to space-charges at the subsurface of a semiconductor, permits one to assemble an appropriate photoelectrolytic cell of the type schematized in Figure 10. The desired oxidation ensues as a

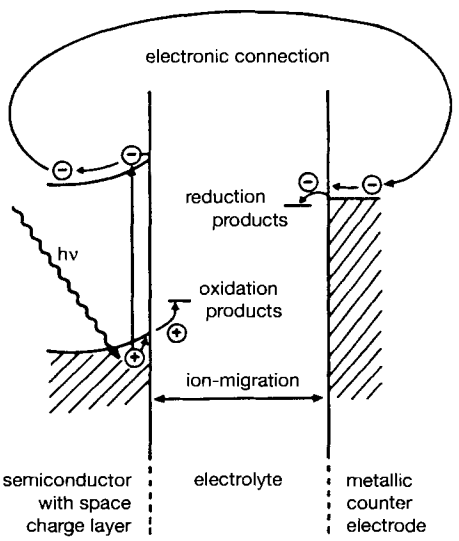


Fig. 10. In photoelectrolysis light is used to create electrons and holes which then serve to effect reduction and oxidation, respectively.

result of the electronic hole created by photo-absorption at the semiconductor–electrolyte interface and reduction by the mobile electron at the counter-electrolyte–electrolyte interface. Microcapsules and other appropriate miniature devices housing a tailored photocatalyst, like the one shown sandwiched between colloidal platinum and RuO_2 microelectrodes in Figure 11 can be so structured, as outlined by the Swiss worker M. Grätzel, for the continuous photocleavage of water, or indeed of a wide range of undesirable pollutants in fresh waters.

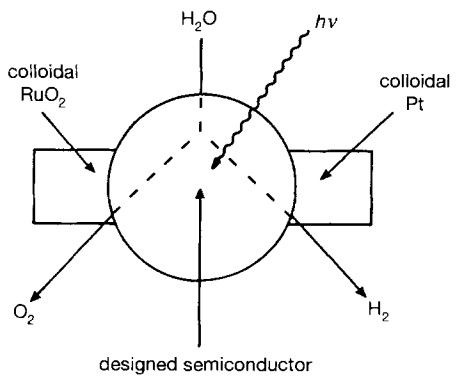


Fig. 11. It should be feasible to design a semiconductor catalyst microcapsule for the photocleavage of water and other abundant meterials (see text).

TiO_2 and ZnO are popular photocatalysts since they each efficiently absorb long wavelength ultraviolet light and are also chemically stable to the reaction conditions. Other semiconductor particles, notably CdS and GaP, absorb larger fractions of the solar spectrum and can form chemically activated surface-bound intermediates: they do, however, tend to degrade during the repeated catalytic cycles that prolonged heterogeneous photocatalysis demands.[114–126] Heterogeneous photocatalysis is used not only for degradation of pollutants and other unwanted organic materials, it can be harnessed for synthetic purposes. Bard et al.[116] have, for example, photocatalytically synthesized methane from acetic acid, and Lehn et al.[127] and Grätzel et al.[123] have demonstrated numerous other syntheses. Semiconductor-catalyzed photoaddition of cyclic enol ethers to 1,2-diazenes to afford hitherto unknown hydrazine derivatives can be effected by using ZnS and CdS.[125]

In designing a good photocatalyst for solar energy conversion of water to hydrogen and oxygen, the band gap between the conduction band and valence band edges must straddle the redox potentials—shown as dashed horizontal lines in Figure 12. The sulfide and selenide of zinc satisfy this condition as bulk solids; silicon and gallium arsenide do not, and neither do the sulfide and selenide of cadmium. However, it is a quantum mechanical fact (see Brus,[128] Nozik et al.,[129] and Henglein and Weller et al.[130]) that the width of the band gap for a given semiconductor widens as the particle size is decreased. Micro- and ultramicrocrystalline specimens of semiconductors may therefore be "tuned" —by the recently developed techniques of nano-technology—so as to yield the required band gap for the solar-driven (or any other light-induced) chemical process, be it synthesis or degradation.

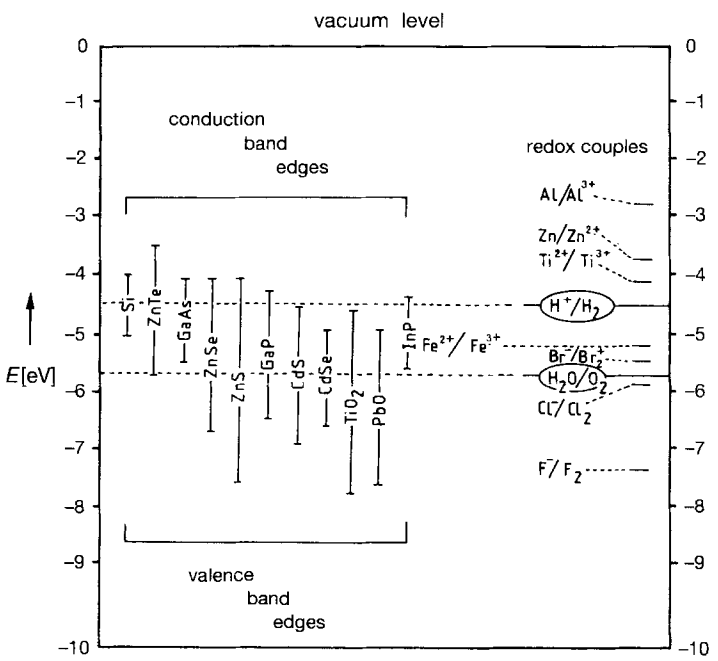


Fig. 12. The lower and upper extremities of the vertical lines denote respectively the top of the valence band and the bottom of the conduction band for several binary photocatalysts. For comparison, the band gap of silicon, as well as the electrochemical potentials of several familiar redox couples are also given (see text).

Elegant work by Parmon and his colleagues[131–133] in Novosibirsk has led to an effective means of harnessing solar energy so as to photosplit naturally occurring impurity hydrogen sulfide in the Black Sea. By ingeniously fashioning a heterojunction between minute particles of the sulfide of copper and the sulfide of solid solutions of zinc and cadmium (Fig. 13) light from the entire solar spectrum may be fruitfully harnessed for the separation of H_2S into hydrogen and water.

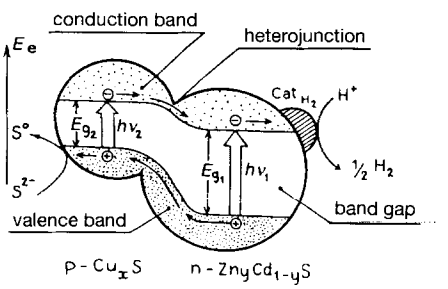


Fig. 13. Energy diagram and scheme (after Parmon et al. [131]) for the photoseparation of charges and catalytic processes in a suspended particle of a semiconductor with microheterojunction $CuS_x/Zn_{1-y}S$, which is one of the most efficient photocatalysts for H_2S cleavage in aqueous solutions. E_e is the electrochemical potential of the electron, E_{g_1} and E_{g_2} are the widths of the band gaps of the respective n- and p-type semiconducors and $h\nu_1$ and $h\nu_2$ are the corresponding light quanta.

Periodic variation in animal and insect population with the passage of time was recognized several decades ago by biologists such as the Australian worker May. In numerous predator–prey situations populations undergo regular bursts of growth followed by rapid decline on time-scales that vary from days to years. May's own work on lemming population (Fig. 14) shows that the mathematics of this periodic or oscillatory phenomenon is well understood. So far as chemists in general are concerned, the most renowned *oscillatory reaction* is the remarkable liquid phase one discovered by Belousov around 1950 and re-discovered by his Russian compatriot Zhabotinokii.[134] (But work at Brooklyn Polytechnic in the 1920s had already identified the

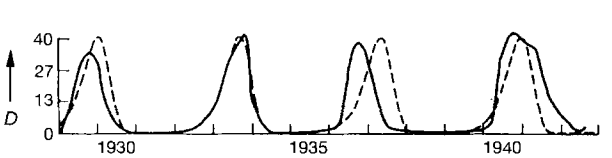


Fig. 14. Variation of the lemming density (D) (solid line) between 1929 and 1943. The dashed curve is the theoretical fit (after R. M. May, *Theoretical Ecology: Principles and Applications*, 2nd ed., Blackwells, Oxford, **1981**, p. 5.

reality and the mathematical basis of oscillatory reactions in chemical phenomena generally.)

Oscillatory reactions in heterogeneous catalysis are now of great interest as the recent reviews of L. D. Schmidt et al., Ertl, and others reveal. Although the existence of such oscillations was not firmly identified until the late 1960s and early 1970s (by Wicke et al.[135, 136] in Germany) it is now believed[137] that probably all bimolecular oxidation reactions catalyzed by transition metals will exhibit oscillations under some sets of experimental conditions. Whereas on the practical side it is rightly felt that oscillatory states of (large-scale) catalytic reactors are potentially dangerous—making it all the more necessary to understand the fundamentals of such processes—it is also appreciated that practical benefits can accrue by operating reactors under unstable regimes (with 'oscillating' input of feed reagents as demonstrated by Matros[138, 139] and Hegedus et al.[140]).

Chemical reactions far from equilibrium on solid catalysts may exhibit the phenomena of nonlinear dynamics, as exemplified by the oxidation of CO on a platinum(110) single-crystal surface (studied by Ertl et al.[141]). Depending on the precise temperature and partial pressure of the reactants, the temporal variation of the reaction rate may become oscillatory and even chaotic. And in a parallel way, the concentration distributions of the adsorbed species on the surface form so-called *spatio-temporal patterns* including propagating and standing waves, rotating spirals, as well as irregular and rapidly changing structures best denoted as "*chemical turbulence*".

The mechanism of the reaction $2CO + O_2 \rightarrow 2CO_2$ as catalyzed by noble metal surfaces is well understood thanks to the work of Engel and Ertl.[142] For the two reactants to be chemisorbed they compete, as it were, on an equal footing. For dissociative chemisorption of O_2, a fairly large ensemble of neighboring unoccupied surface sites is required, and any preadsorbed CO (since it can be bound to every available metal site) acts as an inhibitor for oxygen adsorption. The adsorbed atoms of oxygen, on the other hand, form a relatively open adlayer into which adsorption of CO is still quite feasible. Thus, there is comparatively little influence of preadsorbed oxygen on the adsorption probability for CO. The formation of CO_2 proceeds through recombination of CO_{ad} with O_{ad} (see Fig. 15), which is followed by immediate release into the gas phase. The sticking coefficients of CO and O_2 are functions of the surface coverages of the respective adsorbed species. The kinetics for the overall reaction are described by a set of nonlinear ordinary differential equations for the state variables u_1 and u_2 (which denote the surface coverages of adsorbed CO and O, respectively), the solutions of which depend on the control parameters, temperature, and the partial pressures of the CO and O_2.[143]

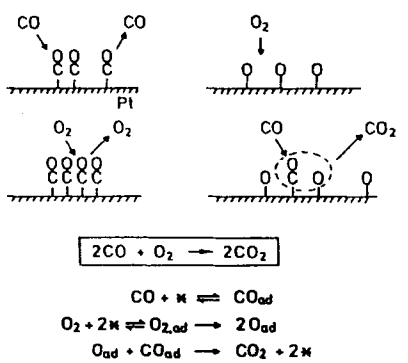


Fig. 15. Schematic representation of the mechanism of the reaction: $2CO + O_2 \rightarrow 2CO_2$ on a platinum surface. The asterisk denotes a free site on the surface [141].

Ertl has shown[141] that, with the Pt(110) surface, when operated under strictly isothermic low-pressure conditions, the reaction rate for a narrow range of control parameters is not stationary but becomes oscillatory as found experimentally[144] (see Fig. 16). The variation of the work function $\Delta\Phi$ (which is proportional to the oxygen coverage, u_2), parallels the oscillatory reaction rate, as indeed does the partial pressure of CO. All this reflects the fact that, with this system, kinetic oscillations are confined to conditions under which adsorption of oxygen is rate-limiting. This observation holds the key for rationalizing the physical mechanism underlying these phenomena.

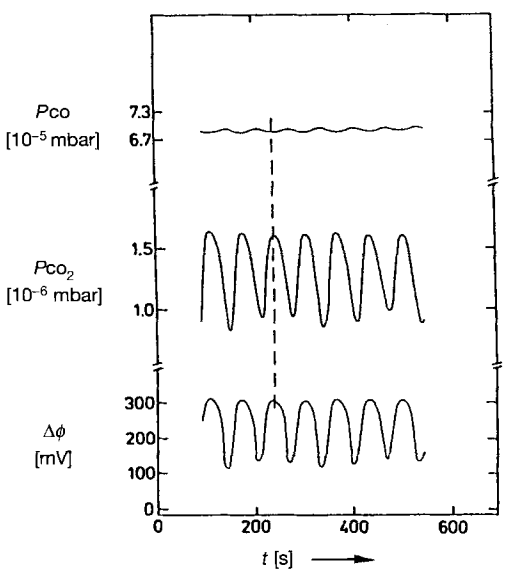


Fig. 16. Oscillatory kinetics with the catalytic CO oxidation at a Pt(110) surface. The recorded CO_2 partial pressure pCO_2 is proportional to the reaction rate; the work function change $\Delta\Phi$ parallels the oxygen coverage u_2. Temperature is 480 K, $pO_2 = 2.1 \times 10^{-4}$ mbar, and $pCO = 6.8 \times 10^{-5}$ mbar as in Figure 10 of ref. [141].

The clean Pt(110) surface does not possess the atomic structure that would correspond to the bulk termination (1×1 mesh as in Fig. 17) but is reconstructed into a 1×2 mesh with a "missing row" that is ostensibly energetically more stable. The heat of adsorption of CO on a 1×1 surface exceeds that on a 1×2 surface so that, as a consequence, a $1 \times 2 \rightarrow 1 \times 1$ transformation—brought about by homogeneous nucleation and

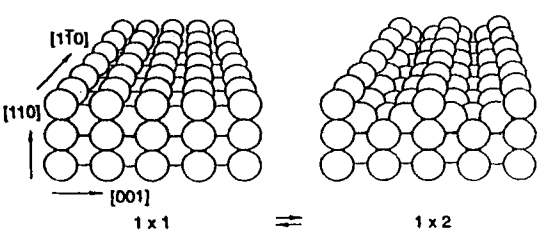


Fig. 17. The two structural modifications of the Pt(110) surface; see text and ref. [141].

minute but spontaneous local displacements of Pt atoms in the topmost layer[145]—takes place as soon as the CO coverage exceeds a critical value of about 0.2. The 1×1 surface exhibits a higher oxygen sticking coefficient than the 1×2 surface. Hence, for a narrow range of control parameters, the surface structure will continuously switch between states of low (1×2) and high (1×1) reactivity.

This is just one explanation for oscillatory phenomena in heterogeneous catalysis. The recent review by Schüth, Henry, and Schmidt,[137] which admirably summarizes over 300 publications dealing with oscillatory phenomena exhibited by a wide range of catalysts in many different forms (films, foils, powders, supported crystallites, and single crystals), gives other, equally valid qualitative and in many cases quantitative explanations for oscillatory reactions in heterogeneous catalysis. Concepts such as "strange" attractors and deterministic chaos, bifurcations, standing and travelling waves as well as turbulence are, it seems, an inherent feature of heterogeneous catalysis. Just as it is recognized for catalysis generally, there is probably no single mechanism that explains all known oscillatory behavior for every heterogeneous system so far studied.

In drawing this section to a close, one may, at the risk of grotesque oversimplification, enumerate some of the key summarizing statements pertaining to the behavior of solid heterogeneous catalysts as in Table 8.

Table 8. Some key generalizations.

In photocatalytic degradation and photocatalytic synthesis there is scope for considerable design by varying both the composition and the physical dimension of appropriate semiconductors.
Bifunctional catalysts, consisting of finely divided metals on oxide or sulfide supports, are of central importance in petrochemical, especially hydro-treating, processes.
Surface reconstructions can be both extensive and ubiquitous; and incommensurate overlayers are by no means rare.
Oscillatory kinetics and spatio-temporal phenomena are widespread in the realm of heterogeneous catalysis; and they encompass propagating or standing waves, bifurciations, determinative chaos and chemical turbulene.
Gross non-stoichiometry within the bulk and at the surfaces of mixed-valence solid catalysts, especially oxides, is of frequent occurrence.

5. Shape-Selective Catalysts

There is overwhelming evidence that molecular biologists and organic chemists concerned with the appreciation and design of biological catalysts are in a much more commanding position than those of us whose pursuits are devoted to the performance and the understanding of the inorganic catalyst.

5.1. Why Are Enzymologists and Immunologists So Well Placed?

Fifty years ago it seemed to Schwab,[146] and doubtless to all his contemporaries, that the complexity of biological catalysis could barely be properly described, let alone adequately explained. It was much easier, as his book revealed (see Fig. 4), to describe and to seek to explain how inorganic catalysts worked. Now, however, the situation is vastly different; and it is instructive for a physical chemist like me, interested in rationally designing inorganic, shape-selective catalysts functioning on principles that have more than a superficial kinship with enzymes and catalytic antibodies, to enquire why.

In a nutshell, it is because the nature of the catalytically active site and its immediate environment along with the geometry of the attachment of the reactant (substrate)[147] in an enzyme or an antibody is known to a high degree of precision. And this has arisen chiefly because of major advances in:

- the (crystal) structure determination of large numbers of enzymes (and an increasing number of antibodies[148–153]);
- the technique of site-specific mutagenesis and
- sophisticated kinetic studies of 'tailored' enzymes.

This has meant that the atomic detail of the active site and the manner in which it undergoes subtle changes upon uptake and conversion of a reactant, or as a result of the delicate modification (by mutagenesis) of the active site, is extraordinarily well appreciated. But enzymes as a class of catalyst are also more amenable to study by a panoply of available techniques and tools because of the convenient (if not anthropomorphic!) fact that chemical conversions occur within them at low temperatures (even at $-20\,^{\circ}C$), highly suited for in situ high-resolution X-ray crystallographic study.

But how has all this come about? A convenient place to begin our answer is by examining recent remarks by one of the founders of molecular biology, Max Perutz[154]:

> *In a Friday Evening Discourse at the Royal Institution in 1948, Linus Pauling said: "I think that enzymes are molecules that are complementary in structure to the activated complexes of the reactions that they catalyse, that is, the molecular configuration that is intermediate between the reacting substances and the products of the reaction".*
>
> *His prediction was borne out in 1965 by lysozyme, the first enzyme structure to be solved. That structure showed the transition state of the substrate to be stabilized by the strong electric field of two carboxylates on either side of the active site cleft. I generalized that finding with the statement: "We may now ask ourselves why chemical reactions, which normally require powerful organic solvents or strong acids and bases, can be made to proceed in aqueous solution near neutral pH in the presence of enzyme catalysts. Organic solvents have the advantage over water of providing a medium of low relative permitivity, in which strong electrical interactions between the reactants can take place. The non-polar interiors of enzymes provide the living cell with the equivalent of the organic solvents used by the chemists. The substrate may be drawn into a medium of low relative permitivity in which strong electrical interactions between it and specific polar groups of the enzyme can occur".*

Perutz's statement in the second half of the citation (taken from ref. [157]) extends well beyond the realm of electrostatics and their role in the catalytic conversion of organic reactants. The notion that the active site of an enzyme is complementary in character to the atomic detail of the activated complex of the reaction catalyzed carries echoes of Paul Ehrlich's proposition, almost a hundred years ago, and Emile Fischer's idea somewhat

later, of a "lock and key" fit between certain molecules. More relevant perhaps is the classic notion that enzymatic action hinges upon transition-state complementarity, a proposition first made by the polymathic English geneticist, J. B. S. Haldane in 1930[158] and then further extended by Linus Pauling (see above and in ref. [155]).

The structure of lysozyme,[156, 159] a proteolytic enzyme closely analogous in its mode of catalytic operation to a solid acid catalyst (see Section 5.6), contains a cleft—a well-defined cavity. Numerous structural determinations of enzymes done subsequently (about 300 in all) show that the cavity active site (which is often synonymous with a hydrophobic pocket) is a recurring structural motif in the architecture of their constitution.

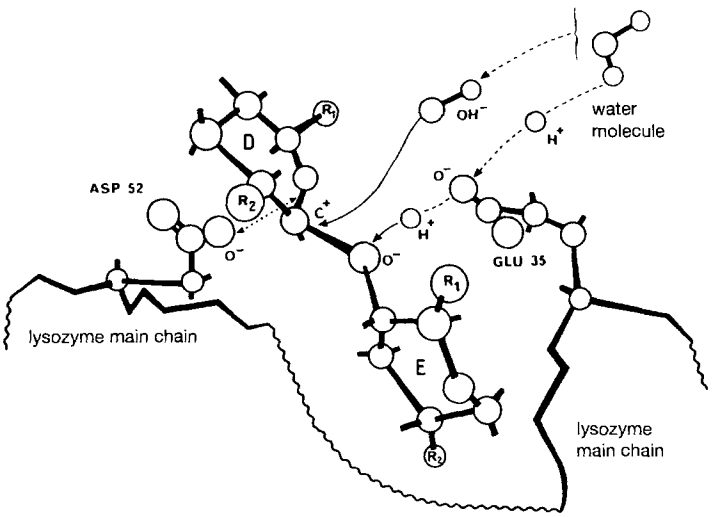


Fig. 19. Schematic illustration of the mechanism of the catalytic action of lysozyme derived from the crystallographic studies of Phillips et al. [156,159].

5.2. Shape-Selectivity in Biocatalysis

The cavity active site, so it has emerged from numerous detailed crystallographic and other structural studies (including NMR spectroscopy and mapping with fluorescence resonance energy transfer[160]), is also a characteristic of central functional importance throughout the immune system (and therefore a major determinant in antibody-antigen interaction[161, 162]) as well as in the behavior of ribozymes.[163]

Figure 18 is a computer graphic representation (to scale) of how a substrate molecule (a polysaccharide) is held as a "tortured victim" (to use Perutz's[154] phrase) inside the cavity active site of lysozyme. A clearer structural picture, based on Phillips' classical study,[156, 159] is shown in Figure 19. In the language of modern enzymology,[162] recognizing that it is a cardinal feature of enzymatic action for the enzyme to bind the substrate rather weakly but for the transition state to be appreciably stabilized by it, we expect there to be physical distortion (hence the torture) of the bound substrate at the cavity active site. The great triumph of X-ray crystallography, and a major turning point in enzymatic catalysis dating from Phillips' work, is that in situ structural studies with substrate and with a range of inhibitor molecules, directly revealed this distortion and, in so doing, suggested a mechanism for the enzyme's action. Catalysis of the hydrolysis of glycosides by lysozyme is brought about by stabilization of a planar, carbenium-ion-like transition state at the anomeric carbon atom for glycoside cleavage by the enzyme. This transition state is also stabilized by the electrostatic interaction between the carboxylate anion at the active site and the developing positive charge on the oxocarbenium ion in the transition state.

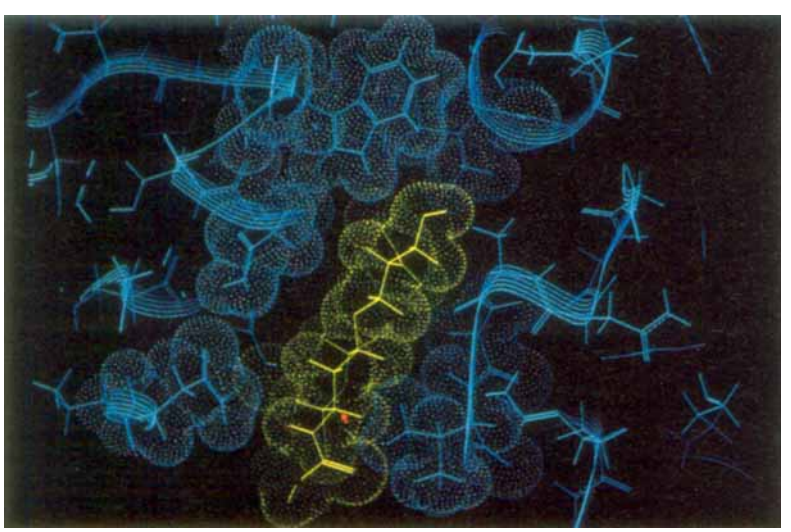


Fig. 18. Computer graphic representation of cavity active site in lysozyme. The polysaccharide (yellow) fits snugly into the hydrophobic pocket of the enzyme (see text). The dotted surfaces represent the surface of the molecule based on the van der Waals radii (prepared by C. M. Freeman, Biosym Inc., San Diego, based on data in [159]).

The elucidation of the mode of catalytic action of lysozyme serves as the archetype for all other proteolytic enzymes, and the majority of all enzymes. Thanks to site-selective mutagenesis, the critical amino acids lining the cavity active site can be precisely identified and the atoms within these fragments, in some instances, located to within a few tenths of an Ångstrom unit. More often than not, it is at a mere triad of amino acids—those that do indeed line the cavity and participate in general acid–base catalysis by the donation and acceptance of protons—where the whole competence of the catalysis resides.

Changing the surface charge of the cavity active site in enzymes by site-directed mutagenesis produces new variants with significantly different catalytic performance. For example, Russell and Fersht[164] were able, by this method, to shift the pH-activity profiles of the enzyme subtilisin, generate higher catalytic activities, and alter the specifities of the enzyme. Their work also afforded insight into the dielectric properties of water in the enzyme, the role of ions in electrostatic shielding and the high-field effects on catalysis. From all this they were able to suggest rules for tailoring pH-activity profiles in enzymatic catalysts.

Armed with site-selective mutagenesis and the consequential power to change the atomic structure of the cavity active site in an enzyme by the merest amount, the enzymologist is able to pinpoint the geometry and entire catalytic apparatus of the critical part of the enzyme in extraordinary

detail. In Knowles'[165] studies of the manner in which triosephosphate isomerase catalyzes the interconversion of the two triosephosphates, dihydroxyacetone phosphate (DHAP), and (*R*)-glyceraldehyde-3-phosphate (GAP) through the intermediate formation of *cis*-enediol, all the skills of structural and kinetic elucidation were brought to bear. A deeper understanding of the mode of catalytic action, to a degree that greatly surpasses what is understood about the mechanism of any reaction catalyzed by a solid inorganic catalyst, is thus achieved. From the crystal structures of the triosephosphate isomerases of both chicken and yeast, with either the substrate or a substrate analogue at the active site, it is clear that the basic catalytic group B^- (Fig. 20) is the oxygen atoms of the carboxylate of

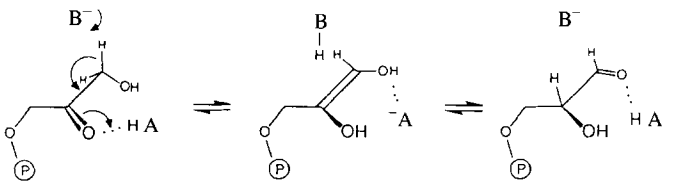


Fig. 20. The reaction catalyzed by triosephosphate isomerase. B is a basic catalytic group which abstracts the pro-(*R*) proton on the carbon of dihyroxyacetone phosphate (DHAP), assisted by an acidic catalytic group HA, to produce the intermediate enediol. This intermediate then collapses to give the product glyceraldehyde 3-phosphate (GAP) and regenerates the enzyme. The same enediol is produced by the enolization of DHAP or of GAP, and the overall reaction simply puts the two enolizations back-to-back (see ref. [165]).

Glu 165, since, in Knowles' words, they "are beautifully positioned for the proton abstraction required".[166] Indeed, when this group is moved by about 1 Å, as in the mutant enzyme where Glu 165 is changed to Asp, for which the structure (determined by X-ray crystallography) shows no other significant alterations, the catalytic power of the enzyme falls by nearly a thousandfold.[167] And when Glu 165 is completely removed and replaced by water, catalytic activity drops by more than a million times. Structural investigation of the crystalline triosephosphate isomerase and its bound substrate also reveal that the electrophile, the proton attached to A in DHAP, is histidine 95. The position of the imidazole ring (that contains the proton) with respect to the substrate being strategically placed for the donation.

Considerable advances[168] towards a detailed understanding of the catalytic mechanism of the zinc enzyme carbonic anhydrase[169] have been made very recently as a result of the application of crystallographic and kinetic methods to wild-type and mutant enzymes. The importance of directed hydrogen bonds for stabilizing the transition state of the catalyzed reaction and for inhibitor selectivity is here again particularly apparent. Thus histidine 64 (His 64) serves as an efficient proton shuttle between the metal center and buffer species (B/BH^+) in the reaction:

$$\begin{array}{ccccc} \text{E-Zn}^{2+}\text{-H}_2\text{O} & \rightleftharpoons & \text{E-Zn}^{2+}\text{-OH}^- & \overset{\text{B}}{\underset{\text{BH}^+}{\rightleftharpoons}} & \text{E-Zn}^{2+}\text{-OH}^- \\ | & & | & & | \\ \text{His} & & \text{His-H}^+ & & \text{His} \end{array}$$

Moreover detailed analysis reveals that His 62, His 67, and His 200, but not His 65, can function as proton shuttles but do so much less efficiently than His 64. The conclusion is inevitable: not only does His 64 have a favorable location providing facile proton transfer pathway but also a physico-chemical environment leading to appropriate acid–base properties.[168] (Just to emphasize the value of spectroscopic as well as crystallographic techniques in elucidating biological catalysis, Krebs et al.[170] were able to observe bound CO_2 by IR spectroscopy.[171])

Looking back, therefore, at the turning point that came with Phillips's work on lysozyme and at the course of events in enzymology subsequently, we may identify some key messages about biocatalysis. Effective enzymatic action entails:

1) accommodating the substrate (reactant) in a stereochemically precise fashion, governed by shape and distances, within the hydrophobic pocket (cavity active site); and
2) having just the right acid–base properties —that is, right pK values and requisite location—as between the lining of the pocket and the bound substrate.

To some degree these desiderata are mirrored in solid acid catalysts of the molecular-sieve kind described in Section 5.5.

5.3. Catalytic Antibodies

But it is not only enzymes that convey significant messages to those of us interested in inorganic shape-selective catalysis, catalytic antibodies do so also. It is a fundamental feature of the immune system that high-specificity binding sites are created spontaneously within the immunoglobin (antibody) protein to eliminate foreign invaders (antigens). The remarkable fact is that the binding sites of the antibody are effectively programmable. The immune system creates within the folds of the polypeptides (immunoglobins) cavity active sites that can recognize a vast array of chemically different invading molecules: each antigen stimulates a specific binding site in the antibody.[161, 173] With the development of *monoclonal antibodies* and genetic engineering techniques antibody catalysts, the creation of which certainly signifies a turning point, are now poised to make major contributions in organic chemistry, biotechnology and medicine, and especially in:

1) Assembling catalysts for disfavored chemical reactions.
2) Devising highly regio- and stereospecific catalysts for the synthesis of enantiomerically pure compounds.
3) The development of catalysts for highly stereoselective proton transfers.

The strategy each time is to choose the right starter molecule, the so-called hapten, to generate an antibody with the appropriate disposition of catalytic groups. The whole philosophy behind catalytic antibodies is that an antibody raised against a transition state will bind it, and thus be a catalyst for the reaction that passes through that state. The haptens are effectively the transition state analogues.

Enzymes and antibodies are self-evidently biological catalysts. In enzymes, molecular evolution over aeons of time has yielded the cavity active site; in the antibodies, because the immune system is 'programmable', the binding site has been forcibly created in a very short time span by the hapten. There

is a third kind of fashioned molecular catalyst, the artificial miniature enzyme (enzyme mimetica) which we consider next.

5.4. Miniature, Artificial Enzymes

In 1985, Bender et al.[174] published a paper of compelling pedagogic elegance describing how, with the aid of a β-cyclodextrin, they assembled a miniature, artificial enzyme, the catalytic performance of which rivalled that of the parent, chymotrypsin, which it mimicked. Chymotrypsin itself is a large (MW 24800 Da) and complicated (245 amino acids) enzyme, the function of which is to catalyze the hydrolysis of a variety of esters and amides. From an X-ray analysis of its structure, the constituents of its active site—the lining of the hydrophobic pocket—were determined. These are an imidazolyl group, a carboxylate group, and a hydroxyl group. These were grafted by Bender et al.[174] in the correct sequence on to the rim of the β-cyclodextrin, which serves as the binding site (Fig. 21).

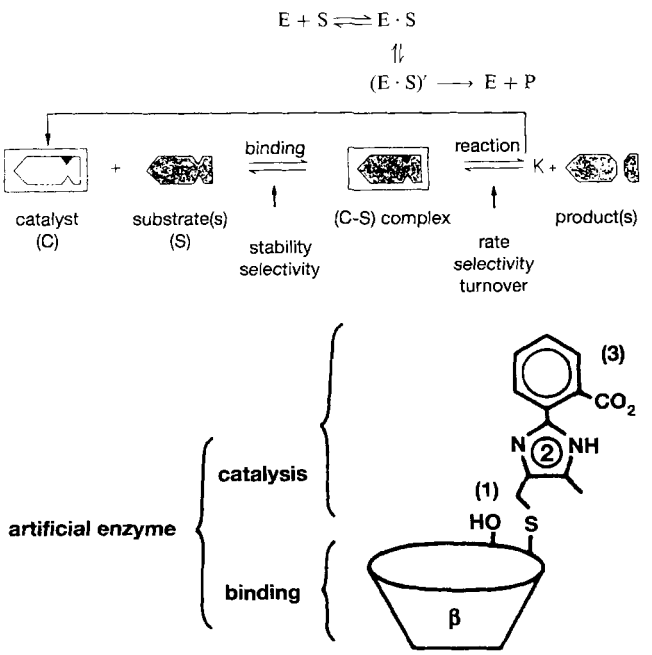
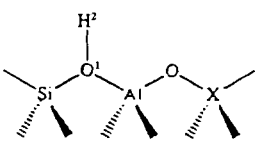


Fig. 21. Top: Schematic representation of the enzymatic process. The enzyme E processes the substrate (reactant) S into product P via the transition state E·S (after Lehn). Bottom: Strategy for the construction of an artificial chymotrypsin (miniature enzyme), based on cyclodextrin (see text; after ref. [174a]).

The artificial chymotrypsin has a relative molecular weight of only 1365, yet the real and artificial enzyme have approximately the same catalytic activity. The development of this miniature enzyme is an example of *supramolecular chemistry*, an area in which Jean-Marie Lehn has played a leading role. The nub of the message is that a sizeable molecular entity, which is nevertheless very much smaller in size and complexity than the natural enzyme, can be so fashioned as to mimic the catalytic performance of the enzyme. It is to be noted that there is a created cavity as well as a created and strategically located Brønsted acid site in this artificial enzyme.[174b]

5.5. Shape-Selective Inorganic Catalysts: Not only Interesting, but also Important

As well as being a crucial determinant of the catalytic performance of enzymes and abzymes (catalytic antibodies), shape-selectivity is also a key feature of molecular-sieve inorganic catalysts described briefly earlier (Sections 2 and 3.1). They are examples of *uniform heterogeneous catalysts*, in the sense previously outlined, and they represent one of the most rapidly growing categories of inorganic catalyst. The dimensions of the pores of the particular molecular sieve under consideration govern the size and shape of the reactant molecules that may enter it, the product molecules that may leave it, and the nature of the reactive intermediates that can form within it. Molecular-sieve solids, typefied by zeolites, are very high-area catalysts (typically 400–500 m^2g^{-1}), with over 99%, depending upon crystallite size, of the surface area inside the bulk. An acidic zeolite such as H^+-ZSM-5[133, 175] may be viewed as a three-dimensional network of corner-sharing SiO_4 tetrahedra, the spaces between these forming molecular-scale micropores of variable shape and dimension dependent upon the precise architecture. A few silicon ions, about one in ten to one in fifty, are replaced by aluminum ions (i.e. AlO_4 replace SiO_4 tetrahedra) and protons are required locally for electroneutrality. The protons are localized at one of the four oxygen atoms of the AlO_4 tetrahedron forming bridging hydroxyl groups. These Brønsted sites, sketched in Scheme 1, have been established to be active in a wide range of catalytic conversions of alkanes, alkenes, and alkanols.



Scheme 1. X = Si, P.

A striking example of the efficacy of solid acid molecular-sieve catalysts is shown in Figures 22 and 23. In Figure 22 the work of Le Bel in France in 1880 on the $ZnCl_2$-assisted dehydration of methanol is set alongside that of the shape-selective catalysis reported by the Mobil Research group nearly a hundred years later. One notes that, with H^+-ZSM-5, no polynuclear aromatic can be formed because the pore dimension (diameter ca. 5.5 Å) does not permit it. Contrast the distribution of products with another molecular-sieve catalyst, mordenite, the pores of which are large enough (diameter ca. 7.5 Å) to accommodate naphthalene and other polynuclear arenes.

Inorganic molecular-sieve catalysts with built-in shape selectivity are of great fundamental interest for a variety of reasons:

1) Microporous microcrystalline catalysts based on the naturally occurring zeolites[19, 20, 176]—an enormously large and growing family— form an open network possessing a porosity such that 30–50% of the solid is void space. About a quarter of the elements of the periodic table can now be incorporated into the framework structure of this kind of solid.
2) By controlling, during or after synthesis, the number of heteroatoms in the framework, finely adjustable concentrations of active sites may be placed, in a spatially uniform fashion, within the inner surface of the catalyst.
3) The precise location and environment of the active sites—be it a proton loosely attached to a framework oxygen, or a

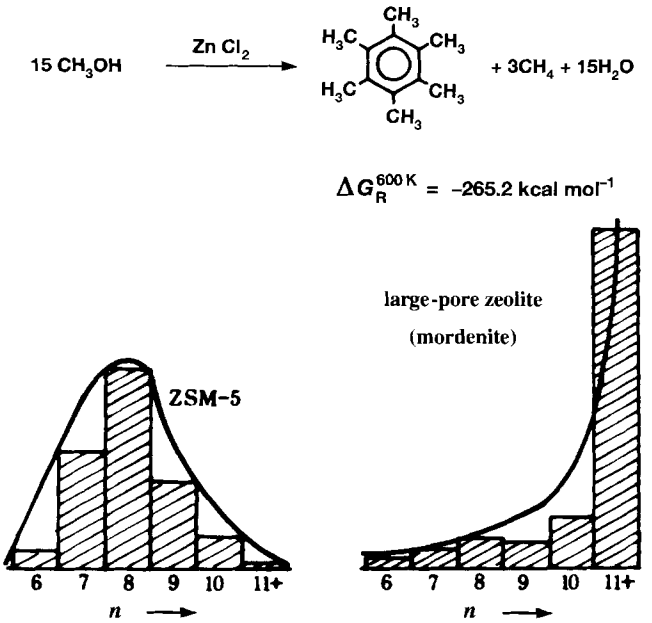


Fig. 22. It has long been known that the dehydration of methanol yields interesting hydrocarbons. Le Bel and Greene, in 1880, using molten $ZnCl_2$, produced hexamethylbenzene this way, along with a soup of other products. With the shape-selective solid acid H^+-ZSM-5, benzene, toluene, and xylene (important constituents of petrol) are among the principal products. With larger pore, molecular-sieve acid catalysts such as mordenite, polynuclear aromatics are also formed.

redox element such as titanium—can be determined experimentally.

4) In situ studies of bound reactants (or inhibitors) within the channels and cavities of the catalysts may be quantitatively followed by IR spectroscopy,[177–179] solid-state NMR,[180–182] X-ray diffraction,[72, 183] X-ray absorption and fluorescence,[60, 184, 185] neutron-scattering,[186, 187] and a range of other techniques (see Table 6).
5) Computational methods[188–194] are very productive and revealing for such catalysts, partly because of the power of quantum chemical techniques allied to classical methods of lattice-energy minimization.

Details are given elsewhere of the considerable progress in deepening our understanding of such factors as catalyst activation;[75] catalytic selectivities,[195] diffusivities and binding energies[50] of reactants and products in molecular sieves, as well

Table 9. Several innovations in applied catalysis since 1980. All processes marked with an asterisk utilize crystalline molecular-sieve catalysts.

Process	Catalyst
1980–1989	
conversion of ethene and benzene to ethyl benzene*	H^+-ZSM-5
methanol to gasoline (petrol)*	H^+-ZSM-5
conversion of ethene and acetic acid to vinyl acetate	Pd
oxidation of *tert*-butyl alcohol to methylmethacrylate	Mo oxides
improved means of liquefying coal	Co, Ni sulfides
production of diesel fuel from CO + H_2 (syngas)	Co
hydrotreating of hydrocarbons*	Pt/zeolite Ni/zeolite H^+ ferrierite
catalytic distillation (in methyl tertiary butyl ether (MTBE) production)	acidic ion exchange resins
vitamin K_4 production	Pd membrane
dehydrocyclization ('Cyclar') of alkanes* conversion of light alkanes to aromatics*	Ga-ZSM5
oxidation of methacrolein hydration of isobutene	Mo-V-P heteropolyacid
polymerization of tetrahydrofuran	phase-transfer catalysis
1990–1993	
production of dimethyl carbonate from acetone	CuCl
conversion of phenol to hydroquinone and catechol*	Ti-silicalite
isomerization of but-1-ene to 2-methylpropene*	H-ferrierite, H-Theta-1 (acidic zeolites)
isomerization of oxime of cyclohexanone to ε-caprolactam*	silico-alumino-phosphate molecular sieve (SAPO-11)
ammoxidation of cyclohexanone to its oxime using H_2O_2*	Ti-silicalite
production of acrylamide from vinyl cyanide	immobilized nitrile hydratase
complete combustion of natural gas (at ca. 1300 °C)	noble metals and/or mixed oxides
'sweetening' of natural gas by selective oxidation of H_2S to S	mixed oxides
oxidation of benzene to phenol via cyclohexene*	zeolites
methanol to light alkenes*	silico-alumino-phosphate molecular sieve
olefin oligomerization ("Shell" polygasoline and kerosene process)*	zeolite
production of L-aspartic acid and L-analine from NH_4 fumarate	immobilized micro-organisms
conversion of toluene to toluene *cis*-1,2-dihydroxy-3-methylbenzene	*Pseudomonas putida*
production of 2,6-diisopropylnaphthalene using propene as alkylating agent*	acidic zeolite (mordenite)
decomposition of hypochlorite	NiO
dehydration of alkanols	heteropolyacid salts

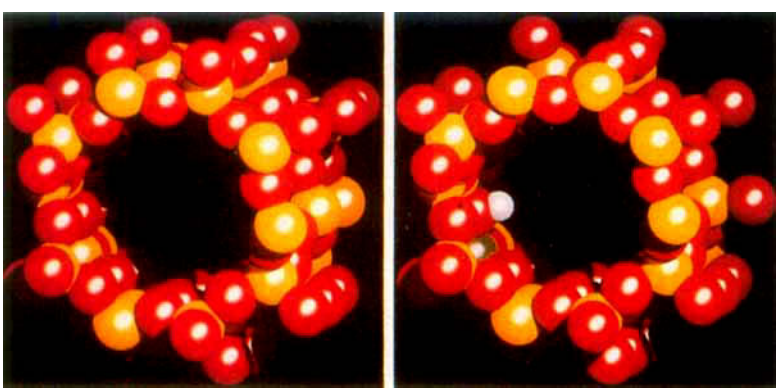


Fig. 23. Scalar representation (left) of the pure, siliceous molecular sieve known as silicalite (SiO_2) the pore diameter of which, as in ZSM-5 (right) is 5.5 Å. H^+-ZSM-5 is a protonated form of the siliceous analogue but with one in ten to one in fifty or so of the silicon atoms in the framework replaced by aluminum atoms. There is one proton loosely attached to framework oxygen atoms for every Al^{3+} ion (or rather trivalent ion such as Fe^{3+}) that substitutes for a Si^{4+}. See also Figures 5 and 24.

as descriptions of fundamentally new types of catalyst structures—some of which can be determined only by a stochastic combination[196] of interlocking techniques such as X-ray powder diffraction, high-resolution electron microscopy,[197, 198] and energy minimization procedures[194] using appropriate interatomic potentials.[199]

Zeolite and related solids now play a very significant role in industrial catalytic processes as may be gleaned from Table 9, where it is seen that a substantial fraction of the innovations in applied catalysis in recent years are based on molecular-sieve catalysts.[18]

5.6. Solid Acid Catalysts and Clean Technology

Clean technology[33] nowadays provides the stimulus for a multitude of new developments and initiatives in applied catalysis, not the least important of which is the growing environmental concern about the use of corrosive liquid acids (such as hydrofluoric acid and 96 percent sulfuric acid) as catalysts for the alkylations or isomerizations of hydrocarbons. Selective and active solid acids are therefore attractive as replacements; and the ever-growing family of molecular-sieve catalysts, with strong proton-donating sites distributed uniformly within the pores and cavities, offer a promising range of viable alternatives.[200–203]

Apart from the substantial family of aluminosilicate zeolitic acids (typefied by H^+-ZSM-5, HY, H-mordenite), the large family of microporous aluminum phosphates[200–205] (ALPOs, signifying $AlPO_4$ polymorphs in a wide range of open tetrahedral network structures) can be controllably modified, usually at synthesis, so as to yield acid SAPOs or acid MAPOs. In a SAPO, silicon atoms replace some of the phosphorus atoms (in tetrahedral coordination) thereby yielding $H[AlP(Si)]O_4$, whereas in the MAPOs, a divalent element M, typically Mg, Zn, Mn, Co, etc, replaces aluminum atoms, giving $H^+[Al(M)P(Si)]O_4$ (metal aluminum phosphate silicate). In a MAPO, such as the fascinating, double-barrelled so-called DAF-1 structure,[206] a divalent atom (Mg) replaces Al. DAF-1 is a very strong solid (Brønsted) acid and has a framework composition $Mg_{0.22}Al_{0.78}PO_4$, the counterbalancing ions being protons loosely bound to the framework oxygen atoms. SAPO-18,[207] on the other hand has a framework composition of typically one silicon per twenty tetrahedral sites. MAPO-18, with M = Mg, Zn, Co, has recently been shown to be highly efficient in converting methanol to mixtures of ethene and propene (Table 10).[208]

Fundamental studies, both experimental and theoretical, of the origins of Brønsted acidity in solid acid catalysts and the nature of the reactive intermediates formed when alkanes are converted by them in processes such as isomerization or cracking, have intensified[209–212] in recent years. It is becoming increasingly apparent from analyses on materials of identical stoichiometry but different framework structures (such as H^+ faujasite and H^+-ZSM-5) that the difference in value of the proton affinity for the bridging hydroxyl oxygen atom,[191] (Fig. 24), and the next oxygen atom is the key to determining the Brønsted acidity of these catalysts. Hydrogen–deuterium exchange reactions, along with dehydrogenation and cracking of

Table 10. Catalytic performance of MAPO-18 (Me = Zn, Co, Mg) for methanol conversion (time on stream: ca. 10 minutues; WHSV = 1.5 h^{-1}) [208] [a].

Catalyst	T [°C]	Methanol conversion [%]	Distribution of products $(CH_3)_2O$	CH_4	C_2H_4	C_3H_6	C_{4+}
	250	31	100	0	0	0	0
ZnAPO-18	300	70	96.4	0.2	0.5	2.1	0
	250	100	0	0.3	17.9	50.7	30.8
	400	100	0	0.3	24.9	46.6	27.5
	250	39	100	0	0	0	0
CoAPO-18	300	87	63.8	1.6	4.6	18.4	11.5
	350	100	0	0.3	14.9	51.8	32.5
	400	100	0	0.3	22.4	51.2	25.6
	250	31	100	0	0	0	0
MgAPO-18	300	88	35.5	1.6	7.2	34.2	21.7
	350	100	0	0.3	13.0	51.0	35.1
	400	100	0	0.3	20.1	49.6	29.7

[a] WHSV = weight hourly space velocity; C_{4+} = higher hydrocarbons.

n-alkanes on Brønsted acid zeolitic catalysts point to the dominance of pentacoordinated carbocations (carbonium ions) as the crucial intermediates for monomolecular conversions of alkanes.[212]

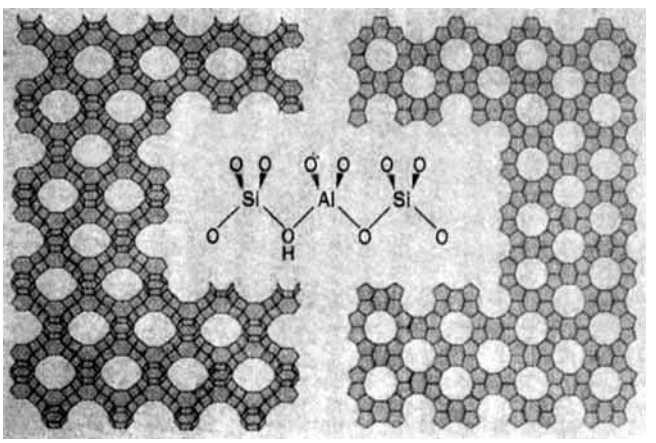
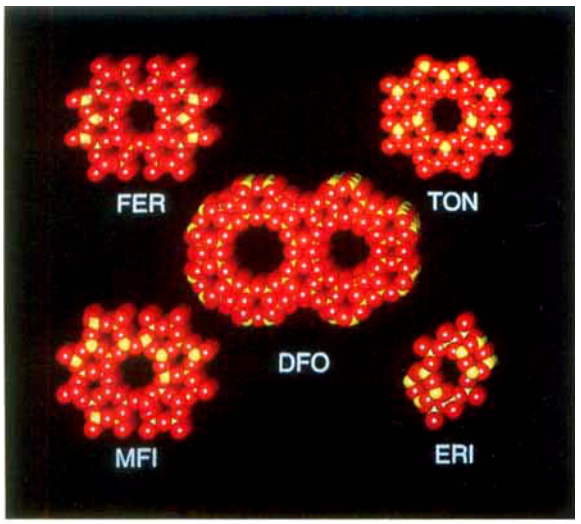


Fig. 24. The acidity of the zeolite catalysts originate from bridging hydroxyl groups (see formula in the center). Zeolite-Y (which has the same framework structure as the mineral faujasite) (left), and ZSM-5 (right) are different structural forms, but can be synthesized with identical compositions. But even with exactly the same number of active sites (Brønsted acid centers as in Fig. 23) they exhibit different catalytic activities. This is because of differences in the proton affinities of bridging hydroxyl oxygen atoms in their framework (see text and refs. [191, 192]).

Given the wide (and subtle) variety of molecular-sieve solids upon which Brønsted acidity may be conveniently conferred,[203, 213, 214] instructive catalytic comparisons may be made between a suitable subset of solid acid catalysts ranging from aluminosilicates to MALPOs (see Fig. 25) using an important isomerization as a probe: the conversion of but-1-ene to 2-methylpropene.[213, 215] (There are powerful factors, again related to "clean technology", why the quest for catalysts for this reaction is so important, see also ref. [216].)

The framework of inorganic molecular sieves of the type discussed here is remarkably flexible: even though these solids do not collapse until very high temperatures are reached, they quiver like a jelly—this was established from ^{29}Si solid-state NMR spectroscopy and molecular dynamics simulation[16, 51]



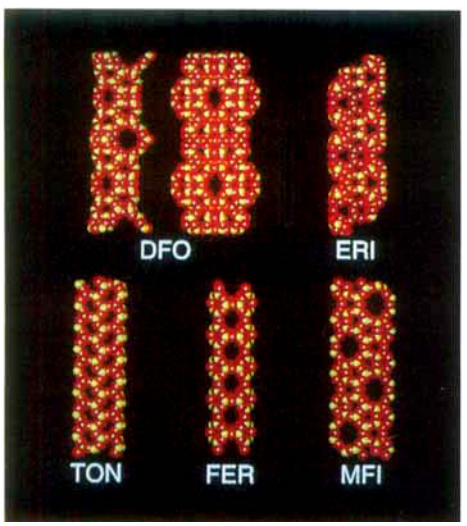


Fig. 25. Plan view (top) and elevation (bottom) of five distinct types of shape-selective molecular-sieve solids that function as solid acid catalysts for the skeletal isomerization of but-1-ene. FER ≡ H^+-ferrierite, TON ≡ H^+ = Theta one, MFI ≡ H^+-ZSM-5 (Mobil five), ERI ≡ H^+-erionite, and DFO ≡ H^+Davy-Faraday One. (DFO (DAF-1) has two distinct kinds of pores [206].)

(Fig. 26) at liquid nitrogen temperature. Using a blend of Monte Carlo and molecular dynamics calculations,[195] we compared the mobility and the binding energy of all four isomers of butene (Fig. 27) inside ZSM-5 and Theta-1, a zeolitic catalyst discovered[217] at the British Petroleum Company. We found that it is much easier for 2-methylpropene than for any of the three other isomers to be released from both these two catalysts. Taking account of spatial considerations, we would expect undesirable by-products—that is, unneeded dimers—to form in the larger cavities where channels intersect. We therefore predicted Theta-1 would be superior to ZSM-5 for the isomerization of but-1-ene to 2-methylpropene (Fig. 28). Our predictions proved true;[213]

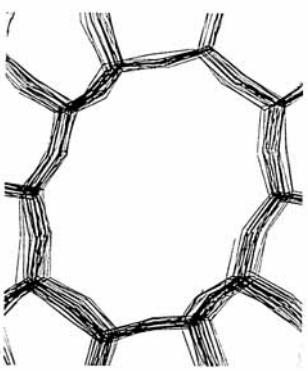


Fig. 26. Superimposed snapshots of a portion of a molecular dynamics simulation of the silicalite framework indicating the degree of structural flexibility [217].

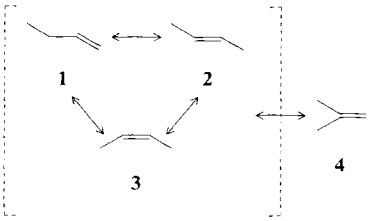


Fig. 27. The four isomers of butene. But-1-ene (**1**) is plentifully available from catalytic oil crackers. 2-methylpropene (**4**) is the desirable product as it may be converted, over another solid acid catalyst, to methyl tertiary butyl ether (MTBE), a replacement for lead-containing constituents of petrol.

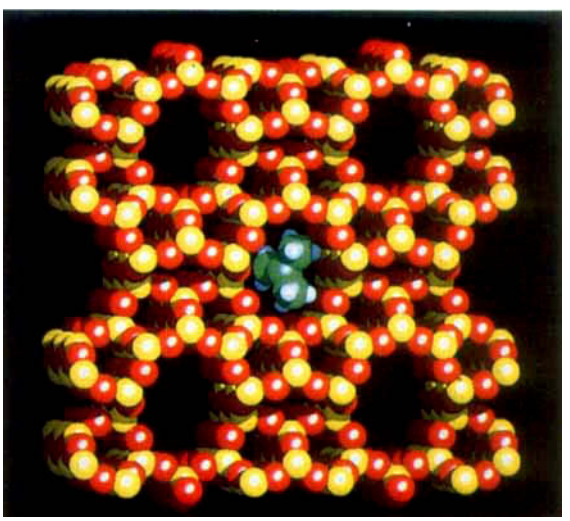


Fig. 28. Using an automated method [195] of blending energy-minimization procedures and Monte Carlo and molecular dynamics calculations it is possible to predict that Theta-1, and other similar molecular sieves with non-intersecting pore structures such as ferrierite, are superior catalysts for the isomerization of but-1-ene to 2-methylpropene than ZSM-5, which has intersecting pores. A 2-methylpropene molecule, shown here in one of the pores of Theta-1, is less strongly bound by, and diffuses more readily out of, the catalyst than any of the other three isomers [33]. (see also Fig. 27).

and they would be equally valid for ferrierite. (We now know [218] that the Shell Company is using H^+ ferrierite and that the BP and Mobil Companies are using H^+ Theta-1 as the basis of their pilot plants for the large-scale production of 2-methylpropene as the precursor for production of methyl tertiary butyl ether (MTBE), that boosts octane rating of (and which dispenses with the need for environmentally harmful lead-containing additives in) petrol.

Less sophisticated computations and modeling suffice to reveal that, in the design of a new solid acid catalyst for the

formation of a valuable precursor for a wide range of polymers and liquid crystals, 2,6-diisopropylnaphthalene (from naphthalene and propene), H^+-mordenite is the catalyst of choice. This is elegantly illustrated in the work of Cusumano et al.,[219] (Fig. 29).

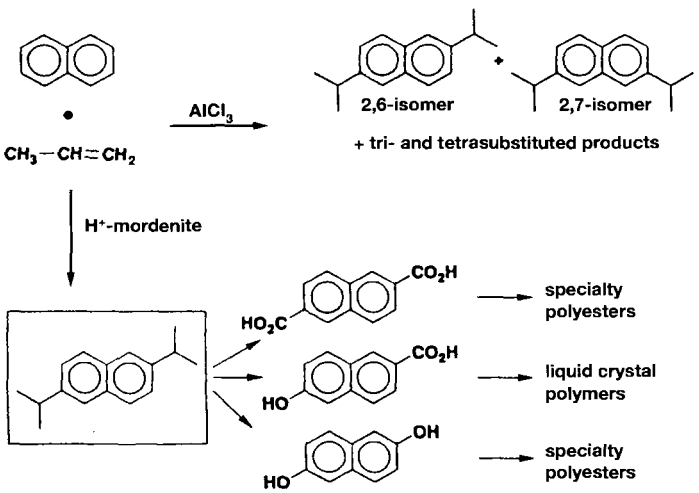


Fig. 29. When naphthalene is alkylated by propene in the presence of aluminum trichloride catalyst, a mixture of the 2,6- and 2,7-diisopropylnaphthalene isomers as well as many tri- and tetrasubstituted naphthalenes is produced. Cusumano [219] has shown that there is overwhelming preference for the 2,6-diisopropyl derivative when H^+-mordenite is used as the acid catalyst, the shape-selectivity of this catalyst being illustrated here.

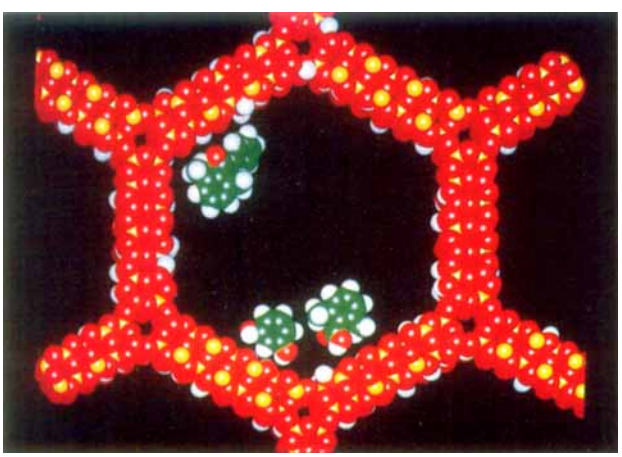
This design strategy for the selection of an optimal catalyst from an already available set of potential molecular-sieve, uniform heterogeneous catalysts or the creation (first on computer and then in the laboratory!) of an altogether new one is likely to gain pace in the near future. As ever, the technical virtuosity of the preparative chemist, now nourished by the input of modeling and computation, will reap rewards. The good news for catalyst engineers in this context as it is for the enzyme designer "is that proper placement of appropriate groups in the right environment seems to be enough".[165] One may now, with optimism, look forward to the day when the degree of prior control required for tailor-made catalysts, such as the water-soluble homogeneous ones now in commercial use[221] for hydrogenation and hydroformylation, will also be achievable with molecular-sieve heterogeneous catalysts. Indeed, as Kirill Zamaraev and I have shown elsewhere[4] there are already industrially demonstrated successes in this regard.

There are definite indications that very many novel microporous solids[220]—like the molecular-sieve cobalt phosphate,[222] or the MCM large-pore structures recently prepared by Beck et al[223] and Stucky et al.,[224] (see Fig. 30) and already used so imaginatively by van Bekkum et al.,[225]—will appear in the near future, providing yet further likely turning points.

In concluding my ruminations here in France, I cannot but reflect the sentiment with which, I believe, everyone would agree, namely that firm and sturdy foundations have been laid for the growth of heterogeneous catalysis (see Fig. 31). There is only one way to go now: upwards!



Fig. 31. A postcard showing the Eiffel Tower under construction. Copyright: Collection Viollet, 1988 (Editions Gerndre, 65 Boulevard Masséna, F-75013 Paris).



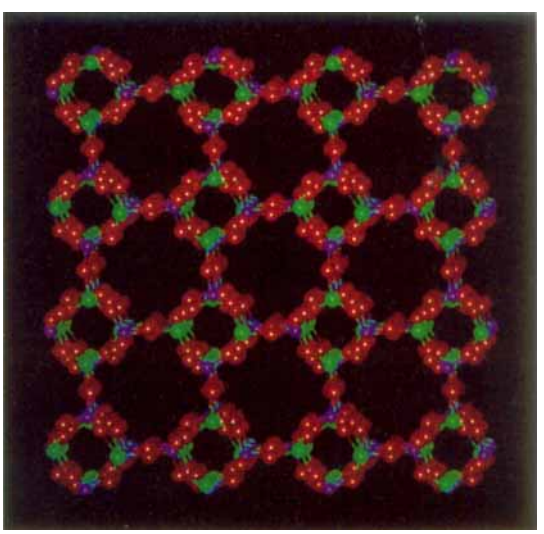


Fig. 30. Left: Graphic illustration of how van Bekkum et al. [225] have used individual members of the newly developed families of large-pore (20 to 50 Å diameter) microcrystalline siliceous solids [222,223] to inject shape-selectivity into organic processes such as the Fries reaction. This hexagonal pore of 31 Å diameter houses various functionalized arenes some of which are initially anchored by pendant Si–OH groups to the walls of the pore (2,6-dimethylbenzoic acid and resorcinol which, by Fries reaction yields a benzophenone derivative). Right: DAF-2 (Davy–Faraday 2) is a recently designed molecular sieve in which the tetrahedral bonded ions of the framework are cobalt (green) and phosphorus (purple) in 1:1 ratio (red: oxygen) [222].

I am grateful to all my colleagues here and to collaborators from other laboratories for their continued cooperation and enthusiasm. Almost all the work bearing my name that is reported in this review was the result of SERC rolling grants.

Received: December 22, 1993. [A 441E]
German version: *Angew. Chem.* **1994**, *106*, 963

[1] Consider how our understanding of the mode of action of biological catalysts was revolutionized by two seemingly trivial discoveries. The first of these, made by the American biochemists J. B. Sumner (in 1926) and J. H. Northrup (in 1931), that enzymes could be crystallized: the second, made in 1934 by Dorothy Crowfoot (as she then was) and J. D. Bernal in England, that crystals of enzymes (notably pepsin) give rise to a glittering profusion of sharp X-ray diffraction spots. These discoveries meant that no longer could the view be sustained, popular until then, that enzymes were a mixture of convoluted macromolecules of variable length, assembled spaghetti-like to yield colloidal dispersions. These two phenomena implied that molecules of enzymes, however complicated, have an extremely well-defined structure, otherwise they would not self-assemble to form a crystal; moreover, the diffraction spots gave the clue, later brilliantly exploited, that the structure, and hence the active site as well as the mode of operation, of an enzyme could be deduced from X-ray crystal analysis. Consider also the simple phase changes that lie at the heart of the humble cloud and bubble chambers and the absolutely pivotal role that they have played in cosmic ray and particle physics.

[2] The intensity and nature of this so-called commercial pressure varies with the passage of time. In one era, the need to produce sulfuric acid or ammonia may stimulate invention or innovation in a given direction. In other eras, production of fuel, fertilizers, foodstuffs, fabrics, or pharmaceuticals lead us to new and hitherto unexplored pastures. These days, environmental issues loom large and there are increasing demands for better catalysts to create a cleaner world [3,4].

[3] L. E. Manzer, *Chem. Sustainable Dev.* **1993**, *1*, 147.

[4] J. M. Thomas, K. I. Zamaraev, *Angew. Chem.* **1994**, *106*, 316; *Angew. Chem. Int. Ed. Engl.* **1994**, *33*, 308.

[5] During the first thirty or so years of the post-phlogiston era several examples of catalytic reactions were discovered or re-examined. These encompassed both homogeneous and heterogeneous reactions. And among the former, the Clément and Desormes mechanism for the manufacture of sulfuric acid by the land chamber process was reported in 1806, and Kirchhoff's investigation of the conversion of starch to sugar by dilute acid in 1814. Dutch chemists studied the catalytic dehydration of alcohol to ethylene as early as 1796, and Thenard's detailed examination of the abilities of five different heated metals to decompose ammonia was published in 1813. Of the metals he studied, iron proved the most effective and platinum the least. It was about 1910 before iron was found (by researchers at BASF) to be the most efficient catalyst for the synthesis of ammonia.

[6] News of Döbereiner's discovery reached England through the French mathematician and physicist, Hachette who wrote to Michael Faraday. Faraday's notebooks (kept at the Royal Institution) contain an entry on 27 September 1823 showing that he verified Döbereiner's discovery. Faraday, with his characteristic thoroughness [8], demonstrated that air was essential to the glowing of the platinum and proved that the powder had the ability to take up hydrogen.

[7] P. Collins, Ambix, **1976**, *23*, 96.

[8] J. M. Thomas, *Michael Faraday and The Royal Institution: The Genius of Man and Place*, Adam Hilger, **1991**.

[9] W. Prandtl, *Deutsche Chemiker in der ersten Hälfte des neunzehnten Jahrhunderts*, Verlag Chemie, Weinheim, **1956**, p. 49.

[10] When urged by the owner of Wallsend Colliery to take out a patent to protect his invention of the miners' safety lamp which would have yielded a large income, Humphry Davy replied to him thus: "*My good friend, I never thought of such a thing; my sole object was to serve the cause of humanity; and if I have succeeded, I am amply rewarded in the gratifying reflection of having done so...*".

[11] J. Schiff, *Unveröffentlichter chemische Dokumente aus dem Goethe- und Schiller -Archiv in Weimar (Chem. Ztg.* **1923**, *47*, 385).

[12] Editorial note: The first comprehensive biography on Fritz Haber has recently been published: D. Stolzenberg, *Fritz Haber*, VCH, Weinheim, **1994**.

[13] R. Schlögl, *Angew. Chem.* **1993**, *105*, 402; *Angew. Chem. Int. Ed. Engl.* **1993**, *32*, 381.

[14] J. M. Thomas, *Angew. Chem.* **1988**, *100*, 1735; *Angew. Chem. Int. Ed. Engl.* **1988**, *27*, 1673.

[15] J. M. Thomas, *Angew. Chem. Adv. Mater.* **1989**, *101*, 1105; *Angew. Chem. Int. Ed. Engl. Adv. Mater.* **1989**, *28*, 1079.

[16] J. M. Thomas, *Philos. Trans. R. Soc. London A.* **1990**, *333*, 173.

[17] *Catalysis: An Integrated Approach to Homogeneous, Heterogeneous and Industrial Catalysis*, (Eds.: J. A. Moulijn, P. W. N. M. van Leeuwen, R. A. van Santen), Elsevier, Amsterdam, **1993**.

[18] J. M. Thomas, W. J. Thomas, *Principles and Practice of Heterogeneous Catalysis*, VCH, Weinheim, **1995**, in press.

[19] R. M. Barrer, *Zeolites and Clay Minerals*, Academic Press, London, **1978**.

[20] D. W. Breck, *Zeolite Molecular Sieves: Structure, Chemistry and Use*, Wiley, New York, **1974**.

[21] J. A. Rabo, *Actes Congr. Int. Catal. 2nd, 1960*, **1961**, 2055.

[22] P. B. Weisz, *Proc. Int. Congr. Catal. 7th*, Tokyo, **1980**, 1.

[23] W. O. Haag, R. M. Lago, P. B. Weisz, *Nature* **1984**, *309*, 589.

[24] E. G. Derouane in *Intercalation Chemistry* (Eds.: A. J. Jacobsen, M. S. Whittingham), Ch. 1, Academic Press, New York, **1982**.

[25] H. Sinn, W. Kaminsky, *Adv. Organomet. Chem.* **1980**, *19*, 99.

[26] W. Kaminsky, K. Külpen, F. R. W. P. Wild, H. H. Brintzinger, *Angew. Chem.* 1985, 97, 507; *Angew. Chem. Int. Ed. Engl.* **1985**, *24*, 507.

[27] E. Katchalski-Katzir, *Trends Biotechnol.* **1993**, *11*, 471.

[28] R. A. Wisdom, P. Dunnill, M. D. Lilly, A. Macral, *Enzyme Microb. Technol.* **1984**, *6*, 443.

[29] R. Noyori in *Modern Synthetic Methods, vol. 5*, (Ed.: R. Scheffold), Springer, Heidelberg, **1989**, p.1.

[30] a) R. A. Johnson, K. B. Sharpless in *Comprehensive Organic Synthesis, vol. 9* (Eds.: B. M. Trost, I. Fleming), Pergamon, New York, **1991**, p. 389; b) J. P. Collman, X. Zhang, V. J. Lee, E. Uffelman, J. I. Brauman, *Science*, **1993**, *261*, 1404; c) recent review: *Catalytic Asymmetric Snythesis* (Ed.: I. Ojima), VCH, New York, **1994**.

[31] G. K. Boreskov, *SU-B*, 826791, **1981**.

[32] G. K. Boreskov, E. A. Levitskii, Z. R. Ismagilov, *Zh. Khin. O-va in D. I. Mendeleeva* **1984**, *29*, 379.

[33] J. M. Thomas, *Sci. Am.* **1992**, *266* (4), 118.

[34] R. Spence ended his distinguished career in the UK as Director of the Atomic Energy Research Establishment, Harewell.

[35] Schwab had an eye for significant developments. He spotted L. H. Germer's important paper in *Z. Phys.* **1929**, on low-energy-electron diffraction of a nickel single crystal exposed to hydrogen; and he reported his fellow countryman's (E. Rupp's) work (*Z. Electrochem.* **1929**) on the same system.

[36] To put things into comparable perspective, it is chastening to recall that theory and experiment in certain realms of astronomy and astrophysical phenomena have recently been reported to agree to eleven significant figures. No theory in chemical kinetics and catalysis can boast such correspondence with experiment.

[37] Present-day novitiates in catalysis need to be constantly reminded of these truths.

[38] R. Car, M. Parrinello, *Phys. Rev. Lett.* **1985**, *55*, or 2471.

[39] W. Kohn, L. J. Sham, *Phys. Rev. Sect. A*, **1965**, *140*, 1133; P. Hohenberg, W. Kohn, *ibid.* **1964**, *136*, 864.

[40] R. Nesper, K. Vogel, P. E. Blöchl, *Angew. Chem.* **1993**, *105*, 786; *Angew. Chem. Int. Ed. Engl.* **1993**, *32*, 701.

[41] J. M. Thomas, *Ultramicroscopy* **1982**, *8*, 11.

[42] J. M. Thomas, *Inorganic Chemistry: Towards the 21st Century* (Ed. M. H. Chisholm) (ACS *Monogr.* **1983**, *211*).

[43] P. L. Gai-Boyes, J. M. Thomas ("*Nanostructure and Chemistry of High Temperature Superconducting Ceramics*") in *Advances in Superconducting Ceramics* (Ed.: C. P. Poole), Gordon and Breach, New York, **1992**.

[44] J. W. Niemantsverdriet, *Spectroscopy in Catalysis*, VCH, Weinheim, **1993**.

[45] R. H. Williams, J. M. Thomas, M. Barber, N. Alford, *Chem. Phys. Lett.* **1972**, *17*, 142. This was the first experimental determination of surface band structure of a solid (molybdenum sulfide) from angular variation of UV-stimulated photoemission.

[46] M. Barber, J. M. Thomas, E. L. Evans, *Chem. Phys. Lett.* **1972**, *18*, 423. This work identified the bonding of oxygen at submonolayer amounts and detected sticking coefficients of impinging oxygen of about 10^{-15}.

[47] J. M. Thomas, E. L. Evans, M. Barber, P. Swift, *Trans. Faraday Soc.* **1971**, *67*, 1875.

[48] M. W. Roberts, *Chem. Soc. Rev.* **1989**, *15*, 451.

[49] G. Ertl, J. Küppers, *Low Energy Electrons and Surface Chemistry*, VCH, Weinheim, **1985**.

[50] C. R. A. Catlow, J. M. Thomas, *Philos. Trans. R. Soc. London A*, **1992**, 341, 255, see also R. A. van Santen, *Chem. Eng. Sci.* **1990**, *45*, 2001.

[51] *Modelling of Structure and Reactivity in Zeolites* (Ed.: C. R. A. Catlow), Academic Press, London, **1992**.

[52] *New Methods of Modelling Processes Within Solids and their Surfaces* (Eds.: C. R. A. Catlow, A. M. Stoneham, J. M. Thomas), Oxford University Press, Oxford, **1993**.

[53] K. Tamaru, *Dynamic Heterogeneous Catalysis*, Academic Press, London, **1978**.

[54] C. Sampson, S. Vasudevan, J. M. Thomas, C. J. Wright, *Bull. Soc. Chim. Belg.* **1982**, *90*, 1215.

[55] P. A. Wright, J. M. Thomas, A. K. Cheetham, A. K. Nowak, *Nature* **1985**, *318*, 611.

[56] A. K. Cheetham, A. P. Wilkinson, *Angew. Chem.* **1992**, *104*, 1594; *Angew. Chem. Int. Ed. Engl.* **1992**, *31*, 1559.

[57] J. H. Sinfelt, G. D. Meitzner, *Acc. Chem. Res.* **1993**, *26*, 1.

[58] *X-ray Absorption* (Eds.: D. C. Koningsberger, R. Prins), Wiley, New York, **1987**.
[59] J. W. Couves, J. M. Thomas, R. H. Jones, B. J. Smith, *Adv. Mater.* **1990**, *2*, 181.
[60] E. Dooryhee, J. M. Thomas, G. N. Greaves, C. R. A. Catlow, R. P. Townsend, A. T. Still, S. W. Carr, *Faraday Disc. Chem. Soc.* **1990**, *89*.
[61] J. W. Couves, J. M. Thomas, G. N. Greaves, R. H. Jones, D. Waller, A. J. Dent, G. E. Derbyshire, *Nature* **1991**, *354*, 465.
[62] J. M. Thomas, G. N. Greaves, *Catal. Lett.* **1993**, *20*, 337.
[63] G. Sankar, P. A. Wright, S. Natarajan, J. M. Thomas, G. N. Greaves, A. J. Dent, B. R. Dobson, C. A. Ramsdale, R. H. Jones, *J. Phys. Chem.* **1993**, *97*, 9550.
[64] B. S. Clausen, L. Gråbek, G. Steffensen, H. Topsøe, *HASYLAB Annu. Rep.* **1991**, 495.
[65] B. S. Clausen, L. Gråbek, G. Steffensen, P. L. Hausen, H. Topsøe, *Catal. Lett.* **1993**, *20*, 23.
[66] J. Stöhr in *NEXAFS Spectroscopy*, Springer, Berlin, **1992**.
[67] J. Haase, A. M. Bradshaw in *Synchrotron Radiation Research Vol. 2* (Ed.: R. Z. Bachrach), Plenum, New York, **1992**, p. 55.
[68] J. M. Thomas, J. Klinowski, *Adv. Catal.* **1985**, *33*, 199.
[69] G. Engelhardt, D. Michel, *High-Resolution Solid-State NMR of Silicates and Zeolites*, Wiley, Chichester, **1987**.
[70] E. R. Andrew, *Int. Rev. Phys. Chem.* **1981**, *1*, 195.
[71] N. Al-Sarraf, J. T. Stuckless, C. E. Wartnaby, D. A. King, *Surf. Sci.* **1993**, *283*, 427.
[72] P. J. Maddox, J. Stahurski, J. M. Thomas, *Catal. Lett.* **1988**, *1*, 191.
[73] I. J. Pickering, P. J. Maddox, J. M. Thomas, *Angew. Chem. Adv. Mater.* **1989**, *101*, 828; *Angew. Chem. Int. Ed. Engl. Adv. Mater.* **1989**, *28*, 808.
[74] A discriminating account of these and other related techniques is given in the admirable monograph by Niemantsverdriet [44].
[75] J. M. Thomas, J. Chen, A. R. George, *Chem. Br.* **1992**, 991.
[76] In industrial practice zeolitic catalysts are very often fashioned into composite particles with the zeolite itself embedded in an amorphous silica (or silica-alumina) matrix. The composite can however be treated as two interpenetrating continua (see P. G. Smirniotis, E. Reicherstein, *Chem. Eng. Sci.* **1993**, *48*, 585) that constitute a uniform whole.
[77] For example, in the synthesis of methanol from $H_2 + CO$ or from $H_2 + CO + CO_2$ mixtures at 10 bar in the 200 to 250 °C range it is convenient to express the rate of methanol formation in Langmuir–Hinshelwood form (see A. Cateron, A. N. Hayhurst, *Chem. Eng. Sci.* **1994**, *49*, 209). Thus, the rate of synthesis of methanol r_M from H_2 and CO is written:

$$r_M = \frac{k_{f1} K_{CO} K_H^2 K_{CH} p_{CO} p_{H_2}^2}{1 + K_{CO} p_{CO} + K_{CO} K_H^{3/2} K_{CH} p_{CO} p_{H_2}^{3/2}}$$

And the rate of synthesis of methanol from $H_2 + CO + CO_2$ is of the form:

$$r_M = \frac{k_{f2} K_{CO_2} K_H K_{HCO_2} p_{CO_2} p_{H_2}^2}{1 + K_{CO_2} p_{CO_2} + K_{CO_2} K_H^{1/2} K_{HCO_2} p_{CO_2} p_{H_2}^{1/2} + \dfrac{K_{CO_2} p_{CO}}{K'_{CO} p_{CO}}}$$

[78] W. J. Thomas in *Perspectives in Catalysis* (Eds.: J. M. Thomas, K. I. Zamaraev), Blackwells, Oxford, **1992**, p. 251.
[79] J. M. Thomas, W. J. Thomas, *Introduction to the Principles of Heterogeneous Catalysis*, Academic Press, London, **1967**.
[80] G. A. Somorjai, *Chemistry in Two Dimensions*, Cornell Univ. Press, Ithaca, NY, **1980**
[81] G. Ertl, *Angew. Chem.* **1990**, *102*, 1258; *Angew. Chem. Int. Ed. Engl.* **1990**, *29*, 1219.
[82] P. Gray, S. K. Scott, *Chemical Oscillations and Instabilities*, Clarendon, Oxford, **1990**.
[83] Notions on catalytic inhibitors and poisons, either explicitly stated or implied were contained in the work of Henry and Faraday in England a hundred years before Taylor.
[84] J. M. Thomas, *Adv. Catal.* **1969**, *19*, 293.
[85] P. Mars, P. van Krevelen, *Chem. Eng. Sci. Suppl.* **1954**, *3*, 41.
[86] I. J. Pickering, J. M. Thomas, *J. Chem. Soc. Faraday Trans.* **1991**, *87*, 3067.
[87] P. A. Wright, S. Natarajan, J. M. Thomas, P. L. Gai-Boyes, *Chem. Mater.* **1992**, *4*, 1053.
[88] M. Boudart, *Adv. Catal.* **1969**, *19*, 153.
[89] G. C. Bond, *Acc. Chem. Res.* **1993**, *26*, 490.
[90] The metal catalysts used for these reactions are particularly susceptible to poisoning. For further details see J. H. Sinfelt, *Bimetallic Catalysts*, Wiley, New York, **1986**.
[91] The effect of poisons on the metal catalysts is relatively minor for structure-insensitive reactions.
[92] S. Berkman, J. C. Morrell, S. Egloff, *Catalysis: Inorganic and Organic*, Reinhold, New York, **1940**. This book contains a full discussion of Boeskens's 'disruptive action' (see *Trans. Faraday Soc.* **1928**, *24*, 611). The 'spatial factors' of Biltz (see *Raumchemie der Festen Stoffe*, Voss, Leipzig, **1934**) and the numerous other ideas which are now either completely atrophied or already buried.
[93] This figure is based on a drawing that appears in *Kinetics of Heterogeneous Catalysis Reactions* (Eds.: M. Boudart, G. Djega-Mariadassou), Princeton Univ. Press, Princeton, NJ, USA, **1984**.
[94] a) F. Solymosi, *Int. Congr. Catal. 8th, Vol. VI*, Verlag Chemie, Weinheim, **1984**, p. 101; b) S. J. Tauster, S. C. Fung, R. L. Garten, *J. Am. Chem. Soc.* **1978**, *100*, 170.
[95] K. C. Taylor in *Catalysis and Automotive Pollution Control* (Eds.: A. Crucq, A. Fressnet), Elsevier, Amsterdam, **1987**.
[96] M. Ichikawa, *Bull. Chem. Soc. Jpn.* **1978**, *51*, 2268.
[97] A. Howie in *Characterization of Catalysts* (Eds.: J. M. Thomas, R. M. Lambert), Wiley, Chichester, **1981**, p. 89.
[98] P. L. Gai-Boyes, *Catal. Rev. Sci. Eng.* **1992**, *34*.
[99] See ref. [44], there particularly chapter 6..
[100] In 1956, Japanese workers, using palladium supported on natural silk, obtained optical yields of about 36 per cent in the hydrogenation of oximes and oxazolones. More recently, W. M. H. Sachtler and Y. Izumi (see *Adv. Catal.* **1983**, *32*, 215) have shown that Raney nickel catalysts, when first modified so as to effect corrosive chemisorption of (*R*,*R*)-tartaric acid, can then smoothly hydrogenate methyl acetoacetate to methyl-3-hydroxylbutyrate:

$$CH_3COCH_2COOH_3 + H_2 \longrightarrow CH_3CH(OH)CH_2COOCH_3$$

American workers using a catalyst similarly modified with chiral tartaric acid "template", hydrogenated 2-methylpyridine to optically active 2-methylpiperidine; and workers at the Zelinskii Institute in Moscow showed that metallic copper, cobalt, and palladium, when modified with chiral amino acids, are also good catalysts for a number of enantioselective hydrogenations.
[101] P. B. Wells, *Faraday Discuss. Chem. Soc.* **1989**, *87*, 1.
[102] Y. Orito, S. Imai, S. Niva, *Nippon Kagaku Kaishi*, **1982**, 137.
[103] R. R. Chianelli, T. A. Pecararo, *J. Catal.* **1981**, *67*, 430.
[104] N. Y. Topsøe, EUROPACAT-1, Keynote Lecture, Montpellier, **1993**.
[105] J. K. Nørskov, B. S. Clausen, H. Topsøe *Catal. Lett.* **1992**, *13*, 1.
[106] F. S. Stone in *Chemistry of the Solid State* (Ed.: W. E. Garner), Butterworths, London, **1955**. Chap. 10.
[107] Ref. [18], Chap. 5.
[108] D. D. Eley, *Catalysis and the Chemical Bond*, University of Notre Dame Press, **1954**.
[109] E. K. Rideal, *Concepts in Catalysis*, Academic Press, London, **1968**.
[110] *Nature of the Surface Chemical Bond*, (Eds.: G. Ertl, T. N. Rhodin), North Holland, Amsterdam, **1979**.
[111] R. Hoffmann, *Solids and Surfaces: Structures of Extended Systems*, VCH, New York, **1988**.
[112] R. A. van Santen, *Theoretical Heterogeneous Catalysis*, World, Singapore, **1993**.
[113] E. Shustorovich, R. C. Baetzield, *Science* **1985**, 227, 876.
[114] H. Gerischer, A. Heller, *J. Electrochem. Soc.* **1992**, *139*, 113.
[115] M. A. Fox, *Acc. Chem. Res.* **1983**, *16*, 314.
[116] B. Kraeutler, A. J. Bard, *J. Am. Chem. Soc.* **1978**, *100*, 2239.
[117] G. Rothenberger, J. Moser, M. Grätzel, N. Serpone, D. K. Sharma, *J. Am. Chem. Soc.* **1985**, 107, 8054.
[118] M. Schiavello, *Photocatalysis and Environment*, Reidel, Dordrecht, **1989**.
[119] J. C. D'Oliveirce, G. Al-Sayyed, P. Pichat, *Environ. Sci. Technol.* **1990**, 24, 990.
[120] H. Hidaka, H. Kubota, M. Grätzel, E. Pillozzetti, N. Serpone, *J. Photochem.* **1986**, *35*, 216.
[121] J. Cunningham, S. Srijarni, *J. Photochem. Photobiol. A* **1991**, *58*, 361.
[122] K. Chandrasekaran, J. K. Thomas, *J. Chem. Soc. Faraday Trans.* **1984**, *80*, 1163.
[123] C. K. Grätzel, M. Jirousek, M. Grätzel, *J. Mol. Catal.* **1990**, *60*, 375.
[124] A. Chimseddine, H. P. Boehm, *J. Mol. Catal.* **1990**, *60*, 295.
[125] R. Künneth, C. Feldmer, H. Kisch, *Angew. Chem.* **1992**, *104*, 1102; *Angew. Chem. Int. Ed. Engl.* **1992**, *31*, 1039.
[126] *Potential Applications of Concentrated Solar Photons*, (Ed.: A. J. Bard), National Academy Press, Washington, **1991**.
[127] J. M. Lehn, *Int. Congr. Catal. 8th Vol. I*, Verlag Chemie, Weinheim, **1984**, p. 110.
[128] L. E. Brus, *J. Chem. Phys.* **1984**, *80*, 4403.
[129] J. M. Nedeljkovic, M. T. Nenadovic, O. I. Micic, A. J. Nozik, *J. Phys. Chem.* **1986**, *90*, 12.
[130] H. Weller, V. Koch, M. Gutierrez, A. Henglein, *Ber. Bunsenges. Phys. Chem.* **1984**, *88*, 649; recent review: H. Weller, *Angew. Chem.* **1993**, *105*, 43; *Angew. Chem. Int. Ed. Engl.* **1993**, *32*, 41.
[131] V. N. Parmon, Z. R. Iamgilov, M. H. Kenzhentsev in *Perspectives in Catalysis* (Eds.: J. M. Thomas, K. I. Zamaraev), Blackwells, Oxford, **1992**, p. 337.
[132] V. N. Parmon, K. I. Zamaraev in *Photochemical Energy Conversion* (Eds.: J. R. Norris, D. Meisel), Elsevier, New York, **1989**, p. 316.
[133] V. N. Parmon, K. I. Zamaraev in *Photocatalysis: Fundamentals and Applications* (Eds.: N. Serpone, E. Pillozzetti), Wiley, New York, **1989**, p. 565.

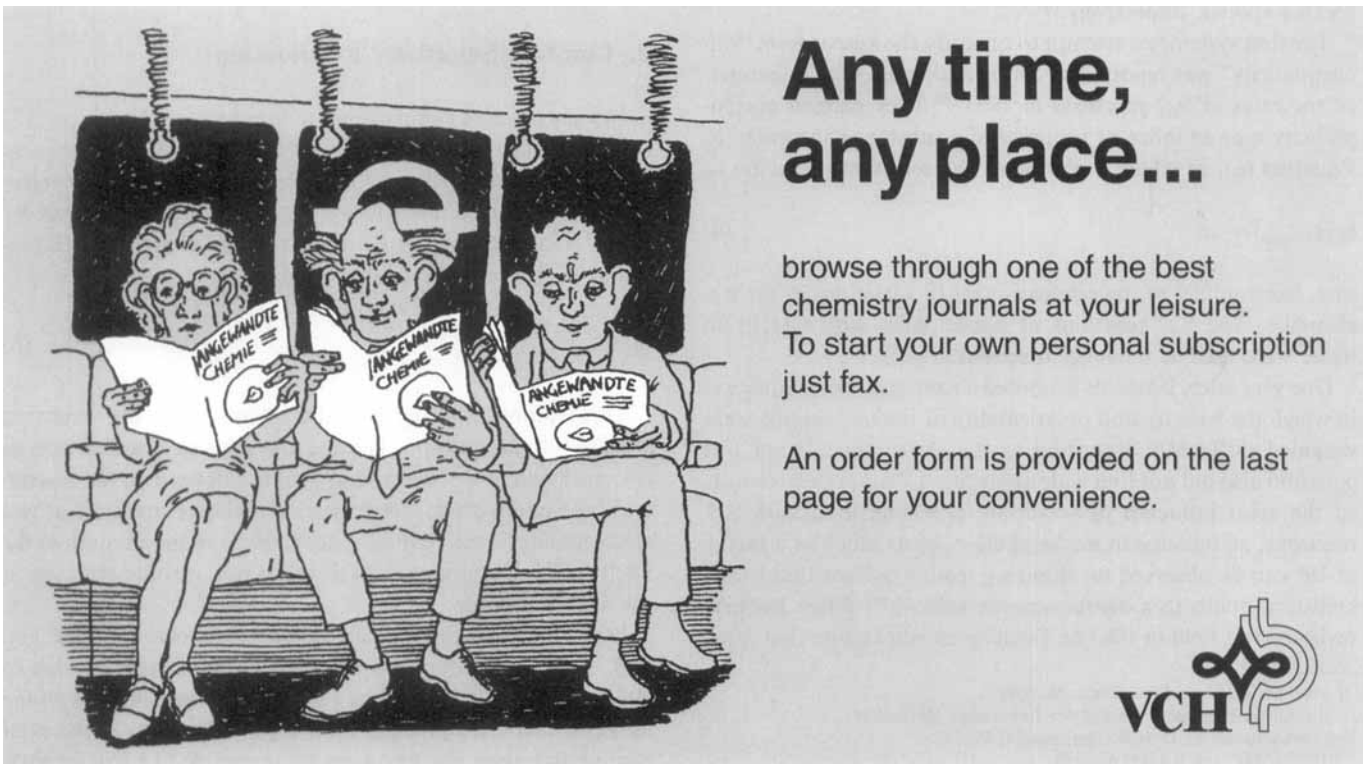
[134] Belousov's first report of his oscillating reaction in 1958 was in such an obscure journal that it failed to catch attention, until Zhobotinskii rediscovered it. The latter's work appeared six years later, coinciding with the arrival of a series of important theoretical advances. See A. M. Zhobotinskii, *Dohl. Akad. Nauk. SSSR.* **1964**, *157*, 392.
[135] H. Beusch, P. Fieguth, E. Wicke, *Chem. Ing. Tech.* **1972**, *44*, 445.
[136] E. Wicke, H. Beusch, P. Fieguth, *ACS Symp. Ser.* **1972**, *109*, 615.
[137] F. Schüth, B. E. Henry, L. D. Schmidt, *Adv. Catal.* **1993**, *39*, 51.
[138] Y. S. Matros, *Chem. Eng. Sci.* **1990**, *45*, 2097.
[139] K. I. Zamaraev in *Perspectives in Catalysis*, (Eds.: J. M. Thomas, K. I. Zamaraev), Blackwells, Oxford, **1992**.
[140] L. L. Hegedus, C. C. Chang, D. J. McEwen, E. M. Sloan, *Ind. Eng. Chem. Fundum.* **1980**, *19*, 367.
[141] G. Ertl, *Science* **1991**, *254*, 1750; see also ref. [81].
[142] T. Engel, G. Ertl, *Adv. Catal.* **1979**, *28*, 1.
[143] The state variables u_1 and u_2 are determined by the sequence of reaction steps in Figure 15 as:

$$du_1/dt = s(CO)p_{CO} - k_d u_1 - k_r u_1 u_2$$

$$du_2/dt = s(O_2)p_{O2} - k_r u_1 u_2$$

and the overall reaction rate R is given by $R = k_r u_1 u_2$, where k_r is the rate coefficient for the surface recombination rate at a particular temperature, and $s(CO)$ and $s(O_2)$ are the sticking coefficients for adsorption of CO and O_2 (normalized to the impingement rates from the gas phase determined by the partial pressures p_{CO} and p_{O2}). k_d is simply the rate coefficient for desorption of CO.
[144] M. Eiswirth, P. Möller, K. Matzl, R. Imbilh, G. Ertl, *J. Chem. Phys.* **1989**, *90*, 510.
[145] T. Gritsch, D. Coulman, R. J. Behm, G. Ertl, *Phys. Rev. Lett.* **1989**, *63*, 1086.
[146] G. M. Schwab, *Catalysis from the Standpoint of Chemical Kinetics*, translated from the German edition by H. S. Taylor, R. Spence, Macmillan, London, **1935**. See also ref. [34]. Original German edition G. M. Schwab, *Katalyse vom Standpunkt der chemischen Kinetic*, Springer, Berlin, **1931**, see page 227ff in particluar.
[147] Biologists, especially biochemists, mean by the word *substrate* the species that is bound to and converted by the enzyme. To the physical scientist, especially physical chemists, the *substrate* (or substratum) generally means the solid upon which a catalyst (or other material) is supported. To conserve conventions and to avoid confusion, we shall in our discussions of biocatalysts gradually adopt the biochemists' use of substrate.
[148] The structure at 3.5 Å resolution of a complete anti-canine lymphoma antibody in which all parts of the distorted Y-shaped molecule with two arms (the so-called Fab fragments) are localized in the crystal and visible in the electron density map has recently been published by L. J. Harris, S. B. Larson, K. W. Hasel, J. Day, A. Greenwood, A. McPherson, *Nature* **1992**, *360*, 369. In the last five years many Fab structures have been crystallographically determined, see, for example, refs. [149–153].
[149] R. C. Stanfield, T. M. Fieser, R. A. Lerner, I. A. Wilson, *Science* **1990**, *248*, 712.
[150] A. G. Amit, R. A. Marvizza, S. E. V. Phillips, R. J. Poljak, *Science* **1986**, *233*, 747.
[151] A. T. Brunger, *Acta Crystallogr. Sect. A* **1991**, *47*, 195.
[152] E. A. Padlan, E. W. Silverton, S. Sheriff, G. H. Cohen, S. J. Smith-Gill, D. R. Davies, *Proc. Natl. Acad. Sci. USA* **1989**, *86*, 5938.
[153] C. Clothia, A. M. Lesk, E. Gherendi, I. M. Tomlinson, G. Walter, J. D. Marks, M. B. Llewellyn, G. Winter, *J. Mol. Biol.* **1992**, *227*, 799.
[154] M. F. Perutz, *Faraday Discuss. Chem. Soc.* **1992**, *93*, 1.
[155] L. Pauling, *Nature* **1948**, 161, 707.
[156] C. C. F. Blake, D. F. Koenig, G. A. Mair, A. C. T. North, D. C. Phillips, V. R. Sarma, *Nature* **1965**, *206*, 757.
[157] M. F. Perutz, *Proc. R. Soc. London B* **1966**, *167*, 448.
[158] J. B. S. Haldane, *Enzymes*, Longmans Green, London, **1930** p. 18.
[159] D. C. Phillips, *Proc. Natl. Acad. Sci. USA* **1967**, *57*, 484.
[160] B. Baird, Y. Zheng, D. Holowka, *Acc. Chem. Res.* **1993**, *26*, 428.
[161] P. G. Schultz, R. A. Lerner, *Acc. Chem. Res.* **1993**, *26*, 391.
[162] See, for example, A. R. Fersht, *Enzyme Structure and Mechanism*, 2nd edition, Freeman, New York, **1985**.
[163] S. Altman, *Angew. Chem.* **1990**, *102*, 735; *Angew. Chem. Int. Ed. Engl.* **1990**, *29*, 749; T. R. Cech, *ibid.* **1990**, *102*, 745 and **1990**, *29*, 759
[164] A. J. Russell, A. K. Fersht, *Nature* **1987**, *328*, 496.
[165] J. R. Knowles, *Nature* **1991**, *350*, 121.
[166] According to Knowles [165] this arrangement is exquisite for several reasons. First, the fit is snug, the distance from the nearer carboxylate oxygen to the substrate's C-1 or C-2 atom being only 2.8 or 3.4 Å. Second, the carboxylate group is bidentate, which means that the proton can be removed from either C-1 or DHAP (from left to right in Fig. 20) or from C-2 of GAP (right to left), with minimal motion of the catalytic base. Third, the stereoelectronic requirement for rapid enolization is nicely satisfied by the active site arrangement of triosephosphate isomerase. And last, advantage is taken of the fact that a *syn* orbital of a carboxylate ion is much more basic than an *anti* orbital.
[167] R. T. Raines, E. L. Sutton, D. R. Strauss, W. Gilbert, J. R. Knowles, *Biochemistry* **1986**, *25*, 7142.
[168] S. Lindskog, A. Liljas, *Curr. Opin. Struct. Biol.* **1993**, *3* (6), 915.
[169] Carbonic anhydrase serves to hydrate CO_2. It has been shown that the rate-limiting step in its mode of operation is the dissociation of water not the formation of the C–H bond to form HCO_3^-. Two hundred and fifty nine amino acids are 'required' to orchestrate this process in carbonic anhydrase.
[170] J. F. Krebs, F. Rana, R. A. Dluhy, C. A. Fierke, *Biochemistry* **1993**, *32*, 4496.
[171] A peak shift from 2343.5 cm^{-1} for dissolved CO_2 to 2340 cm^{-1} indicated [168] that CO_2 is bound without appreciable strain in a hydrophobic environment. According to accepted wisdom [172], an unsolvated CO_2 molecule is loosely held in a hydrophobic pocket and oriented by electrostatic forces from the Zn^{2+} ion and the reactive OH^- ion.
[172] Z. Peng, K. M. Menz, Jr., *J. Am. Chem. Soc.* **1992**, *114*, 2733.
[173] See special issue, devoted to "Chemistry and Immunology", of *Acc. Chem. Res.* **1993**, *26* (August issue), 389-453.
[174] a) V. T. D. Souza, K. Hanahusa, T. O'Leary, R. C. Gradewood, M. L. Bender, *Biochem. Biophys. Res. Commun.* **1985**, 129, 727. See also J. M. Thomas, *Nature* **1986**, 322, 500; b) recent successes in the area of enzyme mimetica are summarized in a highlight by A. J. Kirby (*Angew. Chem.* **1994**, *104*, 573; *Angew. Chem. Int. Ed. Engl.* **1994**, *33*, 551).
[175] ZSM-5 stands for Zeolite Socony Mobil, Number 5. See W. M. Meier, D. H. Olson, *Atlas of Zeolite Structure Types*, 2nd edition, Butterworths, London, **1987**.
[176] Zeolites are a group of aluminosilicate minerals with the general formula $M^{a+}_{n/a} \cdot SiO_{2m} \cdot Al_nO_{2n} \cdot x H_2O$. Here, M is an a-valent cation, and the macroanion has SiO_4^{4-} and AlO_4^{5-} tetrahedra corner-shared with zeolitic water (or other molecules) accommodated in the micropores.
[177] M. A. Makarova, C. Williams, V. N. Romannikov, J. M. Thomas, K. I. Zamaraev, *J. Chem. Soc. Faraday Trans.* **1990**, *86*, 581.
[178] C. Williams, M. A. Makarova, L. V. Malysheva, E. A. Paukshtis, K. I. Zamaraev, J. M. Thomas, *J. Chem. Soc. Faraday Trans.* **1990**, *86*, 3473.
[179] J. M. Thomas, K. I. Zamaraev, *Catal. Lett.* in press.
[180] Y. Xu, C. P. Grey, J. M. Thomas, A. K. Cheetham, *Catal. Lett.* **1990**, *4*, 251; see also *NMR Techniques in Catalysis* (Eds.: A. T. Bell, A. Pines), Dekker, New York, **1994**.
[181] A. G. Stepanov, V. N. Romannikov, K. I. Zamaraev, *Catal. Lett.* **1992**, *13*, 395.
[182] A. G. Stepanov, K. I. Zamaraev, J. M. Thomas, *Catal. Lett.* **1992**, *13*, 407.
[183] J. W. Couves, R. H. Jones, J. M. Thomas, B. J. Smith, *Adv. Mater.* **1990**, *2*, 181.
[184] J. Chen, G. Sankar, J. M. Thomas, R. Xu, G. N. Greaves, D. Waller, *Chem. Mater.* **1992**, *4*, 1373.
[185] A. Zecchina, S. Bordiga, G. Spoto, D. Scarano, G. Petrini, G. Leofanti, M. Padovan, C. Otero Areàn, *J. Chem. Soc. Faraday Trans.* **1992**, *88*, 2959.
[186] P. A. Wright, J. M. Thomas, A. K. Cheetham, A. K. Nowak, *Nature* **1985**, *318*, 6047.
[187] A. K. Cheetham, M. M. Eddy, J. M. Thomas, *J. Chem. Soc. Chem. Commun.* **1984**, 137.
[188] *Modelling of Structure and Reactivity in Zeolites* (Ed.: C. R. A. Catlow), Academic Press, London, **1992**.
[189] J. M. Thomas, C. R. A. Catlow, *Prog. Inorg. Chem.* **1987**, *35*, 1.
[190] G. J. Kramer, R. A. van Santen, *J. Am. Chem. Soc.* **1993**, *115*, 2887.
[191] G. J. Kramer, R. A. van Santen, C. A. Emeis, A. K. Nowak, *Nature* **1993**, *363*, 529-531.
[192] J. Sauer, *Nature* **1993**, *363*, 493.
[193] R. G. Bell, R. A. Jackson, C. R. A. Catlow, *J. Chem. Soc. Chem. Commun.* **1990**, 782.
[194] J. D. Gale, C. R. A. Catlow, W. C. Mackrodt, *Modell. Simul. Mater. Sci. Eng.* **1992**, *1*, 73.
[195] C. M. Freeman, C. R. A. Catlow, J. M. Thomas, S. Brode, *Chem. Phys. Lett.* **1991**, *186*, 137.
[196] P. A. Wright, S. Natarajan, J. M. Thomas, R. G. Bell, P. L. Gai-Boyes, R. H. Jones, J. Chen, *Angew. Chem.* **1992**, *104*, 1526; *Angew. Chem. Int. Ed. Engl.* **1992**, *31*, 1472.
[197] J. M. Thomas in *Zeolites: Facts, Figures, Future* (Eds.: P. A. Jacobs, R. A. van Santen), Elsevier, Amsterdam, **1989**, p. 3.
[198] J. M. Thomas, *Int. Congr. Catal. 8th, Vol. 1*, Verlag Chemie, Weinheim, **1984**, p. 31.
[199] B. W. H. van Beest, G. J. Kramer, R. A. van Santen, *Phys. Rev. Lett.* **1990**, *64*, 1955.
[200] J. A. Rabo, R. J. Pellet, P. K. Coughlin, E. S. Shamshon in *Zeolites as Catalysts and Detergent Builders* (Eds.: H. G. Karge, J. Weitkamp), Elsevier, Amsterdam, **1989**, p. 1.
[201] H. van Bekkum, H. W. Kouwenhoven in *Heterogeneous Catalysis and Fine Chemicals* (Ed.: M. Guisnet), Elsevier, Amsterdam, **1988**, p. 45.
[202] *Guidelines for Mastering the Properties of Molecular Sieves* (Eds.: D. Barthomeuf, E. G. Derouane, W. Hölderich), Plenum Press, **1990**.
[203] *Introduction to Zeolite Science and Practice* (Eds.: H. van Bekkum, E. M. Flanigen, J. C. Jansen), (*Stud. Surf. Sci. Catal.* **1991**, 58).

[204] B. M. Lok, C. A. Messina, R. L. Patton, R. T. Gajek, T. R. Cannan, E. M. Flanigen, *J. Am. Chem. Soc.* **1984**, *106*, 6092.
[205] S. T. Wilson, B. M. Lok, C. A. Messina, T. R. Cannon, E. M. Flanigen, *J. Am. Chem. Soc.* **1982**, *104*, 1146.
[206] P. A. Wright, R. H. Jones, S. Natarajan, R. G. Bell, J. Chen, M. B. Hursthouse, J. M. Thomas, *J. Chem. Soc. Chem. Commun.* **1993**, 633. (DAF-1 stands for *D*avy-*F*araday-1.)
[207] J. Chen, J. M. Thomas, P. A. Wright, S. Natarajan, L. Marchese, S. Bradley, G. Sankar, C. R. A. Catlow, P. L. Gai-Boyes, R. P. Townsend, C. M. Lok, *J. Phys. Chem.* submitted.
[208] J. Chen, J. M. Thomas, *J. Chem. Soc. Chem. Commun.* **1994**, 603.
[209] A. Corma, A. L. Agudo, V. Fornes, *J. Chem. Soc. Chem. Commun.* **1983**, 942.
[210] L. Marchese, J. Chen, P. A. Wright, J. M. Thomas, *J. Phys. Chem.* **1993**, *97*, 8109.
[211] K.-P. Schröder, J. Sauer, M. Leslie, C. R. A. Catlow, J. M. Thomas, *Chem. Phys. Lett.* **1992**, *188*, 320.
[212] J. A. Lercher, R. A. van Santen, H. Vinek, *Catal. Lett.* **1994**, in press. See also S. T. Sie, *Ind. Eng. Chem. Res.* **1992**, *31*, 1881.
[213] S. Natarajan, P. A. Wright, J. M. Thomas, *J. Chem. Soc. Chem. Commun.*, **1993**, 1861.
[214] Review of the applications in synthesis: W. Hölderich, M. Hesse, F. Naumann, *Angew. Chem.* **1988**, **100**, *232*; *Angew. Chem. Int. Ed. Engl.* **1988**, *27*, 226.
[215] H.-L. Zubowa, M. Richter, U. Roost, B. Parlitz, R. Fricke, *Catal. Lett.* **1993**, *19*, 67.
[216] Apart from the factors given earlier, there is, for example, a clamant demand for methyl tertiary butyl ether (MTBE), the high-octane replacement for lead derivatives in petrol. MTBE is made by the catalyzed addition of methanol to 2-methylpropene. See, for example, C. M. Freeman, R. G. Bell, J. Sauer, J. M. Newsam, S. M. Levine, S. M. Tomlinson, J. Brickman, ref. [188], p. 133; G. J. Hutchings, C. P. Nicolaides, M. S. Scurrell, *Catal. Today* **1992**, *15*, 23.
[217] S. A. I. Barri, G. W. Smith, D. White, D. Young, *Nature* **1985**, 312, 533.
[218] H. Mooiweer, K. P. de Jong, B. Kraushaar-Czarnetzki, W. H. J. Stark, P. Granvellet, EUROPACAT-1 Conf. Montpellier, Sept. **1993**; see also J. Haggin, *Chem. Eng. News*, **1993**, *71* (no. 42), 26.
[219] J. A. Cusumano, *Chemtech* **1992**, *22*, 482.
[220] A. R. George, C. R. A. Catlow, J. M. Thomas, *J. Solid State Chem.* **1993**, *104*, 6.
[221] W. A. Herrmann, C. W. Kohlpainter, *Angew. Chem.* **1993**, *105*, 1588; *Angew. Chem. Int. Ed. Engl.* **1993**, *32*, 1524.
[222] J. Chen, R. H. Jones, S. Natarajan, M. B. Hursthouse, J. M. Thomas, *Angew. Chem.* **1994**, *106*, 667; *Angew. Chem. Int. Ed. Engl.* *33*, 639.
[223] a) C. T. Kresge, M. E. Leonowicz, W. J. Roth, J. C. Vartuli, J. S. Beck, *Nature* **1992**, *359*, 710. b) J. S. Beck, J. C. Vartuli, W. J. Roth, M. E. Leonowicz, C. T. Kresge, K. D. Schmitt, C. T.-W. Chu, D. H. Olson, E. W. Sheppard, S. B. McCullen, J. B. Higgins, J. L. Schlenker, *J. Am. Chem. Soc.* **1992**, *114*, 10834.
[224] a) P. Behrens, G. D. Stucky, *Angew. Chem.* **1993**, *105*, 729; *Angew. Chem. Int. Ed. Engl.* **1993**, *32*, 696; b) A. Monnier, F. Schüth, Q. Huo, D. Kumar, D. Margolese, R. S. Maxwell, G. D. Stucky, M. Krishnamurty, P. Petroff, A. Firouzi, M. Janicke, B. F. Chmelka, *Science* **1993**, *261*, 1299.
[225] H. van Bekkum, private communication.



Scales of Nucleophilicity and Electrophilicity: A System for Ordering Polar Organic and Organometallic Reactions

Herbert Mayr * and Matthias Patz

Contrary to widely held opinion, for many reactions in organic and organometallic chemistry it is possible to define nucleophilicity and electrophilicity parameters that are independent of the reaction partners. This phenomenon, discovered by Ritchie during the early 1970s for reactions of highly stabilized carbenium and diazonium ions with n-nucleophiles, also occurs with reactions of carbenium ions with aliphatic and aromatic π-electron systems and in hydride transfer reactions. With the aid of the scales of nucleophilicity and electrophilicity set out here, which extend over eighteen orders of magnitude, forecasts can be made about the feasibility and rate of a given CC bond formation, ionic reduction, or diazo coupling. Linkage with the reactivity scales of Ritchie and Sweigart/Kane-Maguire enables a unified treatment of a large number of polar reactions.

1. Introduction

The foundations of our modern understanding of the course of organic chemical reactions were laid in the mid-1920s, when Lewis's electron theory of valency[1] and the general acid–base theory of Lowry and Brønsted were developed.[2] On this basis, Ingold, in the 1930s, introduced the concepts of "electrophiles" and "nucleophiles", signifying electron-seeking and nucleus-seeking species, respectively.[3]

The first systematic attempt to quantify the kinetic term "nucleophilicity" was reported by Swain and Scott, who investigated the rates of S_N2 reactions in 1953.[4] They defined nucleophilicity n as an inherent property of a substance according to Equation (a), in which s represents the sensitivity (specific to

$$\lg(k/k_{H_2O}) = sn \qquad \text{(a)}$$

each electrophile) of the rate constants to variations in the nucleophile. The S_N2 reactions of nucleophiles with CH_3Br in water were used as reference reactions ($s = 1$).

One year later, Edwards proposed a four-parameter equation in which the basicity and polarizability of the nucleophile were weighted differently according to the electrophile,[5] but this equation also did not find wide application. Parker demonstrated the great influence of solvation, reporting that, with S_N2 reactions, an increase in nucleophilicity by as much as a factor of 10^8 can be observed on changing from a solvent that forms hydrogen bonds to a dipolar aprotic solvent.[6] When Bunnett reviewed this field in 1963 he listed seventeen factors that must be considered in a quantitative representation of nucleophilicity.[7] Because the reactivities of nucleophiles towards *trans*-$[Pt(py)_2Cl_2]$ did not correlate with nucleophilicity parameters known at the time, Pearson et al. concluded that "at present (in 1968) it was not possible to predict quantitatively the rates of nucleophilic displacement reactions if a number of substrates of widely varying properties are considered."[8]

2. Constant Selectivity Relationships

In view of these complexities, a discovery by Ritchie in 1972 attracted much attention. He found that in reactions of carbocations and diazonium ions with nucleophiles, a particular nucleophile system can be characterized by one constant parameter N_+ which is independent of the nature of the electrophile [Equation (b)].[9]

$$\lg(k/k_0) = N_+ \qquad \text{(b)}$$

This relationship (Fig. 1) is also referred to as the "constant selectivity relationship", because the relative reaction rate of two nucleophiles (= selectivity) does not depend on the reactivity of the electrophile. Conversely, the relative reactivity of two electrophiles (= selectivity) is independent of the strength of the nucleophile. Deviations from this behavior are only observed at the diffusion limit.

It was later shown that Equation (b) is not strictly valid, and that better correlations are obtained when different families of electrophiles are treated separately.[10] However, in view of the range of the nucleophilicity scale (approximately 13 orders of magnitude), these discrepancies are negligible to a first approx-

[*] Prof. Dr. H. Mayr, Dipl.-Chem. M. Patz
Institut für Organische Chemie der Technischen Hochschule
Petersenstrasse 22, D-64287 Darmstadt (FRG)
Telefax: Int. code + (6151)16-5591

 © VCH Verlagsgesellschaft mbH, D-69451 Weinheim, 1994 0570-0833/94/0909-0938 $ 10.00+.25/0

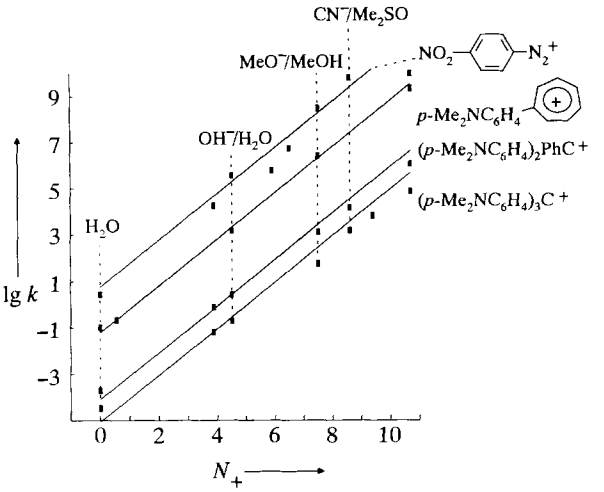


Fig. 1. Constant selectivity relationship according to Ritchie [9].

imation. Furthermore, since the behavior of uncharged electrophiles such as esters,[11] acceptor-substituted ketones,[12] and 2,4-dinitrohalobenzenes[13] is also consistent with Equation (b), its impact increases significantly.

Kane-Maguire, Sweigart et al. observed similar correlations in nucleophilic additions to metal-coordinated π-electron systems.[14] As shown in Figure 2, the relative reactivity of the organometallic complexes $[Mn(CO)_3(C_7H_8)]^+$, $[Fe(CO)_3(2\text{-}MeOC_6H_6)]^+$, and $[Fe(Cp)(C_7H_8)]^+$ is independent of the absolute reaction rates of the reference nucleophiles. Since the relative reactivities of phosphorus and nitrogen nucleophiles towards free carbocations and metal-coordinated π-electron systems are equal,[15] the Kane-Maguire and Sweigart N_{Fe} scale can be considered representative for both classes of electrophiles.

Constant selectivity relationships are also observed in the addition of diarylcarbenium ions (abbreviations defined in Scheme 1) to terminal double bonds, where the new CC bond is

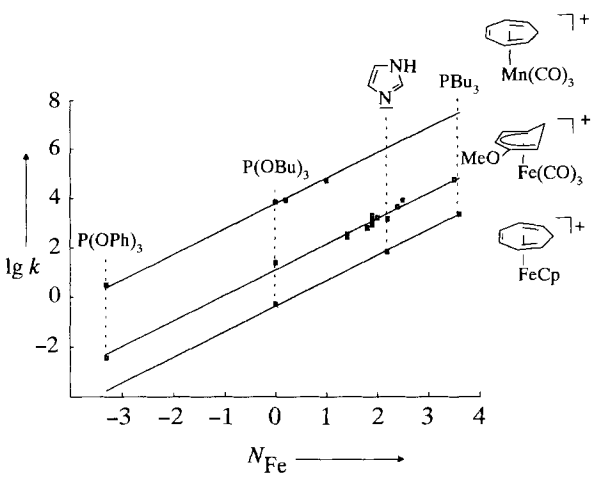
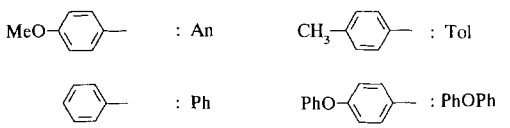


Fig. 2. Constant selectivity relationship according to Kane-Maguire and Sweigart et al. [14].



Scheme 1. Abbreviations used for aryl groups.

formed in the rate-determining step.[16] The relative reactivity of π-nucleophiles is independent of the electrophilicity of the carbenium ions, although the absolute reaction rates vary by more than five orders of magnitude (Fig. 3). If the results of competition experiments[17] are included, it can be shown that, in reactions of compounds containing terminal double bonds with diarylcarbenium ions, the constant selectivity relationship applies over a reactivity range of at least eight orders of magnitude.[16] Diarylcarbenium ions were therefore used as reference electrophiles to establish a scale of nucleophilicity for π-electron systems. As the diarylcarbenium ions so far used, from the bis(*p*-chloro)- to the bis(*p*-dimethylamino)-substituted diphenylcarbenium ion, cover a reactivity range of more than thirteen orders of magnitude, nucleophiles of very different reactivities

Herbert Mayr, born in 1947 in Weilheim, Oberbayern, studied chemistry at the Universität München and gained his doctorate in 1974 under R. Huisgen. After working for one year with G. A. Olah at the Case-Western Reserve University in Cleveland, Ohio, he joined P. von R. Schleyer in Erlangen where he habilitated in 1980. From 1984 to 1991 he headed the Institut für Chemie der Medizinischen Universität at Lübeck. In 1991, he was appointed Professor at the Institut für Organische Chemie in the Technische Hochschule, Darmstadt. His fields of research include syntheses via carbocationic intermediates, kinetics of ion–molecule reactions, linear free energy relationships, carbocationic telomerizations, and unusual cycloadditions.



H. Mayr



M. Patz

Matthias Patz was born in 1965 in Kiel. During his chemistry studies at the University of Hamburg, he spent six months at the University of Southampton. In 1990, he completed his Diploma thesis at the Institut für Anorganische und Angewandte Chemie at Hamburg on anionic effects in potassium crown ether complexes. Early in 1991 he began his doctorate studies in the research group of H. Mayr at the Institut für Chemie der Medizinischen Universität at Lübeck, and moved at the end of 1991 together with the research group to the Technische Hochschule, Darmstadt.

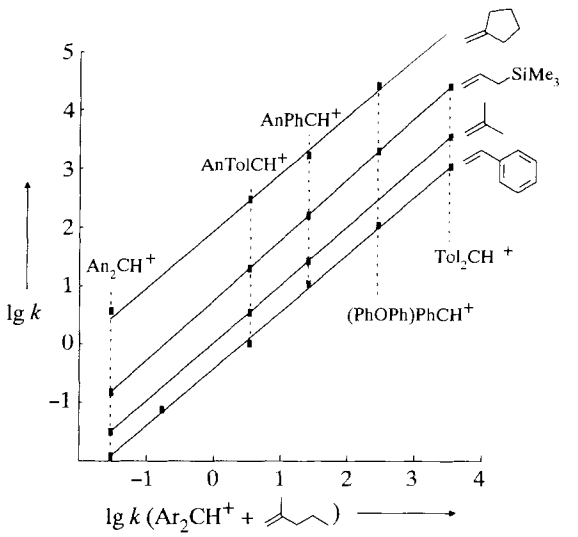


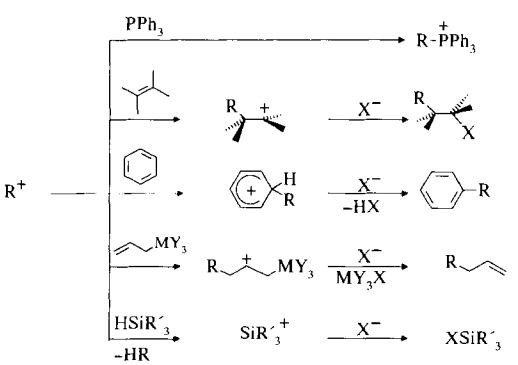
Fig. 3. Constant selectivity relationship in the reactions of benzhydryl cations with alkenes (CH_2Cl_2, $-70\,^{\circ}C$) [16].

can be compared while the steric conditions of the electrophilic centers are kept exactly identical.

3. Rates of Electrophile–Nucleophile Combination Reactions

3.1. Methods of Determination

The majority of the rate constants quoted here have been determined by preparing solutions of stable carbenium ions (or other electrophiles) and monitoring the decrease in concentration after adding the nucleophile. If n-nucleophiles are used, there is a single reaction step (Scheme 2, first reaction), sometimes followed by a deprotonation step. On the other hand, the attack of carbenium ions on alkenes, arenes, allylsilanes, allylgermanes, allylstannanes, or hydrosilanes is the first step in a multiple stage reaction cascade (Scheme 2). The rate constants quoted in this article relate to the first step of this reaction sequence, namely bond formation between electrophile and nucleophile ("electrophile–nucleophile combination"), which is usually rate-determining. In these reactions there is no difference between the reaction rates of free and paired carbenium



Scheme 2. Single-step and multistep reactions of electrophiles (R^+) with nucleophiles. M = Si, Ge, Sn.

ions, which was at first surprising. This observation was explained[18] by the fact that the Gibbs free energy of paired carbocations is more favorable than that of the free ions by an approximately constant amount (about 14 kJ mol^{-1} in CH_2Cl_2, for example) independent of their structure. As this energy difference can also be assumed for the activated complexes, the reaction rate is the same for free and paired carbocations.[18] The reason for the different situation in the chemistry of carbanions has been discussed.[18b]

We determined rate constants of $k < 10^4$ L mol^{-1} s^{-1} conductometrically or photometrically using fiber optics, so that low temperatures and inert gas atmosphere could be employed without problems.[19] The research groups of Ritchie[20] and Kane-Maguire[21] mainly applied stopped-flow techniques (UV/VIS), allowing the measurement of more rapid reactions. In the investigation of carbonyl complexes, IR spectroscopy was also used.[21] With laser pulse methods the diffusion limit could be approached; the carbenium ions are produced by 20 ns laser pulses in the presence of nucleophiles,[22] and the dependence of their decomposition rate on the nucleophile concentration yields the rate constants of the electrophile–nucleophile combination reactions.

Furthermore, the relative reaction rates of alkenes and allylsilanes were determined by competition experiments in which carbenium ions were produced in situ in the presence of a pair of π-nucleophiles.[17, 23] The relative rate constants determined from the ratios of the products agree with the results of absolute rate measurements.[18]

The azide clock technique [24, 63] developed by Jencks exploits the fact that many carbenium ions undergo diffusion-controlled reactions with N_3^- ($k = 5 \times 10^9$ L mol^{-1}s^{-1}).[25] Hence, experiments in which carbenium ions are produced in situ in aqueous azide solutions enable the determination of absolute rate constants from the ratios of the capture products. However, the rate constants calculated from these competition reactions sometimes depend on the azide concentration, so rate constants determined with the azide clock are not always reliable.[26]

For the π-nucleophiles on which this review focuses, we have shown that measurements of absolute rate constants using either salts of stable carbenium ions or carbenium ions produced by laser flash photolysis give consistent results,[27] which have furthermore been verified by product studies in competition reactions. Hence for these nucleophiles there are three completely independent sets of data, whose agreement confirms that the electrophile–nucleophile combination reaction is the rate-determining step.

3.2. Reaction Rate as a Function of Nucleophile, Electrophile, Temperature, and Solvent

The rate constants of the electrophile–nucleophile combination reactions described in this paper are mainly dependent on the four factors mentioned in the heading of this section. A strict separation of these four factors is not possible. In particular, the magnitude of the nucleophilicity and electrophilicity parameters is often linked with the type of the solvent. For the reactions of carbocations with uncharged nucleophiles such as alkenes,[19] neutral hydride donors,[28] and phosphanes,[14] the reaction rate

Table 1. The effect of the solvent on the rate of reaction of carbenium ions with uncharged nucleophiles.

Electrophile (T[°C])	Nucleophile	Solvent	k [L mol^{-1} s^{-1}]	Ref.
An_2CH^+ (−30)	2-Methyl-1-pentene	CH_3NO_2	2.63	[19]
		$(CH_2Cl)_2$	0.958	[19]
		CH_2Cl_2	0.632	[19]
		$CHCl_3$	0.543	[19]
$AnPhCH^+$ (−20)	$HSiMe_2Ph$	CH_3NO_2	71.4	[28]
		CH_3CN	67.5	[28]
		CH_2Cl_2	47.7	[28]
$[Fe(CO)_3(C_6H_7)]^+$ (20)	$PTol_3$	CH_3NO_2	4.1×10^4	[21]
		$(CH_3)_2CO$	2.8×10^4	[21]
	Pyrrol	CH_3NO_2	0.89 [a]	[37]
		CH_3CN	1.34 [a]	[37]

[a] At 45 °C.

is hardly affected by the nature of the solvent (Table 1), because electric charges are neither "created" nor "destroyed" in the rate-determining step. Even the change from the slightly polar chloroform ($\varepsilon = 4.81$) to nitromethane ($\varepsilon = 35.94$) causes the rate of the reaction of bis(*p*-methoxyphenyl)carbenium ion (An_2CH^+) with 2-methyl-1-pentene to increase by a factor of only 4.8. Since the polarities of the solvents used in electrophile–nucleophile reactions normally lie between these two extremes, the influence of the solvent on the rate of such reactions can be neglected to a first approximation.

Reaction rates strongly dependent on the solvent are found, for example, when the reactivities of n-nucleophiles are compared in protic and aprotic solvents (see Section 1). For azo couplings, on the other hand, a correlation between the reaction rate and the donor number[73a] of the solvent is observed.[73b] In such cases, nucleophilicity and electrophilicity is more rationally defined with respect to a particular solvent (see Section 3.3.3).

3.3. Nucleophiles

3.3.1. *Introduction*

Nucleophiles can be classified according to the type of orbital in which the electrons that are available for the new bond with the electrophile are located. Thus, π-nucleophiles (e.g., alkenes), n-nucleophiles (e.g., phosphanes), and σ-nucleophiles (e.g., hydrides) may be distinguished. As it is easier to discuss differences and similarities within these groups, the three classes of nucleophiles are first treated separately.

3.3.2. *Reactivity of π-Nucleophiles*

3.3.2.1. *Alkenes, Dienes, and Alkynes*

Figure 4, which illustrates representative compounds from Table 2, shows that the alkyl-substituted ethenes fall into two groups: those that give secondary carbenium ions on electrophilic attack, and those that give tertiary carbenium ions. *Iso*-butene is 25000 times as reactive as propene, whose reactivity is hardly different from that of the *cis*–*trans* isomers of 2-butene. The steric effect of the *tert*-butyl group causes 2,3,3-trimethyl-1-butene to be 20 times less reactive than *iso*-butene. Consequently, its reactivity is similar to that of norbornene, which is intermediate in reactivity between precursors of secondary and tertiary carbenium ions, in accordance with the S_N1 reactivity of 2-norbornyl derivatives.

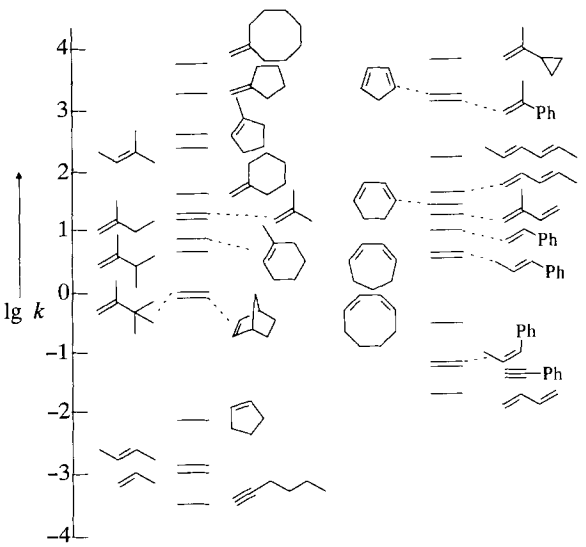


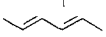
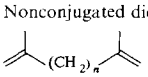
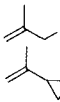
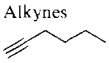
Fig. 4. Rate constants for the reactions of $AnPhCH^+$ with unsaturated hydrocarbons (CH_2Cl_2, −70 °C).

Table 2. Rate constants and activation parameters of the reactions of $AnPhCH^+$ with alkenes, alkynes, and dienes (CH_2Cl_2, −70 °C) [30].

Nucleophile	k [L mol^{-1} s^{-1}]	$\Delta H^{\neq}$ [kJ mol^{-1}]	$\Delta S^{\neq}$ [c] [J mol^{-1} K^{-1}]	s [a]	N [a]
Alkyl-substituted ethenes					
	9.39×10^{-4}	32.6 ± 0.2	−139 ± 1	(0.98)	(−2.36)
	1.85×10^{-3} [b]		(−130)	0.98	−2.02
	1.01×10^{-3}	31.4 ± 0.4	−145 ± 2	(1.20)	(−2.39)
	1.26×10^{-3}	29.9 ± 0.5	−150 ± 2	(1.20)	(−2.38)
	2.33×10^{1}	21.1 ± 0.4	−112 ± 2	1.02	1.07
	1.84×10^{1}	21.4 ± 0.2	−112 ± 1	(1.00)	(1.05)
	6.08		(−115)	(1.00)	(0.67)
	1.21	24.4 ± 0.5	−120 ± 3	(1.00)	(0.10)
	2.58×10^{1}	19.5 ± 1.2	−119 ± 6	1.00	1.02
	2.86×10^{1}	18.6 ± 0.3	−122 ± 1	(1.00)	(1.03)
	2.47×10^{2}	7.5 ± 0.1	−159 ± 0.3	1.16	0.71
	5.62	8.0 ± 0.2	−188 ± 1	1.44	−0.96
Methylenecycloalkanes					
$n = 3$	0.12		(−110)	(1.00)	(−0.44)
$n = 4$	4.01×10^{1}	20.6 ± 0.3	−110 ± 1	(1.00)	(1.30)
$n = 5$	1.72×10^{3}	11.6 ± 0.4	−123 ± 2	1.02	2.31
$n = 6$	4.69×10^{1}	19.8 ± 0.1	−112 ± 1	(1.00)	(1.34)
$n = 7$	4.25×10^{2}	14.2 ± 0.1	−121 ± 1	(1.00)	(1.87)
$n = 8$	5.09×10^{3}	11.2 ± 0.3	−116 ± 2	(1.00)	(2.66)
$n = 9$	1.60×10^{3}	10.7 ± 0.1	−128 ± 1	(1.00)	(2.12)
$n = 10$	2.26×10^{3}	11.7 ± 0.3	−120 ± 1	(1.00)	(2.36)
$n = 11$	7.83×10^{2}	12.0 ± 0.2	−127 ± 1	(1.00)	(1.94)
$n = 12$	1.33×10^{2}	12.5 ± 0.3	−139 ± 1	(1.00)	(1.21)
$n = 15$	8.84×10^{1}	16.7 ± 0.1	−122 ± 1	(1.00)	(1.37)

(Table continues on next page)

Table 2 (continued).

Nucleophile	k [L mol^{-1} s^{-1}]	$\Delta H^{\neq}$ [kJ mol^{-1}]	$\Delta S^{\neq}$ [c] [J mol^{-1} K^{-1}]	s [a]	N [a]
Cyclic alkenes					
	7.0×10^{-3}		(−150)	(1.00)	(−1.93)
	5.2×10^{2}		(−130)	(1.00)	(1.76)
	8.7	17.7 ± 0.2	−136 ± 1	1.10	0.20
	7.82×10^{-1}	23.9 ± 0.3	−126 ± 1	(1.00)	(−0.12)
Conjugated dienes					
	1.93×10^{-2}		(−120)	(1.00)	(−1.15)
	4.62×10^{1}	22.4 ± 0.3	−99 ± 2	(1.00)	(1.55)
	3.06		(−100)	(1.00)	(0.70)
	1.56×10^{1}	23.0 ± 0.4	−106 ± 0.2	0.98	1.12
	2.83×10^{1}		(−100)	(1.00)	(1.37)
	1.82×10^{2}	15.1 ± 0.6	−124 ± 3	(1.10)	(1.22)
	1.74×10^{3}		(−120)	(1.10)	(1.89)
	2.75×10^{1}	18.5 ± 0.7	−123 ± 4	(1.10)	(0.72)
	3.04	22.1 ± 0.7	−123 ± 4	(1.10)	(0.13)
	3.26×10^{-1}		(−120)	(1.10)	(−0.46)
Nonconjugated dienes					
					
$n = 1$	3.42	24.8 ± 0.5	−110 ± 2	(1.00)	(0.55)
$n = 2$	1.51×10^{1}		(−100)	(1.00)	(1.18)
$n = 3$	3.92×10^{1}	26.0 ± 0.1	−83 ± 1	(1.00)	(1.75)
$n = 4$	5.35×10^{1}	22.8 ± 0.5	−97 ± 2	(1.00)	(1.59)
Styrenes					
R = 					
H	1.09×10^{1}	19.3 ± 0.3	−127 ± 1	0.97	0.78
p-F	7.38 [b]		(−120)	(1.00)	(0.64)
p-Cl	1.7 [b]		(−120)	(1.00)	(0.20)
p-Br	1.7 [b]		(−120)	(1.00)	(0.20)
m-NO_2	2.03×10^{-3} [b]		(−120)	(1.00)	(−1.82)
	1.45×10^{3}		(−110)	(1.00)	(2.39)
	3.87	15.5 ± 0.4	−154 ± 2	1.20	−0.47
	8.29×10^{-2}	26.1 ± 0.3	−134 ± 1	(1.20)	(−1.12)
Other alkenes					
	1.13	27.2 ± 1.0	−107 ± 5	(1.00)	(0.28)
	5.65×10^{3}			(1.00)	(2.80)
Alkynes					
	3.03×10^{-4} [b]		(−105)	(0.70)	(−2.19)
	7.2×10^{-2}		(−105)	0.70	0.27
	0.97 [b]		(−110)	(0.80)	(1.11)

[a] The nucleophilicity parameters N and s are defined in Section 4.2 (approximate values in parentheses). [b] From relative reactivities towards Tol_2CH^+ [17, 30d]. [c] Estimated values in parentheses. See Section 3.5.

Unexpectedly large reactivity differences have been observed between the various methylenecycloalkanes.[30c] We found a correlation between the rates of the carbenium ion additions to methylenecycloalkanes and the solvolysis rates of the corresponding cycloalkyl derivatives in S_N1 reactions. Previously the trend in solvolysis was rationalized by a change in the strain (during in $sp^3 \rightarrow sp^2$ hybridization) for the rate-determining step.[31] In the addition reactions discussed here, none of the carbon atoms in the ring undergoes a change in hybridization in the rate-determining step, which throws doubt[30c] on Brown's I-strain theory[32] of the solvolysis of cycloalkyl compounds.[32]

The reactivities of the conjugated dienes and styrenes also reflect the stabilities of the allyl and benzyl cations produced by the electrophilic attack relative to alkylcarbenium ions (as derived from solvolysis data).[30a] In nonconjugated dienes, the additional double bond always causes a decrease in the nucleophilicity; no examples of nucleophilic assistance of the reaction by the second π-bond were found.[30b]

Whereas the nucleophilicities of the CC double-bond systems hitherto studied correlate with the S_N1 reactivities of the addition products, the triple bonds of 1-hexyne and phenylacetylene react much more rapidly than would be expected on the basis of the solvolysis rates of the corresponding vinyl chlorides.[30d] As a consequence of the large energy gain on conversion of a CC triple bond into one CC double bond and one CC single bond (compared with the change C=C → 2 C–C), alkynes are attacked by carbenium ions only slightly more slowly than the correspondingly substituted alkenes, although the vinyl cations produced from alkynes are intermediates of higher energy. Only relative to bridging electrophiles, for example, halogens do alkynes show a significantly lower nucleophilicity than alkenes.[33]

3.3.2.2. *Allylsilanes, Allylgermanes, and Allylstannanes*

The reactivities of allyl–element compounds (Table 3) and alkenes (Table 2) are compared in Figure 5, which shows that

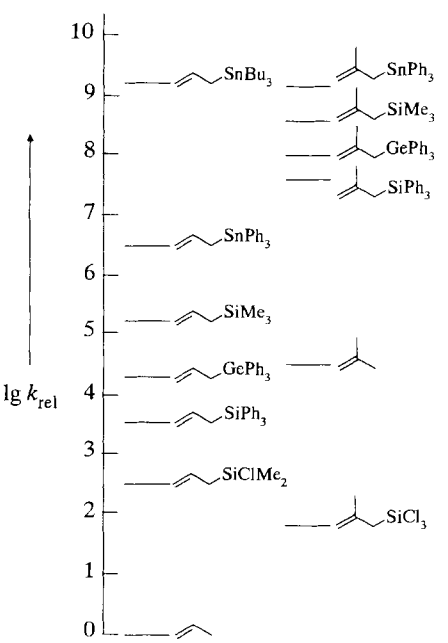
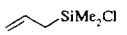
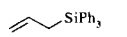
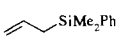
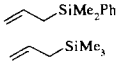
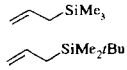
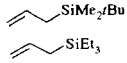
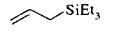
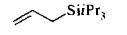
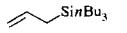
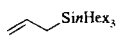
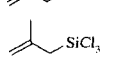
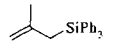
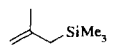
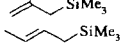
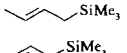
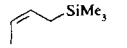
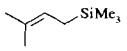
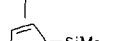
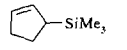
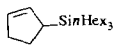
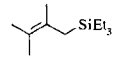


Fig. 5. Reactivities of allylsilanes, allylgermanes, and allylstannanes relative to propene (left) and *iso*-butene (right) [35]. (Reference systems An_2CH^+, $AnPhCH^+$; CH_2Cl_2, −70 °C.)

Table 3. Rate constants of the reactions of allylsilicon, allylgermanium, and allyltin compounds with diarylcarbenium ions (CH_2Cl_2, -70°) [35].

Nucleophile	k with AnPhCH$^+$ [L mol^{-1} s^{-1}]	k with An$_2$CH$^+$ [L mol^{-1} s^{-1}]	s [a]	N [a]
	2.76×10^{-1}		1.07	−0.45
	3.21		0.92	0.46
	3.87×10^{1}		(1.00)	(1.14) [b]
	1.87×10^{2}	2.81×10^{-1}	1.01	1.62
	2.04×10^{2}		(1.00)	(1.65) [b]
	3.13×10^{2}		(1.00)	(1.77) [b]
	4.39×10^{2}		(1.00)	(1.87) [b]
	5.08×10^{2}		(1.00)	(1.92) [b]
	5.42×10^{2}		(1.00)	(1.94) [b]
	6.8×10^{-2}		(1.00)	(−0.77) [b]
	1.91×10^{4}	5.55×10^{1}	0.92	3.68
		4.89×10^{2}	0.89	4.90
	4.19×10^{3}		(1.10)	(1.99) [c]
	1.66×10^{3}		(1.10)	(1.73) [c]
	1.52×10^{3}		1.25	0.84
	1.30×10^{3}		0.90	2.50
	2.81×10^{3}		(0.90)	(2.93)
		1.3×10^{3}	(1.10)	(3.74) [c]
	1.79×10^{1}		(1.00)	(1.07) [d]
	$\approx 2.5 \times 10^{4}$	1.38×10^{2}	0.80	4.80
	5.18×10^{3}	1.01×10^{1}	0.89	3.29
		5.07×10^{3}	0.85	5.72
		2.40×10^{3}	0.82	5.63

[a] Nucleophilicity parameters (N) and s are defined in Section 4.2 (approximate values in parentheses). [b] Estimated values assuming activation entropy of -120 J mol^{-1} K^{-1}. [c] Estimated values assuming activation entropy of -130 J mol^{-1} K^{-1}. [d] Estimated values assuming activation entropy of -110 J mol^{-1} K^{-1}.

the replacement of an allylic hydrogen by a trimethylsilyl group increases the nucleophilicity of the double bond by the factor 200000. A comparison of allyltrimethylsilane with *iso*-butene indicates that a β-trimethylsilyl group in the intermediate carbenium ion increases the reactivity more than an α-methyl group. The series of allyltriphenyl–element compounds shows an increase in nucleophilicity in the order Si < Ge ≪ Sn. The low rates often observed for Lewis acid catalyzed reactions of allylstannanes are therefore a result of the rapid reaction of the allylstannanes with the Lewis acids and the weak nucleophilicity of the intermediates so obtained.[34]

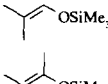
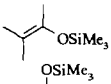
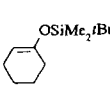
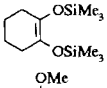
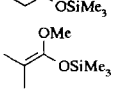
The great influence of the substituents at silicon is apparent on comparing allyltrimethylsilane with allyltriphenylsilane. The difference between the inductive effects of methyl and phenyl causes the triphenylsilyl compound to be a factor of 58 less reactive. A still greater difference in reactivity is observed if a methyl group on the silicon is replaced by chlorine. Thus, allylchlorodimethylsilane is about three orders of magnitude less reactive than allyltrimethylsilane. Finally, replacement of an allylic hydrogen atom by a trichlorosilyl group causes deactivation by a factor of 350 (last two compounds in the right-hand column of Figure 5).[35]

Both columns of Figure 5 show an increase in nucleophilicity along the series $SiPh_3 < GePh_3 < SiMe_3 < SnPh_3 < SnBu_3$. The reactivity differences are smaller in the right-hand group of compounds, because the additional methyl group reduces the electron deficiency in the carbenium center of the intermediate.

3.3.2.3 Alkyl Enol Ethers and Silyl Enol Ethers

Because of the high nucleophilicity of enol ethers, their reactivity towards strong electrophiles such as $(p\text{-}ClC_6H_4)_2CH^+$ and $(p\text{-}MeC_6H_4)_2CH^+$ was determined by the rapid laser flash method (Table 4).[27] As shown by the comparison of 1-(methoxy)cyclopentene with 1-(trimethylsiloxy)cyclopentene, alkyl enol ethers and silyl enol ethers differ only slightly in reactivity. Many of the rate constants measured by laser flash spectroscopy are leveled by the proximity of the diffusion limit, and the differences in reactivity due to activation become more pronounced if the reactivities towards the less electrophilic bis(p-dimethylaminophenyl)carbenium ion are compared.[36] Since alkyl enol ethers polymerize under these conditions, so far only data for silyl enol ethers have been determined against this carbenium ion.

Table 4. Rate constants of the reactions of alkoxy- and siloxy-substituted ethenes with the bis(p-chlorophenyl)methyl cation **A** (CH_3CN), and the bis(p-tolyl)methyl cation **B** (CH_3CN) [27], and the bis(p-dimethylaminophenyl)methyl cation **C** (CH_2Cl_2) [36] at 20 °C.

Nucleophile	Electrophile	k [L mol^{-1} s^{-1}]	Nucleophile	Electrophile	k [L mol^{-1} s^{-1}]
	**A**	1.7×10^{8}			
	B	6.3×10^{6}		**A**	5.5×10^{7}
	**A**	2.0×10^{8}			
	**A**	1.9×10^{8}		**C**	3.53×10^{-2}
	**A**	4.2×10^{8}		**A**	2.1×10^{8}
	A	7.4×10^{8}			
	**B**	3.7×10^{7}		**A**	1.5×10^{9}
				B	4.2×10^{7}
	**A**	7.7×10^{8}		**A**	3.0×10^{9}
	**A**	1.3×10^{9}		**A**	2.5×10^{9}
				B	6.0×10^{8}
	**A**	2.2×10^{9}		**C**	3.61×10^{-1}
	B	2.2×10^{8}			
	**A**	2.7×10^{8}		**A**	2.3×10^{9}
				B	1.3×10^{8}
	**A**	1.3×10^{9}		An_2CH^+	$\approx 1.7 \times 10^{5}$
				C	1.92×10^{-2}
	**A**	3.5×10^{9}			
	B	1.2×10^{8}		**A**	1.4×10^{9}
				**B**	1.1×10^{8}
	A	1.9×10^{9}			
	B	2.2×10^{8}		**C**	1×10^{-3}
	**A**	$\approx 4 \times 10^{9}$			
				A	2.4×10^{9}
				C	8.02×10^{1}

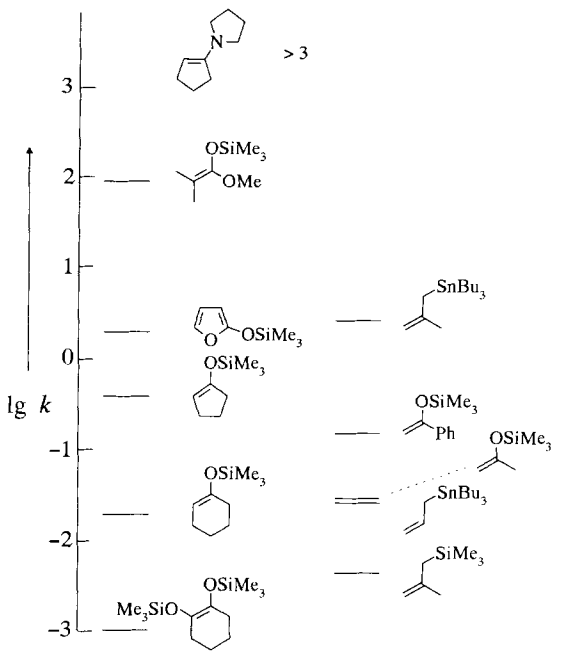


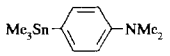
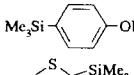
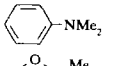
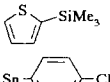
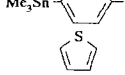
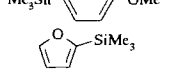
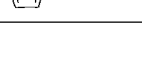
Fig. 6. Rate constants of the reactions of $(p\text{-}Me_2NC_6H_4)_2CH^+$ with electron-rich double-bond systems (CH_2Cl_2, 20 °C) [36, 88].

In Figure 6 the reactivities of silyl enol ethers are compared with those of allylsilanes and allylstannanes. For structurally analogous compounds ($H_2C{=}CMe{-}CH_2{-}SiMe_3$ < $H_2C{=}CMe{-}OSiMe_3 \ll H_2C{=}CMe{-}H_2SnBu_3$), the nucleophilicity of silyl enol ethers lies between that of allylsilanes and allylstannanes.

3.3.2.4. Arenes

The reaction of arenes with the tricarbonylcyclohexadienyl iron cation often does not follow a second order rate law. This behavior has been explained by the reversible formation of an intermediate π-complex.[37] However, second order rate constants were measured for a series of electron-rich arenes (Table 5).

Table 5. Rate constants of the reactions of arenes with the tricarbonylcyclohexadienyl iron cation in nitromethane at 45 °C [14]. Activation parameters $\Delta H^{\neq}$ [kJ mol^{-1}] and $\Delta S^{\neq}$ [J mol^{-1} K^{-1}] in parentheses.

Nucleophile	k [L mol^{-1} s^{-1}]	Nucleophile	k [L mol^{-1} s^{-1}]
	8.9×10^{-1} (47; −96)		9.2×10^{-6}
	5.6×10^{-1} (43.5; −110)		6.4×10^{-6}
	1.0×10^{-1} (71; −43)		4.2×10^{-6}
	6.1×10^{-2} (53; −100)		2.0×10^{-6}
	3.9×10^{-4}		1.0×10^{-6}
	1.7×10^{-4}		2.8×10^{-7}
	1.0×10^{-4}		

We also observed complex kinetics in the reactions of diarylcarbenium ions with benzene derivatives,[38] but attributed this finding to the reversible formation of a σ-complex. In agreement with this assumption, we obtained second order kinetics (Table 6) by adding a tetraalkylammonium salt: the anion, present in high concentration, acts as a base, rapidly deprotonating the intermediate benzenium ion. The relative reactivities of the arenes correlate with their basicities (Fig. 7), as was concluded earlier from the relative arene reactivities determined in competition experiments.[39]

Table 6. Rate constants of the reactions of substituted benzenes with diarylcarbenium ions (CH_2Cl_2, −70 °) [38].

Nucleophile	k with $(p\text{-}ClC_6H_4)_2CH^+$ [L mol^{-1} s^{-1}]	k with $AnPhCH^+$ [L mol^{-1} s^{-1}]	s [a]	N [a]
				
R =				
H	ca. 4×10^{-4}		(1.20)	(−6.29)
Me	7.8×10^{-1}		1.22	−4.22
1,4-Me_2	1.8		(1.20)	(−4.18)
1,3-Me_2	4.2×10^{2}		1.40	−3.31
OMe		3.1×10^{-2}	1.17	−1.56
1-OMe, 3-Me	ca. 5×10^{7} [b]	1.0×10^{1}	1.20	0.02
1,3-$(OMe)_2$		6.4×10^{3}	1.20	2.40
1,3,5-$(OMe)_3$		3.3×10^{7} [b]	1.30	3.40

[a] Nucleophilicity parameters N and s are defined in Section 4.2 (approximate values in parentheses). [b] Laser flash photolysis in acetonitrile at 20 °C. The solvent effect is generally small with these reactions. There is no temperature correction because $\Delta H^{\neq} = 0$

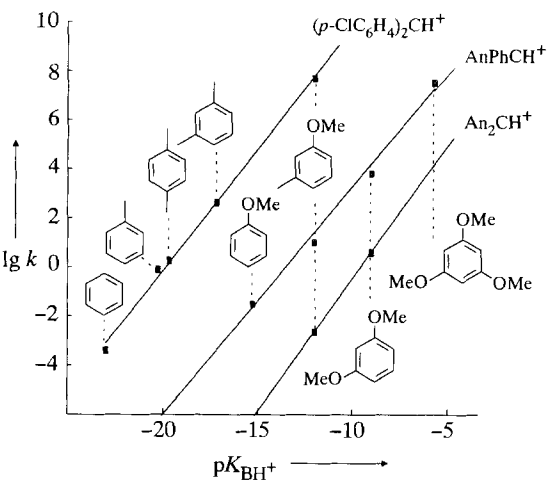


Fig. 7. Correlation between the basicity of arenes and their reactivity towards diarylcarbenium ions (CH_2Cl_2, −70 °C) [38].

3.3.3. Reactivity of n-Nucleophiles

Amines, phosphanes, phosphites, and a number of anions are the most widely investigated representatives of n-nucleophiles. Many reactions with water and hydroxide ions were followed to classify the electrophilicities of carbocations (see Section 3.4.2).

As described in Section 3.2, the rates of the reactions of carbocations with uncharged nucleophiles in aprotic solvents are almost independent of the solvent polarity. Hence the rate constants given in Table 7 for reactions with the tricarbonylcyclohexadienyl iron cation[40] reflect the intrinsic nucleophilicity of phosphanes and phosphites.

Table 7. Rate constants of the reactions of phosphanes and phosphites with the tricarbonylcyclohexadienyliron cation (20 °C, acetone).

Nucleophile	k [L mol^{-1} s^{-1}]	Ref.	Nucleophile	k [L mol^{-1} s^{-1}]	Ref.
P(2-MeOC$_6$H$_4$)$_3$	6.80×10^5	[29, 41]	P(p-ClC$_6$H$_4$)$_3$	9.08×10^2	[29]
PBu$_3$	3.36×10^5	[29]	P(c-C$_6$H$_{11}$)$_3$	1.74×10^2	[29]
	1.3×10^5	[21]	P(2-NCC$_2$H$_4$)$_3$	1.43×10^2	[29]
PEt$_2$Ph	1.55×10^5	[29]		6.39×10^2	[40]
PAn$_3$	6.42×10^4	[29]	P(OBu)$_3$	1.01×10^2	[40]
PTol$_3$	2.83×10^4	[21]		8.44×10^1	[21]
PPh$_2$Tol	8.10×10^3	[29]	P(OEt)$_3$	4.59×10^1	[29]
	1.37×10^4	[40]	P(OMe)$_3$	2.97×10^1	[29]
PPh$_3$	7.46×10^3	[21]	P(2-MeC$_6$H$_4$)$_3$	7.7	[29]
P(2-NCC$_2$H$_4$)Ph$_2$	5.33×10^3	[40]	P(OPh)$_3$	4.13×10^{-2}	[21]
P(p-FC$_6$H$_4$)$_3$	1.57×10^3	[29]			

The higher reactivity of tris(p-tolyl)phosphane and tris(p-anisyl)phosphane relative to triphenylphosphane suggests that the electron density on the phosphorus atom is increased by mesomeric interactions with the substituents. Phosphites are significantly less reactive than phosphanes, because in this case the mesomeric effect is outweighed by the marked negative inductive effect of the oxygen.

Because the rate constants in Tables 7 (phosphanes in acetone) and 8 (amines in acetonitrile) are fairly independent of the solvent, the two sets of data can be compared directly. Amines and phosphanes are thus seen to be similarly nucleophilic in aprotic solvents.

As shown, for example, by McClelland, Steenken et al.,[48] in water-acetonitrile mixtures the nucleophilicity of amines decreases on changing from aprotic to protic solvents, because hydrogen bonds to the nitrogen are formed. For this reason, the nucleophilicity series of amines in water determined by Ritchie (Table 9) differs considerably from the reactivity series in aprotic solvents (Table 8).

Table 8. Rate constants of the reactions of amines with the tricarbonylcyclohexadienyliron cation (20 °C, acetonitrile).

Nucleophile	k [L mol^{-1} s^{-1}]	Ref.	Nucleophile	k [L mol^{-1} s^{-1}]	Ref.
Morpholine	2.65×10^5 [a]	[14]	Phenylalanine methyl ester	5.00×10^3	[40]
2-Methylimidazole	1.40×10^4 [a]	[14]			
N-Methylimidazole	1.00×10^4 [a]	[14]	Aniline	2.78×10^3 [b]	[42]
1-Phenylethylamine	3.62×10^4	[40]	2-Methylpyridine	2.15×10^3 [b]	[44]
Nicotine	2.07×10^4	[40]	o-Methylaniline	2.11×10^3 [b]	[42]
4-Ethylpyridine	1.72×10^4 [b]	[47]	p-Chloroaniline	1.47×10^3 [b]	[45]
p-Methylaniline	1.46×10^4 [b]	[42]	4-Pyridinaldehyde	1.09×10^3	[40]
Imidazole	1.08×10^4	[40, 43]	Nicotinic acid methyl ester	9.80×10^2	[40]
Alanine ethyl ester	9.13×10^3	[40]			
Phenylglycine ethyl ester	6.50×10^3	[40]	2-Ethylpyridine	5.45×10^2	[46]
			4-Pyridinecarbonitrile	3.65×10^2	[40]
Pyridine	7.23×10^3 [b]	[44]		9.37×10^2	[47]
			2,6-Dimethylpyridine	2.80×10^1 [b]	[44]

[a] 0 °C. [b] Extrapolated from Eyring parameters.

Table 9. Rate constants of the reactions of various amines and inorganic anions with malachite green (water, 25 °C).

Nucleophile	k [L mol^{-1} s^{-1}]	Ref.	Nucleophile	k [L mol^{-1} s^{-1}]	Ref.
DABCO [c]	2.6×10^{-3}	[49]	OH^-	1.6	[50]
Et_3N	3.0×10^{-2}	[49]		2.2	[20]
NH_3	3.0×10^{-1}	[50]	CN^-	4.9×10^{-1}	[50]
$MeONH_2$	9.6×10^{-1}	[50]		6.9×10^{-1}	[20]
$HONH_2$	4.34	[50]	ClO^-	1.4×10^3	[50]
H_2NNH_2	4.2×10^1	[50]		5×10^1 [b]	[51]
nPrNH$_2$	1.3×10^1 [a]	[48]	HOO^-	1.3×10^4 [b]	[51]
MeOCH$_2$CH$_2$NH$_2$	3.6 [a]	[48]	SO_3^{2-}	2.8×10^2 [b]	[51]
NCCH$_2$CH$_2$NH$_2$	8.8×10^{-1} [a]	[48]		4.5×10^3	[50]
CF$_3$CH$_2$NH$_2$	5.5×10^{-2} [a]	[48]			

[a] With 33% acetonitrile at 20 °C. [b] 30 °C. [c] DABCO = 1,4-diazabicyclo[2.2.2]octane

The difference in the reactivity of anionic nucleophiles in protic and aprotic solvents, described by Parker for S_N2 reactions,[6] is also observed in the electrophile–nucleophile combination reactions discussed here. Ritchie's N_+ parameters for the azide ion in water (7.6) and in dimethylsulfoxide (DMSO, 10.07) imply, for example, that the azide ion reacts with carbocations in water almost 300 times more slowly than in DMSO.[11] In contrast to the situation for combinations of carbocations with amines discussed above, hydrogen bond formation is not the only factor responsible for the reduced nucleophilicity of anions. Since cation–anion combinations neutralize charge, large reactivity differences on varying solvent polarity are also observed in aprotic solvents.[52] The rates of the combination reactions greatly increase with decreasing solvent polarity, so the reactivity of anionic nucleophiles towards cations can only be defined with respect to a given solvent.

3.3.4. *Reactivity of σ-Nucleophiles (Hydrides)*

In this section, discussion is limited to the abstraction of H^- from hydrides of Main Group 4 elements, which have been studied in detail. In most investigations of hydride abstractions from CH bonds, the triphenylcarbenium ion (= trityl cation) has been employed as the hydride acceptor.[53] Because of their importance in biochemistry, hydride transfers from NADH analogues have been extensively investigated, in particular, N-benzyl-1,4-dihydronicotinamide.[54] Bunton et al. showed that the reactions of cations with this hydride donor obey the N_+ relationship of Ritchie.[55] As these data are primarily used for the characterization of the electrophilicity of carbenium ions, they are discussed in Section 3.4.2.

The reactivity of silanes, germanes, and stannanes towards the hydride acceptor AnPhCH$^+$ increases with increasing metallic character of the central atom and the associated increasing hydride character of the hydrogen (Fig. 8, Table 10). The influence of substituents on the reactivity of the silanes shows that conjugative and hyperconjugative effects assist the formation of the intermediate silicenium ions to a much lesser degree than the formation of carbenium ions. An earlier claim that hydride abstraction from silanes involve a rate-determining one-electron transfer[53a] could be clearly disproved by the H–D isotope effects on reaction rates and products.[28] The transfer of hydride from the silicon to the carbenium center in the rate-determining step was thus confirmed.

Table 10. Rate constants of the reactions of $AnPhCH^+$ with hydride donors (CH_2Cl_2, $-70°$) [28, 56].

Nucleophile	k [$L\,mol^{-1}\,s^{-1}$]	Nucleophile	k [$L\,mol^{-1}\,s^{-1}$]	Nucleophile	k [$L\,mol^{-1}\,s^{-1}$]
$HSiMe_3$	6.37×10^{1}	$HSiPh_3$	8.27	$HSiMe_2(OSiMe_3)$	5.86×10^{1}
$HSiMe_2Et$	9.06×10^{1}	$H_2SiMePh$	5.33	$HSiMe_2(CH_2CMe_3)$	1.65×10^{2}
$HSiMeEt_2$	1.16×10^{2}	$HSiMe_2Ph$	1.49×10^{2}	$HSiMe_2(CH_2SiMe_3)$	4.99×10^{2}
$HSiEt_3$	1.24×10^{2}	$HSiMe_2Tol$	3.30×10^{2}	$HSiMe_2(CH_2GeMe_3)$	8.69×10^{2}
$HSi(n\text{Pr})_3$	2.25×10^{2}	$HSiMe_2An$	8.71×10^{2}	$HSiMe_2(CH_2SnMe_3)$	3.53×10^{3}
$HSi(i\text{Pr})_3$	3.67×10^{2}	$HSiMe_2(p\text{-}ClC_6H_4)$	4.96×10^{1}	$HSiMe(CH_2SiMe_3)_2$	5.12×10^{2}
$HSi(n\text{Bu})_3$	3.85×10^{2}	$HSiMePh_2$	2.24×10^{1}	$HSiMe_2(CH_2SiMe_2n\text{Bu})$	9.79×10^{1}
$H_3Si(n\text{Hex})$	4.79×10^{-2}	$HSiMe_2CH_2Ph$	2.58×10^{1}	$HSiMe_2(CH_2SiMe_2Ph)$	3.44×10^{1}
$H_2Si(n\text{Hex})_2$	7.43	$HSiMe_2CH_2Cl$	2.11×10^{-1}	$HGePh_3$	1.14×10^{2}
$HSi(n\text{Hex})_3$	3.78×10^{2}	$HSiMe_2Cl$	2.1×10^{-1}	$HGe(n\text{Bu})_3$	2.8×10^{4}
H_3SiPh	6.96×10^{-2}	$HSi(SiMe_3)_3$	4.57×10^{2}	$HSnPh_3$	4.98×10^{3}
H_2SiPh_2	1.20				

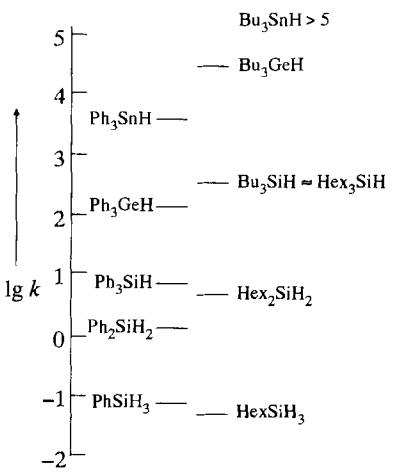


Fig. 8. Rate constants for the reactions of $AnPhCH^+$ with hydride donors (CH_2Cl_2, $-70\,°C$).

The reducing power of *N*-benzyl-1,4-dihydronicotinamide (BDHNA) in water lies between that of BH_4^- and that of BH_3CN^- (Table 11). In less polar solvents the reactivities of the

Table 11. Rate constants of the reactions of the ferrocenyl–anisyl–carbenium ion with 1-benzyl-1,4-dihydronicotinamide (BDHNA) and borohydride anions (25 °C, water) [55].

Nucleophile	k [$L\,mol^{-1}\,s^{-1}$]
BH_4^-	1.5×10^{6}
BDHNA	1.5×10^{5}
BH_3CN^-	7.4×10^{3}

anionic hydride donors BH_4^- and BH_3CN^- are more enhanced than that of BDHNA, with the result that in such solvents the uncharged hydride donor shows the lowest reaction rate of these three reducing agents.[55]

3.4. Electrophiles

3.4.1. The Reactivity-Selectivity Principle as a Basis for Scales of Electrophilicity?

Because of the difficulties in determining absolute reaction rates, the selectivity S_F of electrophiles has been used as an indicator of their reactivity.[39b] S_F expresses the ability of an electrophile to differentiate between the *meta* and *para* positions of a monosubstituted benzene [Eq. (c); m_f, p_f: partial rate factors; b: proportionality constant]. According to the reactivity–selectivity principle, reactive electrophiles are characterized by low selectivity, and less reactive electrophiles by high selectivity. The proportionality between intra- [$\lg(p_f/m_f)$] and intermolecular [$\lg p_f$] selectivity, which is described by Equation (c), is well documented. It is a necessary consequence of the linear free

$$S_F = \lg(p_f/m_f) = b\lg p_f \qquad (c)$$

energy relationships that hold for electrophilic substitutions in the *meta* and *para* positions of a monosubstituted benzene.

The relationship between selectivity S_F and reactivity is less clear, as both slow reactions with low selectivity (mercurations) and rapid reactions with high selectivity (acylations) are known.[57] After the fall of the reactivity–selectivity principle,[58–60] these examples are now no longer exceptions to the rule, and it has become clear that electrophilic reactivities cannot be derived from selectivity data.[16, 26, 59, 60] Scales of electrophilicity must be determined by other means.

3.4.2. Scales of Electrophilicity from "Constant Selectivity Relationships"

Ritchie's N_+ relationship [Equation (b)] contains not only the nucleophilicity parameter N_+, which has been discussed, but also the electrophilicity parameter $\lg k_0$, which is independent of the nucleophile and is the rate constant of the reaction of a given electrophile with water.[9] The parameter $\lg k_0$ can therefore also be represented by E_+ [Eq. (d)].

$$\lg k = E_+ + N_+ \qquad (d)$$

Kane-Maguire, Sweigart et al. analogously obtained a scale of electrophilicity for complexes between transition metals and π-hydrocarbons (Table 12) by using phosphanes and phosphites as reference nucleophiles.[14]

The π-nucleophiles that we have investigated are mostly less reactive than the n-nucleophiles studied by Ritchie, Kane-Maguire, and Sweigart, and are therefore suitable for the characterization of strong electrophiles. Just as the electrophilicity scale of Table 12 is obtained from the y-intercepts in Figure 2, we now obtain the relative electrophilicities of diarylcarbenium

Table 12. Relative reactivities of metal π-complexes towards phosphorus nucleophiles (in acetone, acetonitrile, and nitromethane at 20 °C) [14]. See also Fig. 2.

Electrophile	lg k_{rel}	Electrophile	lg k_{rel}
$[Mn(CO)_3(C_7H_8)]^+$	9.30	$[Fe(CO)_3(C_7H_9)]^+$	5.67
$[Fe(C_6H_6)_2]^{2+}$	8.92	$[Fe(CO)_2(PPh_3)(C_6H_7)]^+$	5.62
$[Fe(CO)_2(NO)(C_4H_4)]^+$	8.15	$[FeCp(CO)_2(C_2H_4)]^+$	5.61
$[Mn(CO)_2(PPh_3)(C_7H_8)]^+$	7.48	$[Mn(CO)(NO)(PPh_3)(C_6H7)]^+$	5.48
$[Fe(CO)_3(C_6H_7)]^+$	7.45	$[FeCp(C_7H_8)]$	5.26
$[Ru(C_6H_6)_2]^{2+}$	7.43	$[Mn(CO)_2(NO)(6\text{-}PhC_6H_6)]^+$	4.78
$[Os(C_6H_6)_2]^{2+}$	6.84	$[Mn(CO)_3(C_6H_6)]^+$	4.70
$[Fe(CO)_3(2\text{-}MeOC_6H_6)]^+$	6.72	$[Re(CO)_3(C_6H_6)]^+$	4.65
$[Fe(CO)(NO)(PPh_3)(C_4H_4)]^+$	6.48	$[Mn(CO)_2(NO)(6\text{-}MeC_6H_6)]^+$	4.60
$[Cr(CO)_3(C_7H_8)]$	6.48	$[CoCp(C_6H_7)]^+$	4.18
$[CoCp(C_8H_{11})]^-$	6.43	$[FeCp(CO)_2(CH_2CHCH_3)]^+$	4.11
$[Mn(CO)_3(NO)(6\text{-}PhC_7H_8)]^+$	6.11	$[Mn(CO)(NO)(PPh_3)(6\text{-}MeC_6H_6)]^+$	2.00
$[Mn(CO)_2(NO)(6\text{-}CNC_6H_6)]^+$	6.08	$[Fe(CO)_2I(C_6H_7)]$	1.95
$[Mo(CO)_3(C_7H_7)]^+$	6.00	$[CoCp(C_7H_9)]^+$	1.88
$[Mn(CO)_2(NO)(C_7H_9)]^+$	5.79	$[Fe(CO)_2I(C_7H_9)]$	0.00
$[W(CO)_3(C_7H_7)]^+$	5.77		

ions from the x-intercepts in Figure 3 and related plots. Since the constant selectivity of diarylcarbenium ions towards terminal vinyl derivatives is also valid for other types of C-electrophiles (Fig. 9),[61] the positions of these electrophiles in Figure 9 reflect their relative electrophilicities.

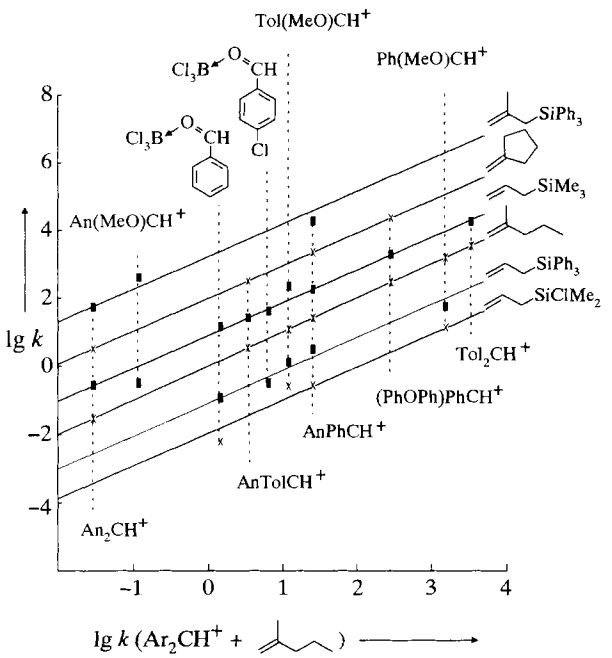
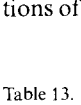
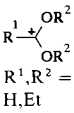
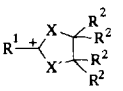
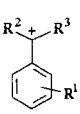
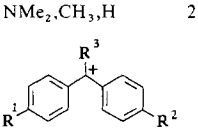


Fig. 9. Rate constants for the reactions of diaryl- and methoxycarbenium ions, and of complexes between aldehydes and Lewis acids with alkenes and allylsilanes (CH_2Cl_2, −70 °C). The rate constants for the reactions of the Lewis acid complexes and the anisyl(methoxy)carbenium ion with 2-methyl-1-pentene were extrapolated from the linear free energy relationship. To facilitate the discussion, the line defined for 2-methyl-1-pentene is also depicted (unity line).

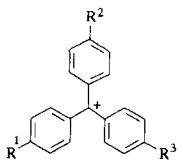
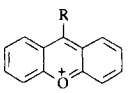
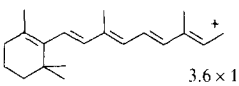
Although the validity of the N_+ relationship has been demonstrated for reactions of some carbenium ions with water, it does not follow that the reactivity order of the electrophiles towards water given in Table 13 exactly reflects their relative reactivity towards other nucleophiles, especially as the k values relate to various mixtures of solvents. The α-methoxybenzyl cation, for example, reacts approximately two orders of magnitude more rapidly with water than the bis(*p*-tolyl)carbenium ion, whereas these two electrophiles hardly differ in their reactivity towards π-nucleophiles (Fig. 9). Possibly the anomeric stabilization of the hemiacetals already affects the transition state of the reactions of carboxonium ions with water. In spite of this discrepan-

Table 13. Pseudo-first-order rate constants for the reactions of carbenium ions with water (20 °C, A = azide clock [24, 68]; B = direct rate measurements); TFE = 2,2,2-trifluoroethanol.

Electrophile	k_w [s^{-1}]	Method	Solvent	Ref.
				
R^1,R^2,R^3 =				
H,Me,H	2×10^9 [a]	A	H_2O	[62]
Me,Me,H	9.5×10^7 [a]	A [d]	TFE/H_2O 1:1	[63]
	5×10^7 [a]	A	H_2O	[62]
Me,Me,OMe	7.0×10^6 [a]	A [d]	TFE/H_2O 2:1	[63]
				
R^1,R^2 =				
H,Et	2×10^7	B	H_2O/CH_3CN	[64]
H,*i*Pr	2.2×10^6	B	H_2O/CH_3CN	[64]
Me,Me	1.8×10^5	B	H_2O/CH_3CN	[64]
Me,-$(CH_2)_3$-	1.8×10^5	B	H_2O/CH_3CN	[64]
Me,Et	2.9×10^4	B	H_2O/CH_3CN	[64]
OMe,-$(CH_2)_3$-	5.4×10^3	B	H_2O	[65]
OMe,Me	1.4×10^3	B	H_2O	[65]
OEt,Et	5.9×10^1	B	H_2O	[65]
				
X,X',R^1,R^2 =				
O,O,H,Me	4.6×10^7	B	H_2O/CH_3CN	[64]
O,O,Me,H	1.4×10^6	B	H_2O/CH_3CN	[64]
O,O,Ph,H	4.0×10^4	B	H_2O/CH_3CN	[64]
O,O,Me,Me	3.8×10^4	B	H_2O/CH_3CN	[64]
O,O,OMe,H	2.7×10^4	B	H_2O	[65]
O,O,An,H	1.2×10^3 [a]	B	CH_3CN/H_2O 1:9	[66]
S,O,An,H	4.6×10^1 [a]	B	CH_3CN/H_2O 1:9	[66]
S,S,Ph,H	5.6×10^{-1} [a]	B	CH_3CN/H_2O 1:1	[67]
S,S,An,H	6.1×10^{-2} [b]	B	CH_3CN/H_2O 1:9	[66]
				
R^1,R^2,R^3 =				
H,Me,H	1×10^{11} [a]	A	TFE/H_2O 1:1	[68]
H,Me,Me	1.7×10^{10} [a]	A	TFE/H_2O 1:1	[69]
Me,Me,H	4×10^9 [a]	A	TFE/H_2O 1:1	[68]
OMe,H,H	2×10^8 [a]	A	TFE/H_2O 1:1	[70]
OMe,Me,H	5×10^7 [a]	A	TFE/H_2O 1:1	[68]
OMe,CO_2Et,H	1.4×10^7 [a]	A	TFE/H_2O 1:1	[71]
NMe_2,CH_3,H	2×10^3 [a]	A	TFE/H_2O 1:1	[68]
				
R^1,R^2,R^3 =				
H,H,H	3×10^8 [a]	A	TFE/H_2O 1:1	[69]
	ca. 9×10^8	B	CH_3CN/H_2O 1:2	[72]
Me,H,H	ca. 1.2×10^8	B	CH_3CN/H_2O 1:2	[72]
H,H,Me	6.8×10^7 [a]	A	TFE/H_2O 1:1	[69]
Me,Me,H	3.2×10^7	B	CH_3CN/H_2O 1:2	[72]
OMe,H,H	2.1×10^6	B	CH_3CN/H_2O 1:2	[72]
OMe,Me,H	9.1×10^5	B	CH_3CN/H_2O 1:2	[72]
OMe,OMe,H	1.3×10^5	B	CH_3CN/H_2O 1:2	[72]
NMe_2,NMe_2,H	2.6×10^{-2}	B	H_2O	[72]

(Table 13 continues on next page)

Table 13 (continued).

Electrophile	k_w [s^{-1}]	Method	Solvent	Ref.
				
R^1,R^2,R^3 =				
NMe_2,NMe_2,NMe_2	3.5×10^{-5} [a]	B	H_2O	[20]
NMe_2,NMe_2,H	2.11×10^{-4} [a]	B	H_2O	[20]
NMe_2,NMe_2,CF_3	2.00×10^{-4} [a]	B	H_2O	[74]
OMe,OMe,OMe	1.00×10^{1}	B	CH_3CN/H_2O 1:2	[72]
H,H,H	1.5×10^{5}	B	CH_3CN/H_2O 1:2	[72]
				
R =				
Ph	4.4×10^{1} [a]	B	H_2O	[75]
An	4.3×10^{1} [a]	B	H_2O	[55]
$(C_5H_5)Fe(C_5H_4)$	2.7×10^{-2} [a]	B	H_2O/CH_3CN 1:1	[55]
				
R =				
H	2.3×10^{4}	B	CH_3CN/H_2O 1:4	[76]
Ph	2.3×10^{1} [a]	B	CH_3CN/H_2O 1:4	[76]
				
R =				
H	2.6 [c]	B	H_2O	[77]
p-ClC_6H_4	1.2 [c]	B	H_2O	[77]
Ph	1.0 [c]	B	H_2O	[77]
An	2.7×10^{-1} [c]	B	H_2O	[77]
p-$Me_2NC_6H_4$	2×10^{-2} [c]	B	H_2O	[77]
	3.6×10^{3}	B	CH_3CN/H_2O 2:3	[78]

[a] At 25 °C. [b] At 30 °C. [c] At 23 °C. [d] Sulfite instead of azide.

cy, the data in Table 13 provide valuable information about the approximate reactivities of numerous synthetically important electrophiles, as shown by the correlation discussed in Section 4.2.

As mentioned in Section 3.3.4, the rate of hydride transfer from *N*-benzyl-1,4-dihydronicotinamide (BDHNA) to many electrophiles has been investigated (Table 14).[54] Because this compound is a relatively strong nucleophile, the investigations focused on electrophiles of very low reactivity, which do not react with water, or do so only sluggishly.

The reaction rates of carbocations with BDHNA were usually determined in water. Because of the possibility of hydrogen bond formation, only the order of magnitude of these rate constants can be compared with those obtained in reactions of BDHNA with cations in aprotic solvents.

3.5. Effect of Temperature

The effect of temperature on selectivity in radical and carbene reactions has been extensively discussed by Giese.[59, 87] The selectivity order of various radicals for a pair of competing reagents above the isoselective temperature is exactly the reverse of that below it, while at the isoselective temperature all the radicals of tbe reaction series show the same selectivity. The isoselective temperature for the reaction of diarylcarbenium ions with the pair allyltrimethylsilane/2-methyl-2-butene, is about 1000 K (Fig. 10), which is far outside the experimental range. In the ideal case of isentropic reaction series, the isoselective temperature is $T = \infty$.

In some cases, the reaction at a particular temperature is completely unselective ($\lg \kappa = 0$), and the relative nucleophilicity of two reaction partners is reversed above and below this temperature. Below -57 °C, for example, the *p*-anisyl(phenyl)carbenium ion reacts more rapidly with 2-methyl-2-butene than with allyltrimethylsilane, while above -57 °C the allyltri-

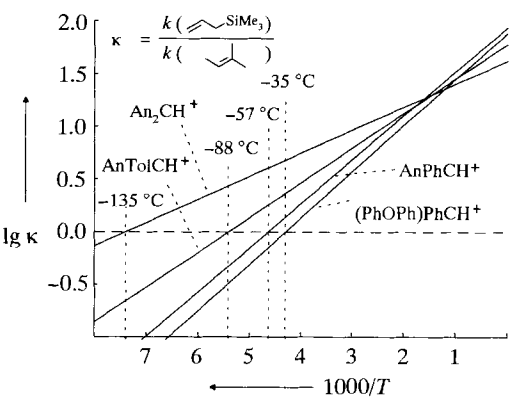


Fig. 10. Selectivity κ of carbenium ions towards the pair allyltrimethylsilane/2-methyl-2-butene as a function of temperature.

Table 14. Rate constants of the reactions of various electrophiles with1-benzyl-1,4-dihydronicotinamide (25 °C, water/acetonitrile; fc = ferrocenyl) [54].

Electrophile	k [$L\,mol^{-1}\,s^{-1}$]	Ref.	Electrophile	k [$L\,mol^{-1}\,s^{-1}$]	Ref.
N-Methylpyridinium	4.2×10^{-7}	[79]	*N*-Methylphthalazinium	4.0×10^{-2}	[83]
3-$CONH_2$	7.5×10^{-4}	[80]	*N*-Methylphenanthridinium	8.0×10^{-2}	[80]
3-NO_2 [d]	7.2×10^{-1}	[80]	*N*-Methyl-3,4-dihydroisoquinolinium	3.3×10^{-3}	[83]
N-methylquinolinium [c]	5.0×10^{-3}	[81]	$[fcAnCH]^+$ [b]	1.5×10^{5}	[55]
3-$CONH_2$	2.8	[81]	$[fc_2CH]^+$	4.7×10^{1}	[55]
3-NO_2	6.5×10^{3}	[81]	$[fc_2PhC]^+$	4.2×10^{-1}	[55]
N-Methylacridinium	4.0×10^{2}	[82]	An_3C^+	2.1×10^{5}	[85]
Tropylium	2.5×10^{4}	[79]	Malachite green	2.7×10^{1}	[85]
Xanthylium	2.7×10^{8}	[79]	Trifluoroacetophenone [c]	8.1×10^{-2}	[86]
N-Methylisoquinolinium	8.0×10^{-4}	[83]	3,10-Dimethyl-5-deazaisoalloxazine [a]	3.4×10^{-2}	[84]
4-$CONH_2$	4.6×10^{-2}	[83]			
5-NO_2	1.2×10^{-1}	[79]			

[a] In isopropanol/water 4:1. [b] In water. [c] 50 °C; in isopropanol/water 1:3. [d] *N*-benzyl compound.

methylsilane is more reactive. At $-57\,^{\circ}C$, the electrophile does not differentiate between the two nucleophiles, and the intersection point with the zero line is termed the aselective temperature.[16b]

A further problem for the construction of reactivity scales is thus encountered. The relative reactivity of the two nucleophiles considered in Figure 10 depends not only on the electrophile but also on the temperature. At low temperatures, 2-methyl-2-butene is always the stronger nucleophile, but above the aselective temperature, which depends on the electrophile, allyltrimethylsilane is more reactive than 2-methyl-2-butene.

The effect of temperature is certainly relatively small in general, with the result that large changes in the electrophilicity and nucleophilicity order do not occur with variations in temperature. If nucleophiles of very similar reactivity but different activation enthalpy (and entropy) are compared, however, a transposition on the reactivity scale may result. How can one judge whether relative reactivities are likely to be affected by such a temperature-dependent reversal?

In almost all the reaction series so far investigated, we have found that the activation entropy is largely dictated by the structural type of the nucleophile, but is influenced only slightly by the nature of the carbocationic electrophile, even when its reactivity changes by about six orders of magnitude (Table 15). If

Table 15. Activation entropies and rate constants ($-70\,^{\circ}C$) for the reactions of carbocations with various nucleophiles (CH_2Cl_2).

Nucleophile	Electrophile	$\Delta S^{\neq}$ [$J\,mol^{-1}\,K^{-1}$]	k [$L\,mol^{-1}\,s^{-1}$]	Ref.
	Tol_2CH^+	−156	6.79×10^{4}	[16]
	$AnTolCH^+$	−151	1.83×10^{1}	[16]
	An_2CH^+	−155	8.38×10^{-2}	[16]
	$(PhOPh)PhCH^+$	−111	1.89×10^{3}	[16]
	$AnPhCH^+$	−122	1.87×10^{2}	[16]
	$AnTolCH^+$	−117	2.63×10^{1}	[16]
	An_2CH^+	−124	2.81×10^{-1}	[16]
	$(p\text{-}Me_2NC_6H_4)_2CH^+$ [b]	−98	1.73×10^{-1}	[88]
	$[Fe(CO)_3(C_6H_7)]^+$ [a, b]	−103	2.55×10^{-2}	[89]
$HSnBu_3$	$(p\text{-}Me_2NC_6H_4)_2CH^+$ [b]	−85	5.22×10^{1}	[56]
	$[Fe(CO)_3(C_6H_7)]^+$ [a, b]	−82	4.87	[89]

[a] In acetone. [b] At 20 °C.

rate constants for electrophile–nucleophile combination reactions are known at only one temperature, the activation parameters and hence the temperature dependence of the reaction rate can therefore be derived from the known rate constant and the estimated activation entropy; $\Delta S^{\neq}$ is assumed to be identical to that for the reaction of the nucleophile concerned (or of a structurally related nucleophile) with any carbocation.

4. Construction of Averaged Scales of Electrophilicity and Nucleophilicity

4.1. The Coexistence of Constant Selectivity Ranges and of Domains of the Reactivity–Selectivity Principle

Strictly speaking, the construction of scales of electrophilicity and nucleophilicity is only meaningful in regions of constant selectivity, as only then is the nucleophilicity series, determined with respect to one electrophile, transferable to another electrophile and vice versa. This situation is almost realized for the systems studied by Ritchie and by Kane-Maguire, Sweigart et al. (cf. Section 2).

In reactions of diarylcarbenium ions with compounds with terminal CC double bonds, the relative reactivity of the π-nucleophiles remains the same while the electrophilicity of the carbenium ions changes by six orders of magnitude ($k = 10^{-2}$–$10^{4}\,L\,mol^{-1}\,s^{-1}$, Fig. 3). For trimethylsiloxycyclohexene and 2-methyl-1-pentene (Fig. 11), the constant selectivity relation-

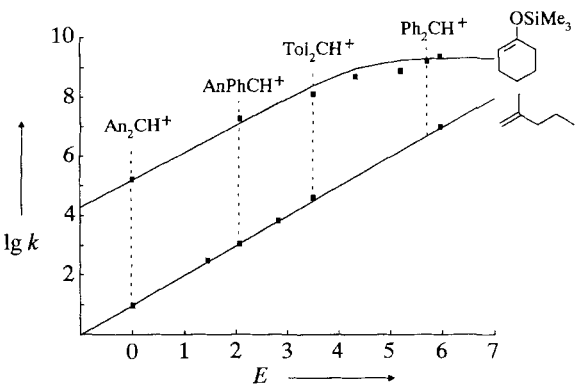


Fig. 11. Comparison of the rate constants of the reactions of diarylcarbenium ions with 2-methyl-1-pentene and trimethylsiloxycyclohexene (20 °C). The electrophilicity parameter E plotted on the x-axis is introduced in Section 4.2.

ship is valid up to rate constants of about $5\times10^{7}\,L\,mol^{-1}\,s^{-1}$. On use of even stronger electrophiles this value of k is exceeded, and the diffusion limit is approached. Then deviations from the linear free energy relationships result, and the ability of the electrophiles to differentiate between the two π-nucleophiles is reduced. An inverse proportionality between reactivity and selectivity can, therefore, only be expected with confidence (see Section 3.5) if the rate constant for at least one of the pair of competing substances is greater than $5\times10^{7}\,L\,mol^{-1}\,s^{-1}$. As the rate constants of the reactions of many reactive intermediates are of this magnitude, the success of the reactivity-selectivity principle in rationalizing the observed carbene and radical reactivities can be explained. Nevertheless, Giese has shown that, even with these systems, violations of the reactivity-selectivity principle often occur.[59]

Our observation that deviations from the linear free energy relationships only occur when the diffusion limit is approached is basically in agreement with the conclusions reached from selectivity studies with carbenium ions produced in solvolysis reactions.[26, 90, 91] It should, however, be noted that in these reactions a narrow transition region has been postulated[91] in which the selectivity is expected to decrease with increasing reactivity because the transition state becomes more similar to the reactants (Hammond region). Our data give no indication of such a region, so in these reactions we question whether a shift of the transition state on the reaction coordinate is the origin of the decreasing selectivity with increasing reactivity.

The relationships between reactivity and selectivity in reactions of carbenium ions with π-nucleophiles do not always have

the simple form shown in Figures 3 and 11. In general, we find that π-nucleophiles with a methyl group at the carbon which forms the new CC bond react more sensitively to a variation in the electrophile than the corresponding unsubstituted compounds. The lines for 2-methyl-2-butene and *trans*-β-methylstyrene in Figure 12, for example, have a greater slope than

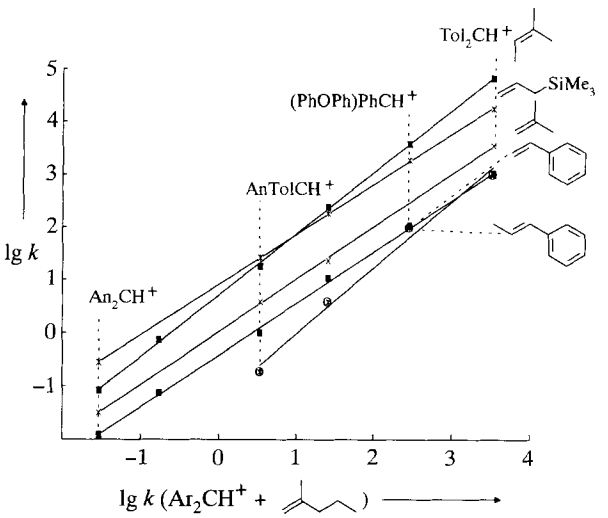


Fig. 12. Rate constants for the reactions of diarylcarbenium ions with various double-bond systems (CH_2Cl_2, −70 °C).

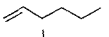
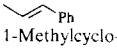
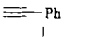
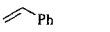
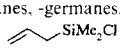
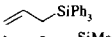
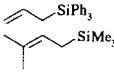
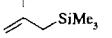
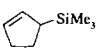
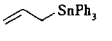
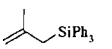
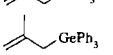
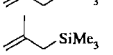
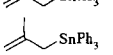
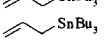
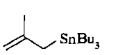
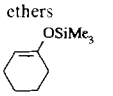
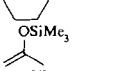
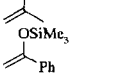
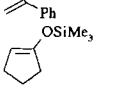
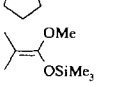
those for *iso*-butene and styrene. Although the reason for the different slopes is not yet clear, it can be excluded that steric factors alone are the cause. Tetramethylethene, 2-methyl-4-trimethylsilyl-2-butene, and 1-methoxy-2-methyl-1-trimethylsiloxy-1-propene, for example, are affected quite differently by variation of the electrophile (Table 16) in spite of the same substituent at the point of attack of the electrophile.

Because of the different slopes (Fig. 12), different types of reactivity-selectivity relationships result in the linear region of the free energy relationships. The bis(*p*-methoxyphenyl)carbenium ion, for example, reacts only a little more rapidly with 2-methyl-2-butene than with *iso*-butene. With increasing electrophilicity of the carbenium ion, the reactivity difference between the two π-nucleophiles initially increases (increasing selectivity) before the approach to the diffusion limit (not shown in Fig. 12) causes it to decrease.

Two reversals of the reactivity–selectivity relationship are observed for the 2-methyl-2-butene/allyltrimethylsilane pair. Carbenium ions with low electrophilicity react more rapidly with allyltrimethylsilane than with 2-methyl-2-butene (Fig. 12). With increasing reactivity of the carbenium ions the selectivity decreases, and the correlation lines cross; on further increase of the electrophilicity, the selectivity increases, now in favor of the 2-methyl-2-butene. If very strong electrophiles are used, the selectivity eventually decreases because the diffusion limit is approached.

The styrene/β-methylstyrene pair behaves similarly. Carbenium ions with low electrophilicity show a preference for styrene; an increase in electrophilicity leads to a reduction in the reactivity difference, the bis(*p*-methylphenyl)carbenium ion reacting with both nucleophiles at equal rates. On further increase in electrophilicity, the reaction rate of the methylated styrene increases to a greater extent, with the result that in competition experiments with the unsubstituted diphenylcarbenium ion, *trans*-β-methylstyrene is favored over styrene by a factor of 4.4.[17b] In this region the selectivity is enhanced in proportion with reactivity, but is reduced on further increase in reactivity, because the two nucleophiles again react with equal rates when the diffusion limit is reached.

Table 16. Nucleophilicity parameters for nonprotic solvents (20 °C, statistically unconfirmed values in parentheses).

No.	Nucleophile Formula	Electrophile [c] (numbers)	s	N	Ref.
Alkenes, alkynes					
1		2, 4, 5, 6	0.98 ± 0.09	−2.02 ± 0.14	[16]
2		1, 6, 7, 9, 10, 11, 12	1.44 ± 0.02	−0.96 ± 0.31	[16, 27]
3		5, 6, 7, 9, 10	1.20 ± 0.05	−0.47 ± 0.10	[16]
4	1-Methylcyclohexene	1, 6, 7, 9, 10, 12	1.10 ± 0.01	0.20 ± 0.19	[16, 27]
5		2, 6, 9	0.70 ± 0.06	0.27 ± 0.11	[30]
6		1, 6, 7, 9, 10, 11, 12, 16, 17	1.16 ± 0.02	0.71 ± 0.31	[16, 27, 93]
7		6, 7, 8, 9, 10, 11, 12, 16, 17	0.97 ± 0.01	0.78 ± 0.05	[16, 93]
8		1, 6, 7, 8, 9, 10, 11, 12, 16, 17, 22, 23	1.00	1.02 ± 0.11	[19, 27, 30, 61, 93]
9		2, 6, 9, 10, 12	1.02 ± 0.01	1.07 ± 0.04	[16, 95]
10		1, 2, 6, 7, 9, 10, 12, 16, 17	0.98 ± 0.02	1.12 ± 0.09	[16, 27, 93, 95]
11		1, 2, 5, 6, 7, 9, 10, 12, 24	1.02 ± 0.03	2.31 ± 0.30	[16, 27, 61]
Allylsilanes, -germanes, and -stannanes					
12		9, 22, 23, 26	1.07 ± 0.07	−0.45 ± 0.10	[35, 61]
13		9, 22, 23, 25, 26	0.92 ± 0.08	0.46 ± 0.05	[35, 61]
14		1, 7, 9, 10, 11, 12	1.25 ± 0.04	0.84 ± 0.13	[35, 96]
15		1,6, 7, 9, 10, 12, 16, 17, 23, 24, 25, 26, 41	1.01 ± 0.03	1.62 ± 0.23	[16, 27, 61, 93, 97]
16		6, 9, 41	0.90 ± 0.05	2.50 ± 0.20	[27, 35, 97]
17		9, 10, 11, 12, 13, 28, 30	0.89 ± 0.01	3.29 ± 0.17	[35, 36, 98]
18		9, 12, 24	0.92 ± 0.04	3.68 ± 0.17	[35, 61]
19		9, 10, 11, 12	0.80 ± 0.04	4.80 ± 0.06	[35]
20		12, 13, 27, 28, 29, 41, 42, 43	0.89 ± 0.03	4.90 ± 0.82	[35, 36, 97, 98]
21		12, 30	(0.82)	5.63	[35, 98]
22		12, 13, 42, 43	0.85 ± 0.04	5.72 ± 0.55	[35, 36, 97]
23		13, 20, 30, 31, 33	0.87 ± 0.10	7.92 ± 0.35	[36, 89, 96]
Silylenol ethers					
24		6, 9, 12, 13, 19, 28, 29, 30	0.92 ± 0.02	5.58 ± 0.18	[27, 36, 89, 96, 98]
25		13, 28, 29	0.90 ± 0.13	5.95 ± 0.24	[88, 98]
26		13, 14, 30, 31, 33	0.89 ± 0.09	6.66 ± 0.28	[88, 89, 99]
27		13, 19, 20, 28, 30	0.93 ± 0.08	6.86 ± 0.46	[36, 89, 96, 98]
28		13, 19, 20, 21, 30, 31, 33	0.93 ± 0.09	9.49 ± 0.45	[36, 89, 96, 100]

(Table 16 continues on facing page)

Table 16 (continued).

No.	Nucleophile Formula	Electrophile [c] (numbers)	s	N	Ref.
Arenes					
	R =				
29	Me	1, 2, 3, 4	1.22 ± 0.21	−4.22 ± 0.10	[38, 101]
30	1,3-Me_2	1, 2, 3, 5, 6	1.40 ± 0.02	−3.31 ± 0.27	[38, 101]
31	OMe	1, 9, 12, 41	1.17 ± 0.08	−1.56 ± 0.49	[38, 97, 101]
32	1-OMe, 3-Me	1, 6, 9, 12, 41	1.20 ± 0.09	0.02 ± 0.50	[38, 97, 101]
33	1,3-$(OMe)_2$	3, 9, 11, 12, 41, 42	1.20 ± 0.05	2.40 ± 0.63	[38, 97, 101]
34	1,3,5-$(OMe)_3$	6, 9, 12	1.30 ± 0.21	3.40 ± 0.45	[38, 101]
35		12, 30	(1.05)	3.86	[14, 97]
Hydride donors					
36	H_3SiPh	5.6, 7, 9	0.76 ± 0.06	−0.05 ± 0.08	[28]
37	$HSiPh_3$	6, 7, 9, 10, 12	0.72 ± 0.01	1.91 ± 0.04	[28]
38	$HSiMe_2Ph$	6, 7, 9, 10, 12, 14, 27, 28, 29	0.72 ± 0.02	3.39 ± 0.15	[28, 53, 98]
39	$HGePh_3$	6, 7, 9, 12	0.66 ± 0.01	3.75 ± 0.03	[56]
40	$HSiBu_3$	9, 10, 11, 12	0.64 ± 0.05	4.48 ± 0.06	[28]
41	$HSnPh_3$	9, 10, 11, 12, 13	0.56 ± 0.01	5.94 ± 0.45	[56]
42	$HGeBu_3$	9, 10, 11, 12, 13	0.69 ± 0.02	6.32 ± 0.15	[56]
43	$HSnBu_3$	13, 21, 30, 31, 33	0.57 ± 0.08	9.29 ± 0.37	[56, 89, 99]
44		14, 18, 19, 21, 29	0.97 ± 0.07	9.45 ± 0.52	[54, 55]
n-Nucleophiles					
45	$P(OPh)_3$	12, 13, 30, 31, 38	0.75 ± 0.14	5.30 ± 0.85	[14, 93]
46	H_2O [a]	2, 5, 6, 9, 10, 12, 13, 14, 15, 18, 28, 29, 42, 43	0.80 ± 0.02	5.80 ± 0.11	[55, 72, 75, 76, 77, 102]
47	MeOH [a]	14, 15	(0.80)	7.73	[103]
48	$H_2NNHCONH_2$ [b]	14, 15	(0.85)	9.39	[104]
49	$F_3CCH_2NH_2$ [b]	10, 12, 14, 15, 18	0.77 ± 0.04	9.55 ± 0.25	[48, 76, 104]
50	$P(OBu)_3$	13, 15, 20, 30, 31, 32, 34, 35, 36, 37, 38, 39, 40	0.70 ± 0.15	10.81 ± 0.16	[14, 15, 93]
51	$EtO_2CCH_2NH_2$ [b]	14, 15	(0.77)	11.68	[104]
52	PPh_3	13, 15, 30, 31, 32, 33, 34, 35, 36, 37, 39, 40	0.80 ± 0.15	13.01 ± 0.19	[14, 15, 93]
53	$PTol_3$	15, 30, 31, 32, 33, 34, 40	0.80 ± 0.14	13.43 ± 0.44	[14, 15]
54		30, 31, 32, 33, 34	0.67 ± 0.02	13.76 ± 0.06	[14]
55		30, 31, 32, 33, 34	0.67 ± 0.21	14.03 ± 0.34	[14]
56	PBu_3	15, 20, 30, 31, 32, 39, 40	0.70 ± 0.11	15.93 ± 0.34	[14, 15]

[a] For pseudo-first-order rate constants with nucleophile as solvent. [b] In water. [c] For the formulas of the electrophiles, see Table 17.

These examples highlight the problems of a single parameter scale of nucleophilicity. If a nucleophilic series is based, for example, on the bis(*p*-methoxyphenyl)carbenium ion as a reference electrophile, the sequence β-methylstyrene < styrene and 2-methyl-2-butene < allyltrimethylsilane is found. If a stronger electrophile (Ph_2CH^+) is used, the sequence becomes styrene < β-methylstyrene and allyltrimethylsilane < 2-methyl-2-butene, and Ph_2CH^+ cannot differentiate at all between strong nucleophiles such as reactive enol ethers.[27] In summary, also for simple electrophile–nucleophile combination reactions, constant selectivity relationships are not strictly fulfilled if a large structural variety of electrophiles and nucleophiles is allowed.

While the problem of diffusion-controlled reactions can be circumvented by using weaker electrophiles for the characterization of strong nucleophiles, the examples discussed above show that even for the electrophile–nucleophile combination reactions illustrated in Figure 12, one single parameter is not sufficient for the characterization of nucleophilic properties. It should rather be borne in mind that in certain cases the *relative* strength of nucleophiles also depends on the electrophile.

4.2. Correlation Analysis

In view of the intersection of correlation lines demonstrated in Section 4.1, it seems expedient not to base the construction of scales of electrophilicity and nucleophilicity on the two-parameter equation of Ritchie [Equation (b)], but also to take into account the different slopes of the correlation lines.

In many investigations of the reactions of diarylcarbenium ions with nucleophiles, the observed rate constants could be represented extremely well by Equation (e) (see also Figs. 3, 9, 12).[16, 28, 35]

$$\lg k = s\lg k_0 + c \qquad \text{(e)}$$

The quantity $\lg k_0$ (rate constant of the reaction of the electrophile with 2-methyl-1-pentene) is a measure of the strength of the electrophile, while the nucleophile is characterized by the quantities c (= 0 for 2-methyl-1-pentene) and s (= 1 for 2-methyl-1-pentene). For nucleophiles stronger than 2-methyl-1-pentene, c adopts a value greater than 0,[92] and for nucleophiles more sensitive than 2-methyl-1-pentene to changes in the electrophile, s is greater than 1.

Problems arise, however, if Equation (e) is used for systems with large absolute values of $\lg k_0$ (very strong or very weak electrophiles), because uncertainties in the value of s have a large effect on the calculated rate constant. We avoid this problem by replacing Equation (e) by Equation (f), which contains,

$$\lg k = s(E + N) \qquad \text{(f)}$$

in addition to an electrophilicity parameter E and a nucleophilicity parameter N, the nucleophile-specific slope parameter s already used in Equation (e). Differences between the s values given in Table 16 and in the literature[16, 28, 35] are mainly due to different reference temperatures.

As most of the experimental values ($\lg k$) used for calculating the correlation lines lie between −4 and +4, inaccuracy in the value of s (= 0.5–1.5) is less serious if Equation (f) is used, because the expression in parentheses ($E + N$) to be multiplied always has a small absolute value. The advantage of using Equation (f) rather than Equation (e) is shown graphically in Figure 13. If the electrophilicity scale is plotted on the x-axis, the nucleophilicity parameter c is obtained, according to Equation (e), from the point of intersection of the correlation lines with perpendiculars at $E = \lg k_0 = 0$, which is sometimes far outside the experimental range. On the other hand, the nucleophilicity parameter N [Eq. (f)] is obtained from the point of intersection of the correlation lines with the horizontal line de-

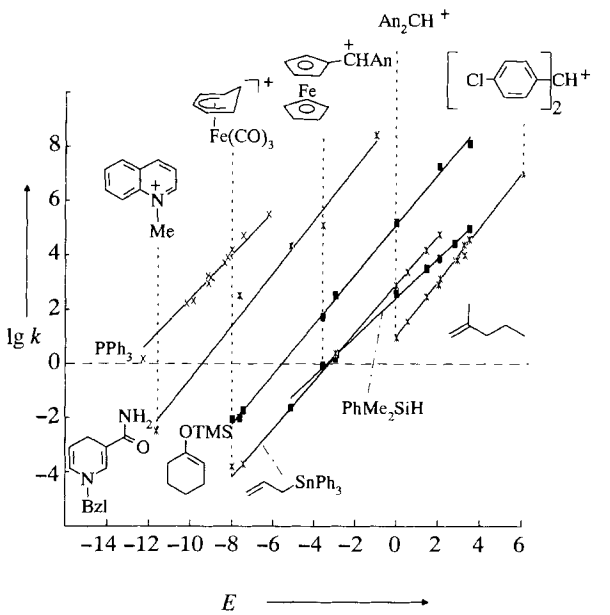


Fig. 13. Rate constants for electrophile–nucleophile combination reactions at 20 °C. Graphical representation of 6 of the 56 correlations listed in Tables 16 and 17.

fined by $\lg k = 0$, which usually lies within or close to the experimental range. The nucleophilicity parameter N then corresponds to the negative value of E for that electrophile with which the nucleophile concerned reacts with a rate constant $k = 1$.

For the correlation analysis, the electrophilicity E of the bis(*p*-methoxyphenyl)methyl cation was set at 0, and the slope parameter s of 2-methyl-1-pentene at 1. Then, the rate constants ($\lg k$) for the combination reactions of diarylcarbenium ions with nucleophiles that have been investigated in detail were subjected to least-squares fitting. The parameters so obtained were kept constant, and other systems were then incorporated by minimizing the squares of the deviations of observed and calculated logarithms of rate constants to yield the data of Table 16.

A standard temperature of 20 °C was chosen for the correlations. In cases where reactions were investigated at another temperature, and activation parameters are not known, the conversion to 20 °C was carried out by estimating the activation entropy (see Section 3.5) which in combination with $\lg k$ allows the activation enthalpy to be calculated.

As the solvent has only a small effect on the rates of most of the electrophile–nucleophile combination reactions discussed here (see Section 3.2), the solvents used in Table 16 are generally not explicitly reported. This information is only given in the case of n-nucleophiles, whose reactivity was frequently investigated in protic solvents, if the nucleophilicity parameters are based on a protic solvent.

Figure 13 illustrates 6 of the 56 lines obtained by correlation analysis. Over the whole reactivity range from very slow reactions ($k \approx 10^{-5}\,\mathrm{L\,mol^{-1}\,s^{-1}}$) up to rate constants of $5 \times 10^{7}\,\mathrm{L\,mol^{-1}\,s^{-1}}$, there are linear relationships. Deviations from linearity only occur as the diffusion limit is approached (see Section 4.1). The series of cationic electrophiles extends from the highly reactive bis(*p*-chlorophenyl)methyl cation ($pK_{R^+} = -14$),[105] which requires very strong Lewis or Brønsted acids for its formation, up to the *N*-methylquinolinium ion ($pK_{R^+} \approx 16.5$),[106] which exists as a cation even in dilute sodium hydroxide solution. A similar reactivity range is covered by nucleophiles, extending from the slightly nucleophilic toluene, through alkylethenes and enol ethers, up to the strongly nucleophilic amines and phosphanes.

Steric effects, which naturally also affect the rate of these reactions, were neglected in our analysis. This is possible because, relative to the enormous reactivity range, the corrections are mostly only small. However, triarylcarbenium ions are excluded from our analysis for the time being to avoid an explicit treatment of the steric effects. It is known that these react significantly more slowly than expected from their Lewis acidity, because of steric shielding.[28, 107]

If the observed pseudo-first-order rate constants for reactions with water (Table 13) are plotted against the electrophilicity parameters E (Table 17), a linear correlation (Eq. (g), and Fig. 14, $r = 0.996$, 13 points plotted) is obtained, from which only the value for the α-methoxybenzyl cation deviates significantly.

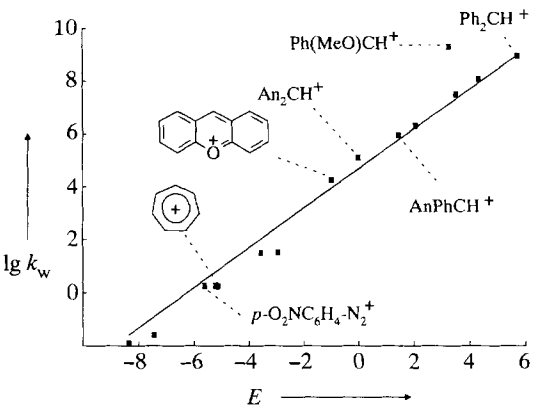


Fig. 14. Correlation between the rate constants of the reactions of electrophiles with water (pseudo-first-order rate constants, Table 13) and the electrophilicity parameters of Table 17.

This correlation equation (g) enables the electrophilicity parameters E to be roughly estimated from known rate constants for the reaction with water. The limits of this method are illustrated by the scatter of the points about the correlation line in Figure 14. As some of the k_w values given in Table 13 are identical to Ritchie's k_0 values, Equation (g) represents the link between our E scale and Ritchie's electrophilicity series.

$$E = 1.24 \lg k_w - 5.80 \quad (k_w \text{ from Table 13}) \qquad \text{(g)}$$

From the overlap of the data in Tables 12 and 17, the correlation equation (h) can be derived, with which Kane-Maguire's k_{rel} values for metal complexes (Table 12) can be converted to electrophilicity parameters E.

$$E = 1.38 \lg k_{rel} - 18.2 \quad (\lg k_{rel} \text{ from Table 12}) \qquad \text{(h)}$$

As the k_{rel} values of Table 12 and the corresponding E values of Table 17 are for the most part based on the same experimental data, the correlation coefficient for Equation (h) is meaningless.

Table 17. Electrophilicity scale for nonprotic solvents (20 °C).

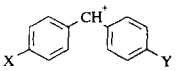
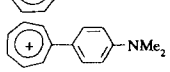
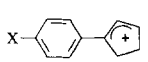
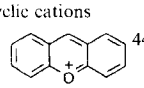
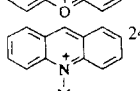
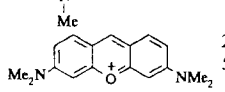
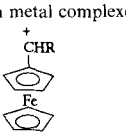
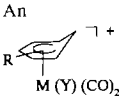
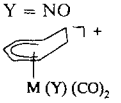
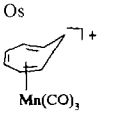
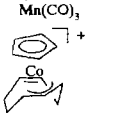
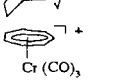
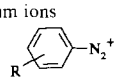
No.	Electrophile Species	Nucleophile [c] No.	E	Ref.
	Benzhydryl cations			
	 X,Y =			
1	Cl,Cl	2, 4, 6, 8, 10, 11, 14, 15, 29, 30, 30, 31, 32	5.96 ± 0.41	[27, 38, 101]
2	H,H	1, 5, 9, 10, 11, 29, 30, 46	5.71 ± 0.21	[16, 27, 30, 72, 95, 101]
3	F,F	29, 30, 33	5.20 ± 0.56	[101]
4	F,H	1, 29	5.37 ± 0.09	[16, 101]
5	Me,H	1, 3, 11, 30, 36, 46	4.33 ± 0.12	[16, 27, 28, 72, 101]
6	Me,Me	1, 2, 3, 4, 5, 6, 7, 8, 9, 10, 11, 15, 16, 24, 30, 32, 34, 36, 37, 38, 39, 46	3.51 ± 0.19	[16, 19, 27, 28, 30, 56, 72, 101]
7	OPh,H	2, 3, 4, 6, 7, 8, 10, 11, 14, 15, 36, 37, 38, 39	2.82 ± 0.06	[16, 19, 28, 35, 56]
8	OPh,Me	7, 8	2.11 ± 0.05	[16, 19]
9	OMe,H	2, 3, 4, 5, 6, 7, 8, 9, 10, 11, 12, 13, 14, 15, 16, 17, 18, 19, 24, 31, 32, 33, 34, 36, 37, 38, 39, 40, 41, 42, 46	2.07 ± 0.19	[16, 19, 27, 28, 30, 35, 38, 56, 72]
10	OMe,Me	2, 3, 4, 6, 7, 8, 9, 10, 11, 14, 15, 17, 19, 37, 38, 40, 41, 42, 46, 49	1.45 ± 0.10	[16, 19, 28, 35, 48, 56, 72]
11	OPh,OMe	2, 6, 7, 8, 14, 17, 19, 33, 40, 41, 42	0.54 ± 0.09	[16, 19, 28, 35, 56, 97]
12	OMe,OMe	2, 4, 6, 7, 8, 9, 10, 11, 14, 15, 17, 18, 19, 20, 21, 22, 24, 31, 32, 33, 34, 35, 37, 38, 39, 40, 41, 42, 45, 46, 49	0	[16, 19, 28, 35, 38, 48, 56, 72, 93, 96, 97, 101]
13	NMe_2, NMe_2	17, 20, 22, 23, 24, 25, 26, 27, 28, 41, 42, 43, 45, 46, 50, 52	−7.45 ± 0.44	[36, 56, 72, 88, 93]
	Allyl and tropylium ions			
14		26, 38, 43, 44, 46, 47, 48, 49, 51	−5.14 ± 0.33	[53, 54, 77, 99, 103, 104]
15		46, 47, 48, 49, 50, 51, 52, 53, 56	−8.36 ± 0.27	[15, 77, 103, 104]
	 X =			
16	Cl	6, 7, 8, 10, 15	3.28 ± 0.42	[93]
17	H	6, 7, 8, 10, 15	2.92 ± 0.28	[93]
	Heterocyclic cations			
18		44, 46, 49	−0.99 ± 0.63	[54, 76]
19		24, 27, 28, 44	−7.63 ± 0.44	[54, 96, 100]
20		23, 27, 28, 50, 56	−9.67 ± 0.60	[15, 96]
21		28, 43, 44	−11.65 ± 0.4	[54, 99, 100]
	Alkoxycarbenium ions			
	 X =			
22	Ph	8, 12, 13	3.26 ± 0.10	[61]
23	Tol	8, 12, 13, 15	2.04 ± 0.11	[61]
24	An	11, 15, 18	0.45 ± 0.24	[61]

Table 17 (continued).

No.	Electrophile Species	Nucleophile [c] No.	E	Ref.
	Carbonyl Lewis acid complexes			
				
25	p-ClC_6H_4 [a]	13, 15	1.03 ± 0.60	[61]
26	Ph [a]	12, 13, 15	0.69 ± 0.60	[61]
	Transition metal complexed cations			
	 R =			
27	Me	20, 38	−2.91 ± 0.05	[98]
28	Ph	11, 17, 20, 24, 25, 27, 38, 46	−2.92 ± 0.42	[75, 98]
29	An	20, 24, 25, 38, 44, 46	−3.70 ± 0.37	[55, 75, 98]
				
30	R = H, M = Fe, Y = CO	17, 21, 23, 24, 26, 27, 28, 33, 35, 43, 45, 50, 52, 53, 54, 55, 56	−8.00 ± 0.47	[14, 89, 98]
31	R = 2-OMe, M = Fe, Y = CO	23, 26, 28, 43, 45, 50, 52, 53, 54, 55, 56	−9.17 ± 0.33	[14, 89]
32	R = 6-Me, M = Mn, Y = NO	50, 52, 53, 54, 55, 56	−12.27 ± 0.4	[14]
				
33	M = Fe, Y = CO	23, 26, 28, 43, 52, 53, 54, 55	−9.88 ± 0.29	[14, 89]
34	M = Mn, Y = NO	50, 52, 53, 54, 55	−10.20 ± 0.1	[14]
	 M =			
35	Fe	50, 52	−6.21 ± 0.15	[14]
36	Ru	50, 52	−8.21 ± 0.13	[14]
37	Os	50, 52	−9.03 ± 0.01	[14]
38		45, 50	−5.12 ± 0.31	[14]
39		50, 52, 56	−8.98 ± 0.23	[14]
40		50, 52, 53, 56	−9.14 ± 0.34	[14]
	Diazonium ions			
	 R =			
41	2,4-$(NO_2)_2$ [b]	15, 16, 20, 31, 32, 33	−2.64 ± 0.56	[97]
42	4-NO_2 [b]	20, 22, 33, 46	−5.62 ± 0.9	[97, 102]
43	H [b]	20, 22	−8.11 ± 1.51	[97]

[a] In dichloromethane. [b] In acetonitrile. [c] For the formulas of the nucleophiles, see Table 16.

In the same way, from the overlap of the entries in Tables 7 and 8 with those in Table 16, Equation (i) is calculated, which

$$N = 1.51 \lg k + 7.53 \ (k \text{ from Tables 7 and 8}) \qquad \text{(i)}$$

represents a link between the nucleophilicity series of Sweigart/Kane-Maguire[14] and the N scale introduced in this article.

Finally, comparison of the data in Table 16 with those in Table 1 of ref. [11] gives Equation (k), which combines Ritchie's N_+ scale with the N scale of Table 16.

$$N = 1.20N_+ + 6.18 \quad \text{(k)}$$

When nucleophilicity parameters derived from Equations (i) and (k) are used in the calculation of rate constants according to Equation (f), the best error compensation is obtained if the slope parameters $s = 0.66$ [Eq. (i)] or $s = 0.83$ [Eq. (k)] are used, these being the reciprocals of the slopes in these equations.

5. Predicting Polar Organic Reactions

If it is assumed that Equation (f) is also valid for combination reactions of nucleophiles and electrophiles given in Tables 16 and 17, but not yet investigated, the rate constants for 2408 electrophile–nucleophile combination reactions can be calculated. If Ritchie and Sweigart/Kane-Maguire scales are incorporated by using Equations (g) to (k), and the extrapolated nucleophilicity parameters of Tables 2, 3, and 6 are included, the forecasting potential is considerably increased.

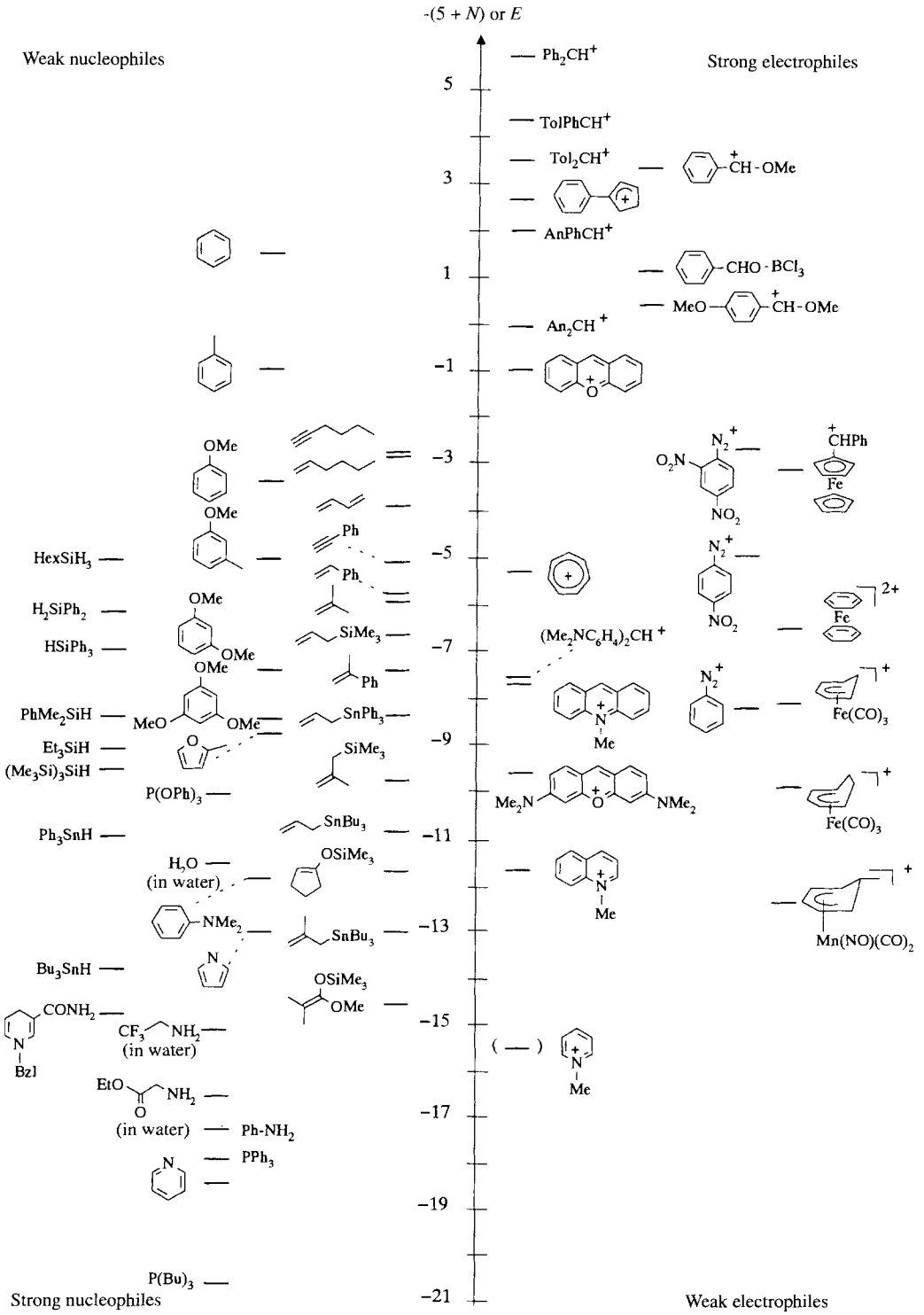


Fig. 15. What reacts with what? Graphical representation of the averaged nucleophilicity and electrophilicity series.

Which electrophile–nucleophile combination reactions take place at 20 °C? In Figure 15 the reaction partners are plotted in such a way that the equation $E = -(5 + N)$ is valid for electrophiles and nucleophiles that are opposite each other. That is, the electrophilicity scale is arranged counter to the nucleophilicity scale. According to Equation (f), for electrophile–nucleophile pairs that are on the same level, $\lg k = -5s$. For most nucleophiles, the limits of s are $0.6 < s < 1.2$ (Table 16); thus for adjacent electrophile–nucleophile pairs, combination rate constants at 20 °C of 10^{-3}–10^{-6} L mol^{-1}s^{-1} are to be expected. If the concentration of the component in excess is 1 mol L^{-1}, half-lives are 12 min to 8 days. To a first approximation, electrophiles will react at 20 °C with all nucleophiles that appear below them in Figure 15. Clearly this can only give a rough picture, and Equation (f) must be used for more precise predictions.

Some examples will illustrate this procedure:

In Figure 15, anisole lies above the tropylium ion; a rapid reaction is unlikely. From Equation (f), a rate constant 10^{-8} L mol^{-1}s^{-1} is calculated, in agreement with the observation that this reaction does not take place at room temperature. Even if tropylium tetrachloroaluminate is heated with anisole to 85 °C, no substitution product is obtained, and the reaction of tropylium chloride with anisole at 85–90 °C for five hours yielded 0.8% *p*-anisylcycloheptatriene.[108] On the other hand, tropylium tetrafluoroborate reacts smoothly at room temperature with allylsilanes,[109] *iso*-butene, and α-methylstyrene,[110] as expected from Figure 15 and Tables 2, 16, and 17.

The tricarbonyl(cyclohexadienyl)iron cation reacts rapidly with silyl enol ethers and allylstannanes even at room temperature.[111] However, the reaction with allyltrimethylsilane required heating for six hours.[112] We are not aware of any reactions of this cation with alkylated ethenes. If these take place at all, they must require more extreme conditions.

Diazo couplings with the benzenediazonium ion are usually carried out with aromatic amines or phenolate ions, whereas phenol ethers are inert. However, the strongly electrophilic 2,4-dinitrobenzenediazonium ion also reacts with anisole, and reaction with the 4-nitrobenzenediazonium ion occurs if the more electron-rich *m*-methylanisole is used.[113] Coupling of 1,3,5-trimethoxybenzene even occurs with the benzenediazonium ion.[113] Likewise, reactions of the 2,4-dinitrobenzenediazonium ion with numerous 1,1-dialkylethenes,[114] styrene,[114] and allylsilanes[115] have been described, but there was no reaction with monoalkylated ethenes.

Equation (f) and the simplified form of Figure 15 not only answers the question whether a reaction proceeds at all, but also helps determine chemoselectivities. If, for example, values of $\lg k$ are calculated to be greater than 8, the diffusion limit is being approached, and hence selectivities in competition reactions will decrease or disappear.

As evident from the derivation, this analysis only considers the kinetic aspects of electrophile–nucleophile combination reactions. Thermodynamic factors are not included, and it is well known that, especially in the coordination of electrophiles with n-nucleophiles, an unfavorable equilibrium often prevents a process that would be expected to take place on kinetic grounds.

6. Conclusions and Future Prospects

The statement made by Pearson 25 years ago that it was then impossible to predict rates of nucleophilic substitutions quantitatively if substrates with very different properties were used is still relevant today.[8] An all-embracing theory of electrophile–nucleophile reactions is still not in sight.

Nevertheless, we have shown in this review that the constant selectivity relationships discovered in the early 1970s by Ritchie, and further developed by Sweigart and Kane-Maguire, are valid with minor modifications in broad areas of organic and organometallic chemistry. These particularly include reactions of cationic carbon electrophiles with nucleophiles in which only one bond is formed in the rate-determining step (no cycloadditions!) and no σ-bonds are broken. However, the fact that hydride transfers (M–H cleavage) and reactions of metallic π-complexes (C–metal cleavage) also obey these simple relationships demonstrates that this is not an indispensable precondition. The behavior of complexes of carbonyl compounds and Lewis acids (Fig. 9) indicates that a positive charge on the electrophile is not essential, in agreement with Ritchie's observation that carboxylic esters or acceptor-substituted ketones show constant selectivity relationships.[11]

We cannot yet offer a conclusive theoretical interpretation of the reactivity relationships presented here. From the MO perturbation method[116] or the configuration-mixing model of Pross and Shaik,[117] a correlation between electron affinity and reactivity of electrophiles would be expected, and also between the ionization potential and the reactivity of nucleophiles. We have shown, however, that in slow reactions ($k = 10^{-4}$–10^{4} L mol^{-1}s^{-1}) of diarylcarbenium ions with π-nucleophiles there is no correlation between ionization potential and nucleophilicity, even if steric factors are held constant.[18a] Nevertheless, we observed a linear relationship between the kinetics ($\Delta G^{\neq}$) and the thermodynamics (ΔG°) of the electrophile–nucleophile combination reactions.[30a]

On the other hand, in rapid reactions ($k \approx 10^{8}$ L mol^{-1}s^{-1}), the relative reactivity of enol ethers is determined mainly by their ionization potential and not by the thermodynamics of the rate-determining step.[27] The transition between the two regions could be explained by a shift of the transition state on the reaction coordinate. According to the Hammond postulate, an early transition state is expected for the more rapid reactions, which accounts for the correlation with the energy of the frontier orbitals. In the slow reactions with a later transition state, the free energy ΔG° of the rate-determining step would play a dominant role. On the other hand, in Section 4.1 we have deduced a constant position for the transition state, based on the absence of the Hammond curvature. This assumption is supported by the observation that the activation entropies, which according to Houk et al. depend on the position of the transition state,[118] are practically constant in our reaction series. Hence, a contradiction arises which we are not able to solve at the present time.

The value of Equation (f) for predicting reactivity is largely dependent on the number of available reactivity parameters. As shown in this review, reliable reactivity data already exist for the most important classes of nucleophiles. Since, for some arenes, absolute rate constants for attack by carbenium ions are now

also known (Tables 5 and 6), the abundant data on electrophilic aromatic substitution reactions can be incorporated into this nucleophilicity scale.[57b, 119] The benefit of this correlation for synthesis design will increase enormously when the well-researched heteroarenes are included.[94]

Our knowledge of the strengths of electrophiles is comparatively scanty. Reliable reactivity data (Table 17) are available for only a few electrophiles, some of which are unimportant for preparative purposes. For some electrophiles whose reaction rates with water are known (Table 13) E-parameters can be estimated, but the range in which Equation (g) is valid is not yet clear. A relationship between electrophilic reactivity and pK_{R^+} values has been reported on several occasions,[54, 72, 120] but the connection between electrophilicity and thermodynamic stability was called into question in a series of more recent papers, which mainly dealt with acceptor-substituted carbocations.[121] For many classes of preparatively important electrophiles, no quantitative reactivity data whatever exists yet, so the determination of more electrophilicity parameters is of the utmost importance for further developments in this area.

Many of the results reported here were obtained by members of this research group during the last decade. Our special thanks are due to them. We thank the Deutsche Forschungsgemeinschaft, not only for support of our work in the past, but also for recently undertaking to fund the continuation of this research within the framework of the "Electrophilicity" project. Financial assistance from the Volkswagen-Stiftung has enabled the expansion into the study of organometallic electrophiles within the framework of the principal program "Organometallic Reactions for Organic Synthesis". Finally, we thank the Fonds der Chemischen Industrie for the general research grant and also for the award of a Kekulé Stipendium to M. Patz.

Received: August 8, 1993 [A 13IE]
German version: *Angew. Chem.* **1994**, *106*, 990
Translated by R. G. Leach, Basingstoke (UK)

[1] G. N. Lewis, *Valence and the Structure of Atoms and Molecules*, The Chemical Catalog Co., **1923**.
[2] a) J. N. Brønsted, *Recl. Trav. Chim. Pays-Bas* **1923**, *42*, 718–728; b) T. M. Lowry, *Chem. Ind. (London)* **1923**, *42*, 43–47.
[3] a) C. K. Ingold, *Recl. Trav. Chim. Pays-Bas* **1929**, *48*, 797–812; b) C. K. Ingold, *J. Chem. Soc.* **1933**, 1120–1127; c) C. K. Ingold, *Chem. Rev.* **1934**, *15*, 225–274.
[4] C. G. Swain, C. B. Scott, *J. Am. Chem. Soc.* **1953**, *75*, 141–147.
[5] a) J. O. Edwards, *J. Am. Chem. Soc.* **1954**, *76*, 1540–1547; b) J. O. Edwards, *ibid.* **1956**, *78*, 1819–1820.
[6] A. J. Parker, *Chem. Rev.* **1969**, *69*, 1–32.
[7] J. F. Bunnett, *Annu. Rev. Phys. Chem.* **1963**, *14*, 271–290; see also: *Nucleophilicity (Adv. Chem. Ser. 215)* (Eds.: J. M. Harris, S. P. McManus), American Chemical Society, Washington DC, **1987**.
[8] R. G. Pearson, H. Sobel, J. Songstad, *J. Am. Chem. Soc.* **1968**, *90*, 319–326.
[9] C. D. Ritchie, *Acc. Chem. Res.* **1972**, *5*, 348–354.
[10] C. D. Ritchie, *Can. J. Chem.* **1986**, *64*, 2239–2250.
[11] C. D. Ritchie, *J. Am. Chem. Soc.* **1975**, *97*, 1170–1179.
[12] a) C. D. Ritchie, J. E. Van Verth, P. O. I. Virtanen, *J. Am. Chem. Soc.* **1982**, *104*, 3491–3497; b) C. D. Ritchie, *ibid.* **1984**, *106*, 7187–7194.
[13] C. D. Ritchie, M. Sawada, *J. Am. Chem. Soc.* **1977**, *99*, 3754–3761.
[14] L. A. P. Kane-Maguire, E. D. Honig, D. A. Sweigart, *Chem. Rev.* **1984**, *84*, 525–543.
[15] T. J. Alavosus, D. A. Sweigart, *J. Am. Chem. Soc.* **1985**, *107*, 985–987.
[16] a) H. Mayr, R. Schneider, U. Grabis, *Angew. Chem.* **1986**, *98*, 1034–1036; *Angew. Chem. Int. Ed. Engl.* **1986**, *25*, 1017–1019; b) *J. Am. Chem. Soc.* **1990**, *112*, 4460–4467.
[17] a) H. Mayr, R. Pock, *Chem. Ber.* **1986**, *119*, 2473–2496; b) R. Pock, H. Mayr, *ibid.* **1986**, *119*, 2497–2509.
[18] a) H. Mayr, *Angew. Chem.* **1990**, *102*, 1415–1428; *Angew. Chem. Int. Ed. Engl.* **1990**, *29*, 1371–1384; b) H. Mayr, R. Schneider, C. Schade, *Makromol. Chem., Macromol. Symp.* **1988**, *13/14*, 43–59.
[19] H. Mayr, R. Schneider, C. Schade, J. Bartl, R. Bederke, *J. Am. Chem. Soc.* **1990**, *112*, 4446–4454.
[20] C. D. Ritchie, G. A. Skinner, V. G. Badding, *J. Am. Chem. Soc.* **1967**, *89*, 2063–2071.
[21] G. R. John, L. A. P. Kane-Maguire, *J. Chem. Soc. Dalton Trans.* **1979**, 873–878.
[22] R. A. McClelland, N. Banait, S. Steenken, *J. Am. Chem. Soc.* **1986**, *108*, 7023–7027.
[23] H. Mayr, R. Pock, *Tetrahedron* **1986**, *42*, 4211–4214.
[24] J. P. Richard, W. P. Jencks, *J. Am. Chem. Soc.* **1982**, *104*, 4689–4691.
[25] R. A. McClelland, V. M. Kanagasabapathy, N. S. Banait, S. Steenken, *J. Am. Chem. Soc.* **1991**, *113*, 1009–1014.
[26] R. Ta-Shma, Z. Rappoport, *J. Am. Chem. Soc.* **1983**, *105*, 6082–6095.
[27] J. Bartl, S. Steenken, H. Mayr, *J. Am. Chem. Soc.* **1991**, *113*, 7710–7716.
[28] H. Mayr, N. Basso, G. Hagen, *J. Am. Chem. Soc.* **1992**, *114*, 3060–3066.
[29] J. G. Atton, L. A. P. Kane-Maguire, *J. Chem. Soc. Dalton Trans.* **1982**, 1491–1498.
[30] a) H. Mayr, R. Schneider, B. Irrgang, C. Schade, *J. Am. Chem. Soc.* **1990**, *112*, 4454–4459; b) B. Irrgang, H. Mayr, *Tetrahedron* **1991**, *47*, 219–228; c) H. Mayr, M. Roth, C. Schade, *J. Org. Chem.* **1994**, *59*, 169–172; d) H. Mayr, J. L. Gonzalez, K. Lüdtke, *Chem. Ber.* **1994**, *127*, 525–531.
[31] H.-J. Schneider, N. Becker, G. Schmidt, F. Thomas, *J. Org. Chem.* **1986**, *51*, 3602–3607.
[32] See, for example, H. C. Brown, M. Borkowski, *J. Am. Chem. Soc.* **1952**, *74*, 1894–1902.
[33] G. Melloni, G. Modena, U. Tonellato, *Acc. Chem. Res.* **1981**, *14*, 227–233.
[34] a) S. E. Denmark, T. Wilson, T. M. Willson, *J. Am. Chem. Soc.* **1988**, *110*, 984–986; b) G. E. Keck, M. B. Andrus, S. Castellino, *ibid.* **1989**, *111*, 8136–8141.
[35] G. Hagen, H. Mayr, *J. Am. Chem. Soc.* **1991**, *113*, 4954–4961; influence of substituents at silicon: M. A. Brook, A. Neuy, *J. Org.Chem.* **1990**, *55*, 3609–3616.
[36] M. Patz, H. Mayr, *Tetrahedron Lett.* **1993**, *34*, 3393–3396.
[37] a) L. A. P. Kane-Maguire, C. A. Mansfield, *J. Chem. Soc. Dalton Trans.* **1976**, 2192–2196; b) G. R. John, L. A. P. Kane-Maguire, *Inorg. Chim. Acta* **1981**, *48*, 179–183; c) G. R. John, C. A. Mansfield, L. A. P. Kane-Maguire, *J. Chem. Soc. Dalton Trans.* **1977**, 574–578.
[38] H. Mayr, J. Bartl, G. Hagen, *Angew. Chem.* **1992**, *104*, 1689–1691; *Angew. Chem. Int. Ed. Engl.* **1992**, *31*, 1613–1615.
[39] a) G. A. Olah, *Acc. Chem. Res.* **1971**, *4*, 240–248; b) L. M. Stock, H. C. Brown, *Adv. Phys. Org. Chem.* **1963**, *1*, 35–154.
[40] T. Ghazy, L. A. P. Kane-Maguire, *J. Organomet. Chem.* **1988**, *338*, 47–53.
[41] J. G. Atton, L. A. P. Kane-Maguire, *J. Organomet. Chem.* **1982**, *226*, C43–C45.
[42] L. A. P. Kane-Maguire, T. I. Odiaka, S. Turgoose, P. A. Williams, *J. Chem. Soc. Dalton Trans.* **1981**, 2489–2495.
[43] D. J. Evans, L. A. P. Kane-Maguire, *Inorg. Chim. Acta* **1982**, *62*, 109–112.
[44] T. I. Odiaka, L. A. P. Kane-Maguire, *J. Chem. Soc. Dalton Trans.* **1981**, 1162–1168.
[45] T. I. Odiaka, *J. Organomet. Chem.* **1987**, *321*, 227–235.
[46] T. I. Odiaka, *J. Chem. Soc. Dalton Trans.* **1986**, 2707–2710.
[47] a) T. I. Odiaka, R. van Eldik, *J. Organomet. Chem.* **1992**, *425*, 89–97; b) *J. Chem. Soc. Dalton Trans.* **1991**, 2215–2218.
[48] R. A. McClelland, V. M. Kanagasabapathy, N. S. Banait, S. Steenken, *J. Am. Chem. Soc.* **1992**, *114*, 1816–1823.
[49] C. D. Ritchie, *J. Am. Chem. Soc.* **1972**, *94*, 3275–3276.
[50] K. Hillier, J. M. W. Scott, D. J. Barnes, F. J. P. Steele, *Can. J. Chem.* **1976**, *54*, 3312–3314.
[51] J. E. Dixon, T. C. Bruice, *J. Am. Chem. Soc.* **1971**, *93*, 6592–6597.
[52] C. Reichardt, *Solvents and Solvent Effects in Organic Chemistry*, VCH, Weinheim, **1988**, pp. 205–207.
[53] a) J. Chojnowski, W. Fortuniak, W. Stańczyk, *J. Am. Chem. Soc.* **1987**, *109*, 7776–7781; b) T. G. Traylor, G. S. Koermer, *J. Org. Chem.* **1981**, *46*, 3651–3656; c) L. M. McDonough, Dissertation, University of Washington, **1960**; d) N. Deno, G. Saines, M. Spangler, *J. Am. Chem. Soc.* **1962**, *84*, 3295–3297; e) G. Giese, A. Heesing, *Chem. Ber.* **1990**, *123*, 2373–2380; f) G. J. Karabatsos, M. Tornaritis, *Tetrahedron Lett.* **1989**, *30*, 5733–5736; g) S. Bradamante, G. A. Pagani, *J. Chem. Soc. Perkin Trans. 2* **1986**, 1035–1046; h) T. G. Traylor, W. Hanstein, H. J. Berwin, N. A. Clinton, R. S. Brown, *J. Am. Chem. Soc.* **1971**, *93*, 5715–5725; i) É. A. Karakhanov, E. A. Dem'yanova, E. A. Viktorova, *Dokl. Akad. Nauk SSSR* **1977**, *233*, 369–370; *Dokl. Chem. Eng. Transl.* **1977**, 144–146.
[54] J. W. Bunting, *Bioorg. Chem.* **1991**, *19*, 456–491; see also S. Fukuzumi, *Adv. Electr. Transfer* **1992**, *2*, 67–175.
[55] C. A. Bunton, N. Carrasco, F. Davoudzadeh, W. E. Watts, *J. Chem. Soc. Perkin Trans. 2* **1980**, 1520–1528.
[56] a) H. Mayr, N. Basso, *Angew. Chem.* **1992**, *104*, 1103–1105; *Angew. Chem. Int. Ed. Engl.* **1992**, *31*, 1046–1048; b) N. Basso, S. Görs, E. Popowski, H. Mayr, *J. Am. Chem. Soc.* **1993**, *115*, 6025–6028.
[57] a) A. Pross, *Adv. Phys. Org. Chem.* **1977**, *14*, 69–132; b) R. Taylor, *Electrophilic Aromatic Substitution*, Wiley, Chichester, **1990**, Chap. 11.

[58] a) O. Exner, *J. Chem. Soc. Perkin Trans. 2* **1993**, 973–979; b) C. D. Johnson, B. Stratton, *ibid.* **1988**, 1903–1907.
[59] B. Giese, *Angew. Chem.* **1977**, *89*, 162–173; *Angew. Chem. Int. Ed. Engl.* **1977**, *16*, 125–136.
[60] E. Buncel, H. Wilson, *J. Chem. Educ.* **1987**, *64*, 475–480.
[61] G. Gorath, H. Mayr, unpublished.
[62] T. L. Amyes, W. P. Jencks, *J. Am. Chem. Soc.* **1989**, *111*, 7888–7900.
[63] P. R. Young, W. P. Jencks, *J. Am. Chem. Soc.* **1977**, *99*, 8238–8248.
[64] S. Steenken, R. A. McClelland, *J. Am. Chem. Soc.* **1989**, *111*, 4967–4973.
[65] S. Steenken, J. Buschek, R. A. McClelland, *J. Am. Chem. Soc.* **1986**, *108*, 2808–2813.
[66] T. Okuyama, *Acc. Chem. Res.* **1986**, *19*, 370–376.
[67] T. Okuyama, N. Haga, S.-y. Takane, K. Ueno, T. Fueno, *Bull. Chem. Soc. Jpn.* **1991**, *64*, 2751–2756.
[68] J. P. Richard, M. E. Rothenberg, W. P. Jencks, *J. Am. Chem. Soc.* **1984**, *106*, 1361–1372.
[69] T. L. Amyes, J. P. Richard, M. Novak, *J. Am. Chem. Soc.* **1992**, *114*, 8032–8041.
[70] T. L. Amyes, J. P. Richard, *J. Am. Chem. Soc.* **1990**, *112*, 9507–9512.
[71] J. P. Richard, T. L. Amyes, I. W. Stevens, *Tetrahedron Lett.* **1991**, *32*, 4255–4258.
[72] R. A. McClelland, V. M. Kanagasabapathy, N. S. Banait, S. Steenken, *J. Am. Chem. Soc.* **1989**, *111*, 3966–3972.
[73] a) Ref. [52], pp. 19–21; b) I. L. Bagal, S. A. Skvortsov, A. V. El'tsov, *J. Org. Chem. USSR (Engl. Transl.)* **1978**, *14*, 328–337.
[74] C. D. Ritchie, D. J. Wright, D.-S. Huang, A. A. Kamego, *J. Am. Chem. Soc.* **1975**, *97*, 1163–1170.
[75] C. A. Bunton, N. Carrasco, W. E. Watts, *J. Organomet. Chem.* **1977**, *131*, C21–C25.
[76] R. A. McClelland, N. Banait, S. Steenken, *J. Am. Chem. Soc.* **1989**, *111*, 2929–2935.
[77] C. D. Ritchie, H. Fleischhauer, *J. Am. Chem. Soc.* **1972**, *94*, 3481–3483.
[78] N. J. Pienta, R. J. Kessler, *J. Am. Chem. Soc.* **1992**, *114*, 2419–2428.
[79] J. W. Bunting, M. M. Conn, *Can. J. Chem.* **1990**, *68*, 537–542.
[80] J. W. Bunting, J. L. Bolton, *Tetrahedron* **1986**, *42*, 1007–1019.
[81] J. W. Bunting, N. P. Fitzgerald, *Can. J. Chem.* **1985**, *63*, 655–662.
[82] J. W. Bunting, V. S. F. Chew, N. P. Fitzgerald, A. Gunasekara, H. T. P. Oh, *Bioorg. Chem.* **1984**, 141–157.
[83] J. W. Bunting, V. S. F. Chew, G. Chu, *J. Org. Chem.* **1982**, *47*, 2303–2307, 2308–2312.
[84] D. Ostović, I.-S. H. Lee, R. M. G. Roberts, M. M. Kreevoy, *J. Org. Chem.* **1985**, *50*, 4206–4211.
[85] C. A. Bunton, S. K. Huang, C. H. Paik, *Tetrahedron Lett.* **1976**, 1445–1448.
[86] J. J. Steffens, D. M. Chipman, *J. Am. Chem. Soc.* **1971**, *93*, 6694–6696.
[87] B. Giese, *Acc. Chem. Res.* **1984**, *17*, 438–442.
[88] M. Müller, H. Mayr, unpublished.
[89] H. Mayr, K.-H. Müller, D. Rau, *Angew. Chem.* **1993**, *105*, 1732–1734; *Angew. Chem. Int. Ed. Engl.* **1993**, *32*, 1630–1632.
[90] R. Ta-Shma, Z. Rappoport, *Tetrahedron Lett.* **1982**, *23*, 781–784.
[91] J. P. Richard, T. L. Amyes, T. Vontor, *J. Am. Chem. Soc.* **1992**, *114*, 5626–5634.
[92] Because of the differences in the slope s, this is strictly valid only for the comparison of the reactivity of nucleophiles towards an electrophile that reacts with 2-methyl-1-pentene at $-70\,^{\circ}C$ with a rate of $\lg k = 0$.
[93] B. Irrgang, H. Mayr, unpublished.
[94] A. R. Katritzky, R. Taylor, *Adv. Heterocycl. Chem.* **1990**, *47*, 1–467.
[95] Y. Wang, L. M. Dorfman, *Macromolecules* **1980**, *13*, 63–65.
[96] M. Patz, H. Mayr, unpublished.
[97] K. Grimm, M. Hartnagel, H. Mayr, unpublished.
[98] D. Rau, H. Mayr, unpublished.
[99] H. Lies, H. Mayr, unpublished.
[100] S. Fukuzumi, M. Fujita, S. Noura, J. Otera, *Chem. Lett.* **1993**, 1025–1028.
[101] J. Bartl, Dissertation, Medizinische Universität, Lübeck, **1990**.
[102] C. D. Ritchie, D. J. Wright, *J. Am. Chem. Soc.* **1971**, *93*, 6574–6577.
[103] C. D. Ritchie, P. O. I. Virtanen, *J. Am. Chem. Soc.* **1972**, *94*, 4963–4965.
[104] C. D. Ritchie, P. O. I. Virtanen, *J. Am. Chem. Soc.* **1973**, *95*, 1882–1889.
[105] N. C. Deno, J. J. Jaruzelski, A. Schriesheim, *J. Am. Chem. Soc.* **1955**, *77*, 3044–3051.
[106] J. W. Bunting, *Tetrahedron* **1987**, *43*, 4277–4286.
[107] a) C. Schade, H. Mayr, *Makromol. Chem. Rapid Commun.* **1988**, *9*, 477–482; b) J.-P. Dau-Schmidt, H. Mayr, *Chem. Ber.* **1994**, *127*, 205–212.
[108] D. Bryce-Smith, N. A. Perkins, *J. Chem. Soc.* **1962**, 5295–5297.
[109] G. Picotin, P. Miginiac, *Tetrahedron Lett.* **1988**, *29*, 5897–5898.
[110] C. Schell, E. Bäuml, H. Mayr, unpublished.
[111] A. J. Birch, L. F. Kelly, A. S. Narula, *Tetrahedron* **1982**, *38*, 1813–1823.
[112] L. F. Kelly, A. S. Narula, A. J. Birch, *Tetrahedron Lett.* **1980**, *21*, 871–874.
[113] K. H. Schündehütte, *Methoden Org. Chem. (Houben-Weyl) 4th ed. 1952–* Bd. X/3, **1965**, p. 232ff.
[114] a) H. Marxmeier, E. Pfeil, *Chem. Ber.* **1964**, *97*, 815–826; b) *Justus Liebigs Ann. Chem.* **1964**, *678*, 28–38.
[115] H. Mayr, K. Grimm, *J. Org. Chem.* **1992**, *57*, 1057–1059.
[116] a) I. Fleming, *Frontier Orbitals and Organic Chemical Reactions*, Wiley, London, **1976**; b) R. F. Hudson, *Angew. Chem.* **1973**, *85*, 63–84; *Angew. Chem. Int. Ed. Engl.* **1973**, *12*, 36.
[117] a) S. S. Shaik, *J. Org. Chem.* **1987**, *52*, 1563–1568; b) A. Pross, *Adv. Phys. Org. Chem.* **1985**, *21*, 99–196; c) S. S. Shaik, A. Pross, *J. Am. Chem. Soc.* **1989**, *111*, 4306–4312.
[118] K. N. Houk, N. G. Rondan, J. Mareda, *Tetrahedron* **1985**, *41*, 1555–1563.
[119] a) *Friedel-Crafts and Related Reactions, Vol 1–4* (Ed.: G. A. Olah), Interscience, New York, **1963–1965**; b) G. A. Olah, *Friedel-Crafts Chemistry*, Wiley, New York, **1973**.
[120] a) E. M. Arnett, K. Molter, *J. Phys. Chem.* **1986**, *90*, 383–389; b) *Acc. Chem. Res.* **1985**, *18*, 339–346.
[121] a) J. P. Richard, T. L. Amyes, L. Bei, V. Stubblefield, *J. Am. Chem. Soc.* **1990**, *112*, 9513–9519; b) J. P. Richard, *J. Org. Chem.* **1994**, *59*, 25–29; c) L. J. Johnston, P. Kwong, A. Shelemay, E. Lee-Ruff, *J. Am. Chem. Soc.* **1993**, *115*, 1664–1669; d) T. L. Amyes, I. W. Stevens, J. P. Richard, *J. Org. Chem.* **1993**, *58*, 6057–6066.

The First Total Syntheses of Taxol

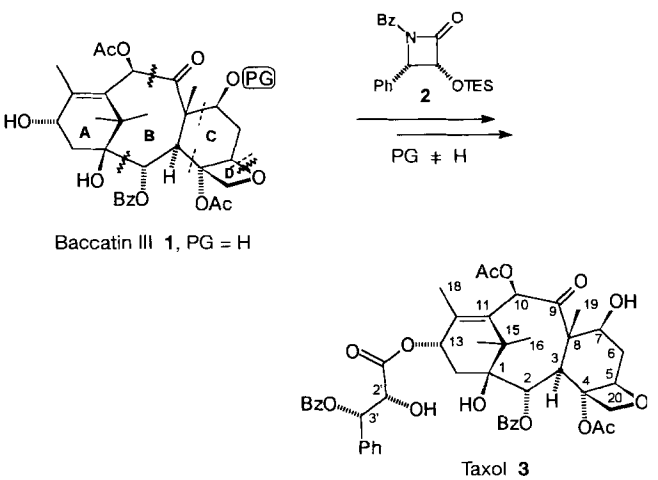
Ludger Wessjohann*

In modern chemistry it is a considerable rarity for the total synthesis of a medicinally and commercially significant natural product not to appear till 22 years after its complete structural elucidation. Though taxol (**3**)[1] is currently the most promising agent against breast cancer and other types of cancer, it took some time before synthetic chemists became interested in it, for several reasons. Thus, nearly a decade elapsed before taxol's biological mode of action—an unusual stabilization of the microtubuli—and its significance for novel cancer therapy were recognized (cf. ref. [1]).

However, from the middle of the 1980s onwards, the number of synthetic attempts increased in an almost explosive manner. Intense competition developed to complete the first total synthesis of this unusual and demanding molecule, a race which involved (and involves) over forty of the best known research groups in the field of natural product synthesis. Taxol and the efforts to complete its synthesis gave rise—at least in the USA and amongst natural product chemists—to at least as much excitement as did fullerenes in physical chemistry, though with the decided difference that taxol did not possess just "potential" applications. Indeed, because of problems with supply and limited possibilities to synthesize derivatives, its full medicinal potential has still only been investigated to a limited extent. For studies of structure–function relationships, the total synthesis is of great importance, especially in preparing the way for the synthesis of derivatives.

An initial highpoint has now been reached with the first two total syntheses by R. A. Holton et al.[2] (Florida State University) and K. C. Nicolaou et al.[3] (University of California, San Diego and Scripps Research Institute).

What was it that made the synthesis of taxol so difficult? For a while, the assertion that every molecule that can exist can today be made, given enough manpower,[4] was almost called into question. To analyse the problem, it is useful to concentrate on the tricyclic A/B/C-ring system of Baccatin III (**1**), which can be treated with **2**, for example, by the method of Holton and Ojima (Scheme 1) to give taxol.[1–3] The oxetane ring (D) is usually treated as a functional group. Apart from this group, the most remarkable feature is the unusual anti-Bredt double bond of the A-ring. However, in contrast to normal doctrine, in this case it leads to a reduction in the total strain (ca. -1.5 kcal mol^{-1}), whereas the very rigid, arched structure of the entire molecule is highly strained from the steric effect of the bridgehead dimethyl groups at C15 (strain energy $\approx +10$ kcal mol^{-1}), in cooperation with the C8-methyl group, which also projects outwards.



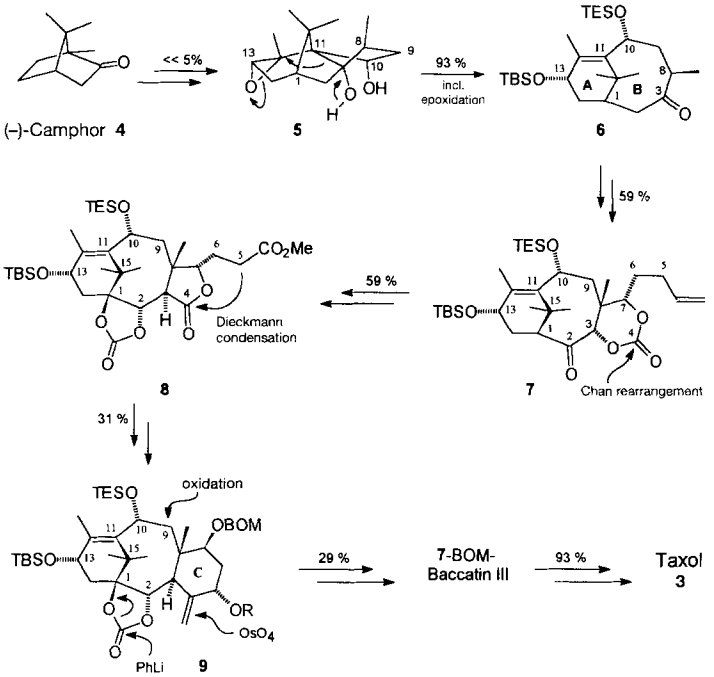
Scheme 1. Semisynthesis of taxol from protected Baccatin III according to Holton and Ojima (cf. ref. [1]); strategic bond cleavages for the syntheses of Holton et al. [2] (– – –) and Nicolaou et al. [3] (∿∿) are indicated. PG = protecting group.

The main problem in taxol synthesis is, then, the construction of the highly functionalized, central, eight-membered ring (B). Although the methyl groups (C16/C19) projecting into this ring are not too close to each other (convex face) in taxol, most reactions with prefabricated A/C rings bring them into too close a proximity during the B-ring closure reaction. In addition, the possibilities for subsequent stereoselective functionalization of the central eight-membered ring are very limited, because of its rigidity and steric shielding, and because of the lability of the oxetane ring and the C7 stereocenter (retroaldol/aldol reaction to the more stable epimer). Till recently, in most syntheses of the taxane skeleton (A/B/C rings) one of the two (or three) central methyl groups have been missing. If all of them were indeed present, it has not been possible to introduce the necessary functional groups afterwards. The two successful research groups have solved these problems very differently, but in part with almost identical reactions.[5]

Holton et al.[2] first constructed the A and B rings, in a linear strategy using the elegant fragmentation of the [3.3.0] system **5** derived from β-patchoulene oxide (Scheme 2), which they had previously used for the synthesis of *ent*-taxusine. However, to

[*] Dr. L. Wessjohann
Institut für Organische Chemie der Universität
Karlstrasse 23, D-80333 München (FRG)
Telefax: Int. code + (89)5902-483

 © VCH Verlagsgesellschaft mbH, D-69451 Weinheim, 1994 0570-0833/94/0909-0959 $ 10.00+.25/0



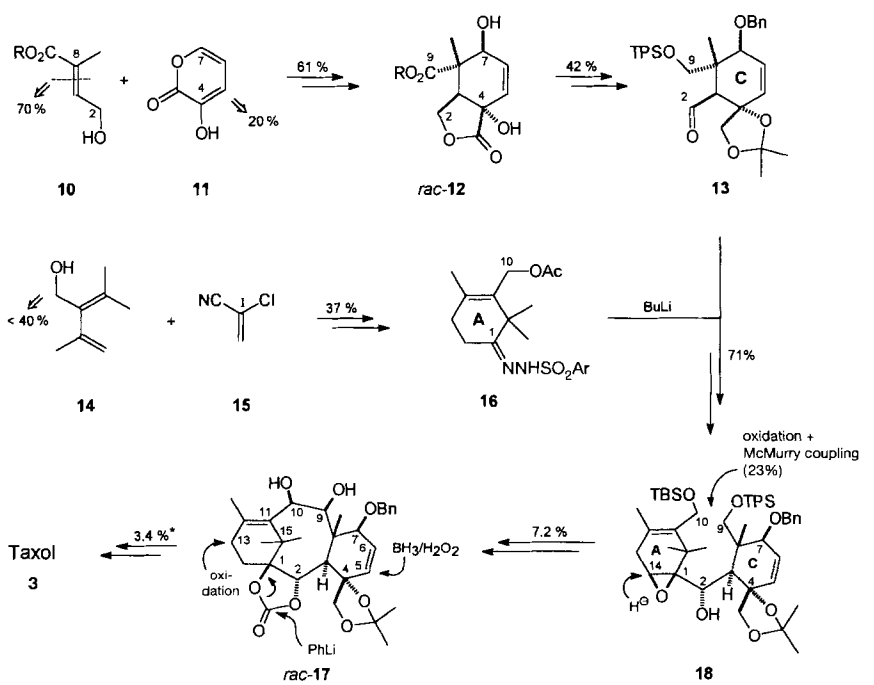
Scheme 2. Total synthesis of taxol according to Holton et al. [2]. Taxol numbering (Scheme 1) used.

obtain the correct enantiomeric series, they had to start extravagantly, using (–)-camphor. The resulting A/B fragment **6** contains the complete, homochiral A-ring and all the methyl groups, as well as one oxygen functional group in both the upper and lower regions for further modifications.

The difficult stereocenter at C7 was constructed early, by using a diastereoselective aldol reaction with magnesium diisopropylamide and 4-pentenal. Since three of the four missing C-ring atoms could be introduced here in a simple manner, derivatizations will later presumably be easy at this step. C4 was provided by a carboxylic ester—also used as a protecting group in intermediate **7**—by an unusual Chan rearrangement. This was followed by a few less elegant steps for deoxygenation at C3 (SmI_2) and oxidation at C1. The latter was only possible with the B/C-*cis* compound, by an unusual, selective enolate formation to the bridgehead C1 rather than to the doubly activated C3—further proof for the unusual steric and conformational characteristics of taxoids. After reduction and isomerization to the *trans* compound, the resulting C1/C2 diol was quantitatively protected with phosgene (cf. **8**) to prepare for the later formation of the benzoate at C2 by addition of phenyllithium and selective fragmentation[6](cf. **9**). First, however, the vinyl group had to be degraded oxidatively to give the ester **8**. The C-ring was then closed by an effective Dieckmann condensation, and decarbalkoxylated.

The remaining keto group at C4 makes possible the oxidation of C5, and conversion to the methylene compound **9**. This last step is sterically problematic and was achieved in moderate yield by a methyl Grignard addition in dichloromethane (instead of ether) and elimination with Burgess' reagent. Dihydroxylation afforded the precursor to the oxetane, which was obtained by nucleophilic substitution of the secondary mesyl or tosyl group at C5, followed by acetylation of the tertiary OH group. These steps, with substitution at the secondary carbon rather than at the primary one (as suggested by the textbooks), were almost identical to those also used by Nicolaou et al.[3] (38%; Holton: 48%). In principle they correspond to the biosynthesis proposed by Halsall and Potier (see ref. [1]). Finally, the upper bridge in the B-ring had to be oxidized, for which benzeneselenic anhydride was very cleverly employed. On the route to 7-BOM-Baccatin III, one should also mention the unusual release of the TBS-protected C13-OH group with tris(dimethylamino)sulfur(difluorotrimethylsilanide).

Nicolaou et al., who only worked on the synthesis of taxol for about two years,[3] follow a much more convergent route (Scheme 3), which begins, however, with achiral precursors. The A-ring precursor was constructed by a Diels–Alder reaction (**14** + **15**) and refunctionalized to the sulfonylhydrazone **16**. This reacted according to Shapiro to give the corresponding alkenyllithium nucleophile, a procedure which is reminiscent of Funk's synthetic route (see ref. [1]). The C2 aldehyde group of **13** served as the electrophile and reacted diastereoselectively in excellent 82% yield to give the A–C coupled alcohol. Chelate-directed epoxidation of this alcohol then led to **18**. Compound **13** was accessible from racemic **12**, the product of the Diels–Alder reaction between 3-hydroxypyrone **11** (from mucic acid) and the dienophile **10**. The epoxide **18** was selectively hydrogenated at C14, and the resulting C1/C2 diol protected as the carbonate (see above).[6]



Scheme 3. Total synthesis of taxol according to Nicolaou et al. [3]. Taxol numbering (Scheme 1) used. * = yield obtained without enantiomer separation. The percentages above the retrosynthetic arrows for the compounds **10**, **11**, and **14** relate to their yields from readily available precursors according to the literature given in reference [3].

After oxidation of C9 and C10 to the aldehyde level, the key step followed. This was a well-established step in constructing strained structures, a McMurry–pinacol coupling to the top B-ring bridge, which afforded the diol **17** in 23% yield. The only other successful eight-membered ring closure starting from an "advanced" A/C system *with* methyl groups is also based on a McMurry reaction at this step, and also led to yields in the lower 20% region. (Kende, also cf. Pattenden). Nicolaou et al., however, only carried out this reaction as far as the diol **17**, permitting further functionalization and enantiomer separation. With Kende's alkene, this is clearly not easily possible.

In order to construct the oxetane ring, the C5–C6 double bond is hydroborated and oxidized with moderate regioselectivity and yield. Oxetane ring closure and benzoate formation at C2[6] follow as already discussed. The late oxidation at C13, the linkage point to the taxol sidechain, is unusual.

When the total yields are directly compared, the more convergent method of Nicolaou et al. is clearly less efficient, especially since the difficulties of enantiomer separation or an—presumably less favorable –asymmetric synthesis are not taken into account (ca. 0.07% compared with 2.7%, or, starting from commercially available materials, about 0.01% against 0.1%).[5] Holton's synthesis shows quite good yields throughout, whereas that of Nicolaou et al. still has room for improvements. At least for the McMurry reaction, these will be very difficult to achieve. In the end, however, a comparison of number of steps and yields in this case is senseless, since for such complex syntheses it tells us very little about the total effort required, or about the practicability of the synthesis.

A more important question concerns which procedure will allow directed synthesis of taxol derivatives. Derivatizations should take place as late as possible in the reaction sequence, in order to minimize the additional labor required. This requirement is better met by a more convergent synthesis such as that of Nicolaou et al. It also more easily permits permutations in the building blocks and the synthesis of A-ring derivatives. C-ring derivatives can, in principle, be provided by both procedures. With Nicolaou's procedure, however, the problem arises that increased steric hindrance with more complex derivatives may lead to even worse yields for the ring closure or in the carbonate formation.[7] Experience has taught us that with taxanes even the tiniest changes in the substituents or the skeleton can cause great problems with the synthesis. It remains to be seen whether the syntheses presented can provide novel taxol derivatives quickly and in significantly improved yields.

A comparison with other syntheses which have not yet been completed must not be forgotten. It is apparent that the route which has probably been chosen most often, fragmentation of bicyclo[4.2.0] systems to yield the B-ring, was not involved in the first success, even though it represents the quickest and, with respect to the reagents, probably simplest (cheapest) entry to the tricycle. As examples I would like to emphasize the elegant synthetic routes of Blechert et al.[8] and of Wender and Mucciaro.[9] The former leads from simple starting materials primarily by aldol and photochemistry to model compounds which are already active. The latter resembles the Holton synthesis in the construction of the A/B ring system, but makes use of a 4/6 precursor of the B-ring instead of a 5/5 one. This allows the use of inexpensive α-pinene to produce the enantiomerically pure tricycle in only six steps. A combination of this procedure with Holton's C-ring annelation is conceivable.

In spite of the fantastic successes from the groups of Holton and Nicolaou, much excitement remains in the race for a total synthesis which is superior to semisynthetic and biological procedures not only with respect to variability, but also to yield, and commercial feasibility.

German version: *Angew. Chem.* **1994**, *106*, 1011

[1] Recently, several excellent review articles on the chemistry and biology of taxol have been published, as well as its history and even politics with the compound. For this reason I have not quoted all the preliminary work and synthetic routes of other authors individually in the text; they are found in K. C. Nicolaou, W.-M. Dai, R. K. Guy, *Angew. Chem.* **1994**, *106*, 38–69; *Angew. Chem. Int. Ed. Engl.* **1994**, *32*, 45; C. S. Swindell, *Org. Prep. Proced. Int.* **1991**, *23*, 465–543; G. M. Gragg, S. A. Schepartz, M. Suffness, M. R. Grever, *J. Nat. Prod.* **1993**, *56*, 1657–1668; T. P. Mucciaro, Dissertation, Stanford University, USA, **1992**.

[2] R. A. Holton, C. Somoza, H.-B. Kim, F. Liang, R. J. Biediger, P. D. Boatman, M. Shindo, C. C. Smith, S. Kim, H. Nadizadeh, Y. Suzuki, C. Tao, P. Vu, S. Tang, P. Zhang, K. K. Murthi, L. N. Gentile, J. H. Liu, *J. Am. Chem. Soc.* **1994**, *116*, 1597; R. A. Holton, H.-B. Kim, C. Somoza, F. Liang, R. J. Biediger, P. D. Boatman, M. Shindo, C. C. Smith, S. Kim, H. Nadizadeh, Y. Suzuki, C. Tao, P. Vu, S. Tang, P. Zhang, K. K. Murthi, L. N. Gentile, J. H. Liu, *ibid.* **1994**, *116*, 1599.

[3] K. C. Nicolaou, Z. Yang, J. J. Liu, H. Ueno, P. G. Nantermet, R. K. Guy, C. F. Claiborne, J. Renaud, E. A. Couladouros, K. Paulvannan, E. J. Sorensen. *Nature* **1994**, *367*, 630–634.

[4] The man years contributed by all the research groups presumably well exceed those required for the synthesis of, for example, vitamin B_{12} or any other single substance.

[5] The addition, alteration, or removal of protecting groups is only included for important steps. Ar = 2,4,6-triisopropylphenyl; Bn = benzyl; BOM = benzyloxymethyl; TBS = *tert*-butyldimethylsilyl; TES = triethylsilyl; TPS = *tert*-butyldiphenylsilyl. Actual yields are given, that is conversions were included in the calculations where necessary, and for precursors the yields from the references given by the authors were used to calculate back to the commercially available starting materials. This leads to lower values than those presented in references [2] and [3].

[6] This important partial reaction has been registered as a patent by Nicolaou et al., and has recently been published: K. C. Nicolaou, P. G. Nantermet, H. Ueno, R. K. Guy, *J. Chem. Soc. Chem. Commun.* **1994**, 295.

[7] Simple taxoids have already been synthesized by Nicolaou's procedure: K. C. Nicolaou, C. F. Claiborne, P. G. Nantermet, E. A. Coulardouros, E. J. Sorensen, *J. Am. Chem. Soc.* **1994**, *115*, 1591. Similar compounds are, however, also accessible by other means (cf. e.g. ref. [8,9]).

[8] S. Blechert, R. Müller, M. Beitzel, *Tetrahedron* **1992**, *48*, 6953-6964, and references therein.

[9] P. A. Wender, T. P. Mucciaro, *J. Am. Chem. Soc.* **1992**, *114*, 5878-5879.

 © *VCH Verlagsgesellschaft mbH, D-69451 Weinheim, 1994* *0570-0833/94/0909-0961 $ 10.00+.25/0*

Molecular Distortion in Reactive Chemical Intermediates

Terry A. Miller*

Chemists have long recognized the intimate connection between a molecule's geometric structure and its reactivity, or in other words the connection between form and function. Historically, the definitive determination of structure, from that of the regular hexagon of benzene to that of the double helix of DNA, has often been followed by significant advances in the understanding and utilization of a molecule's reactivity. Over the years, the structures of most classes of molecules (in their ground electronic state) have been characterized by spectroscopic or crystallographic means.

A major exception to this statement is the class of transient chemical intermediates, which are formed in one step of a complex chemical reaction only to be consumed in a later one. Since it is just these species whose reactivity determine the overall result of the chemical reaction, an accurate understanding of their structure is often critical. Yet their transient nature generally thwarts any structural determinations by crystallographic, or even many spectroscopic, techniques. For lack of better information, the chemical intermediate, often an open-shell radical or radical ion, is typically assumed to be structurally comparable to a closely related "stable" molecule. For example, radical anions or cations, formed by addition or removal of an electron, respectively, are assumed to have roughly the same geometry as their neutral parent. However, such assumptions are inherently dangerous since geometric form ultimately follows electronic structure. Indeed, long ago Jahn and Teller[1] demonstrated by using group theory that any symmetric polyatomic species with an open-shell, degenerate electronic state, such as that of many neutral and charged radicals, would geometrically distort to a configuration of lower energy.

An example of particularly compelling interest is the prototypical aromatic molecule, benzene, and its cation. The closed-shell electronic ground state of benzene has been thought to have the structure of a regular hexagon with the symmetry elements of the D_{6h} point group, since the popularization of the Kekulé electronic structure over a century ago. All reliable experimental observations are consistent[2a] with that structure, the most definitive of which is probably the recently obtained[2b] microwave spectrum of asymmetrically deuterated benzene.

However, matters are much less conclusive concerning the structure of the reactive open-shell radical ions of benzene. Consider, in particular, its radical cation, $C_6H_6^+$, formed by the removal of one of benzene's six π electrons. Since, for D_{6h} benzene, the highest occupied molecular orbital is of e_{1g} symmetry, the ground state of its cation would be expected to be the electronically doubly degenerate $^2E_{1g}$ state, which fulfills the criteria of the above-mentioned Jahn–Teller theorem for distortion. Thus, group theory guarantees that the geometry of $C_6H_6^+$ will not be precisely that of a regular hexagon (D_{6h} in group-theoretical language), but it is the task of experiment to determine whether the molecule's distortion is significant. (Clearly whether a quantity is significant or not depends largely upon the beholder, but pragmatically it is useful to consider that something is significant if it has an observable effect upon a given experiment's results.)

Unlike neutral benzene, the geometry of its cation has been something of a mystery, lacking a definitive experiment owing to its extremely transient existence, or even a real theoretical consensus, due to the unknown magnitude of its Jahn–Teller effect. As will be discussed below, laser-induced fluorescence (LIF) experiments on halo-, particularly fluoro-substituted, derivatives of the benzene cation have given us our best experimental guidance to the structure of $C_6H_6^+$, but similar LIF experiments on the benzene cation $C_6H_6^+$ itself are impossible because of the vanishingly small quantum yield for emission from any of its known excited electronic states. Rather the best *direct* experimental evidence for the structure of the benzene radical cation comes from the photoelectron spectroscopy (PES) of gas-phase benzene[3–5] and from electron paramagnetic resonance (EPR) spectra of $C_6H_6^+$ isolated in a freon matrix.[6] In both studies, the Jahn–Teller distortion of $C_6H_6^+$ was significant, that is, experimentally observable. In the EPR experiment, the H atoms of benzene were found to be not all magnetically equivalent, which would imply chemically, that is, structurally, different environments, which of course is inconsistent with their being attached to equivalent carbon atoms located at the vertices of a regular hexagon. Similarly, the photoelectron spectrum showed a splitting of the components of the lowest excited vibrational level (ν_6 of e_{2g} symmetry), whose motion could lead to distortion of the moleule. Had $C_6H_6^+$ maintained precisely the D_{6h} symmetry of a regular hexagon, these components would be degenerate.

These two direct experiments may seem rather decisive, but they have two major shortcomings. First, although they unambiguously indicate a significant distortion, they do little to quantify it or identify its origin. Second, they do not clearly distinguish between a dynamic and a static distortion. In a static distortion, $C_6H_6^+$ in its vibrationless level would be distorted at all times, that is, permanently. For a dynamic Jahn–Teller effect, at any given instant, $C_6H_6^+$ is distorted from a regular hexagon, but it dynamically samples a number of group-theoretically proscribed distortions, with the mean or average being the undistorted hexagon of D_{6h} symmetry. In principle, the PES experiment could distinguish between these two possibilities by measuring the splittings in a number of excited vibrational levels. In practice, these additional measurements have not been made, primarily because of the spectral congestion at these higher excitations, coupled with the relatively poor spectral resolution (50–100 cm^{-1}) of conventional PES. In principle, the EPR experiment is unambiguously indicative of a *permanent*

[*] Prof. Dr. T. A. Miller
Laser Spectroscopy Facility, Ohio State University
120 W. 18th Avenue, Columbus, OH 43210 (USA)
Telefax: Int. code + (614)292-1948

[**] This work was supported by the National Science Foundation (grant CHE 9005963). I thank Dr. T. G. Wright for useful discussions.

 © VCH Verlagsgesellschaft mbH, D-69451 Weinheim, 1994 0570-0833/94/0909-0962 $ 10.00+.25/0

distortion. However, it is unclear whether this permanent distortion is a property of $C_6H_6^+$ itself or is caused by the freon matrix environment in which the experiment is performed.

The mystery surrounding the structure of $C_6H_6^+$ has recently been diminished significantly by Müller-Dethlefs et al.[7, 8] They have applied the exciting new technique of zero kinetic energy (ZEKE)-PES;[9] as with conventional PES, ZEKE allows the measurement of a cation's quantum levels. However, the resolution of the ZEKE spectrum (ca. 0.2 cm^{-1} in these studies) is 10^2-10^3 higher than conventional PES, allowing the resolution of even the rotational energy levels of the cation.

Observation of rotational structure in the ground state of $C_6H_6^+$ offers an entirely new avenue for determining its structure. In their first work, Lindner et al.[7] show that all the observed rotational transitions are consistent with D_{6h} symmetry for the cation. If distortions reduced the cation's symmetry to D_{3h} or D_{2h}, additional, strong lines would be expected in the rotational spectrum which were not observed. Qualitatively this finding can be interpreted as showing that on the time scale of molecular rotation, the benzene cation has, on average, D_{6h} symmetry.

The result is, of course, consistent with any distortion of $C_6H_6^+$ simply being insignificant (unobservably small in this experiment) and implies that the EPR measurements, on an even slower time scale, have observed a distortion of $C_6H_6^+$ at least in part attributable to its environment. However, this finding does *not* rule out a significantly, but dynamically, distorted cation whose nuclei sample, by pseudorotation, a number of non-D_{6h} configurations whose average does possess D_{6h} symmetry. Indeed if we use the results of LIF investigations[10-12] of 1,3,5-trifluorobenzene ($C_6H_3F_3^+$) and the hexafluorobenzene cation ($C_6F_6^+$), we would expect the latter situation to hold. In those two cases, significant stabilization energy was gained (800–1000 cm^{-1}) through Jahn–Teller distortion, with most of it being apportioned to changes in the C–C bond lengths and C-C-C bond angles. (The Jahn–Teller effect cannot distort any of the benzenoid cations from planarity, though conceivably other effects could.) However, for both fluorobenzenes, it was shown that there are insignificantly small barriers to pseudorotation through configurations averaging to D_{6h} symmetry. Theoretical calculations,[13] shown to be rather accurate for $C_6F_6^+$, predicted a very similar situation for $C_6H_6^+$, that is, the Jahn–Teller distortion of the cations is basically a property of the benzenoid ring and is only affected in a minor way by substituents. Later theoretical predictions for $C_6H_6^+$ would seem to confirm this result.[14]

In principle, even if a dynamic Jahn–Teller distortion is averaged on the rotational time scale, its effects do not entirely vanish from the rotational spectrum. These effects manifest themselves as relatively small, additional terms in the rotational Hamiltonian. In a related five-electron system, the cyclopentadienyl radical, C_5H_5, which similarly pseudorotates, high-resolution LIF spectra have precisely determined the magnitude of these terms and hence the radical's distorted structure.[15] Similar rotational observations are, in principle, possible with $C_6H_6^+$, but the spectral resolution required will severely challenge even the very impressive resolution of the ZEKE variant of PES.

The second paper by Lindner et al.[8] offers an alternative and probably better approach for learning about the likely dynamic Jahn–Teller distortion of $C_6H_6^+$. A direct way to observe this distortion is simply to measure the positions and splittings in a number of Jahn–Teller active vibrational levels. Such results, coupled with the appropriate theory[12] can give a complete description of the geometric distortion of the molecule and the resulting energy stabilization.

As noted earlier, conventional PES typically lacks the resolution to enable an analysis of the congested vibrational structure of a molecule with a number of fundamental, overtone, and combination bands. However, simply being able to resolve all the individual vibrational transitions is not necessarily sufficient. In fact, a recent experiment[16] on $C_6H_6^+$, with a variant of ZEKE in which mass-resolved cations rather than electrons are detected,[17] resolved clearly much of the cation's vibrational structure. Nonetheless, considerable ambiguity remained as to the proper assignment of these distinct vibrational transitions. In the second paper by Lindner et al.,[8] they resolve the rotational structure of an excited vibrational band. This rotational structure serves as a fingerprint of the vibration mode, because rotational selection rules and hence structure depend upon vibronic symmetry.[18] By this approach they positively identify the components of the first excited level of the e_{2g} ν_6 mode of $\tilde{X}^2E_{1g}$ $C_6H_6^+$. In perfect D_{6h} symmetry this level should be fourfold degenerate. However, they find it is strongly split into a doubly degenerate e_{2g} component and b_{1g} and b_{2g} components, the latter two being split by a much smaller amount. These observations clearly indicate that the benzene radical cation is significantly and dynamically distorted along the ν_6 normal coordinate but that it has only a smallish barrier (indicated by the b_{1g}–b_{2g} splitting) to rapid pseudorotation which results in a structure, which is on average a regular hexagon.

The authors do not report in their work any values for the magnitude of the Jahn–Teller geometric distortion nor the energy stabilization derived therefrom. However, continued measurements of a number of rotationally resolved vibrational levels, coupled with the appropriate anaysis, will surely yield such results. At that point another long standing mystery of molecular structure will be solved.

German version: *Angew. Chem.* **1994**, *106*, 1014

[1] H. A. Jahn, E. Teller, *Proc. R. Soc. London Ser. A* **1937**, *161*, 220.

[2] a) See for example O. Ermer, *Angew. Chem.* **1987**, *99*, 791; *Angew. Chem. Int. Ed. Engl.* **1987**, *26*, 782; b) M. Oldoni, R. Widner, G. Grassi, A. Bauder, *J. Mol. Struct.* **1988**, *190*, 31.

[3] L. Åsbrink, E. Lindholm, O. Edqvist, *Chem. Phys. Lett.* **1970**, *5*, 609.

[4] A. W. Potts, W. C. Price, D. G. Streets, T. A. Williams, *Faraday Discuss. Chem. Soc.* **1972**, *54*, 168.

[5] L. Karlsson, L. Mattson, R. Jadrny, T. Bergmark, K. Siegbahn, *Phys. Scr.* **1976**, *14*, 230.

[6] M. Iwasaki, K. Toriyama, K. Nunome, *J. Chem. Soc. Chem. Commun.* **1983**, 320.

[7] R. Lindner, H. Sekiya, B. Beyl, K. Müller-Dethlefs, *Angew. Chem.* **1993**, *105*, 631; *Angew. Chem. Int. Ed. Engl.* **1993**, *32*, 603.

[8] R. Lindner, H. Sekiya, K. Müller-Dethlefs, *Angew. Chem.* **1993**, *105*, 1384; *Angew. Chem. Int. Ed. Engl.* **1993**, *32*, 1364.

[9] For an overview of ZEKE spectroscopy, see, for example: K. Müller-Dethlefs, E. W. Schlag, *Annu. Rev. Phys. Chem.* **1991**, *42*, 109.

[10] T. J. Sears, T. A. Miller, V. E. Bondybey, *J. Chem. Phys.* **1980**, *72*, 6070.

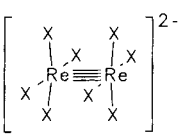
 © *VCH Verlagsgesellschaft mbH, D-69451 Weinheim, 1994* *0570-0833/94/0909-0963 $ 10.00+.25/0*

[11] T. J. Sears, T. A. Miller, V. E. Bondybey, *J. Chem. Phys.* **1981**, *74*, 3240.
[12] T. A. Miller, V. E. Bondybey, *Molecular Ions: Spectroscopy, Structure, and Chemistry* (Eds.: T. A. Miller, V. E. Bondybey), North-Holland, Amsterdam, **1983**.
[13] K. Raghavachari, R. C. Haddon, T. A. Miller, V. E. Bondybey, *J. Chem. Phys.* **1983**, *79*, 1387.
[14] See for example J. Eiding, R. Schneider, W. Domcke, H. Köppel, W. von Niessen, *Chem. Phys. Lett.* **1991**, *177*, 345.
[15] L. Yu, D. W. Cullin, J. M. Williamson, T. A. Miller, *J. Chem. Phys.* **1993**, *98*, 2682.
[16] H. Krause, H. J. Neusser, *J. Chem. Phys.* **1992**, *97*, 5923.
[17] L. Zhu, P. Johnson, *J. Chem. Phys.* **1991**, *94*, 5769.
[18] K. Müller-Dethlefs, *J. Chem. Phys.* **1991**, *95*, 4821.

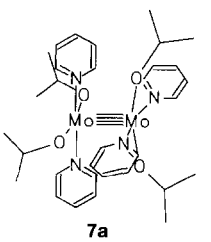
Heterodimetallic Complexes with an Unbridged, Polar Metal–Metal Bond

Max Herberhold* and Guo-Xin Jin

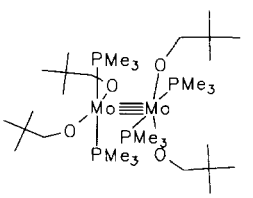
Among the numerous complexes with a direct metal–metal bond[1, 2] those that are stable without bridging ligands are especially fascinating. *Homo*dinuclear complexes with an unsupported metal–metal linkage are known in particular for metals in lower (− I, 0, I) and intermediate oxidation states (II, III). The first group includes dinuclear complexes like **1** and **2** and the cyclopentadienyl metal complexes **3**, **4**, and **5**.



6
X = Cl, Br



7a

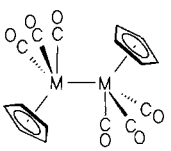


7b

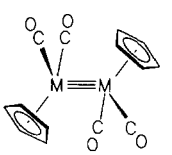
$[(OC)_5M-M(CO)_5]$ $[(Me_3E)(OC)_4Ru-Ru(CO)_4(EMe_3)]$

1a, M = Mn[3a]
1b, M = Tc[3b]
1c, M = Re[3c]

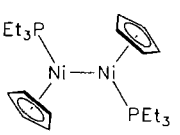
2, E = Si, Ge, Sn[4]



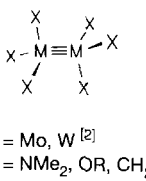
3a, M = Cr [5a]
3b, M = Mo [5b]
3c, M = W [5b]



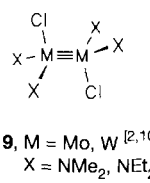
4a, M = Cr [6a]
4b, M = Mo [6b]
4c, M = W



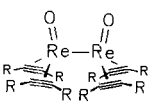
5 [7]



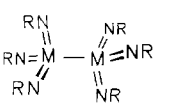
8, M = Mo, W [2]
X = NMe_2, OR, CH_2SiMe_3



9, M = Mo, W [2,10]
X = NMe_2, NEt_2



10, R = Me, Et [11]



11, M = Tc, Re [12]
R = $iPr_2C_6H_3$

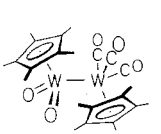
The second group is dominated by dinuclear complexes with metal–metal multiple bonds.[1, 8] Complexes that have been intensively studied owing to their formal quadruple bond—include the homonuclear dirhenate ions $[X_4Re{\equiv}ReX_4]^{2-}$ **6**, whose molecular halves are eclipsed, and the alkoxidomolybdenum complexes **7a**, **b**. The d^3-d^3 dimers **8** and **9**, which contain a formal triple bond, also display a rich chemistry.[2] A related compound with a metal–metal single bond is the alkyne complex **10**. Homodinuclear complexes with unbridged metals in higher oxidation states such as Tc^{VI} and Re^{VI} in complexes **11** are uncommon.

Homodinuclear complexes are generally symmetrical "dimers" with a nonpolar metal–metal bond. Polarity can be introduced to a certain degree, while maintaining the oxidation state of the metal, by "one-sided" exchange of a ligand in homoleptic complexes, which results in compounds like **12** and **13**. The metal–metal bond is yet more polar when the same metal is in different oxidation states in the two centers, as is found in the unexpected products **14** and **15** and in the bis(dithio ether) complexes **16**.

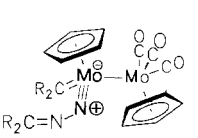
$[(OC)_5Re-Re(CO)_4L]$ $[(Me_2N)_3W{\equiv}W(NMe_2)_2I]$

12[13] **13**[14]

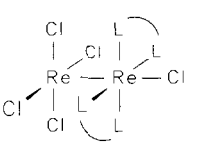
L = C(Me)OMe, CN*t*Bu



14 [15]



15, R = *p*-$CH_3C_6H_4$ [16]



16 [17]
LL = 2,5-dithiahexane, 3,6-dithiaoctane

[*] Prof. Dr. M. Herberhold, Dr. G.-X. Jin
Laboratorium für Anorganische Chemie der Universität
Postfach 101251, D-95440 Bayreuth (FRG)
Telefax: Int. code + (921)552535

For a number of years dinuclear complexes with different metals have been popular subjects of study owing to the reactivity and potential catalytic activity of compounds with metal–metal bonds. The two metals may be adjacent d-block elements as in **17** and **18** or may come from opposite ends of the periodic table as in **19**–**23**.

$[(OC)_5Re-Mo(CO)_4(CPh)]$ **17**[18]

$[(tht)(C_6Cl_5)(C_6F_5)_2Pt-Ag(PPh_3)]$ **18**[19]

tht = tetrahydrothiophene

$[Cp_2(H)_2M-ZnCp]$ **19**, M = Nb, Ta[20]

$[(Ph_3P)_2(H)Pt-Re(H)(CO)_2Cp]$ **20**[21]

$[Cp_2(R)Zr-Ru(CO)_2Cp]$ **21**[22, 23]

$[(Ph_3P)_2(H)Pt-Mo(CO)_3Cp]$ **22**[24]

R = Me, OR, Cl, I

$[(Me_2N)_3Ti-M(CO)_2Cp]$
23, M = Fe, Ru[25]

The concept of "early–late" heterodimetallic compounds, which are formed by combination of a d electron-poor and a d electron-rich transition metal complex fragment, has proved to be especially worthwhile;[26] however, products in which the metal–metal bond is further stabilized by bridging ligands are usually obtained.

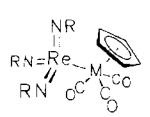
Trinuclear heterodimetallic complexes like **24**–**26** have also been prepared and structurally characterized.

$[Cp(CO)_2Ru-Zr(Cp)_2-Ru(CO)_2Cp]$ **24**[23]

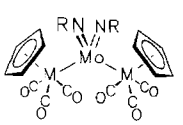
$[(Ph_3P)_2Cu-Fe(CO)_4-Cu(PPh_3)_2]$ **25**[27]

$[(ArN)_3Re-Hg-Re(NAr)_3]$
26, Ar = 2,6-iPr$_2$C$_6$H$_3$[28]

Strongly polar metal–metal bonds can apparently be expected for heterodimetallic complexes in which the metal centers are present in significantly different oxidation states. The importance of the difference in oxidation state for the preparation of unsupported di- and trinuclear complexes with polar metal–metal bonds seems to have been underestimated so far. However, several recent papers[29–32] have focused on the deliberate construction of complexes with polar bonds by the combination of complex fragments with metals in higher and lower oxidation states. Thus the research group of J. Sundermeyer[29] has treated imidometal compounds such as $[Re(N$$t$$Bu)_3Cl]$ and $[Mo(N$-$t$$Bu)_2Cl_2]$ with carbonyl metalate salts like $K[Mn(CO)_5]$ and $K[M(CO)_3Cp]$ (M = Mo, W) to obtain di- and trinuclear complexes of type **27** and **28**, respectively.



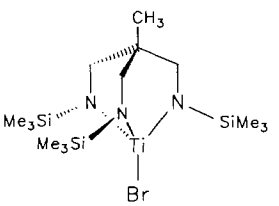
27, M = Mo, W [29]
R = tBu



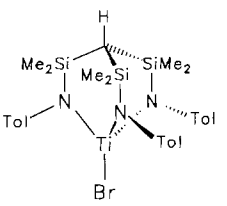
28, M = Mo, W [29]
R = tBu

The synthetic approach of combining a hard "metal acid" ($[Re(N$$t$$Bu)_3]^+$, $[CpM(N$$t$$Bu)_2]^+$ (M = Mo, W), $[Cp_2Nb(N$$t$$Bu)]^+$, $[M(N$$t$$Bu)_2]^{2+}$ (M = Mo, W), $[CpM(N$$t$$Bu)]^{2+}$ (M = Nb, Ta)) with a soft "metal base" ($[Mn(CO)_5]^-$, $[Co(CO)_4]^-$, $[M(CO)_3Cp]^-$ (M = Mo, W), $[Fe(CO)_2Cp]^-$) can certainly be expanded, since plenty of precursors are available for both the high- and the low-valent components.[30] In comparison to the analogous oxometal complexes, imido metal compounds have the advantage that the steric demands of the imido ligand RN can be varied by the choice of the appropriate R group. It remains to be seen whether the subsequent hydrolysis of the metal–imido bonds gives oxometal complexes without affecting the unsupported, polar metal–metal bond.

The significance of steric shielding is also evident in the heterodimetallic complexes synthesized by L. H. Gade et al. starting from the amido-substituted titanium(IV) monobromides **29a**, **b** (Tol = $C_6H_4CH_3$).[31, 32] The tripodal protecting ligand



29a [31]



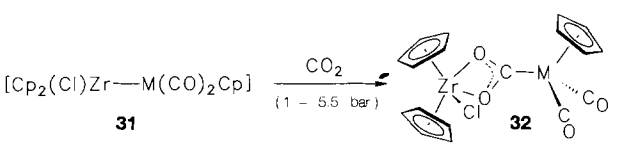
29b [32]

(L_3) stabilizes the titanium(IV) component $[(L_3)TiBr]$ so well, that its reaction with the carbonyl metalates $Na[Co(CO)_3(PPh_3)]$ and $K[M(CO)_2Cp]$ (M = Fe, Ru) leads to stable heterodimetallic complexes with a polar, unsupported metal–metal bond. The Ti–Fe complex of type **30** is much more robust than the related complex **23**.

$[(L_3)Ti-M(CO)_2Cp]$ **30**, M = Fe, Ru[32]

$L_3 = CH_3C(CH_2NSiMe_3)_3$, $HC[SiMe_2N(Tol)]_3$

These new complexes allow the systematic investigation of the chemical reactivity of compounds with a strongly polar, unsupported metal–metal bond. Hitherto there have been few studies on the reactivity of heterodimetallic complexes without bridging ligands, for example the trinuclear compound $[Cp_2Zr\{Ru(CO)_2Cp\}_2]$ analogous to **21**.[22b] A more recent example is the observed insertion of CO_2, but not CS_2, under mild conditions into the metal–metal bond of **31**, which results in the carboxylato complexes **32**.[33] The shielding cyclopentadienyl ligands are apparently important in protecting the metal–metal bond in **31**. In complexes like **27**, **28**, and **30** the bulky ligands



31
M = Fe, Ru

32

 © VCH Verlagsgesellschaft mbH, D-69451 Weinheim, 1994 0570-0833/94/0909-0965 $ 10.00+.25/0

guarantee the kinetic stability of the compounds and apparently prevent the direct electron transfer from the low- to the high-valent component, but they also block access to the metal–metal bond.

German version: *Angew. Chem.* **1994**, *106*, 1016

[1] F. A. Cotton, R. A. Walton. *Multiple Bonds Between Metal Atoms*, 2nd ed., Oxford University Press, London, **1993**.

[2] M. H. Chisholm, *Acc. Chem. Res.* **1990**, *23*, 419–425.

[3] a) M = Mn: A. Almeningen, G. G. Jacobsen, H. M. Seip, *Acta. Chem. Scand.* **1969**, *23*, 685–686; b) M = Tc: M. F. Bailey, L. F. Dahl, *Inorg. Chem.* **1965**, *4*, 1140–1145; c) M = Mn and Re: M. R. Churchill, K. N. Amoh, H. J. Wasserman, *ibid.* **1981**, *20*, 1609–1611.

[4] a) J. D. Cotton, S. A. R. Knox, F. G. A. Stone, *J. Chem. Soc. Chem. Commun.* **1967**, 965–966; b) S. A. R. Knox, F. G. A. Stone, *J. Chem. Soc. A* **1969**, 2559–2565; *ibid.* **1971**, 2874–2880.

[5] a) M = Cr: R. D. Adams, D. M. Collins, F. A. Cotton, *J. Am. Chem. Soc.* **1974**, *96*, 749–754; b) M = Mo and W: R. D. Adams, D. M. Collins, F. A. Cotton, *Inorg. Chem.* **1974**, *13*, 1086–1090.

[6] a) M = Cr: M. D. Curtis, W. M. Butler, *J. Organomet. Chem.* **1978**, *155*, 131–145; b) M = Mo: R. J. Klingler, W. M. Butler, M. D. Curtis, *J. Am. Chem. Soc.* **1978**, *100*, 5034–5039; c) B. J. Morris-Sherwood, C. B. Powell, M. B. Hall, *ibid.* **1984**, *106*, 5079–5084.

[7] U. Denninger, J. J. Schneider, G. Wilke, R. Goddard, C. Krüger, *Inorg. Chim. Acta* **1993**, *213*, 129–140.

[8] R. A. Walton in *Metal-Metal Bonds and Clusters in Chemistry and Catalysis*, (Ed.: J. P. Fackler), Plenum Press, New York, **1990**, pp. 7–18.

[9] M. H. Chisholm, K. Folting, J. C. Huffman, E. F. Putilina, W. E. Streib, R. J. Tatz, *Inorg. Chem.* **1993**, *32*, 3771–3780.

[10] a) M = Mo and W (X = NMe_2): M. Akiyama, M. H. Chisholm, F. A. Cotton, M. W. Extine, C. A. Murillo, *Inorg. Chem.* **1977**, *16*, 2407–2411; b) M = W (X = NEt_2): M. H. Chisholm, F. A. Cotton, M. Extine, M. Millar, B. R. Stults, *J. Am. Chem. Soc.* **1976**, *98*, 4486–4491.

[11] E. Valencia, B. D. Santarsiero, S. J. Greib, A. L. Rheingold, J. M. Mayer, *J. Am. Chem. Soc.* **1987**, *109*, 6896–6898.

[12] A. K. Burrel, J. C. Bryan, *Angew. Chem.* **1993**, *105*, 85–86; *Angew. Chem. Int. Ed. Engl.* **1993**, *32*, 94–95.

[13] a) L = carbene: E. O. Fischer, E. Offhaus, J. Müller, D. Nöthe, *Chem. Ber.* **1972**, *105*, 3027–3035; b) L = isonitrile: M. O. Albers, J. C. A. Boeyens, N. J. Coville, G. W. Harris, *J. Organomet. Chem.* **1984**, *260*, 99–104.

[14] H. Schulz, K. Folting, J. C. Huffman, W. E. Streib, M. H. Chisholm, *Inorg. Chem.* **1993**, *32*, 6056–6066.

[15] H. G. Alt, H. I. Hayen, R. D. Rogers, *J. Chem. Soc. Chem. Commun.* **1987**, 1795–1796; H. G. Alt, H. I. Engelhardt, H. I. Hayen, R. D. Rogers, *J. Organomet. Chem.* **1989**, *366*, 287–295.

[16] L. Messerle, M. D. Curtis, *J. Am. Chem. Soc.* **1982**, *104*, 889–891.

[17] a) M. J. Bennett, F. A. Cotton, R. A. Walton, *J. Am. Chem. Soc.* **1966**, *88*, 3866–3867; b) B. J. Heyen, G. L. Powell, *Polyhedron* **1988**, *7*, 1207–1209.

[18] E. O. Fischer, G. Huttner, T. L. Lindner, A. Frank, F. R. Kreissl, *Angew. Chem.* **1976**, *88*, 163–164; *Angew. Chem. Int. Ed. Engl.* **1976**, *15*, 157–158.

[19] R. Usón, J. Forniés, M. Tomás, I. Ara, J. M. Casas, A. Martin, *J. Chem. Soc., Dalton Trans.* **1991**, 2253–2264.

[20] a) M = Nb: P. H. M. Budzelaar, K. H. den Haan, J. Boersma, G. J. M. van der Kerk, A. L. Spek, *Organometallics* **1984**, *3*, 156–159; b) M = Ta (Cp = C_5H_4Me): P. H. M. Budzelaar, A. A. H. van der Zeijden, J. Boersma, G. J. M. van der Kerk, A. L. Spek, A. J. M. Duisenberg, *Organometallics* **1984**, *3*, 159–163.

[21] C. P. Casey, E. W. Rutter, Jr., K. J. Haller, *J. Am. Chem. Soc.* **1987**, *109*, 6886–6887.

[22] a) C. P. Casey, R. F. Jordan, A. L. Rheingold, *J. Am. Chem. Soc.* **1983**, *105*, 665–667; b) C. P. Casey, *J. Organomet. Chem.* **1990**, *400*, 205–221.

[23] C. P. Casey, R. F. Jordan, A. L. Rheingold, *Organometallics* **1984**, *3*, 504–506.

[24] O. Bars, P. Braunstein, *Angew. Chem.* **1982**, *94*, 319–320; *Angew. Chem. Int. Ed. Engl.* **1982**, *21*, 308–309; O. Bars, P. Braunstein, G. L. Geoffroy, B. Metz, *Organometallics* **1986**, *5*, 2021–2030.

[25] a) M = Fe: W. J. Sartain, J. P. Selegue, *Organometallics* **1987**, *6*, 1812–1815; b) M = Ru: W. J. Sartain, J. P. Selegue, *J. Am. Chem. Soc.* **1985**, *107*, 5818–5820; c) W. J. Sartain, J. P. Selegue, *Organometallics* **1989**, *8*, 2153–2158.

[26] D. W. Stephan, *Coord. Chem. Rev.* **1989**, *95*, 41–107.

[27] G. Doyle, K. A. Eriksen, D. von Engen, *J. Am. Chem. Soc.* **1985**, *107*, 7914–7920.

[28] D. S. Williams, J. T. Anhaus, M. H. Schofield, R. R. Schrock, W. M. Davis, *J. Am. Chem. Soc.* **1991**, *113*, 5480–5481.

[29] J. Sundermeyer, D. Runge, J. S. Field, *Angew. Chem.* **1994**, *106*, 679–682; *Angew. Chem. Int. Ed. Engl.* **1994**, *33*, 678–681.

[30] J. Sundermeyer, D. Runge (Universität Würzburg), personal communication (February 1994).

[31] S. Friedrich, L. H. Gade, A. J. Edwards, M. McPartlin, *Chem. Ber.* **1993**, *126*, 1797–1805.

[32] S. Friedrich, H. Memmler, L. H. Gade, W.-S. Li, M. McPartlin, *Angew. Chem.* **1994**, *106*, 705–708; *Angew. Chem. Int. Ed. Engl.* **1994**, *33*, 676–678.

[33] J. R. Pinkes, B. D. Steffey, J. C. Vites, A. R. Cutler, *Organometallics* **1994**, *13*, 21–23.

 © VCH Verlagsgesellschaft mbH, D-69451 Weinheim, 1994 0570-0833/94/0909-0966 $ 10.00+.25/0

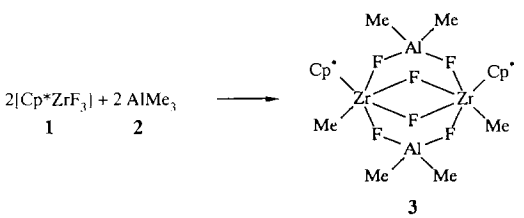
Reactions of $[(C_5Me_5)ZrF_3]$ with $AlMe_3$—Synthesis and Structure of a Zirconium–Aluminum–Carbon Cluster**

Axel Herzog, Herbert W. Roesky,* Zdirad Zak, and Mathias Noltemeyer

Dedicated to Professor Ernst Otto Fischer on the occasion of his 75th birthday

Organometallic fluorides of the elements of Group 4 have been studied very little to date. Our investigations into the reactivity of $[Cp^*ZrF_3]$ (**1**)[1] ($Cp^* = C_5Me_5$) synthesized for the first time recently by us showed that this compound together with methylaluminoxane (MAO) as cocatalyst is suitable for the polymerization of ethylene.[2] Brintzinger, Kaminsky, and Sinn in their fundamental work have been able to show that alkyl derivatives of metallocenes of Group 4 are of crucial importance for such a process.[3]

In order to understand the catalytic activity of **1**, it was necessary to examine whether a selective exchange of the fluorine atoms for alkyl groups is possible for **1**. We have now found that in the reaction of **1** with $AlMe_3$ (**2**) in the mol ratio 1:1, as expected, methyl groups are transferred from aluminum to zirconium and **3** is formed.



The resulting Me_2AlF does not form the known tetramer.[4] The single-crystal X-ray structure analysis of **3** (Fig. 1)[5] shows Me_2AlF for the first time as complex ligand; the fluorine atoms are bridging. Both Zr-F-Zr and Zr-F-Al bridges are formed (Zr–F 211.1–217.9 pm, Al–F 176.5–178.6 pm). The zirconium atoms have a distorted octahedral and the aluminum atoms a distorted tetrahedral environment.

The Zr–C bond length of the ZrMe unit in **3** (mean 228.3 pm) is comparable with those in $[(C_5H_5)_2ZrMe_2]$[6] (227.3(5), 228.0(5) pm), whereas in the $[(Me_2C_5H_3)_2ZrMe]^+$ ion,[7] the corresponding Zr–C bond is, as expected, shorter (225.2(4) pm). This trend can be explained in terms of the decrease in the electron density in the $[(Me_2C_5H_3)_2ZrMe]^+$ ion and the increase in the stength of the ZrMe bond associated with this. In the ^{19}F NMR spectrum of **3**, three signals (ratio of intensities 4:1:1) are observed, that is, the molecular structure known from the solid state is also found in solution.

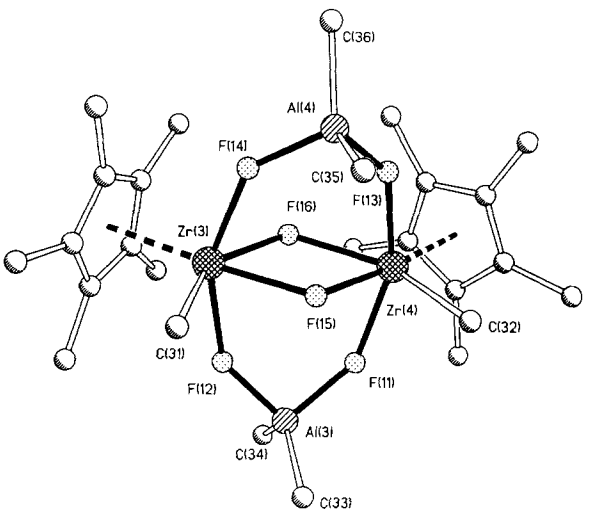


Fig. 1. Crystal structure of **3**. Selected bond lengths [pm] and angles [°]: Zr1–F2 213.9(3), Zr1–F4 211.1(3), Zr1–F6 217.9(3), Zr1–F5 214.1(3), Zr1–C12 228.3(6), Al2–F4 177.6(4), Al2–F3 178.6(4), Al2–C15 191.6(9), Al2–C16 192.1(8); F6-Zr1-F5 67.48(11), Zr1-F6-Zr2 111.67(12), Zr1-F4-Al2 140.2(2).

Remarkably, the *cis* product **3** is formed exclusively. ^1H and ^{19}F NMR measurements on **3** at 70 °C give no indication of an equilibrium with the *trans* isomer. We have also found a stereoselective substitution of this kind for the corresponding hafnium compound, which was hitherto not known for metallocenes.[8]

If **1** or **3** are allowed to react with an excess of $AlMe_3$, methane is eliminated spontaneously at room temperature in *n*-hexane, as detected by IR spectroscopy. In addition to fluorine-containing oil-like products,[9] the $Zr_3Al_6C_7$ cluster **4** is formed. The best yields of **4** (reproducible) are obtained when **1** is treated with $AlMe_3$ in the mol ratio 1:5 [Eq. (a)]. At higher

$$\underset{\mathbf{1}}{3[Cp^*ZrF_3]} + \underset{\mathbf{2}}{15\,AlMe_3} \longrightarrow \underset{\mathbf{4}}{[(Cp^*Zr)_3Al_6Me_8(CH)_5(CH_2)_2]} + 9\,Me_2AlF + 12\,CH_4 \quad \text{(a)}$$

temperatures, the formation of the cluster is accelerated at the expense of the yield; in contrast, **2** and **3** do not react within 4 h at −10 °C. However, **4** is not stable at room temperature and is converted into an insoluble solid.

The group of peaks at *m/z* 1040 (M^+–Me–2H) in the mass spectrum of **4** shows the correct distribution of isotopes. The ion with the greatest intensity is found at *m/z* 965 (M^+–6Me–2H).

Single crystals of **4** are formed from toluene. The X-ray structure analysis[10] at 153 K shows that all fluorine atoms are exchanged in **4** and a $Zr_3Al_6C_7$ cluster has formed (Fig. 2). Six metal atoms form an open cube, which is shielded by Al and C atoms. The cluster is capped by CH and CH_2 groups; some of

[*] Prof. Dr. H. W. Roesky, Dipl.-Chem. A. Herzog, Dr. Z. Zak, Dr. M. Noltemeyer
Institut für Anorganische Chemie der Universität
Tammannstrasse 4, D-37077 Göttingen (FRG)
Telefax: Int. code + (551)393373

[**] This work was supported by the Deutsche Forschungsgemeinschaft, the Volkswagen-Stiftung, Hoechst AG, and the Bundesministerium für Forschung und Technologie. Z. Z. thanks the European Community for a Fellowship.

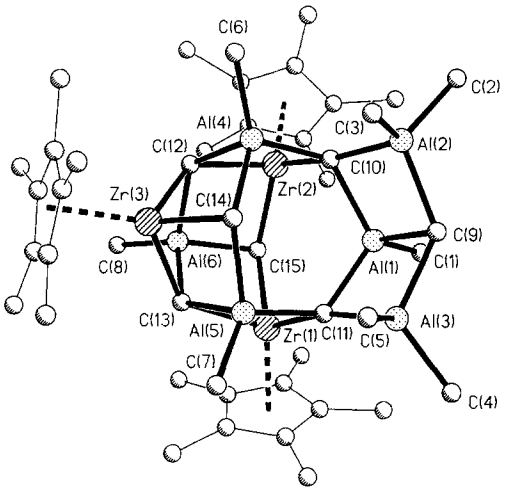


Fig. 2. Crystal structure of **4**. The H atoms are not shown. Selected bond lengths [pm] and angles [°]: Zr1–C15 217.0(7), Zr2–C15 213.9(6), Al6–C15 202.4(7), Zr1–C13 231.1(7), Zr3–C13 221.1(7), Al5–C13 216.7(7), Al6–C13 212.2(7), Zr3–C14 219.1(6), Al5–C14 211.3(7), Al4–C14 213.0(7), Al1–C10 202.8(7), Al2–C10 212.8(6), Al4–C10 200.3(7), Zr2–C10 224.1(6); C11-Zr1-C13 89.8(2), Al5-Zr1-Al1 70.34(10), Al5-C13-Al6 133.6(3), Al6-C13-Zr3 82.4(3), Al5-C13-Zr3 82.2(2), Al5-C13-Zr1 80.0(2), Al6-C13-Zr1 81.9(2), Al6-C13-Zr3 82.4(3).

the C atoms are hypervalently bound. The short metal–metal contacts are remarkable. The average Al–Zr distance (297.8 pm) is shorter than that deduced from the metal radii (303 pm).[11] In this case very long (Al1–Zr1 333.0(2), Al2–Zr2 333.7(2) pm) and very short (Zr1–Al5 288.0(2), Zr2–Al6 287.9(2), Zr3–Al4 284.6(2) pm) Al–Zr distances occur. The average Al–Al distance (268.2 pm) (Al1–Al3 268.7(3), Al1–Al2 267.8(3) pm) is comparable with that in $R_2Al-AlR_2$ ($R = CH(SiMe_3)_2$) (266.0 pm),[12] whereas the average Al–Al bond length in $[Cp^*Al]_4$[13] is 276.9 pm (in the metal 286 pm).[11] Whether the short metal–metal distances in **4** arise because of the electron deficiency, cannot be said with certainty.

As a result of the different metal–carbon bonds, the CH groups are not arranged symmetrically on the (Zr_2Al_2) faces (e.g. C12–Zr2 230.1(7), C12–Zr3 222.9(6), C12–Al6 209.8(6), C12–Al4 216.6(6) pm). The Zr–CH bond lengths lie in a wide range (213.9–231.1 pm). We do not assume that double bond contributions exist in the short Zr–C bonds. Fryzuk et al.[14] have determined a bond length of 202.4(4) pm for an isolated Zr–C double bond in [{1,3-$(SiMe_2CH_2PiPr_2)_2C_5H_3$}Zr=CHPh(Cl)]. The compound $[(C_5H_5)_2Zr(\mu\text{-}C{\equiv}CPh)(\mu\text{-}C'Ph{=}CMe)AlMe_2]$ described by Erker et al.,[15] in which the zirconium and aluminum are linked by the planar-tetracoordinate C′, has a Zr–C′ bond length of 247.0 pm. It is thus significantly longer than that in **4**; in contrast, the Al–C′ bond length is of the same order of magnitude (210.3 pm).

The crystals of **4** obtained by recrystallization from toluene are sparingly soluble in all common solvents; thus, ^{13}C NMR investigations gave no useful information and an unambiguous assignment of the signals in the high-field region of the ^1H NMR spectrum by using 2D methods is not possible.[16] Also the replacement of the Cp* group by C_5Me_4Et fails to solve the problem: the solubility of the resulting cluster analogous to **4** is not improved significantly.[8]

Experimental Procedure

3: **1** (2.00 g, 7.06 mmol) was dissolved in toluene (50 mL) and **2** (3.53 mL, 7.06 mmol, 2 M solution in *n*-hexane) was added dropwise over 0.5 min. The reaction mixture was stirred for a further 0.5 h to complete the reaction. After concentration of the solution under vacuum to a quarter of the original volume, **3** crystallized in the form of colorless crystals. Yield: 1.83 g (70%). M.p. 206 °C; ^1H NMR (C_6D_6, TMS): $\delta = -0.46$ (m, 6H, AlMe), −0.35 (m, 6H, AlMe), 0.5 (m, 3H, ZrMe), 0.54 (m, 3H, ZrMe), 1.76 (s, 30H, Cp*), 2.10 (m, 1.5H, Ph*Me*), 6.95–7.16 (m, 2.5H, *Ph*Me); ^{13}C NMR (C_6D_6, TMS): $\delta = -12.03$ (m, AlMe), −11.08 (m, AlMe), 10.76 (s, C_5Me_5), 21.37 (s, Ph*Me*), 45.17 (dd, $J = 11$ Hz, $J = 30$ Hz, ZrMe), 124.86 (C_5Me_5), 125.63 (s), 128.51 (s), 129.28 (s), 137.83 (s), (*Ph*Me); ^{19}F NMR (C_6D_6, $CFCl_3$): $\delta = -108.18$ (s, 4F, ZrFAl), −69.49 (m, 1F, ZrFZr), −32.52 (m, 1F, ZrFZr); EI-MS (70 eV): *m/z* (%): 696 (100) [$M^+ - Me$]. Correct elemental analysis.

4: **1** (1.00 g, 3.53 mmol) was suspended in *n*-hexane (60 mL) and **2** (8.85 mL, 17.70 mmol, 2 M solution in *n*-hexane) was added dropwise over 0.5 h. After the mixture had been stirred at room temperature for 18 h, no further evolution of gas was observed. The yellow solution was concentrated to a third of the original volume. This led to the precipitation of a yellow, microcrystalline solid, which was filtered off and washed with a little *n*-hexane. This crude solid was taken up in toluene (20 mL), decanted from the insoluble material, and successively concentrated (2 h). In addition to a yellow microcrystalline solid, **4** crystallized in the form of yellow crystals. Yield: 350 mg (28%). ^1H NMR ([D_8]toluene, TMS): $\delta = -1.38$ (d), −0.95 (s), −0.72 (d), −0.52 (s), −0.51 (s), −0.30 (m), −0.171 (s), −0.167 (s), 1.91 (s), 1.94 (s); EI-MS (70 eV): *m/z* (%): 1040 (4) [$M^+ - Me - 2H$], 965 (100) [$M^+ - 6Me - 2H$]. The elemental analysis gave slightly lower values for C and H than those calculated. Fluorine cannot be detected.

Received: August 16, 1993
Revised: January 19, 1994 [Z6288IE]
German version: *Angew. Chem.* **1994**, *106*, 1035

[1] A. Herzog, F.-Q. Lui, H. W. Roesky, A. Demsar, K. Keller, M. Noltemeyer, F. Pauer, *Organometallics* **1994**, in press.
[2] A. Herzog, H. W. Roesky, J. Schimkowiak, unpublished results.
[3] a) W. Kaminsky, A. Ahlers, O. Rabe, W. König in *Organic Synthesis via Organometallics* (Eds.: D. Enders, H.-J. Gais, W. Keim), Vieweg, Braunschweig, **1993**, pp. 151–163; b) H. Sinn, W. Kaminsky, H.-J. Vollmer, R. Woldt, *Angew. Chem.* **1980**, *92*, 396; *Angew. Chem. Int. Ed. Engl.* **1980**, *19*, 390; c) H. Sinn, W. Kaminsky, *Adv. Organomet. Chem.* **1980**, *18*, 99; d) W. Kaminsky, K. Külper, H. H. Brintzinger, F. R. W. P. Wild, *Angew. Chem.* **1985**, *97*, 507; *Angew. Chem. Int. Ed. Engl.* **1985**, *24*, 507.
[4] Structure of $[(Me_2AlF)_4]$: G. Gundersen, T. Haugen, A. Haaland, *J. Organomet. Chem.* **1973**, *54*, 77.
[5] Crystal structure analysis of **3**: $C_{26}H_{48}Al_2F_6Zr_2 \cdot 0.5$ toluene, monoclinic, $P2_1/c$, $a = 2801.5(4)$, $b = 2393.4(4)$, $c = 2302.2(2)$ pm, $\beta = 108.80(1)°$, $Z = 16$, $V = 14.613(4)$ nm^3, $\rho_{calcd} = 1.377$ Mg m^{-3}, $\lambda(Mo_{K\alpha}) = 71.073$ pm, 19236 independent reflections used for stucture solution and refinement. $R = 0.0476$, $wR = 0.1002$ [10b].
[6] W. E. Hunter, D. C. Hrncir, R. Vann Bynum, R. A. Pentilla, J. L. Atwood, *Organometallics* **1983**, *2*, 750.
[7] X. Yang, C. L. Stern, T. J. Marks, *J. Am. Chem. Soc.* **1991**, *113*, 3623.
[8] A. Herzog, H. W. Roesky, unpublished results.
[9] A singlet at $\delta = -145.5$, which corresponds to the ^{19}F NMR shift of the signal of $[(Me_2AlF)_4]$, dominates the ^{19}F NMR spectrum of the oily, unpurified filtrate. The resulting quantity of methane was determined to be 3.5 mol per mol of **1**.
[10] a) Crystal structure analysis of **4**: $C_{45}H_{78}Al_6Zr_3 \cdot 2.5$ toluene, monoclinic, $P2_1/n$, $a = 1275.6(10)$, $b = 3343(4)$, $c = 1553(2)$ pm, $\beta = 96.90(10)°$, $Z = 4$, $V = 6.575(13)$ nm^3, $\rho_{calcd} = 1.298$ Mg m^{-3}, $\lambda(Mo_{K\alpha}) = 71.073$ pm, 8581 independent reflections used for stucture solution and refinement. $R = 0.0535$, $wR = 0.1205$. b) Further details of the crystal structure investigations may be obtained from the Fachinformationszentrum Karlsruhe, D-76344 Eggenstein-Leopoldshafen (FRG) on quoting the depository number CSD-57683.
[11] A. F. Wells, *Structural Inorganic Chemistry*, 5th edition, Clarendon Press, Oxford, **1984**, p. 984.
[12] W. Uhl, *Z. Naturforsch. B* **1988**, *43*, 1113.
[13] C. Dohmeier, C. Robl, M. Tacke, H. Schnöckel, *Angew. Chem.* **1991**, *103*, 593; *Angew. Chem. Int. Ed. Engl.* **1991**, *30*, 564.
[14] M. D. Fryzuk, S. S. H. Mao, M. J. Zaworotko, L. R. MacGillivray, *J. Am. Chem. Soc.* **1993**, *115*, 5336.
[15] G. Erker, M. Albrecht, C. Krüger, S. Werner, *Organometallics* **1991**, *10*, 3791.
[16] The composition of **4** described here with respect to the methine and methylene units is chemically plausible under the assumption of electroneutrality.

Synthesis and Structure of the First Dimeric Iminoalane Containing an Al_2N_2 Heterocycle**

Stephan Schulz, Ludger Häming, Regine Herbst-Irmer, Herbert W. Roesky,* and George M. Sheldrick

Dedicated to Professor M. Frederick Hawthorne on the occasion of his 65th birthday

In the last few years, compounds containing elements of Groups 13 and 15 have attracted a great deal of interest because they are potential single-source precursors for III–V systems that play an important role in semiconductor technology and optoelectronics.[1] We are especially interested in iminoalanes, which previously were only accessible through alkane eliminations, and have reported the preparation of $(MeAlNC_6F_5)_4$, an Al–N heterocubane, formed from $AlMe_3$ and $H_2NC_6F_5$.[2] Besides the heterocubanes $(RAlNR')_x$ ($x = 4$), which are apparently especially stable iminoalane derivatives,[3] compounds with higher degrees of oligomerization are also known.[4] The iminoalane $[MeAlN(2,6\text{-}iPr_2C_6H_3)]_3$ ($x = 3$) synthesized by Power et al. reveals the lowest degree of oligomerization so far. This compound has a six-membered Al_3N_3 ring and can formally be described as being "quasi-aromatic" due to its six π electrons.[5] Despite repeated efforts, iminoalanes with $x = 1$ or 2 could not be prepared. With sterically less demanding groups R′ on the nitrogen atom, products with $x > 3$ are preferred,[6] and as a rule C–H activation takes place when the substituents are larger, as a result of drastic reaction conditions required.[7]

With $(Cp^*Al)_4$ ($Cp^* = C_5Me_5$), first reported by Schnöckel et al.[8] and synthesized by our research group by an easier route,[9] it is possible to synthesize iminoalanes by oxidative addition. The driving force of this reaction is the desire of the aluminum centers to reach the oxidation state III. Due to the high reactivity of $(Cp^*Al)_4$, mild reaction conditions can be employed. By applying sterically demanding substituents on the nitrogen atom, it should be possible to prepare dimeric iminoalanes containing an Al_2N_2 ring.

The reaction of $(Cp^*Al)_4$ with $MesN_3$ ($Mes = Me_3C_6H_2$)[10] in a molar ratio of 1:4 leads to **1** in a good yield. The dimeric iminoalane $(Cp^*AlNMes)_2$ is, however, not formed during the reaction, but rather the cyclic aminoalane **1** as a result of C–H activation of the *ortho*-bonded methyl group and subsequent migration of the proton to the nitrogen atom [Eq. (a)]. This

$$0.5\ (Cp^*Al)_4 + 2\,MesN_3 \longrightarrow \underset{\mathbf{1}}{[Cp^*Al\{\mu\text{-}NH(C_6H_2\text{-}4,6\text{-}Me_2\text{-}2\text{-}CH_2)\}]_2} + 2\,N_2 \quad (a)$$

reaction has been verified by NMR and IR spectroscopic investigations. Power et al. showed that C–H activation can occur during the thermal decomposition of $[RM(Me)N(H)R']_2$ compounds (M = Al, Ga); the Ga compounds reveal a greater tendency towards C–H activation than the corresponding Al compounds.[11]

Compound **1** is a colorless, hydrolysis-sensitive compound which melts at 201 °C. The central core of **1** is a planar four-membered Al_2N_2 ring in which the Al–N bond lengths (197.0–201.3 pm) lie within the expected range. Both the aluminum and the nitrogen atoms are four-coordinate. The hydrogen on the nitrogen atom could be located in the difference electron density synthesis and was refined isotropically. The Al–C distance to the methylene group (198.8 pm) corresponds to the value for an Al–C single bond. The fourth coordination site on the aluminum atom is filled by the Cp* group.[12]

An azide for which C–H activation should be more difficult is Me_3SiN_3. The reaction of $(Cp^*Al)_4$ and Me_3SiN_3 in a molar ratio of 1:4 leads to **2** (m.p. 194 °C) in moderate yield [Eq. (b)].

$$(Cp^*Al)_4 + 4\,Me_3SiN_3 \xrightarrow{-4\,N_2} \underset{\mathbf{2}}{\text{[Me}_3\text{Si–N(Cp*)–Al(Cp*)–N(SiMe}_3\text{)–Al(Cp*)–N(SiMe}_3\text{)]}} \quad (b)$$

In the mass spectrum of **2** we could not distinguish between an Al–N heterocubane and a dimeric iminoalane. However, the X-ray crystal structure determination verified the presence of a dimeric iminoalane (Fig. 1).

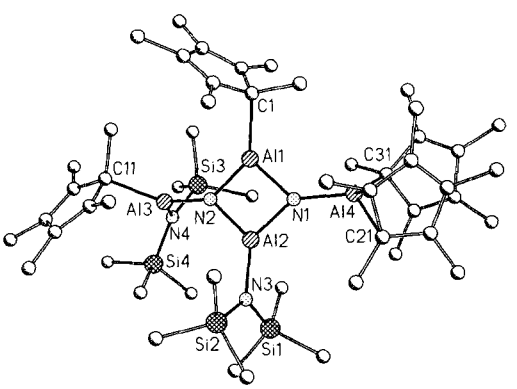


Fig. 1. The structure of **2** in the crystal. Selected bond lengths [pm] and angles [°]: Al1-N1 181.7, Al1-N2 180.3, Al2-N2 181.9, Al2-N1 180.3, N1-Al4 180.4, N2-Al3 178.1, Al3-N4 181.8, Al2-N3 179.0, Al1-C1 198.5; Al1-N1-Al2 84.3, Al1-N2-Al2 84.2, N1-Al1-N2 95.6, N1-Al2-N2 95.5, N2-Al1-C1 138.5, C1-Al1-N1 124.8, N1-Al2-N3 133.5, N3-Al2-N2 130.1, Al1-N1-Al4 132.5, Al4-N1-Al2 142.4, Al2-N2-Al3 134.3, Al3-N2-Al1 139.6.

In **2** the central core is also a four-membered, almost ideally planar Al_2N_2 ring.[13] In contrast to **1**, however, all the aluminum and nitrogen atoms are three-coordinate. Considering the six-membered Al_3N_3 ring of Power et al., **2** could be formally described as anti-aromatic because there are four π electrons available. One can envisage that **2** originates from an Al_4N_4 cube in which the top layer is broken open and the remaining Al_2N_2 ring represents the base. A silyl-group migration and a rearrangement of a Cp* group take place simultaneously.

The Al–N distances lie in the range 178.1–181.9 pm; the average bond lengths in the Al_2N_2 ring are 181.1 pm.[14] The distances are slightly longer than comparable bond lengths in $Al[N(SiMe_3)_2]_3$[15] and $[MeAlN(2,6\text{-}iPr_2C_6H_3)]_3$,[16] which also contain three-coordinate Al and N centers.[17] Higher poly(iminoalane)s with four-coordinate Al and N centers show significantly longer distances.[18] In three cases the Cp* groups in **2** are σ-bonded; one is η^2-bonded.

Apparently the steric demands of the Cp* and the $SiMe_3$ groups are too great to allow for the formation of a cubane;

[*] Prof. Dr. H. W. Roesky, Dipl.-Chem. S. Schulz, L. Häming, Dr. R. Herbst-Irmer, Prof. G. M. Sheldrick
Institut für Anorganische Chemie der Universität
Tammannstrasse 4, D-37077 Göttingen (FRG)
Telefax: Int. code + (551)39-3373

[**] This work was supported by the Deutsche Forschungsgemeinschaft, the Volkswagen-Stiftung, and the Fonds der Chemischen Industrie.

thus, the dimeric iminoalane **2** is generated. By selecting appropriate groups on the azide it should be possible to prepare additional iminoalanes by this method. Perhaps even the synthesis of the first Al–N compound possessing an Al–N double bond may be achieved by oxidative addition to $(Cp^*Al)_4$.

Experimental Procedure

All the reactions were performed under nitrogen atmosphere in dried solvents.

1: $MesN_3$ (0.65 g, 1 mmol) was added to a suspension of $(Cp^*Al)_4$ (0.16 g, 0.25 mmol) in toluene (60 mL) at 25 °C. Subsequently the reaction mixture was heated to 40 °C for about 0.5 h after which time the evolution of gas ended. Over a period of two days, the solvent was condensed off from the orange-colored solution. 0.22 g (74%) of **1** was obtained as colorless crystals. M.p. 201 °C; IR (CsI): $\tilde{\nu}$[cm^{-1}] = 3320, 1305, 1259, 1203, 1068, 1025, 851, 807, 660, 579, 503, 354; ^{1}H NMR (250 MHz, C_6D_6, 25 °C, TMS): δ = 1.64 (s, 15H, C_5Me_5), 1.90 (s, 2H, CH_2), 2.14 (s, 3H, *o*-Me), 2.26 (s, 3H, *p*-Me), 3.26 (s, 1H, N-H), 6.71 (s, 1H, arene-H), 7.01 (s, 1H, arene-H); ^{13}C NMR (100 MHz, C_6D_6, 25 °C, TMS): δ = 10.48 (s, C_5Me_5), 14.20 (s, CH_2), 18.54 (s, *o*-Me), 21.08 (s, *p*-Me), 114.65 (s, C_5Me_5), 129.38 (s, *o*-C), 131.38 (s, *o*-C), 134.41 (s, *p*-C), 136.80 (s, *m*-C), 137.44 (s, *m*-C), 142.18 (s, N-C); MS (EI): *m*/*z* (%): 590 (10) [M^+], 295 (100) [M^+/2]; correct elemental analysis.

2: $(Cp^*Al)_4$ (0.32 g, 0.5 mmol) was suspended in toluene (60 mL) and Me_3SiN_3 (0.23 g, 0.5 mmol) was added. Subsequently, the reaction was heated to 70 °C at which temperature nitrogen evolution was observed. Once the reaction was complete, the mixture was stirred at 80 °C for an additional 10 min. After concentration of the solution to about 5 mL and crystallization at −78 °C, 0.17 g (34%) of **2** was obtained as colorless crystals. M.p. 194 °C; IR (CsI): $\tilde{\nu}$[cm^{-1}] = 1083, 1019, 885, 837, 803, 722, 668, 592, 370, 254; ^{1}H NMR (500 MHz, C_6D_6, 25 °C, TMS): δ = 0.09 (s, 9H, $SiMe_3$), 1.79 (s, 15H, C_5Me_5); ^{13}C NMR (125 MHz, C_6D_6, 25 °C, TMS): δ = 5.90 (s, $SiMe_3$), 13.90 (s, C_5Me_5), 122.0 (s, C_5Me_5); MS (EI): *m*/*z* (%) = 725 (30) [M^+ − 2Cp*], 363 (70) [M^+/2 − Cp*], 322 (80) [$Cp^*AlN(SiMe_3)_2$], 186 (100) [$AlN(SiMe_3)_2$]; correct elemental analysis.

Received: November 29, 1993 [Z 6522 1E]
German version: *Angew. Chem.* **1994**, *106*, 1052

[1] S. M. Sze, *Physics of Semiconductor Devices*, 2nd edition, Wiley, New York, **1981**; C. R. M. Grovenor, *Microelectronic Materials*, Hilger, Philadelphia, PA, **1989**; B. G. Streetman, *Solid State Electronic Devices*, 3rd edition, Prentice Hall, Englewood Cliffs, NJ, **1990**; W. Rockensüss, H. W. Roesky, *Adv. Mater.* **1993**, *5*, 443.

[2] T. Belgardt, H. W. Roesky, M. Noltemeyer, H.-G. Schmidt, *Angew. Chem.* **1993**, *105*, 1101; *Angew. Chem. Int. Ed. Engl.* **1993**, *32*, 1056.

[3] G. Del Piero, M. Cesari, G. Dozzi, A. Mazzei, *J. Organomet. Chem.* **1977**, *129*, 281; T. R. R. McDonald, W. S. McDonald, *Acta Crystallogr. Sect. B* **1972**, *28*, 1619; K. M. Waggoner, P. P. Power, *J. Am. Chem. Soc.* **1991**, *113*, 3385; D. M. Choquette, M. J. Timm, J. L. Hobbs, T. M. Nicholson, M. M. Olmstead, R. P. Planalp, *Inorg. Chem.* **1993**, *32*, 2600.

[4] M. Veith, *Chem. Rev.* **1990**, *90*, 3; M. Cesari, S. Cucinella in *The Chemistry of Inorganic Homo- and Heterocycles, Vol. I* (Eds.: I. Haiduc, D. B. Sowerby), Academic Press, London, **1987**, p. 167.

[5] K. M. Waggoner, H. Hope, P. P. Power, *Angew. Chem.* **1988**, *100*, 1765; *Angew. Chem. Int. Ed. Engl.* **1988**, *27*, 1699.

[6] G. Del Piero, G. Perego, S. Cucinella, M. Cesari, A. Mazzei, *J. Organomet. Chem.* **1977**, *136*, 13; G. Del Piero, M. Cesari, G. Perego, S. Cucinella, E. Cernia, *ibid.* **1977**, *129*, 289; S. Amirkhalili, P. B. Hitchkock, J. D. Smith, *J. Chem. Soc. Dalton Trans.* **1979**, 1206.

[7] P. B. Hitchkock, H. A. Jasim, M. F. Lappert, H. D. Williams, *Polyhedron* **1990**, 245.

[8] C. Dohmeier, C. Robl, M. Tacke, H. Schnöckel, *Angew. Chem.* **1991**, *103*, 594; *Angew. Chem. Int. Ed. Engl.* **1991**, *30*, 564.

[9] S. Schulz, H. W. Roesky, H. J. Koch, G. M. Sheldrick, D. Stalke, A. Kuhn, *Angew. Chem.* **1993**, *105*, 1828; *Angew. Chem. Int. Ed. Engl.* **1993**, *32*, 1729.

[10] I. Ugi, H. Perlinger, L. Behringer, *Chem. Ber.* **1958**, *91*, 2330.

[11] During thermal decomposition $[Me_2GaN(H)Mes]_2$ reacts under C–H activation [19], whereas the corresponding Al compound forms the cubane $(MeAlNMes)_4$. Only when the N atom is coordinated by the sterically more demanding ligand 2,4,6-$tBu_3C_6H_2$ does the Al compound undergo C–H activation [7].

[12] Crystal data of **1**: $C_{38}H_{52}Al_2N_2$, M_r = 590.78, triclinic, space group $P\bar{1}$, a = 1122.5(2), b = 1173.3(2) c = 1370.3(2) pm, α = 92.22(2), β = 109.57(2), γ = 101.25(2)°, V = 1.6572(5) nm^3, Z = 2, ρ_{calcd} = 1.184 Mg m^{-3}; F(000) = 640, λ = 71.073 pm, $\mu(Mo_{K\alpha})$ = 0.117 mm^{-1}. The data were collected on a STOE-Siemens-Huber diffractometer. Intensity measurements were performed by $2\theta/\omega$ scans in the range $8° \le 2\theta \le 50°$ at −120 °C on a rapidly cooled crystal of dimensions 0.30 × 0.20 × 0.15 mm in an oil drop [20]. Of the 11737 measured reflections, 5869 were independent; largest minimum and maximum in the final difference Fourier synthesis: −345 and 729 e nm^{-3}, $R1$ = 0.0733 (for 3715 reflections with $F > 4\sigma(F)$) and $wR2$ = 0.2004 (all data).

[13] The average deviation from the plane is 3.7 pm.

[14] Crystal data of **2**: $C_{52}H_{96}Al_4N_4Si_4$, M_r = 997.61, monoclinic, space group $P2_1/c$, a = 2516.7(7), b = 1942.8(5) c = 1288.5(4) pm, β = 104.50(3)°, V = 6.099(3) nm^3, Z = 4, ρ_{calcd} = 1.086 Mg m^{-3}; F(000) = 2176, λ = 71.073 pm, $\mu(Mo_{K\alpha})$ = 0.190 mm^{-1}. The data were collected on a STOE-Siemens-AED diffractometer. Intensity measurements were performed by $2\theta/\omega$ scans in the range $8° \le 2\theta \le 45°$ at −120 °C on a rapidly cooled crystal of dimensions 0.45 × 0.25 × 0.20 mm in an oil drop [20]. Of the 7405 measured reflections, 7155 were independent; largest minimum and maximum in the final difference Fourier synthesis: −245 and 237 e Å^{-3}, $R1$ = 0.0495 (for 5004 reflections with $F > 4\sigma(F)$) and $wR2$ = 0.1181 (all data). The values of $R1$ and $wR2$ are defined as $R1 = \Sigma||F_o| - |F_c||/[\Sigma|F_o|]$; $wR2 = \{[\Sigma w(F_o^2 - F_c^2)^2]/[\Sigma w(F_o^2)^2]\}^{1/2}$. The structures were solved by direct methods (SHELXS-90) [21] and refined by least-squares against F^2 (SHELX-93) [22]. The hydrogen atoms, except the hydrogen atom located on N1 in **1**, were positioned geometrically and refined by using a riding model in which the Me groups can rotate about their local axes. The hydrogen atom on N1 in **1** was refined by using distance restraints. Further details of the crystal structure investigations may be obtained from the Director of the Cambridge Crystallographic Data Centre, 12 Union Road, GB-Cambridge CB2 1EZ (UK) on quoting the complete literature citation.

[15] G. M. Sheldrick, W. S. Sheldrick, *J. Chem. Soc. A* **1969**, 2279.

[16] In both compounds the bond lengths are 178 pm. These are significantly shorter than the sum of the atomic radii (about 200 pm), but correspond well to the value determined according to the equation of Blom and Haaland (179 pm) [23].

[17] Power et al. reported the monomeric aminoalane tBu_2AlNRR' whose Al–N bond lengths range between 178 and 189 pm. M. A. Petrie, K. Ruhlandt-Senge, P. P. Power, *Inorg. Chem.* **1993**, *32*, 1135.

[18] The bond lengths found in iminoalanes with higher degrees of oligomerization range between 189 and 196 pm [4,6].

[19] P. P. Power, *J. Organomet. Chem.* **1990**, *400*, 49.

[20] T. Kottke, D. Stalke, *J. Appl. Crystallogr.* **1993**, *26*, 615.

[21] G. M. Sheldrick, *Acta Crystallogr. Sect. A* **1990**, *46*, 467.

[22] G. M. Sheldrick, *SHELXL-93*, unpublished results.

[23] R. Blom, A. Haaland, *J. Mol. Struct.* **1985**, *129*, 21.

Synthesis, Crystal and Molecular Structure of Boc-Pro-ΔPhe-Ala-ΔPhe-Ala-OMe; A Pentapeptide with a Novel β-Bend Ribbon Structure**

Kanagalaghatta Ramabhatta Rajashankar, Suryanarayanarao Ramakumar, Tapas Kumar Mal, and Virander Singh Chauhan*

α,β-Dehydroamino acid residues (2,3-didehydroamino acid residues) are found in several naturally occurring peptides from microbial sources as well as in some proteins;[1] their presence in a peptide chain produces remarkable conformational consequences.[2] In addition, dehydropeptides show enhanced resistance to enzymatic degradation.[3] Thus, introduction of α,β-dehydroamino acid residues into bioactive peptide sequences has become an important tool to study structure–function relationships, and to provide analogues of peptide hormones with improved bioactivity.[4] Small peptides containing a single α,β-dehydrophenylalanine (ΔPhe) residue often have β-bend[5] structures,[2b–g] whereas helical structures are stabilized in longer peptides containing more than one ΔPhe residue.[2h–l] In

[*] Prof. V. S. Chauhan, T. K. Mal
International Center for Genetic Engineering and Biotechnology
NII Campus, Aruna Asaf Ali Marg
New Delhi 110 067 (India)
Telefax: Int. code + (11)686-2316
K. R. Rajashankar, Prof. S. Ramakumar
Department of Physics, Indian Institute of Science
Bangalore 560 012 (India)

[**] The authors thank the Department of Biotechnology (India) for access to facilities. One of us (K. R. R.) thanks the Council of Scientific and Industrial Research (India) for a Fellowship.

this regard the behavior of the ΔPhe residue is somewhat similar to that of α-aminoisobutyric acid (Aib), a well-studied helicogenic nonprotein amino acid residue.[6] Recently, we have observed a 3_{10}-helical conformation in a nonapeptide containing three ΔPhe residues.[2j] We report here the synthesis, X-ray crystal and molecular structure of the pentapeptide **1**, which adopts a novel flat (non-helical) β-bend ribbon conformation in contrast to the helical β-bend ribbons observed for other peptides.[7]

Boc-Pro-ΔPhe-Ala-ΔPhe-Ala-OMe **1**

The β-bend ribbon conformation is characterized by interesting hydrogen bond interactions wherein alternating 4→1 hydrogen bonds are absent.[7] This conformation was initially proposed for the $(Aib\text{-}Pro)_n$ peptide sequence on the basis of NMR data[9] and conformational energy calculations,[10] and subsequently observed in several Aib peptides with characteristic sequence.[7] Presumably because β-bend ribbons have almost the same dihedral angles as the 3_{10}-helix backbone, they have been referred to as β-bend ribbon spirals.[7b,f] The β-bend ribbon structures should be of relevance for developing models for peptaibol antibiotics and for the numerous $(Pro\text{-}X)_n$ (with X ≠ Pro) segments found in proteins.[7a,b]

Remarkably, in **1** both the crystallographically independent molecules exhibit novel β-bend ribbon conformations (Fig. 1).

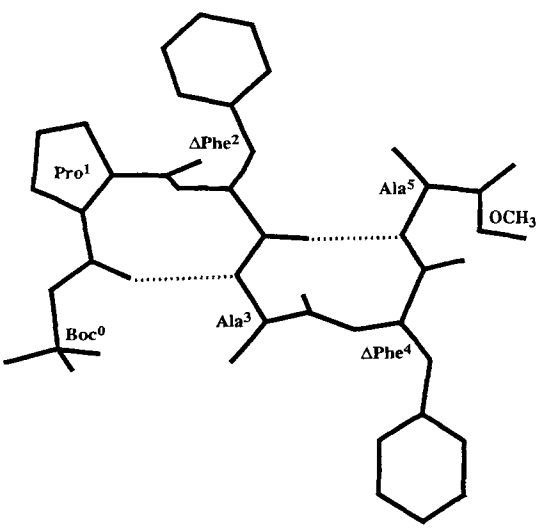


Fig. 1. Molecular structure of **1** in the crystal. Dotted lines indicate the intramolecular 4→1 hydrogen bonds.

This conformation is a consequence of two partially overlapping β-turns.[5] The $Boc^0\text{-}Pro^1\text{-}\Delta Phe^2\text{-}Ala^3$ fragment adopts a type I β-turn conformation (backbone dihedral angles $\phi_{i+1} = -64.6°$, $\psi_{i+1} = -28.5°$ and $\phi_{i+2} = -80.6°$, $\psi_{i+2} = -7.3°$) and the $\Delta Phe^2\text{-}Ala^3\text{-}\Delta Phe^4\text{-}Ala^5$ fragment adopts a type II β-turn conformation ($\phi_{i+1} = -65.8°$, $\psi_{i+1} = 129.9°$ and $\phi_{i+2} = 77.2°$, $\psi_{i+2} = 3.3°$). It should be noted that ΔPhe^2 has a negative ϕ, while ΔPhe^4 has a positive ϕ. This is not surprising in view of the achiral nature of ΔPhe. The above-mentioned β-turns are stabilized by two hydrogen bonds, N3–H···O2(Boc) and N5–H···O2′. The 4→1 hydrogen bond N4–H···O1′ is not observed, which is consistent with the hydrogen bonding features of a β-bend ribbon. However, the hydrogen bonding potential of the O1′ atom as an acceptor is satisfied by intermolecular hydrogen bonding in the two crystallographically independent molecules (Table 1).

Table 1. Intermolecular and intramolecular hydrogen bonds observed in the structure of **1** in the crystal [a].

Donor (D)	Acceptor (A)	D···A [Å]	H···A [Å]	D-H···A [°]	Symmetry
N3A	O2A	3.04	2.04	167.0	0
N5A	O2′A	3.01	2.04	160.4	0
N3B	O2B	2.98	1.99	166.7	0
N5B	O2′B	2.95	1.97	164.7	0
N2A	O1′A	2.92	2.00	149.8	1
N4A	O4′A	2.73	1.75	165.4	2
C1GA	O3′A	3.38	2.47	141.9	1
N2B	O1′B	2.91	1.99	151.6	3
N4B	O4′B	2.75	1.75	167.7	4
C1GB	O3′B	3.24	2.24	152.3	3

Symmetry code:				
	0	x,	y,	z
	1	$-x+1$,	$y+0.5$,	$-z$
	2	$-x+2$,	$y+0.5$,	$-z$
	3	$-x+2$,	$y+0.5$,	$-z+1$
	4	$-x+3$,	$y+0.5$,	$-z+1$

[a] The last letter A or B in the names of the atoms refers to the two crystallographically independent molecules A and B, respectively. C1GA and C1GB represent the γ-carbon atom of the pyrrolidine ring of the Pro^1 residue.

The *trans* conformation of the tertiary urethane Boc–Pro bond in the pentapeptide deviates significantly from planarity ($\omega_0 = -162.6°$). The pyrrolidine ring of the Pro^1 residue which is characterized by $\chi_1 = -10.1°$, $\chi_2 = 7.7°$, $\chi_3 = -2.3°$, $\chi_4 = -5.0°$, and $\theta = 9.3°$, is nearly C^γ-*exo* puckered.[11] The phenyl groups of the two ΔPhe residues are almost planar with olefinic double bond (dihedral angles $\chi_2^2 = -164.5°$, $\chi_4^2 = 4.9°$).

In the β-bend ribbon structures previously reported, the backbone torsion angles are nearly 3_{10}-helical,[7] so that the overall shape of the molecules could grossly be approximated to cylinders. In contrast, in **1** the backbone torsion angles of Ala^3 deviate significantly from 3_{10}-helical values (Table 2), resulting in a relatively flat slablike structure; we designated this structure as a flat β-bend ribbon structure.

Table 2. Torsion angles averaged over the two crystallographically independent molecules of **1**.

Residue	ϕ [°]	ψ [°]	ω [°]
Pro^1	−64.4 [a]	−28.5	179.3
ΔPhe^2	−80.6	−7.3	−173.4
Ala^3	−65.8	129.9	178.8
ΔPhe^4	77.2	3.3	169.8
Ala^5	−63.4	−29.6 [b]	-

[a] C5(Boc)-N1-C1A-C1′. [b] N5-C5A-C5′-O3(OMe).

The peptide molecules reported so far, possessing a β-bend ribbon conformation, invariably have at alternate positions, residues such as proline,[7b,c] *N*-methylaminoisobutyric acid (MeAib),[7d] hydroxyproline (Hyp),[7e] and α-hydroxyisobutyric acid (Hib)[7e,f] which lack the hydrogen bond donating N–H group. In these peptides, therefore, consecutive 4→1 hydrogen bonds are inherently absent at alternate positions, but an approximate 3_{10}-helical conformation is maintained due to conformationally constrained Aib residues, leading to a β-bend ribbon spiral. However, in **1**, a flat β-bend ribbon structure is observed even though the sequence allows the possibility of consecutive 4→1 hydrogen bonds.

The crystal packing of **1** as viewed down the crystallographic *b* axis is shown in Figure 2. The intermolecular hydrogen bonds are listed in Table 1. There are no head-to-tail intermolecular

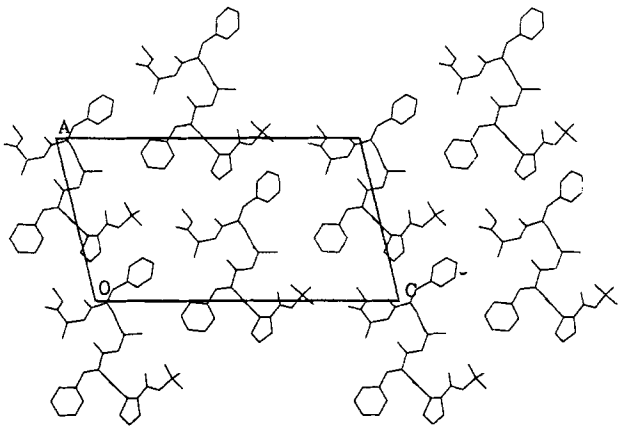


Fig. 2. Crystal packing of **1**. View down the crystallographic *b* axis.

hydrogen bonds, a frequent feature observed in some Aib peptides[6] and α,β-dehydropeptides,[2j] and no hydrogen bonds between the two crystallographically independent molecules; the *ac* plane of the crystal structure is predominantly stabilized by hydrophobic interactions. The intermolecular interactions along the *b* axis are mainly electrostatic in nature. The peptide molecules with an S-shaped backbone are stacked one above the other, along the crystallographic *b* axis and are connected by N–H···O and C–H···O types of hydrogen bonds (Table 1). We observe alternate columns along the *b* axis containing the two crystallographically independent molecules. The interface of the columns contains Boc-methyl groups and dehydrophenylalanine side chains and hence is predominantly hydrophobic. The Phe rings interact in "tilted" configurations,[12] which is in accordance with the observation made in proteins.[12] The O5′ atom does not participate in any hydrogen bond formation.

The structure of **1** now enables a comparison of ΔPhe-containing oligopeptide structures with the corresponding Aib analogues reported earlier, the N-terminal fragments (2-6) of the antibiotic alamethicin, Boc-Pro-Aib-Ala-Aib-Ala-OH[13a] and *Z*(Cl)-Pro-Aib-Ala-Aib-Ala-OMe.[13b] Both Aib peptides have a left-handed 3_{10}-helical structure. Whereas Aib is known to strongly prefer helical backbone dihedral angles, ΔPhe can be accommodated in the 'bridge' region of the conformational space, as the Ala[3]-ΔPhe[4] sequence in **1** shows.

In the crystal structures of ΔPhe-containing peptides reported so far, the ΔF-X1-ΔF-X2 fragment has always exhibited either type III or type III′ β-turn conformations[2i-l] (Table 3), leading to a helical structure, whereas in the crystal structure of **1** the same fragment, for the first time, shows a type II β-turn which is nonhelical (Table 2). Interestingly, the ΔF-X1-ΔF-X2 fragment with X1 = Leu or Val, assumes a right-handed helical conformation (Table 3), whereas, the same fragment with X1 = Ala adopts an entirely different conformation in the present case. There are several examples known, in which the peptide backbone assumes a left-handed helical conformation despite the presence of the chiral L-Ala residue.[13, 14] Thus the Ala residue, presumably, because of the less bulky side chain, appears to permit greater conformational flexibility for the peptide backbone, a result that could be made use of in fine-tuning the designed conformation.

Thus, the solid-state molecular structure of **1** shows how novel conformations such as the flat β-bend ribbon can be obtained by using ΔPhe residues. The comparison with the Aib analogues of the pentapeptide demonstrates that even though Aib and ΔPhe are achiral, conformation constraining residues, different structures may be stabilized by these residues in a given peptide sequence. The conformational variability has been elegantly described in Aib-containing peptides,[13, 15] it has also been observed to some extent in ΔPhe-containing peptides.[14] The comparison of the conformation of the dehydropentapeptide with the other dehydropeptide fragments of the type ΔF-X1-ΔF-X2, shows the role of the amino acid residues X1 and X2 in determining the overall conformation of the dehydrooligopeptide. Clearly, further studies are required to understand the influence of the dehydrophenylalanine residue on the conformation of peptides and to compare its conformation constraining behavior with that of the Aib residue.

Table 3. The conformation exhibited by the X1-ΔF segment of the ΔF-X1-ΔF-X2 fragment in crystal structures studied so far.

Peptide [a]	Ref.	φ [°]	ψ [°]	φ [°]	ψ [°]	β-Turn type
Boc-G-ΔF-L-ΔF-A-NHMe	[2i]	−71.2	−15.4	−58.3	−17.9	III
Boc-V-ΔF-F-A-F-ΔF-V-ΔF-G-OMe	[2j]	−68.6	−15.4	−54.6	−35.1	III
Boc-DA-ΔF-G-ΔF-DA-OMe	[2k]	65.3	5.9	53.0	25.6	III′
Ac-ΔF-V-ΔF-NHMe	[2l]	−62.0	−20.4	−59.2	−24.1	III
Boc-P-ΔF-A-ΔF-A-OMe **1**		−65.8	129.9	77.2	3.3	II

[a] ΔF-X1-ΔF-X2 fragment is underlined.

Experimental Procedure

Synthesis of Boc-Ala-ΔPhe-Ala-OCH_3: A solution of HCl·H-Ala-OCH_3 (0.77 g, 5.5 mM) and triethylamine (0.8 mL, 5.5 mM) in dichloromethane (10 mL) was added to a solution of Boc-Ala-ΔPhe-azlactone [2i] (1.56 g, 5 mM) in dichloromethane (10 mL) and stirred for 48 h at room temperature. After removal of solvent in vacuo, the residue was dissolved in ethyl acetate and washed with saturated $NaHCO_3$ solution, water, 5% citric acid, and saturated NaCl solution and dried over Na_2SO_4. After evaporation and crystallization from diethyl ether/petroleum ether pure tripeptide was obtained. Yield: 1.8 g (87%); m.p. 97–99 °C; R_f ($CHCl_3$/CH_3OH, 9:1) 0.85, R_f (*n*-butanol/acetic acid/H_2O, 4:1:1) 0.89. ^{1}H NMR (270 MHz, $CDCl_3$): δ = 7.76 (1H, s, NH ΔPhe), 7.43 (1H, d, NH Ala(3)), 7.4–7.3 (6H, m, aromatic protons and C^βH ΔPhe), 5.08 (1H, d, NH Ala(1)), 4.68 (1H, m, C^αH Ala(3)), 4.19 (1H, m, C^αH Ala(1)), 3.75 (3H, s, OCH_3), 1.43 (3H, d, $C^\beta H_3$ Ala(3)), 1.41 (12H, d, Boc Me_3 and $C^\beta H_3$ Ala(1)).

1: After deprotection of Boc-Ala-ΔPhe-Ala-OCH_3 with trifluoroacetic acid (TFA)/dichloromethane (1:1, v/v) at room temperature and evaporation, the oily residue was washed with ether to give TFA·H-Ala-ΔPhe-Ala-OCH_3. Boc-Pro-ΔPhe-azlactone [2i] (1.22 mg, 3.5 mM) and TFA·H-Ala-ΔPhe-Ala-OCH_3 (1.5 g, 3.5 mM) were allowed to react as described above. This led to the pure pentapeptide after recrystallization from methanol/water. Yield: 1.7 g (74%); m.p. 236–238 °C; R_f ($CHCl_3$/CH_3OH (9:1)) 0.71, R_f(*n*-butanol/acetic acid/H_2O 4:1:1) 0.93. ^{1}H NMR (270 MHz, in $CDCl_3$ with traces of $(CD_3)_2SO$): δ = 9.49 (1H, s, NH ΔPhe(2)), 8.71 (1H, s, NH ΔPhe(4)), 8.12 (1H, d, NH Ala(3)), 7.3 (1H, d, NH Ala(5)), 7.26–7.09 (12H, m, aromatic protons and 2C^βH ΔPhe(2) and ΔPhe(4)), 4.37 (1H, m, C^αH Ala(5)), 4.26 (1H, m, C^αH Ala(3)), 4.03 (1H, m, C^αH Pro(1)), 3.53 (3H, s, OCH_3), 2.09 (1H, m, C^β H Pro(1)), 1.81 (2H, m, C^γH and C^δH Pro(1)), 1.39 (3H, d, $C^\beta H_3$ Ala(5)), 1.29 (12H, d, Boc Me_3 and $C^\beta H_3$ Ala(3)).

Crystal structure analysis: Single crystals having colorless prismatic morphology were obtained by evaporation of a solution of the peptide ($C_{35}H_{43}N_5O_8$, M_r = 661.75) in methanol/acetone mixture. The crystals belong to the monoclinic space group $P2_1$ with a = 14.365(2), b = 9.931(2), c = 25.787(2) Å, β = 104.03(1)°, V = 3569 Å^3, Z = 4, ρ = 1.23 g cm^{-3}. X-ray intensity data were collected at 21 °C with an Enraf-Nonius CAD4 diffractometer with Ni-filtered $Cu_{K\alpha}$ radiation (λ = 1.5418 Å). The ω-2θ scan technique was used to collect data upto a Bragg angle of 60°. A total of 5881 unique reflections were measured, 5205 of which with $|F_o| > 3\sigma(|F_o|)$ were considered as observed and used in the structure analysis. No significant variation was observed in the intensities of three standard reflections monitored at regular intervals during the data collection, implying electronic and crystal stability. Lorentz and polarization corrections were applied to the data and no absorption corrections were made. The structure was solved by direct methods by using SHELXS86 [8] and refined by full-matrix least-squares technique with anisotropic thermal factors for all non-hydrogen atoms. All the hydrogen atoms were placed at idealized positions on the basis of the stereochemistry and they were included only in structure factor calculations. The final agreement factors are R = 0.056 and R_w = 0.069. There are two crystallographically independent molecules in the asymmetric unit (A and B). The molecular dimensions and the conformation of these two molecules are remarkably similar. Least-squares superposition of the backbone atoms of these two molecules results in an average standard devi-

ation of 0.09 Å, indicating the similarity of the two molecules. Therefore the mean values of the conformational parameters have been used in the discussions. Further details of the crystal structure investigation are available on request from the Director of the Cambridge Crystallographic Data Centre, 12 Union Road, GB-Cambridge CB21EZ (UK), on quoting the full journal citation.

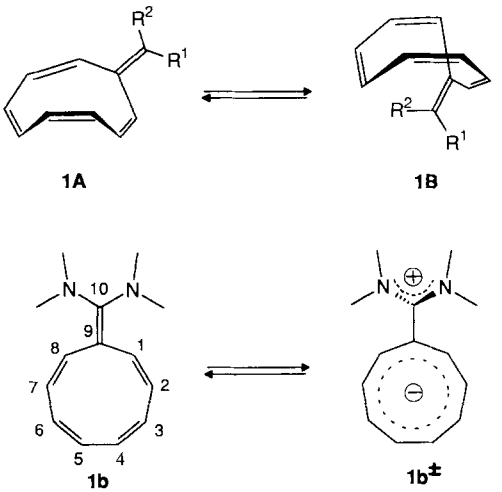
Received: October 26, 1993 [Z6452IE]
German version: *Angew. Chem.* **1994**, *106*, 1048

[1] a) K. Noda, Y. Shimohigashi, N. Izumiya in *The Peptides, Vol. 5*, (Eds. E. Gross, J. Meienhofer), Academic Press, New York, **1983**, p.285; b) G. Jung, *Angew. Chem.* **1991**, *103*, 1067; *Angew. Chem. Int. Ed. Engl.* **1991**, *30*, 1051; c) E. Gross, J. L. Morell, *J. Am. Chem. Soc.* **1971**, *93*, 4634.
[2] a) A. Gupta, A. Bharadwaj, V. S. Chauhan, *J. Chem. Soc. Perkin. Trans. 2* **1990**, 1911; b) E. Ciszak, G. Pietrzynski, B. Rzeszotarska, *Int. J. Peptide Protein Res.* **1992**, *39*, 218; c) A. Gupta, V. S. Chauhan, *ibid.* **1993**, *41*, 421; d) V. Busetti, M. Crisma, C. Toniolo, S. Salvadori, G. Balboni, *Int. J. Biol. Macromol.* **1992**, *14*, 23; e) A. C. Bach II, L. M. Gierasch, *Biopolymers* **1986**, *25*, S175; f) P. Narula, B. Khandelwal, T. P. Singh, *ibid.* **1991**, *31*, 987; g) V. S. Chauhan, K. K. Bhandary *Int. J. Peptide Protein Res.* **1992**, *39*, 223; h) O. Pieroni, A. Fissi, C. Pratesi, P. A. Temussi, F. Ciardelli, *Biopolymers* **1993**, *33*, 1; i) K. K. Bhandary, V. S. Chauhan, *ibid.* **1993**, *33*, 209; j) K. R. Rajashankar, S. Ramakumar, V. S. Chauhan, *J. Am. Chem. Soc.* **1992**, *114*, 9225; k) M. R. Ciajolo, A. Tuzi, C. R. Pratesi, A. Fissi, O. Pieroni, *Biopolymers* **1990**, *30*, 911; l) M. R. Ciajolo, A. Tuzi, C. R. Pratesi, A. Fissi, O. Pieroni, *Int. J. Peptide Protein Res.* **1991**, *38*, 539.
[3] M. L. English, C. H. Stammer, *Biochem. Biophys. Res. Commun.* **1978**, **83**, 1464.
[4] a) P. Kaur, G. K. Patnaik, R. Raghubir, V. S. Chauhan, *Bull. Chem. Soc. Jpn.* **1992**, *65*, 3412; b) Y. Shimohigashi, M. L. English, C. H. Stammer, T. Costa, *Biochem. Biophys. Res. Commun.* **1982**, *104*, 583.
[5] C. M. Venkatachalam, *Biopolymers* **1968**, *6*, 1425.
[6] I. L. Karle, P. Balaram, *Biochemistry* **1990**, *29* 6747.
[7] a) C. Toniolo, E. Benedetti, *Trends. Biochem. Sci.* **1991**, *16*, 350; b) B. D. Blasio, V. Pavone, M. Saviano, A. Lombardi, F. Nastri, C. Pedone, E. Benedetti, M. Crisma, M. Anzolin, C. Toniolo, *J. Am. Chem. Soc.* **1992**, *114*, 6273; c) I. L. Karle, J. Flippen Anderson, M. Sukumar, P. Balaram, *Proc. Natl. Acad. Sci. USA* **1987**, *84*, 5087; d) V. Moretti, G. Valle, M. Crisma, G. M. Bonora, C. Toniolo, *Int. J. Biol. Macromol.* **1992**, *14*, 178; e) G. Valle, R. Bardi, A. M. Piazzesi, M. Crisma, C. Toniolo, G. Cavicchioni, K. Uma, P. Balaram, *Biopolymers* **1991**, *31*, 1669; f) M. Crisma, G. Valle, G. M. Bonora, C. Toniolo, G. Cavicchioni, *Int. J. Peptide Protein Res.* **1993**, *41*, 553.
[8] G. M. Sheldrick, *Acta Crystallogr. Sect. A* **1990**, *46*, 467.
[9] Y. V. Venkatachalapathi, P. Balaram, *Biopolymers* **1981**, *20*, 1137.
[10] B. V. V. Prasad, P. Balaram, *Int. J. Biol. Macromol.* **1982**, *4*, 99.
[11] E. Benedetti in *Proc. Fifth Am. Peptide Symp.* (Eds.: M. Goodman, J. Meienhofer), Wiley, New York, **1977**, p. 257.
[12] J. Singh, J. M. Thornton, *FEBS Lett.* **1985**, *191*, 1.
[13] a) R. Bosch, G. Jung, H. Schmitt, G. M. Sheldrick, W. Winter, *Angew. Chem.* **1984**, *96*, 440; *Angew. Chem. Int. Ed. Engl.* **1984**, *23*, 450; b) T. S. Cameron, A. W. Hanson, A. Taylor, *Cryst. Struct. Commun.* **1982**, *11*, 321.
[14] A. Tuzi, M. R. Ciajolo, G. Guarino, P. A. Temussi, A. Fissi, O. Pieroni, *Biopolymers* **1993**, *33*, 1111.
[15] R. P. Hummel, C. Toniolo, G. Jung, *Angew. Chem.* **1987**, *99*, 1180; *Angew. Chem. Int. Ed. Engl.* **1987**, *26*, 1150.

11,12-Bis(diethylamino)nonatriafulvalene, the First "Aromatic" Nonafulvene**

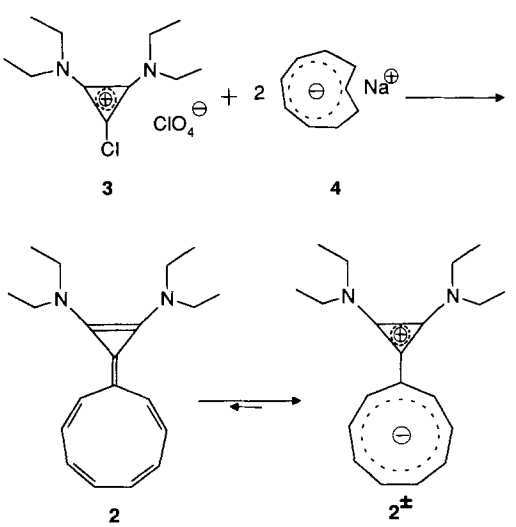
Shengyong Chai and Markus Neuenschwander*

According to NMR investigations, nonpolar nonafulvenes including parent **1a** ($R^1 = R^2 = H$) are olefinic compounds (characterized by strongly alternating bond lengths and a nonplanar ring).[1] As a result of the rapid equilibrium **1A** ⇄ **1B** for $R^1 = R^2$, four pairs of ring protons and four pairs of ring-C atoms are equivalent: H-1/H-8, H-2/H-7, H-3/H-6, H-4/H-5 and C-1/C-8, C-2/C-7, C-3/C-6, C-4/C-5, respectively. Furthermore, ^1H and ^{13}C NMR signals occur at $\delta = 5.4$ to 6.4 and $\delta = 115$ to 132, respectively, and do not significantly change between -100 and $+20\,^\circ C$. Remarkably different behavior is observed for the first isolated nonafulvene **1b**, whose spectra are strongly influenced by solvent polarity and temperature.[2, 3] This is explained reasonably well by an equilibrium between nonplanar olefinic **1b** and planar dipolar **1b**$^\pm$,[4] the latter being favored by polar solvents or low temperatures;[5] very similar behavior is observed for sodium nonafulvenolates.[6]



Hitherto, nonafulvenes which exist in the dipolar form **1**$^\pm$ between -100 and $20\,^\circ C$ in nonpolar solvents were unknown. The ground-state energy of **1**$^\pm$ (characterized by a planarized nine-membered ring) is expected to be considerably lower than that of the nonplanar olefinic structure **1**; thus the structure **1** should not be favored by solvent or temperature effects.

We considered several synthetic pathways to dipolar nonafulvenes;[7] one attractive plan is based on the synthesis of **2**. It is well known from calicenes (pentatriafulvalenes)[8] that a cyclopropene unit, attached to the exocyclic double bond of pentafulvenes, strongly supports or even increases the electron-releasing capacity of exocyclic substituents,[9, 10] while steric effects are



[*] Prof. Dr. M. Neuenschwander, Dr. S. Chai
Institute of Organic Chemistry, University of Bern
Freiestrasse 3, CH-3012 Bern (Switzerland)
Telefax: Int. code + (31)631-4499

[**] Financial support by the Swiss National Foundation (Project No. 20-37336.93) is gratefully acknowledged.

 © VCH Verlagsgesellschaft mbH, D-69451 Weinheim, 1994 0570-0833/94/0909-0973 $ 10.00+.25/0

considerably reduced. In fact, reaction of 1-chloro-2,3-bis(diethylamino)cyclopropenylium perchlorate **3**[11] with two equivalents of Na-(*Z,Z,Z,E*)-cyclononatetraenide (**4**) at −60 °C in THF/CH_2Cl_2 gave pale yellow crystals of **2** (54% yield).[12]

The structure of $\mathbf{2}^{\pm}$ is in agreement with the spectroscopic and analytical results.[13] In the ^1H NMR spectrum (600 MHz, $CDCl_3$, room temperature) the signals of all the ring protons are in the range between $\delta = 7.3$ and 7.0 and are thus shifted by an average $\Delta\delta \approx 1.2$ to low field in comparison with those of nonpolar nonafulvenes.[1] Furthermore, the chemical shifts of the protons of the NEt_2 groups (q at $\delta = 3.68$ and t at $\delta = 1.39$) are very similar to those of **3**.[14] Analysis of the complex AA'BB'XX'YY'-type spectrum of the ring protons of $\mathbf{2}^{\pm}$ (Fig. 1, bottom) gives, after iterative simulation (Fig. 1, top), a set of large and nearly equal ^3J coupling constants as well as a set of surprisingly small long-range coupling constants.[15] In addition, the chemical shifts and the splitting pattern of the ring protons are virtually not influenced by changes of temperature (−50 to +50 °C) or solvents. The ^1H NMR results are convincingly explained with a dipolar cyclopropenylio cyclononatetraenide structure $\mathbf{2}^{\pm}$, which is characterized by a planarized nine-membered ring. This conclusion is supported by the ^{13}C NMR spectra: The signals of all the ring-C atoms experience an average high-field shift of $\Delta\delta = 16$ compared with those of nonpolar nonafulvenes[1] due to the negative π-charge density and moreover, do not alter their positions ($\Delta\delta = 0.9$) between −50 and +50 °C.

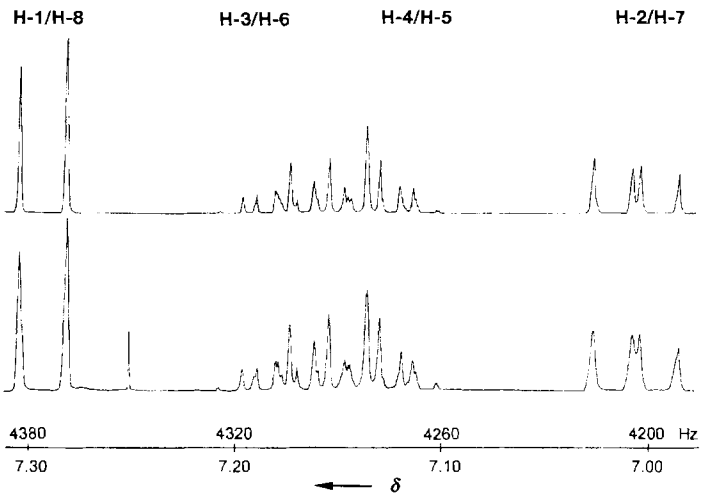


Fig. 1. Expansion of the signals of the ring protons of $\mathbf{2}^{\pm}$; bottom: experimental spectrum; top: simulation with values from [15].

For an illustrative comparison of the surprising NMR spectroscopic similarities between $\mathbf{2}^{\pm}$ and **1b**, for which a temperature-dependent equilibrium of the type $\mathbf{1b} \rightleftarrows \mathbf{1b}^{\pm}$ has been well established, the NMR data of both compounds are summarized in Figure 2.[16] At room temperature and in nonpolar solvents like $CDCl_3$, **1b** behaves like a nonplanar olefinic nonafulvene: The ^1H chemical shifts lie between $\delta = 5.4$ and 6.3[2], the vicinal ^3J coupling constants are strongly alternating,[1, 3] and the ^{13}C chemical shifts of C1 to C8 are in a fairly broad range centered around $\delta = 120$. With decreasing temperature (and increasing importance of $\mathbf{1b}^{\pm}$), ^1H NMR signals shift towards $\delta = 6.9$ to 7.2,[2] the values of the ^3J coupling constants over formal single bonds of **1b** increase dramatically,[1, 2] and the signals of C2 to C8 shift towards $\delta = 110$.[17]

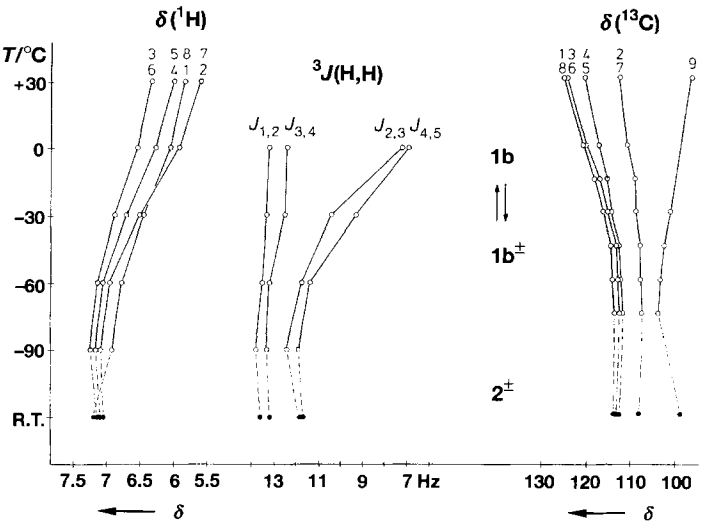


Fig. 2. NMR parameters of nonatriafulvalene **2** compared with those of 10,10-bis-(dimethylamino)nonafulvene **1b** [1–3]. R.T. = room temperature.

All the NMR spectroscopic parameters of the nonatriafulvalene **2** (Fig. 2 bottom) are virtually identical with the values of **1b** in the low-temperature range[18] (which are governed by the influence of dipolar $\mathbf{1b}^{\pm}$). The only difference is that they are not dependent on the solvent polarity or temperature. Thus it is clear that over the temperature range (from −50 to +50 °C) studied and in all the solvents used,[19] 11,12-bis(diethylamino)nonatriafulvalene **2** exists as the dipolar aromatic structure $\mathbf{2}^{\pm}$.

Experimental Procedure

A 50 mL 3-necked flask equipped with a magnetic stirring bar, a thermometer, a septum, and an Ar bubbler was flame-dried while flushed with Ar. The flask was charged with **3** (315 mg, 1 mmol), CH_2Cl_2, (8 mL), and THF (5 mL) and then cooled to −50 °C. At this temperature **4** (2 mL, 2 mmol, 1.001 M solution in THF) was added dropwise under Ar with a syringe over 20 min. The orange reaction mixture was stirred for 4 h at −40 to −50 °C. Then cooled CH_2Cl_2/pentane 1:1 (20 mL) was added. The mixture was stirred for another 10 min at −78 °C, then centrifugated for 10 min (4000 rpm) at −30 °C. The resulting solution was concentrated at −40 °C/0.1 mbar to give yellow crystals. Recrystallization from CH_2Cl_2/Et_2O (2:1) (6 mL) under Ar at −70 °C gave 161 mg (54%) of pale yellow cubic crystals of **2** [20]. Crystals and solutions of **2** are stable for days at room temperature and several hours at +50 °C under Ar, without valence isomerization; however, **2** polymerizes rapidly in the presence of O_2.

Received: November 23, 1993 [Z 6508 IE]
German version: *Angew. Chem.* **1994**, *106*, 1050

[1] A. Otter, G. Sabbioni, M. Neuenschwander, H. P. Kellerhals, *Helv. Chim. Acta* **1986**, *69*, 124; A. Otter, M. Neuenschwander, H. P. Kellerhals, *Magn. Reson. Chem.* **1986**, *24*, 360.
[2] K. Hafner, H. Tappe, *Angew. Chem.* **1969**, *81*, 564; *Angew. Chem. Int. Ed. Engl.* **1969**, *8*, 593.
[3] H. Tappe, Dissertation, Technische Hochschule Darmstadt, **1972**.
[4] G. Boche, F. Heidenhain, B. Staudigl, *Tetrahedron Lett.* **1979**, 4201; *Chem. Ber.* **1982**, *115*, 3191.
[5] Obviously ΔG between **1b** and $\mathbf{1b}^{\pm}$ is so small that solvent or temperature changes may favor either structure. For $\mathbf{1b} \rightarrow \mathbf{1b}^{\pm}$, UV measurements suggest $\Delta H^{\circ} = -6.5\ kcal\,mol^{-1}$ and $\Delta S^{\circ} = -22\ cal\,K^{-1}\,mol^{-1}$ [3].
[6] There is an equilibrium between sodium 10-methylnonafulvenolate and sodium acetylcyclononatetraenide with $\Delta H^{\circ} = -6.9\ kcal\,mol^{-1}$ and $\Delta S^{\circ} = -30\ cal\,K^{-1}\,mol^{-1}$: G. Boche, F. Heidenhain, *J. Am. Chem. Soc.* **1979**, *101*, 738; G. Boche, F. Heidenhain, W. Thiel, R. Eiben, *Chem. Ber.* **1982**, *115*, 3167.
[7] S. Chai, Dissertation, Universität Bern, **1993**.
[8] H. Prinzbach, H. Knöfel, E. Woischnik in *Aromaticity, Pseudo-Aromaticity, Anti-Aromaticity* (Eds.: E. D. Bergmann, B. Pullman), Israel Academy of Sciences, Jerusalem, **1971**, p. 269; H. Prinzbach, H. Knöfel, *Pure Appl. Chem.* **1971**, *28*, 281.
[9] Z. Yoshida, *Pure Appl. Chem.* **1982**, *54*, 1059; S. Araki, Ph. D. Thesis, University of Kyoto, **1978**.

[10] M. Neuenschwander, P. Bönzli, *Helv. Chim. Acta* **1991**, *74*, 1823.
[11] Z. Yoshida, Y. Taiwara, *J. Am. Chem. Soc.* **1971**, *93*, 2573.
[12] It is interesting to note that the similar reaction of **3** with the less nucleophilic Li-(*ZZZZ*)-cyclononatetraenide failed to give **2** [9].
[13] UV($CHCl_3$, 25 °C): λ_{max} (ε) = 407 (8650), 290 (12900), 255 (8590) nm; IR (KBr, 25 °C): ν = 2970m-s, 2930m, 2870w, 1915m, 1538s, 1485w, 1435w-m, 1415m-s, 1380m-s, 1360m-s, 1345m-s, 1300m-s, 1215w-m, 1190m, 1075w, 870w, 685w, 615m cm^{-1}; ^1H NMR (600 MHz, $CDCl_3$, 25 °C): δ = 7.29 (m, 2H), 7.17 (m, 2H), 7.12 (m, 2H), 7.00 (m, 2H), 3.68 (q, 8H); 1.39 (t, 12H) [14, 15]; ^{13}C NMR (100 MHz, $CDCl_3$, 0 °C): δ = 128.9s, 128.7s, 113.5d, 113.2d, 112.4d, 107.4d, 97.8s, 47.4t, 14.7q; MS: high-resolution MS of M^+: 296.2257 (calcd. $C_{18}H_{32}N$: 296.2253).
[14] ^1H NMR of **3** (300 MHz, $CDCl_3$, 25 °C, δ values): N-CH_2: 3.52 (q, 4H), 3.49 (q, 4H); N-CH_2-CH_3: 1.33 (t, 6H), 1.29 (t, 6H). Similar to **3** the N-CH_2 and N-CH_2-CH_3 groups of **2** give two multiplets due to the hindered rotation; τ_c = −25 °C for the N-CH_2 groups, $\Delta G^{\ddagger}$ = 11.5 kcal mol^{-1}. This is the only temperature-dependent process observed in the ^1H NMR spectrum of **2** between −80 and +50 °C.
[15] Results of the ^1H NMR analysis of **2** (600 MHz, $CDCl_3$, 25 °C, δ values): H-1,8: 7.29; H-2,7: 7.00; H-3,6: 7.17; H-4,5: 7.12; ^3J couplings: $J_{1,2} = J_{7,8}$ = 13.58; $J_{2,3} = J_{6,7}$ = 11.78; $J_{3,4} = J_{5,6}$ = 13.16; $J_{4,5}$ = 11.70 Hz; ^4J couplings: $J_{1,3} = J_{6,8}$ = 0.12; $J_{1,4} = 0.21$; $J_{2,4} = J_{5,7}$ = 0.15; $J_{3,5} = J_{4,6}$ = 0.15 Hz.
[16] Note that all the NMR parameters of nonpolar nonafulvenes including **1a** ($R^1 = R^2$ = H) are similar to those **1b** in $CDCl_3$ at room temperature. The only difference is that they are not influenced by solvents or temperature.
[17] C-9 of **1b** is the only ring-C atom showing an opposite trends. This is probably mainly due to the conformational changes involved with **1b** → **1b**$^{\pm}$, which are expected to have a pronounced effect on C-9 (in **1b**$^{\pm}$ the formamidinium unit is supposed to be out of the plane of the ring). Furthermore, the exocyclic "enediamine system" is expected to induce a considerable negative charge at C-9, even in the case of the olefinic stucture **1b**.
[18] Similarly, the UV spectrum of **2** ($CDCl_3$, 25 °C) is nearly identical with that of **1b** (CH_2Cl_2, −80 °C [3]).
[19] CCl_4, $CDCl_3$, [D_6]benzene, [D_8]THF, CD_2Cl_2, [D_6]acetone, CD_3CN.
[20] Several attempts at an X-ray analysis of **2** have failed so far because the compound only crystallizes as polycrystals.

Dibromine Pentoxide Br_2O_5**

Dieter Leopold and Konrad Seppelt*

Recently we synthesized pure Br_2O_3, which according to its crystal structure analysis can be described as $Br-O-BrO_2$.[1] Together with the results of the structure analysis of Br_2O by using EXAFS (*E*xtended *X*-ray *A*bsorption *F*ine *S*tructure),[2] these are the first secure structural data of bromine oxides. After the unequivocal proof of the existence of Br_2O and Br_2O_3, the question arose whether a bromine perbromate ($BrOBrO_3$) identified with the EXAFS method[3] was perhaps in fact Br_2O_3.[1] The basic difficulty of the work with bromine oxides is their thermal instability. This is the reason why in earlier literature additional bromine oxides were postulated, although only elemental analysis and sometimes Raman spectroscopy were used for their characterization, and a review also gave the impression that the syntheses are not always reproducible.[4]

In the synthesis of Br_2O_3 from bromine and ozone in $CFCl_3$ at −78 °C, we have observed a second bromine oxide. This is colorless, and thus should no longer contain an $O-Br^I$ group, and forms on longer ozonization time, therefore a higher oxygen content was to be assumed. In contrast to Br_2O_3, it is insoluble in CH_2Cl_2. In order to synthesize this compound in a pure form, we ozonized elemental bromine in CH_2Cl_2 at −78 °C. In this way the color of the solution lightens from brown (Br_2) via orange (Br_2O_3) to colorless; from the orange-colored step onwards, an initially yellow, then almost colorless powder precipitates [Eq. (a)]. This powder decomposes on warming above

$$Br_2 \xrightarrow[CH_2Cl_2,\ -78\ ^\circ C]{O_3} Br-O-BrO_2 \xrightarrow[CH_2Cl_2,\ -78\ ^\circ C]{O_3} O_2Br-O-BrO_2 \qquad (a)$$

−40 °C, occasionally with detonation. Propionitrile was found to be a suitable solvent from which this compound crystallizes out in the form of large colorless needles; an increase in weight with respect to the amount of powder used indicates the incorporation of solvent in the crystal. These needles melt at about −20 °C with decomposition.

The crystal structure analysis characterized the new oxide as Br_2O_5, which crystallizes with three molecules of propionitrile (Fig. 1). Since the four Br···N contact distances between propionitrile and Br_2O_5 are quite large (278.7(2)–290.1(2) pm), we consider Br_2O_5 in this cocrystallisate as a largely undisturbed molecule. As in Br_2O_3 it is not difficult to differentiate between terminal Br–O double bonds (160.6–161.3(2) pm) and the Br–O single bonds to the bridging oxygen atom (187.5(2), 189.6(2) pm) in Br_2O_5. The bromine atoms are pyramidally surrounded by the oxygen atoms, as to be expected for Br^V centers; the angle at the bridging oxygen atom is with 121.2(1)° likewise in the expected range. The terminal oxygen atoms at the two bromine atoms are eclipsed, the deviations from this are maximally 0.1 pm. This distinguishes Br_2O_5 from I_2O_5. The structure of the latter has been studied both as a pure substance[5] and also as a cocrystallisate $HIO_3 \cdot I_2O_5$ ("HI_3O_8"),[6] and its terminal oxygen atoms are staggered. However, the structure of I_2O_5 is dominated by intermolecular O···I interactions (up to 223 pm). The Raman spectrum of solvate-free Br_2O_5 is in agreement with the structure shown in Figure 1. The valence frequencies of the double bonds, those of the single bonds, and the deformation vibrations are significantly separated from each another. The Raman spectrum, however, differs from that described in 1976 for a Br_2O_5.[7]

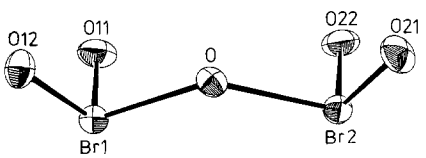


Fig. 1. Structure of the Br_2O_5 molecule in the cocrystallizate $Br_2O_5 \cdot 3C_2H_5CN$ (ORTEP plot, thermal ellipsoids at 50% probability level). Distances [pm] and angles [°]: Br1–O11 160.6(12), Br1–O12 161.1(2), Br1–O 189.6(2), Br2–O21 161.3(2), Br2–O22 160.6(2), Br2–O 187.5; O11-Br1-O12 109.9(1), O-Br1-O11 94.2(1), O-Br-O12 102.6(1), O21-Br2-O22 109.0(1), O-Br2-O21 103.3, O-Br2-O22 94.9(1), Br1-O-Br2 121.2(1)

The unambiguous existence of Br_2O_5, which is mixed with Br_2O_3 if purification is not carried out, questions once again the existence of Br_2O_4, which according to the Raman spectra should occur in two forms, $O_2Br-BrO_2$[8] and $OBr-OBrO_2$,[1b] but according to the EXAFS spectrum should have the structure $BrOBrO_3$.[3]

The structures of Br_2O, Br_2O_3, and Br_2O_5 indicate the building principles for bromine oxides: bromine in the oxidation state +1 occurs in a terminal position with a weak interaction to another bromine atom, and a bromine atom in the oxidation state +5 is pyramidally surrounded with two short and one long

[*] Prof. Dr. K. Seppelt, D. Leopold
Institut für Anorganische und Analytische Chemie der Freien Universität
Fabeckstrasse 34-36, D-14195 Berlin (FRG)
Telefax: Int. code + (30)838-2424

[**] This work was supported by the Fonds der Chemischen Industrie.

bond to the coordination partners. The combination of these two building blocks leads to the least unstable compounds of the system Br/O. The relationship to chlorine is apparent in the oxidation state +1 (e.g. Cl_2O), that to iodine in the oxidation state + 5 (e.g. I_2O_5).

Experimental Procedure

After drying over silica gel, ozone prepared in the ozone generator was introduced into a solution of Br_2 (100 mg) in CH_2Cl_2 (5 mL) at −78 °C. The color of the solution lightened, and this was accompanied by the precipitation of initially an orange-colored, and later an almost colorless solid. When the solution had lost its color, it was decanted and dried under vacuum at −50 °C. Crystallization in the temperature range from −50 °C to −90 °C from C_2H_5CN gave $Br_2O_5 \cdot 3\,C_2H_5CN$ in the form of large colorless needles; the solution had a tendency towards supersaturation. Raman (solid, krypton ion laser, 647.0 nm): $\tilde{\nu}$(Br=O): 868(40), 835(15), 803(90), 774(20); $\tilde{\nu}$(Br–O): 539(30), 511(35); δ: 376(20), 351(100), 161(30), 110(30) cm^{-1}. Crystal structure analysis: $a = 1239.6(2)$, $b = 881.7(1)$, $c = 1452.8(2)$ pm, $\beta = 103.82(1)°$, $V = 1609 \times 10^6$ pm^3, −145 °C, $P2_1/n$, $Z = 4$, $\mu = 49.3$ cm^{-1}. 6988 measured reflections in the range $\theta = 2$–35°, $+h, -k, \pm l$. 6434 independent reflections, $R_{int} = 0.026$, 3617 reflections with $F > 3\sigma(F)$, $R = 0.042$, $R_w = 0.029$, 218 parameters, $W = 1.56/\sigma^2(F)$. Further details of the crystal structure investigation may be obtained from the Fachinformationszentrum Karlsruhe, D-76344 Eggenstein-Leopoldshafen (FRG) on quoting the depository number CSD-57939.

Received: November 29, 1993 [Z 6519 IE]
German version: *Angew. Chem.* **1994**, *106*, 1043

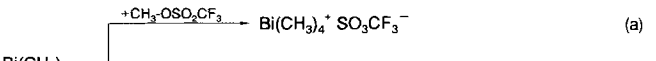
[1] a) R. Kuschel, K. Seppelt, *Angew. Chem.* **1993**, *105*, 1734-1735; *Angew. Chem. Int. Ed. Engl.* **1993**, *32*, 1632-1633. b) Because of the similarity of the Raman spectra, a Br_2O_3 identified by J.-L. Pascal et al. in 1974 is probably identical with the Br_2O_3 investigated by crystal structure analysis. J.-L. Pascal, A. C. Pavia, J. Potier, A. Potier, *C. R. Acad. Sci. Ser. C* **1974**, 43–45; *ibid.* **1975**, 661-664.
[2] W. Levason, J. S. Ogden, M. D. Spicer, N. A. Young, *J. Am. Chem. Soc.* **1990**, *112*, 1019–1022
[3] T. R. Gilson, W. Levason, J. S. Ogden, M. D. Spicer, N. A. Young, *J. Am. Chem. Soc.* **1992**, *114*, 5469–5470.
[4] M. Schmeisser, K. Brändle, *Adv. Inorg. Chem. Radiochem.* **1963**, *5*, 41–89.
[5] K. Selte, A. Kjekshus, *Acta Chem. Scand.* **1970**, *24*, 1912–1924.
[6] Y. D. Feikema, A. Vos, *Acta Crystallogr.* **1966**, *20*, 769–777.
[7] J.-L. Pascal, A. C. Pavia, J. Poitier, A. Poitier, *C. R. Acad. Sci. Ser. C* **1976**, 53–56.
[8] J.-L. Pascal, J. Poitier, *J. Chem. Soc. Chem. Commun.* **1973**, 446–447.

Methylbismuth(v) Compounds**

Stephan Wallenhauer and Konrad Seppelt*

Tetraphenylbismutonium salts,[1] pentaphenylbismuth,[1] and hexaphenylbismutate[2, 3] are compounds which have been known for a long time, for which the relation between light absorption and structure could only be explained recently.[4–8] In contrast, almost nothing is known about alkylbismuth(v) compounds.[9] To our knowledge, there is only one conference report about the preparation of $Bi(C_2H_5)_3CH_3^+$ [9] as well as the detection of $Bi(CH_3)_4^+$ by β decay of $^{210}Pb(CH_3)_4$.[10] The preparation of the bromides (*E*/*Z*) $(CH_3CH{=}CH)_3BiBr_2$ with melting points of 65 and 142 °C, respectively, could not as of yet be reproduced, and this preparation is also questionable in light of the following observations.[11] This lack of knowledge is actually surprising, since the corresponding alkylantimony(v) compounds, in particular $Sb(CH_3)_5$, are prepared readily. The structure of $Sb(CH_3)_5$ was only recently determined to be unequivocally trigonal bipyramidal by an electron diffraction[12] and a single-crystal structure analysis.[13] $As(CH_3)_5$ is equally surprisingly stable, and its vibrational spectra can only be explained in terms of a trigonal bipyramidal structure.[14] Since the phenylbismuth(v) compounds are considerably more unstable than the corresponding antimony(v) compounds, the lacking knowledge on alkylbismuth(v) compounds can be explained by the expected instability. As we shall show in the following, this prediction is only partly true.

Trimethylbismuth can be methylated very easily with $CH_3OSO_2CF_3$ [Eq. (a)]. The resulting tetramethylbismutonium trifluoromethylsulfonate is a colorless compound, which is stable up to over 150 °C. It is surprising that this simple reaction was not reported earlier. According to a crystal structure analysis,[15] the $Bi(CH_3)_4^+$ ion is tetrahedral (Fig. 1a). Weak interactions to the anion and solvate molecule do not distort the structure significantly. The mean Bi–C bond length of 222 pm is



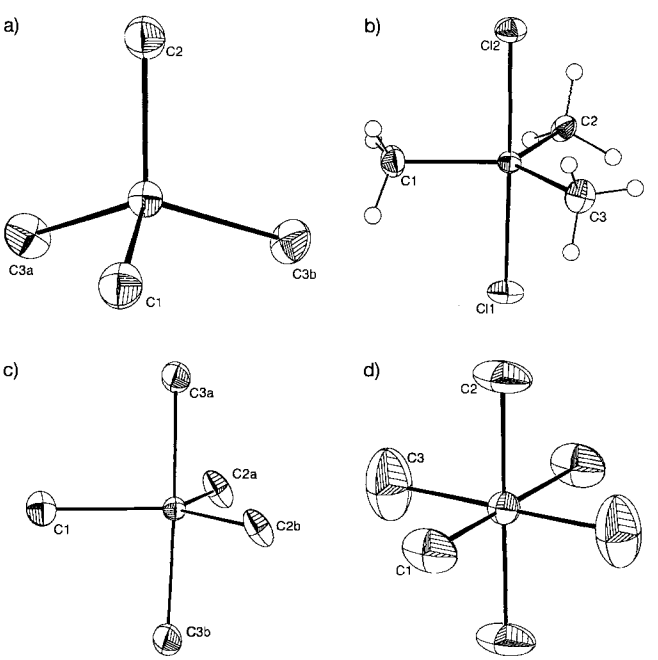


Fig. 1. Structures of the cation of $Bi(CH_3)_4^+SO_3CF_3^- \cdot CH_3CN$ (a), of $Bi(CH_3)_3Cl_2$ (b), of $Bi(CH_3)_5$ (c), and of the anion of $[Li(thf)_4]^+[Bi(CH_3)_6]^-$ (d) in the crystal (ORTEP plots; thermal ellipsoids at the 50% probability level). a) Bond lengths [pm] and angles [°] of $Bi(CH_3)_4^+$: Bi–C 222.0(10), 223.0(10), 221.0(7); C-Bi-C 112.0(4), 109.6(3), 108.9(2). b) The asymmetric unit of $Bi(CH_3)_3Cl_2$ contains one acetone molecule. Bond lengths [pm] and angles [°]: Bi–Cl 260.2(2), 261.7(2), Bi–C 218.9(7), 219.6(6), 220.7(6); Cl1-Bi-Cl2 177.8(1), C-Bi-C 117.4(2), 127.3(2), 115.3(2). The large C-Bi-C bond angle is explained by a long Bi···O contact of 323 pm to the oxygen atom of the acetone molecule. c) As in the structure of $Sb(CH_3)_5$ [13], the $Bi(CH_3)_5$ molecule here is also doubly disordered in the lattice. The second orientation is formed by a 90° rotation about the Bi-C1 axis. Only one orientation is shown for better clarity. Bond lengths [pm] and angles [°]: Bi–C1 230(2), Bi–C2 227(1), Bi–C3 228(2); C1-Bi-C2a 119.3(5), C1-Bi-C3a 89.9(5), C2a-Bi-C2b 121.4(5), C2a-Bi-C3a 90.4(6), C2a-Bi-C3b 89.9(5), C3a-Bi-C3b 179.8(8). d) Bond lengths [pm] and angles [°] of $Bi(CH_3)_6^-$: Bi–C 236(1), 233(1), 230(2); C-Bi-C 89.6(4), 90.0, 90.0, 180.0.

[*] Prof. Dr. K. Seppelt, Dipl.-Chem. S. Wallenhauer
Institut für Anorganische und Analytische Chemie der Freien Universität
Fabeckstrasse 34–36, D-14195 Berlin (FRG)
Telefax: Int. code + (30)838-2424

[**] This work was supported by the Deutsche Forschungsgemeinschaft, the Fonds der Chemischen Industrie, and the Graduiertenkolleg "Synthese und Strukturaufklärung niedermolekularer Verbindungen".

slightly shorter than in the isoelectronic $Pb(CH_3)_4$ (224(1) pm), and the valence force constant calculated (210 Nm^{-1}) is larger than that of tetramethylplumbane (177 Nm^{-1}).[16, 17]

Attempts to halogenate $Bi(CH_3)_3$ proved to be difficult. With Cl_2 and XeF_2, a Bi–C bond cleavage takes place; but chlorination with SO_2Cl_2 to give $Bi(CH_3)_3Cl_2$ is successful, and occurs almost quantitatively [Eq. (b)]. According to a crystal structure analysis,[15] the colorless solid is trigonal bipyramidal (Fig. 1b). This is to be expected, since all compounds known so far of this type R_3YX_2 (R = alkyl, aryl; Y = P, As, Sb, Bi; X = F, Cl, Br) have this structure, in which the halogen atoms adopt the axial-positions. $Bi(CH_3)_3Cl_2$ is, however, thermally unstable and decomposes rapidly at room temperature.

$Bi(CH_3)_3Cl_2$ is the starting material for the syntheses of $Bi(CH_3)_5$ and the anion $[Bi(CH_3)_6]^-$. The reaction with CH_3Li in diethyl ether in the ratio 1:2 at low temperatures gives a blue-violet solution, from which violet crystals of $Bi(CH_3)_5$ precipitate on cooling to $-110\,^{\circ}C$ [Eq. (c)]. According to a crystal

$$Bi(CH_3)_3Cl_2 \xrightarrow[-2\ LiCl]{+2\ CH_3Li\ /\ -95\,^{\circ}C\ /\ Et_2O} Bi(CH_3)_5 \qquad (c)$$

$$Bi(CH_3)_3Cl_2 \xrightarrow[-3\ LiCl]{+3\ CH_3Li\ /\ -78\,^{\circ}C\ /\ THF} [Li(thf)_4]^+[Bi(CH_3)_6]^- \qquad (d)$$

structure analysis[15] at $-163\,^{\circ}C$, the pentamethyl compound is isostructural, perhaps even isomorphous with $Sb(CH_3)_5$,[13] and the bismuth atom is trigonal-bipyramidally surrounded (Fig. 1c). The only noticeable difference is that in crystalline $Sb(CH_3)_5$ the axial bonds (220.9(5) pm) are about 7 pm longer than the equatorial bonds (213.5(6) and 214.5(5) pm). Similar considerations are true for gaseous $Sb(CH_3)_5$.[6]. In contrast, in $Bi(CH_3)_5$, the differences in the bond lengths ($\approx$1 pm) are smaller than the errors in the measurements. This phenomenon can be explained in terms of the reduced ligand repulsion for the larger central atom bismuth, or to put it another way, the differences in the bond lengths in trigonal-bipyramidal compounds require no other theoretical explanation.

It is surprising that $Bi(CH_3)_5$ has this trigonal-bipyramidal structure, since for pentaphenylbismuth the same deep violet color is associated with the square-pyramidal structure. Taking a relativistic correction into consideration for BiH_5, it was calculated that the HOMO–LUMO separation in trigonal-bipyramidal bismuth(V) compounds should be approximately twice as large as it should be for square pyramidal ones, because the LUMO in the latter case is more strongly Bi oriented and is therefore yet lower in energy because of the relativistic effect.[6] The +I effect of the methyl groups in $Bi(CH_3)_5$ eases the charge transfer transition, so that the absorption here also occurs in the visible region for the trigonal-bipyramidal structure. Finally, the color of $Bi(CH_3)_5$ proves that the light absorption of $Bi(C_6H_5)_5$ cannot be attributed to the presence of aromatic rings.

$Bi(CH_3)_5$ is a very unstable compound. In the crystalline state it explodes on rapid warming to room temperature, in solution it decomposes to $Bi(CH_3)_3$. Like $Sb(CH_3)_5$, it is a non-rigid compound, that is, the methyl groups are equivalent in the ^1H NMR spectrum even at $-90\,^{\circ}C$.

The reaction of $Bi(CH_3)_3Cl_2$ with an excess of CH_3Li gives $[Li(thf)_4]^+[Bi(CH_3)_6]^-$ in the form of yellow crystals at $-78\,^{\circ}C$ [Eq. (d)]. Thus, an additional example could be added to the few known compounds, in which six organic groups are bound to a main group element such as in $[Sb(C_6H_5)_6]^-$,[18] $[Bi(C_6H_5)_6]^-$,[2] and $Te(CH_3)_6$.[19] Because of its instability the $[Bi(CH_3)_6]^-$ ion could only be characterized by a crystal structure analysis;[15] the result is shown in Figure 1d. This structure investigation—like that for the isostructural (and possibly isomorphous) $[Li(thf)_4]^+[Sb(CH_3)_6]^-$[7]—proved to be more difficult by a disorder of the Li^+ ion and the THF molecules. The mean Bi–C bond length of the octahedral anion (233(1) pm) is, as expected, significantly larger than the Sb–C bond length in the likewise octahedral $[Sb(CH_3)_6]^-$ ion (224.2(6) pm (mean)).[13] Whereas $[Zr(CH_3)_6]^{2-}$[20] and $W(CH_3)_6$[21] are trigonal prisms, a circumstance which still requires a satisfactory explanation, the main group compounds $[Sb(CH_3)_6]^-$, $[Bi(CH_3)_6]^-$, and $Te(CH_3)_6$ form the expected octahedra.

Experimental Procedure

$Bi(CH_3)_4^+CF_3SO_3^-$: Under an argon atmosphere $Bi(CH_3)_3$ (1.25 g, 4.9 mmol) in CH_3CN (2 mL) was treated with methyl trifluoromethanesulfonate (0.9 g, 5.5 mmol). The mixture was stirred for 6 h at room temperature and concentrated to dryness under high vacuum. This gave 1.5 g of the salt as a colorless solid, which was recrystallized from CH_3CN/Et_2O. Raman (solid, cm^{-1}): $\tilde{\nu}$ = 3054 (m), 2180 (w), 1228 (w), 1210 (w), 1180 (m), 1030 (m), 757 (w), 574.5 (vw), 506 (vs, ν_sBiC), 475.5 (vs, ν_sBiC), 348.5 (w), 315 (w), 211 (vw, δ_eBiC), 157 (m, br, δ_sBiC); IR (solid, cm^{-1}) $\tilde{\nu}$ = 3052 (m), 2946 (m), 2855 (w), 2347 (w), 1684 (w), 1653 (w), 1636 (w), 1605 (w), 1412 (w), 1262, 1225 (s), 1203 (m), 1180 (s), 1167 (s), 1147 (s), 1030 (vs), 849 (s), 757 (m), 639 (s), 574 (m), 518 (m), 503 (s, ν_eBiC), 313 (w), 212 (m, δ_eBiC), 61 (s); NMR (90 MHz, [D$_6$]acetone, 20 °C): ^1H: δ = 2.47, ^{19}F: δ = −78.9.

$Bi(CH_3)_3Cl_2$: Freshly degassed SO_2Cl_2 (1.22 g, 9.0 mmol) at −196 °C was condensed into $Bi(CH_3)_3$ (2.3 g, 9.1 mmol) in dry Et_2O (10 mL). The mixture was stirred at −100 °C, warmed to −78 °C over 2 h, and the Et_2O and SO_2 were pumped off at 10^{-3} mbar to give 2.9 g (95%) colorless solid. NMR (90 MHz, [D$_6$]acetone, −50 °C): ^1H: δ = 3.29, $^{13}C\{^1H\}$: δ = 36.9.

$Bi(CH_3)_5$: CH_3Li (1.3 mL, ca. 1.8 M in Et_2O) was added slowly under argon to a suspension of $Bi(CH_3)_3Cl_2$ (0.3 g, 0.9 mmol) in dry Et_2O (4 mL) at −110 °C. Immediately after the addition of a few drops, the reaction mixture turned violet. After slow heating, the reaction solution was stirred for a short period at −78 °C. The finely distributed LiCl was left to settle overnight at −92 °C. The clear solution was transferred into a sealable glass ampoule with a thin Teflon tube. The volume of the solution was concentrated to a 1/5 of the original volume under the high vacuum at −85 °C. Thereafter the solution was cooled to −115 °C which led to the precipitation of a crystalline violet powder. ^1H NMR (90 MHz, [D$_8$]THF, −90 °C): δ = 1.19.

$[Bi(CH_3)_6]^-$: CH_3Li (ca. 1.8 M in Et_2O) was added to a suspension of $Bi(CH_3)_3Cl_2$ (0.5 g, 1.5 mmol) in dry THF (5 mL) at −95 °C under argon until the violet color of the reaction mixture had turned orange and remained that color. The mixture was slowly warmed to −78 °C, stirred for 30 min at this temperature and the finely distributed LiCl was left to settle out overnight at −92 °C. The resulting clear orange solution was transferred into a sealable ampoule with a thin Teflon tube. Concentration under high vacuum at −65 °C to 1/10 of the original volume and subsequent cooling to −92 °C gave yellow crystals.

Received: November 29, 1993 [Z 6520 IE]
German version: *Angew. Chem.* **1994**, *106*, 1044

[1] G. Wittig, K. Clauss, *Justus Liebigs Ann. Chem.* **1952**, *578*, 136–146.
[2] D. Hellwinkel, G. Kilthau, *Justus Liebigs Ann. Chem.* **1967**, *705*, 66–75.
[3] D. Hellwinkel, M. Bach, *Justus Liebigs Ann. Chem.* **1968**, *720*, 198–200.
[4] A. Schmuck, J. Buschmann, J. Fuchs, K. Seppelt, *Angew. Chem.* **1987**, *99*, 1206–1207, *Angew. Chem. Int. Ed. Engl.* **1987**, *26*, 1180–1182.
[5] A. Schmuck, K. Seppelt, *Chem. Ber.* **1989**, *122*, 803–808.
[6] A. Schmuck, P. Pyykkö, K. Seppelt, *Angew. Chem.* **1990**, *102*, 211–213; *Angew. Chem. Int. Ed. Engl.* **1990**, *29*, 213–215.
[7] A. Schmuck, D. Leopold, S. Wallenhauer, K. Seppelt, *Chem. Ber.* **1990**, *123*, 761–766.
[8] S. Wallenhauer, D. Leopold, K. Seppelt, *Inorg. Chem.* **1993**, *32*, 3948–3951.
[9] R. Dötzer, *3rd Int. Symp. Organometal. Chem., München* **1967**, Abstract, S. 196; *Gmelin*, Bi-Supplementary volume to 8th edition, **1977**, *47*, 14.
[10] J. D. Duncan, F. G. Thomas, *J. Inorg. Nucl. Chem.* **1967**, *29*, 869–890.
[11] A. E. Borisov, M. A. Osipova, A. N. Nesmeyanov, *Izv. Akad. Nauk SSSR Ser. Khim.* **1963**, 1570–1579.
[12] C. Pulham, A. Haaland, A. Hammel, K. Rypdal, H. P. Verne, H. V. Volden, *Angew. Chem.* **1992**, *104*, 1534–1537; *Angew. Chem. Int. Ed. Engl.* **1992**, *31*, 1464–1467.
[13] S. Wallenhauer, D. Leopold, K. Seppelt, unpublished.
[14] K.-H. Mitschke, H. Schmidbaur, *Chem. Ber.* **1973**, *106*, 3645–3651.
[15] Crystal structure analyses: Enraf-Nonius CAD 4 diffractometer, $Mo_{K\alpha}$ radiation, graphite monochromator, direct methods, full-matrix refinement:

 © VCH Verlagsgesellschaft mbH, D-69451 Weinheim, 1994 0570-0833/94/0909-0977 $ 10.00+.25/0

$Bi(CH_3)_4^+ CF_3SO_3^- \cdot CH_3CN$: $a = 940.9(3)$, $b = 737.3(1)$, $c = 1086.8(3)$ pm, $\beta = 110.96(2)^\circ$, $V = 704.1 \times 10^6$ pm^3, $P2_1/m$, $Z = 2$, $T = -143\,^\circ$C, of 4388 measured reflections, 2191 are independent, 1271 of which with $F \geq 3\sigma(F)$, 88 parameters, $R = 0.047$, $R_w = 0.038$. There exists a second crystal form with $a = 1241.9(4)$, $b = 1066.8(3)$, $c = 1112.1(3)$ pm, $\beta = 111.32(2)^\circ$, $V = 1372.7 \times 10^6$ pm^3, $P2_1/c$, with a slightly different interionic arrangement. $Bi(CH_3)_3Cl_2 \cdot (CH_3)_2CO$: $a = 975.91(2)$, $b = 1402.46(3)$, $c = 977.01(2)$ pm, $\beta = 119.90(2)^\circ$, $V = 1159 \times 10^6$ pm^3, $P2_1/c$, $Z = 4$, $T = -143\,^\circ$C, of 3822 measured reflections, 2829 are independent, 2609 of which with $F \geq 3\sigma(F)$, 106 parameters, $R = 0.027$, $R_w = 0.025$. $Bi(CH_3)_5$: $a = 662.5(2)$, $b = 1112.5(3)$, $c = 1131.7(2)$ pm, $V = 834.2(2) \times 10^6$ pm^3, Cmm (no. 63), $Z = 4$, $T = -163\,^\circ$C. Of 1325 measured reflections, 935 are independent, 665 of which with $F \geq 3\sigma(F)$, 27 parameters, $R = 0.055$, $R_w = 0.036$. $[Li(thf)_4]^+[Bi(CH_3)_6]^-$: $a = 1790.9(10)$, $b = 857.1(3)$, $c = 1265.9(7)$ pm, $\beta = 134.68(4)^\circ$, $V = 1382.7(2) \times 10^6$ pm^3, $C2/m$, $Z = 2$, $T = -143\,^\circ$C. Of 2047 measured reflections, 1963 are independent, 1711 of which with $F \geq 3\sigma(F)$, 117 parameters, $R = 0.061$, $R_w = 0.051$. Further details of the crystal structure investigation may be obtained from the Fachinformationszentrum Karlsruhe, D-76344 Eggenstein-Leopoldshafen (FRG) on quoting the depository number CSD-57940.

[16] Calculation under the assumption that the interaction constants between valence and deformation vibrations $g^l - g^{II} = 0$. This is considered to be a good approximation for molecules with a heavy central atom.

[17] For the Pb–C valence force constants of $Pb(CH_3)_4$, values of 178–195 Nm^{-1} are given in the literature depending on the approximation procedure used: H. Siebert, *Z. Anorg. Chem.* **1952**, *268*, 177-190; *ibid.* **1952**, *271*, 75; F. Watari, *Spectrochim. Acta Part A* **1978**, *34*, 1239-1244; J. R. Durig, G. Nagarajan, *Monatsh.Chem.* **1969**, *100*, 1948-1959; K. Shimizu, *Nippon Kagaku Zasshi.* **1956**, *77*, 1284-1287; N. K. Sanyal, D. N. Verma, L. Dixit, *Spectrosc. Lett.* **1976**, *9*, 697-713.

[18] G. Wittig, K. Clauss, *Justus Liebigs Ann. Chem.* **1952**, *577*, 26–39.

[19] L. Ahmed, J. A. Morrison, *J. Am. Chem. Soc.* **1990**, *112*, 7911–7913.

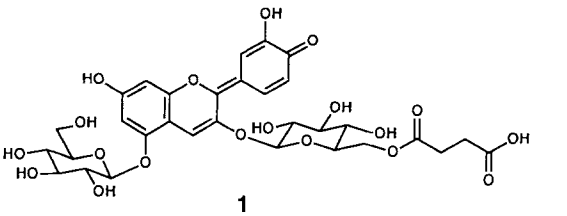
[20] P. G. Marx, G. S. Girolani, *J. Am. Chem. Soc.* **1989**, *111*, 4114–4116.

[21] A. Haaland, A. Hammel, K. Rypdal, H. V. Holden, *J. Am. Chem. Soc.* **1990**, *112*, 4547–4549.

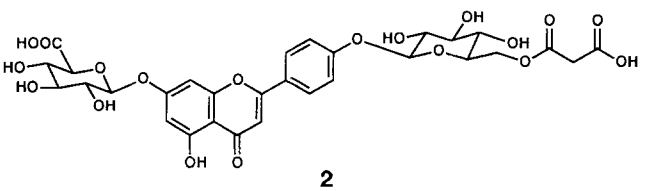
Composition of Protocyanin, A Self-Assembled Supramolecular Pigment from the Blue Cornflower, *Centaurea cyanus***

Tadao Kondo,* Minoru Ueda, Hirotoshi Tamura, Kumi Yoshida, Minoru Isobe, and Toshio Goto†

Willstätter first isolated cyanin from the blue cornflower, *Centaurea cyanus*, in the early part of this century.[1, 2] In 1958 Bayer isolated a blue pigment named protocyanin from the same flower.[3, 4] Just after that, Hayashi obtained it as crystals,[5] as did Asen.[6–8] These three groups proposed protocyanin to be a metal complex, but the reported components contradicted each other, probably because of the complex properties of protocyanin. Protocyanin was described as a metalloanthocyanin analogous to another blue pigment, commelinin.[9] It is not dialyzable, migrates toward the anode on electrophoresis, and dissociates by dilution with water and then quickly decolorizes. We have already determined the complete structure of commelinin.[10] But pure protocyanin could not be obtained directly from cornflower petals since it is much less stable than commelinin. By acid dissociation of an extract, we found that the true anthocyanin and flavone components of protocyanin are succinylcyanin (Sucy, **1**) and a malonylflavone (Mafl, **2**).[11] From these components in addition to metal ions



1



2

we first prepared the true blue pigment of the cornflower. In this paper we report the exact composition of protocyanin.

Protocyanin was carefully purified from the extract of blue cornflower petals by precipitation and gel permeation chromatography (GPC). The resulting pigment shows a blue color in a buffer solution at pH 5,[12] the same as the physiological petal conditions, and exhibits a large negative Cotton effect in the visible region (Fig. 1).[13] The components of the pigment were

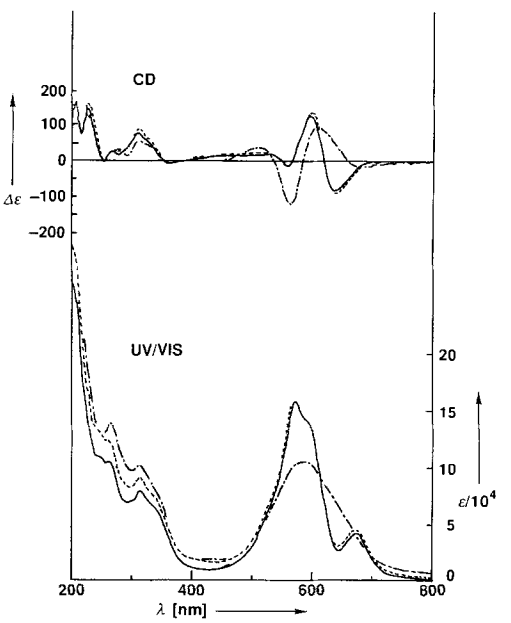


Fig. 1. UV/VIS and CD spectra of natural (——), reconstructed (- - -), and Fe_2-protocyanin (–·–·–) (5×10^{-5} M in 0.1 M acetate buffer (pH 5.0)).

analyzed by HPLC, X-ray fluorescence spectroscopy, and by measurements with inductively coupled plasma (ICP). **1**, **2**, iron, and magnesium ion were always detected, and the ratio of **1** and **2** was almost constant (ca. 1:1), though the proportion of other components changed every time. In order to obtain pure

[*] Prof. Dr. T. Kondo
Chemical Instrument Center, Nagoya University
Chikusa, Nagoya 464-01 (Japan)
Telefax: Int. code + (52) 781-9404

M. Ueda, Dr. H. Tamura, Prof. Dr. M. Isobe, Prof. Dr. T. Goto†
School of Agriculture, Nagoya University

Dr. K. Yoshida
School of Life Studies, Sugiyama Jogakuen University

[**] This research was supported by the Japanese Ministry of Education, Science and Culture of Japan (Grant Aid for Scientific Research of Priority Areas, No. 02250103). We thank Prof. Dr. Y. Kuroda, Nagoya City University, for measurement of the ESR spectra and Prof. Dr. K. Endo, Showa College of Pharmaceutical Sciences, for measurement of the Mössbauer spectra.

protocyanin and determine its exact composition we tried to reconstruct it from the anthocyanin and the flavone components in the presence of various metal ions. To a solution of an equimolar mixture of **1** and **2** was added 10 equivalents of Mg^{2+}, but the color of the resulting solution was purple and differed from that of protocyanin. When 1/6 equivalent of Mohr's salt $(NH_4)_2[Fe(SO_4)_2]$ was added to the purple solution, it turned the same shade of blue as the natural pigment. The reconstructed pigment showed the same UV/VIS and CD spectra (Fig. 1) as the natural protocyanin and moves the same distance to the anode on electrophoresis. An excess of the iron(II) salt (>1/6 equiv) afforded a differently colored pigment,[14] which was also obtained by mixing **1**, **2**, and Fe^{II} ions. Reconstruction without **2** gave another blue pigment.[15] Reconstruction using iron(III) alum resulted in the same product. Therefore, all of the four components were required and sufficient for protocyanin, and no macromolecular components were involved. The ESR spectrum (X-band, 77 K) of protocyanin reconstructed using iron(II) ions displays a signal at $g = 4.26$ indicative of iron(III) ions in the high-spin state ($S = 5/2$) in a rhombic environment;[16] this finding was reconfirmed by Mössbauer spectroscopy.

The pure reconstructed protocyanin was dissociated in 10% trifluoroacetic acid (TFA) in D_2O, and its ^1H NMR spectrum was recorded. The ratio of **1** to **2** in protocyanin was determined to be 1:1, and this result was also confirmed by HPLC. Metal ions were analyzed by atomic absorption and ICP analysis.[17] The ratio of iron(III) to magnesium ions was 1:1, and the ratio of the iron(III) ions to **1** was between 1:6 and 1:8 from quantitative HPLC analysis. We succeeded in measuring the exact molecular weight of protocyanin by using electrospray ionization mass spectrometry (ESI-MS) in the negative-ion mode, which had proved very efficient for commelinin.[18] The molecular ion was observed at m/z 8508 after deconvolution (Fig. 2), and a series of peaks was observed every 22 mass units between m/z 8500 and 8600, which suggests that the carboxyl groups in protocyanin bind Na^+ ions. Therefore, the exact composition of protocyanin is established to be $[Sucy_6Mafl_6Fe^{3+}Mg^{2+}]$ ($C_{366}H_{384}O_{228}FeMg$, $M_r = 8511$). Protocyanin is a metal-complexed anthocyanin. Six molecules each of **1** and **2**, an iron(III) ion, and a magnesium ion self-assemble into a stoichiometric supramolecule. The gross structure should be similar to that of commelinin.

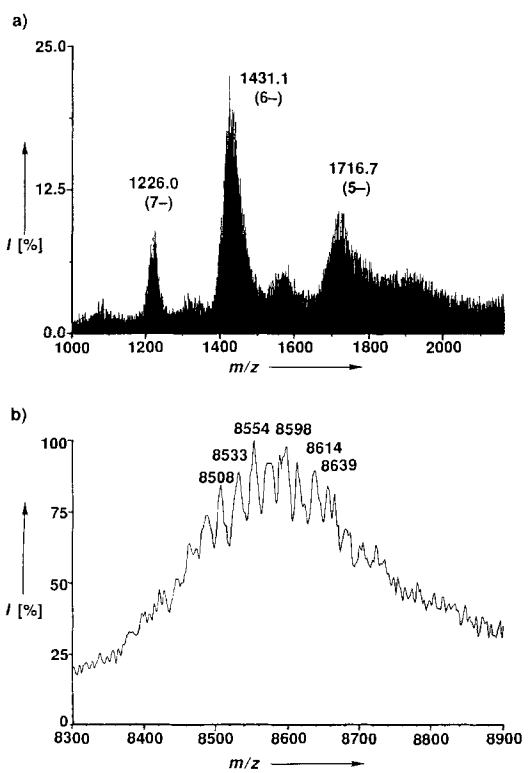


Fig. 2. a) ESI mass spectrum of protocyanin (1 mg protocyanin in 50 μL of H_2O/EtOH (1:1)); API-III PE Sciex triple-quadrupole mass spectrometer in the negative-ion mode; the potential of the interface sprayer was maintained at −105 V at a flow rate of 3 μL min^{-1}. The numbers in parentheses refer to the charge. b) Deconvoluted spectrum of a).

Experimental Procedure

Isolation of protocyanin: Fresh blue petals of *Centaurea cyanus* (3.7 kg) were frozen in liquid N_2 and pulverized, then extracted with water (1.1 L). The blue solution was filtered into EtOH immediately, and the precipitate was collected by centrifugation. The precipitate was dissolved in water then poured into EtOH two more times. The resulting pigment (544 mg) was purified by high-performance GPC (MCI-gel CQS-10, 700 × 7.0 mm, 0.1 M $NaClO_4$), and the blue eluate was passed through a Sephadex G-10 column. The blue fraction was dried in vacuo to afford protocyanin as blue powder (43 mg).—UV/VIS (0.1 M acetate buffer, pH 5.0): λ_{max} (ε) = 676 (4.31×10^4), 569 (1.60×10^5), 315 (8.16×10^4), 262 (1.08×10^5) nm; shoulders at 615 (8.85×10^4), 598 (1.37×10^5), 524 (6.00×10^4) nm. CD: $\lambda(\Delta\varepsilon)$ = 636 (−85.3), 597 (+124.6), 558 (−13.2) nm.

Reconstruction of protocyanin: **1** · TFA (20 mg, 25 μmol) and **2** · TFA (20 mg, 30 μmol) were dissolved in water and neutralized with dilute aqueous ammonia. The solution was concentrated to dryness and redissolved in 250 μL of 0.1 M acetate buffer (pH 5.0). To the purple-colored solution was added 250 μL of 0.5 M $Mg(OAc)_2$ in H_2O (250 μmol) and then 40 μL of 0.1 M Mohr's salt in H_2O (4 μmol). EtOH (1.5 mL) was added to the blue solution, which was allowed to stand at −30 °C for 30 min. After centrifugation the precipitate was collected and purified with Sephadex G-10 column chromatography to give protocyanin (23 mg).—UV/VIS (0.1 M acetate buffer, pH 5.0): λ_{max} (ε) = 676 (4.57×10^4), 569 (1.63×10^5), 315 (9.34×10^4), 262 (1.28×10^5) nm; shoulders at 615 (9.39×10^4), 598 (1.39×10^5), 524 (6.45×10^4) nm. CD: $\lambda(\Delta\varepsilon)$ = 640 (−85.5), 597 (+133.1), 558 (−15.8) nm.

Received: November 15, 1993 [Z 6501 IE]
German version: *Angew. Chem.* **1994**, *106*, 1039

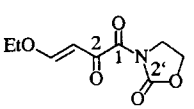
[1] Review: T. Goto, T. Kondo, *Angew. Chem.* **1991**, *103*, 17; *Angew. Chem. Int. Ed. Engl.* **1991**, *30*, 17.
[2] R. Willstätter, A. E. Everest, *Justus Liebigs Ann. Chem.* **1913**, *401*, 189.
[3] E. Bayer, *Chem. Ber.* **1958**, *91*, 1115.
[4] E. Bayer, H. Egeter, A. Fink, K. Nether, K. Wegmann, *Angew. Chem.* **1966**, *78*, 834; *Angew. Chem. Int. Ed. Engl.* **1966**, *5*, 791.
[5] a) K. Hayashi, N. Saito, S. Mitsui, *Proc. Jpn. Acad.* **1960**, *36*, 340; b) N. Saito, S. Mitsui, K. Hayashi, *ibid.* **1961**, *37*, 393.
[6] S. Asen, L. Jurd, *Phytochemistry* **1967**, *6*, 577.
[7] S. Asen, R. M. Horowitz, *Phytochemistry* **1974**, *13*, 1219.
[8] Y. Osawa in *Anthocyanin as Food Colors* (Ed.: P. Markakis), Academic Press, New York, **1982**, pp. 41–68.
[9] K. Hayashi, Y. Abe, S. Mitsui, *Proc. Jpn. Acad.* **1958**, *34*, 373.
[10] T. Kondo, K. Yoshida, A. Nakagawa, T. Kawai, H. Tamura, T. Goto, *Nature* **1992**, *358*, 515.
[11] a) H. Tamura, T. Kondo, Y. Kato, T. Goto, *Tetrahedron Lett.* **1983**, *24*, 5749; b) K. Takeda, S. Tominaga, *Bot. Mag.* **1983**, *96*, 359.
[12] The blue pigment was formed around pH 5.0, in contrast to commelinin which formed at pH > 6.5.
[13] This large negative exciton-type Cotton curve indicates a left-handed screw-stacking of the succinylcyanin chromophores. The same type of stacking is observed in commelinin. See ref. [10].
[14] This pigment, Fe_2-protocyanin, consists of six molecules of **1** and **2**, and two iron ions.—UV/VIS (0.1 M acetate buffer, pH 5.0): λ_{max} (ε) = 588 (1.05×10^5), 314 (1.02×10^5), 266 (1.39×10^5) nm; CD: $\lambda(\Delta)$ = 608 (+73.9), 563 (−101), 512 (+37.0) nm; ESI-MS: (m/z = 8579, $[M + 2Na^+ - 2H^+]$ M_r 8543).
[15] λ_{max} = 688 nm, 544 nm.
[16] a) W. T. Oosterhuis, *Struct. Bonding (Berlin)*, **1974**, *20*, 59; b) L. Que, Jr., *J. Chem. Educ.* **1985**, *62*, 938. Iron(II) ions might be oxidized to iron(III) ions by the air in the solution. Because of the paramagnetic nature of the iron(III) center, protocyanin gave a very broadened ^1H NMR spectrum, and therefore no structural information could be obtained.
[17] Found: Mg, 0.10%; Fe, 0.30% for natural protocyanin, and Mg, 0.19%; Fe, 0.55% for reconstructed protocyanin; Calcd.: Mg, 0.28%; Fe, 0.66% for $C_{366}H_{384}O_{228}FeMg$. Errors might arise from traces of solvent.
[18] T. Kondo, M. Ueda, K. Yoshida, M. Isobe, K. Titani, T. Goto, *J. Am. Chem. Soc.*, submitted.

Asymmetric 1,6-Induction in Hetero-Diels–Alder Reactions of Chiral Oxabutadienes for a De Novo Synthesis of Enantiomerically Pure Carbohydrates: Lewis Acid Dependent Reversal of Facial Selectivity**

Lutz F. Tietze,* Christoph Schneider, and Andrea Montenbruck

Dedicated to Professor Christoph Rüchardt on the occasion of his 65th birthday

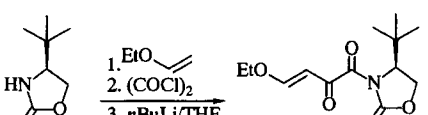
The inverse electron demand hetero-Diels–Alder reaction[1] of 1-oxa-1,3-butadienes with enol ethers is a powerful method for the synthesis of substituted dihydropyrans, which can be easily converted into carbohydrates in a short reaction sequence.[2] Electron-withdrawing substituents in the diene,[1] Lewis acid catalysis,[1] and high pressure[3] considerably accelerate the Diels–Alder reaction. However, problems with low *endo*/*exo* selectivity have often been encountered in these reactions. In addition, no satisfactory asymmetric induction has been achieved to date.[2h, 4] As a result, it has not been possible so far to exploit this highly convergent synthetic strategy for the de novo synthesis of enantiomerically pure carbohydrates.



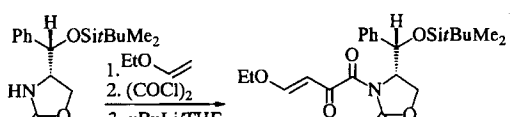
1

We recently reported on the new heterodiene **1**, which undergoes a selective hetero-Diels–Alder reaction promoted by a Lewis acid or trimethylsilyl triflate (TMS-OTf) to give either the *endo* or *exo* product, depending on the activating agent selected.[5]

We now demonstrate that a high degree of asymmetric induction can be achieved in the Diels–Alder reactions of the chiral oxabutadienes **4a** and **4b**, which are readily prepared from ethyl vinyl ether, oxalyl chloride, and the oxazolidinones **2**[6] and **3**, respectively, in a two-step procedure analogous to that used for **1**. The novel compound **3** was prepared in six steps from (1*S*,2*S*)-1-amino-2-phenylpropane-1,3-diol.[7]



2 **4a**



3 **4b**

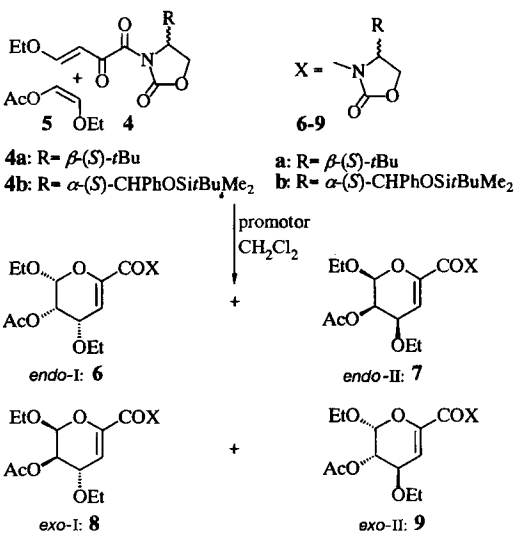
One equivalent of the heterodiene **4a** or **4b** was allowed to react with 1.5 equivalents of Lewis acid or TMS-OTf and two equivalents of the enol ether **5** acting as dienophile at between −30 and −78 °C in dichloromethane (0.1 M) (Table 1). Separate experiments with Lewis acids and TMS-OTf confirmed that the starting materials are configurationally stable under the reaction conditions.[8]

Table 1. Results of the hetero-Diels–Alder reactions of the chiral heterodienes **4a** and **4b** with enol ether **5** in CH_2Cl_2 to yield cycloadducts **6a–9a** and **6b–9b**, respectively.

Diene	Promoter	T [°C]	Products $\Sigma_{endo}/\Sigma_{exo}$ [a] **6+7/8+9**	*endo*-I/*endo*-II [a] **6/7**	Yield [b] **6/7** [%]
4a	Me_2AlCl	−40	>50:1	60:1	84
4a	TMS-OTf	−78	>50:1	1:7.9	90
4a	$SnCl_4$	−78	1:1	50:1 (12:1) [c]	41 (37) [c]
4b	Me_2AlCl	−30	16:1 [d]	1:3.2 [d]	73
4b	TMS-OTf	−78	30:1 [d]	17:1 [d]	88
4b	TBDMS-OTf [e]	−78	17:1 [d]	23:1 [d]	81

[a] Determined by capillary gas chromatography of the crude product. [b] Isolated yield of **6** and **7**. [c] In parentheses **8a/9a**; the *endo* products **6a/7a** could be separated from the *exo* products **8a/9a** by chromatography on silica gel (ethyl acetate/petroleum ether = 1:2). [d] Determined by ^{13}C NMR spectroscopic analysis of the crude product. [e] TBDMS = Si*t*BuMe$_2$.

It is noteworthy that the Me_2AlCl- and TMS-OTf-initiated reactions of diene **4a** with **5** proceed with complete *endo* selectivity ($\Sigma_{endo}/\Sigma_{exo}$ = **(6a + 7a)/(8a + 9a)** = >50:1) and in high yield. The asymmetric induction obtained in the Me_2AlCl-promoted reaction is remarkable, especially considering the distance of the inducing and the newly formed stereogenic centers (1,6-induction) (*endo*-I/*endo*-II = **6a/7a** = 60:1; 97% *de*).[9] The highly stereoselective formation of three new stereogenic centers was thus achieved in 84% chemical yield. When TMS-OTf was used, a reversal of selectivity was observed. Although the selectivity was not as high (*endo*-I/*endo*-II = **6a/7a** = 1:7.9),[10] the major product was now the *endo*-II isomer **7a**, very minor quantities of which were formed in the reaction of **4a** and **5** in the presence of Me_2AlCl. The facial selectivity in these reactions can thus be controlled simply by varying the promotor whilst leaving the auxiliary unchanged.[11] A reduced *endo*/*exo* selectivity (1:1) was observed for the cycloaddition reaction of



5 **4** **6-9**

4a: R = β-(*S*)-*t*Bu
4b: R = α-(*S*)-CHPhOSi*t*BuMe$_2$

a: R = β-(*S*)-*t*Bu
b: R = α-(*S*)-CHPhOSi*t*BuMe$_2$

promotor
CH_2Cl_2

endo-I: **6** + *endo*-II: **7**

exo-I: **8** + *exo*-II: **9**

[*] Prof. Dr. L. F. Tietze, Dr. C. Schneider, Dipl.-Chem. A. Montenbruck
Institut für Organische Chemie der Universität
Tammannstrasse 2, D-37077 Göttingen (FRG)
Telefax: Int. code + (551)39-9476

[**] Inter- and Intramolecular Hetero-Diels–Alder Reactions, Part 47. This work was supported by the Volkswagen-Stiftung and the Fonds der Chemischen Industrie. We thank Degussa AG for providing L-*tert*-leucine. C. S. thanks the Studienstiftung des Deutschen Volkes for a doctoral fellowship. Part 46: L. F. Tietze, H. Geissler, J. Fennen, T. Brumby, S. Brand, G. Schulz, *J. Org. Chem.*, **1994**, *59*, 182.

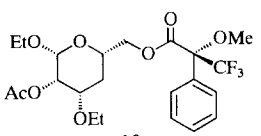
 © VCH Verlagsgesellschaft mbH, D-69451 Weinheim, 1994 0570-0833/94/0909-0980 $ 10.00+.25/0

4a with **5** using $SnCl_4$ as promotor; the induced diastereoselectivity, however, was again very high (50:1 and 12:1, respectively; Table 1).[12]

As expected, formation of **7b** was favored in the Me_2AlCl-promoted reaction of the chiral oxabutadiene **4b** with **5**, whereas **6b** predominated with TMS-OTf as reagent. The *endo* selectivities were once again very high, but the induced diastereoselectivity in the reaction with Me_2AlCl was lower than for the oxabutadiene **4a**, whereas that obtained with TMS-OTf was higher. A further slight improvement in the induced diastereoselectivity was observed with TBDMS-OTf (Table 1).

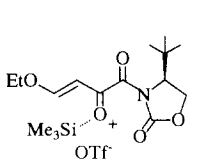
The standard oxazolidinones prepared from L-valine and L-phenylalanine were also examined; they proved to be almost totally unselective in the hetero-Diels–Alder reactions.

In order to establish the absolute configuration of the cycloadducts **6**–**9**, **6a** was stereoselectively hydrogenated in the presence of Pd/C and the carboximide group reduced to a hydroxymethyl group. Acylation gave the crystalline Mosher ester **10**, which was characterized by X-ray structure analysis.[13]

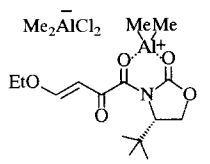


10

In an effort to rationalize the course of the reaction and, in particular, the reversal of selectivity between the reactions promoted by Me_2AlCl and TMS-OTf, we developed the following model.[14] The ^{13}C NMR spectra taken on a solution of the achiral heterodiene **1** and two equivalents of TMS-OTf in dichloromethane at $-78\,^{\circ}C$ clearly show that TMS-OTf binds to the oxygen atom of the oxabutadiene moiety and not to the carbonyl groups of the imide moiety [$\Delta\delta$ (2′-CO) = 0, $\Delta\delta$ (1-CO) = 0, $\Delta\delta$ (2-CO) = 20]. Semiempirical calculations (AM1 and PM3)[15] conducted on the ground state conformations of **1** and its derivative silylated at the 2-CO group reveal that the *anti*-arrangement of the imide carbonyl groups is the more stable conformation in both cases (ΔH_f *anti*/*syn*-**1**: -7.53 and -9.20 kJ mol^{-1}, respectively; *anti*/*syn*-Me_3Si-**1**$^+$: -30.96 and -35.98 kJ mol^{-1} respectively). It is therefore to be expected that heterodiene **4a** favors conformation **A** in the transition state of the reaction promoted by TMS-OTf (non-chelate control).



4a: A



4a: B

In the case of the Diels–Alder reactions of *N*-acryloyloxazolidinones promoted by R_2AlCl, Evans et al.[6a, b] and later Castellino et al.[16] were able to show that a reactive metal-chelate complex is clearly formed in the transition state of the reaction. However, in our case low-temperature ^{13}C NMR measurements on the mixture of **1** and Me_2AlCl failed to yield any information concerning the preferred coordination site of the Lewis acid in the diene. However, by analogy with the earlier studies, we assume that conformation **B** is adopted in the transition state of the Me_2AlCl-promoted reaction (chelate control). The facial differentiations of conformations **A** and **B** are opposite. This means that attack by the enol ether **5** is preferentially directed to opposite faces of the diene, thus inducing the opposite absolute configuration in the dihydropyran unit of the cycloadduct.

Received: November 26, 1993 [Z 6513 IE]
German version: *Angew. Chem.* **1994**, *106*, 1031

[1] a) L. F. Tietze, U. Beifuss, *Angew. Chem.* **1993**, *105*, 137; *Angew. Chem. Int. Ed. Engl.* **1993**, *32*, 131; b) D. L. Boger, *Comprehensive Organic Synthesis, Vol. 5*, Pergamon Press, New York, **1991**, p. 451; c) L. F. Tietze, *J. Heterocycl. Chem.* **1990**, *27*, 47; d) D. L. Boger, S. M. Weinreb, *Hetero-Diels-Alder-Methodology in Organic Synthesis*, Academic Press, San Diego, CA, USA, **1987**; e) S. J. Danishefsky, M. P. De Ninno, *Angew. Chem.* **1987**, *99*, 15; *Angew. Chem. Int. Ed. Engl.* **1987**, *26*, 15; f) T. Kametani, S. Hibino, *Advances in Heterocyclic Chemistry, Vol. 42*, Academic Press, Orlando, FL, USA, **1987**, p. 245; g) G. Helmchen, R. Karge, J. Weetman, *Modern Synthetic Methods, Vol. 4*, Springer, Berlin, **1986**, p. 261; h) R. R. Schmidt, *Acc. Chem. Res.* **1986**, *19*, 250; i) L. F. Tietze in *Selectivity–A Goal for Synthetic Efficiency* (Eds.: W. Bartmann, B. M. Trost), Verlag Chemie, Weinheim, **1984**, p. 299; j) J. Sauer, R. Sustmann, *Angew. Chem.* **1980**, *92*, 773; *Angew. Chem. Int. Ed. Engl.* **1980**, *19*, 779; k) G. Desimoni, G. Tacconi, *Chem. Rev.* **1975**, *75*, 651; l) B. B. Snider, *Acc. Chem. Res.* **1980**, *13*, 426.

[2] a) Overview: D. J. Ager, M. B. East, *Tetrahedron* **1993**, *49*, 5683; b) L. F. Tietze, U. Hartfiel, *Tetrahedron Lett.* **1990**, *31*, 1697; c) D. L. Boger, K. D. Robarge, *J. Org. Chem.* **1988**, *53*, 3373, 5793; d) R. R. Schmidt, B. Haag-Zeino, M. Hoch, *Liebigs Ann. Chem.* **1988**, 885; e) R. R. Schmidt, *Pure Appl. Chem.* **1987**, *59*, 415; f) L. F. Tietze, E. Voss, *Tetrahedron Lett.* **1986**, *27*, 6181; g) L. F. Tietze, E. Voss, K. Harms, G. M. Sheldrick, *ibid.* **1985**, *26*, 5273; h) M. Maier, R. R. Schmidt, *Liebigs Ann. Chem.* **1985**, 2261.

[3] a) L. F. Tietze, T. Hübsch, J. Oelze, C. Ott, W. Tost, G. Wörner, M. Buback, *Chem. Ber.* **1992**, *125*, 2249; b) L. F. Tietze, T. Hübsch, E. Voss, M. Buback, W. Tost, *J. Am. Chem. Soc.* **1988**, *110*, 4065.

[4] a) G. H. Posner, D. G. Wettlaufer, *Tetrahedron Lett.* **1986**, *27*, 667; b) L. F. Tietze, K.-H. Glüsenkamp, *Angew. Chem.* **1983**, *95*, 901; *Angew. Chem. Int. Ed. Engl.* **1983**, *22*, 887; see also: c) L. F. Tietze, P. Saling, *Chirality* **1993**, *5*, 329; d) C. Kaneko in *Organic Synthesis in Japan* (Ed.: R. Noyori), Tokyo Kagaku Dozin, **1992**, p. 175; e) L. F. Tietze, P. Saling, *Synlett* **1992**, 281; f) L. F. Tietze, S. Brand, T. Pfeiffer, J. Antel, K. Harms, G. M. Sheldrick, *J. Am. Chem. Soc.* **1987**, *109*, 921.

[5] L. F. Tietze, C. Schneider, *Synlett* **1992**, 755.

[6] a) D. A. Evans, K. T. Chapman, J. Bisaha, *J. Am. Chem. Soc.* **1988**, *110*, 1238; b) D. A. Evans, K. T. Chapman, D. Tan Hung, A. T. Kawaguchi, *Angew. Chem.* **1987**, *99*, 1197; *Angew. Chem. Int. Ed. Engl.* **1986**, *26*, 1184; c) J. Viret, H. Patzelt, A. Collet, *Tetrahedron Lett.* **1986**, *27*, 5865.

[7] L. F. Tietze, C. Schneider, unpublished results.

[8] (*E*)-1-Acetoxy-2-ethoxyethene cannot be employed because this compound isomerizes under the reaction conditions.

[9] ^1H NMR (200 MHz, C_6D_6) of **6a**/**7a** (60:1): $\delta = 0.60$ (s, 9H, *t*Bu), 1.07 (t, $J = 7.0$ Hz, 3H; CH_3), 1.13 (t, $J = 7.0$ Hz, 3H; CH_3), 1.72 (s, 3H; OAc), 3.17 (dq, $J = 8.5$, 7.0 Hz, 1H; OCH), 3.19 (dd, $J = 9.0$, 8.5 Hz, 1H; 5′-H), 3.46 (dd, $J = 9.0$, 2.2 Hz, 1H; 5′-H), 3.54 (dq, $J = 8.5$, 7.0 Hz, 1H; OCH), 3.69 (dq, $J = 9.5$, 7.0 Hz, 1H; OCH), 3.86 (ddd, $J = 4.5$, 2.5, 1.0 Hz, 1H, 4-H), 4.00 (dq, $J = 9.5$, 7.0 Hz, 1H; OCH), 4.06 (dd, $J = 8.5$, 2.2 Hz, 1H, 4′-H), 5.28 (dd, $J = 1.0$, 0.5 Hz, 1H, 2-H), 5.58 (ddd, $J = 4.5$, 1.7, 0.5 Hz, 1H; 3-H), 5.76 (dd, $J = 2.5$, 1.7 Hz, 1H; 5-H). Cycloadducts **6a**/**7a**, which were isolated in the form of an oil, were not separable by chromatography. However, after reduction with $LiAlH_4$ to yield (2*R*,3*S*,4*S*)-2,4-diethoxy-3,4-dihydro-3-hydroxy-6-hydroxymethyl-2*H*-pyran, separation was possible. A single recrystallization gave the enantiomerically pure product. M.p. 118 °C (ether/petroleum ether); $[\alpha]_D^{20} = -46.5$ ($c = 0.45$, $CHCl_3$).

[10] When two equivalents of the enol ether **5** are used, the imide of 5,7-diacetoxy-6,8,8-triethoxy-2-oxo-3-octenoic acid may be formed as by-product (up to 25%). However, no by-product is formed with 1.1 equivalents of the enol ether and longer reaction times (5 d). A yield of 81% is then obtained with **6a**/**7a** = 1:9 and an *endo*/*exo* ratio of 15:1.

[11] For examples of control of facial selectivity with different Lewis acids, see a) T.-H. Yan, C.-W. Tan, H.-C. Lee, H.-C. Lo, T.-Y. Huang, *J. Am. Chem. Soc.* **1993**, *115*, 2613; b) R. Amoroso, G. Cardillo, P. Sabatino, C. Tomasini, A. Trerè, *J. Org. Chem.* **1993**, 58, 5615; c) S. E. Denmark, M. E. Schnute, *ibid.* **1991**, *56*, 6738; d) H. J. Waldmann, *ibid.* **1988**, *53*, 6133; e) H. Hartmann, A. F. A. Hady, K. Sartor, J. Weetman, G. Helmchen, *Angew. Chem.* **1987**, *99*, 1188; *Angew. Chem. Int. Ed. Engl.* **1987**, *26*, 1143; f) T. Poll, J. O. Metter, G. Helmchen, *ibid.* **1985**, *97*, 116 and **1985**, *24*, 112; g) T. Poll, G. Helmchen, B. Bauer, *Tetrahedron Lett.* **1984**, *25*, 2191.

[12] In addition, the Lewis acids $EtAlCl_2$, $TiCl_4$, $BF_3 \cdot OEt_2$ were employed as catalysts; the results were however unsatisfactory.

[13] Crystal data for **10**: $C_{22}H_{29}O_8F_3$, $M = 478.24$, colorless, platelet-shaped crystals ($0.3 \times 0.8 \times 1.0$ mm^3), monoclinic, space group $P2_1$ with $a = 8.430(3)$, $b = 13.788(5)$, $c = 11.174(4)$ Å, $\beta = 108.64(2)^{\circ}$, $V = 1230.6(6)$ Å^3, $Z = 2$, $\rho_{calcd} = 1.29$ Mg m^{-3}, $F(000) = 504$, $\mu = 0.111$ mm^{-1}, 2697 reflections with $F > 3.0\sigma(F)$, $R = 0.072$, $R_w = 0.088$, Siemens-Stoe AED2 diffractometer. Further

 © VCH Verlagsgesellschaft mbH, D-69451 Weinheim, 1994 0570-0833/94/0909-0981 $ 10.00+.25/0

details of the crystal structure investigation may be obtained from the Fachinformationszentrum Karlsruhe, D-76344 Eggenstein-Leopoldshafen (FRG) on quoting the depository number CSD-58097.

[14] For investigations into the structure of Lewis acid-carbonyl complexes, see a) S. E. Denmark, N. G. Almstead, *J. Am. Chem. Soc.* **1993**, *115*, 3133; b) M. A. McCorrick, Y.-D. Wu, K. N. Houk, *J. Org. Chem.* **1993**, *58*, 3330; c) S. Shambayati, W. E. Crowe, S. L. Schreiber *Angew. Chem.* **1990**, *102*, 273; *Angew. Chem. Int. Ed. Engl.* **1990**, *29*, 256.

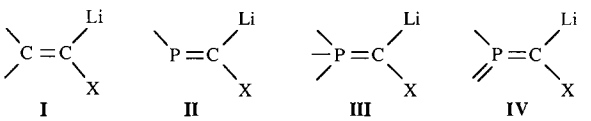
[15] L. F. Tietze, G. Schulz, unpublished results.

[16] S. Castellino, W. J. Dwight, *J. Am. Chem. Soc.* **1993**, *115*, 2986.

Reactions of an Iminophosphoranylidene Carbenoid**

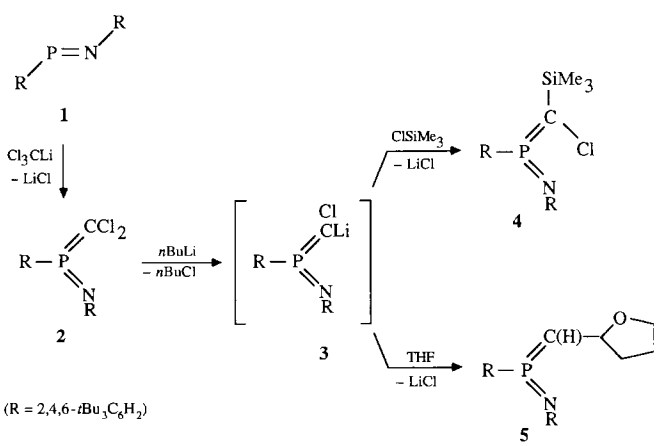
Wolfgang Schilbach, Volker von der Gönna, Dietrich Gudat, Martin Nieger, and Edgar Niecke*

Vinylidene carbenoids **I** are of major significance as synthetic building blocks in organoelement chemistry.[1] However, little is known about this type of carbenoids with phosphorus as heteroatom (**II**–**IV**). Only for the phosphanylidene carbenoid system **II** have several experimental investigations been made.[2] Here we report on the synthesis and reactivity of an iminophosphoranylidene carbenoid of type **IV**, in which the phosphorus atom is in a trigonal-planar coordination environment.



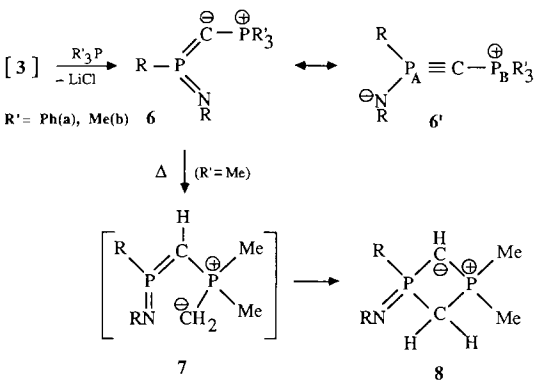
I **II** **III** **IV**

Bis(aryl)iminophosphane[3] (**1**) reacts easily with trichloromethyllithium to give imino(dichloromethylene)phosphorane (**2**); subsequent reaction with *n*-butyllithium in THF at −105 °C results in a deepening of the color of the solution, suggestive of the formation of a carbenoid **3** as an intermediate (^{31}P NMR: $\delta = 83.2$; $J_{PLi} = 25$ Hz). This intermediate can be trapped as the thermally stable, C-silylated substitution product **4** by the subsequent addition of chlorotrimethylsilane. In the absence of an electrophile, **3** reacts with the solvent to give the imino(tetrahydrofuran-2-yl-methylene)phosphorane **5**, which can formally be regarded as an insertion product of an iminophosphorylidene carbene with tetrahydrofuran. Reaction of intermediate **3** and triphenylphosphane yields the "phosphane-adduct" phosphonio(iminophosphoranylidenemethanide) (**6a**) as a stable final product. The compound **6b** obtainable by the corresponding route with trimethylphosphane is, however, not stable in solution but isomerizes[5] by 1,3-H-shift (**7**), followed by ring closure to give the 1,2-dihydro-1,3-diphosphete **8**. Nitrogen derivatives isoelectronic to **6** and **8** are known, a *N*-silylated bis(imino)phosphorane[6] and a 1,2-dihydro-1,2,3λ^5,4λ^5-diazadiphosphete,[7] respectively.



(R = 2,4,6-*t*Bu$_3$C$_6$H$_2$)

1 **2** **3** **4** **5**



6 **6'** **7** **8**

The compositions of compounds **2**, **4**, **5**, **6a**, and **8** are confirmed by elemental analyses and mass spectra. Their constitution in solution is verified by NMR spectra and, in case of compounds **2** and **4** by X-ray structure analysis.[8] In the low-field region of the NMR spectrum the imino(methylene)-phosphoranes **2**, **4**, and **5** show the characteristic resonances for the P=C structural unit [8b] (δ (^{31}P) = 70.1 (**2**), 86.2 (**4**), 75.0 (**5**); δ (^{13}C) = 99.9 (J_{CP} = 245.9 Hz) (**2**), 93.7 (J_{CP} = 119.8 Hz) (**4**), 93.9 (J_{CP} = 184.0 Hz) (**5**)). In the phosphoranes **6a**, **b** the signal (split by the phosphonio group) for the three-coordinate phosphorus atom is shifted drastically to higher field (δ = 20.4 (**6a**), 36.8 (**6b**)); the observed shift lies in the expected range for bis(imino)phosphoranes.[9c, 10] The position of the signal of the phosphonio group and the value of $^2J_{PP}$ correspond with the values reported for carbodiphosphoranes[11] ($\delta = -12.4$, $^2J_{PP}$ = 111.8 Hz (**6a**); $\delta = -21.0$, $^2J_{PP}$ = 63.3 Hz(**6b**)). The position of the signal for the two-coordinate carbon atom (δ = 90.8 (**6a**)) at low field in comparison to carbodiphosphoranes,[12] and the relatively large coupling constants $^1J_{CP}$ (219.7 Hz [P$_A$], 162.1 Hz [P$_B$] (**6a**)) can be interpreted in terms of participation of the limiting dipolar structure **6'** and are also indicative of the formal relationship with alkylidinephosphoranes,[9d] especially the phosphonium salt [(*i*Pr$_2$N)$_2$P=C=PH(*i*Pr$_2$N)$_2$]$^+$[F$_3$CSO$_3$]$^-$.[13]

The composition and constitution of **8** can be deduced from the high-resolution mass spectrum (molecule peak) and from the results of NMR measurements. The four-membered ring structure is verified by the observation of resonance signals for one CH and one CH$_2$ unit, in which each of the carbon atoms (CH: δ = 41.7, $^1J_{CP}$ = 89, 84 Hz; CH$_2$: δ = 40.3, $^1J_{CP}$ = 60, 51 Hz) shows direct coupling to each of the two phosphorus atoms. In contrast to the NMR data obtained for **6a**, the chemical shifts for the ylidic carbon atom and for the proton bonded to it, as

[*] Prof. Dr. E. Niecke, Dr. W. Schilbach, Dr. V. von der Gönna, Dr. D. Gudat, Dr. M. Nieger
Anorganisch-chemisches Institut der Universität
Gerhard-Domagk Strasse 1, D-53121 Bonn (FRG)
Telefax: Int. code + (228)735327

[**] This work was supported by the Deutsche Forschungsgemeinschaft and the Fonds der Chemischen Industrie.

well as the value of the $^2J_{PP}$ coupling constant (25.8 Hz), are quite typical. The unusual steric strain of the molecule hinders rotation of both aryl ligands, this gives rise to temperature-dependent coalescence phenomena in the ^1H and ^{13}C NMR spectra for the signals of the neighboring and non-neighboring substituents. Below temperatures of $-50\,^\circ C$ the rotation is completely "frozen" on the NMR timescale.

Figure 1 shows the structure of compound **4** in the crystal. As in all bis(ylene)phosphoranes that have been structurally investigated, the central phosphorus atom is in a trigonal-planar

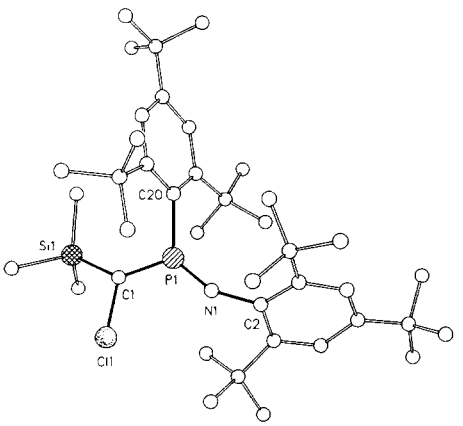


Fig. 1. Structure of imino(methylene)phosphorane **4** in the crystal. Selected bond lengths [pm] and angles [°] (in parentheses the data for **2**): P1=C 167.0(3) [165.5(5)], P1-C_{aryl} 182.5(3) [181.1(6)], P1=N 152.0(2) [152.3(3)], C_{aryl}-P1-C 108.1(1) [107.7(2)], C_{aryl}-P1-N 128.1(1) [128.9(2)], C-P1-N 122.6(1) [121.8(3)].

coordination environment (Σ 358.8°). The atoms Cl1 and Si1 are approximately coplanar with the N1-P1-C1 plane (the angle between the planes P1-C1-Cl1-Si1 and C20-P1-N1-C1 is 15°), whereas the C2 atom is positioned out-of-plane (dihedral angle C20-P1-N1-C2 −58°; C1-P1-N1-C2 137°). In contrast to those in **1**, the two aryl substituents in **4** are *Z*-configurated and orthogonal. The sterically more demanding methylene substituent ($SiMe_3$) occupies the favored *exo* position. The P1–N1 (150.0(2) pm) and P1–C1 distance (167.0(3) pm), and the C1-P1-N1 (122.6(1)°) and C2-N1-P1 angles (145.8(2)°) correspond with typical structural features found for imino(methylene)phosphoranes.[9b] All important parameters for compound **2** deviate only slightly from those of **4**.

Experimental Procedure

2: To a solution of chloroform (1.67 g, 14 mmol) in THF (50 mL) and ether (10 mL), an equimolar amount of nBuLi in n-hexane was added at −105 °C. After the mixture had been stirred for 1 h, **1** (4.3 g, 8 mmol) in ether (20 mL) was added dropwise. After warming the solution to 25 °C the volatile constituents were removed under vacuum and the remaining residue was taken up in hexane, and the insoluble material (LiCl) was separated by filtration. Compound **2** crystallized from the concentrated filtrate at −30 °C. Yield: 45%; m.p. 174–176 °C; MS (70 eV) *m/e* (%): 617 (12) [M^+], 57 (100) [tBu$^+$].

4, **5**: At −105 °C, *n*BuLi (0.63 mL, 1.6 M solution in *n*-hexane) was added to a solution of **2** (620 mg, 1 mmol) in THF (10 mL) and Et_2O (1 mL). After the mixture had been stirred for 1 h, Me_3SiCl (200 mg, 1.8 mmol) was added; the solution was then allowed to warm to room temperature. The volatile constituents were removed under vacuum, the residue was taken up in *n*-hexane, and the LiCl that had formed was filtered off. From the concentrated filtrate **4** crystallized at −30 °C as a pale yellow solid. Yield: 69%; m.p. 175–177 °C. Compound **5** is obtained in a similar fashion in the absence of Me_3SiCl. Yield: 52%. M.p. 148–150 °C.

4: NMR (without aryl) ^1H ($CDCl_3$): $\delta = -0.19$ (s, $SiMe_3$); ^{13}C ($CDCl_3$): $\delta = 93.7$ (d, $J_{CP} = 119.8$ Hz, P=C), −0.8 (d, $^3J_{CP} = 3.6$ Hz, $PCSiC_3$); MS (70 eV) *m/e* (%): 619 (2) [M^+], 57 (100) [tBu$^+$].

5: NMR (without aryl) ^1H ($CDCl_3$): $\delta = 5.26$ (ddt, $^3J_{HP} = 2.0$, $^3J_{HH} = 7.0$, 10.3 Hz, PCC*H*), 3.92 ("q", $^2J_{HH} = {}^3J_{HH} = 7.2$ Hz), 3.57 (dd, $^2J_{HP} = 32.4$, $^3J_{HH} = 10.3$ Hz, PC*H*), 2.21 (m, $OCCH_2$) 1.95 (m, $OCCH_2$); ^{13}C ($CDCl_3$): $\delta = 93.9$ (d, $J_{CP} = 184.0$ Hz, P=C), 75.2 (d, $^2P_{CP} = 1.8$ Hz, PCCO), 67.3, 34.2, 26.5 (s, C_4O framework); MS (70 eV) *m/e* (%): 619 (<1) [M^+], 100 (100) [tBu$^+$].

6, **7**: Reaction of **2** (620 mg, 1 mmol) with *n*BuLi (0.63 mL, 1.6 M in hexane) at −105 °C yielded quantitatively (^{31}P NMR control) the stable phosphorane **6a**, which, following removal of LiCl, was obtained as a pale yellow solid. In contrast, reactions with PMe_3 yielded the unstable intermediate **6b**, which isomerized to **8** during workup of the reaction solution. **6a**: Yield: 83%, m.p. 154 °C (decomp.); MS (70 eV) *m/e* (%): 809 (35) [M^+], 752 (100) [$M^+ - t$Bu$^+$]; **8**: MS (70 eV) *m/e* (%): 623 (0.4) [M^+], 566 (100) [$M^+ - t$Bu$^+$], 608 (3) [$M^+ - CH_3$]

Received: November 26, 1993,
Revised: January 21, 1994 [Z 6514 IE]
German version: *Angew. Chem.* **1994**, *106*, 1037

[1] P. J. Stang in *Methoden Org. Chem. (Houben-Weyl) 4th ed. 1952-*, Bd. E, 19b, **1989**, pp. 84–165; H. Yamamoto in *Comprehensive Organic Synthesis, Vol. 2* (Eds.: I. Fleming, B. Trost), Pergamon, Oxford, **1992**, p. 81.

[2] R. Appel, C. Casser, M. Immenkeppel, *Tetrahedron Lett.* **1985**, *26*, 3551–3554; R. Appel, M. Immenkeppel, *Z. Anorg. Allg. Chem.* **1987**, 7–14; M. Yoshifuji, R. Niitsu, N. Inamoto, *Chem. Lett.* **1988**, 1733–1734; S. J. Geode, F. Bickelhaupt, *Chem. Ber.* **1991**, *124*, 2677–2684; M. Yoshifugi, H. Kawanami, Y. Kawai, K. Toyota, M. Yasunami, T. Nitsu, N. Inamoto, *Chem. Lett.* **1992**, 1053–1056.

[3] M. Lysek, Dissertation, Bielefeld, **1987**.

[4] G. Köbrich, K. Flory, R. H. Fischer, *Chem. Ber.* **1966**, *99*, 1793–1804.

[5] For the formation of **8**, de- and reprotonation of **6** is also conceivable.

[6] A. V. Ruban, A. B. Drapailo, V. D. Romanenko, L. N. Markovskii, *Zh. Obshch. Khim.* **1986**, *56*, 2791–2792.

[7] J. Böske, E. Niecke, B. Krebs, M. Läge, G. Henkel, *Chem. Ber.* **1992**, *125*, 2631–2634.

[8] a) X-ray structure analysis for **2** [4] $C_{37}H_{58}Cl_2NP$ [$C_{40}H_6$,ClNPSi·1/2 toluene]: orange [yellow] crystals, crystal dimensions 0.25 × 0.40 × 0.40 [0.40 × 0.50 × 0.70] mm; $M_r = 618.7$ [702.5 with solvent]; space group $C2/c$ (no. 15) [$P2_1/n$], $a = 36.605(4)$ [9.994(1)], $b = 10.684(1)$ [26.039(2)], $c = 22.571(2)$ [17.034(2)] Å, $\beta = 120.77(1)°$ [90.19(1)°], V = 7.585(1) [4.433(1)] nm^3, Z = 8 [4], $\rho_{calcd} = 1.08$ [1.05] g cm^{-3}, $\mu(Cu_{K\alpha}) = 2.10$ [1.55] mm^{-1}; 5607 [6581] symmetry-independent reflections ($2\theta_{max.} = 120°$ [120°], $T = 293$ [193] K), of which 3473 [6158] reflections with $F > p\sigma(F)$ (p = 3 [4]) were used for structure solution (direct methods) and refinement (368 [434] parameters), non-hydrogen atoms anisotropic, H atoms refined with a "riding" model; $R = 0.067$ [0.062] ($R_w = 0.068$ [0.071], $w^{-1} = \sigma^2(F) = gF^2$, $g = 0.0008$ [0.0001]. Extinction correction (for **4**) and empirical absorption correction (for **2**) was applied by using the program DIFABS. In **2** a *p-tert*-butyl group is disordered (s.o.f. C31, C32, C33 = 0.62(1)). In **4** a toluene molecule is disordered over an inversion center. Further details of the crystal structure investigations may be obtained from the Fachinformationszentrum Karlsruhe, D-76344 Eggenstein-Leopoldshafen (FRG), on quoting the depository number CSD-58059. b) N. Walker, D. Stuart, *Acta Crystallogr. Sect. A* **1993**, *39*, 158–166.

[9] a) *Multiple Bonding and Low Coordination in Phosphorus Chemistry* (Eds.: M. Regitz, O. J. Scherer), Thieme, Stuttgart, **1990**; b) H. Heydt in [9a], pp. 375–390; c) E. Niecke, D. Gudat in [9a], p. 392–403; d) G. Bertrand in [9a], pp. 443–454.

[10] The *endo/endo* bis(imino)phosphorane R–P(=NR)=NSiMe$_3$ (R = 2,4,6-tBu$_3$C$_6$H$_2$), which is isoelectronic to **6** has a ^{31}P NMR shift of $\delta = 66$ [6].

[11] S. O. Grimm in *Phosphorus-31 NMR Spectroscopy in Stereochemical Analysis* (Eds.: J. G. Verkade, L. D. Quin), VCH, Deerfield Beach, FL, **1987**, pp. 645–664.

[12] H. Schmidbaur, O. Gasser, M. Sakhawat Hussain, *Chem. Ber.* **1977**, *110*, 3501–3507.

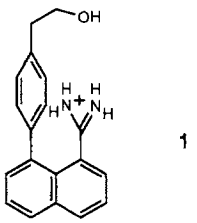
[13] $\delta^{13}C$ (99, $^1J_{CP} = 157.9$ (CP_A), 143.4 (CP_B) Hz); $\delta^{31}P$ (27.2 (P_A), 3.1 (P_B) $^2J_{PP} = 120.8$ Hz). M. Soleilhavoup, A. Baceiredo, O. Treutler, R. Ahlrichs, M. Nieger, G. Bertrand, *J. Am. Chem. Soc.* **1992**, *114*, 10959–10961.

 © VCH Verlagsgesellschaft mbH, D-69451 Weinheim, 1994 0570-0833/94/0909-0983 $ 10.00+.25/0

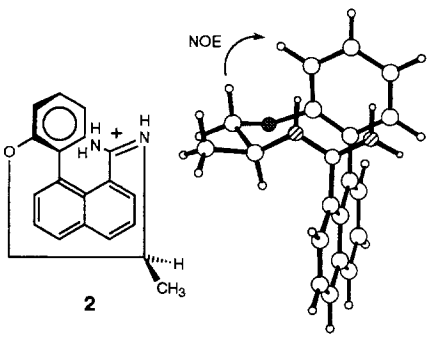
Axially Chiral Amidinium Ions with a Biaryl Skeleton: A New Class of Structure in Host–Guest Chemistry**

Stefan Lehr, Karin Schütz, Markus Bauch, and Michael W. Göbel*

As part of our search for synthetic phosphodiesterases, we reported some time ago[1] on the cationic alcohol **1**. This compound can reversibly coordinate deprotonated phosphoric acid diesters to the amidinium group and react with them in a nucleophilic substitution reaction. On account of its constitutional symmetry, **1** is achiral. We now describe a new stereochemical concept which provides access to novel, axially chiral[2] amidinium ions[3] (**2**, **14**, **15**) starting from the structural type **1** (Fig. 1). These ions are of interest as receptors and catalysts in host–guest chemistry: potential applications include their use as phase transfer catalysts[4] or—in the deprotonated form—as chiral bases.[5]



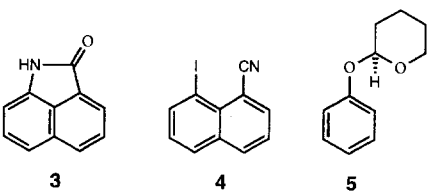
1



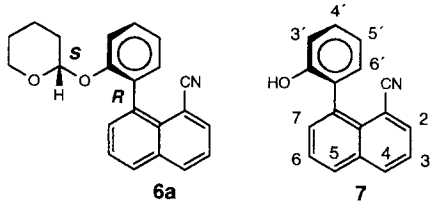
2

Fig. 1. Structural formula and molecular model of the axially chiral amidinium ion **2**.

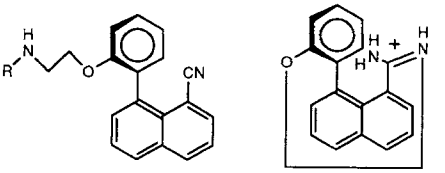
The first step in the synthesis of **2** (Scheme 1) was the conversion of lactam **3** into nitrile **4**. Construction of the biaryl carbon skeleton of **2** was achieved in a palladium-catalyzed coupling of **4** with a copper reagent obtained from the *ortho*-lithiation of *rac*-**5** followed by reaction with copper(I) bromide. The two diastereomeric products formed, *rac*-**6a** ((*S**,*R**) configuration) and *rac*-**6b** ((*S**,*S**) configuration), could be hydrolyzed to give the phenol *rac*-**7** (63% from **4**). The Mitsunobu reaction[6] with *N*-Boc-aminoethanol provided *rac*-**8** (79%). Removal of the protective group gave the aminonitrile *rac*-**9**. Subsequent base-induced cyclization (and protonation) yielded the amidinium ion *rac*-**10** (isolated as the picrate). This ten-membered ring formation was achieved without any problems (78%), even in relatively concentrated solutions. We attribute the surprisingly smooth course of reaction to the fact that seven of the ten atoms in the ring were already fixed in the starting material in a conformation resembling that found in the product.



3 **4** **5**

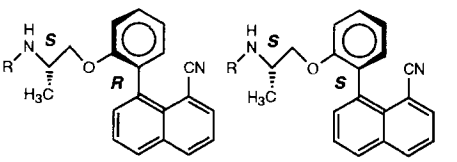


6a **7**



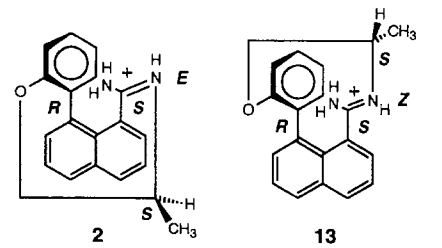
8: R = Boc
9: R = H

10

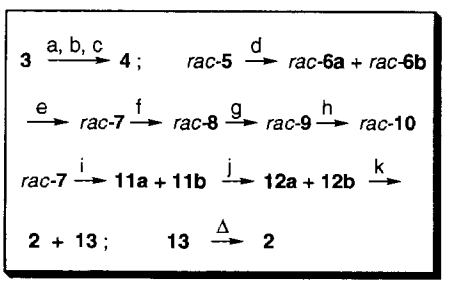


11a: R = Boc
12a: R = H

11b: R = Boc
12b: R = H



2 **13**



Scheme 1. Synthesis of **2**[picrate]: a) 1. NaOH, H_2O, Δ; 2. $NaNO_2$, H_2SO_4; 3. KI (55–60%); b) 1. PCl_5, 2. NH_3 (91%); c)$POCl_3$, pyridine (91%); d) 1.4 equiv *rac*-**5**, 1.4 equiv *n*-butyllithium, *N*,*N*,*N*′,*N*′-tetramethylethylenediamine, THF, 0°C, 50 min; then 1.4 equiv CuBr, −30°C; then 1 equiv **4** and 0.1 equiv $[(Ph_3P)_2PdCl_2]$, −30°C → room temperature, 15 h (68%); e) HCl, MeOH, H_2O (93%); f) *N*-Boc-aminoethanol, diethyl azodicarboxylate, Ph_3P, CH_2Cl_2, room temperature, 20 h (79%); g) HCl, MeOH, H_2O (97%); h) 5 equiv $(Me_3Si)_2NLi$, 1,4-dioxane, Δ, 1 h (*rac*-**10**[picrate]: 78%); i) *N*-Boc-(*S*)-alaninol, diethyl azodicarboxylate, Ph_3P, THF, room temperature, 20 h (56%, 32% *rac*-**7** recovered); j) trifluoroacetic acid, CH_2Cl_2, room temperature (90%); k) 5 equiv $(Me_3Si)_2NLi$, 1,4-dioxane, Δ, 3 h; separation of isomers by fractional crystallization of the picrate from $MeOH/H_2O$ (**2**[picrate]: 61%, **13**[picrate]: 6%).

[*] Dr. M. W. Göbel, Dipl.-Chem. S. Lehr, Dipl.-Chem. K. Schütz, Dr. M. Bauch
Institut für Organische Chemie der Universität
Marie-Curie-Strasse 11, D-60439 Frankfurt am Main (FRG)
Telefax: Int. code + (69)5800-9250

[**] This work was supported by the Fonds der Chemischen Industrie, the Deutsche Forschungsgemeinschaft (Go 545/1-1), and the Graduiertenkolleg "Chemische und Biologische Synthese von Wirkstoffen". We thank Prof. Dr. G. Quinkert for his generous support.

In order to control the absolute configuration at the biaryl axis, the phenol *rac*-**7** was linked with a chiral building block, a side chain synthesized from (*S*)-alanine.[7] Again, two diastereomers were formed, the non-racemic products **11a** ((*S*,*R*) isomer) and **11b** ((*S*,*S*) isomer; total yield of 56%; unreacted phenol *rac*-**7** can be recovered). It was possible to separate **11a** and **11b**, which are interconvertible by rotation about the biaryl axis, by HPLC. A barrier to rotation of 98.3 kJ mol^{-1} (30 °C; ethyl acetate/hexane; ratio of isomers at equilibrium 1.2:1) was calculated from the rate of isomerization. The aminonitriles **12a** and **12b**, obtained by cleavage of the Boc groups, can for steric reasons only undergo the base-induced cyclization when the methyl group of the side chain becomes equatorial and the adjacent methine proton axial (see Fig. 1). This arrangement can only be achieved from the isomer **12a** with the (*S*,*R*) configuration. By raising the reaction temperature we were able to increase the rate of isomerization of **12b** to **12a** to such an extent that both compounds cyclized *stereoconvergently* to give the same amidinium picrate **2**[picrate] with the (*S*,*R*,*S*) configuration (61%).[8] The coupling constants observed in the ^{1}H NMR spectrum and the fact that the axial methylene proton shows a strong nuclear Overhauser effect to the phenyl ring provide evidence for the chair-type conformation in the ten-membered ring of **2**. The (formal) C–N double bond in the amidinium ion **2** has an (*E*) configuration. Compound **2** shows similar binding affinities towards dimethylphosphate ions[9] like cation **1**. From the mother liquor of **2**[picrate] the (*Z*) isomer **13**[picrate] could also be isolated. Conversion of **13**[picrate] to **2**[picrate] was observed on application of heat. Selected physical data for **2**, *rac*-**7**, and *rac*-**10** are given in Table 1.

Table 1. Selected physical data for **2**[picrate], *rac*-**7**, and *rac*-**10**[picrate].

2 [picrate]: M.p. 266–268 °C (ethyl acetate/*n*-hexane). – $[\alpha]_D^{20} = -10.0$ ($c = 0.14$ in methanol). – ^{1}H NMR (270 MHz, [D$_6$]DMSO, locants see **7**): $\delta = 1.10$ (d, $J = 6.7$ Hz, 3H, methyl-H), 3.58 (m, 1H, methine-H$_{ax}$), 3.98 (dd, $J_{gem} = 12.4$ Hz, $J_{vic} = 3.7$ Hz, 1H, methylene-H$_{eq}$), 4.30 (dd, $J_{gem} = 12.3$ Hz, $J_{vic} = 10.7$ Hz, 1H, methylene-H$_{ax}$), 7.12 (dt, $J_t = 7.4$ Hz, $J_d = 0.9$ Hz, 1H, 4′-H), 7.28 (m, 2H, 3′-H and 6′-H), 7.40 (dd, $J = 7.1$ and 1.3 Hz, 1H, 7-H), 7.48 (ddd, 7-line signal, $J = 8.6$, 7.3 and 1.8 Hz, 1H, 5′-H), 7.58 (dd, $J = 7.1$ and 1.4 Hz, 1H, 2-H), 7.72 (t, $J = 7.6$ Hz, 2H, 3-H and 6-H), 7.99 (s, 1H, NH$_{ax}$), 8.13 (dd, $J = 8.3$ and 1.2 Hz, 1H, 5-H), 8.31 (dd, $J = 8.3$ and 1.3 Hz, 1H, 4-H), 8.59 (s, 2H, picrate-H), 8.93 (s, 1H, NH$_{eq}$), 9.13 (d, J = 9.7 Hz, 1H, RNH$_{ax}$)

rac-**7**: M.p. 202–204 °C (ethyl acetate/*n*-hexane). – ^{1}H NMR (250 MHz, [D$_6$]DMSO): $\delta = 6.88$ (m, 2H, 4′-H and 6′-H), 7.16 (dd, $J = 7.9$ and 1.5 Hz, 1H, 3′-H), 7.27 (dt, $J_t = 7.0$ Hz, $J_d = 1.2$ Hz, 1H, 5′-H), 7.45 (dd, $J = 7.1$ and 1.3 Hz, 1H, 7-H), 7.64 (dd, $J = 8.2$ and 7.2 Hz, 1H) and 7.69 (dd, $J = 8.2$ and 7.1 Hz, 1H, 3-H and 6-H), 8.01 (dd, $J = 7.2$ and 1.3 Hz, 1H, 2-H), 8.09 (dd, $J = 8.3$ and 1.3 Hz, 1H, 5-H), 8.33 (dd, $J = 8.3$ and 1.3 Hz, 1H, 4-H), 9.37 (s, 1H, OH)

rac-**10** [picrate]: M.p. 283–286 °C (methanol; decomp. beginning at 275 °C). – ^{1}H NMR (270 MHz, [D$_6$]DMSO): $\delta = 3.35$ (m, superimposed by H_2O, 2H, NCH$_2$), 4.01 (ψd, J about 12 Hz, 1H, OCH$_{eq}$), 4.53 (ddd, 7-line signal, J about 13, 9.5 and 4.5 Hz, 1H, OCH$_{ax}$), 7.12 (t, $J = 7.4$ Hz, 1H, 4′-H), 7.27 (m, 2H, 3′-H and 6′-H), 7.40 (dd, $J = 7.1$ and 1.3 Hz, 1H, 7-H), 7.48 (ddd, $J = 8.6$, 7.3 and 1.7 Hz, 1H, 5′-H), 7.53 (dd, $J = 7.1$ and 1.1 Hz, 1H, 2-H), 7.72 (ψt, J about 7.6 Hz, 2H, 3-H and 6-H), 8.14 (dd, $J = 8.4$ and 1.3 Hz, 1H, 5-H), 8.31 (dd, $J = 8.3$ and 1.2 Hz, 1H, 4-H), 8.44 (s, 1H, NH$_{ax}$), 8.60 (s, 2H, picrate-H), 8.97 (s and d, superimposed, 2H, NH$_{eq}$ and RNH$_{ax}$)

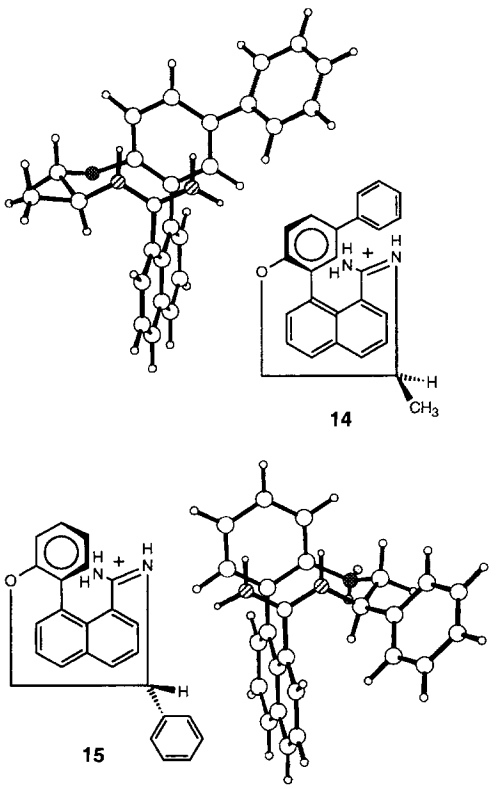


Fig. 2. Structural formulae and molecular models of the amidinium ions **14** and **15**.

above. The synthesis of derivatives of **2** tailor-made for the areas of molecular recognition and catalysis thus appears to be feasible.

The CD spectrum of the picrate salt of **2** (Fig. 3) provides a first impression of how coordination to the amidinium ion influ-

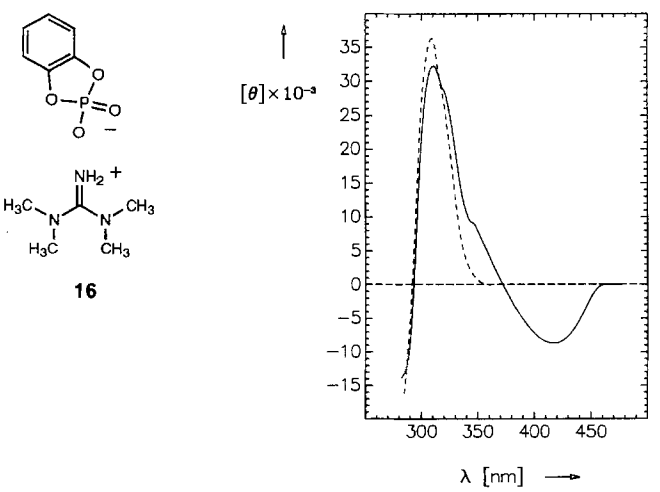


Fig. 3. CD spectrum of **2**[picrate] (50 μM in CH_2Cl_2, room temperature): — without addition, --- with addition of 20 equiv **16**.

The structural principle underlying the stereoconvergent ring closure to **2** is as clear as it is general: It should apply to many types of amino alcohol side chains and should be unaffected by the presence of further substituents, aromatic or heteroaromatic moieties attached to the phenyl ring. Indeed, the synthesis of amidinium ions **14** and **15** (isolated as their picrate salts) (Fig. 2) was achieved following an analogous procedure to that outlined

ences achiral guest molecules. Whereas no signals are recorded beyond 350 nm in the spectrum of the tetraphenylborate salt **2**[BPh_4], a pronounced band is observed at longer wavelengths in the spectrum of **2**[picrate]. The origin of this effect is a chiral disturbance of the picrate chromophore in the host–guest complex. On addition of the salt **16**, whose anion binds to the ami-

dinium ion, the long-wavelength band disappears. Our long-term goal with these investigations is to be able to enantioselectively control not only the spectroscopic behavior but also the reactivity of prochiral guest molecules.

Received: November 29, 1993 [Z 6521 IE]
German version: *Angew. Chem.* **1994**, *106*, 1041

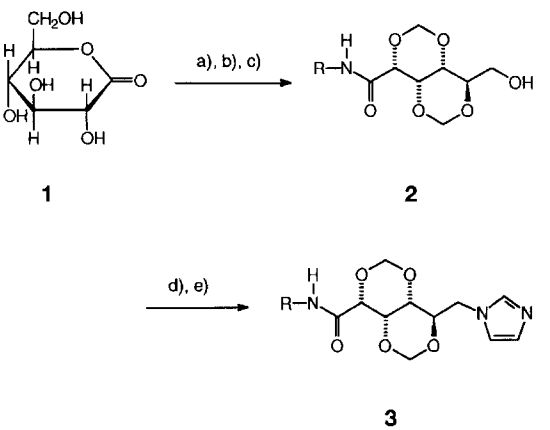
[1] M. W. Göbel, J. W. Bats, G. Dürner, *Angew. Chem.* **1992**, *104*, 217–218; *Angew. Chem. Int. Ed. Engl.* **1992**, *31*, 207–209.
[2] Chiral biaryl structures: a) D. J. Cram, *Angew. Chem.* **1988**, *100*, 1041–1052; *Angew. Chem. Int. Ed. Engl.* **1988**, *27*, 1009–1020; b) R. Noyori, *Chem. Soc. Rev.* **1989**, *18*, 187–208; c) R. Noyori, H. Takaya, *Acc. Chem. Res.* **1990**, *23*, 345–350; d) T. Hayashi, K. Hayashizaki, T. Kioyi, Y. Ito, *J. Am. Chem. Soc.* **1988**, *110*, 8153–8156; e) G. Bringmann, R. Walter, R. Weirich, *Angew. Chem.* **1990**, *102*, 1006–1019; *Angew. Chem. Int. Ed. Engl.* **1990**, *29*, 977; f) G. Bringmann, T. Hartung, *Tetrahedron* **1993**, *49*, 7891–7902.
[3] For preparation and use of non-racemic chiral guanidines in host–guest chemistry, see: a) A. Gleich, F. P. Schmidtchen, P. Mikulcik, G. Müller, *J. Chem. Soc. Chem. Commun.* **1990**, 55–57; b) A. Gleich, F. P. Schmidtchen, *Chem. Ber.* **1990**, *123*, 907–915; c) F. P. Schmidtchen, *Liebigs Ann. Chem.* **1991**, 539–543; d) H. Kurzmeier, F. P. Schmidtchen, *J. Org. Chem.* **1990**, *55*, 3749–3755; e) P. Schiessl, F. P. Schmidtchen, *Tetrahedron Lett.* **1993**, *34*, 2449–2452; f) A. Echavarren, A. Galán, J. de Mendoza, A. Salmerón, J.-M. Lehn, *Helv. Chim. Acta* **1988**, *71*, 685–693; g) A. Echavarren, A. Galán, J.-M. Lehn, J. de Mendoza, *J. Am. Chem. Soc.* **1989**, *111*, 4994–4995; h) A. Galán, E. Pueyo, A. Salmerón, J. de Mendoza, *Tetrahedron Lett.* **1991**, *32*, 1827–1830; i) A. Galán, J. de Mendoza, C. Toiron, M. Bruix, G. Deslongchamps, J. Rebek, *J. Am. Chem. Soc.* **1991**, *113*, 9424–9425; j) A. Galán, D. Andreu, A. M. Echavarren, P. Prados, J. de Mendoza, *ibid.* **1992**, *114*, 1511–1512; k) G. Deslongchamps, A. Galán, J. de Mendoza, J. Rebek, Jr., *Angew. Chem.* **1992**, *104*, 58–60; *Angew. Chem. Int. Ed. Engl.* **1992**, *31*, 61–63; l) E. J. Corey, M. Ohtani, *Tetrahedron Lett.* **1989**, *30*, 5227–5230; m) P. Molina, M. Alajarín, A. Vidal, *J. Org. Chem.* **1993**, *58*, 1687–1695.
[4] For an early example of extraction of anions from water using a nonpolar phase and a lipophilic amidinium ion, see: F. Heinzer, M. Soukup, A. Eschenmoser, *Helv. Chim. Acta* **1978**, *61*, 2851–2874.
[5] For formation and structural characterization of ion pair complexes between nitroalkanes and bicyclic amidines and guanidines, see: a) P. H. Boyle, M. A. Convery, A. P. Davis, G. D. Hosken, B. A. Murray, *J. Chem. Soc. Chem. Commun.* **1992**, 239–242; b) E. van Aken, H. Wynberg, F. van Bolhuis, *ibid.* **1992**, 629–630.
[6] O. Mitsunobu, *Synthesis* **1981**, 1–28.
[7] T. Moriwake, S. Hamano, S. Saito, S. Torii, *J. Org. Chem.* **1989**, *54*, 4114–4120.
[8] For an example of a diastereoselective ring closure reaction of a biaryl derivative leading to kinetic separation of isomers, see: G. Bringmann, J. R. Jansen, H. Busse, *Liebigs Ann. Chem.* **1991**, 803–812; see also [2e,f].
[9] A ^{1}H NMR titration of **2**[picrate] with sodium dimethylphosphate at 30 °C in [D$_6$]DMSO gave a K_a value of 250 ± 30 L mol^{-1}.

Tunable Supramolecular Structures from a Gluconamide Containing Imidazole

Rudi J. H. Hafkamp, Martinus C. Feiters,* and Roeland J. M. Nolte*

In recent years, the interest in supramolecular structures has grown steadily. Self-assembling systems have been prepared from a variety of building blocks including surfactants,[1] polymers,[2] rodlike,[3] and disklike mesogens,[4] etc.[5] As part of our program aimed at the development of novel chiral matrices for catalytic applications, we report here on the synthesis and self-assembling properties of the *n*-octyl-D-gluconamide derivative **3**, which contains a metal-coordinating imidazole group. Our interest in gluconamides and related carbohydrates was raised by the recent studies of Fuhrhop et al. and others,[6] which indicate that these compounds can form a great variety of nanometer-sized structures in water.

Compound **3** was synthesized as shown in Scheme 1. 1,5-D-Gluconolactone was hydrolyzed and protected at its secondary hydroxyl functions in a one-step procedure.[7] The resulting product was esterified to give methyl-2,4;3,5-dimethylene-D-gluconate which was aminolyzed with octylamine to give the amide **2**. The latter compound was tosylated and subsequently converted into **3** by reaction with imidazole in an autoclave at high pressure (15 Kbar).



Scheme 1. a) Trioxane, H_2O/H^+ (74%); b) H^+/MeOH (61%); c) excess of octylamine (no additional solvent used, 77%); d) TsCl/pyridine, 0 °C (87%); e) imidazole, $CHCl_3$, 15 kbar, 50 °C (66%). R = *n*-C_8H_{17}.

Although the polarity of carbohydrate **2** is decreased due to the methylene bridges, it appears that this compound is soluble in water. However, unlike the unprotected derivative,[6a,f] it does not form well-defined aggregates, as judged by electron microscopy (EM). Apparently, the amide bond and the primary hydroxyl function in **2** cannot form hydrogen bonds leading to stable suprastructures in water. The DSC studies (DSC = differential scanning calorimetry) of an aqueous solution of **2** showed only one transition near 53 °C, which can be assigned to the disappearance of amide hydrogen bonds. No transition was observed upon cooling.[8] The thermogram of *n*-octyl-D-gluconamide shows two transitions upon heating,[9] which are attributed to the breaking of a network of intermolecular hydrogen bonds between the hydroxyl groups (at 61 °C), and between the amide hydrogen bonds (at 70 °C).[9]

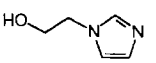
Compound **3** is also soluble in water. From a titration experiment in methanol/water (95/5, v/v), it followed that the apparent pK_a value (pK_a^*) of the imidazole group is 6.28.[10] For comparison, methylimidazole and imidazole were also titrated in this medium and were found to have pK_a^* values of 7.03 and 6.96, respectively, which are comparable to their values in water (6.95 for both compounds[11]).

The copper complexation properties of **3** were investigated by UV/VIS controlled titrations. Addition of $Cu(ClO_4)_2$ to a solution of **3** in water led to the appearance of a broad band at approximately $\lambda = 620$ nm. Unfortunately, the complex $[Cu(\mathbf{3})_n]^{2+}$ was not soluble enough in water to carry out an accurate UV/VIS titration. In mixtures of organic solvents such as chloroform/methanol (1/2, v/v), clear solutions were obtained and the complexation behavior of **3** could be determined. During the titrations of **3** with $Cu(ClO_4)_2$, the λ_{max} gradually shifted from 600 to 780 nm when the ratio [Cu]/[**3**] was increased

[*] Prof. Dr. R. J. M. Nolte, Dr. M. C. Feiters, R. J. H. Hafkamp
Nijmegen SON Research Center
University of Nijmegen
Toernooiveld, NL-6525 ED Nijmegen (The Netherlands)
Telefax: Int. code + (80)55 34 50

 © VCH Verlagsgesellschaft mbH, D-69451 Weinheim, 1994 0570-0833/94/0909-0986 $ 10.00+.25/0

from 1/4 to 1/1. The titrations revealed that at low copper concentrations a 4/1 ligand-to-copper complex[12] is present, whereas at high copper concentrations other complexes, for example [3]/[Cu] = 3, 2, or 1 prevail. For comparison, titrations were also carried out with the non-amphiphilic imidazole compound **4**[13] and with methylimidazole. In both water and methanol/chloroform mixtures the copper complexation curves of **3**, **4**, and *N*-methylimidazole were very similar.



4

The types of aggregates formed by **3** in water were studied by transmission electron microscopy (TEM) and scanning electron microscopy (SEM). In a NaOAc/HOAc buffer of pH 4.5, protonated **3** self-assembles to yield vesicles (100%) with diameters ranging from 160 to 780 nm (Fig. 1A).[14] In a tris(hydroxymethyl)methylamine (TRIS) buffered solution of pH 8.5 long fibers (Fig. 1B and C) and hollow tubuli are formed exclusively (Fig. 1C). The fibers can have a length/width ratio up to 500 (Fig. 1B, the diameters of these fibers are approximately 100 nm).[15] Freeze fracture experiments showed that these fibers are composed of multilayers (not shown). The hollow tubuli have diameters of approximately 3 μm. In a TRIS buffered solution, (pH 8.5), the 1:4 copper complex of amphiphile **3** forms helices (100%, Fig. 1D).[16] The diameters of these helices are approximately 330 nm; much larger than the ropelike structures formed by *N*-octyl-D-gluconamide (diameter of 27 nm).[6f]

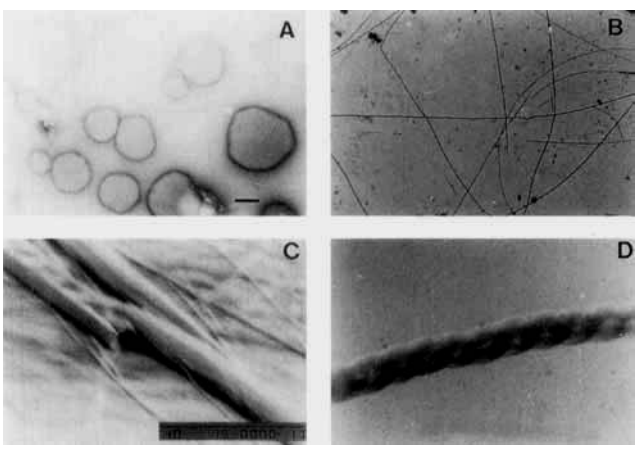


Fig. 1. A: TEM of vesicles of **3** (on a carbon-supported hydrophilic copper grid stained with 2% uranyl acetate; bar is 200 nm). B: TEM of fibers from **3** (Formvar-supported copper gid, stained with 2% uranyl acetate; bar is 5 μm). C: SEM of hollow tubuli and thin fibers of **3** (copper grid from 1B was sputtered with gold; bar is 10 μm). D: TEM of helices from the copper complex of **3** (Formvar-supported copper grid without staining, bar is 200 nm).

In conclusion, we have shown that gluconamide **3** can self assemble to give interesting supramolecular structures which can be tuned by changing the pH or by adding metal ions.

Received: October 28, 1993 [Z 6459 IE]
German version: *Angew. Chem.* **1994**, *106*, 1054

[1] a) J.-H. Fuhrhop, W. Helfrich, *Chem. Rev.* **1993**, *93*, 1565–1582; b) R. Ahuja, P.-L. Caruso, D. Möbius, W. Paulus, H. Ringsdorf, G. Wildburg, *Angew. Chem.* **1993**, *105*, 1082–1085; *Angew. Chem. Int. Ed. Engl.* **1993**, *32*, 1082–1085; c) T. Kunitake, Y. Okahata, M. Shimomura, S.-I. Yasunami, K. Taharabe, *J. Am. Chem. Soc.* **1981**, *103*, 5401–5413; d) J. H. Fendler, *Membrane Mimetic Chemistry*, Wiley, New York, **1982**; e) T. Kunitake, *Angew. Chem.* **1992**, *104*, 692–710; *Angew. Chem. Int. Ed. Engl.* **1992**, *31*, 709–717; f) H. Ringsdorf, B. Schlarb, J. Venzmer, *ibid.* **1988**, *100*, 117–162 and **1988**, *27*, 113–158.

[2] a) V. Perec, D. Tomaros, *Compr. Polym. Sci., Suppl. Vol I* (Ed.: G. Allen), Pergamon, Oxford, **1992**, pp. 300–383; b) D. F. O'Brien, T. Kuo, U. Liman, H. Lamparski, *Polym. J.* **1991**, *23*, 619–628; c) S. L. Kwolak, P. W. Morgan, J. R. Schaefer, *Encycl. Polym. Sci. Eng.* **1985–1987**, *9*, 1–61; d) R. Zentel, *Compr. Polym. Sci Vol. 5*, Pergamon, Oxford, **1989**, 723.

[3] G. A. Jeffrey, L. M. Wingert, *Liq. Cryst.* **1992**, *12*, 179–202.

[4] S. Chandrasekhar, G. S. Ranganath, *Rep. Prog. Phys.* **1990**, *53*, 57–84.

[5] W. Zarges, J. Hall, J.-M. Lehn, *Helv. Chim. Acta* **1991**, *74*, 1843–1852.

[6] a) J.-H. Fuhrhop, P. Schnieder, J. Rosenberg, E. Boekema, *J. Am. Chem. Soc.* **1987**, *109*, 3387–3390; b) J.-H. Fuhrhop, P. Schnieder, E. Boekema, W. Helfrich, *ibid.* **1988**, *110*, 2861–2867; c) C. Boettcher, E. Boekema, J.-H. Fuhrhop, *J. Microsc. Oxford* **1990**, *160*, 173–182; d) J.-H. Fuhrhop, C. Boettcher, *J. Am. Chem. Soc.* **1990**, *112*, 1768–1776; e) J.-H. Fuhrhop, S. Svenson, C. Boettcher, E. Rössler, H.-M. Vieth, *ibid.* **1990**, *112*, 4307–4312; f) J. Köning, C. Boettcher, H. Winkler, E. Zeitler, Y. Talmon, J.-H. Fuhrhop, *ibid.* **1993**, *115*, 693–700; g) D. A. Frankel, D. F. O'Brien, *ibid.* **1991**, *113*, 7436–7437; h) B. Pfannemüller, *Starch/Stärke* **1988**, *40*, 476–486.

[7] M. Zief, A. Scattergood, *J. Am. Chem. Soc.* **1947**, *69*, 2132; C. L. Mehltretter, R. L. Mellies, C. E. Rist, G. E. Hilbert, *ibid.* **1947**, *69*, 2130–2131.

[8] DSC analyses were carried out on a Perkin Elmer DSC 7 using a 4.9% (w/v) aqueous dispersion in a sealed pan, heating and cooling down rate was 5 K min^{-1}.

[9] B. Pfannemüller, I. Kühn, *Makromol. Chem.* **1988**, *189*, 2433–2442.

[10] The titration was carried out under a nitrogen atmosphere and the electrode was calibrated with a sodium succinate/succinic acid and an ammonium oxalate/oxalic acid buffer. D. Perrin, B. Dempsey, *Buffers for pH and Metal Ion Control*, Wiley, London, **1974**.

[11] *CRC Handbook of Chemistry and Physics, 51st ed.* (Ed.: R. C. Weast), CRC, Cleveland, OH, USA, **1970**, D-118.

[12] J. Reedijk, *Recl. Trav. Chim. Pays-Bas* **1969**, 1451.

[13] This compound was synthesized from imidazole and ethylene carbonate (1,3-dioxolan-2-one) as described, cf. H. Komura, T. Yoshino, Y. Ishido, *Carbohydr. Res.* **1973**, *31*, 151–156.

[14] Vesicle samples for EM were prepared by cooling a hot clear solution of **3** in NaOAc/HOAc buffer of pH 4.5 to room temperature. Subsequently, a drop of this solution was placed on a hydrophilic formvar supported grid. The vesicles were stained with uranyl acetate (2%).

[15] For the electron micrographs a hydrophobic Formvar supported grid was used.

[16] To a hot clear solution of **3** (0.5% m/v) in TRIS buffer, 0.25 equiv of $Cu(ClO_4)_2$ was added. The turbid mixture was cooled rapidly to room temperature and allowed to stand for 30 min. No additional staining was used.

Iodine Chains in $(Me_4Sb)_3I_8$ and Discrete Triiodide Ions in Me_4AsI_3**

Ulrich Behrens, Hans Joachim Breunig,* Michael Denker, and Klaus Heinz Ebert

Polyiodides have an extensive structural chemistry,[1] and compounds with discrete iodine chains are of particular interest because of possible unusual electric behavior.[2] Iodine and iodide chains are not rare. They occur, for example, in the iodine–starch complex and in related compounds,[3] in organic metals,[4] in complexes with column structures,[5] and also in saltlike triiodides such as Bu_4NI_3.[6] The iodine chains in these compounds frequently consist of triiodide or iodide ions and iodine molecules.[7] Ordered iodine chains such as in $[Cd(NH_3)_4I_6]$ are unusual;[1] in this complex the iodine chains are not discrete, but are linked three-dimensionally by strong coordinative bonds to

[*] Prof. Dr. H. J. Breunig, M. Denker, K. H. Ebert
Fachbereich 2 der Universität
Postfach 330440, D-28334 Bremen (FRG)
Telefax: Int. code + (421)218-4042
Prof. Dr. U. Behrens
Institut für Anorganische und Angewandte Chemie
der Universität Hamburg (FRG)

[**] This work was supported by the Fonds der Chemischen Industrie. We thank Mrs. L. Akselrod and Dr. S. Roth, Max-Planck-Institut für Festkörperforschung, Stuttgart, for the conductivity measurements. Prof. Dr. O. Jarchow, mineralogisch-petrographisches Institut der Universität Hamburg is thanked for the discussion of the X-ray crystallographic investigations.

 © VCH Verlagsgesellschaft mbH, D-69451 Weinheim, 1994 0570-0833/94/0909-0987 $ 10.00+.25/0

the metal centers. We report here on ordered iodine chains in the golden shining crystals of the compound $(Me_4Sb)_3I_8$ (**1**) and on the structure of the triiodide Me_4AsI_3 **2** with discrete I_3 ions.

The stibonium polyiodide **1** crystallizes from solutions of Me_4SbI and iodine. The compound is air-stable and decomposes first on warming at 136 °C. We were not able to obtain the blue-black triiodide Me_4SbI_3 described by Wittig et al.[8] The results of the X-ray crystal structure analysis[15] show that linear chains of iodine atoms with only slightly alternating distances of 328.3(2) and 329.9(2) pm (Fig. 1 and 2) are present in

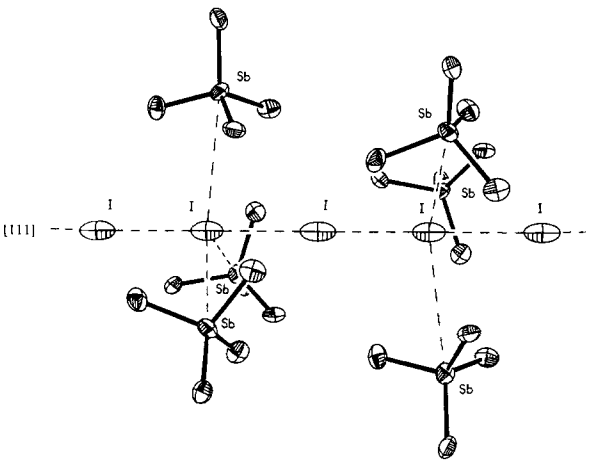


Fig. 1. Environment of a iodine chain in the crystal of **1**.

the crystal of **1**. Rotating crystal and Weissenberg measurements show no indication of a disorder or a superstructure. The iodine chains are arranged parallel to the space-diagonals of the cubic unit cell. Through antimony–iodine contact distances of 412.9(2) pm, every second iodine atom in the chain is surrounded by three stibonium ions, whose tetrahedral faces are each capped by iodine atoms. Similar contact distances and angles as in **1** are also found in the structures of Me_4SbI[9, 10] and $(Me_4Sb)_2(MeSbI_4)$.[10] The distances indicate that a weak interaction exists between every second iodine atom in the chain and the stibonium ions. The unexpected stoichiometry of **1** can be informally explained with coordination numbers.[11] The structure and properties of **1** correspond quite precisely to the criteria presented by Tebbe[1] for compounds with linear triiodide chains, which are constructed from iodine molecules and iodide ions. According to the multicenter bonding model[12, 13] alternating distances in the chain are to be expected, and the chain must be protected from the breakdown into discrete I_3 ions by additional stabilization. This stabilization is apparent from the antimony–iodine interactions. The iodine–iodine distances in the chain are greater than the values normally found in discrete triiodide ions. They correspond to the average distances in the chainlike associated triiodides. The shortest I–I distances between the chains are 570.1(2) pm.

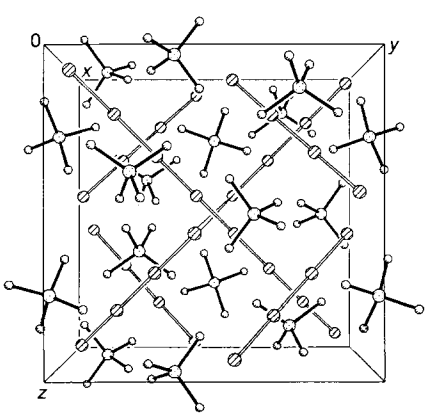


Fig. 2. Unit cell of the crystal structure of **1**. Sb: dotted spheres, I: hatched spheres, C: shaded spheres; projection along [100].

Reaction of Me_4AsI with iodine leads to the known triiodide Me_4AsI_3 **2** in the form of red-violet crystals.[14] The structure of **2** contains stacks of tetrahedral tetramethylarsonium ions, which are surrounded by discrete triiodide ions (Fig. 3). These anions are all linear; however, they differ with respect to their distances. Besides two forms of triiodide ions with equally long iodine–iodine distances of 293.0(2) or 292.3(1) pm, anions also occur with iodine–iodine distances of different lengths (294.8(2) and 290.8(2) pm). Contacts exist between the I_3 anions with iodine–iodine distances ranging from 392 to 405 pm.

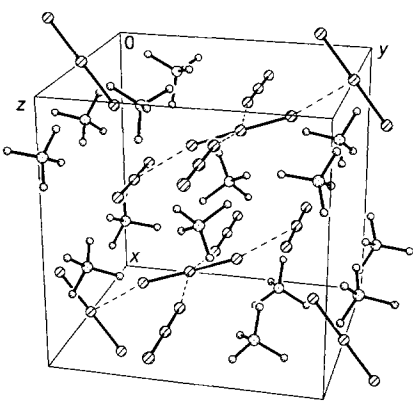


Fig. 3. Unit cell of the crystal structure of **2**. As: dotted spheres, I: hatched spheres, C: shaded spheres.

Solutions of **1** and **2** in ethanol cannot be differentiated by UV/VIS spectroscopy; the typical absorptions of triiodides (290, 357 nm) are observed for both compounds. This shows that the iodine chain in **1** is only stable in the crystal and that it breaks on dissolution with the formation of triiodide and iodide ions. A comparison of the diffuse reflectance spectra clearly shows the visually evident difference in color of **1** and **2**. In the case of **1**, a plateau with little structure covers the entire measurement range up to above 800 nm. In contrast, the absorption of **2** ends in the longwave region with a maximum at 570 nm and a sloping edge, which reaches up to about 750 nm. These results confirm the visual impression and agree qualitatively with the idea that the electron delocalization in **1** is much more extensive than that in **2**. The Raman spectra also confirm the structural differences in the solid state. The spectrum of **1** shows no lines in the expected region for the signals of iodine or of polyiodides. In contrast, for **2**, an intense signal appears at 108 cm^{-1} for the symmetric valence stretch of the triiodide ions with equally long iodine–iodine distances. A separate signal for the asymmetric valence stretch of the I_3 ions with different distances was not observed. Conductivity investigations[16] on crystals of **1** show a significant increase in the conductivity between −50 and 130 °C. The compound is a semiconductor with a band gap of 0.2 eV. At room temperature the conductivity is about 3×10^{-6} $S\,cm^{-1}$.[17]

Experimental Procedure

1: I_2 (0.2 g, 0.79 mmol) was added to Me_4SbI (0.25 g, 0.81 mmol). The mixture was vigorously stirred and dissolved in warm EtOH (5 mL). After slow cooling of the mixture to −25 °C, golden shining compact crystals of **1** were formed in the course

of 5 d. Yield: 0.32 g (67%). M.p. 136 °C (decomp); correct complete elemental analysis.

2: As for the synthesis of **1**, Me_4AsI (0.46 g, 1.76 mmol) and I_2 (0.45 g, 1.77 mmol) were mixed, dissolved in EtOH (25 mL) and cooled to −25 °C. Red-violet needle-like crystals of **2** were obtained after 2 d. Yield: 0.84 g (90%). M.p. 134 °C (ref. [14] 133 °C).

Received: June 25, 1993
Revised version: December 23, 1993 [Z 6169 IE]
German version: *Angew. Chem.* **1994**, *106*, 1023

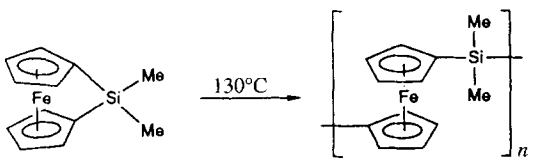
[1] K.-F. Tebbe in *Homoatomic Rings, Chains and Macromolecules of Main-Group Elements* (Ed.: A. L. Rheingold), Elsevier, Amsterdam, **1977**, p. 551.
[2] D. Davis, H. Gutfreund, W. A. Little, *Phys. Rev. B.* **1976**, *13*, 4766.
[3] F. Cramer, U. Bergmann, P. C. Manor, M. Noltemeyer, W. Saenger, *Liebigs Ann. Chem.* **1976**, 1169.
[4] P. Dupuis, S. Flandrois, P. Delhaes, C. Coulon, *J. Chem. Soc. Chem. Commun.* **1978**, 337.
[5] a) H. Endres, H. J. Keller, W. Moroni, J. Weiss, *Acta Crystallogr. Sect. B* **1975**, *31*, 2357; b) H. Endres, H. J. Keller, M. Megnamisi-Belombe, W. Moroni, J. Weiss, R. Comes, *Acta Crystallogr. Sect. A* **1976**, *32*, 954.
[6] F. H. Herbstein, M. Kaftory, M. Kapon, W. Saenger, *Z. Kristallogr.* **1981**, *154*, 11.
[7] P. Coppens in *Extended Linear Chain Compounds* (Ed.: J. S. Miller), Plenum, New York, **1982**, p. 333.
[8] G. Wittig, K. Torsell, *Acta Chem. Scand.* **1953**, *7*, 1293.
[9] G. Burbach, S. Q. Don, A. Weiss, *Ber. Bunsenges. Phys. Chem.* **1989**, *93*, 1302.
[10] H. J. Breunig, K. H. Ebert, S. Gülec, M. Dräger, D. B. Sowerby, M. J. Begley, U. Behrens, *J. Organomet. Chem.* **1992**, *427*, 39.
[11] In consideration of the coordination between Me_4Sb units and iodine atoms with the contact distances of 412.9(2) pm the coordination number 4 results for Me_4Sb and 3 for I and a Me_4Sb/I ratio of 3/4. The observed stoichiometry $(Me_4Sb)_3I_9$ results from the fact that in the iodine chain an additional iodine atom is added to each iodine atom which is coordinated to the antimony atom.
[12] H. Müller, *Theor. Chim. Acta* **1971**, *21*, 110.
[13] H. Müller, *Z. Chem.* **1967**, *7*, 81.
[14] W. R. Cullen, G. B. Deacon, J. H. S. Green, *Can. J. Chem.* **1965**, *43*, 3193.
[15] Crystal data for **1** and **2** at 153 K; $Mo_{K\alpha}$ radiation, **1**: $a = 15.199(2)$ Å, space group $I\bar{4}3d$, 525 independent reflections ($R_{int} = 0.0140$), 447 reflections ($F > 6.0\sigma(F)$). $R = 0.0373$, $\rho_{calcd} = 2.953\ Mg\,m^{-3}$, $V = 3511.2(3)$ Å^3, $Z = 4$. **2**: $a = 14.908(5)$, $c = 13.743(5)$ Å, space group $P4_2/m$, 3675 independent reflections ($R_{int} = 0.0141$), 1626 reflections ($F > 6.0\sigma(F)$), $R = 0.0394$, $\rho_{calcd} = 2.804\ Mg\,m^{-3}$, $V = 3054(2)$ Å^3, $Z = 12$. Further details of the crystal structure investigation may be obtained from the Fachinformationszentrum Karlsruhe, D-76344 Eggenstein-Leopoldshafen (FRG) on quoting the depository number CSD-58088.
[16] Two-contact method.
[17] For comparison: In the two-dimensional semiconductor iodine, the conductivity at room temperature is maximal $1.7 \times 10^{-8}\ Scm^{-1}$ [18].
[18] N. N. Greenwood, A. Earnshaw, *Chemistry of the Elements*, Pergamon, Oxford, **1984**.

Synthesis and Ring-Opening Polymerization of Highly Strained, Ring-Tilted [2]Ruthenocenophanes**

James M. Nelson, Alan J. Lough, and Ian Manners*

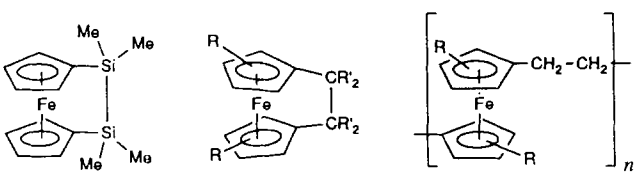
Dedicated to the memory of Dr. Derek S. Manners

Well-defined, soluble polymers which contain transition elements in the main chain are rare but are of considerable interest because of their unusual physical properties and potential applications.[1] As part of our work to develop new routes to these materials we have previously shown that strained [1]ferrocenophanes containing a single silicon (**1**), germanium, or phosphorus atom in the bridge undergo thermal ring-opening polymerization (ROP) to yield high molecular weight polymers (such as **2**).[2–6] These [1]ferrocenophane monomers possess strained structures in which the cyclopentadienyl ligands are significantly tilted by about 18–27° with respect to one another.[3, 7, 8]



1 **2**

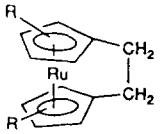
[2]Ferrocenophanes such as **3** with two silicon atoms in the bridge are substantially less strained (tilt angle = 4.19(2)°) than their [1]silaferrocenophane counterparts and appear to be resistant to ROP.[3] However, [2]ferrocenophanes which possess the smaller carbon atoms in the bridge such as **4** (R = H, R′ = Me) are significantly more strained (tilt angles = 21–23°)[9] and have been found to undergo ROP at elevated temperatures to yield poly(ferrocenylethylene)s **5**.[10]



3 **4** **5**

In this paper we report on our attempts to extend this ROP approach to allow the introduction of an alternative transition metal, ruthenium, into the polymer main chain. Since a ruthenium atom is larger than an iron atom, the incorporation of the former into an [*n*]metallocenophane structure would be expected to increase the ring-tilt and provide access to more highly strained species which should be excellent candidates for ROP. In addition, based on the different electrochemical properties of ruthenocene compared to those of ferrocene, access to polymers with modified electrical characteristics would be anticipated.[11]

In contrast to [*n*]ferrocenophanes, few [*n*]ruthenocenophanes have been prepared; none with fewer than three bridging atoms.[12] We found that the reaction of $Li_2[C_5H_4CH_2]_2$ with the Ru^{II} complex *cis*-$[RuCl_2(dmso)_4]$ (dmso = dimethylsulfoxide) yielded **6a**, the first example of a [2]ruthenocenophane, as a pale yellow microcrystalline material after purification by high vacuum sublimation. The identity of this species was verified by NMR spectroscopy, mass spectrometry, and an X-ray diffraction study of a single crystal obtained from hexane at −20 °C. The molecular structure of **6a** is shown in Figure 1.[13, 14]



6

a: R = H
b: R = Me

The most dramatic structural feature of **6a** is the tilt of the virtually planar cyclopentadienyl ligands with respect to one another.

[*] Prof. I. Manners, J. M. Nelson, Dr. A. J. Lough
Department of Chemistry, University of Toronto
80 St. George Street, Toronto M5S 1A1, Ontario (Canada)
Telefax: Int. code + (416)978-8775

[**] This work was supported by the Petroleum Research Fund (PRF), administered by the American Chemical Society, and the Natural Science and Engineering Research Council of Canada (NSERC). We also thank Johnson Matthey PLC for a generous loan of ruthenium salts.

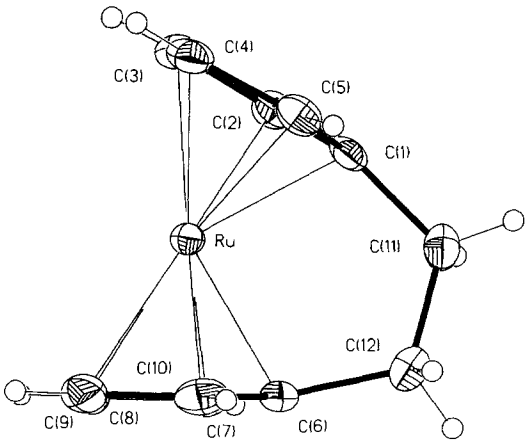


Fig. 1. Molecular structure of **6a**. Selected distances [Å] and angles [°] (estimated standard deviations in parentheses): Ru-C1 2.076(4), Ru-C2 2.156(5), Ru-C3 2.231(5), Ru-C4 2.207(6), Ru-C5 2.143(5), Ru-C6 2.073(6), Ru-C7 2.136(6), Ru-C8 2.206(6), Ru-C9 2.218(5), Ru-C10 2.146(5), C1-C11 1.523(9), C6-C12 1.525(8), C11-C12 1.549(9); C2-C1-C11 124.4(6), C5-C1-C11 127.4(5), C1-C11-C12 114.3(5), C11-C12-C6 111.5(6), C7-C6-C12 130.2(6), C10-C6-C12 121.7(6).

The tilt angle of 29.6(5)° is the largest found for any neutral [*n*]metallocenophane reported to date and is significantly greater than that present in **4** (R = H, R′ = Me) (23°). The degree of tilting in **6a** can also be appreciated by considering the $Cp_{centroid}$-Ru-$Cp_{centroid}$ angle which is 159.3(2)° compared to 180° in ruthenocene, 163.4(6)° for **4** (R = H, R′ = Me), and 164.74(8)° in **1**. Further evidence for a strained structure for **6a** is found in the average angle of 13.4(5)° between the planes of the cyclopentadienyl ligands and the C1–C11 and C6–C12 bonds. These angles reflect the significant distortion from planarity for C1 and C6 which is greater than that in **4** (R = H, R′ = Me), where the corresponding average angle is 9.6(11)°.[3, 9] Another interesting feature of **6a** is the angle between the C11–C12 bond and the plane defined by the centroids of the cyclopentadienyl ring and the ruthenium atom. The value is 21.3(5)°, which is also larger than the value of 18.4(1)° in **4** (R = H, R′ = Me), and indicates that the bridge in **6a** is slightly more twisted. This leads to a slight staggering of the cyclopentadienyl ligands in **6a** with an angle of 8.4(5)° between the projection of the Ru–C bonds on the mean plane of the cyclopentadienyl ligands.

The highly strained molecular framework of **6a** suggested that this species should be a good candidate for ROP. Indeed, when heated in the melt at 220 °C, samples of this material become viscous and then immobile; however, the resulting poly(ruthenocenylethylene) **7a** was insoluble in organic solvents. The soluble, white fibrous poly(ruthenocenylethylene) **7b** was prepared by the ROP of an isomeric mixture of dimethylated [2]ruthenocenophanes of the type **6b**.[15] Compound **6b** was prepared in a similar manner to **6a** using $Li_2[C_5H_3MeCH_2]_2$. A similar strategy was used previously for the preparation of soluble poly(ferrocenylethylene)s.[10] Polymer **7b** was characterized by ^{1}H NMR, ^{13}C NMR, and by gel permeation chromatography (GPC).[16] The ^{1}H NMR spectrum of **7b** (in C_6D_6), for example, showed resonances for the η-C_5H_3 ligand, CH_2 bridge, and Me protons in the correct integration ratio at about $\delta = 4.5$, 2.5, and 1.9, respectively (Fig. 2). The GPC showed that the polymer possessed a bimodal molecular weight distribution with a weight average molecular weight (M_w) of 43100 and a number average molecular weight (M_n) of 12000 for the first fraction, and $M_w = 12700$ and $M_n = 4400$ for the second.

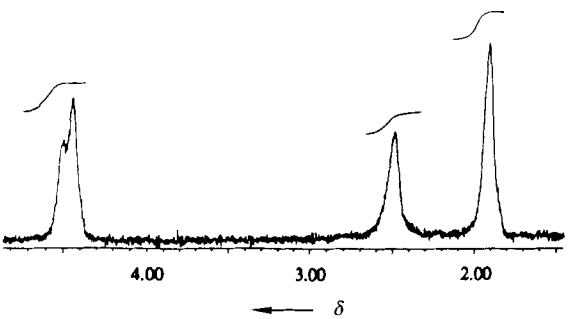
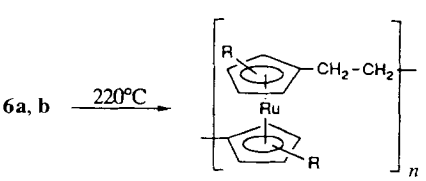


Fig. 2. ^{1}H NMR spectrum of polymer **7b**.

Detailed comparative studies of the physical properties of poly(ruthenocenylethylene)s and poly(ferrocenylethylene)s are in progress. However, even at this stage it is clear that **7b** is noticeably more resistant to oxidation than its iron analogue. This has been confirmed in preliminary cyclic voltammetry experiments which have shown that the poly(ruthenocenylethylene) **7b** possesses an irreversible oxidation wave at 0.60 V,[17] whereas the poly(ferrocenylethylene) **5** (R = Me) undergoes a reversible oxidation at −0.27 V under the same conditions.[5]



7

a : R = H
b : R = Me

Experimental Procedure

6a: A solution of $Li_2[C_5H_4CH_2]_2$ [18] (0.95 g, 5.6 mmol) in THF (40 mL) was added dropwise to a suspension of *cis*-$[RuCl_2(dmso)_4]$ [19] (2.70 g, 5.6 mmol) in the same solvent (40 mL) at −78 °C. The reaction mixture was stirred at this temperature for 3 h and was then allowed to warm to room temperature over a 12 h period. Following solvent removal in vacuo, yellow microcrystalline **6a** was isolated and purified by vacuum sublimation (80 °C, 10 mmHg). Yield 0.60 g (42%); m.p. 130 °C [13].

6b: This species was prepared similarly from $Li_2[C_5H_3MeCH_2]_2$ [10] and was purified by vacuum distillation (bp 80 °C, 10 mmHg) and was isolated as a yellow oil in 42% yield [15].

7b: Compound **6b** (0.61 g, 2.1 mmol) was placed in a sealed, evacuated Pyrex tube and heated at approximately 220 °C for 4 h. The solution gradually became more viscous and eventually immobile. Extraction with THF and precipitation into methanol produced the white fibrous poly(ruthenocenylethylene) **7b**. Yield 0.61 g (100%) [16].

Received: October 21, 1993
Revised: December 7, 1993 [Z 6438 IE]
German version: *Angew. Chem.* **1994**, *106*, 1019

[1] See, for example: S. J. Davies, B. F. G. Johnson, M. S. Khan, J. Lewis, *J. Chem. Soc. Chem. Commun.* **1991**, 187; H. B. Fyfe, M. Mlekuz, D. Zargarian, N. J. Taylor, T. B. Marder, *ibid.* **1991**, 188; M. E. Wright, M. S. Sigman, *Macromolecules* **1992**, *25*, 6055; N. Hagihara, K. Sonogashira, S. Takahashi, *Adv. Polym. Sci.* **1980**, *41*, 149; E. W. Neuse, L. Bednarik, *Macromolecules* **1979**, *12*, 187; P. Bergerat, J. Blumel, M. Fritz, J. Hiermeier, P. Hudeczek, O. Kahn, F. H. Köhler, *Angew. Chem.* **1992**, *104*, 1285; *Angew. Chem. Int. Ed. Engl.* **1992**, *31*, 1258; M. Peuckert, T. Vaahs, M. Bruck, *Adv. Mater.* **1990**, *2*, 398; J. E. Sheats,

C. E. Carraher, C. U. Pittman, *Metal Containing Polymer Systems*, Plenum, London, **1985**.
[2] D. A. Foucher, B. Z. Tang, I. Manners, *J. Am. Chem. Soc.* **1992**, *114*, 6246.
[3] W. Finckh, B. Z. Tang, D. A. Foucher, D. B. Zamble, R. Ziembinski, A. Lough, I. Manners, *Organometallics* **1993**, *12*, 823.
[4] B. Z. Tang, R. Petersen, D. A. Foucher, A. Lough, N. Coombs, R. Sodhi, I. Manners, *J. Chem. Soc. Chem. Commun.* **1993**, 523; D. A. Foucher, B. Z. Tang, P. M. Macdonald, R. Ziembinski, R. Jaeger, J. Massey, G. J. Vancso, I. Manners, *Macromolecules* **1993**, *26*, 2878; I. Manners, *J. Inorg. Organomet. Polym.* **1993**, *3*, 185, and references therein; D. A. Foucher, I. Manners, *Makromol. Chem. Rapid Commun.* **1993**, *14*, 63; I. Manners, *Adv. Mater.* **1994**, *6*, 68.
[5] D. A. Foucher, C. Honeyman, J. M. Nelson, B. Z. Tang, I. Manners, *Angew. Chem.* **1993**, *105*, 1843; *Angew. Chem. Int. Ed. Engl.* **1993**, *32*, 1709.
[6] For other reports of the formation of organometallic polymers from rings containing transition elements see, for example, H. W. Roesky, M. Lücke, *Angew. Chem.* **1989**, *101*, 493; *Angew. Chem. Int. Ed. Engl.* **1989**, *28*, 493. H. W. Roesky, M. Lücke, *J. Chem. Soc. Chem. Commun.* **1989**, 748; P. F. Brandt, T. B. Rauchfuss, *J. Am. Chem. Soc.* **1992**, *114*, 1926.
[7] H. Stoeckli, Evans, A. G. Osborne, R. H. Whiteley, *J. Organomet. Chem.* **1980**, *194*, 91; D. Seyferth, H. P. Withers, *Organometallics* **1982**, *1*, 1275; I. R. Butler, W. R. Cullen, F. W. B. Einstein, S. J. Rettig, A. J. Willis, *ibid.* **1983**, *2*, 128.
[8] The strain energy of **1** has been measured to be about 80 kJ mol^{-1}; see ref. [2].
[9] M. Burke Laing, K. N. Trueblood, *Acta. Crystallogr.* **1965**, *19*, 373.
[10] J. M. Nelson, H. Rengel, I. Manners, *J. Am. Chem. Soc.* **1993**, *115*, 7035.
[11] See for example: U. T. Mueller Westerhoff, A. L. Rheingold, G. F. Swiegers, *Angew. Chem.* **1992**, *104*, 1398; *Angew. Chem. Int. Ed. Engl.* **1992**, *31*, 1352, and references therein; N. G. Connelly, W. E. Geiger, *Adv. Organomet. Chem.* **1984**, *23*, 1.
[12] Several [3]- and [4]ruthenocenophanes have been prepared from ruthenocene by a multistep procedure involving monosubstitution followed by cyclization. S. Kamiyama, T. M. Suzuki, T. Kimura, A. Kasahara, *Bull. Chem. Soc. Jpn.* **1978**, *51*, 909. The [*n*]ruthenocenophanes [Ru(η-C_5H_4)$_2$(CH_2)$_x$] (x = 3 and 4) prepared by this route have been characterized by X-ray diffraction and have ring-tilts of 14.8(2) and 1.7(2)°, respectively. S. Ohba, Y. Saito, S. Kamiyama, A. Kasahara, *Acta Crystallogr. Sect. C* **1984**, *40*, 53.
[13] **6a**: ^{1}H NMR (200 MHz, $CDCl_3$): δ = 4.97 (t, 4H; Cp), 4.59 (t, 4H; Cp), 2.57 (s, 4H; CH_2CH_2), ^{13}C NMR: δ = 93.6 (*ipso*-C, Cp), 73.8, 72.9 (α- and β-C, Cp), 34.8 (CH_2); MS (EI, 70 eV): *m/z* (%): 258 (75) [M^+], in good agreement with isotopic abundance calculations.
[14] For **6a**: a = 6.3506(7), b = 20.7898(14), c = 7.6333(5) Å, β = 113.477(6)°, V = 924.37(14) Å^3, Z = 2, ϱ_{calcd} = 1.85 g cm^{-3}, $P2_1/c$ (no. 14); crystal dimensions 0.30 × 0.15 × 0.13 mm^3; T = 298 K; measuring range $4 < 2\theta < 54°$; 1998 independent reflections, 1581 observed with $F > 6.0\sigma(F)$, 124 refined parameters R = 0.025, Rw = 0.052. Further details of the crystal structure investigation are avaiable on request from the Director of the Cambridge Crystallographic Data Centre, 12 Union Road, GB-Cambridge CB21EZ (UK), on quoting the full journal citation.
[15] **6b**: ^{1}H NMR (200 MHz, C_6D_6): δ = 4.6–5.0 (br m, 3H; Cp), 4.3–4.5 (br m, 3H; Cp), 2.3–2.8 (s, 4H; CH_2CH_2), 1.8–2.2 (s, 6H; Me); ^{13}C NMR (100.5 MHz, C_6D_6): δ = 89.5–95.3 (*ipso*-C, Cp), 71.0–76.7 (α-, β-C, Cp), 32.2–35.3 (CH_2CH_2), 14.0–16.1 (Me). Because of the existence of different isomers the NMR spectra of **6b** consisted of numerous peaks in the regions indicated. MS (EI; 70 eV) *m/z* (%): 286 (100) [M^+] in good agreement with isotopic abundance calculations.
[16] **7b**: ^{1}H NMR (200 MHz, C_6D_6): δ = 4.3–4.6 (br, 6H; Cp), 2.4–2.6 (br, 4H; CH_2CH_2), 1.8–2.0 (br, 6H; Me); ^{13}C NMR (100.5 MHz, C_6D_6): δ = 85.5–92.2 (*ipso*-C, Cp), 74.2–78.8 (α-, β-C, Cp), 30.4–32.1 (CH_2CH_2), 12.7–14.9 (Me). Because of the existence of different isomers, the NMR spectra of **7b** consisted of numerous peaks in the regions indicated. GPC data (see text) were recorded in THF and are relative to polystyrene standards and are therefore considered estimates. The occurrence of a bimodal molecular weight distribution suggests that the polymerization may occur by two different mechanisms. Further work aimed at verifying this hypothesis is underway.
[17] Polymer solutions were 1×10^{-3} M in CH_2Cl_2 with 0.1 M [Bu_4N][PF_6] as a supporting electrolyte and are referenced relative to ferrocene/ferrocenium couple (E = 0 V). See ref. [5] for other details.
[18] H. L. Lentzner, W. E. Watts, *Tetrahedron* **1971**, *27*, 4343; S. Collins, Y. Hong, N. J. Taylor, *Organometallics* **1990**, *9*, 2695.
[19] A. Mercer, J. Trotter, *J. Chem. Soc. Dalton Trans.* **1975**, 2480.

A New Oxygen Tripod Ligand and its First Complexes with p- and d-Block Elements**

Ulrich Kölle,* Thomas Rüther, Nathalie Le Narvor, Ulli Englert, and Wolfgang Kläui

The syntheses and complexation properties of the oxygen tripod ligands [(Cp, Cp*)(Co, Rh){PO(OR)$_2$}$_3$]$^-$ (Tp^l; Cp* = C_5Me_5) have been extensively investigated in recent years.[1, 2] Octahedral [(Tp^l)$_2$M] as well as half-sandwich complexes [Tp^{l}ML$_n$] are formed with s- and d-block metals, in which L may also be an organometallic ligand. To date, only Co^{III}, Rh^{III}, and Ir^{III} have been used as the "carrier" metal for the complexing tris(phosphono) unit, thereby generating a monoanionic ligand. Since the charge influences considerably the complexation properties of the hard tripod ligand, it was desirable to increase this through the use of an M^{II} carrier metal. For this purpose, Ru (possibly Os) is the only feasible option.

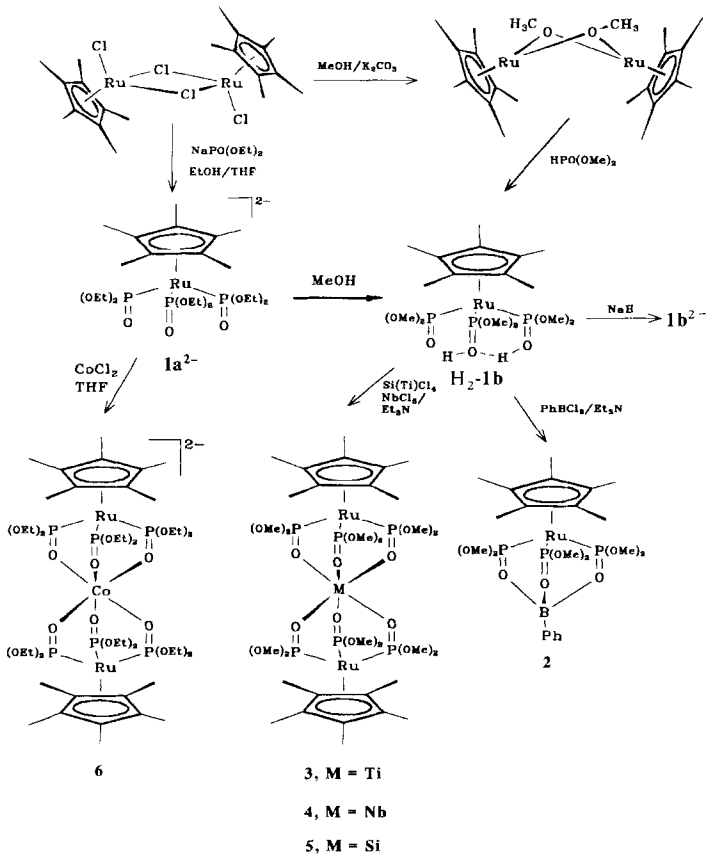
The syntheses of the sodium salts of the new dianionic tripod ligands Tp^{II}, [Cp*Ru^{II}{PO(OR)$_2$}$_3$]$^{2-}$ **1a**$^{2-}$ (R = Et) and **1b**$^{2-}$ (R = Me), proceeds according to Scheme 1, starting from [{Cp*RuCl$_2$}$_2$], by reaction with NaPO(OEt)$_2$ in EtOH/THF, where the alcohol serves as a reducing agent. After the reaction mixture had been evaporated to dryness, the salt Na_2-**1a** was extracted from the solid residue with pentane. The methoxy derivative H_2-**1b** is accessible by treatment of H_2-**1a** with methanol, or from the methoxide [{Cp*Ru(OMe)}$_2$] by reaction in ether with the phosphonic ester HPO(OMe)$_2$. H_2-**1b** is deprotonated by NaH. With alkoxides, an equilibrium mixture of H_2-**1b** and **1b**$^{2-}$ is generated, placing the second pK_a value for H_2-**1b** around that of MeOH.

In the ^{1}H NMR spectrum of H_2-**1b** in C_6D_6, the Cp* signal appears as a quartet (δ = 1.87, $^4J_{H,P}$ = 2.2 Hz) due to coupling to phosphorus; the POMe groups give rise to a virtual quartet (δ = 3.55, vq, $^3J_{H,P}$ = 11.2 Hz). For Na_2-**1a** in benzene, however, only three broad signals are observed for the three sorts of protons, suggesting an asymmetric mode of coordination, probably in the form of an oligomer.[3] In CD_3OD, the spectrum is similar to that of the acid, since the signals are averaged due to partial protonation of the salt. For H_2-**1b** in CD_3OD, the OCH_3 groups are exchanged slowly by OCD_3. If [{Cp*Ru(OMe)}$_2$] is treated with the phosphonic ester HPO(OEt)$_2$ or HPO(O^{i}Pr)$_2$, with workup in the presence of MeOH, only H_2-**1b** is obtained. This facile nucleophilic replacement of the OR groups is responsible for the spontaneous decomposition of H_2-**1** in solvents like water and acetonitrile. Such displacement reactions, however, provide easy access to complexes with different OR groups. In contrast, Tp^l compounds are quite stable.

Metals, nonmetals, and fragments L$_n$M may, under appropriate conditions, be complexed to Tp^{II} (Scheme 1). With $PhBCl_2$, the monotripod phenylborate complex **2** is obtained, by reaction with **1**$^{2-}$, or H_2-**1** (H_2-**1b** as an example) in the presence of Et_3N. Reaction of **1b**$^{2-}$ or H_2-**1b** with $TiCl_4$, $NbCl_5$, or $SiCl_4$

[*] Prof. Dr. U. Kölle, T. Rüther, N. Le Narvor,[+] U. Englert
Institut für Anorganische Chemie der Technischen Hochschule
Prof.-Pirlet Strasse 1, D-52074 Aachen (FRG)
Telefax: Int. code + (241)8888-288
Prof. Dr. W. Kläui
Institut für Anorganische Chemie und Strukturchemie der Universität
Universitätstrasse 1, D-40225 Düsseldorf (FRG)
[+] Permanent address: Laboratoire de Chimie des Organométalliques
Université de Rennes 1
Campus de Beaulieu, F-35042 Rennes (France)

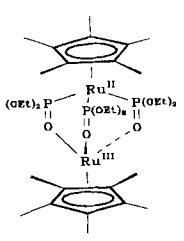
[**] This work was supported by the Deutsche Forschungsgemeinschaft and by the Fonds der Chemischen Industrie. We thank Johnson Matthey, Reading, Great Britain for a loan of $RuCl_3$.



Scheme 1. Synthesis and complexation properties of the oxygen tripod ligands **1a** and **1b**.

affords the neutral bistripod complexes **3**, **4**, and **5**, respectively. The ^{1}H NMR spectrum of the paramagnetic Nb^{IV} complex **4** reveals signals which, though broadened, show virtually no paramagnetic shifting, as was found previously for paramagnetic Tp^I complexes. The Si complex **5** is characterized by a septet in the ^{29}Si NMR spectrum at $\delta = 200$ (sixfold oxygen-coordinated Si[4]), with a ^{29}Si-^{31}P coupling of 14 Hz. Reaction of Na_2-**1a** with $CoCl_2$ in THF yielded the bistripod complex of Co^{II}(**6**), as the disodium salt. Unlike the free ligand, these pentane-soluble complexes are reasonably stable to both air and moisture.

A somewhat different type of complex was formed by the direct reaction of $[\{Cp^*RuCl_2\}_2]$ with $NaOP(OEt)_2$ in THF, in the absence of a reducing agent. Partial reduction of Ru^{III} to Ru^{II}, presumably by the phosphonate, gave rise to the deep green, paramagnetic, mixed-valence monotripod complex **7**.



7

The nonmetal complexes **2** and **5** were characterized by X-ray structure analyses.[5] With **2** (Fig. 1a), bond lengths and angles are comparable to those of the analogous Tp^I complex [CpCo-$\{P(OEt)_2O\}_3BF]BF_4$.[8] In order to obtain the structure of the particularly intriguing Si compound **5**, the more crystallizable Cp^ derivative **5'** (Cp^ = η^5-C_5Me_4Et) was prepared. This crystallizes in the space group $R\bar{3}m$; the threefold rotation axis runs through Ru, Si, and the center of the disordered Cp^ rings (Fig. 1b). Disorder of the $\{P(O)(OR)_2\}_3$ belt occurs in both structures, as is observed for many such tripod complexes.[9] The Si atom is coordinated octahedrally by oxygen; a slight compression along the threefold axis (O-Si-O angles 87.1(1) and 92.9(1)°) is observed. The Si–O distance of 1.787(2) Å is comparable to those in $[Si(1,2\text{-}(O)_2C_6H_4)_3]^{2-}$ (1.813(1), 1.775(3), 1.765(3) Å)[10] and $[HN\{(CH_2)_3O\text{-}2,3\text{-}(O)_2C_6H_3\}_3Si]Cl$,[11] the only structurally characterized examples for sixfold oxygen-coordinated molecular silicon, and are also similar to those found in hexacoordinate silicates (1.73–1.80 Å).[12] This is attributed to the variable "bite" of the tripod ligand. For both **2** and **5**, the P-Ru-P and O-P-Ru angles are, characteristically, very similar, and the variation in central atom radii is compensated solely by the different O-M-O' bond angles.

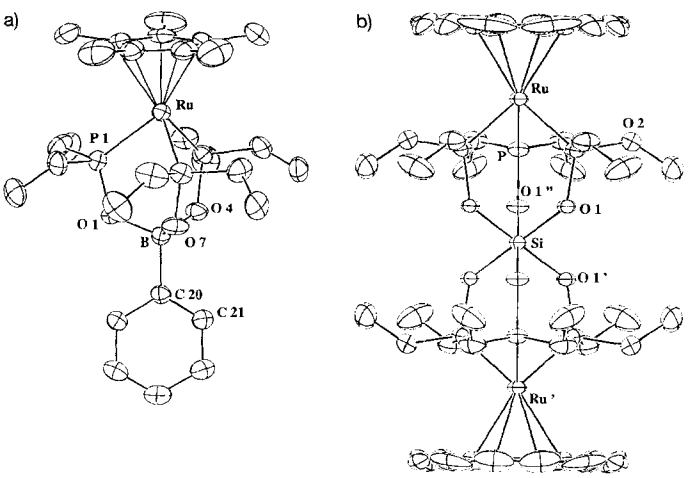


Fig. 1. a) ORTEP representation of $[Cp^*Ru\{P(O)(OMe)_2\}_3BPh]$ **2**. Selected distances [Å] and angles [°]: B-O1 1.484(6), B-O4 1.515(4), B-O7 1.456(4), B-C20 1.609(6), P-O(mean) 1.563(4), Ru-P(mean) 2.237(2), Ru-C_{Cp} 2.236–2.250(5); P-Ru-P(mean) 85.03(6), O-B-O(mean) 109.9(4). b) ORTEP representation of $[\{Cp^*\text{-}Ru[P(O)(OMe)_2]_3\}_2Si]$ **5'**. Selected distances [Å] and angles [°]: Si-O1 1.787(2), O1-P 1.545(4), O2-P 1.594(4), Ru-P 2.221(1); P-Ru-P' 86.06(5), P-O-Si 132.6(1), O1-Si-O1'' 92.9(1), O1-Si-O1' 87.6(1).

Ligand-field properties of Tp^{II} were determined from the Co^{II} complex **6**. Two absorption bands in the visible region of the spectrum, at 18620 and 17150 cm^{-1} were assigned to the transitions $^4A_{2g} \leftarrow {}^4T_{1g}$ and $^4T_{2g} \leftarrow {}^4T_{1g}$. From the ratio of wavenumbers[13] the values $Dq = 902\ cm^{-1}$ and $B = 784\ cm^{-1}$ are obtained. Thus the ligand-field strength of Tp^{II} is somewhat greater than that of Tp^I ($Dq = 825\ cm^{-1}$[12]), though less than that of water ($Dq = 981\ cm^{-1}$). The nephelauxetic parameter B is found to be significantly smaller than that of Tp^I and that of water ($B(Tp^I) = 820$, $B(H_2O) = 872\ cm^{-1}$), implying stronger covalent bonding in Tp^{II}.

The resistance of the central metal towards electrochemical redox changes is surprising. Whereas for the complexes $[(Tp^I)_2M]$, electrode reactions were measured for many d-block metals,[14, 15] the Ti^{IV} center in **3** was inert towards reduction, as was the Co^{II} center in **6** towards oxidation. The cyclic voltammogram of the Si complex **5**[15, 16] shows two almost reversible oxidation peaks ($E^1 = 0.64$, $E^2 = 0.89$ V, $\Delta E_p = 85$ mV) of equal height due to the Ru^{II}/Ru^{III} valence change of the carrier metals. This relative ease of oxidation of the ligand contrasts with the extremely redox-stable Tp^I compounds[14] and limits accordingly observable redox changes of the central metal. The potential difference of 0.25 V between the two oxidation potentials of **5** is too large for a purely electrostatic interaction over a distance of 7.74 Å (Ru ··· Ru distance in **5**) and points to some electronic coupling of the Ru atoms across the P-O-Si-O-P bridge.

The redox behavior of the Ru complex **7** provides information about the relative influence of Tp^I and Tp^{II} on the redox

 © VCH Verlagsgesellschaft mbH, D-69451 Weinheim, 1994 0570-0833/94/0909-0992 $ 10.00+.25/0 Angew. Chem. Int. Ed. Engl. 1994, 33, No. 9

potential of the central metal. An irreversible reduction at $E_p = -1.1$ V shows unequivocally, by comparison with **5**, that the oxidation state III must be assigned to the O-coordinated Ru. The reduction of the latter to Ru^{II}, under analogous conditions, is 0.7 V more negative than the Ru^{II}/Ru^{III} potential for the directly comparable complex [Tp^tRuCp^*].[15] Hence, relative to the Tp^t complexes, the redox potentials in $Tp^{II}M$ complexes again show a cathodic shift.

Thus, with the Tp^{II} system, a new, highly versatile oxygen tripod ligand has become available, whose doubly negative charge makes it particularly suitable for the stabilization of sixfold oxygen-coordinated elements in high oxidation states, and which may prove valuable as a model system for oxoanions of certain elements.

Experimental Procedure

H_2-**1b**: $HP(O)(OMe)_2$ (0.65 mL, 7.08 mmol) was syringed into a solution of $[\{Cp^*Ru(OMe)\}_2]$ (630 mg, 1.18 mmol) in Et_2O (60 mL). After stirring for 4 h at room temperature, the solvent was removed under vacuum, and the dark brown oily residue stirred with pentane (50 mL) and then filtered. Impurities and excess $HP(O)(OMe)_2$ were frozen out at -78 °C, and the pentane solution decanted. After evaporation to dryness, the product was obtained as a light brown powder (1.13 g, 85%).

2: To a solution of H_2-**1** (360 mg, 0.636 mmol) in pentane (20 mL) cooled to -78 °C was added by syringe $PhBCl_2$ (152 mg, 0.13 mL, 0.954 mmol) and Et_3N (206 mg, 0.26 mL, 1.908 mmol). A precipitate of Et_3NHCl formed immediately. After stirring for 2 h at room temperature, the mixture was filtered through cotton wool and washed several times with pentane. After evaporation of the combined pentane extracts to dryness, the product was obtained as a pale yellow powder.

3–**5**: To a solution of H_2-**1b** (623 mg, 1.1 mmol) in Et_2O (25 mL) cooled to -78 °C was added $SiCl_4$, $TiCl_4$, or $NbCl_5$ (1.1 mmol), respectively, and Et_3N (0.61 mL, 4.4 mmol). A precipitate of Et_3NHCl formed immediately. After stirring for 2 h at room temperature, the precipitated salt was filtered off, the solvent removed, the residue washed three times with methanol (10 mL) and dried.

6: To a solution of Na_2-**1a** (200 mg, 0.289 mmol) in THF (15 mL) was added a solution of $CoCl_2$ (19 mg, 0.15 mmol) in THF (4 mL), which caused an immediate decolorization of the blue solution. After 4 h at room temperature, the solvent was removed under vacuum and the solid residue extracted with pentane. The pentane solution was then concentrated to dryness under high vacuum to leave a gray-blue powder.

Na_2-**1a**: 90% Yield; ^{1}H NMR (C_6D_6): $\delta = 2.01$ (br. s; Cp*), 1.31 (br. t; $POCH_2CH_3$), 4.0 (br.; $POCH_2CH_3$); ^{31}P NMR: $\delta = 134.7$ (br. s); IR (KBr): $\tilde{\nu} = 1049$ (P-O-C), 1080 (P=O), 532 cm^{-1} (δ-P=O).

Na_2-**1b**: ^{1}H NMR (C_6D_6): $\delta = 1.98$ (br. s; Cp*), 3.53 (br.; $POCH_3$). H_2-**1b**: 85% Yield; ^{1}H NMR (C_6D_6): $\delta = 1.87$ (q, ^4J(H,P): 2.2 Hz; Cp*), 3.55 (vq, ^3J(H,P) = 11.2 Hz), 10.8 (br.; POH); ^{31}P NMR: $\delta = 144.7$; IR (KBr): $\tilde{\nu} = 1178$ (νP=O), 882 (νP-OH), 534 (δP=O), 595 cm^{-1} (δP-OH); MS: *m/z* (%): 566 (5, M^+), 565 (8, $M-H$), 534 (25, $M-MeOH$), 502 (23, $M-2MeOH$), 424 (40, $Cp^*RuP_2(O)(OH)(OMe)_3$); analysis for $C_{16}H_{35}O_9P_3Ru$ (565.5): calcd.: C, 33.98; H, 6.24; found: C, 32.97; H, 6.38.

2a: 65% Yield; ^{1}H NMR (C_6D_6): $\delta = 1.90$ (q, ^4J(H,P) = 2.2 Hz; Cp*), 3.52 (vq, ^3J(H,P) = 11.3 Hz; OMe); ^{31}P NMR: $\delta = 135.3$; IR (KBr): $\tilde{\nu} = 1056$ (νP-O-C), 1070 cm^{-1} (νP=O); MS: *m/z* (%): 652 (80, M^+), 575 (12, $M-Ph$), 542 (13, $M-P(O)(OMe)_2$); analysis for $C_{22}H_{38}BO_9P_3Ru$ (652.3): calcd.: C, 40.50; H, 5.88; found: C, 41.16; H, 5.92.

3: 48% Yield; ^{1}H NMR (C_6D_6): $\delta = 2.03$ (q, ^4J(H,P) = 2.1 Hz; Cp*), 3.68 (vq, ^3J(H,P) = 10.9 Hz; OMe); ^{31}P NMR: $\delta = 149.6$; IR (KBr): $\nu = 1046$, 1016 (νP-O-C), 1060 (νP=O), 649 cm^{-1} (δP=O); analysis for $C_{32}H_{66}O_{18}P_6Ru_2Ti$ (1174.8): calcd.: C, 32.71; H, 5.67; found: C, 32.70; H 5.76.

4: 58% Yield; ^{1}H NMR (C_6D_6): $\delta = 2.35$ (br. s; Cp*), 3.67 (br. s; OMe); ^{31}P NMR: $\delta = 148.9$; IR (KBr): $\tilde{\nu} = 1051$, 1023 (νP-O-C), 1070 cm^{-1} (P=O), FAB-MS: *m/z* (%): 1175 (44, $M-MeO_2$), 1128 (20, $M-2OMe$), 719 (45, $LNb(OMe)_2$); analysis for $C_{32}H_{66}O_{18}P_6Ru_2Nb$ (1219.8): calcd.: C, 31.51; H 5.45; found: C, 31.44; H, 5.33.

5: 46% Yield; ^{1}H NMR (C_6D_6): $\delta = 2.05$ (q, ^4J(H-P) = 2.1 Hz; Cp*), 3.68 (vq, ^3J(H-P) = 11.1 Hz; OMe); ^{31}P NMR: $\delta = 132.5$; IR (KBr): $\tilde{\nu} = 1057$, 1022 (ν P-O-C), 1090 (P=O), 555 (δP=O), 696 cm^{-1} (νSi-O); analysis for $C_{32}H_{66}O_{18}P_6Ru_2Si$ (1154.8): calcd.: C, 33.28; H, 5.77; found: C, 32.97; H, 5.92.

6: 74% Yield; ^{1}H NMR (C_6D_6): $\delta = 15$ (s, br; Cp*), 2.8 (br; OCH_2CH_3), -1.4 (br; OCH_2CH_3); IR (KBr): $\tilde{\nu} = 1042$, 1030 (νP-O-C), 1096 (P=O), 584 cm^{-1} (δP=O); FAB-MS: *m/z* (%): 1401 (57, M^+), 1355 (50, $M-2Na$), 798 (32, $L(P(O)(OC_2H_4)Co$), 649 (50, LHCo).

7: 96% Yield; ^{1}H NMR (C_6D_6): $\delta = 1.3$ (br, 18H; OCH_2CH_3), 4.08 (br, 12H; OCH_2CH_3), 2.08 (br, 15H; $Cp^*Ru^{II}P_3$), -3.03 (br, 15H; $Cp^*Ru^{III}O_3$); FAB-MS: *m/z* (%): 885 (100, M^+), 839 (20, $M-EtOH_2$), 795 (10, $M-Et_2O_2H$), 467 (20, $Cp^*RuPOH(OEt)_2$).

Received: November 6, 1993 [Z 6481 IE]
German version: *Angew. Chem.* **1994**, *106*, 1028

[1] W. Kläui, H. Otto, W. Eberspach, E. Buchholz, *Chem. Ber.* **1982**, *115*, 1922–1933.
[2] W. Kläui, *Angew. Chem.* **1990**, *102*, 661–670; *Angew. Chem. Int. Ed. Engl.* **1990**, *29*, 627–637.
[3] a) I. Goldberg, H. Shinar, G. Navon, W. Kläui, *J. Inclusion Phenom.* **1987**, *5*, 181; b) W. Kläui, A. Müller, W. Eberspach, R. Boese, I. Goldberg, *J. Am. Chem. Soc.* **1987**, *109*, 164–169.
[4] J. A. Cella, J. D. Cargioli, E. A. Williams, *J. Organomet. Chem.* **1980**, *186*, 13–17.
[5] Crystal structure analyses: ENRAF-Nonius CAD4: $Mo_{K\alpha}$ radiation, graphite monochromator. **2**: Intensity data collected at room temperature with Ω-2θ-scan; pale yellow crystal $0.3 \times 0.3 \times 0.2$ mm, monoclinic, space group $P2_1/n$ (no. 14); $a = 10.352(3)$, $b = 20.067(2)$, $c = 14.323(2)$ Å, $\beta = 98.21(2)°$, $V = 2945(2)$ Å^3, $Z = 4$, $\rho_{calcd} = 1.469$ g cm^{-3}, $\mu(Mo_{K\alpha}) = 7.25$ cm^{-1}, $F(000) = 1344$; 9258 reflections with $\theta < 30°$, of which 4085 symmetry independent with $I > 2\sigma(I)$ for structure resolution and refinement [6], 394 parameters, empirical absorption correction (PSI [7]), split positions with multiplicities of 0.75 and 0.25, respectively, due to disorder of the tripod ligand about the B–Ru axis. $R = 0.058$, $R_w = 0.063$, $w^{-1} = 1/\sigma^2(F_0)$. **5'**·CH_2Cl_2: Crystallized by slow cooling of a concentrated CH_2Cl_2 solution from room temperature to -30 °C; Ω-scan, measurements at -15 °C, colorless crystal, $0.3 \times 0.2 \times 0.2$ mm, rhombohedral, space group $R\bar{3}m$ (no. 166), hexagonal setting; $a = 15.798(6)$, $c = 18.78(1)$ Å, $V = 4060(5)$ Å^3, $Z = 3$, $\rho_{calcd} = 1.556$ g cm^{-3}, $\mu(Mo_{K\alpha}) = 9.04$ cm^{-1}, $F(000) = 1956$; 2886 reflections, with $3 < \theta < 22°$, of which 587 symmetry independent with $I > 1.5\sigma(I)$ for structure resolution and refinement [6], 80 parameters; Si in 3*m*, Ru on 3*m*, P on *m*, Cp disordered about 3, CH_2Cl_2 disordered about 3m; H atoms on the disordered rings disregarded; $R = 0.054$, $R_w = 0.070$, $w^{-1} = 1/\sigma^2(F_0)$. Further details of the crystal structure investigations may be obtained from the Fachinformationszentrum Karlsruhe, D-76344 Eggenstein-Leopoldshafen, on quoting the depository numbers CSD-400684 (**2**) and 400685 (**5'**).
[6] "The ENRAF-NONIUS CAD4-SDP – a Real-Time System for Concurrent X-Ray Data Collection and Crystal Structure Determination": B. A. Frenz in *Computing in Crystallography*. (Eds.: H. Schenk, R. Olthof-Hazekamp, H. van Koningsveld, G. C. Bassi), Universität Delft **1978**; SDP-PLUS, Version 1.1 (1984) and VAXSDP, Version 2.2 (1985).
[7] A. C. T. North, D. C. Phillips, F. S. Mathews, *Acta Crystallogr. Sect. A* **1968**, *24*, 351–359.
[8] a) W. Kläui, *Z. Naturforsch. B* **1979**, *34*, 1403–1407; b) W. Kläui, H. Neukomm, H. Werner, G. Huttner, *Chem. Ber.* **1977**, *110*, 2283–2289.
[9] A. Hörnig, U. Kölle, M. U. Schmidt, G. E. Herberich, U. Englert, *Acta Chim. Hung.* **1993**, *130*, 405–414.
[10] J. J. Flynn, F. P. Boer, *J. Am. Chem. Soc.* **1969**, *91*, 5756–5761.
[11] B. Wolff, A. Weiss, *Angew. Chem.* **1986**, *98*, 173–174; *Angew. Chem. Int. Ed. Engl.* **1986**, *25*, 162–163.
[12] F. Liebau, *Structural Chemistry of Silicates*, Springer, Berlin, **1985**, p. 31.
[13] A. B. P. Lever, *Inorganic Electronic Spectroscopy*, Elsevier, Amsterdam, **1984**, pp. 481 and Anhang V.
[14] N. El Murr, A. Chaloyard, W. Kläui, *Inorg. Chem.* **1979**, *18*, 2629–2631.
[15] U. Kölle, W. Kläui, *Z. Naturforsch. B* **1991**, *36*, 75–83.
[16] Cyclic voltammetry, CH_2Cl_2, Bu_4NPF_6, Pt working electrode, aqueous saturated calomel reference electrode ($E_{1/2}$(ferrocene$^+$/ferrocene^0) = 0.4 V, $v = 100$ mV s^{-1}).

Transannular Addition of Methyllithium to 5,12:6,11-Di[1,2]benzenodibenzo[*a*,*e*]cyclooctene and Its 5,6-Epoxy Derivative

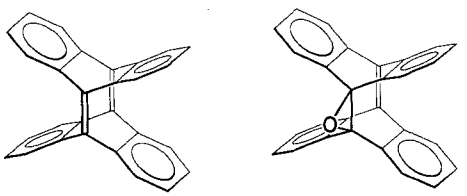
Rainer Herges,* Helfried Neumann, and Frank Hampel

Alkyllithium compounds add stereoselectively to activated double bonds in a *syn* fashion;[1–3] the corresponding ring opening of epoxides proceeds with inversion at the attacked

[*] Priv.-Doz. Dr. R. Herges, Dipl.-Chem. H. Neumann, Dipl.-Chem. F. Hampel
Institut für Organische Chemie der Universität Erlangen-Nürnberg
Henkestrasse 42, D-91054 Erlangen (FRG)
Telefax: Int. code + (9131) 85-9132

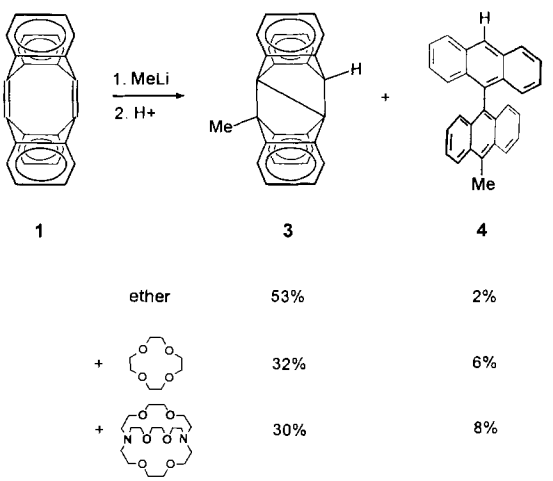
 © VCH Verlagsgesellschaft mbH, D-69451 Weinheim, 1994 0570-0833/94/0909-0993 $ 10.00+.25/0

carbon atom, presumably assisted by coordination of Li^+ to the epoxy oxygen atom.[4, 5] In the case of 5,12:6,11-di[1,2]benzenodibenzo[*a*,*e*]cyclooctene (tetradehydrodianthracene, **1**)[6] and the epoxide **2**, direct attack is only possible from the side away from the molecular framework. The backside is shielded by a double bond which is exactly coplanar with the plane of the π orbitals (or Walsh orbitals). Thus the addition of methyllithium to **1** and **2** leads to products that would not arise from the normal reaction course[7, 8] and provides indications as to the mechanism of the reaction.



1 **2**

Methyllithium reacts with **1** at room temperature in THF, and after aqueous workup two products **3** and **4** are obtained. The initially formed lithium compound, formed by *syn* addition to one of the double bonds, is apparently able to react to give either **3**,[9] by formation of a transannular bond, or **4** through electrocyclic ring opening[10] (Scheme 1). The addition of lithium-complexing ligands such as [12]crown-4 and [2.2.2]cryptand favors the formation of the ring-opened product **4**.



	1	**3**	**4**
ether		53%	2%
+		32%	6%
+		30%	8%

Scheme 1. Addition of methyllithium to **1**.

Epoxide **2**, obtained by oxidation of **1** with *meta*-chloroperbenzoic acid (*m*-CPBA), also reacts with methyllithium at $-5\,^{\circ}C$ to give compound **5**, likewise a product arising from transannular addition. The structure of **5** was confirmed by X-ray crystal structure analysis (Fig. 1).[11] In addition, compound **6** was also formed, which is formally derived from a *syn* addition to the double bond. In this case too, the ratio of products could be shifted away from the transannular compound through addition of lithium complexing ligands (Scheme 2).

The unusual transannular additions of organolithium compounds[7, 8, 12] to **1** and **2** are favored by the exact coplanarity

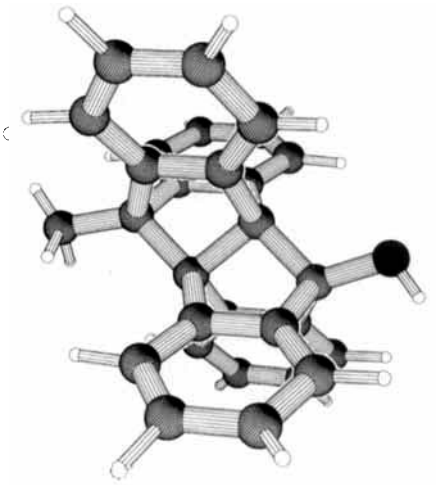
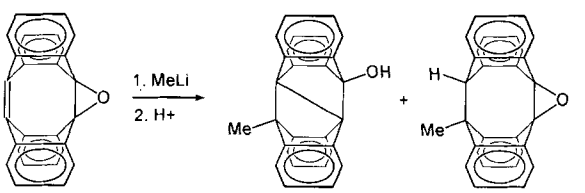


Fig. 1. Crystal structure of **5**.

and the closeness of the π orbitals of the double bonds and the π orbital of the double bond and the Walsh orbitals in the epoxide, respectively. Two possibilities exist which can explain

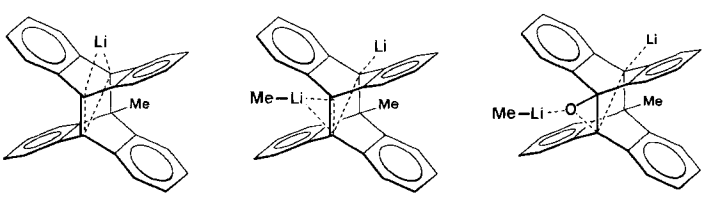


	2	**5**	**6**
ether		45%	6%
+		18%	22%
+		12%	25%

Scheme 2. Addition of methyllithium to **2**.

the alteration in the relative yields of the two products caused by the presence of complexing agents. These are represented in a simplified form as **A** and **B** in Scheme 3.

In the case of addition to **1**, both anionic benzylic positions (one of which is forming in the product, the other which is disappearing in the starting material) could be bridged by lithium in the transition state (transition state **A**). This coordinative stabilization of the transition state would be lost through



A **B** **C**

Scheme 3. Simplified mechanisms of the transannular addition to **1** and **2**.

increasing complexation of the lithium. The yield of **3** is reduced in favor of ring opening leading to **4**. An alternative explanation is that complexation of the double bond by a second equivalent of lithium facilitates the transannular mode of reaction (transition state **B**). Since the reaction was carried out in ether, alternative **A** is more likely.[13]

It is probable that the transannular ring opening of the epoxide proceeds by a mechanism involving transition state **C**, with the participation of a second equivalent of lithium. The "normal" ring opening of the epoxides, which is assisted by coordination of lithium at the epoxide oxygen atom, has been supported by theoretical calculations by von Schleyer et al.,[4] by isolation of the corresponding intermediate by Harder et al.,[5] and by kinetic measurements in several solvents with and without addition of complexing ligands by Chang et al.[14]

Experimental Procedure

2: **1** (1 g, 2.84 mmol) was dissolved in dichloromethane (1.2 L) and cooled to 0 °C. A solution of *m*-CPBA (581 mg, 3.37 mmol) in dichloromethane (70 mL) was then slowly added dropwise. The yellow solution was filtered through a chromatography column filled with silica gel and the eluate distilled off. The residue was suspended in dichloromethane/hexane (1:2), filtered, and washed. A white or pale yellow solid was obtained. Yield 900 mg, (86%); decomp. 276 °C, R_f value: (0.28 in dichloromethane/hexane 1:2). Purity: 80% product. According to GC and ^{13}C NMR the product contained about 10% diepoxide and 10% starting material **1**. These impurities were very difficult to separate by crystallization or chromatography; however, the impurities did not disturb the further reactions, since they were either unreactive or were converted to known products. - IR (KBr): $\tilde{\nu}[cm^{-1}] = 3060$ (w, C–H, arom.), 1450 (m, C=C, arom.), 910, (s, C–O). ^1H NMR (400 MHz, $CDCl_3$): $\delta = 7.1$ (m, 8H), 6.9 (m, 8H); ^{13}C NMR (100.6 MHz, $CDCl_3$): $\delta = 151.3$ (C=C), 146.7 (C, arom.), 139.3 (C,arom.), 126.3 (CH, arom.), 126.0 (CH, arom.), 124.1 (CH, arom.), 122.7 (CH, arom.), 72.1 (CO). MS (70 eV): *m/z* (%): 368 (100, M^+), 339 (35), 337 (27).

3 and **4**: **1** (200 mg, 0.57 mmol) was dissolved in dry THF (220 mL) under an atmosphere of nitrogen. Methyllithium (1.3 mL, 0.75 mmol, 0.58 M solution) was added at room temperature with a syringe to the stirred solution. After 15 min the solution, which had turned brown, was treated with a saturated $NaHCO_3$ solution (ca. 3 mL). This led to an almost complete loss of color. The THF was removed under vacuum to obtain a yellow solid, which was shaken with dichloromethane and water. After concentration of the organic solvent the residue was chromatographed (dichloromethane/hexane, 1:2). Two products could be isolated. **3**: Yield 111 mg (53%), white crystalline solid, decomp.: 232–236 °C, R_f value: 0.3 (dichloromethane/hexane, 1:2). - IR (KBr): $\tilde{\nu}[cm^{-1}] = 3080$ (m, C–H, arom.), 2990 (m, C–H, aliph.), 1430, 1460 (m, C=C, arom.). ^1H NMR (400 MHz, $CDCl_3$): $\delta = 7.21$ (d, $^3J = 6.71$ Hz, 2H; *o*-H, arom.), 7.08 (d, $^3J = 7.3$ Hz, 2H; *o*-H, arom.), 7.02 (d, $^3J = 7.02$ Hz, 2H; *o*-H, arom.), 6.92 (d, $^3J = 7.07$ Hz, 2H; *o*-H, arom.), 6.82 (t, $J = 7.32$ Hz, 4H; *m*-H, arom.), 6.75 (m, $J = 6.10$ Hz, 4.58 Hz, 4H; *m*-H, arom.), 4.95 (s, 1H; CH), 2.36 (s, 3H; CH_3); ^{13}C NMR (100.6 MHz, $CDCl_3$, DEPT): $\delta = 155.6$ (C, arom.), 153.5 (C arom.), 147.2 (C, arom.), 147.2 (C, arom.), 125.4 (CH, arom.), 125.2 (CH, arom.), 127.7 (CH, arom.), 124.7 (CH, arom.), 122.6 (CH, arom.), 122.3 (CH, arom.), 122.1 (CH, arom.), 119.7 (CH, arom.), 97.7 (C, aliph.), 95.0 (C, aliph.), 55.4 (CCH_3), 50.2 (CH, aliph.), 12.0 (CH_3). MS (70 eV): *m/z* (%): 368 (100, M^+), 354 (11), 353 (41), 352 (26), 351 (21), 350 (20).

4: Yield: 4.6 mg (2%), m.p. 238 °C, R_f value: 0.5 (dichloromethane/hexane, 1:2). - ^1H NMR (400 MHz, $CDCl_3$): $\delta = 8.67$ (s, 1H; 9'-H), 8.45 (d, $^3J = 9.16$ Hz, 2H; 1',8'-H), 8.14 (d, $^3J = 8.85$ Hz, 2H; 1,8-H), 7.47 (m, 4H; 2,2',7,7'-H), 7.10 (m, 4H, 4,4',6,6'-H), 3.30 (s, 1H; CH_3); ^{13}C NMR (100.6 MHz, $CDCl_3$): $\delta = 133.7$ (C), 131.8 (C), 131.3 (C), 130.9 (C), 131.5 (10-C), 130.0 (10'-C), 128.5 (9'-CH), 127.6 (9-C), 128.4 (CH), 127.0 (CH), 125.8 (CH), 125.7 (CH), 125.3 (CH), 125.2 (CH), 125.2 (CH), 124.9 (CH), 14.3 (CH_3).

5 and **6**: **2** (200 mg, 0.54 mmol) was dissolved in THF (60 mL) under nitrogen, and cooled to −5 °C with ice/salt. Methyllithium (1.24 mL, 0.72 mmol, 0.58 M solution) was added and the solution slowly darkened. The solution was stirred for a further 15 min to complete the reaction and was then quenched with a saturated $NaHCO_3$ solution until the brown solution became almost colorless. The solvent was removed under vacuum and the residue shaken with dichloromethane and water. The dichloromethane was removed under vacuum and the residue was chromatographed over silica (dichloromethane/hexane, 5:1). Two products could thus be isolated and characterized. **5**: Yield: 90 mg (43%), decomp. 280 °C, white crystalline solid, R_f value: 0.17 (dichloromethane/hexane, 5:1). - IR (KBr): $\tilde{\nu}[cm^{-1}] = 3450$ (b, O–H), 3080 (m, C–H, arom.), 2990 (m, C–H aliph.), 1430, 1460 (m, C=C, arom.). ^1H NMR (400 MHz, $CDCl_3$): $\delta = 7.26$ (d, $^3J = 7.3$ Hz, 2H; *o*-CH), 7.10 (d, $^3J = 6.4$ Hz, *o*-CH), 7.09 (d, $^3J = 4.5$ Hz, 2H; *o*-CH), 6.98 (d, $^3J = 7.3$ Hz, 2H; *o*-CH), 6.78 (m, 8H; *m*-CH), 3.17 (s, 1H; OH), 2.35 (s, 3H; CH_3); ^{13}C NMR (100.6 MHz, $CDCl_3$, DEPT): $\delta = 155.5$ (C, arom.), 153.0 (C, arom.), 146.5 (C, arom.), 145.4 (C, arom.), 125.8 (CH, arom.), 125.4 (CH, arom.), 125.0 (CH, arom.), 124.9 (CH, arom.), 122.7 (CH, arom.), 122.4 (CH, arom.), 119.8 (CH, arom.), 119.0 (CH, arom.), 96.5 (C, aliph.), 93.1 (C, aliph.), 88.4 (C–OH), 55.4 ($C-CH_3$), 12.1 (CH_3). MS (70 eV): *m/z* (%): 384 (100, M^+).

6: The fast running fractions with $R_f > 0.2$ were collected and dried under vacuum. The residue was chromatographed again with dichloromethane/hexane (1:2). The white solid obtained in this way still contained small amounts of diepoxide and **3**. Yield: 12 mg (6%), white crystalline solid, R_f value: 0.27 (dichloromethane/hexane, 1:2). - IR (KBr): $\tilde{\nu}[cm^{-1}] = 3060$ (m, C–H, arom.), 2990, 2940 (m, C–H, aliph.), 1430, 1460 (m, C=C, arom.). ^1H NMR (400 MHz, $CDCl_3$): $\delta = 7.11$ (m, 8H; CH arom.), 6.91 (m, 8H; CH arom.), 4.04 (s, 1H; CH aliph.), 2.15 (s, 3H; CH_3); ^{13}C NMR (100.6 MHz, $CDCl_3$, DEPT): $\delta = 146.3$ (C arom.), 144.0 (C arom.), 140.0 (C arom.), 139.4 (C arom.), 126.7 (CH arom.), 126.3 (CH arom.), 126.0 (CH arom.), 126.0 (CH arom.), 125.7 (CH arom.), 123.6 (CH arom.), 122.2 (CH arom.), 121.9 (CH arom.), 72.5 (CO), 71.7 (CO), 63.0 (CH, aliph.), 52.1 (CCH_3), 25.0 (CH_3). MS (70 eV): *m/z* (%): 384 (100, M^+), 368 (64), 353 (18), 352 (12), 351 (8), 350 (8), 176 (42).

The reactions with complexing agents were carried out analogously; in each case two equivalents of either crown ether or cryptand (with respect to **1** and **2**) were added to the solution before the addition of methyllithium.

Received: November 30, 1993
Revised: December 21, 1993 [Z6526IE]
German version: *Angew. Chem.* **1994**, *106*, 1024

[1] K. N. Houk, N. G. Rondan, P. von R. Schleyer, E. Kaufmann, T. Clark, *J. Am. Chem. Soc.* **1985**, *107*, 2821.
[2] R. D. Bach, K. W. Bair, C. L. Willis, *J. Organomet. Chem.* **1974**, *77*, 31.
[3] J. G. Welch, R. M. Magid, *J. Am. Chem. Soc.* **1967**, *89*, 5300.
[4] S. Harder, J. H. van Lenthe, N. J. R. van E. Hommes, P. von R. Schleyer, *J. Am. Chem. Soc.*, in press.
[5] S. Harder, J. Boersma, L. Brandsma, J. A. Kanters, J. M. Duisenberg, J. H. van Lenthe, *Organometallics* **1990**, *9*, 511.
[6] R. L. Viavatenne, F. D. Greene, L. D. Cheung, R. Majeste, L. M. Trefonas, *J. Am. Chem. Soc.* **1974**, *96*, 4342.
[7] Additional anionically induced transannular reactions of systems containing double bonds arranged parallel: a) D. Hellwinkel, H.-J. Hasselbach, F. Lämmerzahl, *Angew. Chem.* **1984**, *96*, 713; *Angew. Chem. Int. Ed. Engl.* **1984**, *23*, 705; b) G. Wittig, E. Hahn, *Angew. Chem.* **1960**, *72*, 781; c) G. Wittig, J. Otten, *Tetrahedron Lett.* **1963**, 600.
[8] Additional anionically induced transannular ring-opening reactions of epoxides: a) A. P. Davis, G. J. Hughes, P. R. Lowndes, C. M. Robbins, E. J. Thomas, G. H. Witham, *J. Chem. Soc. Perkin Trans 1* **1981**, 1934; b) V. Cere, C. Paolucci, S. Pollicino, E. Sandri, A. Fava, *J. Org. Chem.* **1991**, *56*, 4513.
[9] The parent compound of **3** is known: D. E. Applequist, R. L. Little, E. C. Friedrich, R. E. Wall, *J. Am. Chem. Soc.* **1959**, *81*, 452.
[10] N. M. Weinshenker, F. D. Greene, *J. Am. Chem. Soc.* **1959**, *81*, 452.
[11] Crystal structure analysis of **5**: $C_{29}H_{24}O$, $M = 388.48$, monoclinic, space group $P2(1)/c$, $a = 9.150(4)$, $b = 14.483(9)$, $c = 8.030(4)$ Å, $V = 979.6(9)$ Å^3, $Z = 2$, $\rho_{calcd} = 1.317$ Mg m^{-3}, $F(000) = 412$, $\lambda(Mo_{K\alpha}) = 0.71073$, $T = 200(2)$ K. Data was collected on a Nicolet-R3 four-circle diffractometer with graphite monochromated $Mo_{K\alpha}$ radiation in the range $4° \leq 2\theta \leq 54°$ (4553 reflections measured, of which 2175 were independent). Structure was solved with direct methods (G. M. Sheldrick, *Acta Crystallogr. Sect. A* **1990**, *46*, 467). Full-matrix least squares refinement using F^2 (SHELXL 93, G. M. Sheldrick, Göttingen, **1993**). All non-hydrogen atoms were anisotropically refined; the hydrogen atoms were localized by difference Fourier synthesis and refined isotropically by using the riding model; 139 parameters; *R*-value for $[I > 2\sigma(I)]$: $R1 = 0.0622$; $wR2 = 0.1693$. Further details of the crystal structure investigation can be obtained from The Director of the Cambridge Crystallographic Data Centre, 12 Union Road, GB-Cambridge CB21EZ (UK), on quoting the full literature citation.
[12] The corresponding products were obtained with butyllithium in somewhat lower yields.
[13] Even such an electron-rich double bond as found in didehydrodianthracene should be scarcely capable of competing against an ether donor ligand.
[14] C. J. Chang, R. F. Kiesel, T. E. Hogen-Esch, *J. Am. Chem. Soc.* **1973**, *95*, 8446.

 © VCH Verlagsgesellschaft mbH, D-69451 Weinheim, 1994 0570-0833/94/0909-0995 $ 10.00+.25/0

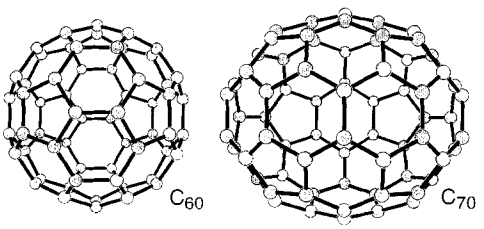
C_{70} Is More Stable than C_{60}: Experimental Determination of the Heat of Formation of C_{70}**

Hans-Dieter Beckhaus, Sergej Verevkin, Christoph Rüchardt,* François Diederich,* Carlo Thilgen, Hans-Ulrich ter Meer, Holger Mohn, and Wolfgang Müller

Before the chemistry of C_{60} took the current fast development,[1] the first two years following the landmark discovery of how to prepare macroscopic amounts of fullerenes by Krätschmer and Huffman[2] were characterized mainly by investigations of the physical properties of fullerenes.[3] However, it took more than a year for a fundamental thermodynamic quantity of C_{60}—its heat of combustion –to be determined.[4–7] This time lapse was due to problems with both the production of highly pure C_{60} in sufficient quantities and the accuracy of calorimetric measurements on small samples—a procedure which is still far from trivial.

Both problems are reflected by large differences among the values published in the literature,[4–7] a fact that led us to reinvestigate the thermodynamic data in question. Reliable values for the heat of formation of the carbon spheres are of great importance not only because they provide an experimental criterion for the quality of theoretical calculations on fullerene structures, but also because they give an insight into the stability of C_{60} and of highly strained molecules in general.

Even though C_{60}, the most strained molecule known so far, is much higher in energy than the other two carbon allotropes graphite and diamond, it exhibits a surprising kinetic stability. With regard to the higher fullerenes C_n ($n \geq 70$), the question arises whether the incorporation of additional six-membered rings into a carbon network with a fixed number (12) of five-membered rings leads to a continuous increase in stability, asymptotically approaching the value of graphite.[8] The determination of the heat of combustion of C_{70} reported here provides the second experimental point on a curve describing the thermodynamic stability of fullerenes as a function of their size.



A redetermination of the heats of formation of C_{60} and C_{70} was made possible because sufficiently large quantities of highly pure samples were provided by Hoechst AG. In order to exclude any contamination by solvent molecules,"gold grade C_{60}" and "gold grade C_{70}" were both subjected to fractional sublimation using helium as the transport gas at 600 and 650 °C/atmospheric pressure, respectively, and stored under argon prior to use. Taking into account the differences in molar extinction coefficients of the two fullerenes, the composition of the C_{60} sample (99.82% C_{60} and 0.18% $C_{60}O$) and the C_{70} sample (0.44% C_{60} and 99.56% C_{70}) was determined by analytical HPLC (Fig. 1).

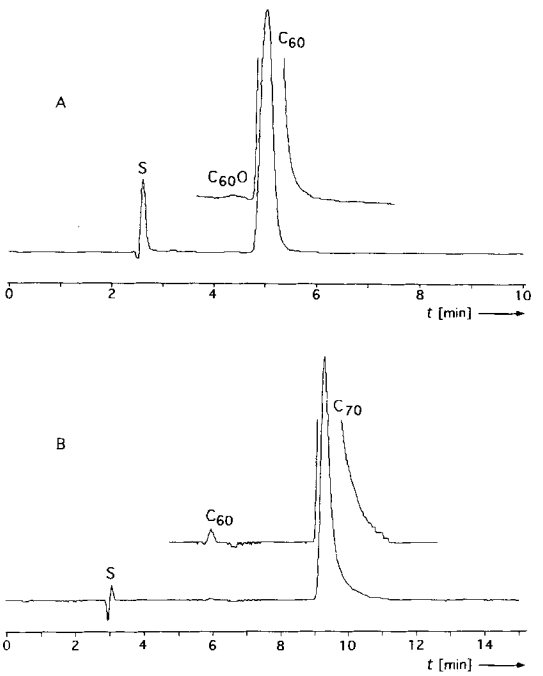


Fig. 1. HPL chromatograms of the sublimed C_{60} (A) and C_{70} (B) samples. Conditions: Vydac 201TP54 C18 reversed-phase column, 250 × 4.6 mm, acetonitrile/toluene 1/1, 1 mL min^{-1}, λ = 310 nm, S = solvent peak.

Chromatographic analysis with pure hexane as the eluent and detection at 254 nm showed that the sublimed samples did not contain any toluene from previous operations.

The heat of combustion measurements were performed in an isoperibolic aneroid microcalorimeter[9] and in a water-stirred isoperibolic macrocalorimeter[10] (Table 1). Adsorbed argon was removed from the pelletized samples by heating at 350 °C/10^{-4} bar for 2 h. The pellets were cooled under vacuum and exposed to N_2 just prior to weighing. Preliminary experiments were used to test the sample stability against oxygen, because under the experimental conditions preceding ignition (30 bar O_2, H_2O saturation), a reversible weight increase was observed. In fact, 1–2 moles of O_2 per mole of fullerene were absorbed in 0.5 h, and after 1 d of exposure, even more than 5 moles of O_2 had been absorbed per mole of C_{70}. According to analytical HPLC, however, this did not lead to a chemical transformation of the fullerenes; in particular, the amount of fullerene oxide did not increase. A control experiment using a C_{60} sample sealed in polyethylene under N_2 gave a $\Delta H_c^{\ominus}$ value within the experimental error of the measurements performed on nonsealed samples (Table 1, Experiment 2). Whereas the combustion of C_{60} was complete in each experiment, that of C_{70}, in some cases, led to the formation of traces of soot which were weighed and taken into account in the calculation.[11] The reduction to the isothermal bomb process with c_p = 0.71 (C_{60}) and 0.79 J K^{-1}g^{-1} (C_{70})

[*] Prof. Dr. C. Rüchardt, Dr. H.-D. Beckhaus, Dr. S. Verevkin
Institut für Organische Chemie und Biochemie der Universität
Albertstrasse 21, D-79104 Freiburg (FRG)
Telefax: Int. code + (761)203-5987
Prof. Dr. F. Diederich, Dr. C. Thilgen
Laboratorium für Organische Chemie, ETH-Zentrum
Universitätstrasse 16, CH-8092 Zürich (Switzerland)
Telefax: Int. code + (1)261-3524
Dr. H.-U. ter Meer, Dr. H. Mohn, Dr. W. Müller
Hoechst AG, D-65926 Frankfurt am Main (FRG)

[**] This work was supported by the Schweizerischen Nationalfonds zur Förderung der wissenschaftlichen Forschung, by the Deutsche Forschungsgemeinschaft, and by the Fonds der Chemischen Industrie.

Table 1. Results from representative combustion experiments for C_{60} and C_{70} [a].

Sample Calorimeter	C_{60} micro [b]	C_{60} macro [c]	C_{70} micro [b]	C_{70} micro [b]	C_{70} macro [c]
ε_{calor} [J K^{-1}]	1481.04	25088.10	1474.78	1474.78	25088.10
($\pm$s) [%] [d]	($\pm$0.018)	($\pm$0.0042)	($\pm$0.020)	($\pm$0.020)	($\pm$0.0042)
m (fullerene) [g]	0.038343	0.025349	0.039070	0.044296	0.260105
m' (fuse) [g]	0.000500	0.000914	0.000697	0.000636	0.000924
m'' (PE) [g] [e]	–	0.474686	–	–	–
ΔT_c [K] [f]	0.93492	0.91327	0.95600	1.08061	0.37177
ε_{color} ($-\Delta T_c$) [J]	−1384.66	−22912.2	−1409.91	−1593.68	9327.07
ε_{cont} ($-\Delta T_c$) [J] [g]	−2.57	−12.67	−2.59	−5.07	−8.1
$\Delta E_{corr.}$ [J] [h]	1.19	7.65	1.22	2.13	7.58
ΔE_{soot} [J] [i]	–	–	–	−1.38	−3.34
$\Delta E_{decomp.}$ (HNO_x) [J] [k]	–	0.03	–	–	–
$-m'\Delta u_c$ (fuse) [J]	8.48	15.48	11.82	10.78	15.65
$-m''\Delta u_c$(PE) [J]	–	21991.2	–	..	-
Δu_c (fullerene) [J g^{-1}]	−35982	−35921	−35780	−35783	−35795
$\Delta H_c^{\ominus}$ (fullerene) [kJ mol^{-1}]	−25928	−25896	−30083	−30086	−30096

[a] Measured and calculated quantities see ref. [12]; buoyancy correction of the weighing carried out with $\rho = 1.76$ (C_{60}) and 1.69 g cm^{-3} (C_{70}), $T_h = 25$ °C, p^i (gas) = 30.00 atm (30.45 bar), $T^f = 25.00 \pm 0.01$ °C, Δu_c(fuse) = -16945 ± 4 J g^{-1}. [b] Aneroid microcalorimeter ref. [9], $V_{bomb} = 0.046$ l, $\Delta E_{ignit} = 1.51$ J, $m^i(H_2O) = 0.23$ g, $m_{platinum} = 2.461$ g. [c] Water-stirred macrocalorimeter ref. [10], $V_{bomb} = 0.266$ l, $\Delta E_{ignit} = 1.46$ J, $m^i(H_2O) = 0.78$ g, $m_{platinum} = 13.13$ g. [d] From calibration measurements with benzoic acid, National Bureau of Standards, ref. sample 39i; s: standard deviation from the mean value. [e] Polyethylene ampoule, Δu_c(PE) = -46372.9 ± 2.9 J g^{-1}. [f] $\Delta T_c = T^f - T^i + \Delta T_{corr.}$ [g] $\varepsilon_{cont}(-\Delta T_c) = \varepsilon^i_{cont}(T^i - T_h) + \varepsilon^f_{cont}(T_h - T^f + \Delta T_{corr})$. [h] Sum of the items 81–85, 87–90, 93 and 94 in ref. [12]. [i] Heat correction for incomplete combustion (33 J per mg soot), ref. [11]. [k] Heat correction on account of the formation of nitrous and nitric acid (titrated).

and to standard conditions was carried out according to the usual procedure.[12] Table 1 shows representative results obtained with both kinds of calorimeters. Table 2 contains the different $\Delta H_c^{\ominus}$ values, their averages, and the resulting standard heats of formation $\Delta H_f^{\ominus}$ of C_{60} and C_{70}.

Table 2. Calorimetrically determined heats of combustion $\Delta H_c^{\ominus}$(c) and standard heats of formation $\Delta H_f^{\ominus}$(c) of C_{60} and C_{70} [kJ mol^{-1}].

	C_{60}	C_{70}
$\Delta H_c^{\ominus}$(c)	−25928	−30083
	−25983	−30128
	−25966	−30086
	−25900	−30124
	−25913	−30096
		−30078
Mean	−25937	−30101
$\pm$s [a]	$\pm$16	$\pm$10
	(= 0.061%)	(= 0.033%)
$\Delta H_f^{\ominus}$(c)	2327	2555
$\pm$s [b]	$\pm$17	$\pm$12
$\Delta H_f^{\ominus}$(c,C) per C atom	38.78 [c]	36.50 [d]
	$\pm$0.28	$\pm$0.17

[a] Standard deviation of the mean value. [b] Standard deviations of all measurements considered. [c] 9.269 $\pm$ 0.068 kcal mol^{-1}. [d] 8.724 $\pm$ 0.041 kcal mol^{-1}.

Since the deviations in the enthalpy of combustion caused by the impurities of 0.44% C_{60} in the C_{70} sample and 0.18% $C_{60}O$ [13] in the C_{60} sample are no larger than 0.7 kJ mol^{-1} and -0.5 kJ mol^{-1}, respectively, no corrections were made to the measured values.

The experimental results were compared to calculated standard gas phase heats of formation $\Delta H_f^{\ominus}$ (g, C) obtained with the use of the enthalpy of sublimation $\Delta H_{sub}^{\ominus}$ determined for C_{60} [14] (Table 3). Iterative MM3[16] force-field-MO calculations on both fullerenes afforded the $\Delta H_f^{\ominus}$(g, C) values given in Table 3.

The redetermination of the heat of formation $\Delta H_f^{\ominus}$ (g, C) per C atom of C_{60} using sublimed samples led to a value (10.16 kcal mol^{-1}) that is slightly higher than the one determined previously by us (10.01 kcal mol^{-1}). Both numbers are in

Table 3. Heat of formation $\Delta H_f^{\ominus}$ (g, C) per C atom of C_{60} and C_{70} [kcal mol^{-1}] [a].

	Method	Ref.	$\Delta H_f^{\ominus}$ (g, C) per C atom	$\pm$s [b]
C_{60}	exp.		10.16	0.06
	exp.	[4]	10.01	0.02
	exp.	[5]	10.58	0.06
	exp.	[6]	9.98	0.06
	exp.	[7]	10.01	0.06
	MM3		9.49	
	increment	[17]	10.57	
	MNDO	[18]	14.5	
C_{70}	exp.		9.65	0.03
	exp.	[6]	9.03	
	MM3		9.10	
	increment	[17]	9.27	
	MNDO	[18]	13.4	
	ab initio	[19]	(Δ −0.91, C_{60} = 0.0) [c]	

[a] With $\Delta H_{sub}^{\ominus}$(c) (298 K, per C atom) = 0.93 kcal mol^{-1} [14]. ΔH_f(298 K, per C atom, graphite) = 0, ΔH_f(298 K, per C atom, diamond) = 0.4 kcal mol^{-1} (1 kcal = 4.184 kJ). [b] From the spread of the heat of combustion of the crystalline samples. [c] Hartree–Fock/double zeta plus polarization (HF/DZP) energy of MNDO structures relative to C_{60}.

relatively good agreement with the results of Kiyobayashi et al.[6] and Diogo et al.[7]. The present experimental data are best reproduced by MM3 and the incremental method, both affording values which are only slightly lower and higher, respectively. In contrast, the numbers derived from MNDO (MNDO = Modified Neglect of Differential Overlap) calculations are much higher. The difference in energy between the two fullerenes is reasonably well reflected by relative ab initio energies (LYP/DZP)(LYP = Lee–Yang–Parr/double zeta plus polarization)[19] obtained from calculations based on MNDO-approximated structures.

The $\Delta H_f^{\ominus}$ (g, C) value determined for C_{70} (9.65 kcal mol^{-1}) is lower by 0.51 kcal mol^{-1} compared to that of buckminsterfullerene. This can be interpreted as the first confirmation of the prediction stating that fullerenes show a decrease in $\Delta H_f^{\ominus}$(g, C) with increasing number of C atoms. It should not be forgotten, however, that higher fullerenes C_n with $n \geq 78$ can exist in a

 © VCH Verlagsgesellschaft mbH, D-69451 Weinheim, 1994 0570-0833/94/0909-0997 $ 10.00+.25/0

number of isomeric forms which may differ considerably in strain and hence in energy content.[20]

Among the theoretical methods used for the calculation of the heat of formation of C_{70}, MM3 and the incremental method give the best results (both providing values which are slightly lower than the experimental ones), whereas the number resulting from MNDO calculations is much higher. From these comparisons it can be concluded that the first two methods mentioned are best suited for the prediction of the heat of formation of higher fullerenes. Due to the lack of availability of these carbon spheres in quantities large enough for experimental measurements, knowledge about their stability will have to rely on theoretical calculations for some time.

Received: December 11, 1993 [Z 6557 IE]
German version: *Angew. Chem.* **1994**, *106*, 1033

[1] a) R. Taylor, D. R. M. Walton, *Nature (London)* **1993**, *363*, 685–693; b) A. Hirsch, *Angew. Chem.* **1993**, *105*, 1189–1192; *Angew. Chem. Int. Ed. Engl.* **1993**, *32*, 1138–1141.
[2] W. Krätschmer, L. D. Lamb, K. Fostiropoulos, D. Huffman, *Nature (London)* **1990**, *347*, 354–358.
[3] a) *Buckminsterfullerenes* (Eds.: W. E. Billups, M. A. Ciufolini), VCH, New York, **1993**; b) *The Fullerenes* (Eds.: H. W. Kroto, J. E. Fischer, D. E. Cox), Pergamon Press, Oxford, **1993**; c) *Acc. Chem. Res.* **1992**, *25*, 98–175.
[4] H.-D. Beckhaus, C. Rüchardt, M. Kao, F. Diederich, C. S. Foote, *Angew. Chem.* **1992**, *104*, 69–70; *Angew. Chem. Int. Ed. Engl.* **1992**, *31*, 63–64.
[5] W. V. Steele, R. D. Chirico, N. K. Smith, W. E. Billups, P. R. Elmore, A. E. Wheeler, *J. Phys. Chem.* **1992**, *96*, 4731–4733.
[6] T. Kiyobayashi, M. Sakiyama, *Annual Report of Microcalorimetry Research Center* (Faculty of Science, Osaka University) **1992**, *13*, 58; *Fullerene Sci. Technol.* **1993**, *1*, 269–273.
[7] H. P. Diogo, M. E. Minas da Pielade, T. J. S. Dennis, J. P. Hara, H. W. Kroto, R. Taylor, D. R. M. Walton, *J. Chem. Soc. Faraday Trans.* **1993**, *89*, 3541–3544.
[8] a) B. L. Zhang, C. H. Xu, C. Z. Wang, C. T. Chan, K. M. Ho, *Phys. Rev. B.* **1992**, *46*, 7333–7336; b) J. Tersoff, *ibid.* **1992**, *46*, 15546–15546.
[9] H.-D. Beckhaus, C. Rüchardt, M. Smisek, *Thermochim. Acta* **1984**, *79*, 149–159.
[10] S. Sunner in *Combustion Calorimetry, Vol. 1* (Eds.: S. Sunner, M. Månsson), Pergamon Press, Oxford, **1979**, Ch. 2. The calorimeter from the Chemical Center, Universität Lund, Sweden, was equipped with a tempering unit for the external bath by BASF AG, Ludwigshafen (temperature stability ±0.001 K). We thank BASF for the generous gift of the calorimeter.
[11] A. J. Head, W. D. Good, C. Mosselman in *Combustion Calorimetry, Vol. 1* (Ed.: S. Sunner, M. Månsson), Pergamon Press, Oxford, **1979**, Ch. 8.
[12] W. N. Hubbard, D. W. Scott, G. Waddington in *Experimental Thermochemistry, Vol. 1* (Ed.: F. D. Rossini), Interscience, New York, **1956**, Ch. 6.
[13] For $C_{60}O$ a value for ΔH_f°(g) of 2110 kJ mol^{-1} may be calculated from the isodesmic reaction (ΔH_f°(g)[kJ mol^{-1}]): $C_{60}H_2$ (2078.5 from MM3 calculation [13a]) + oxirane (−52.6 [13b]) → ethane (−83.8 [13b]) + $C_{60}O$. a) For the preparation of and force-field calculation on hydrogenated fullerenes see: M. Gerst, H.-D. Beckhaus, C Rüchardt, E. E. B. Campbell, R. Tellgmann, *Tetrahedron Lett.* **1993**, *34*, 7729–7732. b) J. B. Pedley, R. D. Naylor, S. B. Kirby, *Thermochemical Data of Organic Compounds*, Chapman and Hall, London, **1986**.
[14] ΔH_{sub} (298 K, per C atom) = 0.93 kcal mol^{-1} extrapolated [15] from the measured enthalpy of sublimation ΔH_{sub} of C_{60} (707 K, per C atom) = 0.67 kcal mol^{-1} [5] with C_p (c, measured) [5] and C_p (g, estimated) [5].
[15] C. Pan, M. P. Sampson, Y. Chai, R. H. Hauge, J. L. Margrave, *J. Phys. Chem.* **1991**, *95*, 2944–2946.
[16] N. L. Allinger, Y. H. Yuh, J.-H. Lii, *J. Am. Chem. Soc.* **1989**, *111*, 8551, 8566, 8576. – Technical Utilisation Corp. Inc., 235 Glen Village Court, Powell, OH 43065, USA
[17] D. A. Armitage, C. W. Bird, *Tetrahedron Lett.* **1993**, *34*, 5811–5812.
[18] D. Bakowies, W. Thiel, *J. Am. Chem. Soc.* **1991**, *113*, 3704–3714.
[19] J. Cioslowski, *Chem. Phys. Lett.* **1993**, *216*, 389–393.
[20] a) F. Diederich, R. L. Whetten, C. Thilgen, R. Ettl, I. Chao, M. M. Alvarez, *Science (Washington)* **1992**, *254*, 1768–1770; b) Z. Slawina, J.-P. François, M. Kolb, D. Bakowies, W. Thiel, *Fullerene Sci. Technol.* **1993**, *1*, 221–230.

Synthesis of Unsaturated Amino Acids by [3,3]-Sigmatropic Rearrangement of Chelate-Bridged Glycine Ester Enolates**

Uli Kazmaier*

Dedicated to Professor Ulrich Schmidt on the occasion of his 70th birthday

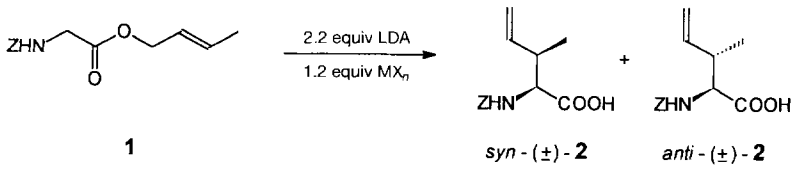
The synthesis of γ,δ-unsaturated amino acids has received a great deal of attention for a long time. Some of these amino acids, which also occur in nature,[1] exhibit pronounced antibiotic activity, and can be used as enzyme inhibitors.[2] These unsaturated amino acids are also very interesting from a synthetic point of view, since more complex compounds can be readily constructed by functionalization of the double bond.[3] In 1975, Steglich et al. described the thermal Claisen rearrangement of *N*-benzoyl-α-amino acid allyl esters on treatment with a dehydrating agent, in which an 5-allyloxazole intermediate was formed.[4] Since the [3,3]-sigmatropic rearrangement takes place highly diastereoselectively, this elegant method found numerous applications, in particular, for the synthesis of α-alkylated amino acids.[5] In 1982, Bartlett et al. investigated the Ireland–Claisen rearrangement[6] of N-acylated glycine allyl esters in detail.[7] In the rearrangement of crotyl esters they found in some cases very high diastereoselectivities. The observed *syn* selectivity can be explained by a preferred formation of the (*E*)-lithium enolate and its chelation by the anionic acylamide group in the α-position. Similar chelate-bridged enolates have also been postulated in sigmatropic rearrangements of α-alkoxy-substituted allyl esters.[8] An interesting asymmetric boron enolate variant of the Claisen rearrangement was described by Corey and Lee in 1991.[9]

Whereas the hitherto described procedures for the Claisen rearrangement of ester enolates of α-amino acid allyl esters make use of the Ireland silylketene acetal variant,[10] we now describe a rearrangement of chelate-bridged metal enolates. Attempts to rearrange lithiated glycine allyl esters directly did not succeed, since the desired rearrangement only occurs at temperatures at which the lithium enolates decompose. However, by adding salts of chelatable metals to the lithium enolate solution, stable glycine enolate chelates are obtained which do not decompose when warmed to room temperature.[11] In fact, copper(II) and nickel(II) salts form very stable chelates with amino acids and peptides;[12] however, the corresponding enolates are not reactive enough to undergo rearrangement.

We have now investigated the influence of a number of metal salts on the yield and diastereoselectivity of the rearrangement of the *N*-benzyloxycarbonylglycine crotyl ester **1** to **2**, and have obtained interesting results (Table 1). The best results with respect to both yield and selectivity were obtained on addition of zinc(II) chloride. If a solution of the zinc enolate (No. 1) is heated from −78 °C to room temperature, the rearrangement begins at −20 °C and is complete after 3 h at room temperature. In the reaction with tetraisopropylorthotitanate (No. 5), the crotyl ester is partially split or even transesterified by titanium(IV) catalysis[13] resulting in lower yields. Otherwise, the metal enolates are clearly superior to silylketene acetals (Nos. 6 and 7) both in terms of their reactivity and selectivity.

[*] Dr. U. Kazmaier
Organisch-chemisches Institut der Universität
Im Neuenheimer Feld 270, D-69120 Heidelberg (FRG)
Telefax: Int. code + (6221)564205

[**] Reactions of Chelated Enolates, Part 1. This work was supported by the Fonds der Chemischen Industrie. I thank Prof. G. Helmchen for his invaluable support.



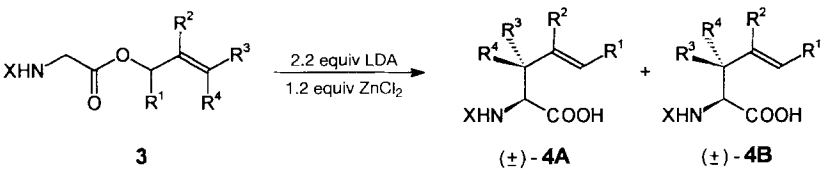
1 *syn*-(±)-**2** *anti*-(±)-**2**

Table 1. Rearrangement of *N*-benzyloxycarbonylglycine crotyl ester **1** after deprotonation with lithium diisopropylamide (LDA) in the presence of metal salts MX_n.

No.	MX_n	Yield [%]	Diastereomer ratio *syn*-(±)-**2**:*anti*-(±)-**2**
1	$ZnCl_2$	90	95:5
2	$CoCl_2$	78	93:7
3	$MgCl_2$	85	91:9
4	$Al(OiPr)_3$	75	90:10
5	$Ti(OiPr)_4$	50	90:10
6	Me_2SiCl_2	50	85:15
7	Me_3SiCl	60	83:17

The driving force for the accelerated rearrangement of the metal enolates is probably the transformation of the high-energy ester enolate into a chelate-bridged, stabilized carboxylate. If the acidic amide proton in crotyl ester **1** is replaced by a methyl group, this chelation does not occur, and no rearrangement is observed. The same applies for *N*-phthaloyl-protected glycine allyl esters.

In view of the good results obtained with zinc(II) chloride, we used this system to carry out a detailed study into the influence of the substituents at the double bond, the olefin configuration, and the N-protective group on the yield and diastereoselectivity of the rearrangement (Scheme 1), since the selectivity for



3 (±)-**4A** (±)-**4B**

Scheme 1. $ZnCl_2$-catalyzed rearrangements of glycine ester enolates. X, R^1-R^4 see Table 2.

silylketene acetals is significantly dependent on these parameters.[7] The results are summarized in Table 2.

All substituted allyl esters **3** show high diastereoselectivities (93–96% *ds*), in which the formation of *syn* products from *trans*-substituted allyl esters (Nos. 3–5, 7–9) and *anti* products from *cis*-substituted allyl esters (Nos. 6, 10) are favored.

This can be explained in terms of a chairlike transition state like that generally postulated for [3,3]-sigmatropic rearrangements of acyclic systems.[14] The particularly high diastereoselectivity in the rearrangement of the silyloxy-substituted *cis*-allyl ester (No. 11) is remarkable. This could be caused by a stabilization of the chairlike transition state by coordination of the silyloxy substituent to the chelated zinc. This is being investigated further. Further investigations into the reasons for this remarkably high diastereoselectivity are in progress.

Table 2. Influence of the substitution, the olefin configuration, and the N-protective group of **3** on the yield and diastereoselectivity of the rearrangement to **4**.

No.	**3** X [a]	R^1	R^2	R^3	R^4 [b]	Yield [%]	Diastereomer ratio (±)-**4A**:(±)-**4B**
1	Z	H	H	H	H	88	
2	Z	H	CH_3	H	H	78	–
3	Z	H	H	C_3H_7	H	76	95:5
4	Z	CH_3	H	CH_3	H	88	93:7
5	Z	C_2H_5	H	CH_3	H	98	95:5
6	Z	C_2H_5	H	H	C_4H_9	73	95:5
7	Boc	CH_3	H	CH_3	H	84	96:4
8	Boc	H	H	C_3H_7	H	78	96:4
9	TFA	H	H	C_3H_7	H	79	95:5
10	TFA	C_2H_5	H	H	C_4H_9	65	94:6
11	Z	H	H	H	$CH_2OTBDPS$	75	98.5:1.5

[a] Z = benzyloxycarbonyl, Boc = *tert*-butyloxycarbonyl, TFA = trifluoroacetyl.
[b] TBDPS = *tert*-butyldiphenylsilyl.

Experimental Procedure

2: Butyllithium (20 mL, 33 mmol, 1.65 M solution in hexane) was added to a solution of diisopropylamine (5.6 mL, 40 mmol) in dry THF (30 mL) at −20 °C under argon. This was stirred for 20 min, cooled to −78 °C, and a solution of **1** (3.95 g, 15 mmol) in THF (15 mL) was added. After 5 min a solution of zinc chloride (2.32 g, 17 mmol) in THF (20 mL) was then added and slowly allowed to warm to room temperature. The clear pale yellow solution was hydrolyzed with 1 N hydrochloric acid, and the organic solvent was removed on a rotary evaporator. The residue was dissolved in ether and washed with 1 N hydrochloric acid. The ether phase was then extracted twice with 1 N sodium hydroxide. The combined aqueous phases were acidified and extracted twice with ether. After the solution had been dried with Na_2SO_4 and concentrated, 3.55 g (90%) of **2** as a white solid was obtained. Recrystallization from ether/petroleum ether gave 3.08 g (78%) of the pure diastereomer *syn*-(±)-**2**, colorless needles, melting point 81–82 °C.

Received: October 27, 1993 [Z 6454 IE]
German version: *Angew. Chem.* **1994**, *106*, 1096

[1] K. Katagiri, K. Tori, Y. Kimura, T. Yoshida, T. Nagasaki, H. Minato, *J. Med. Chem.* **1967**, *10*, 1149; U. Cramer, A. G. Rehfeldt, F. Spener, *Biochemistry* **1980**, *19*, 3074; S. Tsubotani, Y. Funabashi, M. Takamoto, S. Hakoda, S. Harada, *Tetrahedron* **1991**, *47*, 8079.
[2] R. L. Dennis, W. J. Plant, C. G. Skinner, G. L. Sutherland, *J. Am. Chem. Soc.* **1955**, *77*, 2362; J. Edelson, J. D. Fissekis, C. G. Skinner, W. Shive, *ibid.* **1958**, *80*, 2698; P. Shannon, P. Marcotte, S. Coppersmith, C. Walsh, *Biochemistry* **1979**, *18*, 3917; S. Santoso, T. Kemmer, W. Trowitzsch, *Liebigs Ann. Chem.* **1981**, 658.
[3] P. A. Bartlett, D. J. Tanzella, J. F. Barstow, *Tetrahedron Lett.* **1982**, *23*, 619; Y. Ohfune, N. Kurokawa, *ibid.* **1985**, *26*, 5307; N. Kurokawa, Y. Ohfune, *J. Am. Chem. Soc.* **1986**, *108*, 6041; Q. B. Broxterman, B. Kaptein, J. Kamphuis, H. E. Schoemaker, *J. Org. Chem.* **1992**, *57*, 6286.
[4] B. Kübel, G. Höfle, W. Steglich, *Angew. Chem.* **1975**, *87*, 64; *Angew. Chem. Int. Ed. Engl.* **1975**, *14*, 58; N. Engel, B. Kübel, W. Steglich, *ibid.* **1977**, *89*, 408 and **1977**, *16*, 394.
[5] J. Fischer, C. Kilpert, U. Klein, W. Steglich, *Tetrahedron* **1986**, *42*, 2063; K. Burger, K. Geith, K. Kea, *Angew. Chem.* **1988**, *100*, 860; *Angew. Chem. Int. Ed. Engl.* **1988**, *27*, 848; A. L. Castelhano, S. Horne, G. J. Taylor, R. Billedeau, A. Krantz, *Tetrahedron* **1988**, *44*, 5451; L. Colombo, G. Casiraghi, A. Pittalis, *J. Org. Chem.* **1991**, *56*, 3897; M. W. Holladay, A. M. Nadzan, *ibid.* **1991**, *56*, 3900.
[6] R. E. Ireland, R. H. Mueller, A. K. Willard, *J. Am. Chem. Soc.* **1976**, *98*, 2868.
[7] P. A. Bartlett, J. F. Barstow, *J. Org. Chem.* **1982**, *47*, 3933.
[8] S. D. Burke, W. F. Fobare, G. J. Pacofsky, *J. Org. Chem.* **1983**, *48*, 5221; M. Uchikawa, T. Katsuki, M. Yamaguchi, *Tetrahedron Lett.* **1986**, *27*, 4581; H. Uchiyama, M. Kawano, T. Katsuki, M. Yamaguchi, *Chem. Lett.* **1987**, 351; T. J. Gould, M. Balestra, M. D. Wittman, J. A. Gary, L. T. Rossano, J. Kallmerten, *J. Org. Chem.* **1987**, *52*, 3889; H.-J. Altenbach in *Organic Synthesis Highlights* (Eds.: J. Mulzer, H.-J. Altenbach, M. Braun, K. Krohn, H.-U. Reissig), VCH, Weinheim, **1991**, p. 116.
[9] E. J. Corey, D. Lee, *J. Am. Chem. Soc.* **1991**, *113*, 4026.
[10] H. Baumann, R. O. Duthaler, *Helv. Chim. Acta* **1988**, *71*, 1025.
[11] Imine condensations of chelate-bridged glycine ester enolates: F. H. van der Steen, H. Kleijn, G. J. P. Britovsek, J. T. B. H. Jastrzebski, G. van Koten, *J. Org. Chem.* **1992**, *57*, 3906.
[12] H. Sigel, B. Martin, *Chem. Rev.* **1982**, *82*, 385.
[13] D. Seebach, E. Hungerbühler, R. Naef, P. Schnurrenberger, B. Weidmann, M. Züger, *Synthesis* **1982**, 138; M. T. Reetz, *Top. Curr. Chem.* **1982**, *106*, 1.
[14] P. Wipf in *Comprehensive Organic Synthesis, Vol. 5* (Eds.: B. M. Trost, I. Fleming), Pergamon, Oxford, **1991**, p. 827, and references therein.

Synthesis and Structural Characterization of $[\{(Et_2O)Mg\}_6(NPh)_4Br_4]$: A Magnesium–Imide Cage Species Derived from a Dimagnesylamine Solution**

Tony Hascall, Marilyn M. Olmstead, and Philip P. Power*

Dimagnesylamines (imidobis(magnesium halides)) are species in which the two hydrogen atoms from an amine are replaced by MgX moieties (X = halogen).[1] They were first prepared as long ago as 1903[2] by the reaction of a primary amine with two equivalents of Grignard reagent [Eq. (a)].

$$RNH_2 + 2R'MgX \rightarrow \underset{\text{dimagnesylamine}}{\text{"}RN(MgX)_2\text{"}} + 2R'H \qquad (a)$$

(X = halogen; R, R' = alkyl or aryl)

When these compounds are employed as synthetic reagents[3] the formula $RN(MgX)_2$ is normally used but this merely represents the formal stoichiometry required by the reaction scheme. Currently, no structural details for these interesting species are available. In this laboratory, the reactions of Grignard reagents (R'MgX) or diorganomagnesium compounds (MgR'_2) with primary amines (RNH_2) have recently been under investigation. The main objectives of this work were the establishment of the exact formulae of the products and their subsequent synthetic use as imide (NR^{2-}) transfer reagents in main group and transition metal chemistry. It has already been demonstrated that the reaction between $MgEt_2$ and H_2NPh in the presence of THF affords the new magnesium imide cage species **1** which has a

$[(thf)MgNPh]_6$ **1**

hexagonal prismatic Mg_6N_6 structural framework.[4] It is now shown that the reaction between two equivalents of the Grignard reagent EtMgBr and H_2NPh in ether solution gives the novel magnesium–imide aggregate **2**. Compound **2** (see Experimental Procedure) can be isolated from ether solution as a thermally stable, air- and moisture-sensitive, crystalline solid which turns brown upon exposure to air. The crystals are fairly soluble in ethers and slightly soluble in aromatic solvents. In [D_8]toluene at 25 °C the ^1H NMR spectrum shows that only one type of solvating ether molecule or phenyl group is present at room temperature—at least on the NMR time scale. Moreover, integration of the signals for Ph and Et_2O shows that the groups are present in a 2:3 ratio. The ^{13}C NMR spectrum also supports this view.

$[\{(Et_2O)Mg\}_6(NPh)_4Br_4]$ **2**

The stoichiometry and structure of **2** were definitively established by an X-ray crystal structure determination (Fig. 1).[5] The structure of **2** has a slightly distorted Mg_6N_4 adamantane framework composed of four nitrogen atoms (from NPh^{2-} groups) at the bridgehead positions and six ether-solvated Mg^{2+} ions. The four bromide ions, which preserve overall charge balance, are located somewhat asymmetrically[6] above the four fused six-membered Mg_3N_3 rings that form the adamantane core. An alternative view of the structure is that the four μ_3-Br^- ions describe a distorted tetrahedron which circumscribes the Mg_6N_4 cage which is itself composed of an octahedron of Mg^{2+} ions and a tetrahedron of N centers. Thus, each Mg^{2+} ion bridges an edge, and each NPh^{2-} ion caps a face in a μ_3 fashion, of the halide tetrahedron. The geometry at the magnesium centers may be described as distorted trigonal bipyramidal with the axial positions occupied by bromide ions and the equatorial sites occupied by two nitrogen atoms and an oxygen atom. The mean Mg–N and Mg–O distances are 2.041(10) and 2.026(14) Å which are close to those observed in **1**.[4] The Mg–Br distances are in the range 2.76–3.48 Å with an average length of 2.94 Å.[6] The imide nitrogen atoms have distorted tetrahedral environments, and are coordinated to three magnesium atoms and one carbon atom with an average N–C bond length of 1.46 Å.

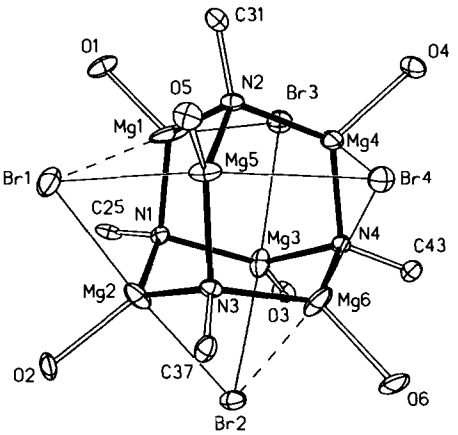


Fig. 1. Molecular structure of $[\{(Et_2O)Mg\}_6(NPh)_4Br_4]$ **2** (computer generated). For clarity, only the oxygen atoms of the ether molecules, the *ipso*-carbon atoms of the Ph substituents, and the $Mg_6N_4Br_4$ framework are shown [5, 6].

The unique formula of **2** probably arises from the disproportionation (b).

$$4RN(MgX)_2 \rightarrow Mg_6(NR)_4X_4 + 2MgX_2 \qquad (b)$$

The structure in the solid appears to closely resemble the solution species. Three crystallizations of **2** from Et_2O did not result in any change in stoichiometry. Furthermore, the addition of 1,4-dioxane (as outlined in the Experimental Procedure) is not required to induce disproportionation since **2** may be isolated by fractional crystallization from the reaction solution. In addition, the use of THF instead of ether gives **3**, which has an

$[\{(thf)Mg\}_6(NPh)_4Br_4]$ **3**

almost identical structure to **2**.[7] The significance of these structures lie in the fact that they demonstrate that the addition of two equivalents of Grignard to aniline results in a completely deprotonated nitrogen center. In this respect it resembles the reaction of $MgEt_2$ with H_2NPh which affords **1**.

Experimental Procedure

All manipulations were carried out under anaerobic and anhydrous conditions. With rapid stirring and cooling in an ice bath, the Grignard reagent EtMgBr was added as a 0.6 M solution in diethyl ether (100 mL, 60 mmol) to aniline (2.8 g, 30 mmol) in 20 mL of the same solvent. When the addition was complete, the solution was allowed to warm to room temperature and stirred for a further 2 h whereupon 1,4-dioxane (1.7 mL, 30 mmol) was added by syringe to afford a white precipitate of $MgBr_2 \cdot 2$ (1,4-dioxane). This was separated by filtration to afford a clear solution which was concentrated under reduced pressure to bring about crys-

[*] Prof. P. P. Power, T. Hascall, Dr. M. M. Olmstead
Department of Chemistry, University of California
Davis, CA 95616 (USA)
Telefax: Int. code + (916) 752-8995

[**] This work was supported by the National Science Foundation and the Petroleum Research Fund.

tallization. Cooling in a freezer to −20 °C afforded the product **2** as colorless crystals. These may be recrystallized by dissolving in refluxing ether and cooling. The yield was about 70%. The crystals rapidly turned brown upon exposure to air and did not melt upon heating to 300 °C. The crystals showed evidence of desolvation and decomposition on heating above 100 °C. ^{1}H NMR: (300 MHz, 25 °C in [D$_8$]toluene: δ = 0.99 (br, 36H, $CH_3(Et_2O)$), 3.6 (br, 24H, $CH_2(Et_2O)$), 6.75 (t, 4H, *p*-H), 7.17 (m, 8H, *m*-H), 7.48 (m, 8H, *o*-H). ^{13}C{^{1}H} NMR: (75.47 MHz, [D$_8$]toluene): δ = 13.16 (s, $CH_3(Et_2O)$) 64.51 ($CH_2(Et_2O)$), 113.21 (s, *o*-C), 124.04 (s, *m*-C). IR: the IR spectrum (nujol mull) of **2** in the metal-ligand stretching region (< 600 cm^{-1}) is characterized by several medium intensity bands at 502, 428, 363, 318, and 245 cm^{-1}.

Received: October 13, 1993 [Z 6415 IE]
German version: *Angew. Chem.* **1994**, *106*, 1056

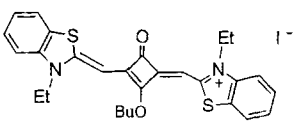
[1] P. A. Petyunin, *Russ. Chem. Rev. Engl. Transl.* **1962**, *31*, 100.
[2] L. Meunier, *C. R. Hebd. Seances Acad. Sci.* **1903**, *136*, 758.
[3] M. Okubo, Y. Inatomi, N. Taniguchi, K. Imamura, *Bull. Chem. Soc. Jpn.* **1988**, *61*, 3581, and references therein.
[4] T. Hascall, K. Ruhlandt-Senge, P. P. Power, *Angew. Chem.* **1994**, *106*, 350; *Angew. Chem. Int. Ed. Engl.* **1994**, *33*, 356.
[5] Crystal data at 130 K with $Cu_{K\alpha}$ (λ = 1.54178 Å) radiation: a = 42.748(7), b = 12.499(2), c = 23.270(3) Å, β = 104.940(10)°, monoclinic, space group $P2_1/c$, Z = 8, 12319 reflections with $I > 2\sigma(I)$, R = 0.063. Further details of the structure may be obtained from the Fachinformationszentrum Karlsruhe, D-76344 Eggenstein-Leopoldshafen (FRG), on quoting the depository number CSD-57836.
[6] In each molecule of the asymmetric unit two of the Br–Mg distances (indicated by dashed lines in Fig. 1) in the structure are significantly longer than the other ten (e.g. Mg1 · · · Br1 = 3.337 Å and Mg6 · · · Br2 = 3.154 Å vs. an average of 2.87 Å for the other Mg–Br distances).
[7] M. M. Olmstead, P. P. Power, unpublished results, **1992**.

Synthesis and Structure of New Cationic Squarylium Dyes

Hiroyuki Nakazumi,* Kazuki Natsukawa, Kazuhisa Nakai, and Kakuzo Isagawa

Squarylium dyes have attracted much attention because of their potential application in xerographic photoreceptors,[1] optical recording media,[2] and organic solar cells,[3] on account of their special properties such as photoconductivity and sharp and intense absorption in the visible (VIS) or near-IR regions (NIR).[4] Generally, known squarylium dyes are 1,3- or 1,2-disubstituted squaric acid derivatives.[5] We have now prepared a hitherto unknown cationic squarylium dye (**1**) and found that it has an extended π-electron system whose two squaric acid subunits are stabilized by formation of an intramolecular hydrogen bond.

The butyl derivative **1a**[6] was prepared in 43% yield by condensation of *N*-butyl-2-methylbenzothiazolium iodide and squaric acid in refluxing butanol/benzene in the absence of a base catalyst such as quinoline. Other alkyl derivatives, **1b** and **1c**, were similarly prepared from the corresponding benzothiazolium iodides. In this reaction, the normal squarylium dye **2** was obtained as a by-product (less than 10% yield). In similar reactions of other heterocyclic compounds with squaric acid, the 2-methyl-quinolinium salt gave a cationic squarylium dye (λ_{max} 856 nm), but the 2-methylindolinium salt gave only the normal squarylium dye. Treatment of **1a** with one equivalent sodium tetraphenylborate in methanol (60 °C, 1 h) afforded the tetraphenylborate salt **3a**. The reaction of *N*-ethyl-2-methylbenzothiazolium iodide with squaric acid in the presence of quinoline was reinvestigated, and was found to yield compound **1c** (deep red squarylium dye) with an absorption maximum in the NIR spectrum (λ_{max} 796 nm), and not the proposed structure **4** previously reported.[7]

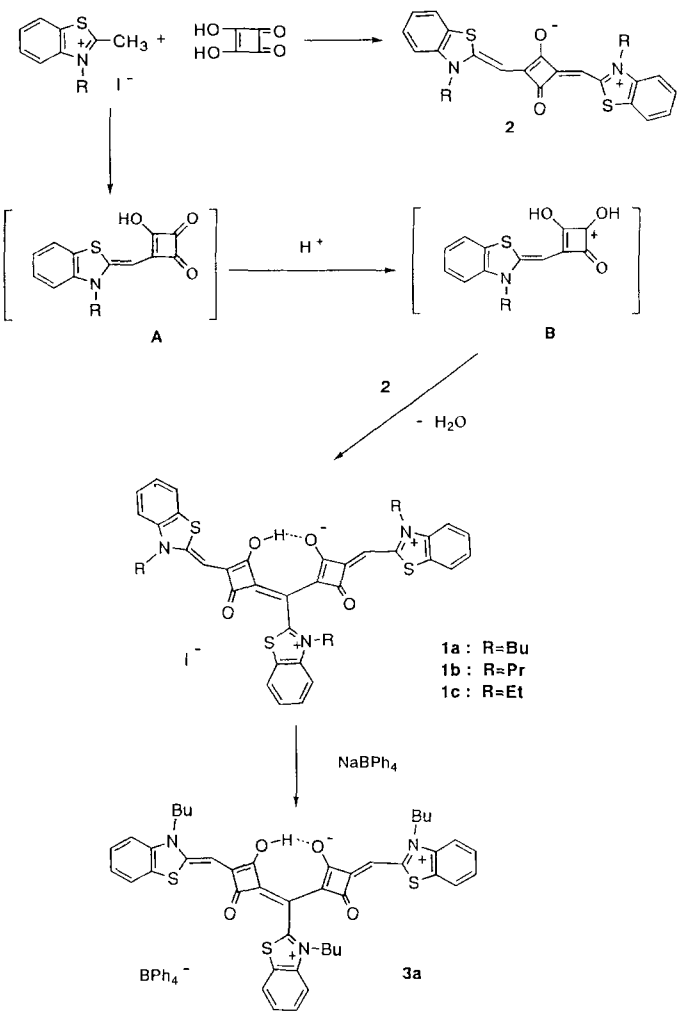


4

The preparation of squarylium dyes is usually carried out under conditions where the enamine 2-methylenebenzothiazole is formed in situ with excess of quinoline. Under such conditions, the main product was the normal squarylium dye **2**; a small amount (less than 10% yield) of the cationic dye **1** was only obtained on prolonged reaction (20 h).

In the absence of quinoline, dye **1** was formed during the early stage of the reaction as a main product (Fig. 1; reaction monitored by VIS/NIR absorption spectroscopy). Initially, the reaction of benzothiazolium iodide with squaric acid gave a mixture of intermediate **A** and the normal squarylium dye **2**. The electrophilic attack of a protonated intermediate **B**, which is easily formed in the presence of an acid, on dye **2** followed by dehydration leads to the cationic dye **1** (Scheme 1).

The X-ray structural analysis[8] of **3a** (Fig. 2) shows a planar polymethine structure, which corresponds to the chromophore



Scheme 1. Synthesis of cationic squarylium dyes **1a–c** as well as the BPh_4 salt **3a**.

[*] Prof. Dr. H. Nakazumi, K. Nakai, K. Isagawa
Department of Applied Material Science, College of Engineering
University of Osaka Prefecture, 1-1 Gakuen-cho, Sakai, Osaka 593 (Japan)
Telefax: Int. Code + (81)722-59-3340
K. Natsukawa
Osaka Prefectural Industrial Technology Research Institute (Japan)

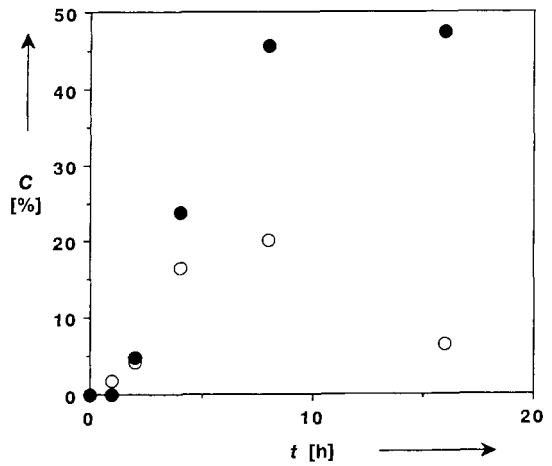


Fig. 1. Product ratios of near-IR absorbed squarylium dye **1a** (●) and blue squarylium dye **2a** (○) prepared from the reaction of squaric acid (0.5 mmol) and *N*-butyl-2-methylbenzothiazolium iodide (1.0 mmol) in the absence of quinoline (*C*: conversion of squaric acid [%] monitored by absorption at 798 and 668 nm, respectively).

in **1**; the largest deviation (0.31 Å) occurs for the O2 atom of the carbonyl group. The positive charge is delocalized over the two squaric acid units and two of the three benzothiazole rings. Two shorter C–C bonds in the cyclobutene (1.43–1.46 Å), and the other C–C as well as the C–N1 and C–N2 bond lengths (1.35–1.43 Å) are indicative of a conjugated polymethine framework in **3a**. The C–O bond (ca. 1.26 Å) in the inner carbonyl groups is longer (ca. 0.06 Å) than the others. An intramolecular hydrogen bond (1.50 Å) between the oxygen atom of the carbonyl group and the hydroxyl group (2.37 Å for O1–O3) leads to an effective delocalization of the π electrons over the polymethine subunit.

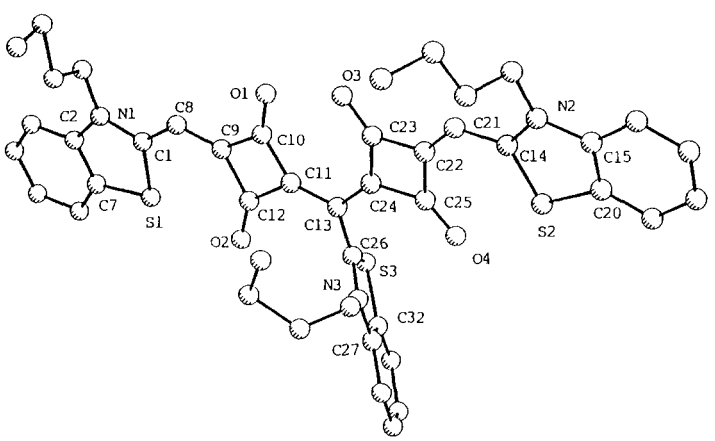


Fig. 2. X-ray crystal structure (PLUTO drawing) of **3a**. Hydrogen atoms and BPh_4^- were omitted for clarity. Selected bond lengths [Å]: N1-C1 1.36(1), N1-C2 1.40(1), C1-C8 1.38(1), S1-C1 1.72(1), S1-C7 1.75(1), C8-C9 1.39(1), C9-C10 1.43(1), C10-O1 1.27(1), C10-C11 1.43(1), C11-C12 1.49(1), C9-C12 1.50(1), C12-O2 1.20(1), C11-C13 1.41(1), C13-C24 1.41(1), N2-C15 1.41(1), N2-C14 1.35(1), S2-C14 1.72(1), S2-C20 1.75(1), C14-C21 1.42(1), C21-C22 1.34(1), C22-C23 1.47(1), C22-C25 1.48(2), C23-O3 1.26(1), C23-C24 1.43(1), C24-C25 1.50(1), C25-O4 1.20(1), C13-C24 1.41(1), C13-C26 1.43(1), S3-C26 1.68(1), S3-C32 1.74(1), N3-C26 1.32(1), N3-C27 1.38(1).

The branched benzothiazolium subunit is not conjugated with the polymethine subunit; the dihedral angle between these two units is 62.5°. The polymethine structure in **1a** or **3a** is also evident from the equivalence of two of the three *N*-butyl groups in the ^1H NMR spectrum, that is, the methylene protons of the NCH_2 group in the polymethine unit and in the branching benzothiazolium subunit of **1a** occur at $\delta = 4.2$ (4H) and 4.73 (2H), respectively. The absorption spectrum of the neutral compound **1a**–HI, which was formed by treatment with sodium hydroxide, exhibits two intense bands in the NIR spectrum ($\lambda_{max} = 845$, 799 nm)[9] for the x and the y band of a typical triarylmethane chromophore. However, the cationic dye **1** showed only a sharp and intense absorption band at 797 nm ($\lg\varepsilon = 5.44$) with a small shoulder; the squarylium dye **2** absorbs at 668 nm. Thus, the chromophore of **1** is a polymethine chromophore which is stabilized by an intramolecular hydrogen bond, and not a triarylmethane chromophore. Although the cationic dye **1** consists of three benzothiazole rings and two squaric acid subunits, the branched benzothiazolium component makes a relatively small contribution to the polymethine chromophore in the solution.

Experimental Procedure

1a: The mixture of *N*-butyl-2-methylbenzothiazolium iodide (1.32 g, 4 mmol) and squaric acid (0.23 g, 2 mmol) in butanol/benzene (4:1)(10 mL) was heated at 110 °C for 7 h. After cooling, chloroform (4 mL), ethyl acetate (3 mL), and methanol (3 mL) were added to the reaction mixture, and the solution was allowed to stand for at least 12 h. The resulting solid was then separated and washed with ethyl acetate to give a black solid, which was purified by recrystallization from CH_2Cl_2/ethyl acetate. Yield: 0.39 g (43%). Other derivatives, **1b** and **1c**, were similarly made from the corresponding *N*-alkyl-2-methylbenzothiazolium iodide in yields of 38–43%.

3a: A CH_2Cl_2 solution of **1a** (20 mL, 0.72 g, 0.8 mmol) was added dropwise to a solution of sodium tetraphenylborate in methanol (5 mL, 0.028 g, 0.8 mmol). The mixture was stirred at 60 °C for 1 h. After cooling, ethyl acetate (3 mL) was added to the reaction mixture, and the solution was allowed to stand for 20 h. The resulting solid was separated and recrystallized from CH_2Cl_2/hexane. Yield: 0.056 g (64%).

Received: November 3, 1993 [Z64741E]
German version: *Angew. Chem.* **1994**, *106*, 1021

[1] A. C. Tam, *Appl. Phys. Lett.* **1980**, *37*, 978; K. Y. Law, F. C. Bailey, *J. Imaging Sci.* **1987**, *31*, 172.
[2] D. J. Gravesteijn, C. Steenbergen, J. Vander Veen, *Proc. SPIE Int. Soc. Opt. Eng.* **1988**, *420*, 327; V. P. Jipson, C. R. Jones, *J. Vac. Sci. Technol.* **1981**, *18*, 105.
[3] V. Y. Merritt, H. J. Hovel, *Appl. Phys. Lett.* **1976**, *29*, 414; R. O. Loutfy, C. K. Hsiao, P. M. Kazmaier, *Photogr. Sci. Eng.* **1983**, *27*, 5.
[4] For reviews on near-infrared absorption spectra of squarylium dyes, see: J. Fabian, H. Nakazumi, M. Matsuoka, *Chem. Rev.* **1992**, *92*, 1197; H. Nakazumi, *J. Soc. Dyes Colour.* **1988**, *104*, 121; M. Emmelius, G. Pawlowski, H. Vollmann, *Angew. Chem.* **1989**, *101*, 1475; *Angew. Chem. Int. Ed. Engl.* **1989**, *28*, 1445.
[5] W. Ziegenbein, H. E. Sprenger, *Angew. Chem.* **1966**, *78*, 937; *Angew. Chem. Int. Ed. Engl.* **1966**, *5*, 893; *ibid.* **1967**, *79*, 581 and **1967**, *6*, 553; A. Treibs, K. Jacob, *Justus Liebigs Ann. Chem.* **1968**, *712*, 123; H. A. Schmidt, *Synthesis.* **1980**, 961; K. Y. Law, F. C. Bailey, *Can. J. Chem.* **1986**, *64*, 2267.
[6] All the compounds gave satisfactory analytical and spectral data. **1a**: Decomp. 258 °C; MS (FAB MS, Xe, 6 kV): *m/z*: 772 ($M^+ - I$); ^1H NMR (270 MHz, [D$_6$]DMSO): $\delta = 8.53$ (dd, $J = 8$, 16 Hz, 2H), 7.25–8.0 (m, 10H), 6.00 (s, 2H, vinyl), 4.73 (b, 2H, NCH_2-), 4.30 (b, 4H, NCH_2-), 1.64–1.98 (m, 6H, -(CH_2)-), 1.28–1.42 (m, 4H, -(CH_2)-), 1.12–1.20 (m, 2H, -(CH_2)-), 0.86 (t, $J = 7.1$ Hz, 6H, Me), 0.73 (t, $J = 7.4$ Hz, 3H, Me); IR (KBr): $\tilde{\nu} = 1740$, 1625 cm^{-1}; VIS ($CHCl_3$): λ_{max} (ε) = 798 (306000), 723 (43500) nm. **1b**: Decomp. 210 °C; MS (FAB MS, Xe, 6 kV): *m/z*: 730 ($M^+ - I$); ^1H NMR (270 MHz, [D$_6$]DMSO): $\delta = 8.48$–8.57 (m, 2H), 7.28–8.01 (m, 10H), 6.07 (s, 2H, vinyl), 4.72 (s, 2H, NCH_2-), 4.32 (b, 4H), 1.70–1.80 (b, 6H), 0.93 (b, 6H), 0.73 (t, $J = 7.04$ Hz, 3H); IR (KBr): $\tilde{\nu} = 1740$, 1625 cm^{-1}; VIS ($CHCl_3$): λ_{max} (ε) = 796 (296000), 722 (44800) nm. **1c**: Decomp. 213 °C; MS (FAB MS, Xe, 6 kV): *m/z* 688 ($M^+ - I$); ^1H NMR (270 MHz, [D$_6$]DMSO): $\delta = 8.52$ (dd, $J = 8.13$ Hz, 2H), 7.35–8.03 (m, 10H), 6.12 (s, 2H, vinyl), 4.77–4.79 (b, 2H, NCH_2-), 4.45–4.50 (b, 4H), 1.20–1.33 (b, 9H); IR (KBr): $\tilde{\nu} = 1740$, 1625 cm^{-1}; VIS ($CHCl_3$): λ_{max} (ε) = 796 (234000), 722 (41400) nm. **3a**: Decomp. 202 °C; MS (FAB MS, Xe, 6 kV): *m/z*: 772 ($M^+ - BPh_4$); ^1H NMR (270 MHz, [D$_6$]DMSO): $\delta = 8.52$ (m, 2H), 7.37–7.98 (m, 10H), 7.15–7.19 (b, 8H), 6.92 (t, $J = 7$ Hz, 4H), 6.78 (t, $J = 7$ Hz, 8H), 6.16 (s, 2H, vinyl), 4.73 (b, 2H, NCH_2-), 4.43 (b, 4H, NCH_2-), 1.68–1.72 (m, 6H, -(CH_2)-), 1.38–1.43 (m, 4H, -(CH_2)-), 1.20 (b, 2H, -(CH_2)-), 0.91 (t, $J = 7.3$ Hz, 6H, Me), 0.74 (t, $J = 7.0$ Hz, 3H, Me); IR (KBr): $\tilde{\nu} = 1740$, 1625 cm^{-1}; VIS ($CHCl_3$): λ_{max} (ε) = 797 (355000), 724 (53800) nm.

[7] N. Kuramoto, K. Natsukawa, K. Asao, *Dyes Pigments* **1989**, *11*, 21.

[8] **3a**: $C_{68}H_{62}N_3O_4S_3B$, $M = 1092.24$, monoclinic, space group $P2_1/a$, $a = 18.162(8)$, $b = 16.20(2)$, $c = 22.117(7)$ Å, $\beta = 107.34(3)^\circ$, $V = 6213(7)$ Å^3, $Z = 4$, $\rho_{calcd} = 1.168$ g cm^{-3}. A total of 12975 unique data points were collected ($Mo_{K\alpha}$, $\lambda = 0.71049$ Å, $\mu = 1.60$ cm^{-1}, $2\theta < 50^\circ$) of which 4386 had $F > 4\sigma(F)$ and were used for structure refinement. These data sets were collected by using a Rigaku AFC-5R diffractometer at 296 K. An absorption correction, using the program DIFABS, was applied which resulted in transmission factors ranging from 0.88 to 1.12. The structure was solved by direct methods and refined by full-matrix least-squares method (TEXSAN, Molecular Structure Corp., USA) with anisotropic thermal parameters for non-hydrogen atoms, except for five carbon atoms of the butyl groups. Because of the disorder of the butyl group, isotropic parameters for these atoms are very large. $R = 0.076$ and $R_w = 0.100$ for 680 parameters. The minimum and maximum residual electron densities are -0.34 and 0.59 e Å^{-3}, respectively. Further details of the crystal structure investigation may be obtained from the Fachinformationszentrum Karlsruhe, D-76344 Eggenstein-Leopoldshafen (FRG), on quoting the depository number CSD-58042.

[9] Neutral species of **1a** (**1a**−HI): VIS ($CHCl_3$): λ_{max} (ε) = 845 (112000), 799 (140000), 697 (30600) nm.

From Triple-Decker to Metallabenzene: A New Generation of Sandwich Complexes

Ulrike Bertling, Ulli Englert, and Albrecht Salzer*

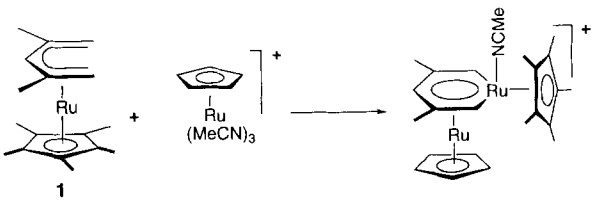
Dedicated to Professor Helmut Werner on the occasion of his 60th birthday

The chemistry of the metallocenes is currently experiencing a true renaissance.[1] Besides complexes with carbocyclic ligands, C_nH_n, metallocenes in which CH is substituted by isoelectronic building blocks (i.e. $C_6H_6 \rightarrow [C_5H_5BR]^-$,[2] or $C_6H_6 \rightarrow C_5H_5P$)[3] are also known. Complete exchange of the CH units leads to pure heteroatom ligands such as P_6.[4] These ligands often act as bridging ligands in triple- and poly-decker complexes. In contrast, this bonding mode has been confirmed, so far, in only two cases for the ubiquitous ligand of metal π complexes, the cyclopentadienyl anion $C_5H_5^-$.[5]

Metallacycles that are isolobal to the previously mentioned element heterocycles act only rarely as π-donor/π-acceptor ligands. The best-known examples are metallacyclopentadienes ("metalloles"), which can form as by-products or intermediates in the metal-catalyzed oligomerization of alkynes.[6] However, this reaction pathway allows only for metallacycles with an even number of C atoms.[7]

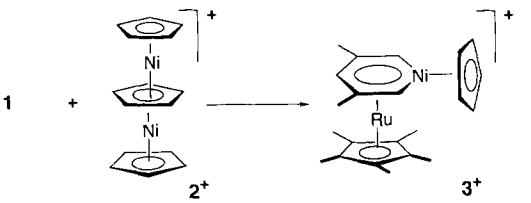
Only in recent years has it become possible to generate mono- and binuclear metallabenzenes. For example, J. Bleeke[8] succeeded in synthesizing binuclear half-sandwich complexes starting from iridabenzene and a $Mo(CO)_3$ moiety. When reacting the "half-open" metallocene **1** with $[CpRu(MeCN)_3]^+$ we obtained a binuclear complex, in which the 14e fragment $[(C_5Me_5)Ru(MeCN)]^+$ complements the pentadienyl ligand to give ruthenabenzene (Scheme 1).[9] Another diruthenium complex with an unsubstituted metallabenzene ring and Me_3Si ligands instead of MeCN has been synthesized just recently by Girolami et al. by a different route.[10]

We now have successfully synthesized the first, simple metal π complex of the composition $[(C_5R_5)_3M_2]^+$, in which the



Scheme 1.

metallabenzene acts as a 6e ligand of a sandwich molecule. Reaction of **1** with the triple-decker cation $\mathbf{2}^+$ as source of the 14e fragment $[CpNi]^+$ gives the cation $\mathbf{3}^+$ (Scheme 2).



Scheme 2.

Complex $\mathbf{3}^+$, isolated as its tetrafluoroborate salt, is essentially air-stable and dissolves in polar solvents such as acetone to give cherry-red solutions without decomposition; the complex can even be purified by chromatography over aluminum oxide. Those CH units of the nickelabenzene ring bonded directly to the metal exhibit a downfield shift in the ^1H and ^{13}C NMR spectra ($\delta = 9.7$ and 167.7, respectively) characteristic for unsaturated metallacycles.[9] A triple-decker complex with a central pentadienyl ligand is conceivable as the initial reaction product that then reacts by insertion of the CpNi moiety into two terminal CH bonds, followed by reductive elimination of hydrogen to give the final product. The mass spectra of "half-open" metallocenes exhibit fragmentation patterns indicative of facile loss of H_2.[11] The thermal ring closure of pentadienyl compounds to give metallocenes by hydrogen elimination is also known.[12]

Single-crystals of **3**-BF_4 were obtained by slow diffusion of propionic anhydride and ether at $-30\,^\circ C$. A single-crystal X-ray structure analysis[13] confirms the presence of a metallabenzene sandwich complex (Fig. 1). The C_5Me_5 ring and the carbon atoms of the nickelabenzene moiety are almost coplanar

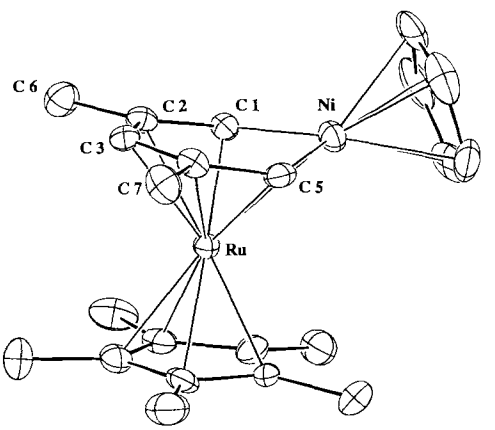


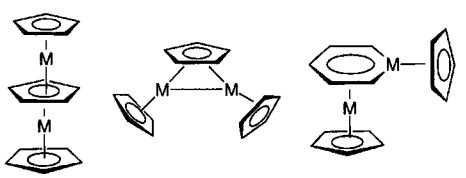
Fig. 1. Structure of $\mathbf{3}^+$ in the crystal (ORTEP). Selected bond lengths [Å]: C1–C2 1.38(1), C2–C3 1.42(1), C3–C4 1.46(1), C4–C5 1.41(1), Ru–Ni 2.554(1), Ni–C1 1.867(9), Ni–C5 1.838(9).

[*] Prof. Dr. A. Salzer, Dipl.-Chem. U. Bertling, Dr. U. Englert
Institut für Anorganische Chemie der Technischen Hochschule
D-52056 Aachen (FRG)
Telefax: Int. code + (241)804646

 © VCH Verlagsgesellschaft mbH, D-69451 Weinheim, 1994 0570-0833/94/0909-1003 $ 10.00+.25/0

(6±1°). The bond lengths within the pentadienyl ligand are mostly identical and are indicative of a high degree of delocalization. The Ni–C distances in the nickelabenzene ring are very short (Ni–C1 1.867(9), Ni–C5 1.839(9) Å) and in accord with a high Ni=C bond character ($Ni-C_{alkyl} \approx 1.99$, $Ni-C_{isonitrile} \approx 1.85$, $Ni-C_{carbonyl} \approx 1.77$ Å[14]). The C-Ni-C angle of 92.4(6)° is similar to that of other heterobenzenes such as arsabenzene (As–C 1.85 Å, C-As-C 97°).[15] Arsenic and nickel have approximately the same atomic radius. The nickel atom is bent out ("upwards") of the plane of the five carbon atoms by 16.4°; this is a result of the short Ru–Ni bond length of 2.55 Å. The angle is markedly smaller than for the ruthenabenzene complex (27.2°), shown in Scheme 1, in which the Ru–Ru distance (2.67 Å) is longer. Consequently, a metallabenzene complex with two 3d metals and an even smaller M–M distance should be completely planar.

In the first publication on $[Cp_3Ni_2]^+$ ($\mathbf{2}^+$) we not only considered the triple-decker structure **I**, later proven correct, but also the structural alternative **II** (Scheme 3),[16] a type of complex



I II III

Scheme 3.

that has in the meantime been confirmed for the compounds $[(\mu\text{-}C_xH_x)Cp_2M_2]^{n+}$ ($x = 6-8$).[17–19] Cp as a ligand bridging a metal–metal bond was first introduced by H. Werner in the complexes $[(\mu\text{-}Cp)Pd_2L_2]$.[20] The metallabenzene complex described here corresponds to type **III** and is an example for the third possible structural isomer with a composition $[(C_5R_5)_3M_2]$.

The aromatic character of metallabenzenes has already been discussed by R. Hoffmann[21] and J. Bleeke.[8] Clearly metallabenzenes are in many respects similar to heteroarenes. This includes structural characteristics such as ring planarity and balanced bond order as well as similar reactivity that allows for formation of remarkably stable metal π complexes of the sandwich-type. Since the bonding mode of the nickelabenzene ligand in $\mathbf{3}^+$ can be described analogous to that of benzene in $[CpRu(C_6H_6)]^+$ the question arises whether detachment or transfer of this ligand to other complex fragments is possible. Bis(metallabenzene) complexes or even triple-decker complexes with a central metallabenzene ring are conceivable.

Experimental Procedure

Synthesis of **3**-BF_4: **1**(1.17 g, 3.5 mmol) and **2**-BF_4 (1.45 g, 3.6 mmol) were stirred in nitromethane (100 mL) for 12 h at 60 °C. After the solvent had been removed under reduced pressure, the residue was chromatographed over Al_2O_3 (activity III) with acetone as eluent. The red fraction gave 0.9 g **3**-BF_4 (48% relative to **1**). Further purification was possible by dissolution in propionic anhydride and precipitation with diethyl ether. ^{13}C NMR (125.7 MHz, CD_3NO_2, 25 °C): $\delta = 167.7$ (C1), 103.8 (C2), 101.5 (C_5Me_5), 96.4 (C_5H_5), 91.9 (C3), 21.0 (Me), 11.0 (C_5Me_5); ^1H NMR (500 MHz, CD_3NO_2, 25 °C): $\delta = 9.7$ (d, $^4J = 1.2$ Hz, 2H; CH), 5.7 (t, $^4J = 1.2$ Hz, 1H; CH), 5.68 (s, 5H; Cp), 2.2 (s, 6H; Me), 1.9 (s, 15H; C_5Me_5).

Received: November 24, 1993 [Z 6509 IE]
German version: *Angew. Chem.* **1994**, *106*, 1026

[1] J. Okuda, *Nachr. Chem. Tech. Lab.* **1993**, *41*, 8.
[2] G. E. Herberich, U. Englert, D. Pubanz, *J. Organomet. Chem.* **1993**, *458*, 1.
[3] C. Elschenbroich, M. Nowotny, B. Metz, W. Massa, J. Graulich, K. Biehler, W. Sauer, *Angew. Chem.* **1991**, *103*, 601; *Angew. Chem. Int. Ed. Engl.* **1991**, *30*, 547.
[4] O. J. Scherer, H. Sitzmann, G. Wolmershäuser, *Angew. Chem.* **1985**, *97*, 358; *Angew. Chem. Int. Ed. Engl.* **1985**, *27*, 351.
[5] G. E. Herberich, U. Englert, F. Marken, P. Hofmann, *Organometallics* **1993**, *12*, 4039.
[6] W.-S. Lee, H. H. Brintzinger, *J. Organomet. Chem.* **1977**, *127*, 93.
[7] M. Green, P. A. Kale, R. J. Mercer, *J. Chem. Soc. Chem. Commun.* **1987**, 375.
[8] J. Bleeke, *Acc. Chem. Res.* **1991**, *24*, 271.
[9] H. W. Bosch, H. U. Hund, D. Nietlispach, A. Salzer, *Organometallics* **1992**, *11*, 2087.
[10] W. Lin, S. R. Wilson, G. S. Girolami, *J. Chem. Soc. Chem. Commun.* **1993**, 284.
[11] M. S. Kralik, A. L. Rheingold, R. D. Ernst, *Organometallics* **1987**, *6*, 2612.
[12] R. U. Kirss, A. Quazi, C. H. Lake, M. R. Churchill, *Organometallics* **1993**, *12*, 4145.
[13] Crystal structure analysis of **3**-BF_4: Enraf-Nonius CAD4; $Mo_{K\alpha}$ radiation; graphite monochromator, empirical absorption correction (PSI [22]); intensity data collected at 258 K with ω scan. Dark red rod $0.1 \times 0.2 \times 0.5$ mm, orthorhombic space group *Pbca* (No. 61); $a = 15.792(5)$, $b = 14.339(4)$, $c = 19.578(4)$ Å, $V = 4433(2)$ Å^3, $Z = 8$, $\rho_{calcd} = 1.618$ g cm^{-3}, $\mu(Mo_{K\alpha}) = 15.60$ cm^{-1}, $F(000) = 2192$; 3475 reflections with $3 < \theta < 24°$, 2070 symmetry-independent reflections with $I > 1.5\sigma(I)$ in structure solution and refinement [23] for 289 parameters; orientational disorder of the BF_4^- ion about a local threefold axis with split positions for three of the four fluorine atoms; $R = 0.057$, $R_w = 0.053$, $w^{-1} = 1/\sigma^2(F_0)$; H atoms in structure factor calculation. Further details of the crystal structure investigation may be obtained from the Fachinformationszentrum Karlsruhe, D-76344 Eggenstein-Leopoldshafen (FRG), on quoting the depository number CSD-58209.
[14] A. G. Orpen, L. Brammer, F. H. Allen, O. Kennard, D. G. Wilson, *J. Che. Soc. Dalton Trans.* **1989**, 1.
[15] C. Elschenbroich, A. Salzer, *Organometallics*, 2nd edition, VCH, Weinheim, **1992**, p. 162.
[16] H. Werner, A. Salzer, *Synth. Inorg. Met. Org. Chem.* **1972**, *2*, 249.
[17] K. Jonas, G. Koepe, L. Schieferstein, R. Mynott, C. Krüger, Y.-H. Tsay, *Angew. Chem.* **1983**, *95*, 637; *Angew. Chem. Int. Ed. Engl.* **1983**, *22*, 620.
[18] A. Salzer, T. Egolf, W. von Philipsborn, *Helv. Chim. Acta* **1982**, *65*, 1145.
[19] J. Bieri, T. Egolf, W. von Philipsborn, U. Piantini, R. Prewo, U. Ruppli, A. Salzer, *Organometallics* **1986**, *5*, 2413.
[20] H. Werner, *Angew. Chem.* **1977**, *89*, 1; *Angew. Chem. Int. Ed. Engl.* **1977**, *16*, 1.
[21] D. L. Thorn, R. Hoffmann, *Nouv. J. Chem.* **1979**, *3*, 39.
[22] A. C. T. North, D. C. Phillips, F. S. Mathews, *Acta Crystallogr. Sect. A* **1968**, *24*, 351.
[23] B. A. Frenz, *The ENRAF-Nonius CAD4-SDP: A Real Time System for Concurrent X-Ray Data Collection and Crystal Structure Determination*, in *Computing in Crystallography* (Eds.: H. Schenk, R. Olthof-Hazekamp, H. van Konigsveld, G. C. Bassi, Universität Delft) **1978**; SDP PLUS, Version 1.1, **1984** and VAXSDP, Version 2.2, **1985**.

Strong, Specific Binding of Six Different DNA Sequences by a Single Conformation-Switching DNA Macrocycle**

Ethel Rubin and Eric T. Kool*

Certain nucleic-acid-binding proteins can recognize varied substrate structures by making use of multiple binding domains or by undergoing conformational changes in a specific binding domain. For example, the *Xenopus* zinc-finger protein TFIIIA recognizes a specific sequence in duplex DNA and a significantly different sequence in ribosomal RNA;[1–5] this switching of binding site is implicated in feedback-type control of gene ex-

[*] Prof. E. T. Kool, E. Rubin
Department of Chemistry, University of Rochester
Rochester, NY 14627 (USA)
Telefax: Int. code + (716)473-6889

[**] This work was supported in part by a grant from the National Institutes of Health (RO1-GM46625). E. T. K. acknowledges awards from the Young Investigator Programs of the Office of Naval Research (1992–1995), the Beckman Foundation (1992–1994), and the Army Research Office (1993–1996), and a Camille and Henry Dreyfus Teacher-Scholar Award (1993).

pression. We have recently begun to examine various approaches for the design of multifunctional DNA-recognizing molecules which can mimic this kind of multisite-binding behavior.[6] The ability to control binding in this way not only serves to mimic a complex biological function, but also may have some practical applications as well. For example, recent studies in the use of oligonucleotides as sequence-specific inhibitors of gene expression have shown that the combination of agents targeted to multiple sites can be more effective in vitro than single-site binding alone.[7–9]

We recently described the design and synthesis of a cyclic oligodeoxynucleotide molecule which can bind strongly to two separate DNA sequences by switching conformation.[6] In that earlier prototypical structure, a cyclic DNA molecule which contained separate pairs of nine-base binding domains (36 nucleotides altogether) was used to recognize two nine-base sequences by interchanging binding and bridging domains (totalling 18 nucleotides of sequence recognition by the 36 nucleotides in the cyclic compound). In order to explore the limits of this kind of multifunctional binding, we now report the synthesis and properties of a new cyclic DNA which is designed to recognize six different sequences by undergoing six conformational changes. At the same time, careful design allows the elimination of duplicated nucleotides, leading to very high economy of function: the molecule selectively recognizes 48 nucleotides of sequence although the molecule itself contains only 35 nucleotides. Several novel design principles are discussed.

The design of the DNA macrocycle **1** involves the combination of several different principles (Fig. 1). First, binding would occur by triplex formation between opposing pyrimidine domains (the Watson–Crick and Hoogsteen domains) in the circle and a complementary sequence of purines in the target molecule. This would result in stronger binding and higher sequence selectivity than is possible for simple Watson–Crick binding.[10, 11] Second, because the two pyrimidine binding domain sequences in such a circle are related by a pseudo-mirror-plane of symmetry, a pair of binding domains might bind the forward (5′ → 3′ direction) or the reverse (3′ → 5′ direction) of a given sequence by switching the roles of the Watson–Crick and Hoogsteen domains. Third, by contiguous alternating placement of three binding domain pairs, this might allow recognition of six different sequences (three in one orientation and three in the reverse). Recognition of a sequence with a given binding domain pair would then make use of the other domains as bridging loops in the complex.[6] Finally, one might achieve this multiple recognition with fewer nucleotides by eliminating those whose function is duplicated in a neighboring domain, thus overlapping the boundaries of the domains. With this approach, many of the individual nucleotides have more than one function.

Specifically, we designed and synthesized the macrocycle **1** with the ability to recognize the six eight-base sequences **2**–**7** (Fig. 1). The total sequence recognition thus encompasses 48 bases of DNA. If the pyrimidine binding domains of the circle were kept separate and incorporated contiguously into a circle, this would require a circle 48 nucleotides in size. By overlapping the ends of the required domains (Fig. 1 bottom), we eliminate the need for 13 of the nucleotides, and so the circle **1** contains only 35 nucleotides.

The structure of **1** should, in principle, retain the high sequence selectivity previously seen for this kind of circular ligand.[10] To test this selectivity, we also synthesized two sequences, **8** and **9** (sequences shown in Fig. 2), which are the same as two of the recognition sequences but with two nucleotides interchanged.

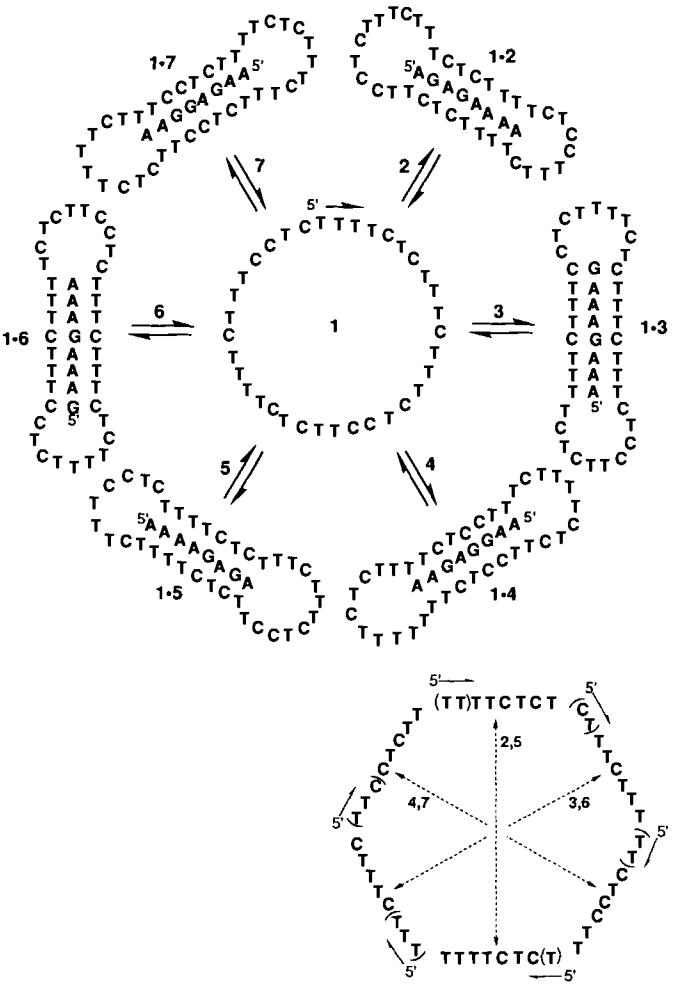


Fig. 1. Top: The sequence of circular oligodeoxynucleotide **1** (in center) and the adducts of **1** with complementary sequences **2**–**7**. Bottom: Strategies for construction of **1**. The three pairs of domains necessary for recognition by triplex formation were placed in alternating configuration such that two halves of a pair oppose one another. (The two domains in each pair are connected by an arrow.) Parentheses indicate nucleotides which are eliminated because they are repeated from the previous domain.

Binding studies of **1** with these eight purine sequences were carried out by optical monitoring of thermal denaturation of the 1:1 mixtures at pH 7.0 (100 mM NaCl, 10 mM $MgCl_2$). Melting curves reveal sharp, apparently two-state transitions at 260 nm for the complexes of **1** with **2**–**7**. As expected for such triple helical complexes,[11] the melting temperatures are considerably higher than those for simple Watson–Crick complements containing the same base pairs (see below). The melting transitions of **1** with **2**–**7** are all within the range 33–37 °C (Fig. 2 top); the hyperchromicities are 18–25%. Also consistent with this mode of binding is the finding that the stability of all six complexes are pH-dependent (data not shown), as expected for triplexes involving C · G · C triads and not duplexes.[12]

By contrast, mismatched sequences **8** and **9** are bound much more weakly than **1**, with T_m values of 18.8 and 19.6 °C, respectively, and are essentially fully dissociated at room temperature. Curve-fitting algorithms[13] allow estimates of free energy for the complexes of **1** with **2**–**9**. Under these conditions, the complexes **1** · **2**–**1** · **7** are bound with free energies ($-\Delta G^\circ_{25}$) of 10.3–12.2 kcal mol^{-1}. By comparison, the complexes of the two mismatched purine sequences (**8**, **9**) are bound much weaker to **1**,

 © VCH Verlagsgesellschaft mbH, D-69451 Weinheim, 1994 0570-0833/94/0909-1005 $ 10.00+.25/0

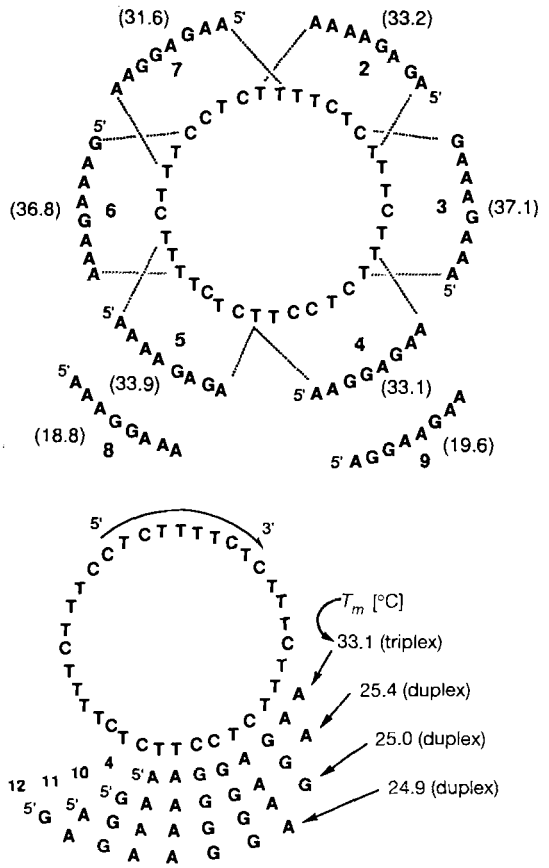


Fig. 2. Top: Melting temperatures T_m [°C] for complexes of **1** with complementary sequences **2**–**7** and mismatched sequences **8** and **9**. Bottom: The relative affinity of **1** for a triple helical complement (**4**) as compared to other Watson–Crick complements (**10**–**12**), as determined by thermal denaturation. The eight-base complements **4** and **10**–**12** are overlapping sequences related by single-nucleotide frameshifts.

with free energies of 6.5 and 6.6 kcal mol^{-1}. Thus, **1** is selective for the complementary sequences over these two mismatched sequences by three to four orders of magnitude in association constant.

A different issue of complementarity and selectivity arises from the structure of **1**. While it is designed to recognize sequences **2**–**7** by triplex formation, it is also complementary in Watson–Crick fashion to 29 additional eight-nucleotide sequences. To test whether the circle **1** binds selectively to the six intended sequences (**2**–**7**) relative to the 29 other sequences, we synthesized three purine octamers, **10**–**12**, which are fully complementary to the circle only in Watson–Crick fashion. The complementary sites for the sequences occur adjacent to the binding domain for the triplex-bound oligomer **4**, and is frameshifted by one, two, or three nucleotides, respectively (Fig. 2 bottom).

Results of these additional binding studies show that while the circle **1** is indeed complementary to the Watson–Crick complements **10**–**12**, it shows considerable selectivity instead for the intended triplex complements **2**–**7**. Thus, **10**–**12** are bound with T_m values of 24.9–25.4 °C and hypochromicity values of 0.10–0.16, while the triplex complements **2**–**7** are bound with T_m values of 33.1–37.1 °C and hypochromicity values of 0.18–0.25. The free energy of formation for these types of complex differs by 2.1–4.3 kcal mol^{-1}. The association constant for **1** · **2**–**1** · **7** is 34- to 1400-fold larger than that for **1** · **10**–**1** · **12**. The sequences which are only complementary in Watson–Crick fashion may thus be viewed as being mismatched sequences, since they are not able to form the full number of stabilizing Hoogsteen bonds that the intended six sequences can. The lower hypochromicitiy values with **1** · **10**–**1** · **12** are consistent with the Hoogsteen strand not being involved in these complexes, although we cannot rule out partial Hoogsteen-type interaction. The selectivity shown by **1** against Watson–Crick binding alone is, in fact, similar in magnitude to the amount of discrimination which a linear oligodeoxynucleotide shows against single-base mismatches.[10] It is clear, therefore, that compound **1** is readily able to distinguish between its six target sequenes and other complementary and partially complementary DNA sequences.

In summary, the results indicate that reasonably complex multifunctional behavior can be successfully designed into synthetic DNA-recognizing molecules. The design of the oligonucleotide macrocycle **1** illustrates ways to control binding properties in DNA molecules by varying more than just the simple primary sequence of nucleotide bases. In this case, the circularity, the use of opposite domains for binding, and the pseudosymmetry of the domains all allow for greater control of secondary and tertiary interactions in the final complexes than is commonly used in Watson–Crick binding. It is possible that this multisite binding might be applied to practical problems of nucleic acid recognition; for example, inhibition of gene expression by targeting more than one site in a gene, or more than one gene in an organism. Further study will be necessary to investigate these possibilities.

Experimental Procedure

Oligodeoxynucleotides **2**–**10** were synthesized by automated methods using β-cyanoethylphosphoramidite chemistry [14] on a Pharmacia LKB instrument, and were purified by preparative denaturing polyacrylamide gel electrophoresis. Quantification was done by measuring absorbance at 260 nm and calculating concentration based on extinction coefficients derived from nearest neighbor analysis [15]. For construction of compound **1**, the linear precursor 5′-dTTTTCTTTC-CTCTTTTCTCTTTCTTTCTCCTTCTCp was synthesized, along with a template for cyclization having the sequence 5′-dAGAAAAGAGAA. Cyclization was carried out with an aqueous nonenzymatic ligation reaction, with 50 μM each of linear precursor and template, 200 mM imidazole · HCl (titrated to pH 7.0 as a stock solution prior to addition to the reaction mixture), 100 mM $NiCl_2$, and 125 mM BrCN for 12 h at 23 °C, as described previously [11, 16]. Workup and isolation were as described previously [11, 17]. The conversion to circular product was about 70% (by gel analysis), and the circular product was isolated in 43% yield by excising, crushing, and elution from the peparative gel followed by dialysis to remove salts. The circular structure was confirmed by complete resistance to cleavage by a combination of T4 DNA polymerase (3′ exonuclease activity) and T4 polynucleotide kinase (3′ phosphatase activity in the absence of ATP) under conditions which cleave the linear precursor to mononucleotides. The cleavage was carried out at 37 °C (1–40 minutes) with 23 μM DNA, 58 mM tris(hydroxymethyl)aminomethane (Tris) · HCl (pH 7.6), 12 mM $MgCl_2$, 6 mM dithiothreitol, 100 μM spermidine, 100 μM EDTA, 0.5 units/μL kinase, and 0.1–0.2 units/μL polymerase. Enzymes were purchased from New England Biolabs (T4 kinase) and United States Biochemical (T4 polymerase).

Thermal denaturation studies on the 1:1 complexes were carried out at 6 μM total oligonucleotide concentration in a buffer containing 100 mM NaCl, 10 mM $MgCl_2$, and 10 mM Na-PIPES (HPIPES = 1,4-piperazinediethanesulfonic acid) at pH 7.0 in stoppered 1 cm pathlength cells. Prior to the denaturation experiment, samples were heated to 90 °C for 2 min and then allowed to cool slowly to room temperature. For the denaturation, a thermocontrolled Varian Cary 1 UV/VIS instrument was used, and temperature was increased at a rate of 0.5 K per minute under nitrogen atmosphere. The reference samples contained the identical buffer without DNA. Curve fitting was carried out as described previously [8, 10]. T_m values are obtained from the first derivative of absorbance with respect to T^{-1}, and are estimated to be accurate to within ±0.5 °C. Precision in free energy measurements is estimated to be ±10–15%.

Received: November 24, 1993 [Z 6510 IE]
German version: *Angew. Chem.* **1994**, *106*, 1057

[1] J. Miller, A. D. McLachan, A. Klug, *EMBO J.* **1985**, *4*, 1609–1614.
[2] N. P. Pavletich, C. O. Pabo, *Science* **1991**, *252*, 809–817.
[3] H. R. B. Pelham, D. D. Brown, *Proc. Natl. Acad. Sci. USA* **1980**, *77*, 4170–4174.
[4] B. M. Honda, R. G. Roeder, *Cell* **1980**, *22*, 119–126.
[5] M. S. Sands, D. F. Bogenhagen, *Nucleic Acids Res.* **1991**, *19*, 1791–1796.
[6] E. Rubin, E. Kool, *J. Am. Chem. Soc.* **1993**, *115*, 301–302.
[7] L. J. Maher III, B. J. Dolnick, *Arch. Biochem. Biophys.* **1987**, *253*, 214–220.
[8] J. Lisziewicz, D. Sun, M. Klotman, S. Agrawal, P. Zamecnik, R. Gallo, *Proc. Natl. Acad. Sci. USA* **1992**, *89*, 11209–11213.
[9] R. Morgan, M. Edge, A. Colman, *Nucleic Acids Res.* **1993**, *21*, 4615–4620.
[10] E. T. Kool, *J. Am. Chem. Soc.* **1991**, *113*, 6265–6266.
[11] G. Prakash, E. T. Kool, *J. Am. Chem. Soc.* **1992**, *114*, 3523–3527.
[12] D. S. Pilch, C. Levenson, R. H. Shafer, *Proc. Natl. Acad. Sci. USA* **1990**, *87*, 1942.
[13] M. Petersheim, D. H. Turner, *Biochemistry* **1983**, *22*, 256–263.
[14] S. L. Beaucage, M. H. Caruthers, *Tetrahedron Lett.* **1981**, *22*, 1859–1862.
[15] P. N. Borer in *Handbook of Biochemistry and Molecular Biology, Vol. I* (Ed.: G. D. Fasman), 3rd edition, CRC, Cleveland, OH, USA, **1985**, p. 589.
[16] S. Rumney, E. T. Kool, *Angew. Chem.* **1992**, *104*, 1686–1689; *Angew. Chem. Int. Ed. Engl.* **1992**, *31*, 1617–1619.
[17] G. Prakash, E. Rubin, E. T. Kool, unpublished.

Courier 12

Angewandte Chemie publishes contributions from all branches of chemistry, from classical to interdisciplinary research. A manuscript should be comprehensible for all chemists, even those who are not specialists in the field.

For the editorial handling of the article, the manuscript must have a **generous spacing** between lines (5 mm at least). Other points in the Instructions for Authors printed in the January 1994 issue should also be observed. Unfortunately an error slipped through in the detail on type size: under item 3a the size given is Courier 10, but should read Courier 12.

This type size is too small.

This type size is ideal.

 © *VCH Verlagsgesellschaft mbH, D-69451 Weinheim, 1994* *0570-0833/94/0909-1007 $ 10.00+.25/0*

Absorbing Free-Radical Chemistry

Half a Century of Free Radical Chemistry. By *D. H. R. Barton* and *S. I. Parekh*. Cambridge University Press, Cambridge, 1993. XI, 164 pp., hardcover £ 30.00, paperback £ 12.95.—ISBN 0-521-44005-X/0-521-44580-9

In six years time free radical chemistry will be celebrating its hundredth birthday. It was Moses Gomberg who announced the birth of the first 'free' radical, the triphenylmethyl radical, in the Journals of the American and German Chemical Societies. Before Gomberg's time, the word 'radical' belonged to the science of nomenclature, and was used to describe those parts of molecules that remained unaltered during chemical reactions. It is interesting to note that Gomberg ended his article by mentioning that his investigations were continuing, and requesting that this research topic should be left to him for a time.

Whether as a result of that statement or because the time was not yet ripe, the fact is that free radical chemistry had only a shadowy existence up to about 1940. It was only with the discoveries of the peroxide effect and, more especially, of free radical polymerization that interest in the topic was reawakened. Nowadays one cannot think of organic synthesis without including free radical chemistry, and new evidence of the importance of free radicals in processes that are vital to living organisms continues to emerge.

1940 was also the time when Derek Barton began work at Imperial College, London, on his dissertation concerning the formation of vinyl chloride during the pyrolysis of 1,2-dichloroethane. In Chapter 1 of the book reviewed here, Barton describes how this work gave him his first contact with free radicals. The first half of the book contains summaries of several lectures given by the author in 1991 as Visiting Professor at the Academia Nazionale dei Lincei in Milan. The second half consists of a new review by S. I. Parekh of the applications of the Barton reaction, discovered ten years ago, whereby free radicals with synthetic potential are generated from carboxylic acids. The first part is a valuable contribution to the history of chemistry between 1940 and 1990. It makes very enjoyable reading and is skillfully written. Derek Barton describes here how the discoveries and developments that were his contribution to free radical chemistry came about. These include the phenolate free radical coupling reaction, the preparation of alkoxy radicals from nitrites (the first 'Barton reaction') and their use in syntheses, the free radical deoxygenation reaction (Barton–McCombie reaction), and the free radical decarboxylation reaction (the third 'Barton reaction'). As one expects from this author, the chapters are written from a very personal standpoint and are enriched by many anecdotes. In Chapter 4, for example, we learn how important a role the game of bridge can have in the discovery of new reactions. The lectures reproduced here are of a quality to stand alongside Sir Derek's talk on the subject "How to Win a Nobel Prize".

The book makes absorbing reading, and (especially in its paperback form) would while away the travelling time in tram, bus, or plane in a very enjoyable way.

Bernd Giese
Institut für Organische Chemie
der Universität Basel (Switzerland)

This section contains book reviews and a list of new books received by the editor. Book reviews are written by invitation from the editor. Suggestions for books to be reviewed and for book reviewers are welcome. Publishers should send brochures or (better) books to the Book Review Editor, Dr. Ralf Baumann, Redaktion Angewandte Chemie, Postfach 101161, D-69451 Weinheim, Federal Republic of Germany. The editor reserves the right of selecting which books will be reviewed. Uninvited books not chosen for review will not be returned.

Supramolecular Architecture. Synthetic Control in Thin Films and Solids. (ACS Symposium Series, Vol. 499.) Edited by *T. Bein*. American Chemical Society, Washington, DC, 1992. XI, 441 pp., hardcover DM 172.—ISBN 0-8412-2460-9

This book is an invaluable resource for those interested in many aspects of porous solids and thin-films synthesis—especially researchers concerned with inclusion or guest–host chemistry. The scope is broad and extremely well-rounded; the editor is to be commended on all aspects of this volume, from the quality of the authors he has attracted to the uniformity of the text, and especially for the inclusion of a very comprehensive index. This latter feature greatly enhances the utility to both the casual reader and the more dedicated user seeking specific material.

The chapters on thin-film synthesis cover self-assembled monolayers of alkanethiols on metal surfaces studied at a fundamental structural level (Whitesides et al.), while synthetic approaches and detailed characterization of self-assembled layers of metal complexes (Ru diimines, Zr phosphonates) are also described in detail. Rieke et al. describe the fascinating concept of biomimetic thin film synthesis, in which organic functionalized surfaces act as a mimic of nucleation proteins designed to direct and control mineral deposition during the formation of bone, shell, etc. in living systems. A major potential for this kind of approach is to use the directing effect of a derivatized surface to produce new materials and composites, and preliminary data are presented here. Finally, a nice review by Parkinson describes the use of scanning tunneling microscopy and atomically flat surfaces to create nanoscale surface modifications and patterning.

The increasingly fashionable area of "soft chemistry" as a new route to solid materials or new phases of known materials is covered in articles by Rouxel et al. (layered solids such as iron phosphonates) and Kaner et al. (MoS_2, ZrN). Pillared clays and related materials for use as catalysts for bromide to nitrile, thiocyanate, sulfide and ether conversions are described by Pinnavaia et al., with high activity ascribed to the stabilization of an organic/aqueous interface on the surface of the clays. Three consecutive chapters describe the use of layered and/or crystalline hosts for polyethers and polyimines to produce ionic conductor materials. The background information provided here, coupled with the authors' own work, provides a nice succinct introduction to this important area.

The remainder of the book is dedicated to three-dimensional frameworks and amorphous networks, a large fraction using zeolite host materials but also covering other microporous nets such as the $Cd(CN)_2$ system. Bein's chapter on clusters, quantum dots, and polymers is a fitting complement to the work presented by other authors on similar themes, providing a wide-ranging yet very readable account of the use of nanovessels as reaction media. Mallouk's work on self-assembled electron transport chains in zeolites is an elegant example of how these principles of zeolite inclusion chemistry can be exploited to help address the problems of photosynthesis mimics. The final two chapters on the production of sol–gel derived glasses are excellent reviews of this exciting area, not only giving background information but also conveying a fine sense of just how versatile this approach can be for the production of functional composite materials and films (e.g. enzyme derivatized materials or glasses for nonlinear optics).

In summary, this book presents a comprehensive overview written in short sections which whet the appetite for further details. It is a must for anyone even remotely interested in inclusion type phenomena, and for those seeking an introduction to the area I can think of no better way to get the feet wet.

Norman Herron
E. I. du Pont de Nemours
Wilmington, DE (USA)

Electrochemical and Electrocatalytic Reactions of Carbon Dioxide. Edited by *B. P. Sullivan, K. Krist* and *H. E. Guard*. Elsevier, Amsterdam, 1993. XVI, 298 pp., hardcover HFl 340.00.—ISBN 0-444-88316-9

The use of carbon dioxide as a source of carbon for chemical reactions in the laboratory or in industry is a highly topical area of research which is of great interest both environmentally and economically. Because of the thermodynamic stability of the CO_2 molecule it is necessary to supply the reaction system with energy by thermal, chemical (through an energy-rich substrate), electrical, or photochemical means. The two last-named methods have attracted growing interest in connection with the development of alternative energy sources, and therefore one especially welcomes this attempt by the editors B. P. Sullivan, K. Krist, and H. E. Guard to put together an account of the present state of research in this field. Regrettably, they have not entirely succeeded in this aim.

The book is a collection of eight review articles in which the respective authors describe their own areas of research and report results from their and other groups' work. The introductory chapter by F. R. Keene is concerned with thermodynamic aspects of the use of CO_2 as a starting material for synthetic purposes, and with the bonding of CO_2 to transition metals, but contains little that has not already been covered in previous reviews. Moreover, the detailed treatment of reactions between CO_2 and transition metal complexes seems superfluous, since the following chapter by C. Creutz is entirely devoted to this subject, giving a detailed survey of the methods of preparation, bonding characteristics, and spectroscopic properties of CO_2 complexes. Methods for detecting and identifying CO_2 adducts are also briefly discussed. However, the widening of the definition of 'CO_2 complexes' to include compounds formed by the reaction of CO_2 with a ligand is unusual and seems rather artificial. Nevertheless, that does not detract from the favorable overall impression of this useful article. Next P. C. Ford deals with the water-gas shift reaction, centered on a discussion of mechanisms. However, it is doubtful whether this topic really deserved a chapter to itself in a book with the above title. In Chapter 4 scientists at the Solar Energy Research Institute review the prospects for electrochemical energy storage based on CO_2, then in Chapter 5 F. R. Keene and B. P. Sullivan return to the topic of transition metal catalysis. Here it would have been better to change the order of the chapters, and at the same time some overlapping of subject matter between Chapter 5 and Chapters 1–3 could have been avoided (e.g., compare p. 123 with pp. 11 and 22, and p. 130 with p. 12). Chapters 6 and 7 are concerned with the electrochemical reduction of CO_2 at metal electrodes; with a total of 118 pages they form the largest part of this book of about 300 pages. Unfortunately the authors get too much immersed in detail, especially in Chapter 6, and the reader will find it difficult to discern general features among the great mass of data, which are partly collected together in tables and diagrams with insufficient accompanying text. The book ends with a brief survey of photochemical and photoelectronic systems for the reduction of CO_2, by N. S. Lewis and G. A. Shreve of Caltech. It might have been helpful to have one or two formula schemes in this article, at least in the general introduction (in 24 pages there is not a single chemical formula!). However, this complex subject is explained in a clearly understandable way, and the published data are critically evaluated.

Unfortunately the book as a whole gives the impression that neither all the authors nor the editors have taken the necessary care with their tasks. For example, a good deal of overlapping could have been avoided by better coordination. Furthermore, in the age of the computer it should have been possible to produce the articles in a more visually appealing form and to ensure some degree of uniformity. Only C. Creutz (Ch. 2) knows how to present her contribution in a really clear and neat style. In contrast, even someone with excellent eyesight will find it scarcely possible to read Chapter 7 without using a magnifying glass.

However, more disturbing than these superficial defects are the many typing errors and inaccuracies that are scattered throughout the book. Even the list of authors at the beginning has not escaped intact. Often one finds that footnotes below tables have no corresponding symbol in the table itself (e.g., pp. 39, 40), and figures and equations are often wrongly numbered and/or do not match the corresponding mention in the text (pp. 176, 177). Sometimes the notation for physical quantities is not consistent, even within a chapter (e.g., pp. 155–160: λ_{el} and λ^{el}; p. 256: M_p and m_p), and one finds incorrect chemical equations (p. 135: Eqns. 24 and 25; p. 259: Fig. 13) or mathematical equations (p. 256: Eqn. 51), even at key points in the book. Just on pages 256 and 257 there are twelve (!) errors, some quite serious. Most annoying is the authors' lack of care in compiling the lists of references for the individual chapters. Some of the errors are of a kind that the interested reader can correct—for example, wrong spellings of names (p. 287: "Cruetz"), wrong years of publication (p. 214: "198" or "19678"), or incorrect literature references (pp. 142, 154)—but vigilance is to no avail when literature references in the text give numbers higher than any contained in the bibliography (as in Chs. 3 and 4).

The shortcomings described above might be partly excused if the articles were exceptionally up-to-date, but here we come to the book's most serious weakness, as all the texts appear to have been written as early as 1989 or 1990. Only the article by C. Creutz was revised and updated at the beginning of 1991, a fact that merited a special mention at the end of her contribution. This general lack of up-to-dateness no doubt explains why, throughout the book, only the reduction of CO_2 is

discussed, with no mention of the electrochemical method for forming C–C bonds, of which there have been numerous reports since 1989.

To summarize, a critical reader with lots of patience and tenacity can extract some interesting information and many useful ideas from this book. Despite the wide-ranging importance of carbon dioxide chemistry that is referred to in the preface, the editors have produced a book that is mainly of interest to the specialist or to the newcomer who is concerned with a relatively narrow, although important, specialized area. However, the main quality that such readers expect from a monograph is up-to-dateness. The contents of this book and the amount of care taken in its preparation seem inadequate to justify the price.

Walter Leitner
Arbeitsgruppe CO_2-Chemie
der Max-Planck-Gesellschaft
an der Universität Jena (FRG)

Chemistry of Iron. Edited by *J. Silver*. Blackie/Chapman & Hall, London, 1993. X, 306 pp., hardcover £ 69.00.—ISBN 0-7514-0062-9

It is not without some initial bias that one approaches a book of a mere 300 pages on the chemistry of iron. One inevitably thinks of the monograph on ruthenium by Seddon and Seddon, which is at least 1000 pages longer. The editor must have anticipated such a reaction, since he states in the preface that "[The book] is not designed to be a dictionary of iron compounds." Nevertheless, it is not exactly reassuring to discover that the book consists of eight articles of greatly differing lengths, from ten pages to about a hundred. This is not to say that a book suffers from having many authors, but it is generally recognized that it is difficult under such circumstances to produce a work that is a unified whole. The combination of differences in form and common subject areas means that overlapping is often unavoidable.

After these prejudiced remarks we return to the book itself. The introductory article, written by the editor J. Silver, is a brief (25 pp.) survey of the chemistry of iron, with examples corresponding to the different oxidation states. Many aspects are only briefly touched on, and thus the level does not extend beyond that of a standard textbook. The rather glib statement that iron occurs in oxidation states up to +8 is, fortunately, qualified a few pages later. The literature references, numbering more than 120, are certainly useful. On the next 15 pages F. J. Berry sets out to introduce the reader to the industrial chemistry of iron. This topic is better covered in "Greenwood and Earnshaw", and no more need be said about this chapter. In the next article E. Sinn has attempted to treat the inorganic chemistry of iron in a mere 25 pages. The lack of success is not entirely due to the shortness of the chapter. The treatment is very superficial. I have rarely come across a text containing so many errors and inaccuracies. The olivine and perovskite structures are confused, $FeCl_2$ is claimed to crystallize in the rutile structure, the "typical" spin state of iron(III) is given as $S = 3/2$, $[Fe(CN_6]^{4-}$ is described as the "ferrocyanide" ion, the author persists in writing "marcosite", and so on. Many compounds are simply ignored: the section on binary halides contains no mention of the fluorides nor of FeI_2. Also the treatment of the subject matter is not balanced; the reason for this becomes obvious on looking through the literature citations.

The longest article (about 90 pp.) is that by P. L. Pauson on organoiron compounds. More than 300 compounds are described under clearly arranged headings, with brief notes on reaction pathways and properties. A further positive feature is the bibliography of over 400 references, including some from 1992. One may question whether a book such as this should contain a separate chapter on spectroscopic methods. However, as there is one (10 pp., B. W. Fitzsimmons), it should certainly have included a few key results obtained by Mössbauer spectroscopy to emphasize the importance of this method, especially for iron studies. The next two articles ("Biological Iron", by J. G. Leigh, G. R. Moore, and M. T. Wilson, 55 pp., and "Models for Iron Biomolecules," by A. K. Powell, 25 pp.) illustrate the fact that in such a collection some overlapping is virtually unavoidable. Apart from that, the two articles together give a very up-to-date survey of the bioinorganic chemistry of iron. The last article by R. C. Hider and S. Singh on iron chelates of clinical importance is peripheral to the book's theme, but nevertheless interesting. The authors describe various multidentate ligands of importance in therapy based on iron chelates, together with their applications, effectiveness, and side effects.

Who ought to buy this book? Although the preface mentions advanced students of all related scientific disciplines, it is too expensive to be recommended for these in its present form. Some of the articles make the book a useful addition for libraries to extend and update their coverage, but here too there is cost-cutting. I regret to say that, despite its attractive silver binding, this book is unlikely to have a glittering future.

Siegfried Pohl
Fachbereich Chemie
der Universität Oldenburg (FRG)

Photodissociation Dynamics. (Series: Cambridge Monographs on Atomic, Molecular and Chemical Physics, Vol. 1. By *R. Schinke*. Cambridge University Press, Cambridge, 1993. 417 pp., hardcover £ 50.00.—ISBN 0-521-38368-4

This book is concerned with the dynamics of photochemical processes, an area of physical chemistry which is of very wide interest. It has undergone rapid development in recent years, owing to the availability of ever more powerful laser systems, new experimental techniques, and new advances in theoretical chemistry. Schinke has written a book which succeeds well in every respect. It is intended not only for specialists with experience in this area but also for advanced students interested in this topic, who will find in it a wealth of relevant information. However, the author's aim is not to give detailed accounts of new experimental methods and results; instead the emphasis is on applying the methods of theoretical chemistry to describe photochemical dissociation processes.

Mathematical equations are limited to those that are absolutely essential, and this will undoubtedly make it much easier for many readers to digest the book. Another positive feature is that instead of reviewing all the reported work on a particular topic, the discussion of experimental and theoretical results is almost always based on a few small model systems (H_2O, H_2O_2, H_2S, ClNO, and CH_3ONO). It is entirely sensible and justifiable to limit the discussion to these model systems, especially as many of the processes described apply equally to larger systems. On the other hand, the bibliography is very extensive (over 750 references), affording easy access to the original publications.

The structure of the book is briefly as follows. A detailed introduction emphasizing the practical questions that need to be addressed is followed by a chapter on light absorption and photodissociation. The next two chapters deal with time-independent and time-dependent quantum mechanical methods, then in Chapter 5 the author turns to the classical description of photodissociation. There then follow chapters on direct and indirect

photodissociation processes and the occupancies of the different quantum states of the dissociation products, which yield important information about the dynamics of such photodissociation processes. The author devotes special attention to dissociation processes in van der Waals molecules and vibrationally excited molecules, and to nonadiabatic processes. Lastly some recent experiments using ultrashort (femtosecond) laser pulses are described.

To summarize, this is a substantial work which is of a high standard throughout. It can be recommended unreservedly, not only for theoretically orientated chemists but also for experimentalists working in the fields of photochemistry, spectroscopy, or chemical kinetics, and for advanced students who wish to become involved in this interesting area of physical chemistry.

Peter Wiesen
Institut für Physikalische Chemie
der Universität-Gesamthochschule
Wuppertal (FRG)

Biocatalysts in Organic Synthesis. (Series: Studies in Organic Chemistry, Vol. 46.) By *J. Halgas*. Elsevier, Amsterdam, 1992. XIV, 334 pp., hardcover $ 180.00.—ISBN 0-444-98698-7

Biocatalytic transformations have led to important advances in asymmetric synthesis, and have now become an indispensable part of the armory of methods in this field. Introductory surveys for nonspecialists are much in demand because biological catalysts occur as a wide variety of special types with unique characteristics and can be used in diverse ways, and because the original publications are scattered throughout many journals of different disciplines. By the nature of the book Halga's this review may be seen to some extent as a postscript to other recent reviews of monographs published on this theme in 1992 (L. Poppe, L. Novák, *Selective Biocatalysis*, VCH Verlagsgesellschaft, Weinheim, **1992**; K. Faber, *Biotransformations in Organic Chemistry*, Springer, Berlin, **1992**; reviews: *Angew. Chem. Int. Ed. Engl.* **1993**, *32*, 920; H. L. Holland, *Organic Synthesis with Oxidative Enzymes*, VCH Verlagsgesellschaft, Weinheim, **1992**; review: *Angew. Chem. Int. Ed. Engl.* **1993**, *32*, 622).

The present book of nine chapters begins with three introductory discussions, first about the fundamental nature of enzymic catalysts (Ch. 1, 12 pp., nomenclature, effects of solvent, temperature, and pH, inhibition), then about the forms in which they are used (Ch. 2, 33 pp., microorganisms and isolated enzymes in both free and immobilized forms), and thirdly about the basic principles of enzymic stereoselectivity (Ch. 3, 12 pp.). The main body of the book, on synthetic applications, begins with Chapter 4 ("Substitution Reactions", 12 pp.). Here the author collects together a miscellany of reactions using enzymes of widely different types (haloperoxidases, transferases, lyases) which can be formally classed as substitutions (methylation, halogenation, transglycosidation; however, glycosyl transferases are not included, despite the fact that an index entry leads one to expect this). Chapter 5 deals with additions at C=C and C=O bonds (21 pp., Michael addition, aldol addition, formation of cyanohydrins and acyloins). Chapter 6 is the longest (97 pp.) in accordance with the preparative importance of its subject, the various aspects of the conversion of esters by hydrolytic enzymes (transesterification, hydrolysis, formation of phosphate esters). Chapter 7 (20 pp.) is devoted to the analogous reactions of amides (including hydrolysis of nitriles). Finally, the last two chapters are focused on the wide range of preparative biocatalytic redox processes, and the methods needed to regenerate cofactors. Chapter 8 (28 pp.) describes the various types of enzymic oxidations of organic compounds (alcohols, amines to carbonyls, Baeyer–Villiger, hydroxylation, dehydrogenation, oxidation at heteroatoms; also included are preparative applications of galactose oxidase, which I did not find in the pertinent monograph by Holland mentioned above). Chapter 9 (65 pp.) concentrates on reductions (mainly of C=O bonds, including reductive amination, but also reduction of C=C, NO_2, and other groups). At the end of the book is a detailed bibliography (939 references extending up to the end of 1989; interestingly, reference [9] is to a monograph that has not yet been published!), together with separate lists of recommended further reading for each chapter (important original publications and recent review articles extending up to 1992, comprising altogether an additional 121 citations). Lastly there is a six-page subject index.

It is already evident from the relative importance given to the individual chapters that Halgas, in noticeable contrast to the authors mentioned above, is especially concerned here to present the full breadth of available methods of enzymic catalysis and the individual potential for synthetic applications. On the one hand he devotes an appropriately large amount of space to the currently most important types of reactions (transesterification/hydrolysis, oxidation and reduction) and enzymes, while on the other hand, by giving a balanced broader survey of the variety of biotransformations used in organic synthesis, he undoubtedly succeeds better in providing readers with ideas for using enzymes to solve their own synthetic problems. Also very useful for beginners are the frequent cross-references to relevant technological processes, e.g., in the synthesis of amino acids.

The text is generously illustrated by formula schemes, although the formulas are unnecessarily large. This often spoils the continuity of flow schemes in relation to page breaks, especially annoying if one must turn the page to find the products of a reaction (pp. 15/16, 67/68, 199/200, 243/244, 285/286). Occasionally one wonders why trivial items (e.g., the depiction of α- and β-methyl glucoside to exemplify glycosides) are presented at the same level as more important matters.

The author's concern for variety and completeness, which is evident from the evaluations of different procedures, and from the wealth of experimental details given, may occasionally cause the reader to lose sight of the wider objective. Although some of the data are summarized in the form of tables, still more use of this form of presentation would definitely have greatly increased the usefulness of the book. Because little systematization has been brought to the varied collection of individual results and preparative details, many important facts will only become apparent after a more thorough reading, rather than allowing a rapid grasp of the salient points. Moreover, this is not helped by the fact that the index is too brief to do justice to the amount of information in the book. Although the reactions described can be well accessed by the many cross-references to the enzymes used to catalyze them, and those to the various microorganisms from which they are derived, this will only be of limited use as a searching aid to the synthetic chemist lacking relevant experience, who is primarily interested not only in reaction types but in compounds, their structural features, and specific conversions.

The book is largely free from typographical and factual errors; the few that remain are of an obvious kind which serve to entertain rather than cause problems, and one is content to overlook them. (Examples: on p. 72 di*chloro*fumaric acid supposedly splits off HF, and on p. 104 an *ee* value of 98% is given for cyclopropanol.) On the other hand it was an-

noying, especially in a fairly expensive book, to find that the review copy had printing defects on several pages, where multiple printing had produced shadow characters making the text difficult to read.

Although the material in this book by Halgas is not especially up-to-date, its particular strength lies in providing a comprehensive and detailed account of enzymic methods in organic synthesis. Thus it is suitable both as an introduction to preparative biocatalysis and as a permanent reference source for research chemists and lecturers with interests in this field.

Wolf-Dieter Fessner
Institut für Organische Chemie
und Biochemie
der Universität Freiburg (FRG)

Liquid Crystal Polymers. (Series: Speciality Polymers. Series editor: *J. M. C. Cowie.*) Edited by *N. A. Platé.* Plenum, New York, 1993. 438 pp., hardcover $ 110.00.—ISBN 0-306-44219-1

This book consists of ten chapters in which twelve Russian authors summarize the rapid developments that have occurred in the field of liquid crystal polymers in the last 15 years or so. Especially noteworthy is the very good coordination that has been achieved between the various specialists with regard to content, consistent use of symbols, and form of presentation. Each chapter has a short introduction linking it to the other authors' contributions and briefly describing the historical development. On the whole the editor has succeeded well in ensuring that the individual authors' reviews of progress in liquid crystal polymers are highly informative and critically presented. It is entirely appropriate that in this area of research the Russian literature should be given special emphasis, as much of it is not sufficiently well known in other countries. However, it must be noted less favorably that there are only sporadic references to work published from 1987 onwards. Brief descriptions of the ten chapters follow.

Chapter 1: Statistical physics of liquid crystalline order in polymeric systems (A. R. Khoklov, 38 pp., 139 refs.). Theoretical models for both rigid and flexible polymers are critically discussed with references to the original papers. Melting behavior and elastic and rheological properties are treated in rather more detail. This chapter provides the fundamental basis for the following chapters. Chapter 2: Phase equilibria in polymer systems with liquid crystalline phases (S. P. Papkov, 32 pp., 58 refs.). After a general classification of the types of phases and explanations of the meaning of thermotropic and lyotropic phases, the author concentrates mainly on the solution behavior of polymers with rigid chains. The predictions of several different models are compared. Chapter 3: Molecular structures of polymers with mesogenic groups (I. N. Shtennikova, 54 pp., 111 refs.). Different conformations are discussed, and the implications in relation to streaming birefringence and the Kerr effect are briefly considered. This is followed by a discussion of these effects as observed in lyotropic polymers and in polymers with main and side chains, from the standpoints of different theories. Chapter 4: The mesomorphic state of polymers with flexible chains (Yu. K. Godovskii and V. S. Papkov, 38 pp., 93 refs.). Various experimental results on linear polyorganosiloxanes, polyphosphazenes, and cyclolinear polyorganosiloxanes are summarized and evaluated. Chapter 5: Thermotropic liquid crystal polymers with mesogenic groups in the main chain (S. S. Skorokhodov, 30 pp., 82 refs.). Continuing the theme of Chapter 4, syntheses of polyesters, polyethers, and polyurethanes are described. Special attention is devoted to the use of texture observations to recognize the liquid-crystalline state, and to the detection of order. The effects of the previous history of the polymer on its physico-chemical properties are discussed. Chapter 6: Comb-like liquid crystal polymers (V. P. Shibaev, 57 pp., 69 refs.). V. P. Shibaev, one of the 'fathers' of polymers with liquid-crystalline side chains, discusses some of his areas of research: methods for the synthesis of polyacrylates, polymethacrylates, polyesters, and polypeptides with various liquid-crystalline side groups. Topics receiving special attention are the glass transitions of the polymers, and related discussions regarding the thermal equilibrium, the effects of chemical variations (including the degree of polymerization) on phase transition temperatures, structural aspects of the phases, and ferroelectric polymers. The survey of nematic polymers and the comparison with smectic polymers in this chapter are some of the most valuable sections of the book. Unfortunately it has only been possible to give a hint here of the start of the rapid developments in the field of elastomers that have occurred in the last few years. Chapter 7: Liquid crystal polymers of the cholesteric type (Ya. S. Freidzon and V. P. Shibaev, 52 pp., 87 refs.). By limiting the topic area to be covered, the authors have been able to give a detailed and comprehensive treatment which is well worth reading, even by specialists. Chapter 8: Structural transformations of thermotropic liquid crystal polymers in electric and magnetic fields (R. V. Talroze and N. A. Platé, 36 pp., 67 refs.). Starting from the fundamental principles, the authors deal mainly with electrooptical effects of dielectric and hydrodynamic origin, and with induced phase transformations and memory effects (information storage). This section should be especially useful to technologists with interests in this area. Chapter 9: Rheological properties of liquid crystal polymers (B. G. Kulichikhin, 44 pp., 119 refs.). The theoretical and experimental aspects of polymer solutions and melts are treated comprehensively. The author also briefly discusses some hitherto unsolved experimental problems and potential technological applications. Chapter 10: High-strength and high-modulus fibers from liquid crystal polymers (A. V. Volokhina and G. I. Kudryavtsev, 36 pp., 94 refs.). The authors discuss the technology and characterization of Aramid fibers, ultra-high-modulus fibers made from heterocyclic monomers, and lyotropic polymers, and predict a bright future for such materials.

The book can be recommended for everyone with interests in mesomorphic phases, and for those concerned with new developments in electrooptics, information storage, sensor technology, and fibers research.

Horst Kresse
Institut für Physikalische Chemie
der Universität Halle-Wittenberg (FRG)

Chirotechnology. Industrial Synthesis of Optically Active Compounds. By *R. A. Sheldon.* Marcel Dekker, New York, 1993. 423 pp., hardcover $ 145.00—ISBN 0-8247-9143-6

Does stereochemistry have any particular implications for the design of an industrial chemical process, and if so, what methodologies with scale-up potential are available for efficient and successful manufacturing of stereoisomers? This simple and straightforward two-fold question well reflects the tremendously increased importance and awareness of industrially related stereochemical issues over the past one or two decades. The three-dimensional concept of molecular species so brilliantly conceived in the mid-1870s and assuming a central role ever since, especially in organic

 © *VCH Verlagsgesellschaft mbH, D-69451 Weinheim, 1994* *0570-0833/94/0909-1013 $ 10.00+.25/0*

chemistry, has now definitely reached the "factory floor", driven to a large extent by the well-established fact that stereoisomers of many chiral compounds differ greatly in their properties when applied in, for example, the pharmaceutical and agrochemical areas, and thus need to be produced in high optical purity. Given this background, it is not entirely surprising to find that this "hot" topic has recently been a focus of attention in journals, books, symposia, and conferences.

It is in this context that one should view the present book entitled with the newly coined word "Chirotechnology" (introduced by Stinson in *Chem. Eng. News* **1992**, *70* (39), 46–79). The approach is comprehensive, aiming to give a broad overview of topics related to stereoisomerism. The ten chapters cover topics ranging from the early landmark discoveries and basic features in "Introduction to Optical Isomerism" via "Chirality and Biological Activity" to "Synthetic Methodology" followed by "Fermentation Processes", "The Chirality Pool", "Racemate Resolution via Crystallization", "Enzymatic Transformations", and "Catalytic Asymmetric Synthesis" up to the present state of the art, ending with about 40 pages on "Industrial Processes", and a short "Epilogue" offering an outlook at possible future developments. Unfortunately the general impression is not very favorable. Firstly, the industrial connection in the methods and processes described is rather feeble, in contrast to the expectation raised by the book's title (which is quite surprising considering that the author has a background in industry). Secondly, more emphasis should be placed on the overridingly important quality aspects (at least for pharmaceutical products), from both the chemical (e.g., residual amounts of transition metals) and optical purity points of view. Thirdly, there are many printing errors (due to the lack of proper proofreading?).

The arrangement of the contents resembles a catalogue in which many methods are presented in a rather superficial way, without enough detailed discussion and in-depth analysis on matters such as process technology and equipment characteristics, comparisons of product outputs per unit reactor volume, process safety, and environmental impact (e.g., by solvents and other waste streams). A recently published "competitor" book (Collins, Sheldrake, Crosby, eds., *Chirality in Industry*, Wiley, 1992) clearly gives a more pronounced industrial edge to the subject. Furthermore, it would be interesting to see some figures comparing the costs of attaining specified optical purities by different methods; and why not give the reader a feeling for the cost increase one would face when shifting from a racemate to a highly enantiomerically pure product? (an industrial factor of great significance indeed!). The ongoing, more or less worldwide regulatory activities in this area constituting a driving force for the industry to pursue the route to stereochemically purer and purer compounds (of course with a concomitant price increase for the final product) should be discussed in more detail than the mere page (69) devoted to the subject.

To name but a few of the flaws found throughout the book, one could mention the structure of Mosher's acid (p. 32) which besides being totally wrong also contains a pentavalent carbon (!), missing heteroatoms (p. 125: nitrogen at C-7 of cephalosporin C; p. 161: carbonyl oxygen; p. 374: penem sulfur and monobactam nitrogen), missing carbon fragments in the molecular backbone or as substituents (p. 131: a propionic acid product is depicted instead of a butyric; p. 390: a five-carbon carbohydrate product instead of one with six), mix-up of formulas (p. 147: D-sorbitol and D-mannitol should change places), the frequent usage of "propanol" for the famous beta-blocker instead of the correct spelling propranolol. In order to save space, unnecessary repetition of information should be avoided, a point which in the present case can be exemplified by a number of more or less identical reaction and formula schemes (p. 59 vs. p. 365; p. 95, Fig. 3–23 vs. p. 226, Fig. 7–12; p. 95, Fig. 3–24 vs. p. 227, Fig. 7–13). Finally, the erroneous statement on page 125 that only penicillins structurally modified at C-6 are useful in therapy ignores the important class of C-2 carboxy-substituted ampicillin pro-drugs (e.g., bacampicillin) produced on the multi-ton scale.

The literature coverage comprised of some 700 references seems to be fairly well updated through 1991; work from 1992 appears only occasionally. Again, one can complain about misspelled author names and errors in volume number and year of publication, but what is even more annoying is the lack of consistency in using both inclusive pagination and first page indication.

In conclusion then, the shortcomings pointed out above need to be corrected in a future edition before this timely book can be recommended for its intended use by chemists in academia at more advanced undergraduate or graduate stages and in industry.

Hans-Jürgen Federsel
Chemical Process Development Laboratory
Astra Production Chemicals AB
Södertälje (Sweden)

Chemical Analysis of Inorganic and Organic Surfaces and Thin Films by Static Time-of-Flight Secondary Ion Mass Spectrometry (TOF-SIMS)

Alfred Benninghoven*

By using mass spectrometry to analyze the atomic and molecular secondary ions that are emitted from a solid surface when bombarded with ions, one obtains detailed information about the chemical composition of the surface. A time-of-flight mass spectrometer is especially suitable for the analysis of secondary ions because of its high transmission, high mass resolution, and ability to detect ions of different masses simultaneously. By using a finely focused primary ion beam it is also possible to analyze microareas and generate surface images with a lateral resolution of 0.1 μm or less. Static time-of-flight secondary ion mass spectrometry (TOF-SIMS) allows monolayer imaging and local analysis of monolayers with high sensitivity, a wide mass range, high mass resolution, and high lateral resolution. Besides information on elements and isotopes, the technique yields direct information on the molecular level and can also be used to analyze surface species of high molecular mass that are thermally unstable and cannot be vaporized. The method can be applied to practically all types of materials and sample forms, including insulators in particular. In this article the basic principles of TOF-SIMS are explained, and its analytical capabilities for both large-area and imaging applications are illustrated by examples. These include silicon surfaces (both uniform and structured), thermally unstable organic molecules on surfaces, synthetic polymers, and synthetically prepared molecular surface films, particles, and fibers. Emitted neutral particles can also be analyzed by post-ionization with a laser, and the possibilities of this technique are discussed.

1. Introduction

1.1. The Scientific and Technical Importance of Solid Surfaces

Many of the technically important properties of solid materials are surface properties and are essentially determined by the chemical composition and structure of the uppermost layer of atoms or molecules. Examples of such properties are adsorption behavior, chemical reactivity, frictional and wear properties, wettability, adhesion, and biocompatibility. Surfaces are therefore of central importance in nearly all areas of advanced technology, in micro- and nanoscale technologies, in microelectronics, in medical technology, and in biotechnology, as well as in chemistry, vehicle manufacture, and mechanical engineering. Accordingly, the study of the relationship between the chemical composition or structure of a surface and the resulting physical and chemical properties is a central theme of basic research.

For both technical applications and scientific studies it is essential that solid surfaces are prepared and modified in a controlled way. Methods used for the modification and structure control of surfaces include not only purely chemical processes but also various physical techniques such as irradiation with ions, electrons, and photons, and treatment by plasmas.

[*] Prof. Dr. A. Benninghoven
Physikalisches Institut der Universität
Wilhelm-Klemm-Strasse 10, D-48149 Münster (FRG)
Telefax: Int. code + (251)83-3682

1.2. Surface Analysis

Effective and powerful methods for surface analysis are necessary for basic research on solid surfaces as well as for technical applications. These analytical methods must be capable of giving detailed information, particularly about the chemical composition in the region of the uppermost atomic or molecular layer, since this essentially determines the physical and chemical properties of the surface.

Selective surface sensitivity is only one of several characteristics necessary for a method to be used for the chemical analysis of surfaces. In addition, the method must be capable of detecting and distinguishing between all elements, including hydrogen, and their isotopes. Also, because of the growing importance of molecular surfaces, it should yield significant information on the molecular level. Since many surface properties can be drastically altered by minute concentrations of certain surface constituents, a surface analytical method must be highly sensitive. Surface constituents are often distributed nonhomogeneously over the surface, for example in the case of a surface

on which a lateral structure has been deliberately created, or where there are natural surface inhomogeneities such as those that occur in corrosion processes, etc. Thus, the method must also have a high lateral resolution combined with high sensitivity and should be universally applicable to surfaces of widely different materials and forms. Lastly, the analytical measurements should be capable of yielding quantitative results, if necessary with the help of external or internal standards.

The methods currently used for surface analysis of solids are nearly all based on energy or mass analysis of electrons, photons, or atomic or molecular components that are emitted from a surface when suitably stimulated.[1] Those that are most important by virtue of their breadth of applicability are Auger electron spectroscopy (AES) and X-ray photoelectron spectroscopy (XPS or ESCA). In AES, surface atoms are excited by electron bombardment so that they emit Auger electrons, which are characteristic of the element concerned. By analyzing their energies one can directly identify the excited surface atoms. In the case of XPS (or ESCA) the surface elements are identified from the energy distribution of the photoelectrons that are emitted when the surface is irradiated by X-rays.

For both techniques the depth analyzed is on the order of a few atomic layers. Both methods give quantitative results. The detection limits are about 10^{-2} of a monolayer for XPS and 10^{-3} of a monolayer for AES. Neither of these methods can be used to detect hydrogen or distinguish between isotopes. Only XPS, through the well-resolved energy distribution of the photoelectrons, yields information about the chemical environments of the emitting atoms; this allows one to detect specific functional groups but not to identify organic molecules, especially when these are large. Several other methods, such as high-resolution electron energy loss spectroscopy (HREELS) and infrared (IR) spectroscopy, also yield a certain amount of information on the molecular level by detecting functional groups, but these too are unable to identify molecules, especially larger ones.

Electron microprobe analysis and the various nanometer probe techniques, such as scanning transmission microscopy (STM) and atomic force microscopy (AFM), also fail to meet the criteria listed above for surface analytical methods. Along with other failings electron microprobe analysis has too great a depth of analysis (about 1 μm),[2] while nanometer probes yield no chemical information.[3]

With regard to the requirements demanded of a surface analytical method, mass spectrometric methods have considerable advantages. They can detect all elements, distinguish between isotopes, yield detailed information about molecules, and are extremely sensitive, even quantitative when standards are used. In principle, therefore, they offer the basis for extremely effective techniques for the analysis of solid surfaces, provided that the surface species can be converted into free ions.

1.3. Surface Mass Spectrometry

Analysis and identification by mass spectrometry is possible only for free ions in the gas phase. Thus two central problems must be solved for any kind of surface mass spectrometry: firstly, the surface constituents to be identified must be transformed into the gas phase, and secondly, these must be ionized. Furthermore, in the case of molecular surface constituents these two operations must be performed in such a way that the probability of fragmentation is acceptably low. The energy needed can in principle be supplied by heating, by applying a strong electric field, or by bombarding the surface with electrons, atomic or molecular particles, or photons. However, most of these methods of excitation are unsuitable for surface analysis. Heating a surface that is to be analyzed will in general cause large changes in its chemical constitution. The detachment and ionization of surface particles by an electric field requires extremely high field strengths which can only be produced at a pointed tip with a very small radius of curvature. The desorption of ions by electron bombardment only occurs very selectively for certain types of surface species in particular bonding situations.

In contrast, bombardment with fast ions or neutral particles,[4] or irradiation with laser light of sufficient intensity[5] results in the removal of material from any type of solid surface. Not only neutral particles but also positive and negative ions are emitted. However, controlled removal of surface material in the monolayer and submonolayer regime, with lateral resolution in the submicron range, in a way that is independent of material type, is only possible with a beam of particles, not with a laser. This is because of the different nature of the energy transfer process from the primary beam to the solid surface, and the difference in the focusing capability of ion beams, which extends down to less than 50 nm; with a laser beam it is very difficult to achieve less than 1 μm.



Alfred Benninghoven was born in 1932 in Frankfurt am Main. He studied physics and mathematics at the Universities of Cologne and Paris from 1952 to 1959. He earned his Ph. D. in physics in 1961 for his research on the flow behavior of alkali metal vapors under ultrahigh vacuum. In 1963 he habilitated at the University of Cologne for his work on the energy distribution of vaporized metal atoms. He accepted a chair for experimental physics at the University of Münster in 1972. His research is focused on the interaction of ions with solid surfaces and the development of surface analytical methods, instruments, and applications, in particular for secondary ion mass spectrometry.

All surface mass-spectrometric methods are in principle material-consuming (destructive) forms of analysis, in which one sacrifices at least those particles that are detected by the mass spectrometer. The total amount of substance available for the analysis is thus limited to the number of atoms or molecules present in the top monolayer of the area that is analyzed. For an area of 1 μm^2 this is somewhere on the order of 10^6 particles (Table 1). When one also takes into consideration that the ionization probabilities for most surface constituents are less than 10^{-4}, it is immediately obvious that for an effective surface analysis one needs a mass spectrometer that detects practically all the ions generated.

Table 1. Order of magnitude of the numbers of particles and amounts of substance in monomolecular films.

Area	1 cm^2	1 mm^2	10 μm^2	1 μm^2	0.1 μm^2
Number of particles	5×10^{14}	5×10^{12}	5×10^8	5×10^6	5×10^4
Amount of substance	1 nmol	10 pmol	1 fmol	10 amol	0.1 amol

The mass spectrum of a mixture of organic molecules—for example, of polymers—can consist of many hundreds or thousands of lines, whose distribution is at first unknown. Thus one needs a wide mass range and high mass resolution, and furthermore it is essential that all ions generated are detected. Consequently, instruments employing a magnetic sector field, and likewise quadrupole spectrometers, are less than ideal as surface mass spectrometers, because of their limited mass range, low transmission, and sequential mass scanning mode. Ion cyclotron resonance mass spectrometers have only a very limited potential for this purpose, owing to their restricted dynamic range, the requirement that the molecular ions must remain stable for a significant time, and the experimental limitations that apply as a consequence of the strong, homogeneous magnetic field required in the sample region. In contrast to these, time-of-flight mass spectrometers offer an almost ideal solution to the requirements for surface mass spectrometry.

From these considerations it can be seen that time-of-flight mass spectrometry of secondary ions generated by bombardment with primary ions is a very effective and universally applicable method for the chemical analysis of surfaces.[6, 7] During the last ten years time-of-flight secondary ion mass spectrometry (TOF-SIMS) has undergone impressive developments. The instrument technology and knowledge of secondary ion emission behavior for a wide variety of material types have now advanced to an extent that allows local monolayer analysis or monolayer imaging of nearly any kind of solid surface with high sensitivity. Detailed information on the molecular level, even for high molecular weight materials, can be obtained with high mass resolution and lateral resolution. Practically every type of material in virtually any form, including especially insulators, is accessible to this method.

In the following sections the fundamentals of time-of-flight secondary ion mass spectrometry will first be described briefly, including the process whereby secondary ions are generated and the principle of time-of-flight mass spectrometry. Then the broad scope of the analytical applications will be illustrated by discussing some typical examples.

2. Basic Principles of Time-of-Flight Secondary Ion Mass Spectrometry (TOF-SIMS)

2.1. Sputtering and the Formation of Secondary Ions

2.1.1. Interaction of Fast Ions with a Solid Surface

When fast ions hit a solid surface they penetrate into the surface region to an appreciable depth.[8] For example, when a metal surface is bombarded with a perpendicular beam of Ar^+ ions with energies in the keV range, the mean depth of penetration is a few tens of nanometers. As it penetrates into the solid the primary ion transfers its kinetic energy to the atoms of the solid in a succession of individual collisions. Through subsequent collisions some of this energy can find its way back to the surface, where it may cause surface particles to be emitted (Fig. 1)[*]. Bombardment by the primary ions not only results in these becoming embedded in the solid near its surface (ion implantation), but also induces changes in the neighborhood of the primary ion tracks. For example, the crystalline or molecular structure may be altered (radiation damage), some of the surface particles may be removed by emission (sputtering), implantation in deeper lying surface regions may occur through recoil, or molecular constituents present at the surface may undergo fragmentation.

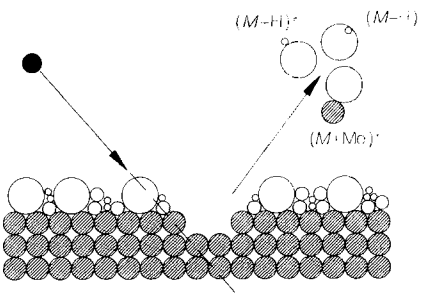


Fig. 1. Formation of secondary ions. When a metal surface Me (Ag, Au, Pt ...; hatched circles) covered by a monolayer of molecules M (white circles) is bombarded with a primary ion (black circle), secondary ions are emitted, typically including the quasi-molecular ions $(M + H)^+$, $(M - H)^-$, and $(M + Me)^+$. The neutral particles, fragment ions, and metal ions also emitted are not shown here.

In addition to these changes of the solid surface, various emission processes are observed. The emission of electrons and photons will not be discussed in detail here, since these processes yield only very limited information about the chemical composition of the emitting surface. The atomic and molecular surface constituents emitted as a result of primary ion bombardment are observed as neutral particles or as positive or negative secondary ions. These particles originate almost entirely from the uppermost layer of atoms or molecules, and therefore they yield direct information about its chemical composition. A fact of great importance for analytical applications is that even molecular surface constituents that are thermally unstable and cannot be vaporized are emitted from the surface as intact neutral particles and as positive or negative secondary ions. This phenomenon of the emission of intact molecular surface constituents, which was at first surprising, provides the basis for molecular surface analysis by SIMS.[9-11] All the surface processes initiat-

[*] In this article Me stands for metal and not for methyl.

ed by a primary ion (changes to the target and all types of emission processes) are completed within less than 10^{-12} s.

When secondary ion emission is used for surface analysis it is desirable that the information obtained should relate to the uppermost monolayer of the solid with as little modification as possible. Thus the total number of primary ions that hit the surface area to be analyzed must be low enough to ensure that the probability of a particular surface region receiving more than one primary ion is negligibly small (SIMS under "static" conditions;[11] see Section 3.1).

2.1.2. Quantitative Description of Sputtering and Secondary Ion Emission

To arrive at a quantitative description of sputtering and secondary ion emission we consider a surface constituent M (either a molecular surface constituent or an atomic species) which is present in the uppermost monolayer with a relative coverage θ(M) (see Fig. 1). The relative coverage θ(M) is the ratio of the number N of such particles present in the uppermost monolayer to the maximum number N_0 that the surface can accommodate in a complete monolayer [Eq. (1)].

$$\theta(\mathrm{M}) = \frac{N}{N_0} \tag{1}$$

The sputtering of a surface particle M can in principle be accompanied by conversion into any of a series of neutral or variously charged secondary particles X_1^q, X_2^q, ... X_i^q .... Here q denotes the charge state of the emitted secondary particle. In the case of a molecular surface constituent the series of species X_i^q will also include fragments of M. The sputtering cross section σ specifies the equivalent area of a monolayer that corresponds to the average number of particles of species M disappearing as a result of the impact of a single primary ion. The reduction of the relative coverage with time θ(M,t) caused by primary ions arriving at a constant rate of v ions per second per cm^2 is given by Equation (2) (see also Fig. 2).

$$\theta(\mathrm{M}, t) = \theta(\mathrm{M},0)^{-v\sigma t} \tag{2}$$

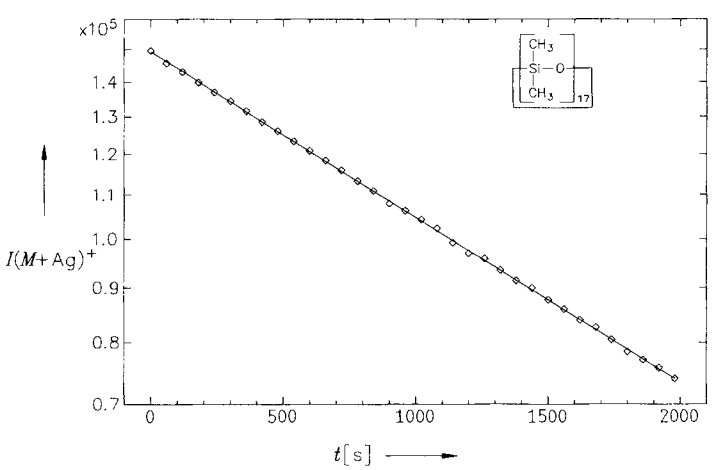


Fig. 2. Stripping of a monolayer of polydimethylsiloxane D17 (m(D17) = 1261u) from a silver substrate by a primary ion beam with a constant and uniform flux density v. The intensity I [cps] (counts per second) of the peak due to the quasi-molecular ion $(M + Ag)^+$ decays with time according to the relationship $I \propto \exp(-\sigma v t)$ [cf. Eq. (2)]. The sputtering cross section σ can be determined directly from the decay plot.

With these simplifying assumptions one can also define the following quantities:

- the sputtering yield Y_s(M), which specifies the average number of surface particles M that would disappear from a closed monolayer of particles of species M (θ(M) = 1) as a result of the impact of one primary ion;
- the secondary particle yield $Y(X_i^q)$, which specifies the average number of secondary particles of a given type X_i^q generated from a closed monolayer of particles M by the impact of one primary ion;
- the transformation probability $P(\mathrm{M} \rightarrow X_i^q)$, which is the probability that the disappearance of a surface particle M as a result of primary ion bombardment will lead to the emission of a given type of secondary particle X_i^q.

These quantities are related according to Equation (3). We

$$P(\mathrm{M} \rightarrow X_i^q) = \frac{Y(X_i^q)}{Y_s(\mathrm{M})} \tag{3}$$

also define the useful yield Y_u according to Equation (4), in which T_r is the overall transmission of the spectrometer.

$$Y_u(\mathrm{M},X_i^q) = P(\mathrm{M} \rightarrow X_i^q)T_r \tag{4}$$

2.1.3. Characteristic Features of Secondary Ion Emission

Secondary ion emission is essentially determined by the nature of the atomic and/or molecular species present at the surface. Conversely, therefore, the secondary ion spectrum enables one to draw direct conclusions about the chemical composition of the uppermost monolayer. The characteristic secondary ion emission spectra for different chemical environments have been investigated in detail for many types of materials, such as metals and semiconductors and their oxides, biopolymers, synthetic polymers, pharmaceuticals, and many other classes of organic compounds. The sputtering yields Y_s(M) for different metals have been found to be quite similar. In the case of bombardment with 10 keV Ar^+ ions, Y_s(M) is typically between 2 and 10.[8] For molecules, depending on the environment and on their nature and size, Y_s(M) can be over ten times greater than for metals. On the other hand, the secondary ion yields $Y(X_i^q)$ and the corresponding transformation probabilities $P(\mathrm{M} \rightarrow X_i^q)$ are much more strongly influenced by the chemical nature of the surface component M and its chemical environment. This matrix effect can cause considerable difficulties in quantitative surface analysis.

When the surface of a pure metal Me is bombarded with ions it emits, in addition to neutral particles, predominantly positive secondary ions Me^+. For most metals the secondary ion yields $Y(Me^+)$ are in the range 10^{-6} to 10^{-4}. $Y(Me^+)$ increases with decreasing ionization energy, and for alkali metals it can reach values approaching 1. The yields of cluster ions Me_n^+ generally fall off very rapidly with increasing n. On going from the metal to the oxide the emission of Me^+ ions is found to increase very sharply, by several orders of magnitude, but this is accompanied by only a relatively small change in the sputtering yield Y_s(Me). At the same time the emission of molecular ions with the general formula $Me_mO_n^+$ is observed. The dependence of this secondary

ion emission on the degree of oxygen coverage has been investigated in detail for many metals.[12, 13] These studies showed that the charge carried by an emitted cluster Me_mO_n is determined by its initial charge state in the oxide lattice at the surface. Thus, metal ions appear predominantly as Me^+, oxygen ions as O^-, and molecular cluster ions as negative ions in those cases where they contain more oxygen ions than metal ions. This conservation of the charge state during sputtering is also observed for other surface constituents, for example for inorganic and organic anion complexes, and has led to the proposal of a general model of "preformed" ions.[14, 15]

In the production of secondary ions from organic molecules, proton transfer and cationization (addition of a cation) both play dominant roles. In addition to the main quasi-molecular ions $(M + H)^+$, $(M - H)^-$, and $(M + \text{cation})^+$ that are formed by these processes, the secondary ion spectrum typically also shows characteristic molecular fragment peaks with quite high intensities. Cationization by Ag^+ ions is a particularly efficient process. This is the basis of a sensitive method for trace analysis of organic compounds, in which the molecules to be analyzed are sputtered from a silver surface on which they have previously been deposited as a monolayer or submonolayer (see Section 4.2).[9, 10, 16]

2.2. Time-of-Flight Secondary Ion Mass Spectrometry

2.2.1. Basic Principle

In secondary ion analysis with a time-of-flight spectrometer it is essential that the ions to be analyzed enter the flight path simultaneously or at least within the shortest possible time interval. To achieve this the area of the surface to be analyzed is bombarded with pulses of primary ions whose duration Δt_p is kept as short as possible (Fig. 3). All the secondary ions that are

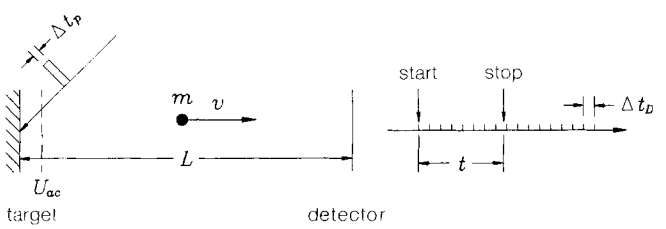


Fig. 3. Principle of a linear time-of-flight mass spectrometer (for explanation see text.)

generated almost simultaneously from one such pulse are then accelerated by passage through a fixed accelerating voltage U_{ac} before entering the flight path of length L. If we neglect the relatively small initial energy of the secondary ions, it follows that all the ions enter the flight path with the same kinetic energy. If T is the measured time of flight we then have the relationship shown in Equation (5).

$$\frac{m}{z} = \frac{2U_{ac}T^2}{L^2} \tag{5}$$

The mass resolution $\Delta m/m$ of a linear time-of-flight spectrometer as described here is limited by the primary pulse duration Δt_p, the time resolution Δt_D of the detection system, the initial energy ΔE of the emitted secondary ions, and the total flight time t, and is given by Equation (6).

$$\frac{\Delta m}{m} = \frac{\Delta E}{E} + \frac{2(\Delta t_p + \Delta t_D)}{t} \tag{6}$$

2.2.2. Practical Spectrometer Design and Performance Data

Figure 4 shows schematically the construction of a modern energy-focusing time-of-flight secondary ion mass spectrometer.[17] The instrument consists of three main components: the primary ion source, the accelerating and flight path system, and

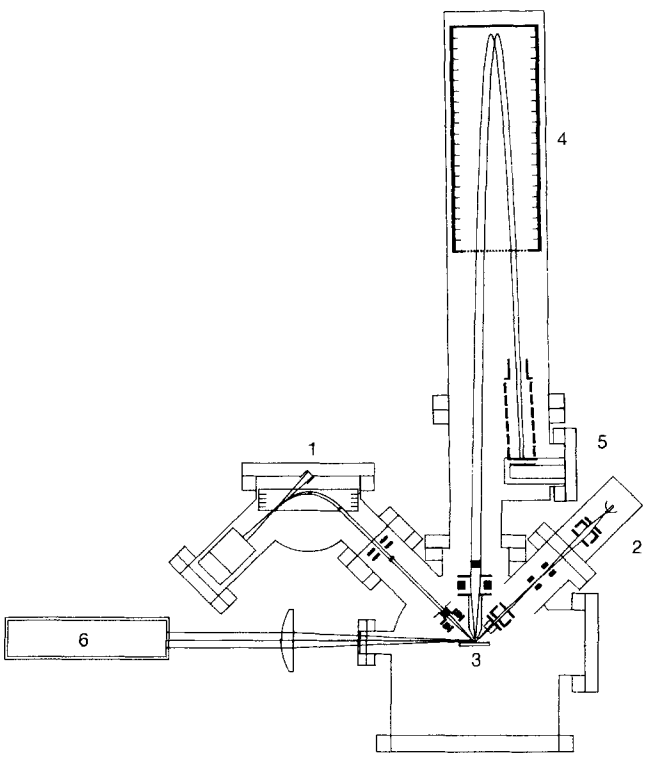


Fig. 4. Construction of a modern high-resolution time-of-flight secondary ion mass spectrometer. The system includes two primary ion sources giving different beam diameters, a pulsed, mass-separating electron impact ion source (1) and a pulsed, fine-focusing liquid metal ion source (2), as well as the target (3), a reflectron for energy focusing the mass-separated secondary ions (4), a detector (5), and a laser for post-ionization of emitted neutral particles (6).

the detector. The primary ion source produces mass-separated pulses of primary ions with a frequency of several kHz; this is achieved by pulsed 90° bending and subsequent compression of a continuous ion beam, which is generated, for example, by an electron impact ion source. This pulsed beam can then be focused by means of an ion-optic lens system to a diameter of less than 5 μm if required. If a liquid metal ion source is used instead, the pulsed ion beam can be reduced to a diameter of less than 0.1 μm.

The beam path contains several ion-optic elements: a beam extractor, an ion lens which focuses the ion beam onto the detector, and a reflectron with a retarding electric field, which has an energy-focusing function on the secondary ions and thus largely eliminates the adverse effect of their initial energy spread on the mass resolution. The detection system consists of a detec-

tor (combining a photoconverter electrode, channel plate, scintillator, and photomultiplier) and a counter giving high time resolution Δt_D [see Eq. (6)].

A spectrometer of this kind can be used in several modes. With a defocused primary ion beam one can record area-integrated secondary ion spectra, especially when high mass resolution is required. Local surface analysis can be performed by using a finely focused primary ion beam. By scanning such a focused beam over a particular area of the surface one can image the lateral distribution of mass-separated secondary ions. For nonconducting samples surface charge effects can easily be eliminated by injecting pulses of slow electrons between successive primary ion pulses.[18]

The performance of a time-of-flight secondary ion mass spectrometer is determined by the characteristics of the primary ion source, the flight path, and the detection system. The quality of the primary ion source is determined by the mass separation, the duration of the primary ion pulse, the average number of primary ions in a pulse, and the focusing of the beam. That of the secondary ion optical system and of the overall flight path is determined by the transmission efficiency and the energy focusing. Lastly, the quality of the detection system depends on its response probability, time resolution, dead time, and maximum data handling rate.[19]

3. Analytical Applications of TOF-SIMS

The main reasons for the remarkably wide range of applications of time-of-flight secondary ion mass spectrometry are its very high surface-specific sensitivity, its universal applicability to practically all types of materials and sample forms, and its ability to give direct molecular information through the emission of molecular ions. This combination of features yields information far exceeding that possible with previously available surface analytical methods.[20] There are four main modes of operation of TOF-SIMS: large-area surface analysis, surface imaging and microarea analysis, depth analysis, and trace analysis of individual substances.

3.1. Large-Area Surface Analysis

In large-area surface analysis the objective is to determine the chemical composition of the uppermost monolayer of a solid as completely as possible and with high sensitivity. For this the primary ion beam should bombard a relatively large area—between 0.01 and several mm^2. This means that the quantity of substance in the uppermost monolayer that is available for analysis and thus the number of secondary ions that can be generated is relatively large. A 1 mm^2 area of a monolayer contains around 5×10^{12} surface particles, which is on the order of 10 pmol (see Table 1). If one assumes a transformation probability of 10^{-4}, these particles can be converted into 5×10^8 analytically useful secondary ions X_i^q. It follows from this that the limit of detection should be less than 10^{-6} of a monolayer (1 ppm), which has been confirmed in practice.

To ensure that the secondary ion spectrum corresponds to the uppermost monolayer, which remains, as far as possible, unaltered by the ion bombardment, only a small fraction of this monolayer should be removed. Application of Equation (2) implies that for this "static" condition[11] the primary ion fluence vt must not be greater than several $10^{11}\,cm^{-2}$. If a value $\sigma = 10^{-12}$ is assumed for the sputtering cross section, about 90% of the analyzed surface should not be altered by the primary ion bombardment. For spectra obtained under these conditions typical recording times are on the order of one minute.

It is not only the uppermost monolayer that becomes altered or removed during ion bombardment. As the primary ions penetrate into the material they also cause severe radiation damage in the underlying layers, so that these can no longer be used for analysis, especially of molecular species. Because of this radiation damage it is not possible to determine molecular depth profiles by sputtering successive layers.

Large-area surface analysis is widely used for the characterization of virtually all types of technically important surfaces, for example in connection with their frictional, wear, corrosion, and adhesion properties, for the control of chemical and physical surface modifications, for identifying defects, for detecting and identifying trace contaminants, for the control of synthetically prepared molecular layer structures, etc.

3.2. Surface Imaging and Microarea Analysis

By reducing the diameter of the primary ion beam and scanning it over the surface region to be analyzed one can measure the lateral distribution of the secondary ion emission, and therefore that of the surface constituents responsible for the emission, with a lateral resolution determined by the beam diameter. The primary beam is positioned at a particular point on the sample surface for a short interval, and the spectrum is recorded and stored with the relevant lateral coordinates. Typical beam diameters vary from a few μm down to 50 nm. If, for example, the surface area analyzed is divided into 256×256 elements (pixels), this mode of operation requires that 65536 complete spectra must be recorded and stored. From these data one can then in principle construct an image for each secondary ion species or group of species showing the distribution on the surface. The recording time needed for such images can vary from a few seconds to several hours. By adding together all the spectra, or only those from a selected region of the imaged surface, one obtains a total spectrum. As another option, one can add together all the positive or negative secondary ions for each image point and thus obtain a total ion image. Images based on the ion-induced emission of secondary electrons can also be recorded by adding an electron detector near the sample. Total ion and electron images are especially useful for giving rapid information about the structure of a sample and for choosing the region to be analyzed or imaged.

Making the beam diameter smaller reduces the amount of substance available per image point in the uppermost monolayer, and thus also the total number of secondary ions that can be generated from the corresponding surface region. This in turn reduces the sensitivity and dynamic range for each individual image point. By subsequently adding together spectra from a sufficiently large surface region the sensitivity and dynamic range can be restored.

The equipment for surface imaging is more complex than that for large-area analysis, and the procedure is more time-consum-

ing. Nevertheless, it is indispensable for analyzing surfaces that are nonhomogeneous, whether by design or by their intrinsic nature, for example in applications in microelectronics and micromechanics, in the control of molecular surface films, and in the analysis of biological sections.

3.3. Determination of Depth Profiles

For small surface areas, for example in particle analysis, it is possible to remove many monolayers in an acceptably short time with a pulsed primary ion beam (dynamic SIMS); in this way one can determine local depth profiles. With a pulsed liquid metal ion source and a typical beam diameter of 1 μm, a primary beam flux of a few million ions per second can be achieved, giving a rate of material removal on the order of ten monolayers per second. However, because of the beam damage produced under these conditions, this dynamic mode of operation is only suitable for elemental analysis, not for molecular analysis. Greater flexibility in the determination of depth profiles is possible by using an additional sputtering ion source that operates continuously and allows rapid sputtering over a larger surface area.

3.4. Trace Analysis

SIMS can detect and identify extremely small amounts of unknown substances in the uppermost monolayer. Therefore the method can also be used for trace analysis, in particular of thermally labile organic compounds that cannot be vaporized. The substance to be analyzed is usually in the form of a solution obtained, for example, from chromatographic separation. To prepare the compound for SIMS analysis it must be applied as a monolayer or sub-monolayer onto a defined area of a suitable target. This can be achieved very simply by depositing a small quantity of the solution onto a suitable substrate with a micropipette and allowing the solvent to evaporate. If 1 μL of a 10^{-3} M solution is applied to an area of 10 mm^2 and uniformly distributed, a closed monolayer is produced. The substrate material is chosen so as to take advantage of the matrix effect, according to which the chemical environment greatly affects the secondary ion yield; by the suitable choice of substrate the yield can be optimized and stabilized. Noble metals, in particular silver, have been found to be especially good substrates.[9, 10] Firstly, they do not modify the molecules deposited on them, and secondly they give very efficient emission of cationizated molecular ions $(M + Me)^+$. This preparative technique has in practice proved to be remarkably simple, rapid, reproducible, and universally applicable. For thermally unstable organic molecules detection limits in the attomolar range (10^{-18} mol) have been achieved.[16]

The first successes in the trace analysis of nonvolatile organic compounds were obtained using quadrupole spectrometers, with consequent limitations on the accessible mass range, mass resolution, and sensitivity. By using a liquid matrix it became possible to employ sector field instruments. In this method the substance to be analyzed is incorporated into a liquid with a low vapor pressure, such as glycerol, in which it usually becomes concentrated at the liquid surface. During sputtering by ion bombardment more substance is supplied to the surface by diffusion from the bulk liquid. In this way the production of secondary ions is not confined to the uppermost monolayer, and a much greater number of substance-specific molecular ions can be generated, although a correspondingly larger quantity of the substance is consumed. This liquid SIMS technique has developed into a standard method of organic mass spectrometry, where it is called fast atom bombardment (FAB), both for historical reasons and because of the experimental details of the method.[21] However, the sensitivity that can be achieved in practice is several orders of magnitude less than that of TOF-SIMS (see Section 4.2), owing to the low transmission of sector field instruments operating at high mass resolution, and the usual sequential method of recording spectra.

4. Examples of Applications

4.1. Surface Analysis of Homogeneous and Structured Silicon Wafers

Silicon is not only the most important material used in microelectronics, it also plays a key role in many other modern technologies, such as solar energy utilization, sensor technology, micromechanics, and nanotechnologies. Silicon surfaces have been studied in great detail with well-established surface analytical methods such as AES and XPS.[22] This section therefore concentrates on the new analytical possibilities opened up by TOF-SIMS by virtue of its high sensitivity and spatial resolution and its ability to yield information on the molecular level. Examples will be provided by analyses of silicon wafer surfaces that are contaminated, modified with molecular substances, or laterally structured.

4.1.1. Detection of Surface Contamination

The secondary ion spectra of oxide-covered silicon surfaces that have been stored in air (Fig. 5) are dominated by peaks due

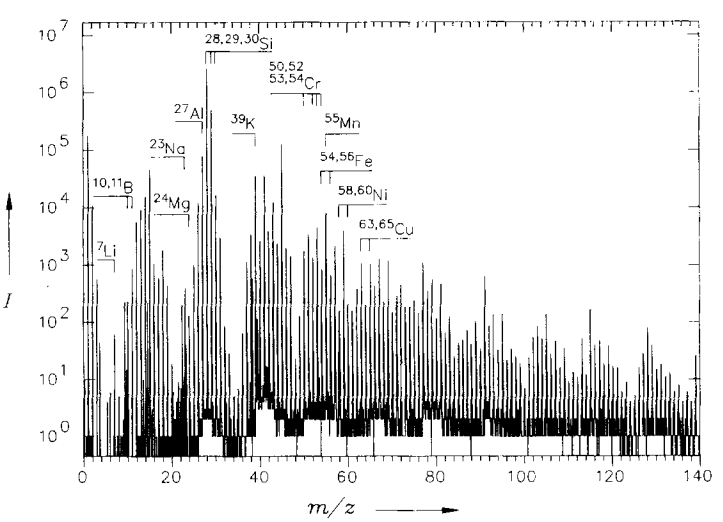
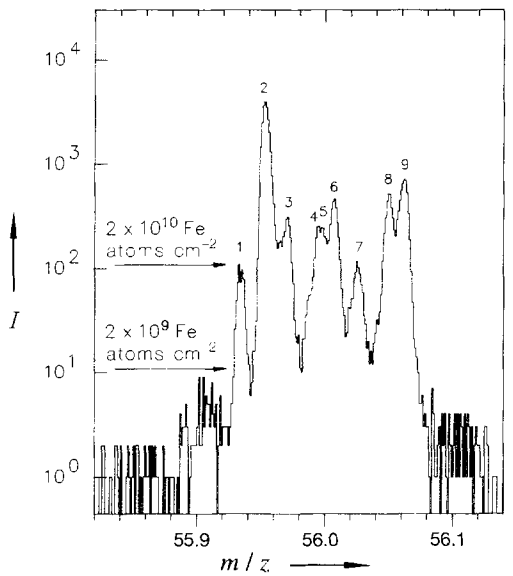


Fig. 5. Positive secondary ion spectrum in the mass range $m/z = 1$–140 for a silicon wafer stored in air. Hydrocarbon ions of the general formula $C_mH_n^+$ are found throughout the mass range. The spectrum shows an intensity range of six orders of magnitude. Additional Me^+ signals are labeled.



Peak no.	Empirical formula	Mass measured	Mass calculated
1	^{56}Fe	55.9341	55.9349
2	$^{28}Si_2$	55.9536	55.9539
3	$^{28}SiCO$	55.9707	55.9718
4	$^{28}SiCNH_2$	55.9952	55.9956
5	$^{29}SiC_2H_3$	55.9996	56.0000
6	$^{28}SiC_2H_4$	56.0074	56.0082
7	C_3NH_4	56.0252	56.0262
8	C_3NH_6	56.0499	56.0500
9	C_4H_8	56.0620	56.0626

Fig. 6. High-resolution positive secondary ion spectrum in the mass region $m/z = 56$ for the sample of Figure 5. The high mass resolution allows one to distinguish nine ion species (cf. table on the right). The positions of the maxima can be determined to an accuracy on the order of ppm, allowing identification of the molecular ions.

to $C_mH_n^+$ ions, which originate from monomolecular contamination layers. Because of the high intensity of these ions, other characteristic secondary ions of interest, such as those from metals, metal oxides, anion complexes, nitrogen-containing compounds, etc., can only be distinguished from hydrocarbon ions $C_mH_n^+$ of identical mass if lines of the same nominal mass are sufficiently separated from each other in the spectrum. Modern time-of-flight mass spectrometers are capable of the high mass resolution needed to achieve this, even in the low-mass region, as Figure 6 illustrates.[23, 24]

In the production of integrated circuit chips, contamination by metals, even at extremely low surface concentrations, can lead to high failure rates. It is therefore of great technical importance to have methods of the highest possible sensitivity for quantitatively detecting any metal contamination that might remain on a wafer surface after the various stages of cleaning and processing. For this reason the detection limits for metals that can be achieved with TOF-SIMS have been systematically investigated. With a primary beam diameter of 30 μm, limits of detectability down to 10^8 atoms per cm^2 have been achieved for metals (Table 2).[25] This corresponds to surface concentrations of less than 1 ppm. To achieve these sensitivities it is necessary to expose the silicon surface to a UV/ozone treatment before the analysis. This oxidizes the metal atoms present on the surface in a reproducible way, thus ensuring high and constant secondary ion yields (cf. Section 2.1.3)[15] and allowing the metals to be determined quantitatively with high sensitivity. With regard to sensitivity and lateral resolution, TOF-SIMS is now the most powerful method available for measuring metal contamination on semiconductor surfaces.

Table 2. Detection limits for various metals on a silicon wafer surface.

Element	Detection limit [atoms per cm^2]	Element	Detection limit [atoms per cm^2]	Element	Detection limit [atoms per cm^2]
Li	2×10^8	Al	3×10^8	Mn	4×10^9
B	2×10^8	K	2×10^{10}	Fe	2×10^9
Na	2×10^8	Ca	3×10^9	Ni	2×10^{10}
Mg	3×10^8	Cr	1×10^9	Cu	1×10^{10}

In the negative ion spectrum one finds, in addition to hydrocarbon ions $C_mH_n^-$, mainly atomic and molecular anions such as F^-, Cl^-, OH^-, CO_3^-, NO_3^-, and SO_4^-. Since the transformation probabilities for their formation are very high, the corresponding surface constituents can be detected down to levels below 1 ppm.[26] Surface constituents of higher molecular mass can also be detected with high sensitivity through their characteristic secondary ion emissions. For example, a silicon wafer surface that has undergone oxidation treatment by a CHF_3/O_2 plasma followed by inefficient cleaning emits $C_mF_n^-$ ions, which originate from plasma polymerization products left on the surface.

4.1.2. Surface Imaging

Figure 7a shows the low-mass region of the positive secondary ion spectrum of an Al/Ti/W structure on a Si test wafer, together with distribution images for ten selected secondary ions and groups of ions, and also the total ion image.[27] Each pixel corresponds to a surface area of about 1 μm^2. In addition to the ions of the main constituents Si, Al, Ti, and W, the positive ion spectrum also contains peaks due to hydrogen and oxygen compounds of these elements as well as hydrocarbon complexes. The images (Fig. 7b) give detailed information about the lateral distribution of the secondary ion emission and therefore of the corresponding surface species, for example the contamination by alkali metals (Na, K) in submonomolecular layers, and the effect of a pre-bombardment with primary ions (seen in the upper left region of the images, e.g. the aluminum image).

4.1.3. Surfaces with Molecular Modification and Lateral Structure

The chemical composition of a silicon surface, and therefore its physical and chemical properties, can be altered in controlled ways by appropriate surface treatments.[28] For example, in HF passivation the oxide layer of a silicon surface is removed, while at the same time a covering of SiH is applied, which is stable under atmospheric conditions and virtually prevents the growth of further oxide. A surface treated in this way is hydrophobic. In contrast, a high concentration of OH groups on a surface results in hydrophilic properties. The surface concentrations of SiH and SiOH can be determined directly by SIMS. The presence of the SiH complex is characterized, for example, by the production of SiH_n^+ ions ($n = 1$ to 3), whereas the SiOH complex gives $SiOH^+$ ions. Figure 8 shows the relationship between

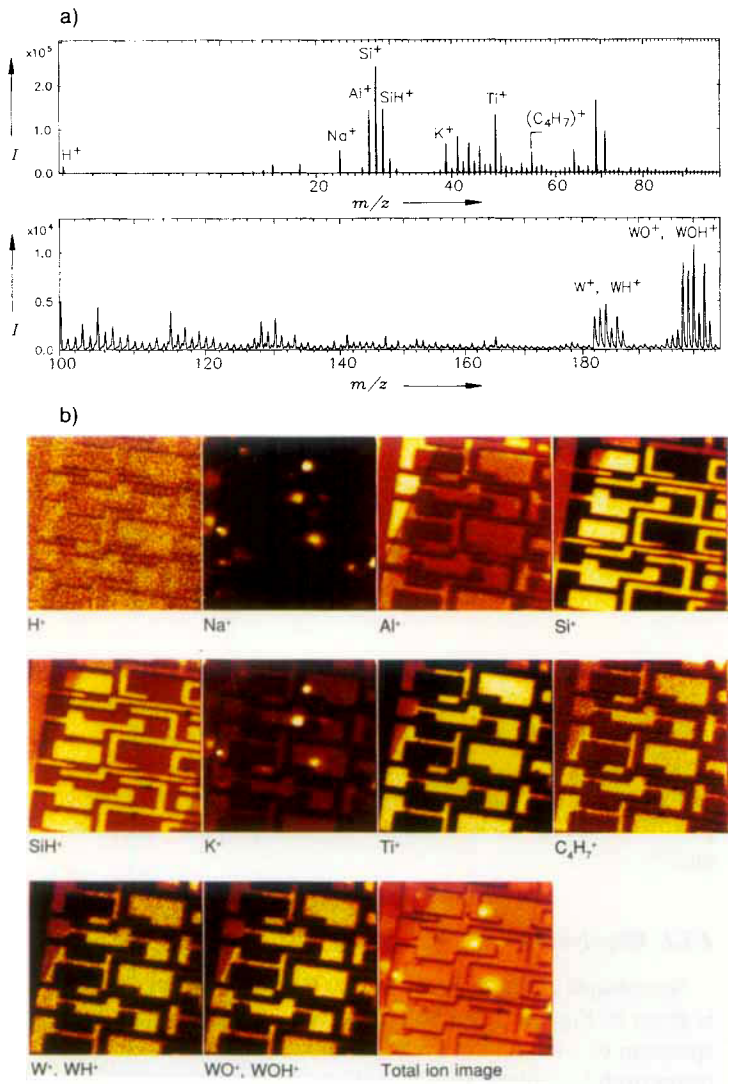


Fig. 7. a) Overall positive ion spectrum of a structured Si/Al/Ti/W test specimen, and b) images ($120 \times 120\ \mu m^2$, 128×128 pixels, 1800 pulses per pixel) showing the distribution of ten secondary ions and groups of ions. The sum image for all the secondary ions is also shown.

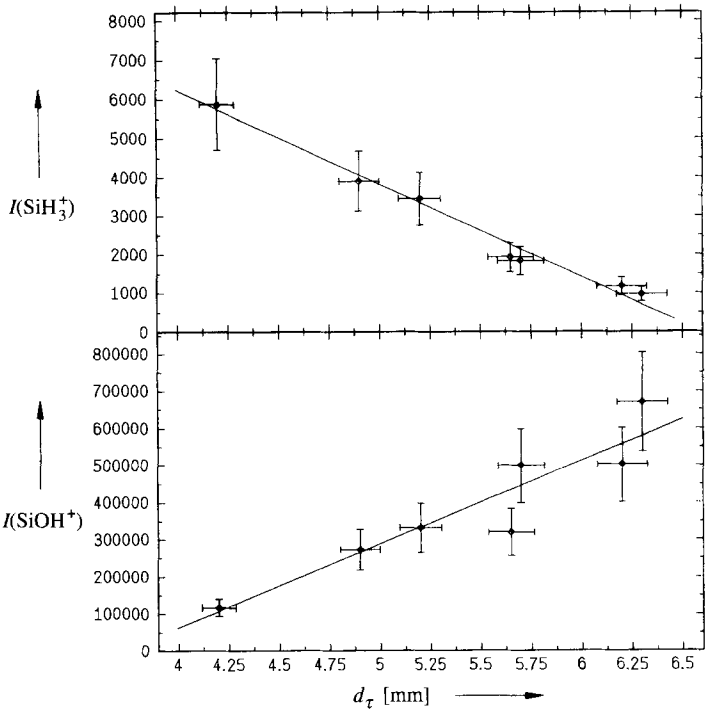


Fig. 8. Relationship between the wettability of a silicon wafer surface and the intensities of the secondary ion peaks for the SiH and SiOH complexes (SiH_3^+ and $SiOH^+$, respectively). The wettability is characterized by the diameter d_τ of a water droplet on the wafer surface.

the wettability of an HF-passivated surface and the emission of SiH_3^+ and $SiOH^+$ ions. The different concentrations of SiH and SiOH on the wafer surface were produced by exposure to UV/ozone for different lengths of time.

By chemical treatment of a silicon surface one can produce a closed monomolecular layer of trimethylsilyl groups, which emit characteristic secondary ions such as $Si(CH_3)_n^+$ $(n = 1-3)$.[29] One can produce a lateral structure in such a molecular monolayer by irradiating locally with electrons or UV light. Figure 9 shows the distribution images for various positive secondary ions emitted from a structured $Si(CH_3)_3$ monolayer.

The attachment of larger organic molecules to silicon surfaces can also be studied by secondary ion mass spectrometry. An example is the covalent linkage of various triethoxysilanes to SiOH groups,[30] and the subsequent attachment of further molecules. Various such systems have been studied in detail by TOF-SIMS, especially in connection with the development of biosensors and biocompatible surfaces.

In a similar way to studies of silicon surfaces, TOF-SIMS can be used to analyze contaminants and to investigate molecular modifications and lateral structures on the surfaces of other materials such as multielement semiconductors (e.g. GaAs), metals, and polymers.[24, 25] As an example Figure 10 shows the lateral distribution of the Ga^+ emission from a very small surface region ($3 \times 3\ \mu m^2$) of a structured GaAs test specimen.

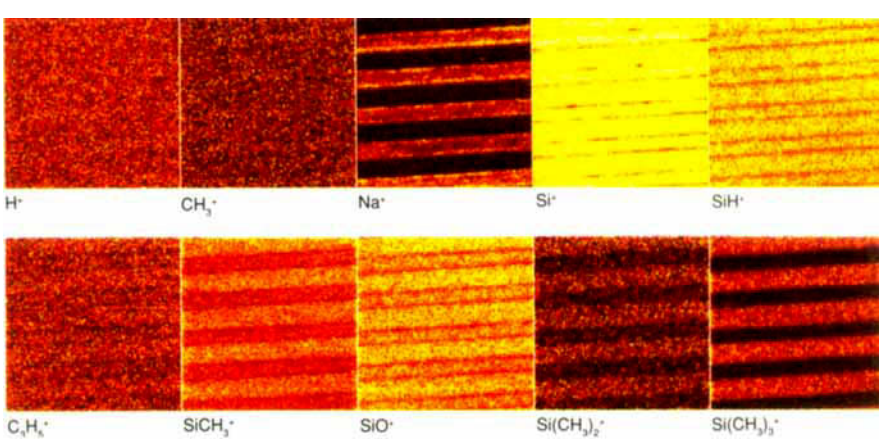


Fig. 9. TOF-SIMS images of a structured trimethylsilyl monolayer on a silicon wafer (field of view: $14 \times 14\ \mu m^2$). The lateral resolution is about 0.1 μm. Primary ion beam: 30 keV, 150 pA; pulse width: 80 us; primary ion fluence: $6.0 \times 10^{14}\ cm^{-2}$; image acquisition time: 10 min; 700 pulses per pixel.

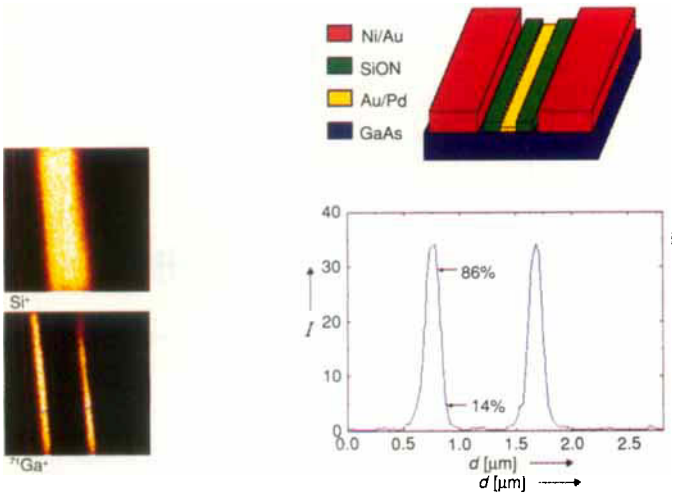


Fig. 10. Lateral distribution of the Si^+ and Ga^+ secondary ion emissions (left) from a GaAs structure (schematic representation, top right). The lateral resolution, as determined from the line scan shown (bottom right), is approximately 80 nm. Field of view: $3 \times 3\ \mu m^2$; sample consumption: 1.5 nm. In the line profile the intensity of the Ga^+ ions is plotted versus the distance coordinate d of the line scan.

Table 3. Transformation probabilities ($P(M \rightarrow X_i^q)$ [Eq. (3)] for quasi-molecular ions X_i^q.

Cmpd. class		Molecule M	Secondary ion X_i^q	Mass [u]	$P(M \rightarrow X_i^q)$
ammonium salts		crystal violet	M^+	372	1×10^{-2}
		cetylmethyl-ammonium bromide (CTAB)	CTA^+	284	5×10^{-2}
amino acids		leucine	$(M + H)^+$	132	7×10^{-4}
			$(M - COOH)^+$	86	3×10^{-4}
			$(M + Ag)^+$	240	1×10^{-3}
peptides		bradykinin	$(M + H)^+$	1060	2×10^{-4}
		gramicidin A	$(M + K)^+$	1919	1×10^{-4}
		melittin	$(M + H)^+$	2846	1×10^{-6}
polymers	mono-layer	polystyrene	$(M + Ag)^+$	1000	5×10^{-3}
			$(M + Ag)^+$	7000	5×10^{-5}
	bulk	polystyrene	$C_7H_7^+$	91	5×10^{-4}
		polydimethyl-siloxane	$Si(CH_3)_3^+$	73	1×10^{-3}
		polypropylene	$C_3H_5^+$	41	2×10^{-4}
		Teflon	CF^+	31	1×10^{-3}
		Krytox	CF_3^+	69	5×10^{-3}

4.2. Organic Molecules

A characteristic feature of the secondary ion spectrum of an organic molecule M is the appearance of the quasi-molecular ions $(M + H)^+$, $(M + \text{cation})^+$, and $(M - H)^-$ (cf. Section 2.1.3). The corresponding transformation probabilities depend on the size and structure of the molecule concerned and its chemical environment on the surface. One also often observes other quasi-molecular ions from which small functional groups have become detached, such as $(M - CH_3)^+$ or $(M - OH)^+$. Besides the above quasi-molecular ions one also finds characteristic fragment ions of various sizes in the low-mass region of both the positive and negative ion spectra. The molecular ions M^+ and M^- are found only rarely.

All the organic compounds investigated up to now, including thermally unstable compounds with masses up to several thousand u, have been found to emit quasi-molecular ions; the transformation probabilities generally decrease with increasing molecular size (Table 3). Systematic studies have been undertaken for many classes of organic compounds, including peptides, nucleotides, other biopolymers, synthetic polymers, organometallic compounds (Fig. 11),[31] inorganic anion complexes, carboxylic acids, amino acids, steroids, barbiturates, sulfonamides, and many other groups of pharmaceuticals, pesticides, dyes, surface active agents, polymer additives, etc.[20]

4.2.1. Biopolymers

An example of the analysis of a high molecular weight peptide is given in Figure 12, which shows the positive secondary ion spectrum of a mixture of cyclosporin A and D (CsA and CsD, respectively) on silver. Protonated and Ag-cationizated molecular ions are observed. The transformation probabilities $P(M \rightarrow (M + Ag)^+)$ for peptides in this mass range are typically on the order of 10^{-4}. The sensitivities achieved (cf. Fig. 13) are correspondingly high. Small fragments of cyclosporin as well as secondary ions arising from the surface contaminants are found in the mass range below 200. The molecular ion yields obtained for

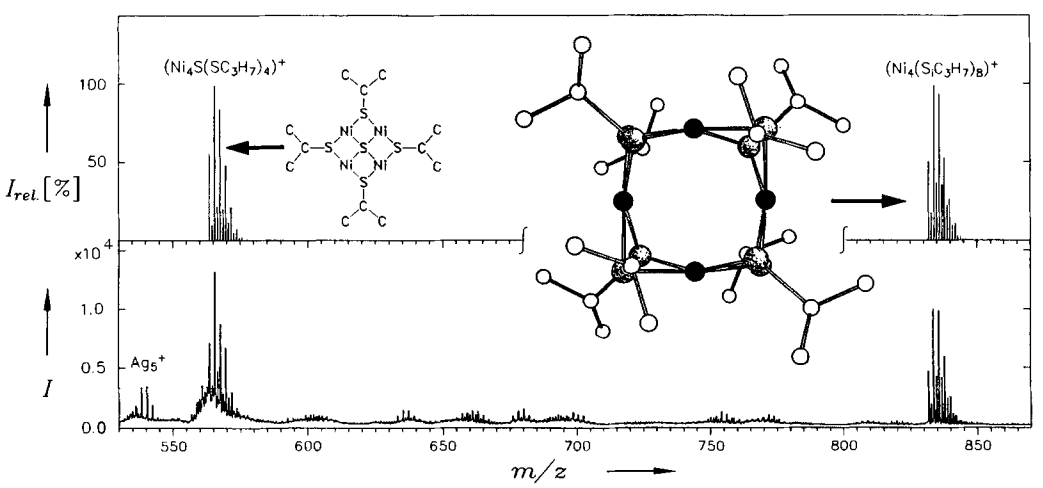


Fig. 11. Characteristic molecular ion emission from an organometallic compound. The molecular structure of the initial compound is shown (nickel: black circles; sulfur: stippled circles; carbon: white circles) together with a proposed structure for a fragment ion that is emitted with high intensity. Calculated (top) and SIMS spectrum (bottom).

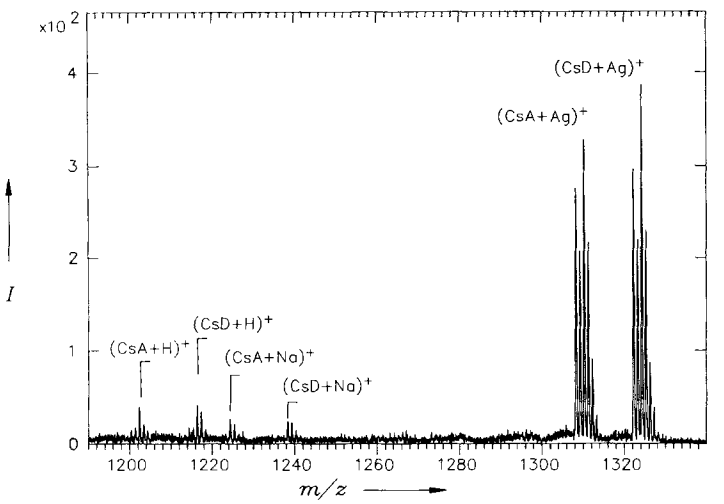


Fig. 12. Emission of protonated and cationizated quasi-molecular ions from a monolayer consisting of an equimolar mixture of cyclosporin A (CsA) and cyclosporin D (CsD). The transformation probability for the silver-cationizated molecular ion is 10^{-4}.

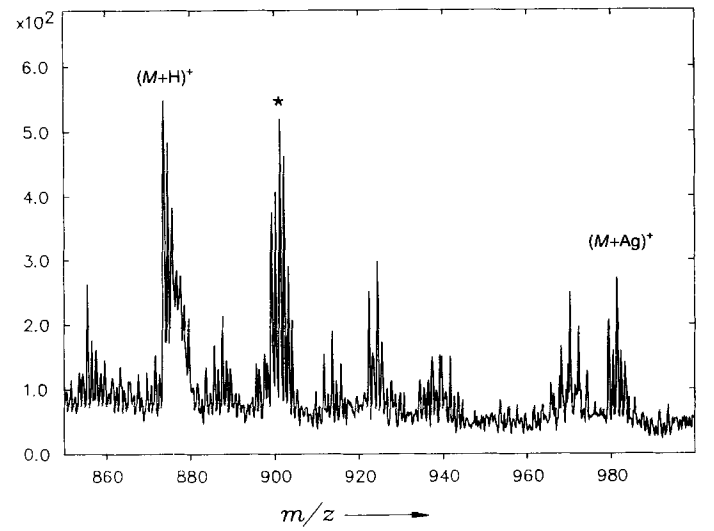
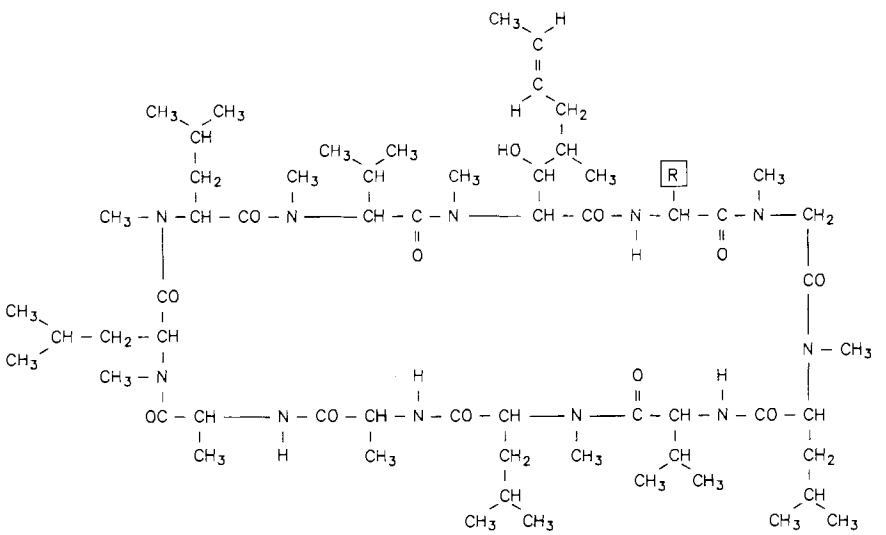


Fig. 13. Emission of $(M + H)^+$ and $(M + Ag)^+$ ions from the structurally modified peptide **1** on silver. The total amount of the peptide used for the analysis was 10^{-14} mol, and the amount in the area actually analyzed (primary ion beam diameter of 100 μm) was about 10^{-18} mol. The peak due to contaminant is marked with a star.

peptides, like those for all other types of organic molecules, depend on the size and primary structure of the molecule concerned and on its chemical environment.



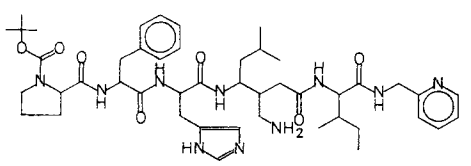
cyclosporin A: R = CH_2–CH_3 $M = 1202$
cyclosporin D: R = $CH(CH_3)_2$ $M = 1216$

Systematic studies of the effects of these variables on the secondary ion emission of small peptides have shown that the highest molecular ion yields are usually obtained with monolayers or submonolayers on noble metal substrates, especially silver. The same applies generally to all types of organic molecules.

Reactive metal substrates greatly reduce the molecular ion yields. For peptides of higher molecular mass ($M > 3000$ u) nitrocellulose has been found to be especially suitable as a substrate. As expected, the sputtering cross sections σ increase with the mass, in other words with the size of the molecule. The σ values for peptides are typically between 10^{-13} and 10^{-12} cm^2. When the transformation probabilities are sufficiently high the distribution of molecules on a surface can be determined in detail. Figure 14 shows an example of this for cyclosporin A on a silver target.

4.2.2. Smaller Molecules

The secondary ion emission of smaller molecules ($M < 500$ u) was investigated in detail using quadrupole mass spectrometers before the development of the more powerful time-of-flight instruments,[32, 33] and therefore a large volume of results on these molecules is available. The earliest systematic studies of secondary ion emission were carried out on amino acids.[9] Since then a vast amount of data has been obtained for many other classes of compounds.[20]



1

4.2.3. Quantification with an Internal Standard

Matrix effects present a serious obstacle to quantitative analysis. Secondary ion emission will only be proportional to the area covered by a particular surface constituent if it is present in the same bonding state throughout. If a solution preparation method is used this cannot be guaranteed. However, calibration

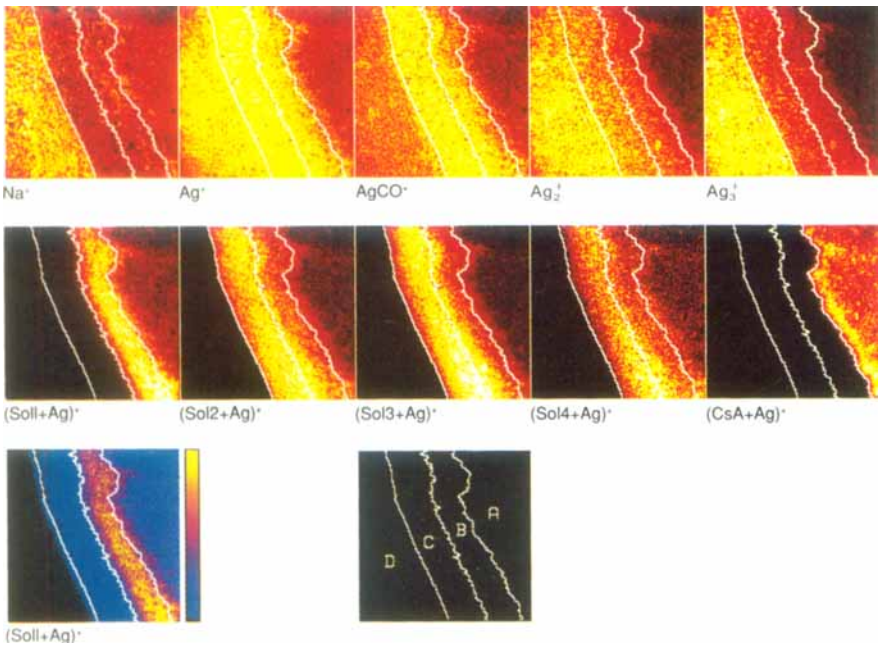


Fig. 14. Images of the edge zone ($400 \times 400\ \mu m^2$, 1800 pulses per pixel) of a Ag surface several mm in diameter on which a solution containing cyclosporin A in several different oils was deposited. These show the distribution of characteristic quasi-molecular ions from the oils (Sol 1–4) and from cyclosporin A (CsA). As the droplet evaporated the different components separated (chromatographic effect). A: $(CsA + Ag)^+$; B: Sol1; C: Sol2, Sol3, Sol4; D: uncovered silver surface.

Experience has also been obtained in quantitative analysis for cyclosporin, which is used for suppressing immune reactions following organ transplant operations. Direct quantitative detection of the therapeutically active cyclosporin A in the blood serum of patients was achieved by using cyclosporin D as a standard.[34] This differs from cyclosporin A only in having an additional CH_2 group in one of the side chains of the ten amino acids. By this method direct determination of cyclosporin A at therapeutically effective concentrations in blood serum was achieved with an accuracy of 20% (Fig. 15).

The results obtained for steroids and cyclosporin show that in many applications chemically similar molecules can be successfully used as standards for molecular SIMS. This method can be used whenever it is possible, during the preparation of the surface, to incorporate a suitable standard compound into the surface at a known concentration simultaneously with the substance to be analyzed.

is possible by introducing a suitable standard of known concentration. By directly comparing the intensities of corresponding quasi-molecular ion peaks of the analyte and the standard, whose concentration on the surface is known, one can determine the concentration of the analyte in the starting solution. The analyte and the standard must behave identically with regard to solubility and deposition on the substrate, and during evaporation of the solvent, sputtering from the surface, and ionization. When isotopically labeled molecules are employed as the standard, these preconditions are fulfilled. However, sufficiently identical behavior can also be expected if the standard used is structurally closely related to the analyte. By applying this method to steroids we have achieved analytical accuracies of about 2%.

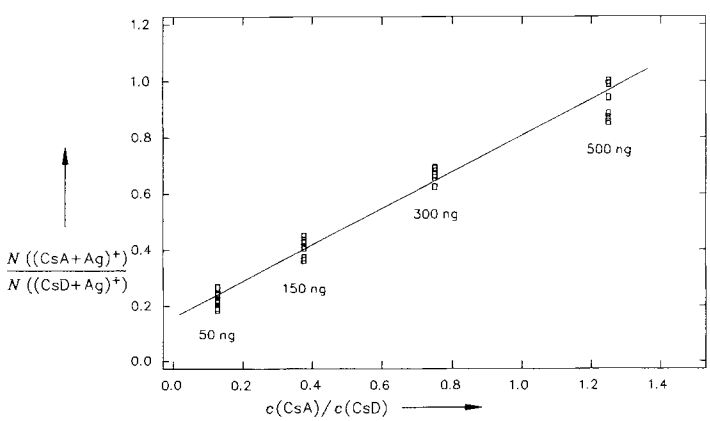


Fig. 15. Quantitative determination of cyclosporin A (50–500 ng) in 1 mL of blood serum. The concentration of the standard, cyclosporin D, was 400 ng mL^{-1}.

4.3. Synthetic Polymers

Synthetic polymers present a special challenge for surface analytical techniques. On the one hand, their technological importance continues to grow as new materials and surface modifications are developed by the incorporation of additives, application of chemical reactions at the surface, plasma treatments, and so on. On the other hand, however, the standard electron spectroscopic methods of AES and XPS are only of limited value for investigating the chemical composition of such surfaces, since they do not give direct information on the molecular level and are relatively insensitive.[35]

Secondary ion spectra of polymers often contain an enormous number of lines, which can extend to masses beyond $m/z = 10000$. At the same time the cross section σ for sputtering and associated radiation damage is typically quite large (up to several 10^{-12} cm^2). For these reasons the potential of secondary ion mass spectrometry for the analysis of polymers can only be fully exploited by using a time-of-flight mass spectrometer. Since the secondary ion emission behavior of polymers as monolayers on metal substrates is very different from that of bulk polymers, these two cases will be discussed separately. Polymer monolayers are prepared from suitable solutions by the method described in Section 3.4. As in the case of organic compounds, the best results are obtained when the substrate is a noble metal, usually silver. Nearly all bulk polymers are insulators, and the analysis of their surfaces by SIMS yielded reproducible and undistorted results only when the technique of pulsed charge compensation was introduced. With this technique it is very important to use only low-energy electrons (< 20 eV) so as to avoid radiation damage.

4.3.1. Polymer Monolayers on Metal Substrates

Most polymers are sufficiently soluble in appropriate solvents to allow the preparation of monolayers by the method described in Section 3.4. Figure 16 shows a typical positive secondary ion

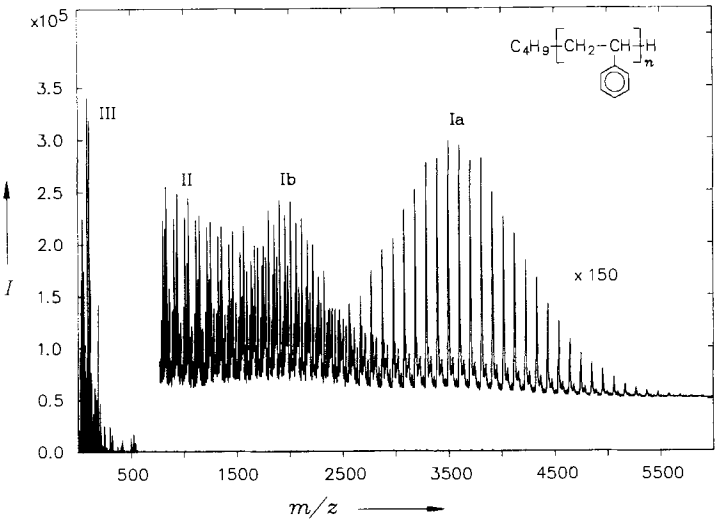
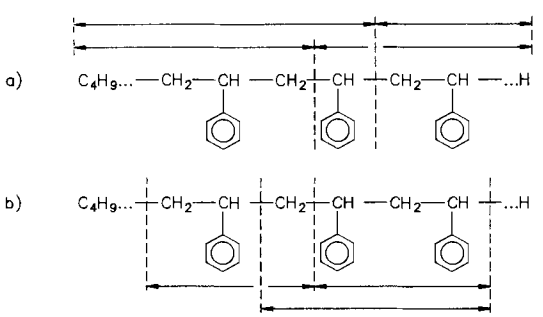


Fig. 16. The positive secondary ion spectrum of polystyrene (M_n = 3770 u) on silver (for explanation see text).

spectrum from a polymer monolayer prepared on silver by this method.[36] In this spectrum one can distinguish three regions: the oligomer region (Ia, Ib), the fragment region (II), and the fingerprint region (III).

The oligomer region arises from the silver-cationizated molecular ions $(M + Ag)^+$ (Ia) and $(M + 2Ag)^{2+}$ (Ib), which are formed by the addition of one and two silver ions, respectively, to intact oligomer molecules emitted from the surface. The fragment region (II), which overlaps with the oligomer region and extends to lower masses, is dominated by silver-cationizated fragments of the oligomers. These are formed by single or double bond cleavages during sputtering and consist of a number of monomer units, with or without one of the two end groups, depending on the position of cleavage in the molecule. The possible fragmentation modes are shown in Scheme 1. The fingerprint region, which extends from the fragment region to lower mass numbers, arises from smaller fragment ions which are emitted with quite high intensities.



Scheme 1. Fragmentation modes for polystyrene.

Systematic studies of the monolayer spectra of a wide variety of polymer types have revealed some general features of their secondary ion emission properties.[37, 38] All polymers give fingerprint spectra (III), which yield information about the mass and structure of the repeat unit and often also about the end groups.[39] The prominence of high molecular mass fragment ions (II) varies between the different polymer types; these too yield information about the repeat units and end groups. Oligomer spectra (Ia, Ib) have generally been observed only for polymers with molecular masses below 10000 u and even then not for all types of polymers; when present they give direct information about the molecular mass distribution of the polymer.

With a time-of-flight spectrometer the masses of the secondary ions can be determined with a precision of a few ppm. An example is given in Figure 17, which shows a portion of the positive ion spectrum of polydimethylsiloxane. The oligomer spectrum contains two series of peaks of different intensities. From exact mass measurements one can construct the molecular formulas for the ions of both series, leading to the conclusion that the main series arises from linear polymer molecules and the weaker series from cyclic polymer molecules.

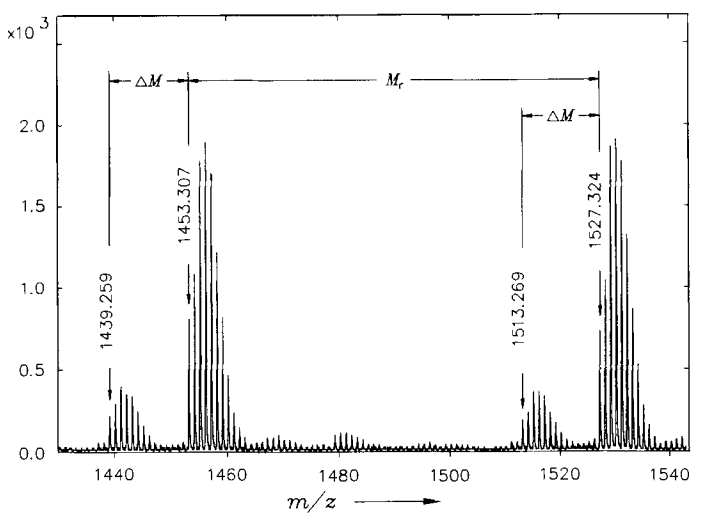


Fig. 17. Part of the high-resolution positive secondary ion spectrum of a polydimethylsiloxane monolayer on silver.

The dependence of the secondary ion emission on variables such as the molecular mass, the presence of different side groups, and the substrate material has been investigated systematically for polystyrene, poly(methyl methacrylate), poly(ethylene glycol), and perfluoroalkyl polyether (Krytox). One result of the study was that all the polymers investigated showed a linear relationship between the molecular mass and the sputtering cross section σ.[40]

As an alternative to preparation from solutions, surface films resembling monolayers have also been successfully produced by mechanically stripping relatively thick polymer films from metal substrates, or by rubbing a bulk polymer specimen against a metal surface. By using the rubbing technique one can produce films that resemble monolayers and have a similar emission

behavior, even when the starting material is insoluble (e.g. films produced by plasma polymerization).

4.3.2. Bulk Polymers

It can be assumed that when a monolayer is prepared the oligomer molecules lie flat on the surface of the substrate. Evidence for this includes the observation that covering a metal substrate with a monolayer always requires the same number of monomer units of a given polymer, regardless of its average molecular mass. Secondly, the sputtering cross section σ increases in proportion to the molecular mass, and thirdly, silver-cationized quasi-molecular ions are observed up to the high-mass region.[40] In contrast to this the molecules in the bulk polymer are more or less entangled, such that ion bombardment does not result in the emission of intact molecular ions but rather only smaller fragments. Cationization is also much less important as an ionization process.

It is in fact found that bulk polymers, with only a few exceptions, give fragment ions mainly in the low-mass region below $m/z = 500$.[41] Often the repeat unit itself is emitted as a secondary ion with high intensity. One can also obtain information about the structure of the repeat unit from the relevant fragment ions. Figure 18 shows typical fragment ion spectra in the low-mass region. The secondary ions observed can be assigned to specific molecular fragments, from which one can identify not only the monomer unit but also its characteristic side groups. The ionization of the fragments can occur through protonation, deprotonation, or charge stabilization at heteroatoms such as oxygen or halogens. If suitable cations are present, the corresponding cationizated fragment ions may also be formed. As expected, the intensities of the peaks that correspond to fragment ions containing end groups decrease as the length of the oligomer molecule increases, whereas the intensities of the peaks of fragment ions that do not contain end groups are independent of the molecular mass of the oligomer. From the ratio of the intensities of these two types of fragment ions one can estimate the average molecular mass for the oligomers, even when no intact quasi-molecular ions are found in the higher mass region.[42] Larger negative fragment ions are most often observed for polymers containing oxygen or halogen atoms, which allow for charge stabilization.

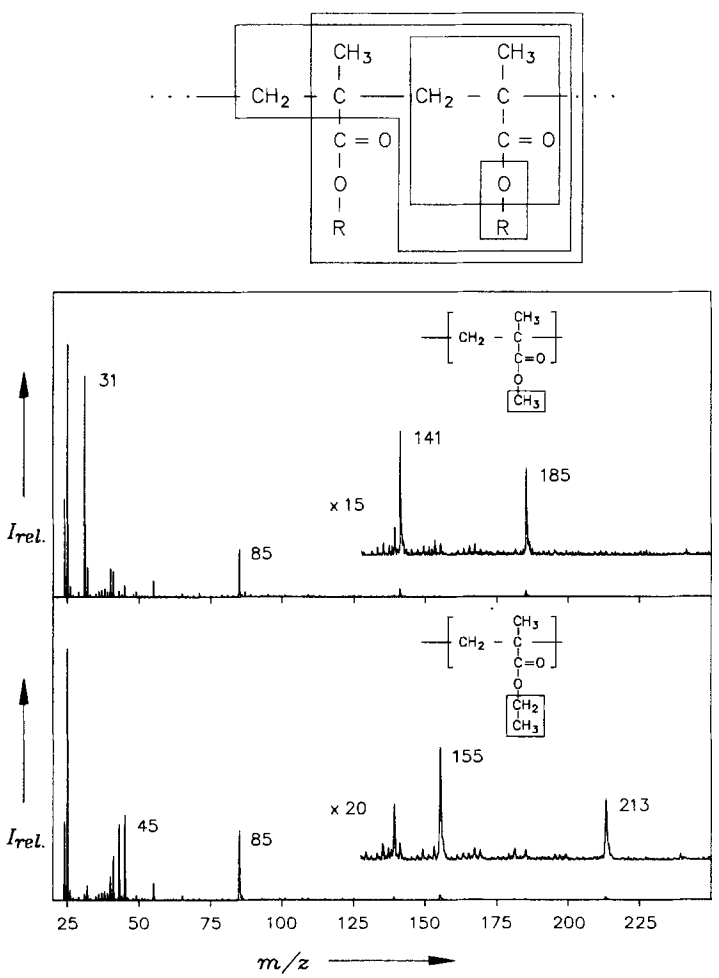


Fig. 18. Negative fragment ion spectra of the surfaces of bulk samples of poly(methyl methacrylate) (top) and poly(ethyl methacrylate) (bottom) in the fingerprint region. Fragment ions corresponding to the monomer units and to the side chains (shown above the spectra) can be identified.

Primary ion bombardment can also destroy or remove molecules of bulk polymers and is accompanied by significant radiation damage to layers below the uppermost monolayer. As a result the signal intensities of characteristic fragment ions diminish during the bombardment. The sputtering cross section for fragment ions in the low-mass region is typically several 10^{-12} cm^2. For a given type of polymer the value is independent of the average initial molecular mass. In special cases where fragment ions of higher mass are observed, the cross sections are significantly greater with values up to 10^{-11} cm^2. In certain cases the emission of characteristic secondary ions actually increases as the primary ion bombardment proceeds; this occurs when the bombardment leads to the formation of fragments that remain on the surface, which are more apt than the oligomer molecules to give rise to secondary ions. Such an increase may typically continue up to a primary ion fluence of about 10^{12} ions per cm^2 and is then followed by a reduction in the emission of the relevant fragment ions at a rate corresponding to the normal sputtering cross section. A striking example of such behavior is observed in the case of Teflon for the fragment ions $(CF_2)_n^-$.[40]

4.3.3. Modified Polymer Surfaces

In general the composition of a polymer at the surface is considerably different from that within the bulk material. For example, one often finds that additives or impurities are concentrated at the surface (Figs. 19 and 20, respectively). The surfaces of polymers are in some cases intentionally modified, for example by chemical reaction, bombardment with ions or electrons, or plasma treatment, to achieve surface properties not normally possessed by the polymer, such as adhesion properties or a degree of surface reactivity. Molecular surface modifications of these kinds can be studied in detail by SIMS. As an example, the modification of the side chain of surface molecules of poly(hydroxyethyl methacrylate) (PHEMA) by reaction with propionyl chloride can be investigated in detail by observing changes in the emission of characteristic fragments in the fingerprint spectrum (Fig. 21). In many cases, such as when oxygen is

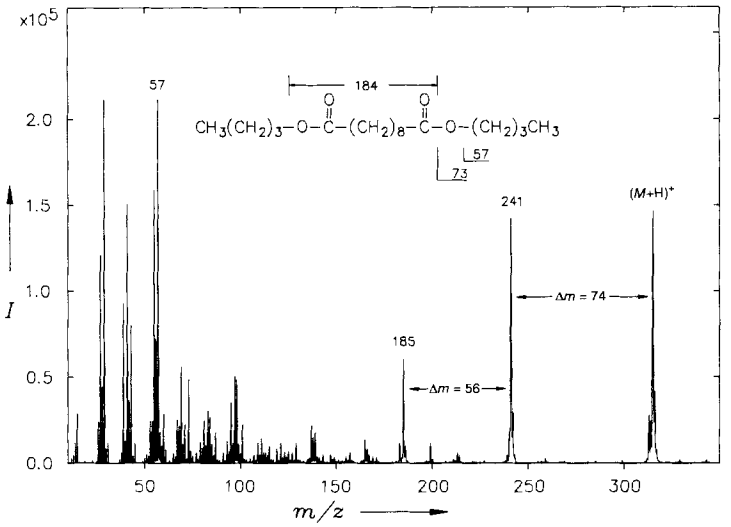


Fig. 19. Detection and identification of an additive (dibutyl sebacate) on a polyvinylchloride surface. Primary ion dose: 3×10^6, positive ion spectrum.

incorporated into the polymer surface, high mass resolution in the fingerprint region is important. For example, treatment of a polystyrene surface with an oxygen or nitrogen plasma causes

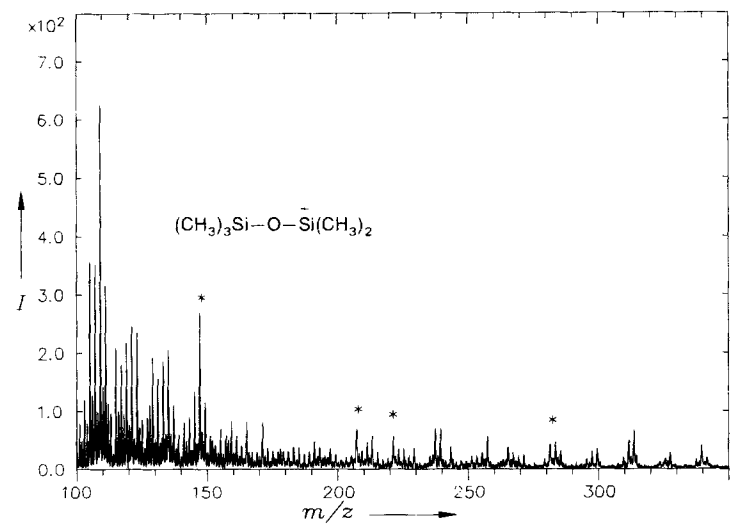


Fig. 20. Detection of silicone oil contamination on a polycarbonate surface. Peaks arising from the contamination are marked with a star.

oxygen or nitrogen to become incorporated into the molecular structure of the surface. This incorporation can be followed by observing changes in the intensities of the relevant secondary ion peaks, provided that the mass resolution is adequate for distinguishing ions of the same mass number that contain one or more atoms of oxygen or nitrogen.[43]

Surface imaging of polymers can be used to investigate the lateral distribution of specific molecular constituents. Figure 22 shows the distribution of lotader inclusions in polypropylene, and Figure 23 shows the location and identification of a particle of Teflon in an ink dot on paper.

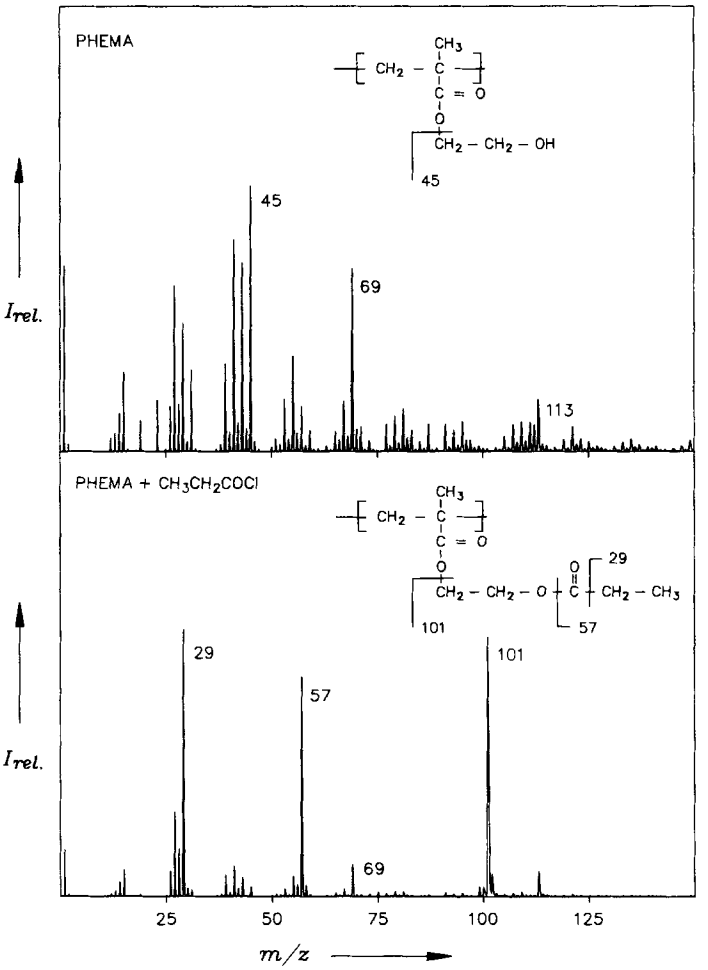


Fig. 21. Chemical modification of a polymer surface. Exposing a poly(hydroxyethyl methacrylate) (PHEMA) surface to gaseous propionyl chloride modifies the side chains, and the fingerprint spectrum then shows secondary ions characteristic of the modified side chains. Positive ion spectrum.

It is not possible to determine molecular depth profiles by the progressive stripping of layers by ion bombardment, owing to the severe radiation damage that would occur. However, such

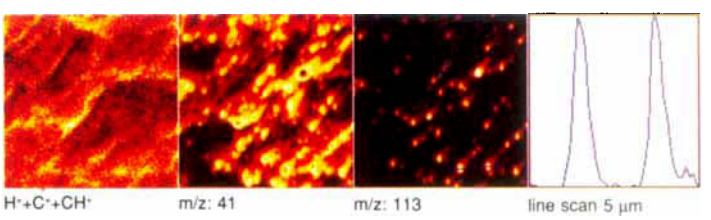
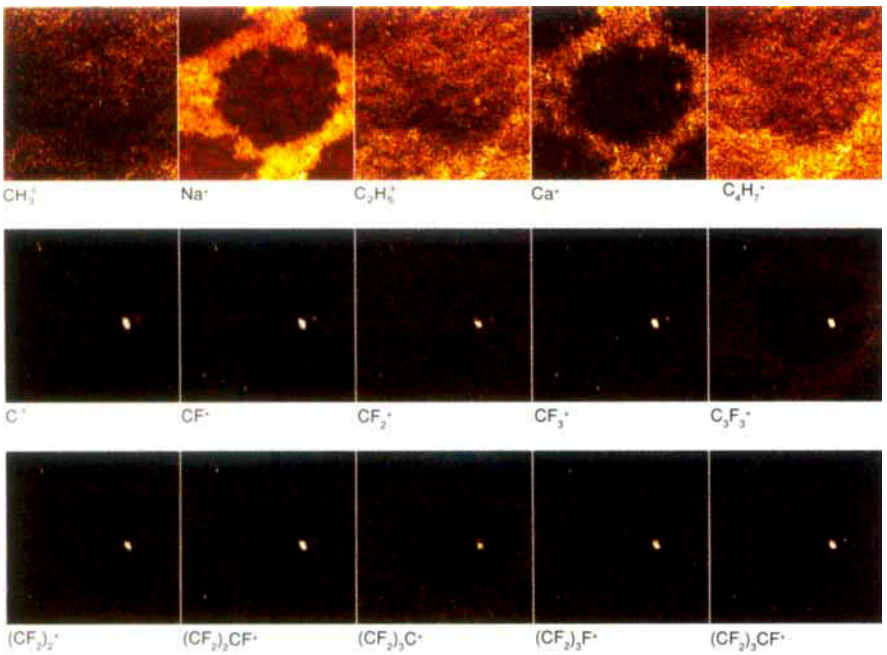


Fig. 22. Imaging of a polymer surface (15×15 µm, 200 pulses per pixel) showing lotader inclusions in polypropylene. The line scan shows that the lateral resolution is about 0.2 µm. The secondary ion with mass $m/z = 113$ is a fragment ion of the lotader. The line profile corresponds to two spots in the image recorded for $m/z = 113$.

profiles can be determined indirectly by imaging suitable polymer sections in combination with image processing techniques.



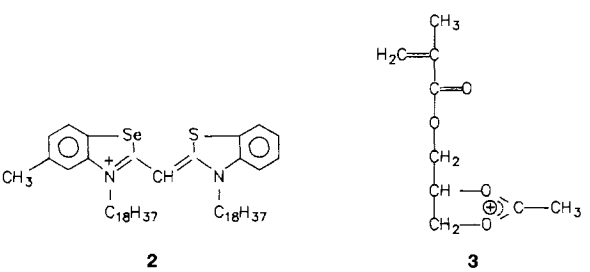
ular layers, and after each step the intensities of one or more of the characteristic secondary ion peaks of the incorporated species are measured. Such experiments have been performed, for example, with a dye, **2** · ClO_4, which was incorporated into a polymethacrylate (PMA) film at high concentration (mixing ratio 1:1). This film was then covered with a gradually increasing number of layers of polyamide (PA), so that the diffusion of the dye through these layers could be measured. Figure 24 shows the sequence of intensities for the signals of the positive dye ion, its negative counterion, and a positive secondary ion (**3**) from PMA as the thickness of the overlying PA film is increased.[46] Both the counterion ClO_4^- and the PMA ion are almost completely excluded by only *one* double monolayer covering of PA. In contrast, the dye molecule itself is still easily detectable after four double monolayers are applied.

4.4. Synthetically Produced Molecular Surface Films

Synthetically produced molecular surface films are becoming increasingly important as passive coatings, as components of sensors and optoelectronic devices, as adhesion promoters, in the modification of membranes, in catalyst development, for making surfaces biocompatible, and for many other purposes. In the development and production of such film systems, and in their routine use for technical applications, an effective and reliable surface analytical method is essential for evaluating film quality (with regard to composition, uniformity, integrity, and contamination), for monitoring the stability of the films under conditions such as high temperatures or storage in aggressive environments, for following diffusion processes in heterogeneous multilayer systems, and so on. Investigations of Langmuir–Blodgett (LB) and self-assembled (SA) films, films of covalently linked amino acids and peptides on polymers, and organosilicon compounds covalently bonded to oxides have shown that for such systems TOF-SIMS gives information that cannot be obtained by any other analytical method.

4.4.1. Langmuir–Blodgett Films

Many polymers form LB films that are very stable and are therefore especially interesting for technical applications. Investigations of the secondary ion emission from such film systems have confirmed that the secondary ions are emitted from a depth of only one to two monolayers.[44, 45] SIMS is therefore an ideal method for studying phenomena such as the vertical diffusion of molecular species that are present only down to a limited depth in a multilayer system. In these experiments a film containing the substance(s) of interest is gradually covered in a stepwise progression with an increasing number of monomolec-



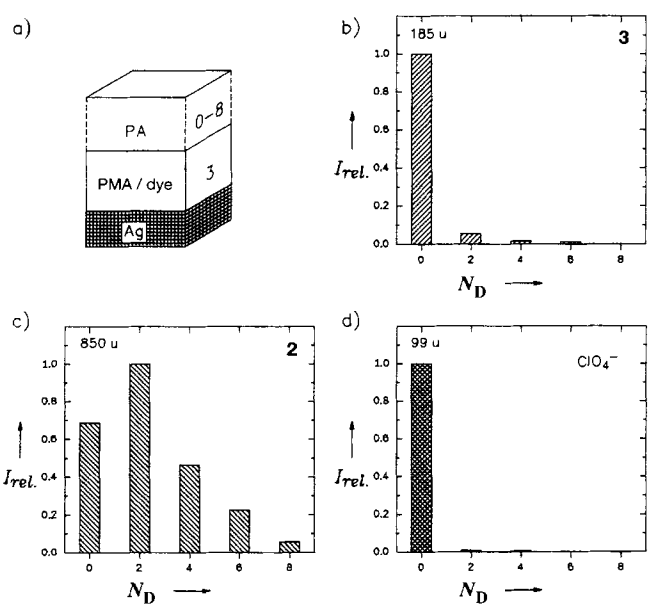


Fig. 24. Diffusion of dye ions through PA LB films of different thicknesses. a) Layer sequence with the number of double layers (the dye ion is present in the initial film in a molar ratio of 1:1). Relative intensities of b) the PMA fragment cation **3**, c) the dye ion **2**, d) the counterion. N_D = number of double layers.

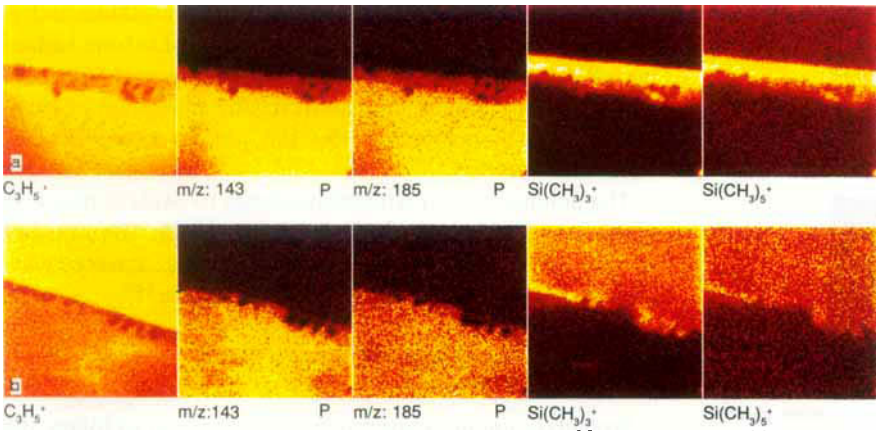


Fig. 25. Location and identification of a silicone oil impurity in a PMA LB film. Masses $m/z = 143$ and 185 correspond to secondary ions characteristic of PMA. The two rows of images (field of view $130 \times 130\ \mu m^2$) relate to different methods of preparation. In series a) the silicone oil impurity is located near the edge of the incomplete LB film, whereas in series b) it is distributed over the entire uncovered area.

Molecular contaminations that can arise, for example, in the production of LB films, can be located and diagnosed by imaging the surface region of interest. For example, it was possible to pinpoint silicone oil contamination in a PMA film by imaging the lateral distribution of the secondary ions $Si(CH_3)_3^+$ and $Si(CH_3)_5^+$ (Fig. 25).

4.4.2. *Self-Assembled Films*

Information of the same kind as for LB films can also be obtained for SA films, such as butylbenzotriazole (BBT) monolayers on metals, by using SIMS. Layers of this type are effective as corrosion inhibitors for copper and nickel. When a metal surface is treated with an aqueous solution of BBT, a closed, passivating monolayer of BBT forms. The formation of the passive layer is affected by the oxidation state of the metal surface and by any contamination that may be present. SIMS imaging of a BBT-treated copper surface yields detailed information about the surface distribution of the species present, including complex molecular species (Fig. 26).

TOF-SIMS studies have also been carried out on the adsorption of organic thiols, sulfides, and disulfides on gold substrates and have provided detailed insight into several surface reac-

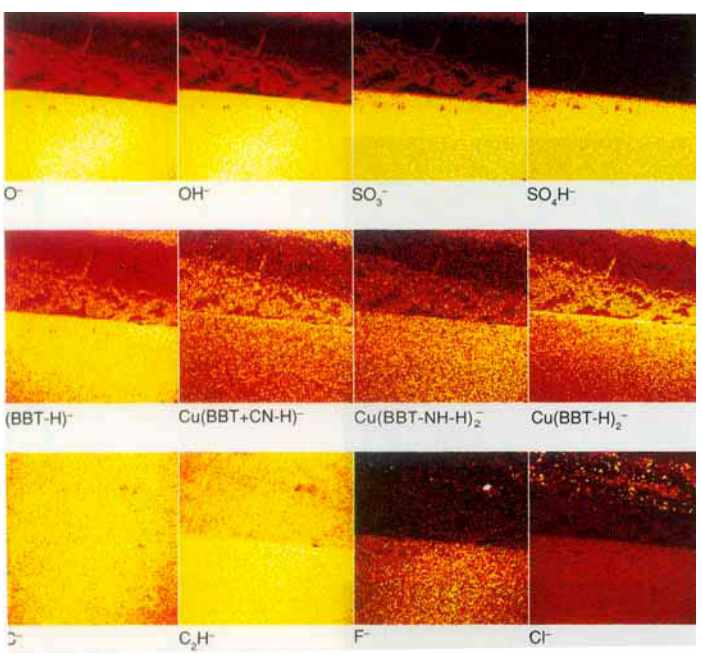


Fig. 26. A self-assembled BBT monolayer on copper. Only the lower part of the imaged area ($250 \times 250\ \mu m^2$, 1100 pulses per pixel) is covered by the BBT monolayer. The secondary ion images for the surface contaminants (F, Cl, SO_4, etc.) show their different lateral distributions. The complex behavior of the BBT molecules near the boundary between the covered and uncovered areas is also evident.

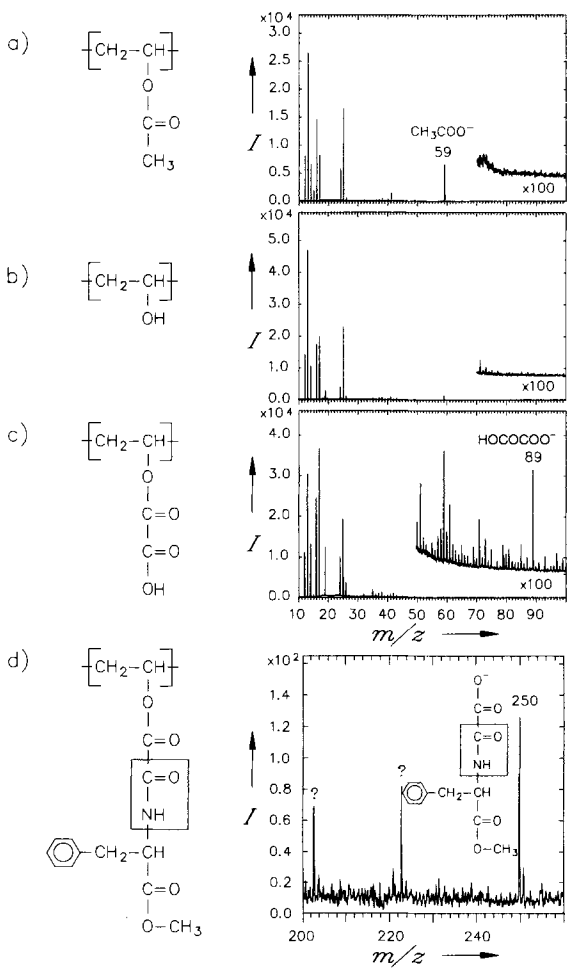


Fig. 27. Immobilization of phenylalanine on poly(vinyl acetate). The separate stages of the process can be studied and monitored by recording the characteristic secondary ion emission of the surface complexes. The spectra correspond to a) the concentration of acetate groups, b) saponification, c) addition of spacer molecules, d) attachment of amino acids.

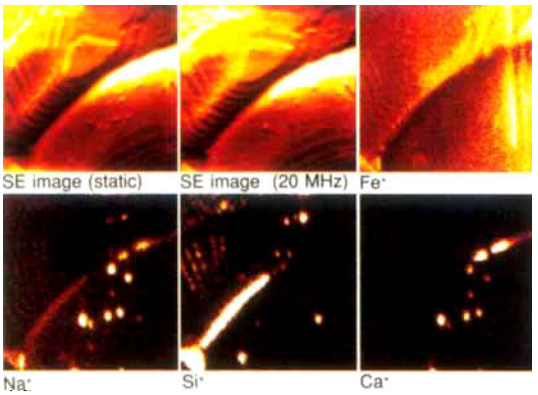


Fig. 28. Images of a $7.5 \times 7.5\ \mu m^2$ area of the surface of a dye carrier particle, obtained by recording images from the ion-induced secondary electrons and the Fe^+, Na^+, Si^+, and Ca^+ secondary ions. Primary ion beam: 140 pA.

tions. For example, SIMS spectra showed that disulfides undergo chemisorption with cleavage of the S–S bond to form surface monosulfides. SIMS has also been successfully used to investigate the most favorable conditions for the adsorption of streptavidin on a monolayer of $HS(CH_2)_{12}$-biotin with optimized stereochemistry.[47]

The bonding of methyltriethoxysilanes to oxide surfaces, in particular SiO_2, has also been studied by SIMS. The structure of the layers formed was characterized; unexpectedly, silsesquioxanes were found on the silica surface.[48]

4.4.3. Immobilized Amino Acids and Peptides on Polymer Surfaces

Secondary ion mass spectrometry can be used to follow the separate stages in the immobilization of amino acids and pep-

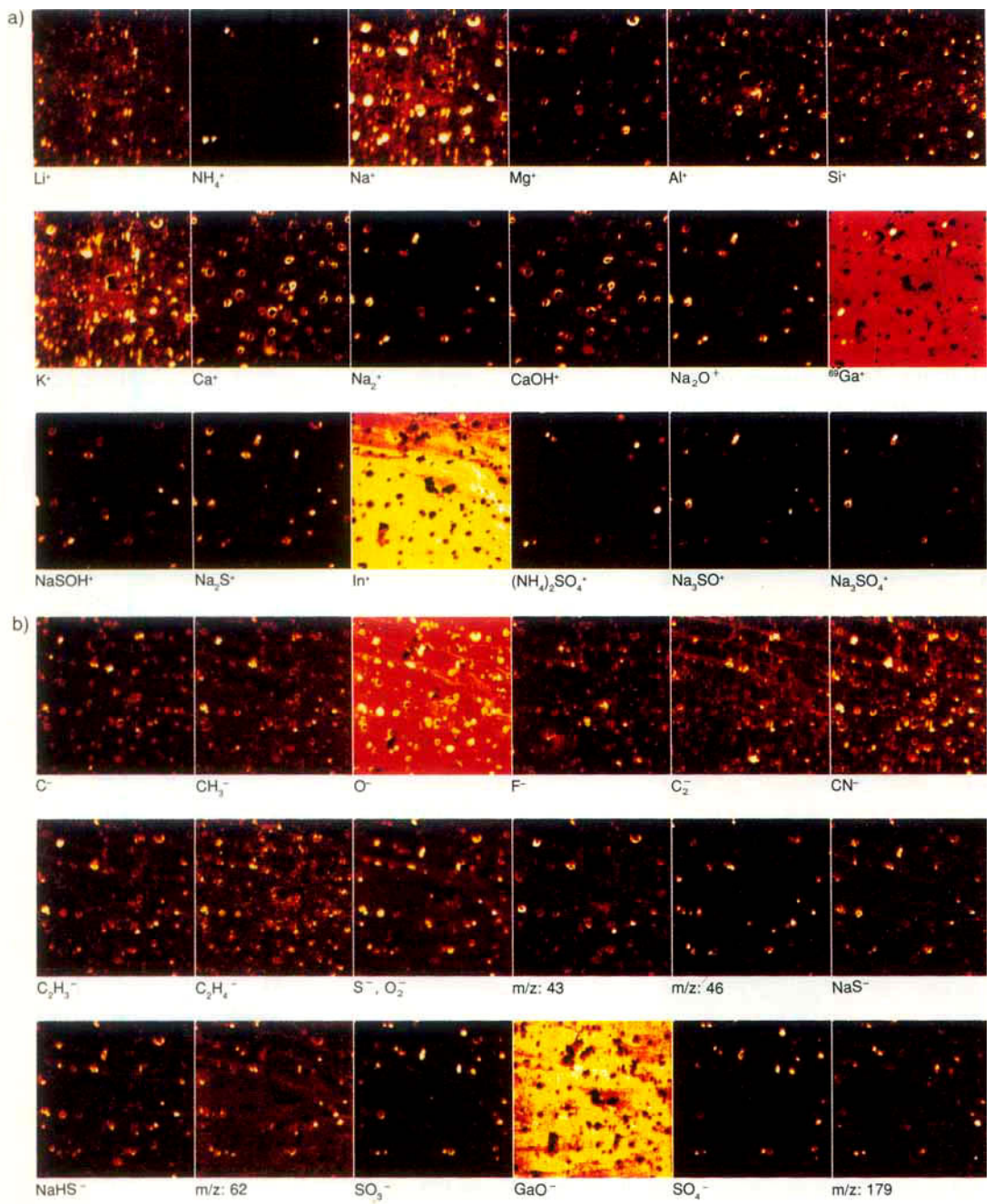


Fig. 29. a) Positive and b) negative secondary ion images of aerosol particles on an indium foil. Field of view: $120 \times 120\ \mu m^2$; 500 pulses per pixel.

tides on surfaces. In one such study the bonding of amino acids and alcohols to polymer surfaces, in particular to copolymers containing vinyl acetate, was investigated. By observing the occurrence and disappearance of characteristic secondary ion peaks it was possible to monitor changes in the concentration of acetate groups at the surface and to follow the saponification of these groups, the addition of spacer molecules, and the attachment of amino acids to these spacers (Fig. 27).[49]

4.5. Particles and Fibers

Since flat or smooth surfaces are not required for SIMS analysis, one can analyze particles and fibers down to submicron dimensions by using a focused primary ion beam. Some examples of such analyses that have been carried out on particles and fibers in recent years include determinations of the surface composition of catalysts in powder form, the elemental and isotopic composition of interplanetary dust particles, the surface composition of dye carrier materials (Fig. 28), and the origin and identity of aerosol particles (Fig. 29), as well as the investigation of polymer particles on silicon wafer surfaces (see Fig. 32), and the determination of the composition of molecular films on carbon, paper (Fig. 30), textile fibers, and hairs, and the incorporation of glass fibers into polymers. In such analyses of particles and fibers, total electron and total ion images are important aids to locating features. Digital image processing and the identification of particular types of particles by computerized comparison of spectra (cluster analysis) are also very important methods.[50] It is also possible in principle to measure depth profiles for particles and fibers, even for molecular species, by imaging sections; if necessary these can be prepared after embedding in a suitable matrix.

SIMS can be used to determine isotope ratios without appreciable distortion by matrix effects, as these affect the ionization of all isotopes of an element to the same extent. Also fluctuations of the primary ion current with time are unimportant with a time-of-flight mass spectrometer, since all secondary ions are detected almost simultaneously. Dead-time effects at high data collection rates can be corrected by suitable evaluation methods. The best accuracies currently obtained with TOF-SIMS for the determination of isotope ratios are on the order of $\pm 2 \times 10^{-3}$ (for $^{107}Ag/^{109}Ag$).[51] For determining isotope ratios with extremely small sample quantities (e.g. microscopic inclusions or interplanetary dust particles) time-of-flight mass spectrometers have a considerable advantage over sector field instruments for a given mass resolution and lateral resolution because of their simultaneous detection of all secondary ions.

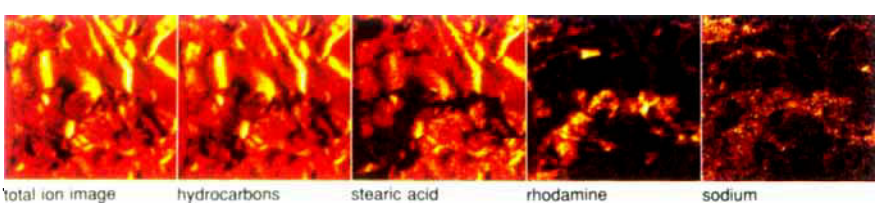


Fig. 30. Characteristic secondary ion images ($250 \times 250\ \mu m^2$; 1000 pulses per pixel) of a paper treated with a mixture of rhodamine and stearic acid.

Mesoscopic particles with dimensions in the nanometer range cannot be directly analyzed as individual particles by TOF-SIMS. However, if they are presented in the form of a sufficiently dense covering on a suitable sample support, the resulting secondary ion spectra yield valuable information about their composition and structure. For example, the negative secondary ion spectra of fullerenes can be used to directly determine the distribution of cluster sizes. For ligand-stabilized Au_{13} superclusters, secondary ions with masses up to $m/z = 150000$ have been observed, yielding important information about the structure of the clusters.[52] However, TOF-SIMS has still to be applied in a systematic way to the study of particles in this mesoscopic size range.

5. Summary and Outlook

Progress in the fundamental understanding of secondary ion emission and in its analytical applications depends critically on the close interaction between basic research, instrument development, and analytical applications. Thus, new analytical problems stimulate fundamental research on novel materials systems, often leading to further advances in knowledge about the ionization process. Analytical problems also directly influence instrument development, as has occurred, for example, in the development of surface imaging, in improvements in transmission and mass resolution, and in the development of techniques to counteract sample charging effects; all these have in turn directly benefited basic research. This review concludes with a summary of the present situation in secondary ion mass spectrometry and some likely future developments in the following three areas: fundamental knowledge (in particular of the generation of secondary ions), instrument technology, and analytical applications.

5.1. Generation of Secondary Ions

We have access to a large body of knowledge about the secondary ion emission behavior of many elements and molecules in diverse chemical environments, such as metals in different oxidation states[12, 13] and organic molecules on different substrate surfaces.[10] Well-founded propositions about secondary ion formation are drawn from these data which are valid either generally or for certain more or less narrowly defined classes of substances. This information on matters such as sputtering rates, the types of secondary ions formed, transformation probabilities, and secondary ion yields is scattered throughout the literature, and the collection and summary of such data is overdue.[52]

A number of experimental findings, including the increase of the metal ion yield by several orders of magnitude on going from a metal to its oxide, and the transformation probabilities close to 1 that are observed for alkali metals, halogens, and many anionic complexes, have led to the hypothesis of charge conservation in secondary ion emission. This states that sur-

face particles are emitted with a charge of the same sign as that which they had at the surface before emission. Such a "precursor" model is also in agreement with the general observation that protonated (deprotonated) molecular ions nearly always give positive (negative) secondary ions.

In order for a molecular ion to be emitted it must survive the sputtering process without disintegrating. This is more likely to occur if the bonding to the surface is weak. Moreover, a molecule ejected from a weakly bonding site will have less vibrational energy, such that the probability of it disintegrating later during its flight time through the spectometer is also small. As yet there is no satisfactory theoretical model to account for the emission of larger molecular secondary particles, in particular those from thermally unstable, nonvaporizable substances. This applies not only to the emission of intact molecules and fragments thereof but also to the processes by which they become ionized. Fundamental studies of precisely defined molecular surface systems of this kind are urgently needed.

5.2. Instrument Technology

The transition from sector field and quadrupole spectrometers to time-of-flight spectrometers was an important breakthrough in surface analysis by secondary ion mass spectrometry. This gave high mass resolution with a mass range that was in principle unlimited, together with a capability for precise mass measurement combined with high transmission and quasi-parallel ion counting, which thus increased the sensitivity by several orders of magnitude. These advantages opened up entirely new possibilities, both in fundamental studies and in applications to practical analytical problems. For these the development of the pulsed charge compensation technique was a very important advance. The buildup of charge on nonconducting specimens is a serious problem with all surface analysis methods such as XPS and AES. Charge compensation by pulsed injection of electrons in the target zone has practically eliminated this problem for TOF-SIMS.

The combination of a high-performance time-of-flight mass spectrometer with a finely focused pulsed ion beam allows surface imaging with a lateral resolution down to 50 nm. The mass analysis of neutral atomic and molecular particles that are emitted is a method of growing importance. With a time-of-flight mass spectrometer the post-ionization needed to make this possible can be carried out efficiently only by laser photoionization.[53] For modular TOF-SIMS instruments it is a straightforward matter to add on a laser system for this purpose (cf. Fig. 4).

During the last ten years time-of-flight secondary ion mass spectrometers have been developed to the stage of mature routine instruments. Several commercial manufacturers now offer reliable high-performance systems. Future instrument developments are likely to be directed towards reducing the time needed to record spectra and images, improving lateral resolution and mass resolution, further improving laser post-ionization facilities, and developing MS/MS techniques. One can also expect to see growth in the use of SIMS in combination with other methods such as XPS, AES, electron microscopy, scanning tunneling microscopy (STM), and atomic force microscopy (AFM).

5.3. Analytical Applications

In addition to the high sensitivity and detailed information on the molecular level possible with TOF-SIMS, an important reason for its widespread and growing use in analysis is that it is universally applicable to real samples of all kinds. Its applications now range from microelectronics through inorganic and organic chemistry, materials development, and environmental analysis to medical technology and clinical analysis. TOF-SIMS made it possible for the first time to obtain images and carry out local analysis of monolayers with high sensitivity, high lateral resolution, and high mass resolution, including measurements

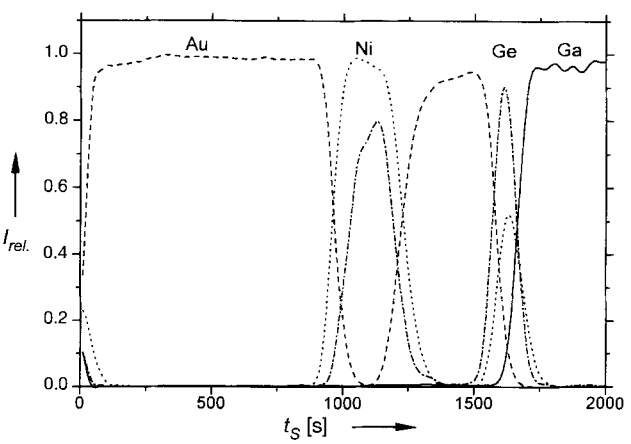


Fig. 31. Depth profile of a gold contact on a microchip, obtained by sputtering (sputter time t_s) over a 1 μm^2 area using a raster-scanned primary ion beam with a diameter of 0.1 μm. To reduce matrix effects the analysis was performed by observing neutral emitted particles after laser ionization.

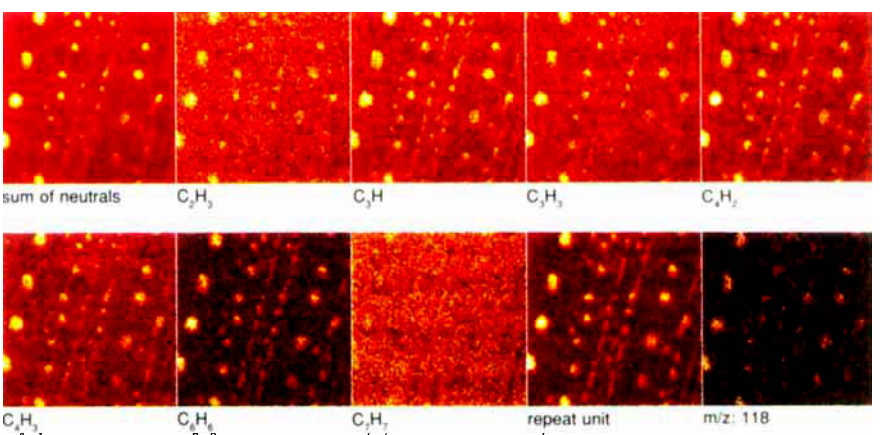


Fig. 32. Laser post-ionization of sputtered neutral particles used here to image polystyrene specks deposited from a solution onto a silicon surface. The emitted neutral particles were ionized by a UV laser before entering the mass analyzer. Field of view: 25 × 25 μm^2; primary ion fluence 10^{13} cm^{-2}; ca. 3500 primary ions per pulse; 128 × 128 pixels; 1 cycle per pixel.

in the high mass range, which gave both molecular and elemental information. The wealth of information yielded by TOF-SIMS for molecular (organic) film systems and surface modifications is particularly important, since these are being developed to replace conventional films (e.g. metals and oxides) for the production of surfaces with specific physical, chemical, and biological properties.

Quantitative SIMS analysis is greatly hindered by matrix effects, which sometimes necessitate very time-consuming comparative measurements and the use of internal or external standards. Calibrations can sometimes be made considerably more easily by measurements on post-ionized neutral particles, especially in elemental analysis (Fig. 31).[53] By using pulsed UV lasers with very short pulse durations (in the picosecond range), transformation probabilities approaching 1 have recently been achieved for metal atoms. With a lateral resolution of 0.1 μm this leads to an extrapolated detection limit of 10^{-4} of a monolayer.[54] Effective post-ionization of molecular surface species has also been achieved for a variety of types of materials (Fig. 32).[54–56]

Future work on the analytical applications of TOF-SIMS is likely to include fundamental studies (e.g. of the interaction of large molecules with precisely defined surfaces), advances in the analysis of particles (e.g. in the environment and in soil), studies of interfaces between organic and inorganic materials (e.g. metal/polymer interfaces, biocompatibility, immobilized molecular layers, lubricants), new materials (e.g. composites, molecular membranes, LB and SA films, catalysts, polymers), and technologies on the micrometer and nanometer scales (e.g. micromechanics, microelectronics, sensors). Biological specimens and sections pose an important challenge for imaging by molecular surface mass spectrometry. The prospect of obtaining molecular information from such materials opens up radically new potential applications. However, further advances in techniques are essential here, for example in the preparation of sections suitable for SIMS analysis, and in the development of "staining" methods.

Received: January 11, 1993
Revised version: December 23, 1993 [A 937 IE]
German version: *Angew. Chem.* **1994**, *106*, 1075
Translated by: Dr. J. K. Becconsall, Gwynedd (UK)

[1] J. C. Rivière, *Surface Analytical Techniques*, Clarendon Press, Oxford, **1990**.
[2] K. F. J. Heinrich, *Electron Beam X-Ray Microanalysis*, Van Nostrand Reinhold, New York, **1981**.
[3] C. Hamsu, M. Hirtschold, *Raster-Tunnel-Mikroskopie*, Akademie Verlag, Berlin, **1991**.
[4] A. Benninghoven, F. G. Rüdenauer, H. W. Werner, *Secondary Ion Mass Spectrometry*, Wiley, New York, **1987**.
[5] *Analysis of Organic and Biological Surfaces* (Eds.: P. J. Elving, J. D. Winefordner), *Chem. Anal. NY*, **1971**, *71*.
[6] E. Niehuis, T. Heller, H. Feld, A. Benninghoven, *J. Vac. Sci. Technol. A* **1987**, *5*, 1243.
[7] E. Niehuis in ref. [20b], p. 269.
[8] *Sputtering by particle bombardment* (Ed.: R. Behrisch), Springer, Berlin, **1981**.
[9] A. Benninghoven, W. Sichtermann, *Org. Mass Spectrom.* **1977**, *12*, 595.
[10] A. Benninghoven, W. Sichtermann, *Anal. Chem.* **1978**, *50*, 1180.
[11] A. Benninghoven, A. Müller, *Thin Solid Films* **1972**, *12*, 439.
[12] A. Benninghoven, E. Löbach, N. Treitz, *J. Vac. Sci. Technol.* **1972**, *9*, 600.
[13] K. H. Müller, P. Beckmann, M. Schemmer, A. Benninghoven, *Surf. Sci.* **1979**, *80*, 325.
[14] A. Benninghoven, *Surf. Sci.* **1975**, *53*, 596.
[15] C. Plog, L. Wiedmann, A. Benninghoven, *Surf. Sci.* **1977**, *67*, 565.
[16] B. Hagenhoff, R. Kock, E. Niehuis, A. Benninghoven, C. Wünsche, H. Musche in ref. [20a], p. 371.
[17] J. Schwieters, H. G. Cramer, T. Heller, U. Jürgens, E. Niehuis, A. Benninghoven, *J. Vac. Sci. Technol. A* **1991**, *9*, 2864.
[18] B. Hagenhoff, D. van Leyen, E. Niehuis, A. Benninghoven, *J. Vac. Sci. Technol. A* **1989**, *7*, 3056.
[19] J. Schwieters, J. F. Zehnpfennig, E. Niehuis, A. Benninghoven, *J. Vac. Sci. Technol. A* **1990**, *8*, 3752.
[20] Reviews of recent development: a) *Secondary Ion Mass Spectrometry, SIMS VII* (Eds.: A. Benninghoven, C. A. Evans, K. D. McKeegan, H. A. Storms, H. W. Werner), Wiley, New York, **1990**; b) *Secondary Ion Mass Spectrometry, SIMS VIII* (Eds.: A. Benninghoven, K. T. F. Janssen, J. Tümpner, H. W. Werner), Wiley, New York, **1992**; c) *Secondary Ion Mass Spectrometry, SIMS IX* (Eds.: A. Benninghoven, Y. Nihei, R. Shimizu, H. W. Werner), Wiley, New York, **1994**.
[21] M. Barber, R. S. Bordoli, G. J. Elliot, R. D. Sedgwick, A. N. Tyler, *Anal. Chem.* **1982**, *54*, 645.
[22] *Analysis of Microelectronic Materials and Devices* (Eds.: M. Grasserbauer, H. W. Werner), Wiley, New York, **1991**.
[23] U. Jürgens, H. G. Cramer, T. Heller, E. Niehuis, Z. Zhang, A. Benninghoven in ref. [20b], p. 277.
[24] E. Niehuis, T. Heller, U. Jürgens, A. Benninghoven, *J. Vac. Sci. Technol. A* **1989**, *7*, 512.
[25] M. Terhorst, R. Möllers, A. Schnieders, A. Benninghoven in ref. [20c], in press.
[26] A. Benninghoven, *Z. Naturforsch. A* **1969**, *24a*, 895.
[27] J. Schwieters, H. G. Cramer, U. Jürgens, E. Niehuis, H. Rulle, T. Heller, J. Zehnpfenning, A. Benninghoven in ref. [20b], p. 497.
[28] *Chemical Surface Preparation, Passivation and Cleaning in Semiconductor Growth and Processing* (Ed.: R. J. Nemanich), *Mater. Res. Soc. Symp. Proc.* **1992**, *259*.
[29] H. van der Wel, J. Lub, P. N. T. van Velzen, A. Benninghoven, *Mikrochim. Acta* **1990**, *II*, 3.
[30] B. Hagenhoff, Dissertation, Universität Münster, Deutscher Universitätsverlag, Wiesbaden, **1994**.
[31] H. Feld, R. Rading, A. Leute, A. Benninghoven, *Org. Mass Spectrom.* **1993**, *28*, 841.
[32] A. Benninghoven, D. Holtkamp, *Surf. Sci.* **1982**, *123*, L 721.
[33] A. Benninghoven, V. Anders, *Org. Mass Spectrom.* **1984**, *19*, 345.
[34] K. Meyer, B. Hagenhoff, M. Deimel, A. Benninghoven, *Org. Mass Spectrom.* **1992**, *27*, 1148.
[35] B. Beamson, A. Bunn, D. Briggs, *SIA Surf. Interface Anal.* **1991**, *17*, 105.
[36] D. van Leyen, B. Hagenhoff, E. Niehuis, A. Benninghoven, *J. Vac. Sci. Technol. A* **1989**, *7*, 1790.
[37] J. Lub, A. Benninghoven, *Org. Mass Spectrom.* **1989**, *24*, 164.
[38] I. V. Bletsos, D. Hercules, *Anal. Chem.* **1991**, *63*, 1953.
[39] B. Hagenhoff, A. Benninghoven, H. Barthel, W. Zoller, *Anal. Chem.* **1991**, *63*, 2466.
[40] D. van Leyen, B. Hagenhoff, E. Niehuis, A. Benninghoven, *J. Vac. Sci. Technol. A* **1989**, *7*, 1790.
[41] D. Briggs, *SIA Surf. Interface Anal.* **1986**, *9*, 391.
[42] D. E. Fowler, R. D. Johnson, D. van Leyen, A. Benninghoven, *SIA Surf. Interface Anal.* **1991**, *17*, 125.
[43] E. Niehuis, P. N. T. van Velzen, J. Lub, T. Heller, A. Benninghoven, *SIA Surf. Interface Anal.* **1989**, *14*, 135.
[44] G. Bolbach, J. C. Blaise in *Secondary Ion Mass Spectrometry, SIMS VI* (Eds.: A. Benninghoven, A. M. Huber, H. W. Werner), Wiley, New York, **1988**, p. 655.
[45] B. Hagenhoff, A. Benninghoven, H. U. Siegmund, D. Holtkamp, *Thin Solid Films* **1992**, *210*, 601.
[46] B. Hagenhoff, M. Deimel, A. Benninghoven, H. U. Siegmund, D. Holtkamp, *J. Phys. D Appl. Phys.* **1992**, *25*, 818.
[47] B. Hagenhoff, A. Benninghoven, J. Spinke, M. Liley, W. Knoll, *Langmuir* **1993**, *9*, 1622.
[48] B. Hagenhoff, A. Benninghoven, K. Stoppek-Langner, J. Grobe, *Adv. Mater.* **1994**, *6*, 142.
[49] A. Leute, Dissertation, Universität Münster, **1994**.
[50] J. Zehnpfennig, H. G. Cramer, T. Heller, E. Niehuis, H. Rulle, T. Stephan, A. Benninghoven in ref. [20c], in press.
[51] T. Stephan in ref. [20b], p. 115.
[52] H. Feld, A. Leute, D. Rading, A. Benninghoven, *Anal. Chem.* **1990**, *62*, 2088.
[53] C. H. Becker, K. T. Gillen, *Anal. Chem.* **1984**, *56*, 1671.
[54] M. Terhorst, R. Möllers, E. Niehuis, A. Benninghoven, *SIA Surf. Interface Anal.* **1992**, *18*, 824.
[55] N. Winograd, *Anal. Chem.* **1993**, *65*, 622A.
[56] M. Terhorst, R. Möllers, E. Niehuis, A. Benninghoven in ref. [20c], in press.

Luminescent Labels—More than Just an Alternative to Radioisotopes?

Andreas Mayer* and Stephan Neuenhofer*

Chemical, chromatographic, or spectrometric methods are generally unsuitable for the detection of molecules in the nano- and subnanogram region because of their low sensitivity. The radioimmunoassay (RIA) developed by Yalow and Berson in 1959 combined the high sensitivity of radioactively labeled substances with the high specificity of immunological reactions for the first time. In this way it was possible to detect quantitatively the tiniest traces of substances in the presence of an excess of other, in some cases, similar foreign substances without prior enrichment. Immunoassays have certainly developed to become the most valuable analytical tool of in vitro diagnostics and are today routinely employed for the detection of endogenous and exogenous substances (e.g. hormones, tumor-associated proteins, bacteria, viruses, toxins, drugs, etc). The many disadvantages of radioactivity such as the required handling licenses, disposal costs, precautions necessary to prevent risks to health, short shelf-life, and limited sensitivity soon led to the search for other nonradioactive labeling methods. Encouraged by the development of light measuring techniques and the commercial availability of highly sensitive apparatus, radioactive isotopes as labels are today being replaced increasingly by enzymes, fluorophores, or luminophores. Some of the new luminescent labels have, however, not only facilitated replacement of radioisotopes, but also a breakthrough into what has until now been unattainable levels of sensitivity. The following article reviews the methods of luminescent labeling and their applications mainly in the area of immunoassays.

1. Introduction

The detection of substances with reagents which bind to the compound to be determined (analyte) is essentially dependent on three conditions if lower detection limits in the pico- to femtomolar region are to be attained and structurally similar substances are not to be measured in addition. First, the detection reagent must have a high affinity for the analyte so that even an analyte present in trace amounts is determined. Second, the binding of the detection reagent to the analyte should be highly specific; this ensures that substances similar to the analyte do not give rise to a deceptively higher concentration of the analyte, or make a time-consuming and labor-intensive prepurification necessary. Third, the reaction product from the analyte and binding reagent must be sensitive to detection, that is, emit a signal which can be quantified exactly by suitable analytical instruments.

[*] Dr. A. Mayer
Hoechst AG, Zentralforschung G 830
D-65926 Frankfurt am Main (FRG)
Telefax: Int. code + (69)331320
Dr. S. Neuenhofer[+]
Hoechst AG, Radiochemisches Laboratorium
D-65925 Frankfurt am Main (FRG)
[+] New address:
Behringwerke AG, Neue Systeme und Gerinnungsdiagnostika
D-35001 Marburg (FRG)
Telefax: Int. code + (6421)394680

The demands for affinity and specificity are ideally fulfilled by antibodies. This involves endogenous glycoproteins, which in organisms of higher life forms, play a decisive role within the immune system by eliminating harmful substances (bacteria, viruses, toxins etc.). In general, affinity constants of antibodies lie between 10^{10} and $10^{12}\,L\,mol^{-1}$. They are capable of recognizing the smallest structural differences at the molecular level, because only then can they distinguish reliably between exogenous and endogenous substances; confusion between the two would have fatal consequences for the host organism.

The first methods used to label detection reagents and thus make them exactly quantifiable employed radioactive isotopes, of which the ^{125}I isotope, in particular, is still in use today. The advantages of this γ emitter are its small size (minimization of steric interference), its "hard" signal, which as a result is less prone to interference, and its lower detection limit of approximately 10 amol (1 amol $= 10^{-18}$ mol).

The combination of antibody/radioactive labeling led to the introduction of radioimmunoassays at the end of the 1950s.[1] These have developed into the most important tool of in vitro diagnostics in medicine.[2] All conceivable endogenous and exogenous substances in the body fluids (e.g. blood or serum) taken from a patient are routinely determined quantitatively by radioimmunoassays. Of considerable importance for routine applicability is that despite the complex composition of the serum medium under investigation, in general, further purifica-

tion steps are not necessary because of the high specificity of the detection reagent "antibody".

Besides the advantages of radioactive labeling there are also, however, a number of disadvantages: The handling of radioactive materials is regulated (official license) and is, thus, limited. The half-life of 60 days for ^{125}I isotope is too short to guarantee a longer shelf-life for labeled reagents. Limited signal emission during measurement due to the natural half-life prevents the high detection sensitivity required for some applications.

In order to overcome these disadvantages the search for nonradioactive labeling methods (nonisotopic methods) in immunodiagnostics had already begun long ago.[3] At the beginning of the 1970s the use of enzymes as labels was described,[4] and in the meantime a large number of stable enzyme labels have become available. In combination with chromogenic or luminogenic substrates, detection of the signal is attributed to the measurement of light as absorption or emission. Emitted light instead of radioactive radiation is also employed in luminogenic direct labeling for the quantification of the analyte concentration. Since the number of photons from samples of luminescent-labeled molecules can be higher than the number of radiation quanta emitted from radioisotopes,[5] initially fluorescence detection seemed to have a good chance of a wide application in nonradioactive labeling;[5, 6] for example, detection of a single fluorescent-labeled protein molecule was successful.[7, 8] However, because of certain disadvantages associated with the first fluorescent label a signifcant replacement of the radioactive label was not forthcoming. This was only achieved by further development of luminescent labels and luminogenic enzyme substrates.[9–15] Luminescent labels not only dispense with having to handle radioactivity but they also allow more precise diagnostic results on account of enhanced sensitivity, and open up new areas of application.

In 1985 the radioimmunoassay (RIA) dominated the German immunoassay market (83% share) with the greatest turnover in the indication fields endocrinology (thyroid gland, fertility) and tumor diagnosis (Fig. 1). The tendency towards the use of methods with nonisotopically labeled compounds is shown in the statistics for 1991; the RIA share of the market has sunk considerably to 55%.[16] The market share of nonradioactive methods comprises luminescence techniques (e.g. fluorescence immunoassay (FIA), chemiluminescence immunoassay (CIA)), enzyme immunoassay (EIA), and other methods such as nephelometry. A further increase in the market share for methods that work without isotopically labeled compounds is to be expected in the future.

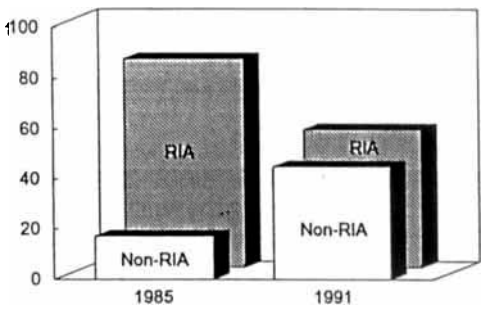


Fig. 1. Market share of radioactive (RIA) and nonradioactive immunoassays (non-RIA).

This review article deals in the broadest sense with luminescent labels and their application. After a definition of the term "label" in Section 2 luminescent processes are presented in a simplified energy-level diagram in Section 3. Section 4 describes the enzyme labels in combination with chromogenic and luminogenic substrates. In Section 5 labels for luminescent direct labeling with special consideration of the underlying mechanisms of chemiluminescent labeling are discussed. Section 6 presents several examples of applications in medicine; further important areas of application are in environmental and food analysis.[17g–h, 18k–p] In addition to the literature already mentioned, the theme of luminescent labels, nonradioactive immunoassays, and gene probes is referred to in several recent books[17] and review articles.[18]

Andreas Mayer, born 1960 in Aschaffenburg, studied chemistry at the Universität Würzburg and received his doctorate under the supervision of H. Quast for work on dicyanosemibullvalenes. In 1989 he entered the main laboratory of the Hoechst AG and strengthened the team working on the development of chemiluminescent labels for diagnostic applications. The main emphasis of his work so far has been the synthesis of functional dyes for applications in the area of diagnostics and information technology.

Stephan Neuenhofer, born 1955 in Mayen/Eifel, studied chemistry and pharmacy in Bonn. After completing his diploma in chemistry (1982) he moved into biochemistry and received his doctorate in 1985 with K. Sandhoff on the topic of gangliosides (Lysogangliosides—Synthesis, Detection in Pathological Brain Tissue and Applications in Biochemical Studies). For his dissertation he received the Edmund-Ter-Meer-Preis. In 1987 he received his approbation as a pharmacist. In August 1987 he began working in the research and development department at the Hoechst AG. His area of interests comprises luminogenic labeling substances, immunoassays, and diagnostic systems as well as their transfer to production. He moved to Behringwerke AG in October 1993 where he has continued with these avenues of research.

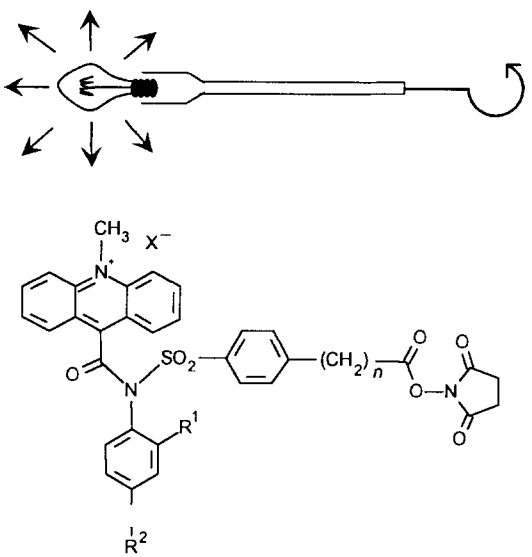


A. Mayer S. Neuenhofer

2. The Label

2.1. Definition and General Structure

A label is a molecule capable of emitting a signal, which is used for labeling proteins and other molecules. It contains, apart from the signal-generating group (fluorescer; more specifically, label), another reactive group (anchor group) which facilitates the covalent bonding to the molecule to be labeled. Between these two groups there is usually a spacer which is supposed to prevent, or at least make difficult, undesirable steric interactions between the signal-generating group of the molecule and the labeled substance. In this way any influences on the immunological reaction ought to be excluded. The schematic structure of a label as well as the chemical formula of a chemiluminescent label from the



Scheme 1. Schematic representation of a luminescent label (top) with the three components: signal-generating unit (fluorescer), spacer, and anchor group as well as a concrete example from the *N*-methylacridinium-9-(*N*-sulfonyl)carboxamide class of compounds (bottom).

class of *N*-methylacridinium-9-(*N*-sulfonyl)carboxamides is shown in Scheme 1. A substance labeled in this way is designated as a tracer.

2.2. Luminescent Labels

2.2.1. *Definitions of Terms*

The term luminescence[19] serves as the generic term for most light emission processes such as fluorescence, phosphorescence, chemiluminescence, electroluminescence etc. Exceptions are, for example, glow emission and coherent scattering processes. In practice, three categories are often used, namely luminescence, fluorescence, and phosphorescence. Luminescence serves as the generic term for chemi- and bioluminescence.

2.2.2. *Requirements for the Suitability as a Luminescent Label*

The suitability of a compound as a luminescent label has certain conditions which must be fulfilled:[20]

Coupling to the compound to be analyzed (analyte) must be simple and quite gentle. A large palette of reactive groups is available for this purpose.

The luminescent properties of the label should not change significantly after the coupling.

The properties of the labeled substance must not be altered significantly by the labeling. The whole spectrum of characteristics must be taken into consideration, for example physico-chemical properties such as solubility and immunological properties. For the duration of the immunoassay, the immunological reactivity, in particular, must remain sufficiently high.

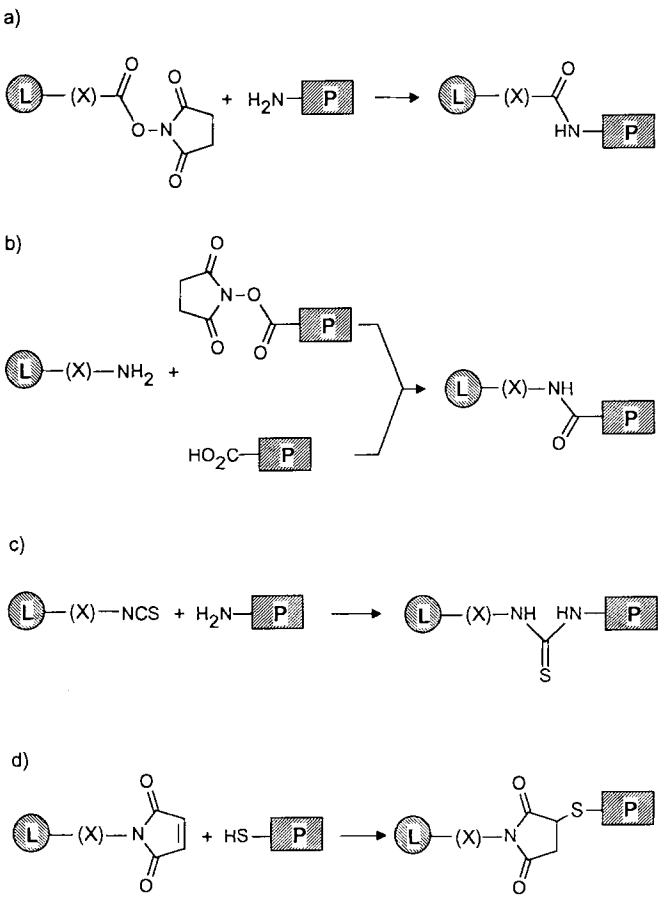
Of course, these general requirements, with the exception of the second point, are also applicable to other labels. The extent to which these points are fulfilled greatly depends on the details of each system and differs from case to case. For instance, small molecules (molecular weight <2 kD) are altered more significantly than large proteins when labeled with a marker of similar size. Proteins, however, are often more sensitive under the labeling conditions; for example, syntheses cannot be carried out in organic solvents. Nevertheless, for most, the conditions to yield suitable conjugates are established by chemical modification of the signal-generating group and/or of the spacer and by choice of the optimal reactive group.

2.2.3. *The Signal-Generating Group*

Fundamentally all luminescent compounds can be considered to be signal-generating groups if they exhibit a sufficient quantum yield in aqueous solutions, are stable enough under the conditions employed, and can be functionalized synthetically in such a way that a reactive group can be bound and the properties can be modified, for example, to increase the solubility in water or to change emission characteristics such as wavelength and decay time. Variability is a prerequisite for the broadest possible application of the label. The most important fluorescent and chemiluminescent labels are considered in more detail in Section 5.[7a, 21]

2.2.4. *The Reactive Group*

As mentioned previously, the reactive or anchor group is used to bind the label to the substance to be labeled. Since coupling to biological material such as proteins, antibodies, hormones etc. is frequently necessary, the formation of an acid amide bond between activated carboxyl groups and amino groups is quite common. Many processes for this are known in peptide chemistry which proceed in aqueous solution under mild conditions.[22, 23] However, only a few reactions have achieved practical significance for labeling processes. Some of the most important coupling reactions are summarized in Scheme 2. Many luminescent labels have an *N*-hydroxysuccinimide (NHS) ester as the reactive group (Scheme 2a).[21, 25] This reactive group has several advantages:[22, 24] it can be readily synthesized from carboxylic acid derivatives;[26] corresponding labels can be purified to a high degree, for example, by HPLC; thus, labeling can be carried out

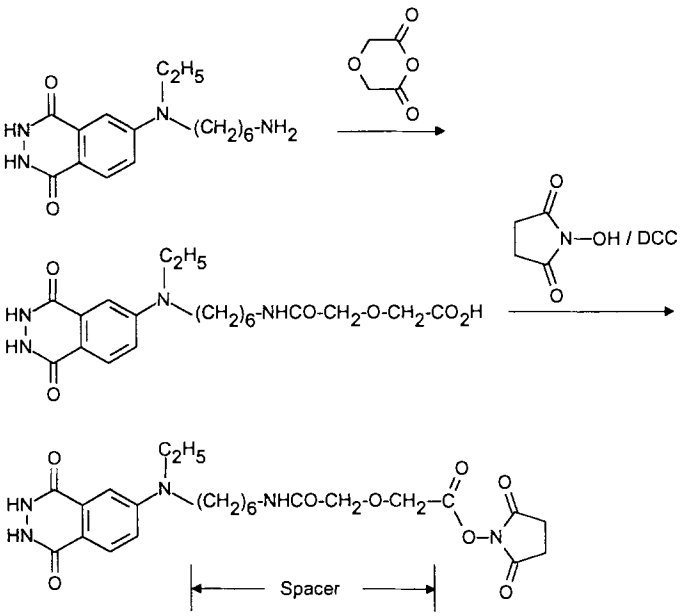


Scheme 2. Important labeling processes; L = label, P = protein, X = spacer.

in a defined and reproducible way. With the exclusion of moisture it is possible to store the label over longer periods of time without the reversal of the coupling activity.[24, 27, 28] The coupling reaction of the succinimide with amino groups proceeds under mild conditions (room temperature) in aqueous solutions; in contrast, alcohols do not react with NHS esters under these conditions.[27] As a variation of this reaction the label can also contain a primary amino functionality as the reactive group for coupling with an NHS ester functionality on the protein (Scheme 2b). The conversion can also be achieved with free carboxyl groups, for example, of proteins, following carbodiimide or "mixed anhydride" methods.[22, 23, 25] Recently acridinium ester labels with imido ester reactive groups were described.[29] Particularly in the case of fluorescent labels, in addition to the the methods already mentioned the isothiocyanate group is often used for coupling with amino groups of proteins to form thiourea derivatives (Scheme 2c).[30] The method shown in Scheme 2d for the coupling by thiol addition to maleic imido groups is well known in peptide chemistry. This reaction is also employed in luminescent labeling[21] and plays a particularly important role in the coupling of enzyme labels to proteins.[31]

2.2.5. *The Spacer*

Usually simple, short alkyl chains or groups which contain aromatic and aliphatic groups (cf. Scheme 1) are employed as

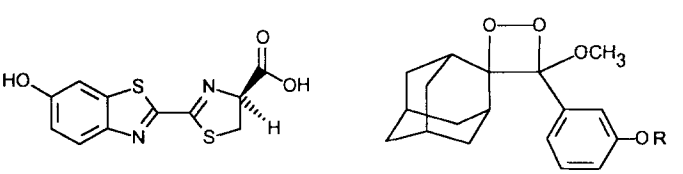


Scheme 3. Synthesis method for a spacer with an NHS reactive group as illustrated by an example of an isoluminol label; DCC = dicyclohexylcarbodiimide.

spacer. An example of the conversion of an amino group of an isoluminol label to give an NHS ester is shown in Scheme 3.[32] By using a spacer of the type shown, which contains several acid amide groups and ether bridges as hydrophilic units, the solubility of immunoconjugates in water can be improved.[33]

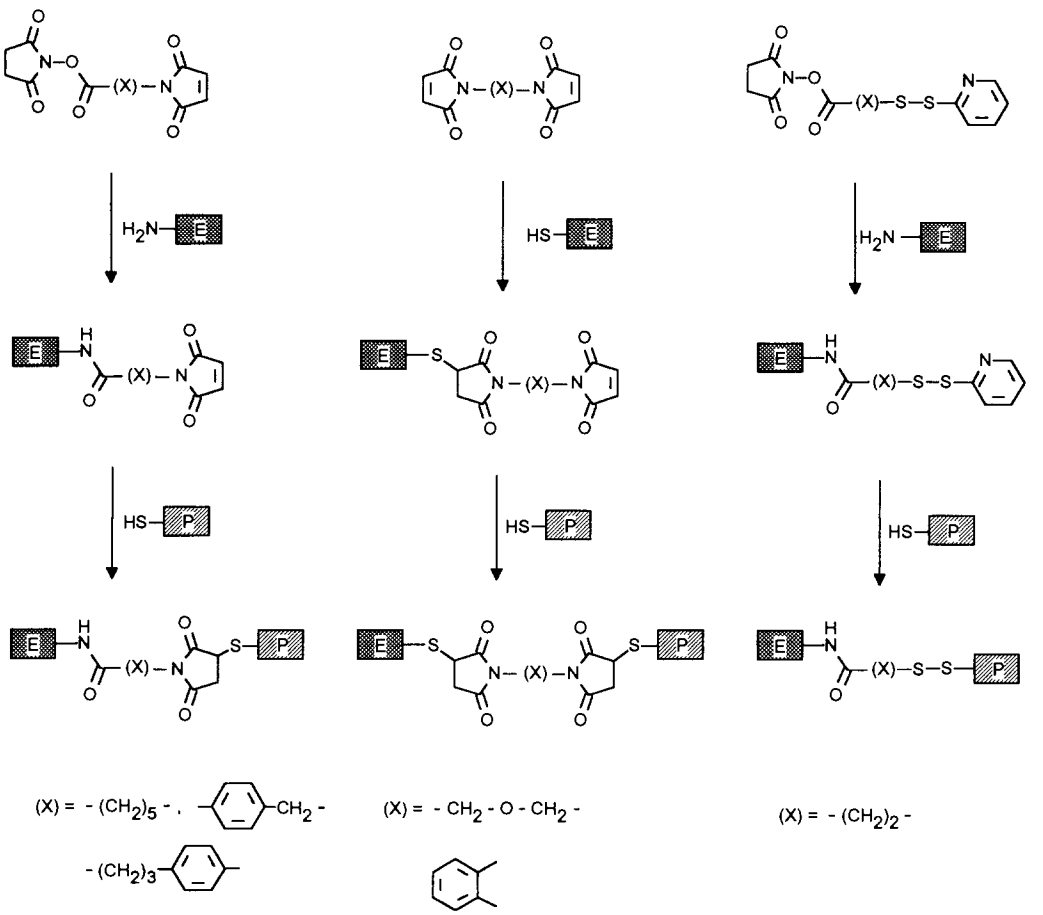
2.3. Enzyme Labels

As a result of their practical significance chromogens and luminogens are also dealt with in this article; these are employed as substrates for the enzyme label (Section 4). The reaction of luciferin derivatives (naturally occurring bioluminescent compounds) with their respective luciferase (enzyme which catalyzes the bioluminescent reaction) leads to luminescent reactions with the highest known quantum yields. The leader in this field is the luciferin (Scheme 4)/luciferase system of the North American



Scheme 4. Firefly luciferin (left) and a stable dioxetane derivative (right).

firefly (*Photinus Pyralis*) with quantum yields around 0.9 Einstein mol^{-1}.[11, 15] Since the end of the 1980s important biogenic luciferases have been genetically engineered and are thus now considered for routine applications.[15] High quantum yields are also obtained by enzyme labels with stable dioxetanes (Scheme 4) as luminogenic substrates. The enzymes often employed are alkaline phosphatase and β-galactosidase (the residue R is phosphate and β-galactose, respectively). Such enzymatic systems are dealt with in more detail in Section 4.



Scheme 5. Bifunctional coupling reagents for labeling of enzymes; E = enzyme, P = protein (e.g. antibody), X = spacer.

Since, in general, enzyme labels are not obtainable as stable universally applicable labels, several methods for enzyme labeling should be addressed. The coupling of enzymes to antibodies or fragments of antibodies is often achieved by bifunctional coupling reagents. Some examples are shown in Scheme 5. The reactions are analogous to the methods already mentioned in Section 2.2.4, and details can be obtained from the references cited in the literature.[24, 31] Coupling methods that exploit the strong noncovalent bonding of the biotin/(strept-)avidin system can only be referred to here.[34]

3. Electromagnetic Radiation as the Measured Signal

3.1. Comparison of Light and Radioactive Radiation

A considerable disadvantage in the use of radioactive isotopes is the necessity to undertake extensive safety precautions against high-energy β- or γ radiation (up to 10^{18} kJ mol^{-1}). Since luminescent labels emit light which is not dangerous—mostly in the visible region of the electromagnetic spectrum ($E \approx$ 200 kJ mol^{-1})—safety measures for the protection from high-energy radiation are no longer required. Furthermore, the specific activity that can be achieved with radioisotopes has an upper limit set by the radiolytic decomposition of the labeled material. Labeling with the isotope ^{125}I is usually limited to one atom per molecule.[21, 35] In addition, the half-life of the radioisotope, which, for example, is only 59.7 days for the frequently used ^{125}I, limits the storability of the labeled material and detection limits. Moreover, radioisotopes emit radiation continuously even when a signal is not necessary for measurement. For the actual measurement, which normally lasts about a minute, only a tiny fraction of the available signal, can be used. An advantage, however, is that a repeat measurement is possible at any time. Luminescent labels, which have a considerably longer lifetime, emit all the available light within a very short space of time once the light reaction has been triggered. In addition, the activity of the tracer can be enhanced further mainly by multiple labelings; in this way the sensitivity of detection is increased. Repeat measurements on the same sample are, however, not possible, at least in the application of chemiluminescent labels with rapid light emission.

3.2. Photophysical Processes

In the simplified energy-level diagram in Figure 2 the most important photophysical processes are summarized with their typical lifetimes τ [s].[36] The radiative transitions shown can be used for the production of detection signals. Since radiationless deactivation leads to less efficiency, especially in long-lived phosphorescence processes in solution, phosphorescence detection plays a minor role for luminescent labels. Finally, the quantification in enzyme systems with chromogenic substrates (cf. Sec-

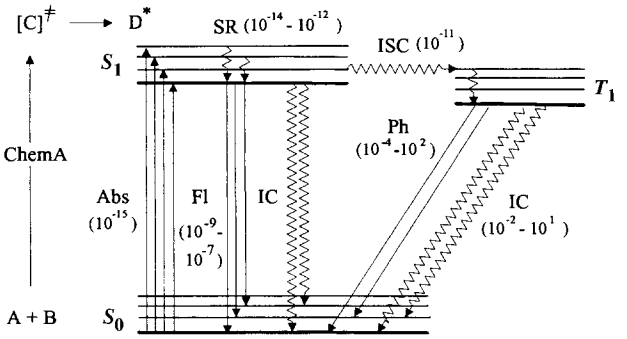


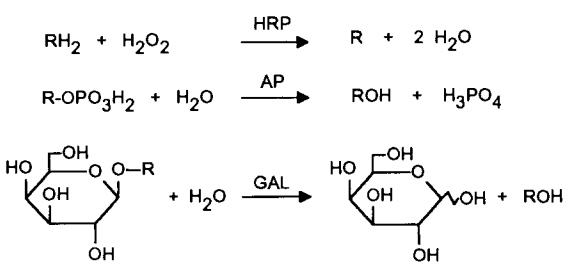
Fig. 2. Simplified energy-level diagram with some photophysical processes. Lifetime τ [s] is given in parentheses; Abs = absorption, Fl = fluorescence, Ph = phosphorescence, SR = vibrational relaxation, ChemA = chemical excitation, IC = internal conversion, ISC = intersystem crossing; straight lines represent radiative processes and wavy lines radiationless processes.

tion 4) is ascribable to absorption measurements. Photoexcitation and evaluation of the fluorescence provide the basis for fluorescent labeling (cf. Section 5.1). The production of excited singlet states (S_1) by chemical reactions is necessary for chemiluminescence detection. The difference in energy between the S_1 and S_0 states for emissions in the visible region lies between 167 (red light) and 293 kJ mol^{-1} (violet light).[11,37] For the effective use of the principles mentioned, in each case, sufficient quantum yields are also a prerequisite. Further details are given for each individual luminophore (see Section 5).

4. Enzyme Labels

The use of enzymes as labels presented the first alternative to radioactive labeling.[38] The basic idea is very promising, because no signal-generating compounds are used, but molecules (enzymes) which produce a lot of signal-generating species. In this way an effective signal amplification mechanism is built in right from the outset.

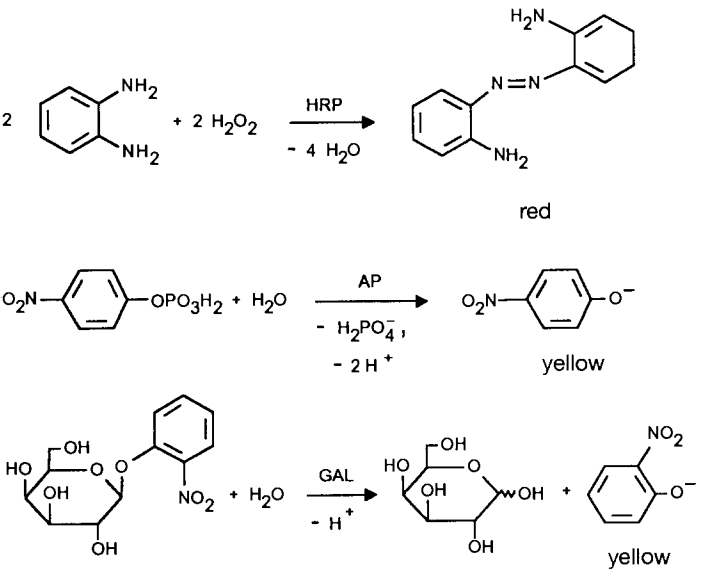
The three most important enzymes that are used as labels are horseradish peroxidase (HRP), alkaline phosphotase (AP), and β-D-galactosidase (GAL). The reactions catalyzed by these enzymes are summarized in Scheme 6. HRP is the smallest enzyme



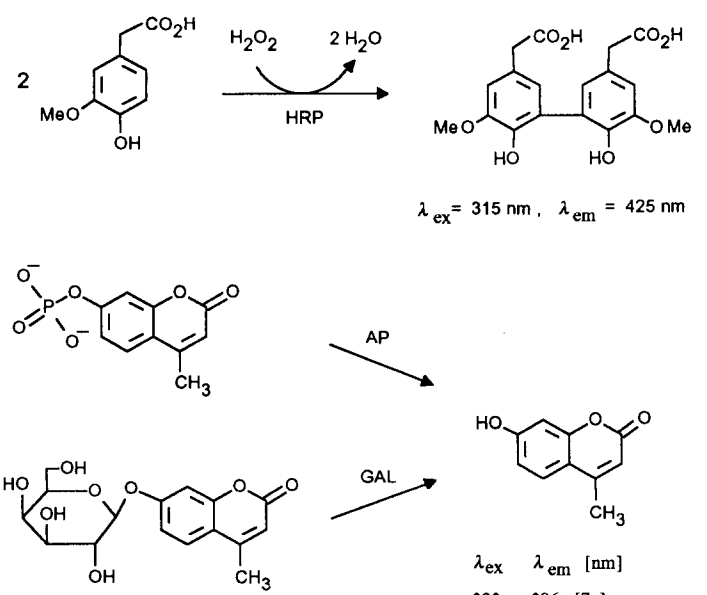
Scheme 6. General representation of the reactions catalyzed by the three most important enzyme labels HRP, AP, and GAL.

of the three with a molecular weight of approximately 40 kD (AP approx. 100 kD, GAL approx. 500 kD) and as a result presents the fewest steric problems. HRP is, however, sensitive towards antimicrobial agents (azide, Thiomersal) frequently employed. AP has the highest catalytic activity; however, it is inhibited by phosphate (product inhibition) and ethylenediaminetetraacetic acid (edta; chelates Zn^{2+} and Mg^{2+} ions which are necessary for enzyme activity).

The oldest enzyme substrates to be employed in analytical methods are the chromogens. These are colorless and are only transformed into colored products by an enzymatic reaction. These products can be quantified photometrically; Scheme 7 shows examples.



Scheme 7. Examples of chromogenic substrates. Apart from *o*-phenylenediamine, 3,3',5,5'-tetramethylbenzidine (TMB) and 2,2'-azinobis(3-ethylbenzothiazoline-6-sulfonic acid) (ABTS) are often employed. Instead of 4-nitrophenylphosphate, 1-napthylphosphate and 5-bromo-4-chloro-3-indolylphosphate are often employed. In addition to 2- or 4-nitrophenyl-β-D-galactopyranoside, chlorophenol red-β-galactopyranoside and 5-bromo-4-chloro-3-indolyl-β-galactopyranoside are often employed.

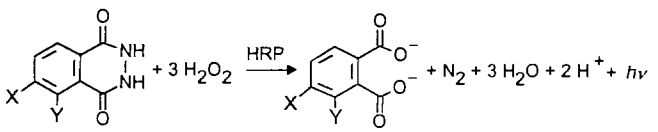


λ_{ex}	λ_{em} [nm]	
323	386	[7a]
380	450	[6]
360	447	[44]

Scheme 8. Examples of fluorogenic substrates. λ_{ex} = excitation wavelength, λ_{em} = emission wavelength.

The most important fluorogenic substrates of the peroxidases contain the same structural element[39, 40, 43] *p*-HO–C_6H_4-C-, whereas in the case of AP and GAL,[41–43] 4-methylumbelliferyl compounds are preferred (Scheme 8).

The chemiluminescent arylhydrazides luminol and isoluminol[45] (Scheme 9) are known substrates for HRP. The quantum

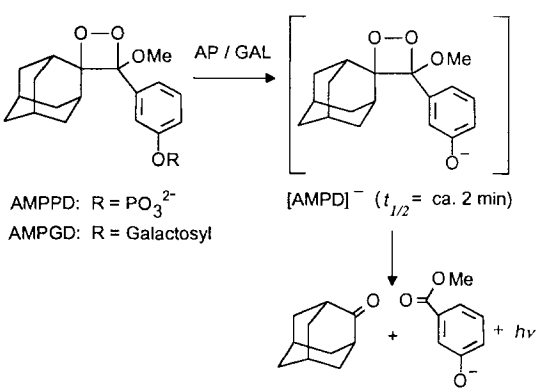


Luminol: X = H, Y = NH_2
Isoluminol: X = NH_2, Y = H

Scheme 9. HRP-catalyzed oxidation of luminol and isoluminol.

yields of the oxidation of these arylhydrazides, that is, the percentage of the molecules of the starting material which at the end of the reaction afford a photon-emitting final product, is approximately 1%. The light intensity can be drastically increased (up to a factor of 1000!) by so-called enhancers such as 6-hydroxybenzothiazole derivatives or *para*-substituted phenols in comparison to a non-enhanced reaction.[46] The underlying mechanism of this enhanced chemiluminescence is not completely understood. The most probable explanation is that one or more of the oxidation steps to generate luminol radicals during the complex reaction pathway of the enzymatic oxidation is accelerated.[46k]

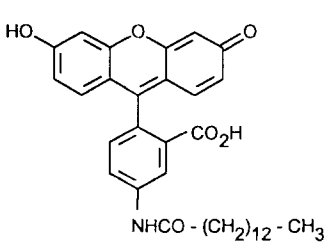
Dioxetane derivatives are the most important chemiluminogenic substrates for AP and GAL[47] (Scheme 10). Also in the



AMPPD: R = PO_3^{2-}
AMPGD: R = Galactosyl

[AMPD]$^-$ ($t_{1/2}$ = ca. 2 min)

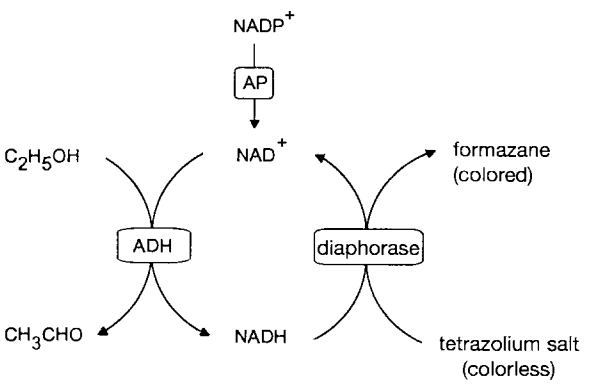
Scheme 10. Adamantylmethoxy(phosphoryloxyphenyl)dioxetane (AMPPD) and adamantylmethoxy(galactopyranosyloxyphenyl)dioxetane (AMPGD) as enzyme substrates. This reaction is catalyzed by AP and GAL.



Scheme 11. Example [5-(*N*-tetradecanoylamino fluorescein)] of a fluorescent tenside.

reactions catalyzed by AP and GAL, the chemiluminescence can be enhanced; for this purpose fluorescent tensides are particularly effective (Scheme 11). Together with normal tenside molecules (e.g. cetyltrimethylammonium bromide) they form micelles into which the substrate diffuses immediately after enzymatic cleavage of the phosphate or galactoside residue. Decomposition of the dioxetane derivative in the micelle leads to an effective transfer of energy to the fluorophore groups of the tenside molecules. This results in a considerable increase in the quantum yield[47j] (Φ_{CL} = approx. 0.005 Einstein per mol; for comparison: Φ_{CL} in tenside-free aqueous buffer solution is ca. 10^{-5} Einstein per mol). According to the literature, as few as 600 different enzyme molecules have so far been detected by employing dioxetane derivatives.[47e]

In the detection systems described previously the signal-generating group forms immediately in the reaction catalyzed by the enzyme label. There is also, however, a series of detection systems in which the signal-generating group is formed only in a subsequent reaction. In analogy to enzyme-catalyzed reactions, considerable increases in the sensitivity can often be achieved by such coupling reactions. In the detection system of Self,[48a] the enzyme label AP catalyzes the formation of NAD^+ from $NADP^+$. The NAD^+ formed catalyzes a specific redox cycle from which a colored substance is produced (Scheme 12).



Scheme 12. Example of a signal amplification: The NAD formed from AP acts as a catalyst in a subsequent redox cycle. ADH = alcohol dehydrogenase.

The lower detection limit for the enzyme label AP with this method was given as 0.01 amol,[48b] and in a more recent publication[48c] even 0.6 zmol (1 zeptomol = 10^{-21} mol); values which would have been inconceivable for direct formation of a dye.

Another method for the highly sensitive detection of AP was described by Christopoulos and Diamandis.[49] AP catalyzes formation of 5-fluorosalicylic acid from 5-fluorosalicylic phosphate. In a subsequent reaction 5-fluorosalicylic acid forms a strongly fluorescing ternary complex with Tb^{3+} and edta the concentration of which can be quantified by time-resolved fluorescence measurements (cf. Section 5.1.4). The lower detection limit was quoted as being 0.6 amol AP per 50 μL sample volume. In the detection system of A. Baret et al.[50] xanthine oxidase is used as the enzyme label. In the presence of oxygen, it oxidizes hypoxanthine to xanthine and uric acid with formation of superoxide radical anions ($O_2^{\cdot-}$). Additional reactive oxygen species (H_2O_2, $^1O_2$, $OH^{\cdot}$) that form in subsequent reactions are suitable for the chemiluminescent oxidation of luminol.

5. Luminescent Labels

5.1. Fluorescent Labeling

Fluorescent labels have been used for a wide range of applications in biology, biomedicine, and analytic methods for a long time.[30] Applications worthy of mention are fluorescence detection with HPLC after precolumn or postcolumn derivatization,[51] flow cytometry,[52] fluorescence microscopy,[53] DNA analysis,[54] and the use as labels in immunoassays, which will be covered in more detail here (see Section 5.1.1). Labeling is usually achieved by the formation of a covalent bond between label—as described, in general, in Section 2—and target substance. Fluorescent dyes without a reactive group can be employed for some purposes. They are only bonded associatively and as a result can accumulate, for example, in cells. A review of fluorochromes that are applied in medicine and biology as well as their spectral data can be found in reference [36].

5.1.1. Special Requirements of Fluorescent Labels for Immunoassays

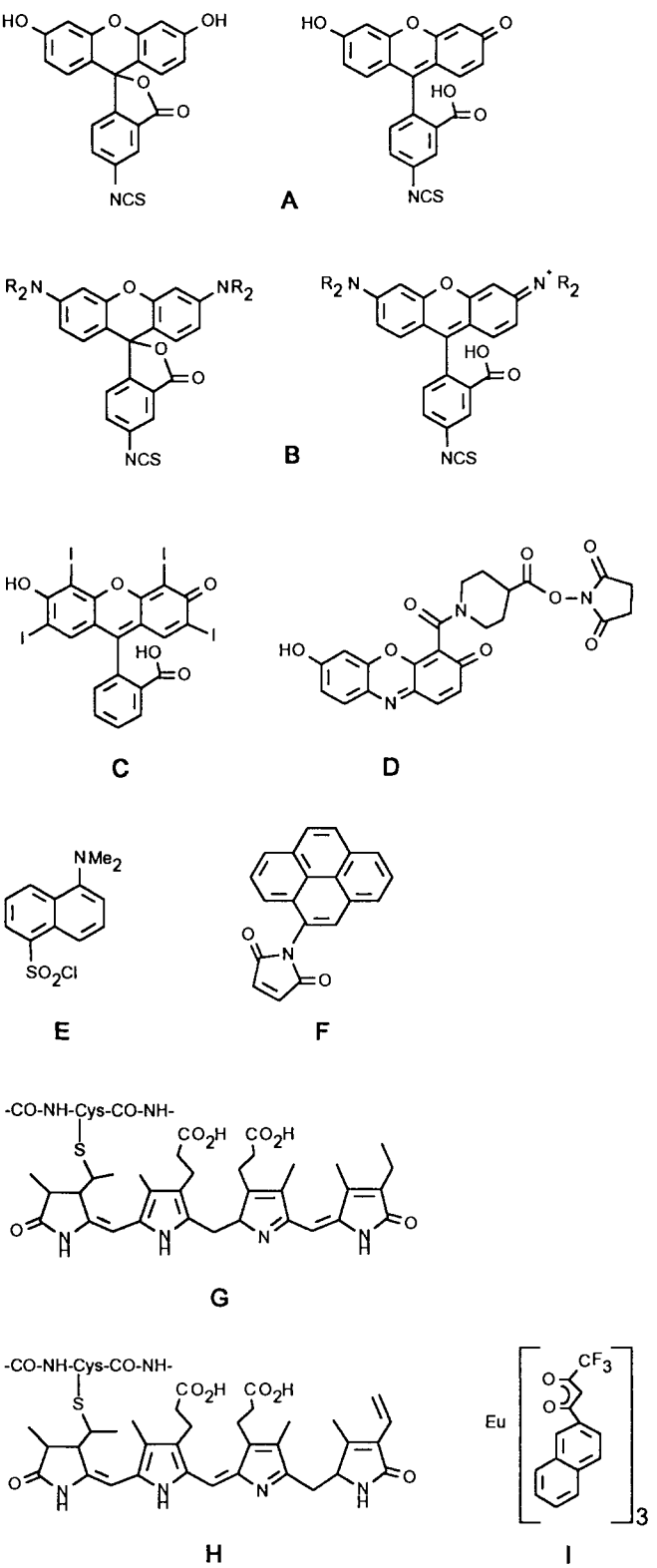
Besides the previously mentioned general requirements for luminescent labels, fluorescent labels for the use in immunoassays should fulfill a few additional conditions which can be derived directly from measured data. In principle, fluorescence measurements of the highest sensitivity are indeed possible,[6, 7, 55] but, in practice, the sensitivity of fluorescent immunoassays (FIAs) is, however, drastically limited by background fluorescence, light scattering and quenching effects. The intrinsic fluorescence of serum components is mainly responsible for the background signal[6, 7] which covers a broad wavelength region. Serum proteins are excited, for example, at 280 nm and emit at 320–350 nm. Other components such as NADH and bilirubin are excited between 330 and 360 nm and 450 and 460 nm, respectively, and fluoresce in the range 430–470 nm and 515 nm, respectively.[7c] The detection limit for immunoconjugates of a fluorescent label with bovine serum albumin or immunoglobulin G (IgG) is on average 10 to 50 times worse in serum than in buffer solution.[6a] Many solid phase materials, for example polystyrene, likewise yield a blank reading. Light scattering is a problem, particularly, in solutions which contain proteins or colloidally dispersed substances. In addition to Rayleigh and Tyndall scattering at the same frequency as the excitation beam, Raman scattering also occurs with a frequency usually shifted by approximately 50 nm. Fluorescence quenching can often result from the smallest changes in the environment of the fluorophore (pH, polarity, oxidation level, proximity of heavy atoms or other absorbing groups). If, for example, a protein is multiply labeled, two fluorophores can become so close that self-quenching of the signal takes place if the absorption and emission spectra overlap.

In order to minimize the influences mentioned the following properties of fluorescent labels are desirable:[56] a) longest possible wavelength emission (500–700 nm), b) large Stoke's shift of > 50 nm, c) long fluorescence lifetime of $\tau > 20$ ns.

A sufficiently long lifetime is particularly significant in applying the principle of fluorescence polarization transfer (cf. Section 5.1.3). Fluorescence lifetimes $\tau > 100$ ns facilitate a significant improvement of the signal-to-noise ratio and thus of the sensitivity, since measurement can only take place after decay of background fluorescence and light scattering. This principle is applied in time-resolved fluorescence measurements which are explained in more detail in Section 5.1.4.

5.1.2. Labels for Direct Fluorescent Labeling

The first compound used for fluorescent labeling of biological material by Coons et al. in 1941 was anthracene isocyanate for the labeling of bacterial proteins.[57] The same group introduced fluoroscein isothiocyanate (FITC, **A**, Scheme 13) as a more ef-



Scheme 13. Selected fluorescent labels **A**–**I**. See Table 1.

fective label soon afterwards.[58] Although judging from its spectral data this xanthene dye (cf. Table 1) does not completely fulfil the above-mentioned requirements for fluorescent labels,

Table 1. Spectral data of selected fluorescent labels **A**–**I**.

	$\lambda_{abs,exc}$ [nm]	λ_{em} [nm]	ε [L mol^{-1} cm^{-1}]	τ [ns]	θ
fluorescein isothiocyanate **A**	492	520	7×10^4	4.5	0.85
rhodamine B isothiocyanate **B** (R = Et)	550	585	[a]	3.0	0.7
TM-rhodamine isothiocyanate **B** (R = Me)	550	580	5×10^4	2.0	
erythrosine **C**	530	558 fl [b] 690 ph [b]	1×10^5	2.7×10^5	0.002
resorufin derivatives **D**	575	590			
dansylchloride **E**	340	480–520	3.4×10^3	14.0	0.3
pyrene maleimide **F**	340	375, 392	3.8×10^4	100	
phycocyanobilin, protein bound **G**	614	643	5.8×10^5	2.2	0.52 [c]
phycoerythrobilin, protein bound **H**	546	576	2.4×10^6	3.2	0.59 [c]
europium-tris[2-naphthoyltrifluoroacetone] **I**	340	590, 613	3.6×10^4	7×10^5	0.8

[a] Unclear literature values: 12300 [6a,b]; 10300 [7a]. b) fl = fluorescence; ph = phosphorescence. c) Most phycobiliproteins afford θ values up to 0.98.

FITC has become the fluorochrome of choice in most applications.[5, 10] Despite the large number of fluorescent labels which have been developed since, FITC still remains the most commonly used in fluorescence immunoassays, possibly due to a high quantum yield and stability. Similar properties are exhibited by rhodamines **B** which belong to the same class of dyes (Scheme 13). Both dyes can exist in the two isomeric forms shown, a spirolactone and quinoid structure.

Efforts to obtain fluorescent labels that can be excited in the longwave region and also emit revealed, for example, that derivatives of the phenoxazin dye resorufin were successful to a certain extent. In the synthesis of fluorescent labels, suitably functionalized resorufins are obtained, for example, from nitroresorcin and 2,6-dihydroxybenzoic acid after reduction of the initially formed resazurine (resorufin-*N*-oxide). Apart from the derivative **D** shown in Scheme 13 which has a succinimidoyl ester as the reactive group, labels based on resorufin with other reactive groups are also known. Compared to fluorescein, resorufin is less affected by the background fluorescence of serum.[59] A longwave shift of excitation and emission wavelengths is also possible with phycobiliproteins,[60] which are obtained from different kinds of red and green algae. The structures of the two prosthetic groups are given in Scheme 13 (**G**, **H**). The compounds exhibit very high molar extinction coefficients and high quantum yields (> 0.8).[61] Not all phycobiliproteins couple with the protein at the A-ring. The substances, which have, in the meantime, become commercially available, were first employed in fluorescence microscopy and flow cytometry, thereafter as labels in immunoassays. When, for example, fluorescein was replaced by phycoerythrin in a sandwich immunoassay, a significant increase in sensitivity (factor 2–10) was achieved; however, this was below that expected from the spectral data.[61, 62] The size of the label and the difficulty in coupling are unfavorable. Since the phycobiliproteins show a broad excitation and emission band, a parallel determination of several parameters is conceivable by the use of different labels with non-overlapping emission bands. This was confirmed in preliminary experiments.

5.1.3. Fluorescence Polarization

The principle of fluorescence polarization,[63] known for a long time, was first employed in the antigen–antibody reaction in 1961.[64] Fluorescence polarization immunoassay is based on the following principle: if a fluorescing compound in solution is excited by polarized light, the observed emission is also polarized. The degree of this polarization depends upon the rotation relaxation time and, thus, on the size of the molecule. If a small (M: 1–10 kD) fluorescent-labeled fast-rotating molecule is bound to an antibody ($M \approx 160$ kD), the result is an increase in the rotating relaxation time of the slowly tumbling immunocomplex and thus also the polarization of the fluorescence. With this principle one can differentiate between unbound labeled antigen and immunocomplex. The method is, however, not suitable for large antigens, since the rotation hardly changes on formation of the immunocomplex. A more exact derivation of the measurement principles is given in reference [63]. The fluorophores mentioned already can be used as labels, although substances with longer fluorescence lifetimes would be more advantageous. In most cases fluorescein isothiocyanate **A** is employed. Accordingly, the sensitivity is limited by factors mentioned already.

Since no separation step is necessary with this principle (homogeneous immunoassay), determinations can be carried out relatively easily provided that sensitivity in the picomolar region is not required. Fluorescence polarization immunoassay is widely used particularly in the area of drug analysis.[59, 63] This method can also be employed in environmental analysis, for example, in the determination of polychlorinated biphenyls (PCBs). Fluorescein derivatives are used as labels.[65]

5.1.4. Time-Resolved Fluorescence

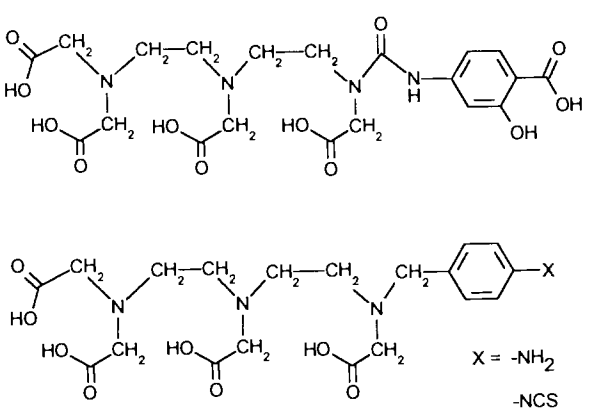
It has already been mentioned that the limiting background fluorescence and the scattering effects can be excluded by the use of labels with very long fluorescence lifetimes and by taking measurements only when the background signal is no longer present. Generally, the lifetime of the unspecific background signal is less than 10 ns. For an interference-free measurement of a specific signal, labels are required whose lifetimes are at least 10 times the decay time of the background.[6a] Suitable organic fluorophores with lifetimes $\tau > 50$ ns are, however, very rare. Pyrene derivatives such as **F** in Scheme 13 exhibit lifetimes of approximately 100 ns, which, however, were shown to be insufficient.[66] The lifetimes of phoshorescence processes are considerably longer. The principle applicability of phosphorescent labels, such as erythrosin derivatives in oxygen-free solutions, could indeed be shown[67] but no progress with phosphores

cence was achieved due to its low quantum yields and high expenditure.

It was not until complexes with rare-earth metal ions, primarily europium(III), were employed as labels that prospects of attaining a drastic improvement in the sensitivity of fluorescence immunoassays by time-resolved measurements and developing more sensitive fluorescent alternatives to RIA were realized.[6, 66] The use of europium trisdiketonates was proposed by Wieder[7b] in 1978 and developed further by other groups.[68]

The chelate complexes of europium(III), terbium(III), samarium(III), and dysprosium(III) are distinguished by unique fluorescent properties (cf. **I** in Scheme 13 and Table 1). Apart from extremely long lifetimes of about 1 μs to 1 ms, a very large Stoke's shift (>200 nm) and sharp emission lines impart the complexes with a high sensitivity (10^{-14} mol L^{-1}).[6, 66] The reason for the observed lifetimes lies in the excitation/emission mechanism. After excitation of the ligand to the S_1 state and intersystem crossing to an energetically suitable triplet state of the ligand, an effective energy transfer to the resonance state of the metal ion occurs, which then gives rise to a sharp emission characteristic of metal ions.[6, 66, 69]

The fluorescent properties of chelates of rare-earth metals alone still do not produce an efficient label for immunoassays. What is essential, also in aqueous buffer solution, is a stable binding to antigens and antibodies. Due to their high stability and solubility in water, polyaminopolycarboxylate chelates, chiefly derivatives of ethylenediaminetetraacetic acid (edta) or diethylenetriaminepentaacetic acid are used for most applications. The use of diazo- and isothiocyanatophenylethylenediaminetriacetate for coordination to europium(III) and terbium(III) has been described.[66, 70] Likewise, mixtures of ethylenediaminetriacetic acid, terbium(III), and 5-sulfosalicylic acid,[7b, 71] mixtures of an edta derivative, europium(III), and a β-diketone[7b, 72] as well as diethylenetriaminetetraacetic acid derivatives with different trivalent lanthanides[7b, 66, 70, 73] were employed for the labeling (Scheme 14).



Scheme 14. Ligands for the coordination of lanthanide ions.

Since many of the very stable lanthanide chelate complexes do not fluorescence with these ligands, a dissociation step must be carried out prior to detection.[74] Furthermore, once the immune reaction is complete, a so-called enhancement solution is added after washing, which leads to the dissociation of the chelate complex and to the formation of fluorescent complexes [DELFIA system (*D*issociation *E*nhanced *L*anthanide *F*luorescence *I*mmuno-*A*ssay)]. The 1,3-diketones β-naphthoyltrifluoroacetone and pivaloyltrifluoroacetone are commonly employed.

The use of chelate complexes with trivalent lanthanide ions facilitated not only the development of highly sensitive immunoassays by time-resolved measurement, but also the simultaneous determination of several parameters, since Eu^{III}, Tb^{III}, Sm^{III}, and Dy^{III} complexes emit at considerably different wavelengths and have different fluorescence lifetimes. Several double determinations have been described;[73, 75] Eu^{III}/Tb^{III} chelates[76] or Eu^{III}/Sm^{III}[76] complexes were used as label pairs. In simultaneous determinations of two parameters from each, the dissociation/enhancement principle was employed. A simultaneous and highly sensitive determination of more than two lanthanide labels is, however, not possible with the simple enhancement solutions.

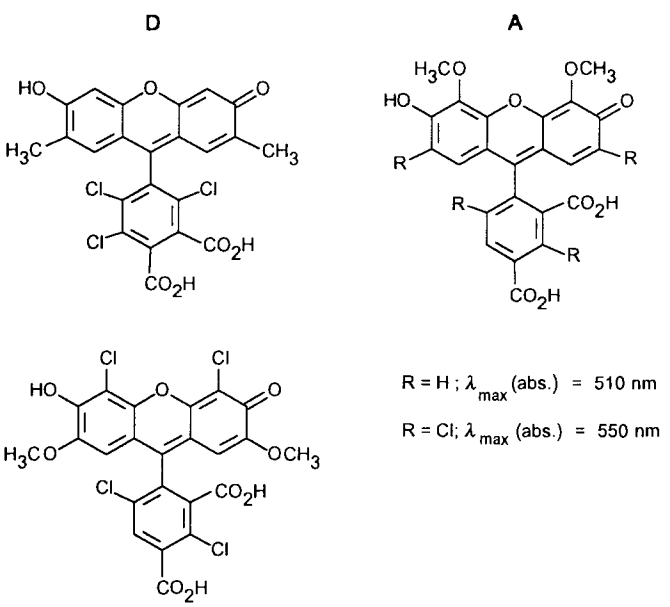
Simultaneous multianalyte determinations are gaining interest,[78] since with the four lanthanide ions mentioned and specially developed enhancement solutions, so-called *co*fluorescence-based *e*nhancement *s*olutions (CFES),[79] four parameters could be determined simultaneously by using time-resolved fluorescence measurements.[73] The enhancement solutions formed in this way consist of a dissociation element, pivaloyltrifluoroacetone and Y^{III}, as well as an element, 1,10-phenanthroline which enhances the fluorescence. Europium(III) and terbium(III) chelates with macrobicyclic ligands that contain α,α′-bipyridine or 1,10-phenanthroline units were already described earlier as efficient luminophores which act as molecular light transformers.[79d]

5.1.5. *Fluorescence Energy Transfer*

In the application of fluorescent labels for immunoassays, the principle of fluorescence-polarization, which facilitated development of homogeneous immunoassays, has already been mentioned. Another method, in which no separation of the unbound labeled molecules from the immunocomplexes is necessary, uses fluorescence energy transfers.[6b, 80] In this case an energy transfer from an electronically excited fluorophore (donor) to a neighboring acceptor dye molecule (quencher) occurs by dipole–dipole coupling. According to Förster[81] the efficiency of the energy transfer is indirectly proportional to the power 6 of the distance. With Förster's theory distance measurements in molecules, for example, can be obtained,[82] and for efficient energy transfer distances must not be greater than 10 nm. This condition is fulfilled in many antigen–antibody complexes. If, for example, the antigen is labeled with the donor and a specific antibody is labeled with the acceptor, quenching of fluorescence (of the donor) occurs in the immunocomplex. In a mixture of labeled and unlabeled antigens the fluorescence signal increases with the quantity of the unlabeled analyte to be determined.

The requirements for the fluorescent labels (donors) that should be employed in energy-transfer immunoassays are the same as those for fluorescent labels already mentioned. Furthermore, the choice of the donor–acceptor pair must be such that the emission spectrum of the donor and the absorption spectrum of the acceptor overlap well. In the beginning the use of the donor–acceptor pair fluorescein isothiocyanate/tetramethyl-

rhodamine isothiocyanate was described.[80b] Since interference from background signals such as background fluorescence from serum are particularly large in homogeneous immunoassay, standard labels such as fluorescein isothiocyanate, umbelliferones, or dansyl chloride certainly are of little significance. For the latter, in addition, the high sensitivity for background effects is disadvantageous. The same can be said for rhodamines such as tetramethylrhodamine. Due to higher absorption and emission wavenumbers, phycobiliproteins and lanthanide chelates are better suited as donors. With the latter, particularly in conjunction with time-resolved measurements, the development of more sensitive fluorescence energy-transfer immunoassays is possible. Also substituted fluoresceins with absorption and emission wavelengths greater than 500 nm (cf. Scheme 15) were used as donors.[80, 83]



Scheme 15. Fluorescein derivatives employed in fluorescent energy transfers; D = donor molecules, A = acceptor molecules.

The energy acceptors (quencher labels) should ideally fulfill the following conditions:[80a] a) high extinction coefficient of the emission wavelength of donor; b) no fluorescence during excitation in the absorption maxima of donor; c) good solubility in water in order to facilitate multiple labeling with the quencher (greater quenching effect); d) the smallest possible background interference in the absorption spectrum.

Since frequently used acceptors such as tetramethylrhodamines do not fulfill these requirements, new non-fluorescent fluorescein derivatives were described which form effective pairs with the donors in Scheme 15.[80, 84]

Fluorescent labeling and the principle of fluorescent energy transfers have recently also found application in the development of biosensors.[85] Detection can be based on the quenching of emission from the donor, new emission from the acceptor, or on the ratio of both emission wavelengths. One biosensor principle based on Langmuir–Blodgett films and fluorescence energy transfer with a cumarin derivative as donor and tetramethylrhodamine as acceptor was recently described.[86]

5.2. Chemiluminescent Labeling

A considerable difference between chemiluminescent detection systems and fluorescent labels is that former do not require the irradiation of the excitation light. With these chemiluminescent systems, in particular, in working with serum, the problems with high background signals, which are mainly responsible for the limited sensitivity of many methods with fluorescence detection, are prevented. However, in several chemiluminescent labels, complex systems comprising oxidation reagents, signal enhancer additives, and catalysts can likewise lead to an unacceptable high background signal, which, of course, has an adverse effect on sensitivity.[87] In the case of chemiluminescence detection in analysis systems, which above all are applied in medical diagnostics, compounds mainly from the following categories are employed:[9, 10–15, 17] luciferins in combination with the corresponding luciferases, cyclic arylhydrazides, acridinium derivatives, stable dioxetanes, and oxalic acid derivatives.

5.2.1. *Bioluminescence*

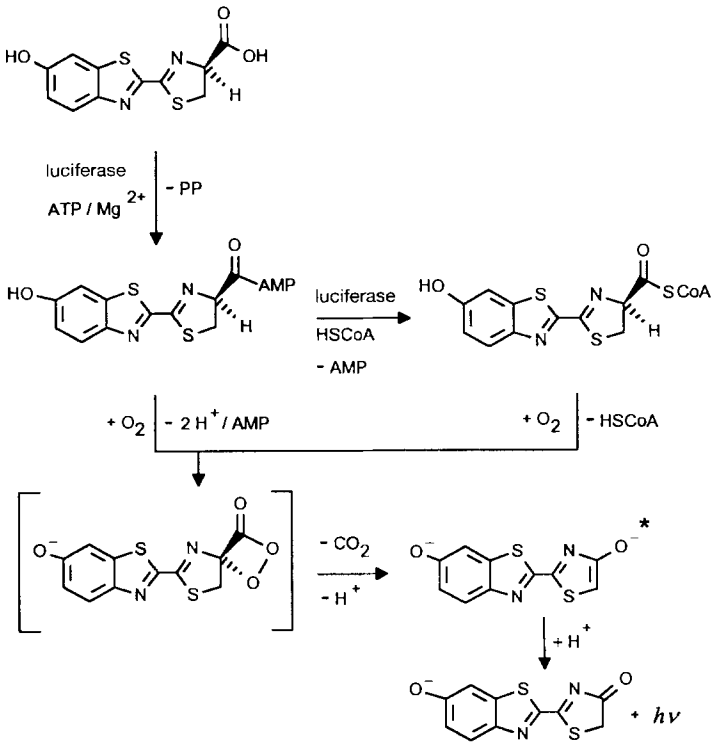
The luciferin/luciferase system of the North American firefly

One of the most well-known and most studied light systems in nature "operates" in the North American firefly (*Photinus Pyralus*). Although the mechanism of bioluminescence has been studied for more than 30 years, and the benzothiazole derivative luciferin became available synthetically and was structurally determined at the beginning of the 1960s, not all the details of the bioluminescence reaction have been elucidated. Since a more detailed description of this and other bioluminescent systems would go beyond the framework of this review article only the latest developments are described briefly.

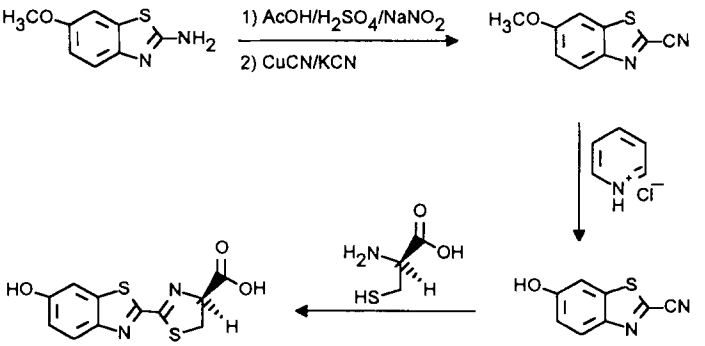
As had been assumed for a long time[88a, b] and to a large extent proven at the end of the 1970s,[88c] the specific luciferase of the firefly catalyzes the oxidation of luciferin in the presence of ATP and magnesium ions (Scheme 16). Initially a complex is formed from the acyl-AMP species of luciferin and luciferase. In the presence of oxygen oxidation ensues to give excited oxyluciferin which returns to the ground state by emitting a photon.[15, 89, 90] In vivo the yellow-green emission (λ_{max} = 565 nm) of the dianion was observed and in vitro an additional red emission (λ_{max} = 615 nm) of the monoanion which was pH-dependent.[88b, 90, 91] The oxidation proceeds presumably via a dioxetanone intermediate[11, 87, 92] which decarboxylates to furnish excited oxyluciferin.

To what extent one can view the often proposed dioxetanone as an intermediate or rather as a transition state is, as in the luminescent systems previously mentioned, still unclear. Instead of the dioxetanone intermediates in the oxidation of luciferins, acridiniumcarboxylic acid derivatives, and oxalic acid esters, the direct formation of excited products by charge-transfer can also be assumed during the decomposition of peroxide intermediates.[93] The mechanistic details cannot be emphasized within the framework of this review and interested readers should refer to the references [11, 87, 92, 93].

All in all, the light reaction of the firefly appears to be elucidated. However, the assumption, first made at the end of the 1950s,[94] that Coenzyme A also plays a role in the light reaction



Scheme 16. Chemistry of the light reaction of the firefly; PP = pyrophosphate; ATP = adenosine triphosphate, AMP = adenosine monophosphate, CoASH = coenzyme A.



Scheme 17. Key step in the synthesis of the firefly luciferin.

has been comfirmed in the past few years.[89, 95] Addition of the coenzyme may further improve the applicability of the firefly luciferin/luciferase system in the near future, since the intensity and duration of the light emission can be increased. The limiting factor for this method until now, in addition to the limited hydrolytic stability of luciferin and the sensitivity of luciferase, was, above all, the poor availability of the enzyme which could be extracted from fireflys. In the meantime the situation has fundamentally changed since the *Photinus Pyralis* luciferase, a protein with a molecular weight of 62 kD, can be expressed in bacteria, for example *E. coli*, by genetic engineering methods.[15, 89, 96, 97] The availability of genetically engineered luciferase and synthetic luciferin has now increased the expectation that this system, which with a quantum yield of up to 0.88 Einstein per mol is the most efficient of all known bio- and chemiluminescence systems, will be more widely applied than previously.

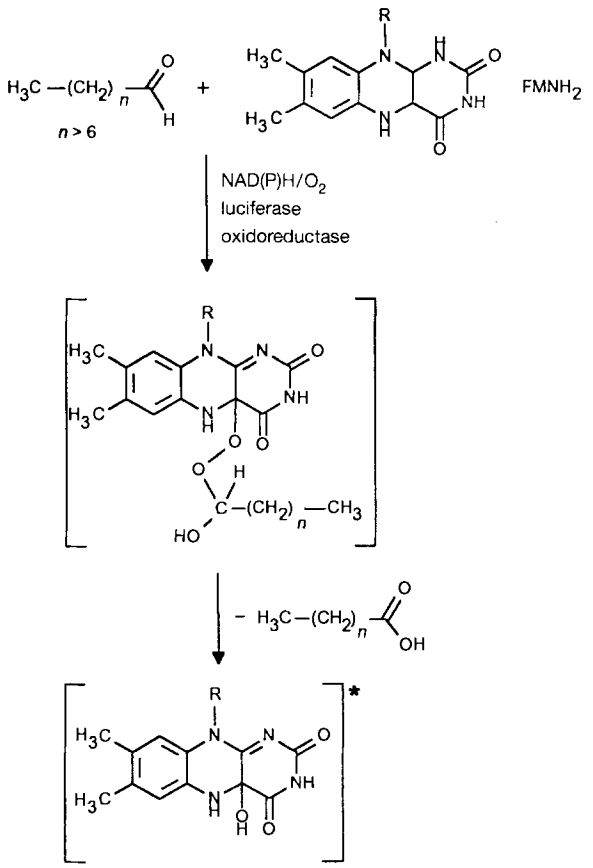
In the last thirty years essentially three synthetic pathways for the construction of firefly luciferin have been described, all of which proceed via the key intermediate 6-methoxybenzothiazole-2-carbonitrile (Scheme 17).[91, 98] The routes differ in the synthesis of the intermediate. Recently a new synthesis[99] has been published in which 6-methoxybenzothiazole-2-carbonitrile is obtained in one step by Sandmeyer cyanation of the commercially available 2-amino-6-methoxybenzothiazole (Scheme 17). The remainder of the synthetic pathway is already well-known: cleavage of the methyl ether and condensation with D-cysteine furnish the luciferin. In reference [99], earlier syntheses are also summarized. The oldest and until now most important application of the firefly luciferin/luciferase system is derived from the ATP-dependence of the bioluminescence reaction. Hence, a sensitive ATP determination can be carried out by using this system. ATP assays[100] are of interest above all in the screening for microorganisms in clinical microbiology in the areas of hygiene and nutrition.[101] A more recent application of steadily increasing significance is the use of the firefly luciferase gene as a reporter gene for the quantification of the gene expression in cells.[89, 102] Here a measurement of the light emission is made after addition of luciferin.

The use of luciferin derivatives,[103] which themselves are not substrates for luciferase, as substrates in enzyme immunoassays offers additional applications. After the luciferin has been released light emission is determined in the presence of luciferase.[103] In this way derivatives in which the phenolic hydroxyl group has been functionalized, such as D-luciferin-*O*-sulfate and -*O*-phosphate, can be cleaved by sulfatases or phosphatases. If the carboxyl group of the luciferin can be functionalized (methyl ester and phenylalanine and arginine amides have been described), the luciferin is released by carboxyesterases or carboxypeptidases.[103] Luciferin-*O*-phosphate as substrate for alkaline phosphatase, in comparison to the chromogenic substrate *p*-nitrophenylphospate, facilitates a sixty-fold increase in sensitivity.[103a] In addition, D-luciferin-β-D-galactopyranoside as substrate for β-galactosidase was described.[104]

Bacterial luciferin derivatives/luciferases

In luminous bacteria such as *Photobacterium fischeri* and *Photobacterium phosphoreum*, light production ensues from the oxidation of long-chain aldehydes in the presence of reduced flavin mononucleotide ($FMNH_2$), oxidoreductase, and bacterial luciferase.[15, 90, 97, 105] The intermediate is assumed to be a peroxide formed from a long-chain aldehyde and a flavin building block (Scheme 18). Depending on the bacterium, light emission occurs in the blue-green to yellow region of the spectrum with quantum yields of up to 0.3. The emitter is presumably a hydroxy derivative of FMN.[11, 15, 105] In vitro blue light (λ_{max} = 492 nm) is emitted.[15, 105c] As with the firefly luciferase, several bacterial luciferases can be obtained by genetic engineering.[97]

The bioluminescence of bacterial luciferases can, in principle, be used to determine all the components that participate in the luminescence reaction, that is, NADH, NADPH, FMN, $FMNH_2$, long-chain aldehydes, and oxygen.[105d] The possibility of determining the concentration of the extremely unstable $FMNH_2$ is theoretical. The use of bacterial luciferases is indeed still less widespread. The bioluminescent determination of long-



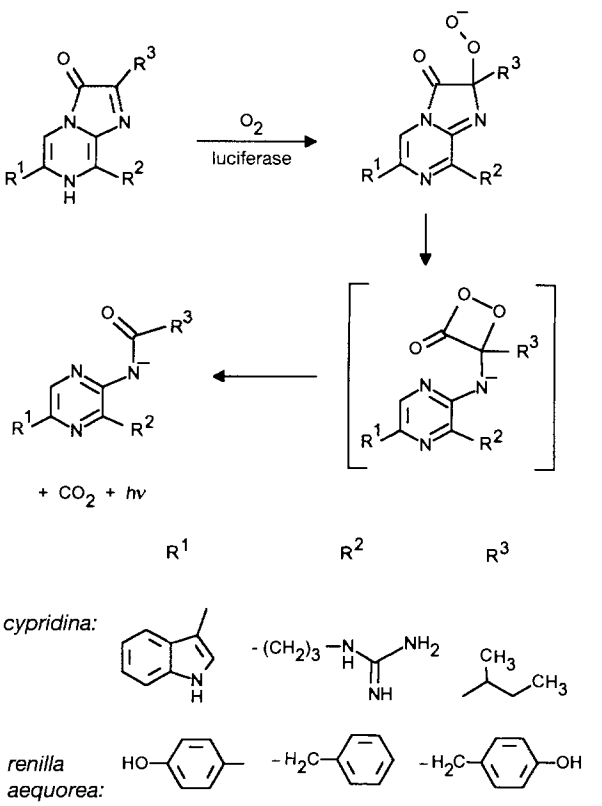
Scheme 18. Bacterial light systems.

chain aldehydes[106] and trace analysis of oxygen[105c] have some significance. A further field of application is in homogeneous DNA hybridization assays.[15, 107] The system for the bioluminescent determination of Papilloma viruses serves as an example.[107]

Luciferin derivatives with imidazopyrazine building blocks and photoproteins

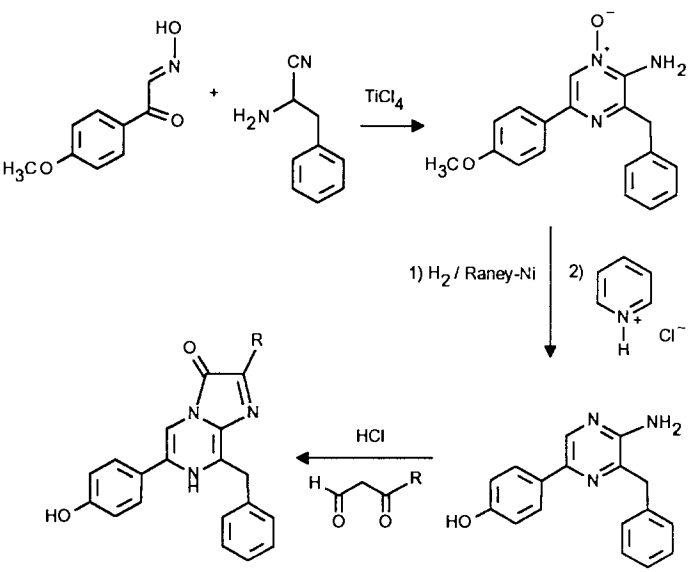
Bioluminescence occurs particularly frequently in marine life such as in crabs, jellyfish, mussels, sponges, fungi, and many fish.[9, 92b, 108] The luciferins of the mussel crab *Cypridina hilgendorfii*, sea pansy *Renilla reniformis*, and of the jellyfish *Aequorea aequorea* show a structural similarity (Scheme 19) which infers a common biosynthetic pathway.[92b] The luminescence mechanism is thought to consist of a catalytic oxygenation followed by ring closure to give an α-peroxylactone. This intermediate decomposes with the formation of the emitter and carbon dioxide (Scheme 19). One should refer to the relevant discussions of the theories concerning the firefly luminescence mechanism in specialist literature.

The photoprotein Aequorin, which was obtained from the jelly fish *Aequorea victoria* in 1962, has aroused particular interest in recent years.[109] It consists of a complex of apoaequorin, coelenterazine (cf. Scheme 19), and molecular oxygen. Addition of calcium or strontium ions to the complex triggers light emission.[110a] One assumes that the binding of calcium ions to the protein induces the decomposition of the resulting oxygenated



Scheme 19. Structures of some imidazolpyrazine luciferin derivatives and an outline of the peroxylactone mechanism.

chromophore. An additional luciferase is not necessary. The emitter was postulated to be the protein-bound anion of the chromophore (cf. Scheme 19).[110b] The active photoprotein is regenerated by incubation of the apoprotein with the coelentarazine in the presence of oxygen, ethylenediaminetetraacetate, and mercaptoethanol.[110c] In the meantime the apoprotein has become accessible by expression in *E. coli*.[111] The synthesis of the coelenterazine was described long ago,[112a, b] and in addi-



Scheme 20. Synthetic route for the construction of coelenterazines. R = CH_3, C_6H_5, $(CH_2)_nC_6H_5$ ($n = 1-3$), $CH_2C_6H_4OH$.

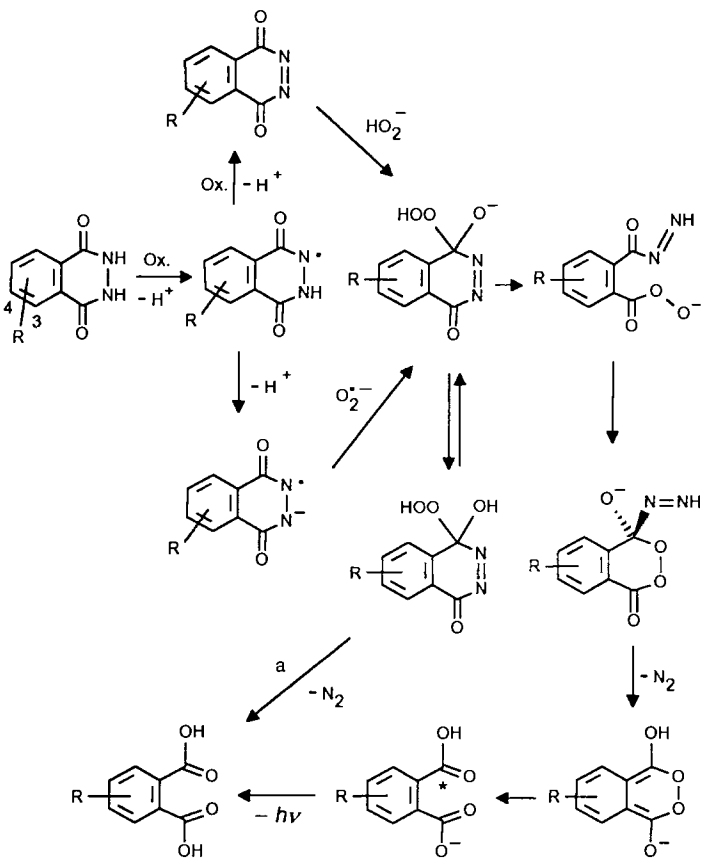
tion the synthesis of some systems with a modified structure was reported.[112c] The synthetic route is summarized in Scheme 20.

Aequorin can be used as a bioluminescent label after biotinylation. The triggering of light emission results from addition of calcium chloride solution. The label can also be detected in the attomol region. This label facilitated, for example, the development of a highly sensitive assay for salmonella determination. With regard to the sensitivity the test was shown to be clearly superior to other ELISA tests (see Section 3.1.2), even those with alkaline phosphotase as label and with chemiluminescent dioxetane AMPPD as substrate.[113a, b] In addition, the use of Aequorin in DNA and protein diagnostics[113c] and in the determination of serum glycoproteins has been described.[113d]

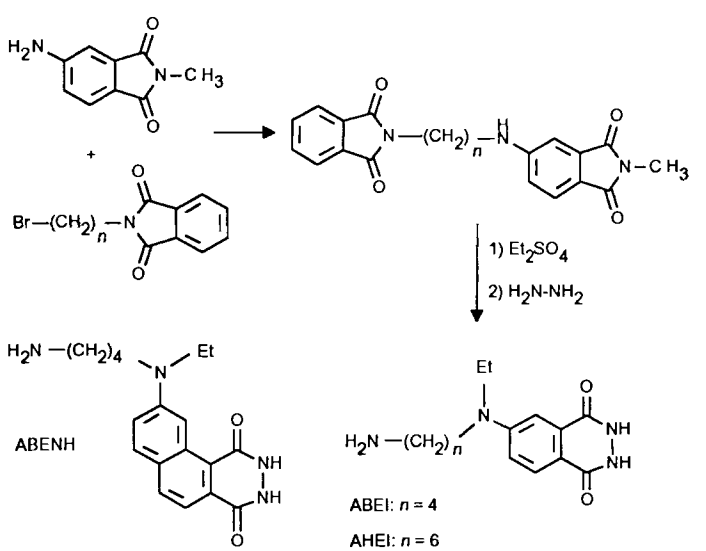
5.2.2. *Cyclic Arylhydrazides*

The chemiluminescence of luminol (3-aminophthalic hydrazide) was observed in 1928 in the form of blue light which was emitted during the oxidation with an alkaline solution of hexacyanoferrate(III) in the presence of hydrogen peroxide.[114] Luminol and carboxylic acid hydrazides have since been extensively studied. A wealth of reagents and catalysts can be employed in the oxidations of luminol and its derivatives. In organic, aprotic solvents, chemiluminescent reactions can be triggered by oxygen in the presence of a strong base. In aqueous solutions hydrogen peroxide is usually employed in the presence of catalysts such as peroxidases, hemin, and cobalt(II) salts.[105] Horseradish peroxidase (HRP)/H_2O_2 is frequently employed. In the course of time, different reaction mechanisms have been discussed.[45v] A simplified reaction mechanism, which is only applicable for a one-electron oxidation and which affords the free luminol radical, is given in Scheme 21. According to a more recent review article it is suggested that the mechanism should be divided into two steps, formation of the key intermediate, an α-hydroxyhydroperoxide, and its decomposition to the excited emitter. Whilst the formation of the hydroperoxide depends considerably on exact reaction conditions, decomposition of the key intermediate is only influenced by pH. Under these conditions the emitter appears to be the monoanion of aminophthalic acid. With other reagents, for example DMSO/base, the dianion of aminophthalic acid functions as the emitter. Intermediates in other proposed mechanisms are azaquinones, endoperoxides, and other peroxidic intermediates.[115b]

One of the oldest applications of luminol, which is still important today, is forensic blood analysis.[116] The application of luminol as a substrate for peroxidases in enzyme immunoassay has already been mentioned. Coupling reactions are necessary for the synthesis of labels for chemiluminescent direct labeling. The study of the chemiluminescent properties of luminol and isoluminol derivatives[117] had revealed that isoluminol only has approximately 10% of the quantum yield of luminol. Since, however, the chemiluminescent quantum yield of luminol decreases significantly[25, 37, 115, 117] if the primary 3-amino group is substituted, isoluminol derivatives, which are not sensitive with regard to substitution of the amino group, or the even more advantageous naphthalenedicarboxylic acid hydrazides which exhibit higher light yields,[21, 117b] were as a rule employed in the synthesis of arylhydrazide labels. The first label based on luminol, diazoluminol,[118] clearly showed the disadvantages outlined and the quantum yield decreased to 1% of that of luminol. Considerable improvements were brought about by isoluminol derivatives in which the coupling group was introduced via the amino functionality.[117b] The structure and the synthesis of some important arylhydrazide labels are summarized in Scheme 22.



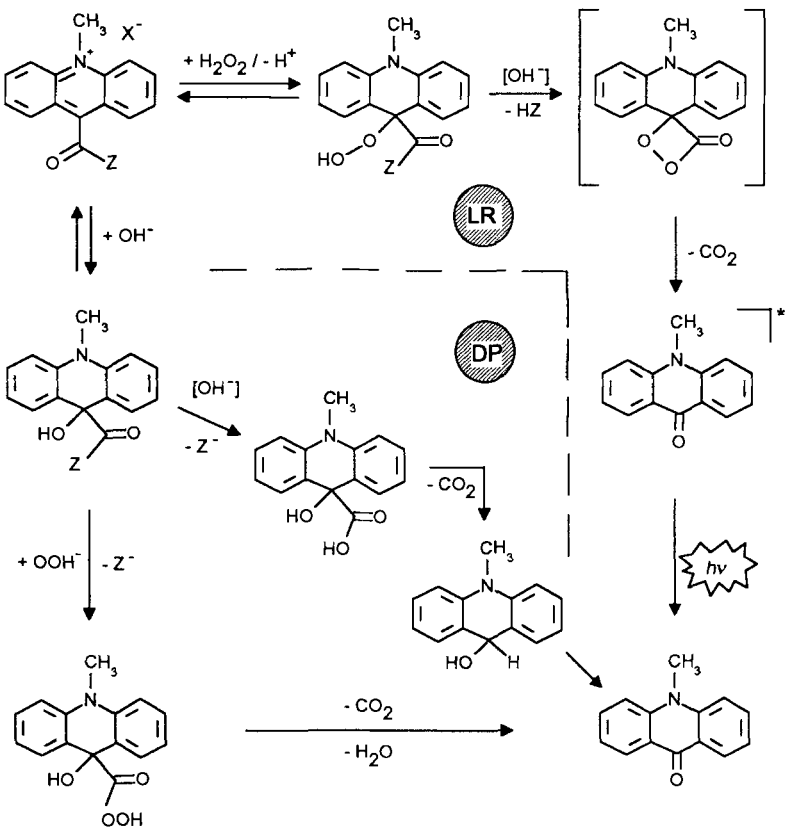
Scheme 21. Simplified mechanism of the chemiluminescence reaction of phthalic hydrazides. Ox = oxidising agent which affords the free luminol radical, for example, HRP. R = 3-NH_2: luminol; R = 4-NH_2: isoluminol. Since the regiochemistry of most processes is unclear, the position of the R residue remains open. a = dark.



Scheme 22. Synthesis and structures of some arylhydrazide labels.

4-Amino-*N*-methylphthalic imide served as the starting material, which was successively alkylated with *N*-(bromoalkyl)phthalic imides and diethylsulfate. The subsequent hydrazinolysis of the bisphthalic imide furnished the frequently used phthalic hydrazide labels ABEI and AHEI (*N*-aminobutyl- or *N*-aminohexyl-*N*-ethylisoluminol), which contain an amino functionality as the coupling group. The phthalic hydrazide label ABENH (*N*-aminobutyl-*N*-ethylnaphthylhydrazide) was obtained by a similar method. The starting material was dimethyl 7-amino-1,2-naphthalenedicarboxylate.[117b] Derivatives of these three labels which contain other reactive groups (isothiocyanate, N-hydroxysuccinimide ester) are also known. Conversion of AHEI to a derivative with a *N*-hydroxysuccinimide-reactive ester was shown previously in Scheme 3.

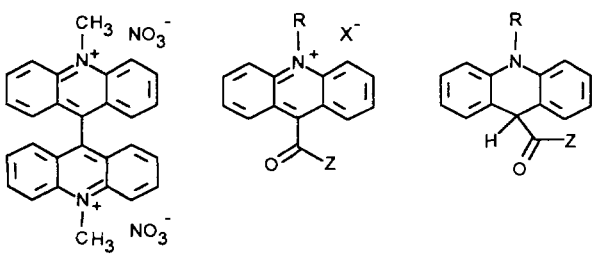
Arylhydrazide labels have and are finding broad application in immunoassays for chemiluminescent labeling of small and large molecules.[119] A distinct disadvantage is the considerable loss of the luminscencent quantum yield of the label after the coupling. Furthermore, these labels are prone to interference since many components catalyze the luminescent reaction. In addition, the reagents which trigger light emission give rise to a large background signal which decreases the sensitivity.[25]



Scheme 24. Chemiluminescence mechanism and pseudo-base equilibrium of 9-acridiniumcarboxylic acid derivatives; DP = dark process, LR = light reaction.

5.2.3. *Acridinium Compounds*

The chemiluminescence of lucigenin [9,9′-bis-(*N*-methylacridinium nitrate); Scheme 23] was reported in 1935.[120] But it was



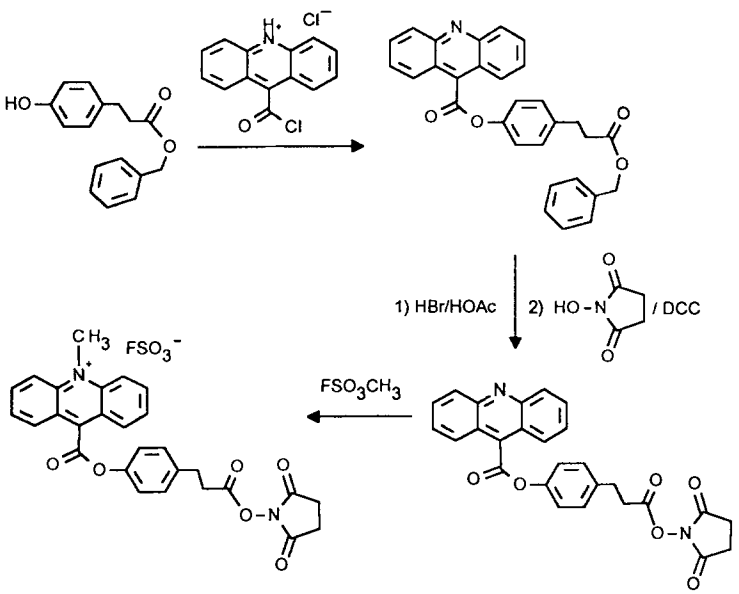
Scheme 23. Examples of chemiluminescent acridinium compounds and acridanes; Z = leaving group.

not until around thirty years later that studies led to other chemiluminescent acridinium compounds. These are specifically, 9-chlorocarbonylacridine hydrochloride,[121] 9-carboxy-10-methylacridinium chloride,[121] and 9-cyano-10-methylacridinium nitrate.[122] Today 9-acridiniumcarboxylic acid derivatives and acridanes are among the best-studied examples of chemiluminescent compounds. No additional reagents, apart from hydrogen peroxide and base, are necessary for the chemiluminescence of acridiniumcarboxylic acid derivatives. Quantum yields of up to approximately 0.05 can be attained with aryl esters;[111] higher still are the light yields which can be attained with acridane aryl esters. The latter exhibit efficient chemiluminescence after treatment with a base in the presence of oxygen.[123] Only the acridiniumcarboxylic acid derivatives that have been more important for the development of luminescent labels will be considered in more detail below. The mechanism of their chemiluminescence shown in Scheme 24 can be considered to be elucidated as far as possible.

First of all, addition of hydrogen peroxide takes place at the electrophilic C-9 position of the acridinium unit. In the case of aryl esters—the leaving group Z then stands for phenolate—the corresponding hydroperoxides could be isolated and characterized.[123] After the addition of hydroxide spontaneous chemiluminescence resulted, usually as intense light flashes. A dioxetanone is often proposed as intermediate, which decomposes to give carbon dioxide and electronically excited *N*-methylacridone, the emitter. The transition to the ground state ensues by emission of a photon at a wavelength of approximately 430 nm. According to more recent studies,[93b] however, no dioxetanone seems to appear as a discrete intermediate. The final product of the light reaction, *N*-methylacridone, can also be formed by other pathways in dark reactions. An important prerequisite for degradation in the dark is the well-known[124] pH-dependant pseudo-base equilibrium of acridinium compounds.[125] The reactions, which for the phenyl ester were studied more accurately in a flow system,[126] are integrated into Scheme 24. It is immediately clear that both the light reaction and the dark process are dependent, for instance, on the properties of the leaving group Z. Other important factors include the peroxide concentration

and the pH value.[126, 127] McCapra et al. showed that for effective chemiluminescence the pK value of the conjugate acid of the leaving group should be less than 12—the pK value of hydrogen peroxide.[108e] Since a good label should exhibit a high chemiluminescent yield in addition to a high stability in the labeled reagent, the discovery of suitable compounds can be equated to a fine balancing act, ending in a compromise between light yield and stability.

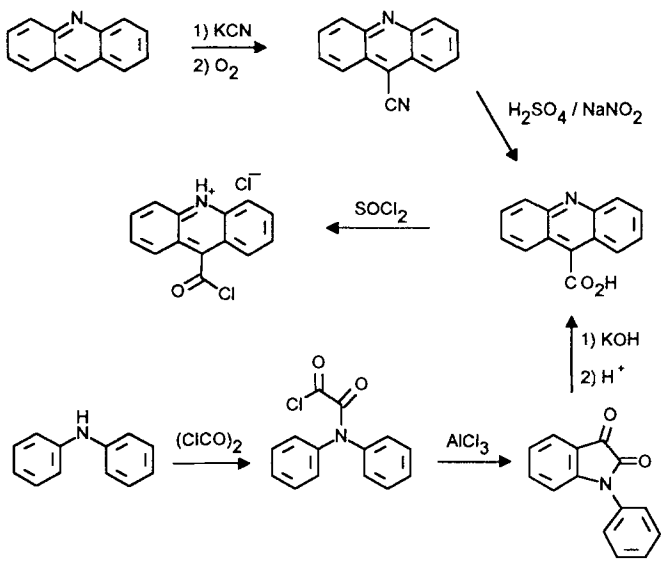
The first attempts to use 9-acridiniumcarboxylate as a label in immunoassays were reported at the beginning of the 1980s. In this an attempt was made to couple aryl esters, which contained free carboxyl groups, to proteins, after activation of the carboxyl groups. These labeling experiments had only limited success.[128] It was not until a phenyl N-methylacridinium-9-carboxylate, containing a hydroxysuccinimide ester on the phenyl group as the reactive group for coupling to proteins, was used that successful labelings could be carried out.[126, 129] The synthesis of this prototype of a chemiluminescent label based on a 9-acridiniumcarboxylic acid derivative,[25, 126, 128–130] the so-called Woodhead label, is summarized in Scheme 25.



Scheme 25. Synthesis of an acridinium ester label.

An important precursor for this and other labels discussed later was 9-acridinecarboxylic acid, whose synthesis is shown in Scheme 26. One reaction route starts from acridine and proceeds via 9-cyanoacridine to give the carboxylic acid.[131] In another synthetic method 9-acridinecarboxylic acid is formed from diphenylamine, which is acylated with oxalyl chloride and is cyclized by using aluminum trichloride to give the N-phenylisatine.[132] The synthesis of substituted acridinecarboxylic acids from substituted N-arylisatines has also been described;[133] however, it appears to work only on a very small scale.

Since the acridinium ester label mentioned was not sufficiently stable for development of commercial chemiluminescence immunoassays[134, 135] (hydrolysis of the ester bond (cf. degradation in the dark in Scheme 24) results in a too rapid a decrease of activity in conjugates), different research groups have been



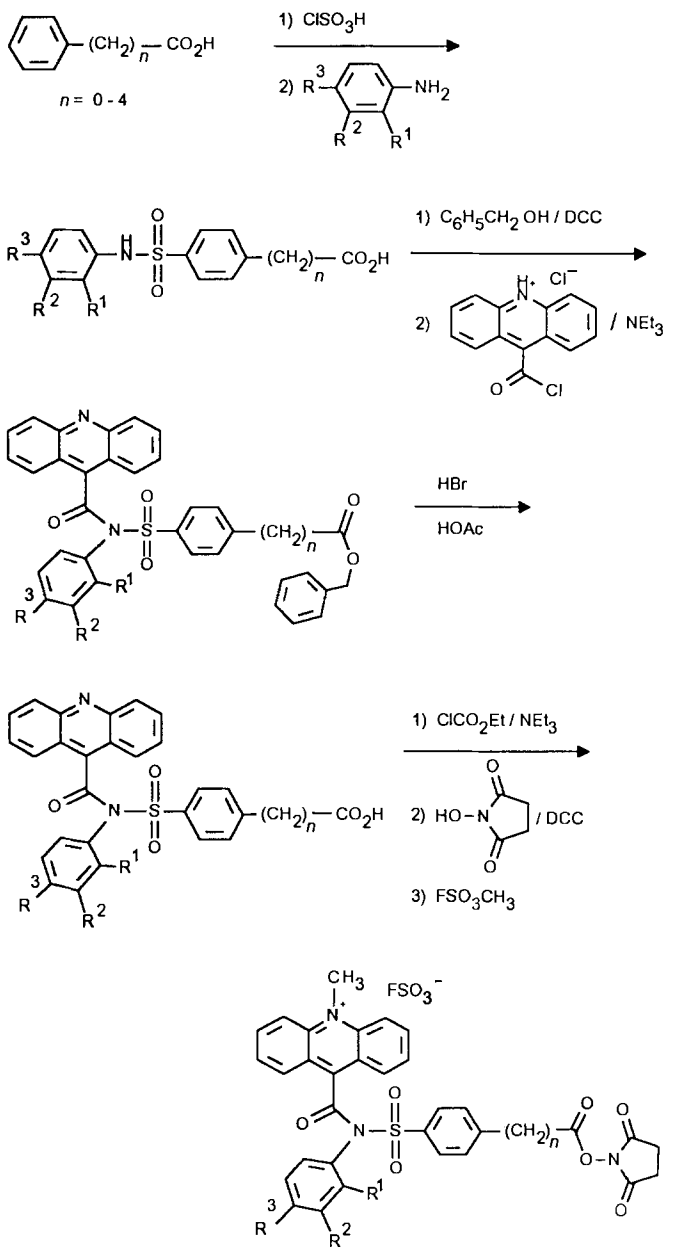
Scheme 26. Possible synthetic routes to 9-acridinecarboxylic acid.

looking for more stable labels based on acridiniumcarboxylic acid. One solution to the problem involved the steric shielding of the ester bond and the C-9 position of the acridine unit, for example, by methyl groups in the 2,6-position of the aryl ring.[134] In addition, other 9-acridiniumcarboxylic acid-(2,6-substituted)aryl esters were described.[136] Here the reactive group can also be bound through a spacer to the acridinium system. To complete the picture one should not forget to mention that aryl N-methylphenanthridinium-6-carboxylates have been described as chemiluminescent labels.[136, 137]

Other research groups have attempted to improve the properties of the acridiniumcarboxylic acid derivatives in comparison to those of the aryl esters, by varying the leaving groups. Thiol esters, indeed, brought about progress in as far as the light yield is concerned, but not, however, as regards to hydrolytic stability.[138] A significant improvement of the stability and very good chemiluminescence quantum yields were achieved when N-sulfonylamide anion was used as the leaving group instead of phenoxide.[138–141] In this class of compounds the spectrum of properties can be influenced much more specifically than for the acridinium ester labels by tailored variations in the structures. For instance, the solubility in water (an important parameter) can be significantly improved by the introduction of suitable substituents.[139, 142] The synthesis of N-methylacridinium-9-(N-sulfonyl)carboxamide labels is summarized in Scheme 27.

In addition, the hydrolysis behavior and the kinetics of emission can be varied to a certain extent.[142, 143] Although phenols and sulfonamides have similar pK values, labels with the latter are usually considerably more stable. This may be attributed to a combination of steric shielding effects and electronic stabilization,[127, 143] through which the dark reaction pathways described are minimized. It is assumed that in N-sulfonylcarboxamides there is an increased bond order of the C–N bond in comparison to the ester C–O bond. This is also evident from the frequencies of the carbonyl stretching vibration in the IR spectrum.[143]

Labels based on 9-acridiniumcarboxylic esters and acridinium-9-(N-sulfonyl)carboxamides have, in the meantime, found

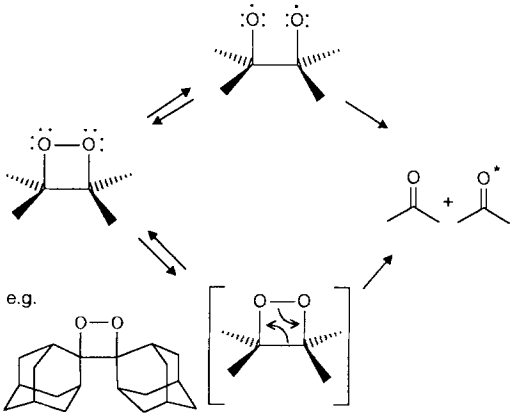


Scheme 27. Synthesis of acridinium-9-(*N*-sulfonyl)carboxamide labels.

broad application in commerical immunoassays (see Section 6).[119c, 144] Up until now only a few applications for other acridinium derivatives have been described. For example, lucigenin can be used in micellular chemiluminescence assays for the determination of reductants (ascorbic acid, uric acid, glucose, and fructose).[145] The micelles are necessary to improve the solubility of lucigenin.

5.2.4. *Dioxetanes*

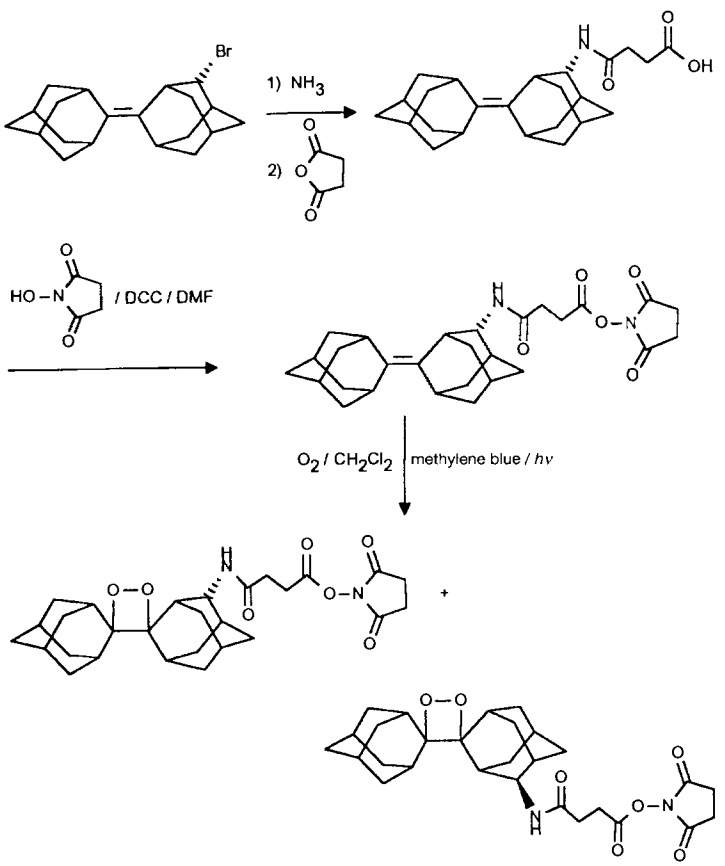
Dioxetanes have for a long time been regarded as merely having curiosity value in the laboratory. Use of the extremely unstable compounds in reagents for diagnostics was not considered. It was not until after adamantylideneadamantane-1,2-dioxetane (an extremely stable compound due to the steric shielding prepared by W. Adam et al.[146] in 1972) became known that the development of dioxetane labels really took off. Light emission could only be triggered thermally for stable dioxetanes of the type mentioned which exhibit a half-life of greater than 20 years at room temperature. In the thermolysis two molecules of adamantone are formed, partly in the S_1 state and partly in the T_1 state (Scheme 28). In principle, cleavage can occur according



Scheme 28. Simplified representation of the decomposition reaction of dioxetanes.

to a diradical or a concerted mechanism.[87] A stepwise pathway, involving homolysis of the O–O bond and formation of a diradical, has been proposed for the decomposition of the stable dioxetanes.[147] The light emission results from the deactivation of the S_1 excited species. Dioxetanes, which, in addition to the steric stabilization by only one adamantyl group, still contain a substituent of low oxidation potential, mostly aryloxy, undergo a different decomposition mechanism. This decomposition route is triggered by cleavage of the O–O bond and by an electron transfer from the oxidizable group into the antibonding orbital of the peroxide bond (CIEEL mechanism, *c*hemically *i*nitiated *e*lectron *e*xchange *l*uminescence).[92e, 148–155] This mechanism for the dioxetanes mentioned which are substrates for enzyme labels is discussed in Section 4.

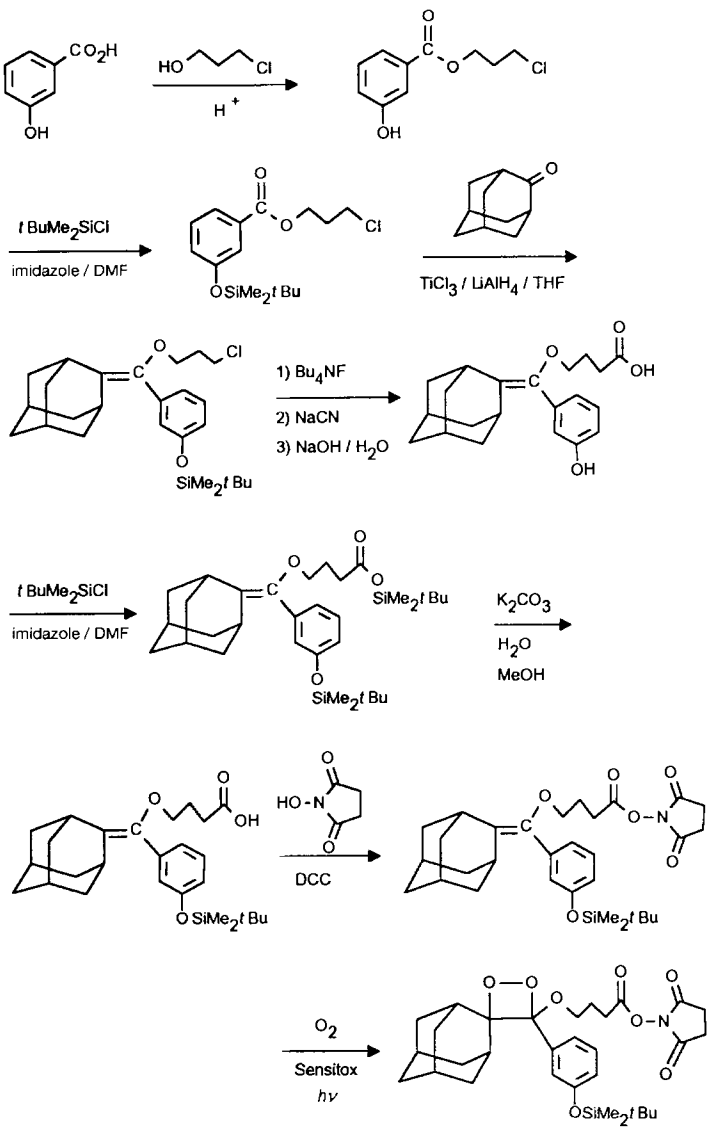
Functionalized adamantylideneadamantanes that contain a reactive group bound to a spacer have been described as a label for thermochemilunescent immunoassays[156] (Hummelen et al., 1986). The synthesis of one such label is given in Scheme 29. The starting material is adamantylideneadamantane, which can be obtained in two steps from adamantanone.[157] In the last step of the synthesis, sensitized (methylene blue) photooxygenation, a mixture (ca. 1:1) of two dioxetane isomers results, which was used in this form in the labeling experiments. The overall yield of the seven-step synthesis, starting from adamantanone is 50%. The triggering of luminescence results from heating the sample adsorbed onto aluminum oxide for a short time at 240 °C. An apparatus for measuring thermochemiluminescence has also been described.[156] Since the efficiency of the direct chemiluminescence of adamantylideneadamantane-1,2-dioxetane is 1×10^{-4} (6×10^{19} photons per mol)[158] under optimal conditions (only 1% of that of luminol), an increase in the energy transfer to a good fluorescent dye is necessary. Bovine serum albumin conjugates with the dioxetane label and 9,10-diphenylanthracene, which, in turn, have been used as labels in



Scheme 29. Synthesis of a thermochemiluminescent dioxetane label. DMF = dimethylformamide.

*f*luorescence *a*mplified *t*hermochemiluminescence *im*muno*a*ssay (FATIMA), have been described. The first assays, for example, for the tumor marker CEA have been described, but the thermochemiluminescence principle appears to be altogether too costly for wider commercial use. The search was then started for model compounds for thermally somewhat less stable dioxetane labels, which could be activated at approximately 150 °C.[159] For example, 9-xanthenylideneadamantane decomposes at around 100 °C (Hummelen et al., 1988). The light emitted from this compound corresponds to the emission from adamantone. Other monoadamantyldioxetane derivatives of the xanthene, naphthalene, and phenyl series, which can be triggered enzymatically and chemically and in which the olefinic starting material contains a methoxy substituent to facilitate dioxetane synthesis, have been described (Schaap et al., 1987).[47c, 47d] Shortly afterwards AMPPD, already mentioned in Section 4, was reported. In contrast to the above-mentioned thermal decomposition, the emitter in the CIEEL decomposition of adamantylidenearyloxy-1,2-dioxetanes, which can be triggered enzymatically or chemically (cf. Scheme 10), is chiefly an excited aryloxy anion.

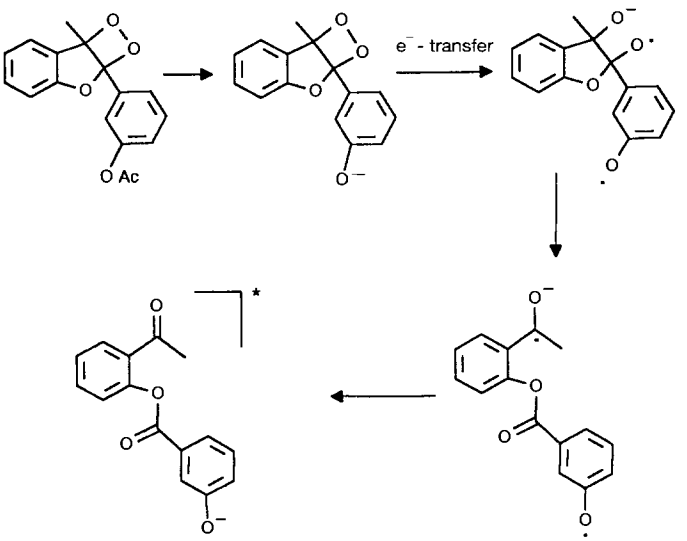
Thus, in less than twenty years since their discovery, dioxetanes have developed from merely being laboratory curiosities to being stable derivatives employed worldwide in immunolgical and biochemical analysis. The development has not yet reached an end. Until a short time ago the 1,2-dioxetanes, which can be triggered enzymatically or chemically, were not known as classical labels with a reactive group for coupling to molecules to be labeled, however, recently also such dioxetane labels for direct labeling methods were introduced.[14, 47p, 160] The synthesis of a selected label is outlined in Scheme 30. Apart from the silyloxy



Scheme 30. Dioxetane labels for chemiluminescent direct labeling which can be triggered chemically. Sensitox = polymer-supported Rose Bengal.

group shown which can be cleaved to trigger luminescence, other substituents can also be employed, for example, phosphate and galactosyl groups. In addition to the hydroxysuccinimide esters shown other common reactive groups should also be considered. A label with a biotin anchor and its use for labeling proteins and antibodies has also been described.[47p] Further applications of this relatively new label are as yet unknown, but judging from the high quantum yields (0.20–0.25 in DMSO)[14] they will presumably not be long in coming.

Finally in this section on dioxetanes another new class of relatively stable dioxetanes should be mentioned namely, phenyl-substituted benzofuran-1,2-dioxetanes.[14, 92e, f] These give quantum yields (up to 4×10^{-6}) similar to those of the enzyme substrates described earlier. The acetoxy-substituted



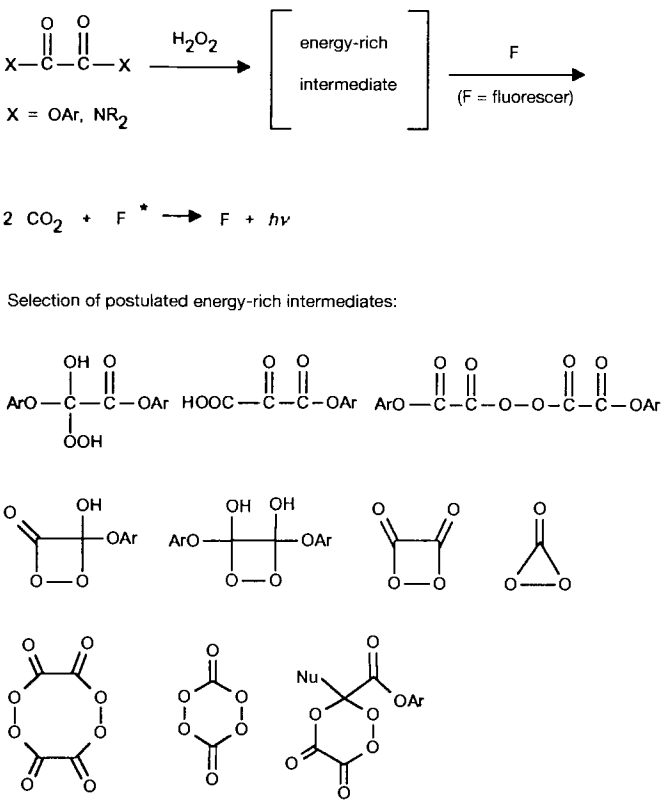
Scheme 31. Structure and decomposition of a benzofurandioxetane.

compound shown in Scheme 31 decomposes, presumably base-induced, according to the CIEEL mechanism. For analogous siloxy-substituted compounds decomposition can, as with similar adamantyl systems, be triggered by fluoride ions.[192f]

5.2.5. Oxalic Acid Derivatives

Oxalic acid derivatives such as oxalyl chloride,[161,162] certain oxalic acid anhydrides,[163] diaryl esters,[164] and oxamides[165] are among the synthetic molecules which exhibit the highest chemiluminescence quantum yields (up to 0.5).[11] Intense luminescence is observed in the presence of a fluorescent dye during the oxidation of oxalic acid derivatives with hydrogen peroxide. Despite extensive studies the complete mechanism of peroxyoxalate chemiluminescence is still not fully understood. A dioxetanedione is often proposed as the energy-rich intermediate which forms the oxalic acid derivative by reaction with hydrogen peroxide (Scheme 32). However, according to the results of more recent work, this highly strained intermediate is not formed;[93b] a large number of possible intermediates is shown in Scheme 32.[14,166–169] As has already been considered in other mechanisms, reaction pathways involving electron transfer or energy transfer are discussed.[14] Finally, either excited carbon dioxide is formed which activates the fluorescent dye by energy transfer, or a charge-transfer complex is formed which decomposes to give CO_2 and a fluorescent dye molecule in the excited state. The luminescence of these systems is relatively long lasting and the emission color can be controlled by choice of dye. The best known application of this are the Cyalume light sticks.[170]

Oxalic acid esters or oxamides cannot be considered for the development of luminescent labels for diagnostic purposes because the solubility of the oxalates and fluorescent dyes requires the use of organic solvents; the compounds are hydrolyzed quickly in aqueous solutions.[11] However, oxalates are employed in chemiluminescence detectors in HPLC or flow injection analysis.[14,171] The appropriate systems allow, inter alia, analysis of environmental toxins, drugs, amino acids, fatty acids, and amines with detection sensitivities ranging from the nanogramm



Scheme 32. Mechanism of chemiluminescence for oxalic acid derivatives.

into the attomol region. Another interesting area of application of oxalate chemiluminescence in diagnostics is the quantitative determination of oxalic acid in urine with detection limits as low as 10 nmol L^{-1}. For this purpose the oxalic acid present is treated with carbodiimide in the presence of hydrogen peroxide and a fluorescent dye. The light emission measured is proportional to the concentration of oxalic acid.[172,173] Even the determination of porphyrins in urine is possible with this method. In this case a fluorescent dye is not necessary because the porphyrins themselves act as sensitizers.[174]

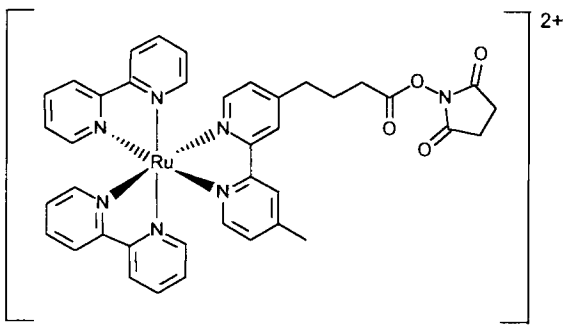
5.2.6. Electrochemiluminescence

The triggering of chemiluminescence by electrochemical processes has been known for a long time but has only gained practical significance in recent years.[175] Radicals produced electrochemically play a significant role in these processes and the electrochemical excitation of luminol/hydrogen peroxide mixtures has been studied in detail.[176] Luminescence is observed with potentials greater than 0.5 V. A mechanism similar to the one presented in Scheme 21 is assumed for potentials of up to 0.7 V. Diazaquinone produced electrochemically reacts with hydrogen peroxide. At higher potentials (1.2 V) the reaction is considerably more complex since the amino group of luminol is involved in oxidation processes.[176] An electrochemical detector based on this system can be used for the determination of hydrogen peroxide.

In addition, the electrochemical processes of acridinium compounds have been investigated.[177] Whilst lucigenin is reduced at −0.3 V and gives rise to luminescence in a subsequent reaction of the radical, acridinium esters show no activity in the range +1

to −1 V. However, the luminescent reaction of the acridinium esters can be initiated electrochemically by hydrogen peroxide produced from oxygen. This principle facilitated development of detectors for labeled analytes without the need for additional reagents. Lysin labeled with the first acidinium ester described earlier could be detected with a sensitivity of 10 fmol.[177]

The chemiluminescence of ruthenium(III) chelate complexes has been known for a long time,[178a, 175a] likewise the electrochemically generated luminescence from trisbipyridineruthenium(II) chelates.[178b] However, the labeling of haptens, proteins, and nucleic acids with ruthenium(II) chelates was only described recently.[179a] The ruthenium complex, which is shown in Scheme 33, uses a hydroxysuccinimide ester sub-



Scheme 33. Structure of an electrochemiluminescent label based on a [tris(bipyridine)]ruthenium chelate.

stituent as the reactive group. The advantages of the label cited are high stability, relatively low molecular weight, high solubility in water, and high sensitivity—the detection limit of the label is 200 fmol L^{-1}. Multiple labeling of proteins and oligonucleotides are possible without being detrimental to immune reactivity, solubility, or ability of the conjugate to hybridize. In the electrochemical reaction $[Ru(bpy)_3]^{2+}$ (bpy = bipyridine) is first oxidized to $[Ru(bpy)_3]^{3+}$ on the electrode surface. Simultaneously, the tripropylamine (TPA) present in a large excess is likewise oxidized to a radical cation $TPA^{\cdot+}$ which spontaneously cleaves a proton. In the reaction of the strong oxidizing reagent $[Ru(bpy)_3]^{3+}$ with the radical $TPA^{\cdot}$, a strong reducing agent, a $[Ru(bpy)_3]^{2+}$ complex is formed in the electronically excited state which returns to the ground state by emission of a photon at 620 nm. The ruthenium(II) complex can re-enter the cyclic process, which automatically causes amplification of the signal.

In addition to an electrochemiluminescent analyser,[179b] immunoassays,[179a] and genetic probe tests[179a, 180] with the, in the meantime, commercially available ruthenium label have been described. The available data is insufficient to evaluate the suitability of electrochemiluminescent detection in diagnostic practice.

6. Applications

6.1. Immunoassays

6.1.1. Introduction

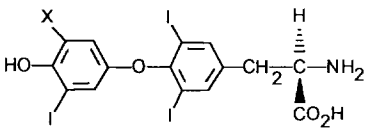
When Yalow and Berson developed the first radioimmunoassay for the in vitro determination of insulin in 1959,[1] they surely could not have envisaged that their method in this or in some other form would become the most important analytical tool of medicinal in vitro diagnostics. It is difficult to overlook the wealth of substances, whose concentrations are today routinely determined in clinical laboratories with immunoassays. A number of these analytes are listed in Table 2 according to diagnostic indications.

Table 2. Some analytes which are routinely determined by immunoassay in different diagnostic areas.

Diseases of the thyroid gland	*Gastrointestinal tract*
TSH (thyroid stimulating hormone, thyrotropin)	calcitonin
T3 (triiodothyronine)	C-peptide
FT3 (free T3, i.e. not bound to binding protein)	gastrin
T4 (tetraiodothyronine)	insulin
FT4 (free T4, i.e. not bound to binding protein)	anti-insulin antibody
TBG (thyroxine binding globulin)	pepsinogen
Tg (thyreoglobulin)	trypsin
Anti-Tg (autoantibody against Tg)	trysin neonatal
TPO (thyroidal peroxidase)	vitamin D
Anti-TPO (autoantibody against TPO)	
TRAK (autoantibody against the TSH receptor)	*Hypertonia and nephrology*
	aldosterone
Tumour growth controls	androstendione
AFP (α-fetoprotein)	angiotensin I (renin)
CA 50 (CA = cancer antigen)	cortisol
CA 125	DHEA (dehyroepiandrosterone)
CA 15-3	17 α-OH-progesterone
CA 19-9	
CA 72-4	*Cardiology*
CA 754	digoxin
calcitonin	myoglobin
CEA (carcinoembryonic antigen)	
cyfra 21-1	*Connective tissue diseases*
ferritin	laminin
HCG (human choriongonadotropin)	NC1 (N-terminal collagen I)
β_2-microglobulin	PIIIP (procollagen-III-peptide)
NCAM (neural cell adhesion molecule)	7S-collagen
NSE (neuron specific enolase)	
osteocalcin	*Infectious diseases*
PAP (prostatic acid phosphatase)	HBsAg (hepatitis B surface antigen)
prolactin	HSV antigens
PSA (prostatic specific antigen)	p24 antigen (HIV antigen)
SCC (squamous cell carcinoma antigen)	rotavirus antigen
TATI (tumor-associated trypsin inhibitor)	antibodies against:
Tg (thyreoglobulin)	– FSME virus
TPA (tissue polypeptide antigen)	– HBsAg
	– HIV1
Pregnancy	– HIV2
AFP (α-fetoprotein)	– HSV
estriol	– measles virus
HCG (human choriongonadotropin)	– rotavirus
progesterone	– rubella virus
	– toxoplasma gondii
Sexual functions	– varicella Zoster
FSH (follicle stimulating hormone, follitropin)	*Inflammatory processes*
LH (luteinizing hormone, lutropin)	α-antitrypsin
progesterone	CRP (C reactive protein)
17α-OH-progesterone	α_1-macroglobulin
prolactin	α_2-acid glycoprotein (Orosomucoid)
testosterone	

The success of immunological assays is owed primarily to their high specificity and sensitivity; antibodies, which are employed in immunoassays as detection reagents, can "recognize" at the molecular level smallest structural differences (much cited "lock-and-key" principle). For example, an antibody raised

against the thyroid hormone thyroxin binds with high affinity (equilibrium constants usually are of the order of 10^{10}–10^{12} L mol^{-1}), whereas triiodothyronine which differs by only one iodine atom is not recognized (Scheme 34).



Scheme 34. Structure of the thyroid hormones T3 (X = H, 3,3'5-triiodo-L-thyronine) and T4 (X = I, 3,3',5,5'-tetraiodo-L-thyronine, L-thyroxine).

As a result of this impressive specificity practically all substances with a molecular weight of greater than 100 D even in complicated liquids such as serum can be determined exactly without prior separation of similar substances. Modern labels can even be traced into the attomolar range (1 amol = 10^{-18} mol). Thus, by labeling antibodies with such labels, the substances to be analyzed can be quantified exactly to the femtomolar range (1 fmol = 10^{-15} mol). A current listing of almost 500 literature references can be found in "Bioluminescence and Chemiluminescence Literature - Immunoassays and Blotting Assays" by O. Nozaki et al.[181]

6.1.2 Categories

Immunoassays can be divided into different groups.

Group I: Competitive immunoassays with analyte tracer:

This group concerns assays in which the detection reagents are an antibody specifically directed against the substance to be determined and an analyte derivative which carries the label (analyte derivative tracer, usually abbreviated to analyte tracer). The analyte tracer should not be too structurally different from the analyte (which under the circumstances only exists in the presence of the label) that it no longer is recognized by the antibody. Furthermore, immunoassays of this group are competitive assays, that is the analyte and analyte tracer compete for a small number of antibody binding sites in an equilibrium reaction (Fig. 3a). The lower the concentration of the analyte-sample to be analyzed, the more antibody–analyte tracer complexes can form as a result. The analyte concentration of an unknown sample can be determined exactly by using a calibration curve drawn up from samples of known concentration (Fig. 3b). As is apparent from Figure 3a, selective measurement of the signal emitted from the antibody–analyte tracer complex requires prior separation of uncomplexed analyte tracer. Separations of this kind are dealt with in Section 6.1.3.

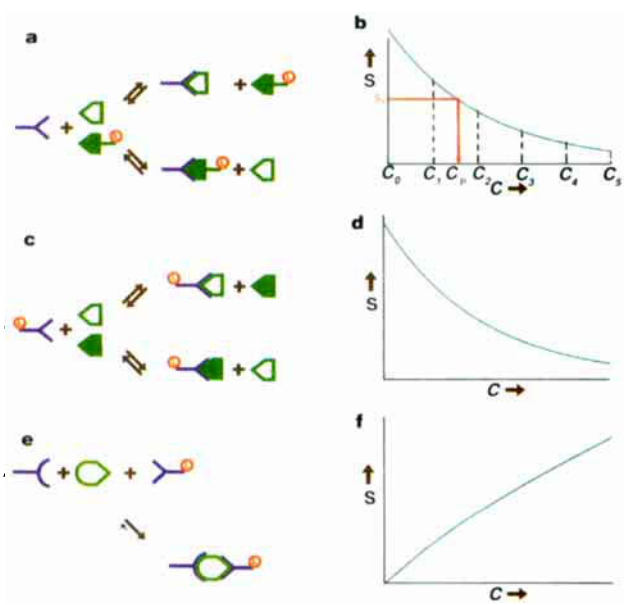


Fig. 3. Principle of the three most important immunoassay methods (left) with the corresponding calibration curves (right). Left: blue = antibody, green = analyte (open) and analyte derivative (closed), red = label. Right: c = concentration, P = unknown sample, S = signal emitted by the antibody–analyte tracer complex (a,b), antibody tracer–analyte derivative complex (c,d) and from the sandwich complex (e,f). This and other schematic representations of an antibody do not take into account the existence of several binding sites (in the case of the IgG antibody: two).

Group II: Competitive immunoassays with antibody tracer:

As in Group I this is also a competitive process. The only difference is that of the two detection reagents (antibody, analyte derivative) it is not the analyte derivative that carries the label but the antibody (antibody tracer also called tracer antibody). As can be seen from Figure 3c, the concentration of the analyte to be determined correlates with the concentration of the antibody tracer-analyte derivative complex after adjusting the equilibrium (Fig. 3d). For the separation of the two labeled complexes which is also necessary in this case see Section 6.1.3.

Group III: Sandwich assays:

Instead of the analyte derivative in competitive assays, in this case a second antibody is the detection reagent. The label is situated on one of the two antibodies. Both antibodies bind to the analyte at different sites (epitopes) and thus form a sandwich complex. An excess of the two antibodies is employed in order to shift the equilibrium in favor of the sandwich complex (Fig. 3e). The favorable equilibrium position in this type of assay due to the excess of reagent leads to a considerably higher sensitivity of detection. Whilst, for example, a competitive assay for the determination of the thyroid hormone thyrotropin is capable of detecting an analyte concentration of about 1–2 fmol mL^{-1}, the lower detection limit in the case of a comparable sandwich assay is about 0.1–0.2 fmol mL^{-1}. The sandwich strategy achieved its breakthrough when it became possible to obtain pure uniform antibodies in virtually any quantity. (Monoclonal antibodies, Nobel Prize, 1984 for Köhler and Milstein).[182, 183]

About the only disadvantage is the limited applicability of this type of assay: small analytes (M < approx. 5 kD) are excluded, since two antibodies cannot bind simultaneously for steric reasons. In the case where the analyte is an antibody (cf. listing in Section 6.1.1; indication: infectious diseases), the sandwich assay can be applied in a slightly modified form: an antigen plays the part of one of the two detection antibodies, thus, for example, a virus particle, against which the analyte antibody is directed. In this case, the resulting sandwich complex consists of antigen, analyte antibody, and detection antibody; the antigen corresponding to its complementary structure binds to the recognition site of the analyte antibody and is, thus, responsible for the specificity of the detection. For the detection antibody it suffices if this is directed against the structure element of the analyte antibody, although this is standard for all

antibodies of the same animal (in this case human) species (Fc portion). The latter presupposes, of course, that the antibodies present in the patient's blood, which are directed against completely different antigens, do not "capture" a significant fraction of the detection anti body. In practice such complications can be easily avoided by the choice of a corresponding high concentration of the detection antibody or by a so-called two-step performance of the assay. The separation of the sandwich complex and excess tracer, also necessary in this case prior to the measurement, is dealt with in Section 6.1.3.

The individual variations within these groups (cold and hot preincubation, one-step and two-step performance, double antibody method) as well as immunoassays which work without a tracer[118a] cannot be dealt with here.

Definitions of Terms:

In scarcely any other area is there such a confusion of terms and abbreviations as in the field of immunoassays. The most well-known expression is the "radioimmunoasssay" (RIA). Unfortunately it is often used for two different circumstances. First, it stands for competitive immunoassays with a radioactive analyte tracer, that is, for the assay type described in Group I, and second it is often employed as the generic term for all immunoassays with a radioactive label. The same can also be said for the enzyme immunoassay (EIA), fluorescence immunoassay (FIA), and luminescence or chemiluminescence immunoassay (LIA and CIA, respectively) which are distinguished from RIA only by the type of label used. A similar ambiguity exists with the acronym ELISA (*e*nzyme-*l*inked *i*mmuno*s*orbent *a*ssay). This term is reserved by some authors for the excess reagent assay (Group III) with the enzyme label and by others is employed quite generally for all immunoassays with enzyme label.

Just as XIA (RIA, EIA, FIA, LIA, CIA) designates specifically assays of Group I, Group II does not have a generally accepted abbreviation. However, in this case one often comes across the expression SPALT (*s*olid *p*hase *a*ntigen *l*uminescence *t*echnique). This describes an assay of Group II with luminogenic label, for which a particular but frequently used technique for separating excess antibody tracer is employed (see Section 6.1.3).

A synonym for sandwich assay (Group III) is the expression 2-site IXMA; this stands for "immuno-x....metric assay" (for example: IRMA: immunoradiometric assay; ILMA: immunoluminometric assay). The expression immunometric means that, in contrast to the competitive assays, one is dealing with an assay with excess reagent. Unfortunately the designation is also not uniform in this case. Hence, Group II, despite its competitive nature, is still designated with the expression "1-site IXMA". Strictly speaking the 1-site IXMA is, however, a very rare type of assay, which uses the same detection reagents as Group II (analyte derivative and antibody tracer), however, uses the antibody tracer in excess, and does not measure the complex formed from the analyte derivative and antibody tracer, but the complex formed from the analyte and antibody tracer.

6.1.3. Separation Methods

As already mentioned the selective measurement of labeled immune complexes necessitate a prior separation of the unbound analyte tracer (in the case of Group I), of antibody tracer not bound to the analyte derivative (Group II), or of unbound antibody tracer (Group III).

The first separation methods involved really difficult purification steps, for example chromatography or electrophoresis. Considerably more manageable, but today regarded as being antiquated, are the methods in which the immune complexes are precipitated by addition of salts or organic solvents, or the unbound analyte tracer is adsorbed on addition of activated charcoal or ion exchange resin. The requisite centrifugation step renders these methods as being no longer able to compete today.

Modern methods usually employ a solid phase. In the simplest case this is a small tube made of synthetic material, whose inner wall is coated with one of the detection reagents (coated tubes). At the same time these tubes serve as the reaction vessel for the immunological detection reaction. The separation immediately prior to measurement is reduced to just merely decanting off or removal of the reaction solution by suction (Fig. 4).

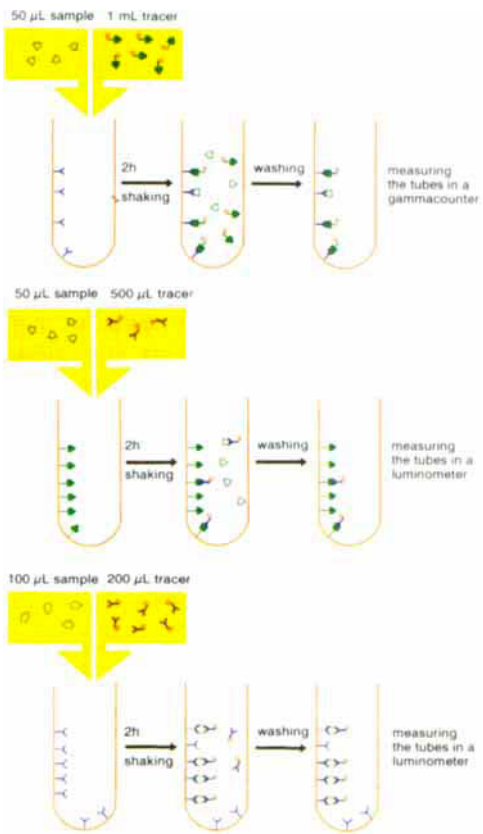


Fig. 4. Examples of commercial immunoassays performed with a coated tube: RIA-gnost T3 (top), a RIA and BeriLux T3 (middle), a SPALT assay for determination of triiodothyronine (T3) and BeriLux TSH (bottom), a 2-site ILMA for the determination of thyroid stimulating hormone (TSH) in serum.

The coating of the solid phase proceeds in the most simple case by direct adsorption of the detection reagent; the solid phase is kept in contact with a solution of the detection reagent for several hours. Under suitable conditions the adsorptive binding is so strong that the immobilized reagent cannot be dissolved by washing the solid phase. Binding can also result through an anchor protein, which adsorbs particularly well onto

the solid phase to which the detection reagent is covalently bonded by bifunctional reagents.[24] Often an antibody, which recognizes a structural element that is common to all antibodies of another animal species, is attached to the solid phase. For instance, antibodies which are directed against the Fc portion of mouse antibodies can be produced in rabbit. In this way antibodies can be anchored onto the solid phase which are less suitable for a direct adsorption. More of these universal solid phases are based on the high affinity binding between biotin and avidin (strept-)avidin[34] as well as between fluorescein and anti-fluorescein antibodies[184] (Fig. 5).

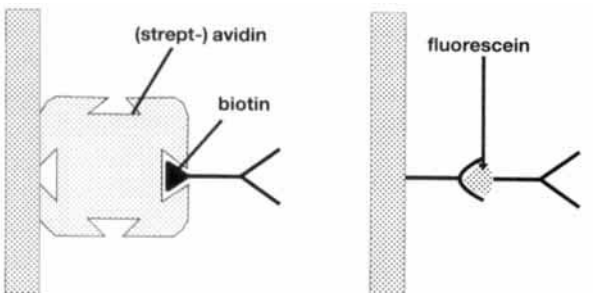


Fig. 5. The binding of a detection reagent (in this case an antibody) to a solid support can be achieved by means of the (strept-)avidin/biotin system (left): The biotinylated antibody is supported by the (strept-)avidin adsorbed onto the solid support. A similar anchoring method is based on the strong bonding between fluorescein groups and antibodies directed against fluorescein (right).

Instead of coated tubes other coated solid phases can also be employed (synthetic spheres, magnetic particles, and membranes). These can also (cf, Fig. 4) participate directly in the immune reaction or merely have a separation function. In the latter case the immune reaction occurs in a homogeneous liquid phase (which has certain advantages with regards to the rate of reaction), and the separation function of the solid phase is only "switched on" once the reaction is completed (Fig. 6).

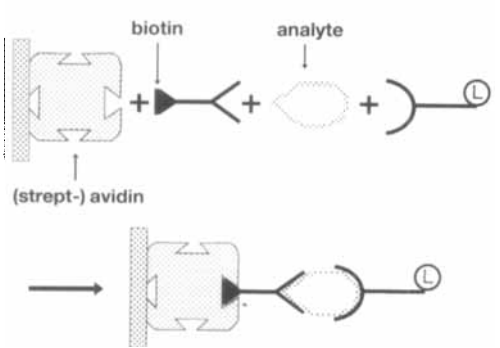


Fig. 6. After completion of the reaction between antibody labeled with either FITC or biotin, analyte, and analyte tracer in the liquid phase, the solid support coated with (strept-)avidin or anti-fluorescein antibodies, respectively, is added, and the sandwich complex is attached to the solid support.

With the OPUS system[185] separation is accomplished without further operation steps. The whole immune reaction takes place in a test module which is about the size of two sugar cubes. An essential component is a transparent polyester film, on the surface of which are three agarose layers. Complexes of the antibody and fluorescent-labeled analyte derivative are embedded in the lower layer (1 μm thick). The serum sample is applied to the top layer (10 μm thick). The analyte molecules contained in the sample diffuse into the lower layer, where they—depending on their concentration—displace more or less tracer molecules from the antibody binding sites. Additional reagents such as aqueous solutions are not necessary here. Whereas antibodies are not able to leave the lower layer because of their size, the unbound tracer molecules are free to diffuse into the two upper layers. The antibody–tracer complexes which remain in the lowest layer are quantified by fluorescence detection. The light source and detector are situated below the test module. The middle agarose layer (10 μm thick) acts as an optical filter due to its iron oxide content and prevents measurement of released tracer molecules which have diffused from the lower layer.

In the purely homogeneous assays there is no separation step because they are based on a changing signal in the formation of the immune complex. The first assay of this type was presented by Rubenstein and Ullman in 1971.[186a] This EMIT method (*e*nzyme-*m*odulated *i*mmunoassay *t*echnology) involves EIA; enzymatic activity of the enzyme label is inhibited by the binding of antibodies (Fig. 7). Another example of a homogeneous assay which employs chemiluminescence energy transfer is shown in Figure 8. Disadvantages of these, at first glance, particularly elegant homogeneous assays are lower sensitivity of detection and a more pronounced susceptibility to interference.

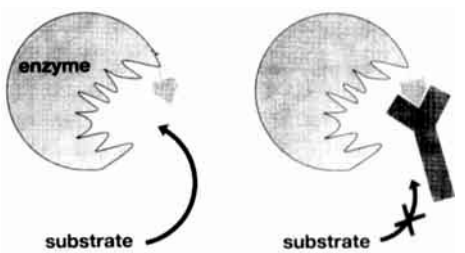


Fig. 7. In the EMIT method an antibody bound to the analyte tracer (analyte derivative labeled with the enzyme) prevents the catalytic conversion of the substrate (e.g. a chromogen) by the enzyme, for example, by steric hindrance at the active site.

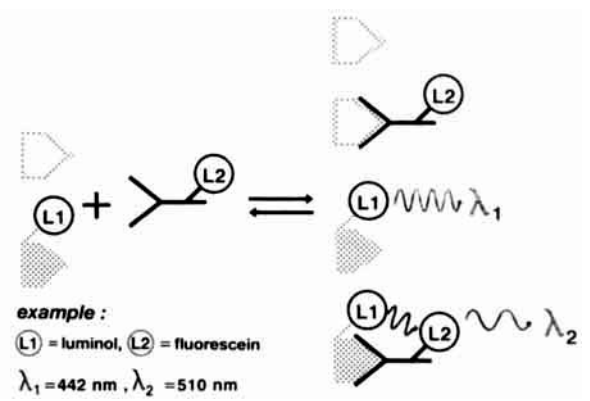


Fig. 8. Example of a homogeneous LIA: The energy transfer across the small distance between the two labels L1 and L2 results in an electronic excitation of L2. The intensity of the light emitted from L2 therefore correlates to the analyte concentration.

6.2. Gene Probes

Whereas analytes in immunological determination methods are after all products of genetic information, nucleic acid sequences are the information itself. The qualitative and quantitative determination at this "primary level" is increasingly gaining significance.

The most important application at present is in the detection of pathogenic organisms (bacteria, viruses).[187] A particular advantage is that not only active viral infections, but also latent ones, are ascertainable by detection of the nucleic acid sequences. Thus, for example, infections with the AIDS virus can be detected already in the incubation phase of seronegative patients. In addition, the control of blood supplies for HIV, HTLV-I, Hepatitis B, etc. is much safer with the detection of the corresponding nucleic acid sequences than with an immunological test.

A series of hereditary diseases, such as diabetes mellitus, Lesch–Nyhan syndrome, phenylketonuria, and sickle cell anemia, can be detected reliably by tracing the mutated genes,[188] likewise the activation of different oncogenes which are involved in the formation of tumors.[189] In forensic medicine the detection of nucleic acid sequences is employed for solving cases involving sexual crimes or in tests for paternity suits.[190]

In contrast to immunoassays no antibodies are employed as direct detection reagents, but relatively short, mostly synthetic nucleic acid sequences (so-called gene probes) which are complementary to part of the analyte (so-called target sequence) (Fig. 9). These hybridize with the target sequence, that is, they

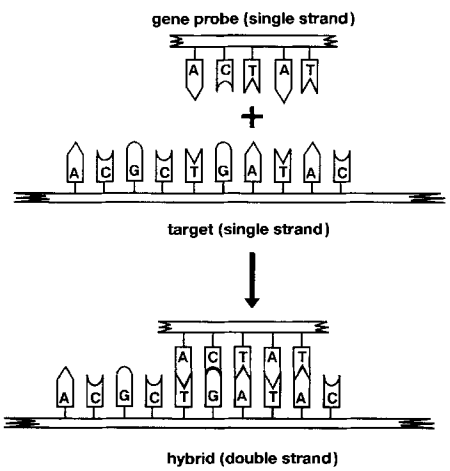


Fig. 9. The affinity of two nucleic acid strands arises from complementary base pairs: adenine (A) bonds to thymine (T) or uracil (U), and cytosine (C) to guanine (G). The gene probes employed are usually chains of 15–30 nucleotides.

bind with it to form a double strand which is held together by hydrogen bonding.

In the Southern–Blot method,[191] named after its founder, the DNA, on which presumably the sequence to be determined lies, is initially cut into defined fragments by restriction enzymes. These are separated by electrophoresis and the bands on the electrophoresis gel are transferred to a suitable carrier (e.g. nitrocellulose), whilst maintaining the relative positions of the bands. The individual DNA fragments (double-stranded) are denatured (that is, they are split into single strands) by heating, in order to make them accessible to a hybridization with the labeled gene probe. One of the advantages of this method is that different probes can be employed simultaneously to trace several nucleic acid sequences.

The visualization of the fragments hybridized with the probes can be accomplished, for example, by applying a photographic film. The exposure times are greatly dependent on the label employed. For the ^{32}P isotope used almost exlusively earlier, it was not unusual to have to wait for several weeks. By employing more modern luminogenic labels the exposure times can be drastically reduced. Methods that use fluorescent labels dispense with need for photographic film and, moreover, there is the advantage that different colored light signals can be received by employing different labels simultaneously. This can make the distinction of DNA fragments which exhibit similar electrophoresis profiles considerably easier.

In analogy to immunoassays there are also corresponding gene probe tests. The pendant of a 2-site IXMA[192] is shown in Figure 10. An analogue of the competitive immunoassay is the

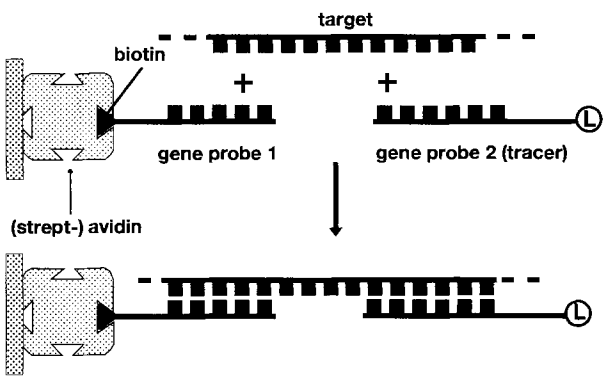


Fig. 10. The counterpart corresponding to the 2-site IXMA on gene probe site.

strand displacement assay[193] (Fig. 11). The only difference, in principle, to the XIA presented in Section 6.1.2. (Group I) is that the labeled gene probe (corresponds to the analyte tracer in XIA) and the target sequence (analyte) do not compete at the same time for the probe bound to the solid phase (corresponds to the antibody in XIA), but that the tracer gains a lead in time (principle of hot incubation; not an unusual experimental variable in XIA).

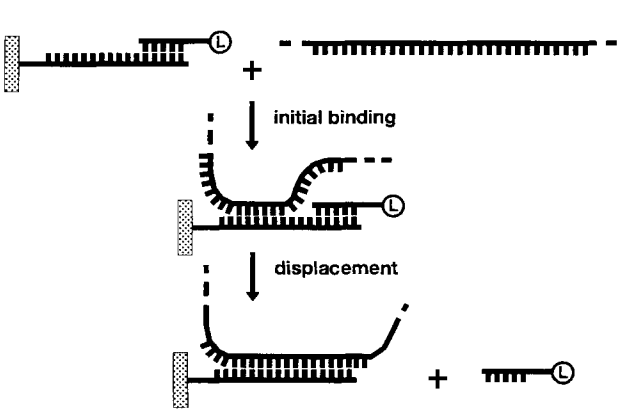


Fig. 11. Principle of the strand displacement assay.

The transfer of techniques from the field of immunoassays has also led to homogeneous gene probe test. In kissing probes (Fig. 12), two labeled probes bind to the target so closely to each other that an interaction is effected between the labels. Thus, only the changes in the signal occurring in this way can be viewed as highly specific.

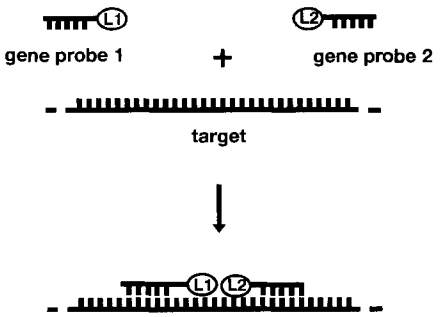


Fig. 12. Principle of the "kissing probes".

The acridinium label is able to intercalate double-stranded DNA and therefore is protected against attack from nucleophilic reagents. In this way it is possible to distinguish between single-stranded and double-stranded bound labels. This has been of use in the "hybridization protection assay".[194]

A revolutionary step for enhancing the sensitivity of gene probe tests was achieved by the PCR methods (polymerase chain reaction).[195] K. B. Mullis received the Nobel prize for the development of this method in 1993. The basic idea is original and at the same time simple. Whereas almost all attempts to improve the lower detection limit were directed at increasing the signal intensity and reducing the background signal, that is, to have the tracer in sight, with the PCR method, the target sequence is selectively replicated(!) and moreover quite simply. First, the target sequence present as a DNA double strand is cleaved into two single strands by denaturing with heat. The two single strands were then hybridized with complementary oligonucleotides and these were subsequently enzymatically

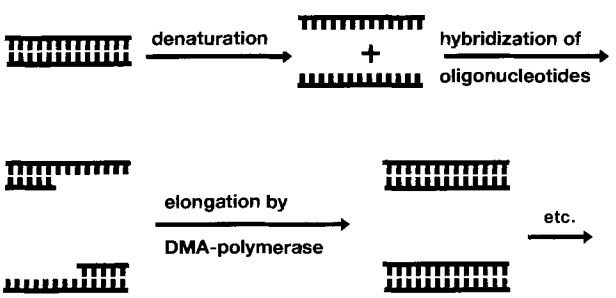


Fig. 13. PCR method.

elongated at the 3'-end with deoxynucleotide triphosphates. This process is repeated several times (Fig. 13) and after 20 cycles the target sequence is amplified by 100 000-fold.

7. Outlook

Even if a γ source which radiates continually for months to emit a signal often only required for a few seconds is everything but modern, there is much to be said, not only on ecological grounds, for the replacement of radioactive labels. With the labeling alternatives available today radioactive labels have, as far as detection sensitivity is concerned, been partly superseded. Why is it then that RIA did not die out long ago? A considerable advantage of RIA is tied up with one of its greatest disadvantages—as seen from an ecological standpoint—the emission of energy-rich radiation. In the thirty years of experience in the field of RIA this method has proved to be extraordinarily "robust". Thus, for example, in the case of the radioactive label the tracer is not influenced by its direct surroundings ("matrix effects") except for in the rarest of cases. Furthermore, the signal is not affected either in terms of its absolute value or in terms of its constancy by most external factors. In addition, the labeling of small analyte derivatives by an isotope inevitably results in fewer changes in properties compared to the introduction of a sterically demanding label. Thus, replacement of radioactive methods will understandably not occur overnight, but is more of a gradual process which is sustained by a steady increase in experience in dealing with nonradioactive labels and the synthesis of more effective labels. Since the most efficient luminescent labels and luminogenic enzyme substrates have only been available for a few years, one can expect an acceleration of this hitherto slow replacement of radioisotopes in the years to come.

We thank all our colleagues for helpful discussions during the drafting and correction of this manuscript as well as Mr. R. Kaske for providing marketing data and Mrs. J. Bruchmann and Mrs. N. Laloi for support during the preparation of the manuscript. Our special thanks go to Mr. A. Kraft for preparing the figures in Section 6.

Received: July 23, 1993 [A 101E]
German version: *Angew. Chem.* **1994**, *106*, 1097
Translated by Dr. S. P. Auguste, Zürich (Switzerland)

[1] R. S. Yalow, S. A. Berson, *J. Clin. Invest.* **1959**, *38*, 1996; *ibid.* **1960**, *39*, 1157.
[2] H. G. Eckert, *Angew. Chem.* **1976**, *88*, 565; *Angew. Chem. Int. Ed. Engl.* **1976**, *15*, 525.
[3] *Nonisotopic Immunoassay* (Ed.: T. T. Ngo), Plenum, New York, **1988**.
[4] a) B. J. Gould, V. Marks in *Nonisotopic Immunoassay* (Ed.: T. T. Ngo), Plenum, New York, **1988**, pp. 3–26; b) E. Engvall, P. Perlmann, *Immunochemistry* **1971**, *8*, 871; *J. Immunol. Methods* **1971**, *10*, 161.
[5] M. E. Jolley, C. J. Wang, S. J. Ekenberg, M. S. Zuelke, D. M. Kelso, *J. Immunol. Methods* **1984**, *67*, 21.
[6] a) E. Soini, I. Hemmilä, *Clin. Chem. Winston-Salem NC* **1979**, *25*, 353; b) I. Hemmilä, *ibid.* **1985**, *31*, 359.
[7] a) I. A. Hemmilä, *App. Fluoresc. Technol.* **1989**, *1* (4), 1; b) I. Wieder in *Immunofluorescence and Related Staining Techniques. Proceedings of the VIth International Conference on Immunofluorescence and Related Staining Techniques* (Eds.: W. Knapp, K. Holubar, G. Wick), Elsevier/North-Holland Biomedical Press, Amsterdam, **1978**, pp. 67–80; c) A. A. Lamola, J. Flores, *J. Am. Chem. Soc.* **1982**, *104*, 2530; G. L. Landen, Y.-T. Tark, D. A. Lightner, *Tetrahedron* **1983**, *39*, 1893.
[8] R. A. Mathies, L. Stryer in *Applications of Fluorescence in the Biomedical Sciences* (Eds.: D. L. Taylor, A. S. Waggoner, R. F. Murphy, F. Lanni, A. S. Birge), Alan R. Liss, New York, **1988**, pp. 129–140.
[9] A. K. Campbell, *Chemiluminescence: Principles and Applications in Biology and Medicine*, 1st edition, VCH/Horwood, Weinheim, Chichester, **1988**.
[10] I. Weeks in *Comprehensive Analytical Chemistry, Chemiluminescence Immunoassay* (Ed.: G. Svehla), Elsevier, New York, **1992**, p. 87.
[11] S. Albrecht, H. Brandl, W. Adam, *Chem. Unserer Zeit* **1990**, *24*, 227.
[12] H. R. Schroeder in *Bioluminescence & Chemiluminescence, Current Status* (Eds.: P. E. Stanley, L. J. Kricka), Wiley, Chichester, **1991**, p. 547.
[13] L. J. Kricka, *Clin. Chem. Winston-Salem NC* **1991**, *37*, 1472.

[14] S. Albrecht, H. Brandl, W. Adam, *Nachr. Chem. Tech. Lab.* **1992**, *40*, 547.

[15] S. Albrecht, H. Brandl, C. Schönfels, W. Adam, *Chem. Unserer Zeit* **1992**, *26*, 63.

[16] Data from the market research at Behringwerke AG, Marburg.

[17] a) *Nonradioactive Labeling and Detection of Biomolecules* (Ed.: C. Kessler), Springer, Berlin, **1992**; b) *Luminescence Techniques in Chemical and Biochemical Analysis* (Eds.: W. R. G. Baeyens, D. De Keukeleire, K. Korkidis), Dekker, New York, **1991**; c) K.-D. Gundermann, F. McCapra, *Chemiluminescence in Organic Chemistry*, Springer, Berlin, **1987**; d) *Bioluminescence and Chemiluminescence: Instruments and Applications, Vol. 1* (Ed.: K. Van Dyke), CRC, Boca Raton, FL, **1985**; e) *Chemi- and Bioluminescence* (Ed.: J. G. Burr) (*Methods Enzymol.* **1978**, *57*), f) S. Bogdanoviv, *Clinica – New Horizons in Immunoassay*, PJB Publications, Richmond, UK, **1990**; g) *Immunoassays for Trace Chemical Analysis – Monitoring Toxic Chemicals in Humans, Food and the Environment* (*ACS Symp. Ser.* **1990**, *451*); h) *Immunochemical Methods for Environmental Analysis* (*ACS Symp. Ser.* **1991**, *442*.).

[18] a) J. P. Gosling, *Clin. Chem. Winston-Salem NC* **1990**, *36*, 1408; b) P. E. Stanley, *J. Biolumin. Chemilumin.* **1992**, *7*, 77; c) *ibid.* **1992**, *7*, 157; d) *ibid.* **1993**, *8*, 51; (review on commercial luminometers; photography of apparatus review on commercial bio- and chemiluminescence-diagnostic kits and reagents); e) W. Adam in *Ullmanns Encyclopedia of Industrial Chemistry, Vol. A 15* (Eds.: B. Elvers, S. Hawkins, G. Schulz), 5th edition, VCH, Weinheim, **1990**, p. 548; f) J. W. Freytag, *J. Clin. Immunoassay* **1991**, *14*, 239; g) K. Miyai, *Adv. Clin. Chem.* **1985**, *24*, 61; h) B. S. Reckmann, *Nachr. Chem. Tech. Lab.* **1989**, *37*, 692; i) E. Wieland, E. Wilder-Smith, H. Kather, *Aerztl. Lab.* **1985**, *31*, 203; j) W. G. Wood, *Laboratoriumsmedizin* **1989**, *13*, 345; k) S. Baudner, R. M. Dreher, *Lebensmittelchem. Gerichtl. Chem.* **1991**, *45*, 53; l) U. Obst, *GIT Fachz. Lab.* **1991**, *35*, 1202; m) J. Sherma, *Anal. Chem.* **1991**, *63*, 118R; n) L. Weil, R. Niessner, *Nachr. Chem. Techn. Lab.* **1991**, *39*, 1277; o) C. Wittmann, B. Hock, *ibid.* **1991**, *39*, M1; p) J. M. Van Emon, V. Lopez-Avila, *Anal. Chem.* **1992**, *64*, 79.

[19] a) *Römpp-Chemie-Lexikon* (Eds.: J. Falbe, M. Regitz), 9th edition, Thieme, Stuttgart, **1990**; b) *McGraw-Hill Encyclopedia of Science & Technology*, 6th edition, McGraw-Hill, New York, **1987**.

[20] See [10] p. 429.

[21] G. Zomer, J. F. C. Stavenuiter, *Anal. Chim. Acta* **1989**, *227*, 11.

[22] E. Wünsch, *Synthese von Peptiden, Teil I* (*Methoden Org. Chem.* (*Houben-Weyl*) *4th ed. 1952–*, Bd. XV/1, **1974**, p. 28).

[23] Y. S. Klausner, M. Bodansky, *Synthesis* **1972**, 453.

[24] H. Ji. Tae, *Enzyme Structure* (*Methods Enzymol.* **1983**, *91*, 580).

[25] See [10] p. 439.

[26] G. W. Anderson, J. E. Zimmerman, F. M. Callahan, *J. Am. Chem. Soc.* **1964**, *86*, 1839.

[27] G. Wendlberger, P. Stelzel, *Synthese von Peptiden, Teil II* (*Methoden Org. Chem.*) (*Houben-Weyl*) *4th ed. 1952–*, Vol. XV/2, **1974**).

[28] Hoechst AG, unpublished.

[29] S. Batmanghelich, R. C. Brown, J. S. Woodhead, I. Weeks, *J. Photochem. Photobiol. B* **1992**, *12*, 193.

[30] E. Koller, *Appl. Fluoresc. Technol.* **1989**, *1* (2), 1.

[31] E. Ishikawa, S. Hashida, T. Kohno, K. Tanaka in *Nonisotopic Immunoassay* (Ed.: T. T. Ngo), Plenum, New York, **1988**, p. 27.

[32] H. R. Schroeder, C. M. Hines, P. O. Vogelhut in *Bioluminescence and Chemiluminescence - Basic Chemistry and Analytical Applications* (Eds.: M. De Luca, W. D. McElroy), Academic Press, New York, **1981**, p. 55.

[33] T. Kinkel, A. Mayer, S. Neuenhofer, R. Oekonomopulos (Hoechst AG), EP-A 0442372, **1991**.

[34] a) J.-L. Guesdon, *J. Histochem. Cytochem.* **1979**, *27*, 1131; b) R. Zahradnik, G. Brennan, J. S. Hutchison, W. D. Odell, *Clin. Chem. Winston-Salem NC* **1989**, *35*, 804; c) E. P. Diamandis, T. K. Christopoulos, *ibid.* **1991**, *37*, 625.

[35] See [10] p. 261.

[36] B. M. Krasovitskii, B. M. Bolotin, *Organic Luminescent Materials*, VCH, Weinheim, **1988**, p. 251.

[37] K.-D. Gundermann, *Top. Curr. Chem.* **1974**, *46*, 61.

[38] a) B. K. van Weeman, A. H. W. M. Schuurs, *FEBS Lett.* **1971**, *15*, 232; b) A. H. W. M. Schuurs, B. K. van Weeman, Akzona, US-A 3791932 **1974**; c) M. Oellerich, *J. Clin Chem. Clin. Biochem.* **1984**, *22*, 895.

[39] G. G. Guilbault, P. J. Brignac, Jr., M. Juneau, *Anal. Chem.* **1968**, *40*, 1256.

[40] K. Zaitsu, Y. Ohkura, *Anal. Biochem.* **1980**, *109*, 109.

[41] E. Ishikawa, M. Imagawa, S. Hashida, *Dev. Immunol.* **1983**, *18*, 219.

[42] M. Imagawa, S. Hashida, Y. Ohta, E. Ishikawa, *Ann. Clin. Biochem.* **1984**, *21*, 3107.

[43] E. Ishikawa, *Clin. Biochem.* **1987**, *20*, 375.

[44] L. K. Pyare in *Nonisotopic Immunoassay* (Ed.: T. T. Ngo), Plenum, New York, **1988**, p. 219.

[45] a) M. J. Cormier, P. M. Prichard, *J. Biol. Chem.* **1968**, *243*, 4706; b) L. Ewetz, A. Thore, *Anal. Biochem.* **1976**, *71*, 546; c) H. Arakawa, M. Maeda, A. Tsuji, *ibid.* **1979**, 248; d) A. D. Pronovost, A. Baumgarten, *Experientia* **1982**, *38*, 304; e) K.-D. Gundermann, K. Wulff, R. Linke, F. Strahler in *Luminescent Assays: Perspectives in Endocrinology and Clinical Chemistry* (Eds.: M. Serio, M. Pazzagli), Raven, New York, **1982**, p. 157; f) J. H. Baxendale, *J. Chem. Soc. Faraday Trans. 1* **1973**, *69*, 1665; g) G. Merenyi, J. Lind, *J. Am. Chem. Soc.* **1980**, *102*, 5830; h) T. E. Eriksen, J. Lind, G. Merenyi, *J. Chem. Soc. Faraday Trans. 1* **1981**, *77*, 2125; i) *ibid.* **1981**, *77*, 2137; j) *ibid.* **1983**, *79*, 1493; k) *ibid.* **1983**, *79*, 1503; l) J. Lind, G. Merenyi, T. E. Eriksen, *J. Am. Chem. Soc.* **1983**, *105*, 7655; m) S. Ljunggren, G. Merenyi, J. Lind, *ibid.* **1983**, *105*, 7622; n) G. Merenyi, J. Lind in *5th Symposium on Radiation Chemistry* (Eds.: J. Dobo, R. Schiller, P. Hedvig), Akademiai Kiado, Budapest, **1983**, p. 103; o) G. Merenyi, J. Lind in *Analytical applications of Bioluminescence and Chemiluminescence* (Eds.: L. J. Kricka, P. E. Stanley, G. H. G. Thorpe, T. P. Whitehead), Academic Press, Orlando, FL, **1984**, p. 569; p) G. Merenyi, J. Lind, T. E. Eriksen, *J. Phys. Chem.* **1984**, *88*, 2320; q) *Photochem. Photobiol.* **1985**, *41*, 203; r) *J. Am. Chem. Soc.* **1986**, *108*, 7716; s) in *6th Symposium on Radiation Chemistry* (Eds.: J. Dobo, R. Schiller, P. Hedvig), Akademiai Kiado, Budapest, **1986**, p. 143; t) G. H. G. Thorpe, L. J. Kricka, *Methods Enzymol.* **1986**, *133*, 331; u) G. Messeri, A. Orlandini, M. Pazzagli, *J. Biolumin. Chemilumin.* **1989**, *4*, 154; v) G. Merenyi, J. Lind, T. E. Eriksen, *ibid.* **1990**, *5*, 53.

[46] a) T. J. N. Carter, C. J. Groucutt, R. A. W. Stott, G. H. G. Thorpe, T. P. Whitehead, (National Institutes of Health) EP-A 0087959, **1982**; L. J. Kricka, G. H. G. Thorpe, T. P. Whitehead, (National Institutes of Health) EP-A 0116454, **1983**; c) G. H. G. Thorpe, E. Gillespie, R. Haggart, L. J. Kricka, T. P. Whitehead in *Analytical Applications of Bioluminescence and Chemiluminescence* (Eds.: L. J. Kricka, P. E. Stanley, G. H. G. Thorpe, T. P. Whitehead), Academic, Orlando, FL **1984**, p. 243; d) G. H. G. Thorpe, R. Haggart, L. J. Kricka, T. P. Whitehead, *Biochem. Biophys. Res. Commun.* **1984**, *119*, 481; e) G. H. G. Thorpe, T. P. Whitehead, R. Penn, L. J. Kricka, *Clin. Chem. Winston-Salem NC* **1984**, *30*, 806; f) G. H. G. Thorpe, L. J. Kricka, E. Gillespie, S. Moseley, R. Amess, N. Baggett, T. P. Whitehead, *Anal. Biochem.* **1985**, *145*, 96; g) G. H. G. Thorpe, L. J. Kricka, S. B. Moseley, T. P. Whitehead, *Clin. Chem. Winston-Salem NC* **1985**, *31*, 1335; h) G. H. G. Thorpe, L. J. Kricka, *Methods Enzymol.* **1986**, *133*, 331; i) C. van Dyke, K. van Dyke, B. Caterson, C. Szustkiewicz, A. Reich, *Fed. Proc.* **1986**, *45*, 732; j) *Bioluminescence and Chemiluminescence: New Perspectives* (Eds.: J. Schölmerich, R. Andreesen, A. Kapp, M. Ernst, W. G. Woods), Wiley, Chichester, **1987**; k) G. H. G. Thorpe, R. A. W. Stott, G. M. Sankolli, D. Catty, C. Raykundalia, A. Roda, L. J. Kricka in [46j], p. 209; l) G. H. G. Thorpe, L. J. Kricka in [46j], p. 199; m) G. H. G. Thorpe, L. J. Kricka, *J. Biolumin. Chemilumin.* **1989**, *3*, 97; n) S. B. Vlasenko, A. A. Arefyev, A. D. Klimov, B. B. Kim, E. L. Gorovits, A. P. Osipov, E. M. Gavrilova, A. M. Yegorov, *ibid.* **1989**, *4*, 164.

[47] a) A. P. Schaap, (Wayne State University, Detroit) US-A 887139, **1986**; b) A. P. Schaap, R. S. Handley, B. P. Giri, *Tetrahedron Lett.* **1987**, *28*, 935; c) A. P. Schaap, T. S. Chen, R. S. Handley, R. De Silva, B. P. Giri, *ibid.* **1987**, *28*, 1155; d) A. P. Schaap, M. P. Sandison, R. S. Handley, *ibid.* **1987**, *28*, 1159; e) I. Bronstein, (Tropix Inc.) "Method of detecting a substance using enzymatically-induced decomposition of dioxetanes", WO 88/00695, GO1N21/76, **1988**; "Synthesis of 1,2-Dioxetanes and Intermediates there from" WO 89/06226, CO7C 41/01, **1989**; f) I. Bronstein, B. Edwards, J. C. Voyta, *J. Biolumin. Chemilumin.* **1989**, *4*, 99; g) I. Bronstein, L. J. Kricka, *J. Clin. Lab. Anal.* **1989**, *3*, 316; h) I. Bronstein, P. McGrath, *Nature* **1989**, *338*, 599; i) I. Bronstein, J. C. Voyta, G. H. Thorpe, L. J. Kricka, G. Armstrong, *Clin. Chem. Winston-Salem NC* **1989**, *35*, 1441; j) A. P. Schaap, H. Akhavan, L. J. Romano, *ibid.* **1989**, *35*, 1863; k) G. H. Thorpe, I. Bronstein, L. J. Kricka, B. Edwards, J. C. Voyta, *ibid.* **1989**, *35*, 2319; l) I. Bronstein in *Luminescence Immunoassay and Molecular Applications* (Eds.: K. van Dyke, R. van Dyke), CRC, Boca Raton, **1990**, 255; m) I. Bronstein, P. Dimond, *Res. Diagn. Clin. Testing* **1990**, *28*, 36; n) I. Bronstein, G. H. G. Thorpe, L. J. Kricka, B. Edwards, J. C. Voyta, *Clin. Chem. Winston-Salem NC* **1990**, *36*, 1087; o) S. Albrecht, H. Ehle, K. Schollberg, R. Bublitz, A. Horn in *Bioluminescence and Chemiluminescence: Current Status* (Eds.: P. E. Stanley, L. J. Kricka), John Wiley, Chichester, **1991**, p. 115; p) A. P. Schaap, L. J. Romano, J. S. Goudar, "1,2-Dioxetane compounds as chemiluminescent labels for organic and biological molecules", (Wayne State University, Detroit) EP-A 0473984, **1992**, US-A 579837, **1992**.

[48] a) C. H. Self, *J. Immunol. Methods* **1985**, *76*, 389; b) A. Johannsson, D. H. Ellis, D. L. Bates, A. M. Plumb, C. J. Stanley, *ibid.* **1986**, *87*, 7; c) D. B. Cook, C. H. Self, *Clin. Chem. Winston-Salem NC* **1993**, *39*, 965.

[49] T. K. Christopoulos, E. P. Diamandis, *Anal. Chem.* **1992**, *64*, 342.

[50] A. Baret, V. Fert, *J. Biolumin. Chemilumin.* **1989**, *4*, 149.

[51] a) H. Lingeman, W. J. M. Underberg, A. Takdate, A. Hulshoff, *J. Liq. Chromatogr.* **1985**, *8*, 789; b) K. Blau, G. S. King, *Handbook of Derivatives for Chromatography*, Heyden & Sons, London, **1978**.

[52] a) D. R. Parks, L. A. Herzenberg, *Methods Enzymol.* **1984**, *108*, 197; b) D. R. Parks, L. L. Lanier, L. A. Herzenberg in *Handbook of Experimental Immunology* (Eds.: D. M. Weir, L. A. Herzenberg, C. C. Blackwell), 4th edition, Scientific Publications, Edinburgh, **1986**; c) D. R. Parks, R. R. Hardy, L. A. Herzenberg, *Cytometry* **1984**, *5*, 159; d) *Flow Cytometry and Cell Sorting* (Ed.: A. Radbruch), Springer, Berlin, **1992**.

[53] a) J. A. Steinkamp, *Rev. Sci. Instrum.* **1984**, *55*, 1375; b) E. Gurr, *Encyclopaedia of Microscopic Stains*, Leonard Hall, London, **1960**; c) D. Kooy, H. Kuypers, *Science* **1979**, *204*, 873.

[54] a) L. M. Smith, J. Z. Sanders, R. J. Kaiser, P. Hughes, C. Dodd, C. R. Connell, C. Heiner, S. B. H. Kent, L. E. Hodd, *Nature* **1986**, *321*, 674; b) P. Heinrich, H. Domdey, *Nachr. Chem. Tech. Lab.* **1988**, *36*, 1196.

[55] N. Ishibashi, T. Ogawa, T. Imasaka, M. Kunitake, *Anal. Chem.* **1979**, *51*, 2096.

[56] F. Watanabe, K. Miyai in *Nonisotopic Immunoassay* (Ed.: T. T. Ngo), Plenum, New York, **1988**, p. 202.

[57] A. H. Coons, H. J. Creech, R. N. Jones, *Proc. R. Soc. Exp. Biol. (N. Y.)* **1941**, *47*, 200.

[58] A. H. Coons, H. J. Creech, R. N. Jones, E. Berliner, *J. Immunol. Methods* **1942**, *45*, 159.

[59] a) R. Herrmann, *Chimia* **1991**, *45*, 317; b) R. Herrmann, C. Klein, M. Junius-Comer, H.-P. Josel, H. G. Batz in *Chemistry of Functional Dyes* (Eds.: Z. Yoshida, T. Kitao), Mita, Tokyo, **1988**, p. 87; c) C. Klein, H.-G. Batz, R. Herrmann (Boehringer Mannheim GmbH), EP-A 209875; **1990**.

[60] M. N. Kronik in *Nonisotopic Immunoassay* (Ed.: T. T. Ngo), Plenum, New York, **1988**, p. 163.

[61] V. T. Oi, A. N. Glazer, L. Stryer, *Cell Biol.* **1982**,*93*, 981.

[62] M. N. Kronick, P. D. Grossman, *Clin. Chem. Winston-Salem NC* **1983**, *29*, 1582.

[63] F. Watanabe, K. Miyai in *Nonisotopic Immunoassay* (Ed.: T. T. Ngo), Plenum, New York, **1988**, p. 199.

[64] W. B. Dandliker, G. A. Feigen, *Biochem. Biophys. Res. Commun.* **1961**, *5*, 299.

[65] P. G. Mattingly, R. J. Brashear (Abbott Laboratories), EP-A 455058, **1991**.

[66] M. P. Bailey, B. F. Rocks, C. Riley in *Nonisotopic Immunoassay* (Ed.: T. T. Ngo), Plenum, New York, **1988**, pp. 187–197.

[67] A. M. Sidki, J. Landon in *Alternative Immunoassays* (Ed.: W. P. Collins), J. Wiley, Chichester, **1985**, pp. 185–201.

[68] I. Hemmilä, S. Dakubu, V.-M. Mukkala, H. Siitari, T. Lövgren, *Anal. Biochem.* **1984**, *137*, 335.

[69] A. P. B. Sinha, *Spectrosc. Inorg. Chem.* **1971**, *2*, 255.

[70] M. W. Sundberg, C. F. Meares, D. A. Goodwin, C. I. Diamanti, *J. Med. Chem.* **1974**, *17*, 1304.

[71] I. Wieder, R. H. Wollenberg (Radiation Corp.) DE-A 3033691, **1981**.

[72] E. Soini, I. Hemmilä (Wallac Oy) SE-A 7902079-8, **1979**; US-A 4374120, **1983**.

[73] Y.-Y. Xu, K. Petterson, K. Blomberg, I. Hemmilä, H. Mikola, T. Lövgren, *Clin. Chem. Winston-Salem NC* **1992**, *38*, 2038.

[74] E. Soini, T. Lövgren in *Nonisotopic Immunoassay* (Ed.: T. T. Ngo), Plenum, New York, **1988**, p. 231.

[75] I. Hemmilä, *Chem. Anal. NY* **1991**, *117*, 244.

[76] a) I. Hemmilä, S. Holttinen, K. Pettersson, T. Lövgren, *Clin. Chem. Winston-Salem NC* **1987**, *33*, 2281; b) H. Silitari, *J. Virol. Methods* **1990**, *28*, 179.

[77] M. Saarma, I. Järvekulg, I. Hemmilä, H. Siitari, R. Sinijärv, *J. Virol. Methods* **1989**, *23*, 47.

[78] a) L. J. Kricka, *Clin. Chem. Winston-Salem NC* **1992**, *38*, 327; b) S. E. Kakabakos, T. K. Christopoulos, E. P. Diamandis, *ibid.* **1992**, *38*, 338; c) R. Ekins, F. Chu, E. Biggart, *Ann. Biol. Clin. Paris* **1990**, *48*, 655.

[79] a) Y.-Y. Xu, I. Hemmilä, *Anal. Chim. Acta* **1992**, *256*, 9; b) Y.-Y. Xu, I. Hemmilä, T. Lövgren, *Analyst* **1992**, *117*, 1061; c) Y.-Y. Xu, I. Hemmilä, *Talanta* **1992**, *39*, 759; d) B. Alpha, J.-M. Lehn, G. Mathis, *Angew. Chem.* **1987**, *99*, 259; *Angew. Chem. Int. Ed. Engl.* **1987**, *26*, 266.

[80] a) P. L. Khanna in *Nonisotopic Immunoassay* (Ed.: T. T. Ngo), Plenum, New York, **1988**, p. 211; b) E. F. Ullman, M. Schwarzberg, K. E. Rubenstein, *J. Biol. Chem.* **1976**, *251*, 4172; US-A 3996345, **1976**; 4199559, **1980**; DE-A 2535574, (Syra Corp) **1976**; GB-A 1560852, **1980**.

[81] T. Förster, *Ann. Phys. Leipzig* **1948**, *2*, 55.

[82] a) L. Stryer, *Annu. Rev. Biochem.* **1978**, *47*, 819; b) Y. Kanaoka, *Angew. Chem.* **1977**, *89*, 142; *Angew. Chem. Int. Ed. Engl.* **1977**, *16*, 137.

[83] a) E. F. Ullman, P. L. Khanna, *Methods Enzymol.* **1981**, *7*, 28; b) R. Rodgers, M. Schwarzenberg, P. L. Khanna, C. H. Chang, E. Ullman, *Clin. Chem. Winston-Salem NC* **1978**, *24*, 1033.

[84] P. L. Khanna, E. F. Ullman, *Anal. Biochem.* **1980**, *108*, 161.

[85] R. D. Schmid, U. Bilitewski, *Chem. Unserer Zeit* **1992**, *26*, 163.

[86] H.-U. Siegmund, A. Becker, H. Ohst, K. Sommer, *Thin Solid Films* **1992**, *207*, 480.

[87] S. Beck, H. Köster, *Anal. Chem.* **1990**, *62*, 2258.

[88] a) W. C. Rhodes, W. D. McElroy, *J. Biol. Chem.* **1978**, *233*, 1528; H. H. Seliger, W. D. McElroy, E. H. White, G. F. Field, *Proc. Natl. Acad. Sci. USA* **1961**, *47*, 1129; b) T. A. Hopkins, H. H. Seliger, E. H. White, M. W. Cass, *J. Am. Chem. Soc.* **1967**, *89*, 7148; c) J. Wannlund, M. DeLuca, K. Stempel, P. D. Boyer, *Biochem. Biophys. Res. Commun.* **1978**, *81*, 987.

[89] A. Hartmann, *Biotec* **1991**, 40.

[90] F. McCapra, *Endeavour* **1973**, *32*, 139.

[91] *Nonisotopic Immunoassay* (Ed.: T. T. Ngo), Plenum, New York, **1988**, p. 277.

[92] a) F. McCapra, Y. C. Chang, V. P. Francois, *J. Chem. Soc. Chem. Commun.* **1968**, 22; b) W. Adam, *J. Chem. Educ.* **1975**, *52*, 138; c) G. B. Schuster, K. A. Horn in *Chemical and Biological Generation of Excited States* (Eds.: W. Adam, G. Cilento), Academic Press, New York, **1982**, Kap. 7; d) J. y-Koo, S. P. Schmidt, G. B. Schuster, *Proc. Natl. Acad. Sci. USA* **1978**, *75*, 30; e) W. Adam, M. H. Schulz, *Chem. Ber.* **1992**, *125*, 2455; f) W. Adam, R. Fell, M. H. Schulz, *Tetrahedron* **1993**, *49*, 2227.

[93] a) K.-D. Gundermann, F. McCapra, *Chemiluminescence in Organic Chemistry*, Springer, Berlin, **1987**, p. 60; b) F. McCapra, *J. Photochem. Photobiol. A* **1990**, *51*, 21; c) *Organic Peroxides* (Ed.: W. Ando), Wiley, Chichester, **1992**; d) W. Adam, M. Heil, T. Mosandl, C. R. Saha-Möller in [93c], p. 521; e) K. Fujimori in [93c], p. 319.

[94] R. L. Airth, W. C. Rhodes, W. D. Mc Elroy, *Biochim. Biophys. Acta* **1958**, *27*, 519.

[95] K. V. Wood in *Bioluminescence & Chemiluminescence, Current Status* (Eds.: P. E. Stanley, L. J. Kricka), Wiley, Chichester, **1991**, pp. 11, 543.

[96] a) J. R. de Wet, K. V. Wood, D. R. Helinski, M. Deluca, *Proc. Natl. Acad. Sci. USA* **1985**, *82*, 7870; b) D. W. Ow, K. V. Wood, M. De Luca, J. R. de Wet, D. R. Helinski, S. H. Howell, *Science* **1986**, *234*, 856–859.

[97] E. A. Meighen in *Bioluminescence & Chemiluminescence, Current Status* (Eds.: P. E. Stanley, L. J. Kricka), Wiley, Chichester, **1991**, p. 3.

[98] a) E. H. White, F. McCapra, G. F. Field, *J. Am. Chem. Soc.* **1961**, *83*, 2402; *ibid.* **1963**, *85*, 337. b) S. Seto, K. Ogura, Y. Nishiyama, *Bull. Chem. Soc. Jpn.* **1963**, *36*, 331; c) E. H. White, H. Wörther, G. F. Field, W. D. McElroy, *J. Org. Chem.* **1965**, *30*, 2344; d) L. J. Bowie, *Methods Enzymol.* **1978**, *57*, 15.

[99] Y. Toya, M. Takagi, H. Nakata, N. Suzuki, *Bull. Chem. Soc. Jpn.* **1992**, *65*, 392.

[100] a) E. Schram in *Bioluminescence & Chemiluminescence, Current Status* (Eds.: P. E. Stanley, L. J. Kricka), Wiley, Chichester, **1991**, p. 407; b) P. E. Stanley, *J. Biolumin. Chemilumin.* **1989**, *4*, 375; c) *ATP Luminescence, rapid methods in microbiology* (Eds.: P. E. Stanley, B. J. McCarthy, R. Smither), Blackwell, Oxford, **1989**.

[101] a) *Bioluminescence & Chemiluminescence, Current Status* (Eds.: P. E. Stanley, L. J. Kricka), Wiley, Chichester, **1991**; b) L. Yu. Brovko, N. N. Ugarova, A. F. Dukhovich in [101a], p. 434; c) W. Gehle, R. Presswood, D. A. Stafford in [101a], p. 437.

[102] D. W. Ow, K. V. Wood, M. Deluca, J. R. DeWet, D. R. Helinski, S. H. Howell, *Science* **1986**, *234*, 856.

[103] a) W. Miska, R. Geiger, *J. Clin. Chem. Clin. Biochem.* **1987**, *25*, 23, 30; b) *J. Biolumin. Chemilumin.* **1989**, *4*, 119.

[104] N. N. Ugarova, Ya. V. Vozny, G. D. Kutuzova, E. I. Dementieva in *Bioluminescence & Chemiluminesence, Current Status* (Eds.: P. E. Stanley, L. J. Kricka), Wiley, Chichester, **1991**, p. 511.

[105] a) A. K. Campbell, *Chemiluminescence: Principles and Applications in Biology and Medicine*, 1st edition, VCH, Weinheim, Horwood, Chichester, **1988**; b) Ch. 3 in [105a], pp. 127–239; c) Ch. 3 in [105a], p. 202; d) Ch. 3 in [105a], pp. 291–302.

[106] E. Wieland, A. David, H. Kather, V. W. Armstrong in *Bioluminescence & Chemiluminescence, Current Status* (Eds.: P. E. Stanley, L. J. Kricka), Wiley, Chichester, **1991**, p. 455.

[107] P. Balaguer, B. Térouanne, A. M. Boussioux, J. C. Nicolas in *Bioluminescence & Chemiluminescence, Current Status* (Eds.: P. E. Stanley, L. J. Kricka), Wiley, Chichester, **1991**, p. 143.

[108] a) W. Adam, *Chem. Unserer Zeit* **1973**, *7*, 182; b) F. McCapra in *Progress in Organic Chemistry, Bd. 8* (Eds.: E. Carruthers, J. K. Sutherland), Butterworth, London, **1973**, p. 231; c) F. McCapra, *Acc. Chem. Res.* **1976**, *9*, 201; d) F. McCapra, *Proc. R. Soc. London* **1982**, *215*, 247.

[109] O. Shimomura, F. H. Johnson, Y. Saiga, *J. Cell. Comp. Physiol.* **1962**, *59*, 223.

[110] a) O. Shimomura, T. Masugi, F. H. Johnson, Y. Haneda, *Biochem. J.* **1978**, *17*, 994; b) O. Shimomura, F. H. Johnson, *Nature (London)* **1979**, *256*, 236; c) *Proc. Natl. Acad. Sci. USA* **1978**, *75*, 2611.

[111] a) S. Inouye, S. Aoyama, T. Miyata, F. I. Tsuji, Y. Sakaki, *Biochem. J.* **1989**, *105*, 473; b) D. Prasher, R. O. McCann, M. J. Cormier, *Biochem. Biophys. Res. Commun.* **1985**, *126*, 1259.

[112] a) Y. Kishi, H. Tanino, T. Goto, *Tetrahedron Lett.* **1972**, 2747; b) S. Inoue, S. Sugiura, H. Kakoi, K. Hazizume, T. Goto, H. Iio, *Chem. Lett.* **1975**, 141; c) C. F. Qi, Y. Gomi, T. Hirano, M. Ohashi, Y. Ohmiya, F. Tsuji, *J. Chem. Soc. Perkin Trans. 1* **1992**, 1608.

[113] a) *Bioluminescence & Chemiluminescence, Current Status* (Eds.: P. E. Stanley, L. J. Kricka), Wiley, Chichester, **1991**; b) D. F. Smith, N. L. Stults, H. Rivera, W. D. Gehle, R. D. Cummings, M. J. Cormier in [113a], p. 530; c) N. L. Stults, N. A. Stocks, R. D. Cummings, M. J. Cormier, D. F. Smith in [113a], p. 533; d) P. F. Zatta, D. F. Smith, M. J. Cormier, R. D. Cummings in [113a], p. 537.

[114] H. O. Albrecht, *J. Phys. Chem.* **1928**, *136*, 321.

[115] a) F. McCapra in *Progress in Organic Chemistry, Bd. 8* (Eds.: E. Carruthers, J. K. Sutherland), Butterworth, London, **1973**, p. 248; b) U. Hantke, *Aerztl. Lab.* **1986**, *32*, 1.

[116] T. E. Yeshion in *Bioluminescence & Chemiluminescence, Current Status* (Eds.: P. E. Stanley, L. J. Kricka), Wiley, Chichester, **1991**, p. 379.

[117] a) R. B. Brundrett, D. F. Roswell, E. H. White, *J. Am. Chem. Soc.* **1972**, *94*, 7536; b) H. R. Schroeder, R. C. Boguslaski, R. J. Carrico, R. T. Buckler, *Methods Enzymol.* **1978**, *57*, 424; c) I. Weeks in *Comprehensive Analytical Chemistry, Chemiluminescence Immunoassay* (Ed.: G. Svehla), Elsevier, New York, **1992**, p. 29.

[118] J. S. A. Simpson, A. K. Campbell, M. E. T. Ryall, J. S. Woodhead, *Nature (London)* **1979**, *279*, 646.

[119] a) I. Weeks in *Comprehensive Analytical Chemistry, Chemiluminescence Immunoassay* (Ed.: G. Svehla), Elsevier, New York, **1992**, Ch. 5, p. 153; b) R. C. Boguslaski, H. R. Schroeder in *Bioluminescence and Chemiluminescence – Basic Chemistry and Analytical Applications* (Eds.: M. De Luca, W. D. McElroy), Academic Press, New York, **1981**, p. 283; c) W. G. Wood, *J. Biolumin. Chemilumin.* **1989**, *4*, 79; d) F. McCapra, I. Beheshti in *Bioluminescence and Chemiluminescence: Instruments and Applications, Vol. 1* (Ed.: K. Van Dyke), CRC, Boca Raton, FL, **1985**, p. 23.

[120] K. Gleu, W. Petsch, *Angew. Chem.* **1935**, *58*, 57.

[121] M. M. Rauhut, D. Sheehan, R. A. Clarke, A. M. Semsel, *J. Org. Chem.* **1965**, *30*, 3587.

[122] F. McCapra, D. G. Richardson, *Tetrahedron Lett.* **1964**, 3167.

[123] F. McCapra, I. Beheshti in *Bioluminescence and Chemiluminescence: Instruments and Applications, Vol. 1* (Ed.: K. Van Dyke), CRC, Boca Raton, FL, **1985**, p. 15.

[124] A. Hantzsch, M. Kalb, *Ber. Dtsch. Chem. Ges.* **1899**, *32*, 3109.

[125] I. Weeks, M. Sturgess, R. C. Brown, J. S. Woodhead, *Methods Enzymol.* **1986**, *133*, 366.

[126] J. S. Littig, T. A. Nieman, *J. Biolumin. Chemilumin.* **1993**, *8*, 25.

[127] M. L. Grayeski, T. J. Novak, A. G. Mohan in *Bioluminescence & Chemiluminescence, Current Status* (Eds.: P. E. Stanley, L. J. Kricka), Wiley, Chichester, **1991**, p. 131.

[128] J. S. Simpson, A. K. Campbell, J. S. Woodhead, A. Richardson, R. Hart, F. McCapra in *Bioluminescence and Chemiluminescence* (Eds.: M. DeLuca, W. D. McElroy), Academic Press, New York, **1981**, p. 673.

[129] a) I. Weeks, I. Beheshti, F. McCapra, A. K. Campbell, J. S. Woodhead, *Clin. Chem. Winston-Salem N. C.* **1983**, *29*, 1474; b) A. K. Campbell, J. S. Woodhead, I. Weeks, (The Welsh National School of Medicine), EP-A 0082636, **1983**.

[130] I. Weeks in *Comprehensive Analytical Chemistry, Chemiluminescence Immunoassay* (Ed.: G. Svehla), Elsevier, New York, **1992**, p. 121.

[131] K. Lehmstedt, E. Wirth, *Ber. Dtsch. Chem. Ges.* **1928**, *61*, 2044.

[132] a) R. Stolle, *J. Prakt. Chem.* **1922**, *105*, 137; b) M. S. Newman, W. H. Powell, *J. Org. Chem.* **1961**, *26*, 812.

[133] J. E. Dombrowski, P. G. Mattingly (Abbott Laboratories), EP-A 0369344, **1990**.

[134] a) S.-J. Law, T. Miller, U. Piran, C. Klukas, S. Chang, J. Unger, *J. Biolumin. Chemilumin.* **1989**, *4*, 88; b) S. J. Law, S. A. Palmacci, S. C. S. Chang, R. S. Cubicciotti (Ciba Corning Diagnostics), EP-B 0263657, **1988**; US-A 4745181, **1981**; c) S. C.-S. Chang, C. K. Klukas, S.-J. Law, C. A. Vitkauskas (Ciba Corning Diagnostics), EP-B 0361817, **1990**.

[135] R. C. Hart, L. R. Taaffe, *J. Immunol. Methods* **1987**, *101*, 91.

[136] F. McCapra, I. Beheshti, R. C. Hart, H. Koelling, A. Patel, K. Ramakrishnan (London Diagnostics), WO-A 89/06231, **1989**; EP-A 0322926, **1989**.

[137] H. T. W. Lin (Mallinckrodt), EP-A 0170415, **1986**.

[138] a) T. Kinkel, H. Lübbers, E. Schmidt, P. Molz, H. J. Skrzipczyk, *J. Biolumin. Chemilumin.* **1989**, *4*, 136; b) P. Molz, H. J. Skrzipzyk, H. Lübbers, H. Strecker, G. Schnorr, T. Kinkel (Hoechst AG), DE-A 3628573, **1986**; EP-B 0257541, **1987**.

[139] T. Kinkel, P. Molz, E. Schmidt, G. Schnorr, H. J. Skrzipczyk (Hoechst AG), DE-A 3805318, **1988**; EP-B 0330050, **1989**.

[140] P. G. Mattingly, L. G. Bennett (Abbott Laboratories), US-A 921979, **1986**; EP-B 0273115, **1987**.

[141] G. Zomer, J. F. C. Stavenuiter (Staat der Niederlande), NL-A 8703075, **1987**; EP-B 0324202, **1988**.

[142] A. Mayer, E. Schmidt, T. Kinkel, P. Molz, S. Neuenhofer, H. J. Skrzipczyk in *Bioluminescence & Chemiluminescence, Current Status* (Eds.: P. E. Stanley, L. J. Kricka) Wiley, Chichester, **1991**, p. 99.

[143] P. G. Mattingly, *J. Biolumin. Chemilumin.* **1991**, *6*, 107.

[144] a) I. Weeks, J. Woodhead in *Bioluminescence & Chemiluminescence, Current Status* (Eds.: P. E. Stanley, L. J. Kricka), Wiley, Chichester, **1991**, p. 553; b) J. Woodhead, I. Weeks, *Clin. Chem. Winston-Salem NC* **1991**, *37*, 472; c) W. Klingler, G. Wiegand, R. Knuppen, *J. Steroid Biochem.* **1987**, *27*, 41.

[145] W. L. Hinze, T. E. Riehl, H. N. Singh, Y. Baba, *Anal. Chem.* **1984**, *56*, 2180.

[146] J. H. Wieringa, J. Strating, H. Wynberg, W. Adam, *Tetrahedron Lett.* **1972**, 169.

[147] W. H. Richardson, G. C. Montgomery, M. B. Yelvington, H. E. O'Neal, *J. Am. Chem. Soc.* **1974**, *96*, 7525.

[148] J.-Y. Koo, G. B. Schuster, *J. Am. Chem. Soc.* **1977**, *99*, 6107.

[149] G. B. Schuster, B. Dixon, J.-Y. Koo, S. P. Schmidt, J. P. Smith, *Photochem. Photobiol.* **1979**, *30*, 17.

[150] R. S. Handley, A. J. Stern, A. P. Schaap, *Tetrahedron Lett.* **1985**, *26*, 3183.

[151] A. P. Schaap, S. D. Gagnon, K. A. Zaklika, *Tetrahedron Lett.* **1982**, *23*, 2943.

[152] C. Lee, L. A. Singer, *J. Am. Chem. Soc.* **1980**, *102*, 3823.

[153] F. McCapra, I. Beheshti, A. Burford, R. A. Hann, K. A. Zaklika, *J. Chem. Soc. Chem. Commun.* **1977**, 944.

[154] F. McCapra, *J. Chem. Soc. Chem. Commun.* **1968**, 155.

[155] N. J. Turro, P. Lechtken, G. Schuster, J. Orell, H.-C. Steinmetz, W. Adam, *J. Am. Chem. Soc.* **1974**, *96*, 1627.

[156] J. C. Hummelen, T. M. Luider, H. Wynberg, *Methods Enzymol.* **1986**, *133*, 531.

[157] a) E. W. Meijer, H. Wynberg, *J. Chem. Educ.* **1982**, *59*, 1071; b) P. D. Bartlett, M. S. Ho, *J. Am. Chem. Soc.* **1974**, *96*, 627.

[158] G. B. Schuster, N. J. Turro, H.-C. Steinmetzer, A. P. Schaap, G. Faler, W. Adam, J. C. Liu, *J. Am. Chem. Soc.* **1975**, *97*, 7110.

[159] A. C. Brouwer, J. C. Hummelen, T. M. Luider, F. van Bolhuis, H. Wynberg, *Tetrahedron Lett.* **1988**, *29*, 3137.

[160] A. P. Schaap, J. S. Goudar, L. J. Romano, *4. Internationales Symposium für quantitative Lumineszenz-Spektrometrie in den biomedizinischen Wissenschaften*, Gent, Belgium, **1991**, Abstracts Volume p. 49.

[161] E. A. Chandross, *Tetrahedron Lett.* **1963**, 761.

[162] M. M. Rauhut, B. G. Roberts, A. M. Semsel, R. A. Clarke, *J. Am. Chem. Soc.* **1966**, *88*, 3604.

[163] L. J. Bollyky, R. H. Whitman, B. G. Roberts, M. M. Rauhut, *J. Am. Chem. Soc.* **1967**, *89*, 6523.

[164] M. M. Rauhut, L. J. Bollyky, B. G. Roberts, M. Loy, R. H. Whitman, A. V. Iannotta, A. M. Semsel, R. A. Clarke, *J. Am. Chem. Soc.* **1967**, *89*, 6515.

[165] S.-S. Tseng, A. G. Mohan, L. G. Haines, L. S. Vizcarra, M. M. Rauhut, *J. Org. Chem.* **1979**, *44*, 4113.

[166] R. E. Milovsky, J. W. Birks, *J. Am. Chem. Soc.* **1991**, *113*, 9715.

[167] F. J. Alvarez, N. J. Parekh, B. Matuszewski, R. S. Givens, T. Higuchi, R. L. Schowen, *J. Am. Chem. Soc.* **1986**, *108*, 6435.

[168] M. F. D. Steinfatt, *Bull. Soc. Chim. Belg.* **1985**, *94*, 85.

[169] M. M. Rauhut, *Acc. Chem. Res.* **1969**, *2*, 80.

[170] L. Y. Bollyky, M. M. Rauhut (American Cyanamid), US-A 3597367, **1971**.

[171] K. W. Singvardson, J. W. Birks, *Anal. Chem.* **1983**, *55*, 432.

[172] S. Albrecht, R. Becker, W.-D. Böhm, *J. Clin. Chem. Clin. Biochem.* **1989**, *27*, 451.

[173] S. Albrecht, W.-D. Böhm, R. Beckert, H. Kroschwitz, V. Neumeister, W. Jaross in *Bioluminescence & Chemiluminescence, Current Status* (Eds.: P. E. Stanley, L. J. Kricka), Wiley, Chichester, **1991**, p. 463.

[174] H. Brandl, S. Albrecht, R. Köstler in *Bioluminescence & Chemiluminescence, Current Status* (Eds.: P. E. Stanley, L. J. Kricka), Wiley, Chichester, **1991**, p. 459.

[175] a) K.-D. Gundermann, *Top. Curr. Chem.* **1974**, *46*, 116; b) L. R. Faulkner, A. J. Bard in *Electroanalytical Chemistry, Vol. 10* (Ed.: A. J. Bard), Marcel Dekker, New York, **1976**, p. 1, c) B. M. Krasovitskii, B. M. Bolotin, *Organic Luminescent Materials*, VCH, Weinheim, **1988**, p. 229, d) H. Tachikawa, L. R. Falkner in *Photoelectrochemistry and Electrochemiluminescence* (Eds.: P. T. Kissinger, W. R. Heineman), Marcel Dekker, New York, **1984**, p. 637.

[176] S. Sakura, *Anal. Chim. Acta* **1992**, *262*, 49.

[177] J. S. Littig, T. A. Nieman, *Anal. Chem.* **1992**, *64*, 1140.

[178] a) F. E. Lyttle, D. M. Hercules, *Photochem. Photobiol.* **1971**, *13*, 123; b) N. E. Tokel, A. J. Bard, *J. Am. Chem. Soc.* **1972**, *94*, 2862.

[179] a) G. F. Blackburn, H. P. Shah, J. H. Kenten, J. Leland, R. A. Kamin, J. Link, J. Peterman, M. J. Powell, A. Shah, D. B. Talley, S. K. Tyagi, E. Wilkins, T.-G. Wu, R. J. Massey, *Clin. Chem. Winston-Salem NC* **1991**, *37*, 1534; b) J. K. Leland, H. P. Shah, J. Kenten (IGEN), US-A 652427, **1991**.

[180] J. H. Kenten, J. Casadei, J. Link, S. Lupold, J. Willey, M. Powell, A. Rees, R. Massey, *Clin. Chem. Winston-Salem NC* **1991**, *37*, 1626.

[181] O. Nozaki, L. J. Kricka, P. E. Stanley, *J. Biolumin. Chemilumin.* **1992**, *7*, 263.

[182] G. Köhler, C. Milstein, *Nature (London)* **1975**, *256*, 495; C. Milstein, *Angew. Chem.* **1985**, *97*, 819; *Angew. Chem. Int. Ed. Engl.* **1985**, *24*, 816; G. Köhler, *ibid.* **1985**, *97*, 829 and **1985**, *24*, 827.

[183] F. R. Seiler, P. Gronski, R. Kurrle, G. Lüben, H.-P. Harthus, W. Ax, K. Bosslet, H.-G. Schwick, *Angew. Chem.* **1985**, *97*, 141; *Angew. Chem. Int. Ed. Engl.* **1985**, *24*, 139.

[184] J. Kang, P. Kaladas, C. Chang, S. Chen, R. Dondero, A. Frank, S. Huhn, P. Lisi, D. Mochnal, J. Nasser, W. Potter, E. Schutt, K. Utberg, H. Graham, *Clin. Chem. Winston-Salem NC* **1986**, *32*, 1682.

[185] a) C. Olive, *J. Clin. Immunoassay* **1991**, *14*, 126; b) F. R. Velazquez, *ibid.* **1992**, *15*, 235.

[186] a) K. E. Rubenstein, E. F. Ullman, (Syra Corp.), US-A 3817837, **1974**; b) F. McCapra, *Chem. Br.* **1989**, 139.

[187] a) D. H. Gilden, A. Vafai, Y. Shtram, Y. Becker, M. Devlin, M. Wellish, *Nature* **1983**, *306*, 478; b) S. L. Moseley, J. W. Hardy, M. I. Huq, P. Echeverria, S. Falkow, *Infect. Immun.* **1983**, *39*, 1167; c) L. Franzen, R. Shabo, L. Aslund, H. Pearlman, T. Persson, H. Wigzell, U. Pettersson, *Lancet* **1984**, 525; d) R. Haas, T. F. Meyer, *Cell* **1986**, *44*, 107; e) *DNA Probes applications in genetic and infectious disease and cancer* (Ed.: L. S. Lerman), Cold Spring Harbor Laboratory, **1986**; f) L. S. Lerman in [187e], p. 1; g) F. C. Tenover in [187e], p. 149; h) J. A. Matthews, L. J. Kricka, *Anal. Biochem.* **1988**, *169*, 1.

[188] a) S. G. Fischer, L. S. Lerman, *Proc. Natl. Acad. Sci. USA* **1983**, *80*, 1579; b) F. S. Collins, S. M. Weissman, *Prog. Nucleic Acid Res. Mol. Biol.* **1984**, *31*, 317; c) V. J. Kidd, M. S. Golbus, R. B. Wallace, K. Itakura, S. L. C. Woo, *N. Engl. J. Med.* **1984**, *310*, 639; d) S. H. Orkin, H. H. Kazazian, Jr., *Annu. Rev. Genet.* **1984**, *18*, 131; e) J. A. Landgale, A. D. B. Malcolm, *Gene* **1985**, *36*, 201; f) S. L. Thein, J. S. Wainscoat, J. M. Old, *Lancet* **1985**, 345; g) A. G. DiLella, J. Marvit, A. S. Lidsky, F. Guettler, S. L. C. Woo, *Nature* **1986**, *322*, 799; h) V. A. McKusick, *Mendelian Inheritance in Man*, 7th edition, Johns Hop-

kins University Press, Baltimore, **1986**; i) D. F. Novack, N. J. Casna, S. G. Fischer, J. P. Ford, *Proc. Natl. Acad. Sci. USA* **1986**, *83*, 586; j) V. A. McKusick, *Molecular Defects in Mendelian Disorders, Newsletter*, 25.3.**1988**.

[189] a) M. Durst, L. Gissmann, H. Ikenberg, H. zur Hausen, *Proc. Natl. Acad. Sci. USA* **1983**, *80*, 3812; b) B. Leder, J. Battey, G. Lenoir, C. Moulding, W. Murphy, H. Potter, T. Stewart, R. Taub, *Science* **1983**, *222*, 765; c) G. M. Brodeur, R. C. Seeger, M. Schwab, H. E. Varmus, J. M. Bishop, *Science* **1984**, *224*, 1121; d) J. Groffen, J. R. Stephenson, N. Heisterkamp, A. de Klein, C. R. Bartram, G. Grosveld, *Cell* **1984**, *36*, 93; e) S. H. Friend, R. Bernard, S. Rogelj, R. A. Weinberg, J. M. Rapaport, D. M. Albert, T. P. Dryja, *Nature* **1986**, *323*, 643; f) J. M. Bishop, *Science* **1987**, *235*, 305; g) J. L. Bos, E. R. Fearon, S. R. Hamilton, M. Verlaan-de Vries, J. H. van Boom, A. J. van der Erb, B. Vogelstein, *Nature* **1987**, *327*, 293; h) R. Reid, M. Greenberg, A. B. Jenson, M. Husain, J. Willet, A. Daoud, G. F. Temple, C. R. Stanhope, A. Sherman, G. Phibbs, A. T. Lorincz, *Am. J. Obstet. Gynecol.* **1987**, *150*, 212.

[190] a) P. Gill, A. J. Jeffreys, D. J. Werett, *Nature* **1985**, *318*, 577; b) A. J. Jeffreys, J. F. Y. Brookfield, R. Semeonoff, *ibid.* **1985**, *317*, 818.

[191] E. M. Southern, *J. Mol. Biol.* **1975**, *98*, 503.

[192] M. Ranki, A. Palva, M. Virtanen, M. Laaksonen, H. Söderlund, *Gene* **1983**, *21*, 77.

[193] a) M. S. Ellwood, M. Collins, E. F. Fritsch, J. I. Williams, S. E. Diamond, J. G. Brewen, *Clin. Chem. Winston-Salem NC* **1986**, *32*, 1631; b) C. P. H. Vary, *Nucleic Acids Res.* **1987**, *15*, 6883.

[194] L. J. Arnold, Jr., P. W. Hammond, W. A. Wiese, N. C. Nelson, *Clin. Chem. Winston-Salem NC* **1989**, *35*, 1588.

[195] a) R. K. Saiki, S. Scharf, F. Faloona, K. B. Mullis, G. T. Horn, H. A. Erlich, *Science* **1985**, *230*, 1350; b) S. C. Kogan, A. B. M. Doherty, J. Gitschier, *N. Engl. J. Med.* **1987**, *317*, 985; c) M. Crescenzi, M. Seto, G. P. Herzig, P. D. Weiss, R. C. Griffith, S. J. Korsmeyer, *Proc. Natl. Acad. Sci. USA* **1988**, *85*, 4869; d) A. J. Jeffreys, V. Wilson, R. Neumann, J. Keyte, *Nucleic Acids Res.* **1988**, *16*, 10953; e) E. S. Kawasaki, S. S. Clark, M. Y. Coyne, S. D. Smith, R. Champlin, O. N. Witte, F. P. McCormick, *Proc. Natl. Acad. Sci. USA* **1988**, *85*, 5698; f) H. Li, U. B. Gyllenstein, X. Cui, R. K. Saiki, H. A. Erlich, N. Arnheim, *Nature* **1988**, *335*, 414; g) C.-H. Ou, S. Kwok, S. W. Mitchell, D. H. Mack, J. J. Sninsky, J. W. Krebs, P. Feorino, D. Warfield, G. Schochetman, *Science* **1988**, *239*, 295; h) R. K. Saiki, G. H. Gelfand, S. Stoffel, S. J. Scharf, R. Higuchi, G. T. Horn, K. B. Mullis, H. A. Erlich, *Science* **1988**, *239*, 487; K. B. Mullis, *Angew. Chem.* **1994**, *106*; *Angew. Chem. Int. Ed. Engl.* **1994**, *33*, in press.

EVENTS

International Symposium

RECOGNITION PROCESSES

The University of Birmingham, UK

24-29 July 1994

THE ROYAL SOCIETY OF CHEMISTRY
PERKIN DIVISION

INVITED SPEAKERS

Y Aoyama	A D Hamilton	R J Roberts
E C Constable	W L Jorgensen	J K M Sanders
F Cramer	G von Kiedrowski	J L Sessler
M J Crossley	J-M Lehn	P Sinaÿ
P B Dervan	R A Lerner	J Stubbe
F N Diederich	D M J Lilley	D M Walba
B Fraser-Reid	G R Newkome	K Wüthrich
J M J Fréchet	V Percec	S C Zimmermann
S E Halford		

Second Circular and Application Form available from

Dr John F Gibson
Secretary (Scientific)
The Royal Society of Chemistry
Burlington House
Piccadilly
London W1V 0BN

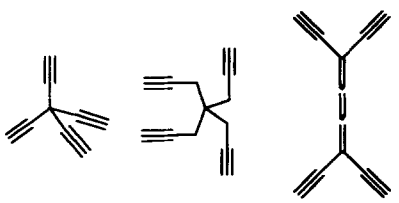
Tel: 44 (0) 71 437 8656
Fax: 44 (0) 71 734 1227

CLOSING DATE FOR APPLICATION:
MONDAY 13 JUNE 1994

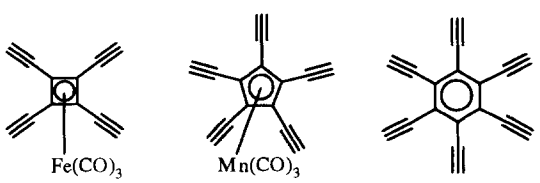
Polyynes—Fascinating Monomers for the Construction of Carbon Networks?**

Uwe H. F. Bunz*

The synthesis of novel carbon modifications and their precursors is currently an area of intensive activity.[1, 2] The discovery of the fullerenes[3] by Krätschmer, Smalley, and Kroto and the all-carbon rings (cyclo[*n*]carbons) by Diederich et al.[4] have fueled interest in this field. Related work has resulted in the synthesis of carbon-rich compounds such as polyethynylenarylene dendrimers by Moore et al.,[5] pericyclynes by Scott et al.,[6] and compounds with a perethynylated π perimeter by Vollhardt et al.[7] (**6**) and by our own research group[8] (**4**, **5**). Molecules **1**–**6** are a selection of monomers reported in the past few years that could be used potentially in the construction of carbon networks.[9]



1 **2** **3**



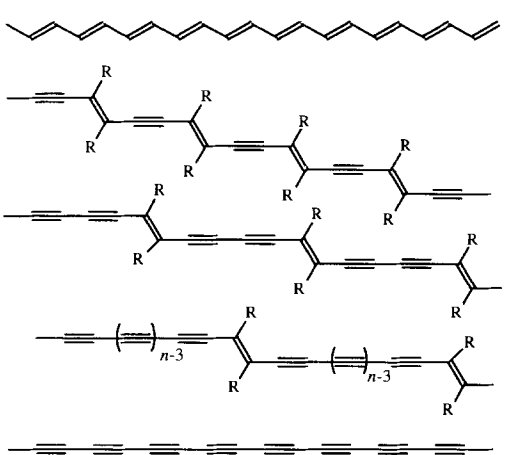
4 **5** **6**

A common feature in the efforts directed towards the preparation of carbon-rich systems is the use of the C–C triple bond as a functional group and linking unit. The alkyne group is the only easily preparable all-carbon building block; terminal alkyne functions can be linked to sp^2-C-Hal molecules readily and in high yields,[10] and are amenable to copper-catalyzed, oxidative Hay or Eglington[11] coupling reactions. Thus, the acetylene function is indispensable not only in the construction of carbon-rich structures but also in the synthesis of larger rings and three-dimensional cages. The relative rigidity and linearity of the C≡C fragment is a further advantage in the synthesis of rigid and uniformly shaped structures.

Strategy for the Construction of Carbon Networks: The stepwise construction of networks, in other words the transformation of appropriate monomers into successively larger oligomers, is the most promising approach. In this way the solubility and stability of the larger systems can be estimated from the properties of smaller molecules. If necessary the monomers can be modified to improve the desired properties of the anticipated network (structural uniformity, solubility, stability).

Linear Systems

The simplest carbon modification conceivable is the polyyne carbon rod **11** with alternating single and triple bonds; this material is referred to in the literature as carbyne or chaoite.[1] Segments of this allotrope with up to 16 conjugated triple bonds were synthesized by Eastmond, Walton, et al. a number of years ago.[12] The stability of these polyynes relies on the bulky triethylsilyl end groups, which effectively prevent the polymerization of the carbon rods. In a recent study Grösser and Hirsch[13] examined the reaction of carbon vapor in the presence of cyanogen under the standard conditions for fullerene synthesis. The authors had intended to generate heteroatom-substituted fullerenes but instead obtained the previously unknown dicyanopolyynes NC–$(C{\equiv}C)_n$–CN ($n = 3$–7).



7 polyacetylene

8 polydiacetylene

9 polytriacetylene

10 poly-*n*-acetylene

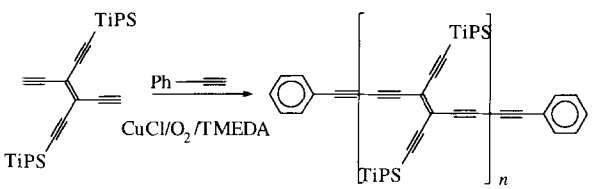
11 carbyne

[*] Dr. U. H. F. Bunz
Max-Planck-Institut für Polymerforschung
D-55021 Mainz (FRG)
Telefax: Int. code: (6131) 379-100

 © VCH Verlagsgesellschaft mbH, D-69451 Weinheim, 1994 0570-0833/94/1010-1073 $ 10.00+.25/0

The insertion of alkene units between the alkyne functions in carbyne **11** can be envisioned to lead to polydiacetylenes **8**,[14a] polytriacetylenes **9**, and poly-*n*-acetylenes **10** in general. Although **11** is likely to polymerize in condensed phase owing to the lack of steric hindrance, it should be possible to synthesize stable hybrid forms intermediate between **7** and **11**. Bulky substituents on the alkene units should be particularly effective in ensuring the stability and solubility of **9** and **10**.

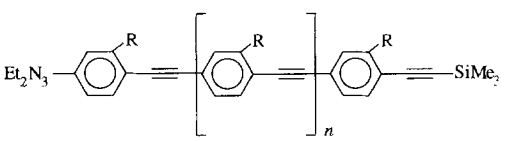
Whereas structures of type **8** were prepared in 1969 by Wegner[14b] by topochemical reaction of appropriate diynes, nothing has been reported on the synthesis of polytriacetylene **9**; the topotactical polymerization of triynes to give **9** has not been successful.[14c] The higher homologue **10** has not been investigated. However, sections of a polytriacetylene structure were recently synthesized by Diederich et al.:[15] Hay coupling of tetrayne **12** (TiPS = triisopropylsilyl) and phenylacetylene produced oligomers **13** ($n = 1-6$). The particular advantage of this



12 **13**

approach is the good solubility and stability of **13** provided by the triisopropylsilyl groups, and the fact that after cleavage of the silyl protecting groups further cross-linking is possible, at least in principle. Calculations conducted by Baughman and Galvao[16] indicate that a three-dimensional carbon network constructed by the cross-linking of **8** should have unusual mechanical properties (auxetes).

Further motivation for the synthesis of oligomers **13** (nanostructures) lies in their potential use as molecular wires in molecular electronics and microlithography: Tour et al.[17] synthesized oligomeric *p*-phenylenethynylenes, which were intended for such applications, by following a strategy developed by Moore et al.[18] Due to solubilizing substituents, chains **14** (R = ethyl, ethylheptyl) with up to 16 phenylethynyl units could be construct-

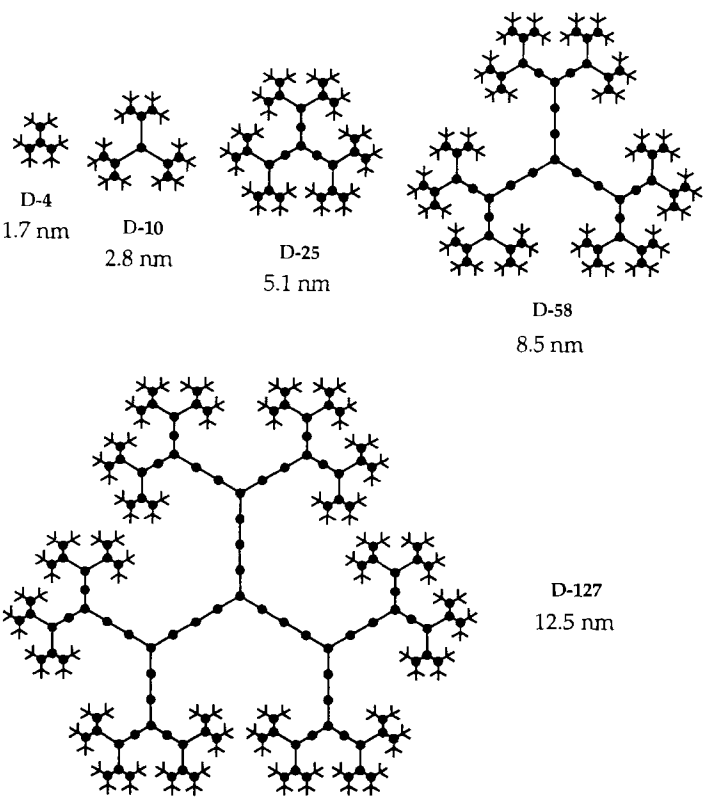


14, $n = 2, 6, 14$

ed as monodisperse particles. The roughly 128 Å long hexadecamer was readily soluble owing to its occurrence as a mixture of diastereomers and the presence of the ethylheptyl group. When the ethylheptyl group was replaced by an ethyl group, even the octameric phenylenethynylene was practically insoluble.

Two-Dimensional Systems

The synthesis of cascade molecules[19] is an established area of research. Molecules with high molecular weights can be obtained in only a few steps by nonlinear growth with high structural control. Recently, Moore et al. reported on the synthesis of the hitherto largest phenylenethynylene dendrimer (Scheme 1).[5] Owing to their rigid components, these molecules have a structurally uniform molecular framework. In the synthesis of classic dendrimers constructed of identical monomeric units growth is halted after several generations, as the spatial demand of the subsequent generation is greater than the volume available. To prepare higher generation dendrimers Moore and Xu used extended monomers of the next generation, which circumvented steric interference. This strategy should allow the synthesis of dendrimers of almost any generation.



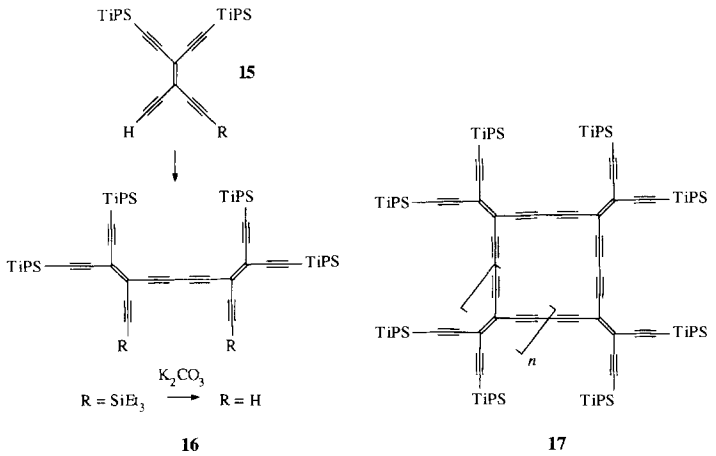
Scheme 1. Dendrimers synthesized by Moore and Xu. ⅄ 1,3,5-substituted benzene ring; —●— : 1,4-substituted phenylene unit; ⋋⋌ 1,3-di-*tert*-butylphenyl unit; — : C≡C unit.

In similar dendrimers, the tetra- and pentaethynyl-substituted organometallic compounds **4** and **5**,[8] respectively, which we prepared from the corresponding iodides, and hexaethynylbenzene (**6**),[7b] generated in 1986 by Vollhardt et al., could also serve as initiator cores.

Rings

The oxidative coupling of diynes under either Hay or Eglington conditions was highlighted by the research of Eglington[11a] and Sondheimer.[11d] Depending on the structure of the monomer,

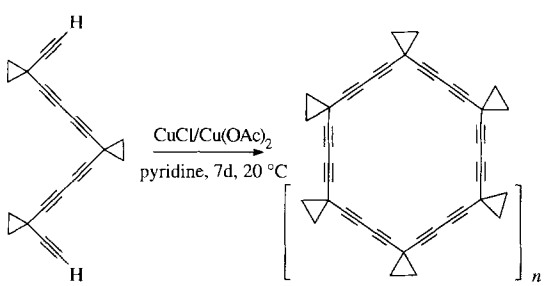
this reaction provides varying amounts of cyclized products with butadiyne units. This reaction has been known and employed for many years, but it still provides fascinating new compounds. Two attractive examples were prepared by Diederich et al.[20] and de Meijere et al.[21] The Diederich group reported on the synthesis of expanded radialenes,[22] which allows access to a new class of cross-conjugated macrocycles. The synthetic approach to **17** is shown in Scheme 2. Attempts to cyclize the



15,16 a (R = SiEt$_3$), **b** (R = H) **a** (n = 1), **b** (n = 2), **c** (n = 3)

Scheme 2. Synthesis of radialenes **17**.

doubly deprotected monomer **15b** by coupling reactions were unsuccessful and gave only acyclic oligomers. However, reaction of dimer **16b** furnished cycles **17a–c**. A novel family of pericyclynes[6] was synthesized by de Meijere et al. The cyclization of trimer **18** under modified Eglington conditions led to three products, two of which were identified unequivocally as the cyclic dimer **19a** and trimer **19b**. The rigid structure and the

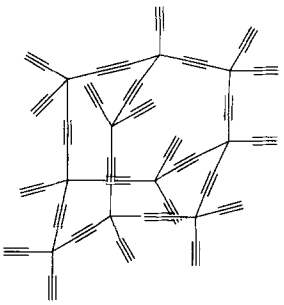


18 **19**
a (n = 1), **b** (n = 2)

electronic interaction between the cyclopropane and butadiyne units is evident in the X-ray structure analysis of **19a**.

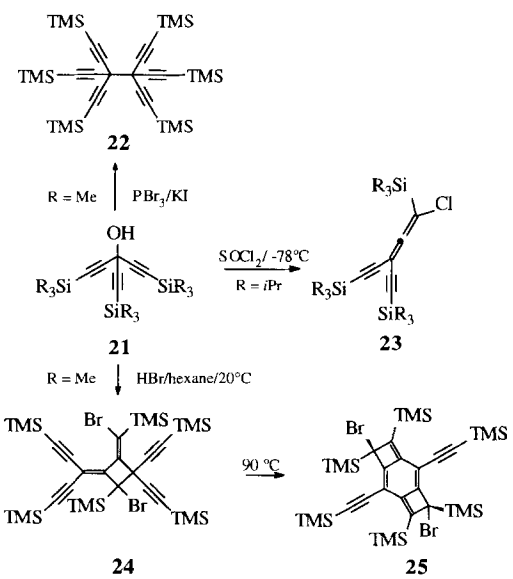
Three-Dimensional Networks

The synthesis of "nonnatural", structurally uniform, three-dimensional carbon networks presents a tremendous challenge and has recently been the focus of intensive research. Hexaethynylbenzene (**6**) synthesized by Vollhardt et al.[7] is a potential building block of supergraphite (graphyne[23]). Tetraethynylmethane **1**, which was postulated by Alberts and Wynberg[24] and prepared recently by Feldman, Kraebel, and Parvez,[25] is a potential monomer for the construction of "superdiamond" **20** (Dutch diamond[23]); here an alkyne unit is inserted between each carbon atom in the diamond lattice (cf. ref.[1]). "Expanded methane" **1** is the smallest member of a new type of "superalkanes" in which an alkyne unit is inserted in every C–H and C–C bond. These structures should be kinetically stable and not explosive (vide infra), since the alkyne units are not conjugated. As a number of research groups were unsuccessful in the synthesis of **1**, Feldman's ten-step "total synthesis" is particularly noteworthy. In contrast to the tetrakis(trimethylsilyl)-protected derivative, unsubstituted **1** is very sensitive towards hydrolysis and decomposes quickly to give a brown oil. Remarkably, the higher homologue tetrapropargylmethane **2**, which we prepared,[26] was unchanged after several weeks at room temperature in air.



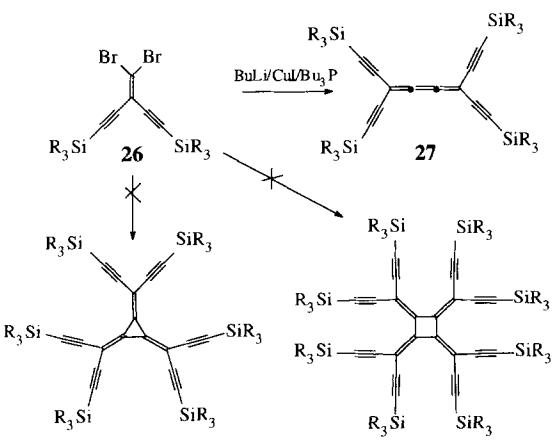
20

Until recently, triethynylmethanol **21**, synthesized by Alberts and Wynberg, was considered to be a possible precursor in the



synthesis of **1**; however, attempts to trap the cation, generated from the reaction of **21** with a Lewis acid, with a metal acetylide were unsuccessful.[27] Attempted halogenation of the OH group in **21** also did not give the desired result. Depending on the combination of reagent and silyl protecting group, completely different products were obtained. The reaction of the trimethylsilyl (TMS)-protected alcohol **21** with a mixture of PBr_3 and KI gave hexaethynylethane **22**,[23] whereas treatment with HBr/CuBr at 20 °C led to cyclobutane **24**. The latter rearranged upon heating to give the surprisingly stable *para*-quinodimethane **25**. On the other hand, when the more sterically hindered TiPS derivative

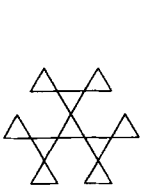
21b was treated with $SOCl_2$ at $-78\,^{\circ}C$, chloroallene **23** was isolated, which did not spontaneously dimerize because of the efficient steric hindrance of the silyl groups. Related and equally promising monomers for the construction of exotic carbon nets include tetraethynylbutatriene **3**, derivatives of which were obtained recently by Diederich et al.[28] by carbenoid dimerization according to the method of Iyoda et al.[29] (Scheme 3). Under



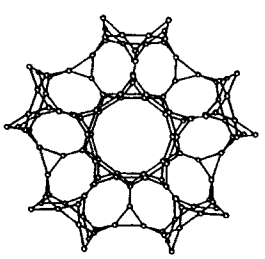
Scheme 3. Synthesis of tetraethynylbutatrienes **27**, R = Me, *i*Pr.

these reaction conditions [3]- and/or [4]radialenes **28** and **29**, respectively, would be expected; however, the steric demand of the TMS and TiPS substituents in these compounds may prevent reactions beyond the dimerization of the intermediate carbenoid, which is formed from **26**, to give **27**. The attempted dimerization of tetraethynylbutatriene **27** with triphenylphosphane catalysis to provide **29** also failed and resulted instead in the hydrogenation of the central double bond in **27**.

One approach to the synthesis of sections of a carbon network without triple bonds was published recently by de Meijere et al.[30] The perspirocyclopropanated [3]rotane **30** obtained is a section of a network type composed exclusively of spirocyclopropane units. A higher oligomer in this series is [80]triangulane **31**, which is an attractive, though not easily achievable, synthetic target.



30



31

The construction of carbon networks is still in its infancy, yet important advances in the synthesis of small sections of such structures are currently being made. The monomers themselves with their unusual structures often display fascinating chemistry. The most difficult problem to be overcome in the synthesis of two- and three-dimensional networks is the rapid drop in the solubility of the higher homologues. Currently, structurally uniform all-carbon networks can be the generated and studied only by computer.[1, 14, 31] This will hopefully change in the future.

German version: *Angew. Chem.* **1994**, *106*, 1127

[1] Review: F. Diederich, Y. Rubin, *Angew. Chem.* **1992**, *104*, 1123; *Angew. Chem. Int. Ed. Engl.* **1992**, *31*, 1101.

[2] R. Gleiter, D. Kratz, *Angew. Chem.* **1993**, *105*, 884; *Angew. Chem. Int. Ed. Engl.* **1993**, *32*, 842.

[3] a) Fullerene formation: H. Schwarz, *Angew. Chem.* **1993**, *105*, 1475; *Angew. Chem. Int. Ed. Engl.* **1993**, *32*, 1412; b) reactions: R. C. Haddon, *Science* **1993**, *261*, 1545, and references therein; A. Hirsch, *Angew. Chem.* **1993**, *105*, 1189; *Angew. Chem. Int. Ed. Engl.* **1993**, *32*, 1138.

[4] See literature cited in [1].

[5] Z. Xu, J. S. Moore, *Angew. Chem.* **1993**, *105*, 1395; *Angew. Chem. Int. Ed. Engl.* **1993**, *32*, 1354, and references therein.

[6] L. T. Scott, M. Unno, *J. Am. Chem. Soc.* **1990**, *112*, 7823; A. de Meijere, F. Jaekel, A. Simon, H. Borrmann, J. Köhler, D. Johnels, L. T. Scott, *ibid.* **1991**, *113*, 3935, and references therein.

[7] a) R. Boese, J. R. Green, J. Mittendorf, D. L. Mohler, K. P. C. Vollhardt, *Angew. Chem.* **1992**, *104*, 1643; *Angew. Chem. Int. Ed. Engl.* **1992**, *31*, 1643; b) R. Diercks, J. C. Armstrong, R. Boese, K. P. C. Vollhardt, *ibid.* **1986**, *98*, 270 and **1986**, *25*, 268.

[8] U. H. F. Bunz, V. Enkelmann, *Angew. Chem.* **1993**, *105*, 1712; *Angew. Chem. Int. Ed. Engl.* **1993**, *32*, 1653; U. H. F. Bunz, V. Enkelmann, J. Räder, *Organometallics* **1993**, *12*, 4745.

[9] Compound **6**, synthesized in 1986 by Vollhardt et al. [7b], is an exception; only protected derivatives of **3** and **5** are known.

[10] C. Lo Sterzo, J. K. Stille, *Organometallics* **1990**, *9*, 687; and references therein; J. K. Stille, J. H. Simpson, *J. Am. Chem. Soc.* **1987**, *109*, 2138; M. Alami, F. Ferri, G. Linstrumentelle, *Tetrahedron Lett.* **1993**, *34*, 6403.

[11] a) Review: *The Chemistry of the Functional Groups. The Chemistry of the Carbon-Carbon Triple Bond* (Ed.: S. Patai), Wiley, New York, **1978**; b) M. Nakagawa in [11a], Chapter 15; c) S. Misumi, T. Kaneda in [11a], Chapter 16; d) F. Sondheimer, *Acc. Chem. Res.* **1972**, *5*, 81.

[12] R. Eastmont, T. R. Johnson, D. R. M. Walton, *Tetrahedron* **1972**, 4601; R. Eastmont, D. R. M. Walton, *ibid.* **1972**, 4591; T. R. Johnson, D. R. M. Walton, *ibid.* **1972**, 5221.

[13] T. Grösser, A. Hirsch, *Angew. Chem.* **1993**, *105*, 1390; *Angew. Chem. Int. Ed. Engl.* **1993**, *32*, 1340.

[14] a) V. Enkelmann, *Adv. Polym. Sci.* **1984**, *63*, 91; b) G. Wegner, *Z. Naturforsch. A* **1969**, *24*, 824; c) V. Enkelmann, Mainz, personal communication.

[15] J. Anthony, C. Boudon, F. Diederich, J.-P. Gisselbrecht, V. Gramlich, M. Gross, M. Hobi, P. Seiler, *Angew. Chem.* **1994**, *106*, 794; *Angew. Chem. Int. Ed. Engl.* **1994**, *33*, 763.

[16] R. H. Baughman, D. S. Galvao, *Nature* **1993**, *365*, 735.

[17] J. S. Schumm, D. L. Pears, J. M. Tour, *Angew. Chem.* **1994**, *106*, No. 13; *Angew. Chem. Int. Ed. Engl.* **1994**, *33*, in press.

[18] J. S. Moore, E. D. Weinstein, Z. Wu, *Tetrahedron Lett.* **1991**, *32*, 2465; J. Zhang, J. S. Moore, Z. Xu, R. A. Aquirre, *J. Am. Chem. Soc.* **1992**, *114*, 2273.

[19] H.-B. Mekelburger, W. Jaworek, F. Vögtle, *Angew. Chem.* **1992**, *104*, 1609; *Angew. Chem. Int. Ed. Engl.* **1992**, *31*, 1571; C. Wörner, R. Mühlhaupt, *ibid.* **1993**, *105*, 1367 and **1993**, *32*, 1367.

[20] J.-D. van Loon, P. Seiler, F. Diederich, *Angew. Chem.* **1993**, *105*, 1817; *Angew. Chem. Int. Ed. Engl.* **1993**, *32*, 1706.

[21] A. de Meijere, S. Kozhushkov, C. Puls, T. Haumann, R. Boese, M. J. Cooney, L. T. Scott, *Angew. Chem.* **1994**, *106*, 934; *Angew. Chem. Int. Ed. Engl.* **1994**, *33*, 869.

[22] For a review on the synthesis of radialenes see H. Hopf, G. Maas, *Angew. Chem.* **1992**, *104*, 953; *Angew. Chem. Int. Ed. Engl.* **1992**, *31*, 931.

[23] R. H. Baughman, H. Eckhardt, M. Kertesz, *J. Chem. Phys.* **1987**, *87*, 6687.

[24] A. H. Alberts, H. Wynberg, *J. Chem. Soc. Chem. Commun.* **1988**, 748.

[25] K. S. Feldman, C. M. Kraebel, M. Parvez, *J. Am. Chem. Soc.* **1993**, *115*, 3846.

[26] U. Bunz, K. P. C. Vollhardt, J. S. Ho, *Angew. Chem.* **1992**, *104*, 11645; *Angew. Chem. Int. Ed. Engl.* **1992**, *31*, 1649.

[27] A. H. Alberts, personal communication.

[28] J.-D. van Loon, P. Seiler, F. Diederich, *Angew. Chem.* **1993**, *105*, 1235; *Angew. Chem. Int. Ed. Engl.* **1993**, *32*, 1187.

[29] M. Iyoda, S. Tanaka, H. Otani, M. Nose, M. Oda, *J. Am. Chem. Soc.* **1988**, *110*, 8494.

[30] S. I. Kozhushov, T. Haumann, R. Boese, A. de Meijere, *Angew. Chem.* **1993**, *105*, 426; *Angew. Chem. Int. Ed. Engl.* **1993**, *32*, 401.

[31] For example R. Nesper, K. Vogel, P. E. Blöchl, *Angew. Chem.* **1993**, *105*, 786; *Angew. Chem. Int. Ed. Engl.* **1993**, *32*, 701.

 © VCH Verlagsgesellschaft mbH, D-69451 Weinheim, 1994 0570-0833/94/1010-1076 $ 10.00+.25/0

Homoleptic Noble Metal Carbonyl Cations**

Lothar Weber*

Homoleptic neutral carbonyl complexes of the noble metals silver, gold, palladium, and platinum have so far only been detected in noble gas and CO matrices at $T \leq 15$ K, and they decompose well below the temperature of liquid nitrogen.[1-3] Thus, it is surprising that after more than a century of metal carbonyl chemistry, thermally stable salts with $[M(CO)_2]^+$ (M = Ag, Au) and $[M(CO)_4]^{2+}$ ions (M = Pd, Pt) were isolated. This is even more remarkable since homoleptic and well-defined stable metal carbonyl cations are rare in comparison to the large number of neutral and anionic metal carbonyls, and since so far they have been limited to the octahedral cations $[M(CO)_6]^+$ (M = Mn, Te, Re).[4-6]

Preparation

In comparison with classic methods the syntheses of noble metal carbonyl cations are unusual. Whereas $[Ag(CO)_2][B(OTeF_5)_4]$ crystallizes from solutions of $Ag[B(OTeF_5)_4]$ in 1,1,2-trichlorotrifluoroethane under about 0.5 bar CO at $T \leq -15\,^\circ C$[7] [Eq. (a)], the considerably more stable $[Au(CO)_2]^+$ salts form in strongly ionizing protic acids or are produced in Lewis acids such as SbF_5. Metallic gold is oxidized by UF_6 in liquid HF in the presence of CO to give $[Au(CO)_2][UF_6]$[8] [Eq. (b)].

$$Ag[B(OTeF_5)_4] \xrightarrow[\leq -15\,^\circ C]{CO} [Ag(CO)_2][B(OTeF_5)_4] \quad (a)$$

$$Au + 2CO + UF_6 \xrightarrow[HF\ liq.]{} [Au(CO)_2][UF_6] \quad (b)$$

The reductive carbonylation of $Au(SO_3F)_3$ in fluorosulfonic acid leads via $[Au(CO)_2]^+$(solv.) to solid $[Au(CO)SO_3F]$, which is carbonylated in pure SbF_5 under solvolysis to give colorless, crystalline $[Au(CO)_2][Sb_2F_{11}]$ with a melting point of 156 °C (decomp.)[9] [Eqs. (c)–(e)].

$$Au(SO_3F)_3 + 3CO \xrightarrow[HSO_3F]{25\,^\circ C} [Au(CO)_2]^+ + CO_2 + S_2O_5F_2 + [SO_3F]^- \quad (c)$$

$$[Au(CO)_2]^+ + [SO_3F]^- \xrightarrow[HSO_3F]{\Delta} [Au(CO)SO_3F] + CO \quad (d)$$

$$[Au(CO)SO_3F] + CO + 4SbF_5 \xrightarrow{SbF_5} [Au(CO)_2][Sb_2F_{11}] + Sb_2F_9(SO_3F) \quad (e)$$

The same strategy has proved to be successful for the preparation of $[Pd(CO)_4][Sb_2F_{11}]_2$ (m.p. 155 °C, decomp.) and $[Pt(CO)_4][Sb_2F_{11}]_2$ (m.p. 200 °C, decomp.)[10] [Eq. (f)]. The necessary starting materials for this reaction *cis*-$[M(CO)_2(SO_3F)_2]$, (M = Pd, Pt) form during the reductive carbonylation of solid

$$[M(CO)_2(SO_3F)_2] + 8SbF_5 + 2CO \xrightarrow[\approx 0.5\ \ 0.6\ bar\ CO]{80\,^\circ C} [M(CO)_4][Sb_2F_{11}]_2 + 2Sb_2F_9(SO_3F) \quad (f)$$

$Pd^{II}[Pd^{IV}(SO_3F)_6]$ and of $Pt(SO_3F)_4$ in HSO_3F, respectively, at 80 °C. If the carbonylation of the latter is carried out at 25 °C, $[Pt(CO)_4][Pt(SO_3F)_6]$ can be isolated as a yellow solid with a melting point of 140 °C (decomp.).[11]

The familiar range of existence (with regard to the metal) of "classic" carbonyl compounds is finally left with the first mercury carbonyl cations $[Hg(CO)_2]^{2+}$ and $[Hg_2(CO)_2]^{2+}$. In this case, too, the solvolysis processes of the corresponding mercury fluorosulfonates in SbF_5 at CO pressures of 0.7–0.9 bar are successful. The colorless salts $[Hg(CO)_2][Sb_2F_{11}]_2$ [m.p. 160 °C, decomp.; Eq. (g)] and $[Hg_2(CO)_2][Sb_2F_{11}]_2$ are formed in almost quantitative yield.[12]

$$Hg(SO_3F)_2 + 8SbF_5 + 2CO \xrightarrow[100\,^\circ C,\ 1\,h]{SbF_5} [Hg(CO)_2][Sb_2F_{11}]_2 + 2Sb_2F_9(SO_3F) \quad (g)$$

Properties

With the exception of $[Ag(CO)_2][B(OTeF_5)_4]$, which decomposes above −15 °C with evolution of CO to give $Ag[B(OTeF_5)_4]$, and $[Hg_2(CO)_2][Sb_2F_{11}]_2$ (the CO decomposition partial pressure at 20 °C is 8 mbar), the salts with noble metal carbonyl cations discussed here are thermally surprisingly stable with melting points between 140 and 200 °C. Without doubt their existence is coupled to the presence of anions with extremely low nucleophilicity such as $[Sb_2F_{11}]^-$ or $[Pt(SO_3F)_6]^{2-}$. The synthesis of derivatives such as $[Au(CO)SO_3F]$ and *cis*-$[M(CO)_2(SO_3F)_2]$ (M = Pd, Pt) from solutions of $[Au(CO)_2]^+$(solv.) and $[M(CO)_4]^{2+}$(solv.) in HSO_3F indicates the substitution lability of these species. In acetonitrile $[Au(CO)_2][Sb_2F_{11}]$ reacts immediately to give $[Au(NCMe)_2][SbF_6]$ [Eq. (h)], whereas the salt is soluble in liquid SO_2 and magic acid (SbF_5/HSO_3F) without decomposition.[9] The mercury carbonyls are only soluble in

$$[Au(CO)_2][Sb_2F_{11}] \xrightarrow[-2CO]{MeCN} [Au(NCMe)_2][SbF_6] \quad (h)$$

magic acid without elimination of CO. In the main, the chemical reactivity of noble metal carbonyl salts has still to be investigated.

Bonding and Structures

Carbon monoxide is the prototype of a very weak donor but excellent acceptor ligand. The synergetic interplay of σ-donor

[*] Prof. Dr. L. Weber
Fakultät für Chemie der Universität
Universitätsstrasse 25, D-33615 Bielefeld (FRG)
Telefax: Int. code + (521)106-6146

 © VCH Verlagsgesellschaft mbH, D-69451 Weinheim, 1994 0570-0833/94/1010-1077 $ 10.00+.25/0

bonding (from occupied 5σ molecular orbital of CO into an empty metal orbital of the σ type) and π-backbonding (from occupied metal d-orbitals into the 2π CO orbitals) is essential for the stability of the classic transition metal carbonyls. The CO valence frequencies in the vibration spectra of the noble metal carbonyl cations (2200–2289 cm^{-1}) are measured relative to the absorption of CO gas (2143 cm^{-1}) at considerably higher wavenumbers (Table 1).[13] The force constants (19.5–21.0 × 10^2 Nm^{-1}) derived herefrom almost reach the value calculated for the HCO^+ ion (21.3 × 10^2 Nm^{-1}) and thus emphasize that the π-backbonding does not play a significant role in the compounds discussed here. The increase of the CO bond order by coordination to a metal cation can be easily explained by the MO scheme of CO: the highest occupied molecular orbital (5σ) of the free CO ligand has antibonding character, which is reduced by bonding to the metal atom.[14]

Table 1. CO vibration frequencies [cm^{-1}], force constants f [10^2 Nm^{-1}], and ^{13}C NMR data [Hz] of binary metal carbonyl cations, CO, and HCO^+.

Species	IR	Raman		NMR	
	$\tilde{\nu}$(CO)	$\tilde{\nu}$(CO)	f(CO)	$\delta(^{13}C)$	$^1J(M-^{13}C)$
CO	2143		18.6	184	
HCO^+	2184		21.3		
$[Ag(CO)_2]^+$	2200		19.5	174	221
$[Au(CO)_2]^+$	2217	2254	20.1	174	
$[Pd(CO)_4]^{2+}$	2248	2278, 2263	20.6		
$[Pt(CO)_4]^{2+}$	2244	2289, 2267	20.6	140	1576
$[Hg(CO)_2]^{2+}$	2278	2281	21.0	169	5220
$[Hg_2(CO)_2]^{2+}$	2247	2248	20.4	189	3350
$[Mn(CO)_6]^+$	2096				
$[Re(CO)_6]^+$	2081				

Whereas in the classic metal carbonyls the ^{13}C NMR resonance signals for the CO ligands are measured in the range $184 \lesssim \delta \lesssim 223$[15] ($\delta^{13}C(CO)g = 184$),[10] the corresponding resonance signals in the cations introduced here generally occur at considerably higher field ($-44 \lesssim \Delta\delta^{13}C \lesssim 5$). These results, too, are in good agreement with the thermal stability of such compounds, which in the main results from the σ-donor bond and which is strengthened by polar contributions and by relativistic effects.

This supports theoretical studies on the structures and bonding energies of linear silver and gold carbonyl cations as well as the cyano complexes isoelectronic to these. It was shown that the metal–ligand bonds are primarily electrostatic in nature and in addition covalent contributions occur through σ-bonds, and at the same time negligible π-backbonding takes place. The greater stability of the corresponding cyano complexes is attributed to the strong σ-donor capability of the CN^- ion.[16] In a similar way to the linear compounds $[M(CO)_2]^+$, $[M(CN)_2]^-$ (M = Ag, Au), $[Hg(CO)_2]^{2+}$, and $Hg(CN)_2$, the square-planar $[M(CO)_4]^{2+}$ and $[M(CN)_4]^{2-}$ ions are also isoelectronic and, in contrast to the classic carbonyl complexes, no longer obey the 18e rule.

Outlook

Stable salts with noble metal carbonyl cations teach us that our view of the transition metal–CO interaction needs revising. Furthermore, once again the fundamental question must be raised at which point the uncritical usage of a familiar and, in general, useful concept leads to preconceived ideas which are an obstacle to further innovation, since in view of the easy access to, in part, considerably stable mercury carbonyl compounds, it is surprising that such "post transition metal carbonyls" were not isolated earlier. The more than 100-year-old chemistry of the metal carbonyls has not lost any of its fascination and still holds further surprises in store.

German version: *Angew. Chem.* **1994**, *106*, 1131

[1] D. McIntosh, G. A. Ozin, *J. Am. Chem. Soc.* **1976**, *98*, 3167–3175.
[2] D. McIntosh, G. A. Ozin, *Inorg. Chem.* **1977**, *16*, 51–59.
[3] E. P. Kündig, D. McIntosh, M. Moskovits, G. A. Ozin, *J. Am. Chem. Soc.* **1973**, *95*, 7234–7241.
[4] E. O. Fischer, K. Fichtel, K. Öfele, *Chem. Ber.* **1962**, *95*, 249–252.
[5] a) W. Hieber, F. Lux, C. Herget, *Z. Naturforsch. B* **1965**, *20*, 1159–1165; b) W. Hieber, T. Kruck, *ibid.* **1961**, *16*, 709–713.
[6] In the complexes $[Cu(CO)][CO_2CF_3]$ (A. F. Scott, L. F. Wilkening, B. Rubin, *Inorg. Chem.* **1969**, *8*, 2533-2534) and $[Cu(CO)][AsF_6]$ (C. D. Desjardins, D. E. Edwards, J. Passmore, *Can. J. Chem.* **1979**, *57*, 2714-2715), which have been described as saltlike, covalent cation–anion contacts cannot be ruled out.
[7] P. K. Hurlburt, J. J. Rack, S. F. Dec, O. P. Anderson, S. H. Strauss, *Inorg. Chem.* **1993**, *32*, 373–374.
[8] M. Adelhelm, W. Bacher, E. G. Höhn, E. Jacob, *Chem. Ber.* **1991**, *124*, 1559–1561.
[9] H. Willner, J. Schaebs, G. Hwang, F. Mistry, R. Jones, J. Trotter, F. Aubke, *J. Am. Chem. Soc.* **1992**, *114*, 8972–8980.
[10] G. Hwang, C. Wang, F. Aubke, H. Willner, M. Bodenbinder, *Can. J. Chem.* **1993**, *71*, 1532–1536.
[11] G. Hwang, M. Bodenbinder, H. Willner, F. Aubke, *Inorg. Chem.* **1993**, *32*, 4667–4669.
[12] H. Willner, M. Bodenbinder, C. Wang, F. Aubke, *J. Chem. Soc. Chem. Commun.*, in press.
[13] In mixed carbonylhalogenoplatinum and -gold complexes, ν(CO) frequencies >2143 cm^{-1} were measured previously: J. Browning, P. L. Goggin, R. J. Goodfellow, M. G. Norton, A. J. M. Rattray, B. F. Taylor, J. Mink, *J. Chem. Soc. Dalton Trans.* **1977**, 2061-2067.
[14] Compare for example: F. A. Cotton, G. Wilkinson, P. L. Gaus, *Basic Inorganic Chemistry*, 2nd edition, **1987**, Wiley; *Grundlagen der Anorganischen Chemie*, VCH, Weinheim, **1990**, pp. 111–112.
[15] H. O. Kalinowski, S. Berger, S. Braun, *^{13}C-NMR-Spektroskopie*, Thieme, Stuttgart, **1984**, pp. 381–383.
[16] A. Veldkamp, G. Frenking, *Organometallics* **1993**, *12*, 4613–4622.

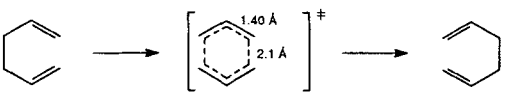
The Pressure Effect in Pericyclic Rearrangements: the Cope Rearrangement, Electrocyclization, and the Intramolecular Diels–Alder Reaction**

Matthias K. Diedrich, Dirk Hochstrate, Frank-Gerrit Klärner,* and Bernd Zimny

Many Diels–Alder reactions are accelerated under high pressure, and this effect is frequently employed in synthetic work. The activation volumes, which can be determined from the dependence of the reaction rate on pressure, are usually very small ($\Delta V^{\neq}$ in the range of -25 to $-45\ cm^3\,mol^{-1}$). Sometimes they are even smaller (i.e., more negative) than the reaction volumes (ΔV_R in the range -30 to $-40\ cm^3\,mol^{-1}$; $(\Delta V^{\neq}/\Delta V_R \geq 1)$.[1] Accordingly, the transition states[2] have volumes similar to, or in some cases smaller than, the products. Competing one-step, pericyclic cycloadditions and multistep cycloadditions that take place via diradical intermediates show relatively large differences in their activation volumes ($\Delta\Delta V^{\neq} \approx 10\ cm^3\,mol^{-1}$), which, at high pressure, has the effect of increased selectivity in favor of pericyclic reactions.[3] Examples are the dimerization of chloroprene,[4] 1,3-cyclohexadiene,[5] and 1,3-butadiene.[3b, 6] The preference for pericyclic reactions under high pressure is because the cyclic transition states—like the ground states—exhibit larger packing coefficients η than the transition states for the corresponding multistep reactions. The packing coefficients of transition states and ground states are defined as the ratio of the van der Waals volumes[7] to the partial molar volumes ($\eta = V_W^{\neq}/V^{\neq}$).

In the reorganization processes mentioned in the title, new interactions occur in the pericyclic transition states. The investigation of the pressure dependence reported here demonstrates a simple relationship between the number of new interactions in the transition state and the size of the activation volume.

On the basis of stereochemical and kinetic investigations, most Cope rearrangements of 1,5-hexadiene derivatives are regarded as pericyclic processes.[8] The van der Waals volumes *calculated* for the parent 1,5-hexadiene (**1**) and the pericyclic transition state $\mathbf{2}^{\neq}$ [9] (Scheme 1) are approximately the same. This is understandable since in the symmetrical transition state $\mathbf{2}^{\neq}$ the bond breaking and making have proceeded to the same extent so that the effects of the two processes on the van der Waals volumes compensate, and no great overall effect of pressure on the Cope rearrangement is to be expected. If it is assumed that, by analogy with the one- and multistep cycloaddition reactions already mentioned, the transition states here also exhibit larger packing coefficients because of their cyclic geometry, the activation volumes ought to be negative, and the Cope rearrangement should be accelerated under pressure. The activation volume can be estimated at approximately $-12\ cm^3\,mol^{-1}$ if the packing coefficient for the transition state is replaced by that for cyclohexene ($\eta = 0.5829$)[3, 7] (Scheme 1). In fact, negative activation volumes of the expected size are found for the Cope rearrangements of 4-cyano-4-ethoxycarbonyl-5-ethyl-1,5-heptadiene[10] and 3-hydroxy-3,5-dimethyl-1,5-hexadiene.[11] However, the compounds are highly polar, so the negative activation volumes could also be due to causes such as electrostriction effects rather than the interactions in the transition state, mentioned above.



	1	**2**$^{\neq}$	**1**
V_w	63.9	62.8	$\Delta V_w^{\neq} = -1.1$
V	119.4	107.7	$\Delta V^{\neq} = -11.7$

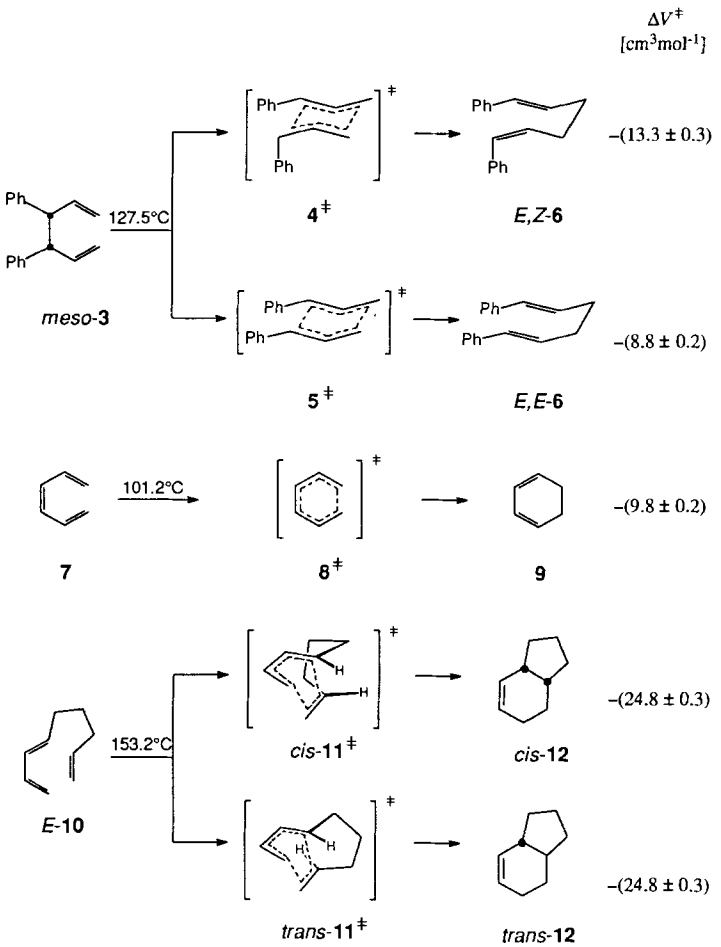
Scheme 1. All volumes are given in $cm^3\,mol^{-1}$. The structural parameters necessary for the calculation of the van der Waals volumes for $\mathbf{2}^{\neq}$ were taken from ab initio calculations [9]. The partial molar volumes for $\mathbf{2}^{\neq}$ were calculated from the equation $V(\mathbf{2}^{\neq}) = V_w(\mathbf{2}^{\neq})/\eta$(cyclohexene).

Because of this we investigated the pressure and temperature dependence of the Cope rearrangement of a pure hydrocarbon, *meso*-3,4-diphenyl-1,5-hexadiene (*meso*-**3**),[12] which reacts at 1 bar and 127.5 °C to form (*E,Z*)- and (*E,E*)-1,6-diphenylhexadienes [(*E,Z*)- and (*E,E*)-**6**] in the ratio of 60.5:39.5. When the pressure was raised an acceleration was observed for both reaction paths as well as an increased selectivity in favor of (*E,Z*)-**6** (127.5 °C, 4.3 kbar:(*E,Z*)-**6**:(*E,E*)-**6** = 73:27). From the pressure dependence of the rate constants (Table 1)[13] the negative activation volumes shown in Scheme 2 were derived. These lie within the order of magnitude expected for the formation of a new ring in the transition state. Dissociation of *meso*-**3** into two 1-phenylallyl radicals (with subsequent recombination to (*E,Z*)-**6** and/or (*E,E*)-**6**) can be excluded, since in this case positive activation volumes, and therefore a pressure-induced retardation, would be expected. On the other hand the pressure effect by itself does not allow a distinction between a pericyclic and a diradical reaction course. In the potential reaction of *meso*-**3** via an intermediate 2,3-diphenylcyclohexa-1,4-diyl, an additional ring is formed in the transition state, just as in the case of the corresponding pericyclic reaction, so both processes should have negative activation volumes of a similar order of magnitude.[14] Thermochemical estimates[15] for the competitive paths from *meso*-**3** to (*E,Z*)-**6** and (*E,E*)-**6**, however, suggest pericyclic processes. A possible explanation for the difference of $\Delta\Delta V^{\neq} = -4.5\ cm^3\,mol^{-1}$ in the activation volumes for competitive reactions is the also volume-reducing, higher steric hindrance[1c] in the chairlike transition state $\mathbf{4}^{\neq}$ compared with that of the boatlike transition state $\mathbf{5}^{\neq}$, caused by the axial position of one phenyl group in $\mathbf{4}^{\neq}$. The concept presented elucidates why the

[*] Prof. Dr. F.-G. Klärner, Dipl.-Chem. M. K. Diedrich, Dr. D. Hochstrate, Dipl.-Chem. B. Zimny
Institut für Organische Chemie der Universität-Gesamthochschule
Universitätsstrasse 5, D-45117 Essen (FRG)
Telefax: Int. code + (201)183-3082

[**] This work was supported by the Deutschen Forschungsgemeinschaft, the Ministerium für Wissenschaft und Forschung des Landes Nordrhein-Westfalen, and the Fonds der Chemischen Industrie.

 © VCH Verlagsgesellschaft mbH, D-69451 Weinheim, 1994 0570-0833/94/1010-1079 $ 10.00+.25/0



Scheme 2. Cope rearrangement of *meso*-**3**, electrocyclization of **7**, and intramolecular Diels–Alder reaction of (*E*)-**10**, and the activation volumes for each of the rearrangements.

degenerate Cope rearrangement in bullvalene, investigated with pressure- and temperature-dependent NMR spectroscopy, shows no significant pressure effect and has an activation volume of virtually zero (19.8 °C: $\Delta V^{\neq} = -0.5\,cm^3\,mol^{-1}$).[16] As a result of the fixed stereochemistry of the bullvalene skeleton, no new interactions in the sense discussed here appear in the transition state.

In the transition state of the electrocyclization of (*Z*)-1,3,5-hexatriene (**7**) to 1,3-cyclohexadiene (**9**),[17] a new interaction develops analogously to that of the Cope rearrangement of *meso*-**3** already discussed. The conversion of **7** to **9** is accelerated by an increase in pressure. The activation volume derived from the pressure dependence of the rate constants[13] at 101.2 °C (Table 1) is $\Delta V^{\neq} = -9.8\,cm^3\,mol^{-1}$ and thereby corresponds to that of the Cope rearrangement in acyclic hexadiene derivatives.

In intramolecular Diels–Alder reactions, bicyclic products are formed from acyclic starting materials. For such reactions examples of relatively large pressure-induced accelerations, which are also useful for preparative purposes, are found in the literature.[18] These compounds, without exception, bear polar groups and are not, therefore, very suitable for the foregoing analysis. We have investigated the pressure and temperature dependence of the intramolecular Diels–Alder reaction of (*E*)-1,3,8-nonatriene to form *cis*- and *trans*-bicyclo[4.3.0]non-2-ene (*cis*- and *trans*-**12**)[19] and determined that the product ratio (at 153.2 °C

Table 1. Pressure dependence of the rate constants k for the pericyclic reactions investigated.

p [bar]	1	230	510	810	990	1540	2750	4340	5850
k(*meso*-**3** → (*E,Z*)-**6**) [a]	1.24	1.21	1.37	1.53	1.62	1.84	2.36	3.03	3.71
k(*meso*-**3** → (*E,E*)-**6**) [a]	0.812	0.693	0.762	0.828	0.879	0.989	1.08	1.11	1.17
p [bar]	1	500	1000	1500	2000	3000	4000	5000	6000
k(**7** → **9**) [b]	0.813	0.946	1.14	1.26	1.45	1.94	2.50	3.17	3.87
p [bar]	1	210	400	800	1100	1600	3100	4600	
k((*E*)-**10** → *cis*-**12**) [c]	0.290	0.757	0.893	1.15	1.36	1.81	3.68	6.13	
k((*E*)-**10** → *trans*-**12**) [c]	0.0951	0.253	0.314	0.388	0.449	0.601	1.28	2.06	

[a] $[10^{-5}\,s^{-1}]$ at 127.5 °C in *n*-hexane. [b] $[10^{-5}\,s^{-1}]$ at 101.2 °C in toluene. [c] $[10^{-5}\,s^{-1}]$ at 153.2 °C in *n*-hexane.

cis-**12**:*trans*-**12** = 74.8:25.2) is not noticeably pressure-dependent. From the temperature dependence of the rate constants, measured at nine points between 195 and 280 °C, the Arrhenius equations (a) and (b) can be derived, which allow the calculation of the activation parameters[20] shown.

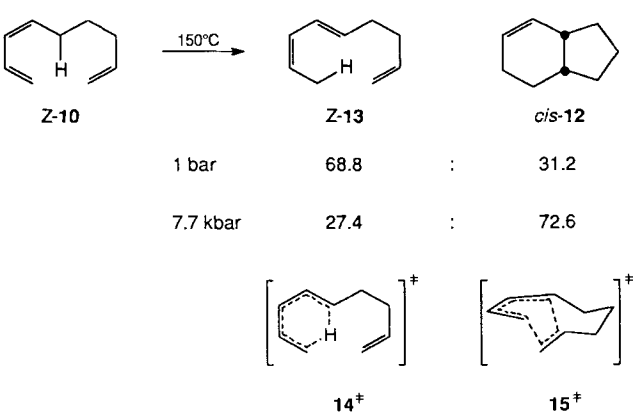
$$k((E)\text{-}\mathbf{10} \rightarrow \textit{cis}\text{-}\mathbf{12}) = 9.12 \times 10^7\,s^{-1} \times \exp[-(26.32 \pm 0.10)\,kcal\,mol^{-1}/RT] \quad (a)$$

238 °C: $\Delta H^{\neq} = (25.30 \pm 0.09)\,kcal\,mol^{-1}$; $\Delta S^{\neq} = -(25.18 \pm 0.19)\,cal\,mol^{-1}\,K^{-1}$

$$k((E)\text{-}\mathbf{10} \rightarrow \textit{trans}\text{-}\mathbf{12}) = 1.70 \times 10^8\,s^{-1} \exp[-(27.79 \pm 0.09)\,kcal\,mol^{-1}/RT] \quad (b)$$

238 °C: $\Delta H^{\neq} = (26.77 \pm 0.09)\,kcal\,mol^{-1}$; $\Delta S^{\neq} = -(23.93 \pm 0.17)\,cal\,mol^{-1}\,K^{-1}$

The activation volumes are determined from the pressure dependence of the rate constants in solution at 153.2 °C (Table 1) to be $\Delta V^{\neq} = -24.8\,cm^3\,mol^{-1}$ for both reactions and are twice as large as that of the Cope rearrangement and the electrocyclization. From this it can be extrapolated that each additional five- or six-membered ring formed in the transition state contributes about -10 to $-12\,cm^3\,mol^{-1}$ to the activation volume. The activation volume therefore yields important information about transition state geometries.



Scheme 3. Thermolysis of (*Z*)-**10** to (*Z*)-**13** or *cis*-**12**. The product ratios at 1 bar and 7.7 kbar are shown.

A particularly instructive example is the thermolysis of (*Z*)-1,3,8-nonatriene [(*Z*)-**10**],[21] in which an intramolecular Diels–Alder reaction leading to *cis*-**12** competes with a sigmatropic [1,5]-hydrogen shift leading to (1,5*E*,7*Z*)-nonatriene (**13**, Scheme 3). The use of high pressure here enables a reversal of the selectivity. At 150 °C and 1 bar the 1,5-hydrogen shift is preferred to the monocyclic transition state **14**‡. At 7.7 bar, on the other hand, the intramolecular Diels–Alder reaction is preferred to the bicyclic transition state **15**‡.

Received: October 28, 1993
Revised version: December 18, 1993 [Z 6464 IE]
German version: *Angew. Chem.* **1994**, *106*, 1135

[1] a) T. Asano, W. J. le Noble, *Chem. Rev.* **1978**, *78*, 407–489; b) R. van Eldik, T. Asano, W. J. le Noble, *ibid.* **1989**, *89*, 549–688; c) G. Jenner, *J. Chem. Soc. Faraday Trans. 1* **1985**, *81*, 2437–2460.

[2] In the Eyring theory activation volumes are defined as reaction volumes of transition states ($\Delta V^{\ddagger} = V^{\ddagger} - \sum V$ (starting materials); $V^{\ddagger}, V$: partial molar volume of transition and ground states, respectively).

[3] a) F.-G. Klärner, *Chem. Unserer Zeit* **1989**, *23*, 53–63; b) F.-G. Klärner, V. Ruster, B. Zimny, D. Hochstrate, *High Pressure Res.* **1991**, *7*, 133–135.

[4] C. A. Steward, Jr., *J. Am. Chem. Soc.* **1971**, *93*, 4815–4821; *ibid.* **1972**, *94*, 635–637.

[5] F.-G. Klärner, B. M. J. Dogan, O. Ermer, W. von E. Doering, M. P. Cohen, *Angew. Chem.* **1986**, *98*, 109–111; *Angew. Chem. Int. Ed. Engl.* **1986**, *25*, 108–110.

[6] F.-G. Klärner, B. Krawczyk, V. Ruster, U. K. Deiters, *J. Am. Chem. Soc.*, submitted.

[7] The van der Waals volumes are represented by the product of the Avogadro constant and the intrinsic volumes of the ground and transition states. The intrinsic volumes can be calculated by means of the program MOLVOL developed by U. Artschwager-Perl and D. Oebels by using the Cartesian coordinates obtained from force field or quantum mechanical calculations together with the van der Waals radii, r_w, of the various atoms obtained from X-ray structure analyses (r_w(C) = 1.80 Å, r_w(H) = 1.17 Å). A copy of MOLVOL is available on request. a) U. Artschwager-Perl, Dissertation, Ruhr-Universität Bochum, **1989**; b) Y. Yoshimura, J. Osugi, M. Nakahara, *Bull. Chem. Soc. Jpn.* **1983**, *56*, 680–683; c) *J. Am. Chem. Soc.* **1983**, *105*, 5414–5418; d) T. Asano, W. J. Le Noble, *Rev. Phys. Chem. Jpn.* **1973**, *43*, 82–91.

[8] W. R. Roth, H. W. Lennartz, W. von E. Doering, L. Birladeanu, C. A. Guyton, T. Kitagawa, *J. Am. Chem. Soc.* **1990**, *112*, 1722–1732, and references therein.

[9] K. Morokuma, W. T. Borden, D. A. Hrovat, *J. Am. Chem. Soc.* **1988**, *110*, 4474–4475; Review: K. N. Houk, Y. Li, J. D. Evanseck, *Angew. Chem.* **1992**, *104*, 711–739; *Angew. Chem. Int. Ed. Engl.* **1992**, *31*, 682–708.

[10] C. Walling, M. Naiman, *J. Am. Chem. Soc.* **1962**, *84*, 2628–2632.

[11] G. A. Stashina, E. N. Vasylvitskaya, G. D. Gamalevich, B. S. El'yanov, E. P. Serebryakov, V. M. Zhulin, *Izv. Akad. Nauk. SSSR Ser. Khim.* **1986**, 329–334.

[12] R. P. Lutz, S. Bernal, R. J. Boggio, R. O. Harris, M. W. McNicholas, *J. Am. Chem. Soc.* **1971**, *93*, 3985–3990; R. P. Lutz, H. A. J. Berg, *J. Org. Chem.* **1980**, *45*, 3915–3916.

[13] The rate of the rearrangements described here were determined at various pressures in a 7 kbar autoclave that could be held at a constant temperature (±0.2 °C). Samples of about 100 µL were removed from the compressed solutions (about 10 mL) by means of a precise dispensing valve and were analyzed by HPLC or GC.

[14] The investigation of the pressure effect in the rearrangement of 2,5-diphenylhexa-1,5-diene, for which a 1,4-diphenylcyclohexa-1,4-diyl intermediate is assumed [8], is under way.

[15] a) The following Arhenius equations were calculated from the temperature dependence of the rate constants k, measured in hexane at five temperatures between 133 and 174 °C: k(*meso*-**3** → (*E,Z*)-**6**) = $4.68 \times 10^{10}\ s^{-1} \exp[-(28.54 \pm 0.33)\ kcal\,mol^{-1}/RT^{-1}]$, from which the following parameters were derived (153.2 °C): $\Delta H^{\ddagger} = (27.69 \pm 0.33)\ kcal\,mol^{-1}$; $\Delta S^{\ddagger} = -(12.43 \pm 0.71)\ cal\,mol^{-1}\,K^{-1}$. k(*meso*-**3** → (*E,E*)-**6**) = $1.58 \times 10^{11}\ s^{-1} \exp[-(29.85 \pm 0.30)\ kcal\,mol^{-1}/RT]$, from which the following parameters were derived (153.2 °C): $\Delta H^{\ddagger} = (29.01 \pm 0.30)\ kcal\,mol^{-1}$; $\Delta S^{\ddagger} = -(9.99 \pm 0.70)\ cal\,mol^{-1}\,K^{-1}$. The activation enthalpies of the rearrangements of *meso*-**3** to (*E,Z*)-**6** and (*E,E*)-**6** are, respectively, 3.7 and 5.0 kcal mol^{-1} larger than those of the Cope rearrangement of *rac*-**3** to (*E,E*)-**6** ($\Delta H^{\ddagger} = 24.0\ kcal\,mol^{-1}$; $\Delta S^{\ddagger} = -12.4\ cal\,mol^{-1}\,K^{-1}$) [12], a fact that is certainly due to steric effects in the *cis*-configured transition state. From the activation enthalpies and the enthalpies of formation calculated with the force field MM2ERW for *meso*-**3** and *rac*-**3** (ΔH_f = 73.8 and 73.5 kcal mol^{-1} respectively)[8], the enthalpies of formation of the transition states for the reactions *meso*-**3** → (*E,Z*)-**6** (ΔH_f° = 101.5 kcal mol^{-1}), *meso*-**3** → (*E,E*)-**6** (ΔH_f° = 102.8 kcal mol^{-1}) and *rac*-**3** → (*E,E*)-**6** (ΔH_f = 97.5 kcal mol^{-1}) could be calculated. The enthalpies of formation thus obtained for the transition states are, without exception, 12 to 17 kcal mol^{-1} lower than the enthalpies of formation, also calculated with the MM2ERW force field, for the potential diradical intermediates *cis*- and *trans*-2,3-diphenylcyclohexa-1,4-diyl (*cis*-chair: ΔH_f° = 118.2 kcal mol^{-1}; twisted *cis*-boat (twist-boat [8]): ΔH_f° = 120.1 kcal mol^{-1}; *trans*-chair: ΔH_f° = 113.8 kcal mol^{-1}) or those of the free radicals resulting from the homolysis of the C-3–C-4 bond (2 × 1-phenylallyl: $\Delta H_f^{\circ} = 2 \times 57.2 = 114.4\ kcal\,mol^{-1}$) [8]. It is, therefore, unlikely that a diradical rearrangement *meso*-**3** → (*E,E*)-**6** occurs as proposed by one of the referees. b) W. von E. Doering, W. R. Roth, R. Breuckmann, L. Figge, H.-W. Lennartz, W.-D. Fessner, H. Prinzbach, *Chem. Ber.* **1988**, *121*, 1–9; c) W. R. Roth, O. Adamczak, R. Breuckmann, H.-W. Lennartz, R. Boese, *ibid.* **1991**, *124*, 2499–2521. We thank Prof. Roth for providing us with a copy of the MM2ERW force field program.

[16] E. M. Schulman, A. E. Merbach, M. Turin, R. Wedinger, W. J. le Noble, *J. Am. Chem. Soc.* **1983**, *105*, 3988–3991.

[17] K. E. Lewis, H. Steiner, *J. Chem. Soc.* **1964**, 3080–3092.

[18] a) N. S. Isaacs, P. Van der Beeke, *Tetrahedron Lett.* **1982**, *23*, 2147–2148; b) B. A. Keay, P. W. Dibble, *ibid.* **1989**, *30*, 1045–1046; c) D. Hocbstrate, Dissertation, Ruhr-Universität Bochum, **1992**; d) L. F. Tietze, C. Ott, K. Gerke, M. Buback, *Angew. Chem.* **1993**, *105*, 1536–1538; *Angew. Chem. Int. Ed. Engl.* **1993**, *32*, 1485–1486.

[19] a) K. N. Houk, Y. T. Lin, *Tetrahedron Lett.* **1985**, *26*, 2269–2272; b) Y. T. Lin, Dissertation, University of Pittsburgh, **1985**; c) F. K. Brown, K. N. Houk, *Tetrahedron Lett.* **1985**, *26*, 2297–2300.

[20] From the activation enthalpies of the reactions (*E*)-**10** → *cis*-**12** and (*E*)-**10** → *trans*-**12** as well as the enthalpy of formation calculated with the force field MM2ERW [15b, c] for (*E*)-**10** (ΔH_f° = 25.9 kcal mol^{-1}), enthalpies of formation for the transition states were calculated: ΔH_f° = 51.7 and 53.0 kcal mol^{-1} respectively. Comparison with the enthalpy of formation of the energetically favored, potential diradical intermediate cyclonon-2-ene-1,6-diyl (ΔH_f° = 67.6 kcal mol^{-1}) also calculated with the MM2ERW force field yielded values of about −16 and −15 kcal mol^{-1} for the transition state resonance energy (TS-RE, energy of concert); thus the two intramolecular Diels–Alder reactions certainly take place by pericyclic processes.

[21] From a mixture of (*Z*)- and (*E*)-**10**, (about 1:1) prepared in a Wittig reaction of (2-propenylidene)triphenylphosphorane [22] and 5-hexenal [23], isomerically pure (*Z*)-**10** was obtained by allowing the (*E*)-**10** to react with maleic anhydride in a selective Diels–Alder reaction and separating the unconverted (*Z*)-**10** from the adduct by column chromatography.

[22] G. Wittig, U. Schöllkopf, *Chem. Ber.* **1954**, *87*, 1318–1330.

[23] D. F. Taber, J. C. Amedio, Jr., K. Raman, *J. Org. Chem.* **1988**, *53*, 2984–2990.

Polymorphism and C=N–N=C Conformational Isomers of Azines: X-ray Crystal and Ab Initio Structures of Two Rotational Isomers of Methyl (*para*-Tolyl) Ketone Azine**

Grace Shiahuy Chen, Mitchell Anthamatten, Charles L. Barnes, and Rainer Glaser*

Azines are important substrates for crisscross additions and their organometallic variants,[2, 3] they react as the "ene" component in [3+2] additions,[4] and they are becoming increasingly important for C–C bond forming reactions.[5] Azines also are receiving increasing attention for their biological,[6] chemical,[7] and physical properties.[8] The characterization of the electronic structure of azines is fundamental to the understanding and the advancement of their chemistry. We have been studying the stereochemistry and stereoelectronics of azines in a systematic fashion,[1] and we report here on the rotamers of methyl (*para*-tolyl) ketone azine, **I**.

Compound **I** was prepared from methyl (*para*-tolyl) ketone and hydrazine hydrate in acidic ethanol.[9] Yellow single

[*] Prof. Dr. R. Glaser, G. S. Chen, M. Anthamatten, Dr. C. L. Barnes
Department of Chemistry, University of Missouri
Columbia, MO 65211 (USA)
Telefax: Int. code + (314) 882-2754

[**] Stereochemistry and Stereoelectronics of Azines, Part 3. This research was supported by the Petroleum Research Fund of the American Chemical Society, the Research Board of the University of Missouri, and the National Science Foundation, and is part of the projected Ph.D. dissertation of G. S. Chen. – Parts 1 and 2: [1].

A particularly instructive example is the thermolysis of (*Z*)-1,3,8-nonatriene [(*Z*)-**10**],[21] in which an intramolecular Diels–Alder reaction leading to *cis*-**12** competes with a sigmatropic [1,5]-hydrogen shift leading to (1,5*E*,7*Z*)-nonatriene (**13**, Scheme 3). The use of high pressure here enables a reversal of the selectivity. At 150 °C and 1 bar the 1,5-hydrogen shift is preferred to the monocyclic transition state **14**‡. At 7.7 bar, on the other hand, the intramolecular Diels–Alder reaction is preferred to the bicyclic transition state **15**‡.

Received: October 28, 1993
Revised version: December 18, 1993 [Z 6464 IE]
German version: *Angew. Chem.* **1994**, *106*, 1135

[1] a) T. Asano, W. J. le Noble, *Chem. Rev.* **1978**, *78*, 407–489; b) R. van Eldik, T. Asano, W. J. le Noble, *ibid.* **1989**, *89*, 549–688; c) G. Jenner, *J. Chem. Soc. Faraday Trans. 1* **1985**, *81*, 2437–2460.

[2] In the Eyring theory activation volumes are defined as reaction volumes of transition states ($\Delta V^{\ddagger} = V^{\ddagger} - \sum V$ (starting materials); $V^{\ddagger}, V$: partial molar volume of transition and ground states, respectively).

[3] a) F.-G. Klärner, *Chem. Unserer Zeit* **1989**, *23*, 53–63; b) F.-G. Klärner, V. Ruster, B. Zimny, D. Hochstrate, *High Pressure Res.* **1991**, *7*, 133–135.

[4] C. A. Steward, Jr., *J. Am. Chem. Soc.* **1971**, *93*, 4815–4821; *ibid.* **1972**, *94*, 635–637.

[5] F.-G. Klärner, B. M. J. Dogan, O. Ermer, W. von E. Doering, M. P. Cohen, *Angew. Chem.* **1986**, *98*, 109–111; *Angew. Chem. Int. Ed. Engl.* **1986**, *25*, 108–110.

[6] F.-G. Klärner, B. Krawczyk, V. Ruster, U. K. Deiters, *J. Am. Chem. Soc.*, submitted.

[7] The van der Waals volumes are represented by the product of the Avogadro constant and the intrinsic volumes of the ground and transition states. The intrinsic volumes can be calculated by means of the program MOLVOL developed by U. Artschwager-Perl and D. Oebels by using the Cartesian coordinates obtained from force field or quantum mechanical calculations together with the van der Waals radii, r_w, of the various atoms obtained from X-ray structure analyses (r_w(C) = 1.80 Å, r_w(H) = 1.17 Å). A copy of MOLVOL is available on request. a) U. Artschwager-Perl, Dissertation, Ruhr-Universität Bochum, **1989**; b) Y. Yoshimura, J. Osugi, M. Nakahara, *Bull. Chem. Soc. Jpn.* **1983**, *56*, 680–683; c) *J. Am. Chem. Soc.* **1983**, *105*, 5414–5418; d) T. Asano, W. J. Le Noble, *Rev. Phys. Chem. Jpn.* **1973**, *43*, 82–91.

[8] W. R. Roth, H. W. Lennartz, W. von E. Doering, L. Birladeanu, C. A. Guyton, T. Kitagawa, *J. Am. Chem. Soc.* **1990**, *112*, 1722–1732, and references therein.

[9] K. Morokuma, W. T. Borden, D. A. Hrovat, *J. Am. Chem. Soc.* **1988**, *110*, 4474–4475; Review: K. N. Houk, Y. Li, J. D. Evanseck, *Angew. Chem.* **1992**, *104*, 711–739; *Angew. Chem. Int. Ed. Engl.* **1992**, *31*, 682–708.

[10] C. Walling, M. Naiman, *J. Am. Chem. Soc.* **1962**, *84*, 2628–2632.

[11] G. A. Stashina, E. N. Vasylvitskaya, G. D. Gamalevich, B. S. El'yanov, E. P. Serebryakov, V. M. Zhulin, *Izv. Akad. Nauk. SSSR Ser. Khim.* **1986**, 329–334.

[12] R. P. Lutz, S. Bernal, R. J. Boggio, R. O. Harris, M. W. McNicholas, *J. Am. Chem. Soc.* **1971**, *93*, 3985–3990; R. P. Lutz, H. A. J. Berg, *J. Org. Chem.* **1980**, *45*, 3915–3916.

[13] The rate of the rearrangements described here were determined at various pressures in a 7 kbar autoclave that could be held at a constant temperature (±0.2 °C). Samples of about 100 µL were removed from the compressed solutions (about 10 mL) by means of a precise dispensing valve and were analyzed by HPLC or GC.

[14] The investigation of the pressure effect in the rearrangement of 2,5-diphenylhexa-1,5-diene, for which a 1,4-diphenylcyclohexa-1,4-diyl intermediate is assumed [8], is under way.

[15] a) The following Arhenius equations were calculated from the temperature dependence of the rate constants k, measured in hexane at five temperatures between 133 and 174 °C: k(*meso*-**3** → (*E,Z*)-**6**) = $4.68 \times 10^{10}\ s^{-1} \exp[-(28.54 \pm 0.33)\ kcal\,mol^{-1}/RT^{-1}]$, from which the following parameters were derived (153.2 °C): $\Delta H^{\ddagger} = (27.69 \pm 0.33)\ kcal\,mol^{-1}$; $\Delta S^{\ddagger} = -(12.43 \pm 0.71)\ cal\,mol^{-1}\,K^{-1}$. k(*meso*-**3** → (*E,E*)-**6**) = $1.58 \times 10^{11}\ s^{-1} \exp[-(29.85 \pm 0.30)\ kcal\,mol^{-1}/RT]$, from which the following parameters were derived (153.2 °C): $\Delta H^{\ddagger} = (29.01 \pm 0.30)\ kcal\,mol^{-1}$; $\Delta S^{\ddagger} = -(9.99 \pm 0.70)\ cal\,mol^{-1}\,K^{-1}$. The activation enthalpies of the rearrangements of *meso*-**3** to (*E,Z*)-**6** and (*E,E*)-**6** are, respectively, 3.7 and 5.0 kcal mol^{-1} larger than those of the Cope rearrangement of *rac*-**3** to (*E,E*)-**6** ($\Delta H^{\ddagger} = 24.0\ kcal\,mol^{-1}$; $\Delta S^{\ddagger} = -12.4\ cal\,mol^{-1}\,K^{-1}$) [12], a fact that is certainly due to steric effects in the *cis*-configured transition state. From the activation enthalpies and the enthalpies of formation calculated with the force field MM2ERW for *meso*-**3** and *rac*-**3** (ΔH_f = 73.8 and 73.5 kcal mol^{-1} respectively)[8], the enthalpies of formation of the transition states for the reactions *meso*-**3** → (*E,Z*)-**6** (ΔH_f° = 101.5 kcal mol^{-1}), *meso*-**3** → (*E,E*)-**6** (ΔH_f° = 102.8 kcal mol^{-1}) and *rac*-**3** → (*E,E*)-**6** (ΔH_f = 97.5 kcal mol^{-1}) could be calculated. The enthalpies of formation thus obtained for the transition states are, without exception, 12 to 17 kcal mol^{-1} lower than the enthalpies of formation, also calculated with the MM2ERW force field, for the potential diradical intermediates *cis*- and *trans*-2,3-diphenylcyclohexa-1,4-diyl (*cis*-chair: ΔH_f° = 118.2 kcal mol^{-1}; twisted *cis*-boat (twist-boat [8]): ΔH_f° = 120.1 kcal mol^{-1}; *trans*-chair: ΔH_f° = 113.8 kcal mol^{-1}) or those of the free radicals resulting from the homolysis of the C-3–C-4 bond (2 × 1-phenylallyl: $\Delta H_f^{\circ} = 2 \times 57.2 = 114.4\ kcal\,mol^{-1}$) [8]. It is, therefore, unlikely that a diradical rearrangement *meso*-**3** → (*E,E*)-**6** occurs as proposed by one of the referees. b) W. von E. Doering, W. R. Roth, R. Breuckmann, L. Figge, H.-W. Lennartz, W.-D. Fessner, H. Prinzbach, *Chem. Ber.* **1988**, *121*, 1–9; c) W. R. Roth, O. Adamczak, R. Breuckmann, H.-W. Lennartz, R. Boese, *ibid.* **1991**, *124*, 2499–2521. We thank Prof. Roth for providing us with a copy of the MM2ERW force field program.

[16] E. M. Schulman, A. E. Merbach, M. Turin, R. Wedinger, W. J. le Noble, *J. Am. Chem. Soc.* **1983**, *105*, 3988–3991.

[17] K. E. Lewis, H. Steiner, *J. Chem. Soc.* **1964**, 3080–3092.

[18] a) N. S. Isaacs, P. Van der Beeke, *Tetrahedron Lett.* **1982**, *23*, 2147–2148; b) B. A. Keay, P. W. Dibble, *ibid.* **1989**, *30*, 1045–1046; c) D. Hocbstrate, Dissertation, Ruhr-Universität Bochum, **1992**; d) L. F. Tietze, C. Ott, K. Gerke, M. Buback, *Angew. Chem.* **1993**, *105*, 1536–1538; *Angew. Chem. Int. Ed. Engl.* **1993**, *32*, 1485–1486.

[19] a) K. N. Houk, Y. T. Lin, *Tetrahedron Lett.* **1985**, *26*, 2269–2272; b) Y. T. Lin, Dissertation, University of Pittsburgh, **1985**; c) F. K. Brown, K. N. Houk, *Tetrahedron Lett.* **1985**, *26*, 2297–2300.

[20] From the activation enthalpies of the reactions (*E*)-**10** → *cis*-**12** and (*E*)-**10** → *trans*-**12** as well as the enthalpy of formation calculated with the force field MM2ERW [15b, c] for (*E*)-**10** (ΔH_f° = 25.9 kcal mol^{-1}), enthalpies of formation for the transition states were calculated: ΔH_f° = 51.7 and 53.0 kcal mol^{-1} respectively. Comparison with the enthalpy of formation of the energetically favored, potential diradical intermediate cyclonon-2-ene-1,6-diyl (ΔH_f° = 67.6 kcal mol^{-1}) also calculated with the MM2ERW force field yielded values of about −16 and −15 kcal mol^{-1} for the transition state resonance energy (TS-RE, energy of concert); thus the two intramolecular Diels–Alder reactions certainly take place by pericyclic processes.

[21] From a mixture of (*Z*)- and (*E*)-**10**, (about 1:1) prepared in a Wittig reaction of (2-propenylidene)triphenylphosphorane [22] and 5-hexenal [23], isomerically pure (*Z*)-**10** was obtained by allowing the (*E*)-**10** to react with maleic anhydride in a selective Diels–Alder reaction and separating the unconverted (*Z*)-**10** from the adduct by column chromatography.

[22] G. Wittig, U. Schöllkopf, *Chem. Ber.* **1954**, *87*, 1318–1330.

[23] D. F. Taber, J. C. Amedio, Jr., K. Raman, *J. Org. Chem.* **1988**, *53*, 2984–2990.

Polymorphism and C=N–N=C Conformational Isomers of Azines: X-ray Crystal and Ab Initio Structures of Two Rotational Isomers of Methyl (*para*-Tolyl) Ketone Azine**

Grace Shiahuy Chen, Mitchell Anthamatten, Charles L. Barnes, and Rainer Glaser*

Azines are important substrates for crisscross additions and their organometallic variants,[2, 3] they react as the "ene" component in [3+2] additions,[4] and they are becoming increasingly important for C–C bond forming reactions.[5] Azines also are receiving increasing attention for their biological,[6] chemical,[7] and physical properties.[8] The characterization of the electronic structure of azines is fundamental to the understanding and the advancement of their chemistry. We have been studying the stereochemistry and stereoelectronics of azines in a systematic fashion,[1] and we report here on the rotamers of methyl (*para*-tolyl) ketone azine, **I**.

Compound **I** was prepared from methyl (*para*-tolyl) ketone and hydrazine hydrate in acidic ethanol.[9] Yellow single

[*] Prof. Dr. R. Glaser, G. S. Chen, M. Anthamatten, Dr. C. L. Barnes
Department of Chemistry, University of Missouri
Columbia, MO 65211 (USA)
Telefax: Int. code + (314) 882-2754

[**] Stereochemistry and Stereoelectronics of Azines, Part 3. This research was supported by the Petroleum Research Fund of the American Chemical Society, the Research Board of the University of Missouri, and the National Science Foundation, and is part of the projected Ph.D. dissertation of G. S. Chen. – Parts 1 and 2: [1].

crystals[10] suitable for X-ray crystallography were formed from a solution of **I** in methylene chloride by vapor diffusion of *n*-hexane. **I** cocrystallizes in two monoclinic racemic modifications,[11] space groups $P2_1/n$ and $P2_1/c$. The two independent molecules **A** and **B** are shown in Figure 1. Both assume the (*E*,*E*) configuration in which the large groups attached to the C=N bonds are *trans*. In general, the configurations of azines are governed by steric factors and result in "*trans*–*trans* structures" which, depending on the priorities of the attached groups, are (*E*,*E*)[12] or (*Z*,*Z*) configured.[1a, 13] The stereochemistry of the azines with regard to the N–N single bond is the focus of the present study.

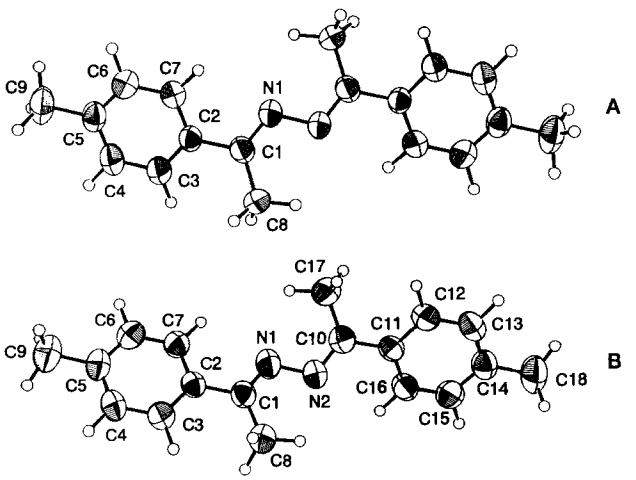
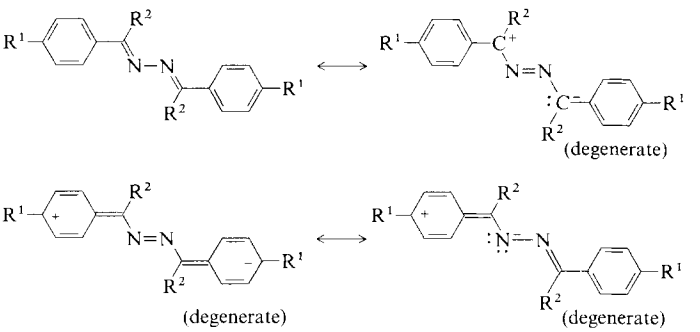


Fig. 1. ORTEPII drawings of the azines **A** (top) and **B** (bottom) with the numbering scheme.

The crystal structures of azines reported previously all show either N–N s-*trans* or *gauche* conformations, and only two cases are known in which *both* conformations occur in polymorphous crystals.[14] In the case of **I** molecule **A** exhibits a *trans* conformation with a C-N-N-C torsion angle τ of 180°, while **B** shows a *gauche* conformation with $\tau = 142.8°$. Similarly, for the azine of 3-acetyl-4-(2-chlorophenyl)-4-hydroxy-2-methoxycrotonic acid lactone, **II**,[15] the *trans* and *gauche* conformers crystallize in different modifications. Our study is of particular significance, as **I** contains phenyl substituents and allows for the first experimental examination of conjugation effects in azines as a function of the N–N conformation. The importance of such solid-state studies has been emphasized by the recent studies by the research groups led by Brock, Grützmacher, and Gompper.[16]

Molecule **A** has a center of inversion, and the phenyl rings are twisted out of the best molecular plane by $\theta_1 = \theta_2 = 23.7°$ (see Table 1 for a definition of the angles). These phenyl conformations would allow for only attenuated conjugation with the azine fragment even though the N–N s-*trans* conformation is best suited for conjugation through the entire azine system (Scheme 1). The C–N bond lengths are 1.279 Å, similar to that in formaldoxime (1.276 Å).[17] The N–N bond lengths of 1.405 Å in **A** are shorter than the generally accepted N–N single bond length of 1.47 Å,[18] but this shortening is expected for N–N bonds between sp^2-hybridized N atoms and cannot be interpreted as an indication of conjugation. Such hybridization effects are also found for the C–C bonds between the azine C and the aromatic C atom; the bond lengths of 1.482 Å agree with the normal $C_{sp^2}-C_{sp^2}$ single bond length of 1.48 Å.[19]



Scheme 1. Is conjugation with the azine fragment (top) or within the Ar-C-N fragment (bottom) important? Not all resonance forms are shown, and only one form is shown for degenerate structures $R^1 = R^2 = CH_3$.

Thus, neither the C–N and N–N bonds nor the C_{ipso}–C bonds show clear structural indications of phenyl conjugation. This result supports the conclusion we made previously by comparative analysis of related phenyl-substituted azines.[1a, 20]

The N–N and C–N bonds in **A** and **B** differ by no more than 0.002 Å, which leads us to the important conclusion that they are essentially independent of the conformation. Thus, conjugation within the azine functional group cannot be significant for **I**.

In **B** one phenyl ring is twisted only slightly ($\theta_1 = 0.5°$), while the torsion angle of the other is more significant ($\theta_2 = 19.9°$). Structure **B** gives us the unique opportunity of examining the possibility of partial conjugation over the fragment Ar–C–N (Scheme 1, bottom) with experimental data. Surprisingly, the C–N bond in the fragment with the N-C-C_{ipso}-C_{ortho} dihedral angle of 0.5° is 0.005 Å *shorter* than that in the fragment with the more marked torsion angle (19.9°). Moreover, the C–C_{ipso} bond in the first fragment is 0.012 Å *longer* than the analogous bond in the second. The latter C–C_{ipso} bond is virtually identical to those in **A**. These structural data provide strong evidence against significant conjugative interactions in the fragment Ar–C–N. We have shown for Ph(HOOC)C=N–N=CH_2[1a] that the barrier to rotation about the Ph–C bond is less than 5 kcal mol^{-1}, and the present analysis corroborates the conclusions of the theoretical study.

Based on the *gauche* preference of formaldazine, according to CNDO/2 calculations, Ishida et al. concluded that *gauche*-**II** would be thermodynamically preferred over *trans*-**II**. However, higher level ab initio studies of the N–N rotational profile of formaldazine[21] show that the *gauche*-**II** structure is over 2 kcal mol^{-1} less stable than *trans*-**II**. Hence, Ishida's conclusion requires revision. We have investigated the energetic preferences of **I** with all-electron ab initio calculations at the RHF/6-31G* level.[22] We completely optimized **I** (C_1) at the RHF/3-21G level, and the de facto D_{2h}-symmetric N–N s-*trans* structure **1** resulted (Fig. 2 and Table 1). Since no *gauche* conformer exists on the potential energy surface, a model for the *gauche* structure, **2**, was obtained by optimizing **I** with the single constraint of $\tau = 142.8$ (τ angle in **B**). The s-*trans* structure **1** is

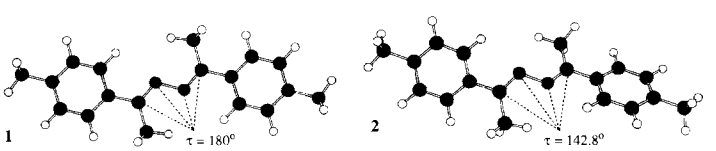


Fig. 2. RHF/3-21G-optimized structures of methyl (*para*-methylphenyl) ketone azine **I**. The planar N–N s-*trans* structure **1** is the minimum; the *gauche* structure **2** was obtained with the constraint C-N-N-C = 142.8°.

Table 1. Selected bond lengths and angles of **A**, **B** [a], **1**, and **2** [b].

Parameter [c, d]	A	B	1	2
N1-N2	1.405(5)	1.407(3)	1.431	1.430
N1-C1	1.279(4)	1.277(4)	1.268	1.267
C1-C2	1.482(4)	1.493(4)	1.491	1.490
C1-C8	1.493(5)	1.494(4)	1.511	1.511
C5-C9	1.509(5)	1.511(4)	1.516	1.516
N2-C10	[e]	1.282(4)	[e]	[e]
C10-C11	[e]	1.481(4)	[e]	[e]
C10-C17	[e]	1.496(4)	[e]	[e]
C14-C18	[e]	1.520(4)	[e]	[e]
N1-N2-C10	[e]	114.17(24)	[e]	[e]
N1-C1-C2	116.0(3)	116.1(3)	117.1	117.2
N1-C1-C8	124.9(3)	123.9(3)	125.3	124.9
N2-N1-C1	114.1(3)	114.97(24)	115.7	116.5
N2-C10-C11	[e]	116.6(3)	[e]	[e]
N2-C10-C17	[e]	123.5(3)	[e]	[e]
C1-N1-N2-C10 = τ	180.0	142.8(3)	180.0	142.8
N2-N1-C1-C8 = ϕ_1	0.5	2.5(2)	0.0	2.2
N1-C1-C2-C7 = θ_1	23.7(2)	0.5(2)	0.0	9.7
N1-N2-C10-C17 = ϕ_2	[e]	3.6(2)	[e]	[e]
N2-C10-C11-C16 = θ_2	[e]	19.9(2)	[e]	[e]
E/E_{rel}(RHF/3-21G): **1**	−797.673044/0.00		**2**: −797.670982/1.29	
E/E_{rel}(RHF/6-31G*): **1**	−802.148751/0.00		**2**: −802.148182/0.36	

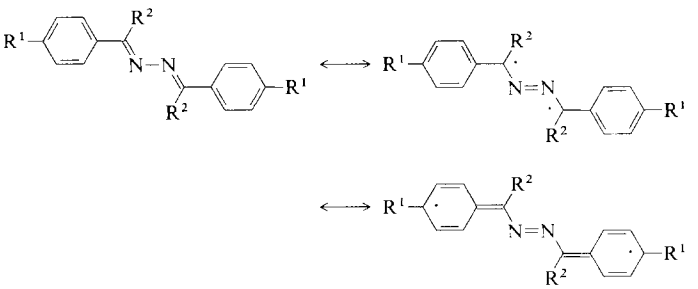
[a] Lengths in Å and angles in degrees. The standard deviations given in parentheses refer to the last digit(s). [b] Structures **1** (optimized in C_1 symmetry, de facto D_{2h} symmetry) and **2** (optimized in C_1 symmetry with C-N-N-C fixed to 142.8°) calculated at the RHF/3-21G level. [c] For atom numbering see Fig. 1. [d] Total and relative energies in Hartrees and kcal mol^{-1}, respectively. Vibrational zero-point energy for the minimum **1** is 227.21 kcal mol^{-1} (RHF/3-21G). [e] Symmetry equivalent to another structural parameter.

preferred over structure **2** by 0.36 kcal mol^{-1} at the RHF/6-31G*//RHF/3-21G level. This theoretical result demonstrates in a compelling fashion that the activation energy required for τ variations between the N–N s-*trans* and *gauche* structures is very small. Hence, small differences in packing interactions in polymorphous crystals suffice to overcome the intrinsic *trans* preference, and solid-state structures with *gauche* molecules also are realized.

Molecule **1** is inversion symmetric and planar, and **2** is C_2-symmetric with azine-phenyl and azine-methyl group twists of 9.7° and 2.2°, respectively. The N–N bonds are about 0.025 Å longer than in the solid-state *trans* and *gauche* conformers, while the C–N bonds are shorter by 0.011 Å.[23] The C–C_{ipso} bond lengths in the gas phase are the same as the corresponding bond in the fragment with $\theta_1 = 0.5°$ in **B** and slightly longer than the others. As was found for the solid-state structures, the important conclusion here is that the conformation dependence of the main structural parameters is minor: for **1** and **2**, all bond lengths are almost the same and the angles differ by less than 1°.

The ^{1}H, ^{13}C, and ^{15}N NMR spectra recorded for **I** show the presence of one isomer in solution. Similarly, the two modifications of **II** give the same ^{1}H NMR spectrum. Therefore, either one centrosymmetric isomer exists in solution or *gauche* enantiomers are found in a fast equilibrium. Our ab initio results favor the former alternative.

Sinha suggested, "there is thus no doubt that ... an excited [diradical] structure ... must also contribute ..." to the ground state of benzaldazine.[24] If the diradical resonance form (Scheme 2) were to contribute to the ground states of phenyl-substituted azines, one would predict that its importance would increase if radical-stabilizing groups were placed in the *para* positions. We examined this prediction by comparison of **1** to the *trans* conformer of unsubstituted methyl phenyl ketone azine[1b] and found that the lengths of the calculated C–N, N–N, and C_{ipso}–C bonds of two D_{2h} structures *are the same.*



Scheme 2. Diradical resonance forms for aryl-substituted azines as suggested by Sinha.

Our analysis thus demonstrates that the resonance form suggested by Sinha plays no major role for the ground state, although other resonance forms may be important for the description of electronically excited states and in discussions of the UV/VIS spectroscopic properties of azines.

Experimental Procedure

Hydrazine hydrate (8 mmol) was added dropwise to a solution of methyl (*para*-tolyl) ketone (10 mmol) in 5 mL of ethanol, and 1 drop of concentrated HCl was then added. The solution was refluxed for 40 min and yellow crystals formed after cooling. M.p. 134–135 °C; ^{1}H NMR (500 MHz, $CDCl_3$): δ = 2.29 (s, 6H; CH_3), 2.38 (s, 6H; CH_3), 7.21 (d, J = 8.1 Hz, 4H; ArH), 7.80 (d, J = 8.1 Hz, 4H; ArH); ^{13}C NMR (125 MHz, $CDCl_3$): δ = 14.8, 21.3, 126.6, 129.0, 135.7, 139.6, 157.6; ^{15}N NMR (51 MHz, CD_2Cl_2): δ = 29.6 [25].

Received: November 30, 1993 [Z 6527 IE]
German version: *Angew. Chem.* **1994**, *106*, 1150

[1] a) R. Glaser, G. S. Chen, C. L. Barnes, *J. Org. Chem.* **1993**, *58*, 7446; b) G. S. Chen, M. Anthamatten, C. L. Barnes, R. Glaser, *J. Org. Chem.*, submitted.
[2] a) Reviews: R. Grashey in *Azomethine Imines, 1,3-Dipolar Cycloaddition Chemistry, Vol. 1* (Ed.: A. Pawda) (*Gen. Heterocycl. Chem. Ser.* **1984**, 733); b) T. Wagner-Jauregg, *Synthesis* **1976**, 349.
[3] C. Kelley, L. A. Mercando, M. R. Terry, N. Lugan, G. L. Geoffrey, Z. Xu, A. L. Rheingold, *Angew. Chem.* **1992**, *104*, 1066; *Angew. Chem. Int. Ed. Engl.* **1992**, *31*, 1053.
[4] a) D. Prajapati, J. S. Sandu, *Heterocycles* **1985**, *23*, 1123; b) E. E. Schweizer, Z. Cao, A. L. Rheingold, M. Bruch, *J. Org. Chem.* **1993**, *58*, 4339.
[5] J. Barluenga, M. J. Iglesias, V. Gotor, *J. Chem. Soc. Chem. Commun.* **1987**, 582, and references therein; I. Ikeda, Y. Kogame, M. Okahara, *J. Org. Chem.* **1985**, *50*, 3640.
[6] V. M. Kolb, A. C. Kuffel, H. O. Spiwek, T. E. Janota, *J. Org. Chem.* **1989**, *54*, 2771.
[7] T. W. Bell, A. T. Papoulis, *Angew. Chem.* **1992**, *104*, 792; *Angew. Chem. Int. Ed. Engl.* **1992**, *31*, 749.
[8] D. S. Dudis, A. T. Yeates, D. Kost, D. A. Smith, J. Medrano, *J. Am. Chem. Soc.* **1993**, *115*, 8770; P. Espinet, J. Etxebarria, M. Marcos, J. Pérez, A. Remón, J. L. Serrano, *Angew. Chem.* **1989**, *101*, 1076; *Angew. Chem. Int. Ed. Engl.* **1989**, *28*, 1065.
[9] E. Flemming, J. Harley-Mason, *J. Chem. Soc.* **1961**, 5560.
[10] X-ray crystal data were collected on an Enraf-Nonius CAD4 diffractometer. **A**: $C_{18}H_{20}N_2$, M_r = 264.37, monoclinic, space group $P2_1/c$, a = 5.6140(20), b = 8.7700(20), c = 15.736(5) Å, β = 98.060(2)°, V = 767.1(4) Å^3, crystal dimensions 0.28 × 0.40 × 0.45 mm^3, T = 298 K, Z = 2, ρ_{calcd} = 1.145 g cm^{-3}, 1113 measured reflections, $\mu(Mo_{K\alpha})$ = 0.06 mm^{-1}, $\theta/2\theta$ scan, λ = 0.70930 Å, 766 observed reflections ($I > 2.0\,\sigma(I)$), 92 parameters; R = 0.065, R_w = 0.085.—**B**: $C_{18}H_{20}N_2$, M_r = 264.37, monoclinic, space group $P2_1/n$, a = 11.4392(10), b = 7.6147(4), c = 17.7270(20) Å, β = 92.289(4)°, V = 1542.90(23) Å^3, crystal dimensions 0.16 × 0.18 × 0.33 mm^3, T = 298 K, Z = 4, ρ_{calcd} = 1.138 g cm^{-3}, 2416 measured reflections, $\mu(Mo_{K\alpha})$ = 0.48 mm^{-1}, $\theta/2\theta$ scan, λ = 1.54056 Å, 1794 observed reflections ($I > 2.0\,\sigma(I)$), 182 parameters; R = 0.060, R_w = 0.095. Further details of the crystal structure investigations are available on request from the Director of the Cambridge Crystallographic Data Centre, 12 Union Road, GB-Cambridge CB21EZ (UK), on quoting the full journal citation.
[11] J. Jacques, A. Collet, S. H. Willen, *Enantiomers, Racemates, and Resolution*, Wiley, New York, **1981**, p. 8ff.
[12] M. C. Garcia-Mina, M. Arrese, M. Martinez-Ripoll, S. Garcia-Blanco, J. L. Serrano, *Acta Crystallogr. Sect. B* **1982**, *38*, 2726; M. R. Ciajolo, A. Sirigu, A. Tuzi, *Acta Crystallogr. Sect. C* **1985**, *41*, 483; L.-Y. Hsu, C. E. Nordman, D. H.

Kenny, *ibid.* **1993**, *49*, 394; B. Mom, G. De With, *Acta Crystallogr. Sect. B* **1978**, *34*, 2785; S. V. Sereda, M. Y. Antipin, T. V. Timofeeva, Y. T. Struchkov, *Sov. Phys. Crystallogr. Engl. Transl.* **1988**, *33*, 66.

[13] E. C. K. Lai, D. Mackay, N. J. Taylor, K. N. Watson, *Can. J. Chem.* **1988**, *66*, 2839.

[14] It is not unusual to find more than one independent molecule in the unit cell. In most cases these symmetry-independent molecules show the same conformation (for recent examples from our group, see R. Glaser, G. S. Chen, C. L. Barnes, *Angew. Chem.* **1992**, *104*, 749; *Angew. Chem. Int. Ed. Engl.* **1992**, *31*, 740; G. S. Chen, R. Glaser, C. L. Barnes, *J. Chem. Soc. Chem. Commun.* **1993**, 1530; R. Glaser, C. L. Mummert, C. J. Horan, C. L. Barnes, *J. Phys. Org. Chem.* **1993**, *6*, 201.); but crystals containing two rotamers are rare.

[15] T. Ishida, M. Inoue, K. Nasu, T. Kurihara, *Acta Crystallogr. Sect. C* **1983**, *39*, 470. In this paper the isomers of **II** are said to have the same NMR spectra in contradiction to previous reports by the same group (T. Kurihara, Y. Sakamoto, M. Mori, T. Sakaki, *Heterocycles* **1978**, *9*, 1041).

[16] C. P. Brock, G. L. Morelan, *J. Phys. Chem.* **1986**, *90*, 5631; H. Grützmacher, H. Pritzkow, *Angew. Chem.* **1992**, *104*, 92; *Angew. Chem. Int. Ed. Engl.* **1992**, *31*, 99; A. Beck, R. Gompper, K. Polborn, H.-U. Wagner, *ibid.* **1993**, *105*, 1424 and **1993**, *32*, 1352.

[17] I. N. Levine, *J. Chem. Phys.* **1963**, *38*, 2326.

[18] C. Standorfy in *General and Theoretical Aspects in the Chemistry of the Carbon-Nitrogen Double Bond* (Ed.: S. Patai), Wiley Interscience, New York, **1970**, p. 2.

[19] A. Streitwieser, C. H. Heathcock, *Organische Chemie*, Verlag Chemie, Weinheim, **1980**, p. 644; *Introduction to Organic Chemistry*, 3rd ed., Macmillan, New York, **1985**, p. 527.

[20] Conjugation might still be important in hetero-substituted azines. a) See literature cited in ref. [1a]; b) K. Hagen, K. Hedberg, *J. Phys. Chem.* **1992**, *96*, 7976; c) G. Kober, P. Rademacher, R. Boese, *J. Chem. Soc. Perkin Trans. 2* **1987**, 761; d) *Acta Chem. Scand. Ser. A* **1988**, *42*, 571.

[21] K. B. Wiberg, P. R. Rablen, M. Marquez, *J. Am. Chem. Soc.* **1992**, *114*, 8654, and references cited in ref. [1a].

[22] W. J. Hehre, L. Radom, P. von R. Schleyer, J. A. Pople, *Ab Initio Molecular Orbital Theory*, Wiley, New York, **1986**.

[23] We found this same feature also in all other azines we have studied; its origin is currently under investigation.

[24] U. C. Sinha, *Acta Crystallogr. Sect. B* **1970**, *26*, 889.

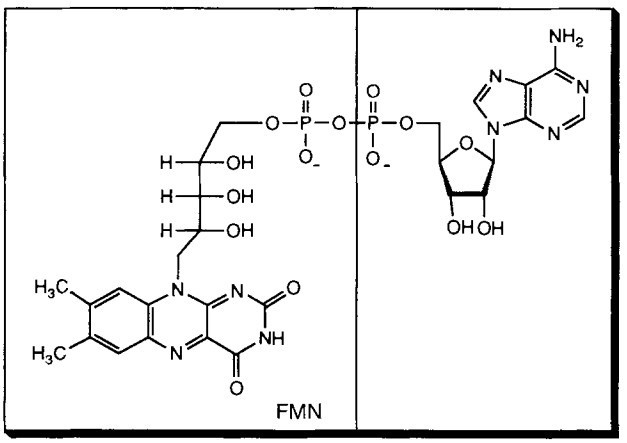
[25] a) Positive chemical shifts reflect increased magnetic shielding relative to the external standard, neat nitromethane. b) M. Witanowski, L. Stefaniak, G. A. Webb, *Nitrogen NMR Spectroscopy* (*Annu. Rep. NMR Spectrosc.* **1981**, *11B*).

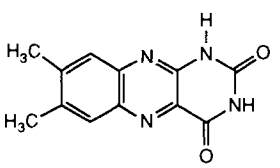
Isolation of RNA Aptamers for Biological Cofactors by In Vitro Selection**

Petra Burgstaller and Michael Famulok*

In vitro selection enables the simultaneous screening of a large number ($\geq 10^{15}$) of different DNA or RNA sequences for certain functionalities. In vitro selection experiments encompass a number of sequential steps, in which the first is always the synthesis of a library of random DNA sequences. After amplification of the DNA by polymerase chain reaction (PCR), an RNA pool is produced by transcription in vitro. Those RNAs (aptamers) that specifically bind to the target molecule are selected from this RNA pool, for example, by affinity chromatography.[1, 2] Such specific ligand-binding nucleic acids not only can have use as potential lead structures for protein inhibitors,[3] but can also help to increase our understanding of the biochemically important recognition processes that involve the interaction of RNA with substrates such as nucleotides, proteins, peptides, amino acids, metal ions, and antibiotics. Furthermore, detailed knowledge of this kind could facilitate the development of new ribozymes.

We report here on the isolation of RNA motifs that bind to the flavin portion of flavin adenine dinucleotide (FAD) and flavin mononucleotide (FMN). In addition, selection experiments were performed in order to isolate RNA aptamers for nicotinamide adenine dinucleotide (NAD^+) and nicotinamide mononucleotide (NMN^+) (Scheme 1).





1

Scheme 1. The FMN, NAD^+, and NMN^+ ligands employed in the selection, and 7,8-dimethylalloxazine which was employed for investigating the binding specificity.

For the selections we used a pool of ^{32}P-labeled RNA 113-mers with a complexity of 10^{15} different sequences which consisted of a random sequence of 74 nucleotides flanked by two defined primer binding sites. By means of affinity chromatography with agarose derivatized with the given cofactor, those RNA sequences were enriched that were bound to agarose and eluted with a solution containing the appropriate ligand (Scheme 2, Table 1).

After six cycles significant amounts of the RNA were bound to the FMN and NAD^+ columns. Binding to the FAD matrix could be detected after four cycles, whereas enrichment of

[*] Dr. M. Famulok, Dipl.-Chem. P. Burgstaller
Fachbereich Chemie, Institut für Biochemie der Universität München
Am Klopferspitz 18a, D-82152 Martinsried (FRG)
Telefax: Int. code + (89)8578-2470

[**] This work was supported by the Deutsche Forschungsgemeinschaft and the European Union (project No. Biot-CT93-0345). We thank E.-L. Winnacker for his support and F. Michel, D. Faulhammer, and T. Luchterhandt for helpful discussions.

a)

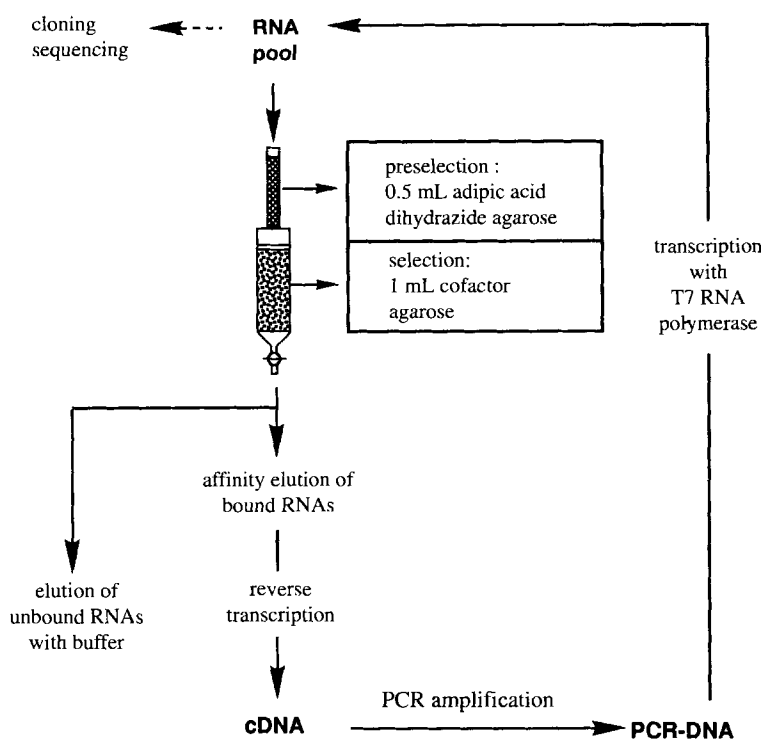
TC TAATACGACTCACTATA GGAGCTCAGCCTTCACTGC →
GGAGCTCAGCCTTCACTGC---(N74)---GGCACCACGGTCGGATCC-3
← CCGTGGTGCCAGCCTAGG

T7-promotor Sac1 Ban1 BamH1

primer sequences:

M27.39: 5′-CCGAATTCTAATACGACTCACTATAGG
M38.27: 5′-TCTAATACGACTCACTATAGGAGCTCAGCCTTCACTGC
M20.106: 5′-GTGGATCCGACCGTGGTGCC

b)



Scheme 2. a) The design of the DNA library for the synthesis of the RNA pools employed. The framed sequence is the T7-promoter, the underlined sequences the restriction sites for the subsequent cloning. b) A schematic representation of the in vitro selection cycle. The RNA was loaded onto the preselection column (0.5 mL adipic acid dihydrazide agarose) and eluted from the column with 1.0 mL of a buffer solution (250 mM NaCl; 50 mM tris-HCL, pH 7.6; 5 mM $MgCl_2$). Nonbinding RNAs were separated by washing with five column volumes of the buffer solution. Bound RNAs were eluted with a buffer solution of the ligand and then treated with reverse transcriptase (50 mM Tris-HCl, pH 8.3; 75 mM KCl; 3 mM $MgCl_2$; 10 mM dithiothreitol (DTT), 0.3% TWEEN 100; 0.4 mM of one of the deoxynucleotide triphosphates dATP, TTP, dGTP, dCTP; 1 μM primer M20.106; 40 U Superscript reverse transcriptase; 45 min reaction at 42 °C). The cDNA was amplified with PCR (10 mM tris-HCL, pH 8.3; 50 mM KCl; 0.01% gelatine; 1.5 mM $MgCl_2$; 0.3% TWEEN 100; 0.2 mM one of the deoxynucleotide triphosphates dATP, TTP, dGTP, dCTP; 3.0 μM primer M38.27; 3.0 μM primer M20.106; 2.5 U 100 μL^{-1} TAQ DNA polymerase; conditions of cycle: 94 °C - 1 min, 55 °C - 2 min, 72 °C - 2 min), the PCR-DNA is transcribed (40 mM tris-HCL, pH 7.9; 6.8 mM spermidine; 22 mM $MgCl_2$; 0.01% Triton X-100; 5 mM of the nucleotide triphosphates ATP, UTP, GTP, CTP; 10 mM DTT; 50 U T7 RNA polymerase; 1–2 μCi α-^{32}P-GTP; reaction for 16 h at 37 °C). The selection cycle can now be repeated with the enriched RNA pool.

NMN^+ was not evident after eight cycles of selection/amplification. The FMN-, FAD-, and NAD^+-selected RNA pools from the last of the respective cycles listed in Table 1 were treated with reverse transcriptase and the cDNA amplified with PCR and cloned. We sequenced 17 clones from the FMN-, 14 from the FAD-, and 16 from the NAD^+-selected RNA pools (Scheme 3).

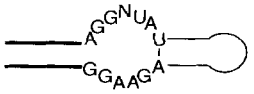
Table 1. Bound fraction [%] of RNA used in the selection cycle. The values represent the fraction of bound RNA that was eluted from the column with the corresponding ligand in the buffer solution; the column was previously washed with five column volumes of buffer solution.

Selection cycle	FMN	FAD	NAD^+	NMN^+
1	0.09	0.11	0.13	0.07
2	1.74	1.20	0.75	0.10
3	1.31	0.14	0.27	0.55
4	0.23	11.09	0.95	0.11
5	0.48	21.38	1.63	0.17
6	33.03		16.07	1.44
7	38.60		36.40	0.12
8				0.33

Thirteen of the FMN-binding RNAs contained two conserved regions with the sequences AGGNUAU and AGAAGG (the sequence of the clone FMN-2 occurred three times). Both consensus sequences are flanked by variable nucleotides, which pair together to form a defined secondary structure. The monoclonal RNAs of the FMN-2, FMN-7, FMN-12, and FMN-15 sequences all have affinity for FMN. By means of analytical affinity chromatography[4] we determined the dissociation constant K_d for the FMN-2 aptamer/FMN complex. The specificity of this RNA was quantified by elution with 7,8-dimethylalloxazine (**1**), FAD, ATP, and GTP. Based on the conserved secondary structure we constructed an RNA sequence of 35 bases (35FMN-2 = 5′-GGCGUGUAGGAUAUCGUGUUCGAGAAGGACACGCC-3′). For the binding of 35FMN-2 and FMN-2 to FMN a K_d of around 0.5 μM was measured. The ribose moiety of FMN was not recognized by the aptamers, as both FMN-2 and 35FMN-2 bind to **1**. Both of these aptamers show very low affinity for adenosine triphosphate (ATP) and do not bind to guanosine triphosphate (GTP) at all. As expected, they bind to FAD with similar values of K_d as for binding to FMN (Table 2).

Four of the fourteen FAD-binding RNAs were identical to the FMN-2 clone. The FAD-3 clone can form the same secondary structure. In comparison to all the other sequences that form this motif, the two consensus sequences are in reversed

FMN Selection



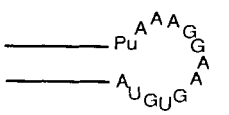
Clone

FMN-2 N_{14}-AGCAGGAUAUG-----N_4-------CAGAAGGGCU-N_3 (3×)
FMN-4 N_{16}-CAUAAGGGUAUUUAAU---N_2---GUUGAGAAGGAUG-N_{20}
FMN-5 N_{16}-GGUGCAGGAUAUG------N_6-------CAGAAGGCACC
FMN-7 N_{44}-UGGUGCAGGUAUUUACG---N_2---CGUUGAGAAGGGCACCA
FMN-9 N_{21}-CGCGCCAGGUAUGCGAA---N_4-UUCUGUCAGAAGGGGUGCG-N_{32}
FMN-10 N_{54}-UCGACUAGGAGGUAUGC-----N_4------GCAGAAGGCCUUUGUCGG-N_{24}
FMN-12 N_{18}-CUUCACUGAAGGGAUAUU------N_4--- ---AACGAAGACUCAGGGGAG-N_{18}
FMN-13 N_{16}-GCAUUCCAGGUAUUUA-----N_2------UAAGAAGGGGAGUGU-N_{15}
FMN-15 N_{62}-CGUUAGGUAUUCU-----N_3------AGAGAAGGAACG-N_{18}
FMN-22 N_{97}-AAGCGUGGUUAGGUAUUGU-----N_4------ACAGAAGGAGCUGCGCUU-N_{28}
FMN-21 N_{14}-GUAAGCCAUAGGAUAUCA-----N_3------UGAGAAGGAUGCUUUAU-N_{18}
FMN-22 N_{54}-UGGUGCUCAGGCUAUC-----N_4------CAGAAGGGGGCACCA
FMN-24 N_{63}-UUUCACGAGGUUAUUG-----N_2------CAGAAGGCGUGAAA-N_{35}

FAD Selection

Clone (Clones 2, 5, 16, and 22 are identical to FMN-2.)

FAD-3 N_{21}-CCCCUCAGAAGGCGCGA------N_{13}---UCGGAGGUAUUGAGUGGG



FAD-1 N_2-UUCGGAAAGGAAGUGUACGAA-N_{12}
FAD-4 N_{40}-UGCGGGCAAAAGGAAGUGUACGUCGCG-N_6
FAD-9 N_{18}-GUCGCUGCGAAAGGAAGGGUAACAGCGGC-N_{26}
FAD-11 N_{34}-AAACAUUAGCAGGAAAGGAAGUGUACUGCAUGUUU-N_4
FAD-20 N_{27}-UGGUGAGGCAGUCGAAAGGAAGUGUAGGUUGCUUCACCA-N_2

Scheme 3. FMN- and FAD-binding RNA sequences. Selected RNAs were treated with reverse transcriptase and amplified by PCR with the M27.39 and M20.106 primers (see Scheme 2a). The M27.39 primer was employed to provide the DNA with *EcoRI* restriction sites. After digestion with *EcoRI* and *BamHI*, the excised fragment was cloned into the vector pGem3z (Promega) [7] and sequenced following the dideoxy method [8]. Only those bases are shown which are relevant in forming the binding motifs shown above each set of sequences. The consensus sequences and a schematic representation of the stem region are also shown.

Table 2. Dissociation constants K_d for the binding of FMN-2, 35FMN-2, FAD-1, and 27FAD-1 to various ligands in solution [a].

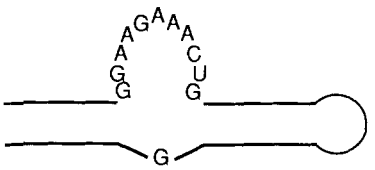
Ligand	K_d [μM]			
	FMN-2	35FMN-2	FAD-1	27FAD-1
FMN	0.5	0.5	84	280
FAD	1.4	0.7	137	273
1	0.5	0.3	23	35
ATP	250	163	4×10^3	2×10^3
GTP	$>5\times10^4$	$>5\times10^4$	3×10^3	3×10^3

[a] The K_d values were determined by elution of ^{32}P-labeled RNA from a column, which contained 1.0 mL of a 0.5 mM FMN or 3 mM FAD agarose, and were calculated according to the equation $K_d = [L]\times\{(V_{el}-V_o)\times(V_e-V_{el})\}$ [1f]. [L] is the concentration of the ligand in the solution, V_{el} the elution volume in the presence of the ligand in solution, V_e the elution volume with buffer solution in the absence of the ligand, V_o the void volume of the column (0.7 mL).

order. This finding in particular strongly supports the proposed secondary structure. The FAD selection provided another binding motif, the conserved 13-mer 5′-PuAAAGGAAGUGUA-3′, which is flanked by pairing base pairs, leading to formation of the stem-loop structure shown in Scheme 3. This motif was found in five sequences (FAD-1, FAD-4, FAD-9, FAD-11, and FAD-20). The affinity of FAD-1 for FAD or FMN is significantly lower than the affinity of the FMN-2 motif for these ligands (Table 2). FAD-1 also recognizes exclusively the flavin portion of FAD, since binding to **1** (K_d = 23 μM) is significantly better than binding to FMN (84 μM), and there is virtually no affinity for the adenosine portion of FAD ($K_d^{ATP} \geq$ 4.0 mM). FAD-1 likewise does not bind to GTP. A minimal 27-mer RNA based on the secondary structure of FAD-1 (27FAD-1 = 5′-GGCAGUCGAAAGGAAGUGUAGACUGCC-3′) and containing the consensus sequence and the stem region exhibits binding constants that are somewhat weaker but on the same order of magnitude as those of the full-length aptamer FAD-1.[5] It is, therefore, one of the smallest specific ligand-binding RNAs known to date. The corresponding DNA sequence of this aptamer has no measurable affinity for FAD.

Why was only one binding motif with affinity for the flavin portion obtained in the FMN selection, whereas in the FAD selection a second motif of significantly lower affinity could also be isolated? This may well be explained by the different concentrations of the ligand in the FMN and the FAD agaroses (FMN: 0.5 mM; FAD: 3.0 mM). A comparison of the elution volumes V_e of FAD-1 for the two derivatized agarose types, V_e = 2 mL for the FMN agarose and V_e = 13 mL for the FAD agarose, provides values of K_d of a similar magnitude. This implies that all FAD-1-type binding species were removed from the FMN agarose with the 5.0 mL washing employed during selection and as a result were not enriched.

All sixteen NAD^+-binding sequences contained the base sequence GGAAGAAACUG. This same consensus sequence is a component of an ATP-binding RNA motif isolated recently by Sassanfar and Szostak.[1d] Indeed, the aptamers that we isolated can fold into the identical motif (Scheme 4). This aptamer binds to the adenosine portion of ATP with a K_d of 4.0 μM and also has affinity for NAD^+. To enrich aptamers, which may be present in small concentrations in the selection pool and which require the NMN^+ portion for binding to NAD^+, we performed three additional selection cycles, in which a negative selection with ATP preceded the elution with NAD^+. However, no further binding species were obtained. This result was confirmed by an NMN^+ selection (Table 1), which likewise did not lead to an enrichment of binding species over eight cycles. The simplest explanation for these results would be that the pool does not contain a single sequence capable of binding to NMN^+.[6]



Scheme 4. RNA-binding motif [1d] for the adenosine portion of ATP or NAD^+.

What is remarkable about this result with NAD^+ and ATP selections[1d] is the fact that two completely independent selections employed for the structurally related, but yet different agaroses and ligands (and nucleic acid pools) led to identical aptamers, and indeed exclusively to those with affinity for the adenosine portion of the ligand. The fact that this motif can be isolated repeatedly from independent pools with a complexity of 10^{14}–10^{15} sequences illustrates the high certainty and precision of this selection technique. Furthermore, this result indicates that the adenosine-specific aptamer is the "optimal sequence solution" for the molecular recognition of adenosine by RNA.

In conclusion, we were able to select new RNA motifs for the specific recognition of biological cofactors from randomized RNA pools. The aptamers described recognize preferentially certain regions of a ligand. Other regions were only poorly bound or not at all. The RNA motifs 35FMN-2 and 27FAF-1 represent a new class of supramolecular systems for the highly specific recognition of flavins based on "irrational receptor design".[9, 10]

Received: November 25, 1993
Revised version: January 18, 1994 [Z6511IE]
German version: *Angew. Chem.* **1994**, *106*, 1163

[1] a) A. D. Ellington, J. W. Szostak, *Nature* **1990**, *346*, 818; b) *ibid.* **1992**, *355*, 850; c) M. Famulok, J. W. Szostak, *J. Am. Chem. Soc.* **1992**, *114*, 3990; d) M. Sassanfar, J. W. Szostak, *Nature* **1993**, *364*, 550; e) D. P. Bartel, J. W. Szostak, *Science* **1993**, *261*, 1411; f) G. J. Connell, M. Illangesekare, M. Yarus, *Biochemistry* **1993**, *32*, 5497; g) M. Famulok, *J. Am. Chem. Soc.*, **1994**, *116*, 1698.

[2] Reviews: a) M. Famulok, J. W. Szostak, *Angew. Chem.* **1992**, *103*, 1001; *Angew. Chem. Int. Ed. Engl.* **1992**, *31*, 979; b) J. W. Szostak, *Trends Biochem. Sci.* **1992**, *17*, 89; c) M. Famulok, J. W. Szostak in *Nucleic Acids and Molecular Biology*, *Vol. 7* (Eds.: F. Eckstein, D. M. J. Lilley), Springer, Berlin, **1993**, p. 271.

[3] a) C. Tuerk, L. Gold, *Science* **1990**, *249*, 505; b) L. C. Bock, L. C. Griffin, J. A. Latham, E. H. Vermaas, J. J. Toole, *Nature* **1992**, *355*, 564; c) C. Tuerk, S. MacDougal, L. Gold, *Proc. Natl. Acad. Sci. USA* **1992**, *89*, 6988; d) D. Schneider, C. Tuerk, L. Gold, *J. Mol. Biol.* **1992**, *228*, 862; e) M. L. Riordan, J. C. Martin, *Nature* **1991**, *350*, 442.

[4] F. H. Arnold, S. A. Scofield, H. W. Blanch, *J. Chromatogr.* **1986**, *355*, 1.

[5] It is striking that FAD-1 and 27FAD-1 bind to **1** more strongly than to FAD or FMN. An explanation for this could be that **1** does not have a negatively charged phosphate group and thus repulsion of the RNA phosphate backbone is not possible. Similar explanations have been given for comparable observations (see ref. [1d]). Other possible explanations include gain or loss of binding entropy as a result of differences in the hydrate shell of **1** and FMN or FAD, aryl stacking interactions, and steric phenomena. Detailed structural investigations would provide a greater insight into such observations.

[6] It is possible that the stringency of the selection conditions did not allow isolation of aptamers that bind NMN^+ or the NMN^+ portion of NAD^+. We are currently examining different buffer conditions, metal ions, and ligand concentrations as well as elution volumes (as with FAD-1), which could lead to isolation of specific motifs. However, the pool certainly did not contain motifs specific for NMN^+ with K_d values comparable to those of the ATP-binding species (1–10 μM).

[7] a) J. Sambrook, E. F. Fritsch, T. Maniatis, *Molecular Cloning*, 2nd ed., Cold Spring Harbor Laboratory Press, Cold Spring Harbor, **1989**; b) F. Asubel, R. Brent, R. E. Kingston, D. D. Moore, J. G. Seidman, J. A. Smith, K. Struhl, *Current Protocols in Molecular Biology*, Wiley, New York, **1987**.

[8] F. Sanger, S. Nicklen, A. R. Coulson, *Proc. Natl. Acad. Sci. USA* **1977**, *74*, 5463.

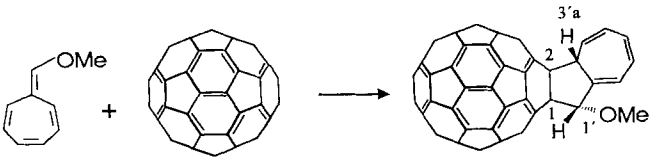
[9] Examples of flavin receptors based on rational receptor design: Y. Aoyama, Y. Tanaka, H. Toi, H. Ogoshi, *J. Am. Chem. Soc.* **1988**, *110*, 634; b) Y. Yano, N. Tamura, K. Mitsui, T. Nabeshima, *Chem. Lett.* **1989**, 1655; c) Y. Aoyama, K. Mizokami, H. Toi, *ibid.* **1990**, 651.

[10] See ref. [2] in G. von Kiedrowski, *Angew. Chem.* **1991**, *103*, 839; *Angew. Chem. Int. Ed. Engl.* **1991**, *30*, 822.

Functionalization of C_{60} Buckminsterfullerene by [8 + 2] Cycloaddition: Spectroscopic and Electron-Transfer Properties of a Tetrahydroazulenofullerene**

Ernst Beer, Michaela Feuerer, Andreas Knorr, Albert Mirlach, and Jörg Daub*

8-Methoxyheptafulvene (**1**) has pronounced π-donor properties[1] and reacts with acceptor-substituted alkenes to form tetrahydroazulenes in a regiospecific [8 + 2] cycloaddition.[2] In contrast, buckminsterfullerene C_{60} (**2**) has a high electron affinity (E_A = 2.6–2.8 eV).[3] This is the reason for the electrophilic nature of the π-system: reactions normally occur at the double bond common to two annulated six-membered rings (6,6 bonds), and **2** can be reduced to the hexaanion.[4, 5] Owing to these properties, the [8 + 2] cycloaddition of **1** with **2** should lead to annulated fullerenes,[6] which would open up a potential route to polyfunctional fullerene derivatives with opto-electronic properties. We report here for the first time on an [8 + 2] cycloaddition of **2** (Scheme 1).



1 **2** **3**

Scheme 1. Reaction of 8-methoxyheptafulvene (**1**) with C_{60} (**2**).

Treatment of 8-methoxyheptafulvene (**1**) with C_{60} (**2**) (in toluene, under a nitrogen atmosphere, at room temperature) gave a mixture of products whose HPLC trace shows more than 90% of one main product. The main fraction from gel permeation chromatography (GPC) on polystyrene gel (eluent: chloroform) was further purified by column chromatography (SiO_2, eluent: toluene/hexane, 6:4).[7] The structure and stereochemistry of the main product were determined by mass spectrometry, and NMR and electron spectroscopy. A peak at *m/z* 854 in the mass spectrum (negative ion, secondary ion mass spectrometry) proves the formation of a monoadduct. In addition, the C_{60} signal at *m/z* 720 indicates that a thermal retro-[8 + 2] cycloaddition occurs. The ^1H NMR spectrum displays the typical resonance signals of a tetrahydroazulene moiety:[8] the signals for 1′-H, 8′-H, 3′a-H in **3** are shifted downfield in comparison to those of structurally related tetrahydroazulenes, reflecting the magnetic anisotropy of the spherical C_{60} unit. In contrast to the C_{60} derivatives studied up to now, the reduced symmetry of **3** (C_1 rather than I_h) results in the separation of all signals in the ^{13}C NMR spectrum. The two signals at δ = 75.13 and 71.58 due to the quaternary aliphatic carbon atoms show conclusively that no bonds within the carbon sphere were broken. Further proof supporting the proposed structure comes from ^{13}C NMR polarization transfer experiments (^{13}C DEPT). The seven methine carbon atoms and the carbon atom of the methoxy group give positive signals. The UV/VIS spectrum shows a band at λ = 432 nm, which is also observed in other C_{60} cycloadducts bridged at a 6,6 bond.[9] The [8 + 2] cycloaddition can take place at either the 6,6 or the 5,6 double bond. Reaction at the 6,6 linkage would produce two *cis*/*trans* diastereomers and at the 5,6 bond up to four diastereomers. Because of the slowness of the [8 + 2] cycloaddition and by analogy with known examples, we assign structure **3** to the major product. In this case the 6,6 double bond in **2** reacts with the sterically less hindered side of **1**, giving **3** with hydrogen atoms C-3′a and C-1′ in the *cis* configuration. The spatial proximity of 3′a-H and 1′-H was confirmed by NOE experiments. The regioselectivity of the reaction is also supported by semiempirical calculations (MNDO, AM1, PM3).[10] The calculated heats of formation H_f of the possible isomers as well as the length of the bridged single bond length in the C_{60} unit are shown in Table 1.

Cyclovoltammetric and spectroelectrochemical studies[11,12] show that the cyclopentane-annulated fullerene **3** is reduced in four reversible or quasi-reversible steps (Table 2, Fig. 1). The radical anion $\mathbf{3}^{\bullet-}$, dianion $\mathbf{3}^{2-}$, and radical trianion $\mathbf{3}^{\bullet 3-}$ were

[*] Prof. Dr. J. Daub, Dipl.-Chem. E. Beer, M. Feuerer, Dipl.-Chem. A. Knorr, Dr. A. Mirlach
Institut für Organische Chemie der Universität
Universitätstrasse 31
D-93040 Regensburg (FRG)
Telefax: Int. code + (941) 943-4984

[**] This work was supported by Hoechst AG. A. K. thanks the Fonds der Chemischen Industrie for a doctoral fellowship. The following colleagues also contributed to this paper: Dr. K. Mayer, J. Kiermeier, Dr. ter Meer (MS), Prof. K. Müllen, Dipl.-Chem. F. Beer (GPC), Dr. E. Eibler, Dipl.-Chem. R. Vasold (HPLC), Dr. T. Burgermeister, and F. Kastner (NMR).

Table 1. Calculated molar heats of formation H_f for the possible regioisomers of **3** and the length of the bridged single bond in the C_{60} unit.

Isomer	Method MNDO	AM1	PM3
		H_f [kcal mol^{-1}]	
cis-6,6	851.51	954.75	797.53
cis-6,5	866.69	972.51	815.32
Δ-*cis*-(6,6-6,5)	15.81	17.76	17.79
		d [Å]	
cis-6,6	1.616	1.580	1.586
cis-6,5	1.640	1.623	1.618

Table 2. Half-step potentials determined by cyclic voltammetry for the reduction of C_{60} (**2**) and the C_{60} derivative (**3**) in different solvents.

Potential [mV][a]	Compound and solvent C_{60} in benzene/CH_3CN 10:1	C_{60} in toluene/CH_3CN 8:2	**3** in THF	**3** in toluene/CH_3CN 8:2
$E^{I}_{1/2}$	−990	−1000	−1090	−1120
$E^{II}_{1/2}$	−1370	−1410	−1640	−1510
$E^{III}_{1/2}$	−1900	−1910	−2260	−2080
$E^{IV}_{1/2}$	−2410	−2380	−2710	−2520

[a] Potentials vs. ferrocene/ferrocenium.

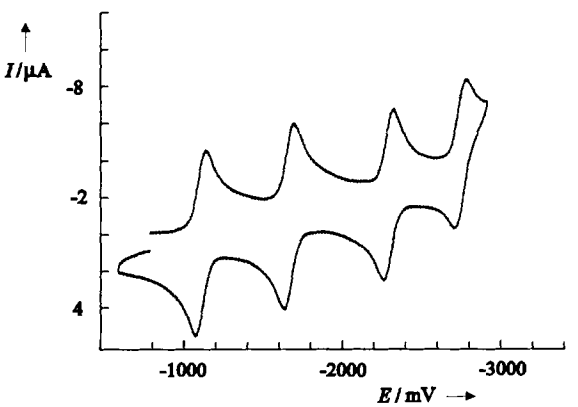


Fig. 1. Cyclic voltammogram of **3** in THF, 0.1 M Bu_4NPF_6, 500 mV s^{-1}; potentials vs. ferrocene/ferrocenium.

clearly identified by UV/VIS/NIR spectroscopy (Fig. 2, Table 3). The reversibility of the reduction steps was confirmed by the isosbestic points. In comparison to the parent compound C_{60} (**2**), compound **3** has a more negative reduction potential for each reduction, in other words, the annulated fullerene derivative **3** is less easily reduced. The longest wavelength bands from the radical anion and radical trianion are the furthest shifted in the NIR region ($\mathbf{3}^{\bullet-}$: 984 nm/1.26 eV; $\mathbf{3}^{\bullet 3-}$: 1342 nm/0.92 eV). In the dianion the lowest energy absorption is at 864 nm/1.43 eV.

This [8 + 2] cycloaddition of buckminsterfullerene C_{60} points out a route to chiral fullerene derivatives containing a tetrahydroazulene unit, making possible the synthesis of fullerenes containing nonalternant substructures with electron-transfer properties. Preliminary studies indicate that the reaction of **3** with triphenylmethylium hexachloroantimonate to give a fullerene tropylium ion proceeds by hydride cleavage. In addition, the cycloheptatriene unit undergoes cycloadditions with 4-methyl-1,2,4-triazol-3,5-diones. We are currently studying C_{60} compounds made from electron-rich fulvenoids and nonfulvenoid π-systems.

Table 3. UV/VIS-NIR data for the radical anion, dianion, and radical trianion of **3** in THF. The lowest energy absorption of C_{60}(**2**) is given for comparison.

Ion	λ [nm]	Isosbestic points [nm]	λ_{max} of **3** [nm]	λ_{max} of C_{60} [nm]
$\mathbf{3}^{\bullet-}$	257, 343 (sh), 563, 984	238, 259, 304, 332	984	1072
$\mathbf{3}^{2-}$	254, 377 (sh), 710, 864	250, 263, 323, 343, 914	864	799
$\mathbf{3}^{\bullet 3-}$	250, 375 (sh), 480, 669, 871, 1342	223, 696, 882	1342	1364

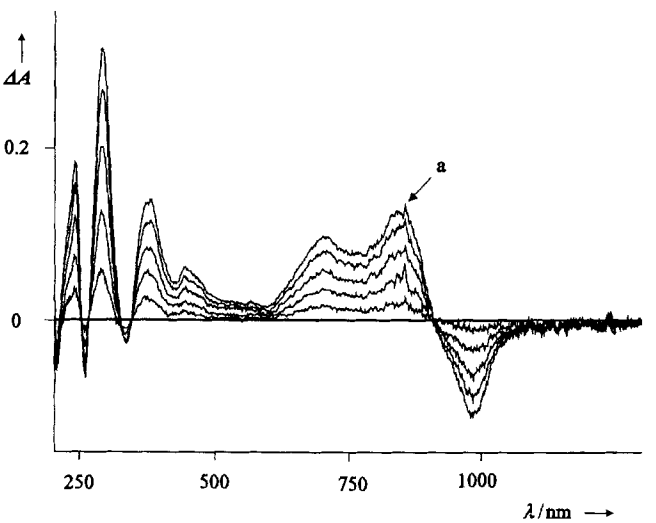


Fig. 2. UV/VIS-NIR potential step difference spectroscopy. Curve a is the spectrum of $\mathbf{3}^{\bullet-}$ subtracted from the spectrum of $\mathbf{3}^{2-}$. The electrochemical uniformity of the conversion of $\mathbf{3}^{\bullet-}$ into $\mathbf{3}^{2-}$ can be seen in the other curves.

Experimental Procedure

8-Methoxyheptafulvene (**1**) (121 mg, 0.9 mmol) was dissolved in 350 mL dry toluene under a nitrogen atmosphere. To this brown solution was added C_{60} (500 mg, 0.7 mmol), and the mixture was stirred for one week at room temperature. The reaction mixture was then concentrated to 50 mL and cooled to 0 °C. This led to precipitation of product, which was isolated by decanting the supernatant, washing with toluene and diethyl ether, and then drying under vacuum (0.01 Torr) at room temperature. This gave 401.4 mg of black-brown powder. The HPLC trace showed C_{60} along with several reaction products, of which the main one was present to >90%. A saturated solution (30 mL) of the crude product in $CHCl_3$ was purified by GPC [7]. The fraction that eluted with a retention time of 30.1 min was chromatographed on a SiO_2 column (3 × 40 cm, toluene/hexane 6:4) under a nitrogen atmosphere to provide pure **3** (17 mg).

NI-LISIMS-MS (*m*-nitrobenzyl alcohol/toluene): *m/z* (%): 886 (13) [$M^{\bullet-}$ + O_2] [13], 854 (20) [$M^{\bullet-}$], 720 (100) [C_{60}^{-}]; UV/VIS (toluene): λ_{max} (lg ε) = 285 (4.70), 308 (4.65) sh, 327 (4.64) sh, 432 (3.65), 483 (3.30) sh, 547 (3.09) sh, 640 (2.69) sh, 706 (2.62); ^{1}H NMR (400 MHz, CS_2/CD_2Cl_2 6:1, 25 °C, TMS) δ = 3.37 (s, 3H; OMe); 3.90 (ddd, ^3J (4',3'a) = 5.2 Hz, ^4J (5',3'a) = 1.4 Hz, ^4J (8',3'a) = 1.4 Hz, 1H; H-3'a); 5.54 (d, ^4J (8',1') = 0.9 Hz, 1H; H-1'); 6.25 (ddd, ^3J (5',4') = 9.3 Hz, ^3J (3'a,4') = 5.2 Hz, ^4J (6',4') = 0.7 Hz, 1H; H-4'); 6.39–6.44 (m, 1H; H-5'); 6.81 (dd, ^3J (7',8') = 4.5 Hz, ^4J (1',8') = 0.9 Hz, 1H; H-8'); 6.91–6.94 (m, 2H; H-7', H-6'); ^{13}C NMR (100 MHz, CS_2/CD_2Cl_2 6:1, 25 °C, TMS): = 156.03, 153.26, 153.03, 152.28, 146.41, 146.36, 146.07, 145.40, 145.38, 145.26, 145.24, 145.20, 145.16, 145.07, 145.05, 145.00, 144.98, 144.73, 144.69, 144.65, 144.61, 144.34, 144.30, 144.21, 144.19, 144.06, 144.04, 143.79, 143.70, 143.67, 143.36, 143.32, 142.21, 142.09, 142.06, 141.70, 141.58, 141.56, 141.44, 141.40, 141.26, 141.25, 141.18, 141.11, 141.10, 140.97, 140.82, 140.72, 140.59, 140.48, 139.20, 139.06, 138.81, 138.80, 137.50, 135.96, 134.85, 132.32 (58 sp^2-C of C_{60}); 133.66 (quaternary C-8a'

in cycloheptatriene): 131.55, 128.74, 124.00, 122.99, 120.74 (sp^2-C in cycloheptatriene); 90.20 (C-3'a), 75.13, 71.58 (2 sp^3-C of C_{60}); 55.42, 55.01 (C-1', OMe).

Received: December 23, 1993 [Z 6577 IE]
German version: *Angew. Chem.* **1994**, *106*, 1140

[1] a) J. Daub, *Chimia* **1987**, *41*, 52–59; b) W. Bauer, I. Betz, J. Daub, L. Jakob, W. Pickl, K. M. Rapp, *Chem. Ber.* **1983**, *116*, 1154–1173.
[2] J. Daub, G. Hirmer, L. Jakob, G. Maas, W. Pickl, E. Pirzer, K. M. Rapp, *Chem. Ber.* **1985**, *118*, 1836–1856.
[3] S. H. Yang, C. L. Pettiette, J. Conceicao, O. Cheshnovsky, R. E. Smalley, *Chem. Phys. Lett.* **1987**, *139*, 233–238.
[4] Reviews: a) R. Taylor, D. R. M. Walton, *Nature* **1993**, *363*, 685–693; b) F. Wudl, *Acc. Chem. Res.* **1992**, *25*, 157–161; c) A. Hirsch, *Angew. Chem.* **1993**, *105*, 1189–1192; *Angew. Chem. Int. Ed. Engl.* **1993**, *32*, 1138–1141.
[5] a) Q. Xie, E. Perez-Cordero, L. Echegoyen, *J. Am. Chem. Soc.* **1992**, *114*, 3978–3980; b) D. Dubois, G. Moninot, W. Kutzner, M. T. Jones, K. M. Kadish, *J. Phys. Chem.* **1992**, *96*, 7137–7145; c) D. Dubois, K. M. Kadish, S. Flanagan, R. E. Haufler, L. P. F. Chibante, L. J. Wilson, *J. Am. Chem. Soc.* **1991**, *113*, 4364–4366; d) G. A. Heath, J. E. McGrady, R. L. Martin, *J. Chem. Soc. Chem. Commun.* **1992**, *17*, 1272–1274; e) M. Baumgarten, A. Gügel, L. Gherghel, *Adv. Mater.* **1993**, *6*, 458–461.
[6] Selected reports [4 + 2] cycloadditions: a) M. Prato, T. Suzuki, H. Foroudian, Q. Li, K. Khemani, F. Wudl, J. Leonetti, R. D. Little, T. White, B. Rickborn, S. Yamago, E. Nakamura, *J. Am. Chem. Soc.* **1993**, *115*, 1594–1595; b) P. Belik, A. Gügel, J. Spickermann, K. Müllen, *Angew. Chem.* **1993**, *105*, 95–97; *Angew. Chem. Int. Ed. Engl.* **1993**, *32*, 78–80; c) F. Diederich, U. Jonas, V. Gramlich, A. Herrmann, H. Ringsdorf, C. Thilgen, *Helv. Chim. Acta* **1993**, *76*, 2445–2453, and references therein.
[7] GPC purification was conducted with a polystyrene gel column (30 × 600 mm, 10 μm, 500 Å) from the company PSS, Mainz (FRG), eluting with $CHCl_3$. The construction of the apparatus is the same as that in ref. [6]. The separation was conducted by co-workers of Prof. Dr. K. Müllen at the Max-Planck-Institut für Polymerforschung in Mainz.
[8] J. Daub, S. Gierisch, T. Knöchel, E. Salbeck, G. Maas, *Z. Naturforsch. Teil B* **1986**, *41*, 1151–1160.
[9] Cf.: L. Isaacs, A. Wehrsig, F. Diederich, *Helv. Chim. Acta* **1993**, *76*, 1231–1250.
[10] All calculations were conducted with the program packages VAMP 4.5 [11] on the restricted Hartree–Fock (RHF) level without symmetry restrictions. The calculated geometries were characterized as minima on the potential energy surface by vibrational analysis.
[11] G. Rauhut, A. Alex, J. Chandrasekhar, T. Clark, *VAMP 4.5, Oxford Molecular Ltd.*, Oxford, **1993**.
[12] J. Salbeck, I. Aurbach, J. Daub, *Dechema Monogr.* **1988**, *112*, 177–191; J. Salbeck, *Anal. Chem.* **1993**, *65*, 2169–2173.
[13] Compound **3** reacts completely within 20 min to produce a very polar species. Treatment of **3** with 4-methyl-3*H*-1,2,4-triazol-3,5-dione gives a mixture of at least three isomers according to the 400 MHz ^{1}H NMR spectrum; only one peak for the molecular ion at *m/z* 968 is seen in the mass spectrum of the reaction mixture.
[14] Dissolved **3** reacts with oxygen.

Regio- and Enantioselective Silane-Terminated Intramolecular Heck Reactions**

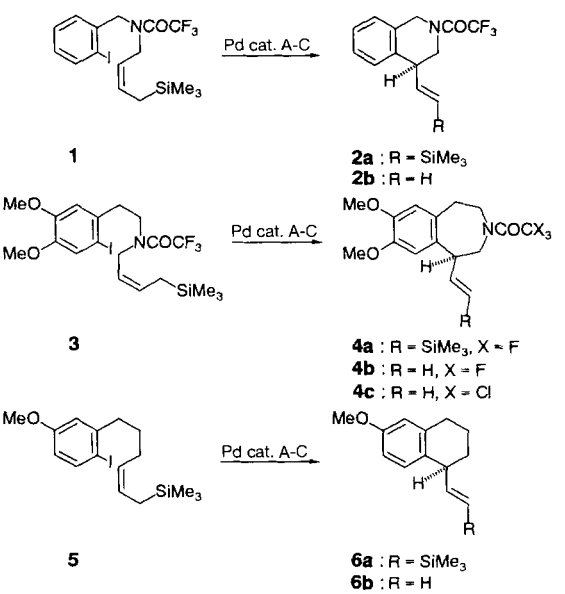
Lutz F. Tietze* and Ralph Schimpf

Dedicated to Professor Wolfgang Lüttke on the occasion of his 75th birthday

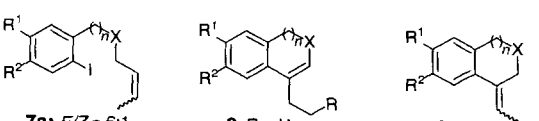
The Pd^0-catalyzed reaction of an aryl or vinyl halide (RX) with an alkene known as the Heck reaction is an important method of C–C bond formation, which has already been used in numerous syntheses of natural products.[1, 2] In addition this reaction is of great significance for the chemical industry. A distinct disadvantage of this C–C bond forming reaction, however, is the frequently low selectivity with regard to the position of the double bond in the product.[2–4] This can be traced back, firstly, to the β-hydride elimination, which occurs in the catalytic cycle, and which can often proceed in different directions; and secondly, to the tendency of the eliminated HPdX species to undergo readdition and subsequently elimination once again.

Thus, the regioselective formation of tertiary sp^3 C centers, which is of importance for the asymmetric Heck reaction, is possible in only a limited number of cases. Enantioselective Heck reactions are therefore currently more or less restricted to cyclic olefins, in which only one direction of elimination is allowed, and to reactions in which quaternary stereogenic centers are formed.[5, 6] We have now been able to demonstrate that tertiary sp^3 centers can be formed in a highly selective manner by using an intramolecular Heck reaction in which the alkene component is an allylsilane.[7] In this way, depending on the reaction conditions, vinyl- or (*E*)-trimethylsilylvinyl-substituted hetero- and carbocycles can be prepared in good yields. Moreover, when (*S*)-2,2'-bis(diphenylphosphino)-1,1'-binaphthyl ((*S*)-BINAP) is used as a ligand, enantioselectivities of up to 90% *ee* can be achieved.

In order to document the significance of the trimethylsilyl group in substrates such as **1**, **3**, and **5** for the direction of



elimination, we have also examined, as a comparison, the Heck reaction of the corresponding compounds **7a–c**, which do not contain a trimethylsilyl group. Three catalyst systems were used: $Pd(OAc)_2/PPh_3/KOAc/NPr_4Br$ (A),[3, 8, 9] $Pd_2(dba)_3/PPh_3/Ag_2O$ (B),[9] and $[Pd_2(dba)_3]$/(*S*)-BINAP/Ag_3PO_4 (C)[6]



7–11	X	*n*	R^1	R^2
a	$NCOCF_3$	1	H	H
b	$NCOCF_3$	2	OMe	OMe
c	CH_2	1	OMe	H

[*] Prof. Dr. L. F. Tietze, Dipl.-Chem. R. Schimpf
Institut für Organische Chemie der Universität
Tammannstrasse 2, D-37077 Göttingen (FRG)
Telefax: Int. code + (551) 39-9476

[**] This work was supported by the Volkswagen-Stiftung and the Fonds der Chemischen Industrie. We also thank Bayer AG and Degussa AG for their generous contributions.

(dba = dibenzylidenacetone). The reaction of compound **1** with catalyst system A yielded exclusively the vinyl-substituted 1,2,3,4-tetrahydroisoquinoline **2b** in 81% yield, whereas with catalyst system B a mixture of **2a** and a small amount of **2b** (93:7) was obtained in 69% yield. Comparable selectivity and yields were also obtained in the conversion of **3** into the 2,3,4,5-tetrahydro-1*H*-3-benzazepine derivatives **4a** and **4b**. Double bond isomers such as **8**–**11** could not be detected in any of these reactions (Table 1). Compound **5** showed somewhat different behavior. In this case reaction with catalyst system A gave a mixture of 1,2,3,4-tetrahydronaphthalenes **6a** and **6b** and 3,4-dihydronaphthalene **9c** in 70% yield; on the other hand, the use of catalyst system B led exclusively to **6a** in 60% yield (Table 1).[10]

Table 1. Heck reactions of **1**, **3**, and **5** with catalyst systems A–C.

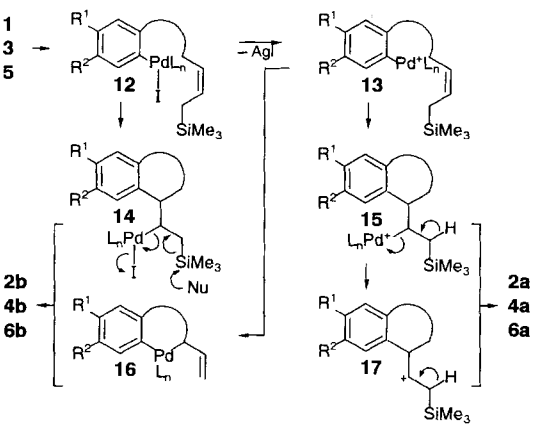
	Cat. [a]	*t* [h]	*T* [°C]	Yield [%] (conversion [%])	Prod.	Product ratios[b] and enantioselectivities[11] a	b	*ee* [%]	8–11
1	A	3	55	81 (100)	**2**	<1	100	–	<1
	B	5	55	69 (100)		93	7	–	<1
	C	48	75	70 (95)		10	90	72[c]	<1
3	A	4	80	56 (70)	**4**	10	90	–	<1
	B	24	80	76 (100)		95	5	–	<1
	C	40	80	79 (100)		9	91	64[d]	<1
5	A	3	65	70 (88)	**6**	44	37		19 (**9c**)
	B	20	65	80 (95)		100	<1	–	<1
	C	24	80	92 (100)		17	83	90[e]	<1

[a] A: 5 mol% $Pd(OAc)_2$/10 mol% PPh_3/3 equiv KOAc/1 equiv NPr_4Br, dimethylformamide (DMF); B: 2.5 mol% $[Pd_2(dba)_3]$/10 mol% PPh_3/1 equiv Ag_2O, DMF; C: 2.5 mol% $[Pd_2(dba)_3]$/7 mol% (*S*)-BINAP /1 equiv Ag_3PO_4, DMF (**1**, **5**) or dimethylacetamide (**3**). [b] The product mixture was separated by chromatography on silica; for **6a** and **6b** silica doped with $AgNO_3$ (10%) had to be used. The ratio of **6a**, **6b**, and **9c** was determined by ^1H and ^{13}CNMR spectra. [c] $[\alpha]_D^{20} = +70.2$ ($c = 1.0$, $CHCl_3$). [d] $[\alpha]_D^{20} = +44.5$ ($c = 1.0$, $CHCl_3$). [e] $[\alpha]_D^{20} = +94.3$ ($c = 1.0$, $CHCl_3$).

The conversions of **1**, **3**, and **5** with the chiral catalyst system C is naturally of particular interest. The highest enantioselectivity of 90% *ee* was obtained for the cyclization of **5** to give **6b**. Similarly, for the formation of **2b** from **1** and **4b** from **3**, respective selectivities of 72% and 64% *ee* were achieved;[11] **4b** could be obtained in enantiomerically pure form by recrystallization.[12] For the determination of absolute configuration **4b** was converted to the trichloroacetyl derivative **4c**. A crystal structure analysis of this derivative indicated that the stereogenic center has the (*S*) configuration.[13] On the basis of the very similar optical rotations of **2b**, **4b**, and **6b**[12] it was assumed that **2b** and **6b** also have the (*S*) configuration. Remarkably, the vinylsilanes **2a**, **3a** and **6a**, which are formed as side products, display very little optical activity. Isomerization experiments proved that **2a**,**b**, **4a**,**b**, and **6a**,**b** are stable under the reaction conditions. Therefore it must be assumed that the cyclization giving vinyl- and trimethylsilylvinyl-substituted compounds follows a different mechanism, at least when catalyst system C is used. It is also surprising that the directing effect of the silver salt is canceled by addition of (*S*)-BINAP. This effect can be seen by comparison of the product ratios obtained from the conversion of **1**, **3**, and **5** with the catalyst systems B and C (Table 1).

The conversion of **7a**–**c** yielded as expected a more or less inseparable mixture of **2b**, **4b**, and **6b**, and **8a**–**c**, **10a**–**c**, and **11a**–**c**, respectively.[14] Remarkably, in contrast to literature results,[15] the addition of silver salts scarcely improved the selectivity. The reaction of **7a** with catalyst system A provided **2b** and **10a**/**11a** in a ratio of 2.5:1, and with catalyst system B in a ratio of 4.1:1. Similar results were obtained for **7b** and **7c** (for **7b**, **4b**:**10b**/**11b**; A = 1:1; B = 1.4:1; for **7c**, **6b**:**8c**; A = 1.2:1; B = 1.3:1).

A conclusive explanation of the different phenomena, in particular the influence of silver salts on the product distribution in the silane-terminated reactions, is not yet possible; nevertheless, we assume that the presence of a silver salt causes the initially formed aryliodopalladium species **12** to give AgI and an aryl Pd^+ intermediate **13**,[16] which reacts further either via **15** or the silylethyl cation **17** (Scheme 1). Owing to the lack of a nucleophile such as I^-, the intermediate undergoes base-induced elimination of a proton with the formation of **2a**, **4a**, and **6a**, respectively.[17] The formation of the vinyl-substituted cycles **2b**, **4b**, and **6b** can be explained by an inter- or intramolecular nucleophilic attack, for example by I^-, on the trimethylsilyl group in **14**. For the reaction with silver salts in the presence of (*S*)-BINAP another intermediate such as **16** may be assumed (Scheme 1).



Scheme 1. Postulated mechanism for the selective formation of **2a**,**b**, **4a**,**b**, and **6a**,**b** from **1**, **3**, and **5**.

The results indicate that the direction of elimination in the intramolecular Heck reaction can be directed through the use of allylsilanes as alkene components and results in the regioselective formation of a tertiary sp^3 center. In addition, when (*S*)-BINAP is used as a chiral ligand, these centers can also be formed with good enantioselectivity.

Experimental Procedure

To 20 mL of degassed DMF under argon was added $[Pd_2(dba)_3]$ (0.025 mmol) and (*S*)-BINAP (0.07 mmol). The reaction mixture was slowly heated to 50 °C with vigorous stirring to achieve a homogeneous system (ca. 30 min). Finally, Ag_3PO_4 (1.1 mmol) and **1**, **3**, or **5** (1 mmol) were added and the mixture heated to the temperature indicated in Table 1. After the reaction was complete (TLC), the solid residue was filtered off and washed with ether (20 mL). Water (20 mL) was added to the filtrate. The ether phase was separated, the aqueous phase washed twice with ether (2 × 5 mL), and the combined ether phases washed with water (10 mL) and saturated aqueous NaCl solution (10 mL). After drying over $MgSO_4$ and removal of the solvent under vacuum, the crude product was chromatographed on silica (petroleum ether/ether = 100:1 [**6**], 20:1 [**2**]; petroleum ether/ethyl acetate = 4:1 [**4**]).

Received: October 8, 1993
Revised: December 17, 1993 [Z6403IE]
German version: *Angew. Chem.* **1994**, *106*, 1138

[1] Two recent examples: K. F. McClure, S. J. Danishefsky, *J. Am. Chem. Soc.* **1993**, *115*, 6094–6100; C. Y. Hong, N. Kado, L. E. Overman, *ibid.* **1993**, *115*, 11028–11029.
[2] L. E. Overman, D. J. Ricca, V. D. Tran, *J. Am. Chem. Soc.* **1993**, *115*, 2042–2044.
[3] L. F. Tietze, R. Schimpf, *Synthesis* **1993**, 876–880.

[4] R. Grigg, V. Santhakumar, V. Sridharan, P. Stevenson, A. Teasdale, M. Thornton-Pett, T. Worakun, *Tetrahedron* **1991**, *46*, 9703–9720.
[5] K. Kondo, M. Sodeoka, M. Mori, M. Shibasaki, *Synthesis* **1993**, 920–930, and references therein; T. Takemoto, M. Sodeoka, E. Sasai, M. Shibasaki, *J. Am. Chem. Soc.* **1993**, *115*, 8477–8478; F. Ozawa, A. Kubo, Y. Matsumoto, T. Hayashi, *Organometallics* **1993**, *12*, 4188–4196; H. Brunner, K. Kramler, *Synthesis* **1991**, 1121–1124.
[6] A. Ashimori, L. E. Overman, *J. Org. Chem.* **1992**, *57*, 4571–4572; A. Ashimori, T. Matsuura, L. E. Overman, D. J. Poon, *ibid.* **1993**, *58*, 6949–6951.
[7] Allyltrimethylsilane has already been used in intermolecular Heck reactions; however, no substantial improvements in the reaction course were possible: C. M. Andersson, K. Karabelas, A. Hallberg, *J. Org. Chem.* **1985**, *50*, 3891–3895; K. Karabelas, C. Westerlund, A. Hallberg, *ibid.* **1985**, *50*, 3896–3900; K. Karabelas, A. Hallberg, *Acta Chem. Scand.* **1990**, *44*, 257–261.
[8] T. Jeffery, *J. Chem. Soc. Chem. Commun.* **1984**, 1287–1289; T. Jeffery, *Tetrahedron Lett.* **1985**, *26*, 2667–2670.
[9] Compounds **2**, **4** and **6** are formed as racemic mixtures when achiral Pd catalyst systems are used.
[10] **4a**: ^{1}H NMR (300 MHz, $CDCl_3$): $\delta = 0.01$ (s, 6.7H; $Si(CH_3)_3$), 0.05 (s, 2.3H; $Si(CH_3)_3$), 2.73 (ddd, $J = 15.5$, 5.5, 1.5 Hz, 0.75H; $ArCH_aH_bCH_2$), 2.83 (ddd, $J = 15.5$, 6.5, 3.0 Hz, 0.25H; $ArCH_aH_bCH_2$), 3.00–3.11 (m, 1H; $ArCH_aH_bCH_2$), 3.23–3.31 (m, 1.5H; CH_2CH_2N), 3.62–3.84 (m, 2H, CH_2CH_2N; $ArCHCH_2N$), 3.85, 3.87, 3.89, 3.90 (4s, 6H; OCH_3), 4.01 (br.d, $J = 13.5$ Hz, 0.75H; $ArCHCH_aH_bN$), 4.66 (dd, $J = 13.5$, 6.0 Hz, 0.75H; $ArCHCH_aH_bN$), 5.38 (dd, $J = 19.0$, 2.0 Hz, 0.75H; $= CH(Si(CH_3)_3)$). 5.63 (dd, $J = 18.5$, 1.5 Hz, 0.25H; $= CH(Si(CH_3)_3)$), 6.15 (dd, $J = 18.5$, 6.5 Hz, 0.25H; CH-CH =), 6.17 (dd, $J = 19.0$, 4.0 Hz, 0.75H; CH-CH =), 6.62 (s, 0.25H; Ar*H*), 6.65 (s, 1.75H; Ar*H*).
[11] The *ee* values were determined with reversed-phase HPLC (separation conditions: **2b**: Baker Chiracel [2 columns in sequence], H_2O/CH_3CN 59:41; **4b** and **6b**: Grom Chiral-AGP, 0.02 M Na_2HPO_4/isopropanol 95:5 and 93:7, respectively. Baseline separation was not achieved for **6b**; the standard error was 2%).
[12] (+)-**4b**: $[\alpha]_D^{20} = +97.0$ ($c = 1.0$, $CHCl_3$). Calculated rotations: **2b**: +97.5; **6b**: +104.8 ($c = 1.0$, $CHCl_3$).
[13] E. Pohl, R. Herbst-Irmer, R. Schimpf, L. F. Tietze, *Acta Crystallogr. Sect. A*, submitted. Reduction of (+)-**4b** with $LiAlH_4$ in THF and subsequent acylation with trichloroacetyl chloride in the presence of Hünig's base in CH_2Cl_2 yielded (+)-**4c**, $[\alpha]_D^{20} = +50.0$ ($c = 1.0$, $CHCl_3$). (+)-**4c** exists in the (*S*) configuration.
[14] The conversion of **7b** with catalyst system A has already been published: see ref. [3].
[15] M. M. Abelman, T. Oh, L. E. Overman, *J. Org. Chem.* **1987**, *52*, 4130–4133.
[16] K. Karabelas, A. Hallberg, *J. Org. Chem.* **1988**, *53*, 4909–4914.
[17] The selective formation of vinylsilanes **2a**, **4a**, and **6a** with the (*E*) configuration can easily be explained by both *syn* and *anti* elimination from the preferred conformation of **15**.

Effects of Metal-Ion Dopants on the Photocatalytic Reactivity of Quantum-Sized TiO_2 Particles**

Wonyong Choi, Andreas Termin, and Michael R. Hoffmann*

Photocatalytic destruction of chemical compounds in the presence of TiO_2 appears to be a viable process for pollution control.[1] In order to enhance the photocatalytic activity of TiO_2 several investigators have attempted doping with metal ions.[2–8] However, many of these investigations have been focused primarily on the photophysical properties of the doped material and less on the photochemical reactivity.[9–11]

In this communication we report on a systematic survey of the photoreactivities of 21 doped TiO_2 colloids with quantum (Q)-sized particles (transparent particle suspensions). Dopant ions that have an ionic radius similar to that of Ti^{4+} (0.75 Å) were chosen for substitution into the lattice. Their ionic radii[12] are given in Figure 1 along with photoreactivity data. The photoreactivity of each metal-doped TiO_2 system was quantified in terms of $CHCl_3$ oxidation[13] by valence band holes (or trapped holes) [Eq. (a)][14] and CCl_4 reduction[15] by conduction band electrons (or trapped electrons) [Eq. (b)]. In these reactions h_{vb}^+ refers to a valence band hole or a trapped hole, $>OH^\bullet$ to a surface-bound OH radical, and e_{cb}^- to a conduction-band electron or a trapped electron. In our experiments the intrinsic quantum yield for each reaction could be measured precisely since transparent colloidal suspensions, which exhibit negligible light-scattering, were used.

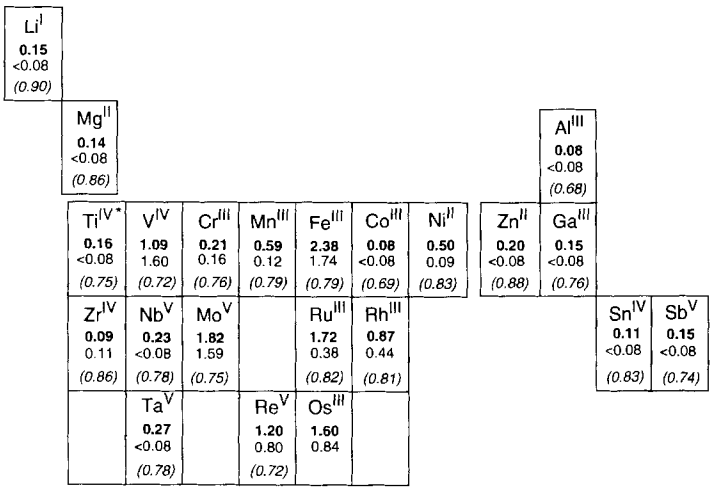


Fig. 1. The metal ions used to dope TiO_2 and their photocatalytic effects. The bold-faced numbers are the quantum yields (%) for the oxidative chloroform degradation ($\Phi_{CHCl_3} = 1/3\{(d[Cl^-]/dt)/I_a\}$) ($I_a$ = absorbed light intensity; the lower numbers are the quantum yields (%) for Cl^- production from the reductive dechlorination of carbon tetrachloride ($\theta_{CCl_4/Cl^-} = (d[Cl^-]/dt)/I_a$). The numbers in the parentheses are the ionic radii (Å) [12] for the metal ion with coordination number 6. All dopant concentrations are 0.5 atom% except Mo^V (0.1%). Ti^{IV}* refers to the undoped TiO_2 (see Experimental Procedure for details).

$$CHCl_3 + h_{vb}^+ (\text{or } >OH^\bullet) \rightarrow H^+ (\text{or } H_2O) + CCl_3^\bullet \quad \text{(a)}$$

$$CCl_4 + e_{cb}^- \longrightarrow Cl^- + CCl_3^\bullet \quad \text{(b)}$$

The measured photoreactivities are summarized in Figure 1 for all of the samples in terms of the quantum yields for $CHCl_3$ oxidation and for CCl_4 reduction. For the majority of dopants the most efficient concentration was 0.5 atom%. However, Mo^V showed a maximum photoreactivity at a doping level of 0.1 atom%. All the dopant concentrations mentioned here are nominal concentrations based upon the assumption of quantitative incorporation of the dopant. The two sets of quantum yields presented in Figure 1 are plotted against each other in Figure 2. Several dopants increased the photoreactivity for the $CHCl_3$ oxidation significantly compared with undoped TiO_2 colloids with Q-sized particles: Fe^{III} (15-fold), Mo^V (11-fold), Ru^{III} (11-fold), Os^{III} (10-fold), Re^V (7.5-fold), V^{IV} (7-fold), and Rh^{III} (5-fold).

Metal-ion dopants may influence the photoreactivity of TiO_2 by acting as electron (or hole) traps and by altering the electron/hole recombination rate.[9, 16] The general correlation between

[*] Prof. M. R. Hoffmann, W. Choi, Dr. A. Termin
W. M. Keck Laboratories, California Institute of Technology
Pasadena, CA 91125 (USA)
Telefax: Int. code + (818)395-2940

[**] This research was supported by the Advanced Research Projects Agency and the Office of Naval Research (N0014-92-J-1901).

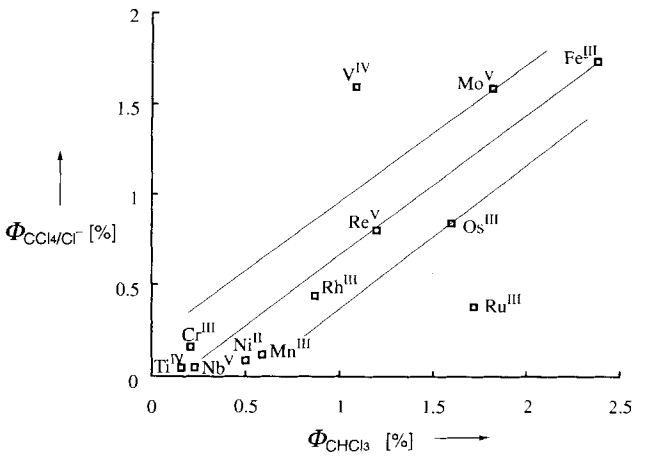


Fig. 2. Correlation plot between the oxidation (chloroform degradation) quantum yield (θ_{CHCl_3}) and the reduction (dechlorination of carbon tetrachloride) quantum yield ($\theta_{CCl_4\text{-}Cl^-}$) from the data of Fig. 1. Some dopants, which show little effect on the photoreactivity, are omitted for clarity. The straight lines are drawn only as a visual guide.

the two quantum yields in Figure 2 suggests that an altered recombination rate influences the interfacial charge transfer of both electrons and holes to a similar extent regardless of the nature of the dopant (i.e. electron trap or hole trap). The significant deviation of V^{IV} and Ru^{III} from the apparent linear correlation indicates that they may act as irreversible hole and electron traps, respectively, and thus prevent the trapped charge carriers from migrating to the solid–solution interface. This irreversibility may arise, in part, from the stable, closed-shell electron configuration of V^{V} (d^0) and the partly filled, low-spin configuration of Ru^{II} (t_{2g}^6 with octahedral coordination). Thus, all of the dopants with closed-shell configurations—Li^{I}, Mg^{II}, Al^{III}, Zn^{II}, Ga^{III}, Zr^{IV}, Nb^{V}, Sn^{IV}, Sb^{V}, and Ta^{V}—have little effect on the observed photoreactivity of TiO_2.

According to the energy level diagram for dopants suggested by Mizushima et al.,[17] V^{IV}, Mn^{III}, and Co^{III} can act as both hole and electron traps, while Fe^{III}, Cr^{III}, and Ni^{II} can serve only as hole traps. However, the energy levels given by Mizushima et al.[17] do not provide a unifying explanation that is consistent with our observations. Even though both Fe^{III} and Cr^{III} have similar energy levels in the TiO_2 lattice (0.2–0.4 eV above the valence band edge), their efficiencies as dopants are substantially different. This suggests that the different electronic configurations (d^5 vs. d^3) may be responsible for the observed photoreactivities. It is interesting to note that all the dopants with d^5 (Fe^{III}, Ru^{III}, and Os^{III}) and d^1 configurations (V^{IV} and Mo^{V}) enhanced the photoreactivity for both oxidation and reduction.

The photoreactivity of doped TiO_2 appears to be a complex function of the dopant concentration, the energy level of dopants within the TiO_2 lattice, their d-electronic configurations, their oxidation states, and the type of defects (substitutional or interstitial) in the host lattice. Some attempts have been made to correlate dopant photoactivity with a simple parameter such as the oxidation state for several dopants.[8, 18] However, we have shown that this simple explanation may be inadequate. In particular the d-electronic configuration and the actual energy level of dopants within the lattice seem to have a significant impact on photoactivity. A more detailed study of the effects of dopants on photoactivity in Q-sized semiconductors is in progress. In conclusion, we feel that the periodic chart of the dopant effects presented here may serve as a useful guide for those who study doping effects of photocatalysts.

Experimental Procedure

Colloid synthesis and characterization: Colloidal Q-sized TiO_2 particles were prepared from the hydrolysis of titanium tetraisopropoxide at pH 1.5 (adjusted with nitric acid) and 5 °C as described previously [19]. The solvent in the resulting transparent colloidal suspension was evaporated to give powders with Q-sized particles. The particle diameters were determined to be in the range of 2–4 nm by transmission electron microscopy (TEM). X-ray diffraction (XRD) and Raman spectroscopy analysis showed that the colloidal TiO_2 was exclusively in the anatase form. These suspensions of Q-sized TiO_2 particles showed an equivalent band-gap transition at 360 nm. The doped systems were prepared according to the above procedure with added metal salts [20] to give a doping level between 0.1 to 3 atom %. Absorption spectra of some doped colloids (e.g. with Fe^{III}, V^{IV}, and Mn^{III}) showed a red-shift in the band-gap transition as we increased the dopant concentration, which verified the incorporation of the doping metal ions into the TiO_2 nanoparticles. In the unique case of Ru^{III} incorporated into the TiO_2 lattice, a strong resolved absorption band centered at 437 nm was observed. No information about the homogeneity of the dopants in the particles was available owing to analytical difficulties.

Photoreactivity measurement: Both reactions (a) and (b) were followed by measuring the Cl^- production after 1 h of UV irradiation with a chloride ion selective electrode. Cl^- production was linear over this time period. Reaction (a) was performed at pH 11.0 ± 0.2 with $[CHCl_3]_0 = 3.15$ mM, and reaction (b) at pH 2.8 ± 0.1 with $[CCl_4]_0 = 5.1$ mM and $[CH_3OH]_0 = 0.1$ M. In each case [TiO] = 0.5 g L^{-1}, $[O_2]_{diss} \approx 0.2$ mM, $I_0 = 1.28 \times 10^{-4}$ Einstein L^{-1} min^{-1} (at 320 nm, full width at half-maximum 15 nm) with a total reactor volume of 35 mL. The light intensity measurement was performed by chemical actinometry using (*E*)-α-(2,5-dimethyl-3-furylethylidene)(isopropylidene)succinic anhydride (Aberchrome 540). [21]

Received: December 3, 1993 [Z 6537 IE]
German version: *Angew. Chem.* **1994**, *106*, 1148

[1] *Photocatalysis – Fundamentals and Applications* (Eds.: N. Serpone, E. Pelizzetti), Wiley Interscience, New York, **1989**.
[2] J. Kiwi, M. Grätzel, *J. Phys. Chem.* **1986**, *90*, 637.
[3] O. A. Ileperuma, K. Tennakone, W. D. D. P. Dissanayake, *Appl. Catal.* **1990**, *62*, L1.
[4] E. Borgarello, J. Kiwi, M. Grätzel, E. Pelizzetti, M. Visca, *J. Am. Chem. Soc.* **1982**, *104*, 2996.
[5] G. N. Schrauzer, T. D. Guth, *J. Am. Chem. Soc.* **1977**, *99*, 7189.
[6] J. Kiwi, C. Morrison, *J. Phys. Chem.* **1984**, *88*, 6146.
[7] J. Soria, J. C. Conesa, V. Augugliaro, L. Palmisano, M. Schiavello, A. Sclafani, *J. Phys. Chem.* **1991**, *95*, 274
[8] K. E. Karakitsou, X. E. Verykios, *J. Phys. Chem.* **1993**, *97*, 1184.
[9] J. Moser, M. Grätzel, R. Gallay, *Helv. Chim. Acta* **1987**, *70*, 1596.
[10] M. Grätzel, R. F. Howe, *J. Phys. Chem.* **1990**, *94*, 2566.
[11] W. K. Wong, M. A. Malati, *Solar Energy* **1986**, *36*, 163.
[12] J. E. Huheey, *Inorganic Chemistry; Principles of Structure and Reactivity*, Harper & Row, New York, **1983**, pp. 73–76.
[13] C. Kormann, D. W. Bahnemann, M. R. Hoffmann, *Environ. Sci. Technol.* **1991**, *25*, 494.
[14] The stoichiometry of the overall reaction is:

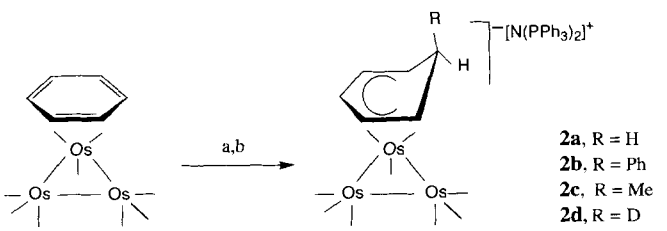
$$CHCl_3 + H_2O + 1/2\ O_2 \longrightarrow CO_2 + 3HCl$$

[15] a) *Encyclopedia of Electrochemistry of the Elements – Organic Section, Vol. XIV* (Eds.: A. J. Bard, H. Lund), Dekker, New York, **1973**, p. 34; b) J. Mönig, D. Bahnemann, K.-D. Asmus, *Chem. Biol. Interact.* **1983**, *47*, 15.
[16] S. T. Martin, H. Herrmann, W. Choi, M. R. Hoffmann, *J. Phys. Chem.*, submitted.
[17] a) K. Mizushima, M. Tanaka, S. Iida, *J. Phys. Soc. Jpn.* **1972**, *32*, 1519; b) K. Mizushima, M. Tanaka, A. Asai, S. Iida, J. B. Goodenough, *J. Phys. Chem. Solids* **1979**, *40*, 1129.
[18] W. Mu, J.-M. Herrmann, P. Pichat, *Catal. Lett.* **1989**, *3*, 73.
[19] a) D. Bahnemann, A. Henglein, J. Lilie, L. Spanhel, *J. Phys. Chem.* **1984**, *88*, 709; b) C. Kormann, D. W. Bahnemann, M. R. Hoffmann, *ibid.* **1988**, *92*, 5196.
[20] The following metal salts served as sources for the dopant ions: LiOH, $Mg(ClO_4)_2$, $AlCl_3$, $(VO)SO_4 \cdot 3H_2O$, $Cr(NO_3)_3$, MnF_3, $Fe(NO_3)_3 \cdot 9H_2O$, CoF_3, $NiCl_2$, $Zn(ClO_4)_2$, $Ga(NO_3)_3$, $Zr(OCH(CH_3)_2)_4$, $NbCl_5$, $MoCl_5$, $RuCl_3$, $Rh(NO_3)_3 \cdot 2H_2O$, $SnCl_4$, $SbCl_5$, $TaCl_5$, $ReCl_5$ and $OsCl_3$.
[21] H. G. Heller, J. R. Langan, *J. Chem. Soc. Perkin Trans. 2* **1981**, 341.

A Triosmium Cluster Complex with a Carbene Ligand in an Unusual Coordination Mode**

Andrew J. Edwards, Mark A. Gallop,
Brian F. G. Johnson, Jochem U. Köhler, Jack Lewis,*
and Paul R. Raithby

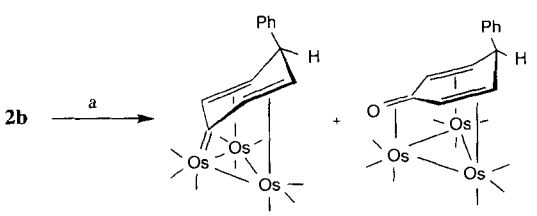
Transition metal clusters which contain π-arene ligands where the arene ligands adopt a face-capping bonding mode are interesting as model compounds for chemisorption of arenes to metal surfaces.[1] This coordination mode was first established for the octahedral Ru_6 carbido cluster $[Ru_6C(CO)_{11}(\eta^6\text{-}C_6H_6)(\mu_3\text{-}\eta^2\text{:}\eta^2\text{:}\eta^2\text{-}C_6H_6)]$[2] and for the trinuclear cluster compounds $[M_3(CO)_9(\mu_3\text{-}\eta^2\text{:}\eta^2\text{:}\eta^2\text{-}C_6H_6)]$ (M = Os[2] (**1**), Ru[3]), and $[(CpCo)_3(\mu_3\text{-arene})]$.[4] Until now little was known about the reactivity of these face-capping arene ligands. The triosmium benzene cluster **1** reacts with carbanions (PhLi, MeLi) and with $LiBHEt_3$ (or $LiBDEt_3$) to form an *exo*-addition product of an anionic cluster (**2a–d**) with a triply bridging cyclohexadienyl ligand (Scheme 1).[5]



1

Scheme 1. Reaction of **1** with carbanions. a) $+R^-$, THF, −78 °C; b) $+[N(PPh_3)_2]Cl$, *i*PrOH.

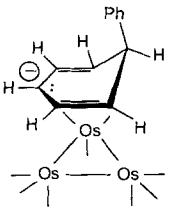
In the case of **2a** hydrogen can be abstracted as a hydride by the triphenylmethyl (trityl) cation to give cleanly the original compound **1**. Labeling with deuterium (**2d**) shows that there is a stereospecific abstraction of the *exo*-hydrogen.[5] Although in the most cases of mononuclear complexes the *exo*-hydrogen is abstracted as well, there are a few reports of *endo*-hydrogen removal from coordinated π-hydrocarbons by the trityl cation.[6] The abstraction of the *endo*-hydrogen from the anionic μ_3-cyclohexadienyl complexes (**2b, c**) would lead to face-capping arene clusters $[Os_3(CO)_9(\mu_3\text{-}\eta^2\text{:}\eta^2\text{:}\eta^2\text{-}C_6H_5R)]$ (R = Ph, Me). However, after reaction at −78 °C between **2b** and the trityl cation, and after purification with thin-layer chromatography (TLC), two different products have been obtained: an orange triosmium carbene complex **3** and an orange triosmium cyclohexadienone complex **4** (Scheme 2).



3 **4**

Scheme 2. Reaction of **2b** with the trityl cation. a) $+Ph_3C^+BF_4^-$, CH_2Cl_2, −78 °C.

It seems that an abstraction of the *endo*-hydride by the sterically demanding trityl cation is not possible, because of the phenyl group in *exo*-position and the CO groups in the equatorial positions on the osmium core. From the resonance structure of **2b** (Scheme 3) it is obvious that an abstraction of the hydride in position 4 results in the carbene structure, and so provides an alternative and novel form of bonding of an isomer of benzene to a transition metal cluster.



2b

Scheme 3. Resonance structure of **2b**.

This carbene carbon is coordinated to the osmium metal core in an unusual bonding mode which has not been observed previously. The structure of **3** has been established by a X-ray analysis (Fig. 1).[7] The distance between the carbene carbon, C12, and Os3 is 2.05(2) Å, which is in the range of usual distances of carbene carbons of the Fischer type coordinated to triosmium clusters (between 1.88(6) Å and 2.14(1) Å).[8] However, this carbene carbon lies above the osmium triangle (as in the face-capping mode), and it is possible that there is a weak interaction to both of the other osmium atoms (Os2–C12 2.582 Å; Os1–C12 2.55(2) Å). The formal double bonds of the ring are also coordinated to these osmium atoms. The six-membered ring is still in a face-capping position ($\mu_3\text{-}\eta^2\text{:}\eta^1\text{:}\eta^2$), but it has a "chairlike" conformation because the carbene carbon has moved out of the plane of C13, C14, C16, and C11 towards the Os3. Nevertheless, the carbene ligand seems to be "side-on" coordinated rather than in the usual end-on way. The second product **4** of the reaction was analyzed by X-ray diffraction and its structure is shown in Figure 2.[9]

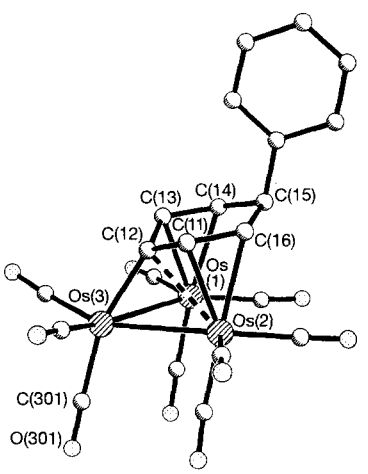


Fig. 1. Crystal structure of **3**: Selected bond lengths [Å]: Os3-C12 2.05(2), Os2-C12 2.58(2), Os1-C12 2.55(2), Os1-C13 2.21(2), Os1-C14 2.33(2), Os2-C11 2.22(2), Os2-C16 2.36(2), C12-C11 1.44(3), C12-C13 1.48(3), C13-C14 1.37(3), C11-C16 1.35(3), C14-C15 1.52(3), C16-C15 1.54(3), Os3-C301 1.93(3), C301-O301 1.17(3).

A side-on coordination of keto functions has been observed rarely. To our knowledge this is the first cyclohexadienone ligand coordinated in this way to a triosmium cluster, and may be viewed as the stabilization of a keto form of an enol of a phenolic group. The cyclohexadienone moiety of the ligand is nearly parallel to and lies above the osmium core. The C–O distance of 1.27(2) Å is between a C=O bond (1.22 Å) and a C–O bond (1.42 Å)[10] and seems to be shorter than distances in η^2-aldehyde/keto ligands of mononuclear complexes.[11] An absorption band in the IR spectrum of **4** at 1515 cm^{-1} (the only addi-

[*] Prof. Lord Lewis, Dr. A. J. Edwards, Dr. M. A. Gallop, Prof. B. F. G. Johnson, Dr. J. U. Köhler, Dr. P. R. Raithby
University Chemical Laboratory
Lensfield Road, GB-Cambridge, CB21EW (UK)
Telefax: Int. code + (223)336-343

[**] This work was supported by the European Community through a Human Capital and Mobility Fellowship (J. U. K.).

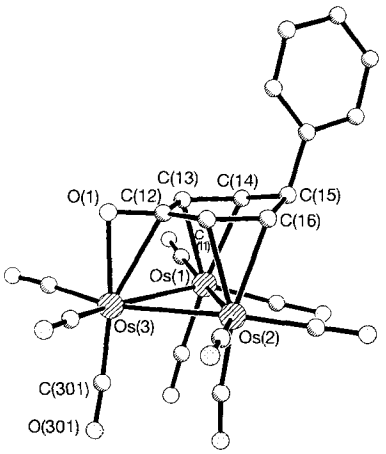


Fig. 2. Crystal structure of **4**: Selected bond lengths [Å]: O1-C12 1.27(2), Os3-O1 2.208(10), Os3-C12 2.45(2), Os1-C13 2.25(2), Os1-C14 2.31(2), Os2-C11 2.28(2), Os2-C16 2.32(2), C12-C11 1.46(2), C12-C13 1.45(2), C13-C14 1.44(2), C11-C16 1.39(2), C14-C15 1.50(2), C16-C15 1.52(2), Os3-C301 1.85(2), C301-O301 1.16(2).

tional band compared to the carbene complex **3**) is assigned to a C=O vibration. This band appears at higher frequencies than those of complexes described in the literature. This is in accordance with the relatively short C–O distance.[11]

There is no hint from the spectroscopic data (IR, NMR) that **4** is present in the reaction solution. Furthermore, the carbene complex **3** is stable in air, even if dissolved in CH_2Cl_2. There is no conversion, when the solution is stored under air for several days. However, if triethylamine is added to this solution or **3** is dissolved in methanol, a fast conversion to **4** takes place (within minutes). We suppose that in the first step the carbene carbon is attacked by a Lewis base, and in the second step there is a reaction with oxygen from the air. This reaction does not proceed under an atmosphere of nitrogen.

During the purification by TLC most probably free electron pairs of silanol and siloxane groups on the surface of the silica gel act as Lewis bases and cause a partial conversion of **3** to **4**. In a related reaction the electrophilic methylidene complex $[(\eta^5\text{-}C_5H_5)Re(NO)(PPh_3)(=CH_2)]^+PF_6^-$ reacts with iodoso benzene ($C_6H_5I^+\text{-}O^-$, an oxygen nucleophile) to form a η^2-formaldehyde complex.[12]

Experimental Procedure

A yellow solution of **2b** (100 mg) in CH_2Cl_2 (10 mL) was cooled to −78 °C and treated dropwise with a solution of $[Ph_3C][BF_4]$ (25 mg, 1.2 mol equiv) in CH_2Cl_2 (3 mL). The color changed to orange. The solution was warmed up to room temperature, and the reaction solution purified by thin layer chromatography (silica gel). Elution with CH_2Cl_2 (40%)/hexane (60%) afforded the major product **3** (high R_f value; 38 mg (60%) yield), and the minor product **4** (low R_f; 8 mg (13%) yield) as orange, air-stable products.

3: ^{1}H NMR (250 MHz, CD_2Cl_2): δ = 7.31–7.42 (m, 5H, Ph), 5.04 (d, ^3J(H, H) = 6.4 Hz, 2H; CH), 4.51 (t, ^3J(H, H) = 2.1 Hz, 1H; CHPh), 3.08 (dd, 2H; CH); ^{13}C {^{1}H} NMR (62.9 MHz, CD_2Cl_2): δ = 206.4 (1C; carbene-C), 190.8 (6C; CO), 177.7 (3C; CO), 144.6 (1C; ipso-C), 129.4 (2C; Ph), 128.5 (1C; Ph), 126.8 (2C; Ph), 54.8 (1C), 52.8 (2C), 39.9 (2C); IR (CH_2Cl_2): $\tilde{\nu}$[cm^{-1}] = 2080(m), 2037(vs), 2031(vs), 2006(m), 1992(m), 1969(w); MS (FAB): *m/z* 982; correct elemental analysis.

4: ^{1}H NMR (250 MHz, CD_2Cl_2): δ = 7.39–7.56 (m, 5H; Ph), 4.97 (t, ^3J(H, H) = 2.4 Hz, 1H; CHPh), 4.2 (dd, ^3J(H, H) = 8 Hz, 2H; CH), 2.99 (d, 2H). ^{13}C {^{1}H} NMR (62.9 MHz, CD_2Cl_2): δ = 181.3 (1C; CO), 177.5 (4C; CO), 175.8 (2C; CO), 170.9 (2C; CO), 147.3 (1C; ipso-C), 138.3 (1C; C=O), 129.6 (2C; Ph), 128.7 (1C; Ph), 126.8 (2C; Ph), 53.8 (2C), 52.3 (2C), 43.1 (1C). IR (CH_2Cl_2): $\tilde{\nu}$[cm^{-1}] = 2087(m), 2047(s), 2032(vs), 2010(m), 1989(m), 1961(w); (KBr): $\tilde{\nu}$[cm^{-1}] = 1515(w); MS (FAB): *m/z* 998. Correct elemental analysis.

Received: January 22, 1994 [Z 6640 IE]
German version: *Angew. Chem.* **1994**, *106*, 1166

[1] G. A. Somorjai, *J. Phys. Chem.* **1990**, *94*, 1013; H. Wadepohl, *Angew. Chem.* **1992**, *104*, 253; *Angew. Chem. Int. Ed. Engl.* **1992**, *31*, 247.
[2] M. P. Gomez-Sal, B. F. G. Johnson, J. Lewis, P. R. Raithby, A. H. Wright, *J. Chem. Soc. Chem. Commun.* **1985**, 1682–1684.
[3] a) B. F. G. Johnson, J. Lewis, M. Martinelli, A. H. Wright, D. Braga, F. Grepioni, *J. Chem. Soc. Chem. Commun.* **1990**, 364–366; b) D. Braga, F. Grepioni, B. F. G. Johnson, J. Lewis, C. E. Housecroft, M. Martinelli, *Organometallics* **1991**, *10*, 1260–1268.
[4] a) H. Wadepohl, K. Büchner, M. Herrmann, H. Pritzkow, *Organometallics* **1991**, *10*, 861–871; b) H. Wadepohl, K. Büchner, H. Pritzkow, *Angew. Chem.* **1987**, *99*, 1294–1295; *Angew. Chem. Int. Ed. Engl.* **1987**, *26*, 1259–1260.
[5] a) M. A. Gallop, B. F. G. Johnson, J. Lewis, A. H. Wright, *J. Chem. Soc. Dalton Trans.* **1989**, 481–487; b) M. A. Gallop, Ph. D. Thesis, University of Cambridge, **1988**.
[6] a) I. U. Khand, P. L. Pauson, W. E. Watts, *J. Chem. Soc. C*, **1969**, 2024–2030; b) N. El Murr, *J. Organomet. Chem.* **1981**, *208*, C9–C11.
[7] a) X-ray crystal structure data of **3**: $C_{21}H_{10}O_9Os_3$, M_r = 976.89, monoclinic, space group $P2_1/n$ (no. 14, nonstandard setting), a = 8.963(2), b = 16.687(3), c = 15.560(3) Å, β = 98.57(3)°, V = 2301.3(8) Å^3, Z = 4, ρ_{calcd} = 2.820 Mgm^{-3}, $F(000)$ = 1744, $\lambda(Mo_{K\alpha})$ = 0.71073 Å, $\mu(Mo_{K\alpha})$ = 16.57 mm^{-1}, T = 293 K. Data were collected on a Stoe four-circle diffractometer, 3069 reflections collected in the range 7.0° < 2θ < 45.0°. A semi-empirical adsorption correction was applied using psi scans with maximum and minimum transmission factors 1.0 and 0.284, respectively. The structure was solved by a combination of direct methods and Fourier difference techniques, and refined by full-matrix least squares on F^2 (SHELXL-93; G. M. Sheldrick, Göttingen, **1993**); Os atoms and C atoms of the phenyl ring were refined anisotropically; all hydrogen atoms in idealized positions [C–H 0.96 Å]) to R_1 = 0.068, wR_2 = 0.188 for 2606 reflections with $I > 2\sigma(I)$. R_1 = 0.077, wR_2 = 0.210 for all data. b) Further details of crystal structure investigation are available on request from the Director of the Cambridge Crystallographic Data Centre, 12 Union Road, GB-Cambridge CB2 1EZ (UK) on quoting the full journal citation.
[8] a) S.-j. Wang, L. L. Miller, R. A. Jacobson, R. J. Angelici, *Inorg. Chim. Acta* **1988**, *145*, 129–137; b) R. D. Adams, G. Chen, J. T. Tanner, *Organometallics* **1990**, *9*, 1530–1538.
[9] X-ray crystal structure data of **4**: $C_{21}H_{10}O_{10}Os_3$, M_r = 992.89, monoclinic, space group $P2_1/c$ (no. 14), a = 9.380(2), b = 13.094(3), c = 17.939(4) Å, β = 95.68(3)°, V = 2192.5(8) Å^3, Z = 4, ρ_{calcd} = 3.01 Mgm^{-3}, $F(000)$ = 1776, $\lambda(Mo_{K\alpha})$ = 0.71073 Å, $\mu(Mo_{K\alpha})$ = 17.40 mm^{-1}, T = 293 K. Data were collected on a Stoe four-circle diffractometer, 2961 reflections collected in the range 7.0 < 2θ < 45.0°. The structure was solved by a combination of direct methods and Fourier difference techniques, and refined by full-matrix least squares on F^2 (SHELXL-93; G. M. Sheldrick, Göttingen, **1993**); Os atoms, C atoms of the phenyl ring, and O coordinated to the cluster framework were refined anisotropically; all hydrogen atoms in idealized positions [C–H 0.96 Å]) to R_1 = 0.054, wR_2 = 0.141 for 2635 reflections with $I > 2\sigma(I)$. R_1 = 0.057, wR_2 = 0.145 for all data, see also [7b].
[10] F. A. Carey, R. J. Sundberg, *Advanced Organic Chemistry, Part A*, 3rd ed., Plenum, New York, **1990**, p. 12.
[11] a) W. D. Harman, D. P. Fairlie, H. Taube, *J. Am. Chem. Soc.* **1986**, *108*, 8223–8227; b) Y.-H. Huang, J. A. Gladysz, *J. Chem. Educ.* **1988**, *65*, 298–303.
[12] a) W. E. Buhro, A. T. Patton, C. E. Strouse, J. A. Gladysz, F. B. McCormick, M. C. Etter, *J. Am. Chem. Soc.* **1983**, *105*, 1056–1058; b) W. E. Buhro, S. Georgiou, J. M. Fernández, A. T. Patton, C. E. Strouse, J. A. Gladysz, *Organometallics* **1986**, *5*, 956–965.

Long-Lived *ipso*-Silylated *p*-Toluenium Ions: Evidence from a Kinetic Isotope Effect**

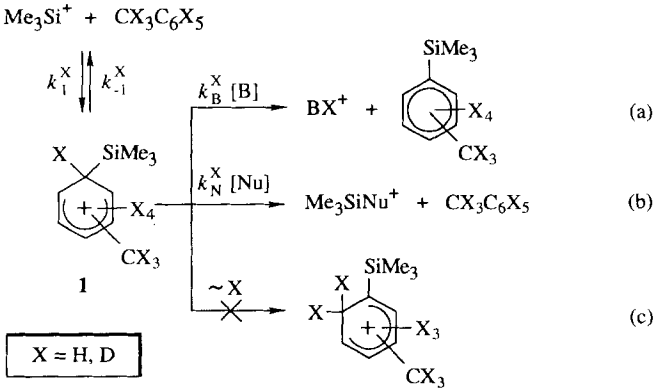
Maria Elisa Crestoni and Simonetta Fornarini*

A recent report[1] in the long-standing search for isolable silyl cations in condensed phase described the crystal structure of an alleged Et_3Si^+ ion, remote from the Ph_4B^- counter ion but within approximate bonding distance (2.18 Å) from the *p*-C atom of a "solvent" toluene molecule. The basis for this interpretation has been questioned after model ab initio calculations

[*] Prof. S. Fornarini, Dr. M. E. Crestoni
Dipartimento di Studi di Chimica e Tecnologia delle
Sostanze Biologicamente Attive
Università di Roma "La Sapienza", P.le A. Moro 5, I-00185 Rome (Italy)
Telefax: Int. code +(6)499 13-888

[**] This work was supported by the Italian Ministero dell'Università e della Ricerca Scientifica e Tecnologica. The authors are grateful to Prof. F. Cacace for his interest and helpful discussions.

favored an $[Et_3Si\text{-toluene}]^+$ σ complex,[2] which emphasizes that the attainment of a free silylium ion is a difficult problem to tackle in condensed phase, despite promising advances.[3] It is also our view, based on a fairly extensive body of experimental data recently made available on the interaction of Me_3Si^+ ions with arenes in the gas phase,[4-8] that the Et_3Si^+–toluene pair is best interpreted as a σ complex. In fact, the gas-phase addition of Me_3Si^+ to toluene, previously observed by high-pressure mass spectrometry,[4] leads to a σ complex, rather than to the originally postulated π complex. We now present positive evidence for the existence of long-lived σ-complex intermediates **1**, that is, silyl-substituted toluene protonated at the silicon-bearing ring carbon, displaying a primary hydrogen kinetic isotope effect (KIE) to deprotonation. This finding follows our studies on aromatic silylation by Me_3Si^+ ions in the gas phase.[7-9] Direct aromatic trimethylsilylation has in fact been accomplished for the first time in the gas phase by the radiolytic technique,[10] operating at about 1 atm, once it was realized that a highly efficient and specific base was necessary to deprotonate the *ipso* arenium ion **1**, in order to compete with an easy desilylation process.[8] In the absence of a suitable base (a nitrogen base, preferably sterically hindered), desilylation of **1** occurs by assistance of trace oxygen nucleophiles. In the fairly detailed mechanistic picture thus obtained, a noteworthy feature is the relative stability of **1** towards isomerization by H-shifts to adjacent ring positions (c), a process normally occurring in other arenium ions, and therefore it undergoes exclusively deprotonation (a) or desilylation (b).



This behavior follows from the significantly high basicity of the silyl-substituted position, which is responsible, inter alia, for the facile *ipso* attack by electrophilic agents and for the acid-induced desilylation processes common in solution as well as in the gas phase.[11] The persistence of the *ipso* hydrogen at the silylated position emerged from the reaction of Me_3Si^+ with selectively deuterated toluenes, which showed practically complete loss of the H or D atom originally bound to the substituted carbon.[9] In order to substantiate this finding and to see if and to what extent the deprotonation step might affect the overall electrophilic substitution sequence, we studied the competitive reaction of PhMe and $[D_8]$PhMe with gaseous Me_3Si^+ ions and observed a primary KIE (Table 1). The overall k_H/k_D values reported in Table 1 show a dependence of the proton affinity (PA)[12] on the structural features and, in certain cases, on the concentration of the added base. The strongest base used, $Me_2N(CH_2)_2NMe_2$, gives a negligible primary KIE, which, however, tends to increase with decreasing PA up to a value of about 4 in the case of NH_3. Ammonia is the closest in proton

Table 1. Gas-phase trimethylsilylation of PhMe/$[D_8]$PhMe by free Me_3Si^+ ions [a].

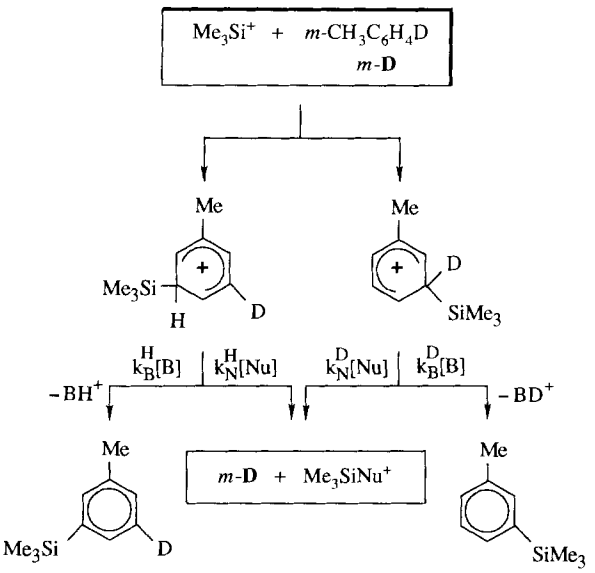
Base (p [Torr])	PA (Base) [b] (kcal mol^{-1})	$Me_3SiC_6X_4CX_3$ (X = H, D) k_H/k_D [c]		Isomeric Distribution [d]	
		para	*meta*	*para*	*meta*
NH_3 (0.60)	204	4.0	3.8	85	15
C_5H_5N (0.82)	221	2.3	2.1	85	15
C_5H_5N (3.5)	221	2.3	2.2	84	16
Et_3N (0.40)	232	1.4	1.3	84	16
Et_3N (0.96)	232	1.3	1.2	84	16
iPr_2NEt (0.55)	235	2.1	2.0	89	11
iPr_2NEt (0.92)	235	2.2	2.1	86	14
iPr_2NEt (4.1)	235	1.7	1.7	89	11
$Me_2N(CH_2)_2NMe_2$ (1.1)	240	1.2	1.1	81	19

[a] All gaseous systems contained PhMe/$[D_8]$PhMe (2–3 Torr), Me_4Si (20 Torr), CH_4 (630–680 Torr) and a radical scavenger (O_2, 10 Torr). [b] Data from Ref. [12a]. In a revised PA scale [12b] the proton affinity of NH_3 is set at 203.5 kcal mol^{-1} and some amines are about 2 kcal mol^{-1} more basic than in Ref. [12a]. [c] Normalized undeuterated to deuterated product ratio: $k_H/k_D = ([CH_3C_6H_4SiMe_3]/[CD_3C_6D_4SiMe_3]) \times ([D_8]PhMe]/PhMe])$. Values affected by approximately ±10% error. [d] ±2% error.

affinity to $Me_3SiC_6H_4Me$, the conjugate base of **1**, whose PA may be estimated at 200 kcal mol^{-1}.[4, 12] Unfortunately, the PA range of the bases used can not be extended further downward because this would require oxygenated compounds, which do not yield neutral silylated products, attacking preferably the silyl group [reaction (b)] rather than the proton [reaction (a)]. Such PA dependence is expected for a primary KIE in the hydron transfer from **1** to the base B (k_B^H/k_B^D).[13] A discontinuity in the trend of the ratio k_H/k_D with PA(B) occurs for $(iPr)_2NEt$, a severely hindered base. Again, the observation of a significant primary KIE involving hindered bases, for example, 2,6-dialkylpyridines, is a common finding, both in the gas phase and in solution.[13-14] Although the k_H/k_D data appear to include a primary KIE, k_B^H/k_B^D, as a major factor, they do not result from a rate-determining hydron transfer, representing instead an example of a hidden isotope effect.[13a, c] In fact, the silylation step, k_1, is by no means reversible under the present experimental conditions. Even if k_1 approached the collision limit of 10^{-9} cm^3 s^{-1}, the known K_1[4] would give $k_{-1} = 0.15$ s^{-1}, vanishingly small in comparison with a $k_B[B]$ term of about 10^8 s^{-1}, typical of collision-controlled deprotonation at base pressures around 1 Torr. The observed k_H/k_D ratio reflects instead the competition of the k_B step, which involves the isotopically labeled hydrogen, in which a common step leads to different products (k_N).[15] Neglecting k_{-1}, the k_H/k_D values reflect the k_B^H/k_B^D ratios [Eq. (1)], modified by two factors.[16] The first (k_1^H/k_1^D)

$$\frac{k_H}{k_D} = \frac{k_A^H}{k_1^D} \times \frac{k_B^H}{k_B^D} \times \frac{(k_N^D[Nu] + k_B^D[B])}{(k_N^H[Nu] + k_B^H[B])} \qquad (1)$$

should include a small inverse secondary KIE due to isotopic substitution at the *ipso*-carbon undergoing change of hybridization, besides higher order KIEs due to H/D substitution of hydrogen atoms farther from reaction site. Similar secondary KIEs may affect k_N^H/k_B^H. Moreover, the k_B^H/k_B^D ratio itself should contain secondary KIE components. To assess the contribution from such secondary KIEs, the silylation of *m*-$CH_3C_6H_4D$ (*m*-**D**) was performed. The *meta*-silylated product arises from attack at either of two *meta* positions, differing in the hydrogen isotope (Scheme 1).



Scheme 1. *meta*-Silylation of *m*-[D_1]toluene with Me_3Si^+.

Whereas the kinetic scheme is essentially the same as for the competition between unlabeled and perdeuterated toluene, the degree of isotopic substitution and hence the incursion of secondary KIEs is vastly reduced. The values of the ratio of deuterated to undeuterated *m*-trimethylsilyl-toluene products, which reflect k_H/k_D, of 2.0 (0.7 Torr pyridine) and 1.5 (0.8 Torr Et_3N) are close to the 2.3 and 1.3–1.4 values obtained for the competition between PhMe and [D_8]PhMe, within the combined error limits, and show that secondary KIEs due to β or more remote hydrogens are minor.

The dependence of k_H/k_D on the base concentration predicted by Eq. (1) does not clearly emerge from Table 1. This may be explained by the narrow concentration range of B explored, which is limited upward by the vanishing amounts of products formed in the presence of excess amine, which interceps Me_3Si^+ or even its precursor ions. On the other hand, the weight of the k_N[Nu] term can not be reduced, as oxygen-containing nucleophiles are unavoidably present as trace impurities in the bulk gas or formed by its radiolysis.[17] A second reason may be traced to the role which may be played by the base itself, especially if sterically unhindered, in the desilylation.[18] It is significant in this respect that when the base cannot conceivably act as a nucleophile, as is the case of $(iPr)_2NEt$, a decrease of k_H/k_D at the highest base concentration distinctly emerges above the error limits. Such base-concentration dependence supports a two-step pathway for the overall silylation reaction via the discrete intermediate **1**.[19]

It follows from the above discussion that the k_H/k_D ratios summarized in Table 1, including the highest value of about 4, represent a lower limit for the k_B^H/k_B^D ratio. Such sizeable KIEs, relatively little affected by secondary contributions, are associated with the deprotonation of **1** and are allowed to manifest themselves by the competition between deprotonation by B and desilylation by Nu (and B). They represent a positive confirmation of the stability of **1** and of the role played by **1** in the cationic aromatic silylation in the gas phase. Finally the ready availability of silylium ions in the gas phase[20] makes the gaseous environment the ideal medium in which their reactivity can be explored, in marked contrast to the strenuous efforts required to obtain isolable silylium ions in the condensed state,[21] and provides the experimental counterpart to theoretical calculations.

Experimental Procedure

The gaseous samples containing accurately weighted amounts of PhMe/[D_8]PhMe were prepared in 135 mL glass vessels by standard vacuum line procedures with research grade gases (Mathesen) and irradiated by ^{60}Co emission in a 220 Gammacell (Nuclear Canada Ltd.) at 35 °C with a total dose of 1×10^4 Gy, which corresponds to less than 1% substrate conversion into silylated toluenes (radiochemical yield ranged from 1×10^{-3} to 0.1 μmol J^{-1}). The radiolytic product mixture was recovered by repeated freeze–thaw cycles with ethyl acetate as solvent. The end solution was analyzed by GLC-MS (60-m long, 0.25 mm i.d., fused silica SPB-20 column (Supelco) coated with a 0.25 μm film of 20% diphenyl – 80% dimethylpolysiloxane; Hewlett Packard 5890 A; Model 5970 B mass selective detector). The relative amounts of isotopomeric products were obtained from the integrated areas of the $[M]^+$ and $[M - CH_3]^+$ ion intensities, which were acquired both in total-ion and in single-ion monitoring mode.

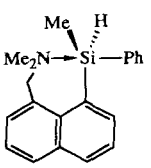
Received: October 12, 1993 [Z 6412 IE]
German version: *Angew. Chem.* **1994**, *106*, 1157

[1] J. B. Lambert, S. Zhang, C. L. Stern, J. C. Huffman, *Science* **1993**, *260*, 1917.
[2] P. von R. Schleyer, P. Buzek, T. Müller, Y. Apeloig, H.-U. Siehl, *Angew. Chem. Int. Ed. Engl.* **1993**, *32*, 1471.
[3] a) C. A. Reed, Z. Xie, R. Bau, A. Benesi, *Science* **1993**, *262*, 402; b) J. B. Lambert, S. Zhang, *J. Chem. Soc. Chem. Commun.* **1993**, 383; c) Z. Xie, D. J. Liston, T. Jelinek, V. Mitro, R. Bau, C. A. Reed, *ibid.* **1993**, 384.
[4] A. C. M. Wojtyniak, J. A. Stone, *Int. J. Mass Spectrom. Ion Processes* **1986**, *74*, 59.
[5] J. M. Stone, J. A. Stone, *Int. J. Mass Spectrom. Ion Processes* **1991**, *109*, 247.
[6] X. Li, J. A. Stone, *Can. J. Chem.* **1992**, *70*, 2070.
[7] F. Cacace, M. E. Crestoni, S. Fornarini, R. Gabrielli, *Int. J. Mass. Spectrom Ion Processes* **1988**, *84*, 17.
[8] S. Fornarini, *J. Org. Chem.* **1988**, *53*, 1314.
[9] F. Cacace, M. E. Crestoni, S. Fornarini, *J. Am. Chem. Soc.* **1992**, *114*, 6776.
[10] a) F. Cacace, *Acc. Chem. Res.* **1988**, *21*, 215; b) M. Speranza, *Mass Spectrom. Rev.* **1992**, *11*, 73.
[11] a) C. Eaborn, *J. Organomet. Chem.* **1975**, *100*, 43; b) F. Cacace, M. E. Crestoni, G. de Petris, S. Fornarini, F. Gradinetti, *Can. J. Chem.* **1988**, *66*, 3099.
[12] a) S. G. Lias, J. E. Bartmess, J. L. Liebman, J. L. Holmes, R. D. Levin, W. G. Mallard, *J. Phys. Chem. Ref. Data Suppl. 1* **1988**, 17; b) J. E. Szuleiko, T. B. McMahon, *J. Am. Chem. Soc.* **1993**, *115*, 7839.
[13] a) L. Melander, W. H. Saunders, Jr. *Reaction Rates of Isotopic Molecules*, Wiley, New York, **1980**; b) R. P. Bell, *The Proton in Chemistry*, Cornell University Press, Ithaca, NY, **1973**; c) A. Thibblin, P. Ahlberg, *Chem. Soc. Rev.* **1989**, *18*, 209.
[14] J. M. Jasinski, J. I. Brauman, *J. Am. Chem. Soc.* **1980**, *102*, 2906.
[15] The KIE observed in elimination reactions from β-substituted silanes derived from a similar branching: S. L. Jones, C. J. M. Stirling, *J. Chem. Soc. Chem. Commun.* **1988**, 1153.
[16] Equation (1) is derived by assuming the steady-state approximation is valid for **1**, and relying on the nearly constant concentrations of $CX_3C_6X_5$, added base (B), and nucleophiles (Nu) in the radiolytic experiments, which typically run to less than 1% substrate conversion, and on the fast deprotonation of **1** (k_B^X[B]), which has to compete with a highly efficient desilylation process (k_N^X[Nu]). See Refs. [4] and [7].
[17] Unfortunately, the branching of reactions (a) and (b) can not be obtained from our radiolysis experiments based on the analysis of neutral final products, since direct silylation of Nu by Me_3Si^+ yields the same products as reaction (b). Thus, a quantitative evaluation of the relative weight of the individual terms of Eq. (1) is prevented, but this does not affect the qualitative conclusions drawn.
[18] According to Equation (1) a decrease of k_H/k_D with increasing base concentration [B] is expected (since when k_B[B] ≫ k_N[Nu], Eq. 1 reduces to $\frac{k_H}{k_D} = \frac{k_1^H}{k_1^D}$). However, if the desilylating reactivity of B overwhelms that of Nu within the explored concentration range, no dependence of k_H/k_D on concentration of B would emerge. Equation (1) would in fact reduce to $k_H/k_D = (k_1^H/k_1^D) \times (k_B^H/k_B^D) \times ((k_B^D + k_{NB}^D)/(k_B^H + k_{NB}^H))$, where k_{NB}^N and k_{NB}^D refer to desilylation by the base B of unlabeled and deuterated **1**, respectively.
[19] R. Taylor, *Electrophilic Aromatic Substitution*, Wiley, Chichester, **1990**, p. 32.
[20] H. Schwarz, *The Chemistry of Organic Silicon Compounds* (Eds.: S. Patai, Z. Rappoport), Wiley, Chichester, **1989**, p. 445.
[21] P. D. Lickiss, *J. Chem. Soc. Dalton Trans.* **1992**, 1333, and references therein.

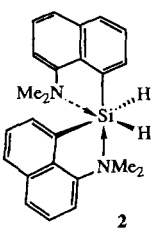
Structure of a (4 + 4)-Coordinate Silicon Compound, a Precursor of Hypercoordinate Silyl Mono- and Dications

Francis Carré, Claude Chuit, Robert J. P. Corriu,* Ahmad Mehdi, and Catherine Reyé

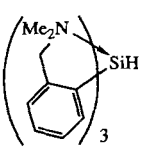
The silicon atom in hydrosilanes is able to expand its coordination number to become penta-[1] (as in compound **1**) or hexacoordinate (as in compound **2**)[2] by formation of donor–acceptor interactions. Moreover, "heptacoordination" at silicon has also been inferred[3] from the molecular structure of silanes **3** and **4**, established by X-ray diffraction analysis. In both compounds, three weak Si ← N interactions are displayed giving rise to the tricapped tetrahedron geometry. In a continuation of our study on silicon species with unusual coordination numbers, we investigated the geometry of organosilanes bearing the potentially bis-chelating ligand **A**[4, 5] and now report the synthesis and the structural determination of a silane with two hydrogen substituents and two such ligands. This compound was found to be a precursor of a silyl cation and by an unexpected reaction, of a silyl dication.



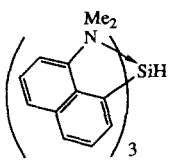
1



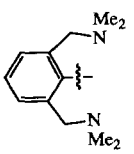
2



3

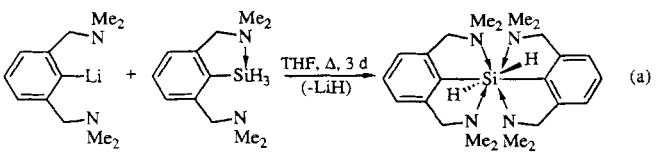


4



A

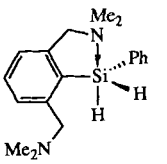
The reactions between the silane **5** and an equimolar amount of 2,6-bis(dimethylaminomethyl)phenyllithium[6] results in the formation of the silane **6** in 68% yield [Eq. (a)]. The equivalence



(a)

5 **6**

of all the NMe_2 groups at 20 °C is shown by the singlet observed for these groups in the ^1H NMR spectrum. A single signal is also observed for all the CH_2N protons. The ^{29}Si NMR chemical shift ($\delta = -61.6$) is upfield of the signal of the silane **7**[7] with only one ligand **A** ($\delta = -51.5$). To establish the nature of the interaction between the NMe_2 groups and the silicon atom a single crystal X-ray diffraction study[8] was performed on **6**. The ORTEP view (Fig. 1) reveals a C_2 axis passing through the silicon atom and bisecting the H-Si-H′ and C1-Si-C′1 angles. The basic tetrahedral structure around the Si atom is maintained, the lone pairs of the NMe_2 groups being directed towards the Si center. The Si–N1 distance, *trans* to the Si–H bond is 3.117 Å, and the N1-Si-H angle 177.5°, whereas the Si–N2 distance *trans* to the Si-C′1 bond is shorter (2.895 Å), and the N2-Si-C′1 angle smaller (168.5°). Thus the molecule can be described as a tetracapped tetrahedron, in which the Si atom is (4 + 4)-coordinated. Interestingly, in contrast with the reported structure of complexes bearing the ligand **A**,[9] the two nitrogen atoms are not in a *trans* arrangement as shown in Figure 1 (right); the N1-Si-N2 angle is 116.7(1)°.



7

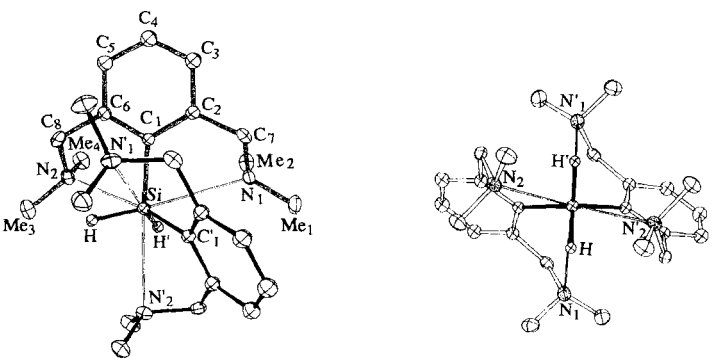


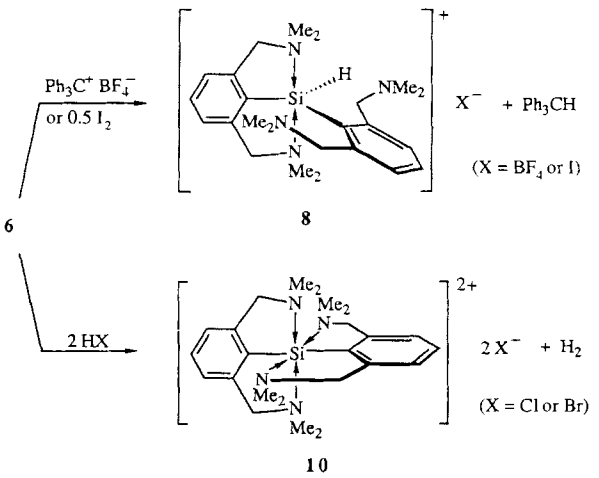
Fig. 1. Left: Crystal structure of **6** (ORTEP representation; hydrogen atoms are omitted for clarity. Ellipsoids are at the 10% probability level). Important bond lengths [Å]: Si–H 1.435(36), Si–C1 1.901(5), Si–N1 3.117(6), Si–N2 2.895(5). Selected angles [°]: H-Si-H′ 114.8 (2.9), C1-Si-C′1 113.2(3), C1-Si-H 108.7 (1.5), C1-Si-H′ 105.8 (1.5). Right: The molecular structure of **6** viewed along its C_2 axis. (Ellipsoids are at the 10% probability level.)

The equivalence of the four NMe_2 groups observed by ^1H NMR at room temperature can be explained by dynamic coordination: the NMe_2 groups displace each other rapidly on the ^1H NMR time scale.

In spite of the steric hindrance around the silicon atom, treatment of the silane **6** with 1 equiv of $Ph_3C^+BF_4^-$ in CH_2Cl_2 solution results in a high yield of Ph_3CH and a silicon-containing species that was identified as the ionic compound **8**. The same silyl cation is obtained by reaction of **6** with 1/2 equiv of I_2 (Scheme 1).

The ^1H NMR spectrum of **8** is reported in Figure 2. The signal at $\delta = 5.07$ was assigned to the SiH protons. By comparison with the ^1H NMR spectrum of the silanium ("siliconium") ion **9**,[7] the two singlets of equal intensity (at $\delta = 2.18$ and 2.65) were assigned to the two NMe_2 groups of one ligand **A**. These two units are magnetically equivalent and exhibit two diastereotopic methyl groups as the result of the coordination of the two nitrogen atoms to the silicon atom. Moreover, a well-defined AB pattern is observed at $\delta = 4.13$ for the corresponding two CH_2N groups. The singlets at $\delta = 1.47$ and 2.25 were assigned to the other two NMe_2 groups, the CH_2N protons appearing as singlets at $\delta = 2.83$ and $\delta = 3.50$, respectively. The existence of

[*] Prof. Dr. R. J. P. Corriu, Dr. F. Carré, Dr. C. Chuit, A. Mehdi, Dr. C. Reyé
Université de Montpellier II
Sciences et Techniques du Languedoc, URA 1097
Place Eugène Bataillon, case 007, F-34095 Montpellier Cédex 5 (France)
Telefax: Int. code + (67)143888.



Scheme 1.

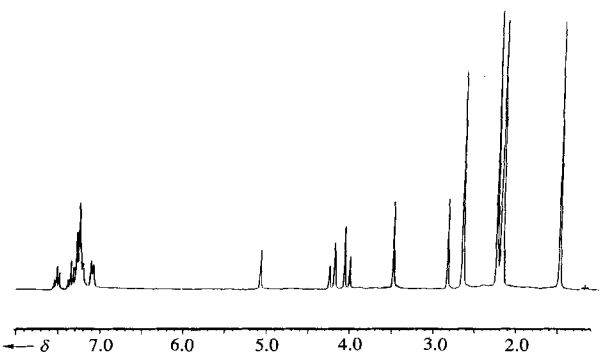
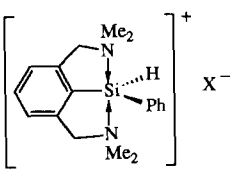


Fig. 2. ^{1}H NMR spectrum ($CDCl_3$, 250 MHz) of **8** at room temperature.

three types of NMe_2 groups was confirmed by ^{15}N NMR spectroscopy. Since the ^{15}N NMR shift of **9** is at $\delta = -337$, the signal at $\delta = -340.4$ is assigned to the two chelating NMe_2 groups, and the other two upfield signals ($\delta = -347.2$ and -348.7) are attributed to the two noncoordinated NMe_2 groups. Thus it can be concluded that cation **8** is pentacoordinated. Moreover, the magnetic nonequivalence of the two noncoordinated NMe_2 groups shown in the ^{1}H NMR spectrum of **8** means that rotation about the corresponding Si–aryl bond is hindered. In the ^{1}H-coupled ^{29}Si NMR spectrum of **8**, a doublet is observed at $\delta = -29$ [$^1J_{Si,H} = 283$ Hz], which is downfield with respect to the corresponding chemical shift observed for the starting silane **6** [$\delta = -61.6$ (t, $^1J_{Si,H} = 213$ Hz)], but in the same range as that for **9** [$\delta = -29.7$, d, $^1J_{Si,H} = 280$ Hz].[7]



9

The IR spectrum of **8** in $CHCl_3$ shows an absorption band for the ν(Si–H) stretch at 2248 cm^{-1} that is at a higher frequency than that for **6** (2174 cm^{-1}) and in the range of other Si–H stretches observed for silyl cations.[7, 10] The positive-ion FAB mass spectrum of **8** shows the parent ion at m/z 411; this corresponds to the mass of the silyl cation.

More surprisingly, the reaction of **6** with two molar equivalents of HCl or HBr gives rise to the dicationic species **10** with loss of H_2 (Scheme 1). Abstraction of two hydrogens is confirmed by ^{1}H and ^{29}Si NMR as well as IR spectroscopy. Moreover, the ^{1}H and ^{29}Si NMR spectra of the products are identical irrespective of the reagent acid used. The ^{1}H NMR spectrum is very simple: there is one signal for all the methyl groups ($\delta = 2.15$) and one signal for the CH_2N protons ($\delta = 3.75$). Absence of a signal corresponding to a Si–H bond was inferred from the ^{1}H-coupled ^{29}Si-NMR spectrum of **10** (a singlet is observed at $\delta = -30.5$) and from the IR spectrum (disappearance of the Si–H stretch). The mass spectrum (EI, 70 eV) shows the parent ion at m/z 410 (corresponding to the mass of the dication). Evidence for the ionic nature of the salts **8** and **10** was provided by conductivity data. The specific conductance of a CH_2Cl_2 solution of **6** increases during the addition of 1/2 equiv of I_2 to give **8** and during the addition of two molar equivalents of HCl to give **10** (Fig. 3).

An interesting feature in the reaction between **6** and HX (X = Cl, Br) is the abstraction of hydrogens with loss of H_2, a reaction which does not occur with Ph_2SiH_2. This redox reaction is an indication of the strong interaction between the NMe_2 groups and the Si center. The addition of one equivalent of HX does not give the silylmonocation **8**, but instead leads to a mixture of the starting compound and the dication **10**.

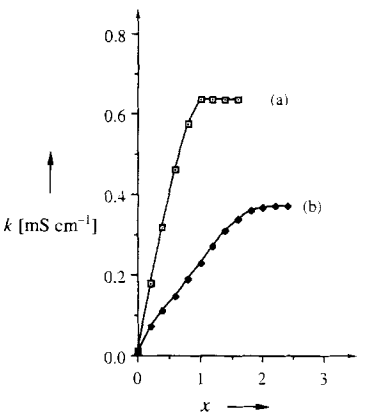


Fig. 3. The conductivity (κ) as a function of the amount of reactant added to a solution of silane **6** in 50 mL of CH_2Cl_2: a) amount of iodine (x [mol equiv I] added to 0.460 mmol of **6**; b) amount of HCl (x [mol equiv]) added to 0.485 mmol of **6**.

In conclusion, use of the 2,6-bis(dimethylaminomethyl)phenyl ligand has permitted the preparation of the novel (4 + 4)-coordinate silicon species **6**, which proves that the Si atom can expand its coordination number beyond six. The very high ability of the ligand **A** to chelate the silicon atom enabled the preparation of not only a silyl cation but also a silyl dication.

Experimental Procedure

6: A THF solution (50 mL) of 2,6-bis(dimethylaminomethyl)phenyllithium [6] (12.4 mmol) was added dropwise at 0 °C to a stirred THF solution of **5** (2.35 g, 12.4 mmol) under argon. The reaction mixture was then heated at reflux for 3 days. After the solvent had been removed, a light brown oil was obtained, which was purified by distillation (115–145 °C/0.025 Torr) followed by recrystallization from pentane to give transparent crystals. Yield: 68%; m.p. 71–74 °C. ^{1}H NMR (250 MHz, $CDCl_3$): $\delta = 1.96$ (s, 12H, $N(CH_3)_2$), 3.24 (s, 4H, CH_2N), 4.87 (s, 2H, SiH), 7.08–7.14 (m, 3H, Ar); ^{29}Si NMR (200 MHz, $CDCl_3$): $\delta = -61.6$ (t, ^1J(Si,H) = 213 Hz), (solid state ^{29}Si NMR: $\delta = -57.2$); IR ($CHCl_3$): $\tilde{\nu}$[cm^{-1}] = 2174.3 (Si–H). Correct elemental analysis for C,H,N.

8: A CH_2Cl_2 solution (10 mL) of $Ph_3C^+BF_4^-$ (0.86 g, 2.6 mmol) was added dropwise at 0 °C under argon to a stirred CH_2Cl_2 solution (15 mL) of silane **6** (1.13 g, 2.73 mmol). Progressive decoloration of the trityl solution occurred during the addition. After addition was complete, the reaction mixture was allowed to warm to 25 °C and stirred for 2 h. The solvent was then removed under vacuum and the residue washed three times with Et_2O to eliminate Ph_3CH. After drying under vacuum a beige powder was obtained (1.2 g, 92% yield). ^{1}H NMR (250 MHz, $CDCl_3$): $\delta = 1.47$ (s, 6H), 2.18 (s, 6H), 2.25 (s, 6H), 2.65 (s, 6H), 2.83 (s, 2H), 3.5 (s, 2H), 4.13 (q, ^2J(H,H) = 15.6 Hz, 4H), 5.07 (s, 1H), 7.07–7.58 (m, 6H); ^{29}Si NMR (200 MHz, $CDCl_3$): $\delta = -29.0$ (d, ^1J(Si,H) = 283 Hz); ^{15}N NMR ($CDCl_3$, ref CH_3NO_2): $\delta = -340.4$, -347.2, -348.7; IR ($CDCl_3$): $\tilde{\nu}$[cm^{-1}] = 2248; positive-ion FAB-MS (2-nitrophenyl octyl ether matrix) m/z 411 $(M - BF_4)^+$; negative-ion FAB-MS m/z: 87 $(BF_4)^-$.

10: 20 mL of a 0.0472 M solution of HCl (0.944 mmol) in CH_2Cl_2 was added dropwise under argon to a stirred CH_2Cl_2 solution (50 mL) of **6** (0.2 g, 0.485 mmol) at room temperature. After 1 h, the solvent was removed to give 0.2 g (92% yield) of

an oily solid: ^{1}H NMR (250 MHz, $CDCl_3$): δ = 2.15 (s, 12H), 3.75 (s, 4H), 7.2–7.45 (m, 3H); ^{29}Si NMR (200 MHz, $CDCl_3$): δ = – 30.5; MS (70 eV): *m/z* 410 $[M - 2Cl]^+$, 38%.

Received: December 7, 1993 [Z 6545 IE]
German version: *Angew. Chem.* **1994**, *106*, 1152

[1] a) S. N. Tandura, M. G. Voronkov, N. V. Alekseev, *Top. Curr. Chem.* **1986**, *131*, 99; b) C. Chuit, R. J. P. Corriu, C. Reyé, J. C. Young, *Chem. Rev.* **1993**, *93*, 1371; c) C. Brelière, F. Carré, R. J. P. Corriu, M. Poirier, G. Royo, *Organometallics* **1986**, *5*, 388; d) J. Boyer, C. Brelière, F. Carré, R. J. P. Corriu, A. Kpoton, M. Poirier, G. Royo, J. C. Young, *J. Chem. Soc. Dalton Trans.* **1989**, 43.

[2] C. Brelière, F. Carré, R. J. P. Corriu, M. Poirier, G. Royo, J. Zwecker, *Organometallics* **1989**, *8*, 1831.

[3] C. Brelière, F. Carré, R. J. P. Corriu, G. Royo, *Organometallics* **1988**, *7*, 1006; N. Auner, R. Probst, F. Hahn, E. Herdtweck, *J. Organomet. Chem.* **1993**, *459*, 25; C. Brelière, F. Carré, R. J. P. Corriu, G. Royo, M. Wong Chi Man, J. Lapasset, *Organometallics* **1994**, *13*, 307.

[4] G. van Koten, *Pure Appl. Chem.* **1989**, *61*, 1681; *ibid.* **1990**, *62*, 1155; J. T. B. H. Jastrzebski, G. van Koten, *Adv. Organomet. Chem.* **1993**, *35*, 241.

[5] F. Carre, C. Chuit, R. J. P. Corriu, A. Mehdi, C. Reyé, *J. Organomet. Chem.* **1993**, *446*, C6.

[6] G. van Koten, J. T. B. H. Jastrzebski, J. G. Noltes, A. L. Spek, J. C. Schoone, *J. Organomet. Chem.* **1978**, *148*, 233.

[7] C. Chuit, R. J. P. Corriu, A. Mehdi, C. Reyé, *Angew. Chem.* **1993**, *105*, 1372; *Angew. Chem. Int. Ed. Engl.* **1993**, *32*, 1311.

[8] X-ray crystal structure data of **6**: monoclinic, space group $C2/c$, a = 18.491(2), b = 9.086(2), c = 16.352(1) Å, β = 111.838(8)°, V = 2550.2(7) Å^3, ρ_{calcd} = 1.075 g cm^{-3}, $\mu(Mo_{K\alpha})$ = 1.01 cm^{-1}, Z = 4.2174, unique reflections up to (sin θ/λ) = 0.639, 849 with $F_0 \leq 2.8\,\sigma(F_0)$. Enraf-Nonius CAD4 diffractometer, $Mo_{K\alpha}$ radiation, λ = 0.71069, T = 22 °C. Solution by direct methods (MULTAN-80). $R(R_w)$ = 0.059 (0.062), $w = 1/(\sigma^2(F_0) + 0.0049\,F^2)$ for 121 refined parameters (anisotropic temperature factors for all atoms; the hydrogen atoms were taken into account in the refinement with isotropic temperature factors and CH_3 as rigid groups. SHELX-76). Residual electron density: 0.72 e Å^{-3}. Further details of the crystal structure investigation are available on request from the Cambridge Crystallographic Data center, University Chemical Laboratory, 12 Union Road, Cambridge CB2 1EZ (UK), on quoting the full journal citation.

[9] a) J. Terheijden, G. van Koten, J. L. de Booys, H. J. C. Ubbels, C. H. Stam, *Organometallics* **1983**, *2*, 1882; b) D. M. Grove, G. van Koten, W. P. Mul, A. A. H. van der Zeijden, J. Terheijden, M. C. Zoutberg, C. H. Stam, *ibid.* **1986**, *5*, 322; c) A. A. H. van der Zeijden, G. van Koten, R. Luijk, K. Vrieze, C. Slob, H. Krabbendam, A. L. Spek, *Inorg. Chem.* **1988**, *27*, 1014.

[10] P. Jutzi, E. A. Bunte, *Angew. Chem.* **1992**, *104*, 1636; *Angew. Chem. Int. Ed. Engl.* **1992**, *31*, 1605.

Synthesis of Enediynes by Diels–Alder Addition**

Henning Hopf* and Marcus Theurig

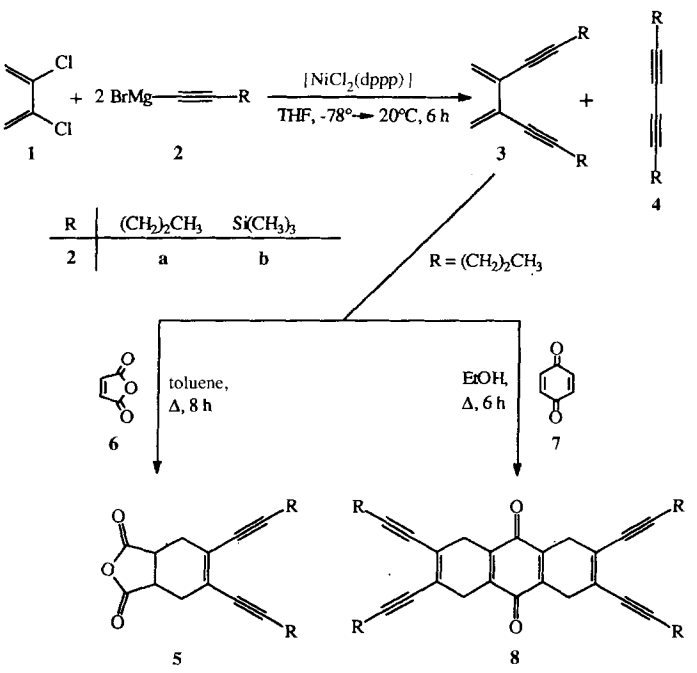
Dedicated to Professor Maximillian Zander on the occasion of his 65th birthday

The hex-3-en-1,5-diyne system forms the core structural element and reaction-initiating component of enediyne antibiotics, which, owing to their DNA-cleaving properties, have catapulted to the forefront in the development of antitumor agents.[1] The synthesis of enediynes has been accomplished to date either through elimination reactions (generation of the central double bond with the ethynyl groups already present[2]) or through coupling reactions (connection of the triple bonds to an existing, usually halogenated olefin[3]).

[*] Prof. H. Hopf, Dipl.-Chem. M. Theurig
Institut für Organische Chemie der Technischen Universität
Hagenring 30, D-38106 Braunschweig (FRG)
Telefax: Int. code + (531)391-5388

[**] New Dienes and Dienophiles, Part 5. This research was supported by the Fonds der Chemischen Industrie. – Part 4: H. Hopf, B. Witulski, *Nachr. Chem. Techn. Lab.* **1991**, *39*, 286.

We now present a fundamentally new route to enediynes, which generates the highly unsaturated system in a simple manner by a [2 + 4] cycloaddition and thereby permits the introduction of (different) substituents in all four positions of the parent hydrocarbon.



Coupling of 2,3-dichloro-1,3-butadiene (**1**) with the terminal alkenes **2**, in the presence of the catalyst [1,3-bis(diphenylphosphino)propane]nickel(II) chloride [$NiCl_2$(dppp)] (tetrahydrofuran, $-78 \rightarrow 20$ °C) generates the 3,4-bis(methylene)-1,5-hexadiyne derivatives **3** in 62–80% yield, in addition to the side products **4**, which arise through dimerization of **2**. The structure of **3** is derived unambiguously from spectroscopic and analytical data.[4] As hoped, the derivatives **3** undergo [2 + 4] cycloadditions smoothly. Thus, reaction with maleic anhydride under the conditions given in the scheme affords the 1:1 cycloadduct **5**, which is obtained as a colorless solid in 36% yield.[4] The double dienophile *p*-benzoquinone (**7**) furnishes the bis(enediyne) system **8** (32%) in the form of yellow needles.[4] Since **7** was used in excess, the formation of this bis(didehydro) derivative of the primary adduct is not surprising. We attribute the comparatively low yields for the unoptimized addition to the susceptibility of the 2,3-functionalized butadienes towards polymerization, which was not taken into account during workup. The cycloadducts are nevertheless conveniently accessible in gram quantities.

We shall report shortly on the use of this synthesis in the preparation of enediynes with additional functionalization in the side chain R, as well as on further reactions of **5** and **8** (aromatization, annelation).

Experimental Procedure

Synthesis of **3b**: A solution of methylmagnesium bromide (3 M, 16.7 mL, 50 mmol) in ether was added dropwise at 0 °C to a solution of trimethylsilylacetylene (4.91 g, 50 mmol) in anhydrous THF (50 mL). The white suspension was allowed to warm to room temperature over 30 min and was then heated at reflux for 1 h. After the reaction mixture was cooled to -78 °C, **1** (2.66 g, 22 mmol) and [$NiCl_2$(dppp)] (0.92 g, 1.7 mmol) were added. The red-brown reaction mixture was allowed to warm to room temperature over 2 h and then stirred for an additional 4 h. Saturated ammonium chloride solution (50 mL) was added to quench the reaction, and the organic phase was separated, washed with water, and then dried over magnesium

sulfate. After the solvent was removed in vacuo, the residue was purified by column chromatography (silica gel, pentane) to give **3b** (3.35 g, 62%) as a yellow solid, m.p. 56 °C.—^{1}H NMR (400 MHz, $CDCl_3$, 25 °C, TMS): $\delta = 0.21$ (s, 18H), 5.71 (d, $J = 2.3$ Hz, 2H), 6.01 (d, $J = 2.3$ Hz, 2H).—^{13}C NMR (100 MHz, $CDCl_3$, 25 °C, TMS): $\delta = -0.11$ (s), 97.88 (s), 101.25 (s), 125.44 (t), 128.55 (s).—IR (KBr): $\tilde{\nu} = 2960$, 2900, 2161, 1698, 1517, 1470, 250 cm^{-1}.—UV/VIS (acetonitrile): $\lambda_{max}(\varepsilon) = 212$ (7800), 220 (9700), 244 (10000), 280 (5900), 292 (5100), 326 nm (750).—MS (70 eV): m/z (%) = 246 (22) [M^+], 231 (40), 108 (18), 73 (100).

Received: December 27, 1993 [Z 6585 1E]
German version: *Angew. Chem.* **1994**, *106*, 1173

[1] Recent reviews on the synthesis of enediyne antibiotics: a) K. C. Nicolaou, W.-M. Dai, *Angew. Chem.* **1991**, *103*, 1453; *Angew. Chem. Int. Ed. Engl.* **1991**, *30*, 1387; b) H. Waldmann, *Nachr. Chem. Tech. Lab.* **1991**, *39*, 211; c) K. C. Nicolaou, A. L. Smith, *Acc. Chem. Res.* **1992**, *25*, 497; d) K. C. Nicolaou, *Angew. Chem.* **1993**, *105*, 1462; *Angew. Chem. Int. Ed. Engl.* **1993**, *32*, 1377.

[2] Generation of the double bond through a) 1,2-elimination: H. Audrain, T. Skrydstrup, G. Uliobarri, D. S. Grierson, *Synlett* **1993**, 20, and references therein; b) McMurry coupling: H. Hopf, C. Horn, W. R. Roth, *Chem. Ber.*, in press; Corey–Winter fragmentation: M. F. Semmelhack, J. Gallagher, *Tetrahedron Lett.* **1993**, *34*, 4121; d) Ramberg–Bäcklund reaction: K. C. Nicolaou, G. Zuccarello, C. Riemer, V. A. Estevez, W.-M. Dai, *J. Am. Chem. Soc.* **1992**, *114*, 7360.

[3] Review: R. Gleiter, D. Kratz, *Angew. Chem.* **1993**, *105*, 884; *Angew. Chem. Int. Ed. Engl.* **1993**, *32*, 842; cf. a) S. L. Schreiber, L. L. Kiessling, *J. Am. Chem. Soc.* **1988**, *110*, 631; b) K. N. Bharucha, R. M. Marsh, R. E. Minto, R. G. Bergman, *ibid.* **1992**, *114*, 3120; c) P. Magnus, P. Carter, J. Elliot, R. Lewis, J. Harling, T. Pitterna, W. E. Bauta, S. Fortt, *ibid.* **1992**, *114*, 2544; d) D. Schinzer, J. Kabbara, *Synlett* **1992**, 766; e) Y.-F. Lu, C. W. Harwig, A. G. Fallis, *J. Org. Chem.* **1993**, *58*, 4202; f) M. E. Maier, T. Brandstetter, *Tetrahedron Lett.* **1992**, *33*, 7511; g) R. Brückner, J. Suffert, *ibid.* **1991**, *32*, 1453.

[4] Selected spectroscopic data for the new compounds: **3a**: ^{1}H NMR (400 MHz, $CDCl_3$, 25 °C, TMS): $\delta = 0.98$ (t, $J = 7.3$ Hz, 6H), 1.56 (m, 4H), 2.32 (t, $J = 7.0$ Hz, 4H), 5.54 (s, 2H), 5.92 (s, 2H).—^{13}C NMR (100 MHz, $CDCl_3$, 25 °C, TMS): $\delta = 13.47$ (q), 21.26 (t), 22.08 (t), 77.34 (s), 93.30 (s), 122.85 (t), 129.55 (s).—MS (70 eV): m/z(%) = 186 (79) [M^+], 171 (4), 158 (48), 141 (56), 130 (88), 128 (100), 115 (67), 91 (41), 77 (40).—**3b**: See Experimental Procedure.—**5**: ^{1}H NMR (400 MHz, [D_6]acetone, 25 °C, TMS): $\delta = 1.00$ (t, $J = 7.2$ Hz, 6H), 1.53 (m, 4H), 2.32 (t, $J = 6.9$ Hz, 4H), 2.63 (m, 4H), 3.08 (m, 2H).—^{13}C NMR (100 MHz, [D_6]acetone, 25 °C, TMS): $\delta = 13.61$ (q), 21.88 (t), 22.86 (t), 31.74 (t), 39.45 (d), 82.6 (s), 94.43 (s), 124.07 (s), 173.93 (s).—IR (KBr): $\tilde{\nu} = 2936$, 2874, 2210, 1706, 1427, 1296, 1256, 1204, 949 cm^{-1}.—UV/VIS (acetonitrile): $\lambda_{max}(\varepsilon) = 200$ (5100), 218 (3900), 256 (10900), 2358 (11500), 264 (13500), 268 (12500), 276 (11400), 290 mm (670).—MS (70 eV): m/z (%) = 284 (100) [M^+], 256 (84), 227 (35), 169 (37), 158 (36), 128 (26), 115 (29), 91 (17), 77 (12).—**8**: ^{1}H NMR (400 MHz, $CDCl_3$, 25 °C, TMS): $\delta = 1.02$ (t, $J = 7.3$ Hz, 12H), 1.58 (m, 8H), 2.36 (t, $J = 6.9$ Hz, 8H), 3.22 (s, 8H).—^{13}C NMR (100 MHz, $CDCl_3$, 25 °C, TMS): $\delta = 13.48$ (q), 21.66 (t), 22.12 (t), 29.29 (t), 80.02 (s), 95.77 (s), 120.66 (s), 137.30 (s), 185.12 (s).—IR (KBr): $\tilde{\nu} = 2964$, 2873, 2212, 1648, 1411, 1335, 1295, 691 cm^{-1}.—UV/VIS (acetonitrile): $\lambda_{max}(\varepsilon) = 192$ (27800), 246 (30500), 266 (27400), 280 (26400), 306 (35700), 328 (7200), 358 nm (4800).—MS (70 eV): m/z (%) = 476 (100) [M^+], 449 (14), 435 (10), 397 (19), 258 (12), 183 (11).

Stable Highly Concentrated Fluorocarbon Gels**

Marie-Pierre Krafft and J. G. Riess*

Highly viscous phases are often found in ternary hydrocarbon/water/surfactant systems. Gels can be found in systems composed of two interlocking continuous phases, one of which is liquid and the other of which consists of long-chain solid or liquid-crystalline material.[1] Both micelles in water and inverted micelles were recently reported to form cylindrical micelles; as the surfactant concentration is increased, they start to entangle and form a dynamic network similar to semidilute polymer solutions.[2–3]

Structures composed of packed, compartmentalized domains can also display a gel-like appearance. Microemulsion gels (so-called ringing gels), which require large amounts of surfactant, were shown to consist of closely packed globular aggregates filled with hydrocarbon, while water forms the continuous phase.[4] Such systems can form cubic phases.[5] When large volumes of a dispersed phase and small amounts of surfactant are used, other viscoelastic gels referred to as high internal phase ratio emulsions (HIPRE) can be obtained. These were shown to consist of polyhedral hydrocarbon cells (polyaphron) delimited by a layer of hydrated surfactant.[6, 7] Gels of this type, which contain up to 99% v/v of a hydrocarbon, were obtained.[4] Their preparation usually requires the use of two surfactants—one oil-soluble and the other water-soluble. As far as water-in-oil emulsions are concerned, concentrated aqueous gels have been reported that contain roughly 50–98% v/v of water as the internal phase and a hydrocarbon or a fluorocarbon as the continuous phase.[8–9]

We wondered whether gels with a high internal fluorocarbon content could be obtained with low amounts of a single fluorinated surfactant and water as components of the cell walls. Such gels would exploit the unique properties of fluorocarbons to spread easily on amphiphilic surfaces and of fluorinated surfactants to stabilize fluorocarbon dispersions, as demonstrated for fluorocarbon emulsions formulated for in vivo oxygen delivery.[10–11]

We found it possible to prepare stable gels consisting of very large amounts of fluorocarbons, exceptionally low amounts of a fluorinated surfactant, and water. We utilized a variety of linear and cyclic fluorocarbons, including some lipophilic ones, with a range of molecular weights, for example perfluorooctyl ethane, perfluorooctyl bromide, perfluorodecalin, a mixture of perfluoro-*n*-butyldecalin (15–20%) and perfluoroperhydrophenanthrene (80–85%) (APF 215), perfluorodiisopropyldecalin (APF-240), and a mixture of perfluorodixylylmethane (60%) and perfluorodixylylethane (40%) (APF-260)[12] Fluorocarbons with a higher boiling point were chosen preferentially to meet the requirement of one of the targeted applications (topical administration of drugs) to prevent the system from rapid evaporation when left open to air. The fluorinated surfactants used were the neutral amine oxide **1** and the zwitterionic phosphocholine derivative **2**.[13, 14] Both were monodispersed, pure, and well defined.

$C_7F_{15}C(O)NH(CH_2)_3N(O)(CH_3)_2$ **1**

$C_8F_{17}C_2H_4OP(O)_2^-C_2H_4N^+(CH_3)_3$ **2**

The new gels were prepared under nitrogen at room temperature by slowly adding the fluorocarbon to a foamy aqueous solution of the fluorinated surfactant. Little energy is required, gentle shaking by hand suffices. As the gel forms, the rate of fluorocarbon addition can be increased. Gels did not form when the surfactant solution was added all at once to a relatively large amount of fluorocarbon. Interestingly, high-energy mechanical homogenization or sonication lead to rapid phase separation. After preparation the gels can be degassed by centrifugation at room temperature (1000 rpm, 15 min).

Typical formulations used for one high molecular weight fluorocarbon, perfluorodiisopropyldecalin, are listed in Table 1. These gels contain up to 99% v/v of the fluorocarbon and

[*] Prof. J. G. Riess, Dr. M.-P. Krafft
Unité de Chimie Moléculaire, associée au CNRS
Université de Nice Sophia Antipolis, Faculté des Sciences
F-06108 Nice Cedex 2 (France)
Telefax: Int. code + 93 52-90 20

[**] This research was supported by the Centre National de la Recherche Scientifique and the ATTA. The authors thank Dr. Gulik-Krzywicki (Gif sur Yvette) for freeze fracture electron microsgraphs and Drs. Ni and Weers (Alliance Pharmaceutical, San Diego, CA) for viscosity measurements.

Table 1. Examples of formulations and viscosities of highly concentrated fluorocarbon gels prepared from perfluorodiisopropyldecalin (APF-240), water, and the neutral amine oxide **1**.

APF-240 [% v/v]	Water [% v/v]	Surfactant [% w/v]	S/W [a]	FC/W [b]	Viscosity [c]
80	20	4	1/5	4	57.9
90	10	3.33	1/3	9	122.7
90	10	2	1/5	9	
95	5	1	1/5	19	56.5
97.5	2.5	0.83	1/3	39	203.5
97.5	2.5	0.5	1/5	39	83.2
99	1	0.2	1/5	99	140.2
99.5	0.5	1	1/5	199	

[a] Surfactant/water ratio. [b] Fluorocarbon/water ratio. [c] Viscosity in Pa s at $0.1\ s^{-1}$.

as little as 0.2% w/v (weight per volume) of the fluorinated surfactant **1** along with roughly 1% v/v of water. Their yield point value is high enough to prevent flow under gravitational forces. Other gels containing larger amounts of water (e.g. 10–20% v/v), have been prepared, since they could incorporate water-soluble drugs. In this case greater amounts of surfactant would also be needed. The gels can be characterized by their fluorocarbon/water (FC/W) and surfactant/water (S/W) ratios. For a given amount of surfactant, the larger the FC/W ratio, the more viscous and elastic (as determined by high yield points) the preparation, in analogy to the gel prepared from hydrocarbon HIPRE.[6] For a given fluorocarbon content, viscosity increases when the S/W ratio increases. A S/W ratio of 1/3 to 1/5 appears to be optimal for gel consistency. Transparency increases with the boiling point of the fluorocarbon.

A freeze fracture electron micrograph of a concentrated (98.5% v/v) fluorocarbon gel shows that its structure consists of a matrix of submicronic polyhedral domains of fluorocarbon surrounded by thin shells of hydrated surfactant (Fig. 1), in agreement with a polyaphron structure.[7] Standard tests with a water-soluble dye or with dry paper impregnated with a 20% cobalt chloride solution confirm that water is the continuous phase.

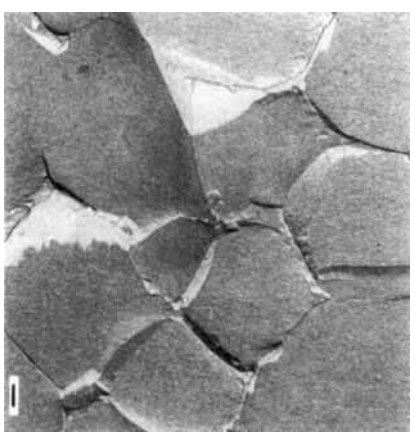


Fig. 1. Freeze fracture transmission electron micrograph of a concentrated fluorocarbon gel (APF-260, 98.5% v/v). The length of the bar corresponds to 220 nm.

It is remarkable that only one water-soluble surfactant is necessary to produce gels when fluorocarbons constitute the dispersed phase. In the case of hydrocarbon polyaphrons, the presence of an oil-soluble surfactant was considered a requirement, so that the oil can spread on the surface of water;[7] however, hydrocarbon polyaphrons were reported which were prepared with only sodium dodecyl sulfate (SDS) as surfactant.[4] In our case we attribute this to the good spreading characteristics of fluorocarbons,[10] as well as to the strong hydrophobic interactions that stabilize the films and vesicles formed by fluorinated surfactants.[15] The gel structure obtained is very similar to that of air bubbles in foams.[16] The easy preparation of fluorocarbon polyaphrons thus calls to mind the analogy drawn between fluorocarbons and gases.[17]

The preparation of the fluorocarbon gels requires a remarkably low amount of energy. The gels are stable enough to withstand heat-sterilization under standard conditions (121 °C, 15 min, $10^5\ Nm^{-2}$). No change in the macroscopic appearance or transparency was observed for both sterilized and nonsterilized gels after one year at room temperature. Neither crystallization of the surfactant nor phase separation was observed.

A thin layer of fluorocarbon can appear with time on the surface of the gel. This is due to the fact that the encapsulating surfactant film is submitted to unbalanced forces at the air interface; thus, the polyhedra tend to burst, releasing the fluorocarbon phase.[7] Once this thin film of fluorocarbon has formed, the system does not change further. The exuded fluorocarbon can easily be reincorporated in the gel by gentle shaking by hand. The gels can be diluted in water to give transparent homogeneous dispersions. After a while, however, the gels tend to form again by sedimentation of the dispersed phase.

The new fluorocarbon gels have potential for topical applications, since they could protect the skin or a wound while remaining permeable to gases. They repel all forms of contaminants, including bacteria. Water-soluble drugs (such as antibiotics), nutrients, and other substances of therapeutic value would be incorporated in the aqueous film, which can also act as a moisturizer. More complex formulations could be designed to allow the simultaneous transport of lipidic and hydrophilic drugs.

Received: December 3, 1993 [Z 6535 IE]
German version: *Angew. Chem.* **1994**, *106*, 1146

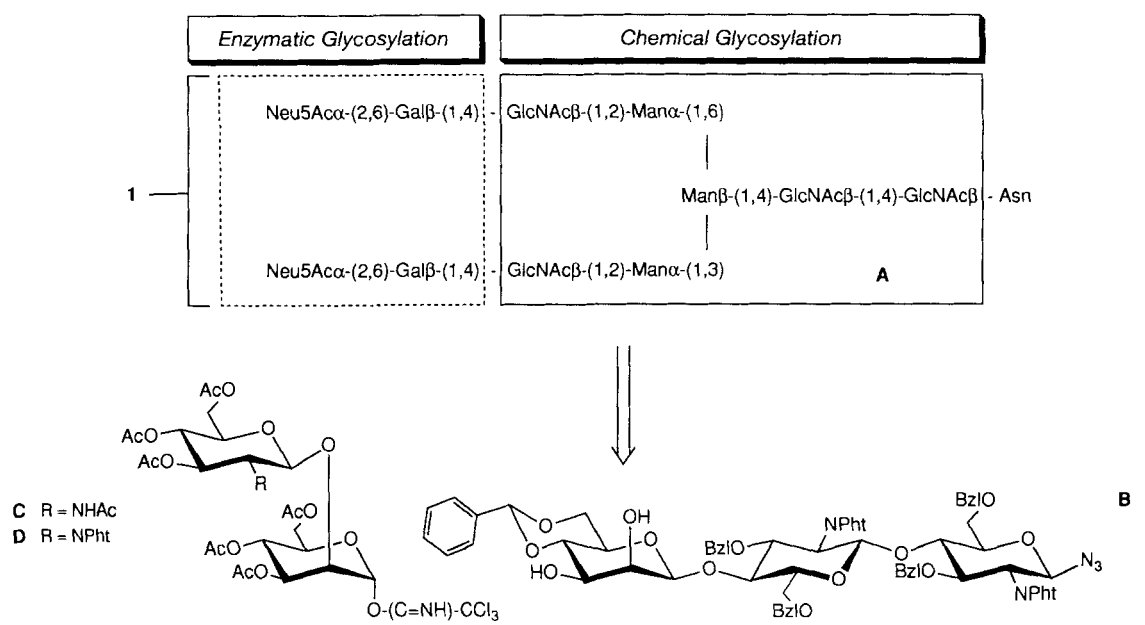
[1] K. J. Lissant in *Emulsion & Emulsion Technology, Vol. 6* (Ed.: K. J. Lissant), Dekker, New York, **1974**, pp. 49–69.
[2] S. J. Candau, E. Hirsch, R. Zana, A. Adam, *J. Colloid Interface Sci.* **1988**, *122*, 430–440.
[3] R. Scartazzini, P. L. Luisi, *J. Phys. Chem.* **1988**, *92*, 829–833.
[4] H. Hoffmann, G. Ebert, *Angew. Chem.* **1988**, *100*, 933–944; *Angew. Chem. Int. Ed. Engl.* **1988**, *27*, 902–912; H. Rehage, G. Platz, G. Ebert, *Ber. Bunsenges. Phys. Chem.* **1988**, *92*, 1158.
[5] K. Fontell, A. Ceglie, B. Lindman, B. Ninham, *Acta Chem. Scand Ser. A* **1986**, *40*, 247–253.
[6] K. J. Lissant, *J. Colloid Interface Sci.* **1966**, *22*, 462–468.
[7] F. Sebba in *Foams and Biliquid Foams-Aphrons* (Ed.: F. Sebba), Wiley, Chichester, **1987**, pp. 103–107.
[8] C. Solans, J. G. Dominguez, J. L. Parra, J. Heuser, S. S. Friberg, *Colloid Polym. Sci.* **1988**, *266*, 570–574; H. Kunieda, C. Solans, N. Shida, J. L. Parra, *Colloids Surf.* **1987**, *24*, 225–227.
[9] J. C. Ravey, M. J. Stébé, *Prog. Colloid. Polym Sci.* **1990**, *82*, 218–228.
[10] J. G. Weers, *J. Fluorine Chem.* **1993**, *64*, 73–93.
[11] J. G. Riess, M. Postel, *Biomater. Artif. Cells Immob. Biotech.* **1992**, *20*, 819–830.
[12] APF-215, APF-240, and APF-260 were obtained from Air Product (Allentown, PA, USA), perfluorodecalin from ISC Chemicals Lim. (Avonmouth, UK). Perfluorooctyl bromide and perfluorooctylethane were a gift from Atochem (Pierre-Bénite, France).
[13] A. Price, (Allied Chemical Corp.), US 3828085, **1974**.
[14] M. P. Krafft, J. P. Rolland, P. Vierling, J. G. Riess, *N. J. Chem.* **1990**, *14*, 869–875.
[15] M. P. Krafft, F. Giulieri, J. G. Riess, *Angew. Chem.* **1993**, *105*, 783–785; *Angew. Chem. Int. Ed. Engl.* **1993**, *32*, 741–743.
[16] In ref. [7], pp. 47–62.
[17] E. Dellacherie, P. Labrude, C. Vigneron, J. G. Riess in *Critical Reviews in Therapeutic Drug Carrier Systems* (Ed.: S. D. Bruck), CRC, Boca Raton, FL, **1987**, pp. 41–94.

 © VCH Verlagsgesellschaft mbH, D-69451 Weinheim, 1994 0570-0833/94/1010-1101 $ 10.00+.25/0

Synthesis of a Biantennary Heptasaccharide by Regioselective Glycosylations **

Carlo Unverzagt*

The oligosaccharides of glycoproteins and glycolipids have been increasingly recognized as carriers of biological information;[1] of special interest are the phenomena of cellular recognition. However, investigations into the function of oligosaccharides found on glycoproteins are at a very early stage. In the case of recombinant erythropoietin, the degree of branching of asparagine-bound carbohydrates (N-glycans) has a great influence on its activity and stability.[2] In cancer cells the occurrence of an additional β-(1 → 6)[3] branch on N-glyans is correlated to the metastatic potential. To study the function of N-glycans in peptides and proteins in detail, it is necessary to provide model compounds like the undecasaccharide-asparagine **1** in sufficient quantity. Compound **1** represents the smallest complete structure of complex type N-glycans frequently found on the glycoproteins of the serum and the cell surface. The isolation of pure N-glycans from glycoproteins is feasible only on a milligram scale. The difficulties caused by the microheterogeneity of the natural material encourage the synthesis of N-glycans with a defined structure. This work describes the synthesis of the branched heptasaccharide **A** as a precursor for compound **1** by two regioselective glycosylations at the β-mannosyl residue of trisaccharide **B** with the disaccharide donors **C** and **D** (Scheme 1).



Scheme 1. The undecasaccharide-asparagine **1** as a model compound for complex type N-glycans. **A** is the branched, core heptasaccharide that was prepared in protected form via the key compounds **B**, **C**, and **D**.

The synthesis of N-glycans and their partial structures[4, 5] is a particular challenge. Already in the mid eighties Ogawa's group synthesized the undecasaccharide **1** without the asparagine moiety by chemical methods.[5] Following the known procedures, many steps are required resulting in a low overall yield. As an alternative to classical chemical approaches in oligosaccharide synthesis, enzymatic methods have become established.[6] A new strategy was developed to obtain the biantennary undecasaccharide-asparagine **1** efficiently. By combining chemical and enzymatic glycosylations, the number of synthetic steps can be reduced. First, the heptasaccharide **A** is synthesized chemically. The protective group pattern is chosen to allow later chemo-enzymatic extension to undecasaccharide-asparagine **1**. Both terminal *N*-acetylglucosamine residues may serve as acceptors for glycosyltransferases.[7] In an enzymatic "one-pot" reaction, glycosides of *N*-acetylglucosamine (GlcNAcβ-R) were elongated to give sialyl-*N*-acetyllactosamine (Neu5Acα-(2 → 6)-Galβ-(1 → 4)-GlcNAcβ-R) in high yields.[8]

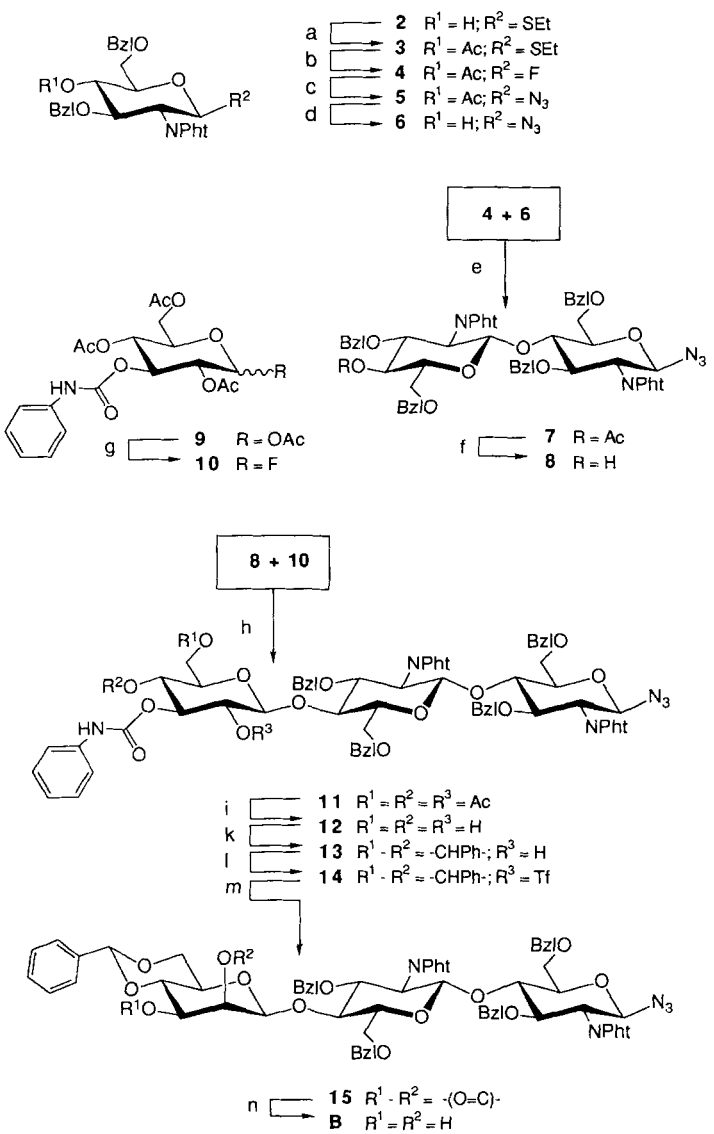
Retrosynthetic analysis of the heptasaccharide **A** suggests a disconnection into trisaccharide acceptor **B** and donors **C** or **D**. The formation of the β-mannosidic bond in **B** is very critical. It can be accomplished by the elegant procedure introduced by Kunz et al. of inverting β-glucosides at C-2 in an intramolecular reaction.[9] To facilitate the connection of aspartic acid to the heptasaccharide **A**, the precursor **B** was equipped with an azide group at the reducing end. The azide group serves as a protective function for the anomeric center[10] and can be transformed to an amine by selective reduction with Raney-nickel.

Trisaccharide **B** was prepared from monosaccharide units, starting at the reducing end. Fluoride **4** is a central compound in the synthesis of chitobiosyl azide **7**, serving as a glycosyl donor and as a precursor of the acceptor **6**. Starting from thioglycoside **2**, prepared in six steps from D-glucosamine hydrochloride,[11] followed by acetylation to **3**, the fluoride **4** can be obtained. Activation of thioglycoside **3** with *N*-bromosuccinimide in the presence of HF–pyridine complex[12] gives the crystalline fluoride **4** in high yield. The latter is converted into azide **5** by reaction with trimethylsilyl azide and catalytic amounts of borontrifluoride–ether. Deacetylation of **5** gives the desired acceptor **6** that was glycosylated with fluoride **4**, to furnish chitobiosyl azide **7** in 83.4 % yield. After removal of the acetate group, the disaccharide acceptor **8** is obtained, whose benzyl ether and phthalimido groups are favorable for the reaction sequence leading to the β-mannoside. As a suitable donor fluoride **10** was chosen, which is accessible from peracetylated 3-phenylcarbamoylglucose[11] (**9**) by reaction with HF–pyridine complex. Glycosylation of disaccharide **8** with **10** gives the β-*gluco*-configurated trisaccharide **11** (85.4%). To perform the intramolecular inversion, the 2″-OH function of the glucose

[*] Dr. C. Unverzagt
Institut für Organische Chemie und Biochemie
der Technischen Universität München
Lichtenbergstrasse 4, D-85748 Garching (FRG)
Telefax: Int. code + (89)3209-3210

[**] This work was supported by the Leonhard-Lorenz-Stiftung and Hoechst AG, and was presented at the seventh European Carbohydrate Symposium 1993 in Krakow (Poland). I thank Prof. Horst Kessler for his generous support.

moiety needs to be free.[8] However, removal of the acetates under basic conditions proved problematic, especially for the acetate in position 2″. During the long reaction times the phthalimido moiety was partly cleaved, which explains the low yield. Acyl groups located between sterically demanding residues tend to be difficult to remove.[13] Triol **12** was benzylidenated with (dimethoxymethyl)benzene (α,α-dimethoxytoluene) and converted into the triflate by trifluoromethanesulfonic anhydride–pyridine. Crude β-*gluco*-triflate **14** is heated to 60 °C and inverts to a β-*manno*-configurated imidocarbonate,[9] which hydrolyzes to the carbonate under mild conditions. Basic methanolysis of the carbonate group furnishes the trisaccharide acceptor **B.** Each step of this inversion sequence can be monitored by thin-layer chromatography. Based on trisaccharide **13** the β-mannoside **B** was obtained after five steps in 70% overall yield. Following this procedure, more than 10 g of trisaccharide **B** were prepared (Scheme 2).



Scheme 2. a) Ac_2O, pyridine (99%); b) *N*-bromosuccinimide, HF/pyridine, CH_2Cl_2, 0 °C (93%); c) trimethylsilylazide, BF_3/OEt_2, CH_2Cl_2 (91%); d) K_2CO_3, MeOH, 0 °C (65%); e) BF_3/OEt_2, molecular sieves 4 Å, CH_2Cl_2 (83%); f) K_2CO_3, MeOH, 0 °C (79%); g) HF/pyridine, (56%); h) BF_3/OEt_2, molecular sieves 4 Å, CH_2Cl_2 (85%); i) K_2CO_3/MeOH, 0 °C; k) α,α-dimethoxytoluene, TosOH, CH_3CN (44% based on **11**); l) Tf_2O, pyridine, CH_2Cl_2, −20 °C; m) 1. dimethylformamide, pyridine, 65 °C; 2. AcOH, dioxane, H_2O, 0 °C; n) NaOMe, MeOH, CH_2Cl_2 (70% based on **13**). – Tf = F_3C-SO_2.

The disaccharide trichloroacetimidates[14] **C** and **D** were synthesized to elongate trisaccharide **B** containing two free hydroxyl groups. Donor **C** was developed in the group of Paulsen[15] and prepared by a modified procedure.[16] A considerably faster route leads to donor **D**[16] in three steps from imidate **16**[17] and tetraacetylmannose **17**.[18]

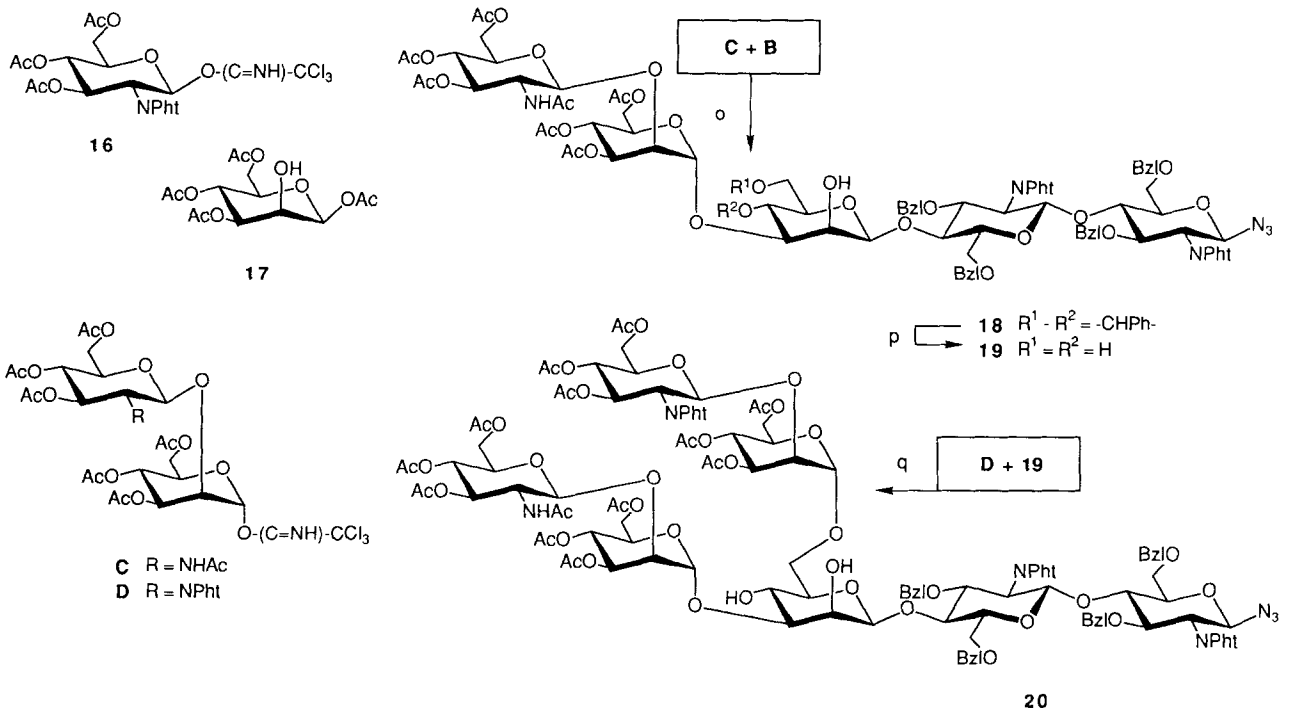
To glycosylate the 3″-OH group of the diol **B** selectively, an acetyl group can be introduced at 2″O by isomerization of a cyclic 2″,3″-orthoester.[11] However, this strategy involving protection at 2″-OH can be circumvented. Diol **B** reacts with the disaccharide imidate **C** selectively at the desired 3″-OH function. Pentasaccharide **18** was isolated in 62% yield; other stereoisomers could not be detected. The α-(1 → 3)-mannosidic linkage formed without neighboring group participation was confirmed by 2D-NMR spectroscopy. The proton-coupled HMQC spectrum yielded a C-1/H-1 coupling constant for the α-mannosyl residue of 177.7 Hz while the β-mannoside expectedly has a lower value of 163.3 Hz.[18] Apparently, the equatorial 3″-OH group is markedly more reactive than the axial 2″-OH function. For β-mannoside acceptor **B**, the observed reactivity corresponds to the preferred glycosylation of the equatorial 3-OH group in galactosides with multiple free hydroxyl functions.

Acidic cleavage of the benzylidene acetal in pentasaccharide **18** gives triol **19** which was examined for a selective elongation of the primary 6″-OH group. Glycosylation of pentasaccharide **19** with 1.7 equiv of disaccharide donor **C** at −10 °C gave only 20% α-(1 → 6)-linked heptasaccharide and 15% of a product with multiple glycosylations, in addition to 55% of unchanged acceptor **19**. Under similar conditions the phthalimido protected donor **D** (1.5 equiv) gave 27% heptasaccharide und 28% of a compound with an additional glycosylation. In contrast, donor **D** (1.2 equiv) reacts highly selectively with **19** at lower temperature (−40 °C) and a diluted reaction mixture, to furnish heptasaccharide **20** (52%), a protected form of the target molecule **A**. The structure of **20**[21] is confirmed by 2D-NMR spectroscopy and FAB-mass spectrometry. Removal of the phthalimido groups from **20** occurs readily following the commonly used procedure with hydrazine hydrate in ethanol (Scheme 3, see next page). Currently the attachment of aspartic acid and the enzymatic elongation to **1** are under investigation.

Crucial to the synthesis of the branched heptasaccharide **20** is the extension of the trisaccharide building block **B**. A temporary protection of the β-mannoside with a benzylidene acetal is sufficient for directing the glycosylation to position 3″. This minimal protection strategy allows the introduction of other branching sugars found in nature at position 2″ and 4″ after reaction of the primary 6″-OH group.

Received: December 20, 1993 [Z 6571 IE]
German version: *Angew. Chem.* **1994**, *106*, 1170

[1] A. Varki, *Glycobiology* **1993**, *3*, 97–130.
[2] M. Takeuchi, N. Inoue, T. W. Strickland, M. Kobuta, M. Wada, R. Shimizu, S. Hoshi, H. Kozutsumi, S. Takasaki, A. Kobata, *Proc. Natl. Acad. Sci. USA* **1989**, *86*, 7819–7822.
[3] J. W. Dennis, S. Laferte, *Cancer Res.* **1989**, *49*, 945.
[4] Review: H. Paulsen, *Angew. Chem.* **1990**, *102*, 851–857; *Angew. Chem. Int. Ed. Engl.* **1990**, *29*, 823–839.
[5] T. Ogawa, M. Sugimoto, T. Kitajma, K. K. Sadozai, T. Nukada, *Tetrahedron Lett.* **1986**, *27*, 5739–5742.
[6] Review: Y. Ichikawa, G. C. Look, C. H. Wong, *Anal. Biochem.* **1992**, *202*, 215–238.
[7] C. Augé, R. Fernandez-Fernandez, C. Gautheron, *Carbohydr. Res.* **1990**, *200*, 257–268.
[8] a) C. Unverzagt, H. Kunz, J. C. Paulson, *J. Am. Chem. Soc.* **1990**, *112*, 9308–9309; b) C. Unverzagt, S. Kelm, J. C. Paulson, *Carbohydr. Res.*, **1994**, *251*, 285–301.
[9] H. Kunz, W. Günther, *Angew. Chem.* **1988**, *100*, 1118–1119; *Angew. Chem. Int. Ed. Engl.* **1988**, 27, 1086–1087.



Scheme 3. o) BF_3/OEt_2, molecular sieves 4 Å, CH_2Cl_2, 0 °C (62%); p) 80% AcOH, 80 °C (70%); q) BF_3/OEt_2, molecular sieves 4 Å, CH_2Cl_2, −40 °C (52%).

[10] a) H. Kunz, C. Unverzagt, *Angew. Chem.* **1988**, *100*, 1763–1765; *Angew. Chem. Int. Ed. Engl.* **1988**, *27*, 1697–1699; b) C. Unverzagt, H. Kunz, *J. Prakt. Chem.* **1992**, *334*, 570–578.

[11] W. Günther, H. Kunz, *Carbohydr. Res.* **1992**, *228*, 217–241.

[12] K. C. Nicolaou, R. E. Dolle, D. P. Papahatjis, J. L. Randall, *J. Am. Chem. Soc.* **1984**, *106*, 4189–4192.

[13] Z. Szurmai, J. Kerekgyarto, J. Harangi, A. Liptak, *Carbohydr. Res.* **1987**, *164*, 313–325.

[14] Review: R. R. Schmidt, *Angew. Chem.* **1986**, *98*, 213–236; *Angew. Chem. Int. Ed. Engl.* **1986**, *25*, 212–235.

[15] H. Paulsen, B. Helpap, *Carbohydr. Res.* **1991**, *216*, 289–313.

[16] Details of the synthesis will be published elsewhere.

[17] G. Grundler, R. R. Schmidt, *Carbohydr. Res.* **1985**, *135*, 203–218.

[18] J. Deferari, E. G. Gros, I. O. Mastronardi, *Carbohydr. Res.* **1967**, *4*, 432–434.

[19] a) K. Bock, C. Pedersen, *J. Chem. Soc. Perkin Trans. 2* **1974**, 293–297; b) S. Wolfe, B. M. Pinto, V. Varma, R. Y. N. Leung, *Can. J. Chem.* **1990**, *68*, 1051–1062.

[20] T. Murase, H. Ishida, M. Kiso, A. Hasegawa, *Carbohydr. Res.* **1988**, *184*, C1–C4.

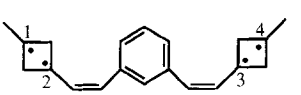
[21] FAB-MS [*o*-nitrobenzylalcohol]: $C_{120}H_{131}N_7O_{50}$ M_r(calcd) = 2469.8; M_r(found) = 2478.2 (M + Li); 2494.5 (M + Na).

Combination of Superexchange and Spin-Polarization Mechanisms Leads to a Novel Hydrocarbon Tetraradical with a High-Spin Ground State**

S. Joshua Jacobs and Dennis A. Dougherty*

An understanding of the factors that control local spin–spin interactions is crucial to the rational development of new magnetic materials.[1] Such insight should allow the design of long-range, three-dimensional interactions that will ultimately produce bulk magnetic ordering. Studies of organic diradicals with triplet ground states have led to the discovery of three separate mechanisms that can produce ferromagnetic (high-spin) coupling between a pair of electrons: A) dynamic spin polarization in delocalized, planar π-systems with appropriate topologies, as in trimethylenemethane and *m*-xylylene; B) superexchange (through-bond) coupling of localized radical centers, as in cyclobutanediyls and cyclopentanediyls; and C) one-center interactions between orthogonal orbitals (analogous to Hund's rule), as in carbenes and nitrenes.

These three mechanisms may also act in concert to produce structures with very large spin quantum numbers. The famous polycarbenes are examples of compounds in which mechanisms A and C are both in effect (CACAC ... structures),[1b, d, 2] and we have recently described high-spin tetraradicals with ABA frameworks.[3] We now provide the first report of a compound with a BAB arrangement, which also leads to a high-spin ground state. In tetraradical **1** the coupling between centers 1 and 2 (and that between 3 and 4) relies on the superexchange mechanism (B), while centers 2 and 3 should be ferromagnetically coupled by the spin-polarization mechanism (A). Alternatively, structure **1** can be viewed as another example of the paradigm shown in Scheme 1[1a, 4] in which *m*-phenylene serves as the FC, and for the first time the spin-containing unit (SC) is a localized diradical, a 1,3-cyclobutanediyl. In addition to establishing a new strategy for the design of high-spin systems, this study illustrates the power of current methods for predicting and analyzing the EPR spectra of very high spin structures such as **1**.

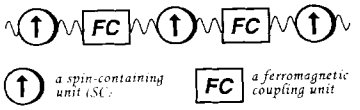


1

Compound **5**, the bisdiazene precursor to **1**, was prepared by an adaptation of transformations developed previously in these laboratories[5–7] via the tricyclic urazole **2** (Scheme 2). Fol-

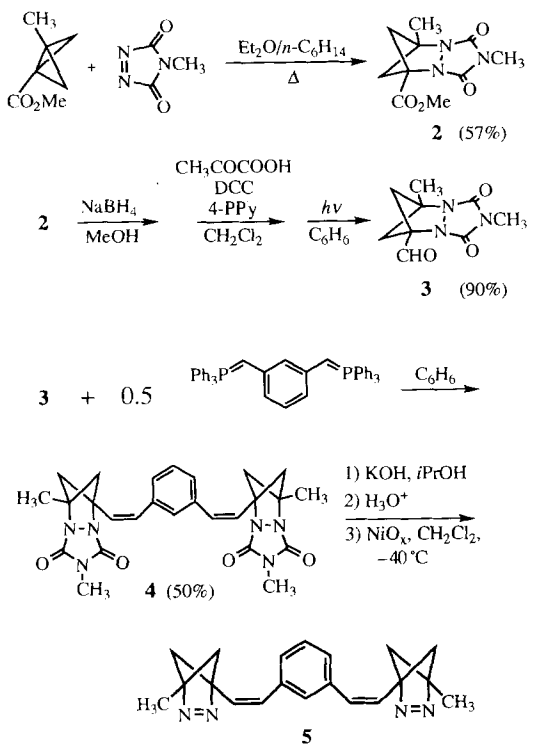
[*] Prof. Dr. D. A. Dougherty, Dr. S. J. Jacobs
Arnold and Mabel Beckman Laboratories of Chemical Synthesis
Division of Chemistry and Chemical Engineering
California Institute of Technology
Pasadena, CA 91125 (USA)
Telefax: Int. code + (818) 564-9297

[**] Contribution No. 8885.



Scheme 1. Representation of a spin system with ferromagnetic coupling.

lowing conversion of **2** into **3** a Wittig reaction gave bisurazole **4** with predominantly (*Z*) configuration.[8] Subsequent transformation of **4** into bisdiazene **5** proceeds under standard hydrolysis conditions was followed by low-temperature oxidation. The high overall yield of this synthesis establishes it as a viable route to many unsymmetrically substituted urazoles.[9]



Scheme 2. Synthesis of **5**. DCC = dicyclohexylcarbodiimide, 4-PPy = 4-pyrrolidinopyridine.

A Heisenberg Hamiltonian may be employed to model the energies of the spin states of tetraradical **1**.[2a, 3] The coupling of electron spins in **1** by mechanism A may be characterized by one magnetic exchange parameter, J_A, while the coupling due to mechanism B is represented by another parameter, J_B. The four-spin system can be described by the Hamiltonian defined in Equation (1). The six covalent electronic states and corresponding state energies resulting from the interactions among the four spins are summarized in Scheme 3.

$$\mathcal{H} = -J_A \boldsymbol{S}_2 \cdot \boldsymbol{S}_3 - J_B((\boldsymbol{S}_2 + \boldsymbol{S}_3) \cdot (\boldsymbol{S}_1 + \boldsymbol{S}_4)) \quad (1)$$

Only if $J_A > 0$ *and* $J_B > 0$ will a high-spin Q ground state result. Results from extensive experimental studies of organic diradicals with triplet ground states employing mechanisms A and B lead one to expect both of these conditions to be satisfied.[1, 2]

In addition, analysis of structure **1** according to established models allows its EPR spectra to be largely foretold. The zero-field splitting (zfs) tensor $\boldsymbol{D}^Q$ for a tetraradical such as **1** can be related to the zfs tensors of the diradical components[2a] according to Equation (2), where $\boldsymbol{D}^B$ represents the dipolar interaction

Quintet (Q): $E_Q = -\frac{J_A}{2} - 2J_B$ Singlet (S_1): $E_{S_1} = -\frac{J_A}{2} + 4J_B$

Triplet (T_1): $E_{T_1} = -\frac{J_A}{2}$ Triplet (T_3): $E_{T_3} = \frac{3J_A}{2}$

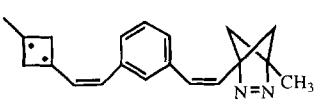
Triplet (T_2): $E_{T_2} = -\frac{J_A}{2} + 2J_B$ Singlet (S_2): $E_{S_2} = \frac{3J_A}{2}$

Scheme 3. Spin states of **1** and corresponding energies.

$$\boldsymbol{D}^Q = \frac{\boldsymbol{D}^B + \boldsymbol{D}^B}{6} + \frac{\boldsymbol{D}^A}{3} \quad (2)$$

across a cyclobutane ring (mechanism B), and $\boldsymbol{D}^A$ represents the dipolar interaction through the *m*-phenylene linker (mechanism A).

Based on previously established[5] substituent effects on the *D* values of cyclobutanediyls, one can predict that $|D^B/hc|$ (and also the *D* value for monodiazene diradical **6**) is approximately 0.060 cm^{-1}.[10] For *m*-xylylene, $|D/hc| = 0.011\ cm^{-1}$,[11] but to obtain D^A this value must be scaled by $\frac{1}{2} \cdot \frac{1}{2}$, since the spin density at the *m*-xylylene centers is only $\frac{1}{2}$.[12] Thus, $|D^B| \gg |D^A|$,[11] and the approximate expression for the *D* value of the tetraradical is $D^Q \approx D^B/3$. This model thus predicts that the *D* value of the quintet state of **1** should be $|D/hc| \approx 0.020\ cm^{-1}$.



6

Since the outer $\Delta m_s = 1$ lines of a triplet EPR spectrum are separated by 2*D*, while the corresponding separation in a quintet spectrum is 6*D*, the outer lines in the $\Delta m_s = 1$ region of the spectra of ^{3}**6** and ^{5}**1** are expected to be coincident. The only features that will allow unambiguous assignment of an observed EPR spectrum to ^{5}**1** will be peaks due to the inner quintet lines, which are associated with transitions between the intermediate magnetic sublevels. Ambiguity in interpreting the experimental spectra can be minimized by full computer simulation of triplet- and quintet-state EPR powder spectra. Such simulations are an indispensable tool in the study of structures such as **1**.[3, 9]

When a frozen solution of **5** in methyltetrahydrofuran is photolyzed in an EPR spectrometer at 4 K, EPR spectra become apparent after brief photolysis (Fig. 1). If the outer four lines the $\Delta m_s = 1$ region are due to a

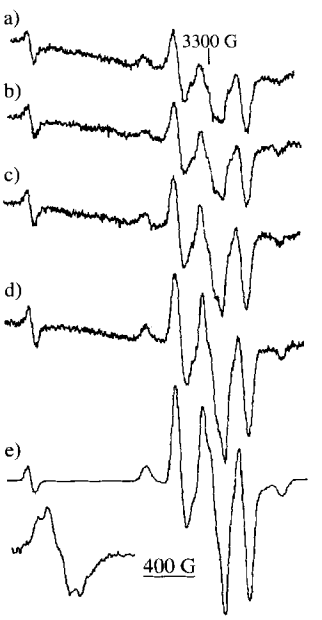


Fig. 1. EPR spectra recorded during photolysis of **5** at 4 K. Photolysis times: a) 75 s, b) 90 s, c) 120 s, d) 180 s, e) 80 min. Inset to e) is an enlargement of the $\Delta m_s = 2$ region.

triplet, $|D/hc| = 0.057\ cm^{-1}$ and $|E/hc| = 0.0009\ cm^{-1}$ is implied, in good agreement with the predictions of for ^{3}**6**. A prominent feature of the spectra recorded after short photolysis times is a $\Delta m_s = 2$ transition (Fig. 1a), a signature of a spin state with $S \geq 1$. The hyperfine splitting observed in this transition is also typical of a cyclobutanediyl and strongly resembles that of the analogous compound 3-ethyl-1-vinylcyclobutanediyl.[5]

As photolysis continues, changes occur throughout the spectrum (Fig. 1b–d), and after extended photolysis, the spectra include a new, large, structured feature in the central region (Fig. 1e). Simulation of a triplet-state EPR spectrum with the zfs parameters assigned above to ^{3}**6** (Fig. 2a) establishes that a triplet state cannot account for all of the fine structure observed. The obvious candidate for the species giving rise to these additional lines is ^{5}**1**.

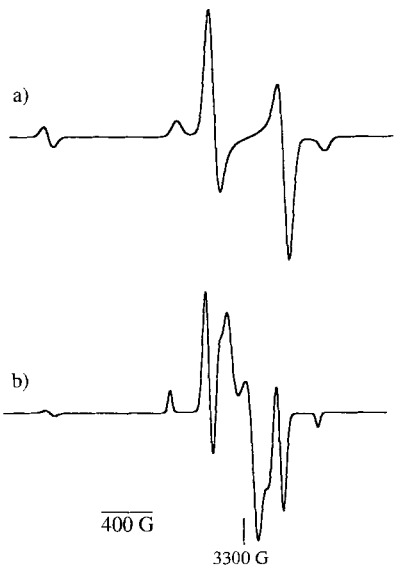


Fig. 2. a) Simulated triplet EPR spectrum with $|D/hc| = 0.057$, $|E/hc| = 0.0009\ cm^{-1}$; b) simulated quintet EPR spectrum with $|D/hc| = 0.0193$, $|E/hc| = 0.00035\ cm^{-1}$.

Several lines of evidence lead us to conclude that the sequence of spectra shown in Figure 1a–e is best interpreted as fitting a system that is initially dominated by ^{3}**6** (Fig. 1a) but evolves on extended photolysis to one that is to a large extent (and perhaps exclusively) ^{5}**1**. First, if Figure 1e is a quintet spectrum, it implies $|D/hc| = 0.019\ cm^{-1}$ and $|E/hc| = 0.00035\ cm^{-1}$, in good agreement with the predicted value for ^{5}**1**. In addition, a computer-simulated spectrum with these zfs values (Fig. 2b) shows good agreement with the observed spectrum in two important regards. First, the $\Delta m_s = 1$ region of the quintet spectrum is much more prominent that the $\Delta m_s = 2$ region, relative to the same comparison for the triplet spectrum (Fig. 2a). A similar relationship is seen in the experimental spectra (Fig. 1e vs. Fig. 1a). Second, the simulation of the quintet spectrum shows a large structured feature in the central region (ca. 3300 G) that is similar to the central feature that grows in on extended photolysis. The general spectral shape is similar to that of other quintet systems we have examined.[13] The fine structure in the central region is not perfectly matched by the simulation, but simulations of powder EPR spectra of quintet systems include a large number of variables, including many linewidth parameters and (possibly) an anisotropic g tensor. We felt no need to attempt to optimize all these and are satisfied with the qualitative agreement.

One could argue that the new central feature is due to monoradical (doublet) impurities or a triplet state with a small D value (e.g., a radical pair), either of which could form on extended photolysis. Several lines of reasoning argue against this. First, the fine structure of the central feature and its breadth (note the 400 G scale bar) are inconsistent with a doublet signal. Second, cyclobutanediyls generally do not produce intense doublet or radical pair signals on generation from diazene precursors (see Fig. 1 or ref. [5]). Third, the asymmetry of the central signal (the low-field component is shorter than its neighbor, while the higher field component is larger than its neighbor), typical of quintet states and reproduced in the simulation is completely inconsistent with doublet or triplet spectra. Fourth, the signals of a secondary photolysis product (doublet system or triplet radical pair) would be expected to grow in at the expense of those of ^{3}**6**. This is clearly not the case, as the growth in the central feature is accompanied by a growth of the outer two pairs of signals (but a relative drop in the $\Delta m_s = 2$ region) as expected for a quintet system.[13] The high intensity of these signals at such low temperatures (4 K) makes it highly probable that the quintet is the ground state of **1**.

The observation of a quintet ground state for tetraradical **1** shows that superexchange and spin-polarization mechanisms can act in concert to produce wholly ferromagnetic coupling in a high-spin organic molecule with a BAB structure. This study further expands the scope of *m*-phenylene as an FC, establishes the suitability of cyclobutanediyls as SCs, and again demonstrates the power of current models and methods in predicting and interpretating the EPR spectra of complex systems.

Received: October 27, 1993
Revised version: January 20, 1994 [Z 6456 IE]
German version: *Angew. Chem.* **1994**, *106*, 1155

[1] For recent overviews see: a) D. A. Dougherty, *Acc. Chem. Res.* **1991**, *23*, 88–94; b) H. Iwamura, *Pure Appl. Chem.* **1993**, *65*, 57–64; c) *Research Frontiers in Magnetochemistry* (Ed.: C. O'Connor), World Scientific Publishing, Singapore, **1993**; d) D. A. Dougherty in [1c], pp. 327–349; e) H. Iwamura in [1c], pp. 303–325.

[2] a) K. Itoh, *Pure Appl. Chem.* **1978**, *50*, 1251–1259; b) in *Magnetic Molecular Materials* (Eds.: D. Gatteschi, O. Kahn, J. S. Miller, F. Palacio), Kluwer, Dordrecht, **1991**, pp. 67–86; c) H. Iwamura, N. Nakamura, N. Koga, S. Sasaki, *Mol. Cryst. Liq. Cryst.* **1992**, *218*, 207–212; d) T. Sugawara, S. Bandow, K. Kimura, H. Iwamura, K. Itoh, *J. Am. Chem. Soc.* **1986**, *108*, 368–371; e) Y. Teki, T. Takui, K. Itoh, H. Iwamura, K. Kobayashi, *ibid.* **1986**, *108*, 2147–2156.

[3] a) S. J. Jacobs, D. A. Shultz, R. Jain, J. Novak, D. A. Dougherty, *J. Am. Chem. Soc.* **1993**, *115*, 1744–1753; b) S. K. Silverman, D. A. Dougherty, *J. Phys. Chem.*, **1993**, *97*, 13273–13283.

[4] D. A. Dougherty, *Mol. Cryst. Liq. Cryst.* **1989**, *176*, 25–32; D. A. Dougherty, D. A. Kaisaki, *ibid.* **1990**, *183*, 71–79; D. A. Dougherty, R. H. Grubbs, D. A. Kaisaki, W. Chang, S. J. Jacobs, D. A. Shultz, K. K. Anderson, R. Jain, P. T. Ho, E. G. Stewart in *Magnetic Molecular Materials* (Eds.: D. Gatteschi, O. Kahn, J. S. Miller, F. Palacio), Kluwer, Dordrecht, **1991**, pp. 105–120.

[5] R. Jain, M. B. Sponsler, F. D. Coms, D. A. Dougherty, *J. Am. Chem. Soc.* **1988**, *110*, 1356–1366.

[6] M. H. Chang, D. A. Dougherty, *J. Org. Chem.* **1981**, *46*, 4092–4093.

[7] G. J. Snyder, D. A. Dougherty, *J. Am. Chem. Soc.* **1989**, *111*, 3927–3942.

[8] E. Vedejs, C. F. Marth, R. Ruggeri, *J. Am. Chem. Soc.* **1988**, *110*, 3940–3948.

[9] For further details on the synthesis of **5** and the simulation of quintet EPR spectra, see S. J. Jacobs, Dissertation, California Institute of Technology, **1994**.

[10] Scaling makes use of the experimental spin densities of cinnamyl radical: A. G. Davies, D. Griller, K. U. Ingold, D. A. Lindsay, J. C. Walton, *J. Chem. Soc. Perkin Trans. 2* **1981**, 633–641.

[11] B. B. Wright, M. S. Platz, *J. Am. Chem. Soc.* **1983**, *105*, 628–630.

[12] For further details of this type of analysis, see ref. [3a].

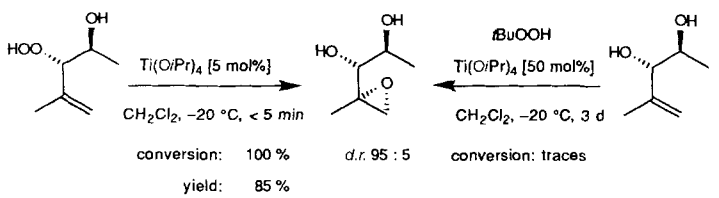
[13] We cannot rule out the presence of ^{3}**6** signals in the final spectrum (Fig. 1e), given the high degree of overlap between the expected spectra of ^{3}**6** and ^{5}**1** (cf. Fig. 2).

Tridentate β-Hydroperoxy Alcohols as Novel Oxygen Donors for the Titanium-Catalyzed Epoxidation of γ,δ-Unsaturated α,β-Diols: A Direct Diastereoselective Synthesis of Epoxy Diols**

Waldemar Adam,* Karl Peters, and Michael Renz

Dedicated to Professor H. Quast on the occasion of his 60th birthday

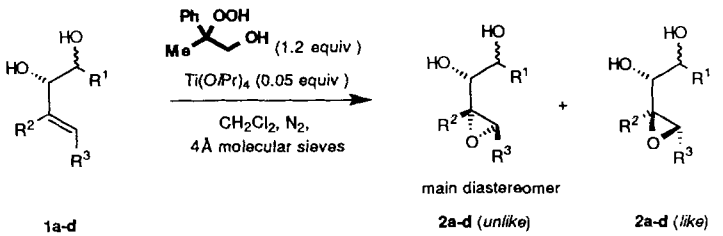
The titanium(IV)-catalyzed expoxidation of allylic alcohols with hydroperoxides, typically *t*BuOOH, is an efficient and convenient method for preparing synthetically valuable epoxy alcohols.[1] In the presence of optically active tartrate as a chiral auxiliary (Sharpless reaction) the oxyfunctionalization can be performed with high enantioselectivity. An attractive extension is our direct hydroxy-epoxidation of allylic hydroperoxides catalyzed by $Ti(OiPr)_4$ (the masked Sharpless reaction), in which the hydroperoxy functionality acts as an oxygen atom donor and the allylic alcohol (generated by reduction of the allylic hydroperoxide) as an oxygen acceptor.[2]



Scheme 1. Two routes to epoxy diols [3]. d.r. = diastereomeric ratio.

The two routes are illustrated in Scheme 1.[3] The direct hydroxy-epoxidation with the unsaturated hydroperoxy alcohol (on the left) proceeds nearly spontaneously (≤ 5 min), whereas the conversion of the analogous enediol with *t*BuOOH as oxygen donor (on the right) is minimal even after three days reaction time and with 50 mol% $Ti(OiPr)_4$. Presumably the bidentate oxidant *t*BuOOH is not able to displace the epoxy diol by ligand exchange to generate the active, so-called *loaded* complex necessary for the catalytic cycle. In contrast, the tridentate hydroperoxy alcohol displaces the epoxy diol readily, and thus oxygen transfer can take place efficiently.

To test the above hypothesis we used a β-hydroperoxy alcohol, 2-hydroperoxy-2-phenyl-1-propanol (easily available by reaction of α-methylstyrene oxide with hydrogen peroxide[4]), as a tridentate oxygen donor for the epoxidation of γ,δ-unsaturated α,β-diols. Such β-hydroperoxy alcohols have not yet been used as oxygen donors in the Sharpless reaction. Indeed, we demonstrate herein that enediols **1** can be epoxidized very efficiently to give epoxy diols **2**, whereby two additional, neighboring stereogenic centers are generated rapidly with high diastereoselectivity (Scheme 2). The configurations of the new chiral centers are determined by that of the β carbon atom.



Scheme 2. Conversion of **1** into **2**; for an explanation of *unlike* and *like* see text.

Generally for the titanium(IV)-catalyzed epoxidation of substrates with more than one hydroxyl functionality it has been necessary to protect all except the allylic hydroxyl group[5] to avoid long reaction times[3b] and irregular stereochemistry.[6] The data in Table 1 show that direct epoxidation of unprotected unsaturated diols **1** with the β-hydroperoxy alcohol proceeds in good yields and with (almost) complete conversion within minutes.

Table 1. Reaction conditions, yields, and diastereomeric ratios for the titanium-catalyzed epoxidation of enediols **1** with 2-hydroperoxy-2-phenylpropan-1-ol to give epoxy diols **2**.

Entry	R^1	R^2	R^3	T [°C]	t [h]	Mass balance [%]	Conversion [%]	Yield [a] [%]	*d.r.* [b]
1 **1a**	H	Me	H	23	2.0	75	81	86	90:10
2 **1b** [c]	Me	Me	H	−25	17.0	83	96	70	89:11
3 **1b** [c]	Me	Me	H	0	3.0	92	88	88	86:14
4 **1b** [c]	Me	Me	H	23	0.5	92	100	88	82:18
5 **1c** [d]	Me	H	nPr	23	0.5	78	100	63	85:15
6 **1d** [e]	Ph	H	Ph	23	0.5	77	100	71 [f]	>90:10

[a] Based on consumed starting material. [b] Diastereomeric ratio (*d.r.*) of *unlike*:*like* products, determined after column chromatography by quantitative analysis of characteristic signals in the ^1H NMR spectrum; error is ±5% of the stated value. [c] A diastereomeric mixture of (1*R**,3*R**):(2*S**,3*R**) = 90:10 was used. [d] Only the (2*R**,3*R**-*E*) diastereomer was analyzed. [e] A diastereomeric mixture of (1*R**,2*R**): (1*S**,2*R**) = 75:25 was used. [f] Isolated in part as tetrol (34%).

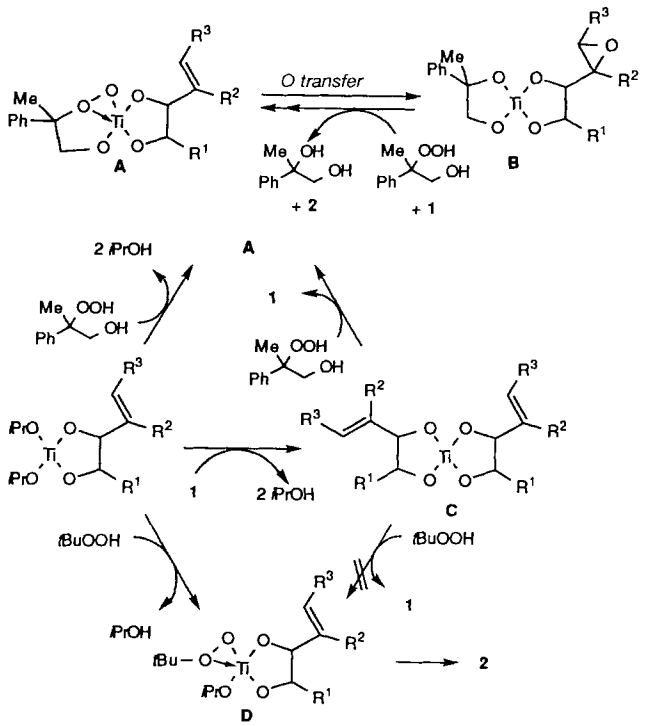
As predicted, the tridentate β-hydroperoxy alcohol (oxygen donor) and the bidentate enediol (oxygen acceptor) are able to regenerate the active, *loaded* complex **A** (Scheme 3) from the inactive complex **B** by efficient displacement of the epoxy diol product and the diol derived from the β-hydroperoxy alcohol. The efficiency of the catalytic cycle is thus ensured. The inactive titanium complex **C** also undergoes ligand exchange to the active, *loaded* titanium complex **A**, and the oxygen transfer proceeds smoothly.

In contrast, bidentate *t*BuOOH displaces the enediol moiety in the coordination step only with difficulty. When only small amounts (ca. 5 mol%) of $Ti(OiPr)_4$ are used, fast formation of the inactive complex **C** ties up all the catalyst (Scheme 3). Since for the latter, ligand exchange to the active, *loaded* complex **D** is slow, the reaction is terminated before it has even started!

Owing to the stronger binding of the epoxy diol product and of the diol derived from the β-hydroperoxy alcohol in the titanium complex **B**, a higher reaction temperature is required for regeneration of the loaded complex **A**. Presumably this is the reason why the oxygen transfer from the β-hydroperoxy alcohol to enediol **1** is very slow at −25 °C (Table 1, entry 2), although this is the temperature of choice for the conventional Sharpless reaction. In our variant substantial acceleration is possible by increasing the reaction temperature to room temperature (Table 1, entry 4).

[*] Prof. Dr. W. Adam, Dipl.-Chem. M. Renz
Institut für Organische Chemie der Universität
Am Hubland, D-97074 Würzburg (FRG)
Telefax: Int.code + (931)888-4606
Dr. K. Peters
Max-Planck-Institut für Festkörperforschung, Stuttgart (FRG)

[**] This research was supported by the Deutsche Forschungsgemeinschaft (SFB 347: "Selektive Reaktionen Metall-aktivierter Moleküle") and the Fonds der Chemischen Industrie.



Scheme 3. Ligand exchange processes for the bi- (*t*BuOOH) and tridentate (β-hydroperoxy alcohol) oxygen donors in the generation of the *loaded* titanium templates **A** and **D** required for the oxygen transfer (**1** → **2**).

The advantage of our modification is the high diastereoselectivity, which ranges from 82:18 up to 90:10 in favor of the *unlike* isomer (see Table 1; *unlike* refers to the β and γ carbon atoms of the substrate). The diastereomeric ratios were determined by quantitative analysis of characteristic signals in the ^{1}H NMR spectra. The main isomer was assigned by comparison with reported spectral data.[3b] The structure of the new epoxy diol **2d** was established by X-ray structure analysis (Fig. 1).[7]

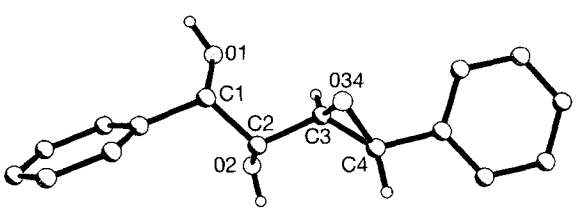


Fig. 1. Crystal structure of (1*S**,2*R**)-1-phenyl-2-[2α(*S**),3β-phenyloxiran-2-yl]-1,2-ethanediol (**2d**) (ORTEP) [7].

The high diastereoselectivity can be traced back to the very rigid transition state for the oxygen transfer, which is stabilized by a number of oxygen–titanium bonds, similar to the active, *loaded* complex **A** (Scheme 3). Unquestionably, the additional homoallylic alcohol functionality of enediol **1** and the hydroxyl group of the β-hydroperoxy alcohol play a decisive role in providing more order through better coordination. Furthermore, the S_N2 mechanism requires that the nucleophilic attack of the π double bond on the oxygen atom to be transferred occurs in the same direction as the activated peroxide bond in the titanium template.[1d] This stereoelectronic requirement and the tighter coordination dictate the high diastereoselectivity. Although it is still uncertain how many titanium atoms are involved in the template, the oxygen donor (β-hydroperoxy alcohol) and acceptor (enediol) must be coordinated to the same titanium atom for effective oxygen transfer.

This epoxidation with a tridentate β-hydroperoxy alcohol offers new preparative perspectives for the direct and stereoselective epoxidation of allylic alcohols bearing additional hydroxyl groups. Such substrates are problematic in the conventional Sharpless epoxidation with bidentate *t*BuOOH and require cumbersome protecting group methodology. It would be of interest to use enantiomerically pure β-hydroperoxy alcohols as oxygen donors, as they have recently become conveniently available through kinetic resolution catalyzed by horseradish peroxidase.[8]

Experimental Procedure

A solution of 1.50 mmol of enediol **1** and 1.80 mmol of the hydroperoxy alcohol in 7 mL of dichloromethane was dried over 4 Å molecular sieves. Ti(O*i*Pr)$_4$ (75.0 μmol) was added under a nitrogen atmosphere. After 30 min the reaction was stopped by addition of 0.1 mL of saturated, aqueous NH_4F solution and the precipitate removed by filtration. The solvent was evaporated by distillation (23 °C, 17 Torr) and the residue purified by column chromatography on silica gel. Conversions, yields, and diastereomeric ratios are given in Table 1.

Received: December 22, 1993 [Z 6575 IE]
German version: *Angew. Chem.* **1994**, *106*, 1159

[1] a) *Asymmetric Synthesis Vol. V: Chiral Catalysis* (Ed.: J. D. Morrison), Academic Press, Orlando, FL, **1985**; b) B. E. Rossiter in [1a], p. 216; c) M. G. Finn, K. B. Sharpless in [1a], p. 247; d) S. S. Woodard, M. G. Finn, K. B. Sharpless, *J. Am. Chem. Soc.* **1991**, *113*, 106–113; e) M. G. Finn, K. B. Sharpless, *ibid.* **1991**, *113*, 113–126.
[2] W. Adam, M. Braun, A. Griesbeck, V. Lucchini, E. Staab, B. Will, *J. Am. Chem. Soc.* **1989**, *111*, 203–212.
[3] a) W. Adam, B. Nestler, *Angew. Chem.* **1993**, *105*, 767–769; *Angew. Chem. Int. Ed. Engl.* **1993**, *32*, 733–735; b) *J. Am. Chem. Soc.* **1993**, *115*, 7226–7231.
[4] a) W. Adam, A. Rios, *J. Chem. Soc. D.* **1971**, 822–823; b) Y. Ogata, Y. Sawaki, H. Shimizu, *J. Org. Chem.* **1978**, *43*, 1760–1763.
[5] a) S. Masamune, W. Choy, *Aldrichimica Acta* **1982**, *15*, 47–64; b) T. Katsuki, A. W. M. Lee, P. Ma, V. S. Martin, S. Masamune, K. B. Sharpless, D. Tuddenham, F. J. Walker, *J. Org. Chem.* **1982**, *47*, 1373–1378; c) P. Ma, V. S. Martin, S. Masamune, K. B. Sharpless, S. M. Viti, *ibid.* **1982**, *47*, 1378–1380.
[6] a) S. Takano, Y. Iwabuchi, K. Ogasawara, *J. Am. Chem. Soc.* **1991**, *113*, 2786–2787; b) *Synlett* **1991**, 548–550.
[7] Experimental details and structural details will be published elsewhere.
[8] W. Adam, U. Hoch, C. R. Saha-Möller, P. Schreier, *Angew. Chem.* **1993**, *105*, 1800–1801; *Angew. Chem. Int. Ed. Engl.* **1993**, *32*, 1737–1739.

Ozone Formation through Decomposition of CFCs in the Stratosphere**

Gustavo A. Argüello, Bernd Jülicher, and Helge Willner*

The first chlorofluorocarbons (CFCs) were synthesized in 1930 in the research labs at General Motors as substitutes for the refrigerants SO_2 and NH_3. These exceedingly useful, nontoxic compounds have received a lot of negative headlines over

[*] Prof. Dr. H. Willner, Prof. Dr. G. A. Argüello,[+] Dipl.-Chem. B. Jülicher
Institut für Anorganische Chemie der Universität
Callinstrasse 9, D-30167 Hannover (FRG)
Telefax: Int. code + (511)762-3006
[+] Fellow of the Alexander von Humboldt Foundation. Permanent address:
INFIQC - Departamento de Fisico-Química, Fac. de Ciencias Químicas
Universidad Nacional de Córdoba, C. C. 61;
Suc. 16, 5016 Córdoba (Argentinia)

[**] This work was supported by the Bundesministerium für Forschung und Technologie, the Deutsche Forschungsgemeinschaft, and the Fonds der Chemischen Industrie.

the last decades because they are partly responsible for the increasing ozone depletion in the stratosphere. The high-energy UV radiation in the stratosphere cleaves the chemically inert CFCs to produce chlorine atoms which convert ozone into oxygen in a photocatalytic cycle.

CF_2Cl_2, a typical chlorofluorocarbon, yields in addition to chlorine atoms [Equations (a) and (b)] a further photolysis frag-

$$CF_2Cl_2 + h\nu(\lambda < 346\ nm) \longrightarrow CF_2Cl + Cl \quad (a)$$

$$CF_2Cl_2 + h\nu(\lambda < 221\ nm) \longrightarrow CF_2 + 2Cl \quad (b)$$

ment, difluorocarbene CF_2[1] [Equation (b)]. In the singlet electronic ground state[2] this fragment has remarkably low reactivity,[3] dimerizing with a rate coefficient of 4.3×10^{-14} cm^3 molecule^{-1} s^{-1},[4] and reacting only rather slowly with oxygen.[5] In contrast, a faster reaction has been suggested for step (c).[6] The formation of F_2CO in the thermal[7] and photochem-

$$^3CF_2 + {}^3O_2 \longrightarrow [CF_2O_2]^* \longrightarrow F_2CO + O \quad (c)$$

ical[5] reaction of C_2F_4 with O_2 has been explained by (c). However, experimental evidence for (c) has been obtained up to now only indirectly by capture reactions involving organic compounds.[8]

During our investigations of the elementary reactions of CF_2 we also examined the reaction with oxygen, which plays a significant role in the chemistry of the stratosphere. We used difluorodiazirine **1** as a clean source of CF_2.[9] CF_2 is produced quantitatively when **1** is irradiated with light of wavelength longer than 320 nm at 15 K in an O_2 matrix. It reacts completely to F_2CO and O_3 in an approximate 1:1 ratio only after excitation of the matrix-isolated CF_2 by light of about 250 nm (absoption maximum of the transition $A\,^1B_1 \leftarrow X\,^1A_1$).[4] Ozone formation was not observed in control experiments with pure solid O_2 at 15 K under the same photolysis conditions. The formation of ozone in the presence of CF_2 can be interpreted as follows:


1

The electronically excited $CF_2(A\,^1B_1)$ is converted by intersystem crossing into $CF_2(^3B_1)$, which then reacts[10] almost without an activation barrier with O_2 to form $F_2CO + O$ [Eq. (c)]. The O atom reacts in turn with the O_2 matrix to ozone. There is no evidence for either the intermediate formation of difluorodioxirane (**2**), which has only recently been synthesized,[11] or for any other CF_2O_2 species.


2

In addition, the observations made for the O_2 matrix were supplemented by those from gas-phase investigations. Mixtures of **1** in O_2 (1:125) were prepared in a UV gas cell at a total pressure of about 1 bar. The UV photolysis was performed through the cell window with a medium pressure mercury lamp in combination with 320 or 225 nm cut-off filters. Photoysis with light of wavelength longer than 320 nm yielded exclusively C_2F_4 through dimerization of the CF_2 formed in the primary process [see Eq. (k)]. This allowed confirmation of the observation described in reference [5], which indicates that singlet CF_2 reacts only slowly if at all with oxygen at room temperature. On the other hand, ozone formation is observed if light of longer wavelength than 225 nm is used (Fig. 1a). Additional products detected by IR spectroscopy include C_2F_4 and F_2CO. Whereas in the matrix experiment only reactions of individual CF_2 molecules can take place, the course of the reaction in the gas phase is more complex.

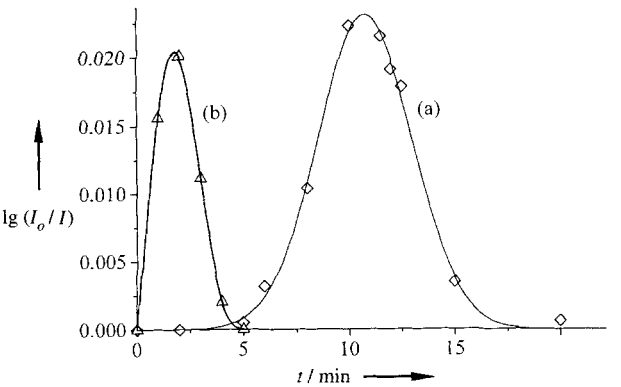


Fig. 1. Time dependence of the O_3 extinction at $\lambda = 258$ nm during the gas-phase photolysis ($\lambda > 225$ nm) of (a) **1** in O_2 and (b) **2** in O_2.

Of particular note is the long induction period of five minutes until the rapid appearance and likewise fast decomposition of O_3 occurs. This reproducible time-behavior could be interpreted in terms of a photochemically controlled cycle (Scheme 1).

$$\mathbf{1}(X\,^1A_1) + h\nu(\lambda = 352\ nm) \longrightarrow CF_2(X\,^1A_1) + N_2 \quad (d)$$

$$CF_2(X\,^1A_1) + h\nu(\lambda = 249\ nm) \longrightarrow CF_2(A\,^1B_1) \quad (e)$$

$$CF_2(A\,^1B_1) \longrightarrow CF_2(^3B_1) \quad (f)$$

$$CF_2(^3B_1) + {}^3O_2 \longrightarrow [CF_2O_2]^* \longrightarrow F_2CO + O \quad (g)$$

$$\downarrow h\nu \quad (h)$$

$$h\nu(\lambda = 225\ nm) + {}^1CF_2 + 2O$$

$$O + O_2 + M \longrightarrow O_3 \quad (i)$$

$$CF_2 + CF_2 \longrightarrow C_2F_4 \quad (k)$$

$$CF_2 + O_3 \longrightarrow F_2CO + O_2 \quad (l)$$

$$C_2F_4 + O_3 \longrightarrow F_2CO + O_2 + {}^3CF_2 \quad (m)$$

$$O_3 + h\nu(\lambda = 255\ nm) \longrightarrow O_2 + O \quad (n)$$

Scheme 1. Photochemically induced reactions likely to occur in the system $\mathbf{1}/O_2$.

A stationary concentration of electronically excited $^1CF_2$ is gradually established through the reactions (d) and (e). As shown by the matrix experiment, intersystem crossing of $CF_2(A\,^1B_1)$ to $CF_2(^3B_1)$ should be possible [Eq. (f)]; the $CF_2(^3B_1)$ then reacts further with O_2 according to Equation (g) [identical to Eq. (c)]. In order to explain the overproportional increase in the O_3 concentration, we postulate that the resulting vibrationally excited CF_2O_2 after photochemical excitation [Eq. (h)] can decay into CF_2 and two O atoms. The energy resulting from the sum of the singlet–triplet energy separation[12] for CF_2 (236.4 kJ mol^{-1}) and the photon energy for $\lambda = 225$ nm (532 kJ mol^{-1}) is sufficient to dissociate O_2 ($D^0 = 498.3$ kJ mol^{-1}) (Fig. 2), which can not be directly cleaved because of its extremely low absorption at wavelengths $\lambda > 225$ nm. The $^1CF_2$ arising from Equation (h) could reenter the cycle at Equation (f), while the O atoms would be captured by O_2 to form O_3 [Eq. (i)]. The sudden increase in the O_3 concentration can thus be understood by such a CF_2-sensitized photochemical cleavage of O_2.

The rapid decay of O_3 results from the reactions (l), (m),[12] and (n). It should be pointed out here that the intensively studied oxidation of carbenes CX_2 (X = H, organic group)[13] can-

 © VCH Verlagsgesellschaft mbH, D-69451 Weinheim, 1994 0570-0833/94/1010-1109 $ 10.00+.25/0

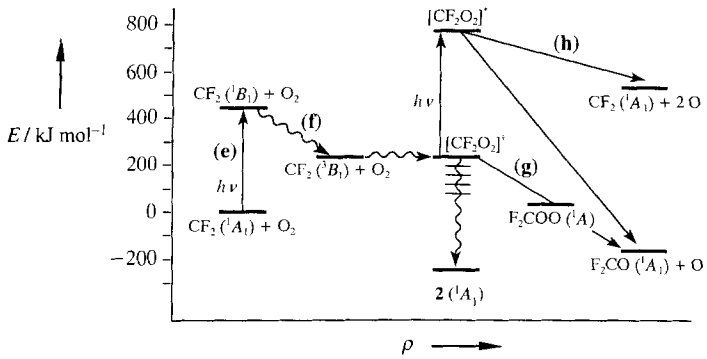


Fig. 2. Energy dependence of the reaction steps (e) to (h), referred to the energy of $CF_2(^1A_1) + O_2$. The thermodynamic data are taken from the refs. [2, 8].

not be compared to the CF_2/O_2 chemistry presented here because of the reversed singlet–triplet sequence.

In order to test for the possible existence of an energetic CF_2O_2 intermediate stage, an analogous experiment with difluorodioxirane **2** ($X\,^1A_1$) has been carried out, and its UV spectrum recorded for the first time. Two absorption bands[14] are apparent in the region of the incident light ($\lambda > 225$ nm) used for the photolysis of **1**, so a photochemical excitation of **2** should also be feasible. Both absorption bands lack any fine structure, which can be considered as evidence for a dissociative excited state. Ozone is formed directly during the photolysis of **2** in an excess of oxygen according to Equations (g) and (i) (Fig. 1b), which indicate that **2** is *one* possible precursor for the ozone formed in the presence of CF_2. Since the rate constants for reactions (f), (g), and (l) are not known, it is not feasible to make an assertion about the branching ratio of the reactions (g) and (h). The ratio (h)/(g) should increase, though, at low pressure and low temperature, since the deactivation of vibrationally excited CF_2O_2 will be slower.[15] Under the conditions used in our work (1 bar, 298 K), reaction (h) still has a certain importance.

The experiments described here show quite clearly that CF_2 can also contribute to ozone formation under stratospheric conditions, regardless which energized CF_2O_2 intermediate is present. This is of importance for the debate over CFC-substitutes, since fluorocarbons are considered as possible replacements. The CF_2 fragment will at least counteract any possible ozone depletion potential. Just how much O_3 is formed through our suggested mechanism can only be calculated when quantitative information over the entire reaction mechanism is available.

Received: October 22, 1993
Revised version: December 10,1993 [Z 6439 IE]
German version: *Angew. Chem.* **1994**, *106*, 1161

[1] R. E. Rebbert, P. J. Ausloos, *J. Photochem.* **1975**, *4*, 419–434; R. Atkinson, D. L. Bauch, R. A. Cox, R. F. Hampson, Jr., J. A. Kerr, J. Troe, *J. Phys. Chem. Ref. Data* **1992**, *21*, 1509.
[2] K. K. Irikura, W. A. Goddard III, J. L. Beauchamp, *J. Am. Chem. Soc.* **1992**, *114*, 48–51.
[3] C. W. Mathews, *Can. J. Phys.* **1967**, *45*, 2355–2374.
[4] S. Sharpe, B. Hartnett, H. S. Sethi, D. S. Sethi, *J. Photochem.* **1987**, *38*, 1–13.
[5] W. J. R. Tyerman, *Trans. Faraday Soc.* **1969**, *65*, 163; F. W. J. Dalby, *J. Chem. Phys.* **1964**, *41*, 2297.
[6] T. Johnston, J. Heicklen, *J. Chem. Phys.* **1967**, *47*, 475.
[7] L. Liu, S. R. Davis, *J. Phys. Chem.* **1992**, *96*, 9719–9724.
[8] M. Rahman, M. L. McKee, P. B. Shevlin, R. Sztyrbicka, *J. Am. Chem. Soc.* **1988**, *110*, 4002–4007.
[9] R. A. Mitsch, *J. Heterocycl. Chem.* **1964**, *1*, 59–60.
[10] The direct reaction of $CF_2(A\,^1B_1)$ with O_2 can be excluded, since O_3 would then be produced immediately. The investigation of the gas phase reaction indicates that O_3 is only formed after a long induction period.
[11] A. Russo, D. D. DesMarteau, *Angew. Chem.* **1993**, *105*, 956–958; *Angew. Chem. Int. Ed. Engl.* **1993**, *32*, 905–907.
[12] S. Toby, F. S. Toby, *J. Phys. Chem.* **1980**, *84*, 206–207.
[13] W. Sander, G. Bucher, S. Wierlacher, *Chem. Rev.* **1993**, *93*, 1583–1621.
[14] $\lambda_{max,1} = 362$ nm, $\sigma_{362} = 0.77 \times 10^{-20}$ cm^2, HWHM = 135 nm; $\lambda_{max,2} < 190$ nm, $\sigma_{200} = 1.00 \times 10^{-20}$ cm^2.
[15] J. T. Herron, R. I. Martinez, R. E. Huie, *Int. J. Chem. Kinet.* **1982**, *14*, 201–224.

[Cp*Fe(η^5-P_5)], a Sandwich Complex with Diverse Ligand Properties**

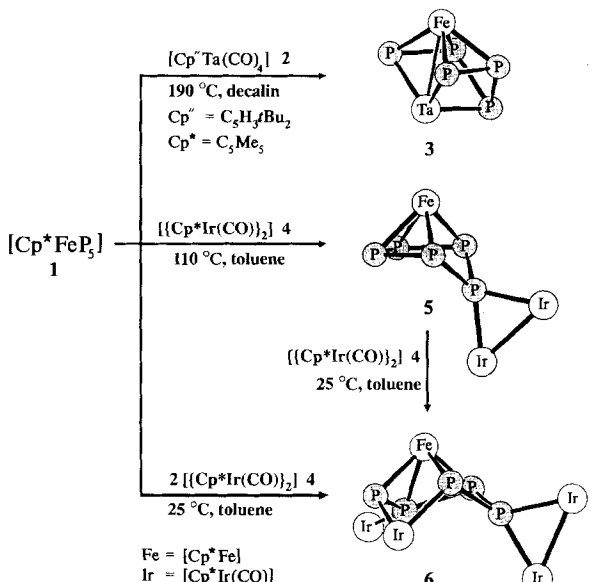
Michaela Detzel, Thomas Mohr, Otto J. Scherer,* and Gotthelf Wolmershäuser

Dedicated to Professor Helmut Werner on the occasion of his 60th birthday

The pentaphosphacyclopentadienyl anion P_5^- holds a key position in the series of *cyclo*-P_n complex ligands.[1] Examples are the sandwich complexes [Cp*M(η^5-P_5)], M = Fe (**1**), Ru[1a] and Os[2] as well as the compounds MP_5, M = Li, Na, K,[3] which can be prepared as stable solutions.

The ferrocene analogue **1**[4] shows diverse ligand properties. The *cyclo*-P_5 building block remains intact and planar both in the terminal coordination of two $Cr(CO)_5$ fragments[5] and in a stacking reaction to give the cationic triple-decker [CpFe(P_5)FeCp*]$^+$ complex[5] with 30 valence electrons.

Two remarkable P_5 ring-opening reactions are observed in the reaction of **1** with the tantalum complex **2** and the iridium binuclear complex **4**.



[*] Prof. Dr. O. J. Scherer, Dipl.-Chem. M. Detzel, Dipl.-Chem. T. Mohr, Dr. G. Wolmershäuser[+]
Fachbereich Chemie der Universität
Erwin-Schrödinger-Strasse, D-67663 Kaiserslautern (FRG)
Telefax: Int. code + (631)205-3200
[+] X-ray structure analyses.
[**] This work was supported by the Graduiertenkolleg "Phosphorchemie als Bindeglied verschiedener chemischer Disziplinen" and the Fonds der Chemischen Industrie. We thank Degussa AG for a gift of $IrCl_3 \cdot 3H_2O$. The help of Dr. Öfele, München, in preparing compound **1** is gratefully acknowledged. Cp* = pentamethylcyclopentadienyl.

The decisive precursor for the formation of **3** is the dimetal complex **7**,[6] which is prepared by a short period photolysis and can be subsequently isolated. In **7** the intact *cyclo*-P_5 ligand is coordinated terminally to the $Ta(CO)_3Cp''$ fragment. The photochemical as well as the thermal elimination of CO from **7** leads to the formation of **3** with cleavage of a P–P bond.

$[Cp^*Fe(\mu\text{-}\eta^5\text{:}\eta^1\text{-}P_5)\{Ta(CO)_3Cp''\}]$ **7**

The compounds **3**, **5**, and **6** form black-green crystals which can be handled in air for a short period; they are sparingly soluble in pentane, soluble in toluene, and very soluble in dichloromethane. The yields of the corresponding reactions lie between 52 and 90%. The ^1H and ^{31}P NMR data for the new complexes[6] are in agreement with the X-ray crystallographic results.[7] The X-ray structure analysis reveals a distorted TaP_5 Dewar benzene as the framework of **3**, whose two P=P bonds (P1–P2 2.150(2), P4–P5 2.152(2) Å) are capped by the 13 valence electron fragment FeCp* (Fig. 1). The iron center

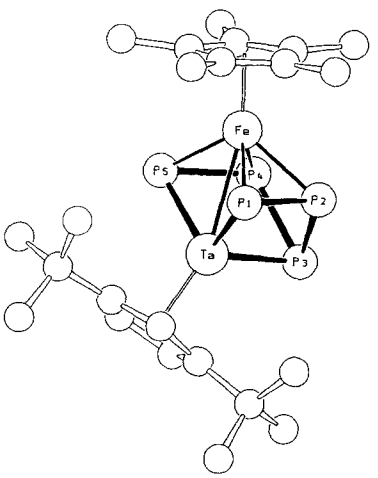
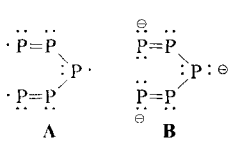


Fig. 1. Crystal structure of **3**. Selected distances [Å] and angles [°]: Ta-Fe 2.854(1), Ta-P1 2.378(2), Ta-P5 2.377(2), Ta-P3 2.391(2), Fe-P1 2.357(2), Fe-P5 2.369(2), Fe-P2 2.300(2), Fe-P4 2.281(2), P1-P2 2.150(2), P4-P5 2.152(2), P2-P3 2.271(2), P3-P4 2.265(2), P2···P4 2.80, P1···P5 3.60, Fe-$Cp^*_{(centr.)}$ 1.723, Ta-$Cp''_{(centr.)}$ 2.106; Ta-P1-P2 74.63(6), Ta-P5-P4 74.56(6), P1-P2-P3 111.40(8), P3-P4-P5 111.23(8), P2-P3-Ta 72.26(6), P4-P3-Ta 72.32(6), P1-Ta-P3 99.99(6), P3-Ta-P5 99.74(6), P1-Ta-P5 98.51(5), P2-P3-P4 76.37(7), sum of the angles of the four-membered rings: Ta,P1,2,3 358.3, Ta,P3,4,5 357.8, Fe,P1,Ta,P5 345.8, Fe,P2,3,4, 352.6, dihedral angle: P1,2,4,5|P2,3,4 108.8.

achieves the 18 valence electron configuration through a Ta–Fe bond (metal–metal distance 2.845(1) Å). The other P–P bonds (P2–P3 2.271(2), P3–P4 2.265(2) Å) are significantly longer. The P_5 ligand of **3** can be described as a triradical pentaphospha-1,4-pentadiene-1,3,5-triyl (**A**) or as a trianion P_5^{3-} (**B**).



In LaP_5 ($La^{3+}P_5^{3-}$), whose P atoms of one layer are linked to give a network comprising condensed twelve-membered rings with a $^2_\infty(P_5^{3-})$ anion lattice, the P–P distances range from 2.16 to 2.22 Å.[8] Whereas in **3** the Ta–P bond lengths (2.377(2)–2.391(2) Å) differ only slightly, the Fe–P distances can be subdivided into two shorter (Fe–P2 2.300(2), Fe–P4 2.281(2) Å) and two longer ones (Fe–P1 2.357(2), Fe–P5 2.369(2) Å). The plane P1,2,4,5 and the plane of the ring-C atoms of the Cp* ligand are arranged almost parallel to each other (deviation 3°), the same is true for the P1,3,5 plane and the plane of the ring-C atoms of the Cp'' ligand (deviation 2.3°).

The X-ray structure analysis[7] shows the P_5 ligand of **5** to be a *cyclo*-P_5 with an envelope conformation (Fig. 2). In addition

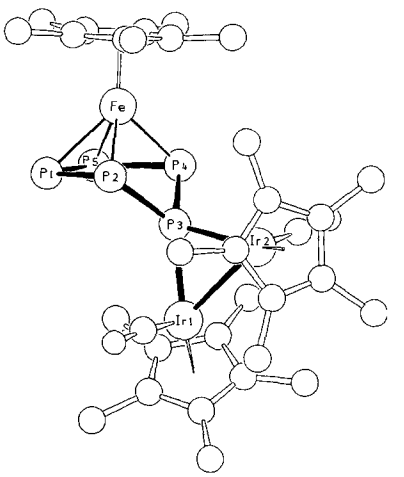


Fig. 2. Crystal structure of **5**. Selected distances [Å] and angles [°]: Fe-P1 2.327(3), Fe-P2 2.310(3), Fe-P4 2.311(3), Fe-P5 2.322(3), Ir1-P3 2.288(2), Ir2-P3 2.305(2), Ir1-Ir2 2.776(1), P1-P2 2.146(4), P2-P3 2.170(3), P3-P4 2.166(3), P4-P5 2.137(4), P1-P5 2.160(5), P2···P4 3.16, Fe-$Cp^*_{(centr.)}$ 1.702, Ir1-$Cp^*_{(centr.)}$ 1.907, Ir2-$Cp^*_{(centr.)}$ 1.903; P2-P1-P5 103.5(2), P1-P5-P4 103.6(2), P5-P4-P3 100.6(2), P1-P2-P3 101.1(2), P2-P3-P4 93.7(1), P2-Fe-P4 86.4(1), sum of the angles: Fe,P2,3,4 359.6, dihedral angles: P2,3,4|P2,1,5,4 121.8, Fe,P2,3,4|P3,Ir1,2 89.0.

to two shorter P–P bonds (P1–P2 2.146(4), P4–P5 2.137(4) Å), two slightly longer ones are observed (P2–P3 2.170(3), P3–P4 2.166(3) Å), which, however, are still considerably shorter than those in the five-membered phosphacycles $(PR)_5$ with an envelope conformation (R = CF_3, C_6H_5, $\bar{d}$(P–P) 2.22 Å).[9] Cp*Fe caps the planar unit P1,2,4,5 almost symmetrically (Fe–P 2.310(3)–2.327(3) Å). In the spirocycle **5** the planes P3,Ir1,2 and P2,3,4,Fe are perpendicular (89°), the ligands at the Ir atoms are arranged *trans*. The $FeIr_2$ complex **5** is diamagnetic, possibly because the Fe atom is negatively and the P3 atom (Fig. 2) is positively charged.

Compound **5** reacts with additional $[\{Cp^*Ir(CO)\}_2]$ (**4**) under mild conditions. In this way a P–P bond of the *cyclo*-P_5 unit and the Ir–Ir bond of the starting material **4** are cleaved, and this in turn leads to the formation of an IrP_5 six-membered ring, which, as the X-ray structure analysis shows,[7] has a strongly distorted chair conformation (Fig. 3) and P–P bonds of considerably different lengths (2.126(6)–2.198(5) Å). This results in an unsymmetrical capping by the Cp*Fe fragment (Fe–P 2.259(6)–2.363(5) Å). Going from **5** to **6** the *trans* configuration of the ligands at Ir1 and Ir2 is retained, the plane of the three-membered ring and the Fe,P2,3,4 plane now form an angle of 84°, thus they deviate more strongly from orthogonality than in complex **5**. The P–Ir distance between terminal Cp*(CO)Ir ligand and P_5 unit (Ir4–P5 2.232(4) Å) is significantly shorter than the corresponding distances between an inserted Cp*(CO)Ir group and a P_5 unit (Ir3–P1,2 2.371(4)–2.408(5) Å); similar

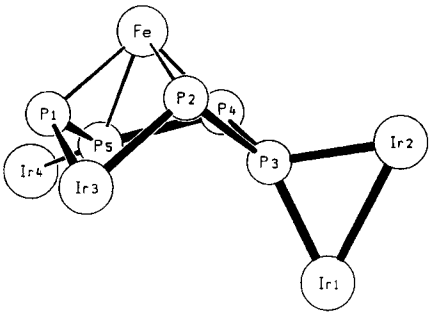


Fig. 3. Crystal structure of **6** (Cp* and CO ligands are not shown). Selected distances [Å] and angles [°]: Fe-P1 2.259(6), Fe-P2 2.322(5), Fe-P4 2.272(5), Fe-P5 2.363(5), Ir1-P3 2.296(4), Ir2-P3 2.312(4), Ir3-P1 2.371(4), Ir3-P2 2.408(5), Ir4-P5 2.232(4), Ir1-Ir2 2.757(1), P2-P3 2.198(5), P3-P4 2.162(6), P4-P5 2.144(7), P1-P5 2.126(6), P1 ··· P2 2.64, P2 ··· P4 3.14, P3 ··· P5 3.40, P3 ··· Ir3 3.73, P5 ··· Ir3 3.84, Fe ··· Ir3 3.86, Fe-$Cp^*_{(centr.)}$ 1.748, Ir1-$Cp^*_{(centr.)}$ 1.918, Ir2-$Cp^*_{(centr.)}$ 1.915, Ir3-$Cp^*_{(centr.)}$ 1.949, Ir4-$Cp^*_{(centr.)}$ 1.932; P2-Ir3-P1 67.2(2), Ir3-P1-P5 117.1(2), P1-P5-P4 111.0(3), P5-P4-P3 104.3(3), P4-P3-P2 92.1(2), P3-P2-Ir3 108.3(2), P2-Ir3-P1 67.2(2), sum of the angles: Fe,P2,3,4 359.3, P1,Ir3,P2,Fe 360.0, dihedral angle: Fe,P2,3,4|P3,Ir1,2 84.0.

relationships are observed in [(triphos)Ir(η^3-P_3)] (triphos = $MeC(CH_2PPh_2)_3$).[10] Compound **6** is also diamagnetic.

Experimental Procedure

3: **1** (64 mg, 0.19 mmol) and **2** (97 mg, 0.21 mmol), dissolved in decalin (30 mL), were heated to reflux and stirred for about 10 h (until the disappearance of the CO band of **2** in the IR spectrum). The color changed from yellow-green to brown-green. After removal of the decalin under vacuum, the residue was taken up in a small amount of CH_2Cl_2, adsorbed onto silica gel (ca. 1 g; 2% H_2O) and dried. The column chromatographic workup (column 16 × 1.5 cm, packed with SiO_2/petroleum ether) gave, after a petroleum ether fraction which contained small amounts of **2**, a dark green fraction (petroleum ether:toluene 10:1) from which green-black crystals of **3** were obtained after removal of the solvent and recrystallization from a saturated *n*-hexane solution at −78 °C. Yield: 68 mg (52%).

5 [**6**]: **1** (138.4 mg, 0.4 mmol) [103.8 mg, 0.3 mmol)] and **4** (284.4 mg, 0.4 mmol) [426.6, 0.6 mmol] were dissolved in toluene (20 [30] mL) and stirred for 20 min at 110 °C [25 °C] (IR control as for the synthesis of **3**). The dark green reaction mixture was concentrated to about half the volume, silica gel (ca. 1 g, 2% water) was added [filtered through filter flakes] and **5** worked up by column chromatography [left standing at −78 °C; the supernatant solution was pipetted off and the black-green crystals of **6** were washed with cold *n*-hexane, yield 323 mg (61%)] (column 20 × 1.5 cm, packed with SiO_2/petroleum ether). Traces of unreacted starting material **1** were eluted with petroleum ether, with toluene a dark green fraction of **5** (380.5 mg, 90%) was obtained, which gave black-green needlelike crystals on crystallization from toluene at room temperature.

Received: December 18, 1993 [Z 6568 IE]
German version: *Angew. Chem.* **1994**, *106*, 1142

[1] Recent reviews: a) O. J. Scherer, *Angew. Chem.* **1990**, *102*, 1137–1155; *Angew. Chem. Int. Ed. Engl.* **1990**, *29*, 1104–1122; b) M. Scheer, E. Herrmann, *Z. Chem.* **1990**, *30*, 41–55.

[2] B. Rink, O. J. Scherer, unpublished results.

[3] M. Baudler, K. Glinka, *Chem. Rev.* **1993**, *93*, 1623–1667, and references therein.

[4] O. J. Scherer, T. Brück, *Angew. Chem.* **1987**, *99*, 59; *Angew. Chem. Int. Ed. Engl.* **1987**, *26*, 59; O. J. Scherer, T. Brück, G. Wolmershäuser, *Chem. Ber.* **1988**, *121*, 935–938; M. Baudler, S. Akpapoglou, D. Ouzounis, F. Wasgestian, B. Meinigke, H. Budzikiewicz, H. Münster, *Angew. Chem.* **1988**, *100*, 288–289; *Angew. Chem. Int. Ed. Engl.* **1988**, *27*, 280–281.

[5] O. J. Scherer, T. Brück, G. Wolmershäuser, *Chem. Ber.* **1989**, *122*, 2049–2054.

[6] ^{1}H NMR (200 and 400 MHz, C_6D_6, 298 K, C_6H_6 int.): **3**: δ = 6.03 (br. 1H), 5.56 (br. 2H), 1.67 (s, 15H), 1.09 (s, 18H) [signals of the ring protons show no splitting even at 200 K]. **5**: δ = 2.10 (s, 15H), 1.87 (s, 15H), 1.70 (s, 15H). **6**: δ = 2.49 (s, 15H), 2.05 (s, 15H), 2.01 (s, 15H), 1.97 (s, 15H), 1.88 (s, 15H). **7**: δ = 5.34 (t, 1H), 5.11 (t, 2H), 1.24 (s, 15H), 1.22 (s, 18H). ^{31}P{^{1}H} NMR (80.82 MHz, C_6D_6, 298 K, 85% H_3PO_4 ext.). **3**: AMM′XX′ spin system. δ = 220.4 (P_A, "t"), 171.0 (P_M, "d"), −286.8 (P_X, "dd"); $^1J_{AX}$ = −199, $^1J_{MX}$ = − 398, $^2J_{AM}$ = 5, $^2J_{XX'}$ = 12, $J_{MX'}$ = − 5 (^3J or ^2J through Fe). **5** (161.64 MHz): AMNXY spin system. δ = 178.0 ($P_A \equiv$ P3 "t"), 25.2 and 14.3 ($P_{M,N} \equiv$ P1,5, each "t"), −65.7 and −70.1 ($P_{X,Y} \equiv$ P2,4, each "dd"); $^1J_{AX}$ = − 364, $^1J_{AY}$ = − 367, $^1J_{MN}$ = − 390, $^1J_{MX}$ = − 395, $^1J_{NY}$ = − 393 Hz, $^2J_{AM}$ = 13, $^2J_{AN}$ = 13, $^2J_{MY}$ = 21, $^2J_{NX}$ = 21, $^2J_{XY}$ = − 5 Hz. **6**: ABCDE spin system. δ = 130.2 ($P_A \equiv$ P3 or P5, ddd), 101.4 ($P_B \equiv$ P1 or P2, dd), 43.0 ($P_C \equiv$ P4, "dd"), −1.6 ($P_D \equiv$ P1 or P2, m), −46.6 ($P_E \equiv$ P3 or P5, m); J_{AB} = 1.8 (^3J or ^2J through Fe), $^1J_{AC}$ = − 356, $^1J_{AD}$ = − 409, $^2J_{AE}$ = − 53, $^2J_{BC}$ = 10, $^2J_{BD}$ = − 41, $^1J_{BE}$ = − 525, $^2J_{CD}$ = −12, $^1J_{CE}$ = − 498, J_{DE} = − 25 (^3J or ^2J through Fe). **7**: AMM′XX′ spin system. δ = 198.7 (P_A, m), 148.7 (P_M, m), 96.0 (P_X, m). $^1J_{AX}$ = − 507, $^1J_{MM'}$ = − 400, $^1J_{MX}$ = − 451, $^2J_{AM}$ = −12, $^2J_{MX'}$ = 38, $^2J_{XX'}$ = − 30). Simulation program: PANIC Version 850501.1, Bruker, Karlsruhe. IR(CH_2Cl_2): **5**: $\tilde{\nu}$(CO)[cm^{-1}] = 1953 (s, br), **6**: 1945 (s, br), 1880 (s), **7** (KBr): 1936 (vs), 1870 (vs), 1835 (vs).

[7] a) **3** crystallizes triclinic, $P\bar{1}$ (no. 2); a = 9.127(3), b = 10.538(3), c = 14.931(5) Å; α = 104.52(2), β = 98.74(2), γ = 94.26(2)°, Z = 2, 6577 measured reflections ($Mo_{K\alpha}$, $2\theta_{max}$ = 55°), of which 6185 observed with $I \geq 2\sigma(I)$; 282 parameters, $R_1(wR_2)$ = 0.032 (0.0678), for all data 0.0444 (0.077). b) **5** crystallizes monoclinic, $P2_1/c$ (no. 14); a = 18.767(1), b = 12.208(1), c = 17.594(2) Å, β = 97.865(6)°, Z = 8, 10883 measured reflections ($Mo_{K\alpha}$, $2\theta_{max}$ = 55°), of which 9100 observed with $I \geq 2\sigma(I)$; $R_1(wR_2)$ = 0.046 (0.091), for all data 0.091 (0.111). c) **6** crystallizes triclinic, $P\bar{1}$ (no. 2); a = 12.551(4), b = 12.925(3), c = 23.660(9) Å; α = 81.61(2), β = 79.62(2), γ = 61.96(3)°, Z = 2, 7944 measured reflections ($Mo_{K\alpha}$, $2\theta_{max}$ = 45°), of which 7593 observed with $I \geq 2\sigma(I)$; 638 parameters, $R_1(wR_2)$ = 0.049 (0.101), for all data 0.086 (0.121). Compound **5** contains 0.5 mol toluene, **6** 0.25 mol *n*-hexane and 0.5 mol toluene, each of which is disordered. R_1 is calculated for F,wR_2 based on F^2. d) Enraf-Nonius CAD-4 diffractometer, T = 293 K, solution and refinement of the structures with the SHELXS-86 and SHELXL-93 programs. Further details of the crystal structure investigations may be obtained from the Fachinformationszentrum Karlsruhe, D-76344 Eggenstein-Leopoldshafen (FRG) on quoting the depository number CSD-57982.

[8] W. Wichelhaus, H. G. von Schnering, *Z. Anorg. Allg. Chem.* **1976**, *419*, 77–86; H. G. von Schnering, W. Hönle, *Chem. Rev.* **1988**, *88*, 243–273, and references therein.

[9] J. J. Daly, *J. Chem. Soc.* **1964**, 6147–6166; C. J. Spencer, W. N. Lipscomb, *Acta Crystallogr.* **1961**, *14*, 250–256.

[10] C. Bianchini, C. Mealli, A. Meli, L. Sacconi, *Inorg. Chim. Acta* **1979**, *37*, L543–544.

High-Pressure Synthesis of K_2PtH_6, a Saltlike Hydride with the K_2PtCl_6 Structure**

Welf Bronger* and Gudrun Auffermann

The hydrides A_2PtH_4 and A_3PtH_5 (A = K, Rb, Cs)[1–4] have been prepared by a reaction of the binary alkali metal hydrides AH with platinum sponge in an extremely pure hydrogen atmosphere according to Equation (a). The reaction temperatures lay between 580 and 700 K, and the hydrogen pressures between 1 and 10 bar.

$$x\,AH + Pt + (z - x)/2\,H_2 \rightarrow A_xPtH_z \qquad (a)$$

The planar $[PtH_4]^{2-}$ building unit is characteristic of the crystal structures of these ternary hydrides. Compounds of the type A_3PtH_5 additionally contain discrete hydride ions, which are coordinated in an octahedral fashion by A^+ ions as in binary alkali metal hydrides. In contrast to analogous halogen compounds, the mobility of the hydrogen atoms within the $[PtH_4]^{2-}$ building units gives rise to phase transitions. Whereas the planar anions are ordered in the low-temperature modifications, the

[*] Prof. Dr. W. Bronger, Dr. G. Auffermann
Institut für Anorganische Chemie der Technischen Hochschule
Prof.-Pirlet-Strasse 1, D-52056 Aachen (FRG)
Telefax: Int. code + (241)8888-288

[**] This work was supported by the Bundesministerium für Forschung und Technologie and by the Fonds der Chemischen Industrie. In addition we were financed by the International Centre for Diffraction Data (ICDD) Grant-in-Aid Program and by the Large Installation Plan of the Commission of the European Community. We thank Dr. P. Müller for performing the neutron diffraction experiments. We are grateful to the Risø National Laboratory for the measurement time made available to us.

averaged structure in the high-temperature modification involves an octahedral coordination of the platinum atoms with an occupation factor of 2/3 for the hydrogen positions.[5] This factor arises because the four hydrogen atoms rapidly change sites within the octahedron. The question whether further hydrogen could be incorporated into the structure under higher H_2 pressure, and thus whether the platinum could be oxidized beyond the oxidation state II, remained unanswered. In the initial experiments with a newly developed high-pressure autoclave capable of a hydrogen reaction pressure of 1500–1800 bar and a temperature of 775 K, we have now synthesized in the potassium/platinum/hydrogen system the compound K_2PtH_6. Potassium hydride[6] and platinum sponge (Degussa, specified purity 99.9%) were employed in a molar ratio of 2:1. The duration of the experiment was 6 h, and its course could be followed directly with a pressure gauge. The uptake of hydrogen, determined from the pressure difference, was 2 mol H_2 per mol Pt. The very air- and moisture-sensitive product is a colorless powder in a uniform phase. To characterize the powder samples, X-ray analyses were performed at room temperature, which showed that the platinum and potassium atoms form an atomic arrangement analogous to that in fluorite. They therefore also correspond to the arrangement in the K_2PtH_4 type. A comparison of the lattice parameters determined by X-ray diffraction for the two phases showed that the unit cell of the new, hydrogen-enriched phase is marginally larger (Table 1).

Table 1. K_2PtH_6 and K_2PtH_4: comparison of the lattice constants [Å] from X-ray diffraction investigations with the low-temperature Guinier camera G645.

Cmpd.	T [K]		
	295	9	
K_2PtH_6	$a = 8.1760(2)$	$a = 8.1116(2)$	
K_2PtH_4	$a = 8.0653(4)$	$a = 5.6215(8)$	$c = 8.122(2)$

Since K_2PtH_4 undergoes a reversible phase change at 195 K as a consequence of the mobility of the hydrogen atoms, comparative X-ray diffraction investigations of K_2PtH_6 and K_2PtH_4 with a low-temperature Guinier camera (model G645, from Huber, Rimsting; temperature range 9–300 K) were conducted to provide further support for the postulated composition K_2PtH_6. The samples were contained in shallow sample holders developed specifically for extremely air- and moisture-sensitive substances during diffractometer imaging. The analysis of the data showed that, as expected, the new phase K_2PtH_6 does not undergo the phase change (cubic → tetragonal) corresponding to that experienced by K_2PtH_4 on cooling (Fig. 1). Furthermore, complementary experiments with a Guinier heating camera showed that K_2PtH_6 can be converted into K_2PtH_4 above 500 K with concomitant H_2 loss. The process is reversible at a suitable H_2 pressure.

For conclusive elucidation of the composition and structure of K_2PtH_6, the corresponding perdeuterated compound, which was synthesized analogously to the hydride, was studied by elastic neutron diffraction at 295 and 8.5 K at the TAS I workstation of the DR 3 reactor in the Risø National laboratory (Denmark). An aluminum tube (inner diameter 10 mm, length 40 mm, wall thickness 0.05 mm) served as sample holder, into which the sample was loaded under argon before closure with a Viton seal. For the low-temperature measurements a closed-cycle, helium-operated refrigerator was used. The analysis of the data was performed with the program DBWS 9006.[7] The neutron experiments confirmed that each platinum is surrounded

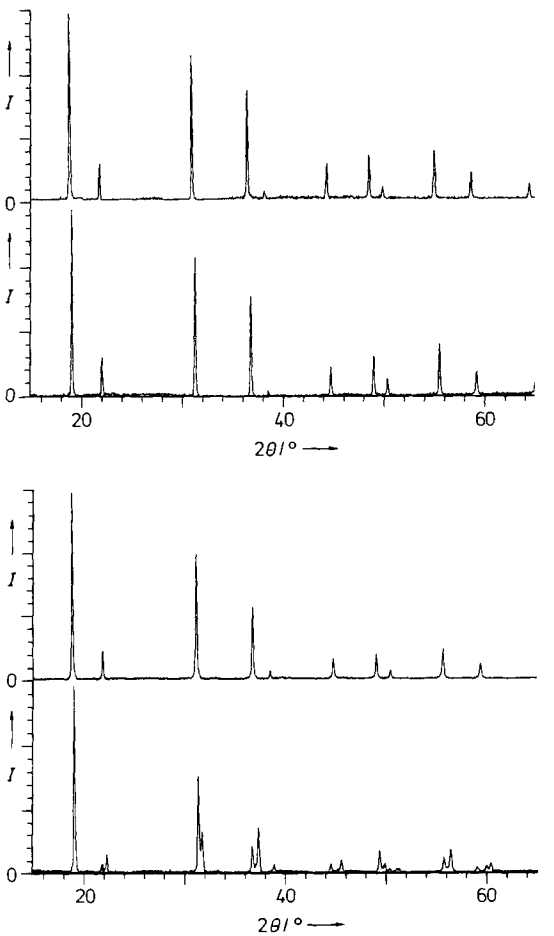


Fig. 1. Sections of the Guinier diffractometer images of K_2PtH_6 and K_2PtH_4 (total range: $10° < 2\theta < 100°$, step size in 2θ:0.004°). Represented from top to bottom are K_2PtH_6 at 295 K, K_2PtH_6 at 9 K, K_2PtH_4 at 295 K, and K_2PtH_4 at 9 K. Both compounds have the same metal-atom arrangement at room temperature, which is maintained at 9 K for K_2PtH_6. In contrast, K_2PtH_4 has undergone a phase change cubic → tetragonal by this temperature. I = measured relative intensity.

by six deuterium atoms in a regular octahedron, and thus the atomic arrangement in K_2PtD_6 is isotypic with that of K_2PtCl_6 (Fig. 2). Final refinements (Table 2) with floating occupation

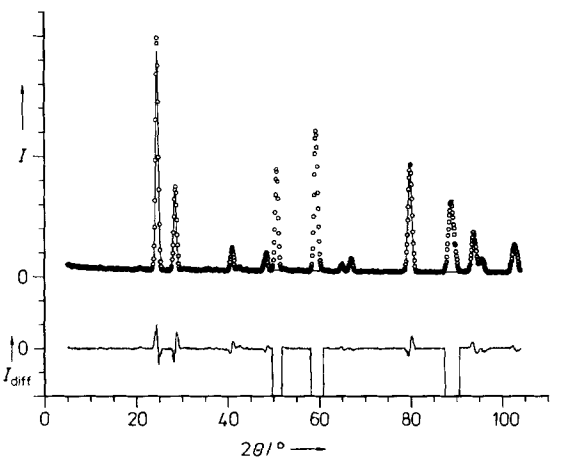


Fig. 2. Neutron diffraction diagram of K_2PtD_6; in addition to the measured (o) and the calculated (—) profiles the difference profile is shown. For the three ranges in which the Bragg reflections of K_2PtD_6 overlap with those of the aluminum tube, only the measured profile is given, since these three regions are also excluded from the refinement. I = measured or calculated relative intensity; I_{diff} = difference between the measured and calculated relative intensities.

Table 2. K_2PtD_6: results of the elastic neutron diffraction at TAS I at room temperature (space group: $Fm3m$, $Z = 4$).

Range					$5° < 2\theta < 105°$
Wavelength					2.01405 Å
Lattice parameter					$a = 8.1399(6)$ Å
Number of reflections considered in the refinement					12
Atomic site parameters and temperature factors					
Pt in (4a)	0	0	0		$B_{iso} = 0.4(5)$ Å^2
K in (8c)	1/4	1/4	1/4		$B_{iso} = 1.0(8)$ Å^2
D in (24e)	x	0	0	x = 0.2015(5)	$B_{iso} = 1.6(4)$ Å^2
R values:	R_{Bragg}: 0.045		$R_{profile}$: 0.097		

parameters for the deuterium positions yielded no deviation from a complete occupation of the octahedral positions. The calculations converged per formula unit K_2PtD_z to a value of $z = 6.00 \pm 0.03$. A phase change at low temperatures was not observed. The structures of K_2PtD_6 and K_2PtD_4 are contrasted in Figure 3. The Pt–D distances at 295 K of 1.640(4) Å in K_2PtD_6 are slightly longer than those in K_2PtD_4 (1.62(1) Å). The phase sequence K_2PtH_4, K_3PtH_5, K_2PtH_6 with increasing hydrogen pressure is in agreement with the trend for the decrease in the volume increment for hydrogen.

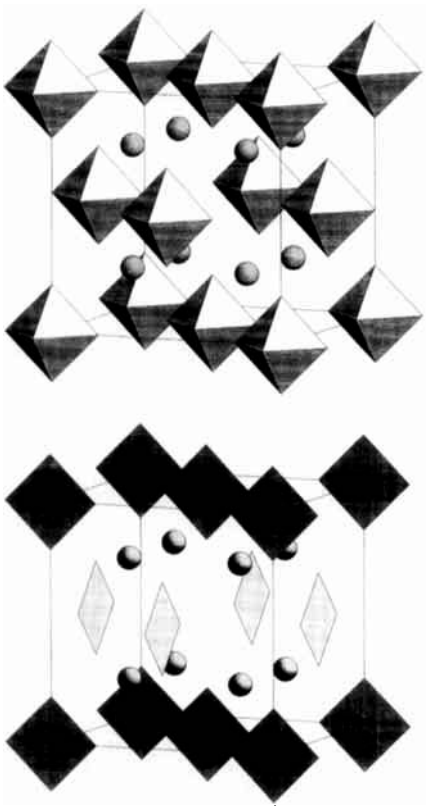


Fig. 3. Comparison of the structures of K_2PtD_6 and the high-temperature modification of K_2PtD_4 (top) with the low-temperature modification of K_2PtD_4 (bottom). Represented are the platinum–deuterium octahedra, whose D-positions are completely occupied for K_2PtD_6 and 2/3 occupied for K_2PtD_4, the platinum–deuterium squares, and the positions of the potassium ions. The structure of the low-temperature form of K_2PtD_4 is shown from the same viewpoint as the high-temperature form, although it may be described by a tetragonal unit cell that is half as large and that has the following cell parameters: $a_{tetr} = a_{cub}/\sqrt{2}$ and $c_{tetr} = a_{cub}$.

The hydride obtained in the high-pressure synthesis enables an extended comparison between metal–hydrogen and metal–halogen complexes. For the hydrogen pressures previously applied, only those hydrides A_xMH_z in which the transition metals M do not attain the highest oxidation states observed for the corresponding ternary fluorides or chlorides were synthesized.[5] Now hydrides are accessible that contain transition metals in the same oxidation states as the halides.

Received: December 18, 1993 [Z 6569 IE]
German version: *Angew. Chem.* **1994**, *106*, 1144

[1] W. Bronger, P. Müller, D. Schmitz, H. Spittank, *Z. Anorg. Allg. Chem.* **1984**, *516*, 35–41.
[2] W. Bronger, G. Auffermann, P. Müller, *J. Less-Common Met.* **1986**, *116*, 9–15.
[3] W. Bronger, G. Auffermann, P. Müller, *J. Less-Common Met.* **1988**, *142*, 243–252.
[4] W. Bronger, G. Auffermann, P. Müller, *Z. Anorg. Allg. Chem.* **1988**, *566*, 31–38.
[5] W. Bronger, *Angew. Chem.* **1991**, *103*, 776–784; *Angew. Chem. Int. Ed. Engl.* **1991**, *30*, 759–768.
[6] Pure potassium hydride was prepared in a steel autoclave by treatment of potassium (Koch Light Laboratories Ltd., specified purity 99.97%) with highly pure hydrogen (specified purity 99.99999%) from a $FeTiH_2$ steel cylinder at 800 K and 3 bar.
[7] A Sathivel, R. A. Young, *Programs DBWS 9006 and DBWS 9006 PC*; School of Physics, Georgia Institute of Technology, Atlanta, GA 30332, USA, **1991**.

A Template Synthesis of Stable Conjugated Primary Enamines from Ketones, Nitriles, and Butadiene**

Luis López, Martin Berlekamp, Dorothee Kowalski, and Gerhard Erker*

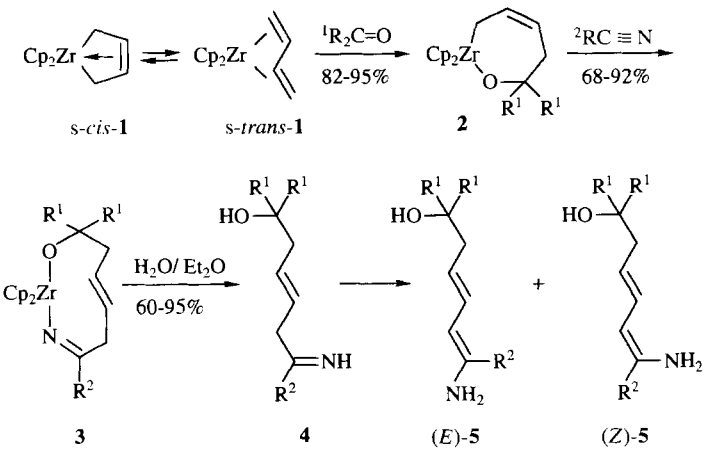
In the 1970s the research groups of H. Ahlbrecht and others showed that β-aryl-substituted primary enamines and their imine tautomers exist in equilibrium at room temperature in an approximately equimolar ratio.[1–3] It is now known that the thermochemical conjugation energy of (heteroatom-free) arylalkenes is about 2 kcal mol^{-1} less than that of the analogous conjugated dienes.[4] If this is also the case for the NH_2-substituted system, simple *conjugated* primary enamines should be significantly favored in this equilibrium over the corresponding imine tautomers. Using a template synthesis[5] we have prepared compounds with which this fundamental relationship can be confirmed experimentally for the nitrogen-substituted frameworks. In this simple fashion stable 1-aminobutadienes that do not contain other enamine-stabilizing substituents[2b] can thus be obtained under thermodynamic control.

During the last few years we have shown that (butadiene)zirconocene reacts with two equivalents of a nitrile to form metallacyclic nine-membered ring compounds that can be hydrolyzed to give 1,6-diaminohexatrienes.[6] We have now treated the (butadiene)zirconocene reagent **1**,[7] first with benzophenone to give the diphenyloxazirconacycloheptene **2a**,[8] and then with one equivalent of 4-methylbenzonitrile. The C-C coupling reaction to give the substituted 1-aza-3-oxa-2-zirconacyclononа-

[*] Prof. Dr. G. Erker, Dr. L. López, Dipl.-Chem. M. Berlekamp, Dipl.-Chem. D. Kowalski
Organisch-chemisches Institut der Universität
Corrensstrasse 40, D-48149 Münster (FRG)
Telefax: Int. code + (251)83-9772

[**] This work was supported by the Deutsche Forschungsgemeinschaft, the Fonds der Chemischen Industrie, and the Alfried Krupp von Bohlen and Halbach Foundation. Dr. L. López thanks the Ministerio de Educacion y Ciencia, Madrid, and the Alexander von Humboldt Foundation for research grants. We thank Prof. Dr. W. R. Roth for interesting discussions and suggestions.

6,9-diene system **3a** took place smoothly at 60 °C within 18 h. The product **3a** contains a *trans* double bond in the ring and is chiral [^{1}H NMR ([D$_6$]benzene, 200 MHz, 300 K): Cp resonance



2a, R^1 = Ph; **2b**, R^1 = –CH$_2$CH$_2$–; **2c**, R^1 = CH$_3$

3–5	**a**	**b**	**c**	**d**	**e**	**f**	**g**	**h**
R^1	Ph	Ph	Ph	Ph	Ph	-CH$_2$CH$_2$-	-CH$_2$CH$_2$-	CH$_3$
R^2	*p*-C$_6$H$_4$CH$_3$	Ph	*p*-C$_6$H$_4$CN	-CH=CHCN	C(CH$_3$)$_3$	Ph	C(CH$_3$)$_3$	Ph

signals at δ = 6.06 and 5.69; diastereotopic methylene protons at C8 and C5 (3.48, 3.13, 2.98, 2.74)]. Compound **3a** is an organometallic/heterocyclic analog of *trans*-cyclononene and exhibits, as expected, a similar activation barrier for the intramolecular enantiomerization by ring inversion ($\Delta G^{\ddagger}_{ent}$(322 K) = 15.6 ± 0.5 kcal mol^{-1}).[9] Hydrolysis of **3a** in the two-phase system Et$_2$O/H$_2$O (room temperature, 1 h), gave (*3E,5Z*)-6-amino-1,1-diphenyl-6-(*p*-tolyl)-3,5-hexadien-1-ol [(*Z*)-**5a**, 60%] as the sole organic product.[10] Compound (*Z*)-**5a** shows the typical ^{13}C NMR signals of the 1-aminobutadiene unit at δ = 146.7, 100.9, 130.5, and 121.8 ([D$_6$]benzene). The ^{1}H NMR signal of the amino group was recorded at δ = 3.69, that of the OH group at δ = 2.71.

With benzonitrile and **2a** we obtained **3b**, hydrolysis of which gave a mixture of ketimine **4b** (about 40%) and the conjugated primary enamines (*Z*)-**5b** and (*E*)-**5b** (4:1). After 2 h in benzene the ketimine component could no longer be detected.

Terephthalic acid dinitrile reacted with **2a** in a 1:1 molar ratio to give mainly the metallacyclic nine-membered ring **3c**, which still contained a free cyano group (IR: $\tilde{\nu}$(C≡N) = 2229 cm^{-1}, Table 1) that was hydrolyzed to a mixture of the (*E*)/(*Z*) isomeric ketimines **4c** in a 4:1 ratio [^{1}H NMR: δ (=NH) = 9.78 and 9.43]. In solution the ketimines tautomerize rapidly even at room temperature to give the thermodynamically favored conjugated primary enamines **5**. After 1 h in benzene at 20 °C only a single aminobutadiene derivative was found by NMR spectroscopy, to which we assign the structure of (*3E,5Z*)-6-amino-6-(4-cyanophenyl)-1,1-diphenyl-3,5-hexadien-1-ol [(*Z*)-**5c**]. It is no longer possible to detect the ketimine in the equilibrium in this system by NMR spectroscopy ([D$_6$]benzene). The reaction of **2a** with fumaric acid dinitrile took a similar course. With an equimolar ratio the reaction cleanly gave the organometallic 1:1 adduct **3d**. Subsequent hydrolysis gave, under kinetic control, a 3:2 mixture of the ketimines (*E*)-**4d** and (*Z*)-**4d**, from which the functionalized aminohexatriene (*2E,4Z,6E*)-4-amino-9-hydroxy-9,9-diphenyl-2,4,6-nonatriene nitrile (*Z*-**5d**) is formed under equilibrium conditions as sole product.

Table 1. Characteristic data for compounds **3**–**8**.

3a: 560 mg (72%), m.p. 101 °C (decomp., DSC); correct analysis (C,H,N); IR(KBr): $\tilde{\nu}$ = 1654 (C=N), 1640 cm^{-1}; ^{1}H NMR (200 MHz, 300 K, [D$_6$]benzene): δ = 7.64–7.11 (several m, 14H, arom.), 6.06, 5.69 (s, each 5H, Cp), 5.28 (m, 2H, 6-H, 7-H), 3.48, 3.13, 2.98, 2.74 (m, each 1H, CH$_2$), 2.20 (s, 3H, CH$_3$); ^{13}C NMR (50 MHz, 300 K, [D$_6$]benzene): δ = 167.6, 139.3, 137.0 (C), 131.8, 130.2, 129.3, 128.5, 128.0, 127.5, 127.1, 110.4 (CH$_2$), 86.3 (C), 47.7, 39.4 (CH$_2$), 21.3 (CH$_3$)

3b: 430 mg (68%), m.p. 108 °C (decomp., DSC); correct analysis (C,H,N); IR(KBr): $\tilde{\nu}$ = 1653 (C=N) cm^{-1}; ^{1}H NMR ([D$_6$]benzene): δ = 7.69–7.10 (m, 15H, arom.), 6.09, 5.68 (s, each 5H, Cp), 5.28 (m, 2H, 6-H, 7-H), 3.36, 3.06, 2.85, 2.66 (m, each 1H, CH$_2$); ^{13}C NMR ([D$_6$]benzene): δ = 167.6, 139.3, 131.8, 130.3, 129.4, 128.6, 128.3, 127.1, 126.8, 110.5, 110.4 (CH), 86.3 (C), 47.8, 39.5 (CH$_2$)

3c: obtained only as a mixture with terephthalic acid dinitrile (ca. 30%) and the bisadduct (ca. 10%); IR(KBr): $\tilde{\nu}$ = 2229 (C≡N), 1654 (C=N) cm^{-1}; ^{1}H NMR ([D$_6$]benzene): δ = 7.40–7.15 (m, 14H, arom.), 6.10, 5.62 (s, each 5H, Cp), 5.19 (m, 2H, 6-H, 7-H), 3.12, 2.68 (m, each 2H, CH$_2$). (The 2:1-adduct from **2a** and terephthalic acid dinitrile shows Cp-signals at δ = 6.09 and 5.72); ^{13}C NMR ([D$_6$]benzene): δ = 165.6 (C9), 141.5 (*ipso*-C, Ph), 132.3, 132.0, 131.1, 130.6, 127.0, 126.8 (C6, C7, C(Ph)), 119.0 (CN), 112.9 (*ipso*-C, Ph), 110.6 (Cp), 86.5 (C4), 47.5, 39.4 (C8, C5)

3d: 570 mg (72%) violet crystals, m.p. 101 °C (decomp., DSC); correct analysis (C,H,N); IR(KBr): $\tilde{\nu}$ = 2220 (C≡N), 1660 (C=N), 1635 cm^{-1}; ^{1}H NMR ([D$_6$]benzene): δ = 7.39–7.08 (m, 10H, arom.), 6.23, 5.17 (AX, ^3J = 16.4 Hz, 2H, CH=CHCN), 5.85, 5.52 (br. s, each 5H, Cp), 5.03 (m, 2H, olef.), 3.02 (m, 1H), 2.61 (m, 2H), 2.38 (m, 1H, CH$_2$); ^{13}C NMR ([D$_6$]benzene): δ = 164.4 (C), 147.1, 131.1, 129.9, 127.9, 126.9 (CH), 118.3 (C), 110.7, 101.0 (Cp), 86.7 (C), 47.3 (CH$_2$), 40.7 (CH$_2$). 1 *ipso*-C not observed

4b: ^{1}H NMR (as a mixture with the enamines, [D$_6$]benzene): δ = 9.61 (s, 1H, =NH), 7.52–6.91 (m, 15H, arom.), 2.8 (m, 4H, CH$_2$), OH not observed

4c: ^{1}H NMR (as a mixture with the second imine isomer [**4c'**] and terephthalic acid dinitrile, ([D$_6$]benzene): δ = 9.78 (s, 1H, =NH) [**4c'**: 9.43], 7.52–6.94 (m, 14H, arom.), 5.34, 5.07 (m, each 1H, CH=CH), 2.82, 2.48 (m, each 2H, CH$_2$), 2.22 (s, 1H, OH)

4d: only characterized spectroscopically, 2 isomers; IR(KBr): $\tilde{\nu}$ = 3444, 3376, 3236 (OH, NH), 2229, 2228 (C≡N), 1644 (C=N), cm^{-1}; ^{1}H NMR (CDCl$_3$, only one isomer observed): δ = 9.76 (s, 1H, =NH), 7.44–7.16 (m, 10H, arom.), 6.93, 5.94 (^3J = 16.8 Hz, 2H, CH=CHCN), 5.43 (m, 2H, olef.), 3.10, 2.95 (m, each 2H, CH$_2$), 2.39 (m, 1H, OH); in [D$_6$]benzene two isomers in the ratio 3:2 were observed (δ(=NH) = 9.77, 8.93); ^{13}C NMR (CDCl$_3$): δ = 172.3 (C), 149.5 (CH), 146.2 (C), 133.8, 128.3, 127.2, 126.0, 125.2 (CH), 121.0 (C), 105.2 (CH), 45.5, 39.5 (CH$_2$), quaternary C under the solvent signal.

5a: 210 mg (60%) oil, which still contains ca. 5% solvent and unidentified impurities; IR: $\tilde{\nu}$ = 3447, 3368, 3270 (NH$_2$, OH), 1617 cm^{-1}; ^{1}H NMR (CDCl$_3$, 200 MHz): δ = 7.49–7.14 (m, 14H, arom.), 6.41, 5.37, 5.31 (m, each 1H, olef.), 3.69 (br. m, 2H, NH$_2$), 3.13 (m, 2H, CH$_2$), 2.71 (br. s, 1H, OH), 2.32 (s, 3H, CH$_3$); ^{13}C NMR (CDCl$_3$): δ = 146.7, 141.8, 138.0, 136.1 (C), 130.5, 129.0, 128.0, 126.7, 126.0, 125.3, 121.8, 100.9 (CH), 77.1 (C), 46.3 (CH$_2$), 21.1 (CH$_3$)

5b: 260 mg (69%) oil, 2 isomers; IR: $\tilde{\nu}$ = 3539–3177, 1610 cm^{-1}; ^{1}H NMR (CDCl$_3$): major component: δ = 7.50–7.08 (m, 15H, arom.), 6.43, 5.42, 5.34 (m, each 1H, olef.), 3.70 (br. s, 2H, NH$_2$), 3.15 (m, 2H, CH$_2$), 2.69 (br. s, 1H, OH); byproduct **5b'**: δ = 6.20 (m, 1H), 5.15 (m, 1H, olef.), 2.94 (m, 2H, CH$_2$), otherwise as for **5b**; ^{13}C NMR (CDCl$_3$, 50 MHz): δ = 146.7, 141.8, 139.0 (C), 130.4, 128.4, 128.2, 128.1, 126.7, 126.0, 125.5, 122.4, 101.6 (CH), 77.2 (C), 46.4 (CH$_2$)

5c: 200 mg (60%) isolated as a mixture with ca. 20% terephthalic acid dinitrile; IR(KBr): $\tilde{\nu}$ = 3467, 3438, 3361 (NH$_2$, OH), 2232 (C≡N), 1602 cm^{-1}; ^{1}H NMR (CDCl$_3$): δ = 7.57–7.1 (m, 14H, arom.), 6.39, 5.52, 5.41 (m, each 1H, olef.), 3.66 (br. s, 2H, NH$_2$), 3.16 (m, 2H, CH$_2$), 2.61 (br. s, 1H, OH); ^{13}C NMR (CDCl$_3$): δ = 146.5 (CNH, 139.5 (*ipso*-C, arom.), 132.7 (CH, arom., double intensity), 132.3 (*ipso*-C, arom.), 132.2 (C4), 128.1, 126.8, 125.9 (CH, arom.), 125.4 (C3), 116.1 (CN), 111.0 (*ipso*-C, arom.), 104.6 C5), 77.2 (C1), 46.3 (C2)

5d: 180 mg (64%) recrystallized from benzene, m.p. 175 °C (DSC); correct analysis (C,H,N); IR(KBr): $\tilde{\nu}$ = 3530, 3460, 3375 (NH$_2$, OH), 2219 (C≡N), 1637 cm^{-1}; ^{1}H NMR (CDCl$_3$): δ = 7.50–7.10 (m, 10H, arom.), 6.66, 5.25 (AX, ^3J = 16.2 Hz, 2H, CH=CHCN), 6.28 (m, 1H), 5.67 (m, 1H), 5.33 (m, 1H, olef.), 3.31 (br. s, 2H, NH$_2$), 3.16 (m, 2H, CH$_2$), 2.39 (br. s, 1H, OH); ^{13}C NMR (CDCl$_3$): δ = 148.2, 146.3, 136.6, 130.9, 128.3, 127.1, 126.0, 118.2, 116.1, 93.1, 77.2, 46.4

5e: from **2a** by treatment with pivalonitrile and subsequent hydrolysis, 170 mg (82%) oil, 2 isomers (9:1); main component: IR(NaCl): $\tilde{\nu}$ = 3527, 3481, 3398 (NH$_2$, OH), 1635 cm^{-1}; ^{1}H NMR ([D$_6$]benzene): δ = 7.57–6.99 (m, 10H, arom.), 6.20, 5.39, 4.92 (m, each 1H, olef.), 3.08 (m, 2H, CH$_2$), 2.89 (br. s, 2H, NH$_2$), 2.56 (br. s, 1H, OH), 0.91 (s, 9H, *t*Bu); ^{13}C NMR ([D$_6$]benzene): δ = 151.1, 147.8 (C), 131.4, 128.5, 126.8, 126.6, 120.1, 96.2 (CH), 47.0 (CH$_2$), 34.9 ((CH$_3$)$_3$C), 28.8 ((CH$_3$)$_3$C)

(Table 1 continued on next page)

Table 1. (continued)

5f: from **1** by treatment with cyclopentanone and benzonitrile and subsequent hydrolysis. 540 mg (95%) oil, 2 isomers (7:3); major component: IR(NaCl): $\tilde{\nu}$ = 3557, 3467, 3364 (NH_2, OH), 1680, 1639, 1620 cm^{-1}; ^1H NMR ($CDCl_3$): δ = 7.6–7.1 (m, 5H, arom.), 6.31, 5.67, 5.44 (m, each 1H, olef.), 3.71 (br., 2H, NH_2), 2.41 (m, 2H, CH_2), 1.9–1.3 (m, 9H, OH, CH_2); ^{13}C NMR ([D$_6$]benzene): δ = 141.6, 140.2 (C), 129.2, 128.6, 128.1, 126.0, 124.7 (CH), 102.4, 81.5 (C), 45.8, 39.7, 24.3 (CH_2)

5g: from **1** by treatment with cyclopentanone and pivalonitrile and subsequent hydrolysis. 1.24 g (89%) oil, 2 isomers (95:5); major component: IR(NaCl): $\tilde{\nu}$ = 3541, 3468, 3375 (NH_2, OH), 1634 cm^{-1}; ^1H NMR ([D$_6$]benzene): δ = 6.18, 5.58, 5.12 (m, each 1H, olef.), 2.97 (br., 2H, NH_2), 2.35 (m, 2H, CH_2), 1.9–1.3 (m, 8H, CH_2), 1.15 (br. s, 1H, OH), 0.99 (s, 9H, H from *t*Bu); ^{13}C NMR ([D$_6$]benzene): δ = 150.2 (C), 129.2, 122.4, 96.6 (CH), 81.5 (C), 45.8 (CH), 39.7 (CH_2), 34.9 (C from *t*Bu), 29.0 (CH_3 von *t*Bu), 24.3 (CH_2)

5h: from **1** by reaction with acetone and benzonitrile and subsequent hydrolysis, 320 mg (81%) oil, 2 isomers (4:1); main component: IR(NaCl): $\tilde{\nu}$ = 3548, 3437, 3364 (NH_2, OH), 1680, 1639, 1618 cm^{-1}; ^1H NMR ([D$_6$]benzene): δ = 7.5–7.0 (m, 5H, arom.), 6.18, 5.62, 5.52 (m, each 1H, olef.), 2.97 (br., 2H, NH_2), 2.24 (m, 2H, CH_2), 1.34 (br. s, 1H, OH), 1.14 (s, 6H, CH_3); ^{13}C NMR ([D$_6$]benzene): δ = 141.6, 140.1 (C), 129.0, 128.6, 128.1, 126.0, 124.5, 102.4 (CH), 70.3 (C), 48.1 (CH_2), 29.4 (CH_3)

6: 160 mg (84%), m.p. 100 °C (DSC); correct high resolution mass spectrum; IR(KBr): $\tilde{\nu}$ = 3479 (OH), 1677 (C=O), 1604 cm^{-1}; ^1H NMR ($CDCl_3$): δ = 7.81–7.19 (m, 14H, arom.), 5.85, 5.44 (m, each 1H, olef.), 3.64, 3.09 (m, each 2H, CH_2), 2.98 (br. s., 1H, OH), 2.41 (s, 3H, CH_3); ^{13}C NMR ($CDCl_3$): δ = 197.7, 146.6, 143.9, 133.9 (C), 129.4, 129.2, 128.8, 128.3, 128.1, 126.7, 125.9 (CH), 76.7 (C), 45.5, 42.1 (CH_2), 21.6 (CH_3)

8: 140 mg (75%) oil; correct high resolution mass spectrum; IR(Film): $\tilde{\nu}$ = 1678(C=O) cm^{-1}; ^1H NMR ($CDCl_3$): δ = 7.90–7.22 (m, 14H, arom.), 4.73 (m, 1H), 3.58 (m, 1H), 3.08 (m, 1H), 2.64 (m, 2H), 2.42 (s, 3H, CH_3), 2.26 (m, 1H), 1.77 (m, 1H); ^{13}C NMR ($CDCl_3$): δ = 198.1, 146.9, 146.3, 143.8, 134.6 (C), 129.2, 128.3, 128.1, 128.0, 126.6, 125.8, 125.7 (CH), 88.1 (C), 75.5 (CH), 45.1, 38.6, 31.6 (CH_2), 21.6 (CH_3)

Aliphatic ketones (cyclopentanone **2b**, acetone **2c**) can also be used as building blocks in this template synthesis (see Table 1, **5f–h**). As expected,[4] the primary enamine with aliphatic substituents in the α-position is also energetically preferred over the corresponding imine tautomer (**5g**) under equilibrium conditions. Also in this case the imine is formed first under kinetic control.

These experiments have shown that the thermochemical conjugation energy of an additional C–C double bond is sufficient to make the formation of simple, conjugated primary enamines under equilibrium conditions energetically much more favorable than that of the corresponding ketimine tautomers. In this fashion 1-aminobutadienes and related compounds have been made accessible by thermodynamic control. Using this basis we have now begun to develop simple new routes to and preparative applications of these interesting synthetic building blocks.[11]

Received: October 8, 1993
Revised version: December 6, 1993 [Z 6402IE]
German version: Angew. Chem. **1994**, *106*, 1168

[1] H. Ahlbrecht, F. Kröhnke, *Justus Liebigs Ann. Chem.* **1967**, *701*, 126; H. Ahlbrecht, *Tetrahedron Lett.* **1968**, 4421; H. Ahlbrecht, S. Fischer, *Tetrahedron* **1970**, *26*, 2837; H. Ahlbrecht, G. Rauchschwalbe, *Tetrahedron Lett.* **1971**, 4897; H. Ahlbrecht, G. Papke, *ibid.* **1972**, 4443; *Tetrahedron* **1974**, *30*, 2571; H. Ahlbrecht, H. Hanisch, W. Funk, R. D. Kalas, *ibid.* **1972**, *28*, 5481; H. Ahlbrecht, S. Fischer, *ibid.* **1973**, *29*, 659; H. Ahlbrecht, J. Blecher, H. Hanisch, G. Papke, M. T. Reiner, *ibid.* **1973**, *29*, 3079; H. Ahlbrecht, W. Funk, M. T. Reiner, *ibid.* **1976**, *32*, 479; H. Ahlbrecht, R.-D. Kalas, *Liebigs Ann. Chem.* **1979**, *102*, and references therein; see also L. Duhamel, P. Duhamel, J.-C. Legal, *Bull. Soc. Chim. Fr.* **1972**, 3230; J. P. Picard, J. M. Aizpurua, A. Elynsuñ, P. Kowalski, *J. Organomet. Chem.* **1990**, *391*, 13. According to this study the $ArCH{=}C(NH_2)R/ArCH_2C(=NH)R$ ratio is solvent dependent; the enamine components are stabilized by polar solvents.

[2] For synthesis of simple primary enamines under *kinetic* control, see a) J.-L. Ripoll, H. Lebrun, A. Thuillier, *Tetrahedron* **1980**, *36*, 2497; b) Y. Vallee, J.-L. Ripoll, D. Maume, *J. Anal. Appl. Pyrolysis* **1988**, *14*, 171.

[3] P. L. Pickard, D. J. Vaughan, *J. Am. Chem. Soc.* **1950**, *72*, 876; P. L. Pickard, G. W. Polly, *ibid.* **1954**, *76*, 5169; R. A. Clark, D. C. Parker, *ibid.* **1970**, *92*, 7257; C. Shin, M. Masaki, M. Onta, *Bull. Chem. Soc. Jpn.* **1971**, *44*, 1657; P. Ollinger, W. Remp, H. Junek, *Monatsh. Chem.* **1974**, *105*, 346; M. Pfau, C. Ribiere, *Bull. Soc. Chim. Fr.* **1971**, 2584; J.-M. Brocas, B. de Jeso, J.-C. Pommier, *J. Organomet. Chem.* **1976**, *120*, 217; B. de Jeso, J.-C. Pommier, *J. Chem. Soc. Chem. Commun.* **1977**, 565; Y. Ohtsuka, *J. Org. Chem.* **1978**, *43*, 3231; P. L. Compagnon, F. Gasquez, T. Kimny, *Synthesis* **1986**, 948; A. Sevin, D. Masure, C. Giessner-Prettre, M. Pfau, *Helv. Chim. Acta* **1990**, *73*, 552; P. J. Walsh, A. M. Baranger, R. G. Bergman, *J. Am. Chem. Soc.* **1992**, *114*, 1708; calculation: B. J. Smith, L. Radom, *ibid.* **1992**, *114*, 36; Review: B. A. Shainyan, A. N. Mirskova, *Russ. Chem. Rev. (Engl. Transl.)* **1979**, *48*, 107.

[4] W. R. Roth, O. Adamczak, R. Breuckmann, H.-W. Lennartz, R. Boese, *Chem. Ber.* **1991**, *124*, 2499, and literature cited therein.

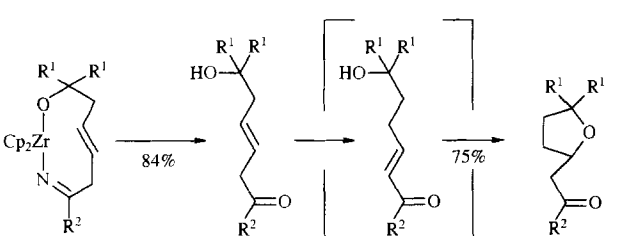
[5] Synthetic principle and examples: H. Yasuda, K. Tatsumi, A. Nakamura, *Acc. Chem. Res.* **1985**, *18*, 120; H. Yasuda, A. Nakamura, *Angew. Chem.* **1987**, *99*, 745; *Angew. Chem. Int. Ed. Engl.* **1987**, *26*, 723; H. Yasuda, T. Okamoto, Y. Matsuoka, A. Nakamura, J. Kai, N. Kanehisa, N. Kasai, *Organometallics* **1989**, *8*, 1139; G. Erker, F. Sosna, P. Betz, S. Werner, C. Krüger, *J. Am. Chem. Soc.* **1991**, *113*, 564; G. Erker, F. Sosna, R. Zwettler, C. Krüger, *Organometallics* **1989**, *8*, 450; G. Erker, F. Sosna, R. Noe, *Chem. Ber.* **1990**, *123*, 821; G. Erker, F. Sosna, R. Zwettler, C. Krüger, *Z. Anorg. Allg. Chem.* **1990**, *581*, 16; G. Erker, F. Sosna, *Organometallics* **1990**, *9*, 1949; G. Erker, F. Sosna, R. Pfaff, R. Noe, C. Sarter, A. Kraft, C. Krüger, R. Zwettler, *J. Organomet. Chem.* **1990**, *394*, 99; G. Erker, R. Pfaff, C. Krüger, S. Werner, *Organometallics* **1991**, *10*, 3559.

[6] G. Erker, R. Pfaff, C. Krüger, M. Nolte, R. Goddard, *Chem. Ber.* **1992**, *125*, 1669; G. Erker, R. Pfaff, *Organometallics* **1993**, *12*, 1921; G. Erker, R. Pfaff, D. Kowalski, E.-U. Würthwein, C. Krüger, R. Goddard, *J. Org. Chem.* **1993**, *58*, 6771.

[7] G. Erker, J. Wicher, K. Engel, F. Rosenfeldt, W. Dietrich, C. Krüger, *J. Am. Chem. Soc.* **1980**, *102*, 6344; G. Erker, J. Wicher, K. Engel, C. Krüger, *Chem. Ber.* **1982**, *115*, 3300; G. Erker, K. Engel, C. Krüger, A.-P. Chiang, *ibid.* **1982**, *115*, 3311; H. Yasuda, Y. Kajihara, K. Mashima, K. Nagasuma, K. Lee, A. Nakamura, *Organometallics* **1982**, *1*, 388; G. Erker, K. Engel, C. Sarter in *Organometallic Synthesis*, Vol. 3 (Eds.: R. B. King, J. J. Eisch), Elsevier, Amsterdam, **1986**, p. 32.

[8] G. Erker, K. Engel, J. L. Atwood, W. E. Hunter, *Angew. Chem.* **1983**, *95*, 506; *Angew. Chem. Int. Ed. Engl.* **1983**, *22*, 494.

[9] *trans*-Cyclononene has a racemization barrier $\Delta G^{\ddagger}_{cm}$ (263 K) of ca. 19 kcal mol^{-1}: A. C. Cope, K. Banholzer, H. Keller, B. A. Pawson, J. J. Wang, H. J. S. Winkler, *J. Am. Chem. Soc.* **1965**, *87*, 3644.



3a **6** **7** **8**

R^1 = Ph, R^2 = *p*-$C_6H_4CH_3$

[10] In contrast hydrolysis of **3a** with 2 N H_2SO_4 (20 °C, 1 d) gave ketone **6**. Treatment of **3a** with 2 N HCl in THF (20 °C, 3 d) on the other hand gave the tetrahydrofuran derivative **8**, which was also obtained from **6** with HCl (see Table 1). We assume that the α,β-unsaturated ketone **7** is formed in situ as an intermediate.

[11] For related reactions of conjugated tertiary enamines see, for example B. Potthoff, E. Breitmeier, *Chem. Ber.* **1987**, *120*, 255; R. L. S. Snowden, R. Brauchli, M. Wüst, *Helv. Chim. Acta* **1990**, *73*, 640; A. C. Braisted, P. G. Schultz, *J. Am. Chem. Soc.* **1990**, *112*, 7430; A. R. Katrizky, Q.-H. Long, P. Lue, *Tetrahedron Lett.* **1991**, *32*, 3597; R. Sustmann, M. Rogge, U. Nüchter, H. Bandmann, *Chem. Ber.* **1992**, *125*, 1647, 1657; review: P. W. Hickmott, *Tetrahedron* **1984**, *40*, 2989.

The Grand Old Man of Polymer Science

Peptide and Protein Hormones. Structure, Regulation, Activity. A Reference Manual. By *W. König*. VCH Verlagsgesellschaft, Weinheim/VCH Publishers, New York, 1993. X, 280 pp., hardcover DM 198.00, $ 135.00.—ISBN 3-527-28417-6/1-56081-211-7

The author of this book is a well-known expert in the field of structure–activity relationships of peptide hormones. It is 25 years since the publication of *The Peptides* by Schröder and Lübke; now at last we again have a handbook which serves as a guide and rapid source of information on most aspects of peptide hormones. The most important qualities that one looks for in a reference book on this extremely active field of research are that it should be clearly set out and up-to-date.

A very brief introduction is followed by nine clearly set out review chapters. The list of references in the appendix mainly covers work published in the period 1985 to 1990. It gives only the first authors, without titles or final page numbers, and in this way the publishers have saved fifty to a hundred pages. To have included the titles of the papers would have been very helpful for readers who want quick access to the original literature without having to make a computer search and read abstracts.

The families of hormones covered in the individual chapters are as follows. Chapter 2: gonadoliberins, thyroliberins, gonadotropines; Chapter 3: parathyroid hormones and calcitonins; Chapter 4: corticoliberin-proopiomelanocortins, opioide peptides, etc.; Chapter 5: blood pressure regulating peptides; Chapter 6: cholecystokinins and gastrins; Chapter 7: the secretin family; Chapter 8: neurotensins; Chapter 9: motilins; Chapter 10: pancreatic spasmolytic peptides. Each of these chapters describes the occurrence and distribution, receptors, and biological effects or functions of the hormones, and also the structure–activity relationships for agonists and antagonists, and the applications. The clearly set out tables showing peptide sequences based on single-letter symbols are especially useful.

It is pleasing to note that the author has had the boldness to be brief. From the many synthetic peptide hormone analogues, which already run into thousands for the well-known examples of oxytocin and vasopressin and into hundreds for the more recently discovered hormones, the author has in nearly every case given only the most important results. He has avoided discussing structure–activity relationships based on molecular geometry, apparently preferring not to give an opinion on the well-worn theme of the relevance of three-dimensional structures in solution and at the receptor. Nevertheless, many readers would have appreciated some references to the literature on hormone studies using NMR spectroscopy and molecular dynamics silmulations (MDS), especially since the book's subtitle refers to "structures", not merely to sequences.

One hopes that this work of reference will be updated every three to five years and enlarged as appropriate. The book will be a valuable resource for all scientists working in relevant interdisciplinary fields and needing to have access to the most recent published work on peptide hormones. However, it is not a substitute for a textbook, nor does it claim to be.

Günther Jung
Institut für Organische Chemie
der Universität Tübingen (FRG)

From Small Organic Molecules to Large: A Century of Progress. (Series: Profiles, Pathways, and Dreams. Series editor: *J. I. Seeman.*) By *H.F. Mark*. American Chemical Society, Washington, DC, 1993. XXVI, 148 pp., hardcover $ 24.95.—ISBN 0-8412-1776-9

Although he was not the world's first polymer chemist, Herman Francis Mark was known as the father of polymer science because of his many contributions to polymer science education and research, first in Europe and then in the United States. His fundamental contributions to science were multidisciplinary. His elder son Hans, a physicist and public official who served as Undersecretary of the U.S. Air Force and Chancellor of the University of Texas, said of him that "My father's greatest accomplishment was as a pioneer in applying modern physics to chemistry." Furthermore, no less an authority than Linus Pauling wrote of Mark, "He was ... one of the leading investigators in ... the use of X-ray diffraction for the determination of the structure of crystals in the years 1923 to 1928, and it was through this work that he developed the feeling for atoms and their interaction with one another that permitted him, later on, to make an effective attack on the problem of the structure and properties of macromolecules. ... I think of him ... as a pioneer in modern structural chemistry and an important early contributor to its development."

Unfortunately, the grand old man of polymer science did not live to see the publication of this autobiography; Mark died on April 6, 1992, less than a month before his 97th birthday. Fortunately, however, his friend and former student Herbert Morawetz not only contributed wonderful anecdotes to this posthumous volume but also edited and proofread the manuscript in its final stages. Furthermore, series editor Seeman has supplemented Mark's account of his life and work by judiciously adding throughout the book material provided by Mark and others that was previously published in *Polymer Science Overview: A Tribute to Herman F. Mark*, edited by G. A. Stahl, American Chemical Soci-

This section contains book reviews and a list of new books received by the editor. Book reviews are written by invitation from the editor. Suggestions for books to be reviewed and for book reviewers are welcome. Publishers should send brochures or (better) books to the Book Review Editor, Dr. Ralf Baumann, Redaktion Angewandte Chemie, Postfach 101161, D-69451 Weinheim, Federal Republic of Germany. The editor reserves the right of selecting which books will be reviewed. Uninvited books not chosen for review will not be returned.

ety, Washington, DC, 1981. Thus the picture of Mark that emerges from the book under review here is a complete and insightful one.

Mark was born in Vienna on May 3, 1895, the oldest of the three children of Dr. Herman Carl Mark, a Jewish surgeon who had become converted to Lutheranism, and his wife Lili (née Mueller), a Lutheran. Most of the elder Mark's friends were Jewish, and some were Zionists; later the younger Mark and his wife Marie (Mimi, née Schramek), a Catholic whom he had married in 1922, became ardent Zionists and traveled to Israel on several occasions. An older friend who was a physics student at the University of Vienna took young Mark to hear lectures by such scientific luminaries as Emil Fischer, Albert Einstein, Ernest Rutherford, and Marie Curie.

After graduating from high school (*Gymnasium*) in July, 1913, Mark decided to discharge his military obligation by enlisting in the Austrian army as a one-year volunteer (*einjährig-Freiwilliger*) in the fall of 1913, intending to begin his university studies in the fall of 1914. The outbreak of World War I frustrated his plans, and he served five years in a mountain infantry regiment on the Italian front, being wounded three times, earning fifteen medals, and becoming Austria's most decorated company-grade officer. At the end of the war, in November 1918, his entire division was captured by the Italians and he spent eleven months in a prison camp at a former convent in Monopoli, where he studied Italian, French, and English and with the help of the Italian textbooks organized a course in general chemistry. Always one to turn adversity to his own advantage, Mark later said of his imprisonment, "I have never since learned so much in so many different areas as in the Convento San Francisco" (p. 13). On returning to Vienna in 1919 he immediately returned to his study of chemistry at the university, which he had begun for one semester in 1915 during his recovery from a war wound. In July, 1921, he received his doctorate *summa cum laude* under Wilhelm Schlenk's direction with a dissertation on the pentaphenylmethyl free radical, the subject of the first of his more than 600 publications.

In 1922 Mark joined the most outstanding scientific institute of the time, the Kaiser-Wilhelm-Institut in Berlin-Dahlem, where he used newly developed experimental methods such as X-ray diffraction to study the molecular structures of natural textile fibers (e.g., cellulose, silk, and wool), which he showed to consist of long-chain molecules with molecular weights above 100,000. On the recommendation of K-W-I Director Fritz Haber, Mark then became an Assistant Director in the largest German chemical corporation of the time, IG Farbenindustrie, at Ludwigshafen am Rhein. There, during the period 1927–1932, he worked on electron diffraction and the synthesis and practical application of his results, but he still continued his fundamental studies of macromolecules and published two books. His process for the catalytic production of styrene from ethylbenzene, developed with Carl Wulff, lowered the cost of styrene and made possible the manufacture of polystyrene and Buna S synthetic rubber.

In view of the growing Nazi threat, Mark left Germany to become Professor of Chemistry at the University of Vienna (1932–1938), where, in addition to teaching physical chemistry, he developed the world's first academic curriculum in polymer science and technology at a time when only a few laboratories, mostly in industry, cultivated the subject and when no organized university courses were available. Here he authored two more books, continued his research, and traveled abroad extensively and routinely lectured at international conferences to publicize both his laboratory and the new discipline of modern polymer science.

Once again fate intervened. After helping Jewish colleagues to leave Austria, including Max Perutz, the future (1962) Nobel chemistry laureate, Mark was arrested on March 12, 1938, the day after Hitler's invasion, and imprisoned and interrogated for several days in a Gestapo prison in Vienna. In April, with only their clothes hung on covered coathangers made of platinum wire as a way of taking their valuables with them, Mark, his wife, two young sons, and his Jewish niece, crossed the border into neutral Switzerland disguised as alpine vacationers. After several months of traveling, the family finally arrived in Hawkesbury, Ontario, where Mark became Research Manager for the Canadian International Pulp and Paper Company (1938–1940). Here he modernized the methods and equipment, trained the laboratory personnel, and applied recent fundamental knowledge to practical production procedures. During this time he initiated the publication of the *Polymer Bulletin* and began the monograph series *High Polymers and Related Substances* (Interscience), which now contains more than forty volumes.

Having successfully completed his mission at Hawkesbury, in 1940 Mark became Adjunct Professor at the Polytechnic Institute of Brooklyn, which also provided a teacher's visa and a consultancy with the DuPont Company. He became Professor in 1942, and during World War II he directed a number of research projects that did not concern polymers for the U.S. government. In 1944 he organized the Institute of Polymer Research, the first of its kind in the United States, and continued as its Director until 1964. He was Dean of the Faculty (1961–1974) and continued to be active as a lecturer and writer long after his formal retirement in 1964 at the age of 69. The recipient of many honorary degrees and numerous honors, including the U.S. National Medal of Science in recognition of a lifetime of achievements in polymer science, Mark continued his extensive travels, visiting throughout his career more than a thousand scientists and engineers in more than a hundred countries (he traveled abroad about 500 times and visited every continent, including Greenland and Antarctica). When one of Mark's many students asked him how he managed to keep up the pace at an advanced age, Mark disclosed the secret of his longevity: "I guess I have no time to get old" (p. 122).

Mark's dominant personality trait was optimism, and although he could have dwelt on the misfortunes and indignities that he suffered during the 1930s, his narrative betrays no trace of bitterness, and he relates his achievements with a great degree of modesty. He prefers to concentrate on the chemistry itself; even his detailed account of his celebrated controversy with Hermann Staudinger over the nature of macromolecules, which Staudinger considered a personal affront, is free of any discussion of personalities, for Mark "had the amazing capacity to see the good side of everything and of everyone" (p. xxiii). Yet this book, which is replete with 41 formal and informal photographs, is an intensely personal one. It abounds with frank confessions that are also good advice for correct behavior. For example, on his concluding page Mark admits, "the treatment of people (scientists, executives, and government representatives) was sometimes so complicated that I never knew whether I was doing the right thing or not. There was only one simple overriding rule: keep cool and never lose your composure!" We warmly recommend this slim volume to scientists (polymer and otherwise), historians of science and technology, and anyone interested in polymers—the substances with which half of all professional chemists work.

George B. Kauffman,
Laurie M. Kauffman
California State University
Fresno, CA (USA)

Organic Superconductors (Including Fullerenes). Synthesis, Structure, Properties, and Theory. By *J. M. Williams* et al. Prentice Hall, Englewood Cliffs, NJ (USA), 1992. 400 pp., hardcover $ 91.10.—ISBN 0-13-640566-5

The authors of this book, most of whom are at the Argonne National Laboratory, Illinois, are international leaders in the field, with complementary expertise in the areas of organic and inorganic materials chemistry, theoretical chemistry, spectroscopy, X-ray crystallography, and solid state physics. They have combined forces to deliver an excellent up-to-date overview of organic superconductors and related highly conducting organic molecular materials (conducting polymers are excluded). This book will be welcomed by active researchers and interested spectators alike. These materials are crystalline charge-transfer salts formed by combinations of specific organic π-donor or π-acceptor molecules. The first organic superconductor was discovered in 1979 and since then there has been vigorous interest in this multi-disciplinary field of research. About 70 organic superconductors are now known, with transition temperatures as high as 33 K in the fullerene series.

The book is divided into eight chapters with three appendices. The main topics are: organic synthesis of the constituent electron donor and acceptor building blocks; structural aspects of these molecules and their derived salts; electrical and superconducting properties; spectroscopic, magnetic, and theoretical studies. A list of well-selected references is given at the end of each chapter. The book is well produced and the reviewer found no factual or typographical errors. Good use is made of diagrams (especially X-ray crystal structures) and tables of data, for ease of correlation of the structural, electrical, and magnetic properties of series of salts where there are minor changes in the constituent moieties. The inter-relationship between different solid-state properties is emphasized. For example, the key role of crystal stacking motifs in determining the transition temperature for the onset of superconductivity is discussed in detail.

The book focuses mainly on tetrachalcogenofulvalene systems; superconducting salts of fulleride anions are described briefly in an appendix which is mainly based on the 1991 literature, so some of this section is rapidly becoming out of date. The book also contains a list of the names and addresses of researchers in the field of organic superconductivity, although it is not quite clear what the criteria are for inclusion in this list! The book concludes with an adequate index of the key materials and subjects covered in the text.

The past decade has witnessed such dramatic, and often unexpected, advances in organic superconductors that it is impossible to predict what the future holds. However, there is no doubt that exciting new experimental and theoretical discoveries could emerge at any time, and that this topic will remain at the forefront of science for a long time. A key goal is to synthesize organic materials with transition temperatures raised to above 100 K, to compete with the ceramic superconductors. This is the best single volume on the subject that has been published, and it has a valuable place in the fast-growing literature on organic superconductors.

Martin R. Bryce
Department of Chemistry
University of Durham
Durham (United Kingdom)

Antibiotics and Antiviral Compounds. Chemical Synthesis and Modification. Edited by *K. Krohn, H. A. Kirst* and *H. Maag*. VCH Verlagsgesellschaft, Weinheim/VCH Publishers, New York, 1993. 482 pp., hardcover DM 128.00, £ 53.00.—ISBN 3-527-29040-0/1-56081-745-3

This book contains a detailed report of an international conference on the synthesis of antibiotics, which has taken place at two-yearly intervals since 1988. The 1992 meeting reported here was held in Kloster Banz, Bavaria (FRG). The subject of antibiotics syntheses is now more topical than ever before. One reason for this is that the synthesis of antibiotics (and other natural products), which initially served to give final proof of a proposed structure, has now developed so that versatile methods for targeted syntheses make it possible to explore variations of essential structural elements and to progress in a systematic way on the basis of structure–activity relationships. A second reason is that there is a growing need to develop ever more effective and selective drugs to combat resistant strains of bacteria, as well as cancer and retroviruses, so as to maintain the present high standard of available therapeutic measures. The subject of antibiotics syntheses as originally understood has therefore been enlarged to include "New Methods" (of making antibiotics) and "Antiviral Agents" (undoubtedly connected with the pressures on the science generated by AIDS), each of these topics being represented by a chapter in the book. The other five chapters are concerned with particular groups of antibiotics, three with the important and well-established areas of macrolides, β-lactams, and carbohydrates (insofar as these are involved in the synthesis of antibiotics), and two with newer areas, firstly peptides and glycopeptides, and secondly the enediyne antibiotics that have become so important in cancer chemotherapy. General aspects, such as synthetic methods and strategies, receptors research, and conformational analyses of bioactive natural products of current interest, are scattered throughout the chapters.

The editors have tried to avoid the heterogeneity usually associated with conference reports by arranging the contents in seven chapters and presenting an outward appearance of uniformity. Nevertheless, the way in which the individual contributions have been assigned to chapters sometimes seems rather forced, and is even wrong in a few cases (for example, the article on echinocandins, which are cyclopeptides, has been allocated to the chapter on macrolides).

The "New Methods" range from organometallic reactions, such as Pd^0-catalyzed allyl substitutions (B. M. Trost), cross-couplings in combination with direct *o*-metallization reactions (V. Snieckus), and the use of Pd^0 reagents to synthesize cyclopropanes which can then be rearranged to give medium-sized O-heterocycles (R. K. Boeckmann), through the use of thiazoles as masked formyl groups in the synthesis of β-amino-α-hydroxyacids (A. Dondoni), to the derivatization of antibiotics using microorganisms (A. Zeeck et al.).

The chapter on macrolides includes descriptions of total syntheses of rutamycin B (J. D. White), erythronolide A (R. W. Hoffmann et al.), and erythronolide B (J. Mulzer et al.). Also some new methods are reported here; for example, White describes the thermal decomposition of ω-hydroxy-*S*-acylxanthates, and Hoffmann describes a stereoselective crotylboration. The convergent synthesis described by Mulzer et al. uses the acetonide of the glyceraldehyde as the only chiral building element; it is a nice example of the modern trend towards versatile synthetic methods mentioned earlier, since in addition to the original target molecule it can be used to prepare various derivatives. To end this chapter G. Höfle and H. A. Kirst discuss new macrolides and their semi-synthetic derivatives, as well as their biological effects, etc.

The chapter on β-lactams describes the penems that are marketed commercially

as antibiotics, followed by new synthetic monobactams, and penicillin and monobactam analogues which act as peptidase inhibitors. This work is being carried out by industrial research teams. The last two articles, one on the chemistry of quinolones (D. Bouzard) and the other on syntheses of cyclopentanoid antibiotics using organophosphorus and organosulfur reagents (M. Mikolajczyk), do not fit well into this chapter.

The topics covered in the peptides chapter include the synthesis of dipeptides with antimycotic activity (H. Wild), studies of structure–activity relationships and mode of action for cyclopeptides with immunosuppressive activity (H. Fliri) and conformational analysis of these agents (H. Kessler et al.), and two contributions on glycopeptides, describing partial syntheses of virus outer shell proteins and tumor-associating antigens (H. Kunz) and attempted total syntheses of vancomycins, an important class of antibiotics (A. V. Rama Rao).

Work by American research groups on the total synthesis of the enediyne antibiotics (antitumor agents) caused a considerable sensation in recent years, so it is unfortunate that none of the eminent chemists who lead these groups attended the Kloster Banz symposium. Consequently the chapter on the enediynes is rather meager. New strategies developed at the Institute Chemie de Substances Naturelles in France and by M. Isobe and T. Nishikawa in Japan for the synthesis of various enediyne antibiotics (esperamicins, calicheamicins, dynemicin) are described. M. Hirama reports on methods for the synthesis of DNA-breaking model substances which contain the ten-membered core ring of neocarcinostatin, and on conformational studies of the neocarcinostatin complex by NMR spectroscopy. Lastly, D. Schinzer describes the use of allylsilanes as the basis of a method that can be used generally in natural products syntheses, and is especially useful for synthesizing calicheamicin model compounds.

The chapter on "Carbohydrates in Antibiotics Research" has as its introduction a contribution by P. Sinay with the same title. This is followed by descriptions of syntheses starting from sugar lactones or sugars as chiral elements (G. W. Fleet, H. J. Altenbach, and Y. Chapleur), and methods for synthesizing common antibiotic sugars, such as amino sugars (J. Jurczak et al.), and deoxy sugars (W. Klaffke), the latter via an enzyme cascade. P. Welzel discusses the role of carbohydrates in the biological activity of various antibiotics, taking the transglycosylase inhibitor moenomycin as an example; much knowledge of structure–activity relationships has been obtained from breakdown and synthesis studies.

Lastly, Chapter 7 is devoted to antiviral agents, especially nucleoside analogues with activity as HIV inhibitors. Here TSAO derivatives seem very promising, and their chemical synthesis, structure–activity relationships, and mode of action are described by J. Balzarini, E. De Clercq, and coworkers. Starting from 4′-azidothymidine as the lead structure, H. Maag has investigated other 4′-substituted nucleosides, whereas G. Jähne and coworkers have concentrated on carbocyclic phosphonate nucleoside analogues and A. Holy and coworkers on acyclic nucleotide analogues. E. Uhlmann discusses antisense technology and oligonucleotides that form triple helices, which offer promise as future alternatives to nucleoside analogues in the areas of antiviral agents and conventional therapies based on small-molecule agents.

The editors have devoted much effort to creating a unified whole from the texts supplied by the authors using a variety of word-processing and formula-drawing systems, resulting in a book which looks far better than most symposium reports, which merely collect together the individual typescripts. Despite this, it has not been possible to completely eradicate a certain amount of nonuniformity: for example, not every article has a summary, and there are differences in the method of giving literature references. Also it would have been useful to include a concise introduction to each of the seven topic areas. The comprehensive subject index is very good, enabling the reader to locate a particular topic without difficulty, and to find information on problems of current importance in the synthesis of active agents. Compared with the report by C. Bleasdale and B. T. Golding on the conference "Molecular Mechanisms in Bioorganic Processes" held in Newcastle upon Tyne (UK), this book is of a similarly high standard but does not go beyond that. It will be of interest to everyone involved in any way with biologically active natural products.

Jürgen Rohr
Institut für Organische Chemie
der Universität Göttingen (FRG)

 © VCH Verlagsgesellschaft mbH, D-69451 Weinheim, 1994 0570-0833/94/1010-1120 $ 10.00+.25/0

Are Polar Organometallic Compounds "Carbanions"? The Gegenion Effect on Structure and Energies of Alkali-Metal Compounds

Christoph Lambert and Paul von Ragué Schleyer*

Dedicated to Professor Ernst Otto Fischer on the occasion of his 75th birthday

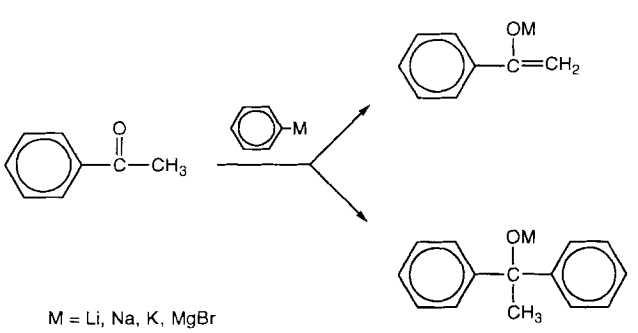
Polar organometallic compounds such as alkyllithium compounds or Grignard reagents often are conceived as "carbanions", although it is well known from experiments that the metal gegenions may have a strong, and often directing, influence on the reactivity (for example, the basicity vs. the nucleophilicity) of the "carbanion". This demonstrates that "carbanions" are tightly associated ion pairs, at least in commonly used less polar or nonpolar solvent systems like ethers or hydrocarbons. However, despite about ninety years of widespread application of these organometallic compounds as bases or nucleophilic reagents, the role of the gegenion is not yet understood fully. The focus of this review is on the inherent influences of the metal gegenion on the structures, reaction energies, and activation barriers of some representative alkali-metal compounds. While most comparisons of physical and chemical properties determined experimentally for Group I compounds are precluded due to different substituents, solvents, ligands, etc., ab initio calculations of model compounds can yield intrinsic data that are useful for a better understanding of chemical behavior. For this reason, most of the data reviewed in this article are based on quantum chemical calculations, which are compared with experimental data where available.

1. Introduction

The term *carbanion* was proposed for the first time in 1933 by E. S. Wallis to designate negatively charged carbon ions in contrast to the positively charged carbonium ions.[1] Most textbooks on Organic Chemistry use this term interchangeably for polar organometallic compounds (like alkyllithium derivatives, Grignard reagents, etc.) and for free carbanions. While this oversimplification may be useful for educational purposes, it hinders the proper insight into the chemistry of polar organometallic (*carbanionoid*) compounds. Very few synthetically important polar organometallic compounds undergo complete ion separation in solution, and even those do not involve "free" carbanions. For example, enolates and even large carbanions without heteroatom substituents are stabilized in alcoholic solvents by hydrogen bonding.[2] The carbanion moiety of most carbanionoid compounds like alkyl- or aryllithium derivatives in ether or hydrocarbon solvents are stabilized electrostatically by the metallic gegenion: contact ion pairs (CIP) with a distinct C–M bonding component are present. Moreover, most polar organometallic compounds do not exist as monomers but as higher aggregated species in which the metal may be associated with more than one carbanion center.[3]

Really free carbanions are present only in the gas phase.[3c, 4] However interesting, the gas phase chemistry of carbanions has not yet achieved any preparative application. In contrast, polar organometallic compounds like alkyllithium bases or Grignard compounds are widely used reagents in both preparative organic and inorganic chemistry.[5] Therefore, chemists are increasingly interested not only in synthetic applications but also in more basic aspects of the chemistry of carbanionoid compounds in condensed phase.

It is often observed that reactions with polar organometallic reagents may take totally different courses with different metal gegenions, even with the alkali metals.[6] For example, the attack of phenyl–M (M = Li, Na, K, MgBr) derivatives on acetophenone can yield two different products (Scheme 1):[7] eno-



Scheme 1. Metalation of acetophenone with phenylmetal compounds.

[*] Prof. Dr. P. von R. Schleyer, Dr. C. Lambert
Institut für Organische Chemie der Universität Erlangen-Nürnberg
Henkestrasse 42, D-91054 Erlangen (FRG)
Telefax: Int. code + (9131)859132

lates (by α-deprotonation) and carbinolates (by addition to the CO double bond).

The ratio enolate/carbinolate strongly depends on the metal gegenion. While phenylpotassium mainly results in enolate formation (enolate/carbinolate 10/1), the lithium and Grignard reagents give carbinolates predominantly (1/23 and $1/\infty$, respectively). Phenylsodium affords a 2:1 mixture. The regiospecificity was explained by the fact that the phenyl compounds of the heavier alkali metals have higher ionicity and thus stronger basicity than the Li derivative. However, as we will see later, the ionicity of all alkali-metal compounds with σ- *and* π-donating substituents (like the phenyl group) is very high and increases only slightly from Li to K.

In general, direct comparison of the gegenion influences on the reactivity suffers from some difficulties: the metal compounds (starting materials and products) may be differently aggregated depending on the metal. The type of solvents may influence the regiospecificity. Additional alkali-metal salts (depending on the experimental procedure used) also may alter the reaction course. The derivatives of the heavier alkali metals are not or only slightly soluble in hydrocarbons, and inhomogenous mixtures form. Unfortunately, more polar solvents are readily attacked by the bases. Complications due to additional coligands or varying substituents also preclude direct comparison of the gegenion influence.

Extensive work has been done to elucidate the gegenion effect on the reactivity in order to achieve specific synthetic purposes.[6] However, much-needed fundamental data are lacking, and there are few general concepts that might provide better insight into gegenion effects. While experimental measurements suffer from the problems associated with the complexity of the reagents, gas-phase investigations, which might yield basic data, are quite rare for polar organometallic compounds. However, ab initio SCF methods enable the behavior of polar organometallic molecules to be computed without interfering influences from solvation or aggregation.[8] This permits the elucidation of *intrinsic* gegenion effects—the prerequisite for the interpretation of experimental data. Ab initio calculations allow derivatives of all Group I metals to be compared on a common basis. This is often difficult or impossible by experimental methods. Therefore, most of data reviewed in this article are based on ab initio calculations. Comparisons are made with experimental data where available.

The following chapters focus on gegenion influences on the polarities, the structures, and the energies of the polar organometallic derivatives R^-M^+ (M = Li, Na, K, Rb, Cs). The polarity of a C–M bond is a basic property, as it is commonly expected that the more ionic the bond of the organometallic derivative the more carbanion-like it will be. The structures of polar organometallic compounds, particularly as demonstrated by X-ray methods, have recently been extensively reviewed.[9] We emphasize here examples that reveal *intrinsic* gegenion effects on the structure of the carbanionic moiety. While R^- is in most cases derived from a C–H acid, we will also regard the alkali-metal derivatives of some N–H acids, as these behave like carbanionoid compounds. Alkali-metal amides are often used as nonnucleophilic alternatives for alkyl- or aryllithium bases in synthetic organic chemistry.[5]



P. von R. Schleyer



C. Lambert

Paul von Ragué Schleyer was born in 1930 in Cleveland, Ohio, USA. After education at Princeton and Harvard Universities he obtained his Ph.D. with P. D. Bartlett at Harvard (1957). He became Full Professor at Princeton in 1965 and finally Eugene Higgins Professor there in 1969. In 1976 he accepted his present position as Professor and Codirector of the Institut für Organische Chemie der Universität Erlangen-Nürnberg. Amongst his many honors he received the Dr. honoris causa of the University of Lyon, the Adolf von Baeyer Memorial medal of the Gesellschaft Deutscher Chemiker, the James Flack Norris Award in Physical Organic Chemistry of the American Chemical Society, the C. K. Ingold Medal and Lectureship of the Royal Society of Chemistry, London, and the A. C. Cope Scholar Award of the American Chemical Society. He is a Fellow of the Bayerische Akademie der Wissenschaften and has been guest professor at nearly 30 universities. He is coauthor and editor of seven books on carbonium ions, quantum chemistry, and lithium chemistry. At present he is the president of the World Association of Theoretical Organic Chemists. His research interest covers experimental and theoretical studies on hydrocarbon cage compounds, carbocations, organic and inorganic lithium compounds as well as boron cage compounds.

Christoph Lambert, born in 1966 in Nürnberg, graduated in chemistry at the University of Erlangen-Nürnberg with a diplom thesis on water-complexed organolithium structures with Professor Schleyer, under whom he completed his Ph.D. degree in 1993. His major interests are experimental and theoretical investigations of the mechanisms of the lithiation of NH, CH, and OH acidic compounds, the solid-state structures of lithiated heterocycles, and the influence of gegenions in alkali-metal compounds. He received the doctoral award of the Hoechst AG as well as a doctoral grant from the Fonds der Chemischen Industrie. Since October 1993 Lambert has held a postdoc position with R. Snaith at the University of Cambridge, England, as a NATO research fellow.

2. The Carbon–Metal Bond in Polar Organometallic Compounds

The nature of the carbon–lithium bond has been examined in many theoretical and experimental investigations.[10] While the degree of ionicity of the C–Li bond is not a measurable quantity, the behavior of organolithium derivatives should be more carbanion-like, if the C–M bond is more polar. After many years of controversy, the highly ionic character of the C–Li bond is now well established.

The erroneous early conclusion that lithium–carbon bonding is predominantly covalent was based on the low melting points, the solubility in nonpolar solvents, and the high volatility of some organolithium compounds.[11] These properties contrasted with those typical of, for examples, the alkyl derivatives of the heavier alkali metals. However, these differences in physical properties reflect the structures of discrete organolithium *aggregates*: the outer sphere of ethyllithium tetramer[12] and *n*-butyllithium hexamer,[13] for instance, offer only hydrocarbon environments externally. Such compounds behave similarly to hydrocarbons, despite the ionic nature of their central cores.

The experimental observation of $^{13}C,^{6}Li$ and $^{13}C,^{7}Li$ NMR coupling[14] and early INDO (INDO = intermediate neglect of differential overlap) calculations (which overestimated the magnitude) of the coupling constants[10c] also provided evidence for at least some covalent bonding: the C,Li coupling is due to the Fermi-contact term, involving s-orbital contributions from both atoms.[15] The small change in the ^{13}C NMR chemical shift of the lithiated carbon, for example, in methyllithium relative to methane also seems to be consistent with a covalent C–Li bond.[16] However, this NMR evidence has been reinterpreted more recently. IGLO chemical shift calculations (IGLO = individual gauge for localized orbitals) shows that ^{13}C chemical shifts of the carbanionic carbons of alkyllithium compounds do not depend on the charge, and differ little from the shifts of the parent hydrocarbons.[17]

The $^{13}C,^{6}Li$ coupling constants depend only on the aggregation and *not* on the carbon hybridization.[18] This contrasts with the behavior of the covalent C–H bonds (see Table 1) and supports an ionic C–Li bonding concept. The very small but decreasing C–Li covalency from sp^3 through sp^2 to sp carbon hybridization compensates for the small but increasing carbon s-orbital contribution from sp^3 through sp^2 to sp: the product of C–Li bond order and s-orbital character in % of the carbon is nearly constant (see Table 2).

Table 1. $^{6}Li,^{13}C$ Coupling constants [Hz] of differently aggregated organolithium compounds [18b] and $^{1}H,^{13}C$ coupling constants [Hz] of some hydrocarbons [15].

		$^{1}J(^{13}C,^{6}Li)$		$^{1}J(^{13}C,^{1}H)$
monomer	$(CH_3)_3CLi$	14.7	CH_4	125
	PhLi	15.6	$H_2C{=}CH_2$	156
			HC≡CH	249
dimer	$(n\text{BuLi})_2$	7.8		
	$(\text{PhLi})_2$	8.0		
	$(t\text{BuC}{\equiv}\text{CLi})_2$	8.3		
tetramer	$(n\text{BuLi})_4$	5.5		
	$(H_2C{=}CHLi)_4$	5.8		
	$(t\text{BuC}{\equiv}\text{CLi})_4$	6.0		

Table 2. Calculated NLMO C–Li bond orders [a] (MP4SDTQ(FC)/6-31++G**//MP2(FU)/6-31G** level) and contributions of s orbitals for some organolithium compounds [19].

	C-Li bond order	s character of the C σ bond orbital [%]	Product of bond order and s character [%]
CH_3Li	0.144	19	2.7
$H_2C{=}CHLi$	0.099	28	2.8
HC≡CLi	0.046	52	2.4

[a] NLMO = Natural Localized Molecular Orbital [24].

The experimentally determined (as well as the computed[46]) high dipole moment (6 D) of methyllithium[20] as well as ESCA shifts (ESCA = electron spectroscopy for chemical analysis)[21] of MeLi and EtLi also support a high degree of ionic character in the C–Li bonding.

Wiberg and Rablan[22] recently reviewed several quantum chemical population analysis procedures critically. While these provide easily obtained estimates of the C–Li bond ionicity, they are based on different definitions. Among others, the Mulliken analysis,[23] Natural Population Analysis (NPA) by Reed and Weinhold et al.,[24] and the AIM topological density analyses by Bader et al.[25] (AIM = atoms in molecules) were applied to calculate the partial charges of methyllithium. While the Mulliken and the NPA analysis are founded on orbital transformations (for NPA the natural atomic orbitals (NAO)) Bader analysis is based on electron density. The partial charges based on partitioning of the basis functions in the Hilbert space as it is performed in the Mulliken or the NPA analysis is not a quantum mechanical observable. Thus, it is not a physical reality but an interpretation.[26] In contrast, the total electron density is an observable and can be measured by X-ray scattering experiments or computed ab initio.

The Mulliken population analyses of organolithium compounds calculated ab initio show a polar but nevertheless predominantly covalent C–Li bonding (16–57% ionic, depending on the basis set used).[8a] This is now recognized as an artifact. The Mulliken population analysis overestimates the electron density on alkali metals and thus underestimates the polar character of the carbon–metal bond.[24a, 27] In contrast, NPA gives a seemingly more realistic picture almost independent of the basis set. This population analysis indicates about 80–90% ionic character for the C–Li bond.[24a, 28]

Both the integrated spacial electron population by Collins and Streitwieser[29] and the Laplacian density analysis (topological density analysis) by Bader et al.[25, 30] are based on electron density. The latter defines regions in a molecule by calculating zero-flux surfaces. Integration of the electron density within these regions gives the charge of the atom. Both analyses also reveal an 80–90% ionic bonding contribution in the C–Li bond of methyllithium.[29, 30]

However, calculations of the electron deformation density $\Delta\rho$ from experimental electron densities ($\Delta\rho = \rho_{exp} - \rho_{calc}$; ρ_{exp}: electron density from X-ray structures; ρ_{calc}: electron density of a "promolecule" with spherical electron densities on the atomic centers[31]) did not allow definite conclusions on the nature of the C–Li bonding, since changes in electron density derived from X-ray diffractions are not significant enough to distinguish between Li^0 and Li^+ atoms.[32]

Streitwieser et al.[33] argued that the small electron density within the C–Li bond is a criterion for a very weak covalent bond contribution (about 80% ionic). However, other ab initio calculations on MeLi by Lipscomb et al.[34] showed that this argument cannot be applied as an indicator for the degree of covalency, since, for example, the purely covalent Li_2 has a lower charge density in the Li–Li bond than MeLi. These authors estimate the ionic contribution in the C–Li bond to be only 55–60%.

Horn and Ahlrichs[35] used a different approach to evaluate the high ionicity of MeLi. The Hartree-Fock/self-consistent field (HF/SCF) energy change ($\Delta E = E^k_{SCF} - E_{SCF}$) when MeLi was forced to have a pure ionic bonding was calculated. The SCF energy (E_{SCF}) of methyllithium was subtracted from the SCF energy (E^k_{SCF}) of a completely ionic methyllithium computed without any 2 s and 2 p valence orbitals on lithium. The small energy difference of $\Delta E = 7.0$ kcal mol^{-1} (compared with the homolytic bond dissociation energy of 46.4 kcal mol^{-1}[46]) reflects the covalent contribution and shows the bond to be highly ionic.

The linear correlation of calculated dimerization energies for some lithium compounds with Pauling electronegativities also implies mainly electrostatic bonding.[36] A nearly identical correlation resulted from a point charge model using the ab initio geometries.[8c, 36] However, electrostatic point charge calculations of tetrameric lithium compounds do not agree with the oligomerization energies derived from ab initio calculations.[37] Purely electrostatic calculations of some aggregates of lithium and cesium compounds (using point charge models and hard sphere electrostatic calculations) resulted in structural conclusions that are in good agreement with experimental observations.[38] Alternative explanations use covalent multicenter bondings (electron-deficient bondings) similar to those in diborane.[8c, d, 39] However, this model is inadequate, since polar organometallic compounds do not seek to fulfill the "octet rule". This becomes obvious in the numerous higher coordination modes of the metal cation in alkali-metal complexes,[40] in which the number of electrons formally assigned to the metal exceeds eight, for example in [CpLi([12]crown-4)],[41] where the number of electrons at Li formally is 14! Hence, "electron counting" plays no role in the discussion of polar organometallic chemistry. Likewise, it is misleading to regard these compounds as being electron-deficient. There is no electron-sufficiency or electron-deficiency in highly ionic species.

The mainly ionic nature with small but not negligible covalent contributions (revealed, for example, by the $^{13}C,^6Li$ coupling) of the C–M bonds in alkali-metal compounds is now widely accepted. The ionicity agrees with the common observation that polar organometallics mostly react by ionic mechanisms.[5] Compounds of alkaline earth metals and some other organometallic derivatives also have strongly ionic C–M bonding. Table 3 shows the natural charges (NPA) calculated ab initio on the metal of the methyl compounds of alkali, alkaline earth, and other main-group and late transition metals.[3c]

The NPA charges reveal an ionic bonding contribution of 74–94% for the M–CH_3 bond in the methyl derivatives of the alkali and alkaline earth metals. The NPA charges on both alkali-metal and alkaline earth methanides are quite similar within each period. However, methyllithium is more ionic than dimethylberyllium and even than methylsodium. Figure 1 shows the NPA metal charges of some alkali-metal compounds MX (X = H, CH_3, NH_2, OH, F, cyclopentadienyl (Cp)).[42]

Table 3. Natural charges [a] on the metal of some methyl metal compounds calculated ab initio. The charges in brackets are the total charges on the metal divided by the number of methyl groups [3c].

MCH_3	$M(CH_3)_2$	$M(CH_3)_2$	$M(CH_3)_3$	$M(CH_3)_4$
Li (0.87)	Be 1.49 (0.74)		B 1.02 (0.36)	C −0.12 (−0.03)
Na (0.79)	Mg 1.55 (0.77)		Al 1.87 (0.62)	Si 1.85 (0.46)
K (0.90)	Ca 1.78 (0.89)	Zn 1.41 (0.71)	Ga 1.68 (0.56)	Ge 1.69 (0.42)
Rb (0.90)	Sr 1.82 (0.91)	Cd 1.36 (0.68)		Sn 1.95 (0.49)
Cs (0.93)	Ba 1.88 (0.94)	Hg 1.17 (0.59)		Pb 1.74 (0.44)

[a] The charges were calculated at the HF level. Ab initio pseudopotential calculations were used for the methyl compounds of Li, Na, K, Rb, Cs, Ca, Sr, Ba, Zn, Cd, Hg, Cd, Sn, and Pb. All other compounds were calculated at the HF/6-31 + G* level.

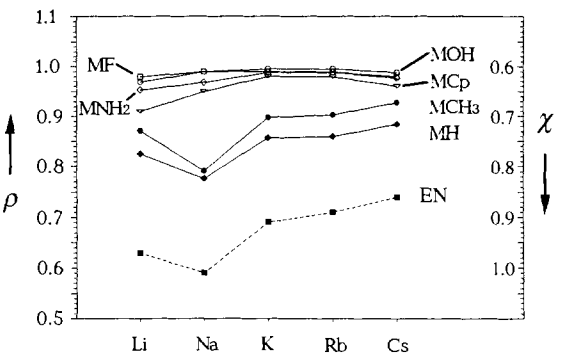


Fig. 1. Natural charges (ρ) on the metal calculated ab initio at the HF level (left scale) for the MX compounds (M = Li–Cs; X = CH_3, H, NH_2, OH, F, Cp) and Allred–Rochow electronegativities EN (χ, right scale) of the alkali metals [43].

While the NPA charges of MX compounds with σ-donor substituents (H, CH_3) follow the nonmonotonous trend of the Allred–Rochow electronegativities χ,[43] the MX derivatives with highly electronegative σ- *and* π-donating substituents (X = NH_2, OH, F, Cp) are distinctly more ionic and do not show any irregular behavior. In the MH and MCH_3 species Li is less electronegative than Na, while the electronegativity decreases from Na to Cs. This was attributed to the better shielded nuclear charge in Li than in Na and in the other heavier alkali metals: the effective nuclear charge eZ_{eff} is lower in lithium, and therefore a relatively small electron-attracting force (= electronegativity) of $F = e^2Z_{eff}/r^2$ (r = covalent radius) is observed for Li. (For a thorough discussion of the "inverted" Na–Li electronegativity, see Ref.[42].) That Li rather than Na behaves irregularly can also be seen in the relatively low IP of Li compared to the general trend for the other alkali metals (Fig. 2).[44]

In derivatives with π-donating substituents the larger polarity of Li compounds is compensated by small π populations on the metal. Thus, a monotonous trend of the ionicity for Li to Cs species results. Two kinds of organo alkali-metal species (σ-bonded such as MCH_3 and σ- + π-bonded such as MCp) must be distinguished, due to their different electronic structures.

Owing to the general high polarity of the organometallic compounds of alkali and alkaline earth metals, it seems reasonable to regard the M–X (X = CR_3, NR_2, OR, F) bond as fully

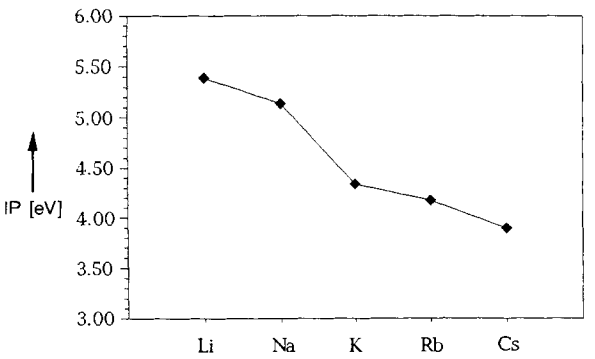


Fig. 2. Experimental ionization potentials (IP) of the alkali metals [44].

ionic. Small σ- and π-back donation from the substituent to the metal slightly reduces the ionicity.

Whereas the methyl derivatives of zinc and cadmium also show significantly polar M–C bonding, the C–Si to C–Pb bonds in $M(CH_3)_4$ have more covalent than ionic character (see Table 3). The bonding of mercury, aluminum, and gallium methanides is intermediate.

The polarity of the Li–C bond increases with the s-orbital contribution to the carbon hybridization: $sp^3 < sp^2 < sp$ (see Table 4).[9b, 45] The NPA charge in methyllithium does not increase monotonously with the degree of aggregation. However, the polarity is slightly higher in the dimer and the tetramer than in the monomer.[28, 45, 46] Ab initio calculations of methyllithium show that the NPA charge on the metal *decreases* upon dimethyl ether solvation. In contrast, the metal charge increases slightly for methylsodium and dimethylmagnesium (Table 4).[47] Therefore, an increase in the polarization of the C–M bond (and thus an increase in the reactivity) upon solvation is not general for all metals.

Table 4. Natural charges ρ on the metal depending on the carbon hybridization, the aggregation [45], and the solvation by dimethyl ether [47].

	ρ_{NPA} (M)		ρ_{NPA} (M)		ρ_{NPA} (M)
CH_3Li	0.853 [a]	CH_3Li	0.853 [a]	CH_3Li	0.841 [c]
$H_2C{=}CHLi$	0.900 [a]	$(CH_3Li)_2$	0.875 [a]	$CH_3Li\cdots O(CH_3)_2$	0.797 [c]
$HC{\equiv}CLi$	0.949 [a]	$(CH_3Li)_3$	0.853 [b]	CH_3Na	0.752 [c]
		$(CH_3Li)_4$	0.857 [a]	$CH_3Na\cdots O(CH_3)_2$	0.796 [c]
				$(CH_3)_2Mg$	1.502 [d]
				$(CH_3)_2Mg\cdots O(CH_3)_2$	1.560 [d]

[a] MP4SDTQ(FC)/6-31++G**//MP2(FU)/6-31G**. [b] MP4SDTQ(FC)/6-31++G**//MP2(FU)/6-31+G*. [c] MP4SDTQ(FC)/6-31+G*//MP2(FU)/6-31(+)G* (no diffuse (+)-functions on the metal in the geometry optimization). [d] MP4SDQ(FC)6-31+G*//MP2(FU)/6-31+G*.

3. Stability of Organo Alkali-Metal Compounds

3.1. Stabilization by Contact Ion Pair Formation

In solution as well as in the solid state, carbanions are stabilized by the gegenion; contact ion pairs (CIP) form often. The stabilization energy is very high and can be estimated by simple electrostatic point charge calculations: a $C^- - Li^+$ distance of 2.0 Å corresponds to a coulombic attraction of 166 kcal mol^{-1},[3c] which is in good agreement with the heterolytic bond dissociation energy of $LiCH_3$ (168.9 kcal mol^{-1}).[48] The stabilization energy is smaller for larger cations and decreases with increasing ionic radius: Li > Na > K > Rb > Cs. Ab initio calculations of the heterolytic bond dissociation energies of the alkali-metal cyclopentadienides ($CpM \rightarrow Cp^- + M^+$) confirm this trend: 182.4 (CpLi), 145.4 (CpNa), 132.2 (CpK), 126.0 (CpRb), and 124.0 kcal mol^{-1} (CpCs).[49] Experimental solvation enthalpies of the alkali-metal cations in water are considerably smaller: Li (119.4), Na (93.2), K (73.1), Rb (67.2), and Cs (59.3 kcal mol^{-1}).[50]

Solvent-separated ion pairs (SSIP) in which the anion and the cation are separated by their solvent shells [Eq. (a)] may form in some cases.[51] This depends on the competition between the

$$\underset{\text{CIP}}{[R^-M^+]_{solv}} \rightleftharpoons \underset{\text{SSIP}}{[R^-||M^+]_{solv}} \rightleftharpoons \underset{\text{dissociated ion pair}}{[R^-]_{solv} + [M^+]_{solv}} \quad \text{(a)}$$

solvation of the cation (solvation of the anion is less important, since the commonly used ether solvents are better at solvating cations than anions) and the electrostatic stabilization of the carbanion by the gegenion. The more delocalized the charge on the anion (this is, the weaker the anion–cation interaction) and the more polar the solvent, (that is, the stronger the cation–solvent interaction) the likelier is the formation of SSIPs. Since the cation–solvent interaction is stronger for smaller cations, lithium salts of resonance-stabilized anions in weakly polar solvents like THF form SSIPs, whereas analogous cesium salts in THF form CIPs. The formation of SSIPs of lithium cations with resonance-stabilized anions is exemplified in some solid-state structures of, for example, fluorenyl anion systems.[52] In some cases, solvent-shared ion pairs form, in which the cation and the carbanion are bridged by solvent molecules. In these ion pairs, the carbanionic moiety is solvated by hydrogen bonding from the solvent molecules.[53] Dissociated ion pairs only occur to a significant extent in very dilute solutions of lithium salts if the negative charge of the carbanion is delocalized and the cations are strongly coordinated by the solvent.[54]

3.2. Relative Metalation Energies

A direct measure for the stability (energy) of an alkali-metal compound is its ion pair acidity relative to a standard compound [Eq. (b)].[55]

$$RH + R'M \rightleftharpoons RM + R'H \quad \text{(b)}$$

The ion pair acidities of many compounds were determined by Streitwieser et al. in various solvent systems like cyclohexylamine[56] and THF[57] by equilibrium or kinetic methods. RM compounds derived from very acidic CH acids and in which the negative charge is delocalized form SSIPs when lithium is the gegenion[57c] and CIPs when cesium is the gegenion (at 10^{-4} M concentration range).[54, 58] The ion pair acidities of these lithium and cesium compounds are very similar.[54, 3c] However, the

acidity of anions with localized charge may be quite different: the acidity of the cesium ion pair of phenylacetonitrile in THF is 22.7 and of the corresponding lithium ion pair, 17.7.[59] This is due to the formation of monomeric CIPs of the lithium salt; the Li^+ ion is attached to the nitrile group.[60] The lithium cation stabilizes the phenylacetonitrile anion better than the cesium cation because of the smaller Li–N distance. Thus, phenylacetonitrile appears to be more acidic as an ion pair with lithium than with cesium. A similar behavior was observed for NH acids. The acidity of the cesium ion pair of carbazole is 19.1, whereas that of the analogous lithium ion pair is 13.8.[61] The enhancement of the acidity of CH acids was considerably weaker because of the formation of aggregates.[62]

Although the results from equilibrium acidity measurements in THF are quite instructive, they only refer to very acidic CH acids. The alkyl and aryl alkali-metal compounds used widely in synthesis are too basic to be measured in THF. The proton transfer is too slow, and solvent decomposition becomes a serious problem. However, the solvating power of less acidic and inert solvent systems like hexane is too weak, and aggregates form. Arnett et al. reported the deprotonation enthalpies of alcohols by many synthetically important lithium and potassium alkyl and aryl compounds, as well as amides and alkoxides (for some examples see Table 5).[63] Since these compounds are aggregated to different extents, direct comparisons are complicated. Figure 3 shows a reasonably good correlation (slope = 1.07) between the experimental stabilization energies (relative to *t*BuOLi) and calculated stabilization energies[92, 94] of some monomeric organolithium bases. Only methyllithium significantly deviates from the correlation, which is certainly due to the different solvent used (diethyl ether). Nevertheless, the deprotonation enthalpies are a valuable estimate of basicity since the data pertain to "realistic" conditions.

Table 5. Enthalpies ΔH [kcal mol^{-1}] for the metalation of isopropyl alcohol by some synthetically important organolithium bases and potassium bis(trimethylsilyl)amide in hexane/ether (90/10) [63], as well as the experimentally determined and calculated (MP2(FU)/6-31G*//MP2(FU)/6-31G* level [92, 94]) stabilization energies ΔE, referred to *t*BuOLi (RLi + *t*BuOH → RH + *t*BuOLi) [kcal mol^{-1}].

Base	$-\Delta H$	$-\Delta E_{exp.}$	$-\Delta E_{calcd}$
tert-butyllithium	56.2 ± 1.8	54.1	56.5
sec-butyllithium	52.8 ± 1.0	50.7	54.9
n-butyllithium	50.0 ± 0.7	47.9	52.4
phenyllithium	42.3 ± 0.3	40.2	42.6
methyllithium	41.6 ± 0.7 [a]	39.5	34.6
lithium diisopropylamide	28.6 ± 1.0	26.5	
lithium 2,2,6,6-tetramethylpiperidide	30.4 ± 1.6	28.3	
lithium bis(trimethylsilyl)amide	15.2 ± 0.5	13.1	
potassium bis(trimethylsilyl)amide	2.9 ± 0.3 [b]	0.8	
lithium *tert*-butoxide	2.1 ± 0.6	0.0	0.0 [c]

[a] In diethyl ether. [b] In THF/toluene (85/15). [c] MP2(FC)/6-31+G*//MP2(FC)/6-31+G*.

However, metalation equilibria of some simple monomeric alkali-metal derivatives calculated ab initio can yield intrinsic C–M bond strengths. As we learned in Section 2, we have to distinguish between two kinds of alkali-metal compounds:[42] slighty covalent MX species with almost exclusively σ-donating substituents (e.g., X = H, CH_3) and almost fully ionic MX compounds with highly electronegative σ- and π-donating substituents (X = NH_2, OH, F, Cp). From these two sets we can form three types of metalation reactions: firstly, reactions between compounds of the σ-donating group [(c)]; secondly, metalation reactions between species from different groups [(d)–(g)]; and thirdly, reactions between compounds of the σ- and π-donating group [(h)].

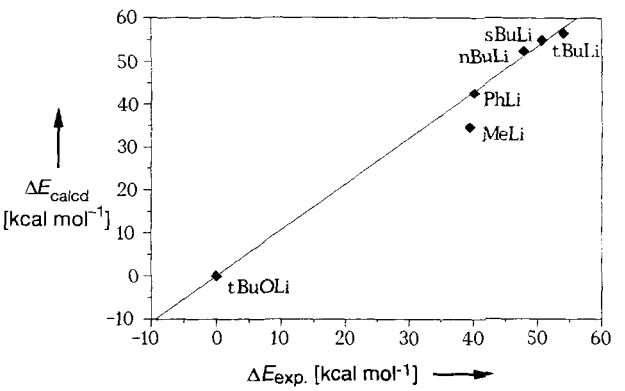


Fig. 3. Calculated (MP2(FU)/6-31G*//MP2(FU)/6-31G* level, ΔE_{calcd}) vs experimental ($\Delta E_{exp.}$) stabilization energies relative to *t*BuOLi. The data are from Table 5; the data point of MeLi was not used for the calculation of the correlation line (slope = 1.07).

$$MCH_3 + H_2 \rightarrow MH + CH_4 \quad (c)$$

$$MCH_3 + NH_3 \rightarrow MNH_2 + CH_4 \quad (d)$$

$$MCH_3 + H_2O \rightarrow MOH + CH_4 \quad (e)$$

$$MCH_3 + HF \rightarrow MF + CH_4 \quad (f)$$

$$MCH_3 + CpH \rightarrow MCp + CH_4 \quad (g)$$

$$MOH + CpH \rightarrow MCp + H_2O \quad (h)$$

The reaction energies for reactions (c) to (h) are displayed in Figure 4. Since covalent contributions strengthen the M–X bonds, the different ionicity (see Fig. 1) directly influences the relative metalation energies of alkali-metal compounds. The reaction energies of (c) are nearly independent of the metal, since the trends in ionicity (and thus the stability) in MH and MCH_3

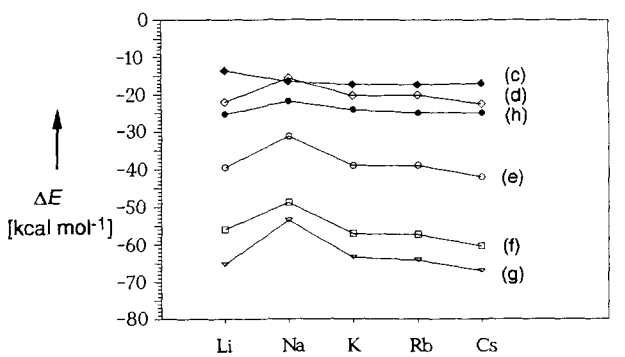


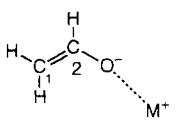
Fig. 4. Metalation energies (ΔE) for the reactions (c) to (h) calculated ab initio at the MP4 level (MP2 for (g) and (h)) [42].

compounds are parallel. In contrast, reaction energies between MCH_3 (σ-donating ligand) and NH_3, H_2O, HF, and CpH (σ- and π-donating ligand) show a nonmonotonous trend along the Li to Cs series [(d) to (g)]. The metalation reactions are more exothermic for Li than for Na since $LiCH_3$ is more ionic (less stable) than $NaCH_3$. Reactions between compounds of the group with σ- and π-donating substituents [e.g. (h)] are also almost independent of the metal.

3.3. Charge Localization by the Gegenion: a Destabilizing Effect

Although the overall coulombic cation–anion interaction is highly favorable (see Section 3.1), the gegenions serve to *localize* the charge of the anion. This competes, in effect, with delocalization by resonance, negative hyperconjugation, and polarization.

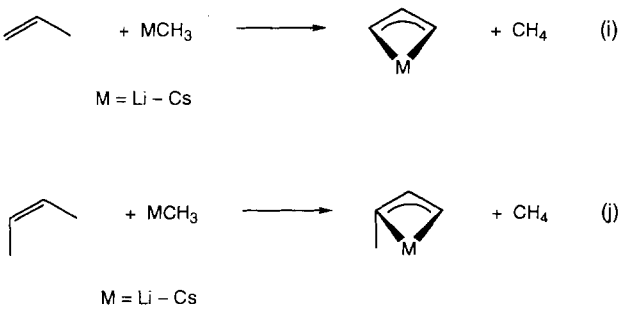
The degree to which the charge-localizing effect of the metal cation destabilizes anions has been evaluated by ab initio calculations of, for example, the geometries, the electronic structures, and the metalation energies of alkali-metal acetaldehyde enolates **1** (Table 6).[64] All the metal ions have near unit charges (0.96 to 1.00). Both the total and the π charges on oxygen are distinctly smaller in the free enolate anion than in the alkali-metal derivatives. The polarizing, charge-localizing influence of the cations is responsible for the larger harges on oxygen in the metal enolates. However, there is only a slight decrease from the Li to the other alkali-metal enolates.



1 M = Li – Cs

The energetic consequences of charge localization are dramatic: the stabilization of the enolate anion relative to that of the hydroxyl anion is very large (about 33 kcal mol^{-1}) (see Table 6). The gegenions in the metalated enolates reduce the stabilization to only 9–14 kcal mol^{-1} relative to MOH. However, the variation in the stabilization along the Li to Cs series is only modest and does *not* reflect the large increase in the O–M distances. Due to the charge-localizing gegenion effect, the resonance stabilization in the alkali-metal enolates is about 19 to 24 kcal mol^{-1} smaller than in the free enolate. The localizing influence is still very effective for long O–M distances (e.g., O–Cs, 2.547 Å).

Similar trends were observed for the metalation of propene and butene with MCH_3, yielding the allyl[65, 66] (e.g. **4**) and the crotyl[66] alkali-metal derivatives, respectively [reactions (i) and (j), Table 7]. Again, the metalation energies show a non-



monotonous trend since a σ-bound alkali-metal derivative (MCH_3) is transformed into a π-bound species (allyl–M) (cf. 3.2). The reaction energies of the metal derivatives are considerably lower than those of the free anions. Even for rubidium the energies do not approach the values for the free anions. The attenuation of charge stabilization in the allyl and crotyl metal

Table 7. Reaction energies ΔE [kcal mol^{-1}] calculated ab initio at the HF/6-31+G level for the metalation of propene [Eq. (i)] and butene [Eq. (j)] with methyl alkali-metal compounds, and for deprotonation with the methyl anion [65, 66].

M	ΔE	
	Eq. (i)	Eq. (j)
Li	−14.4	−12.0
Na	−12.0	−9.7
K	−17.3	−13.4
Rb	−18.9	−14.9
–	−28.2	−27.9

Table 6. Bond lengths [Å], angles [°], and natural charges (ρ) calculated ab initio at the HF level for vinyl alcohol, alkali-metal acetaldehyde enolates (**1**), and the acetaldehyde enolate ion [a] [64], as well as reaction energies ΔE [kcal mol^{-1}] calculated ab initio at the MP2 level for the metalation of vinyl alcohol with alkali-metal hydroxides ($H_2C{=}CHOH + MOH \rightarrow H_2C{=}CHOM + H_2O$) and its deprotonation with the hydroxide ion [64].

M	d(C1-C2)	d(C2-O)	d(O-M)	α(M-O-C)	α(O-C-C)	ρ(C1) [b]	ρ(C1) [b]	ρ(O) [b]	ρ(M) [b]	ΔE
H	1.318	1.340			126.9	−0.498	0.289	−0.749		
						(−0.176)	(0.086)	(−0.913)		
Li	1.332	1.296	1.613	175.2	127.2	−0.571	0.341	−1.131	0.962	−9.4
						(−0.272)	(0.137)	(−0.855)	(0.988)	
Na	1.340	1.286	1.977	179.1	128.0	−0.623	0.365	−1.103	0.988	−12.3
						(−0.331)	(0.163)	(−0.833)	(0.998)	
K	1.342	1.284	2.289 [c]	171.0	128.1	−0.634	0.375	−1.101	0.994	−13.2
						(−0.343)	(0.168)	(−0.826)	(0.997)	
Rb	1.343	1.282	2.447 [c]	170.1	128.2	−0.642	0.378	−1.093	0.994	−13.7
						(−0.352)	(0.172)	(−0.820)	(0.996)	
Cs	1.342	1.284	2.547 [c]	170.0	128.1	−0.635	0.377	−1.097	0.988	−12.9
						(−0.344)	(0.169)	(−0.822)	(0.991)	
–	1.372	1.244			130.4	−0.790	0.424	−0.923		−32.8
						(−0.513)	(0.213)	(−0.702)		

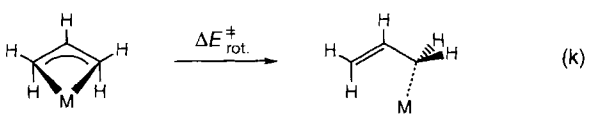
[a] All compounds were optimized using ab initio pseudopotential methods. [b] Values in brackets are natural π charges. [c] MP2(FU) optimized distances.

species is due to charge localization at C1 and C3 by the gegenion (see **4**, Section 4.2). Since the metal cations are situated above the plane of the π system, the charge localization acts *perpendicularly* in the allyl and crotyl derivatives. Hence, the localizing effect (and the destabilization relative to the free anion) is smaller than in the alkali-metal acetaldehyde enolates, where the charge localization acts less symmetrically *in* the plane of the π system.

Charge localization also influences the UV/VIS absorption maxima of alkali-metal compounds. The closer the gegenion is to the anion (i.e., the smaller the cation), the stronger the charge-localizing influence. The electrostatic stabilization of the anion in the ground state relative to the excited state increases with this size trend from Cs to Li. Thus, the excitation energy increases, and a red shift of the absorption maximum is observed in CIPs when going from the Li to the Cs salts. The effect is even more pronounced in SSIPs.[58, 67]

3.4. Rotation and Inversion Barriers in Organometallic Compounds of Alkali Metals

The alkali-metal salts of allyl anions are the prototypes of π-bound polar organometallic species. While allyllithium is an unsymmetrical dimer in THF solution,[68] allylsodium and allylpotassium are symmetrical monomers.[69] NMR studies[70] as well as ab initio calculations[65] were carried out to determine the rotational barrier about the C–C bonds via a *syn*-M–C_3H_5 transition state [Eq. (k)]. Table 8 shows that theoretical and experimental data are in good agreement if a dimeric structure is assumed for allyllithium. With increasing ionic radius of the gegenion, the rotational barriers approach the value of the free allyl anion.



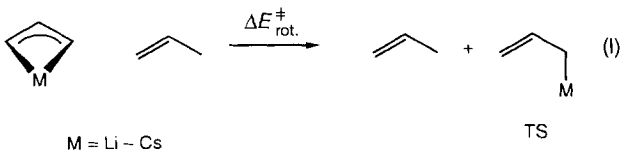
(k)

Table 8. Experimental and calculated rotational barriers [kcal mol^{-1}] of allyl alkali-metal compounds [65].

	Li	Na	K	Rb	Cs	Free anion
$\Delta E^{\ddagger}_{rot.}$ (exp.) [g] (T [°C])	10.7 [a] (– 51)	11.5 [b, e]	16.7 [a] (68)	18.1 [b] (68)	18.0 [a] (68)	
$\Delta E^{\ddagger}_{rot.}$ (calcd)	13.0 [c]	13.4 [d]	17.4 [d]	19.0 [d]	21.8 [d]	21.7 [f]

[a] Ref. [70a]. [b] Ref. [70b]. [c] Dimer, 3-21G. [d] Monomer, MP2(FU)/6-31 + G* (Huzinaga basis set for K, Rb, Cs). [e] ΔE^{*}. [f] MP2(FU)/6-31 + G**. [g] Determined as ΔG.

If the transition state is regarded as a vinylmethyl anion σ-bound to the metal, the rotation refers to a metalation reaction in which a π-bound alkali-metal derivative is converted into a σ-bound species [Eq. (l)]. As mentioned in Section 3.2, this type



(l)

of reaction should result in a *nonmonotonous* trend of the reaction energies along the Li to Cs series. Indeed, this is found for the rotational barriers of the monomeric alkali-metal allyl derivatives (Fig. 5). The example shows very well that the intrinsic course of reaction (activation) energies can be hidden by the formation of aggregates.

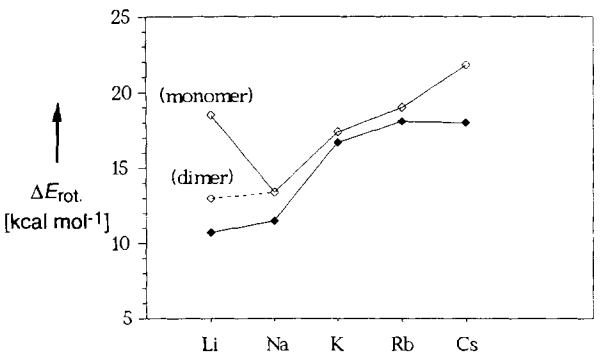


Fig. 5. Experimental (•) and calculated (◇) rotational barriers ($\Delta E^{\ddagger}_{rot.}$) of the allyl alkali-metal compounds (see Table 8) [65].

Whereas the inversion barrier of the free methyl anion is quite low (smaller than 2 kcal mol^{-1}),[71] that of monomeric methyllithium is considerably higher (28.0 kcal mol^{-1}, MP2(FU)/6-31 + G*//MP2(FU)/6-31 + G*).[72] In tetrameric methyllithium the barrier is 14.3 kcal mol^{-1} (combined ab initio/MNDO calculations),[45] in good agreement with the inversion barrier of 2-methylbutyllithium (approximately 15 kcal mol^{-1}).[73] Thus the inversion behavior of monomeric MeLi is not equivalent to that of the methyl anion.

4. Influence of Gegenions on the Structures

4.1. Methyl Derivatives

The solid-state structures of all the alkali-metal methyl compounds were determined by Weiss et al.[74] Both methyllithium[75a–c] and methylsodium[75d–f] crystallize in a cubic space group as tetrameric aggregates. The metal atoms form a tetrahedron and the methyl anions are centered above the tetrahedral faces. In contrast, potassium,[76] rubidium, and cesium methanides[77] crystallize in a hexagonal space group of the NiAs type. Only the cell parameters increase from K to Cs (however, a recent neutron diffraction study including hydrogen atom positions revealed a larger orthorhombic cell for KCH_3[76b]). The deviation in lattice types for $LiCH_3$ and $NaCH_3$ from those for the heavier alkali-metal methanides is rationalized by the different ratios of ionic radii of the alkali-metal cations and the methyl anion. Li^+ (0.69 Å) and Na^+ (0.97 Å) have similar

ionic radii, as do K^+ (1.33 Å), Rb^+ (1.47 Å), and Cs^+ (1.67 Å).[9b]

Although the hydrogen atom positions were determined in some cases by neutron diffraction methods, different aggregation and crystal types preclude direct comparison of the structures of the methyl anion moieties. Ab initio calculations of the monomeric alkali-metal methyl compounds[42] yield C–M distances that are systematically too short due to the monocoordination of the metal cations (Table 9). However, the M-C-H

Table 9. Experimental bond lengths [Å] and calculated bond lengths [Å], angles [°], and natural charges ρ of the methyl alkali-metal compounds [42].

	Li	Na	K	Rb	Cs
experiment (aggregates)					
d(MC)	2.26 [a]	2.53–2.68 [b]	2.95–3.44 [c]	3.36 [d]	3.53 [d]
ab initio [e] (monomers)					
d(M-C)	2.002	2.343	2.698	2.859	2.956
	(2.004)	(2.343)			
d(C-H)	1.090	1.087	1.091	1.092	1.094
	(1.090)	(1.087)			
α(M-C-H)	112.3	111.0	112.4	112.4	112.8
	(111.6)	(110.0)			
ρ_{NPA}(M)	0.87	0.79	0.90	0.90	0.93

[a] Neutron diffraction [75c]. [b] Neutron diffraction [75d, e]. [c] Neutron diffraction [76b]. [d] X-ray analysis [77]. [e] HF geometries for Li and Na (MP2(FU)/6-31+G** in parenthesis), d(M-C) MP2-optimized for K, Rb, Cs. HF-NPA charges. 1-valence-electron effective-core potential (ve-ecp) for Li, Na; 9-ve-ecp for K, Rb, Cs; 4-ve-ecp for C. Basis sets: Li, Na: (2111/31/1); K–Cs: (21111/21111/11); C: (311/311/1); H (311/11).

angles follow the trend of the natural charges on the metal. $CsCH_3$ is the most polar compound and has the widest M-C-H angle (112.8°), that is, the most pyramidal CH_3^- group. $NaCH_3$ shows the smallest angle (111.0°) corresponding to the smallest metal charge. The more polar the C–M bond, the more pyramidal the methyl anion. The M-C-H angle does not approach the value for the angle between the CH bond and the C_{3v} axis in the free methyl anion (109.5°)[78] when going from Na to Cs. Instead, *all* M-C-H angles are wider (the methyl anion is more pyramidal). This is due to the charge-localizing effect of the gegenions: the anionic lone-pair orbital is more localized (has more s character) in the metal species, and thus, the CH_3^- group is more pyramidal than in the free anion. The M-N-H angles of the alkali-metal amides also follow the ionicity of the M–N bond (see Table 10). Parallel with the smooth increase of the polarity from Li to Rb, the smallest M-N-H angle is found in $LiNH_2$ and the widest in $RbNH_2$.[42]

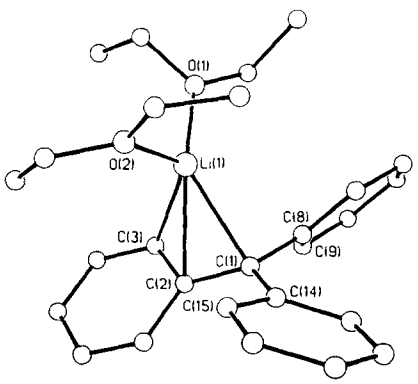
The charge-localizing, pyramidalizing influence can also be observed in the alkali-metal derivatives of triphenylmethane, where charge localization by the gegenion competes with charge delocalization into the phenyl groups. The X-ray structures are known for all the alkali metals (for example, for $Ph_3CLi \cdot 2\,Et_2O$ **2** and for $Ph_3CCs \cdot PMDTA$ **3** (Figs. 6, 7))[79–82] as is a structure of a solvent-separated ion pair with $[Li([12]crown-4)_2]^+$ as the gegenion[83] (Table 11). The monomeric lithium CIP derivatives display a distinctly pyramidal methyl carbon atom (12 pm out of the plane formed by the *ipso* carbon atoms C2, C8, and C14), whereas the triphenylmethyl anion moiety is

Table 10. Calculated bond lengths [Å], angles [°], and natural charges ρ of the alkali-metal amides [a] [42].

	Li	Na	K	Rb	Cs
d(M-N)	1.753	2.107	2.428	2.585	2.668
	(1.755)	(2.120)			
d(N-H)	1.000	1.001	1.003	1.004	1.004
	(1.015)	(1.017)			
α(M-N-H)	127.4	127.8	128.3	128.3	128.2
	(127.6)	(127.7)			
ρ_{NPA}(M)	0.953	0.968	0.988	0.989	0.977

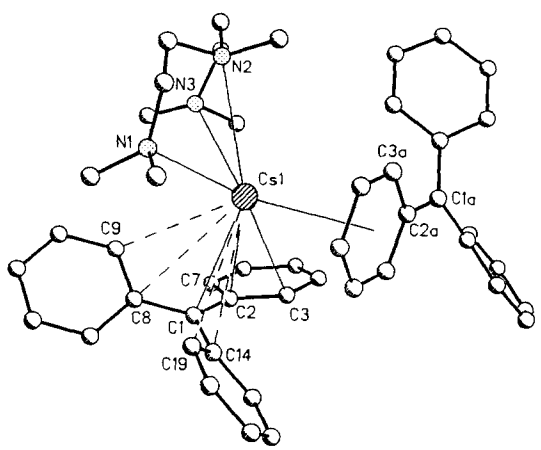
[a] HF geometries for Li and Na (MP2(FU)/6-31+G** values in parenthesis), d(M-N) MP2-optimized for K, Rb, Cs. HF-NPA charges. 1-valence-electron effective-core potential (ve-ecp) for Li, Na; 9-ve-ecp for K, Rb, Cs; 5-ve-ecp for N. Basis sets: Li, Na: (211/31/1); K, Rb, Cs: (21111/21111/11); N: (311/311/1); H (311/11).

essentially planar in the heavier alkali-metal compounds. The compounds with Rb and Cs are polymeric in the solid-state, and the alkali-metal cations are multihapto-coordinated by at least



2

Fig. 6. Crystal structure of **2** [80].



3

Fig. 7. Crystal structure of **3** [82].

one phenyl substituent. This exemplifies the tendency of the heavier alkali-metal derivatives to form multihapto structures. Similar trends in multihapticity were found in alkali-metal carb-

Table 11. Experimentally determined structures of triphenyl alkali-metal salts.

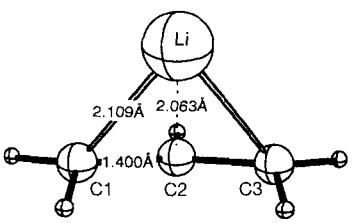
	Ph_3CLi	Ph_3CLi	Ph_3CNa	Ph_3CK	$(Ph_3CRb)_x$	$(Ph_3CCs)_x$	Ph_3C^-
ligand [a]	TMEDA	$2\times Et_2O$	TMEDA	PMDTA/THF	PMDTA	PMDTA	$[Li([12]crown\text{-}4)_2]^+$
C coordination	η^4+2 N	η^3+2 O	$\eta^5+\eta^1+2$ N	η^6+3 N $+1$ O	$2\times\eta^6+3$ N	$\eta^6+\eta^3+3$ N	8 O
d(C1-C2,C8,C14 plane) [Å]	0.12	0.12	0.004	0.01	planar	0.007	planar
d(M-C1) [Å]	2.23	2.31	2.64	-	-	3.35	-
d(M-ring center) [Å]	-	-	-	2.87	3.19	3.33	-
Ref.	[79]	[80]	[81]	[82]	[82]	[82]	[83]

[a] TMEDA = *N,N,N',N'*-tetramethylethylenediamine; PMDTA = pentamethyldiethylenetriamine.

azolides,[84] sulfinimidamides,[85] and pyridyldiphenylmethyl derivatives.[86]

4.2. Allyl Derivatives

Ab initio calculations predict symmetrically bridged structures for the monomeric alkali-metal allyl compounds (e.g. **4**, Fig. 8).[65] In all cases, the hydrogen atoms are bent out of the C1-C2-C3 plane. Because of the antibonding character of the HOMO and the charge repulsion of C1 and C3, a wider C1-C2-C3 angle than in propene is expected in the allyl anion. The C1-C2-C3 angle of the allyl as well as the crotyl alkali-metal compounds increase on going from the Li to the Cs derivatives (Table 12). The electrostatic interaction of the small lithium cation with C1 and C3 results in the smallest C1-C2-C3 angle. The large Cs^+ is further away from C1 and C3. Thus, a C1-C2-C3 angle nearly as wide as that of the free anion results for allylcesium. In contrast, the C1–C2 and C2–C3 distances (1.398–1.400 Å) only vary to a minor extent along the Li to Cs series. Although some solid-state structures are known for allyllithium[87] and sodium[88] derivatives, direct comparison with the calculations is precluded by the different allyl substituents and ligands attached to the metal cation. The experimental values for the C1-C2-C3 angles range between 125° and 132° for the allyllithium derivatives and between 127° and 130° for the sodium species.



4

Fig. 8. Structure of **4** according to ab initio calculations [65].

Table 12. Calculated distances [Å] and angles [°] for propene, the allyl alkali-metal compounds, and the allyl anion [a] [65].

	propene [d]	Li	Na	K	Rb	Cs [b]	free anion [c]
d(M-C1,3)		2.109	2.503	2.811	3.052	3.299	
d(M-C2)		2.063	2.441	2.791	3.025	3.227	
d(C1,3-C2)	1.336 1.496	1.400	1.400	1.398	1.399	1.398	1.396
α(C1-C2-C3)	124.5	126.0	128.7	129.3	130.1	130.4	131.5

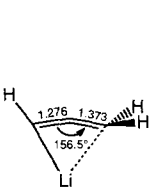
[a] MP2(FU)/6-31G** and Huzinaga basis sets for K, Rb, Cs. [b] MP2(FU)/6-31G*. [c] MP2(FU)/6-31+G**. [d] MP2(FU)/6-31G**, ref. [94].

4.3. Acetaldehyde Enolates

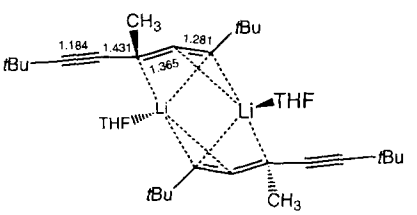
The charge-localizing influence of the gegenion on the geometries of the alkali-metal acetaldehyde enolates (**1**) also is apparent (Table 6; see Section 3.3).[64] The C1–C2 separation is shortest in the vinyl alcohol (1.318 Å) (which has no charge and only modest resonance stabilization). The C–C length increases to 1.332 Å in CH_2CHOLi, but then only approximately an additional 0.01 Å along the Na to Cs series. The free acetaldehyde enolate anion has by far the longest C–C distance (1.372 Å). The variations in the C–O distances are complementary. The shortest separation (1.244 Å) is found in the enolate anion and the largest (1.340 Å) in vinyl alcohol. Due to the partial C–O double-bond character, the values in the metal enolates are intermediate (about 1.29 Å). The known X-ray structures of Li, Na, and K enolates[9c,d] do not show any regular variation in the C–C and C–O bond lengths. Again, different aggregation states, solvation, and substituents are responsible for the irregularities. The quite different structures of the Cs enolate and the free enolate anion show again that the charge-localizing influence is still significant for long M–O separations.

4.4. Allenyl Derivatives

Carbanionoid allenyl compounds exhibit unusual structural features. Allenyllithium compounds are not vinylic derivatives. Instead, a nonclassically 1,3-bridged structure (**5**) with a distinctly bent carbon skeleton is preferred, because the metal cation is



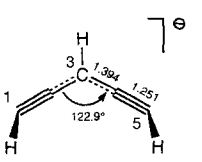
5 C_s MP2(FU)/6-31G*



6



7 C_s MP2(FU)/6-31+G*



8 C_s MP2(FU)/6-31+G*

coordinated to the second double bond.[89] This arrangement is exemplified in the X-ray structure of the dimeric, lithiated 2,2,5,8,8-pentamethyl-3,6-nonadiyne **6**.[9a, 90] In contrast, the free allenyl anion **7** is almost linear.[89c, 91] The vinylic alternative of allenyllithium where the Li^+ is sited in the direction of the former hydrogen atom is not a minimum structure on the hypersurface: optimization of this structure leads without barrier to the bridged structure **5**.[89a] The free parent carbanion (**8**, diethynylmethyl anion) of the lithium compound **6** has a symmetrical C_s structure (MP2(FU)/6-31+G*);[92] the negative NPA-charge is localized at C1, C3, and C5. In contrast, the lithium compound **6** is an unsymmetrically bridged allenyl derivative. The metal cation localizes the negative charge within the allenyl moiety.[93] That the alkynyl substituent does not stabilize the charge effectively by π conjugation is apparent from the similar C–C distances within the allenyl moiety (1.37 and 1.28 Å), but the quite different C–C distances within the alkynyl substituent (1.43 and 1.18 Å). The sodium salt of 2,2,5,8,8-pentamethyl-3,6-nonadiyne is a nonbridged monomer.[93] The C–C distances are analogous to those of **6** (in the allenyl moiety 1.38 and 1.24 Å, in the alkynyl substituent 1.44 and 1.19 Å).

5. Conclusions

The NPA population analyses of several alkali-metal derivatives MX with M = Li, Na, K, Rb, Cs and various X (H, CH_3, NH_2, OH, F, Cp) show that the M–X bond is predominantly ionic in all cases. Moreover, one has to distinguish two different types of organometallic MX species: derivatives with σ-donor substituents (prototype MCH_3) and species with σ- *and* π-donor substituents (prototype MCp). While the former are slightly covalent and show a nonmonotonous trend of ionicity from Li to Cs, the latter are almost fully ionic. Metalation reactions between these groups exhibit a nonmonotonous trend following the (weak) covalency (bond strength) of the σ-donor compounds. Reaction energies within each group are nearly independent of the metal.

Despite the high polarity of the metal derivatives, the energetic properties of these compounds (such as relative metalation energies) do not necessarily tend toward those for the free anions on going from Li to Cs. The energies of some reactions (like the metalation of vinyl alcohol with MOH or the metalation of propene with MCH_3) are smaller than that of the corresponding reaction with the free anion because of charge localization by the gegenion. Even for large cations (e.g. Cs^+), the reaction energies are considerably lower than those of the free anions. In contrast, the rotation barriers of the allyl alkali-metal compounds approach the value of the free anion for larger gegenions (Rb^+ and Cs^+).

The influence of the gegenions on the geometries of the carbanion moiety also is significant. For example, the gegenion localizes the charge and enhances the pyramidalization with respect to the methyl anion in methyl alkali-metal compounds. The allenic structure of salts of the dialkynylmethyl anion also is due to charge localization.

Both the intrinsic structures and energies of polar organometallic compounds are influenced substantially by the gegenion. The description of polar organometallic compounds as "*carbanions*" is inadequate and misleading and should be avoided. Further theoretical and experimental work is needed to elucidate the gegenion influence on the energies of aggregates and solvated species as well as on the activation barriers of reactions of polar organometallic compounds.

This work was supported by the Deutschen Forschungsgemeinschaft, the Convex Computer Corporation, and the Fonds der Chemischen Industrie (scholarship to C. L.).

Received: June 23, 1993 [A 4]
German version: *Angew. Chem.* **1994**, *106*, 1187

[1] E. S. Wallis, F. H. Adams, *J. Am. Chem. Soc.* **1933**, *55*, 3838.
[2] a) L. M. Jackman, B. C. Lange, *Tetrahedron Lett.* **1977**, *33*, 2737; b) I. McEwen, M. Rönnqvist, P. Ahlberg, *J. Am. Chem. Soc.* **1993**, *115*, 3989; see also ref. [53].
[3] General introduction to the chemistry of polar organometallic compounds: a) M. Schlosser, *Struktur und Reaktivität polarer Organometalle*, Springer, Berlin, **1973**; b) J. L. Wardell in *Comprehensive Organometallic Chemistry, Vol. 1* (Eds.: G. Wilkinson, F. G. A. Stone, E. W. Abel), Pergamon Press, Oxford, **1982**, p. 1; c) C. Lambert, P. von R. Schleyer, *Methoden Org. Chem. (Houben-Weyl) 4th Ed. 1952-*, Bd. E19d, **1993**, p. 1.
[4] a) M. J. Pellerite, J. I. Brauman in *Comprehensive Carbanion Chemistry, Vol. A* (Eds.: E. Buncel, T. Durst), Elsevier, Amsterdam, **1980**, p. 55; b) N. M. M. Nibbering, *Adv. Phys. Org. Chem.* **1988**, *24*, 1; c) R. R. Squires, *Acc. Chem. Res.* **1992**, *25*, 461.
[5] a) B. J. Wakefield, *Organolithium Compounds*, Pergamon Press, Oxford, **1974**; b) J. C. Stowell, *Carbanions in Organic Synthesis*, Wiley, New York, **1979**; c) B. J. Wakefield, *Organolithium Methods*, Academic Press, London, **1988**; d) L. Brandsma, H. Verkruijsse, *Preparative Polar Organometallic Chemistry 1*, Springer, Berlin, **1987**; e) L. Brandsma, *Preparative Polar Organometallic Chemistry 2*, Springer, Berlin, **1990**; f) *Comprehensive Organic Synthesis, Vol. 1* (Eds.: B. M. Trost, I. Fleming), Pergamon Press, Oxford, **1991**, g) M. Schlosser in *Modern Synthetic Methods, Vol. 6* (Ed.: R. Scheffold), Verlag Helvetica Chimica Acta, Basel, and VCH, Weinheim, **1992**, p. 227.
[6] a) ref. [3a], Chapter 3.4; b) ref. [5d], Chapter II.14; ref. [5g].
[7] W. I. O'Sullivan, F. W. Swamer, W. J. Humphlett, C. R. Hauser, *J. Org. Chem.* **1961**, *26*, 2306.
[8] a) W. J. Hehre, L. Radom, P. von R. Schleyer, J. A. Pople, *Ab Initio Molecular Orbital Theory*, Wiley, New York, **1986**, Chapter 7.3.2; b) R. H. Nobes, D. Poppinger, W.-K. Li, L. Radom in *Comprehensive Carbanion Chemistry, Vol. C* (Eds.: E. Buncel, T. Durst), Elsevier, Amsterdam, **1987**, p. 1; c) P. von R. Schleyer, *Pure Appl. Chem.* **1983**, *55*, 355; d) *ibid.* **1984**, *56*, 151.
[9] a) W. N. Setzer, P. von R. Schleyer, *Adv. Organomet. Chem.* **1985**, *24*, 353; b) C. Schade, P. von R. Schleyer, *ibid.* **1987**, *27*, 169; c) P. G. Williard in ref. [5f], p. 1; d) D. Seebach, *Angew. Chem.* **1988**, *100*, 1685; *Angew. Chem. Int. Ed. Engl.* **1988**, *27*, 1624; e) G. Boche, *ibid.* **1989**, *101*, 286 and **1989**, *28*, 277; e) P. R. Markies, O. S. Akkerman, F. Bickelhaupt, W. J. J. Smeets, A. L. Spek, *Adv. Organomet. Chem.* **1991**, *32*, 147; f) K. Gregory, P. von R. Schleyer, R. Snaith, *Adv. Inorg. Chem.* **1991**, *37*, 47; g) R. Mulvey, *Chem. Soc. Rev.* **1991**, *20*, 167; T. P. Hanusa, *Chem. Rev.* **1993**, *93*, 1023.
[10] See for example a) ref. [8a]; b) ref. [9b]; c) T. Clark, J. Chandrasekhar, P. von R. Schleyer, *J. Chem. Soc. Chem. Commun.* **1980**, 672, and references therein.
[11] a) U. Schöllkopf, *Methoden Org. Chem. (Houben-Weyl) 4th Ed. 1952-*, Bd. 13/1, **1970**, p. 7; b) G. E. Coates, M. L. H. Green, K. Wade, *Organometallic Compounds, Vol. 1*, Methuen, London, **1967**, p. 1; c) T. L. Brown, *Adv. Organomet. Chem.* **1965**, *3*, 365.
[12] a) H. Dietrich, *Acta Crystallogr.* **1963**, *16*, 681; b) *J. Organomet. Chem.* **1981**, *205*, 291.
[13] T. Kottke, D. Stalke, *Angew. Chem.* **1993**, *105*, 619; *Angew. Chem. Int. Ed. Engl.* **1993**, *32*, 580.
[14] a) L. D. McKeever, R. Waack, M. A. Doran, E. B. Baker, *J. Am. Chem. Soc.* **1968**, *90*, 3244; b) *ibid.* **1969**, *91*, 1057; c) G. Fraenkel, A. M. Fraenkel, M. J. Geckle, F. Schloss, *ibid.* **1979**, *101*, 4745; d) L. D. McKeever, R. Waack, *Chem. Commun.* **1969**, 750.
[15] H.-O. Kalinowski, S. Berger, S. Braun, *^{13}C-NMR-Spektroskopie*, Thieme, Stuttgart, **1984**, Chapter 4.
[16] L. D. McKeever, R. Waack, M. A. Doran, E. B. Baker, *J. Am. Chem. Soc.* **1969**, *91*, 1057.
[17] M. Bühl, N. J. R. van Eikema Hommes, P. von R. Schleyer, U. Fleischer, W. Kutzelnigg, *J. Am. Chem. Soc.* **1991**, *113*, 2459.
[18] a) W. Bauer, W. R. Winchester, P. von R. Schleyer, *Organometallics*, **1987**, *6*, 2371; b) W. Bauer, P. von R. Schleyer, *Adv. Carbanion Chem.* **1992**, *1*, 89.
[19] N. J. R. van Eikema Hommes, C. Lambert, P. von R. Schleyer, unpublished results.
[20] a) L. Andrews, *J. Chem. Phys.* **1967**, *47*, 4834; b) L. Andrews, T. G. Carver, *J. Phys. Chem.* **1968**, *72*, 1743.

[21] a) R. Moberg, Z. C. Yuan, S. Holmberg, F. Bökmann, P. Ahlberg, O. Bohman, H. Siegbahn, *J. Phys. Org. Chem.* **1989**, *2*, 417; b) G. F. Meyers, M. B. Hall, J. W. Chinn, R. J. Lagow, *J. Am. Chem. Soc.* **1985**, *107*, 1413.
[22] K. B. Wiberg, P. R. Rablan, *J. Am. Chem. Soc.*, submitted.
[23] R. S. Mulliken, *J. Chem. Phys.* **1962**, *36*, 3428.
[24] a) A. E. Reed, R. B. Weinstock, F. Weinhold, *J. Chem. Phys.* **1985**, *83*, 735; b) A. E. Reed, L. A. Curtiss, F. Weinhold, *Chem. Rev.* **1988**, *88*, 899.
[25] a) R. F. W. Bader, P. J. McDougall, *J. Am. Chem. Soc.* **1985**, *107*, 6788; b) R. F. W. Bader, *Acc. Chem. Res.* **1985**, *18*, 9; c) R. F. W. Bader, P. L. A. Popelier, T. A. Keith, *Angew. Chem.* **1994**, *106*, 647; *Angew. Chem. Int. Ed. Engl.* **1994**, *33*, 620; d) R. F. W. Bader, *Atoms in Molecules. A Quantum Theory* (*International Series of Monographs on Chemistry, Vol. 22*), Clarendon Press, Oxford, **1990**.
[26] However, the atomic population is an observable of the number operator $\hat{N}$ (integral form of ρ, when ρ is the electron density operator): R. F. W. Bader, P. F. Zou, *Chem. Phys. Lett.* **1992**, *191*, 54.
[27] M. M. Francl, R. F. Hout, W. J. Hehre, *J. Am. Chem. Soc.* **1984**, *106*, 563.
[28] N. J. R. van Eikema Hommes, P. von R. Schleyer, Y.-D. Wu, *J. Am. Chem. Soc.* **1992**, *114*, 1146.
[29] J. B. Collins, A. Streitwieser, *J. Comput. Chem.* **1980**, *1*, 80.
[30] J. P. Ritchie, S. M. Bachrach, *J. Am. Chem. Soc.* **1987**, *109*, 5909.
[31] a) K. Angermund, K. H. Klaus, R. Goddard, C. Krüger, *Angew. Chem.* **1985**, *97*, 241; *Angew. Chem. Int. Ed. Engl.* **1985**, *24*, 237; b) P. Coppens, *ibid.* **1977**, *89*, 33 and **1977**, *16*, 32.
[32] a) R. Amstutz, J. D. Dunitz, D. Seebach, *Angew. Chem.* **1981**, *93*, 487; *Angew. Chem. Int. Ed. Engl.* **1981**, *20*, 465; b) R. Amstutz, T. Laube, W. B. Schweizer, D. Seebach, J. D. Dunitz, *Helv. Chim. Acta* **1984**, *67*, 224.
[33] A. Streitwieser, J. E. Williams, S. Alexandratos, J. M. McKelvey, *J. Am. Chem. Soc.* **1976**, *98*, 4778.
[34] G. D. Graham, D. S. Marynick, W. N. Lipscomb, *J. Am. Chem. Soc.* **1980**, *102*, 4572.
[35] H. Horn, R. Ahlrichs, *J. Am. Chem. Soc.* **1990**, *112*, 2121.
[36] a) E. Kaufmann, T. Clark, P. von R. Schleyer, *J. Am. Chem. Soc.* **1984**, *106*, 1856; b) A.-M. Sapse, E. Kaufmann, P. von R. Schleyer, R. Gleiter, *Inorg. Chem.* **1984**, *23*, 1569.
[37] A.-M. Sapse, K. Raghavachari, P. von R. Schleyer, E. Kaufmann, *J. Am. Chem. Soc.* **1985**, *107*, 6483.
[38] a) A. Streitwieser, *J. Organomet. Chem.* **1978**, *156*, 1; b) R. J. Bushby, H. L. Steel, *ibid.* **1987**, *336*, C25; c) R. J. Bushby, H. L. Steel, *J. Chem. Soc. Perkin. Trans. 2* **1990**, 1143, 1169; d) R. J. Bushby, H. L. Steel, M. P. Tytko, *ibid.* **1990**, 1155.
[39] a) G. Graham, S. Richtsmeier, D. A. Dixon, *J. Am. Chem. Soc.* **1980**, *102*, 5759; b) C. Elschenbroich, A. Salzer, *Organometallchemie*, Teubner, Stuttgart, **1988**, p. 34; *Organometallics*, 2nd ed., VCH, Weinheim, **1992**, p. 22.
[40] a) U. Olsher, R. M. Izatt, J. S. Bradshaw, N. K. Dalley, *Chem. Rev.* **1991**, *91*, 137; b) N. S. Poonia, V. A. Bajaj, *ibid.* **1979**, *79*, 389.
[41] P. Jutzi, *J. Organomet. Chem.* **1990**, *400*, 1.
[42] C. Lambert, M. Kaupp, P. von R. Schleyer, *Organometallics* **1993**, *12*, 853.
[43] A. L. Allred, E. G. Rochow, *J. Inorg. Nucl. Chem.* **1958**, *5*, 264.
[44] C. E. Moore, *Natl. Bur. Stand. Circ. (US)* **1949**, 467. (*Atomic Energy Levels*).
[45] C. Lambert, N. J. R. van Eikema Hommes, P. von R. Schleyer, unpublished results.
[46] E. Kaufmann, K. Raghavachari, A. E. Reed, P. von R. Schleyer, *Organometallics* **1988**, *7*, 1597.
[47] N. J. R. van Eikema Hommes, P. von R. Schleyer, unpublished results.
[48] Determined by using the homolytic bond dissociation energy calculated with ab initio methods ($D(CH_3Li) = 46.4\ kcal\,mol^{-1}$ [46]; see also H. Schiffer, R. Ahlrichs, *Chem. Phys. Lett.* **1986**, *124*, 172), the electron affinity of the methyl radical ($EA(CH_3) = 1.8\ kcal\,mol^{-1}$, G. B. Ellison, P. C. Engelking, W. C. Lineberger, *J. Am. Chem. Soc.* **1978**, *100*, 2556), and the ionization potential of the lithium atom ($IP(Li) = 124.3\ kcal\,mol^{-1}$ [44]).
[49] Ab initio pseudopotential calculations at the HF level: C. Lambert, P. von R. Schleyer, unpublished results.
[50] Experimental hydration enthalpies: N. Wiberg, *Lehrbuch der anorganischen Chemie (Holleman-Wiberg)*, de Gruyter, Berlin, **1985**, p. 954.
[51] a) M. Szwarc, *Ions and Ion Pairs in Organic Reactions, Vol 1, 2*, Wiley, New York, **1972** and **1974**; b) J. Smid, *Angew. Chem.* **1972**, *84*, 127; *Angew. Chem. Int. Ed. Engl.* **1972**, *11*, 112; c) T. E. Hogen-Esch, *Adv. Phys. Org. Chem.* **1977**, *15*, 153; d) Y. Marcus, *Ion Solvation*, Wiley, New York, **1985**; e) G. Boche, *Angew. Chem.* **1992**, *104*, 742; *Angew. Chem. Int. Ed. Engl.* **1992**, *31*, 731.
[52] B. Becker, V. Enkelmann, K. Müllen, *Angew. Chem.* **1989**, *101*, 501; *Angew. Chem. Int. Ed. Engl.* **1989**, *28*, 458.
[53] S. Buchholz, K. Harms, M. Marsch, W. Massa, G. Boche, *Angew. Chem.* **1989**, *101*, 57; *Angew. Chem. Int. Ed. Engl.* **1989**, *28*, 72.
[54] M. J. Kaufmann, S. Gronert, A. Streitwieser, *J. Am. Chem. Soc.* **1988**, *110*, 2829.
[55] a) H. F. Ebel, *Methoden Org. Chem. (Houben-Weyl) 4th Ed. 1952–*, Bd. 13/1, **1970**, p. 31; b) A. Streitwieser, *Acc. Chem. Res.* **1984**, *17*, 353.
[56] a) A. Streitwieser, E. Juaristi, L. L. Nebenzahl in *Comprehensive Carbanion Chemistry, Vol. A* (Eds.: E. Buncel, T. Durst), Elsevier, Amsterdam, **1980**, p. 323; b) A. Streitwieser, J. H. Hammons, E. Ciuffarin, J. I. Brauman, *J. Am. Chem. Soc.* **1967**, *89*, 59; c) A. Streitwieser, E. Ciuffarin, J. H. Hammons, *ibid.* **1967**, *89*, 63.
[57] a) A. Streitwieser, D. A. Bors, M. J. Kaufmann, *J. Chem. Soc. Chem. Commun.* **1983**, 1394; b) D. A. Bors, M. J. Kaufmann, A. Streitwieser, *J. Am. Chem. Soc.* **1985**, *107*, 6975; c) S. Gronert, A. Streitwieser, *ibid.* **1986**, *108*, 7016; d) A. Streitwieser, J. C. Ciula, J. A. Krom, G. Thiele, *J. Org. Chem.* **1991**, *56*, 1074.
[58] a) T. E. Hogen-Esch, J. Smid, *J. Am. Chem. Soc.* **1966**, *88*, 307; b) *ibid.* **1965**, *87*, 669.
[59] M. J. Kaufmann, S. Gronert, D. A. Bors, A. Streitwieser, *J. Am. Chem. Soc.* **1987**, *109*, 602. The pK values were corrected with fluorene ($pK = 22.90$) as standard.
[60] G. Boche, M. Marsch, K. Harms, *Angew. Chem.* **1986**, *98*, 373; *Angew. Chem. Int. Ed. Engl.* **1986**, *25*, 373.
[61] A. Streitwieser, C. Lambert, M. Stratakis, unpublished results.
[62] a) M. J. Kaufmann, A. Streitwieser, *J. Am. Chem. Soc.* **1987**, *109*, 6092; b) J. C. Ciula, A. Streitwieser, *J. Org. Chem.* **1992**, *57*, 431.
[63] a) E. M. Arnett, K. D. Moe, *J. Am. Chem. Soc.* **1991**, *113*, 7068, 7288.
[64] C. Lambert, Y.-D. Wu, P. von R. Schleyer, *J. Chem. Soc. Chem. Commun.* **1993**, 255.
[65] N. J. R. van Eikema Hommes, M. Bühl, P. von R. Schleyer, Y.-D. Wu, *J. Organomet. Chem.* **1991**, *409*, 307.
[66] P. von R. Schleyer, J. Kaneti, Y.-D. Wu, J. Chandrasekhar, *J. Organomet. Chem.* **1992**, *426*, 143.
[67] a) H. E. Zaugg, A. D. Schaefer, *J. Am. Chem. Soc.* **1965**, *87*, 1857; b) J. Smid in *Ions and Ion Pairs in Organic Reactions, Vol. 1* (Ed.: M. Szwarc), Wiley, New York, **1972**, p. 85.
[68] W. R. Winchester, W. Bauer, P. von R. Schleyer, *J. Chem. Soc. Chem. Commun.* **1987**, 177.
[69] R. Pi, W. Bauer, B. Brix, C. Schade, P. von R. Schleyer, *J. Organomet. Chem.* **1988**, *306*, C1.
[70] a) T. B. Thompson, W. T. Ford, *J. Am. Chem. Soc.* **1979**, *101*, 5459; b) S. Brownstein, S. Bywater, D. J. Worsfold, *J. Organomet. Chem.* **1980**, *199*, 1.
[71] W. P. Kraemer, V. Spirko, P.-A. Malmqvist, B. O. Roos, *J. Mol. Spectrosc.* **1991**, *147*, 526.
[72] C. Lambert, P. von R. Schleyer, unpublished results; see also ref. [46].
[73] G. Fraenkel, W. E. Beckenbaugh, P. P. Yang, *J. Am. Chem. Soc.* **1976**, *98*, 6878.
[74] For a review see E. Weiss, *Angew. Chem.* **1993**, *105*, 1565; *Angew. Chem. Int. Ed. Engl.* **1993**, *32*, 1501.
[75] a) E. Weiss, E. A. C. Lucken, *J. Organomet. Chem.* **1964**, *2*, 197; b) E. Weiss, G. Hencken, *ibid.* **1970**, *21*, 265; c) E. Weiss, T. Lambertsen, B. Schubert, J. K. Cockcroft, A. Wiedenmann, *Chem. Ber.* **1990**, *123*, 79; d) E. Weiss, S. Corbelin, J. K. Cockcroft, A. N. Fitch, *Chem. Ber.* **1990**, *123*, 1629; e) *Angew. Chem.* **1990**, *102*, 728; *Angew. Chem. Int. Ed. Engl.* **1990**, *29*, 650; f) E. Weiss, G. Sauermann, G. Thirase, *Chem. Ber.* **1983**, *116*, 74.
[76] a) E. Weiss, G. Sauermann, *Chem. Ber.* **1970**, *103*, 265; b) E. Weiss, T. Lambertsen, B. Schubert, J. K. Cockcroft, *J. Organomet. Chem.* **1988**, *358*, 1; c) E. Weiss, G. Sauermann, *Angew. Chem.* **1968**, *80*, 123; *Angew. Chem. Int. Ed. Engl.* **1968**, *7*, 133.
[77] E. Weiss, H. Köster, *Chem. Ber.* **1977**, *110*, 717.
[78] Analogous basis sets as in [42] used for the alkali-metal species: C. Lambert, P. von R. Schleyer, unpublished results.
[79] J. J. Brooks, G. D. Stucky, *J. Am. Chem. Soc.* **1972**, *94*, 346.
[80] R. A. Bartlett, H. V. R. Dias, P. P. Power, *J. Organomet. Chem.* **1988**, *341*, 1.
[81] H. Köster, E. Weiss, *J. Organomet. Chem.* **1979**, *168*, 273.
[82] D. Hoffmann, W. Bauer, P. von R. Schleyer, U. Pieper, D. Stalke, *Organometallics* **1993**, *12*, 1193.
[83] M. M. Olmstead, P. P. Power, *J. Am. Chem. Soc.* **1985**, *107*, 2174.
[84] K. Gregory, M. Bremer, P. von R. Schleyer, P. A. A. Klusener, L. Brandsma, *Angew. Chem.* **1989**, *101*, 1261; *Angew. Chem. Int. Ed. Engl.* **1989**, *28*, 1224.
[85] F. Pauer, D. Stalke, *J. Organomet. Chem.* **1991**, *418*, 127.
[86] U. Pieper, D. Stalke, *Organometallics* **1993**, *12*, 1201.
[87] a) H. Köster, E. Weiss, *Chem. Ber.* **1982**, *115*, 3422; b) G. Boche, H. Etzrodt, M. Marsch, W. Massa, G. Baum, H. Dietrich, M. Mahdi, *Angew. Chem.* **1986**, *98*, 84; *Angew. Chem. Int. Ed. Engl.* **1986**, *25*, 104; c) U. Schümann, E. Weiss, H. Dietrich, W. Mahdi, *J. Organomet. Chem.* **1987**, *322*, 299; d) D. Seebach, T. Maetzke, R. K. Hynes, M. N. Paddon-Row, S. S. Wong, *Helv. Chim. Acta* **1988**, *71*, 299.
[88] a) S. Corbelin, J. Kopf, N. P. Lorenzen, E. Weiss, *Angew. Chem.* **1991**, *103*, 875; *Angew. Chem. Int. Ed. Engl.* **1991**, *30*, 825; b) H. Bock, K. Ruppert, Z. Havlas, D. Fenske, *ibid.* **1990**, *102*, 1095 and **1990**, *29*, 1042.
[89] a) E. D. Jemmis, J. Chandrasekhar, P. von R. Schleyer, *J. Am. Chem. Soc.* **1979**, *101*, 2848; b) P. von R. Schleyer, E. Kaufmann, G. W. Spitznagel, R. Janoschek, G. Winkelhofer, *Organometallics* **1986**, *5*, 79; c) C. Lambert, P. von R. Schleyer, E.-U. Würthwein, *J. Org. Chem.* **1993**, *58*, 6377.
[90] W. Neugebauer, Dissertation, Universität Erlangen-Nürnberg, **1983**.
[91] W.-K. Li, *Croat. Chem. Acta* **1988**, *61*, 833.
[92] C. Lambert, P. von R. Schleyer, unpublished results.
[93] C. Schade, P. von R. Schleyer, M. Geißler, E. Weiss, *Angew. Chem.* **1986**, *98*, 922; *Angew. Chem. Int. Ed. Engl.* **1986**, *25*, 902.
[94] Quantum chemistry archive of the Universität Erlangen-Nürnberg, unpublished.

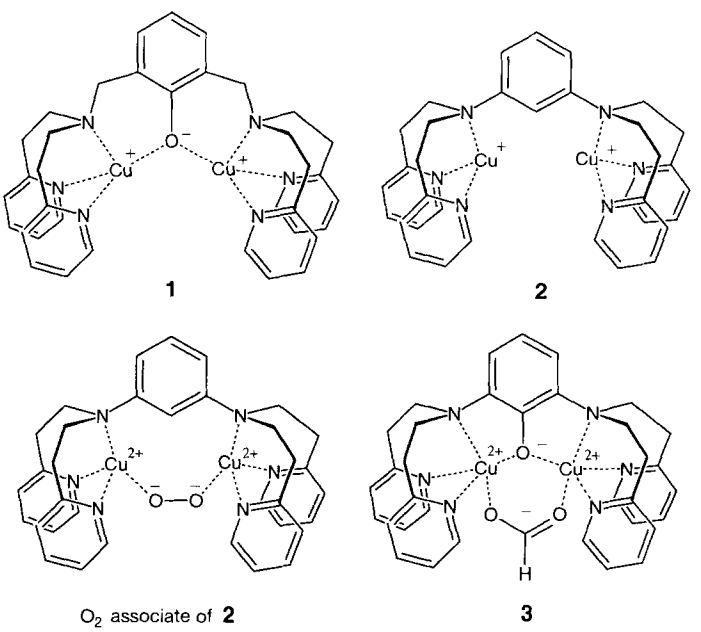
Binuclear Metal Complexes as Efficient Intermediaries in Biochemically Relevant Hydrolysis Reactions

Michael W. Göbel*

Enzymes set chemists a high standard for synthetic catalysts with their often astoundingly high selectivity and simultaneous enormous acceleration of reactions. This goal is very difficult to achieve, let alone to better. The elucidation of enzyme mechanisms is therefore counted among the important tasks of science, to which a wide variety of research disciplines can contribute. In recent years X-ray crystal structure analysis, in particular, has made available a wealth of detailed structural information that can serve a foundation for the formulation of mechanistic proposals. Further refinement of such models is then possible through site-directed mutagenesis and calculations. In the light of the success of scientific methods, which in a certain sense can give a multifaceted view of the problem, the role preparative chemistry may play nowadays in elucidating enzyme catalysis is questioned. Is the synthesis of low molecular weight models of enzymes actually still relevant?

I am convinced that this question can be answered with a decisive yes. One misunderstanding, however, must be avoided. Models of enzymes that describe the complex structure and dynamics of a proteinogenic catalyst are, as a rule, not achieved in the attempts of synthetic chemists. This is also not the goal of such research. The aim of investigations on small, well-defined molecules is far more to probe a particular aspect of the enzyme in question, for example, to consider in isolation the special arrangement of functional groups obtained from crystal structure data and to test the relevance of such an arrangement with respect to the reaction mechanism. In this way individual principles of function are determined, which are useful for a deeper understanding. Another advantage of the reductionistic view lies in the potential for using the principles found in the model to construct totally novel, enzyme-analogous catalysts that could attain practical importance in the future.

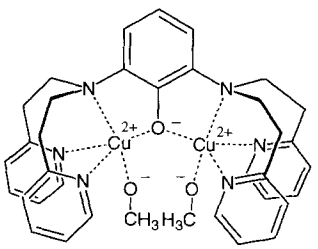
A good example for the value of such model systems is the series of papers that have recently appeared on binuclear metal complexes. Beside the long-known iron–sulfur proteins of the respiratory chain, enzymes and proteins have been described recently in which the active sites contain two or three interacting metal ions (for example, Zn, Fe, Cu).[1] The biological tasks cover oxygen transport to oxygenase and hydrolase activity. Since the structure–function relationship of these enzymes are by no means solved, the synthesis of simplified model complexes is an important goal. Typically, symmetrical ligands linked by *meta*-substituted arene units are used. In this way, with **1** Karlin et al. have prepared a binuclear copper complex along the lines of hemocyanin, the copper-containing O_2-transport protein of molluscs. At low temperature **1** binds O_2 reversibly.[2a] The oxygen associate of complex **2** is more stable.[2b] In the presence of dimethylformamide (DMF) or dimethylacetamide, however, this associate reacts instantaneously to form **3**, whose structure



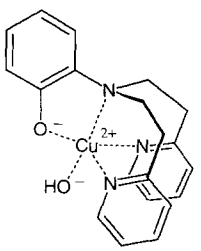
has been solved by X-ray crystallography. In analogous copper complexes the remarkable redox reaction of hydroxylation of the arene and oxidation of the copper ions occurred earlier.[2c] Completely unexpected was the fate of the amide: it was hydrolyzed to the formate ion. In the light of the high kinetic stability of carboxylic amides, whose half-lives in neutral water lies in the range of years, the hydrolysis of DMF within seconds is a new speed record! Where can the reason for this enormous acceleration be found? The presence of both copper ions appears to be essential. While **4** hydrolyzes DMF with a rate constant of about 0.3 h^{-1}, no reaction can be detected with the mononuclear complex **5**.[3] Probably the first Cu ion of **4** coordinates a hydroxide ion, while the second Cu cation binds the

[*] Dr. M. W. Göbel
Institut für Organische Chemie der Universität
Marie-Curie-Strasse 11, D-60439 Frankfurt am Main
Telefax: Int. code + (69)5800-9250

 © VCH Verlagsgesellschaft mbH, D-69451 Weinheim, 1994 0570-0833/94/1111-1141 $ 10.00+.25/0

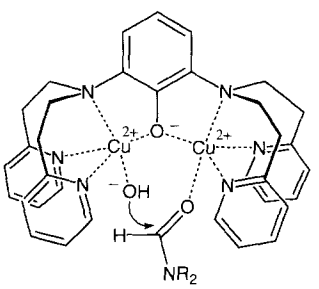


4

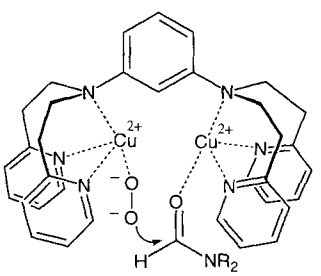


5

oxygen atom of DMF and activates it as Lewis acid for the intramolecular addition of the nucleophile (Scheme 1). With respect to its reactivity, **4** is comparable with the known metal catalysts of amide hydrolysis;[3] nevertheless, the oxygen associate of **2** is unparalleled. As is known, the nucleophilicity of OOH^- ions is drastically enhanced over that of the OH^- ion on account of the α effect. The authors therefore surmise that the species that is responsible for the hydrolysis is a copper complex with peroxido ligand that arises in the primary redox reaction. Scheme 2 depicts the assumed mechanism. The study of complex **2** thus led not only to the answer of the original question on the binding of oxygen in copper complexes, but simultaneously to a novel approach to the construction of artificial peptidases.

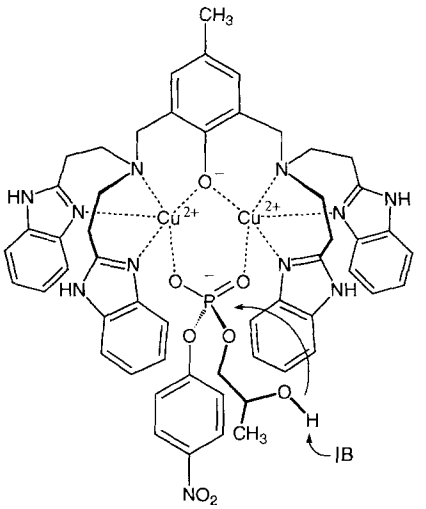


Scheme 1. Postulated mechanism of the amide hydrolysis with **4** as catalyst.



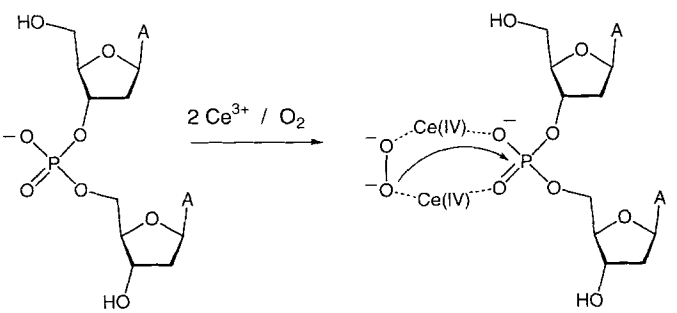
Scheme 2. Postulated mechanism of the amide hydrolysis with **2** as catalyst.

In nature multinuclear metalloenzymes, under which the RNAse H of the HIV reverse-transcriptase is classified, serve as catalysts for several acyl and phosphoryl transfer reactions. Chin et al. chose a binuclear copper complex related to **1** to accelerate the reaction of a phosphoric acid diester anion (Scheme 3).[4] This reaction can be considered a model for the first step of the hydrolysis of RNA, in which the alcohol function of the side chain attacks the phosphoryl center as nucleophile in a ring closure reaction. As in the case already described, the binuclear copper complex was compared with the analogous mononuclear complex: the approximately 50 times larger rate constant of the binuclear complex shows that here, too, the two metal ions probably cooperate.[5] Because on cyclization of the substrate the transition state structures have a higher negative charge density at the phosphoryl group, the interaction with several electrophilic metal sites is advantageous. Analogous zinc complexes have already been used for the hydrolysis of similar model substrates.[6] The ultimate test for every synthetic hydrolase, however, is the phosphoric diester group of DNA. Since an entropically favored intramolecular course of reaction is not



Scheme 3. Model reaction for the first step of the hydrolysis of RNA. B = base.

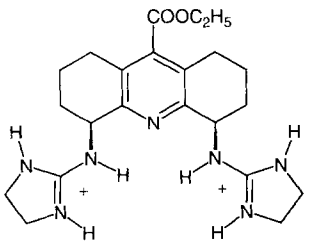
possible, in contrast to RNA, because of the missing hydroxyl function at C2′ in DNA, these phosphoric acid esters show an extreme kinetic stability to substitution. With the redox-active Ce^{3+}/O_2 system, Chin et al. have now been able to perform the *hydrolytic* cleavage of deoxyribodinucleotides as well in convincing style.[7] Although the mechanism of the hydrolysis has not been completely elucidated, the assumption of a reaction of Ce^{3+} ions with oxygen to give a complex of two Ce^{4+} ions and the dianion O_2^{2-} as active agent (Scheme 4) seems plausible. The pathway should be characterized by a similar combination of electrophilic and nucleophilic properties as the intermediate in the amide hydrolysis observed by Karlin et al.



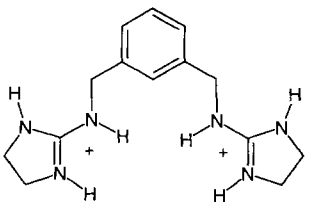
Scheme 4. Conjectured mechanism of the hydrolysis of deoxyribodinucleotides effected by Ce^{3+}/O_2.

To achieve an electrophilic activation (similar to a Lewis acid) of substrates, enzymes are not, however, exclusively dependent on metal ions. Often guanidinium ions of arginine side chains also perform this function. In this way the Staphylokokkus nuclease accelerates the hydrolysis of phosphoric acid diester anions by sixteen orders of magnitude (!), although the active site contains only one calcium ion. The decisive factor is the additional presence of two guanidinium ions that display both the electrostatic and the structural complementarity of the dianionic, trigonal-bipyramidal transition structures of the substrate hydrolysis. To date already three research groups have attempt-

ed to employ the bis(guanidinium) substructure of the Staphylokokkus nuclease as active principle for synthetic catalysts with phosphodiesterase activity.[8] In compounds **6** and **7** the cationic groups are linked to each other in such a way that four hydrogen



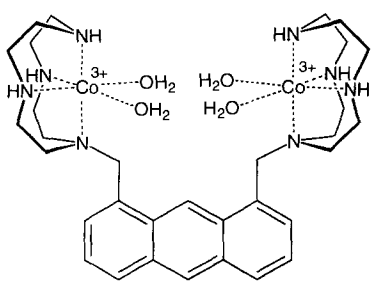
6



7

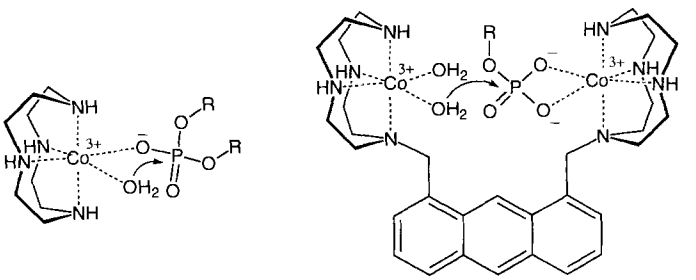
bonds can form simultaneously to a tetrahedral or trigonal-bipyramidal oxo anion to be complexed. As was hoped, **7** and analogous compounds strongly accelerate substitution reactions of phosphoric acid diesters in dipolar, aprotic solvents.[8c, d] Anslyn, Smith et al. could even catalyze the cleavage of RNA in water with **6**.[8b]

The binuclear Co complex **8** described by Czarnik et al.[9] differs from those already mentioned. The two metal ions are held so far apart by the spacer that no direct dimerization of the two subunits through oxygen is possible. Complex **8** accelerates the hydrolysis of phosphoric acid diester anions by seven orders of magnitude, but still does not exceed the activity of mononuclear complexes. In Co^{3+} complexes nucleophile and phosphoric acid diester bind to the same metal ion and react intramolecularly via a four-membered transition state (Scheme 5, left). The high efficiency of **8** is therefore not attributable to a cooperativity of the two Co^{3+} ions. On the other hand **8** increases the rate of hydrolysis of phosphoric acid monoesters about ten times more than the corresponding mononuclear complexes. Probably one metal ion coordinates the nucleophilic water molecule, while the second binds the phosphoryl group in the form of a four-membered ring.[3] The reaction of the phosphoric acid monoester can therefore profit from the special arrangement of the metal ions in **8** (Scheme 5, right).



8

This small selection of examples is intended to demonstrate that synthetic metal complexes provide a plethora of subtle insights into the structure–activity relationships, which may also be valid for enzymes. Finely adjusted modifications are much more difficult to achieve in proteins and still more difficult to test. Moreover, the presented model systems show substantial reactivities in spite of their simple construction. The compounds are indeed of practical interest, perhaps as artificial proteases or as synthetic ribonucleases that—together with antisense oligonucleotides—can effect a hydrolytic deactivation of pathogenic messenger-RNA.



Scheme 5. Postulated mechanism for the hydrolysis of phosphoric acid esters.

German version: *Angew. Chem.* **1994**, *106*, 1201

[1] a) K. D. Karlin, *Science* **1993**, *261*, 701–708; b) B. L. Vallee, D. S. Auld, *Biochemistry* **1993**, *32*, 6493–6500.

[2] a) P. P. Paul, Z. Tyeklár, R. R. Jacobson, K. D. Karlin, *J. Am. Chem. Soc.* **1991**, *113*, 5322–5332; b) N. N. Murthy, M. Mahroof-Tahir, K. D. Karlin, *ibid.* **1993**, *115*, 10404–10405; c) M. S. Nasir, B. I. Cohen, K. D. Karlin, *ibid.* **1992**, *114*, 2482–2494.

[3] The hydrolysis of amides is, however, also possible at mononuclear metal complexes: J. Chin, *Acc. Chem. Res.* **1991**, *24*, 145–152.

[4] M. Wall, R. C. Hynes, J. Chin, *Angew. Chem.* **1993**, *105*, 1696–1697; *Angew. Chem. Int. Ed. Engl.* **1993**, *32*, 1633–1635.

[5] The authors point out, however, that the different kinetics could also be related to different catalyst-substrate affinities.

[6] a) Binuclear Zn complex as model for the active site of the phospholipase C: S. Uhlenbrock, B. Krebs, *Angew. Chem.* **1992**, *104*, 1631–1632; *Angew. Chem. Int. Ed. Engl.* **1992**, *31*, 1647–1648; b) hydrolysis of phosphoric acid esters at binuclear Zn complexes: S. Hikichi, M. Tanaka, Y. Moro-oka, N. Kitajima, *J. Chem. Soc. Chem. Commun.* **1992**, 814–815.

[7] B. K. Takasaki, J. Chin, *J. Am. Chem. Soc.* **1994**, *116*, 1121–1122.

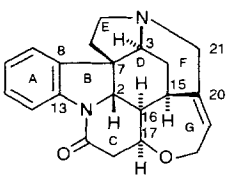
[8] a) D. M. Kneeland, K. Ariga, V. M. Lynch, C.-Y. Huang, E. V. Anslyn, *J. Am. Chem. Soc.* **1993**, *115*, 10042–10055; b) J. Smith, K. Ariga, E. V. Anslyn, *ibid.* **1993**, *115*, 362–364; c) V. Jubian, R. P. Dixon, A. D. Hamilton, *ibid.* **1992**, *114*, 1120–1121; d) R. Groß, G. Dürner, M. W. Göbel, *Liebigs Ann. Chem.* **1994**, 49–58.

[9] D. H. Vance, A. W. Czarnik, *J. Am. Chem. Soc.* **1993**, *115*, 12165–12166.

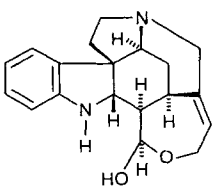
New Total Syntheses of Strychnine

Uwe Beifuss*

Strychnine (**1**), the active component of a notorious arrow poison in Southeast Asia, has a mysterious history. It is a convulsant blocking postsynaptic inhibition in the spinal cord by acting as an antagonist of the inhibitory neurotransmitter, glycine.[2] In therapeutic doses strychnine has a mildly analeptic effect; in toxic doses it leads to uncoordinated tonic convulsions induced by acoustic, tactile, or optical stimuli. Paralysis of the respiratory organ results in death; 100–300 mg is the lethal dose for an adult human.[2c]



1

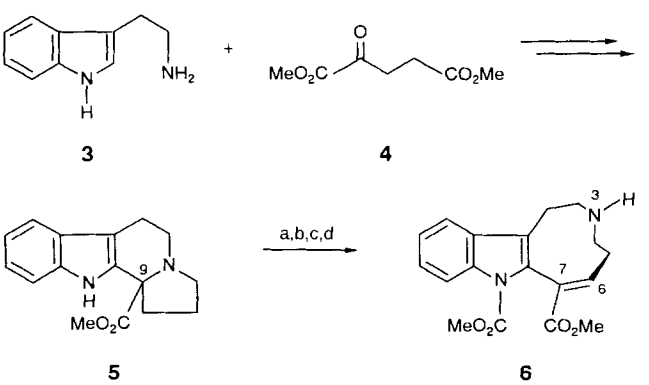


2

In 1818 strychnine (**1**), which occurs in larger amounts in the poison nut (*Strychnos nux vomic L.*) and the Saint-Ignatius's-bean (*Strychnos ignatii Bergius*), was isolated by Pelletier and Caventou[3] and was one of the first alkaloids obtained in pure form. The structure determination by chemical degradation of the natural product, a complex structure with seven rings and six stereogenic centers, proved to be difficult and tedious. Many structural formulas were proposed and rejected before Robinson et al. (1946) and Woodward et al. (1947) presented the correct formula.[4] The relative and absolute configuration was determined by X-ray crystallography a few years later.[5]

The structure determination culminated with the total synthesis of **1** by Woodward et al., which was the only total synthesis of this natural product for nearly forty years.[6] Even today this synthesis is still considered a highlight in the development of modern organic synthesis, since at that time the deliberate design and execution of the synthesis of a molecule of this complexity was unprecedented. Despite the rapid development of organic chemistry since then, strychnine has remained an attractive, challenging synthetic target. A number of novel approaches to the strychnos alkaloids have been devised,[7, 8] but the molecules prepared frequently lack the functionalities required for the construction of the seven-membered allylic ether G ring of strychnine. Recently, almost forty years after Woodward's synthesis, four research groups achieved the total synthesis of strychnine. In 1992 Magnus et al. reported on the successful conclusion of the second total synthesis of strychnine and at the same time the first total synthesis of the so-called Wieland–Gumlich aldehyde **2**.[9] Shortly afterwards Overman et al. published the first, and so far only, enantioselective route to strychnine (**1**),[10] and in the meantime Kuehne et al.[11] and Rawal et al.[12] have also completed their total syntheses. This certainly provides ample grounds for discussing these four new syntheses.

Magnus' synthesis[9] follows the retrosynthetic analysis of the strychnos framework employed successfully by Harley-Mason in the syntheses of several natural products in the 1960s and 1970s.[13] The key step in this strategy is the transannular iminium ion cyclization of a nine-membered ring for the stereoselective construction of rings D and E of the strychnos alkaloids. Magnus follows the classical approach right from the start with the multistep conversion of the tetracyclic amine *rac*-**5**, which is readily accessible from **3** and **4**, into **6** (Scheme 1). A crucial step



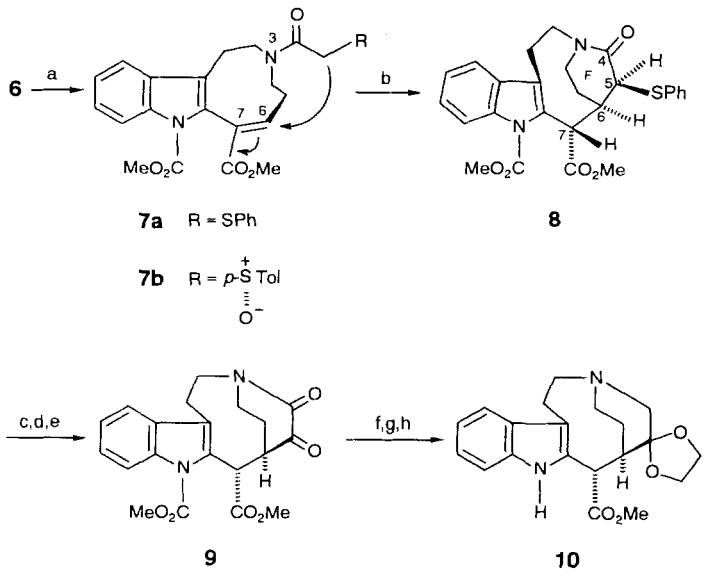
3 **4** **5** **6**

Scheme 1. a) $ClCO_2CH_2CCl_3$, CH_2Cl_2; b) NaOMe, MeOH; c) 50% aq NaOH, CH_2Cl_2, $ClCO_2Me$, benzyltriethylammonium chloride; d) Zn, CH_3COOH, THF.

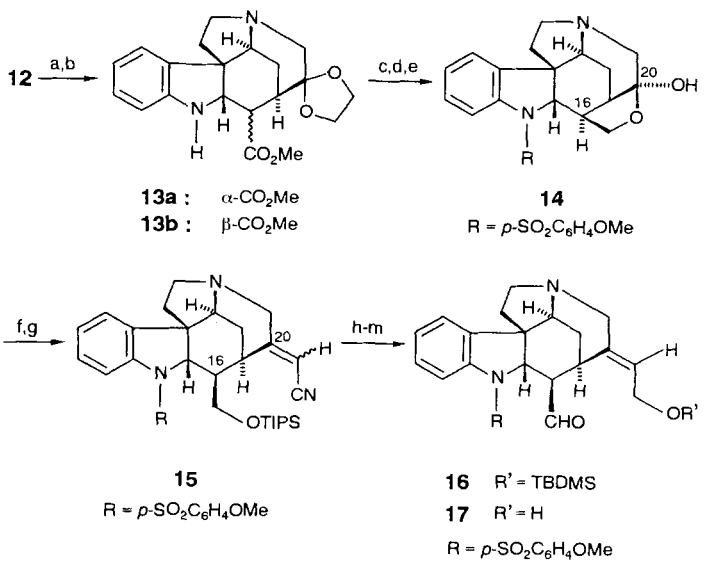
is the β,β,β-trichloroethyl chloroformate induced fragmentation of the tertiary amine *rac*-**5** to provide the expanded nine-membered ring system. One of the most remarkable steps in the remainder of the synthesis is the construction of the F ring by intramolecular conjugate addition. For this purpose amide **7a** is prepared and treated with sodium hydride in THF, which results in the facile, diastereoselective transformation into *rac*-**8**. The stereoselectivity of this 1,4-addition is attributed to the protonation of the intermediate ester enolate from the top face. Oxidation of *rac*-**8** to give the corresponding mixture of sulfoxides is then followed by a Pummerer reaction and Hg^{2+}-mediated hydrolysis to furnish *rac*-**9** (Scheme 2).

Magnus et al. obtained both enantiomers of **9** with considerable effort by acylation of **6** with (+)-(*R*)-*p*-toluenesulfinylacetic acid and cyclization of the resulting sulfoxide **7b**, separation of the four diastereomers formed in this way, combination of the pairs with the same absolute configurations at C-6 and C-7, and subsequent conversion into the two enantiomers **9** and *ent*-**9**.[9a] The cyclization of sulfoxide **7b** yields the two products enantiomeric at C-6 and C-7 in a 55:45 ratio. This is why this route is not only laborious but also only insignificantly more efficient than resolution.

[*] Dr. U. Beifuss
Institut für Organische Chemie der Universität
Tammannstrasse 2, D-37077 Göttingen (FRG)
Telefax: Int. code + (551)39-9660

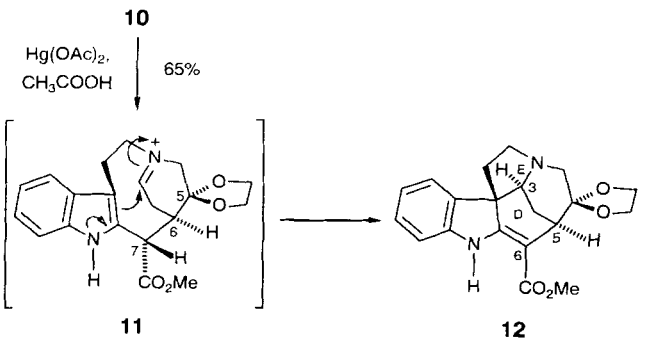


Scheme 2. a) $PhSCH_2CO_2H$, bis(2-oxo-3-oxazolidinyl)phosphinic acid (BOPCl), Et_3N, CH_2Cl_2; b) NaH, THF; c) *m*-chloroperbenzoic acid (MCPBA), CH_2Cl_2, 0 °C; d) trifluoroacetic anhydride (TFAA), 2,6-di-*tert*-butyl-4-methylpiperidine; e) HgO, $CdCO_3$, THF, H_2O; f) $BrCH_2CH_2OH$, 1,8-diazobicyclo[5.4.0]undec-7-ene (DBU), C_7H_8; g) $BH_3 \cdot THF$; h) Na_2CO_3, MeOH, 65 °C.



Scheme 3. a) Zn, H_2SO_4, MeOH; b) MeONa, MeOH; c) *p*-$MeOC_6H_4SO_2Cl$, $EtNiPr_2$, 4-dimethylaminopyridine (DMAP), CH_2Cl_2; d) $LiBH_4$, THF, $HN(CH_2CH_2OH)_2$; e) $HClO_4$; f) triisopropylsilyltrifluoromethanesulfonate (TIPSOTf), DBU, CH_2Cl_2; g) $(EtO)_2P(O)CH_2CN$, potassium hexamethyldisilazide (KHMDS), THF, 25 °C; h) diisobutylaluminum hydride (DIBAL), CH_2Cl_2, H_3O^+; i) $NaBH_4$, MeOH; j) 2 N HCl, MeOH; k) *tert*-butyldimethylsilyltrifluoromethanesulfonate (TBDMSOTf), DBU, CH_2Cl_2, −20 °C; l) $SO_3 \cdot C_5H_5N$, DMSO, Et_3N; m) pyridine, HF.

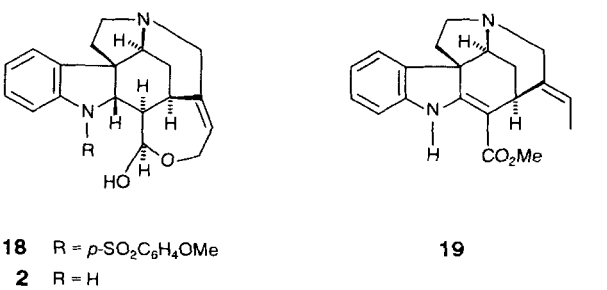
After transformation of *rac*-**9** into acetal *rac*-**10** (Scheme 2) rings D and E are constructed in the most critical step of the entire synthesis. A transannular iminium ion cyclization[7, 13] provides predominantly *rac*-**12** in 65% yield with remarkable regio- and stereoselectivity.[14] It is assumed that treatment of *rac*-**10** with mercury(II) acetate in acetic acid leads primarily to the cyclic iminium ion *rac*-**11** which then gives *rac*-**12**.



A number of steps are required for the conversion of *rac*-**12** into the cyclic hemiacetal *rac*-**14** (Scheme 3). This compound is important for the rest of the synthesis, since it cannot only be prepared from tryptamine (**3**) and dimethyl 2-ketoglutarate (**4**), but can also be obtained readily in substantial amounts and in enantiomerically pure form by degradation of strychnine. Once enough of this relay hemiacetal has been secured, assembly of the G ring can be tackled.

As only a compound with an (*E*)-configurated double bond as in **17** can be used for the synthesis of the G ring, the construction of the hydroxyethylidene double bond must be diastereoselective. This problem had challenged Woodward et al., and like those pioneers Magnus et al. were also foiled: Wittig–Horner reaction furnishes the α,β-unsaturated cyanide **15** as a 2:3 mixture of the (*Z*) and (*E*) isomers. Although the undesired (*Z*) isomer can be isolated and isomerized photochemically to give a mixture of both isomers, this step is far from being optimal.

The next steps in the synthesis include the multistep conversion of (*E*)-**15** into **16**, subsequent cleavage of the silyl ether protecting group, and cyclization of **17**, which cannot be isolated, to provide hexacyclic **18**. With the reductive removal of the



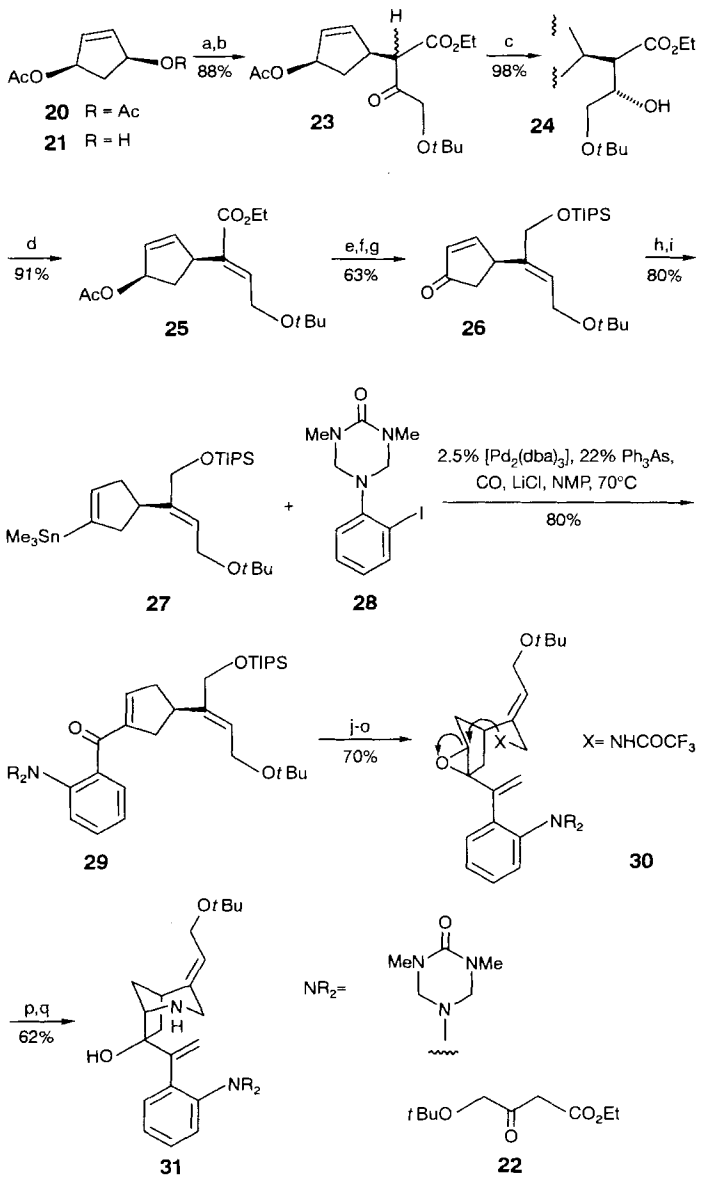
sulfonamide Magnus et al. arrived at their first goal, the total synthesis of the Wieland–Gumlich aldehyde **2**. The conclusion of the total synthesis of strychnine is also within reach; the authors succeeded in converting **2** into the natural product in a one-step reaction with malonic acid, following the method of Robinson et al.[15] With 27 steps this synthesis is only negligibly shorter than Woodward's 28-step synthesis from 1954. But Magnus et al. achieved an overall yield of roughly 0.03%, which is more than 1000 times greater than Woodward's overall yield of 0.00006%. This result would have been impossible without powerful new synthetic methods. Magnus' synthetic strategy has a classical form, and he prepared enantiomerically pure compounds

very effectively by traditional means, namely via a relay compound obtained by degradation of the natural product itself.

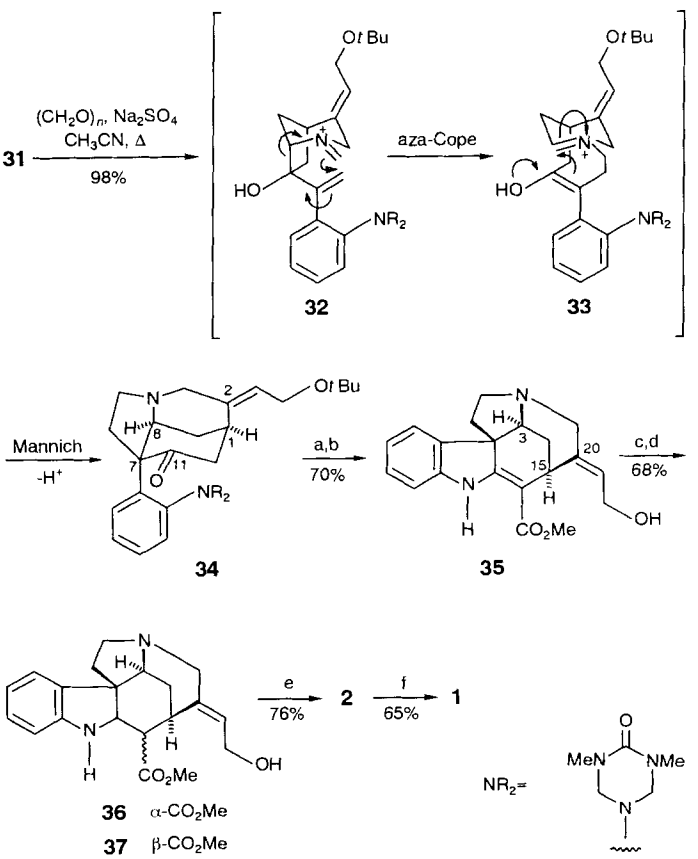
The third total synthesis of strychnine (**1**), so far the only enantioselective route to the natural product, was accomplished by Overman et al.[10] The key to their approach to **1** is the sequential cationic aza-Cope rearrangement/Mannich cyclization, which is frequently employed with success in alkaloid synthesis. With the synthesis of akuammicine *rac*-**19** the authors proved that this strategy offers an efficient route to the strychnos alkaloids.[8g]

The crucial compound in this strychine synthesis is azabicyclo[3.2.1]octane **31**, which is the substrate for the aza-Cope–Mannich sequence (Scheme 4). In the preparation of **31**, *meso*-diester **20** is subjected to acetylcholine esterase catalyzed hydrolysis to yield **21** with high enantiomeric purity. Eighteen ensuing steps then provide **31** in 14% yield. The allylic carbonate obtained from **21** is used in a palladium-catalyzed allylic substitution with **22** to furnish the *cis* products **23**, which are reduced with high diastereoselectivity (>20:1) in accord with the Felkin–Anh model to provide a mixture of the *trans*-β-hydroxy esters **24**. Subsequent *syn* elimination affords the (*E*) isomer **25** almost exclusively (97:3). In this way Overman et al. succeeded in solving the problem of the stereoselective construction of what will become the allylic ether double bond at C-20 of the natural product early in the synthesis. The next important intermediate is the α,β-unsaturated ketone **29**, which is accessible by the palladium-catalyzed, carbonylative cross-coupling of vinyl stannane **27** with the triazone-protected *o*-iodoaniline **28**. In turn, **27** is prepared by the palladium-catalyzed Stille coupling of the enol triflate obtained regioselectively from **26**. The key step in the transformation of **29** into **31** is the stereoselective, intramolecular aminolysis of epoxide **30**, which is the product of the substrate-controlled stereoselective epoxidation and subsequent Wittig methylenation of **29**.

Now the aza-Cope–Mannich cascade must be triggered, in other words, amine **31** must be converted into the corresponding formaldiminiun ion **32** (Scheme 5). This is achieved by reaction with paraformaldehyde without added acid. Intermediate **32** undergoes cationic [3,3] sigmatropic rearrangement under these



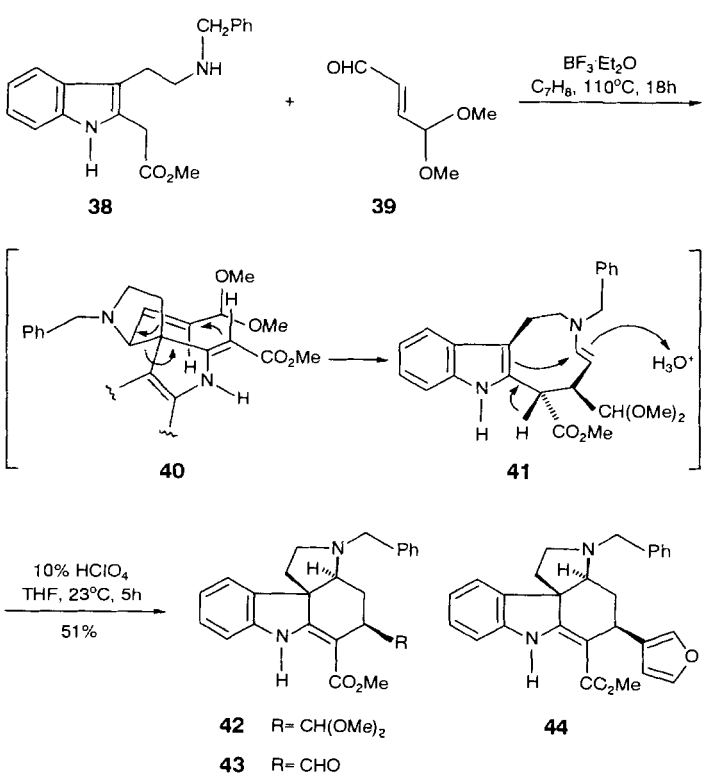
Scheme 4. a) $ClCO_2Me$, pyridine, CH_2Cl_2, 23 °C; b) $tBuOCH_2COCH_2CO_2Et$ (**22**), NaH, 1% $[Pd_2(dba)_3]$, 15% PPh_3, THF, 23 °C; c) $NaCNBH_3$, $TiCl_4$, −78 °C; d) dicyclohexylcarbodiimide (DCC), CuCl, C_6H_6, 80 °C; e) DIBAL, CH_2Cl_2, −78 °C; f) TIPSCl, tetramethylguanidine, *N*-methyl-2-pyrrolidone (NMP), −10 °C; g) Jones oxidation, −5 °C; h) L-Selectride, $PhNTf_2$, THF, −78 → 0 °C; i) Me_6Sn_2, 10% $[Pd(PPh_3)_4]$, LiCl, THF, 60 °C; j) $tBuO_2H$, Triton-B, THF, −15 °C; k) $Ph_3P{=}CH_2$, THF, 0 → 23 °C; l) tetrabutylammonium fluoride (TBAF), THF, −15 °C; m) methanesulfonyl chloride (MsCl), iPr_2NEt, CH_2Cl_2, −23 °C; n) LiCl, DMF, 23 °C; o) NH_2COCF_3, NaH, DMF, 23 °C; p) NaH, C_6H_6, 100 °C; q) KOH, EtOH-H_2O, 60 °C.



Scheme 5. a) Lithium diisopropylamide (LDA), $NCCO_2Me$, THF, −78 °C; b) 5% HCl-MeOH, reflux; c) Zn, 10% H_2SO_4-MeOH, reflux; d) NaOMe, MeOH, 23 °C; e) DIBAL, CH_2Cl_2, −78 °C; f) $CH_2(CO_2H)_2$, Ac_2O, NaOAc, HOAc, 110 °C.

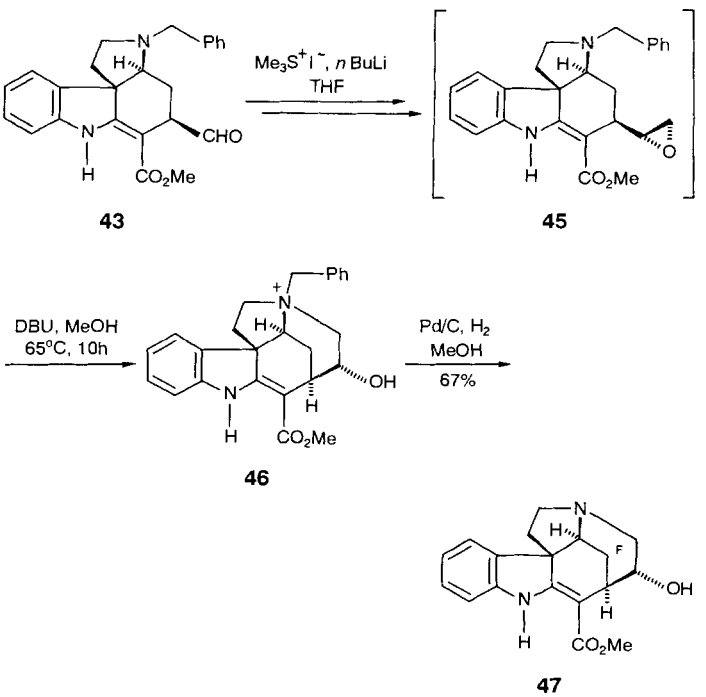
reaction conditions to give **33**, which contains all the structural features that are required for the ensuing intramolecular Mannich cyclization. At the end of the sequence **34** is obtained stereoselectively and almost quantitatively (98% yield)—an outstanding example of the efficiency and flexibility of this synthetic strategy. The cyclization product **34** is then acylated with methyl cyanoformate, and cleavage of the triazone protecting group affords pentacycle **35**, which contains all of the C atoms required for the synthesis of the Wieland–Gumlich aldehyde **2**. The conversion of **36** into strychnine (**1**) by conventional means is the concluding step in the first synthesis of this natural product proceeding without the resolution of racemates and without relay compounds. Overman et al. accomplish this in a total of 25 steps and with an overall yield of approximately 3%. This first enantioselective total synthesis is achieved in excellent yield. But just as impressive is the underlying retrosynthetic analysis, which is then followed by combining several modern palladium-catalyzed reactions and the elegant aza-Cope–Mannich sequence, a distinctive feature of Overman's work.

The beginning of Kuehne's total synthesis of racemic strychnine *rac*-**1**[11] is promising, since the highly diastereoselective construction of the tetracycle *rac*-**42** from tryptamine **38** and butenal **39** proceeds in only one synthetic operation (Scheme 6). The yield for this novel and efficient sequential reaction is 51% after cleavage of the acetal to provide aldehyde *rac*-**43**. Presumably the cyclizing Mannich reaction that leads to *rac*-**40** is followed by a [3,3] sigmatropic rearrangement giving *rac*-**41**, which in turn undergoes acid-catalyzed cyclization to afford *rac*-**42**. This new method also provides access to the indolenine *rac*-**44**,[8e] a compound containing all but two carbon atoms of ring C of the target molecule. However, it has not been possible so far to employ the furan ring in **44** for the construction of rings F and G in strychine. This is why Kuehne et al. relied on *rac*-**42** in their approach to the natural product.



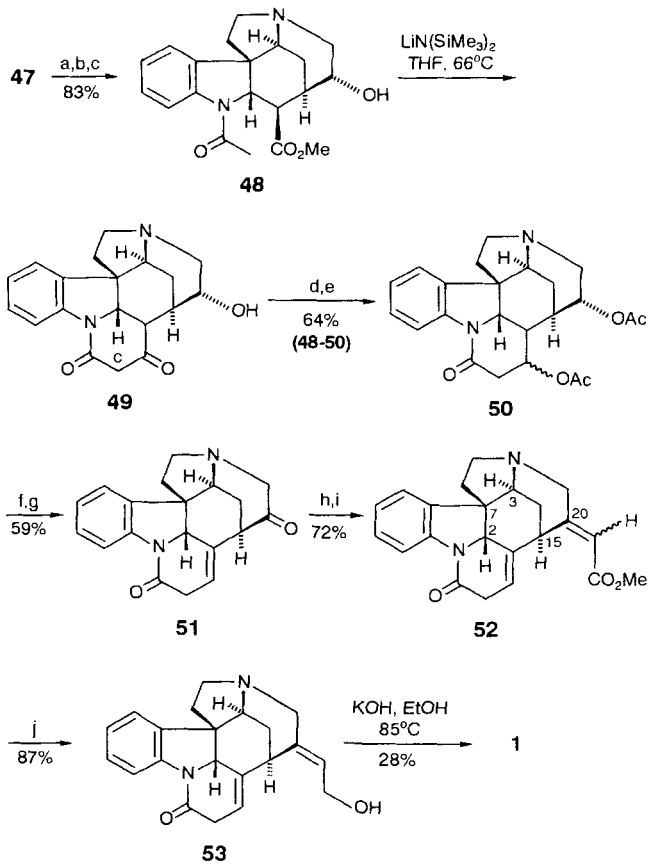
Scheme 6.

This entailed the lengthy and difficult successive construction of the three missing rings F, G, and C. The synthesis of the F ring is the least troublesome, as it succeeds in only three steps and with 67% yield (*rac*-**43** → *rac*-**47**) (Scheme 7). The key step is the intramolecular nucleophilic ring-opening of the unisolated epoxide *rac*-**45**; the thermodynamically controlled reaction yields *rac*-**46** exclusively.



Scheme 7.

In contrast to Magnus and Overman, who directed their syntheses towards the Wieland–Gumlich aldehyde *rac*-**2** and its straightforward conversion into strychnine *rac*-**1**, Kuehne focused on the synthesis of isostrychnine *rac*-**53** (Scheme 8) and had to rely on the isostrychnine–strychnine transformation, which Woodward had already recognized as being exceptionally difficult. First, ring C is assembled. The key step is the intramolecular Claisen reaction of the acetamido ester *rac*-**48** to give ketolactam *rac*-**49**. Although the overall yield for the construction of the C ring is good (*rac*-**47** → *rac*-**51**), the eight steps are relatively laborious. In the next part of the synthesis Kuehne, like Magnus, learned by experience that the (*E*)-selective construction of the allylic ether group at C-20, which is critical for closure of the G ring, is not possible at such a late stage in the synthesis. Wittig olefination of *rac*-**51** provides a 1:1 mixture of the (*E*) and (*Z*) isomers of *rac*-**52**, which can be enriched by irradiation in favor of the required (*E*)-acrylic ester (8:1). The reduction of (*E*)-*rac*-**52** to isostrychnine *rac*-**53** is straightforward; as expected, however, the last step of the synthesis, the problematic conversion of **52** to isostrychnine *rac*-**53** is straightforward; as expected, however, the last step of the synthesis, the problematic conversion of isostrychnine *rac*-**53** into strychnine *rac*-**1**, could not be solved in

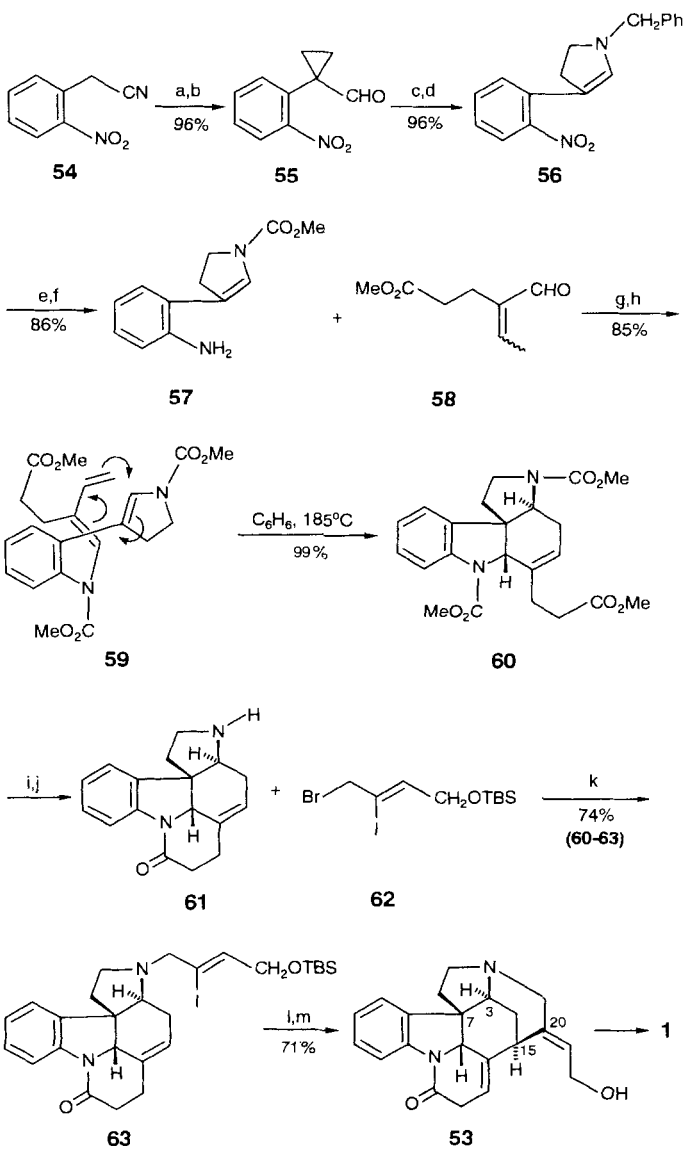


Scheme 8. a) $NaBH_3CN$, HOAc, 23 °C; b) Ac_2O, pyridine; c) NaOMe, MeOH, 0 °C; d) $NaBH_4$, MeOH; e) Ac_2O, pyridine; f) DBU, dioxane-H_2O, 100 °C; g) Swern oxidation; h) $(EtO)_2P(O)CH_2CO_2Me$, $KN(SiMe_3)_2$, THF, 23 °C, 2 h; i) *hv*; j) DIBAL, $BF_3 \cdot Et_2O$, −78 °C.

a satisfactory manner: strychnine *rac*-**1** was isolated in only 28% yield in addition to 61% unreacted starting material. One could argue that not every step in Kuehne's synthesis proceeds with the desired selectivity and yield and that the synthesis is not enantioselective. Yet it should be stressed that this synthesis, designed around a new and efficient key sequence, is one of the shortest routes to strychnine *rac*-**1** with 17 steps and an overall yield of roughly 2%. The efficiency of the synthesis could also be improved by avoiding the isostrychnine–strychnine conversion and the consequent time-consuming assembly of the C ring.

A strategy combining the advantages of both the intramolecular Diels–Alder reaction and the intramolecular Heck reaction was successfully tested in Rawal's synthesis of *rac*-**1**.[12] Heating precursor *rac*-**59**, which is prepared from **54** in eight steps, to 185 °C provides tetracycle *rac*-**60** in 99% yield as the sole product of the Diels–Alder reaction (Scheme 9). The rapid construction of the C ring by intramolecular amide formation in only two steps is also remarkable. Allylation of *rac*-**61** with **62** furnishes *rac*-**63**. Subsequent intramolecular Heck reaction leads to the diastereoselective ring closure providing the bridged piperidine system with retention of the stereochemistry at the double bond of the vinyl iodide. Deprotection concludes this hitherto shortest synthesis of racemic isostrychnine *rac*-**53** which has 14 steps and a 35% yield. But Rawal et al. are confronted with the problem of the inefficient final transformation to give *rac*-**1**. If one assumes Kuehne's reported yield of 28% for this step,[16] then Rawal formally achieves the synthesis of the natural product—albeit in racemic form—in only 15 steps and with almost 10% yield, which is on the order of the results of Overman and Kuehne.

Whether the four new total syntheses represent a *fundamental* improvement over Woodward's strychnine synthesis and the extent of this improvement can certainly be debated. However, it cannot be contested that Overman et al. accomplished the first and only enantioselective synthesis of the natural product, and that Kuehne and Rawal with their respective 17- and 15-step syntheses devised approaches with markedly fewer reaction steps than Woodward's 28-, Magnus' 27-, and Overman's 25-step syntheses. The considerable improvement in the overall yields relative to that of the first total synthesis is also noteworthy. Whereas Magnus improved the yield by a factor 1000, Overman, Kuehne, and Rawal upped the overall yield by a factor of



Scheme 9. a) $BrCH_2CH_2Br$, 50% NaOH, CH_3CN, nBu_4NBr, 23 °C; b) DIBAL, C_7H_8, −78 °C, H_3O^+; c) $BnNH_2$, Et_2O; d) Me_3SiCl, NaI, DMF, 60 °C; e) $ClCO_2Me$, acetone, 23 °C; f) 10% Pd/C, HCO_2NH_4, MeOH; g) 23 °C; h) $ClCO_2Me$, $PhNEt_2$; i) Me_3SiI, $CHCl_3$, 61 °C, 5 h; j) MeOH, 65 °C, 6 h; k) DMF, acetone, K_2CO_3; l) $Pd(OAc)_2$, Bu_4NCl, DMF, K_2CO_3, 70 °C, 3 h; m) 2 N HCl, THF.

100000! These impressive numbers cannot be attributed solely to improved synthetic methods and modern reagents, but emphasize the importance that sequential reactions[17] have achieved in the construction of complex natural products.

The four new total syntheses demonstrate that some of the difficulties in the synthesis of strychnine, such as the diastereoselective construction of the double bond at C-20, can now be solved elegantly, but that others like the isostrychnine–strychnine conversion remain unsolved. Thus it can be expected that the search for improved solutions for the efficient synthesis of strychnine and stychnos alkaloids will continue.

German version: *Angew. Chem.* **1994**, *106*, 1204

[1] L. Lewin, *Die Pfeilgifte*, J. A. Barth, Leipzig, **1923**.

[2] a) H. Betz, *Angew. Chem.* **1985**, *97*, 363; *Angew. Chem. Int. Ed. Engl.* **1985**, *24*, 365; b) E. Teuscher, U. Lindequist, *Biogene Gifte*, Gustav Fischer, Stuttgart, **1987**; c) *Allgemeine und spezielle Pharmakologie und Toxikologie* (Ed.: W. Forth), 5th ed., Bibliographisches Institut & F. A. Brockhaus, Mannheim, **1987**.

[3] P. J. Pelletier, J. B. Caventou, *Ann. Chim. Phys.* **1818**, *8*, 323.

[4] a) H. T. Openshaw, R. Robinson, *Nature* **1946**, *157*, 438; b) R. B. Woodward, W. J. Brehm, A. L. Nelson, *J. Am. Chem. Soc.* **1947**, *69*, 2250.

[5] a) J. H. Robertson, C. A. Beevers, *Acta Crystallogr.* **1951**, *4*, 270; b) C. Bokhoven, J. C. Schoone, J. M. Bijvoet, *ibid.* **1951**, *4*, 275; c) A. F. Peerdeman, *ibid.* **1956**, *9*, 824.

[6] a) R. B. Woodward, M. P. Cava, W. D. Ollis, A. Hunger, H. U. Daeniker, K. Schenker, *J. Am. Chem. Soc.* **1954**, *76*, 4749; b) *Tetrahedron* **1963**, *19*, 247.

[7] Reviews: a) J. Bosch, J. Bonjoch in *Studies in Natural Product Chemistry. Vol 1. Stereoselective Synthesis (Part A)* (Ed.: Atta-ur-Rahman), Elsevier, Amsterdam, **1988**, p. 31; b) G. Massiot, C. Delaude in *The Alkaloids, Vol. 34* (Ed.: A. Brossi), Academic Press, New York, **1988**, p. 211.

[8] a) J. Bonjoch, D. Solé, J. Bosch, *J. Am. Chem. Soc.* **1993**, *115*, 2064; b) M. Amat, J. Bosch, *J. Org. Chem.* **1992**, *57*, 5792; c) M. Amat, A. Linares, J. Bosch, *ibid.* **1990**, *55*, 6299; d) G. A. Kraus, D. Bougie, *Synlett* **1992**, 279; e) R. L. Parsons, J. D. Berk, M. E. Kuehne, *J. Org. Chem.* **1993**, *58*, 7482; f) M. E. Kuehne, D. A. Frasier, T. D. Spitzer, *ibid.* **1991**, *56*, 2696; g) S. R. Angle, J. M. Fevig, S. D. Knight, R. W. Marquis, Jr., L. E. Overman, *J. Am. Chem. Soc.* **1993**, *115*, 3966; h) J. M. Fevig, R. W. Marquis, Jr., L. E. Overman, *ibid.* **1991**, *113*, 5085; i) V. H. Rawal, C. Michoud, R. F. Monestel, *ibid.* **1993**, *115*, 3030; j) H.-J. Teuber, C. Tsaklakidis, J. W. Bats, *Liebigs Ann. Chem.* **1992**, 461; k) J. Nkiliza, J. Vercauteren, J.-M. Léger, *Tetrahedron Lett.* **1991**, *32*, 1787; l) D. B. Grotjahn, K. P. C. Vollhardt, *J. Am. Chem. Soc.* **1986**, *108*, 2091; m) *ibid.* **1990**, *112*, 5653.

[9] a) P. Magnus, M. Giles, R. Bonnert, C. S. Kim, L. McQuire, A. Merritt, N. Vicker, *J. Am. Chem. Soc.* **1992**, *114*, 4403; b) P. Magnus, M. Giles, R. Bonnert, G. Johnson, L. McQuire, M. Deluca, A. Merritt, C. S. Kim, N. Vicker, *ibid.* **1993**, *115*, 8116. I thank Prof. Magnus for sending me a preprint of the publication.

[10] S. D. Knight, L. E. Overman, G. Pairaudeau, *J. Am. Chem. Soc.* **1993**, *115*, 9293.

[11] M. E. Kuehne, F. Xu, *J. Org. Chem.* **1993**, *58*, 7490. I thank Prof. Kuehne for sending me a preprint of the publication.

[12] a) V. H. Rawal, S. Iwasa, C. Michoud, *Abstracts of Papers*, 207th ACS National Meeting, San Diego, CA, American Chemical Society, Washington D. C., **1994**, Abstract 204; *J. Org. Chem.*, **1994**, *59*, 2685–2686. I thank Prof. Rawal for sending me a preprint of the publication.

[13] J. Harley-Mason, *Pure Appl. Chem.* **1975**, *41*, 167.

[14] Typically *rac*-**12** was obtained in 50% yield [9b].

[15] F. A. L. Anet, R. Robinson, *Chem. Ind. (London)* **1953**, 245.

[16] The authors do not give a yield for the conversion of isostrychnine *rac*-**53** into strychnine *rac*-**1**.

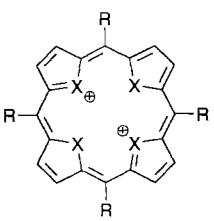
[17] L. F. Tietze, U. Beifuss, *Angew. Chem.* **1993**, *105*, 137; *Angew. Chem. Int. Ed. Engl.* **1993**, *32*, 131.

Tetraoxa[22]porphyrin(2.2.2.2) Dication and Tetraoxa[24]porphyrinogens(2.2.2.2)

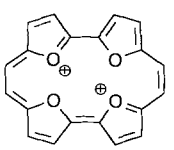
Gottfried Märkl,* Heinrich Sauer, Peter Kreitmeier, Thomas Burgemeister, Fritz Kastner, Georg Adolin, Heinrich Nöth, and Kurt Polborn

Dedicated to Professor Hans Bock

In addition to the porphyrin homologues ([22]porphyrin-(2.2.2.2)[1] and [26]porphyrin(3.3.3.3)[2]) and the porphyrin analogues ([18]porphyrin(2.0.2.0)[3] and [22]porphyrin-(1.3.1.3)[4]), the dicationic [18]porphyrinoids(1.1.1.1) **1** prepared by E. Vogel et al. are among the exciting new developments in porphyrin chemistry.



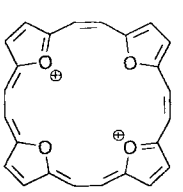
1, X = O
2, X = NMe



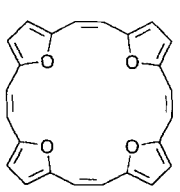
3

E. Vogel et al.[5] described first in 1988 the tetraoxa[18]porphyrin(1.1.1.1)dication **1** (R = H), which is formally analogous to the *N,N',N'',N'''*-tetramethylporphyrin dications **2**,[6] as an aromatic system. Recently, with the synthesis of an octaethyl derivative of **1** (R = H)[7] and tetraalkyl derivatives of **1** (R = alkyl)[7] substituted in the *meso* positions, access to these porphyrinoids has been decisively improved. The porphyrinoid analogue, tetraoxaporphyrin(2.0.2.0) dication **3** (tetraoxaporphycene dication), which is an isomer of **1**, was also prepared by E. Vogel et al.[8]

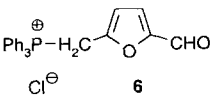
We describe here for the first time the next highest homologue to **1**, the tetraoxa[22]porphyrin(2.2.2.2)dication **4**. Tetraoxaporphyrinogen(2.2.2.2) **5** ([24]annulene tetroxide), the required precursor to **4**, was prepared in 1969 by J. A. Elix[9] by self-condensation of the ylid obtained from 5-formyl-2-furfuryltriphenylphosphonium chloride **6**.



4



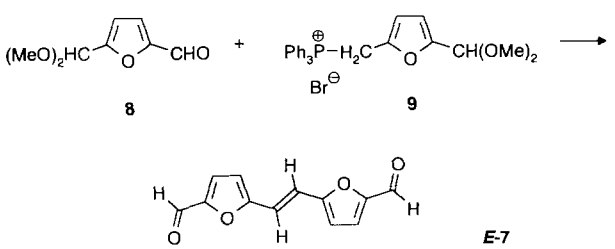
5



6

In addition to traces of a pentamer and a hexamer, he isolated two isomers of **5** each in 0.7% yield, which he assigned the *cis,trans,trans,trans* configuration **5a** (violet-black prisms, m.p. 215–217 °C) and the all-*trans* configuration **5b** (violet prisms, m.p. 269–270 °C).

We synthesized **5** by McMurry dimerization[10] of dialdehyde **7**, which, following the report of H. Saikachi et al.,[11] is accessible by Wittig reaction of the monoacetal **8**[12] of 2,5-furan dialdehyde and phosphonium salt **9**. The pure *trans* isomer (*E*)-**7**



8 **9**

E-7

is obtained from the isomeric mixture (*E*/*Z*)-**7** by recrystallization. McMurry dimerization of (*E*)-**7** was carried out with $TiCl_4$/Zn/Cu in anhydrous tetrahydrofuran. After chromatography on silica gel/CH_2Cl_2 and silica gel/cyclohexane/THF, **5** was obtained in 7% yield (stable black-violet crystals, m.p. > 300 °C). The melting point and spectroscopic data of our compound are not consistent with either of the isomers (**5a, b**) described by J. A. Elix; thus we will refer to the isomer we obtained as **5c**.

In the UV/VIS spectrum of **5c** (Table 1), absorptions with high molar extinctions are evident at short wavelengths (λ_{max} = 346 and 358 nm), and a band with low molar extinction is observed at 471 nm. The deep color of the substance can be attributed to a very broad absorption band with a low extinction centered at approximately 500 nm.

In contrast to tetraoxa[20]porphyrinogen(1.1.1.1),[13] the strong temperature dependence of the ^{1}H NMR spectra of **5c** (400.13 MHz, [D_8]THF, Table 1) points to high molecular dynamics. The ^{1}H NMR spectra at 65 °C and −78 °C are shown in

Table 1. Spectroscopic data (MS, UV/VIS, ^{1}H and ^{13}C NMR) for **5c** [15].

5c: MS (EI, 70 eV): *m/z* 369 (M^+ + H, 26%), 368 (M^+, 100), 184 (M^{2+}, 15); UV/VIS (CH_2Cl_2): λ_{max} [nm] (ε) = 346 (128000), 358 (175000), 471 (2300); ^{1}H NMR (400.13 MHz, [D_8]THF, 65 °C): δ = 8.52 (br. s, H-5,6,17,18), 5.60 and 5.52 (AB, H-3,8,15,20 and H-2,9,14,21, ^3J = 3.5 Hz), 4.81 (s, H-11, 12, 23, 24); ^{1}H NMR (400.13 MHz, [D_8]THF, −78 °C): δ = 12.38 and 5.30 (AX, H-6,18 and H-5,17, ^3J = 16.2 Hz), 5.73 and 5.56 (AB, H-8,20 and H-9, 21, ^3J = 3.6 Hz), 5.50 and 5.45 (AB, H-3,15 and H-2,14, ^3J = 3.5 Hz), 4.72 and 4.66 (AB, H-11,23 and H-12,24, ^3J = 13.8 Hz); ^{13}C NMR (100.61 MHz, [D_8]THF, 21 °C): δ = 157.6 and 155.9 (quat. C), 117.9 (C-5,6,17,18, $^1J(^{13}C,H)$ = 157 Hz), 117.1 (C-2,9,14,21, $^1J(^{13}C,^1H)$ = 174 Hz), 113.4 (C-11,12,23,24, $^1J(^{13}C,^1H)$ = 154 Hz), 111.1 (C-3,8,15,20, $^1J(^{13}C,^1H)$ = 173 Hz); ^{13}C NMR (100.61 MHz, [D_8]THF, −78 °C): δ = 158.0, 157.2, 156.7, 155.6 (quat. C), 118.3 (C-9,21), 118.1 (C-5,17), 117.4 (C-6,18), 117.0 (C-3,15), 114.5 (C-2,14), 114.0 (C-11,23), 112.6 (C-12,24), 108.5 (C-8,20).

[*] Prof. Dr. G. Märkl, H. Sauer, Dr. P. Kreitmeier, Dr. T. Burgemeister, F. Kastner, G. Adolin
Institut für Organische Chemie der Universität
Universitätsstrasse 31, D-93040 Regensburg (FRG)
Telefax: Int. code + (941)943-4505
Prof. Dr. H. Nöth, Dr. K. Polborn
Institut für Anorganische Chemie der Universität München

 © VCH Verlagsgesellschaft mbH, D-69451 Weinheim, 1994 0570-0833/94/1111-1151 $ 10.00+.25/0

Figure 1. The ^{1}H NMR spectra indicate a highly flexible ring system, leading to the rapid equilibration of ring protons H-5/H-6 and H-17/H-18. Semiempirical calculations (AM1, RHF)[14]

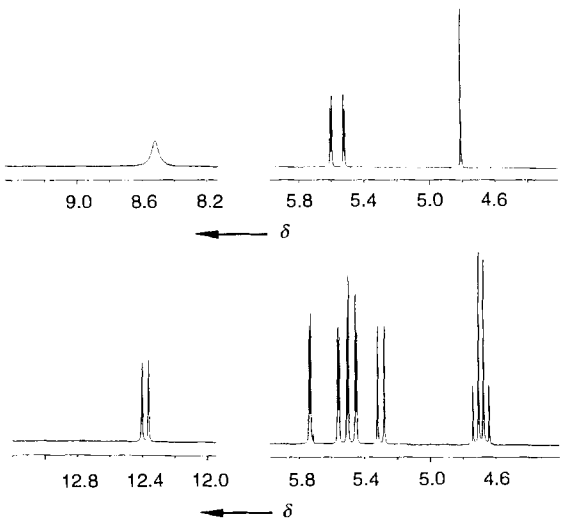
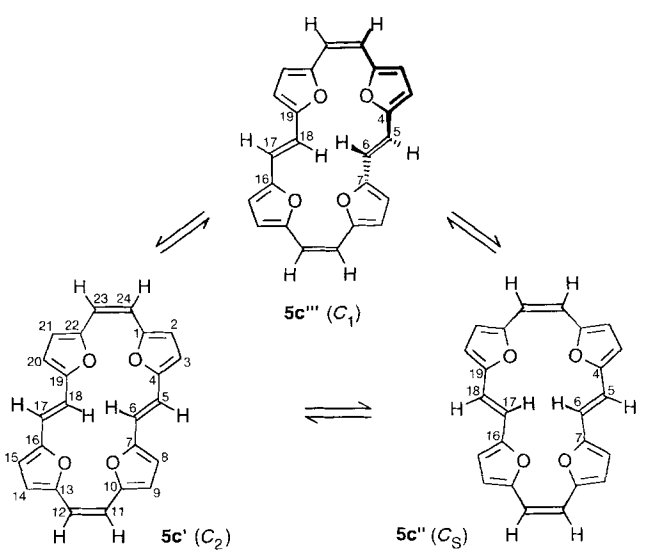


Fig. 1. ^{1}H NMR spectra of *cis,trans,cis-trans*-**5c** at +65 °C (top) and −78 °C (bottom).

indicate a very flat potential energy surface with regard to the rotation of the *trans* double bonds about the 4,5/6,7 and 16,17/18,19 single bonds. Three defined minimum structures are found: **5c′** (approximately C_2-symmetric with boat-type distortion, $\Delta H_f = 95.88$ kcal mol^{-1}), **5c″** (approximately C_s-symmetric with boat-type distortion, $\Delta H_f = 97.13$ kcal mol^{-1}), and **5c‴** (C_1-symmetric with a helical arrangement of the four furan rings, $\Delta H_f = 97.56$ kcal mol^{-1}). A degenerate conversion of **5c′** by synchronous rotation of both *trans* double bonds cannot be discounted based on the potential energy surface. The energy barriers for interconversion of the three conformers **5c′**, **5c″**, and **5c‴**, and the degenerate conversion of **5c′** are less than 10 kcal mol^{-1}.



It can be deduced from the low-temperature spectrum that the *cis,trans,cis,trans*-configurated molecule **5c** is frozen in the **5c′** conformation with C_2 symmetry. In the paratropic 24π ring system the signals of the inner protons H-6, H-18 appear at $\delta = 12.38$, those of the outer protons H-5, H-17 appear at $\delta = 5.30$ as an AX system with $^3J = 16.17$ Hz. With increasing temperature, rotation around the 4,5/6,7 and 16,17/18,19 single bonds occurs, and the inner protons H-6, H-18 equilibrate with the outer protons H-5, H-17. At 65 °C only an averaged signal at $\delta = 8.52$ is observed for H-5, H-6, H-17, H-18 (Fig. 1 b, top). $\Delta G^{\neq}$ is estimated from the coalescence temperature to be approximately 11 kcal mol^{-1}, in good agreement with the results from semiempirical calculations.

The ^{1}H broad-band decoupled ^{13}C NMR spectra of **5c** (100.61 MHz, [D$_8$]THF) at 21 °C and at −78 °C (Table 1) complemented by ^{13}C NMR DEPT measurements at 21 °C and 65 °C and gated decoupling measurements at 21 °C confirm the molecular dynamics of this compound. The ^{1}H NMR signals at 65 °C are assigned based on an NOE difference spectrum measured at 21 °C. The ^{13}C NMR signals at 21 °C and −78 °C are assigned by ^{13}C-^{1}H correlation (Table 1).

X-ray structure analysis[16] confirms that **5c** is in the **5c′** conformation in the solid state. These results are consistent with the conformation found in solution at low temperatures. In the crystal form **5c′** has an inversion center; the nonequivalent furan rings are twisted in opposite directions by approximately 10° (Fig. 2).

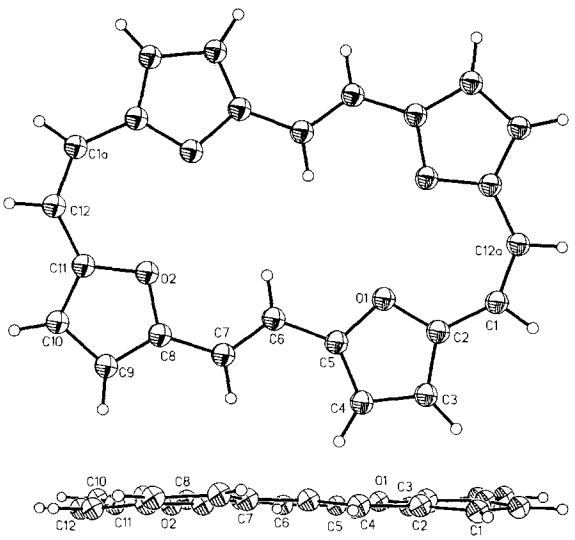
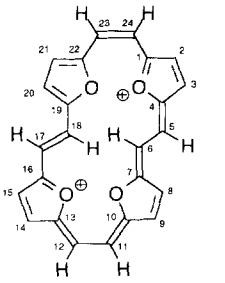


Fig. 2. Crystal structure of **5c′** (ORTEP). Top: view of the molecule from the top; bottom: side view. Selected bond lengths [Å] and angles [°] (standard deviation in parentheses): O1-C2 1.370(2), O1-C5 1.378(2), O2-C8 1.369(2), O2-C11 1.374(2), C1-C2 1.423(3), C1-C12a 1.346(3), C5-C6 1.427(3), C11-C12 1.428(3); C2-O1-C5 107.3(1), C8-O2-C11 107.1(1), O1-C5-C4 108.9(2), O1-C5-C6 117.5(2), C2-C1-C12a 135.6(2), C1-C2-C3 127.7(2), C1-C12a-C11a 134.2(2). Angles formed by the normals to the planes. [°]: O1C2-C5/O2C8-C11 11.5, O2C8-C11/C5-C8 1.2, O1C2-C5/V5-C8 11.1, C5-C8/C11C12C1a-C2a 9.1.

When **5c** is treated with an equimolar amount of bromine in methylene chloride at 0 °C, oxidation to the aromatic tetraoxa[22]porphyrin(2.2.2.2) dication **10** occurs. This compound can be isolated as the bisperchlorate salt in the form of a microcrystalline, blue powder with a metallic sheen (decomp > 300 °C).

The spectroscopic data (Table 2) support the assumption that **10**, like **5c**, has the *cis,trans,cis,trans* configuration with a C_2-symmetric conformation. The assignment of the ^{1}H NMR signals was done with the aid of NOE difference spectroscopy. The results obtained can be applied qualitatively to the ^{1}H NMR



10 (C_2)

spectrum of **5c** at −78 °C. Owing to the low solubility of **10**, ^{13}C-^{1}H correlation spectra could not be measured. In the UV/VIS spectrum of **10** (in 70% perchloric acid) all maxima are red-shifted approximately 100 nm relative to those of **5c**, and the molar extinctions are significantly greater (Fig. 3, Table 2).

The ^{1}H NMR spectrum (400.13 MHz, CF_3COOD, 21 °C) provides clear proof for the configuration of **10**. The protons inside

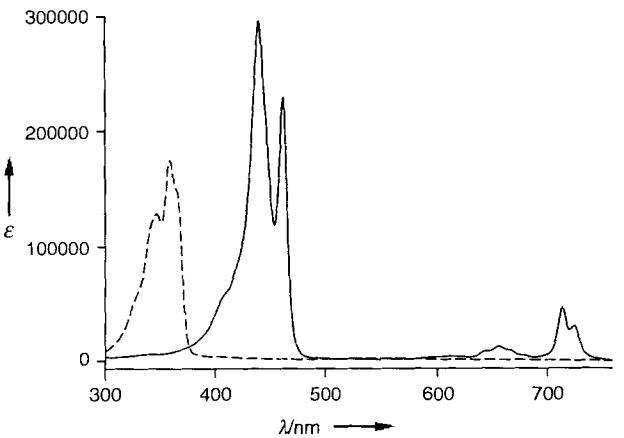


Fig. 3. UV/VIS spectra of **5c** (---) and **10** (—).

the aromatic ring current, H-6 and H-18, are shifted drastically upfield [$\delta = -8.08$ (d, ^{3}J(H,H) = 14.47 Hz)] in comparison with the corresponding protons of **5c** ($\delta = 12.38$). The outer protons

Table 2. Spectroscopic data (MS, UV/VIS, ^{1}H and ^{13}C NMR) for **10** [15].

10: MS(FAB): *m/z* 369 ($(M - 2\,ClO_4 + H)^+$, 49%), 368 ($(M - 2\,ClO_4)^+$, 100); UV/VIS ($HClO_4$): λ_{max} [nm] (ε) = 438 (295600), 460 (229000), 643 (8300), 655 (12600), 666 (9300) sh, 678 (4300) sh, 712 (46000), 723 (30000); ^{1}H NMR (400.13 MHz, CF_3COOD, 21 °C, TMS): δ = 13.66 and −8.08 (AX, H-5,17 and H-6,18, ^{3}J = 14.5 Hz), 12.17 and 11.17 (AB, H-8,20 and H-9,21, ^{3}J = 4.8 Hz), 11.21 and 11.04 (AB, H-3,15 and H-2,14, ^{3}J = 4.6 Hz), 11.50 and 11.42 (AB, H-11,23 and H-12,24, ^{3}J = 13.8 Hz); ^{13}C NMR (100.61 MHz, CF_3COOD, 21 °C, TMS): δ = 166.3, 161.5, 160.4, 159.5 (quart. C), 141.1, 140.3, 136.7, 133.0, 127.4, 126.6, 117.3, 116.7 (CH).

H-5, H-17 are also clearly shifted downfield from $\delta = 5.30$ (d) in **5c** to $\delta = 13.66$ (d) in **10**. In the transition from an antiaromatic to an aromatic system (**5** → **10**) the protons along the inner perimeter are shifted upfield ($\Delta\delta = 20.46$), while the outer protons H-5, H-17 are shifted downfield ($\Delta\delta = 8.36$)! The upfield shift of the protons along the inner perimeter is comparable with the values obtained for octaethyl[22]porphyrin(2.2.2.2)[11] ($\delta = -7.50$) and octaethyl[22]porphyrin(1.3.1.3) ($\delta = -9.54$).[4] The absolute values of the shift on transition from the antiaromatic to the aromatic system are not known in this case, since the [24]porphyrinogens have not yet been described.

The highly dynamic 24 π electron system of **5c** apparently loses its flexibility when it is oxidized to aromatic **10**. In ^{1}H NMR measurements performed on **10** in concentrated D_2SO_4 no dynamic effects are observed up to +180 °C, although the relative integration of the outer protons begins to decrease at 130 °C. This can be attributed to either H/D exchange or sulfonation.

Received: December 27, 1993 [Z 6580 IE]
German version: *Angew. Chem.* **1994**, *106*, 1211

[1] E. Vogel, N. Jux, E. Rodriguez-Val, J. Lex, H. Schmickler, *Angew. Chem.* **1990**, *102*, 1431; *Angew. Chem. Int. Ed. Engl.* **1990**, *29*, 1387; N. Jux, P. Koch, H. Schmickler, J. Lex, E. Vogel, *ibid.* **1990**, *102*, 1429 and **1990**, *29*, 1385.
[2] M. Gosmann, B. Franck, *Angew. Chem.* **1986**, *98*, 1107; *Angew. Chem. Int. Ed. Engl.* **1986**, *25*, 1100.
[3] E. Vogel, M. Köcher, H. Schmickler, J. Lex, *Angew. Chem.* **1986**, *98*, 262; *Angew. Chem. Int. Ed. Engl.* **1986**, *25*, 257.
[4] H. König, C. Eickmeier, M. Möller, U. Rodewald, B. Franck, *Angew. Chem.* **1990**, *102*, 1437; *Angew. Chem. Int. Ed. Engl.* **1990**, *29*, 1393.
[5] E. Vogel, W. Haas, B. Knipp, J. Lex, H. Schmickler, *Angew. Chem.* **1988**, *100*, 445; *Angew. Chem. Int. Ed. Engl.* **1988**, *27*, 406.
[6] B. Frank, C. Wegner, *Angew. Chem.* **1975**, *87*, 419; *Angew. Chem. Int. Ed. Engl.* **1975**, *14*, 424; B. Frank, *ibid.* **1982**, *94*, 327 and **1982**, *21*, 343.
[7] E. Vogel, J. Dörr, A. Herrmann, J. Lex, H. Schmickler, P. Walgenbach, J. P. Gisselbrecht, M. Gross, *Angew. Chem.* **1993**, *105*, 1667; *Angew. Chem. Int. Ed. Engl.* **1993**, *32*, 1600.
[8] E. Vogel, M. Sicken, P. Röhrig, H. Schmickler, J. Lex, O. Ermer, *Angew. Chem.* **1988**, *100*, 450; *Angew. Chem. Int. Ed. Engl.* **1988**, *27*, 411.
[9] J. A. Elix, *Aust. J. Chem.* **1969**, *22*, 1951.
[10] J. E. McMurry, *Chem. Rev.* **1989**, *89*, 1513; J. E. McMurry, M. P. Fleming, K. L. Kees, L. R. Krepski, *J. Org. Chem.* **1978**, *43*, 3255.
[11] H. Saikachi, H. Ogawa, K. Sato, *Chem. Pharm. Bull.* **1971**, *19*, 97.
[12] H. Saikachi, H. Ogawa, Y. Minami, K. Sato, *Chem. Pharm. Bull.* **1970**, *18*, 465.
[13] R. Bachmann, F. Gerson, G. Gscheidt, E. Vogel, *J. Am. Chem. Soc.* **1992**, *114*, 10855.
[14] J. Daub, A. Knorr, Universität Regensburg, personal communication: The calculations were performed with VAMP 4.5.
[15] The ^{1}H and ^{13}C NMR spectra were measured with an ARX 400 spectrometer (Bruker Analytische Messtechnik). The measuring frequencies were 400.13 MHz (^{1}H) and 100.61 MHz (^{13}C). For the ^{1}H NMR spectra TMS was used as internal standard, or when D_2SO_4 was the solvent TMS was used as external standard. For ^{13}C NMR spectra the solvent was used as standard, or if D_2SO_4 was used as solvent, TMS was employed as external standard. The concentrations of the solutions measured were 4 mg **10** in D_2SO_4, 1 mg **10** in CF_3COOD, and 4 mg **5** in [D_8]THF; each sample was prepared with 0.6 mL solvent.
[16] Crystal structure of **5c**': Enraf-Nonius CAD four-circle diffractometer, $Mo_{K\alpha}$ radiation, graphite monochromator. Crystal fragment; size: 0.10 × 0.33 × 0.40 mm. Crystallographic data: $C_{24}H_{24}O_4$, $M_r = 368.39$, $a = 19.330(12)$, $b = 6.765(1)$, $c = 13.603(1)$ Å, $\beta = 97.462(4)°$, $V = 1.7638$ nm^3, monoclinic, space group $C2/m$, $Z = 4$, $\varrho_{calcd} = 1.387$ g cm^{-3}, $\mu = 0.088$ mm^{-1}, $F(000) = 768$. Data collection: 2Φ range: 4–46° in $-h, -k, \pm l$, scan range = 0.65° + 0.35 tan Φ, measuring speed: max. 45 s, 1402 measured reflections, of which 1354 were independent and 966 observed ($F \geq 3\sigma(F)$). Structure solution and refinement: direct methods, anisotropic description of non-hydrogen atoms, H atoms with fixed U_i, 127 variables, $R = 0.0361$, $R_w = 0.0464$. SIR program for structure solution, MolEN program or SHELXTL for refinement. Further details of the crystal structure investigation may be obtained from Fachinformationszentrum Karlsruhe, D-76344 Eggenstein-Leopoldshafen (FRG), on quoting the depository number CSD-58098.

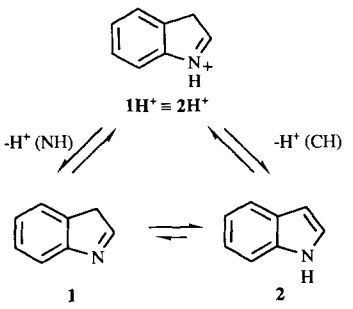
3*H*-Indole**

Ivo G. Gut and Jakob Wirz*

We report on the first spectroscopic identification of 3*H*-indole (**1**) and on its kinetic and thermodynamic stability in aqueous solution. A number of reactions of indole (1*H*-indole, **2**) and its derivatives proceed via the 3*H*-tautomers,[1] for example, the

[*] Prof. Dr. J. Wirz, Dr. I. G. Gut
Institut für Physikalische Chemie der Universität
Klingelbergstrasse 80, CH-4056 Basel (Switzerland)
Telefax: Int. code + (61)267-3855

[**] This work was supported by the Schweizerische Nationalfonds zur Förderung der Wissenschaftlichen Forschung and by Ciba-Geigy SA. We thank P. Renold and G. Strasser, Basel, for experimental cooperation and Profs. A. J. Kresge, University of Toronto, and J. Liebman, University of Maryland, for helpful suggestions.

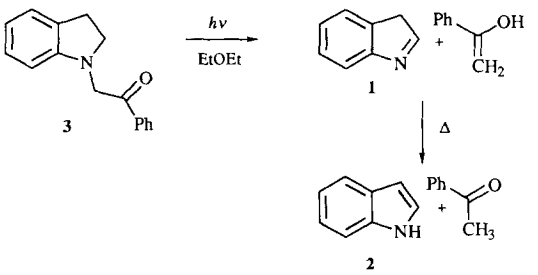


Scheme 1.

acid-catalyzed exchange of the hydrogen atom at C-3 of **2** with the solvent[2] (Scheme 1) and the reactions catalyzed by tryptophanase and tryptophan synthase.[3]

Hill et al. identified **2** and acetophenone as the photoproducts of *N*-indolinylacetophenone (**3**) and proposed that **1** and the enol of acetophenone are the primary photoproducts formed by Norrish type-II fission of **3** (Scheme 2).[4]

When we irradiated (308 or 313 nm) a dilute solution of **3** (10^{-4} M) in anhydrous diethyl ether at room temperature, the



Scheme 2.

changes in the UV spectrum did not correspond to the formation of a 1:1 mixture of acetophenone and **2**. Only when the irradiated mixture was left in the dark did its absorption spectrum change, with a half-life of about 10 h, to that of the final products. This slow reaction is attributed to the ketonization of the enol of acetophenone. The characteristic sharp peak of indole at 287 nm was evident immediately after the irradiation and did not increase in intensity during the dark reaction. Subtraction of the spectrum of indole from the spectrum of the initial photoproduct left a broad, Gaussian-shaped band, λ_{max} = 255 nm, which extended to roughly 300 nm. This spectrum corresponds to that of the enol of acetophenone, which was obtained previously by spectrographic flash photolysis of γ-hydroxybutyrophenone in aqueous solution.[5] Thus, the enol of acetophenone persists for several hours in anhydrous diethyl ether at ambient temperature. In contrast, the tautomerization **1** → **2** appears to be much faster in the same medium.

Completely different UV spectral changes were observed upon irradiation of **3** in anhydrous diethyl ether at −100 °C. In particular, the sharp peak of indole at 287 nm was now absent in the product spectrum. However, when the solution was briefly warmed to −50 °C, the spectrum previously observed shortly after irradiation at room temperature was obtained. These results indicate that 3*H*-indole is stable at −100 °C but is rapidly converted to the 1*H*-tautomer on warming to −50 °C.

Treatment of the solutions with trifluoroacetic acid or ammonia vapor before or after irradiation strongly accelerated the dark reactions. The tautomerization **1** → **2** was less sensitive to base catalysis than the ketonization of the enol of acetophenone: when a solution of **3** in diethyl ether was treated with a trace of ammonia vapor, the spectral changes occurring in the dark at −100 °C indicated ketonization of the enol of acetophenone; the peak of indole at 287 nm was absent. Subtraction of the spectrum of acetophenone provided the absorption spectrum of **1**, which is quite similar to that of 3,3-dimethyl-3*H*-indole[6] (Fig. 1). The tautomerization **1** → **2** now required warming to −20 °C.

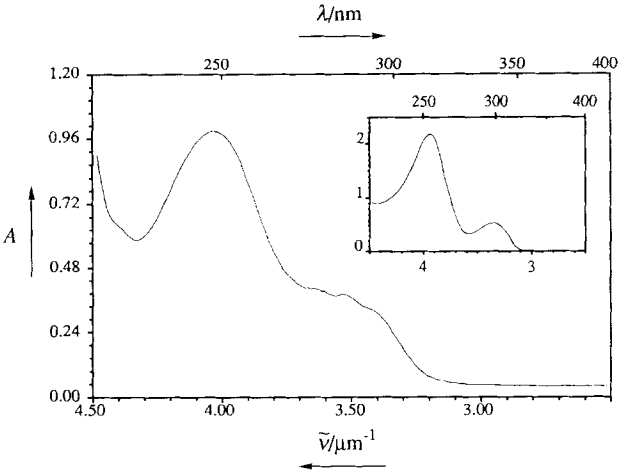
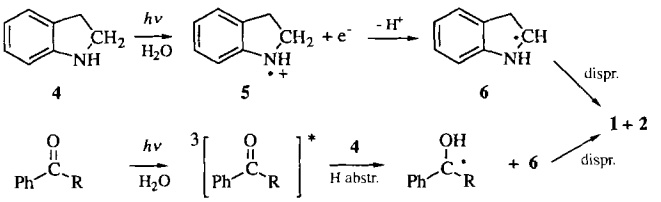


Fig. 1. Absorption spectrum of **1** (diethyl ether, −20 °C); λ_{max}/nm (log ε/($M^{-1}cm^{-1}$)): 248 (4.0), ca. 290 (3.6). Inset: absorption spectrum of 3,3-dimethyl-3*H*-indole (diethyl ether, 25 °C): 255 (4.03), 299 (3.42).

To identify 3*H*-indole by ^{1}H NMR spectroscopy, a solution of **3** (1 mg mL^{-1}) in anhydrous [D_{10}]diethyl ether was treated with a trace of ammonia vapor, irradiated (λ > 345 nm) in an NMR tube at −80 °C, and transferred to the NMR sample chamber, which was also kept at −80 °C. A first spectrum was recorded, the tube was warmed in a bath at −20 °C for 5 min, and a second spectrum was recorded at −80 °C. Finally, the sample was warmed to room temperature for 5 min before a third spectrum was recorded at −80 °C. Comparison of the three spectra with those of authentic samples of **3**, acetophenone, and **2** showed that the first contained predominantly 3*H*-indole (**1**) (δ = 8.40 (s, 1H), 3.79 (s, 2H)) and the enol of acetophenone (δ = 9.8 (s, 1H), 4.64 (s,[7] 1H), 4.31 (s,[7] 1H)). The second spectrum corresponded to a mixture of all tautomers, and the third to one of only **2** and acetophenone. The formation of indole was best monitored by its characteristic peak at δ = 6.49. ^{1}H NMR signals in the aromatic region (δ = 7–8) overlap and could not be analyzed.

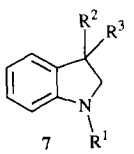
To obtain a reproducible pH–rate profile of the tautomerization **1** → **2** we attempted to generate **1** by flash photolysis in aqueous solution. However, the Norrish type-II photoreaction of **3** is quenched in protic solvents, presumably because an intramolecular charge transfer state is stabilized by solvation.[8] We thus turned to indoline (2,3-dihydroindole, **4**) as an alternative photochemical precursor of **1**; irradiation of a mixture of **4** and acetophenone in ether has been reported to give 2,3-diphenylbutane-2,3-diol and **2**.[4] We found that acetophenone is not necessary for the photo-oxidation of **4** in aqueous solution. Plausible mechanisms for the direct and sensitized photoreactions of **4** are shown in Scheme 3.

Flash photolysis of **4** in aerated aqueous buffer solutions was done with conventional quartz discharge lamps (20 μs pulse width at half intensity). Within 100 μs after irradiation a transient absorption appeared at wavelengths below 320 nm, part of which subsequently decayed by first-order kinetics on the millisecond timescale. The assignment of this transient absorption to 3*H*-indole (**1**) rests on the following observations and is cor-



Scheme 3.

roborated by the kinetic data, which will be discussed later. The absorption onset of the transient coincides with that of **1** (Fig. 1). Variations in alkyl substitution (structures **7**) gave the results expected based on the proposed reaction mechanism (Scheme 3): transients attributable to the corresponding 3*H*-indoles *were* observed with 2,3-dihydrotryptophan (**7**, $R^1 = R^2 = H$, $R^3 = CH_2CHNH_2CO_2H$) and 2,3-dihydroskatol (**7**, $R^1 = R^2 = H$, $R^3 = CH_3$), but *not* with 3,3-dimethylindoline (**7**, $R^1 = H$, $R^2 = R^3 = CH_3$) or *N*-methylindoline (**7**, $R^1 = CH_3$, $R^2 = R^3 = H$). Intermediate **1** was also formed by reaction of indoline with triplet benzophenone or with OH radicals, which were produced by the reaction of triplet benzophenone with an excess of hydrogen peroxide. The transient appeared only in the pH range from about 4.5 to 9. Protonation of **4** ($pK_{a,c} = 5.48 \pm 0.03$)[9] inhibits photoionization in more acidic solutions. In basic solutions the formation of **1** is suppressed by deprotonation of the intermediate radical cation **5** (the pK_a of aniline radical cation is 7.0).[10]



7

The decay rate of **1** depended linearly on proton and on buffer concentrations. Bilinear regression of the rate data obtained with acetic acid buffers versus [HAc] and [Ac^-] as independent variables indicated that only the acid contributes significantly to buffer catalysis. The slopes and extrapolated intercepts of the buffer dilution plots at constant buffer ratio are given in Table 1. Rate constants at zero buffer concentration, which were determined from the intercepts, were accurately proportional to proton concentration throughout the accessible pH range from 4.5 to 9. Contributions from a pH-independent reaction were not detectable down to the lowest proton concentrations, $k_0 \leq 0.01\ s^{-1}$, nor was saturation of acid catalysis apparent at the highest proton concentrations accessible, $[H^+] \cong 10^{-5}$ M. The last result provides an upper limit for the NH dissociation constant of protonated indole, pK_a^{NH} (**2**-H^+) ≤ 4.3, since proton catalysis is expected to reach a plateau when **1** is protonated at nitrogen. The rate constant for catalysis by acetic acid (weighted average of the slopes determined from the buffer dilution plots, Table 1) is $k_{HAc} = (2.2 \pm 0.2) \times 10^3\ M^{-1} s^{-1}$, and that for proton catalysis (weighted average of intercepts divided by [H^+], Table 1) is $k_{H^+} = (4.9 \pm 0.3) \times 10^6\ M^{-1} s^{-1}$. The ratio of these catalytic coefficients, k_{H^+}/k_{HAc}, is $(2.2 \pm 0.3) \times 10^3$.

Table 1. Buffer dilution regression analyses for the decay rates of **1** in aqueous solution at 25 °C. Ionic strength was held at $I = 0.1$ M by the addition of NaCl. Total buffer concentration ranges were 0.02–0.1 M.

Buffer	[HA]/[A]	$[H^+]$/M [a]	No. of date points	Slope k_{HA}/($M^{-1} s^{-1}$)	Intercept $k_{H^+}[H^+]/s^{-1}$
Tris [b]	0.111	8.45×10^{-10}	41	1.9 ± 0.2	< 0.01
Tris	9.00	6.83×10^{-8}	55	3.4 ± 0.1	0.37 ± 0.01
acetate	0.0892	2.51×10^{-6}	55	$(1.8 \pm 0.2) \times 10^3$	11.7 ± 0.5
acetate	0.111	3.15×10^{-6}	44	$(2.5 \pm 0.2) \times 10^3$	13.0 ± 0.9
acetate	0.126	3.55×10^{-6}	57	$(1.9 \pm 0.2) \times 10^3$	20.4 ± 0.8
acetate	0.224	6.31×10^{-6}	30	$(1.4 \pm 0.2) \times 10^3$	37 ± 2
acetate	0.282	7.95×10^{-6}	41	$(3.6 \pm 0.7) \times 10^3$	54 ± 10
acetate	0.295	8.31×10^{-6}	34	$(2.3 \pm 0.3) \times 10^3$	56 ± 4
acetate	0.502	1.41×10^{-5}	36	$(2.5 \pm 0.3) \times 10^3$	88 ± 6
acetate	0.561	1.58×10^{-5}	19	$(3.4 \pm 0.3) \times 10^3$	110 ± 6
acetate	1.00	2.82×10^{-6}	98	$(2.8 \pm 0.3) \times 10^3$	186 ± 8

[a] $[H^+]$ was calculated using the concentration quotients $pK_{a,c}$(HAc, $I = 0.1$ M, 25 °C) = 4.55 [11] and $pK_{a,c}$($TrisH^+$, $I = 0.1$ M, 25 °C) = 8.12 [12]. The calculated values agreed with the readings of a calibrated [13] glass electrode to within 0.02 log units. [b] Tris = tris(hydroxymethyl)methyl amine.

Rate constants for the displacement of deuterium and tritium from the 3-position of [D_1]indole and [T_1]indole, respectively, were determined by Challis and Millar[2] for aqueous acetic acid buffer solutions at 25 °C and ionic strength $I = 0.1$ M. The incidence of general acid catalysis was attributed to protonation at C-3 by the general acid. The same authors have estimated, on the basis of the relation by Swain et al.,[14a] the ratio of the rate constants of proton and deuterium loss from C-3 of protonated indole [D_1]**2**-H^+ as $k_2^H/k_2^D = 5.6 \pm 0.3$ for the reaction with solvent water and $k_2^H/k_2^D = 5.3 \pm 0.4$ for the reaction with acetate ion. They noted explicitly that these estimates did not account for the secondary isotope effects involved. To obtain a more accurate estimate we used the method of Kresge and Chiang,[14b] which gave ${}^Dk_2^H/{}^Hk_2^D = 6.3 \pm 1.3$ for the reaction with solvent water, and ${}^Dk_2^H/{}^Hk_2^D = 6.2 \pm 1.3$ for the reaction with acetate ion. The rate constant for the protonation of indole is then given by ${}^Hk_1^H = (1 + {}^Dk_2^H/{}^Hk_2^D)^D k_{obsd}({}^Hk_1^H/{}^Dk_1^H)$. The kinetic data of Challis and Long for deuterium displacement, ${}^Dk_{obsd}$, thus provide estimates for the rates of protonation of **2** by protons, $k_{H^+} = {}^Hk_1^H(H^+) = 6.2 \pm 1.6\ M^{-1} s^{-1}$, and by acetic acid, $k_{HAc} = {}^Hk_1^H(HAc) = (5.2 \pm 1.4) \times 10^{-3}\ M^{-1} s^{-1}$, in water at 25 °C. The ratio of the two constants is $k_{H^+}/k_{HAc} = (1.2 \pm 0.5) \times 10^3$.

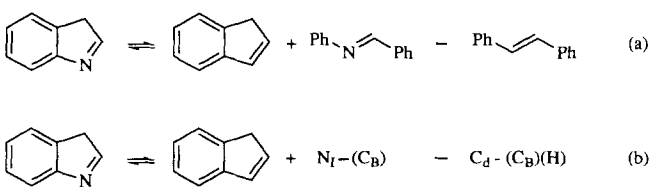
The ratio of the two catalytic coefficients must be the same for the forward and backward reaction **1** ⇄ **2**. The ratio determined from the data of Challis and Long, $k_{H^+}/k_{HAc} = (1.2 + 0.5) \times 10^3$, is, on a purely statistical basis, significantly different from our value of $(2.2 \pm 0.3) \times 10^3$ given above. But considering the various possible sources of systematic errors in both of the completely independent determinations and the necessity of correcting for the unknown secondary isotope effect in the literature data,[2] the near agreement may be considered to be satisfactory. Moreover, catalysis by acetate ion was consistently insignificant in both studies. These results lend further support to the assignment of the transient absorbance observed by flash photolysis of **4** to 3*H*-indole (**1**). The equilibrium constant of tautomerization, $K_T = [\mathbf{1}]/[\mathbf{2}]$, can now be calculated from the ratio of the rates of the forward and backward reactions catalyzed by protons, $K_T = (1.3 \pm 0.4) \times 10^{-6}$, and by acetic acid, $K_T = (2.4 \pm 0.7) \times 10^{-6}$. The average of these values is $K_T = (1.7 \pm 0.6) \times 10^{-6}$, $pK_T = 5.8 \pm 0.2$.

Hinman and Lang estimated the C–H acidity of protonated indole **2**-H^+, $pK_a = -3.5$, by spectrophotometric determination of its ionization ratio in concentrated sulfuric acid solutions.[16] Bunnett and Olson later reevaluated these data by using their improved acidity function which gave $pK_a = -2.5$.[17] We have reevaluated the same data using the *X* acidity function of Cox and Yates[18] and have obtained the same value. Thus the value $pK_a = -2.5$ should be a good approximation of the thermodynamic acidity constant of **2**-H^+ in aqueous solution. The activity coefficients of **2**-H^+ and H^+ should largely cancel at ionic strength $I = 0.1$. We therefore assume the same value for the concentration quotient, $pK_{a,c}^{CH}(I = 0.1\ M) = -2.5 \pm 0.2$, where the error range indicates our estimate of the possible systematic errors involved. The N–H acidity constant of **2**-H^+ may then be calculated from the thermodynamic cycle

 © VCH Verlagsgesellschaft mbH, D-69451 Weinheim, 1994 0570-0833/94/1111-1155 $ 10.00+.25/0

shown in Scheme 1, $pK_{a,c}^{NH}(I = 0.1\,M) = pK_T + pK_{a,c}^{CH}(I = 0.1\,M) = 3.3 \pm 0.4$, which is consistent with the upper limit of 4.3 given above. For comparison, we determined[9] the acidity constant of protonated 3,3-dimethyl-3*H*-indole to be $pK_{a,c}^{NH} = 2.85 \pm 0.01$.

We calculated the enthalpy of isomerization $\mathbf{1} \rightarrow \mathbf{2}$ with the semiempirical methods MNDO,[19a] AM1,[19b] and PM3[19c] of the Spartan 2.0 program package and obtained the values $\Delta_{1\rightarrow 2}H = -9.6$, $+41.8$, and $+78.2\,kJ\,mol^{-1}$, respectively. Much simpler, and probably more reliable estimates of the gas-phase heat of formation of **1** are obtained from the isodesmic reactions shown in Scheme 4. For reaction (a) we used



Scheme 4.

the experimental enthalpies of formation of a) indene, $\Delta_f H_m^{\ominus}(g, 298\,K) = 163.6 \pm 1.5\,kJ\,mol^{-1}$,[20a] *trans*-stilbene, $\Delta_f H_m^{\ominus}(g, 298\,K) = 236\,kJ\,mol^{-1}$,[20b] and *N*-benzylidenaniline, $\Delta_f H_m^{\ominus}(g, 298\,K) = 278.7 \pm 2.2\,kJ\,mol^{-1}$,[20c] and for reaction (b) the first value and Benson's increments for the groups $N_I-(C_B) = 69.9$ and $C_d-(C_B)(H) = 28.4\,kJ\,mol^{-1}$.[21] Both approaches (a) and (b) give nearly identical estimates for the gas-phase heat of formation of **1**, $\Delta_f H_m^{\ominus}(g, 298\,K) = 206 \pm 5\,kJ\,mol^{-1}$. Comparison with the heat of formation of indole, $\Delta_f H_m^{\ominus}(g, 298\,K) = 186.6 \pm 4.6\,J\,mol^{-1}$,[20a] then gives $\Delta_{1\rightarrow 2}H = 19 \pm 10\,kJ\,mol^{-1}$. From the equilibrium constant $pK_T = 5.8 \pm 0.2$ determined in this report we obtain $\Delta_{1\rightarrow 2}G^{\ominus}(aq, 298\,K) = 33 \pm 1\,kJ\,mol^{-1}$ for the Gibbs free energy change in aqueous solution.

In conclusion, the hitherto unknown 3*H*-isomer of indole is remarkably stable in slightly basic aqueous solutions ($\tau \cong 100$ s at pH $\cong$ 9 and 25 °C). The equilibrium constant for the tautomerization of indole **2** to 3*H*-indole (**1**) is $pK_T = 5.8 \pm 0.2$ in aqueous solution; in other words, the equilibrium concentration of **1** is about 1 to 2 ppm. The tautomerization is catalyzed by acid and, less efficiently, by base. The catalytic coefficients for the reaction $\mathbf{1} \rightarrow \mathbf{2}$ are $k_{H^+} = (4.9 \pm 0.3) \times 10^6\,M^{-1}\,s^{-1}$ and $k_{OH^-} \cong 1 \times 10^2\,M^{-1}\,s^{-1}$.[22]

Received: December 27, 1993 [Z 6583 IE]
German version: *Angew. Chem.* **1994**, *106*, 1240

[1] R. J. Sundberg, *The Chemistry of Indoles*, Academic Press, New York, **1970**, pp. 1–82.
[2] B. C. Challis, E. M. Millar, *J. Chem. Soc. Perkin. Trans. 2* **1972**, 1618–1624, 1625–1628.
[3] A. N. Lane, K. Kirschner, *Eur. J. Biochem.* **1983**, *129*, 571–582; R. S. Phillips, E. W. Miles, L. A. Cohen, *Biochemistry* **1984**, *23*, 6228–6234; *J. Biol. Chem.* **1985**, *260*, 14665–14670; R. S. Phillips, *J. Am. Chem. Soc.* **1989**, *111*, 727–730.
[4] J. Hill, M. M. Zakaria, D. Mumford, *J. Chem. Soc. Perkin. Trans. 1* **1983**, 2455–2458.
[5] Y. Chiang, A. J. Kresge, J. Wirz, *J. Am. Chem. Soc.* **1984**, *106*, 6392–6395.
[6] A. H. Jackson, P. P. Lynch, *J. Chem. Soc. Perkin Trans. 2* **1987**, 1215–1219.
[7] The geminal couplings were not resolved: typical values in related enols are $J_{gem} \cong 1$ Hz: B. Capon, B.-Z. Guo, F. C. Kwok, A. K. Siddhanta, C. Zucco, *Acc. Chem. Res.* **1988**, *21*, 135–140.
[8] P. J. Wagner, A. E. Kemppainen, *J. Am. Chem. Soc.* **1969**, *91*, 3085–3087; A. Padwa, W. Eisenhardt, R. Gruber, D. Pashayan, *ibid.* **1969**, *91*, 1857–1859; P. J. Wagner, T. Jellinek, *ibid.* **1971**, *93*, 7328–7330; P. J. Wagner, D. A. Ersfeld, *ibid.* **1976**, *98*, 4515–4518.
[9] Titrations were carried out at 25.0 ± 0.1 °C in the presence of a suitable buffer (acetic acid for **4**, chloroacetic acid for 3,3-dimethyl-3*H*-indole). Ionic strength was held at $I = 0.1$ M by the addition of NaCl. Least squares fitting of the factor-analyzed spectrophotometric data was performed using the program SPECFIT: H. Gampp, M. Maeder, C. J. Meyer, A. D. Zuberbühler, *Talanta* **1985**, *32*, 95–101, 257–264. The resulting acidity constants are concentration quotients, $K_{a,c}$, at $I = 0.1$ M.
[10] E. J. Land, G. Porter, *Trans. Faraday Soc.* **1963**, *59*, 2027–2037.
[11] M. Kilpatrick, R. D. Eanes, *J. Am. Chem. Soc.* **1953**, *75*, 586–587.
[12] R. G. Bates, H. B. Hetzer, *J. Phys. Chem.* **1961**, *65*, 667–671.
[13] H. Sigel, A. D. Zuberbühler, O. Yamauchi, *Anal. Chim. Acta* **1991**, *255*, 63–72.
[14] a) C. G. Swain, E. C. Stivers, J. F. Reuwer, Jr., L. J. Schaad, *J. Am. Chem. Soc.* **1958**, *80*, 5885–5893. b) The consideration of the secondary isotope effect closely follows A. J. Kresge, Y. Chiang, *ibid.* **1967**, *89*, 4411–4417: taking the ratio of equations (11) and (13) from this paper, and making repeated use of the Swain relation, $(k_H/k_D)^{1.442} = k_H/k_T$, gives $({}^{T}k_i/{}^{D}k)_{obsd} = ({}^{H}k_1^{H}/{}^{D}k_1^{H})^{0.442}(1+x)/(1+x^{1.442})$, which can be solved for $x \equiv ({}^{D}k_2^{H}/{}^{H}k_2^{D})$. The quoted error ranges are based on the standard errors of the experimental data [2] and on the assumed range for the secondary isotope effect for protonation of **2**. ${}^{D}k_1^{H}/{}^{H}k_1^{H} = 1.15 \pm 0.05$ [15].
[15] A. Streitwieser, Jr., R. H. Jagow, R. C. Fahey, S. Suzuki, *J. Am. Chem. Soc.* **1958**, *80*, 2326–2332; E. A. Halevi, *Prog. Phys. Org. Chem.* **1963**, *1*, 109–221.
[16] R. L. Hinman, J. Lang, *J. Am. Chem. Soc.* **1964**, *86*, 3796–3806.
[17] J. F. Bunnett, F. P. Olson, *Can. J. Chem.* **1966**, *44*, 1899–1916.
[18] R. A. Cox, K. Yates, *Can. J. Chem.* **1983**, *61*, 2225–2243; R. A. Cox, *Acc. Chem. Res.* **1987**, *20*, 27–31.
[19] a) M. J. S. Dewar, W. Thiel, *J. Am. Chem. Soc.* **1977**, *99*, 4899–4907, 4907–4917; b) M. J. S. Dewar, E. G. Zoebisch, E. F. Healy, J. J. P. Stewart, *ibid.* **1985**, *107*, 3902–3909; c) J. J. P. Stewart, *J. Comput. Chem.* **1989**, *10*, 209–220, 221–264.
[20] a) J. D. Cox, G. Pilcher, *Thermochemistry of Organic and Organometallic Compounds*, Academic Press, London, **1970**; b) E. S. Domalski, E. D. Hearing, *J. Phys. Chem. Ref. Data* **1988**, *17*, 1637–1678; c) J. J. Kirchner, W. E. Acree, Jr., G. Pilcher, L. Shaofeng, *J. Chem. Thermodyn.* **1986**, *18*, 793–799.
[21] S. W. Benson, *Thermochemical Kinetics*, 2nd ed., Wiley, New York, **1976**.
[22] The rate constant for catalysis by hydroxide ions was estimated from the coefficient of base-catalyzed dedeuteration of **2** [2] and the equilibrium constant K_T.

Synthesis, Structures, and Reactions of Two Bis(diaminostannylene)s and a Bis(diaminogermylene) Containing a Central C_6 Ring**

Holger Braunschweig, Peter B. Hitchcock, Michael F. Lappert,* and Luc J.-M. Pierssens

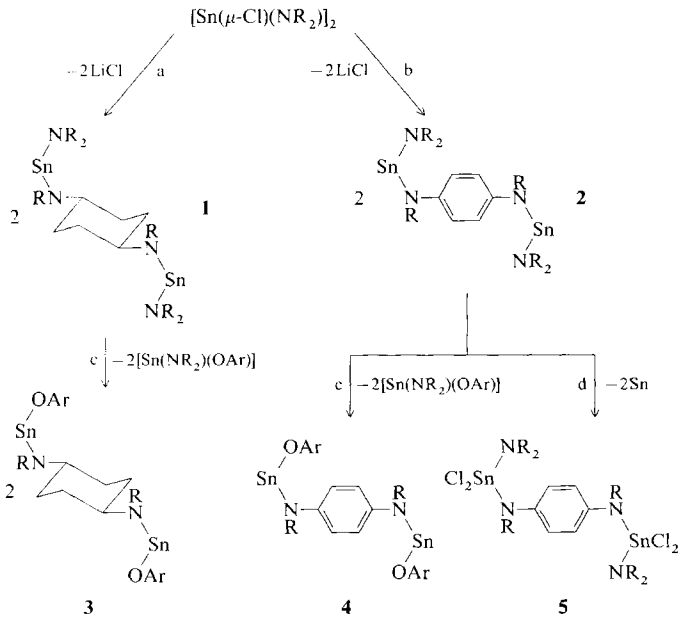
Until about 20 years ago thermally stable bivalent compounds of Ge, Sn, and Pb (=M), the heavier Group 14 element analogues of carbenes, were unknown. Since then a number of mononuclear, homoleptic, thermally stable but highly reactive, colored, diamagnetic compounds MX_2 have been described, in which the monohapto ligand X^- was bulky and free from β-hydrogen atoms. Among those to have been X-ray-characterized are those having X = NR_2,[1, 2] OAr,[3] or SAr,[4] while $M'(CHR_2)_2$ (M' = Ge or Sn) had the same V-shaped (X-M'-X = 88–105°) structure in the gas phase,[5] but were dimeric (*trans*-M'_2X_4) in the crystal.[6] A recent development concerns the first heteroleptic compounds, the stannylenes SnXX', including the structurally authenticated $[Sn(NR_2)(OAr)]$[7a] and the germylene $[Ge(CR_3)(CHR_2)]$.[7b][***]

[*] Prof. M. F. Lappert, Dr. H. Braunschweig, Dr. P. B. Hitchcock, L. J.-M. Pierssens
School of Chemistry and Molecular Sciences
University of Sussex
Brighton BN1 9QJ (UK)
Telefax: Int. code + (273) 677196

[**] We thank Deutsche Forschungsgemeinschaft for the award of a fellowship to H. B., Science and Engineering Research Council for support, and Dr. B. Mathieu for the Mössbauer data.

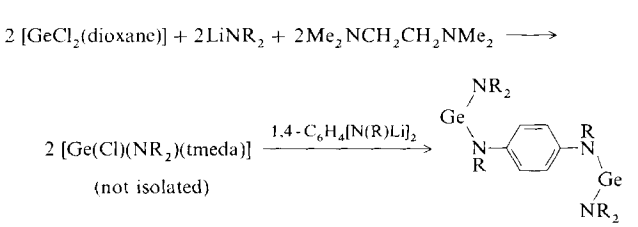
[***] Throughout the communication R stands for $SiMe_3$ and Ar for 2,6-tBu_2-4-MeC_6H_2.

We have now prepared the binuclear compounds XM′–Z–M′X in which the bridging group Z^{2-} is the *N*,*N*′-bis(trimethylsilyl)-*trans*-1,4-cyclohexanediamido or its aromatic equivalent the 1,4-benzenenediamido ligand. The synthesis of such heteroleptic bis(stannylene)s **1** and **2** (X = NR_2) is shown in Scheme 1. Both **1** and **2** could be converted into the corresponding aryloxides [(ArO)M′-Z-M′(OAr)] **3** and **4**, respectively, by treatment with $Sn(OAr)_2$;[3] this metathetical exchange reaction parallels that between $Sn(NR_2)_2$ and $Sn(OAr)_2$ which leads to the formation of $[Sn(NR_2)(OAr)]$.[1] Surprisingly, however, whereas $Sn(NR_2)_2$ and $SnCl_2$ react to give $[Sn(\mu\text{-}Cl)(NR_2)]_2$,[8] treatment of **2** with $SnCl_2$ led to the redox products **5** and tin. A single precedent appears to be in the reaction of $Sn(CHR_2)_2$ with $SnCl_2$ which gave $[Sn(CHR_2)_2Cl_2]$ and tin.[5]



Scheme 1. Synthesis of the bis(diaminostannylene)s **1** and **2** and their conversions into the bis[amino(aryloxy)stannylene]s **3** and **4**, respectively, and into the bis[diamido(dichloro)tin(IV)] compound **5**. Reagents and conditions: a) 1,2-$C_6H_{10}[N(R)Li]_2$ [from *trans*-1,4-$C_6H_{10}(NHR)_2$], C_6H_{14}, 25 °C, 2 h; b) as a) but with 1,4-$C_6H_4[N(R)Li]_2$ [10]; c) (NMR expt. for **3**) $2Sn(OAr)_2$, toluene, 25 °C, 16 h; d) (NMR expt.) $2SnCl_2$, Et_2O, C_6D_6, 20 °C, 7 d.

Although a germanium analogue of $[Sn(\mu\text{-}Cl)(NR_2)]_2$ has not been reported, the reaction in Scheme 2 (tmeda = $Me_2NCH_2CH_2NMe_2$) yielded the bisgermylene **6**, presumably via this intermediate. Some data on **1**–**6** are given in Table 1; ^{119}Sn NMR spectroscopy was diagnostic in following the reactions leading to **1** and **5**, since each compound has a distinct $^{119}Sn\{^1H\}$NMR signal, which differs from those of possible coproducts. Compounds **1**, **2**, **4**, and **6** were also characterized



Scheme 2. Synthesis of the bis(diaminogermylene) **6**.

Table 1. Some analytical and spectroscopic data of **1**–**6**. ^1H NMR: 360 MHz, 305 K, C_6D_6; $^{119}Sn\{^1H\}$ NMR: 186.42 MHz, 300 K, C_6D_6 [a].

1: Yellow; 46% yield; $\delta[^{119}Sn\{^1H\}] = 694$; $\delta(^1H) = 0.25$ (s, 36H; $SiMe_3$), 0.43 (s, 18H; $SiMe_3$), 1.76–1.78 (m, 4H; CH_2), 1.85–1.88 (m, 4H; CH_2), 4.85 (br., 2H; CH)

2: Orange; 70% yield, $\delta[^{119}Sn\{^1H\}] = 606$; $\delta(^1H) = 0.10$ (s, 36H; $SiMe_3$), 0.28 (s, 18H; $SiMe_3$), 6.72 (s, 4H; C_6H_4)

3 [b]: Orange; 100% yield; $\delta[^{119}Sn\{^1H\}] = 283$

4: Yellow; 50% yield; $\delta[^{119}Sn\{^1H\}] = 173$; $\delta(^1H) = -0.86$ (s, 18H; $SiMe_3$), 1.19 (s, 6H; Me), 6.65 (s, 4H; C_6H_4), 6.86 (s, 4H; C_6H_2)

5 [b]: Yellow; 100% yield; $\delta[^{119}Sn\{^1H\}] = 61.1$

6: Orange; 77% yield

[a] $\delta[^{119}Sn\{^1H\}]$ value for $Sn(NR_2)_2$ at 283 K 766, for $Sn(OAr)_2$ −192, for $Sn(NR_2)(OAr)$ 277, for $[Sn(\mu\text{-}Cl)(NR_2)]_2$ 138. [b] This was an NMR experiment; not isolated in the solid state.

by their ^1H and ^{13}C NMR spectra and microanalyses, and **1**, **2**, and **4** by ^{119}Sn Mössbauer spectra (isomer shifts of 2.92 ± 0.6 $mm\,s^{-1}$ and quadrupole splitting of 3.21 ± 0.15 $mm\,s^{-1}$).

The structures of the crystalline bis(stannylene)s **1** (Fig. 1) and **2** (Fig. 2) and the bisgermylene **6** (isomorphous with **2**) (Fig. 2)[9] revealed that the two M′(NR_2) fragments are *trans* to one another. The angle between the aromatic ring and the plane containing M′-N(1)-Si(1) in **2** and **6** is 83°. This conformation is

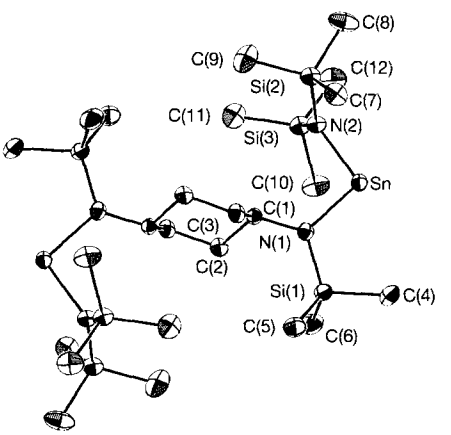


Fig. 1. Molecular structure of **1**. Selected bond lengths [Å] and angles [°]: Sn-N(1) 2.062(2), Sn-N(2) 2.117(2), N(1)-C(1) 1.482(3); N(1)-Sn-N(2) 99.78(8), Sn-N(2)-Si(2) 116.3(1), Sn-N(1)-C(1) 120.7(2).

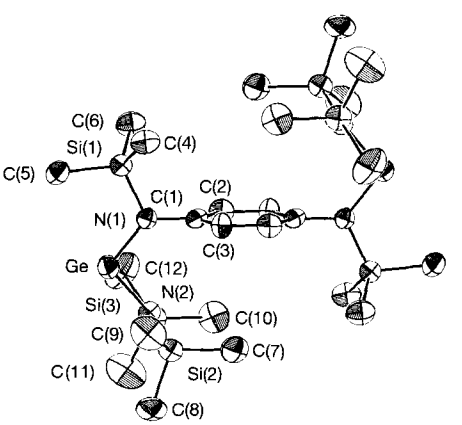


Fig. 2. Molecular structure of **2** and **6** (shown). Selected bond lengths [Å] and angles [°]; data for **6** in square brackets: M′-N(1) 2.066(6) [1.855(2)], M′-N(2) 2.082(7) [1.885(5)], N(1)-C(1) 1.449(11) [1.444(9)]; N(1)-M′-N(2) 101.8(3) [104.7(2)], M′-N(2)-Si(2) 115.3(4) [116.8(3)], M′-N(1)-C(1) 124.8(5) [126.1(4)].

probably retained in C_6D_6 solution because the ^1H and $^{13}C\{^1H\}$ NMR spectra showed a single CH (**2** or **6**) or CH_2 (**1**) environment in the appropriate six-membered ring; alternatively, there may have been fast rotation about the C–N bonds. The M′–N bond lengths and N-M′-N bond angles may be compared with those [2.096(1) and 2.088(6) Å; 104.7(2)°] in crystalline $Sn(NR_2)_2$[2] and [1.878(5) and 1.873(5) Å; 107.1(2)°] in crystalline $Ge(NR_2)_2$.[11] It is noteworthy that the M′–N(aryl) bond in **2** or **6** is significantly shorter than the M′-NR_2 bond, the latter being slightly shorter than in $M'(NR_2)_2$.

The new bridging ligands 1,4-$C_6H_4(NR)_2$ may well prove to have a useful role in a wider range of coordination chemistry, in particular, in the context of determining whether the metal fragment at one nitrogen can "communicate" with the other, as may well be the case for the aromatic system.

Experimental Procedure

2: 1,4-Bis(trimethylsilylamino)benzene [12] (8.0 g, 31 mmol) in hexane (70 mL) was treated with two molar equivalents of an *n*BuLi (41 mL, 62 mmol in *n*-hexane) solution at 25 °C. The mixture was stirred for 12 h. Volatiles were removed in vacuo to yield the yellow solid 1,4-$C_6H_4[N(R)Li]_2$ (8.1 g, 98%). The latter (1.30 g, 4.92 mmol) in *n*-hexane (40 mL) was added to $[Sn(\mu\text{-}Cl)(NR_2)]_2$ [8] (3.09 g, 4.92 mmol) at 25 °C and the mixture was stirred for 2 h, and then filtered. Volatile components were removed from the filtrate in vacuo; the residue was extracted with diethyl ether (10 mL). After 2 d at −30 °C, orange crystals of **2** (2.78 g, 70%) were obtained; correct elemental analysis.

1 and **6**: These were prepared by a similar procedure from *trans*-1,4-$C_6H_{10}[N(R)Li]_2$ and $[Sn(\mu\text{-}Cl)(NR_2)]_2$ (**1**) or for **6** from 1,4-$C_6H_4[N(R)Li]_2$ and $[GeCl(NR_2)$-(tmeda)]. The latter (2.86 g, 86%) (as colorless crystals) was obtained by mixing $[GeCl_2$(dioxane)] (2.00 g, 8.64 mmol), $LiNR_2$ (1.45 g, 8.64 mmol), and $[(Me_2NCH_2)_2$(tmeda)] (1.00 g, 17.28 mmol) in Et_2O (30 mL) by stirring for 16 h at 25 °C, freeing from volatiles in vacuo, and extracting with toluene/hexane (1:1).

4: Toluene (40 mL) was added to **2** (1.5 g, 19 mmol) and $Sn(OAr)_2$ (2.1 g, 37 mmol) at 25 °C. The pale brown reaction mixture was stirred for 16 h, then filtered. The filtrate was concentrated in vacuo and cooled (−5 °C) to yield crystalline **4** (0.86 g, 50%); correct elemental analysis.

Received: January 13, 1994 [Z 6614 IE]
German version: *Angew. Chem.* **1994**, *106*, 1243

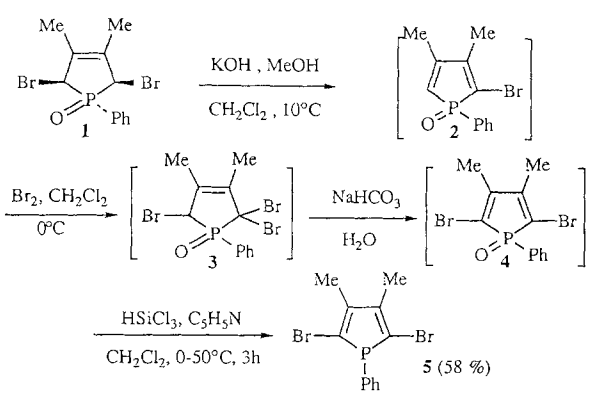
[1] R. W. Chorley, P. B. Hitchcock, M. F. Lappert, W.-P. Leung, P. P. Power, M. M. Olmstead, *Inorg. Chim. Acta* **1992**, *198–200*, 203.
[2] T. Fjeldberg, H. Hope, M. F. Lappert, P. P. Power, A. J. Thorne, *J. Chem. Soc. Chem. Commun.* **1983**, 639.
[3] B. Çetinkaya, I. Gümrükçü, M. F. Lappert, J. L. Atwood, R. D. Rogers, M. J. Zaworotko, *J. Am. Chem. Soc.* **1980**, *102*, 2088.
[4] P. B. Hitchcock, M. F. Lappert, B. J. Samways, E. L. Weinberg, *J. Chem. Soc. Chem. Commun.* **1983**, 1492.
[5] T. Fjeldberg, A. Haaland, B. E. R. Schilling, M. F. Lappert, A. J. Thorne, *J. Chem. Soc. Dalton Trans.* **1986**, 1551.
[6] D. E. Goldberg, P. B. Hitchock, M. F. Lappert, K. M. Thomas, A. J. Thorne, T. Fjeldberg, A. Haaland, B. E. R. Schilling, *J. Chem. Soc. Dalton Trans.* **1986**, 2387.
[7] a) H. Braunschweig, R. W. Chorley, P. B. Hitchcock, M. F. Lappert, *J. Chem. Soc. Chem. Commun.* **1992**, 1311; b) P. Jutzi, A. Becker, H. G. Stammler, B. Neumann, *Organometallics* **1991**, *10*, 1647.
[8] R. W. Chorley, P. B. Hitchcock, B. S. Jolly, M. F. Lappert, G. A. Lawless, *J. Chem. Soc. Chem. Commun.* **1991**, 1302.
[9] Crystal data: **1**: $M = 814.7$, triclinic, $P\bar{1}$, $a = 8.448(3)$, $b = 10.273(4)$, $c = 12.160(5)$ Å, $\alpha = 100.63(3)$, $\beta = 106.73(3)$, $\gamma = 92.53(3)°$, $V = 988.0$ Å^3, $Z = 1$, $\rho_{calcd} = 1.37$ g cm^{-3}, $F(000) = 420$, $\mu = 14.7$ cm^{-1}, $T = 173$ K, 3241 Unique reflections, $R = 0.027$, $R_w = 0.040$, $S = 1.6$, 163 variables. **2**: $M = 808.7$, monoclinic, $C2/c$ (no. 15), $a = 10.891(2)$, $b = 14.229(3)$, $c = 25.747(5)$ Å, $\beta = 94.08(1)°$, $V = 3979.7$ Å^3, $Z = 4$, $\rho_{calcd} = 1.35$ g cm^{-3}, $F(000) = 1656$, $\mu = 14.6$ cm^{-1}, $T = 293$ K, 1924 Unique reflections, $R = 0.058$, $R_w = 0.074$, $S = 2.1$, 163 variables. **6**: $M = 716.5$, monoclinic, $C2/c$ (no. 15), $a = 10.698(5)$, $b = 14.317(8)$, $c = 25.592(7)$, $\beta = 93.39(3)°$, $V = 3912.7$ Å^3, $Z = 4$, $\rho_{calcd} = 1.22$ g cm^{-3}, $F(000) = 1512$, $\mu = 17.1$ cm^{-1}, $T = 293$ K, 3597 Unique reflections, $R = 0.056$, $R_w = 0.065$, $S = 1.7$, 163 variables. For each structure data were measured for $2 < \theta < 25°$ using monochromated $Mo_{K\alpha}$ radiation ($\lambda = 0.71069$ Å) on an Enraf-Nonius CAD4 diffractometer. Structure solution was by heavy atom methods using SHELXS-86, [10]) using data with $I \geq 2\sigma I$. A correction for absorption with DIFABS [11]. Further details of the crystal structure investigations are available on request from the Director of the Cambridge Crystallographic Data Centre, 12 Union Road, GB-Cambridge CB21EZ (UK), on quoting the full journal citation.
[10] G. M. Sheldrick in *Crystallographic Computing 3* (Eds.: G. M. Sheldrick, C. Krüger, R. Goddard), Oxford, **1985**, p. 175.
[11] N. Walker, D. Stuart, *Acta Crystallogr. Sect. A* **1983**, *39*, 158.
[12] L. Birkoffer, H. P. Kuhltal, A. Ritter, *Chem. Ber.* **1969**, *93*, 2810.

Toward Polyphospholes: Synthesis and Structure of an α-Linked Quaterphosphole

Eliane Deschamps, Louis Ricard, and François Mathey*

Among cyclic phosphanes, phospholes display two particular properties that deserve special attention. Firstly, the inversion barrier for the pyramidal phosphorus center, roughly 16 kcal mol^{-1}, is exceptionally low,[1] owing to extensive electronic delocalization within the planar transition state. This means that for phospholes the phosphorus center inverts easily, slightly above room temperature. Secondly, phospholide ions resulting from the cleavage of the P–R exocyclic bond of phospholes are highly aromatic.[2] These two specific properties suggest the possible use of phospholes as building blocks for: a) flexible phosphorus macrocycles that can adapt their conformation at phosphorus to the stereochemical requirements of the metals to be complexed;[3] b) porphyrin-like phosphorus macrocycles with a delocalized π-electron system; and c) electroconducting polyphosphole chains similar to the classical polypyrrole and polythiophene chains.[4] For the preparation of these interesting compounds, a method for the difunctionalization of phospholes on the α and α′ carbon atoms of the ring is essential. Here we report such a technique and its application to the synthesis of 2,2′-biphospholes functionalized at the 5- and 5′-positions and the first α-linked quaterphosphole.

Our approach relies on the quantitative and instantaneous bromine–lithium exchange in 2-bromophospholes.[5] As a first step, we synthesized 2,5-dibromophosphole **5** (Scheme 1; for spectroscopic data for this and other new compounds, see Table 1). The formation of intermediates **2**–**4** was monitored by ^{31}P NMR analysis of the reaction mixtures. All the reactions, except the final reduction step, are almost instantaneous and



Scheme 1. Synthesis of **5**. The overall yield of **5** is given in parentheses.

[*] Prof. Dr. F. Mathey, E. Deschamps, Dr. L. Ricard
Laboratoire Hétéroéléments et Coordination URA 1499 CNRS
DCPH, Ecole Polytechnique, F-91128 Palaiseau Cedex (France)
Telefax: Int. code + (1)69330 10

Table 1. Selected spectroscopic data for compounds **5**–**12**.

5. ^{31}P NMR (CH_2Cl_2): $\delta = +17.04$; ^{1}H NMR ($CDCl_3$): $\delta = 2.22$ (d, ^4J(H-P) = 2.2 Hz, 6H, Me), 7.44–7.54 (m, 5H, Ph); ^{13}C NMR ($CDCl_3$): $\delta = 16.79$ (s, Me), 121.80 (d, ^1J(C-P) = 19.6 Hz, C-Br), 146.76 (d, ^2J(C-P) = 8.2 Hz, Me-*C*=); MS (EI, 70 eV): *m/z*: 345 ($M^+ - H$, ^{79}Br + ^{81}Br, 100%), 265 ($M^+ - Br$, ^{79}Br, 75).

6: ^{31}P NMR (CH_2Cl_2): $\delta = +54.4$; ^{1}H NMR ($CDCl_3$): $\delta = 1.88$ (dq, ^3J(H,P) = 14.1 Hz, ^5J(H-H) = 1.2 Hz, 3H, α Me), 2.07 (dq, ^4J(H-P) = 2.5 Hz, ^5J(H-H) = 1.2 Hz, 3H, β Me), 2.11 (d, ^4J(H-P) = 2.1 Hz, 3H, β' Me); MS: *m/z*: 314 (M^+, ^{81}Br, 57%), 312 (M^+, ^{79}Br, 54), 233 ($M^+ - Br$, 100).

7: ^{31}P NMR ([D$_6$]DMSO): $\delta = +14.96$; ^{1}H NMR ([D$_6$]DMSO): $\delta = 2.09$ (d, ^4J(H-P) = 2.9 Hz, 3H, Me), 2.50 (d, ^4J(H-P) = 4.2 Hz, 3H, Me), 12.4 (br, 1H, CO_2H); ^{13}C NMR ([D$_6$]DMSO): $\delta = 25.23$ (s, Me), 25.73 (s, Me), 139.38 (d, ^1J(C-P) = 13.9 Hz, C-Br), 142.90 (s, *C*-CO_2H), 157.32 (d, ^2J(C-P) = 7.8 Hz, Me-*C*=), 168.18 (d, ^2J(C-P) = 9.8 Hz, Me-*C*=), 174.85 (d, ^2J(C-P) = 19.8 Hz, CO_2H).

8: ^{31}P NMR (THF): $\delta = +12.07$; ^{1}H NMR ($CDCl_3$): $\delta = 2.11$ (d, ^4J(H-P) = 2.9 Hz, 3H, Me), 2.44 (d, ^4J(H-P) = 4.8 Hz, 3H, Me), 9.95 (d, ^3J(H-P) = 11.7 Hz, 1H, CHO); ^{13}C NMR ($CDCl_3$): $\delta = 15.23$ (s, Me), 15.41 (s, Me), 136.23 (d, ^1J(C-P) = 16.0 Hz, C-Br), 143.60 (d, ^1J(C-P) = 4.7 Hz, *C*-CHO), 147.71 (d, ^2J(C-P) = 6.6 Hz, Me-*C*=), 160.57 (d, ^2J(C-P) = 10.0 Hz, Me-*C*=), 185.54 (d, ^2J(C-P) = 15.9 Hz, CHO).

9: ^{31}P NMR (THF): $\delta = +23.5$; ^{1}H NMR ([D$_8$]THF): $\delta = 1.77$ (s, 6H, Me), 1.93 (s, 6H, Me), 7.16 (pseudo s, 10H, Ph); MS: *m/z*: 534 (M^+, ^{81}Br, 55%), 531 (100), 453 ($M^+ - Br$, ^{81}Br, 33), 371 ($M^+ - 2Br - H$, 60).

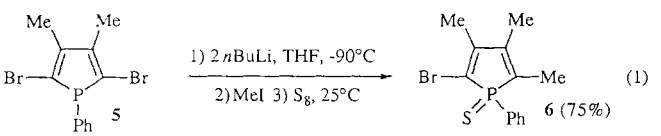
10: ^{31}P NMR (THF): $\delta = +23.3$; ^{1}H NMR ([D$_8$]THF): $\delta = 1.87$ (pseudo t, 6H, Me), 2.42 (pseudo t, 6H, Me); ^{13}C NMR ([D$_8$]THF): $\delta = 15.64$ (s, Me), 16.10 (s, Me), 135.17 (s, *C*-CO_2H), 142.91 (pseudo t, bridge-C?), 148.03 (pseudo t, Me-*C*=), 160.35 (pseudo s, Me-*C*=), 166.53 (pseudo t, CO_2H); IR (Nujol): ν(CO) 1656 (s), 1638 (s) cm^{-1}.

11. ^{31}P NMR ($CDCl_3$): $\delta = +20.05$; ^{1}H NMR ($CDCl_3$): $\delta = 1.95$ (pseudo s, 6H, Me), 2.43 (pseudo t, 6H, Me), 10.00 (pseudo t, $|^3J$(H-P) + ^6J(H-P)$| = 12.3$ Hz, 2H, CHO); MS: *m/z* 430 (M^+, 58%), 252 (100%); IR (Nujol): ν(CO) = 1718(s).

12: ^{31}P NMR (THF): AA'XX' spin system: δ(AA') = +29.69, δ(XX') = +21.29, ^3J(AX) = 61.4 Hz, ^3J(XX') = 55.5 Hz, ^6J(AX') = −0.36 Hz; PD-MS: *m/z*: 904 (M^+, ^{81}Br + ^{79}Br).

quantitative, and none of the intermediates were subjected to extensive purification. The reduction of **4** to **5** is more delicate. The use of pyridine as a cosolvent is absolutely essential to prevent the reduction of the dienic system of the phosphole. When pure, phosphole **5** is reasonably stable and displays good resistance toward oxidation by air.

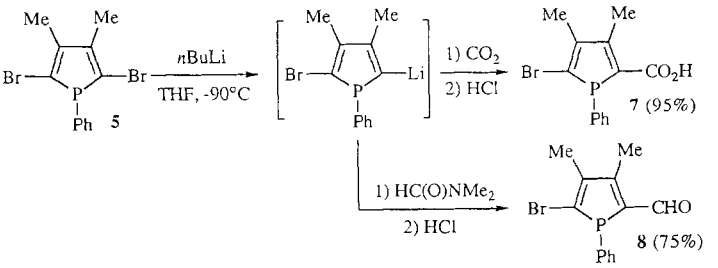
When phosphole **5** is treated with one equivalent of butyllithium in THF at −90 °C, the rapid exchange of one bromine atom by one lithium atom takes place. An excess of butyllithium (2 equiv) does not lead to the exchange of the second bromine atom, as is clear from Eq. (1).



(1)

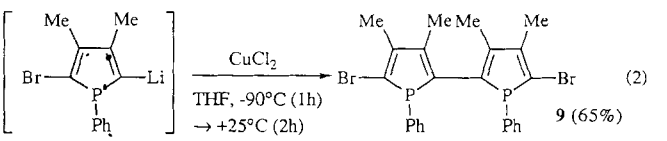
The molecular formula of sulfide **6** was established by mass spectrometry (M^+ at *m/z* 314 (^{81}Br) and *m/z* 312 (^{79}Br)) and by ^{1}H NMR spectroscopy (signal for the α-methyl group at δ = 1.88 (^3J(H−P) = 14.1 Hz)). The monolithio derivative of **5** proved to be an efficient starting material for the synthesis of 5-bromophospholes functionalized in the 2-position (Scheme 2).

In the NMR spectra of **8** in $CDCl_3$, the aldehyde group gives a characteristic ^{1}H resonance at $\delta = +9.95$ (^3J(H−P) = 11.7 Hz) and a ^{13}C resonance at $\delta = +185.54$ (^2J(C−P) = 15.9 Hz). In the ^{13}C NMR spectrum of **7** in [D$_6$]DMSO, the acidic carboxyl group appears at $\delta = +174.85$ (^2J(C−P) = 19.8 Hz). The oxidative coupling of the same monolithio derivative by



Scheme 2.

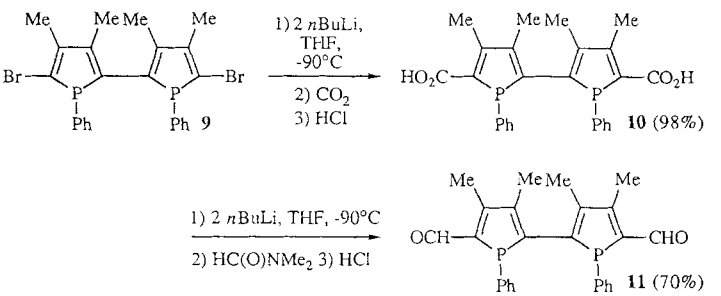
copper(II) chloride affords the 5,5'-dibromo-2,2'-biphosphole **9** [Eq. (2)].



(2)

According to the ^{31}P NMR spectrum (δ^{31}P (**9**) = +23.5 in [D$_8$]THF), only one of the two possible diastereomers of **9** is formed. It is always accompanied by traces of the corresponding 2,2'-biphosphole with H substituents in the 5- and 5'-positions, which has already been described.[5, 6] The molecular formula of **9** was unambiguously established by mass spectrometry; the molecular peaks are found in the range *m/z* 530–534 (^{79}Br and ^{81}Br) with the base peak at *m/z* 531.

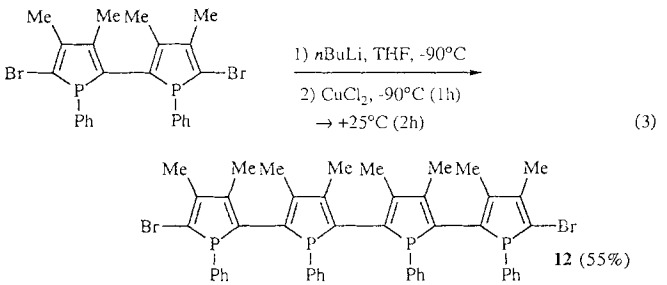
The reactivity of **9** toward butyllithium was studied under our standard conditions (−90 °C, THF). The exchange of the first bromine atom by lithium takes place immediately upon addition of one equivalent of butyllithium. Addition of a second equivalent of butyllithium gives the 5,5'-dilithio derivative. 2,2'-Biphosphole **9** is thus the ideal starting material for the kind of chemistry we evoked in the introduction. As an illustration, we describe the synthesis of two 2,2'-biphospholes functionalized in the 5- and 5'-positions (Scheme 3), which are of potential inter-



Scheme 3.

est for the construction of flexible phosphorus macrocycles, and the synthesis of the first quaterphosphole [Eq. (3)] as a first step en route to polyphospholes.

According to ^{31}P NMR analysis, both **10** and **11** are pure diastereomers (meso or racemates) with the same geometry as **9**. In $CDCl_3$, the carbonyl groups of **11** give rise to a pseudo triplet at $\delta = +10.00$ in the ^{1}H NMR spectrum and at $\delta = +186.13$ in



the ^{13}C NMR spectrum. In THF, the CO_2H carbons of **10** appear as a pseudo triplet at $\delta = +166.53$. The case of **12** is more complex. According to its ^{31}P NMR spectrum, it exists as a mixture of diastereomers, one of which predominates. The simulation of the spectrum of this major diastereomer gave an AA'XX'-type spectrum: (X,X' stand for the "internal" phosphorus atoms): $\delta_{AA'} = +29.69$, $\delta_{XX'} = +21.29$, $^3J_{AX} = 61.4$ Hz, $^3J_{XX'} = 55.5$ Hz. This suggests a highly symmetrical geometry, which was confirmed by X-ray crystal structure analysis (Fig. 1). The molecule possesses a C_2 symmetry axis lying in the

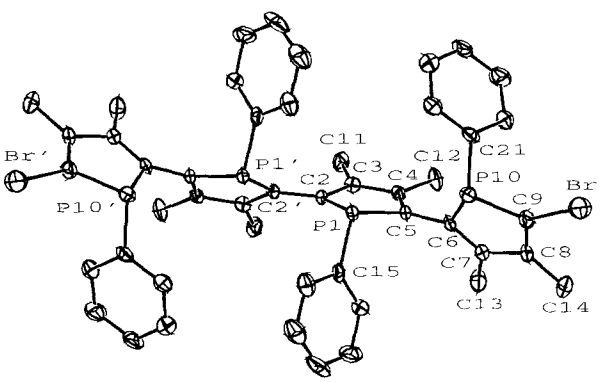


Fig. 1. Crystal structure of **12** [7]. Ellipsoids are scaled to enclose 50% of the electronic density. Hydrogen atoms are omitted for clarity. Important bond lengths [Å] and angles [°]: Br-C9 1.883(7), P1-C2 1.822(6), P1-C5 1.790(6), P1-C15 1.814(7), C2-C2' 1.43(1), C2-C3 1.374(8), C3-C4 1.445(8), C4-C5 1.383(8), C5-C6 1.451(8), C6-C7 1.345(8), C6-P10 1.812(6), C7-C8 1.491(9), C8-C9 1.37(1), C9-P10 1.784(7), P10-C21 1.815(6); C2-P1-C5 91.6(3), C2-P1-C15 106.7(3), C5-P1-C15 106.3(3), P1-C2-C2' 120.1(2), P1-C5-C6 121.8(5), C6-P10-C9 89.7(3), C6-P10-C21 100.3(3), C9-P10-C21 107.4(3), Br-C9-P10 122.3(4); P1'C2'C2P1 25.10(0.43), P1-C5-C6-P10 -49.72(0.60); C2-C5/C6-C9 interplane angle 67.75 ± 0.30.

mean plane of the four rings and bisecting the C2–C2' bond. The geometry of the four phospholes is normal. The C–C bridges (C2–C2' 1.43(1) Å, C5–C6 1.451(8) Å) are not shortened, and thus, conjugation between the phosphole rings is unlikely. With respect to the mean plane, the disposition of the phenyl substituents is up, down, up, down (Fig. 2). Since the coupling method leading to **12** very probably does not alter the conformation at the phosphorus centers, this result suggests that **9**, **10**, and **11** are racemates. Finally, the most surprising observation is that all the four phospholes are pointing in the same direction (Fig. 3); a head-to-tail arrangement was expected.

The recently reported synthesis of the first α-linked quaterpyrrole in three steps and 6.5% overall yield from a 2,2'-bipyrrole[8] well underlines the simplicity and efficiency of our route to difunctionalized α-linked polyphospholes.

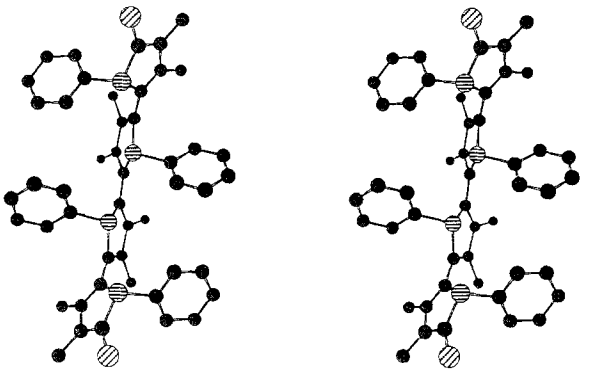


Fig. 2. Stereoview of **12** (C.S.C. Chem3D). The phenyl rings lie almost in the plane of the paper.

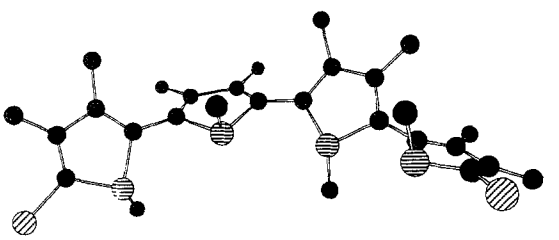


Fig. 3. View of **12** (C.S.C. Chem3D) showing the arrangement of the phosphole rings. Only the *ipso* carbon atoms of the phenyl rings are shown.

Experimental Procedure

5: To **1** [5] (20 g, 5.5×10^{-2} mol) in CH_2Cl_2 (400 mL) at +10 °C was added dropwise a solution of KOH (4.5 g, 8×10^{-2} mol) in methanol (50 mL). At the end of the addition, the quantitative formation of **2** can be monitored by ^{31}P NMR spectroscopy: $\delta^{31}P$ (**1**) = +28, $\delta^{31}P$ (**2**) = +38. The reaction mixture was hydrolyzed at 0 °C and washed with water until neutral. The organic layer was dried over $MgSO_4$. This dry organic layer was kept at 0 °C and treated with bromine (3.5 mL, 6.8×10^{-2} mol) in CH_2Cl_2 (50 mL). At the end of the dropwise addition, the bromination of **2** appeared to be complete according to the ^{31}P NMR spectrum: $\delta^{31}P$ = (**3**) +35. An excess of a solution of $NaHCO_3$ in water was then added all at once to the reaction mixture. The ^{31}P NMR spectrum showed the formation of **4**: $\delta^{31}P$ (**4**) = +32. The solution was treated with $Na_2S_2O_3$, washed with water until neutral, and dried over $MgSO_4$. The solvents were evaporated. Separately, a solution of $HSiCl_3$ (15 mL, 15×10^{-2} mol) in CH_2Cl_2 (30 mL) was added at 0 °C under N_2 to a solution of pyridine (26 mL, 32×10^{-2} mol) in CH_2Cl_2 (40 mL). To the resulting mixture was added dropwise a solution of crude **4** in CH_2Cl_2 (100 mL). At the end of the addition, the mixture was heated at 50 °C for 3 h. Monitoring of the reaction by ^3P NMR spectroscopy showed that the reduction of **4** was complete: $\delta^{31}P$ (**5**) = +17. The resulting suspension was slowly poured onto a mixture of ice and $NaHCO_3$ in water. The resulting thick gel was diluted in CH_2Cl_2 and filtered over celite. After decantation, the water layer was extracted three times with CH_2Cl_2. The organic solution was washed with 3 N HCl (100 mL), then with water until neutral, and dried over $MgSO_4$. After the solvent was removed, the organic residue was quickly chromatographed over silica gel (70–230 mesh) with deoxygenated hexane. The evaporation of hexane yielded 11 g of **5** as white crystals (58%).

6: A solution of phosphole **5** (0.7 g, 2×10^{-3} mol) in anhydrous, freshly distilled THF (10 mL) was prepared under dry N_2 in a Schlenk tube, which was previously dried in an oven at 130 °C. To this solution cooled at −90 °C was added by syringe butyllithium (2.54 mL, 1.6 M, 4×10^{-3} mol), and the mixture was kept at −90 °C an additional hour. Methyl iodide (0.27 mL, 4.4×10^{-3} mol) was then added, and the reaction mixture was kept at −90 °C another hour with stirring. After the reaction mixture was warmed to room temperature, sulfur (0.1 g) was added, and the mixture was stirred at room temperature for 0.5 h. The solvent was removed and the residue chromatographed with toluene. Yield of **6**: 0.48 g (75%) white crystals.

7: The lithium derivative of **5** was prepared as described for **6** from **5** (0.7 g) and butyllithium (1.27 mL, 1.6 M, 2×10^{-3} mol). The solution was kept at −90 °C for 0.5 h with stirring. Then a piece of dry ice was added to the mixture, which was kept at −90 °C for an additional 0.5 h. Hydrochloric acid (0.7 mL, 3 N) in THF (5 mL)

was added by syringe. The mixture was warmed to room temperature. Dichloromethane (50 mL) and aqueous 10% NaOH were added. The aqueous layer was washed several times with CH_2Cl_2, then acidified by 3 N HCl, and extracted six times with CH_2Cl_2. The CH_2Cl_2 extracts were washed with water and dried over $MgSO_4$. Evaporation of the solvent gave 0.6 g (95%) of **7** as white crystals.

8: The lithium derivative of **5** was prepared as described for **7**. After the reaction mixture was kept at $-90\,^{\circ}C$ for 0.5 h, dimethylformamide (0.17 mL, 2.2×10^{-3} mol) was added by syringe. After an additional 0.5 h, 3 N HCl (1.5 mL) in THF (5 mL) was added to the mixture. The reaction mixture was warmed to room temperature, and CH_2Cl_2 (30 mL) and water (30 mL) were mixed with the solution. The aqueous layer was extracted three times with CH_2Cl_2 under N_2. The CH_2Cl_2 layer was washed with water until neutral and dried over $MgSO_4$. After the solvent was evaporated, the organic residue was chromatographed over alumina with toluene to provide 0.46 g of **8** (75%) as yellow crystals. Mass spectrometry and elemental analysis were performed on the more stable P-$W(CO)_5$ complex.

9: The lithium derivative of **5** was prepared as described for **7**. The reaction mixture was kept 0.5 h at $-90\,^{\circ}C$, before copper(II) chloride (0.3 g, 2.2×10^{-3} mol) was added to the solution. After stirring for 1 h at $-90\,^{\circ}C$, the mixture was slowly warmed to room temperature over 2 h. At room temperature, CH_2Cl_2 (50 mL) and ammonia were added, and the mixture was stirred for 20 min. After decantation and extraction of the water layer, the organic phase was washed with water until neutral, dried over $MgSO_4$, and concentrated to dryness. The crude product was chromatographed with hexane/ether 95/5. Biphosphole **9** was obtained as pale yellow crystals in 65% yield (0.69 g).

10: A solution of biphosphole **9** (1.06 g, 2×10^{-3} mol) in THF (50 mL) was prepared in a Schlenk tube. The solution was cooled to $-90\,^{\circ}C$, and butyllithium (2.54 mL, 1.6 M, 4×10^{-3} mol) was added by syringe. After 30 min a piece of dry ice was added and the mixture stirred for another hour. 3 N HCl (1.4 mL) in THF (5 mL) was then added at $-90\,^{\circ}C$, and the mixture was warmed to room temperature. Dichloromethane (150 mL) and 10% NaOH were mixed with the solution. After decantation and washing with CH_2Cl_2, the aqueous layer was acidified by 3 N HCl and extracted several times with CH_2Cl_2 (**10** is poorly soluble in CH_2Cl_2). The CH_2Cl_2 extracts were washed with water, dried over $MgSO_4$, and concentrated to dryness. **10** was obtained in 98% yield (0.9 g) as a deep yellow microcrystalline powder.

11: The dilithio derivative of **9** was prepared as described for **10**. Dimethylformamide (0.34 mL, 4.4×10^{-3} mol) was added to the reaction mixture at $-90\,^{\circ}C$ by syringe. The solution was stirred for 1 h, then 3 N HCl (3 mL) in THF (5 mL) was added dropwise by syringe, and the reaction medium was warmed to room temperature. CH_2Cl_2 (100 mL) and water (20 mL) were mixed with the solution. After decantation, extraction, and neutralization, the organic layer was dried over $MgSO_4$. The organic product was chromatographed with dichloromethane. Yield of **11**: 0.6 g (70%), deep yellow solid.

12: The monolithio derivative of **9** was prepared by the reaction of **9** (2.13 g, 4×10^{-3} mol) with butyllithium (2.5 mL, 1.6 M, 4×10^{-3} mol) in THF (100 mL) at $-90\,^{\circ}C$. After 10 min copper(II) chloride (0.55 g, 4×10^{-3} mol) was added to the solution. After stirring for 1 h at $-90\,^{\circ}C$, the mixture was slowly warmed to room temperature over 2 h. At room temperature, toluene (100 mL) and ammonia were added, and the mixture was stirred for 20 min. After decantation and extraction of the water layer with toluene, the organic phase was washed with water until neutral, dried over $MgSO_4$, and concentrated to dryness. The residue was chromatographed on alumina with hexane/ether (95/5). The quaterphosphole **12** was obtained as deep orange crystals in 55% yield (1 g). Caution: **12** is sensitive to air, thus alumina and the solvents must be deoxygenated and the reaction product handled under nitrogen.

Received: December 14, 1993 [Z 6559 IE]
German version: *Angew. Chem.* **1994**, *106*, 1214

[1] For acyclic phosphanes this barrier is roughly 30–35 kcal mol^{-1}: W. Egan, R. Tang, G. Zon, K. Mislow, *J. Am. Chem. Soc.* **1971**, *93*, 6205.

[2] E. J. Padma Malar, *J. Org. Chem.* **1992**, *57*, 8694.

[3] Some tetraphosphole macrocycles in which the phospholes are connected through phosphorus and α-carbon atoms have already been described: F. Laporte, F. Mercier, L. Ricard, F. Mathey, *J. Am. Chem. Soc.*, in press.

[4] A chain of four thiophene and two phosphole units has been reported: M.-O. Bevierre, F. Mercier, L. Ricard, F. Mathey, *Angew. Chem.* **1990**, *102*, 672; *Angew. Chem. Int. Ed. Engl.* **1990**, *29*, 655.

[5] E. Deschamps, F. Mathey, *Bull. Soc. Chim. Fr.* **1992**, *129*, 486.

[6] F. Mercier, S. Holand, F. Mathey, *J. Organomet. Chem.* **1986**, *316*, 271.

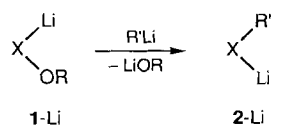
[7] X-ray structure analysis of **7**: Crystals of **7** ($C_{48}H_{44}Br_2P_4$) were grown by slowly cooling a warm solution of the compound in toluene. Data were collected at $-150\pm0.5\,^{\circ}C$ on an Enraf-Nonius CAD4 diffractometer. The crystal structure was solved and refined with the Enraf-Nonius MOLEN package. The compound crystallizes in space group *Pbcn*, $a = 30.254(3)$, $b = 8.164(1)$, $c = 17.608(2)$ Å; $V = 4348.98(1.45)$ Å^3, $Z = 4$, $\varrho_{calc} = 1.382$ g cm^{-3}; $Cu_{K\alpha}$ radiation ($\lambda = 1.54184$ Å), graphite monochromator; $\mu = 40.4$ cm^{-1}; $F(000) = 1848$. A total of 4114 unique reflections were recorded in the range $2^{\circ} \le 2\theta \le 140.0^{\circ}$ of which 779 were considered as unobserved ($F^2 < 3.0\,\sigma(F^2)$), leaving 3335 for solution and refinement. The structure was solved by direct methods. The hydrogen atoms were included as riding contributions in the final stages of least-squares refinement; anisotropic temperature factors were used for all other atoms. A non-Poisson weighting scheme was applied with a p factor equal to 0.08. The final agreement factors were $R = 0.069$, $R_w = 0.110$, G.O.F. = 3.13. The samples we tested have relatively poor quality. This probably results from the random inclusion of another isomer in the lattice and may explain that a large number of systematically absent $0kl$ reflections show a significant intensity and that a large number of medium-intensity reflections have computed structure factors that deviate considerably from the observed values. Further details of the crystal structure investigation may be obtained from the Fachinformationszentrum Karlsruhe, D-76344 Eggenstein-Leopoldshafen (FRG), on quoting the depository number CSD-57975.

[8] H. Ikeda, J. L. Sessler, *J. Org. Chem.* **1993**, *58*, 2340.

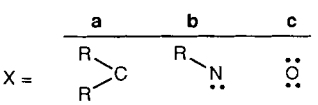
The Oxenoid Character of Metalated Hydroperoxides O(M)OR: Oxidation of Organometallic Compounds R′M′ to R′OH under Mild Conditions**

Gernot Boche,* Ferdinand Bosold, and John C. W. Lohrenz

Recently we reported on the carbenoid nature of α-lithiated ethers ("Li/OR carbenoids") **1a**-Li,[1] in which the C–OR bond is clearly lengthened (by 8–10 pm) in comparison to that of the corresponding ether. This correlates with the surprisingly easy substitution of the RO groups (even when sp^2 bonded) by a nucleophile R′M′ (M′ = Li) (**1a**-Li → **2a**-Li, [Eq. (1)]). An analogous increase of electrophilicity by metalation (!) is found in the N-lithiated hydroxylamines ("Li/OR nitrenoids") **1b**-Li. Owing to the weakening of the N–OR bond,[2a] these compounds can be used as electrophilic aminating agents for R′M′ (M′ = Li) (**1b**-Li → **2b**-Li, [Eq. (1)]).[2b-c]



1-Li **2**-Li (1)



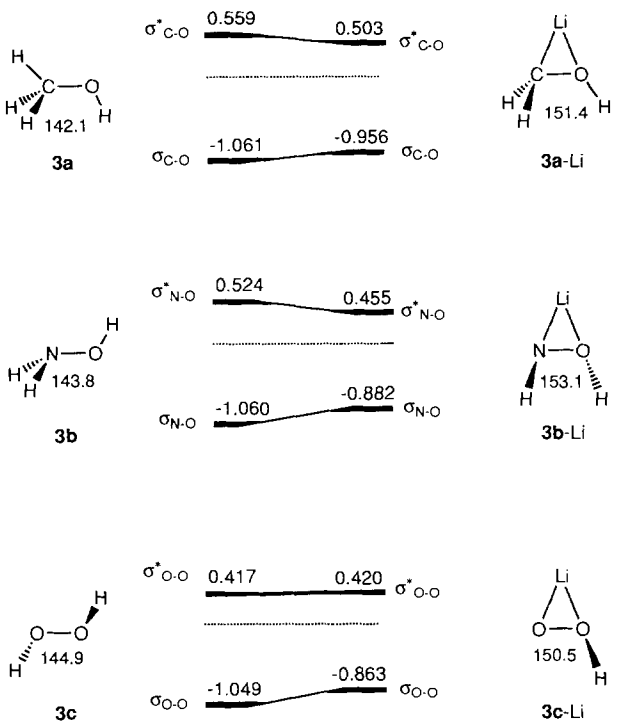
This raises the question as to whether lithiated hydroperoxides **1c**-Li are "Li/OR oxenoids" and therefore especially good electrophiles that will also react with R′M′. This reaction corresponds to an oxidation of organometallic compounds R′M′ to R′OM′ or R′OH (**1c**-Li → **2c**-Li, [Eq. (1)]), a transformation that is still not represented in organometallic chemistry in a general fashion. A recent communication from M. Julia, V. P. Saint-Jalmes, and J.-N. Verpeaux[3] on this subject has encouraged us to report our own results.

Quantum chemical calculations show the close relationship between carbenoids **1a**-Li, nitrenoids **1b**-Li, and **1c**-Li. In

[*] Prof. Dr. G. Boche, F. Bosold, Dr. J. C. W. Lohrenz
Fachbereich Chemie der Universität
D-35032 Marburg (FRG)
Telefax: Int. code + (6421) 28-8917

[**] This work was supported by the Deutsche Forschungsgemeinschaft (SFB 260) and the Fonds der Chemischen Industrie.

Scheme 1 the C(N,O)–OH bond lengths are listed for the model compounds methanol H_3C–OH (**3a**), C-lithiated methanol **3a**-Li, hydroxylamine H_2N–OH (**3b**), N-lithiated hydroxylamine **3b**-Li, hydrogen peroxide HO–OH (**3c**), and monolithiated hydrogen peroxide **3c**-Li (MP2/6-311 + + G(d,p) level). "Natural bond orbital analysis"[4] of the HF/6-311 + + G(d,p) wave function yielded the energies of the σ and σ* orbitals of the C(N,O)–OH bonds.

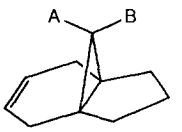


Scheme 1. Structures and bond lengths [pm] for **3a–c** and **3a**-Li to **3c**-Li from calculations at the MP2/6-311 + + G(d,p) level, together with the σ and σ* orbital energies [Hartree] (HF/6-311 + + G(d,p)) for these bonds.

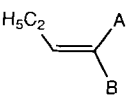
On going from **3c** to **3c**-Li the O–O bond is lengthened by 5.6 pm. Correspondingly, the energy of the σ_{o-o} orbital is raised from −1.049 to −0.863 Hartree. A similar change is observed for the conversions giving carbenoid **3a**-Li[5, 6] and nitrenoid **3b**-Li.[7] In addition, in **3a**-Li and **3b**-Li the $\sigma^*_{C(N)-O}$ orbital is lowered. A similar lowering of the σ^*_{o-o} orbital does not occur in the change from **3c** to **3c**-Li, but the absolute energy of the σ^*_{o-o} orbital in **3c**-Li (0.420 Hartree) is lower compared with that of the σ^*_{c-o} orbital in **3a**-Li (0.503 Hartree) and the σ^*_{N-O} orbital in **3b**-Li (0.455 Hartree), such that an interaction with the nucleophile R′M′ is comparatively favorable. Thus, metalated hydroperoxides should be oxenoids. In addition, the greater tendency of **3c**-Li and methyllithium to form a mixed complex (**3c**·Li·$LiCH_3$: −55.2 kcal mol^{-1} (MP2/6-31G(d)) relative to that of nonlithiated **3c** and CH_3Li (**3c**·$LiCH_3$: −21.4 kcal mol^{-1}) indicates that the reaction of organometallic compounds R′M′ with **3c**-Li is energetically favored over the reaction with **3c**, which serves as a model for nonoxenoid peroxides of the type ROOR.[8, 9]

A search of the literature[10] and our own investigations are in agreement with the results of the quantum chemical calculations. The first suspicion that organometallic compounds R′M′ could react with metalated hydroperoxides O(M)OR (R = alkyl, aryl, etc.) arose during the study of the autoxidation of Grignard compounds R′MgHal with dioxygen O_2.[10d, 11–13] The reaction, which proceeds in two steps (1. R′MgHal + O_2 → O(MgHal)OR′; 2. O(MgHal)OR′ + R′MgHal → 2R′OMgHal), often leads in high yield (> 80%) to R′OMgHal in which R′ can be an alkyl, cycloalkyl, vinyl, aryl, or alkynyl group.[10d]

The first reaction of a lithiated hydroperoxide (lithiated tetralin hydroperoxide) with an organolithium compound (phenyllithium) was reported in 1939.[14] Phenol was obtained in 96% yield. Of special importance is the finding that the oxidation of the isomeric cyclopropyllithium compounds **4a,b**-Li[15] and the vinyllithium compounds **5a,b**-Li[16] with lithio-*tert*-butylhydroperoxide proceed to the corresponding alcoholates and enolates, respectively, with retention of configuration, which makes the intermediate formation of radicals unlikely, at least in these examples.[17]



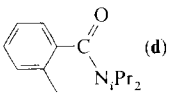
4a-Li : A = H, B = Li[15]
4b-Li : A = Li, B = H



5a-Li : A = Ph, B = Li[16]
5b-Li : A = Li, B = Ph

Our own investigations confirm the easy oxidation of the organolithium compounds R′Li **6a–e** with lithiated cumenyl hydroperoxide O(Li)$OCMe_2$Ph. The corresponding alcohols R′OH were obtained in high yields after hydrolysis[18] (Table 1).

Table 1. Yields [%] for the oxidation of R′Li(MgBr) compounds **6**, cyanocuprates **7**, and "higher order" cyanocuprates **8** with O(Li)$OCMe_2$Ph to give alcohols R′OH.

R′Li(MgBr) **6**	Yield of R′OH from R′Cu(CN)Li **7**	$R'_2Cu(CN)Li_2$ **8**	R′
85	84	82	*n*Bu (**a**)
81	89	90	*t*Bu (**b**)
85	83	78	Ph (**c**)
70 [3]	77	86	 (**d**)
85 (72 [a, b])	56 [c]	67 [d]	$PhCH_2$ (**e**)
95 [a]	-	-	*n*-octyl (**f**)

[a] Grignard compounds R′MgBr. [b] 5% Bibenzyl. [c] 19% Bibenzyl. [d] 14% Bibenzyl.

The Grignard compound **6f** was also oxidized to the alcohol with O(Li)$OCMe_2$Ph. Of particular importance is the oxidation of the cyanocuprates R′Cu(CN)Li **7** corresponding to the lithium compounds **6** and the oxidation of the "higher order" cyanocuprates $R'_2Cu(CN)Li_2$ **8**, which previously could not be converted into alcohols of the type R′OH.[19] The reaction of the benzyl compounds **6e–8e** with O(Li)$OCMe_2$Ph (also) proceeded by electron transfer to give benzyl radicals, as indicated by the formation of bibenzyl.[20, 21]

To sum up: quantum chemical calculations show that metalated (lithiated) hydroperoxides O(M)OR are oxenoid in character and can therefore be regarded as analogues of carbenoids and nitrenoids. In agreement with this is their marked electrophilicity towards nucleophiles such as organometallic compounds of the type R′M′, which are converted into "alcohols"

R'OH under mild conditions. Cyanocuprates R'Cu(CN)Li and "higher order" cyanocuprates $R'_2Cu(CN)Li_2$ provide new examples for this reaction.

Received: December 1, 1993
Revised version: February 11, 1994 [Z 6529 IE]
German version: *Angew. Chem.* **1994**, *106*, 1228

[1] a) G. Boche, F. Bosold, J. C. W. Lohrenz, A. Opel, P. Zulauf, *Chem. Ber.* **1993**, *126*, 1873–1885; b) G. Boche, A. Opel, M. Marsch, K. Harms, F. Haller, J. C. W. Lohrenz, C. Thümmler, W. Koch, *ibid.* **1992**, *125*, 2265–2273; c) the situation with Li/OR carbenoids corresponds exactly to that of Li/Hal carbenoids: G. Boche, M. Marsch, A. Müller, K. Harms, *Angew. Chem.* **1993**, *105*, 1081–1082; *Angew. Chem. Int. Ed. Engl.* **1993**, *32*, 1032–1033.

[2] a) Crystal structure of the nitrenoid [(*N*-lithio-*N*-mesitylsulfonyloxy-*tert*-butylcarbamate)$_2$·thf$_3$]: G. Boche, C. Boie, F. Bosold, K. Harms, M. Marsch, *Angew. Chem.* **1994**, *106*, 90–91; *Angew. Chem. Int. Ed. Engl.* **1994**, *33*, 115–117; b) J. P. Genet, S. Mallart, C. Greck, E. Piveteau, *Tetrahedron Lett.* **1991**, *32*, 2359–2362; c) N. I. Schverdina, Z. Kotscheschkov, *J. Gen. Chem. USSR (Engl. Transl.)* **1938**, *8*, 1825; d) P. Beak, A. Basha, B. Kokko, D. Loo, *J. Am. Chem. Soc.* **1986**, *108*, 6016–6023; e) review article: E. Erdik, M. Ay, *Chem. Rev.* **1989**, *89*, 1947–1980.

[3] M. Julia, V. P. Saint-Jalmes, J.-N. Verpeaux, *Synlett* **1993**, 233–234. We thank Prof. D. Uguen, University of Strasbourg, for bringing this reference to our attention after a lecture on oxenoids in Strasbourg, October 7, 1993. We first reported on oxenoids in a lecture at the Technical University, Munich, on July 27, 1993.

[4] A. E. Reed, L. A. Curtiss, F. Weinhold, *Chem. Rev.* **1988**, *88*, 899–926.

[5] Previous calculations of **3a** and **3a**-Li: a) P. von R. Schleyer, T. Clark, A. J. Kos, G. W. Spitznagel, C. Rohde, D. Arad, K. N. Houk, N. G. Rondan, *J. Am. Chem. Soc.* **1984**, *106*, 6467–6475; and references therein; b) F. Bernardi, A. Bottoni, A. Venturini, A. Mangini, *ibid.* **1986**, *108*, 8171–8175; c) also see ref. [1b].

[6] The significantly higher electrophilicity of a MgCl/Cl carbenoid relative to that of the corresponding alkyl chloride is shown in the reaction of 1-chloropentylmagnesium chloride with n-$C_{11}H_{22}CH(Li)SO_2Ph$, which leads to electrophilic substitution already at −70 to −20 °C. In contrast, in the reaction of 1-chloropentane substitution is not observed even after 2 h at 20 °C: C. De Lima, M. Julia, J.-N. Verpeaux, *Synlett* **1992**, 133–134.

[7] Earlier calculations for **3b** and **3b**-Li: a) G. Boche, H.-U. Wagner, *J. Chem. Soc. Chem. Commun.* **1984**, 1591–1592; b) D. R. Armstrong, R. Snaith, G. T. Walker, *ibid.* **1985**, 789–791; c) M. L. McKee, *J. Am. Chem. Soc.* **1985**, *107*, 859–864.

[8] Analogous complexes have been calculated for the reaction of methyllithium with nitrenoids [7].

[9] The bridging of C(N,O)–OH by Li^+ (in general M^+) found in the calculations of **3a**-c-Li also indicates that the departure of OH^- is enhanced by Li^+ (M^+) during substitution. In the case of carbenoids such enhancement by Li^+ was called metal-assisted ionization: a) M. Duraisamy, H. M. Walborsky, *J. Am. Chem. Soc.* **1984**, *106*, 5035–5037; b) see also G. Köbrich, *Angew. Chem.* **1967**, *79*, 15–27; *Angew. Chem. Int. Ed. Engl.* **1967**, *6*, 41–52.

[10] a) G. Sosnovsky, J. H. Brown, *Chem. Rev.* **1966**, *66*, 529–566; b) M. Maher-Detweiler, *Methoden Org. Chem. (Houben-Weyl) 4th ed. 1952–*, Vol. E13, **1988**, part 1, pp. 176–213; c) U. Schöllkopf, *ibid.* Vol. 13/1, **1970**, pp. 170–253; d) K. Nützel, *ibid.*, Band 13/2a, **1973**, pp. 234–251; e) K.-F. Wedemeyer, *ibid.*, Vol. 6/1c, **1976**, part 1, pp. 141–146; f) K. Geibel, H. Hofmann, H. Kropf, J. Thiem, *ibid.*, Vol. 6/1a, **1979**, part 1, pp. 217–224; g) K. Nützel, *ibid.*, Vol. 13/2a, **1973**, pp. 700–706; h) K. Nützel, *ibid.*, Vol. 13/2a, **1973**, pp. 908–915.

[11] a) C. W. Porter, C. Steel, *J. Am. Chem. Soc.* **1920**, *42*, 2650–2654; b) H. Wuyts, *Bull. Soc. Chim. Belg.* **1927**, *36*, 222; c) H. Wuyts, *C. R. Hebd. Seances Acad. Sci.* **1909**, *148*, 930.

[12] The first use of a "foreign" metalated peroxide O(MgHal)OR for the oxidation of R'MgHal: S. O. Lawesson, N. C. Yang, *J. Am. Chem. Soc.* **1959**, *81*, 4230–4233.

[13] E. Frankland reported on the first reaction of an organometallic compound ($ZnMe_2$) with O_2, in Marburg, in *Justus Liebigs Ann. Chem.* **1853**, *85*, 329–373; see also V. Meyer, R. Demuth, *Ber. Dtsch. Chem. Ges.* **1890**, *23*, 394–398, and ref. [10g].

[14] E. Müller, T. Töpel, *Ber. Dtsch. Chem. Ges.* **1939**, *72*, 273–290.

[15] P. Warner, S.-L. Lu, *J. Org. Chem.* **1976**, *41*, 1459–1461.

[16] E. J. Panek, L. R. Kaiser, G. M. Whitesides, *J. Am. Chem. Soc.* **1977**, *99*, 3708–3713.

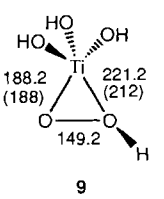
[17] Further examples of reactions of R'Li with O(Li)OR: Li acetylides see ref. [3] (V. Grignard and L. Lepayre reported on the oxidation of R–C≡C–MgBr in *Bull. Soc. Chim. Fr.* **1928**, *43*, 141–142, 930–931; see also C. Walling, S. A. Buckler, *J. Am. Chem. Soc.* **1955**, *77*, 6032–6038); b) aryl Li: M. Nilsson, T. Norin, *Acta Chem. Scand.* **1963**, *17*, 1157–1159; c) M. S. Kemp, R. S. Burden, R. S. T. Loeffler, *J. Chem. Soc. Perkin Trans 1*, **1983**, 2267–2272; d) vinyl Li: H. Neumann, D. Seebach, *Chem. Ber.* **1978**, *111*, 2785–2812; e) reviews: ref. [10c, e, f]; f) $O((RO)_2B)OtBu$ as an oxidizing agent: R. W. Hoffmann, K. Ditrich, *Synthesis* **1983**, 107–109.

[18] Reaction of R'Li **6** with O(Li)$OCMe_2PH$: A solution of *n*BuLi in hexane (1.6 M, 1.25 mL, 2.00 mmol) was added dropwise to a solution of cumyl hydroperoxide (304 mg, 2.00 mmol) in diethyl ether at −78 °C. The solution was stirred for 30 min, and the corresponding R'Li **6** in 2 mL diethyl ether was added. After ca. 12 h the solution was warmed to room temperature. The mixture was hydrolyzed with 2 N HCl, extracted with diethyl ether, and purified by distillation or chromatography. The alcohols R'OH were identified by GC, ^1H and ^{13}C NMR spectroscopy, and mass spectrometry. Reaction of the cuprates **7** and **8**: A solution of the Li compound R'Li **6** in 5 mL THF at −78 °C was allowed to react with CuCN (1 mol equiv for **7**, 0.5 mol equiv for **8**). When the reaction mixture was warmed to −30 °C and stirred, a clear solution formed. The reaction mixture was cooled again to −78 °C, and the solution of the lithiated cumyl hydroperoxide in 5 mL THF was added by means of a cannula. The alcohols were isolated and identified as previously described.

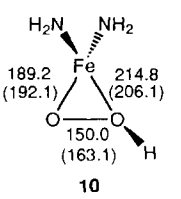
[19] The preparation of unsymmetrical biaryls by the oxidation of the corresponding "higher order" cuprates with O_2 was recently reported: B. H. Lipschutz, K. Siegmann, E. Garcia, F. Kayser, *J. Am. Chem. Soc.* **1993**, *115*, 9276–9282, and references therein.

[20] In the oxidation of R'M' (M' = MgHal, Li) with dialkyl peroxides ROOR, which leads to R'OR, radicals are always formed. In addition this reaction only works with nonbulky residues R, see a) G. A. Baramki, H. S. Chang, J. T. Edward, *Can. J. Chem.* **1962**, *40*, 441–444; b) W. A. Nugent, F. Bertini, J. K. Kochi, *J. Am. Chem. Soc.* **1974**, *96*, 4945–4954; c) see also refs. [10] and [17d]. Oxidations of R'M' with $Me_3SiOOSiMe_3$ were reported by P. Dembech, A. Guerrini, A. Ricci, G. Seconi, M. Taddei, *Tetrahedron* **1990**, *46*, 2999–3006, and references therein; here not only $R'OSiMe_3$ but also $R'SiMe_3$ is formed.

[21] For the compound $(RO)_3TiOOtBu$, which is important in the Sharpless oxidation [22], we have carried out model calculations on $(HO)_3TiOOH$ (**9**) (MP2/O,H: 6-31G(d); Ti (6211111/5111111/3111) [23]) (bond lengths from ref. [24] in parentheses), as have R. D. Bach and H. B. Schlegel et al. [24]. In **9**, which has a bridged structure like that of O(Li)OH **3c**-Li, the O–O bond is 2.2 pm longer than that in HOOH (O–O 147.0 pm (MP2/6-31G(d)). Owing to its oxenoid character, **9** could also exhibit increased electrophilicity like **3c**-Li. Increased electrophilicity was calculated for the Fe^{III} hydroperoxide model **10** and its reaction with NH_3 ((MP2/WH; values in parentheses: CASSCF(7,7)/3-21G) [24]).



9



10

[22] M. G. Finn, K. B. Sharpless, *J. Am. Chem. Soc.* **1991**, *113*, 113–126, and references therein.

[23] a) H. J. H. Wachters, *J. Chem. Phys.* **1970**, *52*, 1033–1036; zusätzlicher Orbitalexponent $d = 0.072$; b) P. J. Hay, *ibid.* **1977**, *66*, 4377–4384.

[24] R. D. Bach, M.-D. Su, J. L. Andrés, H. B. Schlegel, *J. Am. Chem. Soc.* **1993**, *115*, 8763–8769.

Sensitive and Selective Coloration of Cryptand-Type Crown Spirobenzopyrans for Alkaline-Earth Metal Cations**

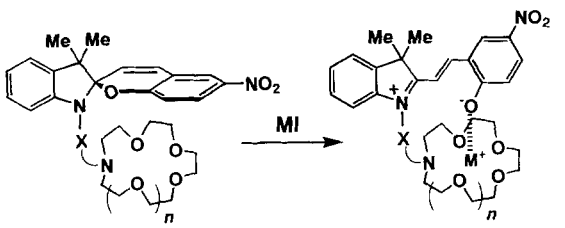
Masahiko Inouye,* Yoshiyuki Noguchi, and Kakuzo Isagawa

The final aim of our research is to create "intelligent" supramolecules and supramolecular systems, in which several conjugated functions are induced by molecular recognition and the whole process is regulated at will.[11] In that connection, we recently developed a new class of spirobenzopyrans possessing a

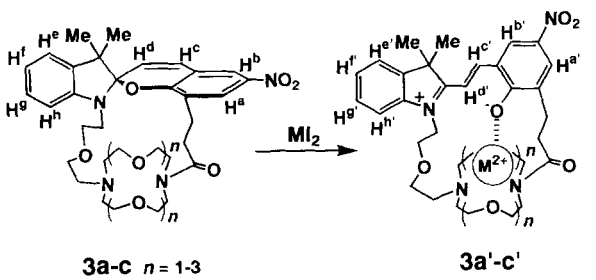
[*] Dr. M. Inouye, Y. Noguchi, Dr. K. Isagawa
Department of Applied Materials Science
University of Osaka Prefecture
Sakai, Osaka 593 (Japan)
Telefax: Int. code + (722)59-3340

[**] We are grateful to Kenichi Takahashi (C. Itoh & Co., Ltd) for a gift of $[(Ph_3P)_3RhCl]$

crown ring as a recognition site, isomerization of which to the open-chain, colored merocyanines was induced by recognition of alkali-metal cations.[2] The spirobenzopyrans bearing a short linkage **1** showed distinctive colors for Li^+ ($n = 2$) and Na^+ ($n = 3$). For larger alkali-metal cations, however, distinctive coloration could not be obtained even in the cases of the $n > 3$ crown spirobenzopyrans. While spirobenzopyrans **2**, in which

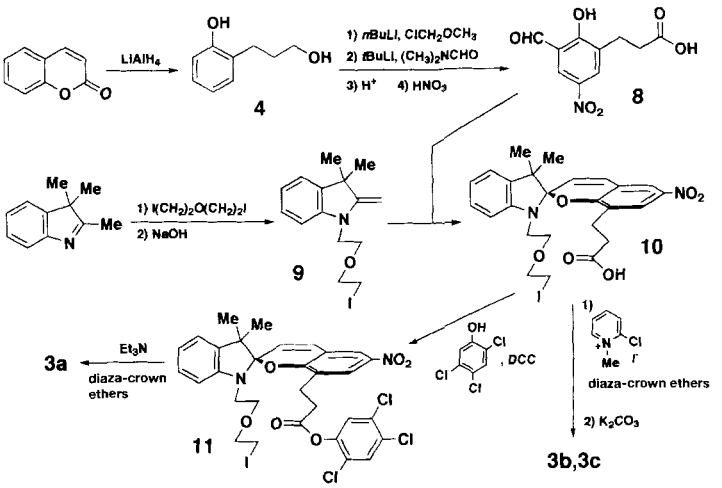


the spiroenzopyran moiety was widely separated from the crown ether units by longer alkyl spacers (X) than in **1**, showed a small selective coloration for larger alkali-metal cations such as K^+ and Cs^+, the molar absorptivities in the presence of alkali-metal iodides were considerably smaller than those of **1**. We thought that the low coloring efficiency might result from unfavorable entropy effects: the probability of the existence of the complexed cations in the neighborhood of the phenolate oxygen of the merocyanines is reduced, and the electrostatic interaction between the complexed large univalent cations and the *p*-nitrophenolate dipole of the merocyanines is weak. Taking into account the above points, we developed cryptand type spirobenzopyran crown ethers (**3**). Here we present the synthesis and selective coloration effects of the new crown spirobenzopyrans on complexation with alkaline-earth metal cations (Scheme 1).



Scheme 1.

The cryptand spirobenzopyrans **3** were synthesized from three components, namely, nitrosalicylaldehyde **8**, indoline **9**, and diaza-crown ethers. The aldol-type cyclization of **8** with **9** gave spirobenzopyran **10** bearing carboxyl and iodoalkyl groups, which on condensation with diaza-crown ethers by Mukaiyama's or activated ester methods, followed by macrocyclization under high-dilution conditions yielded **3**. The key intermediates **8** and **9** were prepared by standard synthetic methods (Scheme 2).[3]



Scheme 2. DCC = dicyclohexylcarbodiimide.

The cryptand spirobenzopyrans **3** showed no absorption bands above 400 nm in aprotic solvents; which indicated closed spiropyran forms. Indeed, this interpretation was verified by NMR studies (see below). The absorption spectra were scarcely affected upon addition of any alkali-metal iodides in CH_3CN.[4] In the ^1H NMR spectra of **3b** in CD_3CN, however, downfield shifts (for aromatic and crown ring protons), splitting (crown ring and alkyl spacer protons), and sharpening (aromatic protons) of the signals in the spiropyran forms were observed after the addition of KI. This result clearly indicated that the alkali-metal cations were bound to the macrocycle of **3**, and that the colorless form was attributable to the weak electrostatic interaction between the complexed univalent cations and the *p*-nitrophenolate dipole of the merocyanines. Addition of alkaline-earth metal iodides to these CH_3CN solutions gave rise to changes in their spectra. Thus, **3a** gave the most intense coloration for Ca^{2+}, and **3b** for Sr^{2+} (Fig. 1). Titration experiments demonstrated that about one equivalent of SrI_2 is enough to obtain the maximum coloration of **3b**. Unfortunately, **3c** showed little changes and poor selectivity in its absorption spectrum under the same conditions. This may be because the crown ring is too flexible to interact strongly with the cations. As expected, little change in the spectra of **1** and **2** occurred under the same conditions.

The isomerization of the cryptand spirobenzopyran **3b** to the open-chain, colored merocyanine **3b'** in the presence of SrI_2 has been studied by ^1H NMR spectroscopy at 500 MHz. In several deuterated solvents ($CDCl_3$, CD_3CN, [D_6]DMSO, etc.), the ^1H NMR signals of **3b** were considerably broadened at room temperature. High-temperature NMR (85 °C) in [D_6]DMSO was able to resolve the identifiable species. (In contrast, spectra of **3a** and **3c** at room temperature in $CDCl_3$ were well-resolved.) To a solution of **3b** (20 μmol) in CD_3CN (0.7 mL) was added SrI_2 (40 μmol), and ^1H NMR spectra were measured as a function of time in the dark. After 30 min, new resonances, which were assigned to a merocyanine (**3b'**), were detected, and the remaining signals of the spiropyran form (**3b**) sharpened and shifted. Equilibrium was reached after 3 h (>80% conversion, Fig. 2). These observations suggested the fast and strong binding of Sr^{2+} by **3b**, and the slow isomerization of the resulting complex (**3b** · Sr^{2+}) to the merocyanine form (**3b'**).[5]

The fast and strong binding of Sr^{2+} by **3b** was corroborated on the basis of FAB mass spectrometry. Before addition of SrI_2, ion peaks for $[M + H]^+$ and $[M + Na]^+$ were detected; after the addition, these signals decreased and finally disappeared, while peaks for $(M - H + Sr)^+$ and $(M + Sr + I)^+$ appeared and increased.

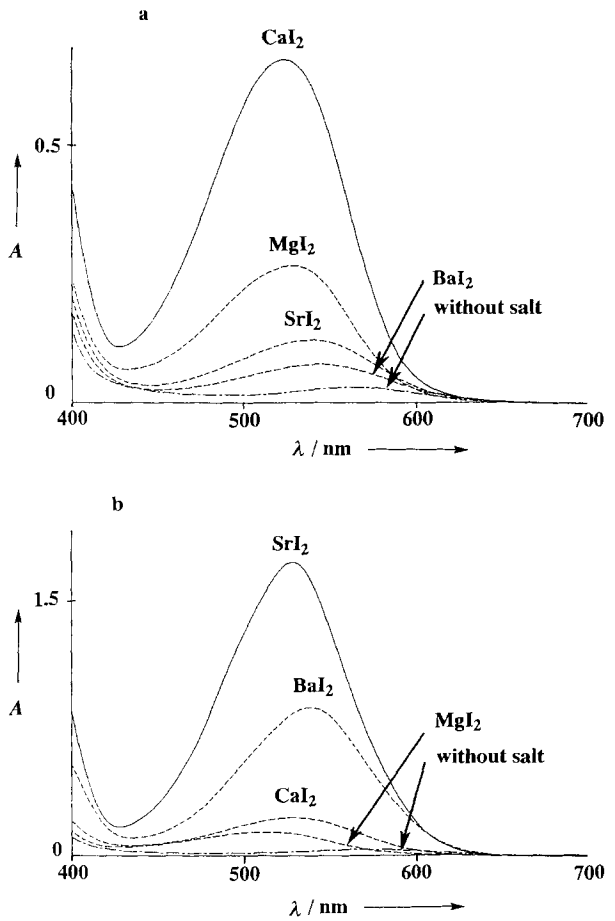


Fig. 1. Electronic absorption spectra of solutions of **3a** (a) and **3b** (b) in acetonitrile in the presence or absence of 1 equiv of alkaline-earth metal iodides [4].

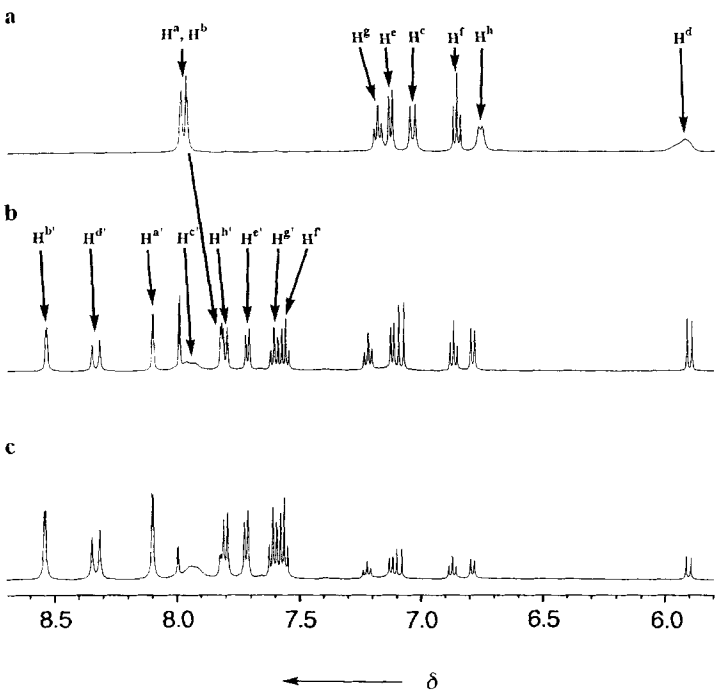


Fig. 2. ^{1}H NMR spectra (500 MHz) of **3b** in CD_3CN. a) Before addition of SrI_2, b) 30 min after the addition, and c) after 3 h. See Scheme 1 for proton labeling.

We have developed new crown spirobenzopyrans, cryptand-type spirobenzopyran. In these spirobenzopyrans, coloration was efficiently induced in the presence of 1 equiv of alkaline-earth metal iodides. The cryptand spirobenzopyrans represent highly sensitive and selective signaling receptors for alkaline-earth metal cations.

Experimental Procedure

4: A suspension of coumarin (17.54 g, 120 mmol), and $LiAlH_4$ (22.77 g, 600 mmol) in THF (300 mL) was heated at reflux for 48 h. A solution of H_2SO_4 (10%) was carefully added dropwise to the mixture at 0 °C until no more hydrogen evolved. The resulting mass was extracted with THF in a Soxhlet extractor (50 h), and the extract was evaporated to dryness. The residue was dissolved in water, extracted with CH_2Cl_2, and the extract evaporated and distilled under reduced pressure to give **4**: yield 57% (10.38 g); b.p. 122–128 °C (0.1 mmHg); IR (KBr): $\tilde{\nu}$ = 3367, 2943, 1593, 1456, 1244, 1107, 1030, 756 cm^{-1}; ^{1}H NMR (270 MHz, $CDCl_3$): δ = 1.88 (quint, J = 6.1 Hz, 2H), 2.78 (t, J = 6.1 Hz, 2H), 3.64 (t, J = 6.1 Hz, 2H), 6.82–6.90 (m, 2H), 7.08–7.14 (m, 2H); ^{13}C NMR (67.8 MHz, $CDCl_3$) δ = 25.22, 32.27, 60.86, 116.16, 120.87, 127.24, 127.61, 130.66, 154.59; EI-MS (70 eV): *m/z* (%): 152 (100) [M^+], 134 (52) [$M^+ - H_2O$], 107 (70) [$M^+ - CH_2CH_2OH$], 77 (56)[$C_6H_4 + H^+$].

8: A solution of *n*-BuLi (103 mmol) in *n*-hexane was added dropwise at 0 °C to a solution of **4** (7.61 g, 50 mmol) in THF (50 mL). The solution was kept at 0 °C under stirring for 1 hr, upon which $ClCH_2OCH_3$ (32.21 g, 400 mmol) was added dropwise, and the reaction mixture was stirred for an additional 1 h at the same temperature, before filtration. The filtrate was evaporated to dryness, the residue dissolved in water, and the solution extracted with CH_2Cl_2 to give 1-(1,3-dioxabutyl)-2-(4,6-dioxaheptyl)benzene (**5**): yield 94% (11.26 g). To a solution of **5** (11.26 g, 47 mmol) in *n*-hexane (100 mL) at 0 °C was added dropwise a solution of *t*-BuLi (66 mmol)in *n*-pentane. At that temperature the solution was stirred for 2 h, and a solution of DMF (5.82 g, 80 mmol) in THF (45 mL) was added dropwise. The reaction mixture was warmed to room temperature and stirred for an additional 12 h. After addition of water (10 mL), the mixture was evaporated to dryness. The residue was dissolved in water and extracted with CH_2Cl_2 to afford 2-(1,3-dioxybutyl)-3-(4,6-dioxaheptyl)benzaldehyde (**6**): yield 93% (11.66 g). A solution of **6** (9.74 g, 36 mmol) in MeOH (150 mL), which contained a small amount of concentrated HCl solution (several drops), was heated at reflux for 9 h. The reaction mixture was neutralized to pH 7 with an aqueous solution of 1 N NaOH and evaporated to dryness. The residue was dissolved in water and extracted with CH_2Cl_2. The extract was evaporated and chromatographed (silica gel; eluent, AcOEt) to give 3-(3-hydroxypropyl)salicylaldehyde (**7**): yield 97% (6.39 g). At 0 °C **7** (1.80 g, 10 mmol) was added dropwise to 60% HNO_3 (15 mL), the reaction mixture stirred for 2 h, and then neutralized to pH 4 with a saturated solution of $NaHCO_3$ in water. The resulting precipitate was filtered and washed with cold (about 0 °C) AcOEt to give **8**: yield 47% (1.14 g); m.p. 175–179 °C (decomp.); IR (KBr): $\tilde{\nu}$ = 3288, 1736, 1662, 1618, 1444, 1346, 1296, 1277, 1209, 1163, 1109, 789, 762, 719 cm^{-1}; ^{1}H NMR (270 MHz, $CDCl_3$): δ = 2.78 (t, J = 7.3 Hz, 2H), 3.09 (t, J = 7.3 Hz, 2H), 8.35 (d, J = 2.4 Hz, 1H), 8.45 (d, J = 2.4 Hz, 1H), 9.99 (s, 1H) 11.96 (s, 1H); ^{13}C NMR (67.8 MHz, [D_6]DMSO): δ = 24.44, 32.73, 120.72, 126.82, 130.54, 131.54, 139.78, 163.58, 173.74, 195.35; EI-MS (70 eV): *m/z* (%): 239 (28) [M^+], 193 (100) [$M^+ - CO_2H - H$], 165 (43) [$M^+ - CH_2CH_2CO_2H - H$]. Correct C,H,N analysis.

10: A solution of **8** (1.29 g, 5.4 mmol) and **9** [2c] (1.93 g, 5.4 mmol) in EtOH (45 mL) was stirred at room temperature for 3 h. After removal of the solvent, the residue was subjected to column chromatography (silica gel; eluent, CH_2Cl_2, AcOEt = 10:1) to give **10**: yield 67% (2.09 g); oil; IR (KBr): $\tilde{\nu}$ = 3450, 3421, 1711, 1651, 1608, 1520, 1483, 1454, 1336, 1273, 1167, 1095, 949, 935, 906, 744 cm^{-1}; ^{1}H NMR (270 MHz, $CDCl_3$): δ = 1.21 (s, 3H), 1.27 (s, 3H), 2.41 (t, J = 7.3 Hz, 2H), 2.65–2.74 (m, 2H), 3.20 (t, J = 6.7 Hz, 2H), 3.28–3.71 (m, 6H), 5.98 (d, J = 10.4 Hz, 1H), 6.61 (d, J = 7.3 Hz, 1H), 6.85 (t, J = 7.3 Hz, 1H), 6.91 (d, J = 10.4 Hz, 1H), 7.08 (d, J = 7.3 Hz, 1H), 7.15 (td, J = 7.3, 1.2 Hz, 1H), 7.90 (d, J = 2.4 Hz, 1H), 7.94 (d, J = 2.4 Hz, 1H); ^{13}C NMR (67.8 MHz, $CDCl_3$): δ = 2.90, 19.88, 24.81, 25.97, 32.46, 43.55, 52.29, 69.08, 71.67, 106.58, 106.99, 118.35, 119.74, 121.30, 121.66, 125.99, 127.28, 127.69, 128.31, 135.81, 140.54, 146.57, 156.98, 177.74; EI-MS (70 eV): *m/z* (%): 578 (30) [M^+], 451 (89) [$M^+ - I$], 393 (88) [$M^+ - CH_2OCH_2CH_2I$].

3b: A solution of **10** (1550 mg, 2.7 mmol) in CH_2Cl_2 (20 mL) was added dropwise to a solution of 1,10-diaza-[18]crown-6 (1760 mg, 6.7 mmol), 2-chloro-1-methylpyridinium iodide (1030 mg, 4.0 mmol), and Et_3N (810 mg, 8.0 mmol) in CH_2Cl_2 (30 mL) at room temperature. The mixture was heated at reflux for 3 h and evaporated. The residue was dissolved in water and extracted with CH_2Cl_2 to yield a mixture of **3b** and noncyclized free monoamine product. A suspension of the mixture described above and finely ground K_2CO_3 (3730 mg, 27 mmol) in THF (250 mL) was heated at reflux for 30 h. After removal of the solvent, the residue was dissolved in water and extracted with CH_2Cl_2. The extract was evaporated to dryness and subjected to column chromatography (silica gel; eluent, AcOEt:Et_3N = 25:1; then ODS (Conmosil. 75C_{18}-OPN, Nacalai Tesque, Inc. Kyoto, Japan) reversed-phase silica gel with MeOH:H_2O = 5:1 as eluent) to afford

3b: yield 18% (334 mg); m.p. 70–72 °C (decomp.); IR (KBr): $\tilde{\nu}$ = 2933, 2889, 2866, 1639, 1606, 1520, 1483, 1452, 1336, 1273, 1119, 1097, 939, 905, 750 cm^{-1}; ^1H NMR (500 MHz, [D$_6$]DMSO, 85 °C) δ = 1.13 (s, 3H), 1.22 (s, 3H), 2.56–2.62 (m, 10H), 3.30–3.57 (m, 26H), 5.97 (d, J = 10.4 Hz, 1H), 6.71 (d, J = 7.3 Hz, 1H), 6.81 (t, J = 7.3 Hz, 1H), 7.12 (t, J = 7.3 Hz, 1H), 7.14 (dd, J = 7.3, 1.2 Hz, 1H), 7.16 (d, J = 10.4 Hz, 1H), 7.97 (d, J = 2.7 Hz, 1H), 8.03 (d, J = 2.7 Hz, 1H); ^{13}C NMR (67.8 MHz, [D$_6$]DMSO, 85 °C): δ = 19.73, 24.15, 25.29, 42.83, 51.91, 54.80, 55.31, 68.51–70.12, 106.31, 118.17, 118.98, 120.48, 121.16, 121.29, 127.29, 128.08, 128.36, 135.34, 140.03, 146.25, 156.20, 170.53; FAB-MS (in 3-nitrobenzyl alcohol): m/z (%): 695 (100) [M + H$^+$], 717 (5) [M + Na$^+$]. Correct elemental analysis.

Received: January 3, 1994 [Z 6596 IE]
German version: *Angew. Chem.* **1994**, *106*, 1226

[1] *Advances in Supramolecular Chemistry, Vol. 1, 2* (Ed.: G. W. Gokel), JAI, Greenwich, **1990**, **1992**. F. Vögtle, *Supramolecular Chemistry*, Wiley & Sons, Chichester, 1991; *Frontiers in Supramolecular Organic Chemistry and Photochemistry* (Eds.: H.-J. Schneider, H. Dürr), VCH, Weinheim, **1991**; M. Inouye, K. Kim, T. Kitao, *J. Am. Chem. Soc.* **1992**, *114*, 778–780; M. Inouye, K. Tsuchiya, T. Kitao, *Angew. Chem.* **1992**, *104*, 198–200; *Angew. Chem., Int. Ed. Engl.* **1992**, *31*, 204–205; M. Inouye, T. Konishi, K. Isagawa, *J. Am. Chem. Soc.* **1993**, *115*, 8091–8095; M. Inouye, *Kagaku to Kogyo (Tokyo)* **1993**, *46*, 214–217.

[2] a) M. Inouye, M. Ueno, T. Kitao, K. Tsuchiya, *J. Am. Chem. Soc.* **1990**, *112*, 8977–8979; b) M. Inouye, M. Ueno, T. Kitao, *J. Org. Chem.* **1992**, *57*, 1639–1641; c) M. Inouye, M. Ueno, K. Tsuchiya, N. Nakayama, T. Konishi, T. Kitao, *J. Org. Chem.* **1992**, *57*, 5377–5383; d) Kimura et al. reported interesting examples of photochemical switching of ionic conductivity utilizing spiropyran crown ethers: K. Kimura, T. Yamashita, M. Yokoyama, *J. Chem. Soc. Perkin Trans. 2* **1992**, 613–619; *J. Phys. Chem.* **1992**, *96*, 5614–5617.

[3] All other new compounds provided spectra (^1H NMR, ^{13}C NMR, IR, MS) and elemental analyses in agreement with their structures. The full data and the experimental details will be reported elsewhere.

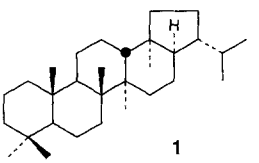
[4] The absorption spectra of 0.1 mM solutions of the spirobenzopyrans in CH_3CN were measured in the presence or absence of metal iodides after the solutions had been allowed to stand in the dark for 3 h.

[5] This tendency was also observed for other spirobenzopyran crown ethers. See Ref. [2b].

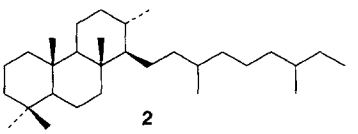
Novel Optically Active Hydrocarbons in Sediments: Evidence for an Extensive Biological Cyclization of Higher Regular Polyprenols**

Philippe Schaeffer, Jacques Poinsot, Véréna Hauke, Pierre Adam, Patrick Wehrung, Jean-Michel Trendel, Pierre Albrecht,* Daniel Dessort, and Jacques Connan

Most polycyclic hydrocarbons occurring in sediments and petroleum are of biological origin. They can, with few exceptions, be related to biological precursors (steroids, terpenoids, etc.) by structural considerations which involve either known, often relatively simple, or hypothetical—but reasonable—geochemical transformations, therefore providing essential information on, for instance, the origin of organic matter in sediments.[1] In some cases, the precise characterization of new biological markers from sediments has had a considerable impact on fields such as microbial biochemistry, as exemplified by the story of geohopanoids, for example **1**.[2a] Thus, the identification and ubiquitous occurrence of geohopanoids in sediments preceded and triggered the discovery of their microbial precursors, the biohopanoids,[2b] a class of procaryotic lipids which play a major role as membrane reinforcers in bacteria. This unexpected pioneering role of geochemistry is further highlighted by the fact that molecular fossils have been found which still remain "orphan", that is, those, whose precursors are unknown as yet in organisms, such as "bacteriosteranes" (3-alkylsteranes)[3] or tricyclopolyprenanes such as **2**.[4, 5]

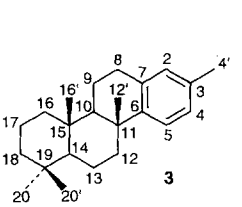


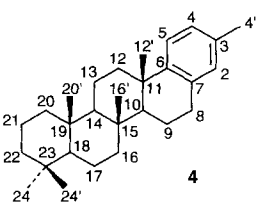
1

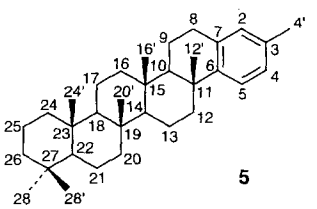

2

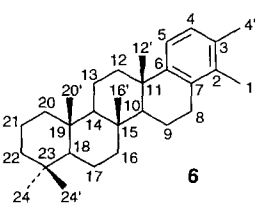
In the course of investigations of various sediments we have encountered a family of polycyclic hydrocarbons which reveal the existence of an unexpected, biological or at least enzyme-initiated, extended polycyclization of higher regular polyprenols (C_{25}–C_{45}).

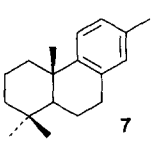
Monoaromatic compounds **3**–**6**[6] were isolated from the organic extract of the Eocene Messel shale (FRG) by a combination of silica gel column chromatography and reverse-phase HPLC.[7] Electron impact (EI) mass spectra of hydrocarbons **3**, **4** and **5** exhibit molecular ion peaks at m/z 310 ($C_{23}H_{34}$), 378 ($C_{28}H_{42}$), and 446 ($C_{33}H_{50}$), respectively. The elemental compositions were confirmed by high-resolution mass spectrometry (HRMS) (Table 1). The mass spectra display a common fragmentation pattern similar to that of the podocarpa-8,11,13-triene derivative **7** which can be interpreted according to Azevedo et al.[8] This fragmentation pattern and the signals of smaller characteristic ions, suggest the presence of closely related polycyclopolyprenic structures differing by C_5 isoprenic units. The structures of the three hydrocarbons were unambiguously established by 1D and 2D NMR studies including homonuclear (^1H-^1H, COSY and NOESY) and heteronuclear (^1H-^{13}C, HMQC and HMBC) correlation experiments which also led to the complete assignment of the signals of the protons and carbon atoms (Table 2). Evidently, especially from the sequences of ^{13}C NMR signals, these compounds form a "preno-


3


4


5


6


7

[*] Dr. P. Albrecht, Dr. P. Schaeffer, J. Poinsot, V. Hauke, Dr. P. Adam, P. Wehrung, Dr. J.-M. Trendel
Laboratoire de Géochimie Organique, associé au CNRS
Institut de Chimie, Université Louis Pasteur
1, rue Blaise Pascal, F-67000 Strasbourg (France)
Telefax: Int. code + (88) 61 00 04
Dr. D. Dessort, Dr. J. Connan
Elf-Aquitaine, CST Jean Feger, F-64018 Pau Cedex (France)

[**] This work was supported by the Centre National de la Recherche Scientifique and the Société Elf-Aquitaine. The authors thank Prof. Dr. G. Ourisson (Strasbourg), Prof. Dr. M. Rohmer (Mulhouse), and Dr. C. Mioskowski (Strasbourg) for helpful discussions, and M.-C. Schweigert and Dr. R. Graff for their assistance in MS and NMR, respectively.

Table 1. Selected analytical data for hydrocarbons **3**–**6** and **8**.

3: Waxy compound; $[\alpha]_D^{23} = -46$ ($c = 0.74$ in $CHCl_3$); ^1H NMR: see ref. [6]; UV (*n*-hexane): $\lambda_{max} = 206$ nm; MS (EI, 70 eV): *m/z* (%): 310 (32) [M^+], 295 (93), 199 (8), 197 (5), 185 (7), 183 (4), 171 (57), 159 (23), 158 (23), 157 (100), 145 (48), 137 (61), 131 (31). HRMS: *m/z* 310.2660 [M^+], calcd for $C_{23}H_{34}$ 310.2660; $\delta^{13}C = -31.1 \pm 0.8$‰

4: M.p. 202–203 °C (needles from CH_2Cl_2/CH_3OH); $[\alpha]_D^{23} = +45$ ($c = 0.77$ in $CHCl_3$); UV (*n*-hexane): $\lambda_{max} = 206$ nm; MS (70 eV): *m/z* (%): 378 (17) [M^+], 363 (54), 239 (2), 225 (3), 205 (13), 199 (3), 197 (4), 191 (5), 185 (3), 183 (5), 171 (100), 159 (14), 158 (12), 157 (28), 145 (17), 137 (9), 131 (15); HRMS: *m/z* 378.3283 [M^+], calcd for $C_{28}H_{42}$ 378.3286; $\delta^{13}C = -33.8 \pm 0.6$‰

5: M.p. 268–269 °C (thin plates from CH_2Cl_2/CH_3OH); $[\alpha]_D^{23} = -38$ ($c = 0.37$ in $CHCl_3$); ^1H NMR: not reported here; UV (*n*-hexane): $\lambda_{max} = 208$ nm; MS (70 eV): *m/z* (%): 446 (10) [M^+], 431 (32), 293 (1), 273 (2), 239 (2), 225 (2), 205 (2), 199 (2), 197 (3), 191 (6), 185 (2), 183 (4), 171 (100), 159 (10), 158 (9), 157 (18), 145 (14), 137 (6), 131 (11); HRMS: *m/z* 446.3917 [M^+], calcd for $C_{33}H_{50}$ 446.3912; $\delta^{13}C = -33.8 \pm 0.3$‰

6: ^1H NMR (assignments by analogy with **4**): $\delta = 7.00$ (d, ^3J(H,H) = 8.0 Hz; H–C(5)), 6.91 (d, ^3J(H,H) = 8.0 Hz; H–C(4)), 2.82 (br. dd, $^{2,3}J$(H,H) = 17.0, 6.0 Hz; Hβ–C(8)), 2.58 (m; Hα–C(8)), 2.36 (ddd, $^{2,3}J$(H,H) = 12.5, 3.0, 3.0 Hz; Hβ–C(12)), 2.22 (s; CH_3(4') or CH_3(1)), 2.09 (s; CH_3(4') or CH_3(1)), 1.20 (dd, ^3J(H,H) = 12.0, 2.0 Hz; H–C(10)), 1.162 (s; CH_3(12')), 1.13 (ddd, $^{2,3}J$(H,H) = 13.0, 13.0, 4.5 Hz; Hα–C(22)), 0.96 (ddd, $^{2,3}J$(H,H) = 12.5, 12.5, 4.0 Hz; Hα–C(16)), 0.929 (s; CH_3(16')), 0.869 (s; CH_3(20')), 0.843 (s; CH_3(24)), 0.825 (s; CH_3(24')); MS (70 eV): *m/z* (%): 392 (21) [M^+], 377 (58), 253 (2), 239 (3), 225 (3), 205 (12), 199 (4), 197 (5), 191 (5), 185 (100), 183 (4), 173 (16), 172 (14), 171 (38), 159 (25), 157 (13), 145 (14), 137 (10); HRMS: *m/z* 392.3436 [M^+], calcd for $C_{29}H_{44}$ 392.3443; $\delta^{13}C = -32.8 \pm 0.1$‰.

8: MS (70 eV): *m/z* (%): 582 (9) [M^+], 567 (27), 429 (6), 355 (10), 341 (6), 239 (7), 225 (5), 191 (13), 171 (100), 159 (9), 158 (11), 157 (18), 145 (11), 137 (5), 131 (10)

logue" series involving the addition of an identical C_5 unit regularly incorporated in the skeleton. These structural relationships are apparent from the striking similarities/analogies shown by the fine structure of the 2D NMR signals and by the coupling patterns of well-resolved signals in the ^1H NMR spectra. In each case, the basic carbon framework was deduced from the HMBC experiment (two- and three-bond heteronuclear correlations, starting from the methyl groups and individual protons). In particular, each methyl group located on a ring junction quaternary carbon atom could be linked to its neighbors (or to the geminal methyl groups) through one common remote connection (^3J) with a methine, therefore establishing the characteristic backbone of the saturated part of the molecule. The chemical shifts of proton and carbon atom signals strongly support a *trans-transoid-trans* stereochemistry with the ring-junction axial methyl groups on the same side of the mean plane of the molecules,[9] which was finally confirmed by the NOEs observed (Fig. 1).

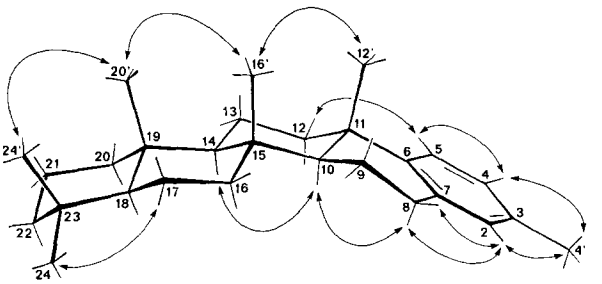
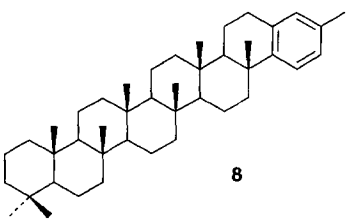


Fig. 1. Spatial representation of **4** (computed by SYBYL 60 software and adapted from a drawing obtained by ALCHEMY III, Tripos Associates Inc., St Louis, Missouri) showing the most important NOEs observed.

Mass spectrometry (including high resolution measurements) showed **6** has the molecular formula $C_{29}H_{44}$. In comparison with **4**, the prominent fragments containing the aromatic nucleus show a shift upwards of 14 Da, suggesting the presence of an additional methyl group on the aromatic moiety. ^1H NMR data of Table 1 unambiguously indicate that the extra methyl group is located at C(2), since compound **6** displays nearly identical resonances to those of **4** (Table 2), and instead of the signal for the aromatic C(2) proton (singlet), the signal for a methyl substituent on the aromatic ring is observed.

Furthermore, hepta- and octacyclic (**8**) analogues (C_{38} and C_{43}, respectively) of hydrocarbons **3**–**5** also occur in Messel shale, as can be inferred from their mass spectra (Table 1).



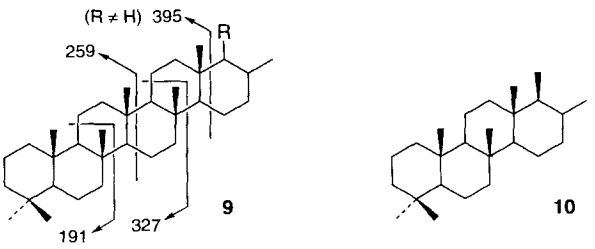
Parallel to the identification of these aromatic products, GC-MS investigations of the alkane fractions from Upper Cretaceous sediments (Lameignère quarry near Orthez, France) revealed a series of homologous highly cyclized hydrocarbons (at least up to seven rings) which, from their extremely informative mass

Table 2. ^{13}C NMR data [a] of hydrocarbons **3**–**5** and ^1H NMR data (500.1 MHz) of hydrocarbon **4** (CD_2Cl_2, δ relative TMS).

C atom [b]	**3** δ(C)	**4** δ(C)	**5** δ(C)	**4** δ(H) [c]	C atom [b]	**3** δ(C)	**4** δ(C)	**5** δ(C)	**4** δ(H) [c]
2	129.56	129.56	129.54	6.82	16'	16.50	17.71	17.60	0.925
3	134.71	134.69	134.67		17	19.04	18.69	17.45	1.43 (β) 1.55 (α)
4	126.80	126.78	126.76	6.89	18	42.46	56.95	61.51	0.82
4'	20.86	20.85	20.84	2.230	19	33.60	37.88	38.13	
5	124.78	124.84	124.83	7.10	20	33.45	40.20	42.13 [f]	0.80 (α) 1.71 (β)
6	148.01	147.95	147.92		20'	21.60	16.40	17.60	0.866
7	135.36	135.38	135.36		21		19.09	18.72	1.39 (α) 1.63 (β)
8	31.21	31.27	31.26	2.75 (α) 2.85 (β)	22		42.52	56.91	1.13 (α) 1.35 (β)
9	18.38	18.28 [d]	18.23 [e]	1.63 (β) 1.82 (α)	23		33.59	37.84	
10	55.90	56.34	56.27	1.23	24		33.43	40.14	0.840
11	38.22	38.04	38.07		24'		21.51	16.31	0.821
12	41.15	41.18	41.16	1.40 (α) 2.35 (β)	25		19.08		
12'	26.36	26.28	26.26	1.145	26		42.52		
13	19.52	18.33 [d]	18.30 [e]	1.51 (β) 1.66 (α)	27		33.56		
14	56.69	61.24	61.60	0.84	28		33.41		
15	38.03	38.30	38.07		28'		21.48		
16	40.18	42.08	42.10 [f]	0.96 (α) 1.89 (β)					

[a] Measured at 100.1 (**3**) and 125.8 MHz (**4** and **5**). [b] "Biogenetic" numbering. [c] Since absolute configurations are unknown, the α/β notation is relative to the configurations represented in the drawings. [d–f] Values with the same letter are interchangeable.

spectra, are clearly related to the previously identified compounds. Indeed, mass spectra[10] of the members of the usually predominant hexacyclic series, for which we propose structures **9** (R = H, alkyl), display two characteristic fragmentation patterns[11] in which the fragments are regularly shifted by 68 Da (unknown C_{34} hexacyclic compounds exhibiting similar mass spectra have also been detected in high abundance in Canadian sediments[12]). Our structural hypotheses are also strongly supported by mass spectral data reported for scalarane **10**[13] which shows a strikingly similar fragmentation pattern.



All these hydrocarbons can be interpreted in terms of "molecular fossils" of polycyclic precursors deriving from the proton-induced cyclization of all-*trans* regular isoprenoids, such as polyprenols or their equivalents. Figure 2 illustrates the formation

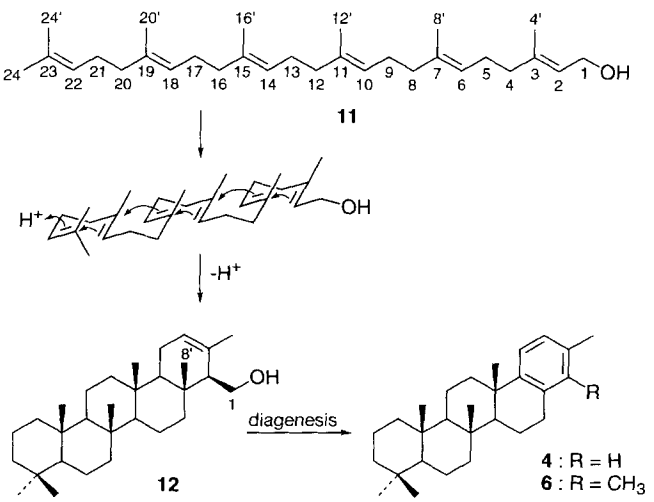


Fig. 2. Proposed biological and diagenetic formation for hydrocarbons **4** and **6**.

of a likely precursor for **4** and **6**, starting from the all-*trans* hexaprenol **11** folded in an all-pre-chair conformation. The resulting pentacyclic triterpenol **12** (or diol if the terminal cationic intermediate is trapped by water) could indeed account for the occurrence of **4** and **6** through well-established geochemical transformations: facultative specific loss of the functionalized C(1) atom (for instance, after oxidation and subsequent decarbonylation or decarboxylation, further facilitated by the presence of a double bond in the β-position, and aromatization starting in the functionalized ring with concomitant loss of the angular methyl group $CH_3(8')$) as commonly observed for pentacyclic triterpenes.[14] Alternatively, reductive processes could explain the presence of the saturated series in sediments. The homologous compounds might be formed by the progressive degradation of a side chain, the latter resulting from an incomplete cyclization of the acyclic precursor.

An important question which remains is whether this cyclization process is biological or not. Indeed, a clay-catalyzed cyclization of polyprenols in sediments such as **11** would, for instance, lead to a compound such as **12**. This can be inferred from the results of biomimetic cyclizations[15] of lower regular polyprenols and of related products catalyzed by acids or superacids as well as of a sesterterpenol (all-*trans* geranylfarnesol), the potential precursor of **3**. Specific rotation measurements (Table 1) showed that the isolated products **3**–**5** are optically active. Hence, if one precludes the very unprobable selective removal of one enantiomer, for instance by biodegradation processes, it is reasonable to assume that the cyclization is enzymatically initiated.[16]

The detection in sediments of high molecular weight biomarkers, which result from the cyclization of regular polyprenols, is not unprecedented, albeit as yet restricted to tricyclic compounds. Indeed, saturated (e.g. **2**) or aromatic (e.g. **7**) tricyclic hydrocarbons in the C_{19} to C_{54} range have been identified or detected in geological sources where they are widely distributed, though not as ubiquitous as the hopanoids.[4] These products have been interpreted as being the molecular fossils of natural as yet unknown tricyclopolyprenols arising from the partial, proton-induced, enzyme-mediated cyclization of higher polyprenols (C_{30} to C_{55}). Remarkably, a cell-free system from the protozoon *Tetrahymena pyriformis*, known to cyclize squalene to tetrahymanol, is also able to cyclize all-*trans* pentaprenyl and hexaprenyl methyl ether into various polycyclic isoprenoids, thus providing direct proof for a proton-induced enzymatic cyclization of higher polyprenol derivatives.[17] The cyclization of hexaprenyl ether led to di-, tri-, tetra-, and pentacyclic skeletons, suggesting the mediation of a rather low-specific enzyme, maybe squalene cyclase itself. With regard to these observations, it appears quite reasonable to envisage that any cyclase capable of (accidentally?) initiating a cyclization process which can proceed stepwise without enzymatic control (as in biomimetic experiments[15c]) might explain the formation of the fossil molecule precursors. Moreover, such a scenario could account for the existence of the diversely cyclized hydrocarbons in sediments, starting from *one* polyprenol precursor (long-chain all-*trans* polyprenoids are widespread in organisms, e.g. side chains of ubiquinones[18]), the side chain having been partially degraded or completely removed during the sedimentation process, as, for example, in the tricyclopolyprenic series. Another possible way of formation could involve an abiotical (clay-catalyzed?) cyclization of biogenic tricyclopolyprenols. In the Messel shale, however, no trace of side chain degradation intermediate products or even of the saturated tricyclopolyprenic series could be detected, making these hypotheses appear highly unlikely, and it is more probable that in this case compounds **3**–**6** and **8** result from the complete cyclization of different polyprenols.

The origin of the hydrocarbons discussed here is unknown. Only compound **3** can eventually be related to known precursors since scalarane derivatives have been described as abundant constituents of sponges (or their symbionts).[19] For the higher cyclized hydrocarbons, neither their presumed biogenic polycyclic precursors (polycyclopolyprenols) nor related biomolecules bearing a potentially adequate framework have as yet been found in living organisms.[20] The postulated precursors of these highly cyclized polyprenic hydrocarbons can be viewed as the representatives of a new class of molecules whose natural distribution and biological significance remains to be determined, although the possibility of "accidental" enzymatic cyclization of regular isoprenoids such as polyprenols by a cyclase with little substrate specificity cannot be ruled out.

Received: December 17, 1993 [Z 6566 IE]
German version: *Angew. Chem.* **1994**, *106*, 1235

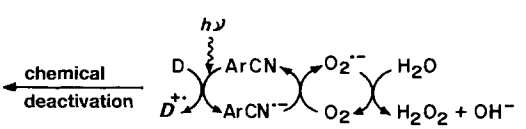
[1] K. E. Peters, J. M. Moldowan, *The Biomarker Guide*, Prentice Hall, Englewood Cliffs, NY, USA, **1993**.
[2] a) G. Ourisson, P. Albrecht, *Acc. Chem. Res.* **1992**, *25*, 398; b) G. Ourisson, M. Rohmer, *ibid.* **1992**, *25*, 403.
[3] J. Dahl, J. M. Moldowan, M. A. McCaffrey, P. A. Lipton, *Nature* **1992**, *355*, 154.
[4] D. Heissler, R. Ocampo, P. Albrecht, J. J. Riehl, G. Ourisson, *J. Chem. Soc. Chem. Commun.* **1984**, 496, and references therein; B. R. T. Simoneit, R. N. Leif, F. R. Aquino Neto, D. A. Azevedo, A. C. Pinto, P. Albrecht, *Naturwissenschaften* **1990**, *77*, 380; S. M. B. De Grande, F. R. Aquino Neto, M. R. Mello, *Org. Geochem.* **1993**, *20*, 1039.
[5] G. Ourisson, P. Albrecht, M. Rohmer, *Trends Biochem. Sci.* **1982**, *7*, 236.
[6] The structure of **3** was presented at the 13th International Symposium on Polynuclear Aromatic Hydrocarbons, Bordeaux, France, October 1–4, 1991: V. Hauke, J. M. Trendel, P. Albrecht in *Polycyclic Aromatic Compounds* (Eds.: P. Garrigues, M. Lamotte), Gordon and Breach Science Publishers, Switzerland, **1993**, p. 451.
[7] For isolation procedure of **3**, see ref. [6]. For isolation of **4**–**6**, the HPLC column used was a Du Pont Zorbax ODS 250 × 9.4 mm, 7 μm, 80 Å (MeOH/$CHCl_3$ 80:20). Compounds **3** (9 mg), **4** (10 mg), and **5** (5 mg) each represent about 10–20 ppm of the total organic extract (35 $g\,kg^{-1}$ shale) and their purity was at least of 94% (GC evaluation). **6** (0.2 mg) was contamined by a known compound (< 10%).
[8] D. A. Azevedo, F. R. Aquino Neto, B. R. T. Simoneit, *Org. Mass Spectrom.* **1990**, *25*, 475, and references therein.
[9] Thus, all methyl groups on ring junctions display high-field ^{13}C chemical shifts $\delta < 20$ (except for the C(12′) methyl: $\delta \approx 26$), which is consistent with their axial orientation on all-*trans* structures (presence of *γ-gauche* effects). The resonances of axial methylene (*J* ca. 13.0, 13.0, 4.0 Hz plus eventually a ^4J W-type coupling ≤ 1 Hz) and axial methine (*J* ca. 12.5, 2.0 Hz) protons which are *trans* relative to the axial methyl groups (i.e. for **4**, Hα–C(12), Hα–C(16), Hα–C(20), Hα–C(22), and H–C(10), H–C(14), H–C(18), respectively) appear at high-field (generally $\delta < 1.15$, less marked for Hα–C(12) and H–C(10) under the deshielding influence of the aromatic moiety). This observation combined with the deshielding of the associated methylene ($37 < \delta < 43$) and methine ($56 < \delta < 62$) carbon atoms point to the absence of *γ-gauche* effects with any of these methyl groups. Conversely, the high-field ^{13}C shifts recorded ($18 < \delta < 20$) for the remaining methylene moieties—C(8) excepted—(i.e. for **4**, C(9), C(13), C(17), and C(21)) together with the deshielding of their attached axial protons ($\delta > 1.2$) reflect double and triple *γ-gauche* interactions with the methyl groups.
[10] MS data (EI 70 eV): *m/z* (%): for **9**, R = H: 466 (25) [M^+], 451 (32), 327 (19), 285 (72), 259 (60), 217 (100), 191 (57), 149 (24); **9**, R = Me: 480 (30) [M^+], 465 (32), 395 (24), 327 (37), 299 (57), 259 (73), 231 (100), 191 (71), 163 (97); **9**, R = Et: 494 (22) [M^+], 479 (30), 395 (100), 327 (15), 313 (23), 259 (36), 245 (39), 191 (36), 177 (51); **9**, R = Pr: 508 (20) [M^+], 493 (25), 395 (100), 327 (45), 259 (70), 191 (59).
[11] The first fragmentation pattern, shown on structures **9**, remains unchanged along the hexacyclic series (the prominent ion peak at *m/z* 395 is present only when R ≠ H and becomes the base peak for R ≥ Et), whereas the second, which concerns the right part of the molecules bearing the side chain, displays ions whose masses are shifted according to the homologue under consideration (*m/z* $149 + n \times 14$, $217 + n \times 14$, $285 + n \times 14$, $n = 0$ and R = H for the C_{34} homologue).
[12] C. L. Riediger, P. W. Brooks, M. G. Fowler, L. R. Snowdon, Poster at the "16th International Meeting on Organic Geochemistry" Stavanger, Norway, September 1993, in *Organic Geochemistry* (Ed.: K. Øygard), Falch Hurtigtrykk, Kalbakken, Norway, **1993**, p. 302.
[13] W. Herz, J. S. Prasad, *J. Org. Chem.* **1982**, *47*, 4173.
[14] C. Spyckerelle, A. C. Greiner, P. Albrecht, G. Ourisson, *J. Chem. Res. (S)* **1977**, 334; *J. Chem. Res. (M)* **1977**, 3829; G. A. Wolff, J. M. Trendel, P. Albrecht, *Tetrahedron* **1989**, *45*, 6721, and references therein.
[15] a) E. E. van Tamelen, R. G. Nadeau, *Bioorg. Chem.* **1982**, *11*, 197; b) W. S. Johnson, *Angew. Chem.* **1976**, *88*, 33; *Angew. Chem. Int. Ed. Engl.* **1976**, *15*, 9; c) M. Nishizawa, H. Takenaka, Y. Hayashi, *J. Am. Chem. Soc.* **1985**, *107*, 522; d) P. F. Vlad, *Pure Appl. Chem.* **1993**, *65*, 1329.
[16] Furthermore, it should be noted that structures differing by a C_5 isoprenic unit have opposite signs of optical rotation. Therefore, if it is assumed that they also have alternate partial enantiomeric structures and that the immediate stereochemical surroundings of the aromatic ring—that is, configurations at C(10) and C(11)—is determinant for the sign of the optical rotation, we can tentatively assign the absolute configurations of the isolated hydrocarbons as being those represented, given that abieta-8,11,13-triene, which has a structure analogous to that of the tricyclic member of the series, **7**, (also present in the Messel shale) and the absolute configuration of which is known, is dextrorotatory (O. Jeger, O. Dürst, G. Büchi, *Helv. Chim. Acta* **1947**, *30*, 1853).
[17] J.-M. Renoux, M. Rohmer, *Eur. J. Biochem.* **1986**, *155*, 125.
[18] M. D. Collins, D. Jones, *Microbiol. Rev.* **1981**, *45*, 316.
[19] J. R. Hanson, *Nat. Prod. Rep.* **1992**, *9*, 481.
[20] Carbon isotopic compositions ($^{13}C/^{12}C$) of aromatic hydrocarbons **3**–**6**, measured by gas chromatography–isotope ratio mass spectrometry and expressed by the $\delta^{13}C$ values, fall within a rather narrow range (−30.5 to −34.5‰), hence indicating a probable common origin. These values are markedly different from those recorded, from the same Messel shale sample, for higher plant pentacyclic triterpene derivatives (−23 to −25‰) and at the boundary of those of aromatic and saturated hopanoid hydrocarbons (−34 to −66‰), a wide range reflecting the diversity of the procaryotic organisms operating in natural environments. It is interesting to note that the monoaromatic-ring-*A* gammacerane derivative, likely originating from protozoa (H. R. Harvey, G. B. McManus, *Geochim. Cosmochim. Acta* **1991**, *55*, 3387, and references therein), has a value (−33.1‰) which would fit well with those of our newly identified compounds. $\delta = 10^3[(R_x - R_s)/R_s]$, where $R = {}^{13}C/{}^{12}C$, x designates sample, s the PDB standard (PDB = Peedee Belemnite; the standard is a belemnite from the Pedee Formation in South Carolina) and $R_s = 0.0112372$. Mean values from at least three replicate measurements.

A Novel Photosystem for Harvesting Visible Light to Drive Photoinduced Electron Transfer (PET) Reductions: β-Activation of α,β-Unsaturated Ketones for Radical Cyclizations**

Ganesh Pandey* and Saumen Hajra

The past decade has witnessed substantial, multidisciplinary research efforts directed towards the conversion of solar light into useful chemical energy; most of the approaches are based on photoinduced electron transfer processes.[1] In organic chemistry several new and synthetically important organic photoreactions have been discovered that employ electron transfer (ET) to or from the substrate in the presence of an electron-rich donor or electron-poor acceptor.[2] Interestingly, remarkable progress has also been made in the area of photoinduced electron transfer (PET) reactions, though the chemistry of the radical cations generated by oxidative reactions remains at the focus.[3] Despite the great synthetic potentials of photosensitized one-electron reductions in organic synthesis, research in this area has been limited, owing to the lack of a suitable photosystem.[4]

Our own interest[3, 5] in this area has been centered on the application of PET oxidation reactions of select donors and cyanoarenes (ArCN) as light-absorbing electron acceptors. Our photosensitization concept relies on the thermodynamic feasibility of ET from $ArCN^{\bullet -}$ to O_2 followed by disproportionation of $O_2^{\bullet -}$ as shown in Scheme 1.



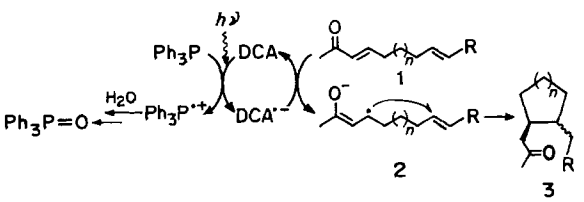
Scheme 1. Mechanism of the PET oxidation of an electron donor D.

The above mechanistic premise led us to envision that photochemical excitation of a system comprising a sacrifical electron donor and ArCN in argon atmosphere should be able to drive a second ET from $ArCN^{\bullet -}$ to another molecule, provided that

[*] Dr. G. Pandey, S. Hajra
Division of Organic Chemistry (Synthesis)
National Chemical Laboratory
Pune 411008 (India)
Telefax: Int. code + (212)330233

[**] This work was supported by the University Grant Commission, New Delhi (Research Fellowship to S.H.). We are grateful to Dr. S. Padhye and A. Kumbhar (University of Poona) for measuring the reduction potentials of the enones.

the redox potentials are matched. For this purpose we have developed a photosystem consisting of triphenylphosphane (Ph_3P) as the sacrificial electron donor and 9,10-dicyanoanthracene (DCA) as the visible-light-absorbing electron acceptor[6] for activating the β position of α,β-unsaturated ketones for radical cyclizations (**1** → **3**) by reductive transfer of one electron (Scheme 2). To our knowledge, the concept[7] described here provides a novel nonreagent-based strategy for the β-activation of enones for radical additions. The generation of radical cations by redox sensitization has been reported.[8] The synthetic potential of this work is comparable to only one other method reported recently[9] which makes use of a toxic and environmentally unfriendly stannyl reagent.



Scheme 2. Mechanism of PET-driven reductions with Ph_3P as a sacrificial electron donor.

The PET phenomena established by our group[6] between Ph_3P and ^{1}ArCN* and the efficient transformation of $Ph_3P^{\bullet+}$ to stable triphenylphosphane oxide (Ph_3PO) by reaction with water led us to select Ph_3P as the sacrificial electron donor. Furthermore, because of the efficiency of the transformation of $Ph_3P^{\bullet+}$ to Ph_3PO, we thought that Ph_3P would be an ideal substrate for controlling the impact of back electron transfer, the intrinsic limitation of PET processes[1] in our photosystem. We chose α,β-unsaturated ketones for the study of sensitized one-electron reduction processes, as they should be suited for testing our concept and for exploring the interesting synthetic avenues of free-radical reactions.

The feasibility of ET from $DCA^{\bullet-}$ to **1** was evaluated by estimating the Gibbs free energy change from the redox potentials of $DCA^{\bullet-}$ (−0.89 eV)[2] and **1** (−0.40 to −0.76 eV)[10, 11] according to $\Delta G_{ET} = E_{1/2}(ox) - E_{1/2}(red)$ (Table 1).

Table 1. Free energy change ΔG_{ET} for electron transfer from $DCA^{\bullet-}$ to enones **1**, **4**, and **7**.

Enone [a]	E_{red} [b, c] [eV]	ΔG_{ET} [kJ mol^{-1}]
1a	−0.40	−47.25
1b	−0.45	−42.43
1c	−0.73	−15.44
1d	−0.68	−20.25
4	−0.76	−12.51
7	−0.70	−18.30

[a] Formulas given in Table 2. [b] Determined by cyclic voltammetry, relative to SCE [10]. [c] Since the reductions are irreversible, the cathodic peak potentials are listed.

A solution of Ph_3P, DCA, and one of the enones **1a–d** in aqueous dimethylformamide (DMF)[12] with isopropyl alcohol as the H• donor was irradiated with visible light (λ = 405 nm) to provide cyclization products **3a–d** formed via free radicals (Table 2); the major diastereomer in each case has the *trans* configuration.[13] An alternative route for the formation of these products involving first [2 + 2]cycloaddition followed by one-electron reductive C–C bond cleavage[14] can be ruled out, since the enones do not absorb light under the experimental conditions. The quantum yields (ϕ = 0.011–0.063) for the product formation clearly indicates that the products are not arising through the chain reactions. Since the transformation of Ph_3P into Ph_3PO is a sequential, two-electron process,[6] Ph_3P can provide two successive electrons for reduction. Therefore, only one molecule of Ph_3P is required to reduce two molecules of enone. Secondary cyclization products such as bicyclo[3.3.0] compounds from the corresponding *cis* isomers of **3a–b** like those observed by Enholm and Kinter[9] were absent in our reactions, possibly because the β-carbon atoms of enolates are less nucleophilic than those of stannyl enolates.

Table 2. Photosensitized reductive cyclizations of enones **1**, **4**, and **7**.

Enone	Product(s) [a] (quantum yield, ϕ) [b]	t[h] [c]	Yield [%] (*trans*/*cis*) [a]
1	**3**		
a, n = 1, R = COOEt	(0.060)	28	98(85/15)
b, n = 1, R = CN	(0.063)	31	97(80/20)
c, n = 2, R = CN	(0.032)	42	94(68/32)
d, n = 2, R = COOEt	(0.030)	40	95(75/25)
4	**5** **6**		
	70:30	50	55
	(0.013) (0.006)		
7	**8** **9**		
	68:32	50	50
	(0.011) (0.005)		

[a] The *cis*/*trans* and product ratios were determined by gas chromatography (Perkin Elmer 8700; HP capillary column, cross-linked methyl silicone, 25 m). [b] Quantum yields were determined with an instrument from Applied Photophysics; light intensities estimated by using uranyl oxalate as a chemical actinometer; product formation measured by HPLC (Perkin Elmer 135C, diode-array detector, C_8 reversed-phase column).

We have also examined the cyclization of enones **4** and **7**, which are nonactivated alkene acceptors. Unlike Enholm and Kinter,[9] we found that these compounds underwent cyclization to produce **5** and **8**, albeit in slower rates, as well as reduction products **6** and **9**.

In summary, we have developed a novel photosystem for converting the photoenergy of visible light into chemical energy. This concept has potential in organic chemistry for a variety of one-electron reduction processes. Further studies are in progress.

Experimental Procedure

A solution of one of the enones **1a–d**, **4**, or **7** (3.60 mmol), Ph_3P (2.1 mmol), and DCA (1.4 mmol) in DMF/*i*PrOH/H_2O (88/10/2) was irradiated in Pyrex tubes under an argon atmosphere with light from a 450 W Hanovia medium-pressure lamp filtered by a $CuSO_4 \cdot 5H_2O \cdot NH_3$ solution (405 nm) [15]. The progress of the

reaction was monitored by GC. After considerable consumption (60–99%) of the starting enone (approximately 28–50 h) the solvent was removed by distillation under reduced pressure. Chromatographic purification (silica gel, 200 mesh) of the reaction mixture eluting with petroleum ether/ethyl acetate gave the cyclization product (**3a**–**d**, **5**, or **8**) along with Ph_3PO. DCA was recovered (98%). The products were characterized by ^1H and ^{13}C NMR spectroscopy and mass spectrometry. **3a** and **3b** were confirmed by comparing with authentic samples [9].

Received: August 18, 1993
Revised version: January 26, 1994 [Z 6292 IE]
German version: *Angew. Chem.* **1994**, *106*, 1217

[1] Selected reviews: I. Willner, B. Willner, *Top. Curr. Chem.* **1991**, *159*, 157, and references therein; S. E. Webber, *Chem. Rev.* **1990**, *90*, 1469; T. J. Meyer, *Coord. Chem. Rev.* **1991**, *111*, 47; M. A. Fox, *Adv. Photochem.* **1986**, *13*, 237.
[2] M. A. Fox, M. Chanon, *Photoinduced Electron Transfer Reactions, Part D*, Elsevier, Amsterdam, **1988**; P. S. Mariano, J. L. Stavinoha, *Synthetic Organic Photochemistry* (Ed.: W. M. Horspool), Plenum Press, New York, **1984**, p. 145; S. L. Mattes, S. Farid, *Org. Photochem.* **1983**, *6*, 223.
[3] G. Pandey, *Top. Curr. Chem.* **1993**, *168*, 175; J. Mattay, *Synthesis* **1989**, 233.
[4] T. Hamada, A. Nishida, O. Yonemitsu, *J. Am. Chem. Soc.* **1986**, *108*, 140; K. Okada, K. Okamoto, M. Oka, *ibid.* **1988**, *110*, 8736. However, the mechanism of the regeneration of the light-absorbing electron donor is not yet known.
[5] G. Pandey, *Synlett* **1992**, 546; G. Pandey, B. B. V. Soma Sekhar, U. T. Bhalerao, *J. Am. Chem. Soc.* **1990**, *112*, 5650; G. Pandey, B. B. V. Soma Sekhar, *J. Org. Chem.* **1992**, *57*, 4019.
[6] G. Pandey, D. Pooranchand, U. T. Bhalerao, *Tetrahedron* **1991**, *47*, 1745; D. Pooranchand, Dissertation, Osmania University, **1992**.
[7] The only analogy to this concept may be found in artificial photosynthesis [1] and glutathione reduction (I. Willner, N. Lapidot, *J. Am. Chem. Soc.* **1991**, *113*, 3625.)
[8] T. Majima, C. Pac, A. Nakasone, H. Sakurai, *J. Am. Chem. Soc.* **1981**, *103*, 4499.
[9] E. J. Enholm, K. S. Kinter, *J. Am. Chem. Soc.* **1991**, *113*, 7784.
[10] Bioanalytical systems, model CV-27; Pt inlay working electrode, Ag/AgCl reference electrode, and Pt wire auxiliary electrode; tetraethyl ammonium perchlorate in DMF as the supporting electrolyte. The DMF solution was degassed by argon bubbling for 10 minutes before each measurement.
[11] Since the reduction potentials are irreversible, the ΔG_{ET} values obtained are only approximate; however, they agree generally quite well with experimental values.
[12] DMF was used as solvent mainly because of the higher solubility of DCA. The reaction can also be performed in acetonitrile, but reaction times are longer owing to the poor solubility of DCA.
[13] Control experiments in the dark or with irradiation (405 nm) but without Ph_3P give no reaction product.
[14] J. Mattay, A. Banning, E. W. Bischof, A. Heidbreder, J. Runsink, *Chem. Ber.* **1992**, *125*, 2119.
[15] J. G. Calvert, J. N. Pitts, *Photochemistry*, Wiley, New York, **1966**, p. 736.

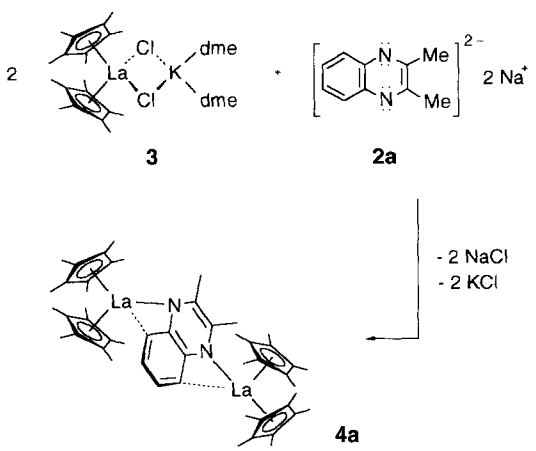
N-Heteroarene Dianions as Antiaromatic Ligands Bridging two Lanthanocene Moieties**

Joachim Scholz,* Annett Scholz, Roman Weimann, Christoph Janiak, and Herbert Schumann

Pyrazine serves as a model ligand for studying magnetic exchange phenomena,[1] electron transfer reactions,[2] or one-dimensional conductors.[3] With its two N-donor functions, this heterocycle can coordinate to Lewis acidic metal centers and at the same time bridge two metal atoms.[4] The π-acceptor characteristics (low-lying LUMOs) of this bridging ligand enable, under suitable conditions, the generation of, for example, stable radical ions from these binuclear complexes.[5]

Quinoxaline and phenazine represent benzo- and dibenzo-annelated derivatives of pyrazine, respectively; in contrast to the parent compound pyrazine, these heterocycles can be reduced to their dianions either electrochemically[6] or by alkali metals.[7] The formally antiaromatic systems with 12-π and 16-π electrons have high charge density and, so far, could be stabilized in only a few cases by presence of alkali and alkaline earth ions.[8] We have found now that the resulting electron-rich N-heteroarene dianions can bridge two lanthanocene moieties. Here we report on the synthesis and crystal structure analysis of complexes **4a** and **4b**, which are the first examples of this new class of compounds.

2,3-Dimethylquinoxaline (**1a**) is rapidly reduced by two equivalents of sodium in THF to give a deep blue solution containing the 12-π dianion **2a**. This dianion reacts with **3** in a 2:1 molar ratio to yield the novel, binuclear lanthanocene complex **4a**, which can be isolated as dark green, extremely air- and moisture-sensitive crystals (Scheme 1). On the basis of the NMR



Scheme 1. dme = dimethoxyethane.

spectra one can already expect unusual bonding properties for this compound. For example, the signals for H atoms H24 and H24a′ ($\delta = 4.22$) and for H25 and H25a′ ($\delta = 5.66$, AA′XX′ spin system, numbering scheme according to Fig. 1) of the 2,3-dimethylquinoxaline heterocycle are shifted to higher field by $\Delta\delta = 3$ and 2.4, respectively, when compared to the free ligand.[9] The nonuniform charge distribution is indicative of a paramagnetic ring current, which is characteristic for systems with $4n$ π electrons such as naphthalene–lithium $Li_2[C_{10}H_8]$.[10b] Atoms C24 and C24′ of the bridging ligand are also strongly shielded ($\delta = 89.9$). In contrast to the ^1H NMR signals, the ^{13}C NMR signal positions are barely influenced by ring-current effects and reflect, for the most part, the actual charge distribution. Hence, the negative charge density in the bridging ligand of **4a** is even higher than in 2,3-diphenylquinoxaline disodium $Na_2[C_8H_4N_2$-(2,3-Ph_2)] (corresponding signal at $\delta = 100.3$).[7] This observation contrasts with those for the recently described 1,4-dihydroquinoxaline derivative 1,4-$[Me_2(tBu)Si]_2(C_8H_6N_2)$ in which the charge density of the $4n$ π electron system is transferred to the stabilizing R_3Si-acceptor substituents through covalent N–Si bonds; moreover, the extent of electron delocalization from the heteroarene to the arene unit is small.[8e]

Figure 1 shows the result of the X-ray structure analysis of **4a**.[11] The two Cp^*_2La moieties face each other and are bound

[*] Dr. J. Scholz, Dipl.-Chem. A. Scholz
Institut für Anorganische Chemie der Universität Halle-Wittenberg
Geusaer Strasse, D-06217 Merseburg (FRG)
Telefax: Int. code + (3461)46-2370
Prof. Dr. H. Schumann, Dr. R. Weimann, Dr. C. Janiak
Institut für Anorganische und Analytische Chemie
der Technischen Universität Berlin (FRG)

[**] This work was supported by the Fonds der Chemischen Industrie. We thank Prof. Dr. K.-H. Thiele for his interest.

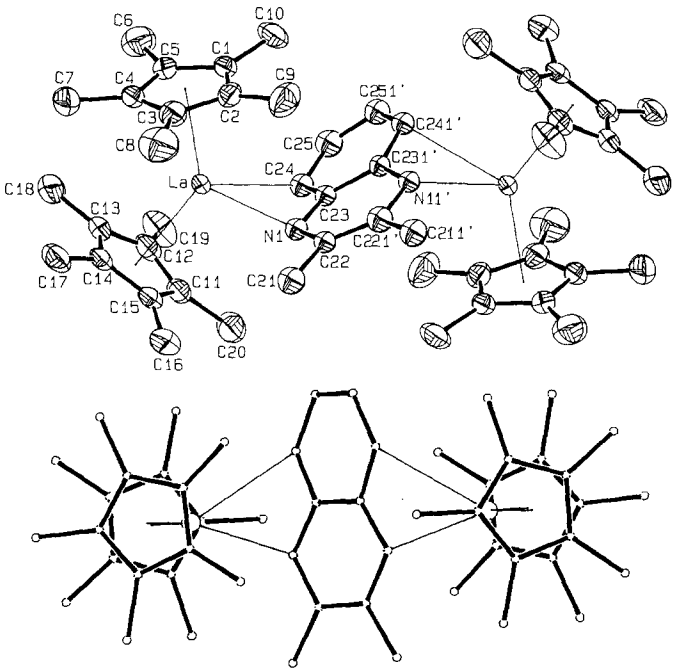


Fig. 1. Structure of **4a** in the crystal. The 2,3-dimethylquinoxaline dianion is disordered and occupies one of two molecular positions. These positions are twisted relative to each other by 180°. For clarity only one of the two arrangements is shown. Top: ORTEP view. Selected bond lengths [Å] and angles [°] (Cp*1 and Cp*2 represent centroid positions of the η^5-bonded cyclopentadienyl ligands C1–C5 and C11–C15): La-N1 2.409(4), La-N1a 2.444(4), La-Cp*1 2.521(1), La-Cp*2 2.537(1), La-C23 2.846(5), La-C23a 2.918(4), La-C24 2.903(5), La-C24a 2.891(5), N1-C22 1.400(6), N1-C23 1.355(6), N1a-C22a 1.391(6), N1a-C23a 1.360(6), C22-C22a 1.37(1), C23-C23a 1.445(8), C24-C25 1.419(7), C24a-C25a 1.453(7), C23-C24 1.376(7), C23a-C24a 1.400(7), C25-C25a 1.37(1), Cp*1-La-Cp*2 136.6(1). Bottom: The complex viewed from above to clarify the bonding.

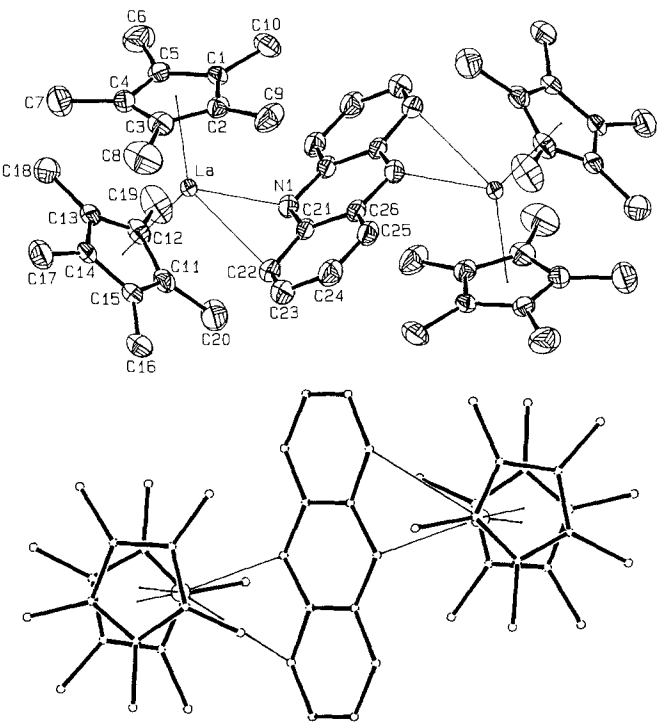
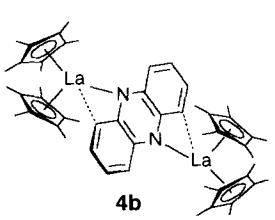


Fig. 2. Structure of **4b** in the crystal. Top: ORTEP view. Selected bond lengths [Å] and angles [°] (Cp*1 and Cp*2 represent the centroid positions of the η^5-bonded cyclopentadienyl ligands C1–C5 and C11–C15): La-N1 2.452(2), La-C21 2.920(2), La-C22 2.931(2), La-Cp*1 2.525(1), La-Cp*2 2.541(1), N1-C21 1.383(3), C21-C22 1.403(3), C22-C23 1.401(4), C23-C24 1.368(4), C24-C25 1.404(4), C25-C26 1.389(3), C21-C26 1.427(3), Cp*1-La-Cp*2 135.9(1). Bottom: The complex as viewed from above in order to clarify the bonding.

to the planar quinoxaline dianion. From an electrostatic point of view the N atoms of the bridging ligand are the more favorable ligating atoms for the lanthanocene moieties; hence, the La–N contacts are short [La–N1 2.409(4), La–N1a 2.444(4) Å] and are of the same magnitude as La–N distances reported previously.[12] The two La atoms are located 1.770(5) Å below and above the quinoxaline plane. This finding is indicative of a partial π character for the La–N interactions. Additional interactions with quinoxaline atoms C24 and C24′ are in line with the tendency of La atoms to attain a higher coordination number. The La–C distances are only marginally larger than the average La–C_{Cp*} distance (2.789 and 2.806 Å) or those reported recently for the $[La(\eta^3\text{-}C_3H_5)_4]^-$ ion (La–$C_{average}$ 2.811 Å).[13] The remarkable high-field positions of the ^{13}C NMR signals of C24 and C24′ and the relatively small $^1J_{C,H}$ coupling constant of only 144.4 Hz indicate that these La–C interactions persist even in solution and that an agostic C–H → La bond is present.

The ^1H NMR spectrum of the phenazine complex **4b** points to a similar bonding arrangement. This complex is obtained in form of orange crystals when a bordeaux-red suspension of $Na_2[C_{12}H_8N_2]$ (**2b**, prepared by reacting phenazine (**1b**) with Na granules in THF for several days) is added to **3**. Complex **4b** is extremely air- and moisture-sensitive and is less soluble in *n*-pentane, diethyl ether, or toluene than **4a**. Figure 2 shows the structure of **4b** in the crystal.[11] The important structural characteristics of **4a** and **4b** are identical. As in **4a**, the La atoms in **4b** are bound to the planar bridging ligand by short contacts with the N atoms and by additional interactions with C22 and C22′. The La atoms are positioned 1.870(5) Å above and below the phenazine plane. The outstanding structural feature of **4b** is, without a doubt, the staggered arrangement of the two Cp^*_2La moieties on the periphery of the bridging ligand. In this arrangement the dipolar repulsion between the two Cp^*_2La moieties is minimized.



4b

The bonding interaction between the La atoms and the carbon atoms of the bridging ligands (i.e., C24 and C24′ in **4a**, C22 and C22′ in **4b**) can easily be rationalized. A PM3 calculation[14] for the phenazine- and the 2,3-dimethylquinoxaline dianion shows not only the expected high charge density on the N atoms but also charge maxima located at exactly those ring carbon atoms (Fig. 3). In contrast, quaternary C atoms (i.e., C23 and C23′ in **4a**, C21 and C21′ in **4b**) adjacent to the N atoms are positively polarized. Their relatively short distance to the La atoms is, therefore, not the result of a bonding interaction with the metal but is apparently forced by the special manner of coordination behavior of the bridging ligands. Relative and absolute bond length variations of the N heterocycles,[9] as determined by crystal structure analysis of **4a** and **4b**, can also be rationalized by PM3 optimization of their respective dianionic structures.

Even in unpolar solvents such as $[D_8]$toluene, the partial La–N π interaction, which explains the deflection of the Cp^*_2La moieties out of the heteroarene plane, is apparently removed. All four Cp* ligands of **4a** and **4b** show only one sharp signal in the ^1H NMR spectrum at room temperature. This Cp* signal, as well as the signals for the H atoms of the 2,3-dimethylquinoxaline in **4a** remain almost unchanged upon cooling the sample

 © VCH Verlagsgesellschaft mbH, D-69451 Weinheim, 1994 0570-0833/94/1111-1172 $ 10.00+.25/0 Angew. Chem. Int. Ed. Engl. 1994, 33, No. 11

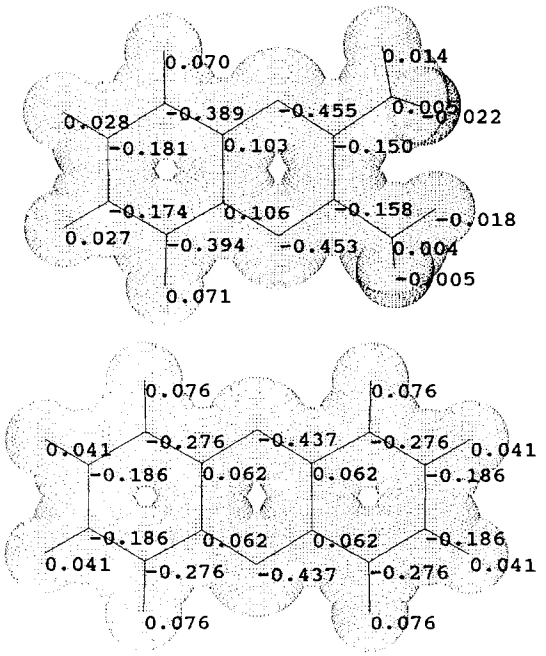


Fig. 3. Charge distribution for the PM3-optimized [14] 2,3-dimethylquinoxaline (top) and phenazine dianions (bottom).

to -80 °C (500 MHz; see Experimental Procedure). However, it cannot be ruled out that even at low temperatures the Cp^*_2La moieties, for example, rotate around the La–N bond. It is worth mentioning that cooling of a toluene solution of **4a** results in a reversible color change from green to dark red.

Complexes **4a** and **4b** represent a novel structural type for organolanthanides, which is reminiscent of the mostly ionic "aromatic alkali-metal amides".[15] Due to their high charge density both the quinoxaline and the phenazine dianions, which can be regarded as heteroatom-modified $4n\,\pi$ anti-Hückel systems, are of special interest as "molecular bridges". We are currently investigating complexes in which two paramagnetic metal centers are connected by these antiaromatic bridging ligands.

Experimental Procedure

All experiments were carried out with thoroughly dried and degassed solvents under an inert argon atmosphere.

4a: In 100 mL THF 2,3-dimethylquinoxaline (1.29 g, 8.15 mmol) was treated with sodium (0.375 g, 16.31 mmol), until all of the metal had been consumed and a deep blue solution was formed. This solution was then added dropwise at -50 °C to a solution of $[Cp^*_2La(\mu\text{-}Cl)_2K(dme)_2]$, prepared by adding $LaCl_3$ (4.0 g, 16.31 mmol) to [Cp*K(dme)] (8.61 g, 32.6 mmol) in 200 mL THF). After warming the reaction mixture to room temperature and removing the solvent under vacuum, **4a** was isolated by extraction of the residue with 100 mL diethyl ether. Recrystallization from *n*-pentane yielded 2.77 g (17%) of dark green crystals, which were suitable for crystal structure analysis. $T_{decomp.} \approx 115$ °C. Correct elemental analysis.—^{1}H NMR (300 MHz, C_6D_6, 20 °C): $\delta = 5.66$ (m, $^3J(H_A,H_X) = 6.0$ Hz, $^4J(H_A,H_X) = 1.3$ Hz, 2H; $C_8H_4N_2$-2,3-Me_2), 4.22 (m, $^3J(H_A,H_X) = 6.0$ Hz, $^4J(H_A,H_X) = 1.3$ Hz, 2H; $C_8H_4N_2$-2,3-Me_2), 2.22 (s, 60H; C_5Me_5), 1.50 (s, 6H; $C_8H_4N_2$-2,3-Me_2); ^{1}H NMR (500 MHz, [D$_8$]toluene, -80 °C): $\delta = 5.73$ (m, 2H; $C_8H_4N_2$-2,3-Me_2), 4.23 (m, 2H; $C_8H_4N_2$-2,3-Me_2), 2.04 (s, 60H; C_5Me_5), 1.50 (s, 6H; $C_8H_4N_2$-2,3-Me_2); ^{13}C NMR (75 MHz, C_6D_6, 25 °C): $\delta = 150.7$ (s, $C_8H_4N_2$-2,3-Me_2), 122.2 (s, $C_8H_4N_2$-2,3-Me_2), 119.8 (dd, $^1J(C,H) = 159.3$ Hz; $C_8H_4N_2$-2,3-Me_2) 119.1 (s, C_5Me_5), 89.9 (ddd, $^1J(C,H) = 144.4$ Hz; $C_8H_4N_2$-2,3-Me_2), 18.5 (q, $^1J(C,H) = 124.6$ Hz; $C_8H_4N_2$-2,3-Me_2), 9.6 (q, $^1J(C,H) = 125.2$ Hz; C_5Me_5).

4b: In 100 mL THF, phenazine (1.47 g, 8.15 mmol) was treated with sodium (0.375 g, 16.31 mmol). The resulting bordeaux-red suspension was then added dropwise at -50 °C to a solution of $[Cp^*_2La(\mu\text{-}Cl)_2K(dme)_2]$, prepared by adding $LaCl_3$ (4.0 g, 16.31 mmol) to [Cp*K(dme)] (8.61 g, 32.6 mmol) in 200 mL THF. After warming the reaction mixture to room temperature and removing the solvent under vacuum, the residue was extracted with diethyl ether. From this extract, **4b** separated in the form of orange-red crystals (yield 1.63 g, 10%). Recrystallization of this material from diethyl ether gave single crystals suitable for crystal structure analysis. $T_{decomp.} \approx 80$ °C. Correct elemental analysis.—^{1}H NMR (300 MHz, C_6D_6, 20 °C): $\delta = 6.19$ (m, AA'XX', 4H; $C_{12}H_8N_2$), 5.29 (m, AA'XX', 4H; $C_{12}H_8N_2$), 2.06 (s, 60H; C_5Me_5); ^{13}C NMR (75 MHz, C_6D_6, 25 °C): $\delta = 145.5$ ($C_{12}H_8N_2$), 121.1 (C_5Me_5), 119.9, 106.4 ($C_{12}H_8N_2$), 10.6 (C_5Me_5).

Received: December 14, 1993 [Z 6560 IE]
German version: *Angew. Chem.* **1994**, *106*, 1220

[1] D. Kahn, *Angew. Chem.* **1985**, *97*, 837–853; *Angew. Chem. Int. Ed. Engl.* **1985**, *24*, 834–850.

[2] a) W. Kaim, *Angew. Chem.* **1984**, *96*, 609–610; *Angew. Chem. Int. Ed. Engl.* **1984**, *23*, 613–614; b) W. Kaim, *Acc. Chem. Res.* **1985**, *18*, 160–166.

[3] O. Schneider, M. Hanack, *Angew. Chem.* **1982**, *94*, 68–69; *Angew. Chem. Int. Ed. Engl.* **1982**, *21*, 79–80.

[4] Numerous examples of such structural variations exist for both main group and transition metals. Of special interest are complexes in which the N heteroarene acts as a π bridging ligand and enables charge transfer between two metal atoms, as is the case in the Creutz–Taube ion $[(NH_3)_5Ru(\mu\text{-}C_4H_4N_2)Ru(NH_3)_5]^{5+}$: C. Creutz, H. Taube, *J. Am. Chem. Soc.* **1969**, *91*, 3988–3989; b) *ibid.* **1973**, *95*, 1086–1094; c) U. Fürholz, H. B. Bürgi, F. E. Wagner, A. Stebler, J. H. Ammeter, E. Krausz, R. J. H. Clark, M. J. Stead, A. Ludi, *ibid.* **1984**, *106*, 121–123; additional examples: d) $[(Cp_3Yb)_2(\mu\text{-}C_4H_4N_2)]$: E. C. Baker, K. N. Raymond, *Inorg. Chem.* **1977**, *16*, 2710–2714; e) $[(Cp^*_2Ba)_2(\mu\text{-}C_4H_4N_2)]$: R. A. Williams, T. P. Hanusa, J. C. Huffman, *J. Organomet. Chem.* **1992**, *429*, 143–152.

[5] a) W. Kaim, *Chem. Ber.* **1982**, *115*, 910–918; b) R. Groß, W. Kaim, *Angew. Chem.* **1984**, *96*, 610–611; *Angew. Chem. Int. Ed. Engl.* **1984**, *23*, 614–615; c) R. Groß, W. Kaim, *Inorg. Chem.* **1986**, *25*, 498–506.

[6] R. M. Crooks, A. J. Bard, *J. Phys. Chem.* **1987**, *91*, 1274–1284.

[7] a) A. Minsky, Y. Cohen, M. Rabinovitz, *J. Am. Chem. Soc.* **1985**, *107*, 1501–1505; b) Y. Cohen, A. Y. Meyer, M. Rabinovitz, *ibid.* **1986**, *108*, 7039–7044.

[8] a) $[Mg_2Br_2(\mu\text{-}C_{12}H_8N_2)(thf)_6]$: P. C. Junk, C. L. Raston, B. W. Skelton, A. H. White, *J. Chem. Soc. Chem. Commun.* **1987**, 1162–1164; b) $[Li_2(\mu\text{-}Cl)(\mu\text{-}NC_{12}H_8NH)(thf)_4]$: L. M. Engelhardt, G. E. Jacobsen, A. H. White, C. L. Raston, *Inorg. Chem.* **1991**, *30*, 3978–3980; 1,4-dihydropyrazine, 1,4-dihydroquinoxaline, and 1,4-dihydrophenazine compounds that are stabilized by π acceptor substituents (e.g., SiR_3) in the 1,4 position have not been taken into consideration: c) W. Kaim, *Angew. Chem.* **1981**, *93*, 621–622; *Angew. Chem. Int. Ed. Engl.* **1981**, *20*, 600–601; d) 1,4-$(Me_3M)_2C_4H_4N_2$ (M = Si, Ge): H.-D. Hausen, O. Mundt, W. Kaim, *J. Organomet. Chem.* **1985**, *296*, 321–337; e) 1,4-[(*t*Bu)Me_2Si]$C_8H_6N_2$: A. Lichtblau, H.-D. Hausen, W. Kaim, *Z. Naturforsch. B* **1993**, *48*, 713–718; f) 1,4-[(*t*Bu)Me_2Si]$C_4Me_4N_2$: W. Kaim, A. Lichtblau, H.-D. Hausen, *J. Organomet. Chem.* **1993**, *456*, 167–173.

[9] **1a**: ^{1}H NMR (C_6D_6): $\delta = 8.04$ (m, AA'XX', 2H; $C_8H_4N_2$-2,3-Me_2), 7.21 (m, AA'XX', 2H; $C_8H_4N_2$-2,3-Me_2), 2.16 (s, 6H; $C_8H_4N_2$-2,3-Me_2); ^{13}C NMR (C_6D_6): $\delta = 153.5$, 141.9, 128.9, 128.6 ($C_8H_4N_2$-2,3-Me_2), 22.8 ($C_8H_4N_2$-2,3-Me_2).—**1b**: ^{1}H NMR (C_6D_6): $\delta = 8.13$ (m, AA'XX', 4H; $C_{12}H_8N_2$), 7.17 (m, AA'XX', 4H; $C_{12}H_8N_2$); ^{13}C NMR (C_6D_6): $\delta = 144.0$, 130.9, 130.3; see also A. E. A. Porter in *Comprehensive Heterocyclic Chemistry, Vol. 3*, Part 2B, (Eds.: A. J. Boulton, A. McKillop), Pergamon Press, Oxford, **1988**, Chap. 2.14; cited references.

[10] a) $[C_{10}H_8]^{2-}$: R. Benken, H. Günther, *Helv. Chim. Acta* **1988**, *71*, 694–702; b) $[C_{14}H_{10}]^{2-}$: K. Müllen, *ibid.* **1976**, *59*, 1357–1359.

[11] a) Crystal data for **4a**: formula $C_{50}H_{70}N_2La_2 \cdot OC_4H_{10}$, $M_r = 976.93$ g cm^{-1} (without Et_2O), crystal dimensions $0.30 \times 0.25 \times 0.50$ mm^3, $a = 1034.8(1)$, $b = 1102.2(2)$, $c = 1148.7(3)$ pm, $\alpha = 81.71(2)$, $\beta = 78.01(2)$, $\gamma = 88.74(1)$°, $V = 1268.2(4) \times 10^6$ pm^3, $Z = 1$, $\rho_{calc.} = 1.356$ g cm^{-3}, $\mu = 15.82$ cm^{-1}, $F(000) = 543$, triclinic crystal system, space group $P\bar{1}$ (No. 2), Enraf–Nonius CAD4 diffractometer, $Mo_{K\alpha}$ radiation, $\lambda = 71.069$ pm, graphite monochromator, temperature 160 K, 4694 measured reflections, 4330 independent ($R_{int} = 0.0179$) and 4187 observed reflections [$F_o \geq 2\sigma(F_o)$], empirical absorption correction (Ψ scans), 393 parameters refined, $R = 0.021$, $R_w = 0.024$, residual electron density: max. 0.49, min. -0.49 eÅ^{-3}. b) **4b**: formula $C_{52}H_{68}N_2La_2 \cdot OC_4H_{10}$, $M_r = 998.94$ g cm^{-1} (without Et_2O), crystal dimensions $0.30 \times 0.26 \times 0.50$ mm^3, $a = 1029.0(1)$, $b = 1114.9(2)$, $c = 1142.1(3)$ pm, $\alpha = 82.15(2)$, $\beta = 78.58(2)$, $\gamma = 87.32(1)$°, $V = 1271.9(5) \times 10^6$ pm^3, $Z = 1$, $\rho_{calc.} = 1.400$ g cm^{-3}, $\mu = 15.72$ cm^{-1}, $F(000) = 543$, triclinic crystal system, space group $P\bar{1}$ (No. 2), Enraf–Nonius CAD4 diffractometer, $Mo_{K\alpha}$ radiation, $\lambda = 71.069$ pm, graphite monochromator, temperature 160 K, 4696 measured reflections, 4404 independent ($R_{int} = 0.0199$) and 4263 observed reflections [$F_o \geq 2\sigma(F_o)$], empirical absorption correction (Ψ scans), 335 parameters refined, $R = 0.019$, $R_w = 0.021$, residual electron density: max. 0.48, min. -0.48 eÅ^{-3}. Further details of the crystal structure investigation may be obtained from the Fachinformationszentrum Karlsruhe, D-76344 Eggenstein-Leopoldshafen (FRG), on quoting the depository number CSD-57974 and the journal citation.

[12] Examples for La–N σ bonds: a) $[(MeC_5H_4)La(NPh_2)_3][Li(dme)_3]$ La-N 2.443(7)···2.469(8) Å, average 2.459(7) Å, J. Guan, S. Jin, Y. Lin, Q. Shen,

Organometallics **1992**, *11*, 2483–2847; b) $[Cp^*_2LaNHCH_3(NH_2CH_3)]$ La-N 2.323(1) and 2.302(10) Å, La ← N 2.70(1) Å. M. R. Gagné, C. L. Stern, T. J. Marks, *J. Am. Chem. Soc.* **1992**, *114*, 275–294.

[13] R. Taube, H. Windisch, F. H. Görlitz, H. Schumann, *J. Organomet. Chem.* **1993**, *445*, 85–91.

[14] J. J. P. Stewart, *J. Comput. Chem.* **1989**, *10*, 209–221; b) J. J. P. Stewart in *Reviews in Computational Chemistry* (Eds.: K. B. Lipkowitz, D. B. Boyds), VCH, Weinheim, **1990**, p. 45ff.

[15] a) R. Hacker, E. Kaufmann, P. von Ragué Schleyer, W. Mahdi, H. Dietrich, *Chem. Ber.* **1987**, *120*, 1533–1538; b) K. Gregory, M. Bremer, P. von Ragué Schleyer, P. A. A. Klusener, L. Brandsma, *Angew. Chem.* **1989**, *101*, 1261–1264; *Angew. Chem. Int. Ed. Engl.* **1989**, *28*, 1224–1226.

Catalytic Pt^+-Mediated Oxidation of Methane by Molecular Oxygen in the Gas Phase**

Ralf Wesendrup, Detlef Schröder, and Helmut Schwarz*

Dedicated to Professor Heinz-Georg Wagner on the occasion of his 65th birthday

The activation of methane represents a fundamental challenge in chemistry, and the catalytic conversion of methane to methanol or formaldehyde is both of scientific and economic interest.[1] At metal surfaces activation of methane often commences with a homolytic C–H bond cleavage and proceeds by reactions of the so-formed methyl radicals with an oxidant. Alternately, the reaction of methane with a transition metal center [M] may lead either to a metal-bonded hydrido methyl fragment, $H-M-CH_3$, or a carbene species, $M=CH_2$, with subsequent O-atom transfer to form the oxygenated products. Furthermore, direct oxidation of methane can be achieved by reactive oxo species, for example, high-valent transition metal oxides, which are recovered in the catalytic process. In a more classical fashion, methane functionalization may also proceed by ionic mechanisms in which either a proton or a hydride is abstracted or protonation take place.[2]

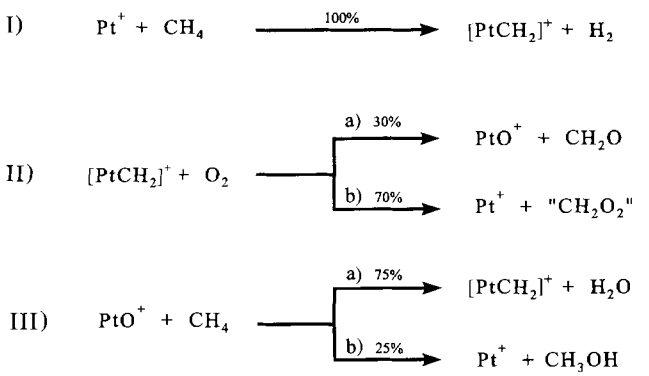
The high catalytic activity of platinum has been known since the last century, and platinum-based catalysts are widely used in reduction as well oxidation processes.[3] Although heterogeneous catalysis is one of the most actively pursued research areas, this approach often fails to provide an understanding of the chemistry at a molecular level. In contrast, more direct mechanistic information may be obtained in gas-phase experiments in which the reactions of "naked" metal ions with neutral substrates can be probed under relatively well-defined conditions.[4]

Recently, Irikura and Beauchamp[1b, 5] discovered that "naked" third-row transition metal cations are capable of dehydrogenating methane in a stoichiometric fashion in the gas phase to yield the methylene complexes $[M=CH_2]^+$.[6] Here, we report the design and realization of a catalytic cycle[7] for the gas-phase oxidation of methane under the conditions of Fourier transform ion cyclotron resonance (FT-ICR) mass spectrometry.[8]

[*] Prof. Dr. H. Schwarz, Dr. D. Schröder, R. Wesendrup
Institut für Organische Chemie der Technischen Universität
Strasse des 17. Juni 135, D-10623 Berlin (FRG)
Telefax: Int. code + (30)314-21102

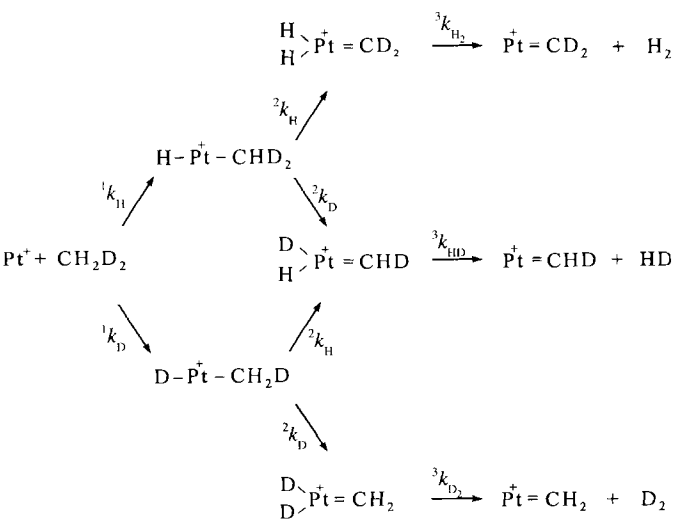
[**] This work was supported by the Deutsche Forschungsgemeinschaft and the Fonds der Chemischen Industrie. We are grateful to Spectrospin AG, Fällanden, for the loan of a glow-discharge ion source, and Degussa AG, Hanau, for the generous supply of platinum targets.

As reported earlier,[5] thermalized Pt^+ ions dehydrogenate methane to yield the carbene complex $[PtCH_2]^+$ (Scheme 1, process I). Although the rate constant k_R ($k_R = 8.2 \times 10^{-10}$ cm^3 molecule^{-1} s^{-1}) is somewhat smaller than the collision rate constant k_{ADO} ($k_{ADO} = 9.8 \times 10^{-10}$ cm^{-3} molecule^{-1} s^{-1}; ADO = average dipole orientation),[9] the reaction is quite efficient if one takes into account that CH_4 is a small, symmetric molecule with low polarizability and strong C–H bonds. Thermochemical considerations[10] lead to the conclusion that, since reaction I occurs at thermal energies, the reaction enthalpy (ΔH_r) for methane dehydrogenation is negative, and, thus, the heat of formation (ΔH_f) of $[PtCH_2]^+$ is smaller than 316 kcal mol^{-1}; furthermore, the observation of reaction II (see below) sets a lower limit for $\Delta H_f[PtCH_2]^+$ at 308 kcal mol^{-1}; in the following, we will use an averaged value of $\Delta H_f[PtCH_2^+] = 312 \pm 4$ kcal mol^{-1}; from this one derives a Pt^+-CH_2 bond dissociation energy of $BDE(Pt^+-CH_2) = 115 \pm 4$ kcal mol^{-1}.[10b]



Scheme 1. Formation and reactions of $[PtCH_2]^+$ and $[PtO]^+$, as well as the formation of the methane oxidation products CH_3OH, CH_2O, and "CH_2O_2".

The intramolecular kinetic isotope effects (KIEs) associated with the Pt^+-mediated dehydrogenation of CH_2D_2 can be deduced from the relative abundance of $[PtCD_2]^+$, $[PtCHD]^+$, and $[PtCH_2]^+$, which are formed in a 2.5:6.5:1.0 ratio. Because formation of $[PtCHD]^+$ from CH_2D_2 is favored by a factor of 4 over the other two isotopomers, the statistically weighted ratio is 2.5:1.6:1.0 for H_2, HD, and D_2 losses, respectively. According to the mechanism depicted in Scheme 2, these data can be



Scheme 2. Scheme for the kinetics of the reactions of Pt^+ and CH_2D_2.

analyzed in terms of intramolecular kinetic isotope effects associated with the rates of the insertion step (^1k), the α-hydrogen transfer (^2k), and the reductive elimination of dihydrogen (^3k),[11] as described in Equations (a)–(c).

$$k_{H_2}/k_{HD} = 0.5(^1k_H/^1k_D + {}^2k_H/{}^2k_D) \times {}^3k_{H_2}/{}^3k_{HD} = 1.6 \quad \text{(a)}$$

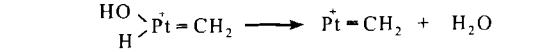
$$k_{H_2}/k_{D_2} = (^1k_H/^1k_D)(^2k_H/{}^2k_D)(^3k_{H_2}/{}^3k_{D_2}) = 2.5 \quad \text{(b)}$$

$$k_{HD}/k_{D_2} = 0.5(^1k_H/^1k_D + {}^2k_H/{}^2k_D) \times {}^3k_{HD}/{}^3k_{D_2} = 1.6 \quad \text{(c)}$$

Although an exact solution of the set of equations (a)–(c) is not possible, from (a) and (c) we can conclude that $^3k_{HD} = (^3k_{H_2} \times {}^3k_{D_2})^{1/2}$. Such a correlation is typical for a rate-determining reductive elimination of molecular hydrogen from a symmetrical transition structure.[12] Accordingly, $^1k_H/^1k_D$ as well as $^2k_H/^2k_D$ are close to unity, and the observed intramolecular kinetic isotope effect associated with the rate-determining reductive elimination step (^3k) is about 1.6 per H atom. It is noteworthy that in contrast to other methane activation processes,[1] for Pt^+ the initial C–H bond insertion does not contribute to the rate-determining step. In view of the differences usually expected for intra- and intermolecular kinetic isotope effects,[13] our findings are in good agreement with the minor KIE associated with the Pt^+-mediated activation of CD_4 ($k_H/k_D = 1.3$).[5]

A catalytic process for the gas-phase oxidation of methane must regenerate the consumed Pt^+ for further cycles. The $[PtCH_2]^+$ intermediate must therefore be oxidized by an appropriate reagent. Interestingly, and in contrast to other examples,[14] nitrous oxide does not serve as an oxidant donating a single O atom, and N_2O is completely unreactive towards $PtCH_2^+$, although the formation of Pt^+, formaldehyde, and nitrogen is exothermic by 24 kcal mol^{-1}. However, $[PtCH_2]^+$ reacts with molecular oxygen to form Pt^+ and the monoxide PtO^+ as the ionic products (Scheme 1, reaction II); thermalized Pt^+ does not react with O_2, but with N_2O yields the monoxide cation PtO^+. Although reaction II is exothermic for both products (see below), it is relatively slow relative to the collision rate ($k_R = 0.2 \times 10^{-10}$ cm^3 molecule^{-1} s^{-1}; $k_{ADO} = 5.6 \times 10^{-10}$ cm^3 molecule^{-1} s^{-1}), which indicates that a barrier is associated with the activation of dioxygen by $[PtCH_2]^+$. We cannot deduce the structures of the neutral products in our experimental ICR setup; however, thermodynamic considerations imply that formaldehyde is formed in reaction IIa ($\Delta H_R = -4 \pm 4$ kcal mol^{-1}). In reaction IIb the situation is not as straightforward, since several possibilities such as formic acid or its thermolysis products carbon monoxide/water or carbon dioxide/dihydrogen are thermochemically accessible ($\Delta H_R = -69 \pm 4$ kcal mol^{-1} (HCO_2H), -63 ± 4 kcal mol^{-1} (CO/H_2O), and -73 ± 4 kcal mol^{-1} (CO_2/H_2O)).[15]

The PtO^+ cation also contributes to the catalytic cycle, since it is recovered as Pt^+ after reaction with methane (Scheme 1, reaction III). Not unexpected for a transition metal oxide cation (e.g. FeO^+),[16] reaction III is collision-controlled ($k_R = 10.5 \pm 10^{-10}$ cm^3 molecule^{-1} s^{-1}; $k_{ADO} = 9.8 \times 10^{-10}$ cm^3 molecule^{-1} s^{-1}) and gives rise to $[PtCH_2]^+$ and neutral water ($\Delta H_R = -61 \pm 4$ kcal mol^{-1}), or Pt^+ and methanol ($\Delta H_R = -30$ kcal mol^{-1}). When CH_2D_2 is employed as reaction partner, reaction III leads to $[PtCD_2]^+$, $[PtCHD]^+$, and $[PtCH_2]^+$, which are formed in a ratio of 2.1:5.3:1.0. An analysis similar to that performed for the reactions in Scheme 2 indicates that in reaction IIIa the reductive elimination of water from a $[(HO)(H)PtCH_2]^+$ intermediate contributes most to the rate-determining step; however, contributions of the other steps to the measured intramolecular isotope effect cannot be ignored entirely (Scheme 3).



Scheme 3. Formation of $[PtCH_2]^+$ from $[PtO]^+$ and CH_4.

Combining reactions I–III of Scheme 1 leads to a catalytic cycle under FT-ICR conditions in which Pt^+ ions mediate the oxidation of methane by molecular oxygen. This is the first successful demonstration of *catalytic* methane activation by a naked metal ion under oxidative conditions. Since the conversion of $[PtCH_2]^+$ (reaction II) is the slowest step in the cycle and $[PtCH_2]^+$ is also formed in reaction III, a large excess of oxygen is necessary for a satisfactory catalytic rate (typically, a ratio of $CH_4:O_2 = 1:20$ is sufficient).

The deviation of the Pt^+ concentration from the pseudo-first order exponential decrease (Fig. 1) clearly demonstrates the operation of a catalytic process in the present system; this supposition is further substantiated by the steady state concentrations for the reactive species Pt^+, $[PtCH_2]^+$, and $[PtO]^+$ at longer reaction times (>80 s). The slow reaction of $[PtCH_2]^+$ with methane[5] ($k_R = 0.2 \times 10^{-10}$ versus $k_R = 8.2 \times 10^{-10}$ cm^3 molecule^{-1} s^{-1} for the activation of methane by naked Pt^+) that generates $Pt[C_2,H_4]^+$ (Scheme 4) and, after subsequent oxidation, $[PtCO]^+$, $Pt[C,O,H]^+$, and $[PtH]^+$, which neither react with oxygen nor with methane, limits the turnover of the overall process by the irreversible formation of unreactive products.

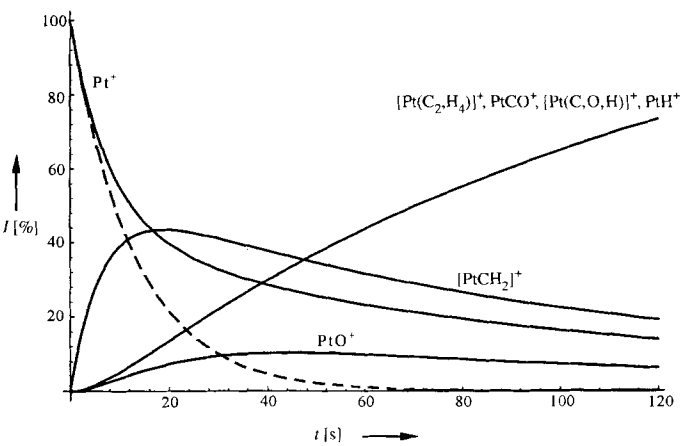
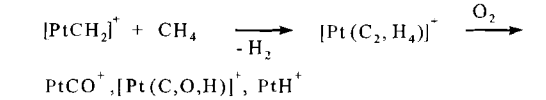


Fig. 1. Temporal evolution of the species involved in the Pt^+-catalyzed methane oxidation ($CH_4:O_2 = 1:20$). The dashed curve shows the decrease of the Pt^+ signal in the presence of methane only. All curves are based on a numerial solution of the appropriate differential equations on use of the k_R values given in the text. For the sake of clarity the experimentally measured data are omitted; these data agree with the computed ion abundancies within experimental error (± 5%). Ion losses at long storage time (>80 s) are taken into account.

By an iterative modeling of the kinetic data with the rate constants for the reactions depicted in Schemes 1 and 4, at a certain pressure[7c,i] ($p(CH_4) = 4 \times 10^{-9}$ mbar, $p(O_2) = 8 \times 10^{-8}$ mbar) a turnover number of about 6 is computed. Further-



Scheme 4. Formation and oxidation of $[Pt(C_2,H_4)]^+$.

 © VCH Verlagsgesellschaft mbH, D-69451 Weinheim, 1994 0570-0833/94/1111-1175 $ 10.00+.25/0

more, this analysis reveals that in the Pt^+-mediated oxidation, methane is converted into methanol (10%), formaldehyde (25%), and "CH_2O_2" (65%). The turnover of the system may be enhanced by increasing the oxygen excess to favor reactions II and III; however, this will result in a lowering of the overall rate of conversion. Similar to the effect observed in the reaction of Ir^+ with methane in the presence of oxygen,[5] reaction II accelerates slightly during the course of the catalysis; this may indicate the formation of excited $[PtCH_2]^+$ ions or of the presence of a structural isomer in reaction IIIa. This point will be addressed in forthcoming, more detailed kinetic studies.

In conclusion, the reaction sequence reported here describes for the first time a relatively efficient catalytic system for the gas-phase oxidation of methane by a bimolecular ion–molecule process. However, even in the gas phase the well-known problem of over-oxidation cannot yet be circumvented: the formation of "CH_2O_2" is observed as main reaction channel.

Experimental Procedure

Pt^+ ions were generated in the external ion source of a Spectrospin CMS 47X FT-ICR mass spectrometer [17] by either laser desorption/laser ionization by focusing a beam of a Nd:YAG laser ($\lambda = 1064$ nm) onto a platinum target [18] or glow-discharge ionization of a platinum wire in an argon plasma [19]. The cations were extracted from the source and transferred to the analyzer cell by a system of electric potentials and lenses. The isolation of the $^{195}Pt^+$ isotope and all subsequent isolation steps were performed by using FERETS [20], a computer-controlled ion-ejection protocol that combines single frequency ejection pulses with frequency sweeps to optimize ion isolation. After isolation the ions of interest were thermalized by collisions with either pulsed-in argon gas or the reaction gases, and the thermalized ions were subsequently reisolated. The degree of thermalization was assumed to be complete if no further change in reactivity occurs upon increasing the amount of pulsed-in argon gas [7*i*]. Methane and oxygen were admitted to the FTICR cell through leak valves (typical pressures about 4×10^{-9} mbar and 8×10^{-8} mbar, respectively). The pseudo-first order rate constants were derived from the decay of the precursor ion signals and converted to absolute rate constants by calibrating the ionization gauge measurements with rates of well-known ion–molecule processes [14b, 21, 22]; the error in the absolute rates is $\pm 25\%$ [14b]. All functions of the instrument were controlled by a Bruker Aspect 3000 minicomputer. Methane (Linde AG, 99.999%), [D_2]methane (Cambridge Isotope Laboratories, >98 atom% D), and oxygen (Linde AG, 99.995%) were used without further purification.

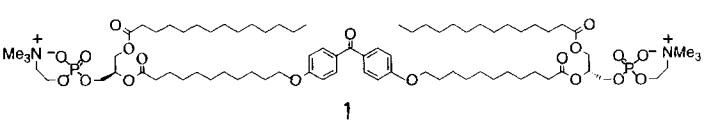
Received: December 15, 1993 [Z 6562 IE]
German version: *Angew. Chem.* **1994**, *105*, 1232

[1] a) H. Schwarz, *Angew. Chem.* **1991**, *103*, 837; *Angew. Chem. Int. Ed. Engl.* **1991**, *30*, 820; b) K. K. Irikura, J. L. Beauchamp, *J. Phys. Chem.* **1991**, *95*, 8344; c) J. M. Fox, *Catal. Rev. Sci. Eng.* **1993**, *35*, 169.
[2] J. Sommer, J. Bukula, *Acc. Chem. Res.* **1993**, *26*, 370.
[3] See for example a) M. A. Benvenuto, A. Sen, *J. Chem. Soc. Chem. Commun.* **1993**, 970; b) M. Del Todesco Frisone, F. Pinna, G. Strukul, *Organometallics* **1993**, *12*, 148; c) J. A. Labinger, A. M. Herring, D. K. Lyon, G. A. Luinstra, J. E. Bercaw, I. T. Horváth, K. Eller, *ibid.* **1993**, *12*, 895, and references therein.
[4] Recent reviews on gas-phase transition metal chemistry: a) K. Eller, H. Schwarz, *Chem. Rev.* **1991**, *91*, 1121; b) P. B. Armentrout, *Annu. Rev. Phys. Chem.* **1990**, *41*, 313.
[5] K. K. Irikura, J. L. Beauchamp, *J. Am. Chem. Soc.* **1991**, *113*, 2769.
[6] Further examples of cationic Pt species in the gas phase: a) T. F. Magnera, D. E. David, J. Michl, *J. Am. Chem. Soc.* **1987**, *109*, 936; b) D. J. Trevor, D. M. Cox, A. Kaldor, *ibid.* **1990**, *112*, 3742; c) M. Hada, H. Nakatsuji, H. Nakai, S. Gyobu, S. Miki, *J. Mol. Struct.* (Theochem) **1993**, *281*, 207.
[7] Other catalytic process under FT-ICR conditions: a) M. M. Kappes, R. H. Staley, *J. Am. Chem. Soc.* **1981**, *103*, 1286; b) S. W. Buckner, B. S. Freiser, *ibid.* **1988**, *110*, 6606; c) D. Schröder, H. Schwarz, *Angew. Chem.* **1990**, *102*, 1468; *Angew. Chem. Int. Ed. Engl.* **1990**, *29*, 1433; d) P. Schnabel, M. P. Irion, K. G. Weil, *J. Phys. Chem.* **1991**, *95*, 9688; *Chem. Phys. Lett.* **1992**, *190*, 255; e) M. P. Irion, *Int. J. Mass Spectrom. Ion Processes* **1992**, *121*, 1; f) M. P. Irion, P. Schnabel, *Ber. Bunsenges. Phys. Chem.* **1992**, *96*, 1101; g) P. Schnabel, K. G. Weil, M. P. Irion, *Angew. Chem.* **1992**, *104*, 633; *Angew. Chem. Int. Ed. Engl.* **1992**, *31*, 636; h) S. Karraß, D. Schröder, H. Schwarz, *Chem. Ber.* **1992**, *125*, 751; i) D. Schröder, A. Fiedler, M. F. Ryan, H. Schwarz, *J. Phys. Chem.*, **1994**, *98*, 68; j) R. Wesendrup, Diplomarbeit, Technische Universität Berlin, 1994.
[8] *FT-ICR/MS: Analytical Applications of Fourier Transform Ion Cyclotron Resonance Mass Spectrometry* (Ed.: B. Asamoto), VCH, Weinheim, **1991**.
[9] T. Su, M. T. Bowers, *Int. J. Mass Spectrom. Ion Phys.* **1973**, *12*, 347.
[10] a) If not mentioned otherwise, all thermochemical data were taken from: S. G. Lias, J. E. Bartmess, J. F. Liebman, J. L. Holmes, R. D. Levin, W. G. Mallard, *J. Phys. Chem. Ref. Data* **1988**, *17*, Suppl. 1. b) In two recent theoretical studies, the BDE (Pt^+-CH_2) were calculated at 123 ± 5 and 119 kcal mol^{-1}: K. K. Irikura, W. A. Goddard III, *J. Am. Chem. Soc.*, submitted. C. Heinemann, R. Hartwig, R. Wesendrup, W. Koch, H. Schwarz, *J. Am. Chem. Soc.*, submitted.
[11] D. Schröder, H. Schwarz, *Chimia* **1989**, *43*, 317.
[12] a) G. Hvistendahl, D. H. Williams, *J. Chem. Soc. Chem. Commun.* **1975**, 4; b) H. Schwarz, W. Franke, J. Chandrasekhar, P. von R. Schleyer, *Tetrahedron* **1979**, *35*, 1969, and references therein.
[13] a) P. J. Derrick, K. F. Donchi in *Comprehensive Chemical Kinetics, Vol. 24* (Eds.: C. H. Bamford, C. F. H. Tipper), Elsevier, Amsterdam, **1983**, p. 53; b) D. Schröder, D. Sülzle, O. Dutuit, T. Baer, H. Schwarz, *J. Am. Chem. Soc.*, in press.
[14] a) Ref. [7a–c]; b) D. Schröder, Dissertation, Technische Universität Berlin, **1993**.
[15] Even if HCO_2H is formed in a highly vibrationally excited state, in view of the significant barriers (>60 kcal mol^{-1}) associated with its dehydration or dehydrogenation, it is likely to survive: a) P. G. Blake, H. H. Davies, G. E. Jackson, *J. Chem. Soc. B* **1971**, 1923; b) P. Ruelle, *J. Am. Chem. Soc.* **1987**, *109*, 1722.
[16] a) Ref. [7c]; b) D. Schröder, A. Fiedler, J. Hrusák, H. Schwarz, *J. Am. Chem. Soc.* **1992**, *114*, 1215.
[17] a) K. Eller, H. Schwarz, *Int. J. Mass Spectrom. Ion Processes* **1989**, *93*, 243; b) K. Eller, W. Zummack, H. Schwarz, *J. Am. Chem. Soc.* **1990**, *112*, 621.
[18] B. S. Freiser, *Talanta* **1985**, *32*, 697; *Anal. Chim. Acta* **1985**, *178*, 137.
[19] Recent examples: a) W. S. Taylor, W. R. Everett, L. M. Babcock, T. L. McNeal, *Int. J. Mass Spectrom. Ion Processes* **1993**, *125*, 45; b) D. M. Chambers, S. A. McLuckey, G. L. Glish, *Anal. Chem.* **1993**, *65*, 778.
[20] R. A. Forbes, F. H. Laukien, J. Wronka, *Int. J. Mass Spectrom. Ion Processes* **1988**, *83*, 23.
[21] J. E. Bartmess, R. M. Georgiadis, *Vacuum* **1983**, *33*, 149.
[22] For example: Y. Lin, D. P. Ridge, B. Munson, *Org. Mass Spectrom.* **1991**, *26*, 550.

Increased Selectivity of a Simple Photosensitive Probe in the Presence of Large Proportions of Cholesterol**

Siw Bodil Fredriksen, Valérie Dollé, Masakuni Yamamoto, Yoichi Nakatani,* Maurice Goeldner and Guy Ourisson

We have recently described a photoactivatable phospholipidic transmembrane probe **1**,[1,2] which had a marked advantage over the simpler membrane probes described earlier by Khorana et al.[3] and Breslow et al.[4] It was much more site-selective and



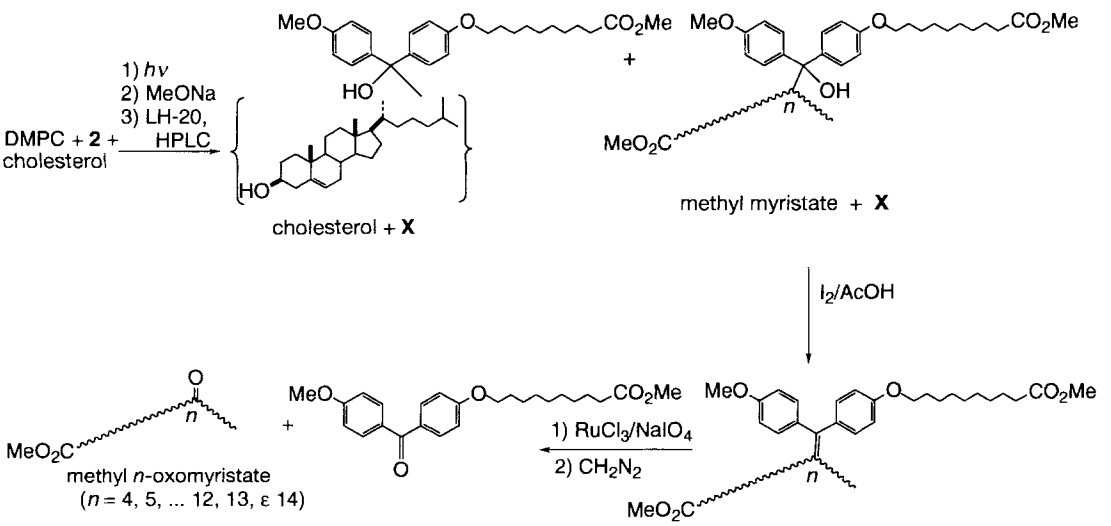
1

attacked preferentially the terminal carbons of neighboring phospholipids. This selectivity was excellent in the presence of the near-physiological concentrations (33 mol%) of cholesterol, a normal constituent of eucaryotic membranes, which it reinforces by favoring a compact and regular arrangement of the phospholipids. The probe **1**, when used together with choles-

[*] Prof. Y. Nakatani, S. B. Fredriksen, V. Dollé, M. Yamamoto, Prof. M. Goeldner
Prof. G. Ourisson
Laboratoire de Chimie Organique des Substances Naturelles associé au CNRS,
Université Louis Pasteur
5 rue Blaise Pascal, F-67084 Strasbourg (France)
Telefax: Int. code +(88)607620

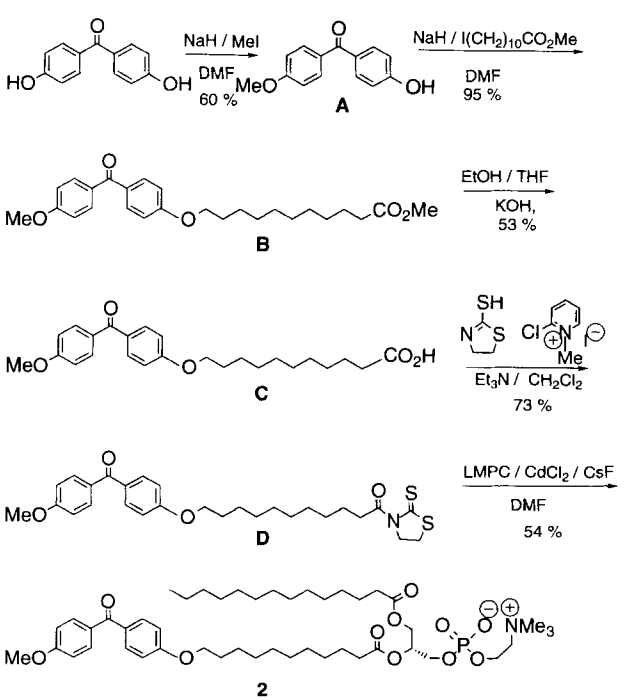
[**] This work was supported by the CNRS (Action Incitative de l'Interface Chimie-Biologie), by the Supermolecules Research Project of the Research Development Corporation of Japan and Université Louis Pasteur.

terol, is therefore a useful new tool for the investigation of the topography of membranes. However, its synthesis is not easy. Furthermore, we noted that our predecessors had not attempted to improve the very low selectivity of their simpler probes by adding cholesterol. The same is true of two studies recently published: one describing a different type of photoactivatable membrane - spanning probe,[5] and the other[6] dealing with simple benzophenone probes very similar to the one described below, but not more selective than those of Khorana or Breslow for the same reason.



Scheme 2. Reaction sequence for the determination by the photoreaction of the functionalized positions in the myristoyl chains in DMPC. **X** = probe fragment linked by photoactivation to cholesterol or methyl myristate.

We have synthesized the phospholipidic photoactivatable "half-probe" **2** by the route shown in Scheme 1 (all products have been fully characterized by ^{1}H NMR and ^{13}C NMR spectrometry and, for the end product, by MS and microanalysis). In analogy to its transmembrane counterpart **1**, addition of 5 mol% of the new probe **2** to 1,2-dimyristoyl-*sn*-glycero-3-phosphocholine (DMPC) and organization by freeze–thaw cycles in water hardly depresses the phase-transition temperature T_m, which shows that **2** indeed does not perturb the double layers to be investigated. We then tested its behavior upon irradiation in vesicles of DMPC containing varying proportions of cholesterol. The products of the reaction were analyzed, as in ref. [2], by the reaction sequence summarized in Scheme 2, and the results obtained with increasing cholesterol content are reported in Figure 1; in Figure 2 they are compared at 33 mol% cholesterol content[7] with those previously obtained with the transmembrane probe **1**.



Scheme 1. Synthesis of the half-probe **2**. **A**: m.p. 139–140 °C; **B**: m.p. 93–94 °C; **C**: m.p. 138–139 °C; **D**: m.p. 127–128 °C; **2**: T_M = 46.3 °C (pure); 23.6 °C (5 mol% in DMPC). DMF = dimethylformamide, LMPC = 2-lysomyristoylphosphocholine.

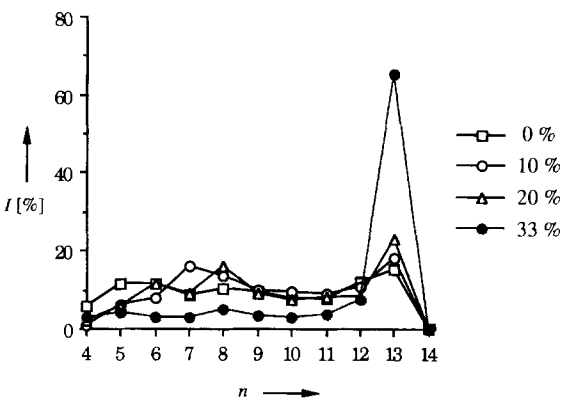


Fig. 1. Effect of cholesterol (mol% indicated on the right) on the distribution of DMPC positions functionalized by irradiation of the half-probe **2**. *I*: Percentage functionalization at carbon atom number *n* of the myristoyl chain.

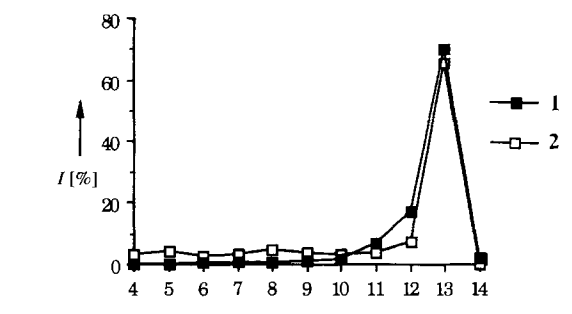


Fig. 2. Comparison of the effect of 33 mol% cholesterol on the distribution of DMPC positions functionalized by irradiation of the probes **1** and **2**. *I* and *n* as for Fig. 1.

 © VCH Verlagsgesellschaft mbH, D-69451 Weinheim, 1994 0570-0833/94/1111-1177 $ 10.00+.25/0

Without cholesterol or with low proportions of this membrane reinforcer, the selectivity is very low: all the carbon atoms of the chain up to C-4 are attacked, and there is no marked preference for the end of the chain, as expected by analogy with the results of Khorana, of Breslow, or of Lala.[3, 4, 6] However, near 33 mol% cholesterol, the picture changes drastically, and the selectivity becomes nearly as good as that observed with the transmembrane probe.

The loss of selectivity observed in all cases by halving the probe is in agreement with expectation: the transmembrane probe *must* be more ordered than the half probe. However, the difference of selectivity is so low at high cholesterol concentrations, and the synthesis of the half-probe is so much more straightforward, that its use, or that of analogues, will probably be warranted for the exploration of the topography of the inside of membranes, in particular of membrane-inserted proteins. The radius around a photoexcited benzophenone carbonyl group within which hydrogen can be abstracted to oxygen has been evaluated by Winnik[8] to be about 2 Å. Thus, our results indicate in both cases highly ordererd bilayer systems; the selectivity can probably not be increased with this chromophore.

The effect of added cholesterol should lead also unavoidably to its attack. This is indeed the case: we have isolated small amounts of products which, after transmethylation, were separated and analyzed by mass spectrometry and ^{1}H NMR and ^{13}C NMR spectroscopy. Three of these products have the expected mass for the dehydrated cholesterol + probe photoproduct. Their NMR spectra suggest they are substituted in the side chain, but they have not yet been more precisely characterized.

The structure of the half-probe leads necessarily, in its photoreaction with chiral substrates such as cholesterol or proteins, to diastereomeric heterogeneity. This, and the relative inconvenience of the necessarily complex handling of the photoproducts, justifies improvements in the design of future analogues.

Received: November 29, 1993 [Z 6524IE]
German version: *Angew. Chem.* **1994**, *106*, 1230

[1] Y. L. Diyizou, A. Genevois, T. Lazrak, G. Wolff, Y. Nakatani, G. Ourisson, *Tetrahedron Lett.* **1987**, *28*, 5743–5746.
[2] a) M. Yamamoto, W. A. Warnok, A. Milon, Y. Nakatani, G. Ourisson, *Angew. Chem.* **1993**, *105*, 302–304; *Angew. Chem. Int. Ed. Engl.* **1993**, *32*, 259–261. b) M. Yamamoto, V. Dollé, W. A. Warnock, Y. Diyizou, M. Yamada, Y. Nakatani, G. Ourisson, *Bull Soc. Chim. Fr.*, in press.
[3] A. H. Ross, R. Radhakrishnan, R. J. Robson, H. G. Khorana, *J. Biol. Chem.* **1982**, *257*, 4152–4161, and references therein.
[4] M. F. Czarniecki, R. Breslow, *J. Am. Chem. Soc.* **1979**, *101*, 3675–3676, and references therein.
[5] J. M. Delfino, S. L. Schreiber, F. M. Richards, *J. Am. Chem. Soc.* **1993**, *115*, 3458–3474.
[6] A. K. Lala, E. R. Kumer, *J. Am. Chem. Soc.* **1993**, *115*, 3982–3988.
[7] Up to 33 mol% cholesterol does not perturb DMPC bilayers: R. A. Demel, B. de Kruyff, *Biochim. Biophys. Acta* **1976**, *457*, 109–132.
[8] M. A. Winnik, *Acc. Chem. Res.* **1977**, *10*, 173–179.

Synthesis and Characterization of Thiolato Complexes with Two-Coordinate Iron(II)**

Jeffrey J. Ellison, Karin Ruhlandt-Senge, and Philip P. Power*

Stable complexes with two-coordinate, open shell, transition metal centers are quite rare and, almost without exception, are confined to derivatives of bulky alkyl or amido ligands.[1] For ligands with bonding atoms from the third period, for example, sulfur or phosphorus, twofold coordination is currently unknown in the condensed phase and three-coordinate species are very rare.[2] Transition metal complexes with low coordination numbers (2 or 3) have recently assumed a new importance owing mainly to the disclosure of the crystal structure of the nitrogen-fixing FeMo cofactor of *Azotobacter vinelandii* in which six of the seven iron centers are, most probably, three-coordinate and ligated by sulfur atoms (sulfido ligands)[3a] (Fig. 1). Moreover,

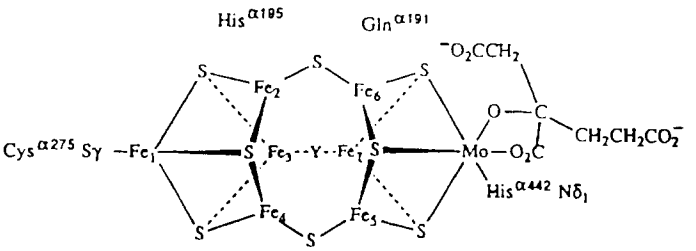


Fig. 1. Schematic drawing (from ref. [3b]) for the binding of nitrogen to MoFe cofactor of nitrogenase.

it has been proposed that the dinitrogen molecule coordinates to the six iron centers within the central Fe_6 cage which is in its reduced form.[3b] The, as yet incompletely defined,[3c, d] site Y (Fig. 1) may also involve an N or O species. The participation of this ligand site in facilitating access of the dinitrogen molecule to the core irons is also a possibility. In this case, it is conceivable that an iron center coordinated by two sulfido ligands may be involved as an intermediate during the reduction process. In this paper the first two thiolato complexes **1** and **2** (Mes = 2,4,6-$Me_3C_6H_2$) which have essentially two-coordinate iron centers are now described.

Compounds **1** and **2** were synthesized by the reaction of one or two equivalents of the new thiol HS(2,6-$Mes_2C_6H_3$) with

$[Fe\{S(2,6\text{-}Mes_2C_6H_3)\}\{N(SiMe_3)_2\}]$ **1** $[Fe\{S(2,6\text{-}Mes_2C_6H_3)\}_2]$ **2**

$[Fe\{N(SiMe_3)_2\}_2]$. The X-ray crystallographic data[4] show that **1** (Fig. 2) and **2** (Fig. 3) are monomers with no close interactions between neighboring molecules. Two crystallographically independent, but chemically identical, monomers and two toluene molecules are observed in each asymmetric unit in the case of **1**. Both **1** and **2** possess a bent geometry at the iron center; the S-Fe-N angles in **1** are 118.9(2) and 120.8(2)°, while in **2** the S-Fe-S angle is very similar, 121.8(1)°. The Fe–S and Fe–N bond lengths in **1** are 2.308(2) and 2.314(2), and 1.913(6) and 1.923(5) Å, respectively; in **2** the Fe–S distances are 2.277(2) and

[*] Prof. P. P. Power, J. J. Ellison, Dr. K. Ruhlandt-Senge
Department of Chemisty, University of California
Davis, CA 95616 (USA)
Telefax: Int. code + (916) 752-8995

[**] This work was supported by the National Science Foundation and the Petroleum Research Fund.

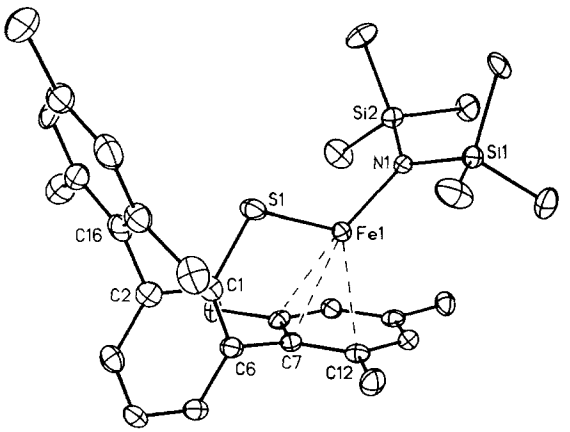


Fig. 2. Crystal structure of **1**. H atoms are not shown for clarity. Selected bond lengths [Å] and angles [°] with values for the second molecule of the asymmetric unit in square brackets: Fe-S 2.314(2) [2.308(2)], Fe-N 1.913(6) [1.923(5)], Fe···C7 2.457 [C37 2.423], Fe···C8 2.551 [C38 2.518], Fe···C12 2.519 [C42 2.533], S-Fe-N 118.9(2) [120.8(2)], Fe-S-C 107.8(3) [105.7(2)].

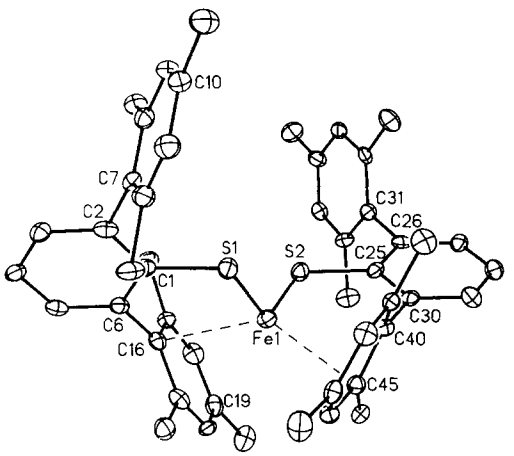


Fig. 3. Crystal structure of **2**. H atoms are not shown for clarity. Bond lengths [Å] and angles [°]: Fe-S 2.277(2), 2.275(2), Fe···C16 2.535, Fe···C45 2.470, S-Fe-S 121.8(1), Fe-S-C 106.2(2), 108.7(3).

2.275(2) Å. Thus, the Fe–S bonds in **1** and **2** are somewhat shorter than those observed for four-coordinate anionic thiolatoiron(II) complexes $[Fe(SPh)_4]^{2-}$[5] (2.338(2)–2.360(2) Å and $[Fe_2(SEt)_6]^{2-}$[6] (2.304(4) Å); however, those in **2** (2.277(2), 2.275(2) Å) are similar to the terminal Fe–S bond lengths observed in the three-coordinate iron thiolate dimers $[\{Fe[S(2,4,6\text{-}tBu_3C_6H_2)]_2\}_2]$[7a] (2.262(3) Å) and $[\{Fe[S(2,4,6\text{-}Ph_3C_6H_2)]_2\}_2]$[7b] (2.256(3) Å). Further metal–ligand interactions with an *ortho*-mesityl group of a thiolato ligand are observed in both **1** and **2**. For **1**, the shortest of these distances are Fe1···C7 (2.457) and Fe2···C37 (2.423 Å). Interactions with other C atoms in the mesityl group lie in the range 2.518–2.730 Å. In **2** the closest contacts are Fe···C45 (2.470) and Fe···C16 (2.535 Å). It is notable that these distances are well outside the sum of the radii of iron (1.25 Å)[8a] and sp^2-hybridized carbon (0.74 Å).[8b] Furthermore, they are significantly longer than the Fe–C distances observed (usually in the range 1.9–2.25 Å) in iron complexes that have η^2–η^6 π-bonded hydrocarbyl ligands.[9] The weakness of these interactions is confirmed by a variable temperature ^{1}H NMR spectroscopic study of **2** in [D_8]toluene, since the paramagnetically shifted peaks show no splitting at temperatures as low as −95 °C. A significant (ca. 8–10 kcal mol^{-1}) Fe···Mes interaction should have been apparent (through splitting of the Mes ^{1}H NMR peaks) at this low temperature. The ^{1}H NMR spectrum of **1** in [D_8]toluene solution is more complex and indicates that **1** disproportionates to a significant extent (ca. 10%) in solution to give **2** and $[Fe\{N(SiMe_3)_2\}_2]$. The magnetic moments of **1** and **2** show that the Fe^{II} centers in both complexes possess a high-spin configuration. The UV/VIS spectra of the two compounds are featureless and display a slow rise in absorption toward higher energy. The IR spectra of **1** and **2** and the precursor thiol indicate that the ligand C–H stretching frequencies are not significantly altered by coordination of the thiolato ligand to the iron center.

The structural and spectroscopic data support the view that the iron centers in **1** and **2** are primarily two-coordinate with minor interactions with the π-electron density of the *ortho*-mesityl group of the thiolato ligand. The relatively small (ca. 120°) ligand-metal-ligand angle in **1** and **2** is probably a consequence of the following: 1) the low valence electron count (10 e$^-$) at the iron center, which leaves several empty metal orbitals available to accept electron density; 2) the "soft" interligand angle at the iron atom, which can be relatively easily distorted from the idealized 180° geometry; and 3) ease of rotation around the M–S bond, which permits the organic substituent to adopt a variety of orientations (subject to steric constraints) thereby permitting the Fe···C interactions to occur.

Clearly, the unique steric and electronic properties of the ($S(2,6\text{-}Mes_2C_6H_3)$) ligand enable twofold coordination at the iron centers in **1** and **2** to be observed. Although the FeMo cofactor does not contain bulky nonprotein substituents, and only one thiolato (cysteine) ligand, the environment provided by the protein apparently produces a similar effect in the stabilization of low coordination numbers at iron.[3] Compound **2** does not, of course, represent a model for a nitrogen-fixing site in the MoFe cofactor; however, both **1** and **2** show that it is feasible to prepare stable complexes with two-coordinate iron centers in which sulfur is the main ligating atom.

Experimental Procedure

All reactions were performed under anaerobic and anhydrous conditions. I(2,6-$Mes_2C_6H_3$) [10] and $[Fe\{N(SiMe_3)_2\}_2]$ [1c] were prepared by published procedures:

HS(2,6-$Mes_2C_6H_3$): I(2,6-$Mes_2C_6H_3$) (4.4 g, 10 mmol) was dissolved in THF (80 mL) and cooled in a dry-ice bath. *n*BuLi (10 mmol, 6.25 mL of a 1.6 M solution in hexanes) was added by syringe. The solution was stirred at −78 °C for 1 h whereupon a threefold excess of sulfur (0.86 g, 30 mmol) was added. After stirring for 2 h at −78 °C, the deep red solution was allowed to warm to room temperature. It was then added slowly to $LiAlH_4$ (2.5 g) suspended in ether (10 mL) with cooling in an ice bath. After stirring for 10 h the excess $LiAlH_4$ was destroyed with water (10 mL) and 10% HCl (50 mL) was added. The organic layer was separated and the aqueous layer was extracted with diethyl ether (2 × 70 mL). The combined phases were dried (1 h) over K_2CO_3 and filtered. The solvent was removed under reduced pressure and the residue was crystallized from ethyl acetate as a colorless solid in about 60% yield: M.p. 213–215 °C. IR (Nujol) $\tilde{\nu}$[cm^{-1}] = 2545 w (ν(S-H)), 585 m, 570 w, 545 w, 505 w, 482 w, 457 w, 345 m; ^{1}H NMR (200 MHz, [D_8]toluene, 25 °C): δ = 2.05 (s, 12H, *o*-Me), 2.36 (s, 6H, *p*-Me), 3.05 (s, 1H, S-H), 7.00 (s, 4H, *m*-H (Mes)), 7.06 (2H, d, *m*-H(Ph), ^4J = 9 Hz), 7.26 (1H, *p*-H ^4J = 9 Hz).

1: HS(2,6-$Mes_2C_6H_3$) (0.69 g, 2 mmol) was dissolved in a 1:1 mixture of hexane and toluene (40 mL). This solution was added dropwise with a cannula to $[Fe\{N(SiMe_3)_2\}_2]$ [1c] (0.75 g, 2 mmol) in hexane (10 mL) with stirring. After 2 h the solution had become pale yellow. It was then filtered and the volume was reduced to about 3 mL. Cooling overnight in a freezer at −20 °C produced large yellow crystals of **1** in 60% yield. M.p. 150 °C. μ = 4.5 μ_B at 25 °C. IR (Nujol) $\tilde{\nu}$[cm^{-1}] = 695 s, 665 s, 630 w, 610 w, 585 w, 460 m, 410 w, 355 m.

2: HS(2,6-$Mes_2C_6H_3$) (0.69 g, 2 mmol) was suspended in hexane (25 mL) and $[Fe\{N(SiMe_3)_2\}_2]$ (4.0 mL of a 0.247 M solution in toluene) was added dropwise with a syringe. The solution became dark red upon stirring for 2 h, whereupon it was concentrated to incipient crystallization under reduced pressure. The mixture was then filtered and cooled for 24 h in a freezer at −20 °C to afford **2** as red needles in

 © VCH Verlagsgesellschaft mbH, D-69451 Weinheim, 1994 0570-0833/94/1111-1179 $ 10.00+.25/0

quantitative yield. M.p. 250–253 °C. $\mu = 4.3\ \mu_B$ at 25 °C. IR (Nujol) $\tilde{\nu}$[cm^{-1}] = 585 m, 565 w, 542 w, 462 m, 387 m, 339 m. ^{1}H NMR (200 MHz, [D$_8$]toluene, isotropic shifts at ca. 25 °C): δ = 49.48 (br. s, 2H), 41.28 (br. s, 6H), 6.9 (br. s, 12H), −22.36 (br. s, 4H), −24.55 (br. s, 1H).

Received: October 28, 1993 [Z 6463 IE]
German version: *Angew. Chem.* **1994**, *106*, 1248

[1] a) N. H. Buttrus, C. Eaborn, P. B. Hitchcock, J. D. Smith, A. C. Sullivan, *J. Chem. Soc. Chem. Commun.* **1985**, 1300; b) R. A. Andersen, A. Haaland, K. Rypdal, H. V. Volden, *ibid.* **1985**, 1807; c) R. A. Andersen, K. Faegri, J. C. Green, A. Haaland, M. F. Lappert, W. P. Leung, K. Rypdal, *Inorg. Chem.* **1988**, *27*, 1782; d) P. P. Power, *Comments Inorg. Chem.* **1989**, *3*, 77.

[2] a) P. G. Eller, D. C. Bradley, M. B. Hursthouse, D. W. Meek, *Coord. Chem. Rev.* **1977**, *24*, 1; b) D. C. Bradley, M. B. Hursthouse, R. J. Smallwood, A. J. Welch, *J. Chem. Soc. Chem. Commun.* **1972**, 872; c) Y. W. Yared, S. L. Miles, R. Bau, C. Reed, *J. Am. Chem. Soc.* **1977**, *99*, 7076; d) H. L. M. Van Gaal, F. L. A. Van Den Bekerom, *J. Organomet. Chem.* **1977**, *134*, 237; e) T. Yoshida, T. Okano, S. Otsuka, *J. Chem. Soc. Chem. Commun.* **1978**, 855; f) J. Hvoslef, H. H. Hope, B. D. Murray, P. P. Power, *ibid.* **1983**, 1438; g) D. M. Roddick, T. D. Tilley, A. L. Rheingold, S. J. Geib, *J. Am. Chem. Soc.* **1987**, *109*, 945; h) H. Chen, M. M. Olmstead, D. C. Pestana, P. P. Power, *Inorg. Chem.* **1991**, *30*, 1783; i) S. C. Goel, M. Y. Chiang, D. J. Rauscher, W. E. Buhro, *J. Am. Chem. Soc.* **1993**, *115*, 160.

[3] a) J. Kim, D. C. Rees, *Nature* **1992**, *360*, 553; b) J. Kim, D. C. Rees, *Science* **1992**, *257*, 1677; c) M. K. Chan, J. Kim, D. C. Rees, *ibid.* **1993**, *260*, 792; d) Mo and Fe edge EXAFS studies on crystalline nitrogenase are in agreement with the X-ray crystal structure: J. Chen, J. Christiansen, N. Campobasso, J. T. Bolin, R. C. Titsworth, B. J. Hales, J. J. Rehr, S. P. Cramer, *Angew. Chem.* **1993**, *105*, 1661; *Angew. Chem. Int. Ed. Engl.* **1993**, *32*, 1592.

[4] Crystal data at 130 K with Mo$_{K_\alpha}$ radiation (λ = 0.71069 Å, **1**) or Cu$_{K_\alpha}$ radiation (λ = 1.54178 Å, **2**); **1**: a = 9.162(4), b = 17.564(9), c = 46.720(14) Å, orthorhombic, space group $Pbc2_1$, Z = 8, 5796 ($I > 2\sigma(I)$ data, R = 0.058. **2**: a = 10.324(3), b = 11.142(3), c = 18.551(5) Å, α = 80.78(2), β = 85.53(2), γ = 70.59(2), Z = 2, space group $P\bar{1}$, 3530 $I > 2\sigma(I)$ data, R = 0.083. Further details of the crystal structure investigations may be obtained from the Fachinformationszentrum Karlsruhe, D-76344 Eggenstein-Leopoldshafen (FRG) on quoting the depository number CSD-58172.

[5] D. Coucouvanis, D. Swenson, N. C. Baenziger, C. Murphy, D. G. Holah, N. Sfarnas, A. Simopoulos, A. Kastikas, *J. Am. Chem. Soc.* **1981**, *103*, 3350.

[6] K. S. Hagen, R. H. Holm, *Inorg. Chem.* **1984**, *23*, 418.

[7] a) P. P. Power, S. C. Shoner, *Angew. Chem.* **1991**, *103*, 308; *Angew. Chem. Int. Ed. Engl.* **1991**, *30*, 330; b) P. P. Power, K. Ruhlandt-Senge, *Bull. Chim. Soc. Fr.* **1992**, *129*, 594.

[8] a) J. E. Huheey, *Inorganic Chemistry*, 3rd edition, Harper and Row, New York, **1983**, p. 283; b) J. E. March, *Advanced Organic Chemistry*, 3rd edition, Wiley, New York, **1985**, p. 19.

[9] A. J. Deeming in *Comprehensive Organometallic Chemistry, Vol. 4* (Eds.: G. Wilkinson, F. G. A. Stone, E. W. Abel), Pergamon, Oxford, **1984**, Chapter 31.3.

[10] C. F. Du, H. Hart, K. D. Ng, *J. Org. Chem.* **1986**, *51*, 3162.

A Convergent Synthesis of 2,5-*trans*-Linked Oligo(tetrahydrofuran)s: Potential Building Blocks for a Polyether Helix with Ion Channel Activity**

Ulrich Koert,* Matthias Stein, and Klaus Harms

Examination of the structure, function, and regulation of membrane-bound ion channels is the focus of an interdisciplinary research area.[1] Through the design and synthesis of artificial ion channels,[2] chemists have access to model systems that may lead to a better understanding of biological ion channels. Polyether-based structures are particularly suitable for the transport of Na^+ and K^+ ions. Figure 1 shows a comparison of various ion channel models based on polyethers.

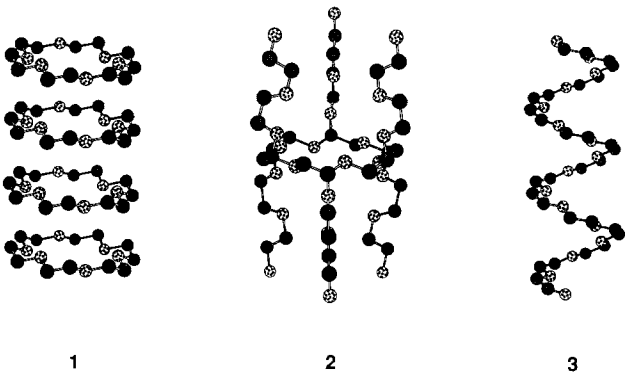
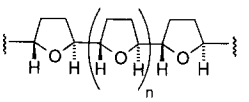


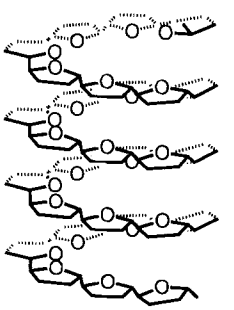
Fig. 1. Ion channel models based on polyethers. **1**: cylindrical arrangement of crown ethers, **2**: polyether strands. **3**: polyether helix. Dark spheres: carbon atoms; stippled spheres: oxygen atoms.

To date, ion channels have been formed by the cylindrical packing of crown ether molecules **1**[3] or by the bundling together of polyethylene glycol strands **2**.[4] In a cylindrical arrangement of crown ethers **1** a cation is relatively strongly bound within one crown ether unit. An energy barrier must be overcome in order for this cation to jump to the neighboring crown ether molecule. The unfavorable energy associated with discontinuous transport is largely avoided in polyether helix **3**. Here we report on a new synthesis of oligo(tetrahydrofuran)s,[5] a class of polyethers that could be used as building blocks for polyether helices.

CPK models show that oligomer **4a** (Scheme 1) formed from *trans*-linked tetrahydrofuran units will adopt a helical confor-



4a



4b

Scheme 1. 2,5-Linked oligo(tetrahydrofuran)s **4a** with the relative configuration *trans-anti-trans* and a schematic illustration of a polyether helix **4b**.

mation (**4b**) if the relative configuration of the tetrahydrofuran oligomer is *trans-anti-trans*.[6] This type of polyether helix is expected to be a functional ion channel when located within a membrane.

X-ray structural analysis (Fig. 2)[7] of the dimeric THF lactone **5**, with its 2,5-*trans*-linkage, supports this idea of a polyether helix constructed from 2,5-*trans*-linked oligo(tetrahydrofuran)s. The two oxygen atoms of the THF units in **5** are

[*] Dr. U. Koert, Dipl.-Chem. M. Stein, Dr. K. Harms
Fachbereich Chemie der Universität
Hans-Meerwein-Strasse, D-35043 Marburg (FRG)
Telefax: Int. code + (6421)288917

[**] This work was supported by the Deutsche Forschungsgemeinschaft and the Fonds der Chemischen Industrie. We thank Wacker AG and BASF AG for donations of chemicals. M. S. thanks the Studienstiftung des Deutschen Volkes for a graduate fellowship.

gauche to each other. This *gauche* conformation of the C4–C5 bond is a prerequisite for a THF helix structure. A THF-polyether helix can be further stabilized in a membrane through hydrophobic interactions between the THF methylene groups and the alkyl chains of the membrane lipids. A helix coiled four to five times with seven oxygen atoms per spiral should be sufficiently long to traverse a membrane 5 nm thick.

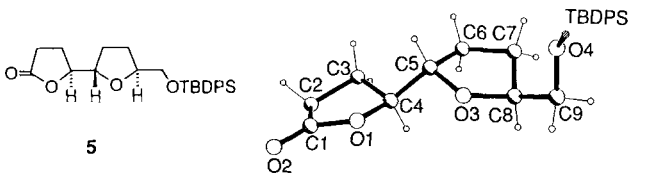
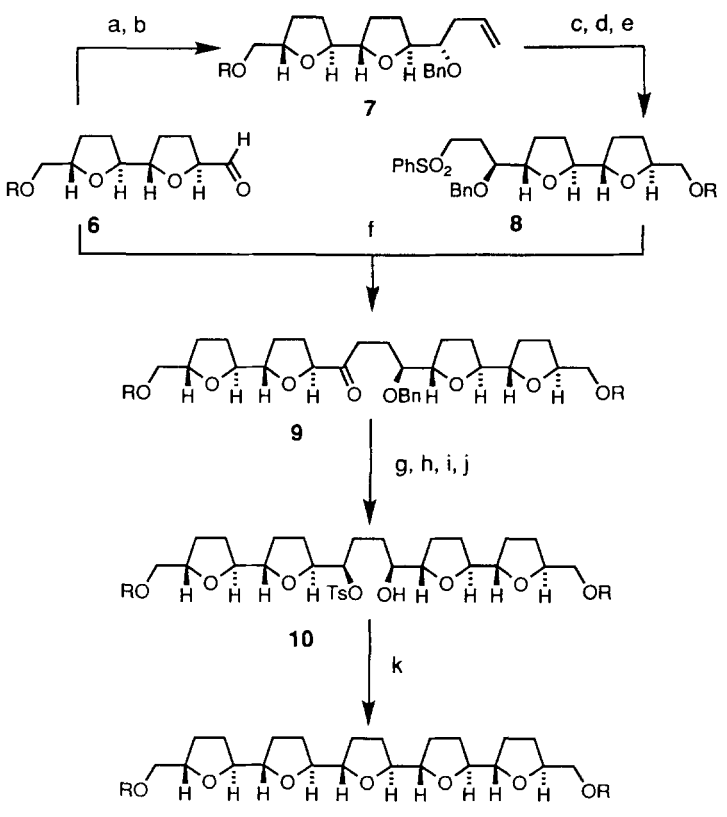


Fig. 2. Crystal structure of the dimeric tetrahydrofuran derivative **5**. For clarity the three alkyl groups on the Si atom of the protective group are not shown. TBDPS = *t*-butyldiphenylsilyl.

A helix can exist in the form of either of its enantiomers (the *P* or *M* isomer). The helical sense of the THF-polyether helix is determined by the absolute configuration of the chiral THF unit. In order to form a polyether helix with a predictable conformation, it is first necessary to synthesize an enantiomerically pure oligo(tetrahydrofuran) of type **4**. Here we report on a convergent method for obtaining enantiomerically pure 2,5-*trans*-linked oligo(tetrahydrofuran)s.[8]



Scheme 2. Convergent synthesis of tetrahydrofuran pentamer **11**. R = TBDPS. Bn = benzyl. Ts = tosyl. a) (−)-*B*-Allyldiisopinocampheylborane, THF, −78 °C, 73%; b) BnBr, NaH, THF, 90%; c) O_3, CH_2Cl_2, Ph_3P, then $NaBH_4$, MeOH, 87%; d) PhSSPh, Bu_3P, CH_2Cl_2, 98%; e) magnesium monoperoxophthalate, EtOH, 90%; f) 1: lithium diisopropylamide, THF, −78 °C; 2: $(COCl)_2$, DMSO, Et_3N, CH_2Cl_2; 3: Al/Hg, THF/*n*PrOH, 4:1, 73%; g) $NaBH_4$, MeOH, *ds*: 50:50, epimers separated by chromatography, 45%; h) tosyl chloride, pyridine 20 °C, 81%; j) H_2, Pd/C, MeOH, 75%; k) NaH, THF, 50 °C, 2 h, 60%.

The starting point for the synthesis of the tetrahydrofuran pentamer **11** was the enantiomerically pure aldehyde **6** (Scheme 2).[8] A reagent-controlled allyl boration as described by H. C. Brown et al.[9] gave the homoallyl alcohol (*ds*: 85:15), which was converted into the benzyl-protected compound **7**. The relative configuration of the newly formed stereocenter was determined by using reference compounds[8] whose relative configurations had been previously established by X-ray structural analysis. The terminal double bond of compound **7** was ozonized. Reductive workup of the alcohol obtained from the ozonolytic cleavage gave an alcohol that was then converted into sulfone **8**. The lithiated sulfone was coupled with aldehyde **6**. After Swern oxidation and desulfonation the stereochemically pure ketone **9** was obtained. In preparation for the ring closure of the tetrahydrofuran ring the keto group was reduced and the resulting alcohol tosylated. The benzyl protective group was cleaved by catalytic hydrogenation to provide compound **10**. Finally, the tetrahydrofuran ring was closed by an intramolecular substitution reaction proceeding with inversion. The C_2 symmetry of the tetrahydrofuran pentamer **11** was verified by the half signal set of the ^1H and ^{13}C NMR spectra (Table 1).

Table 1. Selected analytical and spectroscopic data of compounds **8**, **9**, and **11**.

8: colorless oil; $[\alpha]_D^{20} = -14.5$ ($c = 4.00$, $CHCl_3$); ^1H NMR [a]: $\delta = 1.01$ (s, 9H), 1.66–2.00 (m, 10H), 3.02–3.10 (m, 1H), 3.19–3.29 (m, 1H), 3.41–3.47 (m, 1H), 3.59 (dd, $J = 10.4$, 5.3 Hz, 1H), 3.66 (dd, $J = 10.4$, 4.5 Hz, 1H), 3.82–3.90 (m, 2H), 3.98–4.04 (m, 1H), 4.05–4.13 (m, 1H), 4.45 (d, $J = 11.7$ Hz, 1H), 4.66 (d, $J = 11.7$ Hz, 1H), 7.20–7.37 (m, 10H), 7.46–7.67 (m, 8H), 7.81–7.84 (m, 2H); ^{13}C NMR [b]: $\delta = 19.3$ (s), 24.1 (t), 26.9 (q), 27.0 (t), 28.1 (t), 28.2 (t), 28.4 (t, 2C), 52.9 (t), 66.7 (t), 72.7 (t), 78.8 (d), 79.9 (d), 81.6 (d, 2C), 81.8 (d), 127.6 (d), 127.7 (d), 128.0 (d), 128.1 (d), 128.4 (d), 129.3 (d), 129.5 (d), 129.6 (d), 133.6 (d), 133.8 (s), 135.7 (d), 138.5 (s), 139.3 (s); correct elemental analysis for $C_{41}H_{50}O_6SSi$

9: colorless oil; $[\alpha]_D^{20} = -15.4$ ($c = 1.20$, $CHCl_3$); ^1H NMR [a]: $\delta = 1.01$, 1.02 (each s, 18H), 1.58–1.99 (m, 16H), 2.29–2.55 (m, 4H), 3.32–3.36 (m, 2H), 3.60–3.67 (m, 4H), 3.71–3.77 (m, 1H), 3.87–3.91 (m, 2H), 4.02–4.15 (m, 4H), 4.50 (d, $J = 11.7$ Hz, 1H), 4.73 (d, $J = 11.7$ Hz, 1H), 7.29–7.36 (m, 17H), 7.63–7.65 (m, 8H); ^{13}C NMR [b]: $\delta = 19.4$ (s), 20.0 (s), 24.8 (t), 27.0 (q), 27.1 (q), 28.4 (t), 28.5 (t), 28.6 (t), 33.1 (t), 38.9 (t), 42.6 (t), 66.5 (t), 66.7 (t), 72.8 (t), 73.8 (d), 79.7 (d), 79.9 (d), 80.5 (d), 81.8 (d), 82.1 (d), 82.6 (d), 127.5 (d), 127.7 (d), 127.8 (d), 128.0 (d), 128.1 (d), 128.3 (d), 128.4 (d), 129.6 (d), 129.7 (d), 133.9 (s), 135.7 (d), 139.2 (s), 210.9 (s); correct elemental analysis for $C_{61}H_{78}O_8Si_2$

11: colorless oil; $[\alpha]_D^{20} = -10.4$ ($c = 0.60$, $CHCl_3$); ^1H NMR [c]: $\delta = 1.04$ (s, 18H), 1.60–2.03 (m, 20H), 3.60 (dd, $J = 10.4$, 5.7 Hz, 2H), 3.69 (dd, $J = 10.4$, 4.3 Hz, 2H), 3.85–3.97 (m, 8H), 4.10–4.15 (m, 2H), 7.35–7.37 (m, 12H), 7.65–7.68 (m, 8H); ^{13}C NMR [d]: $\delta = 19.3$ (s), 26.9 (q), 28.0 (t), 28.1 (t), 28.2 (t), 28.3 (t), 28.5 (t), 66.6 (t), 79.7 (d), 81.6 (d, 2C), 81.8 (d), 81.9 (d), 127.6 (d), 129.5 (d), 133.8 (s), 135.6 (d), 135.7 (d); HR-MS for $C_{54}H_{72}O_7Si_2$: calcd.: 888.4816; found: 888.4951

[a] 300 MHz ($CDCl_3$), 20 °C; [b] 75 MHz ($CDCl_3$), 20 °C; [c] 500 MHz ($CDCl_3$), 20 °C; [d] 126 MHz ($CDCl_3$) 20 °C.

Seven oxygen atoms from compound **11** would suffice to form one full turn in a helical spiral. In order to traverse a membrane, molecules with a length encompassing four to five helical turns are required, and thus longer oligo(tetrahydrofuran)s are necessary. To this end two approaches appear particularly promising: the use of a bidirectional synthetic strategy and the coupling of oligo(tetrahydrofuran) units through amide linkages.

Received: December 22, 1993 [Z 6572 IE]
German version: *Angew. Chem.* **1994**, *106*, 1238

[1] R. B. Gennis in *Biomembranes, Molecular Structure and Function*. Springer, New York, **1989**, pp. 270–306.
[2] a) G. G. Cross, T. M. Files, T. D. James, M. Zojaji, *Synlett* **1993**, 449–460; b) C. J. Stankovic, S. L. Schreiber, *Chemtracts: Org. Chem.* **1991**, *4*, 1–20; c) J. D. Lear, Z. R. Wassermann, W. F. DeGrado, *Science* **1988**, *240*, 1177–1181.

[3] a) R. J. M. Nolte, A. J. M. VanBeijnen, J. G. Neeve, J. W. Zwikker, A. J. Verkley, W. Drenth, *Isr. J. Chem.* **1984**, *24*, 297; b) A. Nakano, Q. Xie, J. V. Mallen, L. Echegoyen, G. W. Gokel, *J. Am. Chem. Soc.* **1990**, *112*, 1287; c) V. E. Carmichael, P. J. Dutton, T. M. Fyles, T. M. James, J. A. Swan, M. J. Zojaji, *ibid.* **1989**, *111*, 767; d) N. Voyer, *ibid.* **1991**, *113*, 1818.

[4] M. J. Pregel, L. Jullien, J.-M. Lehn, *Angew. Chem.* **1992**, *104*, 1695–1697; *Angew. Chem. Int. Ed. Engl.* **1992**, *31*, 1637–1639.

[5] a) Overview of poly(epoxide) cyclizations as an approach to oligo(tetrahydrofuran)s: H.-J. Altenbach in *Organic Synthesis Highlights* (Eds.: J. Mulzer, H.-J. Altenbach, M. Braun, K. Krohn, H.-J. Reissig), VCH, Weinheim, **1991**, pp. 145–150; b) T. R. Hoye, J. Suhadolnik, *Tetrahedron* **1986**, *42*, 3309–3362; c) T. R. Hoye, P. R. Hanson, A. C. Kovelesky, T. D. Ocain, Z. Zhuang, *J. Am. Chem. Soc.* **1991**, *114*, 9369–9371; e) overview of the synthesis of 2,5-disubstituted tetrahydrofurans: J.-C. Harmange, B. Figadere, *Tetrahedron: Asymmetry* **1993**, *4*, 1711–1754; f) even poly(ethylene oxide) displays helical domains in the crystalline state, which can be used for ion transport: R. Dupon, B. L. Papke, M. A. Ratner, D. H. Whitmore, D. F. Shriver, *J. Am. Chem. Soc.* **1982**, *104*, 6247–6251; g) investigations of related structures in the polymer field: W. J. Schultz, M. C. Etter, A. V. Pocius, S. Smith, *ibid.* **1980**, *102*, 7982–7984; h) oligo(tetrahydropyran)s: X. Wang, S. D. Erickson, T. Iimori, W. C. Still, *ibid.* **1992**, *114*, 4128–4137.

[6] This assumption is supported by the results of force field calculations carried out on the tetrahydrofuran trimer; MacroModel V3.5X/MM2*, **1992**, Columbia University, New York: F. Mohamadi, N. G. J. Richards, W. C. Guida, R. Liskamp, C. Caufield, M. Lipton, G. Chang, T. Hendrickson, W. C. Still, *J. Comput. Chem.* **1980**, *11*, 440.

[7] Crystallographic data for **5** ($C_{25}H_{32}O_3Si$, $M = 408.60$): monoclinic, space group $P2_1$, $a = 1055.5(2)$, $b = 798.3(2)$, $c = 1493.6(3)$ pm, $\beta = 109.12(3)^\circ$, $Z = 2$, $\rho_{calcd} = 1.141\ g\,cm^{-3}$, $\mu(Cu_{K\alpha}) = 10.34\ cm^{-1}$. Data measured at room temperature with an Enraf-Nonius CAD4 diffractometer; 3532 measured reflections, of which 3392 were independent ($R_{int.} = 0.0231$), and all of which were used for data refinement. Solution with direct methods with the Siemens SHELXTL-PLUS(VMS) program package, refinement of F^2 with SHELXL-93, $wR2 = 0.1197$ for all data: weight $w = 1/[\sigma^2(F_o^2) + (0.0739P)^2 + 0.4065P]$ with $P = (F_o^2 + 2F_c^2)/3$, GOF = 1.032, the conventional R value for 2701 reflections with $I > 2\sigma(I)$ is 0.0471; all non-hydrogen atoms were refined anisotropically, the H atoms were refined with the "riding model" and fixed temperature factors. Calculations were conducted on a Micro-VAX II and on a VAX-6000-420. Further details of the crystal structure investigation may be obtained from the Fachinformationszentrum Karlsruhe, D-76344 Eggenstein-Leopoldshafen (FRG), on quoting the deposity number CSD-400533.

[8] For a linear approach to dimeric and trimeric oligo(tetrahydrofuran)s: U. Koert, M. Stein, K. Harms, *Tetrahedron Lett.* **1993**, *34*, 2299–2302.

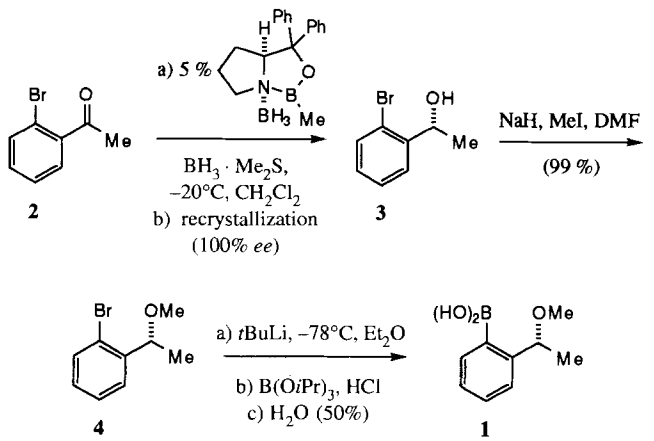
[9] P. K. Jadhav, K. S. Bhat, P. T. Perumal, H. C. Brown, *J. Org. Chem.* **1986**, *51*, 432–439.

A Reagent for Determining Optical Purities of Diols by Formation of Diastereomeric Arylboronate Esters

Kevin Burgess* and Alexander M. Porte

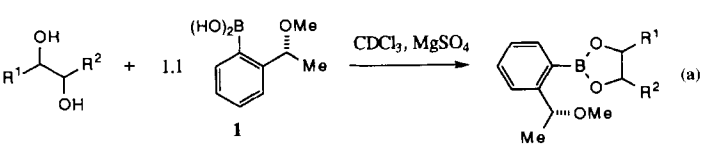
Optical purities of alcohols are often determined by forming diastereomeric methoxyphenyltrifluoromethyl acetates ("Mosher's esters"),[1] mandelates,[2] trivalent phosphorus derivatives,[3] and organoboron[4] or organosilicon compounds.[5] None of these methods is particularly suitable for diols. Syntheses of bis-Mosher's esters, for instance, are especially susceptible to kinetic resolutions, and substrate diols with inequivalent OH functionalities give two sets of NMR marker peaks in narrow regions of the ^1H and ^{19}F NMR spectra. Moreover, some of the commercial derivatizing agents are not optically pure (97.9–99.7% *ee* for Mosher's acid)[6] hence significant cumulative errors occur when two such groups are introduced. Despite this, formation of bis-Mosher's esters is used,[7–10] presumably because there has been no alternative derivatizing agent that is clearly superior. We report here a synthesis of the optically pure boronic acid **1**, and simple applications of this for determining enantiomeric excesses of 1,2- and 1,3-diols.

Scheme 1 shows the asymmetric synthesis of **1**. Optical activity was introduced by the reduction of *ortho*-bromoacetophenone **2** with BH_3 in the presence of a chiral catalyst.[11] The asymmetric induction obtained in this step was not critical since samples of alcohol **3** of about 85% *ee* were upgraded to optically pure form after one or two recrystallizations from hexane; enantiomeric trifluoroacetates of **3** were nicely resolved by capillary GC with a chiral stationary phase, thus the optical purity of **3** is easily confirmed. Methyl ether **4** was made from **3**, and a transmetalation procedure was used to convert **4** into the corresponding boronic acid **1**,[12] which was purified by recrystallization. No chromatographic separations were required in this synthesis.



Scheme 1. Asymmetric synthesis of boronic acid **1**.

Derivatization of diols using the arylboronic acid **1** is simple. A slight excess of **1** was mixed with the diol in toluene, THF, or $CDCl_3$ in the presence of a dehydrating agent (ground molecular sieves or $MgSO_4$) [Eq. (a)]. The reaction mixture was filtered and the ^1H NMR spectrum of the filtrate was recorded. Complete conversion of the substrate to a boronic ester was observed for all the substrates tested, so kinetic resolutions were not a concern. In most cases the position of the OCH_3 signal of the excess reagent **1** was distinct from that of the OCH_3 signal of the diastereomeric boronic ester products, and the enantiomeric excesses were deduced immediately by integration. Sometimes, overlap of the product and reagent OCH_3 signals complicated the spectra. If this occurred, the crude reaction mixture was loaded onto a short column of silica gel and eluted with diethyl ether containing a trace of triethylamine. Excess reagent **1** was retained on the column, and the ^1H NMR spectrum of the material which passed through was analyzed without difficulty.



[*] Dr. K. Burgess, A. M. Porte
Department of Chemistry, Texas A & M University
College Station, TX 77843-3255 (USA)
Telefax: Int. code + (409)845-8839

[**] This work was supported by The Robert Welch Foundation and The National Science Foundation. K. B. thanks The National Institutes of Health for a Career Development Award, and the Alfred P. Sloan Foundation.

Figure 1 shows an expanded region of the ^{1}H NMR spectrum of the diastereomeric boronate ester from racemic 2,3-butanediol. The resolution of the OCH_3 resonance signals is representative. Table 1 summarizes the data obtained for all the substrates. Six 1,2-diols (entries 1–6), two 1,3-diols (entries 7 and 8), a 2-hydroxy acid (entry 9), and a 2-amino alcohol (entry 10) were analyzed in this way. Generally, baseline resolution was obtained by using a 400 MHz instrument and $CDCl_3$ as solvent, although occasionally 200 MHz was sufficient (entry 2). Better resolution of the two diastereomers may be observed when C_6D_6 is used as solvent (entry 2). An attractive feature of this derivatization technique is that the OCH_3 resonance used for the analyses originated from the reagent, thus it is a probe which is independent of the spectroscopic properties of the substrate. This reagent-derived OCH_3 resonance was baseline-resolved for entries 1–9, and almost baseline-resolved for entry 10. Resonances derived from the substrate were also resolved in some experiments (entries 4, 5, and 10), and can be a better marker of the enantiomeric excess than the OCH_3 signal (cf. entry 10). Entries 9 and 10 suggest this technique may also be useful for substrates other than diols.

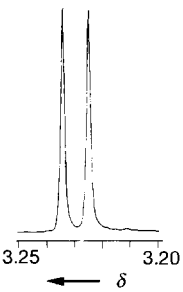
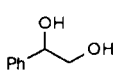
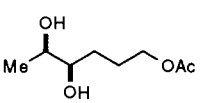
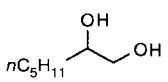
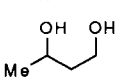
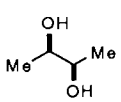
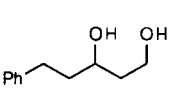
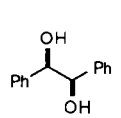
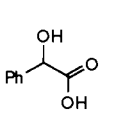
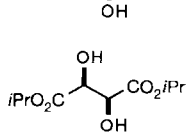
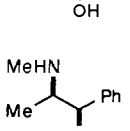


Fig. 1. Expanded region of the ^{1}H NMR spectrum showing the OCH_3 signals of the diastereomeric boronate esters from **1** and racemic 2,3-butanediol (at 400 MHz in $CDCl_3$).

Table 1. Results from the ^{1}H NMR spectra of racemic substrates derivatized with **1** [a].

Entry	Racemic substrate	$\Delta\delta$ (OCH_3) [ppb] (MHz) [$\Delta\delta$ (other protons) [ppb]]	Entry	Racemic substrate	$\Delta\delta$(OCH_3) [ppb] (MHz) [$\Delta\delta$ (other protons) [ppb]]
1		7.4 (400)	6		14.0 (500)
2		9.7 (200) 11.4 in C_6D_6	7		9.7 (400)
3		9.3 (400)	8		9.3 (400)
4		11.8 (400) [30.0 (PhC*H*)]	9		20.3 (500)
5		14.0 (400) [21.1 (C*H*OH)]	10 [b]		5.4 (400) [6.3 (NCH_3)]

[a] In $CDCl_3$. [b] Diastereomeric oxazaborolidines were formed in this case by mixing the amino alcohol and boronic acid **1** (1.1 equiv) in toluene at 110 °C, and azeotropic removal of water.

The value of diols as chirons is increasing as enantioselective bishydroxylations[13–15] become standard techniques in organic synthesis. Methods for determining optical purities of diols therefore have assumed greater significance. Chromatographic methods to measure optical activities have the advantage of high accuracy but they are not always convenient, particularly if the required stationary phases are unavailable or the compound has inconvenient physical properties. Consequently, derivatization methods for accessing optical purities by NMR spectroscopy have considerable appeal. Boronic acid **1** can be obtained in optically pure form, it is easily converted to arylboronate esters, and kinetic resolutions are easily avoided. We do not claim that this reagent will be suitable for determining enantiomeric excesses of all diols, but Table 1 contains a comprehensive list of the 1,2- and 1,3-diols screened by us so far.[16]

Experimental Procedure

3: Neat *ortho*-bromoacetophenone **2** (9.085 g, 4.5 mmol) was added dropwise to a solution of catalyst, 4,5,6,7-tetrahydro-1-methyl-3,3-diphenyl-1*H*,3*H*-pyrrolo[1,2-*c*]-[1,3,2]oxazaborole-borane, (0.655 g, 2.25 mmol) and BH_3·Me_2S (4.5 mL, 45 mmol) in dichloromethane (3 mL) at −20 °C. The mixture was allowed to stand for 8 h at −20 °C. The mixture was added carefully to methanol (10 mL) precooled to −20 °C; evolution of gas occurred. After removal of the solvent additional methanol (10 mL) was added and removed, thus eliminating $B(OMe)_3$ and $MeB(OMe)_2$ [11]. The residual oil was dissolved in methanol and passed quickly through Amberlyst 15 (NH_4^+ form) eluted with methanol. The product was crystallized from *n*-hexane (6.9 g, 39.4 mmol, 84%). ^{1}H NMR (200 MHz, $CDCl_3$): δ = 7.60 (m, 2H), 7.35 (m, 1H), 7.10 (m, 1H), 5.23 (q, J = 6.4 Hz, 1H), 2.30 (s, 1H), 1.47 (d, J = 6.4 Hz, 2H).

4: The alcohol, **3**, (1.00 g, 4.90 mmol) was added to a slurry of NaH (0.176 g, 7.35 mmol) in dimethylformamide (4 mL). After gas evolution ceased, MeI (2.78 g, 19.6 mmol) was added, and the solution was stirred for 12 h. Et_2O (30 mL) was added, and the solution washed with brine (4 × 10 mL). The organic layer was dried over Na_2SO_4 and the solvent was evaporated. The product was used in the next step without further purification (1.05 g, 11.95 mmol, 100%). ^{1}H NMR (200 MHz, $CDCl_3$): δ = 7.50 (dt, J = 7.9 Hz, 1.3 Hz, 2H), 7.3 (m, 1H), 7.12 (m, 1H), 4.71 (q, J = 6.4 Hz, 1H), 3.25 (s, 3H), 1.40 (d, J = 6.4 Hz, 2H); ^{13}C NMR: δ = 143.3, 133.2, 129.2, 128.4, 127.5, 123.2, 78.6, 57.0, 22.7; $[\alpha]_D^{20}$ = −100.8 (c = 6.4, CH_2Cl_2).

1: The ether **4** (0.500 g, 2.33 mmol) in Et_2O (5 mL) at −78 °C was transmetalated by the addition of *tert*-butyllithium (3.89 mL, 5.4 mmol, 1.4 M in pentane). After warming to room temperature for 0.5 h the solution was again cooled to −78 °C. This orange solution was cannulated into a solution of triisopropylborate (0.438 g, 2.33 mmol) in Et_2O (5 mL) also at −78 °C. The mixture was stirred for 3 h while allowing it to warm to 25 °C. A solution of HCl (1 M) in Et_2O (3.00 mL, 3.00 mmol) was added at 0 °C to the above mixture and then stirred for 1 h. The solution was cannulated from the solid and the solvent evaporated. The boronate ester was distilled (90–100 °C, 0.5 Torr). Following the distillation the boronate ester was hydrolyzed to the boronic acid **1** in water (2 mL) and stirred for 0.5 h giving a white solid. The boronic acid was recrystallized from *n*-hexane (0.209 g, 1.16 mmol, 50%). ^{1}H NMR (200 MHz, $CDCl_3$): δ = 8.05 (m, 1H), 7.36 (m, 2H), 7.19 (m, 1H), 6.90 (s, 2H), 4.45 (q, J = 6.72 Hz, 1H), 3.30 (s, 3H), 1.56 (d, J = 6.72 Hz, 2H); ^{13}C NMR: δ = 146.5, 137.7, 130.4, 128.9, 127.8, 83.5, 56.3, 22.6; m.p. 72–74 °C; $[Ga]_D^{25}$ = +27 (c = 0.5, CH_2Cl_2).

Derivatization method: Boronic acid **1** (0.055 mmol), racemic mandelic acid (0.05 mmol), and $MgSO_4$ (300 mg) were placed in $CDCl_3$ (2 mL). The solution was stirred for 3 h, filtered, and the NMR spectrum was recorded. In this case the OCH_3 resonance of the excess reagent was well resolved from the product. For some other substrates it was necessary to remove the excess boronic acid by passing the product through a small plug of silica with diethyl ether/triethylamine, and subsequently to rerecord the NMR spectrum.

Received: January 19, 1994 [Z 6632 IE]
German version: *Angew. Chem.* **1994**, *106*, 1218

[1] J. A. Dale, H. S. Mosher, *J. Am. Chem. Soc.* **1973**, *95*, 512.
[2] B. M. Trost, J. L. Belletire, S. Godleski, P. G. McDougal, J. M. Balkovec, J. J. Baldwin, M. E. Christy, G. S. Ponticello, S. L. Varga, J. P. Springer, *J. Org. Chem.* **1986**, *51*, 2370.
[3] D. Parker, *Chem. Rev.* **1991**, *91*, 1441.
[4] J. M. Brown, S. W. Leppard, G. C. Lloyd-Jones, *Tetrahedron Asymmetry* **1993**, *3*, 261.
[5] T. H. Chan, Q.-J. Peng, D. Wang, J. A. Guo, *J. Chem. Soc. Chem. Commun.* **1987**, *5*, 325.
[6] W. A. Konig, K.-S. Nippe, P. Mischnick, *Tetrahedron Lett.* **1990**, *31*, 6867.
[7] E. N. Jacobsen, I. Markó, W. S. Mungall, G. Schröder, K. B. Sharpless, *J. Am. Chem. Soc.* **1988**, *110*, 1968.

 © *VCH Verlagsgesellschaft mbH, D-69451 Weinheim, 1994* *0570-0833/94/1111-1183 $ 10.00+.25/0*

[8] B. B. Lohray, T. H. Kalantar, B. M. Kim, C. Y. Park, T. Shibata, J. S. M. Wai, K. B. Sharpless, *Tetrahedron Lett.* **1989**, *30*, 2041.
[9] K. B. Sharpless, W. Amberg, M. Beller, H. Chen, J. Hartung, Y. Kawanami, D. Lübben, E. Manoury, Y. Ogino, T. Shibata, T. Ukita, *J. Org. Chem.* **1991**, *56*, 4585.
[10] K. B. Sharpless, W. Amberg, Y. L. Bennani, G. A. Crispino, J. Hartung, K. Jeong, H. Kwong, K. Morikawa, Z. Wang, D. Xu, X. Zhang, *J. Org. Chem.* **1992**, *57*, 2768.
[11] D. J. Mathre, A. S. Thompson, A. W. Douglas, K. Hoogsteen, J. D. Carroll, E. G. Corley, E. J. J. Grabowski, *J. Org. Chem.* **1993**, *58*, 2880.
[12] H. C. Brown, T. E. Cole, *Organometallics* **1983**, *2*, 1316.
[13] K. Morikawa, J. Park, P. G. Andersson, T. Hashiyama, K. B. Sharpless, *J. Am. Chem. Soc.* **1993**, *115*, 8463.
[14] G. A. Crispino, K.-S. Jeong, H. C. Kolb, Z.-M. Wang, D. Xu, K. B. Sharpless, *J. Org. Chem.* **1993**, *58*, 3785.
[15] L. Wang, K. B. Sharpless, *J. Am. Chem. Soc.* **1992**, *114*, 7568.
[16] After this paper had been submitted we became aware of another method wherein 1,2-diols were derivatized with a boronic acid derivative (W. Tokles and J. K. Snyder, *Tetrahedron Lett.*, **1988**, *29*, 6063). However, no resolution of protons was obtained in that work, instead enantiomeric excesses were measured by integration of resonances in ^{13}C spectra.

Structural and Magnetic Characterization of a Novel Heptanuclear Hydroxo-Bridged Copper(II) Cluster of the Corner-Sharing Dicubane Type**

José Antonio Real, Giovanni De Munno, Rosaria Chiappetta, Miguel Julve,* Francesc Lloret, Yves Journaux,* Jean-Christophe Colin, and Geneviève Blondin

Transition metal clusters with a cubane-like structure are a very important class of compounds.[1] In the case of copper(II), several examples of alkoxo-bridged Cu^{II} tetramers with cubane-like cores are known, and their magnetic properties were adequately described by considering exchange interactions between all four metal ions.[2, 3] Their structure can be viewed as the result of the association of two planar dinuclear di(μ-alkoxo)-copper(II) complexes through weak Cu–alkoxo apical interactions. The structural similarity of these alkoxo-bridged and the hydroxo-bridged copper(II) compounds is illustrated in the first hydroxo-bridged $Cu_4(OH)_4$ tetramer, $[Cu(bpy)(OH)]_4(PF_6)_4$ (bpy = 2,2′-bipyridine),[4] where two almost planar di(μ-hydroxo)-copper(II) dimers are held together by long out-of-plane Cu–OH bonds. The spin ground state in the $Cu_4(OH)_4$ cubane is a quintet arising from a weak ferromagnetic interaction between the two low-lying triplet states of the two dimers. In fact, all examples of di(μ-hydroxo)copper(II) species containing bpy as terminal ligand exhibit ferromagnetic coupling between the dimers. A similar situation occurs when bpy is replaced by 2,2′-bipyrimidine (bpym), as illustrated by $[Cu_2(bpym)_2(OH)_2]X_2 \cdot 6H_2O$ ($X = ClO_4^-$, NO_3^-).[5, 6] In this case, the bischelating ability of bpym led to the polymerization of the dinuclear unit to yield one-dimensional chains of Cu^{II} ions alternately bridged by bpym and two hydroxo groups. The chains exhibit a regular alternation of ferro- and antiferromagnetic interactions.[6, 7]

In the scope of our continuous research in this field we prepared the compound **1**, which, as far as we are aware, is the first

$[Cu_7(bpym)_6(OH)_8(H_2O)_2](NO_3)_6 \cdot H_2O$ **1**

hydroxo-bridged $Cu_7(OH)_8$ dicubane-like compound. It was characterized by elemental analysis, variable-temperature magnetic measurements, and X-ray structural analysis.[8]

The crystal structure of **1** consists of a discrete centrosymmetric hydroxo-bridged $[Cu_7(bipym)_6(OH)_8(H_2O)_2]^{6+}$ heptameric entity exhibiting core of two corner-sharing cubane-like units (Fig. 1), six uncoordinated nitrate groups, and a water molecule of crystallization. The cationic complex can be described in terms of three fragments: a central centrosymmetric trinuclear unit containing the Cu(3), Cu(4), and Cu(3a) copper atoms, and two symmetry-related Cu(1)–Cu(2) and Cu(1a)–Cu(2a) dinuclear entities in which bpym acts as terminal ligand in both cases. The two dimeric units are connected to the trinuclear one

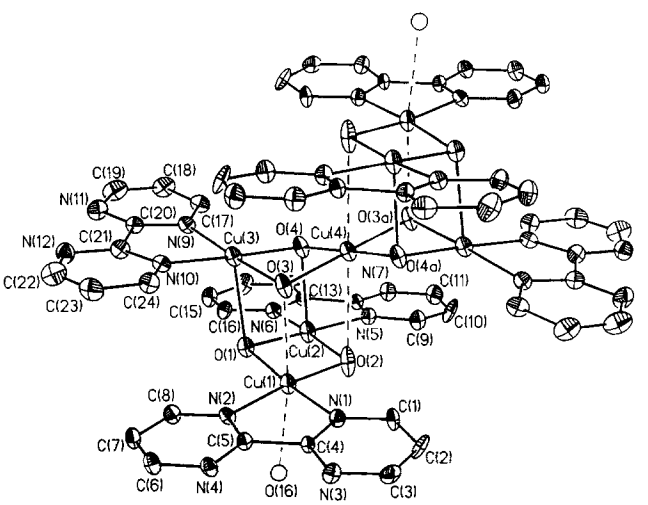


Fig. 1. The structure and the atomic labeling of the $[Cu_7(bipym)_6(OH)_8(H_2O)_2]^{6+}$ ion in **1** (ellipsoids at the 30% probability level). Selected distances [Å] and angles [°] with standard deviations in parentheses: Cu(1)-N(1) 2.030(7), Cu(1)-N(2) 1.991(11), Cu(1)-O(1) 1.969(6), Cu(1)-O(2) 1.924(12), Cu(1)-O(3) 2.494(8), Cu(1)-O(16) 2.485(15), Cu(2)-N(5) 1.998(12), Cu(2)-N(6) 2.012(7), Cu(2)-O(1) 1.982(10), Cu(2)-O(2) 1.919(7), Cu(2)-O(4) 2.425(8), Cu(3)-N(9) 1.988(8), Cu(3)-N(10) 1.997(12), Cu(3)-O(3) 1.936(7), Cu(3)-O(4) 1.946(10), Cu(3)-O(1) 2.437(8), Cu(4)-O(3) 1.916(10), Cu(4)-O(4) 1.927(6), Cu(4)-O(2) 2.951(10); N(1)-Cu(1)-N(2) 80.9(4), N(1)-Cu(1)-O(1) 175.5(4), N(1)-Cu(1)-O(2) 94.2(4), N(1)-Cu(1)-O(3) 97.6(3), N(1)-Cu(1)-O(16) 91.4(5), N(2)-Cu(1)-O(1) 101.4(4), N(2)-Cu(1)-O(2) 173.8(4), N(2)-Cu(1)-O(3) 96.2(3), N(2)-Cu(1)-O(16) 82.4(5), O(1)-Cu(1)-O(2) 83.7(4), O(1)-Cu(1)-O(3) 78.4(3), O(1)-Cu(1)-O(16) 92.7(4), O(2)-Cu(1)-O(3) 88.3(4), O(2)-Cu(1)-O(16) 93.9(5), O(3)-Cu(1)-O(16) 170.6(5), N(5)-Cu(2)-O(2) 94.3(4), N(5)-Cu(2)-O(1) 177.2(3), N(5)-Cu(2)-N(6) 81.3(4), N(5)-Cu(2)-O(4) 98.1(3), N(6)-Cu(2)-O(1) 101.2(4), N(6)-Cu(2)-O(2) 171.6(4), N(6)-Cu(2)-O(4) 97.3(3), O(1)-Cu(2)-O(2) 83.4(4), O(1)-Cu(2)-O(4) 80.3(3), O(2)-Cu(2)-O(4) 90.4(3), N(9)-Cu(3)-N(10) 81.0(4), N(9)-Cu(3)-O(3) 177.3(3), N(9)-Cu(3)-O(4) 98.7(4), N(9)-Cu(3)-O(1) 102.0(3), N(10)-Cu(3)-O(3) 99.8(4), N(10)-Cu(3)-O(4) 177.8(3), N(10)-Cu(3)-O(1) 101.6(3), O(3)-Cu(3)-O(4) 80.4(3), O(3)-Cu(3)-O(1) 80.4(3), O(4)-Cu(3)-O(1) 80.6(3), O(3)-Cu(4)-O(4) 81.4(3), O(3)-Cu(4)-O(3a) 180.0(1), O(3)-Cu(4)-O(4a) 98.6(3), O(3)-Cu(4)-O(2) 75.9(3), O(3)-Cu(4)-O(2a) 104.1(3), O(4)-Cu(4)-O(3a) 98.6(3), O(4)-Cu(4)-O(4a) 180.0(1), O(4)-Cu(4)-O(2) 75.8(3), O(4)-Cu(4)-O(2a) 104.2(3), O(2)-Cu(4)-O(2a) 180.1(1) (symmetry code: (a) $-x, 1-y, 1-z$) [12].

[*] Prof. M. Julve, Dr. J. Real, Dr. F. Lloret
Departament de Química Inorgànica
Facultat de Química de la Universitat de València
Dr. Moliner 50, E-46100-Burjassot, València (Spain)
Telefax: Int. code + (6)386-4322
Prof. G. De Munno, R. Chiappetta
Dipartimento di Chimica, Università della Calabria
87030 Arcavacata di Rende, Cosenza (Italy)
Dr. Y. Journaux, J.-C. Colin, Dr. G. Blondin
Laboratoire de Chimie Inorganique, URA CNRS 420
Université de Paris Sud, F-91405 Orsay (France)

[**] This work was supported by the Spanish Dirección General de Investigación Científica y Técnica (DGICYT) (PB91-0807-C02-01), the Italian Ministero dell'Università e della Ricerca Scientifica e Tecnologica, and the Spanish–French Integrated Actions.

by long axial Cu–O bonds ranging from 2.425(8) [Cu(2)–O(4)] to 2.951(10) Å [Cu(4)–O(2)] in such a way that a $Cu_7(OH)_8$ double cubane-like core results.

The Cu^{II} centers have the geometry expected as a result of vibronic Jahn–Teller forces [strongly axially elongated octahedra for Cu(1) and Cu(4) and square pyramids for Cu(2) and Cu(3)]. The three copper atoms from the central centrosymmetric fragment are held together by four hydroxo groups in equatorial positions. Two nitrogen atoms from bpym and two hydroxo groups occupy the basal positions around Cu(3), whereas four hydroxo groups build the equatorial plane around Cu(4). The axial position of Cu(3) is occupied by the O(1) hydroxo atom from the doubly hydroxo-bridged dimer, and the copper atom is displaced by 0.041(2) Å from the mean basal plane towards this axial oxygen. The axial positions around Cu(4) are filled by the O(2) and O(2a) hydroxo atoms from the two symmetry-related dimers. Cu(4) is forced by symmetry to be in the basal plane defined by the O(3), O(4), O(3a), and O(4a) atoms. The dihedral angle between the basal planes of Cu(3) and Cu(4) is 26.6(2)°. The values of the Cu(3)-O(4)-Cu(4) and Cu(3)-O(3)-Cu(4) angles are 96.3(3) and 95.6(3)°, respectively. The Cu(2) and Cu(1) atoms from the dimeric fragment are (4 + 1) and (4 + 2)-coordinated, respectively. Their equatorial planes are formed by two nitrogen atoms from bpym and two hydroxo groups, and the axial positions are filled by the hydroxo O(4) oxygen in the former and the O(3) hydroxo and O(16) water oxygens in the latter. Both copper atoms are slightly displaced from their mean basal planes [0.008(2) and 0.040(3) Å, respectively]. The dihedral angle between the equatorial planes of Cu(1) and Cu(2) of 8.7(2)° reveals that bending within the dimer is smaller than that within the trinuclear unit. The values of the Cu(1)-O(1)-Cu(2) and Cu(1)-O(2)-Cu(2) angles are 94.5(4) and 98.0(5)°, respectively. The bending around the O(1)···O(2) axis in the $Cu(1)(OH)_2Cu(2)$ unit contrasts with the situation found in the related compounds $[Cu_2(bpym)_2(OH)_2]X_2 \cdot 6H_2O$ ($X = ClO_4^-$, NO_3^-) mentioned above, which exhibit a planar, centrosymmetric $Cu(OH)_2Cu$ network.

The Cu(1)···Cu(2), Cu(1)···Cu(3), Cu(1)···Cu(4), Cu(2)···Cu(3), Cu(2)···Cu(4), and Cu(3)···Cu(4) intracluster metal–metal separations are 2.901(3), 3.407(3), 3.520(3), 3.360(3), 3.467(3), and 2.869(2) Å, respectively.

Figure 2 shows the magnetic behavior of **1** in the form of the dependence of $\chi_M T$ on temperature and of M on the magnetic field H. A Curie law corresponding to seven uncoupled copper(II) ions is valid between room temperature and 60 K. Below this temperature, $\chi_M T$ steadily increases and reaches a value of 5.20 $cm^3 mol^{-1} K$ at 1.8 K. This value, which is greater than that expected for one quadruplet and two triplets that do not

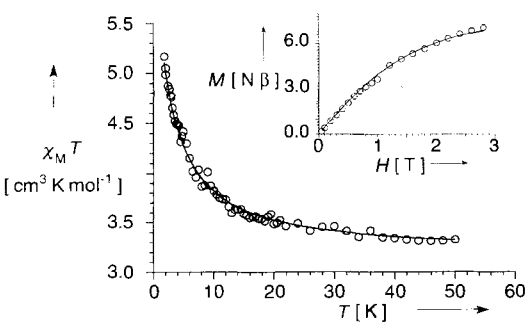


Fig. 2. Temperature dependence of $\chi_M T$ (χ_M: the magnetic susceptibility per seven copper(II) ions) for **1**: (○) experimental data; (—) best theoretical fit. The inset shows the magnetization data of **1** at 2.0 K; the solid line represents the behavior of a cluster with an $S = 7/2$ ground state with a Landé factor of 2.20.

interact, reveals that ferromagnetic interactions between the dinuclear and trinuclear entities occur. The experimental magnetic data were analyzed with the Hamiltonian operator $\mathcal{H} = -J_1[S_1S_2 + S_{1a}S_{2a}] - J_2[S_3(S_1 + S_2) + S_{3a}(S_{1a} + S_{2a})] - J_3[S_4(S_3 + S_{3a})] - J_4[S_4(S_1 + S_2 + S_{1a} + S_{2a})]$. A schematic drawing showing the distribution of the exchange interaction parameters in **1** is given in Figure 3. The expressions of the

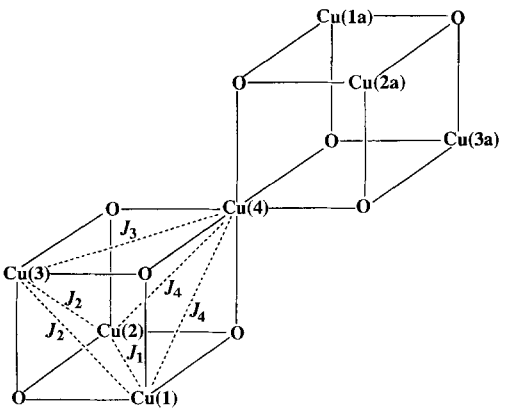


Fig. 3. Diagram of the $Cu_7(OH)_8$ core showing half of the exchange parameters.

magnetic susceptibility and magnetization were obtained by diagonalization in the subspaces of spin S varying between $S = 7/2$ and $S = 1/2$. The final values of the exchange parameters and the Landé g factor were determined with a least-square fit of both susceptibility and magnetization data; the reliability factor R was defined as in Equation (a). The correlation ob-

$$R = (\Sigma[(\chi_M T)_{obsd} - (\chi_M T)_{calcd}]^2 + \Sigma[(M)_{obsd} - (M)_{calcd}]^2)/(\Sigma[(\chi_M T)_{obsd}]^2 + \Sigma[(M)_{obsd}]^2) \quad (a)$$

served among the J values makes the fit difficult, and therefore an iterative procedure was used.[13] The best fit values ($R = 1.4 \times 10^{-5}$) of $J_1 = 5.1\ cm^{-1}$, $J_2 = 0.4\ cm^{-1}$, $J_3 = 5.4\ cm^{-1}$, and $g = 2.20$ were obtained by setting $J_4 = 0$. This set of values are reliable in the light of the structural data. The average θ values in the $Cu(1)(OH)_2Cu(2)$ (dinuclear) and $Cu(3)(OH)_2Cu(4)$ (trinuclear) networks are smaller than 97.5°, and consequently, ferromagnetic interactions within these entities are expected according to the known J versus θ relationship.[14] The significant bending that they display accounts for their reduced values.[4] On the other hand, the small spin density of the d_{z^2} orbital causes the weak ferromagnetic interaction between the dinuclear and the trinuclear fragments through the long out-of-plane Cu–(OH) bonds which connect them. Finally, the magnetization studies at 2 K supports the occurrence of an energetically low-lying octet state in **1**. The present compound provides us with an example of a high-spin complex with ferromagnetic interactions between seven copper(II) ions in a double cubane arrangement. More efforts are justified to prepare more complex high-spin systems taking advantage of the bridging capability of bpym.

Experimental Procedure

A mixture of polyhedral emerald green crystals of **1** and blue-green rhombohedral crystals of $[Cu_2(bpym)_2(H_2O)_2(OH)_2](NO_3)_2 \cdot 4H_2O$ were grown by slow evaporation of blue aqueous solutions containing copper(II) nitrate trihydrate, bpym, and

sodium carbonate in a 1:0.85:0.6 molar ratio. The crystals of **1** were handpicked for X-ray diffraction and magnetic measurements. Correct elemental analysis (C, H, N, Cu).

Received: January 3, 1994 [Z 6594 IE]
German version: *Angew. Chem.* **1994**, *106*, 1223

[1] J. M. Berg, R. H. Holm in *Iron-Sulfur Proteins, Vol. 4* (Ed.: T. G. Spiro), Wiley-Interscience, New York, **1982**, Chap. 1; R. H. Holm, S. Ciurli, J. A. Weigel, *Prog. Inorg. Chem.* **1990**, *38*, 1.

[2] R. Mergehenn, W. Haase, *Acta Crystallogr. Sect B* **1977**, *33*, **1877**, 2734; L. Merz, W. Haase, *J. Chem. Soc. Dalton Trans.* **1978**, 1594; *ibid.* **1980**, 875; H. Astheimer, F. Nepveu, L. Walz, W. Haase, *ibid.* **1985**, *315*; L. Schawabe, W. Haase, *ibid.* **1985**, 1909.

[3] J. W. Hall, W. E. Estes, E. D. Estes, R. P. Scaringe, W. E. Williams, *Inorg. Chem.* **1977**, *16*, 1572; N. Matsumoto, T. Tsutsumi, A. Ohyoshi, H. Okawa, *Bull. Chem. Soc. Jpn.* **1983**, *56*, 1388.

[4] J. Sletten, A. Sørensen, M. Julve, Y. Journaux, *Inorg. Chem.* **1990**, *29*, 5054.

[5] I. Castro, M. Julve, G. De Munno, G. Bruno, J. A. Real, F. Lloret, J. Faus, *J. Chem. Soc. Dalton Trans.* **1992**, 1739.

[6] G. De Munno, M. Julve, F. Lloret, J. Faus, M. Verdaguer, A. Caneschi, *Angew. Chem.* **1993**, *105*, 1122; *Angew. Chem. Int. Ed. Engl.* **1993**, *32*, 1046.

[7] M. L. Kirk, W. E. Hatfield, M. S. Lah, D. Kessissoglou, V. Pecoraro, L. W. Morgan, J. D. Petersen, *J. Appl. Phys.* **1991**, *69*, 6013.

[8] X-ray structure analysis: Siemens R3m/V automatic diffractometer, $Mo_{K\alpha}$, $\lambda = 0.71073$ Å, graphite monochromator, 298 K, Lorentz polarization and Ψ-scan absorption correction [9]. Data collection, solution, and refinement: ω-2θ, standard Patterson methods with subsequent Fourier recycling, SHELXTL-PUS [10]. Two nitrate groups and a water molecule are disordered. The disorder of each nitrate anion has been treated assuming a population factor of 0.5 for the nitrogen and for one of the oxygens. The oxygen of the disordered water was also given a 0.5 population factor. Data collection on a different crystal of **1** was also carried out at 120 K in order to reduce the degree of disorder and to get a more accurate description of its structure. Unfortunately, the disorder was not reduced by cooling, thus proving that it is mainly statistical. Only the structural data at room temperature are reported because the final discrepancy indices at low temperature were not better. All non-hydrogen atoms, except the oxygen atoms of water molecules, and oxygen and nitrogen atoms of disordered nitrate groups, were refined anisotropically. The hydrogen atoms of the bpym ligand were set in calculated positions and refined as riding atoms. They were all refined isotropically. Final geometrical calculations and graphical manipulations were performed with the PARST program [11] and the XP utility of the SHELX-PLUS system, respectively. **1**: $C_{48}H_{50}N_{30}Cu_7O_{29}$ ($M_r = 1937.9$), triclinic, space group $P\bar{1}$, $a = 11.553(7)$, $b = 13.164(7)$, $c = 13.419(8)$ Å, $\alpha = 70.66(4)$, $\beta = 82.21(5)$, $\gamma = 64.14(4)^\circ$, $V = 1733(2)$ Å^3, $Z = 1$, $\rho_{calcd.} = 1.857$ g cm^{-3}, $\mu = 22.13$ cm^{-1}, 2θ range 3–54°, crystal size $0.34 \times 0.18 \times 0.08$ mm^3, $F(000) = 967.7581$ unique reflections, 3862 observed with $I > 3\sigma(I)$, 498 parameters, $R(F_o) = 0.0744$, $R_w(F_o) = 0.0795$ and $S = 1.735$ with $w^{-1} = \sigma^2(F_o) + 0.0021\,(F_o)^2$. Further details of the crystal structure investigations are available on request from the Fachinformationszentrum Karlsruhe, D-76344 Eggenstein-Leopoldshafen (FRG), on quoting the depository number CSD-58070 and the journal citation.

[9] A. C. T. North, D. C. Philips, F. S. Mathews, *Acta Crystallogr. Sect. A* **1968**, *24*, 351.

[10] SHELXTL PLUS, Version 4.21/V. Siemens Analytical X-Ray Instruments Inc., Madison, WI, 1990.

[11] M. Nardelli, *Computer. Chem.* **1983**, *7*, 95.

[12] Bond distances and angles in the bpym ligands are in agreement with those reported in the literature. The pyrimidyl rings of bpym are planar. However, the bpym as a whole is not planar: the dihedral angles between the pyrimidyl rings of the bpym ligands bound to Cu(1), Cu(2) and Cu(3) are 3.6(3), 2.5(3), and 4.6(4)°, respectively.

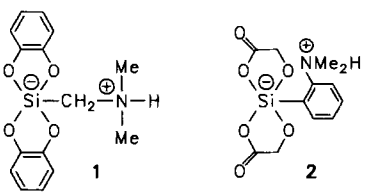
[13] At first we considered only the interactions within the two dimers and the trinuclear entity and the best fit was made on J_1 and J_3 as variables with $J_2 = J_4 = 0$. Then we kept these J_1 and J_3 values constant and fit on J_2 and J_4. This procedure is continued until self-consistent values for all parameters are found.

[14] W. E. Hatfield in *Magneto-Structural Correlations in Exchange Coupled Systems* (Eds.: R. D. Willett, D. Gatteschi, O. Kahn), *NATO ASI Ser., Ser. C* **1985**, *140*, 555.

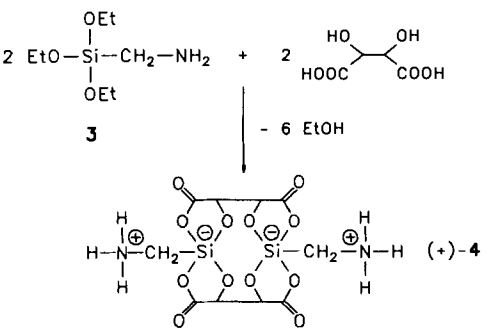
The First Zwitterionic, Optically Active Disilicate with Pentacoordinate Silicon**

Reinhold Tacke,* Mathias Mühleisen, and Peter G. Jones

The study of compounds with higher coordinate silicon atoms is currently one of the main areas of research in silicon chemistry.[1] In the past few years, *ionic* λ^5Si-silicates have been investigated particularly intensively. With the systematic elaboration of a new class of substances, the spirocyclic *zwitterionic* λ^5Si-silicates, this area of research has recently expanded.[2, 3] These compounds are neutral molecular λ^5Si-silicates in which two diolato(2−) ligands and one ammonio-substituted organic group are bound to the Si coordination center. The bidentate diolato(2−) ligands thus far employed are derived from diols of the catechol and glycolic acid types. The zwitterions **1**[2e] and **2**,[2h] which may be classified as molecular mononuclear complexes of pentacoordinate silicon, are typical examples of this class of compounds.



With the synthesis of (+)-bis[(ammonio)methyl]bis[μ-(*R*,*R*)-tartrato(4−)-O^1,O^2:O^3,O^4]disilicate (+)-**4**, we have now succeeded in obtaining a molecular binuclear λ^5Si,λ^5Si′-silicon complex for the first time (Scheme 1). In this compound, two tetradentate (*R*,*R*)-tartrato(4−) ligands bridge the two Si atoms, and each ligand bonds to each of the Si atoms at two coordination sites. The disilicate (+)-**4** has a pentacyclic molecular framework and contains two pentacoordinate (formally negatively charged) Si atoms and two tetracoordinate (formally positively charged) N atoms. To the best of our knowledge, this is the first



Scheme 1. Synthesis of the disilicate (+)-**4** from (aminomethyl)triethoxysilane **3** and (*R*,*R*)-(+)-tartaric acid.

[*] Prof. Dr. R. Tacke, Dipl.-Chem. M. Mühleisen
Institut für Anorganische Chemie der Universität
Engesserstrasse, Geb. 30.45
D-76128 Karlsruhe (FRG)
Telefax: Int. code (721) 608-4290
Prof. Dr. P. G Jones
Institut für Anorganische und Analytische Chemie
der Technischen Universität Braunschweig

[**] This work was supported by the Deutsche Forschungsgemeinschaft and the Fonds der Chemischen Industrie.

 © VCH Verlagsgesellschaft mbH, D-69451 Weinheim, 1994 0570-0833/94/1111-1186 $ 10.00+.25/0

optically active compound of pentacoordinate silicon. Its optical activity results from the presence of the two chiral (*R*,*R*)-tartrato(4−) ligands and the two chiral $Si(\overline{OO}')_2C$ units.

Compound (+)-**4** was prepared by reaction of (aminomethyl)triethoxysilane[4] **3** with (*R*,*R*)-(+)-tartaric acid (molar ratio 1:1) in aqueous solution and isolated as a 2:1 mixture of (+)-**4** and (+)-**4**·3 H_2O (yield approx. 88%). The formation of (+)-**4** (100% *ee*, 100% *de*) occurred stereospecifically. Compounds (+)-**4** and (+)-**4**·3 H_2O were obtained in pure form by mechanical sorting and then characterized.[5] The trihydrate was structurally characterized by X-ray diffraction on a single crystal;[6] this was not possible in the case of the water-free compound because of its poor crystal quality.

The molecular structure of (+)-**4** in the crystal of (+)-**4**·3 H_2O is shown in Figure 1. The coordination polyhedra sur-

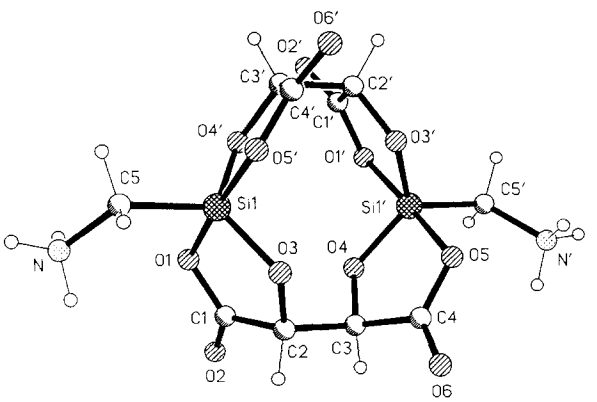


Fig. 1. Molecular structure of (+)-**4** in the crystal of (+)-**4**·3 H_2O. Selected distances [pm] and angles [°] (standard deviations in parentheses): Si1-O1 179.1(2), Si1-O3 167.5(2), Si1-O4′ 166.5(2), Si1-O5′ 182.0(2), Si1-C5 188.5(3), Si1′-O1′ 182.5(2), Si1′-O3′ 166.9(2), Si1′-O4 166.6(2), Si1′-O(5) 179.7(2), Si1′-C5′ 188.4(3); O1-Si1-O3 89.07(9), O1-Si1-O4′ 90.06(10), O1-Si1-O5′ 175.56(9), O1-Si1-C5 95.45(11), O3-Si1-O4′ 121.18(10), O3-Si1-O5′ 87.85(9), O3-Si1-C5 120.04(12), O4′-Si1-O5′ 88.79(9), O4′-Si1-C5 118.58(12), O5′-Si1-C5 88.87(11), O1′-Si1′-O3′ 88.21(9), O1′-Si1′-O4 88.87(9), O1′-Si1′-O5 175.13(9), O1′-Si1′-C5′ 89.28(11), O3′-Si1′-O4 122.57(10), O3′-Si1′-O5 88.68(9), O3′-Si1′-C5′ 120.23(11), O4-Si1′-O5 89.64(9), O4-Si1′-C5′ 117.06(11), O5-Si1′-C5′ 95.52(11).—The molecular symmetry of (+)-**4** may be described as approximately D_2 if the ammoniomethyl groups are ignored.

rounding the atoms Si1 and Si1′ can be described to a first approximation as slightly distorted trigonal bipyramids [transition trigonal bipyramid → square pyramid: 7.7% Si1; 10.6% Si1′],[7] in which each of the axial positions is occupied by carboxylate oxygen atoms. Several intermolecular N−H···O and O−H···O hydrogen bonds are present in the crystal structure of (+)-**4**·3 H_2O. The construction of the three-dimensional H-bonding system is complicated and characterized by a large acceptor excess (D/A ratio 12:30), such that generally only one of the acceptor sites on the oxygen atoms is used (exceptions: use of two acceptor sites by the carbonyl oxygen atoms O2, O2′, and O6′ as well as nonparticipation of the atoms O4, O4′, and O5′ in hydrogen bonding).

It follows from NMR spectroscopic investigations[8] that the zwitterionic binuclear complex (+)-**4** is also present in solution ([D_6]DMSO, D_2O). The presence of pentacoordinate Si atoms of the type SiO_4C is clearly indicated by the characteristic ^{29}Si chemical shifts ([D_6]DMSO: $\delta = -91.7$; D_2O: $\delta = -90.0$), and the presence of tetracoordinate N atoms of the ammonium type can be indirectly confirmed by the identification of the NH_3 group by ^1H NMR spectroscopy ([D_6]DMSO: $\delta = 7.1$).

The results presented here suggest that a rich complex chemistry of higher coordinate silicon in aqueous solution may be developed, in which diolato ligands derived from natural products (such as tartaric acid in this case) are of particular interest: it has been speculated in the literature[9] that silicon transport in biological systems might be based on higher coordinate Si species, and complexes such as the title compound could be of interest as model systems in this respect.

Experimental Procedure

(+)-**4**/(+)-**4**·3 H_2O: **3** [4] (800 mg, 4.14 mmol) was added to a stirred solution of (*R*,*R*)-(+)-tartaric acid (622 mg, 4.14 mmol) in water (120 mL) at room temperature. The resulting clear solution was concentrated at 60 °C/40 Torr to a volume of 100 mL and then allowed to stand undisturbed at room temperature for 96 h (formation of the first crystals ca. 24 h after the reactants were mixed). The solid formed was filtered off and washed with ethanol (3 × 10 mL) and then dried at room temperature in a nitrogen stream; yield 780 mg (ca. 88%) of a crystal mixture composed of (+)-**4** (colorless, thin needles) and (+)-**4**·3 H_2O (colorless rhombuses) in a ratio of roughly 2:1 (^1H NMR spectroscopic determination of the proportion of H_2O in the mixture). (+)-**4** and (+)-**4**·3 H_2O were isolated in pure form by mechanical sorting under the microscope.

(+)-**4**: M.p. > 350 °C; $[\alpha]_{589}^{20} = +86$ (DMSO, $c = 1.00$); correct C, H, N analysis; ^1H NMR ([D_6]DMSO): $\delta = 2.05$ (br. s, 2H; $SiCH_2N$), 4.15 (s, 4H; CH), 7.1 (br. s, 6H; NH); ^1H NMR (D_2O): $\delta = 2.56$ (br. s, 2H; $SiCH_2N$), 4.68 (s, 4H; CH); ^{13}C NMR ([D_6]DMSO): $\delta = 28.2$ ($SiCH_2N$), 75.5 (CH), 173.3 (C=O); ^{13}C NMR (D_2O): $\delta = 29.3$ ($SiCH_2N$), 77.7 (CH), 178.2 (C=O); ^{29}Si NMR ([D_6]DMSO): $\delta = -91.7$; ^{29}Si NMR (D_2O): $\delta = -90.0$; FAB-MS (glycerol as matrix, xenon as neutral gas), *m*/*z* (%): 409 (100) [$M - H^+$], 411 (100) [$M + H^+$].

(+)-**4**·3 H_2O: M.p. > 350 C; $[\alpha]_{589}^{20} = +84$ (DMSO, $c = 1.14$); correct C, H, N analysis. The ^1H, ^{13}C, and ^{29}Si NMR data and the FAB-MS data were identical with those obtained under the same measurement conditions as used for (+)-**4** [exception: an additional resonance signal in the ^1H NMR spectrum ([D_6]DMSO) at $\delta = 3.35$ (s, 6H; H_2O)].

Received: January 12, 1994 [Z 6609 IE]
German version: *Angew. Chem.* **1994**, *106*, 1250

[1] Reviews: a) W. S. Sheldrick in *The Chemistry of Organic Silicon Compounds, Part 1* (Eds.: S. Patai, Z. Rappoport), Wiley, Chichester, **1989**, pp. 227–303; b) R. R. Holmes, *Chem. Rev.* **1990**, *90*, 17–31; c) C. Chuit, R. J. P. Corriu, C. Reye, J. C. Young, *ibid.* **1993**, *93*, 1371–1448.

[2] Original publications: a) C. Strohmann, R. Tacke, G. Mattern, W. F. Kuhs, *J. Organomet. Chem.* **1991**, *403*, 63–71; b) R. Tacke, J. Sperlich, C. Strohmann, G. Mattern, *Chem. Ber.* **1991**, *124*, 1491–1496; c) R. Tacke, J. Sperlich, C. Strohmann, B. Frank, G. Mattern, *Z. Kristallogr.* **1992**, *199*, 91–98; d) R. Tacke, F. Wiesenberger, A. Lopez-Mras, J. Sperlich, G. Mattern, *Z. Naturforsch. B* **1992**, *47*, 1370–1376; e) R. Tacke, A. Lopez-Mras, J. Sperlich, C. Strohmann, W. F. Kuhs, G. Mattern, A. Sebald, *Chem. Ber.* **1993**, *126*, 851–861; f) R. Tacke, A. Lopez-Mras, W. S. Sheldrick, A. Sebald, *Z. Anorg. Allg. Chem.* **1993**, *619*, 347–358; g) J. Sperlich, J. Becht, M. Mühleisen, S. A. Wagner, G. Mattern, R. Tacke, *Z. Naturforsch. B* **1993**, *48*, 1693–1706; h) R. Tacke, A. Lopez-Mras, P. G. Jones, *Organometallics*, in press.

[3] Review: R. Tacke, J. Becht, A. Lopez-Mras, J. Sperlich, *J. Organomet. Chem.* **1993**, *446*, 1–8.

[4] Synthesis: J. E. Noll, J. L. Speier, B. F. Daubert, *J. Am. Chem. Soc.* **1951**, *73*, 3867–3871.

[5] The levorotatory antipode (−)-**4** [(−)-**4**·3 H_2O] can be obtained by the reaction of **3** with (*S*,*S*)-(−)-tartaric acid in an analogous manner.

[6] Crystal data for (+)-**4**·3 H_2O: $C_{10}H_{20}N_2O_{15}Si_2$, monoclinic, space group $P2_1$, $a = 815.2(3)$, $b = 1045.1(4)$, $c = 1089.1(3)$ pm, $\beta = 103.06(3)°$, $V = 0.9039(5)$ nm^3, $Z = 2$, $T = -130$ °C. A colorless prism (0.90 × 0.15 × 0.15 mm) was mounted in inert oil (type RS3000; donation from Riedel de Haën). 5624 Intensities were measured on a diffractometer (Stoe, type STADI-4) ($Mo_{K\alpha}$ radiation, $2\theta_{max} = 60°$), of which 5299 were independent ($R_{int} = 0.035$). The structure was solved by direct methods and refined on F^2 (program SHELXL-93, G. M. Sheldrick, Universität Göttingen). The final $R_w(F^2)$ value was 0.111, the conventional $R(F)$ value was 0.043 (for 282 parameters). The absolute configuration of (+)-**4** was confirmed by means of an *x* refinement [$x = 0.02(11)$] (cf. H. D. Flack, *Acta Crystallogr. Sect. A* **1983**, *39*, 876–881). Further details of the crystal structure investigation may be obtained from the Fachinformationszentrum Karlsruhe, D-76344 Eggenstein-Leopoldshafen (FRG) on quoting the depository number CSD-400670.

[7] The quantification of the distortion in this form relates to the transition from the ideal trigonal bipyramid toward the ideal square pyramid along the reaction coordinate of the Berry pseudorotation. The degree of distortion was calculated according to the dihedral angle method described in the literature [10], using the values given there for the reference geometry of the ideal square pyramid.

[8] Measurement conditions: 250.1 (^{1}H), 62.9 (^{13}C), and 49.7 MHz (^{29}Si); approx. 22 °C; [D$_5$]DMSO ($\delta = 2.49$) and $(CH_3)_3Si(CH_2)_3SO_3Na$ ($\delta = 0$) as internal ^{1}H standards in [D$_6$]DMSO or D$_2$O; [D$_6$]DMSO ($\delta = 39.90$) and $(CH_3)_3Si(CH_2)_3SO_3Na$ ($\delta = 0$) as internal ^{13}C standards in [D$_6$]DMSO or D$_2$O; TMS ($\delta = 0$) and $(CH_3)_3Si(CH_2)_3SO_3Na$ ($\delta = 0$) as internal ^{29}Si standards in [D$_6$]DMSO or D$_2$O.

[9] C. W. Sullivan in *Silicon Biochemistry* (Eds.: D. Evered, M. O'Connor), Wiley, Chichester, **1986**, pp. 59–89, and references therein.

[10] R. R. Holmes, J. A. Deiters, *J. Am. Chem. Soc.* **1977**, *99*, 3318–3326.

[$Zr_3Cp_2(O_2CNiPr_2)_6(\mu_3$-O)($\mu_2$-CCO)], the First Crystallographically Established Ketenylidene Complex; A Model for CO Reductive Cleavage on Metal Surfaces**

Fausto Calderazzo, Ulli Englert, Alessandro Guarini, Fabio Marchetti, Guido Pampaloni,* and Annalaura Segre

The formation of carbon–carbon bonds from the C_1 feedstock, CO, is a fundamental reaction in organometallic chemistry. Reductive coupling of CO to give fragments containing C-C multiple bonds has been reported.[1] In these reactions exhaustive transfer of oxygen from CO to cations of early transition metals, lanthanides, or actinides occurs. On the other hand, less extensive reductions of carbon monoxide occurs with alkali metals or solutions of them to yield $(CO)_n^{m-}$ species, $n = m = 2$;[2] $n = 4$, $m = 2$;[3] $n = m = 6$.[4] To our knowledge, only one case exists[5a] of the intermediate reduction of CO to the ketenylidene ligand, namely in the reaction of [Ta(tBu$_3$SiO)$_3$] with CO at low temperature and pressure, which gives an almost equimolar mixture of [TaO(tBu$_3$SiO)$_3$] and [Ta(CCO)(tBu$_3$SiO$_3$]; the latter compound is not isolated, but contains a terminal ketenylidene ligand according to spectroscopic data. The reaction of [Sm(C$_5$Me$_5$)$_2$(thf)$_2$] with CO was reported to yield the metal-substituted ketenecarboxylic acid in [Sm$_2$(C$_5$Me$_5$)$_4$(O$_2$CCCO)(thf)]$_2$.[5b]

In continuation of our studies on redox reactions with *N*,*N*-dialkylcarbamato complexes of transition elements,[6] we now report[7] that the reaction of [Cp$_2$Zr(CO)$_2$] with [Zr(O$_2$CNR$_2$)$_4$] (R = Et, *i*Pr) in refluxing toluene affords colorless crystals of the diamagnetic compounds **1a** (R = Et) and **1b** (R = *i*Pr) in satisfactory yields [Eq. (a)].

$$[Cp_2Zr(CO)_2] \xrightarrow{[Zr(O_2CNR_2)_4]} \underset{\mathbf{1}}{[Zr_3Cp_2(O_2CNR_2)_6(\mu_3\text{-}O)(\mu_2\text{-}CCO)]} \quad (a)$$

Compounds **1** are poorly soluble in aliphatic hydrocarbons and slightly soluble in aromatic hydrocarbons and THF. The μ-ketenylidene derivatives **1** are characterized by a sharp IR absorption at 2013 cm^{-1} (in toluene or as nujol mull), which shifts to 1951 cm^{-1} in the ^{13}C-labeled compound prepared from [Cp$_2$Zr(^{13}CO)$_2$] and [Zr(O$_2$CNiPr$_2$)$_4$], thus showing that the carbon atoms of the μ-ketenylidene ligand come from the carbonyl groups of the zirconium(II) complex. No shift of the 2013 cm^{-1} band is observed in the compound obtained from the reaction of [Cp$_2$Zr(CO)$_2$] with [Zr(O$_2$^{13}CNiPr$_2$)$_4$].

The ^{13}C NMR spectrum of the ^{13}C-labeled product [Zr$_3$Cp$_2$(O$_2$CNiPr$_2$)$_6$(μ_3-O)(μ_2-^{13}C^{13}CO)] shows two doublets at $\delta = 181.5$ and 112.4 ($J_{C,C} = 78.9$ Hz); the former resonance is assigned to the carbon adjacent to the oxygen atom of the ketenylidene ligand, in agreement with the reported values for bridging ketenylidene groups.[8]

Figure 1 shows the molecular structure[9] of **1b**, which consists of a μ_3-O-bridged triangle of zirconium atoms. Two of the metal atoms (Zr2 and Zr3) are coordinated to bridging carbamates and to the cyclopentadienyl and μ-CCO ligands; the third zirconium atom (Zr1) has bridging and terminal carbamato ligands. A similar essentially planar Zr_3 (μ_3-O) moiety has been observed[10] in [Zr$_3$Cp$_3$(μ_2-OH)(μ_3-O)(μ_2-PhCOO)$_3$]$^+$PhCOO$^-$ [Zr–O (mean value) 2.071(11) Å, Zr-O-Zr (mean value) 108.1(8)°; Zr···Zr (mean value) 3.354(12) Å; see caption to Fig. 1 for the corresponding values for **1b**]. The μ-ketenylidene ligand is substantially linear [C1-C2-O2, 179(1)°]; the C1-C2 and the C2-O2 bond lengths of 1.31(2) and 1.24(1) Å, respectively, are in accord with the reported values.[8]

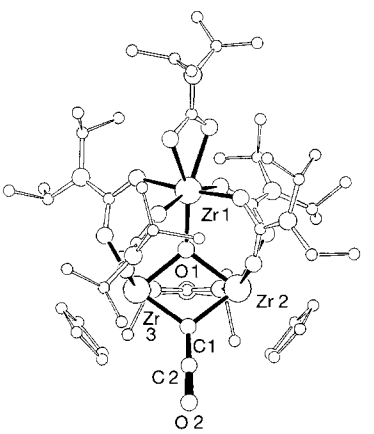


Fig. 1. Crystal structure of **1b** [19]. Selected distances [Å] and angles [°]: Zr1–O1 2.049(5), Zr2–O1 2.140(5), Zr3–O1 2.126(5), Zr2–C1 2.122(8), Zr3–C1 2.138(8), Zr···Zr (mean value) 3.597(1); Zr1-O1-Zr2 125.0(2), Zr1-O1-Zr3 130.0(3), Zr2-O1-Zr3 103.8(2), O1-Zr2-C1 73.7(2), O1-Zr3-C1 73.6(2), Zr2-C1-Zr3 104.0(4), Zr2-C1-C2 126.8(8), Zr3-C1-C2 128.1(8).

The ketenylidene ligand has been assembled around a transition metal cation by four synthetic methods: a) reductive dehalogenation or dehalogenation of a metal-coordinated C–X_n fragment, such as the dehalogenation[11] of [Co$_3$(CO)$_9$C–Cl] by AlCl$_3$ in the presence of CO; b) reductive cleavage (by an external reducing agent such as an alkali metal) in a trinuclear or tetranuclear metal cluster of a CO *single* bond obtained by a preliminary electrophilic activation of a metal-coordinated carbonyl group;[12] c) reaction of a low-valent metal complex with C_3O_2;[13] d) carbonylation of a diazomethyl complex.[14] Furthermore, a silver ketenylidene complex has been prepared[15] from a silver salt and ketene or ketene precursors. The isolation of compounds **1** corresponds to a new preparative method by which the Zr-coordinated carbonyl groups are reduced to the μ_2-ketenylidene ligand without addition of an external reducing agent. The four reducing equivalents required by this process ($2CO \rightarrow C_2O + O$) are provided by zirconium(II).

The proximity of the metal atoms in **1** may establish similar conditions to those at a metal surface on which an analogous process might take place. The simplicity and the high chemoselectivity of the reaction reported in this paper, and the high

[*] Prof. G. Pampaloni, Prof. F. Calderazzo, Dr. F. Marchetti
Dipartimento di Chimica e Chimica Industriale,
Sezione di Chimica Inorganica
Via Risorgimento 35, I-56126 Pisa (Italy)
Telefax: Int. code + (50) 20237

Dr. U. Englert
Institut für Anorganische Chemie der Technischen Hochschule Aachen (FRG)

Dr. A. Guarini
ENIChem, Istituto Guido Donegani, Novara (Italy)

Dr. A. Segre
Istituto C. N. R. di Strutturistica Chimica "G. Giacomello", Roma (Italy)

[**] This work was supported by the Consiglio Nazionale delle Ricerche (CNR, Roma), Progetto Finalizzato Chimica Fine II. The authors wish to thank Prof. A. Zecchina, Università di Torino, for helpful discussions.

stability of the μ_2-*bridged* ketenylidene ligand characterized by a strong IR stretching band in the same region as that of terminal metal-coordinated carbonyl groups suggest that metal surfaces or reduced metal oxides may lead more frequently than originally thought to surface-coordinated ketenylidene groups as intermediates or end products of the CO chemisorption process.[16] Thus the earlier suggestions[5, 8, 12] that ketenylidene might be a surface-bonded species are considerably strengthened by these novel findings. IR-active $\geq C=C=O$ sequences absorbing around 2100 cm^{-1} were postulated for carefully dehydrated MgO exposed to carbon monoxide.[17]

In agreement with the nucleophilic character of the α carbon atom in organic ketenes,[18] the zirconium(IV) complex **1b** reacts with substrates containing the $\geq C=O$ group. With carbon dioxide, after appropriate workup, the μ-oxo derivative **2** was isolated and characterized by elemental analysis, ^{13}C NMR spectroscopy, and mass spectrometry (protonated molecular ion: $m/z = 1297$). X-ray diffraction data on **2** show the com-

$[Zr_3Cp_2(O_2CN\mathit{i}Pr_2)_6(\mu_3\text{-}O)(\mu_2\text{-}O)]$ **2**

pound to have a substantially similar structure to **1b** in which the μ_2-CCO group of **1b** is replaced by the μ_2-oxo ligand. The reaction of the ^{13}C-labeled **1b**, $[Zr_3Cp_2(O_2CN\mathit{i}Pr_2)_6(\mu_3\text{-}O)(\mu_2\text{-}{}^{13}C{}^{13}CO)]$, with acetone led, inter alia, to the same $(\mu_3\text{-}O)(\mu_2\text{-}O)$ derivative as in the reaction with CO_2, and to the compounds $Me_2C={}^{13}CH{}^{13}C(O)N\mathit{i}Pr_2$, $\mathit{i}Pr_2N{}^{13}C(O){}^{13}CH_3$, and $\mathit{i}Pr_2N{}^{13}C(O){}^{13}CH_2C(OH)Me_2$ detected by GC-MS, which clearly contain the ketenylidene fragment. Mesityloxide was found among the volatile products.

Experimental Procedure

All experiments were performed under an inert atmosphere of argon, unless otherwise stated. IR, ^1H and ^{13}C NMR spectra, and mass spectra (desorption chemical ionization with isobutane as the reagent gas) were measured with Perkin Elmer FT 1725X, Varian Gemini 200, Bruker AM 200, and Finnigan MAT 8400 double-focusing reverse-geometry instruments, respectively. Satisfactory elemental analyses were obtained for all compounds reported in this paper.

1: Only the preparation of the compound with R = *i*Pr is described in detail. The ethyl derivative was prepared analogously. A solution of $[ZrCp_2(CO)_2]$ (8.08 g, 29.1 mmol) and $[Zr(O_2CN\mathit{i}Pr_2)_4]$ (19.3 g, 28.9 mmol) in toluene (250 mL) was heated at reflux for 1.5 h. After cooling to room temperature, an IR spectrum of the solution revealed a strong absorption band at 2013 cm^{-1}. After filtration of some dark insoluble material and evaporation of about 150 mL of toluene under reduced pressure, a colorless crystalline solid precipitated, which was filtered off, washed with toluene (5 × 10 mL), and dried in vacuo at room temperature (8.67 g). The diamagnetic solid was identified as **1b**. IR (Nujol and polychlorotrifluoroethylene mulls): $\tilde{\nu}$ = 3110 m-w, 2970 m-s, 2930 m, 2870 w, 2013 s, 1964 w, 1580 w, 1530 vs, 1510 vs, 1385 s, 1360 vs, 1210 m, 1160 m-w, 1135 w, 1075 m, 1020 m-w, 900 w, 870 w, 820 m, 800 m-s, 785 vs, 730 m-w, 680 m-s, 660 w, 600 m-s, 570 m-s, 530 m-s and 470 m-w cm^{-1}; IR(THF): $\tilde{\nu}$ = 2015 cm^{-1}; IR(CH_2Cl_2): $\tilde{\nu}$ = 2010 cm^{-1}. ^1H NMR ([D_6]-benzene, 20 °C, TMS): 6.7 (10 H, s), 3.8 (6 H, multiplet), 1.2 (72 H, multiplet). ^{13}C NMR ([D_8]toluene, 20 °C, TMS): 181.5 (d, *C*CO); 169.5, 162.4, 161.0 (s, CO_2); 112.4 (d, *C*CO); 114 (s, Cp); 46.9, 45.7 [s, $CH(CH_3)_2$]; 22 (s, CH_3, partial overlap with the solvent). A further corp (2.3 g) of the spectroscopically pure compound was obtained from the filtrate by reduction of the volume of the solution to 25 mL and addition of heptane (25 mL). The resulting pale brown solid was filtered and washed with heptane (about 10 × 30 mL) (43% overall yield based on the total zirconium). The average yield on a set of fifteen preparations is around 50%.

Received: June 4, 1993
Revised: December 29, 1993 [Z 6125 IE]
German version: *Angew. Chem.* **1994**, *106*, 1254

[1] E. M. Carnahan, J. D. Protasiewicz, S. J. Lippard, *Acc. Chem. Res.* **1993**, *26*, 90–97; J. D. Protasiewicz, S. J. Lippard, *J. Am. Chem. Soc.* **1991**, *113*, 6564–6570; R. N. Vrtis, S. J. Lippard, *Isr. J. Chem.* **1990**, *30*, 331–341; P. A. Bianconi, I. D. Williams, M. P. Engeler, S. J. Lippard, *J. Am. Chem. Soc.* **1986**, *108*, 311–313, and references therein.

[2] E. Weiss, W. Büchner, *Helv. Chim. Acta* **1963**, *46*, 1121–1127; W. Büchner, *ibid.* **1965**, *48*, 1229–1236.

[3] G. Silvestri, S. Gambino, G. Filardo, M. Guainazzi, R. Ercoli, *Gazz. Chim. Ital.* **1972**, *102*, 818–821; P. W. Lednor, P. C. Versloot, *J. Chem. Soc. Chem. Commun.* **1983**, 284–285.

[4] J. Liebig, *Ann. Chem. Pharm.* **1834**, *11*, 82; A. Joannis, *C. R. Hebd. Seances Acad. Sci.* **1914**, *158*, 874–879.

[5] a) D. R. Neithamer, R. E. Lapointe, R. A. Wheeler, D. R. Richerson, G. D. Van Duyne, P. T. Wolczanski, *J. Am. Chem. Soc.* **1989**, *111*, 9056–9072; b) W. J. Evans, J. W. Grate, L. A. Hughes, H. Zhang, J. L. Atwood, *ibid.* **1985**, *107*, 3728–3730.

[6] F. Calderazzo, G. Pampaloni, M. Sperrle, U. Englert, *Z. Naturforsch. B* **1992**, *42*, 389–394, and references therein.

[7] A preliminary account of this work has been reported: F. Calderazzo, G. Pampaloni, F. Marchetti, *Primo Congresso del Gruppo Interdivisionale di Chimica Organometallica*, Camerino, Italy, September 9–12, **1992**, p. 21.

[8] G. L. Geoffroy, S. L. Bassner, *Adv. Organomet. Chem.* **1992**, *28*, 1–83.

[9] **1b**: Crystal data: $C_{54}H_{94}N_6O_{14}Zr_3 \cdot 0.5$ toluene, $M = 1371$, triclinic, space group $P\bar{1}$ (no. 2), $a = 13.636(5)$, $b = 13.634(5)$, $c = 20.882(5)$ Å, $\alpha = 92.55(2)$, $\beta = 97.61(2)$, $\gamma = 114.56(2)°$, $V = 3478(4)$ Å^3, $Z = 2$, $\rho = 1.309$ g cm^{-3}. Enraf-Nonius CAD4 diffractometer; $\lambda = 0.7107$ Å; $\mu(MoK_\alpha) = 4.90$ cm^{-1}, $F(000) = 1434$, $T = 263$ K, $R = 0.064$, $R_w = 0.076$, GOF = 1.897 for 5340 independent absorption-corrected intensities with $I > 3\,\sigma(I)$ and $3 < \theta < 25.0°$ for 739 parameters. One of the carbamate ligands (N4, C41–C47) is disordered [19].

[10] U. Thewalt, K. Döppert, W. Lasser, *J. Organomet. Chem.* **1986**, *308*, 303–309.

[11] D. Seyferth, G. H. Williams, C. L. Nivert, *Inorg. Chem.* **1977**, *16*, 758–765.

[12] D. F. Shriver, M. J. Sailor, *Acc. Chem. Res.* **1988**, *21*, 374–379, and references therein.

[13] G. Paiaro, L. Pandolfo, *Comments Inorg. Chem.* **1991**, *12*, 213–235, and references therein.

[14] E. Deydier, M. J. Menu, M. Dartiguenave, Y. Dartiguenave, *J. Organomet. Chem.* **1993**, *458*, 225–228.

[15] D. Bryce-Smith, *Chem. Ind.* **1975**, 154–157; E. T. Blues, D. Bryce-Smith, R. Shaoul, H. Hirsch, M. J. Simons, *J. Chem. Soc. Perkin Trans. 2* **1993**, 1631–1642.

[16] R. R. Ford, *Adv. Catal.* **1970**, *21*, 51–150. For recent studies on the chemistry of CO on surfaces: P. Basu, D. Panayotov, J. T. Yates, *J. Am. Chem. Soc.* **1988**, *110*, 2074–2081; T. Mizushima, K. Tohji, Y. Udagawa, A. Ueno, *ibid.* **1990**, *112*, 7887–7893; S. L. Yan, X. Gao, S. C. Chang, B. C. Schardt, M. J. Weaver, *ibid.* **1991**, *113*, 6049–6056; J. Lin, P. Jones, E. I. Salomon, *ibid.* **1991**, *113*, 8312–8326; J.-W. He, W. K. Kuhn, D. W. Goodman, *ibid.* **1991**, *113*, 6416–6419; G. Blyholder, M. Lawless, *ibid.* **1992**, *114*, 5828–5832; A. Goursot, I. Papai, D. R. Salahub, *ibid.* **1992**, *114*, 7452–7458; P. A. Paredes Olivera, E. P. M. Leiva, E. A. Castro, A. J. Arvia, *J. Electroanal. Chem.* **1993**, *351*, 65–79.

[17] A. Zecchina, S. Coluccia, G. Spoto, D. Scarano, L. Marchese, *J. Chem. Soc. Faraday Trans.* **1990**, *86*, 703–709.

[18] *The Chemistry of Ketenes, Allenes and Related Compounds* (Ed.: S. Patai), Wiley, New York, **1980**.

[19] Further details of the crystal structure determination may be obtained from the Fachinformationszentrum Karlsruhe, D-76344 Eggenstein-Leopoldshafen (FRG), on quoting the depository number CSD-58071.

The Determination of Maximum Common Substructures by a Genetic Algorithm: Application in Synthesis Design and for the Structural Analysis of Biological Activity

Markus Wagener and Johann Gasteiger*

The comparison of the structures of two compounds is a widespread problem in chemistry, for instance, in the analysis of biological activity, in the search for promising starting materials for the synthesis of a target compound, in the elucidation of biosynthetic pathways, and in the determination of the atoms and bonds directly involved in a reaction. An essential task for the comparison is the determination of the largest substructure common to the two structures (maximum common substruc-

[*] Prof. Dr. J. Gasteiger, Dr. M. Wagener
Computer-Chemie-Centrum der Universität Erlangen-Nürnberg
Nägelsbachstrasse 25, D-91052 Erlangen (FRG)
Telefax: Int. code + (9131)85-6566

 © VCH Verlagsgesellschaft mbH, D-69451 Weinheim, 1994 0570-0833/94/1111-1189 $ 10.00+.25/0

ture; MCSS). Therefore, the search for an MCSS plays an important role in the computer-assisted processing of chemical information. This is reflected by the high number of publications suggesting solutions to this problem.[1] In the end, all methods have to explore the set of all possible solutions and provide different heuristics to keep the search within bounds. We will show here that the MCSS problem can also be solved by a genetic algorithm. This allows one to avoid a time-consuming systematic search and is thus particularly advantageous for larger structures.

Genetic algorithms (GA) are optimization methods that model mechanisms used by nature to adjust to a changing environment.[2] Initially, a number of randomly determined solutions (population) for a problem is given. These solutions are all approximations to the optimum sought, but differ in their "fitness". A set of genetic operators usually having an analogy in natural genetics is then iteratively applied to this population (Fig. 1).

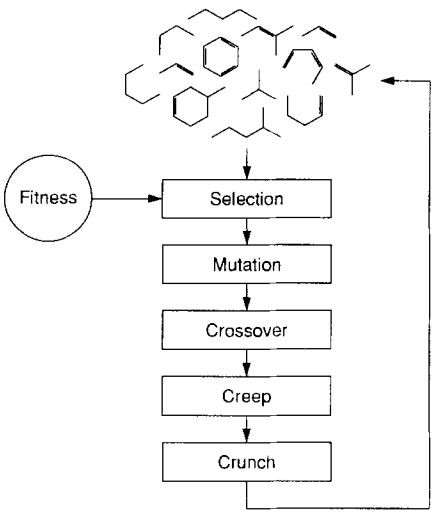


Fig. 1. Overview of the genetic algorithm used here. The boxes represent the genetic operators, and the population is indicated by the structure fragments.

The selection operator favors those solutions (individuals) for the next generation that have a high fitness value. This progressively reduces the number of unfavorable solutions, that is, those with a low fitness value, in the population. The other operators form new individuals with potentially better properties from the present population.

Genetic algorithms are robust and can therefore be applied to a host of problems.[2] However, in chemistry they have not yet found much use except in chemometric methods[3] and for the determination of the minimum chemical distance.[4]

In our method for searching for the maximum common substructure of two compounds by a genetic algorithm, bonds in the two molecules considered are assigned to each other. Such an assignment corresponds to an individual of the GA-population. This bond matching might represent a common substructure but need not. The fitness of such a bond matching is calculated by Equation (a).

$$F = N - V - (T_1 + T_2 - 2) \qquad \text{(a)}$$

N is the total number of bonds in the two structures that participate in the bond matching. V specifies how often two adjacent bonds in one structure are assigned to two nonadjacent bonds in the other structure. Thus, the higher the value of V, the worse the matching of the two substructures. T_1 and T_2 give the number of unconnected parts in the two structures. The value of 2 was introduced to ensure that F gives the number of matching bonds if a coherent and fitting substructure is found. The upper part of Figure 2 shows a comparison of cyclobutane and methylbutane. Bonds shown in bold are assigned to each other. Thus, bond b is assigned to bond 2 and bond c to bond 4, as also shown in the table to the right of the two structures. The other bonds of cyclobutane are not assigned to any bonds of methylbutane (indicated by an asterisk). The fitness value of -1 is calculated as follows: Altogether, four bonds are assigned to each other ($N = 4$). The two bonds are adjacent in cyclobutane but not in methylbutane and thus all four violate the neighborhood relationship ($V = 4$). The substructure in cyclobutane consists of only one part ($T_1 = 1$), but in methylbutane there are two fragments ($T_2 = 2$).

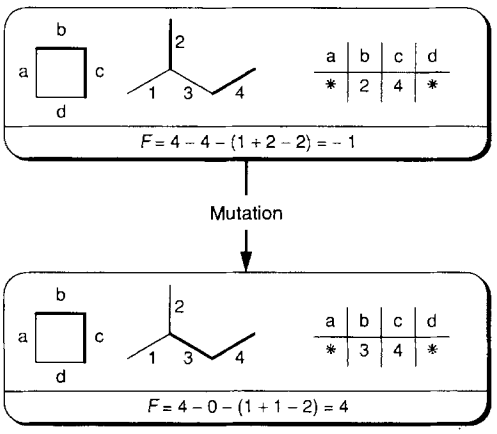


Fig. 2. The mechanism of the mutation operator: the assignment of bond b in cyclobutane to bond 2 in methylbutane is changed to an assignment to bond 3, which raises the fitness (F) from -1 to $+4$.

A population of such individuals consisting of pairs of mutually assigned structures is converted into a new population by five genetic operators: selection, mutation, crossover, creep, and crunch.[5] Selection uses a procedure[6] that reduces the number of stochastic errors relative to other selection methods. Mutation arbitrarily changes the assignment of one bond pair. Figure 2 shows how bond b is reassigned by mutation from bond 2 to bond 3 of methylbutane. This increases the fitness from -1 to $+4$. Crossover exchanges partial solutions in the form of partial structure assignments between two individuals. Figure 3 shows how the assignment of bond c to bond 4 is transferred from the right to the left individual and thus increases the common substructure.

Two additional operators, creep and crunch, that are specifically tailored to the problem at hand were developed to increase the efficiency of the MCSS search. They use information on the constitution of the structures investigated, quite in contrast to the classical operators mutation and crossover, and aim at individuals with higher fitness values. The creep operator increases the assignment of bonds by one bond pair if this is possible without violating neighborhood relationships in the two structures investigated (cf. the quantity V in the fitness function (a)). This is particularly helpful if only one bond pair is missing to the maximum common substructure. Thus, the last step of the global maximum can be made with the creep operator particularly easily.

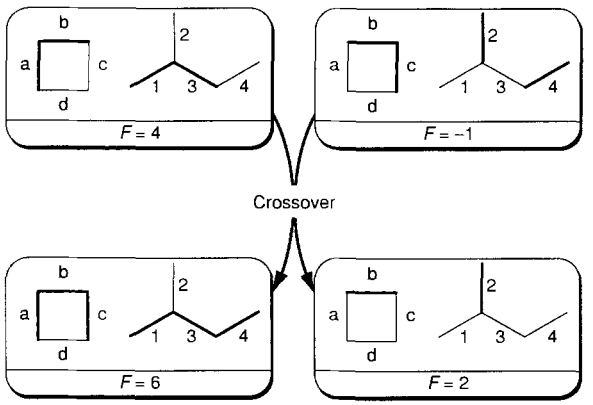


Fig. 3. The mechanism of the crossover operator: the assignment of bond c to bond 4 is transferred from the second pair of structures (individual) to the first.

The crunch operator, on the other hand, decreases the number of assigned bonds. If a partial structure is not contiguous the crunch operator will delete all bonds of the smallest fragment. In this way, local maxima that are quite often characterized by small disconnected fragments can safely be escaped.

Strong competition between the individuals of a population particularly in the initial phases of the optimization can result in finding only a local maximum due to early convergence. In order to avoid such a situation the population is divided into separate partial populations called niches. Competition then mainly occurs within a niche but is reduced between niches.

Genetic algorithms are methods that are driven by chance and consequently do not necessarily lead to the global optimum. Therefore, each substructure assignment problem was separately treated 50 times with different initializations of the populations in the following three examples. The results of these 50 separate runs allow an estimate of how safely the genetic algorithm finds the global optimum. The bond order (single, double, or triple bonds) of the assigned bonds was not considered in these studies in order to find substructures that are as large as possible. A single run of a genetic algorithm was performed for 400 generations. Each population comprised 100 individuals; the size of an individual was determined by the number of bonds in the larger of the two structures. Each of the following examples illustrates a different field of application.

The structural prerequisites of biological activity can be analyzed with this method. Figure 4 shows the two strong analgesics morphine (**1**) and methadone (**2**), and the MCSS (in bold, fitness 34.0) found in 48 of the 50 program runs. A program run took 20 s on a Sparc Station 10/20. The average fitness of the 50 runs was 33.9. Clearly, final conclusions on the biological activity can only be drawn by comparison of the three-dimensional structures. We are therefore working on an extension of the method for the determination of the maximum common three-dimensional substructure by a genetic algorithm.

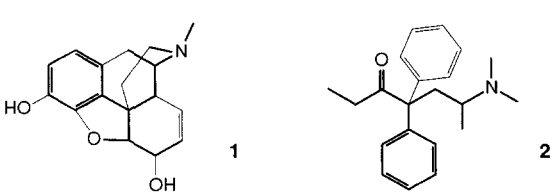


Fig. 4. The maximum common substructure of the two analgesics morphine (**1**) and methadone (**2**) indicated in bold.

The method can also be used for the analysis of biosynthetic pathways. Geissoschizine (**4**) is an important intermediate in the biosynthesis of the monoterpene alkaloids.[7] Figure 5 shows the largest substructure common to strychnine (**3**) and geissoschizine (**4**) (fitness 48.0) that was obtained in 31 of the 50 optimization experiments. The average fitness attained in 50 runs was 44.0. All details of the transformation of geissoschizine into the strychnos alkaloids are not yet known; the common substructure found here can give important hints worthy of further experimental investigations.

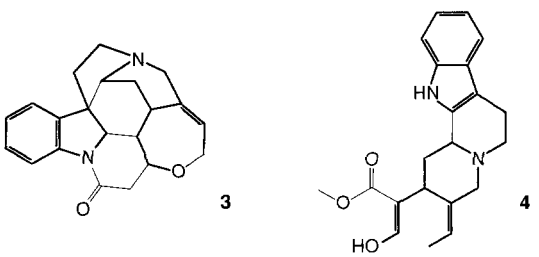


Fig. 5. The largest substructure common to strychnine (**3**) and geissoschizine (**4**).

The synthesis of strychnine by Woodward et al.[8] serves as an illustration of a search for appropriate starting materials for the synthesis of a desired target compound. Figure 6 shows the maximum common substructure between strychnine (**3**) and 2-veratrylindole (**5**) which was used as a starting material in the synthesis. A substructure of this size (fitness 34.0) was found 35 times in 50 program runs with an average fitness of 32.1. The common substructure nearly covers the entire skeleton of **5**, and therefore this compound is an attractive starting material. This high similarity was also utilized by Woodward et al. in their synthesis: all atoms of the MCSS in veratrylindole except the one marked by an asterisk were used as assigned by the genetic algorithm to build the skeleton of strychnine.

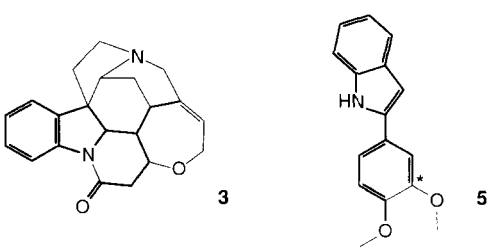


Fig. 6. The largest common substructure of strychnine (**3**) and 2-veratrylindole (**5**), a starting material in the synthesis of **3**.

The search for appropriate starting materials for a synthesis can also benefit from a search for duplicate substructures in one and the same molecule. This can indicate that instead of two different starting materials only one has to be made and used twice in the course of the synthesis. The larger the structure of the precursor that is used several times, the more efficient the synthesis strategy. Nature also often utilizes this principle; the most notable examples are the terpenes constructed from isoprene units.

The described genetic algorithm was extended to find the largest substructure contained twice in a molecule. The extended procedure works with the same fitness function [Eq. (a)] and with the genetic operators selection, mutation, crossover, creep and crunch as previously described. However, the way the sub-

structure is represented had to be changed in order to allow both substructures to be contained in a single molecule. This requires restrictions to prevent an atom or a bond from appearing in both substructures.

The search for the largest two identical substructures in badion A (**6**), the natural dye in the cap of *Xerocomus badius*,[9] with the extended genetic algorithm provides the result shown in Figure 7. The substructure contained twice in this molecule is highlighted in bold. This substructure corresponds to pulvinic acid (**7**), also found in *Xerocomus badius* and presumably an intermediate in the biosynthesis of badion A, which can be formed from it by oxidative dimerization.[10] The substructure shown in Figure 7 (fitness 54.0) was found 27 times in 50 runs of the genetic algorithm (average fitness 48.1).

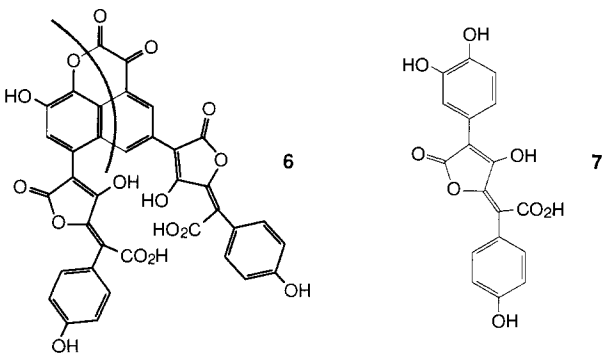


Fig. 7. Badion A (**6**) and the potential intermediate in its biosynthesis, pulvinic acid (**7**). The substructures shown in bold and separated by an arc were found by the genetic algorithm.

A systematic search in a reaction database was made to investigate how often this synthesis principle is used and which types of structures and reactions are employed. Six hundred reactions were selected randomly from the update 1991 of the Chem Inform-RX reaction database.[11] Among these the genetic algorithm found 30 reactions where a starting material was incorporated twice into the reaction product. One of these reactions, the condensation of an arene with formaldehyde, is shown in Figure 8. This example shows that the method also allows the analysis of reactions in which a molecule contains parts from starting materials other than the matching substructures.

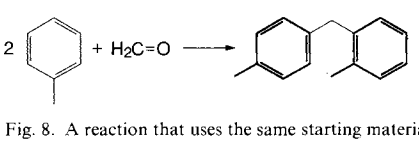


Fig. 8. A reaction that uses the same starting material twice. It is representative of the 30 reactions found in a systematic search in a randomly chosen part of the ChemInform-RX reaction database.

The example also illustrates that considerations of symmetry in a molecule do not suffice to decipher this synthesis strategy. It is only the search for the maximum matching substructures that enables planning of such syntheses.

Received: October 15, 1993
Revised: December 27, 1993 [Z 6421/6422 IE]
German version: *Angew. Chem.* **1994**, *106*, 1245

[1] G. Levi, *Calcolo* **1972**, *9*, 1–12; M. M. Cone, R. Venkataraghavan, F. W. McLafferty, *J. Am. Chem. Soc.* **1977**, *99*, 7668–7671; T. H. Varkony, Y. Shiloach, D. H. Smith, *J. Chem. Inf. Comput. Sci.* **1979**, *19*, 105–111; M. Bersohn, K. Mackay, *ibid.* **1979**, *19*, 137–141; J. J. McGregor, P. Willett, *ibid.* **1981**, *21*, 137–140; J. J. McGregor, *Software – Practice and Experience* **1982**, *12*, 23–34; M. Bersohn, *J. Chem. Soc. Perkin Trans 1* **1982**, 631–637; H. Scribrany, K. Varmuza, *Fresenius J. Anal. Chem.* **1992**, *334*, 220–222; L. Chen, W. Robien, *J. Chem. Inf. Comput. Sci.* **1992**, *32*, 501–506.

[2] D. E. Goldberg, *Genetic Algorithms in Search, Optimization, and Machine Learning*, Addison-Wesley, Reading, MA, **1989**.

[3] D. Wienke, C. Lucasius, G. Kateman, *Anal. Chim. Acta* **1992**, *265*, 211–225; M. Bos, H. T. Weber, *ibid.* **1991**, *247*, 97–105; T. Li, C. Lucasius, G. Kateman, *ibid.* **1992**, *268*, 123–134; C. Lucasius, G. Kateman, *TrAC Trends Anal. Chem. Pers. Ed.* **1991**, *10*, 254–261.

[4] E. Fontain, *Anal. Chim. Acta* **1992**, *265*, 227–232; *J. Chem. Inf. Comput. Sci.* **1992**, *32*, 748–752.

[5] Details of the optimization of this method will be published in *J. Comput. Chem.*

[6] J. E. Baker in *Genetic Algorithms and their Applications: Proceedings of the Second International Conference on Genetic Algorithms* (Ed.: J. J. Grefenstette), Lawrence Erlbaum, Hillsdale, NJ, **1987**, p. 14.

[7] D. R. Dalton, *The Alkaloids*, Marcel Dekker, New York, **1979**.

[8] R. B. Woodward, M. P. Cava, W. D. Ollis, A. Hunger, H. U. Daeniker, K. Schenker, *Tetrahedron* **1963**, *19*, 247–288.

[9] B. Steffan, W. Steglich, *Angew. Chem.* **1984**, *96*, 435–437; *Angew. Chem. Int. Ed. Engl.* **1984**, *23*, 445–447.

[10] W. Steglich, H.-T. Huppertz, B. Steffan, *Angew. Chem.* **1985**, *97*, 716–717; *Angew. Chem. Int. Ed. Engl.* **1985**, *24*, 711–712.

[11] A. Parlow, C. Weiske, J. Gasteiger, *J. Chem. Inf. Comput. Sci.* **1990**, *30*, 400–402; J. Gasteiger, C. Weiske, *Nachr. Chem. Tech. Lab.* **1992**, *40*, 1114–1120; the ChemInform-RX reaction database is produced by FIZ CHEMIE, Berlin, and by Bayer AG, Leverkusen.

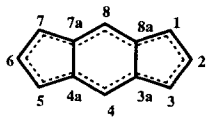
s-Indacene: A Delocalized, Formally Antiaromatic 12 π Electron System**

Roland H. Hertwig, Max C. Holthausen, Wolfram Koch,* and Zvonimir B. Maksić

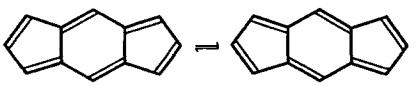
s-Indacene is a planar, conjugated, tricyclic hydrocarbon with 12 π electrons. Formally it can be considered as a [12]annulene perturbed by two cross links or alternatively as a molecule obtained by fusion of two fulvenes (Scheme 1). According to the Hückel ($4n + 2$) rule it is an antiaromatic system.[1] Thus, the equilibrium structure of the lowest energy singlet state is expected to be C_{2h}-symmetric with localized double bonds (**2**) and not D_{2h}-symmetric with a delocalized π electron system (**1**).[2] Indeed, in early HMO[3] and semiempirical studies[4] on the equilibrium structure of *s*-indacene the localized structure was found to be more stable than the delocalized one. This conclusion was very recently supported by Gellini et al. by Hartree–Fock (HF) MO calculations using medium-sized basis sets.[5] The authors arrive at an energy difference of 5.6 kcal mol^{-1} in favor of the C_{2h} structure **2**. However, unsubstituted *s*-indacene is extremely reactive and decomposes immediately,[6] and structural investigation by X-ray diffraction is not possible. In addition, the

[*] Prof. Dr. W. Koch, Dipl.-Chem. R. H. Hertwig,
Dipl.-Chem. M. C. Holthausen
Institut für Organische Chemie der Technischen Universität
Strasse des 17. Juni 135, D-10623 Berlin (FRG)
Telefax: Int. code + (30)314-21102
Prof. Dr. Z. B. Maksić
Ruđer Bošković Institute
Bijenička 54, HR-41001 Zagreb (Croatia)

[**] This research was supported by the Gesellschaft von Freunden der TU Berlin and the Fonds der Chemischen Industrie. Excellent service, in particular by Dr. T. Steinke, and a generous amount of computing time was provided by the Konrad-Zuse Zentrum für Informationstechnik Berlin.



1, D_{2h}



2, C_{2h} **2**, C_{2h}

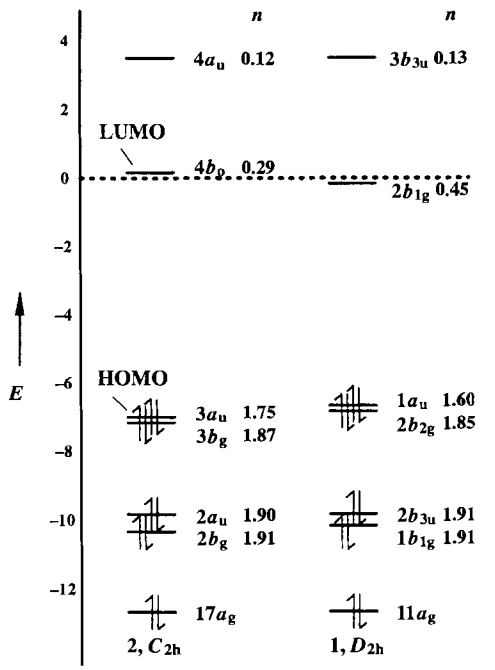
Scheme 1. Delocalized (D_{2h}-symmetric) and localized (C_{2h}-symmetric) forms of *s*-indacene.

reported calculations are not at a level high enough to allow for an unambiguous conclusion, and hence the exact equilibrium structure of *s*-indacene is still not known. It was pointed out that substitution at symmetry-equivalent positions can lead to greater delocalization of the π electrons.[1, 4, 7] The most prominent example is 1,3,5,7-tetra-*tert*-butyl-*s*-indacene, whose carbon skeleton has effective D_{2h} symmetry according to the X-ray structure analysis reported by Hafner et al.;[4] this structure was later confirmed by Dunitz et al.[8] In addition, only four peaks appear in ^{13}C NMR spectrum for the 12 carbon atoms in the ring system, even at −130° C.[4] It is possible that the crystal structure obtained does not correspond to the ground state, but to the saddle of the valence isomerization, owing to the stabilization afforded by crystal packing effects.[8] However, the NMR results can be explained only by a very low energy barrier between the two degenerate C_{2h} valence isomers or by a completely delocalized π electron system.

A qualitative rationalization of the substituent effect on the delocalization in such systems has recently been given by Heilbronner and Yang using simple HMO theory.[7] Their model indeed shows that 1,3,5,7-tetra-*tert*-butyl-*s*-indacene should have a stronger tendency towards delocalization than the parent *s*-indacene; however this model provides no clear-cut answer to whether *s*-indacene prefers a localized or delocalized structure. *s*-Indacene is a borderline case, and it appears that its geometrical structure depends on subtle details of the electron density distribution.

We report here on our high-level quantum chemical calculations on the equilibrium structure of the lowest energy singlet state of *s*-indacene. We tackled this problem using two independent theoretical approaches: conventional ab initio methods with inclusion of correlation effects,[9] and methods based on density functional theory, in which electron correlation is implicitly contained in the functional used.[10]

Inspection of the computed (HF/6-31G*[11]) orbital energies shows that the simple, one determinant based picture of HF theory is probably not adequate for a proper description of the electronic structures of **1** and **2**. The energy of the highest occupied molecular orbital (HOMO) is relatively high, whereas the energy of the lowest unoccupied molecular orbital (LUMO) is around 0 eV and thus very low. Hence, the Slater determinant corresponding to the excitation of two electrons from the HOMO to the LUMO can be expected to be an important contributor to the ground-state wave function. Complete active space SCF (CASSCF) calculations for MP2-6-31G* optimized geometries[12] in which all possible distributions of 12 π electrons are considered for the 12 MOs constructed from the carbon $2p_z$ orbitals revealed that the electronic structure of both isomers of *s*-indacene is indeed very complex. The HF determinants of **1** and **2** have a weight of only 64 and 71%, respectively. Excitations to the LUMO are very prominent; this formally empty orbital is occupied with 0.45 (**1**) and 0.29 electrons (**2**), and the next orbital is also partially occupied (>0.1 electrons; Scheme 2). At the CASSCF level **2** is predicted to be 5.7 kcal mol^{-1} more stable than **1**.[13]



Scheme 2. Orbital energies *E* [eV] (HF/6-31G*), symmetries, and occupation numbers *n* [electrons] of natural orbitals (CASSCF/6-31G*) of **1** and **2**.

The qualitative implication of this result is that **1** and **2** are not pure closed-shell systems but have substantial singlet diradical character. The CASSCF treatment, however, accounts only for the energetic near-degeneracy of Slater determinants, the so-called nondynamic electron correlation, but not for dynamic electron correlation. Further refinement of the level of theory is required for accurate results. Thus, in a subsequent step we computed the energies of **1** and **2** by using the CASPT2 method, a multireference version of second-order many-body perturbation theory developed recently by Roos et al.,[14] in which all but the carbon 1s electrons are correlated. The full CASSCF wavefunction was used as reference space in the CASPT2 calculations. At this level both the multireference character of the wavefunction and the dynamic electron correlations are included. At this highest ab initio MO level the delocalized, D_{2h}-symmetric form **1** of *s*-indacene is 3.1 kcal mol^{-1} *more* stable than its localized, C_{2h} counterpart.[15]

In our second set of calculations we used density functional theory employing the local density approximation (LDA) with local Slater exchange functional and correlation functional parametrization on the homogeneous electron gas of Vosko, Wilk, and Nusair.[16] Nonlocal gradient corrections according to Becke[17] and Perdew[18] (LDA + BP) for exchange and correlation, respectively, were also added. Here, nondynamic as well as dynamic electron correlation is implicitly accounted for through the form of the functional used. For example, whereas HF calculations on azulene erroneously give a localized, C_s-symmetric equilibrium structure, LDA plus nonlocal corrections yields the

correct, delocalized structure.[19] With both approximations, LDA and LDA + BP, optimizations of **1** and **2** starting from the MP2/6-31G* structures lead only to the delocalized structure **1**. A C_{2h}-symmetric minimum structure corresponding to **2** was not found. Determination of the harmonic frequencies at the LDA + BP level by numerical differentiation of the analytical gradients showed that **1** is indeed a minimum structure with only real frequencies.

The structural parameters of **1** as determined by MP2/6-31G* and LDA + BP are summarized in Table 1 and compared to the X-ray structure data of 1,3,5,7-tetra-*tert*-butyl-*s*-indacene. Even though the *tert*-butyl substituents certainly influence the geometry of 1,3,5,7-tetra-*tert*-butyl-*s*-indacene, the agreement between the experimental and computed data is excellent. The root mean square deviations for the C–C bonds are only 0.005 Å (MP2) and 0.006 Å (LDA + BP), and the differences between the two methods are only marginal.

Table 1. Calculated bond lengths [Å] and angles [°] of **1** and the data from the X-ray structure analysis of 1,3,5,7-tetra-*tert*-butyl-*s*-indacene [8].

Parameter	MP2/6-31G*	LDA + BP/TZP	Exp. [a]
C(1)-C(2)	1.404	1.408	1.406, 1.408
C(3)-C(3a)	1.429	1.427	1.434, 1.438
C(3a)-C(4)	1.397	1.401	1.394, 1.395
C(3a)-C(8a)	1.437	1.445	1.442
C(1)-H	1.087	1.091	
C(2)-H	1.085	1.089	
C(4)-H	1.092	1.095	
C(1)-C(2)-C(3)	108.6	108.5	110.8
C(2)-C(3)-C(3a)	108.5	108.7	106.8, 106.9
C(3)-C(3a)-C(8a)	107.2	107.1	107.6, 107.9
C(4)-C(3a)-C(8a)	120.9	120.9	120.4
C(3a)-C(4)-C(4a)	118.1	118.2	119.2
C(8a)-C(1)-H	125.5	125.5	
C(1)-C(2)-H	125.7	125.8	
C(3a)-C(4)-H	120.9	120.9	

[a] Since the X-ray structure does not show strict D_{2h} symmetry, two values are given for one parameter where necessary.

Since the conventional ab initio MO method and the approach based on density functional theory converge to give the same answer concerning the structure of *s*-indacene, we conclude that the equilibrium structure of *s*-indacene has D_{2h} symmetry and a completely delocalized 12 π electron system, despite its formal classification as a $4n$ π antiaromatic system. It follows that the D_{2h}-symmetric X-ray structure of 1,3,5,7-tetra-*tert*-butyl-*s*-indacene is not a "frozen transition state"[8] but corresponds to the ground state structure of this molecule. The high reactivity and elusiveness of *s*-indacene can most likely be explained by its considerable singlet diradical character.

Received: December 15, 1993 [Z 6563 IE]
German version: *Angew. Chem.* **1994**, *106*, 1252

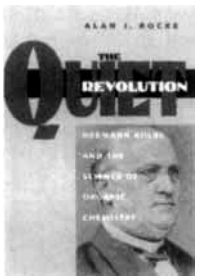
[1] Reviews on nonbenzoid, polycyclic, conjugated π electron systems: K. Hafner, *Angew. Chem.* **1963**, *75*, 1041; *Angew. Chem. Int. Ed. Engl.* **1964**, *3*, 165; *Pure Appl. Chem. Suppl.* **1971**, *2*, 1. For a recent, systematic, theoretical investigation of nonalternant hydrocarbons, including *s*-indacene, see: M. C. Böhm, J. Schütt, *J. Phys. Chem.* **1992**, *96*, 3674.
[2] We use the term "delocalized" in the sense that alternating single and double bonds are not present. It does not imply that *all* C–C bonds have equal lengths, as in benzene.
[3] T. Nakajima, T.Saijo, H. Yamaguchi, *Tetrahedron* **1964**, *20*, 2119.
[4] K. Hafner, B. Stowasser, H.-P. Krimmer, S. Fischer, M. C. Böhm, H. J. Lindner, *Angew. Chem.* **1986**, *98*, 646; *Angew. Chem. Int. Ed. Engl.* **1986**, *25*, 630.
[5] C. Gellini, G. Cardini, P. R. Salvi, G. Marconi, K. Hafner, *J. Phys. Chem.* **1993**, *97*, 1286.
[6] K. Hafner, K. H. Häfner, C. König, M. Kreuder, G. Ploss, G. Schulz, E. Sturm, K. H. Vöpel, *Angew. Chem.* **1963**, *75*, 35; *Angew. Chem. Int. Ed. Engl.* **1963**, *2*, 123.
[7] E. Heilbronner, Z.-z. Yang, *Angew. Chem.* **1987**, *99*, 369; *Angew. Chem. Int. Ed. Engl.* **1987**, *26*, 360; E. Heilbronner, *J. Chem. Educ.* **1989**, *66*, 471.
[8] J. D. Dunitz, C. Krüger, H. Irngartinger, E. F. Maverick, Y. Wang, M. Nixdorf, *Angew. Chem.* **1988**, *100*, 415; *Angew. Chem. Int. Ed. Engl.* **1988**, *27*, 387.
[9] The Hartree-Fock and MP2 calculations were performed using Gaussian 92 [20] with a standard 6-31G* basis set. The CASSCF and CASPT2 energy determinations used the same basis set and were performed with the MOLCAS-2 program package [21]. The number of configuration state functions included in the CASSCF wavefunction was 56928 for **1** and 113456 for **2**. Since geometry optimizations were not possible at these levels, the CASSCF and CASPT2 energy calculations were based on the MP2/6-31G* geometries.
[10] The density functional calculations were performed using ADF, Version 1.0.2 [22]. An uncontracted triple ζ-STO basis set, which was augmented with one 3d (2p) and one 4f (3d) polarization function for carbon (hydrogen) was used (TZP). The carbon 1s electrons were treated in the frozen core approximation. The total molecular electron density was fitted in each SCF iteration by an auxiliary basis set of s, p, d, f, and g STO functions.
[11] At the HF/6-31G* level **2** is computed to be more stable than **1** by 9.2 kcal mol^{-1}; E_{tot} (**2**) = −459.00322 Hartree.
[12] At the MP2/6-31G* level **2** is computed to be more stable than **1** by 0.7 kcal mol^{-1}; E_{tot} (**2**) = −460.52091 Hartree.
[13] The total energy of **2** at this this level is −459.16212 Hartree.
[14] K. Anderson, P.-Å. Malmqvist, B. O. Roos, A. J. Sadlej, K. Wolinksi, *J. Phys. Chem.* **1990**, *94*, 5483; K. Anderson, P.-Å. Malmqvist, B. O. Roos, *J. Chem. Phys.* **1992**, *96*, 1218.
[15] The total energy of **1** at this this level is −460.53367 Hartree.
[16] S. H. Vosko, L. Wilk, M. Nusair, *Can. J. Phys.* **1980**, *58*, 1200.
[17] A. D. Becke, *Phys. Rev. A* **1988**, *38*, 2398.
[18] J. P. Perdew, *Phys. Rev. B* **1986**, *33*, 8822.
[19] N. C. Handy, personal communication; N. C. Handy, R. D. Amos, *Science*, in press.
[20] M. J. Frisch, G. W. Trucks, M. Head-Gordon, P. M. W. Gill, M. W. Wong, J. B. Foresman, B. G. Johnson, H. B. Schlegel, M. A. Robb, E. S. Replogle, R. Gomperts, J. L. Andres, K. Raghavachari, J. S. Binkley, C. Gonzalez, R. L. Martin, D. J. Fox, D. J. DeFrees, J. Baker, J. J. P. Stewart, J. A. Pople, *Gaussian 92*, Rev. A; Gaussian Inc. Pittsburgh, PA, **1992**.
[21] K. Andersson, M. R. A. Blomberg, M. P. Fülscher, V. Kellö, R. Lindh, P.-A. Malmqvist, J. Noga, J. Olsen, B. O. Roos, A. J. Sadlej, P. E. M. Siegbahn, M. Urban, P.-O. Widmark, *MOLCAS*, Version 2, University of Lund, Sweden, **1991**.
[22] G. te Velde, E. J. Baerends, *Amsterdam Density Functional (ADF)*, Release 1.0.2, Dept. of Theoretical Chemistry, Vrije Universiteit, Amsterdam, The Netherlands, **1993**.

 © VCH Verlagsgesellschaft mbH, D-69451 Weinheim, 1994 0570-0833/94/1111-1194 $ 10.00+.25/0

Controversial Life Now Acclaimed

The Quiet Revolution: Hermann Kolbe and the Science of Organic Chemistry. By *A. J. Rocke*. University of California Press, Berkeley, 1993. XIII, 501 pp., hardcover $ 50.00.—ISBN 0-520-08110-2

Adolf Wilhelm Hermann Kolbe (1818–1884) is primarily known today for his scathing and ridiculing attacks on August Kekulé and Jacobus Henricus van't Hoff and for his polemical criticisms of other contemporaries in the pages of the *Journal für praktische Chemie*, which he edited from 1870 until his death. His vituperative writings were so intemperate that many contemporary and later observers believed that he may have been mentally ill. Yet such a view of Kolbe is woefully incomplete. He was a brilliant experimenter who discovered many important organic compounds and reactions. He helped develop the German system of science education, and his laboratory in Leipzig, the largest and best equipped of his day, attracted numerous students from many countries. He was the leader of synthetic organic chemistry during the 1850s and 1860s, and his synthesis of acetic acid from its elements in 1844 provided a significant attack on the concept of vitalism, which had not been completely overthrown by Wöhler's earlier (1828) and better known synthesis of urea.



Kolbe was the influential, pivotal figure in what Alan J. Rocke, Professor of History at Case Western Reserve University and a leading authority on 19th-century chemistry, calls the "quiet revolution". This change emerged during the 1850s from the turbulent disputes about theories of chemical types, radicals, and constitutions, which during the 1860s gave birth to the new science of structural organic chemistry, the last major transition leading to modern chemistry. Kolbe employed all his talents and characteristics—his aggressive intellectual debate, political influence, violent temper, ardent chauvinism, and anti-French xenophobia—to maintain his position in the German academic world. A profound conservative, he vigorously attacked structural formulas and structural chemistry; he considered himself as bearing the mantle of the great classical chemists, especially Berzelius, whose copula theory he retained as the last major element of dualism left in organic chemistry.

Although Rocke's volume (the 11th in the California *History of Science* series) is the first book-length biography of Kolbe in any language, it is much more. The author has used Kolbe's life and career to highlight and chronicle an important period of chemistry in more depth than has hitherto been attempted: "By looking at the field through Kolbe's eyes we see the transformations of this period from the perspective of a man who was at once both an insider and an outsider" (p. 5). Rocke has made extensive use of hitherto unexploited documents from many archives, German and otherwise, as well as literally hundreds of blunt revealing letters from Kolbe and other chemists, to endow his account of the "quiet revolution" with a thrilling immediacy. He also details the social, educational, institutional, and cultural milieu in the various German states in which Kolbe worked, as well as in France and Great Britain (Kolbe spent the period 1845–1847 in London as Lyon Playfair's assistant and was a close friend of Edward Frankland and other English chemists).

Rocke's multifaceted and interpretative account includes biographies of figures pertinent to his story, such as von Baeyer, Berzelius, Bunsen (Kolbe's *Doktorvater*), Dumas, Erlenmeyer, Frankland, Gerhardt, von Hofmann, Kekulé, Laurent, Liebig, Volhard, Williamson, Wöhler, and Wurtz. He explores the influence of these and other personalities, patterns of state support, laboratory organization, teaching methods, and academic publishing (Kolbe was associated with the publishers Eduard and Heinrich Vieweg many years). Eighteen photographs, numerous formulas, equations, tables, notes (83 pp.), a glossary of German and chemical terms (9 pp.), a bibliography (11 pp.), and an index (17 pp., 2 cols. per page) are also provided. This important contextualized study will not only be useful to historians of chemistry and of 19th-century German science as well as to chemists, but should also be of interest to the history of science community in general, because of its novel aspects and historiographic richness.

George B. Kauffman
California State University
Fresno, CA (USA)

Applied Laser Spectroscopy. Techniques, Instrumentation, and Applications. Edited by *D. L. Andrews*. VCH Verlagsgesellschaft, Weinheim/VCH Publishers, New York, 1992. IX, 471 pp., hardcover DM 198.00.—ISBN 3-527-28027-3/1-56081-023-8

Spectroscopy in the visible, ultraviolet, and infrared spectral regions is nowadays performed, almost as a matter of course, using lasers, and there are probably more lasers than monochromators and spectrographs in the laboratories. The well-known properties of lasers as light sources, such as spatial resolution limited only by diffraction, narrow spectral bandwidth, and short pulse duration with high peak intensity, have in the last ten years become more easily and cheaply available. Rapid strides have also been made in the development of detectors (whether for charged particles or for photons). Lastly, the high electric field strengths generated by lasers allow the study of nonlinear processes in the samples under investigation. The combination of a wide variety of laser light sources, of materials investigated, and of light-induced processes, together with appropriate detection methods, has led to a plethora of spectroscopic techniques

This section contains book reviews and a list of new books received by the editor. Book reviews are written by invitation from the editor. Suggestions for books to be reviewed and for book reviewers are welcome. Publishers should send brochures or (better) books to the Book Review Editor, Dr. Ralf Baumann, Redaktion Angewandte Chemie, Postfach 101161, D-69451 Weinheim, Federal Republic of Germany. The editor reserves the right of selecting which books will be reviewed. Uninvited books not chosen for review will not be returned.

 © VCH Verlagsgesellschaft mbH, D-69451 Weinheim, 1994 0570-0833/94/1111-1195 $ 10.00+.25/0

known to insiders by their corresponding acronyms. Thus, the beginner needs an introductory overview of the fascinating capabilities of laser spectroscopy.

That is the purpose of the book reviewed here. The authors of its ten chapters report on the present situation in their special fields. In their treatment of molecular spectroscopy there is a definite emphasis on smaller molecules in the gas phase. In accordance with the aims of the book, the basic principles of each spectroscopic method are simply described rather than explained in detail, referring the interested reader to more advanced publications. This is usually followed by descriptions of practical layouts and instrumentation with specific examples. The literature coverage extends to about the end of 1990; however, a beginner interested in a particular topic could certainly locate important recent publications by intelligent forward searching.

The book begins with two introductory chapters giving an overview of laser properties, the achievable photon fluxes, the probability of multiphoton processes, types of lasers, and instrumental aspects such as wavelength calibration. Electronic spectroscopy is then treated in two extensive chapters: "Electronic Photoabsorption Spectroscopy" (W. Demtröder) and "Laser-Induced Fluorescence Spectroscopy" (J. Pfab), the second of these emphasizing the role of the dynamics of photodissociation. In the chapter "High-Resolution Infrared Spectroscopy" B. J. Howard and J. M. Brown describe the use of tunable IR lasers, for example in studies of hollow cathodes, cold jets, and photolysis products. This is followed by chapters on "Modern Techniques in Raman Spectroscopy" (M. D. Morris), "Nonlinear Raman Spectroscopy" (H. Berger, B. Lavorel, G. Millot), "Multiphoton Absorption Spectroscopy" (L. Goodman, J. Philis), and "Laser Mass Spectroscopy" (K. W. D. Ledingham, R. P. Singhal). The contribution on "Ultrafast Spectroscopic Methods" (P. A. Anfinrud, C. K. Johnson, R. Sension, R. M. Hochstrasser) is very up-to-date.

A consequence of this form of treatment is that the special research interests of the authors are strongly represented in their contributions. Also, as already mentioned, condensed phases are only considered in a few of the chapters. A chapter on the topical subject of hole-burning spectroscopy could usefully have been included to complement the others.

The quality of the figures is very mixed. Figures afford a simple way of conveying a lot of information, and for this reason a wasted opportunity is a double cause for regret. For example, the CW laser shown in Figure 2.7 will have poor mode quality, the DFDL lasers in Figures 2.9 and 2.10 will produce mainly amplified spontaneous emission, and in Figure 6.3 we find an optical path which is truly a "black box". However, these criticisms are fairly trivial in view of the wealth of material on methods and examples.

To summarize, this book provides a very useful description of spectroscopic principles, the relevant techniques, and their applications in the area of molecular spectroscopy, especially of small molecules in the gas phase. It offers the reader a quick overview of all the topics covered, and some chapters provide easy access to more detailed treatments.

Niko Ernsting
Max-Planck-Institut
für Biophysikalische Chemie
Göttingen (FRG)

Inorganic Biochemistry. An Introduction. By *J. A. Cowan.* VCH Publishers, New York/VCH Verlagsgesellschaft, Weinheim, 1993. XII, 349 pp., hardcover DM 69.00.— ISBN 1-56081-537-X/3-527-89537-X

If Alfred Werner were alive today, what branch of chemistry would he choose? Possibly inorganic biochemistry. This modern version of coordination chemistry is becoming increasingly popular, as is shown by the ever growing number of publications. During the last twenty years Werner's 'descendants', whose interests lie in the overlapping regions of inorganic chemistry, bioscience, and physics, have worked in collaboration with spectroscopists, theoreticians, electrochemists, biochemists, and molecular biologists to open up a fascinating new field of research. Although the importance of metals in life processes is still only incompletely understood, the subject is ripe for textbooks to be written. Nowadays every modern textbook of inorganic chemistry contains a chapter on inorganic biochemistry. But surprisingly, despite the obviously good market prospects for textbooks devoted solely to this subject, very few are available. In this introductory text J. A. Cowan has set out to remedy the situation. The book is intended mainly for advanced students and interested nonspecialists from other areas of chemical research. It can be said at the outset that it meets the needs of these readers very well and is a significant addition to the range.

The first two chapters, which make up about a quarter of the book, equip the reader with the necessary toolkit, i.e., the basic principles of the chemistry of complexes. Chapter 1 deals first with the concepts of crystal field theory and the kinetics and mechanisms of reactions of transition metal complexes. This is followed by a short excursion into basic principles of biochemistry, in which the author sketches the essential features of the structures of proteins and nucleotides, cell biology, and molecular biology. Chapter 2 describes the spectroscopic and biochemical techniques needed for characterizing metalloproteins. The presentation of these topics is excellent. The basic principles of each spectroscopic or electrochemical method are described in such a way that the reader can easily work through the chapters that follow.

The main part of the book is concerned with the role of metals in life processes, which is treated on the basis of the concepts already introduced. The subject matter is arranged according to biochemical functionality. Chapter 3 describes the uptake, transport, and storage of metals in organisms. Chapters 4 and 5 then deal with the functions of metalloproteins as oxygen carriers, hydrolases, and redox systems. Chapter 6 describes the functions of alkali metals in the regulation of membrane potentials, the activation of enzymes, and biomineralization, and Chapter 7 the role of alkaline-earth metals in the regulation of biochemical processes. Chapter 8 is concerned with the toxic effects of oxygen and heavy metals. Chapter 9 describes the use of metals in conjunction with chemical or spectroscopic methods to elucidate the structures and reactive properties of compounds. Lastly, Chapter 10 discusses two particular examples in detail, namely cytochrome-C-oxidase and mercury(II)-reductase.

The book is well structured from a learning standpoint. Each chapter begins by describing the basic features of the biochemical processes concerned. This conceptual framework is then brought to life by discussing suitably chosen examples. The excellent illustrations and the brief summaries at the ends of the chapters help the reader to assimilate the new material. A selected bibliography, mainly references to monographs and reviews covering results up to 1992, is given at the end of each chapter, thus enabling the reader to refer to the original literature. As an example of this structure, Chapter 3 begins with a general description of the metal balance of cells. This is followed by a section on ion transport through membranes, subdivided into the topics of the structure of membranes, ion transport, ionophores, siderophores and ion chan-

 © VCH Verlagsgesellschaft mbH, D-69451 Weinheim, 1994 0570-0833/94/1111-1196 $ 10.00+.25/0

nels, and lastly ion pumping. The chapter ends by discussing metal transport and storage in vivo, illustrated by the examples of transferrin and ferritin.

The publishers too have done what is necessary to ensure a successful final result. The good typesetting and print quality make the book a pleasure to read. The price of DM 69.00 is not exactly cheap for a textbook of this size, but is appropriate for this quality. How well the book will become accepted is largely a question of how it compares with the competition. Two other textbooks are to be published soon, one by Berg and Lippard and the other by Lippard and Bertini. The only comparable book available at present is that by Kaim and Schwederski, which offers more material at a lower price, but is published in 'copy-ready' form. For my taste the arrangement of the subject matter in 'Kaim and Schwederski' seems less clear and convincing, whereas in Cowan's book the essential nature of the role of metals in life processes is brought out more clearly by a deliberate avoidance of too much detail.

Who will benefit most from this book? It can definitely be recommended for reading by final-year students, organic chemists, and biochemists with interests in inorganic complexes; it will certainly also be a welcome additional resource for readers working in the biosciences or medicine.

Wolfgang Tremel
Institut für Anorganische
und Analytische Chemie
der Universität Mainz (FRG)

Conjugate Addition Reactions in Organic Synthesis. (Tetrahedron Organic Chemistry Series, Vol. 9, series editor: *J. E. Baldwin.*) By *P. Perlmutter.* Pergamon, Oxford, 1992. XIX, 373 pp., paperback £ 28.50, hardcover £ 58.95.—ISBN 0-08-0370675 (paperback), 0-08-0370667 (hardcover)

Conjugate additions of nucleophiles to acceptor systems are among the most useful reactions of organic chemistry. This book treats the subject under the headings of the various acceptor groups, with special emphasis on stereoselectivity. The individual chapters also contain descriptions of many natural products syntheses.

The author has taken much care in the writing of the introduction. An account of the history of the Michael addition reaction is followed by a precise and detailed treatment of the classification of reaction types, the nomenclature, and the mechanisms of 1,4 addition reactions. Adequate attention is given here to regio- and stereochemical aspects including chiral systems and chiral catalysis. The role of the nucleophile is also clearly explained, with an especially detailed discussion of cuprate chemistry. Control of reactions by the addition of Lewis acids, polar reagents, or metal salts is described. This extensive and very useful introduction concludes with the Baldwin rules, and general statements about stereoselective ring closure and tandem reactions.

Chapter 2 deals with alkenals and alkenones. A detailed discussion of the Robinson anellation, an important reaction for forming bi- or polycyclic enones, also draws attention to its disadvantages. The author goes on to treat acyclic systems, and discusses stereochemical models relating to stereoselectivity in such systems. Cyclic 1,3-diketones are also discussed as important intermediates in syntheses. On the subject of 1,3-diketones, asymmetric induction is also considered, of course. Next the author deals with cuprates, organozinc, and organosilicon compounds (Sakurai reactions). Here again special attention is given to stereochemical yields, so that the reader gets a good idea of the possibilities for stereoselective syntheses in a variety of systems. The author discusses all the relevant models that have been proposed for transition states in Lewis acid catalyzed addition reactions of allyl silanes. Free radical additions and reactions involving silyl enol ethers are then described. The chapter ends with a discussion of heteroatoms as nucleophiles, covering N, P, S, Si, and Sn.

Chapter 3 is concerned with cycloalkenones, beginning with additions of stabilized carbanions. Here again the main emphasis is on stereochemical effects. After reporting the findings their applications are well illustrated by examples in syntheses of natural products, notably of prostaglandins. Next stereochemical aspects of cuprate addition reactions are discussed in detail, including even medium-sized and large rings, as also are additions to bicycloenones. After the cuprates an assortment of other organometallic compounds follows, including those of zinc and silicon. Chiral systems are treated next, followed by intramolecular processes involving stabilized carbanions and intramolecular Sakurai reactions for the stereoselective synthesis of bicycloketones. Both methods of activation, using fluoride ions or Lewis acids, are described. This is followed by free radical reactions and addition reactions of heteronucleophiles such as oxygen or sulfur. An important class of natural products, the cytotoxic calicheamicins, are described; here an intramolecular 1,4 addition with sulfur as nucleophile serves as activator for a subsequent Bergmann cyclization.

Chapter 4 is devoted to addition reactions involving unsaturated acids and their derivatives, beginning with ketone enolates and their reactions with unsaturated esters, nitriles, and amides. Next the author describes reactions involving ester enolates, then further sections deal with nitro- and sulfur-stabilized additions. Here again the focus is on stereochemical aspects. Special attention is given to cuprate additions, and tandem reactions yielding cyclic compounds are also treated. Even such "exotic" compounds as unsaturated acyl-iron complexes are discussed in detail, so that the reader is given a complete overview. Also included, of course, are double Michael additions, which allow the diastereoselective synthesis of cyclic compounds with useful functionalities. Considerable space is devoted to intramolecular processes, and even complex functionalized systems are included. Following the pattern already seen in earlier chapters, Chapter 4 ends with free radical cyclizations, enamine reactions, and additions involving heteronucleophiles.

Chapter 5 deals with addition reactions of lactones and lactams. The section on cuprate additions also covers reactions of bicyclic and macrocyclic lactones. This is followed by reactions of heteronucleophiles; these include the very useful silyl cuprates, which can be regarded as masked (partly blocked) alcohols. The book ends with two short chapters on nitroalkenes and alkenyl sulfoxides and phosphonates (Chapter 6) and on alkyne additions (Chapter 7). Here, as before, the reactions of stabilized carbanions are followed by those of cuprates, other organometallic compounds, and heteronucleophiles.

To summarize, this book is the first comprehensive monograph on conjugate addition reactions and fills a genuine gap; it should therefore be in every chemical library. Moreover, it will please every research chemist since it contains an almost unlimited abundance of important methods for bond formation. The arrangement of the material is logical throughout, and the importance of the book is further enhanced by the well chosen examples, in which there is a strong emphasis on stereoselective reactions. Many interesting examples from the area of natural products syntheses are described and thoroughly discussed, thus giving the reader a very broad overview of the appli-

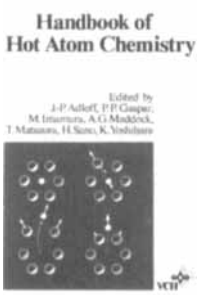
 © *VCH Verlagsgesellschaft mbH, D-69451 Weinheim, 1994* *0570-0833/94/1111-1197 $ 10.00+.25/0*

cations. The reasonable price should enable students to afford the book. As a final comment, the standard of production is excellent and attractive.

Dieter Schinzer
Institut für Organische Chemie
der Technischen Universität
Braunschweig (FRG)

Handbook of Hot Atom Chemistry. Edited by *J.-P. Adloff, P. P. Gaspar, M. Imamura, A. G. Maddock, T. Matsuura, H. Sano* and *K. Yoshihara*. VCH Verlagsgesellschaft, Weinheim/VCH Publishers, New York/Kodansha, Tokyo, 1992. XVIII, 702 pp., hardcover DM 330.00.—ISBN 3-527-29001-X/1-56081-271-0/4-06-205851-0

The "Handbook of Hot Atom Chemistry" is essentially a revised and updated version of the book "Hot Atom Chemistry" published in 1984 with T. Matsuura as editor. In the preface the editors regret the fact that this wide-embracing field of study has been little recognized up to now, despite the important contributions that it has made to fundamental knowledge and applications in many areas of chemistry. Moreover, they point out that financial support for and interest in hot atom chemistry research have been severely reduced throughout the world in the last few years. This phenomenon, also shared by its parent disciplines of radiochemistry and nuclear chemistry, is a temporary situation resulting from the current debate about nuclear energy. For many radiochemists their first contact with their chosen area of research came from investigating the chemical effects of nuclear reactions, briefly described as the "chemistry of hot atoms" or "recoil chemistry". Following a nuclear reaction the newly formed "hot" atoms are able, due to their high energy, to take part in unusual processes leading sometimes to unusual products. Radioactive recoil atoms are easy to detect through their subsequent decay, and can therefore serve as probes yielding information about their chemical environment.



The handbook sets out, in about 700 pages, to provide a wider readership with a survey of the aims, current state of knowledge, techniques, and applications of hot atom chemistry, and to draw attention to some hitherto unsolved questions and potential further applications. The editors hope thereby to reawaken interest in this field of research, and also to help avert a possible future shortage of people with the technical skills for dealing competently with radioactive materials. The initiative for preparing the book has come from T. Matsuura of the Nuclear Institute of Rikko University, Japan. Four of the editors and 30 of the authors are Japanese scientists, while a further 16 authors are from the USA and 14 from Europe.

The book begins with several short reviews outlining the origins of hot atom chemistry and some important developments. The second section then deals with the behavior of hot atoms of halogens and of tritium, and of recoiling atoms of C, O, N, and S, which are of special importance for organic chemistry. The third section introduces some fundamental aspects of theoretical models for describing the processes that occur. Next the behavior of recoil atoms in solids and liquids is considered from several different viewpoints, including the effects of radiochemical and related processes on the reaction medium. A further section discusses the ways in which other nuclear techniques, such as Mössbauer spectroscopy, measurements of the effects of chemical processes on the angular distribution of the emitted nuclear radiation, or positronium chemistry, can contribute to studies of recoil atoms. The last group of articles deals with applications of knowledge of recoil chemistry and with techniques used in nuclear medicine, geochemistry, cosmic chemistry, nuclear engineering, and environmental science.

In a work described as a handbook one expects to find a comprehensive, balanced, and systematically arranged survey. With 56 individual contributions this can only be achieved by applying strict guidance to the authors, since only in this way can one avoid frequent overlapping. Here the wide variations between contributions in the amount of detail (with lengths varying from three to 24 pages) and the use of different typefaces emphasizes the overall impression of a lack of uniformity. Also the grouping of the articles into topic areas has not been achieved in a convincing way. In view of the wide-ranging and heterogeneous variety of topics that are embraced by the term "hot atom chemistry", especially those concerned with radiochemistry and nuclear chemistry, one can appreciate the difficulty of devising a clear and meaningful subdivision of the subject matter. In fact the handbook is more a loose collection of review articles in which leading experts have summarized the current state of knowledge in their own or closely related fields. The literature references enable the interested reader to explore in greater depth. It is not practicable here to describe the individual contributions in detail, nor is it necessary. As well as articles aimed at enabling even those without previous knowledge to understand the most important relationships, there are others that inform specialists about comparatively recent results in particular areas.

Although one's expectations, from the description "handbook", of a systematic, comprehensive, and balanced treatment are not realized, this collection of articles nevertheless provides an up-to-date insight into some of the most important research areas, methods, and applications of recoil chemistry. Furthermore, reading selected articles could give advanced students of chemistry or physics the awakened interest in this special field that the editors desire, and may stimulate some scientists to use the knowledge and methods of recoil chemistry in their own research. In a few years time it will undoubtedly again become necessary to present the status of this field to a wider circle of people for reconsideration. Then it will certainly be possible, with a tighter and more systematic arrangement of the heterogeneous subject matter, a smaller number of review articles treating clearly defined areas, and (as in the 1984 version) a uniform and easily readable typeface, to make hot atom chemistry attractive to a wider readership.

Edmund Henrich
Institut für Heiße Chemie
Kernforschungszentrum
Karlsruhe (FRG)

 © VCH Verlagsgesellschaft mbH, D-69451 Weinheim, 1994 0570-0833/94/1111-1198 $ 10.00+.25/0

The Polymerase Chain Reaction (Nobel Lecture)**

Kary B. Mullis*

In 1944 Erwin Schrödinger, stimulated intellectually by Max Delbruck, published a little book called *What is Life?* It was an inspiration to the first of the molecular biologists, and has been, along with Delbruck himself, credited for directing the research during the next decade that solved the mystery of how "like begat like".

Max was awarded the Nobel Prize in 1969, and rejoicing in it, he also lamented that the work for which he was being honored before all the peoples of the world was not something which he felt he could share with more than a handful. Samuel Beckett's contributions in literature, honored at the same time, seemed to Max somehow universally accessible to anyone. But not his. In his Nobel lecture Max imagined his imprisonment in an ivory tower of science.

"The books of the great scientists," he said, "are gathering dust on the shelves of learned libraries. And rightly so. The scientist addresses an infinitesimal audience of fellow composers. His message is not devoid of universality but its universality is disembodied and anonymous. While the artist's communication is linked forever with its original form, that of the scientist is modified, amplified, fused with the ideas and results of others, and melts into the stream of knowledge and ideas which forms our culture. The scientist has in common with the artist only this: that he can find no better retreat from the world than his work and also no stronger link with his world than his work."

Well, I like to listen to the wisdom of Max Delbruck. Like my other historical hero, Richard Feynman, who also passed through here, Max had a way of seeing directly into the core of things and clarifying it for the rest of us. But I am not convinced with Max that the joy of scientific creation must remain completely mysterious and unexplainable, locked away from all but a few esoterically informed colleagues. I lean toward Feynman in this matter. I think Feynman would have said, if you can understand it, you can explain it.

So I'm going to try to explain how it was that I invented the polymerase chain reaction (PCR). There's a bit of it that will not easily translate into normal language. If that part weren't of some interest to more than a handful of people here, I would just leave it out. What I will do instead is let you know when we get to that and also when we are done with it. Don't trouble yourself over it. It's esoteric and not crucial. I think you can understand what it felt like to invent PCR without following the details.

In 1953 when Jim Watson and Francis Crick published the structure of DNA, Schrödinger's little book and I were eight years old. I was too young to notice that mankind had finally understood how it might be that "like begat like". The book had been reprinted three times. I was living in Columbia, South Carolina, where no one noticed that we didn't have a copy. But my home was a few blocks away from an undeveloped wooded area with a creek, possums, racoons, poisonous snakes, dragons, and a railroad track. We didn't need a copy. It was a wilderness for me and my brothers, an unknown and unregimented place to grow up. An if we got bored of the earth, we could descend into the network of storm drains under the city. We learned our way around that dark, subterranean labyrinth. It always frightened us. And we always loved it.

By the time Watson and Crick were being honored in Stockholm in 1962, I had been designing rockets with my adolescent companions for three years. For fuel, we discovered that a mixture of potassium nitrate and sugar could be very carefully melted over a charcoal stove and poured into a metal tube in a particular way with remarkable results. The tube grew larger with our successive experiments until it was about four feet long. My mother grew more cautious, and often her head would appear out of an upstairs window, and she would say things that were not encouraging. The sugar was reluctantly furnished by her own kitchen, and the potassium nitrate we purchased from the local druggist.

Back then in South Carolina young boys seeking chemicals were not immediately suspect. We could even buy dynamite fuse from the hardware store with no questions asked. This was good, because we were spared from early extinction on one occasion when our rocket exploded on the launch pad, by the very reliable, slowly burning dynamite fuses we could employ, coupled with our ability to run like the wind once the fuse had been lit. Our fuses were in fact much improved over those Alfred Nobel must have used when he was frightening his own mother. In one of our last experiments before we became so interested in the maturing young women around us that we would not think deeply about rocket fuels for another ten years, we blasted a frog a mile into the air and got him back alive. In another, we inadvertently frightened an airline pilot, who was preparing to land a DC-3 at the Columbia airport. Our mistake.

At Dreher High School we were allowed free, unsupervised access to the chemistry lab. We spent many an afternoon there tinkering. No one got hurt and no lawsuits resulted. They

[*] Dr. K. B. Mullis
6767 Neptune Place, Apartment 4
La Jolla, CA 92037 (USA)

[**] Copyright © The Nobel Foundation 1993.—We thank the Nobel Foundation, Stockholm, for permission to print this lecture.

wouldn't let us in there now. Today we would be thought of as a menace to society. If I'm not mistaken, Alfred Nobel for a time was not allowed to practice his black art on Swedish soil. Sweden, of course, was then and still is way ahead of the United States in these matters.

I never tired of tinkering in labs. During the summer breaks from Georgia Tech, Al Montgomery and I built an organic synthesis lab in an old chicken house on the edge of town where we made research chemicals to sell. Most of them were either noxious or explosive. No one else wanted to make them, somebody wanted them, and so their production became our domain. We suffered no boredom and no boss. We made enough money to buy new equipment. Max Gergel, who ran Columbia Organic Chemicals Company, and who was an unusually nice man, encouraged us and bought most of our products, which he resold. There were no government regulators to stifle our fledgling efforts, and it was a golden age, but we didn't notice it. We learned a lot of organic chemistry.

By the time I left Georgia Tech for graduate school in biochemistry at the University of California at Berkeley, the genetic code had been solved. DNA did not yet interest me; I was excited by molecules. DNA before PCR was long and stringy, not really molecular at all. Six years in the biochemistry department didn't change my mind about DNA, but six years of Berkeley changed my mind about almost everything else.

I was in the laboratory of Joe Neilands who provided his graduate students with a place to work and very few rules. I'm not even sure that Joe knew any rules except the high moral ground of social responsibility and tolerance. Not knowing that the department did have rules, I took courses in astrophysics instead of in molecular biology, which I figured I could learn from my molecular biologist friends. I published my first scientific paper in *Nature* in 1968. It was a sophomoric astrophysical hypothesis called "The Cosmological Significance of Time Reversal." I think *Nature* is still embarrassed about publishing it, but it was immensely useful to me when it came time for my qualifying examination. The committee would decide whether or not I would be allowed to earn a PhD without coursework in molecular biology. And my paper in *Nature* helped them to justify a "yes". In retrospect, the membership of that committee is intriguing.

Don Glaser, who received the Nobel Prize in physics in 1960 at age 34, would later be one of the founders of Cetus Corporation, where I was working when I invented PCR. Henry Rapoport, who discovered psoralens, would be the scientific advisor to my department at Cetus, and would coauthor two patents with me. Alan Wilson, now sadly passed away, would be the first researcher outside of Cetus to employ PCR. And Dan Koshland would be the editor of *Science* when my first PCR paper was rejected from that journal and also the editor when PCR was three years later proclaimed "Molecule of the Year". I passed. None of us, I think, as we walked out of that room, had any conscious inkling of the way things would turn out among us.

In Berkeley it was a time of social upheaval, and Joe Neilands was the perfect mentor to see his people through it with grace. We laughed a lot over tea at four every afternoon around a teakwood table that Joe had brought from home and oiled once a month. Our lab had an ambience that was special. I decided to become a neurochemist. Joe was the master of microbial iron transport molecules. Our lab was different than most, where the head of the lab would prefer that you help advance his career by elaborating on some of his work. Not so with Neilands. As long as I wrote a thesis and got a degree, he didn't care what else did, and I stayed in his lab happily, following my own curiosity even if it carried me into music courses, for as long as Joe thought we could get away with it. The department was paying me a monthly stipend from the National Institutes of Health, and eventually we knew I would have to leave.

After six years I headed east with a PhD and confidence in my education. My wife of a few months went to Kansas to go to medical school, and I followed her there. That was 1972.

I had made no professional plans that would work in Kansas, so I decided to become a writer. I discovered pretty quickly that I was far too young. I didn't know anything yet about tragedy, and my characters were flat. I didn't know how to describe a mean spirit in terms someone else could believe.

So I had to get a job as a scientist. I found a job at the medical school working with two pediatric cardiologists and a pathologist. It was a very fortunate accident. For one thing pediatricians are always the nicest doctors, and for another thing these doctors were very special: Leone Mattioli, whose wife could cook, Agostino Molteni, and Richard Zakheim. For two years I did medical research, learned how to appreciate old-world values from two Italians and a New York Jew, and learned human biology for the first time.

Marriage over, I returned to Berkeley, working for a time in a resturant and then at the University of California at San Francisco killing rats for their brains. I heard Max Delbruck lecture, but I don't think I understood the significance of who he was, nor was I influenced by him to go into molecular biology. I was working on the enkephalins.

But then there was a seminar describing the synthesis and cloning of a gene for somatostatin. That impressed me. For the first time I realized that significant pieces of DNA could be synthesized chemically and that they were likely to be very exciting. I started studying DNA synthesis in the library. And I started looking for a job making DNA molecules.

Cetus hired me in the fall of 1979. I worked long hours and enjoyed it immensely. DNA synthesis was much more fun than killing rats, and the San Francisco Bay Area was a good place to be doing it. There were a number of biotechnology companies and several academic groups working on improving the synthesis methods for DNA. Within two years, there was a machine in my lab from Biosearch of San Rafael, California, turning out oligonucleotides much faster than the molecular biologists at Cetus could use them. I started playing with the oligonucleotides to find out what they could do.

The lab next door to me was run by Henry Erlich and was working on methods for detecting point mutations. We had a number of oligonucleotides for them. I started thinking about their problem and proposed an idea of my own which they ended up calling oligomer restriction. It worked as long as the target sequence was fairly concentrated, like a site on a purified plasmid, but it didn't work if the site was relatively rare, like a single copy gene in human DNA.

I apologize to those of you who just got lost, but I do have to say a few things now that are going to be difficult. I will get back to the story in a few minutes.

The oligomer restriction method also relied on the fact that the target of interest contained a restriction site polymorphism, which kept it from being universally applicable to just any point mutation. I started thinking about doing some experiments wherein an oligonucleotide hybridized to a specific site could be extended by DNA polymerase in the presence of only dideoxynucleoside triphosphates. I reasoned that if one of the dideoxynucleoside triphosphates in each of four aliquots of a reaction was radioactive, then an analysis of the aliquots on a gel could indicate which of the dideoxynucleoside triphosphates had added to the hybridized oligonucleotide and therefore which base was adjacent to the 3'-end of the oligonucleotide. It would be like doing Sanger sequencing at a single base pair.

On human DNA it would not have worked because the oligonucleotide would not have specifically bound to a single site. On a DNA as complex as human DNA it would have bound to hundreds or thousands of sites depending on the sequence involved and the conditions used. What I needed to make this work was some method of raising the relative concentration of the specific site of interest. What I needed was PCR, but I had not considered that possibility. I knew the difference numerically between five thousand base pairs as in a plasmid and three billion base pairs as in the human genome, but somehow it didn't strike me as sharply as it should have. My ignorance served me well. I kept on thinking about my experiment without realizing that it would never work. And it turned into PCR.

One Friday night I was driving, as was my custom, from Berkeley up to Mendocino where I had a cabin far away from everything off in the woods. My girlfriend, Jennifer Barnett, was asleep. I was thinking. Since oligonucleotides were not that hard to make anymore, wouldn't it be simple enough to put two of them into the reaction instead of only one, such that one of them would bind to the upper strand and the other to the lower strand with their 3'-ends adjacent to the opposing bases of the base pair in question. If one oligonucleotide were made longer than the other, then their single-base extension products could be separated on a gel from each other and one could act as a control for the other. I was going to have to separate them on a gel anyway from the large excess of radioactive nucleoside triphosphate. What I would hope to see is that one of them would pick up one radioactive nucleotide and the other would pick up its complement. Other combinations would indicate that something had gone wrong. It was not a perfect control, but it would not require a lot of effort. It was about to lead me to PCR.

I liked the idea of a control that was nearly free in terms of cost and effort. And also, it would help use up the oligonucleotides that my lab could now make faster than they could be used.

As I drove through the mountains that night, the stalks of the California buckeyes heavily in blossom leaned over into the road. The air was moist and cool and filled with their heady aroma.

Encouraged by my progress on the thought experiment, I continued to think about it and about things that could possibly go wrong. What if there were deoxynucleoside triphosphates in the DNA sample, for instance? What would happen? What would happen, I reasoned, is that one or more of them would be added to the oligonucleotide by the polymerase prior to the termination of chain elongation by addition of the dideoxynucleoside triphosphate; it could easily be the wrong dideoxynucleoside triphosphate, and it surely would result in an extension product that would be the wrong size, and the results would be spurious. It would not do. I needed a way to ensure that the sample was free from contamination from deoxynucleoside triphosphates. I could treat the sample before the extension reaction with bacterial alkaline phosphatase. The enzyme would degrade any triphosphates present down to nucleosides, which would not interefere with the main reaction. But then I would need to deactivate the phosphatase before adding the dideoxynucleoside triphosphates, and everyone knew at that time that BAP, as we called it, was not irreversibly denaturable by heat. The reason we knew this was that the renaturation of heat-denatured BAP had been demonstrated in classic experiments that had shown that a protein's shape was dictated by its sequence. In the classical experiments the renaturation had been performed in a buffer containing lots of zinc. What had not occurred to me or apparently many others was that BAP could be irreversibly denatured if zinc was omitted from the buffer, and that zinc was not necessary in the buffer if the enzyme was only going to be used for a short time and had its own tightly bound zinc to begin with. There was a product on the market at the time called matBAP wherein the enzyme was attached to an insoluble matrix that could be filtered out of a solution after it had been used. The product sold because people had the impression that you could not irreversibly denature BAP. We'd all heard about, but not read, the classic papers.

This says something about the arbitrary way that many scientific facts get established, but for this story, its only importance is that, had I known then that BAP could be heat-denatured irreversibly, I may have missed PCR. As it was, I decided against using BAP and tried to think of another way to get rid of deoxynucleoside triphosphates. How about this, I thought. What if I leave out the radioactive dideoxynucleoside triphosphates, mix the DNA sample with the oligonucleotides, drop in the polymerase, and wait? The polymerase should use up all the deoxynucleoside triphosphates by adding them to the hybridized oligonucleotides. After this was complete I could heat the mixture, causing the extended oligonucleotides to be removed from the target, then cool the mixture allowing new, unextended oligonucleotides to hybridize. The extended oligonucleotides would be far outnumbered by the vast excess of unextended oligonucleotides and therefore would not rehybridize to the target to any great extent. Then I would add the dideoxynucleoside triphosphate mixtures, and another aliquot of polymerase. And now things would work.

But what if the oligonucleotides in the original extension reaction had been extended so far that they could now hybridize to unextended oligonucleotides of the opposite polarity in this second round. The sequence that they had been extended into would permit that. What would happen?

EUREKA!!! The result would be exactly the same, only the signal strength would be doubled.

EUREKA again!!! I could do it intentionally, adding my own deoxynucleoside triphosphates, which were quite soluble in water and legal in California.

And again, EUREKA!!! I could do it over and over again. Every time I did it I would double the signal. For those of you who got lost, we're back to the story.

I stopped the car at mile marker 46.7 on Highway 128. In the glove compartment I found some paper and a pen. I confirmed that two to the tenth power was about a thousand and that two to the twentieth power was about a million and that two to the thirtieth power was around a billion—close to the number of base pairs in the human genome. Once I had cycled this reaction thirty times I could read the sequence of a sample with an immense signal and almost no background.

Jennifer wanted to get moving. I drove on down the road. In about a mile it occurred to me that the oligonucleotides could be placed at some arbitrary distance from each other, not just flanking a single base pair and that I could make an arbitrarily large number of copies of any sequence I chose, and what's more, most of the copies after a few cycles would be the same size. That size would be up to me. They would look like restriction fragments on a gel. I stopped the car again.

"Dear Thor!" I exclaimed. I had solved the two most annoying problems in DNA chemistry in a single lightening bolt. Abundance and distinction. With two oligonucleotides, DNA polymerase, and the four nucleoside triphosphates I could make as much of a DNA sequence as I wanted and I could make it on a fragment of a specific size that I could distinguish easily.

Somehow, I thought, it had to be an illusion. Otherwise it would change DNA chemistry forever. Otherwise it would make me famous. It was too easy. Someone else would have done it, and I would surely have heard of it. We would be doing it all the time. What was I failing to see? "Jeniffer, wake up. I've thought of something incredible."

She wouldn't wake up. I had thought of incredible things before that somehow lost some of their sheen in the light of day. This one could wait till morning. But I didn't sleep that night. We got to my cabin, and I starting drawing little diagrams on every horizontal surface that would take pen, pencil, or crayon until dawn, when with the aid of a last bottle of good Mendocino County cabernet, I settled into a perplexed semiconsciousness. Afternoon came, along with new bottles of celebratory red fluids from Jack's Valley Store, but I was still puzzled and alternated between being absolutely pleased with my good luck and clever brain, and being mildly annoyed at myself and Jennifer Barnett for not seeing the flaw that must have been there. I had no phone at the cabin, and there were no other biochemists besides Jennifer and me in Anderson Valley. The conundrum which lingered throughout the weekend and created an unprecedented desire in me to return to work early was compelling. If the cyclic reactions which by now were symbolized in various ways all over the cabin really worked, why had I never heard of them being used? If they had been used, I surely would have heard about it, and so would everybody else including Jennifer, who was presently sunning herself by the pond and taking no interest in the explosions that were rocking my brain.

Why wouldn't these reactions work?

Monday morning I was in the library. The moment of truth. By afternoon it was clear. For whatever reasons, there was nothing in the abstracted literature about the success or failure of amplifying DNA by the repeated reciprocal extension of two primers hybridized to the separate strands of a particular DNA sequence. By the end of the week I had talked to enough molecular biologists to know that I wasn't missing anything really obvious. No one could recall such a process ever being tried.

However, shocking to me, not one of my friends or colleagues would get excited over the potential for such a process. True, I was always having wild ideas, and this one maybe looked no different than last week's. But it was different. There was not a single unknown in the scheme. Every step involved had been done already. Everyone agreed that you could extend a primer on a DNA template, and everyone knew you could melt double-stranded DNA. Everyone agreed that what you could do once, you could do again. Most people don't like to do things over and over, I in particular. If I had to do a calculation twice, I preferred to write a program instead. But no one thought it was impossible. It could be done, and there was always automation. The result on paper was so obviously fantastic that even I had little irrational lapses of faith that it would really work in a tube. Most everyone, who would take a moment to talk about it with me felt compelled to come up with some reason why it wouldn't work. It was not easy in that postcloning, prePCR year to accept the fact that you could have all the DNA you wanted. And that it would be easy.

I had a directory full of untested ideas in the computer. I opened a new file and named this one polymerase chain reaction. I didn't immediately try an experiment, but all summer I kept talking to people in and out of the company. I described the concept around August at an in-house seminar. Every Cetus scientist had to give a talk twice a year. But no one had to listen. Most of the talks were dry descriptions of labor performed, and most of the scientists left early without comment.

One or two technicians were interested, and on the days when she still loved me, Jennifer thought it might work. On the increasingly numerous days when she hated me, my ideas and I suffered her scorn together.

I continued to talk about it, and by late summer had a plan to amplify a 400 base pair fragment from human nerve growth factor, which Genentech had cloned and published in *Nature*. I would start from whole human placental DNA from Sigma, taking a chance that the cDNA sequence had derived from a single exon. No need for a cDNA library. No colonies, no nothing. It would be dramatic. I would shoot for the moon. Primers were easy to come by in my lab, which made oligonucleotides for the whole company. I entered the sequences I wanted into the computer and moved them to the front of the waiting list.

My friend Ron Cook, who had founded Biosearch, and produced the first successful commercial DNA synthesis machine, was the only person I remember during that summer who shared my enthusiasm for the reaction. He knew it would be good for the oligonucleotide business. Maybe that's why he believed in it. Or maybe he's a rational chemist with an intact brain. He's one of my best friends now, so I have to disqualify myself from claiming any really objective judgement regarding him. Perhaps I should have followed his advice, but then things would have worked out differently, and I probably wouldn't be here on the beach in La Jolla writing this, which I enjoy. Maybe I would be rich in Tahiti. He suggested one night at his house that since no one at Cetus had taken it seriously, I should resign my job, wait a little while, make it work, write a patent, and get rich. By rich he wasn't imagining 300 million dollars. Maybe one or two million. The famous chemist Albert Hofmann was at Ron's that night. He synthesized LSD in 1943. At the time he didn't realize what he had done. It only dawned on him slowly, and then things worked their way

out over the years like no one would have ever predicted, or could have controlled by forethought and reason.

I responded weakly to Ron's suggestion. I had already described the idea at Cetus, and if it turned out to be commercially successful they would have lawyers after me forever. Ron was not sure that Cetus had rights on my ideas unless they were directly related to my duties. I wasn't sure about the law, but I was pretty happy working at Cetus and assumed innocently that if the reaction worked big-time I would be amply rewarded by my employer.

The subject of PCR was not yet party conversation, even among biochemists, and it quickly dropped. Albert was much more interesting, even for me. He had given a fine talk that afternoon at Biosearch.

Anyhow, my problems with Jennifer were not getting any better. That night was no exception to the trend. I drove home alone feeling sad and unsettled, not in the mood for leaving my job or for any big change in what was left of stability in my life. PCR seemed distant and very small compared to our very empty house.

In September I did my first experiment. I like to try the easiest possibilities first. So one night I put human DNA and the nerve growth factor primers in a little screw-cap tube with an O-ring and a purple top. I boiled the mixture for a few minutes, cooled it, added about 10 units of DNA polymerase, closed the tube, and left it at 37 °C. It was exactly midnight on the ninth of September. I poured a cold Beck's into a 400 mL beaker and contemplated my notebook for a few minutes before leaving the lab.

Driving home I figured that the primers would be extended right away, and I hoped that at some finite rate the extension products would come unwound from their templates, be primed, recopied, and so forth. I did not relish the idea of heating, cooling, and adding polymerase over and over again, and held this for a last-resort method of accomplishing the chain reaction. I was thinking of DNA–DNA interactions as being reversible with all the ramifications thereof. I wasn't concerned about the absolute rate of dissociation, because I didn't care how long the reaction took as long as nobody had to do anything. I assumed there would always be some finite concentration of single strands, which would be available for priming by a relatively high concentration of primer with pseudo-first-order kinetics.

For a reaction with the potential which I dreamed of for this one, especially in light of the absence of anything else that could do the same thing, time was only a very secondary consideration. If it would work at all was important. The next most important thing was, would it be easy to do? Then came time.

At noon the next day I went to the lab to take a 12-hour sample. There was no sign by ethidium bromide of any 400 base pair bands. I could have waited another hundred years, as I had no idea what the absolute rates might be. But I succumbed slowly to the notion that I couldn't escape much longer the unpleasant prospect of cycling the reaction between temperatures for the single- and double-stranded states. This also meant adding the thermally unstable polymerase after every cycle.

For three months I did sporadic experiments while my life at home and in the lab with Jennifer was crumbling. It was slow going. Finally I retreated from the idea of starting with human DNA, I wasn't even absolutely sure that the Genentech sequence from *Nature* that I was using was from a single exon. I settled on a target of more modest proportions, a short fragment from pBR 322, a purified plasmid. The first successful experiment happened on December 16th. I remember the date. It was the birthday of Cynthia, my former wife from Kansas City, who had encouraged me to write fiction and bore us two fine sons. I had strayed from Cynthia eventually to spend two tumultous years with Jennifer. When I was sad for any other reason, I would also grieve for Cynthia. There is a general place in your brain, I think, reserved for "the melancholy of relationships past". It grows and prospers as life progresses, forcing you finally, against you will, to listen to country music.

And now as December threatened Christmas, Jennifer, that crazy, wonderful woman chemist, had dramatically left our house and the lab, and headed to New York and her mother, for reasons that seemed to have everything to do with me but which I couldn't fathom. I was beginning to learn tragedy. It differs a great deal from pathos, which you can learn from books. Tragedy is personal. It would add strength to my character and depth someday to my writing. Just right then, I would have preferred a warm friend to cook with. Hold the tragedy lessons. December is a rotten month to be studying your love life from a distance.

I celebrated my victory with Fred Faloona, a young mathematician and a wizard of many talents whom I had hired as a technician. Fred had helped me that afternoon set up this first successful PCR reaction, and I stopped by his house on the way home. As he had learned all the biochemistry he knew directly from me he wasn't certain whether or not to believe me when I informed him that we had just changed the rules in molecular biology. "Okay, Doc, if you say so." He knew I was more concerned with my life than with those cute little purple-topped tubes.

In Berkeley it drizzles in the winter. Avocados ripen at odd times, and the tree in Fred's front yard was wet and sagging from a load of fruit. I was sagging as I walked out to my little silver Honda Civic, which never failed to start. Neither Fred, empty Beck's bottles, or the sweet smell of the dawn of the age of PCR could replace Jenny. I was lonesome.

Received: January 17, 1994 [A49 IE]
German version: *Angew. Chem.* **1994**, *106*, 1271

Synthetic DNA and Biology (Nobel Lecture)**

Michael Smith*

Most of the significant work has been summarized in a number of reviews and articles. In these there was, of necessity, a good deal of simplification and omission of detail.... With the passage of time, even I find myself accepting such simplified accounts.
F. Sanger[1]

Introduction

I had the good fortune to arrive in the laboratory of Gobind Khorana, in September 1956, just one month after he had made the accidental discovery of the phosphodiester method for the chemical synthesis of deoxyribooligonucleotides,[2] a synthetic approach whose full exploitation led to elucidation of the genetic code and the first total synthesis of a gene.[3-5] An identifying characteristic of the Khorana approach to the production of synthetic polynucleotides for the solution of biological problems has been a willingness to use both chemical and enzymatic tools as appropriate,[5, 6] and this catholic approach is the foundation of all the molecular technology employed in modern molecular genetics.[7-9] It had a major impact on my thinking.

During my post-doctoral time in the Khorana group I was mainly involved in small molecule synthesis: nucleoside-5′ triphosphates[10] and nucleoside-3′,5′ cyclic phosphates.[11] However, I was able to contribute to the technology of polynucleotide synthesis by the development of the methoxytrityl series of 5′-hydroxyl protecting groups[12] and with a first approach to the chemical synthesis of ribooligonucleotides.[13]

In 1961 I left the Khorana group to join the Fisheries Research Board of Canada Vancouver Laboratory. Whilst much of my research effort was directed at studies on salmonid physiology and endocrinology, it was possible to continue studies on the chemistry of phosphodiester synthesis, and this resulted in a new method for nucleoside-3′5′ cyclic phosphate synthesis by alkaline transesterification under anhydrous conditions, a reaction which obviated the need for chemical protecting groups on the heterocyclic bases.[14, 15]

In 1966, I became a faculty member in the Department of Biochemistry of the University of British Columbia, which has been my academic home ever since. Studies on oligonucleotide synthesis continued, directed at the reaction of deoxyribonucleoside phosphorofluoridates in anhydrous alkaline conditions.[16] Although this method, in making base protecting groups redundant, represented a significant advance, it did not have the generality required of a universal synthetic method.[17, 18]

An approach to deoxyribooligonucleotide synthesis that did prove to be versatile, simple, and useful, although inefficient, involved the extension of short primers using *E. coli* polynucleotide phosphorylase, in the presence of Mn^{2+} and NaCl, with deoxyribonucleoside-5′ diphosphates as substrate.[19-22] This procedure, which made possible the synthesis of deoxyribooligonucleotides up to 12 to 13 nucleotides in length, proved to be a significant breakthrough for our small group, because it allowed us to undertake a number of fairly ambitious molecular biological projects at a time (between 1970 and 1980) when oligonucleotides were not generally accessible. Of course, it has been displaced as a routine synthetic procedure with the advent of automated chemical synthesis (which still uses the methoxytrityl protecting group) with nucleoside-3′ phosphoroamidites as the key intermediates.[23-25]

Model Studies on Oligonucleotide Double Helix Stability and Specificity

In 1968 planned studies on the biosynthesis of salmonid protamine[26] and on the sequence of dA,dT-rich crab DNA[27] became impossible for personal or for technical reasons. Casting around for a new project, I suggested to Caroline Astell, who was studying for her Ph.D, a series of model studies with chemically synthesized oligonucleotides directed at defining the stability and specificity of oligonucleotide duplexes of defined sequence. The objective was to see if a synthetically accessible oligonucleotide could be a tool for identifying and isolating a specific messenger RNA based on Watson–Crick hydrogen bonding. From the statistical point of view it should be possible, since the length required of an oligonucleotide in order for it to be unique in a given genome size ranges from 9 nucleotides for λ phages with a genome of 4.6×10^4 base pairs to 18 for the higher plants, such as *A. cepa* with a genome of 1.5×10^{10} base pairs (Table 1). Also relevant was the work of Michelson and Monny[28] and of Niyogi and Thomas[29] on interactions of ribooligonucleotides with ribopolynucleotides, which indicated that stable double helices can be formed with as few as seven base pairs and, equally importantly, which demonstrated that

[*] Prof. M. Smith
Biotechnology Laboratory and Department of Biochemistry
The University of British Columbia
237-6174 University Boulevard, Vancouver, B.C. V6T 1Z3 (Canada)

[**] Copyright © The Nobel Foundation 1994. We thank the Nobel Foundation, Stockholm, for permission to print this lecture.

Table 1. DNA content of haploid genomes and oligonucleotide length required for unique recognition [a].

Organism	Z [b]	N [c]	Organism	Z [b]	N [c]
Viruses			Plants		
λ-Phage	4.6×10^4	9	*C. reinhardtii*	10^8	14
Bacteria			*A. thaliana*	10^8	14
D. pneumoniae	1.7×10^6	11	*Z. mays*	6.6×10^9	17
E. coli	4.1×10^6	12	*A. cepa*	1.5×10^{10}	18
Fungi			Animals		
S. cerevisiae	1.7×10^7	13	*C. elegans*	10^8	14
N. crassa	2.1×10^7	13	*D. melanogaster*	1.3×10^8	14
			B. rerio	10^9	16
			M. musculus	2.2×10^9	17
			H. sapiens	3.3×10^9	17

[a] Recognition by the nucleotide is unique when $4^N \geq 2 \times Z$. [b] Z = the number of base pairs in the genome. [c] N = number of nucleotides in the oligonucleotide.

there is a significant increase in duplex stability for each additional base pair up to about 16 base pairs (Fig. 1). The work of Gilham et al. with random length oligothymidylates covalently attached to cellulose demonstrated their potential power for affinity chromatography,[30, 31] which led to an important procedure for isolation of eukaryote mRNAs.[32] However, although data was available on duplex stability involving *mixtures* of oligonucleotides of defined length with DNA,[33, 34] there was no systematic data obtained with pure oligonucleotides of defined sequence and length.

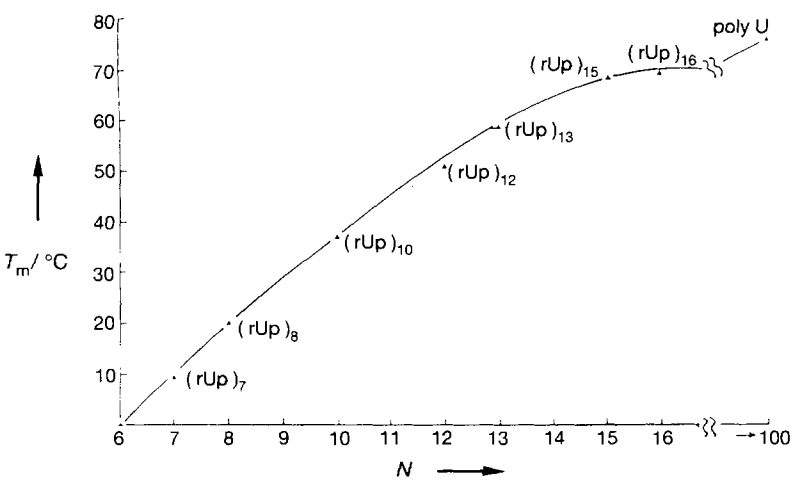


Fig. 1. The relationship between oligouridylate length and the T_m of double helices with polyadenylate in 0.02 M NaCl, 0.01 M sodium cacodylate ($Me_2As(O)O^-Na^+$), pH 7.0 [28]. N = number of uridine residues.

Our approach was to prepare deoxyribooligonucleotide celluloses by using simple oligonucleotides of defined length and sequence synthesized by the Khorana method and to employ these oligonucleotide celluloses, in the form of thermally eluted columns, to establish the stability of duplexes with a variety of complementary, or partially complementary, deoxyribo- and ribooligonucleotides.[35–38] The results and conclusions of this time-consuming but critical series of experiments has been summarized in more detail elsewhere,[39] and only some highlights will be discussed here.

First, it was clear that, under appropriate conditions of ionic strength, stable duplexes containing as few as six dA–dT base pairs can be formed (Fig. 2). Further, additional base pairs increase duplex stability significantly, but in a nonlinear manner; the incremental increase in stability diminishes with increased length. Also, a single base-pair mismatch of dT with dT or of dT with dG decreases duplex stability by the same amount (equivalent to removing about two base pairs), but duplex formation is still possible at low temperature (Fig. 2). In addition, it was obvious that oligonucleotide duplexes form rapidly at low temperatures, conditions under which denatured double-strand DNA does not reanneal.

These experiments convinced me that it would be possible to use a synthetic oligonucleotide to identify an RNA or a DNA containing the exact Watson–Crick complement of its sequence and to differentiate it from similar but not identical sequences. An opportunity to demonstrate this principle was provided by mutants in the lysozyme-encoding locus of phage T4.[40] Also, at a later date, the data made me realize that it should be possible to use short synthetic deoxyribooligonucleotides as specific mutagens and to differentiate between a point mutant and wild-type DNA.

Experiments on the interaction of deoxyribooligonucleotide celluloses and ribooligonucleotides confirmed the results of earlier studies on the relative stabilities of DNA–DNA and DNA–RNA double strands.[39, 41] They also demonstrated a further important principle: a dT, rG



Michael Smith, born in Blackpool, Great Britain, on April 26, 1932, studied Chemistry at the University of Manchester from 1950 to 1953. He finished his Ph.D. there in 1956 with H. B. Henbest on cyclohexane diols and then joined the group of Gobind Khorana in Vancouver, Canada, as Postdoctoral Fellow to work on biologically important organophosphates. In 1960 he moved with the group to the Institute for Enzyme Research at the University of Wisconsin and worked on the synthesis of ribooligonucleotides. In 1961 he accepted a post at the Fischeries Research Board of Canada Laboratory in the grounds of the University of British Columbia in Vancouver. He was awarded the position of Medical Research Associate of the Medical Research Council of Canada at this university in 1966. A new interdisciplinary Institute, the Biotechnology Laboratory, came into being in 1986 with his help. After a heavy load of administrative tasks recently, he is looking forward to returning to the bench.

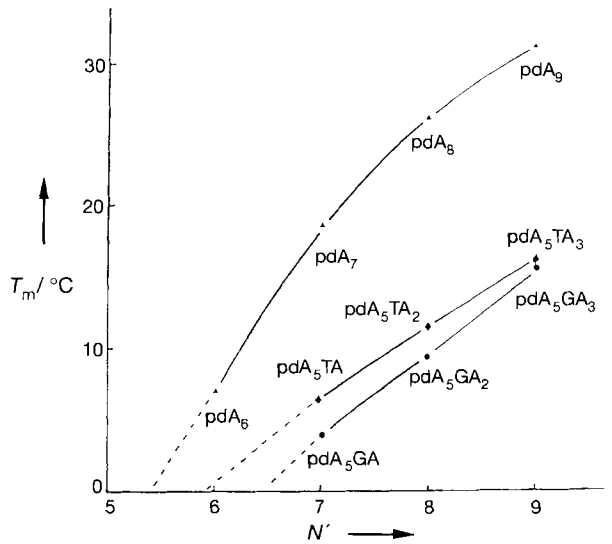


Fig. 2. The T_m values of the duplexes of complementary oligodeoxyribonucleotides with cellulose-pdTq in 1 M NaCl, 0.01 M sodium phosphate, pH 7.0 [38]. The oligodeoxyribonucleotides of the two lower curves each contain a single base-pair mismatch. N' = number of the deoxyribonucleotide residues.

base pair is relatively stable (Fig. 3). Differences in the stability of dT, dG and dT, rG base pairs (compare Figs. 2 and 3), presumably, reflect differences in the base pairing allowed in the B forms and the A forms of double helix.[42] The observation has two practical implications. First, the most specific and stringent interaction of an oligonucleotide probe will be the one between a deoxyribooligonucleotide and DNA. Second, one cannot assume that duplex structures that are formed by RNA will be formed by DNA or by deoxyribooligonucleotides. In connection with this, I have always been puzzled by the widespread acceptance of the idea that deoxyinosine is precocious in base pairing because inosine behaves in a precocious manner in tRNA duplex interactions. Studies on deoxyinosine, in fact, indicate that it functions as a specific analog of deoxyguanosine, although it does not self-aggregate as does deoxyguanosine.[7, 8, 42]

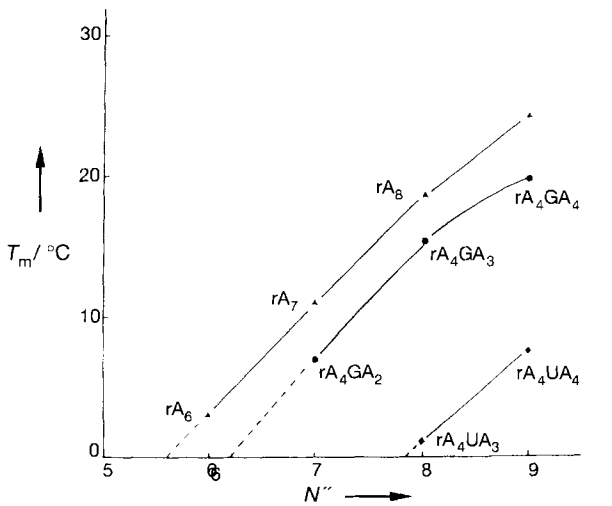


Fig. 3. The T_m values of the duplexes with cellulose-pdTq in 1 M NaCl, 0.01 M sodium phosphate, pH 7.0 [38]. The oligoribonucleotides of the two lower curves each contain a single base-pair mismatch. N'' = number of ribonucleotide residues.

The above empirical studies and related ones not discussed here[39] provided the direct inspiration for and commitment to our use of synthetic deoxyribooligonucleotides as probes for isolation of specific DNA fragments, as primers for the direct sequencing of double-stranded DNA, as primers for precise definition of the ends of mRNAs, as specific mutagens, and as tools for the identification and isolation of point mutations.

Deoxyribooligonucleotides as DNA Probes

When the model studies described in the foregoing section were commenced, in 1968, the intent was to develop a method for isolation of specific mRNAs by affinity chromatography. However, the development of the full panoply of DNA cloning techniques in the early 1970s[9] made it clear that the prime target for work with synthetic deoxyribooligonucleotides should be a method for monitoring gene isolation. Discussions with Dr. Benjamin D. Hall made me aware of the important studies of F. Sherman on double-frameshift mutants of yeast cytochrome *c*.[44] Knowledge of the amino acid sequence of these mutants allowed the unambiguous prediction of the N-terminal coding sequence and, hence, provided a specific target for an oligonucleotide of defined sequence. A second attractive feature about a yeast gene as a first target was the fact that the length of oligonucleotide required for a specific probe (13 nucleotides, Table 1) was close to the limit for our enzymatic method of synthesis.[19, 21, 22] The required probe was synthesized by means of the enzymatic method[45] and was used to isolate the gene, albeit with some difficulty,[46] thus clearly validating the principle that a synthetic oligonucleotide could function as a probe for gene isolation. The subsequent generalization of the method using mixtures of oligonucleotides[47, 48] has made this approach to gene isolation into a powerful tool in molecular genetics.[7, 8]

Sequencing Double-Stranded DNA with Oligonucleotide Primers

At the time when the iso-1-cytochrome *c* gene was isolated, the chemical method for DNA sequence determination[49] and the chain terminating enzymatic method[50] had newly been developed; the former is applicable to double-stranded DNA and the latter to single-stranded DNA. The sequences of the ends of the Eco RI-Hind III DNA fragment containing the cytochrome *c* coding sequence were obtained by the chemical method.[46] Based on my conviction that an oligonucleotide should hybridize *at low temperature* with a complementary DNA strand of a denatured DNA double helix in solution, even though the second DNA strand was present and capable of producing a thermodynamically much more stable structure, I decided to investigate the possibility of directly sequencing double-stranded DNA by the enzymatic method with synthetic oligonucleotide primers. The critical question was whether the second DNA strand would displace a short oligonucleotide from a complex with the complementary DNA strand under the conditions of the Sanger enzymatic sequencing method.[51] The first experiment was completely successful, an enormously excit-

ing event. As a consequence, the sequence of the gene was completed by "walking" along the sequence with a series of short oligonucleotide primers nine or ten nucleotides in length.[52] I believe that the full potential of this approach to gene sequencing has yet to be realized.

Another important application of oligonucleotide-primed sequencing of double-stranded DNA is the precise identification of point mutations produced by classical genetic techniques at a given locus. A particular good example was in the analysis of a large number of independently isolated point mutations in a yeast suppressor tRNA gene.[53, 54]

Defining the Ends of mRNAs Precisely

It is important to define the sequences at the 5'- and 3'-ends of mRNAs exactly. For the 3'-end of an mRNA, this can be done by oligonucleotide-primed sequencing with reverse transcriptase for the Sanger sequencing method with RNA enriched for the desired mRNA as template. The family of 12 deoxyribooligonucleotides consisting of a tract of dT residues terminated at the 3'-end by two other deoxyribonucleotides can be annealed to the 3'-end of polyladenylated eukaryotic mRNA. If the transcribed sequence has a unique 3'-end, only one of the twelve oligonucleotides should act as a specific primer. This strategy was used to define the sequence of the unique 3'-end of bovine growth hormone mRNA[55] and to demonstrate and precisely define the microheterogeneity at the 3'-end of the bovine prolactin mRNA transcript.[56] The iso-1-cytochrome *c* proved to have a unique 3'-end,[57] while the 5'-end of the same mRNA is very disperse indeed, as was shown by oligonucleotide primed extension using the mRNA as template.[58] There are no other methods for defining the 5'- and 3'-ends of mRNAs with this precision, a degree of precision that is essential to the accurate definition of transcription initiation and termination signals.[57, 58]

Oligonucleotide-Directed Mutagenesis

I strongly believe that, through the products of organic synthesis, it will be possible to gain influence over the development of organisms and to produce changes that surpass all that can be achieved by conventional breeding.
Emil Fischer[59]

"The ignis fatuus *of Genetics has been the specific mutagen, the reagent that would penetrate to a given gene, recognize it, and modify it in an specific way."*
J. Lederberg[60]

Initiation of the project to isolate the yeast cytochrome *c* gene made me realize that I needed to learn about DNA sequence determination. I was lucky to be able to spend a year, starting in the fall of 1975, in Fred Sanger's laboratory working with the "plus-minus" sequencing method as part of the team that was attacking the sequence of the *E. coli* phage ΦX174.[61, 62] There are three pairs of overlapping genes in the 5386 nucleotide genome.[63–65] All genes are encoded on the same DNA strand, and each overlapping pair uses different codon reading frames. An essential integral component of defining the position and reading frame of these genes was the availability of nonsense mutants suppressible by amber or ochre suppressors. This use of precisely located mutants of a particular phenotype highlighted the need for a very specific mutagenic method that would define the target to a specific base pair in the genome and introduce a predetermined change with sufficiently high efficiency to allow genomic screening in order to identify phenotypically silent mutants. Since the DNA of phage ΦX174 is single stranded and the complete sequence of its genome was known from our earlier studies, the demonstration that small oligonucleotides as short as seven nucleotides in length could form stable duplexes at low temperature even with a mismatch (Fig. 2) suggested that oligonucleotide-directed mutagenesis should be possible. There was additional useful information: *Point mutants can be reverted*, albeit with low efficiency, by annealing mutant phage ΦX174 DNA with fragments from the complementary strand of wild-type DNA prior to transfection.[66, 67] However, fragments very much longer than those that we could readily synthesize were needed, and the low efficiency precluded genotypic screening.[66, 67] In discussing these issues, Clyde Hutchison (who, also was spending one year in Fred Sanger's group and whose biological knowledge of ΦX174 was invaluable to the sequencing project) and I realized that the studies of Kornberg and Goulian.[43, 68–70] provided an obvious route to a mutagenic method, since they had demonstrated that an oligonucleotide as short as nine nucleotides in length could act as a primer for *E. coli* DNA polymerase I on a circular single-strand template, and that the product could be converted into a closed circular duplex by enzymatic ligation. It was also known that most of the primer molecule is excised from the product,[72] presumably due to the 5'-exonuclease activity of *E. coli* DNA polymerase I.[71] With this information and our knowledge that the stability of duplexes involves a mismatched oligonucleotide, we decided to use a 12 nucleotide oligomer, with a centrally positioned single nucleotide mismatch, as primer and with ΦX174 DNA as template and *E. coli* DNA polymerase I in which the 5'-exonuclease had been inactivated by subtilisin[73–75] to construct a closed, circular, double-stranded DNA with the oligonucleotide in one strand. Transfection of *E. coli* with this DNA should produce wild-type and mutant phage. The specific mutations chosen for the first experiment were the production and reversion of a known nonsense mutation *am3* in the lytic function, gene E, of ΦX174, since convenient phenotypic screens for these mutations were available. The mutations involved the interconversion of a Trp codon TGG and an amber codon TAG by G–T and A–C mismatches.[76] In the first experiments, mutation was achieved but at low efficiency. This was increased to a very encouraging level of about 15% after removal of incompletely closed duplexes by adsorption to nitrocellulose or treatment with a single-strand specific nuclease under conditions in which a single base-pair mismatch was not degraded.[76] Further studies directed at optimizing the mutagenic conditions resulted in efficiencies of up to 39% with a 12 nucleotide mutagenic primer and significant mutation with a heptamer mutagenic primer.[77] The wisdom of using subtilisin-treated DNA polymerase is evident from comparison of these results with those of another study which employed intact *E. coli* DNA polymerase I.[78]

Further studies on the mutagenesis of phage ΦX174 demonstrated that, in addition to the two transition mutations of the first experiments, it was possible to produce transversion mutations and single nucleotide deletions, also by using very short oligonucleotides.[79] Clearly, the method was highly specific, efficient, and general within the context of the genome of ΦX174. It was time to generalize the method further so that it could be applied to any cloned fragment of DNA. The icosahedral bacteriophages, such as ΦX174, are not potential vectors for recombinant DNA because the amount of DNA that can be accommodated in the viral particle is limited. The filamentous bacteriophages, on the other hand, can accommodate additional DNA incorporated into the genome. At the time when Mark Zoller and I were planning the generalization of the method, there were those that argued in favor of a methodology applied to double-stranded recombinant plasmids. It seemed to us that the biology of a filamentous bacteriophage, which produces single-stranded, circular DNA and then purifies it as phage particles, argued overpoweringly in favor of phage DNA as vector. Subsequent developments in recombinant phage biology and in the construction of phagemids[7, 8] have vindicated this strategic decision, although viable procedures for plasmid mutagenesis are available.[80–82] Oligonucleotide mutagenesis with filamentous phage DNA as template proved to be more difficult than with ΦX174 DNA, presumably because of a greater degree of secondary structure that inhibited the production of full-length, double-stranded circles. Consequently, new procedures for enhancing the efficiency of the mutagenic procedure had to be developed.[83–86] The power of the methodology was graphically illustrated by our first involvement in protein engineering in collaboration with Greg Winter and Alan Fersht.[87] This, of course, presaged the enormous use of the methodology in protein structure–function analysis that has become a feature of modern biochemistry.

Genotypic Selection or Screening for Mutants

Because the immediate product of the enzymatic incorporation of a mutagenic oligonucleotide into a double-stranded recombinant DNA is a heteroduplex, biological replication of the DNA will produce mutated and unmutated progeny DNAs, providing there is no asymmetry in the mechanism of DNA replication or providing there is not an asymmetric mismatch-repair mechanism. In fact, it is possible to achieve mutagenic efficiencies of close to 50% by using standard procedures[77, 85] With this level of efficiency, screening by DNA sequence determination is the most effective procedure for detecting the desired mutant DNA. However, often the yield of mutant is considerably less than 50%. It is my opinion that the predominant reason for this is the use of template DNA that is contaminated with random oligonucleotides resulting from bacterial DNA degradation; others ascribe it to biological mismatch-repair favoring the sequence of the template DNA.[80] Whatever the cause of the reduced yield of mutant, procedures other than sequence determination are required for mutant identification. The ones that are available fall into two categories: those using the mutagenic oligonucleotide as a tool for identifying mutant DNA and those which select for progeny derived from the newly synthesized, oligonucleotide-containing DNA strand.

The significantly enhanced stability of a perfectly matched oligonucleotide duplex relative to one with a mismatch (see Fig. 2) suggested that a mutagenic oligonucleotide should be able to identify mutant complementary DNA. This principle was used to develop a method for *selection* of mutant DNA. In this procedure the mixture of wild-type and mutant single-stranded phage DNA produced by oligonucleotide mutagenesis acts as a template for double-stranded DNA synthesis with the mutagenic oligonucleotide as primer under conditions that should not form a mismatched duplex.[88] Following transfection into *E. coli*, this procedure can select mutant DNA with close to 100% efficiency.

An alternative procedure is to use the mutagenic oligonucleotide as a probe to screen for mutant DNA in plaques produced by *E. coli* with mutagenized phage.[83, 84] Again, this procedure is very reliable in the identification of mutant DNA. The same principle is used in the identification of point mutations in human DNA[89] where, of course, the complexity of the human genome requires a probe containing a minimum of 17 nucleotides (see Table 1).

A number of procedures for selection of progeny derived from the DNA strand containing the mutagenic oligonucleotide have been developed.[80] Two of these, one based on in vivo selection and the other on in vitro selection have proved most popular and are widely used. In vivo selection involves a template DNA in which about 1% of the deoxythymidine residues have been replaced by deoxyuridine residues. This template is incorporated into double-stranded DNA in which the mutagenic oligonucleotide is part of the in vitro synthesized second strand. On transfection of an appropriate *E. coli* host, the deoxyuridine strand is selectively degraded by the bacterium's DNA damage-repair system, resulting in progeny derived primarily from the mutant strand.[90] In vitro selection involves a normal recombinant phage template DNA with the mutagenic oligonucleotide incorporated in the second strand that contains enzymatically synthesized thiophosphate internucleotide linkages. These are resistant to cleavage by restriction endonuclease, which, as a consequence nicks the template. The nicked template is partially degraded with an exonuclease and then repaired by a DNA polymerase and DNA ligase. The result is a double-stranded DNA which, predominantly, is mutant in both strands and which produces, predominantly, mutant recombinant phage on transfection of *E. coli*.[91]

Conclusion

This concludes my account of our studies on the use of synthetic deoxyribooligonucleotides as tools for characterizing naturally occurring nucleic acids, which is as accurate as I can make it, bearing in mind the caveat of Fred Sanger[1] cited at the beginning of this article. Clearly, many other applications of oligonucleotide in biology exist, notably the polymerase chain reaction[92] and its multitudinous variations, but also in double-strand DNA synthesis and in the use of oligonucleotide probes in vitro and in vivo. In the latter area there is the potential for development of a whole new chemistry directed at pharmaceuti-

cals that block the expression of specific genes and at diagnostic agents.[93, 94]

With regard to our own work, it is very satisfying that the model studies started in 1968 provided the inspiration for so many applications and scientific collaborations (only a few of which are cited in this article). The potential of oligonucleotide-directed site-specific mutagenesis was apparent from the outset as confirmed by the following quote:

> *"This new method of mutagenesis has considerable potential...to define the role of... origins of DNA replication, promoters, and the sequences for ribosome-building sites ... specific mutation within protein structural genes ... will allow precise studies of protein structure–function relationships"*
> Hutchison et al.[76]

However, we could not have anticipated the explosion of gene isolations, the improvements in DNA sequence determination methodology, and the advances in the chemistry of nucleic acids synthesis that have occurred since 1978. This has resulted in an amazing increase in the use of site-directed mutagenesis as an analytical tool in biochemistry and biology. And it has been accompanied by continual improvements in the basic methodologies and versatility of site-directed mutagenesis[80–82] and the initiation of new scientific publications such as Protein Engineering and Protein Science. It would not be too much of an exaggeration to say that the prediction of Emil Fischer in 1917[59] has been fulfilled, and the dilemma posed by Joshua Lederberg in 1959[60] has been resolved.

My career in nucleic acid research would not exist without the example and inspiration of Gobind Khorana. Also, I am indebted to the many young scientists who have been members of my group over the past 30 years, but especially to Caroline Astell, Shirley Gillam, Patricia Jahnke, and Mark Zoller, who were the individuals primarily responsible for the studies discussed in this article, as well as to Tom Atkinson who undertook the arduous task of manual chemical synthesis of oligonucleotides in the time immediately prior to the introduction of automated synthesizers. Two crucial, indispensible collaborators, whose biological expertise and commitment were essential to these studies, were Ben Hall in the studies on the isolation of the yeast cytochrome c gene and Clyde Hutchison in the development of oligonucleotide-directed mutagenesis. And my year in Fred Sanger's laboratory was wonderful in its excitment and in its timeliness. Research funding support by the U.S. National Institutes of Health was essential in allowing me to continue synthetic nucleotide chemistry in the years immediately after I left the Khorana group. Since 1966, the Medical Research Council of Canada has continuously provided me with the salary support and research grants that have been the stable and very much appreciated foundation for my more speculative research activities. I have also received, for more limited periods, research support from the British Columbia Health Research Foundation and from the National Cancer Institute of Canada. For the past four years I have been Scientific Leader of the Canadian Protein Engineering Network of Centres of Excellence, a country-wide collaboration on protein structure-function analysis, generously funded by the Network of Centres of Excellence program. Finally, firstly at the British Columbia Research Council, then at the Fisheries Research Board of Canada Vancouver Laboratory, mostly in the Department of Biochemistry and more recently in the Biotechnology Laboratory, the campus of the University of British Columbia has been my scientific home since 1956. I am very grateful for the environment that it has provided, especially in the Department of Biochemistry where the studies described in this article were carried out.

Received: January 19, 1994 [A 50 IE]
German version: *Angew. Chem.* **1994**, *106*, 1277

[1] *Sequences, sequences and sequences:* F. Sanger, *Annu. Rev. Biochem.* **1988**, *57*, 1–28.
[2] *A new approach to the synthesis of polynucleotides:* H. G. Khorana, G. M. Tener, J. G. Moffatt, E. H. Pol, *Chem. Ind. London* **1956**, 1523.
[3] H. G. Khorana, *Some Recent Developments in the Chemistry of Phosphate Esters of Biological Interest*, J. Wiley, New York, **1961**.
[4] *Nucleic acid synthesis in the study of the genetic code*: H. G. Khorana in *Les Prix Nobel en 1968*, P. A. Nerstedt, Stockholm, **1969**, p. 196–200.
[5] *Total synthesis of a gene*: H. G. Khorana, *Science* **1979**, *203*, 614–625.
[6] *A new synthesis of guanosine-5'-phosphate*: R. W. Chambers, J. G. Moffatt, H. G. Khorana, *J. Am. Chem. Soc.* **1957**, *79*, 3747–3752.
[7] F. M. Ausubel, R. Brent, R. E. Kingston, D. D. Moore, J. G. Seidman, J. A. Smith, K. Struhl, *Current Protocols in Molecular Biology*: (two volumes, supplemented quarterly), Wiley Interscience, New York, **1987**.
[8] J. Sambrook, E. F. Fritsch, T. Maniatis, *Molecular Cloning. A Laboratory Manual*, 2nd ed. (three volumes), Cold Spring Harbor Laboratory Press, Cold Spring Harbor, NY, **1989**.
[9] J. D. Watson, M. Gilman, J. Witkawski, M. Zoller, *Recombinant DNA*, 2nd ed., Scientific American Books, New York, **1993**.
[10] *An improved and general method for the synthesis of ribo- and deoxyribo-nucleoside-5' triphosphates*: M. Smith, H. G. Khorana, *J. Am. Chem. Soc.* **1958**, *80*, 1141–1145.
[11] *The synthesis and properties of ribonucleoside-3',5' cyclic phosphates*: M. Smith, G. I. Drummond, H. G. Khorana, **1961**, *83*, 698–706.
[12] *Synthesis of uridylyl-(3' → 5')-Uridine and uridylyl-(3' → 5')-adenosine*: M. Smith, D. H. Rammler, I. H. Goldberg, H. G. Khorana, *J. Am. Chem. Soc.* **1962**, *84*, 430–440.
[13] *Specific synthesis of the C5'-C3' interribonucleotide linkage: the synthesis of uridylyl-(3' → 5')-uridine*: M. Smith, H. G. Khorana, *J. Am. Chem. Soc.* **1959**, *81*, 2911.
[14] *Synthesis of deoxyribonucleoside-3',5' cyclic phosphates by base-catalysed transesterification*: M. Smith, *J. Am. Chem. Soc.* **1964**, *86*, 3586.
[15] *Preparation of nucleoside-3',5' cyclic phosphates in strong base*: R. K. Borden, M. Smith, *J. Org. Chem.* **1966**, *31*, 3247–3253.
[16] *Oligodeoxyribo-nucleotides: chemical synthesis in anhydrous base*: R. von Tigerstrom, M. Smith, *Science* **1970**, *167*, 1266–1268.
[17] *The synthesis of the internucleotide bond by a base-catalysed reaction*: R. von Tigerstrom, P. Jahnke, M. Smith, *Nucleic Acids Res.* **1975**, *2*, 1727–1736.
[18] *Application of base-catalysed reaction to the synthesis of dinucleotides containing the four common deoxyribonucleosides and of oligodeoxythymdylates*: R. von Tigerstrom, P. Jahnke, M. Smith, *Nucleic Acids Res.* **1975**, *2*, 1737–1743.
[19] *Enzymatic synthesis of deoxyribo-oligonucleotides of defined sequence*: S. Gillam, M. Smith, *Nature (London) New Biol.* **1972**, *238*, 233–234.
[20] *Enzymatic synthesis of deoxyribo-oligonucleotides of defined sequence. Properties of the enzyme*: S. Gillam, M. Smith, *Nucleic Acids Res.* **1974**, *1*, 1631–1648.
[21] *Use of E. coli polynucleotide phosphorylase for the synthesis of oligodeoxyribonucleotides of defined sequene*: S. Gillam, M. Smith, *Methods Enzymol.* **1980**, *65*, 687–701.
[22] *Enzymatic synthesis of oligo-deoxyribonucleotides of defined sequence*: S. Gillam, P. Jahnke, M. Smith, *J. Biol. Chem.* **1978**, *253*, 2532–2539.
[23] *Hindered dialkylamino nucleoside phosphite reagents in the synthesis of two DNA 51-mers*: S. P. Adams, K. S. Kavka, E. J. Wykes, S. B. Holder, G. R. Galluppi, *J. Am. Chem. Soc.* **1983**, *105*, 661–663.
[24] *Solid-phase synthesis of oligodeoxyribo-nucleotides by the phosphite-triester method*: T. Atkinson, M. Smith in *Oligonucleotide Synthesis. A Practical Approach* (Ed.: M. J. Gait), IRL, Oxford, **1984**, p. 35–81.
[25] *An investigation of several deoxyribonucleoside phosphoramidates useful for synthesizing deoxyoligonucleotides*: L. J. McBride, M. H. Caruthers, **1983**, *24*, 245–248.
[26] *Biosynthesis of protamine during spermatogenesis in salmonid fish*: C. J. Ingles, J. R. Trevithick, M. Smith, G. H. Dixon, *Biochem. Biophys. Res. Commun.* **1966**, *22*, 627–634.
[27] *The intracellular location of the adenine- and thymine-rich component of deoxyribonucleate in testicular cells of the crab, Cancer productus*: C. R. Astell, D. T. Suzuki, R. P. Klett, M. Smith, I. H. Goldberg, *Exp. Cell Res.* **1969**, *54*, 3–10.

[28] *Oligonucleotides and their association with polynucleotides*: A. M. Michelson, C. Monny, *Biochim. Biophys. Acta* **1967**, *149*, 107–126.

[29] *The stability of oligoadenylate-polyuridylate complexes as measured by thermal chromatography*: S. K. Niyogi, C. A. Thomas, Jr., *J. Biol. Chem.* **1968**, *243*, 1220–1223.

[30] *Complex formation in polynucleotides and its application to the separation of polynucleotides*: P. T. Gilham, *J. Am. Chem. Soc.* **1962**, *84*, 1311–1312.

[31] *The use of polynucleotide-celluloses in sequence studies of nucleic acids*: P. T. Gilham, W. E. Robinson, *J. Am. Chem. Soc.* **1964**, *86*, 4985–4989.

[32] *Purification of biologically active globin messenger RNA by chromatography on oligothymidylic acid-cellulose*: H. Aviv, P. Leder, *Proc. Natl. Acad. Sci. USA* **1972**, *69*, 1408–1412.

[33] *The interaction of oligodeoxyribonucleotides with denatured DNA*: B. L. McConaughy, B. J. McCarthy, *Biochim. Biophys. Acta* **1967**, *149*, 180–189.

[34] *The influence of chain length and base composition on the specific association of oligoribonucleotides with denatured deoxyribonucleic acid*: S. K. Niyogi, *J. Biol. Chem.* **1969**, *244*, 1576–1581.

[35] *Further studies on the properties of oligonucleotide cellulose columns*: C. R. Astell, M. T. Doel, P. A. Jahnke, M. Smith, *Biochemistry* **1973**, *12*, 5068–5074.

[36] *Thermal elution of complementary sequences of nucleic acids from cellulose columns with covalently attached oligonucleotides of known length and sequence*: C. R. Astell, M. Smith, *J. Biol. Chem.* **1971**, *246*, 1944–1946.

[37] *Synthesis and properties of oligonucleotide-cellulose columns*: C. R. Astell, M. Smith, *Biochemistry* **1972**, *11*, 4114–4120.

[38] *The base-pairing specificity of cellulose-pdT_9*: S. Gillam, K. Waterman, M. Smith, *Nucleic Acids Res.* **1975**, *2*, 625–634.

[39] *Synthetic oligodeoxyribonucleotides as probes for nucleic acids and as primers in sequence determination*: M. Smith in *Methods of DNA and RNA Sequencing* (Ed.: S. M. Weissman), Praeger, New York, **1983**, pp. 23–68.

[40] *The chemical synthesis of deoxyribo-oligonucleotides complementary to a portion of the lysozyme gene of phage T4 and their hybridization to phage-specific RNA and phage DNA*: M. T. Doel, M. Smith, *FEBS Lett.* **1973**, *34*, 99–102.

[41] *Cooperative properties of DNA, RNA and hybrid homopolymer pairs*: M. J. Chamberlin, *Fed. Proc.* **1965**, *24*, 1446–1457.

[42] J. D. Watson, N. H. Hopkins, J. W. Roberts, J. A. Steitz, A. M. Weiner, *Molecular Biology of the Gene*, 4th ed., Benjamin/Cummings, Menlo Park, CA, **1987**.

[43] A. Kornberg, W. H. Freeman, *DNA Replication*, San Francisco, CA, **1980**.

[44] *Yeast frameshift mutations identified by sequence changes in iso-1-cytochrome c*: J. W. Stewart, F. Sherman, in *Molecular and Environmental Aspects of Mutagenesis* (Ed.: L. Prakash, F. Sherman, M. W. Miller, C. W. Lawrence, H. W. Taber), Charles C. Thomas, Springfield, IL, **1974**, pp. 102–107.

[45] *Enzymatic synthesis of oligonucleotides of defined sequence: synthesis of a segment of yeast iso-1-cytochrome c gene*: S. Gillam, F. Rottman, P. Jahnke, M. Smith, *Proc. Natl. Acad. Sci. USA* **1977**, *74*, 96–100.

[46] *Identification and isolation of the yeast cytochrome c gene*: D. L. Montgomery, B. D. Hall, S. Gillam, M. Smith, *Cell* **1978**, *14*, 673–680.

[47] *Hybridization of oligonucleotides of mixed sequence to rabbit β-globin DNA*: R. B. Wallace, M. J. Johnson, T. Hirose, T. Miyake, E. H. Kawashima, K. Itakura, *Nucleic Acids Res.* **1981**, *9*, 3647–3656.

[48] *Use of synthetic oligonucleotides as hybridization probes: isolation of cloned cDNA sequences for human β_2-microglobulin*: S. V. Suggs, R. B. Wallace, T. Hirose, E. H. Kawashima, K. Itakura, *Proc. Natl. Acad. Sci. USA* **1981**, *78*, 6613–6617.

[49] *A new method for sequencing DNA*: A. M. Maxam, W. Gilbert, *Proc. Natl. Acad. Sci. USA* **1977**, *74*, 560–564.

[50] *DNA sequencing with chain terminating inhibitors*: F. Sanger, S. Nicklen, A. R. Coulson, *Proc. Natl. Acad. Sci. USA* **1977**, *74*, 5463–5467.

[51] *Determination of nucleotide sequences in DNA*: F. Sanger in *Les Prix Nobel En 1980*, Norstedt, Stockholm, **1981**, p. 143–159.

[52] *Sequence of the gene for iso-1-cytochrome c in Saccharomyces cerevisae*: M. Smith, D. W. Leung, S. Gillam, C. R. Astell, D. L. Montgomery, B. D. Hall, *Cell* **1979**, *16*, 753–761.

[53] *Mutations at the yeast SUP4 tRNA*Tyr *locus; transcription of the mutant genes in vitro*: R. A. Koski, S. G. Clarkson, J. Kurjan, B. D. Hall, M. Smith, *Cell* **1980**, *22*, 415–425.

[54] *Mutations at the yeast SUP4 $tRNA^{Tyr}$ locus: DNA sequence changes in mutants lacking suppresor activity*: J. Kurjan, B. D. Hall, S. Gillam, M. Smith, *Cell* **1980**, *20*, 701–709.

[55] *Use of oligodeoxynucleotide primers to determine poly(adenylic acid) adjacent sequences in messenger ribonucleic acid*: N. L. Sasavage, M. Smith, S. Gillam, C. Astell, J. H. Nilson, F. Rottman, *Biochemistry* **1980**, *19*, 1737–1743.

[56] *Variation in the polyadenylation site of prolactin messenger RNA*: N. L. Sasavage, M. Smith, S. Gillam, R. P. Woychik, F. M. Rottman, *Proc. Natl. Acad. Sci. USA* **1982**, *79*, 223–227.

[57] *Sequence of the yeast iso-1-cytochrome c mRNA*: J. M. Boss, S. Gillam, R. S. Zitomer, M. Smith, *J. Biol. Chem.* **1981**, *256*, 12958–12961.

[58] *Saccharomyces cerevisiae CYC1 mRNA 5'-end positioning: analysis by in vitro mutagenesis, using synthetic duplexes with random mismatch base pairs*: J. B. McNeil, M. Smith; *Mol. Cell Biol.* **1985**, *5*, 3545–3551.

[59] E. Fischer, **1917**.

[60] *A view of genetics*: J. Lederberg in *Les Prix Nobel En 1958*, Norstedt, Stockholm, **1959**, pp. 170–189.

[61] *A rapid method for determining sequences in DNA by primed synthesis with DNA polymerase*: F. Sanger, A. R. Coulson, *J. Mol. Biol.* **1975**, *94*, 441–448.

[62] *The nucleotide sequence of bacteriophage ΦX174*: F. Sanger, A. R. Coulson, T. Friedmann, B. G. Barrell, N. L. Brown, J. C. Fiddes, C. A. Hutchison III, P. M. Slocombe, M. Smith, *J. Mol. Biol.* **1978**, *125*, 225–246.

[63] *Overlapping genes in bacteriophage ΦX174*: B. G. Barrell, G. M. Air, C. A. Hutchison III, *Nature* **1976**, *264*, 34–41.

[64] *The sequence of a region of bacteriophage ΦX174 coding for parts of genes A and B*: N. L. Brown, M. Smith, *J. Mol. Biol.* **1977**, *116*, 1–28.

[65] *Gene K of bacteriophage ΦX174 codes for a protein which affects the burst size of phage production*: S. Gillam, T. Atkinson, A. Markham, M. Smith, *J. Virol.* **1985**, *53*, 708–709.

[66] *Genetic assay for small fragments of bacteriophage ΦX174 deoxyribonucleic acid*: C. A. Hutchison III, M. H. Edgell, *J. Virol.* **1971**, *8*, 181–189.

[67] *Biological activity of ΦX174 replicative form DNA fragments*: P. J. Weisbeek, J. H. van de Pol, *Biochim. Biophys. Acta* **1970**, *224*, 328–338.

[68] *Incorporation of oligodeoxynucleotides into DNA*: M. Goulian, *Proc. Natl. Acad. Sci. USA* **1968**, *61*, 284–291.

[69] *Synthesis of infectious phage ΦX174 DNA*: M. Goulian, A. Kornberg, R. L. Sinsheimer, *Proc. Natl. Acad. Sci. USA* **1967**, *58*, 2321–2328.

[70] *Properties of oligodeoxynucleotides that determine priming activity with Escherichia coli deoxyribonucleic acid polymerase I*: M. Goulian, S. H. Goulian, E. E. Codd, A. Z. Blumenfield, *Biochemistry* **1973**, *12*, 2893–2901.

[71] *Exonuclease VI, a new nuclease activity associated with E. coli DNA polymerase*: R. P. Klett, A. Cerami, E. Reich, *Proc. Natl. Acad. Sci. USA*, **1968**, *60*, 943–950.

[72] *Initiation of the replication of single-stranded DNA by Escherichia coli DNA polymerase*: M. Goulian, *Cold Spring Harbor Symp. Quant. Biol* **1968**, *33*, 11–20.

[73] *An active fragment of DNA polymerase produced by proteolytic cleavage*: D. Brutlag, M. R. Atkinson, P. Setlow, A. Kornberg, *Biochem. Biophys. Res. Commun.* **1969**, *37*, 982–989.

[74] H. Klenow, I. Henningsen, *Selected elimination of the exonuclease activity of the deoxyribonucleic acid polymerase from Escherichia coli B by limited proteolysis*: H. Klenow, I. Henningsen, *Proc. Natl. Acad. Sci. USA* **1970**, *65*, 168–175.

[75] *Proteolytic cleavage of native DNA polymerase into two different catalytic fragments. Influence of assay conditions on the change of exonuclease activity and polymerase activity*: H. Klenow, K. Overgaard-Hansen, S. A. Patkar, *Eur. J. Biochem.* **1971**, *22*, 371–381.

[76] *Mutagenesis at a specific position in a DNA sequence*: C. A. Hutchison III, S. Phillips, M. H. Edgell, S. Gillam, P. Jahnke, M. Smith, *J. Biol. Chem.* **1978**, *253*, 6551–6560.

[77] *Site-specific mutagenesis using synthetic oligodeoxyribonucleotide primers: optimum conditions and minimum oligodeoxyribonucleotide length*: S. Gillam, M. Smith, *Gene* **1979**, *8*, 81–97.

[78] *Efficient correction of a mutation by use of chemically synthesized DNA*: A. Razin, T. Hirose, K. Itakura, A. D. Riggs, *Proc. Natl. Acad. Sci. USA* **1978**, *75*, 4268–4270.

[79] *Constructed mutants using synthetic oligodeoxyribonucleotides as site-specific mutagens*: M. Smith, S. Gillam in *Genetic Engineering. Principles and Methods, Vol. 3* (Ed.: J. K. Setlow, A. Hollaender), Plenum, New York, **1981**, pp. 1–52.

[80] *In vitro mutagenesis*: M. Smith, *Annu. Rev. Genet.* **1985**, *19*, 423–462.

[81] *New molecular biology methods for protein engineering*: M. J. Zoller, *Curr. Opin. Biotechnol.* **1991**, *2*, 526–531.

[82] *New recombinant DNA methodology for protein engineering*: M. J. Zoller, *Curr. Opin. Biotechnol.* **1992**, *3*, 348–354.

[83] *Oligonucleotide-directed mutagenesis using M13-derived vectors: an efficient and general procedure for the production of point mutations in any fragment of DNA*: M. J. Zoller, M. Smith, *Nucleic Acids Res.* **1982**, *10*, 6487–6500.

[84] *Oligonucleotide-directed mutagenesis of fragments cloned in M13 vectors*: M. J. Zoller, M. Smith, *Methods Enzymol.* **1983**, *100*, 468–500.

[85] *Oligonucleotide-directed mutagenesis: a simple method using two oligonuleotide primers and a single-stranded DNA template*: M. J. Zoller, M. Smith, *DNA* **1984**, *3*, 479–488.

[86] *Oligonucleotide-directed mutagenesis: a simple method using two oligonucleotide primers and a single-stranded DNA template*: M. J. Zoller, M. Smith, *Methods Enzymol.* **1987**, *154*, 329–350.

[87] *Redesigning enzyme structure by site-directed mutagenesis: tyrosyl t-RNA synthetase and ATP binding*: G. Winter, A. R. Fersht, A. J. Wilkinson, M. J. Zoller, M. Smith, *Nature* **1982**, *299*, 756–758.

[88] *Site-specific mutagenesis using synthetic oligodeoxyribonucleotide primers: in vitro selection of mutant DNA*: S. Gillam, M. Smith, *Gene* **1979**, *8*, 99–106.

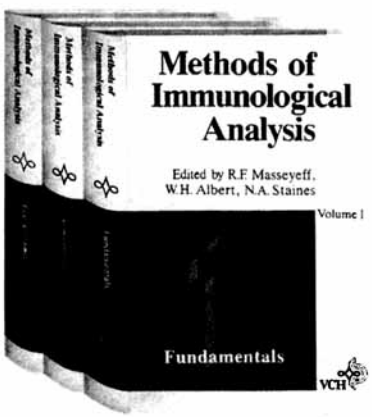
[89] *Detection of sickle-cell β^S-globin allele by hybridization with synthetic oligonucleotides*: B. J. Conner, A. A. Reyes, C. Morin, K. Itakura, R. L. Teplitz, R. B. Wallace, *Proc. Natl. Acad. Sci., USA* **1983**, *80*, 278–282.
[90] *Rapid and efficient site-specific mutagenesis without phenotypic selection*: T. A. Kunkel, *Proc. Natl. Acad. Sci. USA* **1985**, *82*, 488–492.
[91] *The rapid generation of oligonucleotide-directed mutations at high frequency using phosphothioate-modified DNA*: J. W. Taylor, J. Ott, F. Eckstein, *Nucleic Acids Res.* **1985**, *13*, 1451–1455.
[92] K. Mullis in *Les Prix Nobel en 1993*, Norstedt, Stockholm, **1994**; *Angew. Chem.* **1994**, *106*, 1271; *Angew. Chem. Int. Ed. Engl.* **1994**, *33*, 1209.
[93] *Peptide nucleic acids and their potential applications in biotechnology*: O. Buchardt, M. Egholm, R. H. Berg, P. E. Nielsen, *Trends Biotechnol.* **1993**, *11*, 384–386.
[94] *Oligonucleotide therapy*: S. T. Crooke, *Curr. Opin. Biotechnol.* **1993**, *3*, 656–661.

Lapses in the lab?
No longer with...

LIFE SCIENCES

In every laboratory you need your set of

Methods of Immunological Analysis
edited by R. Masseyeff, W. Albert, and N.A. Staines



Now available! A complete practice-oriented introduction to immunoanalysis. Three detailed volumes packed with the most comprehensive and up-to-date collection of analytical techniques employing immunological methods.

Indispensable for both specialists and non-specialists!

Volume 1: Fundamentals
ISBN 3-527-27906-7

Volume 2: Samples and Reagents
ISBN 3-527-27907-5

Volume 3: Cells and Tissues
ISBN 3-527-27908-3

Save 20% by ordering the whole set!

Single volume price: DM 410.00 each. Set price: DM 330.00 per volume. Series ISBN 3-527-27905-9.
Please write for our comprehensive prospectus!

A Growing Collection for a Growing Science!

Human Protein Data
edited by A. Haeberli

First Installment. 1992. XLV, 424 pages with 59 figures. Ring Binder. DM 275.00. Subscription price DM 225.00. ISBN 3-527-28211-4

Second Installment. 1993. LVII, 192 pages with 30 figures. Ring Binder. DM 175.00. Subscription price: DM 150.00. ISBN 3-527-30015-5

Third Installment. 1994. Ca 200 pages. Looseleaf. Ca DM 175.00. Subscription price: ca DM 150.00. ISBN 3-527-30056-2

A unique compendium of data on human proteins, collected from leading laboratories worldwide.
With the Third Installment now available, this superb reference work covers over 300 human proteins!
Condensed and still comprehensive (contains physico-chemical data, structures, and physiological and pathological mechanisms), the work is extraordinarily up-to-date.
In addition, the convenient loose-leaf format facilitates regular updating.

Special feature: a computer retrieval program on diskette which allows easy searches through the data.

Journal

European Journal of Immunology

1995. Volume 25. Published monthly. Annual subscription rate DM 1255.00 including postage and handling charges. Membership rates available upon request.
ISSN 0014-2980

To order please contact your bookseller or:

VCH, P.O. Box 10 11 61, D-69451 Weinheim
VCH, 8 Wellington Court, Cambridge CB1 1HZ, UK
VCH, Hardstrasse 10, P.O. Box, CH-4020 Basel
VCH, 220 East 23rd Street, New York, NY 10010-4606, USA (toll free: 1-800-367-8249)
VCH, Eikow Building, 10-9 Hongo 1-chome, Bunkyo-ku, Tokyo 113, Japan

VCH

An Amazing Distortion in DNA Induced by a Methyltransferase (Nobel Lecture)**

Richard J. Roberts*

Much of my work in biology has been driven by my early training in chemistry. In the study of a new chemical compound, the first and most important thing is to determine its detailed molecular structure. For a molecular biologist that usually means determining some DNA sequence, since an accurate knowledge of sequence will then allow the proper design of experiments to examine function. I was first exposed to the idea of macromolecular sequences while I was a postdoctoral fellow with Jack Strominger at Harvard. During that time I briefly visited Fred Sanger's laboratory in Cambridge, England, to learn the methodology of RNA fingerprinting and sequencing.

Shortly before moving to Cold Spring Harbor Laboratory, I learned of restriction enzymes from a lecture by Dan Nathans and immediately decided that here was the key to DNA sequencing. The idea was that by mapping restriction sites and sequencing small fragments, longer gene-sized sequences could be put together. My laboratory set out to isolate and characterize as many restriction enzymes as possible.[1] We began to use these enzymes to map Adenovirus-2 DNA[2] and to identify small fragments that might be worth sequencing. One such fragment would contain the 5'-end of an Adenovirus-2 mRNA and the eukaryotic promoter that controlled its expression. It was the hunt for this promoter-containing fragment that led to our discovery of split genes and RNA splicing.[3-6] By this time, Fred Sanger and Walter Gilbert had developed DNA sequencing methods, and we focused our attention on the sequence requirements for RNA splicing. Joe Sambrook, Walter Keller, and others cloned the tripartite leader that was present on Adenovirus-2 late mRNAs, and Sayeeda Zain determined its sequence.[7] Soon we undertook the complete sequencing of the Adenovirus-2 genome, which was eventually finished as a collaborative effort with Ulf Pettersson's laboratory.[8]

We realized early on that computational help would be essential for the sequencing project, and we developed many programs for assembling and analyzing DNA sequences.[9-14] During this time we and others began to clone and sequence the genes for restriction enzymes and their companion methyltransferases (MTases).[15,16] Our initial naive assumption was that in any given restriction–modification system there would be a common region in the protein sequence of the restriction enzyme and the MTase that would pinpoint the region responsible for DNA sequence recognition. This was based on the fact that both enzymes had to recognize exactly the same DNA sequence. Once this common protein sequence had been recognized, we thought it likely that in vitro manipulation would allow us to change the DNA sequence recognized and so create new restriction enzymes by protein engineering. This proved hopelessly naive. Not only was there no similarity between the sequences for restriction enzyme and MTase genes, there was also no similarity between the genes for different restriction enzymes. There was, however, considerable sequence similarity among the genes for MTases, which was especially strong for the enzymes forming 5-methylcytosine. This observation has shaped the last few years of my research efforts and has led to our latest discovery, which is the topic of this lecture.

Methylation of adenine and cytosine residues is commonly found in prokaryotes, and cytosine methylation is widespread in eukaryotes. In bacteria, DNA methylation serves as a component of restriction–modification systems[17] and also as part of mismatch repair systems.[18] In higher eukaryotes, methylation of cytosine residues appears to be essential[19] and is involved in the control of gene expression, developmental regulation, genomic imprinting, and X-chromosome inactivation.[20]

There are three kinds of methylation that bacteria use to protect their DNA against the action of restriction enzymes: at the 5- (m5C) and N4-positions of cytosine (m4C), and at the N6-position of adenine (m6A). To date, 50 different m5C-MTase genes have been sequenced.[21] When we first began comparing the sequences of these genes in 1987, the available computer software was unable to provide good alignments of many of these sequences because the similarity between them was limited to short patches, which we now call motifs, that were separated by quite dissimilar regions. The similarity could be detected by eye, however. Janos Pósfai in my laboratory began developing algorithms that could find these small patches of similarity among proteins.[22] The program searched for the presence of small triplet patterns (Fig. 1) and then combined them into motifs that represented well-conserved regions within each of the set of proteins being aligned. These motifs then anchored the inital alignment. By reducing the stringency of the triplet search and limiting it to the regions between the main motifs, weaker motifs could be found, which enabled a more complete alignment.

[*] Prof. Dr. R. J. Roberts
New England Biolabs
32 Tozer Road, Beverly, MA 01915 (USA)
Telefax: Int. code + (508)921-1527

[**] Copyright © The Nobel Foundation 1994.—We thank the Nobel Foundation, Stockholm, for permission to print this lecture.

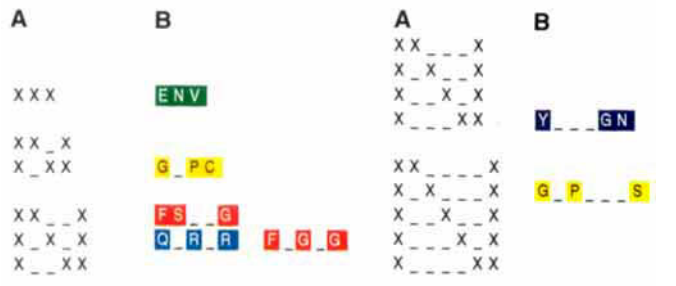


Fig. 1. A) Examples of the triplet patterns used to align multiple sequences. Each pattern contains three specific amino acids each at a set position X; any amino acid is allowed at positions _. The simplest pattern (top) consists of all possible simple tripeptides ($20 \times 20 \times 20 = 8000$ combinations). All sequences are searched for each of these patterns (224000 total for 10 amino acids) and their frequencies recorded. B) Examples of common patterns found in the m5C-MTases.

Finally gaps could be introduced to complete the alignment. We have since refined these programs and included a user interface with graphic output that enables the overall architecture of a group of proteins to be visualized. The relationships among the m5C-MTases is illustrated schematically in Figure 2. There are six regions of strong similarity and four more regions of lesser similarity that can be used to anchor the alignments between these sequences. Connecting these motifs are regions that vary in length and sequence. Similar analyses of the m5C-MTase have been reported by others.[23]

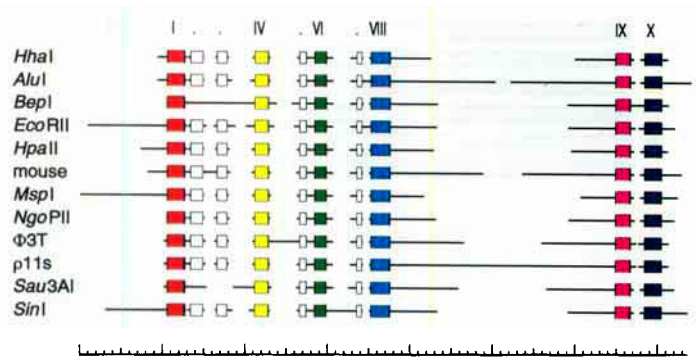


Fig. 2. Schematic representation of the alignment of twelve representative m5C-MTases. The six well-conserved motifs that anchored the original alignment are shown in color (light red: motif I, F-G-G; yellow: motif IV, PC; green: motiv VI, ENV; light blue: motif VIII, Q-R-R; dark red: motif IX, RE; dark blue: motif X, GN). The open boxes represent the four weakly conserved motifs. The organisms from which these enzymes were obtained are listed on the left.

Among the six well-conserved motifs, two could be assigned functional significance. Motif IV, which is shown in block form in Figure 3a, contains a cysteine residue that was postulated by Santi and Danenberg to be a key catalytic residue.[24] They had proposed (Fig. 3b) that an initial step in the reaction involved the formation of a covalent complex between this cysteine residue in the MTase and the 6-position of cytosine in a Michael reaction. This activates the 5-position of cytosine and permits transfer of the methyl group from the cofactor *S*-adenosylmethionine (AdoMet). Much biochemical evidence was available to support this mechanism, including the important observation that 5-fluorocytosine was a mechanism-based inhibitor.[25] Later work has enabled the isolation of the covalent intermediate,[26–28] and the cysteine within motif IV has been shown directly to be the site of covalent bond formation.[26] Recent experiments have shown that mutation of this cysteine residue to glycine, serine, or other amino acids blocks MTase action.[29–31]

Motif I could also be assigned a functional role. It contained three highly conserved residues FGG (Fig. 4a). Importantly, it

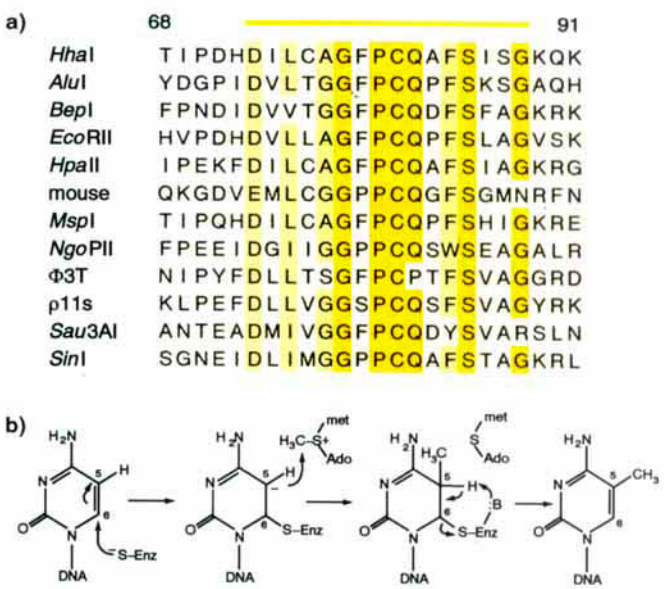


Fig. 3. a) Block diagram showing the well-conserved motif IV (PC). Residues conserved among all m5C-MTase sequences are strongly highlighted in yellow, and those that show three or fewer variants are lightly shaded. b) Schematic representation of the reaction pathway for the methylation of cytosine.



Richard J. Roberts, born in 1943 in Derby, England, obtained his Ph.D. in organic chemistry at Sheffield University in 1968. Following a postdoctoral stay with J. L. Strominger at Harvard University, he worked at Cold Spring Harbor Laboratory from 1972 to 1992, where he advanced to be Assistant Director of Research. He is currently Director of Eukaryotic Research at New England Biolabs in Beverly, Massachusetts. In addition to intensive studies on the type-II restriction enzymes, his research has focused on Adenovirus-2. In recent years his work has centered around DNA methyltransferases. He was one of the pioneers in the development of computer-aided sequence analysis for proteins and nucleic acids.

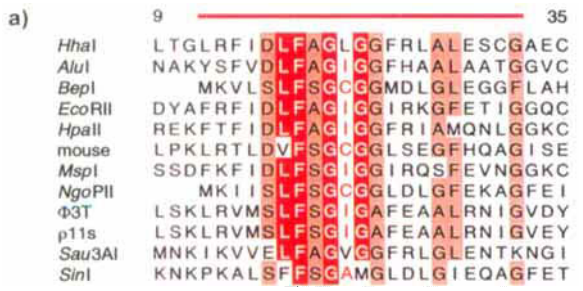


Fig. 4. a) Block diagram showing the well-conserved motif I (FGG). Residues conserved among all m5C-MTase sequences are strongly highlighted in red, and those that show three or fewer variants are lightly shaded. b) Consensus sequences for motif I and its relatives in other MTases (based on ref. [32]).

shows distinct similarities to motifs found in other MTases (Fig. 4b). It can be seen that all three classes of DNA MTases, m5C-, m4C-, and m6A-MTases as well as protein and RNA MTases contain a related motif. The common functional feature is that each MTase uses AdoMet as the methyl donor, and so motif I was suggested to be involved in binding to the cofactor.[32, 33]

We were interested in trying to define the region within the m5C-MTases that was responsible for sequence-specific recognition of the DNA substrate. Because the shared function of this group of MTases was the chemistry of the reaction, we argued that each of the common regions, exemplified by motifs I and IV, must be directly involved, either by interacting with the cofactor or providing residues important for catalysis. Since the precise DNA sequence recognized by each enzyme was different, we expected that this recognition would be mediated by a region that differed among the sequences. Only one region, the so-called variable segment located between motifs VIII and IX, appeared a reasonable candidate. Examination of these variable regions shows that not only the amino acid sequence but also the lengths of the segments vary considerably from MTase to MTase.

Although most of the known m5C-MTases are monospecific, that is, they recognize a single sequence, some MTases are known that recognize more than one specific sequence. These are the so-called "multispecific" MTases that are encoded by several *Bacillus* bacteriophages. These enzymes are single polypeptides like the monospecific enzymes, but they have the unusual property of methylating several quite different sequences. One example is M.Φ3TI, which recognizes and methylates the sequences GGCC and GCNGC.[34] This enzyme is included in Figure 2, and there it can be seen that its variable region is extraordinarily long. A series of elegant studies carried out in Tom Trautner's laboratory has showed convincingly that single mutations within the variable regions of M.Φ3TI and other multispecific MTases knock out the ability of the enzyme to recognize one of the specific sequences, while still allowing the others to be recognized.[35, 36] In the case of the monospecific MTases, a comparable experiment was not possible, since mutations that prevented DNA recognition would also block MTase activity. Saulius Klimasauskas and Janise Nelson in my laboratory undertook a series of experiments in which they swapped domains between two of the monospecific MTases.[37] We chose M.*Hpa*II (recognition sequence: CmCGG) and M.*Hha*I (recognition sequence: GmCGC), because they both recognize tetranucleotide sequences and because the base methylated is located at an equivalent position within the recognition sequences. The variable regions, with or without flanking sequences, were swapped as illustrated in Figure 5. In several cases, active MTases resulted, and comparison of the hybrids showed clearly that sequence specificity lay entirely within the variable region. Surprisingly, hybrids in which the variable region plus its adjacent motif IX were transferred showed much higher methylation activity than hybrids in which just the variable region had been swapped.

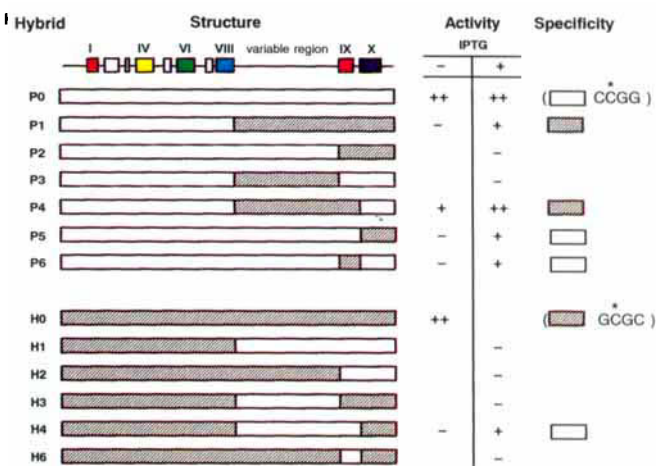


Fig. 5. Schematic representation of the hybrids P1–P6 and H1–H6 between M.*Hpa*II (P0) and M.*Hha*I (H0). The MTases were under the control of an IPTG-inducible promoter on a pBR322 derivative. Sequences derived from M.*Hpa*II are shown by open boxes; those from M.*Hha*I are shown by shaded boxes. The column labeled Activity shows the extent of protection of plasmid DNA in vivo, as measured by restriction enzyme cleavage in vitro, either before (−) or after IPTG induction (+) (− indicates no protection, + indicates weak protection, ++ indicates > 90% protection). The specificity of the hybrid methyl transferase is shown on the right.

In another series of experiments, Mi Sha swapped the variable regions from M.*Hpa*II and M.*Msp*I. These enzymes both recognize the sequence CCGG, but M.*Msp*I transfers the methyl group to the first cytosine residue in the sequence,[38] whereas M.*Hpa*II transfers the group to the second cytosine residue.[39] The results of these experiments showed that the choice of base to be methylated also depends upon the variable region.[40]

While we were pursuing our studies of the biochemistry and molecular biology of MTases, it became apparent that a crystal structure would be essential if we were to understand fully the reaction mechanism. Ashok Dubey in my lab began a collaboration with Xiaodong Cheng, who was working in Jim Pflugrath's laboratory at Cold Spring Harbor. They purified and attempted to crystallize M.*Msp*I, which we had studied extensively.[41–43] Later they tried to crystallize M.*Hpa*II, on which we had also worked.[44] In both cases, the efforts were unsuccessful. How-

ever, the third attempt with M.*Hha*I was quite successful. This enzyme forms part of the *Hha*I restriction system from *Haemophilus haemolyticus*, which had been discovered in my laboratory.[45] It is one of the smallest of the m5C-MTases, containing 327 amino acids ($M_r \approx 37$ kDa). Its gene has been cloned and sequenced,[46] and the protein was overexpressed in *E. coli*[37, 46a] and subjected to detailed kinetic studies.[25] Sanjay Kumar purified the enzyme, and in December 1991 it crystallized readily—a wonderful Christmas present! Within eleven months Xiaodong Cheng had a structure for the binary complex between M.*Hha*I and AdoMet at 2.5 Å resolution.[48]

The structure was most revealing (Fig. 6); it was composed of a large domain and a small domain forming a cleft that appeared ideal for accomodating a DNA helix. Motif I (FGG) was confirmed to be involved in AdoMet binding, while another of the conserved motifs, X (GN), was also implicated in AdoMet binding. Motif IV (PC) was positioned close to the AdoMet-binding site on the same side of the cleft. Motif VIII (QRR) lay at the base of the cleft, where one could imagine that the positively charged residues of the motif could play a role in binding to the phosphodiester backbone of the DNA helix. Conserved motif IX (RE) threaded its way through the small domain, which otherwise consisted of almost the entire variable region. Motif IX appeared to form a backbone responsible for bracing the structure of the small domain. Finally, conserved motif VI (ENV) was clearly involved in correctly positioning motif IV.

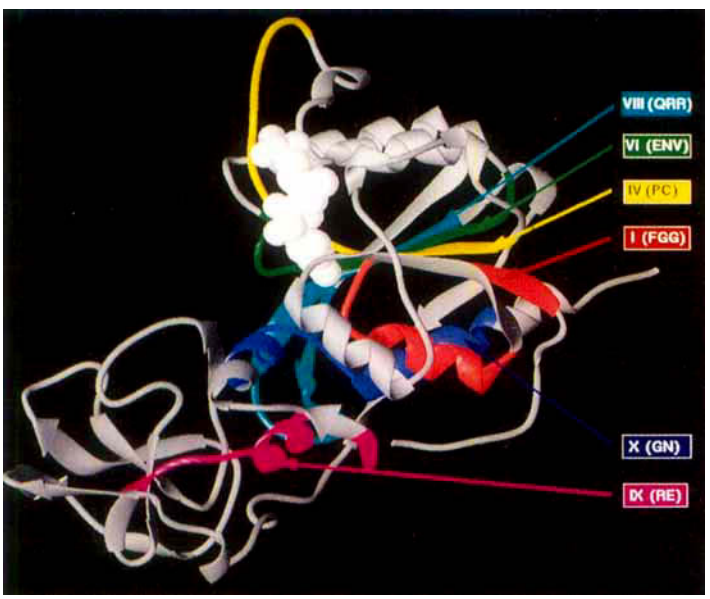
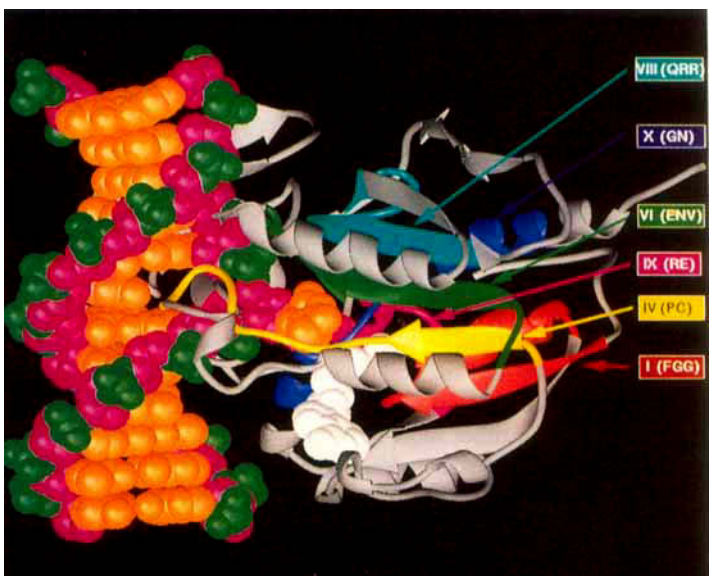


Fig. 6. The structure of M.*Hha*I in a binary complex with its cofactor AdoMet. The motifs are colored as in Figure 2. The cofactor, AdoMet, is shown in white as a space-filling model.

The structure provided a clear explanation for our earlier observation that domain swaps that included both motif IX and the variable region gave more active MTases than those involving just the variable region.[37, 40] Although motif IX is quite highly conserved among the MTases, there are differences from one MTase to another, and these could be expected to influence the ability of a heterologous motif IX to brace the structure of the small domain.

Soon after we obtained crystals of the binary complex between M.*Hha*I and AdoMet, we set about trying to obtain cocrystals that would also include DNA. Two kinds of complexes were envisioned. One would contain M.*Hha*I together with native DNA and *S*-adenosylhomocysteine (AdoHcy), while another would contain M.*Hha*I with AdoMet and a DNA duplex substituted with 5-fluorocytosine at the target. The latter would be expected to form a covalent intermediate in which the methyl group had transferred to the 5-position of cytosine, but release

a)



b)

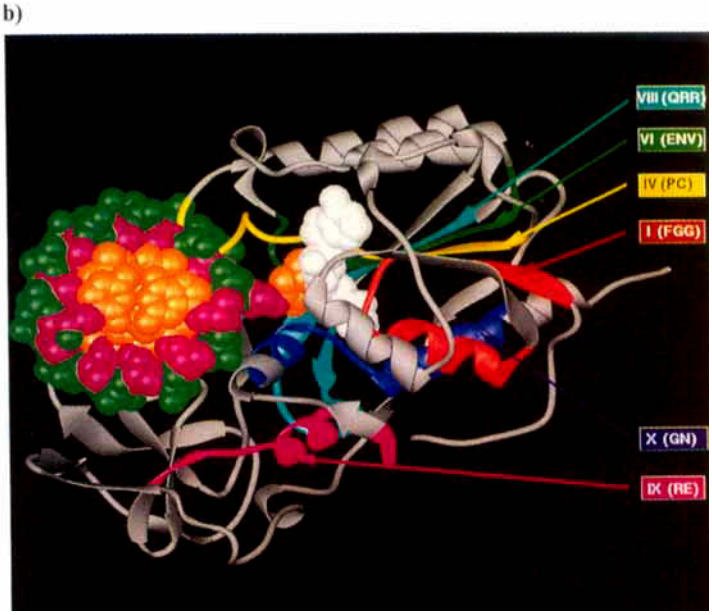


Fig. 7. The structure of M.*Hha*I in a ternary complex with a substrate duplex DNA–oligonucleotide and the end product of the reaction, AdoHcy. The motifs are colored as in Figure 2. AdoHcy is white, the DNA bases are orange, the deoxyribose is pink, and the phosphates are green. a) View from the side of the DNA axis. b) View looking down the DNA axis.

of the DNA from the covalent complex with the protein would be inhibited by the presence of the fluorine atom, which is a poor leaving group. Such a complex could almost be viewed as a model of the transition state in DNA methylation.

Saulius Klimasauskas jointed the project for the cocrystallization, and we were fortunate in obtaining good crystals fairly readily with both native DNA and DNA containing 5-fluorocytosine. Xiaodong Cheng, who now has his own laboratory at Cold Spring Harbor, has solved the cocrystal structure at 2.8 Å resolution (Fig. 7).[49] We had expected to find that the DNA helix would be distorted in some way to allow the chemical reaction to take place, because the chemistry requires that the cysteine residue must approach the cytosine in a direction perpendicular to the plane of the ring. We imagined at most some extreme bending of the DNA. Unexpectedly, the distortion is much greater than a bend and much more elegant. The target cytosine flips right out of the axis of the DNA helix and into a pocket in the enzyme that contains the catalytically important cysteine residue. The rest of the helix is relatively undistorted. Another large conformational shift has taken place in the active site loop which encompasses motif IV. The entire 20-residue loop rotates through almost 180° from its original position to bring the catalytically active cysteine into contact with the target cytosine (Fig. 8).

The position in the DNA helix that was occupied by the target cytosine is now filled by two residues. One is a glutamine residue from the small domain, and the other is a serine residue from the active site loop. Surprisingly, neither of these residues is conserved among other m5C-MTases, which suggests that many residues could assist in opening a helix in this manner. As can be seen from Figure 7, the interaction between M.*Hha*I and DNA can be thought of as the enzyme embracing the DNA with two arms that penetrate the helix during the embrace and assisting in the extrusion of the target cytosine.

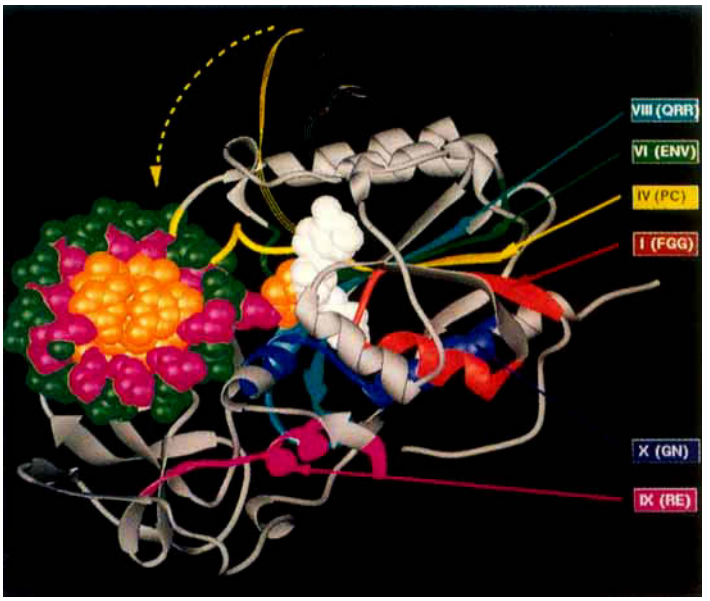


Fig. 8. Composite of the M.*Hha*I structures with and without DNA showing the conformational changes that take place upon binding to DNA (colors as in Fig. 7). The active site loop (yellow) is shown as a solid line to indicate its position in the ternary complex structure (with DNA) and as a triple-stranded ribbon in the binary complex structure (no DNA).

The sequence-specific interactions between M.*Hha*I and its substrate mainly involve two distinct loops (the sequence recognition loops) from the small domain. One loop is responsible for interactions with the orphan guanosine that is left after the cytosine has flipped and makes specific contacts with the adjacent bases on the same strand. It also provides the glutamine residue that fills the hole left after the target cytosine is flipped. The second recognition loop interacts predominantly with the

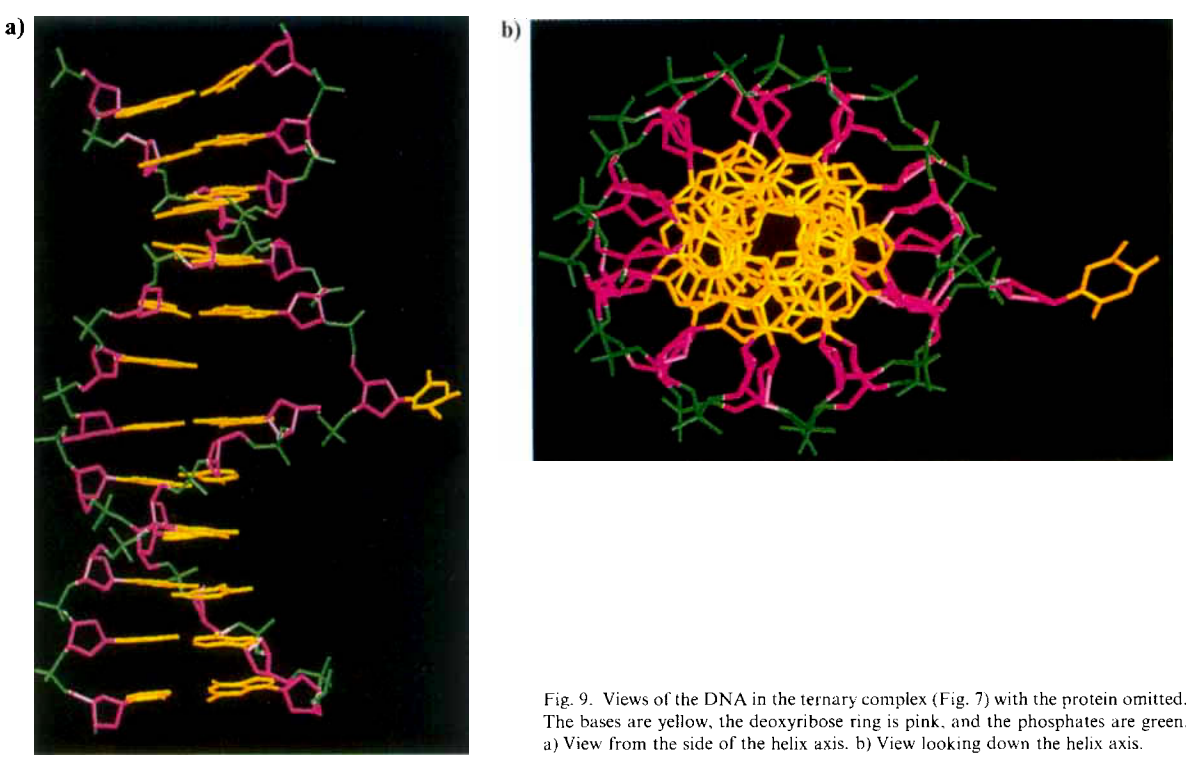


Fig. 9. Views of the DNA in the ternary complex (Fig. 7) with the protein omitted. The bases are yellow, the deoxyribose ring is pink, and the phosphates are green. a) View from the side of the helix axis. b) View looking down the helix axis.

strand containing the target cytosine. However, the interactions in the covalent complex should be viewed as an end point of a more complicated interaction. They may not be an accurate reflection of the initial events that led to recognition. More information on these initial events may be provided by studies of mutant proteins or DNA analogues that can form complexes without flipping the target cytosine. It should be noted that none of the well-characterized DNA binding motifs[50] appear to play a role in this system.

Previous studies of DNA–protein interactions have shown quite dramatic distortions induced in DNA by proteins, but usually these have involved bends or kinks; one of the most dramatic was the flattening and bending of DNA induced by the TATA-box binding protein.[51, 52] There have been no previous examples of proteins interacting with DNA and causing a base to flip out of the helix. Since the DNA bases lie buried in the inside of the helix in normal DNA, the mechanism presented here provides an elegant means by which complete access to the base becomes possible. We anticipate that other proteins performing chemistry on DNA bases also use this mechanism. Obvious candidates would be the MTases that form N^6-methyladenine or N^4-methylcytosine. Some of the enzymes, such as DNA glycosylases, that repair DNA damage might also flip the damaged base out of the helix prior to its excision. Many proteins that interact with DNA need to open up the helix. Some examples are topoisomerases, helicases, DNA polymerases and/or their auxiliary proteins that operate at replication origins, RNA polymerases, and recombination enzymes. In the structure shown in Figure 9 the phosphodiester bonds adjacent to the target cytosine are distorted from their positions in normal B DNA, and one might imagine that the continued unzipping of the helix would be easy.

Surprisingly, the interaction between M.*Hha*I and DNA requires no external energy source. Conformational rearrangements within the protein combined with specific interactions between protein and DNA likely provide the energy to open the helix. The energy is then stored for use during the return of the target cytosine. It would be surprising if this mechanism is not used elsewhere. Split genes were discovered unexpectedly but proved to be easily found once we knew they were there. This mechanism of flipping a base out of the DNA helix might also prove to be of widespread importance as a first step in opening up a DNA helix. We should lose no time in exploring the possibility.

I am most grateful to all of my colleagues who have worked so hard in my laboratory to ensure our success. None of this would have been possible without their input. In addition to those mentioned explicitly in the text I thank Phyllis Myers, Kathy O'Neill, Margaret Wallace, Louise D'Allessandro, Jodie Freyer, Carol Marcincuk, Dana Macelis, and Ching Lin, whose dedication has been especially important in making my life easier. I thank Jim Watson for persuading me to go to Cold Spring Harbor Laboratory and for many stimulating conversations. Among many colleagues, Ashok Bhagwat, Mike Botchan, Don Comb, Greg Freyer, Rich Gelinas, Tom Gingeras, David Helfman, Winship Herr, Adrian Krainer, Stu Linn, and Ira Schildkraut have been good friends and valuable sources of criticism and advice. I thank the National Institutes of Health and the National Science Foundation for much support over the years. Finally, I am indebted to my wife, Jean, and my children, Alison, Andrew, Christopher, and Amanda, who have been supportive and understanding of my addiction to science.

Received: January 17, 1994 [A 48 IE]
German version: *Angew. Chem.* **1994**, *106*, 1285

[1] R. J. Roberts, *Crit. Rev. Biochem.* **1976**, *4*, 123–164.
[2] C. Mulder, J. R. Arrand, H. Delius, W. Keller, U. Pettersson, R. J. Roberts, P. A. Sharp, *Cold Spring Harbor Symp. Quant. Biol.* **1974**, *39*, 397–400.
[3] R. E. Gelinas, R. J. Roberts, *Cell* **1977**, *11*, 533–544.
[4] L. T. Chow, R. E. Gelinas, T. R. Broker, R. J. Roberts, *Cell* **1977**, *12*, 1–8.
[5] R. E. Gelinas, L. T. Chow, R. J. Roberts, T. R. Broker, D. F. Klessig, at the *Brookhaven Symposium in Genetic Interaction and Gene Transfer* (*Brookhaven Symp. Biol.* **1977**, *29*, 345–347).
[6] T. R. Broker, L. T. Chow, A. R. Dunn, R. E. Gelinas, J. A. Hassell, D. F. Klessig, J. B. Lewis, R. J. Roberts, B. S. Zain, *Cold Spring Harbor Symp. Quant. Biol.* **1978**, *42*, 531–553.
[7] B. S. Zain, J. Sambrook, R. J. Roberts, W. Keller, M. Fried, A. R. Dunn, *Cell* **1979**, *16*, 851–861.
[8] R. J. Roberts, G. Akusjarvi, P. Alestrom, R. E. Gelinas, T. R. Gingeras, D. Sciaky, U. Pettersson in *Adenovirus DNA. The Viral Genome and Its Expression* (Ed.: W. Doerfler), Martinus Nijhoff, Boston, MA, **1986**, pp. 1–51.
[9] T. R. Gingeras, J. P. Milazzo, R. J. Roberts, *Nucleic Acids Res.* **1978** *5*, 4105–4127.
[10] T. R. Gingeras, J. P. Milazzo, D. Sciaky, R. J. Roberts, *Nucleic Acids Res.* **1979**, *7*, 529–545.
[11] T. R. Gingeras, P. I. Rice, R. J. Roberts, *Nucleic Acids Res.* **1982**, *10*, 103–114.
[12] T. R. Gingeras, R. J. Roberts, *Science* **1980**, *209*, 1322–1328.
[13] R. M. Blumenthal, P. R. Rice, R. J. Roberts, *Nucleic Acids Res.* **1982**, *10*, 91–101.
[14] C. Keller, M. Corcoran, R. J. Roberts, *Nucleic Acids Res.* **1984**, *12*, 379–386.
[15] A. Kiss, G. Pósfai, C. C. Keller, P. Venetianer, R. J. Roberts, *Nucleic Acids Res.* **1985**, *13*, 6403–6421.
[16] A. S. Bhagwat, A. Sohail, R. J. Roberts, *J. Bacteriol.* **1986**, *166*, 751–755.
[17] R. J. Roberts, S. S. Halford in *Nucleases* (Eds.: S. M. Linn, R. S. Lloyd, R. J. Roberts), Cold Spring Harbor Laboratory Press, Cold Spring Harbor, NY, **1993**.
[18] P. Modrich, *Annu. Rev. Genet.* **1991**, *25*, 229–253.
[19] E. Li, T. H. Bestor, R. Jaenisch, *Cell* **1992**, *69*, 915–926.
[20] J. P. Jost, H. P. Saluz, *DNA Methylation: Molecular Biology and Biological Significance*, Birkhäuser, Basel, **1993**.
[21] S. Kumar, X. Cheng, S. Klimasauskas, S. Mi, J. Pósfai, R. J. Roberts, G. G. Wilson, *Nucleic Acids Res.*, **1994**, *22*, 1–10.
[22] J. Pósfai, A. S. Bhagwat, G. Pósfai, R. J. Roberts, *Nucleic Acids Res.* **1989**, *17*, 2421–2435.
[23] R. Lauster, T. A. Trautner, M. Noyer-Weidner, *J. Mol. Biol.* **1989**, *206*, 305–312.
[24] D. V. Santi, P. V. Danenberg in *Folates and Pterins, Vol. 1* (Eds.: R. L. Blakely, S. J. Benkovic), Wiley-Interscience, New York, **1984**, pp. 343–396.
[25] J. C. Wu, D. V. Santi, *J. Biol. Chem.* **1987**, *262*, 4778–4786.
[26] L. Chen, A. M. MacMillan, W. Chang, K. Ezaz-Nikpay, W. S. Lane, G. L. Verdine, *Biochemistry* **1991**, *30*, 11018–11025.
[27] S. Friedman, N. Ansari, *Nucleic Acids Res.* **1992**, *20*, 3241–3248.
[28] S. S. Smith, B. E. Kaplan, L. C. Sowers, E. M. Newman, *Proc. Natl. Acad. Sci. USA* **1992**, *89*, 4744–4748.
[29] M. W. Wyszynski, S. Gabbara, A. S. Bhagwat, *Nucleic Acids Res.* **1992**, *20*, 319–326.
[30] S. Mi, R. J. Roberts, *Nucleic Acids Res.* **1993**, *21*, 2459–2464.
[31] L. Chen, A. M. MacMillan, G. L. Verdine, *J. Am. Chem. Soc.* **1993**, *115*, 5318–5319.
[32] D. Ingrosso, A. V. Fowler, J. Bleibaum, S. Clarke, *J. Biol. Chem.* **1989**, *264*, 20130–20139.
[33] S. Klimasauskas, A. Timinskas, S. Menkevicius, D. Butkiene, V. Butkus, A. A. Janulaitis, *Nucleic Acids Res.* **1989**, *17*, 9823–9832.
[34] M. Noyer-Weidner, S. Jentsch, B. Pawlek, U. Gunthert, T. A. Trautner, *J. Virol.* **1983**, *46*, 446–453.
[35] T. S. Balganesh, L. Reiners, R. Lauster, M. Noyer-Weidner, K. Wilke, T. A. Trautner, *EMBO J.* **1987**, *6*, 3543–3549.
[36] K. Wilke, E. Rauhut, M. Noyer-Weidner, R. Lauster, B. Pawlek, B. Behrens, T. A. Trautner, *EMBO J.* **1988**, *7*, 2601–2609.
[37] S. Klimasauskas, J. E. Nelson, R. J. Roberts, *Nucleic Acids Res.* **1991**, *19*, 6183–6190.
[38] R. Y. Walder, C. J. Langtimm, R. Catterjee, J. A. Walder, *J. Biol. Chem.* **1983**, *258*, 1235–1241.
[39] M. B. Mann, H. O. Smith, *Nucleic Acids Res.* **1977**, *4*, 4211–4221.

[40] S. Mi, R. J. Roberts, *Nucleic Acids Res.* **1992**, *20*, 4811–4816.
[41] P. M. Lin, C. H. Lee, R. J. Roberts, *Nucleic Acids Res.* **1989**, *17*, 3001–3011.
[42] A. K. Dubey, B. Mollet, R. J. Roberts, *Nucleic Acids Res.* **1992**, *20*, 1579–1585.
[43] A. K. Dubey, R. J. Roberts, *Nucleic Acids Res.* **1992**, *20*, 3167–3173.
[44] C. O. Card, G. G. Wilson, K. Weule, J. Hasapes, A. Kiss, R. J. Roberts, *Nucleic Acids Res.* **1990**, *18*, 1377–1383.
[45] R. J. Roberts, P. A. Myers, A. Morrison, K. Murray, *J. Mol. Biol.* **1976**, *103*, 199–208.
[46] M. Caserta, W. Zacharias, D. Nwankwo, G. G. Wilson, R. D. Wells, *J. Biol. Chem.* **1987**, *262*, 4770–4777.
[47] a) J. C. Wu, D. V. Santi, *Nucleic Acids Res.* **1988**, *16*, 703–717; b) S. Kumar, X. Cheng, J. W. Pflugrath, R. J. Roberts, *Biochemistry* **1992**, *31*, 8648–8653.
[48] X. Cheng, S. Kumar, J. Pósfai, J. W. Pflugrath, R. J. Roberts, *Cell* **1993**, *74*, 299–307.
[49] S. Klimasauskas, S. Kumar, R. J. Roberts, X. Cheng, *Cell*, **1994**, *76*, 357–369.
[50] S. C. Harrison, *Nature* **1991**, *353*, 715–719.
[51] Y. Kim, J. H. Geiger, S. Hahn, P. B. Sigler, *Nature* **1993**, *365*, 512–520.
[52] J. L. Kim, D. B. Nikolov, S. K. Burley, *Nature* **1993**, *365*, 520–527.

A stop-gap solution?



If the latest library copy of Angewandte spends more time off the shelf than on, stop the gap with a personal subscription.

Just call or fax

VCH

USA: Tel. 1-(800) 422-8824; Fax (305) 428-8201
UK: Tel. (0223) 321111, Fax (0223) 313221

Split Genes and RNA Splicing (Nobel Lecture)**

Phillip A. Sharp*

Introduction

By the late 1970s the physical structure of a gene was firmly established from work in bacteria. The sequences of the gene, the RNA, and the protein were colinearly organized and expressed. Since the science of genetics suggested that genes in eukaryotic organisms behaved similarly to those of prokaryotic organisms, it was naturally assumed that this bacterial gene structure was universal. It followed that if the gene structure was the same, the mechanisms of regulation were probably very similar, and thus what was true of a bacterium would be true of an elephant.

However, many descriptive biochemical aspects of the genetic material and its expression in cells with nuclei suggested that the simple molecular biology of gene expression in bacteria might not be universal. First, obviously, RNAs transcribed from nuclear genes are physically separated from the translational machinery in the cytoplasm. Thus, the nuclear compartment could be the site of selective RNA processing and transport. Second, the DNA content of eukaryotic germ cells varied significantly between organisms without an apparent variation in the number of genes. Some organisms appeared to have ten times as much DNA as was required to encode all of the proteins. Third, the previously described phenomenon of heterogeneous nuclear RNA (hnRNA) suggested that long RNAs were transcribed from diverse nuclear sequences.[1] These hnRNAs had a short half-life relative to cytoplasmic mRNAs and thus could potentially be precursors to mRNAs. Furthermore, both the long hnRNA and the shorter mRNA appeared to have modified 5′ and 3′ termini in common, a ^{7}mGpppX cap[2-4] and polyadenylation tracts,[5-7] respectively. The meaning of these observations concerning hnRNAs remained controversial as it was not possible to establish a precursor–product relationship between the nuclear RNA population and the cytoplasmic mRNA.

Whether or not the structure of genes in eukaryotic cells was the same as that in bacteria was not really questioned at that time. The important issue was to establish the exact biochemical pathway between a gene in the nucleus and its mRNA in the cytoplasm. This hypothetical pathway was pictured as beginning with initiation of transcription by RNA polymerase II(B) which would proceed through completion of transcription beyond the terminus of the gene. The nuclear precursor RNA transcribed from the gene was potentially processed, and the mRNA selectively transported to the cytoplasm. Regulation of gene expression, the basis of almost all interesting biology, including cancer, cellular responses to infection, and development would primarily result from changes in the rates or efficiencies of the various steps in the pathway. Thus, understanding the pathway of eukaryotic gene expression promised new insights into the mechanisms of regulation and the biochemical events controlling both diverse biological and biochemical phenomena.

Background

The late stage of adenovirus infection was chosen as the best system for studying the pathway of nuclear gene → nuclear precursor RNA → cytoplasmic mRNA → protein. We had previously established several restriction endonuclease cleavage maps of the viral genome (Fig. 1)[8] and had used fragments of the genome to map the positions of cytoplasmic mRNAs generated during the early and late stages of infection.[9] We had also determined the abundance (in copies per cell) of both nuclear and cytoplasmic RNAs,[10] and this suggested that RNAs from both compartments could be obtained in adequate amounts to compare their structures directly by using the electron microscope and the then recently developed RNA · DNA hybridization methods. Furthermore, these earlier studies established that sets of viral RNA sequences were restricted to the nucleus,

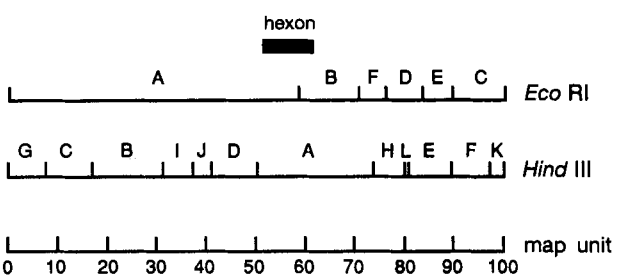


Fig. 1. Maps of cleavage sites for restriction endonucleases *Eco*RI (top) and *Hind*III (middle). The approximately 35000 base pairs of adenovirus 2 DNA was assigned as 100 map units (bottom). The positions of cleavage sites are denoted by vertical lines and fragments are lettered on the basis of length. The r and l viral strands are transcribed to the right and left, respectively. The sequences constitituting the body of mRNA specifying the abundant hexon (II) protein are encompassed by the bar about the boundary of *Eco*RI fragments A and B.

[*] Prof. P. A. Sharp
Department of Biology and the Center for Cancer Research
Massachusetts Institute of Technology
Cambridge, MA 02139 (USA)
Telefax: Int. code + (617)253-3867

[**] Copyright © The Nobel Foundation 1994.—We thank the Nobel Foundation, Stockholm, for permission to print this lecture.

suggesting a selection in processing and/or transport of only certain RNA sequences to the cytoplasm.[11] Finally, several studies had established that long nuclear RNA was transcribed from the adenovirus genome during the late stages of infection[12] and the stable cytoplasmic RNAs were shorter than the predominant nuclear RNAs. Thus, the production of RNAs during the late stage of adenovirus infection presented a paradigm for the heterogeneous nuclear RNA phenomenon associated with cellular genes.

Discovery of RNA Splicing

Comparison of the structure of a cytoplasmic mRNA with that of a nuclear precursor RNA[13] required the purification of a specific homogeneous mRNA. The most abundant mRNA, which encoded the adenovirus hexon protein, was separated from other viral mRNAs by gel electrophoresis and used in electron microscope mapping studies.[14] Ray White, as a fellow at Stanford, was the first to recognize that RNA · DNA hybrids were more stable than DNA · DNA duplexes in high concentrations of formamide.[15] This phenomenon was characterized physically by Davidson et al.[16] and was the basis of a convenient R-looping technique in which RNA forms a hybrid with a DNA strand, displacing the other strand of DNA into an easily observed loop. The adenovirus mRNA for hexon protein was mapped by the R-loop method to the *Hind*III A fragment of adenovirus 2 (see Fig. 1).[13]

Inspection of the R-loops between the hexon-mRNA and the *Hind*III A DNA fragment with an electron microscope revealed the presence of RNA tails at both the 5′ and 3′ ends of the hybrid (Figs. 2A, B and C). The single-strand RNA tail at the 3′ end was expected, as the RNA was known to be polyadenylated post-transcriptionally. The single-strand RNA tail at the 5′ end of the hybrid was not expected; however, this 5′ tail of RNA could have been displaced from the RNA · DNA hybrids by formation of duplex DNA by a process called branch migration. In fact, similar 5′ tails had been observed previously in R-loop mapping of adenovirus mRNA and had been ascribed to such branch migration.[17, 18] Arguing against branch migration however was the finding that the lengths of the 5′ tails were relatively uniform, namely 170 nucleotides. To eliminate this potential of competing DNA sequences displacing RNA se-

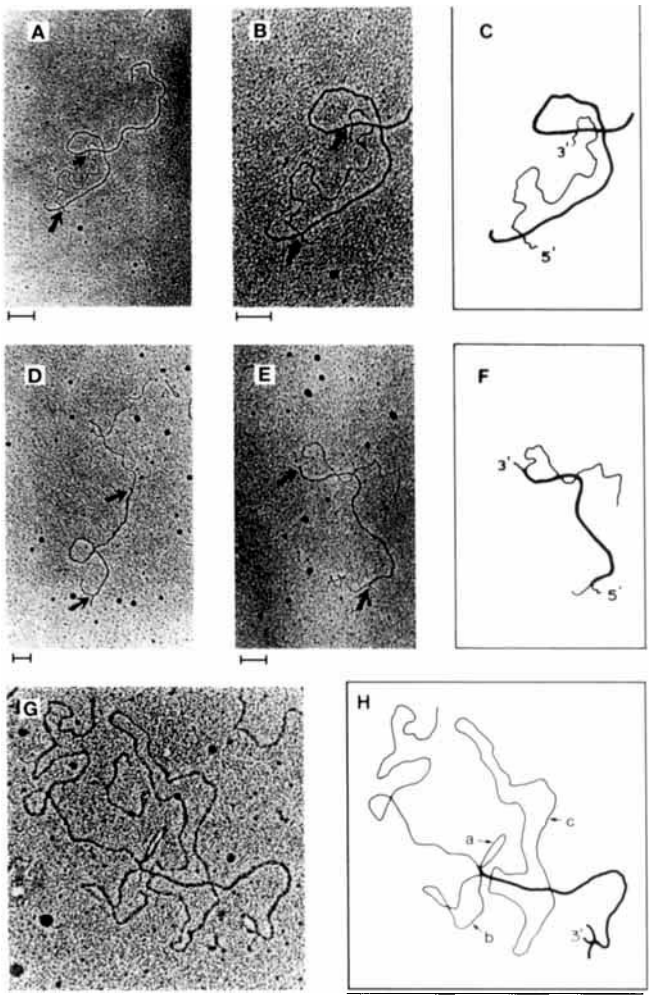


Fig. 2. Electron micrographs of hybrids of hexon mRNA and fragments of adenovirus 2 (Ad2) DNA [13]. A, B) Examples of R-loop hybrids observed after incubation of hexon mRNA and duplex *Hind*III A fragment DNA. C) Schematic representation of A and B. D, E) Two examples of hybrids of hexon mRNA and the single-stranded *Hind*III A fragment. F) A schematic representation of E. The single-stranded RNA at the end of the hybrid region is represented by a wavelike line. In A, B, D, and E the positions of the RNA tails at the 5′ and 3′ ends of the hybrids are denoted by arrows. G) An example of a hybrid between single-stranded *Eco*RI A DNA and hexon RNA. H) Schematic representation of G. The hybrid region is indicated by a heavy line; loops a, b, and c (single-stranded unhybridized DNA) are joined by hybrid regions resulting from annealing of upstrem DNA sequences to the 5′ tail of hexon mRNA. Bars on micrographs represent 0.1 μm.



Professor P. A. Sharp was born on June 6, 1944 in Kentucky. He obtained a B. A. in chemistry and mathematics from Union College, Kentucky, and a Ph.D. in chemistry from the University of Illinois, Champaign-Urbana. He carried out postdoctoral research with Prof. N. Davidson at the California Institute of Technology and with Prof. J. Watson at the Cold Spring Harbor Laboratory. Subsequently, he joined the Center for Cancer Research and Department of Biology at the Massachusetts Institute of Technology in 1974. In 1985 he succeeded Prof. S. E. Luria as Director of the Center for Cancer Research. He is currently Head of the Department of Biology, a position he assumed in 1991. His research interests have centered on the molecular biology of tumor viruses and the mechanisms of RNA splicing, which he discovered in 1977. His work provided one of the first indications of the startling phenomenon of split genes in the cells of mammals. His scientific achievements have resulted in numerous awards, the most prestigious of which was the Nobel Prize for Medicine in 1993.

quences, we used a denatured single strand of the *Hind*III fragment (Fig. 2D, E, and F) to form a RNA · DNA hybrid. Surprisingly, the 5′ RNA tail still did not form a hybrid with the adjacent viral sequences, suggesting that these RNA sequences were derived from other DNA sequences.

Could the DNA sequences transcribed to form the 5′ tail sequence, the leader RNA sequence, be located upstream of the body of the hexon mRNA, perhaps as part of the long nuclear RNA? To test this possibility, a strand of the *Eco*RI A DNA fragment was hybridized with the hexon mRNA. This DNA fragment contained all of the linear viral sequences which could have been transcribed by the polymerase before encountering the body of the hexon mRNA. Surprisingly, and wonderfully, the leader RNA sequences hybridized to three short tracts of DNA sequences, creating three different size loops a, b, and c of intervening single-strand DNA (Figs. 2G and H). The length of these loops mapped the positions of the leader sequences, L1, L2, and L3, to approximately 16.9, 19.8, and 26.9 map units on the genome, respectively. The distances between the bases of the three loops permitted an estimate of the lengths of the two internal leaders to be 80 and 110 nucleotides, respectively. The 5′ proximal leader was estimated to be quite short, but longer than fifteen nucleotides.

RNA splicing was the mechanism we proposed for generation of the final hexon mRNA.[13] It was known that the nucleus of virus-infected cells contained long RNAs transcribed from the viral sequences between the 5′ leader L1, located at 17 map units, and the body of the hexon mRNA, located between 51.7 and 61.3 map units.[19, 20] Thus the long nuclear RNA probably contained sequences for all three leaders, L1, L2, and L3, as well as for the body of the mRNA. These sequences were conjectured to be joined by excision of the intervening sequences and ligation of the flanking RNAs, a process dubbed RNA splicing (Fig. 3). In fact, the nuclear RNAs were quite abundant and were easily visualized by electron microscopy of the RNA · DNA hybrids.[21] Analysis of the structure of these RNA · DNA hybrids revealed the presence of potential intermediates, in which only L1 had been spliced to L2 or L1, L2, and L3 had been joined by splicing.

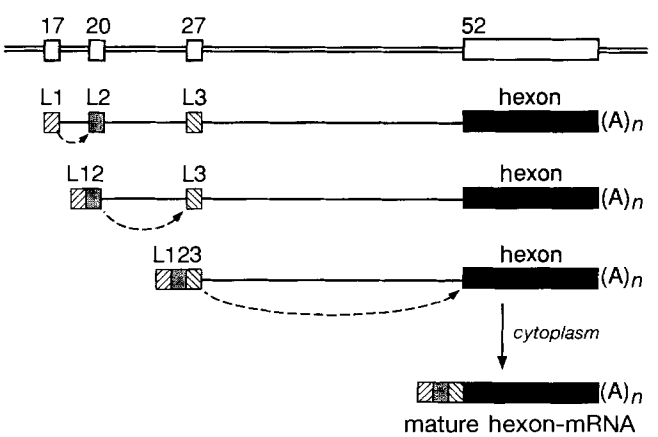


Fig. 3. Proposed RNA splicing mechanism for synthesis of mRNA for hexon protein. A long nuclear precursor RNA is transcribed from 16.9 map units through the polyA addition site at the end of the body of hexon mRNA. The region of the Ad2 genome from which the precursor RNA is transcribed is shown at the top of the figure. The four RNA segments in the cytoplasmic mRNA are processed from this precursor by excision of intervening sequences and ligation (denoted by dashed arrows).

The RNA splicing hypothesis reconciled many paradoxes. Both the longer nuclear RNAs and the shorter cytoplasmic mRNAs could share 5′ cap termini, ^{7}mGpppX, and 3′ polyadenosine tracts,[22] because internal sequences were removed from the nuclear precursor. More specifically for adenovirus, previous evidence had suggested that many different viral mRNAs appeared to share a common 5′ terminal sequence.[23] This sequence, a long T1 oligonucleotide, contained the cap and an apparently unique sequence eleven residues in length. If many of the late viral mRNAs were processed by splicing from the same type of precursor RNA, they could share a common sequence at their 5′ termini. More importantly, the RNA splicing hypothesis provided an explanation for the hnRNA phenomenology associated with cellular genes. Heterogeneous nuclear RNA transcribed from diverse cellular genes could be processed by RNA splicing into shorter cytoplasmic mRNAs. Thus, most cellular genes probably contained sequences which were removed by RNA splicing, that is they were split genes.

Split Genes: Intervening Sequences or Introns in Cellular Genes

Shortly after the discovery of RNA splicing and split genes in adenovirus, a number of cellular genes were also shown to have introns or intervening sequences. For example, the globin genes contained two intervening sequences,[24, 25] the ovalbumin gene was split into eight sets of sequences,[26] and the immunoglobulin genes contained both short and long introns.[27] In fact, the average cellular gene contains approximately eight introns and the primary transcription unit is typically four times larger than the final mRNA. Shortly thereafter, it was recognized that there was a limited set of conserved sequences at each intron boundary.[28] Interestingly, these consensus sequences were common of vertebrate, plant, and yeast cells[29] suggesting the splicing process was evolutonarily general. Introns in the latter organisms are generally shorter and have more highly conserved sequences at their boundaries.

Phylogenetic comparison of the sequences of homologous genes from a variety of organisms revealed that intron sequences had drifted much more rapidly than exon sequences. This suggested that intron sequences are generally not functional, at least in the context of requiring long tracts of specific sequences. Furthermore, the length of introns in homologous genes varied significantly during evolution, suggesting little constraint. Finally, it was clear that specific introns could be lost during evolution. The mechanism responsible for the exact deletion of introns is probably related to gene conversion using a cDNA copy of the mRNA or a partially spliced intermediate RNA. This process has been documented for the removal of introns from yeast genes[30] and raises the question of why introns persisted during evolution.

Mutations in Cellular Genes

Many human diseases are caused by mutations that interfere with RNA splicing. Approximately one quarter of all mutations

in the human globin genes underlying thalassemia are mutations in sequences specifying correct RNA splicing. Thus, conserving information for accurate splicing is a constraint on genetic systems. The limited nature of the mutations altering splicing in the globin family is interesting.[31] All of the characterized mutations either alter the conserved 5′ or 3′ splice site sequences at the boundaries of the intron, or are changes within introns that generate new consensus splice sites (Fig. 4). The former is simple: mutation of the highly conserved GU or AG sequences at the boundaries of the intron commonly inactivates splicing at that site, and this frequently leads to the activation of a nearby cryptic splice site. The latter is more complicated. In this case, a mutational change within an intron—CT → GT activates this site as a 5′ splice site and, as a consequence, an upstream AG is activated as a 3′ splice site for further splicing. This results in the generation of a short exon from the previous intron sequences (Fig. 4). Thus, mutations can alter both the position of splice sites and the number of exons to generate novel proteins.

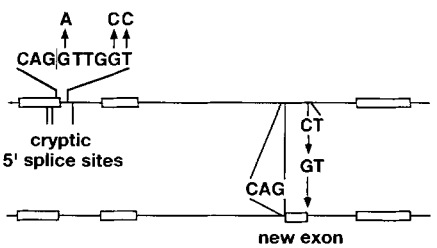


Fig. 4. β-Globin mutations. β-Globin genes of thalassemia patients possessing mutations which affect RNA splicing [31]. The single base changes in four independent patients are indicated by arrows from the diagram of the two intron structure of the β-globin gene. Three of the mutations alter conserved sequences of the 5′ splice site (left) and a fraction of the mRNA from these mutant genes is processed at the cryptic 5′ splice sites. The fourth mutation is within the sequences of the second intron (right) and creates a 5′ splice site at this position. This results in the induction of the indicated sequences as a new exon. Exon sequences are represented by rectangles, intron sequences by lines.

Mistakes are probably not uncommon in splicing of RNA from complex genes. Exons can occasionally be skipped and, in some cases, circular RNAs can be generated.[32, 33] Since specific functions have not been assigned to many of these RNAs, their generation may reflect noise in the system. Interestingly, it has recently been proposed that an mRNA surveillance system exists in cells which destroys RNAs as they enter the cytoplasm if they contain an open reading frame interrupted by a translational termination signal.[34] This system would probably degrade most mRNAs with splicing errors as they are transported to the cytoplasm.

Why Split Genes and RNA Splicing?

It is difficult to confidently account for why introns have been conserved during evolution within the genes of most, if not all, eukaryotes. Clearly the intron–exon structure of genes has been very important in the generation of new genes during evolution. For example, the fibronectin gene of man is composed of three types of exons, each of which encodes a specific type of protein folding domain (Fig. 5).[35] These same three protein-folding domains and corresponding exon structures are found in other

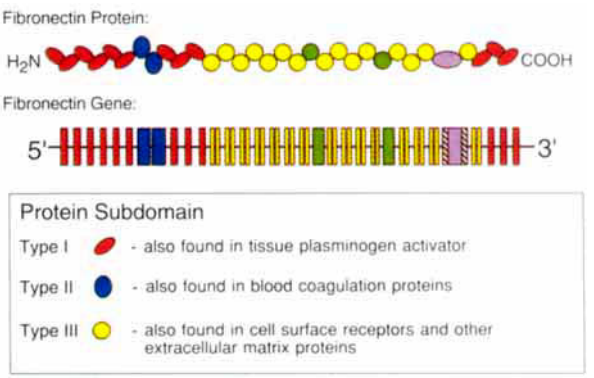


Fig. 5. Fibronectin gene evolved by exon duplication. The large extracellular matrix protein, fibronectin, is primarily composed of three types of protein subdomains, I, II, and III denoted as tilted red ellipsoids, vertical blue ellipsoids, and yellow circles, respectively. Each of these domains are encoded by a defined exon pattern, one or two exons, denoted as vertical rectangles. These exon units are duplicated in the fibronectin gene and also in the other genes containing these domains. In two cases, large green rectangles, the intron separating the typical two exon structures of the type III subdomain, have been deleted. These patterns suggest that descendants of a common progenitor exon configuration were used to generate parts of these genes [36].

genes, some of which encode cell surface receptors and blood coagulation proteins. Thus, the fibronectin gene was created by tandem and dispersed duplication of exon units using breakage and joining within the intron sequences. Since these exon units are assembled precisely by RNA splicing and encode functional protein domains, the final protein is stable and has multiple functions. Duplication and utilization of an exon unit has been a common mechanism for the generation of new genes encoding many cell surface receptors and other types of proteins in vertebrates. Thus, the presence of exon units which correspond to functional protein domains has been critical for the evolution of complex organisms.

The ability to alternatively select different combinations of exons at the stage of RNA splicing to generate proteins with different functions is clearly critical for the viability of many vertebrate organisms. Approximately, one of every twenty genes is expressed by alternative pathways of RNA splicing in different cell types or growth states. For example, nuclear precursor RNAs from the fibronectin gene are alternatively spliced into mRNAs that encode 20 different proteins. These proteins have slightly different functions reflecting their variant structures. Furthermore, a set of exons is not included in mRNAs processed in liver cells but is included in mRNAs in other cell types (Fig. 6). The fibronectin secreted by the liver more readily circulates in the blood stream because it has fewer protein domains which are recognized by receptors on the cell surface than the other forms of fibronectin.[36] The fibronectin secreted by other cells is more typically found in the intracellular matrix of solid tissue. A similar variation in cellular adhesion is observed with alternative splicing patterns in another part of the fibronectin mRNA. Thus, through alternative splicing, the same set of gene sequences can be utilized for different functions.

Alternative splicing of precursor RNAs in different cell types must reflect differences in the factors regulating the splicing process. Only in few cases have these factors been identified, primarily by the analysis of mutants which are defective in the regulatory step. The development of sexual dimorphism in the fruit fly *Drosophila* is regulated at the level of alternative RNA

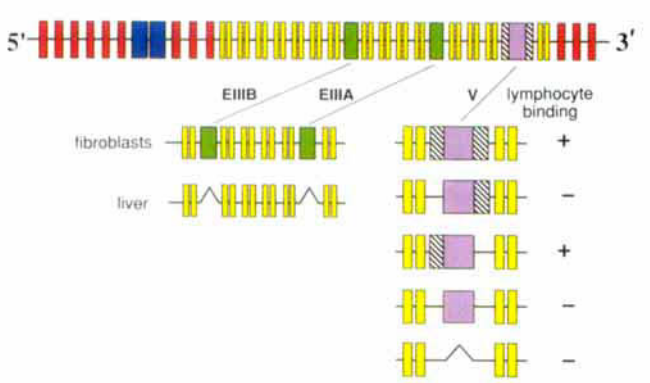


Fig. 6. Alternative splicing of RNA encoding fibronectin. The exons denoted as EIIIB and EIIIA are spliced into the mature RNA synthesized in many cell types including fibroblasts. However, in the liver, these two exons are not included, are skipped, in synthesis of the mRNA. Furthermore, five variations for the splicing patterns of the V region are shown. All of these variations on splicing are found in most cell types. The fibronectin proteins encoded by the first and third mRNA bind differentially to receptors on lymphocytes. In total, at least twenty different proteins are synthesized from the single fibronectin gene.

splicing by expression of a cascade of genes. Early in development, the female or male specific pattern of splicing is set by a reading of the ratio of sex chromosomes to autosomal chromosomes. After setting this switch, the developmental process is controlled by an autoregulatory process which maintains the male or female splicing pattern in many if not all cells.[37] Interestingly, most of the proteins encoded by these sex regulating genes are members of a family whose common features are one or more RNA recognition subdomains and a pronounced tract of the repeating amino acid sequence Arg-Ser.[38] It is likely that these factors directly interact through the Arg-Ser tract with other proteins critical for formation of the splicing machinery.

Split Genes in the Progenote?

The split gene structure must be very old, clearly predating the divergence of organisms that gave rise to plants, yeast, and man.[29] First, as will be described later, a complex splicing machinery, which involves greater than 50–100 proteins and five small RNAs, exists in the nucleus of all eukaryotes. This machinery is highly conserved and could not have arisen spontaneously in the various lineages. Second, introns are conserved in positions within homologous genes found in the lineages of plants and animals. This evidence established that split genes and RNA splicing were present in common progenitor organisms a billion years ago. Several scientists have speculated that genes originally evolved as exons and that the progenote organism from which current prokaryotic and eukaryotic organisms evolved may have had a split gene structure.[39–42] These primordial exons are pictured as encoding sequences for stable protein folding domains. Assembly of a number of exon sequences by RNA splicing would be expected to produce a protein composed of stable folding domains which have a high probability of being functional either structurally or catalytically. If genes originally evolved in this fashion, the positions of introns in relationship to protein secondary structure might not be random. Evidence to support this hypothesis has been sought in the exon–intron structure of evolutionarily old proteins critical for energy metabolism. For example, the enzyme pyruvate kinase is conserved in structure and functions in bacteria, yeast, and chicken (Fig. 7).[43] The gene is not interrupted with introns in bacteria and yeast, but contains ten introns in chicken, nine within the coding sequences. The positions of these nine



Fig. 7. The structure of pyruvate kinase and the intron positions [44] (reprinted with permission, Copyright © 1993, Cell Press, Cambridge, MA, USA). Pyruvate kinase is shown schematically as a protein with secondary and tertiary structure on the left. On the right, this structure is expanded at the positions of introns in the tertiary structure of the protein. Note that the first three introns all fall between α-helix (barrels) and β-sheet (arrows) repeats. Intron 8 is positioned in approximately equivalent positions in the mononucleotide binding fold of pyruvate kinase and maize alcohol dehydrogenase.

introns are not random when compared to the protein structure. First, in the N-terminal part of the protein, the first three introns are positioned between repeating structural motifs of α helix-β sheet. Second, in the mononucleotide binding fold, pyruvate kinase shares a common intron position with one other old metabolic enzyme, alcohol dehydrogenase. In pyruvate kinase, the eighth intron occupies a position similar to that of an intron in the dehydrogenase. Since the generation of these two enzymes from a common protein subdomain clearly predated the evolutionary divergence of prokaryotic and eukaryotic organisms, these results suggest that the progenitor organisms for both prokaryotic and eukaryotic organisms may have had a split gene structure more typical of a current eukaryotic cell (for discussion see ref. [44]).

Is the Gene an Exon?

The gene was first genetically defined as a unit of inheritance associated with a locus on a chromosome. The chemical definition of a gene has become much more difficult, however, as the complexity of genetic information and its modifications are discovered. The existence of alternative splicing of exons, where information at an exon unit can be optionally expressed in some cells and not in others, suggests that an exon might correspond to a gene. That is, an exon corresponds to the minimal amount of information which is expressed as a discrete unit. This concept becomes particularly relevant when the *trans*-splicing process is considered.[45] In this case, exons transcribed from different loci, and in many cases different chromosomes, are joined by RNA splicing. *Trans*-splicing of exons and introns has been established in the parasite trypanosomes,[46] the flat worm *C. elegans*,[47] and suggested for some human genes.[48] Clearly, in the case of *trans*-splicing, both the unit of inheritance and the locus on a chromosome can correspond to a single exon.

It is unlikely, however, that the current working definition of a gene as a linear collection of exons which are joined by RNA splicing will be radically altered in near future. This is probably wise, as the existence of multiple processes collectively called RNA editing further complicates the biochemical definition of a gene.[49] However, given the possibility that the earliest unit of genetic information may have evolved as an exon, the general concept of exons as gene units may be more valid than any other proposal.

Splicing of Nuclear Precursor RNAs to mRNAs

The development of a reaction composed of soluble cellular components which accurately processed precursor RNAs (pre-mRNAs) to mRNAs was critical for advancing our understanding of splicing.[50] When combined with the use of highly radioactive pre-mRNA substrates, a biochemical analysis of the splicing process became feasible.[51, 52] Not surprisingly, kinetic RNA intermediates in the splicing reaction were soon identified.[53, 54] Surprisingly, however, these intermediates had a lariat structure in which the 5′ nucleotide of the intron was joined in a 2′,5′-phosphodiester bond to an adenosine unit within the intron.)[55] Since the adenosine unit is covalently bonded through both 3′,5′- and 2′,5′-phosphodiester linkages, this forms an RNA branch. The existence of such branches was described from nuclease digestion studies of total nuclear RNA from human cells.[56] Formation of the branch appears simultaneously with cleavage at the 5′ splice site and generates the lariat RNA which typically migrates more slowly than the pre-mRNA during electrophoresis through a tight porosity polyarylamide gel.

The splicing of pre-mRNA proceeds in two steps (Fig. 8, left). As mentioned above, the first step consists of cleavage at the 5′ splice site with the concomitant formation of the branch. At this stage, the 5′ exon RNA has a 3′ hydroxyl group and the lariat intermediate RNA contains the intron and 3′ exon. The second step consists of cleavage of the RNA at the 3′ splice site with concomitant joining of the two exons. The intron is released as a lariat RNA and is reasonably stable in reactions in vitro. This contrasts with the situation in vivo where intron RNAs are almost always rapidly degraded.

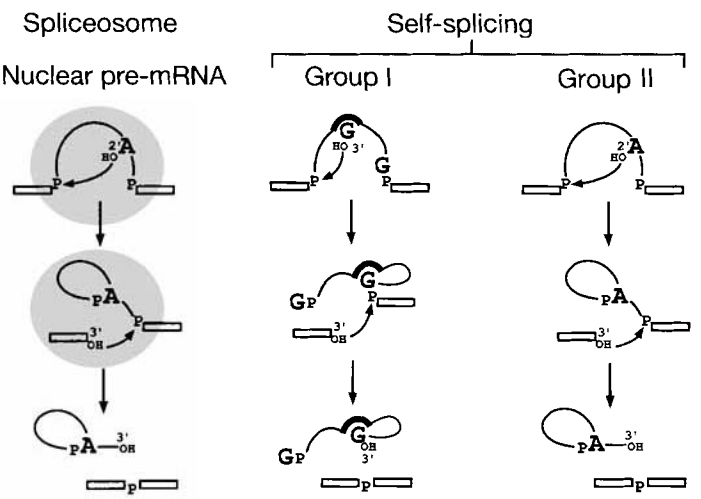


Fig. 8. Comparison of self-splicing and nuclear pre-mRNA splicing mechanisms. The first column outlines the mRNA precursor splicing mechanism. The shaded circle represents a multicomponent complex, the spliceosome, which promotes the splicing reaction. The second column outlines the splicing mechanism of self-splicing introns of the group I type. This process is catalyzed by RNA structures within the intron (dark semicircle), which contains a guanosine binding site, and utilizes a guanosine (G) factor in the first step. The third column outlines the splicing mechanism of self-splicing introns of the group II type. This process is also catalyzed by RNA structures within the intron but utilizes, instead of a cofactor, an adenosine residue (A) within the intron to form a lariat RNA. All three mechanisms proceed by two steps, reaction at the 5′ splice site and then reaction at the 3′ splice site.

The fact that the intermediate state, consisting of two RNAs, was efficiently converted to the final products strongly suggested that these RNAs remain bound in a complex. The complex was identified by its rate of sedimentation in a glycerol gradient (60S) and was designated to be a spliceosome or splicing body.[57, 58] As anticipated from earlier work which suggested the importance of small nuclear ribonucleoprotein particles in splicing, the spliceosome contained the small nuclear RNAs (snRNAs) U2, U4, U5, and U6 and, under certain conditions, U1.[59] Thus, the spliceosome, much like a ribosome, contains a substrate RNA and a number of stable cellular RNA-protein components.

Group I, Group II, and the Spliceosome

Comparison of the two steps in splicing by the spliceosome to the RNA-catalyzed self-splicing reactions of group I and II introns shows some striking similarities (Fig. 8). In all three cases, the first step is cleavage at the 5′ splice site. In group I introns, this cleavage requires a guanosine which specifically occupies a binding site in the catalytic intron sequences.[60] The 3′ hydroxyl group on this guanosine is activated and through a transesterification reaction displaces the 3′ hydroxyl of the 5′ exon. Group II self-splicing introns cleave at the 5′ splice site by activating the 2′ OH at the branch site, producing a lariat RNA[61, 62] much like that produced by the spliceosome. The second step for all three processes involves a reaction at the 3′ splice site to join the exons and displace the intron. The simplest mechanism for the second step of splicing of the group I and II introns is a single transesterification. This has been proven to be the case for reactions by group I introns.

The similarities between the spliceosomal process and the self-splicing introns suggested that these reactions might be

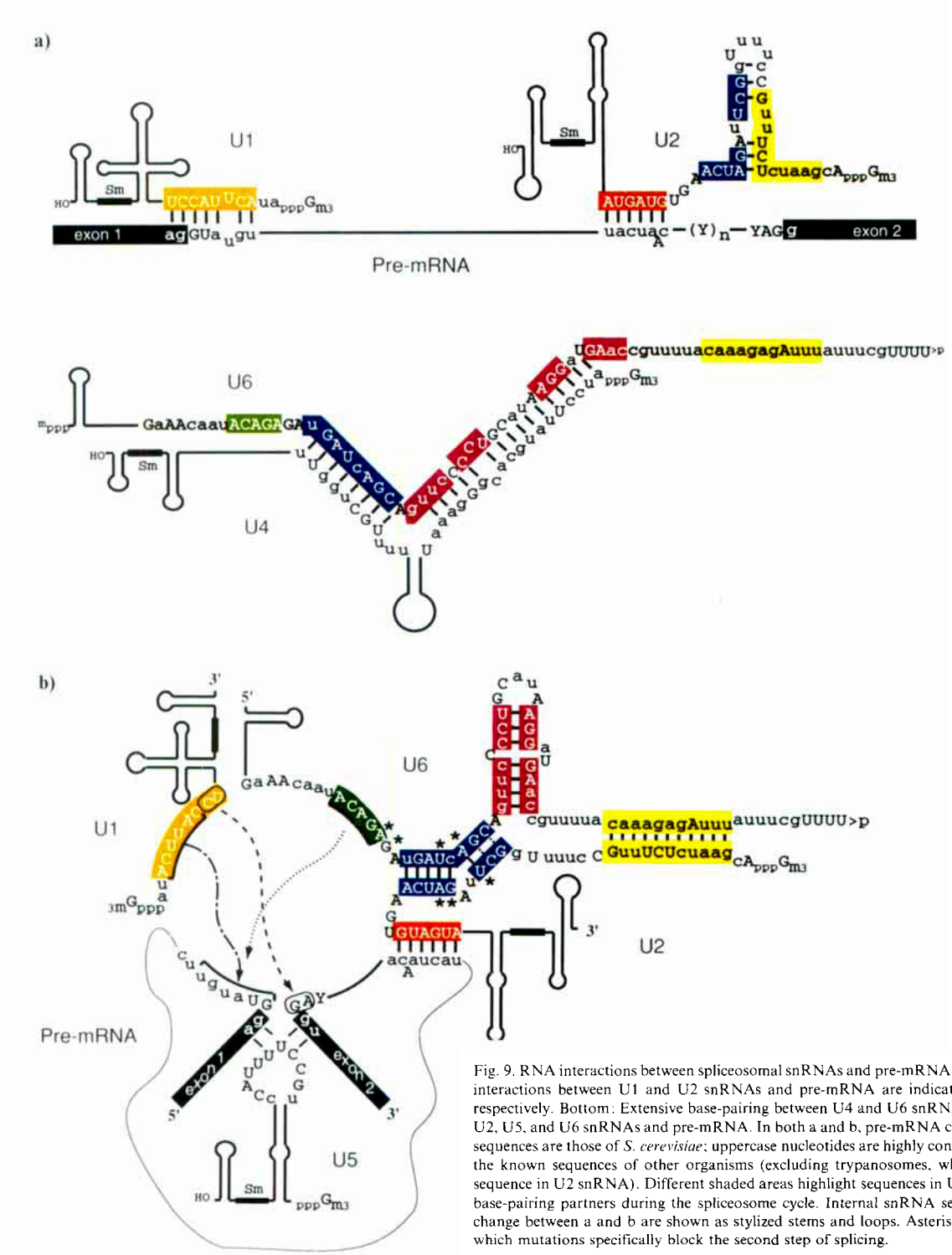


Fig. 9. RNA interactions between spliceosomal snRNAs and pre-mRNA substrates. a) Top: Base-pairing interactions between U1 and U2 snRNAs and pre-mRNA are indicated on left and right of intron, respectively. Bottom: Extensive base-pairing between U4 and U6 snRNAs. b) Interactions between U1, U2, U5, and U6 snRNAs and pre-mRNA. In both a and b, pre-mRNA consensus sequences and snRNA sequences are those of *S. cerevisiae*; uppercase nucleotides are highly conserved between *S. cerevisiae* and the known sequences of other organisms (excluding trypanosomes, which do not have a GUAGUA sequence in U2 snRNA). Different shaded areas highlight sequences in U2 and U6 snRNAs that change base-pairing partners during the spliceosome cycle. Internal snRNA secondary structures that do not change between a and b are shown as stylized stems and loops. Asterisks indicate snRNA positions at which mutations specifically block the second step of splicing.

evolutionarily related. This is particularly the case for the group II and spliceosome reactions. Thus, the snRNAs in the spliceosome might be pictured as a group II intron in pieces, where these RNAs form the catalytic sites for both reactions. The proteins in the spliceosomes could be necessary for recognition of the precursor RNA, arranging the snRNAs in catalytic structures and rearrangement of the components to facilitate completion of the process. Early in evolution all introns might have been self-splicing. Then, during the passage of time, *trans*-acting components may have developed which executed the splicing of introns by recognition of sequences at the splice sites, thus permitting atrophy of the *cis*-sequence within each intron.[63] *Trans*-acting segments of group II introns which complement the splicing of introns with partial catalytic structure have been documented (see ref. [63]).

Years after the discovery of the lariat intermediate in the *cis*-splicing process, studies of the *trans*-splicing reaction revealed a branched intermediate state. Thus, the chemistry of the *trans*-splicing reaction is very similar to that of the *cis*-splicing process.[64] It is therefore highly likely that the *cis*- and *trans*-splicing processes are variations of a single fundamental mechanism. Trypanosome parasites which exclusively synthesize mRNA by *trans*-splicing of a short leader RNA do not apparently express U1 snRNA or U5 snRNA, but do express U2, U4, and U6 snRNAs.[65]

The sequence complementarity between the 5′ end of U1 snRNA and the consensus sequences at the 5′ splice site led to the hypothesis that this interaction was critical for splicing.[66, 67] This hypothesis has been confirmed by a number of studies including the inhibition of splicing in vitro by addition of anti-sera specific for U1 snRNP.[68] After the discovery of lariat RNA, a consensus sequence was recognized in the region flanking the branch site. This consensus sequence is complementary to a conserved internal sequence in U2 snRNA, and mutational analysis has shown that this interaction is also critical in splicing.[69] U1 and U2 snRNAs recognize consensus sequences at the 5′ splice site and branch site as early steps in the splicing reaction (Fig. 9a). At the same stage of splicing U4 and U6 snRNAs are bound to one another through an extended region of complementarity.[70] SnRNA U6 is unique relative to the other snRNAs in that: it is not bound by core peptides recognized by the Sm lupus antisera, it is transcribed by a different polymerase, and it has a different type of modification at its 5′ terminus. U6 snRNA is also the most conserved member of the snRNA family and may have a unique catalytic role. The U4/6 snRNP forms a specific complex with U5 snRNP and this tri-snRNP complex is thought to bind to the other components in formation of the spliceosome.[71]

After formation of the spliceosome, there are major rearrangements of the snRNAs (Fig. 9b). Both genetic and biochemical experiments show that U6 and U2 snRNAs are paired through an extensive tract of complementarity in the spliceosome.[72, 73] Formation of the U2 and U6 structure requires dissociation of U4 snRNA from U6 snRNA. In fact, U4 snRNA can be released from the active spliceosome after this transition. The complementarity between U1 snRNA and the 5′ splice site sequence is probably also dissociated before the first step of splicing. The 5′ splice site almost certainly pairs with another region of U6 snRNA.[74, 75] U5 snRNA is thought to be important in recognition of the exon sequences immediately flanking the splice sites. Mutations in these flanking sequences frequently have significant effects on splicing efficiency and these effects can be reduced by complementary changes in U5 snRNSs.[76] It is possible that there are further rearrangements in the secondary structures formed by the snRNAs between the first and second steps in splicing. There are mutational changes in U2 and U6 (positions denoted by * in Fig. 9) which only inactivate the second step.[72, 73] Inspection of the network of complementarity formed between snRNAs and the pre-mRNA in the spliceosome reveals a concentration of snRNA structure, perhaps tertiary, near the branch site and 5′ splice site sequences. This arrangement of snRNAs might form the catalytic site for the first step. Perhaps further rearrangements would form another catalytic site for the second step.

Formation of the Spliceosome

A number of stable complexes containing snRNAs and pre-mRNA have been partially characterized and placed in a spliceosome cycle (Fig. 10).[77] The commitment complex CC

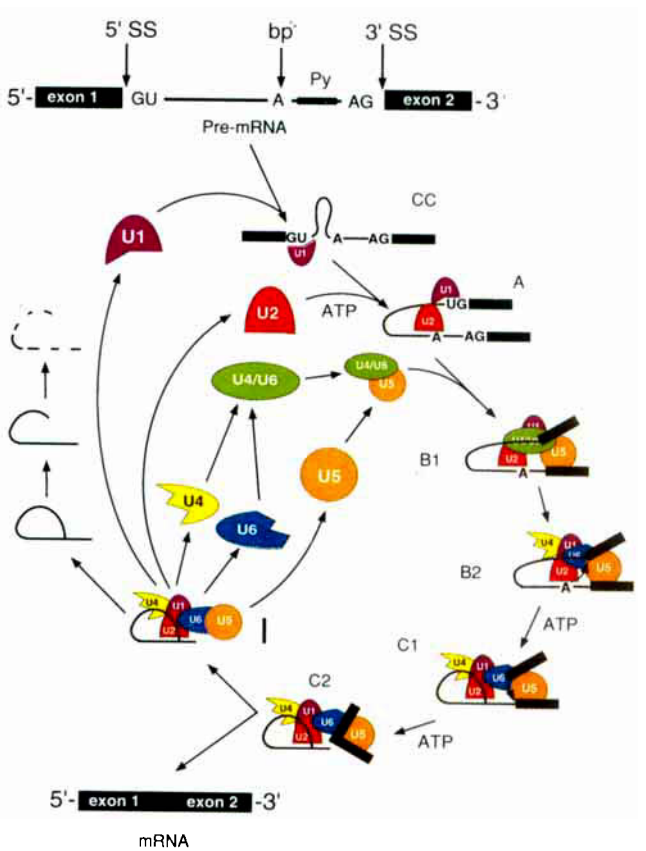


Fig. 10. Schematic representation of the spliceosome cycle in terms of the role of small nuclear ribonucleoprotein (snRNP) particles in pre-mRNA splicing. Pre-mRNA (top), containing two exons separated by an intron, enters splicing complexes with snRNPs and exits as mRNA (bottom) and excised lariat intron (left). Other, non-snRNP factors are required for spliceosome formation, but have been omitted for simplicity. CC, A, B1, B2, C1, C2, and I represent complexes within the splicing pathway that have been distinguished biochemically and/or genetically. 5′ SS, 3′ SS, bs, and Py indicate 5′ and 3′ splice sites, branch site, and polypyrimidine tract, respectively. The individual snRNPs indicated are U1, U2, U4, U5, and U6.

forms on the pre-mRNA by recognition of the 5′ splice site sequence by U1 snRNP and sequences encompassing the branch site and 3′ splice sites.[78–80] For mammalian systems, a pyrimidine tract near the 3′ splice site and branch site is particularly important. The subsequent binding of U2 snRNP to the pre-mRNA results in formation of the very stable A complex. The stable binding of U2 snRNP to the pre-mRNA depends critically on a protein U2AF,[81] which recognizes the polypyrimidine tract through prototypical RNA-binding domains and signals interactions with the other splicing components through a tract of Arg-Ser amino acid repeats. Interestingly, U1 snRNP which is also required for stable U2 snRNP binding, has a bound protein with a tract of Arg-Ser repeats, the U1-70 kd polypeptide. Whether U2AF and U1-70 kd directly communicate across the intron is not clear.

The B1 spliceosome forms when the U4/U6/U5 tri-snRNA complex binds the A complex. It is probably in the B1 complex that U4 snRNA dissociates from U6 snRNA and perhaps U1 snRNA from the 5′ splice site. These events define the B2 complex which is the precursor of the C1 complex. The first step of splicing has occurred in the C1 complex. In generation of the C2 complex, it is likely that there are further rearrangements that are necessary to catalyze the second step in splicing. The C2 complex dissociates and the newly joined exons are released from the snRNP · intron complex I. In the cell, the spliced product migrates to the cytoplasm. The lariat intron is retained with the snRNPs and this complex I turns over. The snRNPs are recycled for further splicing in vivo, while the intron RNA is degraded. Since all snRNAs are very stable, a particular snRNA likely participates in many splicing cycles.

Assembly and rearrangements of complexes as elaborate as those in the spliceosome cycle would be expected to require a number of proteins. Sophisticated genetic analysis has identified a number of yeast gene products that are important for splicing either in vivo or in vitro.[82, 83] Temperature-sensitive mutations in *p*recursor *R*NA *p*rocessing (PRP) genes cause the accumulation of unspliced pre-mRNA in the nucleus and/or generate extracts defective for splicing in vitro (Fig. 11). Surprisingly, it is estimated that at least a hundred different genes encode products important for RNA splicing, about 2% of the total yeast genome. Thus, the splicing apparatus is a significant component of the nucleus. The amino acid sequences predicted for some of the PRP genes suggest that they have functions such as RNA binding, RNA helicase and protein–protein interaction properties. Matching these hypothetical functions to processes in spliceosomes will be challenging.

Reassuringly, the steps in the spliceosome cycle where particular PRP proteins are required (Fig. 11) are consistent with the cycle as defined by kinetic and biochemical methods. Most transitions between specific forms of the spliceosome require one or more specific proteins. Furthermore, a number of PRP mutants are defective in splicing because of their inability to reassemble snRNPs for further splicing. Thus, both genetic and biochemical results prove that the spliceosome cycle is the process responsible for excision of introns from split genes.

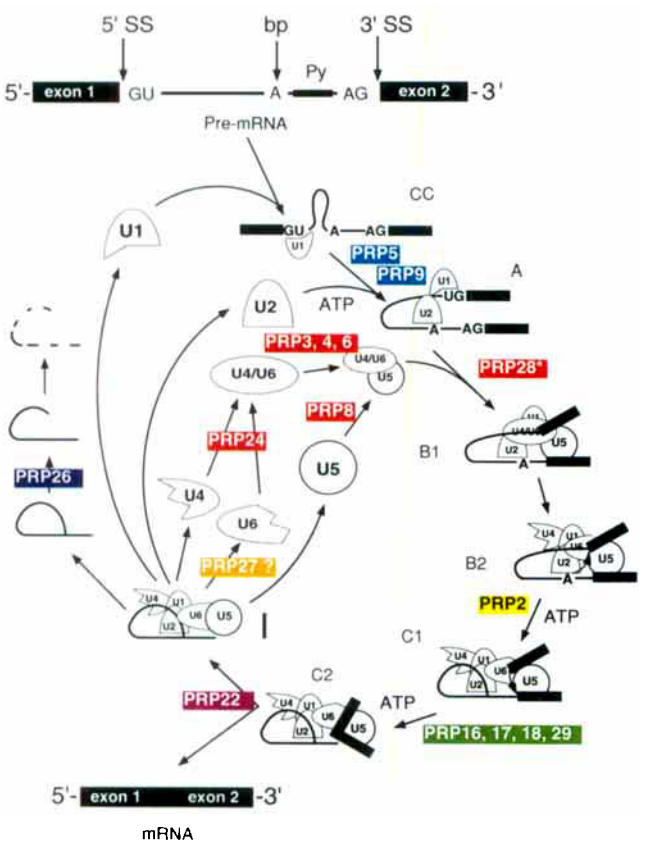


Fig. 11. Transitions in the spliceosome cycle which require a PRP protein. The particular PRP mutant is listed beside the arrow indicating the transition in the cycle in vitro requires the mutant protein.

The Chemistry of the Spliceosome

Both steps in the spliceosome process involve reactions between hydroxyl groups and a phosphodiester bond. The products and substrates in both steps contain the same number of covalent bonds and thus each step could be accomplished with a single transesterification reaction. This has been shown to be the case for group I self-splicing introns by analysis of the stereochemistry of the two reactions (Fig. 12).[84–86] Phosphorothioates in diester bonds of RNA are chiral, having either R_p or S_p stereochemistry depending upon the position of the sulfur

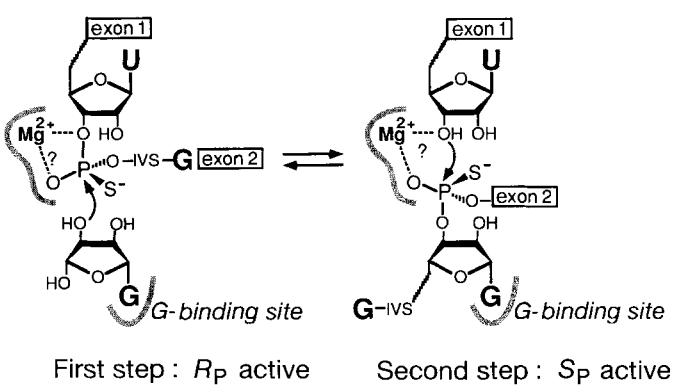


Fig. 12. The stereochemistry of the first and second step reactions of the group I self-splicing site. A sulfur atom is indicated at the positions where it does not inhibit the reactions, R_p and S_p positions for the first and second steps, respectively [84–86]. The interactions between the oxygen group on the phosphate and the Mg^{2+} groups are hypothetical, proposed to explain why a phosphorothioate with the sulfur atom in this position is not reactive.

atom. The specific stereochemistry can be determined by its sensitivity to particular nucleases. If a chiral phosphorothioate group participates in a single transesterification reaction, its stereochemistry is inverted, for example, from R_p to S_p. This fact permits counting of the number of transesterification reactions in a process and, thus, the detection of any potential transient intermediate.

As implied above, R_p and S_p phosphorothioates are not equally active in many catalytic sites. This is commonly interpreted as reflecting the unique role of one of the oxygen groups on the phosphate in interaction with a metal ion, a role which could not be equally well-fulfilled by a sulfur group. These principles of phosphorothioate chemistry have been analyzed for the group I self-splicing intron and now have been studied in the spliceosome.

The two steps of splicing by the group I intron are probably executed as forward and reverse reactions at a single catalytic site (Fig. 12). In the first step, the guanosine cofactor is bound to the G binding site and its 3′ OH group is activated for the transesterification reaction. In this reaction, the R_p configurated phophorothioate is active while the S_p is not. This suggests that the oxygen group in the equivalent S_p position is uniquely recognized in this reaction, perhaps by a metal ion. Consistent with a single transesterification mechanism during the first step, the R_p chiral center is converted to a S_p phosphorothioate product.[84] In the second step, the guanosine group at the 3′ splice site occupies the G binding site and the 3′ OH of the 5′ exon is activated for the transesterification reaction. As would necessarily be the case by the principle of microscopic-reversibility, the S_p configurated phosphorothioate is active in this reaction and the R_p is not.[86] The S_p substrate phosphodiester bond generates a R_p product. Thus, stereochemical analysis of the group I process strongly supports the hypothesis of a single catalytic center for both steps.

The stereochemistry of the two steps in the spliceosome process was investigated by synthesis of substrate RNAs containing either a R_p or S_p phosphorothioate at either the 5′ or 3′ splice site.[87] The particular stereoisomer was incorporated by a combination of chemical synthesis, oligo-primed transcription, and ligation of RNAs by use of a bridging oligodeoxynucleotide and T4 DNA ligase).[88] Splicing of the phosphorothioate-containing RNA substrates was tested in nuclear extracts after different periods of incubation. Analysis of the substrate and product RNAs showed that a) both steps in splicing involve a single transesterification reaction with inversion of the chiral center of the active phosphorothioate, and b) the S_p diastereomer was the active phosphorothioate in both steps, while the R_p diastereomer was not.[87]

A comparison of the stereochemistry and critical components in the two steps in splicing for the group I self-splicing process and the spliceosome process is informative (Fig. 13). As discussed before, the two steps in the group I case are forward and reverse reactions within a single catalytic center. This is almost certainly not the situation for the spliceosome process. In both steps of the latter process, the S_p phosphorothioate was active; thus, the second step is not a reverse of the first step. These results are most consistent with the proposal that the spliceosome generates two different catalytic centers for the two steps. The constituents in these centers may partially overlap but

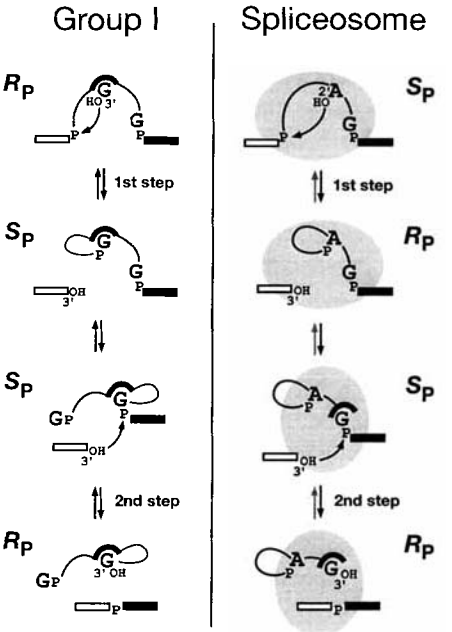


Fig. 13. Chemical mechanisms and stereochemical configurations of the two steps of pre-mRNA splicing (right) and group I intron self-splicing (left). First-step differences between spliceosomal and group I splicing include opposite phosphorothioate diastereomer preferences, different reaction nucleophiles (2′-OH versus 3′-OH), differential placement (5′ versus 3′) of the conserved guanosine (G) with respect to the phosphate at the 5′ splice site. Second-step similarities include preference for the S_p phosphorothioate diastereomer, use of a 3′-OH as the nucleophile and a conserved guanosine (G) attached through a 3′ oxygen to the phosphate at the 3′ splice site. The phosphorothioate diastereomer (R_p or S_p), which is not significantly inhibitory, is indicated for the substrate for each step. The diastereomer that results is indicated for the product of each step. Small dashed arrows indicate the potential (but not yet observed) reversibility of each step of nuclear pre-mRNA splicing. The dark hemicircle, indicated in the spliceosome for the second step, designates a hypothetical site similar to that of group I introns.

the centers must be distinct. This is also consistent with the different chemical nature of reaction components in the two steps. A 2′ hydroxyl group on an adenosine is activated in the first step, while a 3′ hydroxyl group on the 5′ exon is activated during the second step. Furthermore, the conserved guanosine residue is linked to the activated phosphate by a 5′ bond in the first step and a 3′ bond in the second. Thus, the spliceosome process, and probably the group II self-splicing process, must involve two distinct catalytic sites.

The catalytic site in the spliceosome responsible for the second step is probably similar to that of the group I self-splicing introns. These two sites share several common characteristics. Both catalyze the transesterification reaction using a) an S_p, and not R_p, phosphorothioate at the active site, b) the activated phosphate is linked to the 3′ position to a conserved guanosine residue, and c) both activate a 3′ hydroxyl group on the 5′ exon. These similarities are probably determined by some common chemical structure among the two catalytic sites. Perhaps this common microstructure reflects a shared RNA tertiary structure for the catalytic centers and a shared evolutionary origin.

Nuclear Structure and RNA Splicing

The processing of introns occurs from both nascent RNA which is being extended by polymerase and from post-transcrip-

tional precursor RNA.[89] Thus, the splicing apparatus must be located proximal to the gene, as well as in the regions between the gene and the nuclear pores. After completion of splicing, the mRNA is transported to the cytoplasm through one of the approximately 4000 nuclear pores of a typical mammalian cell.[90] The mechanism by which nuclear RNAs are transported from sites of transcription and splicing to pores remains a mystery.

The subnuclear locations of a number of proteins and RNAs important for RNA splicing have been studied by light and electron microscopy. The most striking feature is the concentration of snRNPs, U2, U4/6, and U5 in 20–50 speckled structures and also in 1–5 foci called coiled bodies (Fig. 14).[91, 92] This

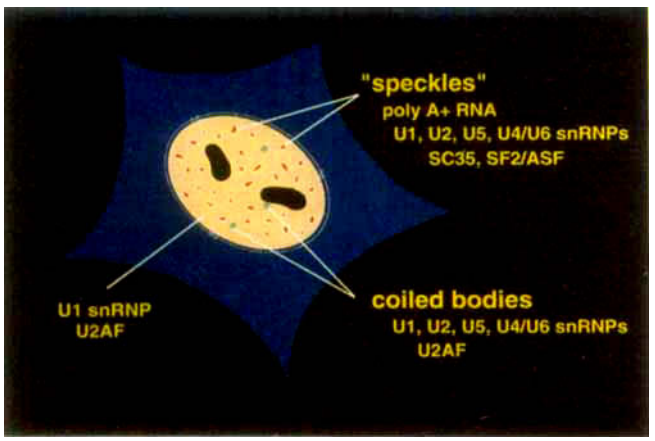


Fig. 14. Subnuclear localization of splicing factors in the nucleus. Specific antisera and in situ hybridization methods have been used to localize components of the spliceosome and splicing factors in the nucleus of mammalian cells. The outline of the cell is shown without structure in the cytoplasm. Three nuclear pores are diagrammed in the nuclear membrane. The large dark structures are nucleoli, site of ribosomal RNA synthesis. Some of the components of the speckles, regions containing pre-mRNA, are listed. The coiled bodies are different and do not appear to contain pre-mRNAs [93]. The general pink shadowing represents the nuclear distribution of U1 snRNP and U2AF.

contrasts with the subnuclear location of U1 snRNP, which, although also concentrated in speckles and foci, is more uniformly dispersed throughout the nucleus. These speckled structures correspond to regions described by electron microscopists as interchromatin granule clusters and the perichromatin fibril network. High-resolution in situ hybridization methods and pulse labeling studies locate newly synthesized RNA in the speckled regions and also in curvilinear tracks which extend from the gene toward the nuclear periphery.[93, 94] The further the nuclear precursor RNA is located along the tracks which lead from its gene of origin, the lower the relative concentration of intron sequences as compared to exon sequences. This suggests that the precursor RNA moves through the speckled structures as it is being processed and transported.[94] Active spliceosomes are probably concentrated in these regions.

Several proteins important for RNA splicing are also concentrated in speckled structures with the snRNPs. These include the Arg/Ser proteins SF2/ASF[95, 96] and SC35.[97] Surprisingly, these proteins, as well as the snRNPs in active spliceosomes, are probably attached to an operationally defined nuclear matrix. This matrix is the structure that remains in the nucleus after almost all of the chromatin proteins and DNA are extracted by sequential treatments with DNase 1 and high salt concentration.[98] The integrity of the fibrillar matrix which remains is sensitive to RNase, suggesting a major role for RNA in its structure. Spliceosomes have been shown to be associated with the nuclear matrix as it has been possible to process pulse-labeled endogenous precursor RNA extracted as part of the matrix.[98]

Active spliceosomes may be associated with the nuclear matrix through interactions with proteins in the Arg/Ser family.[99, 100] A panel of monoclonal antibodies has been generated to components in the nuclear matrix of human cells. Three of these monoclonal antibodies specifically stain the matrix and extensively colocalize with the snRNPs in the speckled structures. Surprisingly, these three antibodies specifically immunoprecipitate spliceosome complexes which contain exon sequences.[101] Thus, the antibodies immunoprecipitate a fraction of the precursor RNA, the lariat intermediate RNA and the associated 5′ exon, and the spliced exon product RNAs. The antibodies do not immunoprecipitate the intron containing spliceosome complex I even though it contains most of the snRNPs and associated protein components. These remarkable results suggest that the matrix components bind to exon RNA sequences that are specifically assembled into splicing complexes.

The proteins recognized by the monoclonal antibodies to the nuclear matrix are most likely members of the Arg/Ser family of proteins or are associated with the Arg/Ser proteins. Precursor RNAs are not immunoprecipitated from reactions containing nuclear extracts depleted of Arg/Ser proteins. Further addition of preparations of purified Arg/Ser proteins will block specific immunofluorescence staining of subnuclear structures. These results are consistent with a model where the Arg/Ser family of proteins are associated with or form the nuclear matrix.[101] Newly synthesized RNA sequences are recognized by the Arg/Ser proteins such as SC35, ASF, the U1 70 kd, and U2AF and become associated with the matrix, perhaps, through interactions of the Arg/Ser tracts. On this structure, complete spliceosomes would form, encompassing the matrix proximal splice sites and execute splicing. The exon product RNAs would remain matrix bound and move by some unknown mechanism to the nuclear pore.

Conclusion

The discovery of split genes and RNA splicing has been critical for studies of the biology of eukaryotic organisms. Gene regulation is central to all biological phenomena and RNA splicing is important in the regulation of genes, particularly when precursor RNAs are pocessed by alternative pathways to generate mRNAs encoding different proteins. The mechanism of splicing by the spliceosome is probably related to the self-splicing process of group I and II introns. The spliceosome process is old in an evolutionary sense, perhaps as old as the ribosomal process responsible for translation. Thus, the eukaryotic cell can be conjectured as consisting of two compartments, the nucleus where the spliceosome processes RNA precursors by RNA catalysis and the cytoplasm where the ribosome translates mRNAs by RNA catalysis. The distinct subnuclear locations of spliceosome-related components suggest a compartmentalized

organization for the nucleus. Further studies of RNA splicing and transport hold promise of revealing the nature of the organizational specificity of the nucleus.

I thank my collaborators over the years (listed in alphabetical order): A. S. Baldwin, S. M. Berget, A. J. Berk, K. Berkner, B. Blencowe, M. A. Brown, S. Buratowski, C. Carr, R. W. Carthew, C. Cepko, D. Chang, D. Chasman, L. A. Chodosh, G. Chu, R. G. Clerc, J. D. Crispino, D. J. Donoghue, A. Z. Fire, D. E. Fisher, S. J. Flint, M. Garcia-Blanco, A. Gil, S. Gilbert, P. J. Grabowski, H. Handa, U. Hansen, S. Hardy, S. Harper, T. Harrison, M. Horowitz, P. S. Jat, R. Kaufman, J. Kim, R. Kingston, J. Kjems, T. Kobayashi, M. M. Konarska, T. Kristie, A. I. Lamond, F. Laski, J. LeBowitz, K. LeClair, F. Lee, I. Lemischka, A. MacMillan, R. Marciniak, P. McCaul, R. Meyers, C. Moore, M. Moore, M. Morton, M. Murata, R. Padgett, J. Parvin, J. L. Pomerantz, C. Query, M. E. Samuels, J. Sedivy, S. Seiler, S. Shykind, H. Singh, H. Skolnik-David, M. Timmers, A. Virtanen, J. Weinberger, and Q. Zhou.

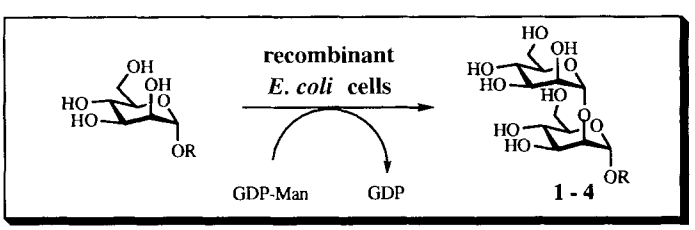
Received: January 12, 1994 [A 461E]
German version: *Angew. Chem.* **1994**, *106*, 1292

[1] J. E. Darnell, Jr., *Harvey Lectures* **1975**, *69*, 1–47.
[2] Y. Furuichi, M. Morgan, S. Muthukrishnan, A. J. Shatkin, *Proc. Natl. Acad. Sci. USA* **1975**, *72*, 362–366.
[3] C. M. Wei, B. Moss, *Proc. Natl. Acad. Sci. USA* **1974**, *71*, 3014–3018.
[4] F. Rottman, A. Shatkin, R. P. Perry, *Cell* **1974**, *3*, 197–199.
[5] M. Edmonds, M. H. Vaughan, Jr., H. Nakazoto, *Proc. Natl. Acad. Sci. USA* **1971**, *68*, 1336–1340.
[6] S. Y. Lee, J. Mendecki, G. Brawerman, *Proc. Natl. Acad. Sci. USA* **1971**, *68*, 1331–1335.
[7] J. E. Darnell, Jr., R. Wall, R. J. Tushinski, *Proc. Natl. Acad. Sci. USA* **1971**, *68*, 1321–1325.
[8] U. Pettersson, C. Mulder, H. Delius, P. A. Sharp, *Proc. Natl. Acad. Sci. USA* **1973**, *70*, 200–204.
[9] P. A. Sharp, P. H. Gallimore, S. J. Flint, *Cold Spring Harbor Symp. Quant. Biol.* **1974**, *34*, 457–474.
[10] S. J. Flint, P. H. Gallimore, P. A. Sharp, *J. Mol. Biol.* **1975**, *96*, 47–68.
[11] S. J. Flint, P. A. Sharp, *J. Mol. Biol.* **1976**, *106*, 749–771.
[12] S. Bachenheimer, J. E. Darnell, *Proc. Natl. Acad. Sci. USA* **1975**, *72*, 4445–4449.
[13] S. M. Berget, C. Moore, P. A. Sharp, *Proc. Natl. Acad. Sci. USA* **1977**, *74*, 3171–3175.
[14] J. Lewis, J. F. Atkins, C. Anderson, P. R. Baum, R. F. Gesteland, *Proc. Natl. Acad. Sci. USA* **1975**, 4445–4449.
[15] M. Thomas, R. L. White, R. W. Davis, *Proc. Natl. Acad. Sci. USA* **1976**, *73*, 2294–2298.
[16] J. Casey, N. Davidson, *Nucleic Acid Res.* **1977**, *4*, 1539–1552.
[17] H. Westphal, J. Meyer, J. Maizel, *Proc. Natl. Acad. Sci. USA* **1976**, *73*, 2069–2071.
[18] L. T. Chow, J. M. Roberts, J. B. Lewis, T. R. Broker, *Cell* **1977**, *11*, 819–836.
[19] S. Goldberg, J. Weber, J. E. Darnell, Jr., *Cell* **1977**, *10*, 617–622.
[20] J. Weber, W. Jelinek, J. E. Darnell, Jr., *Cell* **1977**, *10*, 611–616.
[21] S. M. Berget, P. A. Sharp, *J. Mol. Biol.* **1979**, *129*, 547–565.
[22] R. P. Perry, D. E. Kelley, *Cell* **1976**, *8*, 433–442.
[23] R. E. Gelinas, R. J. Roberts, *Cell* **1977**, *11*, 533–544.
[24] A. J. Jeffreys, R. A. Flavell, *Cell* **1977**, *12*, 1097–1108.
[25] S. M. Tilghman, D. C. Tiermeier, J. G. Seidman, B. M. Peterlin, M. Sullivan, J. V. Maizel, P. Leder, *Proc. Natl. Acad. Sci. USA* **1978**, *75*, 725–729.
[26] R. Breathnach, J-L. Manel, P. Chambon, *Nature* **1977**, *270*, 314–319.
[27] S. Tonegawa, A. M. Maxam, R. Tizard, O. Bernard, W. Gilbert, *Proc. Natl. Acad. Sci. USA* **1978**, *75*, 1485–1489.
[28] R. Breathnach, P. Chambon, *Annu. Rev. Biochem.* **1981**, *50*, 349–384.
[29] R. A. Padgett, P. J. Grabowski, M. M. Konarska, S. Seiler, P. A. Sharp, *Annu. Rev. Biochem.* **1986**, *55*, 1119–1150.
[30] G. R. Fink, *Cell* **1987**, *49*, 5–6.
[31] R. Treisman, S. Orkin, T. Maniatis, *Nature* **1983**, 591–596.
[32] J. M. Nigro, K. R. Cho, E. R. Fearson, S. E. Kern, J. M. Ruppert, J. D. Oliver, D. W. Kinzler, B. Vogelstein, *Cell* **1991**, *64*, 607–613.
[33] C. Cocquerelle, P. Daubersies, M.-A. Majerus, J.-P. Kerckaert, B. Bailleul, *EMBO J.* **1992**, *11*, 1095–1098.
[34] R. Pulok, P. Anderson, *Genes Dev.* **1993**, *7*, 1885–1897.
[35] R. S. Patel, E. Odermatt, J. E. Schwarzbauer, R. O. Hynes, *EMBO J.* **1986**, *6*, 2565–2572.
[36] R. O. Hyens, *Fibronectin*, Springer, New York, **1989**.
[37] B. S. Baker, *Nature* **1989**, *340*, 521–524.
[38] M. Tian, T. Maniatis, *Science* **1992**, *256*, 237–240.
[39] W. Gilbert, *Nature* **1978**, *271*, 501.
[40] J. E. Darnell, Jr. *Science* **1978**, *202*, 1257.
[41] W. F. Doolittle, *Nature* **1978**, *272*, 581.
[42] C. C. F. Blake *Nature*, **1978**, *273*, 267.
[43] *Intervening Sequences in Evolution and Development* (Ed.: E. M. Stone, R. J. Schwartz), Oxford University Press, New York, **1990**.
[44] N. Lonberg, W. Gilbert, *Cell* **1985**, *40*, 81–90.
[45] N. Agabian, *Cell* **1990**, *61* 1157–1160.
[46] P. Borst, *Ann. Rev. Biochem.* **1986**, *55*, 701–732.
[47] M. Krause, D. Hirsh, *Cell* **1987**, *49*, 753–761.
[48] M. Vellard, A. Sureau, J. Soret, C. Martinerie, B. Perbal, *Proc. Natl. Acad. Sci. USA* **1992**, *89*, 2511–2515.
[49] R. Benne, J. van den Burg, J. P. J. Branhenhoff, P. Sloof, J. H. van Boom, M. C. Tramp, *Cell* **1986**, *46*, 819–826.
[50] R. A. Padgett, S. F. Hardy, P. A. Sharp, *Proc. Natl. Acad. Sci. USA* **1983**, *80*, 5230–5234.
[51] M. R. Green, T. Maniatis, D. A. Melton, *Cell* **1983**, *32*, 681–694.
[52] N. Hernandez, W. Keller, *Cell* **1983**, *35*, 89–99.
[53] P. J. Grabowski, R. A. Padgett, P. A. Sharp, *Cell* **1984**, *37*, 415–427.
[54] A. R. Krainer, T. Maniatis, B. Ruskin, M. R. Green, *Cell* **1984**, *36*, 993–1005.
[55] M. M. Konarska, P. J. Grabowski, R. A. Padgett, P. A. Sharp, *Nature* **1985**, *313*, 552–557.
[56] J. C. Wallace, M. Edmonds, *Proc. Natl. Acad. Sci. USA* **1983**, *80*, 950–954.
[57] P. J. Grabowski, S. R. Seiler, P. A. Sharp, *Cell* **1985**, *42*, 345–353.
[58] E. Brody, J. Abelson, *Science* **1985**, *228*, 963–967.
[59] J. A. Steitz, D. L. Black, V. Gerke, K. A. Parker, A. Krämer, D. Frendeway, W. Keller, in *Structure and function of major and minor small nuclear ribonucleoprotein particles* (Ed.: M. L. Birnstiel), pp. 115–154, Springer, New York, **1988**.
[60] T. R. Cech, *Cell* **1985**, *43*, 713–716.
[61] C. L. Peebles, P. S. Perlman, K. L. Mecklenburg, M. L. Petrillo, J. H. Tabor, K. A. Jarrell, H.-L. Cheng, *Cell* **1986**, *44*, 213–223.
[62] R. van der Veen, A. C. Arnberg, G. van der Horst, L. Bonen, H. F. Tabak, L. A. Grivell, *Cell* **1986**, *44*, 225–234.
[63] P. A. Sharp, *Science* **1991**, *254*, 663.
[64] G. J. Hannon, P. A. Maroney, J. A. Denker, T. W. Nilsen, *Cell* **1990**, *61*, 1247–1255.
[65] K. R. Watkins, J. M. Dungan, N. Agabian, *Cell* **1993**, in press.
[66] M. R. Lerner, J. A. Boyle, S. M. Mount, S. L. Wolin, J. A. Steitz, *Nature* **1980**, *283*, 220–224.
[67] J. Rogers, R. Wall, *Proc. Natl. Acad. Sci. USA* **1980**, *77*, 1877–1879.
[68] R. A. Padgett, S. M. Mount, J. A. Steitz, P. A. Sharp, *Cell* **1983**, *35*, 101–107.
[69] R. Parker, P. G. Siliciano, C. Guthrie, *Cell* **1987**, *49*, 229–239.
[70] C. Guthrie, B. Patterson, *Annu. Rev. Genet.* **1988**, *22*, 387–419.
[71] M. M. Konarska, P. A. Sharp, *Cell* **1987**, *49*, 763–774.
[72] H. D. Madhani, C. Cuthrie, *Cell* **1992**, *71*, 803–817.
[73] D. S. McPheeters, J. Abelson, *Cell* **1992**, *71*, 819–831.
[74] H. Sawa, J. Abelson, *Proc. Natl. Acad. Sci. USA* **1992**, *89*, 11269–11273.
[75] D. A. Wassarman, J. A. Steitz, *Science* **1992**, *257*, 1918–1925.
[76] A. Newman, C. Norman, *Cell* **1992**, *68*, 743–754.
[77] M. J. Moore, C. C. Query, P. A. Sharp, in *The RNA World* (R. F. Gesteland, J. F. Atkins), Cold Spring Harbor Laboratory Press, **1993**, p. 303–357.
[78] B. Seraphin, M. Rosbash, *EMBO J.* **1991**, *10*, 1209–1216.
[79] S. Michaud, R. Reed, *Genes Dev.* **1991**, *5*, 2534–2546.
[80] S. F. Jamison, M. A. Garcia-Blanco, *Proc. Natl. Acad. Sci. USA* **1992**, *89*, 5482–5486.
[81] B. Ruskin, P. D. Zamore, M. R. Green, *Cell* **1988**, *52*, 207–219.
[82] S. W. Ruby, J. Abelson, *Trends Genet.* **1988**, *7*, 79–85.
[83] C. Guthrie, *Science* **1991**, *253*, 157–163.
[84] J. A. McSwiggen, T. R. Cech, *Science* **1989**, *244*, 679–683.
[85] J. Rajagopal, J. A. Doudna, J. W. Szostak, *Science*, **1989**, *244*, 692–694.
[86] E.-R. Suh, R. B. Waring, *Nucleic Acids Res.* **1992**, *20*, 6303–6309.
[87] M. J. Moore, P. A. Sharp, *Nature* **1993**, *365*, 364–368.
[88] M. J. Moore, P. A. Sharp, *Science* **1992**, *256*, 992–997.
[89] A. L. Beyer, Y. N. Osheim, *Genes Dev.* **1988**, *2*, 754–765.
[90] H. Mehlin, B. Daneholt, U. Skoglund, *Cell* **1992**, *69*, 605–613.
[91] D. L. Spector, *Annu. Rev. Cell. Biol.* **1993**, *9*, 265–315.
[92] U. Nyman, H. Hallman, G. Hadloczky, I. Pettersson, G. Sharp, N. R. Ringertz, *J. Cell. Biol.* **1986**, *102*, 137–144.
[93] K. C. Carter, D. Bowman, W. Carrington, K. Fogarty, J. A. McNeil, F. S. Fay, J. B. Lawrence, *Science* **1993**, *259*, 1330–1334.
[94] Y. Xing, C. V. Johnson, P. R. Dobner, J. B. Lawrence, *Science* **1993**, *259*, 1326–1330.
[95] H. Ge, J. L. Manley, *Cell* **1990**, *62*, 25–34.
[96] A. R. Krainer, G. C. Conway, D. Kozak, *Cell* **1990**, *62*, 35–42.
[97] X.-D Fu, T. Maniatis, *Nature* **1990**, *343*, 437–441.
[98] S. Zeitlin, R. C. Wilson, A. Efstratiadis, *J. Cell. Biol.* **1989**, *108*, 765–777.
[99] M. B. Roth, C. Murphy, J. G. Gall, *J. Cell. Biol.* **1990**, *111*, 2217–2223.
[100] M. B. Roth, A. M. Zahler, J. A. Stolk, *J. Cell. Biol.* **1991**, *115*, 587–596.
[101] B. J. Blencowe, J. A. Nickerson, R. Issner, S. Penman, P. A. Sharp, unpublished.

Recombinant Whole Cells as Catalysts for the Enzymatic Synthesis of Oligosaccharides and Glycopeptides**

Guido F. Herrmann, Peng Wang, Gwo-Jenn Shen, and Chi-Huey Wong*

Syntheses of oligosaccharides[1] using isolated glycosidases[2] or glycosyl transferases,[3] or a combination of both,[4] have been studied extensively during the last decade. A general limitation of this methodology is the low availability and the high cost of glycosyl transferases, though some glycosyl transferases can be obtained in sufficient amounts for synthesis by cloning and overexpression.[5] Recently we reported on the expression of a cloned α-1,2-mannosyl transferase (α-1,2-ManT) in *E. coli* XL1-Blue strain at the level of ≈ 1 U L^{-1} for use in the mannosylation of saccharides and glycopeptides.[6] Since isolation of the enzyme and other glycosyl transferases in general is not trivial, we decided to exploit the feasibility of using whole cells of the recombinant *E. coli* as catalysts. Although biotransformations based on whole cells such as bakers' yeast[7] are common, no example has been reported in which recombinant cells are used for glycosyl transfer reactions. To demonstrate the feasibility of the concept, we examined several acceptors for the enzymatic mannosylation reaction with GDP-Man as mannosyl donor (Fig. 1).



1, R = H, 75% (α/β = 7/3)

2, R = Me, 53%

3, R = , 72%

4, R = , 42%

Fig. 1. Enzymatic synthesis of disaccharides **1** and **2**, and glycopeptides **3** and **4** by using recombinant *E. coli* whole cells. Man = mannose, GDP = guanosine diphosphate. Cbz = benzyloxycarbonyl, Boc = *tert*-butoxycarbonyl.

The disaccharides Manα1,2Man **1** and Manα1,2ManOMe **2**, and the dimannosylated glycopeptides Cbz-α[Manα1,2Man]Thr-OMe **3** and Boc-Tyr-α(Man(α1,2Man]-Thr-Val-OMe **4** were obtained in moderate to good yields. As inhibition of the reaction by the released guanosine diphosphate (GDP) was not observed, addition of alkaline phosphatase to decompose GDP was omitted. While it is not clear how mannosylation takes place, the cell walls of *E. coli* XL1-Blue strain used in this study might be leaking, which would allow the transport of products and substrates. Leakage of α-1,2-ManT from the periplasmic space of *E. coli* into the medium was dismissed, as no mannosylation activity was detected in the fermentation broth after isolation of cells.

In summary, this report illustrates the convenient use of recombinant glycosyl transferase in oligosaccharide and glycopeptide synthesis without the tedious procedure of enzyme purification. Immobilization (e.g. by gel entrapment)[8] of the recombinant cells may permit a feasible reactor design for large-scale synthesis. Additionally, the use of two or more recombinant *E. coli* strains expressing different glycosyl transferases may allow the one-pot synthesis of oligosaccharides.

Experimental Procedure

Cultivation of recombinant E. coli [ATTC #77379]

The *E. coli* strain containing the plasmid pManflag20 was grown in shaking flasks as described elsewhere in detail [6]. Usually 2 - 4 g of wet cells can be obtained per liter of fermentation broth. The cells were isolated by centrifugation. The resulting pellet was washed once with 10 mM HEPES buffer (pH 7). Subsequently the cells were stored in a 50% (w/w) suspension in 10 mM HEPES (pH 7) at −20 °C. Storage of the cells at −20 °C did not affect the activity of α-1,2-ManT over a period of several months.

Enzyme Assay

α-1,2-ManT activity was determined using the following assay conditions: A solution containing 1 mM GDP-Man [9], 15.6 nCi GDP-[^{14}C]-Man (Amersham, UK), 100 mM ManOMe, 50 mM HEPES (pH 7.2), 0.1% Triton X, 10 mM $MnCl_2$, phosphatase inhibitors [10] (5 mM ATP, 3 mM Theophylline, 3 mM Cimetidine) and 10 μL ca. 50% (w/w) intact recombinant *E. coli* cells in a total volume of 40 μL was incubated for 15–60 min at 37 °C. The reaction was stopped by adding 400 μL of ice-cold QAE Sephadex A-25 in H_2O (50% (v/v)). The mixture was centrifuged for 10 min at 10000 g, and a 200-μL aliquot of the supernatant was used to determine the radioactivity in 10 mL Scinti Verse SX 1-4 (Fisher, USA).

1 [11]: To 1.5 mL of the buffer described above was added GDP-Man (24.2 mg, 20 mM), Man (72 mg, 200 mM), and recombinant *E. coli* cells (0.5 mL, 50% (w/w)). The mixture was stirred for 23 h at room temperature, and the reaction was followed by TLC (system I: $CHCl_3$/MeOH/H_2O = 6/2.5/0.25 (v/v/v): R_f(Man) = 0.18, R_f(**1**) = 0.08; system II: *i*PrOH/H_2O/NH_3 = 7/2/1 (v/v/v): R_f(Man) = 0.36, R_f(**1**) = 0.26, R_f(GDP-Man) = 0.16). Subsequently the *E. coli* cells were removed by centrifugation at 10000 g for 15 min. The pellet was washed twice with 3 mL H_2O, and the combined supernatants were combined with 40 mL MeOH and stirred for 15 min. The precipitated proteins were centrifuged at 10000 g for 20 min, and the supernatant was lyophilized and applied to a Biogel P4 column (120 × 4 cm) with water as the eluent. The desired fractions were lyophilized to yield product **1** as a 71/29 mixture of the α and β anomers (10.3 mg, 75% yield). The ^{1}H NMR (500 MHz, D_2O) data were consistent with those reported [12]. The ^{1}H NMR spectrum of **1** indicates the α-selectivity of α-1,2-ManT, as signals corresponding to a α-mannosidic linkage were not detected. This finding confirms our previous results with purified α-1,2-ManT [6].

2: The reaction was carried out in analogy to that giving **1** except that ManOMe (38.8 mg, 100 mM) was used as acceptor. The mixture was stirred for 20 h at room temperature and the reaction followed by TLC (system I: R_f(ManOMe) = 0.39, R_f(**2**) = 0.12; system II: R_f(ManOMe) = 0.48, R_f(**2**) = 0.32). Following the same workup procedure as for **1**, the supernatant obtained was lyophilized and the product purified by silica gel column chromatography (system I) to yield **2** (7.6 mg, 53% yield). ^{1}H NMR (500 MHz, D_2O) and ^{13}C{^{1}H} NMR (D_2O) spectra were identical with those reported previously [6]. HRMS for $C_{13}H_{24}O_{11}Cs^+$ [$M + Cs^+$]: calcd. 489.0373; found 489.0370.

3a: To a solution of 2,3,4,6-tetra-*O*-acetyl-D-mannopyranosyl bromide (2.0 g, 4.86 mmol) in dry dichloromethane (30 mL) was added at −20 °C Cbz-Thr-OMe

[*] Prof. Dr. C.-H. Wong, G. F. Herrmann, Dr. P. Wang, Dr. G.-J. Shen
Department of Chemistry, The Scripps Research Institute
10666 North Torrey Pines Road, La Jolla, CA 92037 (USA)
Telefax: Int. code + (619) 554 6731

[**] This research was supported by the National Institutes of Health (GM 44154). G. F. H. thanks the German Academic Exchange Service for financial support (Doktorandenstipendium HSP II/AUFE).

(1.3 g, 4.86 mmol), silver triflate (1.5 g, 1.2 equiv, 5.84 mmol), and triethylamine (0.59 g, 1.2 equiv, 5.84 mmol). The suspension was stirred at −20 °C for 4 h and then filtered through a bed of Celite. The filtrate was washed twice with water and twice with saturated sodium bicarbonate. The organic layer was dried over anhydrous $MgSO_4$ and concentrated in vacuo, and the residue was chromatographed with silica gel (eluted with EtOAc/hexane = 6/1 (v/v)) to give the desired product **3a** as a white solid (1.9 g, 68% yield). ^{1}H NMR (500 Hz, $CDCl_3$) δ = 1.30 (d, J = 6.5 Hz, 3H), 1.91 (s, 3H), 1.98 (s, 3H), 2.01 (s, 3H), 2.02 (s, 3H), 3.77 (s, 3H), 4.00 (m, 1H), 4.06 (dd, J = 2.5, 12.5 Hz, 1H), 4.21 (dd, J = 6.0, 12.5 Hz, 1H), 4.35 (dd, J = 2.5, 6.5 Hz, 1H), 4.43 (dd, J = 2.5, 9.5 Hz, 1H), 4.82 (d, J = 1.5 Hz, 1H), 4.96 (s, 1H), 5.12 (s, 2H), 5.21 (dd, J = 1.5, 4.5 Hz, 2H), 5.46 (d, J = 9.5 Hz, 1H), 7.25–7.32 (m, 5H); ^{13}C{^{1}H} NMR ($CDCl_3$) δ = 17.6, 20.4, 20.6, 52.6, 58.3, 62.1, 62.2, 65.9, 67.0, 68.2, 68.3, 69.3, 98.5, 127.7, 127.9, 128.0, 128.3, 135.7, 156.3, 169.4, 169.6, 170.3; HRMS for $C_{27}H_{35}N_1O_{14}Cs^+$ [M + Cs^+]: calcd. 829.1796; found 829.1796.

3b: To a solution of **3a** (300 mg, 0.28 mmol) in 20 mL of anhydrous methanol at 0 °C was added 1% MeONa in anhydrous methanol (about 500 μL). The solution was stirred at 0 °C for 1.5 h, and then Dowex H^+ was added until the mixture reached pH 4.0. After filtration the solvent was removed in vacuo to give the desired product **3b** as a colorless liquid (152 mg, 82% yield). $[\alpha]_D^{20}$ = + 44.11 (c = 0.045 in MeOH); ^{1}H NMR (500 MHz, CD_3OD) δ = 1.12 (d, J = 6.0 Hz, 3H), 3.19 (m, 1H), 3.43–3.48 (m, 2H), 3.52–3.58 (m, 3H), 3.63 (s, 3H), 3.68 (dd, J = 1.5, 11.5 Hz, 1H), 4.22 (m, 2H), 4.65 (s, 1H), 5.00 (s, 2H), 7.20–7.28 (m, 5H); ^{13}C{^{1}H} NMR (CD_3OD) δ = 18.9, 52.8, 60.3, 62.9, 67.9, 68.5, 72.1, 72.2, 75.1, 77.0, 103.1, 128.9, 129.0, 129.5, 138.1, 159.1, 172.6; HRMS for $C_{19}H_{27}N_1O_{10}Cs^+$ [M + Cs^+]: calcd. 562.0073; found 562.0098.

3: To 0.375 mL of buffer [10] containing GDP-Man (6.15 mg, 20 mM) and **3b** (4.29 mg, 20 mM) was added 25 μL of acetone and 10 μL of 50 mM phenylmethylsulfonyl fluoride (PMSF) dissolved in DMF. Recombinant *E. coli* cells (0.125 mL, 50% (w/w)) were added, and the mixture was stirred for 20 h at room temperature. The reaction was followed by TLC (system I: R_f(**3b**) = 0.68, R_f(**3**) = 0.36; system II: R_f(**3b**) = 0.8, R_f(**3**) = 0.65). The product obtained from the supernatant was purified by silica gel column chromatography (system I) to yield **3** (4.29 mg, 72% yield). ^{13}C{^{1}H}NMR (CD_3OD) δ = 18.7, 30.2, 30.8, 53.1, 60.4, 62.9, 63.0, 67.9, 68.5, 68.9, 71.7, 71.8, 72.4, 74.9, 75.1, 77.0, 77.3, 80.9, 101.4, 104.3, 128.9, 129.1, 129.5; HRMS for $C_{25}H_{37}NO_{15}Na^+$ [M + Na^+]): calcd. 614.2061; found 614.2078.

4: To 0.375 mL buffer [10] containing GDP-Man (6.15 mg, 20 mM) and **4a** (6.57 mg, 20 mM) [6] was added 10 μL of the PMSF solution and 25 μL of acetone. Recombinant *E. coli* cells (0.125 mL, 50% (w/w)) were added, and the mixture was stirred for 17.5 h at room temperature. The reaction was monitored by TLC (system I: R_f(**4a**) = 0.81, R_f(**4**) = 0.5). The solid product obtained from the supernatant was purified by silica gel column chromatography (system I) to yield **4** (3.4 mg, 42% yield). ^{13}C{^{1}H}NMR (CD_3OD) δ = 18.6, 19.5, 28.7, 31.8, 38.3, 42.1, 52.7, 57.5, 58.4, 59.3, 63.0, 63.4, 68.9, 69.1, 71.8, 72.4, 75.1, 76.6, 80.5, 101.3, 101.7, 104.1, 116.2, 129.2, 131.4, 143.5, 157.2, 171.1, 173.52; HRMS for $C_{36}H_{57}N_3O_{18}H^+$ [M + H^+]: calcd. 820.3715; found 820.3710.

Received: January 31, 1994 [Z 6659 IE]
German version: *Angew. Chem.* **1994**, *106*, 1346

[1] a) Y. Ichikawa, G. C. Look, C.-H. Wong, *Anal. Biochem.* **1992**, *202*, 215; b) E. J. Toone, E. S. Simon, M. D. Bednarski, G. M. Whitesides, *Tetrahedron* **1989**, *45*, 5365; c) S. David, C. Augé, C. Gautheron, *Adv. Carbohydr. Chem. Biochem.* **1991**, *49*, 175; d) U. Korf, J. Thiem, *Kontakte (Darmstadt)* **1992**, 3.

[2] a) K. G. I. Nilsson, *TIBTECH* **1988**, *6*, 256; b) G. F. Herrmann, U. Kragl, C. Wandrey, *Angew. Chem.* **1993**, *105*, 1399; *Angew. Chem. Int. Ed. Engl.* **1993**, *32*, 1342; c) S. Bay, A. Namane, D. Cantacuzene, *Bioorg. Med. Chem. Lett.* **1993**, *3*, 2515–2520.

[3] a) Y. Ichikawa, Y.-C. Lin, D. P. Dumas, G.-J. Shen, E. Garcia-Junceda, M. A. Williams, R. Bayer, K. Ketcham, L. E. Walker, J. C. Paulson, C.-H. Wong, *J. Am. Chem. Soc.* **1992**, *114*, 9283; b) C. Augé, C. Mathieu, C. Merienne, *Carbohydr. Res.* **1986**, *151*, 147; c) J. Thiem, T. Wiemann, *Synthesis* **1992**, 141.

[4] G. F. Herrmann, Y. Ichikawa, C. Wandrey, F. C. A. Gaeta, J. C. Paulson, C.-H. Wong, *Tetrahedron Lett.* **1993**, *34*, 3091–3094.

[5] a) K. Nakazawa, K. Furukawa, H. Narimatsu, A. Kobata, *J. Biochem.* **1993**, *113*, 747–753; b) C. Krezdorn, G. Watzele, R. B. Kleene, S. X. Ivanov, E. G. Berger, *Eur. J. Biochem.* **1993**, *212*, 113–120; c) W. Gillespie, S. Kelm, J. C. Paulson, *J. Biol. Chem.* **1992**, *267*, 21004.

[6] P. Wang, G.-J. Shen, Y.-F. Wang, Y. Ichikawa, C.-H. Wong, *J. Org. Chem.* **1993**, *58*, 3985–3990.

[7] a) S. M. Roberts, K. Wiggins, G. Casy, *Preparative Biotransformations: Whole Cells and Isolated Enzymes in Organic Chemistry*; Wiley, Chichester, **1992**; b) S. Servi, Synthesis **1990**, 1; c) R. Csuk, B. I. Glänzer, *Chem. Rev.* **1991**, *91*, 49–97; d) W. Charney, H. L. Herzog, *Microbial Transformations of Steroids*; Academic, New York, **1967**; e) F. Zilliken, P. N. Smith, C. S. Rose, P. György, *J. Biol. Chem.* **1954**, *208*, 299–305; f) F. Zilliken, P. N. Smith, C. S. Rose, P. György, *ibid.* **1955**, *217*, 79–82. Zilliken et al. report the activity of a β-galactosidase from whole cells of *Lactobacillus bifidus var. pennsylvanicus*. *N*-acetyllactosamine was obtained in 5.4% yield when lactose and *N*-acetylglucosamine were incubated with whole cells of *L. bifidus* under anaerobic conditions.

[8] M. A. Mazid, *Bio/Technology* **1993**, *11*, 690–695.

[9] J. E. Heidlas, K. W. Williams, G. M. Whitesides, *Acc. Chem. Res.* **1992**, *25*, 307.

[10] For the use of phosphatase inhibitors see: T. Metaye, Y. Mettey, J. Lehuede, J. M. Vierfond, P. Lalegerie, *Biochem. Pharmacol.* **1988**, *37*, 4263.

[11] For the formation of **1** with other α-1,2-mannosyl transferases see: a) H. Ankel, E. Ankel, J. S. Schutzbach, J. C. Garancis, *J. Biol. Chem.* **1970**, *245*, 3945–3955; b) J. S. Schutzbach, H. Ankel, *ibid.* **1971**, *246*, 2187–2194; c) A. K. Verma, M. K. Raizada, J. S. Schutzbach, *ibid.* **1977**, *252*, 7235–7242; d) Y.-C. Lee, C. E. Ballou, *Biochem.* **1965**, *4*, 257–264.

[12] a) A. Allerhand, E. Berman, *J. Am. Chem. Soc.* **1984**, *106*, 2400–2412; b) H. Kobayashi, N. Shibata, S. Konno, K. Hisamichi, S. Suzuki, *Carbohydr. Res.* **1992**, *229*, 369–375.

Remarkable Stereoselectivity in the Inhibition of α-Galactosidase from Coffee Bean by a New Polyhydroxypyrrolidine Inhibitor**

Yi-Fong Wang, Yoshikazu Takaoka, and Chi-Huey Wong*

Many naturally occurring and synthetic polyhydroxypyrrolidines and piperidines (referred to hereafter as azasugars) have been developed as inhibitors of glycosidases and glycosyl transferases.[1] Of these azasugars, six-membered derivatives in both chair and flattened-chair conformations,[2, 3] and five-membered derivatives have been commonly used.[1, 3] These inhibitors are considered to mimic the high-energy intermediate in the cleavage of a glycosidic bond that presumably proceeds through a transition state with substantial sp^2 character and positive charge at the anomeric center.[1]

In general, the six-membered azasugars with a chair conformation specifically inhibit the enzymes that catalyze hydrolysis of the corresponding structurally related glycosides[1] (e.g. 1-deoxynojirimycin inhibits α-glucosidase with K_i = 8.7 μM but not α-galactosidase).[4] The flattened-chair six-membered[2] and five-membered[1, 5] azasugars are, however, more flexible: different stereoisomers may exhibit the same degree of inhibition toward one enzyme, and one stereoisomer may inhibit several glycosidases equally well. It was postulated that the shape recognition and electrostatic interaction between the enzyme and inhibitor play more important roles than the stereochemical differentiation in the stabilization of the transition state.[2, 4] Contrary to this hypothesis, we report here that α-galactosidase is inhibited by a new five-membered azasugar (K_i = 5 × 10^{-8} M) at least 1000-fold more effectively than by diastereomers **2** and **3** (Fig. 1).

We describe two routes for the synthesis of **1** (Schemes 1 and 2). Compound **6** prepared from 5-keto-D-fructose[6] or **2**[5a] was treated with 1.25 equivalents of 2-methoxypropene in the presence of *p*-toluenesulfonic acid to give the *cis*-monoacetonide **7** as the only product. Protection of the primary hydroxyl function as a *tert*-butyldiphenylsilyl ether, oxidation of the secondary hydroxyl group with periodinane,[7] and stereospecific reduction with diisobutylaluminum hydride gave the inverted isomer **10**. After treatment with tetrabutylammonium fluoride and *p*-

[*] Prof. Dr. C.-H. Wong, Dr. Y.-F. Wang, Dr. Y. Takaoka[+]
Department of Chemistry, The Scripps Research Institute
10666 N. Torrey Pines Road, La Jolla, CA 92037 (USA)
Telefax: Int. code + (619) 554-6731

[+] Additional address: Frontier Research Program on Glycotechnology
RIKEN (The Institute of Physical and Chemical Research)
Wako City, Saitama 351-01 (Japan)

[**] This research was supported by the National Institutes of Health (GM44154). We thank Dr. W.-D. Fessner for a sample of fuculose-1-phosphate aldolase. We also thank Dr. A. B. Reitz for a sample of **6**.

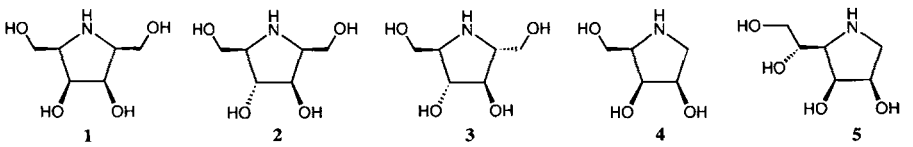
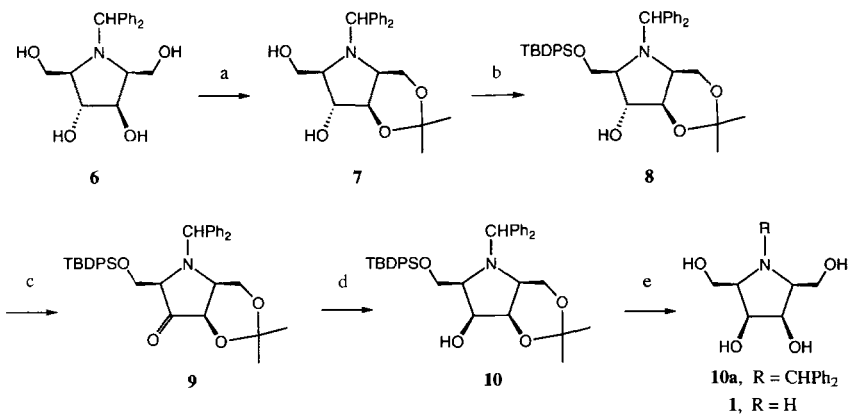
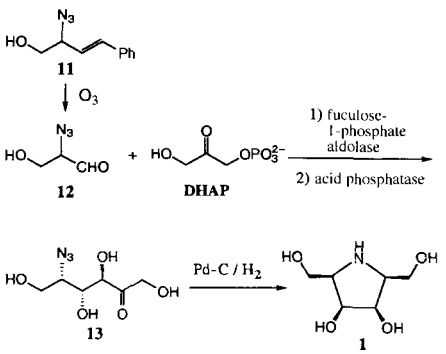


Fig. 1. Inhibition of α-galactosidase by polyhydroxypyrrolidones 1–5. Compound **2** is described in ref. [5], compounds **3**–**5** in ref. [5d].



Scheme 1. Synthesis of **1**. Reagents and conditions: a) 2-methoxypropene/cat. *p*-TsOH, 65%; b) *tert*-butyldiphenylsilyl chloride/pyridine, 92%; c) periodinane, 80%; d) diisobutylaluminum hydride/toluene, −78 °C, 91%; e) 1) Bu_4NF/THF, 2) cat. *p*-TsOH/MeOH, 3) $Pd(OH)_2/H_2$, 75%.



Scheme 2. Chemoenzymatic synthesis of **1**.

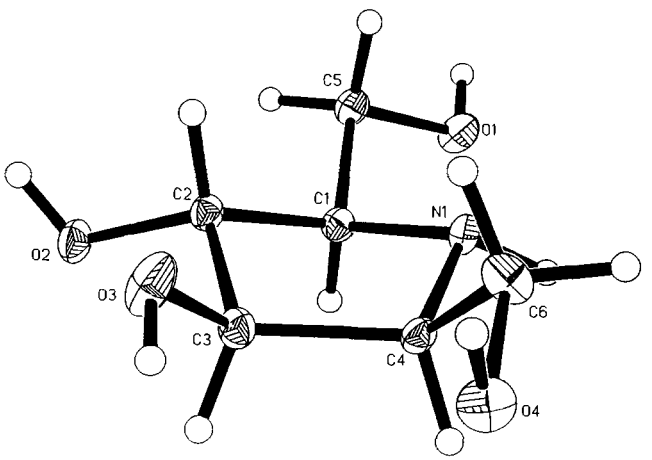


Fig. 2. Crystal structure of **2** (ORTEP representation). See also ref. [11].

toluenesulfonic acid, and hydrogenation on $Pd(OH)_2$, **1** was obtained in 38% yield from **6**.

A much shorter synthesis of **1** is illustrated in Scheme 2. Fuculose-1-phosphate aldolase[8] was used to catalyze the aldol reaction of dihydroxyacetone phosphate (DHAP)[9] and aldehyde **12**. After dephosphorylation the aldol product was converted into **1** by reductive amination. Inhibition analysis[4] of **1** against α-galactosidase from coffee bean at pH 5.5 indicated a competitive type of inhibition with $K_i = 5 \times 10^{-8}$ M. To our knowledge, this is the best pyrrolidine inhibitor of α-galactosidase known to date. It appears that the stereocenters at the 2- and 4-positions are very critical. A marked decrease of inhibition activity was observed when either one of these two centers was inverted. Since pyrrolidines exist in an envelope conformation, as shown by the X-ray structure of **2** (an inhibitor of α-glucosidase, $K_i = 2.8\,\mu$M;[5a] Fig. 2), compound **1** may mimic the conformation and charge distribution of the transition state structure for the cleavage of the glycosidic bond (Fig. 3). It is noted, however, that **1** binds the enzyme less

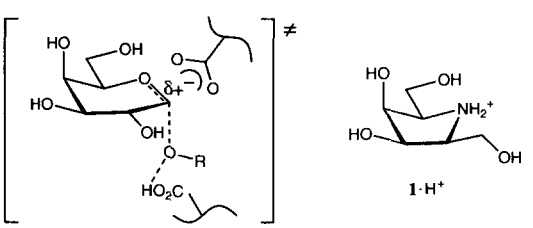


Fig. 3. Proposed transition state structure for the α-galactosidase reaction. Compound **1** is a mimic of the galactosyl cation.

tightly than does 1-deoxy-D-galactonojirimycin, which has a chair conformation ($K_i = 1.6 \times 10^{-9}$ M).[4b]

In summary, we have shown that five-membered azasugars can act as potent glycosidase inhibitors and that the inhibition rently using chemoenzymatic methods to prepare other pyrrolidines for evaluation of their inhibition.

Experimental Section

7: To a solution of **6** (9.9 g, 30 mmol) in 180 mL anhydrous dichloromethane/tetrahydrofuran (1:1) was added 2-methoxypropene (2.4 mL, 25 mmol) and *p*-toluenesulfonic acid (3 g) under N_2. The solution was stirred at room temperature. After 20 h, another 1.2 mL of 2-methoxypropene was added, and the solution was allowed to stir for an additional 26 h. Saturated $NaHCO_3$ solution (10 mL) was added to terminate the reaction. The organic solvent was removed under reduced pressure. Water (50 mL) was then added, and the mixture was extracted with ethyl acetate (3 × 50 mL). The organic layer was dried over Na_2SO_4 and then concentrated to give a residue which was purified by silica gel column chromatography (ethyl acetate/hexane = 1/1 to 1/0) to yield 4.8 g of **7** and 3.2 g of recovered substrate. **7**: $[\alpha]_D^{23} = -63$ ($c = 1.1$, MeOH); $R_f = 0.18$ (ethyl acetate/hexane = 1/1); ^{1}H NMR (500 MHz, $CDCl_3$/TMS): $\delta = 1.29$ (3H, s), 1.30 (3H, s), 3.08 (1H, dd, $J = 5.0$, 10.3 Hz), 3.25 (1H, ddd, $J = 5.2$, 5.9, 6.4 Hz), 3.32 (1H, dd, $J = 5.9$, 11.7 Hz), 3.37 (1H, dd, $J = 6.4$, 11.7 Hz), 3.51 (1H, dd, $J = 5.0$, 10.5 Hz), 3.66 (1H, t, $J = 10.5$ Hz), 4.18 (1H, s), 4.20 (1H, d, $J = 5.2$ Hz), 5.11 (1H, s), 7.17–7.53 (10H, m); ^{13}C NMR (125 MHz, $CDCl_3$): $\delta = 21.9$, 26.5, 63.0, 64.0, 64.3, 72.3, 74.0, 78.4, 79.4, 99.8, 128.1, 128.3, 129.3, 129.5, 129.9, 144.8, 145.3.

8: To 450 mg (1.22 mmol) of compound **7** was added 2 mL pyridine. The mixture was stirred at room temperature and then 549 mg (2 mmol) of *tert*-butyldiphenylsilyl chloride was added by syringe. The mixture was stirred at room temperature for 1 h. After addition of ethyl acetate (15 mL) the mixture was washed with H_2O, 1 N HCl, and saturated aqueous $NaHCO_3$, and then dried over Na_2SO_4. The organic solvent was removed under vacuum. The residue was purified by silica gel column chromatography (ethyl acetate/hexane = 1/10 to 1/5) to furnish 683 mg of **8** in 92% yield; $[\alpha]_D^{23} = -54.8$ ($c = 0.61$, MeOH); $R_f = 0.63$ (ethyl acetate/hexane = 1/2); ^{1}H NMR (500 MHz, $CDCl_3$): $\delta = 0.96$ (2, 9H), 1.25 (s, 3H), 1.29 (s, 3H), 3.09 (ddd, 1H, $J = 10$, 10, 10 Hz), 3.29 (m, 3H), 3.59 (m, 1H), 3.80 (dd, 1H, $J = 10$, 10 Hz), 4.19 (dd, 1H, $J = 2.0$, 4.5 Hz), 4.48 (dd, 1H, $J = 2.0$, 2.0 Hz), 4.95 (s, 1H), 7.38 (m, 20H); ^{13}C NMR (125 MHz, $CDCl_3$): $\delta = 22.3$, 25.7, 26.0, 26.8, 61.7, 62.9, 65.6, 71.4, 74.0, 77.5, 79.0, 98.8, 127.1, 127.3, 127.6, 128.1, 128.2, 128.3, 128.6, 129.5, 129.6, 135.3, 135.5, 143.3, 143.4; HRMS for $C_{38}H_{45}O_4NSiCs$ [$M + Cs^+$]: calcd 740.2172, found 740.2168.

9: To a solution of periodinane [7] (548 mg, 0.9 mmol) in 10 mL CH_2Cl_2 was added 548 mg of **8** in 2 mL CH_2Cl_2. The mixture was stirred at room temperature for 3.5 h, 2 mL of 1 N NaOH was added, and the mixture was stirred for additional 10 min. The organic layer was then washed with 1 N NaOH and dried over $MgSO_4$, and the solvent was removed under vacuum to give 438 mg of **9** in 80% yield; $[\alpha]_D^{23} = -19.0$ ($c = 1.05$, MeOH); $R_f = 0.41$ (ethyl acetate/hexane = 1/4). ^{1}H NMR (500 MHz, $CDCl_3$): $\delta = 1.06$ (s, 9H), 1.33 (s, 6H), 3.39–3.46 (m, 1H), 3.48 (dd, 1H, $J = 6.0$, 11 Hz), 3.50 (dd, 1H, $J = 3.0$, 10.5 Hz), 3.53 (ddd, 1H, $J = 8.5$, 6, 8.5 Hz), 3.81 (dd, 1H, $J = 11$, 8.5 Hz), 3.87 (dd, 1H, $J = 10.5$, 3.5 Hz), 4.31 (dd, 1H, $J = 8.5$, 1 Hz), 4.74 (s, 1H), 7.07–7.74 (m, 20H); ^{13}C NMR (125 MHz, $CDCl_3$): $\delta = 25.3$, 25.5, 26.8, 54.1, 62.0, 64.0, 67.3, 71.7, 71.8, 127.5, 127.6, 127.7, 128.3, 128.3, 128.7, 129.7, 129.7, 135.8.

10: To a solution of **9** (400 mg, 0.66 mmol) in 5 mL toluene at −78 °C was added diisobutylaluminum hydride (0.5 mL, 1.0 M in hexane) dropwise by syringe. After the addition was complete, the mixture was stirred at −78 °C for 0.5 h. The reaction was then quenched with 400 μL methanol followed by addition of 4 mL of 10% aqueous solution of Rochelle's salt (potassium sodium tartrate) and 16 mL ether. The mixture was stirred at room temperature for 1 h, and the organic layer was washed with 1 N HCl and saturated aqueous $NaHCO_3$, and dried over $MgSO_4$. The solvent was removed under vacuum and the residue purified by silica gel column chromatography (ethyl acetate/hexane = 1/10 to 1/3) to give 366 mg of **10** in 91% yield; $[\alpha]_D^{23} = -7.2$ ($c = 1.15$, MeOH); $R_f = 0.59$ (ethyl acetate/hexane = 1/2); ^{1}H NMR (500 MHz, $CDCl_3$): $\delta = 0.96$ (s, 9H), 1.33 (s, 3H), 1.40 (s, 3H), 3.05–3.08 (m, 1H), 3.30–3.41 (m, 3H), 3.74 (dd, 1H, $J = 10$, 5.5 Hz), 4.27 (t, 1H, $J = 5.5$ Hz), 4.37–4.45 (m, 2H), 4.79 (s, 1H), 7.47 (m, 20H); ^{13}C NMR (125 MHz, $CDCl_3$): $\delta = 21.8$, 26.5, 26.7, 59.8, 62.5, 63.3, 66.9, 71.4, 73.8, 73.9, 127.2, 127.3, 127.8, 128.3, 128.4, 128.5, 129.6, 129.7, 135.3, 135.4; HRMS for $C_{38}H_{45}O_2NSiCs$ [$M + Cs^+$]: calcd 740.2172, found 740.2170.

1: To a solution of **10** (296 mg, 0.49 mmol) in 8 mL THF was added 1 mL of 1.0 M tetrabutylammonium fluoride in THF. The mixture was stirred at room temperature for 30 min. The solvent was then removed under reduced pressure, and the residue was dissolved in 15 mL methanol treated with 200 mg of *p*-TsOH·H_2O. The mixture was stirred at room temperature overnight. After 2 mL of saturated aqueous $NaHCO_3$ was added, the resulting mixture was stirred for another 10 min. The methanol was removed under vacuum and the residue extracted with ethyl acetate and purified by silica gel column chromatography (ethyl acetate) to give 121 mg of **10a** in 75% yield. $[\alpha]_D^{25} \pm 0$ ($c = 1.0$, CH_3OH); $R_f = 0.18$ (ethyl acetate); ^{1}H NMR (500 MHz, CD_3OD): $\delta = 3.1–3.2$ (m, 2H), 3.40 (dd, 2H, $J = 3.0$, 11.0 Hz), 3.45 (dd, 2H, $J = 6.0$, 11.0 Hz), 4.05–4.15 (m, 2H), 5.11 (s, 1H), 7.1–7.5 (m, 10H); ^{13}C NMR (125 MHz, CD_3OD): $\delta = 61.5$, 65.8, 72.8, 73.1, 128.3, 129.2, 130.2, 143.4; HRMS for $C_{19}H_{23}NO_4$ [$M + H^+$]: calcd 330.1713, found 330.1711.

1: A solution of **10a** (90 mg, 0.27 mmol) in 10 mL methanol was hydrogenated with 30 mg of $Pd(OH)_2$ under hydrogen atmosphere at room temperature. After 6 h the catalyst was filtered off and washed with methanol. The combined methanol solutions were concentrated and the oily residue purified by silica gel column chromatography ($CHCl_3/CH_3OH/H_2O/NH_4OH$ = 5/4/1/0.08) to give **1**: ^{1}H NMR (500 MHz, CD_3OD): $\delta = 3.55–3.65$ (m, 2H), 3.88 (dd, 2H, $J = 8.0$, 12.0 Hz), 3.92 (dd, 2H, $J = 5.0$, 12.0 Hz), 4.3–4.4 (m, 2H); ^{13}C NMR (125 MHz, CD_3OD): $\delta = 59.45$, 63.08, 71.69; HRMS for $C_6H_{13}NO_4$ [$M + H^+$]: calcd. 164.0923, found 164.0911; correct C,H,N analysis.

Chemoenzymatic synthesis of **1**: Ozone was bubbled through a solution of **11** [10] (302 mg, 1.6 mmol) in methanol (10 mL) at −78 °C until the reaction solution became pale blue. After nitrogen was passed through the solution to remove excess ozone, the ozonide was treated with dimethylsulfide (1 mL) and water (1 mL) for 12 h at room temperature. Methanol was removed under vaccuum, and the residue was then purified by chromatography on Amberlite XAD-II (3.0 × 10 cm, H_2O) to yield **12**, which was added to an aqueous solution of dihydroxyacetone phosphate (DHAP, 11 mL, 0.3 mmol). The pH of the solution was adjusted to 7.5 with 0.5 N NaOH. Fuculose-1-phosphate aldolase (2.0 mL, 70 U) was added to this solution and the mixture stirred slowly for 1 d at room temperature. After an enzymatic assay indicated that DHAP was completely consumed, the mixture was adjusted to pH 4.7 with 1 N HCl, acid phosphatase (from sweet potato, type XA, 0.8 mL, 200 U) was added, and the mixture was then stirred slowly at room temperature for 1 d. The mixture was adjusted to pH 7.0 with 0.5 N NaOH, and water was removed under reduced pressure. The residue was treated with methanol, and the soluble portion was collected and purified by silica gel chromatography ($CHCl_3/MeOH/H_2O$ = 8/2/0.1) to yield compound **13** (50.4 mg, 82%). $[\alpha]_D^{23} = -13.5$ ($c = 0.60$, MeOH); ^{1}H NMR (400 MHz, D_2O): $\delta = 3.50$ (1H, d of AB type, $J = 11.8$ Hz), 3.60 (1H, t, $J = 10.8$ Hz), 3.71 (1H, d of AB type, $J = 11.80$ Hz), 3.75 (1H, ddd, $J = 10.80$, 9.92, 5.60 Hz), 3.84 (1H, dd, $J = 10.80$, 5.60 Hz), 3.88 (1H, d, $J = 3.24$ Hz), 3.92 (1H, dd, $J = 9.92$, 3.24 Hz); ^{13}C NMR (100 MHz, D_2O): $\delta = 58.70$, 60.85, 64.25, 69.68, 70.37, 98.65; HRMS for $C_6H_{11}N_3O_5Na$ [$M^+ + Na$]: calcd 228.0596, found 228.0590.

A solution of **13** (28.4 mg, 0.14 mmol) in ethanol (10 mL) was hydrogenated with 10% Pd-C (10 mg) under 50 psi of hydrogen for 12 h. The catalyst was removed by filtration, and the solvent was evaporated under vacuum. The residue was purified by silica gel chromatography ($CHCl_3/MeOH/H_2O/NH_4OH$ = 6/4/1/0.1) to yield compound **1** (14 mg, 61%). The NMR data (^{1}H and ^{13}C) are the same as those for **1** prepared chemically.

Received: February 14, 1994 [Z 6692 IE]
German version: *Angew. Chem.* **1994**, *106*, 1343

[1] a) M. L. Sinnott, *Chem. Rev.* **1990**, *90*, 1171; b) B. Winchester, G. W. Fleet, *Glycobiology* **1992**, *2*, 199; c) G. C. Look, C. H. Fotsch, C.-H. Wong, *Acc. Chem. Res.* **1993**, *26*, 182.

[2] G. Papandreou, M. K. Tong, B. Ganem, *J. Am. Chem. Soc.* **1993**, *115*, 11682.

[3] a) L. Gzollnev, J. Kuszmann, A. Vasella, *Helv. Chim. Acta.* **1990**, *73*, 1338; b) K. Wallitnann, A. Vasella, *ibid.* **1991**, *74*, 1520.

[4] a) T. Kajimoto, K. K.-C. Liu, R. L. Pederson, Z. Zhong, Y. Ichikawa, J. A. Porco, C.-H. Wong, *J. Am. Chem. Soc.* **1991**, *113*, 6187; b) G. Legler, S. Pohl, *Carbohydr. Res.* **1986**, *155*, 119.

[5] a) K. K.-C. Liu, T. Kajimoto, L. Chen, Z. Zhong, Y. Ichikawa, C.-H. Wong, *J. Org. Chem.* **1991**, *56*, 6280; b) Y.-F. Wang, D. P. Dumas, C.-H. Wong, *Tetrahedron Lett.* **1992**, *34*, 403; c) Y. Takaoka, T. Kajimoto, C.-H. Wong, *J. Org. Chem.* **1993**, *58*, 4809; d) G. W. J. Fleet, S. J. Nicholas, P. W. Smith, S. V. Evans, L. E. Fellows, R. L. Nash, *Tetrahedron Lett.* **1985**, *26*, 3127.

[6] A. B. Reitz, E. W. Baxter, *Tetrahedron Lett.* **1990**, *31*, 6777.

[7] D. B. Dess, J. C. Martin, *J. Org. Chem.* **1983**, *48*, 4156.

[8] Recombinant fuculose-1-phosphate aldolase from *E. coli* was used. Procedure for overexpression of the enzyme will be published separately. We have deposited the microbial strain with the American Type Culture Collection (ATCC 86984), and it is available to the public. For other reports on the overexpression of this enzyme, see A. Ozaki, E. J. Toone, C. H. von der Osten, A. Sinskey, G. M. Whitesides, *J. Am. Chem. Soc.* **1990**, *112*, 4970; W.-D. Fessner, G. Sinerius, A. Schneider, M. Dreyer, G. E. Schultz, J. Badia, J. Aguilar, *Angew. Chem.* **1991**, 103, 596; *Angew. Chem. Int. Ed. Engl.* **1991**, *30*, 555.

[9] R. L. Pederson, J. Esker, C.-H. Wong, *Tetrahedron* **1991**, *47*, 2643.

[10] R. R. Hung, J. A. Straub, G. M. Whitesides, *J. Org. Chem.* **1991**, *56*, 3849.

[11] Crystal data for **2** ($C_6H_{13}NO_4S$): orthorhombic, space group $P2_12_12_1$ (No. 19; D_2^4), $a = 5.946(1)$, $b = 7.272(1)$, $c = 17.484(2)$ Å, $V = 756.0(2)$ Å^3, $Z = 4$, $\rho_{calcd} = 1.434$ g cm^{-3}, $M_r = 163.2$ g mol^{-1}, measurement at 293 K in the 2θ-θ mode, $Cu_{K\alpha}$ radiation, $\lambda = 1.54018$ Å, $\mu Cu_{K\alpha} = 0.112$ mm^{-1}, 741 reflections measured ($4.0° < 2\theta < 120°$), of which 671 were independent and 633 with $F > 2.0\,\sigma(F)$ were used for refinement, 120 parameters, GOF = 1.54, $R = 4.10$, $R_w = 5.13$. Further details on the crystal structure investigation will be provided elsewhere.

Synthesis and Structure of the First Organometallic Galloxane Hydroxide $Mes_6Ga_6O_4(OH)_4$**

Jens Storre, Thomas Belgardt, Dietmar Stalke, and Herbert W. Roesky*

Dedicated to Professor Hubert Schmidbaur on the occasion of his 60th birthday

Recently structural investigations by Barron et al. revealed that the controlled hydrolysis of alkylaluminum compounds can afford both hydroxides and oxides.[1] The formation of a mixed

[*] Prof. Dr. H. W. Roesky, Dipl.-Chem. J. Storre, Dipl.-Chem. T. Belgardt, Priv.-Doz. Dr. D. Stalke
Institut für Anorganische Chemie der Universität
Tammannstrasse 4, D-37077 Göttingen (FRG)
Telefax: Int. code + (551)39-3373

[**] This work was supported by the Deutsche Forschungsgemeinschaft and the Fonds der Chemischen Industrie. Mes = mesityl.

hydroxide oxide was not observed. The commercially used, partially hydrolyzed alkylaluminum compounds[2] and the corresponding gallium compounds[3] are important cocatalysts for metallocenes of group 4 of the periodic table. In considering polymerization reactions with metallocenes containing fluorine and methylaluminoxane as cocatalyst[4] we were chiefly interested in the function and structure of the cocatalyst systems.

$$\underset{\mathbf{1}}{Mes_2GaCl} + KOH \xrightarrow[-KCl]{} Mes_2GaOH \qquad (a)$$

$$6\,Mes_2GaOH + 2\,H_2O \xrightarrow[-6\,MesH]{} \underset{\mathbf{3}}{Mes_6Ga_6O_4(OH)_4} \qquad (b)$$

$$6\,\underset{\mathbf{2}}{Mes_3Ga} + 6\,H_2O \xrightarrow[-6\,MesH]{\text{toluene}} 6\,Mes_2GaOH \xrightarrow[-6\,MesH]{+H_2O} \mathbf{3} \qquad (c)$$

In order to obtain crystalline products, we carried out hydrolysis with Mes_2GaCl (**1**) and Mes_3Ga (**2**) (Mes = mesityl). Compound **1** reacts with hydrated KOH in THF leading to the formation of KCl and probably Mes_2GaOH [Eq. (a)], which condenses to give $Mes_6Ga_6O_4(OH)_4$ (**3**) [Eq. (b)]. The resulting KCl could be separated by filtration and MesH could be detected by ^{1}H NMR spectroscopy. In order to confirm this reaction pathway, we treated **2** with water in toluene [Eq. (c)], since the hydrolysis of organogallium compounds affords the corresponding gallium hydroxides.[5] The reaction led to the formation of **3** and MesH. The condensation of the homologous aluminum compounds[6] has so far not been explained unambiguously.

The IR spectrum of $[\mathbf{3}(thf)_4]$ shows the characteristic OH vibrations: a sharp band at 3671 for free and a broad band at 3521 cm^{-1} for bridging OH groups, which can be explained by partial release of the coordinating THF molecules. The EI mass spectrum shows the peak for the molecular ion at $m/z = 1264$ and that of the hydroxide-free hexameric galloxane at $m/z = 1228$ (100% rel. intensity, $M^+ - 2H_2O$). In the ^{1}H NMR spectrum, two signals each are observed for the ring protons ($\delta = 6.73-6.71$) as well as for the *ortho* ($\delta = 2.57-2.53$) and the *para* ($\delta = 2.18$) methyl protons of the mesityl group. Thus, the mesityl groups are arranged differently. This is confirmed by the distorted octahedral structure in the solid state. The OH protons occur at $\delta = 6.37$.

Single crystals suitable for X-ray structure analysis[7] were obtained from THF. In addition to the four THF molecules coordinated to **3**, six uncoordinated THF molecules are present per formula unit. As a result of the latter the crystals disintegrate very rapidly as soon as the mother liquor is removed. The selection of the crystal and subsequent application was therefore carried out at $-50\,^\circ$C.[8] The hexanuclear mesitylgalloxane hydroxide **3** crystallizes in the space group *R*3*c*. The oxygen atoms O4 and O3 lie on the threefold axis (Fig. 1). To a first approximation the structure can be described as a distorted octahedron of six gallium atoms. Each face of this octahedron per hemisphere is capped alternately by an μ_3-oxygen atom and a μ_3-hydroxide group. All gallium atoms are formally in the oxidation state + III and are five-coordinate. This degree of coordination is not unusual for gallium compounds (e.g. in $Me_2GaO_2C_7H_5$; $O_2C_7H_5$ = α-tropolyl).[12] The hydroxidic oxygen atoms form significantly longer Ga–O distances than the oxidic oxygen atoms (221 and 245 pm for O1 and O3, respectively, in contrast to 187 and 189 pm for O2 and O4, respectively). Furthermore, the environment of the hydroxidic oxygen atoms is more pyramidalized than that of the oxidic oxygen atoms (Ga-O-Ga for O1 and O3 88.1 and 78.6°, respectively; in contrast for O2 and O4 110.7 and 108.9°, respectively). This observation is consistent with the one made for $Mes_6Ga_6F_4O_4$,[13] namely that the oxidic oxygen atoms form a comparable mean angle of 111.6° (105.9–117.7°) with the two bound gallium atoms. The average Ga–C distance of 196 pm is in the range typical for arylgallium compounds.[14] THF molecules in the spaces left by the six mesityl ligands coordinate by hydrogen bonds to the four OH functions of the $Ga_6O_4(OH)_4$ framework (O1···O5 273 and O3···O6 252 pm). Coordination of this sort has already been described for $[(tBu_2AlOH)_3 \cdot 2thf]$.[11]

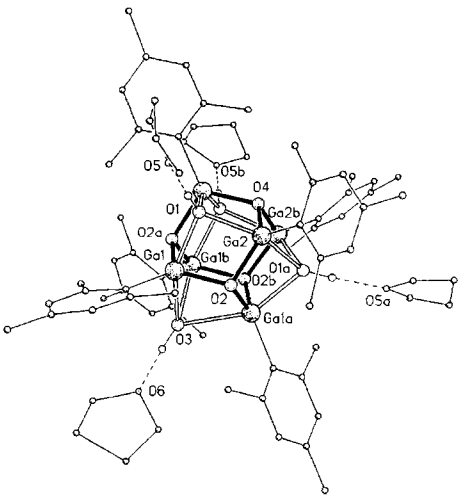


Fig. 1. Crystal structure of $[\mathbf{3}(thf)_4] \cdot 6$THF. The six noncoordinated THF molecules are not shown. The bond lengths [pm] and angles [°] labeled with an * are average values, the numbers in square brackets are the range of values, the standard deviations are extreme values: O1–Ga 221(1)* [213(1)–230(1)], O3–Ga 245(1), O2–Ga 187(1)* [185.5(9)–189(1)], O4–Ga 189.3(5), Ga–C 196(1)* [195(1)–197(1)]; Ga-O1-Ga 88.1(4)* [87.5(3)–88.6(3)], Ga-O3-Ga 78.6(4), Ga-O2-Ga 110.7(5)* [107.6(4)–113.0(5)], Ga-O4-Ga 108.9(5).

It is thus possible to prevent condensation through reaction of all hydroxide groups by the use of sterically demanding substituents. In addition Neumüller and Gahlmann observed the formation of the hexanuclear organogallium fluoride oxide $Mes_6Ga_6F_4O_4$, isoelectronic to **3**,[13] in the partial hydrolysis of Mes_2GaF. It may well be possible that OH–metal interactions play a role not only in the polymerization, but also in the water-accelerated zirconium-catalyzed carbalumination of alkynes.[15]

Experimental Procedure

3: a) A solution of $GaMes_3$ (1.4 g, 3.3 mmol) in THF (20 mL) was added dropwise to a solution of $GaCl_3$ (0.3 g, 1.7 mmol) in THF (20 mL) and stirred for 30 h at room temperature. Subsequently KOH (0.28 g, 5.00 mmol, not dried) was added to this solution and the resulting mixture was stirred for 5 d at room temperature under an inert atmosphere. After the KCl had been filtered off, the filtrate was concentrated under vacuum and the white solid obtained was washed with *n*-hexane (20 mL). Crystallization from THF afforded 0.9 g (66%) $[\mathbf{3}(thf)_4]$. The decomposition temperature of the THF-free compound **3** lay above 350 °C. Correct elemental analysis for C, H, Ga.

^{1}H NMR (250 MHz, [D$_8$]THF, TMS$_{ext}$): $\delta = 6.73-6.71$ (m, Ar-H), 6.37 (s, OH), 2.57–2.53 (m, 2,6-CH$_3$), 2.19–2.17 (m, 4-CH$_3$); IR (nujol): $\tilde{\nu}$[cm^{-1}] = 3671 s, 3521 s, br., 3015 s, 1719 m, 1601 vs, 1558 s, 1412 m, 1292 m, 1056 vs, 1028 vs, 848 s, 703 s, 589 m, 543 s.

b) Degassed water (106 μL, 5.9 mmol) was added by syringe to a solution of $GaMes_3$ (2.52 g, 5.9 mmol) in toluene (100 mL) at $-78\,^\circ$C and the mixture was stirred and slowly allowed to warm to room temperature. Subsequently it was stirred for 3 d, the volatiles were removed under vacuum, the white residue washed with *n*-hexane (20 mL) and filtered. The residue was dried under vacuum (10^{-4} mbar) for about 15 h. Yield of **3** (0.72 g, 58%). Correct elemental analysis of C and H for $Mes_6Ga_6O_4(OH)_4$. IR and NMR spectra in [D$_8$]THF were consistent with those for the product prepared according to method a).

Received: January 21, 1994 [Z66371E]
German version: *Angew. Chem.* **1994**, *106*, 1365

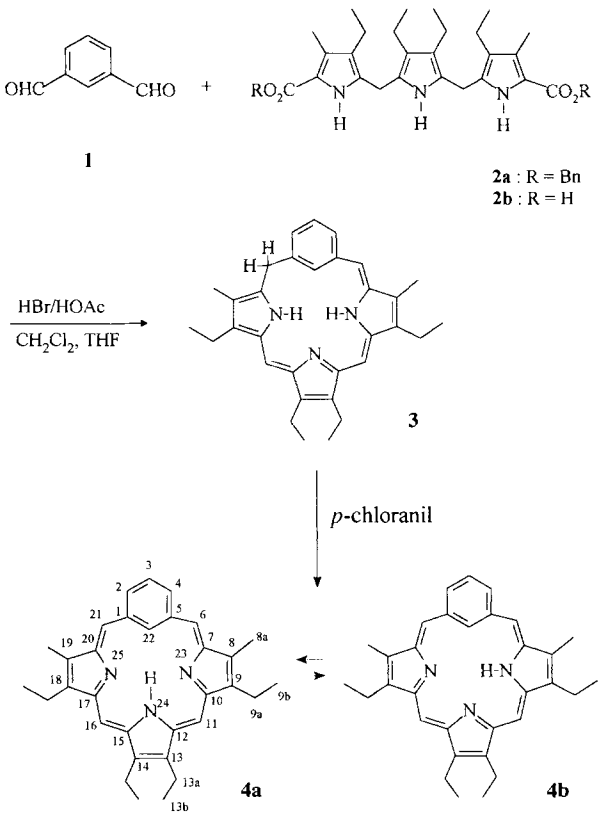
[1] M. R. Mason, J. M. Smith, S. G. Bott, A. R. Barron, *J. Am. Chem. Soc.* **1993**, *115*, 4971.
[2] H. Sinn, W. Kaminsky, *Adv. Organomet. Chem.* **1980**, *18*, 99.
[3] K. Ziegler, GB-B 775384, **1957**; *Chem. Abstr.* **1958**, *52*, 12893e.
[4] A. Herzog, H. W. Roesky, Z. Zak, M. Noltemeyer, *Angew. Chem.* **1994**, *106*, 1035; *Angew. Chem. Int. Ed. Engl.* **1994**, *33*, 967.
[5] D. A. Atwood, A. H. Cowley, P. R. Harris, R. A. Jones, S. U. Koschmieder, C. M. Nunn, *Organometallics* **1993**, *12*, 24.
[6] S. Pasynkiewicz, *Polyhedron* **1990**, *9*, 429.
[7] Crystal data of $[3(thf)_4]\cdot 6THF$: $M = 1986.46$, rhombohedral, space group $R\bar{3}c$, $a = b = 2353.6(3)$, $c = 3133.0(6)$ pm, $V = 15.030(4)$ nm^3, $Z = 6$, $\rho_{calcd} = 1.317$ Mgm^{-3}, $F(000) = 6264$, $\lambda = 71.073$ pm, $T = -120\,^{\circ}C$, $\mu(Mo_{K\alpha}) = 1.651$ mm^{-1}, crystal dimensions: $0.7 \times 0.5 \times 0.5$ mm, $6^{\circ} \le 2\theta \le 40^{\circ}$; of the 6127 collected reflections, 2440 are independent, and these were used for the refinement of 164 parameters with the help of 198 restraints; maximal residual electron density: 899 e nm^{-3}, $R1(F > 4\sigma(F)) = 0.069$ and $wR2 = 0.199$ (all data) with $R1 = \Sigma||F_o| - |F_c||/\Sigma|F_o|$ and $wR2 = (\Sigma w F_o^2 - F_c^2)^2/\Sigma w(F_o^2)^2)^{0.5}$. The data were collected on a Stoe-Huber diffractometer. Intensities of a rapidly cooled crystal in an oil drop [8] were collected by $2\theta/\omega$ method. Semiempirical absorption corrections were carried out on all data. The structure was solved by direct methods (SHELXS-90) [9] and refined by least squares on F^2 [10]. The disorders of the THF solvent molecules were refined with distance restraints. The refinement of the inversion twinning paramter [11] ($x = 0.00(4)$ for $x = 0$ for the correct absolute structure and $x = +1$ for the inverted structure) confirmed the absolute structure of **3**. The solution of the structure and the refinement in the space group $R\bar{3}c$ were unsuccessful. The structure could be solved in the space group Cc, but a refinement was also here unsuccessful. Further details of the crystal structure investigation may be obtained from the Director of the Cambridge Crystallographic Data Centre, 12 Union Road, GB-Cambridge CB2 1EZ, on quoting the full journal citation.
[8] T. Kottke, D. Stalke, *J. Appl. Crystallogr.* **1993**, *26*, 615.
[9] G. M. Sheldrick, *Acta Crystallogr. Sect. A* **1990**, *46*, 467.
[10] G. M. Sheldrick, SHELXL-93, program for crystal structure refinement, Göttingen, **1993**.
[11] H. D. Flack, *Acta Crystallogr. Sect. A* **1983**, *39*, 876.
[12] I. Waller, T. Halder, W. Scharz, J. Weidlein, *J. Organomet. Chem.* **1982**, *232*, 99.
[13] B. Neumüller, F. Gahlmann, *Angew. Chem.* **1993**, *105*, 1770; *Angew. Chem. Int. Ed. Engl.* **1993**, *32*, 1701.
[14] O. T. Beachley, Jr., M. R. Churchill, J. C. Pazik, J. W. Ziller, *Organometallics* **1986**, *5*, 1814.
[15] P. Wipf, S. Lim, *Angew. Chem.* **1993**, *105*, 1095; *Angew. Chem. Int. Ed. Engl.* **1993**, *32*, 1068.

Benziporphyrin, a Benzene-Containing, Nonaromatic Porphyrin Analogue

Kurt Berlin and Eberhard Breitmaier*

An interesting approach for modifying the basic porphyrin framework for the most varied applications[1] is replacing the pyrrole ring by another five-membered ring heteroarene such as furan and thiophene,[2] or by pyridine[3, 4] or benzene. When 1,3-disubstituted six-membered rings are incorporated, the macrocycle can achieve 18 π aromaticity only at the expense of the 6 π aromatic system. The obvious question is which of the two rings wins this competition. Recently we reported on the synthesis of a modified porphyrinogen in which a pyrrole is replaced by a pyridine unit.[4] However, we could not obtain the 18 π aromatic tautomer with maximum unsaturation which corresponds to a porphyrin. The oxidation of the pyriporphyrinogen[4] leads to the ketone instead.

We report here on the first benzene-containing macrocycle that is a porphyrin analogue, which in contrast to the pyriporphyrins,[4] was obtained simply by oxidation of the appropriate porphyrinogen **3**. Tripyrranedicarboxylic acid **2b**[5] was decarboxylated in situ and condensed with isophthalaldehyde (**1**) in dichloromethane/THF with 33% HBr in glacial acetic acid as the catalyst. The resulting macrocycle was then oxidized in situ with *p*-chloranil to give **4**. In analogy to pyriphorphin we propose the name benziporphin for the unsubstituted framework and the numbering shown for **4a**.



The spectroscopic data for the compound give no indication of 18 π aromaticity and cyclic conjugation in the tautomer. The UV spectrum, for example, does not display the Soret band (420 nm, $\lg\varepsilon > 4$) characteristic of porphyrins, and in the ^{1}H NMR spectrum the pyrrole-NH protons ($\delta = 8.90$) and the inner benzenoid protons ($\delta = 7.88$) do not show the shielding typical for the inner protons of an [18]annulene. Thus the tautomers **4a/b** (4:1 in $CDCl_3$) have an intact benzenoid arene unit. It is apparent that the aromatic 18 π tautomer does not exist even when only one 6 π arene would have to be sacrificed. Thus **4**, a prototype of macrocycles in which benzenoid rings successively replace the pyrrole rings of porphyrin, indicates that porphyrin analogues with more than one 6 π arene[6] cannot be [18]annulenes.

The successful preparation of **4** also implies that the surprising behavior of the "pyriporphyrinogens"[4] towards oxidants results from the side reaction of the reactive α-alkyl group of the pyridine rings and is not a consequence of the unattainable 18 π aromaticity.

Experimental Procedure

Diester **2a** (635 mg, 1 mmol) was dissolved in 80 mL of anhydrous THF and treated with 200 mg of Pd/C (10% Pd) and 0.1 mL of triethylamine. After 3 h of hydrogenation at ambient pressure the catalyst was removed by vacuum filtration and the filtrate (**2b**) added dropwise to a solution of isophthalaldehyde (**1**) (134 mg, 1 mmol) in 800 mL of dichloromethane. Argon was then bubbled through the reaction mixture for 15 min, and then 1.8 mL of a solution of HBr in glacial acetic acid (33%) was added. The reaction mixture was stirred for 4 h with exclusion of light, 750 mg of *p*-chloranil was added, and 15 min later the reaction mixture was neutralized with 2.5 mL of triethylamine and left to stand ca. 15 h. The solvent was removed under

[*] Prof. Dr. E. Breitmaier, Dipl.-Chem. K. Berlin
Institut für Organische Chemie und Biochemie der Universität
Gerhard-Domagk-Strasse 1, D-53121 Bonn (FRG)
Telefax: Int. code + (228)73-5683

vacuum and the residue purified by column chromatography on neutral alumina under argon: eluent: a) ethyl acetate/cyclohexane 2:3, b) dichloromethane/petroleum ether (b.p. 40–60 °C) 1:2, $R_f = 0.21$. The dark green fraction provided 27 mg (58.6 μmol, 5.9%) of black-blue crystals. Selected physical and spectroscopic data of **4**: m.p. 135–138 °C (decomp); MS (70 eV): *m/z* (%): 463.2985 (53), calcd 463.2988 [$M^+ + 2H$], 462.3 (48) [$M^+ + H$], 461.2841 (100), calcd 461.2831 [M^+]; ^{1}H NMR (400 MHz, $CDCl_3$): $\delta = 1.27$, 1.36 (2 t, 12H; 9b-H/13b-H), 2.34, 2.42 (2 s, 6H (1:4); 8a-H), 2.77, 2.85 (2 q, 8H; 9a-H, 13a-H), 6.57 (s, 2H; 11-H), 7.25, 7.28 (s, 2H (1:4); 6-H), 7.74 (t, $^3J(H,H) = 8.2$ Hz, 1H; 3-H), 7.88 (m br, 1H; 22-H), 7.98 (d, 2H; 2-H), 8.90 (br. s, 1H; NH); ^{13}C NMR (100 MHz, $CDCl_3$, data for **4a**): $\delta = 10.3$ (C-8a), 15.3, 16.0 (C-9b/C-13b), 18.0, 18.4 (C-9a/C-13a), 92.9 (C-11), 122.4 (C-6), 124.8 (C-22), 128.7 (C-3), 133.9 (C-12), 137.2 (C-2), 140.4 (C-13), 141.0 (C-9), 141.2 (C-8), 147.7 (C-1), 156.9 (C-7), 168.8 (C-10); UV/VIS (CH_2Cl_2): λ_{max} (lg ε) = 243 nm (4.19), 315 (4.39), 381 (4.49), 610 (3.49), 632 (3.50), 716 (3.24); IR (KBr): $\tilde{\nu} = 3309$, 3040, 2960, 2928, 2865, 1618, 1587, 1572, 1434, 1101, 809, 687 cm^{-1}.

Received: February 9, 1994 [Z 6681 IE]
German version: *Angew. Chem.* **1994**, *106*, 1356

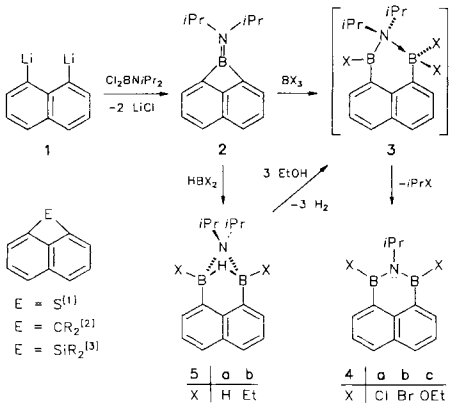
[1] J. L. Sessler, A. K. Burrell, *Top. Curr. Chem.* **1991**, *161*, 177–273, and references therein.
[2] M. J. Broadhurst, R. Grigg, A. W. Johnson, *J. Chem. Soc. C* **1971**, *21*, 3681–3690.
[3] D. Jacoby, C. Floriani, A. Chiesi-Villa, C. Rizzoli, *J. Am. Chem. Soc.* **1993**, *115*, 7025–7026.
[4] K. Berlin, E. Breitmaier, *Angew. Chem.* **1994**, *3*, 229–230; *Angew. Chem. Int. Ed. Engl.* **1994**, *33*, 219–220, and references therein.
[5] J. L. Sessler, M. R. Johnson, V. Lynch, *J. Org. Chem.* **1987**, *52*, 4394–4397.
[6] G. R. Newkome, Y. J. Joo, D. W. Evans, S. Pappalardo, F. R. Fronczek, *J. Org. Chem.* **1988**, *53*, 786–790, and references therein.

Synthesis and Reactivity of a Naphtho[1,8-*bc*]boret**

Achim Hergel, Hans Pritzkow, and Walter Siebert*

Dedicated to Professor Helmut Werner on the occasion of his 60th birthday

1,8-Bridged naphthalene derivatives are interesting not only structurally because of the distortion of their arene framework, but also because of their synthetic potential owing to the strained four-membered ring. Up to now compounds of this type have been synthesized with sulfur, carbon, and silicon in the bridging position;[1–3] all attempts to prepare the corresponding nitrogen and oxygen analogues have failed.[4, 5]



[*] Prof. Dr. W. Siebert, Dr. A. Hergel, Dr. H. Pritzkow
Anorganisch-chemisches Institut der Universität
Im Neuenheimer Feld 270, D-69120 Heidelberg (FRG)
Telefax: Int. code + (6221) 56-4197

[**] This work was supported by the Deutsche Forschungsgemeinschaft (Sonderforschungsbereich 247), the Fonds der Chemischen Industrie, and BASF AG.

We have now succeeded in synthesizing the first boron-bridged naphthalene, **2**, in a yield of 89% by the reaction of 1,8-dilithionaphthalene (**1**) with Cl_2BNiPr_2. Colorless, crystalline **2** is thermally stable and can be sublimed without decomposition. On the basis of spectroscopic data the molecule appears to have C_2 symmetry, which is confirmed by a crystal structure analysis (Fig. 1).[6] The slightly shortened B–N bond (1.37 Å) lies almost in the plane of the naphthalene framework, and the angles within the boret ring indicate that the ring is very strained.

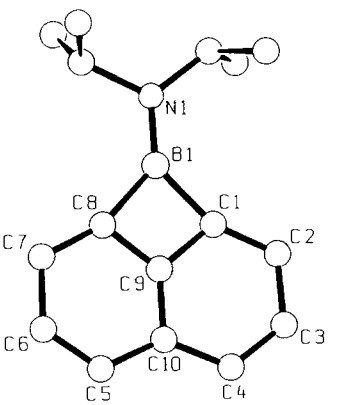


Fig. 1. Molecular structure of **2**. Selected distances [Å] and angles [°]: B1-N1 1.375, 1.369(5), B1-C1 1.599, 1.601(5), B1-C8 1.602, 1.601(5), C1-C9 1.404, 1.403(4), C8-C9 1.397, 1.406(4); C1-B1-C8 86.2, 86.7(3), B1-C1-C9 85.6, 85.2(3), B1-C8-C9 85.7, 85.1(3), C1-C9-C8 102.6, 103.0(3).

Compound **2** reacts under mild conditions with BX_3 (X = Cl, Br) to give naphtho[1,8-*cd*][1,2,6]azadiborinin **4a, b** by a novel ring expansion. The first step is assumed to be the cleavage of a B–C bond in **2** by BX_3 leading to the nonisolable intermediate **3**, which gives rise to the naphthoannelated heterocycle **4** by elimination of *i*PrX (or propene + HX). Reaction of **2** with diborane and diethylborane (X = H, Et) provides the μ-diisopropylaminodiboranes **5a, b**. In this case a B–H–B bridge forms which prevents further reaction. Compound **5a** is thus a stabilized isomer of **3** (X = H). The proof for this is provided by the replacement of the three hydrogen atoms bound to boron in **5a** by ethoxy groups. **3** (X = OEt) reacts with elimination of ethyl isopropyl ether (or propene + EtOH) and formation of **4c**.

The crystal structure analysis[7] of **5b** (Fig. 2) indicates that the boron atoms lie almost in the plane of naphthalene. The B-N-B angle (75.5(3)°) is remarkably small, and the atoms B-N-H form approximately a right angle.

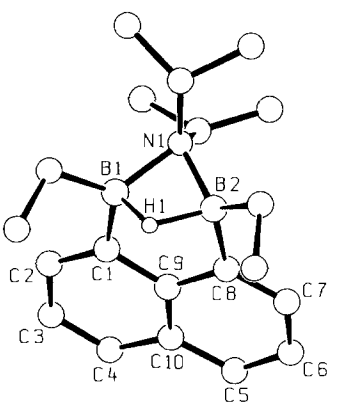


Fig. 2. Molecular structure of **5b**. Selected distances [Å] and angles [°]: N1-B1 1.615(6), N1-B2 1.613(5), B1-C1 1.606(6), B2-C8 1.609(6), B1-H1 1.25(3), B2-H1 1.35(3), C1-C9 1.424(5), C8-C9 1.419(5); B1-N1-B2 75.8(3), N1-B1-C1 111.8 (3), N1-B2-C8 112.3(3), B1-C1-C9 114.3(3), B2-C8-C9 114.0(3), C1-C9-C8 116.1(3).

Compound **5a** displays temperature-dependant molecular dynamics; the ^{1}H NMR spectrum at 220 K confirms the constitu-

tion in the solid state. Besides the splitting pattern for the signals of the naphthalene protons, the spectrum exhibits two doublets and two septets for the two isopropyl groups. At higher temperatures the signals in the aliphatic region coalesce, and at 370 K one doublet and one septet are evident. Compound **5a**, in contrast to **5b**, undergoes an exchange process at higher temperatures, in which the two methine protons and the four methyl groups are equivalent on the NMR timescale. We assume that a transition state **3** (X = H) is formed by opening of the μ-bridge; both hydrogen atoms of the BH_2 unit are now capable of forming a new bridge, and thus on the NMR timescale both isopropyl groups become equivalent. The temperature-dependent ^{11}B NMR spectrum confirms this. At room temperature a slightly broadened doublet can be seen (coupling of μ-H—B is not resolved) which is converted into a quartet at higher temperatures (370 K). This observation can be explained by the rapid, oscillating motion of the three hydrogen atoms around the boron atoms, such that they appear equivalent to the boron nucleus. This phenomenon is comparable to the exchange process of the hydrogen atoms in μ-dimethylaminodiborane(6).[8] In this case the ^{11}B NMR spectrum displays a doublet of triplets at 283 K and a sextet at 377 K.

Experimental Procedure

2: A solution of **1** (28.05 mmol) in ether (70 mL) at −30 °C was added to a solution of Cl_2BNiPr_2 (84.15 mmol) in hexanes (60 mL) cooled to −20 °C. Filtration and sublimation (52 °C, 0.001 Torr) yielded **2** in 89% yield, m.p. 84 °C. ^1H NMR (200 MHz, $CDCl_3$): δ = 7.70 (dd, 2H), 7.60 (dd, 2H), 7.45 (dd, 2H), 3.90 (sept, 2H), 1.47 (d, 12H); ^{13}C NMR (50 MHz, $CDCl_3$): δ = 163 (br.), 148 (br.), 129.4, 126.0, 122.6, 121.8, 49.3, 24.3; ^{11}B NMR (29 MHz, $CDCl_3$): δ = 37; Electron Impact (EI)-MS: *m/z* (%): 237 (26) [M^+], 194 (56) [$M^+ - i$Pr].

4a: BCl_3 was treated with **2** in hexane at −20 °C. Workup by recrystallization provided **4a** in 92% yield, m.p. 89 °C (decomp). ^1H NMR (200 MHz, C_6D_6): δ = 8.49 (dd, 2H), 7.60 (dd, 2H), 7.23 (dd, 2H), 4.96 (sept, 1H), 1.48 (d, 6H); ^{13}C NMR (75 MHz, C_6D_6): δ = 139.7, 137.6, 133.8, 126.8, 51.6, 22.6; ^{11}B NMR (29 MHz, C_6D_6): δ = 43.9; EI-MS: *m/z* (%): 275 (43) [M^+], 260 (100) [M^+ − Me].

4b: Preparation analogous to **4a**, yield 53%, m.p. 75 °C (decomp). ^1H NMR (300 MHz, $CDCl_3$): δ = 8.71 (dd, 2H), 8.12 (dd, 2H), 7.66 (dd, 2H), 5.25 (sept, 1H), 1.73 (d, 6H); ^{13}C NMR (75 MHz, $CDCl_3$): δ = 142.2, 136.5, 133.3, 131.0, 126.2, 55.7, 22.7; ^{11}B NMR (29 MHz, $CDCl_3$): δ = 43.6; EI-MS: *m/z* (%): 365 (68) [M^+], 350 (100) [M^+ − Me].

5a: **2** and $LiBH_4$ in hexanes were treated with boron trifluoride–ether in ether. Filtration and recrystallization from hexane yielded **5a** in 93% yield, m.p. 110 °C (decomp). ^1H NMR (200 MHz, $CDCl_3$, 220 K): δ = 7.76 (dd, 2H), 7.71 (dd, 2H), 7.45 (dd, 2H), 2.7 (sept, br., 1H), 2.58 (sept, 1H), 2.0 (br., 1H), 1.49 (d, 6H), 0.98 (d, 6H); ^1H NMR (200 MHz, C_7D_8, 370 K): δ = 7.59 (dd, 2H), 7.51 (dd), 2H), 7.23 (dd, 2H), 2.68 (sept, 2H), 2.0 (br, 1H), 0.88 (d, 12H); ^{13}C NMR (75 MHz, C_6D_6): δ = 146.9, 143 (br.), 131.2, 130.7, 126.9, 126.5, 59 (br.), 50 (br.), 21.8; ^{11}B NMR (64 MHz, C_7D_8, 270 K): δ = −10.3 (d, br.); ^{11}B NMR (64 MHz, C_7D_8, 350 K): δ = −10.3 (q); EI-MS: *m/z* (%): 251 (23) [M^+], 208 (100) [$M^+ - i$Pr].

5b: Diethylborane was slowly added to **2** in hexane. **5b** was obtained after recrystallization in 82% yield, m.p. 108 °C (decomp). ^1H NMR (200 MHz, C_6D_6): δ = 7.69 (dd, 2H), 7.61 (dd, 2H), 7.43 (dd, 2H), 3.10 (sept, 1H), 2.77 (sept, 1H), 2.11 (br., 1H), 1.3–1.7 (m, 4H), 1.22 (t, 6H), 1.07 (t, 6H), 0.59 (d, 6H); ^{13}C NMR (50 MHz, C_6D_6): δ = 147.4, 144 (br.), 131.8, 129.7, 126.9, 126.1, 56.5, 51.1, 25 (br.), 23.1, 14.7, 8.8 (br.); ^{11}B NMR (29 MHz, C_6D_6): δ = 1.0; EI-MS: *m/z* (%): 307 (6) [M^+], 236 (100) [M^+ − Et − iPr].

4c: **5a** was treated with ethanol and recrystallized from hexane. Yield : 95%, m.p. 85 °C. ^1H NMR (200 MHz, C_6D_6): δ = 8.40 (dd, 2H), 7.72 (dd, 2H), 7.35 (dd, 2H), 4.1 (q, br., 4H), 2.59 (sept, 1H), 1.23 (t, br., 6H), 0.90 (d, 6H); ^{13}C NMR (50 MHz, C_6D_6): δ = 142.3, 134.5, 132.2, 132.0, 125.8, 59 (br.), 47.9, 18.9, 17 (br.); ^{11}B NMR (29 MHz, C_6D_6): δ = 29.4.

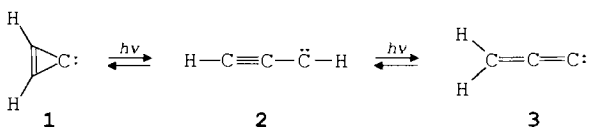
Received: January 29, 1994 [Z 6655 IE]
German version: *Angew. Chem.* **1994**, *106*, 1342

[1] R. W. Hoffmann, W. Sieber, *Justus Liebigs Ann. Chem.* **1967**, *703*, 96; J. Meinwald, S. Knapp, *J. Am. Chem. Soc.* **1974**, *96*, 6532.
[2] R. J. Bailey, H. Shechter, *J. Am. Chem. Soc.* **1974**, *96*, 8116; M. Gessner, P. Card, H. Shechter, G. G. Christoph, *ibid.* **1977**, *99*, 2371; P. J. Card, F. E. Friedli, H. Shechter, *ibid.* **1983**, *105*, 6104; A. Kumar, F. E. Friedli, L. Hsu, P. J. Card, N. Mathur, H. Shechter, *J. Org. Chem.* **1991**, *56*, 1663.
[3] L. S. Yang, H. Shechter, *J. Chem. Soc. Chem. Commun.* **1976**, 775.
[4] W. D. Crow, C. Wentrup, *J. Chem. Soc. Chem. Commun.* **1968**, 1026; P. Flowerday, M. J. Perkins, *J. Chem. Soc. C* **1970**, 298; D. L. DeJongh, G. N. Evenson, *J. Org. Chem.* **1972**, *37*, 2152.
[5] A. J. Gordon, *J. Org. Chem.* **1970**, *35*, 4261; D. C. DeJongh, G. N. Evenson, *Tetrahedron Lett.* **1971**, 4093.
[6] Crystal structure analysis of **2**: triclinic, space group $P\bar{1}$, a = 8.108(4), b = 14.204(7), c = 14.288(7) Å, α = 74.35(4), β = 76.08(3), γ = 76.04(3)°, V = 1510 Å^3, Z = 4; 4979 independent reflections measured (four-circle diffractometer, $Mo_{K\alpha}$ radiation, ω scan); refinement against F^2 [9] with all reflections, C, B, and N anisotropic, H atoms isotropic in calculated positions (342 parameters), $R1$ = 0.066 (for 2350 observed reflections $I > 2\sigma(I)$) $wR2$ = 0.207 (for all reflections) [10].
[7] Crystal structure analysis of **5b**: monoclinic, space group $P2_1/n$, a = 8.762(11), b = 15.35(2), c = 14.20(2) Å, β = 91.51(10)°, V = 1909 Å^3, Z = 4; 3329 independent reflections measured (four-circle diffractometer, $Mo_{K\alpha}$ radiation, ω scan); refinement against F^2 [9] with all reflections, C, B, and N anisotropic, H atoms isotropic in calculated positions (230 parameters), $R1$ = 0.076 (for 1560 observed reflections $I > 2\sigma(I)$) $wR2$ = 0.217 (for all reflections) [10].
[8] D. F. Gaines, R. Schaeffer, *J. Am. Chem. Soc.* **1964**, *86*, 1505; R. E. Schirmer, J. H. Noggle, D. F. Gaines, *ibid.* **1969**, *91*, 6240.
[9] G. M. Sheldrick, SHELXL93, Universität Göttingen, **1993**.
[10] Further details of the crystal structure investigation may be obtained from the Fachinformationszentrum Karlsruhe, D-76344 Eggenstein-Leopoldshafen (FRG) on quoting the depository numbers CSD-400825 (**2**), -400824 (**5b**).

C_2H_2Si Isomers: Generation by Pulsed Flash Pyrolysis and Matrix-Spectroscopic Identification**

Günther Maier,* Hans Peter Reisenauer, and Harald Pacl

The matrix-spectroscopic identification[1] and photochemical interconversion[1] of the isomeric carbenes cyclopropenylidene (**1**), propynylidene (**2**), and propadienylidene (**3**) are of interest in many ways. For one, the isolation of **1**–**3** as well as their chlorinated[2] and fluorinated[3] derivatives serves to illustrate the potential of matrix isolation spectroscopy. In addition, the structural assignments for these species are based on the comparison of the experimentally observed and calculated IR spectra and therefore emphasize the importance of simultaneously applying quantum chemical calculations and spectroscopic measurements. Moreover, reactions **1** ⇌ **2** ⇌ **3** are carbene–carbene rearrangements, and only few examples exist for this class of reactions. Lastly, **1**[4] and **3**[5] have also been shown to play a decisive role in the chemistry of interstellar clouds.[6]

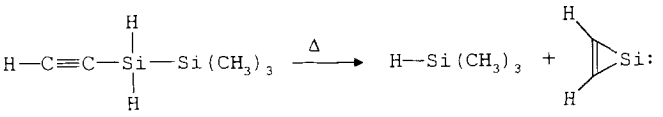


According to calculations by H. F. Schäfer et al.[7] **6** is expected to be the most stable C_2H_2Si species. Thus, it has been discussed as the adduct of a Si atom with acetylene.[8, 9] H. Schwarz et al. have shown[10] that if one ionizes chlorotrimethylsilane in the gas phase, neutralization–reionization mass spectrometry allows

[*] Prof. Dr. G. Maier, Dr. H. P. Reisenauer, Dipl.-Chem. H. Pacl
Institut für Organische Chemie der Universität
Heinrich-Buff-Ring 58, D-35392 Giessen (FRG)
Telefax: Int. code + (641) 702-5712

[**] Hetero π Systems, Part 20. This work was supported by the Fonds der Chemischen Industrie and the Deutsche Forschungsgemeinschaft. – Part 19: ref. [17].

detection of a particle whose connectivities are indicative of structure **6**.

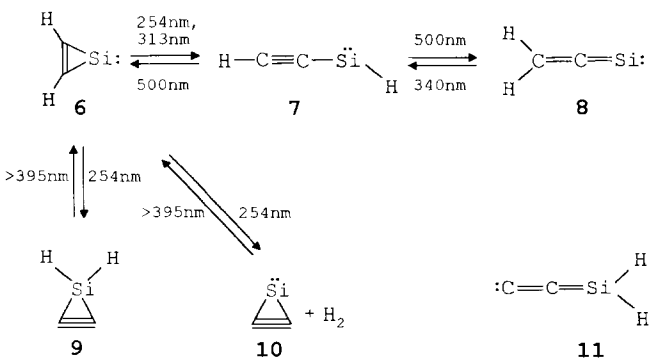


4 **5** **6**

Better experimental access to the C_2H_2Si potential energy surface is offered by pyrolysis of 2-ethynyl-1,1,1-trimethyldisilane (**4**). Compound **4** can be prepared by reaction of 1,1,1-trimethyl-2-phenyldisilane[11] with trifluoromethanesulfonic acid (toluene, 4 h, room temperature)[12] to give the corresponding triflate. The triflate is then treated with mesityllithium (15 min, −40 °C) to form 2-mesityl-1,1,1-trimethyldisilane (44%), which upon further reaction with trifluoromethanesulfonic acid (pentane, 4 h, 0 °C)[13] and treatment with sodium acetylide (suspension in diethyl ether) yields **4**. The reaction product is distilled under vacuum and isolated by preparative gas chromatography [silicon phase OV 101, 175 °C; yield: 25%; ^{1}H NMR (capillary): $\delta = 0.89$ (s, 9H, $Si(CH_3)_3$), 3.00 (t, $^4J(H,H) = 1.5$ Hz, 1H, H–C), 4.34 (d, $^4J(H,H) = 1.5$ Hz, 2H, SiH_2); ^{13}C NMR: $\delta = -1.0$ ($Si(CH_3)_3$), 80.4 ($CSiH_2$), 98.3 (HC); ^{29}Si NMR: $\delta = -85.7$ (SiH_2), −16.3 ($Si(CH_3)_3$)].

Gaseous mixtures of disilane **4** and argon (1:1000–2000) were subjected to flash pyrolysis at various temperatures and pressures. After leaving the hot zone the reaction products were directly condensed onto a CsI or BaF_2 window at 10 K. The matrix-isolated products were studied by IR and UV/VIS spectroscopy. Under the conditions of *high-vacuum* flash pyrolysis (quartz tube: diameter 8 mm, length of heated zone 5 cm; ca. 10^{-3} mbar, 600 °C) only trimethylsilane (**5**) and small amounts of acetylene were detected. Any C_2H_2Si isomer that might have formed was too unstable to be detected under these pyrolysis conditions.

Pulsed flash pyrolysis proved more successful. The gaseous mixture (regulated by a pulsed magnetic valve) was expanded through a corundum tube (inner diameter 1 mm, length of heated zone 10 mm, heated to ca. 1100 °C by a tungsten resistance wire)[14] directly into the high vacuum of the cryostat. The products were condensed onto the matrix window at 10 K.



6 **7** **8**

9 **10** **11**

Under these pyrolysis conditions the IR spectrum shows, apart from the bands for trimethylsilane (**5**), those of another compound. This compound is identified as 1-silacyclopropenylidene (**6**)—even though the structure of reactant **4** suggests formation of ethynylsilanediyl (ethynylsilylene) (**7**)—by comparison with the IR spectra for **6**, **7**, and **8** calculated by ab initio methods in 1986.[7a] Furthermore, **6** exhibits a weak, broad UV absorption between 320 and 260 nm ($\lambda_{max} = 286$ nm). Irradiation into this band with monochromatic light of wavelength 313 nm results in a rearrangement to give ethynylsilanediyl (**7**). During this photoreaction only the absorbances of **6** and **7** change, and thus the IR and UV/VIS spectra of both compounds can be determined by subtraction. Figure 1 shows the difference IR spectrum and the calculated spectra for **6** and **7**.[7a]

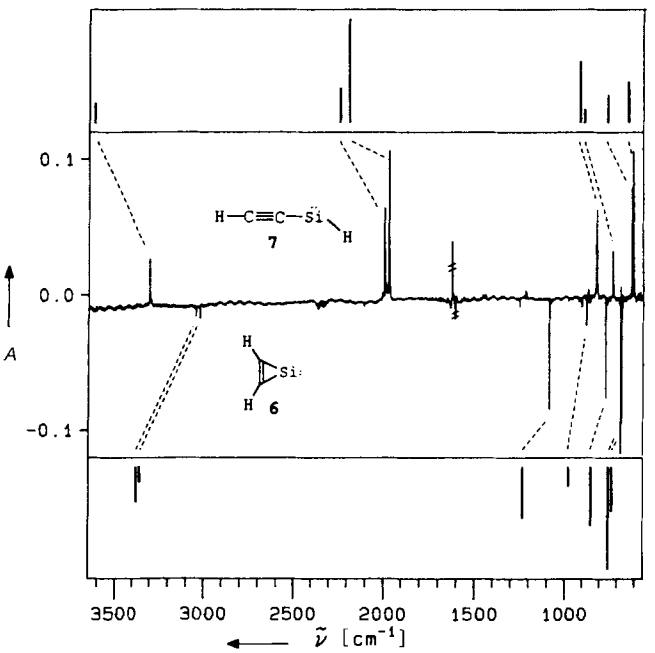


Fig. 1. IR spectra of **6** and **7**. Middle: difference IR spectrum for the photoreaction **6** → **7** (Ar matrix, 10 K). Top: calculated [7a] IR spectrum for **7**. Bottom: calculated [7a] IR spectrum for **6**; IR bands due to water have been crossed.

Particularly characteristic for **7** are the bands of the CH (3304.1 cm^{-1}), the CC (1995.5 cm^{-1}), and the SiH (1969.5 cm^{-1}) stretching vibrations. The spectral pattern of the remaining bands at lower wavenumbers (cf. Table 1) is also in satisfactory agreement with the calculation.

Table 1. Experimentally determined IR absorptions (argon matrix, 10 K) of **6**–**9** ([cm^{-1}]; relative integrated intensities in parentheses).

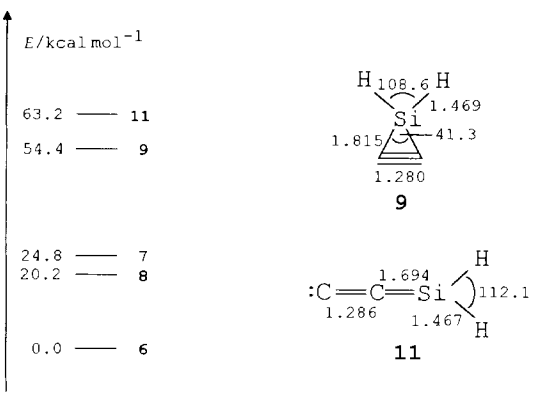
6	**7**	**8**	**9**
3048.5 (10)	3304.1 (31)	1667.5 (100)	2228.9 (49)
3026.3 (9)	1995.5 (27)	957.5 (100)	2214.4 (49)
1085.8 (87)	1969.5 (100)		1769.9 (7)
875.1 (26)	1216.0 (3)		1023.1 (100)
761.8 (56)	814.8 (49)		836.5 (50)
677.4 (100)	722.7 (14)		600.7 (7)
672.1 (90)	613.8 (32)		
	605.1 (41)		

This is also true for 1-silacyclopropenylidene (**6**) (cf. Table 1). In accordance with the calculation its IR spectrum shows two bands for the CH stretching vibrations (3048.5 and 3026.3 cm^{-1}) and five additional absorptions between 1100 and 600 cm^{-1}, which, by calculation, can be attributed to HCSi bending vibrations and SiC stretching vibrations. A band for the CC stretching vibration is not observed; theory[7b] predicts a corresponding

band at 1569 cm^{-1} in the IR spectrum with a relative intensity of $<1\%$, which is apparently too weak to be detected.

For silanediyl (**7**) a broad absorption band is recorded in the visible region of the spectrum ($\lambda_{max} = 500$ nm). It is therefore not surprising that irradiation of **7** with visible light of wavelength 500 nm mainly leads to reisomerization to give 1-silacyclopropenylidene (**6**). A small amount of a new species is also formed, and two weak IR bands at 1667.5 and 957.5 cm^{-1} and a UV band with fine structure (λ = 340, 325, and 310 nm) are recorded. Irradiation into this absorption (λ = 340 nm) leads to reisomerization to **7**; hence, this species is another isomer of C_2H_2Si. By comparison with the calculated IR spectra this isomer is identified as vinylidenesilanediyl (**8**), for which the strongest IR band (CC stretching vibration) is predicted at 1859 cm^{-1}.[7a]

Irradiation of **6** with light of wavelength λ = 254 nm leads to the formation of **7** and two new compounds. One of these can easily be identified by its characteristic IR bands at 1745.3/1741.0 and 826.4 cm^{-1} (ref. [15a–c]: 1741 and 824 cm^{-1}) and by its electronic transition band[15c] as the well-known,[15d] cyclic C_2Si (**10**). The second compound shows IR absorptions at 2228.9 and 2214.4 cm^{-1}, which are typical for SiH_2 groups (symmetric and asymmetric SiH stretching vibrations). Furthermore, a weak band at 1769.9 cm^{-1} and additional bands at 1023.1, 836.5, and 600.7 cm^{-1} are observed. Therefore, the fourth isomer must either be of constitution **9** or **11**. Silacyclopropyne (**9**) was initially dismissed as an unlikely candidate, as calculations[7a] indicate that this structure represents a transition state. Thus, it was important to calculate IR spectra for **9** and **11**, something that had not previously been done. Calculations at the MP2/6-31G** level[16] led to two important findings. Firstly, when the electron correlation energy is taken into account (cf. Scheme 1) **9** is a minimum. Secondly, the experimentally



Scheme 1. Relative energies E[kcal mol^{-1}] calculated at the MP2/6-31G** level for the isomers **6**–**9** and **11** (energy minima) and optimized geometries (bond lengths [Å] and angles [°]) for **9** and **11**.

measured and calculated spectra are in satisfactory agreement for **9**, but not for **11** (cf. Scheme 1 and Table 2). We therefore prefer the structure of silacyclopropyne (**9**) for the fourth isomer.

Table 2. IR absorptions for **9** and **11** ([cm^{-1}], absolute intensities [km mol^{-1}] in parentheses) calculated at the MP2/6-31G** level.

9		**11**	
2371 (148)	819 (88)	2391 (100)	690 (78)
2362 (127)	697 (68)	2374 (74)	684 (73)
1779 (<1)	420 (114)	1967 (345)	122 (<1)
1102 (214)	375 (0)	1052 (126)	120 (<1)
858 (106)		798 (10)	

This is also supported by the observation that the bands at 1769.9 (CC stretching vibration) and 836.5 cm^{-1} (symmetric CSi stretching vibration) have similar positions in the C_2Si molecule **10** (1745.3/1741.0 and 826.4 cm^{-1}, respectively). The band at 836.5 cm^{-1} is assigned to the calculated absorption at 858 cm^{-1}. Theory predicts a second, relatively intense band at 819 cm^{-1}. As this absorption is missing in the experimentally recorded spectrum, the question arises whether further calculations at a higher level are necessary. We will attempt to definitively assign the structure of **9** by studying a ^{13}C isotopomer. To the best of our knowledge **9** would represent the first example of a cyclopropyne.

Upon irradiation ($\lambda > 395$ nm) compound **9** is transformed into **6** (therefore, both compounds are indeed isomers). Simultaneously, C_2Si (**10**), which is formed concurrently with **9**, reacts with eliminated hydrogen that is trapped in the same matrix cage to also give **6**. Trapping reactions of this kind have also been observed for various other unsaturated silicon compounds.[17]

Received: January 27, 1994 [Z 6651 IE]
German version: *Angew. Chem.* **1994**, *106*, 1347

[1] a) H. P. Reisenauer, G. Maier, A. Riemann, R. W. Hoffmann, *Angew. Chem.* **1984**, *96*, 596; *Angew. Chem. Int. Ed. Engl.* **1984**, *23*, 641; b) G. Maier, H. P. Reisenauer, W. Schwab, P. Čársky, B. A. Hess, Jr., L. J. Schaad, *J. Am. Chem. Soc.* **1987**, *109*, 5183–5188; c) G. Maier, H. P. Reisenauer, W. Schwab, P. Čársky, V. Špirko, B. A. Hess, Jr., L. J. Schaad, *J. Chem. Phys.* **1989**, *91*, 4763–4773.

[2] G. Maier, T. Preiss, H. P. Reisenauer, B. A. Hess, Jr., L. J. Schaad, *J. Am. Chem. Soc.*, **1994**, *116*, 2014–2010.

[3] G. Maier, T. Preiss, H. P. Reisenauer, *Chem. Ber.*, **1994**, *127*, 779–782.

[4] a) P. Thaddeus, J. M. Vrtilek, C. A. Gottlieb, *Astropyhs. J.* **1985**, *299*, L63–L66; b) N. G. Adams, D. Smith, *ibid.* **1987**, *317*, L25–L27.

[5] a) J. Cernicharo, C. A. Gottlieb, M. Guélin, T. C. Killian, G. Paubert, P. Thaddeus, J. M. Vrtilek, *Astrophys. J.* **1991**, *368*, L38–L41; b) C. A. Gottlieb, T. C. Killian, P. Thaddeus, P. Botschwina, J. Flügge, M. Oswald, *J. Chem. Phys.* **1993**, *98*, 4478–4485.

[6] For the interstellar chemistry of Si-containing molecules, see ref. [10].

[7] a) G. Frenking, R. B. Remington, H. F. Schäfer III, *J. Am. Chem. Soc.* **1986**, *108*, 2169–2173; b) G. Vacek, B. T. Colgrave, H. F. Schäfer III, *ibid.* **1991**, *113*, 3192–3193. c) For the calculation of energies and rotational constants see: D. L. Cooper, *Astrophys. J.* **1990**, *354*, 229-231; for additional literature see ref. [10].

[8] a) D. Husain, P. E. Norris, *J. Chem. Soc. Faraday Trans. 2* **1978**, *74*, 106–114; b) S. C. Basu, D. Husian, *J. Photochem. Photobiol. A* **1988**, *42*, 1–12.

[9] M.-D. Su, R. D. Amos, N. C. Handy, *J. Am. Chem. Soc.* **1990**, *112*, 1499–1504.

[10] R. Srinivas, D. Sülzle, T. Weiske, H. Schwarz, *Int. J. Mass Spectrom. Ion Processes* **1991**, *107*, 369–376.

[11] a) E. Hengge, G. Bauer, H. Marketz, *Z. Anorg. Allg. Chem.* **1972**, *394*, 93–100; b) D. Littmann, Dissertation, Universität Gießen, **1985**.

[12] W. Uhlig, *Chem. Ber.* **1992**, *125*, 47–53.

[13] This "detour" is necessary in order to achieve sufficiently different boiling points during workup between the split-off benzene derivative (mesitylene), ethynyldisilane (**4**), and the solvent.

[14] Pulsing is imperative in order to achieve the high vacuum necessary in the matrix apparatus, which is directly flanged to the pyrolysis tube, and to generate a sufficiently high particle density at the moment of pyrolysis so that energy is not transferred via the wall of the reaction vessel (species **6**–**9** would stick to the vessel wall) but instead by molecule collisions. Experimental parameters: duration of pulse: 0.2 s, equivalent to ca. 1 mL gas mixture at 1000 mbar per pulse; pulse frequency: 10 pulses per minute.

[15] a) R. A. Shepherd, W. R. M. Graham, *J. Chem. Phys.* **1985**, *82*, 4788–4790; b) *ibid.* **1988**, *88*, 3399–3401; c) W. Weltner, Jr., D. McLeod, Jr., *ibid.* **1964**, *41*, 235–245; d) B. Kleman, *Astrophys. J.* **1956**, *123*, 162–165.

[16] Gaussian 92, Revision B: M. J. Frisch, G. W. Trucks, M. Head-Gordon, P. M. W. Gill, M. W. Wong, J. B. Foresman, B. G. Johnson, H. B. Schlegel, M. A. Robb, E. S. Replogle, R. Gomperts, J. L. Andres, K. Raghavachari, J. S. Binkley, C. Gonzales, R. L. Martin, D. J. Fox, D. J. Defrees, J. Baker, J. J. P. Stewart, J. A. Peple, Gaussian Inc., Pittsburgh, PA, USA, **1992**.

[17] G. Maier, J. Glatthaar, *Angew. Chem.* **1994**, *106*, 486–488; *Angew. Chem. Int. Ed. Engl.* **1994**, *33*, 473–475.

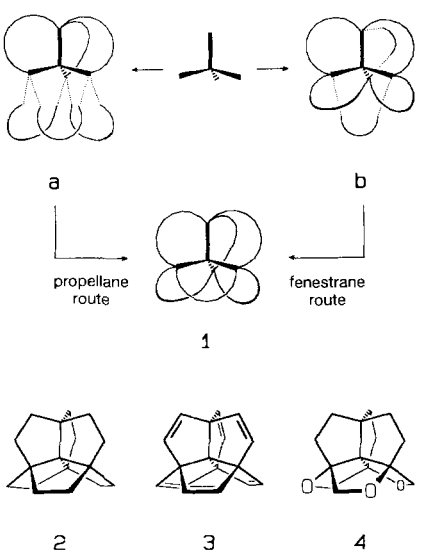
 © VCH Verlagsgesellschaft mbH, D-69451 Weinheim, 1994 0570-0833/94/1212-1250 $ 10.00+.25/0

Synthesis of Centrohexacyclic Hydrocarbons by the Propellane Route: Centrohexaindan and Tribenzocentrohexaquinane**

Dietmar Kuck,* Bernd Paisdor, and Detlef Gestmann

Dedicated to Dr. Howard E. Simmons, Jr. on the occasion of his 65th birthday

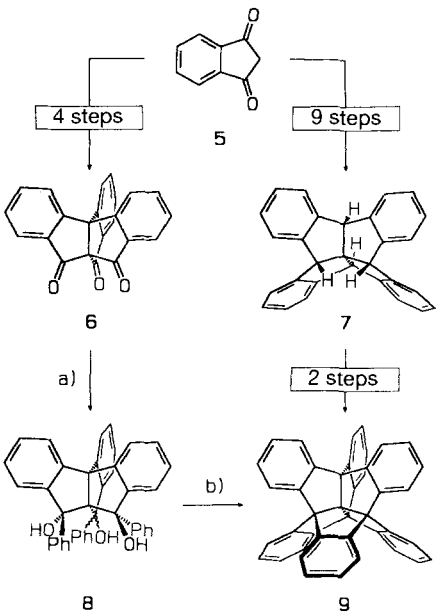
The construction of centrohexacyclic hydrocarbon frameworks with the general structure **1** (centrohexacyclanes;[1] Scheme 1) continues to present a challenge in organic polycycle chemistry. In these types of structures six annelated carbocycles share a central neopentane unit of five quaternary carbon atoms and form a microlattice with nonplanar topology.[2] The compounds with six centrally annelated cyclopentane rings should be relatively strain-free.[1, 3] Thus relatively undistorted frameworks of, for example, perhydrotriquinacene and all-*cis*-[5.5.5.5]fenestrane can be found in the yet unknown parent structure, centrohexaquinane **2**, which can be considered to be the condensation center of four pentagon dodecahedrane units.[1] Nevertheless, synthetic routes to **2** and centrohexaquinacene **3**, which was first



Scheme 1.

proposed in 1978,[4] must take into account considerable steric compression and/or fragmentation between the components that are to be joined. Therefore, not surprisingly, centrohexacyclic hydrocarbons[5, 6] and the corresponding heterocycles[7–9] have remained quite rare. Only one directed synthesis of a centrohexacyclic hydrocarbon framework was reported previously, namely the synthesis of the sixfold benzoannelated derivative of **2**, centrohexaindan **9**.[5] We have now discovered a new route to **9** and centrohexacyclic triethers related to the "Simmons–Paquette molecule" **4**[8, 9] and have developed a synthesis of the novel tribenzocentrohexaquinanes.

In our first synthesis of **9** the already highly condensed fenestrindan **7**, which is thus protected against fragmentation, was bridged twice (route **b** to **1** in Scheme 1 and route **5** → **7** → **9** in Scheme 2). A newer alternative synthesis, the propellane route, starts with 9,10,11-triptindantrione **6**,[10] a [3.3.3]propellane accessible from 1,3-indandione **5** in only four steps (route **a** to **1** in Scheme 1 and route **5** → **6** → **8** → **9** in Scheme 2).



Scheme 2. Synthesis of centrohexaindan **9** by the propellane route and by the fenestrane route. **5** → **6**: ref. [10]; **5** → **9**: ref. [5]. a) PhLi (20 mol) in benzene/Et_2O/c-C_6H_{12}; H_2O; b) H_3PO_4/xylene, Δ; yield 40% of **6**.

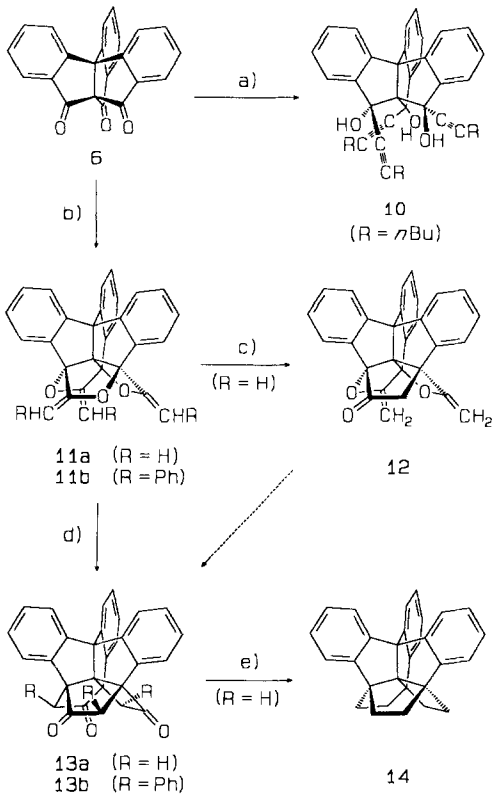
Three equivalents of aliphatic Grignard compounds like CH_3MgBr and $C_6H_5CH_2MgBr$ can be added to triptindantrione **6** with remarkable ease and without ring opening. Only two equivalents of phenylmagnesium bromide react with **6**;[10] however, threefold addition is possible if phenyllithium is employed in a poorly solvating medium. After hydrolysis a mixture of isomeric triols **8** is obtained, which can be cyclodehydrated with acid catalysis to give **9**. These two steps, in which a total of six C–C bonds are formed, conclude the synthesis of centrohexaindan **9** from **5** in only six steps and with a total yield of up to 24%.[11]

The propellane route was then used for the first construction of centrohexaquinanes with *partial* benzoannelation. The synthesis of tribenzocentrohexaquinane **14** is shown in Scheme 3. In this synthesis a C_2 synthon was required which, in analogy to the sequence **6** → **8** → **9**, would undergo threefold nucleophilic addition to **6** and subsequent cyclization to yield the triquinacene framework complementary to the [3.3.3]propellane unit. Neither the application of the strategies used by Simmons III and Maggio,[8] and by Paquette et al.[9] (e.g. rearrangement of a trispiro[[3.3.3]propellanetris(oxirane)] to **4**) to the triptindan system nor other approaches of our own were successful.[10, 12, 13] A surprisingly direct route to **14** and interesting derivatives is based on the threefold reaction of **6** with lithium acetylides.

Unexpectedly, the reaction of triptindantrione **6** with three equivalents of lithium acetylide in THF furnishes not triol **10** (R = H) but tris(enol ether) **11a**, the first derivative of the "Simmons–Paquette molecule" **4**. The excessive steric bulk of the neopentane core of the triptindan framework apparently favors the nucleophilic addition of the intermediate alcoholate to the *syn*-1,3-ethynyl group.[14] The intramolecular additions can be completed by treating the reaction mixture with aqueous sodi-

[*] Dr. D. Kuck, Dr. B. Paisdor, Dipl.-Chem. D. Gestmann
Fakultät für Chemie der Universität
Universitätsstrasse 25, D-33615 Bielefeld (FRG)
Telefax: Int. code + (521) 106-6146

[**] Benzoannelated Centropolyquinanes, Part 18. This work was supported by the Deutsche Forschungsgemeinschaft. – Part 17: [7b].



Scheme 3. a) *n*BuCCH/*n*BuLi, THF, 20 °C, then H_2O, Na_2CO_3; b) C_2H_2 or PhCCH/*n*BuLi, THF, $T = -80$ °C → 20 °C or $T = 20$ °C, respectively, then H_2O, Na_2CO_3; c) decalin, 300 °C, 4 h; d) decalin, 300 °C, 24 h; e) $N_2H_4 \cdot H_2O$, diethylene glycol, KOH, $T = 140$ → 210 °C.

Table 1. Physical and spectroscopic data for compounds **11**, **13**, and **14**.

11a: Colorless crystals, m.p. >360 °C; ^{1}H NMR (300 MHz, $CDCl_3$, TMS): δ = 4.61, 4.67 (AB spectrum, ^2J = 2.8 Hz, 6H), 7.38 (m, 6H), 7.54 (d, 3H), 7.78 (d, 3H); IR (KBr): $\tilde{\nu}$ = 1656 cm^{-1} (C=C); MS (EI, 70 eV): *m/z*: 414 ($M^{+\cdot}$, 36), 386 (36), 358 (42), 330 (100); HRMS: ($C_{29}H_{18}O_3$) calcd 414.1256; found 414.1265

11b: Colorless crystals, m.p. 272 °C; ^{1}H NMR (300 MHz, $CDCl_3$, TMS): δ = 5.97 (s, 3H), 7.14 (t, 3H), 7.30 (t, 6H), 7.41 (m, 6H), 7.66 (d, 6H), 7.74 (m, 3H), 7.80 (m, 3H); IR (KBr): $\tilde{\nu}$ = 1671 cm^{-1} (C=C); MS (EI, 70 eV): *m/z*: 642 ($M^{+\cdot}$, 100), 614 (20), 586 (35), 558 (16); HRMS: ($C_{47}H_{30}O_3$) calcd 642.2195; found 642.2186

13a: Colorless crystals, m.p. >360 °C; ^{1}H NMR (300 MHz, $CDCl_3$, TMS): δ = 2.84, 3.27 (AB spectrum, $|^2J|$ = 19.6 Hz, 6H), 7.30 (m, 9H), 7.84 (d, 3H); IR (KBr): $\tilde{\nu}$ = 1745 cm^{-1} (C=O); MS (EI, 70 eV): *m/z*: 414 ($M^{+\cdot}$, 49), 386 (41), 358 (39), 330 (100); HRMS: ($C_{29}H_{18}O_3$) calcd 414.1256; found 414.1257

13b: Colorless crystals, m.p. 298 °C; ^{1}H NMR (300 MHz, $CDCl_3$, TMS): δ = 4.74 (s, 3H), 6.34 (d, ^3J = 7.8 Hz, 3H), 6.50 (br. d, ^3J = 7.0 Hz, 6H), 6.90 (td, ^3J = 7.5 Hz, ^4J = 0.8 Hz, 3H), 7.05 (t, $^3J \approx 7.5$ Hz, 6H), 7.14 (d, $^3J \approx 7.4$ Hz, 3H), 7.27 (td, ^3J = 7.5 Hz, ^4J = 0.9 Hz, 3H), 7.82 (d, ^3J = 7.8 Hz, 3H); IR (KBr): $\tilde{\nu}$ = 1741 cm^{-1} (C=O); MS (EI, 70 eV): *m/z*: 642 ($M^{+\cdot}$, 100), 614 (53), 586 (75), 558 (32); HRMS: ($C_{47}H_{30}O_3$) calcd 642.2195; found 642.2194

14: Colorless crystals, m.p. 264 °C; ^{1}H NMR (250 MHz, $CDCl_3$, TMS): δ = 1.93, 2.17 (AA'BB' spectrum, 12H), 7.10 7.25 (m, 9H), 7.67 (d, ^3J = 7.4 Hz, 6H); MS (EI, 70 eV): *m/z*: 372 ($M^{+\cdot}$, 100), 358 (13), 343 (15), 329 (13), 316 (15); ^{13}C NMR (62.9 MHz, $CDCl_3$, TMS): δ = 39.83 (t, CH_2), 65.88 [s, *C*(C)(Ar)(CH_2)$_2$)], 77.22 [s, C(Ar)$_3$], 123.58 (t), 124.25 (t), 127.58 (t), 127.63 (t), 148.36 (s), 150.34 (s), the signal of the centro-C atom is missing; HRMS: ($C_{29}H_{24}$) calcd 372.1878; found 372.1879

um carbonate; unfortunately, the yield of **11a** is only 25%. The analogous reaction with phenylacetylene provides **11b** in 27% yield, but so far the reaction with 1-hexyne has only given triol **10** (R = *n*Bu).

Tris(enol ether)s **11** are characterized by mass spectrometry and IR and NMR spectroscopy (Table 1). The high molecular symmetry is reflected in the simple ^{1}H and ^{13}C NMR spectra; the AB pattern of the signals for the olefinic methylene protons of **11a** (^2J = 2.8 Hz) is particularly characteristic. In the mass spectra of the enol ethers the elimination of up to three equivalents of CO is evident in the upper mass range. This indicates that heterocycles **11a** and **11b** rearrange to the corresponding carbocycles **13a** and **13b** not only in the mass spectrometer, but possibly also on the preparative scale. Whereas attempts with Brønsted and Lewis acids (H_2SO_4/H_2O/THF, $AlBr_3/CH_2Cl_2$) and with $LiCl_4$/ether[15] were not successful, the thermolysis[16] of **11a** in decalin at 300 °C provided the desired trione **13a** in 30%; **11b** was converted diastereoselectively into the triphenyl derivative **13b** in even 60% yield.[17] As expected, the mass spectra of the two triones are very similar to those of compounds **11**, but features typical of cyclopentanone rings are observed in the ^{1}H and ^{13}C NMR, and IR spectra, for example an AB spectrum with $^2J = -19.6$ Hz (**13a**). Thermolysis of **11a** for shorter periods resulted in the product of a single rearrangement, monoketone **12**. The parent compound of the new centrohexacycles, tribenzohexaquinane **14**, was obtained by Wolff–Kishner reduction of **13a** and also characterized unequivocally (Table 1).

We are currently trying to convert centrohexaquinanetrione **13** into the corresponding (unsaturated) tribenzocentrohexaquinacenes. These types of triquinanetriones and triquinacenes, which have their convex molecular faces completely shielded,[18, 19] may be key intermediates in new, promising approaches to pentagon dodecahedranes from two triquinacene units.[18c, 18d, 20–22]

In conclusion we note that the propellane route described here for the construction of centrohexacyclic hydrocarbons may serve as an example of how the a priori unfavorable steric relations mentioned at the beginning of this report may also be advantageous for such compact structures. The remarkably facile formation of tris(enol ether) **11** is apparently a result of a proximity effect, and the subsequent consecutive rearrangements do not provide any possibility for the fragmentation of the molecular framework. The next particularly challenging step is determining whether the new propellane route leading to benzoannelated centrohexaquinanes like **9** and **14** may also be useful in the synthesis of the parent compound, centrohexaquinane **2**.

Experimental Procedure

9: A suspension of **6** (3.36 g, 10.0 mmol) in 250 mL of benzene was prepared with exclusion of air and moisture. A solution of phenyllithium (2 M, 100 mL) in diethyl ether/cyclohexane was then added and the reaction mixture heated at 40 °C for 12 h. After hydrolysis the organic phase was dried and concentrated, and the biphenyl formed removed by Kugelrohr distillation. The remaining triol **8** was dissolved in 250 mL of xylene and treated with 5 mL of orthophosphoric acid, and the reaction mixture was heated for 24 h with a water separator. After the reaction mixture had cooled, the organic layer was decanted off, dried over sodium sulfate, and concentrated. The brown residue was filtered over silica gel ($CHCl_3$) and recrystallized from dichloromethane/hexane. Pure **9** (MS, NMR [5]) was obtained as colorless needles (2.07 g, 40%).

11a and **11b**: A suspension of **6** (3.36 g, 10.0 mmol) in 200 mL of THF was added dropwise over 30 min to a solution of lithium acetylide [23] (1.06 g, 33.0 mmol) in 200 mL of THF cooled at −90 °C. The temperature was not allowed to exceed −80 °C during the addition. After the addition was complete, the red-brown solution was stirred for 60 min before it was allowed to warm to room temperature. Water (80 mL) and then solid Na_2CO_3 were added until the aqueous layer had a pulpy consistency. After a further 12 h of stirring, the organic layer was decanted off and the residue washed with $CHCl_3$ (2 × 200 mL). The combined organic layers were dried with Na_2SO_4 and concentrated. Column chromatography on silica gel ($CHCl_3$/hexane) provided **11a** (1.04 g, 25%). – When lithium phenylacetylide (3.57 g, 33.0 mmol) was used and the reaction conducted at room temperature, **11b** (1.73 g, 27%) was obtained after analogous workup.

13a and **13b**: A mixture of **11a** (200 mg, 480 μmol) or **11b** (200 mg, 310 μmol), 8 mg of hydroquinone, and 10 mL of anhydrous decalin was sealed under nitrogen in a thick-walled glass ampule and heated at 300 °C in an oven for 24 h. After cooling to room temperature, the light brown reaction solution was treated with pentane to precipitate the product as a beige powder, which was washed with pentane and

purified by column chromatography (silica gel, CH_2Cl_2/ethyl acetate 60:1) to give **13a** (60 mg, 30%) or **13b** (120 mg, 60%).

14: Triketone **13** (16.0 mg, 38.6 μmol) was heated with 5 mL of diethylene glycol, 1 mL of hydrazine hydrate, and 50 mg of KOH at 140 °C for 3 h and then at 210 °C for 4 h. The reaction mixture was allowed to cool, 5 mL of water was added, and the mixture was extracted with $CHCl_3$ (2 × 10 mL). Filtration through silica gel ($CHCl_3$) gave **14** (3.0 mg, 21%).

Received: January 26, 1994 [Z6645IE]
German version: *Angew. Chem.* **1994**, *106*, 1326

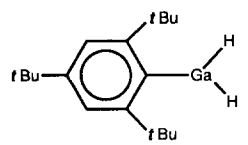
[1] P. Gund, T. M. Gund, *J. Am. Chem. Soc.* **1981**, *103*, 4458–4465.
[2] Topologically nonplanar means nonplanar according to graph theory. a) D. M. Walba, *Tetrahedron* **1985**, *41*, 3161–3212; b) F. Harary in *Chemical Applications of Graph Theory* (Ed.: A. T. Balaban), Academic Press, London, **1976**, Chapter 2; c) J. Simon in *Graph Theory and Topology in Chemistry* (Eds.: R. B. King, D. H. Rouvray), Elsevier, Amsterdam, **1987**, p. 43.
[3] a) O. Ermer, *Aspekte von Kraftfeldrechnungen*, Wolfgang Baur, München, **1981**, Chapter 4.6.3; b) W. Luef, R. Keese, *Helv. Chim. Acta* **1987**, *70*, 543–553.
[4] L. A. Paquette, R. A. Snow, J. L. Muthard, T. Cynkowski, *J. Am. Chem. Soc.* **1978**, *100*, 1600–1602.
[5] a) D. Kuck, A. Schuster, *Angew. Chem.* **1988**, *100*, 1222–1224; *Angew. Chem. Int. Ed. Engl.* **1988**, *27*, 1192–1194; b) D. Kuck, A. Schuster, B. Paisdor, D. Gestmann, unpublished.
[6] R. Eckrich, D. Kuck, *Synlett* **1993**, *4*, 344–347.
[7] a) D. Kuck, A. Schuster, R. A. Krause, *J. Org. Chem.* **1991**, *56*, 3472–3475; b) D. Kuck, A. Schuster, D. Gestmann, *J. Chem. Soc. Chem. Commun.* **1994**, 609–610.
[8] a) H. E. Simmons III, J. E. Maggio, *Tetrahedron Lett.* **1981**, *22*, 287–290; b) H. E. Simmons III, PhD Thesis, Harvard University, **1980**; c) S. A. Benner, J. E. Maggio, H. E. Simmons III, *J. Am. Chem. Soc.* **1981**, *103*, 1581–1582; d) J. E. Maggio, H. E. Simmons III, *ibid.* **1981**, *103*, 1579–1581.
[9] a) L. A. Paquette, M. Vazeux, *Tetrahedron Lett.* **1981**, *22*, 291–294; b) L. A. Paquette, R. V. Williams, M. Vazeux, A. R. Browne, *J. Org. Chem.* **1984**, *49*, 2194–2197.
[10] B. Paisdor, D. Kuck, *J. Org. Chem.* **1991**, *56*, 4753–4759.
[11] We recently developed a third synthesis of **9**; see ref. [5b,7b].
[12] Three equivalents of 2-(trimethylsilyl)vinylmagnesium bromide add to triketone **6** in good yield; attempts to cyclize the resulting triptindantriol were not successful. B. Paisdor, Dissertation, Universität Bielefeld, **1989**.
[13] All attempts at the oxidative removal of several benzene rings from **9** with the goal of the conversion **9** → **2** (or **3**) have failed so far; see ref. [5b].
[14] For similar intramolecular additions see: J. S. Swenton, A. Callinan, S. Wang, *J. Org. Chem.* **1992**, *57*, 78–85.
[15] a) P. A. Grieco, *Aldrichimica Acta* **1991**, *24*, 59–66; b) P. A. Grieco, J. D. Clark, C. T. Jagoe, *J. Am. Chem. Soc.* **1991**, *113*, 5488–5489.
[16] a) Examples of the thermal rearrangement of enol ethers into ketones: S. Wang, G. W. Morrow, J. S. Swenton, *J. Org. Chem.* **1989**, *54*, 5364–5371, and references therein; b) β-phenyl substitution of the enol ethers facilitates the [1.3] rearrangement, see ref. [16a].
[17] The marked upfield shift of the three *ortho* protons of the triptindan framework of **13b** (to $\delta = 6.34$) besides that of six *ortho* protons of the phenyl groups (to $\delta = 6.50$) provides unequivocal proof of their "*exo*" orientation relative to the perhydrotriquinacene unit.
[18] Centrosubstituted triquinacenes: a) A. K. Gupta, G. S. Lannoye, G. Kubiak, J. Schkeryantz, S. Wehrli, J. M. Cook, *J. Am. Chem. Soc.* **1989**, *111*, 2169–2179; b) A. K. Gupta, U. Weiss, J. M. Cook, *Tetrahedron Lett.* **1988**, *29*, 2535–2538; c) X. Fu, J. M. Cook, *J. Org. Chem.* **1992**, *57*, 5121–5128; d) X. Fu, J. M. Cook, *Tetrahedron Lett.* **1990**, *31*, 3409–3412; e) B. Bengtson, Dissertation, Universität Hamburg, **1986**; f) see also ref. [6]; g) X. Fu, J. M. Cook, *Aldrichimica Acta* **1992**, *25*, 43–54.
[19] Centrosubstituted tribenzotriquinacenes: a) A. Schuster, D. Kuck, *Angew. Chem.* **1991**, *103*, 1717–1720; *Angew. Chem. Int. Ed. Engl.* **1991**, *30*, 1699–1702; b) D. Kuck, T. Lindenthal, A. Schuster, *Chem. Ber.* **1992**, *125*, 1449–1460, and references therein.
[20] a) D. M. Müller, *Chem. Weekbl.* **1963**, *59*, 334; b) R. B. Woodward, T. Fukunaga, R. C. Kelly, *J. Am. Chem. Soc.* **1964**, *86*, 3162–3164; c) I. T. Jacobsen, *Acta Chem. Scand.* **1967**, *21*, 2235–2246.
[21] E. Carceller, M. L. García, A. Moyano, M. A. Pericàs, F. Serratosa, *Tetrahedron* **1986**, *42*, 1831–1839.
[22] Reviews: a) *Cage Hydrocarbons* (Ed.: G. A. Olah), Wiley, New York, **1990**; b) L. A. Paquette in [22a], Chapter 9, pp. 331–335; c) W. D. Fessner, H. Prinzbach in [22a], Chapter 10, pp. 355–357; d) L. A. Paquette, *Chem. Rev.* **1989**, *89*, 1051–1065; e) P. E. Eaton, *Tetrahedron* **1979**, *35*, 2189–2223.
[23] M. M. Midland, *J. Org. Chem.* **1975**, *40*, 2250–2252.

Base-Free Monomeric Organogallium Hydrides**

Alan H. Cowley,* François P. Gabbaï, Harold S. Isom, Carl J. Carrano, and Marcus R. Bond

Information on neutral gallium mono- and dihydrides is quite sparse.[1] Structurally characterized examples of such species are confined to the dimers $[Me_2Ga(\mu\text{-}H)]_2$,[2] $[H_2Ga(\mu\text{-}Cl)]_2$,[3] $[H_2Ga(\mu\text{-}NMe_2)]_2$,[4] and $[H_2Ga(\mu\text{-}H)_2BH_2]$[5] and the novel monomer $[HGa(BH_4)_2]$ with a pentacoordinate gallium atom.[6, 7] However, the recent detection of the tricoordinate monomers $GaHCl_2$ and GaH_2Cl in argon matrices[8] suggested that monomeric organogallium hydrides might become isolable if sufficiently bulky substituents were employed.

Treatment of $[Ga(Ar)Cl_2]$[9] (Ar = 2,4,6-$tBu_3C_6H_2$) with $LiGaH_4$ in Et_2O at −78 °C afforded a 73% yield of colorless crystalline **1**. In the CI mass spectrum of **1** the base peak appears at *m/z* 315 and corresponds to $[Ga(Ar)H]^+$. This assignment was confirmed by a high-resolution mass spectrum (HRMS).[10] The detection of a terminal GaH_2 moiety in the neutral molecule was evident from the presence of infrared peaks in the terminal Ga–H stretching region ($\nu_s = 1908\ cm^{-1}$(sh), $\nu_{as} = 1887\ cm^{-1}$) and the relative intensities of the GaH_2 resonance and those of the aryl substituent in the ^1H NMR spectrum.[10] Moreover, the deshielded position of the GaH_2 resonance ($\delta = 6.41$) was suggestive of a base-free product since, for example, amine-gallane adducts exhibit hydride resonances in the range $\delta = 4.5–5.0$.[11] The monomeric nature of **1** was confirmed by an X-ray structure analysis.[12] Individual molecules of **1** (Fig. 1) reside on a crys-



1

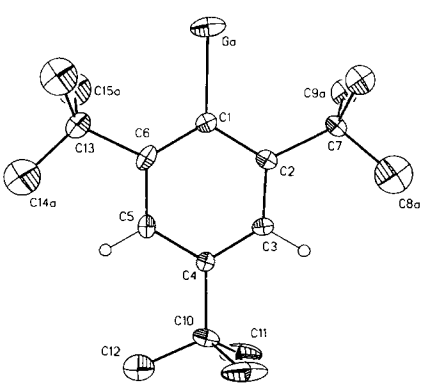


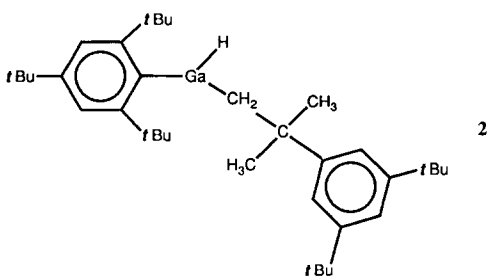
Fig. 1. View of **1** showing the atom labeling scheme. The *t*Bu groups at C2 and C6 are disordered and only the two highest occupancy methyl carbon atoms are shown. The hydrogen atoms on the gallium atom were not located. Selected distances [Å]: Ga–C1 1.942(7), Ga···C8 and Ga···C14 2.56(2).

[*] Prof. A. H. Cowley, F. P. Gabbaï, H. S. Isom
Department of Chemistry & Biochemistry
The University of Texas at Austin
Austin, TX 78712 (USA)
Telefax: Int. code + (512)471-6822
Prof. C. J. Carrano, Dr. M. R. Bond
Department of Chemistry
Southwest Texas State University
San Marcos, TX 78666 (USA)
Telefax: Int. code + (512) 245-2374

[**] This work was supported by the National Science Foundation and the Robert A. Welch Foundation.

tallographic mirror plane located at $y = 1/4$ in the space group $P2_1/m$; there are no unduly short intermolecular contacts. The *t*Bu groups at C2 and C6 are disordered about two orientations which are related by 180° rotations around the C2–C7 and C6–C13 bonds. Because of this disorder and weak scattering it was not possible to locate the hydrogen atoms on gallium in the Fourier difference map. The Ga–C bond length in **1** (1.942(7) Å) is virtually identical to that in $[Ga(Ar)Cl_2]$;[9] the Ga···C8 and Ga···C14 contacts are both short (2.56(2) Å). Compound **1** survives sublimation at 80 °C (10^{-2} Torr); however, solutions of **1** in benzene undergo rapid photolysis with 254 nm light to give Ga^0, H_2, and 1,3,5-$tBu_3C_6H_3$.

The expected product of the reaction of $[Ga(Ar)_2Cl]$[13] with $LiGaH_4$ in Et_2O at −78 °C was the monohydride $[Ga(Ar)_2H]$. However, while peaks attributable to $[Ga(Ar)_2H]^+$ and $[Ga(Ar)_2]^+$ were evident in the CI mass spectrum and a terminal Ga–H moiety was detected in the IR spectrum, the *t*Bu and aromatic C–H regions of the ^1H NMR spectrum of **2** were



2

considerably more complex than anticipated.[10] X-ray structure analysis revealed that the colorless, crystalline product is, in fact, an isomer of the target compound (Fig. 2).[12]

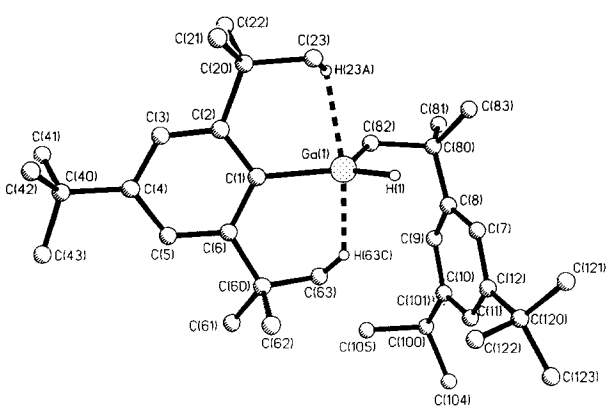
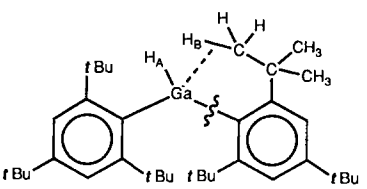


Fig. 2. View of **2** showing the atom labeling scheme. All hydrogen atoms except H(1), H(23A), and H(63C) are omitted for clarity. The *t*Bu groups at C(4) and C(10) are disordered. Important distances [Å] and angles [°]: Ga(1)–C(1) 1.983(17), Ga(1)–C(82) 1.972(17), Ga(1)–H(1) 1.43(10), C(80)–C(82) 1.551(23) Ga(1)···H(23A) 2.28(2), Ga(1)···H(63C) 2.03(2); C(1)-Ga(1)-C(82) 120.2(6), C(1)-Ga(1)-H(1) 131(5), C(82)-Ga(1)-H(1) 108(5), Ga(1)-C(82)-C(80) 119.2(11), H(23A)-Ga(1)-H(63C) 168.4(7).

The hydride **2** is monomeric in the solid state and there are no unusual intermolecular interactions. In this case it was possible to detect the hydrogen atom attached to gallium in the final Fourier difference map. Although the metric parameters are not very accurate, it is clear that the environment of the gallium atom is trigonal planar. There are no previous experimental values for a terminal Ga–H bond length involving tricoordinate gallium. The Ga–H bond length in **2** (1.43(10) Å) may be compared with the range of bond lengths (1.487–1.586 Å) established for tetra- and pentacoordinate species by gas-phase electron diffraction[2–6] and the value of 1.527 Å for $GaHCl_2$ calculated by ab initio methods.[8] The Ga–C(Ar) bond length in **2** (1.983(17)Å) is slightly longer than that in **1** (1.942(7) Å), ostensibly due to the more sterically encumbered environment in the former. A further point of structural interest relates to the short contacts between the gallium atom and one of the hydrogen atoms on each of the two *ortho*-*t*Bu groups (Fig. 2). One of these distances (Ga(1)···H(63C) = 2.03(2) Å) is shorter than the other (Ga(1)···H(23A) = 2.28(2) Å), and the calculated position of H(63C) is such that this atom points directly at the gallium center. On the other hand H(23A), which was located in the final Fourier difference map, adopts a location that places the mid-point of the C(23)–H(23A) bond near the quasi threefold axis of the gallium atom, thus suggesting the presence of an agostic interaction. Such interactions may, in fact, explain the isomerization of $[Ga(Ar)_2H]$ to **2**. As shown in Scheme 1, an agostic interaction between the gallium atom and a C–H bond of one of the *ortho*-*t*Bu methyl groups ($C-H_B$) could result in transfer of the H_B atom to the gallium atom and formation of a new Ga–C bond in concert with the cleavage of a Ga–C(*ipso*) bond and 1,2 transfer of H_A to the aryl ring.



Scheme 1. Postulated rearrangement mechanism for the isomerization to give **2**.

It is germane to point out that Meller et al.[13] have reported that $[Ga(Ar_2)Cl]$ is converted to $[Ga(CH_2CMe_2C_6H_3\{3,5\text{-}tBu_2\})(Ar)(Cl)]$ and a benzo[*b*]gallolane by heating in high vacuum at 140–160 °C. Presumably, the mechanism of this reaction is different because we do not observe gallolane formation. Moreover, the putative isomerization of $[Ga(Ar_2)H]$ to **2** takes place under significantly milder conditions (ambient pressure and a maximum temperature of 25 °C).

Finally, attempts to prepare the analogous indium hydrides have been unsuccessful so far. For example, reaction of the new monomeric indium chloride $[In(Ar)_2Cl]$ (**3**) with $LiGaH_4$ in Et_2O at −78 °C results in **1** by aryl cleavage and transmetalation.

Experimental Procedure

1: A solution of $LiGaH_4$ (8 mmol) in Et_2O (20 mL) was added to a solution of $[Ga(Ar)Cl_2]$ [8] (0.39 g, 1.0 mmol) in Et_2O (3 mL) at −78 °C. The resulting reaction mixture was allowed to warm slowly to 25 °C and was stirred for a further 20 h at this temperature. The solvent and volatiles were removed under reduced pressure and the resulting white residue was extracted with hexane (10 mL). After 3 h this stirred solution was filtered, and the volume of the filtrate reduced to 3 mL. X-ray quality crystals of **1** were grown by cooling the saturated solution to −20 °C. The yield of **1** was 73% (0.23 g). (M.p. 134 °C). Compound **2** was prepared in 42% yield by a similar procedure. (M.p. 180 °C, decomp.).

3: A slurry of $InCl_3$ (1.11 g, 5.0 mmol) in hexane (50 mL) was added to a suspension of ArLi (2.52 g, 10 mmol) in hexane (200 mL). The reaction mixture was heated to reflux for 18 h. The solvent and volatiles were removed under reduced pressure and the resulting residue was washed with pentane (3 × 20 mL). The pentane extracts were filtered through diatomaceous earth and the volume of the filtrate was reduced

by 50%. Small colorless crystals of **3** formed in 18% yield (0.58 g) after storage of this solution at −20 °C for several days. (M.p. 170 °C).

Received: January 20, 1994 [Z6636IE]
German version: *Angew. Chem.* **1994**, *106*, 1354

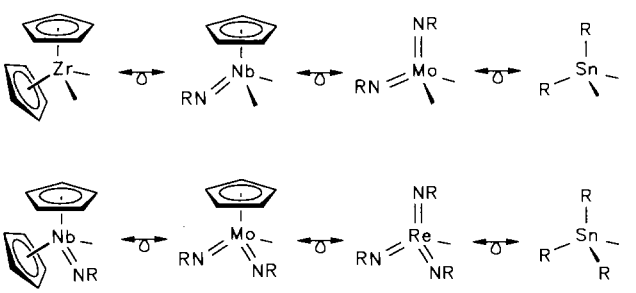
[1] *Gmelin Handbook of Inorganic Chemistry. Organogallium Compounds, Part 1*, Springer, Berlin, **1987**.
[2] P. L. Baxter, A. J. Downs, M. J. Goode, D. W. H. Rankin, H. E. Robertson, *J. Chem. Soc. Chem. Commun.* **1986**, 805.
[3] M. J. Goode, A. J. Downs, C. R. Pulham, D. W. H. Rankin, H. E. Robertson, *J. Chem. Soc. Chem. Commun.* **1988**, 768.
[4] P. L. Baxter, A. J. Downs, M. J. Goode, D. W. H. Rankin, H. E. Robertson, *J. Chem. Soc. Dalton Trans.* **1985**, 807.
[5] C. R. Pulham, P. T. Brain, A. J. Downs, D. W. H. Rankin, H. E. Robertson, *J. Chem. Soc. Chem. Commun.* **1990**, 177.
[6] M. T. Barlow, C. J. Dain, A. J. Downs, G. S. Laurensen, D. W. H. Rankin, *J. Chem. Soc. Dalton Trans.* **1982**, 597.
[7] For interesting polycycles with gallium hydride moieties, see M. J. Henderson, C. H. Kennard, C. L Raston, G. Smith, *J. Chem. Soc. Chem. Commun.* **1990**, 1203; J. L. Atwood, S. G. Bott, C. Jones, C. L. Raston, *Inorg. Chem.* **1991**, *30*, 4868.
[8] R. Köppe, M. Tacke, H. Schnöckel, *Z. Anorg. Allg. Chem.* **1991**, *605*, 35; R. Köppe, H. Schnöckel, *J. Chem. Soc. Dalton Trans.* **1993**, 3393.
[9] S. Schulz, S. Pusch, E. Pohl, S. Dielkus, R. Herbst-Irmer, A. Meller, H. W. Roesky, *Inorg. Chem.* **1993**, *32*, 3343; M. A. Petrie, P. P. Power, H. V. Rasika Dias, K. Ruhlandt-Senge, K. M. Waggoner, R. J. Wehmschulte, *Organometallics* **1993**, *12*, 1086.
[10] ^{1}H NMR (300.15 MHz, C_6D_6, 295 K, TMS): **1**: $\delta = 1.29$ (s, 18 H, *o*-*t*Bu), 1.35 (s, 9 H, *p*-*t*Bu), 6.41 (br, 2 H, GaH_2), 7.40 (s, 2 H, H-aryl). **2**: $\delta = 1.46$ (br, 2 H, CH_2), 1.70 (s, 6 H, 2 CH_3), 6.62 (br, 1 H, GaH); 3,5-*t*$Bu_2C_6H_3$: 1.23 (s, 18 H, *m*-*t*Bu), 7.40 (t, 1 H, *p*-H-aryl, *J* 1.8 Hz), 7.57 (d, 2 H, *o*-H-aryl, *J* 1.8 Hz); 2,4,6-*t*$Bu_3C_6H_2$: 1.34 (s, 9 H, *p*-*t*Bu), 1.38 (s, 18 H, *o*-*t*Bu), 7.42 (s, 2 H, H-aryl). **3**: $\delta = 1.31$ (s, 9 H, *p*-*t*Bu), 1.58 (s, 18 H, *o*-*t*Bu), 7.62 (s, 2 H, H-aryl); IR (KBr): **1**; $\tilde{\nu}$[cm^{-1}] = 2961 s, 2905 m, 2867 m, 2818 w sh, 1908 m sh, 1887 s, 1584 s, 1540 m, 1530 w, 1476 m, 1461 m, 1392 s, 1361 s, 1255 m, 1217 m, 1202 w, 1190 w, 1145 m, 1106 s br, 992 w sh, 965 m, 811 m, 767 m; **2**: $\tilde{\nu}$[cm^{-1}] = 2963 s, 2905 m, 2867 m, 1843 m, 1596 m, 1477 m, 1460 w, 1393 w, 1362 m, 1261 s, 1245 w sh, 1202 w br, 1099 s; 1023 s, 899 w, 872 m, 802 s, 725 w sh, 714 m br; **3**: ν[cm^{-1}] = 2966 s, 2901 m br, 2875 s, 1786 w, 1769 w, 1596 s, 1539 w, 1486 w sh, 1462 s, 1404 s, 1365 s, 1271 m sh, 1258 s, 1210 m, 1128 m, 1101 s, 1022 m br, 930 w, 906 m, 881 s, 811 s, 745 m. MS (CI, CH4): **1**: *m*/*z* 315 (M^+ − H, 100%); HRMS: Calculated for $C_{18}H_{30}{}^{69}Ga$ 315.1603; found 315.1590. **2**: *m*/*z* 559 (M^+ − H, 100%), 315 (M^+ − *t*$Bu_3C_6H_2$, 47%); HRMS: Calculated for $C_{36}H_{58}{}^{69}Ga$ 559.3794; found 559.3778; **3**: *m*/*z* 676 (M^- + Cl), 605 (M^+ − Cl), 395 (M^- − Ar); HRMS: Calculated for $C_{36}H_{58}InCl_2$ (M^- + Cl) 675.2954; found 675.2945. The X-ray crystal structure of **3** has been determined and will be published elsewhere.
[11] C. Jones, G. A. Koutsantonis, C. L. Raston, *Polyhedron* **1993**, *12*, 1829.
[12] Crystal structure data for **1**, $C_{18}H_{31}Ga$, monoclinic, space group $P2_1/m$, $Z = 2$, $a = 9.927(1)$, $b = 9.694(2)$, $c = 10.273(1)$ Å, $\beta = 112.58(1)°$, $V = 912.9(3)$ Å^3, $\rho_{calcd} = 1.15$ g cm^{-3}, $Mo_{K\alpha}$, $\lambda = 0.71073$ Å, $\mu = 1.489$ mm^{-1}. 1711 unique data were collected at 173 K on a Nicolet P 3 diffractometer (ω scan technique, $4.0 < 2\theta < 50.0°$). Of these, 907 have $I > 4\sigma(I)$ and were used for structure solution and refinement, $R = 0.095$. The *ortho* *t*Bu groups are disordered. The site occupation factors for C8 and C9 are 69(1)%; those for C14 and C15 are 55(1)%. The hydrogen atoms on gallium could not be located and were not included in the refinement; the other hydrogen atoms were calculated in idealized positions (C–H 0.96 Å). Crystal structure data for **2**, $C_{36}H_{59}Ga$, monoclinic, space group $P2_1/n$, $Z = 4$, $a = 9.355(2)$, $b = 27.930(6)$, $c = 14.110(3)$ Å, $\beta = 107.14(3)°$, $V = 3523.0(1)$ Å^3, $\rho_{calcd} = 1.059$ g cm^{-3}, $Mo_{K\alpha}$, $\lambda = 0.71073$ Å, $\mu = 0.801$ mm^{-1}. 4485 unique data were collected on a Siemens R 3m/V diffractometer at 298 K (2θ-θ scan technique, $3.5 > 2\theta < 45.0°$). Of these, 1567 had $I > 4\sigma(I)$ and were used for structure solution and refinement, $R = 0.0813$. Two of the *t*Bu groups are disordered. The site occupation factors are 71(3)% for C(41), C(42), and C(43); those for C(101), C(104), and C(105) are 47(2)%. Further details of the crystal structure investigations may be obtained from the Fachinformationszentrum Karlsruhe, D-76344 Eggenstein-Leopoldschafen (FRG), on quoting of depository number CSD-58075.
[13] A. Meller, S. Pusch, E. Pohl, L. Häming, R. Herbst-Irmer, *Chem. Ber.* **1993**, *126*, 2255.

The Bonding Capability of Imido Complex Fragments of Groups 5–7 with Regard to the Isolobal Relationship**

Jörg Sundermeyer* and Diane Runge

Dedicated to Professor Helmut Werner on the occasion of his 60th birthday

In bond theory organoimido and cyclopentadienyl ligands show surprising parallels.[2] If they are considered as anionic ligands, they both make a maximum of six electrons available for bonding with a metal cation.[3] Both are σ,2π-bonding ligands,[4] which form σ and π bonds with metal orbitals of the same symmetry.[5] If the $C_5R_5^-$ anion binds to a d^n-M metal center (e.g., d^0-W^{6+}) and the dianion NR^{2-} to an isoelectronic d^n-M′ metal center from the following group in the periodic table (e.g., d^0-Re^{7+}), two entities with the same electron count and comparable valence orbitals result (e.g., $[W(\eta^5\text{-}C_5R_5)]^{5+}$ or $[Re(NR)]^{5+}$). Schrock et al.[6] have already pointed out parallels in the chemistry of complexes with the entity $[M(NAr)_2]$ (M = Mo, W; Ar = 2,6-*i*$Pr_2C_6H_3$) and those containing the metallocene unit $[Cp_2M]$ (M = Ti, Zr, Hf; Cp = η^5-C_5H_5). Gibson et al. extended this relationship to the linking fragments [CpM(NR)] (M = Nb, Ta) and confirmed the isolobal character of these three complex fragments by quantum-mechanical calculations[7] and reactivity studies[8] (Scheme 1, top). Recently we reported on M–M′ coupling reactions of the two homoleptic imidoyl cations $[Re(NR)_3]^+$ and $[Mo(NR)_2]^{2+}$ (R = *t*Bu) with carbonyl metalates $[Cp_nM(CO)_m]^-$ of Groups 6–8.[9] It was shown that a direct metal–metal interaction is possible between high- and low-valent metal centers. These results prompted us to the question whether the bonding capability (concept according to R. Hoffmann[10a]) of imido complex fragments $[Cp_nM'(NR)_m]$ (M from Groups 5, 6, or 7) can be determined along the route of selective M–M′ coupling reactions, by binding representative complex fragments with these entities to the classic 17 valence electron unit $[CpFe(CO)_2]$. Extrapolation of these studies could lead to the derivation of a new isolobal relationship between carbonyl and imido complex fragments $[Cp_nM'(NR)_m]$.



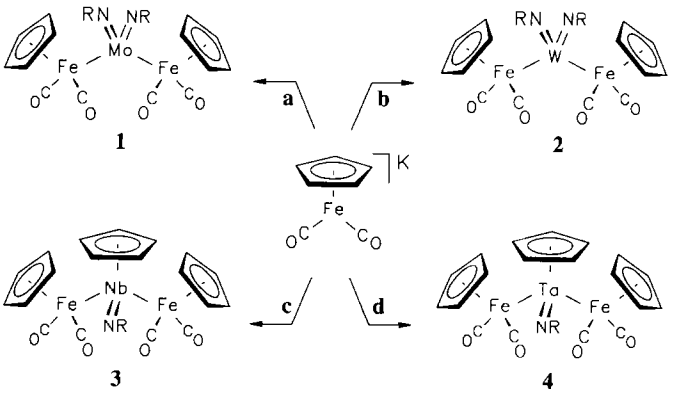
Scheme 1. Isolobal relationships in imido complex fragments.

According to the cyclopentadienyl–imido analogy, not only the homoleptic imido complex fragments $[Mo(NtBu)_2]^{2+}$ and

[*] Dr. J. Sundermeyer, Dipl.-Chem. D. Runge
Institut für Anorganische Chemie der Universität
Am Hubland, D-97074 Würzburg (FRG)
Telefax: Int. code + (931)-888-4605

[**] High-valent derivatives of the d-metal acids. Part 11. This work was supported by the Fonds der Chemischen Industrie and the Deutsche Forschungsgemeinschaft (SFB 347). We thank Professor Helmut Werner for his support and the company H. C. Starck, Goslar, for a gift of high purity grade metal oxides and chlorides. Part 10: Ref. [1].

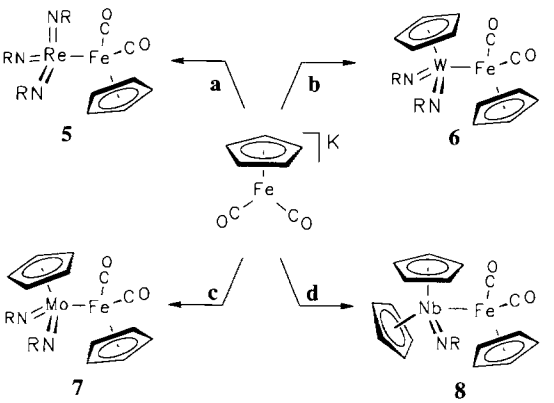
$[W(NtBu)_2]^{2+}$ can be used as building blocks for the synthesis of trinuclear complexes [Fe]–[M″]–[Fe] ([Fe] = $[CpFe(CO)_2]$), but also the metal Lewis acids of Group 5 $[CpNb(NtBu)]^{2+}$ and $[CpTa(NtBu)]^{2+}$[1] (Scheme 2). The reactions indicate that



Scheme 2. The bonding capability of electronically related imidoyl complex fragments $[Cp_nM'(NR)_m]$ of Groups 5 and 6. a) $[Mo(NtBu)_2Cl_2]$, b) $[W(NtBu)_2Cl_2(py)_2]$, c) $[CpNb(NtBu)Cl_2]$, d) $[CpTa(NtBu)Cl_2]$. R = *t*Bu, py = pyridine.

these d-metal acids are electronically related, and the isolobal relationship with the carbonyl complex fragments is thereby established. On the basis of the spectroscopic data of **1**–**4** (Table 1), the presence of bridging ligands can be excluded. On the other hand, according to the isolobal principle[10] the characterization of **1**–**4** sets up a conceptual bridge between the doubly metalated zirconocene [Ru]–$[Cp_2Zr]$–[Ru], described by Casey et al. ([Ru] = $[CpRu(CO)_2]$[11]) and stannylene-bridged complexes of the type [M]–$[SnR_2]$–[M] (M = Fe, Ru, Mo, etc).[12]

We now contrast this series of—in the broadest sense—carbene-like[13] imido complex fragments with a series of radical complex fragments (Scheme 1, bottom). The radical fragments have not yet been isolated as monomeric d^1 species; however, they form homonuclear, diamagnetic dimers by direct M–M coupling,[1, 14] similar to 17VE metal carbonyl complex fragments. Cross dimerization of these metal radicals with the 17VE complex fragment $[CpFe(CO)_2]$ has now led to a series of diamagnetic, mixed-valent imido complexes that we were able to characterize. The formal principle of the series rests upon the cyclopentadienyl–imido analogy. Like the parent compound **5**,[9] **6**–**8** can be synthesized by reaction of the metal nucleophile $[CpFe(CO)_2]^-$ with the organometallic Lewis acids $[CpW(NtBu)_2]^+$,[15] $[CpMo(NtBu)_2]^+$,[15] and $[Cp_2Nb(NtBu)]^+$[1] (Scheme 3). The spectroscopic data of **6**–**8** clearly indicate a nonbridged metal–metal bond, as is present in $[(tBuN)_3Re–Mo(CO)_3Cp]$[9] and $[Cp^*(O)_2W–W(CO)_3Cp^*]$ ($Cp^* = \eta^5$-C_5Me_5) (Table 1).[16] The results make it seem plausible that the imido complex fragments depicted at the bottom of Scheme 1 are not only isolobal to one another, but that they should also have similar valence orbitals to a (R_3E) group (E = Si, Ge, Sn) or the 17VE carbonyl complex fragments.[17]



Scheme 3. The bonding capability of electronically related imidoyl complex fragments $[Cp_nM'(NR)_m]$ of Groups 5–7. a) $[Re(NtBu)_3Cl]$, b) $[CpW(NtBu)_2Cl]$, c) $[CpMo(NtBu)_2Cl]$, d) $[Cp_2Nb(NtBu)Cl]$. R = *t*Bu.

Table 1 summarizes selected spectroscopic data of the complexes **1**–**8**, which have also been characterized by elemental analysis. A comparison of the position of the IR bands ν_s(C=O) and ν_{as}(C=O) in complexes of the type [M″]–$[Fe(CO)_2Cp]$ allows conclusions to be drawn about the decrease of electron den-

Table 1. Experimental data of **1**–**8**.

Cmpd. (R = *t*Bu)	ν(CO) [a]	ν(M=NC) [b]	$\delta(C_\alpha)$	$\delta(C_\beta)$	$\Delta\delta$ [c]	M^+ [d]	Color, yield, m.p.
$[(RN)_2Mo\{Fe(CO)_2Cp\}_2]$ **1**	1978 s, 1969 vs, 1926 vs	1247 s 1204 s	68.78	31.83	36.95	593.8	orange, 71%, 144 °C [f]
$[(RN)_2W\{Fe(CO)_2Cp\}_2]$ **2**	1983 s, 1976 vs, 1930 vs	1281 s 1241 s	67.60	32.45	35.15	681.3	yellow, 79%, 226 °C [f]
$[Cp(RN)Nb\{Fe(CO)_2Cp\}_2]$ **3**	1952 vs, 1916 vs, 1900 s	1235 s	70.02	32.20	37.82	584.0	orange-red, 71%, 120 °C [f]
$[Cp(RN)Ta\{Fe(CO)_2Cp\}_2]$ **4**	1950 vs, 1915 vs, 1901 s	1253 s	68.24	32.20	36.04	671.6	orange-yellow, 21%, 170 °C [f]
$[(RN)_3Re–Fe(CO)_2Cp]$ **5**	1994 vs 1949 vs	1229 s 1211 s	67.63	31.34	36.29	577.2	yellow, 83%, 105 °C
$[Cp(RN)_2W–Fe(CO)_2Cp]$ **6**	1977 vs 1927 vs	1282 s 1244 s	66.95	31.89	35.06	568.0	yellow, 56%, 74 °C
$[Cp(RN)_2Mo–Fe(CO)_2Cp]$ **7**	1972 vs 1925 vs	1246 s 1219 s	68.43	31.07	37.36	481.8	orange-yellow, 66%, 53 °C [f]
$[Cp_2(RN)Nb–Fe(CO)_2Cp]$ **8**	1956 vs 1908 vs	1231 s	69.72	31.05	38.67	470.7	orange-yellow, 35%, 102 °C [f]

[a] In cm^{-1}; **1**, **5**, and **7** in *n*-hexane, all others in methylcyclohexane; for comparison: $[Me_2Sn\{Fe(CO)_2Cp\}_2]$ 1989, 1978, 1946, 1935 in cyclohexane [12a]; $[H–Fe(CO)_2Cp]$ 2013, 1949 in MeCN [18]; $[Me_3Sn–Fe(CO)_2Cp]$ 1994, 1943 in hexane [17b]; $[(Me_2N)_3Ti–Fe(CO)_2Cp]$ 1948, 1898 in octane [19]. [b] In cm^{-1}; Nujol mull. [c] $^{13}C\{^1H\}$ NMR (100.6 MHz); **1**, **5**, and **7** in $CDCl_3$, all others in C_6D_6. $C_\alpha = CMe_3$, $C_\beta = CMe_3$, $\Delta\delta = \delta(C_\alpha)-\delta(C_\beta)$; relative measure for the M≡N character [24]. [d] EI-MS (70 eV); highest peak of the pattern reported, correct isotope distribution. [f] Decomposition.

 © VCH Verlagsgesellschaft mbH, D-69451 Weinheim, 1994 0570-0833/94/1212-1256 $ 10.00+.25/0

sity induced by the metal acid [M″] at the neighboring metal center. The following qualitative ordering of the acceptor character of the cationic Lewis acids $[M'']^{n+}$ can be derived from the extent of the backbonding to the CO ligands (Scheme 4, Table 1, cf. footnote [a]). A similar comparative look at the CO vibra-

$$[SnMe_2]^{2+} > [W(N\mathit{t}Bu)_2]^{2+} \cong [Mo(N\mathit{t}Bu)_2]^{2+} > [CpTa(N\mathit{t}Bu)]^{2+} \cong [CpNb(N\mathit{t}Bu)]^{2+}$$

$$[H]^{+} > [SnMe_3]^{+} \cong [Re(N\mathit{t}Bu)_3]^{+} > [CpW(N\mathit{t}Bu)_2]^{+} \cong [CpMo(N\mathit{t}Bu)_2]^{+} > [Ti(NMe_2)_3]^{+} > [Cp_2Nb(N\mathit{t}Bu)]^{+}$$

Scheme 4. The acceptor character decreases from left to right.

tional bands shows that the oxidation state, despite its formal nature, makes a larger contribution to the Lewis acidity of cationic metal acids—for example $[(\mathit{t}BuN)_3Re]^{+}$ in contrast with $[(Me_2N)_3Ti]^{+}$[19]—than the position of the central atom in the periodic system. It is, after all, the ligands that influence the acceptor character of a metal center decisively by their π-donor ability. In this context the amido (NMe_2) and cyclopentadienyl ligands (η^5-C_5H_5) are stronger donors than the imido ligand ($N\mathit{t}Bu$).

It is worth mentioning that the reactivity of the anion $[Re(NAr)_3]^{-}$ (Ar = 2,6-iPr$_2$C$_6$H$_3$) resembles that of the carbonyl metalates $[Cp_nM(CO)_m]^{-}$.[20] As a result protonation yields a hydride complex with an acidic hydrogen atom. In this regard a comparison with $[R_3Sn-H]$ is also obvious. The hydride complexes $[(\eta^5\text{-}C_5Me_5)_2(PhN)Ta-H]$,[21] $[(\eta^5\text{-}C_5H_5)_2(\mathit{t}BuN)Nb-H]$,[22] and $[(\eta^5\text{-}C_5Me_5)_2(ArN)W-H]$[23] that are isoelectronic with $[(ArN)_3Re-H]$ in the sense of the thesis presented here were also described recently.

Both the reviewed results on hydrides and our own suggest the isolobal relationship formulated in Scheme 1, which is derived from the following rule: If in a complex fragment $[(\eta^5\text{-}C_5R_5)M]$ the ligand η^5-C_5R_5 is substituted for NR and the central atom d^n-M (n = 0, 1, 2) is replaced by an isoelectronic metal center d^n-M′ from the next higher group of the periodic table, a complex fragment [(RN)M′] that has the same number of valence orbitals and valence electrons, and valence orbitals of similar symmetry and energy results.

Received: December 9, 1993
Revised version: January 28, 1994 [Z 6549 IE]
German version: *Angew. Chem.* **1994**, *106*, 1328

[1] S. Schmidt, J. Sundermeyer, *J. Organomet. Chem.*, in press.
[2] D. S. Glueck, J. C. Green, R. I. Michelman, I. N. Wright, *Organometallics* **1992**, *11*, 4221–4225.
[3] The "closed-shell anion" RN^{2-} is considered a six-electron donor to a d^n-metal cation, and the "nitrene" RN a four-electron ligand to a metal atom. Irrespective of whether the hetero- or homolytic view is favored, a maximum of one σ and two π bonds to the metal is possible. A comparable statement is valid for the six- and five-electron donors $(\eta^5\text{-}C_5H_5)^{-}$ and $(\eta^5\text{-}C_5H_5)^{\cdot}$. In complexes with several competing π donors, the bond order deviates from the maximum value of 3 depending on the molecular symmetry. The bond description M=NR chosen consistently in this paper includes the high triple-bond component M≡NR that is typical for d-electron-poor complexes: W. A. Nugent, J. M. Mayer, *Metal-Ligand Multiple Bonds*, Wiley, New York, **1988**.
[4] a) T. R. Cundari, *J. Am. Chem. Soc.* **1992**, *114*, 7879–7888; b) K. A. Jørgensen, *Inorg. Chem.* **1993**, *32*, 1521–1522; c) T. R. Cundari, *J. Am. Chem. Soc.* **1992**, *114*, 10557–10563; d) M. H. Schofield, T. P. Kee, J. T. Anhaus, R. R. Schrock, K. H. Johnson, W. M. Davis, *Inorg. Chem.* **1991**, *30*, 3595–3640; e) see also [6], [7] and [20].
[5] If the two ligands approach the metal center along the z axis, orbitals of the same symmetry interact: σ, 2π-donor RN^{2-}: N(sp hybrid, p_z, s) → M(d_{z^2}, p_z, s); N(p_x) → M(d_{xz}, p_x); N(p_y) → M(d_{yz}, p_y). σ, 2 π-Donor $C_5H_5^{-}$: $C_5(a_1, a_2)$ → M(d_{z^2}, p_z, s); $C_5(e_1)$ → M(d_{xz}, p_x); $C_5(e_1)$ → M(d_{yz}, p_y). A δ-backbond M(d_{xy}, $d_{x^2-y^2}$) → $C_5(e_2)$ has no or a comparatively small significance in d-electron-poor complexes of d^n (n = 0, 1, 2) configuration.
[6] a) D. S. Williams, M. H. Schofield, J. T. Anhaus, R. R. Schrock, *J. Am. Chem. Soc.* **1990**, *112*, 6728–6729; b) D. S. Williams, M. H. Schofield, R. R. Schrock, *Organometallics* **1993**, *12*, 4560–4571.
[7] D. N. Williams, J. P. Mitchell, A. D. Poole, U. Siemeling, W. Clegg, D. C. R. Hockless, P. A. O'Neil, V. C. Gibson, *J. Chem. Soc. Dalton Trans.* **1992**, 739–751.
[8] a) A. D. Poole, V. C. Gibson, W. Clegg, *J. Chem. Soc. Chem. Commun.* **1992**, 237–239; b) P. W. Dyer, V. C. Gibson, J. A. K. Howard, B. Whittle, C. Wilson, *ibid.* **1992**, 1666–1668; c) J. K. Cockcroft, V. C. Gibson, J. A. K. Howard, A. D. Poole, U. Siemeling, C. Wilson, *ibid.* **1992**, 1668–1670.
[9] J. Sundermeyer, D. Runge, J. S. Field, *Angew. Chem.* **1994**, *106*, 679–682; *Angew. Chem. Int. Ed. Engl.* **1994**, *33*, 678–681.
[10] a) M. Elian, R. Hoffmann, *Inorg. Chem.* **1975**, *14*, 1058–1076; b) R. Hoffmann, *Angew. Chem.* **1982**, *94*, 725–739; *Angew. Chem. Int. Ed. Engl.* **1982**, *21*, 711–725; c) F. G. A. Stone, *ibid.* **1984**, *96*, 85–96 and **1984**, *24*, 89–100.
[11] P. P. Casey, R. F. Jordan, A. L. Rheingold, *Organometallics* **1984**, *3*, 504–506; the directly comparable iron complex [M] = $[CpFe(CO)_2]$ decomposes thermally at as low a temperature as −20 °C.
[12] a) N. Flitcroft, D. A. Halbourne, U. Paul, P. M. Tucker, F. G. A. Stone, *J. Chem. Soc. A* **1966**, 1130–1133; b) K. Triplett, D. Curtis, *Inorg. Chem.* **1976**, *15*, 431–433, and references therein.
[13] The carbene-like character of $[\eta^5\text{-}C_5H_5)_2Ti]$ was underpinned by EHMO calculations: H. H. Brinzinger, L. S. Bartell, *J. Am. Chem. Soc.* **1970**, *92*, 1105–1107. In contrast to a carbene, the inorganic carbene analogues in Scheme 1 have a third, energetically low-lying orbital (a_1 in the case of titanocene), that can be available for an additional interaction with concomitant increase in the coordination number at the metal center (Ti, Nb, Mo, Sn, etc.): J. W. Lauher, R. Hoffmann, *ibid.* **1976**, *98*, 1729–1742; see also [7].
[14] a) A. K. Burrell, J. C. Bryan, *Angew. Chem.* **1993**, *105*, 85–86, *Angew. Chem. Int. Ed. Engl.* **1993**, *32*, 94–95; b) A. A. Danopoulos, C. J. Longley, G. Wilkinson, B. Hussain, M. B. Hursthouse, *Polyhedron* **1989**, *8*, 2657–2670; c) J. Sundermeyer, U. Radius, P. Mountford, unpublished.
[15] a) J. Sundermeyer, *Chem. Ber.* **1991**, *124*, 1977–1979; b) U. Radius, J. Sundermeyer, *ibid.* **1992**, *125*, 2183–2186; c) J. Sundermeyer, U. Radius, C. Burschka, *ibid.* **1992**, *125*, 2379–2384.
[16] H. G. Alt, H. I. Hayen, R. D. Rogers, *J. Chem. Soc. Chem. Commun.* **1987**, 1795–1796.
[17] Representative examples of comparable [M]-ER_3 complexes (E = Si, Ge, Sn): a) W. Malisch, M. Kuhn, *Chem. Ber.* **1974**, *107*, 979–995; b) J. W. Faller, B. V. Johnson, C. D. Schaeffer, Jr., *J. Am. Chem. Soc.* **1976**, *98*, 1395–1400, and references therein.
[18] E. J. Moore, J. M. Sullivan, J. R. Norton, *J. Am. Chem. Soc.* **1986**, *108*, 2257–2263.
[19] W. J. Sartain, J. P. Selegue, *Organometallics* **1987**, *6*, 1812–1815. The metal acidity of $[(R_2N)_3Ti]^{+}$ can be enhanced, for example by *N*-silyl and *N*-arylamido ligands: S. Friedrich, H. Memmler, L. H. Gade, W.-S. Li, M. McPartlin, *Angew. Chem.* **1994**, *106*, 705–708; *Angew. Chem. Int. Ed. Engl.* **1994**, *33*, 676–678.
[20] D. S. Williams, R. R. Schrock, *Organometallics* **1993**, *12*, 1148–1160.
[21] G. Parkin, A. van Asselt, D. J. Leahy, L. Winnery, N. G. Hua, R. W. Quan, L. M. Henling, W. P. Schaefer, B. D. Santarsiero, J. E. Bercaw, *Inorg. Chem.* **1992**, *31*, 82–85.
[22] A. N. Chernega, M. L. H. Green, A. G. Suárez, *J. Chem. Soc. Dalton Trans.* **1993**, 3031–3034.
[23] S. R. Huber, T. C. Baldwin, D. E. Wigley, *Organometallics* **1993**, *12*, 91–97.
[24] W. A. Nugent, R. J. McKinney, R. V. Kasdovski, F. A. Van-Catledge, *Inorg. Chim. Acta* **1982**, *65*, L91–L93.

A Novel Organomagnesium Compound Consisting of Two Triple-Decker Cations $[LMg(\mu\text{-}Me)_3MgL]^{+}$ and an Octamethyltrimagnesate Anion: $[\{Me_2Mg(\mu\text{-}Me)_2\}_2Mg]^{2-}$**

Heiko Viebrock, Ulrich Behrens, and Erwin Weiss*

Dedicated to Professor Hansjörg Sinn on the occasion of his 65th birthday

The polymer chains $[MgR_2]_n$ (R = Me, Et, Ph) found in solvent-free diorganomagnesium compounds are disrupted by bases L (L = ether, amine) with the formation of primarily

[*] Prof. Dr. E. Weiss, Dr. H. Viebrock, Prof. Dr. U. Behrens
Institut für Anorganische und Angewandte Chemie der Universität
Martin-Luther-King-Platz 6, D-20146 Hamburg (FRG)
Telefax: Int. code + (40) 7222247

[**] Alkyl- and Arylmetal Compounds, Part 52. This research was supported by the Fonds der Chemischen Industrie. We thank Prof. K. Weighardt, Universität Bochum, for the gift of *N,N′,N″*-trimethyl-1,4,7-triazacyclononane L. – Part 51: [1].

monomeric or dimeric adducts $[MgR_2L_n]_m$ ($m = 1,2$).[1-4] In a few cases[5, 6] treatment with cryptands or crown ethers leads to disproportionation into organomagnesium cations and anions (organomagnesates).[4]

As part of our ongoing systematic investigations we tested the cyclic tripod amine ligand *N*,*N*′,*N*″-trimethyl-1,4,7-triazacylononane (tacn),[7] introduced into coordination chemistry by K. Wieghardt et al., for its suitability as a basic solvent for dimethylmagnesium. The nonequimolar reaction[8] of $[MgMe_2]_n$ with tacn (7:4) in benzene [Eq. (a)] also proceeded by

$$7\,MgMe_2 + 4\,tacn \xrightarrow{C_6H_6} \underset{\mathbf{1}}{[(tacn)Mg(\mu\text{-}Me)_3Mg(tacn)]_2^+[Mg_3Me_8]^{2-}] \cdot 1.5\,C_6H_6} \quad (a)$$

disproportionation and unexpectedly yielded the product bis[tri-μ-methyl-bis(tacn)-dimagnesium] octamethyltrimagnesate · 1.5 benzene **1**, which provided the crystal structure shown in Figures 1 and 2 (cited in ref.[2]).

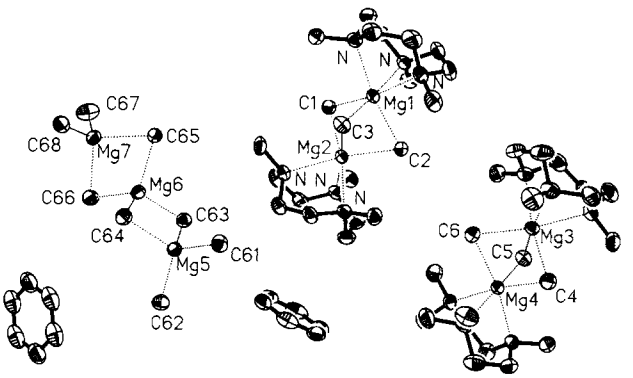


Fig. 1. Crystal stucture of **1** [10] (asymmetric unit with benzene molecules). Selected distances [pm] and angles [°] in the anion: Mg5-C61 217.4(2), Mg5-C62 216.0(3), Mg5-C63 235.7(2), Mg5-C64 234.5(3), Mg6-C63 222.6(3), Mg6-C64 224.2(2), Mg6-C65 223.8(3), Mg6-C66 222.9(2), Mg7-C65 236.5(2), Mg7-C66 235.4(3), Mg7-C67 216.1(3), Mg7-C68 215.7(3); C63-Mg6-C64 108.4(1), C63-Mg6-C65 103.5(1), C63-Mg6-C66 112.0(1), C64-Mg6-C65 120.1(1), C64-Mg6-C66 107.2(1), C65-Mg6-C66 105.8(1), C61-Mg5-C62 117.7(1), C67-Mg7-C68 123.4(1).

Recently, similar disproportionation products, namely $[MgR(14N4)]^+[MgRX_2]^-$ and $[MgR(14N4)]^+X^-$ (R = *i*Pr, *i*Bu, etc., 14N4 = 1,4,8,11-tetramethyl-1,4,8,11-tetraazacyclotetradecane, X = halogen) were described but were only characterized by NMR spectroscopy.[9]

The asymmetric structural unit of **1**[10] (Fig. 1) contains two cations that are only slightly different crystallographically, which may be described as triple-decker complexes: two Mg atoms coordinated to tacn ligands are bridged by three central methyl groups. The latter are arranged in staggered positions with respect to the N atoms of the tacn ligands as is shown in a projection along the Mg–Mg axis (Fig. 2). This structure type is new for organomagnesium compounds; a similar cation is found only in $[(pmdta)Mg(\mu\text{-}Me)_2Mg(pmdta)]^{2+}(fluorenide)_2^-$ (pmdta = $Me_2N(C_2H_4)N(Me)(C_2H_4)NMe_2$) described recently by us which contains only doubly bridged and pentacoordinated Mg atoms.[11] By contrast, in **1** the Mg atoms of the cation are bridged by three methyl groups and have octahedral coordination (C-Mg-C angle ca. 90°). The Mg-C-Mg angle is very small in the cations of **1** (ca. 68°) compared with those in $[MgR_2]_n$. The Mg–Mg distance (262.9 pm) is the smallest yet observed in organomagnesium compounds characterized by X-ray analysis.[4, 11-13, 15] Recently a metal–metal interaction was considered for a Mg–Mg distance of 276.8 pm.[15]

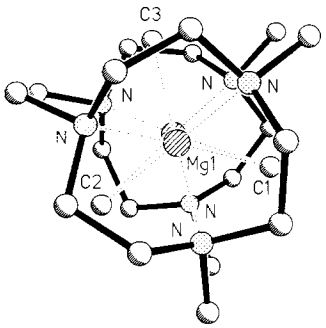


Fig. 2. Triple-decker cation of **1**; view along Mg1–Mg2 (similar to Mg3–Mg4). Selected distances [pm] and angles [°]: Mg1-C1 232.3(2), Mg1-C2 237.8(3), Mg1-C3 237.8(2), Mg2-C1 235.7(2), Mg2-C2 232.5(2), Mg2-C3 236.8(2), Mg-N 230.6(2)–231.9(2), Mg-Mg 262.9(1); C-Mg1-C 90.8(1)–92.2(1), C-Mg2-C 91.6(1)–92.4(1), Mg1-C-Mg2 67.3(1)–68.4(1).

The anion $[Mg_3Me_8]^{2-}$ is the first trimagnesate.[2] It can be described as a section of a polymer chain $[MgMe_2]_n$; however, there are three different groups of Mg–C distances in the anion. Only the distances from Mg6 to the neighboring C atoms (223–224 pm) correspond to the value in $[MgMe_2]_n$ (224 pm[11]). On the one hand, the Mg–C distances between terminal atoms Mg5 and Mg7 and the bridging methyl groups (ca. 235 pm) are clearly longer and correspond to the values in the cations. On the other hand, the Mg–C distances between the terminal Mg atoms and the terminal methyl groups (ca. 216 pm) are shortened and comparable to those in simple dimethylmagnesium compounds $MgMe_2L$.[3, 14]

The C-Mg-C bond angles at Mg6 are clearly different (103.5 to 120.1°) but correspond, on the average, to those reported for the polymer. The angle between the terminal methyl groups and their Mg atoms (123.4 and 117.7°) is greatly expanded in comparison to the tetrahedral angle (109.5°). The Mg–Mg distances, 280.6 and 277.6 pm, are larger than those in the cations and in the dialkylmagnesium polymers.

Experimental Procedure

Dimethylmagnesium (0.5 g, 9 mmol) and tacn (1.0 mL, 0.85 g, 5 mmol) were dissolved in 50 mL of benzene with rigorous exclusion of air and water. After the solution had been stirred for three days it was filtered, concentrated to the saturation point, and kept at 7 °C during crystallization. Colorless crystals, yield 0.7 g (46% based on $MgMe_2$), soluble in benzene, very sensitive to air and hydrolysis. Correct analytical values were obtained for C, H, N, Mg.

Received: January 13, 1994 [Z6615IE]
German version: *Angew. Chem.* **1994**, *106*, 1364

[1] H. Viebrock, E. Weiss, *Z. Naturforsch. B* **1994**, *49*, 89, and references therein.
[2] E. Weiss, *Angew. Chem.* **1993**, *105*, 1565; *Angew. Chem. Int. Ed. Engl.* **1993**, *32*, 1501, and references therein.
[3] H. Viebrock, E. Weiss, *J. Organomet. Chem.* **1994**, *464*, 121, and references therein.
[4] P. R. Markies, O. S. Akkerman, F. Bickelhaupt, W. J. J. Smeets, A. L. Spek, *Adv. Organomet. Chem.* **1991**, *32*, 147, and references therein.
[5] $[MgEt([2.2.1]crytand)]_2^+[Mg_2Et_6]^{2-}$, $[Mg(neopentyl)([2.1.1]cryptand)]^+[Mg(neopentyl)_3]^-$: E. P. Squiller, R. R. Whittle, H. G. Richey, Jr., *J. Am. Chem. Soc.* **1985**, *107*, 432.
[6] $[\{MgMe([15]crown\text{-}5)\}^+(Mg_2Me_5)^-]_n$: A. D. Pajersky, M. Parvez, H. G. Richey, Jr., *J. Am. Chem. Soc.* **1988**, *110*, 2660.
[7] K. Wieghardt, P. Chaudhuri, B. Nuber, J. Weiss, *Inorg. Chem.* **1982**, *21*, 3086.
[8] It has not yet been checked whether the equimolar reaction of tacn with MgR_2 gives a base adduct $MgR_2(tacn)$ or, by disproportionation, a cation $[MgR(tacn)]^+$ with tetracoordinated magnesium.
[9] R. M. Fabicon, A. D. Pajerski, H. G. Richey, Jr., *J. Am. Chem. Soc.* **1993**, *115*, 9333.
[10] Crystal structure data for **1** ($C_{59}H_{135}Mg_7N_{12}$, $M = 1182.96$): triclinic, space group $P\bar{1}$, $a = 1471.9(2)$, $b = 1680.8(2)$, $c = 1791.9(4)$ pm, $\alpha = 67.30(3)$, $\beta = 66.34(3)$, $\gamma = 78.32(3)°$, $V = 3740 \times 10^6$ pm^3, $Z = 2$, ρ (from X-ray analysis) = 1.050 g cm^{-3}; crystal size $0.3 \times 0.3 \times 0.15$ mm; measured reflections: 13450 symmetry independent, of which 12732 have $F_o^2 \geq 0$; anisotropic refinement for the nonhydrogen atoms; 735 refined parameters; $R1 = 0.052$, [$F_o > 4\sigma(F_o)$;

10349 reflections], $wR2 = 0.141$; Enraf-Nonius CAD4 four-circle diffractometer: 173 K; $Cu_{K\alpha 1}$ radiation; $\mu = 1.00\ mm^{-1}$; $2.85 < \theta < 69°$; empirical absorption correction (DIFABS [18]); structure solution with SHELX-86 [16], refinement with SHELXL-93 [17]; the torsion angles were refined for all the methyl groups, the remaining H atoms were calculated in ideal positions and treated as "riding" in further refinements. **1** crystallizes with two formula units per unit cell in the triclinic space group $P\bar{1}$. The asymmetric unit contains two cations, one anion, and one and a half molecules of benzene. Further details of the crystal structure investigation may be obtained from the Fachinformationszentrum Karlsruhe, D-76344 Eggenstein-Leopoldshafen (FRG) on quoting the depository number CSD-57976.

[11] E. Weiss, *J. Organomet. Chem.* **1964**, *2*, 314.
[12] E. Weiss, *J. Organomet. Chem.* **1965**, *4*, 101.
[13] J. Toney, G. D. Stucky, *J. Organomet. Chem.* **1970**, *22*, 241.
[14] T. Greiser, J. Kopf, D. Thönnes, E. Weiss, *J. Organomet. Chem.* **1980**, *191*, 1.
[15] A. J. Arduengo III, H. V. R. Dias, F. Davidson, L. R. Harlow, *J. Organomet. Chem.* **1993**, *462*, 13.
[16] G. Sheldrick, SHELXS-86, Program for Crystal Structure Solution, *Universität Göttingen*, **1986**.
[17] G. Sheldrick, SHELXL-93, Program for Crystal Structure Determination, *Universität Göttingen*, **1993**.
[18] N. Walker, D. Stewart, *DIFABS, An Empirical Method of Correcting Diffractometer Data for Absorption Coefficients* (*Acta Crystallogr. Sect. A* **1983**, *39*, 158).

A Kinetic Study of the Hydrolysis of Phosgene in Aqueous Solution by Pulse Radiolysis**

Ralf Mertens, Clemens von Sonntag,* Johan Lind, and Gabor Merenyi

Phosgene is a very important industrial product with an annual production of approximately 2 million tons.[1] Phosgene is also an end product of the free radical induced degradation of chlorinated hydrocarbons (this is well-documented in the gas phase).[2] In recent years "advanced oxidation processes", which are based on the formation of OH radicals (e.g. UV/hydrogen peroxide, UV/ozone, ozone/hydrogen peroxide), have been gaining in importance for the treatment of not only wastewater but also polluted drinking water.[3] The mechanism of the OH•-induced degradation of chlorinated hydrocarbons can be readily studied by pulse radiolysis using conductometric detection, since the liberation of chloride ions (and concomitantly protons) in the course of the oxidative degradation cascade is accompanied by a conductance change. In order to assign one of the kinetic components of this conductance change to a given elementary step, for example the hydrolysis of phosgene, the kinetic parameters of the reaction must be determined independently. Two reports focus on the rate of reaction of phosgene with water,[4, 5] but only one of them is relevant to the present work.[5] In that study, pure phosgene gas was dissolved in short laminar jets of aqueous solutions, the hydrochloric acid taken up by the aqueous solutions titrated, and the results interpreted within the framework of nonsteady-state absorption-plus-reaction theory. The reported rate constants extrapolated to 25 °C were $6\ s^{-1}$ for the spontaneous and $1.6 \times 10^4\ dm^3\ mol^{-1}\ s^{-1}$ for the OH^--induced hydrolysis. We report here on our determination of these rate constants by a different approach: the pulse radiolysis technique. This technique is largely used for the investigation of free-radical reactions.[6, 7] However, our results show that pulse radiolysis is also suitable for studying the kinetics of nonradical reactions, which are of wider interest.

In the radiolysis of water, OH radicals, solvated electrons, and H atoms are formed as free-radical intermediates [reaction (1)]. Hydroxyl radicals and solvated electrons are formed in about equal amounts [$G(^{\bullet}OH) \approx G(e_{aq}) \approx 2.8 \times 10^{-7}\ mol\ J^{-1}$; G = amount of a given species formed in mol relative to the absorbed energy of ionizing radiation in J], while the formation of H atoms is less significant [$G(H^{\bullet}) \approx 0.6 \times 10^{-7}\ mol\ J^{-1}$].[8] The OH radicals do not react with carbon tetrachloride in solution, but solvated electrons and the H atoms readily yield trichloromethyl radicals [reactions (2) and (3), $k_2 = 1.6 \times 10^{10}\ dm^3\ mol^{-1}\ s^{-1}$, $k_3 = 3.8 \times 10^7\ dm^3\ mol^{-1}\ s^{-1}$].[9] Two conceivable routes lead from the trichloromethyl radical to phosgene via the (potentially very shortlived) intermediate, trichloromethanol: the trichloromethyl radical can react with the OH radical [reaction (4)], or the trichloromethyl radical can react with O_2 to give the trichloromethylperoxyl radical [reaction (5)], which is then reduced with the iodide ion [reaction (6)].[10] In reactions (4)–(7) trichloromethanol and phosgene are formed in situ very rapidly, and their hydrolysis [reactions (7)–(9)] can be followed by changes in conductivity. We will discuss both routes.

$$H_2O \xrightarrow[\text{radiation}]{\text{ionizing}} e_{aq}, {}^{\bullet}OH, H^{\bullet}, H^+, OH^-, H_2O_2, H_2 \quad (1)$$

$$CCl_4 + e_{aq} \longrightarrow {}^{\bullet}CCl_3 + Cl^- \quad (2)$$

$$CCl_4 + H^{\bullet} \longrightarrow {}^{\bullet}CCl_3 + H^+ + Cl^- \quad (3)$$

$${}^{\bullet}CCl_3 + {}^{\bullet}OH \longrightarrow CCl_3OH \quad (4)$$

$${}^{\bullet}CCl_3 + O_2 \longrightarrow CCl_3OO^{\bullet} \quad (5)$$

$$CCl_3OO^{\bullet} + 3I^- + 3H^+ \longrightarrow CCl_3OH + I_2 + I^- + H_2O \quad (6)$$

$$CCl_3OH \longrightarrow Cl_2C{=}O + H^+ + Cl^- \quad (7)$$

$$Cl_2C{=}O + H_2O \longrightarrow CO_2 + 2H^+ + 2Cl^- \quad (8)$$

$$Cl_2C{=}O + OH^- \longrightarrow CO_2 + H^+ + 2Cl^- \quad (9)$$

Argon-purged, aqueous solutions saturated with CCl_4 were subjected to 1-μs pulses of high-energy electrons (2.7 MeV). Right after the pulse, when the excess conductivity due to the formation of H^+ and OH^- during the pulse had decayed, an increase in conductivity was observed which was equivalent to $3.4 \times 10^{-7}\ mol\ J^{-1}$ (based on the formation of a proton and an anion) (Fig. 1). This increase in conductivity can be accounted

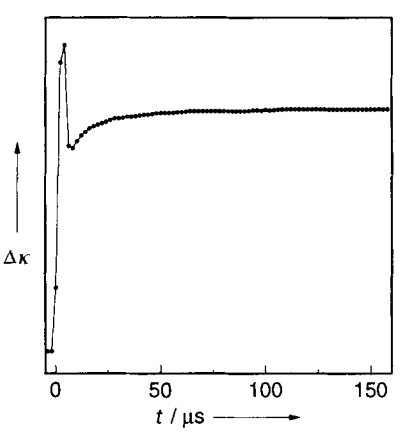


Fig. 1. Pulse radiolysis of an Ar-purged aqueous CCl_4 solution at 25 °C. The change of conductivity κ as a function of time (up to 150 μs) reflects the reaction of solvated electrons and H atoms with CCl_4 and the formation and (instantaneous) decay of CCl_3OH.

[*] Prof. Dr. C. von Sonntag, Dipl.-Chem. R. Mertens
Max-Planck-Institut für Strahlenchemie
Postfach 101365, D-45413 Mülheim an der Ruhr (FRG)
Telefax: Int. code + (208) 304-3951
Dr. G. Merenyi, Dr. J. Lind
Department of Nuclear Chemistry, Royal Institute of Technology
S-10044 Stockholm (Sweden)

[**] This work was supported by the Bundesministerium für Forschung und Technologie (Projects 02-WT-9078 and 02-WT-9288).

for by reactions (2) and (3). The radicals formed, $^{\bullet}CCl_3$ and $^{\bullet}OH$, react bimolecularly according to reactions (4), (10), and (11). The rate constants of reactions (10) and (11) are known ($2k_{10} = 7.4 \times 10^8$ dm^3 mol^{-1} s^{-1};[11] $2k_{11} = 1.1 \times 10^{10}$ dm^3 mol^{-1} s^{-1}[9]). Considering the large rate constant for dimeriza-

$$2\,^{\bullet}CCl_3 \longrightarrow C_2Cl_6 \quad (10)$$

$$2\,^{\bullet}OH \longrightarrow H_2O_2 \quad (11)$$

tion of the OH radical, we may assume k_4 to be 6×10^9 dm^3 mol^{-1} s^{-1}. For applied doses of 12 to 60 Gy per pulse this leads to a first half-life of radical decay in the order of 5 to 16 μs and the formation of CCl_3OH of about 30% of the primary CCl_3 radicals (estimated by computer simulation). After the neutralization of H^+ and OH^- formed during the pulse [reaction (1)] there is an increase in conductivity between 5 and 16 μs (Fig. 1). An exact evaluation of the yield of this conductivity increase is not possible, since decay by neutralization and buildup overlap. An increase in conductivity means that at the given pH (ca. 5.5–6.0) CCl_3OH is either fully deprotonated [reaction (12)] or it hydrolyzes as soon as it formed ($k_7 \geq 8 \times 10^4$ s^{-1}).

Assuming $pK_a(CH_3OH) = 16$ and using the reported[12] increments for the electron-withdrawing effect of Cl substituents, one estimates $pK_a(CCl_3OH)$ to be 3.5–4 [equilibrium (12)/(−12)]. Even this very rough estimate indicates that at the pH of the above experiments the observed increase in conductivity may in fact be due to reaction (12). However, after the deprotonation of CCl_3OH, the subsequent chloride ion loss must be very fast, and hence we conclude that CCl_3OH must hydrolyze very rapidly indeed. The previously mentioned value of $k_7 \geq 8 \times 10^4$ s^{-1} is, of course, only a lower limit. The hydrolysis of CCl_3OH can, in fact, be much faster. A geminal chlorohydrin similar to trichloromethanol (albeit with an unpaired electron in the β position) is formed when the OH radical reacts with tetrachloroethene [reaction (13)]. In this case HCl is liberated within 3 μs [reaction (14)],[13] which implies $k_{14} \geq 7 \times 10^5$ s^{-1}. We thus conclude that phosgene is produced in situ at times ≤ 50 μs. Any further increase of conductivity in this system must then be due to its hydrolysis.

$$CCl_3OH \rightleftharpoons CCl_3O^- + H^+ \quad (12/-12)$$

$$CCl_2{=}CCl_2 + {}^{\bullet}OH \longrightarrow {}^{\bullet}CCl_2{-}CCl_2OH \quad (13)$$

$$^{\bullet}CCl_2{-}CCl_2OH \longrightarrow {}^{\bullet}CCl_2{-}C(O)Cl + H^+ + Cl^- \quad (14)$$

As can be seen from Figure 2 there is a third conductivity increase in the 100-ms time range. This increase is equivalent to 2.2×10^{-7} mol J^{-1}, and its half-life is independent of the dose rate (dose per pulse). From these data it follows that the rate constant of the spontaneous hydrolysis of phosgene at 25 °C is $k_8 = 9$ s^{-1}.

Additional experiments have been conducted in basic solutions. There, formation of H^+ and Cl^- leads to a decrease in conductivity, since the strongly conducting OH^- ions are replaced by the less conducting Cl^- ions. The conductivity decrease in the third time domain was measured as a function of the OH^- concentration, and it was found that the rate of conductivity change increases with increasing OH^- concentration. In basic solutions the kinetics of the conductivity change are not monoexponential. This was expected, since the reported[5] value of $k_9 = 1.6 \times 10^4$ dm^3 mol^{-1} s^{-1} is close to that of the reaction of OH^- with CO_2 [$k(OH^- + CO_2 \rightarrow HCO_3^-) = 6.9 \times 10^3$ dm^3 s^{-1}].[14] The conductivity in the present experiments was evaluated by fitting only the first (faster) part of the conductivity change to a first-order reaction. The results are shown graphically in the inset in Figure 2 (○). The data fall on a straight line, whose slope yields $k_9 = 2.8 \times 10^4$ dm^3 mol^{-1} s^{-1} which is in very reasonable agreement with the literature value.[5]

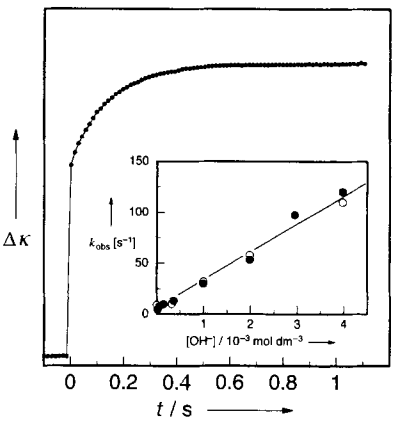


Fig. 2. Pulse radiolysis of an Ar-purged aqueous CCl_4 solution at 25 °C. The change of conductivity as a function of time (up to 1 s) reflects the hydrolysis of phosgene. Inset: Hydrolysis of phosgene in basic solution; observed rate of conductivity change as a function of the OH^- concentration. ○: $^{\bullet}CCl_3$ plus $^{\bullet}OH$ route; ●: $CCl_3O_2^-$ plus I^- route.

We conducted some γ-radiolysis and product analysis studies to confirm the formation of phosgene in the present system. We found that CO_2 [$G(CO_2) = 1.0 \times 10^{-7}$ mol J^{-1}], C_2Cl_6 [$G(C_2Cl_6) = 0.5 \times 10^{-7}$ mol J^{-1}], and Cl^- [$G(Cl^-) = 6.8 \times 10^{-7}$ mol J^{-1}] form. These data are not expected to fully reflect the pulse radiolysis results, since under the conditions of γ-radiolysis the OH radicals not only undergo reactions (4) and (11) but also react with the products, bicarbonate and H_2O_2. Strong evidence for the scavenging of OH radicals by the radiolysis products is given by the low H_2O_2 yield, $G(H_2O_2) = 0.55 \times 10^{-7}$ mol J^{-1}, which is only one-third of the value expected based on the total amount of H_2O_2 [from reactions (1) and (11)]. These side reactions do not play a role in the single-pulse experiments described previously and do not affect the kinetic data.

Trichloromethylperoxide radicals that form in oxygen-containing aqueous solutions react readily with iodide ions.[10] An adduct forms [reaction (15)], which reacts with a further iodide ion, whereby a trichloromethoxyl radical is formed and a molecule of iodine is liberated [reaction (16)]. In a subsequent step the trichloromethoxyl radical is reduced by an iodide ion to the trichloromethanol anion [reaction (17)], which loses a chloride ion to form phosgene [reaction (18)].

$$CCl_3OO^{\bullet} + I^- \longrightarrow [CCl_3OOI]^{\bullet -} \quad (15)$$

$$[CCl_3OOI]^{\bullet -} + H^+ + I^- \longrightarrow CCl_3O^{\bullet} + I_2 + OH^- \quad (16)$$

$$CCl_3O^{\bullet} + I^- \longrightarrow CCl_3O^- + I^{\bullet} \quad (17)$$

$$CCl_3O^- \longrightarrow Cl_2C{=}O + Cl^- \quad (18)$$

Under our experimental conditions (CCl_4 and iodide ions both 10^{-3} mol dm^{-3}, pH 4, Ar:O_2 = 10:1) the OH radical generated by radiolysis is scavenged by the iodide ion [reaction (19)]. Although both molecular iodine and iodine atoms form complexes with iodide ions [reactions (20) and (21)], this

$$^{\bullet}OH + I^- \longrightarrow OH^- + I^{\bullet} \quad (19)$$

$$I_2 + I^- \rightleftharpoons I_3^- \quad (20/-20)$$

$$I^{\bullet} + I^- \rightleftharpoons I_2^{\bullet -} \quad (21/-21)$$

 © VCH Verlagsgesellschaft mbH, D-69451 Weinheim, 1994 0570-0833/94/1212-1260 $ 10.00+.25/0

does not cause a change in conductivity. This whole sequence of reactions proceeds at times $\leq 40\ \mu s$,[10] much faster than the subsequent hydrolysis of phosgene. Hence the kinetics of this reaction can be studied fairly easily.

Following radiolysis carbon dioxide was also measured ($G(CO_2) = 2.45 \times 10^{-7}\ mol\,J^{-1}$). Considering that under our experimental conditions all H atoms and 5% of the solvated electrons are scavenged by O_2, one would expect CO_2 to be formed with $G(CO_2) = 2.65 \times 10^{-7}\ mol\,J^{-1}$. The measured value agrees well with that calculated and thus supports the proposed mechanism.

In acid solutions the sum of reactions (1), (2), (5), and (15)–(19) leads to a drop in conductivity (consumption of 2 mol equiv of H^+). The hydrolysis of phosgene [liberation of 2 mol equiv of H^+, reaction (8)] causes the conductivity to return to its prepulse value (Fig. 3).

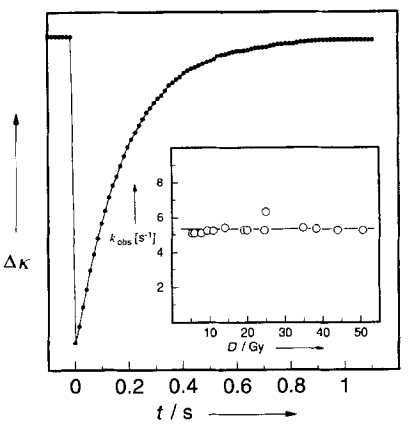


Fig. 3. Pulse radiolysis of aqueous CCl_4 solutions containing O_2 and iodide ions at 20 °C. The recovery of the conductivity drop reflects the hydrolysis of phosgene. Inset: The observed rate constant of phosgene hydrolysis as a function of dose D.

A series of experiments were also conducted at high pH to obtain additional data for the OH^--induced hydrolysis of phosgene [reaction (9)]. These data are included in the inset in Figure 2 (●). They agree well with the values determined with the $^{\bullet}CCl_3 + {}^{\bullet}OH$ method (○).

The data shown in Figure 3 are from experiments carried out at 20 °C, that is, at a lower temperature than those in Figure 2. Since the rate of the spontaneous hydrolysis of phosgene strongly increases with increasing temperature,[5] it is not surprising that at 20 °C $k_8 = 5.3\ s^{-1}$ is found (cf. inset in Fig. 3).

In the earlier study[5] the hydrolysis of phosgene was studied at only two temperatures (open circles in Fig. 4). The pulse-radiolysis technique allows a larger temperature range, and hence more reliable kinetic parameters can be obtained. Figure 4 shows an Arrhenius plot covering the temperature range from 13 to 59 °C. The slope of the straight line drawn through the experimental points yields $A = 1.4 \times 10^{10}$ and $E_a = 53\ kJ\,mol^{-1}$.

Figure 4 shows that the data from the two different approaches we used agree very well, and that the data obtained by the laminar jet method[5] are not very far off. This was not expected, since many assumptions were made in the evaluation of the laminar jet data.[5] Our value for the hydrolysis of phosgene is also in the range of activation energies reported for the gas-phase reaction ($14-60\ kJ\,mol^{-1}$).[1] It is noted that in the gas phase this activation energy is much more difficult to determine[1] and fraught with larger errors (e.g. wall effects) than those encountered in our pulse-radiolysis experiments.

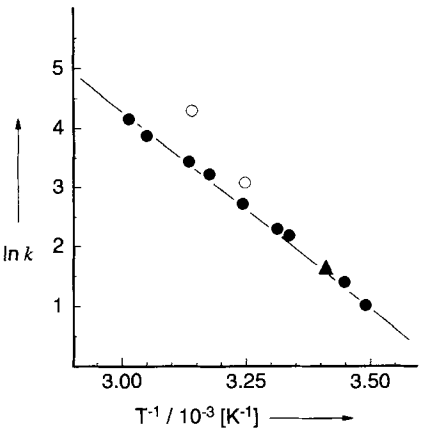


Fig. 4. Arrhenius plot of phosgene hydrolysis. ●: pulse radiolysis, $CCl_3O_2^-$ plus I^- approach; ▲: pulse radiolysis, $^{\bullet}CCl_3$ plus $^{\bullet}OH$ approach; ○: laminar jet method [5].

Experimental Procedure

Aqueous solutions saturated with CCl_4 (>99% Merck), which contained an excess of CCl_4 to guarantee saturation, were purged with argon (99.99%) to free the solutions from oxygen. For pulse radiolysis a 2.7 MeV Van de Graaff electron accelerator delivering electron pulses of 1-μs duration was used. Details have been described in ref. [7]. For measuring the temperature dependence of the kinetics of the phosgene hydrolysis, the solution was kept in a thermostated reservoir. A thermocouple was inserted into the waste tube of the conductivity cell [7] to measure the temperature as closely as possible. The dose rate of the γ-radiolysis experiments was $0.19\ Gy\,s^{-1}$. Hydrogen peroxide was determined according to ref. [15], carbon dioxide according to ref. [16], and chloride ions by ion chromatography (Dionex 2010i).

Received: December 11, 1993 [Z 6553 IE]
German version: *Angew. Chem.* **1994**, *106*, 1320

[1] H. Keiser, E. Reichold, *Staub Reinhalt. Luft* **1988**, *48*, 239.
[2] H. Scheytt, H. Esrom, L. Prager, R. Mehnert, C. von Sonntag in *Non-thermal Plasma Techniques for Pollution Control, Part B: Electron Beam and Electrical Discharge Processing* (Eds.: B. M. Penetrante, S. E. Schultheis) (*NATO ASI Ser. Ser. G* **1993**, *34B*, 91).
[3] a) C. von Sonntag, G. Mark, R. Mertens, M. N. Schuchmann, H.-P. Schuchmann, *Aqua (London)* **1993**, *42*, 201; b) O. Legrini, E. Oliveros, A. M. Braun, *Chem. Rev.* **1993**, *93*, 671.
[4] I. Ugi, F. Beck, *Chem. Ber.* **1960**, *94*, 1839.
[5] W. H. Manogue, R. L. Pigford, *Am. Inst. Chem. Eng. J.* **1960**, *6*, 494.
[6] a) K.-D. Asmus, *Methods Enzymol.* **1984**, *105*, 167; b) *Pulse radiolysis* (Ed.: Y. Tabata), CRC, Boca Raton, FL, USA, **1991**.
[7] C. von Sonntag, H.-P. Schuchmann in *Oxygen Radicals in Biological Systems, Part C* (Ed.: L. Packer) (*Methods Enzymol.* **1993**, *233*, 3).
[8] a) C. von Sonntag, *The Chemical Basis of Radiation Biology*, Taylor and Francis, London, **1987**; b) G. V. Buxton in *Radiation Chemistry: Principles and Applications* (Eds.: Farhataziz, M. A. J. Rodgers), VCH, Weinheim, **1987**, p. 321.
[9] G. V. Buxton, C. L. Greenstock, W. P. Helman, A. B. Ross, *J. Phys. Chem. Ref. Data* **1988**, *17*, 513.
[10] M. Bonifacic, C. Schöneich, K.-D. Asmus, *J. Chem. Soc. Chem. Commun.* **1991**, 1117.
[11] B. Lesigne, L. Gilles, R. J. Woods, *Can. J. Chem.* **1974**, *52*, 1135.
[12] D. D. Perrin, B. Dempsey, E. P. Serjeant, *pK_a Prediction for Organic Acids and Bases*, Chapman and Hall, New York, **1981**.
[13] R. Köster, K.-D. Asmus, *Z. Naturforsch. B* **1971**, *26*, 1108.
[14] M. N. Schuchmann, C. von Sonntag, *Z. Naturforsch B* **1982**, *37*, 1184.
[15] A. O. Allen, C. J. Hochanadel, J. A. Ghormley, T. W. Davis, *J. Phys. Chem.* **1952**, *56*, 575.
[16] M. I. Al-Sheikhly, H.-P. Schuchmann, C. von Sonntag, *Int. J. Radiat. Biol.* **1985**, *47*, 457.

 © VCH Verlagsgesellschaft mbH, D-69451 Weinheim, 1994 0570-0833/94/1212-1261 $ 10.00+.25/0

Determination of the Kinetics of Vinyl Radical Reactions by the Characteristic Visible Absorption Spectra of Vinylperoxyl Radicals**

Ralf Mertens and Clemens von Sonntag*

Vinyl radicals are quite ubiquitous. They are formed, for example, when vinyl halides are photolyzed [e.g. reaction (1)][1]

$$Cl_2C{=}CCl_2 + h\nu \longrightarrow Cl_2C{=}CCl^{\bullet} + Cl^{\bullet} \quad (1)$$

and are thus important intermediates in the photodegradation of anthropogenic environmental pollutants such as tetrachloroethene, trichloroethene, and vinyl chloride. *cis*-Dichloroethene and vinyl chloride also arise from the bacterial degradation of tetrachloro- and trichloroethene contaminants in the soil. 5-Bromouracil (5-BrUra) may be used to substitute thymine in DNA. This renders the 5-BrUra-substituted strand photolabile, and again vinyl radicals play an important role.[2] Vinyl radicals are also generated when free radicals add to acetylene and its derivatives.[3]

For our ongoing studies on the UV photolysis of vinyl halides in air[4] and in oxygenated aqueous solutions[5] we required further kinetic data concerning the fate of these radicals in the presence of oxygen. To ascertain whether these radicals react readily with oxygen, as nearly all carbon-centered radicals do,[6] we used the pulse radiolysis technique[7, 8] which has proven to be an excellent tool for studying the formation and reactivity of peroxyl radicals in aqueous solutions.[9]

Carbon-centered peroxyl radicals usually show noncharacteristic UV absorption spectra in the range $\lambda < 300$ nm and no significant absorption in the visible region. Surprisingly, the vinylperoxyl radicals, especially the chlorine-substituted ones, showed a strong absorption in the visible region, which can be used to study the kinetics of vinylperoxyl radical reactions as well as of the reactions of the vinyl radicals and their competing reaction with oxygen.

Vinylperoxyl radicals were generated by pulse radiolysis.[8] A short pulse (1 μs) of high-energy electrons (2.8 MeV) applied to an O_2-containing aqueous solution of vinyl halides (10^{-3} mol dm^{-3}) gives rise to solvated electrons (e_{aq}), OH radicals, and H atoms [reaction (2)]. Their radiation chemical yields are $G(e_{aq}) \approx G(^{\bullet}OH) \approx 2.8 \times 10^{-7}$ mol J^{-1} and $G(H^{\bullet}) \approx 0.6 \times 10^{-7}$ mol J^{-1}. The solvated electrons react rapidly with the vinyl halides by dissociative electron capture, yielding vinyl radicals and chloride ions[10] [e.g. reaction (3); $k_3 = 1.3 \times 10^{10}$ dm^3 mol^{-1} s^{-1}],[11] in competition with their reaction with oxygen [reaction (4); $k_4 = 1.9 \times 10^{10}$ dm^3 mol^{-1} s^{-1}].[11] The OH radicals and the H atoms add to the double bond of the vinyl halide [e.g. reaction (5); $k_5 = 2.6 \times 10^9$ dm^3 mol^{-1} s^{-1}];[11] in other words, about half of the radical yield consists of vinyl radicals. It is not possible to study the fate of the vinyl radicals separately from that of the OH-adduct radicals generated in reaction (5); however, if the solvated electrons are converted into further OH radicals by saturating the solution with N_2O [reaction (6); $k_6 = 9.1 \times 10^3$ dm^3 mol^{-1} s^{-1}],[11] vinyl radicals are no longer formed.

$$H_2O \xrightarrow{\text{ionizing radiation}} e_{aq}, {}^{\bullet}OH, H^{\bullet}, H^+, H_2O_2, H_2 \quad (2)$$

$$e_{aq} + Cl_2C{=}CCl_2 \longrightarrow Cl_2C{=}CCl^{\bullet} + Cl^- \quad (3)$$

$$e_{aq} + O_2 \longrightarrow O_2^{\bullet -} \quad (4)$$

$$^{\bullet}OH(H^{\bullet}) + Cl_2C{=}CCl_2 \longrightarrow HOCCl_2{-}CCl_2^{\bullet}\ (HCCl_2{-}CCl_2^{\bullet}) \quad (5)$$

$$H_2O + N_2O + e_{aq} \longrightarrow {}^{\bullet}OH + N_2 + OH^- \quad (6)$$

The OH-adduct radicals formed in reaction (5) are known to lose HCl rapidly [reaction (7); $k_7 > 7 \times 10^5$ s^{-1}].[10] The absorption spectrum of the resulting intermediate is shown in Figure 1. In the presence of oxygen this spectrum changes owing to the formation of the corresponding peroxyl radicals [reaction (8)].

$$HOCCl_2{-}CCl_2^{\bullet} \longrightarrow HCl + Cl(O)C{-}CCl_2^{\bullet} \quad (7)$$

$$Cl(O)C{-}CCl_2^{\bullet} + O_2 \longrightarrow Cl(O)C{-}CCl_2O_2^{\bullet} \quad (8)$$

These peroxyl radicals display the typical noncharacteristic UV absorption ≤ 260 nm. The rate of their buildup as a function of the O_2 concentration (inset in Fig. 1) yields a bimolecular

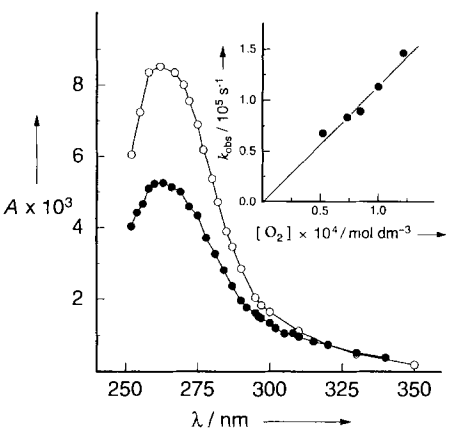


Fig. 1. Pulse radiolysis of N_2O- (○) and N_2O/O_2-saturated (●) aqueous solutions of tetrachloroethene (10^{-3} mol dm^{-3}). Inset: Rate of buildup of the peroxyl radical absorption at 260 nm as a function of the O_2 concentration.

rate constant $k_8 = 1.2 \times 10^9$ dm^3 mol^{-1} s^{-1}. Thus there is nothing unexpected in the behavior of these peroxyl radicals.

When Ar/O_2-saturated, N_2O-free tetrachloroethene solutions are pulse-irradiated, the absorption spectrum shown in Figure 2

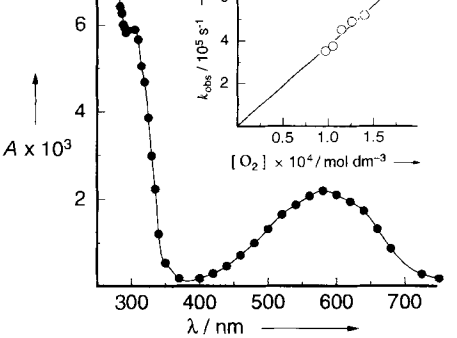


Fig. 2. Pulse radiolysis of Ar/O_2 (9/1)-saturated aqueous solution of tetrachloroethene. Absorption spectrum after completion of the reactions with O_2. Inset: Rate of buildup of the trichlorovinylperoxyl radical absorption at 580 nm as a function of the O_2 concentration.

[*] Prof. Dr. C. von Sonntag, Dipl.-Chem. R. Mertens
Max-Planck-Institut für Strahlenchemie
Postfach 101365, D-45413 Mülheim an der Ruhr (FRG)
Telefax: Int. code + (208) 304-3951

[**] This work was supported by the Bundesministerium für Forschung und Technologie (Projects 02-WT-9078 and 02-WT-9288).

develops. Besides an absorption in the UV there is now also a strong absorption in the visible. The data in Figure 2 (inset) yield a rate constant $k_9 \approx 3.8 \times 10^9\ dm^3\,mol^{-1}\,s^{-1}$. Since this absorption did not occur in the absence of trichlorovinyl radicals (see above), we assume that the trichlorovinyl radical reacts very rapidly with oxygen [reaction (9)] and that the species with

$$Cl_2C{=}CCl^{\bullet} + O_2 \longrightarrow Cl_2C{=}CClO_2^{\bullet} \quad (9)$$

the absorption maximum at 580 nm is the trichlorovinylperoxyl radical. The shoulder at 305 nm is also assigned to this radical, as the peroxyl radicals resulting from OH and H addition [reactions (5)–(8)] absorb at shorter wavelengths (cf. Fig. 1). Further vinylperoxyl radicals are produced from trichloroethene, *cis*- and *trans*-1,2-dichloroethene, 1,1-dichloroethene, vinyl bromide, and 5-bromouracil. Pulse-irradiation of trichloroethene generates 1,2- and 1,1-dichlorovinyl radicals in a ratio of 4:1, (R. Mertens, C. von Sonntag, unpublished results); in the other cases only one vinyl radical species is generated. The absorption spectra of the corresponding peroxyl radicals are shown in Figure 3; the absorption maxima and molar absorption coefficients are compiled in Table 1. The dichlorovinylperoxyl radical, like

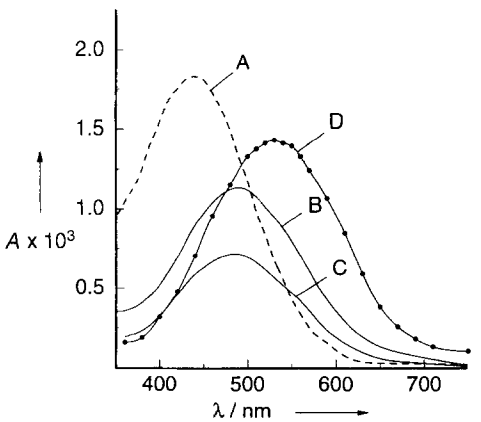


Fig. 3. Absorption spectra of halogenated vinylperoxyl radicals in the visible: A: vinylperoxyl, B: 2-chlorovinylperoxyl, C: 1-chlorovinylperoxyl, D: 1,2-dichlorovinylperoxyl/1,1-dichlorovinylperoxyl (4/1).

are compiled in Table 1. The dichlorovinylperoxyl radical, like the trichlorovinylperoxyl radical, displays a shoulder in the UV [$\varepsilon(300\ nm) \approx 3000\ dm^3\,mol^{-1}\,cm^{-1}$]. The absorptions of the other vinylperoxyl radicals also increase in the UV (< 330 nm) without exhibiting well-defined maxima or shoulders at $\lambda > 280$ nm. The vinyl halides and oxygen compete for the solvated electron [cf. reactions (3) and (4)]. On account of the high volatility of most of the vinyl halides used in this study, their concentrations are not known as exactly as would be required for assessing the molar absorption coefficients with an accuracy of better than 10%.

Table 1. Absorption maxima of vinylperoxyl radicals in the visible region and the corresponding molar absorption coefficients.

Radical	λ_{max} [nm]	ε [$dm^3\,mol^{-1}\,cm^{-1}$]	Radical	λ_{max} [nm]	ε [$dm^3\,mol^{-1}\,cm^{-1}$]
$H_2C{=}CHO_2^{\bullet}$	440	1100 [a]	$Cl_2C{=}CClO_2^{\bullet}$	580	1300
$ClHC{=}CHO_2^{\bullet}$ [b]	480	890	uracil-5-$O_2^{\bullet}$	570	950
$ClHC{=}CHO_2^{\bullet}$ [c]	480	900	phenyl-$O_2^{\bullet}$	490	1600
$H_2C{=}CClO_2^{\bullet}$	480	530	anisyl-$O_2^{\bullet}$	600	2100
$ClHC{=}CClO_2^{\bullet}/Cl_2{=}CHO_2^{\bullet}$ (4/1)	540	1100			

[a] Lower limit; the vinyl bromide concentration was difficult to control because of the high volatility of vinyl bromide. [b] From *cis*-dichloroethene. [c] From *trans*-dichloroethene.

With an increasing number of chlorine substituents the absorption maximum of the peroxyl radicals undergoes a red-shift. It can be readily calculated that the energy of the transition drops by about 22 $kJ\,mol^{-1}$ per Cl substituent; it does not seem to matter whether the Cl atom is α or β to the peroxyl radical function.

The nature of the transitions that cause these surprising spectra is not yet known. It is noted, however, that the arylcarbinyloxyl radicals $ArCR_2O^{\bullet}$,[12] analogues of the arylperoxyl radicals $ArO_2^{\bullet}$ (cf. Table 1, see also ref. [13]), and the alkylthioperoxyl radicals RSO_2[14] both show absorption in the visible. Thus it may well be possible that these transitions are made possible by the interaction of the unpaired electron with the π system or the d orbitals at sulfur, respectively. These transitions are then possibly a kind of charge transfer band (cf. ref. [12]).

When the inverse of the first half-life of the decay of the vinylperoxyl and the chlorinated vinylperoxyl radicals is plotted as a function of the dose per pulse (i.e. initial peroxyl radical concentration), a straight line with an intercept close to zero is obtained. This means that they largely decay by reacting with one another and with the other peroxyl radicals present in these systems. Rate constants for the bimolecular termination on the order of $10^9\ dm^3\,mol^{-1}\,s^{-1}$ are calculated from this kind of plot. They are not much different from those found for the OH$^{\bullet}$ addition reaction [reaction (5); cf. Table 2].

However, very different behavior is displayed by the 5-bromouracil-derived vinylperoxyl radical, which undergoes very rapid unimolecular decay ($k = 6 \times 10^4\ s^{-1}$). In view of such a high rate it is not expected that bimolecular decay processes could compete significantly, given the relatively low peroxyl radical concentrations obtainable in our pulse-radiolysis experiments. Hence its decay is practically independent of the dose rate, in contrast to the other vinylperoxyl radicals. In agreement with the existence of a true unimolecular reaction the half-life is independent of the 5-bromouracil concentration. The final product of this reaction has been reported to be isodialuric acid.[15] It had in fact been postulated[15] to arise from some kind of an unimolecular decay process, but experimental evidence was lacking until now; further details still remain to be elucidated.

The addition of halogenated alkylperoxyl radicals such as trichloromethylperoxyl radicals to olefins has been reported recently, and the rate of this reaction has been shown to depend strongly on the Taft σ^* values of the substituents on the olefin.[16] No such first-order decay component was observed in the present systems at a concentration of the chlorinated olefin of about $10^{-3}\ mol\,dm^{-3}$. This is not surprising, since with chlorine substituent(s) at the C=C double bond the rate constant of peroxyl radical addition should be drastically reduced. Product analyses of the degradation of chlorinated olefins in aqueous solutions at low dose rates ($0.25\ Gy\,s^{-1}$) and upon UV photolysis (fluence at 254 nm $9\ Wm^{-2}$) indicate that the addition reaction of vinylperoxyl radicals to the chlorinated olefin must be very slow indeed and does not compete with the bimolecular decay of the peroxyl radicals.

Vinyl radicals do not show an appreciable absorption in the easily accessible spectral region[10] (confirmed in the present study); hence it is not possible to measure by spectroscopy their rate of reaction with a substrate as long as the ensuing substrate

Table 2. Compilation of rate constants determined by pulse radiolysis. The starred values were determined by product analysis.

Reaction	k [$dm^3 mol^{-1} s^{-1}$]	Reaction	k [$dm^3 mol^{-1} s^{-1}$]
$H_2C=CH^{\bullet} + O_2$	4.6×10^9	ClHC=CCl•/$Cl_2C=CH^{\bullet}$ (4/1) + propan-2-ol	6.3×10^6
$ClHC=CH^{\bullet}$ [a] + O_2	4.6×10^9		8.4×10^6
ClHC=CCl•/$Cl_2C=CH^{\bullet}$ (4/1) + O_2	4.3×10^9	$ClHC=CH^{\bullet}$ [a] + propan-2-ol	5.6×10^6
$Cl_2C=CCl^{\bullet} + O_2$	3.8×10^9	$H_2C=CH^{\bullet}$ + propan-2-ol	2.0×10^5
phenyl + O_2	4.6×10^9	phenyl + propan-2-ol	1.2×10^7
p-anisyl + O_2	4.3×10^9	*p*-anisyl + propan-2-ol	1.4×10^7
$COCl-CCl_2O_2^{\bullet} + COCl-CCl_2O_2^{\bullet}$	1.0×10^9	$Cl_2C=CCl^{\bullet}$ + methanol	2.9×10^6
$H_2C=CHO_2^{\bullet} + RO_2^{\bullet}$	1.1×10^9	ClHC=CCl•/$Cl_2C=CH^{\bullet}$ (4/1) + methanol	6.3×10^5
$ClHC=CHO_2^{\bullet}$ [a, b] + $RO_2^{\bullet}$ [c]	8.8×10^8	$ClHC=CH^{\bullet}$ + methanol	2.1×10^5
$ClHC=CClO_2^{\bullet} + RO_2^{\bullet}$ [c]	9.6×10^8	$Cl_2C=CCl^{\bullet}$ + 2-methylpropan-2-ol	1.6×10^5
$H_2C=CClO_2^{\bullet} + RO_2^{\bullet}$ [c]	9.0×10^8	$H_2C=CHO_2^{\bullet}$ + ascorbate	1.9×10^8
$Cl_2C=CClO_2^{\bullet} + RO_2^{\bullet}$ [c]	8.0×10^8	$HCCl=CHO_2^{\bullet}$ + ascorbate	1.6×10^8
uracil-5-$O_2^{\bullet}$ (unimolecular decay)	6.0×10^4 [d]	$HCCl=CClO_2^{\bullet}$ + ascorbate	2.9×10^8
$Cl_2C=CCl^{\bullet}$ + propan-2-ol	4.1×10^7	$H_2C=CClO_2^{\bullet}$ + ascorbate	2.6×10^8
	2.4×10^7	$Cl_2C=CClO_2^{\bullet}$ + ascorbate	2.3×10^8

[a] From *trans*-dichloroethene. [b] From *cis*-dichloroethene. [c] $RO_2^{\bullet}$ results from the bimolecular decay of vinylperoxyl radicals or from the peroxyl radical that arises from the addition of 'OH to the vinyl halide [reaction (5)]. [d] Dimension: s^{-1}.

radical also has no significant absorption. Alcohols are another example. Their radicals resulting from H-abstraction do not absorb strongly in either the UV or the visible.[17] Vinyl radicals undergo rapid H-abstraction reactions [e.g. reaction (10)];[18]

$$Cl_2C=CCl^{\bullet} + HC(CH_3)_2OH \longrightarrow Cl_2C=CHCl + {}^{\bullet}C(CH_3)_2OH \quad (10)$$

now, despite the poor detectability of both the starting and product radical species in reactions such as (10), rate constants can be determined by competition experiments with O_2 [cf. reaction (9)]. Rate constants can be determined in two ways: a) by product analysis: at a fixed O_2 concentration and increasing propan-2-ol concentration the yield of trichloroethene must go up; b) by pulse radiolysis: the absorbance of the vinylperoxyl radical must go down. Rate constants obtained from such measurements are compiled in Table 2.

It can be seen that the rate of reaction of vinyl radicals with alcohols increases with the number of chlorine substituents. The H atoms in methanol and 2-methylpropan-2-ol are more strongly bound than the tertiary one in propan-2-ol. Hence the reactivity of the vinyl radicals with these alcohols is much lower. This competition experiment does not allow the determination of rate constants smaller than 10^6 $dm^3 mol^{-1} s^{-1}$ as long as O_2-saturated solutions ($[O_2] = 1.25 \times 10^{-3}$ $mol\,dm^{-3}$) are used and the alcohol concentration is not increased much above 1 $mol\,dm^{-3}$. However, the range may be extended downward by an order of magnitude when the O_2 concentration is reduced to one-tenth by saturating the solutions with Ar/O_2 in a ratio of 10:1. The rate constants that fall into the range of 10^5–10^6 $dm^3 mol^{-1} s^{-1}$ were determined under these conditions.

Vinylperoxyl radicals are oxidants and may undergo electron transfer reactions, for instance with ascorbate ions. The rate constants were determined by following the buildup of the ascorbate radical absorption at 360 nm. It had been ascertained with the 2-chlorovinylperoxyl radical that its decay corresponds to the buildup of the ascorbate radical. It is noted that these rate constants (Table 2) are similar to those reported for chlorinated alkylperoxyl radicals.[19]

Experimental Procedure

For pulse radiolysis, purified (Millipore Milli-Q) water was saturated with Ar/O_2 mixtures, prior to the addition of appropriate amounts of the (volatile) halides, which were dissolved by prolonged stirring. The purity of the commercially available halides was ≥98%. Because of the high rate constants for the reaction of the halides with solvated electrons [cf. reaction (3)], impurities do not have a material impact on the spectra observed. The pulse-radiolysis setup has been described recently [8]. Some additional experiments were done conducted with ^{60}Co γ-radiation at a dose rate of 0.26 $Gy\,s^{-1}$.

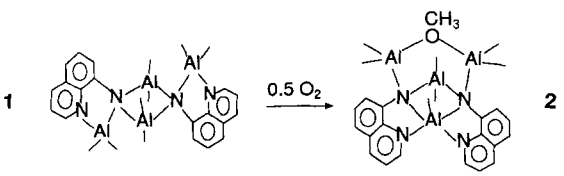
Received: December 11, 1993 [Z 6554 IE]
German version: *Angew. Chem.* **1994**, *106*, 1323

[1] a) J. G. Calvert, J. N. Pitts, Jr., *Photochemistry*, Wiley, New York, **1966**; b) P. G. Sammes in *The Chemistry of the Carbon–Halogen Bond, Part 2* (Ed.: S. Patai), Wiley, London, **1973**, p. 747.
[2] a) F. Hutchinson, W. Köhnlein, *Prog. Mol. Subcell. Biol.* **1980**, *7*, 1; b) C. von Sonntag, *The Chemical Basis of Radiation Biology*, Taylor and Francis, London, **1987**.
[3] a) R. F. Anderson, D. Schulte-Frohlinde, *J. Phys. Chem.* **1978**, *82*, 22; b) D. Schulte-Frohlinde, R. Anker, E. Bothe in *Oxygen and Oxy Radicals in Chemistry and Biology* (Eds.: M. A. J. Rodgers, E. L. Powers), Academic Press, New York, **1981**, p. 61.
[4] H. Scheytt, H. Esrom, L. Prager, R. Mehnert, C. von Sonntag in *Non-thermal Plasma Techniques for Pollution Control, Part B: Electron Beam and Electrical Discharge Processing* (Eds.: B. N. Penetrante, S. E. Schultheis) (*NATO ASI Ser. Ser. G* **1993**, *34 B*, 91).
[5] C. von Sonntag, G. Mark, R. Mertens, M. N. Schuchmann, H.-P. Schuchmann, *Aqua (London)* **1993**, *42*, 201.
[6] P. Neta, R. E. Huie, A. B. Ross, *J. Phys. Chem. Ref. Data* **1990**, *19*, 413.
[7] a) K.-D. Asmus, *Methods Enzymol.* **1984**, *105*, 167; b) *Pulse Radiolysis* (Ed.: Y. Tabata), CRC Press, Boca Raton, FL, USA, **1991**.
[8] C. von Sonntag, H.-P. Schuchmann in *Oxygen Radicals in Biological systems, Part C* (*Methods Enzymol.* **1994**, *233*, 3).
[9] C. von Sonntag, H.-P. Schuchmann, *Angew. Chem.* **1991**, *103*, 1255; *Angew. Chem. Int. Ed. Engl.* **1991**, *30*, 1229.
[10] R. Köster, K.-D. Asmus, *Z. Naturforsch. B* **1971**, *26*, 1108.
[11] G. V. Buxton, C. L. Greenstock, W. P. Helman, A. B. Ross, *J. Phys. Chem. Ref. Data* **1988**, *17*, 513.
[12] D. V. Avila, J. Lusztyk, K. U. Ingold, *J. Am. Chem. Soc.* **1992**, *114*, 6576.
[13] M. P. Sommeling, P. Mulder, R. Louw, D. V. Avila, J. Lusztyk, K. U. Ingold, *J. Phys. Chem.* **1993**, *97*, 8361.
[14] G. G. Jayson, D. A. Stirling, A. J. Swallow, *Int. J. Radiat. Biol.* **1971**, *19*, 143.
[15] E. Gilbert, D. Schulte-Frohlinde, *Z. Naturforsch. B* **1970**, *25*, 492.
[16] Z. B. Alfassi, R. E. Huie, P. Neta, *J. Phys. Chem.* **1993**, *97*, 6835.
[17] K.-D. Asmus, A. Henglein, A. Wigger, G. Beck, *Ber. Bunsenges. Phys. Chem.* **1966**, *70*, 756.
[18] a) E. Gilbert, G. Wagner, D. Schulte-Frohlinde, *Z. Naturforsch. B* **1971**, *26*, 209; b) E. Gilbert, G. Wagner, *ibid.* **1972**, *27*, 644; c) E. Gilbert, C. Cristallini, *ibid.* **1973**, *28*, 615.
[19] a) J. E. Packer, R. L. Willson, D. Bahnemann, K.-D. Asmus, *J. Chem. Soc. Perkin Trans. 2* **1980**, *296*; b) M. Lal, C. Schöneich, J. Mönig, K.-D. Asmus, *Int. J. Radiat. Biol.* **1988**, *54*, 773.

Oxygen-Induced Structural Transformation of the Polynuclear Organoaluminum Complex $[Al_4(\mu_3\text{-8-quinolylimide})_2(CH_3)_8]$ to $[Al_4(\mu_3\text{-8-quinolylimide})_2(CH_3)_7(\mu\text{-}OCH_3)]$**

Steven J. Trepanier and Suning Wang*

Organoaluminum amido and imido complexes have attracted much attention on account of their rich structural and bonding features and potential applications.[1-3] Most of the previous studies focused on the synthesis, structures, and thermal properties of alkylaluminum compounds with monodentate amido or imido ligands, although a few alkylaluminum complexes with bidentate amido ligands have been reported.[2-4] The extensive investigations into the chemical reactivities of trialkylaluminum were promoted by their valuable industrial applications.[5] In contrast, little is known about the reactivity of alkylaluminum amido or imido compounds. We report here the synthesis and structures of two novel tetranuclear alkylaluminum complexes with 8-quinolylimide ligands (**1** and **2**) and their unusual reactivities with oxygen.



The reaction of $Al(CH_3)_3$ with 8-quinolylamine in a 2:1 ratio in toluene at 23 °C produced the colorless compound **1** in high yield. This compound has been fully characterized by ^{1}H NMR and single-crystal X-ray diffraction analyses.[6] The structure of **1** (Fig. 1) has an inversion center. The imido nitrogen atom N2 has tetrahedral geometry and bridges three aluminum atoms with nearly equal Al–N2 bond lengths. The Al2–N1 distance of 1.993(6) Å lies within the same range. Each aluminum atom is also coordinated to two methyl groups, thus attaining tetrahedral geometry. The Al1–Al1′ separation of 2.788(5) Å is similar to those observed previously in dinuclear aluminum amido complexes.[1-3] If **1** retains the same structure in solution as that in the solid state, four methyl signals should have been observed in the ^{1}H NMR spectrum. Because only two methyl signals with nearly equal intensity appear in the ^{1}H NMR spectrum of **1** at 298 K we conclude that in solution compound **1** has C_{2h} symmetry with the two quinoline rings in the mirror plane.

Reactions between trialkylaluminum and primary amines usually yield amido complexes.[1-4] Tetranuclear aluminum complexes with monodentate imido ligands and cubane structures were typically obtained by heating the corresponding dinuclear amido complexes.[2c, 3b] In contrast, tetranuclear **1** was obtained readily by the direct reaction of $Al(CH_3)_3$ with 8-quinolylamine at 23 °C, perhaps promoted by the presence of the pyridyl group. Such a reactivity has not been observed in monodentate aromatic primary amines such as 8-naphthylamine, which forms a dinuclear aluminum amido complex[3a] upon reaction with $Al(CH_3)_3$.

[*] Prof. Dr. S. Wang, S. J. Trepanier
Department of Chemistry and Biochemistry, University of Windsor
Windsor, Ontario N9B 3P4 (Canada)
Telefax: Int. code + (519)973-7098

[**] This work was supported by the Natural Sciences and Engineering Research Council of Canada.

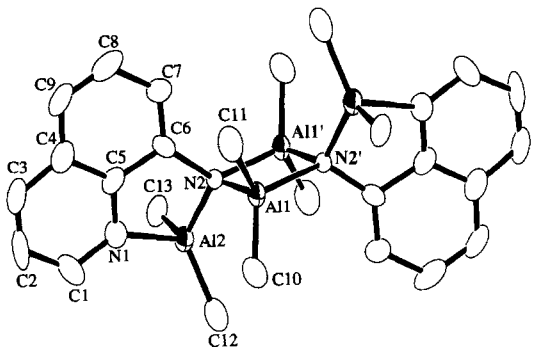


Fig. 1. An ORTEP diagram showing the molecular structure of **1** with labeling scheme (50% thermal ellipsoids). Selected bond lengths and angles: Al1-N2 1.992(7), Al1-N2′ 1.941(6), Al1-C10 1.97(1), Al1-C11 1.969(9), Al2-N1 1.993(6), Al2-N2 1.930(7), Al2-C12 1.946(9), Al2-C13 1.98(1); N2-Al1-N2′ 89.7(2), C10-Al1-C11 109.3(4), N1-Al2-N2 85.6(3), C12-Al2-C13 117.5(4), C6-N2-Al2 103.8(4), Al1-N2-Al1′ 90.3(3).

The most interesting property of **1** is its reaction with oxygen and transformation to **2**. Compound **2** was initially isolated in the synthesis of **1** as a minor orange product. NMR and single-crystal X-ray diffraction analyses[6] revealed that there is a methoxy ligand in **2**, which was confirmed by independent synthesis by reaction of $Al(CH_3)_3$ with 8-quinolylamine and methanol in a 4:2:1 ratio in toluene at 23 °C (yield 40%). Since there were no sources of methanol available in the original synthesis of **1**, we postulate that the methoxy group was produced by the reaction of the methyl ligand with a trace amount of oxygen present in the reaction medium; thus, **1** may be the direct precursor to **2**. In fact, when **1** was exposed to 0.5 equiv. of O_2 in toluene at 23 °C, it was converted into **2** nearly quantitatively after about 24 h (monitored by ^{1}H NMR spectroscopy).

As shown in Figure 2, the oxidation has caused a dramatic change in the coordination environments and the arrangement of the four aluminum centers, from a butterfly structure in **1** to a tetrahedron in **2**. Although it is not unexpected that the re-

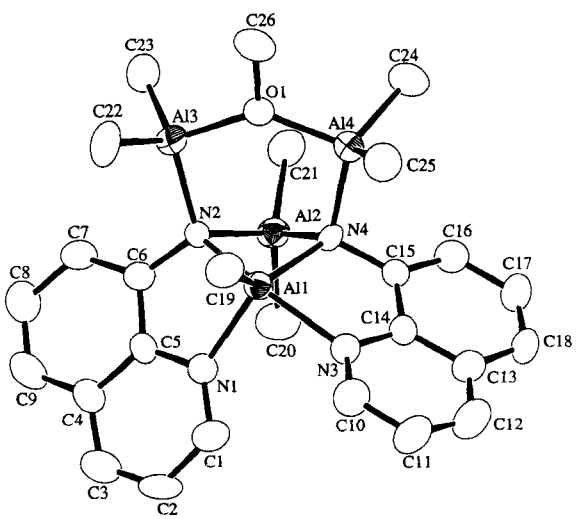


Fig. 2. An ORTEP diagram showing the molecular structure of **2** with labeling scheme (50% thermal ellipsoids). Selected bond lengths and angles: Al1-N1 2.039(6), Al1-N2 2.014(5), Al1-N3 2.122(5), Al1-N4 1.943(5), Al1-C19 1.953(7), Al2-N2 1.958(5), Al2-N4 1.923(5), Al2-C20 1.967(7), Al2-C21 1.950(7), Al3-N2 1.929(5), Al3-O1 1.868(4), Al3-C22 1.955(7), Al3-C23 1.952(7), Al4-N4 1.949(5), Al4-O1 1.857(4), Al4-C24 1.958(8), Al4-C25 1.941(8); N1-Al1-N4 125.0(2), N2-Al1-N3 154.3(2), N1-Al1-C19 104.4(3), N4-Al1-C19 130.6(3), N2-Al1-N4 81.0(2), N2-Al2-N4 83.0(2), C20-Al2-C21 115.2(3), Al3-O1-Al4 136.6(3), N2-Al3-O1 97.4(2), C22-Al2-C23 112.1(3), N4-Al4-O1 99.0(2), C24-Al4-C25 111.9(4).

 © VCH Verlagsgesellschaft mbH, D-69451 Weinheim, 1994 0570-0833/94/1212-1265 $ 10.00+.25/0

placement of a methyl group by a methoxy group causes a significant structural change since the methoxy group has a stronger tendency than a methyl group to be a bridging ligand, structural evidence for this type of transformation, especially that induced by oxidation with oxygen, is scarce in organoaluminum amido and imido complexes. As in **1**, the imido nitrogen atom in **2** bridges three aluminum centers with nearly equal Al–N distances. Both pyridyl nitrogen atoms are coordinated to the Al1 atom with slightly longer Al–N distances than those of imido nitrogen–aluminum bonds. The complex contains three types of aluminum centers, a five-coordinate Al1 with one carbon and four nitrogen atoms, a four-coordinate Al2 with two carbon and two nitrogen atoms, and four-coordinate Al3 and Al4 with two carbon atoms and one nitrogen and one oxygen atom. The environment about the five-coordinate Al1 could be described as a distorted trigonal bipyramid in which N2 and N3 occupy the axial positions. Although such a geometry is not very common for organoaluminum complexes, it has been reported previously.[1–3] The four aluminum atoms have an approximate tetrahedral arrangement. The shortest separation (2.801(3) Å) is between Al1 and Al2, which is apparently caused by the two imido nitrogen bridges. The longest separation (3.460(3) Å) is between Al3 and Al4, which are bridged by the methoxy ligand.

The crystal structure of **2** is asymmetric. Every one of the seven methyl groups bonded to the aluminum centers have different chemical environments in the solid state. If the structure of **2** is the same in solution as in the solid state, seven chemical shifts due to the seven methyl groups bonded to the aluminum centers should be detected in the ^{1}H NMR spectrum. Since for these methyl groups the ^{1}H NMR spectrum at 186–197 K shows only five chemical shifts in the region of $\delta = 0.5$ to -2.0 with a ratio of 1:2:1:2:1, we deduce that in solution **2** has a symmetric structure with a mirror plane containing Al1, Al2, and the methoxy group.

Compound **2** is much more stable toward oxygen oxidation than **1**. After the toluene solution of **2** had been exposed to one atmosphere of O_2 for about 12 h at 23 °C, no decomposition could be detected by ^{1}H NMR spectroscopy. Significant decomposition of **2** was observed only after the soluton was exposed to oxygen for several days. The decomposition products have not been characterized.

The behavior of **1** and **2** toward oxygen is unusual. Trialkylaluminum complexes react rapidly with oxygen to produce alkoxide products via the peroxide intermediate, and very often these reactions are so fast that little control of the desired products is possible unless extreme reaction conditions such as low temperature are employed.[7] Both imido and methyl ligands in **1** are susceptible to oxidation, but only one of the methyl ligands was oxidized by oxygen, and **2** was the only product. This implies that the alkyl group in alkylaluminum imido complexes is more susceptible to oxygen than the imido ligand. The high stability of **2** toward oxygen could be attributable to the bridging and electronic effects of the methoxy and imido ligands.

Experimental

All synthetic manipulations were performed under an inert atmosphere (dried argon).

1: $Al(CH_3)_3$ (2.0 M, 2.0 mL) in toluene (0.004 mol) was added to 8-quinolylamine (0.29 g, 0.002 mol) in toluene (10 mL) at 23 °C. The mixture was stirred for 30 minutes. Upon concentration of the solution colorless crystals of compound **1** precipitated in nearly quantitative yield. ^{1}H NMR ([D$_8$]toluene, 25 °C): $\delta = -0.22$ (s, 12H, CH_3), -0.06 (s, 12H, CH_3), 6.35 (m, 2H, CH), 6.82 (d, 2H, CH), 7.30 (m, 4H, CH), 7.62 (m, 2H, CH), 8.24 (m, 2H, CH). Elemental analysis: Calcd for $C_{26}H_{36}Al_4N_4$: C, 60.98; H, 7.03; N, 10.95. Found: C, 60.79; H, 7.08; N, 10.65.

2: $Al(CH_3)_3$ (2.0 M, 2.0 ml) in toluene (0.004 mol) was added to 8-quinolylamine (0.29 g, 0.002 mol) in toluene (10 mL) at 23 °C. After the mixture was stirred for 10 min, methanol (0.032 g, 0.001 mol) was added. The resulting orange-brown solution was stirred for 30 minutes. Upon concentration of the solution yellow-orange crystals of **2** were obtained in nearly quantitative yield. ^{1}H NMR ([D$_6$]benzene, 25 °C): $\delta = -1.83$ (s, 3H, CH_3), -0.60 (s, 6H, CH_3), 0.01 (s, 3H, CH_3), 0.13 (s, 6H, CH_3), 0.27 (s, 3H, CH_3), 3.59 (s, 3H, CH_3), 6.46 (m, 2H, CH), 6.81 (d, 2H; CH), 7.12 (m, 2H, CH), 7.42 (m, 2H, CH), 7.75 (m, 4H, CH). ^{13}C NMR ([D$_6$]benzene, 25 °C): $\delta = -9.13$; -6.02; -4.11 (CH_3), 50.17 (OCH_3), 117.80; 120.66; 122.73; 129.65; 130.49; 140.96; 143.88; 145.41; 149.60 (aromatic C). Elemental analysis: Calcd. for $C_{26}H_{36}Al_4ON_4$: C, 59.14; H, 6.82; N, 10.61. Found: C, 57.08; H, 6.31; N, 10.25. The low C, H, and N content of this sample are probably caused by the partial decomposition of this material during analysis.

Transformation of **1** to **2**: O_2 (4.80 cm^3 at 1 atm; 0.196 mmol) was introduced to a toluene solution (15 mL) containing **1** (0.20 g, 0.391 mmol) by syringe at 23 °C. After 48 h **1** was completely converted into **2**, as shown by ^{1}H NMR spectra.

Received: December 6, 1993 [Z 6542 IE]
German version: *Angew. Chem.* **1994**, *106*, 1357

[1] a) Z. Jian, L. V. Interrante, D. Kwon, F. S. Tham, R. Kullnig, *Inorg. Chem.* **1992**, *31*, 4815; b) Z. Jian, L. V. Interrante, *Chem. Mater.* **1990**, *2*, 439; c) K. J. L. Paciorek, J. H. Nakahara, L. A. Hoferkamp, C. George, J. L. Flippen-Anderson, R. Gilardi, *ibid.* **1991**, *3*, 82; d) D. C. Boyd, R. T. Haasch, D. R. Mantell, R. K. Schutze, J. F. Evans, W. L. Gladfelter, *ibid.* **1989**, *1*, 119; e) F. C. Sauls, L. V. Interrante, *Coord. Chem. Rev.* **1993**, *128*, 193.

[2] a) S. J. Schauer, W. T. Pennington, G. H. Robinson, *Organometallics* **1992**, *11*, 3287; b) J. J. Byers, B. Lee, W. T. Pennington, G. H. Robinson, *Polyhedron* **1992**, *11*, 967; c) K. M. Waggoner, P. P. Power, *J. Am. Chem. Soc.* **1991**, *113*, 3385; d) D. M. Choquette, M. J. Timm, J. L. Hobbs, M. M. Rahim, K. J. Ahmed, R. P. Planalp, *Organometallics* **1992**, *11*, 529; e) J. F. Janik, E. N. Duesler, R. T. Paine, *Inorg. Chem.* **1988**, *27*, 4335.

[3] a) M. G. Davidson, D. Elilio, S. J. Less, A. Martin, P. R. Raithby, R. Snaith, D. S. Wright, *Organometallics* **1993**, *12*, 1; b) D. M. Choquette, M. J. Timm, J. L. Hobbs, T. M. Nicholson, M. M. Olmstead, R. P. Planalp, *Inorg. Chem.* **1993**, *32*, 2600; c) S. Cucinella, T. Salvatori, C. Busetto, M. Cesari, *J. Organomet. Chem.* **1976**, *121*, 137; d) P. B. Hitchcock, J. D. Smith, K. M. Thomas, *J. Chem. Soc. Dalton Trans.* **1976**, 1433; e) Z. Jian, L. V. Interrante, D. Kwon, F. S. Tham, R. Kullnig, *Inorg. Chem.* **1991**, *30*, 995.

[4] O. T. Beachley, Jr., K. C. Racette, *Inorg. Chem.* **1976**, *15*, 2110; b) *ibid.* **1975**, *14*, 2534; c) G. Dozzi, C. Busetto, T. Salvatori, S. Cucinella, *J. Organomet. Chem.* **1980**, *192*, 17.

[5] J. J. Eisch in *Comprehensive Organometallic Chemistry, Vol. 1* (Eds.: G. Wilkinson, F. G. A. Stone, E. W. Abel), Pergamon, Oxford, **1982**, Chap. 6.

[6] Crystal data for **1**: $C_{26}H_{36}Al_4N_4$, monoclinic, space group $P2_1/n$, $a = 8.637(3)$, $b = 14.056(4)$, $c = 12.396(6)$ Å, $\beta = 108.17(3)°$, $V = 1429.8(9)$ Å^3, $Z = 2$, $\rho_{calcd} = 1.190$ g cm^{-3}, $T = 298$ K. Crystal data for **2**: $C_{26}H_{36}Al_4N_4O$, monoclinic, space group $P2_1/c$, $a = 13.741(3)$, $b = 14.040(3)$, $c = 15.175(2)$ Å, $\beta = 92.02(2)°$, $V = 2925.7(9)$ Å^3, $Z = 4$, $\rho_{calcd} = 1.200$ g cm^{-3}, $T = 298$ K. Data were collected on a Rigaku AFC6-S diffractometer with graphite-monochromated $Mo_{K\alpha}$ radiation operated at 50 kV and 35 mA. The structure solution and refinement for both compounds were carried out by using the TEXSAN software program on a Silicon Graphics Computer. Convergence to the final R values of $R = 0.074$ and $R_w = 0.082$ was achieved for **1** by using 1093 reflections ($I > 3.00\,\sigma(I)$) and 154 parameters. Convergence to the final R values of $R = 0.065$ and $R_w = 0.049$ was achieved for **2** by using 2487 reflections ($I > 3.00\,\sigma(I)$) and 316 parameters. Further details of the crystal structure analysis may be obtained from the Fachinformationszentrum Karlsruhe, D-76344 Eggenstein-Leopoldshafen (FRG), on quoting the depository number CSD-58077 and the journal citation.

[7] a) T. G. Brilkina, V. A. Shushunov, *Reactions of Organometallic Compounds with Oxygen and Peroxides*, Iliffe, London, **1969**; b) W. M. Cleaver, A. R. Barron, *J. Am. Chem. Soc.* **1989**, *111*, 8966.

The First Cycloaddition Reactions of Dimeric Arsenium Cations**

Neil Burford,* Trenton M. Parks, Pradip K. Bakshi, and T. Stanley Cameron*

Small molecules containing coordinatively unsaturated centers are excellent foundations from which to develop new directions in synthetic chemistry. The *carbenes* **1** are perhaps the best known examples,[1] and recently a number of new reactions have been reported.[2] The chemistry of the analogous *phosphenium cations* **2** is also extensive and represents a principal direction in the development of modern phosphorus chemistry.[3] We have recently synthesized simple compounds containing *arsenium* centers and shown them, in the absence of a π-delocalized framework,[4] to adopt weakly associated dimeric structures **3** in the solid state.[5] Here we report the first cycloaddition reactions for these cations, demonstrating dramatic contrasts to observations for phosphenium cations. Additionally, we show surprising differences between the reactivity of **3a** and **3b**.

1 **2**

3a: X = NMe
b: X = S

The tetrachlorogallate salts of **3a** and **3b** each react rapidly with 2,3-dimethyl-1,3-butadiene in CH_2Cl_2 to give bicyclic cationic products. Reaction of **3a**-$(GaCl_4)_2$ gives the ammonium salt **4**-$GaCl_4$[6] in essentially quantitative yield (as shown by ^1H NMR spectroscopy of the reaction mixture).

4 **5** **6**

Crystallographic characterization of **4**-$GaCl_4$ confirms the bicyclic structure of the cation, and an expected pyramidal geometry for arsenic (Fig. 1).[7] The cross-ring As1–N2 bond is significantly longer [2.056(10) Å] than that of As1–N1 [1.797(11) Å], and both are slightly longer than those observed in the dication **3a** [tetracoordinate As to N, 1.949(4) Å; tricoordinate As to N, 1.752(5) Å]. Published values for As–N bonds are limited, but are typically in the range of 1.82 to 1.88 Å.[8] For further comparison we have also determined the structure of the neutral dimethyldiazarsolidine **5**[5] [As–N: 1.830(8) and 1.77(1) Å].[9]

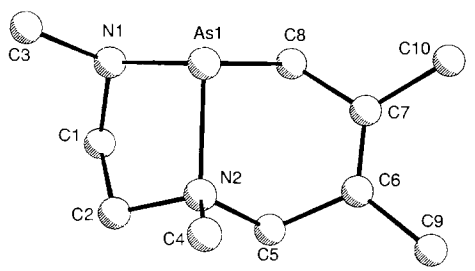


Fig. 1. PLUTO plot of cation **4**. Hydrogen atoms omitted for clarity.

2,3-Dimethylbuta-1,3-diene reacts with **3b**-$(GaCl_4)_2$ to give a mixture (^1H and ^{13}C NMR spectra show a multitude of complex and broad signals) from which we have isolated the $GaCl_4^-$ salt of 1-thionia-4,6-dithia-5-arsabicyclo[3.3.0]octane (**6**).[10] Crystallographic characterization[11] reveals a bicyclic structure for cation **6** (Fig. 2), reminiscent of **4**. The unexpected structure of **6** can be considered in terms of an extrusion of an As–S^+ moiety from the dimer **3b**, perhaps by an initial interaction with butadiene in a fashion similar to its analogous reaction with **3a**. We have also been able to synthesize **6**-$GaCl_4$ quantitatively (as shown by ^1H and ^{13}C NMR spectroscopy of the reaction mixture) from **7**[12] with $GaCl_3$. Comparison of the cross-ring bonds in **6** [As1–S2, 2.390(4); As2–S5, 2.347(4) Å] and **7** [As–S, 2.719(3) Å][13] reveals that heterolytic As–Cl bond cleavage of **7** enhances the S → As cross-ring donation. The long cross-ring bonds in both **4** and **6** allow a classification of these compounds as intramolecular base-stabilized[14] arsenium cations.

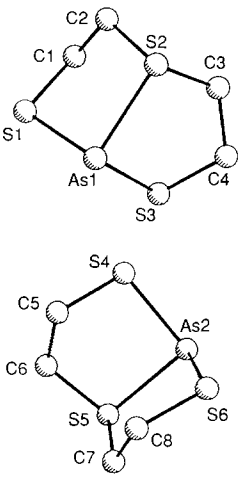


Fig. 2. PLUTO plot of cation **6**. Two molecules are present in the asymmetric unit. Hydrogen atoms are omitted for clarity.

Reactions of **3** with 2,3-dimethylbutadiene are in dramatic contrast to the corresponding established cycloaddition chemistry of this butadiene with phosphenium cations, which provide the spirocyclic phosphonium cation **8**.[15] Although the nature of the arsenium cations in solution is not clear,[5] the quantitative formation of **4** implies a concerted process, possibly a Diels–Alder type cycloaddition involving the As–N bond of either the dimer or the monomer as dienophile. We conclude that the electronic structure of the arsenium cations differs significantly from the phosphenium analogues in terms of the relative energy of the LUMO and of the nonbonding electron pair at the arsenic center. However, the reactivity of the arsenium cations may be biased by the penchant for dimer formation, which is not observed for phosphenium cations.[16]

7

8

Experimental Procedure

NMR: Bruker AC250 (250 MHz for ^1H, 62.89 for ^{13}C) and Bruker AMX400 spectrometers (400 MHz for ^1H, 100.6 for ^{13}C). Shifts are reported relative to TMS and referenced to the internal solvent signal. IR: Nicolet 510P FT-IR spectrometer. All reactions were performed in evacuated vessels [17].

4-$GaCl_4$: 2,3-Dimethylbutadiene (0.11 g, 1.3 mmol) in CH_2Cl_2 (about 7 mL) was added dropwise (8 min) to a stirred solution of **3a**-$(GaCl_4)_2$ (0.32 g, 0.42 mmol) in CH_2Cl_2 (about 37 mL). Slow removal of solvent in vacuo gave colorless crystals of **4**-$GaCl_4$ (55% yield). Very air-sensitive.

[*] Dr. N. Burford, T. M. Parks, P. K. Bakshi, Dr. T. S. Cameron
Department of Chemistry
Dalhousie University
Halifax, Nova Scotia B3H 4J3 (Canada)
Telefax: Int. code + (902)494-1310

[**] In this paper the terms phosphenium and arsenium ion are used instead of phospharylium and arsanylium ion recommended by IUPAC.

6-$GaCl_4$: 2,3-Dimethylbutadiene (0.14 g, 1.7 mmol) in CH_2Cl_2 (about 10 mL) was added dropwise (8 min) to a stirred solution of **3b**-$(GaCl_4)_2$ (0.35 g, 0.46 mmol) in CH_2Cl_2 (about 50 mL). Slow removal of solvent (>75%) in vacuo gave pale yellow crystals and a dark brown powder. The crystals were characterized as **6**-$GaCl_4$ (crude yield 57%). Very air-sensitive. The brown powder was not characterized.

6-$GaCl_4$: $GaCl_3$ (0.27 g, 1.5 mmol) in CH_2Cl_2 (about 24 mL) was added dropwise (55 min) to a stirred solution of **7** (0.40 g, 1.5 mmol) in CH_2Cl_2 (about 36 mL). Precipitation resulted in a white powder. Characterized as **6**-$GaCl_4$ (78% yield). Very air-sensitive.

Received: December 30, 1993
Revised: February 28, 1994 [Z 6591 IE]
German version: *Angew. Chem.* **1994**, *106*, 1332

[1] See, for example, a) G. L. Clos, P. P. Gaspar, G. S. Hammond, H. D. Hartzler, C. Mackay, D. Seyferth, A. M. Trozollo, E. Wassermann in *Carbenes* (Eds.: R. A. Moss, M. Jones), Wiley, New York, **1975**; b) W. Kirmse, *Carbene Chemistry*, 2nd ed., Academic Press, New York, **1971**; c) J. Hine, *Divalent Carbon*, Ronald Press, New York, **1964**.

[2] a) G. R. Gillette, A. Baceiredo, G. Bertrand, *Angew. Chem.* **1990**, *102*, 1486; *Angew. Chem. Int. Ed. Engl.* **1990**, *29*, 1429; b) A. J. Arduengo III, M. Kline, J. C. Calabrese, F. Davidson, *J. Am. Chem. Soc.* **1991**, *113*, 9704; c) A. J. Arduengo III, H. V. Rasika Dias, J. C. Calabrese, F. Davidson, *ibid.* **1992**, *114*, 9724; d) *Inorg. Chem.* **1993**, *32*, 1541.

[3] M. Sanchez, M. R. Mazières, L. Lamandé, R. Wolf in *Multiple Bonds and Low Coordination in Phosphorus Chemistry* (Eds.: M. Regitz, O. J. Scherer), Thieme, Stuttgart, **1990**, p. 129–149.

[4] N. Burford, T. M. Parks, B. W. Royan, J. F. Richardson, P. S. White, *Can. J. Chem.* **1992**, *70*, 703.

[5] N. Burford, T. M. Parks, B. W. Royan, T. S. Cameron, J. F. Richardson, E. J. Gabe, R. Hynes, *J. Am. Chem. Soc.* **1992**, *114*, 8147.

[6] **4**-$(GaCl_4)$: M.p. 139–140 °C. ^{1}H NMR (CD_2Cl_2): δ = 1.95 (m, 6H), 2.67 (d, 1H), 2.97 (s, 3H), 3.10 (d, 1H), 3.15 (t of d, 1H), 3.22 (s, 3H), 3.49 (d of d, 1H), 3.55 (d, 1H), 3.69 (d of d, 1H), 3.85 (d, 1H), 3.90 (d of d of d, 1H); ^{13}C NMR (CD_2Cl_2): δ = 20.3, 20.7, 37.6, 41.8, 52.2, 59.1, 62.2, 62.8, 128.8, 130.4. Peaks assigned by 2D NMR techniques (cosy, inverse H,X-COSY (HETCOR)). IR (Nujol): $\tilde{\nu}$[cm^{-1}] = 1657(w), 1413(m), 1325(w), 1300(w), 1270(m), 1241(m), 1171(m), 1116(m), 1073(m), 1058(w), 1009(m), 984(m), 967(s), 940(w), 924(w), 885(w), 867(m), 798(w), 784(m), 737(w), 655(w), 597(w), 581(m), 569(m), 525(w), 453(w), 423(w), 383(vs), 366(s), 349(m), 313(w), 228(w). Correct C,H analysis. NMR of the reaction mixture is essentially identical to that of the redissolved pure material.

[7] a) Crystal data for $C_{10}H_{20}AsCl_4GaN_2$: M = 454.74, orthorhombic, $Pca2_1$, a = 18.471(2), b = 7.000(2), c = 13.738(1) Å, V = 1776.2(8) Å^3, Z = 4, ρ_{calcd} = 1.70 Mg m^{-3}, μ = 39.84 cm^{-1}. Data were collected at 18 ± 1 °C on a Rigaku AFC5R diffractometer with graphite monochromated $Mo_{K\alpha}$ radiation (λ = 0.71069 Å) using the ω-2θ scan technique ($2\theta_{max.}$ = 46.0°). The structure was solved by direct methods and refined by block-matrix least squares to R = 0.0437, R_w = 0.0437 for 951 observed reflections with $I > 3.00\sigma(I)$ and with 162 parameters. All calculations were performed on a VAX computer using the SHELX 76 crystallographic software package of Crystal Structure Determination, G. M. Sheldrick, SHELX 76. Program for Crystal Structure Determination, University of Cambridge, Cambridge (UK) 1976. b) Further details of the crystal structure investigations are available on request from the Director of the Cambridge Crystallographic Data Centre, 12 Union Road, GB-Cambridge CB2 1EZ (UK), on quoting the full journal citation.

[8] See, for example, a) J. Weiss, W. Eisenhuth, *Z. Anorg. Allg. Chem.* **1967**, *350*, 9; b) A. Gieren, H. Betz, T. Hübner, V. Lamm, M. Herberhold, K. Guldner, *ibid.* **1984**, *513*, 160; c) M. Veith, B. Bertsch, *ibid.* **1988**, *557*, 7; d) R. Bohra, H. W. Roesky, M. Noltemeyer, G. M. Sheldrick, *Acta Crystallogr. Sect. C* **1984**, *40*, 1150; e) H. Grützmacher, H. Pritzkow, *Chem. Ber.* **1989**, *122*, 1417.

[9] Crystal data for $C_4H_{10}AsClN_2$: M = 196.51, monoclinic, $P2_1/n$, a = 6.959(7), b = 9.23(2), c = 12.14(2) Å, β = 95.4(1)°, V = 777(4) Å^3, Z = 4, ρ_{calcd} = 1.681 Mg m^{-3}, μ = 46.24 cm^{-1}. Data were collected at −60 ± 1 °C (melts at 19 °C) on a Rigaku AFC5R diffractometer with graphite monochromated $Mo_{K\alpha}$ radiation (λ = 0.71069 Å) using the ω-2θ scan technique ($2\theta_{max.}$ = 46°). The structure was solved by direct methods and refined by full-matrix least squares on F to R = 0.0431, R_w = 0.0587 for 814 observed reflections with $I > 3.00\,\sigma(I)$ and with 73 parameters. All calculations were performed on a VAX computer using the TEXSAN crystallographic software package of Molecular Structure Corporation (TEXSAN—TEXRAY Single Crystal Structure Analysis Package, Version 5.0, Molecular Structure Corporation, The Woodlands, Texas, **1989**). See also [7b].

[10] **6**-$(GaCl_4)$: Chars 200 °C, M.p. 218–221 °C. ^{1}H NMR (CD_2Cl_2): δ = 4.10 (m, 4H), 3.85 (m, 4H); ^{13}C NMR (CD_2Cl_2): δ = 49.8, 43.2; IR(Nujol): $\tilde{\nu}$[cm^{-1}] = 1416(m), 1282(w), 1252(m), 1149(w), 1137(w), 941(w), 932(w), 907(m), 831(m), 811(m), 668(w), 652(w), 597(w), 441(w), 429(w), 377(vs), 370(vs); correct C,H analysis.

[11] Crystal data for $C_4H_8AsCl_4GaS_3$: M = 438.74, monoclinic, $P2_1/n$, a = 14.669(2), b = 12.647(5), c = 15.112(2) Å, β = 100.20(1)°, V = 2759(2) Å^3, Z = 8, ρ_{calcd} = 2.112 Mg m^{-3}, μ = 55.44 cm^{-1}. Data were collected at 18 ± 1 °C on a Rigaku AFC5R diffractometer with graphite monochromated $Mo_{K\alpha}$ radiation (λ = 0.71069 Å) using the ω-2θ scan technique ($2\theta_{max.}$ = 46.0°). The structure was solved by direct methods and refined by full-matrix least squares to R = 0.0468, R_w = 0.0583 for 2210 observed reflections with $I > 3.00\sigma(I)$ and with 236 parameters. All calculations were performed on a VAX computer using the TEXSAN crystallographic software package of Molecular Structure Corporation (TEXSAN—TEXRAY Structure Analysis Package, Molecular Structure Corporation, **1989**). See also [7b].

[12] R. Engler, *Z. Anorg. Allg. Chem.* **1974**, *406*, 74.

[13] M. Dräger, *Chem. Ber.* **1974**, *107*, 2601.

[14] See, for example, M. Veith, S. Becker, V. Huch, *Angew. Chem.* **1989**, *101*, 1287; *Angew. Chem. Int. Ed. Engl.* **1989**, *28*, 1237.

[15] a) C. K. SooHoo, S. G. Baxter, *J. Am. Chem. Soc.* **1983**, *105*, 7443; b) A. H. Cowley, R. A. Kemp, J. G. Lasch, N. C. Norman, C. A. Stewart, *ibid.* **1983**, *105*, 7444; c) A. H. Cowley, R. A. Kemp, J. G. Lasch, N. C. Norman, C. A. Stewart, B. R. Whittlesey, T. C. Wright, *Inorg. Chem.* **1986**, *25*, 740.

[16] N. Burford, P. Losier, C. MacDonald, V. Kyrimis, P. K. Bakshi, T. S. Cameron, *Inorg. Chem.*, **1994**, *33*, 1434.

[17] N. Burford, J. Müller, T. M. Parks, *J. Chem. Educ.*, in press.

Metalation of Tris(trimethylsilyl)- and Tris(dimethylphenylsilyl)methane with Methylsodium: The First Dialkylsodate**

Salih S. Al-Juaid, Colin Eaborn, Peter B. Hitchcock, Keith Izod, Michael Mallien, and J. David Smith*

The diorganolithate $[Li(thf)_4][LiR_2]$, where R = $C(SiMe_3)_3$, the first example of a species that had been postulated many years earlier but never observed, was obtained in 1983 by metalation of $(Me_3Si)_3CH$ with MeLi in tetrahydrofuran.[1] Two further salts, $[Li(tmen)_2][LiR_2]$[2] (tmen = $Me_2N(CH_2)_2NMe_2$) and [(pmdeta)Li(μ-Cl)Li(pmdeta)][LiR_2],[3] pmdeta = $Me_2N(CH_2)_2NMe(CH_2)_2NMe_2$, were subsequently isolated, but no other diorganolithate or diorganosodate has been reported, although organosodium compounds have been known for more than 70 years.[4] We now describe the preparation and structural characterization of such a species.

The metalation of $(Me_3Si)_3CH$ by MeNa in Et_2O[5] was rather slow, and complicated by reaction between the alkylsodium and the solvent. However, in the presence of tmen reaction was rapid. The product was isolated as colorless plates that were air- and moisture-sensitive and was shown by X-ray diffraction to be **1**.[6] The ether was rapidly lost in vacuum; no trace of it

$[Na(tmen)_2(Et_2O)]\,[Na\{C(SiMe_3)_3\}_2]$ **1**

was detected in the ^{1}H NMR spectrum of a sample that had been pumped on for about 30 s.

As shown in Figure 1 the structure consists of discrete cations and anions. The sodium atoms in both ions are in special positions: the anion lies across a center of symmetry and is therefore linear, and the cation is on a two-fold axis along Na2–O. The Na–C bond length of 247.9(6) pm is unusually short;[7] that in polymeric $NaCH(SiMe_3)_2$,[8] in which the Na is also two-coordinate but with weak interactions to adjacent hydrogen atoms, is 255.5(10) pm. Most other organosodium compounds have

[*] Dr. J. D. Smith, Dr. S. S. Al-Juaid, Prof. C. Eaborn, Dr. P. B. Hitchcock, Dr. K. Izod, Dr. M. Mallien
School of Chemistry and Molecular Sciences, University of Sussex
Brighton, BN1 9QJ (UK)
Telefax: Int. code + (273)/677-196

[**] This work was supported by the Science and Engineering Research Council and a scholarship from the Saudi Arabian Government (S. S. Al-J.).

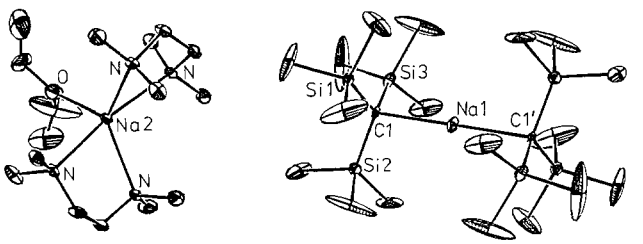


Fig. 1. Structure of the ions in **1** [6]. Important distances [pm] and angles [°] with values for $[Mg\{C(SiMe_3)_3\}_2]$ [9] in parentheses: mean Si–C(M) 181.7(8) (187.7(3)), Si–Me 183.4(10) (188.1(4)), Si-C-Si 115.9(3), (112.6(1)), Me-Si-Me 103.0(5) (105.4(2)).

structures in which the sodium has a coordination number of between 4 and 6.

Comparison of the structure of the anion in **1** with the neutral isoelectronic MgR_2[9] is revealing. As expected the Na–C bond is longer than the Mg–C bond [211.6(2) pm]. The outstanding feature is that the Na atom in **1** is sterically much less shielded than the Mg atom in MgR_2. In the latter (as in the related neutral species MR_2 with M = Hg,[10] Zn,[11] or Mn[12]) one of the Me groups of each Me_3Si group projects in towards the center of the molecule, and the carbon atoms of the six Me_3Si groups interlock, effectively hiding the metal. In **1** one Me of each Me_3Si group points directly away from the metal, and the other two point only slightly inwards. Because of this and the relatively long metal–C bond, the metal is considerably more exposed. The presence of the negative charge (and possibly its partial delocalization over the R groups) may be responsible for the fact that the mean Si–C(M) bond length in **1** is markedly shorter than that in MgR_2, and the mean Si-C-Si angle substantially larger than the corresponding angle in MgR_2. (The mean Si–Me bond length in **1** is also apparently shorter than that in MgR_2, and the mean Me-Si-Me angle is apparently narrower than that in MgR_2, but this may be an artefact arising from the large libration indicated by the elongated thermal ellipsoids of the carbon atoms of the Me groups in **1**.) It is noteworthy that short Si–C(Na) bond lengths (180.6(3) pm) are also found in $[NaCH(SiMe_3)_2]_n$.[8]

In contrast, **2** is readily formed in Et_2O and isolated as solvent-free yellow plates. An X-ray study[13] shows that the solid contains pairs of molecules linked together into chains (Fig. 2).

$Na[C(SiMe_2Ph)_3]$ **2**

The molecules within each pair have similar but not quite identical dimensions; each Na atom is close to the central carbon

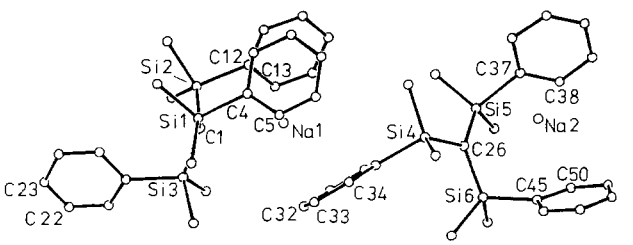


Fig. 2. Molecular structure of **2** [13]. Important distances [pm] and angles [°]: Na1–Cl 275.4(14), Na1–C4 280.9(13), Na1–C5 291.5(14), Na1–C12 280.1(13), Na1–C13 282.0(15), Na1–C32 293.3(13), Na1–C33 286.5(14), Na1–C34 306.7(13), Na2–C22′ 290(2), Na2–C23′ 281(2), Na2–C26 298.3(14), Na2–C37 282.0(13), Na2–C38 290(2), Na2–C45 283.1(14), Na2–C50 301(2), all other Na–C > 310, mean Si–C 181.2(12), Si–Me 187.2(12), Si–Ph 191.4(14), Si1-C1-Si2 119.6(6), Si1-C1-Si3 120.3(6), Si2-C1-Si3 115.0(6), Si4-C26-Si5 120.7(7), Si4-C26-Si6 117.8(7), Si5-C26-Si6 119.8(7). Adjacent pairs of molecules along the chain are related by the *c* glide plane.

atom of the same molecule and to three asymmetrically coordinated Ph groups, two from the same molecule (closest Na–C contact to the *ipso* carbon) and one from an adjacent molecule (closest Na–C contact to *meta* and *para* carbon atoms). The coordination at the central carbon is almost planar (sum of angles 355° for C(1) and 358° for C(26)), as found in [Na(tmen)][CPh_3][14] and $[NaCH(SiMe_3)_2]_n$;[8] in contrast, the methyl anions in solid NaMe are pyramidal.[5]

The structure of **2** may be compared with those of **3**,[15] isolated as a thf adduct, and **4**.[16] In all cases there are significant

$(Me_2PhSi)_3CLi$ **3** $(Me_2PhSi)_3CK$ **4**

interactions between the metal and the phenyl groups of the ligand. As the size of the metal increases these interactions become progressively more important (η^1 in **3**, η^2 or η^4 in **2**, or η^6 in **4**) relative to interactions with the central carbon. This is reflected in physical properties: the sodium compound is more soluble in ether or toluene than the potassium derivative, which suggests that the chains are more readily broken by solvation. The coordination around sodium **2** can be viewed as that of a distorted tetrahedron with one bond to the central carbon and three to Ph groups. As far as we are aware, such a coordination sphere has not been observed in other organosodium compounds, but two η^6-Ph ligands are found in $[Ph_2C{=}CHCPh_2Na]\cdot OEt_2$,[17] two η^6-Ph, and one η^2-Ph ligand in $[(Et_2O)_2Na_2][Ph_2C{-}CPh_2]$,[18] and two η^3- and two η^1-Ph ligands in $K[(PhCH)_2PMe_2]$.[19] One η^6-Ph ligand is found in 1-phenylcyclohexenylsodium · pmdeta.[20]

Experimental Procedure

1: A solution of MeLi (20 cm³, 0.7 M) in Et_2O was added to a cold (0 °C) solution of NaO*t*Bu (13.8 mmol) in Et_2O. The mixture was allowed to warm to 5 °C and kept at that temperature for 10 min. The white precipitate of MeNa was then filtered off, washed three times with 20 cm³ Et_2O at 0 °C, and stirred with Et_2O (30 cm³), tmen (10.0 mmol), and $(Me_3Si)_3CH$ (11.0 mmol) at 0 °C. The mixture was allowed to warm to 20 °C, and stirred for 12 h. The slightly cloudy solution was filtered, solvent removed in vacuum from the filtrate, and the colorless residue washed with petrol (b.p. 40–60 °C, 25 cm³) and recrystallized from cold ether. M.p. 128–130 °C. ^{1}H NMR (C_6D_6, chemical shifts relative to $SiMe_4$, 25 °C): δ = 0.43 (s, 18H, Me_3Si), 1.54 (s, 4H), and 1.69 (s, 12H, tmen); ^{13}C NMR: δ = 3.9 (CSi_3), 8.3 (Me_3Si), 45.4, and 56.6 (tmen); ^{29}Si NMR: δ = −11.1.

2: A solution of $(Me_2PhSi)_3CH$ (5.6 g, 13 mmol) in cold (−10 °C) diethyl ether (40 cm³) was added to solid methylsodium (0.49 g, 13 mmol), and the mixture allowed to warm slowly to 20 °C and then stirred for 12 h. The slightly turbid solution was filtered, and solvent removed under vacuum. The pale yellow solid residue was washed with petrol (b.p. 40–60 °C, 4 × 40 cm³) and recrystallized from hot toluene to give yellow hexagonal plates of **2**. M.p. 195° (decomp). ^{1}H NMR ([D_8]thf, 25 °C): δ = 0.00 (s, 18H, $SiMe_2$), 6.93 (m, 3H, *p*-C, Ph); 7.03 (m, 6H, *m*-C, Ph), 7.79 (m, 6H, *o*-C, Ph). ^{13}C NMR: δ = − 6.4 (CSi_3) 6.93 ($SiMe_2$), 125.4, 126.3, 135.3, 155.1 (Ph). ^{29}Si NMR: δ = −13.9.

Received: December 6, 1993 [Z 6541 IE]
German version: *Angew. Chem.* **1994**, *106*, 1336

[1] C. Eaborn, P. B. Hitchcock, J. D. Smith, A. C. Sullivan, *J. Chem. Soc. Chem. Commun.* **1983**, 827.
[2] C. Eaborn, P. B. Hitchcock, J. D. Smith, A. C. Sullivan, *J. Organomet. Chem.* **1984**, *263*, C23.
[3] N. H. Buttrus, C. Eaborn, P. B. Hitchcock, J. D. Smith, J. G. Stamper, A. C. Sullivan, *J. Chem. Soc. Chem. Commun.* **1986**, 969.
[4] E. Krause, A. von Grosse, *Die Chemie der Metallorganischen Verbindungen*, Bontraeger, Berlin, **1937**, p. 76.
[5] E. Weiss, S. Corbelin, J. K. Cockcroft, A. N. Fitch, *Chem. Ber.* **1990**, *123*, 1629; E. Weiss, *Angew. Chem.* **1993**, *105*, 1565; *Angew. Chem. Int. Ed. Engl.* **1993**, *32*, 1501.
[6] **1**: Crystal data $C_{36}H_{96}ON_4Na_2Si_6$. M = 815.7, monoclinic, space group $C2/c$, a = 13.986(4), b = 18.767(7), c = 20.895(4) Å, β = 93.15(2)°, V = 5476.1 Å³ $Mo_{K\alpha}$ radiation, λ = 0.71069 Å, Z = 4, ρ = 0.99 g cm⁻³, $F(000)$ = 1816, $\mu(Mo_{K\alpha})$ 1.90 cm⁻¹, T = 173 K. 4966 unique reflections measured and 2403 with $|F^2| > 2\sigma(F^2)$ used. No absorption or decay correction. Structure analysis by direct methods with SHELXS-86. Full-matrix least squares refinement with Enraf-Nonius MOLEN programs, non-H atoms anisotropic and H at

calculated positions with $U_{iso} = 1.3\ U_{eq}$ for parent atoms. Final $R = 0.095$, $R' = 0.070$. Further details of the crystal structure investigations are available on request from the Director of the Cambridge Crystallographic Data Centre, 12 Union Road, Cambridge CB21EZ (UK) on quoting the full journal citation.

[7] C. Schade, P. von R. Schleyer, *Adv. Organomet. Chem.* **1987**, *27*, 169.

[8] P. B. Hitchcock, M. F. Lappert, W.-P. Leung, L. Diansheng, T. Shun, *J. Chem. Soc. Chem. Commun.* **1993**, 1386.

[9] S. S. Al-Juaid, C. Eaborn, P. B. Hitchcock, C. A. McGeary, J. D. Smith, *J. Chem. Soc. Chem. Commun.* **1989**, 273.

[10] F. Glockling, N. S. Hosmane, V. B. Mahale, J. J. Swindall, L. Magos, T. J. King, *J. Chem. Res.* **1977**, (S) 116, (M) 1201.

[11] M. Westerhausen, B. Rademacher, W. Poll, *J. Organomet. Chem.* **1991**, *421*, 175.

[12] N. H. Buttrus, C. Eaborn, P. B. Hitchcock, J. D. Smith, A. C. Sullivan, *J. Chem. Soc. Chem. Commun.* **1985**, 1380.

[13] **2**: Crystal data $C_{25}H_{33}NaSi_3$, $M = 440.8$, monoclinic, space group Cc, $a = 9.413(5)$, $b = 15.749(9)$, $c = 33.211(18)$, $\beta = 91.46(5)$, $V = 4921.8$, $Z = 8$, $\rho = 1.19\ g\,cm^{-3}$, $F(000) = 1888$, $Mo_{K\alpha}$ radiation, $\lambda = 0.71069$ Å, $\mu = 2.1\ cm^{-1}$, $T = 173$ K, 4707 unique reflections measured and 2742 with $|F^2| > 2\sigma(F^2)$ used. Absorption correction (DIFABS) 1.36 max., 0.65 min. Structure analysis and refinement as for **1**. Final $R = 0.082$, $R' = 0.075$.

[14] H. Köster, E. Weiss, *J. Organomet. Chem.* **1979**, *168*, 273.

[15] C. Eaborn, P. B. Hitchcock, J. D. Smith, A. C. Sullivan, *J. Chem. Soc. Chem. Commun.* **1983**, 1390.

[16] C. Eaborn, P. B. Hitchcock, K. Izod, A. J. Jaggar, J. D. Smith, *Organometallics*, **1994**, *13*, 753.

[17] H. Bock, K. Ruppert, Z. Havlas, D. Fenske, *Angew. Chem.* **1990**, *102*, 1095; *Angew. Chem. Int. Ed. Engl.* **1990**, *29*, 1042.

[18] H. Bock, K. Ruppert, D. Fenske, *Angew. Chem.* **1989**, *101*, 1717; *Angew. Chem. Int. Ed. Engl.* **1989**, *28*, 1685.

[19] H. Schmidbaur, U. Deschler, B. Milewski-Mahrla, B. Zimmer-Gasser, *Chem. Ber.* **1981**, *114*, 608.

[20] S. Corbelin, J. Kopf, N. P. Lorenzen, E. Weiss, *Angew. Chem.* **1991**, *103*, 875; *Angew. Chem. Int. Ed. Engl.* **1991**, *30*, 825.

Efficient Synthesis of Heteroradialenes by SN′ Reaction**

Rolf Gleiter,* Harald Röckel, Hermann Irngartinger, and Thomas Oeser

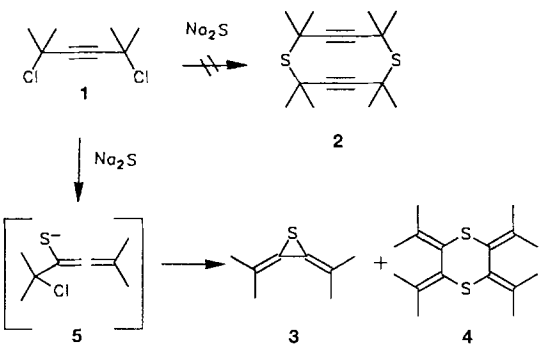
Dedicated to Professor Margot Becke-Goehring on the occasion of her 80th birthday

Radialenes, a relatively new class of compounds first mentioned in the sixties, are not only aesthetically pleasing, but are also interesting objects of study for theoretical chemists or researchers in material science because of their electronic properties.[1] Over the last few years new and simple synthesis have made alicyclic radialenes readily accessible. Photoelectron spectroscopic studies have shown that permethylated alicyclic radialenes have energetically high-lying occupied molecular orbitals.[2] They should therefore be suitable as electron donors in donor–acceptor complexes. These complexes have aroused interest as conductors and organic ferromagnetics.[3] Heteroradialenes have been investigated by Maercker et al.[4] and Ando et al.[5] Thiaradialenes, however, could so far only be synthesized by a multistep procedure,[5] which may be the reason why so little is known about their physical-chemical properties. We now report a synthesis affording thiaradialenes from simple and easily accessible starting materials.

[*] Prof. Dr. R. Gleiter, Dipl. Chem. H. Röckel, Prof. Dr. H. Irngartinger, Dr. T. Oeser,
Organisch-chemisches Institut der Universität
Im Neuenheimer Feld 270, D-69120 Heidelberg (FRG)
Telefax: Int. code +(6221) 564205

[**] This work was supported by the Deutsche Forschungsgemeinschaft, the Fonds der Chemischen Industrie, and the BASF AG, Ludwigshafen.

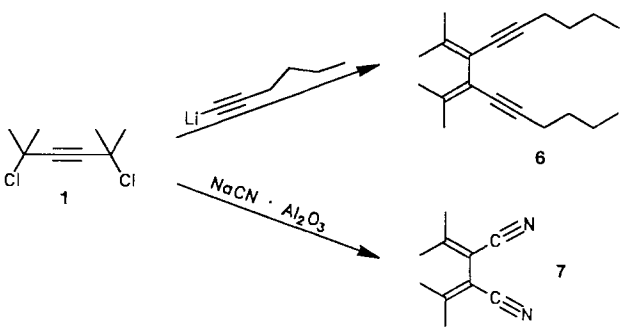
Treatment of 2,5-dimethyl-2,5-dichloro-3-hexyne (**1**) with $Na_2S \cdot Al_2O_3$[6] does not react by nucleophilic substitution at the propargyl C atom to the expected octamethyl-1,6-dithia-3,8-cyclodecadiyne (**2**), but to the methyl derivatives of thia[3]radialene (**3**) and dithia[6]radialene (**4**). These two compounds were first synthesized by Ando et al. by another procedure.[5] This unexpected result can be explained by an SN′ mechanism (Scheme 1). We assume that substitution of chloride



Scheme 1.

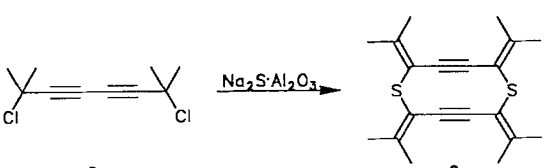
with the sulfide anion by the SN′ reaction leads to compound **5** as an intermediate, which cyclizes in a further step either intramolecularly to **3** or intermolecularly to **4**.

The reaction of **1** with other nucleophiles yields 2,3-disubstituted 1,1,4,4-tetramethyl-1,3-butadienes. As an example the reactions of 1-lithio-1-hexyne and $NaCN \cdot Al_2O_3$ are shown in Scheme 2. They lead exclusively to the SN′ products **6** and **7**.



Scheme 2.

Consequently now, in addition to earlier work of Hopf,[7] 2,3-dialkynyl-substituted 1,3-butadienes are readily available by this easy synthesis. Both products **6** and **7** have interesting cross-conjugated multiple-bond systems and are promising starting materials for reactions at the conjugated triple bonds, or at the diene system.



Scheme 3.

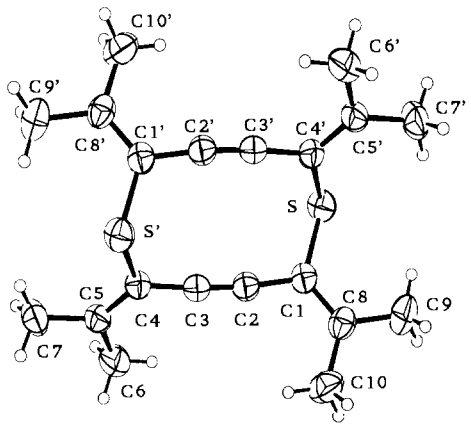
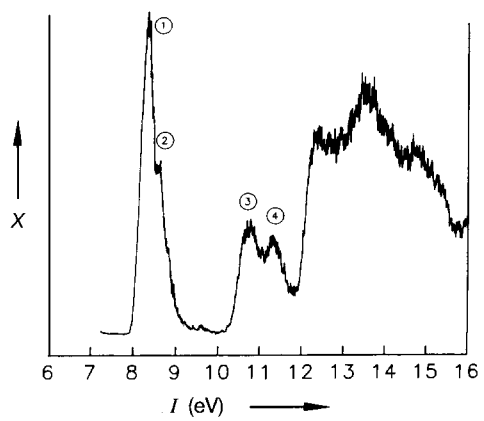


Fig. 1. Crystal structure of **9**; selected bond lengths [Å] and angles [°]: C1–C2 1.430(3), C2–C3 1.201(3), C3–C4 1.426(3), C4–C5 1.346(3), C1–C8 1.346(2), S–C1 1.792(2), S–C4′ 1.798(2); C1-S-C4′ 102.6(1), S-C4′-C5′ 121.4(1), S-C1-C8 121.9(1), S-C1-C2 115.0(1), S-C4′-C3′ 115.1(1), C1-C2-C3 173.9(2), C2-C3-C4 173.6(2), C2-C1-C8 123.0(2), C3-C4-C5 123.3(2), C6-C5-C7 115.6(2), C9-C8-C10 115.2(2).

We consider that the reaction of 2,7-dimethyl-2,7-dichloro-3,5-octadiyne (**8**) with $Na_2S \cdot Al_2O_3$ has particular scope. It is similar to the preceding reactions and furnishes 2,5,7,10-tetra-isopropylidene-1,6-dithia-3,8-cyclodecadiyne (**9**) (Scheme 3). Diyne **9** may also be considered as an expanded dithia[6]radialene. As is apparent from Figure 1 the ten-membered ring in **9** adopts chair conformation.[8] The transannular distance between the triple bonds is 3.085(2) Å. The minor decrease in this distance relative to that in the structurally related 1,6-dithia-3,8-cyclodecadiyne,[9] for which a transannular distance of 3.102(2) Å is reported, is probably due to the exchange of the four sp^3-carbon atoms for sp^2-carbon atoms in **9**. The bond angles at the sp centers are 173.6(2)° and 173.9(2)°; hence, the linear arrangement of the triple bonds is bent by 6.4(2)° and 6.1(2)°, respectively. Similar deformations have been observed for all ten-membered diyne systems known to date.[10] The torsion angle of the two isopropylidene groups along the triple bond is 66.9(3)° (C5–C4···C1–C8).

By photoelectron spectroscopy (PE) and cyclic voltammetry (CV) it is possible to verify that the obtained radialenes, especially **3** and **4**, are indeed electron-rich π systems. At the top of Figure 2 the He(I)-PE spectrum of **3** is shown and at the bottom the cyclic voltammograms of **3** and **4**. In Table 1 the first vertical ionization energies are listed.



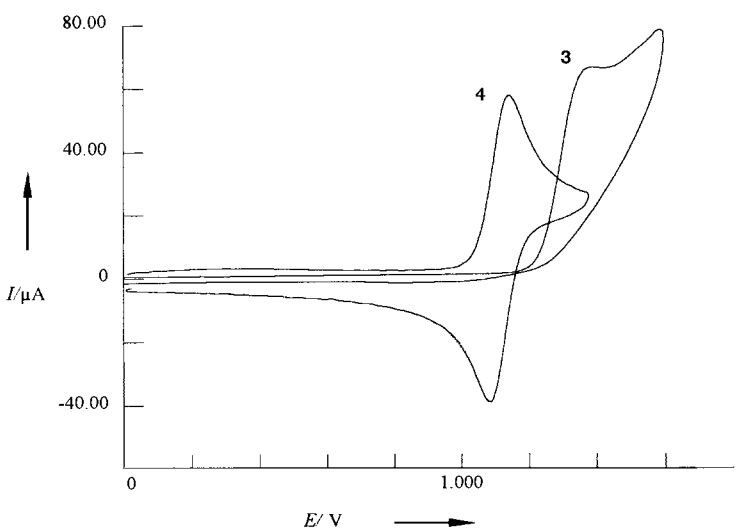


Fig. 2. Top: He(I)-PE spectrum of **3**. x = count rate. Bottom: Cyclic voltammograms of **3** and **4** in $CH_2Cl_2/(n\text{Bu})_4N\ PF_6$; scan rate: 100 mV/s^{-1}, reference electrode: saturated calomel electrode.

Table 1. Vertical ionization energies and oxidation potentials of radialenes **3** and **4**.

thia[3]radialene (**3**)	dithia[6]radialene (**4**)
ionization energies	
8.0 eV	7.1 eV
8.3 eV	7.5 eV
10.5 eV	8.3 eV
11.1 eV	9.1 eV
oxidation potentials [a]	
1600 mV	1115 mV

[a] The oxidation potentials were measured with a HEKA potentiostat (PG 28) in CH_2Cl_2 as solvent and $(n\text{Bu})_4N\ PF_6$ as electrolyte. The working electrode was a Metrohm disk electrode (radius = 3 mm) and reference electrode a saturated calomel electrode (SCE), which was separated from the call by a frit and a luggin capillary. The oxidation potential of ferrocene/ferrocenium (480 mV) was taken as standard.

The PE spectrum of **3** shows a sharp band at 8.0 eV, assigned to the sulfur 3p lone pair. The following band at 8.3 eV represents the HOMO of the tetramethyl butadiene fragment. The next two bands at 10.5 and 11.1 eV are assigned to Walsh-like orbitals arising from the 3p orbital of sulfur and the two carbon atoms of the three-membered ring. While the first ionization energy of **3** is similar to that of other sulfides,[11] there is a significant decrease to 7.1 eV in the case of **4** that can be explained by interaction of the sulfur 3p lone pairs with the butadiene system. The relatively high-lying HOMO is also observable by cyclic voltammetry. Thia[3]radialene **3** shows an irreversible oxidation at 1600 mV, as is common for alicyclic radialenes,[1] but **4** shows a reversible single-electron oxidation at 1115 mV (vs SCE).

The reactions described in this paper allow the investigation of the chemistry of a number of new radialenes. Furthermore they have made possible the simple synthesis of 2,3-dialkynyl-1,3-butadienes, a class of interesting compounds that have thus far been difficult to investigate.

Experimental Procedure

3 and **4**: To a suspension of $Na_2S \cdot Al_2O_3$ (19.2 g) [6] in 80 mL THF/DMPU (10:1, DMPU = *N*,*N*′-dimethyl-2,6-diazacyclohexanone) was added dropwise under reflux **1** (1.78 g, 10 mmol) dissolved in 30 mL of the solvent. After 12 h the solution was distilled under reduced pressure to recover the starting material (50%). After chromatography of the residue (silica/cyclohexane) **3** (420 mg, 3 mmol) and **4**

(300 mg, 1.07 mmol) were isolated. **3**: ^{1}H NMR: δ = 1.98 (s, 6H), 2.07 (s, 6H); ^{13}C NMR: δ = 22.64, 23.00, 111.37, 115.00; EI-MS: *m/z*: 140 (M^+); **4**: ^{1}H NMR: δ = 1.84 (s, 6H), 1.67 (s, 6H); ^{13}C NMR: δ = 21.06, 21.90, 125.55, 130.43; EI-MS: *m/z*: 280 (M^+)

6 (see also ref. [12]): 1-Hexyne (1.64 g, 20 mmol) was dissolved in THF (50 mL) at -78 °C and deprotonated with *n*-butyllithium (1.6 M in *n*-hexane). This solution was added dropwise to a refluxing solution **1** (890 mg, 5 mmol) in THF/DMPU (5:2) 60 mL. After 12 h the reaction was quenched with water and extracted with ether (3 × 50 mL), dried over Na_2SO_4, and purified by chromatography (silica/cyclohexane). Isolated yield of **b**: 150 mg (0.55 mmol, 11%). ^{1}H NMR: δ = 0.89 (t, 6H, ^3J = 7.1 Hz), 1.38–1.59 (m, 8H), 1.64 (s, 6H), 1.93 (s, 6H), 2.33 (t, 4H, ^3J = 6.9 Hz); ^{13}C NMR: δ = 13.66, 19.39, 20.62, 21.97, 22.62, 31.15, 79.54, 92.20, 116.56, 141.12; EI-MS: *m/z* 270 (M^+)

7: Hexyne **1** (1.78 g, 10 mmol) dissolved in 30 mL of the solvent mixture was added to a suspension of NaCN · Al_2O_3 (1:1 4.0 g) in THF/DMPU (10:1) 80 mL under reflux within 5 h. After 12 h the solution was worked up as above. After chromatography (silica/cyclohexane) **7** was isolated as a colorless liquid. Yield: 976 mg (6.2 mmol, 61%). ^{1}H NMR: δ = 1.88 (s, 6H), 2.16 (s, 6H); ^{13}C NMR: δ = 21.36, 24.04, 103.05, 116.06, 160.45; EI-MS: *m/z*: 160 (M^+)

9: To a suspension of Na_2S · Al_2O_3 in the solvent mixture described above, **8** (2.03 g, 10 mmol) in 30 mL of the solvent was added, and the mixture was heated at reflux for 12 h. **9** was isolated as above in 10% yield (328 mg) after chromatography (silica/cyclohexane). ^{1}H NMR: δ = 2.04 (s, 12H), 2.08 (s, 12H); ^{13}C NMR: δ = 21.97, 24.11, 93.56, 111.58, 147.14; CI-MS: *m/z* 328 (M^+). The crystals for X-ray analysis precipitated from CH_2Cl_2 at −30 °C.

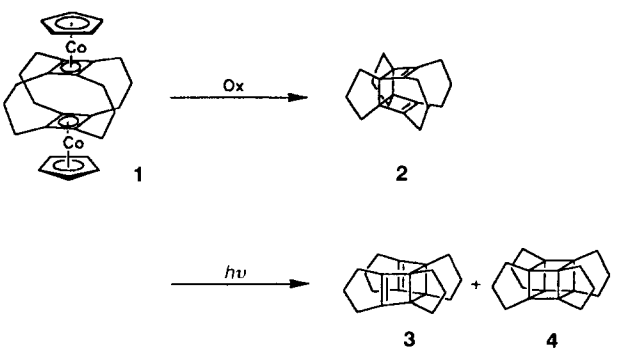
Received: January 4, 1994 [Z 6670 IE]
German version: *Angew. Chem.* **1994**, *106*, 1340

[1] H. Hopf, G. Maas, *Angew. Chem.* **1992**, *104*, 953–1122; *Angew. Chem. Int. Ed. Engl.* **1992**, *31*, 931–954.
[2] T. Bally, E. Haselbach, *Helv. Chim. Acta* **1978**, *61*, 754–761.
[3] T. Sugimoto, H. Awaji, Y. Misaki, Z. Yoshida, Y. Kai, H. Nakagawa, N. Kasai, *J. Am. Chem. Soc.* **1985**, *107*, 5792–5793.
[4] A. Maercker, W. Brieden, *Chem. Ber.* **1991**, *124*, 933–938, and references therein.
[5] W. Ando, Y. Haniu, T. Takata, *Tetrahedron Lett.* **1981**, *22*, 4815–4816; W. Ando, Y. Haniu, T. Takata, K. Ueno, *ibid.* **1985**, *26*, 3019–3022.
[6] B. Czech, S. Quici, S. L. Regen, *Synthesis* **1980**, *113*.
[7] H. Hopf, H. Lipka, *Chem. Ber.* **1991**, *124*, 2075–2084.
[8] X-Ray analysis of **9**: colorless crystals from CH_2Cl_2; crystal size 0.45 × 0.45 × 0.15 mm; monoclinic; space group $P2_1/c$; Z = 2; the molecule is positioned upon a crystallographic center of symmetry; a = 9.042(1) Å, b = 12.713(2) Å, c = 8.248(1) Å, β = 99.54(1)°; V = 934.9(4) Å^3; ρ_{calcd} = 1.17 Mgm^{-3}; $2\theta_{max}$ = 56°; $Mo_{K\alpha}$; λ = 0.71071 Å; graphite monochromator; ω 2θ scan; T = 293 K; 2371 measured reflections, 2371 independent reflections, 1477 observed [$I > 2.5\sigma(I)$]; Lp-correction, numerical absorption correction μ = 0.268 mm^{-1} (T_{min} = 0.958, T_{max} = 0.807); direct methods (MULTAN), MolEN program package (Enraf Nonius); full-matrix least squares refinement (F^2), S and C atoms were refined anisotropically, H atoms were refined isotropically, variables = 148, R = 0.037, R_W = 0.045, S = 1.734, $(\Delta/\sigma)_{max}$ = < 0.01, $(\Delta\rho)_{max}$ = 0.175 e Å^{-3}; $(\Delta\rho)_{min}$ = 0.159 e Å^{-3}. Further details of the structure investigation are available on request from the Fachinformationszentrum Karlsruhe, D-76344 Eggenstein-Leopoldshafen on quoting the depository number CSD-380017.
[9] G. Eglinton, I. A. Lardy, R. A. Raphael, G. A. Sim, *J. Chem. Soc.* **1964**, 1154–1158; R. Gleiter, S. Rittinger, H. Irngartinger, *Chem. Ber.* **1991**, *124*, 365–369.
[10] R. Gleiter, *Angew. Chem.* **1992**, *104*, 29–46, *Angew. Chem. Int. Ed. Engl.* **1992**, *31*, 27–44.
[11] R. Gleiter, J. Spanget-Larsen, *Top. Curr. Chem.* **1979**, *86*, 139–195, and references therein.
[12] Another synthesis of 2,3-dialkynyl-1,3-butadienes and some reactions of these new types of compounds have been reported recently: H. Hopf, M. Theurig, *Angew. Chem.* **1994**, *106*, 1173; *Angew. Chem. Int. Ed. Engl.* **1994**, *33*, 1099.

New Types of Metal-Stabilized Cyclobutadiene Superphanes**

Rolf Gleiter,* Heinrich Langer, and Bernhard Nuber

The metal-catalyzed trimerization of alkynes to aromatic compounds is a useful reaction.[1–3] Cobalt-catalyzed [2 + 2 + 2] cycloadditions are sometimes accompanied by a side reaction, the dimerization to metal-stabilized cyclobutadiene complexes. These complexes are considered inert towards further cycloaddition reactions.[4] If cyclic diynes are used as starting materials, the tricyclic cyclobutadiene complexes are usually the main product.[5, 6] In the case of the reaction of [CpCoL$_2$] (Cp = η^5-cyclopentadienyl; L$_2$ = 2CO, 1,5-cyclooctadiene (cod)) with 1,6-cyclodecadiyne, 1,8-cyclotetradecadiyne, or 1,10-cyclooctadecadiyne an intermolecular reaction is even possible, which leads to CpCo-stabilized superphanes such as **1**.[6] These species are not only aesthetically attractive, but also useful for preparing cage compounds such as the fourfold bridged derivatives of tricyclo[4.2.0.0^{2,5}]octa-3,7-diene (**2**), its isomer (**3**), and the cubane derivative (**4**).[6]



Scheme 1. Ox = oxidation.

In connection with mechanistic investigations of the photochemistry of **2** we wanted to synthesize superphanes with different chain lengths. To this end the recently published stepwise path to metal-stabilized superphanes seemed appropiate.[7] In this paper we report on the first verification of this concept to yield a CpCo-stabilized cyclobutadiene superphane with different chain lengths. In addition we describe another new type of superphane and a novel CpCo complex of a fourfold bridged bicyclo[4.2.0]octa-2,4,7-triene.

Starting point of our synthesis is 6-undecynol (**5**),[8] which was converted into the tricyclic cyclobutadiene complexes (**6**) by reaction with [CpCo(cod)] in 70% yield (Scheme 2). The mixture of the isomeric alcohols **6** was oxidized to the diketone **7** by the Oppenauer procedure with acetone in 83% yield. In the next step the diketone **7** was transformed into the bisselenadiazoles **8a**/**8b** in 35% yield with a procedure first devised by Lalezari et al.[9] Without further purification the mixture **8a**/**8b** was treated with *n*BuLi at −40 °C to give a 1:1 mixture of the tricyclic diynes **9a**/**9b** in 70% yield.

[*] Prof. Dr. R. Gleiter, Dipl.-Chem. H. Langer
Organisch-chemisches Institut der Universität
Im Neuenheimer Feld 270, D-69120 Heidelberg (FRG)
Telefax: Int. code + (6221)56-4205
Dr. B. Nuber
Anorganisch-chemisches Institut der Universität Heidelberg

[**] This work was supported by the Deutsche Forschungsgemeinschaft (SFB 247), the Fonds der Chemischen Industrie, and the BASF Aktiengesellschaft (Ludwigshafen).